985/ V.23/pt. 1

VOLUME 23
1985
ACC. NOS N85-10001 TO N85-36162

S & T REFERENCE
LD C
U.S. DOCUMENTS
NEWARK PUBLIC LIBRARY

STAR

AN ABSTRACT JOURNAL

Scientific and Technical Aerospace Reports

Annual Index 1985

Part One
SUBJECT

PRODUCED BY THE
SCIENTIFIC AND TECHNICAL
INFORMATION
BRANCH

NASA

NAS 1.9/5:

NATIONAL AERONAUTICS AND SPACE ADMINISTRATION

WHAT YOU CAN DO FOR *STAR*

All users of this abstract service are urged to forward reports to be considered for announcement in *STAR*. This will aid NASA in its efforts to provide the fullest possible coverage of all scientific and technical publications that might support aeronautics and space research and development. If you have prepared relevant reports (other than those that you will transmit to NASA, DoD, or DOE through the usual contract- or grant-reporting channels), please send them for consideration to the NASA Scientific and Technical Information Facility, P.O. Box 8757, B.W.I. Airport, Maryland 21240.

Reprints of journal articles, book chapters, and conference papers are also welcome. These will be considered for announcement in *STAR's* companion journal, *International Aerospace Abstracts*.

You may specify a particular source to be included in a report announcement if you wish; otherwise the report will be placed on public sale at the National Technical Information Service. Copyrighted publications will be announced but not distributed or sold.

PURCHASE OF *STAR*

The semimonthly issues are available postpaid on subscription and in single copy from the Superintendent of Documents, United States Government Printing Office, Washington, D.C. 20402, United States of America.

PUBLISHED BY:

UNITED STATES GOVERNMENT
NATIONAL AERONAUTICS AND SPACE ADMINISTRATION
SCIENTIFIC AND TECHNICAL INFORMATION BRANCH

Scientific and Technical Aerospace Reports, Volume 23, is prepared by the NASA Scientific and Technical Information Facility operated for the National Aeronautics and Space Administration by RMS Associates.

The Administrator of the National Aeronautics and Space Administration has determined that the publication of this periodical is necessary in the transaction of the public business required by law of this Agency. Use of funds for printing this periodical has been approved by the Director of the Office of Management and Budget through March 22, 1988.

US ISSN 0036-8741

SPECIAL NOTICE

The abstract sections of the semimonthly *STAR* journals can be bound separately. Individual abstracts can be located readily be means of the page numbers given at each entry, e.g., p 2207. To assist the user in binding *STAR* Volume 23, four (4) title pages are included in the back of Part I of the Annual Index.

For sale by the Superintendent of Documents, U.S. Government Printing Office Washington, D.C. 20402

READEX FICHE best copy available

VOLUME 23 NUMBERS 1-24

Scientific and Technical Aerospace Reports

Annual Index (Part I) January – December 1985

TABLE OF CONTENTS

Page

PART I

Introduction iii
Subject Index A-1

PART II

Introduction iii
Personal Author Index B-1
Corporate Source Index C-1
Contract Number Index D-1
Report/Accession Number Index E-1

INTRODUCTION

WHAT STAR ANNUAL INDEXES ARE

This Annual Index is an edited consolidation of the indexes to the individual issues of *Scientific and Technical Aerospace Reports (STAR)* for the calendar year 1985 (Volume 23 Numbers 1 through 24). For the convenience of the user, it is divided into two parts, each bound separately. Part I contains the Subject Index. Part II contains the Personal Author Index, Corporate Source Index, Contract Number Index, and Report/Accession Number Index. The Annual Index supersedes the semimonthly indexes previously issued during 1985.

Each entry in this index includes a group of identifying numbers in the following form: 23 p 3906 N85-34200. The first two digits (23) identify the issue in which the document was announced. The "p" and the four digits that follow (3906) refer to the page number, in the designated issue, on which the abstract of the document appears. The next group of numbers (N85-34200) is the NASA Accession Number, a unique identification number assigned by NASA to each document that was acquired, indexed, and announced in *STAR* during the year.

In addition to these identifying numbers each entry in the Subject Index contains a title or title and title extension. Each entry in the Personal Author and Corporate Source Indexes contains the title of the document.

At the beginning of each index in this cumulation, a typical listing is illustrated with each of its elements identified to assist the reader in using the different types of index entries.

HOW TO USE THE SUBJECT INDEX

Subject terms in this cumulative index are arranged alphabetically, and are supplemented with cross-references which are intended to serve as directions that will enable the user to modify, enlarge, or narrow his search in accordance with his specific interests. The subject headings have been selected from the latest revision of the *NASA Thesaurus*. Two types of cross-references are used:

1. Use (U) references direct the user to alternate headings under which material on the subject may be found. For example:

   ANNULAR JETS
   U ANNULAR FLOW
   U JET FLOW
   COLUMBIAN
   U NIOBIUM

2. Narrower Term (NT) references refer the user to more specific headings in the same subject area, under which additional material on the subject may be found. For example:

   EMISSION
   NT ELECTRON EMISSION
   NT NEUTRON EMISSION
   NT THERMAL EMISSION

Finally, a searcher should use the titles and title extensions in the index to narrow further his quest for particular items. This is because subject terms can readily refer to more than one class of document. For example:

CATHODES
Cesium plasma cathodes as sources of high intensity electron beams
Cathode material testing in electrochemical half cells

This illustrates a case where two references on different topics are listed under the same subject term.

HOW TO USE THE PERSONAL AUTHOR INDEX

All personal authors identified in the abstract-section citations in the individual *STAR* issues appear in this index. Differences in transliteration schemes may require multiple searching of the index for variants of an author's name. For example:

EMELIANOV, M. D.
YEMELYANOV, M. D.

HOW TO USE THE CORPORATE SOURCE INDEX

The corporate source index entries are abridged versions of the corporate sources used in the abstract-section citations in the individual issue supplements. The corporate source supplementary (organizational component) does not appear in the index. For example:

PRINCETON UNIV., N.J. DEPT. OF CHEMICAL ENGINEERING.
(Corporate source at citation)
PRINCETON UNIV., N.J.
(Corporate source index entry)

HOW TO USE THE CONTRACT NUMBER INDEX

All contract numbers that are identified in the abstract-section citations in the individual *STAR* issues appear in this index. Changes by agencies in the style in which contract numbers are presented may require multiple searching for variants. For example:

AF 33(615)-67-C-1758
F33615-67-C-1758

HOW TO USE THE REPORT/ACCESSION NUMBER INDEX

All report numbers that have been assigned by the corporate source, monitoring activity, or cataloging activity appear in this index. Variations in initial input may result in different report number series. For example:

TP-924
ONERA-TP-924

A COMPREHENSIVE INFORMATION SERVICE

The National Aeronautics and Space Administration makes the results of worldwide research and development activities in aeronautics, space, and supporting disciplines promptly available to participants in its programs. NASA's scientific and technical information system now contains over two million documents, which are abstracted, indexed, and obtained through retrieval and dissemination services. These services which include the abstract journal, *Scientific and Technical Aerospace Reports (STAR)*, are described fully in a bulletin, *The NASA Scientific and Technical Information System ... and How to Use It*, available at no charge from the NASA Scientific and Technical Information Facility, P.O. Box 8757, B.W.I. Airport, Maryland 21240.

AVAILABILITY OF DOCUMENTS

Information concerning the availability of documents announced in the *STAR* issues covered in this index is found in the Introduction to the most currently issued semimonthly issue.

PUBLIC COLLECTIONS OF NASA DOCUMENTS

DOMESTIC: NASA and NASA-sponsored documents and a large number of aerospace publications are available to the public for reference purposes at the library maintained by the American Institute of Aeronautics and Astronautics, Technical Information Service, 555 West 57th Street, 12th Floor, New York, New York 10019.

EUROPEAN: An extensive collection of NASA and NASA-sponsored publications is maintained by the British Library Lending Division, Boston Spa, Wetherby, Yorkshire, England for public access. The British Library Lending Division also has available many of the non-NASA publications cited in *STAR*. European requesters may purchase facsimile copy or microfiche of NASA and NASA-sponsored documents, those identified by both the symbols # and * from ESA — Information Retrieval Service European Space Agency, 8-10 rue Mario-Nikis, 75738 CEDEX 15, France.

FEDERAL DEPOSITORY LIBRARY PROGRAM

In order to provide the general public with greater access to U.S. Government publications, Congress established the Federal Depository Library Program under the Government Printing Office (GPO), with 50 regional depositories responsible for permanent retention of material, inter-library loan, and reference services. Over 1,300 other depositories also exists. A list of the regional GPO libraries appears on the inside back cover.

SUBJECT INDEX

SCIENTIFIC AND TECHNICAL AEROSPACE REPORTS VOLUME 23 NUMBERS 1-24

Typical Subject Index Listing

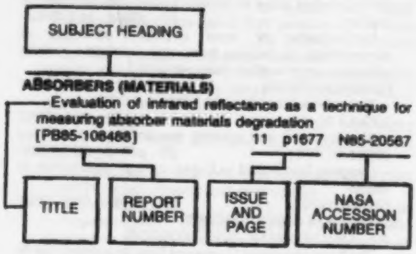
SUBJECT HEADING
ABSORBERS (MATERIALS)
Evaluation of infrared reflectance as a technique for measuring absorber materials degradation
[PB85-108488] 11 p1677 N85-20567
TITLE
REPORT NUMBER
ISSUE AND PAGE
NASA ACCESSION NUMBER

The subject heading is the key to the subject content of the document. Titles, issues, page numbers, report numbers, and accession numbers of pertinent documents are provided under each subject heading. When the title is insufficiently descriptive of the document content, a title extension has been added, separated by three hyphens. The report number helps to indicate the type of document cited (e.g., NASA report, translation, NASA contractor report). The issue and page identify the *STAR* issue in which the document was announced and the page number on which the citation appears. The accession number denotes the number by which the citation is identified on that page. The titles are arranged under each subject heading in ascending accession number order. The subject headings have been selected from the latest revision of the *NASA Thesaurus* (NASA SP-7051).

A

A STARS
Hyades moving group 05 p0740 N85-14757
The velocity-age relation for B and A stars 05 p0740 N85-14762
Kinematics of B and A stars 05 p0741 N85-14766
A type stars as probes of the local interstellar medium 06 p0874 N85-15550

A-7 AIRCRAFT
The development of a performance and mission planning program for the A-7E aircraft
[AD-A151717] 15 p2471 N85-25258

A-10 AIRCRAFT
Peripheral vision horizon display on the single seat night attack A-10 01 p0009 N85-10053
Performance evaluation of A-10 aircraft mainteance units and aircraft using constrained facet analysis
[AD-A146955] 07 p0893 N85-15680

A-310 AIRCRAFT
Statistical study of the dynamic analysis of the workload in the A310 certification campaign 16 p2844 N85-27531

A-320 AIRCRAFT
Description of MBB computerized design techniques for A320 06 p1141 N85-17194
Design of the nacelle for the A-320 aircraft
[SNIAS-851-111-111] 20 p3393 N85-31046

ABEL FUNCTION
A continuous Helson surface in R3 11 p1698 N85-20674

ABERRATION
Effect of aberration in optical system on illuminance distribution over image of strip in semicoherent light 06 p0777 N85-14970
Light scattered from polished optical surfaces: Wings of the point spread function 08 p1252 N85-17911
Aberration characteristics of plane-parallel compensator plate 14 p2276 N85-24100
Stimulated Brillouin scattering reflectivity in the presence of various aberrators
[AD-A151750] 15 p2563 N85-25812
Method of measuring spherical aberration and apparatus therefor
[AD-D011706] 19 p3367 N85-30882
Theoretical modeling of laser induced optical degradation
[AD-A155302] 21 p3592 N85-32323
New method for correcting chromatism of mirror-lens objectives 21 p3696 N85-32965

ABILITIES
An investigation of the effect of correlated abilities on observed test characteristics
[AD-A144869] 01 p0113 N85-10765
Trends in skill and accuracy of National Weather Service pop forecasts
[PB84-229053] 06 p0840 N85-15335
Training high performance skills: Fallacies and guidelines
[AD-A148574] 08 p1198 N85-17545
A theorem on the optimal allocation of effort
[AD-A148028] 08 p1211 N85-17623

ABIOGENESIS
Estuaries of the Cape. Part 2: Synopses of available information on individual systems. Report 13: Silvermine (CSW 3)
[CSIR-RR-412-PT-2] 01 p0086 N85-10582
Estuaries of the Cape. Part 2: Synopses of available information on individual systems. Report no. 16: Eerste (CSW 6)
[CSIR-RR-415-PT-2] 01 p0087 N85-10585

ABLATION
A T-matrix theory of galactic heavy-ion fragmentation
[NASA-TP-2363] 08 p1221 N85-17690
Laser ablation studies using RIS
[DE85-001118] 09 p1326 N85-18336
Atmospheric profile imprint in firewall ablation coefficient 11 p1662 N85-20473
Charge-to-mass dispersion methods for abrasion-ablation fragmentation models
[NASA-TM-86340] 11 p1726 N85-20857
Alternate nozzle ablative materials program
[NASA-CR-175658] 14 p2246 N85-23924
Examination of a method for predicting the properties of railgun plasmas
[AR-004-322] 17 p3039 N85-28799
Numerical studies of ablation and ionization of railgun materials
[DE85-010741] 19 p3223 N85-29983
One method of solving the problem of unsteady heat exchange of a body and its ablation 22 p3733 N85-33146
Laser effects on opaque targets. Part 2C: Thermal effects of a time-variable beam intensity
[ISL-R-105/84-PT-2C] 22 p3791 N85-33486
Thermal transport measurements of UV laser irradiated spherical targets
[DE85-011038] 23 p3931 N85-34365
A study of the chemistry of alkali metals in the upper atmosphere
[AD-A156349] 24 p4117 N85-35524

ABLATIVE MATERIALS
Thermal design of the space shuttle solid rocket booster 06 p1103 N85-16976
Adequacy of metal ablation process with laser radiation and a shock-compressed plasma 13 p2026 N85-22706
Experimental study of enthalpy of quasimonocrystal of graphite and carbon glass in temperature range of 2890-3818 deg K 13 p2036 N85-22751
Seven-wavelength pyrometer for determining surface temperature of ablation materials
[NASA-TM-77832] 14 p2305 N85-24268
Thermal protection systems for reentry vehicles
[CNES-NT-113] 23 p3900 N85-34157

ABORT TRAJECTORIES
Study of several factors affecting crew escape trajectories from the Space Shuttle Orbiter at low-subsonic speeds
[NASA-TM-86303] 10 p1428 N85-19008

ABRASION
Structure and wear workshop colloquium 01 p0054 N85-10356
The influence of the carbide distribution on the abrasive wear of ledeburitic chromium steels 01 p0054 N85-10359
Structure and abrasive resistance of iron based alloys rich in hardening components 01 p0054 N85-10360
Microstructural effects in abrasive wear
[DE84-016155] 04 p0509 N85-13247
A T-matrix theory of galactic heavy-ion fragmentation
[NASA-TP-2363] 08 p1221 N85-17690
Effect of microstructure on solid particle erosion in multiphase materials
[DE85-000426] 11 p1608 N85-20109
Charge-to-mass dispersion methods for abrasion-ablation fragmentation models
[NASA-TM-86340] 11 p1726 N85-20857
A comparison of terrestrial saltation flux in the laboratory and the field 13 p2189 N85-23582
Abrasive cutting-off wheel 15 p2568 N85-25843
Microstructure-abrasive wear characteristics of low carbon dual phase steels
[DE85-010968] 19 p3239 N85-30083
Impact dynamics research on composite transport structures
[NASA-TM-86391] 19 p3264 N85-30367
Three body abrasive wear in various metal combinations 23 p3906 N85-34200

ABRASION RESISTANCE
Experimental AC (Asphalt Concrete) overlays of PCC pavement
[PB84-218171] 03 p0342 N85-12203
Effects of B, Ti and Ta implantation on the wear resistance of Fe and Ni-plated Fe
[AD-A149947] 12 p1806 N85-21330
Effect of zero-wear in friction pairs operating in abrasive media 13 p2045 N85-22801
Role of fluid lubricant-coolant in fine grinding of optical glass by diamond tool 14 p2290 N85-24125
Wear improvement in titanium alloys by ion implantation
[AD-D011694] 19 p3239 N85-30081

ABRASIVES
Abrasive products study
[PB84-223635] 01 p0033 N85-10205
Effect of microstructure on solid particle erosion in multiphase materials
[DE85-000426] 11 p1608 N85-20109
The effect of abrasive blasting on the fatigue and corrosion of an aluminium-copper alloy
[AD-A154954] 21 p3566 N85-32182

ABSORBENTS
Desorption efficiences of vapor phase polynuclear aromatic compounds on solid adsorbents
[DE85-001303] 10 p1436 N85-19052
The effects of water and hydrogen on materials used in integrated circuit packages
[AD-A151893] 15 p2518 N85-25529
Flight-service program for advanced composite rudders on transport aircraft
[NASA-CR-174537] 19 p3217 N85-29950
Improved catalysts for liquid hydrocarbon fuels from syngas
[DE85-011062] 20 p3421 N85-31234
Molecular and macromolecular sieving by asymmetric ultrafiltration membranes
[PB85-157766] 24 p4077 N85-35266

ABSORBERS (MATERIALS)
Evaluation of infrared reflectance as a technique for measuring absorber materials degradation
[PB85-108488] 11 p1677 N85-20567
Correctness of reflection characteristics of radio absorbent materials 13 p2081 N85-22995
Capture of liquid hydrogen boiloff with metal hydride absorbers
[NASA-CR-175677] 14 p2249 N85-23939
Measured acoustic properties of variable and low density bulk absorbers
[NASA-TM-87065] 19 p3351 N85-30770
Choice of optimum saturating absorber for YAG passive mode-locking laser 21 p3685 N85-32893

ABSORPTANCE
Changes in spectral properties of detached leaves
[E85-10042] 07 p0963 N85-16243
Effect of integration time on precision of absorbances measured with a diode array UV-VIS spectrophotometer
[AD-A146952] 07 p1043 N85-16624
A calorimetric approach for measuring emittance and normal spectral absorptance at elevated temperatures
[AD-A151292] 15 p2651 N85-26351
Thermal consequences of localized SAR from RFR exposures 16 p2775 N85-27130
ABSORPTION
Water absorption and conductivity in poly(ethylene oxide)-lithium tetrafluoroborate films
[AD-A147969] 10 p1450 N85-19138
Nebulization reflux concentrator
[NASA-CASE-LAR-13254-1] 11 p1615 N85-20154
Collaborative shock tube studies of benzene pyrolysis
[DE85-006347] 14 p2253 N85-23962
Process for clarification of water
[DE85-007864] 17 p2923 N85-28023
Chromophores with auxochrome-like function
[NASA-TM-77849] 20 p3421 N85-31233
Quasi-steady-state melting mode during combined laser irradiation of semiconductor materials
21 p3682 N85-32874
ABSORPTION BANDS
U ABSORPTION SPECTRA
ABSORPTION COEFFICIENT
U ABSORPTIVITY
ABSORPTION COOLING
Mathematical models for the boiling diagram of the ideal two-component mixture
[DFVLR-FB-84-22] 04 p0471 N85-13000
Performance evaluation of an active solar cooling system utilizing low cost plastic collectors and an evaporatively-cooled absorption chiller
[DE84-010813] 12 p1880 N85-21798
Testing and further development of a solar absorption cooling plant
[BMFT-FB-T-84-264] 15 p2588 N85-25954
Ten degree Kelvin hydride refrigerator
[NASA-CASE-NPO-16393-1-CU]
18 p3065 N85-29084
ABSORPTION CROSS SECTIONS
Remote sensing of atmospheric gases with CO2 lasers. Continuation and conclusion of spectroscopic investigations
[BMFT-FB-W-84-030] 07 p0989 N85-16285
MSG-7: Molecular absorption processes related to the penetration of ultraviolet solar radiation into the middle atmosphere 11 p1658 N85-20449
Chemical kinetics and photochemical data for use in stratospheric modeling. Evaluation number 6
[NASA-CR-175564] 12 p1888 N85-21849
Workshop report on new directions in soft X-ray photoabsorption
[DE85-006150] 14 p2419 N85-24923
Tables of nuclear cross sections for galactic cosmic rays: Absorption cross sections
[NASA-RP-1134] 16 p2864 N85-27665
Hydrogen absorption in metals: A field ion microscopy study
[DE85-010299] 18 p3076 N85-29026
Opticals constant at X-ray wavelengths
[DE85-009743] 19 p3355 N85-30795
Absorption of 10.6 micrometer laser radiation in electron-hole condensate in germanium
21 p3681 N85-32870
An attempt to detect induced neutron capture in laser radiation field 21 p3690 N85-32928
Determination of band oscillator strengths of atmospheric molecules from high resolution vacuum ultraviolet cross section measurements
[NASA-CR-176150] 22 p3814 N85-33624
Monte Carlo learning-biasing experiment with intelligent random numbers
[DE85-010713] 22 p3834 N85-33742
Dissociative and double photoionization cross sections of NO from threshold to 120 A
[NASA-CR-176185] 24 p4147 N85-35713
ABSORPTION SPECTRA
NT FRAUNHOFER LINES
Middle infrared spectral studies of geologic materials in their natural state using photothermal beam deflection spectroscopy
[AD-A144694] 01 p0120 N85-10620
Nonlinear absorption of laser radiation in InP and in GaAs 02 p0266 N85-11740
Simultaneous measuring absorption spectrometer
[BMFT-FB-T-84-132] 03 p0365 N85-12339
Ice-soil mixtures: Visual and near-infrared remote sensing tuchniques
[NASA-CR-174067] 04 p0525 N85-13358
Saturation phenomena in LIF measurements, appendix B 05 p0676 N85-14339
Evidence for pairing of implanted nitrogen in silicon
[DE84-015622] 06 p0866 N85-15517
Absorption line studies and the distribution of neutral gas in the local interstellar medium
06 p0873 N85-15544
A type stars as probes of the local interstellar medium
06 p0874 N85-15550
Optical observations of nearby interstellar gas
06 p0875 N85-15557
Observations of absorption lines from highly ionized atoms 06 p0876 N85-15562
Detection of narrow C 4 and Si 4 absorption features in spectra of stars within 200 pc f the Sun
06 p0876 N85-15564
The smallest sizes of diffuse interstellar clouds
06 p0878 N85-15578
Stromgren trails of hot white dwarfs
06 p0879 N85-15589
Measurement of soft X-ray absorption spectra with a fluorescent ion chamber detector
[AD-A142213] 07 p0922 N85-1583
Narrow absorption components in Be star winds
08 p1232 N85-17760
Low excitation absorptions in the spectrum of the quasar PKS 1327-206 due to the galaxy MCG 03-34-085
08 p1237 N85-17801
The extragalactic nature of H0323+022
08 p1237 N85-17802
A study of the K-edge absorption spectra of selected vanadium compounds
[AD-A149334] 10 p1435 N85-19045
Quantum mechanical and semiclassical approaches to molecular dynamics
[DE85-003458] 10 p1555 N85-19603
IUE absorption line studies of highly ionized interstellar gas 11 p1743 N85-20962
Galactic absorption lines measured from the IUE low dispersion spectra of active galaxies
11 p1745 N85-20977
High-velocity interstellar gas in the line-of-sight to HD 50896 11 p1749 N85-20999
An episodic red-wing structure of SiIV, lambda 1394A, in gamma Cas 11 p1750 N85-21009
FP Cygni profiles in HL CMa
11 p1752 N85-21022
Ultraviolet spectroscopy of the interacting binary U Sagittae 11 p1755 N85-21042
Ultraviolet observations of circumstellar matter in Algol type binary systems 11 p1756 N85-21043
Ultraviolet, radio and X-ray observations of hybrid stars 11 p1759 N85-21063
The effects of atmospheric water vapor on infrared propagation
[AD-A150030] 12 p1934 N85-22150
Below-room-temperature water-vapor continuum absorption within the 8- to 10 micron atmospheric transmission window
[TR-0084(4945-09)-1] 13 p2132 N85-23266
Studies of galactic HI in 21-centimeter absorption
13 p2170 N85-23486
First direct detection of clay minerals on Mars
13 p2194 N85-23612
Reassignment of the iron (3) absorption bands in the spectra of Mars 13 p2195 N85-23614
Determination of mineral type, abundance, and grain size with remotely obtained reflectance spectra
13 p2196 N85-23623
An atlas of pure water vapor spectra from 500 to 5000/cm, volume 1
[AD-A151756] 15 p2505 N85-25454
X-ray spectroscopy of solids under pressure
[DE85-006939] 15 p2507 N85-25465
Possible uses of tunable diode lasers in infrared spectroscopy
[ESA-TT-869] 15 p2564 N85-25818
High-frequency microwave observations of convective precipitation 15 p2596 N85-26000
A measurement of the vibrational band strength for the upsilon sub 3 band of the HO2 radical
[NASA-CR-175856] 16 p2744 N85-26936
An atlas of pure water vapor spectra from 500 to 5000/cm, Volume 2
[AD-A151757] 16 p2745 N85-26940
Effects of temperature on remotely sensed mafic mineral absorption features 16 p2809 N85-27323
Hydrogen absorption in metals: A field ion microscopy study
[DE85-010299] 18 p3076 N85-29026
Thermal donor removal by rapid thermal annealing: Infrared absorption
[DE85-010092] 18 p3081 N85-29059
The development of new techniques in laser spectroscopy 19 p3233 N85-30041
Separation of Drude and band-to-band spectra in polyvalent metals
[DE85-010247] 19 p3240 N85-30093
A study of Co and Mn in ZnO varistors
[DE85-011193] 19 p3263 N85-30233
Combustion control with smart sensors
[DE85-009419] 19 p3274 N85-30303
Sensitive detection of tunable diode laser absorption by polarization rotation
[DE85-009621] 19 p3277 N85-30322
Structure and chemistry of sol-gel derived transparent silica aerogel
[DE85-009902] 20 p3434 N85-31303
Doppler spectrometer for measuring narrow photochemical gaps in inhomogeneously broadened spectra 21 p3689 N85-32921
Determination of band oscillator strengths of atmospheric molecules from high resolution vacuum ultraviolet cross section measurements
[NASA-CR-176150] 22 p3814 N85-33624
The universal spectrum of AGNs and QSOs
[OG-2.7-9] 22 p3872 N85-33962
Time-resolved and infrared spectroscopy of excitons
[DE85-011879] 23 p3912 N85-34235
Dangling bonds and sub-gap optical absorption in silicon
[DE85-011752] 24 p4082 N85-35302
ABSORPTION SPECTROSCOPY
NT OPTOGALVANIC SPECTROSCOPY
The X-ray Absorption Coefficient Fine Structure (EXAFS) study on precipitates in AlCu
[DESY-SR-84-15] 01 p0025 N85-10153
Experimental capabilities and prospects for measuring soft X-ray photoabsorption
[DE84-015466] 02 p0278 N85-11813
Mossbauer spectroscopic investigations of the diffusion and correlation of lattice defects (complementary to neutron spectroscopic investigations)
03 p0429 N85-12736
Direct measurements of nitrous acid, nitrogen dioxide and formaldehyde in auto exhaust by differential optical absorption spectroscopy
[PB84-229269] 06 p0767 N85-14905
Effect of ultraviolet radiation on transparent polymer films as determined using in situ FTIR-RA spectroscopy. Volume 2: Photophysics of poly(vinylidene fluoride) films
[DE84-013040] 09 p1299 N85-18159
Carbon monoxide adsorption on a platinum electrode studied by polarization modulated FT-IRRAS (Fourier Transform-IR Reflections Adsorption Spectroscopy). Part 1: CO adsorbed in the double layer potential region and its oxidation in acids
[AD-A149751] 12 p1800 N85-21288
Effect of ultraviolet radiation on transparent polymer films as determined using in situ FTIR-RA spectroscopy. Volume 1: Photodegradation of transparent polymer films
[DE84-013039] 12 p1814 N85-21377
Spectroscopic studies of lead oxide in a flow tube
[AD-A151849] 15 p2505 N85-25455
High resolution spectroscopy of C13O16 in gas mixtures
[AD-A152625] 17 p2919 N85-27991
Spectroscopy of surface adsorbed molecules
[DE85-009452] 17 p3034 N85-28768
Recent advances in optical measurement methods in physics and chemistry
[DE85-008695] 17 p3037 N85-28792
Digital control of diode laser for atmospheric spectroscopy
[NASA-CASE-NPO-16000-1] 18 p3112 N85-29264
Formation and fate of toxic chemicals in California's atmosphere
[PB85-172609] 18 p3134 N85-29414
Structural and physical studies on a new class of low-dimensional conducting material: FeOCl intercalated with TTF and related molecules
[DE85-009701] 18 p3196 N85-29824
Clay identification and amount measured by laboratory techniques compared to well log responses: Application to tight gas sands and shales
[DE85-010411] 19 p3362 N85-30843
Differential optical absorption techniques for diagnostics of coal gasification
[DE85-010177] 19 p3368 N85-30890
X-ray spectroscopy of solids under pressure
[DE85-011466] 22 p3745 N85-33213
ABSORPTIVE INDEX
U ABSORPTIVITY
ABSORPTIVITY
In vivo dermal absorption method and system for laboratory animals
[AD-D011231] 01 p0094 N85-10635
Change in Venusian atmosphere absorption coefficient with altitude 02 p0163 N85-11103
Laboratory investigation of coefficients of absorption of air at Lambda = 10.6 microns 02 p0263 N85-11723

Characteristics of absorption and frequency filtration of ULF electromagnetic waves in the ionosphere
03 p0376 N85-12402

Ice-soil mixtures: Visual and near-infrared remote sensing techniques
[NASA-CR-174087] 04 p0525 N85-13358

GaAs material properties and models
05 p0665 N85-14277

Anti-reflection coatings materials and models
05 p0665 N85-14278

Analysis of optical and electrical performance of a TCP-coated solar cell 06 p0832 N85-15293

Absorption and emission of EUV radiation by the local ISM 06 p0876 N85-15563

Optical properties of composite materials
[AD-A146768] 07 p0920 N85-15828

Continuum absorption by H2O in the 700-1200 cm(-1) and 2400-280 cm(-1) windows
[AD-A147391] 07 p0997 N85-16334

Estimate of sound absorption due to magnetoelastic interactions
[AD-A148216] 08 p1218 N85-17671

USSR report: Physics and mathematics
[JPRS-UPM-85-001] 11 p1715 N85-20786

Phonon-impurity relaxation and acoustic wave absorption in yttrium-aluminum garnet crystals with impurities 11 p1715 N85-20790

Effect of impurities on absorption in semiconductors and lasing of semiconductor lasers 11 p1716 N85-20797

A method for determining in situ the absorption coefficient of particulate media using pulsed laser technique
[AD-D011548] 12 p1799 N85-21281

Investigation of absorptive electrochemical systems for display applications
[BMFT-FB-T-84-301] 15 p2507 N85-25467

Kinetic studies following state selective laser excitations
[DE85-007173] 15 p2564 N85-25816

Submillimeter-band solid state distributed feedback laser 15 p2644 N85-26307

Comprehensive silicon solar cell computer modeling
[NASA-CR-175959] 17 p2987 N85-28461

Selective radiative cooling with MgO and/or LiF layers
[DE85-011595] 19 p3262 N85-30228

Optical stability, atmospheric transparency and aerosol absorption 19 p3297 N85-30442

Variability of rural aerosols under stable weather conditions 21 p3647 N85-32663

Absorption of laser radiation in substance with absorption coefficient depending linearly upon temperature 21 p3694 N85-32953

Coefficient of optical absorption and scattered light capture effect 21 p3695 N85-32959

Aluminum work function: Effect of oxidation, mechanical scraping and ion bombardment
[NASA-TM-87079] 23 p3915 N85-34265

Acoustical absorption coefficient in a diffuse field of a plane, rectangular material of finite dimensions placed on an infinite perfectly reflecting surface
[NRC/CNR-TT-2113] 23 p3968 N85-34599

X-ray spectra of bursting neutron stars
23 p3981 N85-34686

Underwater measurements of muon intensity
[HE-5.1-16] 24 p4202 N85-36078

ABSTRACTS

Center for Electronics and Electrical Engineering Technical Bulletin covering center programs with 1984 CEEE events calendar
[PB84-222785] 01 p0045 N85-10292

Center for Electronics and Electrical Engineering Technical Bulletin covering center programs with 1984 CEEE events calendar
[PB84-223684] 01 p0045 N85-10293

Center for Electronics and Electrical Engineering Technical Bulletin covering center programs
[PB84-219716] 01 p0045 N85-10295

Center for Electronics and Electrical Engineering Technical Bulletin covering center programs
[PB84-218056] 01 p0045 N85-10296

Geology and geomorphology of the southern central Blue Ridge: An indexed bibliography
[PB84-225119] 01 p0072 N85-10480

Publications of the National Bureau of Standards, 1983 catalog
[PB84-218031] 01 p0126 N85-10869

European Scientific Notes, Number 38-9
[AD-A145683] 02 p0306 N85-11975

National Photovoltaics Program Annual Review Meeting, abstracts
[DE84-013003] 04 p0530 N85-13390

Abstract and index collection
[PB85-119501] 10 p1569 N85-19892

Model of information-reference dialogue system for working with document abstracts
12 p1903 N85-21949

Aerospace Medicine and Biology: A continuing bibliography with indexes, supplement 267, January 1985
[NASA-SP-7011(267)] 12 p1904 N85-21959

Evaluation of the vocabulary switching systems
[PB85-127157] 12 p1951 N85-22260

Schema theory in the representation and analysis of text 14 p2433 N85-25004

Air Force Office of Scientific Research (AFOSR): Technical report summaries. Fourth quarter (CY)
[AD-A150860] 14 p2456 N85-25167

A summary of the Naval Postgraduate School research program
[AD-A151721] 16 p2875 N85-27738

Compilation of abstracts of theses submitted by candidates for degrees
[AD-A151722] 16 p2875 N85-27739

Summary of Research, Academic Departments, 1983 - 1984
[AD-A151724] 16 p2875 N85-27741

Bibliography of Lewis Research Center technical publications announced in 1984
[NASA-TM-87012] 17 p3049 N85-28876

Proceedings of the 19th Annual Conference of the Finnish Physical Society
[REPT-104] 20 p3532 N85-31974

Seventh Symposium on Biotechnology for Fuels and Chemicals: Program and abstracts
[DE85-011197] 22 p3742 N85-33192

1985 Amorphous Silicon Review Meeting
[DE85-008794] 22 p3807 N85-33582

A hierarchy of knowledge levels implemented in a rule-based production system to calculate bounds on the size of intersections and unions of simple sets
[AD-A155291] 22 p3848 N85-33836

NASA patent abstracts bibliography: A continuing bibliography. Section 1: Abstracts (supplement 27)
[NASA-SP-7039(27)-SECTION-1]
22 p3849 N85-33840

Monitoring building energy performance: An informal review and characterization of research in progress
[BNL-51765] 23 p3923 N85-34308

Center for Electronics and Electrical Engineering technical progress bulletin covering center programs, July-September with 1985 CEEE events calendar
[PB85-191393] 24 p4091 N85-35363

ABUNDANCE

Giacobini-Zinner comet: Polarimetric and physical observations
[NASA-TM-77771] 01 p0130 N85-10894

Contribution to the radiogeology of Sao Roque, SP, granites
[INPE-3079-PRE/492] 03 p0391 N85-12503

Ge abundances in the lunar mantle and implications for the origin of the Moon 04 p0582 N85-13721

Origin of the Moon 04 p0587 N85-13745

Pioneer 10 and Voyager observations of the interstellar medium in scattered emission of the He 584 A and H Lya 1216 A lines 06 p0873 N85-15541

Deuterium abundance in the local interstellar medium
06 p0874 N85-15552

Boron cosmochemistry 06 p0886 N85-15642

Differentiated meteorites and the components of chondrites
[NASA-CR-174201] 06 p0890 N85-15649

The abundance of deuterium in the outer solar system from ground-based measurements of monodeuterated methane 07 p1060 N85-16725

Measurements of H2O in Jupiter's atmosphere from 5 microns airborne observations 08 p1244 N85-17854

Elemental abundances of mercury-manganese stars and the population 2 type star HD 109995
[NASA-CR-174298] 08 p1255 N85-17913

Boundary conditions for the paleoenvironment: Chemical and physical processes in the pre-solar nebula — molecular clouds, interstellar matter, and abundance
[NASA-CR-174370] 10 p1570 N85-19901

IUE observations of planetary nebulae in the Magellanic Clouds 11 p1747 N85-20986

The Jovian Stratosphere in the ultraviolet
11 p1760 N85-21069

Cosmic ray composition and origin
12 p1955 N85-22287

A Jamin interferometer to determine the helium abundance in the atmosphere of Jupiter
[BONN-IR-83-17] 12 p1961 N85-22329

Relative abundances of sub-iron to iron nuclei in low energy (50-250 MeV/N) cosmic rays as observed in the Skylab experiment
[OG-4.1-4] 22 p3876 N85-34010

Cosmic ray charge and energy spectrum measurements using a new large area Cerenkov x dE/dx telescope
[OG-4.1-5] 22 p3876 N85-34011

The energy dependence of the neon-22 excess in the cosmic radiation
[OG-4.3-7] 22 p3879 N85-34032

Initial results from the Caltech/DRSI balloon-borne isotope experiment
[OG-4.3-8] 22 p3879 N85-34033

Ariel 6 measurements of ultra-heavy cosmic ray fluxes in the region 34 or = Z or = 48
[OG-4.4-3] 22 p3879 N85-34036

Ariel 6 measurements of ultra-heavy cosmic ray fluxes in the region Z or = 48
[OG-4.4-4] 22 p3880 N85-34037

Elemental abundances of cosmic rays with Z 33 as measured on HEAO-3
[OG-4.4-5] 22 p3880 N85-34038

Abundances of secondary elements among the ultra heavy cosmic rays: Results from HEAO-3
[OG-4.4-6] 22 p3880 N85-34039

Capabilities of the LDEF-2 heavy nuclei collection
[OG-4.4-8] 22 p3880 N85-34040

Ultraheavy cosmic ray tracks in meteorites: A reappraisal, based on calibrations with relativistic ions
[OG-4.4-10] 22 p3880 N85-34041

Solar Coronal and photospheric abundances from solar energetic particle measurements
[SH-2.1-5] 23 p3998 N85-34786

Variations in elemental composition of several MEV/nucleon ions observed in interplanetary space
[SH-2.1-7] 23 p3998 N85-34788

Anomalous abundances of solar energetic particles and coronal gas: Coulomb effects and First Ionization Potential (FIP) ordering
[SH-2.1-10] 23 p3999 N85-34791

Abundances from solar-flare gamma-ray line spectroscopy
[SH-2.1-13] 23 p3999 N85-34794

Solar flare gamma-ray line spectroscopy
[SH-2.1-14] 23 p3999 N85-34795

Elemental abundance differences between nuclei acclerated in CIR shocks and solar flares
[SH-2.2-6] 23 p4000 N85-34801

The heavy ion composition in 3HE-rich solar flares
[SH-2.2-7] 23 p4000 N85-34802

Germanium and lead: Significant differences between meteoritic and photospheric abundances?
[OG-7.1-2] 23 p4012 N85-34864

Lead and uranium group abundances in cosmic rays
[OG-7.1-3] 23 p4013 N85-34865

Implications of source abundances of ultraheavy cosmic rays
[OG-7.1-4] 23 p4013 N85-34866

Alfven wave scattering and the secondary to primary ratio
[OG-7.2-9] 23 p4015 N85-34878

Do supernovae of type 1 paly a role in cosmic-ray production?
[OG-8.2-5] 23 p4019 N85-34905

Bursting star formation and the overabundance of Wolf-Rayet stars
[OG-8.2-8] 23 p4019 N85-34907

Measurement of low energy cosmic rays aboard Spacelab-1
[SH-10.1-6] 23 p4053 N85-35137

AC (CURRENT)

U ALTERNATING CURRENT

AC GENERATORS

The microprocessor control of a motor-alternator
[RAE-TM-NAV-ENG-1023(L)] 02 p0244 N85-11591

Vibroacoustic control diagnostics of selected machines based on research on the slide bearing of an automobile engine and the alternator
[ISSN-0208-5658] 05 p0641 N85-14112

Two-rotor alternators with superconductor field winding 06 p0795 N85-15082

The ferrite permanent magnet AC motor: A technical and economical assessment
[DE85-002480] 13 p2066 N85-22903

Batteryless magneto-driven portable radiac
[DE85-011622] 22 p3760 N85-33300

ACCELERATED LIFE TESTS

Cyclic endurance testing of the RB211-22B cast HP turbine blade — high pressure (HP)
[PNR-90210] 03 p0320 N85-12063

Accelerated viscoelastic characterization of T300/5208 graphite-epoxy laminates 03 p0325 N85-12091

Accelerated stress facility 1976-1983
[AD-A146101] 03 p0359 N85-12303

NBS (National Bureau of Standards) solar collector durability-reliability test program
[PB85-113603/GAR] 09 p1346 N85-18469

Forced corrosion tests of construction components of passenger aircraft fuselages 11 p1600 N85-20062

A note on some simple influence diagnostics in accelerated life testing
[AD-A149593] 12 p1882 N85-21677

Life testing of rubber seals — aircraft hydraulic systems
[AD-A143193] 13 p2098 N85-23086

Advanced life analysis methods. Volume 2: Crack growth analysis methods for attachment lugs
[AD-A150420] 13 p2103 N85-23109
Parallel test method for LSI (Large Scale Integration) microprocessors
[AD-A150237] 13 p2144 N85-23310
Advanced life analysis methods. Volume 3: Experimental evaluation of crack growth analysis methods for attachment lugs
[AD-A151058] 14 p2317 N85-24319
Module performance and failure analysis area: Flat-plate solar array project
[NASA-CR-175689] 15 p2585 N85-25936
Natural and accelerated aging of plastics
17 p2936 N85-28123
A test methodology for an automated and interactive software development environment
[AD-A152857] 17 p3011 N85-28618
Accelerated and real-time geosynchronous life cycling test performance of nickel-hydrogen batteries
20 p3448 N85-31405
Understanding and laboratory prediction of the atmospheric corrosion behavior of steels and of non-ferrous metals and alloys
[AD-A154842] 21 p3566 N85-32179
High temperature electronics technology: Life test report
[AD-A154681] 21 p3580 N85-32257
Accelerated stress factors and failure/degradation mechanisms in terrestrial solar cells
21 p3613 N85-32451
Degradation mechanisms and accelerated aging test design
[TI85-003251] 23 p3940 N85-34420

ACCELERATION
What is being done to control motion sickness?
15 p2687 N85-26599
Accelerator experiments on the contribution of secondary particles to the production of cosmogenic nuclides in meteorites
[SH-7.1-8] 23 p4048 N85-35100

ACCELERATION (PHYSICS)
NT ANGULAR ACCELERATION
NT DECELERATION
NT ELECTRON ACCELERATION
NT HIGH ACCELERATION
NT HIGH GRAVITY ENVIRONMENTS
NT IMPACT ACCELERATION
NT PARTICLE ACCELERATION
NT PLASMA ACCELERATION
NT SPIN REDUCTION
NT TRANSVERSE ACCELERATION
Design of a digital ride quality augmentation system for commuter aircraft
[NASA-CR-172419] 01 p0006 N85-10037
The Reports of Aeromedical Laboratory, volume 25, no. 1/2
[ISSN-0023-2858] 01 p0090 N85-10605
The effects of isotonic training on +Gz tolerance
01 p0090 N85-10607
Acceleration waves 02 p0207 N85-11367
Study of the solar corona using radio and space observations
[NASA-CR-174034] 02 p0304 N85-11963
Magnetospheric plasma studies using data from the dynamics high and low altitude plasma instruments
[AD-A145751] 03 p0392 N85-12505
Geomagnetic secular variation: A jerk in 1970
04 p0521 N85-13329
Acceleration of bluff bodies through fluids
05 p0593 N85-13786
Diffusion in metals under high mechanical strain and acceleration
[JUEL-1913] 07 p0928 N85-15887
Superconducting rotor dynamics
[AD-A147176] 07 p0947 N85-16000
Comparative visualization of accelerating flow around various bodies, starting from rest
[AD-P004159] 09 p1264 N85-17944
Primer for mass metrology
[PB85-121424/GAR] 09 p1305 N85-18199
Acceleration responses of typical LRU's subjected to bench handling and installation shock
09 p1334 N85-18385
Alternative shock characterizations for consistent shock test specifications 09 p1335 N85-18396
Numerical simulations of liquid propellant combustion instability: Onset and growth
[DE85-000743] 10 p1458 N85-19186
Tether fundamentals 11 p1643 N85-20345
Artificial gravity: Tethers and containers
11 p1645 N85-20367
Development of high field Nb-Ti accelerator dipoles
[DE85-000621] 11 p1714 N85-20782
Averaging of equations of cometary orbital motion with allowance for nongravitational effects
13 p1978 N85-22411
Physics of the inner heliosphere: Mechanisms, models and observational signatures
[NASA-CR-175632] 13 p2205 N85-23677
Problems of space biology. Volume 50: Nystagmometry for evaluation of the status of the vestibular function
[NASA-TM-77616] 14 p2385 N85-24694
Comets and nongravitational forces
14 p2437 N85-25038
Unsteady Navier-Stokes calculations in an accelerated reference frame
[AD-A151751] 15 p2557 N85-25774
Effects of magnetic shear on lower hybrid waves in the suprauroral region
[AD-A151980] 15 p2656 N85-26392
Empirical development of ground acceleration, velocity and displacement for accidental explosions at J5 or the proposed large altitude rocket cell at Arnold Engineering Development Center
[DE85-008324] 16 p2758 N85-27020
Acceleration resistant combination of opposite-handed piezoelectric crystals
[AD-D011626] 16 p2778 N85-27143
Acceleration-resistant crystal resonator
[AD-D011627] 16 p2778 N85-27144
Acceleration sensitivity reduction method
[AD-D011631] 16 p2778 N85-27146
Acceleration insensitive oscillator
[AD-D011621] 17 p2953 N85-28236
A counterpart of Faxen's formula in potential flow
[REPT-84-09] 17 p2960 N85-28279
Design of SC cut 10 MHZ H.Q. crystals with G. sensitivity better than 2.10(-10)/G 17 p2966 N85-28319
Wake fields and wake field acceleration
[DE85-008054] 17 p3031 N85-28750
Multiple time-scale methods in particle simulations of plasmas
[DE85-007519] 17 p3040 N85-28808
Spacecraft, straight-tube evaporator design
[AD-A154462] 19 p3226 N85-30003
Seakeeping and vibration tests of the Coast Guard 110 foot surface effect ship SEA BIRD class (WSES)
[AD-A154150] 19 p3252 N85-30166
Effect of periodic accelerations on physiochemical properties and Ca2 + reactivity of actomyosin in white rat myocardium and skeletal muscles
19 p3324 N85-30594
Physics with low temperature antiproton
[DE85-009627] 19 p3355 N85-30798
Recovery of pyroshock data from distorted acceleration records
[NASA-TP-2494] 20 p3407 N85-31141
Update on the evolution of the LAGEOS orbit
20 p3491 N85-31698
Pulsed hydrojet propulsion
[DE85-010771] 22 p3784 N85-33446
Acceleration of polarized H(-) in the BNL 200 MeV linac
[DE85-011836] 22 p3840 N85-33777
Long term variability of the cosmic ray intensity
[OG-3.1-11] 22 p3874 N85-33999
Injection of energetic particles following the gamma-ray flares on June 7, 1980, as observed on Helios 1
[SH-1.3-9] 23 p3993 N85-34756
The cosmic-ray shock structure problem for relativistic shocks
[OG-8.1-1] 23 p4017 N85-34891
Time-dependent nonlinear cosmic ray shocks confirming abstract
[OG-8.1-3] 23 p4017 N85-34893
Relativistic cosmic ray spectra in the full non-linear theory of shock acceleration
[OG-8.1-6] 23 p4018 N85-34896
Acceleration of cosmic rays in supernova-remnants
[OG-8.1-9] 23 p4018 N85-34899
Evaluation of parameters for particles acceleration by the zero-point field of quantum electrodynamics
[OG-8.2-16] 23 p4020 N85-34912
Matched filtering of visual evoked potentials to detect acceleration (+Gz) induced blackout
[AD-A155912] 24 p4131 N85-35609

ACCELERATION PROTECTION
Improving inflight negative Gz restraint for aircrewmen
[AD-A151909] 16 p2703 N85-26688

ACCELERATION STRESSES (PHYSIOLOGY)
NT CENTRIFUGING STRESS
Frequency and nature of electrocardiographic disturbances in dogs during single and repeated exposure to +G sub z accelerations 01 p0092 N85-10619
Analysis of the transient response of temporal artery blood flow data relative to various anti-G suit pressure schedules 10 p1533 N85-19660
Space adaptation syndrome: Incidence and operational implications for the space transportation system program
11 p1695 N85-20655
Homeostasis in primates in the hyperdynamic environment — circadian timekeeping and effects of lower body positive pressure on sleep
15 p2610 N85-26065
The European vestibular experiments of the Spacelab-1 mission 20 p3508 N85-31808
Some results of the European vestibular experiments in the Spacelab-1 mission 20 p3508 N85-31809
Oxygenation and regional circulation in gingival mucosa during exposure to lower body negative pressure
23 p3953 N85-34498
The effect of +Gx acceleration on platelet activation as determined by plasma platelet factor 4 levels
[AD-A155881] 24 p4131 N85-35608

ACCELERATION TOLERANCE
The Reports of Aeromedical Laboratory, volume 25, no. 1/2
[ISSN-0023-2856] 01 p0090 N85-10605
The effects of isotonic training on +Gz tolerance
01 p0090 N85-10607
Assessment of the inflating characteristics of the modified anti-G suit 01 p0090 N85-10609
Effect of fluid and salt supplements to food allowance on endurance of head-to-pelvis accelerations following 7-day dry immersion and under ordinary motor activity conditions 01 p0092 N85-10618
Frequency and nature of electrocardiographic disturbances in dogs during single and repeated exposure to +G sub z accelerations 01 p0092 N85-10619
Random pattern tracking acceleration tolerance tester
[AD-D011404] 07 p1017 N85-16459
Tolerance, fatigue, physiological and performance effects of sustained and oscillating lateral accelerations
10 p1533 N85-19659
Positive Gz accelerations tolerance of individuals 41 to 58 years of age 19 p3323 N85-30588
Analysis of the transient response of temporal artery blood flow data relative to various anti-G suit pressure schedules
[AD-A155242] 21 p3666 N85-32775
Tolerance to +Gz and +Gx accelerations of individuals in older age groups in good health and with early signs of arteriosclerosis 23 p3952 N85-34496
Effect of hypokinesia and +Gz accelerations on transport function of human blood
23 p3952 N85-34497
Matched filtering of visual evoked potentials to detect acceleration (+Gz) induced blackout
[AD-A155912] 24 p4131 N85-35609
Simulation of high +Gz onset in the dynamic environment simulator
[AD-A155963] 24 p4131 N85-35610

ACCELERATORS
Superconducting magnet technology for accelerators
[DE85-004192] 12 p1926 N85-22102

ACCELEROMETERS
NT STRAIN GAGE ACCELEROMETERS
Keeping up with operational loads in the French Air Force: Defining new equipment
07 p0696 N85-15681
Flight simulation for inertial navigation system
14 p2273 N85-24081
Preguidance and piloting with the aid of composite inertial sensors 16 p2696 N85-26646
Low cost two gimbal inertial platform and its system integration 16 p2698 N85-26661
Simulation of a low orbit restitution. Covariance analysis of the position-velocity by Doppler and accelerometer measurements
[CNES-CT/DTI/MS/AE/166] 16 p2728 N85-26836
Research and development of subsurface acoustic wave devices for sensor applications
[AD-A152197] 16 p2861 N85-27642
Principles of designing digital compensating accelerometers 17 p2944 N85-28172
Uniaxial angular accelerometers
17 p2944 N85-28173
Study on a flexure hinged pendulum accelerometer
[NAL-TR-844] 18 p3104 N85-29220
Passivation on high Q acoustic strain sensor for accelerometer
[AD-A153565] 18 p3177 N85-29695
Investigation of fast reaction SAW (Surface Acoustic Wave) accelerometer
[AD-A153876] 19 p3216 N85-29943
The DREO (Defence Research Establishment Ottawa) inertial Navigation Laboratory: Development and test capabilities
[AD-A154425] 19 p3216 N85-29945
R and D activities of the Systems Engineering Division
20 p3540 N85-32027

Application of satellite accelerometer data to improve density models
[AD-A154904] 21 p3631 N85-32558
Multiple-stage integrating accelerometer
[DE85-006505] 23 p3935 N85-34368

ACCEPTABILITY
Development of acceptance criteria for batches of silane primer for external tank thermal protection system bonding applications
[NASA-CR-171436] 15 p2518 N85-25523
Development of acceptance criteria for batches of silane primer for external tank thermal protection system bonding applications
[NASA-CR-175850] 16 p2754 N85-26995
A critique of Deming's discussion of acceptance sampling procedures
[AD-A154305] 19 p3348 N85-30751
Atmospheric modeling of organics for risk assessment: A Chemist's view
[DE85-009770] 23 p3909 N85-34217

ACCEPTANCE
U ACCEPTABILITY

ACCEPTOR MATERIALS
Electrochemistry of polymer films. Applications to chemical analysis and energy conversion
[AD-A147737] 08 p1132 N85-17136

ACCESS CONTROL
Throughput characteristics of Carrier Sense Multiple Access (CSMA) networks
[FUB-25-1983] 01 p0106 N85-10713
Heterogeneous data base access
05 p0735 N85-14724
Some experiences of testing protocol implementations — open systems interconnection
[NPL-DITC-48/84] 08 p1204 N85-17574
Performance evaluation and control of distributed computer communication networks
[AD-A148103] 08 p1208 N85-17598
Analytical modeling of a polling protocol — airline information network
[ENST-84H001] 09 p1277 N85-18029
Design and analysis of an access control system for a multi-backend database system
[AD-A148750] 09 p1367 N85-18586
AID: Access to Informal Documentation
[DE85-000418] 11 p1740 N85-20939
Access path optimization for network database retrieval 16 p2877 N85-27749
Optimizing data access in the LAMPF control system
[DE85-012653] 24 p4140 N85-35663

ACCIDENT INVESTIGATION
NT AIRCRAFT ACCIDENT INVESTIGATION
Structural design guidelines for heliports
[FAA-PM-84-23] 02 p0149 N85-11010

ACCIDENT PREVENTION
Development and certification of a new stall warning and avoidance system 05 p0702 N85-14507
A manual control test for the detection and deterrence of impaired drivers 05 p0709 N85-14550
The use of falconry as mean to persuade the birds to stay out of the airport vicinity 11 p1580 N85-19956
Safety with industrial manufacturing lasers
14 p2306 N85-24281
MELCOR Accident Consequence Code System (MACCS)
[DE85-009712] 19 p3339 N85-30669
A review of the SIMMER-2 analyses of liquid-metal-cooled fast breeder reactor core-disruptive accident fuel escape
[DE85-010803] 19 p3366 N85-30876
General Aviation Airworthiness Alerts, no. 85
[FAA-AC-43-16] 22 p3729 N85-33117
Transient three-phase three-component systems. Part 1: Formulation of the system of differential equations
[DE85-013267] 24 p4095 N85-35384

ACCIDENT PRONENESS
Calculation of trajectories of detached wind turbine blades and prediction of site risk levels associated with failures of HAWT's 24 p4110 N85-35475

ACCIDENTS
NT BIRD-AIRCRAFT COLLISIONS
Volatility of vanadium from a candidate fusion tractor alloy
[DE84-015277] 05 p0618 N85-13955
HS and E environmental sciences
[DE84-016183] 05 p0672 N85-14314
Ballistic/detonic transition of propellants
08 p1117 N85-17041
Control of tractors on sloping ground
[AD-P004292] 09 p1408 N85-18869
The medical results of human exposures to radio frequency radiation
[AD-A149718] 12 p1905 N85-21962
Two phase discharge of liquefied gases through pipes. Field experiments with ammonia and theoretical model
[FOA-B-40139-C1] 18 p3103 N85-29209
Hazardous air pollutants
[GPO-43-064] 21 p3613 N85-32456
The 1983 international intercomparison of nuclear accident dosimetry systems at Oak Ridge National Laboratory
[DE85-011303] 23 p3934 N85-34382
Computer code calculations of the TMI-2 accident: Initial and boundary conditions
[DE85-012613] 24 p4140 N85-35666
Thermal hydraulic features of the TMI accident
[DE85-014569] 24 p4152 N85-35747

ACCLIMATIZATION
NT ALTITUDE ACCLIMATIZATION
NT COLD ACCLIMATIZATION
NT HEAT ACCLIMATIZATION
Introduction to human biometeorology
05 p0687 N85-14415
Aerobic and anaerobic exercise tolerance in the heat: Effect and acclimatization 14 p2388 N85-24707
Exercise-heat strain during hypohydration: Interaction with heat acclimation and aerobic fitness
[AD-A151023] 14 p2389 N85-24717

ACCOUNTING
The analysis of tank calibration data from several runs
[DE84-015529] 02 p0200 N85-11337
Management control systems and interdependencies: An empirical study
[AD-A152280] 16 p2876 N85-27746
Computer center policy
[AD-A154416] 19 p3338 N85-30661
Energy accounting software
[DE85-010612] 19 p3340 N85-30694
DOD Value Engineering Conference report. Value Engineering (VE): A tool that benefits line management held at Leesburg, Virginia on 1-2 November 1984. Part 1. Executive summary
[AD-A156067] 24 p4163 N85-35810

ACCRETION
U DEPOSITION

ACCRETION DISKS
Spherical accretion onto a protostellar core
03 p0442 N85-12817
The lunar angular momentum problem
04 p0588 N85-13752
Formation of the prelunar accretion disk
04 p0588 N85-13755
X-ray spectra of accretion disks — active galactic nuclei 08 p1239 N85-17814
Shock acceleration in active galactic nuclei and quasars 08 p1241 N85-17828
Models of nonkeplerian accretion disks based on dynamo magnetic field: Application to Active Galactic Nuclei (AGN) 08 p1242 N85-17834
X-ray spectra of accretion disks — active galactic nuclei 08 p1242 N85-17838
Circumstellar dust disks around young stars
08 p1247 N85-17870
The vertical structure and stability of alpha model accretion disks 09 p1417 N85-18938
EXOSAT observations of the galactic bulge X-ray source GX17+2 — X ray binary star 11 p1742 N85-20951
Thermal convection and magnetic fields in accretion disks of black holes 12 p1955 N85-22285
Drift-accretion theory of the spiral structure of galaxies
12 p1957 N85-22298
Hydrodynamics of astrophysical jets — active galactic nuclei 12 p1958 N85-22307
Formation of optical-line emitting regions in the jets of SS433 12 p1959 N85-22316
Evolution of grains in a turbulent solar nebula
13 p2179 N85-23525
A numerical study of nonspherical black hole accretion 16 p2881 N85-27780
Ultra high energy gamma rays, cosmic rays and neutrinos from accreting degenerate stars
[OG-2.2-5] 22 p3864 N85-33931
500 TeV gamma rays from Hercules X-1
[OG-2.2-7] 22 p3865 N85-33933
A model for the UHE gamma-rays from Hercules X-1
[OG-2.2-8] 22 p3865 N85-33934

ACCUMULATORS
NT DUST COLLECTORS
NT SOLAR COLLECTORS
NT SOLAR REFLECTORS
Development and evaluation of cloud water collectors
[PB84-232529] 04 p0540 N85-13437
Power transfer from natural emitters to collection apertures at microwave wavelengths
[NASA-CR-174275] 07 p0945 N85-15989
Application of fiber optics and compound collectors
08 p1253 N85-17912
Antiproton source beam position system
[DE84-016716] 09 p1360 N85-18679
Development of a second-generation linear Fresnel Photovoltaic and Thermal (PVT) concentrator array, including fabrication and installation of a 200 square meter collector field
[DE85-008473] 17 p2988 N85-28465
Integrated current collector and catalyst support
[DE85-011618] 22 p3761 N85-33311
Multistage spent particle collector and a method for making same
[NASA-CASE-LEW-13914-1] 22 p3791 N85-33489
Vapor phase heat transport concepts
[DE85-009550] 23 p3931 N85-34366

ACCURACY
NT GEODETIC ACCURACY
NT GEOMETRIC ACCURACY
Research on large, highly accurate, inflatable reflectors
[AD-A145080] 01 p0016 N85-10099
Economic model of calibration improvements for automatic test equipment
[PB84-217827] 01 p0051 N85-10335
Evaluation of laser profile and deflection measuring system
[FAA-PM-84-24] 02 p0201 N85-11341
Observations of lightweight Doppler system accuracy
[AD-A145968] 03 p0317 N85-12049
Portable real-time clock
[AD-A146218] 03 p0364 N85-12336
Comparability and accuracy of industry codes in different data systems
[PB84-215607] 04 p0548 N85-13482
Magnetic constraints on early lunar evolution revisited: Limits on accuracy imposed by methods of paleointensity measurements 04 p0582 N85-13716
Improvement of the accuracy of reflection factor measurements by a computer 05 p0629 N85-14033
Treatment and expression of measurement uncertainties 05 p0630 N85-14042
The Georges Bank monitoring program 1983: Analysis of trace metals in bottom sediments
[CIRC-915] 05 p0688 N85-14423
Reducing numerical diffusion for incompressible flow calculations
[NASA-TM-83621] 06 p0756 N85-14840
Resolution and accuracy of radar measurements
06 p0789 N85-15044
Summary of photovoltaic performance models
06 p0832 N85-15296
Trends in skill and accuracy of National Weather Service pop forecasts
[PB84-229053] 06 p0840 N85-15335
Power of deterministic thinking in machine tool accuracy
[DE85-001751] 07 p0974 N85-16186
Development of a Helicopter integrated navigation system 08 p1073 N85-16802
High accuracy Doppler navigation employing optimum integrated position fix information
08 p1073 N85-16803
An application of discriminant analysis to the selection of software cost estimating models
[AD-A147632] 08 p1204 N85-17580
Study on steerability of articulated tracked vehicles
[AD-P004308] 09 p1410 N85-18885
Geometric accuracy of LANDSAT-4 MSS image data
11 p1667 N85-20503
Influence of individual reflections on the precision of parameter estimates in least squares refinement
[DE85-000830] 11 p1735 N85-20909
Modal control of structural systems
[AD-A149734] 12 p1790 N85-21235
Speed and accuracy in automated manufacture
[DE85-003913] 12 p1819 N85-21410
Accuracy of typhoon center determined by GMS imagery 12 p1894 N85-21887
AFOS (Automation of Field Operations and Services)-ERA forecast verification, September 1984
[PB85-137578] 12 p1897 N85-21912
Method for determining the number of correlative measurements required to validate the SBUV/2 ozone retrievals 13 p2105 N85-23114
Measurement requirements for the detection of ozone trends 13 p2105 N85-23115
Automated extraction of absorption bands from reflectance special 13 p2197 N85-23624
Innovation in earthquake and natural hazards research: Determining soil liquefaction potential
[PB85-149573] 14 p2374 N85-24678
Arithmetic and elementary functions on mini and microcomputers 14 p2396 N85-24761
Accuracy of the calculated stress field around a craze
[DE85-005520] 16 p2801 N85-27272
Optimal relative data weights
16 p2805 N85-27296
Studies into location accuracy — ARGOS system
16 p2811 N85-27334

Evaluation of the PROFS (Program for Regional Observing and Forecasting Services) 1982, real-time forecast experiment
[PB85-159747] 16 p2697 N85-27495
Separating the variances of noise components in the Global Positioning System
[AD-P004578] 17 p2983 N85-28295
An empirical comparison of the accuracy of univariate and multivariate corrections for range restriction
[AD-A153071] 17 p3019 N85-28670
Study of the accuracy of astrometric observations of comets
[ESA-CR(P)-1964] 17 p3054 N85-28903
On the accuracy of Cs beam primary frequency standards 18 p3105 N85-29224
Time transfer techniques: Historical overview, current practices and future capabilities
18 p3106 N85-29245
New GOES satellite synchronized time code generation 18 p3109 N85-29247
Accepting error to make less error
[AD-A153949] 18 p3171 N85-29651
Accuracy in determining velocity of fluid movement by Doppler method 19 p3293 N85-30419
Study of the interferences of 2 GHz radio beams with a DORIS system — precise low orbit determination system (DORIS)
[CNES-CT/DRT/TIT/RL-84/140-T]
20 p3442 N85-31362
TOPEX error budget 20 p3493 N85-31717
Accuracy and operational use of medium and extended range numerical atmospheric forecasts: A review
[AD-A155027] 21 p3635 N85-32579
Medium range atmospheric forecast system: Evaluation report
[AD-A155240] 21 p3637 N85-32589
Resource allocation in cerebral specialization of function: Behavioral and electrophysiological studies
[AD-A155062] 21 p3664 N85-32759
A method of accurizing rail guns
[LA-10028-MS] 22 p3737 N85-33166
Art of programming programmable microcalculators, part 4: errors of calculations 22 p3778 N85-33411
Determining an azimuth with a north seeking gyro
[AD-A155880] 24 p4063 N85-35180
Accuracy and error analysis — airborne instruments
24 p4123 N85-35557

ACEE PROGRAM
Fuel efficiency through new airframe technology
[NASA-TM-84548] 02 p0133 N85-10909
Energy efficient engine combustor test hardware detailed design report
[NASA-CR-167945] 02 p0140 N85-10950
Energy efficient engine component development and integration program
[NASA-CR-170034] 02 p0146 N85-10990
Energy efficient engine. Volume 2. Appendix A: Component development and integration program
[NASA-CR-173085] 02 p0146 N85-10991
Energy efficient engine. Volume 1: Component development and integration program
[NASA-CR-173084] 02 p0146 N85-10992
Energy efficient engine. Low pressure turbine test hardware detailed design report
[NASA-CR-167958] 02 p0147 N85-10994
Energy efficient engine high pressure turbine test hardware detailed design report
[NASA-CR-167955] 02 p0147 N85-10995
Energy efficient engine high pressure turbine ceramic shroud support technology report
[NASA-CR-168036] 02 p0147 N85-10996
Energy efficient engine ICLS engine bearings, drives and configuration: Detail design report
[NASA-CR-167871] 02 p0147 N85-10997
Energy efficient engine. High pressure compressor detail design report
[NASA-CR-165558] 02 p0147 N85-10998
Investigation of toughened neat resins and their relations to advanced composite mechanical properties
04 p0464 N85-12949
Steady- and unsteady-pressure measurements on a supercritical-wing model with oscillating control surfaces at subsonic and transonic speeds
[NASA-TM-84543] 06 p1077 N85-16831
Transonic steady- and unsteady-pressure measurements on a high-aspect-ratio supercritical-wing model with oscillating control surfaces
[NASA-TM-81888] 09 p1273 N85-18003
Subsonic and transonic pressure measurements on a high-aspect-ratio supercritical-wing model with oscillating control surfaces
[NASA-TM-83201] 09 p1273 N85-18004
Energy efficient engine high-pressure turbine component rig performance test report
[NASA-CR-168189] 19 p3218 N85-29955
Energy efficient engine integrated core/low spool test hardware design report
[NASA-CR-168137] 19 p3218 N85-29956
Energy Efficient Engine (E3) controls and accessories detail design report
[NASA-CR-168017] 19 p3218 N85-29957
Energy efficient engine component development and integration program
[NASA-CR-172946] 19 p3219 N85-29958
Energy efficient engine. Fan and quarter-stage component performance report
[NASA-CR-168070] 23 p3897 N85-34141
Energy efficient engine, high pressure turbine thermal barrier coating. Support technology report
[NASA-CR-168037] 24 p4066 N85-35199

ACETALDEHYDE
(Vinyloxy)fluorocyclotriphosphazenes
[AD-A147448] 07 p0924 N85-15850

ACETATES
Fatal hemorrhagic shock and acetate solutions
[AD-A146754] 07 p1014 N85-16444
1-Fluoro-1,1,5-Trinitro-3-Oxa-5-Azahexane and method of preparation
[AD-D011421] 08 p1136 N85-17158
Pre-flight report on cultured human embryonic kidney cell handling and cell electrophoresis. Prepared prior to continuous-flow electrophoretic separation experiments aboard space shuttle flight STS-8
20 p3503 N85-31775
Microbiological and biochemical studies towards optimization of substrate utilization by methanogenic bacteria
[PB85-166332] 24 p4084 N85-35310

ACETONE
Biocatalyzed processes for production of commodity chemicals: Assessment of future research advances for N-butanol production
[NASA-CR-174264] 07 p0919 N85-15819
ECUT, Energy Conversion and Utilization Technologies program: Technical and economic assessment of processes for the production of butanol and acetone. Phase 2: Analysis of research advances
[NASA-CR-175471] 10 p1434 N85-19034
Brittle fracture resistance of electron beam-welded joints in titanium Alpha alloys 15 p2500 N85-25419
Microstructural characteristics during the controlled solidification of a binary system
[DE85-005200] 15 p2507 N85-25461

ACETYL COMPOUNDS
Method of obtaining polychalcones
[AD-A145051] 01 p0018 N85-10107
Use and disuse and the control of acetylcholinesterase activity in fast and slow twitch muscle of rat
[NASA-CR-175717] 15 p2614 N85-26109
Phenoxy resins containing pendent ethynyl groups and cured resins obtained therefrom
[NASA-CASE-LAR-13262-1] 18 p3068 N85-28973

ACETYLACETONE
Investigation of the Ostwald ripening of separated particles in liquid-liquid systems under microgravity conditions
[BMFT-FB-W-84-037] 05 p0615 N85-13927

ACETYLENE
Preparation of polymers of functionalized acetylenes
[AD-D011296] 06 p0771 N85-14935
Vibrational spectroscopy of chemisorption phenomena on model catalyst surfaces
[AD-A146753] 07 p0922 N85-15840
Conduction in polymerized polyfunctional diacetylenes
[AD-A149104] 10 p1451 N85-19145
Characterization of acetylene-terminated resin cure states
[AD-A149463] 10 p1452 N85-19146
Synthesis and thermomechanical properties of new AT-Phenylene R systems
[AD-A149961] 12 p1813 N85-21372
Collaborative shock tube studies of benzene pyrolysis
[DE85-006347] 14 p2253 N85-23962
The mechanisms of phenylacetylene polymerization by molybdenum and titanium initiators
[AD-A150993] 14 p2260 N85-24007
C2H(n) fragments on metal surfaces
[AD-A151474] 15 p2505 N85-25449
Crossed molecular beam studies of the reactions of oxygen and fluorine atoms
[AD-A153302] 17 p2921 N85-28006
Lifetime and quenching measurements of C2H emission produced by vacuum ultraviolet photolysis of C2H2
[DE85-010769] 19 p3278 N85-30330
Metal alkoxides: Models for metal oxides. Alkoxide ligands in early transition metal organometallic chemistry
[DE85-011368] 23 p3916 N85-34269
The photodissociation of acetylene at 193.3 NM
[AD-A155775] 24 p4075 N85-35255

ACHIEVEMENT
The impact of group processing on achievement in cooperative learning groups
[AD-A153168] 17 p3001 N85-28551
Oral discussion, group-to-individual transfer and achievement in cooperative learning groups
[AD-A153209] 17 p3001 N85-28552

ACID BASE EQUILIBRIUM
A potentiometric study of chloroaluminate equilibria in the aluminum chloride - 1-methyl-2-ethylimidazolium chloride ionic liquid
[AD-A144729] 01 p0023 N85-10144
Monitoring approaches for assessing quality of high altitude lakes: Colorado Flat Tops Wilderness Area
[PB85-117232] 11 p1679 N85-20579

ACID RAIN
Acid rain and transported air pollutants: Implications for public policy
[PB84-222967] 01 p0071 N85-10469
Analysis of potential combustion sorce impacts on acid deposition using an independently derived inventory, volume 1
[DE84-012005] 02 p0225 N85-11471
Estimation of the potential and probable source regions for acid precipitation
[DE84-015119] 02 p0225 N85-11472
Potential for acidification of six remote ponds in the White Mountains of New Hampshire
[PB84-207349] 02 p0225 N85-11475
Selection, procurement and description of Salem Limestone samples used to study the effects of acid rain
[PB84-231067] 04 p0484 N85-13066
Effects of acid rain on plant microbial associations in California
[PB84-242122] 04 p0532 N85-13404
Transformation processes and wet deposition on the urban scale
[DE84-015294] 04 p0539 N85-13432
Acid rain and tree physiology: Some hypotheses for observed changes in forest productivity
[DE84-016568] 05 p0672 N85-14318
Analysis of terrestrial conditions and dynamics
[E85-10063] 08 p1174 N85-17401
Mesoscale storm and dry period parameters from hourly precipitation data: Program documentation
[DE85-001366] 09 p1357 N85-18538
Sequential precipitation chemistry sampling program at Brookhaven National Laboratory with an analytical summary of 1976-1982 data
[DE85-002788] 10 p1513 N85-19545
Non-photochemical interactions of sulfur and nitrogen compounds in acid deposition
[DE84-016141] 10 p1513 N85-19546
National Acid Precipitation Assessment Program. Report to the President and Congress (1983)
[PB85-116713] 11 p1679 N85-20581
National Performance Audit Program ambient air audits of analytical proficiency
[PB85-138204] 11 p1680 N85-20586
Effects of air pollution and acid rain on forest decline
[GPO-37-459] 12 p1883 N85-21818
Report on the Second Annual Review Meeting of the National Acid Precipitation Assessment Program. Research to assist decisionmaking: Summary
[DE85-003003] 12 p1884 N85-21820
Combined effects of atmospheric deposition, internal acid production, and harvesting on nutrient gains and losses from forest ecosystems
[DE85-002325] 12 p1884 N85-21821
Gas-liquid chemistry of natural waters, volume 1
[DE85-002803] 12 p1884 N85-21822
Rationale and basic design for experimental acidification of a lake ecosystem in Northern Wisconsin
[PB85-116077] 12 p1885 N85-21829
Non-precipitating cumulus cloud study
[DE85-002352] 12 p1896 N85-21902
Studies of the mechanisms and rates with which nitrogen species are incorporated into cloud water and precipitation
[PB85-144350] 12 p1898 N85-21914
Areas with forest soils sensitive to acidic deposition under alternative damage hypotheses
[DE85-005257] 13 p2130 N85-23257
PLUVIUS: A generalized 1-dimensional model of reactive pollutant behavior, including dry deposition, precipitation formation, and wet removal, 2nd edition
[DE85-005542] 14 p2353 N85-24538
MAP3S precipitation chemistry network
[DE85-005324] 14 p2353 N85-24539
An analysis of issues concerning acid rain, report to the Congress of the United States
[TI85-901070] 15 p2589 N85-25959
A comparative evaluation of the effects of acid precipitation, natural acid production and harvesting of cation removal from forests
[DE85-005254] 15 p2589 N85-25961

Emission inventory applications to regional acid deposition modeling
[PB85-157398] 16 p2760 N85-27033

Interactive effects of acid rain and gaseous air pollutants on natural terrestrial vegetation
[DE85-005255] 16 p2821 N85-27401

Acid rain: Effects on fish and wildlife
[PB85-154672] 16 p2821 N85-27402

Acid precipitation in North America: 1980, 1981 and 1982 annual data summaries from acid deposition system data base
[PB85-162477] 16 p2822 N85-27410

Acid rain: Towards automated monitoring
16 p2829 N85-27444

Oxygen isotopic study of the oxidation of SO2 by H2O2 in the atmosphere
[DE85-004017] 17 p2988 N85-28468

Chemical transformations in acid rain. Volume 2: Investigation of kinetics and mechanism of aqueous-phase peroxide formation
[PB85-173433] 18 p3135 N85-29416

North American acid deposition data base system (ADS) and its use in spatial analysis
[PB85-173235] 18 p3201 N85-29856

Evaluation of methods used for the determination of acidity in acid rain samples
[PB85-178309] 19 p3237 N85-30070

Environmental Sciences Division report
[DE85-010452] 19 p3306 N85-30506

A comparative evaluation of the effects of acid precipitation, natural acid production and harvesting on cation removal from forests
[DE85-010821] 19 p3309 N85-30511

Chemical transformation in acid rain. Volume 1: New methodologies for sampling and analysis of gas-phase peroxide
[PB85-173425] 19 p3311 N85-30527

An interim user's manual for the advanced scavenging module version 1.2
[PB85-173904] 19 p3318 N85-30572

Design of the National Trends Network for monitoring the chemistry of atmospheric precipitation
[GS-CIRC-964] 20 p3486 N85-31664

Atmospheric Tracer Workshop
[DE85-010573] 20 p3486 N85-31668

Historic emissions of sulfur and nitrogen oxides in the U.S. from 1900 to 1980. Volume 1: Results
[PB85-191195] 20 p3487 N85-31674

Historic emissions of sulfur and nitrogen oxides in the U.S. from 1900 to 1980. Volume 2: Data
[PB85-191203] 20 p3487 N85-31675

EPA (Environmental Protection Agency) research program guide, FY-1985, October 1, 1984 - September 30, 1985
[PB85-181881] 20 p3487 N85-31676

Acid rain in Europe
[COMMITTEE-PRINT-99-F] 22 p3810 N85-33601

Practical consequences of the assessment of different energy health risks
[DE85-004538] 22 p3825 N85-33696

Effects of acid rain on forest nutrient status
[DE85-012486] 23 p3947 N85-34463

Throughfall rate and chemistry studies: Whiteface Mountain
[DE85-012407] 23 p3947 N85-34484

ACIDITY

Acid Deposition: Processes of Lake Acidification
[PB84-216175] 01 p0070 N85-10466

Potential for acidification of six remote ponds in the White Mountains of New Hampshire
[PB84-207349] 02 p0225 N85-11475

Monitoring approaches for assessing quality of high altitude lakes: Colorado Flat Tops Wilderness Area
[PB85-117232] 11 p1679 N85-20579

Evidence that resorption of bone by rat peritoneal macrophages occurs in an acidic environment
15 p2612 N85-26098

Evaluation of methods used for the determination of acidity in acid rain samples
[PB85-178309] 19 p3237 N85-30070

Granulometric study of the acidity and sulfate excess in marine aerosols 21 p3652 N85-32691

ACIDS

NT ALANINE
NT AMINO ACIDS
NT ASPARTIC ACID
NT BENZOIC ACID
NT BUTYRIC ACID
NT CARBOXYLIC ACIDS
NT CHROMIC ACID
NT CITRIC ACID
NT DEOXYRIBONUCLEIC ACID
NT DICARBOXYLIC ACIDS
NT FATTY ACIDS
NT GLUTAMINE
NT GLUTATHIONE
NT GLYCINE
NT HYDROBROMIC ACID
NT HYDROCHLORIC ACID
NT HYDROFLUORIC ACID
NT METHIONINE
NT NITRIC ACID
NT OXIDASE
NT PEPTIDES
NT PHOSPHORIC ACID
NT RIBONUCLEIC ACIDS
NT SULFURIC ACID
NT TRYPTOPHAN

Spectrophotometric studies of iodine complexes in an aluminum chloride - butylpyridinium chloride ionic liquid
[AD-A145074] 01 p0024 N85-10150

Computer-assisted Gran titration procedure for strong acid determination
[DE85-006801] 15 p2507 N85-25482

A comparative evaluation of the effects of acid precipitation, natural acid production and harvesting of cation removal from forests
[DE85-005264] 15 p2589 N85-25961

Correlation of zeolite ZSM-5 acid strength with catalytic activity and selectivity
[DE85-005415] 17 p2922 N85-28013

Improved acid electrolytes for fuel cells
[PB85-176053] 18 p3132 N85-29397

An interim user's manual for the advanced scavenging module version 1.2
[PB85-173904] 19 p3318 N85-30572

Method for extracting lanthanides and actinides from acid solutions by modification of Purex solvent
[DE85-006763] 23 p3909 N85-34220

Origin of sedimentary humic acids, potential carriers of ore-forming elements 24 p4104 N85-35443

ACOUSTIC ATTENUATION

NT SHOCK WAVE ATTENUATION

The role of dislocations in ultrasonic attenuation
[AERE-R-11384] 12 p1804 N85-21317

Surface forward scattering and reflection
[AD-A150115] 12 p1926 N85-22112

Long range downwind propagation of low-frequency sound
[NASA-TM-86409] 15 p2645 N85-26318

Interaction of finite-amplitude sound with air-filled porous materials
[NASA-CR-174885] 16 p2860 N85-27637

Study of sound attenuation in sediments
[AD-A153690] 18 p3177 N85-29697

Airborne sound transmission loss characteristics of wood-frame construction
[AD-A154174] 20 p3524 N85-31919

Overground Excess Sound Attenuation (ESA). Volume 3: Application of ESA data in NOISEFILE
[AD-A154820] 21 p3699 N85-32984

Lateral attenuation of aircraft flight noise
[AD-A154958] 21 p3700 N85-32986

Acoustical absorption coefficient in a diffuse field of a plane, rectangular material of finite dimensions placed on an infinite perfectly reflecting surface
[NRC/CNR-TT-2113] 23 p3968 N85-34599

ACOUSTIC COMBUSTION

U COMBUSTION STABILITY

ACOUSTIC DUCTS

Investigations of reactive and non reactive acoustic boundary layers in porous walled ducts
13 p2000 N85-22535

On the solution for the sound field in a semi-infinite uniform duct with sheared mean flow
20 p3523 N85-31912

Models for describing active noise control in ducts
[ISVR-TR-127] 20 p3525 N85-31922

ACOUSTIC EMISSION

Acoustic emission linear pulse holography
[DE84-014519] 01 p0050 N85-10330

Detection of hydrogen assisted crack growth by measurement of modulus changes and acoustic emission
[DE84-015752] 02 p0184 N85-11236

Contributions to the 7th International Acoustic Emission Symposium
[AD-A145368] 02 p0275 N85-11792

Acoustic emission monitoring of fatigue in 7010 aluminum alloys
[AERE-R-11167] 03 p0334 N85-12152

Technical activities 1983, Office of Nondestructive Evaluation
[PB84-217074] 03 p0370 N85-12360

Rotary-wing aircraft noise measurements: Analysis of variations and proposed measurement standard
[AD-A146207] 03 p0416 N85-12662

Acoustic emission waveforms in a half space
[AD-A146322] 03 p0417 N85-12664

Three-dimensional crack location by acoustic emission
[AERE-R-11277] 06 p0818 N85-15193

Identification of leaks: Internal acoustic method, phase 2
[PB85-101947/GAR] 07 p0936 N85-15927

Quantitative acoustic emission techniques
[AERE-R-11262] 07 p0977 N85-16203

In-situ stress determination in soil and rock using the acoustic emission method
[AD-A147459] 07 p0979 N85-16215

Journal of Research of the National Bureau of Standards, Volume 89, Number 1, January-February, 1984
[PB84-235530] 08 p1262 N85-17931

Contribution of the study of light aircraft propeller noise
[ESA-TT-865] 09 p1378 N85-18667

Leak monitoring in high pressure preheaters by a noninvasive ultrasonic method
[CISE-2373] 11 p1650 N85-20394

Leak detection by acoustic emission monitoring in power plant high pressure preheaters
[CISE-2392] 11 p1650 N85-20395

Defect characterisation and monitoring by acoustic emission
[AERE-R-11409] 12 p1863 N85-21683

Characterisation of fatigue crack extension by quantitative acoustic emission
[AERE-R-11289] 12 p1866 N85-21721

Method and apparatus for detecting acoustic emissions from metal matrix wire
[AD-D011556] 12 p1927 N85-22107

Use of acoustical emission method to study specifics of fracture of boron reinforced plastic structural elements 13 p2026 N85-22606

Optimal synthesis of surface acoustic wave filters
13 p2070 N85-22933

Sound emission by particle beam passing through hole in rigid shield 15 p2525 N85-25570

Acoustic emission of semiconductor devices
15 p2529 N85-25593

Contribution to the study of equivalent noise source identification in fast cold jets
[ISL-R-114/83] 16 p2861 N85-27645

Method of assessment of start of slow crack growth by acoustic emission technique
[BLL-BISI-TRANS-21762-(9022.06)]
17 p3027 N85-28722

Acoustic emission study of fatigue crack extension position in a stress cycle 19 p3263 N85-30355

Propagation of acoustic pulse in atmospheric waveguide 19 p3297 N85-30443

Production verification of the acoustic emission weld monitor
[AD-A154168] 20 p3464 N85-31519

Simulation model of acoustic emission due to microscopic fracture in metals
[BLL-BISI-TRANS-22367-(9022.06)]
20 p3523 N85-31909

Source characterization of point-like and distributed sources of acoustic emission 20 p3523 N85-31910

Acoustic emission during transformation of austenite in 38KhN3MF steel
[BLL-M-35825-(5828.4)] 23 p3914 N85-34258

Contribution to the properties of carbon fiber reinforced composites — structural mechanics
[ESA-TT-849] 24 p4074 N85-35246

ACOUSTIC EXCITATION

Behavior of charged particles in lower ionosphere with acoustical effects 02 p0161 N85-11069

Optoacoustic spectroscopy
[AD-A145995] 03 p0419 N85-12679

Response measurements for two building structures excited by noise from a large horizontal axis wind turbine generator
[NASA-CR-172482] 04 p0558 N85-13552

Spacecraft structural acoustic studies: Development of structural acoustic design guides
[ESA-CR(P)-1916] 05 p0604 N85-13849

Preliminary analysis of tone-excited two-stream jet velocity decay
[NASA-TM-86951] 12 p1770 N85-21114

Acoustic agglomeration methods and apparatus
[NASA-CASE-NPO-15466-1] 12 p1927 N85-22104

Vibroacoustic study of the NASA Goddard Space Flight Center OSS-1 payload
[NASA-CR-175320] 13 p1986 N85-22465

Acoustic noise associated with the MOD-1 wind turbine: its source, impact, and control
[DE85-002947] 18 p3178 N85-29700

Acoustic radiation from concentric shells containing an inner fluid
[AD-A155476] 21 p3700 N85-32991

ACOUSTIC GENERATORS

U SOUND GENERATORS

ACOUSTIC IMPEDANCE

Determination of the pressure sensitivity of 1 inch condenser microphones
[PTB-AK-26] 05 p0633 N85-14058

The effect of grazing flow on the impedance of the Helmholtz resonator 05 p0636 N85-14076
Characteristic impedance of a porous center during transmission of quasi-static sinusoidal vibrations
[ISSN-0208-5658] 05 p0647 N85-14155
On the long range propagation of sound over irregular terrain
[NASA-CR-3862] 07 p1038 N85-16589
Interaction of finite-amplitude sound with air-filled porous materials
[NASA-CR-174885] 16 p2860 N85-27637
Reactanceless synthesized impedance bandpass amplifier
[NASA-CASE-GSC-12786-1] 18 p3093 N85-29145
Method for thermal monitoring subcutaneous tissue
[NASA-CASE-LAR-13028-1] 19 p3326 N85-30616
Spectral methods for the estimation of acoustic intensity, energy density, and surface velocity using a multimicrophone probe 20 p3524 N85-31916
ACOUSTIC INSTABILITY
Theoretical study of collective ion acceleration in the Luce diode
[AD-A150107] 12 p1929 N85-22116
Acoustic energy balance method
13 p2000 N85-22537
Investigation of the characteristics of the velocity-coupled response functions of solid propellants
13 p2001 N85-22540
Measurements of distributed combustion
13 p2001 N85-22542
Distributed combustion: A mechanism of acoustic suppression 13 p2001 N85-22543
ACOUSTIC LEVITATION
Development of the sonic pump levitator
[NASA-CR-171382] 12 p1782 N85-21186
High temperature acoustic levitator
[NASA-CASE-NPO-16022-1] 12 p1927 N85-22105
Gravity enhanced acoustic levitation method and apparatus
[NASA-CASE-NPO-16147-1-CU]
18 p3177 N85-29693
ACOUSTIC MEASUREMENT
NT NOISE MEASUREMENT
YO-3A acoustics research aircraft systems manual
[NASA-TM-85968] 01 p0012 N85-10074
Electromagnetic-acoustic-transducer
a system for thick-weld inspection
[PB84-219492] 01 p0051 N85-10336
Low-frequency sound absorption measurements in air
[NASA-RP-1128] 02 p0275 N85-11789
Pulse-echo method for flaw detection in concrete
[PB84-234509] 06 p0775 N85-14953
Analytical and physical modeling program for the NASA Lewis Research Center's Altitude Wind Tunnel (AWT)
[NASA-TM-86919] 07 p0909 N85-15757
Acoustic transducers for fast reactor instrumentation
[BLL-RISLEY-TR-4979-(9091.9F)]
07 p0961 N85-16091
External cavity diode laser sensor
[AD-D011341] 07 p0969 N85-16152
Quantitative acoustic emission techniques
[AERE-R-11262] 07 p0977 N85-16203
Acoustic tomographic reconstrution of anomalies in three-dimensional bodies
[DE84-017035] 09 p1378 N85-18686
USSR report: Physics and mathematics
[JPRS-UPM-85-001] 11 p1715 N85-20786
Nondestructive method for detecting machine damage in beryllium
[DE85-001074] 12 p1862 N85-21681
Defect characterisation and monitoring by acoustic emission
[AERE-R-11409] 12 p1863 N85-21683
The measurement of residual stresses using ultrasonics
[AERE-R-11415] 12 p1866 N85-21722
Calibration method for acoustic scattering measurements using a spherical target
[AD-D011521] 12 p1927 N85-22106
Numerical results of acoustic radiation, transmission and reflection of steel plate in water
[AMTE(N)-TM-84037] 13 p2155 N85-23378
Properties of materials using acoustic waves
[AD-A150486] 13 p2155 N85-23382
Surface pressure produced by Space Transportation System flight 41B
[AD-A150793] 14 p2242 N85-23901
Investigation of errors of acoustic goniometer information-measurement systems on rocking base
14 p2283 N85-24139
Optical monitoring of photo-acoustic pulse propagation in silicon wafers
[AD-A151333] 15 p2651 N85-26352
Development of a modified time delay spectrometry technique for underwater acoustic measurements in a multipath environment
[AD-A152111] 16 p2860 N85-27639
Experimental investigation of the pulsed photoacoustic effect produced on a solid surface
[AD-A152114] 16 p2860 N85-27640
Measurement of cochlear acoustic pressure in guinea pigs
[ISL-CO-234/83] 16 p2861 N85-27644
The Shock and Vibration Digest, volume 17, no. 1
[AD-A151061] 17 p2977 N85-28397
Sound intensity measurement
17 p2977 N85-28398
Correlation of predicted and measured sonic boom characteristics from the reentry of STS-1 orbiter
[NASA-TP-2475] 18 p3177 N85-29694
Study of sound attenuation in sediments
[AD-A153690] 18 p3177 N85-29697
Crosswell acoustic surveying in gas sands: Travel-time pattern recognition, seismic Q and channel waves
[DE85-010777] 19 p3352 N85-30778
On the solution for the sound field in a semi-infinite uniform duct with sheared mean flow
20 p3523 N85-31912
Gas sensing with surface acoustic wave devices
[DE85-009125] 20 p3524 N85-31921
Ultrasonic position reference systems for an autonomous sentry robot and a robot manipulator arm
[AD-A155481] 21 p3596 N85-32336
FAA/GAMA (Federal Aviation Administration/General Aviation Manufacturer's Association) propeller aircraft noise test program, Salina Municipal Airport, Salina, Kansas
[AD-A154818] 21 p3699 N85-32983
Acoustic cross-correlation flowmeter for solid-gas flow
[DE85-005968] 23 p3936 N85-34391
Acoustical absorption coefficient in a diffuse field of a plane, rectangular material of finite dimensions placed on an infinite perfectly reflecting surface
[NRC/CNR-TT-2113] 23 p3966 N85-34599
Search for acoustic signals from high energy cascades
[HE-7.1-1] 24 p4213 N85-36155
Experimental investigation of radiative-acoustic effects in the water by the thermodynamical conditions of Dumand
[HE-7.1-2] 24 p4213 N85-36156
Exploring results of the possibility on detecting cosmic ray particles by acoustic way
[HE-7.1-3] 24 p4213 N85-36157
Acoustic detection of air shower cores
[HE-7.1-4] 24 p4213 N85-36158
ACOUSTIC MICROSCOPES
High resolution acoustic microstructural characterization of titanium with interstitial contamination
[AD-P004128] 08 p1127 N85-17103
Research on nondestructive testing
[AD-A148375] 08 p1171 N85-17380
Acoustic microscopy at cryogenic temperatures
[AD-A146755] 09 p1384 N85-18704
Scanning photoacoustic microscopy of aluminum with aluminum oxide, roughness standards and rubber
[AD-A149460] 10 p1441 N85-19081
Nondestructive method for detecting machine damage in beryllium
[DE85-001074] 12 p1862 N85-21681
Reliability of void detection in structural ceramics using scanning laser acoustic microscopy
[NASA-TM-87035] 21 p3597 N85-32337
ACOUSTIC PROPAGATION
A description and discussion of FREDDEX oceanographic measurements
[AD-A145032] 01 p0066 N85-10596
Behavior of charged particles in lower ionosphere with acoustical effects 02 p0161 N85-11069
The numerical solution of the Helmholtz equation for wave propagation problems in underwater acoustics
[NASA-CR-172454] 02 p0250 N85-11634
The acoustic pressure in a wedge-shaped water layer overlying a fast fluid bottom
[AD-A145517] 02 p0276 N85-11795
The S-matrix and acoustic signal structure in simple and compound waveguides
[PP-583] 03 p0415 N85-12652
Deep water mass circulation in the Western Alboran Basin: Measurements in July and September 1980 (Alboran I experiment)
[AD-A146586] 08 p1191 N85-17504
SAI (Science Applications, Inc.) Interim Scattering Model/Ice (SISM/ICE)
[AD-A146596] 08 p1213 N85-17636
A critical analysis of ocean thermal analysis models in operation at FNOC (Fleet Numerical Oceanography Centers)
[AD-A146731] 09 p1359 N85-18547
Preliminary results of study of space-time variability of shallow sea on steady acoustical path
10 p1469 N85-19459
Arctic acoustic propagation model with ice scattering
[AD-A149430] 10 p1553 N85-19795
A stochastic-mechanical approach to acoustic pulse propagation in the deep ocean sound channel
[AD-A149698] 12 p1928 N85-22110
Acoustic energy exchange in sheared mean flows — solid rocket motors 13 p1990 N85-22534
Transmission of gear noise to aircraft interiors prediction methods 14 p2223 N85-23766
Abatement of noise and vibration in pipelines of hydro systems 14 p2276 N85-24102
Acoustic radiation from bilaminar plates
14 p2415 N85-24903
Propagation of sound in matter
[AD-A151013] 14 p2416 N85-24907
Propagation of sound in matter
[AD-A151052] 14 p2416 N85-24908
Recent progress in the development and application of the parabolic equation
[AD-A151475] 15 p2637 N85-26265
Long range downwind propagation of low-frequency sound
[NASA-TM-86409] 15 p2645 N85-26318
Acoustic propagation in a thermally stratified atmosphere
[NASA-CR-175767] 16 p2860 N85-27636
Propagation of acoustic pulse in atmospheric waveguide 19 p3297 N85-30443
Microwave SAW (Surface Acoustic Wave) monochromator
[AD-D011718] 21 p3590 N85-32311
ACOUSTIC PROPERTIES
NT ACOUSTIC IMPEDANCE
NT ACOUSTIC INSTABILITY
NT ACOUSTIC SCATTERING
NT ACOUSTIC VELOCITY
NT REVERBERATION
NT SOUND INTENSITY
Vibration, acoustic, and shock design and test criteria for components on the Solid Rocket Boosters (SRB), Lightweight External Tank (LWT), and Space Shuttle Main Engines (SSME)
[NASA-RP-1127] 01 p0061 N85-10405
Nonlinear acoustics
[AD-A145580] 02 p0276 N85-11796
Sources, paths, and concepts for reduction of noise in the test section of the NASA Langley 4x7m wind tunnel
[NASA-CR-172446-VOL-1] 05 p0726 N85-14666
Comparison of options for reduction of noise in the test section of the NASA Langley 4x7m wind tunnel, including reduction of nozzle area
[NASA-CR-172446-VOL-2] 05 p0726 N85-14667
Noise measurement flight test: Data-analyses, Sikorsky S-76A helicopter
[AD-A148525] 08 p1218 N85-17673
Effect of sealants of the sound absorption coefficients of acoustical friable insulating materials
[AD-A148541] 08 p1218 N85-17674
Methods of computer-aided analysis of non-Gaussian noise and application to robust adaptive detection, part 2
[AD-A148670] 10 p1539 N85-19704
Acoustic scaling: A re-evaluation of the acoustic model of Manchester Studio 7
[BBC-RD-1984/18] 12 p1822 N85-21432
Interaction of a turbulent vortex with a lifting surface
15 p2464 N85-25214
Phase-lock fiber optic interferometer
[AD-D011603] 16 p2786 N85-27191
Geoacoustic models: Washington state continental margin
[AD-A153761] 18 p3177 N85-29699
Chemical-acoustic interactions in combustion systems
[AD-A153657] 19 p3233 N85-30046
Measured acoustic properties of variable and low density bulk absorbers
[NASA-TM-87065] 19 p3351 N85-30770
Airborne sound transmission loss characteristics of wood-frame construction
[AD-A154174] 20 p3524 N85-31919
Acoustic scaling: The development of improved instrumentation
[BBC-RD-1985/7] 24 p4145 N85-35694
Analysis of two-parameter constant background born inversion for acoustic synthetic data
[AD-A156394] 24 p4145 N85-35696
Acoustic resonances in cylinder bundles oscillating in a compressible fluid
[DE85-004066] 24 p4145 N85-35699
ACOUSTIC RADIATION
U SOUND WAVES

ACOUSTIC RETROFITTING
Noise in small portable motocompressors. Experiments on limited-cost acoustic treatments to obtain progressive improvements
[CETIM-11-H-445] 04 p0558 N85-13557
Aircraft cabin noise prediction and optimization
[NASA-CR-175982] 19 p3350 N85-30768
Design of sidewall treatment of cabin noise control of a twin engine turboprop aircraft
[NASA-CR-172245] 19 p3351 N85-30771

ACOUSTIC SCATTERING
NT REVERBERATION
Analytical modeling of random thermal fluctuations in the NORDA high-frequency sound scattering facility
[AD-A145024] 01 p0116 N85-10790
High-frequency asymptotic behavior of reflected and transmitted waves during scattering of sound by hollow elastic sphere filled with fluid 02 p0266 N85-11738
Acoustic scattering cross sections for truly composite wind-wave surfaces. Scattering without bubbles
[AD-A145672] 03 p0415 N85-12655
Selective observation of elastic-body resonances via their ringing in transient acoustic scattering
[AD-A145868] 03 p0416 N85-12658
USSR report: Physics and mathematics
[JPRS-UPM-84-007] 05 p0723 N85-14651
Resonant scattering of acoustic waves by elastic spherical shell in fluid 06 p0778 N85-14972
Research on acoustical and optical scattering, optics of bubbles, diffraction catastrophes, laser generation of sound, and shock induced cavitation
[AD-A146703] 06 p0860 N85-15466
SAI (Science Applications, Inc.) Interim Scattering Model/Ice (SISM/ICE)
[AD-A148596] 08 p1213 N85-17636
Arctic acoustic propagation model with ice scattering
[AD-A149430] 10 p1553 N85-19795
Calibration method for acoustic scattering measurements using a spherical target
[AD-D011521] 12 p1927 N85-22106
Surface forward scattering and reflection
[AD-A150115] 12 p1928 N85-22112
Surface scattering
[AD-A150252] 13 p2153 N85-23366
Elastic wave scattering from cavities and sound inclusions analyzed by the resonance method
[AD-A150315] 13 p2155 N85-23381
Properties of materials using acoustic waves
[AD-A150465] 13 p2155 N85-23382
Scattering of sounds by piezoceramic cylindrical shell near rigid surface 17 p2943 N85-28168
Toward the theory of acoustic scattering on uneven free surface 21 p3680 N85-32862
Understanding coherence losses incurred by bottom-retained signals
[AD-A155559] 21 p3701 N85-32992
Second Colloquim on the Scattering of Ultrasonic Waves
[AD-A156298] 24 p4145 N85-35697

ACOUSTIC SOUNDING
Characterization of stressed metals using acoustic shear waves 05 p0648 N85-14159
Influence of refraction effects on informativeness of bistatic acoustical atmospheric sounding systems
06 p0825 N85-15237
Specifics of backscattering of sound by bottom of bank in open sea 10 p1499 N85-19460
Average sound intensity decrease rule in irregular hydroacoustical waveguide 10 p1499 N85-19461
Ultrasonic large-diameter pipe weld testing installations 11 p1603 N85-20081
Quantitative non-destructive evaluation of damage in composite materials using transmitted and reflected ultrasound
[NASA-CR-175550] 12 p1796 N85-21269
Experimental results of temperature-wind soundings of the atmosphere by the radio acoustical method
14 p2340 N85-24471

ACOUSTIC STABILITY
U FREQUENCY STABILITY

ACOUSTIC VELOCITY
Active remote sensing of ocean parameters, an engineering study 02 p0213 N85-11403
CHORDS: A new temperature or sound speed profile thinning algorithm
[AD-A145464] 02 p0275 N85-11793
Project review on geophysical and ocean sound speed profile inversion
[AD-A145717] 02 p0276 N85-11797
Influence of pressure on speed of sound in single-phase region of stratifying mixtures 11 p1715 N85-20788
Sound velocity of carbon at high pressures
[DE85-002016] 12 p1926 N85-22113
Coupling between velocity oscillations and solid propellant combustion 13 p2000 N85-22536
Coupled acoustic and hydrodynamic wave instabilities
13 p2000 N85-22538
Investigation of the characteristics of the velocity-coupled response functions of solid propellants
13 p2001 N85-22540
Coupling between velocity oscillations and solid propellant combustion
[AD-A151081] 14 p2247 N85-23927
Field of point source of low-frequency sound in atmosphere with altitudinally nonuniform wind
15 p2524 N85-25566
Wave description of sound propagation through stratified moving atmosphere 15 p2525 N85-25567
Apparatus for measuring velocity of sound in fluids
17 p2944 N85-28175
Spectral methods for the estimation of acoustic intensity, energy density, and surface velocity using a multimicrophone probe 20 p3524 N85-31916
Trailing edge flow and aerodynamic sound. Part 1: Tonal pressure and velocity fluctuations. Part 2: Random pressure and velocity fluctuations
[AD-A154947] 21 p3552 N85-32097
Toward the propagation of waves in unsteady media
21 p3683 N85-32881
Sound speed measurements in liquid oxygen-liquid nitrogen mixtures
[NASA-TP-2464] 24 p4083 N85-35307
Experimental investigation of radiative-acoustic effects in the water by the thermodynamical conditions of Dumand
[HE-7.1-2] 24 p4213 N85-36156

ACOUSTIC VIBRATIONS
U SOUND WAVES

ACOUSTICAL HOLOGRAPHY
Heterodyne holographic interferometry for visualization of surface acoustic waves
[AD-A155405] 22 p3636 N85-33753

ACOUSTICS
NT AEROACOUSTICS
NT GEOMETRICAL ACOUSTICS
NT MAGNETOACOUSTICS
NT PSYCHOACOUSTICS
NT UNDERWATER ACOUSTICS
Scattering of plane wave on cylindrical shell in low-frequency region 02 p0256 N85-11677
Influence of radiation wavelength on elastic pulse shape during laser excitation 02 p0257 N85-11681
Laminar-to-turbulent flow transition under influence of acoustic oscillations 02 p0260 N85-11701
USSR report: Physics and mathematics
[JPRS-UPM-84-004] 02 p0266 N85-11737
Coupling of airborne sound into the Earth
[AD-A146231] 03 p0416 N85-12663
Research activities of the Illinois University Coordinated Science Laboratory
[AD-A145589] 03 p0449 N85-12856
USSR report: Electronics and electrical engineering
[JPRS-UEE-84-010] 04 p0485 N85-13095
Perceptibility of nonlinear distortions in power amplifier
06 p0789 N85-15041
A miniature urethane molded acoustic transducer
[AD-A146459] 06 p0804 N85-15114
An extension of the Born inversion method to a depth dependent reference profile
[AD-A146469] 06 p0859 N85-15461
Human engineer's guide to auditory displays. Volume 2: Elements of signal reception and resolution affecting auditory displays
[AD-A146513] 06 p0859 N85-15462
Basic research in electronic (JSEP): Joint Services Electronics Program
[AD-A147891] 07 p0948 N85-16007
Statistical filtering as method for detecting transcrustal acoustic anomalies 07 p0962 N85-16237
Analysis of the surface load and radiated sound of a vibrating airfoil with application to the experiment of Brooks
[NASA-CR-3864] 07 p1036 N85-16590
Estimate of sound absorption due to magnetoelastic interactions
[AD-A148216] 08 p1218 N85-17671
Digital sound: Programme-modulated noise levels in sound signals subjected to a number of digital companding processes
[BBC-RD-1984/11] 09 p1310 N85-18233
On the interaction of a sound pulse with the shear layer of an axisymmetric jet. Part 3: Nonlinear effects
[NASA-CR-172512] 09 p1378 N85-18863
Acoustic resonance in heat exchanger tube banks
[DE85-004395] 11 p1632 N85-20281
USSR report: Electronics and electrical engineering
[JPRS-UEE-85-004] 12 p1837 N85-21531
Methods of progressing waves in turbulent media with applications to acoustics
[AD-A149599] 12 p1920 N85-22055
Ice statistics and acoustic scattering in the Arctic basin
[AD-A150141] 13 p2140 N85-23269
Noise measurement flight test: Data/Analyses, hughes 500 D/E helicopter
[AD-A148110] 14 p2219 N85-23758
Propagation of sound in matter
[AD-A151013] 14 p2416 N85-24907
Propagation of sound in matter
[AD-A151052] 14 p2416 N85-24908
Psychological and physiological basis of stereophonic effect 15 p2526 N85-25574
An evaluation of proposed acoustic treatments for the NASA LaRC 4 x 7 meter wind tunnel
[NASA-CR-172577] 15 p2648 N85-26319
Analysis of combustion oscillations in heterogeneous systems
[AD-A151999] 16 p2745 N85-26942
Phase-lock fiber optic interferometer
[AD-D011603] 16 p2766 N85-27191
Acoustic oscillations of rods and plates
17 p2944 N85-28170
Theoretical investigations of the propagation and interactions of surface waves
[AD-A153548] 18 p3185 N85-29753
Activities of Istituto Elettrotecnico Nazionale Galileo Ferraris 18 p3199 N85-29845
Hot Dry Rock Geothermal Energy Developement Program
[DE85-010570] 19 p3268 N85-30264
Acoustic particle separation
[NASA-CASE-NPO-155559-1] 19 p3350 N85-30765
Acoustic imaging systems (for robotic object acquisition)
[AD-A154043] 19 p3351 N85-30772
USSR report: Physics and mathematics
[JPRS-UPM-85-004] 21 p3680 N85-32860
Lateral attenuation of aircraft flight noise
[AD-A154958] 21 p3700 N85-32986
Heterodyne holographic interferometry for visualization of surface acoustic waves
[AD-A155405] 22 p3636 N85-33753
Applications of the Kirchoff-Helmholtz integral to problems in body wave seismology
24 p4116 N85-35515
Acoustic scaling: The development of improved instrumentation
[BBC-RD-1985/7] 24 p4145 N85-35694

ACOUSTO-OPTICS
Guided-wave optic devices for integrated optic information processing
[AD-A145695] 02 p0280 N85-11827
Characteristics of light diffraction by two acoustic waves, one with complex frequency composition
03 p0348 N85-12243
USSR report: Physics and mathematics
[JPRS-UPM-84-007] 05 p0723 N85-14651
Laser excitation of coupled surface electromagnetic and acoustic waves and of static structures in solids
05 p0723 N85-14652
A single optical fiber telephone system
[AD-D011293] 06 p0799 N85-15107
USSR report: Electronics and electrical engineering
[JPRS-UEE-84-018] 07 p0949 N85-16014
Optimization piezoelectric transducer width of acousto-optical devices 07 p0950 N85-16024
Study of optical sound generation and amplification
[AD-A147359] 07 p1039 N85-16592
Tunable heterodyne receiver from 100 micron to 1,000 micron for airborne observations
08 p1249 N85-17888
Optical data processing for missile guidance
[AD-A149346] 10 p1422 N85-18972
Photoacoustic effect and its applications
12 p1820 N85-21421
Acousto-optically addressed Fourier transform matched filters
[AD-A150298] 13 p2063 N85-22889
USSR report: Electronics and electrical engineering
[JPRS-UEE-85-002] 13 p2066 N85-22907
Space-time response characteristics of acoustooptic filter for compression of linearly frequency-modulated signal 13 p2071 N85-22937
Integrated optical components utilizing acoustooptic and electrooptic diffraction in micro-waveguides
13 p2089 N85-23044
Acoustooptic demodulation of frequency-modulated signals 13 p2090 N85-23050
Acoustooptic cell as space-frequency filter
13 p2090 N85-23051
Accuracy of random signal spectral parameter estimation against interference background in acoustooptical spectrum analyzers
13 p2090 N85-23052
Optoacoustic receiver with semiconductor-type radiator and photodetector 14 p2274 N85-24066

Photoacoustic imaging
[AD-A150623] 14 p2416 N85-24905
Optical monitoring of photo-acoustic pulse propagation in silicon wafers
[AD-A151333] 15 p2651 N85-26352
The development and implementation of an optical communications laboratory
[AD-A151882] 16 p2772 N85-27111
Acousto-optical spectrometers at Itapetinga Radio Observatory
[INPE-3479-PRE/722] 16 p2881 N85-27776
An introductory view of Raman-Nath type equations
[PREPRINT-422] 18 p3172 N85-29664
High accuracy digital acousto-optic matrix computer
[AD-D011692] 19 p3343 N85-30716
Acoustic imaging systems (for robotic object acquisition)
[AD-A154043] 19 p3351 N85-30772
The sound field of a moving laser-induced acoustic array (theory)
[AD-A154553] 21 p3699 N85-32961
Fundamentals of radio optical theory of resonant and directional quasi-optical devices
22 p3780 N85-33420
Binary signal detection in acoustooptic receivers
22 p3782 N85-33430
Asymmetry of diffraction orders with light diffraction at surface acoustic wave 22 p3782 N85-33431

ACQUISITION
NT DATA ACQUISITION
NT TARGET ACQUISITION
Systems analysis for microcomputer acquisitions
[AD-A145447] 02 p0239 N85-11556
Survey relating to the implementation of cost/schedule control systems criteria within the Department of Defense and industry
[AD-A146684] 06 p0870 N85-15526
Acquisition planning at the Defense Communications Agency
[AD-A146877] 07 p1051 N85-16669
Food acquisition: Food ingredients, raw materials and supply 14 p2393 N85-24737
Capital investment motivational techniques used by prime contractors on subcontractors
[AD-A153660] 18 p3196 N85-29837
Producibility Engineering and Planning (PEP): Program management guidelines
[AD-A153730] 19 p3379 N85-30966
Second Colloquim on the Scattering of Ultrasonic Waves
[AD-A156298] 24 p4145 N85-35697

ACRYLATES
Properties of ultra-violet cured poly(dimethylsiloxane)-urea acrylates
[AD-A148570] 08 p1134 N85-17146
Chiral polymers
[AD-A150366] 13 p2037 N85-22760
New air-curing lacquer systems with high solids content
[BMFT-FB-T-85-005] 17 p2936 N85-28124

ACRYLIC RESINS
Fluorinated diacrylic esters
[AD-D011326] 07 p0929 N85-15669
Process for preparation of crosslinked poly(tri-n-butyltin) methacrylate with simultaneous particle size reduction
[AD-D011313] 07 p0932 N85-15905
Study for a large area acrylic scintillator detector — magnetic monopoles
[NOTA-INTERNA-827] 18 p3097 N85-29174
Measurement of the attenuation length of an acrylic scintillator — magnetic monopoles
[NOTA-INTERNA-828] 18 p3097 N85-29175
New corrosion protection concept for very high voltage line towers
[BLL-OA-TRANS-2691-(6196.300)]
20 p3429 N85-31270
Effect of polymer additives on characteristics of direct-current motor with liquid dielectric filler
22 p3772 N85-33376

ACRYLONITRILES
Morphology and dynamic mechanical properties of diglycidyl ether of bisphenol-A toughened with carboxyl-terminated butadiene-acrylonitrile
04 p0466 N85-12958
Properties of polycaproamide fibers modified by grafted polyacrylonitrile 06 p0761 N85-14867
The adsorption of acrylonitrile at a gold electrode: An EMIRS measurement of the electrochemical stark effect
[AD-A148664] 08 p1123 N85-17062

ACTH
U ADRENOCORTICOTROPIN (ACTH)

ACTINIDE SERIES
NT AMERICIUM
NT AMERICIUM ISOTOPES
NT AMERICIUM 241
NT CALIFORNIUM ISOTOPES
NT CURIUM
NT CURIUM 244
NT PLUTONIUM
NT PLUTONIUM ISOTOPES
NT PLUTONIUM 238
NT PLUTONIUM 239
NT RADIUM
NT THORIUM
NT THORIUM ISOTOPES
NT TRANSURANIUM ELEMENTS
NT URANIUM
NT URANIUM ISOTOPES
NT URANIUM 235
Influence of 5f electrons on structures and bonding in the actinide-hydrogen intermetallics
[DE84-013893] 01 p0118 N85-10807
Actinides, the narrowest bands
[DE84-016483] 05 p0733 N85-14710
Method for fluorination of actinide fluorides and oxyfluorides using O2F2
[DE85-011646] 22 p3743 N85-33202
Capabilities of the LDEF-2 heavy nuclei collection
[OG-4.4-8] 22 p3680 N85-34040

ACTINIDE SERIES COMPOUNDS
NT NEPTUNIUM COMPOUNDS
NT PLUTONIUM OXIDES
NT URANIUM CARBIDES
NT URANIUM COMPOUNDS
NT URANIUM FLUORIDES
Mossbauer effect and contactless conductivity studies of superconducting actinides intermetallics and hydrides. Mossbauer high pressure studies
03 p0430 N85-12743
Method for extracting lanthanides and actinides from acid solutions by modification of Purex solvent
[DE85-005763] 23 p3909 N85-34220

ACTINOGRAPHS
U ACTINOMETERS

ACTINOMETERS
NT INFRARED DETECTORS
NT INFRARED SCANNERS
NT INFRARED SPECTROMETERS
NT INFRARED SPECTROPHOTOMETERS
NT MICROWAVE RADIOMETERS
NT PASSIVE L-BAND RADIOMETERS
NT PYRANOMETERS
NT RADIOMETERS
NT SOLAR SPECTROMETERS
NT SPECTROHELIOGRAPHS
NT SPECTROPHOTOMETERS
NT SPECTRORADIOMETERS
NT ULTRAVIOLET SPECTROMETERS
NT ULTRAVIOLET SPECTROPHOTOMETERS
Impact of fluctuations in optical properties of atmosphere on the ratio of spectral brightness from remote sensing of agricultural land 22 p3734 N85-33149

ACTIVATED CARBON
A study of the chemical interaction of gases with activated carbon
[AD-A147342] 07 p0923 N85-15846
Versatility of peat emphasized
07 p0994 N85-16316
The reaction of oxygen-nitrogen mixtures with granular activated carbons below the spontaneous ignition temperature
[AD-A149041] 10 p1434 N85-19039
Low pressure storage of methane on interlayered clays for potential vehicular applications
[DE85-006949] 16 p2758 N85-27017
Radiocarbon content in the annual tree rings during last 150 years and time variation of cosmic rays
[SH-7.1-15] 23 p4048 N85-35106

ACTIVATION
Study of proton and neutron activation of metal samples in low Earth orbit
[NASA-CR-171183] 01 p0026 N85-10164
A comment on Rosen's comments on activation and inhibition
[CTH-MATH-1984-24] 06 p0719 N85-14617
Impact of activation optimization on the Vandenberg Ground Support System using Q-GERT analysis
[AD-A148446] 08 p1105 N85-16966
Activation of Si-N modes in silicon by pulsed laser annealing
[DE85-003969] 13 p2097 N85-23082
CO adsorption on (111) and (100) surfaces of the Pt sub 3 Ti alloy. Evidence for parallel binding and strong activation of CO
[NASA-CR-176077] 21 p3565 N85-32176
A simple model to investigate the activation process in waterclouds 21 p3649 N85-32675
Measurements of the critical supersaturation of 0.029 to 0.035 micron radius particles at Washington, District of Columbia 21 p3649 N85-32676
Fog activation and supersaturation
21 p3650 N85-32678
Luminescence and absorption of indium-activated potassium-borate glasses subjected to high-power excitation 21 p3681 N85-32966
The effect of +Gx acceleration on platelet activation as determined by plasma platelet factor 4 levels
[AD-A155661] 24 p4131 N85-35606

ACTIVATION ANALYSIS
NT NEUTRON ACTIVATION ANALYSIS
Non-invasive techniques for determining musculoskeleton body composition
[DE84-015718] 04 p0545 N85-13470
Measurement and evaluation of selected 14-MeV neutron cross sections for fusion
[DE85-010295] 19 p3385 N85-30667
NBS (National Bureau of Standards) reactor: Summary of activities Jul. 1983 through Jun. 1984
[PB85-164836] 20 p3522 N85-31907
Study of proton and neutron activation of metal samples in low Earth orbit
[NASA-CR-171596] 21 p3558 N85-32130

ACTIVATION ENERGY
Fire retardant cellulosehydrate fibers
06 p0761 N85-14870
Deer control using 7 strand vertical fence
11 p1581 N85-19958
Detonations of solid explosives
[AD-A152012] 15 p2521 N85-25540
Thermoelectric properties of beta-boron and some boron compounds
[DE85-011978] 21 p3582 N85-32270
Activation analysis of natural water using neutrons of various energies 21 p3690 N85-32924
Three-dimensional hydrodynamic hot-spot model
[DE85-009587] 23 p3922 N85-34301
Grain boundary and surface diffusion in oxide systems
[DE85-007291] 23 p3985 N85-34715

ACTIVE CONTROL
Active control technology experience with the Space Shuttle in the landing regime
[NASA-TM-85910] 01 p0012 N85-10071
Fuel efficiency through new airframe technology
[NASA-TM-84548] 02 p0133 N85-10909
Energy efficient engine. Low pressure turbine test hardware detailed design report
[NASA-CR-167956] 02 p0147 N85-10994
Integrated Application of Active Controls (IAAC) technology to an advanced subsonic transport project-longitudinal handling qualities study of a relaxed-stability airplane
[NASA-CR-3660] 02 p0148 N85-11005
Development and flight evaluation of an augmented stability active controls concept: Executive summary
[NASA-CR-168009] 02 p0149 N85-11006
The microprocessor control of a motor-alternator
[RAE-TM-NAV-ENG-1023(L)] 02 p0244 N85-11591
Flying qualities and control system characteristics for superaugmented aircraft
[NASA-CR-170419] 05 p0596 N85-13600
Active sticks: A new dimension in controller design
06 p0706 N85-14531
Integrated Application of Active Controls (IAAC) technology to an advanced subsonic transport project. ACT/Control/Guidance System study, volume 1
[NASA-CR-165963-VOL-1] 06 p0754 N85-14837
Integrated Application of Active Controls (IAAC) technology to an advanced subsonic transport project. ACT/Control/Guidance System study. Volume 2: Appendices
[NASA-CR-165963-VOL-2] 06 p0754 N85-14838
Efficiency in integral active antennas
06 p0792 N85-15060
Study to eliminate ground resonance using active controls
[NASA-CR-166609] 07 p0902 N85-15715
Helicopter active control with rotor blades relaxation
08 p1075 N85-16819
Challenges in the development of the orbiter active thermal control subsystem 08 p1096 N85-16923
Active control of forward swept wings with divergence and flutter aeroelastic instabilities
09 p1282 N85-18063
The experimental performance of an off-road vehicle utilizing a semi-active suspension — off-road motorcyles
09 p1339 N85-18421
Ground and flight testing for aircraft guidance and control
[AGARD-AG-262] 13 p1966 N85-22350
Dynamic wind tunnel testing for active control research 13 p1966 N85-22352
Dynamic wind-tunnel testing of active controls by the NASA Langley Research Center
13 p1968 N85-22353
Passive and Active Control of Space Structures (PACOSS) 14 p2234 N85-23848
ACOSS 11 (Active Control Of Space Structures)
[AD-A150639] 14 p2246 N85-23922

Active dispersion control for a Doppler broadened laser
[AD-D011570] 14 p2310 N85-24297
The design and operation of a simple low-speed flutter-suppression model
[AD-A151610] 15 p2474 N85-25269
Active control of forward swept wings with divergence and flutter aeroelastic instabilities
[AD-A151637] 15 p2474 N85-25270
The ONERA establishment at Cannes in the service of aeronautical research
[ESA-TT-875] 15 p2475 N85-25276
Numerical simulation of boundary layer excitation by surface heating/cooling
[NASA-CR-172575] 15 p2554 N85-25756
Technical evaluation report on the Flight Mechanics Symposium on Active Control Systems: Review, Evaluation and Projections
[AGARD-AR-220] 16 p2711 N85-26730
Active control technology: Past, present, future
16 p2711 N85-26731
The state-of-the-art and future of flight control systems 16 p2712 N85-26732
A perspective on superaugmented flight control advantages and problems 16 p2712 N85-26733
Aspects of application of ACT systems for pilot workload alleviation 16 p2712 N85-26734
Application of AFTI/F-16 task-tailored control modes in advanced multirole fighters 16 p2712 N85-26735
X-29A digital flight control system design
16 p2712 N85-26736
The evaluation of ACS for helicopters: Conceptual simulation studies to preliminary design
16 p2712 N85-26737
ACT applied to helicopter flight control
16 p2712 N85-26738
An update on experience on the fly by wire Jaguar equipped with a full-time digital flight control system
16 p2712 N85-26740
ACT flight research experience
16 p2713 N85-26741
Operational and developmental experience with the F/A-18A digital flight control system
16 p2713 N85-26742
OLGA: An open loop gust alleviation
16 p2713 N85-26744
Active control technology experience with the Space Shuttle in the landing regime 16 p2713 N85-26747
The aerodynamics of controls
16 p2713 N85-26748
Active control landing gear for ground loads alleviation
16 p2714 N85-26749
Wing buffeting active control testing on a transport aircraft configuration in a large sonic tunnel
16 p2714 N85-26750
How to handle failures in advanced flight control systems of future transport aircraft 16 p2714 N85-26752
The certification of airborne complex digital systems
16 p2714 N85-26754
Automatic flight control modes for the AFTI/F-111 mission adaptive wing aircraft 16 p2714 N85-26756
The evolution of active control technology systems for the 1990's helicopter 16 p2715 N85-26758
Active Control Systems: Review, Evaluation and Projections
[AGARD-CP-384] 17 p2901 N85-27883
Active Control Technology (ACT): Past, present and future 17 p2901 N85-27884
The state-of-the-art and future of flight control systems 17 p2901 N85-27885
A perspective on superaugmented flight control advantages and problems 17 p2901 N85-27886
Aspects of application of ACT systems for pilot workload alleviation 17 p2901 N85-27887
X-29 digital flight control system design
17 p2901 N85-27889
The evolution of ACS for helicopters: Conceptual simulation studies to preliminary design
17 p2902 N85-27890
Some flight test results with redundant digital flight control systems 17 p2902 N85-27892
ACT flight research experience
17 p2902 N85-27894
Flight testing and development of the F/A-18A digital flight control system 17 p2902 N85-27896
OLGA: An open loop gust alleviation system
17 p2903 N85-27897
Demonstration of relaxed static stability on a commercial transport 17 p2903 N85-27898
Active control technology experience with the Space Shuttle in the landing regime 17 p2903 N85-27900
Active control landing gear for ground load alleviation
17 p2903 N85-27902
Wing buffeting active control testing on a transport aircraft configuration in a large sonic windtunnel
17 p2904 N85-27903
A modular dissimilar redundant computer designed for high integrity control 17 p2904 N85-27904
How to handle failures in advanced flight control systems of future transport aircraft 17 p2904 N85-27905
The evolution of active control technology systems for the 1990's helicopter 17 p2905 N85-27911
Vibration control of rotor shaft
[NASA-TM-87053] 18 p3117 N85-29292
NASA Space controls research and technology program 20 p3408 N85-31149
Characteristic elastic systems of time-limited optimal maneuvers 20 p3413 N85-31184
Models for describing active noise control in ducts
[ISVR-TR-127] 20 p3525 N85-31922
R and D activities of the Systems Engineering Division
20 p3540 N85-32027

ACTIVE GLACIERS
U GLACIERS

ACTIVE VOLCANOES
U VOLCANOES

ACTIVITY (BIOLOGY)
Primary light harvesting system: The relationship of phycobilisomes to photosystem 1 and 2
[DE85-003075] 11 p1689 N85-20622
Sulfur Cycle 21 p3662 N85-32748

ACTIVITY CYCLES (BIOLOGY)
Biogeochemical cycles: Interactions in global metabolism 05 p0652 N85-14184
Spontaneous motility of goldfish in absence of terrestrial zeitgebers: Space flight simulation in a mine
06 p0689 N85-14432
Circadian dynamics of potassium excretion in urine as related to working on one and two shifts
19 p3325 N85-30598

ACTUATION
Systems study for an Integrated Digital-Electric Aircraft (IDEA)
[NASA-CR-3840] 07 p0902 N85-15714
Space shuttle rudder/speedbrake actuation subsystem
08 p1102 N85-16965
Development of the space shuttle body flap actuation subsystem 08 p1102 N85-16966
Magnetically actuated compressor
[NASA-CASE-GSC-12799-1] 12 p1818 N85-21404

ACTUATOR DISKS
Turbine blade damping study
[NASA-CR-171255] 04 p0456 N85-12890
Users manual for a computer program for dynamic response analysis of bladed systems
[UDR-TR-84-38] 04 p0456 N85-12893

ACTUATORS
Development and flight evaluation of an augmented stability active controls concept: Executive summary
[NASA-CR-166009] 02 p0149 N85-11006
Autonomous momentum management for space station, exhibit A
[NASA-CR-171256] 04 p0462 N85-12933
Overview of magnetic bearing control and linearization approaches for annular magnetically suspended devices
05 p0607 N85-13872
Precise control of flexible manipulators
[NASA-CR-174210] 07 p0973 N85-16178
Mirror actuator control system
[AD-D011383] 07 p1042 N85-16619
Space shuttle rudder/speedbrake actuation subsystem
08 p1102 N85-16965
Development of the space shuttle body flap actuation subsystem 08 p1102 N85-16966
Design and test of a four channel motor for electromechanical flight control actuation
[NASA-CR-171838] 08 p1156 N85-17294
Neural compensation, muscle load distribution and muscle function in control of biped models
09 p1314 N85-18257
The development of a microprocessor-controlled linearly-actuated valve assembly
[NASA-CR-174437] 10 p1491 N85-19415
Fine figuring actuator
[AD-D011478] 10 p1557 N85-19819
Solar optical telescope primary mirror controller
[NASA-CR-174416] 10 p1570 N85-19903
Laser Doppler Anemometry (LDA) signal triggering and effective particle size range
[KU-SFB-210/E/5] 11 p1634 N85-20290
Slow opening valve — valve design for shuttle portable oxygen system
[NASA-CASE-MSC-20112-1] 11 p1642 N85-20336
Solar powered actuator with continuously variable auxiliary power control
[NASA-CASE-MFS-25637-1] 12 p1876 N85-21769
A quantitative comparison of active and passive damping for large space structures
[UTIAS-TN-249] 13 p1996 N85-22524
Optimum design of electrical motors for multilink manipulators and automated manufacturing systems
13 p2062 N85-22880
Analysis and design of hydraulic servo systems within the scope of the improvement of a fatigue testing installation of the Royal Dutch Army
[LEOK-TR-1984-09] 14 p2265 N85-24033
Vibration isolator actuator
[AD-D011574] 14 p2321 N85-24343
Surveillance program for the dissection and analysis of explosive and pyrotechnic components
[DE85-006105] 16 p2757 N85-27016
Fully redundant mechanical release actuator
[NASA-CASE-LAR-13196-1] 18 p3116 N85-29257
The effect of sensor and actuator errors on static shape control for large space structures
[NASA-TM-86446] 19 p3225 N85-29998
Thermal expansion coefficients of a 30% glass fiber filled PEEK pyrotechnic charge holder
[DE85-010805] 19 p3251 N85-30155
Thermo-electric valve
[AD-D011682] 19 p3252 N85-30165
Spillover minimization: An approach for actuators and sensors placement in distributed parameter study
[INPE-3525-PRE/748] 19 p3272 N85-30289
Experiments in structural dynamics and control using a grid 20 p3410 N85-31165
The experimental computer control of a two-dimensional hyperbolic system 20 p3411 N85-31166
Stiffness control of large space structures
20 p3414 N85-31189
Wideband disturbance accomodation in precision flexible space structures 20 p3415 N85-31194
Self-tuning adaptive-controller using online frequency identification 20 p3417 N85-31205
Comparison of the response of shape memory alloy actuators using air-cooling and water-cooling
[AD-A155216] 21 p3567 N85-32185
Automatic rotary valve actuator
[DE85-012797] 22 p3794 N85-33505
Design and development of a linear thermal actuator
22 p3796 N85-33518
A dual, fault-tolerant aerospace actuator
22 p3796 N85-33530
Design of a dual fault tolerant space shuttle payload deployment actuator 22 p3796 N85-33531
Intelligent redundant actuation system requirements and preliminary system design
[NASA-CR-177366] 23 p3896 N85-34136
Actuator rigging test set electromagnetic interference test (CE03)
[AD-A155819] 24 p4086 N85-35327
Computer simulation of a cruise missile using brushless dc motor fin control
[AD-A155935] 24 p4089 N85-35349

ACUITY
NT VISUAL ACUITY
Quantitative measurement of human auditory acuity
10 p1524 N85-19614

ADA (PROGRAMMING LANGUAGE)
Ada (trademark) training curriculum. Using the Ada language reference manual I402 teacher's guide
[AD-A143582] 01 p0103 N85-10686
Ada (trademark) training curriculum. Basic Ada programming I202 teacher's guide. Laboratory manual and exercises
[AD-A143583] 01 p0103 N85-10687
Ada (trademark) training curriculum. Real-time concepts I303 teacher's guide
[AD-A145093] 01 p0104 N85-10694
Ada (trademark) training curriculum. Software engineering for managers m101 teacher's exercise guide
[AD-A145094] 01 p0104 N85-10695
Advanced Ada (trademark)
[AD-A146257] 03 p0407 N85-12602
Real-time Ada (trademark)
[AD-A146258] 03 p0407 N85-12603
Experimenting with the Rolm Ada language workshop for specifying and designing 03 p0408 N85-12607
A proposal for standard basic functions in Ada
[NPL-DITC-45/84] 05 p0715 N85-14584
Ada compiler validation summary report: New York University (NYU Ada/Ed) compiler, version 1.4 for VAX 11/780, using VMS 3.5
[AD-A146924] 07 p1022 N85-16483
Ada compiler validation summary report: TeleSoft (TeleSoft Ada) compiler, version 2.0a for Sun 120 Motorola M68010, using 4.2 BSD UNIX-Sun Version 1.1
[AD-A146925] 07 p1022 N85-16484
NYU Ada/Ed user's guide: Version 1.4 for VAX/VMS systems
[AD-A146759] 07 p1024 N85-16495
Ada training curriculum. Real-time systems in Ada I401 teacher's guide, volume 1
[AD-A146782] 07 p1024 N85-16496
Ada training curriculum. Real-time systems in Ada I401 teacher's guide, volume 2
[AD-A146783] 07 p1024 N85-16497

Software testing in an Ada programming environment
08 p1065 N85-16748

Concept paper for the development of a DOD Ada (trademark) software engineering education and training plan
[AD-A148774] 08 p1206 N85-17592

Ada (trademark) primer
[AD-A148855] 10 p1539 N85-19703

Ada compiler validation summary report, Dansk Datamatik Center, VAX 11 compiler version 1.1
[AD-A149340] 11 p1699 N85-20881

A Gypsy-to-Ada program compiler
[TR-39] 12 p1913 N85-22005

Selection and use of general-purpose programming-language: Program examples, volume 2
[PB85-122008] 12 p1917 N85-22039

Selection and use of general-purpose programming language: Overview, volume 1
[PB85-122016] 12 p1917 N85-22040

Software library: A reusable software issue
[AD-A150722] 14 p2403 N85-24816

Reusable software: A concept for cost reduction
16 p2697 N85-26655

Evaluation of Ada (trademark) as a communications programming language, volume 1
[AD-A152314] 16 p2848 N85-27559

Evaluation of Ada (trademark) as a communications programming language. Volume 2: Communications protocols application
[AD-A152315] 16 p2848 N85-27560

Evaluation of Ada (trademark) as a communications programming language. Volume 3: Trusted software application
[AD-A152316] 16 p2848 N85-27561

Automatic distribution of programs in MASCOT and Ada (trademark) environments: A feasibility study
[AD-A152665] 17 p3010 N85-28614

AFIT GKS: A GKS implementation in the Ada programming language
[AD-A152954] 17 p3012 N85-28620

Evaluation and Validation (E/V) team public report, volume 1
[AD-A153609] 18 p3161 N85-29584

Ada validation summary report. ALS AdaVAX version 1.1 VAX-11/780 using VAX/VMS release 3.6
[AD-A153684] 18 p3162 N85-29588

Ada (trademark) compiler validation summary report. Honeywell information systems GCOS6 Ada version 1.1
[AD-A153746] 18 p3162 N85-29590

Ada compiler validation summary report, University of Karlsruhe-GMD/German MOD Siemens - BS 2000 version 7.30
[AD-A153747] 18 p3163 N85-29591

Ada (trademark) compiler validation summary report: ALSYS ALSYCOMP-0001
[AD-A153750] 18 p3163 N85-29592

Ada developments
[REPT-84-28] 18 p3164 N85-29604

Ada compiler validation summary report: University of Karlsruhe-GMD/German MOD VAX 11 compiler, version v1.0
[AD-A154370] 19 p3337 N85-30678

Survey of Ada (Trademark)-based PDLs (Program Design Language)
[AD-A154402] 19 p3338 N85-30680

Study of the applicability of higher order languages for on-board satellite software production
[ESA-CR(P)-2024] 20 p3516 N85-31864

Artificial intelligence in Ada (trademark): Pattern-directed processing
[AD-A156230] 24 p4141 N85-35671

ADAPTATION
NT ACCLIMATIZATION
NT ALTITUDE ACCLIMATIZATION
NT COLD ACCLIMATIZATION
NT DARK ADAPTATION
NT HEAT ACCLIMATIZATION
NT LIGHT ADAPTATION
NT RETINAL ADAPTATION

Functional capacities of elderly subjects exposed to simulated spaceflight factors 01 p0091 N85-10617

Assessment of lift- and blockage-induced wall interference in a three-dimensional adaptive-wall tunnel
03 p0312 N85-12016

A data base for three-dimensional all-interference code evaluation 03 p0312 N85-12017

Wall adaptation at Mach 1.2 — wind tunnel tests
[ONERA-RTS-26/3075-AY-402]
04 p0453 N85-12873

Loss of bone substance in consequence of amputation as a model for the adaptation to microgravity
05 p0694 N85-14484

Effects of external loads on human head movement control systems 06 p0707 N85-14534

Use of shanks transformation for speeding up adaptation process in antenna arrays 07 p0951 N85-16029

Vityaz specialists study human adaptability to ocean depths 07 p0980 N85-16225

Research on adaptive antenna techniques 6
[AD-A149341] 11 p1624 N85-20228

Prediction of the space adaptation syndrome
11 p1693 N85-20646

Space adaptation syndrome: Incidence and operational implications for the space transportation system program
11 p1695 N85-20655

Multiple regression method used to assess animal adaptation to hypoxic hypoxia 12 p1902 N85-21947

Plans for adaptation research during Antarctic expedition 14 p2333 N85-24426

Biological investigations of adaptive networks. Neuronal control of conditioned responding
[AD-A150959] 14 p2385 N85-24695

Principal patterns of functional changes of human respiratory system in adaptation to high pressure
14 p2387 N85-24704

Fluid-electrolyte responses during prolonged space flight: A review and interpretation of significant findings
[NASA-CR-171878] 15 p2617 N85-26124

Mathematical modeling of fluid-electrolyte alterations during weightlessness
[NASA-CR-171881] 15 p2617 N85-26125

The design of an adaptive predictive coder using a single-chip digital signal processor
[AD-A152461] 17 p2952 N85-28231

Predictors of transfer adjustment: A longitudinal study
[AD-A152462] 17 p3000 N85-28548

Adaptive aiding for symbiotic human-computer control: Conceptual model and experimental approach
[AD-A153870] 19 p3332 N85-30644

The European vestibular experiments of the Spacelab-1 mission 20 p3508 N85-31808

Some results of the European vestibular experiments in the Spacelab-1 mission 20 p3508 N85-31809

Learning and self adaptation applied to the simulation of a human pilot
[ONERA-RT-24/5122-SY] 20 p3511 N85-31828

Intracardiac hemodynamics and human heart function in simulated weightlessness 22 p3733 N85-33140

Mathematical analysis of heart rhythm assessment of distinctive features in adaptation to spaceflight conditions 22 p3733 N85-33142

Effect of hypokinesia and +Gz accelerations on transport function of human blood
23 p3952 N85-34497

Lipid hydrolysis in man during antiorthostatic hypokinesia 23 p3953 N85-34500

ADAPTERS

Low voltage two wire to four wire telephone circuit converter apparatus
[AD-D011449] 10 p1468 N85-19261

Structure of SYLDA double launch system for Ariane
17 p2946 N85-28185

ADAPTIVE CONTROL
NT ACTIVE CONTROL
NT LEARNING MACHINES
NT SELF ADAPTIVE CONTROL SYSTEMS

Robotization of electric welding processes
03 p0345 N85-12225

Architecture of adaptive space-frequency-time signal processing system 04 p0486 N85-13103

Evaluation of automated decisionmaking methodologies and development of an integrated robotic system simulation
[NASA-CR-172401] 04 p0552 N85-13516

Adaptive mutual interference suppression method
[AD-D011268] 05 p0628 N85-14024

Phase only adaptive nulling in a monopulse antenna
[AD-D011269] 05 p0628 N85-14026

An apparatus for and a method of controlling multiple time-varying processes
[AD-D011253] 05 p0631 N85-14045

Improvement of electromechanical systems by utilization of microelectronic technology 07 p0955 N85-16053

Logic elements for systems with variable structure
07 p0955 N85-16054

Precise control of flexible manipulators
[NASA-CR-174210] 07 p0973 N85-16178

Bibliography of adaptive control
[OUEL-1544/84] 08 p1209 N85-17602

Research on optimal control, stabilization and computational algorithms for aerospace applications
[NASA-CR-174318] 08 p1209 N85-17603

Simplified grasping and manipulation with dextrous robot hands
[AD-A148962] 10 p1492 N85-19419

Dual adaptive control based upon sensitivity functions
[NASA-CR-169331] 10 p1543 N85-19727

Research in adaptive and decentralized control
[AD-A148964] 10 p1543 N85-19728

Adaptive regulation of transmitter radiation power in radio lines during delays of control signals
12 p1841 N85-21551

System dynamics and network control
[AD-A149420] 13 p2054 N85-22863

Electronics Engineering Department EE Technical Review
[UCRL-50025-84-1] 13 p2063 N85-22887

Adaptive control of airborne radar antennas
13 p2080 N85-22980

Adaptive techniques for control of large space structures
[AD-A150957] 14 p2246 N85-23923

Construction of high speed guaranteed regulators
14 p2270 N85-24063

Synthesis of hyperstable control system with adaptive model 14 p2273 N85-24084

Noise cancellation using adaptive arrays
[AD-A150721] 14 p2292 N85-24206

Practical methods for the compensation and control of multivariable systems
[AD-A151047] 14 p2407 N85-24841

Feasibility analysis of moving bank multiple model adaptive estimation and control algorithms
[AD-A152015] 15 p2641 N85-26292

Algorithms for determining the relative complexity of dynamic signals
[BLL-M-36111-(5826.4)] 16 p2851 N85-27574

Automatic flight control modes for the AFTI/F-111 mission adaptive wing aircraft 17 p2905 N85-27909

Adaptive nulling at HF using a compact array of active parasitic antennas
[AD-A152582] 17 p2946 N85-28203

In orbit infrastructure
[DM-51/CC-FL-044-83] 18 p3066 N85-28966

A simulation study of jammer nulling trade-offs in a reactively steered adaptive array
[AD-A153461] 18 p3090 N85-29124

Standard Generic approach for Spacecraft Autonomy and Automation, phase 2 (SGASA-2). Volume 1: Executive summary
[ESA053-1-VOL-1] 18 p3167 N85-29623

Standard Generic Approach for Spacecraft Autonomy and Automation, phase 2 (SGASA-2). Volume 2: Technical report
[ESA053-1-VOL-2] 18 p3167 N85-29624

Standard Generic Approach for Spacecraft Autonomy and Automation, phase 2 (SGASA-2). Volume 3: Appendices
[ESA053-1-VOL-3] 18 p3167 N85-29625

Research on optimal control, stabilization and computational algorithms for aerospace applications
[NASA-CR-172528] 19 p3221 N85-29970

Adaptive aiding for symbiotic human-computer control: Conceptual model and experimental approach
[AD-A153870] 19 p3332 N85-30644

High gain adaptive control of decentralized systems
[DE85-001566] 19 p3343 N85-30717

Adaptive identification and control of structural dynamics systems using recursive lattice filters
[NASA-TP-2371] 20 p3407 N85-31142

NASA Space controls research and technology program 20 p3408 N85-31149

Space station dynamic modeling, disturbance accommodation, and adaptive control
20 p3409 N85-31154

New directions in asymptotically stable finite-dimensional adaptive control of linear distributed parameter systems 20 p3412 N85-31177

Proceedings of the Workshop on Identification and Control of Flexible Space Structures, volume 3
[NASA-CR-176053] 20 p3415 N85-31195

Adaptive control: Actual status and trends
20 p3416 N85-31202

A nonlinear dual-adaptive control strategy for identification and control of flexible structures
20 p3416 N85-31203

Stable direct adaptive control of linear infinite-dimensional systems using a command generator tracker approach 20 p3416 N85-31204

Self-tuning adaptive-controller using online frequency identification 20 p3417 N85-31205

Robust adaptive control 20 p3417 N85-31207

Fixed gain and adaptive techniques for rotorcraft vibration control
[NASA-CR-177344] 22 p3728 N85-33111

Gradiental adaptive corrector with optimum tuning step 22 p3776 N85-33403

Recursive partitioning estimation
24 p4141 N85-35670

ADAPTIVE CONTROL SYSTEMS
U ADAPTIVE CONTROL

ADAPTIVE FILTERS

Noise removal in multichannel images
[NASA-CR-174116] 04 p0554 N85-13526

Suppression of biodynamic interference by adaptive filtering 06 p0706 N85-14530

Studies in statistical signal processing
[AD-A147130] 07 p0940 N85-15959

Multiple channel adaptive filtering using a fast orthogonalization network: An application to efficient pulsed Doppler radar processing
[AD-A147929] 08 p1211 N85-17619
One-dimensional processing for adaptive image restoration
[AD-A149314] 10 p1557 N85-19815
Synthesis of optimum algorithms for secondary processing 13 p2080 N85-22992
Methods of digital correction for channels of multichannel radar receivers 13 p2082 N85-23005
Noise cancellation using adaptive arrays
[AD-A150721] 14 p2292 N85-24206
Basic research in electronics (JSEP)
[AD-A151002] 14 p2298 N85-24230
The performance of a new adaptive filter for digital communications
[AD-A151890] 15 p2543 N85-25702
Correlating and adaptive digital filters
[BMFT-FB-T-84-299] 15 p2551 N85-25744
Transform domain adaptive filtering using a recursive DFT
[DE85-008965] 18 p3172 N85-29656
Adaptive filtering for large space structures: A closed-form solution 20 p3417 N85-31206
Application of adaptive noise cancellation to Coast Guard voice communications
[AD-A154798] 21 p3574 N85-32230
Introduction to adaptive techniques for voice signal processing
[FUB-52-1983] 22 p3756 N85-33287
Synthesis of adaptive filters for tracking radio systems 22 p3763 N85-33325
High-speed adaptation algorithm for harmonic corrector 22 p3765 N85-33336
Adaptive corrector operating in frequency domain 22 p3765 N85-33337
Transformation of spectrum of phase-code keyed signal for scanning in time 22 p3765 N85-33338

ADAPTIVE OPTICS
Fast Hartmann method for problems in astronomical adaptive optics 02 p0161 N85-11094
Investigations relating to the simultaneous use of Combined Optical Adaptive Techniques (COAT) and angle-tracking
[ESA-TT-844] 09 p1385 N85-18712
Bibliography of Soviet Laser Developments, Number 67, September-October 1983
[AD-A151199] 15 p2562 N85-25805
Solar adaptive optics
[AD-A155434] 21 p3724 N85-33101

ADDERS (CIRCUITS)
U ADDING CIRCUITS

ADDING CIRCUITS
Hardware realization of digital filters without multipliers 22 p3766 N85-33340

ADDITION RESINS
NT ACRYLIC RESINS
NT VINYL COPOLYMERS

ADDITIVES
NT ADMIXTURES
NT ANTIFREEZES
NT ANTIKNOCK ADDITIVES
NT PLASTICIZERS
NT PROPELLANT ADDITIVES
NT PROPELLANT BINDERS
NT SOLID ROCKET BINDERS
An investigation of the solubility and diffusivity of chromium in gallium arsenide
[AD-A144940] 01 p0024 N85-10148
Eutectic explosives containing ammonium nitrate
[DE84-015705] 01 p0034 N85-10213
Effects of additives and KOH electrolyte concentration on dissolution of iron electrodes
[DE84-014840] 02 p0173 N85-11162
P-doping of (CH)x to the metallic regime with gaseous oxygen. Application to oxygen fuel cell type electrodes
[AD-A145477] 02 p0186 N85-11242
The concept of doping of conducting polymers. The role of reduction potentials
[AD-A145480] 02 p0186 N85-11243
A study of defects in neutron transmutation doped silicon: Gallium by hall effect analysis
[AD-A146047] 03 p0433 N85-12758
Effect of doping on the voltage holdoff performance of alumina insulators in vacuum
[DE84-017163] 04 p0480 N85-13060
Effect of lubricant extreme-pressure additives on surface fatigue life of AISI 9310 spur gears
[NASA-TP-2408] 04 p0507 N85-13234
Synthesis of transit practice: Diesel fuel quality and effects of fuel additives
[PB84-235688] 05 p0621 N85-13973
Fluorinated aliphatic polyalkylether lubricant with an additive composed of an aromatic phosphine substituted with perfluoroalkylether groups
[AD-D011286] 06 p0770 N85-14927
Development of technology of silicon single-crystal production semiconductor power devices: State of art outlook 06 p0795 N85-15078
Process research of non-Cz silicon material 06 p0830 N85-15275
Effect of five lubricants on life of AISI 9310 spur gears
[NASA-TP-2419] 07 p0962 N85-16099
An investigation of chemiluminescent reactions
[AD-A148460] 08 p1122 N85-17073
Tensile test of pressureless-sintered silicon nitride at elevated temperature
[NASA-TM-77777] 08 p1172 N85-17390
Densification of submicron YSZ (Yttria-Stabilized Zirconia) powders with alumina and borate additives
[AD-A149520] 10 p1452 N85-19150
Investigation of fuel additive effects on sooting flames
[AD-A149154] 10 p1457 N85-19179
Improved operation of transversely exited N2O lasers
[AD-D011468] 10 p1490 N85-19409
Development of AK18 alloy production technology based on electrothermic silumin 11 p1598 N85-20048
Effect of rhodamine-B on the electrodeposition of lead on copper, revision
[DE85-000674] 11 p1606 N85-20101
Characterization of lubricated bearing surfaces operated under high loads
[NASA-TM-86964] 12 p1811 N85-21357
Plasmachemical evaporation and doping of amorphous silicon 12 p1879 N85-21790
Investigation of the effects of NaOH dopant level on the physical and mechanical properties of carbon/phenolic composite material 12 p1945 N85-22213
Effects of HMX addition on the combustion of energetic binders 13 p2004 N85-22560
The effects of lithium counterdoping on radiation damage and annealing in n(+)p silicon solar cells 13 p2007 N85-22586
Microstructure and properties of ferrous alloy weldments
[DE85-005582] 14 p2257 N85-23987
Dopant incorporation in silicon during nonequilibrium solidification: Comparison of 2 processes
[DE85-005568] 14 p2430 N85-24986
Status of French research in plastic batteries 15 p2530 N85-25603
Effect of nickel addition on the thermal, magnetic and magnetomechanical properties of Fe(80)B(15)Si(5)
[AD-A152281] 16 p2749 N85-26967
Jet fuel instability mechanisms
[NASA-CR-175856] 17 p2936 N85-28127
Lubricant and additive effects on spur gear fatigue life
[NASA-TM-87044] 17 p2974 N85-28373
The microstructural state of Nb3Sn in a multifilamentary titanium doped bronze-process wire
[DE85-010979] 19 p3240 N85-30069
High-temperature oxidation of reaction-roasted silicon nitride with various additives 19 p3244 N85-30114
A method for predicting additive drag reduction from small-diameter pipe flows
[AD-A154411] 19 p3266 N85-30254
Improved catalysis for liquid hydrocarbon fuels from syngas
[DE85-011062] 20 p3421 N85-31234
Phenomena simulation for heavy doping and surface recombination velocity 20 p3482 N85-31638
Process and design considerations for high-efficiency solar cells 20 p3482 N85-31641
The effect of alloy additions on superplasticity in thermomechanically processed high magnesium aluminum-magnesium alloys
[AD-A155142] 21 p3567 N85-32184
Z-contrast imaging and electron channeling analysis of dopants in semiconductors
[DE85-011410] 21 p3582 N85-32269
Thermoelectric properties of beta-boron and some boron compounds
[DE85-011978] 21 p3582 N85-32270
Injection of drag reducing additives into turbulent water flows: Two-component velocity measurements and mixing length model predictions
[AD-A154804] 21 p3583 N85-32274
Experimental test for interpreting the increase in sensibility of doped CR-39
[OG-4.4-11] 22 p3880 N85-34042

ADDRESSING
Thin film transistors for addressing flat panel displays
[BMFT-FB-T-84-210] 08 p1227 N85-17726
Automatic multi-banking of memory for microprocessors
[NASA-CASE-NPO-15295-1] 12 p1911 N85-21992
A secure high-speed transaction protocol
[CWI-CS-R8417] 17 p3009 N85-28605

ADENINES
NT RIBONUCLEIC ACIDS

ADENOSINE DIPHOSPHATE
The DNA metabolism and poly-(ADP-ribose) synthesis in lymphocytes of persons exposed to low doses of ionizing radiation
[OEFZS-4307] 20 p3507 N85-31800

ADENOSINE TRIPHOSPHATE
Neutron small angle scattering of the free and membrane-bound ATPase --- adenosine triphosphate (ATP) 03 p0431 N85-12746
Chemical, biological, and physical measurements from the subtropical western North Atlantic Ocean. Summer 1982, USNS Lynch, cruise 710-82
[AD-A153823] 18 p3201 N85-29857
Influence of underwater volcanic mountains of Atlantic on microplankton distribution 19 p3294 N85-30424
Radioprotective efficacy of ATP and adenosine with exposure to high energy protons 19 p3325 N85-30602

ADENOSINES
NT ADENOSINE DIPHOSPHATE
NT ADENOSINE TRIPHOSPHATE
Radioprotective efficacy of ATP and adenosine with exposure to high energy protons 19 p3325 N85-30602
Molecular toxicology of chromatin: The role of Poly(ADP-Ribose) in gene control
[AD-A154415] 19 p3327 N85-30611

ADHEROMETERS
U ADHESION TESTS

ADHESION
Zero adhesion system
[AD-D011237] 01 p0015 N85-10093
Optical contacting for gravity probe star tracker
[NASA-TM-86475] 01 p0120 N85-10819
The adhesion of hard and wear resistant coatings 02 p0179 N85-11203
The role of molecular diffusion in the adhesion of elastomers
[AD-A145576] 02 p0186 N85-11245
Universal binding energy relations in metallic adhesion
[NASA-TM-86889] 03 p0331 N85-12132
Polyimide-glass multilayer printed wiring boards
[DE84-015092] 05 p0631 N85-14048
Fundamental tribological properties of ceramics
[NASA-TM-86915] 07 p0930 N85-15893
Cryogenic glass-to-metal seal
[AD-D011370] 07 p0933 N85-15911
Application of electrochemical engineering methods and theory to solving corrosion and adhesion problems with organic coatings
[AD-A147799] 08 p1129 N85-17115
Mod silver metallization for photovoltaics
[NASA-CR-174444] 10 p1509 N85-19518
Humidity effects on adhesion of nickel-zinc ferrite in elastic contact with magnetic tape and itself
[NASA-TP-2449] 12 p1811 N85-21359
Monte Carlo lattice models for adsorbed polymer conformation
[NASA-TP-2453] 14 p2426 N85-24961
Aging of gold thick-film solder joints
[DE85-008847] 18 p3077 N85-29037
Adherence of ash particles from the combustion of micronized coal
[DE85-008600] 19 p3229 N85-30023

ADHESION TESTS
An improved torsional method for determining the fracture toughness of stiff materials and of adhesive joints
[AD-A152091] 16 p2800 N85-27267
A study of adherent oxide scales
[AD-A155554] 21 p3567 N85-32188
Study of an ultrasonic detection method to inspect bonding effects in light alloy bonded structures, test report no. 43-954/F --- aircraft structures
[PV-43-954/F] 22 p3795 N85-33510

ADHESIVE BONDING
Ceramic microstructure and adhesion
[NASA-TM-83804] 01 p0031 N85-10186
Deformations and strains in adhesive joints by moire interferometry
[NASA-CR-172474] 02 p0185 N85-11236
Evaluation of the alkaline peroxide pre-bond surface treatment for titanium
[AD-A147352] 07 p0928 N85-15881
Laboratory investigation on adhesives for Naval facilities construction
[AD-A147453] 07 p0932 N85-15909
Mechanical properties of adhesively bonded aluminum structures protected with hydration inhibitors
[AD-A148123] 08 p1133 N85-17139

The development of a method for the shock-resistant securing of large batteries in submarines
09 p1335 N85-16391
Single crystal silicon as a low-temperature structural material
[DE84-017409] 09 p1400 N85-18810
Procedures for the bonding of the E.M.C. mirror onto its INVAR mirror flange --- United Kingdom Infrared Telescope
[UKIRT-19] 09 p1414 N85-18917
Characterization of a thermoplastic polyimidesulfone
[NASA-TM-86358] 10 p1450 N85-19135
Reliability of adhesive bonds under severe environments. Report of the Committee on Reliability of Adhesive Bonds in Severe Environments
[AD-A149010] 10 p1451 N85-19140
Adhesive joint formation under field conditions
[AD-D011478] 10 p1453 N85-19153
Characterization and adhesive bonding of poly(etheretherketone) resins and composites
[DE85-002526] 11 p1593 N85-20023
Hot melt adhesive attachment pad
[NASA-CASE-LAR-12894-1] 11 p1610 N85-20125
Characterization of mode 1 and mixed-mode failure of adhesive bonds between composite adherends
[NASA-TM-86355] 12 p1797 N85-21270
On the stress analysis of bonded inserts
[ARL/STRUC-R-407] 12 p1865 N85-21698
Study of character of adhesive interaction and breaking of polyimid-aluminum foil junction during process of hardening 13 p2014 N85-22637
The characterisation of oxide films on treated aluminium alloys
[MOAD-R-849] 13 p2022 N85-22687
Elasticity solution of an adhesively bonded joint
[NASA-CR-175591] 13 p2101 N85-23097
Development of acceptance criteria for batches of silane primer for external tank thermal protection system bonding applications
[NASA-CR-171429] 14 p2259 N85-23998
Fracture surface analysis in composite and titanium bonding: Part 1: Titanium bonding
[NASA-CR-175750] 15 p2502 N85-25434
Development of acceptance criteria for batches of silane primer for external tank thermal protection system bonding applications
[NASA-CR-171436] 15 p2518 N85-25523
A study of the time dependence in fracture processes relating to service prediction of adhesive joints and advanced composites
[AD-A152064] 15 p2579 N85-25910
Bond test data acquisition and analysis system
[DE85-007021] 16 p2780 N85-27158
Mechanical properties of adhesively bonded aluminum structures protected with hydration inhibitors
[AD-A153755] 18 p3079 N85-29047
Adhesive evaluation of LARC-TPI and a water-soluble version of LARC-TPI
[NASA-TM-86428] 19 p3248 N85-30136
Influence of interface ply orientation on fatigue damage of adhesively bonded composite joints
[NASA-TM-86443] 19 p3284 N85-30365
Fundamental studies related to failure of adhesively bonded structures
[AD-A154072] 19 p3285 N85-30374
Description of an holographic interferometry nondestructive test installation: Application to bond tests
[SNIAS-851-430-101] 20 p3454 N85-31521
Improved materials for composites and adhesive joints
[AD-A154918] 21 p3561 N85-32152
Improved materials for composite and adhesive joints
[AD-A155065] 21 p3562 N85-32153
Experimental and theoretical assessment of a new technique for the non-destructive evaluation of laminated panels
[AD-A155822] 21 p3582 N85-32155
Molecular orbital studies in oxidation: Sulfate formation and metal-metal oxide adhesion
[NASA-CR-176070] 21 p3585 N85-32174
A cracked orthotropic sheet stiffened by a semi-infinite orthotropic sheet
[NASA-TP-2455] 21 p3597 N85-32339
Method of bonding silver to glass and mirrors produced according to this method
[DE85-011642] 22 p3792 N85-33495
Study of an ultrasonic detection method to inspect bonding effects in light alloy bonded structures, test report no. 43-854/F --- aircraft structures
[PV-43-854/F] 22 p3795 N85-33510
Nonlinear adhesive behavior effects in a cracked orthotropic sheet stiffened by a semi-infinite orthotropic sheet
[NASA-TM-87584] 23 p3941 N85-34426

ADHESIVES
NT GLUES
NT PASTES
Volatile organic emissions from adhesives with indoor applications
[DE84-015965] 05 p0620 N85-13966
Encapsulation materials and processing
06 p0830 N85-15269
Laboratory investigation on adhesives for Naval facilities construction
[AD-A147453] 07 p0932 N85-15909
Corrosion properties of second-generation conductive materials 07 p1000 N85-16348
Evaluation and prediction of long-term environmental effects of nonmetallic materials
[NASA-CR-171353] 10 p1450 N85-19137
Elastomer toughened polyimide adhesives --- bonding metal and composite material structures for aircraft and spacecraft
[NASA-CASE-LAR-12775-2] 12 p1809 N85-21349
Rubber modified epoxy adhesive
[AD-D011527] 12 p1810 N85-21354
Study of character of adhesive interaction and breaking of polyimid-aluminum foil junction during process of hardening 13 p2014 N85-22637
Research on composite materials for structural design
[AD-A150802] 14 p2260 N85-24004
Prediction of the long term stability of polyester-based recording media
[PB85-160133] 14 p2262 N85-24019
Development of a polystyrene insulation system
[DE85-006950] 16 p2784 N85-27180
Adhesive evaluation of LARC-TPI and a water-soluble version of LARC-TPI
[NASA-TM-86428] 19 p3248 N85-30136
Working with flammable solvents, thinners, paints and adhesives
[HSE-TRANS-11066] 19 p3250 N85-30154
Optical effects of thin film adhesives in multijunction solar cells
[DE85-010120] 19 p3305 N85-30488
Synthesis and characterization of copolyimides with varying flexibilizing groups
[NASA-TM-86418] 20 p3433 N85-31296
STPI/LARC: A 200 deg C polyimide adhesive
[NASA-TM-86447] 20 p3433 N85-31297
Influence of the resin on interlaminar mixed-mode fracture
[NASA-TM-87571] 21 p3561 N85-32150

ADIABATIC CONDITIONS
Further developments of a nongradient theory of premixed turbulent flames
[NAL-TR-802T] 01 p0023 N85-10143
On the cause of X-line formation in the near-Earth plasma sheet: Results of adiabatic convection of Plasma-Sheet-Plasma
[AD-A145835] 03 p0396 N85-12525
Generation of available potential energy and other diagnostic studies during FGGE
05 p0683 N85-14388
Estimations of diabatic heating for an explosively-developing maritime cyclone
[AD-A147676] 08 p1188 N85-17483
Acceleration of an electron ring in a modified betatron with transverse pressure
[AD-A148626] 08 p1221 N85-17688
The Adiabatic invariant: A tool for the study of the dynamics of the solar system 15 p2676 N85-26519
Investigations of the material factors in the adiabatic shearing of steels
[AD-A153084] 17 p2979 N85-28418
A numerical study of the mean trajectory approximation in a non-adiabatic process
[AD-A152763] 17 p3030 N85-28737
Adiabatic approach in the theory of polyatomic photodissociation: Application to C2N2
[DE85-008515] 18 p3071 N85-28996
Some recent developments in numerical modelling at ECMWF 18 p3147 N85-29481
Study of intermediate velocity penetration of steel spheres into deep aluminum targets
[DE85-010419] 19 p3267 N85-30385
Diagnostics of severe convection and subsynoptic scale ageostrophic circulations
[NASA-CR-171581] 21 p3634 N85-32571
Spectral evolution of gamma-rays from adiabatically expanding sources in dense clouds
[OG-2.5-2] 22 p3869 N85-33950
A theoretical study of non-adiabatic surface effects for a model in the NTF cryogenic wind tunnel
[NASA-CR-3824] 23 p3929 N85-34352
Why do leaky-box models work so fine?
[OG-7.2-8] 23 p4014 N85-34877
Relativistic transport theory for cosmic-rays
[OG-8.3-8] 23 p4022 N85-34926

ADIABATIC EQUATIONS
An interactive computer code for calculation of gas-phase chemical equilibrium (EQLBRM)
[NASA-CR-168337] 02 p0140 N85-10948
Adiabatic thermal models for planetary bodies
22 p3857 N85-33881

ADJOINTS
Use of adjoint equations in problems of evaluating state of random hydrodynamic fields
19 p3289 N85-30398
Monte Carlo techniques for analyzing deep penetration problems
[DE85-011426] 23 p3968 N85-34598

ADJUSTING
A strategy for the adjustment and analysis of densification networks --- geodetic networks
[SER-C-295] 01 p0063 N85-10420
Impact tests of adjusters for the HBU-12 lap belt
[AD-A148021] 06 p1060 N85-16843
Adjustment structure
[AD-D011461] 10 p1459 N85-19193
The 1980 diagnostic adjustment of the German main triangulation network. 4: Network adjustment (part 3)
[SER-B-267-PT-3-MITT-168] 11 p1665 N85-20494
The 1980 diagnostic adjustment of the German main triangulation network. 4: Network adjustment (part 1)
[SER-B-267-PT-1-MITT-168] 11 p1670 N85-20525
The 1980 diagnostic adjustment of the German main triangulation network. 4: Network adjustment (part 2)
[SER-B-267-PT-2-MITT-168] 11 p1670 N85-20526
Adjustment of the national dispersion model for air pollution from elevated sources
[KNMI-TR-57] 14 p2353 N85-24540
Adjustment of the frequency-temperature characteristics of crystal oscillators
[AD-D011588] 15 p2548 N85-25726
Predictors of transfer adjustment: A longitudinal study
[AD-A152462] 17 p3000 N85-28548

ADJUSTMENT
U ADJUSTING

ADMINISTRATION
U MANAGEMENT

ADMITTANCE
U ELECTRICAL IMPEDANCE

ADMIXTURES
On the co-variant formulation of the law of motion of passive particles in a field of turbulence
[REPT-564] 03 p0377 N85-12407
Algebra of hydrodynamic flows of an ideal fluid and the prediction of the behaviour of a system of particles of a passive admixture on Riemann surfaces with a variable curvature
[REPT-565] 03 p0377 N85-12408
Influence of background electrically neutral argon admixture on mechanical strength of silicon crystals
21 p3683 N85-32878
High temperature polymer concrete
[DE85-005756] 23 p3920 N85-34290

ADOBE FLATS
U FLATS (LANDFORMS)

ADP
U ADENOSINE DIPHOSPHATE

ADRENAL GLAND
Skeletal muscle metabolism in hypokinetic rats
[NASA-CR-174059] 02 p0233 N85-11520
Biochemical status of adrenocortical dysfunction following spaceflight 12 p1901 N85-21935
Distinctive morphological manifestations of acute stress reaction in adrenal cortex of hypokinetic rats
12 p1902 N85-21944
Primate adrenal reactions to antiorthostatic hypokinesia 19 p3324 N85-30591

ADRENAL METABOLISM
Role of glucocorticoids in the response to unloading of muscle protein and amino acid metabolism
15 p2609 N85-26077
Primate adrenal reactions to antiorthostatic hypokinesia 19 p3324 N85-30591

ADRENALINE
U EPINEPHRINE

ADRENERGICS
The effect of beta adrenergic blockade on ratings of perceived exertion
[AD-A148053] 08 p1195 N85-17530

ADRENOCORTICOTROPIN (ACTH)
Biochemical status of adrenocortical dysfunction following spaceflight 12 p1901 N85-21935
Rat plasma hormone levels following flight aboard Cosmos-1129 biosatellite 22 p3823 N85-33681

ADSORBENTS
A study of gas solid reactions using coated piezoelectric detectors
[AD-A153047] 17 p2920 N85-28001

ADSORPTION
NT CHEMISORPTION

Inhibition of hydrogen absorption during plating of high strength steels
[AD-A144862] 01 p0028 N85-10174

The use of fixed-bed adsorber models to predict the fluxes of toxic substances in groundwaters and soil environments
[PB84-202563] 01 p0071 N85-10468

Reversible change in parameters of GaAs-based surface-barrier metal-semiconductor diodes induced by hydrogen absorption-desorption
02 p0258 N85-11690

Calculation of the scattering function of rotating molecules with emphasis on the tunnel spectra of absorbed molecules 03 p0427 N85-12725

Structure and kinetics of physisorption, properties of helium during reduction of the dimension
03 p0432 N85-12749

USSR report: Chemistry
[JPRS-UCH-84-012] 06 p0761 N85-14865

Polymer-carbon black interaction in electrically conducting fiber-forming composites
06 p0762 N85-14875

Structure determination of molecular adsorbates with dynamical LEED and HREELS
[DE85-002007] 06 p0861 N85-15473

The adsorption of CO and oxygen on Cu layers on a W(110) surface
[AD-A147345] 07 p0923 N85-15847

Modulated surface vibrational spectroscopies at electrode/electrolyte interfaces
[AD-A148665] 08 p1123 N85-17083

Effect of microstructure and trapping on the hydrogen embrittlement susceptibility of a ti-bearing HSLA steel
[AD-A148610] 08 p1130 N85-17122

Metal-support interactions: Their effects upon adsorption, electronics, and activity/selectivity properties of cobalt in hydrogenation
[DE85-003316] 09 p1292 N85-18113

Mechanisms of gas permeation through polymer membranes
[DE84-017423] 09 p1293 N85-18117

Prediction of retention indices of polynuclear aromatic hydrocarbons. Part 2: Capillary gas chromatography
[DE85-001301] 10 p1437 N85-19053

Separation of gas mixtures with coordination complexes
[DE85-000363] 10 p1438 N85-19062

Adsorption thermodynamics and surface transport of metal catalyst poisons
[DE85-002688] 10 p1441 N85-19084

Optical second harmonic generation for surface studies
[DE85-000670] 11 p1640 N85-20333

Adsorption thermodynamics and surface transport of metal catalyst poisons
[DE85-003750] 12 p1802 N85-21301

In situ monitoring of electrochemical reactions by surface enhanced Raman scattering
[PB85-149789] 12 p1803 N85-21312

Some unique aspects of fouling on copper as compared to titanium or nickel
[AD-A150072] 12 p1806 N85-21332

Critical events in inelastic deformation of glassy polymers in adsorptive medium
13 p2014 N85-22634

Adsorption behaviour of nitrogen compounds on to porous polymer beads and applications to atmospheric sampling
[BLL-DRIC-TRANS-7399-(3623.66)]
13 p2036 N85-22753

Determining adsorption of surface-active substances by sea bottom deposits 13 p2107 N85-23126

Adsorption site, adsorption energy and normal vibration frequency of H/Ni(100) via total energy calculations
[AD-A150555] 13 p2156 N85-23388

Hydrogen on impurity-covered iron surfaces
14 p2254 N85-23968

Interaction of low energy electrons with surface lattice vibrations
[DE85-005475] 14 p2426 N85-24975

Experimental testing of cooling by low pressure adsorption in a zeolite
[DE85-007509] 16 p2716 N85-26783

Correlation of zeolite ZSM-5 acid strength with catalytic activity and selectivity
[DE85-005415] 17 p2922 N85-28013

Methanol adsorption on Pt(111)
[DE85-006802] 17 p2923 N85-28017

Theory of laser-stimulated surface process. 2: A generalized-master-equation approach to energy transfer between an IR laser, an aspecties and phonons
[AD-A153083] 17 p2970 N85-28344

Multiple scattering effects in low energy alkali ion scattering: Application to the analysis of adsorbate ordering and bonding geometry
[DE85-007575] 17 p3032 N85-28757

Spectroscopy of surface adsorbed molecules
[DE85-009452] 17 p3034 N85-28768

Adsorption of Hg on lunar samples
[DE85-007948] 17 p3054 N85-28906

Coadsorption studies on transition metals
[PB85-183713] 18 p3072 N85-29003

Technique for measuring surface diffusion by laser-beam-localized surface photochemistry
[DE85-007685] 18 p3113 N85-29273

Electronic structure calculations for low coverage adlayers
[DE85-007733] 18 p3179 N85-29709

Cation promotion effects in zeolite-supported F-T catalysts
[DE85-009969] 19 p3233 N85-30044

Method for production of ceramic oxide and carbide bodies by polymer inclusion and decomposition
[DE85-011668] 19 p3250 N85-30152

Statistical mechanics of adsorption and wetting
[DE85-010093] 19 p3269 N85-30271

Adsorption of O2, SO2, and SO3 on nickel oxide. Mechanism for sulfate formation
[NASA-CR-176072] 21 p3565 N85-32175

CO adsorption on (111) and (100) surfaces of the Pt sub 3 Ti alloy. Evidence for parallel binding and strong activation of CO
[NASA-CR-176077] 21 p3565 N85-32176

Cloud condensation on insoluble particles
21 p3648 N85-32670

Characterization of catalysts with metal-support effects and of the species adsorbed on their surfaces
[DE85-012254] 24 p4096 N85-35394

Size and shape dependence of CO adsorption sites on sapphire supported Fe microcrystals
[NASA-CR-176171] 24 p4160 N85-35794

ADSORPTIVITY

Functional and structural changes in human erythrocyte surface after irradiation by UV waves of various wavelenights. Report 2: Adsorption of alcyan blue by external premembranous components
09 p1361 N85-18565

ADVANCED X RAY ASTROPHYSICAL FACILITY
U X RAY ASTROPHYSICS FACILITY

ADVANCED X RAY ASTROPHYSICS FACILITY
U X RAY ASTROPHYSICS FACILITY

ADVANCING GLACIERS
U GLACIERS

ADVANCING SHORELINES
U BEACHES

ADVECTION

The development of objective forecast techniques based on advection of surface weather parameters
01 p0078 N85-10522

Pointwise iterations of finite element modeling of advection-diffusion equations
[DE84-015284] 02 p0253 N85-11656

Generalized formulation of TVD Lax-Wendroff schemes
[NASA-CR-172478] 04 p0554 N85-13528

Razrezy program research in the tropical Atlantic
07 p0981 N85-16229

An evaluation of an advection fog prediction model
[AD-A147436] 07 p1008 N85-16403

A scheme for short-term prediction of hydrometeors using advection and physical forcing
[AD-A148011] 08 p1188 N85-17487

Measurements of sediment temperatures, conductivity and heat flow in the North Atlantic and their relevance to radioactive waste disposal
[IOS-172] 09 p1359 N85-18551

Evaluation of two numerical integrator schemes
[PB85-138196] 11 p1683 N85-20603

Two-dimensional numerical model of sensible and latent heat transport in an irrigated field under advective conditions 13 p2131 N85-23261

Variation of Arctic cloud cover in summer
[DE85-004507] 13 p2139 N85-23265

Fog advection in the Namib 16 p2831 N85-27454

A multilevel-multigrid method for recirculating flows
21 p3583 N85-32271

Mesoscale features and atmospheric refraction conditions of the Arctic marginal ice zone
[AD-A155139] 21 p3636 N85-32584

New semi-implicit method for solving the time-dependent conservation equations for incompressible flow
[DE85-010926] 23 p3931 N85-34367

AE-C SATELLITE
U EXPLORER 51 SATELLITE

AEOLIAN TONES

Statistics of Aeolian surface of Mars
13 p2199 N85-23637

AERATION

In-lake water quality management for Lake Eureka: Highlights of third year (1983) operation
[PB85-104149/GAR] 07 p0990 N85-16289

AERIAL EXPLOSIONS

The HEMP (High-altitude Electromagnetic Pulse) response of a long transmission line buried in the earth
[AD-A148517] 06 p0800 N85-15108

Long-distance propagation of infrasound in atmosphere near Earth's surface 06 p0825 N85-15238

Environmental airblast around large shock tubes
[DE85-010654] 20 p3463 N85-31512

Explosion in flight 21 p3683 N85-32883

Study to assess the effects of magnetohydrodynamic electromagnetic pulse on electric power systems, phase 1, volume 3
[DE85-011301] 24 p4156 N85-35771

AERIAL IMAGERY
U AERIAL PHOTOGRAPHY

AERIAL PHOTOGRAPHY

Remote sensing for landforms and soils in the arid southwest United States 03 p0378 N85-12410

Some principles of plant resources evaluation using remotely sensed data 04 p0543 N85-13459

EARSeL/ESA Symposium on Integrative Approaches in Remote Sensing
[ESA-SP-214] 05 p0655 N85-14202

Integrative investigation on forest damage detection based on airborne Multispectral Scanner data
05 p0656 N85-14215

Landform evaluation through integrated remote sensing methods. A case study in parts of Haryana, India
05 p0657 N85-14221

The need for integrating ground thermal measurements with thermal aircraft imagery 05 p0660 N85-14243

Photo-reconnaissance system
[AD-D011287] 06 p0826 N85-15245

Evidence accumulation for spatial reasoning
07 p0985 N85-16261

Forest area estimates from LANDSAT MSS and forest inventory plot data
[PB85-105617/GAR] 07 p0990 N85-16290

Interactive digital image processing for terrain data extraction
[AD-A148580] 08 p1176 N85-17417

Exploring the solar system with stellar occultations
08 p1245 N85-17857

Geoindication method for interpreting aerial and space photographs: Status and prospects
13 p1984 N85-22445

Combined analysis of the dynamics of complex ecosystems based on repeated remote measurements
13 p1985 N85-22450

Comprehensive, integrated, remote sensing at DOE sites
[DE85-004867] 13 p2126 N85-23240

Accomplishments of Institute of Cartography summarized 13 p2166 N85-23435

Calculation of image shift in panoramic photography
15 p2486 N85-25357

Identification of structure of soil-vegetation cover using aerial and space photographs 16 p2726 N85-26826

Diffusion coefficients for coastal water determined from aerial photographs
[INPE-3413-PRE/679] 16 p2810 N85-27331

Comparative study of the digital analysis of areas of the Earth's surface prepared for planting using different classification algorithms
[INPE-3359-PRE/637] 16 p2846 N85-27545

Airphoto interpretation of vegetation and landforms for soil mapping 17 p2983 N85-28436

Air photo analysis, photo interpretation logic, and feature extraction
[AD-A153926] 18 p3124 N85-29347

Handbook for obtaining and using aerial photography to map aquatic plant distribution
[AD-A154584] 21 p3605 N85-32386

Coastal erosion along Monterey Bay
[AD-A155610] 21 p3655 N85-32707

Cataloging the spectral brightness coefficients of the forested region of the European territory of the USSR
22 p3735 N85-33155

AERIAL RECONNAISSANCE

Satellite, airborne remote sensing development outlined 03 p0342 N85-12199

Earth Resources, A Continuing Bibliography with Indexes
[NASA-SP-7041(43)] 03 p0376 N85-12411

Measurements of atmospheric carbon disulfide using aircraft platforms and a GC/MS isotopic dilution analysis technique 03 p0381 N85-12500

The need for a dedicated public service helicopter design 06 p0753 N85-14828

Geological effectiveness of automated processing of highly precise aeromagnetic surveys in Caspian region
06 p0821 N85-15216

Photo-reconnaissance system
[AD-D011287] 06 p0826 N85-15245

Hybrid state estimation approach to multiobject tracking for airborne surveillance radars
[AD-A149459] 08 p1153 N85-17279
Earth resources: A continuing bibliography with indexes
[NASA-SP-7041(44)] 10 p1503 N85-19484
1981 wC-130 airborne lightning characterization program data review
[AD-A150230] 13 p2138 N85-23275
A constant altitude flight survey method for mapping atmospheric ambient pressures and systematic radar errors
[NASA-TM-86733] 19 p3217 N85-29951
Electronic reconnaissance aircraft of the Soviet Union Navy
[AD-A154706] 21 p3551 N85-32091

AERIAL RUDDERS
Space shuttle rudder/speedbrake actuation subsystem
08 p1102 N85-16965
Translating rudder pedal system
[AD-D011510] 12 p1780 N85-21172

AEROACOUSTICS
Results of tests of advanced flexible insulation vortex and flow environments in the North American Aerodynamics Laboratory lowspeed wind tunnel using 0.0405-scale Space Shuttle Orbiter model 16-0 (test OA-309)
[NASA-CR-167692] 01 p0015 N85-10096
Turbofan noise generation. Volume 2: Computer programs
[NASA-CR-167952] 02 p0275 N85-11791
Aeroacoustic data for high Reynolds number supersonic axisymmetric jets
[NASA-TM-86296] 07 p1038 N85-16587
Aeroacoustics at the DFVLR Brunswick Research Center: A survey on recent and current activities
[DFVLR-MITT-84-14] 08 p1219 N85-17677
Analysis of selected problems involving vortical flows
[NASA-CR-177347] 15 p2463 N85-25212

AEROASSIST
OTV Propulsion issues
[NASA-CP-2347] 08 p1106 N85-16989
NASA OAST perspective 08 p1106 N85-16990
Performance assessment of aero-assisted orbital transfer vehicles 08 p1106 N85-16993
Low lift-to-drag aero-assisted orbit transfer vehicles
08 p1107 N85-16994
Moderate lift-to-drag aeroassist
08 p1107 N85-16995
Benefits of high aerodynamic efficiency to orbital transfer vehicles 08 p1107 N85-16996
Space science and applications
11 p1644 N85-20362
Nonequilibrium air radiation (Nequair) program: User's manual
[NASA-TM-86707] 19 p3353 N85-30780

AEROBES
Aerobic sulfur-oxidizing bacteria: Environmental selection and diversification 21 p3656 N85-32712
Distribution and abundance of organic thiols
21 p3657 N85-32717

AEROBIOLOGY
Growth of soil bacteria in presence of Martian soil analog, carbon dioxide and hydrogen peroxide
09 p1361 N85-18560

AEROBRAKING
An optimization method for the preliminary design of interplanetary aerobraking missions
08 p1076 N85-16822
Design study of an integrated aerobraking orbital transfer vehicle
[NASA-TM-58264] 12 p1795 N85-21262

AERODYNAMIC AXIS
U AERODYNAMIC BALANCE

AERODYNAMIC BALANCE
Data input, processing and presentation — helicopter rotor balance measurement
[NASA-TM-77739] 01 p0125 N85-10856
Aerodynamic research efforts at SERI Wind Energy Research Center at Rocky Flats
[DE85-000529] 12 p1881 N85-21805
Dispersion sensitivity of the eight inch advanced ramjet munitions technology projectile due to wind and minor thrust errors
[AD-A152145] 16 p2727 N85-26835
Recent developments in rotary-balance testing of fighter aircraft configurations at NASA Ames Research Center
[NASA-TM-86714] 21 p3551 N85-32090

AERODYNAMIC BRAKES
NT DRAG CHUTES
NT LEADING EDGE SLATS
NT TRAILING EDGE FLAPS
NT WING FLAPS
An experimental study of airfoil-spoiler aerodynamics
[NASA-CR-177328] 06 p0748 N85-14796

AERODYNAMIC BUZZ
U FLUTTER

AERODYNAMIC CENTER
U AERODYNAMIC BALANCE

AERODYNAMIC CHARACTERISTICS
NT AERODYNAMIC BALANCE
NT AERODYNAMIC DRAG
NT AERODYNAMIC STABILITY
NT INTERFERENCE DRAG
NT INTERFERENCE LIFT
NT LIFT
NT STATIC AERODYNAMIC CHARACTERISTICS
NT ZERO LIFT
A study of aerodynamic characteristics of wing-body combinations. Part 2: Low-wing airplane
[NAL-TR-796] 01 p0002 N85-10010
Inlet and airframe compatibility for a V/STOL fighter/attack aircraft with top-mounted inlets
[NASA-TM-84252] 01 p0003 N85-10015
Prediction of aerodynamic characteristics of fighter wings at high angles of attack
[AD-A145107] 01 p0003 N85-10017
Experimental data base for computers program assessment. Report of the Fluid Dynamics Panel Working Group 04: Addendum
[AGARD-AR-138-ADD] 01 p0004 N85-10020
Pressure distribution on a swept wing aircraft in flight
01 p0004 N85-10025
Design and wind tunnel evaluation of a symmetric airfoil series for large wind turbine applications
[NASA-CR-174764] 02 p0135 N85-10919
VORCOR: A computer program for calculating characteristics of wings with edge vortex separation by using a vortex-filament and-core model
[NASA-CR-165902] 02 p0135 N85-10921
Results of winglet development studies for DC-10 derivatives
[NASA-CR-3677] 02 p0136 N85-10936
Energy efficient engine ICLS Nacelle detail design report
[NASA-CR-167870] 02 p0146 N85-10993
Definition of acceptable levels of mismatch for equivalent systems of augmented CTOL (Conventional Take-Off and Landing) aircraft
[AD-A145619] 02 p0149 N85-11007
The lateral-directional characteristics of a 74-degree Delta wing employing gothic planform vortex flaps
[NASA-CR-3848] 03 p0311 N85-12009
Flow visualization study of a vortex-wing interaction
[NASA-TM-86656] 03 p0316 N85-12040
Nonlinear system identification methodology development based on F-4S flight test data analysis
[AD-A146289] 03 p0318 N85-12053
Numerical simulation of the subsonic wing-rock phenomenon 03 p0320 N85-12064
A study of flow past an airfoil with a jet issuing from its lower surface
[NASA-CR-166610] 04 p0451 N85-12660
Application of the ONERA model of dynamic stall
[NASA-TP-2399] 04 p0451 N85-12662
Space Shuttle Orbiter trimmed center-of-gravity extension study. Volume 8: Effects of configuration modifications on the aerodynamic characteristics of the 140 A/B Orbiter at a Mach number of 5.97
[NASA-TM-72661-VOL-8] 04 p0452 N85-12667
Evaluation of the unsteady effects for a class of wind turbines 05 p0592 N85-13772
Influence of stationary components on unsteady flow in industrial centrifugal compressors
05 p0645 N85-14140
Aerodynamic characteristics of some lifting reentry concepts applicable to transatmospheric vehicle design studies
[NASA-TM-86331] 06 p0747 N85-14787
Details of export A-5 close-support aircraft given --- Qiang-5 aircraft 06 p0748 N85-14793
PROGRAM VSAERO: A computer program for calculating the non-linear aerodynamic characteristics of arbitrary configurations: User's manual
[NASA-CR-166476] 06 p0749 N85-14802
Aerodynamic and thermal characteristics of stellate bodies in hypersonic flow of rarefied gas at angle of attack 06 p0778 N85-14974
Effects of body shape on the aerodynamics of a body of revolution at Mach numbers from 1.6 to 4.6
[NASA-TM-86345] 07 p0893 N85-15657
Analytical modeling of circuit aerodynamics in the new NASA Lewis wind tunnel
[NASA-TM-86912] 07 p0897 N85-15686
An investigation of vortex-induced aerodynamic characteristics of supersonic cruise configurations
[NASA-CR-174299] 07 p0898 N85-15690
Downwash in the plane of symmetry of an elliptically loaded wing
[NASA-TP-2414] 07 p0898 N85-15693
Aileron effectiveness for a subsonic transport model with a high-aspect-ratio supercritical wing
[NASA-TM-86674] 07 p0898 N85-15695
Effect of aerodynamic and angle-of-attack uncertainties on the May 1979 entry flight control system of the Space Shuttle from Mach 8 to 1.5
[NASA-TP-2365] 07 p0913 N85-15778
Designer on civil aircraft design trends in USSR
08 p1066 N85-16768
Improvement of Aerodynamic Performance Through Boundary Layer Control and High Lift Systems
[AGARD-CP-365] 08 p1066 N85-16771
Operational requirements versus technological capabilities 08 p1072 N85-16798
Study of winglets applied to biplanes
[NASA-TM-86350] 08 p1083 N85-16862
Airworthiness and flight characteristics test of the RC-12D Guardrail V
[AD-A148046] 08 p1084 N85-16864
Optimum performance parameters for ski-jump operations of USAF fighter aircraft
[AD-A148532] 08 p1084 N85-16867
The aerodynamic challenges of the design and development of the space shuttle orbiter
08 p1093 N85-16909
The development and application of aerodynamic uncertainties: And flight test verification for the space shuttle orbiter 08 p1093 N85-16910
Performance assessment of aero-assisted orbital transfer vehicles 08 p1106 N85-16993
Benefits of high aerodynamic efficiency to orbital transfer vehicles 08 p1107 N85-16996
Exploratory investigation of the aerodynamic characteristics of a biwing vehicle at Mach 20.3
[NASA-TM-86314] 08 p1113 N85-17021
Proceedings of the workshop on unsteady separated flow held at the United States Air Force Academy on August 10-11, 1983
[AD-A148249] 09 p1263 N85-17937
Calculations for aerodynamic characteristics on a 3-D lifting body in a subsonic flow using boundary element method
[NAL-TR-835] 09 p1272 N85-17998
Icing flight research: Aerodynamic effects of ice and ice shape documentation with stereo photography
[NASA-TM-86906] 09 p1279 N85-18049
Theory of wing rock 09 p1282 N85-18064
The Altitude Wind Tunnel (AWT): A unique facility for propulsion system and adverse weather testing
[NASA-TM-86921] 09 p1283 N85-18067
The S2MA wind tunnel at the Modane-Avrieux aerodynamic test center
[ESA-TT-862] 09 p1284 N85-18071
Influence of normalized frequency on time-dependent aerodynamic characteristics of vane blading profiles
09 p1306 N85-18204
Computation of noise radiation from a free jet perpendicular to its axis via laser anemometry measurements
[ESA-TT-870] 09 p1379 N85-18669
Some fighter aircraft trends
[NASA-TM-86352] 10 p1420 N85-18954
Space Shuttle Orbiter trimmed center-of-gravity extension study. Volume 9: Effects of configuration modifications on the aerodynamic characteristics of the 140 A/B Orbiter at Mach numbers of 1.5, 2.0, and 2.5 --- wind tunnel tests
[NASA-TM-72661-VOL-9] 10 p1420 N85-18956
A method for estimating the rolling moment due to spin rate for arbitrary planform wings
[NASA-TM-86365] 10 p1425 N85-18990
Noise constraints effecting optimal propeller designs
[NASA-TM-86967] 11 p1575 N85-19923
Wind-tunnel investigation of a full-scale canard-configured general aviation airplane
[NASA-TP-2382] 11 p1575 N85-19925
STS-1 Pogo analysis
[NASA-TM-87433] 11 p1591 N85-20007
Measured unsteady transonic aerodynamic characteristics of an elastic supercritical wing with an oscillating control surface
[NASA-TM-86376] 12 p1771 N85-21116
A calculation of slender delta wing with leading-edge separation by quasi-vortex-lattice method
12 p1821 N85-21423
Supersonic Tactical Missile (STM) radome development
[AD-P004360] 12 p1825 N85-21454
Aerodynamic behavior of ventilated wind tunnel walls
13 p1966 N85-22363
The application of some lifting-body reentry concepts to missile design
[NASA-TM-86394] 13 p1969 N85-22366
Calculation of vortex-flap aerodynamic characteristics
[NASA-CR-175624] 13 p1969 N85-22367

Large-scale Advanced Propfan (LAP) performance, acoustic and weight estimation, January, 1984
[NASA-CR-174782] 13 p1969 N85-22368
Determination of aerodynamic and propulsion parameters of general aviation aircraft using steady state flight test data 13 p1971 N85-22377
Redesign of fuselage compartments by method of special contours 13 p2042 N85-22784
Oscillating airfoils and their wake
[NASA-TM-77831] 14 p2209 N85-23701
Missions and vehicle concepts for modern, propelled, lighter-than-air vehicles
[NASA-TM-87461] 15 p2457 N85-25170
Transonic Unsteady Aerodynamics and its Aeroelastic Applications
[AGARD-CP-374] 15 p2457 N85-25171
Analysis of transonic aerodynamic characteristics for a supercritical airfoil oscillating in heave, pitch and with oscillating flap 15 p2458 N85-25175
A semi-empirical unsteady transonic method with supersonic free stream 15 p2458 N85-25179
Special course on V/STOL aerodynamics: An assessment of European jet lift aircraft
[AGARD-R-710-ADDENDUM] 15 p2460 N85-25186
Unsteady analysis of rotor blade tip flow
[NASA-CR-3866] 15 p2462 N85-25202
Transonic aerodynamic and aeroelastic characteristics of a variable sweep wing
[NASA-TM-86677] 15 p2462 N85-25203
Effects of side-stick controllers on rotorcraft handling qualities for terrain flight
[NASA-TM-86688] 15 p2473 N85-25267
Mach-10 high Reynolds number development in the NSWC (Naval Surface Weapons Center) hypervelocity facility
[AD-A151241] 15 p2474 N85-25274
Numerical analyses in aerodynamic design of aero-engine fan 16 p2692 N85-26618
Low Reynolds number vehicles
[AGARD-AG-288] 16 p2699 N85-26666
Rotor blade flap-lag stability and response in forward flight in turbulent flows 16 p2705 N85-26698
Low-speed aerodynamic test of an axisymmetric supersonic inlet with variable cowl slot
[NASA-TM-87039] 16 p2708 N85-26710
OLGA: An open loop gust alleviation
16 p2713 N85-26744
The aerodynamics of controls
16 p2713 N85-26748
Observations, theoretical ideas and modeling of turbulent flows: Past, present and future
[NASA-TM-86679] 16 p2762 N85-27167
Analyses of orderly structures in jets and the relationship with emitted noise
[ISL-R-117/83] 16 p2861 N85-27646
Some effects of sweep direction and strakes for wings with sharp leading edges
[CA-8421] 17 p2892 N85-27826
A method to calculate the parameters of wings of arbitrary planform
[AD-A152889] 17 p2892 N85-27831
Design of robust controllers for a multiple input-multiple output control system with uncertain parameters application to the lateral and longitudinal modes of the KC-135 transport aircraft
[AD-A153100] 17 p2900 N85-27877
The aerodynamics of control
17 p2903 N85-27901
Wind-tunnel evaluation of a 21-percent-scale powered model of a prototype advanced scout helicopter
[NASA-TP-2420] 18 p3058 N85-28923
Wake effects on the aerodynamic performance of horizontal axis wind turbines
[NASA-CR-174920] 18 p3127 N85-29364
Nonlinear potential analysis techniques for supersonic-hypersonic configuration design
[NASA-CR-166078] 19 p3212 N85-29917
High Reynolds number tests of a NASA SC(3)-0712(B) airfoil in the Langley 0.3-meter transonic cryogenic tunnel
[NASA-TM-86371] 19 p3213 N85-29926
Two approaches for the prediction of plume-induced seperation
[AD-A154098] 19 p3215 N85-29935
Low-speed tests of a high-aspect-ratio, supercritical-wing transport model equipped with a high-lift flap system in the Langley 4- by 7-meter and Ames 12-foot pressure tunnels
[NASA-TP-2097] 20 p3388 N85-31010
Real scale test of the Petit Canard aircraft in the number 3 section, 47 sqm, of the SIMA wind tunnel, May 1984
[ONERA-PV-1/0772-GY] 20 p3389 N85-31018
Aerodynamic measurement of the wind flow in the number two section of the SIMA wind tunnel
[ONERA-PV-1/8138-GY] 20 p3389 N85-31019
Compendium of unsteady aerodynamic measurements, addendum 1
[AGARD-R-702-ADD-1] 20 p3390 N85-31028
Heat transfer in aeropropulsion systems
[NASA-TM-87066] 20 p3453 N85-31444
Quest for performance: The evolution of modern aircraft
[NASA-SP-468] 21 p3551 N85-32089
Trailing edge flow and aerodynamic sound. Part 1: Tonal pressure and velocity fluctuations. Part 2: Random pressure and velocity fluctuations
[AD-A154947] 21 p3552 N85-32097
Flight control system for a computer controlled aircraft with limited sensors
[AD-A155107] 21 p3555 N85-32115
Conceptual design and analysis of high-speed electronic imaging
[LA-10072-MS] 22 p3758 N85-33292
Aerodynamic analysis of a horizontal axis wind turbine by use of helical vortex theory. volume 2: Computer program users manual
[NASA-CR-174921] 22 p3804 N85-33563
The aerodynamic characteristics of a GU25-5(11)8 aerofoil for low Reynolds numbers
[GU-AERO-8410] 23 p3894 N85-34121

AERODYNAMIC CHORDS
U AIRFOIL PROFILES

AERODYNAMIC COEFFICIENTS
Fitting aerodynamic forces in the Laplace domain: An application of a nonlinear nongradient technique to multilevel constrained optimization
[NASA-TM-86317] 02 p0134 N85-10917
An investigation of vortex-induced aerodynamic characteristics of supersonic cruise configurations
[NASA-CR-174299] 07 p0898 N85-15690
Transport processes in the upper atmosphere
11 p1646 N85-20375
Unsteady aerodynamic characterization of a military aircraft in vertical gusts
[NASA-TM-77810] 12 p1770 N85-21110
Flight-measured laminar boundary-layer transition phenomena including stability theory analysis
[NASA-TP-2417] 12 p1771 N85-21118
Low-speed characteristics of a circulation control airfoil with AFT camber and a spiral trailing edge
[AD-A150851] 14 p2213 N85-23725
Design of apparatus for the determination of aerodynamic drag coefficients of automobiles
[AD-A151842] 15 p2464 N85-25219
A study of transonic flutter of a two-dimensional airfoil using the U-g and p-k methods
[AD-A151463] 15 p2473 N85-25266
Wind tunnel wall interference
[AD-A151212] 15 p2474 N85-25273
La Recherche Aerospatiale Bimonthly Bulletin Number 1984-3, 220/May-June
[ESA-TT-882] 16 p2695 N85-26636
Measurements of the symmetric aerodynamic coefficients for flat faced cylinders in the angle of attack regime 0 to 90 deg for transonic and supersonic speeds
[FFA-TN-1984-04] 16 p2700 N85-26675
Subsonic and transonic aerodynamics of a wraparound fin configuration
[AD-A153846] 18 p3059 N85-28927

AERODYNAMIC CONFIGURATIONS
NT WING NACELLE CONFIGURATIONS
Inlet and airframe compatibility for a V/STOL fighter/attack aircraft with top-mounted inlets
[NASA-TM-84252] 01 p0003 N85-10015
Experimental data base for computers program assessment. Report of the Fluid Dynamics Panel Working Group 04: Addendum
[AGARD-AR-138-ADD] 01 p0004 N85-10020
DFVLR rotorcraft: Construction and engineering
[NASA-TM-77740] 01 p0006 N85-10035
Stress-derivative control of keystoning deformation in finite element codes 01 p0058 N85-10385
PAN AIR: A computer program for predicting subsonic or supersonic linear potential flows about arbitrary configurations using a higher order panel method. Volume 3: Case manual (version 1.0)
[NASA-CR-3253] 02 p0135 N85-10922
Role of research aircraft in technology development
[NASA-TM-85913] 02 p0137 N85-10932
Energy efficient engine ICLS Nacelle detail design report
[NASA-CR-167870] 02 p0146 N85-10993
Simulator study of flight characteristics of several large, dissimilar, cargo transport airplanes during approach and landing
[NASA-TP-2357] 02 p0148 N85-11002
Comparative flow calculation on transonic cone/cylinder standard models in connection with the wall interference problem
[FW-FO-1689] 04 p0453 N85-12878
The preliminary checkout, evaluation and calibration of a 3-component force measurement system for calibrating propulsion simulators for wind tunnel models
[NASA-CR-174113] 04 p0458 N85-12903
An overview of some monoplanar missile programs
[NASA-TM-86330] 06 p0747 N85-14786
The aerodynamics of some guided projectiles
[NASA-TM-86334] 06 p0747 N85-14789
F-7 supersonic day fighter viewed --- Jian-7 aircraft
06 p0747 N85-14791
A-5 supersonic attack aircraft described --- Qiang-5 aircraft 06 p0747 N85-14792
Hypersonic flow of mixture around blunt body
06 p0779 N85-14979
A collection of flow visualization techniques used in the Aerodynamic Research Branch
[NASA-TM-85998] 06 p0808 N85-15135
Systems study for an Integrated Digital-Electric Aircraft (IDEA)
[NASA-CR-3840] 07 p0902 N85-15714
Aircraft drag reduction technology
08 p1070 N85-16782
Theoretical study of boundary-layer control
08 p1070 N85-16784
Aerodynamic-structural study of canard wing, dual wing, and conventional wing systems for general aviation applications
[NASA-CR-172529] 08 p1077 N85-16829
Study of winglets applied to biplanes
[NASA-TM-86350] 08 p1083 N85-16862
The space shuttle ascent vehicle aerodynamic challenges configuration design and data base development 08 p1093 N85-16906
The aerodynamic challenges of the design and development of the space shuttle orbiter
08 p1093 N85-16909
Exploratory investigation of the aerodynamic characteristics of a biwing vehicle at Mach 20.3
[NASA-TM-86314] 08 p1113 N85-17021
Generation of 3-dimensional body fitted coordinates using hyperbolic partial differential equations
[AD-A148059] 09 p1274 N85-18006
The S2MA wind tunnel at the Modane-Avrieux aerodynamic test center
[ESA-TT-862] 09 p1284 N85-18071
Effects of airfoil shape, thickness, camber, and angle of attack on calculated transonic unsteady airloads
[NASA-TM-86320] 10 p1420 N85-18957
Space Shuttle orbiter trimmed center-of-gravity extension study
[NASA-TP-2284] 10 p1428 N85-19003
Parametric study of a canard-configured transport using conceptual design optimization
[NASA-TP-2400] 11 p1584 N85-19979
Semianalytic modeling of aerodynamic shapes
[NASA-TP-2413] 12 p1771 N85-21120
Calculation of vortex-flap aerodynamic characteristics
[NASA-CR-175624] 13 p1969 N85-22367
The generation of three-dimensional body-fitted coordinate systems for viscous flow problems
[AD-A150861] 14 p2408 N85-24848
Experience with transonic unsteady aerodynamic calculations 15 p2458 N85-25176
Automatic Dynamic Aircraft Modeler (ADAM) for the computer program NASTRAN 15 p2574 N85-25875
Computational aerodynamics in designing aircraft
16 p2693 N85-26622
Numerical example of three-dimensional flying object in shockless transonic flow 16 p2693 N85-26623
Navier-Stokes solution of hypersonic blunt-nosed body flowfields 16 p2693 N85-26624
Recent progress in computational aerodynamics
16 p2693 N85-26626
Computational aerodynamics for aircraft wing design
16 p2693 N85-26627
Comparison of computational results of a few representative three dimensional transonic potential flow analysis programs 16 p2693 N85-26628
A numerical design method for three-dimensional transonic wings 16 p2694 N85-26631
ESP (External-Stores Program): A pilot computer program for determining flutter-critical external-store configurations. Volume 1: User's manual
[AD-A152268] 16 p2710 N85-26725
ESP (External-Stores Program): A pilot computer program for determining flutter-critical external-store configurations. Volume 2: Final report on program enhancement and delivery
[AD-A152269] 16 p2711 N85-26726
ESP (External-Stores Program): A pilot computer program for determining flutter-critical external-store configurations. Volume 3, part 1: Program compilation
[AD-A152270] 16 p2711 N85-26727
The evaluation of ACS for helicopters: Conceptual simulation studies to preliminary design
16 p2712 N85-26737

Supersonic aerodynamic characteristics of canard, tailless, and aft-tail configurations for 2 wing planforms
[NASA-TP-2434] 17 p2891 N85-27822
Static and dynamic pressure measurements on a NACA 0012 airfoil in the Ames High Reynolds Number Facility
[NASA-TP-2485] 17 p2891 N85-27823
Methods for design aerodynamics of modern transport aircraft
[DFVLR-FB-85-05] 17 p2893 N85-27836
Addition of flexible body option to the TOLA computer program, part 1
[NASA-CR-132732-1] 17 p2896 N85-27855
The flight control system for the Experimental Aircraft Programme (EAP) demonstration aircraft
17 p2904 N85-27908
Propulsion efficiency of vibrating bodies in subsonic gas stream 17 p2942 N85-28159
Nonlinear potential analysis techniques for supersonic-hypersonic configuration design
[NASA-CR-166078] 19 p3212 N85-29917
Performance comparison between NACA 23024 and NACA 64(3)-618 airfoil configurated rotors for horizontal-axis wind turbines
[NASA-TM-83471] 19 p3303 N85-30477
Compendum of unsteady aerodynamic measurements, addendum 1
[AGARD-R-702-ADD-1] 20 p3390 N85-31028
Data set 8: ZKP wing, oscillating aileron
20 p3390 N85-31029
Data set 9: LANN wing. Pitching oscillation
20 p3390 N85-31030
Recent developments in rotary-balance testing of fighter aircraft configurations at NASA Ames Research Center
[NASA-TM-86714] 21 p3551 N85-32090
Wind tunnel drag evaluations of helicopter nose sections
[AD-A155489] 21 p3553 N85-32100
Study of an efficient long-range Mach 2.7 supersonic transport configuration concept
[NASA-TM-86414] 21 p3554 N85-32110
Aerodynamic characteristics of a distinct wing-body configuration at Mach 6: Experiment, theory, and the hypersonic isolation principle
[NASA-TP-2467] 22 p3727 N85-33107
Energy efficient transport technology: Program summary and bibliography
[NASA-RP-1135] 22 p3729 N85-33116
Proceedings of the 14th Army Science Conference. Volume 2: Principal authors I through O
[AD-A149201] 24 p4144 N85-35690

AERODYNAMIC DRAG
Optimum design of nonplanar wings: Minimum induced drag for a given lift and wing root bending moment
[NAL-TR-797] 01 p0002 N85-10011
Airworthiness and Flight Characteristics (A and FC) test of the EH - 1X/EH - 1H helicopter configurations
[AD-A144881] 01 p0007 N85-10039
A comparison of Wortmann airfoil computer-generated lift and drag polars with flight and wind tunnel results
[NASA-TM-86035] 04 p0452 N85-12868
Investigations into the effects of scale and compressibility on lift and drag in the RAE 5m pressurized low-speed wind tunnel 08 p1066 N85-16773
An optimization method for the preliminary design of interplanetary aerobraking missions
08 p1076 N85-16822
Profile design for wings and propellers
[NASA-TM-77785] 10 p1419 N85-18953
Hypothetical zero yaw drag trajectory of spinning projectiles between M = 5 and M = 10
[AD-A146899] 10 p1421 N85-18963
Techniques to analyze vehicle coastdown data
[DE85-005159] 12 p1772 N85-21127
Determination of the drag of free flying particles in supersonic flow with a pulsed laser
12 p1773 N85-21129
Technical evaluation report on the FDP Symposium on Flight Test Techniques
[AGARD-AR-208] 12 p1777 N85-21157
Investigations into the effects of scale and compressibility on lift and drag in the RAE 5m pressurised low-speed wind tunnel
[RAE-TM-AERO-2006] 13 p1969 N85-22372
Preliminary assessment of power-generating tethers in space and of propulsion for their orbit maintenance
13 p1997 N85-22520
Investigation of the Vortex Tab
[NASA-CR-172566] 15 p2463 N85-25209
Flow past a flat plat with a vortex/sink combination
[JIAA-TR-58] 15 p2464 N85-25215
Design of apparatus for the determination of aerodynamic drag coefficients of automobiles
[AD-A151842] 15 p2464 N85-25219
The development of a performance and mission planning program for the A-7E aircraft
[AD-A151717] 15 p2471 N85-25258
Mercedes-Benz auto 2000 achieves low drag coefficient 15 p2530 N85-25602
A computer program for the drag prediction of subsonic, turbine powered aircraft in the en-route configuration
[VTH-LR-412] 16 p2701 N85-26681
Atmospheric density model 16 p2805 N85-27297
Aerodynamic performance of a wing in ground effect using the PANAIR program
[AD-A153303] 17 p2892 N85-27832
Ice shapes and the resulting drag increase for a NACA 0012 airfoil
[NASA-TM-83556] 17 p2894 N85-27839
Urban vehicle research project
[DE85-005444] 17 p3052 N85-28889
Consummative expressions for satellite drag perturbations in a spherically symmetrical atmosphere
[AD-A154230] 19 p3222 N85-29961
SANDRAG: A computer code for predicting drag of bodies of revolution at zero angle of attack in incompressible flow
[DE85-011170] 19 p3338 N85-30664
Wind tunnel drag evaluations of helicopter nose sections
[AD-A155489] 21 p3553 N85-32100
The influence of helicopter tail shape on drag: An aerodynamic study using a low speed wind tunnel
[AD-A156304] 24 p4062 N85-35174

AERODYNAMIC FORCES
NT AERODYNAMIC DRAG
NT AERODYNAMIC INTERFERENCE
NT AERODYNAMIC LOADS
NT BLAST LOADS
NT GUST LOADS
NT INTERFERENCE LIFT
NT LIFT
NT WING LOADING
NT ZERO LIFT
Integral equation of lifting surfaces in Laplace domain and analytic continuation of its pressure kernel
[NAL-TR-795T] 01 p0002 N85-10009
Fitting aerodynamic forces in the Laplace domain: An application of a nonlinear nongradient technique to multilevel constrained optimization
[NASA-TM-86317] 02 p0134 N85-10917
Force and moment measurements on a 74 deg delta wing with an apex flap
[NASA-CR-166081] 02 p0134 N85-10918
Unsteady aerodynamic response of cascades and turborotors 03 p0319 N85-12058
Effect of a variable camber and twist wing at transonic Mach numbers
[NASA-TM-86261] 04 p0452 N85-12869
A preliminary study of using a strain-gauged balance and parameter estimation techniques for the determination of aerodynamic forces on a model in a very short duration wind tunnel
[AD-A146473] 06 p0810 N85-15145
An exploratory study of finite difference grids for transonic unsteady aerodynamics
[NASA-TM-84583] 07 p0699 N85-15696
Theoretical study of non-linear unsteady aerodynamics of a non-rigid lifting body
[AD-P004169] 09 p1266 N85-17954
Experimental study of aerodynamic shielding of turbojet engine air intake against exhaust gases
09 p1307 N85-18210
Flight dynamics of axisymmetrical rotating bodies in air medium 13 p2043 N85-22791
Estimating unsteady aerodynamic forces on a cascade in a three-dimensional turbulence field
[NASA-TM-86701] 14 p2209 N85-23704
Investigation of the aerodynamic forces on bluff bodies at high Reynolds numbers
[DFVLR-MITT-84-19] 14 p2213 N85-23727
Effect of drag behind nozzle array on its force and energy characteristics 14 p2277 N85-24107
Calculation of harmonic aerodynamic forces of aerofoils and wings from the Euler equations
15 p2458 N85-25177
Application of CFD techniques toward the validation of nonlinear aerodynamic models
[NASA-TM-86715] 16 p2700 N85-26671
Preliminary wind tunnel study of the influence of a jet on the unsteady aerodynamics of a turbojet engine
[ONERA-RT-12/5115-RY-230-R-231G]
16 p2701 N85-26679
Flow around rotating and nonmoving circular cylinder near flat screen. Report 1: Aerodynamic forces in cylinder 16 p2765 N85-27059
Aerodynamic forces developing in channels between vases in turbine drive wheels 16 p2765 N85-27062
Turbine blade-tip clearance excitation forces
[NASA-CR-171534] 19 p3220 N85-29963
A review of shock waves around aeroassisted orbital transfer vehicles
[NASA-TM-86769] 22 p3739 N85-33177

AERODYNAMIC HEAT TRANSFER
NT HYPERSONIC HEAT TRANSFER
Results of a M = 5.3 heat transfer test of the integrated vehicle using phase-change paint techniques on the 0.0175-scale model 56-OTS in the NASA/Ames Research Center 3.5-foot hypersonic wind tunnel
[NASA-CR-167695] 13 p1966 N85-22466
Unsteady transonic heat transfer in a transient facility
[NASA-CR-176145] 23 p3930 N85-34354
Mach 14 flow restrictor thermal stress analysis
[AD-A156215] 24 p4067 N85-35208

AERODYNAMIC HEATING
NT SHOCK HEATING
Experimental and predicted heating distributions for biconics at incidence in air at Mach 10
[NASA-TP-2334] 03 p0361 N85-12313
Columbia: The first 5 flights entry heating data series. Volume 1: An overview
[NASA-CR-171820] 07 p0913 N85-15777
Challenges in the development of the orbiter radiator system 08 p1096 N85-16925
Shuttle system ascent aerodynamic and plume heating 08 p1103 N85-16975
Aerothermal tests of a 12.5 percent cone at Mach 6.7 for various Reynolds numbers, angles of attack and nose shapes — conducted in Langley 8-foot high temperature tunnel
[NASA-TP-2345] 08 p1161 N85-17322
Aerodynamic heating rate distributions induced by trailing edge controls on hypersonic aircraft configurations at Mach 8
[NASA-TM-87453] 13 p1969 N85-22370
Results of aeroheating DFI and ET design-data test on a 0.0175-scale model 60-OTS conducted in the Von Karman Gas Dynamics Facility (VKF) 40' supersonic and the 50' hypersonic wind tunnels A and C
[NASA-CR-167693] 13 p1966 N85-22466
Navier-Stokes solution of hypersonic blunt-nosed body flowfields 16 p2693 N85-26624
Unsteady heat transfer due to time-dependent free stream velocity 17 p2911 N85-27947
The role of thermal motions of air particles for fireballs
[PUBL-59] 17 p3053 N85-28900
SRB thermal protection systems materials test results in an arc-heated nitrogen environment
[NASA-CR-170881] 24 p4072 N85-35236
Results of tests of weathered K5NA closeout material in the MSFC Hot Gas Facility
[NASA-CR-170893] 24 p4073 N85-35239
Study of NSI and related cable performance during tests performed in the NASA Hot Gas Facility
[NASA-CR-170888] 24 p4101 N85-35423

AERODYNAMIC INTERFERENCE
Wind Tunnel Wall Interference Assessment and Correction, 1983
[NASA-CP-2319] 03 p0311 N85-12011
Wall interference measurements for three-dimensional models in transonic wind tunnels: Experimental difficulties 03 p0311 N85-12012
Survey of ONERA activities on adaptive-wall applications and computation of residual corrections
03 p0312 N85-12013
Wind tunnel wall interference in closed, ventilated and adaptive test sections 03 p0312 N85-12014
Two- and three-dimensional model and wall data from a flexible-walled transonic test section
03 p0312 N85-12015
Assessment of lift- and blockage-induced wall interference in a three-dimensional adaptive-wall tunnel
03 p0312 N85-12016
Interference from slotted walls
03 p0314 N85-12028
An inerference assessment approach for a three-dimensional slotted tunnel with sparse wall pressure data 03 p0314 N85-12030
Determination of equivalent model geometry for tunnel wall interference assessment/correction
03 p0314 N85-12031
Adaptation of a four-wall interference assessment/correction procedure for airfoil tests in the 0.3-m TCT 03 p0315 N85-12035
Modeling of propulsive jet plumes--extension of modeling capabilities by utilizing wall curvature effects
[AD-A146262] 03 p0362 N85-12324
Detection, classification, and extraction of helicopter-radiated noise
[AD-A145993] 03 p0416 N85-12661
Flow separation induced by periodic aerodynamic interference
[AD-P004174] 09 p1266 N85-17959
Unsteady transonic flow calculations for two-dimensional canard-wing configurations with aeroelastic applications
[NASA-TM-86375] 10 p1420 N85-18960

Experimental study of main rotor tip geometry and tail rotor interactions in hover. Volume 1. Text and figures
[NASA-CR-177336-VOL-1] 13 p1965 N85-22344

Experimental study of main rotor tip geometry and tail rotor interactions in hover. Volume 2: Run log and tabulated data
[NASA-CR-177336-VOL-2] 13 p1965 N85-22345

Study for prediction of rotor/wake/fuselage interference, part 1
[NASA-CR-177340-VOL-1] 13 p1965 N85-22346

Study for prediction of rotor/wake/fuselage interference. Part 2: Program users guide
[NASA-CR-177340-VOL-2] 13 p1966 N85-22347

F-14A aircraft high-speed flow simulations
[NASA-CR-172559] 14 p2209 N85-23702

Approximate neutral point of a subsonic canard aircraft
[NASA-TM-86694] 15 p2462 N85-25205

Unsteady gas dynamics problems related to flight vehicles
[AD-A151187] 15 p2464 N85-25218

Wind tunnel wall interference
[AD-A151212] 15 p2474 N85-25273

An experimental and analytical study of the aerodynamic interference effects between two Sears-Haack bodies at Mach 2.7
[NASA-TM-85729] 16 p2700 N85-26673

Synthesis study: Validation of a gust generator in the presence of a model in a wind tunnel
[ONERA-RT-16/5108-RY-051]
16 p2701 N85-26678

Adaptive wall wind tunnels and wall interference correction methods
[DFVLR-IB-222-84-A-37] 17 p2905 N85-27912

Effect of ground and/or ceiling planes on thrust of rotors in hover
[NASA-TM-86754] 20 p3388 N85-31014

AERODYNAMIC LIFT
U LIFT

AERODYNAMIC LOADS
NT BLAST LOADS
NT GUST LOADS

An experimental study on the induced normal force on tail-fins due to wing-tail interference
[NAL-TR-814] 03 p0318 N85-12051

Low power laminar aircraft structures
04 p0451 N85-12857

Operational loads measurement: A philosophy and its implementation 07 p0894 N85-15665

Navy operational loads data sources and systems
07 p0895 N85-15668

Operational loads data evaluation for individual aircraft fatigue monitoring 07 p0895 N85-15669

Structural flight load measurement demonstration of structural integrity 07 p0895 N85-15670

Aeroelastic analysis and the identification of flight loads — Mirage 2000 aircraft 07 p0896 N85-15679

Keeping up with operational loads in the French Air Force: Defining new equipment
07 p0896 N85-15681

Loads and Aeroelasticity Division research and technology accomplishments for FY 1984 and plans for FY 1985
[NASA-TM-86356] 07 p0898 N85-15691

Comparison of analytical and experimental steadyand unsteady-pressure distributions at Mach number 0.78 for a high-aspect-ratio supercritical wing model with oscillating control surfaces
[NASA-TM-84589] 07 p0899 N85-15697

Speed benefits of tilt-rotor designs for LHX
[NASA-CR-166437] 07 p0902 N85-15717

Flutter control with unsteady aerodynamic models
[AD-A147858] 07 p0909 N85-15753

Unsteady aerodynamic loading of an airfoil due to vortices released intermittently from its upper surface
[AD-P004162] 09 p1265 N85-17947

Modeling stochastic wind loads on vertical axis wind turbines
[DE85-001148] 09 p1340 N85-18426

Airbus fatigue tests 11 p1618 N85-20186

A study for calculating rotor loads using free vortex concept 11 p1620 N85-20194

Parachute inflation dynamics
11 p1715 N85-20792

Calculation of the flow around thick wings with separation vortices 12 p1821 N85-21424

Determination of stresses and deformations in linearly elastic conical shell subjected to aerodynamic loading and heating 13 p2047 N85-22812

Preliminary study of inphase gusts and moment force wind loads over the first 150 meters at KSC, Florida
[NASA-TM-86501] 13 p2137 N85-23273

Advanced life analysis methods. Volume 3: Experimental evaluation of crack growth analysis methods for attachment lugs
[AD-A151058] 14 p2317 N85-24319

Prediction of vortex-induced loads on wind-tunnel turning vanes
[NASA-TM-86678] 15 p2462 N85-25204

Description of a computer program treating transonic steady state aeroelastic effects for a canard or tail airplane
[FFA-TN-1983-23] 16 p2700 N85-26674

The effect of load factor on aircraft handling qualities
[AD-A152118] 16 p2710 N85-26724

Application of AFTI/F-16 task-tailored control modes in advanced multirole fighters 16 p2712 N85-26735

Some flight test results with redundant digital flight control systems 16 p2712 N85-26739

Study of stresses on surface of flat barrier immersed in under expanded jet of rarefied gas
16 p2765 N85-27061

Overview of aerothermodynamic loads definition study
17 p2910 N85-27942

Research on structures and materials — aircraft structures
[B8580060] 17 p2981 N85-28432

Acrosswind response of towers and stacks of circular cross-section 19 p3282 N85-30354

A new finite element approach: Progress in inviscid flow computations
[NASA-TM-86434] 20 p3454 N85-31450

Flight control system for a computer controlled aircraft with limited sensors
[AD-A155107] 21 p3555 N85-32115

AERODYNAMIC MOMENTS
U STABILITY DERIVATIVES

AERODYNAMIC NOISE

Analysis of noise measured from a propeller in a wake
[NASA-TP-2358] 02 p0274 N85-11788

Noise constraints effecting optimal propeller designs
[NASA-TM-86967] 11 p1575 N85-19923

Noise transmission loss of a rectangular plate in an infinite baffle
[NASA-TP-2398] 12 p1927 N85-22109

Large-scale Advanced Propfan (LAP) performance, acoustic and weight estimation, January, 1984
[NASA-CR-174782] 13 p1969 N85-22368

Laboratory studies of spacecraft response to transient discharge pulses 13 p1995 N85-22506

An experimental study of the noise generated by vaporous cavitation in turbulent shear flows produced by confined orifice plates 15 p2645 N85-26316

La Recherche Aerospatiale Bimonthly Bulletin Number 1984-3, 220/May-June
[ESA-TT-882] 16 p2695 N85-26636

Rotorcraft noise 18 p3057 N85-28916

Trailing edge flow and aerodynamic sound. Part 1: Tonal pressure and velocity fluctuations. Part 2: Random pressure and velocity fluctuations
[AD-A154947] 21 p3552 N85-32097

Nozzle wall roughness effects on free-stream noise and transition in the pilot low-disturbance tunnel
[NASA-TM-86389] 23 p3930 N85-34355

Optimally designed propellers constrained by noise
24 p4065 N85-35196

AERODYNAMIC STABILITY

Some considerations on Aeroelastic instabilities caused by coupling between propeller-type rotor and its supporting structure
[NAL-TR-804] 01 p0003 N85-10013

Aircrew-aircraft integration: A summary of US Army research programs and plans
[NASA-TM-85991] 02 p0148 N85-11004

Oil-flow study of a Space Shuttle orbiter tip-fin controller
[NASA-TM-86276] 04 p0460 N85-12920

Flutter parametric studies of cantilevered twin-engine transport type wing with and without winglet. Volume 2: Transonic and density effect investigations
[NASA-CR-172410-VOL-2] 04 p0513 N85-13270

Flutter control with unsteady aerodynamic models
[AD-A147858] 07 p0909 N85-15753

Active control of forward swept wings with divergence and flutter aeroelastic instabilities
09 p1282 N85-18063

Viscous effects on transonic airfoil stability and response
[NASA-TM-86374] 10 p1421 N85-18961

Acta Aeronautica et Astronautic Sinica (selected articles)
[AD-A148830] 11 p1575 N85-19922

An experimental study of aerodynamic damping characteristics of a compressor annular cascade in high speed flow and the visualization of annular cascade flow
[NAL-TR-838] 15 p2554 N85-25759

Aerodynamic detuning analysis of an unstalled supersonic turbofan cascade
[NASA-TM-87001] 16 p2700 N85-26670

Optimum parameters of aerogyroscopic satellite orientation system 16 p2718 N85-26782

Dynamic and aeroelastic action of guy cables
[VTT-18] 16 p2802 N85-27276

Static and dynamic pressure measurements on a NACA 0012 airfoil in the Ames High Reynolds Number Facility
[NASA-TP-2485] 17 p2891 N85-27823

Proceedings of the 9th US Air Force and the Federal Republic of Germany Data Exchange Agreement Meeting, Viscous and Interacting Flow Field Effects
[AD-A153020] 17 p2958 N85-28266

Research on optimal control, stabilization and computational algorithms for aerospace applications
[NASA-CR-172528] 19 p3221 N85-29970

Ground effect on helicopter aerodynamics and stability
20 p3395 N85-31063

Interactive aircraft flight control and aeroelastic stabilization
[NASA-CR-176035] 20 p3396 N85-31064

Aerodynamic characteristics of the standard dynamics model in coning motion at Mach 0.8
[NASA-TM-86717] 21 p3552 N85-32094

The physical and empirical basis for a specific clear-air turbulence risk index
[NASA-CR-178522] 24 p4120 N85-35540

AERODYNAMIC STALLING

Application of the ONERA model of dynamic stall
[NASA-TP-2399] 04 p0451 N85-12862

Development and certification of a new stall warning and avoidance system 05 p0702 N85-14507

Flight test results on stall characteristics of a large jet transport
[NAL-TR-817] 06 p0754 N85-14835

Prediction of dynamic stall characteristics using advanced non-linear panel methods
[AD-A148453] 08 p1078 N85-16836

Supermaneuverability
[AD-P004153] 09 p1263 N85-17938

Wing rock flow phenomena
[AD-P004154] 09 p1264 N85-17939

Unsteady stall penetration of an oscillating swept wing
[AD-P004156] 09 p1264 N85-17941

A Navier-Stokes calculation of the airfoil dynamic stall process
[AD-P004163] 09 p1265 N85-17948

Theoretical investigation of dynamic stall using a momentum integral method
[AD-P004170] 09 p1266 N85-17955

Synthesized airfoil data method for prediction of dynamic stall and unsteady airloads
[NASA-CR-3672] 09 p1274 N85-18005

Rocky Flats Wind Energy Research Center FY 1983 report
[DE85-004500] 10 p1511 N85-19535

The unsteady boundary layer on an elliptic cylinder following the impulsive onset of translational and rotational motion — dynamic stall 14 p2209 N85-23699

Nonlinear problems in flight dynamics involving aerodynamic bifurcations
[NASA-TM-86706] 15 p2462 N85-25206

Flight investigation of stall, spin and recovery characteristics of a low-wing, single-engine, T-tail light airplane
[NASA-TP-2427] 15 p2470 N85-25248

Simulator study of the stall departure characteristics of a light general aviation airplane with and without a wing-leading-edge modification
[NASA-TM-86309] 15 p2470 N85-25250

Investigation of potential and viscous flow effects contributing to dynamic stall
[AD-A151696] 15 p2557 N85-25773

Unsteady Navier-Stokes calculations in an accelerated reference frame
[AD-A151751] 15 p2557 N85-25774

Preliminary airworthiness evaluation of a National Aeronautics and Space Administration automated stall warning system for an OV-1 aircraft
[AD-A152010] 16 p2707 N85-26708

Wing tunnel investigation of dynamic stall of an NACA 0018 airfoil oscillating in pitch
[NAE-AN-27] 17 p2892 N85-27830

Turbulence structure in the boundary layers of an oscillating airfoil
[AD-A153631] 18 p3059 N85-28926

Calculation of steady and unsteady airfoil flow fields via the Navier-Stokes equations
[NASA-CR-3899] 22 p3727 N85-33105

Flutter clearance of the Schweizer 1-36 deep-stall sailplane
[NASA-TM-85917] 22 p3729 N85-33118

A design procedure to modify the trailing edge upper surface pressure gradient of a given aerofoil
[GU-AERO-8408] 23 p3894 N85-34120

An investigation into the three-dimensional stall development on a modified NACA 23012 aerofoil
[GU-AERO-8414] 23 p3894 N85-34124

Comments on the prediction of dynamic stall
[GU-AERO-8501] 23 p3894 N85-34125

AERODYNAMIC VEHICLES
U AIRCRAFT

AERODYNAMICS
NT AEROTHERMODYNAMICS
NT ROTOR AERODYNAMICS
NT SUPERSONICS

Aerodynamics of airfoils subject to 3-dimensional periodic gusts
[AD-A145149] 01 p0003 N85-10018

Rotor systems research aircraft airplane configuration flight-test results
[NASA-TM-85911] 01 p0006 N85-10034

Characteristic boundary conditions for three-dimensional transonic unsteady aerodynamics
[NASA-TM-86292] 02 p0134 N85-10915

Energy efficient engine combustor test hardware detailed design report
[NASA-CR-167945] 02 p0140 N85-10950

Aeronautical Engineering. A Continuing Bibliography With Indexes
[NASA-SP-7037(179)] 03 p0307 N85-11976

Inverse design technique for cascades
[NASA-CR-3836] 03 p0311 N85-12008

Estimation of helicopter performance using a program based on blade element analysis
[AD-A146341] 03 p0318 N85-12055

Aeronautical Engineering, a continuing bibliography with indexes
[NASA-SP-7037(180)] 04 p0451 N85-12858

Development of computational fluid dynamics at NASA Ames Research Center
[NASA-TM-86021] 04 p0452 N85-12866

Autonomous momentum management for space station
[NASA-CR-174065] 04 p0462 N85-12931

Subsynchronous vibrations in a high pressure centrifugal compressor: A case history 05 p0642 N85-14118

Performance measures for aircraft landings as a function of aircraft dynamics 05 p0712 N85-14565

Closing the design loop on HiMAT (highly maneuverable aircraft technology)
[NASA-TM-85923] 06 p0754 N85-14836

Circulation control: A bibliography of DTNSRDC research and selected outside references: Update
[AD-A146966] 07 p0893 N85-15661

Aero-optics experimental techniques
[AD-A146755] 07 p0957 N85-16067

Aeronautical Engineering: A continuing bibliography with indexes (supplement 182)
[NASA-SP-7037(182)] 08 p1057 N85-16758

International aviation (selected articles)
[AD-A148704] 08 p1067 N85-16762

Aerodynamic issues in the design of high-lift systems for transport aircraft 08 p1069 N85-16780

Joined wing transonic design and test validation
[AD-A148355] 08 p1078 N85-16834

Aeronautical engineering, a continuing bibliography with indexes
[NASA-SP-7037(181)] 09 p1263 N85-17932

Numerical approach for the aerodynamic analysis if airfoils with laminar separation
[NASA-CR-172496] 09 p1273 N85-18001

A first-order Green's function approach to supersonic oscillatory flow: A mixed analytic and numeric treatment
[NASA-CR-172207] 09 p1273 N85-18002

Generation of 3-dimensional body fitted coordinates using hyperbolic partial differential equations
[AD-A148059] 09 p1274 N85-18006

Aeronautical engineering: A continuing bibliography with indexes
[NASA-SP-7037(184)] 10 p1419 N85-18949

LOVEL-84: A LOw-VELocity aerodynamic heating code for flat plates, wedges, and cones
[DE85-002604] 11 p1576 N85-19933

New air supply-prime mover facility for engine tests detailed 11 p1621 N85-20204

A locally linearized panel method fur tran-/subsonic flow past an oscillating wing 11 p1622 N85-20212

Air Force Academy Aeronautics Digest
[AD-A149614] 12 p1769 N85-21104

An investigation of aerowindows for solar receivers
[DE84-010831] 12 p1677 N85-21772

List of RAE (Royal Aircraft Establishment) translations issued during the period 1 March 1983 - 31 March 1984
[AD-A149787] 12 p1951 N85-22257

Aeronautical Engineering: A continuing bibliography with indexes, supplement 185
[NASA-SP-7037(185)] 13 p1965 N85-22342

Aeronautical Engineering: A cumulative index to the 1984 issues of the continuing bibliography
[NASA-SP-7037(183)] 13 p1965 N85-22343

Absolute stability of unsteady movement of axisymmetrical rotating flight vehicle
13 p2044 N85-22793

Aeronautical engineering, a continuing bibliography with indexes
[NASA-SP-7037(186)] 14 p2207 N85-23682

Problem of reduction to ideal tube in experimental aerodynamics 14 p2286 N85-24179

A fundamental study of liquid phase particle breakup. Revision
[AD-A150791] 14 p2301 N85-24249

Nonlinear problems in flight dynamics involving aerodynamic bifurcations
[NASA-TM-86706] 15 p2462 N85-25206

Three-Dimensional Boundary Layers
[AGARD-R-719] 15 p2558 N85-25784

A perspective on superaugmented flight control advantages and problems 16 p2712 N85-26733

Wind energy technology program summary
[DE85-007349] 16 p2820 N85-27392

Adaptive grid generation for numerical solution of Burger's equation
[AD-A152217] 16 p2856 N85-27606

Research and development. Technical and scientific reports 1984 16 p2873 N85-27724

New flow physical aspects in aerodynamics
[MBB-FE-122/S/PUB/133] 16 p2873 N85-27725

Upwind-difference methods for aerodynamic problems governed by the Euler equations
[REPT-84-23] 17 p2893 N85-27834

Test devices for aeronautical research and technology
[NASA-TM-77651] 17 p2906 N85-27914

Helicopter aeromechanics: Introduction and historical review 18 p3057 N85-28914

Subsonic and transonic aerodynamics of a wraparound fin configuration
[AD-A153646] 18 p3059 N85-28927

A computational method for wings of arbitrary planform
[AD-A153788] 18 p3059 N85-28929

Acoustic noise associated with the MOD-1 wind turbine: its source, impact, and control
[DE85-002947] 18 p3178 N85-29700

Aeronautical Engineering: A continuing bibliography with indexes
[NASA-SP-7037(187)] 19 p3211 N85-29911

Aerodynamic analysis of a horizontal axis wind turbine by use of helical vortex theory. Volume 1: Theory
[NASA-CR-168054] 19 p3212 N85-29916

A first-order time-domain Green's function approach to supersonic unsteady flow
[NASA-CR-172208] 19 p3214 N85-29930

Compendium of unsteady aerodynamic measurements, addendum 1
[AGARD-R-702-ADD-1] 20 p3390 N85-31028

Data set 8: ZKP wing, oscillating aileron
20 p3390 N85-31029

Data set 9: LANN wing. Pitching oscillation
20 p3390 N85-31030

R and D programmes at the National Aeronautical Laboratory
[AR-22] 20 p3539 N85-32022

R and D activities of the Aerodynamics Division
20 p3539 N85-32023

Aeronautical engineering: A continuing bibliography with indexes (supplement 189)
[NASA-SP-7037(189)] 22 p3727 N85-33104

Nineteenth Aerospace Mechanisms Symposium
[NASA-CP-2371] 22 p3795 N85-33512

Aeronautical engineering: A continuing bibliography with indexes, supplement 190
[NASA-SP-7037(190)] 24 p4059 N85-35152

Analysis of incompressible cascade flows using state-of-the-art computer programs
[AD-A155850] 24 p4062 N85-35173

AEROELASTIC RESEARCH WINGS

Transonic calculations for a flexible supercritical wing and comparison with experiment
[NASA-TM-86439] 20 p3388 N85-31012

AEROELASTICITY

Some considerations on Aeroelastic instabilities caused by coupling between propeller-type rotor and its supporting structure
[NAL-TR-804] 01 p0003 N85-10013

Characteristics of controlled-oscillating annular cascade test facility with Freon gas
[NAL-TR-812] 01 p0003 N85-10014

Aeroelastic stability analysis with interacting structural nonlinearities 02 p0207 N85-11364

Extended aeroelastic analysis for helicopter rotors with prescribed hub motion and blade appended pendulum vibration absorbers
[NASA-CR-172455] 03 p0315 N85-12038

Unsteady aerodynamic response of cascades and turborotors 03 p0319 N85-12058

Propulsive efficiency of vibrating wing in supersonic flow 05 p0724 N85-14656

Verification of a computer program for vibration analysis of composite wing cores
[NAL-TR-825] 06 p0817 N85-15187

Aeroelastic analysis and the identification of flight loads -- Mirage 2000 aircraft 07 p0898 N85-15679

Stereo Electro-optical Tracking System (SETS)
[NASA-CR-172471] 07 p0962 N85-16096

Active control of forward swept wings with divergence and flutter aeroelastic instabilities
09 p1262 N85-18063

Unsteady transonic flow calculations for two-dimensional canard-wing configurations with aeroelastic applications
[NASA-TM-86375] 10 p1420 N85-18960

Viscous effects on transonic airfoil stability and response
[NASA-TM-86374] 10 p1421 N85-18961

Three-dimensional unsteady lifting surface theory in the subsonic range
[NASA-TM-77812] 12 p1770 N85-21111

A study of transonic flutter of a two-dimensional airfoil using the U-g and p-k methods
[LR-615] 12 p1771 N85-21121

Study for the optimization of a transport aircraft wing for maximum fuel efficiency. Volume 1: Methodology, criteria, aeroelastic model definition and results
[NASA-CR-172551] 13 p1971 N85-22378

Simple theoretical models for composite rotor blades
[NASA-CR-175620] 13 p1971 N85-22382

Structural response of a rotating bladed disk to rotor whirl
[NASA-CR-175605] 13 p1973 N85-22391

Oscillating airfoils and their wake
[NASA-TM-77831] 14 p2209 N85-23701

A research program in active control/aeroelasticity
[NASA-CR-175674] 14 p2218 N85-23752

Flutter taming: A new tool for the aeroelastic designer
[AD-A150834] 14 p2226 N85-23802

Some optimization problems in static aeroelasticity for wings made of composite materials
14 p2277 N85-24104

Transonic Unsteady Aerodynamics and its Aeroelastic Applications
[AGARD-CP-374] 15 p2457 N85-25171

Experience with transonic unsteady aerodynamic calculations 15 p2458 N85-25176

Computation of unsteady transonic flows about two-dimensional and three-dimensional AGARD standard configurations 15 p2459 N85-25183

Calculation of unsteady transonic flow around a high swept wing 15 p2459 N85-25184

The development of unsteady transonic 3-D full potential code and its aeroelastic applications
15 p2460 N85-25187

Transonic aerodynamic and aeroelastic characteristics of a variable sweep wing
[NASA-TM-86677] 15 p2462 N85-25203

Unsteady gas dynamics problems related to flight vehicles
[AD-A151187] 15 p2464 N85-25218

Active control of forward swept wings with divergence and flutter aeroelastic instabilities
[AD-A151837] 15 p2474 N85-25270

Description of a computer program treating transonic steady state aeroelastic effects for a canard or tail airplane
[FFA-TN-1983-23] 16 p2700 N85-26674

Dynamic and aeroelastic action of guy cables
[VTT-18] 16 p2802 N85-27276

An assessment of the suitability of the BHGA structural test rig for aerodynamic testing of hang gliders
[CA-8505] 17 p2896 N85-27853

Flight trials of a modified gulfstream commander carrying external stores
[AD-A153376] 17 p2896 N85-27859

On the wind-induced vibrations of a mass-spring system
[REPT-84-04] 17 p2981 N85-28428

Helicopter Aeromechanics
[AGARD-LS-139] 18 p3057 N85-28913

Recent developments in the dynamics of advanced rotor systems 18 p3057 N85-28917

The static aeroelasticity of a composite wing
18 p3121 N85-29321

Selected topics in experimental aeroelasticity at the NASA Langley Research Center
[NASA-TM-86436] 19 p3284 N85-30364

Interactive aircraft flight control and aeroelastic stabilization
[NASA-CR-176035] 20 p3396 N85-31064

Aeroelastic constraints for a wing weight minimization procedure
[FFA-TN-1985-4] 23 p3895 N85-34126

The application of bispectral analyses to aeroelastic phenomena 24 p4060 N85-35157

Analysis of flexible aircraft longitudinal dynamics and handling qualities. Volume 1: Analysis methods
[NASA-CR-177943-VOL-1] 24 p4066 N85-35202

Analysis of flexible aircraft longitudinal dynamics and handling qualities. Volume 2: Data
[NASA-CR-177943-VOL-2] 24 p4067 N85-35203

AEROLOGY

Optimization of system for observing Northern Hemisphere atmospheric pressure field
15 p2485 N85-25338

Lightweight aerological radiosonde MARZ
16 p2807 N85-27309

Reports from the German Meteorological Service. No. 167: Results of aerological soundings in the model area upper Rhine: Heat release project upper Rhine area, part 3
[ISBN-3-88148-216-4] 23 p3950 N85-34479

AEROMAGNETISM

Long-wavelength magnetic and gravity anomaly correlations on Africa and Europe
20 p3476 N85-31597

AEROMAGNETO FLUTTER
U FLUTTER

AEROMANEUVERING

Report of the Transportation Panel
11 p1645 N85-20364

AERONAUTICAL ENGINEERING

Aeronautical systems technology needs: Escape, rescue and survival, test facilities and test equipment and training-simulation equipment
[AD-A145059] 01 p0001 N85-10002

ACEE program rationale and implementation
[NASA-TM-84549] 02 p0133 N85-10908

Characteristics of systems engineering in aviation science research
[AD-A145602] 02 p0292 N85-11899

Research and technology
[NASA-TM-86321] 02 p0305 N85-11973

Aeronautical Engineering, A Continuing Bibliography With Indexes
[NASA-SP-7037(179)] 03 p0307 N85-11976

Activities report of the Department of Engineering
03 p0342 N85-12202

Aeronautical Engineering, a continuing bibliography with indexes
[NASA-SP-7037(180)] 04 p0451 N85-12858

USSR report: Engineering and equipment
[JPRS-UEQ-84-007] 06 p0775 N85-14954

Aeronautical Engineering: A continuing bibliography with indexes (supplement 182)
[NASA-SP-7037(182)] 08 p1067 N85-16758

Aeronautical engineering, a continuing bibliography with indexes
[NASA-SP-7037(181)] 09 p1263 N85-17932

The Prandtl Hergesell project of a national research establishment for aeronautics
[ESA-TT-835] 09 p1272 N85-17993

Aeronautical engineering: A continuing bibliography with indexes
[NASA-SP-7037(184)] 10 p1419 N85-18949

Calendar of selected aeronautical and space meetings
[AGARD-CAL-84/2] 10 p1573 N85-19917

Air Force Academy Aeronautics Digest
[AD-A149614] 12 p1769 N85-21104

Bibliography of Lewis Research Center technical publications announced in 1983
[NASA-TM-83693] 12 p1951 N85-22255

List of RAE (Royal Aircraft Establishment) translations issued during the period 1 March 1983 - 31 March 1984
[AD-A149787] 12 p1951 N85-22257

Aeronautical Engineering: A continuing bibliography with indexes, supplement 185
[NASA-SP-7037(185)] 13 p1965 N85-22342

Aeronautical Engineering: A cumulative index to the 1984 issues of the continuing bibliography
[NASA-SP-7037(183)] 13 p1965 N85-22343

Aeronautical engineering, a continuing bibliography with indexes
[NASA-SP-7037(186)] 14 p2207 N85-23682

Model research: The National Advisory Committee for Aeronautics, 1915-1958, volume 1
[NASA-SP-4103-VOL-1] 14 p2207 N85-23683

Model research, the National Advisory Committee for Aeronautics, 1915-1958, volume 2
[NASA-SP-4103-VOL-2] 14 p2207 N85-23684

Future directions in aeropropulsion technology
[NASA-TM-87010] 14 p2207 N85-23685

USSR report: Engineering and equipment
[JPRS-UEQ-84-005] 14 p2285 N85-24157

Fiscal year 1986 technical objective document
[AD-A151039] 14 p2432 N85-25000

Research and technology
[NASA-TM-86662] 14 p2456 N85-25166

The 1985 long-range program plan
[NASA-TM-87464] 15 p2664 N85-26440

Activities of the Aeronautics and Space Engineering Board
[NASA-CR-175825] 16 p2691 N85-26610

Alternatives for jet engine control
[NASA-CR-175832] 16 p2709 N85-26714

Alternatives for jet engine control
[NASA-CR-175833] 16 p2709 N85-26715

Guide for the execution of reliability tests in the laboratory --- aeronautical equipment
16 p2796 N85-27237

Simulation for human factors research. A central question: Fidelity 18 p3159 N85-29568

Aeronautical Engineering: A continuing bibliography with indexes (supplement 188)
[NASA-SP-7037(188)] 19 p3211 N85-29910

Aeronautical Engineering: A continuing bibliography with indexes
[NASA-SP-7037(187)] 19 p3211 N85-29911

The economics of private sector R and D decisionmaking in aeronautics
[NASA-CR-176007] 19 p3379 N85-30962

National aeronautical R and D goals: Technology for America's future 19 p3379 N85-30964

Some applications of aeronautical engineering in the construction of yachts
[NLR-MP-83042-U] 20 p3394 N85-31052

The Naval Postgraduate School Flight Mechanics Laboratory: A feasibility study
[AD-A154578] 21 p3557 N85-32127

DYNA3D, INGRID, and TAURUS: An integrated, interactive software system for crashworthiness engineering
[DE85-010928] 21 p3677 N85-32846

Aeronautical engineering: A continuing bibliography with indexes (supplement 189)
[NASA-SP-7037(189)] 22 p3727 N85-33104

Aeronautical engineering: A continuing bibliography with indexes, supplement 190
[NASA-SP-7037(190)] 24 p4059 N85-35152

AERONAUTICAL SATELLITES

Experimental satellite system for determining coordinates of maritime distress
09 p1308 N85-18216

AERONAUTICS

Large scale computing in aeronautical design
01 p0007 N85-10043

AGARD Highlights
[AGARD-HIGHLIGHTS-84/2] 02 p0305 N85-11972

Natural laminar flow airfoil design considerations for winglets on low-speed airplanes
[NASA-CR-3853] 04 p0452 N85-12863

Operation of aviation support bases
04 p0544 N85-13461

Research and technology highlights of the Lewis Research Center
[NASA-TM-86899] 08 p1261 N85-17928

On the frontier: Flight research at Dryden 1946-1981
[NASA-SP-4303] 09 p1263 N85-17934

The Prandtl Hergesell project of a national research establishment for aeronautics
[ESA-TT-835] 09 p1272 N85-17993

National airspace system: Operational requirements
[AD-A149349] 10 p1422 N85-18973

Flight investigation of stall, spin and recovery characteristics of a low-wing, single-engine, T-tail light airplane
[NASA-TP-2427] 15 p2470 N85-25248

West European report: Science and technology
[JPRS-WST-84-036] 18 p3066 N85-28960

AEV local verification for aviation, precipitation, and temperature programs: AV, REL, TEM
[PB85-179125] 19 p3318 N85-30568

Aeronautical engineering: A continuing bibliography with indexes (supplement 189)
[NASA-SP-7037(189)] 22 p3727 N85-33104

Aeronautical engineering: A continuing bibliography with indexes, supplement 190
[NASA-SP-7037(190)] 24 p4059 N85-35152

AERONOMY

Aeronomy 02 p0298 N85-11930

Summary presentation of the Science Applications Panel 11 p1644 N85-20355

Aeronomical aspects of mesospheric photodissociation: Processes resulting from the solar H Lyman alpha line
[AERONOMICA-ACTA-A-285-1984]
11 p1680 N85-20587

Sounding rocket program Aeronomie. The payload M-I in the project MAP-WINE
[BMFT-FB-W-84-046] 12 p1790 N85-21238

Atmospheric chemistry
[INPE-3190-PRE/554] 16 p2826 N85-27430

Equitorial scintillations: Advances since ISEA-6
[AD-A154962] 21 p3631 N85-32559

Activities report of the Aeronomy Department
[G-774-1984] 21 p3633 N85-32569

AEROPHYSICS
U ATMOSPHERIC PHYSICS

AEROS SATELLITE

Sources of information concerning the ionosphere
04 p0521 N85-13334

AEROSOLS
NT FOG

Gravitational effects on premixed particle cloud flames
02 p0171 N85-11144

Spectroradiometric calibration of the Thematic Mapper and Multispectral Scanner system
[E85-10026] 02 p0218 N85-11439

Aerosol sampling bias from differential electrostatic charge and particle size 02 p0224 N85-11467

A dispersion model for airborne particulates inside a building
[DE84-014961] 02 p0225 N85-11473

Development of a global model for atmospheric backscatter at CO2 wavelengths
[NASA-CR-174053] 02 p0228 N85-11489

Arctic haze: Meteorological aspects of long-range transport 02 p0230 N85-11499

Evaluation of an aerosol prediction model for coastal regions using marine aerosol generation and transport data
[AD-A145443] 02 p0231 N85-11510

Laboratory investigation of coefficients of absorption of air at Lambda = 10.6 microns 02 p0263 N85-11723

Ultraviolet observations of Uranus and Neptune below 3000 Angstrom 02 p0298 N85-11932

Organic aerosol formation: OH(hydroxyl radical) versus ozone oxidation pathways
[PB84-219860] 03 p0386 N85-12484

A system for monitoring radon and its decay products in the atmosphere
[INPE-3085-PRE/494] 03 p0391 N85-12502

Atmospheric extinction in critical environments
[AD-A146102] 03 p0396 N85-12527

Characteristics of aerosol volume distributions measured at Meppen, W. Germany
[AD-A146138] 03 p0396 N85-12528

Deposition in the human lung during respiration of small particles suspended in the air
[BLL-RISLEY-TR-5021-(9091.9F)]
03 p0400 N85-12549

Intermediate results of a 1-year study of a laser spectrometer in the DOE filter test facilities
[DE84-016478] 04 p0506 N85-13228

Urban aerosol modeling
[PB84-233469] 04 p0532 N85-13401

Parallel flow diffusion battery
[DE84-005964] 05 p0631 N85-14047

Certain optimal parameters of high-velocity Venturi ejection tubes
[BLL-M-35924-(5828.4)] 05 p0634 N85-14066

Utilization of SAGE aerosol profiles in the analysis of Mauna Loa stratospheric lidar data
[NASA-CR-174198] 05 p0675 N85-14332

Assessment of Techniques for Measuring Tropospheric H sub x O sub y: Summary 05 p0675 N85-14337

Aerosol reactor for silicon processing
06 p0832 N85-15292

Comparison measurements on optical particle counters
[BLL-DOUNREAY-TR-934-(9091.9F)]
07 p0961 N85-16092

Middle Atmosphere program. Handbook for MAP. Volume 13: Ground-based techniques
[NASA-CR-174345] 08 p1183 N85-17452

Lidar systems for aerosol studies: An outline
08 p1183 N85-17457

Satellite stratospheric aerosol measurement validation
[NASA-TM-86003] 08 p1187 N85-17479

Optical wave propagation and imaging in the atmosphere 08 p1222 N85-17694

Carbon dioxide laser radar for monitoring atmospheric transmittance and atmospheric aerosol
09 p1354 N85-18516

Condensational transformation of atmospheric aerosol particle distribution functions 10 p1500 N85-19468

Airborne lidar measurements of El Chichon stratospheric aerosols, October 1982 to November 1982
[NASA-RP-1136] 10 p1514 N85-19550

Upper atmosphere research at INPE
[INPE-3281-PRE/604] 10 p1515 N85-19557

Aerosol limb absorption --- stratosphere
[NASA-TM-77733] 10 p1515 N85-19562

Imaging through a multiple scattering medium
[DE85-002051] 10 p1557 N85-19821

Effect of water vapor and water droplets on the RAM-1 (Real-Time Aerosol Monitor): Preliminary results
[PB85-109429] 11 p1637 N85-20313

MAP in Japan: Organization and projects
11 p1655 N85-20425

The Middle Atmosphere Program: A special project for the Antarctic Middle Atmosphere (AMA)
11 p1656 N85-20430

The concentration of sulfate in broken cloud layers
[DE85-000228] 11 p1678 N85-20574

Continued research in mesoscale air pollution simulation modeling. Volume 7. Mathematical modeling of urban aerosol dynamics
[PB85-137388] 11 p1679 N85-20584

Continued research in mesoscale air pollution simulation modeling. Volume 5: Refinements in numerical analysis, transport, chemistry, and pollutant removal
[PB85-137362] 11 p1680 N85-20585

Lidar observations of stratospheric aerosol over Mauna Loa Observatory, 1974 - 1981
[PB85-115061] 11 p1682 N85-20597

Novel photo-thermal technique for flow and spectroscopic measurements in a dense aerosol stream
[AD-A149745] 12 p1800 N85-21287

Photo-thermal detection of the onset of photo-chemical nucleation (laser-snow) in vapor
[AD-A150111] 12 p1801 N85-21295

Aerosol multiple-scanning code, ASCAT
[LA-10046-MS] 12 p1823 N85-21440

Study of electric field and ion effects on HVDC lines
[DE85-002975] 12 p1833 N85-21503

Transmission and reflection of laser beams propagating through aerosol clouds in space
[LA-9998-MS] 12 p1856 N85-21638

Spectroradiometric calibration of the Thematic Mapper and Multispectral Scanner system
[E85-10094] 12 p1874 N85-21756

Phase function, backscatter, extinction, and absorption for standard radiation atmosphere and El Chichon aerosol models at visible and near-infrared wavelengths
[NASA-TM-86379] 12 p1892 N85-21874

Impact of aerosols on visibility and climate: A report prepared for Panel 3, Environmental Impact, of the NATO/CCMS Air Pollution Pilot Study on Air Pollution Control Strategies and Impact Modelling
[PB85-106744] 12 p1897 N85-21906

Studies of the mechanisms and rates with which nitrogen species are incorporated into cloud water and precipitation
[PB85-144350] 12 p1898 N85-21914

Chemical characterization and toxicologic evaluation of airborne mixtures. Inhalation toxicology of diesel fuel obscurant aerosol in Sprague-Dawley rats. Phase 3. Subchronic exposures
[AD-A150100] 12 p1905 N85-21966

Microstructure of Venus cloud layer based on spectrophotometric data from Venera-11 spacecraft
13 p1982 N85-22436

Effects of temperature variation among droplets in an evaporating fuel spray 13 p2004 N85-22562

Multiple element neutron-activation analysis of atmospheric aerosols with X-ray and gamma-spectrometric recording of radionuclides formed
13 p2013 N85-22631

One mechanism of formation of organic fraction in atmospheric aerosol 13 p2014 N85-22632

Size and velocity distributions of particles and droplets in spray combustion systems
[AD-A150355] 13 p2017 N85-22648

The orientation distribution of nonspherical aerosol particles within a cloud
[AD-A150600] 13 p2092 N85-23061

Infrared aerosol absorption index
13 p2110 N85-23147

The relationship between marine aerosol particles and satellite-detected radiance 13 p2131 N85-23263

Cumulus cloud venting of mixed layer ozone
[NASA-TM-87429] 13 p2132 N85-23269

Analysis of biological particles by mass spectrometry
[AD-A149952] 13 p2141 N85-23291

Physical chemistry of exothermic gas-aerosol calorimetry
[AD-A150672] 14 p2251 N85-23950

The detonation of aerosols and vapors of combustible substances under controlled conditions. Part 1: Construction of a test installation
[ISL-R-109/83-PT-1] 14 p2254 N85-23966

The significance for laser anemometry of particles carried along in a gas flow
[ISL-CO-205/83] 14 p2301 N85-24251

Measurement of the expansion velocity of an aerosol cloud during pyrotechnical dispersion
[ISL-R-125/83] 14 p2303 N85-24262

Classification of atmospheric aerosol for evaluation of its effect on climate 14 p2333 N85-24428

Chemical composition of coastal haze aerosol
14 p2338 N85-24456

Study of integral and spectral direct solar radiation over Atlantic 14 p2341 N85-24475

Visibility of small objects in turbid atmosphere
14 p2342 N85-24482

Influence of aerosol on formation of outgoing thermal radiation 14 p2342 N85-24483

Characteristics and behavior of atmospheric aerosols: application to prediction of infrared extinction
[AD-A150891] 14 p2372 N85-24665

Sea surface temperatures from VAS MSI data
[NASA-CR-175706] 14 p2382 N85-24689

Computer-assisted Gran titration procedure for strong acid determination
[DE85-006801] 15 p2507 N85-25462

Skywave radar detectability of volcanic aerosols
[AD-A151448] 15 p2542 N85-25694

Particle curtain generator for optical property measurements of solid particles
[DE85-005784] 15 p2560 N85-25797

Results of recent large-scale NH3 and N2O4 dispersion experiments
[DE85-004968] 15 p2589 N85-25960

Size distributions of elemental carbon in atmospheric aerosols
[PB85-153534] 15 p2589 N85-25963

SAM 2 measurements of the polar stratospheric aerosol, volume 5
[NASA-RP-1140] 15 p2590 N85-25970

Development of global model for atmospheric backscatter at CO2 wavelengths
[NASA-CR-175679] 15 p2591 N85-25971

Development of algorithms for using satellite meteorological data sets to study global transport of stratospheric aerosols and ozone
[NASA-CR-172540] 15 p2591 N85-25974

Aerosol deposition along the respiratory tract at zero gravity: A theoretical study
[DE85-006703] 15 p2619 N85-26136

Studies of electro-optical attenuation in the vicinity of cloud base
[AD-A151745] 15 p2653 N85-26360

French and West German equipment for Vega Project
16 p2722 N85-26805

SAM II measurements of the polar stratospheric aerosol. Volume 6: April to October 1981
[NASA-RP-1141] 16 p2825 N85-27422

Atmospheric radon measurements in the Antarctic Penninsula: A preliminary report
[INPE-3398-PRE/667] 16 p2827 N85-27436

Evolution of stratospheric aerosol size distribution from ground-based radiometric measurements: A study of El Chichon aerosol
[DE85-007555] 16 p2827 N85-27439

Geophysical monitoring for climatic change, number 12
[PB85-172278] 16 p2837 N85-27496

Study of the formation of sulfuric acid aerosols
[DE85-008102] 17 p2922 N85-28011

Equipment development for rapid detection of microorganisms in air and water
[FOA-A-40046-B2] 18 p3134 N85-29410

Optical stability, atmospheric transparency and aerosol absorption 19 p3297 N85-30442

Clearing of polydisperse aqueous aerosol by laser radiation pulses 19 p3298 N85-30445

Haze over eastern North America. Part 1: Haze properties
[PB85-181857] 19 p3311 N85-30526

Effects of relative humidity gradients on the evaluation of submicron aerosol flux measurements in the atmospheric surface layer
[DE85-010510] 19 p3316 N85-30555

Satellite measurements of atmospheric aerosols
[AD-A153607] 19 p3316 N85-30556

Source Term Experiments Project (STEP): Aerosol characterization system
[DE85-010248] 19 p3361 N85-30839

Modeling of chemical transformations of SO(x) and NO(x) in the polluted atmosphere: An overview of approaches and current status
[PB85-173169] 20 p3487 N85-31677

Function of a device for detection of biological aerosols in field testing
[FOA-C-40194-B2] 20 p3504 N85-31782

Efficiency tests of samplers for microbiological aerosols, a review
[FOA-C-40199-B1] 20 p3504 N85-31783

Investigation of variation in the concentration of bacteria in outdoor testing, with the use of a detector for aerosols of bacteria
[FOA-C-40201-B2] 20 p3504 N85-31784

Aerosol analysis and emission spectrometry with free jets
[DE85-010576] 21 p3564 N85-32168

Silicon production in an aerosol reactor
21 p3609 N85-32416

Data analysis for lidar and quartz crystal microbalance systems
[NASA-CR-172601] 21 p3615 N85-32464

Nuclear thermal transmittance in the atmosphere using LOWTRAN-6 computer code
[AD-A154869] 21 p3630 N85-32563

Absorption and scattering properties of aerosols of aggregated particles in the infrared spectral region
[AD-A155475] 21 p3637 N85-32591

Eleventh International Conference on Atmospheric Aerosols, Condensation and Ice Nuclei, volume 2
[PB85-182418] 21 p3638 N85-32596

Mechanism of heterogeneous deposition ice nucleation near water-saturation 21 p3638 N85-32597

Inactivation of silver iodide by atmospheric nucleation inhibitors 21 p3638 N85-32599

Ice nucleation by silver iodine particles with nearly critical sizes 21 p3638 N85-32600

Photoinduced active sites on ice nucleating aerosol of silver iodide 21 p3639 N85-32601

Experimental investigation of properties of ice-forming reagents 21 p3639 N85-32602

The effect of supersaturation, temperature and particle size on ice-nucleating ability of atmospheric aerosol
21 p3639 N85-32604

Ice crystal nucleation on hygroscopic aerosols
21 p3639 N85-32605

On the efficiency of the mechanism of ice particles formation in the vapor supersaturation field around a freezing droplet 21 p3639 N85-32606

Generation of lead, lead iodide and iodide aerosols and their ice nucleation 21 p3639 N85-32607

Aircraft observations of condensation and ice nuclei at a tropical station 21 p3640 N85-32613

A statistical analysis of ice nuclei concentrations at urban and rural sites in Valladolid, Spain
21 p3640 N85-32614

Supersaturation spect A of Ice Nuclei at different locations in Europe and over the North-Atlantic
21 p3640 N85-32615

The capture of ice nucleating and non ice-nucleating aerosols by ice phase precipitation
21 p3641 N85-32620

The 100 years of Aitken Nuclei (AN) study-reminiscence, current and future problems 21 p3641 N85-32621

Properties of aerosol particles detected by satellites in coastal regions 21 p3641 N85-32622

Multi-channel electric aerosol spectrometer
21 p3642 N85-32623

Supersaturation obtained in a condensation nucleus counter 21 p3642 N85-32624

The investigation of natural and artificial ice nuclei by the improved membrane filter method
21 p3642 N85-32626

Stable generation of highly monodisperse aerosols
21 p3642 N85-32628

Eleventh International Conference on Atmospheric Aerosols, Condensation and Ice Nuclei, volume 1
[PB85-182400] 21 p3644 N85-32636

Photochemical aerosol formation in polluted atmosphere 21 p3644 N85-32642

The influence of Brownian coagulation on the size distributions of atmospheric aerosols
21 p3645 N85-32643

A study of time transformation of natural photochemical aerosols 21 p3645 N85-32644

A new hypothesis for the observed vertical distribution of atmospheric aerosols 21 p3645 N85-32646

On the mechanisms responsible for the formation of typical size spectra and vertical distribution of tropospheric aerosol particles 21 p3645 N85-32647

On the transformation regularities of time series of solid aerosol concentrations in the surface atmospheric layer
21 p3645 N85-32648

Our knowledge about the atmospheric aerosol
21 p3646 N85-32650

Characteristics of aerosol composition in a nonurban area, north China 21 p3646 N85-32651

Trace element concentrations in atmospheric aerosol over Hungary 21 p3646 N85-32652

Chemical composition of atmospheric aerosol at Delhi
21 p3646 N85-32653

Mineral aerosols and source identification
21 p3646 N85-32654

Physical and chemical aerosol characteristics in extremely clean air masses at Cape Grim, Tasmania
21 p3646 N85-32655

Aitken particle size distribution in Antarctica
21 p3646 N85-32656

Airborne measurements of the vertical distribution of Arctic haze 21 p3647 N85-32657

Condensation nuclei and aerosol size distribution measurements in Arctic haze 21 p3647 N85-32658

Aircraft investigations of the distribution of aerosols in the lower troposphere 21 p3647 N85-32659

The variability of aerosol microstructure in continental and oceanic surface layers of the atmosphere in anticyclones 21 p3647 N85-32660

Variation of the submicron aerosol structure 21 p3647 N85-32661

Some considerations about the natural atmospheric radioactive aerosol 21 p3647 N85-32662

Variability of rural aerosols under stable weather conditions 21 p3647 N85-32663

Marine aerosols at the Dutch North Sea coast: Size distributions and fractionation of trace elements 21 p3648 N85-32664

Application of Particle Induced X-ray Emission analysis (PIXE) to aerosol long range transport studies 21 p3648 N85-32665

Scavenging of submicron aerosol particles by snow crystals: Theory and experiments 21 p3648 N85-32667

A probabilistic method for particle size analysis of aerosols 21 p3648 N85-32669

Cloud condensation on insoluble particles 21 p3648 N85-32670

Observations of cloud droplets, aerosol particles and cloud condensation nuclei in continental air masses 21 p3649 N85-32671

Condensation properties of atmospheric aerosol 21 p3649 N85-32672

Investigation of the formation of cloud particle spectrum on natural condensation nuclei 21 p3649 N85-32674

A simple model to investigate the activation process in waterclouds 21 p3649 N85-32675

Measurements of the critical supersaturation of 0.029 to 0.035 micron radius particles at Washington, District of Columbia 21 p3649 N85-32676

On the question to the effect of surfactants on the spectrum of cloud drops in the process of their condensation growth 21 p3650 N85-32679

Influence on an industrial site on the characteristics of CCN supersaturation with air masses of different origin 21 p3650 N85-32683

Theoretical studies of structure and stability of hydrates of atmospheric sulfur species 21 p3650 N85-32684

A review on the formation of aerosol particles in the atmosphere 21 p3651 N85-32687

Aerosol formation by wave action over Ross Sea, Antartica 21 p3651 N85-32688

An electron microscopic study of urban aerosol 21 p3651 N85-32689

Sulfates in marine aerosols over the tropical Western Pacific Ocean 21 p3651 N85-32690

Granulometric study of the acidity and sulfate excess in marine aerosols 21 p3652 N85-32691

Variations of particulate sulfur concentrations in a coastal atmospheric environment in connection with the change of air masses origin 21 p3652 N85-32692

Characterization of insoluble particles associated with cloud droplets 21 p3652 N85-32693

The measured rate of condensation nucleation to droplets using the techniques of chemical kinetics 21 p3652 N85-32694

Development of a microorifice uniform deposit cascade impactor
[DE85-006765] 22 p3812 N85-33614

Nordic Association for Aerosol Research (NOSA) Aerosol Symposium: Program and abstracts
[FOA-E-40019] 22 p3812 N85-33616

Evaluation of source strength and dispersion model predications with data from large nitrogen tetroxide field experiments
[DE85-011855] 23 p3947 N85-34465

MATADOR (Methods for the Analysis of Transport And Deposition Of Radionuclides) code description and user's manual
[TI85-901402] 23 p3966 N85-34592

Downstream behavior of volatile fission product species
[DE85-012124] 23 p3971 N85-34617

System for the continuous generation of phosphorous aerosols from red phosphorus-butyl rubber
[DE85-013527] 24 p4072 N85-35232

Experimental lithium system
[DE85-013252] 24 p4094 N85-35382

Linear absorption and scattering of laser beams
[AD-A156167] 24 p4098 N85-35401

Incorporating meteorological data into receptor analysis: RAPS (Regional Air Pollution Study) revisited
[PB85-186944] 24 p4114 N85-35503

Literature search for new physical methods for biological aerosol detection
[AD-A155863] 24 p4128 N85-35592

Calculation of the diffusion of light by aerosols: Description of the MIELOR software and results obtained
[REPT-80] 24 p4137 N85-35638

AEROSPACE ENGINEERING
NT AERONAUTICAL ENGINEERING

Aerospatiale's experimentations of vectorization on supercomputers for aircraft structural problems 01 p0007 N85-10041

Impact of new computing systems on computational mechanics and flight-vehicle structures technology 01 p0007 N85-10042

Large scale computing in aeronautical design 01 p0007 N85-10043

Development of space instrumentation of Intercosmos member countries 02 p0163 N85-11106

Report of the Department of Aerospace Engineering 03 p0307 N85-11977

NSSDC and WDC-A-R and S document availability and distribution services
[NASA-TM-87374] 03 p0438 N85-12787

Reduction method for thermal analysis of complex aerospace structures
[NASA-TP-2373] 07 p0957 N85-16066

SNAP (Space Nuclear Auxiliary Power) reactor overview
[AD-A146831] 07 p1041 N85-16612

Activities report of the aerospace industry in West Germany
[ISSN-0722-3838] 07 p1053 N85-16686

Activities report of the aerospace industry in West Germany
[ISSN-0722-3838] 07 p1054 N85-16687

Random equations in aerodynamics
[NASA-CR-174279] 08 p1077 N85-16825

S-3A ballast block final design and engineering tests
[AD-A147685] 08 p1080 N85-16842

Orbiter processing facility: Access platforms Kennedy Space Center, Florida, from challenge to achievement 08 p1102 N85-16968

Summary of activities of Aeronautics and Space Engineering Board
[NASA-CR-174294] 08 p1228 N85-17729

Scientific and technical information output of the Langley Research Center for calendar year 1984
[NASA-TM-86336] 08 p1229 N85-17740

Space Station engineering and technology development
[NASA-CR-174383] 09 p1287 N85-18079

Activities report in aerospace in West Germany
[ISSN-0070-3966] 09 p1418 N85-18947

West Europe report: Science and technology
[JPRS-WST-85-004] 10 p1460 N85-19204

Calendar of selected aeronautical and space meetings
[AGARD-CAL-84/2] 10 p1573 N85-19917

West Europe report: Science and technology
[JPRS-WST-85-008] 11 p1617 N85-20174

China report: Science and technology
[JPRS-CST-84-032] 11 p1621 N85-20202

Biomechanics finds practical applications in aerospace research 11 p1621 N85-20205

Where are we going in tethers 11 p1644 N85-20354

Space science and applications 11 p1644 N85-20362

Bibliography of Lewis Research Center technical publications announced in 1983
[NASA-TM-83693] 12 p1951 N85-22255

USSR report: Engineering and equipment
[JPRS-UEQ-85-003] 13 p2042 N85-22782

Authorizing appropriations to the National Aeronautics and Space Administration for fiscal year 1986
[H-REPT-99-32] 13 p2168 N85-23452

Spatial acquisition algorithms and systems for intersatellite optical communication links
[AD-A150794] 14 p2282 N85-24207

Technology for large space systems: A bibliography with indexes, supplement 11
[NASA-SP-7046(11)] 15 p2475 N85-25277

A decision support methodology for space technology advocacy
[AD-A151895] 15 p2476 N85-25283

USSR report: Space
[JPRS-USP-85-003] 15 p2476 N85-25284

West Europe report: Science and technology
[JPRS-WST-85-014] 15 p2489 N85-25362

In-plane shear properties of graphite Fibre/Epoxy composites for aerospace applications: Evaluation of test methods by the decision analysis technique
[AD-A151599] 15 p2503 N85-25440

West Europe report: Science and technology
[JPRS-WST-84-007] 15 p2530 N85-25600

West Europe report: Science and technology
[JPRS-WST-84-010] 15 p2535 N85-25644

Multikilowatt hydrogen-nickel oxide battery system
[DE85-003339] 15 p2550 N85-25737

IPAD: Integrated Programs for Aerospace-vehicle Design
[NASA-CR-3890] 15 p2632 N85-26221

The 1985 long-range program plan
[NASA-TM-87464] 15 p2664 N85-26440

Application of space methods in geodesy 16 p2724 N85-26817

A study of spacecraft technology and design concepts, volume 1
[NASA-CR-172579-VOL-1] 16 p2730 N85-26844

A study of spacecraft technology and design concepts. Volume 2: Appendices
[NASA-CR-172579-VOL-2] 16 p2730 N85-26845

Space Station Engineering and Technology Development
[NASA-CR-175806] 16 p2731 N85-26851

Space Station Spartan study
[NASA-TM-86215] 16 p2731 N85-26852

Activities in aerospace 17 p2891 N85-27821

Technical services at NLR
[B8561896] 17 p3049 N85-28871

West Europe report: Science and technology
[JPRS-WST-84-031] 18 p3066 N85-29069

West Europe report: Science and technology
[JPRS-WST-84-035] 18 p3067 N85-29102

Research on structural analysis at the DFVLR, Brunswick 18 p3120 N85-29314

Space research at NLR 20 p3397 N85-31075

Visualization of computation results. Definition of a graphics satellite computer
[ONERA-RT-2/3587-CY] 20 p3514 N85-31845

USSR report: Space
[JPRS-USP-84-006] 22 p3731 N85-33128

Special tools used by cosmonauts in EVA 22 p3731 N85-33129

AEROSPACE ENVIRONMENTS
NT DEEP SPACE
NT INTERPLANETARY SPACE
NT INTERSTELLAR SPACE

Metal oxide semiconductors power transistors
[CNES-84/QPE/FT/190] 04 p0496 N85-13166

Effects of the solar and extraterrestrial environments on space power systems 05 p0610 N85-13896

Environmental interactions working group report 05 p0611 N85-13908

Spacelab 1 experiment: Microorganisms in space hard environment 05 p0691 N85-14443

Activities report in Earth and planetary environments physics
[CRPE-NT-134] 05 p0734 N85-14720

Testing changes in visual function due to orbital environment
[AD-A147259] 07 p1016 N85-16453

Evaluation and prediction of long-term environmental effects of nonmetallic materials
[NASA-CR-171353] 10 p1450 N85-19137

Instrumentation for Application Number 1: Mass spectrometric analysis of the boundary layer associated with the tethered satellite 11 p1646 N85-20372

Study proposal for the possible use of ISS as an aerodynamic facility for aerospace applications 11 p1646 N85-20374

Earth observations and the polar platform
[NOAA-TR-NESDIS-18] 11 p1669 N85-20517

Aviation medicine's role in modern airforce discussed 11 p1696 N85-20662

Assessment of satellite collision hazards by simulated sampling in space 12 p1784 N85-21195

Transmission and orbital constraints in space-related programs: Briefing summary 12 p1787 N85-21216

Natural environment design criteria for the Space Station definition and preliminary design
[NASA-TM-86498] 12 p1789 N85-21232

On the P1 data from GMS-SEM 12 p1894 N85-21890

Interactions between large space power systems and low-Earth-orbit plasmas 13 p1992 N85-22490

The Giotto spacecraft impact-induced plasma environment
[ESA-SP-224] 14 p2243 N85-23905

Spacecraft environment during the Giotto-Halley encounter: A summary 14 p2246 N85-23921

A FORTRAN program for deep space sensor analysis
[AD-A151700] 15 p2489 N85-25366

Analysis of space station operations in the space debris environment
[AD-A151872] 15 p2493 N85-25380

West Europe report: Science and technology
[JPRS-WST-84-006] 15 p2531 N85-25606

Space brain research in China reported 15 p2537 N85-25657

Nondestructive equipment study
[NASA-CR-171865] 15 p2571 N85-25853

Structural development and gravity 15 p2608 N85-26071

Research on zero-gravity botany apparatus 16 p2723 N85-26811

Forecasts on long-range development of space programs 16 p2727 N85-26830

Solar activity monitoring satellite (SAMSAT): Impact on space environment services
[PB85-165066] 16 p2888 N85-27818
Spray applicator for spraying coatings and other fluids in space
[NASA-CASE-MSC-18852-1] 18 p3115 N85-29283
Current concepts and future directions of CELSS
18 p3155 N85-29532
Survey of CELSS concepts and preliminary research in Japan 18 p3155 N85-29533
Human productivity experience and undersea habitat design 18 p3159 N85-29563
Considerations for space station interior architecture
18 p3159 N85-29564
Human factors in space station architecture: The ECLSS module concept 18 p3159 N85-29565
Ion beam sputter-deposited thin film coatings for protection of spacecraft polymers in low Earth orbit
[NASA-TM-87051] 19 p3246 N85-30137
Measurement of material damping in a simulated space environment 20 p3397 N85-31070
On the measurement of material damping in a simulated space environment 20 p3411 N85-31169
Evaluation of Results of Space Experiments in Physiology and Medicine and Informal Briefings by the F-16 Medical Working Group 20 p3506 N85-31806
Three-dimensional ballistocardiography in microgravity
20 p3510 N85-31818
Special tools used by cosmonauts in EVA
22 p3731 N85-33129
Effects of environment on spacecraft materials
22 p3733 N85-33144
Microorganisms in space flight
23 p3951 N85-34490
Effect of seeds of heavy charged particles of galactic cosmic radiation 23 p3954 N85-34505
Problems of aviation and space medicine and psychology discussed at 14th Gagarin lectures
23 p3954 N85-34509
Determination of characteristic values for fiber reinforced materials 24 p4074 N85-35247

AEROSPACE INDUSTRY
NT AIRCRAFT INDUSTRY
Comments on the commercialization of expendable launch vehicles 02 p0153 N85-11034
Space know-how, twenty years' space experience
04 p0461 N85-12926
Electronic components for space applications
[CNES-NT-109] 04 p0496 N85-13169
Component reliability and assembling technologies
[CNES-NT-108] 04 p0511 N85-13258
An electronic documentation system
[SNIAS-842-111-101] 04 p0577 N85-13683
BDLI memorandum on the future of space flight in the Federal Republic of Germany
[NASA-TM-77624] 07 p0911 N85-15765
Activities report in aerospace in West Germany
[ISSN-0070-3966] 09 p1418 N85-18947
Activities in French aerospace
11 p1587 N85-19995
Aerospace Safety Advisory Panel
[NASA-TM-87426] 13 p1970 N85-22373
Welcome to the Saclay Propeller Testing Center
[NASA-TM-77648] 14 p2225 N85-23799
West Europe report: Science and technology
[JPRS-WST-84-008] 15 p2531 N85-25606
Characteristics and applications of superplastic materials for aeronautics
[MBB-BB-565/84-O] 16 p2873 N85-27727
Managerial benefits of Helios for the European industry 16 p2887 N85-27809
The technological gains of Helios for the European industry 16 p2887 N85-27810
Activities in aerospace 17 p2891 N85-27821
Note for a research feasibility project: High reliability design in the aeronautical field
[REPT-84-RR-350] 20 p3387 N85-31005
Description of an holographic interferometry nondestructive test installation: Application to bond tests
[SNIAS-851-430-101] 20 p3464 N85-31521
Philosophy of nondestructive control in aeronautics quality control. Knowledge of and improvements to nondestructive test safety
[SNIAS-851-551-101] 20 p3465 N85-31522
Management of Corrosion
[AGARD-LS-141] 22 p3749 N85-33238
Corrosion management strategies for aircraft and related systems 22 p3749 N85-33239
Theoretical aspects of corrosion and practical implications for aircraft and related systems
22 p3749 N85-33240
Environmental factors in corrosion and deterioration of materials 22 p3750 N85-33241
Investment justification of robotic technology in aerospace manufacturing. User's manual
[AD-A156193] 24 p4099 N85-35410

AEROSPACE MEDICINE
Personal experience with the PVHD and opinion of situations in which a wide Field Of View (FOV) PVHD might be helpful 01 p0006 N85-10045
USSR report: Space Biology and Aerospace Medicine, volume 18, no. 4, July - August 1984
[JPRS-USB-84-006] 01 p0091 N85-10611
Potential use of dialogue with computers in biomedical research 01 p0091 N85-10614
Space medicine and biology, continuing bibliography (supplement 263)
[NASA-SP-7011(263)] 01 p0094 N85-10636
USSR report: Space
[JPRS-USP-84-005] 02 p0156 N85-11060
Cosmonauts complete 4th month aboard Salyut-7
02 p0157 N85-11065
Applications of aerospace technology in biology and medicine
[NASA-CR-165872] 02 p0234 N85-11521
Aerospace Medicine and Biology, a continuing bibliography with indexes
[NASA-SP-7011(264)] 02 p0234 N85-11525
AGARD bulletin technical programme, 1985
[AGARD-BUL-84-2] 02 p0305 N85-11971
The effects of helicopter vibration on the spinal system
[AD-A148274] 03 p0402 N85-12562
USSR report: Life sciences. Biomedical and behavioral sciences
[JPRS-UBB-84-025] 04 p0543 N85-13453
USSR report: Life Sciences: Biomedical and behavioral sciences
[JPRS-UBB-84-026] 04 p0543 N85-13457
Impact of space medicine on Earth-based medicine: Academician Ye. I. Chazov comments on the work in orbit of physician O. Atkov 04 p0543 N85-13458
A survey of space biology and space medicine
[ESA-BR-17] 04 p0545 N85-13466
Aerospace Medicine and Biology, a continuing bibliography with indexes
[NASA-SP-7011(265)] 04 p0545 N85-13467
Space medicine research publications: 1983-1984
[NASA-CR-3860] 04 p0545 N85-13469
Overview of German microgravity activities in the field of life science 05 p0696 N85-14476
USSR report: Life sciences. Biomedical and behavioral sciences
[JPRS-UBB-84-015] 07 p1010 N85-16416
USSR report: Life sciences. Biomedical and behavioral sciences
[JPRS-UBB-84-027] 07 p1012 N85-16426
Aerospace medicine and biology: A continuing bibliography with indexes
[NASA-SP-7011(266)] 08 p1194 N85-17525
Aerospace medicine and biology: A continuing bibliography with indexes, supplement 268
[NASA-SP-7011(268)] 08 p1194 N85-17526
Efforts to improve aviation medical examiner performance through continuing medical education and annual performance reports
[AD-A148078] 08 p1195 N85-17531
Health examination findings among active civil airmen
[AD-A148325] 08 p1195 N85-17533
USSR report: Life sciences. Biomedical and behavioral sciences
[JPRS-UBB-85-002] 09 p1360 N85-18559
USSR report: Life sciences. Biomedical and behavioral sciences
[JPRS-UBB-85-011] 10 p1525 N85-19616
Be healthy, pilot 10 p1526 N85-19626
Aerospace medicine and biology: A continuing bibliography with indexes
[NASA-SP-7011(269)] 10 p1526 N85-19628
Report of the Artificial Gravity Panel
11 p1645 N85-20365
Motion Sickness: Mechanisms, Prediction, Prevention and Treatment
[AGARD-CP-372] 11 p1693 N85-20642
Susceptability to kinetoses and the amplitude perceived from sensory illusions 11 p1694 N85-20651
China report: Science and technology
[JPRS-CST-84-036] 11 p1696 N85-20661
Aviation medicine's role in modern airforce discussed
11 p1696 N85-20662
Symposium on Military Aviation Medicine summarized
11 p1696 N85-20663
Research and technology activities at Ames Research Center's Biomedical Research Division
[NASA-TM-86692] 12 p1899 N85-21925
USSR report: Space Biology and Aerospace Medicine, volume 18, no. 6, November - December 1984
[JPRS-USB-85-002] 12 p1900 N85-21931
Review of US manual of clinical aviation medicine
12 p1904 N85-21957
Review of US guide on medication and flying
12 p1904 N85-21958
Aerospace Medicine and Biology: A continuing bibliography with indexes, supplement 267, January 1985
[NASA-SP-7011(267)] 12 p1904 N85-21959
Second generation USAFSAM (United States Air Force School of Aerospace Medicine) microprocessor audiometer
[AD-A149638] 12 p1905 N85-21963
The clinical and biomedical evaluation of trauma and fatalities associated with aircrew ejection and crash. A Working Group report
[AGARD-AR-194] 12 p1906 N85-21969
Lyakhov and Aleksandrov on 150-day flight
13 p1977 N85-22405
China report: Science and technology
[JPRS-CST-84-030] 13 p2041 N85-22777
Research opportunities in human behavior and performances
[NASA-CR-3886] 13 p2142 N85-23299
USSR report: Life sciences. Biomedical and behavioral sciences
[JPRS-UBB-85-012] 14 p2386 N85-24697
Second Soviet-French Symposium on Space Cytology
14 p2386 N85-24699
Results of a longitudinal study of airsickness during naval flight officer training: Executive summary
[AD-A150887] 14 p2388 N85-24712
Second Soviet-French Symposium on Space Technology 15 p2483 N85-25326
Aerospace Medicine and Biology: A continuing bibliography with indexes
[NASA-SP-7011(270)] 15 p2615 N85-26114
Computer simulation studies in fluid and calcium regulation and orthostatic intolerance
[NASA-CR-171869] 15 p2616 N85-26117
Psychometric evaluation of head injury among fliers referred to the AF School of Aerospace Medicine
[AD-A151479] 15 p2617 N85-26129
Cardiovascular effects of weightlessness
15 p2688 N85-26607
Aerospace medicine and biology: A continuing bibliography with indexes, supplement 271, May 1985
[NASA-SP-7011(271)] 16 p2840 N85-27514
USSR report: Space Biology and Aerospace Medicine, volume 18, no. 5, September - October 1984
[JPRS-USB-84-007] 19 p3322 N85-30583
Development of guidelines for setting physiological and hygienic standards for noise levels in aerospace medicine 19 p3323 N85-30584
Applications of aerospace technology in biology and medicine
[NASA-CR-166100] 19 p3328 N85-30619
Aerospace Medicine and Biology: A continuing bibliography with indexes (supplement 272)
[NASA-SP-7011(272)] 19 p3328 N85-30620
Space-flight simulations of calcium metabolism using a mathematical model of calcium regulation
[NASA-CR-171883] 19 p3328 N85-30621
Longitudinal study of cardiovascular disease in US Navy pilots
[AD-A154331] 19 p3328 N85-30623
Effects of coating rectangular microscopic electrophoresis chamber with methylcellulose
20 p3496 N85-31748
Results of Space Experiments in Physiology and Medicine and Informal Briefings by the F-16 Medical Working Group
[AGARD-CP-377] 20 p3507 N85-31805
Spatial orientation in weightlessness and readaptation to Earth's gravity 20 p3509 N85-31811
Cardiovascular research in space: Problems and results 20 p3510 N85-31817
Sleep and wake physiology in weightlessness
20 p3510 N85-31819
USSR Space Life Sciences Digest
[NASA-CR-3922] 21 p3656 N85-32709
USSR report: Life sciences. Biomedical and behavioral sciences
[JPRS-UBB-85-020] 21 p3663 N85-32752
Remote medical diagnosis 21 p3663 N85-32753
Aerospace medicine and biology: A continuing bibliography with indexes, supplement 273
[NASA-SP-7011(273)] 21 p3663 N85-32755
Air force technical objective document, Aerospace Medical Division, Fiscal Year 1986
[AD-A155195] 21 p3664 N85-32762
Results and prospects of physiological research during spaceflights 22 p3732 N85-33139
Mechanisms of osteodystrophy in weightlessness
22 p3733 N85-33143

USSR report: Space Biology and Aerospace Medicine, volume 19, no. 2, March - April 1985
[JPRS-USB-85-004] 22 p3820 N85-33867

Labyrinthine and extralabyrinthine mechanisms of development of motion sickness in weightlessness
22 p3821 N85-33868

Aerospace Medicine and Biology: A continuing bibliography with indexes (supplement 274)
[NASA-SP-7011(274)] 23 p3952 N85-34491

USSR report: Space Biology and Aerospace Medicine, vol. 19, no. 3, May - June 1985
[JPRS-USB-85-005] 23 p3952 N85-34494

Problems of aviation and space medicine and psychology discussed at 14th Gagarin lectures
23 p3954 N85-34509

Proceedings of a Scientic Meeting on the Occasion of the Inauguration of New Buildings for the DFVLR Institute for Aerospace Medicine
[ESA-TT-857] 24 p4129 N85-35595

The research programme of the Institute for Aerospace Medicine
24 p4129 N85-35596

Simulation of high +Gz onset in the dynamic environment simulator
[AD-A155963] 24 p4131 N85-35610

AEROSPACE SAFETY

Space Nuclear Safety Program
[DE84-016973] 05 p0728 N85-14679

FAA (Federal aviation administration) assessment of satellite concepts and aviation spectrum requirements
[AD-A152336] 17 p2946 N85-28199

Space station crew safety alternatives study. Volume 3: Safety impact of human factors
[NASA-CR-3856] 19 p3223 N85-29984

Space Station crew safety alternatives study. Volume 2: Threat development
[NASA-CR-3855] 21 p3558 N85-32133

AEROSPACE SCIENCES

Canada report to COSPAR 01 p0131 N85-10906

USSR report: Space
[JPRS-USP-84-005] 02 p0156 N85-11060

AEROSPACE SYSTEMS

Material problems for high-temperature, high-power space energy-conversion systems
[AD-A145940] 03 p0385 N85-12466

Conceptual design for scaled truss antenna flight experiment
[NASA-TM-85804] 04 p0462 N85-12932

Robotic technology: An assessment and forecast
[AD-A146672] 06 p0815 N85-15171

SNAP (Space Nuclear Auxiliary Power) reactor overview
[AD-A146831] 07 p1041 N85-16612

Space System Applications to Tactical Operations
[AGARD-CP-344] 11 p1709 N85-20751

Tactical operations and space applications
11 p1709 N85-20752

Fiscal year 1986 technical objective document
[AD-A151039] 14 p2432 N85-25000

Research and technology
[NASA-TM-86662] 14 p2456 N85-25166

Application of space methods in geodesy
16 p2724 N85-26817

The replacement of precious metal thick film inks using conductive polymer technology
[AD-A152002] 16 p2749 N85-26965

European Science Notes, Volume 39, Number 3
[AD-A152446] 17 p3027 N85-28717

Air Force technical objective document FY 86
[AD-A152730] 17 p3047 N85-28855

Overhead management guide for aerospace procurements
[AD-A153626] 18 p3198 N85-29835

Space research at NLR 20 p3397 N85-31075

Robust control of multivariable and large space systems
[AD-A155117] 21 p3559 N85-32140

Ninteenth Aerospace Mechanisms Symposium
[NASA-CP-2371] 22 p3795 N85-33512

A spacefaring people: Perspectives on early spaceflight
[NASA-SP-4405] 23 p4056 N85-35142

Space science and exploration: A historical perspective
23 p4056 N85-35143

The next assignment: The state of the literature on space
23 p4057 N85-35146

Evaluation of nuclear detonation location capability under high attack scenario
[AD-A155761] 24 p4149 N85-35729

AEROSPACE TECHNOLOGY TRANSFER

Aeronautics Technology Possibilities for 2000: Report of a workshop
[NASA-CR-174018] 01 p0001 N85-10001

Rotor systems research aircraft airplane configuration flight-test results
[NASA-TM-85911] 01 p0006 N85-10034

West Europe report: Science and technology
[JPRS-WST-84-004] 03 p0309 N85-11996

Fokker wants to start new Netherlands space program
03 p0310 N85-11999

Loads and Aeroelasticity Division research and technology accomplishments for FY 1984 and plans for FY 1985
[NASA-TM-86356] 07 p0896 N85-15691

West Europe report: Science and technology
[JPRS-WST-84-039] 07 p0936 N85-15929

West Europe report: Science and technology
[JPRS-WST-85-001] 08 p1141 N85-17190

Space research in the Federal Republic of Germany
09 p1265 N85-18074

Activities report in aerospace in West Germany
[ISSN-0070-3966] 09 p1418 N85-18947

European Scientific Notes. Volume 39, number 1
[AD-A149496] 10 p1566 N85-19696

Authorizing appropriations to the National Aeronautics and Space Administration for fiscal year 1986
[H-REPT-99-32] 13 p2168 N85-23452

Technology and Economics, Inc. Technology Application Team
[NASA-CR-175630] 13 p2168 N85-23454

AGARD bulletin: Meetings, publications, membership
[AGARD-BUL-85-1] 15 p2696 N85-26589

Symbiosis between postgraduate training and research projects: A successful experience
[INPE-3216-PRE/569] 16 p2810 N85-27330

The technological gains of Helios for the European industry
16 p2867 N85-27810

European Science Notes, Volume 39, Number 3
[AD-A152446] 17 p3027 N85-28717

West Europe report: Science and technology
[JPRS-WST-84-037] 18 p3066 N85-29108

FRG weighs ESA participation, budget issues
18 p3068 N85-29110

Some applications of aeronautical engineering in the construction of yachts
[NLR-MP-83042-U] 20 p3394 N85-31052

NASA Space controls research and technology program
20 p3408 N85-31149

Civilian Space Stations and the US future in Space
[OTA-STI-242] 20 p3418 N85-31215

USSR report: Life sciences. Biomedical and behavioral sciences
[JPRS-UBB-85-020] 21 p3663 N85-32752

USSR report: Space
[JPRS-USP-84-006] 22 p3731 N85-33128

Product definition: Technical specification of needs
[SNIAS-851-430-104] 23 p3910 N85-34228

New technologies at the forefront of industrial developments
24 p4061 N85-35166

AEROSPACE VEHICLES

NT FLEXIBLE SPACECRAFT

Aerodynamic characteristics of some lifting reentry concepts applicable to transatmospheric vehicle design studies
[NASA-TM-86331] 06 p0747 N85-14787

A theoretical method for selecting space craft and space suit atmospheres
[AD-A148219] 08 p1200 N85-17559

An overview of the MIL-HDBK-5 program
[AD-A147788] 14 p2254 N85-23970

AEROSTATS

U AIRSHIPS

AEROTHERMOCHEMISTRY

Sandia Cooperative Group on the Aerothermochemistry of Turbulent Combustion. Discussion record of fourth meeting
[DE85-004720] 20 p3423 N85-31248

Intermittency, conditional sampling and turbulent combustion
20 p3424 N85-31249

Conditional modelling in turbulent shear flows
20 p3424 N85-31250

Non-equilibrium effects in turbulent diffusion flames
20 p3425 N85-31258

Sandia Cooperative Group on the Aerothermochemistry of Turbulent Combustion
[DE85-004720] 20 p3455 N85-31453

Sandia Cooperative Group on the Aerothermochemistry of Turbulent Combustion
[DE85-007493] 20 p3455 N85-31454

Sandia Cooperative Group on the Aerothermochemistry of Turbulent Combustion. Discussion record of the second meeting
[DE85-007493] 22 p3743 N85-33203

AEROTHERMODYNAMICS

Aerothermal modeling program
02 p0145 N85-10983

Space Shuttle wind tunnel testing program
[NASA-RP-1125] 02 p0167 N85-11127

Experimental and predicted heating distributions for biconics at incidence in air at Mach 10
[NASA-TP-2334] 03 p0361 N85-12313

Optimum thermogasdynamic design of gas turbine engines by characteristics of element prototypes
06 p0777 N85-14965

Heat transfer results and operational characteristics of the NASA Lewis Research Center Hot Section Cascade Test Facility
[NASA-TM-86890] 06 p0808 N85-15133

Analytical and physical modeling program for the NASA Lewis Research Center's Altitude Wind Tunnel (AWT)
[NASA-TM-86919] 07 p0909 N85-15757

Columbia: The first 5 flights entry heating data series. Volume 1: An overview
[NASA-CR-171820] 07 p0913 N85-15777

Shuttle system ascent aerodynamic and plume heating
08 p1103 N85-16975

Orbiter entry aerothermodynamics
08 p1104 N85-16978

Orbiter thermal protection system
08 p1104 N85-16979

Combustion research for gas turbine engines
[NASA-TM-86983] 12 p1778 N85-21164

Results of aeroheating DFI and ET design-data test on a 0.0175-scale model 60-OTS conducted in the Von Karman Gas Dynamics Facility (VKF) 40' supersonic and the 50' hypersonic wind tunnels A and C
[NASA-CR-167693] 13 p1968 N85-22486

Results of a M = 5.3 heat transfer test of the integrated vehicle using phase-change paint techniques on the 0.0175-scale model 56-OTS in the NASA/Ames Research Center 3.5-foot hypersonic wind tunnel
[NASA-CR-167695] 13 p1968 N85-22488

Space Shuttle aerothermodynamic data report, phase C
[NASA-CR-171858] 14 p2241 N85-23697

NASA R and T aerospace plane vehicles: Progress and plans
[NASA-TM-86429] 15 p2491 N85-25366

Future fundamental combustion research for aeropropulsion systems
[NASA-TM-87049] 17 p2896 N85-27870

Structural Integrity and Durability of Reusable Space Propulsion Systems
[NASA-CP-2381] 17 p2910 N85-27941

Overview of aerothermodynamic loads definition study
17 p2910 N85-27942

Heating parameter estimation using coaxial thermocouple gages in wind tunnel test articles
[AD-A153039] 17 p2968 N85-28328

A new finite element approach: Progress in inviscid flow computations
[NASA-TM-86434] 20 p3454 N85-31450

AFC (CONTROL)

U AUTOMATIC FREQUENCY CONTROL

AFCS (CONTROL SYSTEM)

U AUTOMATIC FLIGHT CONTROL

AFFECTS

U EFFECTS

AFFINITY

Thermally modulated electron affinity detector for priority pollutant analysis
[PB85-158145] 15 p2506 N85-25469

AFRICA

Operating experiences of reverse osmosis plants treating Rand Water Board (RWB) water: Pitfalls and problems
01 p0023 N85-10142

Mineral nutrients in Mediterranean ecosystems
[REPT-71] 01 p0069 N85-10456

Short period forecasts in West Africa using Meteosat data
01 p0079 N85-10526

Estuaries of the Cape. Part 2: Synposes of available information on individual systems. Report no. 19: Groot (WES) (CMS 23) and Sout (CMS 22)
[CSIR-RR-418] 01 p0087 N85-10568

The identification of rain-bearing synoptic systems through principal component analysis
02 p0212 N85-11394

The application of principal component analysis in a study of rainfall
02 p0212 N85-11396

Archean sedimentation and tectonics in southern Africa
[NASA-CR-174156] 04 p0533 N85-13408

The mineralogy of global magnetic anomalies
[E85-10061] 07 p0987 N85-16272

Satellite definition of the bio-optical and thermal variation of coastal eddies associated with the African current
[AD-A147910] 07 p0989 N85-16282

Synthesis of proterozoic data as a prerequisite for tectonic and thermal modeling
[NASA-CR-174252] 07 p0995 N85-16323

Reduced to pole long-wavelength magnetic anomalies of Africa and Europe 20 p3475 N85-31595

Euro-African MAGSAT anomaly-tectonic observations
20 p3475 N85-31596

Long-wavelength magnetic and gravity anomaly correlations on Africa and Europe
20 p3476 N85-31597

Microwave hydrology: A trilogy
[NASA-CR-176042] 20 p3477 N85-31603

AFTERBODIES
Navier-Stokes solution of 3-dimensional hypersonic afterbody flowfields over capsule-type vehicles
[NAL-TR-819] 03 p0311 N85-12010
Empirical formulas for the prediction of the base pressure of missile bodies at subsonic velocities
[DFVLR-FB-84-23] 03 p0316 N85-12044
Effects of body shape on the aerodynamics of a body of revolution at Mach numbers from 1.6 to 4.6
[NASA-TM-86345] 07 p0893 N85-15657
On the evaluation of boundary layer measurements on boattailed bodies of revolution in axisymmetric compressible subsonic flow
[ESA-TT-883] 20 p3457 N85-31471
SRB TPS closeout materials characterization
[NASA-CR-170885] 24 p4070 N85-35222
Study of NSI and related cable performance during tests performed in the NASA Hot Gas Facility
[NASA-CR-170886] 24 p4101 N85-35423

AFTERBURNERS
U AFTERBURNING

AFTERBURNING
Flameholder with integrated air mixer
[AD-D011549] 12 p1778 N85-21161
Some unique features in operation of two-stage turbojet engine with afterburner 13 p2049 N85-22828
Effect of water injection into air for turbine cooling on economy of operation of gas turbine engine with afterburning 13 p2050 N85-22830

AFTERGLOWS
Ionic reactions of atmospheric importance
[AD-A147354] 07 p0997 N85-16333
Gas phase ion-molecule chemistry of carbon, nitrogen and oxygen compounds
[AD-A152876] 17 p2919 N85-27996

AGC (CONTROL)
U AUTOMATIC GAIN CONTROL

AGE DETERMINATION
U CHRONOLOGY

AGE FACTOR
Functional capacities of elderly subjects exposed to simulated spaceflight factors 01 p0091 N85-10617
The dynamical behavior of the age-size-distribution of a cell population
[CWI-AM-R8414] 17 p2996 N85-28538
Positive Gz accelerations tolerance of individuals 41 to 58 years of age 19 p3323 N85-30588

AGE HARDENING
U PRECIPITATION HARDENING

AGENTS
Optical 3-D signature device for detecting chemical agents
[AD-D011669] 19 p3272 N85-30293

AGGLOMERATION
Acoustic agglomeration methods and apparatus
[NASA-CASE-NPO-15466-1] 12 p1927 N85-22104
Gasification of boron oxide drops and boron slurry agglomerates in combustion gases
13 p1999 N85-22529

AGGLUTINATION
Functional and structural changes in human erythrocyte surface after irradiation by UV waves of various wavelengths. Report 1: Expression of ABO and Rhesus system antigen 09 p1361 N85-18564
Functional and structural changes in human erythrocyte surface after irradiation by UV waves of various wavelenights. Report 2: Adsorption of alcyan blue by external premembranous components
09 p1361 N85-18565

AGGREGATES
Unexplained Fe, Ni and S anomalies in CV chondrite components 06 p0884 N85-15618
Electrochemical features of the ferric sulfate leaching of CuFeS2/C aggregates
[AD-A148661] 08 p1123 N85-17081
Field validation of statistically-based acceptance plan for bituminous airport pavements. Volume 1: Correlation analysis of Marshall properties of laboratory-compacted specimens
[FAA-PM-84-12-VOL-1] 12 p1781 N85-21180
Texture independent determination of residual stress in polycrystalline aggregates using Rayleigh waves
[AERE-R-11483] 12 p1943 N85-22203
Characterization of atomic defects and their aggregates using positron annihilation spectroscopy
[DE85-006206] 14 p2418 N85-24918
High temperature polymer concrete
[DE85-005756] 23 p3920 N85-34290

AGING (BIOLOGY)
Blood pressure levels of active pilots compared with those of air traffic controllers
[AD-A146845] 06 p0846 N85-15373
Changes in spectral properties of detached leaves
[E85-10042] 07 p0983 N85-16243
Toxicity, mutagenesis and aging due to endogenous oxygen radicals
[AD-A150121] 12 p1900 N85-21928
Sleep deprivation and performance: Older age performance and limited sleep period use
[AD-A153102] 17 p2999 N85-28540
Tolerance to +Gz and +Gx accelerations of individuals in older age groups in good health and with early signs of arteriosclerosis 23 p3952 N85-34496

AGING (MATERIALS)
NT AGING (METALLURGY)
Weldability of aged heat resistant nickel alloys
01 p0021 N85-10125
System engineering and integration contract for implementation of the National Airspace System plan, volume 1, sections 1.0-4.0, 6.0
[AD-A145763] 03 p0317 N85-12048
Long-term thermal aging of 2 graphite-polyimide composite materials
[NASA-TP-2369] 03 p0325 N85-12094
Free volume considerations in thermoplastic and thermosetting resins 04 p0465 N85-12952
Influence of relaxation on the mechanical characteristics of a carbon-epoxy composite. Report no. 45.427/1
04 p0468 N85-12980
Solidification and aging behavior of types 308 and 308CRE stainless steel welds
[DE84-016552] 04 p0476 N85-13029
Encapsulation materials and processing
06 p0830 N85-15269
Photothermal degradation of encapsulants
06 p0830 N85-15270
Determination of the decomposition behavior of double base propellants at low temperatures
08 p1117 N85-17045
Compressive strength-maturity relationships of mortar containing fly ash
[AD-A148705] 09 p1339 N85-18423
Accelerated aging of aluminized acrylic solar mirror materials
[DE85-002683] 11 p1612 N85-20138
Chemical and photographic evaluation of rigid explosive transfer lines
[AD-A149303] 11 p1613 N85-20145
Sol-gel-derived AR coatings for solar receivers
[DE85-000192] 11 p1673 N85-20541
Synthesis and thermomechanical properties of new AT-Phenylene R systems
[AD-A149961] 12 p1813 N85-21372
NBS solar collector durability/reliability test program
[DE85-003469] 12 p1881 N85-21801
TEM/FIM study of modulated microstructures in the Fe-Be system
[DE85-005379] 13 p2023 N85-22678
Effect of alternative aging and accident simulations on polymer properties
[DE85-002642] 13 p2037 N85-22762
Stability of highly nonlinear oxide-zinc resistors under continuous voltage of industrial frequency
13 p2087 N85-23030
Synthesis and properties of elevated temperature P/M aluminum alloys
[AD-A151031] 14 p2256 N85-23981
Influence of short-range order on deformation mechanisms in solid solutions
[DE85-006374] 14 p2258 N85-23989
Retroreflective armbands: Influences of wearing mode, aging and other factors on the visibility distance
[IZF-1984-28] 14 p2422 N85-24942
Characterization-curing-property studies of HBRF 55A resin formulations
[NASA-CR-175836] 16 p2753 N85-26989
Damage caused to polyurethane foams by aging, simulated sunlight exposure, heat and fire
[AD-A152040] 16 p2754 N85-26998
Natural and accelerated aging of plastics
17 p2936 N85-28123
Qualitative and quantitative determination of aging by mechanical tests — plastics 17 p2977 N85-28393
Recycling agent selection and tentative specification
[AD-A153529] 18 p3070 N85-28988
Aging study of copper alloy 172
[DE85-009646] 18 p3075 N85-29023
Aging of gold thick-film solder joints
[DE85-009647] 18 p3077 N85-29037
Investigation of fast reaction SAW (Surface Acoustic Wave) accelerometer
[AD-A153876] 19 p3216 N85-29943
Study of the kinetics of hydrogenation using aged catalysts
[DE85-010427] 19 p3230 N85-30025
Ten year environmental test of glass fiber/epoxy pressure vessels
[NASA-TM-87058] 19 p3231 N85-30034
Internal structure of GP zones in dilute Al-Cu alloys
19 p3238 N85-30073
CP DDT detonators. 4: Thermal aging
[DE85-011172] 19 p3251 N85-30160
Long-term thermal aging of Celion/V378A composite materials
[NASA-TM-86362] 20 p3421 N85-31236
Thermomechanical deformation in the presence of metallurgical changes 20 p3466 N85-31533
Hot isostatically pressed Sm(2)(TM)17 magnets
[AD-A155479] 21 p3582 N85-32267
Near-threshold fatigue: An overview of the role of microstructure and environment
[DE85-009903] 23 p3941 N85-34431
Conduction and aging of piezoelectric PZT ceramics
24 p4069 N85-35346
A kinetic model for predicting oxidative degradation rates in combined radiation-thermal environments
[TI85-002629] 24 p4100 N85-35414

AGING (METALLURGY)
Thermal ageing studies of 9%Cr 1%Mo steel
[AERE-R-11109] 03 p0333 N85-12149
Investigation of the isothermal precipitation behavior of nickel-base alloys using electrochemical phase extraction
[JUEL-1903] 05 p0619 N85-13958
Strength and aging behaviour of soft soldered joints
[BLL-T6385/BG/WH800/84] 07 p0925 N85-15862
On reversion phenomena in Cu-Zr-Cr alloys
[NASA-TM-77791] 08 p1125 N85-17092
Reversion phenomena of Cu-Cr alloys
[NASA-TM-77780] 08 p1125 N85-17094
Comparison of property regeneration techniques and life prediction procedures applied to laboratory tested and service exposed Ni-Cr alloys
[NPL-DMA(A)-91] 09 p1333 N85-18374
Initial aging phenomena in copper-chromium alloys
[NASA-TM-77790] 10 p1439 N85-19070
Study of influence of cold plastic deformation on aging of VT30 alloy 10 p1448 N85-19124
Evaluation of 7010 aluminium alloy extruded tube in the T76 condition
[BR92019] 11 p1596 N85-20039
Mechanism of titanium impact on brittle tendency in delayed deformation of martensite-aging steels
11 p1604 N85-20087
Effects of neutron irradiation at 450(0)C and 16 dpa on the properties of various commercial copper alloys
[DE85-005716] 13 p2024 N85-22684
Decomposition of VTAN alloy solid solution upon irradiation and thermal aging 13 p2029 N85-22712
Structure and aging of amorphous chromium-germanium alloys 15 p2497 N85-25401
Structural changes with one- and two-stage aging of alloys Ti-Al-Mo-Fe and Ti-Zr-V-Al-Sn
15 p2499 N85-25415
Effect of thermal ageing on the mechanical properties of PWR pressure vessel steels and weldments
[AERE-R-11460] 24 p4078 N85-35275

AGREEMENTS
The structures and the role of an international agency for the control of satellites
[NASA-TM-76765] 03 p0441 N85-12806
The effects of controversy and concurrence seeking on effective decision making
[AD-A153370] 17 p3002 N85-28555

AGRICULTURAL AIRCRAFT
Effectiveness of agricultural aviation
04 p0544 N85-13460
Director on institute's civil aviation projects
08 p1067 N85-16764
Improved sprayer for AN-2 cropdusting work
08 p1068 N85-16769

AGRICULTURE
Agribusiness and space: No limits to growth
02 p0152 N85-11029
USSR report: Life sciences. Biomedical and behavioral sciences
[JPRS-UBB-84-025] 04 p0543 N85-13453
USSR report: Life Sciences: Biomedical and behavioral sciences
[JPRS-UBB-84-026] 04 p0543 N85-13457
A field control methodology of remotely sensed data for statistical purposes: An example of SPOT simulated data in eastern Belgium — land use statistics
05 p0660 N85-14241
Renewable energy: Energy from agricultural products
[TI84-901769] 05 p0669 N85-14307
Detecting agricultural to urban land use change from multi-temporal MSS digital data — Salt Lake County, Utah
[E85-10049] 07 p0983 N85-16245
Exploring the use of structural models to improve remote sensing agricultural estimates 07 p0985 N85-16259
Image variance and spatial structure in remotely sensed scenes — South Dakota, California, Missouri, Kentucky, Louisiana, Tennessee, District of Columbia, and Oregon
07 p0986 N85-16265

USSR report: Life sciences. Biomedical and behavioral sciences
[JPRS-UBB-84-018] 07 p1010 N85-16416

An investigation of the driving wheel thrust of paddy field tractors
[AD-P004284] 09 p1407 N85-18861

Study of the motion of agricultural vehicles on steep grass-covered slopes
[AD-P004290] 09 p1408 N85-18867

Pressure tests in soil below tires of agricultural vehicles
[AD-P004294] 09 p1408 N85-18871

Turning behaviour of articulated frame steering tractor
[AD-P004304] 09 p1409 N85-18881

An integrated GIS/remote sensing data base in North Cache soil conservation district, Utah: A pilot project for the Utah Department of Agriculture's RIMS (Resource Inventory and Monitoring System)
[E85-10073] 10 p1504 N85-19487

Analysis of the quality of image data required by the LANDSAT-4 Thematic Mapper and Multispectral Scanner — agricultural and forest cover types in California
[E85-10074] 10 p1504 N85-19488

Birds and airport agriculture in the conterminous United States: A review of literature
[AD-P004208] 11 p1583 N85-19975

Remote sensing technology now playing practical roles 11 p1619 N85-20190

Moisture variation in northern hemisphere temperate latitudes 13 p2105 N85-23119

Characterization of LANDSAT-4 TM and MSS image quality for the interpretation of California's agricultural resources — Central Valley 13 p2118 N85-23190

Atlas of archived vegetation, land-use and seasonal Albedo data sets
[NASA-TM-86199] 14 p2346 N85-24508

NASTRAN's application in agricultural engineering
15 p2575 N85-25880

Function of remote sensing in Brazil
[INPE-3314-PRE/621] 16 p2810 N85-27329

Symposium on Atmospheric Sciences in South Africa
[CSIR-S-331] 16 p2829 N85-27442

A weather service for agriculture
16 p2830 N85-27450

Genetic engineering of plants: Agricultural research opportunities and policy concerns
[DE85-006771] 16 p2840 N85-27513

Preliminary technology utilization assessment of the robotic fruit harvester
[NASA-CR-175834] 16 p2844 N85-27532

Meteorology and food production: The theme of the 16 meteorology day
[AD-A152372] 17 p2996 N85-28518

Earth Resources: A continuing bibliography with indexes, issue 45
[NASA-SP-7041(45)] 18 p3123 N85-29336

Screening Prosopis (mesquite) species for biofuel production on semi-arid lands
[DE85-010048] 19 p3302 N85-30471

Agricultural weather report for the Ijsselmeer polders in the 1984 summer season; a verification report
[KNMI-TR-61] 20 p3496 N85-31737

USSR report: Life sciences. Biomedical and behavioral sciences
[JPRS-UBB-85-017] 20 p3504 N85-31785

Deficit irrigation feasibility study and demonstration project
[DE85-011531] 22 p3802 N85-33555

Salinity driven oceanographic upwelling
[DE85-011664] 22 p3818 N85-33652

USSR report: Life sciences. Biomedical and behavioral sciences
[JPRS-UBB-85-018] 22 p3819 N85-33660

Snow cover in the Siberian forest-steppe
[NASA-TM-77914] 23 p3943 N85-34435

AGRISTARS PROJECT

Shortwave infrared detection of vegetation
[E85-10064] 08 p1174 N85-17402

Analysis of data acquired by synthetic aperture radar and LANDSAT Multispectral Scanner over Kershaw County, South Carolina, during the summer season
[E85-10071] 10 p1503 N85-19485

NOAA-AISC user's guide for implementing CERES maize model for large area yield estimation
[E85-10063] 12 p1873 N85-21748

NOAA-AISC user's guide for implementing CERES wheat model for large area yield estimation
[E85-10065] 12 p1873 N85-21750

Estimating solar radiation for plant simulation models
[E85-10069] 12 p1873 N85-21751

Thematic Mapper data quality and performance assessment in renewable resources/agriculture/remote sensing 13 p2120 N85-23201

Supplement to evaluation of satellite derived estimates of solar radiation
[E85-10066] 14 p2346 N85-24506

Evaluation of satellite derived estimates of solar radiation
[E85-10067] 14 p2346 N85-24507

AGROCLIMATOLOGY

An integrated remote sensing approach for identifying ecological range sites — parker mountain
[E85-10050] 07 p0983 N85-16248

The climate in food production in Latin America
07 p1001 N85-16359

Crop yield forecasting 07 p1001 N85-16360

The challenge of food production: The importance of climate 07 p1001 N85-16361

Socio-economic impact of climate — Mexico
07 p1003 N85-16372

Evaluation of the climatic resources of Cuba applied to agricultural work 07 p1004 N85-16380

AGROMETEOROLOGY

Short period forecasts in West Africa using Meteosat data 01 p0079 N85-10626

Frost nowcasting in the agricultural area of Valencia (Spain) — meteorological satellites
05 p0658 N85-14225

Climate Conference for Latin America and the Caribbean
[WMO-632] 07 p1000 N85-16352

Crop yield forecasting 07 p1001 N85-16360

The challenge of food production: The importance of climate 07 p1001 N85-16361

The management of atmospheric resources in food production 07 p1002 N85-16362

Water and climate, study of one case
07 p1002 N85-16369

Evaluation of the climatic resources of Cuba applied to agricultural work 07 p1004 N85-16380

The El Nino phenomenon and its agrometeorological implications 07 p1004 N85-16382

Agricultural weather report for the Ijsselmeer polders in the 1984 summer season; a verification report
[KNMI-TR-61] 20 p3496 N85-31737

AGT

U AUTOMATED GUIDEWAY TRANSIT VEHICLES

AILERONS

NT FLAPERONS

Aileron controls for wind turbine applications
[NASA-TM-86867] 02 p0222 N85-11458

Aileron effectiveness for a subsonic transport model with a high-aspect-ratio supercritical wing
[NASA-TM-85674] 07 p0898 N85-15695

Shutdown characteristics of the Mod-O wind turbine with aileron controls
[NASA-TM-86918] 07 p0992 N85-16299

Flight service evaluation of advanced composite ailerons on the L-1011 transport aircraft
[NASA-CR-172483] 08 p1118 N85-17049

Gust load alleviation of a cantilevered rectangular elastic wing. Wind tunnel experiment and analysis
[NAK-TR-86] 18 p3063 N85-28950

Compendium of unsteady aerodynamic measurements, addendum 1
[AGARD-R-702-ADD-1] 20 p3390 N85-31028

Data set 8: ZKP wing, oscillating aileron
20 p3390 N85-31029

Reflection plane tests of a wind turbine blade tip section with ailerons
[NASA-TM-87018] 23 p3945 N85-34444

AIR

NT COMPRESSED AIR
NT EXPIRED AIR
NT LIQUID AIR

Electron energy loss rates in N-2, O-2 and air
[AD-A145158] 01 p0072 N85-10476

Diagnostics of ionization in air produced by infrared radiation from A pulse CO2 laser
[AD-A145376] 02 p0201 N85-11342

Laboratory investigation of coefficients of absorption of air at Lambda = 10.6 microns 02 p0263 N85-11723

Low-frequency sound absorption measurements in air
[NASA-RP-1128] 02 p0275 N85-11789

Pathogenesis and treatment of cerebral air embolism and associated disorders
[AD-A146723] 07 p1014 N85-16443

Theoretical studies of the ignition and combustion of silane-hydrogen-air mixtures
[NASA-CR-3876] 10 p1433 N85-19032

Self-Optimized Sector (SOS) model of self-consistent energy loss and scattering for an electron beam propagating in air
[DE85-003161] 11 p1722 N85-20831

Hydrogen flame acceleration and transition to detonation
[DE85-000611] 12 p1802 N85-21299

Continuous measurement of zircaloy corrosion in air with an ultrasonic corrosion monitor
[DE85-003660] 12 p1807 N85-21337

Pseudo-stationary oblique-shock-wave reflections in a polyatomic gas, sulfur hexafluoride
[UTIAS-TN-253] 12 p1845 N85-21577

The effect of air holes on combustor liner wall temperature profile: Experiments
[NAL-TR-840] 15 p2504 N85-25443

Modeling the role of radicals in the ignition of and flame propagation in hydrogen-air and methane-air mixtures
16 p2744 N85-26935

Aluminum-air power cell research and development
[DE85-008117] 17 p2966 N85-28456

Air Weather Service (AWS) climatic briefs: Europe
[AD-A152526] 17 p2996 N85-28519

Research test facility for evaporation and combustion of alternative jet fuels at high air temperatures
[AD-A153830] 18 p3083 N85-29073

A model for the combustion of polymethyl methacrylate in air in a laminar diffusion flame
[VTH-LR-439] 18 p3165 N85-29606

Air bag restraint system
[AD-D011671] 19 p3215 N85-29936

Rayleigh scattering for density measurements in premixed flames: One point, time series data
20 p3424 N85-31253

Supersaturation obtained in a condensation nucleus counter 21 p3642 N85-32624

Recombination and ionization in a nitrogen plasma
[AD-A155426] 22 p3845 N85-33813

Influence of technology of atomization of naturally alloyed iron on grain-size characteristics of powder material
[BLL-M-35810-(5828.4)] 23 p3914 N85-34257

Cerenkov radiation from periodic electron bunches for finite emission length in air
[AD-A156156] 24 p4090 N85-35352

Proton-air and proton-proton cross sections from air shower data
[HE-1.1-1] 24 p4170 N85-35849

Proton-air inelastic cross section at S(1/2) = 30 TeV
[HE-1.1-2] 24 p4170 N85-35850

AIR BEARINGS

U GAS BEARINGS

AIR BLASTS

U AERIAL EXPLOSIONS

AIR BREATHING BOOSTERS

Integral boost, heat protection, port covers and transition 07 p0918 N85-15813

AIR BREATHING ENGINES

NT GAS TURBINE ENGINES
NT J-85 ENGINE
NT JET ENGINES
NT RAMJET ENGINES
NT SUPERSONIC COMBUSTION RAMJET ENGINES
NT TURBOFAN ENGINES
NT TURBOJET ENGINES
NT TURBOPROP ENGINES

An experimental investigation of two-dimensional thrust augmenting ejectors, part 1
[NASA-CR-174111] 04 p0456 N85-12894

An experimental investigation of two-dimensional thrust augmenting ejectors, part 2
[NASA-CR-174110] 04 p0456 N85-12895

Combustion in high speed air flows
[AD-A148371] 08 p1122 N85-17070

A study of air breathing rockets. Part 4: Direct fuel injection into a secondary combustor
[NAL-TR-832] 09 p1287 N85-18063

An air-breathing ballistic space transporter for Europe
[NASA-TM-77645] 12 p1792 N85-21244

Status of boron combustion research
13 p1998 N85-22528

Fiscal year 1986 technical objective document
[AD-A151039] 14 p2432 N85-25000

Status of boron combustion research
[AD-A154762] 21 p3563 N85-32160

AIR CONDITIONING

An assessment of ground-coil heat-pump technology
[DE85-002567] 10 p1486 N85-19362

Performance evaluation of an active solar cooling system utilizing low cost plastic collectors and an evaporatively-cooled absorption chiller
[DE84-010813] 12 p1880 N85-21798

Latent heat storage in cooling systems
[DE85-005355] 13 p2129 N85-23248

A review of development and application of heat pump technology
[CSIR-RR-585] 14 p2300 N85-24241

Evaporatively cooled chiller for solar air conditioning systems design and field test
[DE84-014154] 20 p3484 N85-31652

AIR CONDITIONING EQUIPMENT
Modeling of a second-generation solar-driven Rankine air conditioner
[DE84-016132] 01 p0006 N85-10223
Turbine test report, addendum
[DE84-016130] 02 p0205 N85-11353
New control design principles based on measured performance and energy analysis of HVAC (Heating, Ventilating, and Air-Conditioning) systems
[AD-A151706] 15 p2522 N85-25546
The influence of oil contamination on the nucleate pool-boiling behavior of R-114 from a structured surface
[AD-A158809] 21 p3585 N85-32284
AIR CONDUCTIVITY
Natural convection in square partitioned enclosures
[AD-A153767] 18 p3197 N85-29829
AIR COOLING
Cooling system investigation of the 3-kW MEP models 016A, 021A, and 026A (60Hz, 400-Hz and 28-V dc) gasoline-engine-driven generator sets
[AD-A147571] 07 p0974 N85-16185
Improvement of gas turbine engine performance by water injection into turbine cooling air
09 p1307 N85-18209
Method for refining microstructures of cast titanium articles
[AD-D011518] 12 p1804 N85-21318
Effect of water injection into air for turbine cooling on economy of operation of gas turbine engine with afterburning 13 p2050 N85-22830
effect of gas stream sweeping past the effluent of a perforated plate on heat transfer inside the perforations
13 p2051 N85-22836
Comparison of the response of shape memory alloy actuators using air-cooling and water-cooling
[AD-A155216] 21 p3567 N85-32185
AIR CURRENTS
NT JET STREAMS (METEOROLOGY)
NT MERIDIONAL FLOW
NT VERTICAL AIR CURRENTS
Numerical calculations of stratified Ekman layer flow over ridges with a finite element model
[DE84-014482] 04 p0499 N85-13179
High-frequency wind wave spectrum in storm basin
14 p2336 N85-24444
Radon concentration inversion in the troposphere: Still unexplained
[INPE-3360-PRE/638] 16 p2526 N85-27431
The physical and empirical basis for a specific clear-air turbulence risk index
[NASA-CR-176522] 24 p4120 N85-35540
AIR CUSHION VEHICLES
U GROUND EFFECT MACHINES
AIR DEFENSE
NT ANTIMISSILE DEFENSE
A methodology for the determination of rotary wing aircraft vulnerabilities in air-to-air combat simulation
[AD-A148964] 10 p1424 N85-18984
Close air support mission: Development of a unitary measure of pilot performance
[AD-A149285] 11 p1697 N85-20665
Visual simulation requirements for aircraft aspect recognition at real world distances
[AD-A151040] 14 p2228 N85-23810
Inertial navigation system - LAS II for SGT YORK testing
[AD-A154204] 19 p3216 N85-29944
Program Manager: The journal of the defense systems management college, volume 14, number 2, March-April 1985
[AD-A154219] 20 p3540 N85-32031
Assured information flow capping architecture
[AD-A155392] 22 p3756 N85-33283
AIR DROP OPERATIONS
60,000 pound capacity extraction system
[AD-A145841] 03 p0318 N85-12052
AIR DUCTS
A numerical procedure on three-dimensional parabolic flow in duct 16 p2692 N85-26620
AIR FILTERS
Fabric filter system study
[PB84-229749] 03 p0342 N85-12206
Electrostatic augmentation of fabric filtration: Reverse-air pilot unit experience
[PB84-230002] 03 p0343 N85-12207
Development of a mass transfer machine for gas/liquid operations in the absence of gravity
[BMFT-FB-W-84-027] 05 p0637 N85-14091
Gas contamination detection device
[AD-D011386] 07 p0921 N85-15833
Diffusion deposition in fibrous filters for parallel and transverse flow models
[DE85-006149] 13 p2093 N85-23066
The investigation of natural and artificial ice nuclei by the improved membrane filter method
21 p3642 N85-32626
AIR FLOW
NT AIR CURRENTS
NT JET STREAMS (METEOROLOGY)
NT MERIDIONAL FLOW
NT VERTICAL AIR CURRENTS
Stall elimination and restart enhancement device
[AD-D011217] 01 p0010 N85-10062
Turbine heat transfer 02 p0142 N85-10964
Energy efficient engine. High pressure compressor detail design report
[NASA-CR-168558] 02 p0147 N85-10998
A dispersion model for airborne particulates inside a building
[DE84-014861] 02 p0225 N85-11473
Microburst wind structure and evaluation of Doppler radar for wind shear detection
[DOT/FAA/PM-84/29] 02 p0230 N85-11501
Problem of reduction to ideal wind tunnel in experimental aerodynamics 02 p0260 N85-11702
Investigation of heat exchange on models in subsonic jets of induction plasmatron 02 p0269 N85-11756
Aircraft flow effects on cloud droplet images and concentrations
[AD-A146176] 03 p0306 N85-12529
Simple mesoscale models for operational use in regions of topographic and thermal forcing: Development and evaluation
[AD-A146867] 06 p0839 N85-15325
The 500 millibar sign frequency teleconnection charts: Winter
[PB85-106276/GAR] 07 p1009 N85-16410
Combustion in high speed air flows
[AD-A148371] 08 p1122 N85-17070
Studies on reactive mufflers. Part 2: Mufflers with air flow 09 p1303 N85-18184
Control technology for fiber reinforced plastics industry at AMF Hatteras Yachts, New Bern Division, New Bern, North Carolina
[PB85-109015] 10 p1460 N85-19196
New air supply-prime mover facility for engine tests detailed 11 p1621 N85-20204
A probe for direct measurement of flow direction
[ESA-TT-853] 11 p1637 N85-20310
Flameholder with integrated air mixer
[AD-D011549] 12 p1776 N85-21161
Liquid fuel spray processes in high-pressure gas flow
[NASA-TM-86944] 12 p1844 N85-21570
Surface-slip equations for multicomponent nonequilibrium air flow
[NASA-TM-85820] 12 p1845 N85-21573
Multi-year plan for Experimental Systems Research: Passive and hybrid solar energy program
[DE85-004698] 12 p1882 N85-21810
Study for prediction of rotor/wake/fuselage interference, part 1
[NASA-CR-177340-VOL-1] 13 p1965 N85-22346
Study for prediction of rotor/wake/fuselage interference. Part 2: Program users guide
[NASA-CR-177340-VOL-2] 13 p1966 N85-22347
Diffusion deposition in fibrous filters for parallel and transverse flow models
[DE85-006149] 13 p2093 N85-23066
The ASCOT Data Analysis Workshop
[DE85-004407] 13 p2139 N85-23283
Planning of air cushion transport vehicles
14 p2285 N85-24160
A computer program to calculate the supersonic flow over a solid cone in air or water
[AD-A151102] 15 p2464 N85-25217
Air flow of the western coastal boundary of South Africa and its influence on the ocean 16 p2831 N85-27459
Aerodynamic performance of a wing in ground effect using the PANAIR program
[AD-A153303] 17 p2892 N85-27832
On Long's solution to hydrostatic flow over mountains
[DFVLR-MITT-84-02] 17 p2994 N85-28503
Multiple equilibria of the barotropic vorticity equation on a sphere 18 p3146 N85-29475
Approximate factorization method for computation of nonhydrostatic mesoscale flows
[DE85-007259] 19 p3313 N85-30537
A study of the adequacy of quasi-geostrophic dynamics for modeling the effect of frontal cyclones on the larger scale flow
[NASA-CR-176065] 20 p3495 N85-31731
Mesoscale features and atmospheric refraction conditions of the Arctic marginal ice zone
[AD-A155139] 21 p3636 N85-32584
The influence of helicopter tail shape on drag: An aerodynamic study using a low speed wind tunnel
[AD-A156304] 24 p4062 N85-35174
Experimental study of free and mixed convective flow of air in a heated cavity
[DE85-012536] 24 p4094 N85-35380
AIR INLETS
U AIR INTAKES
AIR INTAKES
NT ENGINE INLETS
NT INLET AIRFRAME CONFIGURATIONS
NT SUPERSONIC INLETS
Variable inlet vane assembly for a gas turbine combustion
[AD-D011220] 01 p0010 N85-10063
Interest of internal bleed for a two-dimensional air intake operating in a wide Mach number range (1.8-3 plus)
08 p1071 N85-16793
Selection of air intake parameters for supersonic-flow operation 13 p2051 N85-22837
West Europe report: Science and technology
[JPRS-WST-84-012] 15 p2523 N85-25552
MBB uses new CFC form tool for titanium alloy air intake 15 p2523 N85-25553
Low-speed aerodynamic test of an axisymmetric supersonic inlet with variable cowl slot
[NASA-TM-87039] 16 p2706 N85-26710
AIR JETS
Jet array impingement flow distributions and heat transfer characteristics: Effects of initial crossflow and nonuniform array geometry 02 p0142 N85-10967
Rayleigh and Raman scattering for density in a swirling flow combustor 08 p1120 N85-17060
Flow visualization study of the effect of injection hole geometry on an inclined jet in crossflow
[NASA-TM-86936] 11 p1631 N85-20260
Improved silicon grinding method and apparatus
[NASA-CASE-NPO-16336-1-CU]
12 p1819 N85-21407
Comparison of measured and computed boundary layers at the tail-end of an axisymmetric body in an air-jet
[AMTE(N)-TM-83053] 14 p2209 N85-23700
Experimental investigation of annular air curtain domes
[UTIAS-288] 15 p2521 N85-25543
Study of stresses on surface of flat barrier immersed in under expanded jet of rarefied gas
16 p2765 N85-27061
Moist barotropic instability in the tropics
20 p3469 N85-31683
Mean and large-scale turbulence characteristics of the noise-producing region of an acoustically excited round jet 20 p3523 N85-31911
Jets in air-jet family
[HE-3.2-1] 24 p4179 N85-35812
AIR LAND INTERACTIONS
Boundary layer-cloud interactions as potential storm predictors 01 p0081 N85-10543
Biosphere/atmosphere interactions
05 p0679 N85-14364
Theory and modeling of the interaction between subgrid scale orography and large scale flow
[DM-43] 16 p2827 N85-27440
Quasi stationary states in the Southern Hemisphere
18 p3144 N85-29465
Global model of transport of pollutants in atmosphere
19 p3297 N85-30439
An atmospheric boundary layer model forced by the operational ECMWV-model
[WSR-3] 24 p4120 N85-35541
AIR LAUNCHING
An artificial intelligence based framework for planning air launched cruise missile missions
[AD-A154466] 19 p3344 N85-30722
AIR LAW
Civil air code international flights section explained
15 p2460 N85-25194
Rotterdam Airport and the Common Market
17 p2894 N85-27840
Thirty years' activities for aircraft safety
20 p3391 N85-31033
The 121.5 MHz ELT: Past, present and future -- Emergency Locator Transmitter (ELT)
20 p3401 N85-31105
AIR LOCKS
Fokker wants to start new Netherlands space program
03 p0310 N85-11999
AIR MASSES
The atmospheric extinction problem
08 p1251 N85-17901
Variation of Arctic cloud cover in summer
[DE85-004507] 13 p2139 N85-23285
Atmospheric cross sections for the Arctic gas and aerosol sampling program, March - April 1983
[NASA-CR-176027] 19 p3314 N85-30541
A statistical analysis of ice nuclei concentrations at urban and rural sites in Valladolid, Spain
21 p3640 N85-32614
Observations of cloud droplets, aerosol particles and cloud condensation nuclei in continental air masses
21 p3649 N85-32671
Variations of particulate sulfur concentrations in a coastal atmospheric environment in connection with the change of air masses origin 21 p3652 N85-32692

AIR NAVIGATION
NT ALL-WEATHER AIR NAVIGATION
NT AREA NAVIGATION
NT NAP-OF-THE-EARTH NAVIGATION

National airspace review 02 p0136 N85-10926

National airspace system: Operational requirements [AD-A149349] 10 p1422 N85-18973

Terrain following without use of forward looking sensors 16 p2698 N85-26859

Low cost two gimbal inertial platform and its system integration 16 p2698 N85-26861

The AFTI/F16 terrain-aided navigation system [DE85-008411] 18 p3060 N85-28935

Simulations of strapdown-system errors and error compensation methods — transport aircraft navigation [DFVLR-MITT-84-22] 20 p3392 N85-31040

Flight testing the Litton LTN 90 laser gyro strapdown system for civil aviation [ESA-TT-904] 20 p3392 N85-31042

AIR PIRACY

Semiannual report to Congress on the effectiveness of the civil aviation security program [AD-A149522] 10 p1421 N85-18967

AIR POLLUTION
NT GLOBAL AIR POLLUTION
NT INDOOR AIR POLLUTION

Demonstrating air quality improvements: A review of alternatives [DE84-014274] 01 p0070 N85-10462

Acid rain and transported air pollutants: Implications for public policy [PB84-222967] 01 p0071 N85-10469

Size specific total particulate emission factors for mobile sources [PB84-226653] 01 p0071 N85-10471

Mobile source exposure estimation [PB84-224518] 01 p0095 N85-10643

Aerosol sampling bias from differential electrostatic charge and particle size 02 p0224 N85-11467

The changing pattern of fossil fuel CO2 emissions [DOE/OR-21400/2] 02 p0224 N85-11469

Green River air quality model development: Meteorological and tracer data, July/August 1982. Field study in Brush Valley, Colorado [DE84-014975] 02 p0225 N85-11474

Arctic haze: Meteorological aspects of long-range transport 02 p0230 N85-11499

Bibliography of climate textbooks and studies [WCP-84] 02 p0231 N85-11505

Review of the NAAQS (National Ambient Air Quality Standards) for carbon monoxide: Reassessment of scientific and technical information [PB84-231315] 03 p0388 N85-12485

Analysis of Santa Barbara oxidant study [PB84-229277] 03 p0388 N85-12486

Review of the attributes and performance of six urban diffusion models [PB84-236650] 04 p0484 N85-13087

Thermodynamic conditions of the Earth's atmosphere with pollution processes 04 p0523 N85-13345

Outline of a new emissions model for military and civilian aircraft facilities [DE84-016455] 04 p0531 N85-13394

Aircraft measurements of tracer gas during the 1983 cross Appalachian tracer experiment (CAPTEX) [DE84-015292] 04 p0531 N85-13395

Impact of alcohol fuels on urban air pollution: Methanol photochemistry study [DE84-012950] 04 p0531 N85-13397

Regional-scale (1000 KM) model of photochemical air pollution. Part 2: Input processor network design [PB84-232651] 04 p0532 N85-13400

Atmospheric tracer experiments in a deep narrow valley [PB84-234590] 04 p0532 N85-13402

VOC emissions from volatile organic liquid storage tanks: Background information for proposed standards [PB84-237320] 04 p0532 N85-13403

Climatological variability in modeling of long-term regional transport and deposition of air pollutants [DE84-014726] 04 p0539 N85-13430

Calms processor (CALMPRO) user's guide [PB84-229467] 04 p0540 N85-13439

Fundamental molecular physics and chemistry, part 1 [DE84-009127] 04 p0561 N85-13571

Carbon cycle: Terrestrial interactions 05 p0652 N85-14187

Global carbon - nitrogen - phosphorus cycle interactions: A key to solving the atmospheric CO2 balance problem? 05 p0652 N85-14188

Mean maximum mixing heights for northern Asia for the winter of 1978 [DE84-015980] 05 p0672 N85-14315

Portable instrument for the detection and identification of air pollutants [DE84-014767] 05 p0672 N85-14316

Carbon monoxide study, Anchorage, Alaska, November 22, 1982 to February 11, 1983 [PB84-238595] 05 p0673 N85-14321

Cross-Appalachian Tracer Experiment (CAPTEX '83) [PB84-238641] 06 p0834 N85-15307

NAAQS (National Ambient Air Quality Standards) Exposure Model (NEM) applied to carbon monoxide [PB84-242551] 06 p0834 N85-15310

Climate and water quality 07 p1002 N85-16368

Determination of the laws governing the changes in the standard deviations of the distribution of pollution based on observations of the atmospheric turbulence spectrum and the possibility of simulating it in the laboratory [BLL-TR-T6373/BG/MRS14663/84] 08 p1179 N85-17431

Air quality assessment model validation in complex terrain [AD-A147690] 08 p1180 N85-17434

Impact of aircraft emissions on air quality in the vicinity of airports. Volume 3: Air quality and emission modeling needs [AD-A147851] 08 p1180 N85-17435

Modeling of turbulent dispersion of neutral and buoyant contaminents released from two dimensional sources — air pollution [VKI-TN-150] 08 p1180 N85-17438

Atmospheric photochemical modeling of turbine engine fuels. Phase 1: Experimental studies. Volume 2: Environmental chamber data tabulations [AD-A147786] 08 p1185 N85-17470

The application of emissions trading to DoD installations [AD-P004136] 09 p1348 N85-18472

Quality assurance for environmental analytical chemistry, 1983 [DE84-016045] 09 p1349 N85-18489

Meteorological factors responsible for high CO (carbon monoxide) levels in Alaskan cities [PB85-115137/GAR] 09 p1350 N85-18493

Stratospheric concentration of nitric acid, ozone and carbonyl sulfide: Measurement of nitric acid absorption in the Q branch of the V4 band as a function of temperature [ESA-TT-864] 09 p1355 N85-18524

Laser air pollution monitoring system planned for Moscow 10 p1500 N85-19465

TRAN-STAT: Statistics for environmental studies [DE85-000829] 10 p1513 N85-19547

Application of SIMCA (Soft Independent Modeling of Class Analogy) pattern recognition to air pollutant analytical data [PB85-124683] 10 p1513 N85-19549

Evaluation of recent SO/sub x/and NO/sub x/ emission inventories [DE85-002649] 11 p1677 N85-20570

The concentration of sulfate in broken cloud layers [DE85-000226] 11 p1678 N85-20574

Meteorological support for the 1983 Deep Creek, Maryland experiment [DE85-002616] 11 p1678 N85-20575

Air quality for ozone and other photochemical oxidants. External review draft, volume 1 [PB85-126035] 11 p1679 N85-20582

Continued research in mesoscale air pollution simulation modeling. Volume 7. Mathematical modeling of urban aerosol dynamics [PB85-137388] 11 p1679 N85-20584

Continued research in mesoscale air pollution simulation modeling. Volume 5: Refinements in numerical analysis, transport, chemistry, and pollutant removal [PB85-137362] 11 p1680 N85-20585

Lidar observations of stratospheric aerosol over Mauna Loa Observatory, 1974 - 1981 [PB85-115061] 11 p1682 N85-20597

Turbulence parameters impacting dispersion in an urban convection boundary layer [PB85-116036] 11 p1682 N85-20598

User's guide for the Photochemical Box Model (PBM) [PB85-137164] 11 p1682 N85-20602

Evaluation of two numerical integrator schemes [PB85-138196] 11 p1683 N85-20603

Effects of air pollution and acid rain on forest decline [GPO-37-459] 12 p1883 N85-21818

Atlantic Coast Unique Regional Atmospheric Tracer Experiment (ACURATE) [PB85-128460] 12 p1886 N85-21839

Hazardous air pollutants: Wet removal rates and mechanisms [PB85-138626] 12 p1887 N85-21842

Hazardous air pollutants: Dry-deposition phenomena [PB85-138279] 12 p1887 N85-21843

Continued research in mesoscale air pollution simulation modeling. Volume 6. Further studies in the modeling of microscale phenomena [PB85-137370] 12 p1887 N85-21844

Sector analysis of relevant meteorological parameters for long range transport of air pollutants [NR-27] 12 p1893 N85-21882

Impact of aerosols on visibility and climate: A report prepared for Panel 3, Environmental Impact, of the NATO/CCMS Air Pollution Pilot Study on Air Pollution Control Strategies and Impact Modelling [PB85-108744] 12 p1897 N85-21906

Adsorption behaviour of nitrogen compounds on to porous polymer beads and applications to atmospheric sampling [BLL-DRIC-TRANS-7399-(3623.66)] 13 p2036 N85-22753

Spectroscopic study of gas pollutants in atmosphere over large cities: A review 14 p2341 N85-24478

Adjustment of the national dispersion model for air pollution from elevated sources [KNMI-TR-57] 14 p2353 N85-24540

Field validation of 6-particle puff model [DE85-004073] 15 p2589 N85-25882

Analytical methods for determination of POHC (Principal Organic Hazardous Constituents) in combustion products [PB85-161578] 16 p2747 N85-26955

Emission inventory applications to regional acid deposition modeling [PB85-157386] 16 p2760 N85-27033

Interactive effects of acid rain and gaseous air pollutants on natural terrestrial vegetation [DE85-005255] 16 p2821 N85-27401

Acid rain: Effects on fish and wildlife [PB85-154672] 16 p2821 N85-27402

Review of national emission standards for mercury [PB85-153906] 16 p2822 N85-27406

Utilization of remote sensing data in the evaluation of air pollution characteristics in the south coast/Southeast Desert Air Basin [PB85-162063] 16 p2822 N85-27407

Symposium on Atmospheric Sciences in South Africa [CSIR-S-331] 16 p2829 N85-27442

Elemental analysis of aerosols in Transvaal urban and power-producing areas using time and size-resolved samples 16 p2829 N85-27443

A wind-bivane/microprocessor system for on-line prediction and display of pollutant distributions 16 p2830 N85-27449

Effect of traffic and meteorology on air pollution 16 p2830 N85-27452

Ground-based remote sensing of atmospheric pollution 16 p2832 N85-27462

Testing of materials and coatings for jet engine components under simulated operational conditions [B8580073] 17 p2899 N85-27873

A study of gas solid reactions using coated piezoelectric detectors [AD-A153047] 17 p2920 N85-28001

Investigation of air pollution impact in Eastern Bavaria: Measurement results from August and September, 1984 [DFVLR-FB-85-03] 17 p2988 N85-28471

DFVLR measuring system for the determination of the spatial distribution of environmental parameters of the atmosphere by means of mobile instrumented platforms [DFVLR-FB-85-09] 17 p2989 N85-28472

Quality assurance for RESOLVE (Research on Operations-Limiting Visual Extinction). A visibility study in the California desert [AD-A152383] 17 p2992 N85-28494

Impact of alcohol fuels on urban air pollution: Methanol photochemistry study [DE85-009539] 18 p3133 N85-29403

Environmental Research Division report: Atmospheric physics [DE85-009659] 18 p3133 N85-29404

Analysis and model/data comparisons of large-scale releases of nitrogen tetroxide [DE85-009989] 18 p3133 N85-29406

Elemental tracers of source regions of contaminants in precipitation [DE85-007366] 18 p3133 N85-29407

Equipment development for rapid detection of microorganisms in air and water [FOA-A-40046-B2] 18 p3134 N85-29410

Formation and fate of toxic chemicals in California's atmosphere [PB85-172609] 18 p3134 N85-29414

Hellmut Berg issue — meteorology [MITT-39] 18 p3147 N85-29483

Urban climate and air hygiene before, during, and after the lifework of Hellmut Berg. Overview of a branch of applied meteorology 18 p3147 N85-29487

Diffusion of trace gases in the ground level boundary layer 18 p3148 N85-29489

Application of climatological analysis to minimize air pollution impacts in California [PB85-172963] 18 p3149 N85-29502

Ambient air contamination: Characterization and detection techniques 18 p3157 N85-29546
Internal contamination in the space station
18 p3157 N85-29549
Control of acid deposition precursors through dry scrubbing
[DE85-010261] 19 p3235 N85-30056
Institute works on modeling thermonuclear plasma processes 19 p3296 N85-30435
Reduction of pollutant formation in combustion processes
[DE85-010181] 19 p3309 N85-30512
The Terrain-Responsive Atmospheric Code (TRAC) for plume growth and dispersion in complex terrain
[DE85-010541] 19 p3309 N85-30513
Technical guide for estimating fugitive dust impacts from coal handling operations, volume 2
[DE85-010939] 19 p3309 N85-30514
Technical guide for estimating fugitive dust impacts from coal handling operations. Volume 1: Project summary
[DE85-010948] 19 p3309 N85-30515
MELSAR: A mesoscale air quality model for complex terrain. Volume 2: Appendices
[DE85-010991] 19 p3310 N85-30519
Sources of copper air emissions
[PB85-191138] 19 p3310 N85-30523
Factor analysis of atmospheric pollution by polycyclic aromatic hydrocarbons
[HSE-TRANS-10968] 19 p3311 N85-30528
Analysis of aldehydes and ketones in the gas phase
[PB85-181865] 20 p3426 N85-31261
New corrosion protection concept for very high voltage line towers
[BLL-OA-TRANS-2691-(6196.300)]
20 p3429 N85-31270
Environmental concerns related to natural gas vehicles
[DE85-010246] 20 p3486 N85-31666
State of knowledge of environmental concerns related to natural-gas-fueled vehicles
[DE85-009746] 20 p3486 N85-31667
Atmospheric Tracer Workshop
[DE85-010573] 20 p3486 N85-31668
Organic air pollutants during manufacturing and handling of PVC floor tiles
[FOA-E-40018] 20 p3487 N85-31669
Historic emissions of sulfur and nitrogen oxides in the U.S. from 1900 to 1980. Volume 1: Results
[PB85-191195] 20 p3487 N85-31674
Historic emissions of sulfur and nitrogen oxides in the U.S. from 1900 to 1980. Volume 2: Data
[PB85-191203] 20 p3487 N85-31675
EPA (Environmental Protection Agency) research program guide, FY-1985, October 1, 1984 - September 30, 1985
[PB85-181881] 20 p3487 N85-31676
Modeling of chemical transformations of SO(x) and NO(x) in the polluted atmosphere: An overview of approaches and current status
[PB85-173169] 20 p3487 N85-31677
Manual for the computer program for the Gaussian plume model with percentile calculations
[KNMI-TR-60] 20 p3517 N85-31867
Hazardous air pollutants
[GPO-43-064] 21 p3613 N85-32458
VALMET: A valley air pollution model
[DE85-010620] 21 p3614 N85-32463
Eleventh International Conference on Atmospheric Aerosols, Condensation and Ice Nuclei, volume 2
[PB85-182418] 21 p3638 N85-32596
Observations of the atmospheric ice nucleus at northwest China 21 p3641 N85-32618
Photochemical aerosol formation in polluted atmosphere 21 p3644 N85-32642
Human activity and production rate of secondary nuclei 21 p3645 N85-32645
Characteristics of aerosol composition in a nonurban area, north China 21 p3646 N85-32651
Trace element concentrations in atmospheric aerosol over Hungary 21 p3646 N85-32652
Physical and chemical aerosol characteristics in extremely clean air masses at Cape Grim, Tasmania
21 p3646 N85-32655
Condensation nuclei and aerosol size distribution measurements in Arctic haze 21 p3647 N85-32658
Some considerations about the natural atmospheric radioactive aerosol 21 p3647 N85-32662
Influence on an industrial site on the characteristics of CCN supersaturation with air masses of different origin
21 p3650 N85-32663
Variations of particulate sulfur concentrations in a coastal atmospheric environment in connection with the change of air masses origin 21 p3652 N85-32692
on the transport of large condensation nuclei in the atmosphere at various altitudes over the territory of the USSR 21 p3653 N85-32698
Laser Elektronika-01 for air pollution control lidar
21 p3684 N85-32867
Acid rain in Europe
[COMMITTEE-PRINT-99-F] 22 p3810 N85-33601
The 1984 effluent and environmental monitoring report for the Bettis Atomic Power Laboratory
[DE85-011533] 22 p3810 N85-33602
ARAC status report, 1985
[DE85-012635] 22 p3810 N85-33603
Environmental summary for calendar year 1984
[DE85-012020] 22 p3810 N85-33604
Environmental monitoring at Lawrence Livermore National Laboratory: 1984 report
[DE85-011593] 22 p3811 N85-33606
The 1984 environmental monitoring report, Sandia National Laboratories, Albuquerque, New Mexico
[DE85-011175] 22 p3811 N85-33607
Control technology for radioactive emissions to the atmosphere at US Department of Energy facilities: The Los Alamos Meson Physics Facility
[DE85-011402] 22 p3811 N85-33609
Technology of off-gas treatment for liquid-fed ceramic melters
[DE85-012467] 22 p3812 N85-33610
The 1984 environmental monitoring program report for Idaho National Engineering Laboratory site
[DE85-011209] 22 p3812 N85-33611
Evaluation of the 2DFLOW and hybrid complex-terrain dispersion models with the 1980 ASCOT data base from the Geysers
[DE85-012960] 22 p3812 N85-33613
Atmospheric reaction products from hazardous air pollutant degradation
[PB85-185841] 22 p3813 N85-33620
Practical consequences of the assessment of different energy health risks
[DE85-004538] 22 p3825 N85-33696
Atmospheric modeling of organics for risk assessment: A Chemist's view
[DE85-009770] 23 p3909 N85-34217
Description of a test site for large-scale heavy gas dispersion and combustion experiments
[DE85-004987] 23 p3911 N85-34231
Forecasting future industrial SO2 and NC/sub x/ emissions, revised 23 p3947 N85-34461
User's guide to the MATHEW/ADPIC models
[DE85-012952] 23 p3966 N85-34587
Basic research on pulse-combustion phenomena
[PB85-200228] 24 p4077 N85-35265
Studies in photochemical smog chemistry. 1: Atmospheric chemistry of toulene. 2: Analysis of chemical reaction mechanisms for photochemical smog
24 p4113 N85-35497
Incorporating meteorological data into receptor analysis: RAPS (Regional Air Pollution Study) revisited
[PB85-188944] 24 p4114 N85-35503

AIR PURIFICATION
Ventilation flow: Submerged
18 p3156 N85-29545
Space shuttle revitalization system
18 p3157 N85-29548
Third US/USSR Symposium on Particulate Control
[PB85-190690] 19 p3310 N85-30522

AIR QUALITY
Space Shuttle Environmental Effects: The First 5 Flights
[NASA-CR-171812] 01 p0069 N85-10457
Demonstrating air quality improvements: A review of alternatives
[DE84-014274] 01 p0070 N85-10462
Review of the NAAQS (National Ambient Air Quality Standards) for carbon monoxide: Reassessment of scientific and technical information
[PB84-231315] 03 p0388 N85-12485
Analysis of Santa Barbara oxidant study
[PB84-229277] 03 p0388 N85-12486
Airliner cabin air quality
[S-REPT-98-468] 03 p0402 N85-12560
Outline of a new emissions model for military and civilian aircraft facilities
[DE84-016455] 04 p0531 N85-13394
Proceedings of a Workshop on Atmospheric Research Needs for the Western United States
[DE84-015069] 04 p0534 N85-13412
Relationship between model complexity and data base quality for complex terrain tracer experiments
[DE84-015022] 04 p0539 N85-13429
Calms processor (CALMPRO) user's guide
[PB84-229467] 04 p0540 N85-13439
NAAQS (National Ambient Air Quality Standards) Exposure Model (NEM) applied to carbon monoxide
[PB84-242551] 06 p0834 N85-15310
Visibility monitoring in the southern California desert for the Department of Defense: Research on operations-limiting visual extinction, RESOLVE protocol
[AD-A146617] 06 p0835 N85-15315
Air quality assessment model validation in complex terrain
[AD-A147690] 08 p1160 N85-17434
Impact of aircraft emissions on air quality in the vicinity of airports. Volume 3: Air quality and emission modeling needs
[AD-A147951] 08 p1160 N85-17435
Impact of aircraft emissions on air quality in the vicinity of airports. Volume 4. Nitrogen dioxide and hydrocarbons
[AD-A148253] 08 p1160 N85-17436
Atmospheric photochemical modeling of turbine engine fuels. Phase 1: Experimental studies. Volume 2: Environmental chamber data tabulations
[AD-A147786] 08 p1165 N85-17470
The application of emissions trading to DoD installations
[AD-P004136] 09 p1346 N85-18472
Measurement and analysis of ambient carbon monoxide concentrations for project-level air quality impact studies
[PB85-104602/GAR] 09 p1350 N85-18492
Atmospheric science and power production
[DE84-005177] 09 p1354 N85-18521
Laser air pollution monitoring system planned for Moscow 10 p1500 N85-19465
Evaluation of recent SO/sub x/and NO/sub x/ emission inventories
[DE85-002649] 11 p1677 N85-20570
Air quality for ozone and other photochemical oxidants. External review draft, volume 1
[PB85-126035] 11 p1679 N85-20582
Air quality criteria for ozone and other photochemical oxidants. External review draft, volume 5
[PB85-126076-VOL-5] 11 p1679 N85-20583
Continued research in mesoscale air pollution simulation modeling. Volume 7. Mathematical modeling of urban aerosol dynamics
[PB85-137388] 11 p1679 N85-20584
Legislation to improve airline safety
[GPO-38-222] 12 p1773 N85-21132
Evaluation of complex terrain air quality simulation models
[PB85-119485] 12 p1886 N85-21835
Air quality criteria for ozone and other photochemical oxidants. External review draft, volume 2
[PB85-126043] 12 p1886 N85-21836
Air quality criteria for ozone and other photochemical oxidents, external review draft, volume 3
[PB85-126050] 12 p1886 N85-21837
Air quality criteria for ozone and other photochemical oxidants. External review draft, volume 4
[PB85-126068] 12 p1886 N85-21838
Papers from the Symposium on Emissions: The Value of Incentives and Guidelines for Control
[S-336] 15 p2590 N85-25967
Air quality benefit analysis for Los Angeles and San Francisco based on housing values and visibility
[PB85-168049] 16 p2822 N85-27409
Urban climate and air hygiene before, during, and after the lifework of Hellmut Berg. Overview of a branch of applied meteorology 18 p3147 N85-29487
Environmental Research Laboratories (of the National Oceanic and Atmospheric Administration) programs and plans: FY 1984 programs and FY 1985 plans
[PB85-171494] 18 p3149 N85-29501
Qualitative and quantitative examination of the performance of regional air quality models representing different modeling approaches
[DE85-010508] 19 p3310 N85-30518
MELSAR: A mesoscale air quality model for complex terrain. Volume 2: Appendices
[DE85-010991] 19 p3310 N85-30519
Assessment of the role of nitrogen oxides in nonurban ozone formation
[PB85-173680] 19 p3311 N85-30524
Identification and quantification of nitropolynuclear aromatic hydrocarbons in ambient and indoor air particulate samples
[PB85-176790] 19 p3311 N85-30525
Annual environmental monitoring report, January-December 1984
[DE85-011689] 20 p3486 N85-31665
Environmental concerns related to natural gas vehicles
[DE85-010246] 20 p3486 N85-31666
State of knowledge of environmental concerns related to natural-gas-fueled vehicles
[DE85-009746] 20 p3486 N85-31667
Soil extraction kit
[AD-D011736] 22 p3742 N85-33190
Environmental surveillance at Los Alamos during 1984
[DE85-011686] 22 p3811 N85-33605
The 1984 environmental monitoring report, Sandia National Laboratories, Albuquerque, New Mexico
[DE85-011175] 22 p3811 N85-33607

MELSAR: A mesoscale air quality model for complex terrain. Volume 1: Overview, technical description and user's guide
[DE85-010943] 22 p3811 N85-33608
Evaluation of the 2DFLOW and hybrid complex-terrain dispersion models with the 1980 ASCOT data base from the Geysers
[DE85-012960] 22 p3812 N85-33613
Modeling of auto exhaust smog chamber data for EKMA development
[PB85-186492] 22 p3813 N85-33619
Review of US NOx abatement technology
[PB85-193522] 24 p4114 N85-35501
AIR SAMPLING
Aerosol sampling bias from differential electrostatic charge and particle size 02 p0224 N85-11467
Aircraft measurements of tracer gas during the 1983 cross Appalachian tracer experiment (CAPTEX)
[DE84-015292] 04 p0531 N85-13395
Integrated global background monitoring network
[DE84-016996] 04 p0532 N85-13398
Portable instrument for the detection and identification of air pollutants
[DE84-014767] 05 p0672 N85-14316
Carbon monoxide study, Anchorage, Alaska, November 22, 1982 to February 11, 1983
[PB84-236595] 05 p0673 N85-14321
Direct measurements of nitrous acid, nitrogen dioxide and formaldehyde in auto exhaust by differential optical absorption spectroscopy
[PB84-229269] 06 p0767 N85-14905
Attempted measurement of gaseous H-2O-2 in the ambient atmosphere
[DE85-001937] 06 p0834 N85-15306
The CSIRO (Australia) atmospheric carbon dioxide monitoring program: Surface data
[CSIRO-TP-6] 07 p0996 N85-16324
Methodology for the collection and analysis of trace metals in atmospheric precipitation
[CM-67] 09 p1350 N85-18491
Measurement and analysis of ambient carbon monoxide concentrations for project-level air quality impact studies
[PB85-104602/GAR] 09 p1350 N85-18492
Comparative evaluation of GC/MS (Gas Chromatography/Mass Spectrometry) data analysis processing
[PB85-125664] 11 p1596 N85-20037
Solid sorbent air sampler
[NASA-CASE-MSC-20653-1] 11 p1636 N85-20301
The concentration of sulfate in broken cloud layers
[DE85-000228] 11 p1678 N85-20574
Evaluation of complex terrain air quality simulation models
[PB85-119485] 12 p1886 N85-21835
Atlantic Coast Unique Regional Atmospheric Tracer Experiment (ACURATE)
[PB85-128460] 12 p1886 N85-21839
Acid rain: Towards automated monitoring
16 p2829 N85-27444
SCPP (Sierra Cooperative Pilot Project) data collection and analysis. Volume 1: Executive summary
[PB85-156065] 16 p2837 N85-27494
Theoretical basis for the determination of the concentration of radon decay products in air from the activity of a particulate air sample
[IRI-190-83-07] 17 p3035 N85-28774
Program RNTHR/2: An HP-41 C program for the calculation of RaA, RaB, and RaC concentrations in air based on three measurements of an air-dust sample
[IRI-190-83-10] 18 p3134 N85-29412
Density and confinement effects on mixing characteristics of an axisymmetrical CO(2) jet
[AD-A154468] 19 p3267 N85-30258
Optical waveguide sensor for methane gas
[AD-D011691] 19 p3273 N85-30294
Mathematical model of global processes in the biosphere 19 p3295 N85-30431
Quasi non-intrusive sampling and analysis of gases associated with the boundary layer on the tethered satellite and similar supersonic and hypersonic research vehicles
[NASA-CR-176075] 20 p3407 N85-31140
On the design of a global detection system for airborne radioactivity
[CM-68] 20 p3487 N85-31670
Particulate contamination control in clean rooms by particle fallout (PFO) measurements
[ESA-PSS-01-204-ISSUE-1] 20 p3487 N85-31673
Ames Laboratory measurements of alkali levels in the Curtiss-Wright PFBC gas stream
[DE85-011357] 22 p3745 N85-33214
Control technology for radioactive emissions to the atmosphere at US Department of Energy facilities: The Los Alamos Meson Physics Facility
[DE85-011402] 22 p3811 N85-33609
The 1984 environmental monitoring program report for Idaho National Engineering Laboratory site
[DE85-011209] 22 p3812 N85-33611
Development of a microorifice uniform deposit cascade impactor
[DE85-006765] 22 p3812 N85-33614
AIR SEA ICE INTERACTIONS
Ice dynamics
[AD-A147376] 07 p0988 N85-16278
Southern ocean sea-ice morphology and kinematics
08 p1144 N85-17217
MIZEX. A program for mesoscale Air-Ice-Ocean interaction experiments in arctic marginal ice zones. 4: Initial results and analysis from MIZEX 83
[AD-A148255] 08 p1173 N85-17399
Passive microwave remote sensing for sea ice research
[NASA-CR-175570] 12 p1874 N85-21756
Carbonate chemistry of the Weddell Sea
[DOE/EV-110611/4] 12 p1898 N85-21916
Large space antenna technology applied to radar-imaging, rain-rate measurements, and ocean wind sensing 14 p2230 N85-23820
Possible sea ice impacts on oceanic deep convection
15 p2603 N85-26041
Results of the MIZEX preliminary campaign: 29 June to 19 July 1983 — Marginal Ice Zone Experiment (MIZEX), satellite observation
[CNES-84/142/T/CT/DRT/TIT/RL]
20 p3478 N85-31609
AIR SEA INTERACTIONS
U AIR WATER INTERACTIONS
AIR SICKNESS
U MOTION SICKNESS
AIR TO AIR MISSILES
NT SIDEWINDER MISSILES
AIR TO AIR REFUELING
Technical evaluation report on the FDP Symposium on Flight Test Techniques
[AGARD-AR-208] 12 p1777 N85-21157
AIR TO SURFACE MISSILES
Cost-effective missile guidance through distributed architecture and standard processes
16 p2698 N85-26662
Next generation gunship
[AD-A156361] 24 p4065 N85-35193
AIR TRAFFIC
MERIT: A man/computer data management and enhancement system for upper air nowcasting/forecasting in the United States — Minimum Energy Routes using Interactive Techniques (MERIT)
01 p0083 N85-10556
Activities report in air traffic control
03 p0317 N85-12047
TCAS 2 logic performance during phase one operational evaluation
[DOT/FAA/PM-84/20] 05 p0595 N85-13793
Activities report of the aerospace industry in West Germany
[ISSN-0176-5086] 05 p0734 N85-14718
FAA (Federal Aviation Administration) statistical handbook of aviation, calendar year 1983
[AD-A148171] 08 p1067 N85-16760
Airport activity statistics of certificated route air carriers
[AD-A148472] 08 p1081 N85-16846
Air traffic management concepts for the UK in the 1990's: A review of recent RSRE work
[AD-A147850] 08 p1082 N85-16853
Ultralight aircraft technology and public safety
[GPO-38-948] 12 p1773 N85-21131
Disturbance to the population due to flight operations at landing fields. Questionnaire on community reaction to non-commercial and sporting aviation
[NASA-TM-76531] 14 p2353 N85-24537
National airspace review. Implementation plan. Revised
[AD-A151412] 15 p2468 N85-25238
Air traffic: Instruments, airports, companies, post, cargo and passengers 18 p3060 N85-28932
Traffic alert and collision avoidance system: Operational simulation
[FAA-PM-85-10] 19 p3216 N85-29941
FAA air traffic activity, fiscal year 1984
[AD-A154318] 19 p3216 N85-29942
Status of air traffic control system
[S-HRG-98-1197] 20 p3391 N85-31036
System safety study of minimum TCAS 2 for instrument weather conditions
[FAA-PM-85-12] 22 p3728 N85-33113
The contribution made by flight mechanics to civil aviation 24 p4061 N85-35169
AIR TRAFFIC CONTROL
NT AUTOMATED EN ROUTE ATC
NT RADAR APPROACH CONTROL
National airspace review 02 p0136 N85-10926
Enhanced TCAS 2/CDTI traffic Sensor digital simulation model and program description
[NASA-CR-172445] 02 p0136 N85-10927
System engineering and integration contract for implementation of the National Airspace System Plan. Volume 2: Section 5.0
[AD-A145710] 02 p0137 N85-10929
A proof-of-principle getaway special free-flying satellite demonstration 02 p0155 N85-11051
New airport ground traffic control system planned
03 p0310 N85-12006
Activities report in air traffic control
03 p0317 N85-12047
System engineering and integration contract for implementation of the National Airspace System plan, volume 1, sections 1.0-4.0, 6.0
[AD-A145763] 03 p0317 N85-12048
Aircraft navigation and landing technology: Status of implementation
[GPO-38-615] 04 p0454 N85-12883
Closely spaced independent parallel runway simulation
[DOT/FAA/CT-84/45] 04 p0457 N85-12902
The construction of auditive tests of attention and spatial orientation and their factorial structure
[DFVLR-FB-84-21] 05 p0699 N85-14485
Predictions of cockpit simulator experimental outcome using system models 05 p0702 N85-14504
National airspace review: Airport radar service area operational confirmation report
[DOT/FAA/AT-84/2] 07 p0901 N85-15707
A bird strike handbook for base-level managers
[AD-A147928] 07 p0948 N85-16008
Designer on Aeroflot automated COMMO system development 08 p1067 N85-16765
National airspace review enhancement plan, revision 3
[AD-A150743] 08 p1082 N85-16852
Air traffic management concepts for the UK in the 1990's: A review of recent RSRE work
[AD-A147850] 08 p1082 N85-16853
A cockpit-display concept for executing a multiple glide-slope approach for wake-vortex avoidance
[NASA-TP-2386] 08 p1085 N85-16869
Test of dispersal of turbojet aircraft departure tracks at washington National Airport (1983-84), volume 1 report
[AD-A148111] 08 p1218 N85-17669
Research at automated ATC Scientific-Experimental Center 09 p1278 N85-18037
Improvements in Kazan airport equipment, facilities
09 p1278 N85-18039
Improvements under way at Gorkiy airport
09 p1278 N85-18040
Design and realization of a multiradar tracking system for air traffic control
[ENST-84E010] 09 p1279 N85-18044
Denver ARTCC (Air Route Traffic Control Center) evaluation of PROFS (Program for Regional Observing and Forecasting Services) mesoscale weather products
[PB85-120301/GAR] 09 p1279 N85-18045
Prototype concept design for US Army type 3A Air Traffic Control Tower (ATCT)
[AD-A148840] 09 p1284 N85-18070
National airspace system: Operational requirements
[AD-A149349] 10 p1422 N85-18973
Collision avoidance for Naval training aircraft
[FAA-PM-84-4] 12 p1774 N85-21136
The evolution of methods of air traffic control
[AD-A149606] 12 p1774 N85-21137
Operations concept for the advanced automation system man-machine interface
[AD-A149797] 12 p1774 N85-21139
A radome for air traffic control SSR radar systems
[AD-P004373] 12 p1827 N85-21467
Civil avionics flight testing with the RAE(B) BAC1-11
13 p1967 N85-22354
A flight management algorithm and guidance for fuel-conservative descents in a time-based metered air traffic environment: Development and flight test results
13 p1967 N85-22356
Planned office and facility consolidations: To improve system effectiveness and efficiency, FY 1985-87
[AD-A150441] 13 p1970 N85-22376
Analysis of estimation algorithms for CDTI and CAS applications
[NASA-CR-172444] 13 p1973 N85-22387
FAA aviation forecasts: Fiscal years 1985-1996
[AD-A151050] 14 p2216 N85-23747
Safety recommendation(s). A-84-82 through -84
[REPT-3957] 14 p2217 N85-23748
An analysis of the impacts of the Airport Radar Service Area (ARSA)
[AD-A150954] 14 p2217 N85-23749
Development concerns for satellite-based air traffic control surveillance systems 14 p2230 N85-23816

Multiple resources and display formatting: The implications of task integration in a simulated air traffic control task
[AD-A150713] 14 p2292 N85-24205
Administration chief on air traffic control improvements
15 p2460 N85-25193
Calculation and display of stack departure times for aircraft inbound to Heathrow Airport
[AD-A151991] 15 p2469 N85-25241
Wind modelling for increased aircraft operational efficiency 16 p2697 N85-26652
National Airspace System Plan: Facilities, equipment and associated development 16 p2704 N85-26692
Probabilistic computer model of optimal runway turnoffs
[NASA-CR-172549] 16 p2715 N85-26760
National airspace review, change 1
[AD-A152369] 17 p2894 N85-27844
Developments in the area of air traffic control systems and the relation with meteorology
[NLR-MP-84029-U] 17 p2895 N85-27848
A general area air traffic controller simulation using colour graphics
[AD-A153634] 18 p3060 N85-28933
FAA air traffic activity, fiscal year 1984
[AD-A154318] 19 p3216 N85-29942
Definition and layout of a traffic generator for an air traffic control simulation
[ESA-TT-886] 20 p3391 N85-31034
Status of air traffic control system
[S-HRG-98-1197] 20 p3391 N85-31036
A feasibility study for the use of electronic flight strips in ATC controller workstations
[DFVLR-FB-85-08] 20 p3392 N85-31039
Simulation studies of time-control procedures for the advanced air traffic control system
[NASA-TP-2493] 21 p3553 N85-32101
Status of the air traffic control system
[GPO-40-343] 21 p3554 N85-32107
System safety study of minimum TCAS 2 for instrument weather conditions
[FAA-PM-85-12] 22 p3728 N85-33113
Performance of rolling ball and isometric joystick on a 2-D target alignment task
[RSRE-MEMO-3695] 22 p3826 N85-33699
Effect of interference on the performance of a minimum TCAS 2
[FAA-PM-84-33] 23 p3895 N85-34131
Introduction to European air traffic control
[AD-A156326] 24 p4062 N85-35176
FAA requirements for model to support capacity, delay, noise and energy programs
[AD-A155815] 24 p4063 N85-35179
Analogies of control mechanisms in flight guidance and medicine 24 p4129 N85-35597

AIR TRAFFIC CONTROLLERS (PERSONNEL)
The Reports of Aeromedical Laboratory, volume 25, no. 1/2
[ISSN-0023-2858] 01 p0090 N85-10605
A study of fatigue of shiftworkers in air traffic control and weather service groups in JASDF
01 p0090 N85-10610
Blood pressure levels of active pilots compared with those of air traffic controllers
[AD-A146645] 06 p0846 N85-15373
Training high performance skills: Fallacies and guidelines
[AD-A148574] 08 p1198 N85-17545
Operations concept for the advanced automation system man-machine interface
[AD-A149797] 12 p1774 N85-21139
Administration chief on air traffic control improvements
15 p2460 N85-25193
Calculation and display of stack departure times for aircraft inbound to Heathrow Airport
[AD-A151991] 15 p2469 N85-25241
Construction of a job-oriented test for the selection of air traffic controllers
[DFVLR-FB-84-51] 17 p3002 N85-28558
Investigation of biochemical and psychological parameters of air traffic controllers in prestart state before beginning to work 19 p3325 N85-30599
A feasibility study for the use of electronic flight strips in ATC controller workstations
[DFVLR-FB-85-08] 20 p3392 N85-31039
Status of the air traffic control system
[GPO-40-343] 21 p3554 N85-32107
Performance of rolling ball and isometric joystick on a 2-D target alignment task
[RSRE-MEMO-3695] 22 p3826 N85-33699
U.S. Civil airmen statistics for calendar year 1984
[AD-A156326] 24 p4059 N85-35153

AIR TRANSPORTATION
Activities report in air traffic control
03 p0317 N85-12047
German domestic scheduled air transport in the year 2000
[ESA-TT-828] 05 p0595 N85-13792
FAA (Federal Aviation Administration) statistical handbook of aviation, calendar year 1983
[AD-A148171] 08 p1067 N85-16760
Utilization of Increased Airlift Capability (UIAC) study
[AD-A148669] 08 p1081 N85-16847
Tolerance endpoint for evaluating the effects of heat stress in dogs
[AD-A148104] 08 p1192 N85-17511
Issues in air transport
[PB85-121374/GAR] 09 p1277 N85-18030
Semiannual report to Congress on the effectiveness of the civil aviation security program
[AD-A149522] 10 p1421 N85-18967
Airport system development
[PB85-127793] 11 p1587 N85-19993
Assessing the behavior and performance of teams in organizations: The case of air transport crews
[AD-A150359] 13 p2143 N85-23302
USSR report: Transportation
[JPRS-UTR-84-008] 14 p2208 N85-23694
Bugayev on civil aviation ministry's 1983 achievements 14 p2208 N85-23696
FAA aviation forecasts: Fiscal years 1985-1996
[AD-A151050] 14 p2216 N85-23747
USSR report: Transportation
[JPRS-UTR-85-008] 15 p2460 N85-25189
Civil air code international flights section explained
15 p2460 N85-25194
Aviation system delays
[S-HRG-98-1241] 21 p3553 N85-32102
The research programme of the Institute for Aerospace Medicine 24 p4129 N85-35596

AIR WATER INTERACTIONS
NT AIR SEA ICE INTERACTIONS
Large-scale ocean-atmosphere interactions in the mid-latitudes and equatorial regions: A literature review
[CSIR-T/SEA-8302] 01 p0073 N85-10482
Excitation of quasi-static magnetic fields with axial structure 02 p0259 N85-11696
Dynamics of coupled ice-ocean system in the marginal ice zone: Study of the mesoscale processes and of constitutive equations for sea ice
[NASA-CR-174171] 04 p0542 N85-13448
Biogeochemical cycles: Interactions in global metabolism 05 p0652 N85-14184
Global biogeochemical cycles: Studies of interaction and change, some views on the strategy of approach
05 p0652 N85-14185
Some aspects of understanding changes in the global carbon cycle 05 p0652 N85-14186
Interactions of the marine phosphorus and carbon cycles 05 p0653 N85-14190
Air-sea heat exchange, an element of the water cycle
05 p0653 N85-14195
An investigation of the marine boundary layer during cold air outbreak 05 p0680 N85-14368
Structure and growth of the marine boundary layer
05 p0680 N85-14369
Numerical modeling of the atmosphere
05 p0680 N85-14370
Air-sea interaction during cold air outbreaks
05 p0685 N85-14401
Cage regional energy budgets from the GLAS ATH order model 05 p0685 N85-14402
Diagnostics of rainfall anomalies in the nordeste during the global weather experiment 05 p0685 N85-14405
Energy active areas of ocean
06 p0820 N85-15204
Studies of the ocean surface and the coupling between the sea and the atmosphere
[AD-A146546] 06 p0841 N85-15339
Spectral model for subtidal variability in the Chesapeake Bay
[PB84-226679] 06 p0842 N85-15345
Razrezy program research in the tropical Atlantic
07 p0981 N85-16229
Frazil ice formation
[AD-A147425] 07 p0988 N85-16279
Meteorological aspects of the 1982-83 El Nino/southern oscillation episode 07 p1001 N85-16356
The ocean and the dynamics of the tropical atmosphere; its possible predicability 07 p1002 N85-16366
A one dimensional dynamical model of ocean/atmosphere interactions
09 p1358 N85-18545
Analysis of flow within the coastal boundary layer off Long Island, New York
[DE85-001384] 09 p1359 N85-18550
The effect of stochastic surface heat fluxes on the climatology of the seasonal thermocline
[AD-A149957] 12 p1889 N85-21857
Intensification of tropical instabilities
[AD-A149965] 12 p1896 N85-21899
Oceanic role in terrestrial climate
[DE85-004422] 12 p1896 N85-21904
Modeling of mechanism of positive feedback between mean Earth surface temperature and atmospheric carbon dioxide in geologic time scale 13 p2106 N85-23122
Numerical investigation of evolution of energy spectrum of slightly nonlinear Rossby waves
13 p2106 N85-23124
Contribution to theory of ocean-atmosphere gas exchange 13 p2108 N85-23134
Sea-ice motion in response to geostrophic winds
14 p2323 N85-24357
A large-scale air sea interaction project over the Pacific basin 14 p2326 N85-24373
Atmosphere ice-ocean interactions in the Antarctic (IAGO) 14 p2326 N85-24375
The French Ocean Climate in Equatorial Atlantic (FOCAL) Drifter Program, 1983-1984
14 p2329 N85-24399
The Tropical Ocean and Global Atmosphere program (TOGA) 14 p2330 N85-24411
Applications of ARGOS measurements in equatorial Pacific Ocean-atmosphere interaction studies
14 p2331 N85-24414
An overview of NDBC drifting buoy development programs — NOAA Data Buoy Center (DBC)
14 p2332 N85-24422
Influence of interaction between ocean and atmosphere on intensity of moving tropical cyclone
14 p2333 N85-24431
Influence of bubbles formed upon breaking of waves on gas exchange between ocean and atmosphere
14 p2335 N85-24439
Structure of cold film in water-air boundary layer
14 p2335 N85-24443
Parameterization of apparent and latent heat fluxes above water surface in calm weather under natural conditions 14 p2337 N85-24454
A study of the turbulent layer in the water at an air-water interface 14 p2378 N85-24679
Sensitivity analysis of a coupled atmospheric-oceanic boundary layer model
[AD-A150760] 14 p2382 N85-24690
Analysis of the inflow and air-sea interactions in hurricane Frederic 15 p2595 N85-25990
North Atlantic Deep Water Formation
[NASA-CP-2367] 15 p2601 N85-26028
Changes in the high-latitude ocean as possible causes of atmosphere CO2 variations 15 p2602 N85-26038
Climatic impact of a change in North Atlantic Deep Water formation 15 p2603 N85-26045
Deepwater wind wave growth with fetch and duration
[AD-A151604] 15 p2604 N85-26051
China's integrated circuit production
16 p2806 N85-27302
Tropical Oceans-Global Atmosphere (TOGA) experiment planning for the Brazilian participation in TOGA global climate program
[INPE-3499-PRE/735] 16 p2834 N85-27477
Simulation of a synchronously coupled atmosphere-ocean prediction model
[AD-A152020] 16 p2835 N85-27482
NASA Oceanic Processes Program annual review
[NASA-TM-87565] 16 p2838 N85-27503
Time-dependence of CO2-induced climate change
[DE85-007568] 17 p2997 N85-28525
On the global distribution of three-dimensional Eliassen-Palm fluxes by stationary waves
18 p3145 N85-29469
A GCM study of the atmospheric response to tropical SST anomalies 18 p3146 N85-29477
Global model of transport of pollutants in atmosphere
19 p3297 N85-30439
Northeast Brazil droughts and Atlantic SST anomalies
[INPE-3538-PRE/754] 19 p3316 N85-30553
Atmospheric chlorofluromethanes as tracers of ocean circulation and mixing: Measurement and calibration techniques and studies in the Greenland and Norwegian Seas 19 p3319 N85-30573
Experiments using atmospheric forcing from a FGGE analysis to drive an upper ocean model
[INPE-3503-PRE/738] 19 p3319 N85-30576
A study of the turbulent layer in the water at an air-water interface
[AD-A154117] 19 p3319 N85-30578
Some remarks on the constitutive equations of stratified gas-liquid flow
[EME-137] 20 p3456 N85-31466
Geodynamics Branch research program
[NASA-TM-86223] 20 p3489 N85-31688
Southern oscillation/El Nino excitation of the Earth's Chandler wobble 20 p3490 N85-31695
Tropical Ocean and Global Atmosphere (TOGA) heat exchange project: A summary report
[NASA-CR-176036] 20 p3496 N85-31738

Mesoscale features and atmospheric refraction conditions of the Arctic marginal ice zone
[AD-A155139] 21 p3636 N85-32584

Bacterial ice nuclei of marine origin: Some recent observations 21 p3640 N85-32611

Properties of aerosol particles detected by satellites in coastal regions 21 p3641 N85-32622

Numerical simulations of the response of intense ocean currents to atmospheric forcing
[AD-A155161] 21 p3655 N85-32704

Simulation of the coupled atmospheric and oceanic boundary layer model during MILDEX
[AD-A155166] 21 p3655 N85-32705

Study of molecular diffusivity influence on mass transfer rate at a water-atmosphere interface
22 p3747 N85-33222

Air-sea interaction with SSM/I and altimeter
[NASA-CR-176105] 22 p3818 N85-33650

Meteorological data from the OPTOMA (Ocean Prediction Through Observations, Modeling and Analysis) program OPTOMA 2, leg D2. 30 Jun. - 10 Jul. 1984
[AD-A156134] 24 p4123 N85-35560

Mean cloudiness over the global tropics from satellite observations
[AD-A156188] 24 p4123 N85-35561

AIRBORNE EQUIPMENT

NT AIRBORNE/SPACEBORNE COMPUTERS

Effectiveness of agricultural aviation
04 p0544 N85-13460

USAF approach to airborne structural data recording: Airborne Data Acquisition Multifunction System (ADAMS)
07 p0697 N85-15683

Realization and testing of an experimental color display system for general aviation helicopters and aircraft
[BMFT-FB-W-84-042] 08 p1086 N85-16872

Optical studies of nitrogen oxides in the stratosphere
08 p1183 N85-17455

A far infrared Echelle spectrometer for the Kuiper Airborne Observatory 08 p1249 N85-17886

A 150 micron heterodyne spectrometer for airborne astronomy 08 p1249 N85-17887

Tunable heterodyne receiver from 100 micron to 1,000 micron for airborne observations
08 p1249 N85-17888

Instrumentation for submillimeter polarimetry
08 p1250 N85-17889

Design and analysis of airborne scanning optical systems 11 p1623 N85-20218

Airborne remote sensing CCD imaging system
11 p1623 N85-20220

MAP-related activities in the United States
11 p1655 N85-20427

Atmospheric research aircraft — conductivity/charge measurements
[ONERA-RS-87/7154/PY] 11 p1682 N85-20596

A subaperture approach to the calculation of flashlobes introduced by airborne radomes
[AD-P004355] 12 p1825 N85-21449

Intra-eruption geologic map from an x-band radar image during the May 18, 1980 eruption of Mount St. Helens, Washington 13 p2199 N85-23639

Radar observations of fissure-fed basaltic lava flows, Craters of the Moon, Idaho 13 p2199 N85-23640

DFVLR measuring system for the determination of the spatial distribution of environmental parameters of the atmosphere by means of mobile instrumented platforms
[DFVLR-FB-85-09] 17 p2989 N85-28472

Convective storm downdraft outflows detected by NASA/MSFC's Airborne 10.6 micron pulsed Doppler Lidar System
[NASA-CR-3898] 17 p2995 N85-28511

Dynamic rectification of airborne scanner digital image recordings 18 p3124 N85-29344

Altitude variations of cosmic-ray soft and hard components observed by airborne detectors
[SH-6.1-5] 23 p4045 N85-35079

The principles of wind measurement with the help of aircraft 24 p4123 N85-35558

AIRBORNE RADAR APPROACH

Development and flight test of a helicopter, X-band, portable precision landing system concept
[NASA-TM-86710] 16 p2710 N85-26721

Investigation of imaging and flight guidance concepts for rotorcraft zero visibility approach and landing
[NASA-CR-166571] 17 p2894 N85-27843

AIRBORNE/SPACEBORNE COMPUTERS

Analytical redundancy management mechanization and flight data analysis for the F-8 digital fly-by-wire aircraft flight control sensors
[NASA-CR-170396] 06 p0757 N85-14844

NOAA (National Oceanic and Atmospheric Administration) Aircraft Satellite Data Link (ASDL)
[PB84-243773] 07 p0942 N85-15976

Investigation of semiautomatic aircraft control processes employing time redundancy in on-board digital trajectory control computers 07 p0954 N85-16048

Data and results of a laboratory investigation of microprocessor upset caused by simulated lightning-induced analog transients
07 p0999 N85-16345

Documentation and separate test program development is most important for test/maintenance
08 p1065 N85-16745

Experience in using on-aircraft software for testing integrated systems 08 p1065 N85-16747

Automatic error detection and recovery techniques in onboard intelligent units for space and avionic application 08 p1066 N85-16756

The design and development of an integrated core system for battlefield helicopters
08 p1074 N85-16811

Development and implementation of the verification process for the shuttle avionics system
08 p1091 N85-16896

Satellite description 09 p1412 N85-18900

Feasibility of self-structured current accessed bubble devices in spacecraft recording systems
[NASA-CR-172554] 13 p1998 N85-22525

Spaceborne automatic data processing
14 p2397 N85-24769

A cost-efficient control procedure for the benefit of all airspace users 16 p2697 N85-26651

The interactive generation of specifications for an onboard software series (GISELE)
17 p2904 N85-27906

Certifying complex digital systems on civil aviation aircraft 17 p2904 N85-27907

The Department of Defense statement on the Science and Technology Program by Colonel Donald I. Carter, USAF Acting Deputy Under Secretary of Defense for Research and Advanced Technology before the Subcommittee on Research and Development of the Committee on Armed Services of the United States House of Representatives, 99th Congress, first session
[AD-A152467] 17 p3046 N85-28850

Space station automation study-satellite servicing. Volume 1: Executive summary
[NASA-CR-171512] 19 p3226 N85-29999

Development and evaluation of a Fault-Tolerant Multiprocessor (FTMP) computer. Volume 2: FTMP software
[NASA-CR-166072] 19 p3341 N85-30706

Development and evaluation of a Fault-Tolerant Multiprocessor (FTMP) computer. Volume 3: FTMP test and evaluation
[NASA-CR-166073] 19 p3341 N85-30707

A micro/PDP-11 system for 406 MHz COSPAS/SARSAT processing 20 p3403 N85-31117

Informatics Division 20 p3449 N85-31416

Microprocessor AirborneData Acquisition and Replay (MADAR) system
[AD-A151728] 20 p3514 N85-31843

Comparative study on data system architectures --- spacecraft data processing
[ESA-CR(P)-2015] 21 p3675 N85-32828

Effects of space radiation on advanced semiconductor devices. Part 3: Further cosmic ray simulation studies of single event upsets and latch-up in CMOS memories
[AERE-G-3368-PT-3] 22 p3848 N85-33833

Development and operation of a measuring data acquisition system for use in light airplanes
24 p4123 N85-35556

AIRBUS

U EUROPEAN AIRBUS

AIRCRAFT

Three degree of freedom steady state point performance program: Updated version 1
[CSIR-NIAST-83/48] 01 p0001 N85-10005

Auditory information systems in military aircraft: Current configurations versus the state of the art
[AD-A145469] 02 p0275 N85-11794

Logistics support costs for the B-1B aircraft can be reduced
[AD-A145646] 03 p0309 N85-11996

The beginnings of airborne astronomy, 1920 - 1930: An historical narrative 08 p1244 N85-17849

On the frontier: Flight research at Dryden 1946-1981
[NASA-SP-4303] 09 p1263 N85-17934

Advanced life analysis methods. Volume 1: Cracking data survey and NDI (nondestructive inspection) assessment for attachment lugs
[AD-A150419] 13 p2103 N85-23108

Low-profile fastener
[AD-D011667] 19 p3280 N85-30343

Removable cleanable antireflection shield
[AD-D011735] 22 p3644 N85-33810

AIRCRAFT ACCIDENT INVESTIGATION

Review of aircraft accident data: US General Aviation
[PB84-230960] 01 p0005 N85-10027

Aircraft accident report. Central Airlines flight 27, Hughes Charter Air, Gates Learjet model 25 (N51CA) Newark International Airport, Newark, New Jersey, March 30, 1983
[PB84-910411] 02 p0136 N85-10924

Aircraft accident report, Western Helicopters, Inc., Bell UH-1B, N87701, Valencia, California, July 23, 1982
[PB84-910414] 05 p0594 N85-13789

Aircraft accident report Air Canada, Lockheed L-1011, C-FTNJ, near Charleston, South Carolina, November 24, 1983
[PB84-910413] 05 p0594 N85-13790

Annual review of aircraft accident data: US general aviation, calendar year, 1981
[PB84-230960] 06 p0750 N85-14805

Proceedings of the 6th Human Factors Workshop on Aviation
[AD-A150043] 12 p1909 N85-21982

Safety recommendation(s), A-84-128 through -133
[REPT-3996C/41] 15 p2466 N85-25221

Safety recommendation(s), A-84-123 and -124
[REPT-3894B/93] 15 p2466 N85-25222

Safety recommendation(s), A-84-96
[REPT-3983A/217] 15 p2466 N85-25223

Safety recommendation(s), A-84-76 through -78
[REPT-3751E] 15 p2466 N85-25224

Aircraft accident report: United Airlines Flight 663, Boeing 727-222, N7647U, Denver, Colorado, May 31, 1984
[PB85-910405] 16 p2703 N85-26886

General Aviation Crashworthiness Project. Phase 2: Impact severity and potential injury prevention in general aviation accidents
[PB85-917002] 19 p3215 N85-29938

AIRCRAFT ACCIDENTS

NT BIRD-AIRCRAFT COLLISIONS

Review of aircraft accident data: US General Aviation
[PB84-230960] 01 p0005 N85-10027

Proceedings of the Aviation Accident Investigation Symposium
[PB84-917004] 01 p0005 N85-10029

Aircraft accident report. Central Airlines flight 27, Hughes Charter Air, Gates Learjet model 25 (N51CA) Newark International Airport, Newark, New Jersey, March 30, 1983
[PB84-910411] 02 p0136 N85-10924

Aircraft accident report: Flying Tigers, Inc., Flight 2468, McDonell Douglas DC8-63, N797FT, Chambers Field, Naval Air Station, Norfolk, Virginia, October 25, 1983
[PB84-910408] 02 p0136 N85-10925

Aircraft accident report, Scandinavian Airlines System, Flight 901, McDonnell Douglas DC-10-30, John F. Kennedy International Airport, Jamaica, New York, February 28, 1984
[PB84-910415] 05 p0594 N85-13788

Crew communication as a factor in aviation accidents
05 p0710 N85-14555

Communication on the flight deck
05 p0711 N85-14557

Annual review of aircraft accident data: US general aviation, calendar year, 1981
[PB84-230960] 06 p0750 N85-14805

Human factors in cockpit automation
06 p0752 N85-14819

Establishment of posture and working movements of pilot in air crash enquiries 07 p1010 N85-16417

FAA (Federal Aviation Administration) statistical handbook of aviation, calendar year 1983
[AD-A148171] 08 p1067 N85-16760

SPH-4 US Army flight helmet performance, 1972 - 1983
[AD-A148674] 08 p1201 N85-17562

Safety awareness, pilot education, and incident reporting programs 09 p1276 N85-18020

The aviation safety reporting system
09 p1276 N85-18021

Annual review of aircraft accident data: US air carrier operations calendar year 1981
[NTSB/ARC-85/01] 12 p1774 N85-21134

TCAS II: Design and validation of the high-traffic-density surveillance subsystem
[DOT/FAA/PM-84/5] 13 p1970 N85-22375

Safety recommendation(s), A-84-93 through -95
[REPT-3963/33] 14 p2216 N85-23746

Safety recommendation(s), A-84-96
[REPT-3983A/217] 15 p2466 N85-25223

Aircraft accident report: United Airlines Flight 663, Boeing 727-222, N7647U, Denver, Colorado, May 31, 1984
[PB85-910405] 16 p2703 N85-26886

Frangibility of obstacles at airports
[NLR-MP-84002-U] 17 p2961 N85-28431

DYNA3D, INGRID, and TAURUS: An integrated, interactive software system for crashworthiness engineering
[DE85-010928] 21 p3677 N85-32846

AIRCRAFT ANTENNAS

Measurements of polarization characteristics of radiation field of on-board aircraft antennas 03 p0346 N85-12230

On aircraft antennas and basic scattering studies [AD-A146017] 03 p0355 N85-12282

Microstrip antenna for multichannel radiometer 06 p0791 N85-15056

Proceedings of the Symposium on Electromagnetic Windows (17th) held at Georgia Inst. of Technology, Engineering Experiment Station, Atlanta, Georgia on 25-27 July 1984. Part 2 [AD-A149125] 12 p1824 N85-21444

Comparison of spherical wave ray tracing and exact boundary value solutions for spherical radomes [AD-P004353] 12 p1824 N85-21447

Coordinate determination errors in measuring characteristics of radiation field of airborne antennas 13 p2068 N85-22919

Simulation and analysis of airborne antenna radiation patterns 20 p3439 N85-31342

AIRCRAFT APPROACH SPACING

National airspace review enhancement plan, revision 3 [AD-A150743] 08 p1062 N85-16652

AIRCRAFT BASES

U MILITARY AIR FACILITIES

AIRCRAFT BRAKES

NT LEADING EDGE SLATS

NT TRAILING EDGE FLAPS

NT WING FLAPS

AIRCRAFT CABINS

U AIRCRAFT COMPARTMENTS

AIRCRAFT CARRIERS

An update of the functional requirements of the Naval Aviation Logistics Command Management Information System (NALCOMIS) [AD-A146565] 06 p0871 N85-15532

An interactive environment for the development of an expert system in ZOG [AD-A149954] 12 p1915 N85-22025

Visual and part-task manipulations for teaching simulated carrier landings [AD-A153622] 18 p3154 N85-29529

AIRCRAFT COMMUNICATION

Ministry wants better commo facilities for agroaviation 03 p0310 N85-12003

Designer on Aeroflot automated COMMO system development 06 p1067 N85-16765

Tactical HF communication for military helicopters using the NVIS mode 08 p1074 N85-16807

National airspace system: Operational requirements [AD-A149349] 10 p1422 N85-18973

EHF air-to-air communications 10 p1469 N85-19273

Spectrum resource assessment of the Aeronautical Mobile Service between 400 MHz and 17.7 GHz [PB85-125995] 11 p1626 N85-20241

The effects of atmospheric turbulence on an air-to-air optical communication link [AD-A151640] 15 p2543 N85-25700

Survey of narrow band vocoder technology [AD-A151919] 16 p2773 N85-27114

AIRCRAFT COMPARTMENTS

Aircraft cabin pressurization control system tester [AD-D011225] 01 p0013 N85-10081

The pyrolysis toxic gas analysis of aircraft interior materials [AD-A146285] 03 p0328 N85-12115

Airliner cabin air quality [S-REPT-98-468] 03 p0402 N85-12560

Modeling of aircraft cabin fires [NBS-GCR-84-473] 04 p0454 N85-12880

An improved source model for aircraft interior noise studies [NASA-CR-172517] 08 p1217 N85-17666

Modeling of aircraft cabin fires [PB85-137695/GAR] 09 p1277 N85-18031

Pathophysiological study of poisoning due to thermal degradation of materials — aircraft cabins [CERMA-84-15] 11 p1692 N85-20640

Legislation to improve airline safety [GPO-38-222] 12 p1773 N85-21132

Suppression and control of Class C cargo compartment fires [FAA-CT-84-21] 12 p1773 N85-21133

Simultaneous cabin and ambient ozone measurements on two Boeing 747 airplanes. Volume 3: October 1978 - July 1979 [NASA-TM-86683] 12 p1892 N85-21872

Thermal response of aircraft cabin ceiling materials during a post-crash, external fuel-spill, fire scenario [PB85-145647] 14 p2220 N85-23764

Transmission of gear noise to aircraft interiors prediction methods 14 p2223 N85-23788

A study of interior noise levels, noise sources and transmission paths in light aircraft [NASA-CR-172152] 19 p3350 N85-30766

Effects of propeller rotation direction on airplane interior noise levels [NASA-TP-2444] 19 p3350 N85-30767

Design of sidewall treatment of cabin noise control of a twin engine turboprop aircraft [NASA-CR-172245] 19 p3351 N85-30771

The role of aircraft panel materials in cabin fires and their properties [FAA-CT-84-30] 21 p3553 N85-32104

Aviation safety (aircraft passenger survivability and cabin safety) [GPO-39-847] 23 p3895 N85-34130

AIRCRAFT CONFIGURATIONS

Preliminary airworthiness evaluation of the Rutan Aircraft Factory (RAF), Inc. LONG-EZ airplane with external sight [AD-A145381] 02 p0138 N85-10937

Second sailplane project: The RP-2 04 p0488 N85-12977

An in-flight investigation of a twin fuselage configuration in approach and landing [NASA-CR-172366] 05 p0596 N85-13801

Design of an airfoil leading edge slat using an inverse aerodynamic calculation method 08 p1069 N85-16777

Integrated digital/electric aircraft concepts study [NASA-CR-3841] 08 p1083 N85-16861

A first-order Green's function approach to supersonic oscillatory flow: A mixed analytic and numeric treatment [NASA-CR-172207] 09 p1273 N85-18002

Over the wing propeller [NASA-CASE-LAR-13134-1] 11 p1584 N85-19980

Study for prediction of rotor/wake/fuselage interference, part 1 [NASA-CR-177340-VOL-1] 13 p1965 N85-22346

Study for prediction of rotor/wake/fuselage interference. Part 2: Program users guide [NASA-CR-177340-VOL-2] 13 p1966 N85-22347

Boundary layer transition control for takeoff and landing configurations 14 p2211 N85-23714

Experiences with transition fixation in the high-speed regime at NLR 14 p2211 N85-23715

Recent developments in the dynamics of advanced rotor systems [NASA-TM-86669] 14 p2317 N85-24320

Computation of unsteady transonic flows about two-dimensional and three-dimensional AGARD standard configurations 15 p2459 N85-25183

The application of transonic unsteady methods for calculation of flutter airloads 15 p2460 N85-25186

Tensile and fracture toughness properties of Mirage III spars [AR-003-019] 15 p2578 N85-25899

A first-order time-domain Green's function approach to supersonic unsteady flow [NASA-CR-172208] 19 p3214 N85-29930

Calculation of transonic flows around an aircraft configuration with motorized nacelle [SNIAS-851-111-106] 20 p3387 N85-31008

Quest for performance: The evolution of modern aircraft [NASA-SP-468] 21 p3551 N85-32089

Flight testing the fixed-wing configuration of the Rotor Systems Research Aircraft (RSRA) [NASA-TM-86762] 23 p3896 N85-34135

AIRCRAFT CONSTRUCTION

U AIRCRAFT STRUCTURES

AIRCRAFT CONSTRUCTION MATERIALS

NT AIRFRAME MATERIALS

Near-threshold fatigue crack growth and crack closure in 17-4 precipitation hardening steel and 2043-T3 aluminum alloy [FFA-TN-1984-16] 02 p0210 N85-11385

The pyrolysis toxic gas analysis of aircraft interior materials [AD-A146285] 03 p0328 N85-12115

Tensile and crack propagation tests on aluminum alloys of the 2000 and 7000 series in laminated plate and forged products [M2-678300] 03 p0373 N85-12383

Low power laminar aircraft structures 04 p0451 N85-12857

Modern structural materials. Present situation and evolution prospects — aircraft materials [SNIAS-842-551-101] 04 p0455 N85-12886

Characterizing delamination resistance of toughened resin composites 04 p0464 N85-12943

Electroforming of nickel [SNIAS-841-501-101] 04 p0484 N85-13085

Preliminary evaluation of an improved flammability test method for aircraft materials [FAA-CT-84-22] 08 p1080 N85-16840

Composite structure repair, addendum [AGARD-R-716-ADD] 08 p1120 N85-17057

Repair of composites 08 p1120 N85-17058

FRG firms jump into market for auto, aircraft ceramics 09 p1309 N85-18225

Fatigue-creep interaction in + or - 45 deg carbon-resin composites — aircraft construction materials [ONERA-RT/40/7086/M] 11 p1594 N85-20027

High-strength composite materials for aircraft, body armor 11 p1599 N85-20057

Forced corrosion tests of construction components of passenger aircraft fuselages 11 p1600 N85-20062

Composite structural materials [NASA-CR-175515] 12 p1796 N85-21268

Corrosion of aircraft Al and Al-Zn ion plated steel fasteners 13 p2021 N85-22686

An overview of the MIL-HDBK-5 program [AD-A147788] 14 p2254 N85-23970

Development of a field repair technique for mini-sandwich Kevlar/epoxy aircraft skin [AD-A151369] 15 p2503 N85-25439

Mechanical properties of cast Martensitic high-strength multicomponent titanium alloys 15 p2514 N85-25514

Pechiney strategy includes development of new materials 15 p2531 N85-25607

Aluminum-lithium alloys: The answer of the aluminum industry to the threat of advanced fiber-reinforced materials [VTH-LR-406] 17 p2932 N85-28102

Research on structures and materials — aircraft structures [B8580060] 17 p2981 N85-28432

DFVLR research in aluminum-lithium alloys 18 p3087 N85-29105

Study of the influence of metallurgical factors on fatigue and fracture of aerospace structural materials [AD-A153913] 18 p3122 N85-29328

Mechanical properties of aligned short carbon fiber reinforced PES and PI laminates [ESA-TT-898] 20 p3422 N85-31240

Influence of recrystallization and solution on the tenacity of the 7010 and 7475 alloys. Olygocyclic fatigue of the 7010 alloy [ONERA-RT-19/5069-M] 20 p3432 N85-31289

R and D activities of the Materials Science Division 20 p3539 N85-32024

R and D activities of the Structural Sciences Division 20 p3539 N85-32026

New materials needs in aeronautics [SNIAS-851-502-101] 22 p3729 N85-33120

AIRCRAFT CONTROL

NT HELICOPTER CONTROL

Aircraft accident report: Flying Tigers, Inc., Flight 2468, McDonell Douglas DC8-63, N797FT, Chambers Field, Naval Air Station, Norfolk, Virginia, October 25, 1983 [PB84-910406] 02 p0136 N85-10925

High-temperature optically activated GaAs power switching for aircraft digital electronic control [NASA-CR-174711] 04 p0457 N85-12901

Accounting for error stochasticity in terminal homing of aircraft 04 p0489 N85-13115

A unified method for evaluating real-time computer controllers: A case study — aircraft control [NASA-CR-174168] 04 p0547 N85-13478

Integrated Application of Active Controls (IAAC) technology to an advanced subsonic transport project. ACT/Control/Guidance System study, volume 1 [NASA-CR-165963-VOL-1] 06 p0754 N85-14837

Integrated Application of Active Controls (IAAC) technology to an advanced subsonic transport project. ACT/Control/Guidance System study. Volume 2: Appendices [NASA-CR-165963-VOL-2] 06 p0754 N85-14838

Aircraft thrust control scheme for terrain following system [AD-D011387] 07 p0901 N85-15711

Investigation of semiautomatic aircraft control processes employing time redundancy in on-board digital trajectory control computers 07 p0954 N85-16048

Integrated digital/electric aircraft concepts study [NASA-CR-3841] 08 p1083 N85-16861

Time series analysis of closed-loop pilot vehicle dynamics 08 p1087 N85-16876

Use of airplanes for loft training 09 p1276 N85-18019

Preliminary performance of a vertical-attitude takeoff and landing, supersonic cruise aircraft concept having thrust vectoring integrated into the flight control system [NASA-CR-172530] 10 p1423 N85-18977

Pilot workload, performance and aircraft control automation 10 p1534 N85-19670

Acta Aeronautica et Astronautic Sinica (selected articles) [AD-A148830] 11 p1575 N85-19922

Leading edge flap system for aircraft control augmentation
[NASA-CASE-LAR-12787-2] 11 p1585 N85-19985

Robustness of continuous multivariable flight controls
[ONERA-RT-12/7224-SY] 11 p1586 N85-19987

Robustness of continuous multivariable flight controls
[ONERA-RT-11/7224-SY] 11 p1586 N85-19988

In-flight investigation of the effects of time delay in control system on flying qualities in landing approach
[DFVLR-FB-84-35] 11 p1586 N85-19939

Optimal symmetric flight studies
[NASA-CR-172508] 12 p1780 N85-21176

Aeronautical Engineering: A continuing bibliography with indexes, supplement 185
[NASA-SP-7037(185)] 13 p1965 N85-22342

Reference systems for the evaluation of dead-reckoning navigation equipment 13 p1967 N85-22358

Relative control effectiveness technique with application to airplane control coordination
[NASA-TP-2416] 14 p2218 N85-23753

Multivariable control law design for the AFTI/F-16 with a failed control surface
[AD-A151908] 15 p2474 N85-25271

Cost Effective and Affordable Guidance and Control Systems
[AGARD-CP-360] 16 p2695 N85-26638

A method of estimating aircraft attitude from fly by wire flight control system data 16 p2697 N85-26653

Application of linear optimal control theory to the design of the elevator control system of the DHC-2 Beaver experimental aircraft
[VTH-LR-411] 16 p2711 N85-26729

Controller requirements for uncoupled aircraft motion, volume 1
[AD-A153173] 17 p2900 N85-27878

In-flight investigation of the influence of pitch damping and pitch control effectiveness on landing approach flying qualities of statically unstable transport aircraft
[DFVLR-FB-84-12] 17 p2900 N85-27880

Proposals for the determination of necessary elevator handling characteristics of sailplanes in high speed range
[DFVLR-FB-84-52] 17 p2900 N85-27882

Active Control Technology (ACT): Past, present and future 17 p2901 N85-27884

The state-of-the-art and future of flight control systems 17 p2901 N85-27885

Aspects of application of ACT systems for pilot workload alleviation 17 p2901 N85-27887

Some flight test results with redundant digital flight control systems 17 p2902 N85-27892

An update of experience on the fly by wire Jaguar equipped with a full-time digital flight control system
17 p2902 N85-27893

Demonstration of relaxed static stability on a commercial transport 17 p2903 N85-27898

The aerodynamics of control
17 p2903 N85-27901

The STOL and maneuver technology program integrated control system development 17 p2905 N85-27910

A survey of the turbulence in the marine surface layer for the operation of low-Reynolds number aircraft
[AD-A154133] 19 p3316 N85-30558

Learning and self adaptation applied to the simulation of a human pilot
[ONERA-RT-24/5122-SY] 20 p3511 N85-31828

R and D activities of the Systems Engineering Division
20 p3540 N85-32027

Seat experiments for the full-scale transport aircraft controlled impact demonstration
[AD-A155024] 21 p3553 N85-32106

Flight control system for a computer controlled aircraft with limited sensors
[AD-A155107] 21 p3555 N85-32115

Development of control laws for a flight test maneuver autopilot for an F-15 aircraft
[NASA-TM-86736] 22 p3730 N85-33122

Energy management of three-dimensional minimum-time intercept
[NASA-CR-176174] 24 p4064 N85-35186

Control variables in vertical wind determination using simple flight-mechanical equations
24 p4121 N85-35546

AIRCRAFT DESIGN

NT HELICOPTER DESIGN

Optimum design of nonplaner wings: Minimum induced drag for a given lift and wing root bending moment
[NAL-TR-797] 01 p0002 N85-10011

The Influence of Large Scale Computing on Aircraft Structural Design
[AGARD-R-706] 01 p0007 N85-10040

Observations from varying the lift and drag inputs to a noise prediction method for supersonic helical tip speed propellers
[NASA-TM-83797] 01 p0115 N85-10788

ACEE program rationale and implementation
[NASA-TM-84549] 02 p0133 N85-10908

Energy efficient engine component development and integration program
[NASA-CR-169496] 02 p0146 N85-10989

Energy efficient engine component development and integration program
[NASA-CR-170034] 02 p0146 N85-10990

Energy efficient engine. Volume 2. Appendix A: Component development and integration program
[NASA-CR-173085] 02 p0146 N85-10991

Effect of stress concentrations in composite structures
[NASA-CR-173976] 02 p0170 N85-11140

Low power laminar aircraft structures
04 p0451 N85-12857

Natural laminar flow airfoil design considerations for winglets on low-speed airplanes
[NASA-CR-3853] 04 p0452 N85-12863

Physics on aircraft wakes
[NASA-CR-174105] 04 p0453 N85-12871

Solvent resistant thermoplastic composite matrices
04 p0466 N85-12960

Increase in the economy of design and process planning by integrated and graphic data processing, phase 2 --- aircraft design
[BMFT-FB-W-84-026] 05 p0716 N85-14589

Aerodynamic characteristics of some lifting reentry concepts applicable to transatmospheric vehicle design studies
[NASA-TM-86331] 06 p0747 N85-14787

New fighter aircraft reported --- Jian-8 aircraft
06 p0747 N85-14790

F-7 supersonic day fighter viewed --- Jian-7 aircraft
06 p0747 N85-14791

A-5 supersonic attack aircraft described --- Qiang-5 aircraft 06 p0747 N85-14792

Details of export A-5 close-support aircraft given --- Qiang-5 aircraft 06 p0748 N85-14793

Civil law enforcement missions
06 p0751 N85-14812

HH-65A Dolphin digital integrated avionics
06 p0751 N85-14815

Integrated cockpit design for the Army helicopter improvement program 06 p0751 N85-14816

United States Air force aircraft modification process: A system dynamics analysis
[AD-A146954] 07 p0893 N85-15659

Design study of technology requirements for high performance single-propeller-driven business airplanes
[NASA-CR-3863] 07 p0896 N85-15692

Missions and vehicle concepts for modern, propelled, lighter-than-air vehicles
[NASA-TM-86672] 08 p1066 N85-16757

Computer sizing of fighter aircraft
[NASA-TM-86351] 08 p1067 N85-16759

International aviation (selected articles)
[AD-A148704] 08 p1067 N85-16762

Designer on civil aircraft design trends in USSR
08 p1068 N85-16768

Recent progress of development and understanding of high lift systems 08 p1068 N85-16772

Design of an airfoil loading edge slat using an inverse aerodynamic calculation method
08 p1069 N85-16777

Aerodynamic issues in the design of high-lift systems for transport aircraft 08 p1069 N85-16780

Design studies of thick laminar flow airfoils for low speed flight employing turbulent boundary layer suction over the rear part 08 p1070 N85-16786

Technology developments for laminar boundary layer control on subsonic transport aircraft
08 p1071 N85-16787

Integrated digital/electric aircraft concepts study
[NASA-CR-3841] 08 p1083 N85-16861

Study of winglets applied to biplanes
[NASA-TM-86350] 08 p1083 N85-16862

A description of a logistically ideal aircraft
[AD-A148425] 08 p1084 N85-16866

The aircraft engine of the future
[PNR-90226] 08 p1087 N85-16875

Description of MBB computerized design techniques for A320 08 p1141 N85-17194

The development of a dynamic model of a generalised combat aircraft with forward wings for the identification of stability and control characteristics
[CAR-84-33] 09 p1280 N85-18050

Profile design for wings and propellers
[NASA-TM-77785] 10 p1419 N85-18953

Some fighter aircraft trends
[NASA-TM-86352] 10 p1420 N85-18954

Deployment sequence mode selection system for aircraft ejection seat
[AD-D011464] 10 p1422 N85-18968

The design of sport and touring aircraft
[NASA-TM-77783] 10 p1423 N85-18975

Preliminary performance of a vertical-attitude takeoff and landing, supersonic cruise aircraft concept having thrust vectoring integrated into the flight control system
[NASA-CR-172530] 10 p1423 N85-18977

Details of export A-5 close-support aircraft given
10 p1424 N85-18983

Study of advanced fuel system concepts for commercial aircraft and engines
[NASA-CR-174752] 10 p1456 N85-19176

Noise constraints effecting optimal propeller designs
[NASA-TM-86967] 11 p1575 N85-19923

Parametric study of a canard-configured transport using conceptual design optimization
[NASA-TP-2400] 11 p1584 N85-19979

Current development, applications of airships in USSR
12 p1769 N85-21109

Towards a renewal of the propeller in aeronautics
[NASA-TM-77803] 12 p1779 N85-21169

Translating rudder pedal system
[AD-D011510] 12 p1780 N85-21172

Some aspects of the design of a fly-by-wire flying control system for a supersonic V/STOL fighter aircraft
[COLL-AERON-8413] 12 p1780 N85-21175

Lubrication and performance of high-speed rolling-element bearings
[NASA-TM-86958] 12 p1859 N85-21658

Introduction: The clinical and biomedical evaluation for trauma and fatalities associated with aircrew ejection and crash 12 p1906 N85-21970

Aeronautical Engineering: A continuing bibliography with indexes, supplement 185
[NASA-SP-7037(185)] 13 p1965 N85-22342

Dynamic wind-tunnel testing of active controls by the NASA Langley Research Center
13 p1966 N85-22353

Study for the optimization of a transport aircraft wing for maximum fuel efficiency. Volume 1: Methodology, criteria, aeroelastic model definition and results
[NASA-CR-172551] 13 p1971 N85-22378

China report: Science and technology
[JPRS-CST-84-008] 13 p1972 N85-22384

Uses of composite materials
13 p2027 N85-22698

Redesign of fuselage compartments by method of special contours 13 p2042 N85-22784

Problems of the application of wind tunnel results to aerodynamic performance of large aircraft
14 p2211 N85-23713

The design of high-performance gliders
[NASA-TM-77772] 14 p2217 N85-23750

Design considerations for high-altitude, long-endurance, microwave-powered aircraft
[NASA-TM-86403] 14 p2218 N85-23751

Transmission error measurements in gearbox development 14 p2224 N85-23794

Do new aircraft need new technologies and certification rules? 14 p2224 N85-23795

Missions and vehicle concepts for modern, propelled, lighter-than-air vehicles
[NASA-TM-87461] 15 p2457 N85-25170

Special course on V/STOL aerodynamics: An assessment of European jet lift aircraft
[AGARD-R-710-ADDENDUM] 15 p2460 N85-25188

USSR report: Transportation
[JPRS-UTR-84-014] 15 p2467 N85-25229

Flying objects
[CH-634516-A5] 15 p2469 N85-25242

Aircraft
[CH-642598-A5] 15 p2470 N85-25246

Simulator study of the stall departure characteristics of a light general aviation airplane with and without a wing-leading-edge modification
[NASA-TM-86309] 15 p2470 N85-25250

The ONERA establishment at Cannes in the service of aeronautical research
[ESA-TT-875] 15 p2475 N85-25276

MBB cost-reduction plan for Airbus construction described 15 p2532 N85-25616

YAV-8B Harrier 15 p2686 N85-26605

Computer software for aerodynamic design of aircraft developed within the National Aerospace Laboratory
16 p2691 N85-26613

Numerical analyses in aerodynamic design of aero-engine fan 16 p2692 N85-26618

Computational aerodynamics in designing aircraft
16 p2693 N85-26622

Numerical example of three-dimensional flying object in shockless transonic flow 16 p2693 N85-26623

Computational aerodynamics for aircraft wing design
16 p2693 N85-26627

Comparison of computational results of a few representative three-dimensional transonic potential flow analysis programs 16 p2693 N85-26628

Three-dimensional wing boundary layer analysis program BLAY and its application
16 p2694 N85-26632

ACT flight research experience
16 p2713 N85-26741
The introduction of new cockpit technology: A human factors study
[NASA-TM-86659] 16 p2843 N85-27528
Research and development. Technical and scientific reports 1984 16 p2873 N85-27724
Utilization of an automated riveting system in aircraft construction
[MBB-UT-11/84-O] 16 p2875 N85-27736
Methods for design aerodynamics of modern transport aircraft
[DFVLR-FB-85-05] 17 p2893 N85-27836
Test flight of IL-76TD long-range transport variant
17 p2894 N85-27842
Technical services at NLR
[B8561896] 17 p3049 N85-28871
Future of V/STOL aircraft systems: A survey of opinions
[NASA-TM-86689] 18 p3061 N85-28937
MBB expands CADAM system for a 320 program
18 p3067 N85-29099
Aeronautical Engineering: A continuing bibliography with indexes (supplement 188)
[NASA-SP-7037(188)] 19 p3211 N85-29910
Impact dynamics research on composite transport structures
[NASA-TM-86391] 19 p3264 N85-30367
Avionics and civil aircraft systems: The present and the future
[SNIAS-851-111-104] 20 p3392 N85-31038
Design of the nacelle for the A-320 aircraft
[SNIAS-851-111-111] 20 p3393 N85-31046
Design of a basic airfoil for a slightly swept wing. Part 1: Theoretical transonic airfoil design
[ESA-TT-892] 20 p3394 N85-31054
Corrosion in civil aircraft structures
[SNIAS-851-111-105] 20 p3432 N85-31291
Preliminary sizing and performance of aircraft
[NASA-TM-86357] 21 p3554 N85-32111
Design of an expert-system flight status monitor
[NASA-TM-86739] 21 p3669 N85-32794
Energy efficient transport technology: Program summary and bibliography
[NASA-RP-1135] 22 p3729 N85-33116
Qualification needs for advanced integrated aircraft
[NASA-TM-86731] 22 p3729 N85-33119
New materials needs in aeronautics
[SNIAS-851-502-101] 22 p3729 N85-33120
Maintenance and the military environment
22 p3750 N85-33243
A guide to USAF helicopter instrument flight procedures
[AD-A156102] 24 p4063 N85-35182
Design and testing of an energy-absorbing crewseat for the F/FB-111 aircraft. Volume 2: Data from seat testing
[NASA-CR-3917] 24 p4064 N85-35184
Proceedings of the 14th Army Science Conference. Volume 2: Principal authors I through O
[AD-A149201] 24 p4144 N85-35690
A research program to reduce the interior noise in general aviation aircraft, index and summary
[NASA-CR-176178] 24 p4145 N85-35695

AIRCRAFT DETECTION
National airspace system: Operational requirements
[AD-A149349] 10 p1422 N85-18973

AIRCRAFT ENERGY EFFICIENCY PROGRAM
U ACEE PROGRAM

AIRCRAFT ENGINES
NT J-52 ENGINE
NT TF-34 ENGINE
NT VARIABLE CYCLE ENGINES
A study of bird ingestions into large high bypass ratio turbine aircraft engines
[DOE/FAA/CT-84/13] 01 p0005 N85-10028
Turbine Engine Hot Section Technology (HOST)
[NASA-TM-83022] 02 p0140 N85-10951
Equivalent damage: A critical assessment
02 p0140 N85-10952
Benchmark notch test for life prediction
02 p0140 N85-10953
Nonlinear structural and life analyses of a turbine blade 02 p0141 N85-10954
Nonlinear structural and life analyses of a combustor liner 02 p0141 N85-10955
Pre-HOST high temperature crack propagation
02 p0141 N85-10956
Structural analysis 02 p0143 N85-10969
Burner liner thermal/structural load modelling
02 p0143 N85-10970
Component-specific modeling
02 p0143 N85-10971
The 3-D inelastic analysis methods for hot section components: Brief description 02 p0143 N85-10972
Constitutive model development for isotropic materials
02 p0144 N85-10975
Airfoil deposition model 02 p0144 N85-10979
Effects of surface chemistry on hot corrosion life: Overview 02 p0145 N85-10980
Combustion hot section technology
02 p0145 N85-10981
Combustion system for radiation investigations
02 p0145 N85-10986
Energy efficient engine component development and integration program
[NASA-CR-170034] 02 p0146 N85-10990
Energy efficient engine. Low pressure turbine test hardware detailed design report
[NASA-CR-167956] 02 p0147 N85-10994
Energy efficient engine high pressure turbine test hardware detailed design report
[NASA-CR-167955] 02 p0147 N85-10995
Energy efficient engine. High pressure compressor detail design report
[NASA-CR-165558] 02 p0147 N85-10996
Air force engine repair - Oklahoma City Air Logistics Center, Propulsion Division
[AD-P003999] 03 p0307 N85-11980
Performance deterioration of cascades exposed to solid particles 03 p0319 N85-12057
Basic study of bladed disk structural response
[AD-A146226] 03 p0319 N85-12061
Propulsion — jet aircraft engines
[PNR-90208] 03 p0320 N85-12062
Cyclic endurance testing of the RB211-22B cast HP turbine blade — high pressure (HP)
[PNR-90210] 03 p0320 N85-12063
The applications of fibre optics in gas turbine engine instrumentation
[PNR-90209] 03 p0420 N85-12687
Static jet noise test results of four 0.35 scale-model QCGAT mixer nozzles
[NASA-TM-86871] 04 p0556 N85-13551
Random vibrations of aircraft engine blades
06 p0777 N85-14967
Predicted performance benefits of an adaptive digital engine control system of an F-15 airplane
[NASA-TM-85916] 07 p0905 N85-15729
Monitoring engine thermal stresses
07 p0906 N85-15735
Accelerated Mission Endurance Testing (AMET)
07 p0906 N85-15736
Design and test requirements for development of today's engines 07 p0906 N85-15737
Contamination and distortion of steady flow field induced by discrete frequency in aircraft gas turbines
[AD-A147092] 07 p0958 N85-16073
The aircraft engine of the future
[PNR-90226] 08 p1087 N85-16875
Rolls-Royce experience with thermal barrier coatings — in aircraft engines
[PNR-90222] 08 p1135 N85-17152
Flow measurement device
[AD-D011432] 08 p1168 N85-17369
An improved source model for aircraft interior noise studies
[NASA-CR-172517] 08 p1217 N85-17668
Design description of a microprocessor based Engine Monitoring and Control unit (EMAC) for small turboshaft
[NASA-TM-86860] 09 p1263 N85-17935
Research and development for semi-spherical inflow control device
[NAL-TR-833] 09 p1281 N85-18056
Improvement of gas turbine engine performance by water injection into turbine cooling air
09 p1307 N85-18209
On limits of applicability of linear models to dynamics of gas channels in aircraft engines
09 p1308 N85-18219
FRG firms jump into market for auto, aircraft ceramics
09 p1309 N85-18225
NASA Lewis Research Center/University Graduate Research Program on Engine Structures
[NASA-TM-86916] 09 p1333 N85-18375
Preliminary performance of a vertical-attitude takeoff and landing, supersonic cruise aircraft concept having thrust vectoring integrated into the flight control system
[NASA-CR-172530] 10 p1423 N85-18977
Analytical fuel property effects: Small combustors, phase 2
[NASA-CR-174848] 10 p1456 N85-19175
Study of advanced fuel system concepts for commercial aircraft and engines
[NASA-CR-174752] 10 p1456 N85-19176
Study of advanced fuel system concepts for commercial aircraft
[NASA-CR-174751] 11 p1584 N85-19978
Over the wing propeller
[NASA-CASE-LAR-13134-1] 11 p1584 N85-19980
Assuring structural integrity in Army systems
[NASA-CR-175482] 11 p1651 N85-20398
A theory of post-stall transients in multistage axial compression systems
[NASA-CR-3878] 12 p1771 N85-21117
Description of a technique to measure spray distribution in an air stream
[AD-A149780] 12 p1771 N85-21122
Stratified charge rotary aircraft engine technology enablement program
[NASA-CR-174812] 12 p1776 N85-21163
Tribological systems as applied to aircraft engines
[NASA-TM-86965] 12 p1858 N85-21657
Effects of inlet distortion on a static pressure probe mounted on the engine hub in an F-15 airplane
[NASA-TP-2411] 13 p1974 N85-22394
Hydrodynamic simulation of transient processes in injection system of aircraft engines during pump unswirling 13 p2050 N85-22829
Effect of water injection into air for turbine cooling on economy of operation of gas turbine engine with afterburning 13 p2050 N85-22830
T700 cuttar life improvement program
[AD-A150450] 13 p2099 N85-23089
Welcome to the Saclay Propeller Testing Center
[NASA-TM-77648] 14 p2225 N85-23799
High frequency estimation of 2-dimensional cavity scattering
[AD-A151697] 15 p2542 N85-25696
Advanced smoke meter development survey and analysis
[NASA-CR-168287] 15 p2560 N85-25792
Nondestructive tests of ceramic components for aircraft turbines 16 p2709 N85-26718
Test devices for aeronautical research and technology
[NASA-TM-77651] 17 p2905 N85-27914
An investigation into the soot production processes in a gas turbine engine
[AD-A152710] 17 p2919 N85-27992
Compressor and turbine models - numerical stability and other aspects
[AD-A153811] 18 p3063 N85-28948
Hold-time effects in elevated temperature fatigue crack propagation
[AD-A154146] 19 p3286 N85-30376
Component-specific modeling
[NASA-CR-174925] 21 p3556 N85-32119
Elevated temperature crack growth
[NASA-CR-174957] 22 p3799 N85-33540
Performance improvements from surfacing in aero engine components
[PNR-90257] 23 p3897 N85-34142
Directionally solidified gas turbine alloys
[PNR-90264] 23 p3917 N85-34279
Towards the year 2000: Developments in inspection and product assurance to be anticipated during the next 15 years — aircraft engines
[PNR-90258] 23 p3940 N85-34421
Cost effective single crystals: The Rolls Royce approach — gas turbine components
[PNR-90262] 23 p3965 N85-34717

AIRCRAFT EQUIPMENT
NT AIRCRAFT HYDRAULIC SYSTEMS
NT AIRCRAFT LIGHTS
NT AIRCRAFT TIRES
NT BOMBING EQUIPMENT
NT EJECTION SEATS
Moving object detection system using infrared scanning
[AD-D011222] 01 p0120 N85-10822
Flares and photoflash items
[AD-A145442] 02 p0187 N85-11253
Electronics/avionics depots in the United States Air Force Warner Robins Air Logistics Center
[AD-P004000] 03 p0307 N85-11981
Wear and corrosion of components under stress and subjected to motion
[AD-A145781] 03 p0372 N85-12372
The effect of aircraft generated electromagnetic interference (EMI) on future avionics systems: A compendium
[AD-A148380] 06 p0799 N85-15101
Voice command weapons launching system
[AD-D011378] 07 p0937 N85-15940
cost and benefits optimization model for fault-tolerant aircraft electronic systems
[NASA-CR-166043] 07 p0946 N85-15993
Military vital sign monitor
[AD-A147257] 07 p1016 N85-16452
Managing recoverable aircraft components in the PPB and related processes: Executive summary
[AD-A148808] 07 p1050 N85-16667
Design for Tactical Avionics Maintainability
[AGARD-CP-361] 08 p1063 N85-16731
Objectives in studying the maintainability of aircraft systems 08 p1063 N85-16732

Joint service design for testability program
08 p1063 N85-16733
Study and realisation of a 3rd level maintenance center based on ATE systems utilization
08 p1063 N85-16735
A practical example of reducing life cycle costs and increased availability 08 p1063 N85-16736
Director on institute's civil aviation projects
08 p1067 N85-16764
Impact tests of automatic lap belt configurations
[AD-A148034] 08 p1081 N85-16844
NASA three-laser airborne differential absorption lidar system electronics
[NASA-CR-174293] 08 p1166 N85-17353
Improvements under way at Gorkiy airport
09 p1278 N85-18040
FRG firms jump into market for auto, aircraft ceramics
09 p1309 N85-18225
The susceptibility of aeronautical navigational aids to interference from adjacent-band broadcast transmissions
[BBC-RD-1984/12] 09 p1311 N85-18234
Laser clock
[AD-D011513] 12 p1855 N85-21634
Advanced life analysis methods. Volume 3: Experimental evaluation of crack growth analysis methods for attachment lugs
[AD-A151058] 14 p2317 N85-24319
US Army Aviation Engineering Flight Activity (USAAEFA) report bibliography update 1983 - 1984
[AD-A151381] 15 p2457 N85-25168
Managing recoverable aircraft components in the PPB (Planning, Programming and Budgeting) and related processes. Technical volume
[AD-A152014] 15 p2457 N85-25169
A description of the process of elaborating man-machine dialog in an aircraft equipped with cathode tubes: Roles and specifications of piloted simulation methods
16 p2698 N85-26658
Terrain following without use of forward looking sensors 16 p2698 N85-26659
Improving inflight negative Gz restraint for aircrewmen
[AD-A151909] 16 p2703 N85-26688
Earth Resources: A continuing bibliography with indexes, issue 45
[NASA-SP-7041(45)] 18 p3123 N85-29336
Aeronautical Engineering: A continuing bibliography with indexes (supplement 188)
[NASA-SP-7037(188)] 19 p3211 N85-29910
Air bag restraint system
[AD-D011671] 19 p3215 N85-29936
Simulation studies of time-control procedures for the advanced air traffic control system
[NASA-TP-2493] 21 p3553 N85-32101
General Aviation Airworthiness Alerts, no. 85
[FAA-AC-43-16] 22 p3729 N85-33117

AIRCRAFT FUEL SYSTEMS
Aircraft wing fuel tank environmental simulator tests for evaluation of antimisting fuels
[FAA-CT-84-15] 07 p0934 N85-15920
Flow measurement device
[AD-D011432] 08 p1168 N85-17369
Study of advanced fuel system concepts for commercial aircraft and engines
[NASA-CR-174752] 10 p1456 N85-19176
Study of advanced fuel system concepts for commercial aircraft
[NASA-CR-174751] 11 p1584 N85-19978
Interactions between F-111 fuselage fuel tank sealants. Part 2: Variation in performance properties of polysulfides after contact with polyester degradation products
[AD-A149777] 12 p1812 N85-21368
Hydrodynamic simulation of transient processes in injection system of aircraft engines during pump unswirling 13 p2050 N85-22629

AIRCRAFT FUELS
Variability of major organic components in aircraft fuels. Volume 1: Technical discussion
[AD-A145574] 02 p0188 N85-11256
Variability of major organic components in aircraft fuels. Volume 2: Illustrations
[AD-A145831] 04 p0481 N85-13067
Distribution and storage of aviation turbine fuel for military operations in northern Australia
[AD-A147180] 07 p0935 N85-15921
Study of advanced fuel system concepts for commercial aircraft
[NASA-CR-174751] 11 p1584 N85-19978
A study of intumescent reaction mechanisms
[AD-A149605] 12 p1812 N85-21365
A standard aircraft diffusion flame: Spectral characteristics and a feasibility study for developing an alternate calibration source for aircraft optical fire detection systems
[AD-A150231] 13 p2039 N85-22768
FAA aviation forecasts: Fiscal years 1985-1996
[AD-A151050] 14 p2216 N85-23747
Applications of high pressure differential scanning calorimetry to aviation fuel thermal stability research
[NASA-TM-87002] 14 p2249 N85-23941
Trends of petroleum fuels
[DE85-000116] 14 p2263 N85-24023
USSR report: Transportation
[JPRS-UTR-84-017] 15 p2461 N85-25196
Chronic fuel shortages in Volga civil aviation administration 15 p2461 N85-25198
Ilyushin bureau designer on fuel conservation research
15 p2467 N85-25231
Aviation turbine fuels from tar sands bitumen and heavy oils. Part 1: Process analysis
[AD-A151319] 15 p2521 N85-25539
Realisation of relaxed static stability on a commercial transport 16 p2713 N85-26746
Jet fuel property changes and their effect on producibility and cost in the U.S., Canada, and Europe
[NASA-CR-174840] 16 p2757 N85-27012
Fuel freeze point investigations
[AD-A152601] 17 p2937 N85-28129
Heat management system for aircraft
[AD-D011658] 18 p3061 N85-28936
Detailed studies of aviation fuel flowability
[NASA-CR-174936] 20 p3435 N85-31308
A comparison of two bench scale tests of fuel low temperature flow properties
[AD-A154477] 20 p3435 N85-31311
Observations of the use of the setapoint detector
[AD-A154533] 21 p3571 N85-32206
Comparative analysis of operational forecasts versus actual weather conditions in airline flight planning, volume 1
[NASA-CR-167862] 24 p4119 N85-35534
Comparative analysis of operational forecasts versus actual weather conditions in airline flight planning, volume 4
[NASA-CR-167865] 24 p4120 N85-35537
Comparative analysis of operational forecasts versus actual weather conditions in airline flight planning: Summary report
[NASA-CR-167866] 24 p4120 N85-35538

AIRCRAFT GUIDANCE
Guidance and navigation programs and plans
06 p0751 N85-14809
Helicopter Guidance and Control Systems for Battlefield Support
[AGARD-CP-359] 08 p1072 N85-16797
Implications of guidance and control technology on human factors considerations 10 p1532 N85-19656
Algorithms for automatic four-dimensional aircraft guidance, considering the momentary wind situation
[DFVLR-FB-84-40] 12 p1775 N85-21146
Optimal symmetric flight studies
[NASA-CR-172508] 12 p1780 N85-21176
A flight management algorithm and guidance for fuel-conservative descents in a time-based metered air traffic environment: Development and flight test results
13 p1967 N85-22356
Reference systems for the evaluation of dead-reckoning navigation equipment 13 p1967 N85-22358
Cost Effective and Affordable Guidance and Control Systems
[AGARD-CP-360] 16 p2695 N85-26638
Investigation of imaging and flight guidance concepts for rotorcraft zero visibility approach and landing
[NASA-CR-166571] 17 p2894 N85-27843
Simulation studies of time-control procedures for the advanced air traffic control system
[NASA-TP-2493] 21 p3553 N85-32101

AIRCRAFT HAZARDS
The microburst as a hazard to aviation: Structure, mechanisms, and nowcasting 01 p0074 N85-10491
Automated aircraft icing forecast technique
[AD-A144853] 01 p0085 N85-10571
A bird strike handbook for base-level managers
[AD-A147928] 07 p0948 N85-16006
A study of the effects of triggered lightning
[AD-A148296] 08 p1189 N85-17494
Don't fowl out
[AD-P004179] 11 p1578 N85-19941
Accidents and serious incidents to civil aircraft due to birstrikes
[AD-P004180] 11 p1578 N85-19942
Analysis of bird strikes reported by European airlines, 1976 - 1980
[AD-P004181] 11 p1578 N85-19943
1983 Air Force bird strikes
[AD-P004182] 11 p1579 N85-19944
Birds and aircraft engine strike rates
[AD-P004184] 11 p1579 N85-19946
Review of engine ingestions to wide body transport aircraft
[AD-P004185] 11 p1579 N85-19947
Reducing gull use of some attractions near airports
[AD-P004195] 11 p1581 N85-19962
Evaluation of effectiveness of bird scaring operations at a sanitary landfill site near CFB Trenton, Ontario, Canada
[AD-P004201] 11 p1582 N85-19968
Development of bird hazard reduction for airport operational safety
[AD-P004202] 11 p1582 N85-19969
The bird strike situation and its ecological background in the Copenhagen Airport, Kastrup
[AD-P004203] 11 p1582 N85-19970
Bird control program Orlando International Airport
[AD-P004204] 11 p1583 N85-19971
Staff assistance to bases for bird hazards
[AD-P004205] 11 p1583 N85-19972
Bird strike avoidance system for Dover AFB, Delaware
[AD-P004206] 11 p1583 N85-19973
The potential of the NEXRAD radar system for warning of bird hazards
[AD-P004210] 11 p1583 N85-19977
Annual review of aircraft accident data: US air carrier operations calendar year 1981
[NTSB/ARC-85/01] 12 p1774 N85-21134
Direct-strike lightning photographs, swept-flash attachment patterns, and flight conditions for storm hazards 1982
[NASA-TM-86347] 12 p1892 N85-21877
Wind shear detection technology
[GPO-38-920] 12 p1893 N85-21879
Aircraft skin penetrator and agent applicator. Volume 1: Working model development and construction
[AD-A150498] 13 p1970 N85-22374
Thermal response of aircraft cabin ceiling materials during a post-crash, external fuel-spill, fire scenario
[PB85-145647] 14 p2220 N85-23764
USSR report: Transportation
[JPRS-UTR-84-017] 15 p2461 N85-25196
Effects of lightning on aircraft studied at Sheremetyevo 15 p2461 N85-25199
Safety recommendation(s), A-84-96
[REPT-3983A/217] 15 p2466 N85-25223
Safety recommendation(s), A-84-76 through -78
[REPT-3751E] 15 p2466 N85-25224
The impact of weather on aviation safety
[GPO-35-520] 16 p2703 N85-26685
Lightning strikes on aircraft. The TRIP 82 experiment and 3-dimensional electromagnetic interferometry
[ONERA-RF-88/7154-PY] 16 p2703 N85-26690
Status of air traffic control system
[S-HRG-98-1197] 20 p3391 N85-31036
On the state of knowledge on meteorologically caused icing of aircraft in clouds
[ESA-TT-861] 20 p3496 N85-31736

AIRCRAFT HYDRAULIC SYSTEMS
Space shuttle rudder/speedbrake actuation subsystem
08 p1102 N85-16965
Life testing of rubber seals — aircraft hydraulic systems
[AD-A143193] 13 p2098 N85-23086

AIRCRAFT INDUSTRY
Development of a production order release methodology
[AD-A145213] 01 p0124 N85-10852
For the sacred air space of our motherland; an interview with our country's famous aircraft designer, Lu Hsiao-Peng
[AD-A146291] 03 p0309 N85-11997
The embedded test (BIT): Impact on the total cost of possession 08 p1063 N85-16734
Innovation in British industry (notably the aircraft industry) and its value: Collected papers
[BAE-KRS-N-GEN-286] 09 p1263 N85-17933
FAA aviation forecasts: Fiscal years 1985-1996
[AD-A151050] 14 p2216 N85-23747
Aviation workers plenum reviews fuel conservation progress 15 p2461 N85-25197
National airspace review. Implementation plan. Revised
[AD-A151412] 15 p2468 N85-25238
Characterization of solderless miniwrapping connections
[CNES-NT-112] 16 p2798 N85-27238
The evolution of the U.S. helicopter industry
[AD-A154290] 19 p3211 N85-29913
Automated fabrication of composite structures for helicopters
[SNIAS-851-210-104] 20 p3393 N85-31049
DOD Value Engineering Conference report. Value Engineering (VE): A tool that benefits line management held at Leesburg, Virginia on 1-2 November 1984. Part 2. Plenary session
[AD-A156068] 24 p4183 N85-35811

AIRCRAFT INSTRUMENTS
NT ALTIMETERS
NT ANEMOMETERS
NT APPROACH INDICATORS
NT ATTITUDE INDICATORS

NT AUTOMATIC PILOTS
NT COMPASSES
NT GYRO HORIZONS
NT GYROCOMPASSES
NT HOT-WIRE ANEMOMETERS
NT MAGNETIC COMPASSES
NT PLAN POSITION INDICATORS
NT POSITION INDICATORS
NT RADIO ALTIMETERS
NT RADIO DIRECTION FINDERS
NT SPACECRAFT POSITION INDICATORS
NT SPEED INDICATORS
NT TACHOMETERS

Realistic localizer courses for aircraft instrument landing simulators
[NASA-CR-172333] 04 p0455 N85-12885

System status display information
[NASA-CR-172347] 04 p0455 N85-12889

Airspeed sensing pressure valve system
[AD-D011472] 10 p1425 N85-18987

Electronic displays: Their strengths and weaknesses for advanced high performance aircraft
10 p1533 N85-19664

Changing system and display concepts and their impact on aircrew performance 10 p1533 N85-19665

Combinatorial performance/cost analysis of an autonomous navigation system for aircraft
16 p2695 N85-26640

Navigation and flight director guidance for the NASA/FAA helicopter MLS curved approach flight test program
[NASA-CR-177350] 16 p2704 N85-26691

Geomagnetic velocimeter
[AD-D011672] 19 p3218 N85-29953

MIZEX, 1984, NASA CV-990 flight report
[NASA-TM-86216] 19 p3299 N85-30451

The development and evaluation of color display systems for airborne applications. Phase 1: Fundamental visual, perceptual, and display system considerations
[FAA/PM-85-19] 22 p3626 N85-33700

Determination of instrument errors by compatibility checking: Results from dynamic flight test data
[ARL/AERO-R-162] 23 p3896 N85-34137

AIRCRAFT LANDING
NT CRASH LANDING
NT DITCHING (LANDING)
NT SKID LANDINGS

Aircraft accident report: Flying Tigers, Inc., Flight 2468, McDonell Douglas DC8-63, N797FT, Chambers Field, Naval Air Station, Norfolk, Virginia, October 25, 1983
[PB84-910406] 02 p0136 N85-10925

Preliminary airworthiness evaluation of the Rutan Aircraft Factory (RAF), Inc. LONG-EZ airplane with external sight
[AD-A145381] 02 p0138 N85-10937

Aircraft accident report, Scandinavian Airlines System, Flight 901, McDonnell Douglas DC-10-30, John F. Kennedy International Airport, Jamaica, New York, February 28, 1984
[PB84-910415] 05 p0594 N85-13788

To take off and to land safely. Hoechst 1678 for ice and snow free runways 05 p0595 N85-13791

An in-flight investigation of a twin fuselage configuration in approach and landing
[NASA-CR-172366] 05 p0596 N85-13801

Alternatives for runway rubber removal from porous friction surfaces
[DOT/FAA/PM-84/28] 05 p0597 N85-13803

Performance measures for aircraft landings as a function of aircraft dynamics 05 p0712 N85-14565

Multi-crew model analytic assessment of landing performance and decision-making demands
05 p0712 N85-14567

Guidance and navigation programs and plans
06 p0751 N85-14809

Critical conditions for the automatic control of landing from decision height in variable winds
[UTIAS-284] 06 p0753 N85-14830

Simulation evaluation of two VTOL control/display systems in IMC approach and shipboard landing
[NASA-TM-85996] 06 p0756 N85-14841

The effect of changes in the angle of incidence in the event of a richochet at a float step
[RAE-TRANS-2120] 07 p0902 N85-15712

Development of a preliminary ALRS stabilized material pavement analysis system (SPAS)
[AD-A147116] 07 p0910 N85-15760

Aircraft barricade
[AD-D011316] 07 p0910 N85-15761

Testing solution for IL-76 braking system problem
08 p1067 N85-16766

Airport activity statistics of certificated route air carriers
[AD-A148472] 08 p1081 N85-16846

Evaluation of arctic test of improved tritium radioluminescent lighting
[AD-A148215] 08 p1089 N85-16884

Why vertical landing — aircraft
[BAE-KRS-N-GEN-301] 09 p1279 N85-18048

In-flight investigation of the effects of time delay in control system on flying qualities in landing approach
[DFVLR-FB-84-35] 11 p1586 N85-19989

New runway enables IL-76 flights to Tenkeli in far north 12 p1769 N85-21108

Runway rubber removal specification development field evaluation procedures development
[FAA-PM-84-27] 12 p1781 N85-21179

Boundary layer transition control for takeoff and landing configurations 14 p2211 N85-23714

Total energy-rate feedback for automatic glide-slope tracking during wind-shear penetration
[NASA-TP-2412] 14 p2226 N85-23801

Trajectory measurements for take-off and landing tests and other short-range applications, volume 16
[AGARD-AG-160-VOL-16] 15 p2561 N85-25801

The use of pressure sensing taps on the aircraft wing as sensor for flight control systems
16 p2698 N85-26660

Study of longitudinal landing flying qualities evaluation using pilot model theory
[AD-A152194] 16 p2706 N85-26702

A system for take-off and landing measurements (STALINS)
[B8580072] 17 p2895 N85-27849

Addition of flexible body option to the TOLA computer program, part 1
[NASA-CR-132732-1] 17 p2896 N85-27855

Addition of flexible body option to the TOLA computer program. Part 2: User and programmer documentation
[NASA-CR-132732-2] 17 p2896 N85-27856

In-flight investigation of the influence of pitch damping and pitch control effectiveness on landing approach flying qualities of statically unstable transport aircraft
[DFVLR-FB-84-12] 17 p2900 N85-27880

Visual and part-task manipulations for teaching simulated carrier landings
[AD-A153622] 18 p3154 N85-29529

Application of frequency domain handling qualities criteria to the longitudinal landing task
[NASA-TM-86728] 22 p3730 N85-33124

The integrated manual and automatic control of complex flight systems
[NASA-CR-176166] 24 p4066 N85-35201

AIRCRAFT LIGHTS

Flares and photoflash items
[AD-A145442] 02 p0187 N85-11253

AIRCRAFT MAINTENANCE

Aircraft cabin pressurization control system tester
[AD-D011225] 01 p0013 N85-10081

Expert systems in maintenance diagnostics for self-repair of digital flight control systems
[AD-P003933] 02 p0247 N85-11613

DoD Robotics Application Workshop Proceedings
[AD-A145867] 03 p0307 N85-11978

Air force engine repair - Oklahoma City Air Logistics Center, Propulsion Division
[AD-P003999] 03 p0307 N85-11980

Electronics/avionics depots in the United States Air Force Warner Robins Air Logistics Center
[AD-P004000] 03 p0307 N85-11981

Air force landing gear repair - Ogden Air Logistics Center Industrial Products and Landing Gear Division
[AD-P004001] 03 p0307 N85-11982

Jet engine blade repair at the Oklahoma Air Logistics Center, Propulsion Division
[AD-P004003] 03 p0307 N85-11983

Air Force honeycomb shaping at SM-ALC (Sacramento Air Logistics Center)
[AD-P004005] 03 p0308 N85-11985

Laser paint removal
[AD-P004009] 03 p0308 N85-11989

Future robotics program at San Antonio ALC (Air Logistics Center)
[AD-P004011] 03 p0309 N85-11991

Robotics in nondestructive inspection at Sacramento Air Logistics Center
[AD-P004012] 03 p0309 N85-11992

USSR report: Transportation
[JPRS-UTR-84-028] 03 p0310 N85-12002

Editorial urges improved aviation repair work quality
03 p0310 N85-12004

Maintenance Management Information and Control System (MMICS): Administrative boon or burden
[AD-A145782] 03 p0438 N85-12790

DYNA-SIM: A nonstationary queuing simulation with application to the automated test equipment problem
[AD-A146984] 06 p0667 N85-15450

An update of the functional requirements of the Naval Aviation Logistics Command Management Information System (NALCOMIS)
[AD-A146565] 06 p0671 N85-15532

Performance evaluation of A-10 aircraft maintenance units and aircraft using constrained facet analysis
[AD-A146955] 07 p0893 N85-15660

Parametric estimates of propulsion system maintenance manhours
[AD-A147120] 07 p0894 N85-15662

A Q-GERT network simulation model for examining pipeline time in the Navy's J-52 intermediate level jet engine repair cycle
[AD-A147269] 07 p0894 N85-15663

Operational Loads Data
[AGARD-CP-375] 07 p0894 N85-15664

F-16 force management, yesterday, today and tomorrow 07 p0895 N85-15674

Managing recoverable aircraft components in the PPB and related processes: Executive summary
[AD-A146806] 07 p1050 N85-16667

Design for Tactical Avionics Maintainability
[AGARD-CP-361] 08 p1063 N85-16731

Objectives in studying the maintainability of aircraft systems 08 p1063 N85-16732

Joint service design for testability program
08 p1063 N85-16733

Study and realisation of a 3rd level maintenance center based on ATE systems utilization
08 p1063 N85-16735

A practical example of reducing life cycle costs and increased availability 08 p1063 N85-16736

Avionics fault tree analysis and artifical intelligence for future aircraft maintenance 08 p1066 N85-16755

International projects, other work of Aeroproyekt Institute 08 p1068 N85-16767

Composite structure repair, addendum
[AGARD-R-716-ADD] 08 p1120 N85-17057

Composite repair of aircraft structures
08 p1120 N85-17059

Mobile accelerator neutron radiography system
[AD-A148808] 09 p1323 N85-18311

National airspace system: Operational requirements
[AD-A149349] 10 p1422 N85-18973

Transportation
[JPRS-UTR-85-004] 12 p1769 N85-21105

Aviation repair plant directors on quality control measures 12 p1769 N85-21106

Proceedings of the 6th Human Factors Workshop on Aviation
[AD-A150043] 12 p1909 N85-21982

Aviation maintenance computerized management information systems: Perspective for the future
[AD-A150637] 13 p1966 N85-22349

Ministry officials on improving aircraft technical servicing 14 p2208 N85-23697

Development of a field repair technique for mini-sandwich Kevlar/epoxy aircraft skin
[AD-A151369] 15 p2503 N85-25439

Graphic simulation of a machine-repairman model
[AD-A151761] 16 p2694 N85-26633

Deployable Core Automated Maintenance System (DCAMS)
[AD-A153695] 18 p3198 N85-29839

Air Force bid sample testing 20 p3437 N85-31323

Corrosion management strategies for aircraft and related systems 22 p3749 N85-33239

Relating corrosion maintenance to environmental factors 22 p3750 N85-33247

Implications of artificial intelligence on the design of future onboard systems
[SFENA-OPS/C/S3/84252A] 23 p3967 N85-34596

AIRCRAFT MANEUVERS

Directional solidification of flake and nodular cast iron during KC-135 low-g maneuvers
02 p0154 N85-11040

Measuring workload differences between short-term memory and long-term memory scenarios in a simulated flight environment 05 p0703 N85-14513

Algorithm for tracking maneuvering object with ambiguous measurements 06 p0791 N85-15057

Evaluation of operational loads to verify structural design 07 p0896 N85-15677

Modeling of aircraft performance from flight test results using quasi steady-state test techniques
09 p1279 N85-18047

Coordinate determination errors in measuring characteristics of radiation field of airborne antennas
13 p2066 N85-22919

Minimum time turns using vectored thrust
[AD-A151693] 15 p2471 N85-25256

High specific power aircraft turn maneuvers: Tradeoff of time-to-turn versus change in specific energy
[AD-A151701] 15 p2471 N85-25257

Application of CFD techniques toward the validation of nonlinear aerodynamic models
[NASA-TM-86715] 16 p2700 N85-26671

Autofocus motion compensation for synthetic aperture radar and its compatibility with strapdown inertial navigation sensors on highly maneuverable aircraft
[AD-A151940] 16 p2704 N85-26693

Piloted simulation of one-on-one helicopter air combat at NOE flight levels
[NASA-TM-86686] 16 p2710 N85-26720

Parameter identification results of tests in nonsteady symmetric flight with the Hawker Hunter Mk 7
[NLR-TR-83042-U] 17 p2897 N85-27860

The STOL and maneuver technology program integrated control system development 17 p2905 N85-27910

System safety study of minimum TCAS 2 for instrument weather conditions
[FAA-PM-85-12] 22 p3728 N85-33113

Development of control laws for a flight test maneuver autopilot for an F-15 aircraft
[NASA-TM-86736] 22 p3730 N85-33122

Control variables in vertical wind determination using simple flight-mechanical equations
24 p4121 N85-35546

AIRCRAFT MODELS

Wind tunnel wall interference correction for aircraft models 03 p0314 N85-12029

On aircraft antennas and basic scattering studies
[AD-A146017] 03 p0355 N85-12282

Differences in health risks by aircraft model among US Navy pilots
[AD-A146147] 03 p0401 N85-12556

Unsteady aerodynamic characterization of a military aircraft in vertical gusts
[NASA-TM-77810] 12 p1770 N85-21110

Structural design of the Sandia 34-M Vertical Axis Wind Turbine
[DE85-002631] 13 p2129 N85-23247

Hover test results of a small-scale twin-tilt nacelle model
[NASA-TM-86665] 14 p2210 N85-23706

Automatic Dynamic Aircraft Modeler (ADAM) for the computer program NASTRAN 15 p2574 N85-25875

Wing buffeting active control testing on a transport aircraft configuration in a large sonic tunnel
16 p2714 N85-26750

Parameter identification results of tests in nonsteady symmetric flight with the Hawker Hunter Mk 7
[NLR-TR-83042-U] 17 p2897 N85-27860

Pressure distribution data from tests of 2.29 M (7.5 feet) span EET high-lift transport aircraft model in the Ames 12-foot pressure tunnel
[NASA-TM-84517] 19 p3211 N85-29912

Flight-mechanics test with a restricted flying aircraft model in a wind tunnel
[ESA-TT-885] 20 p3394 N85-31053

Design and implementation of input signals for identification of pilot/aircraft model
[ESA-TT-880] 20 p3394 N85-31055

Development and validation of a general purpose linearization program for rigid aircraft models
[NASA-TM-86737] 21 p3556 N85-32122

AIRCRAFT NOISE
NT JET AIRCRAFT NOISE
NT SONIC BOOMS

Jet noise suppression by porous plug nozzles
[NASA-CR-3613] 02 p0275 N85-11790

Airport noise impact prediction and measurement
03 p0387 N85-12476

Prediction and modeling of helicopter noise
[AD-A145764] 03 p0415 N85-12656

Detection, classification, and extraction of helicopter-radiated noise
[AD-A145993] 03 p0416 N85-12661

Rotary-wing aircraft noise measurements: Analysis of variations and proposed measurement standard
[AD-A146207] 03 p0416 N85-12662

Static jet noise test results of four 0.35 scale-model QCGAT mixer nozzles
[NASA-TM-86671] 04 p0556 N85-13551

Evaluation of the Langley 4- by 7-meter tunnel for propeller noise measurements
[NASA-TM-85721] 04 p0558 N85-13553

NOISEMAP 4.4 computer program update, operator's manual, addendum 1
[AD-A147091] 07 p1025 N85-16503

Helicopter noise survey performed at Las Vegas, Nevada, 19-21 January, 1984
[AD-A147392] 07 p1039 N85-16593

Noise measurement flight test: Data-analyses aerospatiale AS-355F TwinStar helicopter
[AD-A147497] 07 p1039 N85-16595

Helicopter model rotor-blade vortex interaction impulsive noise: Scalability and parametric variations
[NASA-TM-86007] 08 p1077 N85-16826

An improved source model for aircraft interior noise studies
[NASA-CR-172517] 08 p1217 N85-17668

Test of dispersal of turbojet aircraft departure tracks at washington National Airport (1983-84), volume 1 report
[AD-A148111] 08 p1218 N85-17669

Noise measurement flight test for Boeing Vertol 234/CH 47-d helicopter: Data/analyses
[AD-A148172] 08 p1218 N85-17670

Noise measurement flight test: Data-analyses Aerospatiale AS 350D AStar helicopter
[AD-A148496] 08 p1218 N85-17672

Noise measurement flight test: Data-analyses, Sikorsky S-76A helicopter
[AD-A148525] 08 p1218 N85-17673

Aeroacoustics at the DFVLR Brunswick Research Center: A survey on recent and current activities
[DFVLR-MITT-84-14] 08 p1219 N85-17677

Aircraft noise effects: An interdisciplinary study of the effects of aircraft noise on man. Part 1: Basic report
[NASA-TM-75819] 10 p1526 N85-19629

Aircraft noise effects: An interdisciplinary study of the effect of aircraft noise on man. Part 2: Appendix
[NASA-TM-75818] 10 p1527 N85-19630

Aircraft noise effects: An inter-disciplinary study of the effect of aircraft noise on man. Part 3: Supplementary analyses of the social-scientific portion of the study on aircraft noise conducted by the DFG
[NASA-TM-75802] 10 p1527 N85-19631

Fluctuating pressures on fan blades of a turbofan engine, flight test investigation
[NASA-TP-2381] 10 p1553 N85-19790

A community survey of helicopter noise annoyance conducted under controlled noise exposure conditions
[NASA-TM-86400] 13 p2154 N85-23374

Research on the effect of noise at different times of day: Models, methods and findings
[NASA-CR-3888] 13 p2154 N85-23375

An experimental investigation of the chopping of helicopter main rotor tip vortices by the tail rotor
[NASA-CR-177338] 13 p2154 N85-23376

Wind tunnel acoustic study of a propeller installed behind an airplane empennage: Data report
[NASA-CR-177335] 13 p2154 N85-23377

Noise measurement flight test: Data/Analyses, hughes 500 D/E helicopter
[AD-A148110] 14 p2219 N85-23758

Disturbance to the population due to flight operations at landing fields. Questionnaire on community reaction to non-commercial and sporting aviation
[NASA-TM-76531] 14 p2353 N85-24537

Interaction of a turbulent vortex with a lifting surface
15 p2464 N85-25214

Fundamental studies of structure borne noise for advanced turboprop applications
[NASA-CR-175737] 15 p2646 N85-26320

Prediction of free-field noise levels from aircraft flyover measurements
[VTH-LR-427] 16 p2861 N85-27647

Effects of propeller rotation direction on airplane interior noise levels
[NASA-TP-2444] 19 p3350 N85-30767

Aircraft cabin noise prediction and optimization
[NASA-CR-175982] 19 p3350 N85-30768

Data on noise environments at different times of day around airports
[NASA-CR-172612] 19 p3351 N85-30769

Design of sidewall treatment of cabin noise control of a twin engine turboprop aircraft
[NASA-CR-172245] 19 p3351 N85-30771

Aviation noise effects
[AD-A154319] 19 p3352 N85-30776

Impulsive noise due to transonic blade-vortex interactions 20 p3523 N85-31913

FAA/GAMA (Federal Aviation Administration/General Aviation Manufacturer's Association) propeller aircraft noise test program, Salina Municipal Airport, Salina, Kansas
[AD-A154818] 21 p3699 N85-32983

Overground Excess Sound Attenuation (ESA). Volume 3: Application of ESA data in NOISEFILE
[AD-A154820] 21 p3699 N85-32984

Helicopter noise survey for selected cities in the contiguous US
[AD-A154893] 21 p3699 N85-32985

Lateral attenuation of aircraft flight noise
[AD-A154958] 21 p3700 N85-32986

A theoretical appraisal of the use of ground-plane microphones for aircraft noise measurements
[NPL-AC-103] 22 p3838 N85-33752

Langley aeronautics and space test highlights, 1984
[NASA-TM-87585] 23 p4057 N85-35151

AIRCRAFT NOISE PREDICTION
U NOISE PREDICTION (AIRCRAFT)

AIRCRAFT PARTS

Determination of parameters of cupped aircraft landing ski 06 p0775 N85-14956

US Army helicopter operational flight loads
07 p0895 N85-15675

Helicopter data acquisition in WHL
07 p0896 N85-15676

All-composite Airbus empennage
07 p0936 N85-15931

Managing recoverable aircraft components in the PPB and related processes: Executive summary
[AD-A146806] 07 p1050 N85-16667

The Air Force can improve its forecasts of aircraft spare parts requirements
[AD-A147911] 07 p1053 N85-16682

Estimating wartime support resource requirements. Statistical and related policy issues
[AD-A147923] 07 p1053 N85-16685

Alternative shock characterizations for consistent shock test specifications 09 p1335 N85-18396

Flexible manufacturing system for the production of aircraft parts
[PNR-90237] 14 p2207 N85-23687

Fiber optics applications for MIL-STD-1760
[AD-A151113] 15 p2470 N85-25251

AIRCRAFT PERFORMANCE
NT HELICOPTER PERFORMANCE

Performance capabilities of the C-5 and C-17 cargo aircraft
[AD-A145518] 02 p0138 N85-10939

Airborne performance measurement system design: C-5 aircraft
[AD-A145436] 02 p0236 N85-11539

Speed benefits of tilt-rotor designs for LHX
[NASA-CR-166437] 07 p0902 N85-15717

Missions and vehicle concepts for modern, propelled, lighter-than-air vehicles
[NASA-TM-86672] 08 p1066 N85-16757

Modeling of aircraft performance from flight test results using quasi steady-state test techniques
09 p1279 N85-18047

The design of sport and touring aircraft
[NASA-TM-77783] 10 p1423 N85-18975

Preliminary performance of a vertical-attitude takeoff and landing, supersonic cruise aircraft concept having thrust vectoring integrated into the flight control system
[NASA-CR-172530] 10 p1423 N85-18977

Details of export A-5 close-support aircraft given
10 p1424 N85-18983

Acta Aeronautica et Astronautic Sinica (selected articles)
[AD-A148830] 11 p1575 N85-19922

AIRLAB: A laboratory for flight-crucial-electronics system research 13 p1968 N85-22362

Boundary layer control by transition fixing — conference
[DFVLR-MITT-84-17] 14 p2211 N85-23712

Problems of the application of wind tunnel results to aerodynamic performance of large aircraft
14 p2211 N85-23713

The design of high-performance gliders
[NASA-TM-77772] 14 p2217 N85-23750

Simulation of aircraft behaviour on and close to the ground
[NASA-TM-87460] 14 p2218 N85-23754

Glider Nimbus 3-24.5. Partial certification test results for importation in the U category
[REPT-CEV/IS/SE/AV/84] 14 p2220 N85-23763

Structures and Dynamics Division research and technology plans for FY 1985 and accomplishments for FY 1984
[NASA-TM-86417] 15 p2577 N85-25895

Parameter identification results of tests in nonsteady symmetric flight with the Hawker Hunter Mk 7
[NLR-TR-83042-U] 17 p2897 N85-27860

Demonstration of relaxed static stability on a commercial transport 17 p2903 N85-27898

Realisation of relaxed static stability on a commercial transport 17 p2903 N85-27899

Mission analysis of solar powered aircraft
[NASA-CR-172583] 20 p3597 N85-31072

Qualification needs for advanced integrated aircraft
[NASA-TM-86731] 22 p3726 N85-33119

Comparative analysis of operational forecasts versus actual weather conditions in airline flight planning, volume 1
[NASA-CR-167662] 24 p4119 N85-35534

AIRCRAFT PILOTS

Effects of foveal information processing
01 p0009 N85-10052

The Reports of Aeromedical Laboratory, volume 25, no. 1/2
[ISSN-0023-2858] 01 p0090 N85-10605

Psychological states (mood, affect or emotion) experienced by JASDF pilots through flying duties. 3: Flying conditions causing pilots psychological disturbances 01 p0090 N85-10606
The relationship between emotional tension scale and psychological uneasiness of JASDF pilots in flying situations 01 p0090 N85-10608
Assessment of the inflating characteristics of the modified anti-G suit 01 p0090 N85-10609
Air-to-air visual acquisition performance with TCAS 2
[FAA-PM-84-17] 02 p0236 N85-11537
What pilots like (and don't like) about the new cockpit technology 05 p0710 N85-14554
Management training for cockpit crews at Piedmont flight 09 p1276 N85-18013
Video concepts in CRM training
09 p1276 N85-18015
Be healthy, pilot 10 p1526 N85-19626
Grasp of information by the pilot in future combat aircraft 10 p1533 N85-19662
Traffic alert and collision avoidance system: Operational simulation
[FAA-PM-85-10] 19 p3216 N85-29941
Psychophysiological nature of aircraft feel
19 p3323 N85-30587
A systematic determination of skill and simulator requirements for airline transport pilot certification
[AD-A154135] 19 p3330 N85-30630
Learning and self adaptation applied to the simulation of a human pilot
[ONERA-RT-24/5122-SY] 20 p3511 N85-31826
AIRCRAFT POWER SOURCES
U AIRCRAFT ENGINES
AIRCRAFT POWER SUPPLIES
Advanced secondary power system for transport aircraft
[NASA-TP-2463] 18 p3062 N85-28944
AIRCRAFT PRODUCTION
Flexible manufacturing system for the production of aircraft parts
[PNR-90237] 14 p2207 N85-23687
AIRCRAFT PRODUCTION COSTS
MBB automates aircraft production in many FRG facilities 14 p2289 N85-24186
FRG journal analyzes state, prospects of airbus programs: General analysis 15 p2535 N85-25638
AIRCRAFT RELIABILITY
Airworthiness and flight characteristics test of the JOH-6A light combat helicopter configured with a wire strike protection system
[AD-A144880] 01 p0006 N85-10038
Airworthiness and Flight Characteristics (A and FC) test of the EH - 1X/EH - 1H helicopter configurations
[AD-A144881] 01 p0007 N85-10039
Preliminary airworthiness evaluation of the Rutan Aircraft Factory (RAF), Inc. LONG-EZ airplane with external sight
[AD-A145381] 02 p0138 N85-10937
The DG400 propulsed glider
[CEV/IS/SE/AV/84] 05 p0595 N85-13795
Nondestructive inspection: Improved capabilities of technicians
[AD-A147388] 07 p0975 N85-16196
Airworthiness and flight characteristics test of the RC-12D Guardrail V
[AD-A148046] 08 p1084 N85-16864
Preliminary airworthiness evaluation AH-1S (MC) helicopter with external fuel tanks installed
[AD-A148091] 08 p1084 N85-16865
Standardization of helicopter certification requirements in the western world
[SNIAS-851-210-103] 20 p3393 N85-31048
AIRCRAFT SAFETY
Study of effects of lightning on aircraft systems stressed 03 p0310 N85-12005
Flight phase status monitor study. Phase 1: Systems concepts
[DOT/FAA/PM-84/18] 03 p0317 N85-12048
Crew communication as a factor in aviation accidents
05 p0710 N85-14555
A bird strike handbook for base-level managers
[AD-A147928] 07 p0948 N85-16006
Safety awareness, pilot education, and incident reporting programs 09 p1276 N85-18020
Why vertical landing — aircraft
[BAE-KRS-N-GEN-301] 09 p1279 N85-18048
Bird Strike Committee Europe
[AD-P004207] 11 p1583 N85-19974
The FAA grant-in-aid assurances: FAR part 139, and airport hazards
[AD-P004209] 11 p1583 N85-19976
Pathophysiological study of poisoning due to thermal degradation of materials — aircraft cabins
[CERMA-84-15] 11 p1692 N85-20640
Legislation to improve airline safety
[GPO-38-222] 12 p1773 N85-21132
Annual review of aircraft accident data: US air carrier operations calendar year 1981
[NTSB/ARC-85/01] 12 p1774 N85-21134
A safety evaluation of the relocation of the ACM (Air Combat Maneuver) panel in the F-14 ( )/AIP (Avionics Integration Program)
[AD-A149596] 12 p1777 N85-21158
Wind shear detection technology
[GPO-38-920] 12 p1893 N85-21879
FTASUM: Aviation forecast summaries
[PB85-112977] 12 p1897 N85-21908
Safety recommendation(s), A-84-65
[REPT-3906] 14 p2216 N85-23743
Safety recommendation(s), A-84-103
[REPT-3909B/101B] 14 p2216 N85-23745
Safety recommendation(s), A-84-93 through -95
[REPT-3983/33] 14 p2216 N85-23746
Safety recommendation(s), A-84-82 through -84
[REPT-3957] 14 p2217 N85-23748
Preliminary design of a limb restraint evaluator
[AD-A151749] 15 p2466 N85-25226
Aircraft safety improvement 15 p2688 N85-26602
Generalized escape system simulation: Its purpose, recent modifications and potential
[DE85-005571] 16 p2703 N85-26689
Flying in spite of the weather
[NLR-MP-84021-U] 17 p2895 N85-27847
Traffic alert and collision avoidance system: Operational simulation
[FAA-PM-85-10] 19 p3216 N85-29941
Thirty years' activities for aircraft safety
20 p3391 N85-31033
The 121.5 MHz ELT: Past, present and future — Emergency Locator Transmitter (ELT)
20 p3401 N85-31105
The role of aircraft panel materials in cabin fires and their properties
[FAA-CT-84-30] 21 p3553 N85-32104
General Aviation Airworthiness Alerts, no. 85
[FAA-AC-43-16] 22 p3729 N85-33117
Aviation safety (aircraft passenger survivability and cabin safety)
[GPO-39-847] 23 p3895 N85-34130
Investigation of experimental lightweight firewall materials for A/C engine bay applications
[AD-A155765] 24 p4062 N85-35175
AIRCRAFT SPECIFICATIONS
Details of export A-5 close-support aircraft given
10 p1424 N85-18983
An overview of the MIL-HDBK-5 program
[AD-A147786] 14 p2254 N85-23970
US Army Aviation Engineering Flight Activity (USAAEFA) report bibliography update 1983 - 1984
[AD-A151381] 15 p2457 N85-25168
NASA/aircraft industry standard specification for graphite fiber toughened thermoset resin composite material
[NASA-RP-1142] 16 p2742 N85-26923
AIRCRAFT SPIN
Determination of corrections to flow direction measurements obtained with a wing-tip mounted sensor
[NASA-CR-174412] 10 p1421 N85-18962
Extended moment arm anti-spin device
[NASA-CASE-LAR-12979-1] 12 p1776 N85-21147
Flight investigation of stall, spin and recovery characteristics of a low-wing, single-engine, T-tail light airplane
[NASA-TP-2427] 15 p2470 N85-25248
Dual towline spin-recovery device
[NASA-CASE-LAR-13076-1] 24 p4086 N85-35200
AIRCRAFT STABILITY
Preliminary airworthiness evaluation of the Rutan Aircraft Factory (RAF), Inc. LONG-EZ airplane with external sight
[AD-A145381] 02 p0138 N85-10937
Preliminary performance of a vertical-attitude takeoff and landing, supersonic cruise aircraft concept having thrust vectoring integrated into the flight control system
[NASA-CR-172530] 10 p1423 N85-18977
Acta Aeronautica et Astronautic Sinica (selected articles)
[AD-A148830] 11 p1575 N85-19922
A Lagrange-D'Alembert formulation of the equations of motion of a helicopter carrying an externally suspended load
[NASA-TM-85864] 12 p1776 N85-21149
Aeronautical Engineering: A continuing bibliography with indexes, supplement 185
[NASA-SP-7037(185)] 13 p1965 N85-22342
Relative control effectiveness technique with application to airplane control coordination
[NASA-TP-2416] 14 p2218 N85-23753
A perspective on superaugmented flight control advantages and problems 17 p2901 N85-27886
Demonstration of relaxed static stability on a commercial transport 17 p2903 N85-27898
Realisation of relaxed static stability on a commercial transport 17 p2903 N85-27899
Experimental and theoretical determination of the wing-induced lateral wind on the tail surfaces in oscillating rolling motion. Part 1: Application of the Mobile Oscillating Derivatives (MOD) on an experimental part
[IFD-1/84-PT-1] 18 p3061 N85-28939
Experimental and theoretical determination of the wing-induced lateral wind on the tail surfaces in oscillating rolling motion. Part 2: Theoretical investigations for calculation of the lateral wind
[IFD-1/84-PT-2] 18 p3061 N85-28940
Contributions on the subject of longitudinal movements of aircraft in wind shears
[NASA-TM-77837] 18 p3139 N85-29432
AIRCRAFT STRUCTURES
NT AFTERBODIES
NT AIRFRAMES
NT FOREBODIES
NT FUSELAGES
NT NOSES (FOREBODIES)
Method for measuring haze in transparencies
[AD-D011233] 01 p0120 N85-10823
Quasi-steady analysis of aircraft panel flammability
[AD-A145461] 02 p0136 N85-10938
Advanced manufacturing development of a composite empennage component for L-1011 aircraft
[NASA-CR-165885] 02 p0170 N85-11141
Development of powder metallurgy 2XXX series Al alloys for high temperature aircraft structural applications
[NASA-CR-172408] 02 p0182 N85-11220
Measurement of the inertial constants of a rigid or flexible structure of arbitrary share through a vibration test
[NASA-TM-77557] 02 p0209 N85-11381
Air Force honeycomb shaping at SM-ALC (Sacramento Air Logistics Center)
[AD-P004005] 03 p0308 N85-11985
Crack resistance of pressed and rolled semifinished goods of aluminum alloys used in load-bearing aircraft wing structures 03 p0348 N85-12245
Low power laminar aircraft structures
04 p0451 N85-12857
Graphics software for the display of body deformation motion
[FW-FO-1640] 04 p0455 N85-12888
Composite fracture toughness and impact characterization 04 p0466 N85-12963
Composite structural materials
[NASA-CR-174077] 04 p0467 N85-12966
Defect detection threshold in riveted joints, test report no.44-833/F — in aircraft 04 p0511 N85-13260
Increase in the economy of design and process planning by integrated and graphic data processing, phase 2 — aircraft design
[BMFT-FB-W-84-028] 05 p0716 N85-14589
A study of crashworthiness of light aircraft fuselage structures: A numerical and experimental investigation
[UTIAS-266] 06 p0750 N85-14803
Analytical construction of flight vehicle surfaces
06 p0775 N85-14957
Verification of a computer program for vibration analysis of composite wing cores
[NAL-TR-825] 06 p0817 N85-15187
Operational Loads Data
[AGARD-CP-375] 07 p0894 N85-15664
Operational loads data evaluation for individual aircraft fatigue monitoring 07 p0895 N85-15669
Structural flight load measurement demonstration of structural integrity 07 p0895 N85-15670
Advanced fatigue monitoring on service aircraft
07 p0895 N85-15671
F-16 force management, yesterday, today and tomorrow 07 p0895 N85-15674
US Army helicopter operational flight loads
07 p0895 N85-15675
Evaluation of operational loads to verify structural design 07 p0896 N85-15677
Tornado: Structural Usage Monitoring System (SUMS) 07 p0896 N85-15680
All-composite Airbus empennage
07 p0936 N85-15931
The influence of fastener flexibility on load transfer and fatigue life predictions for multirow bolted and riveted joints — aircraft structures
[LBF-FB-172/84] 07 p0979 N85-16219
Composite structure repair, addendum
[AGARD-R-716-ADD] 08 p1120 N85-17057
Composite repair of aircraft structures
08 p1120 N85-17059
Flexible manufacturing system for the production of aircraft parts
[BLL-PNR-90237-(8019.3153)]
08 p1137 N85-17159
Icing flight research: Aerodynamic effects of ice and ice shape documentation with stereo photography
[NASA-TM-86906] 09 p1279 N85-18049

USSR report: Engineering and equipment
[JPRS-UEQ-85-001] 09 p1305 N85-18200

On solving nonlinear problems of aircraft structural mechanical design 09 p1309 N85-18223

Some fighter aircraft trends
[NASA-TM-86352] 10 p1420 N85-18954

Integrated paratroop door
[AD-D011507] 12 p1776 N85-21148

Fatigue crack propagation in mirage 1110 wing main spar specimens and the effects of spectrum truncation on life
[ARL/STRUC-R-405] 12 p1776 N85-21152

A history of full-scale testing of aircraft structures at the National Aeronautical Establishment
[NAE-AN-24] 12 p1777 N85-21153

Elastomer toughened polyimide adhesives — bonding metal and composite material structures for aircraft and spacecraft
[NASA-CASE-LAR-12775-2] 12 p1809 N85-21349

Finite element analysis of problems associated with life enhancement techniques
[ARL/STRUC-R-404] 12 p1862 N85-21676

Normal mode calculations for fuselage type intricate structures by regarding them as systems with superposed constraints 13 p2048 N85-22817

Operational loads measurement: A philosophy and its implementation — aircraft structures
[AD-A149445] 13 p2144 N85-23306

Durability calculation of wing panel element
14 p2285 N85-24159

Two recent cases of marker load applications on cargo/fighter aircraft fatigue tests
14 p2318 N85-24325

Aircraft structure for application to training aircraft
[CH-635286-A5] 15 p2469 N85-25244

Automatic Dynamic Aircraft Modeler (ADAM) for the computer program NASTRAN 15 p2574 N85-25875

Protective coatings for aircraft structures: A review
[VTH-LR-413] 16 p2706 N85-26704

ESP (External-Stores Program): A pilot computer program for determining flutter-critical external-store configurations. Volume 3, part 1: Program compilation
[AD-A152270] 16 p2711 N85-26727

Investigation of the influence of some paint systems and water displacing corrosion inhibitors on anodic undermining corrosion of aluminum 2024 clad alloy — aircraft structures
[VTH-LR-443] 16 p2756 N85-27009

The application of computer aided structural optimization to the design of aircraft components
[MBB-UT-21/84-O] 16 p2873 N85-27728

New materials and techniques for aircraft structures
[B8580074] 17 p2897 N85-27861

Heat resistant Carbon Fiber Reinforced Plastics (CFRP) hardening equipment
[MBB/LFA33/CFK/PUB/007] 17 p2916 N85-27976

Proceedings of the 9th US Air Force and the Federal Republic of Germany Data Exchange Agreement Meeting. Viscous and Interacting Flow Field Effects
[AD-A153020] 17 p2958 N85-28266

Research on structures and materials — aircraft structures
[B8580080] 17 p2961 N85-28432

Further investigations to improve the fatigue life of the Mirage 1110 wing main span
[ARL/STRUC-TM-397] 18 p3061 N85-28938

MBB expands CADAM system for a 320 program
18 p3087 N85-29099

Structural Analysis
[DFVLR-MITT-84-21] 18 p3120 N85-29313

Research on structural analysis at the DFVLR, Brunswick 18 p3120 N85-29314

Activities of the Department of Aerospace Engineering
18 p3199 N85-29844

Aeronautical Engineering: A continuing bibliography with indexes (supplement 188)
[NASA-SP-7037(188)] 19 p3211 N85-29910

Fuel containment and damage tolerance in large composite primary aircraft structures
[NASA-CR-166083] 19 p3231 N85-30032

Automated fabrication of composite structures for helicopters
[SNIAS-851-210-104] 20 p3393 N85-31049

Elastomers used in aeronautics industry
[SNIAS-851-551-103] 20 p3434 N85-31304

Influence of the molding joint plane on the fatigue resistance of the alloys 7010 and 7050. Test Report No. M1-631600
[PV-M1-631600] 20 p3470 N85-31562

R and D programmes at the National Aeronautical Laboratory
[AR-22] 20 p3539 N85-32022

R and D activities of the Materials Science Division
20 p3539 N85-32024

R and D activities of the Structural Sciences Division
20 p3539 N85-32026

Quest for performance: The evolution of modern aircraft
[NASA-SP-468] 21 p3551 N85-32089

Preliminary sizing and performance of aircraft
[NASA-TM-86357] 21 p3554 N85-32111

Study of an ultrasonic detection method to inspect bonding effects in light alloy bonded structures, test report no. 43-954/F — aircraft structures
[PV-43-954/F] 22 p3795 N85-33510

Flight service evaluation of composite helicopter components
[NASA-CR-172562] 23 p3909 N85-34222

An automated technique for encasing specific payloads with low-drag fairings 24 p4063 N85-35183

Fatigue lives of specimens representing critical locations in Mirage 3 spars under Australian and Swiss test spectra
[ARL-STRUC-R-415] 24 p4064 N85-35187

Analysis of flexible aircraft longitudinal dynamics and handling qualities. Volume 1: Analysis methods
[NASA-CR-177943-VOL-1] 24 p4066 N85-35202

Analysis of flexible aircraft longitudinal dynamics and handling qualities. Volume 2: Data
[NASA-CR-177943-VOL-2] 24 p4067 N85-35203

AIRCRAFT SURVIVABILITY

F-16 force management, yesterday, today and tomorrow 07 p0895 N85-15674

An empirical self-protection chaff model
[AD-A151928] 16 p2773 N85-27115

General Aviation Crashworthiness Project. Phase 2: Impact severity and potential injury prevention in general aviation accidents
[PB85-917002] 19 p3215 N85-29938

AIRCRAFT TIRES

Aircraft chocks
[AD-A145135] 01 p0012 N85-10077

Alternatives for runway rubber removal from porous friction surfaces
[DOT/FAA/PM-84/28] 05 p0597 N85-13803

The space shuttle program from challenge to achievement: Space exploration rolling on tires
06 p1101 N85-16960

Selection of effective arrangement of heavy undercarriage systems for use with concrete runways
14 p2285 N85-24156

A feasibility study for using low boiling point fluids to change aircraft tire deflection
[AD-A152096] 16 p2706 N85-26701

AIRCRAFT WAKES
NT HELICOPTER WAKES
NT PROPELLER SLIPSTREAMS
NT SLIPSTREAMS

Preliminary results using a rapid photographic wake traverse system — in a wind tunnel
[RAE-TM-AERO-1987] 02 p0200 N85-11332

Analysis of noise measured from a propeller in a wake
[NASA-TP-2358] 02 p0274 N85-11788

Recent advances in computational methods to solve the high-lift multi-component airfoil problem
06 p1068 N85-16774

AIRCREWS
U FLIGHT CREWS

AIRFIELD SURFACE MOVEMENTS

New airport ground traffic control system planned
03 p0310 N85-12006

Simulation of aircraft behaviour on and close to the ground
[NASA-TM-87460] 14 p2218 N85-23754

AIRFIELDS
U AIRPORTS

AIRFOIL CHARACTERISTICS
U AIRFOILS

AIRFOIL FENCES

An exploratory study of apex fence flaps on a 74 deg delta wing
[NASA-CR-172463] 15 p2463 N85-25208

AIRFOIL PROFILES
NT WING PROFILES
NT WING SPAN

First cryogenic test of the CAST 7 profile in the T2 wind tunnel. Comparison with calculations — airfoils
[ONERA-RTS-58/1635-AY-035-D]
04 p0577 N85-13682

Effects of aircraft and flight parameters on energy-efficient profile descents in time-based metered traffic
[NASA-CR-172338-ADD] 07 p0901 N85-15706

Detailed study of the flow around a multi-element airfoil. Comparison with calculations 06 p1069 N85-16775

Laminar separation bubble with transition: Prediction test with local interaction — airfoils
[PNR-90231] 09 p1274 N85-18008

Profile design for wings and propellers
[NASA-TM-77785] 10 p1419 N85-18953

Skin friction measurements for 2 relatively thick airfoil sections at high Reynolds number
[AD-A150021] 12 p1772 N85-21125

Investigation of the aerodynamic forces on bluff bodies at high Reynolds numbers
[DFVLR-MITT-84-19] 14 p2213 N85-23727

Airfoil wing with flap
[CH-634787-A5] 15 p2469 N85-25243

Investigation of potential and viscous flow effects contributing to dynamic stall
[AD-A151696] 15 p2557 N85-25773

Design of a basic profile for a low sweep airfoil. Part 2: Experimental investigation on the DFVLR-W1 airfoil profile in the Brunswick transonic wind tunnel
[DFVLR-FB-85-01-PT-2] 17 p2892 N85-27833

Integral profile method for production of carbon fiber sheets
[MBB/LFA34/CFK/PUB/006] 17 p2916 N85-27975

Experimental investigations on airfoils with different geometries in the domain of high angles of attack-flow separation
[NASA-TM-77892] 22 p3726 N85-33110

An investigation into the three-dimensional stall development on a modified NACA 23012 aerofoil
[GU-AERO-8414] 23 p3894 N85-34124

AIRFOIL SECTIONS
U AIRFOIL PROFILES

AIRFOIL THICKNESS
U AIRFOIL PROFILES

AIRFOILS
NT AERIAL RUDDERS
NT AEROELASTIC RESEARCH WINGS
NT AILERONS
NT AIRFOIL FENCES
NT BEARINGLESS ROTORS
NT CAMBERED WINGS
NT CIRCULATION CONTROL AIRFOILS
NT DELTA WINGS
NT ELEVATORS (CONTROL SURFACES)
NT ELEVONS
NT FIXED WINGS
NT FLAPERONS
NT FLAPS (CONTROL SURFACES)
NT FLEXIBLE WINGS
NT HORIZONTAL TAIL SURFACES
NT JET FLAPS
NT LAMINAR FLOW AIRFOILS
NT LEADING EDGE SLATS
NT LIFTING ROTORS
NT LOW ASPECT RATIO WINGS
NT PROPELLER BLADES
NT RECTANGULAR WINGS
NT RIGID ROTORS
NT RIGID WINGS
NT ROTARY WINGS
NT SLENDER WINGS
NT SPOILERS
NT SUPERCRITICAL AIRFOILS
NT SUPERCRITICAL WINGS
NT SUPERSONIC AIRFOILS
NT SWEPT FORWARD WINGS
NT SWEPT WINGS
NT SWEPTBACK WINGS
NT TABS (CONTROL SURFACES)
NT THIN AIRFOILS
NT THIN WINGS
NT TILTING ROTORS
NT TIP DRIVEN ROTORS
NT TRAILING EDGE FLAPS
NT TWISTED WINGS
NT UNSWEPT WINGS
NT VARIABLE SWEEP WINGS
NT VORTEX FLAPS
NT WING FLAPS
NT WINGS

Development and applications of algorithms for calculating the transonic flow about harmonically oscillating wings
[NASA-CR-172376] 01 p0002 N85-10007

Computational methods for complex flowfields
[AD-A145219] 01 p0004 N85-10019

Embedded-grid generation with complete continuity across interfaces for multi-element airfoils
02 p0133 N85-10911

Design and wind tunnel evaluation of a symmetric airfoil series for large wind turbine applications
[NASA-CR-174764] 02 p0135 N85-10919

Turbine heat transfer 02 p0142 N85-10964

Gas side heat transfer: 2-D flow
02 p0142 N85-10965

Jet array impingement flow distributions and heat transfer characteristics: Effects of initial crossflow and nonuniform array geometry 02 p0142 N85-10967

Life prediction and constitutive models for anisotropic materials 02 p0144 N85-10976

AIRFOILS

Interactive aircraft flight control and aeroelastic stabilization
[NASA-CR-174025] 02 p0148 N85-11003

Performance of two transonic airfoil wind tunnels utilizing limited ventilation 03 p0313 N85-12020

Experiments suitable for wind tunnel wall interference assessment/correction 03 p0313 N85-12021

Asymptotic methods for wind tunnel wall corrections at transonic speed 03 p0313 N85-12022

Progress in wind tunnel wall interference assessment/correction procedures at the NAE
03 p0314 N85-12025

Review of the advanced technology airfoil test program in the 0.3-meter transonic cryogenic tunnel
03 p0315 N85-12033

Some experience with Barnwell-Sewall type correction to two-dimensional airfoil data 03 p0315 N85-12034

Interaction between an airfoil and a streamwise vortex
[AD-A145823] 03 p0316 N85-12041

Design of a basic airfoil for a slightly swept wing. Part 1: Theoretical transonic airfoil design
[DFVLR-FB-84-19-PT-1] 03 p0316 N85-12043

An experimental study on the induced normal force on tail-fins due to wing-tail interference
[NAL-TR-814] 03 p0318 N85-12051

Unsteady aerodynamic response of cascades and turborotors 03 p0319 N85-12058

Numerical studies of unsteady transonic flow over an oscillating airfoil
[NASA-TM-86011] 03 p0361 N85-12316

A study of flow past an airfoil with a jet issuing from its lower surface
[NASA-CR-166610] 04 p0451 N85-12860

Natural laminar flow airfoil design considerations for winglets on low-speed airplanes
[NASA-CR-3853] 04 p0452 N85-12863

A comparison of Wortmann airfoil computer-generated lift and drag polars with flight and wind tunnel results
[NASA-TM-86035] 04 p0452 N85-12868

Effect of a variable camber and twist wing at transonic Mach numbers
[NASA-TM-86261] 04 p0452 N85-12869

The role of freestream turbulence scale in subsonic flow separation
[NASA-CR-174172] 04 p0452 N85-12870

Tailored airfoils for vertical axis wind turbines
[DE84-013618] 04 p0529 N85-13380

Simulation of separated transonic airfoil flow by finite-difference viscous-inviscid interaction
05 p0591 N85-13768

Evaluation of the unsteady effects for a class of wind turbines 05 p0592 N85-13772

Experimental studies of transonic airfoil trailing edge and wake flowfield properties 05 p0592 N85-13773

An experimental study of airfoil-spoiler aerodynamics
[NASA-CR-177328] 06 p0748 N85-14796

Comparison of uniform perturbation solutions and numerical solutions for some potential flows past slender bodies
[NASA-CR-172485] 06 p0749 N85-14799

Development of the code NSFOIL for analyzing high Reynolds number transonic flow around an airfoil
[NAL-TR-816] 06 p0749 N85-14801

Laminar separation bubble with transition: Prediction test with local interaction
[BLL-PNR-90231-(8019.3153)]
06 p0808 N85-15132

Unsteady pressure measurements on a biconvex airfoil in a transonic oscillating cascade
[NASA-TM-86914] 07 p0898 N85-15689

Aircraft wing fuel tank environmental simulator tests for evaluation of antimisting fuels
[FAA-CT-84-15] 07 p0934 N85-15920

Some important problems in unsteady boundary layers including separation. 1: Nature of singularity on oscillating airfoils
[AD-A147897] 07 p0960 N85-16087

High temperature thermocouple and heat flux gauge using a unique thin film-hardware hot juncture
[NASA-TM-86898] 07 p0962 N85-16096

Analysis of the surface load and radiated sound of a vibrating airfoil with application to the experiment of Brooks
[NASA-CR-3864] 07 p1038 N85-16590

Recent advances in computational methods to solve the high-lift multi-component airfoil problem
08 p1068 N85-16774

Inviscid compressible flow past a multi-element aerofoil 08 p1069 N85-16776

Turbulent bubbles behind airfoils and wings at high angle of attack 08 p1069 N85-16779

Design studies of thick laminar flow airfoils for low speed flight employing turbulent boundary layer suction over the rear part 08 p1070 N85-16786

Pneumatic turbulators: A device for drag reduction at Reynolds numbers below 5 million
08 p1071 N85-16791

Results of S5 CH tests with an ARL (Aerospace Research Laboratory) cascade
[NASA-TM-77510] 08 p1089 N85-16882

Unsteady aerodynamic loading of an airfoil due to vortices released intermittently from its upper surface
[AD-P004162] 09 p1265 N85-17947

A Navier-Stokes calculation of the airfoil dynamic stall process
[AD-P004163] 09 p1265 N85-17948

Unsteady separated flow: Forced and common vorticity about oscillating airfoils
[AD-P004167] 09 p1265 N85-17952

Leading edge separation criterion for an oscillating airfoil
[AD-P004175] 09 p1267 N85-17960

Corrections for attached sidewall boundary-layer effects in 2-dimensional airfoil testing
[NASA-CR-3873] 09 p1272 N85-17997

Flow instabilities in transonic small disturbance theory
[NASA-TM-86251] 09 p1273 N85-18000

Numerical approach for the aerodynamic analysis if airfoils with laminar separation
[NASA-CR-172496] 09 p1273 N85-18001

Synthesized airfoil data method for prediction of dynamic stall and unsteady airloads
[NASA-CR-3672] 09 p1274 N85-18005

Study of controlled diffusion stator blading
[NASA-CR-167995] 09 p1281 N85-18058

The boundary layer on compressor cascade blades
[NASA-CR-174369] 09 p1319 N85-18282

On the flow processes in sharply inclined and stalled airfoils in parallel movement and rotation
[NASA-TM-77509] 10 p1419 N85-18952

Analysis of inviscid transonic flow around an airfoil by diagonal form of IAF scheme
[NAL-TR-831] 10 p1420 N85-18955

Effects of airfoil shape, thickness, camber, and angle of attack on calculated transonic unsteady airloads
[NASA-TM-86320] 10 p1420 N85-18957

Viscous effects on transonic airfoil stability and response
[NASA-TM-86374] 10 p1421 N85-18961

Wall interference estimation of the NAL's two-dimensional wind tunnel
[NAL-TR-829] 10 p1426 N85-18992

A multistage time-stepping scheme for the Navier-Stokes equations
[NASA-CR-172527] 10 p1483 N85-19365

Post stall airfoil data for wind turbines: Wind tunnel test results
[DE85-004052] 10 p1511 N85-19534

Rocky Flats Wind Energy Research Center FY 1983 report
[DE85-004500] 10 p1511 N85-19535

A fast algorithm of the finite difference method for computation of the transonic flow past an arbitrary airfoil with the conservative full-potential equation
11 p1619 N85-20191

On relaxation of transonic flows around zero-lift airfoils and convergence of self-correcting wing tunnels
11 p1622 N85-20214

Finite difference computation of the flow around airfoils in two-dimensional transonic slotted wall wind tunnel
11 p1623 N85-20216

The Satellite sail 11 p1647 N85-20376

Three-dimensional unsteady lifting surface theory in the subsonic range
[NASA-TM-77812] 12 p1770 N85-21111

A study of transonic flutter of a two-dimensional airfoil using the U-g and p-k methods
[LR-615] 12 p1771 N85-21121

Tailored airfoils for vertical axis wind turbines
[DE85-004628] 12 p1772 N85-21128

Numerical integration of the unsteady full-potential equation with applications to transonic flow about a two-dimensional airfoil
[NLR-MP-84022-U] 12 p1773 N85-21130

Hypersonic flow about triangular airfoil at large angles of attack 13 p2044 N85-22792

T700 cutter life improvement program
[AD-A150450] 13 p2099 N85-23089

Structural design of the Sandia 34-M Vertical Axis Wind Turbine
[DE85-002631] 13 p2129 N85-23247

Oscillating airfoils and their wake
[NASA-TM-77831] 14 p2209 N85-23701

The structure of separated flow regions occurring near the leading edge of airfoils, including transition
[NASA-CR-175670] 14 p2209 N85-23703

Computations of two-dimensional airfoil-vortex interactions — helicopter rotor flowfields
[NASA-CR-3885] 14 p2210 N85-23709

Flutter taming: A new tool for the aeroelastic designer
[AD-A150834] 14 p2226 N85-23802

Transonic Unsteady Aerodynamics and its Aeroelastic Applications
[AGARD-CP-374] 15 p2457 N85-25171

Numerical studies of unsteady transonic flow over oscillating airfoil 15 p2458 N85-25174

Experience with transonic unsteady aerodynamic calculations 15 p2458 N85-25176

Calculation of harmonic aerodynamic forces of aerofoils and wings from the Euler equations
15 p2458 N85-25177

Unsteady transonic aerodynamic and aeroelastic calculations about airfoils and wings
15 p2459 N85-25185

A study of transonic flutter of a two-dimensional airfoil using the U-g and p-k methods
[AD-A151463] 15 p2473 N85-25268

Transient technique for measuring heat transfer coefficients on stator airfoils in a jet engine environment
[NASA-TM-87005] 15 p2560 N85-25794

Investigation to optimize the passive shock wave/boundary layer control for supercritical airfoil drag reduction
[NASA-CR-175788] 16 p2699 N85-26665

Low Reynolds number vehicles
[AGARD-AG-288] 16 p2699 N85-26666

Automatic flight control modes for the AFTI/F-111 mission adaptive wing aircraft 16 p2714 N85-26756

Static and dynamic pressure measurements on a NACA 0012 airfoil in the Ames High Reynolds Number Facility
[NASA-TP-2485] 17 p2891 N85-27823

Users manual for coordinate generation code CRDSRA
[NASA-CR-172584] 17 p2891 N85-27824

User's manual for airfoil flow field computer code SRAIR
[NASA-CR-172585] 17 p2891 N85-27825

Numerical study of porous airfoils in transonic flow
[NASA-TM-86713] 17 p2892 N85-27828

Wing tunnel investigation of dynamic stall of an NACA 0018 airfoil oscillating in pitch
[NAE-AN-27] 17 p2892 N85-27830

Ice shapes and the resulting drag increase for a NACA 0012 airfoil
[NASA-TM-83556] 17 p2894 N85-27839

Proposals for the determination of necessary elevator handling characteristics of sailplanes in high speed range
[DFVLR-FB-84-52] 17 p2900 N85-27882

New facility to study unsteady wake effects on turbine airfoil heat transfer 17 p2911 N85-27948

Constitutive cyclic deformation behavior in single-crystal and directionally solidified SSME high-pressure fuel turbopump airfoil materials 17 p2914 N85-27965

A 5-year research plan, 1985-1990. Wind energy technology: Generating power from the wind
[DE85-008427] 17 p2967 N85-28463

Turbulence structure in the boundary layers of an oscillating airfoil
[AD-A153631] 18 p3059 N85-28926

A study of aerodynamic control in stalled flight leading-edge vortex formation analysis
[AD-A153758] 18 p3059 N85-28928

A study of aerodynamic control in stalled flight long laminar separation bubble analysis
[AD-A153850] 18 p3059 N85-28930

Post-stall wind tunnel data for NACA 44XX series airfoil sections
[DE85-002948] 18 p3060 N85-28931

Inviscid analysis of two supercritical laminar-flow-control airfoils at design and off-design conditions
[NASA-TM-84657] 19 p3212 N85-29920

Application of two-dimensional unsteady aerodynamic to a free-tip rotor response analysis
[NASA-CR-177348] 19 p3215 N85-29933

Aircraft rotor blade with passive tuned tab
[NASA-CASE-ARC-11444-1] 19 p3217 N85-29947

Performance comparison between NACA 23024 and NACA 64(3)-618 airfoil configurated rotors for horizontal-axis wind turbines
[NASA-TM-83471] 19 p3303 N85-30477

Computer programs for smoothing and scaling airfoil coordinates
[NASA-TM-84666] 20 p3386 N85-31011

Interactive aircraft flight control and aeroelastic stabilization
[NASA-CR-176035] 20 p3396 N85-31064

Sidewall boundary-layer effects in two-dimensional airfoil testing
[NASA-CR-176034] 20 p3396 N85-31065

Heat transfer in aeropropulsion systems
[NASA-TM-87066] 20 p3453 N85-31444

An evaluation of four methods of numerical analysis for two-dimensional airfoil flows
[AD-A155202] 21 p3552 N85-32098

Calculation of steady and unsteady airfoil flow fields via the Navier-Stokes equations
[NASA-CR-3899] 22 p3727 N85-33105
Experimental investigations on airfoils with different geometries in the domain of high angles of attack-flow separation
[NASA-TM-77892] 22 p3728 N85-33110
Generation by conformal mappings of aerofoil sections and of certain other simple shapes suitable for both aerodynamic and stress-concentration problems
[AD-A154901] 22 p3728 N85-33112
Local heat-transfer measurements on a large, scale-model turbine blade airfoil using a composite of a heater element and liquid crystals
[NASA-TM-86900] 22 p3782 N85-33435
An evaluation of three helicopter rotor sections
[NASA-TM-86719] 23 p3893 N85-34115
A design procedure to modify the trailing edge upper surface pressure gradient of a given aerofoil
[GU-AERO-8406] 23 p3894 N85-34120
Modelling of unsteady, incompressible separation on an aerofoil using an inviscid flow algorithm
[GU-AERO-8412] 23 p3894 N85-34122
The collected data for ramp function tests on a NACA 23012 aerofoil. Volume 1: Description and pressure data
[GU-AERO-8413-VOL-1] 23 p3894 N85-34123
A comparison of laser Doppler anemometry and probe measurements within the boundary layer of an airfoil at subsonic flow
[ISL-CO-219/84] 23 p3895 N85-34127
A stream function approach to solving the conservative Euler equations for transonic flows
24 p4059 N85-35156
Heat transfer characteristics for two-dimensional arrays of impinging jets with initial crossflow
24 p4092 N85-35365

AIRFRAME MATERIALS
Fuel efficiency through new airframe technology
[NASA-TM-84548] 02 p0133 N85-10909
Full-scale crash-test evaluation of two load-limiting subfloors for general aviation airframes
[NASA-TP-2380] 04 p0512 N85-13267
A comparison of fatigue lives under a complex and a much simplified flight-by-flight testing sequence --- Mirage 3 aircraft
[ARL/STRUC-TM-386] 09 p1280 N85-18052
Fatigue Crack Topography
[AGARD-CP-376] 14 p2318 N85-24321
New materials and techniques for aircraft structures
[B8580074] 17 p2897 N85-27861

AIRFRAMES
The Influence of Large Scale Computing on Aircraft Structural Design
[AGARD-R-706] 01 p0007 N85-10040
Fuel efficiency through new airframe technology
[NASA-TM-84548] 02 p0133 N85-10909
Iterative method of calculating strength of airframe members using finite element method
06 p0775 N85-14955
Analysis of thin-walled airframe members in geometrically nonlinear statement
06 p0780 N85-14985
Some aspects of engine and airframe integration for Ramjet and Ramrocket powered missiles
07 p0918 N85-15812
High-strength composite materials for aircraft, body armor 11 p1599 N85-20057
Aircraft skin penetrator and agent applicator. Volume 2: Test and evaluation
[AD-A151609] 15 p2466 N85-25225
Design, fabrication and test of composite curved frames for helicopter fuselage structure
[NASA-CR-172436] 15 p2470 N85-25247
Tensile and fracture toughness properties of Mirage III spars
[AR-003-019] 15 p2578 N85-25899
Initial quality of advanced joining concepts
[AD-A152241] 16 p2759 N85-27027
USAF damage tolerant design handbook: Guidelines for the analysis and design of damage tolerant aircraft structures, revision B
[AD-A153161] 17 p2896 N85-27858

AIRGLOW
NT GEOCORONAL EMISSIONS
NT NIGHTGLOW
NT TWILIGHT GLOW
Nocturnal increases of ionization in the ionospheric F region in the low latitude of Brazil during magnetic storms
[INPE-3271-PRE/596] 05 p0675 N85-14334
Study of infrared atmospheric emission
[AD-A147517] 07 p0998 N85-16336
Application of Fabry-Perot spectrometers for measurement of upper atmosphere temperatures and winds 08 p1183 N85-17454
Upper atmosphere research at INPE
[INPE-3281-PRE/604] 10 p1515 N85-19557
Analysis and interpretation of observations of airglow at 297 nm in the Venus thermosphere
13 p2172 N85-23473
A measurement of the intensity of the cosmic background radiation at 3.9 cm
13 p2206 N85-23681
Determination of total moisture content in cloud-free atmosphere by relative radio emission measurements
14 p2340 N85-24472
Fabry-Perot interferometer and skymapping photometer determinations of midlatitude f-region neutral winds and temperatures and airglow enhancement/depletions
[AD-A150730] 14 p2373 N85-24666
Observations of airglow O2(1-Sigma) atmospheric band at 8645 A and the rotational temperature at 23 deg S
[INPE-3378-PRE/653] 16 p2626 N85-27435
Thermospheric winds observed by OI6300A Doppler shifts at 23 deg S in the Brazilian sector
[INPE-3384-RPE/470] 16 p2634 N85-27479
SCRIBE data of October 23, 1983 flight
[AD-A154864] 21 p3705 N85-33012
Atmospheric Emission Photometric Imaging (AEPI)
23 p3902 N85-34170

AIRLINE OPERATIONS
Activities report of the aerospace industry in West Germany
[ISSN-0176-5066] 05 p0734 N85-14718
Activities report of the aerospace industry in West Germany
[ISSN-0722-3838] 07 p1053 N85-16686
Activities report of the aerospace industry in West Germany
[ISSN-0722-3838] 07 p1054 N85-16687
Simulation 09 p1277 N85-18024
Analytical modeling of a polling protocol --- airline information network
[ENST-84H001] 09 p1277 N85-18029
First deputy minister on 1984 civil aviation performance 09 p1277 N85-18033
Finnair, LOT, SAS reps in USSR on present operations, plans 09 p1278 N85-18035
Sunset of the Civil Aeronautics Board
[S-HRG-98-940] 09 p1403 N85-18829
Digest of the Deutsche Lufthansa report, 1983
[ISSN-0415-603X] 09 p1418 N85-18948
Rotterdam Airport and the Common Market
17 p2894 N85-27840

AIRPORT LIGHTS
NT RUNWAY LIGHTS

AIRPORT PLANNING
Airport site selection and design
[AD-P004193] 11 p1581 N85-19959
Landscape management on airports for reduction of bird populations
[AD-P004194] 11 p1581 N85-19960
Airport system development
[PB85-127793] 11 p1587 N85-19993
Deputy minister on civil aviation construction projects
14 p2208 N85-23692
OWEMA report: A project study concerning the possibilities and the desirability of a east-west runway for Maastricht Airport (Netherlands) as a Euro-regional air freight center
[B8476490] 18 p3064 N85-28955
Aviation system delays
[S-HRG-98-1241] 21 p3553 N85-32102

AIRPORT TOWERS
Prototype concept design for US Army type 3A Air Traffic Control Tower (ATCT)
[AD-A148840] 09 p1284 N85-18070
Planned office and facility consolidations: To improve system effectiveness and efficiency, FY 1985-87
[AD-A150441] 13 p1970 N85-22376

AIRPORTS
NT HELIPORTS
Evaluation of laser profile and deflection measuring system
[FAA-PM-84-24] 02 p0201 N85-11341
New airport ground traffic control system planned
03 p0310 N85-12006
Start-2 ATC system installation progresses at Leningrad 03 p0311 N85-12007
Airport noise impact prediction and measurement
03 p0367 N85-12476
Operation of aviation support bases
04 p0544 N85-13461
TAF verification (airport weather forecasts)
[GEOPHYSSDBW-FM-205] 05 p0687 N85-14420
FAA (Federal Aviation Administration) statistical handbook of aviation, calendar year 1983
[AD-A148171] 08 p1067 N85-16760
International projects, other work of Aeroproyekt Institute 08 p1068 N85-16767
Activities report on West German civil airports. Part 1: Text
[ISBN-3-87977-055-7-PT-1] 08 p1090 N85-16887
Activities report for the West German Civil Airports. Part 2: Tables
[ISBN-3-87977-055-7-PT-2] 08 p1090 N85-16888
Impact of aircraft emissions on air quality in the vicinity of airports. Volume 3: Air quality and emission modeling needs
[AD-A147951] 08 p1180 N85-17435
Impact of aircraft emissions on air quality in the vicinity of airports. Volume 4. Nitrogen dioxide and hydrocarbons
[AD-A148253] 08 p1180 N85-17436
Test of dispersal of turbojet aircraft departure tracks at washington National Airport (1983-84), volume 1 report
[AD-A148111] 08 p1218 N85-17669
Improvements in Kazan airport equipment, facilities
09 p1278 N85-18039
Improvements under way at Gorkiy airport
09 p1278 N85-18040
Denver ARTCC (Air Route Traffic Control Center) evaluation of PROFS (Program for Regional Observing and Forecasting Services) mesoscale weather products
[PB85-120301/GAR] 09 p1279 N85-18045
Aircraft noise effects: An inter-disciplinary study of the effect of aircraft noise on man. Part 3: Supplementary analyses of the social-scientific portion of the study on aircraft noise conducted by the DFG
[NASA-TM-75802] 10 p1527 N85-19631
The use of small mobile radars to detect, monitor, and quantify bird movements
[AD-P004188] 11 p1580 N85-19951
Blackbirds and starlings: Population ecology and habits related to airport environments
[AD-P004190] 11 p1580 N85-19953
Birds on airports: The reason for their presence
11 p1580 N85-19955
The use of falconry as mean to persuade the birds to stay out of the airport vicinity 11 p1580 N85-19956
Control of mammals at airports
[AD-P004192] 11 p1580 N85-19957
Inexpensive multipurpose landscaping
11 p1581 N85-19961
Reducing gull use of some attractions near airports
[AD-P004195] 11 p1581 N85-19962
FAA policy regarding solid waste disposal facilities
[AD-P004196] 11 p1581 N85-19963
Airport bird hazards associated with solid waste disposal facilities
[AD-P004197] 11 p1581 N85-19964
Successful control of gulls and other birds at a sanitary landfill
[AD-P004198] 11 p1582 N85-19965
Development of bird hazard reduction for airport operational safety
[AD-P004202] 11 p1582 N85-19969
The bird strike situation and its ecological background in the Copenhagen Airport, Kastrup
[AD-P004203] 11 p1582 N85-19970
Bird control program Orlando International Airport
[AD-P004204] 11 p1583 N85-19971
Birds and airport agriculture in the conterminous United States: A review of literature
[AD-P004208] 11 p1583 N85-19975
The FAA grant-in-aid assurances: FAR part 139, and airport hazards
[AD-P004209] 11 p1583 N85-19976
Light your runways and taxiways without electricity
[DE85-000269] 11 p1586 N85-19991
International airport study: How to improve the effect of airports on trade and on export-related industries
[PB85-124923] 11 p1586 N85-19992
Airport system development
[PB85-127793] 11 p1587 N85-19993
Examination of the feasibility for demonstration and use of radioluminescent lights for Alaskan remote runway lighting
[DE85-002503] 12 p1782 N85-21185
FTASUM: Aviation forecast summaries
[PB85-112977] 12 p1897 N85-21906
An analysis of the impacts of the Airport Radar Service Area (ARSA)
[AD-A150954] 14 p2217 N85-23749
Disturbance to the population due to flight operations at landing fields. Questionnaire on community reaction to non-commercial and sporting aviation
[NASA-TM-76531] 14 p2353 N85-24537
A study of the methods for evaluating the noise impact of a proposed airport on a community
15 p2588 N85-25957
Probabilistic computer model of optimal runway turnoffs
[NASA-CR-172549] 16 p2715 N85-26760

Study of acceptance criteria for joint densities in bituminous airport pavements [FAA-PM-85-5] 16 p2715 N85-26761

Radioluminescent lighting for rural Alaskan runway lighting and marking [DE85-007022] 16 p2716 N85-26764

Acceptability testing of radioluminescent lights for VFR-night air taxi operations [DE85-007303] 16 p2716 N85-26765

Rotterdam Airport and the Common Market 17 p2894 N85-27840

Airport and airway system cost allocation model. Volume 7: User's manual [AD-A152877] 17 p2906 N85-27917

Frangibility of obstacles at airports [NLR-MP-84002-U] 17 p2981 N85-28431

Air traffic: Instruments, airports, companies, post, cargo and passengers 18 p3060 N85-28932

Data on noise environments at different times of day around airports [NASA-CR-172612] 19 p3351 N85-30769

AIRSHIPS

Missions and vehicle concepts for modern, propelled, lighter-than-air vehicles [NASA-TM-86672] 06 p1066 N85-16757

Current development, applications of airships in USSR 12 p1769 N85-21109

Missions and vehicle concepts for modern, propelled, lighter-than-air vehicles [NASA-TM-87461] 15 p2457 N85-25170

AIRSPACE

System engineering and integration contract for implementation of the National Airspace System Plan. Volume 2: Section 5.0 [AD-A145710] 02 p0137 N85-10929

System engineering and integration contract for implementation of the National Airspace System plan, volume 1, sections 1.0-4.0, 6.0 [AD-A145763] 03 p0317 N85-12048

National airspace review: Airport radar service area operational confirmation report [DOT/FAA/AT-84/2] 07 p0901 N85-15707

National airspace review enhancement plan, revision 3 [AD-A150743] 08 p1082 N85-16852

National airspace review. Implementation plan. Revised [AD-A151412] 15 p2468 N85-25238

Airport and airway system cost allocation model. Volume 7: User's manual [AD-A152877] 17 p2906 N85-27917

Introduction to European air traffic control [AD-A156328] 24 p4062 N85-35176

AIRSPEED

Critical conditions for the automatic control of landing from decision height in variable winds [UTIAS-284] 06 p0753 N85-14830

Recent methods for calibrating the anemometry of helicopters at low speeds 08 p1074 N85-16809

Simulating speed and height cues in the C-130 weapon system trainer [AD-P004313] 09 p1268 N85-17967

Determination of corrections to flow direction measurements obtained with a wing-tip mounted sensor [NASA-CR-174412] 10 p1421 N85-18962

Airspeed sensing pressure valve system [AD-D011472] 10 p1425 N85-18967

Miniature electrooptical air flow sensor [NASA-CASE-LAR-13065-1] 11 p1635 N85-20295

Safety recommendation(s), A-84-123 and -124 [REPT-3894B/93] 15 p2466 N85-25222

High specific power aircraft turn maneuvers: Tradeoff of time-to-turn versus change in specific energy [AD-A151701] 15 p2471 N85-25257

Formulation and implementation of nonstationary adaptive estimation algorithm with applications to air-data reconstruction [NASA-TM-86727] 16 p2706 N85-26699

Using regression analysis for determining air data sensor errors by means of an inertial navigation system [ESA-TT-886] 20 p3392 N85-31041

AIRWORTHINESS

U AIRCRAFT RELIABILITY

AIRWORTHINESS REQUIREMENTS

U AIRCRAFT RELIABILITY

AIRY FUNCTION

Brownian motion with a parabolic drift and Airy functions [CWI-MS-R8413] 12 p1925 N85-22097

AITKEN NUCLEI

Eleventh International Conference on Atmospheric Aerosols, Condensation and Ice Nuclei, volume 2 [PB85-182418] 21 p3638 N85-32596

Inactivation of silver iodide by atmospheric nucleation inhibitors 21 p3638 N85-32599

Ice nucleus measurements 21 p3640 N85-32609

The 100 years of Aitken Nuclei (AN) study-reminiscence, current and future problems 21 p3641 N85-32621

Analysis of performance of dynamic thermal diffusion chamber 21 p3642 N85-32625

Eleventh International Conference on Atmospheric Aerosols, Condensation and Ice Nuclei, volume 1 [PB85-182400] 21 p3644 N85-32636

The first condensation nucleus conference 21 p3644 N85-32637

Study of the formation of particles from natural hydrocarbons released by vegetation 21 p3644 N85-32640

Experimental studies of the formation of Aitken nuclei in the atmosphere 21 p3644 N85-32641

Human activity and production rate of secondary nuclei 21 p3645 N85-32645

Aitken particle size distribution in Antarctica 21 p3646 N85-32656

Properties of forest derived cloud condensation nuclei 21 p3650 N85-32682

The nuclei of cloud formation 21 p3651 N85-32685

Transport and formation of summertime cloud condensation nuclei over the Arctic Ocean 21 p3651 N85-32686

A review on the formation of aerosol particles in the atmosphere 21 p3651 N85-32687

The interaction of polynuclear aromatic hydrocarbons PAH's with water vapor and their role as condensation nuclei in the formation of haze and fog 21 p3652 N85-32695

Applicability of surface CCN measurements 21 p3652 N85-32696

on the transport of large condensation nuclei in the atmosphere at various altitudes over the territory of the USSR 21 p3653 N85-32698

ALABAMA

Operational evaluation of 5 cm Doppler radar. Two contributions: Review of WSR-74C Doppler radar operations at WSO Montgomery, Alabama (April 1982 - August 1983). The Johnson-Effect resolving ambiguous Doppler velocities [PB84-207521] 01 p0041 N85-10269

Alabama Tin Belt: Metallogenesis and mineral resource evaluation. Year-end report [DE84-901335] 07 p0969 N85-16283

Water resources data for Alabama, water year 1983 [PB85-123842] 10 p1507 N85-19507

Geodetic accuracy of LANDSAT 4 Multispectral Scanner and Thematic Mapper data --- Washington, DC, California, Alabama, South Dakota, and Illinois 11 p1667 N85-20504

ALADIN 2 AIRCRAFT

Presentation of the acoustic and aerodynamic results of the Aladin 2 concept qualification testing [NASA-TM-77883] 24 p4060 N85-35161

ALANINE

Response of amino acids in hindlimb muscles to recovery from hypogravity and unloading by tail-cast suspension [NASA-CR-176183] 24 p4128 N85-35589

Response of rat hindlimb muscles to 12 hours recovery from tail-cast suspension [NASA-CR-176182] 24 p4128 N85-35590

ALARMS

U WARNING SYSTEMS

ALASKA

The Alaskan mineral resources assessment program: Guide to information contained in the folio of geologic and mineral-resource maps of the Medfra Quadrangle, Alaska [GS-CIRC-928] 02 p0219 N85-11443

A paleomagnetic study of the Prince William terrane and Nixon Fork terrane, Alaska 02 p0226 N85-11478

Late quarterly glaciolacustrine and vegetational history of the Copper River Basin, south-central Alaska 03 p0391 N85-12499

The United States Geological Survey in Alaska: Accomplishments during 1981 [USGS-CIRC-868] 04 p0515 N85-13283

Summary of LANDSAT quadrangle studies in Alaska 04 p0515 N85-13284

Digital elevation models improve processing of Alaskan gravity data 04 p0515 N85-13285

Seismic studies in southern Alaska 04 p0515 N85-13286

Horizontal-strain observations in the Shumagin Island and Yakataga seismic gaps, Alaska 04 p0515 N85-13287

Computer-generated latitude and longitude templates for rapid determination of geographic positions in Alaska 04 p0516 N85-13288

The Kanayut Conglomerate in the westernmost Brooks Range, Alaska 04 p0516 N85-13289

Geothermal studies in Alaska: Conditions at Prudhoe Bay 04 p0516 N85-13290

Reconnaissance geology of the northern part of the Unalakleet quadrangle 04 p0516 N85-13291

Newly recognized sedimentary environments in the Shelikof Formation, Alaska 04 p0516 N85-13292

New ages of radiolarian chert from the Rampart district, east-central Alaska 04 p0516 N85-13293

Concordant bands of augen gneiss within metasedimentary rocks in the Big Delta C-2 quadrangle, east-central Alaska 04 p0516 N85-13294

Metamorphic petrology of the Table Mountain area, Circle quadrangle, Alaska 04 p0516 N85-13295

Paleozoic limestones of the Crazy Mountains and vicinity, Circle quadrangle, east-central Alaska 04 p0517 N85-13296

Late Paleozoic and early Mesozoic radiolarians in the Circle quadrangle, east-central Alaska 04 p0517 N85-13297

Structural observations in the Circle quadrangle, Yukon-Tanana Upland, Alaska 04 p0517 N85-13298

Lacustrine and eolian deposits of Wisconsin age at Riverside Bluff in the upper Tanana River valley, Alaska 04 p0517 N85-13299

The northern coast plutonic-metamorphic complex, southeastern Alaska and northwestern British Columbia 04 p0518 N85-13305

Cretaceous plutonic rocks, Mitkof and Kupreanof Islands, Petersburg quadrangle, southeastern Alaska 04 p0518 N85-13306

Late oligocene gabbro near Ketchikan, southeastern Alaska 04 p0518 N85-13307

Geology and geochemical evolution of the Lost River, Alaska, tin deposit 04 p0533 N85-13405

Carbon monoxide study, Anchorage, Alaska, November 22, 1982 to February 11, 1983 [PB84-236595] 05 p0673 N85-14321

Revised Uniform Summary of Surface Weather Observations (RUSSWO). Shemya AFB, Alaska, parts A-F [AD-A146917] 07 p1005 N85-16366

Shore ice ride-up and pile-up features. Part 2. Alaska's Beaufort Sea coast, 1983 - 1984 [AD-A148428] 08 p1190 N85-17501

Meteorological factors responsible for high CO (carbon monoxide) levels in Alaskan cities [PB85-115137/GAR] 09 p1350 N85-18493

Mountain barrier baroclinity effects on surface winds along the Alaskan Arctic coast 14 p2238 N85-23877

Characteristics of fast sea ice collected near Barrow, Alaska 15 p2582 N85-25925

The ecology of tundra ponds of the Arctic coastal plain: A community profile [TI85-900650] 15 p2589 N85-25958

Glossary of landscape and vegetation ecology for Alaska [PB85-153831] 16 p2816 N85-27372

Structural analysis of terrane accretions in the eastern Brooks Range and adjacent areas in central Alaska and Canada [DE85-008279] 17 p2993 N85-28501

Deep source gas [DE85-001984] 18 p3126 N85-29358

The U.S. Geological Survey in Alaska: Accomplishments during 1982 [US-GEOL-SURV-CIRC-939] 20 p3493 N85-31719

Pacific Northwest and Alaska bioenergy program glossary [DE85-011740] 22 p3808 N85-33591

The United States Geological Survey in Alaska: Accomplishments during 1983 [USGS-CIRC-945] 23 p3948 N85-34468

Some geophysical guides to ore in southern and southwestern Alaska 24 p4103 N85-35438

ALBEDO

NT COSMIC RAY ALBEDO

NT EARTH ALBEDO

Ultraviolet observations of Uranus and Neptune below 3000 Angstrom 02 p0298 N85-11932

Satellite masses in the Uranus and Neptune systems [PSI-CONTRIB-196] 02 p0301 N85-11947

Dust properties determined from backscattering in the interplanetary and interstellar medium 03 p0446 N85-12838

Influence of the atmosphere on remotely sensed reflection from vegetation surfaces [DE85-000658] 11 p1670 N85-20521

Atlas of relectance patterns for uniform earth and cloud surfaces (NIMBUS-7ERB-61 days) [PB85-116382] 12 p1891 N85-21870

GMS operational calibration procedure and status 12 p1895 N85-21893

Snow reflectance from Thematic Mapper 13 p2120 N85-23205

Seasonal and secular variation of the Solis Lacus albedo feature: Relation to the Martian dust-transport cycle 13 p2188 N85-23576

Accurate albedos of the brightest regions on Io
13 p2195 N85-23618
Determination of mineral type, abundance, and grain size with remotely obtained reflectance spectra
13 p2196 N85-23623
Mars planimetric mapping 13 p2203 N85-23666
Atlas of archived vegetation, land-use and seasonal Albedo data sets
[NASA-TM-86199] 14 p2346 N85-24508
Current ideas on the nature of comets
14 p2435 N85-25017
Evaluating radiation distortions of optical image of Earth's surface in horizontally inhomogeneous atmosphere 15 p2486 N85-25345
Selection of a model of Earth's albedo radiation, practical calculation of its effect on the trajectory of a satellite
[NASA-TM-77870] 15 p2591 N85-25972
Sea ice, climate and Fram Strait
15 p2603 N85-26042
Earth Albedo and the orbit of LAGEOS
[NASA-TM-86210] 21 p3558 N85-32131
The distribution of compositional classes in the asteroid belt: A cosmochemical fingerprint?
22 p3852 N85-33856
Interpretation of photometric measurements of airless bodies 22 p3855 N85-33871
Monte Carlo techniques for analyzing deep penetration problems
[DE85-011426] 23 p3968 N85-34598
Additional flux of particles and albedo-electrons in upper atmosphere
[SH-6.1-6] 23 p4045 N85-35080
Observation of energy spectrum of electron albedo in low latitude region at Hyderabad, India
[SH-6.1-7] 23 p4045 N85-35081
Proton albedo spectrum observation in low latitude region at Hyderabad, India
[SH-6.1-8] 23 p4045 N85-35082

ALCOHOLS
NT ETHYL ALCOHOL
NT GLYCOLS
NT METHYL ALCOHOLS
NT PHENOLS
NT POLYVINYL ALCOHOL
Workload demand and CNS depressant stressor effects on spatial orientation information processing
[AD-A145211] 01 p0098 N85-10651
Converting gasoline farm tractors to run efficiently on farm-produced alcohol
[DE84-015796] 02 p0205 N85-11350
Development of acceptance criteria for batches of silane primer for external tank thermal protection system bonding applications
[NASA-CR-171266] 04 p0478 N85-13043
DOE supported research in alcohol fuel technology development
[DE84-007686] 06 p0774 N85-14948
Research and development of alcohol fuel usage in spark ignited engines 09 p1301 N85-18175
ECUT, Energy Conversion and Utilization Technologies program: Technical and economic assessment of processes for the production of butanol and acetone. Phase 2: Analysis of research advances
[NASA-CR-175471] 10 p1434 N85-19034
Fluorinated polyurethanes
[AD-D011528] 12 p1810 N85-21353
Trifunctional catalysts for conversion of syngas to alcohols
[DE85-004577] 13 p2040 N85-22771
Urban vehicle research project
[DE85-005444] 17 p3052 N85-28889
Alcohol: An alternate energy resource for community use
[DE85-007731] 18 p3084 N85-29075
Alkaline battery containing a separator of a cross-linked copolymer of vinyl alcohol and unsaturated carboxylic acid
[NASA-CASE-LEW-13102-1] 18 p3093 N85-29144
Impact of alcohol fuels on urban air pollution: Methanol photochemistry study
[DE85-009539] 18 p3133 N85-29403
Galactose oxidase in stereospecific oxidation of primary alcohols
[AD-A154059] 19 p3234 N85-30048
Phase behavior and QLS (Quasielastic Light Scattering) in potassium linoleate/n-alkanol microemulsions
[AD-A155028] 21 p3563 N85-32163
Metal alkoxides: Models for metal oxides. Alkoxide ligands in early transition metal organometallic chemistry
[DE85-011368] 23 p3916 N85-34269
Air university commander's and supervisor's guide on substance abuse
[AD-A158336] 24 p4133 N85-35622

ALDEHYDES
NT ACETALDEHYDE
NT FORMALDEHYDE
Highly dispersed metal atoms in zeolites
[DE85-010515] 19 p3354 N85-30792
Analysis of aldehydes and ketones in the gas phase
[PB85-181866] 20 p3426 N85-31261

ALDOSTERONE
Biochemical status of adrenocortical dysfunction following spaceflight 12 p1901 N85-21935

ALERTNESS
Shape with and without redundant colour as coding mechanism for simulated radar displays in a time-extended simple vigilance task
[AD-A151683] 16 p2844 N85-27533
Effects of low level carbon monoxide (CO) on tracking and monitoring. An attempt to replicate the findings of Putz et al. (1976) protocol 2
[AD-A155722] 22 p3825 N85-33694

ALEUTIAN ISLANDS (US)
Geology and geochemistry of early Tertiary submarine volcanic rocks of the Aleutian Islands, and their bearing on the development of the Aleutian Island Arc
03 p0389 N85-12493
Kuril-Aleutian subduction 19 p3290 N85-30402

ALFALFA
Multi crop area estimation in Idaho using EDITOR
[E85-10054] 06 p0827 N85-15251
Two-dimensional numerical model of sensible and latent heat transport in an irrigated field under advective conditions 13 p2131 N85-23261

ALFVEN WAVES
U MAGNETOHYDRODYNAMIC WAVES

ALGAAS
U ALUMINUM GALLIUM ARSENIDES

ALGAE
NT BLUE GREEN ALGAE
Response of algal populations to changes in stream water quality
[PB84-202464] 01 p0070 N85-10465
Modeling effects of toxicants on aquatic systems
[DE84-016594] 04 p0531 N85-13396
Cultivation and conversion of marine macroalgae — biomass energy production
[DE84-004522] 04 p0544 N85-13464
Problems associated with the utilization of algae in bioregenerative life support systems
[NASA-CR-166615] 07 p1019 N85-16469
Algal culture studies related to a Closed Ecological Life Support System (CELSS)
[NASA-CR-177322] 07 p1019 N85-16470
Petrography, sedimentology, diagenesis, and reservoir characteristics of some Pennsylvanian phylloid algal limestones: Kansas and Utah, USA
09 p1352 N85-18507
Artificial photosynthesis with algal and reconstituted systems
[DE85-002557] 10 p1523 N85-19604
Research and development of shallow algal mass culture systems for the production of oils
[DE85-000518] 11 p1690 N85-20624
Microalgae culture collection, 1984-1985
[DE84-013035] 11 p1690 N85-20626
Photosynthetic water splitting
[DE85-002460] 11 p1690 N85-20627
Characteristic vector analysis of inflection ratio spectra: New technique for analysis of ocean color data
[NASA-TP-2428] 13 p2126 N85-23237
Studies of photosynthetic Energy Conversion
[DE85-005973] 15 p2586 N85-25944
Technical and economic analysis of liquid fuel production from microalgae
[DE85-002926] 16 p2758 N85-27018
The role of sulfur in osmoregulation and salinity tolerance in cyanobacteria, algae, and plants
21 p3660 N85-32736
Salinity driven oceanographic upwelling
[DE85-011664] 22 p3818 N85-33652
Production of liquid fuels and chemicals by microalgae
[DE85-008780] 22 p3819 N85-33658
Composition and dynamics of bacteriocenosis associated with algae in human life-support systems
22 p3823 N85-33684
Resource evaluation and site selection for microalgae production systems
[DE85-008807] 23 p3951 N85-34485
Screening and characterizing oleaginous microalgal species from the southeastern United States
[DE85-008787] 23 p3951 N85-34488

ALGAL BLOOM
U ALGAE

ALGEBRA
NT ADJOINTS
NT AUTOMORPHISMS
NT BANACH SPACE
NT BINOMIALS
NT CANONICAL FORMS
NT CURRENT ALGEBRA
NT DETERMINANTS
NT EIGENVALUES
NT EIGENVECTORS
NT GROUP THEORY
NT HERMITIAN POLYNOMIAL
NT HILBERT SPACE
NT HOMOMORPHISMS
NT JORDAN FORM
NT LIE GROUPS
NT LINEAR EQUATIONS
NT LINEAR EVOLUTION EQUATIONS
NT LINEAR TRANSFORMATIONS
NT MATRICES (MATHEMATICS)
NT MONGE-AMPERE EQUATION
NT NONLINEAR EQUATIONS
NT NONLINEAR EVOLUTION EQUATIONS
NT POLYNOMIALS
NT QUADRATIC EQUATIONS
NT SOBOLEV SPACE
NT SPINOR GROUPS
NT STATE VECTORS
NT STIFFNESS MATRIX
NT STOKES THEOREM (VECTOR CALCULUS)
NT STRESS TENSORS
NT TENSORS
NT VECTOR SPACES
NT VECTORS (MATHEMATICS)
NT VORTICITY
Mathmatics and Computer Science Division activities
[DE84-014842] 01 p0104 N85-10701
PASCAL-MP algebraic and numerical manipulator for polynomials
[INPE-3229-TDL/176] 02 p0240 N85-11562
Algebraic functions of H-functions with specific dependency structure
[AD-A145598] 02 p0252 N85-11647
United States Air Force on research on algebraic manipulation
[AD-A145737] 02 p0253 N85-11655
Process algebra for communication and mutual excitation
[CWI-CS-R8409] 05 p0720 N85-14622
Algebraic techniques in systolic array design
[AD-A146417] 06 p0857 N85-15451
The algebraic structure of convolutional codes with application to code construction and decoding
[AD-A148770] 08 p1206 N85-17591
Computing the Kac determinant using dual mode techniques and more about the No-ghost theorem
[DE85-001329] 09 p1375 N85-18640
Towards the construction of periodic solutions of pseudodifferential equations with the aid of algebraic operators 10 p1535 N85-19674
MACSYMA usage at Langley
[NASA-CR-172518] 10 p1537 N85-19688
Checking microcode algebraically
[AD-A149441] 10 p1547 N85-19759
Process algebra with asynchronous communication mechanisms
[CWI-CS-R8410] 11 p1625 N85-20235
Generalization of Beurling algebras
11 p1698 N85-20675
Object-oriented algebraic specification: Proposal for a notation and 12 examples
[CWI-CS-R8411] 11 p1707 N85-20744
Accidental degeneracies, hidden supersymmetries, and spectrum-generating superalgebras
[DE85-003547] 11 p1738 N85-20930
Parallel linear algebra library for the Denelcor HEP
[DE85-004685] 12 p1917 N85-22034
An algebraic specification language and a syntax directed editor
[AD-A150664] 14 p2403 N85-24815
BLAS (Basic Linear Algebra Subroutines), linear algebra modules and supercomputers
[AD-A151504] 15 p2628 N85-26199
Alternatives for jet engine control
[NASA-CR-175831] 16 p2709 N85-26713
Proposal for an extended set of FORTRAN Basic Linear Algebra subprograms
[DE85-007241] 16 p2848 N85-27562
Schubert varieties are arithmetically Cohen-Macaulay
16 p2853 N85-27592
Quadratic spaces over discrete Hodge algebras
16 p2853 N85-27593
Algebra of communicating processes
[CWI-CS-R8421] 17 p2950 N85-28214
Boundary to constructive solid geometry mappings: A focus on 2-D issues 17 p3004 N85-28570
A complete inference system for regular processes with silent moves
[CWI-CS-R8420] 17 p3014 N85-28638
A high-accuracy optical linear algebra processor for finite element applications
[NASA-CR-175894] 17 p3017 N85-28658
Discrete mathematics for communications systems
[AD-A152814] 17 p3018 N85-28664

Tenth-order expansion formulae for the orbital eccentricity function K (sub lpq)(e) obtained using a symbolic algebraic manipulation system
[AD-A153754] 18 p3170 N85-29647
On MGR (Upsilon) multigrid methods
[AD-A153887] 19 p3345 N85-30733
Parametric stiffness control of flexible structures
20 p3414 N85-31187
Symposium on Computational Mathematics-State-of-the-Art: Informal Proceedings
[DE85-006122] 20 p3516 N85-31858
A cracked orthotropic sheet stiffened by a semi-infinite orthotropic sheet
[NASA-TP-2455] 21 p3597 N85-32339
Gradient scaling for nonuniform meshes
[DE85-009625] 22 p3784 N85-33443
A study of the second and third order closure models of turbulence for prediction of separated shear flows
[NASA-CR-176127] 23 p3929 N85-34353
Stress analysis of axisymmetric sandwich shells of variable thickness 24 p4101 N85-35419

ALGORITHMS
NT PARSING ALGORITHMS
NT SIMPLEX METHOD
Computational methods for complex flowfields
[AD-A145219] 01 p0004 N85-10019
Impact of new computing systems on computational mechanics and flight-vehicle structures technology
01 p0007 N85-10042
Comparison of numerical techniques for integration of stiff ordinary differential equations arising in combustion chemistry
[NASA-TP-2372] 01 p0011 N85-10065
CREKID: A computer code for transient, gas-phase combustion of kinetics
[NASA-TM-83806] 01 p0011 N85-10068
Planarity criteria in electromagnetic topology
[AD-A145279] 01 p0038 N85-10241
Augmented weak forms and element-by-element preconditioners: Efficient iterative strategies for structural finite elements. A preliminary study
01 p0056 N85-10384
A Monte Carlo comparison of the recovery of winds near upwind and downwind from the SASS-1 model function by means of the sum of squares algorithm and a maximum likelihood estimator
[NASA-CR-3839] 01 p0064 N85-10421
Function algorithms for MPP scientific subroutines, volume 1
[NASA-CR-175246] 01 p0102 N85-10678
Numerical algorithms and parallel tasking
[AD-A145090] 01 p0104 N85-10693
Markovian control problems: Functional equations and algorithms
[MCTH-57] 01 p0107 N85-10717
Recursive algorithms for adaptive arrays based on estimates
[REPT-5-84] 01 p0107 N85-10718
A comparative evaluation of algorithms for generalized network problems
[TWISK-289] 01 p0107 N85-10721
Vertical compression algorithms
[DE84-015040] 01 p0126 N85-10884
Shock capturing finite difference algorithms for supersonic flow past fighter and missile type configurations
[NASA-CR-174051] 02 p0134 N85-10913
Accelerated convergence for incompressible flow calculations
[NASA-TM-86863] 02 p0140 N85-10949
Routing the power and ground wires on a VLSI chip
[AD-A145356] 02 p0194 N85-11296
An automated immittance measuring system for electroacoustic transducers
[AD-A145701] 02 p0200 N85-11336
Efficient methods for mechanical and structural reliability analysis and design 02 p0205 N85-11355
Quasi-Newton algorithms for large scale nonlinear systems 02 p0208 N85-11370
Parallel searching and merging on ZMOB
[AD-A145424] 02 p0241 N85-11574
Research on distributed languages and algorithms
[AD-A145661] 02 p0242 N85-11580
Research topics: Multiprocessing algorithms for computational logic
[DE84-015500] 02 p0242 N85-11583
A fast, compact assignment algorithm
[NRIMS-TWISK-331] 02 p0250 N85-11632
Inverse problems, optimization and algorithms
[AD-A145397] 02 p0250 N85-11638
An algorithm for least squares projections onto the intersection of shifted, convex cones
[AD-A145426] 02 p0251 N85-11640
Rapidly convergent algorithms for nonsmooth optimization
[AD-A145556] 02 p0251 N85-11643
Control and identification of time varying systems
[AD-A145636] 02 p0252 N85-11649
Likelihood estimation for generalized mixed exponential distributions
[AD-A145675] 02 p0252 N85-11651
Design of edge detectors for reduced images
[AD-A145700] 02 p0252 N85-11653
CHORDS: A new temperature or sound speed profile thinning algorithm
[AD-A145464] 02 p0275 N85-11793
Active regions — and the Solar Maximum Mission
[NASA-CR-170628] 02 p0304 N85-11965
A digital algorithm for composite laminate analysis: FORTRAN, Revised
[AD-A145833] 03 p0326 N85-12096
Multielement bend discontinuities in oversize rectangular waveguides
[PR-200] 03 p0354 N85-12275
Signal processing algorithms
[AD-A145748] 03 p0406 N85-12590
A sequential quadratic programming algorithm for solving large, sparse nonlinear programs
[AD-A145854] 03 p0407 N85-12597
Analysis and design methodology for VLSI computing networks
[AD-A146030] 03 p0409 N85-12611
A decomposable algorithm for contour surface display generation
[AD-A145783] 03 p0410 N85-12619
Statistical analysis of some traveling salesman algorithms
[AD-A145786] 03 p0410 N85-12620
The ML (Maximum Likelihood) method for frequency estimation of real sinusoids in noise
[AD-A146053] 03 p0411 N85-12628
A two-segment approximation algorithm for separable convex programming with linear constraints
[AD-A146215] 03 p0412 N85-12634
Designing optimal AOQL sampling plans a computerized approach
[AD-A146266] 03 p0413 N85-12639
Algorithm for astronomical, extended source, signal-to-noise radio calculations
[NASA-TP-2396] 03 p0445 N85-12833
Algorithm for astronomical, point source, signal to noise ratio calculations
[NASA-TP-2397] 03 p0445 N85-12834
Microprocessor implementation of algorithms of nonlinear filtration 04 p0486 N85-13104
Comparison analysis of algorithm for construction of functional tests for combined large-scale integrated circuits 04 p0490 N85-13121
Quasi-three dimensional modeling of functionally-integrated elements of large-scale integrated circuits 04 p0490 N85-13122
Long-range predictive control using weighting-sequence models
[OUEL-1542/84] 04 p0553 N85-13521
On the formal development of graph theoretical algorithms by transformation
[TUM-I8403] 04 p0553 N85-13522
Restoration of multichannel microwave radiometric images
[NASA-CR-174115] 04 p0554 N85-13527
Generalized formulation of TVD Lax-Wendroff schemes
[NASA-CR-172478] 04 p0554 N85-13528
Transformation of two and three-dimensional regions by elliptic systems
[NASA-CR-174176] 04 p0554 N85-13529
Parallel processing of numerical transport algorithms
[DE84-016825] 04 p0555 N85-13534
TCAS 2 logic performance during phase one operational evaluation
[DOT/FAA/PM-84/20] 05 p0595 N85-13793
A generalized LQG approach to self-tuning control. Part 1: Aspects of design. Part 2: Implementation and simulation
[OUEL-1536/84] 05 p0622 N85-13976
The adaptive spectrum analyser
05 p0622 N85-13978
On estimating the phase of periodic waveform in additive Gaussian noise, part 2 05 p0622 N85-13982
VLSI architectures for the multiplication of integers modulo a Fermat number 05 p0624 N85-13993
Documentation of earthquake algorithms
[PB84-235324] 05 p0677 N85-14351
Applications of sequential estimation to numerical weather prediction 05 p0681 N85-14374
Determining training device requirements in Army aviation systems 05 p0711 N85-14556
Research in computer science
[NASA-CR-174088] 05 p0713 N85-14572
Fast algorithms and specialized architectures
05 p0714 N85-14579
Integrated resource management algorithms for computer systems 05 p0715 N85-14582
Efficient sorting routines in FORTRAN 77
[OUEL-1529/84] 05 p0716 N85-14590
Automatic determination of motion in an image sequence. The interest for interpretation
[ENST-84E012] 05 p0716 N85-14592
On an algorithm for Pythagorean sums and its connection with continued fractions
[NPL-DITC-42/84] 05 p0718 N85-14603
Most wanted factorizations using the quadratic sieve
[DE84-016208] 05 p0718 N85-14609
Some implementations of multigrid linear system solvers
[CWI-NM-R8401] 05 p0720 N85-14626
Numerical method for computing supersonic flow over wings of flight vehicles 05 p0725 N85-14659
Molarity principle: Foundation for parallel digital signal processes 05 p0725 N85-14663
Multi-disciplinary techniques for understanding time-varying space-based imagery
[AD-A144357] 05 p0726 N85-14681
Analytical redundancy management mechanization and flight data analysis for the F-8 digital fly-by-wire aircraft flight control sensors
[NASA-CR-170396] 06 p0757 N85-14844
Primary data processing in very long baseline radiointerferometer 06 p0783 N85-15006
Asymptotically optimal ranking algorithms for quasi-determinate signal detection
06 p0792 N85-15064
A geometric approach to high resolution TVD schemes
[NASA-CR-172484] 06 p0857 N85-15449
Selecting a leader in a clique in O(N log N) messages
[AD-A146581] 06 p0857 N85-15453
Tristatic tracking filter used by the multistatic measurement system
[AD-A146865] 07 p0911 N85-15769
cost and benefits optimization model for fault-tolerant aircraft electronic systems
[NASA-CR-166043] 07 p0946 N85-15993
Influence of Faraday effect in ionosphere on nonmutuality of meteor radio channel
07 p0952 N85-16037
A second-order accurate parabolized Navier-Stokes algorithm for internal flows
[NASA-CR-174258] 07 p0956 N85-16059
An evaluation and comparison of vertical profile data from the VISSR Atmospheric Sounder (VAS)
[NASA-TP-2425] 07 p1000 N85-16351
Decentralized control of scheduling in distributed systems
[AD-A147446] 07 p1022 N85-16487
An algorithm for assembly of stiffness matrices into a compacted data structure
[AD-A146727] 07 p1023 N85-16492
Monotone operators in mathematical programming
[AD-A147309] 07 p1025 N85-16506
Continuity of the null space basis and constrained optimization
[AD-A147038] 07 p1030 N85-16538
Techniques for vector quantization
[AD-A147052] 07 p1030 N85-16539
A dual quadratic programming algorithm
[AD-A147237] 07 p1031 N85-16547
Extracting embedded generalized networks from linear programming problems
[AD-A147565] 07 p1033 N85-16558
Structural optimization and other large-scale processes
[AD-A147895] 07 p1034 N85-16564
Efficient computation of optimal time for transaction processing in a database system
[AD-A147568] 07 p1054 N85-16693
High accuracy Doppler navigation employing optimum integrated position fix information
08 p1073 N85-16803
Vectorizable multigrid algorithms for transonic flow calculations
[NASA-CR-174326] 08 p1077 N85-16827
Research into topics in transonic flow theory
[AD-A148526] 08 p1078 N85-16837
Information extraction and transmission techniques for spaceborne synthetic aperture radar images
[NASA-CR-174341] 08 p1150 N85-17256
Coding for reliable satellite communications
[NASA-CR-174315] 08 p1150 N85-17257
Hierarchical data structures and algorithms for digital stereoscopical mensuration 08 p1175 N85-17410
An efficient algorithm for the computation of the inverse in bundle adjustment systems — photogrammetry
08 p1175 N85-17411
The algebraic structure of convolutional codes with application to code construction and decoding
[AD-A148770] 08 p1206 N85-17591

Asynchronous distributed flow control algorithms
[AD-A148452] 08 p1208 N85-17600

Research on optimal control, stabilization and computational algorithms for aerospace applications
[NASA-CR-174318] 08 p1209 N85-17603

Algorithm for space-time analysis of data on geomagnetic field
[NASA-TM-77804] 08 p1209 N85-17609

Signal reconstruction from Fourier transform sign information
[AD-A148039] 08 p1211 N85-17624

The EM algorithm for censored data
[AD-A148136] 08 p1212 N85-17626

Use of iterative linear and nonlinear algebraic methods for solving large stiff systems of ODEs
[AD-A148516] 08 p1213 N85-17636

Probabilistic analysis of algorithms for NP-Complete problems
[AD-A148207] 08 p1215 N85-17653

A variable span smoother
[AD-A148241] 08 p1215 N85-17655

Decentralized control of scheduling in distributed systems
[AD-A147688] 08 p1228 N85-17731

On one design principle of surge protector for gas turbine engine compressor 09 p1306 N85-18206

A public key cryptographic algorithm based on a generalization of the knapsack problem
[FUB-7-1984] 09 p1313 N85-18250

Development of multigrid algorithms for problems from fluid dynamics
[GMD-111] 09 p1321 N85-18305

The optimal control and design of a flexible manipulator arm 09 p1327 N85-18340

An optimal parallel processing method for inverting sparse matrices 09 p1367 N85-18586

Modeling relationships using groups and items
09 p1367 N85-18591

Parallel algorithms for robot dynamics
[DE84-016583] 09 p1369 N85-18605

Where are the parallel algorithms?
[NASA-CR-172516] 09 p1373 N85-18627

Initialization of Thompson-Pisarenko's algorithm — sinusoidal signal parameter estimation
[FUB-46-1983] 09 p1375 N85-18641

Methodology for evaluating related databases and a computerized algorithm for merging their output
09 p1401 N85-18821

A multistage time-stepping scheme for the Navier-Stokes equations
[NASA-CR-172527] 10 p1483 N85-19365

A generalized ordering constraint for stereo correspondence
[AD-A149182] 10 p1487 N85-19390

Planning of minimum-time trajectories for robot arms
[AD-A148956] 10 p1492 N85-19418

Cyclone diagnostics — rainfall estimation, backscatter, and lidar
[NASA-CR-171337] 10 p1518 N85-19567

Equations and algorithms for meteorological applications in air weather service
[AD-A148894] 10 p1519 N85-19575

Relative performance of micro and mainframe computers
[AD-A149281] 10 p1538 N85-19695

Algorithms for the Euler and Navier-Stokes equations for supercomputers
[NASA-CR-172543] 10 p1539 N85-19701

Efficient algorithm for fuzzy linear programming with multiple objectives
[AD-A149012] 10 p1544 N85-19736

Smoothing with split linear fits
[AD-A149032] 10 p1545 N85-19740

Vectorization and implementation of an efficient multigrid algorithm for the solution of elliptic partial differential equations
[AD-A149049] 10 p1545 N85-19743

Blunder detection using a sequential least squares adjustment
[AD-A149514] 10 p1548 N85-19765

Order picking in an aisle
[AD-A149553] 10 p1548 N85-19766

Robust Kalman filtering and its applications
[AD-A149044] 10 p1550 N85-19775

One-dimensional processing for adaptive image restoration
[AD-A149314] 10 p1557 N85-19815

Optical implementation of the synthetic discriminant function
[AD-A149562] 10 p1557 N85-19817

Finite-(beta) optimization of tandem mirrors
[DE85-002658] 10 p1560 N85-19835

Distribution of hydrogen in multi-layer welded joints of alloyed steels 11 p1603 N85-20079

Simulation of the electrochemical machining process
[DE85-003797] 11 p1616 N85-20159

Guidepost routing algorithm for distributed computer networks 11 p1622 N85-20210

Numerical simulation of turbulent reacting flows
[DE84-016777] 11 p1632 N85-20278

Real time algorithms for robotic control of teleoperators
[DE85-001137] 11 p1647 N85-20360

Continued research in mesoscale air pollution simulation modeling. Volume 5: Refinements in numerical analysis, transport, chemistry, and pollutant removal
[PB85-137362] 11 p1680 N85-20565

Parallel processing experiences on the Denelcor HEP computer
[DE85-000653] 11 p1702 N85-20703

Three algorithms for parametric frequency domain system identification
[DE85-002801] 11 p1706 N85-20735

New approach for solving large residual nonlinear least squares problems
[DE85-002555] 11 p1707 N85-20742

Bayesian analysis of time series 1: Householder transformation analyses
[DE85-004449] 11 p1708 N85-20749

Precise measurements of radial velocities of emission lines in the far-ultraviolet spectra of late-type stars
11 p1758 N85-21062

Cometary atmospheres: Modeling the spatial distribution of observed neutral radicals
[NASA-CR-175465] 11 p1765 N85-21098

A study of transonic flutter of a two-dimensional airfoil using the U-g and p-k methods
[LR-615] 12 p1771 N85-21121

Algorithms for automatic four-dimensional aircraft guidance, considering the momentary wind situation
[DFVLR-FB-84-40] 12 p1775 N85-21146

A comparison of the efficiency of numerical methods for integrating chemical kinetic rate equations
[NASA-TM-83590] 12 p1778 N85-21162

Modal control of structural systems
[AD-A149734] 12 p1790 N85-21235

Estimating algorithmic error of digital recursive filters
12 p1839 N85-21543

Algorithm for statistical simulation of electromagnetic compatibility characteristics of high-frequency transmission channels in radioelectronic facilities
12 p1842 N85-21560

Synthesis of digital control for object with lag
12 p1843 N85-21562

Mathematical simulation of thermal prrocesses involved in electron-beam treatment 12 p1843 N85-21565

Modeling of transient heat pipe operation
[NASA-CR-175496] 12 p1844 N85-21571

A three-dimensional spectral algorithm for simulations of transition and turbulence
[NASA-CR-172561] 12 p1845 N85-21575

Algorithm for the simulation of transient viscoelastic flows with free surfaces
[DE85-002713] 12 p1848 N85-21590

Robust calculation of three-dimensional transonic potential flow based on the nonlinear gas multigrid method and a mixed incomplete lower upper decomposition/strongly implicit procedure (ILU/SIP) algorithm
[NLR-MP-84003-U] 12 p1848 N85-21593

Velocity inversion using a stratified reference
[AD-A150082] 12 p1889 N85-21858

RAPIDbus: Design of an extensible multiprocessor structure
[AD-A150061] 12 p1912 N85-21998

A linear characteristic-nodal transport method for the two-dimensional (X,Y)-geometry multigroup discrete ordinates equations over an arbitrary triangle mesh
[LA-10092-T] 12 p1913 N85-22006

User's guide for NPSOL (Version 2.1): A FORTRAN package for quadratic programming
[AD-A150078] 12 p1916 N85-22028

Software for special functions
[DE85-004684] 12 p1917 N85-22033

Parallel linear algebra library for the Denelcor HEP
[DE85-004685] 12 p1917 N85-22034

Determining conductivity by boundary measurements. Part 2: Interior results
[AD-A149750] 12 p1921 N85-22063

Parallel processing of encoded bit strings
[AD-A149612] 12 p1921 N85-22064

Distributed asynchronous deterministic and stochastic gradient optimization algorithms: Revision
[AD-A149997] 12 p1921 N85-22068

Statistics for the maximum of several positive random variables with application to networking
[AD-A150005] 12 p1922 N85-22069

A review of some aspects of robust inference for time series
[AD-A149706] 12 p1923 N85-22082

Needs, opportunities, and options for large scale systems research
[DE85-004642] 12 p1925 N85-22091

Determining object orientation from a single image using multiple information sources
[AD-A149960] 12 p1933 N85-22146

Multiple resolution representation and probabilistic matching of 2-D gray-scale shape
[AD-A149961] 12 p1933 N85-22147

Evaluation of expert systems
12 p1947 N85-22229

Problems in decentralized decision making and computation
[AD-A150025] 12 p1950 N85-22251

A flight management algorithm and guidance for fuel-conservative descents in a time-based metered air traffic environment: Development and flight test results
13 p1967 N85-22356

On the solution of the three-dimensional flowfield about a flow-through nacelle
[NASA-TM-87448] 13 p1969 N85-22371

Analysis of estimation algorithms for CDTI and CAS applications
[NASA-CR-172444] 13 p1973 N85-22387

Computation of elliptical functions in problems of celestial mechanics 13 p1979 N85-22418

Algorithm for determining optimal three impulse point-to-orbit transfer with limited transfer time
13 p1979 N85-22419

Assembly robot control algorithms
13 p2046 N85-22806

Nonlinear behavior and stability of thin spherical shells subjected to non-axisymmetrical loading
13 p2048 N85-22821

Efficiency of algorithms for gas-air channel diagnostics in gas turbine engines based on gas thermodynamic parameters 13 p2048 N85-22823

Advanced mixed-mode simulation techniques
13 p2062 N85-22883

Factorized algorithms for combined spatial and temporal processing of radar signals 13 p2081 N85-22997

Algorithm in Walsh function basis for analysis of integrated microcircuits on MOS-structures
13 p2083 N85-23006

Use of Bigaussian approximation to describe fading in scattering communications channel
13 p2084 N85-23017

Computing convolution of multifrequency signal employing truncated fast Fourier transform algorithms
13 p2085 N85-23019

Synthesis of quasi-optimum algorithms for signal recognition against background of correlated noise employing discrete spectral transformations
13 p2085 N85-23020

New convolution and discrete Fourier transformation algorithms based on rectangular transformations over field of roots of unity 13 p2085 N85-23022

Discrimination of normal and anomalous magnetic and electric fields in geoelectromagnetic variations
13 p2114 N85-23166

Polynomial parameterization in inverse gravimetric problem 13 p2115 N85-23174

Primary processing of experimental magnetovariation sounding data using spline functions
13 p2115 N85-23175

Orphan detection in the Argus system
[AD-A150562] 13 p2148 N85-23331

Implementation of some concurrent algorithms
[DE85-004687] 13 p2148 N85-23334

Algorithms for reconstruction of partially known, band limited Fourier transform pairs from noisy data
[AD-A150194] 13 p2150 N85-23347

Image data compression using uneven knots selection
[AD-A150602] 13 p2152 N85-23359

Algorithm for singular decomposition
[DE85-016488] 13 p2152 N85-23361

Motion planning with six degrees of freedom
[AD-A150312] 13 p2165 N85-23432

Quantitative analyses of planetary reflectance spectra
13 p2197 N85-23625

Progress in planetary radarclinometry
13 p2198 N85-23630

Thermal response of aircraft cabin ceiling materials during a post-crash, external fuel-spill, fire scenario
[PB85-145647] 14 p2220 N85-23764

An eigensystem realization algorithm for application to modal testing 14 p2233 N85-23842

Linearization of digital derived rate algorithm for use in linear stability analysis
[NASA-TM-87000] 14 p2243 N85-23904

Quaternion algorithms of 3-dimensional inertial navigational systems 14 p2287 N85-24173

Spatial acquisition algorithms and systems for intersatellite optical communication links
[AD-A150794] 14 p2292 N85-24207

ALGORITHMS

An improved battery state-of-charge indicator
[NASA-CR-175701] 14 p2298 N85-24227

Some methods of computing platform transmitter terminal location estimates -- ARGOS system; whale tracking 14 p2332 N85-24420

Perceptual organization and visual recognition
[AD-A150826] 14 p2391 N85-24723

Finite element methods in space mathematics
14 p2396 N85-24757

Propagation of numerical errors in computers and numerical quality 14 p2396 N85-24760

Execution of cellular logic operations in spatially continuous, bit slice processor 14 p2401 N85-24798

Nonlinear 0-1 programming. 1: Linearization techniques, revision
[AD-A150960] 14 p2405 N85-24826

A simple and efficient algorithm to compute tail probabilities from transforms
[AD-A150928] 14 p2409 N85-24849

Probalistic analysis of combinatorial algorithms: An annotated bibliography
[CWI-OS-R8411] 14 p2411 N85-24864

Disproof of the Mertens conjecture
[CWI-NM-R8412] 14 p2414 N85-24896

Some historical and other notes about the Mertens conjecture and its recent disproof
[CWI-NM-R8415] 14 p2414 N85-24898

Parametric coherence estimation via convolved correlations
[DE85-003946] 14 p2416 N85-24909

A fast ray tracing routine for laterally inhomogeneous media
[AD-A150964] 14 p2421 N85-24936

On the orbit improvement results obtained by referring old cometary observations to the SAO Star Catalog
14 p2438 N85-25042

Implementation of an inertial navigation algorithm using a limited wordlength microprocessor for a strapdown navigation computer
[BAE-BT-12792] 15 p2468 N85-25234

Multistep orbital correction algorithms for an Earth satellite using low thrust engine
15 p2479 N85-25303

Calculation of image shift in panoramic photography
15 p2488 N85-25357

An analysis of grid-based line drawing quantization methods
[AD-A151847] 15 p2522 N85-25547

Margin leveling algorithm for fully saturated satellite transponder with CDMA (Code Division Multiple Access) signaling
[AD-A151710] 15 p2543 N85-25699

Development of robots and application to industrial processes
[NASA-CR-175754] 15 p2567 N85-25840

Control of a flexible beam
[DE85-007243] 15 p2580 N85-25914

Effective microinstruction pipeline organization in a high-capacity microprocessor 15 p2625 N85-26176

Care 3 model overview and user's guide, first revision
[NASA-TM-86404] 15 p2627 N85-26192

The design and analysis of a complete hierarchical interface for the multi-backend database system
[AD-A151550] 15 p2629 N85-26203

On the throughput of channel access algorithms with limited sensing
[AD-A151984] 15 p2630 N85-26208

Censored observations, repeated measures and mixed effects models: An approach using the EM algorithm and normal errors
[MATHEMATICS-RESEARCH-183]
15 p2636 N85-26256

Vortex dynamics
[AD-A151278] 15 p2637 N85-26260

Communication complexity of the Gaussian elimination algorithm on multiprocessors
[AD-A151891] 15 p2638 N85-26267

Solution of coupled system of PDE by the transistorized multigrid method
[DE85-006377] 15 p2639 N85-26276

Sliding interfaces with contact-impact in large scale Lagrangian computations
[DE85-006451] 15 p2639 N85-26277

Construction of efficient algorithms for the estimation of multivariate probability densities
[AD-A151509] 15 p2640 N85-26285

Feasibility analysis of moving bank multiple model adaptive estimation and control algorithms
[AD-A152015] 15 p2641 N85-26292

Design and implementation of the digital engineering laboratory distributed database management system
[AD-A151694] 15 p2665 N85-26450

Developing an automated technique for translating a relational database into an equivalent network one
[AD-A151844] 15 p2666 N85-26451

Generation of flight paths using heuristic search
[AD-A151949] 16 p2704 N85-26694

Formulation and implementation of nonstationary adaptive estimation algorithm with applications to air-data reconstruction
[NASA-TM-86727] 16 p2706 N85-26699

Method for evaluating perturbation in algorithms for solving navigational problems 16 p2718 N85-26783

The effect of inaccuracies in structural models on the control of large space structures
[AD-A151794] 16 p2732 N85-26856

Control of motion of manipulator robots on basis of first-order kinematic algorithms
16 p2762 N85-27047

Optimal control of electric drive with simultaneous control inputs for motor current and flux
16 p2763 N85-27049

Approximate solution of the problem of fluid oscillations in cavities of revolution 16 p2764 N85-27056

Automation of the process of speech signal segmentation in an analogic-numeric system
[REPT-5/1984] 16 p2768 N85-27082

Development and application of optimum sensitivity analysis of structures
[NASA-CR-175857] 16 p2799 N85-27257

Basic research for the geodynamics program
[NASA-CR-175751] 16 p2825 N85-27424

Parallel time 0(log N) acceptance of deterministic CFLs
[AD-A152255] 16 p2845 N85-27539

A general purpose scatter storage subsystem and a comparison of hashing methods
[NASA-CR-175814] 16 p2845 N85-27542

Comparative study of the digital analysis of areas of the Earth's surface prepared for planting using different classification algorithms
[INPE-3359-PRE/637] 16 p2846 N85-27545

Character recognition using correlation techniques
[AD-A152006] 16 p2847 N85-27549

A data based algorithm for choosing the window width when estimating the integral of f2(x)
[AD-A152093] 16 p2847 N85-27553

Numerical optimization algorithm for engineering problems using microcomputer
[AD-A152135] 16 p2847 N85-27554

Multigrid algorithms on the hypercube multiprocessor
[AD-A152200] 16 p2847 N85-27556

Squeezing the most out of Eigenvalue solvers on high-performance computers
[DE85-007569] 16 p2849 N85-27565

Local uniform mesh refinement on loosely-coupled parallel processors
[AD-A152199] 16 p2850 N85-27571

Corrective-predictive systems
[BLL-M-36063-(5828.4)] 16 p2851 N85-27573

Algorithms for determining the relative complexity of dynamic signals
[BLL-M-36111-(5828.4)] 16 p2851 N85-27574

A fast hidden line algorithm with contour option
[NASA-CR-175803] 16 p2852 N85-27582

Finite elements and the method of conjugate gradients on a concurrent processor
[NASA-CR-175812] 16 p2853 N85-27588

Born inversion with a stratified reference velocity
[AD-A149222] 16 p2853 N85-27594

Scene analysis using recursive frequency domain correlation with energy normalization
[AD-A151777] 16 p2854 N85-27596

Complexity of dense linear system solution on a multiprocessor ring
[AD-A151970] 16 p2854 N85-27598

Evaluation of an algorithm for the solution of the time-dependent Euler equations
[AD-A151993] 16 p2854 N85-27600

A heuristic solution to the spacing problem: Maximizing the minimum Euclidean distance among N points in a convex region
[AD-A152116] 16 p2855 N85-27603

Efficient parallel pseudo-random number generation
[AD-A152235] 16 p2855 N85-27606

Probabilistic algorithms in group theory
[AD-A152253] 16 p2859 N85-27630

Computing the singular value decomposition of a product of two matrices
[DE85-006977] 16 p2859 N85-27631

On the choice of coordinates for semiconductor simulation
[AD-A152214] 16 p2870 N85-27706

Discrete foundation for physics and experience
[DE85-008172] 16 p2872 N85-27720

An adaptive technique and its application in database design 16 p2877 N85-27748

Access path optimization for network database retrieval 16 p2877 N85-27749

Incorporating control into the optimal structural design of large flexible space structures
[AD-A152858] 17 p2909 N85-27937

Enhacements to the TTS-502 time transfer system
17 p2963 N85-28286

The steering of GPS time 17 p2964 N85-28301

Automatic detection of gust fronts
[FAA-PM-85-11] 17 p2995 N85-28516

A comparison of three curve intersection algorithms
17 p3007 N85-28592

Tracking algorithm performance analysis program (TRAPP)
[DE85-007304] 17 p3009 N85-28601

The addition of advanced scene rendering techniques to a general purpose graphics package
[AD-A153323] 17 p3012 N85-28625

Evidential reasoning in expert systems for image analysis
[AD-A153379] 17 p3013 N85-28627

Ray tracing general sweep defined objects
[REPT-84-36] 17 p3014 N85-28636

Efficient parallel solution of linear systems with hyperbolic rotations
[AD-A152355] 17 p3018 N85-28661

Numerical methods for stiff ordinary and elliptic partial differential equations
[AD-A153247] 17 p3020 N85-28675

Parallel Cholesky factorization on a multiprocessor
[DE85-008762] 17 p3021 N85-28682

Montonicity preserving bicubic interpolation, revision 1
[DE85-007976] 17 p3021 N85-28683

A greedy algorithm for the transhipment along a single road problem
[AD-A152343] 17 p3025 N85-28709

Maximum flow in planar networks with exponentially distributed arc capacities
[AD-A153158] 17 p3026 N85-28710

Kirchhoff modeling via wave equation datuming
[AD-A152399] 17 p3028 N85-28727

The AFTI/F16 terrain-aided navigation system
[DE85-008411] 18 p3060 N85-28935

Piloted simulation of an algorithm for onboard control of time-optimal intercept
[NASA-TP-2445] 18 p3063 N85-28949

Application of model following control and estimation techniques to attitude control of maneuvering spacecraft. Part 1: Theory and simulation results
[NLR-TR-82116-U-PT-1] 18 p3065 N85-28957

Computer-aided thermohydraulic design of TEMA type E shell and tube heat exchangers for use in low pressure, liquid-to-liquid, single phase applications
[AD-A153779] 18 p3100 N85-29191

Automatic volume calibration system
[DE85-008955] 18 p3102 N85-29204

Recent developments in nonlinear normal mode initialization 18 p3142 N85-29451

Three-dimensional data display on the two-dimensional screen
[AD-A153699] 18 p3160 N85-29577

A global optimization algorithm using stochastic differential equations
[AD-A153526] 18 p3161 N85-29583

Parallel computation of multiple-scale problems, revision 1
[DE85-009447] 18 p3164 N85-29598

Solving elliptic partial differential equations on the hypercube multiprocessor
[AD-A153464] 18 p3168 N85-29629

A quadratic programming algorithm
[AD-A153476] 18 p3168 N85-29631

Finding the largest l(p)-ball in a polyhedral set
[AD-A153542] 18 p3170 N85-29643

High performance asynchronous limited sensing algorithms for CSMA and CSMA-CD channels
[AD-A153919] 18 p3171 N85-29650

Pipelined Givens method for computing the QR factorization of a sparse matrix
[DE85-009772] 18 p3171 N85-29653

Monotonicity preserving bicubic interpolation
[DE85-004206] 18 p3172 N85-29657

Constructing a bit string universe
[DE85-008317] 18 p3197 N85-29829

Distributed database design tool
[AD-A153760] 18 p3200 N85-29850

On the numerical computation of nonlinear force-free magnetic fields 18 p3203 N85-29871

Research on optimal control, stabilization and computational algorithms for aerospace applications
[NASA-CR-172528] 19 p3221 N85-29970

Study of second order upwind differencing in a recirculating flow
[NASA-CR-174939] 19 p3264 N85-30243

A probabilistic forecasting model of tropical cyclone-generated storm surge for a straight coastline
19 p3314 N85-30544

Performance envelopes and optimal appropriateness measurement
[AD-A154129] 19 p3330 N85-30629
On the step size in Karmarkar's algorithm
[AD-A154040] 19 p3335 N85-30661
An algorithm to test for confluence in a system of left to right rewrite rules
[AD-A154066] 19 p3335 N85-30662
An algorithm for the influence numbers in the expansion of the lumped gravitational potential coefficients in the presence of resonant inclination variation
[AD-A154229] 19 p3336 N85-30669
The origin of the binary-search paradigm
[AD-A154367] 19 p3337 N85-30677
A parallelized point successive over-relaxation method on a multiple instruction multiple data stream computer
[AD-A154377] 19 p3337 N85-30679
A dynamic programming approach to time-staged convex programs
[DE85-010616] 19 p3340 N85-30700
High gain adaptive control of decentralized systems
[DE85-001586] 19 p3343 N85-30717
An iterative method for indefinite systems of linear equations
[NASA-CR-172345] 19 p3345 N85-30728
On MGR (Upsilon) multigrid methods
[AD-A153887] 19 p3345 N85-30733
Numerical algorithms for solving linear algebra problems
[DE85-010310] 19 p3346 N85-30736
An extension to complex-valued functions of an algorithm for numerically inverting the Laplace transform
[DE85-010701] 19 p3347 N85-30743
Bayesian factor analysis
[AD-A154184] 19 p3347 N85-30747
A critique of Deming's discussion of acceptance sampling procedures
[AD-A154305] 19 p3348 N85-30751
Target discrimination using infrared techniques: Theoretical considerations
[AD-A154070] 19 p3350 N85-30762
Measurement problem in PROGRAM UNIVERSE
[DE85-008179] 19 p3378 N85-30959
Modified dynamic hashing
[DE85-011166] 19 p3381 N85-30974
Approximation techniques for parameter estimation and feedback control for distributed models of large flexible structures 20 p3413 N85-31179
An integrated control and minimum mass structural optimization algorithm for large space structures
20 p3413 N85-31183
Experimental verification of identification algorithms for control of flexible structures 20 p3418 N85-31211
An Eigensystem Realization Algorithm (ERA) for modal parameter identification and model reduction
20 p3418 N85-31212
Self-adaptive echo cancellation for telephony
[ENST-84E013] 20 p3441 N85-31353
Computer methods in manipulator kinematics, dynamics and control: A comparative study
20 p3462 N85-31506
Study of new computing algorithms for supercomputers. Application to parallel processing computation
[SNIAS-440-070/84] 20 p3516 N85-31860
Inference in hierarchic classification — data bases
[ENST-84E014] 20 p3518 N85-31873
Efficient solution methods for nonlinear finite element analysis 20 p3519 N85-31886
Time-implicit Monte-Carlo collision algorithm for particle-in-cell electron transport models
[DE85-010758] 20 p3521 N85-31900
New O(6) region near A = 130 and the interplay of triaxiality and gamma-softness in the IBA
[DE85-010957] 20 p3530 N85-31961
Globally-asynchronous locally-synchronous systems
[AD-A154624] 21 p3573 N85-32222
Routing algorithms and stochastic analysis for large communications networks
[AD-A154654] 21 p3573 N85-32225
A multilevel-multigrid method for recirculating flows
21 p3583 N85-32271
Non-model based estimation with applications to sensor calibration using multiple sensors
[AD-A154736] 21 p3589 N85-32306
Emergency modeling of hazardous air pollutants
[AD-A155441] 21 p3614 N85-32461
Practical use of a tropopause height determination algorithm on an MST radar data set, part 1.8B
21 p3618 N85-32479
Criteria and algorithms for spectrum parameterization of MST radar signals 21 p3626 N85-32527
Automated cell detection as a mesocyclone precursor tool
[AD-A154952] 21 p3635 N85-32577
Real-time automated detection of mesocyclones and tornado vortex signatures
[AD-A154966] 21 p3635 N85-32578
Consensus in the presence of partial synchrony (Preliminary version)
[AD-A154705] 21 p3670 N85-32799
SIGMA - A stochastic-integration global minimization algorithm
[AD-A154878] 21 p3671 N85-32806
A comparison and analysis of Vintr's global routing algorithm with the Lee routing algorithm in two-layer printed circuit boards
[AD-A155600] 21 p3673 N85-32816
A practical approach to Karmarkar's algorithm
[AD-A155714] 21 p3673 N85-32818
Evaluation and implementation of a functional microprogram generator
[AD-A155164] 21 p3674 N85-32823
Broadcasting topology and routing information in computer networks
[AD-A155668] 21 p3674 N85-32827
On the dependence of the convergence of Gummel's algorithm on the regularity of the solution
[AD-A154628] 21 p3675 N85-32832
A new fault-tolerant algorithm for clock synchronization
[AD-A154771] 21 p3676 N85-32836
A vectorized nearest-neighbors algorithm of order N using a monotonic logical grid
[AD-A155169] 21 p3679 N85-32853
Poisson formula for radon transformation and numerical image reconstruction algorithm
21 p3697 N85-32973
An image compression survey and algorithm switching based on scene activity
[NASA-TP-2458] 22 p3727 N85-33106
Implementation of the SITAN algorithm in the digital terrain management and display system
[DE85-010659] 22 p3729 N85-33115
Enhancing precision of remote temperature sensing data from satellites under cloudy atmospheric conditions
22 p3734 N85-33148
High-speed adaptation algorithm for harmonic corrector 22 p3765 N85-33336
State of art and development problems in computer-aided design of electronic circuits
22 p3766 N85-33342
Modeling of electronic circuits with high degree of component integration 22 p3766 N85-33343
Diakoptic calculation of characteristics for optimization of linear circuits with respect to parameters of individual branches 22 p3767 N85-33346
Algorithms for constructing models of circuit elements in input language of computer-aided design software
22 p3768 N85-33356
Algorithm for determination of isomorphic graphs
22 p3769 N85-33357
Method of estimating convergence of Haar coefficients in message compression problems
22 p3769 N85-33358
Determination of sensitivity functions for discrete dynamic systems from results of function modeling on digital computer 22 p3769 N85-33359
Analysis of crosstalk in nonhomogeneous multiconductor lines 22 p3769 N85-33360
Gradiental adaptive corrector with optimum tuning step 22 p3776 N85-33403
Multishaker modal testing
[NASA-CR-176139] 22 p3800 N85-33544
Solar energy meteorological research and training program: Region 4
[DE85-011783] 22 p3816 N85-33640
Optimal Bayesian estimators for image segmentation and surface reconstruction
[AD-A155732] 22 p3827 N85-33704
DECODE: A software manual for use with the Serial ASCII Instrumentation Loop (SAIL) system
[AD-A155358] 22 p3828 N85-33709
Parallel Cholesky factorization in message-passing multiprocessor environments
[DE85-012079] 22 p3830 N85-33717
An algorithm for the generation of primitive polynomials
[FUB-17-1984] 22 p3831 N85-33730
Research on distributed artificial intelligence
[AD-A155356] 22 p3833 N85-33733
Some ideas for decomposing the domain of elliptic partial differential equations in the Schwarz process
[DE85-011844] 22 p3834 N85-33739
Modelling of unsteady, incompressible separation on an aerofoil using an inviscid flow algorithm
[GU-AERO-8412] 23 p3894 N85-34122
A versatile computer package for mechanism analysis, part 2: Dynamics and balance
23 p3924 N85-34315
The improved display of 625-line television pictures: Adaptive interpolation
[BBC-RD-1985/5] 23 p3925 N85-34328
Sequential regularization solution of the inverse heat conduction problem
[DE85-010657] 23 p3931 N85-34362
Algorithm for calculation of strain state from measurements of node coordinates of arbitrary curvilinear grid
[BLL-M-36304-(5828.4)] 23 p3940 N85-34422
Short-time creep of ice
[NRC/CNR-TT-2111] 23 p3941 N85-34428
Reordering computations for parallel execution
[NASA-CR-177961] 23 p3957 N85-34522
A theoretical and empirical analysis of coherent ray-tracing 23 p3957 N85-34524
Computer analysis techniques for the temporal evaluation of cardiac wall motion
23 p3958 N85-34530
An analysis and algorithm for filling propagation
23 p3961 N85-34551
A curvilinear coordinate method for the solutions of initial value problems using the third-order upwind differencing scheme
[IPPJ-734] 23 p3975 N85-34642
Cubic interpolated pseudo-particle method (CIP) for solving hyperbolic-type equation
23 p3979 N85-34673
Numerical simulation in astrophysics: Smoothed particle methods 23 p3979 N85-34674
Vector calculation of particle code
23 p3981 N85-34688
Energy management of three-dimensional minimum-time intercept
[NASA-CR-176174] 24 p4064 N85-35186
Communication complexity of distributed shortest path algorithms
[AD-A156049] 24 p4087 N85-35332
An evaluation of a class of practical optimization techniques for structural dynamics applications
[PB85-195766] 24 p4103 N85-35434
Optimal estimation of a high degree gravity field from a global set of 1 deg x 1 deg anomalies to degree and order 250
[AD-A156006] 24 p4117 N85-35519
Comparative analysis of operational forecasts versus actual weather conditions in airline flight planning, volume 2
[NASA-CR-167863] 24 p4119 N85-35535
Reachable grasps on a polygon: The convex rope algorithm
[AD-A155913] 24 p4138 N85-35647
L-step sequential decoding
[AD-A156121] 24 p4138 N85-35649
Pruned error-trellis decoding of certain non-systematic convolutional codes
[AD-A156122] 24 p4138 N85-35650
Three-dimensional finite deformation viscoelastic model accounting for damage effects
[DE85-012951] 24 p4139 N85-35660
Recursive partitioning estimation
24 p4141 N85-35670
Algorithmic approaches in sets of good answers in inverse problems
[PM/84/18] 24 p4142 N85-35677
Smoothing surface data by spline functions
[AD-A155829] 24 p4142 N85-35678

ALIGNMENT
NT SELF ALIGNMENT
Linac quadrupole connections
[DE84-014694] 01 p0118 N85-10810
Gyrodynamic fixture for measuring thrust force components
[AD-D011258] 06 p0760 N85-14860
Measurement of parameters defining orientation of liquid crystals in electrooptic cells 06 p0777 N85-14971
Magnetic alignment theory and the interpretation of polarization 06 p0880 N85-15590
Upgrading flexible infrared waveguides
[AD-A146763] 07 p0970 N85-16160
An alignment fixture for a 2-Degree-of-Freedom (TDF) gyroscope
[AD-A148885] 10 p1422 N85-18969
An evaluation of the 64-meter antenna radial bearing for use on the 70-meter antenna
10 p1464 N85-19238
Mask aligner for solar cell fabrication
[AD-D011450] 10 p1510 N85-19529
Ingot slicing machine and method
[NASA-CASE-NPO-15483-1] 12 p1857 N85-21650
Error analysis of heliostat alignment methods
14 p2281 N85-24128
Modernization of running gear of crane
14 p2286 N85-24163

Non-linear methods for inertial navigation system alignment
[BAE-BT-12683] 15 p2488 N85-25232
Assessment of a nonlinear method of INS alignment — inertial navigation systems (INS)
[BAE-BT-12684] 15 p2488 N85-25233
Surveying and optical tooling technologies combined to align a skewed beamline at the LAMPF accelerator
[DE85-005802] 16 p2804 N85-27664
Alignment and assembly tool for very large diameter cylinders
[NASA-CASE-MFS-28001-1] 18 p3116 N85-29289
Accelerator vibration issues
[DE85-010766] 22 p3842 N85-33791

ALIPHATIC COMPOUNDS
NT ACETALDEHYDE
NT ACETONE
NT ACETYL COMPOUNDS
NT ACETYLACETONE
NT ACETYLENE
NT ACRYLATES
NT ACRYLONITRILES
NT ADENOSINE DIPHOSPHATE
NT ADENOSINE TRIPHOSPHATE
NT ADENOSINES
NT ALKANES
NT ALKENES
NT ALKYL COMPOUNDS
NT ALKYNES
NT ANTHRACENE
NT BUTADIENE
NT BUTANES
NT BUTENES
NT CARBON TETRACHLORIDE
NT CARBON TETRAFLUORIDE
NT CELLULOSE
NT CHLOROETHYLENE
NT CHLOROFORM
NT CHOLINE
NT CITRIC ACID
NT CYANOGEN
NT CYCLIC HYDROCARBONS
NT CYCLOPROPANE
NT DDT
NT DIISOCYANATES
NT ETHANE
NT ETHYL ALCOHOL
NT ETHYLENE
NT ETHYLENEDIAMINE
NT FATTY ACIDS
NT GALACTOSE
NT GLUCOSE
NT GLUTAMATES
NT GLUTAMINE
NT GLUTATHIONE
NT GLYCOGENS
NT GLYCOLS
NT HEXENES
NT HYDRAZINES
NT KETONES
NT MALEATES
NT METHANE
NT METHYL ALCOHOLS
NT METHYL COMPOUNDS
NT NITRATE ESTERS
NT NITROPROPANE
NT NUCLEOSIDES
NT PARAFFINS
NT PENTANES
NT PENTOSE
NT PROPANE
NT PROPYL COMPOUNDS
NT PROPYLENE
NT RIBOSE
NT STARCHES
NT SUCROSE
NT SUGARS
NT THIOLS
NT TRIAMINOGUANIDINIUM AZIDE
NT TRIMETHYL COMPOUNDS
NT URETHANES
NT VINYLIDENE
Converting gasoline farm tractors to run efficiently on farm-produced alcohol
[DE84-015796] 02 p0205 N85-11350
Fluorinated polyurethanes
[AD-D011526] 12 p1810 N85-21353

ALKALI HALIDES
NT CESIUM IODIDES
NT SODIUM CHLORIDES
NT SODIUM IODIDES
Thresholds of optical breakdown in alkali-halide crystals under pulses from CO2-laser 14 p2262 N85-24134
Polarimetric image recorder
[AD-D011605] 16 p2787 N85-27192
Perturbative treatment of quasi-resonant proton neutralization at alkali-halide surfaces
[AD-A154143] 19 p3358 N85-30606

ALKALI METALS
NT CESIUM
NT CESIUM ISOTOPES
NT CESIUM 134
NT CESIUM 137
NT LIQUID LITHIUM
NT LIQUID POTASSIUM
NT LIQUID SODIUM
NT LITHIUM
NT POTASSIUM
NT POTASSIUM 40
NT RUBIDIUM
NT RUBIDIUM ISOTOPES
NT SODIUM
NT SODIUM ISOTOPES
NT SODIUM VAPOR
Corrosion in alkali metal/molybdenum heat pipes
[DE84-014039] 02 p0184 N85-11233
Electrochemical investigations of novel electrode materials
[DE84-014352] 04 p0495 N85-13158
Origin of the Moon: Constraints from volatile elements 04 p0584 N85-13727
The effect of temperature and pressure on the composition density of alkaline metals
[BLL-M-35940-(5828.4)] 05 p0816 N85-13934
Homogeneous reaction involving components of different redox couples. 2: Polarographic studies of the interactions of alkali metal cations with anthracene and fluoroanthene dianions in N,N-dimethylformamide and acetonitrile
[AD-A148667] 08 p1124 N85-17085
S-11 and S-20 photocathode research activity, revision 1
[DE84-017164] 09 p1326 N85-18335
Calorimetric investigation into the possibility of a charge density wave ground state in alkali metals
[DE85-002006] 09 p1397 N85-18795
Classical rainbow scattering of alkali ions on metal surfaces. Application to the investigation of unknown surface structures
[MPIS-10/1984] 11 p1726 N85-20654
Heterocontact effects in point contact electron-phonon spectroscopy of the alkali metals
[AD-A149760] 12 p1800 N85-21290
Studies of metal/carbon surface chemistry
[DE85-005513] 15 p2507 N85-25463
Analysis of alkali liquid metal Rankine space power systems
[DE85-005089] 16 p2741 N85-26917
Ames Laboratory measurements of alkali levels in the Curtiss-Wright PFBC gas stream
[DE85-011357] 22 p3745 N85-33214
Infrared studies of the influence of alkali metals on the C-O bond in chemisorbed carbon monoxide
[DE85-005306] 23 p3911 N85-34232
Metal alkoxides: Models for metal oxides. Alkoxide ligands in early transition metal organometallic chemistry
[DE85-011368] 23 p3916 N85-34269
A study of the chemistry of alkali metals in the upper atmosphere
[AD-A156349] 24 p4117 N85-35524

ALKALIES
NT POTASSIUM HYDROXIDES
Optical detection of alkali compounds
[DE84-015506] 03 p0328 N85-12117
Laser spectroscopy of alkali atom-tetrahaloethylene reactions
[AD-A147431] 07 p0923 N85-15848
Lidar studies of the alkali metals
08 p1184 N85-17460
Resistance of optical coatings to alkali solutions and sea water 14 p2281 N85-24129
Bifunctional oxygen electrodes
[DE85-006871] 17 p2955 N85-28248
Multiple scattering effects in low energy alkali ion scattering: Application to the analysis of adsorbate ordering and bonding geometry
[DE85-007575] 17 p3032 N85-28757
Cation promotion effects in zeolite-supported F-T catalysts
[DE85-008869] 19 p3233 N85-30044
Alkali atom - SbCl(5) reactions: Blue-green chemiluminescence from an inverted population in SbCl
[AD-A154371] 19 p3276 N85-30315
Photofragment fluorescence as a sensitive probe for gas-phase alkali compounds and their photochemistry
[DE85-010707] 22 p3746 N85-33219
Photoionization of alkali and alkaline earth atoms: Na and Mg
[DE85-011812] 22 p3837 N85-33755

ALKALINE BATTERIES
Research on separators for alkaline zinc batteries
[DE85-003062] 12 p1836 N85-21523
Alkaline battery containing a separator of a cross-linked copolymer of vinyl alcohol and unsaturated carboxylic acid
[NASA-CASE-LEW-13102-1] 18 p3093 N85-29144
Low-rate discharge of various electrochemical batteries for use with oceanographic instruments
[AD-A153965] 18 p3095 N85-29159
Electrochemical and morphological study of the effect of temperature on the restructuring and loss of capacity of alkaline battery electrodes
[DE85-006869] 18 p3129 N85-29378

ALKALINE EARTH METALS
Inoculation of non-metallic inclusions in steel 17GS
[BLL-BISI-TRANS-22431-(9022.06)]
17 p2925 N85-28042

ALKALINE EARTH OXIDES
NT BARIUM OXIDES
NT BERYLLIUM OXIDES
NT CALCIUM OXIDES
NT MAGNESIUM OXIDES
Electronically excited alkaline earth oxides: Chemical production and collisional energy transfer processes
[AD-A153172] 17 p3044 N85-28833

ALKALINITY
Tectonic position and formation of young alkaline provinces of continents and oceans
10 p1502 N85-19480
Carbonate chemistry of the Weddell Sea
[DOE/EV-110611/4] 12 p1898 N85-21916
Ohmic potential drop and gas bubble radius distribution in alkaline water electrolysis 17 p2924 N85-28025

ALKALOIDS
NT ATROPINE
NT QUINOLINE

ALKALOSIS
Respiratory chain of alkalophilic bacteria
[DE84-012558] 09 p1360 N85-18556

ALKANES
NT BUTANES
NT ETHANE
NT HEXENES
NT METHANE
NT NITROPROPANE
NT PARAFFINS
NT PENTANES
NT PROPANE
Liquid phase products and solid deposit formation from thermally stressed model jet fuels
[NASA-TM-86874] 04 p0481 N85-13066
Review of the toxicokinetics of n-hexane
[AD-P004016] 06 p0843 N85-15352
Molecular mechanisms of n-hexane neurotoxicity
[AD-P004020] 06 p0843 N85-15354
Electrochemistry at very high potentials: The use of ultramicroelectrodes in the anodic oxidation of short chain alkanes
[AD-A148654] 08 p1123 N85-17078
Fuels combustion research
[AD-A149106] 10 p1457 N85-19178
Transitional metal activation and functionalization of C-H bonds
[DE85-006816] 16 p2746 N85-26949
The distribution of higher n-alkanes in partially frozen middle distillate fuels
[AD-A153940] 18 p3063 N85-29074
Phase behavior and QLS (Quasielastic Light Scattering) in potassium linoleate/n-alkanol microemulsions
[AD-A155028] 21 p3563 N85-32163
Soil extraction kit
[AD-D011736] 22 p3742 N85-33190

ALKENES
NT BUTADIENE
NT BUTENES
NT ETHYLENE
NT HEXENES
NT PROPYLENE
NT VINYLIDENE
A metal-catalyzed rearrangement of alkene-alkynes and the stereochemistry of metallacyclobutene ring opening
[AD-A149084] 10 p1435 N85-19042
Rep rated long life capacitor development: Phase 1 and 2
[DE85-000719] 11 p1629 N85-20258

ALKYD RESINS
New air-curing lacquer systems with high solids content
[BMFT-FB-T-85-005] 17 p2936 N85-28124

ALKYL COMPOUNDS
NT TRIMETHYL COMPOUNDS
Fluorinated aliphatic polyalkylether lubricant with an additive composed of an aromatic phosphine substituted with perfluoroalkylether groups
[AD-D011286] 06 p0770 N85-14927

Super hydrides
[AD-A153499] 18 p3070 N85-28986
Pyrophoric alkylaluminum compounds in decoy flares
[FOA-C-20562-E4] 18 p3078 N85-29039
Improved acid electrolytes for fuel cells
[PB85-178053] 18 p3132 N85-29397
Spray pyrolysis as a synthetic tool
[AD-A153891] 19 p3234 N85-30047
Self-developing polysilane deep-UV resists: Photochemistry, photophysics and submicron lithography
[DE85-007808] 19 p3237 N85-30067

ALKYLATION
Study of application of organic semiconductors to electronic components
[BMFT-FB-T-84-142] 02 p0289 N85-11890
Effects of introduction of alkyl groups into aluminium anodized coatings
[DRIC-T-7244] 03 p0331 N85-12133

ALKYNES
NT ACETYLENE
A metal-catalyzed rearrangement of alkene-alkynes and the stereochemistry of metallacyclobutene ring opening
[AD-A149084] 10 p1435 N85-19042

ALL SKY PHOTOGRAPHY
The ROSAT all-sky survey in X-rays
08 p1243 N85-17843
The ROSAT XUV wide field camera
08 p1243 N85-17844

ALL-WEATHER AIR NAVIGATION
Coverage and buildup of the Navstar constellation
11 p1711 N85-20764
Flying in spite of the weather
[NLR-MP-84021-U] 17 p2895 N85-27847

ALL-WEATHER LANDING SYSTEMS
Development and flight test of a helicopter compact, portable, precision landing system concept
08 p1076 N85-16821

ALLENDE METEORITE
Minor elements and cathodoluminescence of Mg-rich olivines from Murchison and Allende carbonaceous meteorites 06 p0884 N85-15619
X-radiography of slices of the Allende Meteorite
06 p0885 N85-15622
Dynamic thermal episodes in the protosolar nebula: Development of models from observations on CAI's
06 p0887 N85-15633
Mineralogical investigations of lunar samples and meteorites
[NASA-CR-174291] 08 p1258 N85-17918
Lunar sample analysis — Allende meteorite
[NASA-CR-171851] 10 p1572 N85-19911
Interstellar Al-26 and excess Mg-26
15 p2680 N85-26551

ALLOCATIONS
NT RESOURCE ALLOCATION
Spectrum resource assessment of the 1530-1660.5 MHz band
[NTIA/REPT-84/160] 10 p1469 N85-19268
Summary of activities of the Committee on Science and Technology
[H-REPT-98-1189] 12 p1964 N85-22341
An analysis of a dynamic project cost problem
[CSIR-TWISK-338] 13 p2149 N85-23341
Criteria for qualifying for FRG federal CAD/CAM subsidies 15 p2536 N85-25651
Airport and airway system cost allocation model. Volume 7: User's manual
[AD-A152877] 17 p2906 N85-27917
Geostationary orbit capacity study
[REPT-44-3558] 18 p3091 N85-29134
Department of Housing and Urban Development-Independent Agencies Appropriation Act, 1986 20 p3542 N85-32041
National Aeronautics and Space Administration research and development 20 p3542 N85-32042
Progress report on implementing the recommendations of the White House Science Council's Federal Laboratory Review Panel, volume 1
[PB85-185072] 24 p4184 N85-35819

ALLOYS
NT ALUMINUM ALLOYS
NT ANTIMONY ALLOYS
NT ARSENIC ALLOYS
NT AUSTENITIC STAINLESS STEELS
NT BARIUM ALLOYS
NT BEARING ALLOYS
NT BERYLLIUM ALLOYS
NT BINARY ALLOYS
NT BISMUTH ALLOYS
NT BORON ALLOYS
NT BRASSES
NT BRONZES
NT CARBON STEELS
NT CAST ALLOYS
NT CESIUM ALLOYS
NT CHROMIUM ALLOYS
NT CHROMIUM STEELS
NT COBALT ALLOYS
NT COPPER ALLOYS
NT EUTECTIC ALLOYS
NT FERRITIC STAINLESS STEELS
NT GERMANIUM ALLOYS
NT GOLD ALLOYS
NT HAFNIUM ALLOYS
NT HASTELLOY (TRADEMARK)
NT HEAT RESISTANT ALLOYS
NT HIGH STRENGTH ALLOYS
NT HIGH STRENGTH STEELS
NT INCONEL (TRADEMARK)
NT IRON ALLOYS
NT KOVAR (TRADEMARK)
NT LEAD ALLOYS
NT LIGHT ALLOYS
NT LIQUID ALLOYS
NT LITHIUM ALLOYS
NT LOW CARBON STEELS
NT MAGNESIUM ALLOYS
NT MANGANESE ALLOYS
NT MARAGING STEELS
NT MARTENSITIC STAINLESS STEELS
NT MOLYBDENUM ALLOYS
NT MONEL (TRADEMARK)
NT NEODYMIUM ALLOYS
NT NICKEL ALLOYS
NT NICKEL STEELS
NT NIOBIUM ALLOYS
NT NITINOL ALLOYS
NT PALLADIUM ALLOYS
NT PLATINUM ALLOYS
NT POTASSIUM ALLOYS
NT QUATERNARY ALLOYS
NT RARE EARTH ALLOYS
NT REFRACTORY METAL ALLOYS
NT RENE 95
NT RHENIUM ALLOYS
NT RUTHENIUM ALLOYS
NT SELENIUM ALLOYS
NT SHAPE MEMORY ALLOYS
NT SILICON ALLOYS
NT SILVER ALLOYS
NT SODIUM ALLOYS
NT SOLDERS
NT STAINLESS STEELS
NT STEELS
NT TANTALUM ALLOYS
NT TERNARY ALLOYS
NT TIN ALLOYS
NT TITANIUM ALLOYS
NT TUNGSTEN ALLOYS
NT UDIMET ALLOYS
NT URANIUM ALLOYS
NT VANADIUM ALLOYS
NT WASPALOY
NT WROUGHT ALLOYS
NT ZINC ALLOYS
NT ZIRCALOYS (TRADEMARK)
NT ZIRCONIUM ALLOYS
Effects of cobalt, boron, and zirconium on the microstructure of Udimet 738
[NASA-CR-174762] 01 p0027 N85-10166
Minor element effects on gas tungsten arc weld penetration
[PB84-222579] 01 p0056 N85-10370
Materials studies for magnetic fusion energy applications at low temperatures, 7
[DE84-013487] 01 p0122 N85-10837
Method for calculating linear shrinkage and expansion of metals and alloys
[BLL-M-35747-(5828.4)] 02 p0175 N85-11173
Alloying effects of reactive elements in ferritic stainless steels 02 p0178 N85-11196
Erosion of sintered WC-Co alloys
02 p0179 N85-11201
The influence of metallurgical aspects on the pitting corrosion behaviour of high alloy stainless steels
02 p0179 N85-11202
Recent developments on the role of molybdenum in irons and steels 02 p0180 N85-11206
Metastable phase formation in ion implanted metals
[DE84-014945] 02 p0183 N85-11229
Use of magnetic compression based on amorphous alloys as a drive for induction linacs
[DE84-014524] 02 p0277 N85-11805
The modification of metallic corrosion by ion implantation: Engineering applications and fundamentals studies
[AD-P003954] 02 p0286 N85-11870
Application of positron annihilation in materials science
[DE84-014733] 02 p0288 N85-11883
Structural uses for ductile ordered alloys. Report of the committee on application potential for ductile ordered alloys
[AD-A146313] 03 p0332 N85-12139
USSR report: Materials science and metallurgy
[JPRS-UMS-84-007] 03 p0348 N85-12244
Parameters of structural relaxation and mechanical properties of amorphous alloys
03 p0349 N85-12246
HgCdTe surface and defect study program
[AD-A146343] 03 p0434 N85-12764
Change in the nitrogen content when nitrided alloys are heated
[BLL-M-35946-(5828.4)] 05 p0615 N85-13929
Testing of production of silicon-titanium-magnesium alloying composition
[BLL-M-35904-(5828.4)] 05 p0616 N85-13937
Material selection consideration for solar ponds
05 p0686 N85-14284
Modelling of deformation and fracture in high-temperature structural materials
[DE84-016906] 06 p0818 N85-15191
The growth of metastable peritectic compounds
[NASA-CR-171290] 07 p0920 N85-15825
The influence of porosity on the deformation and fracture of alloys
[AD-A148766] 08 p1130 N85-17124
Structural studies of amorphous Mo-Ge alloys using synchrotron radiation
[DE85-002061] 08 p1131 N85-17125
Alloying effects and microstructure of iron aluminides
[DE85-000903] 09 p1295 N85-18137
Behavior of pressurized tubes of candidate alloys in a simulated low-Btu environment
[DE85-003403] 09 p1296 N85-18141
Ion beam studies of hydrogen in metals
[DE84-017422] 09 p1297 N85-18145
Advanced artificial dielectric materials for millimeter wavelength applications
[AD-A148960] 10 p1431 N85-19027
Characterization of erosion of metallic materials under cavitation attack in a mineral oil
[NASA-TM-86934] 10 p1440 N85-19075
Cobalt-free permanent magnet alloys
[AD-A149272] 10 p1441 N85-19079
Radiation-induced compositional redistribution and local phase transformation in irradiated alloys
[DE85-000080] 10 p1441 N85-19082
Kinetics of reaction of metals and non-metals during diffusion welding 11 p1602 N85-20076
Weldability of alloy ABM1 to alloy 1201
11 p1603 N85-20080
Structure of transient zone in diffusion welding of TsTS-19 piezoceramic with AMg6 alloy
11 p1603 N85-20082
Alloys based on NiAl for high temperature applications
[NASA-TM-86976] 12 p1805 N85-21322
Advanced thin film thermocouples
[NASA-CR-175541] 12 p1850 N85-21607
Viscoplastic constitutive relationships with dependence on thermomechanical history
[NASA-CR-174836] 12 p1864 N85-21691
Creep crack growth in ductile alloys
[DE85-003937] 13 p2023 N85-22676
New tooling for plasma cutting technology
13 p2061 N85-22942
Annealing effects in ferromagnetic amorphous alloys
[AD-A150648] 14 p2255 N85-23972
Exploratory corrosion tests on alloys in molten salts at 900(0)C
[DE85-000511] 14 p2257 N85-23983
Tracer diffusion in an ordered alloy: Application of the path probability and Monte Carlo methods
[DE85-002768] 14 p2257 N85-23986
Influence of short-range order on deformation mechanisms in solid solutions
[DE85-006374] 14 p2258 N85-23989
Exploratory corrosion tests on materials and fluids for advanced high-temperature molten-salt storage
[DE85-002911] 14 p2258 N85-23991
Measurements of radiation-induced segregation and diffusion in ion irradiated alloy using implanted manganese
[AERE-R-11526] 14 p2258 N85-23994
Characterization of atomic defects and their aggregates using positron annihilation spectroscopy
[DE85-006208] 14 p2418 N85-24916
USSR report: Materials science and metallurgy
[JPRS-UMS-85-001] 15 p2496 N85-25395
Structural changes with one- and two-stage aging of alloys Ti-Al-Mo-Fe and Ti-Zr-V-Al-Sn
15 p2499 N85-25415
Effects of surface chemistry on hot corrosion life
[NASA-CR-174915] 16 p2708 N85-26711

Properties and microstructures for dual alloy combinations of three superalloys with alloy 901
[NASA-TM-86887] 16 p2749 N85-28963

On the feasibility of Ab Initio calculations of ordering alloy phase diagrams
[DE85-007073] 16 p2751 N85-26979

The influence of melting practice and of microalloying, with rare earth metals and with boron, on the quality of low-carbon steel
[BLL-BISI-22467-(9022.06)] 17 p2925 N85-28036

Powder-metallurgy alloys and steels
[BLL-BISI-TRANS-22239-(9022.06)] 17 p2926 N85-28050

New process for production of bimetal with corrosion-resistant cladding layer
[BLL-BISI-TRANS-22371-(9022.06)] 17 p2927 N85-28056

Production and compaction of amorphous metal powders
[BLL-BISI-TRANS-22367-(9022.06)] 17 p2929 N85-28080

In situ HVEM studies of electron beam-driven composition changes in thin film alloys: Displacement-rate gradient effects
[DE85-007992] 17 p2931 N85-28092

Temperature and manganese content dependences of tensile deformation in iron-high manganese binary alloys
[DE85-007656] 17 p2932 N85-28098

Submerged arc welding of new Czechoslovak micro-alloy steels
[BLL-BISI-TRANS-22193-(9022.06)] 17 p2972 N85-28356

Unalloyed and alloyed line wires of improved properties
[BLL-BISI-TRANS-21930-(9022.06)] 18 p3073 N85-29006

Interfacial segregation and fracture
[DE85-009779] 18 p3075 N85-29019

Local density theory of heats of formation and short-range order parameters in substitutionally disordered alloys
[DE85-008811] 18 p3075 N85-29021

Cavitation erosion of plasma sprayed alloys
[DE85-009542] 18 p3077 N85-29036

Theory of positron annihilation in vacancies in concentrated disordered alloys
[DE85-010267] 18 p3183 N85-29734

Alloy development for irradiation performance
[DE85-010454] 19 p3240 N85-30091

Structure and properties of VT23 alloy welded joints after thermocyclic processing 19 p3246 N85-30125

Fatigue-crack propagation behavior of alloy A-286
[DE85-007460] 19 p3288 N85-30391

Durability of reinforced hard-alloy draw plates
[BLL-M-36278-(5828.4)] 20 p3465 N85-31526

Determination of deformation speed during high-speed deformation of cylindrical shells
[BLL-M-36280-(5828.4)] 20 p3465 N85-31527

Thermomechanical deformation in the presence of metallurgical changes 20 p3466 N85-31533

Results of an interlaboratory fatigue test program conducted on alloy 800H at room and elevated temperatures
[NASA-CR-174940] 21 p3587 N85-32340

Management of Corrosion
[AGARD-LS-141] 22 p3749 N85-33236

Corrosion management strategies for aircraft and related systems 22 p3749 N85-33239

Maintenance and the military environment
22 p3750 N85-33243

Protective systems and maintenance policies for marine environments 22 p3750 N85-33245

The study of the effect of residual microimpurities on the fatigue strength of 55S2 steel
[BLL-M-36317-(5828.4)] 23 p3913 N85-34246

Pitting corrosion of ferrous alloys
[AERE-R-11490] 24 p4078 N85-35273

Fatigue damage detection in steels by optical correlation
[AD-A155830] 24 p4079 N85-35277

X-ray fluorescence analysis of 304L stainless steel
[DE85-013254] 24 p4080 N85-35286

ALLUVIUM

Attenuation of seismic waves at regional distances
[AD-A150198] 13 p2132 N85-23267

ALMUCANTAR

U ELEVATION ANGLE

ALOUETTE SATELLITES

NT ALOUETTE 2 SATELLITE

ALOUETTE 2 SATELLITE

Actual altitudes of radioacoustic sounding in decimeter wavelength band 06 p0826 N85-15243

ALPHA DECAY

International program to improve decay data for transactinium nuclides
[DE85-011258] 20 p3529 N85-31954

Production of stable embryo particles in dense ion tracks of alpha particle emissions in the atmosphere
21 p3644 N85-32638

ALPHA PARTICLES

A system for monitoring radon and its decay products in the atmosphere
[INPE-3065-PRE/494] 03 p0391 N85-12502

Alpha-particle diagnostics with high energy neutral beams
[IPPJ-695] 06 p0863 N85-15485

Feasibility of alpha particle measurement by CO2 laser Thomson scattering
[DE85-001764] 09 p1326 N85-18334

Effect of alpha particles on the stability of Elmo Bumpy Torus (EBT) reactor
[DE84-017266] 09 p1392 N85-18759

Feasibility of alpha particle measurement by CO2 laser Thomson scattering
[DE85-004936] 13 p2097 N85-23081

Noninductive current drive in Tokamaks
[DE85-005427] 14 p2424 N85-24951

An alpha particle diagnostic beam line system to generate an intense Li(O) beam with an ORNL SITEX source
[DE85-010584] 18 p3182 N85-29730

New concept for a wall detector for alpha particles
[DE85-009037] 18 p3183 N85-29740

Effect of polarized radiative transfer on the Hanle magnetic field determination in prominences: Analysis of hydrogen H alpha line observations at Pic-du-Midi
18 p3207 N85-29894

The effects of alpha particle production on the stability of an Elmo Bumpy Torus (EBT) reactor
19 p3369 N85-30895

Production of stable embryo particles in dense ion tracks of alpha particle emissions in the atmosphere
21 p3644 N85-32638

Calculated neutron-induced cross sections for /sup 63,65/Cu/sup 58,60/Ni and (52) Cr from 1 to 20 MeV and comparisons with experiments
[DE85-011928] 22 p3844 N85-33808

Injection of energetic particles following the gamma-ray flares on June 7, 1980, as observed on Helios 1
[SH-1.3-9] 23 p3993 N85-34756

Observations of solar energetic particles at a synchronous orbit
[SH-3.1-1] 23 p4001 N85-34806

Calculation of heavy-ion tracks in liquid water
[DE85-012101] 24 p4149 N85-35725

Gamma-ray production cross sections for alpha-particle induced reactions on F-19 and Na-23
[DE85-012603] 24 p4150 N85-35732

Some nuclear data needs in astrophysics
[DE85-012916] 24 p4168 N85-35842

Determination of primary energy in nucleus-nucleus collisions and the high P(sub)T tail of alpha-particles
24 p4173 N85-35875

ALPHA RADIATION

U ALPHA PARTICLES

ALPHABETS

Character recognition using correlation techniques
[AD-A152006] 16 p2847 N85-27549

ALPHANUMERIC CHARACTERS

NT BINARY DIGITS

Plotting TDL coastal wind forecasts
[PB84-220789] 03 p0397 N85-12533

Axial representations of shape
[AD-A150367] 13 p2151 N85-23356

Comparative study of the digital analysis of areas of the Earth's surface prepared for planting using different classification algorithms
[INPE-3359-PRE/637] 16 p2846 N85-27545

ALPINE METEOROLOGY

Frontal motion in mountainous terrain: Analysis and implications for 0 to 12 hour forecasts
01 p0076 N85-10502

Simple methods in very short-range forecasting based on data from a mesoscale network of automatic stations (ANETZ) and from satellite (Meteosat) and radar — Swiss Alps 01 p0082 N85-10548

Some aspects of matching nowcasting and Very-Short-Range Forecasting (VSRF) products with the need of a multilingual community of a mountainous country — Swiss Alps 01 p0084 N85-10566

Alpine meteorology: Translations of classic contributions by Wagner, A., Ekhart, E. and Defant, F.
[DE84-014929] 01 p0085 N85-10574

Data catalog for the 1982 DFVLR observational Foehn experiment — alpine wind
[DFVLR-FB-84-33] 09 p1358 N85-18543

Measurement of water equivalent of mountain snow cover — ARGOS system 14 p2327 N85-24386

Observation of precipitating clouds by a vertically pointing radar at Morino in the Iburi District, Hokkaido, Japan 15 p2582 N85-25922

Statistical comparison of radar echoes of convective precipitation between the northern Alps and its foreland
[DFVLR-FB-85-07] 17 p2950 N85-28215

ALPS MOUNTAINS (EUROPE)

Alpine meteorology: Translations of classic contributions by Wagner, A., Ekhart, E. and Defant, F.
[DE84-014929] 01 p0085 N85-10574

Crustal stretching and subsidence in sedimentary eastern Switzerland and permo-carboniferous basins in the continental United States
[DE85-000622] 11 p1681 N85-20592

ALTERATION

U REVISIONS

ALTERNATING CURRENT

Induction voidmeter
[DE84-014321] 01 p0050 N85-10329

High-current measurement techniques
[PB85-100444] 11 p1637 N85-20311

Power control for ac motor
[NASA-CASE-MFS-25861-1] 13 p2062 N85-22877

Dynamic characteristics of ac arc in welding aluminum alloys 15 p2500 N85-25424

The performance of an alternating-current thyristor-controlled motor 15 p2546 N85-25716

Induction heating gun
[NASA-CASE-LAR-13161-1] 18 p3065 N85-29063

Alternating current OHMIC heating in a toroidal stellerator 20 p3534 N85-31988

Tailored vacuum chambers for ac magnets
[DE85-010767] 21 p3591 N85-32319

Optimization of design parameters for alternating current stabilizer based on magnetic suspension
22 p3772 N85-33374

ALTERNATING CURRENT GENERATORS

U AC GENERATORS

ALTERNATIVES

Diesel fuel alternatives for engines in civil works prime movers
[AD-A149738] 12 p1817 N85-21400

ALTERNATORS (GENERATORS)

U AC GENERATORS

ALTIMETERS

NT RADIO ALTIMETERS

TCAS 2 logic performance during phase one operational evaluation
[DOT/FAA/PM-84/20] 05 p0595 N85-13793

Theoretical and experimental analyses of laser altimeters for barometric measurements over the ocean
08 p1165 N85-17351

A method for determining mesoscale dynamic topography
[AD-D011412] 08 p1191 N85-17506

Along-track deflection of the vertical from SEASAT: GEBCO (General Bathymetric Chart of the Oceans) overlays
[PB85-129641] 12 p1876 N85-21767

Application of space methods in geodesy
16 p2724 N85-26817

Global mean sea surface based upon a combination of the GEOS-3 and SEASAT altimeter data
20 p3492 N85-31710

SEASAT altimetry for surface height of inland seas
20 p3493 N85-31714

TOPEX error budget 20 p3493 N85-31717

Global geoid and gravity anomaly predictions using the collocation and point mass techniques
[AD-A154517] 21 p3605 N85-32367

ALTITUDE

NT FLIGHT ALTITUDE
NT HIGH ALTITUDE
NT LOW ALTITUDE
NT SEA LEVEL

Change in Venusian atmosphere absorption coefficient with altitude 02 p0163 N85-11103

Critical conditions for the automatic control of landing from decision height in variable winds
[UTIAS-284] 06 p0753 N85-14830

Analytical and physical modeling program for the NASA Lewis Research Center's Altitude Wind Tunnel (AWT)
[NASA-TM-86919] 07 p0909 N85-15757

On the altitudinal distribution of birds and bird strikes in the Netherlands
[AD-P004189] 11 p1580 N85-19952

Atmospheric environment for Space Shuttle (STS-51A) launch
[NASA-TM-86497] 12 p1892 N85-21875

Altitude of auroral scattering observed along auroral electrojets 14 p2339 N85-24465

Statistical comparison of pooled nitrogen washout data of various altitude decompression response groups
[NASA-TM-58265] 15 p2639 N85-26278

A constant altitude flight survey method for mapping atmospheric ambient pressures and systematic radar errors
[NASA-TM-86733] 19 p3217 N85-29951

Comparison of tropopause altitude determination by the Platteville Radar, Sunset Radar and the NWS Rawinsonde
21 p3617 N85-32477

Observations of mesospheric turbulence by rocket probe and VHF radar, part 2.4A
21 p3619 N85-32484

Terrain illumination conditions when taking scanning photographs from space
22 p3736 N85-33159

Altitude variations of cosmic-ray soft and hard components observed by airborne detectors
[SH-6.1-5] 23 p4045 N85-35079

Long-period cosmic ray variations and their altitude dependence
[SH-6.1-19] 23 p4046 N85-35091

Particle distributions in approximately 10(13) - 10(16) eV air shower cores at mountain altitude and comparison with Monte Carlo simulations
[HE-4.2-18] 24 p4190 N85-35994

ALTITUDE ACCLIMATIZATION

Results of study of hypoxia problems
04 p0544 N85-13482

Dynamics of external respiration and gas metabolism under combined effect of hypoxia and hypercapnia
08 p1193 N85-17519

Multiple regression method used to assess animal adaptation to hypoxic hypoxia
12 p1902 N85-21947

Structural changes in thyroid due to high-altitude adaptation in Kirghizia
22 p3820 N85-33666

Effect of dibazol on parameters of nonspecific resistance of subjects in pressurized cabins
23 p3954 N85-34504

ALTITUDE CONTROL

Altitude control using action-demanding interactive displays: Toward an active psychophysics
[AD-P004311] 09 p1267 N85-17965

ALTITUDE SICKNESS

The effect of naproxen on acute mountain sickness and vascular responses to hypoxia
[AD-A145144] 01 p0095 N85-10638

Simulator sickness: Sensorimotor disturbances induced in flight simulators
[AD-P004334] 09 p1271 N85-17988

Airsickness control using biofeedback to self-regulate psychophysiological responses
[AD-A151167] 15 p2617 N85-26126

Effect of spironolactone on acute mountain sickness
[AD-A153780] 18 p3153 N85-29525

ALTITUDE SIMULATION

Analytical modeling of circuit aerodynamics in the new NASA Lewis wind tunnel
[NASA-TM-86912] 07 p0897 N85-15688

The NASA Altitude Wind Tunnel (AWT): Its role in advanced icing research and development
[NASA-TM-86920] 07 p0910 N85-15758

An environmentally-controlled extended-use small animal hypobaric chamber
[AD-A153735] 19 p3221 N85-29974

ALTITUDE TESTS

NT HIGH ALTITUDE TESTS

The KZD-85 engine test. Engine type: 1 cylinder, 2 stroke motor 2100 Husquarna
[FWE-FO-1717] 02 p0205 N85-11354

Oxygen uptake as an indicator of animal adaptation to altitude hypoxia
19 p3324 N85-30595

ALTITUDE TOLERANCE

Hemodynamics and neurodynamics of the human brain during exposure to moderate hypoxic hypoxia
01 p0094 N85-10630

Effect of acute hypoxia on coronary and systemic hemodynamics
23 p3953 N85-34503

ALU (COMPUTER COMPONENTS)

U ARITHMETIC AND LOGIC UNITS

ALUMINA

U ALUMINUM OXIDES

ALUMINATES

Glass corrosion in liquid lithium
[DE85-002086] 09 p1299 N85-18162

Alloys based on NiAl for high temperature applications
[NASA-TM-86976] 12 p1805 N85-21322

Ionic conduction and water diffusion in Li (BETA)-alumina
[DE85-007548] 16 p2755 N85-27005

ALUMINIZING

U ALUMINUM COATINGS

ALUMINUM

NT ALUMINUM ISOTOPES

NT ALUMINUM 26

NT POWDERED ALUMINUM

NT SINTERED ALUMINUM POWDER

The influence of aluminum on the qualities of low and medium carbon steel
[BLL-M-35754-(5828.4)] 03 p0330 N85-12123

Influence of aluminum oxide film on thermocompression bonding of gold wire to evaporated aluminum film
[NASA-TM-77503] 03 p0330 N85-12127

Universal binding energy relations in metallic adhesion
[NASA-TM-86889] 03 p0331 N85-12132

Effects of introduction of alkyl groups into aluminium anodized coatings
[DRIC-T-7244] 03 p0331 N85-12133

Research approaches to qualify aluminum for Ocean Thermal Energy Conversion (OTEC) systems
[DE84-013007] 04 p0476 N85-13034

Thermite and Fe/KClO4: Some thermodynamic calculations
[DE84-018945] 04 p0573 N85-13653

Abundancies of Ni, Cr, CO and major elements in the silicate portion of the Moon: Constraints from primary lunar magmas
04 p0582 N85-13720

Investigation of materials for inert electrodes in aluminum electrodeposition cells
[DE84-015036] 05 p0617 N85-13947

Multiaxial yield behavior of 1100 aluminum following various magnitudes of prestrain
[DE84-013904] 05 p0617 N85-13949

Development and testing of TiB2, used as cathode material in Al-electrolysis cells
[BMFT-FB-T-84-176] 05 p0633 N85-14060

Thermal conductivity of aluminum, copper, iron and tungsten for temperature from 1 K to the melting point
[PB84-235878] 06 p0770 N85-14924

Microstructure, texture and formability of thin aluminium sheets
06 p0796 N85-15086

Recommended aluminum pipe welding procedures for corps of engineers construction
[AD-A146712] 06 p0815 N85-15172

Ultrasonic girth weld evaluation for aluminum substrate of spherical Kevlar-epoxy test specimens
[DE85-001592] 06 p0816 N85-15181

Bulk compositions of Al-rich chondrules in ordinary and carbonaceous chondrites: Variations and similarities
06 p0881 N85-15601

The growth of metastable peritectic compounds
[NASA-CR-171289] 07 p0920 N85-15824

Optimization of the NiCrAl-Y/ZrO-Y2O3 thermal barrier system
[NASA-TM-86905] 07 p0927 N85-15878

Experimental compliance calibration of the NASA Lewis Research Center Mode 2 fatigue specimen
[NASA-TM-86908] 07 p0977 N85-16205

A study of constitutive relations for polycrystalline aluminum during finite dynamic plastic deformation
08 p1172 N85-17388

Advanced NMR characterization of zeolite catalysts
[DE85-000456] 09 p1291 N85-18104

Alloying effects and microstructure of iron aluminides
[DE85-000903] 09 p1295 N85-18137

Beam-foil spectroscopy of highly ionized aluminum atoms
09 p1390 N85-18746

High temperature properties of equiatomic FeAl with ternary additions
[NASA-TM-86938] 10 p1439 N85-19072

Chemistry Institute's advances in making extra-pure aluminum
10 p1443 N85-19093

Mechanical properties of Be-Al composite
10 p1443 N85-19094

Aluminum in biogenic cycle and forms of its occurence in ocean
10 p1499 N85-19463

USSR report: Materials science and metallurgy
[JPRS-UMS-84-005] 11 p1597 N85-20044

Study of phase composition of Al-B plasma coatings
11 p1598 N85-20050

Structure and properties of copper-titanium-aluminum composites obtained by thermoreactive sintering
11 p1600 N85-20061

Patterns in the occurrence of the brittle topologically close-packed phases: Al
[DE85-000592] 11 p1607 N85-20106

Chemically amplified laser direct-writing of aluminum
[DE85-000306] 11 p1639 N85-20324

A computerized study of rigid cones penetrating aluminum targets
[FOA-C-20561-D4] 11 p1648 N85-20384

Effects of chromium and aluminum on mechanical and oxidation properties of iron-nickel-base superalloys based on CG-27
[NASA-TP-2443] 12 p1805 N85-21323

Measurements of distributed combustion
13 p2001 N85-22542

Study of character of adhesive interaction and breaking of polyimid-aluminum foil junction during process of hardening
13 p2014 N85-22637

Directional dependent engineering properties of aluminum-aramid-epoxy laminates
[CCMS-85-02] 13 p2015 N85-22638

An electrochemical study of the corrosion behavior of primer coated 2219-T87 aluminum
[NASA-TP-2459] 13 p2021 N85-22662

Dependence of superplastic flow on state of grain boundaries
13 p2025 N85-22689

Method of calculating strength of joint produced by cold welding of aluminum under discrete loading
13 p2034 N85-22743

AL-124 light-emitting diode in 30 Mbit/s fiber-optic communication line
13 p2060 N85-22925

Microstructure and properties of ferrous alloy weldments
[DE85-005582] 14 p2257 N85-23987

Use of optical techniques in studies of wear rates of anodized aluminum and polymer coatings on aluminum
14 p2259 N85-23997

Fatigue crack topography and crack growth analysis — wrought and cast aluminum
14 p2319 N85-24333

Development of coating for protection of backside of seam in welding of titanium alloys
15 p2500 N85-25421

Ultrasonic SH wave velocity in textured aluminum plates
[AERE-R-11516] 15 p2509 N85-25475

Ion beam mixing of marker layers in Al and Si
[DE85-006227] 15 p2511 N85-25490

Temperature, velocity, and species mapping in an induction plasma
[DE85-004005] 15 p2512 N85-25499

Structure of condensed aluminum thin film metallizations
15 p2512 N85-25501

Reduced-chromium stainless steel substitutes containing silicon and aluminum
[PB85-160786] 15 p2513 N85-25502

Measurement of material properties to Mbar pressures using time-resolved shock wave techniques
[DE85-007319] 15 p2558 N85-25780

Ultrasonic characterization of porosity: Theory
[DE85-005922] 15 p2646 N85-26325

Spectroscopic studies of a railgun muzzle flash
[MRL-R-952] 16 p2728 N85-26837

Ignition of metals in high pressure oxygen
16 p2735 N85-26874

Effect of low-velocity or ballistic impact damage on the strength of thin composite and aluminum shear panels
[NASA-TP-2441] 16 p2742 N85-26924

Microscopic study of the influence of impurities on interface bonding
[AD-A151725] 16 p2743 N85-26928

The application of BRILES rivets for mechanical jointing of Aramid Reinforced Aluminum Laminate (ARALL)
[VTH-LR-387] 16 p2802 N85-27279

Friction and wear behavior of aluminum and composite I-beam stiffened airplane skins
[NASA-TM-86418] 17 p2895 N85-27852

Influence of manganese and heat treatment on structure and properties of Fe-0.1 percent-C-14 percent Cr-based steels
[BLL-BISI-TRANS-22299-(9022.06)] 17 p2928 N85-28071

Preventing the formation of an anomalous structure in chemically sealed low carbon steel
[BLL-BISI-TRANS-22373-(9022.06)] 17 p2930 N85-28085

Research on design of cryotransformers and its prospects for the future
[AD-A152400] 17 p2952 N85-28230

Aluminum-air power cell research and development
[DE85-008117] 17 p2986 N85-28456

Possible indication of an A-dependence of R in deep-inelastic electron scattering from nuclei
[DE85-008174] 17 p3033 N85-28783

Strain fields for aluminum at different tooling temperatures and extrusion ratios
[DE85-008257] 18 p3075 N85-29020

Mechanical properties of adhesively bonded aluminum structures protected with hydration inhibitors
[AD-A153755] 18 p3079 N85-29047

Aluminum-air power cell: The M3-3 experiment
[DE85-008878] 18 p3096 N85-29168

Establishment of a methodology for predicting lifetimes in active solar systems
[DE85-008629] 18 p3130 N85-29383

Study of the equilibrium vacancy ensemble in aluminum using 1D- and 2D-angular correlation of annihilation radiation
[DE85-008967] 18 p3194 N85-29813

Characteristics of charge transfer in the dispersed phase of electrorheological suspensions
[RAE-TRANS-2125] 19 p3233 N85-30040

Separation of Drude and band-to-band spectra in polyvalent metals
[DE85-010247] 19 p3240 N85-30093

Producing titanium-sapphire items by solid-phase bonding through aluminum gasket
19 p3246 N85-30127

Diffusion welding of aluminum with vacuum-tight corundum ceramic
19 p3247 N85-30130

Effect of confinement on failure in 95 TATB/5 KEL-F
[DE85-010790] 19 p3251 N85-30156

Impact dynamics research on composite transport structures
[NASA-TM-86391] 19 p3284 N85-30367

Study of intermediate velocity penetration of steel spheres into deep aluminum targets
[DE85-010419] 19 p3287 N85-30365
Environmental background measurement program
[AD-A153880] 19 p3319 N85-30577
Magnetoconductance in aluminum films, wires, and cylinders 19 p3374 N85-30929
An update of the JPL program to develop Li-SOCl2 cells 20 p3445 N85-31384
Excitation of some alkaline Earth-like ions
[DE85-010737] 20 p3529 N85-31951
Defect production and recovery in FCC metals irradiated at 4.2 K
[DE85-010477] 20 p3536 N85-32014
Thermoelectric properties of beta-boron and some boron compounds
[DE85-011678] 21 p3582 N85-32270
Plasma mass and effective inductance in a small railgun
[AD-A154944] 21 p3589 N85-32304
Laser beam interactions with vapor plumes during Nd:YAG laser welding on aluminum
[DE85-009793] 21 p3593 N85-32328
Properties of Ti-6Al-4V spun formed fuze supports
[DE85-011968] 22 p3792 N85-33498
A new analysis of cosmic ray isotopes at 3 GeV/n from HEAO3-C2 data
[OG-4.3-8] 22 p3879 N85-34031
Fracture behavior of aluminum composites reinforced with fiber 23 p3907 N85-34207
Enthalpies of formation of liquid Fe-Ce-Si and Fe-Ce-Al three-component alloys
[BLL-M-36296-(5828.4)] 23 p3913 N85-34247
The properties of VSt3sp inoculated steel
[BLL-M-35884-(5828.4)] 23 p3915 N85-34263
Aluminum work function: Effect of oxidation, mechanical scraping and ion bombardment
[NASA-TM-87079] 23 p3915 N85-34265
Electrically conductive containment vessel for molten aluminum
[DE85-008518] 23 p3939 N85-34415
Elliptical X-ray analyzer spectrograph application to a laser-produced plasma
[DE85-013790] 24 p4097 N85-35398
Few-particles generation channels in inelastic hadron-nuclear interactions at energy approximately equals 400 GeV
[HE-3.2-9] 24 p4179 N85-35917

ALUMINUM ALLOYS
USSR report: Materials science and metallurgy, no. 93
[JPRS-84810] 01 p0018 N85-10110
Effect of scandium on the structure and properties of Al-Zn-Mg alloys 01 p0018 N85-10111
Influence of parameters of aluminun alloy anodizing process on oxide coating thickness
01 p0018 N85-10113
Suppressing porosity in weld joints of 1420 aluminum alloy 01 p0020 N85-10123
Effect of welding method on corrosion resistance of welded compositions made of 1201 alloy
01 p0020 N85-10124
Implantation of ionized monomer into aluminum alloy 6061 for marine corrosion protection
[AD-A144874] 01 p0028 N85-10172
Biofouling and corrosion studies at the Seacoast Test Facility in Hawaii
[DE84-014643] 01 p0029 N85-10180
Effect of penetrant on fatigue of aluminum alloy lap joints
[NLR-TR-82104-U] 01 p0056 N85-10373
Flight simulation fatigue crack propagation in metal/carbon-epoxy laminates
[NLR-TR-83006-U] 01 p0063 N85-10416
Containerless drop tube solidification and grain refinement of NiAl3 02 p0154 N85-11042
A study of environmental characterization of conventional and advanced aluminum alloys for selection and design. Phase 1: Literature review
[NASA-CR-172387-PHASE-1] 02 p0181 N85-11218
A study of environmental characterization of conventional and advanced aluminum alloys for selection and design. Phase 2: The breaking load test method
[NASA-CR-172387-PHASE-2] 02 p0182 N85-11219
Development of powder metallurgy 2XXX series Al alloys for high temperature aircraft structural applications
[NASA-CR-172408] 02 p0182 N85-11220
The transient oxidation of single crystal NiAl + Zr
[NASA-CR-174796] 02 p0182 N85-11221
Near-threshold fatigue crack growth and crack closure in 17-4 precipitation hardening steel and 2043-T3 aluminum alloy
[FFA-TN-1984-16] 02 p0210 N85-11386
Short cracks and crack closure in AL 2024-T3
[FFA-TN-1984-40] 02 p0210 N85-11387
Plastic deformation and microstructural transformations of metals under shock waves 02 p0272 N85-11775
Feasibility of the electrochemical method of determining nitrogen content in metallic melts
[BLL-M-35730-(5828.4)] 03 p0330 N85-12124
Observation of oxide skin in powder metallurgy aluminum alloys
[AD-A145919] 03 p0331 N85-12135
Acoustic emission monitoring of fatigue in 7010 aluminum alloys
[AERE-R-11167] 03 p0334 N85-12152
Crack resistance of pressed and rolled semifinished goods of aluminum alloys used in load-bearing aircraft wing structures 03 p0348 N85-12245
One-dimensional model of thin films. Analysis of aluminum surface 03 p0350 N85-12254
Study of deformation and fracture of AMg6N weldable aluminum alloy by method of acoustic emission
03 p0352 N85-12266
Tensile and crack propagation tests on aluminum alloys of the 2000 and 7000 series in laminated plate and forged products
[M2-678300] 03 p0373 N85-12383
The Al-Be system: The effects of RSP on structure and phase relating
[DE84-015604] 04 p0474 N85-13019
Electrochemical pitting evaluation of aluminum alloy 7075 in machining coolant
[DE84-016844] 04 p0475 N85-13026
Nondestructive determination of mechanical properties — aluminum alloys 04 p0512 N85-13266
Characterization of aluminum alloy 7010 in moderate width plate and T651 and T7651 metallurgical states
[REPT-44-606/F] 05 p0619 N85-13961
The variable polarity plasma arc welding process: Its application to the Space Shuttle external tank
[NASA-TM-86482] 05 p0641 N85-14115
Evaluation of the crack initiation life behavior of fatigue loaded automotive components made from high strength aluminium alloys
[ESA-TT-733] 05 p0651 N85-14181
Carbon fibre reinforced aluminum matrix composites: A critical review
[AD-A146367] 06 p0764 N85-14883
Phase equilibria of stored chemical energy reactants
[AD-A146527] 06 p0765 N85-14896
Fractographic observation and estimation of crack growth curve of aluminum alloy under ramdom flight simulation loading
[NAL-TR-824] 06 p0768 N85-14913
Wear of anodic oxide films on aluminum alloys in cryogenic liquids
[NAL-TR-818] 06 p0768 N85-14914
The effect of potential on the corrosion fatigue behavior of a precipitation hardened aluminum alloy
[AD-A146537] 06 p0768 N85-14916
Application of solidification theory to rapid solidification processing
[AD-A146619] 06 p0769 N85-14917
Improvement of the ladle deoxidizing of Al-killed steel
[BMFT-FB-T-84-172] 06 p0769 N85-14923
Three-dimensional crack location by acoustic emission
[AERE-R-11277] 06 p0818 N85-15193
Mechanical property data 7050-t736511 alloy
[AD-A147365] 07 p0928 N85-15882
Design of ordered intermetallic alloys for high-temperature structural use
[DE85-000697] 07 p0928 N85-15885
Influence of constant amplitude and variable amplitude loading on crack initiation and micro crack propagation in Al 2024-T3
[DFVLR-FB-84-29] 07 p0979 N85-16220
Electronic structure and properties of magnetic defects in Co(1 + x)Al(1-x) and Fe(1 + x)Al(1-x) alloys
[NASA-TM-77498] 07 p1047 N85-16648
Application of electrochemical engineering methods and theory to solving corrosion and adhesion problems with organic coatings
[AD-A147799] 08 p1129 N85-17115
Fluctuation phenomena studies in chemically sensitive field effect transistor. Part 1: Corrosion of aluminum
[AD-A148240] 08 p1129 N85-17118
Rapid solidification processing and powder metallurgy of Al alloys
[AD-A148427] 08 p1130 N85-17120
Engineering property comparisons of PM and IM aluminum alloy forgings
[AD-B088148L] 08 p1173 N85-17398
A study of spectrum fatigue crack propagation in two aluminum alloys. 1: Spectrum simplification
[NASA-TM-86929] 09 p1293 N85-18124
A study of spectrum fatigue crack propagation in two aluminum alloys. 2: Influence of microstructures
[NASA-TM-86930] 09 p1294 N85-18125
Ion implantation of surgical Ti-6Al-4V alloy
[DE85-000943] 09 p1296 N85-18142
Ti-6Al-4V alloy castings prepared in zircon sand molds and the effect of hot isostatic pressing
[PB85-108532/GAR] 09 p1298 N85-18150
Antifriction nickel-phosphorous coatings on aluminum alloy products 09 p1309 N85-18221
Laser-initiated combustion studies on metallic alloys in pressurized oxygen
[PB85-128114] 10 p1438 N85-19068
Radiation-induced compositional redistribution and local phase transformation in irradiated alloys
[DE85-000080] 10 p1441 N85-19082
Characterization of Nb-8 wt % Al wires by analytical electron microscopy
[DE85-002726] 10 p1442 N85-19086
Development of surface cracks in AMg6 alloy under low-cycle loading conditions 10 p1442 N85-19089
K sub 1* -n diagram of cyclical crack resistance of aluminum alloys 10 p1442 N85-19090
Influence of excess phases on fracture toughness of cast alumiun-magnesium-zinc alloy
10 p1442 N85-19091
Study of superplastic alloys based on Al-Zn-Ca
10 p1442 N85-19092
Excitation modes and parameters of stress waves in metal exposed to single laser pulses
10 p1446 N85-19109
Estimate of quality of aluminum alloy surface preparation for arc welding 10 p1449 N85-19128
Computation of thermal shock-free straightening conditions for aluminum-magnesium alloy welded structures 10 p1449 N85-19131
Evaluation of 7010 aluminium alloy extruded tube in the T76 condition
[BR92019] 11 p1596 N85-20039
Rapidly solidified NiAl and FeAl
[NASA-TM-86941] 11 p1597 N85-20042
USSR report: Materials science and metallurgy
[JPRS-UMS-84-005] 11 p1597 N85-20044
Effect of ingot structure of failure ductility of pressed semifinished products of high-durability aluminum alloys
11 p1597 N85-20045
Structure-phase state and properties of high-durability VAL8 alloy 11 p1597 N85-20046
Mechanism and pattern of fatigue crack growth in aluminum alloys 11 p1597 N85-20047
Development of AK18 alloy production technology based on electrothermic silumin
11 p1598 N85-20048
Estimating deformability upon pressing of aluminum alloys based on results of mechanical testing
11 p1598 N85-20049
Study of microstructure of aluminum and copper alloys after processing with continuous CO2 laser beam
11 p1601 N85-20066
Bending two-layer metal-polymer plates
11 p1604 N85-20085
Effect of form memory in alloys based on Cu-Al systems 11 p1604 N85-20088
Influence of work-hardening on the Portevin-LeChatelier effect
[DE85-002505] 11 p1605 N85-20093
Initial development of nickel and nickel-iron aluminides for structural uses
[DE84-016641] 11 p1608 N85-20108
Effect of mill run and temper variations on barrier anodic film format ion on 6061 aluminum alloy
[DE85-000447] 11 p1608 N85-20112
Micrographic and fractographic examination of alloys 2214 and 2024 for conditions which would cause burning of the metal on being put into solution. trial 17/175
[DGT-23.419] 11 p1609 N85-20117
Fatigue crack growth in Aramid Reinforced Aluminum Laminates (ARALL): Mechanisms and predictions
[DFVLR-FB-84-37] 11 p1609 N85-20118
Crack growth geometry in aluminum alloy sheet material under flight simulation loading. 1: A comparison between TWIST and miniTWIST FALSTAFF and short FALSTAFF. 2: Effect of truncating high loads
[VTH-LR-441] 11 p1609 N85-20119
Carbon filter plates for aluminum filtration at casting
[BMFT-FB-T-84-242] 12 p1808 N85-21343
Performance of Chromel versus Alumel and Nicrosil versus Nisil thermocouple assemblies in vacuum and argon between 1000 deg C and 1200 deg C
[DE85-000810] 12 p1853 N85-21624
Defect characterisation and monitoring by acoustic emission
[AERE-R-11409] 12 p1863 N85-21683
Characterisation of fatigue crack extension by quantitative acoustic emission
[AERE-R-11289] 12 p1866 N85-21721
The strength and characteristics of VPPA welded 2219-T87 aluminum alloy 12 p1946 N85-22224
Ignition phenomena of bulk aluminum alloy as a function of oxygen pressure 13 p1999 N85-22531

Structures of ordered linear dislocation multipoles in Cu-Al alloys
[ISSN-0379-6906] 13 p2021 N85-22664

The characterisation of oxide films on treated aluminium alloys
[MOAD-R-849] 13 p2022 N85-22667

Magnetic studies of Ni3Al(Fe) compounds
[DE85-005262] 13 p2025 N85-22686

USSR report: Materials science and metallurgy
[JPRS-UMS-85-002] 13 p2025 N85-22688

Dependence of superplastic flow on state of grain boundaries 13 p2025 N85-22689

Fatigue and corrosion fatigue resistance of aluminum casting alloy VAL10 and forging alloy AK8
13 p2025 N85-22690

Structural strenght of strip D16T aluminum alloy with low copper and magnesium content
13 p2025 N85-22691

Temperature effects of heterogenizated annealing on structure and properties of V95 aluminum alloy
13 p2025 N85-22692

Anomalies of aluminum structure and properties
13 p2026 N85-22693

New deformable secondary aluminum alloys
13 p2026 N85-22694

Study of processes of modification of Al-Si alloys
13 p2026 N85-22695

Aluminum alloy ATs5K5 (5% Zn + 5% Ca) for superplastic forming 13 p2026 N85-22697

Segregation of silicon in alumin-carbon fiber composites 13 p2028 N85-22706

Composition and thickness of oxide coatings on granule surfaces of aluminum alloys 13 p2030 N85-22719

Basis and pyramidal slipping in single crystals of alpha-alloy Ti-Al-Sn 13 p2032 N85-22730

Problem of pore formation mechanism in welded joints of aluminum alloys in the system aluminum-magnesium-lithium 13 p2032 N85-22732

Analysis of strength and ductility of welded joints in AMtsS and AMg5 aluminum alloys
13 p2033 N85-22737

Effect of moisture in inert gases on density of seam metal and on mechanical characteristics of welded joints of aluminum and aluminum alloys
13 p2034 N85-22744

Characteristics of surface crack development in ATtsS aluminum alloy during slow-cycle loading
13 p2034 N85-22745

China report: Science and technology
[JPRS-CST-84-030] 13 p2041 N85-22777

Experimental investigation of crippling strength of Chinese aluminum alloy (LY12CZ) sections
13 p2041 N85-22779

Use of ferrofluids in machining of metals
13 p2045 N85-22802

The effect of notch acuity on the fracture toughness of silicon carbide/aluminum metal matrix composites
[AD-A150970] 14 p2248 N85-23936

The role of hydrogen in the stress corrosion failure of high strength Al-Zn-Mg alloys
[AD-A150691] 14 p2256 N85-23978

Synthesis and properties of elevated temperature P/M aluminum alloys
[AD-A151031] 14 p2256 N85-23981

Fatigue crack propagation and fracture in 7050 and 7091 aluminum alloy forgings 14 p2318 N85-24324

Effect of deep cooling on crack resistance and low-temperature hardening of aluminum alloys
15 p2496 N85-25396

Fatigue of clad aluminum materials D16T and 2024-T3 with stepped loading 15 p2496 N85-25397

Dynamic characteristics of ac arc in welding aluminum alloys 15 p2500 N85-25424

Pressure welding of corrosion-resistant steel with AMg6 aluminum 15 p2501 N85-25426

Thermocompression welding of parts made from AMts and VT1 alloys 15 p2501 N85-25430

Mechanical properties of welded joints of 1201 aluminum alloy 15 p2502 N85-25431

Mechanisms of corrosion fatigue in high strength I/M (Ingot Metallurgy) and P/M (Powder Metallurgy) aluminum alloys
[AD-A151177] 15 p2509 N85-25478

Mossbauer spectrometry: Testing of a new computer based system and its application to a study of an aluminum-iron-cerium alloy
[AD-A151826] 15 p2510 N85-25483

Metallurgical characterization of aluminum powder consolidation
[AD-A151990] 15 p2510 N85-25484

Superplasticity in a thermo-mechanically processed Aluminum-10.2%Mg-0.52%Mn alloy
[AD-A152016] 15 p2510 N85-25485

Design of ductile polycrystalline Ni3Al alloys
[DE85-005572] 15 p2511 N85-25491

Weldability of Ni3Al-type aluminide alloys
[DE85-006932] 15 p2512 N85-25496

Oxidation of nickel-aluminum and iron-aluminum alloys
[DE85-006930] 15 p2512 N85-25497

USSR report: Materials science and metallurgy
[JPRS-UMS-85-004] 15 p2513 N85-25503

Effect of zirconium on forming ultrafine-grained structure in Al-Mg-Zr alloy 15 p2513 N85-25504

Corrosion behavior of Al4 aluminum alloy hardened by CO2 laser radiation 15 p2514 N85-25512

Pechiney strategy includes development of new materials 15 p2531 N85-25607

Fatigue life, fatigue crack propagation and fracture toughness study of 7075 aluminum alloy subjected to thermomechanical processing 15 p2573 N85-25852

Tensile and fracture toughness properties of Mirage III spars
[AR-003-019] 15 p2578 N85-25899

Transition region for corner cracks at holes
[AD-A151835] 15 p2579 N85-25908

Experimental studies of the electronic structure of 1-2 and 1-3 intermetallic compounds
[DE85-006078] 15 p2682 N85-26432

Durability of Aramid reinforced aluminum laminate (ARALL)
[VTH-LR-423] 16 p2744 N85-26933

Microstructures and properties of rapidly solidified alloys
[NASA-CR-172377] 16 p2748 N85-26961

Evaluation of the corrosion properties of aluminum alloy 5083 weldments
[DE85-007729] 16 p2751 N85-26977

The effect of low sheet thicknesses on the fracture toughness of an Al alloy (7075-T6) — Aramid Reinforced Aluminum Laminate (ARALL)
[VTH-LR-425] 16 p2752 N85-26984

Influence of pretreatment, environment and strain rate on stress corrosion cracking of the aluminum alloy 7075-T6
[VTH-LR-433] 16 p2752 N85-26985

Investigation of the pitting potential of rapidly solidified aluminum-lithium alloys
[VTH-LR-434] 16 p2752 N85-26986

Investigation of the influence of some paint systems and water displacing corrosion inhibitors on anodic undermining corrosion of aluminum 2024 clad alloy — aircraft structures
[VTH-LR-443] 16 p2756 N85-27009

Special features of the one-sided automatic welding of structures of Al-Mg alloys 16 p2792 N85-27222

Aluminum-lithium alloys: The answer of the aluminum industry to the threat of advanced fiber-reinforced materials
[VTH-LR-406] 17 p2932 N85-28102

Erosion of multiphase materials
[DE85-008895] 18 p3066 N85-28978

Evaluation of 7XXX-series aluminum alloys for the W87 aft support ring
[DE85-009067] 18 p3076 N85-29027

Age hardening and atomic structure of an aluminum-6 at. % silver alloy
[DE85-009977] 18 p3077 N85-29031

The precipitation mechanism in a metallic solid solution crystal: Case of the aluminum-copper and aluminum-silver systems
[DE85-009961] 18 p3077 N85-29032

West Europe report: Science and technology
[JPRS-WST-84-035] 18 p3087 N85-29102

Study of the influence of metallurgical factors on fatigue and fracture of aerospace structural materials
[AD-A153913] 18 p3122 N85-29328

Studies of strain rate effects in the deformation of solids by means of stress pulses and ultrasonic methods
[DE85-009463] 18 p3122 N85-29329

Aluminum pressure die casting process for the production of low porosity castings and new casting alloys
[BMFT-FB-T-84-286] 18 p3123 N85-29335

Anisotropic electron-impurity scattering in dilute AlLi: (Small) corrections to the local density approximation
[DE85-002946] 19 p3238 N85-30076

Corrosion fatigue cooperative testing program statistical analysis
[AD-A153886] 19 p3238 N85-30077

Effects of annealing treatments on superplasticity in a thermomechanically processed Aluminum-10.2%Mg-0.52%Mn
[AD-A154414] 19 p3239 N85-30080

USSR report: Materials Science and Metallurgy
[JPRS-UMS-85-005] 19 p3241 N85-30095

Effect of ScAl3 phase dispersion on hardening of alloy Al-6.3 percent Mg-0.21 percent Sc
19 p3241 N85-30096

Mechanical modification of friction surfaces of aluminum alloys by friction transfer 19 p3241 N85-30097

Study of phase equilibria and crystallization processes in Al-Zn-Mg alloy systems 19 p3241 N85-30098

Possible causes of modification and strengthening of aluminum by scandium 19 p3241 N85-30099

Action of plasma and explosion products on alumina
19 p3242 N85-30100

Crystallization of aluminum-based alloys in weightlessness 19 p3242 N85-30101

Specifics of fine structure of pressed aluminum alloys manufactured by plasma atomization
19 p3242 N85-30102

Physical-mechanical characteristics and wear resistance of coatings applied by microarc oxidation
19 p3242 N85-30104

Resistance to corrosion fatigue in aluminum alloy 1561 in sea water 19 p3243 N85-30108

Atomized magnetism-aluminum protective coatings
19 p3244 N85-30116

Welding of steel-aluminum cooling panels for the holds of refrigerator vessels 19 p3246 N85-30120

Chemical composition and kinetics of libration of gases upon welding of aluminum alloys
19 p3247 N85-30131

Means for reducing hydrogen concentration upon surfacing of antifriction aluminum alloys with powder electrode 19 p3247 N85-30132

Properties of heat resistant Ni-Al-Nb alloys with unidirectional eutectic structure
19 p3247 N85-30133

concentration variation of work function of alloys in the system nickel-titanium-aluminum
19 p3247 N85-30134

Optimisation of MCr Al coating compositions for marine gas turbines
[BR91159] 20 p3394 N85-31066

Crack growth data for two aluminum alloys 7050-T73651 and 2024-T3
[FFA-TN-1984-51] 20 p3432 N85-31290

Influence of the molding joint plane on the fatigue resistance of the alloys 7010 and 7050. Test Report No. M1-631600
[PV-M1-631600] 20 p3470 N85-31562

Modifications of flight-by-flight load sequences to provide for good fracture surface readability
[NLR-MP-84012-U] 20 p3472 N85-31577

Understanding and laboratory prediction of the atmospheric corrosion behavior of steels and of non-ferrous metals and alloys
[AD-A154642] 21 p3566 N85-32179

The effect of abrasive blasting on the fatigue and corrosion of an aluminium-copper alloy
[AD-A154954] 21 p3566 N85-32182

The effect of alloy additions on superplasticity in thermomechanically processed high magnesium aluminum-magnesium alloys
[AD-A155142] 21 p3567 N85-32184

Experimental studies of the geometric and electronic structure of chemisorption bonding
[PB85-192250] 22 p3747 N85-33228

Mechanical properties of plasma arc cut steel
23 p3905 N85-34188

The influence of temperature on static and dynamic SCC crack growth behavior in aluminum alloy
23 p3905 N85-34190

A fractographic study on mode 2 and mode 3 SCC crack growth in an Al-Zn-Mg alloy 23 p3905 N85-34191

Fatigue crack retardation phenomenon caused by single-multiple overloads in 2017-T3 aluminum allow
23 p3906 N85-34196

Method for preparing high purity vanadium
[DE85-006412] 23 p3913 N85-34242

Influence of particle erosion on the microstructural changes in metals and alloys
[TI85-901384] 23 p3917 N85-34276

Fatigue lives of specimens representing critical locations in Mirage 3 spars under Australian and Swiss test spectra
[ARL-STRUC-R-415] 24 p4064 N85-35187

Studies of the crystallization process of aluminum-silicon alloys using a high temperature microscope
[NASA-TM-77869] 24 p4078 N85-35272

Development of a mathematical model for predicting the percentage fatigue life increase resulting from shot peened components
[AD-A155774] 24 p4101 N85-35425

Prediction of plasticity characteristics for three-dimensional fracture specimens comparison with experiment
[AD-A156425] 24 p4102 N85-35430

ALUMINUM ARSENIDES

AlAs/GaAs superlattice barrier unipolar diode structure
[DE85-001904] 11 p1736 N85-20921

A study of Ga(.47)In(.53)As and Al(.48)In(.52)As for very high frequency device applications
[AD-A151995] 16 p2870 N85-27706

Summary of recent studies on AlGaAs/GaAs radiation hardened photodiodes
[DE85-008601] 18 p3194 N85-29812

ALUMINUM BORON COMPOSITES

Influence of 3% NaCl solution on rate of accumulation of damage and residual strength of aluminum-boron composite 13 p2027 N85-22699

Division boundary in Al-B composite material with boron in contact with solid and liquid aluminum
13 p2027 N85-22704

Estimating degree of development of physical-chemical interaction among components in Al-B fiber composite material 13 p2027 N85-22705

Effect of operating medium on cyclic durability of AD33-W composite 13 p2020 N85-22716

Effect of surface state on durability of aluminized boron fibers 19 p3244 N85-30115

Features of the interaction between fibers and matrix in production of aluminum-boron composite material
19 p3244 N85-30117

ALUMINUM CARBIDES

Segregation of silicon in alumin-carbon fiber composites 13 p2028 N85-22706

ALUMINUM CHLORIDES

A potentiometric study of chloroaluminate equilibria in the aluminum chloride - 1-methyl-2-ethylimidazolium chloride ionic liquid
[AD-A144729] 01 p0023 N85-10144

Spectrophotometric studies of iodine complexes in an aluminum chloride - butylpyridinium chloride ionic liquid
[AD-A145074] 01 p0024 N85-10150

Electrochemistry and electrochemical methodology in molten salts
[AD-A149613] 12 p1799 N85-21284

ALUMINUM COATINGS

Influence of aluminum metallization coatings on corrosion fatigue properties of steel
01 p0018 N85-10112

The experimental mod 3 firefighters' aluminized crash-rescue, fire-proximity hood
[AD-A144883] 01 p0098 N85-10855

Qualitative and quantitative compositional analysis of shale derived by gas chromatography and combined gas Chromatography/Mass spectrometry. Executive summary
[AD-A148360] 07 p0924 N85-15851

Accelerated aging of aluminized acrylic solar mirror materials
[DE85-002883] 11 p1612 N85-20138

Corrosion of aircraft Al and Al-Zn ion plated steel fasteners 13 p2021 N85-22666

Impact ionization from gold, aluminum and PCB-Z — Giotto spacecraft paint PCB-Z 14 p2244 N85-23910

Mechanisms of buildup and properties of aluminum coatings on heat-resistant nickel alloys
15 p2513 N85-25506

Technology development for thin-film-trace humidity sensors
[BMFT-FB-T-84-288] 17 p2969 N85-28338

Action of wear-inhibiting Al2O3-coatings when applied to hard metal cutting tools
[BLL-RISLEY-TR-5041-(9091.9F)]
24 p4081 N85-35292

ALUMINUM COMPOUNDS
- NT ALUMINATES
- NT ALUMINUM ARSENIDES
- NT ALUMINUM CARBIDES
- NT ALUMINUM CHLORIDES
- NT ALUMINUM NITRIDES
- NT ALUMINUM OXIDES
- NT ALUMINUM SILICATES
- NT BERYL
- NT FELDSPARS
- NT SAPPHIRE

The X-ray Absorption Coefficient Fine Structure (EXAFS) study on precipitates in AlCu
[DESY-SR-84-15] 01 p0025 N85-10153

The B2 aluminides as alternative materials
[NASA-TM-86937] 10 p1440 N85-19076

ALUMINUM GALLIUM ARSENIDES

Effect of liquid phase composition on thickness of epitaxial Ga sub (1-x) Al sub x As films
02 p0257 N85-11683

Thin film (Al, Ga)As heterojunction solar cells
02 p0258 N85-11691

Gallium arsenide/AlGaAs multilayer structures with special doping profiles for microwave and optoelectronic devices
[BMFT-FB-T-84-207] 08 p1227 N85-17725

Fabrication and I-V characterization of AlGaAs/GaAs MODFETs with P-type surface layers grown by molecular beam epitaxy
[AD-A151695] 15 p2660 N85-26415

ALUMINUM GRAPHITE COMPOSITES

Localized corrosion currents from graphite/aluminum and welded SiC/Al metal matrix composites
[AD-A150866] 14 p2256 N85-23980

ALUMINUM ISOTOPES
- NT ALUMINUM 26

Cosmogenic Na-22 and Al-26 in Luna-24 lunar drill core soil samples 13 p1981 N85-22427

SMM detection of interstellar Al-26 gamma radiation
[OG-3.2-1] 22 p3874 N85-34001

Galactic distribution of interstellar Al-26
[OG-3.2-3] 22 p3874 N85-34002

ALUMINUM NITRIDES

Aluminum nitride insulator for 3-5 MIS (Metal-Insulator-Semiconductor) applications
[AD-A147842] 07 p1049 N85-16662

AlN insulator for 3-5 MIS applications
[AD-A150674] 14 p2426 N85-24962

Passivation on high Q acoustic strain sensor for accelerometer
[AD-A153585] 18 p3177 N85-29695

ALUMINUM OXIDES
- NT SAPPHIRE

Fundamental studies of structure property relationship in transformation toughened ceramics
[DE84-015344] 01 p0033 N85-10204

Trivalent ion exchange in beta alumina
[AD-A145373] 02 p0172 N85-11151

The transient oxidation of single crystal NiAl+Zr
[NASA-CR-174756] 02 p0182 N85-11221

Influence of aluminum oxide film on thermocompression bonding of gold wire to evaporated aluminum film
[NASA-TM-77503] 03 p0330 N85-12127

Annealing of implanted Al-2O-3 in a reducing environment
[DE84-015370] 03 p0332 N85-12140

Reinforcement of molybdenum disilicide with nematic crystals of aluminum oxide 03 p0353 N85-12269

Phase transformations of AlPO4 with SiO2 structures
03 p0425 N85-12713

Structural changes during milling of aluminum oxide powders
[NASA-TM-77488] 04 p0472 N85-13008

Tests and modeling for sintering theory
[DE84-015110] 04 p0473 N85-13012

Erosion of multiphase materials
[DE84-015816] 04 p0474 N85-13018

Formation of subsurface Al2O3 layers in aluminum by oxygen ion implantation
[DE84-015529] 04 p0474 N85-13020

Surface diffusion of high temperature vapors in porous alumina
[DE84-015968] 04 p0479 N85-13053

Effect of doping on the voltage holdoff performance of alumina insulators in vacuum
[DE84-017163] 04 p0480 N85-13060

An optical and mass spectrometric study of the aluminum-oxygen flame
[AD-A147434] 07 p0923 N85-15849

Microbiological method for the desiliconization of high-silica bauxites
[BLL-MINTEK-TR-1168-(5810.5759)]
07 p0925 N85-15864

Fundamental tribological properties of ceramics
[NASA-TM-86915] 07 p0930 N85-15893

Dispersed metal-toughened ceramics and ceramic brazing
[NASA-CR-174284] 07 p0933 N85-15916

Transformation toughened ceramics for the heavy duty diesel engine technology program
[NASA-CR-174889] 07 p1055 N85-16696

Mechanical properties of adhesively bonded aluminum structures protected with hydration inhibitors
[AD-A148123] 08 p1133 N85-17139

Ionic and molecular transport in beta- and beta"-alumina
[DE85-000984] 09 p1380 N85-18680

High temperature laser interferometric studies of solid electrolytes 09 p1396 N85-18785

Formation of amorphous layers in Al2O3 by ion implantation
[DE85-001289] 09 p1397 N85-18794

Sub-eutectic densification and second phase formation in Al2O3 - CaO
[DE85-002085] 09 p1398 N85-18796

Scanning photoacoustic microscopy of aluminum with aluminum oxide, roughness standards and rubber
[AD-A149480] 10 p1441 N85-19081

Amorphization of ceramics by ion beams
[DE85-000936] 10 p1453 N85-19156

Modeling thermal plasma material processing experiments
[DE85-001561] 10 p1560 N85-19838

Material growth and characterization for solid state devices
[NASA-CR-174410] 10 p1561 N85-19847

Laser processing of ceramics
[DE85-001184] 11 p1612 N85-20135

Slit-ring test for evaluating fracture in tubular cross sections
[DE85-003550] 11 p1654 N85-20416

Electrochemical processes at the sodium (BETA)" alumina interface
[DE85-004653] 12 p1802 N85-21305

The Valence- and conduction-band structure of the sapphire (1102) surface
[AD-A150001] 12 p1940 N85-22184

Distributed combustion: A mechanism of acoustic suppression 13 p2001 N85-22543

Formation of alumina layers on iron-base alloys
[BLL-T6418/BG/LRS/LRST737/84]
13 p2020 N85-22657

Composition and thickness of oxide coatings on granule surfaces of aluminum alloys 13 p2030 N85-22719

Dispersed-metal-toughened alumina
[NASA-CR-174687] 13 p2037 N85-22758

Research directed advanced high temperature coating system beyond current state-of-the art systems
[AD-A150696] 14 p2255 N85-23974

Density and thermal expansion measurements of several mixed oxide glasses in the solid and liquid regions
[DE85-006134] 14 p2261 N85-24014

Structure and properties of ion-implanted Al sub 2 O sub 3
[DE85-005374] 14 p2430 N85-24987

Temperature, velocity, and species mapping in an induction plasma
[DE85-004005] 15 p2512 N85-25499

France develops own aluminum-based composite ceramic 15 p2534 N85-25636

Degradation phenomena in solid electrolytes
[DE85-007066] 15 p2587 N85-25949

Particulate and whisker toughened alumina composites
[DE85-005239] 16 p2743 N85-26930

Thermal annealing of Fe implanted Al2O3 in oxidizing and reducing environment: Revised version
[DE85-007546] 16 p2752 N85-26983

Test and modeling for sintering theory
[DE85-007761] 16 p2755 N85-27004

Microstructure-mechanical property relationships in transformation-toughened ceramics
[DE85-009722] 17 p2935 N85-28117

Diffusion welding of aluminum with vacuum-tight corundum ceramic 19 p3247 N85-30130

Vibrational properties of disordered solids: Far infrared studies
[DE85-010400] 19 p3377 N85-30951

Improved materials for composite and adhesive joints
[AD-A155065] 21 p3562 N85-32153

The Faraday affect in ruby and corundum in strong magnetic fields 21 p3697 N85-32967

Method for preparing Pb-(beta)-aluminum ceramic
[DE85-011665] 22 p3752 N85-33256

Preparation and use of very pure o-D2
[DE85-009415] 22 p3843 N85-33800

Electrolytic synthesis of colored eta alumina film
23 p3906 N85-34201

Rotating bending fatigue strength of silicon carbide and alumina-fiber reinforced aluminum
23 p3907 N85-34208

Grain boundary and surface diffusion in oxide systems
[DE85-007291] 23 p3985 N85-34715

Action of wear-inhibiting Al2O3-coatings when applied to hard metal cutting tools
[BLL-RISLEY-TR-5041-(9091.9F)]
24 p4081 N85-35292

Noise in silver beta alumina ceramics
[AD-A156135] 24 p4082 N85-35297

Size and shape dependence of CO adsorption sites on sapphire supported Fe microcrystals
[NASA-CR-176171] 24 p4160 N85-35794

Noise in sodium beta alumina crystals
[AD-A156025] 24 p4161 N85-35798

ALUMINUM SILICATES

Modified aluminosilicide coating for heat-resistant nickel alloys 15 p2514 N85-25509

Conditions for formation of parageneses containing kyanite-orthoclase in region of Mount Provender and Pratt Peak (Shackleton Range, Antarctica)
19 p3298 N85-30447

ALUMINUM 26

Interstellar Al-26 and excess Mg-26
15 p2680 N85-26551

Gamma-ray line emission from Al-26 produced by Wolf-Rayet stars
[OG-3.2-5] 22 p3875 N85-34003

ALVEOLI

Pulmonary blood flow and oxygenation of arterial blood in a healthy subject upon 7 days hypokinesia
07 p1014 N85-16439

AMAZON REGION (SOUTH AMERICA)
Systematic data interpretation of remote sensing in the reception of hydrocarbons, volume 1
[E85-10008] 02 p0215 N85-11421
Eddy correlation measurements of energy partition for Amazonian forest
[INPE-3195-PRE/559] 06 p0827 N85-15252
Water and climate, study of one case
07 p1002 N85-16369
The water balance and climate — Amazon region
07 p1003 N85-16370
Ecological impacts of hydroelectric projects in Amazonia 07 p1003 N85-16374
The Amazon and climate 07 p1003 N85-16376
Deforestation, floodplain dynamics, and carbon biogeochemistry in the Amazon Basin
08 p1144 N85-17216
Information for space radar designers: Required dynamic range vs resolution and antenna calibration using the Amazon rain forest 08 p1147 N85-17239
Meridional penetration of frontal systems in South America and its relation to organized convection in the Amazon
[INPE-3407-PRE/676] 10 p1518 N85-19572
System of interpretation of remote sensing data when hydrocarbons are present, volume 2
[INPE-3087-TDL/162-VOL-2] 16 p2810 N85-27326
The ARGOS system in Brazil — hydrology
16 p2813 N85-27349
The micrometeorology of an Amazonian rainforest
[INPE-3515-PRE/740] 19 p3315 N85-30551
On the dynamical climatology of the Amazon Basin and associated rain producing mechanisms
[INPE-3531-RPE/477] 19 p3315 N85-30552
AMBIENCE
Characterization of material surfaces exposed to atomic oxygen on space shuttle missions
12 p1946 N85-22220
AMBIENT TEMPERATURE
Advances in room-temperature solid-state gamma-ray spectrometry
[DE84-015944] 04 p0469 N85-12987
Attempted measurement of gaseous H-2O-2 in the ambient atmosphere
[DE85-001937] 06 p0834 N85-15306
NBS (National Bureau of Standards) daylight availability database
[PB84-245745] 07 p1054 N85-16688
Microwave surface resistivity of several materials at ambient temperature 10 p1463 N85-19226
Short duration winter-time performances of different passive solar systems
[DE85-000850] 11 p1675 N85-20557
The temperature of a glass-encapsulated solar cell estimated from ambient air temperature and global radiation
[GKSS-84-E-36] 11 p1676 N85-20563
Portable Automated Mesonet (PAM) data from the 1980 experiment in Anderson Creek Valley
[DE85-004361] 13 p2139 N85-23282
Soil temperature extrema recovery rates after precipitation cooling 20 p3491 N85-31697
Results of an interlaboratory fatigue test program conducted on alloy 800H at room and elevated temperatures
[NASA-CR-174940] 21 p3597 N85-32340
Improved Nominal Operating Cell Temperature (NOCT) test procedure 21 p3612 N85-32449
Lake ice occurence as a possible detector of atmospheric CO2 effects on climate
[DE85-012987] 23 p3950 N85-34480
AMBIGUITY
About ambiguity and Q-functions
[AD-A145283] 02 p0250 N85-11636
Ambiguity and uncertainty in probabilistic inference
[AD-A147378] 07 p1035 N85-16572
The ambiguity function of random binary-phase-coded waveforms
[AD-A148906] 10 p1466 N85-19249
The ambiguity function and the Wigner distribution
[AD-A150095] 12 p1829 N85-21482
Language design, computers and brains
[AD-A152819] 17 p3008 N85-28594
AMBIPOLAR DIFFUSION
Breakdown of intrinsic ambipolarity for the radial diffusion due to a rotating RF field 23 p3977 N85-34660
Effect of ECH and ICH on ambipolar potential in NBT-1M 23 p3978 N85-34661
Analytic and numerical calculations of the ambipolar electric field in a stellarator 23 p3978 N85-34665
AMBIT
U FIELD THEORY (PHYSICS)
AMERICIUM
NT AMERICIUM ISOTOPES
NT AMERICIUM 241
Americium thermodynamic data for the EQ3/6 database
[DE84-017065] 04 p0573 N85-13656
Americium metal preparation on the multigram scale
[DE85-003735] 13 p2024 N85-22683
Thermodynamic systematics of oxides of americium, curium and neighboring elements
[DE85-009704] 18 p3197 N85-29831
AMERICIUM ISOTOPES
NT AMERICIUM 241
Historical review of californium-252 discovery and development
[DE85-010223] 19 p3362 N85-30844
AMERICIUM 241
Role of natural dissolved organic compounds in determining the concentrations of americium in natural waters
[DE85-010266] 19 p3229 N85-30022
Determination of the average neutron activation cross section with an annular-shaped 241 Am/Be neutron source and a NaI(T1) detector for the 27 Al (n,p)27 Mg-reaction
[REPT-4/1984] 20 p3532 N85-31975
The 1984 environmental monitoring program report for Idaho National Engineering Laboratory site
[DE85-011209] 22 p3812 N85-33611
AMIDES
NT POLYIMIDES
NT UREAS
Properties of polycaproamide fibers modified by grafted polyacrylonitrile 06 p0761 N85-14867
Low temperature synthesis of polycaproamide copolymers grafted with polydimethylaminothylmethacrylate
06 p0761 N85-14868
Preparation of fire-resistant infusible polycaproamide fiber 06 p0763 N85-14877
Working medium for sorption heat pumps
[BLL-T6360/BG/WH785/84] 06 p0807 N85-15131
AMINES
NT ANILINE
NT CATECHOLAMINE
NT DIAMINES
NT ETHYLENEDIAMINE
NT TRIAMINOGUANIDINIUM AZIDE
The 7-Amino-4,6-Dinitrobenzofuroxan, an insensitive high explosive
[AD-A145665] 02 p0188 N85-11257
Study of reaction kinetics and development of elastic properties in network polymerization systems by the impulse technique
[AD-A148187] 08 p1133 N85-17141
Molecular dynamics in nitramines and modified nitramines
[AD-A148515] 08 p1220 N85-17686
Amine salts as bonding agents
[AD-D011543] 12 p1817 N85-21396
Chemical interpretation of the relaxed permittivity during epoxy resin cure
[AD-A150955] 14 p2260 N85-24005
Polyamines as possible modulators of gravity induced calcium transport in plants 15 p2606 N85-26060
Processable and stable conductive polymers
[AD-D011684] 19 p3249 N85-30143
Nuclear magnetic resonance study of the intramolecular rearrangement of 2-(5-cyanotetrazolato)pentaammine cobalt (III) perchlorate
[DE85-010610] 22 p3839 N85-33772
Metal (2) 4,4',4',4'' phthalocyanine tetraamines as curing agents for epoxy resins
[NASA-CASE-ARC-11424-1] 23 p3919 N85-34281
AMINO ACIDS
NT ALANINE
NT ASPARTIC ACID
NT GLUTAMINE
NT GLUTATHIONE
NT GLYCINE
NT METHIONINE
NT PEPTIDES
NT POLYPEPTIDES
NT TRYPTOPHAN
Skeletal muscle metabolism in hypokinetic rats
[NASA-CR-174069] 02 p0233 N85-11520
Effects of hyperthermia on free amino acids in rat brain and in subcellular fractions 11 p1691 N85-20631
USSR report: Space Biology and Aerospace Medicine, volume 18, no. 6, November - December 1984
[JPRS-USB-85-002] 12 p1900 N85-21931
Cosmonauts' blood plasma free amino acid levels during preflight training 12 p1901 N85-21937
Remarks on preparation of indandione detection reagents
[NASA-TM-77905] 21 p3580 N85-32146
Cytochromes and iron sulfur proteins in sulfur metabolism of phototrophic bacteria
21 p3657 N85-32718
Investigation of some aspects of amino acid metabolism in man during brief exposure to antiorthostatic hypokinesia combined with ultraviolet radiation
22 p3822 N85-33678
AMMETERS
Pulsed-power system diagnostics: Electromagnetic data interpretation along pulse lines
[AD-A146607] 06 p0810 N85-15148
High-current measurement techniques
[PB85-100444] 11 p1637 N85-20311
Beam current sensor
[DE85-011600] 20 p3459 N85-31482
AMMONIA
NT LIQUID AMMONIA
Electrochemistry in near-critical and supercritical fluids. I. Ammonia
[AD-A146429] 06 p0765 N85-14894
Silazane precursors to silicon nitride
[AD-A146791] 07 p0931 N85-15899
Photosynthesis of ammonia
[DE85-001482] 11 p1595 N85-20029
Studies of the kinetics and mechanisms of ammonia synthesis and hydrodesulfurization on metal single crystal surfaces
[DE85-001650] 11 p1595 N85-20030
Meteorological support for the 1983 Deep Creek, Maryland experiment
[DE85-002616] 11 p1678 N85-20575
Effect of high ammonia content in closed environment on some parameters of human nitrogen and carbohydrate metabolism against background of a controlled diet
12 p1903 N85-21948
Ammonia formation caused by the presence of water in the wet grinding of silicon nitride powder
[NASA-TM-77746] 14 p2249 N85-23937
Results of recent large-scale NH3 and N2O4 dispersion experiments
[DE85-004988] 15 p2589 N85-25960
Cation promotion effects in zeolite-supported F-T catalysts
[DE85-009969] 19 p3233 N85-30044
Facility for large-scale hazardous gas testing
[DE85-011852] 21 p3564 N85-32169
Metal alkoxides: Models for metal oxides. Alkoxide ligands in early transition metal organometallic chemistry
[DE85-011368] 23 p3916 N85-34269
Determination of properties of zeolite/refrigerant combinations for solar refrigeration systems
[DE85-012009] 23 p3945 N85-34448
AMMONIUM COMPOUNDS
NT AMMONIUM NITRATES
NT AMMONIUM PERCHLORATES
Additives for heat engine coal slurry fuels
[DE84-016434] 05 p0621 N85-13971
Synthesis of antimicrobial chemical fibers and fibrous materials containing quaternary ammonium compounds and their utilization 06 p0762 N85-14872
Michelle-derived catalysts for extended Schulz-Flory
[DE85-005656] 17 p2922 N85-28012
Throughfall rate and chemistry studies: Whiteface Mountain
[DE85-012407] 23 p3947 N85-34464
AMMONIUM NITRATES
Eutectic explosives containing ammonium nitrate
[DE84-015705] 01 p0034 N85-10213
The IMX double direct process
[AD-A146250] 03 p0340 N85-12188
Application of Monte Carlo and molecular dynamics methods to the calculation of thermodynamic properties of molten salts
[AD-A148897] 10 p1565 N85-19869
Explosibility of ammonium nitrate
[HSE-TRANS-11111] 19 p3252 N85-30164
AMMONIUM PERCHLORATES
The heat sensitivity of solid propellants
08 p1117 N85-17043
Mechanism of burning rate enhancement by ferric oxide 13 p2002 N85-22546
AMMUNITION
Effects of perforation L/D ratio and slotting on stick propellant combustion
[AD-A148654] 10 p1456 N85-19177
Laboratory vibration schedules
[AD-A155856] 24 p4064 N85-35186
AMOR ASTEROID
The discovery circumstances of Earth-approaching asteroids
[NASA-CR-174327] 08 p1258 N85-17920
AMORPHOUS MATERIALS
Deuteron NMR (Nuclear Magnetic Resonance) in relation to the glass transition in polymers
[AD-P003910] 01 p0032 N85-10196
Studies of laser melting and rapid solidification using amorphous silicon
[DE84-014737] 02 p0202 N85-11345

Use of magnetic compression based on amorphous alloys as a drive for induction linacs
[DE84-014524] 02 p0277 N85-11805

Characterization of amorphous surface layers in Fe implanted with Ti and C
[DE84-014980] 02 p0289 N85-11885

USSR report: Materials science and metallurgy
[JPRS-UMS-84-007] 03 p0348 N85-12244

Parameters of structural relaxation and mechanical properties of amorphous alloys
03 p0349 N85-12246

Effect of annealing in transverse magnetic field on magnetic permeability of amorphous Fe5Co70Si15B10 alloy 03 p0349 N85-12247

Magnetic properties of and superfine interactions in amorphous Fe-Cr-Co-Si-B alloys
03 p0349 N85-12248

Static and dynamic disordering in amorphous magnets and crystals 03 p0422 N85-12699

Radiation effects in amorphous metallic alloys
[DE84-014302] 04 p0475 N85-13025

Structural properties of amorphous metals by Raman scattering
[DE84-016947] 04 p0475 N85-13027

Development of rapidly quenched alloys with special physical properties and of processes for their continuous production
[BMFT-FB-T-84-179] 04 p0477 N85-13039

Advanced amorphous materials for photovoltaic conversion
[DE84-017198] 04 p0529 N85-13384

Amorphous metallic layers in Si metallization systems
06 p0830 N85-15277

Advances and opportunities in the amorphous silicon research field
[DE84-004526] 06 p0833 N85-15304

Recent developments in photovoltaics
[DE84-004526] 06 p0833 N85-15305

Application of the diffraction model to amorphous magnesium zinc alloys
[AD-A147369] 07 p0928 N85-15883

Structural relaxation and isoconfigurational flow of a metallic glass near equilibrium
[AD-A147888] 07 p0933 N85-15915

Electronic properties of intercalated graphite and amorphous metals
[AD-A147664] 08 p1225 N85-17716

Plasma deposition of amorphous metal alloys
[DE85-000768] 09 p1295 N85-18132

Amorphous materials and recrystallization
[DE85-001873] 09 p1398 N85-18801

Reactivity of ion implanted silicon carbide
[DE85-001543] 09 p1399 N85-18802

Amorphization of ceramics by ion beams
[DE85-000936] 10 p1453 N85-19156

Electron-diffraction structural examination of amorphous iron-tin alloys 11 p1604 N85-20084

Amorphous Ni-Ti alloys: A new method of synthesis
[DE85-002744] 11 p1605 N85-20094

Structural studies of sputtered Ni-As-O films
[DE85-003229] 11 p1605 N85-20095

Properties and thermal stabilities of amorphous transition metal hydrides
[DE85-002117] 11 p1607 N85-20104

Effects of hydrogen on magnetic properties of amorphous zirconium alloys
[DE85-003303] 11 p1607 N85-20107

Moessbauer study of amorphous Fe(67)Co(18)B(14)S(1)
[AERE-R-11526] 11 p1737 N85-20928

Corrosion-resistant amorphous alloys
13 p2035 N85-22748

Structure of amorphous films of alloys based on Fe, condensed from laser erosion products
13 p2035 N85-22749

Energy spectrum of processes of structural relaxation of amorphous alloy FeCo70Si15B10
13 p2035 N85-22750

Electronic transport in hydrogenated amorphous silicon films
[DE85-002901] 13 p2164 N85-23426

Annealing effects in ferromagnetic amorphous alloys
[AD-A150648] 14 p2255 N85-23972

SEM (Scanning Electron Microscopy) studies of magnetic domains in amorphous metals
[AD-A150963] 14 p2256 N85-23979

Characterization of poly(ethylene oxide) drawn by solid state extrusion
[AD-A150987] 14 p2260 N85-24006

USSR report: Materials science and metallurgy
[JPRS-UMS-85-001] 15 p2496 N85-25395

Determination of symmetry of immediate surroundings in amorphous Co-P alloys 15 p2496 N85-25398

Temperature variation of resistivity of certain alloys based on transition and simple metals in amorphous and crystalline states 15 p2496 N85-25399

Conversions in amorphous zirconium-vanadium alloy
15 p2496 N85-25400

Structure and aging of amorphous chromium-germanium alloys 15 p2497 N85-25401

Study of amorphous strips and microconductors by ferromagnetic resonance method
15 p2497 N85-25402

Optical properties of hydrogenated amorphous carbon films grown from methane plasma
[NASA-TM-86995] 15 p2658 N85-26406

Structural inhomogeneities in amorphous nickel-phosphorus alloy
[BLL-M-36103-(5828.4)] 16 p2748 N85-26960

Solid state hydrogen pumping and storage material
[AD-D011610] 16 p2757 N85-27011

Electrical resistivity in amorphous metals: Consequences of phonon ineffectiveness in the diffraction model
[AD-A152130] 16 p2779 N85-27150

Glassy metals: New highly resistant material
[BLL-BISI-TRANS-21764-(9022.06)]
17 p2926 N85-28049

Obtaining amorphous coatings of FeW and Fe-Cr-P-B alloys using laser sputtering
[BLL-BISI-22493-(9022.06)] 17 p2927 N85-28057

Production and compaction of amorphous metal powders
[BLL-BISI-TRANS-22387-(9022.06)]
17 p2929 N85-28080

Thermal expansion effects in electrical transport in amorphous metals
[AD-A152477] 17 p2930 N85-28089

Corrosion resistant coating
[NASA-CASE-NPO-15928-1] 18 p3073 N85-29005

Application of the reference intensity method to coal analysis
[DE85-009528] 19 p3228 N85-30015

Investigation for low-cost permanent magnets
[AD-A154387] 19 p3260 N85-30212

Amorphous alloys of ion-implanted Fe-Ti-C
[DE85-010656] 19 p3360 N85-30834

Amorphous metallic films in silicon metallization systems 21 p3610 N85-32427

Mirror reflection of charged particles from amorphous and polycrystalline surfaces 21 p3690 N85-32927

The development and evaluation of point defect models for the growth of passive films on single crystal, polycrystalline, and amorphous metal surfaces
[AD-A154665] 21 p3709 N85-33023

Long-term research in Japan: Amorphous metals, metal oxide varistors, high-power semiconductors and superconducting generators
[DE85-010827] 22 p3748 N85-33230

In-situ observations of the development of heavy-ion damage in semiconductors
[DE85-010289] 22 p3761 N85-33307

1985 Amorphous Silicon Review Meeting
[DE85-008794] 22 p3807 N85-33582

Process for improving the quality of epitaxial silicon films grown on insulating substrates
[AD-D011730] 22 p3847 N85-33828

The effect of liquid-liquid phase separation of glass on the properties and crystallization behavior
[NASA-TM-77890] 23 p3919 N85-34285

Size and shape dependence of CO adsorption sites on sapphire supported Fe microcrystals
[NASA-CR-176171] 24 p4160 N85-35794

AMORPHOUS SEMICONDUCTORS

Studies of hydrogenated amorphous silicon
[DE84-013038] 01 p0067 N85-10443

Solar generators made of amorphous silicon
05 p0662 N85-14257

Laser annealing of ion implanted semiconductors
[AD-A146979] 07 p1047 N85-16652

Density of states and recombination in amorphous silicon (a-Si:H)
[BMFT-FB-T-84-216] 08 p1135 N85-17151

Stability of amorphous metals on semiconductor substrates
[DE84-017256] 09 p1295 N85-18134

Infrared modulation of photoluminescence in glow discharge amorphous silicon
[DE85-016993] 11 p1737 N85-20922

International Congress Centrum Berlin report on photovoltaics 12 p1877 N85-21773

Pin solar cells made of amorphous silicon
12 p1879 N85-21787

Development of an amorphous silicon panel
12 p1879 N85-21788

Amorphous silicon solar cells with a view to cheap production processes 12 p1879 N85-21789

Plasmachemical evaporation and doping of amorphous silicon 12 p1879 N85-21790

Production and characterization of amorphous silicon (a-Si:H) as base material for solar cells
12 p1879 N85-21791

Thin-film solar cells from sputtered and vapor-deposited amorphous silicon 12 p1879 N85-21792

Chemical vapor deposition of amorphous semiconductor films
[DE85-002917] 15 p2661 N85-26421

Investigation of a Si and related semiconductors as materials for photovoltaic conversion
[DE85-002932] 18 p3096 N85-29163

Carrier loss in dispersive transport in amorphous semiconductors
[DE85-009122] 18 p3194 N85-29811

Drift mobilities by time-of-flight methods and time-dependent phototransport in the nanosecond regime in amorphous semiconductors
[DE85-008729] 18 p3194 N85-29815

Glow discharge deposition at high rates using disilane
[DE85-010236] 19 p3263 N85-30235

Microscopic structure of two-dimensional electron glass
[DE85-010265] 19 p3376 N85-30942

Chemistry and physics of silicon-based amorphous semiconductors
[DE85-001931] 19 p3377 N85-30949

Defects in tetrahedrally coordinated amorphous semiconductors
[AD-A155150] 21 p3581 N85-32263

Thin-film reliability and engineering overview
21 p3612 N85-32450

Raman scattering studies in solids
[AD-A155528] 21 p3710 N85-33032

1985 Amorphous Silicon Review Meeting
[DE85-008794] 22 p3807 N85-33582

Formation of amorphous silicon by light ion damage
[DE85-012605] 23 p3972 N85-34623

AMOUNT

Models for mixture experiments when the response depends on the total amount
[DE85-000370] 09 p1374 N85-18637

AMPERAGE

U ELECTRIC CURRENT

AMPHIBIA

NT FROGS

The development of the vestibular apparatus under conditions of weightlessness
[NASA-TM-77517] 07 p1011 N85-16422

Simulated microgravity as a probe for understanding the mechanisms of early pattern specification
15 p2611 N85-26092

Report of Amphibian Development Group
24 p4127 N85-35583

AMPLIFICATION

NT SOUND AMPLIFICATION
NT WAVE AMPLIFICATION

Transverse field interaction multibeam amplifier
[AD-D011241] 01 p0043 N85-10282

Narrowband tunable dye laser with amplifier pumped by powerful nitrogen laser 02 p0262 N85-11716

Calculation of energy characteristics of double-passage amplifier 03 p0347 N85-12238

Vorticity amplification in viscous flow around a body
03 p0360 N85-12309

Investigation of effect of photocurrent amplification in meta-dielectric-semiconductor structures based on silicon 04 p0488 N85-13110

Analysis of a coded, M-ary orthogonal input optical channel with random-gain photomultiplier detection
05 p0624 N85-13990

Coherent amplification of ultrasonic pulses in activated crystals 05 p0724 N85-14653

The dc SQUID as a tuned radiofrequency amplifier
[DE85-000701] 06 p0805 N85-15123

Array sidelobes, error tolerance, gain, and beamwidth
[AD-A147004] 07 p0940 N85-15956

New construction principles for oscillator power summing devices 07 p0949 N85-16016

Adaptive antenna arrays for weak interfering signals
[NASA-CR-174336] 08 p1150 N85-17258

Gain instabilities in photomultipliers: How accurate are photon counting measurements?
08 p1251 N85-17903

Resonance between betatron and synchrotron oscillations in a free electron laser: A 3-D numerical study
[AD-A150059] 12 p1857 N85-21645

Design and testing of gyroklystron amplifiers
[AD-A151026] 14 p2298 N85-24231

Earth station antenna sidelobe characteristics
[PB85-164986] 16 p2780 N85-27159

Conversion efficiencies of charged particle beam driven free electron lasers
[AD-A154404] 19 p3276 N85-30316

Fin-line horn antennas
[AD-A154597] 21 p3580 N85-32255

Fixed gain and adaptive techniques for rotorcraft vibration control
[NASA-CR-177344] 22 p3728 N85-33111

AMPLIFICATION FACTOR
U AMPLIFICATION
AMPLIFIER DESIGN
Feasibility study for a 34 GHz (Ka band) gyroamplifier
[NASA-CR-174439] 10 p1477 N85-19325
A circuit grammar for operational amplifier design
[AD-A149566] 10 p1481 N85-19346
Cascode and differential amplifier using field-effect transistors 15 p2529 N85-25591
Reactanceless synthesized impedance bandpass amplifier
[NASA-CASE-GSC-12788-1] 18 p3093 N85-29145
Design and fabrication of monolithic broadband microwave GaAs low noise FET amplifiers
20 p3443 N85-31370
Thirty GHz low noise GaAs FET amplifiers — satellite-ground communication
[CD.6500686] 20 p3449 N85-31413
AMPLIFIERS
NT BROADBAND AMPLIFIERS
NT CURRENT AMPLIFIERS
NT DIFFERENTIAL AMPLIFIERS
NT FEEDBACK AMPLIFIERS
NT FLUID AMPLIFIERS
NT LIGHT AMPLIFIERS
NT LIMITER AMPLIFIERS
NT MICROWAVE AMPLIFIERS
NT OPERATIONAL AMPLIFIERS
NT PARAMETRIC AMPLIFIERS
NT PHOTOMULTIPLIER TUBES
NT POWER AMPLIFIERS
NT PREAMPLIFIERS
NT TRANSISTOR AMPLIFIERS
Transverse field interaction multibeam amplifier
[AD-D011241] 01 p0043 N85-10282
An optically isolated amplifier
[CSIR-SR-ELEK-257] 01 p0049 N85-10321
Calculation of energy characteristics of double-passage amplifier 03 p0347 N85-12236
Forced oscillations theory for resonant extended interaction electron devices
[PR-206] 03 p0358 N85-12296
The 30 GHz solid state amplifier for low cost low data rate ground terminals
[NASA-CR-174795] 03 p0358 N85-12300
Design, construction, and operational results of an 800-A, 10-kV hot deck amplifier
[DE84-014044] 04 p0496 N85-13162
China report: Science and technology
[JPRS-CST-84-001] 04 p0557 N85-13545
Present status, future prospects of domestic acoustical instruments 04 p0557 N85-13548
The dc SQUID as a tuned radiofrequency amplifier
[DE85-000701] 06 p0805 N85-15123
Feasibility study for a 34 GHz (Ka band) gyroamplifier
[NASA-CR-174439] 10 p1477 N85-19325
Enhancing the performance of a high-gain free electron laser operating at millimeter wavelengths
[DE85-000862] 12 p1857 N85-21646
Transient processes in tuned amplifier during phase-shift keying with smooth phase variation
15 p2527 N85-25581
Temperature sensitive oscillator
[NASA-CASE-GSC-12958-1] 19 p3258 N85-30201
Development and application of a high power ND-glass laser instrument
[AD-A154366] 19 p3276 N85-30314
Comparative characteristics of optical multiposition pulse signals with intersymbol distortion
22 p3764 N85-33329
Synthesis of high-speed devices using integrated operational amplifiers 22 p3781 N85-33428
Wide-band phase locked loop amplifier apparatus
[AD-D011720] 23 p3927 N85-34337
Solid state high power amplifier for driving the SLC injector klystron
[DE85-013063] 24 p4090 N85-35356
AMPLITUDE DISTRIBUTION ANALYSIS
The estimation of persistance statistics from cumulative probabilities of wave height
[NMI-R183] 03 p0397 N85-12534
Piezoelectric filter with low-Q inductances
13 p2070 N85-22932
Cosmic ray variations with the period close to 27 days and their connection with solar activity longitudinal distribution
[SH-4.4-19] 23 p4035 N85-35015
AMPLITUDE MODULATION
The spectral distribution of field components for a sinusoidal power modulated monofrequency optical carrier source
[FI-44-TBR-94] 04 p0565 N85-13601
Parameters of amplitude-modulated signal upon reflections 13 p2076 N85-22966
Transient processes in tuned amplifier during phase-shift keying with smooth phase variation
15 p2527 N85-25581
The distortion of AM broadcast antenna patterns as caused by nearby towers and highrise buildings
[CRC-1379] 15 p2538 N85-25668
A sampling phasemeter design for pulsed continuous wave signals
[AD-A155237] 21 p3581 N85-32264
A new description of combined trellis coding with asymmetric modulation
[NASA-CR-176197] 24 p4086 N85-35323
AMPLITUDE PROBABILITY ANALYSIS
U AMPLITUDE DISTRIBUTION ANALYSIS
AMPLITUDES
NT PULSE AMPLITUDE
NT SCATTERING AMPLITUDE
Pattern reversal visual evoked potentials and reaction time
[CSIR-SR-PERS-354] 01 p0097 N85-10644
Nonlinear propagation in a depth-dependent ocean
[AD-A145079] 01 p0116 N85-10791
Local photometric standards for CaII emission stars
01 p0128 N85-10883
The investigation of short wave signal structure in the vicinity of the caustic by means of a high-directed antenna
[PR-194] 03 p0354 N85-12277
Standardization of amplitude characteristics of galvanometric seismographs in the KAPG network
[REPT-552] 03 p0375 N85-12395
Shear-layer correction after Amiet under consideration of additional temperature gradient. Working diagrams for correction of signals
[NASA-TM-77741] 03 p0415 N85-12654
Accurate measurement of heat capacity by differential scanning calorimetry 04 p0488 N85-12975
On derivation and significance of geomagnetic equivalent amplitude indices 04 p0520 N85-13321
Recent observations of tides and tidal currents from the northeastern Bering Sea shelf
[PB84-241785] 04 p0543 N85-13452
Helicopter pilot performance for discrete-maneuver flight tasks 05 p0702 N85-14502
Artificial defocusing lens in ionosphere
05 p0724 N85-14654
Measuring large amplitudes of mechanical vibrations with laser interferometers 06 p0787 N85-15028
The use of an optical data acquisition system for bladed disk vibration analysis
[NASA-TM-86891] 06 p0817 N85-15184
Spectral model for subtidal variability in the Chesapeake Bay
[PB84-226679] 06 p0842 N85-15345
Low noise multiple crystal-controlled oscillator
[AD-D011401] 07 p0948 N85-16010
An analytical model of periodic waves in shallow water
[AD-A147501] 07 p0960 N85-16085
An analytical model of periodic waves in shallow water
[AD-A147502] 07 p0960 N85-16086
Real-time estimation of amplitude and group delay distortion in a PSK line-of-sight communications channel
[AD-A147735] 08 p1151 N85-17266
The atmospheric extinction problem
08 p1251 N85-17901
The Midway Atoll coral cap: Meteoric diagenesis, amplitude of sea-level fluctuation and dolomitization
09 p1351 N85-18499
Coherent receiver phase and amplitude alignment circuit
[AD-D011487] 10 p1468 N85-19265
Autumn and winter anomalies in ionospheric absorption as measured by riometers 11 p1660 N85-20460
Resonance between betatron and synchrotron oscillations in a free electron laser: A 3-D numerical study
[AD-A150059] 12 p1857 N85-21645
Surface forward scattering and reflection
[AD-A150115] 12 p1928 N85-22112
Reduction of amplitude-phase distortions of movable microwave coupling circuit for antenna field measurements 13 p2068 N85-22920
Programmable filter with fanned interdigital surface acoustic wave transducer 13 p2083 N85-23008
Nature of seismic images with amplitude and time fluctuations of recorded oscillations
13 p2112 N85-23156
A theoretical study of the ozone quasi-biennial oscillation in the tropical stratosphere 13 p2132 N85-23264
Analytical studies and experimental measurements of amplitude and phase of near-field range antenna probes
[AD-A150922] 14 p2283 N85-24212
Determining geometrical divergence using seismic observation data 14 p2343 N85-24489
Observations of intermediate-degree solar oscillations
14 p2442 N85-25069
Fatigue damage and small crack growth during biaxial loading 16 p2797 N85-27247
Studies of collisional and nonlinear radiative process for development of coherent UV and XUV sources
[AD-A152001] 16 p2865 N85-27670
High voltage power supply
[NASA-CASE-GSC-12818-1] 18 p3093 N85-29147
Interaction of large amplitude stress waves in layered elastic-plastic materials
[AD-A153519] 18 p3121 N85-29323
Mechanistic experiments to determine the origin of Southern Hemisphere stationary waves
18 p3143 N85-29461
An objective analysis technique for extrapolating tidal fields 20 p3493 N85-31715
Huffman-coded pulse compression waveforms
[AD-A155322] 21 p3576 N85-32243
Amplitude stabilization of pulse signals
22 p3762 N85-33320
Synthesis of high-speed devices using integrated operational amplifiers 22 p3781 N85-33428
Generalized string amplitude and wave equation for hadrons
[DE85-011492] 22 p3842 N85-33796
Cosmic ray intensity variations at primary rigidities near 1900 GV
[OG-5.3-0] 22 p3885 N85-34075
Reducing grating lobes due to subarray amplitude tapering
[AD-D011723] 23 p3927 N85-34339
Applications of the Kirchoff-Helmholtz integral to problems in body wave seismology
24 p4116 N85-35515
Average features of the muon component of EAS or = 10(17) eV
[HE-4.3-10] 24 p4191 N85-36004
AMPOULES
Reusable thermal cycling clamp
[NASA-CASE-LAR-12866-1] 12 p1658 N85-21651
ANAEROBES
Anaerobic digestion of biomass: status summary and research development needs, 1983
[PB85-161925] 13 p2040 N85-22772
Comparative anaerobic power of males and females
[AD-A151960] 16 p2842 N85-27523
Anaerobic reduction of elemental sulfur by Chromatium vinosum and Beggiatoa alba 21 p3660 N85-32739
Anaerobic microbial transformations in subsurface environments
[DE85-012790] 22 p3819 N85-33659
ANALOG CIRCUITS
Analog voice processing for FM transmission in a telephone channel
[INPE-2798-PRE/359] 03 p0354 N85-12279
Ensuring required metrological reliability of analog instrument channels by parametric compensation
07 p0955 N85-16050
A general theory of circuit analogy in fracture diagnosis
[AD-A147177] 07 p0978 N85-16212
System for computer-aided design of analog electronic circuits 22 p3768 N85-33353
Microcomputer controlled image processor
[AD-D011734] 22 p3833 N85-33735
Analog, still without fear
[AD-A155920] 24 p4089 N85-35348
ANALOG COMPUTERS
NT UNIVAC 1100 SERIES COMPUTERS
Microcomputer: Controlled statistics analyzer
[BLL-CE-TRANS-7971-(9022.09)]
13 p2144 N85-23306
ANALOG DATA
Optical waveguide spatial filters
[AD-A145674] 02 p0280 N85-11825
Analog disc recorder system: Operator's reference manual
[DE84-016926] 04 p0503 N85-13209
A scanning alarm electronic processor
[AD-D011419] 08 p1158 N85-17309
Complexity, testability, and fault analysis of digital, analog and hybrid systems
[AD-A148465] 08 p1213 N85-17634
Solid state research
[AD-A147640] 08 p1225 N85-17714
A description of the NRL oblique-incidence-ionogram data base
[AD-A148625] 08 p1230 N85-17748
Study on steerability of articulated tracked vehicles
[AD-P004308] 09 p1410 N85-18885
Photonic methods of high speed analog data recording
[DE84-016723] 11 p1637 N85-20306
Electrical characterization of analog microprocessors
[AD-A149629] 12 p1911 N85-21995

User's guide to calibration of analog electronic controllers in HVAC systems
[AD-A150803] 14 p2298 N85-24229
Parallel programmable charge domain device
[AD-D011599] 15 p2540 N85-25733
Pipelined programmable charge domain device
[AD-D011598] 17 p2951 N85-28225
Investigation and construction of the Mini Remote Terminal Unit (mRTU-M) Analog Processor Module (AP-M), volume 1
[MR-DS-01-VOL-1] 18 p3166 N85-29619
Investigation and construction of the Mini Remote Terminal Unit (mRTU-M), Analog Processor Module (AP-M), volume 2
[MR-DS-01-VOL-2] 18 p3166 N85-29620
Analog frequency modulated laser using magnetostriction
[AD-D011701] 19 p3276 N85-30318
Defense Mapping Agency (DMA) raster-to-Vector analysis
[AD-A154153] 19 p3336 N85-30668
Self-adaptive echo cancellation for telephony
[ENST-84E013] 20 p3441 N85-31353
Development of a dedicated speech work station
[AD-A155465] 21 p3674 N85-32824
Solid state research
[AD-A154783] 21 p3709 N85-33025
Design of high-order analog and digital filters with identical sections 22 p3766 N85-33341

ANALOG SIMULATION
Estimating algorithmic error of digital recursive filters
12 p1839 N85-21543
Experimental simulation of the flows in front of and behind a projectile with and without gas slippage
[ISL-CO-232/83] 14 p2302 N85-24258
The utilization of a light-gas gun to simulate interior ballistic flow
[ISL-CO-233/83] 14 p2303 N85-24259
Feasibility study of an installation to simulate the flow of propellant gases in a gun barrel, part 2
[ISL-R-128/83-PT-2] 14 p2303 N85-24263
Stress in axially symmetrical heavy metal projectiles during discharge — numerical simulation
[ISL-CO-219/83] 14 p2321 N85-24345

ANALOG TO DIGITAL CONVERTERS
Digital radio receivers and problems of analog-to-digital conversion of narrow-band signals
04 p0486 N85-13101
Development of components for micro-C oriented sensor systems
[BMFT-FB-T-84-126] 04 p0504 N85-13215
User-oriented development and production of integrated circuits in small and medium quantities
[BMFT-FB-T-84-171] 05 p0633 N85-14059
Formation of reference signals in laser-type gas analyzers with mechanical switching of optical channels
06 p0787 N85-15027
Analog to digital converter
[AD-D011338] 07 p0945 N85-15983
Power spectrum analysis of astronomical photographs digitised with small apertures 07 p0965 N85-16127
Medium speed computer interface (digitizer) for general purpose data acquisition
[DE85-001585] 09 p1367 N85-18587
Low voltage two wire to four wire telephone circuit converter apparatus
[AD-D011449] 10 p1468 N85-19261
Some propagation experimental results on protection techniques for line-of-sight digital systems
10 p1472 N85-19286
RELTIM: A library of routines used in real time machine control applications
[PB85-116507] 10 p1542 N85-19725
Quantization study for ERS-1 wave mode
[DFVLR-FB-84-39] 11 p1625 N85-20234
The study of certain aspects of probability with applications in communications theory
[AD-A149820] 12 p1829 N85-21476
Multichannel digital processing of wideband signals
12 p1840 N85-21548
EZPIX: A tablet entry method for computer-generated slides, drawings, and graphs
[DE85-005234] 12 p1916 N85-22030
The use of a high-speed 12-bit A/D converter for digital sampling of communication signal carriers
[AD-A150578] 13 p2056 N85-22872
Synthesis of quasi-optimum two-level signal discriminator with level changing at unknown point
13 p2083 N85-23010
Microcomputer controlled image acquisition system
15 p2537 N85-25654
Microcomputer controlled automatic peak locking of laser circuit 15 p2537 N85-25655
A portable pulse analyzer for nuclear geophysics using a Sinclair-TK microcomputer
[INPE-3278-PRE/801] 16 p2864 N85-27666
The HURRA high resolution experimental radar system sampling unit
[FOA-C-30376-E1] 18 p3091 N85-29133
A stored data acquisition system: Update
[DE85-010534] 18 p3166 N85-29616
R, L, C, G measurement 21 p3668 N85-32784
Development of a dedicated speech work station
[AD-A155465] 21 p3674 N85-32824
Method of and apparatus for generating an interstitial point in a data stream having an even number of data points
[NASA-CASE-MFS-25319-1] 22 p3827 N85-33701
Microcomputer controlled image processor
[AD-D011734] 22 p3833 N85-33735
Using an LSI-11/23 and RT-11 to digitize analog tapes
[DE85-012736] 24 p4139 N85-35656
The structure of the shower disk observed at Mt. Norikura
[HE-4.7-1] 24 p4198 N85-36052
Thickness of the particle swarm in cosmic ray air showers
[HE-4.7-14] 24 p4200 N85-36064
Search for acoustic signals from high energy cascades
[HE-7.1-1] 24 p4213 N85-36155

ANALOGIES
NT HYDRAULIC ANALOGIES
A similarity analysis of phase change heat conduction in corners 05 p0634 N85-14069
A general theory of circuit analogy in fracture diagnosis
[AD-A147177] 07 p0978 N85-16212
Explorations into thermodynamics analogies and critical points in reference to gas-solid transport
[DE85-000816] 11 p1738 N85-20929
Terrestrial analogs for planetary wrinkle ridges
13 p2199 N85-23644
On the absence of strike-slip faults from the planets and satellites 13 p2200 N85-23645
Application of field similitude theory to calculation of stripline heating 22 p3780 N85-33419
Some plant location problems — computer networks
[FUB-14-1984] 22 p3835 N85-33746
Analogies of control mechanisms in flight guidance and medicine 24 p4120 N85-35597

ANALOGS
A total dose characterization of five commercial analog multiplexors
[AD-A146886] 07 p0946 N85-15997
Growth of soil bacteria in presence of Martian soil analog, carbon dioxide and hydrogen peroxide
09 p1361 N85-18560

ANALYSIS
U ANALYZING

ANALYSIS (MATHEMATICS)
NT ABEL FUNCTION
NT AIRY FUNCTION
NT ANALYTIC FUNCTIONS
NT APPROXIMATION
NT ASYMPTOTES
NT ASYMPTOTIC SERIES
NT BANACH SPACE
NT BESSEL FUNCTIONS
NT BETHE-SALPETER EQUATION
NT BIHARMONIC EQUATIONS
NT BLASIUS EQUATION
NT BOREL SETS
NT BORN APPROXIMATION
NT BURGER EQUATION
NT CALCULUS
NT CALCULUS OF VARIATIONS
NT CHANDRASEKHAR EQUATION
NT CHEBYSHEV APPROXIMATION
NT COLLINEARITY
NT COMBINATIONS (MATHEMATICS)
NT COMBINATORIAL ANALYSIS
NT COMPLEX VARIABLES
NT COMPOSITE FUNCTIONS
NT COMPUTATIONAL CHEMISTRY
NT COMPUTATIONAL FLUID DYNAMICS
NT CONFORMAL MAPPING
NT CONJUGATE GRADIENT METHOD
NT CONJUGATE POINTS
NT CONTINUITY (MATHEMATICS)
NT CONVOLUTION INTEGRALS
NT COPLANARITY
NT DELTA FUNCTION
NT DEPENDENT VARIABLES
NT DIFFERENCE EQUATIONS
NT DIFFERENTIAL CALCULUS
NT DIFFERENTIAL EQUATIONS
NT EDDINGTON APPROXIMATION
NT EINSTEIN EQUATIONS
NT ELLIPTIC DIFFERENTIAL EQUATIONS
NT ELLIPTIC FUNCTIONS
NT ENTIRE FUNCTIONS
NT ERROR ANALYSIS
NT EULER-CAUCHY EQUATIONS
NT EXISTENCE THEOREMS
NT EXPONENTIAL FUNCTIONS
NT EXTREMUM VALUES
NT FACTORIALS
NT FALKNER-SKAN EQUATION
NT FINITE DIFFERENCE THEORY
NT FINITE ELEMENT METHOD
NT FOKKER-PLANCK EQUATION
NT FOURIER ANALYSIS
NT FOURIER SERIES
NT FOURIER TRANSFORMATION
NT FREDHOLM EQUATIONS
NT FUNCTION SPACE
NT FUNCTIONAL ANALYSIS
NT GAMMA FUNCTION
NT GAUSS EQUATION
NT GREEN'S FUNCTIONS
NT HALF PLANES
NT HALF SPACES
NT HARMONIC ANALYSIS
NT HARMONIC FUNCTIONS
NT HARTREE APPROXIMATION
NT HELMHOLTZ VORTICITY EQUATION
NT HILBERT SPACE
NT HILBERT TRANSFORMATION
NT HYPERBOLIC DIFFERENTIAL EQUATIONS
NT HYPERBOLIC FUNCTIONS
NT HYPERGEOMETRIC FUNCTIONS
NT INTEGRAL CALCULUS
NT INTEGRAL EQUATIONS
NT INTEGRAL TRANSFORMATIONS
NT INTERPOLATION
NT ITERATION
NT J INTEGRAL
NT JACOBI MATRIX METHOD
NT KERNEL FUNCTIONS
NT LAGUERRE FUNCTIONS
NT LAME WAVE EQUATIONS
NT LAPLACE TRANSFORMATION
NT LEAST SQUARES METHOD
NT LEGENDRE FUNCTIONS
NT LIAPUNOV FUNCTIONS
NT LIMITS (MATHEMATICS)
NT LINEAR EQUATIONS
NT LINEAR EVOLUTION EQUATIONS
NT LIOUVILLE EQUATIONS
NT LIPSCHITZ CONDITION
NT LOGARITHMS
NT MAXIMA
NT MEAN SQUARE VALUES
NT MEASURE AND INTEGRATION
NT MEROMORPHIC FUNCTIONS
NT MONGE-AMPERE EQUATION
NT MONTE CARLO METHOD
NT NEUMANN PROBLEM
NT NEWTON-RAPHSON METHOD
NT NOMOGRAPHS
NT NONLINEAR EQUATIONS
NT NONLINEAR EVOLUTION EQUATIONS
NT NUMERICAL ANALYSIS
NT NUMERICAL DIFFERENTIATION
NT NUMERICAL INTEGRATION
NT ORTHOGONAL FUNCTIONS
NT PADE APPROXIMATION
NT PARABOLIC DIFFERENTIAL EQUATIONS
NT PARTIAL DIFFERENTIAL EQUATIONS
NT PARTICLE IN CELL TECHNIQUE
NT PARTITIONS (MATHEMATICS)
NT PERIODIC FUNCTIONS
NT PHASE-SPACE INTEGRAL
NT POISSON EQUATION
NT POWER SERIES
NT QUADRATIC EQUATIONS
NT REAL VARIABLES
NT RELAXATION METHOD (MATHEMATICS)
NT RITZ AVERAGING METHOD
NT RUNGE-KUTTA METHOD
NT SERIES (MATHEMATICS)
NT SINGULAR INTEGRAL EQUATIONS
NT SINGULARITY (MATHEMATICS)
NT SOBOLEV SPACE
NT SPHERICAL HARMONICS
NT STURM-LIOUVILLE THEORY
NT TANGENTS
NT TAYLOR SERIES
NT TESSERAL HARMONICS
NT VECTOR ANALYSIS
NT VLASOV EQUATIONS
NT VOLTERRA EQUATIONS
NT VORTICITY
NT WEIGHTING FUNCTIONS
NT WIENER HOPF EQUATIONS
NT ZONAL HARMONICS

Performance of the h, p and h-p versions
01 p0056 N85-10383
Numerical methods for solving systems of linear equations
[INPE-3240-RPE/463] 02 p0250 N85-11633
USSR report: Physics and mathematics
[JPRS-UPM-84-004] 02 p0266 N85-11737
Nonlinear semigroups and evolution governed by accretive operators
[AD-A147556] 07 p1033 N85-16557
Complexity, testability, and fault analysis of digital, analog and hybrid systems
[AD-A148465] 08 p1213 N85-17634
Optical flow and texture variables useful in detecting decelerating and accelerating self-motion
[AD-A148718] 09 p1384 N85-18703
Symmetry breaking for a class of semi-linear elliptic problems
[AD-A149093] 10 p1546 N85-19748
Effects of assuming independent component failure times, if they are actually dependent, in a series system
[AD-A150582] 13 p2101 N85-23092
Interaction of metals and metalloids with biomembranes
[DE85-004902] 13 p2141 N85-23293
Twenty questions on ordered spaces
14 p2413 N85-24880
A note on perfect normality in generalized ordered spaces 14 p2413 N85-24881
Metrization theorems for continuous images of compact ordered spaces 14 p2413 N85-24882
A pathological homogeneous subspace of the real line
14 p2413 N85-24883
A note on topological groups with dense orderable subspaces 14 p2413 N85-24884
The Kappa sub n property in small Omega sub 1 trees
14 p2413 N85-24885
On compactifications of generalized order GO-spaces
14 p2413 N85-24886
The orderability of compact scattered spaces
14 p2413 N85-24887
Submetrizable topologies on the ordinals
14 p2414 N85-24888
Local bases and product partial order II
14 p2414 N85-24890
Mappings of finite oscillations at local separating points 14 p2414 N85-24891
Orderable subspaces of compact F-spaces
14 p2414 N85-24892
The nonlinear analysis of thick composite plates using a cubic spline function
[AD-A152115] 16 p2801 N85-27268
Symbiosis between postgraduate training and research projects: A successful experience
[INPE-3216-PRE/569] 16 p2810 N85-27330
Impact of ozone on vegetation
[PB85-159937] 16 p2821 N85-27403
An interactive computer package for use with simulation models which performs multidimensional sensitivity analysis by employing the techniques of response surface methodology
[AD-A151956] 16 p2846 N85-27548
Performance evaluation of stochastic timed decision-free Petri Nets
[AD-A153987] 18 p3171 N85-29652
Symposium on Computational Mathematics-State-of-the-Art: Informal Proceedings
[DE85-008122] 20 p3516 N85-31858
USSR report: Physics and mathematics
[JPRS-UPM-85-004] 21 p3680 N85-32860
Stability of two-dimensional immiscible flow to viscous fingering
[DE85-011403] 23 p3931 N85-34364
Analytic and numerical calculations of the ambipolar electric field in a stellarator 23 p3978 N85-34665
Polylith: The early goals
[DE85-012534] 24 p4139 N85-35658

ANALYSIS OF VARIANCE
Individual geopotential coefficients of order 15 and 30, from resonant satellite orbits
[AD-A146687] 06 p0828 N85-15256
Estimation of variance of the regression estimator
[AD-A149407] 10 p1551 N85-19780
On the characterization of nonnegatively estimable linear combinations of variance components
[AD-A153786] 18 p3174 N85-29678
Overhead management guide for aerospace procurements
[AD-A153626] 18 p3198 N85-29835
Corrosion fatigue cooperative testing program statistical analysis
[AD-A153886] 19 p3238 N85-30077
The distribution and dynamics of planetary nebulae in M32 and the Andromeda Galaxy
20 p3546 N85-32068

ANALYTIC FUNCTIONS
NT ENTIRE FUNCTIONS
Some families of near-orthonormal analytic and harmonic functions
[AD-A144722] 01 p0110 N85-10748
On the rate of mean convergence of finite linear predictors of multivariate stationary stochastic processes
[AD-A145609] 02 p0254 N85-11664
Interpolating sequences for H to infinity in the ball
[CTH-MATH-1984-15] 04 p0556 N85-13542
Annuals of the Finnish Academy of Sciences, series A. 1: Mathematics, volume 8, part 2
[ISSN-0066-1953] 10 p1535 N85-19673
On the spherical derivative of a meromorphic function with a Nevanlinna deficient value
10 p1535 N85-19676
On harmonic functions with integrable maximum modulus 10 p1536 N85-19681
Close-to-convex functions and linear-invariant families
10 p1536 N85-19683
Annals of the Fourier Institute, volume 34, no. 4
11 p1698 N85-20668
An extension of the Gleason problem in pseudoconvex domains 11 p1698 N85-20671
Contribution of the cup-product of Milnor's fiber with /1/ sup 2 lambda poles 11 p1698 N85-20672
Classic Fourier microdistributions in the real analytic case 11 p1698 N85-20673
Annals of the Scientific Academy of Finland, series A. 1: Mathematics, volume 9
[ISSN-0066-1953] 15 p2633 N85-26229
Harmonic univalent functions
15 p2633 N85-26230
Fourier-Stieltjes coefficients and continuation of functions 15 p2633 N85-26231
On meromorphic functions continuous on the Stoilow boundary 15 p2633 N85-26232
Remarks of the maximal dilatation of the Beurling-Ahlfors extension 15 p2634 N85-26239
Entire functions with spiral limits
15 p2634 N85-26241
Conditions for the possibility of conformal sewing
[ST-AASF-IMD-58] 16 p2856 N85-27625
Analysis of two-parameter constant background born inversion for acoustic synthetic data
[AD-A156394] 24 p4145 N85-35698

ANALYTIC GEOMETRY
NT CATENARIES
NT CIRCUMFERENCES
NT CONICS
NT ELLIPSES
NT EPICYCLOIDS
NT HYPERBOLAS
NT LOCI
NT MERCATOR PROJECTION
NT OBLATE SPHEROIDS
NT PARABOLAS
NT SPHEROIDS
NT TANGENTS
NT TORUSES
COM-GEOM Interactive Display Debugger (CIDD)
[AD-A145001] 01 p0104 N85-10692
Numerical improvement of asymptotic solutions and nonlinear shell analysis 05 p0648 N85-14158

ANALYTICAL CHEMISTRY
USSR report: Chemistry
[JPRS-UCH-84-012] 06 p0761 N85-14865
Ion microscopy of metals and semiconductors
[AD-A147116] 07 p1043 N85-16626
Chemical information from ion scattering spectrometry
[AD-A148287] 08 p1121 N85-17069
Background detection and correction in multicomponent analysis
[AD-A148251] 08 p1212 N85-17628
Multicomponent calibration and quantitation methods
[AD-A148252] 08 p1212 N85-17629
Quality assurance for environmental analytical chemistry, 1983
[DE84-016045] 09 p1349 N85-18489
Two-dimensional measurements of OH concentration and temperature in reactive flows
[AD-A149849] 12 p1800 N85-21292
Compositional and structural analysis of Air Force materials
[AD-A150992] 14 p2252 N85-23957
Abstracts of the 36th Southeastern Regional Meeting of the American Chemical Society
[AD-A151506] 15 p2496 N85-25304
The development of laser analytical methods for the characterization of solid-liquid and solid-high pressure gas interfaces
[AD-A152382] 17 p2918 N85-27966
Analytical Chemistry Division
[DE85-010585] 18 p3068 N85-28974
Principles of quality assurance of chemical measurements
[PB85-177947] 18 p3072 N85-28997
The determination of dinitrotoluene in single base propellants
[AD-A154672] 21 p3571 N85-32209
Marine environmental quality assessment program, five-year plan (FY 1984 - 1988)
[AD-A154715] 21 p3613 N85-32459

ANALYZERS
NT ENGINE ANALYZERS
NT SIGNAL ANALYZERS
Program flow analyzer, volume 1
[AD-A145320] 02 p0241 N85-11572
Bragg cell spectrum analyzer specification
[AD-D011320] 07 p1044 N85-16629
Battery charger
[AD-D011420] 08 p1178 N85-17425
Calculation and computer simulation of the Paraboloidal Mirror Analyzer (PMA)
[DE85-001417] 09 p1384 N85-18705
Microcomputer: Controlled statistics analyzer
[BLL-CE-TRANS-7971-(9022.09)]
13 p2144 N85-23306
Possiblity of developing charged-particle energy analyzer based on hyperboloidal axisymmetrical lens
21 p3691 N85-32933

ANALYZING
Analyzing two-level fractional factorial experiments for possible dispersion effects
[AD-A149455] 10 p1548 N85-19760
Using a logic analyser and trigger unit to de-bug a program
[BAE-881/ELO/1487] 15 p2626 N85-26180

ANATOMY
NT ADRENAL GLAND
NT ARM (ANATOMY)
NT ARTERIES
NT BLADDER
NT BLOOD VESSELS
NT BONES
NT BRAIN
NT BRAIN STEM
NT BRONCHI
NT CARDIAC VENTRICLES
NT CARDIOVASCULAR SYSTEM
NT CEREBELLUM
NT CEREBRAL CORTEX
NT CEREBRAL VENTRICLES
NT CEREBRUM
NT CHEMORECEPTORS
NT CIRCULATORY SYSTEM
NT COCHLEA
NT DIAPHRAGM (ANATOMY)
NT EAR
NT ELBOW (ANATOMY)
NT ERYTHROCYTES
NT EYE (ANATOMY)
NT FEET (ANATOMY)
NT FEMUR
NT FINGERS
NT GASTROINTESTINAL SYSTEM
NT GRAVIRECEPTORS
NT HAND (ANATOMY)
NT HEAD (ANATOMY)
NT HEART
NT HEMATOPOIESIS
NT HEMATOPOIETIC SYSTEM
NT HUMAN BODY
NT INTESTINES
NT JOINTS (ANATOMY)
NT KIDNEYS
NT KNEE (ANATOMY)
NT LABYRINTH
NT LEG (ANATOMY)
NT LIMBS (ANATOMY)
NT LIVER
NT LUNGS
NT LYMPHOCYTES
NT MARROW
NT MECHANORECEPTORS
NT MUSCULOSKELETAL SYSTEM
NT MYOCARDIUM
NT NECK (ANATOMY)
NT OCULOMOTOR NERVES
NT ORGANS
NT OTOLITH ORGANS
NT PANCREAS
NT PARATHYROID GLAND
NT PELVIS
NT PHOTORECEPTORS
NT PITUITARY GLAND
NT PROPRIOCEPTORS
NT RECTUM
NT RESPIRATORY SYSTEM
NT RETINA

NT SCIATIC REGION
NT SKULL
NT SPLEEN
NT TEETH
NT THYMUS GLAND
NT THYROID GLAND
NT TORSO
NT VASCULAR SYSTEM
NT VEINS
NT VERTEBRAE
NT VERTEBRAL COLUMN
NT VESTIBULES
NT WRIST

ANCHORS (FASTENERS)
Vehicle anchoring system
[AD-D011262] 06 p0815 N85-15173
Expedient runway surfacing with post tensioning system for expeditionary airfields
[AD-D011677] 19 p3222 N85-29976

ANDES MOUNTAINS (SOUTH AMERICA)
Mesoscale lee cyclogenesis 09 p1355 N85-18527

ANDROMEDA GALAXIES
The distribution and dynamics of planetary nebulae in M32 and the Andromeda Galaxy
20 p3546 N85-32068

ANECHOIC CHAMBERS
Near-field effects on radome boresight errors
[AD-P004356] 12 p1825 N85-21450
Acoustic detection of air shower cores
[HE-7.1-4] 24 p4213 N85-36158

ANEMIAS
Research opportunities in loss of red blood cell mass in space flight
[NASA-CR-175808] 16 p2641 N85-27517

ANEMOMETERS
NT HOT-FILM ANEMOMETERS
NT HOT-WIRE ANEMOMETERS
NT LASER ANEMOMETERS
Hot section laser anemometry
02 p0142 N85-10962
Laser anemometer optimization
02 p0142 N85-10963
Laser Doppler Anemometry (LDA) signal triggering and effective particle size range
[KU-SFB-210/E/5] 11 p1634 N85-20290
Wind: Measuring for energy
[DE85-900227] 11 p1687 N85-20607
Flow measurement by laser Doppler anemometry in a nuclear fuel assembly
[DE85-003260] 12 p1848 N85-21592

ANEMOMETRY
U VELOCITY MEASUREMENT

ANESTHESIA
NT ELECTROANESTHESIA
Smith predictor and self-tuning control of muscle relaxant drug administration
[RR-257] 02 p0235 N85-11534

ANESTHESIOLOGY
Smith predictor and self-tuning control of muscle relaxant drug administration
[RR-257] 02 p0235 N85-11534

ANESTHETICS
NT CHLOROFORM
NT CYCLOPROPANE
NT METHYL CHLORIDE
Changes in the impedance and bioelectrical activity of the cerebral cortex of rats under the action of anaesthetic drugs
[HSE-TRANS-10371] 19 p3327 N85-30617
Studies of circulatory and metabolic changes during ketamine narcosis
[AD-A154512] 21 p3663 N85-32756

ANGLE OF ATTACK
Wind tunnel calibration of a hemispherical head angle of attack and angle of sideslip indicator
[FFA-TN-1984-11] 02 p0135 N85-10923
Navier-Stokes solution of 3-dimensional hypersonic afterbody flowfields over capsule-type vehicles
[NAL-TR-819] 03 p0311 N85-12010
Heat transfer and pressure drop in blade cooling channels with turbulence promoters
[NASA-CR-3837] 03 p0361 N85-12315
Review of requirements and status of simulation and scaling of transonic, viscous flows
[AD-A146357] 06 p0808 N85-15137
Experiences with the use of a side-strut model support system for high angles of attack in the Trinsonik wind tunnel TMK
[DFVLR-MITT-84-09] 07 p0910 N85-15763
Effect of aerodynamic and angle-of-attack uncertainties on the May 1979 entry flight control system of the Space Shuttle from Mach 8 to 1.5
[NASA-TP-2365] 07 p0913 N85-15778
Unsteady stall penetration of an oscillating swept wing
[AD-P004156] 09 p1264 N85-17941
Theoretical investigation of dynamic stall using a momentum integral method
[AD-P004170] 09 p1266 N85-17955
Determination of corrections to flow direction measurements obtained with a wing-tip mounted sensor
[NASA-CR-174412] 10 p1421 N85-18962
Study of several factors affecting crew escape trajectories from the Space Shuttle Orbiter at low-subsonic speeds
[NASA-TM-86303] 10 p1428 N85-19006
Effect of inclination, transverse intertip spacing, and logitudinal pitch on crossflow heat transfer from an array of finned tubes 10 p1482 N85-19359
Implications of guidance and control technology on human factors considerations 10 p1532 N85-19656
Hypersonic flow about triangular airfoil at large angles of attack 13 p2044 N85-22792
The structure of separated flow regions occurring near the leading edge of airfoils, including transition
[NASA-CR-175670] 14 p2209 N85-23703
Low-speed stability and control wind-tunnel investigations of effects of spanwise blowing on fighter flight characteristics at high angles of attack --- Langely 12-ft low-speed tunnel and 30- by 60-ft tunnel
[NASA-TP-2431] 14 p2210 N85-23706
Performance and surge limits of a TF30-P-3 turbofan engine/axisymmetric mixed-compression inlet propulsion system at Mach 2.5
[NASA-TP-2461] 15 p2472 N85-25261
Investigation of potential and viscous flow effects contributing to dynamic stall
[AD-A151696] 15 p2557 N85-25773
Measurements of the symmetric aerodynamic coefficients for flat faced cylinders in the angle of attack regime 0 to 90 deg for transonic and supersonic speeds
[FFA-TN-1984-04] 16 p2700 N85-26675
Experiences with the use of a side-strut model support system for high angles for attack in the TMK Trinsonik Wind Tunnel
[ESA-TT-895] 20 p3396 N85-31069
Recent developments in rotary-balance testing of fighter aircraft configurations at NASA Ames Research Center
[NASA-TM-86714] 21 p3551 N85-32090
Aerodynamic characteristics of the standard dynamics model in coning motion at Mach 0.6
[NASA-TM-86717] 21 p3552 N85-32094
Numerical solutions of turbulent models for flow over a flat plate with angle of attack
[DE85-010380] 21 p3585 N85-32286
Experimental investigations on airfoils with different geometries in the domain of high angles of attack-flow separation
[NASA-TM-77892] 22 p3728 N85-33110

ANGLES (GEOMETRY)
NT ANGLE OF ATTACK
NT BRAGG ANGLE
NT ELEVATION ANGLE
NT GRAZING INCIDENCE
Design sensitivity analysis of an antisymmetric angle-ply laminate
[CSIR-TWISK-318] 01 p0021 N85-10128
The effect of changes in the angle of incidence in the event of a richochet at a float step
[RAE-TRANS-2120] 07 p0902 N85-15712
Tolerance synthesis of multilayer radome walls
07 p0953 N85-16041
Quantitative use of multiincidence-angle SAR for geologic mapping 08 p1145 N85-17220
Investigation of SIR-B images for lithologic mapping
08 p1148 N85-17241
Australian Multiexperimental Assessment of SIR-B (AMAS) 08 p1148 N85-17243
German Radar Observation Shuttle Experiment (ROSE) 08 p1148 N85-17245
Influence of setting angle of jet cooling nozzles on temperature and stress state of a turbine wheel
09 p1306 N85-18208
Forces on undriven, angled wheels
[AD-P004303] 09 p1409 N85-18880
Polarization angles of linearly polarized antennas and radio waves in satellite communications
[PB85-131613] 11 p1626 N85-20240
Angular measurement system
[NASA-CASE-MFS-25825-1] 11 p1635 N85-20296
Detection of angular modulated electromagnetic signals
[AD-D011563] 12 p1823 N85-21437
Mathematical model of discriminator for signals with fluctuations and thermal noise 13 p2072 N85-22943
Examination of the contact wetting angle in the vicinity of critical temperature
[BLL-T6416/BG/CRS/LR-ST735/84]
13 p2091 N85-23054
Characterization of terrestrial solar cells for space applications: Electrical characteristics of thin Westinghouse dendritic web cells as a function of solar intensity, temperature, and incidence angle
[NASA-CR-175642] 14 p2349 N85-24516
Free-surface phenomena under low- and zero-gravity conditions
[NASA-CR-175835] 16 p2782 N85-27168
Measurement and interpretation of electron angle at MABE beam stop
[DE85-006583] 17 p3032 N85-28755
Two-degree-of-freedom linear and planar microwave array lenses
[AD-A153701] 18 p3095 N85-29156
Inherent angular tracking error in an amplitude comparison monopulse radar
[AD-A154212] 19 p3255 N85-30185
Integrated dual beam line scanning antenna and negative resistance diode oscillator
[AD-D011717] 19 p3261 N85-30223
On design of off-axis specimens
[AD-A154328] 19 p3286 N85-30379
Aerodynamic measurement of the wind flow in the number two section of the SIMA wind tunnel
[ONERA-PV-1/8138-GY] 20 p3389 N85-31019
Solid surface characterization by contact angle measurements
[FOA-C-40209-C,B2] 20 p3459 N85-31483
Intersatellite optical links: The point ahead angle
[CNES-83/DRT/TIT/TR/150] 20 p3533 N85-31984
Arrival directions of cosmic rays of E .4 EeV
[OG-5.3-4] 22 p3884 N85-34071
Comprehensive fracture diagnostics experiement. Part 2: Comparison of seven fracture azimuth measurements
[DE85-011707] 23 p3948 N85-34470
OMEGA: Optoelectronic measurement of the incidence angle of a projectile
[ISL-CO-223/84] 23 p3974 N85-34634
The response of ionization chambers to relativistic heavy nuclei
[OG-9.1-13] 23 p4024 N85-34939
Reachable grasps on a polygon: The convex rope algorithm
[AD-A155913] 24 p4138 N85-35647
Geophysical searches for three-neutrino oscillations
[HE-5.3-9] 24 p4205 N85-36103

ANGULAR ACCELERATION
Influence of gravitoinertial force level on apparent magnitude of coriolis cross-coupled angular accelerations and motion sickness 11 p1693 N85-20644
Results of a longitudinal study of airsickness incidence during Naval flight officer training
11 p1694 N85-20649
Uniaxial angular accelerometers
17 p2944 N85-28173
Effect of experimental motion sickness on postrotory nystagmus and counterrotation illusion
22 p3824 N85-33690

ANGULAR CORRELATION
Electronic structure and lattice dynamics of solid state substances from gamma nuclear resonance absorption and angular correlation measurements
03 p0427 N85-12728

ANGULAR DISTRIBUTION
Focusing beam of 1-GeV protons with volumetric capture to the mode of channeling by bent single crystal
02 p0268 N85-11750
Structural studies of sputtered MOS(2) films by angle-resolved photoelectron spectroscopy
[AD-A146052] 03 p0433 N85-12759
Fast neutron capture with a white neutron source
[DE84-016799] 04 p0562 N85-13580
Coincidence techniques to study electron emission in ion-atom collisions
[DE85-003635] 11 p1724 N85-20846
Angular dependence of the Rayleigh-surface wave velocity in polycrystalline metals with small anisotropy
[AERE-R-11595] 15 p2509 N85-25476
Theoretical studies of heavy ion scattering processes
[DE85-008623] 17 p3032 N85-28753
SPECTER: Neutron damage calculations for materials irradiations
[DE85-005791] 18 p3180 N85-29716
Electron multiple, plural and single scattering
[DE85-010325] 18 p3181 N85-29721
Fast-neutron-spectrum measurements for the thick-target (9)Be(d/ = 7 MeV
[DE85-010481] 18 p3183 N85-29735
Investigation of thick-target neutron emission from Be-9(d,n)B-10 at E(d) = 7 MeV for angles other than zero degrees
[DE85-010254] 20 p3528 N85-31947
Evaluated nuclear-data file for niobium
[DE85-012095] 21 p3704 N85-33009

Low-energy sputterings with the Monte Carlo Program ACAT
[IPPJ-AM-40] 23 p3982 N85-34890
On the angular and energy distribution of solar neutrons generated in P-P reactions
[SH-1.4-9] 23 p3995 N85-34769
Additional flux of particles and albedo-electrons in upper atmosphere
[SH-6.1-6] 23 p4045 N85-35080
Neutron production by Ne and Si ions on a thick Cu target at 670 MeV/A with application to radiation protection
[DE85-014526] 24 p4152 N85-35746
1Single particle momentum and angular distributions in hadron-hadron collisions at ultrahigh energies
[HE-1.2-1] 24 p4171 N85-35860
Angular distribution and multiplicity of backward hadrons in hFe interactions at 0.5-5.0 TeV energies (PION Experiment)
[HE-1.2-8] 24 p4172 N85-35866
Anuglar distribution of shower particles produced in the collisions of 20-GeV/c and 300-GeV negative pions with emulsion nuclei 24 p4172 N85-35868
Inclusive angular distribution of alpha and Li fragments produced in the Fe-C and Fe-Pb collisions at 1.88 GeV/u
[HE-1.4-11] 24 p4177 N85-35898
Characteristics of anomalously high multiplicity cosmic ray interactions
[HE-3.3-1] 24 p4180 N85-35920
Peculiarities of gamma-quanta distribution at 20 TeV energy
[HE-3.7-10] 24 p4186 N85-35967
The thickness of the shower disc as observed in showers produced by primaries above 10 (19)eV
[HE-4.7-6] 24 p4199 N85-36057
Thickness of the particle swarm in cosmic ray air showers
[HE-4.7-14] 24 p4200 N85-36064
Measurement of neutrino oscillations in MACRO experiment
[HE-5.3-10] 24 p4206 N85-36104

ANGULAR MOMENTUM
A packed storage program for angular momentum coupling coefficients
[TWISK-316] 01 p0102 N85-10680
A reappraisal of Darwin's fission hypothesis and a possible limit to the primordial angular momentum of the Earth 04 p0585 N85-13736
Numerical simulations of fission
04 p0585 N85-13737
Models of angular momentum input to a circumterrestrial swarm from encounters with heliocentric planetesimals
04 p0587 N85-13750
The lunar angular momentum problem
04 p0588 N85-13752
Formation of the prelunar accretion disk
04 p0588 N85-13755
Description of a laboratory model Annular Momentum Control Device (AMCD) 05 p0606 N85-13863
Winds from rotating, magnetic, hot stars
08 p1234 N85-17775
Suspension torques on a gimballed electrostatically supported gyroscope and requirements on the gyroscope and spacecraft for the relativity gyroscope experiment
12 p1851 N85-21606
Models of angular momentum input to a circum-terrestrial swarm from encounters with heliocentric planetesimals 13 p2179 N85-23521
Flight investigation of stall, spin and recovery characteristics of a low-wing, single-engine, T-tail light airplane
[NASA-TP-2427] 15 p2470 N85-25248
Microscopic analysis of angular momentum projected HFB-states in terms of interacting bosons
[DE85-007629] 16 p2863 N85-27661
Mutli-particle quantum mechanics obeying fractional statistics
[DE85-007630] 16 p2873 N85-27723
Spin distributions in heavy ion fusion at and below the Coulomb barrier
[DE85-007817] 17 p3031 N85-28751
Analysis and modeling of variations in length of day
19 p3340 N85-30761
Interacting Boson approximation
[DE85-003016] 22 p3837 N85-33756
Duality of two-point functions for confined non-relativistic quark-antiquark systems
[DE85-012334] 23 p3971 N85-34618

ANGULAR MOTION
U ANGULAR VELOCITY

ANGULAR RESOLUTION
Limitation of VLBI angular resolution
07 p1057 N85-16710
Opportunities for high angular and temporal resolutions of galactic objects at radio frequencies — QUASAT
07 p1059 N85-16723
Image processing instrumentation for speckle interferometry and imaging
[AD-A149308] 11 p1762 N85-21084
Determination of angular resolution of coded aperture gamma-ray telescope 13 p1981 N85-22432
Spectra and positions of galactic gamma-ray sources
[OG-2.5-7] 22 p3869 N85-33963
A search for sources of ultra high energy gamma rays at air shower energies with Ooty EAS array
[OG-2.6-8] 22 p3870 N85-33970
The gamma-ray telescope Gamma-1
[OG-9.2-10] 23 p4026 N85-34949
Lapex: A Phoswich balloon experiment for hard X-ray astronomy
[OG-9.3-1] 23 p4027 N85-34956
A new ultra high energy gamma ray telescope at Ohya mine
[OG-9.4-3] 23 p4029 N85-34970
An EAS experiment at mountain altitude for the detection of gamma-ray sources
[OG-9.4-5] 23 p4029 N85-34972
A new array for the study of ultra high energy gamma-ray sources
[OG-9.4-7] 23 p4029 N85-34974
Shower disc sampling and the angular resolution of gamma-ray shower detectors
[OG-9.5-2] 23 p4030 N85-34980
A method to improve observations of gamma-ray sources near 10 (15) eV
[OG-9.5-5] 23 p4030 N85-34982
Angular resolution of air-shower array-telescopes
[OG-9.5-6] 23 p4030 N85-34983
Astrophysical applications of high angular resolution array-telescopes
[OG-9.5-7] 23 p4031 N85-34984
Angular resolution of an EAS array for gamma ray astronomy energies 5 x 10 (13) eV
[OG-9.5-8] 23 p4031 N85-34985
Note on the detection of high energy primary cosmic gamma rays by air shower observation
[OG-9.5-9] 23 p4031 N85-34986
The angular resolution of air shower gamma ray telescopes
[OG-9.5-14] 23 p4031 N85-34990
Measurement of low energy cosmic rays aboard Spacelab-1
[SH-10.1-6] 23 p4053 N85-35137
Preliminary results of the Cerenkov EAS flashes the Crimean Astrophysical Observatory
[HE-4.4-17] 24 p4194 N85-36023
Thickness of the particle swarm in cosmic ray air showers
[HE-4.7-14] 24 p4200 N85-36064

ANGULAR VELOCITY
Rotational motion of a satellite
13 p1981 N85-22428
Status of and outlook for producing means of transmitting units of plane angle, angular velocity and acceleration with ring lasers 13 p2074 N85-22955
Investigation of errors of acoustic goniometer information-measurement systems on rocking base
14 p2283 N85-24130
Models of solar differential rotation
14 p2446 N85-25097
Optimum rotation of solid body with 1 axis of symmetry 16 p2718 N85-26781
Fluidic angular velocity sensor
[NASA-CASE-NPO-16479-1-CU]
18 p3104 N85-29219

ANHYDRIDES
NT INORGANIC PEROXIDES
NT ORGANIC PEROXIDES
NT PEROXIDES
Condensation of anhydrides or dicarboxylic acids with compounds containing active methylene groups. Part 19: Condensation of phthalic and substituted phthalic anhydrides with benzoylacetic ester
[NASA-TM-77865] 19 p3227 N85-30009
Condensation of anhydrides or dicarboxylic acids with compounds containing active methylene groups. Part 1: Condensation of phthalic anhydride with acetoacetic and malonic ester
[NASA-TM-77866] 19 p3227 N85-30010
Remarks on preparation of indandione detection reagents
[NASA-TM-77605] 21 p3560 N85-32146

ANIK SATELLITES
SLIM TDMA ANIK B pilot project
[CRC-REPT-1366] 03 p0354 N85-12278

ANILINE
Homogeneous reaction involving components of different redox couples. 1: Theoretical considerations and digital simulation
[AD-A148666] 06 p1124 N85-17064
Supersonic molecular jet study of the liquid state
[AD-A147416] 09 p1379 N85-18671
Influence of pressure on speed of sound in single-phase region of stratifying mixtures 11 p1715 N85-20758
Resistance of polyaniline films as a function of electrochemical potential and the fabrication of polyaniline-based microelectronic devices
[AD-A154999] 21 p3569 N85-32201

ANIMALS
NT AMPHIBIA
NT BABOONS
NT BEARS
NT BIRDS
NT CATS
NT DEER
NT DOGS
NT DOLPHINS
NT FISHES
NT FROGS
NT GUINEA PIGS
NT HETEROTROPHS
NT HUMAN BEINGS
NT INSECTS
NT INVERTEBRATES
NT LARVAE
NT MAMMALS
NT MICE
NT MONKEYS
NT PRIMATES
NT PROTOZOA
NT RABBITS
NT RATS
NT SEALS (ANIMALS)
NT SHARKS
NT SHEEP
NT SPIDERS
NT TURTLES
NT WHALES
NT WILDLIFE
Estuaries of the Cape. Part 2: Synopses of available information on individual systems. Report 13: Silvermine (CSW 3)
[CSIR-RR-412-PT-2] 01 p0086 N85-10582
Estuaries of the Cape. Part 2: Synopses of available information on individual systems. Report no. 16: Eerste (CSW 6)
[CSIR-RR-415-PT-2] 01 p0087 N85-10585
Estuaries of the Cape. Part 2: Synopses of available information on individual systems. Report no. 17: Lourens (CSW 7)
[CSIR-RR-416-PT-2] 01 p0087 N85-10586
In vivo dermal absorption method and system for laboratory animals
[AD-D011231] 01 p0094 N85-10635
Small animal hypobaric chamber
[AD-A146196] 03 p0364 N85-12335
Oxygen delivery during exercise: Limitations to maximum flow 05 p0686 N85-14424
Effect of broad-band constant noise on some systems of animal body 14 p2367 N85-24705
NASA Space Biology Program: 9th Annual Symposium
[NASA-CP-2336] 15 p2605 N85-26054
Effects of weightlessness of Aurelia Ephyra differentiation and statolith synthesis
15 p2605 N85-26056
Gravity perception in a Cladoceran-Zooplankter: Anatomy of antennal socket setae of Daphnia magna
15 p2605 N85-26057
Review and annotated bibliography of benthic studies in coastal and estuarine areas of Florida with a selected compilation of worldwide benthic methodological references and southeastern United States benthic taxonomic references
[PB85-151041] 16 p2822 N85-27405
MARMAP survey of the continental shelf from Cape Hatteras, North Carolina to Cape Sable, Nova Scotia (1977 - 1983). Atlas 1: Summary of operations
[PB85-150865] 16 p2839 N85-27506
An environmentally-controlled extended-use small animal hypobaric chamber
[AD-A153735] 19 p3221 N85-29974
The 1984 environmental monitoring report, Sandia National Laboratories, Albuquerque, New Mexico
[DE85-011175] 22 p3811 N85-33607
Antihypertensive neutral lipid
[DE85-011625] 22 p3819 N85-33656
The 1984 biotic studies of Yucca Mountain, Nevada test site, Nye County, Nevada
[DE86-011715] 23 p3951 N85-34487

ANIMATION
U MOTION

ANIONS

Electronic and redox properties of stacked-ring silicon phthalocyanines from molecular orbital theory
[AD-A147161] 07 p0922 N85-15844

Homogeneous reaction involving components of different redox couples. 1: Theoretical considerations and digital simulation
[AD-A148666] 08 p1124 N85-17084

Microstructural analysis of ion containing polymers
[DE85-001594] 10 p1453 N85-19157

The synthesis, structural characterization and reactions of closo-Rhodacarborane Anions containing a formal d8 metal vertex 1,2
[AD-A149640] 12 p1799 N85-21285

Theoretical studies of kinetic mechanisms of negative ion formation in plasmas
[AD-A150820] 14 p2423 N85-24946

The electronic spectra of phthalocyanine radical anions and cations
[AD-A152328] 17 p2318 N85-27986

Gas phase ion-molecule chemistry of carbon, nitrogen and oxygen compounds
[AD-A152876] 17 p2919 N85-27996

An alpha particle diagnostic beam line system to generate an intense Li(O) beam with an ORNL SITEX source
[DE85-010584] 18 p3182 N85-29730

Method of reducing impurity and antisite defects in semiconductor crystal materials, and device and apparatus respectively produced from and utilizing same
[AD-D011688] 19 p3260 N85-30216

Electron photoejection in carbanions
[DE85-011747] 23 p3911 N85-34230

Electron photoejection in carbanions
[DE85-011748] 23 p3912 N85-34237

Throughfall rate and chemistry studies: Whiteface Mountain
[DE85-012407] 23 p3947 N85-34464

ANISOTROPIC MEDIA

Identification of pulse-echo rays in austenitic steels
[AERE-R-11265] 03 p0369 N85-12356

Microwave measurement of the complex dielectric tensor at anisotropic slab materials
[DE84-017050] 04 p0493 N85-13144

Reflection theorems for some anisotropic media
07 p0953 N85-16038

Angular dependence of the Rayleigh-surface wave velocity in polycrystalline metals with small anisotropy
[AERE-R-11595] 15 p2509 N85-25476

Multiple scattering of electromagnetic waves in discrete random media
[AD-A151766] 16 p2772 N85-27112

Examination of anisotropic films by resonance method
22 p3778 N85-33412

ANISOTROPIC PLATES

Quantification of Saint-Venant's principle for a general prismatic member 04 p0467 N85-12972

A refinement of the transverse shear deformation theory for multilayered anisotropic plates
[STN-5] 20 p3471 N85-31571

ANISOTROPIC SHELLS

Normal mode method of solving problem forced oscillations of rib-reinforced shell of revolution in liquid
02 p0273 N85-11781

Stability of anisotropic cylindrical sandwich shells
16 p2786 N85-27065

ANISOTROPY

Theory of nuclear magnetic relaxation
[AD-P003911] 01 p0082 N85-10197

Fracture, failure, and fragmentation
01 p0059 N85-10390

A finite element projection method for the solution of particle transport problems with anisotropic scattering
[AD-A145382] 02 p0250 N85-11637

Improved beam theory for anisotropic materials
04 p0466 N85-12973

Collective processes and formation of star clusters
05 p0736 N85-14743

Anisotropy and microstructure of rare earth permanent magnet materials
[AD-A148549] 06 p0859 N85-15460

Irradiation creep induced anisotropy in a/2110 dislocation populations
[DE84-016823] 06 p0866 N85-15520

Low cycle fatigue of MAR-M 200 single crystals at 760 and 870 deg C
[NASA-TM-86933] 10 p1440 N85-19074

On shrinkage and molecular extension
[AD-A149100] 10 p1451 N85-19144

Imaging through a multiple scattering medium
[DE85-002051] 10 p1557 N85-19821

Ferromagnetic resonance in a Ni-Mo superlattice
[DE85-000096] 11 p1736 N85-20911

Calculation of ionospheric profiles by inverting VLF/LF reflection data. 2. Anisotropic propagation
[AD-A150105] 12 p1890 N85-21859

Correlation of interplanetary medium parameters in transition region of high-velocity solar wind streams
13 p1978 N85-22412

Orientation and temperature dependence of some mechanical properties of the single-crystal nickel-base superalloy Rene N4. 3: Tension-compression anisotropy
[NASA-TM-86982] 13 p2021 N85-22660

Investigations of ultrasonic wave interactions at boundaries separating anisotropic materials
[DE85-003506] 13 p2155 N85-23384

Measurement of the large-scale anisotropy of the cosmic background radiation at 3 MM 13 p2206 N85-23680

Solid/melt interface studies of high-speed silicon sheet growth
[NASA-CR-175698] 14 p2350 N85-24525

Energetic electron anisotropy and ELF waves onboard GEOS. How does quasi-linear diffusion work
14 p2366 N85-24623

Models of solar differential rotation
14 p2446 N85-25097

Effect of nickel addition on the thermal, magnetic and magnetomechanical properties of Fe(80)B(15)Si(5)
[AD-A152281] 16 p2749 N85-26967

Polarimetric image recorder
[AD-D011605] 16 p2787 N85-27192

Active and passive remote sensing of ice
[AD-A151741] 16 p2815 N85-27369

The soft X-ray background as a supernova blast wave viewed from inside: Solar abundance models
[NASA-CR-175787] 16 p2887 N85-27813

Investigation for low-cost permanent magnets
[AD-A154387] 19 p3260 N85-30212

Investigation of thick-target neutron emission from Be-9(d,n)B-10 at E(d) = 7 MeV for angles other than zero degrees
[DE85-010254] 20 p3528 N85-31947

Drift anisotropy instability of a finite Beta magnetospheric plasma
[IFSI-84-12] 20 p3536 N85-32005

Anisotropy of the permittivity field inferred from aspect-sensitive radar echoes 21 p3620 N85-32492

Influence of mirror anisotropy and Brewster window orientation on radiation characteristics of ring lasers
21 p3684 N85-32889

Low frequency instabilities driven by an ion temperature anisotropy
[AD-A154902] 21 p3707 N85-33016

Shear wave transducer for boreholes
[DE85-011662] 22 p3787 N85-33461

The effect of anisotropic emission on the log N-log S curve of gamma-ray bursts
[OG-1.2-4] 22 p3862 N85-33914

Search for ultra high energy gamma-rays from various sources
[OG-2.6-7] 22 p3870 N85-33969

Long term variability of the cosmic ray intensity
[OG-3.1-11] 22 p3874 N85-33999

Arrival directions of large air showers, low-mu showers and old-age low-mu air showers observed at St. Chacaltaya
[OG-5.3-2] 22 p3884 N85-34069

Anisotropy of cosmic rays of energy 10 (15) eV to 10 (17) eV observed at Akeno
[OG-5.3-3] 22 p3884 N85-34070

Arrival directions of cosmic rays of E 4 EeV
[OG-5.3-4] 22 p3884 N85-34071

The sidereal anisotropy of cosmic rays around 3 x 10 (15) eV observed at a middle north latitude
[OG-5.3-6] 22 p3884 N85-34072

Arrival direction distribution of cosmic rays of energy 10 (18) eV
[OG-5.3-7] 22 p3885 N85-34073

Air shower arrival directions measured at Buckland Park
[OG-5.3-11] 22 p3885 N85-34077

A simulation of high energy cosmic ray propagation 2
[OG-5.4-2] 22 p3885 N85-34079

Implications of the experimental results on high energy cosmic rays with regard to their origin
[OG-5.4-5] 22 p3886 N85-34082

Virgo cluster as a high energy cosmic rays source
[OG-5.4-8] 22 p3886 N85-34085

Modeling cosmic ray anisotropies near 10(18) eV
[OG-5.4-9] 22 p3886 N85-34086

Anisotropy and the knee of the energy spectrum
[OG-5.4-10] 22 p3887 N85-34087

A model for the proton spectrum and cosmic ray anisotropy
[OG-5.4-12] 22 p3887 N85-34089

On galactic origin of cosmic rays with energy up to 10(19) eV
[OG-5.4-16] 22 p3887 N85-34091

Flux-line lattice anisotropy in V3Si: Observation and interpretation
[DE85-011935] 23 p3985 N85-34713

Helios 1 energetic particle observations of the solar gamma ray flare events of 7, 21 June 1980 and 3 June 1982
[SH-1.3-8] 23 p3993 N85-34755

Ultrarelativistic electrons and solar flare gamma-radiation
[SH-1.3-11] 23 p3993 N85-34757

Cosmic ray north-south anisotropy 1961 - 1983
[SH-4.2-8] 23 p4007 N85-34844

Effects of a wavy neutral sheet on cosmic ray anisotropies
[SH-4.2-11] 23 p4008 N85-34849

The expected cosmic ray density and stream distributions at the heliolatitudinal asymmetry of solar wind
[SH-4.2-14] 23 p4008 N85-34852

The effect of the neutral sheet structure of the interplanetary magnetic field on cosmic ray distribution in space
[SH-4.2-18] 23 p4008 N85-34855

On the cosmic ray diffusion in a violent interstellar medium
[OG-7.2-14] 23 p4015 N85-34881

Gradients and anisotropies of high energy cosmic rays in the outer heliosphere
[SH-4.3-7] 23 p4032 N85-34992

IMF-sense-dependent cosmic ray anisotropy produced from diffusion-convection in heliosphere
[SH-4.3-9] 23 p4032 N85-34994

Influence of the neutral sheet on the Swinson's type north-south anisotropy of cosmic rays
[SH-4.3-10] 23 p4032 N85-34995

Characteristics of cosmic ray pole-equator anisotropy derived from spherical harmonic analysis of neutron monitor data
[SH-4.3-12] 23 p4032 N85-34996

First zonal harmonic component of cosmic ray neutron intensity
[SH-4.3-13] 23 p4032 N85-34997

The corotating variation of the north-south anisotropy of cosmic rays
[SH-4.3-15] 23 p4033 N85-34999

Sidereal anisotropies in the median rigidity range 60-600GV in 1978-1983
[SH-4.4-3] 23 p4033 N85-35001

The effect of the interplanetary magnetic field on sidereal variations observed at medium depth underground detectors
[SH-4.4-5] 23 p4033 N85-35003

The sidereal semi-diurnal variation observed at high zenith angles at Mawson, 1968-1984, and the polarity of the solar main field
[SH-4.4-6] 23 p4033 N85-35004

Sidereal anisotropy of cosmic rays
[SH-4.4-8] 23 p4034 N85-35006

Formulation of cosmic-ray solar daily variation and its seasonal variation, produced from generalized stationary anisotropy of solar origin
[SH-4.5-2] 23 p4036 N85-35020

Solar tri-diurnal variation of cosmic rays in a wide range of rigidity
[SH-4.5-3] 23 p4036 N85-35021

Upper cut-off rigidity for corotation anisotropy during solar activity cycles 20 and 21
[SH-4.5-4] 23 p4036 N85-35022

Diurnal anisotropy during solar activity cycle twenty and diffusion-convection model
[SH-4.5-7] 23 p4036 N85-35025

Comparative study of the phase of diurnal anisotropy on quiet and disturbed days on a long term basis up to recent period
[SH-4.5-9] 23 p4037 N85-35027

Study of spectral exponent on quiet and disturbed days
[SH-4.5-10] 23 p4037 N85-35028

The modulation features of the long-period cosmic ray variations in connection with the sign change of the general magnetic field of the Sun
[SH-4.5-15] 23 p4037 N85-35032

Cosmic ray density gradient and its dependence on the north-south asymmetry in solar activity
[SH-4.5-17] 23 p4038 N85-35034

Anomalous increase of solar anisotropy above 150GV in 1981-1983
[SH-4.5-18] 23 p4038 N85-35035

Diagnostic of electromagnetic conditions in space using cosmic rays
[SH-4.5-19] 23 p4038 N85-35036

Change of cosmic ray anisotropy with solar activity
[SH-4.5-20] 23 p4038 N85-35037

Magnetic fluctuation and cosmic ray diurnal variations
[SH-4.5-21] 23 p4038 N85-35038

The theoretical and experimental investigation of cosmic ray Forbush-effects
[SH-5.1-20] 23 p4044 N85-35072

Peculiarities of Galactic Cosmic Ray (GCR) anisotropy variation in connection with the recurrent and sporadic Forbush effects
[SH-5.1-21] 23 p4044 N85-35073

A comparative analysis of gamma and hadron families at the superhigh energies recorded in experiment Pamir
[HE-3.7-1] 24 p4185 N85-35960

Character of energy flow in air shower core
24 p4189 N85-35985

An underground cosmic ray muon telescope for observation of cosmic ray anisotropy
24 p4196 N85-36037

Underground measurements on secondary cosmic rays
[HE-5.4-1] 24 p4207 N85-36116

ANNEALING

NT LASER ANNEALING

NT PULSE HEATING

Influence of annealing on properties of AT3 alloy welded joints
01 p0019 N85-10118

Kinetics of short-range ordering in metallic glasses: Analysis of the crossover effect
[DE84-015524] 02 p0187 N85-11251

Complex formation and temperature stability of electrophysical properties of GaAs seminsulating single crystals
02 p0258 N85-11689

The effect of heat treatment on wear resistance of gas-plasma eutectic coatings
[BLL-M-35756-(5828.4)] 03 p0329 N85-12122

Annealing of implanted Al-2O-3 in a reducing environment
[DE84-015370] 03 p0332 N85-12140

Parameters of structural relaxation and mechanical properties of amorphous alloys
03 p0349 N85-12246

Effect of annealing in transverse magnetic field on magnetic permeability of amorphous Fe5Co70Si15B10 alloy
03 p0349 N85-12247

Structural recrystallization in titanium
03 p0351 N85-12258

A study of defects in neutron transmutation doped silicon: Gallium by hall effect analysis
[AD-A146047] 03 p0433 N85-12758

On the origins of structural defects in BF2(+)-implanted and rapid thermally annealed silicon: Conditions for defect free regrowth
[DE84-016060] 04 p0572 N85-13650

Impact toughness of wire after cold deformation and annealing
[BLL-M-35941-(5828.4)] 05 p0615 N85-13930

Multiaxial yield behavior of 1100 aluminum following various magnitudes of prestrain
[DE84-013904] 05 p0617 N85-13949

Development of technology of silicon single-crystal production semiconductor power devices: State of art outlook
06 p0795 N85-15076

Oxide charge characteristics of low temperature MOS (Metal-Oxide-Silicon) oxide films
[AD-A146447] 06 p0803 N85-15113

Atmospheric heating of meteorites: Results from nuclear track studies
06 p0862 N85-15607

Defective nature of the crystalline lattice of nickel ferrite-based solid solutions
[BLL-WH-595-(9091.9F)] 07 p1046 N85-16645

X-ray and backscattering analysis of ion implantation phenomena in GaAs and related compounds
[AD-A147449] 07 p1048 N85-16659

Study of the mechanism for annealing embrittlement of an iron-based metallic glass
[DE84-016856] 08 p1300 N85-18164

Radiation effects in Straind-Layer Superlattice (SLS) structures
[DE85-001713] 09 p1398 N85-18799

Ion beam processes in Si
[DE85-001254] 09 p1399 N85-18808

Damage to boron fibers during thermal cycling and annealing
10 p1445 N85-19107

Study of the volumetric changes in VT23 alloy upon heating
10 p1448 N85-19123

Mod silver metallization for photovoltaics
[NASA-CR-174444] 10 p1509 N85-19518

Pulsed excimer laser processing for cost-effective solar cells
[NASA-CR-175465] 10 p1509 N85-19520

Dependence of mechanical properties of large VT3-1 alloy forgings on microstructure parameters
11 p1602 N85-20072

Low cost, sprayed CuInSe2 solar cell research
[DE85-003487] 12 p1881 N85-21799

Investigation of device and electronic interactions in GaAs device processing
[AD-A149747] 12 p1940 N85-22182

The effects of lithium counterdoping on radiation damage and annealing in n(+)p silicon solar cells
13 p2007 N85-22586

Temperature effects of heterogenizated annealing on structure and properties of V95 aluminum alloy
13 p2025 N85-22692

Influence of annealing on cyclic and short-term strength of thin sheets of VT1-0 titanium and OTR4 alloy
13 p2031 N85-22727

Thermal hardening of welded joints in titanium alloys with various structures 13 p2032 N85-22734

Investigation of the effect of annealing on the dislocation and sub-grain boundary content of solvent-evaporation-grown CdTe
[AD-A144087] 13 p2162 N85-23415

Influence of substrate heating and thermal annealing on the surface crystallinity in single Si crystals implanted with high doses of (16)O
[DE85-005264] 13 p2164 N85-23428

Annealing effects in ferromagnetic amorphous alloys
[AD-A150648] 14 p2255 N85-23972

Possible use of rapid heating for improving mechanical properties of titanium alloys 15 p2498 N85-25409

Effect of annealing procedures on structure and properties of VT6 alloy with initial large-grained structure
15 p2498 N85-25410

Effect of aluminum on nature of titanium alloy failure
15 p2498 N85-25411

Study of oxidized surface coating on titanium after annealing 15 p2498 N85-25412

Brittle fracture resistance of electron beam-welded joints in titanium Alpha alloys 15 p2500 N85-25419

Structure and properties of VT20L titanium alloy with 0.1-0.3 percent content 15 p2515 N85-25517

Characterization of thin films and layered structures using X-ray absorption and reflection at grazing incidence
[DE85-006560] 15 p2662 N85-26429

Relationships between microstructure and microfissuring in alloy 718 16 p2735 N85-26876

Solution softening in molybdenum-rhenium alloys
[DE85-006706] 16 p2750 N85-26972

Thermal annealing of Fe implanted Al2O3 in oxidizing and reducing environment: Revised version
[DE85-007546] 16 p2752 N85-26983

Thermomechanical softening treatment for bearing and tool steels
[BLL-BISI-TRANS-22432-(9022.06)]
17 p2925 N85-28035

Influence of preliminary cold deformation on fineness of pearlite
[BLL-BISI-TRANS-22409-(9022.06)]
17 p2927 N85-28054

The characteristic structure of weld metal of high temperature alloy X20CrMoV 121
[BLL-BISI-TRANS-21623-(9022.06)]
17 p2928 N85-28069

Kinetics of the formation of a complex alloyed boride coating on iron and its properties
[BLL-BISI-TRANS-22303-(9022.06)]
17 p2930 N85-28084

Activities of the Solid State Physics Research Institute
[NASA-CR-175899] 17 p3042 N85-28818

Thermal donor removal by rapid thermal annealing: Infrared absorption
[DE85-010082] 18 p3081 N85-29059

Post-deposition heat treatments of CdS/CuInSe2 solar cells
[DE85-002943] 18 p3128 N85-29373

Electronic states in silicon and on its interfaces
[AD-A153664] 18 p3193 N85-29807

Effects of annealing treatments on superplasticity in a thermomechanically processed Aluminum-10.2%Mg-0.52%Mn
[AD-A154414] 19 p3239 N85-30080

Fatigue resistance of homogeneous and heterogeneous welded joints of TS5 titanium alloy
19 p3246 N85-30126

Investigation for low-cost permanent magnets
[AD-A154387] 19 p3260 N85-30212

Method for producing high quality germanium-germanium nitride interfaces for germanium semiconductors and device produced thereby
[AD-D011702] 19 p3260 N85-30218

Electrical properties of bulk grown nitrogen doped silicon
[AD-A155471] 21 p3581 N85-32288

Metallic glass composition
[DE85-011594] 22 p3751 N85-33253

Ultra-trace analysis of sinter tantalum with SIMS
[BLL-RARDE-TR-1220-(7291.7985)]
23 p3913 N85-34245

Changes in lattice cell parameter of film intermetallic compounds RT2
[BLL-M-35874-(5828.4)] 23 p3915 N85-34261

An X-ray diffraction study of titanium oxidation
[NASA-CR-176263] 23 p3915 N85-34264

Rapid annealing of temperature-compensated, precision voltage references following fast-neutron irradiation
[DE85-009821] 23 p3970 N85-34609

Decomposition of martensite in R6M5 and R6AM5 steels after direct immersion in liquid nitrogen
[BLL-M-36305] 24 p4077 N85-35268

Advanced detectors and signal processing
[NASA-CR-176193] 24 p4088 N85-35343

Size and shape dependence of CO adsorption sites on sapphire supported Fe microcrystals
[NASA-CR-176171] 24 p4160 N85-35794

Laser and electron beam processing of semiconductors
[AD-A155914] 24 p4161 N85-35796

ANNIHILATION REACTIONS

NT POSITRON ANNIHILATION

Performance of a large area flash chamber prototype
[NOTA-INTERNA-807] 02 p0201 N85-11336

Experimental medium energy physics
[DE84-014625] 02 p0278 N85-11807

Fermilab research program workbook
[DE84-012566] 06 p0862 N85-15476

Experimental investigations in particle physics at intermediate energies
[DE85-001481] 11 p1722 N85-20832

Parton dynamics in hadronic processes
[DE85-006072] 14 p2418 N85-24922

Experimental methods of heavy quark detection
[DE85-006316] 17 p3036 N85-28781

Control technology for radioactive emissions to the atmosphere at US Department of Energy facilities: The Los Alamos Meson Physics Facility
[DE85-011402] 22 p3811 N85-33609

Annihilation radiation in cosmic gamma-ray bursts
[OG-1.1-3] 22 p3861 N85-33905

Unthermalized plasma in bursts sources
[OG-1.1-5] 22 p3861 N85-33907

Neutrino-antineutrino annihilation around collapsing star
[OG-1.1-10] 22 p3861 N85-33911

Diffuse galactic annihilation radiation from supernova nucleosynthesis
[OG-3.2-8] 22 p3875 N85-34004

Galactic cosmic ray antiprotons and supersymmetry
[OG-6.1-9] 22 p3888 N85-34100

ANNUAL VARIATIONS

Predictor model for seasonal variations in skid resistance, volume 1
[PB84-226612] 01 p0036 N85-10229

Predictor model for seasonal variations in skid resistance. Volume 2: Comprehensive report
[PB84-226620] 01 p0037 N85-10230

The climate of Denmark. Summaries of observations from light vessels. 3: Sea temperature
[ISBN-87-7478-215-0] 01 p0073 N85-10481

Return wave heights off South Uist estimated from seven years of data
[IOS-164] 01 p0089 N85-10601

Observations of the pulsating hydrogen: Deficient star BD+13 deg 3224, during 1980 - 1981
01 p0128 N85-10882

Remote sensing as a mineral prospecting technique
[E85-10010] 02 p0216 N85-11423

Northern Hemisphere atlas of 1-minute rainfall rates
[AD-A145411] 02 p0231 N85-11508

Seasonal variations in Triton's atmospheric mass and composition 02 p0301 N85-11948

Seasonal variations of reflexibility and transmissibility of ULF waves propagating through the ionosphere of geomagnetic mid-latitudes
[REPT-560] 03 p0376 N85-12403

On the annual and semiannual variation of S sub R at l'Aquila — geomagnetism 04 p0520 N85-13326

On some new features of semiannual variation of the geomagnetic field 04 p0520 N85-13327

Image texture study for the operational meteorological satellites NOAA 6 and NOAA 7 and its variation with time. Application to the Beauce region
[ENST-84E009] 05 p0681 N85-14249

Solar pond research at Argonne National Laboratory
05 p0687 N85-14291

Interannual variability in the observed circulation
05 p0686 N85-14409

The influence of synoptic scales on low-frequency modes of variability 05 p0687 N85-14412

Annual energy spectrum for tracking arrays
06 p0832 N85-15297

Monthly and seasonal climatology over the global tropics and subtropics for the decade 1973 to 1983. Volume 1: 200 mb winds
[AD-A146521] 06 p0838 N85-15322

Diurnal and seasonal patterns of temperature and wind flow in the planetary boundary layer for ten locations in complex terrain
[PB85-108696/GAR] 06 p0640 N85-15333

Satellite definition of the bio-optical and thermal variation of coastal eddies associated with the African current
[AD-A147910] 07 p0869 N85-16262

The problem of climate and climate variation
07 p1001 N85-16353

Evaluation of the climatic resources of Cuba applied to agricultural work 07 p1004 N85-16360

The use of hydrometeorological data in explaining shrimp cycles in Guyana 07 p1004 N85-16361

Interrelationship of atmospheric parameters in Honduras
[AD-A147371] 07 p1007 N85-16401

North American vegetation patterns observed with the NOAA-7 advanced very high resolution radiometer — North America
[E85-10062] 08 p1174 N85-17400

Regional and seasonal variations in snow-cover density in the USSR
[AD-A148429] 08 p1169 N85-17496

The atmospheric extinction problem
08 p1251 N85-17901

An analysis of the seasonal variations in the water vapor transport fields over the Southern Hemisphere
09 p1356 N85-18531

Weather data for simplified energy calculation methods. Volume 3. Western United States: TRY data
[DE85-000495] 09 p1358 N85-18540

Calculation of optical characteristics of shelf ecological system based on its mathematical model
10 p1496 N85-19453

Growth and reflectance characteristics of winter wheat canopies
[E85-10080] 10 p1505 N85-19494

Study of low energy density photovoltaic applications under varying rate structures
[DE85-000185] 10 p1511 N85-19538

Sequential precipitation chemistry sampling program at Brookhaven National Laboratory with an analytical summary of 1976-1982 data
[DE85-002788] 10 p1513 N85-19545

Interannual variations of the winter circulation in the Northern Hemisphere and in the southern oscillation (meridian) and their possible connections with the climate of Northeast Brazil
[INPE-3333-TDL/182] 10 p1519 N85-19573

Cut-off lows and their influence on the weather in Switzerland
[REPT-45] 10 p1519 N85-19574

The Middle Atmosphere Program: Winter In Northern Europe (MAP/WINE) 11 p1655 N85-20429

Autumn and winter anomalies in ionospheric absorption as measured by riometers 11 p1660 N85-20460

A model of the influence of neutral air dynamics on the seasonal variation in the low ionosphere
11 p1660 N85-20462

Explanation of the normal winter anomaly from the seasonal variation of short wave absorption
11 p1660 N85-20463

Seasonal characteristics of mesospheric plasma and their transitions 11 p1660 N85-20464

Spring changeover of the middle atmosphere circulation compared with rocket wind data up to 80 km
11 p1661 N85-20466

Monthly and seasonal weather outlook for October 1984, volume 38, number 19. 29 September 1984
[PB85-113538] 11 p1687 N85-20610

OSCAR experiment high-density network data report
[DE85-004907] 12 p1884 N85-21826

The effect of stochastic surface heat fluxes on the climatology of the seasonal thermocline
[AD-A149957] 12 p1889 N85-21857

Solar-geophysical data number 479, July 1984. Part 1: (Prompt reports). Data for June 1984, May 1984 and later data
[NASA-CR-175542] 12 p1962 N85-22333

Empirical and modeled synoptic cloud climatology of the Arctic Ocean
[NASA-CR-175626] 13 p2137 N85-23272

Seasonal and secular variation of the Solis Lacus albedo feature: Relation to the Martian dust-transport cycle
13 p2188 N85-23576

Water-ice clouds on Mars: Location and seasonal variation 13 p2194 N85-23611

The Tropical Ocean and Global Atmosphere program (TOGA) 14 p2330 N85-24411

Small component spectral model of annual course of zonal atmospheric circulation 14 p2337 N85-24453

Ionospheric effects of seasonal and diurnal variations of electric fields in equatorial F-region
14 p2338 N85-24459

Diurnal variations in terrestrial magnetic field and structure of magnetosphere 14 p2344 N85-24493

MAP3S precipitation chemistry network
[DE85-005324] 14 p2353 N85-24539

Monthly and Seasonal Weather Outlook for mid-December 1984 mid-January 1985, volume 38, number 24, 14 December 1984
14 p2379 N85-24667

Analysis of hydrometeorological conditions in Antarctic coastal waters according to data from hydrological and satellite observations 15 p2487 N85-25354

Development of algorithms for using satellite meteorological data sets to study global transport of stratospheric aerosols and ozone
[NASA-CR-172540] 15 p2591 N85-25974

Annual cycle. Part 1: The annual variation of surface temperatures over the United States and Canada
[PB85-147676] 15 p2600 N85-26026

Annual cycle. Part 2: The annual variation of precipitation over the United States and Canada
[PB85-147684] 15 p2600 N85-26027

Oceanographic variations in recent decades and their impact on the fertility of the Iceland Sea
15 p2602 N85-26034

Mars: Seasonally variable radar reflectivity
15 p2683 N85-26570

Year-to-year variability of components of Earth's radiation budget according to satellite measurement data 16 p2725 N85-26821

The seasonal cycle of atmospheric CO in the Southern Hemisphere 16 p2830 N85-27447

Fog advection in the Namib 16 p2831 N85-27454

Air flow of the western coastal boundary of South Africa and its influence on the ocean 16 p2831 N85-27459

Forecast of Atlantic seasonal hurricane activity for 1985 16 p2833 N85-27470

AWS (Air Weather Service) climatic briefs: North America
[AD-A152161] 16 p2835 N85-27483

Solar-Geophysical Data Number 484, December 1984. Part 1 (prompt reports): Data for November 1984, October 1984 and late data
[NASA-CR-175829] 16 p2888 N85-27819

Precipitation and snow cover data, 1977
[ISBN-951-697-215-2] 17 p2995 N85-28514

Observations of surface water temperature in the Netherlands since 1860: Statistics
[KNMI-WR-84-3] 17 p2997 N85-28531

Observations of surface water temperature in the Netherlands since 1860: Tables for light vessels
[KNMI-WR-84-4] 17 p2998 N85-28532

Observations of surface water temperature in the Netherlands since 1860: Series from KNMI-RWS
[KNMI-WR-84-5] 17 p2998 N85-28533

Measurements of VHF/UHF radio propagation in a maritime temperate climate
[CRC-1380] 18 p3089 N85-29119

Permafrost, seasonally frozen ground, snow cover and vegetation in the USSR
[AD-A153628] 18 p3124 N85-29346

The seasonal cycle of storminess as measured by band-pass fluctuations 18 p3144 N85-29467

The contrasting Northern Hemisphere winters of 1980-81 and 1981-82 18 p3144 N85-29468

Monthly and seasonal weather outlook for mid-February to mid-March 1985, volume 39, number 4, February 14, 1985
[PB85-164580] 18 p3149 N85-29500

Application of climatological analysis to minimize air pollution impacts in California
[PB85-172983] 18 p3149 N85-29502

The influence of global dust storms on the mean seasonal daily insolations at the Martian surface
[AERONOMICA-ACTA-A-289-1984]
18 p3203 N85-29868

Categorization of nocturnal drainage flows within the Brush Creek valley in western Colorado and the variability of sigma theta in complex terrain
[DE85-011291] 19 p3300 N85-30461

Calibration of relevant measuring sensors
[DE85-009620] 19 p3306 N85-30492

Tropical ozone: Seasonal variations in the troposphere at 6 deg S
[INPE-3555-PRE/766] 19 p3313 N85-30535

Atmospheric cross sections for the Arctic gas and aerosol sampling program, March - April 1983
[NASA-CR-176027] 19 p3314 N85-30541

On the dynamical climatology of the Amazon Basin and associated rain producing mechanisms
[INPE-3531-RPE/477] 19 p3315 N85-30552

Northeast Brazil droughts and Atlantic SST anomalies
[INPE-3536-PRE/754] 19 p3316 N85-30553

On the interannual variability of the Indian monsoon and the Southern Oscillation 20 p3495 N85-31728

The worldwide distribution of the seasonal cycle of mean sea level
[IOS-190] 20 p3497 N85-31743

Insolation changes on Pluto caused by orbital element variations
[AERONOMICA-ACTA-A-290-1984]
20 p3546 N85-32070

Trace element concentrations in atmospheric aerosol over Hungary 21 p3646 N85-32652

Chemical composition of atmospheric aerosol at Delhi
21 p3646 N85-32653

The variability of aerosol microstructure in continental and oceanic surface layers of the atmosphere in anticyclones 21 p3647 N85-32660

Numerical modeling of sea ice dynamics and ice thickness characteristics
[AD-A154600] 21 p3654 N85-32700

Comparisons of the North Polar Cap of Mars and the Earth's Northern Hemisphere snow cover
[NASA-TM-86191] 23 p3869 N85-34728

Characteristics of cosmic ray pole-equator anisotropy derived from spherical harmonic analysis of neutron monitor data
[SH-4.3-12] 23 p4032 N85-34996

Cosmic ray intensity distribution perpendicular to solar equatorial plane at 1 A.U. during 1978-83
[SH-4.3-14] 23 p4032 N85-34998

The corotating variation of the north-south anisotropy of cosmic rays
[SH-4.3-15] 23 p4033 N85-34999

Cosmic ray intensity variations observed at Matsushiro (220 M.W.E. in depth)
[SH-4.4-9] 23 p4034 N85-35007

Cosmic ray biennual variation
[SH-4.4-15] 23 p4034 N85-35011

Cosmic ray modulation by high-speed solar wind fluxes
[SH-5.1-22] 23 p4044 N85-35074

The influence of quiet asymmetric magnetosphere on the cutoff rigidities of the main cone
[SH-6.1-10] 23 p4045 N85-35083

A possible mechanism to cause the quasi-biennial variability on the solar neutrino flux
[SH-8.1-5] 23 p4049 N85-35110

Subseasonal variability in a two-level atmospheric general circulation model 24 p4114 N85-35504

ANNULAR DUCTS

Stall elimination and restart enhancement device
[AD-D011217] 01 p0010 N85-10062

Unsteady free-convection heat transfer inside an annular cavity
[CFD/84/16] 08 p1163 N85-17339

High-pressure rocket engine turnaround duct computational fluid dynamics analysis
13 p2003 N85-22556

ANNULAR FLOW

Characteristics of controlled-oscillating annular cascade test facility with Freon gas
[NAL-TR-812] 01 p0003 N85-10014

Stability of fluid flow in a cylindrical annulus
[NASA-TM-77720] 01 p0046 N85-10300

Identification of dynamic coefficients of annular turbulent seals 05 p0644 N85-14133

Analysis and testing for rotordynamic coefficients of turbulent annular seals with different, directionally homogeneous surface-roughness treatment for rotor and stator elements 05 p0644 N85-14134

Analysis for leakage and rotordynamic coefficients of surface roughened tapered annular gas seals
05 p0644 N85-14135

An improved computer model for prediction of axial gas turbine performance losses
[NASA-CR-174246] 07 p0904 N85-15724

Unsteady free-convection heat transfer inside an annular cavity
[CFD/84/16] 08 p1163 N85-17339

Determination of total pressure losses in stepped annular diffusors with curvilinear outer walls and uniform velocity field at inlet 09 p1306 N85-18203

An experimental study of aerodynamic damping characteristics of a compressor annular cascade in high speed flow and the visualization of annular cascade flow
[NAL-TR-838] 15 p2554 N85-25759

Flow visualization study of inverted annular flow of post dryout heat transfer region
[DE85-010482] 19 p3269 N85-30275

ANNULAR NOZZLES

Experimental investigation of shock-cell noise reduction for single stream nozzles in simulated flight
[NASA-CR-3845] 04 p0557 N85-13550

ANNULI

Birkhoff orbits for non-monotone twist maps
[AD-A144718] 01 p0110 N85-10747

ANODES

NT CELL ANODES
NT SHELL ANODES
NT TUBE ANODES

Advanced fuel cell development
[DE84-014847] 01 p0044 N85-10289

The driving-force dependence of electrochemical rate parameters: Origins of anodic-cathodic asymmetries for metal aquo redox couples
[AD-A145605] 02 p0172 N85-11153
Oxygen diffusion from anodic surface oxide films on titanium subhydride studies by auger electron spectroscopy and electron energy loss spectroscopy
[DE84-016942] 04 p0572 N85-13645
Behaviour of lead-silver anodes in zinc electrodeposition from sulphuric acid baths
[BLL-MINTEK-TR-1180-(5810.5759)]
06 p0764 N85-14887
The anode mechanism of a thermal argon arc
[NASA-TM-77754] 07 p0921 N85-15835
The development and test of ultra-large-format multi-anode microchannel array detector systems
[NASA-CR-174247] 07 p1043 N85-16622
Electrochemistry at very high potentials: The use of ultramicroelectrodes in the anodic oxidation of short chain alkanes
[AD-A148654] 08 p1123 N85-17078
Photometry with Multi-Anode Microchannel Arrays (MAMAs) and Charge Injection Devices (CIDs)
08 p1252 N85-17909
Thermal investigation of an electrical high-current arc with porous gas-cooled anode
[NASA-TM-77769] 11 p1627 N85-20245
Development of a low cost electrochemical CO monitor based on anodic scanning voltammetry in nonaqueous electrolyte
[PB85-113488] 11 p1637 N85-20314
Alternative anodic reactions in water splitting
[DE85-004159] 12 p1802 N85-21300
Review of anode phenomena in vacuum arcs
[DE85-002736] 12 p1926 N85-22101
Application of modulated hydrodynamic voltammetry to the study of anodic electrocatalysis
[DE85-004182] 13 p2018 N85-22653
Molten carbonate fuel cell performance model update, draft
[DE85-005423] 13 p2129 N85-23252
Oxygen evolution on NiCo2O4 electrodes
17 p2924 N85-28026
Bifunctional oxygen electrodes
[DE85-006871] 17 p2955 N85-28248
Streak tube characterization
[DE85-009874] 17 p2956 N85-28255
Molten carbonate fuel cell performance model update
[DE85-003356] 17 p2986 N85-28454
Spectrographic investigation of low-voltage arc discharge in argon atmosphere
[BLL-M-36276-(5828.4)] 20 p3422 N85-31242
Method of production of metals by cathodic solution of their compounds in electrolytic cells
[BLL-OA-TRANS-3207-(6198.300)]
20 p3429 N85-31266
Deposition of nickel-cobalt alloys by controlled-potential electrolysis
[PB85-198562] 24 p4081 N85-35291

ANODIC COATINGS
Influence of parameters of aluminum alloy anodizing process on oxide coating thickness
01 p0018 N85-10113
Effects of introduction of alkyl groups into aluminium anodized coatings
[DRIC-T-7244] 03 p0331 N85-12133
Wear of anodic oxide films on aluminum alloys in cryogenic liquids
[NAL-TR-818] 06 p0768 N85-14914
Method for bonding insulator to insulator
[AD-D011340] 07 p0929 N85-15891
Improved ceramic anodes for corrosion protection
[AD-A149482] 10 p1452 N85-19149
Effect of mill run and temper variations on barrier anodic film format ion on 6061 aluminum alloy
[DE85-000447] 11 p1608 N85-20112
Resistance of polyaniline films as a function of electrochemical potential and the fabrication of polyaniline-based microelectronic devices
[AD-A154999] 21 p3569 N85-32201

ANODIC STRIPPING
Microprocessor-controlled anodic stripping voltammeter for trace metal analysis in tap water
[DE85-002781] 12 p1852 N85-21619

ANODIZING
Effect of mill run and temper variations on barrier anodic film format ion on 6061 aluminum alloy
[DE85-000447] 11 p1608 N85-20112
Corrosion characteristics of some steels produced through a self-cleaning rotating electrode
[BLL-BISI-TRANS-22046-(9022.06)]
17 p2925 N85-28034
Electrolytic synthesis of colored eta alumina film
23 p3906 N85-34201

ANOMALIES
NT GEOMAGNETIC HOLLOW
NT GEOTHERMAL ANOMALIES
NT GRAVITY ANOMALIES
NT MAGNETIC ANOMALIES
The de Tilini star pointer characterization and conclusions on the 1982 transmediterranean flight
[CESR-83-1070] 02 p0139 N85-10946
Systematic data interpretation of remote sensing in the reception of hydrocarbons, volume 1
[E85-10009] 02 p0215 N85-11421
Remote sensing as a mineral prospecting technique
[E85-10010] 02 p0216 N85-11423
Digital Terrain Elevation Data (DTED) anomaly removal through the use of an interactive Fourier frequency filtering process
[AD-A145433] 02 p0219 N85-11445
Anomalies in frequency characteristics of solid-state ring laser 02 p0271 N85-11765
Anomalon search — heavy cosmic ray interactions
[NOTA-INTERNA-825] 02 p0305 N85-11970
The winter anomaly in ionospheric absorption (with special reference to the results obtained in Spain)
04 p0522 N85-13336
Possible anomaly prediction system for the middle atmosphere — ionospheric absorption
04 p0522 N85-13339
Heat sources in the tropics and large scale flow anomalies associated with precipitation anomalies in northeast Brazil
[INPE-3211-TDL/175] 04 p0536 N85-13421
Kohn anomaly in metastable fcc lanthanum at low temperatures
[DE84-015459] 04 p0569 N85-13628
Implications of the chiral anomaly for quantum Hall effect devices
[NUB-2662] 05 p0629 N85-14029
Diagnostics of rainfall anomalies in the nordeste during the global weather experiment 05 p0685 N85-14405
Linear studies of stationary, extratropical anomalies in the troposphere 05 p0686 N85-14410
Unexplained Fe, Ni and S anomalies in CV chondrite components 06 p0884 N85-15619
Chemical evolution of the solar nebula: A new model
06 p0887 N85-15631
Statistical filtering as method for detecting transcrustal acoustic anomalies 07 p0982 N85-16237
Ocean and climate, an example. The interannual variability of the tropical Pacific Ocean
07 p1002 N85-16365
Climate and fisheries: A Peruvian case study
07 p1003 N85-16373
The 500 millibar sign frequency teleconnection charts: Winter
[PB85-106276/GAR] 07 p1009 N85-16410
Solid rocket motor certification to meet space shuttle requirements from challenge to achievement
08 p1098 N85-16941
An investigation of ionospheric irregularity effects on SIR-B image processing and information extraction
08 p1149 N85-17247
Droughts and floods in South America due to the 1982-83 El Nino-southern oscillation episode
[INPE-3408-PRE/677] 09 p1357 N85-18535
Acoustic tomographic reconstrution of anomalies in three-dimensional bodies
[DE84-017035] 09 p1379 N85-18666
Nonlinear seismology 10 p1503 N85-19482
Recent investigations at INPE in magnetospheric physics and geomagnetism
[INPE-3280-PRE/603] 10 p1514 N85-19555
Planetary scale circulation anomalies associated with droughts over northeast Brazil
[INPE-3351-PRE/630] 10 p1518 N85-19570
Large scale circulation anomalies and prediction of northeast Brazil droughts
[INPE-3405-PRE/674] 10 p1518 N85-19571
Winter anomaly of the lower ionosphere and its possible causes 11 p1660 N85-20459
Winter anomaly 1982/83 in comparison with earlier winters (1980-82) 11 p1660 N85-20461
Explanation of the normal winter anomaly from the seasonal variation of short wave absorption
11 p1660 N85-20463
Dependence of the high latitude middle atmosphere ionization on structures in interplanetary space
11 p1664 N85-20487
Interacting binary systems 11 p1744 N85-20967
Workshop on Remote Sensing/Lineament Applications for Energy Extraction
[DE84-009291] 12 p1875 N85-21763
Moisture variation in northern hemisphere temperate latitudes 13 p2105 N85-23119
El Nino, the capricious child 13 p2106 N85-23121
Diurnal variations in terrestrial magnetic field and structure of magnetosphere 14 p2344 N85-24493
Temperature anomalies above ore bodies
14 p2345 N85-24500
A study of terrain reductions, density anomalies and geophysical inversion methods in gravity field modelling
[AD-A150788] 14 p2373 N85-24666
Real-time enhancement of a climatology or forecast of ocean thermal structure using observed ocean temperatures
[AD-A151118] 15 p2604 N85-26049
On geoid heights and flexure of the lithosphere at seamounts
[AD-A151220] 15 p2604 N85-26050
A spectacular nitrogen isotope anomaly in Bencubbin
15 p2663 N85-26559
Effect of nickel addition on the thermal, magnetic and magnetomechanical properties of Fe(80)B(15)Si(5)
[AD-A152261] 16 p2749 N85-26967
Quasi stationary states in the Southern Hemisphere
18 p3144 N85-29465
Northeast Brazil droughts and Atlantic SST anomalies
[INPE-3538-PRE/754] 19 p3316 N85-30553
The nature of the anomalies on the polytherms of the properties of molten metallic alloys
[BLL-M-36265-(5828.4)] 20 p3430 N85-31277
Short meridional scale anomalies in the lower stratosphere and upper troposphere
20 p3489 N85-31684
Dynamic compensation of Venus's geoid: A comparison with Earth 22 p3858 N85-33686
Anomalous abundances of solar energetic particles and coronal gas: Coulomb effects and First Ionization Potential (FIP) ordering
[SH-2.1-10] 23 p3999 N85-34791
Search for anomalous C-jets in Chacaltaya emulsion chamber experiment
[HE-3.2-5] 24 p4179 N85-35913
Anomalous correlation between hadron and electromagnetic particles in hadron and gamma-ray families
[HE-3.3-6] 24 p4180 N85-35924
Anomalies in cosmic rays: New particles versus charm?
[HE-5.4-9] 24 p4206 N85-36120

ANOMALOUS TEMPERATURE ZONES
Thermal energy resources of thermal waters in Kazakhstan 06 p0820 N85-15208
Temperature anomalies above ore bodies
14 p2345 N85-24500
A GCM study of the atmospheric response to tropical SST anomalies 18 p3146 N85-29477

ANORTHOSITE
Particle velocity experiments in anorthosite and gabbro
[NASA-CR-174158] 04 p0533 N85-13407
Primordial magmaspheres and their lasting consequences 22 p3857 N85-33682

ANOXIA
Armed forces special Symposium on Medicine of Altitudes 13 p2166 N85-23441

ANTARCTIC ENVIRONMENT
U ICE ENVIRONMENTS

ANTARCTIC REGIONS
NT ROSS ICE SHELF
South African Antarctic research report to SCAR, no. 24, 1982. 1: Record of activities: April 1981 - September 1982. 2: Planned activities: October 1982 - September 1983. 3: Recent publications: 1981/1982
[CSIR-SR-SCAR-24] 01 p0063 N85-10417
Sea ice data buoys in the Weddell Sea
[AD-A144953] 01 p0088 N85-10594
Marine geological and geophysical investigations of the Antarctic Continental Margin, 1984
[GS-CIRC-935] 02 p0212 N85-11400
MIZEX. A program for mesoscale air-ice-ocean interaction experiments in arctic marginal ice zones. III: Modeling the marginal ice zone
[AD-A145351] 02 p0233 N85-11517
Feasibility of long duration ballooning in Antarctica
[PB84-240571] 04 p0541 N85-13443
Report on United States Antarctic research activities, February 1983 - October 1984 and United States Antarctic research activities planned for October 1984 - September 1985
[PB84-231265] 05 p0677 N85-14352
Environmental data inventory for the antarctic area
[PB85-107944] 06 p0819 N85-15195
USSR report: Earth sciences
[JPRS-UES-84-007] 06 p0819 N85-15196
Surging as a potential response of ice sheets to CO2-induced changes in the polar environment (SPICAE)
[DE84-016472] 06 p0841 N85-15341
Peculiar spherules from Antarctica and their origin
06 p0883 N85-15612
Meteorite concentrations in Antarctica: How complete is the picture? 06 p0889 N85-15644

Earth science investigations in the United States Antarctic Research Program (USARP)
[PB84-240506] 07 p0990 N85-16288

The visibility climatology of McMurdo Sound-Williams Field, Antarctica
[AD-A148108] 08 p1189 N85-17492

Survey of VLF-OMEGA transmissions received during summer at Antarctic peninsula
[INPE-3399-PRE/686] 10 p1482 N85-19223

USSR report: Earth sciences
[JPRS-UES-85-003] 10 p1497 N85-19446

Brazil future plans in upper atmosphere research in Antarctica
[INPE-3400-PRE/699] 10 p1515 N85-19559

Some aspects of atmospheric circulation near South America and interactions with the Antarctic regions
[INPE-3306-PRE/618] 10 p1515 N85-19561

MAP in Japan: Organization and projects
11 p1655 N85-20425

The Middle Atmosphere Program: A special project for the Antarctic Middle Atmosphere (AMA)
11 p1658 N85-20430

Proceedings of a Workshop on Environment of West Antarctica: Potential CO2-induced changes
[PB85-110757] 11 p1671 N85-20527

Los Alamos Mini-Review: Tracking Antarctic winds
[DE85-004597] 12 p1896 N85-21903

USSR report: Earth sciences
[JPRS-UES-85-002] 13 p2105 N85-23116

Antarctic glaciation, or what are catastrophes in Earth's history 13 p2105 N85-23118

China report: Science and technology
[JPRS-CST-85-003] 13 p2166 N85-23433

Planetary analogs in Antarctica: Mars
13 p2193 N85-23604

Planetary analogs in Antarctica: Icy satellites
13 p2193 N85-23605

Chemical weathering of soils from the dry valleys of Antarctica: A terrestrial analog of Martian weathering processes 13 p2197 N85-23628

The use of the ARGOS system for the study of the drift of Antarctic icebergs 14 p2240 N85-23690

Automatic weather stations in Antarctica
14 p2324 N85-24360

Main features of Antarctic Ocean circulation as revealed by satellite tracking of icebergs
14 p2325 N85-24372

Atmosphere ice-ocean interactions in the Antarctic (IAGO) 14 p2326 N85-24375

Antarctic automatic weather stations
14 p2329 N85-24397

Plans for adaptation research during Antarctic expedition 14 p2333 N85-24426

Results of comparison of long-wave radiation fluxes measured by Soviet and Japanese actinometric radiosonde 14 p2333 N85-24427

Observations of the MF-HF plasma wave emissions in active auroras by the sounding rocket experiments at Syowa station 14 p2366 N85-24620

VLF wave-particle interaction experiments by EXOS-B/Siple station transmissions
14 p2366 N85-24622

Whistler mode waves near the plasmapause: Results from the IMS VLF experiment at Halley, Antarctica
14 p2367 N85-24628

Designer O. K. Antonov on new AN-74 arctic transport
15 p2467 N85-25230

Analysis of hydrometeorological conditions in Antarctic coastal waters according to data from hydrological and satellite observations 15 p2487 N85-25354

North Atlantic Deep Water formation: Information from ice cores 15 p2502 N85-26035

USSR report: Earth sciences
[JPRS-UES-85-005] 16 p2807 N85-27307

Atmospheric radon measurements in the Antarctic Penninsula: A preliminary report
[INPE-3296-PRE/667] 16 p2827 N85-27436

Information relative to cartography and geodesy. Series 2: Translations, Number 42, Volume 2 — maps
[ISSN-0469-4244] 18 p3123 N85-29337

Digital image mapping of Antarctica using NOAA-7 AVHRR imagery 18 p3124 N85-29340

German contributions to the cartography of Antarctica by means of photogrammetry and remote sensing
18 p3124 N85-29342

Microbial ecology of extreme environments: Antarctic yeasts and growth in substrate-limited habitats
[NASA-CR-176005] 19 p3326 N85-30609

Antarctica
[S-HRG-98-1181] 20 p3473 N85-31584

Petroleum and mineral resources of Antarctica
[US-GEOL-SURV-CIRC-909] 20 p3477 N85-31605

Use of the synoptic view: Examples from Earth and other planets 21 p3602 N85-32371

Aerosol formation by wave action over Ross Sea, Antartica 21 p3651 N85-32668

ANTARCTICA
U ANTARCTIC REGIONS

ANTENNA ARRAYS
NT LINEAR ARRAYS
NT STEERABLE ANTENNAS

Nowcasting using lightning location techniques
01 p0084 N85-10568

Recursive algorithms for adaptive arrays based on estimates
[REPT-5-84] 01 p0107 N85-10718

The study of microstrip antenna arrays and related problems
[NASA-CR-174054] 02 p0189 N85-11265

Possibility of realization of highly-directional antenna arrays 03 p0344 N85-12220

A dynamical model for a towed linear sonar antenna
[REPT-6-84] 04 p0512 N85-13263

Modern radioastronomical aperture synthesis systems (review) 06 p0782 N85-14997

Phase problem in aperture synthesis systems
06 p0782 N85-15002

Synthesis of zeros in radiation pattern of linear antenna array 06 p0784 N85-15015

Remote sounding of fields in feed radiators of multi-element antenna system with allowance for interaction with sounding device
06 p0790 N85-15047

Characteristics of circular-polarized printed radiators in planar phased antenna array 06 p0790 N85-15049

Investigation of characteristics of phased antenna array considering interaction between radiators and properties of power divider 06 p0790 N85-15051

Scattering matrix of antenna array with Joule losses in radiators 06 p0791 N85-15053

Characteristics of two-frequency combined dipole antenna arrays 06 p0791 N85-15055

Peculiarities of microprocessor implementation of algorithms for processing radio signals and noise in large antenna arrays 06 p0792 N85-15059

Characterization of MMIC devices for active array antennas
[NASA-TM-86907] 07 p0913 N85-15779

Array sidelobes, error tolerance, gain, and beamwidth
[AD-A147004] 07 p0940 N85-15956

Parallel processor configuration for adaptive antenna arrays
[AD-D011347] 07 p0942 N85-15970

Basic research in electronic (JSEP): Joint Services Electronics Program
[AD-A147691] 07 p0948 N85-16007

Use of shanks transformation for speeding up adaptation process in antenna arrays 07 p0951 N85-16029

Analysis of effectiveness of partial optimization of spatial processing systems 07 p0952 N85-16031

Determination of row-and-column control principle of phase antenna array from amplitude-phase distribution of field in aperture 07 p0952 N85-16033

Infrared technology for satellite power conversion — antenna arrays and bolometers
[NASA-CR-174286] 07 p0991 N85-16293

Dual mode radio frequency-infrared frequency system
[AD-D011402] 08 p1081 N85-16850

Adaptive antenna arrays for weak interfering signals
[NASA-CR-174336] 08 p1150 N85-17258

Spaceborne distributed SAR antenna
[NASA-CR-171835] 08 p1150 N85-17259

Millimeter wave antenna technology
[AD-A148694] 08 p1155 N85-17291

Partial reflection spaced antenna wind measurements
08 p1186 N85-17467

Broad-band UHF dipole array
[NASA-TM-86373] 10 p1462 N85-19222

Condensed antenna structural models for dynamics analysis 10 p1463 N85-19230

Conformal phased array antenna pattern corrector
[AD-D011489] 10 p1468 N85-19266

Overview of RADC adaptive antenna developments for communications 10 p1474 N85-19299

Interleaved array antenna technology development
[NASA-CR-171845] 10 p1477 N85-19326

Research on adaptive antenna techniques 6
[AD-A149341] 11 p1624 N85-20228

Multiple loop sidelobe canceller
[AD-D011530] 12 p1823 N85-21434

Method and apparatus for self-calibration and phasing of array antenna
[NASA-CASE-NPO-15820-1] 12 p1832 N85-21493

Wide angle phased array dome lens antenna with a reflection/transmission switch
[AD-D011562] 12 p1833 N85-21502

Phased antenna array for wind profiling applications
[PB85-132884] 12 p1837 N85-21529

KAM-250 antenna switch 13 p2068 N85-22916

Studies of galactic HI in 21-centimeter absorption
13 p2170 N85-23466

Microstrip comb array design
[R-NIAS-24] 14 p2290 N85-24195

An examination of signal-to-noise enhancement at the Edzell CDAA (Circular Disposed Antenna Array)
[AD-A150708] 14 p2291 N85-24204

Noise cancellation using adaptive arrays
[AD-A150721] 14 p2292 N85-24206

Interference immunity of optical radar system with phased antenna array 15 p2526 N85-25575

Cophasal horizontal wideband array antennas for transmitting with asymmetric output
15 p2526 N85-25576

Design and swept-frequency measurement of printed circuit board log-periodic dipole arrays
[R-NIAS-23] 15 p2539 N85-25671

Mobile antenna and beam pointing studies for satellite mobile communications
[NASA-CR-175736] 15 p2540 N85-25679

Trade-off between land vehicle antenna cost and gain for satellite mobile communications
[NASA-CR-175732] 15 p2540 N85-25681

Land vehicle antennas for satellite mobile communications
[NASA-CR-175735] 15 p2540 N85-25682

A study of computational techniques for noncanonical microstrip antennas and arrays
[AD-A152216] 16 p2774 N85-27123

Performance analysis of the DSN baseband assembly (Bba) Real-Time Combiner (RTC)
[NASA-CR-175878] 17 p2946 N85-28190

Performance analysis of the DSN baseband assembly (Bba) Real-Time Combiner (RTC)
[NASA-CR-175877] 17 p2947 N85-28193

Adaptive nulling at HF using a compact array of active parasitic antennas
[AD-A152582] 17 p2948 N85-28203

Two-degree-of-freedom linear and planar microwave array lenses
[AD-A153701] 18 p3095 N85-29156

Computer simulation of the effects of a distributed array antenna on synthetic aperture radar images
[NASA-CR-171888] 19 p3254 N85-30176

Theoretical investigation of single-frequency 8-element localizer signal scattering for critical area determination
[FAA-PM-85-4] 20 p3391 N85-31037

Antenna pointing of large flexible telecommunications spacecraft 20 p3409 N85-31156

Phase synchronizing large antenna arrays using the spatial correlation properties of radar clutter
20 p3439 N85-31344

ECM multiple-target retrodirective antenna
[AD-D011528] 20 p3439 N85-31346

New concepts in free electron lasers
20 p3460 N85-31493

New VLBI technology developments
20 p3491 N85-31702

Null synthesis with phase and amplitude controls at the subarray outputs
[AD-A155187] 21 p3576 N85-32241

Evaluation of the effects of roll angle on the natural convection heat transfer from an array of cylindrical spines
[AD-A154594] 21 p3583 N85-32273

A simple model for testing the effects of gravity-wave-produced vertical oscillations of scattering irregularities on spaced-antenna, horizontal drift measurements 21 p3619 N85-32489

Criteria for optimum spacing of spaced antenna, part 3.2A 21 p3620 N85-32491

Increase of antenna area instead of transmitter power, part 6.3A 21 p3624 N85-32517

Summary of progress at the Poker Flat Observatory in Alaska 21 p3628 N85-32539

Radio telescope with 256 antennas built in Siberia
22 p3732 N85-33136

Digital holographic synthesis of pattern-forming transparencies for ring antenna arrays
22 p3763 N85-33326

Adaptive synthesis of antennas with separation of signals by direction of arrival 22 p3764 N85-33328

USSR report: Electronics and electrical engineering
[JPRS-UEE-84-003] 22 p3773 N85-33361

Frequency independent parabolic phased antenna array of log periodic antennas 22 p3774 N85-33387

Minimizing field scattered by slender dipoles
22 p3774 N85-33388

Adaptive antenna arrays for satellite communications: Design and testing
[NASA-CR-176162] 23 p3926 N85-34329

A planar version of a 4.0 gigahertz reactively steered adaptive array
[AD-A156029] 24 p4087 N85-35330

Signal space models for antenna arrays
[AD-A156063] 24 p4087 N85-35335

Theory of mutual impedances and multiple reflections in an N-element array environment
[PB85-191419] 24 p4092 N85-35364

ANTENNA COMPONENTS
NT ANTENNA COUPLERS
NT ANTENNA FEEDS
NT DIRECTIONAL COUPLERS
Invariance of mean-square effective area of synthesized apertures 06 p0784 N85-15009
Antenna matching device tuning for type ZhRU radiostations 06 p0786 N85-15017
Characterization of MMIC devices for active array antennas
[NASA-TM-86907] 07 p0913 N85-15779
Feasibility study for a 34 GHz (Ka band) gyroamplifier
[NASA-CR-174439] 10 p1477 N85-19325
The 60 GHz antenna system analyses for intersatellite links, phase A
[NASA-CR-175285] 12 p1823 N85-21439
Deployable folded antenna apparatus
[AD-D011503] 12 p1832 N85-21495
System of light protection of antenna-mast structures of radio-relay lines 15 p2527 N85-25583
Two-degree-of-freedom linear and planar microwave array lenses
[AD-A153701] 18 p3095 N85-29156
A simplified GPS C/A reciever front end with low noise performance 18 p3109 N85-29251

ANTENNA COUPLERS
NT COUPLING CIRCUITS
NT DIPLEXERS
NT DIRECTIONAL COUPLERS
Hardwire missile receiver coupler
[AD-D011350] 07 p0937 N85-15936
Mutual coupling analysis for conformal microstrip antennas 20 p3439 N85-31343

ANTENNA DESIGN
A generalized solution to a class of printed circuit antennas
[AD-A145626] 02 p0191 N85-11276
Some considerations on the capacitive calibration used for the 2.3 ton cryogenic antenna at CERN --- gravitational antennas
[NOTA-INTERNA-809] 02 p0192 N85-11284
Possibility of realization of highly-directional antenna arrays 03 p0344 N85-12220
Conceptual design for scaled truss antenna flight experiment
[NASA-TM-85804] 04 p0462 N85-12932
Workshop on Mechanical Technology for Antennas --- conferences; satellite antennas
[ESA-SP-225] 05 p0625 N85-13999
Antenna mechanical technologies within ESA
05 p0625 N85-14000
High performance deployable antenna structures
05 p0625 N85-14001
Offset unfurlable antenna concepts
05 p0625 N85-14002
The UK and Netherlands millimetre-wave telescope --- Netherlands (NL) 05 p0625 N85-14003
Electrical consequences of mechanical antenna characteristics 05 p0625 N85-14006
Structural aspects of SAR antenna for Japanese Earth Resources Satellite 1 05 p0626 N85-14007
Technology for the ERS-1 SAR antenna
05 p0626 N85-14008
Mechanical/thermal design of a polarization sensitive reflector --- communication satellites
05 p0626 N85-14009
CASA technological effort in the field of antennas --- satellite radar antennas 05 p0626 N85-14010
BAe antenna hardware technology for current satellite projects 05 p0626 N85-14011
Technology and performances of structural thermal mechanical equipment used for antenna of TV.SAT-TDF 1 program 05 p0626 N85-14012
CASA activities in antenna technology --- satellite antennas 05 p0627 N85-14015
ARABSAT spacecraft: Rx and Tx antenna mechanisms 05 p0628 N85-14022
Characteristics of circular-polarized printed radiators in planar phased antenna array 06 p0790 N85-15049
Green function in theory of microstrip antennas
06 p0790 N85-15050
Efficiency in integral active antennas
06 p0792 N85-15060
Broadband pillbox antennas
[AD-A146569] 06 p0799 N85-15104
The 20 GHz proof-of-concept test model results for a multiple scan beam dual reflector antenna
[NASA-CR-174288] 07 p0938 N85-15944
A low-sidelobe space feed lens
[AD-A147983] 07 p0942 N85-15972
Dual band, low sidelobe, high efficiency mirror antenna
[AD-D011329] 07 p0944 N85-15980
Compact wideband multiple conductor monopole antenna
[AD-D011331] 07 p0944 N85-15981
Configuration study for a 30 GHz monolithic receive array: Technical assessment
[NASA-CR-174697] 09 p1311 N85-18238
Configuration study for a 30 GHz monolithic receive array, volume 1
[NASA-CR-174697-VOL-1] 09 p1311 N85-18239
Configuration study for a 30 GHz monolithic receive array, volume 2
[NASA-CR-174697-VOL-2] 09 p1311 N85-18240
The effects of mode impurity of Ka-band system performance 10 p1463 N85-19227
Condensed antenna structural models for dynamics analysis 10 p1463 N85-19230
Design procedure for the new 70-meter antenna subreflector positioner 10 p1463 N85-19232
HF broadband whip antenna evaluation
[AD-A149527] 10 p1467 N85-19258
Shuttle S-band high gain switched beam breadboard antennas
[NASA-CR-171852] 10 p1478 N85-19327
Compensator development and examination of performance and robustness
[NASA-CR-175470] 11 p1627 N85-20244
Monte Carlo studies of tandem mirror plasmas interacting with waves in the Ion Cyclotron Range of Frequencies (ICRF)
[DE85-002988] 11 p1731 N85-20883
The 60 GHz antenna system analyses for intersatellite links, phase A
[NASA-CR-175285] 12 p1823 N85-21439
Image lobe analysis for large radomes
[AD-P004359] 12 p1825 N85-21453
3-D Dome/Rotman lens antenna breadboard demonstration
[AD-A149809] 12 p1828 N85-21475
Wide angle phased array dome lens antenna with a reflection/transmission switch
[AD-D011562] 12 p1833 N85-21502
Performance ranges of helical antenna made of conductor with extra bends 12 p1838 N85-21536
Computer aided antenna design and frequency selection for HF communications
[AD-A150485] 13 p2056 N85-22869
Variational and moment method solutions of the fields in a parallel-plate waveguide-aperture system
[DE85-006289] 13 p2057 N85-22876
A generalized solution to a class of printed circuit antennas 13 p2062 N85-22882
Experimental verification of beam deflection from hybrid reflector antenna within wide-angle sector
13 p2079 N85-22984
Large Space Antenna Systems Technology, 1984
[NASA-CP-2368-PT-1] 14 p2229 N85-23813
NASA mobile satellite program
14 p2229 N85-23814
Application of pushbroom altimetry from space using large space antennas 14 p2230 N85-23817
LDR system concepts and technology
14 p2231 N85-23823
Development of the 15-meter hoop-column antenna system 14 p2231 N85-23825
Box truss development and its application
14 p2231 N85-23826
Synchronously deployable tetrahedral truss reflector
14 p2231 N85-23827
Antenna Technology for QUASAT application --- radio antenna for very long base interferometry missions
14 p2231 N85-23828
Cable-catenary large antenna concept
14 p2231 N85-23829
Extreme precision antenna reflector study results
14 p2232 N85-23830
Large Space Antenna Systems Technology, 1984
[NASA-CP-2368-PT-2] 14 p2233 N85-23840
Large antenna control methods: Current status and future trends 14 p2234 N85-23845
Design and measured performance of a broadband Archimedes spiral antenna
[R-NIAS-22] 14 p2290 N85-24194
A compact, aperture-matched, balanced transmission line antenna
[R-NIAS-28] 14 p2290 N85-24196
Prime-focus parabolic reflector antenna: Theory and measurement
[R-NIAS-20] 14 p2291 N85-24199
Spheroidal functions: Properties and tabulation. Application to antenna synthesis
14 p2396 N85-24758
Antenna with outboard exciter for 3.4-13.25 GHz frequency range 15 p2526 N85-25577
Design and swept-frequency measurement of printed circuit board log-periodic dipole arrays
[R-NIAS-23] 15 p2539 N85-25671
Compensator development and examination of performance and robustness
[NASA-CR-175703] 15 p2540 N85-25678
Concepts and cost trade-offs for land vehicle antennas in satellite mobile communications
[NASA-CR-175731] 15 p2540 N85-25680
A simplified GPS C/A reciever front end with low noise performance 18 p3109 N85-29251
A special antenna for SARSAT EPIRBs providing circular polarization and hemispheric coverage for reliable transmission to satellites --- Emergency Position Indicating Radio Beacon (EPIRB) 20 p3404 N85-31122
Dynamic performance of several large antenna concepts 20 p3409 N85-31155
Design and evaluation of control systems for large communications satellites 20 p3409 N85-31157
Control of large antennas based on electromagnetic performance criteria 20 p3409 N85-31158
Large space structure flight experiment
20 p3410 N85-31163
Design of a shuttle-borne SAR for the DFVLR's planning study
[ERYS-019/84] 20 p3419 N85-31218
Fin-line horn antennas
[AD-A154597] 21 p3580 N85-32255
Most desirable terrain, e.g., flat vs valley location, part 5.1B 21 p3624 N85-32513
Summary of session on optimum transmitter and antenna configuration for MST radar, part 6
21 p3624 N85-32514
Frequency independent parabolic phased antenna array of log periodic antennas 22 p3774 N85-33367
Polarization diversity addition to the 10 centimeter Doppler weather radar
[AD-A156062] 24 p4087 N85-35334

ANTENNA FEEDS
Remote sounding of fields in feed radiators of multi-element antenna system with allowance for interaction with sounding device
06 p0790 N85-15047
Hardwire missile receiver coupler
[AD-D011350] 07 p0937 N85-15936
Dual offset reflector antenna systems with rotationally symmetric aperture distributions
[AD-A147346] 07 p0940 N85-15961
A low-sidelobe space feed lens
[AD-A147983] 07 p0942 N85-15972
The effects of mode impurity of Ka-band system performance 10 p1463 N85-19227
A reflectometer unit for a 500 kW HF balanced screened feeder
[BBC-RD-1984/13] 10 p1477 N85-19322
Printed circuit balun with a dipole antenna
[AD-D011534] 12 p1833 N85-21498
Wide angle phased array dome lens antenna with a reflection/transmission switch
[AD-D011562] 12 p1833 N85-21502
KAM-250 antenna switch 13 p2068 N85-22916
Measured performance of a broadband matching section for peripherally fed helical antennas
[R-NIAS-25] 15 p2539 N85-25670
Beam forming network
[NASA-CASE-NPO-15743-1] 18 p3089 N85-29118
MMIC devices for active phased array antennas
[NASA-CR-176015] 19 p3254 N85-30177
A hardware demonstration of distributed control for a flexible offset-feed antenna 20 p3410 N85-31160
Multitrunk high-frequency multiplexing of antenna-waveguide channels 22 p3774 N85-33385
Method of constructing folding umbrella-type antenna
22 p3774 N85-33386
Minimizing field scattered by slender dipoles
22 p3774 N85-33388

ANTENNA FIELDS
U ANTENNA RADIATION PATTERNS

ANTENNA RADIATION PATTERNS
NT SIDELOBES
An error analysis for the use of presently available lunar radio flux data in broadbeam antenna-system measurements
[PB84-218361] 01 p0016 N85-10097
Case study of sample spacing in planar near-field measurement of high gain antennas
[NASA-TM-86872] 01 p0037 N85-10234
A proof-of-principle getaway special free-flying satellite demonstration 02 p0155 N85-11051
Apparatus of short baseline centimetric wave radiointerferometer with cable communication lines for astrophysical research 06 p0782 N85-15001
Invariance of mean-square effective area of synthesized apertures 06 p0784 N85-15009
Synthesis of zeros in radiation pattern of linear antenna array 06 p0784 N85-15015
Measurement of external antenna characteristics with allowance for distorting factors (review)
06 p0790 N85-15046

Remote sounding of fields in feed radiators of multi-element antenna system with allowance for interaction with sounding device
06 p0790 N85-15047

Fast method for calculating radiation patterns of nonequidistant radiator systems
06 p0791 N85-15052

System of equations for finding antenna radiation pattern from near-field samples 06 p0791 N85-15054

Efficiency in integral active antennas
06 p0792 N85-15060

The 20 GHz proof-of-concept test model results for a multiple scan beam dual reflector antenna
[NASA-CR-174266] 07 p0936 N85-15944

Dual offset reflector antenna systems with rotationally symmetric aperture distributions
[AD-A147346] 07 p0940 N85-15961

Efficient computation of reflector antenna aperture distributions and far field patterns
[AD-A147367] 07 p0940 N85-15962

Tactical HF communication for military helicopters using the NVIS mode 08 p1074 N85-16807

Information for space radar designers: Required dynamic range vs resolution and antenna calibration using the Amazon rain forest 08 p1147 N85-17239

The effects of soil moisture on bistatic clutter power
[AD-A147636] 08 p1150 N85-17261

Loop radiating elements
[AD-D011409] 08 p1158 N85-17306

Propagation measurements for land-mobile satellite services in the 800 MHz band
[CRC-TN-724] 09 p1310 N85-18231

Radiation patterns of a pyramidal horn antenna
09 p1311 N85-18236

Multivariable Autoregressive Moving Average (ARMA) models: A time approach to antenna processing
[ENST-84E015] 09 p1313 N85-18252

Measurement procedures for the radar spectrum engineering criteria
[PB85-119022/GAR] 09 p1313 N85-18254

The effects of mode impurity of Ka-band system performance 10 p1463 N85-19227

Subreflector focusing techniques applied to new DSS-15 and DSS-45 34-meter antennas
10 p1464 N85-19233

Conformal phased array antenna pattern corrector
[AD-D011489] 10 p1468 N85-19266

Comparison of measured and calculated mutual coupling in the near field between microwave antennas
[PB85-105963] 11 p1625 N85-20237

Landing control centrals
[AD-A149800] 12 p1775 N85-21140

Technical evaluation report on the FDP Symposium on Flight Test Techniques
[AGARD-AR-208] 12 p1777 N85-21157

The 60 GHz antenna system analyses for intersatellite links, phase A
[NASA-CR-175285] 12 p1823 N85-21439

A subaperture approach to the calculation of flashlobes introduced by airborne radomes
[AD-P004355] 12 p1825 N85-21449

Automated radome testing
[AD-P004362] 12 p1826 N85-21456

USSR report: Electronics and electrical engineering
[JPRS-UEE-85-002] 13 p2066 N85-22907

Coordinate determination errors in measuring characteristics of radiation field of airborne antennas
13 p2068 N85-22919

Reduction of amplitude-phase distortions of movable microwave coupling circuit for antenna field measurements 13 p2068 N85-22920

Experimental verification of beam deflection from hybrid reflector antenna within wide-angle sector
13 p2079 N85-22984

Synthesis of multistep directional couplers with nonminimum-phase characteristics
13 p2079 N85-22986

Scattering of waves by axisymmetrical edge
13 p2080 N85-22987

Electromagnetic analysis for surface tolerance effects on large space antennas 14 p2234 N85-23850

Microstrip comb array design
[R-NIAS-24] 14 p2290 N85-24195

Prime-focus parabolic reflector antenna: Theory and measurement
[R-NIAS-20] 14 p2291 N85-24199

Analytical studies and experimental measurements of amplitude and phase of near-field range antenna probes
[AD-A150922] 14 p2293 N85-24212

Spheroidal functions: Properties and tabulation. Application to antenna synthesis
14 p2396 N85-24758

COSPAS-SARSAT satellite orbit predictor, volume 5
[NASA-TM-85015-VOL-5] 14 p2439 N85-25052

Space processing of acoustic signals in plane-parallel waveguide — antenna arrays 15 p2525 N85-25572

Interference immunity of optical radar system with phased antenna array 15 p2526 N85-25575

Cophasal horizontal wideband array antennas for transmitting with asymmetric output
15 p2526 N85-25576

Antenna with outboard exciter for 3.4-13.25 GHz frequency range 15 p2526 N85-25577

The distortion of AM broadcast antenna patterns as caused by nearby towers and highrise buildings
[CRC-1379] 15 p2538 N85-25666

Mobile antenna and beam pointing studies for satellite mobile communications
[NASA-CR-175736] 15 p2540 N85-25679

Land vehicle antennas for satellite mobile communications
[NASA-CR-175735] 15 p2540 N85-25682

Null generation using discs on a reflector
[AD-A151897] 15 p2544 N85-25703

Radiation and scattering of spiral antennas
[AD-A151929] 16 p2773 N85-27118

Earth station antenna sidelobe characteristics
[PB85-164986] 16 p2780 N85-27189

Performance analysis of the DSN baseband assembly (Bba) Real-Time Combiner (RTC)
[NASA-CR-175877] 17 p2947 N85-28193

A simulation study of jammer nulling trade-offs in a reactively steered adaptive array
[AD-A153461] 18 p3090 N85-29124

Computer simulation of the effects of a distributed array antenna on synthetic aperture radar images
[NASA-CR-171866] 19 p3254 N85-30176

Inherent angular tracking error in an amplitude comparison monopulse radar
[AD-A154212] 19 p3255 N85-30185

Theoretical investigation of single-frequency 8-element localizer signal scattering for critical area determination
[FAA-PM-85-4] 20 p3391 N85-31037

Phase synchronizing large antenna arrays using the spatial correlation properties of radar clutter
20 p3439 N85-31344

Offset reflector with horn feed array, used as an experimental sensor for radiometric measurements
[ESA-TT-830] 20 p3443 N85-31369

Deterministic and random phase noise of oscillators — synthetic aperture radar
[ESA-TT-848] 20 p3449 N85-31415

Null synthesis with phase and amplitude controls at the subarray outputs
[AD-A155187] 21 p3576 N85-32241

Anisotropy of the permittivity field inferred from aspect-sensitive radar echoes 21 p3620 N85-32492

Effects of line-of-sight velocity on spaced-antenna measurements, part 3.5A 21 p3621 N85-32496

Problems and solutions in analyzing partial-reflection drift data by correlation techniques
21 p3626 N85-32529

Comprehensive radio direction finder with electronically stabilized radiation pattern 22 p3762 N85-33318

Method of constructing folding umbrella-type antenna
22 p3774 N85-33385

Minimizing field scattered by slender dipoles
22 p3774 N85-33386

Box truss analysis and technology development. Task 1: Mesh analysis and control
[NASA-CR-172570] 23 p3900 N85-34156

Adaptive antenna arrays for satellite communications: Design and testing
[NASA-CR-176162] 23 p3926 N85-34329

Characteristic modes for slots in a ground plane TE case
[AD-A155757] 24 p4086 N85-35326

A planar version of a 4.0 gigahertz reactively steered adaptive array
[AD-A156029] 24 p4087 N85-35330

Theory of mutual impedances and multiple reflections in an N-element array environment
[PB85-191419] 24 p4092 N85-35364

ANTENNAS
NT AIRCRAFT ANTENNAS
NT CASSEGRAIN ANTENNAS
NT CYLINDRICAL ANTENNAS
NT DIPOLE ANTENNAS
NT DIRECTIONAL ANTENNAS
NT FURLABLE ANTENNAS
NT GRAVITATIONAL WAVE ANTENNAS
NT HELICAL ANTENNAS
NT HOOP COLUMN ANTENNAS
NT HORN ANTENNAS
NT LENS ANTENNAS
NT LOG PERIODIC ANTENNAS
NT LOOP ANTENNAS
NT MICROWAVE ANTENNAS
NT MISSILE ANTENNAS
NT MONOPOLE ANTENNAS
NT MONOPULSE ANTENNAS
NT MULTIPLE BEAM INTERVAL SCANNERS
NT PARABOLIC ANTENNAS
NT RADAR ANTENNAS
NT RADIO ANTENNAS
NT RECTENNAS
NT RHOMBIC ANTENNAS
NT SATELLITE ANTENNAS
NT SLOT ANTENNAS
NT SPACECRAFT ANTENNAS
NT SPACETENNAS
NT SPIRAL ANTENNAS
NT STEERABLE ANTENNAS
NT TWO REFLECTOR ANTENNAS
NT WAVEGUIDE ANTENNAS
NT WHIP ANTENNAS

Case study of sample spacing in planar near-field measurement of high gain antennas
[NASA-TM-86672] 01 p0037 N85-10234

Center for Electronics and Electrical Engineering Technical Bulletin covering center programs
[PB84-216058] 01 p0045 N85-10296

RF characteristics of the hoop column antenna for the land mobile satellite system mission
[NASA-CR-3842] 02 p0189 N85-11264

A generalized solution to a class of printed circuit antennas
[AD-A145626] 02 p0191 N85-11278

USSR report: Electronics and electrical engineering
[JPRS-UEE-84-014] 03 p0344 N85-12215

Conceptual design for scaled truss antenna flight experiment
[NASA-TM-85804] 04 p0482 N85-12932

Fundamental limitations in antenna resolution by maximum entropy methods
[DE84-017052] 04 p0493 N85-13145

Active nutation control of spacecraft using a magnetic bearing momentum wheel with Vernier gimballing capability
[NAL-TR-8201] 06 p0759 N85-14867

USSR report: Electronics and electrical engineering
[JPRS-UEE-84-012] 06 p0781 N85-14891

Antenna matching device tuning for type ZhRU radiostations 06 p0785 N85-15017

USSR report: Electronics and electrical engineering
[JPRS-UEE-84-011] 06 p0789 N85-15042

Fast method for calculating radiation patterns of nonequidistant radiator systems
06 p0791 N85-15052

MMIC devices for active phased array antennas
[NASA-CR-174281] 07 p0936 N85-15943

Data appendix: F-number = 1.0 EMR with a flexible back electrode
[NASA-CR-172477] 07 p0946 N85-15994

USSR report: Electronics and electrical engineering
[JPRS-UEE-84-017] 07 p0951 N85-16025

Reduction method for thermal analysis of complex aerospace structures
[NASA-TP-2373] 07 p0957 N85-16066

Integrated defense communications system antijamming antenna system
[AD-D011423] 08 p1154 N85-17285

Antenna axis drive torques for the 70-meter antenna
10 p1464 N85-19237

An evaluation of the 64-meter antenna radial bearing for use on the 70-meter antenna
10 p1464 N85-19238

Elevation bearing maximum load, 70-meter antenna
10 p1464 N85-19239

Characteristics of the elevation drive suspension of the 64-meter antennas 10 p1464 N85-19240

Hydrostatic bearing pad maximum load and overturning conditions for the 70-meter antenna
10 p1465 N85-19241

A technical solution to fadings in tactical satellite digital transmissions 10 p1473 N85-19297

Overview of RADC adaptive antenna developments for communications 10 p1474 N85-19299

Direction finder set, radio
[AD-A149958] 12 p1775 N85-21142

A computer analysis of the RF performance of a ground-mounted, air-supported radome
[AD-P004352] 12 p1824 N85-21446

Generalized radome BSE (radome boresight error) characterization using superposition techniques
[AD-P004354] 12 p1825 N85-21448

A radome for air traffic control SSR radar systems
[AD-P004373] 12 p1827 N85-21467

Gain enhancement methods for printed circuit antennas
[AD-A150090] 12 p1835 N85-21517

Preliminary investigation into using the sun as a source for G/T (Gain to System Noise Temperature) measurements
[PB85-126148] 12 p1952 N85-22265

USSR report: Electronics and electrical engineering
[JPRS-UEE-85-002] 13 p2066 N85-22907

KAM-250 antenna switch 13 p2068 N85-22916

Large space antenna technology applied to radar-imaging, rain-rate measurements, and ocean wind sensing 14 p2230 N85-23820
Advanced 2-frequency ocean sensing radar using high resolution antenna beams 14 p2230 N85-23821
WRAP-RIB antenna technology development
14 p2231 N85-23824
Development of the 15-meter hoop-column antenna system 14 p2231 N85-23825
Box truss development and its application
14 p2231 N85-23826
Precision space structures 14 p2232 N85-23833
An eigensystem realization algorithm for application to modal testing 14 p2233 N85-23842
Electromagnetic analysis for surface tolerance effects on large space antennas 14 p2234 N85-23850
Feed system design considerations for large space antenna systems. Part 2: Single aperture with overlapping feeds 14 p2235 N85-23853
Diffraction analysis of mesh deployable reflector antennas 14 p2235 N85-23854
Shuttle attached antenna Flight Experiment Definition Study (FEDS) 14 p2237 N85-23865
Electro-science requirements for shuttle-attached antenna flight experiments 14 p2237 N35-23866
Analytical studies and experimental measurements of amplitude and phase of near-field range antenna probes
[AD-A150922] 14 p2293 N85-24212
Ways of optimization of light energy transformation in primary stages of photosynthesis. Necessity of optimization of photosynthetic unit structure and method for calculating efficiency 14 p2386 N85-24700
Ways of optimization of light energy transformation in primary stages of photosynthesis. Optimization of lattice structure of uniform photosynthetic unit
14 p2386 N85-24701
ANTENA user guide
[DE85-004961] 14 p2424 N85-24953
Electromagnetic scattering by arbitrarily shaped reflectors: Subreflector efficiency
[AD-A149224] 15 p2541 N85-25687
Calibration methods in millimeter-wave radioastronomy
[INPE-3461-PRE/724] 16 p2681 N85-27776
Avionics data base
[AD-A152415] 17 p2897 N85-27863
Mathematical modeling and control of a large space structure as applied to a shuttle-antenna configuration
[AD-A153269] 17 p2910 N85-27939
LFMR definition study
[AD-A153691] 18 p3090 N85-29126
Upgrade of the LLNL EM transient range monocone antenna
[DE85-006639] 18 p3097 N85-29172
The effect of sensor and actuator errors on static shape control for large space structures
[NASA-TM-86446] 19 p3225 N85-29996
High switching speed electrically tuned microwave magnetic resonance devices
[AD-D011699] 19 p3260 N85-30217
ICRF antenna coupling and wave propagation in a tokamak plasma 19 p3369 N85-30893
Proceedings of the Workshop on Identification and Control of Flexible Space Structures, volume 3
[NASA-CR-176053] 20 p3415 N85-31195
Mutual coupling analysis for conformal microstrip antennas 20 p3439 N85-31343
The use of the glistening surface concept in rough surface scattering
[AD-A154922] 21 p3575 N85-32234
Field antenna handbook
[AD-A155204] 21 p3576 N85-32242
Numerical modeling of subsurface communication
[DE85-012818] 21 p3577 N85-32249
Middle Atmosphere Program. Handbook for MAP. Volume 14: URSI/SCOSTEP Workshop on Technical Aspects of MST Radar
[NASA-CR-176085] 21 p3615 N85-32466
USSR report: Electronics and electrical engineering
[JPRS-UEE-84-015] 22 p3702 N85-33314
Multitrunk high-frequency multiplexing of antenna-waveguide channels 22 p3774 N85-33385
Method of constructing folding umbrella-type antenna
22 p3774 N85-33386
High-field launch electron cyclotron heating experiments in the ELMO Bumpy Torus
[DE85-012069] 22 p3846 N85-33825
Reducing grating lobes due to subarray amplitude tapering
[AD-D011723] 23 p3927 N85-34339
Moment-method formulation of the cavity-probe aperture antenna
[DE85-013264] 24 p4088 N85-35338
Center for Electronics and Electrical Engineering technical progress bulletin covering center programs, July-September with 1985 CEEE events calendar
[PB85-191393] 24 p4091 N85-35363

ANTHRACENE
Homogeneous reaction involving components of different redox couples. 2: Polarographic studies of the interactions of alkali metal cations with anthracene and fluoroanthene dianions in N,N-dimethylformamide and acetonitrile
[AD-A148667] 08 p1124 N85-17065
Studies on organic semiconductors. 15: Effects of the substituents on the photoconductivities of substituted anthracenes
[NASA-TM-77768] 08 p1225 N85-17712
Thermal reactions of aromatics with CaO
[DE85-010088] 22 p3742 N85-33193
ANTHROPOMETRY
Anthropometric cockpit compatibility assessment of US Army aircraft for large and small personnel wearing a training, warm-weather clothing configuration
[AD-A145208] 01 p0099 N85-10656
Anthropometric cockpit compatibility assessment of US Army aircraft for large and small personnel wearing A cold weather, armored vest, chemical defense protective clothing configuration
[AD-A145472] 02 p0236 N85-11547
Challenges of developing an electro-optical system for measuring man's operational envelope
08 p1095 N85-16921
Technique for measuring body circumferences and skinfold thicknesses
[AD-A148166] 08 p1195 N85-17532
An investigation of spinal injury potential from the use of the ACES 2 ejection seat by lower weight female pilots
[AD-A148449] 08 p1196 N85-17537
Crewstation assessment of reach as applied to the OH-58A helicopter
[AD-A149413] 10 p1531 N85-19650
The application of anthropometric survey data to aircrew clothing sizing
[AD-A150545] 13 p2143 N85-23304
Preliminary design of a limb restraint evaluator
[AD-A151749] 15 p2466 N85-25226
Comparative anaerobic power of males and females
[AD-A151960] 16 p2842 N85-27523
Relationship between the Army two mile run test and maximal oxygen uptake
[AD-A153914] 18 p3154 N85-29526
ANTIADRENERGICS
The effect of beta adrenergic blockade on ratings of perceived exertion
[AD-A148053] 08 p1195 N85-17530
ANTIAIRCRAFT MISSILES
NT SIDEWINDER MISSILES
ANTIBODIES
Induction of immunity to toxins with anti-idiotypic antibody
[AD-A146793] 07 p1014 N85-16445
Armed forces special Symposium on Medicine of Altitudes 13 p2166 N85-23441
Isolation of hybridomas for golgi-associated proteins and a plant calmodulin 15 p2613 N85-26103
Rapid rate-kinetic turbidometric assay for quantitation of antiviral complement-fixing antibodies
[AD-A153644] 18 p3152 N85-29516
ANTICHOLINERGICS
Effects of pyridostigmine on psychomotor and visual performance
[AD-A148553] 08 p1196 N85-17539
ANTICLINES
Structural development of the west-central Grant Range, Nye County, Nevada 24 p4115 N85-35508
ANTICLINORIA
U ANTICLINES
ANTICOAGULANTS
Management of microcirculatory disorders in vibration sickness 10 p1524 N85-19611
ANTICYCLONES
Mesoscale features and atmospheric refraction conditions of the Arctic marginal ice zone
[AD-A155139] 21 p3636 N85-32584
The variability of aerosol microstructure in continental and oceanic surface layers of the atmosphere in anticyclones 21 p3647 N85-32660
Maintenance of blocking anticyclones in a general circulation model
[PB85-190866] 24 p4124 N85-35567
ANTIEMETICS AND ANTINAUSEANTS
Medication interference with space research: An example from a mass-discrimination experiment on Spacelab 1 05 p0695 N85-14472
ANTIFERROMAGNETISM
Fermi surface study of CeSb
[DE85-002532] 10 p1564 N85-19862
Investigation of electric and magnetic properties of intercalated graphite
[AD-A148801] 12 p1797 N85-21274
Coexistence of antiferromagnetism and spin-glass ordering in the Ising system FeO 55MgO 45Cl2
[DE85-004164] 12 p1942 N85-22197
Peltier heat of a small polaron in a magnetic semiconductor
[DE85-000470] 14 p2430 N85-24989
ANTIFOULING
An electrochemical approach to the prevention of biofouling phenomena
[PB84-202613] 01 p0025 N85-10156
Process for preparation of crosslinked poly(tri-n-butyltin) methacrylate with simultaneous particle size reduction
[AD-D011313] 07 p0932 N85-15905
ANTIFREEZES
Development of a high-temperature coolant for advanced diesel engines
[AD-A153680] 18 p3117 N85-29297
ANTIFRICTION BEARINGS
NT BALL BEARINGS
NT ROLLER BEARINGS
Testing the antifriction properties of alloys for heavily loaded bearings 06 p0780 N85-14990
Applications of vibration analysis to the condition monitoring of rolling element bearings
[ARL/AERO-R-163] 12 p1859 N85-21663
Powder metallurgy bearings for advanced rocket engines 16 p2736 N85-26881
ANTIGENS
Functional and structural changes in human erythrocyte surface after irradiation by UV waves of various wavelengths. Report 1: Expression of ABO and Rheaus system antigen 09 p1361 N85-18564
Functional and structural changes in human erythrocyte surface after irradiation by UV waves of various wavelenights. Report 2: Adsorption of alcyan blue by external premembranous components
09 p1361 N85-18565
Differences in susceptibility of inbred mice to bacillus anthracis
[AD-A155646] 21 p3662 N85-32750
Genetic and physiological control of protective antigen synthesis by bacillus anthracis
[AD-A156324] 24 p4133 N85-35617
ANTIGRAVITY
Analysis of the transient response of temporal artery blood flow data relative to various anti-G suit pressure schedules 10 p1533 N85-19660
Simulation of high +Gz onset in the dynamic environment simulator
[AD-A155963] 24 p4131 N85-35610
ANTIKNOCK ADDITIVES
Knock syndrome: its cures and its victims
[NASA-CR-174395] 10 p1458 N85-19185
ANTIMATTER
NT ANTINEUTRINOS
NT ANTINUCLEONS
NT ANTIPARTICLES
NT ANTIPROTONS
NT POSITRONS
On the nature of the baryon asymmetry
[NASA-TM-86156] 05 p0746 N85-14784
Gravitational properties of antimatter
[DE85-009601] 18 p3197 N85-29832
ANTIMISSILE DEFENSE
Directed energy missile defense in space
[PB84-210111] 01 p0015 N85-10095
ANTIMISSILE MISSILES
Arms control and The President's Strategic Defense Initiative
[AD-A156334] 24 p4068 N85-35212
ANTIMISTING FUELS
Aircraft wing fuel tank environmental simulator tests for evaluation of antimisting fuels
[FAA-CT-84-15] 07 p0934 N85-15920
A brief review of the technology of microemulsions and other micellar systems
[AD-A149759] 12 p1800 N85-21289
Practical real-time quality control of antimisting kerosene
[DE/FAA/CT-85/1] 18 p3083 N85-29072
ANTIMONIDES
NT GALLIUM ANTIMONIDES
NT INDIUM ANTIMONIDES
ANTIMONY
Dopant incorporation in silicon during nonequilibrium solidification: Comparison of 2 processes
[DE85-005568] 14 p2430 N85-24986
Optically bistable devices using InSb
18 p3186 N85-29758
Control of acid deposition precursors through dry scrubbing
[DE85-010281] 19 p3235 N85-30056

ANTIMONY ALLOYS
Comparative analysis of laboratory and fullscale experimental data for metal flow displacements and speeds
[BLL-M-36266-(5828.4)] 20 p3430 N85-31276
ANTIMONY COMPOUNDS
NT GALLIUM ANTIMONIDES
NT INDIUM ANTIMONIDES
Fermi surface study of CeSb
[DE85-002532] 10 p1564 N85-19862
Alkali atom - SbCl(5) reactions: Blue-green chemiluminescence from an inverted population in SbCl
[AD-A154371] 19 p3276 N85-30315
ANTINEUTRINOS
Neutrino-antineutrino annihilation around collapsing star
[OG-1.1-10] 22 p3851 N85-33911
QCD analysis of neutrino charged current structure function F2 in deep inelastic scattering
[HE-5.3-23] 24 p4207 N85-36114
ANTINUCLEONS
Discussion session: Nucleon- and antinucleon-nucleus inelastic scattering and charge exchange
[DE85-010723] 19 p3364 N85-30660
ANTIPARTICLES
NT ANTINEUTRINOS
NT ANTINUCLEONS
NT ANTIPROTONS
NT POSITRONS
Search for heavy antinuclei in the cosmic radiation
[OG-6.1-2] 22 p3887 N85-34093
The flux of secondary anti-deuterons and antihelium produced in the interstellar medium
[OG-6.1-5] 22 p3888 N85-34096
ANTIPROTONS
Antiproton source beam position system
[DE84-010716] 09 p1380 N85-18679
Bunch coalescing in the main ring to form intense proton and antiproton bunches without RF counterphasing
[DE85-001364] 09 p1382 N85-18692
High energy physics study
[DE84-015803] 09 p1383 N85-18700
Low energy antiproton interaction studies at Brookhaven
[DE85-001226] 11 p1720 N85-20820
Gravitational properties of antimatter
[DE85-009601] 18 p3197 N85-29832
Physics with low temperature antiproton
[DE85-009627] 19 p3355 N85-30798
Spectral evolution of gamma-rays from adiabatically expanding sources in dense clouds
[OG-2.5-2] 22 p3869 N85-33959
Nineteenth International Cosmic Ray Conference. OG sessions, volume 2
[NASA-CP-2376-VOL-2] 22 p3875 N85-34006
Abundance of low energy (50-150 MeV) antiprotons in cosmic rays
[OG-6.1-1] 22 p3887 N85-34092
Propagation and secondary production of low energy antiprotons in the atmosphere
[OG-6.1-3] 22 p3887 N85-34094
Secondary antiproton production in relativistic plasmas
[OG-6.1-4] 22 p3888 N85-34095
The flux of secondary anti-deuterons and antihelium produced in the interstellar medium
[OG-6.1-5] 22 p3888 N85-34096
Analysis of experimental data on interstellar antiprotons in the light of measurements of high-energy electrons and He-3 nuclei
[OG-6.1-6] 22 p3888 N85-34097
Observed antiprotons and energy dependent confinement of cosmic rays: A conflict?
[OG-6.1-7] 22 p3888 N85-34098
Antiparticles in the extragalactic cosmic radiation
[OG-6.1-8] 22 p3888 N85-34099
Galactic cosmic ray antiprotons and supersymmetry
[OG-6.1-9] 22 p3888 N85-34100
Galactic antiprotons of 0.2-2 GeV energy
[OG-6.1-11] 22 p3888 N85-34101
The design of an experiment to detect low energy antiprotons
[OG-9.1-1] 23 p4022 N85-34928
An experiment to measure the energy spectrum of cosmic ray antiprotons from 100 to 1000 MeV
[OG-9.1-3] 23 p4022 N85-34929
Studies of relativistic heavy ion collisions
[DE85-014686] 24 p4152 N85-35745
P(P bar)P elastic scattering and cosmic ray data
[HE-1.1-6] 24 p4170 N85-35854
Some remarks about simulation of cosmic ray phenomena with use of nuclear interaction models based on the current SPS proton-antiproton data
[HE-1.2-6] 24 p4172 N85-35864
A test of the Feynman scaling in the fragmentation region
[HE-1.2-9] 24 p4172 N85-35867
ANTIRADIATION DRUGS
Chemical protection against ionizing radiation
[AD-A147822] 07 p1016 N85-16457
Radioprotective efficacy of ATP and adenosine with exposure to high energy protons
19 p3325 N85-30802
ANTIREFLECTION COATINGS
Effect of an underlayer of cadmium telluride on the reflection-reducing properties of zinc sulfide on mercury cadmium telluride
[AD-A146195] 03 p0414 N85-12649
Material models and device structures for GaAs solar cells, introduction 05 p0665 N85-14276
Anti-reflection coatings materials and models
05 p0665 N85-14278
Effective antireflection coatings of transparent polymeric materials by gas-phase surface fluorination
[DE84-013027] 09 p1385 N85-18711
Sol-gel-derived AR coatings for solar receivers
[DE85-000192] 11 p1673 N85-20541
1.5 to 1.7 micrometers LEDs (Light-Emitting Diode)
[AD-A149683] 12 p1834 N85-21508
Resistance of optical coatings to alkali solutions and sea water 14 p2281 N85-24129
Nonuniform interference coatings with thickness-dependent refractive index
14 p2281 N85-24131
Gyrotron traveling-wave device including quarter wavelength anti-reflective dielectric layer to enhance microwave absorption
[AD-D011690] 19 p3271 N85-30285
Technical and historical overview of the study at Lawrence of porous antireflection coatings
[DE85-010825] 20 p3434 N85-31302
Process and design considerations for high-efficiency solar cells 20 p3482 N85-31641
Los Alamos optical materials reliability, maintainability, and exposure testing program
[DE85-011894] 21 p3613 N85-32456
Effects of laser radiation on surfaces and coatings
[DE85-010475] 22 p3790 N85-33484
Removable cleanable antireflection shield
[AD-D011735] 22 p3844 N85-33810
ANTISEPTICS
Synthesis of antimicrobial chemical fibers and fibrous materials containing quaternary ammonium compounds and their utilization 06 p0762 N85-14872
ANTISHIP WARFARE
Optimizing the specifications for an air-surface laser system 16 p2696 N85-26844
ANTISUBMARINE WARFARE
Development of a Helicopter integrated navigation system 08 p1073 N85-16802
Real-time enhancement of a climatology or forecast of ocean thermal structure using observed ocean temperatures
[AD-A151118] 15 p2604 N85-26049
The NAVTAG (Naval Tactical Game) system and its modification to include the SH-60B helicopter
[AD-A152004] 16 p2856 N85-27624
ANTISUBMARINE WARFARE AIRCRAFT
NT P-3 AIRCRAFT
The NAVTAG (Naval Tactical Game) system and its modification to include the SH-60B helicopter
[AD-A152004] 16 p2856 N85-27624
ANTISYMMETRY
Design sensitivity analysis of an antisymmetric angle-ply laminate
[CSIR-TWISK-318] 01 p0021 N85-10128
ANTONOV AIRCRAFT
Designer O. K. Antonov on new AN-74 arctic transport
15 p2467 N85-25230
ANVIL CLOUDS
Anvil structure of severe thunderstorms
15 p2595 N85-25993
ANVILS
Electrical resistance measurements of metals to 40 GPa in the diamond cell
[DE85-001009] 11 p1629 N85-20262
ANXIETY
Psychological states (mood, affect or emotion) experienced by JASDF pilots through flying duties. 3: Flying conditions causing pilots psychological disturbances 01 p0090 N85-10606
AO-1 AIRCRAFT
U OV-1 AIRCRAFT
AOIPS
U ATMOSPHERIC & OCEANOGRAPHIC INFORM SYS
APATITES
U CALCIUM PHOSPHATES
U MINERALS
APERTURES
NT SYNTHETIC APERTURES
RF characteristics of the hoop column antenna for the land mobile satellite system mission
[NASA-CR-3842] 02 p0169 N85-11264
Formation of radio images by scanning around circle
02 p0264 N85-11727
Comparison of wide aperture and short residence time ion lenses
[DE84-015274] 03 p0420 N85-12685
Characterization of MMIC devices for active array antennas
[NASA-TM-86907] 07 p0913 N85-15779
Dual offset reflector antenna systems with rotationally symmetric aperture distributions
[AD-A147346] 07 p0940 N85-15961
Efficient computation of reflector antenna aperture distributions and far field patterns
[AD-A147367] 07 p0940 N85-15962
Power transfer from natural emitters to collection apertures at microwave wavelengths
[NASA-CR-174275] 07 p0945 N85-15989
Aperture studies with PATRICIA and RACETRACK on simple attices containing SSC dipoles
[DE85-004163] 11 p1724 N85-20842
An investigation of aerowindows for solar receivers
[DE84-010931] 12 p1877 N85-21772
Beam loss due to the aperture limitation resulting from intrabeam scattering
[DE85-005138] 12 p1930 N85-22124
Determination of angular resolution of coded aperture gamma-ray telescope 13 p1981 N85-22432
Variational and moment method solutions of the fields in a parallel-plate waveguide-aperture system
[DE85-006298] 13 p2057 N85-22876
Application of modern Aperture Integration (AI) and Geometrical Theory of Diffraction (GTD) techniques for analysis of large reflector antennas
14 p2234 N85-23851
Feed system design considerations for large space antenna systems. Part 1: Multiple apertures with non-overlapping feeds 14 p2234 N85-23852
Feed system design considerations for large space antenna systems. Part 2: Single aperture with overlapping feeds 14 p2235 N85-23853
Small aperture analysis of the dual TEM (transverse electromagnetic) cell and an investigation of test object scattering in a single TEM cell
[PB85-159952] 14 p2306 N85-24277
Development of the microwave antenna range of the national antenna test facility at Paardefontein
[R-NIAS-21] 15 p2539 N85-25669
Modeling and analysis of pinhole occulter experiment: Initial study phase
[NASA-CR-175978] 19 p3272 N85-30287
Method of precisely modifying predetermined surface layers of a workpiece by cluster ion impact therewith
[DE85-006519] 23 p3984 N85-34710
Hexagonal uniformly redundant arrays for coded-aperture imaging
[OG-9.2-1] 23 p4024 N85-34940
SONTRAC: A solar neutron track chamber detector
[SH-8.1-12] 23 p4052 N85-35127
Moment-method formulation of the cavity-probe aperture antenna
[DE85-013264] 24 p4068 N85-35338
APEXES
An experimental study of the pressure in a fast bottom beneath the apex of an overlying fluid wedge
[AD-A153618] 18 p3177 N85-29696
APNEA
U RESPIRATION
APOLLO APPLICATIONS PROGRAM
The evolution of civilian in-space infrastructure, i.e., space station concepts in the United States
07 p0914 N85-15788
APOLLO ASTEROIDS
The discovery circumstances of Earth-approaching asteroids
[NASA-CR-174327] 08 p1256 N85-17920
APOLLO PROJECT
The evolution of civilian in-space infrastructure, i.e., space station concepts in the United States
07 p0914 N85-15788
Feoktistov says manned lunar, Mars flights lack justification 13 p1985 N85-22452
APOLLO SPACECRAFT
On the Apollo subsatellite evidence for a lunar core
04 p0581 N85-13714
Ground man-machine interfaces for orbiter checkout
08 p1091 N85-16897
Challenges in the development of the shuttle extravehicular mobility unit 08 p1095 N85-16922
Hypervelocity impacts on Skylab 4/Apollo windows
12 p1785 N85-21202
Hypervelocity impact investigations and meteoroid shielding experience related to Apollo and Skylab
12 p1785 N85-21206
Analysis of systematic errors in systems of selenodetic coordinates 13 p1982 N85-22436

APPALACHIAN MOUNTAINS (NORTH AMERICA)
Aircraft measurements of tracer gas during the 1983 cross Appalachian tracer experiment (CAPTEX)
[DE84-015292] 04 p0531 N85-13395
Late precambrian to ordovician metamorphism and orogenesis in the Blue Ridge and western Piedmont, Virginia Appalachians 09 p1352 N85-18503
Lithologic and environmental atlas of Berea Sandstone (Mississippian) in the Appalachian Basin
[PB85-129039] 11 p1682 N85-20600

APPARATUS
U EQUIPMENT

APPENDAGES
NT ARM (ANATOMY)
NT ELBOW (ANATOMY)
NT HAND (ANATOMY)
NT KNEE (ANATOMY)
NT LEG (ANATOMY)
The design and development of a spacecraft appendage tie down mechanism 22 p3797 N85-33522

APPLICATION
U UTILIZATION

APPLICATIONS OF MATHEMATICS
Complexity, testability, and fault analysis of digital, analog and hybrid systems
[AD-A148465] 08 p1213 N85-17634
Computing environments for data analysis. Part 1. Introduction
[AD-A148677] 09 p1373 N85-18632
Sensitivity of inferred subphotospheric velocity field to mode selection, analysis technique and noise
14 p2442 N85-25065
Compilation of abstracts of theses submitted by candidates for degrees
[AD-A151722] 16 p2875 N85-27739

APPLICATIONS PROGRAMS (COMPUTERS)
Toward an improved FIPS cost-benefit methodology. Phase 2: Descriptive models, general purpose application software development and maintenance
[PB84-226943] 06 p0870 N85-15527
METC VAX-IBM guide to ASPEN
[DE85-001974] 12 p1916 N85-22031
Executive control systems in the engineering design environment
[NASA-CR-172582] 14 p2406 N85-24635
Mapping principles for the standards interface for computer aided design
[PB85-177905] 16 p2849 N85-27566

APPLICATIONS TECHNOLOGY SATELLITES
U ATS

APPROACH
NT AIRBORNE RADAR APPROACH
NT INSTRUMENT APPROACH
Aircraft accident report. Central Airlines flight 27, Hughes Charter Air, Gates Learjet model 25 (N51CA) Newark International Airport, Newark, New Jersey, March 30, 1983
[PB84-910411] 02 p0136 N85-10924
An in-flight investigation of a twin fuselage configuration in approach and landing
[NASA-CR-172368] 05 p0596 N85-13801
A cockpit-display concept for executing a multiple glide-slope approach for wake-vortex avoidance
[NASA-TP-2386] 08 p1085 N85-16869
A frozen vorticity approach to the axisymmetric strong interaction problem
[AD-A149101] 10 p1484 N85-19369
Safety recommendation(s), A-84-82 through -84
[REPT-3957] 14 p2217 N85-23748
An IKBS approach to image understanding
[AD-A151992] 16 p2854 N85-27599
Ground-based and in-flight simulator studies of flight characteristics of a twin-fuselage passenger transport airplane during approach and landing
[NASA-TP-2451] 23 p3896 N85-34144

APPROACH AND LANDING TESTS (STS)
Aerodynamic challenges of ALT
06 p1094 N85-16911
The orbiter air data system 06 p1094 N85-16912

APPROACH CONTROL
NT RADAR APPROACH CONTROL
Aspects of application of ACT systems for pilot workload alleviation 16 p2712 N85-26734
Construction of a job-oriented test for the selection of air traffic controllers
[DFVLR-FB-84-51] 17 p3002 N85-28558
A preliminary investigation of handling qualities requirements for helicopter instrument flight during decelerating approach maneuvers and overshoot
[AD-A154650] 21 p3557 N85-32125
Guidelines for the evaluation of visual approach slope indicators
[ARL/SYS-R-32] 23 p3896 N85-34132
The integrated manual and automatic control of complex flight systems
[NASA-CR-176166] 24 p4066 N85-35201

APPROACH INDICATORS
Evaluation of arctic test of improved tritium radioluminescent lighting
[AD-A148215] 08 p1089 N85-16884
Safety recommendation(s), A-84-123 and -124
[REPT-3894B/93] 15 p2466 N85-25222

APPROPRIATIONS
Department of Housing and Urban Development, and certain independent agencies appropriations for fiscal year 1985, part 2
[S-REPT-98-869-PT-2] 01 p0127 N85-10870
An agenda for a study of government science policy
[GPO-40-860] 12 p1949 N85-22245
National Telecommunications and Information Administration authorization
[GPO-38-660] 16 p2879 N85-27766
National Aeronautics and Space Administration Authorization Act, 1986
[S-REPT-99-91] 17 p3051 N85-28885
National Aeronautics and Space Administration Authorization Act, 1986
[S-REPT-99-91] 19 p3381 N85-30978
Department of Housing and Urban Development-Independent Agencies Appropriation Bill, 1986
[H-REPT-99-212] 19 p3382 N85-30979
National Aeronautics and Space Administration
19 p3382 N85-30980
Department of Housing and Urban Development-Independent Agencies Appropriation Act, 1986 20 p3542 N85-32041
National Aeronautics and Space Administration research and development 20 p3542 N85-32042
Testimony of Robert A. Frosch before the Subcommittee on HUD and Independent Agencies of the Senate Committee on Appropriations
[NASA-TM-87496] 22 p3738 N85-33173
Department of Housing and Urban Development Independent Agencies Appropriation Bill, 1986
[S-REPT-99-129] 23 p3987 N85-34720
National Aeronautics and Space Administration research and development: Program description
23 p3987 N85-34721

APPROXIMATION
NT BORN APPROXIMATION
NT CHEBYSHEV APPROXIMATION
NT EDDINGTON APPROXIMATION
NT FINITE DIFFERENCE THEORY
NT FINITE ELEMENT METHOD
NT HARTREE APPROXIMATION
NT LEAST SQUARES METHOD
NT MEAN SQUARE VALUES
NT NEWTON-RAPHSON METHOD
NT NUMERICAL DIFFERENTIATION
NT PADE APPROXIMATION
NT PARTICLE IN CELL TECHNIQUE
NT RELAXATION METHOD (MATHEMATICS)
NT RITZ AVERAGING METHOD
Design proposals for torsional buckling of stiffeners
[AD-A144783] 01 p0062 N85-10409
On the treatment of material laws for approximate J-estimation methods
[GKSS-84-E-15] 01 p0062 N85-10414
Normal approximation for response time in a processor-shared computer system model
[AD-A144997] 01 p0103 N85-10690
Approximating hierarchical normal priors using a vague component
[CSIR-TWISK-284] 01 p0107 N85-10720
Some concepts in multi-criteria optimization
[CSIR-TWISK-299] 01 p0108 N85-10722
The approximation of nonsmooth solutions of hyperbolic partial differential equations
[CSIR-TWISK-297] 01 p0108 N85-10723
Simultaneous rational approximation of a function and its derivatives in the complex plane
[CSIR-TWISK-311] 01 p0109 N85-10733
Sensitivity analysis in generalized rational approximation with restricted denominator
[CSIR-TWISK-319] 01 p0109 N85-10734
The convergence of Garlerkin approximation schemes for second-order hyperbolic equations with dissipation
[CSIR-TWISK-325] 01 p0109 N85-10736
Spline-Galerkin solution of integral equations for 3-body scattering above break-up
[TWISK-327] 01 p0109 N85-10738
Legendre-Tau approximation for functional differential equations. Part 3: Eigenvalue approximations and uniform stability
[NASA-CR-172447] 01 p0110 N85-10744
Partitions of unity and approximation
[AD-A144717] 01 p0110 N85-10746
Some families of near-orthonormal analytic and harmonic functions
[AD-A144722] 01 p0110 N85-10748
Methods for numerical differentiation
[AD-A145058] 01 p0112 N85-10758
Credibility approximations for Bayesian prediction of second moments
[AD-A144996] 01 p0113 N85-10768
Comment on the validity of an L2 treatment of the center of mass problem
[CSIR-TWISK-324] 01 p0114 N85-10779
Fast Fourier transform for unequally spaced data
01 p0128 N85-10876
Fitting aerodynamic forces in the Laplace domain: An application of a nonlinear nongradient technique to multilevel constrained optimization
[NASA-TM-86317] 02 p0134 N85-10917
Approximation methods for inverse problems involving the vibration of beams with tip bodies
[NASA-CR-172468] 02 p0209 N85-11379
Approximation of discontinuous solutions of hyperbolic partial differential equations
[NRIMS-TWISK-302] 02 p0250 N85-11631
Sinc method of solution of singular integral equations
[AD-A146155] 03 p0411 N85-12631
A two-segment approximation algorithm for separable convex programming with linear constraints
[AD-A146215] 03 p0412 N85-12634
Coherent amplification of ultrasonic pulses in activated crystals 05 p0724 N85-14653
A geometric approach to high resolution TVD schemes
[NASA-CR-172484] 06 p0857 N85-15449
Determination of moments of initial estimate during linear approximation of distribution of ejected impurity
07 p0954 N85-16045
Numerical methods and approximation and modelling problems in stochastic control theory
[AD-A146927] 07 p1029 N85-16533
A counterexample to a result of Strang and Fix concerning controlled approximation
[AD-A147360] 07 p1032 N85-16550
Spline methods for approximating quantile functions and generating random samples
[NASA-TP-2389] 07 p1035 N85-16565
Multivariable flight control with time-scale separation
[NASA-CR-174320] 08 p1087 N85-16873
Computer subroutines for estimation of human exposure to radiation in low Earth orbit
[NASA-TM-86324] 08 p1199 N85-17550
Improved stability and performance bounds using approximate models — control system design
[RR-260] 08 p1209 N85-17606
Asymptotic methods for the analysis, estimation, and control of stochastic dynamic systems
[AD-A147758] 08 p1211 N85-17618
The performance of variable sampling plans when the normal distribution is truncated
[AD-A147717] 08 p1215 N85-17649
Electronic structure of liquid metal alloys
[DE85-000904] 09 p1295 N85-18136
Resistivity of alloys
[DE85-000906] 09 p1296 N85-18138
Modeling of real UT transducer field/flaw interactions
[DE85-000341] 09 p1329 N85-18351
A 3-dimensional mass conserving element for compressible flows
[NASA-CR-172513] 09 p1373 N85-18626
On the connection between multigrid and cyclic reduction
[NASA-TM-86020] 09 p1373 N85-18629
Simple approximate variances for b-letter values. A sampling enquiry: Supplement
[DE85-001410] 09 p1376 N85-18647
Nonlocal and nonlinear effects on solar oscillations
09 p1416 N85-18934
Diffeomorphic approximation of quasiconformal and quasisymmetric homeomorphisms
10 p1536 N85-19678
A Galerkin method for the estimation of parameters in hybrid systems governing the vibration of flexible beams with tip bodies
[NASA-CR-172537] 10 p1544 N85-19734
Controlled approximation and a characterization of the local approximation order
[AD-A149095] 10 p1546 N85-19750
A new method of approximating normal and t-tail areas
[AD-A149457] 10 p1548 N85-19761
A remark on regularization in Hilbert spaces
[AD-A149046] 10 p1552 N85-19787
Imaging through a multiple scattering medium
[DE85-002051] 10 p1557 N85-19821
Theoretical and experimental study of crack resistance and macrocrack growth rate in organic fiber reinforced plastic under pure shear condition
11 p1598 N85-20053

The eigenvalues of the pseudospectral Fourier approximation to the operator sin (2x) d/dx
[NASA-CR-172538] 11 p1706 N85-20729
Alternative approximation concepts for space frame synthesis
[NASA-CR-172526] 12 p1776 N85-21150
Recovering pointwise values of discontinuous data within spectral accuracy
[NASA-CR-172535] 12 p1919 N85-22049
A two-dimensional smoothing spline and a regression problem
[AD-A149824] 12 p1921 N85-22067
Inference for censored matched pairs using signed ranks
[MATHEMATICS-RESEARCH-182]
12 p1923 N85-22078
Rates of convergence of semistochastic approximation procedures for solving stochastic optimization problems
12 p1924 N85-22088
Approximation order from certain spaces of smooth bivariate splines on a 3-direction mesh
[AD-A149633] 12 p1925 N85-22092
Preliminary development of an approximation procedure for supercritical wing design optimization applications
[AD-A150177] 13 p1972 N85-22383
Computing convolution of multifrequency signal employing truncated fast Fourier transform algorithms
13 p2085 N85-23019
Significance of the thin-layer Navier-Stokes approximation
[DE85-002630] 13 p2092 N85-23063
Confidence intervals using the regenerative method for simulation output analysis
[AD-A150147] 13 p2149 N85-23343
Approximation in optimal control and identification of large space structures
[AD-A150323] 13 p2151 N85-23351
Accumulation of the terrestrial planets
13 p2179 N85-23524
Some approximations of geophysical hydrodynamics
14 p2336 N85-24448
Properties of systems which lead to efficient computation of reliability
[AD-A151033] 14 p2409 N85-24853
Algorithms and approximations for queueing systems
[CWI-TRACT-8] 14 p2410 N85-24859
On the stability of predictor-corrector methods for parabolic equations with delay
[CWI-NM-R8410] 14 p2410 N85-24860
Estimation of optimum scores for partition detectors using stochastic approximation techniques
14 p2411 N85-24865
One method for constructing model of point masses of planetary gravity field 15 p2479 N85-25300
Natural convection in cylindrical containers
15 p2555 N85-25763
Approximating posterior distributions of system reliability derived from component test data
[AD-A152057] 15 p2572 N85-25857
Truncated nonlinear filters 15 p2635 N85-26249
Scattered data interpolation and approximation
[DE85-007495] 15 p2641 N85-26290
An approximation theory for nonlinear evolution equations and single conservation laws
16 p2691 N85-26614
A numerical procedure on three-dimensional parabolic flow in duct 16 p2692 N85-26620
Application of conformal mapping to grid generation
16 p2692 N85-26621
Approximate solution of the problem of fluid oscillations in cavities of revolution 16 p2764 N85-27056
An incremental multigrid strategy for the fluid dynamics equations
[AD-A151953] 16 p2783 N85-27172
An approximation to the problem of a pin-loaded hole in an orthothropic plate
[VTH-LR-386] 16 p2802 N85-27278
Solving the minimal least squares problem subject to bounds on the variables
[TRITA-NA-8215] 16 p2852 N85-27580
Uniformly high-order accurate non-oscillatory schemes, 1
[NASA-CR-175768] 16 p2853 N85-27589
Eigenvalue approximation methods for quantum lattice Hamiltonians 16 p2858 N85-27627
Characteristics of steady-state hypersonic flow about blunted bodies with discontinuities in generators
17 p2941 N85-28155
SC filters and design centering of integrated circuits. Part 2: Design centering of integrated circuits
[BMFT-FB-T-84-265-PT-2] 17 p2956 N85-28257
Curved finite elements and curve approximation
17 p3007 N85-28590
An inequality and its application to the truncated distributions 17 p3020 N85-28673
Spatial differencing for finite difference codes
[DE85-008902] 17 p3021 N85-28684
On the accuracy of the Poincare-Lindstedt method
[REPT-84-37] 17 p3022 N85-28690
On the condition number of modified moment matrices arising from least squares approximation in the complex plane
[AD-A152353] 17 p3026 N85-28714
A numerical study of the mean trajectory approximation in a non-adiabatic process
[AD-A152763] 17 p3030 N85-28737
The mean trajectory approximation for charge and energy transfer processes at surfaces
[AD-A152708] 17 p3043 N85-28830
Quantum model of dephasing-enhanced laser desorption: Master equation approach
[AD-A153789] 18 p3112 N85-29289
Sigma filter 18 p3142 N85-29450
The vertical structure of global rotational normal modes 18 p3144 N85-29464
Effect of some estimators on a large sample approximation to the non-null distribution of the pearson chi-square statistic
[AD-A153515] 18 p3173 N85-29673
Development of the relativistic impulse approximation
[DE85-008505] 18 p3179 N85-29711
Evaluation of the eigenvalue method in the solution of transient heat conduction problems
[AD-A154434] 19 p3266 N85-30256
Well-posedness of one-way wave equations and absorbing boundary conditions
[NASA-CR-172619] 19 p3345 N85-30727
Calculation of Franck-Condon factors for diatomic molecules
[AD-A154463] 19 p3353 N85-30784
Activities of Rutgers - The State University Department of Mathematics
[AD-A154158] 19 p3370 N85-30904
Plasma radiation sources. Quasi-adiabatic theory and numerical modeling in the electro-diffusive approximation
[AD-A154375] 19 p3370 N85-30906
Tables of generalized hydrogen diffusion profiles and permeating fluxes for fusion applications
[DE85-008876] 19 p3372 N85-30919
Approximation techniques for parameter estimation and feedback control for distributed models of large flexible structures 20 p3413 N85-31179
Approximation of optimal infinite dimensional compensators for flexible structures
20 p3413 N85-31181
Influence of error of determination of moire isotach orders on the stability of their approximation
[BLL-M-36277-(5828.4)] 20 p3450 N85-31423
Reduced order models and simulation data in control systems design
[RR-267] 20 p3483 N85-31516
Memory effects in dynamical many-body systems: The isomnesic (constant-memory) approximation
[AD-A154160] 20 p3520 N85-31869
Improved Nominal Operating Cell Temperature (NOCT) test procedure 21 p3612 N85-32449
Toward the propagation of waves in unsteady media
21 p3683 N85-32881
On the problem of linear programming with approximate data 21 p3698 N85-32978
Discrete-element acoustic analysis of submerged structures using doubly asymptotic approximations
[AD-A154959] 21 p3700 N85-32987
Maximally flat approximation of attenuation characteristics of coupled-line filters
22 p3775 N85-33393
Interacting Boson approximation
[DE85-003016] 22 p3837 N85-33756
Multiaxial stress analysis taking account of penetration depth of X-rays. A solution by means of polynomial approximation 23 p3907 N85-34204
Building an octree from a set of parallelepipeds
23 p3964 N85-34572
Guiding center distribution function and longitudinal invariant 23 p3978 N85-34663
The role of cosmic rays in magnetic hydrodynamics of interstellar medium
[OG-7.2-15] 23 p4015 N85-34882
Finite analytic solutions of supersonic flows in two-dimensional non-symmetrical channels
24 p4059 N85-35154
Prediction of turbulent internal recirculating flows with K-epsilon models 24 p4092 N85-35366
Vibrations of free hollow circular cylindrical bodies
24 p4100 N85-35418
An evaluation of a class of practical optimization techniques for structural dynamics applications
[PB85-195766] 24 p4103 N85-35434
A new theory for multistep discretizations of stiff ordinary differential equations: Stability with large step sizes
[NASA-CR-177941] 24 p4142 N85-35675
Model robust response surface designs: Scaling two-level factorials
[AD-A156218] 24 p4143 N85-35686
Applications and misapplications of the channel-capture formalism of direct neutron capture
[DE85-013992] 24 p4152 N85-35748
Optical receivers using rough reflectors
[NASA-CR-176200] 24 p4154 N85-35750
Study of the parameters affecting the collapse of a rotating protostellar cloud 24 p4168 N85-35837

APPROXIMATION METHODS
U APPROXIMATION

APSIDAL ANGLES
U APSIDES

APSIDES
NT PERIGEES
NT PERIHELIONS
The stellar wind in the BO V-type eclipsing binary Y Cygni 11 p1755 N85-21040

APTITUDE
The application of basic control laws to human medicine
[DFVLR-MITT-84-13] 05 p0697 N85-14482
Cognitive asymmetry and occupation. Computer programmers, students, and bank personnel, part 1 and part 2
[AD-A147125] 08 p1197 N85-17540
Technical evaluation of the Naval Automated Pilot Aptitude Measurement System (NAPAMS)
[AD-A152361] 17 p3000 N85-28547
Estimating ability with the wrong model
[AD-A154071] 19 p3335 N85-30683
Equipercentile test equating: The effects of presmoothing and postsmoothing on the magnitude of sample-dependent errors
[AD-A154110] 19 p3347 N85-30746

AQUATIC PLANTS
Aquatic plant control research program. Evaluation of Fusarium roseum Culmorum as a biological control agent for Hydrilla verticillata
[AD-A145228] 01 p0069 N85-10459
Estuaries of the Cape. Part 2: Synopses of available information on individual systems. Report 13: Silvermine (CSW 3)
[CSIR-RR-412-PT-2] 01 p0086 N85-10582
Estuaries of the Cape. Part 2: Synopses of available information on individual systems. Report no. 16: Eerste (CSW 6)
[CSIR-RR-415-PT-2] 01 p0087 N85-10585
Effects of low temperatures on the growth and unfrozen water content of an aquatic plant
[AD-A147107] 07 p1011 N85-16424
Review and annotated bibliography of benthic studies in coastal and estuarine areas of Florida with a selected compilation of worldwide benthic methodological references and southeastern United States benthic taxonomic references
[PB85-151041] 16 p2822 N85-27405
Handbook for obtaining and using aerial photography to map aquatic plant distribution
[AD-A154584] 21 p3605 N85-32388

AQUEOUS SOLUTIONS
Experiments on turbulent mixing and chemical reactions in a liquid mixing layer 02 p0134 N85-10912
Transport phenomena in the boundary layer during solution solidification under microgravity. Ice growth from a water-salt solution
[BMFT-FB-W-84-031] 03 p0329 N85-12121
Electrokinetic potential and stability of SiC suspensions in electrolyte solutions
[NASA-TM-77492] 04 p0469 N85-12984
Investigations regarding process analysis of liquids in the 1 to 2 micrometer spectral range
[BMFT-FB-T-84-169] 05 p0614 N85-13926
Current and potential transients during localized corrosion of stainless steel
[DE84-014100] 05 p0618 N85-13954
Measuring system with ion selective electrodes
[BMFT-FB-T-84-170] 05 p0639 N85-14100
Photoacoustic spectroscopy at electrode-solution interface
[DE85-001872] 09 p1292 N85-18111
Thermodynamic properties of aqueous NaCl from 273 to 823 K with estimates for higher temperatures
[DE85-000392] 09 p1292 N85-18116
Contributions of segregated phosphorus to the intergranular stress corrosion cracking of nickel
[DE85-003112] 11 p1606 N85-20099
Compiled and thermodynamic data sources for aqueous and biochemical systems: An annotated bibliography, 1930 - 1983
[PB85-137693] 12 p1944 N85-22206
Applications of photoinduced electron transfer and hydrogen abstraction reactions to chemical and electrochemical conversion processes
[DE85-006068] 15 p2506 N85-25459

Kinetics of hydrolysis and products of hydrolysis and photolysis of tetryl
[AD-A153144] 17 p2921 N85-28005
Properties of nitrogen containing stainless alloy designed for high resistance to pitting
[DE85-008282] 17 p2931 N85-28095
Corrosion Research Center of the University of Minnesota
[DE85-009418] 18 p3075 N85-29022
Chemical transformations in acid rain. Volume 2: Investigation of kinetics and mechanism of aqueous-phase peroxide formation
[PB85-173433] 18 p3135 N85-29416
Systematic view of transition intensities in the spectra of actinides and lanthanides in condensed phases
[DE85-010272] 19 p3354 N85-30789
Experimental evaluation of the thermodynamic properties of concentrated aqueous potassium hydroxide solutions
[DE85-010628] 23 p3912 N85-34238

AQUICULTURE

Cultivation and conversion of marine macroalgae — biomass energy production
[DE84-004522] 04 p0544 N85-13464
Research and development of shallow algal mass culture systems for the production of oils
[DE85-000518] 11 p1690 N85-20624
Aquatic Invertebrate Development Working Group
24 p4127 N85-35585

AQUIFERS

Definition of global dispersion coefficients — aquifers
[PSE-83/4-B] 01 p0064 N85-10426
Water resources by orbital remote sensing: Examples of applications
[E85-10015] 02 p0217 N85-11428
Geothermal resource assessment for North Dakota
[DE84-016128] 04 p0526 N85-13367
Steady flow model user's guide
[DE85-002001] 08 p1163 N85-17337
Field testing of aquifer thermal energy storage
[DE85-000399] 09 p1344 N85-18457
Protocol for aquifer cleanup decision making at military installations
[AD-P004151] 09 p1349 N85-18487
Evaluation of subsurface fracture geometry using fluid pressure response to solid earth tidal strain
[DE85-003294] 12 p1890 N85-21864
Determining deep heat flow and rate of horizontal percolation from temperature measurements in aquifer
13 p2116 N85-23180
Report on regional groundwater flow modeling for the Palo Duro Basin, Texas
[DE85-007490] 16 p2815 N85-27370
Central solar heating plants with seasonal storage. Evaluation of systems concepts based on heat storage in aquifers
[DE85-006788] 16 p2820 N85-27396
Groundwater model for an island aquifer: Bribie Island groundwater study
[CE-44] 16 p2821 N85-27398
Occurrence of uranium in ground water in the vicinity of the US Department of Energy Feed Materials Production Center, Fernald, Ohio
[DE85-010340] 19 p3364 N85-30862
State-of-the-art of aquifer restoration. Volume 1: Sections 1 through 8
[PB85-181071] 20 p3478 N85-31612
State-of-the-art of aquifer restoration. Volume 2: Appendices A through G
[PB85-181089] 20 p3478 N85-31613
Detailed validation of a liquid and heat flow code against field performance
[DE85-008801] 23 p3932 N85-34368
Depletion modeling of liquid dominated geothermal reservoirs
[DE85-009923] 23 p3943 N85-34437
The geostatistical approach to the inverse problem in two-dimensional steady state groundwater modeling
24 p4107 N85-35462
Hydrogeology of the lower Glen Rose Aquifer, south-central Texas 24 p4108 N85-35466

ARABIAN SEA

Arabian gulf circulation — pollution monitoring
14 p2331 N85-24412
Mineralogical-geochemical characteristics of ferromanganese formations in Arabian-Indian Ocean Ridge 19 p3293 N85-30416
On the interannual variability of the Indian monsoon and the Southern Oscillation 20 p3495 N85-31726

ARABSAT

ARABSAT spacecraft: Rx and Tx antenna mechanisms 05 p0629 N85-14022

ARC CHAMBERS

Study of a constricted electric arc cooled by transpiration
[NASA-TM-77846] 17 p3038 N85-28796

ARC CLOUDS

The arc cloud complex: A case study
[AD-A145384] 02 p0231 N85-11507

ARC DISCHARGES

Gas pressure and electron density at the level of the active zone of hollow cathode arc discharges
[NASA-TM-77477] 03 p0414 N85-12848
The discharge mechanism of the high-temperature arc
[NASA-TM-77794] 07 p0922 N85-15837
Gas pressure and electron density in the active zone level of hollow cathode arc discharges
[NASA-TM-77488] 07 p0945 N85-15988
An investigation of arc discharging on negatively biased dielectric conductor samples in a plasma
13 p1994 N85-22496
Phenomenology of discharges in space: Application to a solar generator — SPOT satellite
13 p2007 N85-22583
Electrostatic discharge testing on a carbon fiber solar panel structure 13 p2007 N85-22584
The loss of material from the cathode of metal arcs
[NASA-TM-77845] 17 p2918 N85-27985
Spectrographic investigation of low-voltage arc discharge in argon atmosphere
[BLL-M-36276-(5828.4)] 20 p3422 N85-31242
High pressure working mode of hollow cathode arc discharges
[NASA-TM-77880] 20 p3535 N85-31992
Hollow cathodes in high pressure arc discharges
[NASA-TM-87098] 23 p3903 N85-34179

ARC GENERATORS

Experimental research on electric propulsion. Note 7: Analysis of the performance of an arc-jet driven by means of hydrogen and nitrogen
[NASA-TM-77473] 06 p0760 N85-14861
Experimental research on electrical propulsion. Note 2: Experimental research on a plasma jet with vortex type stabilization for propulsion
[NASA-TM-77874] 18 p3067 N85-28968

ARC JET ENGINES

Experimental research on electric propulsion. Note 7: Analysis of the performance of an arc-jet driven by means of hydrogen and nitrogen
[NASA-TM-77473] 06 p0760 N85-14861
Axisymmetric electromagnetic field influence on the characteristic velocity of an arc-jet
[NASA-TM-77475] 07 p0938 N85-15942
Electrode erosion in arc discharges at atmospheric pressure
[NASA-TM-87087] 23 p3903 N85-34178
Hollow cathodes in high pressure arc discharges
[NASA-TM-87098] 23 p3903 N85-34179

ARC LAMPS

Investigation of light source and scattering medium related to vapor-screen flow visualization in a supersonic wind tunnel
[NASA-TM-86290] 06 p0810 N85-15144
Life study of RF excited Hg arc lamps and CO2 waveguide lasers
[AD-A149618] 12 p1856 N85-21640
Electrodeless HID lamp study
[DE85-010626] 18 p3096 N85-29167
Optical output stabilization method for direct current arc lamps
[AD-A154867] 21 p3705 N85-33013

ARC SPRAYING

Arc spray fabrication of metal matrix composite monotape
[NASA-CASE-LEW-13828-1] 19 p3230 N85-30027

ARC WELDING

NT GAS TUNGSTEN ARC WELDING
NT PLASMA ARC WELDING
Utility of the M.I.T. (Massachusetts Institute of Technology) underwater stud welding gun
[AD-A144793] 01 p0055 N85-10365
Optical seam tracking of robotic arc welding
[VTT-272] 01 p0055 N85-10368
Design, construction, demonstration and delivery of an automated narrow gap welding system
[AD-A145497] 02 p0204 N85-11348
New welding equipment for mechanized welding and trends in further development 03 p0352 N85-12264
Prediction of weld defects using welding condition data
[VTT-RR-264] 03 p0370 N85-12359
Optimization of toughness properties of HSCA shielded metal arc welding electrodes
[BMFT-FB-T-84-186] 05 p0646 N85-14148
ONR (Office of Naval Research) Far East Scientific Bulletin, volume 9, number 3, July to September 1984
[AD-A147282] 08 p1262 N85-17930
Effect of tempering on the strength and toughness of 2 1/4 Cr-1 Mo steel weldments
[DE85-003818] 09 p1296 N85-18140
Mechanical properties of Shielded Metal Arc (SMA) and Submerged Arc (SA) welded joints for quenched and tempered steel StE 470.
[VTT-319] 09 p1328 N85-18346
Estimate of quality of aluminum alloy surface preparation for arc welding 10 p1449 N85-19128
The effect of filler wire and flux compositions on the microstructure and properties of microalloyed steel weld metal
[AD-A149529] 10 p1492 N85-19423
Weldability of alloy ABM1 to alloy 1201
11 p1603 N85-20080
Properties of welded joints in argon arc welding of titanium alloy using a protective coating
13 p2032 N85-22733
Reliability of robotized welding apparatus
13 p2034 N85-22741
Structure and mechanical characteristics of heterogeneous joints produced by laser welding
13 p2034 N85-22742
Study of experimental robotized system for arc welding based on Universal-15 manipulator
15 p2500 N85-25423
Dynamic characteristics of ac arc in welding aluminum alloys 15 p2500 N85-25424
Effectiveness of use of heat-dissipating clamps to reduce deformation during argon arc welding of thin sheets of AMg6 alloy 15 p2501 N85-25427
Hardening of titanium alloy electric-arc welded joints
15 p2514 N85-25513
Welding technology and organisation in steel construction 15 p2566 N85-25828
Robotic arc welding 15 p2566 N85-25830
Automation and robotics in welding
15 p2566 N85-25831
Recent advances in arc welding equipment and their application 15 p2566 N85-25832
A critical review of selected recent advancements in arc welding equipment and processes
15 p2566 N85-25833
Underwater pipeline: Welding by high frequency induction
[BLL-WI-TRANS-682-(9312.57)]
16 p2792 N85-27221
Welder training/welder testing
[BLL-WI-TRANS-683-(9312.57)]
16 p2792 N85-27223
Submerged arc welding of new Czechoslovak micro-alloy steels
[BLL-BISI-TRANS-22193-(9022.06)]
17 p2972 N85-28356
Application of 4-wire submerged arc method to welding UOE pipe
[BLL-BISI-TRANS-22417-(9022.06)]
17 p2972 N85-28358
High-speed longitudinal welding of pipes by automatic submerged arc process
[BLL-BISI-TRANS-22340-(9002.06)]
17 p2973 N85-28366
Effect of protective method on cyclic durability and nature of failure of titanium alloy welded joints
19 p3245 N85-30122
Low pressure arc butt welding of dissimilar metals
19 p3248 N85-30128
Welding of steel-aluminum cooling panels for the holds of refrigerator vessels 19 p3248 N85-30129
Hot cracking of austenitic stainless steels: The debut of the Sigmajig
[DE85-010560] 20 p3431 N85-31287
Chromium-base powder alloys for welding cladding layer of bimetal
[BLL-M-35776-(5828.4)] 23 p3915 N85-34260
Electronic imaging system and technique
[DE85-005740] 23 p3935 N85-34393

ARCHAEOLOGY

Methodological research in connection with the handling of LANDSAT satellite data for archaeology
05 p0655 N85-14207
Multivariate analyses of sedimentological data at two early Bronze age sites, Bab edh-Dhra and Numeira, southeast Dead Sea Graben, Jordan
05 p0674 N85-14326
Paleoenvironmental investigations at seed cave (Windust cave H-45FR46), Franklin County, Washington
[AD-A154777] 21 p3635 N85-32576

ARCHES

Investigation of internal friction of free-flowing material during discharge
[BLL-M-36141-(5828.4)] 15 p2553 N85-25752

ARCHITECTURE

Patterns of behavior in lodgings exposed to traffic noise
[NASA-TM-77750] 03 p0387 N85-12479
The human role in space. Volume 3: Generalizations on human roles in space
[NASA-CR-171225] 04 p0546 N85-13475

Seismic performance of low-rise light-framed wood buildings 08 p1171 N85-17384
Prototype concept design for US Army type 3A Air Traffic Control Tower (ATCT)
[AD-A148840] 09 p1284 N85-18070
Report of the Artificial Gravity Panel
11 p1645 N85-20365
Photovoltaic roofing tile systems
12 p1878 N85-21783
Evaluating wind flow around buildings on heliport placement
[FAA-PM-84-25] 12 p1893 N85-21881
Progress through cooperation and exchange of ideas and experiences 15 p2626 N85-26186
Design of computer-related workstations in relation to job functions and productivity
[AD-A151938] 16 p2844 N85-27534
Overview: Human factors issues in space station architecture 18 p3158 N85-29558
Assured information flow capping architecture
[AD-A155392] 22 p3756 N85-33283
Generative design in architecture using an expert system 23 p3965 N85-34582

ARCHITECTURE (COMPUTERS)
Aerospatiale's experimentations of vectorization on supercomputers for aircraft structural problems
01 p0007 N85-10041
Impact of new computing systems on computational mechanics and flight-vehicle structures technology
01 p0007 N85-10042
Electronics Engineering Department: EE technical review
[DE84-016124] 01 p0044 N85-10286
The FLEX/32 multicomputing environment
01 p0057 N85-10378
Performance of the h, p and h-p versions
01 p0058 N85-10383
Activities of the MIT Laboratory for Computer Science
[AD-A145134] 01 p0100 N85-10661
Data flow computer architecture
[DE84-014362] 01 p0100 N85-10664
Analysis of three database system architectures using benchmarks
[PB84-217512] 01 p0105 N85-10706
A technique to model and design physical database systems
[DE84-015337] 01 p0126 N85-10863
The computer-communication link for the innovative use of Space Station 02 p0150 N85-11016
Supercomputers and VLSI: The effect of large scale integration on computer architecture
[AD-A145408] 02 p0239 N85-11555
Design and descriptive tools for systolic architectures
[DE84-015521] 02 p0239 N85-11557
Parallel searching and merging on ZMOB
[AD-A145424] 02 p0241 N85-11574
Parallel, iterative solution of sparse linear systems: Models and architectures
[NASA-CR-172457] 02 p0243 N85-11586
Fault tolerant computing research
[AD-A145640] 02 p0244 N85-11590
Application of the CSRL language to the design of expert diagnosis systems: The Auto-Mech experience
[AD-P003922] 02 p0245 N85-11602
Study on the conversion and test of protocols
[ENST-84E005] 03 p0356 N85-12293
Application of a silicon compiler to VLSI (Very Large Scale Integrated circuits) design of digital pipelined multipliers
[AD-A146328] 03 p0403 N85-12569
Analysis and design methodology for VLSI computing networks
[AD-A146030] 03 p0409 N85-12611
A decomposable algorithm for contour surface display generation
[AD-A145783] 03 p0410 N85-12619
USSR report: Electronics and electrical engineering
[JPRS-UEE-84-010] 04 p0485 N85-13095
Architecture of adaptive space-frequency-time signal processing system 04 p0486 N85-13103
A control scheme for microcomputers being used in multiprocessor arrays
[DE84-014590] 04 p0547 N85-13479
Physical database processor preliminary interface specifications
[PB84-217561] 04 p0548 N85-13483
New directions in software for advanced computer architectures
[DE84-017435] 04 p0550 N85-13502
A distributed expert system for Space Shuttle flight control 05 p0602 N85-13836
VLSI architectures for the multiplication of integers modulo a Fermat number 05 p0624 N85-13993
Massively parallel processor 05 p0680 N85-14366
Memory hierarchies for Directly Executed Language microprocessors 05 p0713 N85-14570
Requirements and overview of the LINCS distributed operating system architecture
[DE84-013721] 05 p0714 N85-14577
Fast algorithms and specialized architectures
05 p0714 N85-14579
S-MICRO: A system for simulating a microprogrammed control unit
[INPE-3224-PRE/575] 05 p0715 N85-14585
Avionics/crew station integration
06 p0752 N85-14818
Internal structure of microprocessor
06 p0785 N85-15020
Workshop on Computer Architecture
[AD-A146455] 06 p0847 N85-15378
Architecture, design, and system; performance assessment and development methodology for computer-based systems. Volume 1: Methodology description, discussion, and assessment
[AD-A146577] 06 p0847 N85-15379
Distributed database components in a DBMS (Database Management System) component architecture
[PB84-217546] 06 p0848 N85-15382
Specialized silicon compilers for language recognition
[AD-A146528] 06 p0853 N85-15425
A framework for the development of Navy computer-based systems: Combat system architecture and combat system engineering put into perspective
[AD-A146460] 06 p0856 N85-15445
Algebraic techniques in systolic array design
[AD-A146417] 06 p0857 N85-15451
Two-dimensional signal processing and storage and theory and applications of electromagnetic measurements. Supplemental appendix
[AD-A146648] 07 p0939 N85-15953
Upset susceptibility study employing circuit analysis and digital simulation --- digital systems and electromagnetic interference 07 p0999 N85-16344
Future database machine architectures
[AD-A146786] 07 p1022 N85-16481
Computer science research in Europe
[AD-A146905] 07 p1022 N85-16482
Local area network evaluation by MICROSS extensions
[AD-A146773] 07 p1027 N85-16521
Built-in test and self repair mechanisms in a digital correlator integrated circuit 08 p1064 N85-16741
Hardware/software codesign for maintainable systems
08 p1066 N85-16753
Evolution toward a multi-bus architecture for Army helicopter avionic systems 08 p1074 N85-16812
Restructurable VLSI program
[AD-A148145] 08 p1157 N85-17301
Kernel Ada Programming Support Environment (KAPSE) interface team public report, volume 4
[AD-A147648] 08 p1205 N85-17581
Matrix-matrix multiplication using an electrooptical systolic-engagement array processing architecture
[AD-D011410] 08 p1223 N85-17704
Raster graphics extensions to the core system
[NASA-CR-174348] 09 p1367 N85-18580
Integrating heterogeneous non-geometric information systems using RIM
[DE84-017600] 09 p1402 N85-18823
The feasibility of a multiprocessor architecture for real-time contour surface display generation
[AD-A149427] 10 p1538 N85-19697
Meta-level control through fault detection and diagnosis
[AD-A149064] 10 p1540 N85-19709
Siemens introduces fast computer with pipeline architecture 11 p1618 N85-20178
ESOP expert system model described
11 p1619 N85-20187
PASLIB programmer's guide for the finite element machine, revision 2.1-A
[NASA-CR-172281] 11 p1706 N85-20727
Needs, opportunities, and options for large scale systems research
[DE85-002664] 11 p1709 N85-20750
RAPIDbus: Design of an extensible multiprocessor structure
[AD-A150061] 12 p1912 N85-21996
Towards the generation of efficient code from verified programs
[TR-40] 12 p1914 N85-22017
Feasibility of self-structured current accessed bubble devices in spacecraft recording systems
[NASA-CR-172554] 13 p1998 N85-22525
Periodic binary sequence generators: VLSI circuits considerations
[NASA-CR-175649] 13 p2063 N85-22986
Synthesis of tree-structured computing systems through use of closures
[AD-A150502] 13 p2147 N85-23326
Performance evaluation of distributed systems with unbalanced flows: An analysis of the INFOPLEX data storage hierarchy
[AD-A150526] 13 p2147 N85-23328
General design considerations of an Air Force information system
[AD-A150611] 13 p2168 N85-23449
Multidimensional digital signal processing
[AD-A150833] 14 p2292 N85-24209
Comparative architectures for a multiple function speech processor
[AD-A150873] 14 p2292 N85-24211
USSR report: Cybernetics, computers, and automation technology
[JPRS-UCC-85-002] 14 p2400 N85-24794
Systems design and application of computers with flexible architecture 14 p2401 N85-24800
The Multimission Image Processing Laboratory's virtual frame buffer interface
[NASA-CR-175655] 14 p2402 N85-24805
Executive control systems in the engineering design environment
[NASA-CR-172582] 14 p2406 N85-24835
Design and analysis of ordering and join for a multi-backed database system
[AD-A150711] 14 p2433 N85-25006
Rotorcraft digital advanced avionics system (RODAAS) functional description
[NASA-CR-166611] 15 p2468 N85-25237
Conversion of algorithms to custom integrated circuit devices
[AD-A151288] 15 p2547 N85-25720
Posing of the problem, status, and future of parallel computer architecture for image processing
15 p2622 N85-26155
The EGPA multiprocessor system and its possible application for pattern recognition tasks --- computer architecture 15 p2622 N85-26156
Computer architecture for image processing and pattern recognition in the Federal Republic of Germany. Status 1983, a review 15 p2623 N85-26161
Supercomputers and symbolic computation
[AD-A151376] 15 p2623 N85-26166
Role of supercomputers in energy research programs
[DE85-006865] 15 p2624 N85-26172
Computer technology advances exhibited
15 p2625 N85-26175
High-capacity real-time computer system for processing hydrophysical data 15 p2625 N85-26178
Mini- and microcomputer local control network architecture and design principles
15 p2625 N85-26179
Communication complexity of the Gaussian elimination algorithm on multiprocessors
[AD-A151691] 15 p2638 N85-26267
Recent advances in supercomputers
16 p2693 N85-26625
Navigation: Accounting for copy
16 p2695 N85-26641
A modular dissimilar redundant computer designed for high integrity control 16 p2714 N85-26751
Design and specification of a local area network architecture for use in real-time flight simulation
[AD-A152242] 16 p2716 N85-26762
Reliability models for dataflow computer systems
[NASA-CR-175813] 16 p2846 N85-27543
Evaluation of Ada (trademark) as a communications programming language, volume 1
[AD-A152314] 16 p2848 N85-27559
Evaluation of Ada (trademark) as a communications programming language. Volume 3: Trusted software application
[AD-A152316] 16 p2848 N85-27561
Continued development and implementation of the Universal Network Interface Device (UNID) 2, Digital Engineering Laboratory Network (DELNET), volume 1
[AD-A151935] 16 p2850 N85-27569
Continued development and implementation of the Universal Network Interface Device (UNID) 2 in the Digital Engineering Laboratory Network (DELNET), volume 2
[AD-A151947] 16 p2850 N85-27570
Complexity of dense linear system solution on a multiprocessor ring
[AD-A151970] 16 p2854 N85-27596
Multiple array processors for ocean acoustic problems
[AD-A152174] 16 p2860 N85-27641
Computational plasma physics and supercomputers, revision 1
[DE85-007228] 16 p2867 N85-27687
A modular dissimilar redundant computer designed for high integrity control 17 p2904 N85-27904
VLSI workshop and project: February - November 1982
[WSRL-0374-TR] 17 p2951 N85-28223

System Analysis for the Huntsville Operation Support Center, Distributed Computer System
[NASA-CR-171506] 17 p3015 N85-28642
Synchronization and fault-masking in redundant real-time systems
[NASA-TM-87476] 17 p3015 N85-28644
Interfacing the VAX 11/780 using Berkeley Unix 4.2.BSD and Ethernet based Xerox network systems, volume 1
[AD-A152953] 17 p3015 N85-28645
Interfacing the VAX 11/780 using berkeley UNIX 4.2BSD and Ethernet based Xerox Network Systems
[AD-A153174] 17 p3016 N85-28647
A high-accuracy optical linear algebra processor for finite element applications
[NASA-CR-175894] 17 p3017 N85-28658
Efficient parallel solution of linear systems
[AD-A152683] 17 p3018 N85-28663
France's use of Cray 1, plans for national supercomputer 18 p3086 N85-29093
Distributed database design tool
[AD-A153760] 18 p3200 N85-29850
A single chip VLSI architecture for radar signal processing 19 p3257 N85-30195
The BLAZE language: A parallel language for scientific programming
[NASA-CR-172615] 19 p3334 N85-30656
A parallelized point successive over-relaxation method on a multiple instruction multiple data stream computer
[AD-A154377] 19 p3337 N85-30679
Fault-tolerant computing research
[AD-A154082] 19 p3342 N85-30710
MECA: A multiprocessor concept specialized to Monte Carlo
[DE85-010791] 19 p3346 N85-30737
Design and implementation of an intelligence database
[AD-A154095] 19 p3361 N85-30973
Distributed implementation of functional program evaluation
[DE85-009573] 20 p3514 N85-31844
PIPE-1000: An implementation of piping on an HP-1000 minicomputer
[PB85-191955] 20 p3514 N85-31847
Proceedings of the 1st Workshop for the Design of Expert System Partial Differential Equation Solvers
[AD-A154192] 20 p3515 N85-31853
Globally-asynchronous locally-synchronous systems
[AD-A154624] 21 p3573 N85-32222
Secure digital voice communications in the Defense Data Network (DDN)
[AD-A154677] 21 p3574 N85-32226
Characteristics of a numerical fluid dynamics simulator
[DE85-009602] 21 p3586 N85-32290
Resource management for the tagged token dataflow architecture
[AD-A154773] 21 p3667 N85-32779
Real-time contour surface display generation
[AD-A155232] 21 p3668 N85-32780
Software for interactive on-line conferences
[AD-A154742] 21 p3670 N85-32801
HLLM software support
[AD-A154826] 21 p3671 N85-32805
Comparative study on data system architectures --- spacecraft data processing
[ESA-CR(P)-2015] 21 p3675 N85-32828
Simulation of complex three-dimensional flows
[NASA-TM-86773] 21 p3675 N85-32831
New developments on the core function for efficient implementation of the difficult residue number system operations
[AD-A154678] 21 p3676 N85-32834
Basic features of personal computers
22 p3766 N85-33344
Flat is not necessarily good
[DE85-012819] 22 p3830 N85-33723
Modular digital holographic fringe data processing system
[NASA-CR-177952] 23 p3933 N85-34376
The parser generator as a general purpose tool
[NASA-CR-177955] 23 p3957 N85-34521
Architecture of languages for large CAD systems development 23 p3962 N85-34557
A methodology for the design of testable custom large-scale integrated circuits
[AD-A156098] 24 p4090 N85-35351
Design for MISP: A multiple instruction stream shared pipeline processor
[AD-A156314] 24 p4136 N85-35635
Distribution of computer functionality for accelerator control at the Brookhaven AGS
[DE85-012520] 24 p4141 N85-35669
Report on the SLC control system
[DE85-013076] 24 p4148 N85-35722

ARCTIC ENVIRONMENTS
U ICE ENVIRONMENTS

ARCTIC OCEAN
Sea-level in the world ocean. Part 5. The North-East Pacific and Arctic Oceans, a catalogue of measurements
[CSIR-T/SEA-6303-5] 01 p0067 N85-10589
Active microwave measurements of sea ice under fall conditions: The RADARSAT/FIREX fall experiment --- in the Canadian Arctic
[E85-10019] 02 p0217 N85-11432
One-year records of current and bottom pressure in the strait between Nordaustlandet and Kvitoeya and Svalbard, 1980 - 1981
[AD-A145594] 02 p0233 N85-11518
Eastern-Western Arctic Sea ice analysis 1983
[AD-A146133] 03 p0398 N85-12541
Arctic ice island and sea ice movements and mechanical properties
[DE84-016323] 04 p0542 N85-13450
Satellite photographs suggest arctic volcano
07 p0982 N85-16239
Arctic marine acoustics
[AD-A147492] 07 p1039 N85-16594
Data report on variations in the composition of sea ice during MIZEX/East'83 with the Nimbus-7 SMMR
[NASA-TM-86170] 09 p1342 N85-18443
Ice statistics and acoustic scattering in the Arctic basin
[AD-A150141] 13 p2140 N85-23289
Sea-ice motion in response to geostrophic winds
14 p2323 N85-24357
Sea ice, climate and Fram Strait
15 p2603 N85-26042
Arctic mixed layer dynamics
[AD-A153582] 18 p3150 N85-29505
Transport and formation of summertime cloud condensation nuclei over the Arctic Ocean
21 p3651 N85-32686

ARCTIC REGIONS
Response of arctic ecosystems to elevated carbon dioxide regimes, volume 2
[DE84-015236] 01 p0069 N85-10460
Forecasting of polar lows 01 p0075 N85-10495
Arctic haze: Meteorological aspects of long-range transport 02 p0230 N85-11499
MIZEX. A program for mesoscale air-ice-ocean interaction experiments in arctic marginal ice zones. III: Modeling the marginal ice zone
[AD-A145351] 02 p0233 N85-11517
Evaluation of arctic test of improved tritium radioluminescent lighting
[DE84-014887] 05 p0597 N85-13805
USSR report: Earth sciences
[JPRS-UES-84-007] 06 p0819 N85-15196
Development of radar to measure sea ice merits prize nomination 06 p0826 N85-15244
Satellite photographs suggest arctic volcano
07 p0982 N85-16239
Parachute expedition to Arctic
07 p0982 N85-16240
MIZEX. A program for mesoscale Air-Ice-Ocean interaction experiments in arctic marginal ice zones. 4: Initial results and analysis from MIZEX 83
[AD-A148255] 08 p1173 N85-17399
Regional and seasonal variations in snow-cover density in the USSR
[AD-A148429] 08 p1189 N85-17496
Technology development for unmanned untethered submersible vehicle systems
[AD-A148794] 09 p1304 N85-18190
USSR report: Earth sciences
[JPRS-UES-85-003] 10 p1497 N85-19446
Types of placer formation of eastern Arctic shelf
10 p1498 N85-19452
MIZEX (Marginal Ice Zone Program): A program for mesoscale air-ice-ocean interaction experimemts in Arctic marginal ice zones. 5. MIZEX 84. Summer experiment PI (Principal Investigator) preliminary reports
[AD-A148986] 10 p1521 N85-19594
Arctic acoustic propagation model with ice scattering
[AD-A149430] 10 p1553 N85-19795
Cold Arctic Mesopause Project (CAMP): Scientific objectives 11 p1656 N85-20433
High time resolution thermospheric temperature and wind studies in the Arctic
[AD-A150114] 12 p1890 N85-21860
USSR report: Earth sciences
[JPRS-UES-85-002] 13 p2105 N85-23116
Arctic-North Atlantic rift megasystem
13 p2105 N85-23117
Application of field X-ray: Radiometric analysis in exploratory geology and means for its improvement
13 p2115 N85-23176
Empirical and modeled synoptic cloud climatology of the Arctic Ocean
[NASA-CR-175628] 13 p2137 N85-23272
Variation of Arctic cloud cover in summer
[DE85-004507] 13 p2139 N85-23285
Ice statistics and acoustic scattering in the Arctic basin
[AD-A150141] 13 p2140 N85-23289
High-frequency acoustic variability in the arctic
[AD-A150550] 13 p2155 N85-23363
Applications of ARGOS data collection systems in Arctic regions 14 p2238 N85-23875
Mountain barrier baroclinity effects on surface winds along the Alaskan Arctic coast 14 p2238 N85-23877
Applications of ARGOS data collection system for automatic meteorological observatories in Arctic regions
14 p2240 N85-23893
MI-8 helicopter cargo loading experiment for Arctic shipping 14 p2332 N85-24425
Substorm associated Pc 1 emission in the morning sub-cleft latitudes 14 p2368 N85-24637
Designer O. K. Antonov on new AN-74 arctic transport
15 p2467 N85-25230
The ecology of tundra ponds of the Arctic coastal plain: A community profile
[TI85-900650] 15 p2589 N85-25958
Mining cosmic dust from the blue ice lakes of Greenland 15 p2682 N85-26563
USSR report: Earth sciences
[JPRS-UES-85-005] 16 p2807 N85-27307
Operational experiences with the ARGOS system in Greenland 16 p2813 N85-27353
An assessment of atmospheric refractivity in the northern marginal ice zone
[AD-A152346] 17 p2992 N85-28493
Atmospheric cross sections for the Arctic gas and aerosol sampling program, March - April 1983
[NASA-CR-176027] 19 p3314 N85-30541
Arctic acoustic tomography MIZEX 84
[AD-A154426] 19 p3320 N85-30580
The COSPAS/SARSAT local user terminal in Tromso, Norway. Special considerations and experience with high latitude location (69 deg, 43 min N)
20 p3402 N85-31109
Mesoscale features and atmospheric refraction conditions of the Arctic marginal ice zone
[AD-A155139] 21 p3636 N85-32584
Condensation nuclei and aerosol size distribution measurements in Arctic haze 21 p3647 N85-32658
Arctic and offshore research
[DE85-001995] 22 p3818 N85-33653

AREA NAVIGATION
Evaluation of radio navigation systems and their configuration with respect to minimum cost
[ESA-TT-847] 20 p3392 N85-31043

ARGENTINA
Tectonic, volcanic, and climatic geomorphology study of the Sierras Pampeanas Andes, northwestern Argentina 08 p1144 N85-17215
Meteorological and oceanographic support during the Falklands conflict 11 p1712 N85-20769

ARGON
NT ARGON ISOTOPES
Experimental studies of atomic inner shell ionization phenomena
[DE84-013448] 01 p0118 N85-10805
Diffusion of gases in porous solids: Simulation and measurements
[DE84-016292] 04 p0500 N85-13191
The discharge mechanism of the high-temperature arc
[NASA-TM-77794] 07 p0922 N85-15837
Study of opacity effects on line radiation from pellet implosions
[DE85-000380] 10 p1491 N85-19413
The effect of inert gases on ion transport across the erythrocyte membrane
[AD-A148889] 10 p1527 N85-19635
Pseudo-stationary oblique-shock-wave reflections in a polyatomic gas, sulfur hexafluoride
[UTIAS-TN-253] 12 p1845 N85-21577
Performance of Chromel versus Alumel and Nicrosil versus Nisil thermocouple assemblies in vacuum and argon between 1000 deg C and 1200 deg C
[DE85-000810] 12 p1853 N85-21624
Argon ion pollution of the magnetosphere
13 p1998 N85-22523
Properties of welded joints in argon arc welding of titanium alloy using a protective coating
13 p2032 N85-22733
Threshold double photoionization of argon with synchrotron radiation
[AD-A150615] 13 p2157 N85-23369
Effectiveness of use of heat-dissipating clamps to reduce deformation during argon arc welding of thin sheets of AMg6 alloy 15 p2501 N85-25427
Spectroscopy of quasimolecular X-rays with H-like decelerated ions
[DE85-006565] 15 p2649 N85-26337
Welding of 11 458.1 steel in shielding atmospheres
[BLL-BISI-TRANS-21763-(9022.06)]
17 p2972 N85-28353

Hall mobility in fluid argon
[DE85-007288] 17 p3045 N85-28840
Structure and properties of VT23 alloy welded joints after thermocyclic processing 19 p3248 N85-30125
Environmental monitoring at Argonne National Laboratory
[DE85-010613] 19 p3309 N85-30516
Vibrational energy transfer in benzene-argon collisions
[DE85-009603] 19 p3355 N85-30797
Energy transfer and excimer formation in rare gas solids 19 p3374 N85-30930
Spectrographic investigation of low-voltage arc discharge in argon atmosphere
[BLL-M-36276-(5828.4)] 20 p3422 N85-31242
New metal coating method developed
21 p3568 N85-32191
Supersaturation obtained in a condensation nucleus counter 21 p3642 N85-32624
Influence of background electrically neutral argon admixture on mechanical strength of silicon crystals
21 p3683 N85-32878
Measurements of Fe and Ar fragmentation cross sections
[PAPER-OG-7.2-20] 21 p3714 N85-33047
Liquid crystal light valve structures
[NASA-CASE-MSC-20036-1] 22 p3847 N85-33826
Apparatus and method for the horizontal, crucible-free growth of silicon sheet crystals
[DE85-011586] 22 p3847 N85-33829
Thermodynamics of the corrosion of chromium in molten carbonates
[DE85-011407] 24 p4079 N85-35282
Size and shape dependence of CO adsorption sites on sapphire supported Fe microcrystals
[NASA-CR-176171] 24 p4160 N85-35794

ARGON ISOTOPES
Investigation of the daytime lunar atmosphere
[NASA-CR-175636] 14 p2440 N85-25057
The degassing history of the Earth: Noble gas studies of Archean cherts and zero age glassy submarine basalts 21 p3718 N85-33072
The 1984 environmental monitoring report, Sandia National Laboratories, Albuquerque, New Mexico
[DE85-011175] 22 p3811 N85-33607
Control technology for radioactive emissions to the atmosphere at US Department of Energy facilities: The Los Alamos Meson Physics Facility
[DE85-011402] 22 p3811 N85-33609
Measurements of the fragmentation of (40)Ar, (28)Si and (12)C in CH2C and H targets between 300 and 1500 MeV/nuc at the Bevalac
[OG-7.2-19] 23 p4016 N85-34886
Measurements of Fe and Ar fragmentation cross sections
[OG-7.2-20] 23 p4016 N85-34887
Correlation between solar neutrino flux and other solar phenomena 23 p4049 N85-35109
The conjecture concerning time variations in the solar neutrino flux
[SH-8.1-6] 23 p4049 N85-35111

ARGON LASERS
Excimer laser photofragmentation of organophosphonates. 1: Detection of the PO radical from dimethyl methyl phosphonate (DMMP)
[AD-A149471] 10 p1490 N85-19407
Linewidth and bandwidth measurements of the q-branch of h2 using CW coherent anti-Stokes Raman spectroscopy
[AD-A151868] 15 p2506 N85-25456
Fiber optic Raman thermometer for Space Shuttle main engine preburner profiling 16 p2739 N85-26904
A study of mode-locked argon ion-dye laser systems
16 p2789 N85-27205
Photochemical ignition studies. 1: Laser ignition of flowing premixed gases
[AD-A153046] 17 p2920 N85-28002
Investigation of several low-lying levels of X doublet pi state of NCO using argon laser excited fluorescence
[AD-A153693] 18 p3071 N85-28994

ARGON PLASMA
Spatial resolution of small particles in silane discharge
[AD-A150953] 14 p2423 N85-24948
Temperature, velocity, and species mapping in an induction plasma
[DE85-004005] 15 p2512 N85-25499
Experiments in plasma initiation and laser absorption in flowing gases
[AD-A154303] 19 p3276 N85-30313
Synthesis of ultrafine ceramic and metallic powders in a thermal argon rf plasma
[DE85-009634] 23 p3983 N85-34696

ARGUMENTS (MATHEMATICS)
U INDEPENDENT VARIABLES

ARIANE LAUNCH VEHICLE
View of Ariane countdown procedures, Kourou launch facilities 03 p0310 N85-12001
Launching systems
[CNES-NT-111] 04 p0460 N85-12917
Relationships between Ariane trajectories and satellite orbits 05 p0599 N85-13815
British aerospace studies HOTOL satellite launcher
10 p1460 N85-19206
The ARIANE family 11 p1712 N85-20774
Ignition, separation of boosters, stages in Ariane 3
14 p2289 N85-24185
Studies on rocket engines for future European launchers
[SEP-TPRL/K-19572/84] 15 p2495 N85-25393
Calender of Ariane launches 1984 - 1987
15 p2523 N85-25554
Costs, payload of Ariane, US Space Shuttle compared
15 p2530 N85-25601
West Europe report: Science and technology
[JPRS-WST-84-027] 15 p2532 N85-25612
France officially proposes development of Ariane 5 to ESA 15 p2532 N85-25613
SEP of France to make Ariane HM-60 cryogenic engine 15 p2532 N85-25614
West Europe report: Science and technology
[JPRS-WST-84-026] 15 p2532 N85-25617
French CNES official describes Ariane V launcher
15 p2532 N85-25619
The Ariane launch vehicle is the key of the Europeans to the space market 17 p2906 N85-27931
Structure of SYLDA double launch system for Ariane
17 p2946 N85-28185
Documentation for the West German Federal Cabinet's space policy decision 17 p3051 N85-28886
Space insurance firms view shuttle, Ariane reliability
18 p3086 N85-29090
Ariane space general director on satellite launcher market 18 p3087 N85-29103
FRG weighs ESA participation, budget issues
18 p3088 N85-29110
DFVLR study recommends European independence in space systems 18 p3088 N85-29111
Ariane launcher system. Pyrotechnics subsystem: Definition of chains and pyrotechnic components
[CNES-84/CT/DRT/SST/SE/242(1)]
20 p3398 N85-31081

ARID LANDS
Australian Multiexperimental Assessment of SIR-B (AMAS) 08 p1146 N85-17243
Vegetation analysis for arid lands geobotany
[NASA-CR-175455] 10 p1506 N85-19500
Work physiology of operating personnel at power plants in arid regions 10 p1523 N85-19606
Evaluation of carrying capacity and landscape damage in northern Kenya by multistage remote sensing
[DFVLR-FB-84-47] 14 p2347 N85-24514
Screening Prosopis (mesquite) species for biofuel production on semi-arid lands
[DE85-010048] 19 p3302 N85-30471
Comprehensive mapping of arid territories of Arizona using space photography 22 p3737 N85-33164
Resource evaluation and site selection for microalgae production systems
[DE85-006807] 23 p3951 N85-34485
Remote sensing of hydrologic transport processes using spot simulation data
[DE85-012412] 24 p4106 N85-35467

ARIETID METEOROIDS
Observations of RR Lyrae and X Arietis with the IUE satellite 11 p1754 N85-21030

ARIP (IMPACT PREDICTION)
U COMPUTERIZED SIMULATION
U IMPACT PREDICTION

ARITHMETIC
NT FIXED POINT ARITHMETIC
NT FLOATING POINT ARITHMETIC
Electrooptical matrix multiplication using the twos complement arithmetic for improved accuracy
[AD-D011252] 05 p0728 N85-14682
Digital high speed programmable convolver
[AD-D011455] 10 p1481 N85-19348
Propagation of numerical errors in computers and numerical quality 14 p2396 N85-24760
Arithmetic and elementary functions on mini and microcomputers 14 p2396 N85-24761
Numerical optical computing at the Ohio State University 18 p3188 N85-29775

ARITHMETIC AND LOGIC UNITS
Hardware multiplier processor
[DE84-006174] 05 p0713 N85-14574

ARIZONA
Hydrogeochemical investigation of thermal springs in the Black Canyon-Hoover Dam area, Nevada and Arizona
[PB84-202472] 01 p0064 N85-10428
Control aspects of the Schuchuli Village stand-alone photovoltaic power system
[NASA-TM-83790] 04 p0495 N85-13157
CO-2-silica geothermometer for low temperature geothermal resource assessment, with application to resources in the Safford Basin, Arizona
[DE84-013958] 04 p0534 N85-13411
Intraband radiometric performance of the LANDSAT 4 Thematic Mapper — Washington, DC, Arkansas, Massachusetts, Virginia, and Arizona
12 p1871 N85-21738
The geology of Mt. Hope, a silicic volcanic center in West Central Arizona 13 p2187 N85-23571
Preliminary assessment of climatic change during late Wisconsin time, southwest Great Basin and vicinity, Arizona, California and Nevada
[DE85-008343] 16 p2838 N85-27488

ARKANSAS
Sedimentary petrology and provenance of the upper Jackforth Sandstone (Morrowan) Quachita Mountains, Arkansas, USA 08 p1182 N85-17447
Scan angle and detector effects in Thematic Mapper radiometry — Iowa and Arkansas
12 p1871 N85-21735
Intraband radiometric performance of the LANDSAT 4 Thematic Mapper — Washington, DC, Arkansas, Massachusetts, Virginia, and Arizona
12 p1871 N85-21738

ARM (ANATOMY)
NT ELBOW (ANATOMY)
Simple nonrestrictive arm restraint system
[AD-D011216] 01 p0005 N85-10026
Electromyographic patterns associated with discrete limb movements 05 p0710 N85-14551
Windblast arm protector assembly
[AD-D011512] 12 p1909 N85-21984
Postural adjustments associated with arm movements in weightlessness 20 p3509 N85-31813

ARMATURES
Metal armatures for railguns
[AD-A152129] 16 p2728 N85-26838

ARMED FORCES
NT ARMED FORCES (FOREIGN)
NT ARMED FORCES (UNITED STATES)
NT NAVY
Maintenance and the military environment
22 p3750 N85-33243

ARMED FORCES (FOREIGN)
Conceptual model of critical requirements for effective pilot performance in high performance aircraft
10 p1533 N85-19663
A review of fatality, impairment of consciousness and head and neck injury on Royal Air Force ejections 1968-1981 12 p1907 N85-21975
Correlations between selection ratings and success as army aviators
[FOA-C-53020-H2] 15 p2620 N85-26144
Investigation of the requirement for auxiliary heating of Canadian forces personnel
[AD-A151950] 16 p2841 N85-27522
Soviet weapons development and the scientific community
[AD-P004562] 17 p3047 N85-28857
The revolution in military affairs and the Soviet system
[AD-P004568] 17 p3048 N85-28863

ARMED FORCES (UNITED STATES)
Self-paced instruction. Factors critical to implementation in Air Force technical training: A preliminary inquiry
[AD-A145098] 01 p0097 N85-10647
Air Force Human Resources Laboratory report: Fiscal year, 1983
[AD-A145647] 02 p0238 N85-11548
AFHRL (Air Force Human Resources Laboratory) program for artificial intelligence applications to maintenance and training
[AD-P003931] 02 p0247 N85-11611
United States Air Force on research on algebraic manipulation
[AD-A145737] 02 p0253 N85-11655
NEO robotic application development at Letterkenny Army Depot: The application of robotics to agricultural blast cleaning
[AD-P004007] 03 p0308 N85-11987
Air Force Materials Laboratory plans/projects
[AD-P004010] 03 p0308 N85-11990
Potential application of robotics and state-of-the art end effectors at Letterkenny Army Depot
[AD-P004015] 03 p0309 N85-11994
Field applications for robotic materiel handling
[AD-P004016] 03 p0309 N85-11995
The role of physical and physiological capacities and their modification on the tolerance to various stress experienced by Air Force personnel
[AD-A145779] 03 p0400 N85-12550
Cardiovascular disease among U.S. Navy pilots
[AD-A145871] 03 p0400 N85-12552
An update on the capabilities of the Air Force Computerized Occupational Health Program (COHP)
[AD-P004037] 06 p0845 N85-15367

The Air Force stock fund and aircraft availability
[AD-A148868] 08 p1067 N85-16761
Utilization of Increased Airlift Capability (UIAC) study
[AD-A148869] 08 p1081 N85-16847
Design of an evaluation system to measure performance degradation due to continuous operations
[AD-A148186] 08 p1200 N85-17556
Reflections on trends in dynamics: The Navy's perspective 09 p1334 N85-18382
Compatible goals: Defense and environmental protection
[AD-P004137] 09 p1347 N85-18473
Closed-loop concepts for the Army: Water conservation, recycle, and reuse
[AD-A148639] 09 p1365 N85-18581
Catalog of completed studies, US Army health care studies and clinical investigation activity
[AD-A149450] 10 p1566 N85-19885
Air Force Office of Scientific Research (AFOSR) technical report summaries. Third quarter (CY)
[AD-A149965] 10 p1573 N85-19918
1983 Air Force bird strikes
[AD-P004182] 11 p1579 N85-19944
Tactical operations and space applications
11 p1709 N85-20752
US MILSATCOM: Present and future
11 p1709 N85-20753
Military applications of meteorological satellite (METSAT) data 11 p1711 N85-20767
Air Force Academy Aeronautics Digest
[AD-A149614] 12 p1769 N85-21104
A review of fatality, impairment of consciousness, and head/neck injury on USAF ejections 1971 - July 1983
12 p1906 N85-21974
Fiscal year 1986 technical objective document
[AD-A151039] 14 p2432 N85-25000
Air Force Office of Scientific Research (AFOSR): Technical report summaries. Fourth quarter (CY)
[AD-A150660] 14 p2456 N85-25167
Manufacturing methods and technology CAD/CAM (Computer-Aided Design/Computer-Aided Manufacturing) related efforts (FY 1980 - 1986)
[AD-A151617] 16 p2846 N85-27547
Continued development and implementation of the Universal Network Interface Device (UNID) 2 in the Digital Engineering Laboratory Network (DELNET), volume 2
[AD-A151947] 16 p2850 N85-27570
Computer assisted flight schedule optimization
[AD-A151689] 16 p2858 N85-27623
Summary of Research, Academic Departments, 1983 - 1984
[AD-A151724] 16 p2875 N85-27741
Rome Development Center Air Force technical objective document C3I FY-86
[AD-A152476] 17 p3047 N85-28851
Air Force technical objective document FY 86
[AD-A152730] 17 p3047 N85-28855
Air Force Federal Photovoltaic Utilization Program
[DE85-010612] 20 p3484 N85-31648
Air force technical objective document, Aerospace Medical Division, Fiscal Year 1986
[AD-A155195] 21 p3664 N85-32762
Feasibility of applications of Competition Decision Assist Package (CDAP) to spare parts
[AD-A154716] 21 p3712 N85-33036
Air Force Office of Scientific Research (AFOSR). Technical report summaries: First quarter (CY)
[AD-A154757] 21 p3713 N85-33041
U.S. Civil airmen statistics for calendar year 1984
[AD-A156326] 24 p4059 N85-35153
Laboratory vibration schedules
[AD-A155856] 24 p4084 N85-35188
United States Army welding research and development topical and coordination meeting
[AD-A155834] 24 p4099 N85-35409
Solar pond technology for Navy applications
[AD-A155877] 24 p4112 N85-35488
Air university commander's and supervisor's guide on substance abuse
[AD-A156336] 24 p4133 N85-35622

ARMOR
Penetrator/armour interactions: Background to Australian work
[MRL-R-936] 03 p0367 N85-12353
Thermal contact conductance measurements on Doublet 3 armor tile traphite
[DE84-013554] 05 p0613 N85-13916
Production verification of the acoustic emission weld monitor
[AD-A154168] 20 p3464 N85-31519

AROMATIC COMPOUNDS
Liquid phase products and solid deposit formation from thermally stressed model jet fuels
[NASA-TM-86874] 04 p0481 N85-13066
Prediction of retention indices of polynuclear aromatic hydrocarbons. Part 1: HPLC on nitrogen containing normal phase packing materials
[DE85-001302] 10 p1436 N85-19051
Desorption efficiences of vapor phase polynuclear aromatic compounds on solid adsorbents
[DE85-001303] 10 p1436 N85-19052
Fuels combustion research
[AD-A149106] 10 p1457 N85-19178
Quantitative determination of compound classes in jet turbine fuels by high performance liquid Chromatography/Differential refractive index detection: Part 2
[AD-A149296] 11 p1613 N85-20144
Electrostatic potentials: A new method for interpreting and predicting molecular reactivities and for designing synthetic pathways. Applications to nitroaromatics, nitramines and nitrated
[AD-A150120] 12 p1801 N85-21296
Spray pyrolysis as a synthetic tool
[AD-A153691] 19 p3234 N85-30047
Experimental studies of chemical reactivity during shock initiation of hexanitrostilbene
[DE85-011726] 22 p3754 N85-33270

ARRAYS
NT ANTENNA ARRAYS
NT LINEAR ARRAYS
NT MULTISPECTRAL LINEAR ARRAYS
NT PHASED ARRAYS
NT SOLAR ARRAYS
NT SOLAR BLANKETS
NT STEERABLE ANTENNAS
Data flow computer architecture
[DE84-014362] 01 p0100 N85-10664
Automated installation methods for photovoltaic arrays 2
[SAND-84-7035] 02 p0222 N85-11453
Modular photovoltaic array field
[SAND-83-7026] 02 p0222 N85-11454
Modular detonator device
[AD-D011232] 03 p0340 N85-12184
Chemical derivatization of an array of three gold microelectrodes with polypyrrole: Fabrication of a molecule-based transistor
[AD-A146221] 03 p0359 N85-12304
Heatsink requirements for coherent operation of high-power semiconductor laser arrays
[AD-A146184] 03 p0366 N85-12346
Use of monitors in FORTRAN: A tutorial on the barrier, self-scheduling DO-loop and Askfor monitors
[DE84-016506] 05 p0715 N85-14587
Fly's eye sensor nonlinear signal processing
[AD-D011290] 05 p0729 N85-14684
Algebraic techniques in systolic array design
[AD-A146417] 06 p0857 N85-15451
Transmission line biased coherent array of Josephson oscillators
[AD-D011323] 07 p0944 N85-15979
RF laser array driver apparatus
[AD-D011375] 07 p0969 N85-16155
Phased locked array laser systems
[AD-D011317] 07 p0971 N85-16164
The development and test of ultra-large-format multi-anode microchannel array detector systems
[NASA-CR-174247] 07 p1043 N85-16622
Switchable zero order diffraction gratings as light valves
[AD-A147575] 07 p1044 N85-16633
A variable length and sensor spacing thermistor array
[AD-D011416] 08 p1113 N85-17017
Coherent array of Josephson oscillators with external bias leads
[AD-D011367] 08 p1156 N85-17293
The use of self-scanned silicon photodiode arrays for astronomical spectrophotometry
08 p1252 N85-17907
Photometry with Multi-Anode Microchannel Arrays (MAMAs) and Charge Injection Devices (CIDs)
08 p1252 N85-17909
Signal Hill solar-powered repeater report and recommendations
[DE85-000487] 09 p1316 N85-18273
An electronically controlled array for simulation of passive target/background signatures at millimeter wavelengths
[AD-D011456] 10 p1468 N85-19263
An evaluation of wind measurements by four Doppler sodars
[PB85-115301] 10 p1520 N85-19586
Natural convection heat transfer between arrays of horizontal cylinders and their enclosure
[DE85-003773] 11 p1632 N85-20260
Double pinhole spatial phase correlator apparatus
[AD-D011495] 11 p1729 N85-20872
Experimental test of the three subaperture method for estimating target elevation angle
[AD-A149887] 12 p1851 N85-21614
Monolithic short wave infrared (SWIR) detector array
[NASA-CR-175284] 12 p1874 N85-21759
Stability of vortex structures during separation flow past array of wings 14 p2278 N85-24110
Bipolar nonswitching logic arrays: Universal components of function expanders for computation of elementary functions 14 p2400 N85-24787
A multi-element ultrasonic ranging array
[AD-A150898] 14 p2416 N85-24908
Performance of charge-injection-device infrared detector arrays at low and moderate backgrounds
[NASA-TM-86667] 15 p2560 N85-25793
Method and apparatus for generating a structured light beam array
[AD-D011580] 15 p2652 N85-26357
Maintenance of photovoltaic power systems
[AD-A152299] 16 p2819 N85-27390
Analysis and modeling for thermal focal plane arrays
[AD-A153156] 17 p2968 N85-28329
Chemometric analysis of multisensor arrays
[AD-A153605] 18 p3174 N85-29660
Physiochemically controlled scour jet array system
[AD-D011668] 19 p3306 N85-30505
Nested dissection on a mesh-connected processor array
[AD-A154088] 19 p3342 N85-30711
Hierarchical beamforming with application to a large aperture array system 20 p3439 N85-31345
A multiplying slot array
[AD-A155570] 21 p3576 N85-32245
The dynamics of slack marine cables
[AD-A155022] 21 p3599 N85-32349
The Norwegian seismic array (NORSAR)
[AD-A154751] 21 p3631 N85-32555
The moving thermoacoustic array: A theoretical feasibility study
[AD-A154510] 21 p3699 N85-32980
Estimating angular position of optical radiation source when received by array of photodetectors
22 p3778 N85-33413
Synthesis of metrico-topological model for layout of topology of large-scale-integration arrays
22 p3781 N85-33427
Mosaic Infrared Sensor for Space Astronomy (MIRSSA)
[NASA-CR-176154] 22 p3786 N85-33456
Electromagnetic inspection of wire ropes using sensor arrays
[AD-A155412] 22 p3795 N85-33509
MORSE-CGA: A Monte Carlo radiation transport code with array geometry capability
[DE85-012063] 22 p3830 N85-33718
Air shower arrival directions measured at Buckland Park
[OG-5.3-11] 22 p3885 N85-34077
Hexagonal uniformly redundant arrays for coded-aperture imaging
[OG-9.2-1] 23 p4024 N85-34940
Mini and super mini arrays for the study of highest energy cosmic rays
[OG-9.4-9] 23 p4029 N85-34976
Angular resolution of air-shower array-telescopes
[OG-9.5-6] 23 p4030 N85-34983
Astrophysical applications of high angular resolution array-telescopes
[OG-9.5-7] 23 p4031 N85-34984
Angular resolution of an EAS array for gamma ray astronomy energies 5 x 10 (13) eV
[OG-9.5-8] 23 p4031 N85-34985
The ISAVF opto-mechanical test bed
[NASA-TM-87505] 24 p4067 N85-35206
Heat transfer characteristics for two-dimensional arrays of impinging jets with initial crossflow
24 p4092 N85-35365
Measurement of shower electrons and muons using a small air shower array
[HE-4.3-11] 24 p4192 N85-36005

ARRESTING GEAR
Aircraft barricade
[AD-D011316] 07 p0910 N85-15761

ARRHYTHMIA
Mapping of mammalian arrhythmias with the cardiac laser scanner 03 p0399 N85-12545

ARSENIC
The influence of manganese on intercrystalline internal adsorption of arsenic in low carbon steel
[BLL-M-35965-(5828.4)] 05 p0615 N85-13931
Environmental surveillance at Los Alamos during 1984
[DE85-011886] 22 p3811 N85-33605

ARSENIC ALLOYS
Structural studies of sputtered Ni-As-O films
[DE85-003229] 11 p1605 N85-20095

ARSENIC COMPOUNDS
NT ALUMINUM GALLIUM ARSENIDES
NT GALLIUM ARSENIDES
NT INDIUM ARSENIDES
Effect of light pulses on film of chalcogenide vitreous semiconductors 02 p0258 N85-11687
Compositional, structural, and physical studies of some graphite hexafluoroarsenates and their relatives
[DE85-000855] 10 p1432 N85-19030

ARSENIDES
NT ALUMINUM ARSENIDES
NT ALUMINUM GALLIUM ARSENIDES
NT GALLIUM ARSENIDES
NT INDIUM ARSENIDES

ARTERIES
Pulmonary blood flow and oxygenation of arterial blood in a healthy subject upon 7 days hypokinesia
07 p1014 N85-16439
Analysis of the transient response of temporal artery blood flow data relative to various anti-G suit pressure schedules 10 p1533 N85-19660
Analysis of the transient response of temporal artery blood flow data relative to various anti-G suit pressure schedules
[AD-A155242] 21 p3686 N85-32775

ARTERIOSCLEROSIS
Tolerance to +Gz and +Gx accelerations of individuals in older age groups in good health and with early signs of arteriosclerosis 23 p3952 N85-34496

ARTHROPODS
NT INSECTS
NT LARVAE
NT SPIDERS

ARTIFICIAL CLOUDS
NT BARIUM ION CLOUDS

ARTIFICIAL GRAVITY
Proceedings of a Workshop on Applications of Tethers in Space, Volume 2
[NASA-CR-171197] 03 p0322 N85-12077
Tethers open new space options
11 p1642 N85-20340
Physiological considerations of artificial gravity
11 p1643 N85-20351
Summary presentation to the Artificial Gravity Panel
11 p1644 N85-20356
Physiological considerations of artificial gravity
11 p1645 N85-20366
Artificial gravity: Tethers and containers
11 p1645 N85-20367

ARTIFICIAL INTELLIGENCE
NT COGNITIVE PSYCHOLOGY
NT EXPERT SYSTEMS
Terrain navigation concepts for autonomous vehicles
[AD-A144994] 01 p0005 N85-10031
A review of selected studies of computerized speech recognition conducted at the Naval Postgraduate School
[AD-A144841] 01 p0037 N85-10235
Feature discovery by competitive learning
[AD-A145052] 01 p0097 N85-10646
Office of Technology Assessment
01 p0127 N85-10672
Toward a computational neuropsychology of high-level vision
[AD-A145711] 02 p0236 N85-11540
Artificial Intelligence in Maintenance: Proceedings of the Joint Services Workshop
[AD-A145349] 02 p0244 N85-11592
The need for improvements in weapon system maintenance: What can AI (Artificial Intelligence) contribute?
[AD-P003913] 02 p0244 N85-11593
Artificial intelligence applications to maintenance
[AD-P003914] 02 p0244 N85-11594
On applying AI (Artificial Intelligence) to maintenance and troubleshooting
[AD-P003915] 02 p0244 N85-11595
Overview of training and aiding
[AD-P003917] 02 p0245 N85-11597
AI (Artificial Intelligence) approaches to troubleshooting
[AD-P003918] 02 p0245 N85-11598
Failure detection processes by pattern recognition and expert systems
[AD-P003924] 02 p0246 N85-11604
GUIDON
[AD-P003925] 02 p0246 N85-11605
Designing an expert system for training automotive electrical troubleshooting
[AD-P003926] 02 p0246 N85-11606
Models of natural intelligence in fault diagnosis tasks: Implications for training and aiding of maintenance personnel
[AD-P003927] 02 p0246 N85-11607
The psychology of technical devices and technical discourse
[AD-P003929] 02 p0246 N85-11609
Artificial intelligence approaches to monitoring system integrity
[AD-P003930] 02 p0246 N85-11610
AFHRL (Air Force Human Resources Laboratory) program for artificial intelligence applications to maintenance and training
[AD-P003931] 02 p0247 N85-11611
Artificial intelligence contributions to training and maintenance
[AD-P003934] 02 p0247 N85-11614
NAVAIR's (Naval air systems command) AI (Artificial Intelligence) program for ATE (Automated Test Equipment)
[AD-P003935] 02 p0247 N85-11615
Artificial intelligence applications to automatic test equipment
[AD-P003936] 02 p0247 N85-11616
Model-based probabilistic reasoning for electronics troubleshooting
[AD-P003937] 02 p0247 N85-11617
Implications of artificial intelligence for a user defined technical information system
[AD-P003938] 02 p0248 N85-11618
Application of artificial intelligence to equipment maintenance
[AD-P003939] 02 p0248 N85-11619
DELTA: An expert system for diesel electric locomotive repair
[AD-P003941] 02 p0248 N85-11621
An effective graphics user interface for rules and inference mechanisms
[AD-P003942] 02 p0248 N85-11622
The ACE (Automated Cable Expert) experiment: Initial evaluation of an expert system for preventive maintenance
[AD-P003943] 02 p0248 N85-11623
The application of artificial intelligence to a maintenance and diagnostic information system
[AD-P003945] 02 p0249 N85-11625
Intelligent information retrieval from on-line technical documentation
[AD-P003946] 02 p0249 N85-11626
On the requirements of expert systems for fault isolation
[AD-P003947] 02 p0249 N85-11627
Memory-based expert systems
[AD-A145612] 02 p0249 N85-11628
Constraint-based scheduling in an intelligent logistics support system: An artificial intelligence approach
[AD-A145613] 02 p0293 N85-11900
Air Force Materials Laboratory plans/projects
[AD-P004010] 03 p0308 N85-11990
Status and prospects of computational fluid dynamics for unsteady transonic viscous flows
[NASA-TM-86018] 03 p0315 N85-12037
West Europe report: Science and technology, no. 166
[JPRS-84845] 03 p0341 N85-12190
French firms develop artificial intelligence robot
03 p0341 N85-12192
East Europe report: Scientific affairs, no. 791
[JPRS-84624] 03 p0341 N85-12195
Technological institute director views artificial intelligence 03 p0341 N85-12197
The search for regularity: Four aspects of scientific discovery
[AD-A145939] 03 p0366 N85-12355
Research in knowledge representation for natural language understanding
[AD-A145807] 03 p0409 N85-12613
Test-bed for programmable automation research. Phase 1
[AD-A145872] 03 p0409 N85-12614
Knowledge representation and natural-language semantics
[AD-A146025] 03 p0409 N85-12615
Psychological issues in the design of expert systems
[AD-A146081] 03 p0436 N85-12792
Technologies for space station autonomy
[NASA-CR-174112] 04 p0458 N85-12906
Definition of technology development missions for early Space Station satellite servicing. Volume 1: Executive summary
[NASA-CR-171228] 04 p0460 N85-12922
Soviet robot exhibition reviewed
04 p0491 N85-13128
Development, new application of Soviet robots
04 p0491 N85-13129
Expert systems in design and manufacture
[DE84-005522] 04 p0550 N85-13496
Minimal cut-set methodology for artificial intelligence applications
[DE84-016674] 04 p0553 N85-13518
Real-time planning by an intelligent robot
[DE84-016669] 04 p0553 N85-13519
Induction of fuzzy decision rules
[INPE-3053-PRE/474] 04 p0554 N85-13525
Getting mental models and computer models to cooperate 05 p0709 N85-14548
Knowledge-based communication and management support in a system development environment
05 p0717 N85-14586
Use of artificial intelligence and simple mathematics to analyze a physiological model 05 p0717 N85-14597
Multi-disciplinary techniques for understanding time-varying space-based imagery
[AD-A144357] 05 p0728 N85-14681
Interpretation of natural language database queries using optimization methods 05 p0735 N85-14723
Crewstation design and validation
06 p0752 N85-14822
Recent advances in data compression
[DE85-001133] 06 p0854 N85-15432
Research on introspective systems
[AD-A146406] 06 p0870 N85-15530
Vision by man and machine: How the brain processes visual information may be suggested by studies in computer vision (and vice versa)
[AD-A147890] 07 p1017 N85-16458
Interaction of human cognitive models and computer based models in supervisory control
[AD-A142547] 07 p1020 N85-16474
Implementation of a constraint machine for prism - A parallel problem solver
[AD-A147844] 07 p1026 N85-16512
Avionics fault tree analysis and artifical intelligence for future aircraft maintenance 08 p1066 N85-16755
New applications for robot loaders, unloaders
08 p1139 N85-17175
East Europe report: Science and technology
[JPRS-ESA-84-046] 08 p1139 N85-17176
Researchers on third generation robotics development
08 p1140 N85-17184
Robotics research, integration overview presented. Application objectives cited 08 p1142 N85-17201
Probabilistic analysis of algorithms for NP-Complete problems
[AD-A148207] 08 p1215 N85-17653
The optimal control and design of a flexible manipulator arm 09 p1327 N85-18340
Strategy planning by an intelligent machine
[DE84-016609] 09 p1372 N85-18624
Researchers, projects at French intelligent machine center 10 p1460 N85-19207
French firm develops 2D, 3D computer vision system
10 p1461 N85-19208
Dean of Kiev State University on impact of robots
10 p1461 N85-19213
On motion planning with uncertainty: Revised
[AD-A149521] 10 p1492 N85-19421
Research on knowledge delivery
[AD-A149505] 10 p1538 N85-19696
Qualitative process theory
[AD-A148967] 10 p1543 N85-19729
French plans for fifth generation computer systems
[AD-A149435] 10 p1544 N85-19732
Proceedings of the 14th Army Science Conference. Volume 1: Principal Authors A through H
[AD-A149200] 10 p1573 N85-19920
A functional vehicle for autonomous mobile robot research
[AD-A150052] 12 p1860 N85-21666
Dynamic visual servo control of robots: An adaptive image-based approach
[AD-A150057] 12 p1860 N85-21667
The automated reasoning system ITP
[ANL-84-27] 12 p1914 N85-22016
Characterizing the parallelism in rule-based expert systems
[DE85-002432] 12 p1919 N85-22047
Aviation maintenance computerized management information systems: Perspective for the future
[AD-A150637] 13 p1966 N85-22349
Advancing automation and robotics technology for the Space Station and for the US economy. Volume 1: Executive overview
[NASA-TM-87566-VOL-1] 13 p1986 N85-22460
Advancing automation and robotics technology for the Space Station and for the US economy, volume 2
[NASA-TM-87566-VOL-2] 13 p1987 N85-22461
The potential for advanced computerized aids for comprehensible writing of technical documents
[AD-A150501] 13 p2055 N85-22870
Artificial Intelligence and Bionics Workshop held at Stowe, Vermont on 11-15 June 1984
[AD-A150463] 13 p2149 N85-23339
Research needs for artificial intelligence applications in support of C3 (Command, Control, and Communication)
[AD-A150867] 14 p2292 N85-24210
Some critical factors that limit the effectiveness of machine intelligence technology in military systems applications
[AD-A150684] 14 p2407 N85-24838

Artificial intelligence applications to testability
[AD-A150694] 14 p2407 N85-24839
Semantic networks and neural nets
[AD-A150750] 14 p2407 N85-24840
Our future in the cosmos: Computers
14 p2432 N85-24997
Documentation for the machine-readable version of the Stellar Spectrophotometric Atlas, 3130 A lambda 10800 A of Gunn and Stryker (1983)
[NASA-TM-87437] 14 p2438 N85-25045
Documentation for the machine-readable version of A Library of Stellar Spectra (Jacoby, Hunter and Christian 1984)
[NASA-TM-87438] 14 p2438 N85-25046
Documentation for the machine-readable version of A Finding List for the Multiplet Tables of NSRDS-NBS 3, Sections 1-10 (Adelman, Adelman, Fischel and Warren 1984)
[NASA-TM-87440] 14 p2438 N85-25048
Documentation for the machine-readable version of the Cordoba Durchmusterung (CD)
[NASA-TM-87441] 14 p2439 N85-25049
Documentation for the machine-readable version of the Cape Photographic Durchmusterung (CPD)
[NASA-TM-87442] 14 p2439 N85-25050
Documentation for the machine readable version of the Yale Catalogue of the Positions and Proper Motions of Stars between Declinations -60 deg and -70 deg (Fallon 1983)
[NASA-TM-87443] 14 p2439 N85-25051
Status and prospects of computational fluid dynamics for unsteady transonic flow 15 p2459 N85-25180
An approach to planning in the inflight emergency domain
[AD-A151869] 15 p2467 N85-25226
Artificial intelligence based control of a sensor-driven machine
[DE85-006972] 15 p2633 N85-26227
Generation of flight paths using heuristic search
[AD-A151949] 16 p2704 N85-26694
Symbiosis between postgraduate training and research projects: A successful experience
[INPE-3216-PRE/569] 16 p2810 N85-27330
Diagnosis: Using automatic test equipment and an artificial intelligence expert system
[AD-A151916] 16 p2851 N85-27576
Artificial intelligence in space platforms
[AD-A152078] 16 p2851 N85-27578
Research in knowledge representation for natural language understanding
[AD-A152260] 16 p2851 N85-27579
Application of artificial intelligence (AI) to radar image understanding
[AD-A152519] 17 p3017 N85-28654
A study of user-defined searching requirements for the on-line version of the directory of DOD-sponsored R and D data bases on the Defense Gateway computer system
[AD-A153000] 17 p3050 N85-28878
Applications of some artificial intelligence methods to satellite soundings 18 p3141 N85-29446
Hybrid uncertainty theory
[DE85-008357] 18 p3167 N85-29622
The application of artificial intelligence techniques to large distributed networks
[NASA-CR-177346] 19 p3344 N85-30721
An artificial intelligence based framework for planning air launched cruise missile missions
[AD-A154466] 19 p3344 N85-30722
Data communications-Oriented Production System Language (CPSL)
[DE85-011457] 20 p3440 N85-31352
Distributed implementation of functional program evaluation
[DE85-009573] 20 p3514 N85-31844
Proceedings of the 1st Workshop for the Design of Expert System Partial Differential Equation Solvers
[AD-A154192] 20 p3515 N85-31853
The documentation assistant: An intelligent system for documentation
[AD-A154709] 21 p3670 N85-32800
Space station automation and robotics study. Operator-systems interface
[NASA-CR-176095] 22 p3738 N85-33172
Space robot simulator vehicle
[NASA-CR-176133] 22 p3739 N85-33176
Future of robots in nuclear plants and processes
[DE85-011505] 22 p3793 N85-33500
Machine intelligence for robotics applications
[DE85-011430] 22 p3793 N85-33503
Flat is not necessarily good
[DE85-012819] 22 p3830 N85-33723
Knowledge engineering application in image processing 23 p3965 N85-34583
Heuristic rules for visualization
23 p3965 N85-34584
Robot environment expert system
[NASA-CR-3915] 23 p3967 N85-34593
Implications of artificial intelligence on the design of future onboard systems
[SFENA-DPS/C/S3/84252A] 23 p3967 N85-34596
Monte Carlo techniques for analyzing deep penetration problems
[DE85-011426] 23 p3968 N85-34598
Testbed for sensory control of intelligent machines
[DE85-012355] 24 p4099 N85-35412
Justified generalization: Acquiring procedures from examples
[AD-A156408] 24 p4135 N85-35626
Polylith: The early goals
[DE85-012534] 24 p4139 N85-35658
Artificial intelligence in Ada (trademark): Pattern-directed processing
[AD-A156230] 24 p4141 N85-35671

ARTIFICIAL RESPIRATION
U RESUSCITATION

ARTIFICIAL SATELLITES
NT AERONAUTICAL SATELLITES
NT AEROS SATELLITE
NT ALOUETTE 2 SATELLITE
NT ANIK SATELLITES
NT ARABSAT
NT ASTRONOMICAL SATELLITES
NT ATS
NT BIOSATELLITES
NT COMMUNICATION SATELLITES
NT COMMUNICATIONS TECHNOLOGY SATELLITE
NT COS-B SATELLITE
NT COSMOS SATELLITES
NT COSMOS 936 SATELLITE
NT COSMOS 1129 SATELLITE
NT COSPAS
NT DYNAMICS EXPLORER 1 SATELLITE
NT EOSS
NT ERS-1 (ESA SATELLITE)
NT EUROPEAN COMMUNICATIONS SATELLITE
NT EXOSAT SATELLITE
NT EXPLORER SATELLITES
NT EXPLORER 10 SATELLITE
NT EXPLORER 43 SATELLITE
NT EXPLORER 46 SATELLITE
NT EXPLORER 50 SATELLITE
NT EXPLORER 51 SATELLITE
NT EXTREME ULTRAVIOLET EXPLORER SATELLITE
NT FAR UV SPECTROSCOPIC EXPLORER
NT GEODETIC SATELLITES
NT GEOPHYSICAL SATELLITES
NT GEOS SATELLITES (ESA)
NT GEOS 1 SATELLITE
NT GEOS 2 SATELLITE
NT GEOS 3 SATELLITE
NT GOES SATELLITES
NT GOES 5
NT GRAVITY GRADIENT SATELLITES
NT HEAO 1
NT HEAO 2
NT HEAO 3
NT HELIOS SATELLITES
NT HELIOS 1
NT HELIOS 2
NT HEOS B SATELLITE
NT HUBBLE SPACE TELESCOPE
NT IMP
NT INFRARED ASTRONOMY SATELLITE
NT INTELSAT SATELLITES
NT INTERCOSMOS SATELLITES
NT INTERNATIONAL SUN EARTH EXPLORER 1
NT INTERNATIONAL SUN EARTH EXPLORER 2
NT INTERNATIONAL SUN EARTH EXPLORER 3
NT INTERNATIONAL SUN EARTH EXPLORERS
NT ISIS SATELLITES
NT IUE
NT L-SAT
NT LAGEOS (SATELLITE)
NT LANDSAT SATELLITES
NT LANDSAT 1
NT LANDSAT 4
NT LANDSAT 5
NT LONG DURATION EXPOSURE FACILITY
NT LUNAR SATELLITES
NT MAGSAT SATELLITES
NT MARISAT SATELLITES
NT MARITIME SATELLITES
NT METEOROLOGICAL SATELLITES
NT METEOSAT SATELLITE
NT MIRANDA SATELLITE
NT MULTISPECTRAL RESOURCE SAMPLER
NT NAVIGATION SATELLITES
NT NAVSTAR SATELLITES
NT NIMBUS SATELLITES
NT NIMBUS 5 SATELLITE
NT NIMBUS 7 SATELLITE
NT NOAA SATELLITES
NT NOAA 6 SATELLITE
NT NOAA 7 SATELLITE
NT NOAA 8 SATELLITE
NT OAO 3
NT OGO
NT ORBITAL SPACE STATIONS
NT OTS (ESA)
NT PASSIVE SATELLITES
NT PROGNOZ SATELLITES
NT QUASAT
NT ROSAT MISSION
NT SAGE SATELLITE
NT SARSAT
NT SCATHA SATELLITE
NT SCIENTIFIC SATELLITES
NT SEASAT SATELLITES
NT SEASAT 1
NT SIRIO SATELLITE
NT SIRS B SATELLITE
NT SKYNET SATELLITES
NT SOLAR MESOSPHERE EXPLORER
NT SOLAR POWER SATELLITES
NT SPACE INFRARED TELESCOPE FACILITY
NT SPARTAN SATELLITES
NT SPOT (FRENCH SATELLITE)
NT STORMSAT SATELLITE
NT SYMPHONIE SATELLITES
NT SYNCHRONOUS SATELLITES
NT TETHERED SATELLITES
NT TIROS N SERIES SATELLITES
NT TIROS SATELLITES
NT TRANSIT SATELLITES
NT UK SATELLITES
NT VELA SATELLITES
NT VENERA SATELLITES
NT VENERA 11 SATELLITE
Development of the Engineering Test Satellite-3 (ETS-3) ion engine system
[NASA-TM-77538] 01 p0017 N85-10101
Problem of determining highly accurate coordinates of artificial satellites by photographic methods
02 p0162 N85-11096
Space research benefits national economy
02 p0163 N85-11107
NESDIS international activities, appendix 2
02 p0296 N85-11917
Sweden's Kiruna may be future launch site for satellites 03 p0310 N85-12000
Study of instrument design options for the Columbus spectroscopy mission
[NASA-CR-174072] 04 p0502 N85-13205
Theory of the orbital motion of an artificial Earth satellite
[NAL-TR-807] 06 p0758 N85-14847
Aerodynamic and thermal characteristics of satellite bodies in hypersonic flow of rarefied gas at angle of attack 06 p0778 N85-14974
Upper Atmosphere Research Satellite (UARS) trade analysis
[NASA-CR-175269] 07 p0912 N85-15774
Theory of the orbital motion of an artificial Earth Satellite
[NAL-TR-807] 09 p1285 N85-18075
Study of factors affecting an HF/VHF direct broadcasting satellite service
[PB85-120889/GAR] 09 p1313 N85-18256
Transdigitizer for relaying signals from Global Positioning System (GPS) satellites
[AD-D011442] 10 p1422 N85-18970
A semianalytical, artificial satellite orbit propagation procedure based on optimal parameter estimation
[INPE-3301-PRE/613] 10 p1427 N85-18997
One rocket multiple satellite launch technology
[AD-A149228] 10 p1427 N85-19002
Telemetry systems of Interkosmos satellites
11 p1617 N85-20173
A system simulator for the solar generator of artificial satellites
[INPE-3320-TDL/180] 11 p1672 N85-20534
NORAD's PARCS small satellite tests (1976 and 1978) 12 p1783 N85-21191
NASA/JSC orbital debris study: Debris model
12 p1783 N85-21193
The long term behaviour of Earth orbits and the implications for debris control 12 p1786 N85-21213
Passive microwave remote sensing for sea ice research
[NASA-CR-175570] 12 p1874 N85-21758
Plans for Interbol satellite experiment
13 p1977 N85-22407
Nontraditional method for determining unperturbed orbits of unknown space objects using incomplete optical observational data 13 p1979 N85-22417
China report: Science and technology
[JPRS-CST-84-030] 13 p2041 N85-22777

Nation said to rank high with 15 satellites
13 p2041 N85-22776

Periodic movements of axisymmetrical satellite about center of mass due to gravitational moment
13 p2042 N85-22780

Development, prospect of satellite dynamics discussed
13 p2052 N85-22847

Multistep orbital correction algorithms for an Earth satellite using low thrust engine
15 p2479 N85-25303

Electric potential of satellite in electron emitting experiments in initial stage of electron beam injection in steady-state mode
15 p2480 N85-25309

Czech institute develops microcomputer for satellites
15 p2484 N85-25331

Selection of optimal control program for solar cell panels of Earth satellites
15 p2484 N85-25335

Application of perturbation theory to problem in orbital theory
15 p2537 N85-25656

Margin leveling algorithm for fully saturated satellite transponder with CDMA (Code Division Multiple Access) signalling
[AD-A151710] 15 p2543 N85-25669

Positions of relative equilibrium of satellite-gyrostat
16 p2718 N85-26777

Observability in problem of correction of inertial navigation systems using additional information from artificial Earth satellite
16 p2719 N85-26785

Satellite selection criteria 16 p2804 N85-27266

Atmospheric density model 16 p2805 N85-27267

Simultaneous Earth observations from 2 satellites
[NASA-TM-86204] 16 p2810 N85-27325

Altimetry data and the elastic stress tensor of subduction zones
[NASA-CR-175796] 16 p2825 N85-27425

West Europe report: Science and technology
[JPRS-WST-84-024] 17 p2945 N85-28183

Structure of SYLDA double launch system for Ariane
17 p2946 N85-28185

Swedish space program includes research satellites
18 p3088 N85-29113

Balanced system for ranging and synchronization between satellite pairs
[AD-D011697] 19 p3224 N85-29992

Global geoid and gravity anomaly predictions using the collocation and point mass techniques
[AD-A154517] 21 p3605 N85-32367

Far travelers: The exploring machines
[NASA-SP-480] 22 p3731 N85-33126

On the principle of uniformity of satellite communications systems
22 p3773 N85-33382

Magnetospheric multiprobes: MMP/CHEMSAT
23 p3902 N85-34171

ARTILLERY

The electronic typesetting program programmer's manual
[AD-A147500] 07 p1025 N85-16506

ARTS

NT ABILITIES

NT GRAPHIC ARTS

ARYABHATA

U INDIAN SPACECRAFT

ARYL COMPOUNDS

U AROMATIC COMPOUNDS

ASBESTOS

Early detection of environmental exposure
[AD-P004039] 06 p0845 N85-15369

Effect of sealants of the sound absorption coefficients of acoustical friable insulating materials
[AD-A148641] 08 p1218 N85-17674

Substitution of asbestos by aramid fibers and fiber blends in industrial textiles and composites with organic binders
[BMFT-FB-T-85-006] 23 p3920 N85-34294

ASCENT

NT CLIMBING FLIGHT

ASCENT PROPULSION SYSTEMS

The space shuttle ascent vehicle aerodynamic challenges configuration design and data base development
08 p1093 N85-16906

ASCENT TRAJECTORIES

The space shuttle launch vehicle aerodynamic verification challenges
08 p1093 N85-16907

ASHES

NT FLY ASH

Ash contents of Costa Rican peat deposits
[DE85-010734] 19 p3301 N85-30462

Ice nucleating characteristics of Capparis Aphylla, an Indian herb
21 p3641 N85-32519

ASIA

Mean maximum mixing heights for northern Asia for the winter of 1978
[DE84-015980] 05 p0672 N85-14315

Lateral inhomogeneity of mantle surface in western Eurasia
14 p2344 N85-24497

Location of continental Permian volcanites of central Asia and its tectonic interpretation
14 p2346 N85-24505

Frequency dependence of Q in the mantle underlying the shield areas of eurasia
[AD-A151367] 15 p2592 N85-25978

AWS (Air Weather Service) climatic briefs: Asia
[AD-A151944] 16 p2935 N85-27481

The 2nd World Meteorological Association Regional Association (Asia), 8th session
[WMO-642] 22 p3817 N85-33643

ASPARTATES

Responses of rat hindlimb muscles to 12 hours recovery from tail-cast suspension
[NASA-CR-176182] 24 p4126 N85-35590

ASPARTIC ACID

Blood amino acids of cosmonauts before and after 211-day spaceflight 12 p1900 N85-21933

ASPECT RATIO

NT HIGH ASPECT RATIO

NT LOW ASPECT RATIO

Blind zones and aspect ratio bias in acquisition of discontinuity orientation data
[DE84-002718] 04 p0533 N85-13410

Detailed pressure distribution measurements obtained on several configurations of an aspect-ratio-7 variable twist wing
[NASA-TM-86306] 10 p1419 N85-18950

Basic studies of multiple free and confined jets
[AD-A149556] 10 p1485 N85-19374

Visual simulation requirements for aircraft aspect recognition at real world distances
[AD-A151040] 14 p2228 N85-23810

Some optimization problems in static aeroelasticity for wings made of composite materials
14 p2277 N85-24104

Wind tunnel wall interference
[AD-A151212] 15 p2474 N85-25273

Visual search strategy predictions: The use of aspect ratio as a cue
[BAE-BT-12565] 15 p2619 N85-26138

Hypersonic nonequilibrium gas flow past zero-aspect wing 16 p2765 N85-27063

Multiple scattering of electromagnetic waves in discrete random media
[AD-A151706] 16 p2772 N85-27112

Aerodynamic performance of a wing in ground effect using the PANAIR program
[AD-A153303] 17 p2892 N85-27832

Solution to eigenvalue problems of antisymmetric cross-ply and antisymmetric angle-ply laminated plates using affine transformations
[AD-A153040] 17 p2917 N85-27980

A numerical study of Taylor-Vortex flow
[AD-A154787] 21 p3584 N85-32277

Object identification and manipulation using silhouette moments
[AD-A154755] 21 p3705 N85-33011

Neoclassical diffusion including ellipticity in a heliotron-like configuration 23 p3978 N85-34667

Generalized reduced fluid model with finite ion-gyroradius effects
[DE85-013123] 24 p4157 N85-35777

ASPHALT

Design of alternate launch and recovery surfaces for environmental effects
[AD-A145800] 03 p0320 N85-12066

Related studies to cathodic protection of reinforced concrete structures
[PB84-218114] 03 p0333 N85-12145

Experimental AC (Asphalt Concrete) overlays of PCC pavement
[PB84-218171] 03 p0342 N85-12203

Development of a rapid test method for asphalt concrete content determination in hot-mix paving mixtures
[PB84-218692] 03 p0342 N85-12204

Evaluation of moduli and thicknesses of pavement systems by spectral-analysis-of-surface-waves method
[PB84-219112] 03 p0342 N85-12205

Alternatives for runway rubber removal from porous friction surfaces
[DOT/FAA/PM-84/28] 05 p0597 N85-13803

Field validation of statistically-based acceptance plan for bituminous airport pavements. Volume 1: Correlation analysis of Marshall properties of laboratory-compacted specimens
[FAA-PM-84-12-VOL-1] 12 p1781 N85-21180

Field validation of statistically-based acceptance plan for bituminous airport pavements. Volume 2: Statistical analysis of Marshall properties of plant-produced bituminous materials
[FAA-PM-84-12-VOL-2] 12 p1781 N85-21181

Field validation of statistically-based acceptance plan for bituminous airport pavements. Volume 3: Statistical analysis of 3 methods for determining maximum specific gravity of bituminous concrete mixtures
[FAA-PM-84-12-VOL-3] 12 p1781 N85-21182

Field validation of statistically-based acceptance plan for bituminous airport pavements. Volume 5: Summary of validation studies
[FAA-PM-84-12-VOL-5] 12 p1782 N85-21184

Overlays for plain jointed concrete pavements
[PB85-156287] 15 p2523 N85-25557

Anticorrosion protection of reinforcing steel in prestressed gypsum and anhydrite concrete
[BLL-BISI-TRANS-22079-(9022.06)]
17 p2926 N85-28044

Recycling agent selection and tentative specification
[AD-A153529] 18 p3070 N85-29968

Pycnometer shaker
[PB85-174985] 20 p3460 N85-31481

ASPHYXIA

Basic cryogenics and materials. Phase 1
[NASA-CR-177932] 21 p3572 N85-32215

ASPIRATION

U VACUUM

ASSAULTING

U ATTACKING (ASSAULTING)

ASSAYING

Development of a new class of chemical and biological ultrasensors: Ribonuclease contamination and control
[NASA-CR-175466] 11 p1635 N85-20296

Compact L-edge densitometer for uranium concentration assay
[DE85-010344] 18 p3110 N85-29261

Quantitative passive technique for assay of near-surface tritium in materials
[DE85-010661] 19 p3360 N85-30833

Carcinogenesis of nitrated toluenes and benzenes skin and lung tumor assays in mice
[AD-A155723] 22 p3818 N85-33655

Improved flow cytometer measurement of binding assays
[DE85-006407] 23 p3935 N85-34390

ASSEMBLER ROUTINES

MC68CRX cross-assembler users manual
[AD-A148031] 08 p1205 N85-17584

ASSEMBLIES

NT SUBASSEMBLIES

NT TAIL ASSEMBLIES

The development of an optoelectronic assembly applied to computer systems
[AD-A145028] 01 p0120 N85-10621

SMP: A solid modeling program
[NASA-CR-172473] 02 p0241 N85-11570

Emitted vibration measurement device and method
[NASA-CASE-MFS-25961-1] 11 p1635 N85-20299

Performance of Chromel versus Alumel and Nicrosil versus Nisil thermocouple assemblies in vacuum and argon between 1000 deg C and 1200 deg C
[DE85-000810] 12 p1853 N85-21624

Releasable cable connector assembly for use between a mobile and stationary object
[AD-D011536] 12 p1858 N85-21655

Development of a sintered shim
[DE85-006183] 13 p2025 N85-22665

Direct transient analysis of a fuze assembly by axisymmetric solid elements 15 p2576 N85-25890

A Gimbal sizing analysis for an IPACS rotating assembly
[NASA-CR-172524] 16 p2741 N85-26913

Fully redundant mechanical release actuator
[NASA-CASE-LAR-13196-1] 18 p3116 N85-29287

Self-locking mechanical center joint
[NASA-CASE-LAR-12864-1] 19 p3279 N85-30336

Voyager 0.2-lbf thruster valve assembly short pulse test report
[NASA-CR-176121] 22 p3741 N85-33185

Latch assembly
[DE85-011660] 22 p3792 N85-33492

Two-plane balance and slip-ring design
22 p3799 N85-33536

ASSEMBLING

NT ORBITAL ASSEMBLY

Automation of assembly of elecirical products
03 p0346 N85-12228

Mathematical modeling of assembly processes involving use of sensitized robots 04 p0488 N85-13111

Component reliability and assembling technologies
[CNES-NT-106] 04 p0511 N85-13258

External tank processing from barge to pad
08 p1096 N85-16927

Automated assembly of Gallium Arsenide and 50-micron thick silicon solar cell modules
[NASA-CR-174331] 08 p1168 N85-17364

Ground test article for deployable space structure systems
[NASA-CR-171301] 10 p1429 N85-19011

Double pinch-push contact insertion end-effector
[AD-D011485] 10 p1459 N85-19196
Investigation of dynamics of manipulator with elastic sections 13 p2048 N85-22819
Advanced life analysis methods. Volume 2: Crack growth analysis methods for attachment lugs
[AD-A150420] 13 p2109 N85-23109
Extreme precision antenna reflector study results
14 p2232 N85-23630
Large Deployable Reflector (LDR) requirements for space station accommodations
14 p2236 N85-23658
Classification of holding jigs for objects of robotized assembly 14 p2266 N85-24039
Construction in space 15 p2484 N85-25328
Robot use in FRG increases but sensor technology lags 15 p2531 N85-25605
Robots, automatic devices inside VW's Wolfsburg plant 17 p2946 N85-28186
Alignment and assembly tool for very large diameter cylinders
[NASA-CASE-MFS-28001-1] 18 p3116 N85-29269
X-ray satellite
[NASA-TM-77896] 20 p3407 N85-31144
Automatic assembly of space stations
20 p3409 N85-31153
Field testing of a lightweight relocatable structure in a temperate environment
[AD-A155171] 21 p3599 N85-32350
Multi-robot assembly of IC's 23 p3964 N85-34577

ASSEMBLY LANGUAGE
MC68CRX cross-assembler users manual
[AD-A148031] 08 p1205 N85-17584
Topics in optical materials and device research, 3. Volume 2
[AD-A149727] 12 p1911 N85-21096
ZTL: A subroutine package for the IBM personal computer to support the Ziatech ZT1488 IEEE-488 controller
[LA-10141-MS] 12 p1913 N85-22010
HGRAPH: A subroutine package for the IBM personal computer to support the Hercules Graphic Card
[LA-10144-MS] 12 p1914 N85-22013
ZTLCK: A subroutine package for the IBM personal computer to support the Ziatech ZT1488 real time clock
[LA-10146-MS] 12 p1914 N85-22014
TRANIO: A subroutine package for the IBM personal computer to support the transfer 6002 CAMAC crate controller
[LA-10145-MS] 12 p1914 N85-22015
A quickly tested Pascal random number generator for microcomputers
[AD-A156059] 24 p4136 N85-35633

ASSESSMENTS
NT DAMAGE ASSESSMENT
NT TECHNOLOGY ASSESSMENT
DC-10 winglet flight evaluation
[NASA-CR-3704] 19 p3217 N85-29949
Description of a test site for large-scale heavy gas dispersion and combustion experiments
[DE85-004967] 23 p3911 N85-34231
The role of regional subsurface geochemistry in resource assessment in the central United States
24 p4104 N85-35440
Some recent deposit modeling efforts
24 p4106 N85-35453

ASSIGNMENT
U ALLOCATIONS

ASSIMILATION
A simulation experiment on the impact of geostationary temperature retrievals in numerical models
15 p2597 N85-26005
VAS/model impact study 15 p2597 N85-26006
Users guide for optimum interpolation method of global data assimilation
[AD-A155929] 24 p4138 N85-35648
Two methods of global data assimilation
[AD-A155981] 24 p4143 N85-35684

ASSOCIATIONS
U ORGANIZATIONS

ASSOCIATIVE PROCESSING (COMPUTERS)
Linear associative mapping
[ESA-TT-856] 05 p0719 N85-14611
Evaluation of the RSTN (Regional Seismic Test Network) network and further improvement to automatic association
[AD-A146395] 06 p0835 N85-15312
Toward a model of attention and the development of automatic processing
[AD-A149348] 10 p1567 N85-19882

ASSURANCE
Measurement assurance programs. Part 2: Development and implementation
[PB84-217876] 01 p0051 N85-10338
Measurement assurance programs. Part 1: General introduction
[PB84-217868] 01 p0051 N85-10339
The ESA product assurance specification system: Explanatory note 04 p0511 N85-13259
Toward a non-bureaucratic approach to quality assurance in data processing
[DE84-007484] 04 p0550 N85-13497
Quality assurance for environmental analytical chemistry, 1983
[DE84-016045] 09 p1349 N85-18469
Characteristics of quality data
[DE85-001203] 10 p1568 N85-19889
Examination of stuels by chemical analysis for quality assurance
[BLL-BISI-TRANS-22068-(9022.06)]
17 p2929 N85-28074
Principal quality assurance measures in the manufacture of HF-welded high-pressure linepipe
[BLL-BISI-TRANS-21690-(9022.06)]
17 p2976 N85-28389
Principles of quality assurance of chemical measurements
[PB85-177947] 18 p3072 N85-28907
Towards the year 2000: Developments in inspection and product assurance to be anticipated during the next 15 years — aircraft engines
[PNR-90258] 23 p3940 N85-34421

ASTEROID BELTS
NT AMOR ASTEROID
NT APOLLO ASTEROIDS
NT ASTEROIDS
NT VESTA ASTEROID
The asteroid ring 15 p2678 N85-26536
Asteroid compositional rings: Clues to the compositions of primordial planetesimals in the middle solar system
15 p2678 N85-26537
Collisional outcomes in the asteroid belt
15 p2678 N85-26538
The distribution of compositional classes in the asteroid belt: A cosmochemical fingerprint?
22 p3852 N85-33856

ASTEROID MISSIONS
Asteroid amphitrite: Surface composition and prospects for the possible Galileo flyby 15 p2680 N85-26549
Space ventures and society long-term perspectives
[NASA-CR-176012] 19 p3379 N85-30963

ASTEROIDS
NT AMOR ASTEROID
NT APOLLO ASTEROIDS
NT VESTA ASTEROID
The asteroidal source region of ordinary chondrites
06 p0881 N85-15600
How many Earth-approaching asteroids are there?
[NASA-CR-174209] 06 p0890 N85-15650
The discovery circumstances of Earth-approaching asteroids
[NASA-CR-174327] 08 p1258 N85-17920
The geology of the terrestrial planets
[NASA-SP-469] 09 p1410 N85-18886
Asteroids, comets and planet formation
09 p1410 N85-18889
Asteroid taxonomy from cluster analysis of photometry
09 p1411 N85-18897
Research in planetary studies and operation of Mauna Kea Observatory
[NASA-CR-175618] 13 p2169 N85-23460
Study and estimation of planet-crossing asteroid populations: Discoveries and analysis
13 p2175 N85-23498
The olivine asteroids: Discovery, mineralogy, and relationship to palasites 13 p2175 N85-23500
Convex-profile inversion of asteroid lightcurves
13 p2176 N85-23502
Surfaces of asteroids and cometary nuclei
13 p2176 N85-23503
The asteroid ring 15 p2678 N85-26536
Asteroid compositional rings: Clues to the compositions of primordial planetesimals in the middle solar system
15 p2678 N85-26537
Collisional outcomes in the asteroid belt
15 p2678 N85-26538
Asteroid amphitrite: Surface composition and prospects for the possible Galileo flyby 15 p2680 N85-26549
Mining cosmic dust from the blue ice lakes of Greenland 15 p2682 N85-26563
A search for evidence of large body Earth impacts associated with biological crisis zones in the fossil record 15 p2682 N85-26567
An analysis of alternate hydrogen sources for lunar manufacture
[DE85-007234] 16 p2884 N85-27792
Speckle interferometry applied to asteroids and other solar system objects
[NASA-CR-175976] 19 p3384 N85-30995
The 13 November 1984 occultation of BD +08 deg 0471 by (1) Ceres
[NASA-CR-176106] 23 p3987 N85-34725
The nature and origin of outer solar system asteroids from reflectance spectrophotometry
24 p4168 N85-35838

ASTHMA
Short-term human respiratory effects of nitrogen dioxide: Determination of quantitative dose-response profiles. Phase 2: Exposure of asthmatic volunteers to 4 PPM NO2
[PB85-104388/GAR] 07 p1017 N85-16462

ASTRO MISSIONS (STS)
The 1986 National Aeronautics and Space Administration authorization
[GPO-47-635] 24 p4166 N85-35829

ASTROBIOLOGY
U EXOBIOLOGY

ASTRODYNAMICS
Method for prompt modeling of quasiperiodic movement of solid near-axisymmetrical body in atmosphere
13 p2043 N85-22790
Application of quaternions to problems of solid body dynamics in the atmosphere 15 p2481 N85-25313
Solved und unsolved problems in planetary ring dynamics 15 p2674 N85-26502
Dynamics of neutral small particles — in the solar system 15 p2676 N85-26521
Accuracy in predicting orbital motion of artificial Earth satellite 16 p2720 N85-26793
Optimal relative data weights
16 p2805 N85-27296

ASTROGRAPHY
NGC 2024: Multi-wavelength infrared and radio observations 08 p1246 N85-17865
Far-infrared photometry of low-mass pre-main-sequence stars with broad CO wings 08 p1246 N85-17866
The astrometry programme at Mt. John Observatory
14 p2436 N85-25026
The astrometry network of observers in China
14 p2436 N85-25027
Obtaining accurate comet positions despite some inaccurate catalog stars 14 p2437 N85-25032
Reduction of astrographic catalogues
14 p2437 N85-25033

ASTROLABES
Timing-system design considerations for a mobile astrolabe 17 p2965 N85-28309

ASTROMASTS
U LONGERONS

ASTROMETRY
The present state of the International Star Cluster Photometry Programme 06 p0737 N85-14741
Plate measurements and reductions at Muenster — astronomical photography 07 p0966 N85-16129
First tests on the astrometric performance of the new PDS1010G at Hamburg Observatory — granite microdensitometer 07 p0966 N85-16135
Astrometric applications of the Mt. Stromlo PDS 1010A — microdensitometer 07 p0967 N85-16136
Automated star counts in nebulous areas
07 p0967 N85-16137
Cometary Astrometry
[NASA-CR-175680] 14 p2435 N85-25015
The astrometry network of the IHW and the P/Crommelin trial run results 14 p2435 N85-25016
Remarks on cometary astrometry
14 p2435 N85-25019
Cometary astrometry with Schmidt cameras
14 p2435 N85-25020
Astrometry of comets using hypersensitized type 2415 film 14 p2435 N85-25021
Astrometric plates obtained at the primary focus of large aperture reflectors 14 p2436 N85-25022
Kitt Peak measurements of P/Halley positions
14 p2436 N85-25023
Problems and procedures of cometary astometry
14 p2436 N85-25024
Astometry at La Silla 14 p2436 N85-25025
The astrometry programme at Mt. John Observatory
14 p2436 N85-25026
The astrometry network of observers in China
14 p2436 N85-25027
The astrometry network of observers in Japan
14 p2436 N85-25028
The astrometry network of observers in USSR
14 p2436 N85-25029
Desired characteristics of catalogs for cometary astrometry 14 p2436 N85-25030
The IHW reference star catalogs for Comets Halley and Giocobini-Zinner 14 p2436 N85-25031
Obtaining accurate comet positions despite some inaccurate catalog stars 14 p2437 N85-25032
Measuring: The quantifying art
14 p2437 N85-25035

Least squares reduction technique 14 p2437 N85-25036

Reduction of astrometric plates 14 p2437 N85-25037

The work on Comet Halley's orbit at ESOC 14 p2438 N85-25041

Study of the accuracy of astrometric observations of comets [ESA-CR(P)-1964] 17 p3054 N85-28903

ASTRONAUT PERFORMANCE

Ultrasonic study of early cardiovascular adaptation to zero gravity 05 p0691 N85-14445

NASA: Model development for human factors interfacing [NASA-CR-175584] 12 p1910 N85-21985

Psychological issues relevant to astronaut selection for long-duration space flight: A review of the literature [AD-A154051] 19 p3330 N85-30627

ASTRONAUT TRAINING

25th anniversary of the Gagarin Cosmonaut Training Center [NASA-TM-77644] 09 p1266 N85-18076

ASTRONAUTS

Approaches to radiation guidelines for space travel [DE85-001248] 09 p1363 N85-18576

Astronaut hazard during free-flight polar EVA 13 p1997 N85-22522

Psychological issues relevant to astronaut selection for long-duration space flight: A review of the literature [AD-A154051] 19 p3330 N85-30627

Experience of science astronaut on the Spacelab-1 mission 20 p3508 N85-31807

Results of microbiological studies conducted during operation of Salyut-6 orbital station 22 p3823 N85-33682

The effect of +Gx acceleration on platelet activation as determined by plasma platelet factor 4 levels [AD-A155881] 24 p4131 N85-35608

ASTRONAVIGATION

Optimization of orientation in navigation by two heavenly bodies 07 p0951 N85-16027

Errors of analog of inertial coordinate systems modeled in astronavigation system 07 p0951 N85-16028

ASTRONOMICAL CATALOGS

The catalogue of the discrete sources in the declination range from -13 deg to -2 deg [NASA-TM-77594] 01 p0129 N85-10887

Documentation for the machine-readable version of A Catalogue of Extragalactic Radio Source Identifications (Veron-Cetty and Veron 1983) [NASA-TM-87373] 03 p0405 N85-12587

Documentation for the machine-readable version of The Revised AFGL Infrared Sky Survey Catalog (Price and Murdock 1983) [NASA-TM-87377] 03 p0405 N85-12588

Documentation for the machine-readable version of the MK classification extension catalogue Morris-Kennedy (1983) [NASA-TM-87372] 04 p0549 N85-13491

Documentation for the machine-readable version of the Perth 75: A Catalogue of Positions of 2589 FK4 and FK4S Stars (Nikoloff and Hog 1982) [NASA-TM-87376] 04 p0549 N85-13492

Documentation for the machine-readable version of the AGK3 Star Catalogue of Positions and Proper Motions North of -2 deg .5 declination (Dieckvoss and Collaborators 1975) [NASA-TM-87378] 04 p0549 N85-13493

The Lund catalogue of open cluster parameters 05 p0738 N85-14742

Catalogue of observations of total occultations of stars by the Moon for the years 1972 to 1980 and of grazing occultations for the years 1963 to 1980 [BULL-192] 05 p0741 N85-14768

Dark cloud and globule distribution for galactic longitudes 230 to 360 degrees 06 p0678 N85-15575

Data reduction 09 p1412 N85-18903

Flux reconstruction and calibration 09 p1412 N85-18904

Analysis of processing 09 p1412 N85-18905

Sky coverage, confusion, completeness and reliability 09 p1412 N85-18906

The formats of the IRAS catalogs and atlases 09 p1413 N85-18908

IUE low-dispersion reference atlas 11 p1760 N85-21073

Statistical classification of IUE low-dispersion stellar spectra: Progress report 11 p1760 N85-21075

Herstmonceux observations of the Sun, planets and Moon, 1957 - 1982 [BULL-193] 11 p1762 N85-21087

Materialization of a reference system via a star catalog 14 p2399 N85-24787

Desired characteristics of catalogs for cometary astrometry 14 p2436 N85-25030

The IHW reference star catalogs for Comets Halley and Giocobini-Zinner 14 p2436 N85-25031

Obtaining accurate comet positions despite some inaccurate catalog stars 14 p2437 N85-25032

Reduction of astrographic catalogues 14 p2437 N85-25033

On the orbit improvement results obtained by referring old cometary observations to the SAO Star Catalog 14 p2438 N85-25042

Documentation for the machine-readable version of the Stellar Spectrophotometric Atlas, 3130 A lambda 10800 A of Gunn and Stryker (1983) [NASA-TM-87437] 14 p2438 N85-25045

Documentation for the machine-readable version of A Library of Stellar Spectra (Jacoby, Hunter and Christian 1984) [NASA-TM-87438] 14 p2438 N85-25046

Documentation for the machine-readable version of the Revised S210 Catalog of Far-Ultraviolet Objects (Page, Carruthers and Heckathorn 1982) [NASA-TM-87439] 14 p2438 N85-25047

Documentation for the machine-readable version of the Cordoba Durchmusterung (CD) [NASA-TM-87441] 14 p2439 N85-25049

Documentation for the machine-readable version of the Cape Photographic Durchmusterung (CPD) [NASA-TM-87442] 14 p2439 N85-25050

Documentation for the machine readable version of the Yale Catalogue of the Positions and Proper Motions of Stars between Declinations -60 deg and -70 deg (Fallon 1983) [NASA-TM-87443] 14 p2439 N85-25051

A second catalog of gamma ray bursts: 1978 - 1980 localizations from the interplanetary network [OG-1.2-1] 22 p3861 N85-33912

Limits to the burster repetition rate as deduced from the 2nd catalog of the interplanetary network [OG-1.2-5] 22 p3862 N85-33915

ASTRONOMICAL COORDINATES

Optimization of orientation in navigation by two heavenly bodies 07 p0951 N85-16027

Data reduction 09 p1412 N85-18903

Analysis of processing 09 p1412 N85-18905

Reduction of astrographic catalogues 14 p2437 N85-25033

On the orbit improvement results obtained by referring old cometary observations to the SAO Star Catalog 14 p2438 N85-25042

Basic formulae for the computation of the deflection of the vertical from astronomical star observations [AD-A154912] 21 p3605 N85-32390

Jets in air-jet family [HE-3.2-1] 24 p4179 N85-35912

ASTRONOMICAL MAPS

Infrared mapping of galaxian centers: Star forming regions with kiloparsec scale sizes 03 p0444 N85-12827

Synthesis of radio image on RATAN-600 radiotelescope 06 p0783 N85-15004

Automated star counts in nebulous areas 07 p0967 N85-16137

The formats of the IRAS catalogs and atlases 09 p1413 N85-18908

Infrared observations of the Uranian rings 15 p2672 N85-26488

Far-infrared observations of young clusters embedded in the R Coronae Austrinae and RHO Ophiuchi dark clouds [NASA-TM-86681] 24 p4167 N85-35834

ASTRONOMICAL MODELS

NT DENSITY WAVE MODEL

NT STELLAR MODELS

Time-dependent chemistry of molecular clouds 03 p0443 N85-12822

The Martian climate: Energy balance models with CO2/H2O atmospheres [NASA-CR-174073] 03 p0448 N85-12849

Far-infrared photometry of compact extragalactic sources: OJ 187 and BL Lac [NASA-TM-86022] 04 p0580 N85-13701

Galaxy and cluster formation in a universe dominated by cold dark matter [DE84-015879] 04 p0580 N85-13706

Bulk composition of the Moon in the context of models for condensation in the solar nebula 04 p0583 N85-13725

Tidal disruption and the origin of the Moon 04 p0586 N85-13739

A numerical investigation of planetesimal collision trajectories with a Moon accumulating in Earth orbit 04 p0586 N85-13740

Stochastic does not equal ad hoc --- theories of lunar origin 04 p0586 N85-13741

A testable gravitational capture model for the origin of the Earth's Moon 04 p0586 N85-13742

Directional properties of circular Maria: Interpretation in the context of a testable gravitational capture model for lunar origin 04 p0586 N85-13743

The problem of iron partition between Earth and Moon during simultaneous formation as a double planet system 04 p0587 N85-13744

An integrated dynamical and geochemical approach to lunar origin modelling 04 p0587 N85-13748

Lunar origin from impact on the Earth 04 p0588 N85-13757

Stability of stellar disk and ratio of halo to disk masses in the galaxy 05 p0740 N85-14763

Structure and evolution of the large scale solar and heliospheric magnetic fields 05 p0746 N85-14782

Local Interstellar Medium. International Astronomical Union Colloquium No. 81 [NASA-CP-2345] 06 p0672 N85-15539

Supersymmetric inflationary cosmology [DE85-001331] 06 p0681 N85-15598

BL Lacertae objects: Multifrequency observations and model applications 08 p1236 N85-17792

Shock acceleration in active galactic nuclei and quasars 08 p1241 N85-17828

On the hydrodynamical equations of astrophysical jets --- active galactic nuclei 08 p1241 N85-17831

An alternative to relativistic beaming in AGN --- Active Galactic Nuclei (AGN) 08 p1242 N85-17833

Models of nonkeplerian accretion disks based on dynamo magnetic field: Application to Active Galactic Nuclei (AGN) 08 p1242 N85-17834

Macroscopic currents and wind perturbations in the frame of the wind and shock model --- galactic nuclei 08 p1242 N85-17836

Duelling winds: A model for broad-line regions --- galactic nuclei 08 p1242 N85-17837

Theoretical studies of emission line variability in type 1 Seyfert galaxies 08 p1242 N85-17839

A model for the climatic behavior of water on Mars 09 p1415 N85-18931

Coordinated multifrequency observations of the BL LAC objects MRK 180, MRK 421, and MRK 501 11 p1746 N85-20983

A model for the variable continuum of the Seyfert 1 galaxy NGC 5548 11 p1747 N85-20985

The changing ultraviolet spectrum of Herbig-Haro object No. 1 11 p1747 N85-20989

Accretion in the zeta Aurigae and 32 Cygni shock cones 11 p1754 N85-21036

Consequences of hot gas in the broad line region of active galactic nuclei [NASA-TM-86176] 11 p1763 N85-21090

The axisymmetric pulsar magnetosphere 12 p1955 N85-22279

Dynamics of elliptical galaxies and the r sup 1/4 luminosity law 12 p1955 N85-22282

Nonlinear evolution of astrophysical Alfven waves 12 p1956 N85-22294

About static and dynamic solutions of the aligned rotator model --- pulsar magnetospheres 12 p1958 N85-22306

Hydrodynamics of astrophysical jets --- active galactic nuclei 12 p1958 N85-22307

Equilibrium model of thin magnetic flux tubes --- solar atmosphere 12 p1958 N85-22310

An analytic model for hydromagnetospheres --- stellar winds; pulsars; cosmic jets 12 p1959 N85-22313

The influence of the local solar wind structures on the propagation of low energy particles 12 p1959 N85-22314

Small scale structure and the Spinar model for active galactic nuclei 12 p1959 N85-22316

Viking radio science data analysis and synthesis [NASA-CR-175631] 13 p2171 N85-23471

An idealized short period comet model: Surface insolation, H2O flux, dust flux and mantle evolution 13 p2176 N85-23504

Planetary Rings. Colloquium 75 --- conferences [ISBN-2-85428-100-4] 15 p2670 N85-26473

A model containing blobs for the A ring of Saturn 15 p2671 N85-26479

The rings of Uranus 15 p2672 N85-26486

Evolution of collisional systems --- planetary disks 15 p2674 N85-26505

A simple model of Saturn's rings revisited 15 p2674 N85-26506

Viscosity in Saturn's rings 15 p2674 N85-26507

Comments on collision mechanics in ring systems --- planetary rings [PSI-CONTRIB-186] 15 p2675 N85-26510

Diffusion instability in a bimodal disc --- planetary rings 15 p2675 N85-26513

Stochastic modeling of planetary ring systems 15 p2675 N85-26516

The Adiabatic invariant: A tool for the study of the dynamics of the solar system 15 p2676 N85-26519

The formation of the terrestrial planets from lunar sized planetesimals 15 p2678 N85-26533
The evolution of meteor streams 15 p2678 N85-26539
Some features of the interplanetary medium during Forbush decreases
[NOTA-INTERNA-836] 18 p3202 N85-29866
First-order shock acceleration in solar flares
[SH-1.1-5] 23 p3989 N85-34732
Variations in the propagation of UH-nuclei
[OG-7.1-1] 23 p4012 N85-34863
An experiment to measure the energy spectrum of cosmic ray antiprotons from 100 to 1000 MeV
[OG-9.1-3] 23 p4022 N85-34929

ASTRONOMICAL OBSERVATORIES
NT ASTRONOMICAL SATELLITES
NT GAMMA RAY OBSERVATORY
NT HEAO
NT HEAO 1
NT HEAO 2
NT HEAO 3
NT HUBBLE SPACE TELESCOPE
NT INFRARED ASTRONOMY SATELLITE
NT IUE
NT OAO 3
NT QUASAT
NT ROSAT MISSION
NT SPACE INFRARED TELESCOPE FACILITY
NT SPARTAN SATELLITES
Study of instrument design options for the Columbus spectroscopy mission
[NASA-CR-174072] 04 p0502 N85-13205
The Ebro Observatory and international scientific organizations 04 p0518 N85-13309
Aperture synthesis for radioastronomy 06 p0781 N85-14992
Pointing and control system design study for the space infrared telescope facility (SIRTF)
[NASA-CR-166612] 07 p0915 N85-15795
Recalibration of the KPNO spot sensitometers --- Kitt Peak National Observatory 07 p0963 N85-16103
Some nonatlas work at the European Southern Observatory (ESO) Sky Atlas Laboratory --- astronomical photography 07 p0964 N85-16117
The work of the photolabs at the Royal Observatory, Edinburgh --- astronomical photography 07 p0965 N85-16122
SIRTF: The next step
[NASA-TM-86663] 07 p1059 N85-16724
Airborne Astronomy Symposium. A symposium commemorating the tenth anniversary of operations of the Kuiper Airborne Observatory
[NASA-CP-2353] 08 p1244 N85-17848
The Lear Jet Observatory: Fifteen years of discovery and rebirth 08 p1244 N85-17850
Simultaneous determination of the xi and eta components of vertical deflection with a prism astrolabe
[SER-B-270-MITT-171] 09 p1343 N85-18450
Astronomy and sodium lighting
[RAND/N-2069-RC] 09 p1413 N85-18914
The astrometry network of observers in China 14 p2436 N85-25027
The astrometry network of observers in Japan 14 p2436 N85-25028
The astrometry network of observers in USSR 14 p2436 N85-25029
A program of ground-based astronomy to complement einstein observations
[AD-A151111] 15 p2668 N85-26466
A priority of space exploration: Observation of Saturn's rings from a Saturn orbiter 15 p2679 N85-26542
Program for observations of Halley's comet 22 p3732 N85-33138
Research of advanced techniques for X-ray detectors and telescopes with applications to rockets and the LAMAR facility
[NASA-CR-176161] 23 p4054 N85-35141

ASTRONOMICAL PHOTOGRAPHY
Problem of determining highly accurate coordinates of artificial satellites by photographic methods 02 p0162 N85-11096
Astronomical photography 1984 --- conferences
[ROE-OR-14] 07 p0962 N85-16102
SENSIT.FOR: A program for sensitometric reduction 07 p0963 N85-16105
A spectrosensitometer with an absolute calibration 07 p0963 N85-16106
Comparison of the fine grain compensation hypersensitization (FAH) process with gas hypersensitizing techniques --- astronomical photography plates 07 p0963 N85-16107
The results of hydrogen hypersensitization of photoemulsions --- astronomical photography 07 p0963 N85-16108
Nitrogen flushing during exposure of large Schmidt telescope plates 07 p0963 N85-16109
The most effective astronomical photographic emulsions for recording of faint and low-contrast objects 07 p0963 N85-16110
Astronomical applications of new infrared films 07 p0964 N85-16111
The 3a-F emulsion and the quasar redshift cut-off 07 p0964 N85-16112
Microspots on spectroscopic plates --- astronomical photography 07 p0964 N85-16113
Where to next in astronomical photography? --- tabular grain emulsions 07 p0964 N85-16114
What do we want: Increased speed, resolution, contrast or DOE? --- astronomical photography 07 p0964 N85-16115
Some aspects of photography with a small Schmidt camera --- astronomical photography 07 p0964 N85-16116
Some nonatlas work at the European Southern Observatory (ESO) Sky Atlas Laboratory --- astronomical photography 07 p0964 N85-16117
Using a Gossen light meter to produce enlarged interpositive film copies from glass plates --- astronomical photography 07 p0964 N85-16118
Unsharp masking at the enlarger --- astronomical photography 07 p0964 N85-16119
Processing of photographic observing material at the National Astronomical Observatory Rozhen 07 p0965 N85-16120
The UK Schmidt telescope and the facilities in Edinburgh 07 p0965 N85-16121
The work of the photolabs at the Royal Observatory, Edinburgh --- astronomical photography 07 p0965 N85-16122
An investigation into the fidelity of reproduction of UKST original objective prism plates on to film --- United Kingdom Schmidt Telescope (UKST) 07 p0965 N85-16123
Power spectrum analysis of astronomical photographs digitised with small apertures 07 p0966 N85-16127
Recent developments on the COSMOS plate-scanning machine --- microdensitometer 07 p0966 N85-16128
Plate measurements and reductions at Muenster --- astronomical photography 07 p0966 N85-16129
The Torun measuring system for astronomical spectra 07 p0966 N85-16130
The Malin effect in stellar photography 07 p0966 N85-16131
Some applications of signal-to-noise in photographic stellar photometry 07 p0966 N85-16132
Stellar photographic photometry using a double wedge technique with a focal reducer system 07 p0966 N85-16133
Design and fabrication of a CCD camera for use with relay optics in solar X-ray astronomy
[NASA-CR-174334] 08 p1164 N85-17344
An objective prism quasar survey with the Schmidt telescope on Calar Alto (Spain) 08 p1243 N85-17845
Development of a portable zenith chamber and its use on the 47th parallel
[SER-C-267] 11 p1741 N85-20946
Analysis of white dwarf Lyman alpha profiles 11 p1752 N85-21018
Evaluating accuracy in orientation of topographic photograph and satellite-centered direction from star photograph 13 p1983 N85-22442
Remarks on cometary astrometry 14 p2435 N85-25019
Cometary astrometry with Schmidt cameras 14 p2435 N85-25020
Astrometry of comets using hypersensitized type 2415 film 14 p2435 N85-25021
Astrometric plates obtained at the primary focus of large aperture reflectors 14 p2436 N85-25022
Problems and procedures of cometary astometry 14 p2436 N85-25024
Astometry at La Silla 14 p2436 N85-25025
Least squares reduction technique 14 p2437 N85-25036
Variability of the structure of the granulation over the solar activity cycle 14 p2447 N85-25100
One aspect of determination of direction of space survey base from photographs of planetary surface and star sky 15 p2487 N85-25352
Summary of optical groundbased E ring observations at the University of Arizona 15 p2671 N85-26482
Analysis and modeling of variations in length of day 19 p3349 N85-30761
A star camera aspect system suitable for use in balloon experiments
[OG-9.3-10] 23 p4028 N85-34965

ASTRONOMICAL PHOTOMETRY
NT STELLAR SPECTROPHOTOMETRY
South African Astronomical Observatory Circulars, no. 7
[SAAOC-7] 01 p0127 N85-10875
Observations of the pulsating hydrogen: Deficient star BD+13 deg 3224, during 1980 - 1981 01 p0128 N85-10882
Spectral components at visual and infrared wavelengths in active galactic nuclei
[NASA-CR-174133] 03 p0445 N85-12832
Time series photometry with a CCD camera 08 p1252 N85-17906
The use of self-scanned silicon photodiode arrays for astronomical spectrophotometry 08 p1252 N85-17907
Photodiodes for astronomical stellar radiometry 08 p1252 N85-17908
Photometry with Multi-Anode Microchannel Arrays (MAMAs) and Charge Injection Devices (CIDs) 08 p1252 N85-17909
Filter and passband problems 08 p1252 N85-17910
Light scattered from polished optical surfaces: Wings of the point spread function 08 p1252 N85-17911
Application of fiber optics and compound collectors 08 p1253 N85-17912
Asteroid taxonomy from cluster analysis of Photometry 09 p1411 N85-18897
Study of the pulsations of the ZZ Ceti stars 09 p1414 N85-18923
Improved continuum definition in high-background IUE images 11 p1761 N85-21078
Convex-profile inversion of asteroid lightcurves 13 p2176 N85-23502
Offerings of the Astronomical Institute of Bonn 15 p2667 N85-26459
Photoelectric observations of contact binary stars
[REPT-96] 15 p2667 N85-26460
Photoelectric observations of the dwarf nova VW Hydri during the November 1977 supermaximum
[REPT-97] 15 p2667 N85-26461
Photoelectric observations of the eclipsing binary V 836 Cygni
[REPT-98] 15 p2668 N85-26462

ASTRONOMICAL SATELLITES
NT HEAO
NT HEAO 1
NT HEAO 2
NT HEAO 3
NT HUBBLE SPACE TELESCOPE
NT INFRARED ASTRONOMY SATELLITE
NT IUE
NT OAO 3
NT QUASAT
NT SPACE INFRARED TELESCOPE FACILITY
NT SPARTAN SATELLITES
QUASAT: An orbiting very long baseline interferometer program using large space antenna systems 14 p2230 N85-23822
China report: Science and technology
[JPRS-CST-85-007] 15 p2533 N85-25621
Professional Committee on Solid Propulsion hold conference 15 p2533 N85-25623
Mapping with QUASAT (quasar satellite) using short observation times
[AD-A155155] 21 p3559 N85-32141

ASTRONOMICAL SPECTROSCOPY
A spectroscopic survey of 113 nearby red dwarf stars 01 p0129 N85-10886
Forbidden lines of oxygen in comet spectra 02 p0163 N85-11105
Solar neutrino spectroscopy
[DE84-015518] 02 p0304 N85-11968
Fr. Angelo Secchi, a pioneer in the study of solar-terrestrial relationships 04 p0519 N85-13312
Oblique focus ICCD laboratory evaluation
[NASA-CR-174205] 06 p0862 N85-15480
Optical and UV emission of active galactic nuclei 08 p1236 N85-17791
The 1.5 - 3.5 micron spectroscopy of the Orion H2 source 08 p1246 N85-17864
High sensitivity, high angular resolution far-infrared photometry from the KAO 08 p1246 N85-17867
Carbon stars: There is no such thing as a dead leg 08 p1247 N85-17871
Mid-infrared spectroscopy of planetary nebulae 08 p1247 N85-17872
Interstellar grain mantles 08 p1247 N85-17874
Far-infrared spectroscopy of galaxies: The 158 micron C(+) line 08 p1249 N85-17882
High precision measurement of stellar radial velocity variations 08 p1250 N85-17896
International Ultraviolet Explorer observations of amorphous hot galaxies
[NASA-CR-174354] 10 p1571 N85-19904
A new generation of spectrometer designs for ultraviolet astronomy 11 p1761 N85-21079
The multi-anode microchannel array detector system: Current status and future prospects 11 p1761 N85-21080

Interactions of galaxies and their nuclear activity
20 p3545 N85-32060
Development of observational and instrumental techniques in hard X-ray and medium energy gamma-ray astronomy
[NASA-CR-176172] 24 p4168 N85-35841

ASTRONOMICAL TELESCOPES
NT HELIOMETERS
NT INFRARED TELESCOPES
NT PYROHELIOMETERS
NT SPACE INFRARED TELESCOPE FACILITY
NT SPECTROSCOPIC TELESCOPES
NT ULTRAVIOLET TELESCOPES
NT X RAY TELESCOPES
Study of a coded mask telescope for astronomical measurements in the hard X-ray domain
[MPE-182] 01 p0129 N85-10889
Construction of a superheterodyne receiver for 10 micron waves to be put on a Cassegrain optics telescope for spectroscopic research on the Mars and Venus atmospheres
[MPE-183] 06 p0872 N85-15538
Image quality on the KAO 08 p1249 N85-17885
A 150 micron heterodyne spectrometer for airborne astronomy 08 p1249 N85-17887
A new generation of sub mm telescopes, made of carbon fiber reinforced plastic 08 p1250 N85-17890
The ground based photometric limitations to the search for light variations due to 5-minute solar-type oscillations in other stars 08 p1251 N85-17898
Light scattered from polished optical surfaces: Wings of the point spread function 08 p1252 N85-17911
Dall-Null tester for spaceborne applications
[AD-A151772] 16 p2881 N85-27779
Optical observations of HEAO-B objects
17 p3052 N85-28895
Radio telescope with 256 antennas built in Siberia
22 p3732 N85-33136
High energy neutrino astronomy with MACRO
[HE-5.3-12] 24 p4206 N85-36106

ASTRONOMY
NT GAMMA RAY ASTRONOMY
NT INFRARED ASTRONOMY
NT RADAR ASTRONOMY
NT RADIO ASTRONOMY
NT SPACEBORNE ASTRONOMY
NT ULTRAVIOLET ASTRONOMY
NT X RAY ASTRONOMY
NT X RAY BINARIES
NT X RAY SOURCES
National Science Foundation grants and awards for fiscal year 1983, volume 2
[PB84-212323] 01 p0125 N85-10854
South African Astronomical Observatory Circulars, no. 7
[SAAOC-7] 01 p0127 N85-10875
Observations of four Beta Cephei stars in NGC6231
01 p0128 N85-10877
Research and technology, 1984: Marshall Space Flight Center
[NASA-TM-86476] 04 p0590 N85-13765
The beginnings of airborne astronomy, 1920 - 1930: An historical narrative 08 p1244 N85-17849
Global meteor observation system (GLOBMET)
11 p1656 N85-20438
Research and technology: Fiscal year 1984 report
[NASA-TM-85231] 12 p1964 N85-22340
Activities report of the Institute for Astronomy and Astrophysics
[MITT-5] 14 p2434 N85-25012
Cometary Astrometry
[NASA-CR-175660] 14 p2435 N85-25015
USSR report: Space
[JPRS-USP-85-003] 15 p2476 N85-25284
Astrometric method advances Astronomy, geodesy
16 p2806 N85-27306
Basic formulae for the computation of the deflection of the vertical from astronomical star observations
[AD-A154912] 21 p3605 N85-32390
Space research in the United Kingdom: An assessment
[AD-A155334] 21 p3712 N85-33038
The 13 November 1984 occultation of BD +08 deg 0471 by (1) Ceres
[NASA-CR-176106] 23 p3987 N85-34725
Neutrino astronomy and the atmospheric background
[HE-5.3-17] 24 p4207 N85-36111

ASTROPHYSICS
NT COMPUTATIONAL ASTROPHYSICS
NT SOLAR PHYSICS
South African Astronomical Observatory Circulars, no. 7
[SAAOC-7] 01 p0127 N85-10875
Observations of four Beta Cephei stars in NGC6231
01 p0128 N85-10877
USSR report: Space
[JPRS-USP-84-005] 02 p0156 N85-11060
Cosmonauts complete 4th month aboard Salyut-7
02 p0157 N85-11065
Salyut-7 crew in orbit 150 days
02 p0157 N85-11066
Tass reports astrophysical, atmospheric studies on Salyut-7 02 p0158 N85-11075
The solar wind at 20-30 AU 02 p0301 N85-11960
Study of the solar corona using radio and space observations
[NASA-CR-174034] 02 p0304 N85-11983
RS CV sub n binary systems
[NASA-CR-174164] 04 p0580 N85-13704
Evolution of globular clusters
05 p0738 N85-14745
Investigation of central parts of globular clusters, performed in PUlkovo 05 p0738 N85-14747
The distribution of dust in the region of the Rosette Nebula and MON OB2 association
05 p0739 N85-14753
Proper motions and kinematical properties of Orion trapezium type stellar systems 05 p0739 N85-14755
Research in nuclear astrophysics: Stellar collapse and supernovae
[DE84-015559] 05 p0743 N85-14776
Method of aperture synthesis: Fundamental relations and data processing in aperture synthesis systems (review) 06 p0781 N85-14994
Interferometry with decametric waves (review)
06 p0781 N85-14996
Metric-wave and decimetric-wave aperture synthesis systems (review) 06 p0782 N85-14998
Testing theories of superluminal motion --- QUASAT
07 p1058 N85-16714
Comments on the physics of active galactic nuclei
08 p1240 N85-17823
Experimental determination of the 1 sigma(+) state electron-dipole-moment function of carbon monoxide up to a large internuclear separation
[NASA-TM-85979] 09 p1379 N85-18670
Molecular hydrogen and thermal phases in astrophysics 09 p1414 N85-18022
Cosmic axions
[DE85-001330] 09 p1418 N85-18944
Report of the Electrodynamic Interactions Panel
11 p1645 N85-20363
National solar-terrestrial research program, part 1. Solar-terrestrial research for the 1980's, part 2
[AD-A149542] 11 p1681 N85-20591
JPL highlights, 1983
[NASA-CR-175558] 12 p1951 N85-22256
Plasma Astrophysics --- conference
[ESA-SP-207] 12 p1953 N85-22270
Research in particles and fields
[NASA-CR-175472] 12 p1963 N85-22337
Research and technology: Fiscal year 1984 report
[NASA-TM-85231] 12 p1964 N85-22340
Theoretical and observational studies of stellar activity
13 p2171 N85-23468
Giant planets and their satellites: Cosmochemistry, evolution and structure 13 p2175 N85-23494
The structure and composition of Uranus and Neptune
13 p2175 N85-23495
Introduction to the Space Physics Analysis Network (SPAN)
[NASA-TM-86499] 14 p2290 N85-24198
Activities report of the Institute for Astronomy and Astrophysics
[MITT-5] 14 p2434 N85-25012
Cometary Astrometry
[NASA-CR-175660] 14 p2435 N85-25015
The structure and angular momentum content of dark clouds 14 p2439 N85-25054
X-ray polarimetry: The measurement of the polarization of solar flare X-rays and the design of a Compton polarimeter 14 p2441 N85-25059
Rotational inversion from global solar oscillations
14 p2442 N85-25064
Satellite research on solar flares
16 p2717 N85-26776
The soft X-ray background as a supernova blast wave viewed from inside: Solar abundance models
[NASA-CR-175767] 16 p2887 N85-27813
Activities report of the Institute for Extraterrestrial Physics
[MPI-PAE/EXTRATERR-187] 17 p3053 N85-28896
Institute works on modeling thermonuclear plasma processes 19 p3296 N85-30435
Slow tearing modes: Transitions to instability
20 p3534 N85-31989
Activities report of the Department of Astrophysics
20 p3546 N85-32064
Solar-geophysical data no. 485, January 1985. Part 1 (prompt reports): Data for December 1984, November 1984 and late data
[PB85-181360] 20 p3548 N85-32079
Space research in the United Kingdom: An assessment
[AD-A155334] 21 p3712 N85-33038
Research in particles and fields
[NASA-CR-176060] 21 p3724 N85-33103
Yakutsk Institute's cosmic ray research facility
22 p3732 N85-33135
Program for observations of Halley's comet
22 p3732 N85-33138
Numerical simulation in astrophysics: Smoothed particle methods 23 p3979 N85-34674
Research of advanced techniques for X-ray detectors and telescopes with applications to rockets and the LAMAR facility
[NASA-CR-176161] 23 p4054 N85-35141
Pulsed-neutron-source models for the astrophysical s-process
[DE85-012927] 24 p4151 N85-35740
Development of observational and instrumental techniques in hard X-ray and medium energy gamma-ray astronomy
[NASA-CR-176172] 24 p4168 N85-35841
Some nuclear data needs in astrophysics
[DE85-012916] 24 p4168 N85-35842
The research program of the Liquid Scintillation Detector (LSD) in the Mont Blanc Laboratory
[HE-5.3-6] 24 p4205 N85-36100
A search for cosmic sources of high energy neutrinos with small underground detectors
[HE-5.3-16] 24 p4206 N85-36110
Monopole, astrophysics and cosmic ray observatory at Gran Sasso
[HE-6.1-4] 24 p4209 N85-36130

ASYMMETRY
Cognitive asymmetry and occupation. Computer programmers, students, and bank personnel, part 1 and part 2
[AD-A147125] 08 p1197 N85-17540
Multiple resources and brain laterality
[AD-A148912] 10 p1530 N85-19643
Skewed stable variables and processes
[AD-A150549] 13 p2153 N85-23372
Stability of permanent rotation modes of asymmetric heavy solid body 14 p2279 N85-24118
Attempts to localize and identify the gravity sensing device of plant seedlings 15 p2607 N85-26064
Plant growth biophysics: The basis for growth asymmetry induced by gravity 15 p2611 N85-26089
Asymmetric flux generation and its relaxation in reversed field pinch
[IPPJ-712] 15 p2656 N85-26387
Predicting fully plastic mode 2 crack growth from an asymmetric defect
[AD-A152227] 16 p2801 N85-27269
Theoretical prediction of stationary positions in the rectangular chamber during asymmetric electroosmotic flow 20 p3499 N85-31750
The longitudinal asymmetry of the interplanetary perturbation producing Forbush decreases
[IFSI-84-18] 20 p3546 N85-32065
Search for the north-south asymmetry in solar activity
[AD-A155525] 21 p3724 N85-33102
Multidiode integrated-circuit protective device
22 p3781 N85-33425
Assessment of magnetic field asymmetries in ELMO Bumpy square
[DE85-011905] 22 p3846 N85-33819
Model of azimuthal non-uniformities induced by RF heating in RFC-XXM 23 p3977 N85-34658
Assessment of magnetic field asymmetries in ELMO Bumpy square
[DE85-011559] 23 p3984 N85-34705
North-south asymmetry in activity on the Sun and cosmic ray density gradients
[SH-4.2-7] 23 p4007 N85-34845
The expected cosmic ray density and stream distributions at the heliolatitudinal asymmetry of solar wind
[SH-4.2-14] 23 p4008 N85-34852
The influence of quiet asymmetric magnetosphere on the cutoff rigidities of the main cone
[SH-6.1-10] 23 p4045 N85-35083
New Matsushiro underground cosmic ray station (220 M.W.E. in depth)
[SH-9.1-14] 23 p4052 N85-35129
A new description of combined trellis coding with asymmetric modulation
[NASA-CR-176197] 24 p4086 N85-35323

ASYMPTOTES
Numerical improvement of asymptotic solutions and nonlinear shell analysis 05 p0848 N85-14158

A limit theorem for the superposition of renewal processes
[CWI-MS-R8409] 05 p0722 N85-14636

On the global asymptotic stabilization of nonlinear systems
[PREPRINT-836] 08 p1209 N85-17604

Velocity inversion using a stratified reference
[AD-A150082] 12 p1889 N85-21858

Asymptotic behavior of matrix coefficients related to reductive symmetric spaces
[CWI-PM-R8410] 12 p1925 N85-22095

Extended semiclassical calculations
[DE85-007824] 19 p3346 N85-30736

ASYMPTOTIC METHODS

Singular asymptotic expansions in nonlinear rotordynamics
[NASA-CR-174012] 01 p0017 N85-10100

Estimates of Freud-Christoffel functions for some weights with the whole real line as support
[CSIR-TWISK-323] 01 p0114 N85-10775

An asymptotic theory for logistic regression when some predictors are measured with error
[AD-A145673] 02 p0254 N85-11666

Asymptotic methods for wind tunnel wall corrections at transonic speed 03 p0313 N85-12022

Least squares estimation of conditionally heteroscedastic autoregressions
[AD-A145904] 03 p0411 N85-12626

Analysis and testing for rotordynamic coefficients of turbulent annular seals with different, directionally homogeneous surface-roughness treatment for rotor and stator elements 05 p0644 N85-14134

Approximating the percentage points of Greenwood's statistic with Cornish-Fisher expansions
[CWI-MS-R8405] 05 p0721 N85-14634

An operator method for computing the asymptotics of a collision resolution interval
[AD-A146837] 07 p1028 N85-16528

Local likelihood estimation
[AD-A1473317] 07 p1035 N85-16571

Asymptotic methods for the analysis, estimation, and control of stochastic dynamic systems
[AD-A147758] 08 p1211 N85-17618

Robust linear filtering for multivariable stationary time series, part 3
[AD-A148169] 08 p1212 N85-17627

Low-dimensional behavior of the pattern formation Cahn-Hilliard equation
[DE85-003727] 12 p1922 N85-22072

Singular asymptotic expansions in nonlinear rotordynamics 12 p1945 N85-22218

Investigation of dynamics of manipulator with elastic sections 13 p2048 N85-22819

Domain of applicability of asymptotic description of radio pulse fields near critical frequency
13 p2073 N85-22949

Scattering of waves by axisymmetrical edge
13 p2080 N85-22987

Asymptotically optimum multialternative sequential procedures for discernment of processes minimizing average length of observations
13 p2084 N85-23012

Confidence intervals using the regenerative method for simulation output analysis
[AD-A150147] 13 p2149 N85-23343

Asymptotic methods especially in combustion
[AD-A151505] 15 p2505 N85-25450

Point processes associated with extreme value theory
[AD-A151211] 15 p2640 N85-26280

Asymptotic solutions of MHD equations with finite conductivity
[REPT-12/1984] 16 p2852 N85-27581

Comments on the paper by F. Pegoraro, L. Sugiyama: Spatial diffusion of charged high-energy fusion products by shear Alfven perturbations
[INPE-3291-PRE/606] 16 p2866 N85-27675

On the accuracy of the Poincare-Lindstedt method
[REPT-84-37] 17 p3022 N85-28690

Extrapolation methods in the finite element method
[BONNER-MATHE-SCHR-158]
19 p3345 N85-30729

Asymptotic expansions for finite element eigenvalues and finite element solution 19 p3345 N85-30730

Asymptotic expansions for the finite element approximation of parabolic functions
19 p3345 N85-30731

Some asymptotic problems in the optimal control of distributed systems 20 p3412 N85-31175

Turbulent mixing and combustion
22 p3744 N85-33207

ASYMPTOTIC PROPERTIES

Estimates of Freud-Christoffel functions for some weights with the whole real line as support
[CSIR-TWISK-323] 01 p0114 N85-10775

On the coupling of an anchored flame with an acoustic field
[COLL-AERON-8434] 12 p1790 N85-21282

Accuracy of approximation of Bayes estimates in presence of noninformative parameters
13 p2084 N85-23015

On the length of asymptotic paths of meromorphic functions of order zero 15 p2833 N85-26234

On asymptotic joint distribution of the eigenvalues of the noncentral manova matrix for nonnormal populations
[AD-A151886] 15 p2842 N85-26294

Asymptotic expansion of Jacobi polynomials
[REPT-84-35] 17 p3021 N85-28689

Error-correcting codes for computer memories
24 p4136 N85-35636

ASYMPTOTIC SERIES

Scattering by a parabolic cylinder: A uniform asymptotic expansion
[AD-A145688] 02 p0252 N85-11652

Asymptotically optimal ranking algorithms for quasi-determinate signal detection
06 p0792 N85-15064

An asymptotic analysis of a transient p-n junction model
[AD-A147270] 07 p0947 N85-16004

Asymptotic representation of solutions of the basic semiconductor device equations
[AD-A149040] 10 p1545 N85-19741

The asymptotic behavior of the likelihood ratio statistic for testing a shift in mean in a sequence of independent normal variates
[AD-A149329] 10 p1550 N85-19779

Asymptotic distributions of the sample mean, autocovariances and autocorrelations of long-memory time series
[AD-A149409] 10 p1551 N85-19781

Tests of fit based on normalized spacings
[AD-A149749] 12 p1921 N85-22062

Asymptotics for configural estimators
[AD-A150106] 12 p1924 N85-22087

Theory of oriented nucleation with asymmetric single elements. 2: Effects of rotational diffusion
[IFTR-32/1984] 12 p1939 N85-22179

Asymptotic expansions of the distribution of test statistics associated with several two parameter exponential distributions
[AD-A151906] 15 p2641 N85-26289

Asymptotic expansion of Jacobi polynomials
[REPT-84-35] 17 p3021 N85-28689

A class of polynomials related to those of Laguerre
[CWI-AM-R8411] 17 p3022 N85-28693

Uniform asymptotic expansions of integrals
[CWI-AM-R8412] 17 p3022 N85-28694

Instability at the interface between two shearing fluids in a channel
[AD-A153532] 18 p3099 N85-29185

Towards a statistical analysis of genetic sequences data with particular reference to protein sequences
[AD-A153605] 18 p3152 N85-29515

Least-squares approximation to minimum chi-square estimators of location and scale parameters and their effect on the Pearson chi-square test
[AD-A153534] 18 p3169 N85-29638

Limit behaviour for stochastic monotonicity and applications
[AD-A153614] 18 p3170 N85-29648

Nonparametric renewal function estimation
[AD-A153474] 18 p3173 N85-29672

Extent to which least-squares cross-validation minimizes integrated square error in nonparametric density estimation
[AD-A153789] 18 p3174 N85-29679

Discrete-element acoustic analysis of submerged structures using doubly asymptotic approximations
[AD-A154959] 21 p3700 N85-32987

ASYNCHRONOUS MOTORS

Full load testing in the platform module prior to tow-out: A case history of subsynchronous instability
05 p0642 N85-14117

ATHEROSCLEROSIS

U ARTERIOSCLEROSIS

ATHLETES

Influence of geomagnetic disturbances on cardiovascular function of athletes
08 p1193 N85-17516

ATHODYDS

U RAMJET ENGINES

ATLANTIC OCEAN

Sea-level in the world ocean. Part 6: The South Atlantic and South Pacific Oceans, a catalogue of measurements
[CSIR-T/SEA-8303-6] 01 p0087 N85-10590

Late quaternary glacial cycles in the Bahamian deep basins and in the adjacent Atlantic Ocean
02 p0226 N85-11476

Submarine sand ridges: Geology and development, New Jersey, USA 02 p0227 N85-11482

Summary of 1984 Atlantic seasonal tropical cyclone activity and verification of author's forecast
03 p0395 N85-12520

The structure of the Iceland-Faeroe ridge, derived from geophysical measurements
[DRIC-T-7255] 03 p0397 N85-12535

The Long Term Upper Ocean Study (LOTUS). Cruise summary
[AD-A145767] 03 p0397 N85-12536

Variations with time of the carbon dioxide partial pressure in central and south Atlantic surface waters
[AD-A145825] 03 p0398 N85-12537

Heat sources in the tropics and large scale flow anomalies associated with precipitation anomalies in northeast Brazil
[INPE-3211-TDL/175] 04 p0538 N85-13421

Measurements of electric fields obtained by stratospheric balloons in the region of the South Atlantic anomaly
[INPE-3218-PRE/571] 05 p0675 N85-14335

Razrezy program research in the tropical Atlantic
07 p0981 N85-16229

Conditions governing the formation of stratocumulus clouds over the western Atlantic during cold air outbreaks
[AD-A146780] 07 p1004 N85-16383

A compilation of moored current meter and wind recorder data. Volume 35: Long-Term Upper Ocean Study (LOTUS) (Moorings 764, 765, 766, 767, 770), May 1982 - April 1983
[AD-A147103] 07 p1009 N85-16412

The long term upper ocean study (LOTUS). Cruise summary and hydrographic data report, OCEANUS 154, May 1984
[AD-A147908] 07 p1009 N85-16414

Oceanographic data for development of the US exclusive economic zone
[PB85-106458/GAR] 07 p1010 N85-16415

Detailed oceanic crustal modeling
[AD-A148589] 08 p1191 N85-17507

Preliminary post-emplacement safety analysis of the subseabed disposal of high-level nuclear waste
[DE84-011162] 08 p1221 N85-17692

Measurements of sediment temperatures, conductivity and heat flow in the North Atlantic and their relevance to radioactive waste disposal
[IOS-172] 09 p1359 N85-18551

Benthic boundary layer, IOS observational programme: Discovery Gap measurements, March 1984 --- Institute of Oceanographic Sciences (IOS)
[ISO-180] 09 p1359 N85-18552

Hurricane experience levels of coastal county populations: Texas to Maine
[PB85-111383] 10 p1520 N85-19581

The imaging of internal waves by the SEASAT-A synthetic aperture radar
[AD-A149806] 12 p1875 N85-21761

Atlantic Coast Unique Regional Atmospheric Tracer Experiment (ACURATE)
[PB85-128460] 12 p1886 N85-21839

Report of the International Ice Patrol Services in the North Atlantic Ocean, season of 1982
[AD-A149595] 12 p1898 N85-21917

The imaging of internal waves by the SEASAT-A synthetic aperture radar
[ARE(PORTLAND)TN-720/84]
13 p2054 N85-22860

Automatic buoys to assist the tuna fishery off the Azores 14 p2238 N85-23879

Circulation pattern of the North Atlantic, part of the warmwater sphere research effort at Kiel University
14 p2239 N85-23888

Evaluation of wave energy resources on the French Atlantic seaboard 14 p2325 N85-24369

Transatlantic migration study of the leathery turtle using the ARGOS system. Transatlantic turtle race
14 p2326 N85-24379

The French Ocean Climate in Equatorial Atlantic (FOCAL) Drifter Program, 1983-1984
14 p2329 N85-24399

Most important geochemical barrier zones in ocean (with example of Atlantic Ocean basin)
14 p2343 N85-24491

North Atlantic Deep Water Formation
[NASA-CP-2367] 15 p2601 N85-26028

Review of North Atlantic source waters
15 p2601 N85-26029

Deep water formation 15 p2601 N85-26030

Temporal and spatial scales of Labrador Sea water formation 15 p2601 N85-26031

Chemical signatures associated with the freshening of Northern Atlantic waters between 1972 and 1981
15 p2601 N85-26032

North Atlantic Deep Water and the world ocean 15 p2602 N85-26033

Oceanographic variations in recent decades and their impact on the fertility of the Iceland Sea 15 p2602 N85-26034

Quaternary North Atlantic surface paleoceanography in regions of potential deep-water formation 15 p2602 N85-26036

Glacial-to-interglacial changes in NADW fluxes? 15 p2602 N85-26037

Ocean modeling of the North Atlantic 15 p2602 N85-26039

Numerical simulation of North Atlantic Sea ice variability, 1951 - 1980 15 p2603 N85-26040

Climatic impact of a change in North Atlantic Deep Water formation 15 p2603 N85-26045

Ocean circulation and meteorology off the Georgia coast. Part 1: Real-time telemetry system for data collection [PB85-155935] 15 p2605 N85-26052

ARGOS-tracked drifters in the Rockall Trough 16 p2812 N85-27340

Contribution of the NOAA-7 and 8 and ARGOS partnership to white tuna fishing in the northeast Atlantic 16 p2813 N85-27355

X-ray intensification at balloon altitudes of the South Atlantic magnetic anomaly in association with geomagnetic activity [INPE-3469-PRE/712] 16 p2827 N85-27437

The sea level response to weather along the coast of southern Africa 16 p2829 N85-27446

On the 1983 drought in northeast Brazil [INPE-3412-PRE/676] 16 p2834 N85-27476

Tropical Oceans-Global Atmosphere (TOGA) experiment planning for the Brazilian participation in TOGA global climate program [INPE-3499-PRE/735] 16 p2834 N85-27477

An evaluation of discretized conditional probability and linear regression threshold techniques in model output statistics forecasting of visibility over the north Atlantic Ocean [AD-A151955] 16 p2857 N85-27619

Summary of archived Atlantic coast wave information study pressure, wind, wave, and water level data [AD-A153782] 18 p3151 N85-29508

Chemical, biological, and physical measurements from the subtropical western North Atlantic Ocean. Summer 1982, USNS Lynch, cruise 710-82 [AD-A153823] 18 p3201 N85-29857

Density characteristics of asthenosphere in Atlantic Ocean 19 p3294 N85-30423

Influence of underwater volcanic mountains of Atlantic on microplankton distribution 19 p3294 N85-30424

Tectonic structure features of some deep faults in Atlantic and Pacific Oceans (according to deep seismic sounding-reflected waves method data) 19 p3295 N85-30428

Mariners weather log, volume 29, number 1, winter 1985 [PB85-177483] 19 p3318 N85-30570

Research, progress and the mark A box model for physical, biological and chemical transports [DE85-010574] 19 p3320 N85-30581

Forecast of Atlantic seasonal hurricane activity for 1985 20 p3495 N85-31732

An evaluation of discretized conditional probability and linear regression threshold techniques in model output statistics forecasting of cloud amount and ceiling over the North Atlantic Ocean [AD-A155100] 21 p3636 N85-32581

Research at the Institute of Oceanographic Sciences related to the possible disposal of radioactive waste on or beneath the seafloor [IOS-204] 23 p3973 N85-34628

Marine phosphorite deposits model for exploration, with emphasis on deposits in the US Atlantic coastal plain 24 p4104 N85-35439

Atlantic coast hindcast. Phase 2: Wave information, additional extremal estimates [AD-A156137] 24 p4125 N85-35575

ATLAS CENTAUR LAUNCH VEHICLE

Assessment of candidate-expendable launch vehicles for large payloads [NASA-CR-175540] 14 p2237 N85-23867

ATLAS LAUNCH VEHICLES

NT ATLAS CENTAUR LAUNCH VEHICLE

ATMOSPHERE EXPLORER C

U EXPLORER 51 SATELLITE

ATMOSPHERES

On the angular and energy distribution of solar neutrons generated in P-P reactions [SH-1.4-9] 23 p3995 N85-34769

ATMOSPHERIC & OCEANOGRAPHIC INFORM SYS

A wind-bivane/microprocessor system for on-line prediction and display of pollutant distributions 16 p2830 N85-27449

ATMOSPHERIC ABSORPTION

U ATMOSPHERIC ATTENUATION

ATMOSPHERIC ATTENUATION

Atmospheric channel performance measurements at 10 to 100 GHz [PB84-211325] 01 p0042 N85-10271

Using measured variance of skywave radar sea-echo power spectra to estimate ionospheric Doppler broadening of mean spectra [PB84-214071] 03 p0399 N85-12544

Multiple scattering effects on transmission through the atmosphere [AD-A147527] 07 p0941 N85-15969

Propagation and scattering considerations for the 0.2-3.0 GHz frequency range for a space-based radar [AD-A148504] 08 p1153 N85-17282

Atmospheric wind and diffusion from analysis of an SF6 release at 350 km altitude [AD-A147965] 08 p1185 N85-17471

Carbon dioxide laser radar for monitoring atmospheric transmittance and atmospheric aerosol 09 p1354 N85-18516

Digital controller for the Wave Propagation Laboratory's VHF and UHF wind-profiling radars [PB85-112142] 11 p1626 N85-20238

MSG-7: Atmospheric penetration of solar radiation in the range of Schumann-Runge bands 11 p1657 N85-20443

Synopsis of mid-latitude radio wave absorption in Europe 11 p1659 N85-20454

Evaluation of the radiometric integrity of LANDSAT 4 Thematic Mapper band 6 data 12 p1869 N85-21726

Spectroradiometric calibration of the Thematic Mapper and Multispectral Scanner system [E85-10094] 12 p1874 N85-21756

Atmospheric handbook: Atmospheric data tables available on computer tape [PB85-108512] 12 p1891 N85-21867

The effects of atmospheric water vapor on infrared propagation [AD-A150030] 12 p1934 N85-22150

Infrared aerosol absorption index 13 p2110 N85-23147

Below-room-temperature water-vapor continuum absorption within the 8- to 10 micron atmospheric transmission window [TR-0084(4945-09)-1] 13 p2132 N85-23266

Applicability of vertically homogeneous atmospheric models for remote soundings 14 p2341 N85-24477

Development of an auroral absorption substorm 14 p2360 N85-24586

Rain rate determinations from electronic weight measurements: Instrument description and data reduction techniques [AD-A150765] 14 p2378 N85-24681

Sound propagation studies for a large horizontal axis wind turbine [NASA-CR-172564] 14 p2415 N85-24904

Evaluating radiation distortions of optical image of Earth's surface in horizontally inhomogeneous atmosphere 15 p2486 N85-25345

Field of point source of low-frequency sound in atmosphere with altitudinally nonuniform wind 15 p2524 N85-25566

Wave description of sound propagation through stratified moving atmosphere 15 p2525 N85-25567

ILUM code: Solar and lunar flux calculations for multi-cloud layered atmospheres [DE85-005578] 15 p2600 N85-26025

Studies of electro-optical attenuation in the vicinity of cloud base [AD-A151745] 15 p2653 N85-26360

Meteorological factors in Earth-Satellite propagation [NASA-CR-175764] 16 p2769 N85-27089

Synchronizing heavily encoded data in bad weather 16 p2770 N85-27099

EHF attenuation derived from emission temperatures in light rain [AD-A151166] 16 p2772 N85-27110

Radar study of the melting layer [ESA-CR(P)-1974] 17 p2997 N85-28527

Atmospheric limitations to clock synchronization at microwave frequencies 18 p3107 N85-29236

Comparison of 8 to 12 micrometer and 3 to 5 micrometer CVF transmissometer data with LOWTRAN calculations [AD-A154218] 19 p3350 N85-30763

Radiometry: A useful prediction tool — atmospheric attenuation [ESA-SP-1071] 20 p3399 N85-31084

Ship-to-ship propagation: Maritime data analyses [AD-A155484] 21 p3592 N85-32325

Linear absorption and scattering of laser beams [AD-A156167] 24 p4098 N85-35401

Sensitivity of depth of maximum and absorption depth of EAS to hadron production mechanism 24 p4188 N85-35982

EAS development curve at energy of 10(16) - 10(18) eV measured by optical Cerenkov light [HE-4.4-7] 24 p4193 N85-36015

ATMOSPHERIC BOUNDARY LAYER

Evaluation of an integrated mixed-layer model for single station prediction in a marine regime 01 p0060 N85-10535

Boundary layer-cloud interactions as potential storm predictors 01 p0061 N85-10543

The lifting condensation level and its relation to convective cloud base [AD-A145654] 02 p0232 N85-11513

Development of a microcomputer coupled atmospheric and oceanic boundary layer prediction model [AD-A146334] 03 p0397 N85-12530

Energy diagnostics and impact studies of FGGE global data sets and GLAS GCM simulations 05 p0683 N85-14390

Air-sea interaction during cold air outbreaks 05 p0685 N85-14401

Mixed layers and satellite retrievals 05 p0686 N85-14411

Study of low-frequency sound with point source in stream with shear 06 p0825 N85-15239

Modeling influence of three layer cloud cover on outgoing thermal radiation 06 p0825 N85-15242

Indirect estimation of convective boundary layer structure for use in routine dispersion models [PB84-238260] 06 p0834 N85-15308

Simulation of entrainment at the top of the atmospheric boundary layer for use in General Circulation Models (GCM) [DM-42] 09 p1355 N85-18525

Radiosodar system for remote synchronous measurements of wind speed, temperature and its fluctuations 13 p2110 N85-23145

The BALSAMINE experiment 14 p2238 N85-23876

Statistical/Trend analysis of the marine atmospheric boundary layer model [AD-A151053] 14 p2374 N85-24673

Deepwater wind wave growth with fetch and duration [AD-A151604] 15 p2604 N85-26051

Study of the functions of similarity of the planetary boundary layer. Part 2: Results [INPE-3130-PRE/521-VOL-2] 16 p2626 N85-27429

Three powered sailplanes as meteorological instrumentation for atmospheric boundary layer studies at DFVLR [DFVLR-FB-84-50] 17 p2897 N85-27862

On the improvement of satellite temperature retrievals by means of boundary layer models 18 p3140 N85-29443

On Fofonoff's mode 18 p3145 N85-29471

Use of radar with frequency modulation for studying atmospheric boundary layer 19 p3296 N85-30437

Excitation of turbulence by density waves [NASA-CR-3905] 19 p3314 N85-30546

Effects of relative humidity gradients on the evaluation of submicron aerosol flux measurements in the atmospheric surface layer [DE85-010510] 19 p3316 N85-30555

A survey of wind and turbulence modeling methods [AD-A154470] 20 p3496 N85-31733

Facility for large-scale hazardous gas testing [DE85-011852] 21 p3564 N85-32169

Properties of aerosol particles detected by satellites in coastal regions 21 p3641 N85-32622

Simulation of the coupled atmospheric and oceanic boundary layer model during MILDEX [AD-A155166] 21 p3655 N85-32705

Verification of Doppler sodar measurements — atmospheric boundary layer [KNMI-WR-85-2] 22 p3817 N85-33645

An atmospheric boundary layer model forced by the operational ECMWV-model [WSR-3] 24 p4120 N85-35541

Measurements for the determination of the vertical structure of the convective boundary layer — atmospheric boundary layer 24 p4122 N85-35550

Partitioning of the vertical turbulent energy transport into positive and negative contributions — meteorology 24 p4122 N85-35551

Aircraft measurements during the Bonn Experiment (BONEX 1) — meteorology 24 p4122 N85-35552

ATMOSPHERIC CHEMISTRY

Estimation of the potential and probable source regions for acid precipitation [DE84-015119] 02 p0225 N85-11472

Organic aerosol formation: OH(hydroxyl radical) versus ozone oxidation pathways [PB84-219880] 03 p0388 N85-12484

Thermodynamic conditions of the Earth's atmosphere with pollution processes 04 p0523 N85-13345

Impact of alcohol fuels on urban air pollution: Methanol photochemistry study [DE84-012950] 04 p0531 N85-13397
Regional-scale (1000 KM) model of photochemical air pollution. Part 2: Input processor network design [PB84-232651] 04 p0532 N85-13400
Proceedings of a Workshop on Atmospheric Research Needs for the Western United States [DE84-015069] 04 p0534 N85-13412
Fundamental molecular physics and chemistry, part 1 [DE84-009127] 04 p0561 N85-13571
Research and technology, 1984: Marshall Space Flight Center [NASA-TM-86476] 04 p0590 N85-13765
The use of tracers for the study of atmospheric chemical and physical transformation processes [DE84-015287] 05 p0671 N85-14313
Determination of Toluene's degradation products under simulated atmospheric conditions 05 p0674 N85-14331
Assessment of Techniques for Measuring Tropospheric H sub x O sub y [NASA-CP-2332] 05 p0675 N85-14336
Assessment of Techniques for Measuring Tropospheric H sub x O sub y: Summary 05 p0675 N85-14337
Chemical kinetics and Earth's atmosphere 06 p0822 N85-15216
Application of quantum chemistry of atmospheric chemistry [AD-A147035] 07 p0922 N85-15843
Remote sensing of atmospheric gases with CO2 lasers. Continuation and conclusion of spectroscopic investigations [BMFT-FB-W-84-030] 07 p0989 N85-16285
Ionic reactions of atmospheric importance [AD-A147354] 07 p0997 N85-16333
Electronically excited atomic and molecular oxygen [AD-A147732] 08 p1121 N85-17064
A new fast response probe for diffusion studies in atmospheric air — pollution modeling [IC-AERO-84-01] 08 p1180 N85-17437
Atmospheric photochemical modeling of turbine engine fuels. Phase 1: Experimental studies. Volume 2: Environmental chamber data tabulations [AD-A147786] 08 p1185 N85-17470
On the importance of light hydrocarbons in multiphase atmospheric systems [JUEL-1942] 08 p1190 N85-17498
Atmospheric acidification chemistry: A review [PB84-215490] 09 p1350 N85-18495
Atmospheric science and power production [DE84-005177] 09 p1354 N85-18521
Sequential precipitation chemistry sampling program at Brookhaven National Laboratory with an analytical summary of 1976-1982 data [DE85-002788] 10 p1513 N85-19545
Non-photochemical interactions of sulfur and nitrogen compounds in acid deposition [DE84-016141] 10 p1513 N85-19546
Upper atmosphere research at INPE [INPE-3281-PRE/604] 10 p1515 N85-19557
Infrared excitation of clusters and ions of atmospheric interest [DE85-002098] 10 p1516 N85-19564
MAP in India 11 p1655 N85-20424
Cold Arctic Mesopause Project (CAMP): Scientific objectives 11 p1656 N85-20433
MAP activities in Hungary 11 p1657 N85-20440
Ozone measurements in the mesosphere during a solar proton event 11 p1665 N85-20490
The concentration of sulfate in broken cloud layers [DE85-000228] 11 p1678 N85-20574
Meteorological support for the 1983 Deep Creek, Maryland experiment [DE85-002616] 11 p1678 N85-20575
Middle atmosphere NO and NO2 observed by means of the Spacelab one grille spectrometer [AERONOMICA-ACTA-A-293-1984] 11 p1680 N85-20588
Applicability of laboratory kinetics studies to the evaluation of aqueous phase atmospheric oxidation of sulfur-4 [DE85-000586] 12 p1883 N85-21819
Gas-liquid chemistry of natural waters, volume 1 [DE85-002603] 12 p1884 N85-21822
Gas-liquid chemistry of natural waters, volume 2 [DE85-002457] 12 p1884 N85-21823
OSCAR experiment high-density network data report [DE85-004907] 12 p1884 N85-21826
Continued research in mesoscale air pollution simulation modeling. Volume 6. Further studies in the modeling of microscale phenomena [PB85-137370] 12 p1887 N85-21844
Chemical kinetics and photochemical data for use in stratospheric modeling. Evaluation number 6 [NASA-CR-175564] 12 p1888 N85-21849
Global tropospheric chemistry: A plan for action [NASA-CR-175545] 12 p1891 N85-21865
Non-precipitating cumulus cloud study [DE85-002352] 12 p1896 N85-21902
Multiple element neutron-activation analysis of atmospheric aerosols with X-ray and gamma-spectrometric recording of radionuclides formed 13 p2013 N85-22631
One mechanism of formation of organic fraction in atmospheric aerosol 13 p2014 N85-22632
One-dimensional nonstationary model of photochemical transformations of gas impurities in stratosphere 14 p2342 N85-24484
PLUVIUS: A generalized 1-dimensional model of reactive pollutant behavior, including dry deposition, precipitation formation, and wet removal, 2nd edition [DE85-005542] 14 p2353 N85-24536
Magnetospheric effects on the upper atmosphere 14 p2365 N85-24616
High altitude sampling program: Radioactivity in the stratosphere [DE85-005924] 14 p2374 N85-24676
Emission inventory applications to regional acid deposition modeling [PB85-157386] 16 p2760 N85-27033
Measurement of elements in the stratosphere [NASA-CR-175691] 16 p2823 N85-27414
Free radicals in the stratosphere: A new observational technique 16 p2824 N85-27415
Atmospheric chemistry [INPE-3190-PRE/554] 16 p2826 N85-27430
Oxygen isotopic study of the oxidation of SO2 by H2O2 in the atmosphere [DE85-004017] 17 p2988 N85-28468
Homogeneous processes of atmospheric interest [NASA-CR-175770] 17 p2989 N85-28475
Absolute calibrations of SO2 and NO analyzers by photographic methods [DFVLR-MITT-85-02] 17 p2994 N85-28504
Reconstruction of past atmospheric CO/sub 2/ contents from the chemistry of the contemporary ocean: An evaluation [DE85-008426] 18 p3133 N85-29401
Environmental Research Division report: Atmospheric physics [DE85-009659] 18 p3133 N85-29404
Kinetics and intensity of photochemical processes in the atmosphere [BPT-10/84] 18 p3134 N85-29411
Formation and fate of toxic chemicals in California's atmosphere [PB85-172609] 18 p3134 N85-29414
Chemical transformations in acid rain. Volume 2: Investigation of kinetics and mechanism of aqueous-phase peroxide formation [PB85-173433] 18 p3135 N85-29416
Conceptual Design for a Gulf Coast Oxidant Transport and Transformation Experiment: Workshop proceedings and recommendations [PB85-173789] 18 p3135 N85-29417
Investigation of the reaction system NOX/ClOX/HOX under tropospheric and stratospheric conditions [BPT-11/84] 18 p3137 N85-29427
Atmosphere monitoring requirements 18 p3158 N85-29553
Quantitative studies for photoabsorption and fluorescence of HCl [NASA-CR-175965] 19 p3233 N85-30043
Evaluation of methods used for the determination of acidity in acid rain samples [PB85-178309] 19 p3237 N85-30070
Applied Science Division's Environmental Research Program [DE85-010637] 19 p3308 N85-30510
Analysis of aldehydes and ketones in the gas phase [PB85-181865] 20 p3426 N85-31261
Modeling of chemical transformations of SO(x) and NO(x) in the polluted atmosphere: An overview of approaches and current status [PB85-173169] 20 p3487 N85-31677
Activities report of the Aeronomy Department [G-774-1984] 21 p3633 N85-32569
Eleventh International Conference on Atmospheric Aerosols, Condensation and Ice Nuclei, volume 2 [PB85-182418] 21 p3636 N85-32596
Ice nucleation by silver iodine particles with nearly critical sizes 21 p3638 N85-32600
Airborne measurements of atmospheric ice nuclei 21 p3640 N85-32612
A statistical analysis of ice nuclei concentrations at urban and rural sites in Valladolid, Spain 21 p3640 N85-32614
Experimental studies of the formation of Aitken nuclei in the atmosphere 21 p3644 N85-32641
Photochemical aerosol formation in polluted atmosphere 21 p3644 N85-32642
The influence of Brownian coagulation on the size distributions of atmospheric aerosols 21 p3645 N85-32643
The nuclei of cloud formation 21 p3651 N85-32685
Characterization of insoluble particles associated with cloud droplets 21 p3652 N85-32693
Sulfur Cycle 21 p3662 N85-32748
Evaluation of the 2DFLOW and hybrid complex-terrain dispersion models with the 1980 ASCOT data base from the Geysers [DE85-012980] 22 p3812 N85-33613
Ozone during sudden stratospheric warming: A three-dimensional simulation [AERONOMICA-ACTA-A-292-1984] 22 p3813 N85-33621
Acetonitrile in the Earth's atmosphere: An upper limit deduced from infrared solar spectra [AERONOMICA-ACTA-A-295-1985] 22 p3813 N85-33623
Middle Atmosphere Program. Handbook for MAP, volume 11 [NASA-CR-176107] 22 p3814 N85-33625
Elemental tracers of source regions of contaminants in precipitation [DE85-012858] 24 p4113 N85-35499
Atmospheric nitrogen oxides: Their detection and chemistry [PB85-193910] 24 p4114 N85-35502
Air chemistry measurements 2 [AD-A156041] 24 p4117 N85-35520
A study of the chemistry of alkali metals in the upper atmosphere [AD-A156349] 24 p4117 N85-35524
Time-dependent response of the climate to increasing atmospheric carbon dioxide 24 p4119 N85-35532

ATMOSPHERIC CIRCULATION
Large-scale ocean-atmosphere interactions in the mid-latitudes and equatorial regions: A literature review [CSIR-T/SEA-8302] 01 p0073 N85-10482
About the influence of nonadiabatic processes on frontogenesis near the ground 01 p0075 N85-10498
Evaluation of surface sensible heat flux effects on the generation and modification of mesoscale circulations 01 p0079 N85-10527
Development of an operational system for Very-Short-Range Forecasting (VSRF) at Swedish Meteorological and Hydrological Institute (SMHI) 01 p0083 N85-10559
Some aspects of post-frontal convective areas along the west coast of the united states [AD-A144895] 01 p0085 N85-10572
Quasi-stationary atmospheric responses to large-scale forcing 02 p0227 N85-11484
A comparison of 2- and 3-dimensional transport within a stratosphereic circulation model 02 p0227 N85-11485
Arctic haze: Meteorological aspects of long-range transport 02 p0230 N85-11499
Atmospheric dynamics of Uranus and Neptune: Theoretical considerations 02 p0299 N85-11936
Conditional symmetric instability and mesoscale rainbands 05 p0678 N85-14356
Global Scale Atmospheric Processes Research Program Review [NASA-CP-2344] 05 p0679 N85-14360
GLAS fourth order model 05 p0679 N85-14361
Orographic effects in atmospheric circulation 05 p0679 N85-14362
Spectral general circulation model development 05 p0679 N85-14363
Biosphere/atmosphere interactions 05 p0679 N85-14364
Fully implicit numerical methods for the baroclinic primitive equations 05 p0679 N85-14365
A vertically resolved planetary boundary layer 05 p0680 N85-14367
Generation of available potential energy and other diagnostic studies during FGGE 05 p0683 N85-14388
Comparison of forecast and observed energetics 05 p0683 N85-14389
Energy diagnostics and impact studies of FGGE global data sets and GLAS GCM simulations 05 p0683 N85-14390
Spectral energetics diagnoses and FGGE spectral observing periods and energetics analyses of forecast experiments with GLAS GCM 05 p0683 N85-14391
Jet stream errors and tropospheric-stratospheric interactions in the GLAS general circulation model 05 p0683 N85-14392
Analysis of diabatic heating during FGGE 05 p0683 N85-14393
Global scale diagnosis of FGGE data 05 p0683 N85-14394

best copy available

ATMOSPHERIC CIRCULATION

Theoretical modeling for numerical weather prediction
05 p0684 N85-14395

Large scale rossby waves during FGGE
05 p0684 N85-14396

Planetary scale interactions 05 p0684 N85-14397

Structure and energetics of medium-scale atmospheric waves in the southern hemisphere summer
05 p0685 N85-14403

Investigation of cloud feedback in the GLAS model
05 p0685 N85-14404

Diagnostics of rainfall anomalies in the nordeste during the global weather experiment 05 p0685 N85-14405

Application of the bounded derivative initialization method 05 p0686 N85-14407

Implicit numerical methods in meteorology
05 p0686 N85-14408

Interannual variability in the observed circulation
05 p0686 N85-14409

Linear studies of stationary, extratropical anomalies in the troposphere 05 p0686 N85-14410

The influence of synoptic scales on low-frequency modes of variability 05 p0687 N85-14412

A new physical Lagrangian tracer
[DE84-016212] 05 p0687 N85-14419

Polar regions and climatic change
[PB84-237023] 05 p0688 N85-14421

Characteristic scale of inner mixing layers in stably stratified atmosphere 06 p0824 N85-15235

Simple mesoscale models for operational use in regions of topographic and thermal forcing: Development and evaluation
[AD-A146667] 06 p0839 N85-15325

Towing tank studies of stratified flow over ridges and valleys
[DE84-011418] 06 p0839 N85-15329

The 500 millibar sign frequency teleconnection charts: Winter
[PB85-106276/GAR] 07 p1009 N85-16410

A 2-dimensional second order closure model of the upper atmosphere 08 p1182 N85-17450

Spectral modeling of a potential vorticity equation for a barotropic flow on a beta-plane
[CWI-AM-R8408] 08 p1186 N85-17478

Dynamics of the low-latitude thermosphere and ionosphere 09 p1351 N85-18501

Simulation of entrainment at the top of the atmospheric boundary layer for use in General Circulation Models (GCM)
[DM-42] 09 p1355 N85-18525

Behavior and characteristics of storm cold outflows
09 p1356 N85-18529

Global scale diagnoses of FGGE data
[NASA-CR-174356] 09 p1356 N85-18533

Discovery about temperature fluctuations in turbulent air flows 10 p1500 N85-19466

Some aspects of atmospheric circulation near South America and interactions with the Antarctic regions
[INPE-3308-PRE/618] 10 p1515 N85-19561

Planetary scale circulation anomalies associated with droughts over northeast Brazil
[INPE-3351-PRE/630] 10 p1518 N85-19570

Large scale circulation anomalies and prediction of northeast Brazil droughts
[INPE-3405-PRE/674] 10 p1518 N85-19571

Interannual variations of the winter circulation in the Northern Hemisphere and in the southern oscillation (meridian) and their possible connections with the climate of Northeast Brazil
[INPE-3333-TDL/182] 10 p1519 N85-19573

PMP-2: Equatorial wave dynamics
11 p1655 N85-20422

French activities relevant to middle atmosphere research 11 p1655 N85-20423

UK participation in the Middle Atmosphere Programme
11 p1655 N85-20426

The global meteor observation system (GLOBMET)
11 p1656 N85-20432

MAP activities in Hungary 11 p1657 N85-20440

Middle Atmosphere Program. Handbook for MAP, volume 10
[NASA-CR-175477] 11 p1658 N85-20450

Middle atmosphere temperature and dynamics as revealed from D-region observations
11 p1659 N85-20453

Abnormal circulation changes in the winter stratosphere, detected through variations of D region ionospheric absorption 11 p1659 N85-20458

Seasonal characteristics of mesospheric plasma and their transitions 11 p1660 N85-20464

Spring changeover of the middle atmosphere circulation compared with rocket wind data up to 80 km
11 p1661 N85-20466

Large scale winter time disturbances in meteor winds over central and eastern Europe
11 p1661 N85-20467

Changes in the ozone content over central Europe during reversals of stratospheric circulation in late winter
11 p1661 N85-20469

Some aspects of general circulation and tides in the middle atmosphere 11 p1661 N85-20470

Meteor wind results from Atlanta, USA, and Ramey, Puerto Rico 11 p1662 N85-20474

Basic features of global circulation in the mesopause lower thermosphere region 11 p1662 N85-20475

Winds and waves (4 min - 11 yrs) in the upper middle atmosphere (60-110 km) at Saskatoon, Canada (52 deg N, 107 deg W): MF radar (2.2 MHz) soundings 1973 - 1983 11 p1662 N85-20476

The dynamics of ionospheric D region over East Siberia 11 p1662 N85-20477

Stratwarm effects in the ionospheric D region wind field 11 p1663 N85-20479

Investigation of aeronomic processes on the basis of ionospheric sporadic E 11 p1663 N85-20482

Comparison of MESOI atmospheric dispersion estimates with data and estimates from other models
[DE85-002372] 11 p1678 N85-20572

A study of eddy-mean flow interactions using Eliassen-Palm diagnostics: FGGE SOP-1 data and the NASA GLAS general circulation model compared
[NASA-CR-175506] 11 p1686 N85-20604

The 500 millibar sign frequency teleconnection charts: Fall
[PB85-110930] 11 p1687 N85-20612

The 500 millibar sign frequency teleconnection charts: Summer
[PB85-111359] 11 p1688 N85-20613

The 500 millibar sign frequency teleconnection charts: Spring
[PB85-111367] 11 p1688 N85-20614

Structure and forcing of teleconnection patterns occuring in general circulation model simulations
[DE85-002434] 12 p1890 N85-21862

Analysis of the NASA/MSFC Airborne Doppler Lidar results from San Gorgonio Pass, California
[NASA-CR-171355] 12 p1892 N85-21873

Navy tactical applications guide. Volume 4. Part 1. Eastern North Pacific weather analysis and forecast applications
[AD-A150097] 12 p1896 N85-21900

Non-precipitating cumulus cloud study
[DE85-002352] 12 p1896 N85-21902

Empirical and modeled synoptic cloud climatology of the Arctic Ocean
[NASA-CR-175628] 13 p2137 N85-23272

Variation of Arctic cloud cover in summer
[DE85-004507] 13 p2139 N85-23285

Mountain barrier baroclinity effects on surface winds along the Alaskan Arctic coast 14 p2236 N85-23877

Atmosphere ice-ocean interactions in the Antarctic (IAGO) 14 p2326 N85-24375

Considering zonal wind in semidiurnal tide problem
14 p2335 N85-24440

Small component spectral model of annual course of zonal atmospheric circulation 14 p2337 N85-24453

Comparison of observations of orographic disturbances in the troposphere and upper atmosphere
14 p2341 N85-24479

PLUVIUS: A generalized 1-dimensional model of reactive pollutant behavior, including dry deposition, precipitation formation, and wet removal, 2nd edition
[DE85-005542] 14 p2353 N85-24538

A study of the turbulent layer in the water at an air-water interface 14 p2378 N85-24679

Circulation statistics based on FGGE (First GARP Global Experiment) level 3-B analyses produced by GFDL (Geophysics Fluid Dynamics Laboratory)
[PB85-149318] 14 p2379 N85-24688

Cyclic flows in the solar convection zone due to the dynamo reaction 14 p2451 N85-25137

Field validation of 6-particle puff model
[DE85-004073] 15 p2569 N85-25962

The South Pacafic convergence zone and energy balance of the southern hemisphere
15 p2593 N85-25980

Monitoring tropical cyclone growth using GOES VISSR/VAS and Nimbus-7 TOMS data
15 p2595 N85-25989

Analysis of the inflow and air-sea interactions in hurricane Frederic 15 p2595 N85-25990

Role of jet streaks and boundary layer processes in organizing a pre-convective environment
15 p2597 N85-26008

Impact of soil moisture in organizing a severe storm outbreak 15 p2597 N85-26009

Role of frontal circulations and gravity waves in initiating convective storm systems 15 p2598 N85-26010

Meso-8 scale numerical simulations of the jet streak adjustments which organized the Carolina tornado outbreak and the subsequent explosive coastal cyclogenesis 15 p2598 N85-26011

A study of the effect of gently varying terrain on atmospheric flow near the surface
16 p2823 N85-27411

Wave dynamics and transport in the stratosphere
[NASA-CR-175789] 16 p2823 N85-27413

Study of the functions of similarity of the planetary boundary layer. Part 1: Theory
[INPE-3129-PRE/520-PT-1] 16 p2826 N85-27428

Study of the functions of similarity of the planetary boundary layer. Part 2: Results
[INPE-3130-PRE/521-VOL-2] 16 p2826 N85-27429

Radon concentration inversion in the troposphere: Still unexplained
[INPE-3380-PRE/638] 16 p2826 N85-27431

Upper-air data collection during CAPTEX
[DE85-006300] 16 p2827 N85-27438

Evolution of stratospheric aerosol size distribution from ground-based radiometric measurements: A study of El Chichon aerosol
[DE85-007555] 16 p2827 N85-27439

Theory and modeling of the interaction between subgrid scale orography and large scale flow
[DM-43] 16 p2827 N85-27440

Geophysical monitoring for climatic change, number 12
[PB85-172278] 16 p2837 N85-27496

Circulation statistics from January and July: Simulation with the NCAR (National Center for Atmospheric Research) community climate model (CCMOB)
[PB85-165637] 16 p2837 N85-27497

Great Lakes winter weather and ice conditions for 1982-83
[PB85-165009] 16 p2837 N85-27498

NASA Oceanic Processes Program annual review
[NASA-TM-87565] 16 p2838 N85-27503

Potential climatic impacts of increasing atmospheric CO2 with emphasis on water availability and hydrology in the United States
[NASA-TM-87479] 17 p2995 N85-28517

Mathematical modeling and simulation of climate and climatic change
[DE85-008974] 17 p2997 N85-28526

Conceptual Design for a Gulf Coast Oxidant Transport and Transformation Experiment: Workshop proceedings and recommendations
[PB85-173789] 18 p3135 N85-29417

Propagation of gravity waves in the atmosphere and around critical levels
[KNMI-WR-85-1] 18 p3137 N85-29428

Variability of short term eddy-correlation estimates of mass exchange
[PB85-172641] 18 p3138 N85-29431

Specification of surface roughness over oceans in the GLAS Fourth Order GCM 18 p3142 N85-29455

Model development highlight for 1984: The GLA Fourth Order GCM 18 p3143 N85-29457

Response of winter forecasts made with the GLA Fourth Order GCM to Changes in the horizontal grid resolution
18 p3143 N85-29458

Comparison of forecast and observed energetics
18 p3143 N85-29459

Mechanistic experiments to determine the origin of Southern Hemisphere stationary waves
18 p3143 N85-29461

Energy sources of the dominant frequency dependent 3-dimensional atmospheric modes
18 p3143 N85-29462

The vertical structure of global rotational normal modes 18 p3144 N85-29464

Quasi stationary states in the Southern Hemisphere
18 p3144 N85-29465

On the global distribution of three-dimensional Eliassen-Palm fluxes by stationary waves
18 p3145 N85-29469

Transient eddies in the UCLA GCM
18 p3145 N85-29470

A new CO2 transmittance parameterization and its impact on the GLA GCM 18 p3146 N85-29476

A GCM study of the atmospheric response to tropical SST anomalies 18 p3146 N85-29477

Influence of land surface processes on the Indian monsoon: A numerical study 18 p3146 N85-29478

Influence of land-surface roughness on atmospheric circulation and rainfall: A sensitivity study with a GCM
18 p3146 N85-29479

The structure and dynamics of an observed moist front 18 p3146 N85-29480

Large-eddy simulation in planetary boundary-layer research 18 p3147 N85-29482

Circulation and transport in the middle atmosphere: Troposphere and lower atmosphere
18 p3148 N85-29491

Circulation and transport in the middle atmosphere: Mesosphere and lower thermosphere
18 p3148 N85-29492

Diagnostic verification of the GLAS (Goddard Laboratory for Atmospheric Sciences) general circulation model as applied to a case of extratropical maritime explosive cyclogenesis
[AD-A153666] 18 p3146 N85-29494
Approximate method for computing wind velocity in atmosphere 19 p3296 N85-30444
Atmospheric planetary wave response to external forcing
[NASA-CR-176000] 19 p3315 N85-30548
On the dynamical climatology of the Amazon Basin and associated rain producing mechanisms
[INPE-3531-RPE/477] 19 p3315 N85-30552
Northeast Brazil droughts and Atlantic SST anomalies
[INPE-3538-PRE/754] 19 p3316 N85-30553
Some studies in filtering of atmospheric turbulence
[AD-A154042] 19 p3316 N85-30557
Experiments using atmospheric forcing from a FGGE analysis to drive an upper ocean model
[INPE-3503-PRE/736] 19 p3319 N85-30576
An examination of the Southern Oscillation in the upper troposheric tropical and subtopical wind field
20 p3488 N85-31680
Errors and parameterizations of sub-grid scale processes in regional-scale atmospheric models
20 p3488 N85-31682
Structure and energetics of medium-scale atmospheric waves in the Southern Hemisphere
20 p3489 N85-31685
Troposphere-stratosphere (surface-55 km) monthly general circulation statistics for the Northern Hemisphere-four year averages
[NASA-TM-86182] 20 p3495 N85-31730
Carbon dioxide and climate: Potential impacts
[DE85-009473] 20 p3496 N85-31734
Hadley circulation in planetary atmospheres
20 p3546 N85-32067
Middle Atmosphere Program. Handbook for MAP. Volume 14: URSI/SCOSTEP Workshop on Technical Aspects of MST Radar
[NASA-CR-176065] 21 p3615 N85-32466
Tropospheric-stratospheric exchange, part 1.1A
21 p3615 N85-32468
Gravity waves from the stratosphere to the mesosphere, part 1.3B 21 p3616 N85-32471
A numerical analysis of transient planetary waves and the vertical structure in a meso-strato-troposphere model, part 1.4A 21 p3617 N85-32473
General circulation of the middle atmosphere, part 1.4B 21 p3617 N85-32474
Performance of the Colorado wind-profiling network, part 1.5A 21 p3617 N85-32475
Vertical transport in the atmosphere: Measurement capabilities and requirements of VHF radars, part 1.6A
21 p3617 N85-32476
Synoptic-scale dynamics with vertical velocity, part 1.8A 21 p3617 N85-32478
Determination of billows and other turbulent structures, part 4.1A 21 p3621 N85-32500
Spectral measurements of turbulence and gravity waves, part 4.2A 21 p3622 N85-32501
Gravity-wave spectra in the atmosphere observed by MST radar, part 4.2B 21 p3622 N85-32502
Estimation of vertical diffusion from observations of Atmospheric turbulence layers, part 4.4B
21 p3623 N85-32507
Momentum flux measurements: Techniques and needs, part 4.5A 21 p3623 N85-32508
MST radar data management
21 p3627 N85-32532
Data base for the Colorado profiling network
21 p3627 N85-32533
Generation of available potential energy and the energy cycle during the global weather experiment
[NASA-CR-175301] 21 p3634 N85-32572
Circulation analysis of two snowstorms during the SNOW-TWO program
[AD-A155225] 21 p3637 N85-32587
Notes on atmospheric stability, turbulence, and its measurements
[AD-A155230] 21 p3637 N85-32588
Sahara Desert dust transport to the south
21 p3648 N85-32666
Measurements of giant salt nuclei from inland in east China 21 p3648 N85-32668
Observations of cloud droplets, aerosol particles and cloud condensation nuclei in continental air masses
21 p3649 N85-32671
Condensation properties of atmospheric aerosol
21 p3649 N85-32672
Numerical simulations of the response of intense ocean currents to atmospheric forcing
[AD-A155161] 21 p3655 N85-32704
A mixed pseudospectral/finite difference method for a thermally driven fluid in a nonuniform gravitational field
[NASA-TM-87581] 22 p3783 N85-33436
Airborne cloud tracking measurements during the Three Mile Island nuclear station accident, Middletown, Pennsylvania. Date of survey: March - June 1979
[DE85-012060] 22 p3816 N85-33638
Radar wind profilers in the Colorado network
[PB85-185486] 22 p3817 N85-33647
Development of an adjustable buoyancy balloon tracer of atmospheric motion. Phase 1: Systems design and demonstration of feasibility
[PB85-185817] 22 p3817 N85-33648
Subseasonal variability in a two-level atmospheric general circulation model 24 p4114 N85-35504
A strategy for calibrating atmospheric transport models
[CSIRO-DAR-TP-9] 24 p4116 N85-35518
The kinematic structure of cold frontal rainbands
24 p4119 N85-35531
Case studies for flux measurements along a low-flying route to the south of Munich 24 p4121 N85-35548
The determination of lee circulation during the foehn wind 24 p4122 N85-35554
Maintenance of blocking anticyclones in a general circulation model
[PB85-190866] 24 p4124 N85-35567
Airborne Investigations of Mesoscale Convective Systems (AIMCS), 1984: Operational summary and data inventory
[PB85-187904] 24 p4125 N85-35571

ATMOSPHERIC COMPOSITION
NT ATMOSPHERIC MOISTURE
NT IONOSPHERIC COMPOSITION
Effect of hyperoxia and increased gas atmosphere density on contractile function of the right ventricle
01 p0093 N85-10628
Model of atmospheric ozone for middle latitudes
02 p0161 N85-11091
A study of greenhouse effects using zero, 1 and 2 dimensional climate models 02 p0230 N85-11498
Atmospheres of Uranus and Neptune
02 p0298 N85-11929
Aeronomy 02 p0298 N85-11930
Physical properties of the Uranian satellites
02 p0300 N85-11946
STS natural environment analysis
[NASA-CR-171221] 03 p0322 N85-12079
A proposed reference set of scenarios for radiatively active atmospheric constituents
[DOE/NBB-0066] 03 p0388 N85-12483
Measurements of atmospheric carbon disulfide using aircraft platforms and a GC/MS isotopic dilution analysis technique 03 p0391 N85-12500
Carbon dioxide, the greenhouse effect and climate: A primer
[GPO-33-444] 03 p0395 N85-12519
Atmospheric extinction in critical environments
[AD-A146102] 03 p0396 N85-12527
Variations with time of the carbon dioxide partial pressure in central and south Atlantic surface waters
[AD-A145825] 03 p0398 N85-12537
The Jovian atmospheric window at 2.7 microns: A search for H2S
[NASA-TM-86661] 03 p0445 N85-12836
Thermodynamic conditions of the Earth's atmosphere with pollution processes 04 p0523 N85-13345
Trends in ozone and temperature structure: Comparison of theory and measurements
[DE84-016201] 04 p0539 N85-13428
Global carbon - nitrogen - phosphorus cycle interactions: A key to solving the atmospheric CO2 balance problem?
05 p0652 N85-14188
Fundamental equations of the LIF hydroxyl measurements, appendix A 05 p0676 N85-14338
Studies of radiative transfer in planetary atmospheres
[NASA-CR-174194] 05 p0745 N85-14778
Lower atmospheric composition of Jupiter from Voyager infrared measurements
[NASA-CR-174196] 05 p0745 N85-14779
Analysis and characterization of organic carbon compounds in atmospheric particulate matter
[PB84-232636] 06 p0766 N85-14903
Simple formula to estimate carbon dioxide gas effect in radiation balance of underlying surface
06 p0823 N85-15226
The CSIRO (Australia) atmospheric carbon dioxide monitoring program: Surface data
[CSIRO-TP-6] 07 p0996 N85-16324
Middle Atmosphere program. Handbook for MAP. Volume 13: Ground-based techniques
[NASA-CR-174345] 08 p1183 N85-17452
Microwave radiometric studies of composition and structure 08 p1183 N85-17456
Lidar systems for aerosol studies: An outline
08 p1183 N85-17457
Active optical sounding of ozone and minor constituents in the middle atmosphere: A review of ground-based lidar measurements 08 p1183 N85-17458
Lidar studies of the alkali metals
08 p1184 N85-17460
Guidelines for atmospheric measurements in support of electro-optical systems testing
[AD-A148090] 08 p1186 N85-17474
On the importance of light hydrocarbons in multiphase atmospheric systems
[JUEL-1942] 08 p1190 N85-17496
Stratospheric concentration of nitric acid, ozone and carbonyl sulfide: Measurement of nitric acid absorption in the Q branch of the V4 band as a function of temperature
[ESA-TT-864] 09 p1355 N85-18524
Near infrared modeling of the equatorial regions of Jupiter and Saturn 09 p1415 N85-18930
Airborne lidar measurements of El Chichon stratospheric aerosols, October 1982 to November 1982
[NASA-RP-1136] 10 p1514 N85-19550
Development of a low cost electrochemical CO monitor based on stripping voltammetry
[PB85-113470] 11 p1637 N85-20312
UK participation in the Middle Atmosphere Programme
11 p1655 N85-20426
The Middle Atmosphere Program: A special project for the Antarctic Middle Atmosphere (AMA)
11 p1656 N85-20430
Cold Arctic Mesopause Project (CAMP): Scientific objectives 11 p1656 N85-20433
Middle Atmosphere Program. Handbook for MAP, volume 8
[NASA-CR-175478] 11 p1657 N85-20445
MAP/GLOBUS campaign 1983
11 p1658 N85-20447
Carbon dioxide and the greenhouse effect
[GPO-39-043] 11 p1677 N85-20569
Middle atmosphere NO and NO2 observed by means of the Spacelab one grille spectrometer
[AERONOMICA-ACTA-A-293-1984]
11 p1680 N85-20588
The Jovian Stratosphere in the ultraviolet
11 p1760 N85-21069
Atlantic Coast Unique Regional Atmospheric Tracer Experiment (ACURATE)
[PB85-128460] 12 p1886 N85-21839
Multiple element neutron-activation analysis of atmospheric aerosols with X-ray and gamma-spectrometric recording of radionuclides formed
13 p2013 N85-22631
One mechanism of formation of organic fraction in atmospheric aerosol 13 p2014 N85-22632
Possible role of ocean biota in global carbon balance — phytoplankton production 13 p2107 N85-23129
Sulfur oxygen processes on Io
13 p2173 N85-23481
Photometric analysis of Jupiter-illuminated images of Io 13 p2196 N85-23620
Chemical composition of coastal haze aerosol
14 p2338 N85-24456
Spectroscopic study of gas pollutants in atmosphere over large cities: A review 14 p2341 N85-24478
Magnetospheric effects on the upper atmosphere
14 p2365 N85-24616
Extended atmospheres of outer planet satellites and comets
[NASA-CR-175673] 14 p2440 N85-25058
Research on atmospheric dust formations using satellite observation data 15 p2485 N85-25339
Operational methods for calculating atmospheric dispersion
[BLL-CE-TRANS-8040-(9022.09)]
15 p2588 N85-25955
Size distributions of elemental carbon in atmospheric aerosols
[PB85-153534] 15 p2589 N85-25963
Changes in the high-latitude ocean as possible causes of atmosphere CO2 variations 15 p2602 N85-26036
One approach to remote sensing of total ozone content 16 p2725 N85-26822
Comparison of observed and predicted short-term tracer-gas concentrations in the atmosphere
[DE85-007566] 16 p2821 N85-27399
Interactive effects of acid rain and gaseous air pollutants on natural terrestrial vegetation
[DE85-005255] 16 p2821 N85-27401
Acid precipitation in North America: 1980, 1981 and 1982 annual data summaries from acid deposition system data base
[PB85-162477] 16 p2822 N85-27410
Measurement of elements in the stratosphere
[NASA-CR-175891] 16 p2823 N85-27414
Stratospheric ClO: In-situ detection with a new approach 16 p2824 N85-27416
The copper vapor laser 16 p2824 N85-27417
In-situ stratospheric ozone measurements: Recent results and their implications 16 p2824 N85-27419
Water vapor 16 p2824 N85-27420

Role and fate of ozone in the atmosphere 16 p2824 N85-27421

Atmospheric radon measurements in the Antarctic Penninsula: A preliminary report
[INPE-3398-PRE/667] 16 p2827 N85-27436

Elemental analysis of aerosols in Transvaal urban and power-producing areas using time and size-resolved samples 16 p2829 N85-27443

Geophysical monitoring for climatic change, number 12
[PB85-172278] 16 p2837 N85-27496

Cometary atmospheres: Modeling the spatial distribution of observed neutral radicals
[NASA-CR-175852] 16 p2882 N85-27781

Absolute calibrations of SO2 and NO analyzers by photographic methods
[DFVLR-MITT-85-02] 17 p2994 N85-28504

Theoretical basis for the determination of the concentration of radon decay products in air from the activity of a particulate air sample
[IRI-190-83-07] 17 p3035 N85-28774

Improvement of the basic knowledge of the climatology of the vertical ozone layer by enhanced balloon sounding
[BPT-6/84] 18 p3137 N85-29426

Geothermal hydrogen and health in Rotorua, New Zealand
[DE85-901283] 19 p3301 N85-30467

Volatiles in the outer solar system. 1: Thermodynamics of clathrate hydrates. 2: Ethane ocean on Titan. 3: Evolution of primordial Titan atmosphere
19 p3382 N85-30984

Ozone in the 21st century: Increase or decrease
[AERONOMICA-ACTA-A-291-1984]
20 p3489 N85-31687

Concentrations of ice nuclei of different modes of activities 21 p3641 N85-32616

Observations of the atmospheric ice nucleus at northwest China 21 p3641 N85-32618

The investigation of natural and artificial ice nuclei by the improved membrane filter method
21 p3642 N85-32626

A thermal diffusion chamber for the measurement of cloud condensation nuclei 21 p3642 N85-32627

Concentration and source areas of ice nuclei in the Alaskan atmosphere 21 p3643 N85-32634

Eleventh International Conference on Atmospheric Aerosols, Condensation and Ice Nuclei, volume 1
[PB85-182400] 21 p3644 N85-32636

Study of the formation of particles from natural hydrocarbons released by vegetation
21 p3644 N85-32640

Experimental studies of the formation of Aitken nuclei in the atmosphere 21 p3644 N85-32641

Photochemical aerosol formation in polluted atmosphere 21 p3644 N85-32642

The influence of Brownian coagulation on the size distributions of atmospheric aerosols
21 p3645 N85-32643

A study of time transformation of natural photochemical aerosols 21 p3645 N85-32644

Human activity and production rate of secondary nuclei 21 p3645 N85-32645

A new hypothesis for the observed vertical distribution of atmospheric aerosols 21 p3645 N85-32646

On the transformation regularities of time series cf solid aerosol concentrations in the surface atmospheric layer
21 p3645 N85-32648

Our knowledge about the atmospheric aerosol
21 p3646 N85-32650

Chemical composition of atmospheric aerosol at Delhi
21 p3646 N85-32653

Aitken particle size distribution in Antarctica
21 p3646 N85-32656

Condensation nuclei and aerosol size distribution measurements in Arctic haze 21 p3647 N85-32658

Aircraft investigations of the distribution of aerosols in the lower troposphere 21 p3647 N85-32659

The variability of aerosol microstructure in continental and oceanic surface layers of the atmosphere in anticyclones 21 p3647 N85-32660

Theoretical studies of structure and stability of hydrates of atmospheric sulfur species 21 p3650 N85-32664

A review on the formation of aerosol particles in the atmosphere 21 p3651 N85-32667

The evolution of complex and higher organisms
[NASA-SP-478] 21 p3656 N85-32706

Origin of life 21 p3657 N85-32713

Evolution of the atmosphere 21 p3658 N85-32725

Participation of singlet oxygen in photodestruction of air-saturated solutions of coumarin dyes
21 p3665 N85-32691

The possibilities of remote analysis of atmospheric gases based on Raman scattering spectroscopy
21 p3665 N85-32692

Constraints on early atmosphere from planetary accretion processes 21 p3717 N85-33064

The composition of the primitive atmosphere and the synthesis of organic compounds on the early Earth
21 p3717 N85-33065

The problem of the Earth's CO2 content and the iron core 21 p3718 N85-33069

Water loss from Venus: Implications for the Earth's early atmosphere 21 p3721 N85-33087

MELSAR: A mesoscale air quality model for complex terrain. Volume 1: Overview, technical description and user's guide
[DE85-010943] 22 p3811 N85-33608

Atmospheric reaction products from hazardous air pollutant degradation
[PB85-185841] 22 p3813 N85-33620

Ozone during sudden stratospheric warming: A three-dimensional simulation
[AERONOMICA-ACTA-A-292-1984]
22 p3813 N85-33621

Acetonitrile in the Earth's atmosphere: An upper limit deduced from infrared solar spectra
[AERONOMICA-ACTA-A-295-1985]
22 p3813 N85-33623

Middle Atmosphere Program. Handbook for MAP, volume 11
[NASA-CR-176107] 22 p3814 N85-33625

Potential spin-offs of the carbon dioxide observational platform system (CO-OPS) for remote sensing opportunities
[NASA-TP-2510] 23 p3899 N85-34149

Agents and effects of ozone trends in the atmosphere
[AERONOMICA-ACTA-A-287-1984]
23 p3946 N85-34466

Climate modeling: A retrospective-prospective view with consideration for the atmospheric carbon dioxide-climate issue
[DE85-011532] 23 p3950 N85-34481

ATMOSPHERIC CONDITIONS
U METEOROLOGY

ATMOSPHERIC CONDUCTIVITY
NT IONOSPHERIC CONDUCTIVITY

An improved rocket-borne electric field meter for the middle atmosphere
[NASA-CR-175510] 12 p1868 N85-21851

Distribution of atmospheric electric current in the global circuit
[CONTRIB-87] 12 p1868 N85-21852

Field validation of 6-particle puff model
[DE85-004073] 15 p2569 N85-25962

The Martian climate: Energy balance models with CO2/H2O atmospheres
[NASA-CR-175722] 15 p2679 N85-26547

Effect of vertical shear on regional-scale trajectories in near-frontal conditions
[DE85-007554] 19 p3317 N85-30561

The electric current densities beneath thunderstorms
20 p3494 N85-31726

Application of Particle Induced X-ray Emission analysis (PIXE) to aerosol long range transport studies
21 p3648 N85-32665

ATMOSPHERIC CORRECTION

Fast Hartmann method for problems in astronomical adaptive optics 02 p0161 N85-11094

Correction for atmospheric refraction in an airborne, operational environment
[AD-A146552] 06 p0835 N85-15314

LANDSAT-4 Thematic Mapper calibration and atmospheric correction 12 p1870 N85-21734

LANDSAT 4 band 6 data evaluation
[E85-10093] 12 p1874 N85-21755

Preliminary investigation into using the sun as a source for G/T (Gain to System Noise Temperature) measurements
[PB85-128146] 12 p1952 N85-22265

Investigating statistical characteristics of atmospheric background brightness and star background density in equatorial region of celestial sphere
15 p2478 N85-25298

ATMOSPHERIC DENSITY

Effect of hyperoxia and increased gas atmosphere density on contractile function of the right ventricle
01 p0093 N85-10628

Global matrix of thermospheric density values for selected solar/geomagnetic conditions and spacecraft orbital attitudes
[NASA-TM-86478] 04 p0533 N85-13409

Continuum absorption by H2O in the 700-1200 cm(-1) and 2400-280 cm(-1) windows
[AD-A147391] 07 p0997 N85-16334

Atmospheric profile imprint in firewall ablation coefficient 11 p1662 N85-20473

Consummative expressions for satellite drag perturbations in a spherically symmetrical atmosphere
[AD-A154230] 19 p3222 N85-29961

Applied research and development for falling-sphere air density measuring systems
[AD-A155227] 21 p3552 N85-32099

Application of satellite accelerometer data to improve density models
[AD-A154904] 21 p3631 N85-32558

Studies of the solar mesosphere explorer: Dynamics and horizon sensor performance. Part A: Spin axis precession and atmospheric drag. Part B: Clouds
[NASA-CR-175306] 24 p4069 N85-35213

ATMOSPHERIC DIFFUSION

Observed rate of tropospheric diffusion
[DE84-016047] 02 p0224 N85-11470

Review of the attributes and performance of six urban diffusion models
[PB84-236850] 04 p0484 N85-13087

A new fast response probe for diffusion studies in atmospheric air — pollution modeling
[IC-AERO-84-01] 08 p1160 N85-17437

Atmospheric wind and diffusion from analysis of an SF6 release at 350 km altitude
[AD-A147965] 08 p1165 N85-17471

Atmospheric diffusion in hilly region on middle reaches of the Chang Jiang 11 p1620 N85-20196

Atmospheric dispersion of hypergolic liquid rocket fuels, volume 1
[AD-A149597] 12 p1817 N85-21399

Adjustment of the national dispersion model for air pollution from elevated sources
[KNMI-TR-57] 14 p2353 N85-24540

The Terrain-Responsive Atmospheric Code (TRAC) for plume growth and dispersion in complex terrain
[DE85-010541] 19 p3309 N85-30513

Modeling of chemical transformations of SO(x) and NO(x) in the polluted atmosphere: An overview of apprcaches and current status
[PB85-173169] 20 p3487 N85-31677

Impact of fluctuations in optical properties of atmosphere on the ratio of spectral brightness from remote sensing of agricultural land 22 p3734 N85-33149

The first three harmonics of solar daily variation caused by the diffusive propagation of galactic cosmic rays through the heliosphere
[SH-4.5-1] 23 p4035 N85-35019

ATMOSPHERIC EFFECTS

Distribution of atmospheric radio interference
06 p0792 N85-15063

Limits of the propagation medium with respect to digital signal transmission 10 p1469 N85-19270

Propagation of wide bandwidth signals in a tropospheric ducting system 10 p1469 N85-19271

The effect of the arbitrary level assignment of satellite cloud motion wind vectors on wind analyses in the pre-thunderstorm environment
[NASA-TM-86186] 10 p1517 N85-19565

Lake ice occurrence as a possible detector of atmospheric CO2 effects on climate
[DE85-002951] 11 p1687 N85-20606

Proposed preliminary design criteria model environment for the 1990's 12 p1784 N85-21194

Atmospheric environment for Space Shuttle (STS-51A) launch
[NASA-TM-86497] 12 p1892 N85-21875

Thematic Mapper data quality and performance assessment in renewable resources/agriculture/remote sensing 13 p2120 N85-23201

The Terrain-Responsive Atmospheric Code (TRAC) for plume growth and dispersion in complex terrain
[DE85-010541] 19 p3309 N85-30513

Factor analysis of atmospheric pollution by polycyclic aromatic hydrocarbons
[HSE-TRANS-10988] 19 p3311 N85-30528

One-dimensional model hindcasts of warm anomalies in the North Pacific Ocean
[AD-A154128] 19 p3320 N85-30579

Understanding and laboratory prediction of the atmospheric corrosion behavior of steels and of non-ferrous metals and alloys
[AD-A154642] 21 p3566 N85-32179

A review of shock waves around aeroassisted orbital transfer vehicles
[NASA-TM-86769] 22 p3739 N85-33177

Lake ice occurence as a possible detector of atmospheric CO2 effects on climate
[DE85-012987] 23 p3950 N85-34480

Atmospheric effects on the underground muon intensity
[SH-6.1-3] 23 p4044 N85-35078

Determination of characteristic values for fiber reinforced materials 24 p4074 N85-35247

ATMOSPHERIC ELECTRICITY
NT AURORAL ELECTROJETS
NT ELECTROJETS
NT EQUATORIAL ELECTROJET
NT IONOSPHERIC CURRENTS

NASA thunderstorm overflight program: Atmospheric electricity research. An overview report on the optical lightning detection experiment for spring and summer 1983
[NASA-TM-86468] 03 p0363 N85-12330
Measurements of electric fields obtained by stratospheric balloons in the region of the South Atlantic anomaly
[INPE-3218-PRE/571] 06 p0675 N85-14335
Synoptic observations of the radio noise background in the frequency range 150-180 kHz to provide design data for the low frequency communications designer
[AD-A147436] 07 p0941 N85-15965
A study of the effects of triggered lightning
[AD-A148296] 08 p1189 N85-17494
Atmospheric research aircraft — conductivity/charge measurements
[ONERA-RS-87/7154/PY] 11 p1682 N85-20596
Effects of lightning on aircraft studied at Sheremetyevo 15 p2461 N85-25199
Measuring methods of atmospheric electric elements at the Earth's surface during snowfall and investigation of these relationships 15 p2581 N85-25920
Some considerations about the natural atmospheric radioactive aerosol 21 p3647 N85-32682

ATMOSPHERIC EMISSION
U AIRGLOW

ATMOSPHERIC ENERGY SOURCES
Cage regional energy budgets from the GLAS ATH order model 05 p0685 N85-14402
Comments on the measurements of multiple muon phenomena
[HE-5.2-13] 24 p4203 N85-36089

ATMOSPHERIC ENTRY
NT HYPERSONIC REENTRY
NT REENTRY
NT SPACECRAFT REENTRY
NT UNCONTROLLED REENTRY (SPACECRAFT)
The orbiter air data system 08 p1094 N85-16912
Approximate analytic method of calculating trajectories of movement of a flight vehicle in the atmosphere
14 p2279 N85-24121
Natural reentry of satellites 14 p2397 N85-24774
Results of tests of the SRB aft skirt heat shield curtain in the MSFC Hot Gas Facility
[NASA-CR-170888] 24 p4070 N85-35223

ATMOSPHERIC ENTRY SIMULATION
Method for prompt modeling of quasiperiodic movement of solid near-axisymmetrical body in atmosphere
13 p2043 N85-22790

ATMOSPHERIC GENERAL CIRCULATION EXPERIMENT
Computer studies of baroclinic flow — Atmospheric General Circulation Experiment
[NASA-CR-171338] 10 p1517 N85-19566

ATMOSPHERIC HEAT BUDGET
Combining Heat Capacity Mapping Mission (HCMM) LANDSAT and thematic map information into a unique high precision merged multichannel system — climatology 05 p0660 N85-14239
The first winter of MAP-dynamics, 1982-1983: A winter with three different warming periods
11 p1657 N85-20446
Influence of aerosol on formation of outgoing thermal radiation 14 p2342 N85-24483
Partitioning of the vertical turbulent energy transport into positive and negative contributions — meteorology
24 p4122 N85-35551
Aircraft measurements during the Bonn Experiment (BONEX 1) — meteorology 24 p4122 N85-35552
Motor glider measurements during the Urban Atmosphere Energy Budget Experiment (EESA 1)
24 p4122 N85-35553

ATMOSPHERIC HEATING
Analysis of diabatic heating during FGGE
05 p0683 N85-14393
Global scale diagnosis of FGGE data
05 p0683 N85-14394
Planetary scale interactions 05 p0684 N85-14397
Atmospheric heating of meteorites: Results from nuclear track studies 06 p0882 N85-15807
The Middle Atmosphere Program: Winter in Northern Europe (MAP/WINE) 11 p1655 N85-20429
Middle Atmosphere Program. Handbook for MAP, volume 8
[NASA-CR-175476] 11 p1657 N85-20445
The first winter of MAP-dynamics, 1982-1983: A winter with three different warming periods
11 p1657 N85-20446
Stratwarm effects in the ionospheric D region wind field 11 p1663 N85-20479
Outer atmospheres of cool stars observed with IUE
11 p1744 N85-20968
Anomalous heating of ionospheric components (thermal e- and He+) via intense Ion Cyclotron Waves (ICW's)
14 p2368 N85-24633
Sensitivity of planetary waves to initial conditions and forcing
[AD-A154111] 19 p3345 N85-30734
Ozone during sudden stratospheric warming: A three-dimensional simulation
[AERONOMICA-ACTA-A-292-1984]
22 p3813 N85-33621

ATMOSPHERIC IMPURITIES
U AIR POLLUTION

ATMOSPHERIC IONIZATION
NT AURORAL IONIZATION
Analysis of ionization sources in D region based on theoretical models 06 p0825 N85-15240
MWR, Meteor Wind Radars 08 p1184 N85-17462
MAP activities in Hungary 11 p1657 N85-20440
Investigation of aeronomic processes on the basis of ionospheric sporadic E 11 p1663 N85-20482
High energy particle effects in the D region during and after geomagnetic storms 11 p1664 N85-20485
Dependence of the high latitude middle atmosphere ionization on structures in interplanetary space
11 p1664 N85-20487
Dependence of equatorial F-region plasma bubble rise velocity and dynamo electric field on solar cycle
[INPE-3439-PRE/696] 16 p2826 N85-27434
X-ray intensification at balloon altitudes of the South Atlantic magnetic anomaly in association with geomagnetic activity
[INPE-3469-PRE/712] 16 p2827 N85-27437
Shuttle Molecular Gun: Smog. Potential experiment for the electrodynamic Tethered Satellite System (TSS) mission
[IFSI-84-17] 20 p3419 N85-31221
Rocket measurements of mesospheric ionization irregularities
[NASA-CR-176056] 20 p3494 N85-31721

ATMOSPHERIC LASERS
Linear absorption and scattering of laser beams
[AD-A156167] 24 p4096 N85-35401

ATMOSPHERIC LOADING
U POLLUTION TRANSPORT

ATMOSPHERIC MODELS
NT REFERENCE ATMOSPHERES
Processing and display of atmospheric phenomenaa data
[NASA-CR-171178] 01 p0072 N85-10475
The mesoscale-beta-scale evolution of mid-latitude meso-alpha-scale convective complexes
01 p0073 N85-10488
Automated analysis and nowcasting of mesoscale convective systems 01 p0074 N85-10492
Three-dimensional mesoscale analysis of serial soundings 01 p0074 N85-10493
Rain bands and symmetric instability
01 p0075 N85-10496
A short-term forecast model for thunderstorm rotation
01 p0081 N85-10542
A system for meteorological satellite, radar, conventional data and model analysis 01 p0082 N85-10551
Interactive computer display systems in nowcasting
01 p0083 N85-10557
Model of atmospheric ozone for middle latitudes
02 p0161 N85-11091
Quasi-stationary atmospheric responses to large-scale forcing 02 p0227 N85-11484
A comparison of 2- and 3-dimensional transport within a stratosphereic circulation model
02 p0227 N85-11485
Development of a global model for atmospheric backscatter at CO2 wavelengths
[NASA-CR-174053] 02 p0228 N85-11489
A study of greenhouse effects using zero, 1 and 2 dimensional climate models 02 p0230 N85-11498
Statistical interpretation of NWP model output: An overview of techniques used and results achieved
[REPT-551.509.313] 02 p0231 N85-11503
Report of the Third Session of the International Working Group on Data Management for the International Satellite Cloud Climatology Project (ISCCP)
[WCP-82] 02 p0231 N85-11504
Properties of the upper tropospheres of Uranus and Neptune derived from observations at visible to near-infrared wavelengths 02 p0298 N85-11933
Laboratory evaluation of microwave absorption properties under simulated conditions for planetary atmospheres
[NASA-CR-174060] 02 p0303 N85-11960
A proposed reference set of scenarios for radiatively active atmospheric constituents
[DOE/NBB-0066] 03 p0388 N85-12483
A 2-dimensional description of potential perturbations to the ozone layer due to NOx and H-2-O aircraft emissions
[AD-A148292] 03 p0392 N85-12511
Development of a microcomputer coupled atmospheric and oceanic boundary layer prediction model
[AD-A146334] 03 p0397 N85-12530
The Martian climate: Energy balance models with CO2/H2O atmospheres
[NASA-CR-174073] 03 p0448 N85-12849
Thermodynamic conditions of the Earth's atmosphere with pollution processes 04 p0523 N85-13345
China report: Science and technology
[JPRS-CST-84-001] 04 p0557 N85-13546
Theoretical and observed dispersion of acoustic-gravity waves in atmosphere 04 p0557 N85-13547
The Interaction of Global Biochemical Cycles
[NASA-CR-174184] 05 p0652 N85-14183
Global biogeochemical cycles: Studies of interaction and change, some views on the strategy of approach
05 p0652 N85-14185
Three dimensional global modeling of atmospheric CO2 05 p0652 N85-14189
GLAS fourth order model 05 p0679 N85-14361
Orographic effects in atmospheric circulation
05 p0679 N85-14362
Spectral general circulation model development
05 p0679 N85-14363
Biosphere/atmosphere interactions
05 p0679 N85-14364
A vertically resolved planetary boundary layer
05 p0680 N85-14367
Normal mode initialization 05 p0680 N85-14372
Forecast impact of components of the FGGE observing system 05 p0681 N85-14373
Water vapor profile retrievals from the HIRS/MSU satellite sounder 05 p0681 N85-14378
Jet stream errors and tropospheric-stratospheric interactions in the GLAS general circulation model
05 p0683 N85-14392
Global scale diagnosis of FGGE data
05 p0683 N85-14394
Theoretical modeling for numerical weather prediction
05 p0684 N85-14395
Numerical prediction of the president's day cyclone
05 p0684 N85-14399
Cage regional energy budgets from the GLAS ATH order model 05 p0685 N85-14402
Investigation of cloud feedback in the GLAS model
05 p0685 N85-14404
Application of the bounded derivative initialization method 05 p0686 N85-14407
Implicit numerical methods in meteorology
05 p0686 N85-14408
Linear studies of stationary, extratropical anomalies in the troposphere 05 p0686 N85-14410
The influence of synoptic scales on low-frequency modes of variability 05 p0687 N85-14412
Internal gravity waves in real atmosphere
06 p0825 N85-15236
Analysis of ionization sources in D region based on theoretical models 06 p0825 N85-15240
Modeling influence of three layer cloud cover on outgoing thermal radiation 06 p0825 N85-15242
Indirect estimation of convective boundary layer structure for use in routine dispersion models
[PB84-236260] 06 p0834 N85-15306
Large-eddy simulation. Guidelines for its application to planetary boundary layer research
[AD-A146381] 06 p0890 N85-15651
Fluctuations during observations of extraterrestrial sources from outer space through Earth's atmosphere
07 p0953 N85-16040
Research in geodesy based upon radio interferometric observations of extragalactic radio sources
[AD-A147581] 07 p0988 N85-16280
Atmospheric Modeling And Sensor Simulation (AMASS) study
[NASA-CR-171283] 07 p0996 N85-16325
The role of finite parallel length on the stability of barium clouds
[AD-A146972] 07 p0996 N85-16328
The effects of long-periodic forcing in a zero-dimensional climate model 07 p1002 N85-16363
Index cycles simulated by a low order forced barotropic model 07 p1002 N85-16364
Experiments in forecasting atmospheric marine horizontal visibility using model output statistics with conditional probabilities of discretized parameters
[AD-A147574] 07 p1008 N85-16404
Sensor-atmosphere-target simulation. Computer program SENSAT
[DFVLR-FB-84-32] 08 p1176 N85-17419
Determination of the laws governing the changes in the standard deviations of the distribution of pollution based on observations of the atmospheric turbulence spectrum and the possibility of simulating it in the laboratory
[BLL-TR-T6373/BG/MRS14663/84]
08 p1179 N85-17431

Modeling of turbulent dispersion of neutral and buoyant contaminants released from two dimensional sources — air pollution
[VKI-TN-150] 08 p1180 N85-17438

Plasma and magnetospheric research
[NASA-CR-171290] 08 p1183 N85-17451

Atmospheric photochemical modeling of turbine engine fuels. Phase 1: Experimental studies. Volume 2: Environmental chamber data tabulations
[AD-A147786] 08 p1185 N85-17470

Radiation parameterization programs for use in general circulation models
[AD-A148015] 08 p1188 N85-17486

Development of guidance forecasts at the Royal Netherlands Metorological Institute (KNMI). Part 1: General information
[KNMI-TR-54-PT-1] 08 p1190 N85-17499

Atmospheric acidification chemistry: A review
[PB84-215490] 09 p1350 N85-18495

A turbulent closure model for the free atmosphere
09 p1351 N85-18502

Atmospheric science and power production
[DE84-005177] 09 p1354 N85-18521

Simulation of entrainment at the top of the atmospheric boundary layer for use in General Circulation Models (GCM)
[DM-42] 09 p1355 N85-18525

Global scale diagnoses of FGGE data
[NASA-CR-174356] 09 p1356 N85-18533

The influence of soil moisture distribution on the severe-storm environment of the southern Great Plains: A numerical study of the SESAME 4 case
09 p1357 N85-18534

Mesoscale storm and dry period parameters from hourly precipitation data: Program documentation
[DE85-001366] 09 p1357 N85-18538

Combined effects of baroclinic and barotropic instability in a nonlinear low order model
[DM-41] 09 p1358 N85-18544

Near infrared modeling of the equatorial regions of Jupiter and Saturn 09 p1415 N85-18930

PMP-1: A coordinated study of the behavior of the middle atmosphere in winter 11 p1654 N85-20421

MAP in Japan: Organization and projects
11 p1655 N85-20425

UK participation in the Middle Atmosphere Programme
11 p1655 N85-20426

Soviet National Middle Atmosphere Program
11 p1655 N85-20428

The global meteor observation system (GLOBMET)
11 p1656 N85-20432

MAP activities in Hungary 11 p1657 N85-20440

Basic features of global circulation in the mesopause lower thermosphere region 11 p1662 N85-20475

Study of pollutant dispersion in an urban street canyon
[DE85-002648] 11 p1677 N85-20571

Comparison of MESOI atmospheric dispersion estimates with data and estimates from other models
[DE85-002372] 11 p1678 N85-20572

Continued research in mesoscale air pollution simulation modeling. Volume 7. Mathematical modeling of urban aerosol dynamics
[PB85-137388] 11 p1679 N85-20584

Atmospheric properties of RU Lupi derived from high- and low-resolution IUE spectra
11 p1754 N85-21031

The physical implications of an isothermal model for the hot intracluster medium
[NASA-TM-86174] 11 p1763 N85-21089

Wind-tunnel research on the mechanics of plumes in the atmospheric surface layer
[AD-A150019] 12 p1846 N85-21584

Spectroradiometric calibration of the Thematic Mapper and Multispectral Scanner system
[E85-10094] 12 p1874 N85-21756

Distribution of atmospheric electric current in the global circuit
[CONTRIB-87] 12 p1888 N85-21852

Substorms in the Earth's atmosphere
[DE85-000654] 12 p1890 N85-21861

Structure and forcing of teleconnection patterns occurring in general circulation model simulations
[DE85-002434] 12 p1890 N85-21862

21 Layer troposphere-stratosphere climate model
[NASA-TM-86183] 12 p1892 N85-21871

Research Reports: 1984 NASA/ASEE Summer Faculty Fellowship Program
[NASA-CR-171317] 12 p1944 N85-22210

New atmospheric sensor analysis study
[NASA-CR-171426] 13 p2094 N85-23069

Modeling of mechanism of positive feedback between mean Earth surface temperature and atmospheric carbon dioxide in geologic time scale 13 p2106 N85-23122

Numerical experiments with simple model of ocean climate 13 p2106 N85-23123

Possibility of determining atmospheric weather parameters by radio and radiooptical measurements of refraction of cosmic sources 13 p2110 N85-23146

Stagnation zone impaction on a simple terrain feature in stable flow 13 p2130 N85-23255

Ground-up-to-Space (GUTS) laser propagation code description and manual
[AD-A150783] 14 p2309 N85-24295

Classification of atmospheric aerosol for evaluation of its effect on climate 14 p2333 N85-24428

Lyapunov stability of very simple steady solutions of prognostic systems 14 p2333 N85-24429

Influence of interaction between ocean and atmosphere on intensity of moving tropical cyclone
14 p2333 N85-24431

Small component spectral model of annual course of zonal atmospheric circulation 14 p2337 N85-24453

Applicability of vertically homogeneous atmospheric models for remote soundings 14 p2341 N85-24477

Influence of aerosol on formation of outgoing thermal radiation 14 p2342 N85-24483

One-dimensional nonstationary model of photochemical transformations of gas impurities in stratosphere
14 p2342 N85-24484

Adjustment of the national dispersion model for air pollution from elevated sources
[KNMI-TR-57] 14 p2353 N85-24540

Ionosphere-magnetosphere coupling and convection
14 p2364 N85-24609

Analysis of atmospheric interferometer data
[AD-A150682] 14 p2372 N85-24663

Characteristics and behavior of atmospheric aerosols; application to prediction of infrared extinction
[AD-A150691] 14 p2372 N85-24665

Statistical/Trend analysis of the marine atmospheric boundary layer model
[AD-A151053] 14 p2374 N85-24673

Sensitivity analysis of a coupled atmospheric-oceanic boundary layer model
[AD-A150760] 14 p2382 N85-24690

Investigation of the daytime lunar atmosphere
[NASA-CR-175636] 14 p2440 N85-25057

A model for the dynamics of the deep photosphere
14 p2450 N85-25129

Linear models of acoustic waves in sunspot umbrae
14 p2450 N85-25130

Use of atmospheric models in predicting artificial Earth satellite motion 15 p2478 N85-25296

One method for constructing model of point masses of planetary gravity field 15 p2479 N85-25300

Evaluating radiation distortions of optical image of Earth's surface in horizontally inhomogeneous atmosphere 15 p2486 N85-25345

Experimental investigation of annular air curtain domes
[UTIAS-288] 15 p2521 N85-25543

Operational methods for calculating atmospheric dispersion
[BLL-CE-TRANS-8040-(9022.09)]
15 p2588 N85-25955

Development of global model for atmospheric backscatter at CO2 wavelengths
[NASA-CR-175679] 15 p2591 N85-25971

The physics of the marine stratocumulus-capped mixed layer 15 p2593 N85-25979

An Earth longwave radiation climate model
[NASA-CR-175749] 15 p2594 N85-25984

Convection modeling and application to severe storms
15 p2595 N85-25991

Modeling of cloud systems 15 p2595 N85-25992

Modeling of midwest severe thunderstorms
15 p2596 N85-25995

Estimation of convective rainfall from visible and infrared satellite data 15 p2596 N85-25999

Mesoscale analysis and modeling group
15 p2596 N85-26001

ILUM code: Solar and lunar flux calculations for multi-cloud layered atmospheres
[DE85-005578] 15 p2600 N85-26025

Studies of electro-optical attenuation in the vicinity of cloud base
[AD-A151745] 15 p2653 N85-26360

Is there more than one steady state for NOx?
15 p2687 N85-26593

Wind modelling for increased aircraft operational efficiency 16 p2697 N85-26652

Modeling plasma mantle of Earth's magnetosphere
16 p2720 N85-26790

Emission inventory applications to regional acid deposition modeling
[PB85-157386] 16 p2760 N85-27033

Theory and modeling of the interaction between subgrid scale orography and large scale flow
[DM-43] 16 p2827 N85-27440

Use of a network of telemetered meteorological stations for prediction of the distribution of an atmospheric tracer
16 p2831 N85-27456

The problem of atmospheric turbulence
[NASA-CR-175783] 16 p2832 N85-27464

Tropical Oceans-Global Atmosphere (TOGA) experiment planning for the Brazilian participation in TOGA global climate program
[INPE-3499-PRE/735] 16 p2834 N85-27477

Simulation of a synchronously coupled atmosphere-ocean prediction model
[AD-A152020] 16 p2835 N85-27482

Circulation statistics from January and July: Simulation with the NCAR (National Center for Atmospheric Research) community climate model (CCMOB)
[PB85-165637] 16 p2837 N85-27497

Test of lidar inversion algorithm sensitivity to atmospheric backscatter and extinction parameters, revision A
[AD-A152082] 16 p2865 N85-27671

Monodeurated methane in the outer solar system. 2. Its detection on Uranus at 1.6 microns
[NASA-CR-175762] 16 p2882 N85-27782

Homogeneous processes of atmospheric interest
[NASA-CR-175770] 17 p2989 N85-28475

Geophysical plasmas and atmospheric modeling
[AD-A152805] 17 p2993 N85-28497

Time-dependence of CO2-induced climate change
[DE85-007566] 17 p2997 N85-28525

Ozone and temperature trends due to the injection of trace species in the atmosphere
[AERONOMICA-ACTA-A-286-1984]
18 p3132 N85-29399

Methods for simulating gas phase SO2 oxidation in atmospheric models
[PB85-173110] 18 p3135 N85-29418

Research Review, 1983
[NASA-TM-86219] 18 p3139 N85-29433

The impact of scatterometer data on limited-area model predictions of the QE 2 storm 18 p3139 N85-29436

Preliminary results from numerical experiments on the summer 1980 heat wave and drought
18 p3140 N85-29438

Experiments on the assimilation of patches of data using a barotropic model 18 p3140 N85-29441

High-latitude filtering in a global grid-point model using model normal modes 18 p3140 N85-29442

On the improvement of satellite temperature retrievals by means of boundary layer models
18 p3140 N85-29443

Development and testing of the variable vertical resolution Fourth Order GCM 18 p3142 N85-29453

Parameterization of surface fluxes in the VVR Fourth Order GCM 18 p3142 N85-29454

Model development highlight for 1984: The GLA Fourth Order GCM 18 p3143 N85-29457

Response of winter forecasts made with the GLA Fourth Order GCM to Changes in the horizontal grid resolution
18 p3143 N85-29458

Energy sources of the dominant frequency dependent 3-dimensional atmospheric modes
18 p3143 N85-29462

A comparison of the bounded derivative and the normal mode initialization methods using real data
18 p3144 N85-29463

The vertical structure of global rotational normal modes 18 p3144 N85-29464

Transient eddies in the UCLA GCM
18 p3145 N85-29470

Analysis of a simulated cloud climatology
18 p3145 N85-29472

A new CO2 transmittance parameterization and its impact on the GLA GCM 18 p3146 N85-29476

A GCM study of the atmospheric response to tropical SST anomalies 18 p3146 N85-29477

Influence of land surface processes on the Indian monsoon: A numerical study 18 p3146 N85-29478

Influence of land-surface roughness on atmospheric circulation and rainfall: A sensitivity study with a GCM
18 p3146 N85-29479

The structure and dynamics of an observed moist front 18 p3146 N85-29480

Some recent developments in numerical modelling at ECMWF 18 p3147 N85-29481

Global model of transport of pollutants in atmosphere
19 p3297 N85-30439

Areal coverage of storm precipitation
[NASA-CR-176013] 19 p3315 N85-30550

Atmospheric Tracer Workshop
[DE85-010573] 20 p3486 N85-31668

Spectral methods for limited area models
20 p3488 N85-31679

Strongly nonlinear dynamics of baroclinic waves
20 p3488 N85-31681

Errors and parameterizations of sub-grid scale processes in regional-scale atmospheric models
20 p3486 N85-31682

A survey of wind and turbulence modeling methods
[AD-A154470] 20 p3496 N85-31733

Carbon dioxide and climate: Potential impacts
[DE85-009473] 20 p3496 N85-31734

Lightcurve CCD spectrophotometry of Pluto
20 p3545 N85-32057

VALMET: A valley air pollution model
[DE85-010820] 21 p3614 N85-32463

A numerical analysis of transient planetary waves and the vertical structure in a meso-strato-troposphere model, part 1.4A 21 p3617 N85-32473

Nuclear thermal transmittance in the atmosphere using LOWTRAN-6 computer code
[AD-A154669] 21 p3630 N85-32553

Application of satellite accelerometer data to improve density models
[AD-A154904] 21 p3631 N85-32558

Generation of available potential energy and the energy cycle during the global weather experiment
[NASA-CR-175301] 21 p3634 N85-32572

Accuracy and operational use of medium and extended range numerical atmospheric forecasts: A review
[AD-A155027] 21 p3635 N85-32579

Mean flow and turbulence in complex terrain
[AD-A155136] 21 p3636 N85-32583

Simulation of the coupled atmospheric and oceanic boundary layer model during MILDEX
[AD-A155166] 21 p3655 N85-32705

A mixed pseudospectral/finite difference method for a thermally driven fluid in a nonuniform gravitational field
[NASA-TM-87581] 22 p3783 N85-33436

Atmospheric modeling of organics for risk assessment: A Chemist's view
[DE85-009770] 23 p3909 N85-34217

User's guide to the MATHEW/ADPIC models
[DE85-012952] 23 p3966 N85-34587

Millimeter-wave propagation in moist air: Model versus path data
[AD-A156040] 24 p4087 N85-35331

Application of a turbulent closure model to the parameterization of the vertical diffusion of heat, momentum, and humidity in the ECMWF model — European Center for Medium Term Weather Forecasting (ECMWF)
[MITT-41] 24 p4095 N85-35387

Subseasonal variability in a two-level atmospheric general circulation model 24 p4114 N85-35504

A strategy for calibrating atmospheric transport models
[CSIRO-DAR-TP-9] 24 p4116 N85-35518

Maintenance of blocking anticyclones in a general circulation model
[PB85-190666] 24 p4124 N85-35567

ATMOSPHERIC MOISTURE

Experiment on nowcasting of heavy rainfall and severe storms in central China in 1979-1981
01 p0081 N85-10545

H2O profile in lower atmosphere of Venus based on effective radiation flux measurements
02 p0163 N85-11102

Effects of atmospheric water vapor and clouds on NOAA (National Oceanic and Atmospheric Administration) AVHRR (Advanced Very High Resolution Radiometer) satellite data
[AD-A145425] 02 p0280 N85-11824

Air-sea heat exchange, an element of the water cycle
05 p0653 N85-14195

A diagnostic approach to obtaining planetary boundary layer winds using satellite-derived thermal data
05 p0674 N85-14330

Conditional symmetric instability and mesoscale rainbands 05 p0678 N85-14356

Studies of atmospheric water in storms with the Nimbus 7 scanning multichannel microwave radiometer
05 p0682 N85-14382

Atmospheric environment for Space Shuttle (STS-41G) launch
[NASA-TM-86486] 07 p0995 N85-16320

Condensational transformation of atmospheric aerosol particle distribution functions 10 p1500 N85-19468

Electrochemical cell to measure corrosion rates in noncondensing environments
[DE85-003148] 12 p1807 N85-21338

TRAJ: Single station trajectory plot
[PB85-135002] 12 p1897 N85-21911

Dependence of combustion of homogeneous kerosene-air mixtures on humidity of air
13 p2051 N85-22835

Possibility of determining atmospheric weather parameters by radio and radiooptical measurements of refraction of cosmic sources 13 p2110 N85-23146

Response of Earth's atmosphere to increases in solar flux and implications for loss of water from Venus
13 p2178 N85-23518

Determination of total moisture content in cloud-free atmosphere by relative radio emission measurements
14 p2340 N85-24472

Determining atmosphere moisture content from differences in two-frequency microwave radiation measurements 14 p2341 N85-24474

Ice multiplication in summertime cumulus clouds in the BEWMEX area 16 p2829 N85-27445

Precipitable water in the atmosphere, determined from surface dewpoint values 16 p2831 N85-27457

Atmospheric frontal zone studies
[NASA-CR-175293] 16 p2833 N85-27469

The moist available energy of a conditionally unstable atmosphere 18 p3145 N85-29473

The structure and dynamics of an observed moist front 18 p3146 N85-29480

Variability of air humidity profiles over ocean determined by lidar sounding 19 p3296 N85-30436

Influence of moisture and elevated temperature on the fatigue properties of WTS-3 glass fiber blade material — wind turbine blade (WTS-3)
[FFA-TN-1984-58] 20 p3470 N85-31558

Water loss from Venus: Implications for the Earth's early atmosphere 21 p3721 N85-33067

Throughfall rate and chemistry studies: Whiteface Mountain
[DE85-012407] 23 p3947 N85-34464

Program for Regional Observing and Forecasting Services (PROFS)
[PB85-188050] 24 p4124 N85-35569

ATMOSPHERIC NOISE

U ATMOSPHERICS

ATMOSPHERIC OPTICS

Fast Hartmann method for problems in astronomical adaptive optics 02 p0161 N85-11094

Some statistical characteristics of atmospheric optical thickness in visible spectral range
02 p0164 N85-11109

Methods for determining atmospheric optical parameters using results of space survey of Earth's surface
02 p0165 N85-11117

Relation between atmospheric scattering and backscattering coefficient
[ESA-TT-837] 05 p0677 N85-14350

Guidelines for atmospheric measurements in support of electro-optical systems testing
[AD-A148090] 08 p1186 N85-17474

Time spectra of intensity fluctuations along reflecting path 13 p2079 N85-22981

Mean free path lenght of photons with broken cloud cover 14 p2338 N85-24455

Error in laser correlation wind speed meters resulting from variable atmospheric transparency
14 p2338 N85-24457

Diffuse reflection of light from turbid conservative medium of finite thickness with incidence of beam on surface of scattering glancing 14 p2342 N85-24481

Visibility of small objects in turbid atmosphere
14 p2342 N85-24482

A brief comparison of Egyptian with West German atmospheric transmission data in the 8 to 11.5 micron waveband
[BAE-BT-12829] 15 p2594 N85-25983

La Recherche Aerospatiale Bimonthly Bulletin Number 1984-3, 220/May-June
[ESA-TT-882] 16 p2695 N85-26636

Airborne measurements of the vertical distribution of Arctic haze 21 p3647 N85-32657

ATMOSPHERIC PHYSICS

NT CLOUD PHYSICS

Research study: Studies in atmospheric processes from Space Platforms
[NASA-CR-171176] 01 p0072 N85-10473

Trapping for Newtonian diffusion processes
[REPT-73] 01 p0130 N85-10893

Seminar on Principal Components Analysis in the Atmospheric and Earth Sciences
[CSIR-S-334] 02 p0211 N85-11386

A review of the millimeter and centimeter observations of Uranus 02 p0299 N85-11935

Atmospheric dynamics of Uranus and Neptune: Theoretical considerations 02 p0299 N85-11936

Report of the Division of Atmospheric Physics, 1980-1983 03 p0391 N85-12501

Millimeter-wave propagation and remote sensing of the atmosphere
[AD-A146339] 03 p0393 N85-12512

Carbon dioxide, the greenhouse effect and climate: A primer
[GPO-33-444] 03 p0395 N85-12519

Proceedings of a Workshop on Atmospheric Research Needs for the Western United States
[DE84-015069] 04 p0534 N85-13412

Structure and energetics of medium-scale atmospheric waves in the southern hemisphere summer
05 p0685 N85-14403

Activities report in Earth and planetary environments physics
[CRPE-NT-134] 05 p0734 N85-14720

USSR report: Earth sciences
[JPRS-UES-84-007] 06 p0819 N85-15196

USSR report: Earth sciences
[JPRS-UES-84-008] 07 p0980 N85-16223

Continuum absorption by H2O in the 700-1200 cm(-1) and 2400-280 cm(-1) windows
[AD-A147391] 07 p0997 N85-16334

Study of infrared atmospheric emission
[AD-A147517] 07 p0998 N85-16336

Electronically excited atomic and molecular oxygen
[AD-A147732] 08 p1121 N85-17084

The use of principal components analysis techniques Nimbus-7 coastal zone color scanner data to define mesoscale ocean features through a warm humid atmosphere
[AD-A148567] 08 p1176 N85-17416

A new fast response probe for diffusion studies in atmospheric air — pollution modeling
[IC-AERO-84-01] 08 p1180 N85-17437

Plasma and magnetospheric research
[NASA-CR-171293] 08 p1183 N85-17451

Atmospheric science and power production
[DE84-005177] 09 p1354 N85-18521

USSR report: Earth sciences
[JPRS-UES-85-003] 10 p1497 N85-19446

Recent investigations at INPE in magnetospheric physics and geomagnetism
[INPE-3280-PRE/603] 10 p1514 N85-19555

Brazil future plans in upper atmosphere research in Antarctica
[INPE-3400-PRE/669] 10 p1515 N85-19559

Science Applications, part 1 11 p1643 N85-20346

PMP-1: A coordinated study of the behavior of the middle atmosphere in winter 11 p1654 N85-20421

French activities relevant to middle atmosphere research 11 p1655 N85-20423

Soviet National Middle Atmosphere Program
11 p1655 N85-20428

Middle Atmosphere Program. Handbook for MAP, volume 10
[NASA-CR-175477] 11 p1658 N85-20450

Atmospheric transmissometer
[AD-D011540] 12 p1932 N85-22140

USSR report: Earth sciences
[JPRS-UES-85-002] 13 p2105 N85-23116

USSR report: Earth sciences
[JPRS-UES-85-004] 14 p2332 N85-24424

Error in laser correlation wind speed meters resulting from variable atmospheric transparency
14 p2338 N85-24457

Observations of auroras and related plasma phenomena by the Kyokko and Jikiken satellite in IMS — EXOS-A and B satellite 14 p2354 N85-24547

The Earth's magnetopause — International Magnetospheric Study 14 p2355 N85-24549

Observations of the magnetospheric boundary layers — International Magnetospheric Study
14 p2355 N85-24551

Magnetospheric effects on the upper atmosphere
14 p2365 N85-24616

Resonance generation of inertial waves (in the atmosphere) by Doppler-shift of inertio-gravity modes
15 p2590 N85-25968

Academician Zuyev notes plans for lasers on spacecraft for atmospheric research 16 p2717 N85-26775

Conceptual Design for a Gulf Coast Oxidant Transport and Transformation Experiment: Workshop proceedings and recommendations
[PB85-173789] 18 p3135 N85-29417

Applied Science Division's Environmental Research Program
[DE85-010637] 19 p3308 N85-30510

Sensitivity of planetary waves to initial conditions and forcing
[AD-A154111] 19 p3345 N85-30734

Comparison of 8 to 12 micrometer and 3 to 5 micrometer CVF transmissometer data with LOWTRAN calculations
[AD-A154218] 19 p3350 N85-30763

Activities report of the Aeronomy Department
[G-774-1984] 21 p3633 N85-32569

Photochemical aerosol formation in polluted atmosphere 21 p3644 N85-32642

Middle Atmosphere Program. Handbook for MAP, volume 11
[NASA-CR-176107] 22 p3814 N85-33625

National Center for Atmospheric Research
[PB85-191237] 22 p3848 N85-33835

Proceedings of Meteorological Motor Glider (MEMO) Workshop '84
[DFVLR-MITT-85-04] 24 p4121 N85-35542

The measurement of nitrogen oxide (NO, NO2) exchange over plant/soil surfaces
[CSIRO-DAR-TP-8] 24 p4127 N85-35587
ATMOSPHERIC PRESSURE
NT CYCLOGENESIS
Numerical forecast of pressure field by considering the mutual influence of orography, thermal nonhomogeneity and surface friction 01 p0060 N85-10534
Effect of hyperoxia and increased gas atmosphere density on contractile function of the right ventricle
01 p0093 N85-10626
Atmospheric environment for Space Shuttle (STS-41G) launch
[NASA-TM-86486] 07 p0995 N85-16320
Revised Uniform Summary of Surface Weather Observations (RUSSWO). Shemya AFB, Alaska, parts A-F
[AD-A146917] 07 p1005 N85-16388
Revised Uniform Summary of Surface Weather Observations (RUSSWO). Pope AFB, Fayetteville, North Carolina, parts A-F
[AD-A146918] 07 p1005 N85-16389
Revised Uniform Summary of Surface Weather Observations (RUSSWO). Sondestrom AB, Greenland, parts A-F
[AD-A146919] 07 p1005 N85-16390
Revised Uniform Summary of Surface Weather Observations (RUSSWO). England AFB, Alexandria, Lousiana, parts A-F
[AD-A146920] 07 p1006 N85-16391
Revised Uniform Summary of Surface Weather Observations (RUSSWO). Parts A-F: Homestead AFB, Florida
[AD-A147203] 07 p1007 N85-16396
Limited surface observations climatic summary (LISOCS). Camp Casey, Tong Du Chon, Korea
[AD-A147204] 07 p1007 N85-16397
Limited surface observatins climatic summary (LISOCS). Ansback AHP, Germany
[AD-A147205] 07 p1007 N85-16398
Revised Uniform Summary of Surface Weather Observations (RUSSWO). O'Hare International Airport, Chicago, parts A-F
[AD-A147206] 07 p1007 N85-16399
Theoretical and experimental analyses of laser altimeters for barometric measurements over the ocean
08 p1165 N85-17351
Isentropic objective analysis
[PB85-112167] 11 p1686 N85-20617
Method of and apparatus for measuring temperature and pressure — atmospheric sounding
[NASA-CASE-GSC-12558-1] 12 p1856 N85-21639
Evaluation of ettringite and related compounds for use in solar energy storage
[PB85-146876] 12 p1883 N85-21816
Seismic observation of infrasonic signals
[AD-A149574] 12 p1889 N85-21853
TRAJ: Single station trajectory plot
[PB85-135002] 12 p1897 N85-21911
A computer controlled mass spectrometer system for investigating the decomposition of non-metallic materials under atmospheric conditions 12 p1946 N85-22237
Portable Automated Mesonet (PAM) data from the 1980 experiment in Anderson Creek Valley
[DE85-004361] 13 p2139 N85-23282
Observations of current pulsations of characteristics in atmosphere with period of about 1.5 hours
14 p2341 N85-24480
Ocean circulation and meteorology off the Georgia coast. Part 1: Real-time telemetry system for data collection
[PB85-155935] 15 p2605 N85-26052
The sea level response to weather along the coast of southern Africa 16 p2829 N85-27446
Summary of Meteorological Observations, Surface (SMOS), Dallas, Texas
[AD-A150599] 16 p2835 N85-27480
Study of synthesis gas conversion over metal oxides
[DE85-010136] 18 p3072 N85-28999
Trends in the Southern Hemisphere
18 p3144 N85-29466
A constant altitude flight survey method for mapping atmospheric ambient pressures and systematic radar errors
[NASA-TM-85733] 19 p3217 N85-29951
Mechanism of the catalytic gasification and reactivity of graphite
[DE85-009932] 19 p3229 N85-30020
The mobile phase in coals: Its nature and modes of release
[DE85-011696] 19 p3230 N85-30026
Approximate method for computing wind velocity in atmosphere 19 p3298 N85-30444
Atmospheric environment for space shuttle (STS-51C) launch
[NASA-TM-86506] 19 p3315 N85-30547
A global low order spectral model designed for climate sensitivity studies
[NASA-CR-175999] 19 p3315 N85-30549
Two-phase flow visualization in a transparent, atmospheric pressure, boiling water loop
[DE84-016857] 21 p3586 N85-32288
Air-sea interaction with SSM/I and altimeter
[NASA-CR-176105] 22 p3818 N85-33650
Electrode erosion in arc discharges at atmospheric pressure
[NASA-TM-87067] 23 p3903 N85-34176
Monitoring dosage of volatile compounds in tests at low barometric pressure 23 p3954 N85-34506
Comparative study of the phase of diurnal anisotropy on quiet and disturbed days on a long term basis up to recent period
[SH-4.5-9] 23 p4037 N85-35027
Atmospheric effects on the underground muon intensity
[SH-6.1-3] 23 p4044 N85-35078
The neutron moderated detector and groundbased cosmic ray modulation studies
[SH-9.1-13] 23 p4052 N85-35126
Air chemistry measurements 2
[AD-A156041] 24 p4117 N85-35520
Maintenance of blocking anticyclones in a general circulation model
[PB85-190666] 24 p4124 N85-35567
ATMOSPHERIC RADIATION
NT AIRGLOW
NT AURORAL ARCS
NT AURORAS
NT DAWN CHORUS
NT GEOCORONAL EMISSIONS
NT IONOSPHERIC NOISE
NT NIGHTGLOW
NT RADIO AURORAS
NT SKY RADIATION
NT TWILIGHT GLOW
NT WHISTLERS
A sphere-scanning radiometer for rapid directional measurements of sky and ground radiance: The PARABOLA field instrument
[NASA-TM-86171] 03 p0363 N85-12329
Investigation of cloud feedback in the GLAS model
05 p0685 N85-14404
Nature of short-period variations of cosmic rays in stratosphere 06 p0823 N85-15224
Simple formula to estimate carbon dioxide gas effect in radiation balance of underlying surface
06 p0823 N85-15226
MAP activities in Hungary 11 p1657 N85-20440
Altitude of auroral scattering observed along auroral electrojets 14 p2339 N85-24465
The keV electrons and 80 keV protons in the vicinity of the high latitude magnetosphere and at the bow shock 14 p2355 N85-24554
Glow of ionospheric F-layer in Line 630 nm determined from photographs taken aboard Salyut-6 orbital station: Interpretation of results 16 p2721 N85-26799
One approach to remote sensing of total ozone content 16 p2725 N85-26822
Analysis of a simulated cloud climatology
18 p3145 N85-29472
Atmospheric X-rays at 11 deg S geomagnetic latitude
[INPE-3539-PRE/755] 19 p3386 N85-31004
Some consideration about the natural atmospheric radioactive aerosol 21 p3647 N85-32662
Determination of altitude of cloud cover top from Meteor satellite data 22 p3734 N85-33150
Propagation and secondary production of low energy antiprotons in the atmosphere
[OG-6.1-3] 22 p3887 N85-34094
Application of imaging to the atmospheric Cherenkov technique
[OG-9.5-4] 23 p4030 N85-34981
Three dimensional calculation of flux of low energy atmospheric neutrinos
[SH-8.1-11] 23 p4050 N85-35116
Nucleon decay and atmospheric neutrinos in the Mont Blanc experiment
[HE-6.2-6] 24 p4211 N85-36142
ATMOSPHERIC REFRACTION
NT RADIO WAVE REFRACTION
A radar sea clutter model for atmospheric ducting conditions
[AD-A145321] 02 p0190 N85-11268
Autonomous navigation of USAF spacecraft
03 p0321 N85-12074
Correction for atmospheric refraction in an airborne, operational environment
[AD-A146552] 06 p0835 N85-15314
Practical application of IREPS (Integrated Refractive Effects Prediction System)
[AD-A146528] 06 p0838 N85-15323
Fluctuations during observations of extraterrestrial sources from outer space through Earth's atmosphere
07 p0953 N85-16040
C2 sub n (optical) studies in the free atmosphere based on rawinsonde data
[AD-A147307] 07 p0997 N85-16332
Statistical/Trend analysis of the marine atmospheric boundary layer model
[AD-A151053] 14 p2374 N85-24673
An assessment of atmospheric refractivity in the northern marginal ice zone
[AD-A152348] 17 p2992 N85-28493
A review of tropospheric refraction effects on Earth-to-satellite systems 18 p3107 N85-29235
Gravity waves from the stratosphere to the mesosphere, part 1.3B 21 p3616 N85-32471
Some recent developments in the interpretation of MST radar returns from clear air (keynote paper), part 2
21 p3618 N85-32480
Mesoscale features and atmospheric refraction conditions of the Arctic marginal ice zone
[AD-A155139] 21 p3636 N85-32584
ATMOSPHERIC SCATTERING
NT TROPOSPHERIC SCATTERING
Characterization of atmospheric conditions along transmission paths from a remotely piloted vehicle
[AD-A145527] 02 p0232 N85-11511
Mars polar volatiles: Topographic and geologic setting
[NASA-CR-174089] 04 p0581 N85-13708
Relation between atmospheric scattering and backscattering coefficient
[ESA-TT-837] 05 p0677 N85-14350
Multiple scattering effects on transmission through the atmosphere
[AD-A147527] 07 p0941 N85-15969
Middle Atmosphere program. Handbook for MAP. Volume 13: Ground-based techniques
[NASA-CR-174345] 08 p1183 N85-17452
The radiation temperature of a cloud of particles
[FOA-C-30367-E4] 08 p1190 N85-17497
Description of amplitude scintillations on a 11 GHz slant path in terms of forward scattering from turbulent layers
[FI-455-TBR-76] 11 p1625 N85-20232
Prospective investigations with DFVLR radar of possible relevance in the assessment of radio interference due to scattering from precipitations — meteorological radar
[DFVLR-FB-84-42] 12 p1830 N85-21485
Atmospheric handbook: Atmospheric data tables available on computer tape
[PB85-108512] 12 p1891 N85-21867
Radio scintillations observed during atmospheric occultations of Voyager: Internal gravity waves at Titan and magnetic field orientations at Jupiter and Saturn
[NASA-CR-175554] 12 p1961 N85-22327
Mean free path lenght of photons with broken cloud cover 14 p2338 N85-24455
Experimental study of anisotropy of scattering of radar signals by clouds and precipitation
14 p2340 N85-24473
Modeling of radiothermal radiation of rain by Monte-Carlo method 14 p2341 N85-24476
Applicability of vertically homogeneous atmospheric models for remote soundings 14 p2341 N85-24477
Specifics of polarization structure of repeated scattering background in optical laser sounding signals
14 p2342 N85-24485
Test of lidar inversion algorithm sensitivity to atmospheric backscatter and extinction parameters, revision A
[AD-A152082] 16 p2865 N85-27671
Earth observation modeling based on layer scattering matrices
[NLR-MP-84015-U] 17 p2984 N85-28440
Lidar system using polarization discrimination techniques for molecular air pollution monitoring
19 p3308 N85-30504
Meteorological and aeronomical requirements for MST radar networks (keynote paper), part 1
21 p3615 N85-32467
Properties of aerosol particles detected by satellites in coastal regions 21 p3641 N85-32622
Calculation of the diffusion of light by aerosols: Description of the MIELOR software and results obtained
[REPT-80] 24 p4137 N85-35638
Atmospheric interactions detected in both the upper and the lower chambers at Chacaltaya
[HE-3.3-7] 24 p4180 N85-35925
ATMOSPHERIC SHELLS
U ATMOSPHERIC STRATIFICATION
ATMOSPHERIC SOUNDING
Satellite observations 01 p0013 N85-10069
The past, present, and anticipated future contributions of geosynchronous satellites to short range prediction
01 p0076 N85-10503

Use of satellite soundings and imagery for nowcasting and very-short-range forecasting
01 p0076 N85-10504

Remote sensing of atmospheric particulates: Technological innovation and physical limitations in applications to short-range weather prediction
[NSF ATM-82-09664] 01 p0077 N85-10511

Characterization of atmospheric conditions along transmission paths from a remotely piloted vehicle
[AD-A145527] 02 p0232 N85-11511

A case study of a convective outbreak using VAS-derived thermodynamic parameters
[AD-A145560] 02 p0232 N85-11512

Multifrequency lidar based on dye laser
02 p0262 N85-11715

Influence of refraction effects on informativeness of bistatic acoustical atmospheric sounding systems
06 p0625 N85-15237

Actual altitudes of radioacoustic sounding in decimeter wavelength band 06 p0626 N85-15243

Convective scale weather analysis and forecasting
[NASA-CR-174185] 06 p0638 N85-15320

Binary pulse compression techniques for MST radars
08 p1184 N85-17464

The analysis of spaced sensor records by correlation techniques 08 p1184 N85-17465

The MST radar technique 08 p1185 N85-17466

The influence of deep cumulus convection on large-scale flow during AVE/SESAME 1, 10-11 April 1979
09 p1355 N85-18526

Meteorological Sounding System (MSS) standard operating procedures
[AD-A149513] 10 p1519 N85-19578

Space and time variations and turbopause dynamical structure 11 p1663 N85-20483

Middle Atmosphere Program. Handbook for MAP. Volume 12: Coordinated Study of the Behavior of the Middle Atmosphere in Winter (PMP-1) Workshops
[NASA-CR-175475] 11 p1665 N85-20492

Microstructure of Venus cloud layer based on spectrophotometric data from Venera-11 spacecraft
13 p1982 N85-22436

Results of comparison of long-wave radiation fluxes measured by Soviet and Japanese actinometric radiosounds 14 p2333 N85-24427

Experimental results of temperature-wind soundings of the atmosphere by the radio acoustical method
14 p2340 N85-24471

Applicability of vertically homogeneous atmospheric models for remote soundings 14 p2341 N85-24477

Specifics of polarization structure of repeated scattering background in optical laser sounding signals
14 p2342 N85-24485

Results of the Langmuir-probe experiment on board Intercosmos-18 — ionosphere-magnetosphere interaction 14 p2362 N85-24596

Case studies of snow clouds by means of snow crystal sondes 15 p2581 N85-25921

Resonance generation of inertial waves (in the atmosphere) by Doppler-shift of inertio-gravity modes
15 p2590 N85-25968

Mesoscale analysis and modeling group
15 p2596 N85-26001

Review of VAS demonstration
15 p2596 N85-26002

Nowcasting applications of VAS
15 p2597 N85-26003

Recent VAS imaging/sounding research
15 p2597 N85-26004

A simulation experiment on the impact of geostationary temperature retrievals in numerical models
15 p2597 N85-26005

VAS/model impact study 15 p2597 N85-26006

Utilization of satellite data in mesoscale modeling of severe weather 15 p2597 N85-26007

Assessment of VAS soundings in the analysis of a preconvective environment
[NASA-TM-86205] 16 p2625 N85-27427

Improvement of the basic knowledge of the climatology of the vertical ozone layer by enhanced balloon sounding
[SPT-6/84] 18 p3137 N85-29428

Combined catalog of ionosphere vertical soundings data
[PB85-166494] 18 p3138 N85-29430

Small-scale structure of ionospheric F-region
19 p3297 N85-30440

Specifics of laser sounding of atmosphere along horizontal and slightly slanting paths over water surface
19 p3297 N85-30441

Diagnosis of vertical motions from VAS retrievals during a convective outbreak
[NASA-CR-171569] 19 p3316 N85-30554

Atmospheric X-rays at 11 deg S geomagnetic latitude
[INPE-3539-PRE/755] 19 p3386 N85-31004

The role of scientific ballooning for exploration of the magnetosphere
[TRITA-EPP-84-07] 20 p3494 N85-31724

Laser Elektronika-01 for air pollution control lidar
21 p3664 N85-32887

The use of TOMS data in evaluating and improving the total ozone from TOVS measurements
[NOAA-TR-NESDIS-23] 22 p3614 N85-33626

ATMOSPHERIC STRATIFICATION

Layered sloping mesoscale structures and rainbands in atmospheric frontal regions and their relation to symmetric instability 01 p0075 N85-10497

Evaluation of an integrated mixed-layer model for single station prediction in a marine regime
01 p0080 N85-10535

Mixed layers and satellite retrievals
05 p0686 N85-14411

Generation and evolution of diabatic planetary waves in continuously stratified atmosphere with Ekman dissipation 09 p1354 N85-18515

Long nonlinear waves in layers of sudden changes in wind velocity 14 p2340 N85-24470

Coronal structures 14 p2448 N85-25110

Waves in inhomogeneous media — magnetohydrodynamic waves; solar atmosphere
14 p2449 N85-25116

A model for the dynamics of the deep photosphere
14 p2450 N85-25129

Effects of atmospheric stratification on dissipative acoustic and Alfven waves — solar atmosphere
14 p2453 N85-25149

Applications of fuzzy clustering techniques to stratified by tropopause MSU temperature retrievals
18 p3141 N85-29444

Propagation of acoustic pulse in atmospheric waveguide 19 p3297 N85-30443

ATMOSPHERIC TEMPERATURE

NT IONOSPHERIC TEMPERATURE

Use of ground based microwave radiometers for nowcasting 01 p0078 N85-10517

On probability forecasts for temperature
01 p0084 N85-10565

Alpine meteorology: Translations of classic contributions by Wagner, A., Ekhart, E. and Defant, F.
[DE84-014929] 01 p0085 N85-10574

The extremeness of the cold front of December 31, 1978 over the CSR
[REPT-566] 03 p0377 N85-12409

A temperature climatology for New York State
03 p0394 N85-12517

Calibration and use of filter test facility orifice plates
[DE84-016851] 04 p0500 N85-13190

Trends in ozone and temperature structure: Comparison of theory and measurements
[DE84-016201] 04 p0539 N85-13428

NOAA/NASA joint simulation of AMTS and HIRS
05 p0682 N85-14384

Air-sea interaction during cold air outbreaks
05 p0685 N85-14401

Structure of temperature field based on observations of refraction from high meteorological mast
06 p0819 N85-15199

Atmospheric environment for Space Shuttle (STS-41G) launch
[NASA-TM-86486] 07 p0995 N85-16320

The effects of long-periodic forcing in a zero-dimensional climate model 07 p1002 N85-16363

Revised Uniform Summary of Surface Weather Observations (RUSSWO). Alconbury RAF United Kingdom, parts A-F
[AD-A146913] 07 p1004 N85-16384

Revised Uniform Summary of Surface Weather Observations (RUSSWO). McChord AFB, Washington, parts A-F
[AD-A146914] 07 p1005 N85-16385

Revised Uniform Summary of Surface Weather Observations (RUSSWO). Mildenhall RAF, United Kingdom, parts A-F
[AD-A146915] 07 p1005 N85-16386

Revised Uniform Summary of Surface Weather Observations (RUSSWO). Dobbins AFB, Georgia, parts A-F
[AD-A146916] 07 p1005 N85-16387

Revised Uniform Summary of Surface Weather Observations (RUSSWO). Shemya AFB, Alaska, parts A-F
[AD-A146917] 07 p1005 N85-16388

Revised Uniform Summary of Surface Weather Observations (RUSSWO). Pope AFB, Fayetteville, North Carolina, parts A-F
[AD-A146918] 07 p1005 N85-16389

Revised Uniform Summary of Surface Weather Observations (RUSSWO). Sondestrom AB, Greenland, parts A-F
[AD-A146919] 07 p1005 N85-16390

Revised Uniform Summary of Surface Weather Observations (RUSSWO). England AFB, Alexandria, Lousiana, parts A-F
[AD-A146920] 07 p1006 N85-16391

Revised Uniform Summary of Surface Weather Observations (RUSSWO). Parts A-F: Homestead AFB, Florida
[AD-A147203] 07 p1007 N85-16396

Limited surface observations climatic summary (LISOCS). Camp Casey, Tong Du Chon, Korea
[AD-A147204] 07 p1007 N85-16397

Limited surface observatins climatic summary (LISOCS). Ansbach AHP, Germany
[AD-A147205] 07 p1007 N85-16398

Revised Uniform Summary of Surface Weather Observations (RUSSWO). O'Hare International Airport, Chicago, parts A-F
[AD-A147206] 07 p1007 N85-16399

Climate at CRREL (Cold Regions Research and Engineering Laboratory) Hanover, New Hampshire
[AD-A148400] 08 p1189 N85-17495

A catalogue of dynamic parameters describing the variability of the middle stratosphere during the northern winters 11 p1656 N85-20435

Middle Atmosphere Program. Handbook for MAP, volume 7
[NASA-CR-175479] 11 p1656 N85-20437

PMP-1 report: The fourth winter of PMP-1, 1981 - 1982: A winter with several interesting features
11 p1657 N85-20441

Workshop on Comparison of Data and Derived Dynamical Quantities During Northern Hemisphere (PMP-1) Winters 11 p1657 N85-20444

The first winter of MAP-dynamics, 1982-1983: A winter with three different warming periods
11 p1657 N85-20446

Variation of derived mesospheric nitric oxide in relation to wind and temperature in winter
11 p1658 N85-20452

Middle atmosphere temperature and dynamics as revealed from D-region observations
11 p1659 N85-20453

Stratwarm effects in the ionospheric D region wind field 11 p1663 N85-20479

Middle Atmosphere Program. Handbook for MAP. Volume 12: Coordinated Study of the Behavior of the Middle Atmosphere in Winter (PMP-1) Workshops
[NASA-CR-175475] 11 p1665 N85-20492

Carbon dioxide and the greenhouse effect
[GPO-39-043] 11 p1677 N85-20569

Method of and apparatus for measuring temperature and pressure — atmospheric sounding
[NASA-CASE-GSC-12558-1] 12 p1856 N85-21639

High time resolution thermospheric temperature and wind studies in the Arctic
[AD-A150114] 12 p1890 N85-21880

On the relationship between maximum surface temperature and various parameters; with reference to objective forecasting
[KNMI-TR-58] 12 p1897 N85-21905

TRAJ: Single station trajectory plot
[PB85-135002] 12 p1897 N85-21911

Monthly and seasonal weather outlook for January 1985, volume 39, number 1
[PB85-148799] 12 p1898 N85-21915

Small component spectral model of annual course of zonal atmospheric circulation 14 p2337 N85-24453

Experimental results of temperature-wind soundings of the atmosphere by the radio acoustical method
14 p2340 N85-24471

Observations of current pulsations of characteristics in atmosphere with period of about 1.5 hours
14 p2341 N85-24480

Fabry-Perot interferometer and skymapping photometer determinations of midlatitude f-region neutral winds and temperatures and airglow enhancement/depletions
[AD-A150730] 14 p2373 N85-24666

Low Temperature Science. Series A: Physical Sciences
[ISSN-0439-3538] 15 p2581 N85-25917

The temperature fluctuation in stable stratification above snow cover 15 p2581 N85-25918

Greenhouse effect in Earth's primordial atmosphere
16 p2607 N85-27310

Regularities in recent changes in surface air temperature and atmospheric precipitation fields
16 p2607 N85-27311

Proper quality of anticorrosion work no matter how bad the atmospheric conditions
[BLL-BISI-TRANS-22080-(9022.08)]
17 p2975 N85-28383

Ozone and temperature trends due to the injection of trace species in the atmosphere
[AERONOMICA-ACTA-A-288-1984]
18 p3132 N85-29399

Objective determination of heat wave patterns
18 p3140 N85-29437
Approximate method for computing wind velocity in atmosphere 19 p3298 N85-30444
Utilization of satellite data and regional scale numerical models in short range weather forecasting
[NASA-CR-175960] 19 p3314 N85-30545
Monthly and seasonal weather outlook for mid-March to mid-April 1985, March 14, 1985, volume 39, no. 6
[PB85-174751] 19 p3317 N85-30565
Influence of moisture and elevated temperature on the fatigue properties of WTS-3 glass fiber blade material — wind turbine blade (WTS-3)
[FFA-TN-1984-58] 20 p3470 N85-31558
Short meridional scale anomalies in the lower stratosphere and upper troposphere
20 p3489 N85-31664
Monthly and seasonal weather outlook for April 1985, March 30, 1985, volume 39, no. 7
[PB85-183604] 22 p3817 N85-33646
Reports from the German Meteorological Service. No. 167: Results of aerological soundings in the model area upper Rhine: Heat release project upper Rhine area, part 3
[ISBN-3-88148-216-4] 23 p3950 N85-34479
Variations of the cosmic ray general component in Antarctica
[SH-4.4-17] 23 p4035 N85-35013
Program for Regional Observing and Forecasting Services (PROFS)
[PB85-188050] 24 p4124 N85-35569
Connection between variations of the atmosphere temperature profile and variations of the meson component intensity
[HE-3.1-12] 24 p4178 N85-35910

ATMOSPHERIC TIDES
The Moon's orbit history and inferences on its origin
04 p0585 N85-13735
Considering zonal wind in semidiurnal tide problem
14 p2335 N85-24440

ATMOSPHERIC TURBULENCE
NT CLEAR AIR TURBULENCE
NT GUSTS
NT LOW LEVEL TURBULENCE
Processing and display of atmospheric phenomenaa data
[NASA-CR-171178] 01 p0072 N85-10475
Thermosonde and UHF radar measurements of C2 sub n at Westford, Massachusetts - July 1981
[AD-A145398] 02 p0190 N85-11270
Fluctuations in parameters of light beam along path with reflection in turbulent atmosphere
02 p0263 N85-11722
Stochastic motor blade dynamics
[AD-A146312] 03 p0318 N85-12054
Aircraft accident report Air Canada, Lockheed L-1011, C-FTNJ, near Charleston, South Carolina, November 24, 1983
[PB84-910413] 05 p0594 N85-13790
Variability of short-term eddy-correlation estimates of mass exchange
[DE84-007271] 05 p0677 N85-14349
Air-sea interaction during cold air outbreaks
05 p0685 N85-14401
Field coherence function in layerwise nonhomogeneous troposphere 06 p0784 N85-15012
Lidar measurements of structural characteristics of atmospheric turbulence 06 p0824 N85-15229
Large-eddy simulation. Guidelines for its application to planetary boundary layer research
[AD-A146361] 06 p0890 N85-15651
Determination of the laws governing the changes in the standard deviations of the distribution of pollution based on observations of the atmospheric turbulence spectrum and the possibility of simulating it in the laboratory
[BLL-TR-T6373/BG/MRS14883/84]
08 p1179 N85-17431
Thermosonde C2N measurements in Hawaii--August 1982
[AD-A148016] 08 p1189 N85-17489
Description of amplitude scintillations on a 11 GHz slant path in terms of forward scattering from turbulent layers
[FI-455-TBR-76] 11 p1625 N85-20232
Middle Atmosphere Program. Handbook for MAP, volume 4
[NASA-CR-175482] 11 p1654 N85-20420
Investigation of aeronomic processes on the basis of ionospheric sporadic E 11 p1663 N85-20482
Space and time variations and turbopause dynamical structure 11 p1663 N85-20483
Study of pollutant dispersion in an urban street canyon
[DE85-002648] 11 p1677 N85-20571
Turbulence parameters impacting dispersion in an urban convection boundary layer
[PB85-116036] 11 p1682 N85-20596
Investigations of micro-turbulence in the bottom of the boundary layer
[AD-A149823] 12 p1696 N85-21697
A spatially incoherent and temporally coherent source
[AD-A151281] 13 p2157 N85-23390
Energy structure of atmospheric boundary layer above waves 14 p2335 N85-24442
The effects of atmospheric turbulence on an air-to-air optical communication link
[AD-A151840] 15 p2543 N85-25700
Radar turbulence estimates. Effects of wind shear and reflectivity factor gradients
[AD-A151876] 15 p2599 N85-26023
Mean conditions and turbulence statistics at Vandenberg AFB, California
[AD-A151366] 15 p2665 N85-26449
Response of a wind turbine blade to seismic and turbulent wind excitations 16 p2817 N85-27375
Air flow of the western coastal boundary of South Africa and its influence on the ocean 16 p2831 N85-27459
Analysis of the NASA/MSFC airborne Doppler lidar results from San Gorgonio Pass, California
[NASA-CR-3901] 16 p2832 N85-27463
The problem of atmospheric turbulence
[NASA-CR-175783] 16 p2832 N85-27464
Large-eddy simulation in planetary boundary-layer research 18 p3147 N85-29482
Radio wave scattering and intermittency of turbulence in the atmosphere 19 p3288 N85-30392
Radio wave scattering and turbulence intermittence in atmosphere 19 p3298 N85-30446
Some studies in filtering of atmospheric turbulence
[AD-A154042] 19 p3316 N85-30557
The influence of a turbulent region on the flux of auroral electrons
[KGI-PREPRINT-072] 20 p3494 N85-31723
Comparison of wind and turbulence measurements from Doppler lidar and instrumented aircraft
[NASA-CR-171535] 20 p3495 N85-31729
A survey of wind and turbulence modeling methods
[AD-A154470] 20 p3496 N85-31733
Middle Atmosphere Program. Handbook for MAP. Volume 14: URSI/SCOSTEP Workshop on Technical Aspects of MST Radar
[NASA-CR-176065] 21 p3615 N85-32466
Excerpts from the paper: Research Status and Recommendation from the Alaska Workshop on Gravity Waves and Turbulence in the Middle Atmosphere, part 1.3A 21 p3616 N85-32470
Morphology of the scattering targets: Fresnel and turbulent mechanisms, part 2.1A
21 p3618 N85-32481
Interpretation of radar returns from the mesosphere, part 2.3A 21 p3619 N85-32485
Radar echoes at 2.66 and 40.92 MHz from the mesosphere, part 2.6A 21 p3619 N85-32486
Network ST radar and related measurements at Pennsylvania State University 21 p3629 N85-32544
Notes on atmospheric stability, turbulence, and its measurements
[AD-A155230] 21 p3637 N85-32588
A numerical and analytical investigation of lee cyclogenesis
[AD-A155607] 21 p3638 N85-32594
Size spectra for the source-enhanced coagulation with the turbulent mass transfer 21 p3645 N85-32649
Fog activation and supersaturation
21 p3650 N85-32678
Environmental-physical measurements and determination of atmospheric turbulence with the ASK-16 motor glider 24 p4122 N85-35549

ATMOSPHERIC WINDOWS
Absorption of radiation by water vapor in windows of relative transparency of 95-145 micrometer range
13 p2076 N85-22968
Below-room-temperature water-vapor continuum absorption within the 8- to 10 micron atmospheric transmission window
[TR-0084(4945-09)-1] 13 p2132 N85-23266
Choice of optimum pairs of spectral intervals for IR-range survey of Earth's surface 15 p2486 N85-25344
High-frequency microwave observations of convective precipitation 15 p2596 N85-26000

ATMOSPHERICS
NT DAWN CHORUS
NT HISS
NT WHISTLERS
Tass reports astrophysical, atmospheric studies on Salyut-7 02 p0158 N85-11075
Prospective investigations with DFVLR radar of possible relevance in the assessment of radio interference due to scattering from precipitations — meteorological radar
[DFVLR-FB-84-42] 12 p1830 N85-21485
Comparison of 8 to 12 micrometer and 3 to 5 micrometer CVF transmissometer data with LOWTRAN calculations
[AD-A154218] 19 p3350 N85-30763
A high-speed digital signal processor for atmospheric radar, part 7.3A 21 p3626 N85-32525

ATOLL REEFS
U CORAL REEFS

ATOM CONCENTRATION
Grain boundary structure in NiO
[DE84-016242] 06 p0868 N85-15519
The influence of temperature on the composition density of the transition metals
[BLL-M-35896-(5826.4)] 23 p3915 N85-34262

ATOMIC BATTERIES
U RADIOISOTOPE BATTERIES

ATOMIC BEAMS
Laser cooling and trapping of neutral atoms
[AD-A146048] 03 p0366 N85-12345
Multiphoton ionization of cesium atoms above and below the two-photon ionization threshold
[DE85-000976] 09 p1381 N85-18682
Measurements of integral yields of charged secondary particles using neutral beams simulating a cometary fly-by — Giotto mission 14 p2244 N85-23908
Hydrogen vibrational population distributions and negative ion generation in tandem high-density hydrogen discharges
[DE85-006764] 16 p2863 N85-27657
High efficiency ionizer using a hollow cathode discharge plasma
[DE85-006690] 16 p2868 N85-27693
An examination of the use of wave packets for the calculation of atom diffraction by surface
[AD-A152760] 17 p3029 N85-28735
Cooling high intensity atomic hydrogen beams to liquid helium temperatures
[DE85-012515] 24 p4146 N85-35718

ATOMIC CLOCKS
Clock synchronization by the Symphonie and Laser Synchronization from Stationary Orbit (LASSO) geostationary satellites 14 p2396 N85-24778
Lifetime and reliability of rubidium discharge lamps for use in atomic frequency standards
[AD-A150787] 14 p2417 N85-24915
Recent improvements in the atomic time scales of the National Bureau of Standards 17 p2962 N85-28290
Timing-system design considerations for a mobile astrolabe 17 p2965 N85-28309
Methods for optimal recursive estimation of non-stationary time series, applications to atomic time and frequency metrology 17 p2965 N85-28312
Kalman filtering with a two-state clock model
17 p2965 N85-28314
Kalman filter estimates of the NAVSTAR satellite clock parameters 17 p2965 N85-28315
Physics element design aspects for a tactical rubidium frequency standard 17 p2967 N85-28321
Prospects for atomic frequency standards
18 p3105 N85-29222
On the accuracy of Cs beam primary frequency standards 18 p3105 N85-29224
Methods to recover the narrow Dicke sub-Doppler feature in evacuated wall-coated cells without restrictions on cell size 18 p3105 N85-29225
Diode laser 87Rb optical pumping in an evacuated wall-coated cell 18 p3105 N85-29226
On-orbit frequency stability analysis of the GPS NAVSTAR-1 quartz clock and the NAVSTARs-6 and -8 rubidium clocks 18 p3105 N85-29227
Rubidium and cesium frequency standards status and performance on the GPS program
18 p3106 N85-29228
A low noise synthesizer for autotuning and performance testing of hydrogen masers 18 p3106 N85-29242
Performance data of US Naval Observatory VLG-11 hydrogen masers since September, 1983
18 p3106 N85-29244
Maser and secondary clock in telecommunications networks 18 p3108 N85-29246
The time and frequency comparisons via Loran-C and National TV Network in Yugoslavia
18 p3109 N85-29248
Using GPS and VLBI technology to maintain 14 digit synchronization 18 p3109 N85-29250
Time comparisons using the Global Positioning System (GPS). Method and first results obtained using the DFVLR C/A receiver
[ESA-TT-894] 20 p3480 N85-31490
Elemental technetium as a cosmic-ray clock
[OG-7.1-9] 23 p4013 N85-34870

ATOMIC COLLISIONS
The Berkeley mini-collider
[DE84-014594] 01 p0118 N85-10808
Linac quadrupole connections
[DE84-014694] 01 p0118 N85-10810
Velocity-changing collisional effects in nonlinear atomic spectroscopy and photon echo decay in gases
[NASA-CR-174159] 04 p0559 N85-13559

Energy transfer in atom-molecule scattering experiments in the 1eV region with SF6-Ar, CF4-Ne and Xe-CO2 systems as examples
[REPT-11/1983] 04 p0563 N85-13588
Laboratory studies of atomic collision processes of importance in planetary atmospheres
[NASA-CR-174142] 04 p0589 N85-13758
Scattering experiments on interactions of excited atoms: Differential cross sections of the system Na (3P)+K(4S)
[MPIS-8/1984] 05 p0728 N85-14677
Inclusion of electron transfer in the calculation of K(n)L(v) multiple vacancy production by ion impact
[DE84-016596] 05 p0733 N85-14711
Progress in numerical calculations of ion-atom collisions
[DE84-016598] 06 p0861 N85-15474
Electron capture by multiply charged ions from hydrogen atoms at low energies
[DE84-016560] 06 p0861 N85-15475
Theoretical studies relating to the interaction of radiation with matter: Atomic collision processes occuring in the presence of radiation fields
[AD-A146854] 07 p1040 N85-16602
Theoretical studies of Rydberg atom collisions
[AD-A148558] 08 p1220 N85-17687
ORNL ECR multicharged ion source
[DE85-001283] 09 p1380 N85-18681
Atomic and molecular collision processes
[DE85-001604] 09 p1382 N85-18690
Compilation of atomic data for diagnostics of Tokamak
09 p1390 N85-18744
The coordinated research program at IAEA on atomic collision data for plasma diagnostics
09 p1390 N85-18747
Time dependent Hartree-Fock theory of ion-atom collisions: Application to F(9+) + Ne
[DE85-003063] 11 p1723 N85-20838
Inner shell contribution to multiple ionization in ion-atom collisions
[DE85-003107] 11 p1723 N85-20839
Coincidence techniques to study electron emission in ion-atom collisions
[DE85-003635] 11 p1724 N85-20846
Coincidence studies of secondary electron emission in light ion-atom collisions
[DE85-002373] 11 p1725 N85-20852
Recent advances in forward electron production studies in ion-atom and ion-solid collisions
[DE85-001255] 11 p1726 N85-20853
Atomic processes involving impurities in the plasma edge
[DE85-001277] 11 p1730 N85-20882
Bibliography of atomic and molecular processes, 1983
[DE85-000662] 12 p1929 N85-22121
Mean delta-ray energies in ion molecule collisions
[DE85-005524] 13 p2157 N85-23395
Observation of pure resonance and threshold effects in electron impact experiments in high intensity laser fields
[AD-A150725] 14 p2309 N85-24293
Numerical solution of a first kind Fredholm integral equation arising in electron-atom scattering
[CWI-NM-R8414] 14 p2414 N85-24897
Kinetics and structure of excited states
[AD-A151902] 15 p2648 N85-26334
Atomic physics aspects of a Relativistic Nuclear Collider
[DE85-006867] 15 p2650 N85-26342
Space station as quark matter factory
[DE85-004606] 15 p2685 N85-26585
Ionization coefficient for atomic collisions in meteor trail 16 p2720 N85-26792
Electronically excited alkaline earth oxides: Chemical production and collisional energy transfer processes
[AD-A153172] 17 p3044 N85-28633
Atomic hydrogen maser measurements with wall surfaces of carbon tetrafluoride
18 p3108 N85-29243
Electron-proton collider option for the superconducting super collider
[DE85-010146] 18 p3196 N85-29822
Polarized internal target apparatus
[DE85-011611] 19 p3354 N85-30793
Vibrational energy transfer in benzene-argon collisions
[DE85-009603] 19 p3355 N85-30797
Resonant-transfer-and-excitation for highly charged ions (16 or = Z or = 23) in collisions with helium
[DE85-010550] 19 p3359 N85-30823
A theoretical study of electron capture in ion-ion and ion-atom collisions
[DE85-011154] 19 p3362 N85-30842
Electron-atom collision studies using optically state selected beams
[DE85-010848] 19 p3368 N85-30888
Inelastic Near-Surface Interactions. Proceedings of the Werner Brandt Workshop on Penetration Phenomena
[DE85-010579] 20 p3526 N85-31928
Nuclear data needs for fusion energy development
[DE85-010445] 20 p3536 N85-32000
Multiple vacancy production by high energy heavy ions
[DE85-004428] 24 p4182 N85-35805

ATOMIC ENERGY
U NUCLEAR ENERGY

ATOMIC ENERGY LEVELS
Radiation data and standards for Tokamak diagnostics
09 p1390 N85-18742
Optogalvanic measurement of even parity Rydberg levels in krypton gas
[AD-A152113] 16 p2745 N85-26943
Photophysical studies of triplet exciton processes in pure polymer films
[DE85-008571] 18 p3080 N85-29056

ATOMIC EXCITATIONS
Photoconductivity and emission from the impurity excited states in silicon
[DE84-015583] 04 p0479 N85-13052
Multiphoton ionization of atomic cesium
[DE85-001266] 09 p1380 N85-18678
Laser-induced-fluorescence-spectroscopy of atomic processes under a high magnetic field
09 p1389 N85-18740
Study of light shifts in laser pumped quantum discriminator frequency 11 p1716 N85-20798
Kinetics and structure of excited states
[AD-A151902] 15 p2648 N85-26334
Double photon excitation of high-Rydberg atoms as a long-lived submillimeter detector
[NASA-CASE-NPO-16372-1] 19 p3352 N85-30779
The SLC program
[DE85-011433] 19 p3357 N85-30813
Experimental level-structure determination in odd-odd actinide nuclei
[DE85-010476] 19 p3360 N85-30835
Contributions to the 19th International Cosmic Ray Conference
[NASA-CR-176049] 20 p3543 N85-32044
Energy spectra of elements with 18 less than or equal to Z less than or equal to 28 between 10 and 300 GeV/amu 20 p3543 N85-32045
Elemental abundances of cosmic rays with Z33 as measured on HEAO-3 20 p3543 N85-32046
Abundances of secondary elements among the ultra heavy cosmic rays: Results from HEAO-3
20 p3543 N85-32047
Implications of source abundances of ultraheavy cosmic rays 20 p3543 N85-32049
Study of proton and neutron activation of metal samples in low Earth orbit
[NASA-CR-171596] 21 p3558 N85-32130
Pairing correction of particle-hole state densities for two kinds of fermions
[DE85-011549] 23 p3971 N85-34620

ATOMIC EXPLOSIONS
U NUCLEAR EXPLOSIONS

ATOMIC INTERACTIONS
NT ATOMIC COLLISIONS
Exchange and correlation effects and pair potentials of inter-atomic interaction
[BLL-M-35745-(5828.4)] 02 p0277 N85-11800
Bibliography of atomic and molecular processes, 1983
[DE85-000662] 12 p1929 N85-22121

ATOMIC MASS
U ATOMIC WEIGHTS

ATOMIC PHYSICS
Fundamental molecular physics and chemistry, part 1
[DE84-009127] 04 p0561 N85-13571
Parity and time-reversal non-conversation in atoms
[DE84-016924] 04 p0562 N85-13581
Activities report in nuclear physics
05 p0728 N85-14680
Theoretical issues involving traps for neutral spin-polarized atoms
[AD-A148035] 08 p1220 N85-17682
French activities relevant to middle atmosphere research 11 p1655 N85-20423
Studies of silicon-refractory metal interfaces: Photoemission study of interface formation and compound nucleation
[AD-A150075] 12 p1800 N85-21293
Potential at atomic boundaries in the TF (or TFD) model and equations of states 12 p1820 N85-21419
Laboratory for laser energetics report
[DE85-007235] 15 p2563 N85-25814
Atomic physics aspects of a Relativistic Nuclear Collider
[DE85-006867] 15 p2650 N85-26342
Research activities of the Physics Division
[DE85-006958] 19 p3357 N85-30811
Atomic, Molecular and Solid-State Theory, and Computational Quantum Chemistry, part 1
[DE85-009401] 20 p3526 N85-31929
Activities report in nuclear physics and particle acceleration 20 p3532 N85-31977
Activities of the Physics Division
[DE85-000784] 21 p3702 N85-33002
The 2nd European Conference on Atomic and Molecular Physics
[AD-A155863] 24 p4146 N85-35715

ATOMIC RECOMBINATION
NT OXYGEN RECOMBINATION
Laser-induced-fluorescence-spectroscopy of atomic processes under a high magnetic field
09 p1389 N85-18740
Molecular orbital studies in oxidation: Sulfate formation and metal-metal oxide adhesion
[NASA-CR-176070] 21 p3565 N85-32174

ATOMIC SPECTRA
Velocity-changing collisional effects in nonlinear atomic spectroscopy and photon echo decay in gases
[NASA-CR-174159] 04 p0559 N85-13559
Spectra of highly-ionized atoms for the diagnostics of the new generation of Tokamaks
09 p1388 N85-18730
Impact of atomic data on Tokamak modeling
09 p1390 N85-18743
Sample introduction methods for improving the particle detection capability of the spectrometric oil analysis program
[AD-A150139] 13 p2156 N85-23390
Kinetics and structure of excited states
[AD-A151902] 15 p2648 N85-26334
Optogalvanic measurement of even parity Rydberg levels in krypton gas
[AD-A152113] 16 p2745 N85-26943

ATOMIC STRUCTURE
Relationships between electronic structure and stability of metallic glasses
[AD-A145141] 01 p0028 N85-10176
Influence of 5f electrons on structures and bonding in the actinide-hydrogen intermetallics
[DE84-013893] 01 p0118 N85-10807
Relationships between electronic structure and stability of metallic glasses
[AD-A145506] 02 p0267 N85-11874
Electronic structure and lattice dynamics of solid state substances from gamma nuclear resonance absorption and angular correlation measurements
03 p0427 N85-12728
Paramagnetic impurity effects in NMR determinations of hydrogen diffusion and electronic structure in metal hydrides. Cerium in YH-2 and LaH-2.25
[DE84-014127] 04 p0472 N85-13005
Surface structure determination with ARPEFS
[DE84-016904] 04 p0571 N85-13644
The atomic structure of Si-SiO2 interfaces suggesting a ledge mechanism of silicon oxidation
[DE84-016057] 05 p0731 N85-14703
Theoretical methods for the study of transition metals in crystals
[DE84-015606] 05 p0732 N85-14709
Electronic and magnetic properties of transition-metal surfaces, interfaces and overlayers
[DE84-016886] 05 p0733 N85-14713
Electronic bandstructure of an incommensurate crystal
[DE84-016891] 05 p0733 N85-14714
Structure of adsorbed monolayers. The surface chemical bond
[DE84-016879] 06 p0861 N85-15471
Electron spectrometry experiments with the use of synchrotron radiation
[DE85-001266] 07 p1041 N85-16610
Electronic structure and properties of magnetic defects in Co(1+x)Al(1-x) and Fe(1+x)Al(1-x) alloys
[NASA-TM-77498] 07 p1047 N85-16648
Replacement of Fe-3+ ions in nickel ferrites by nonmagnetic Al-3+ and Sc-3+ ions
[BLL-WH-594-(9091.9F)] 08 p1125 N85-17090
Theoretical research program to study transition metal trimers and embedded clusters
[NASA-CR-174296] 08 p1125 N85-17093
Electronic structure, chemical bonding, and superconductivity of silver films on germanium
[AD-A147720] 08 p1128 N85-17112
Silicon superlattices. 2: Si-Ge heterostructures and MOS systems
[NASA-CR-174287] 08 p1224 N85-17711
Electronic structure of semiconductor interfaces
[AD-A147663] 08 p1225 N85-17715
Electronic structure, chemical bonding, and electron conductivity of thin-film transition-metal silicides
[AD-A147721] 08 p1226 N85-17718
Quantum Monte Carlo for molecules
[AD-A148159] 08 p1227 N85-17727

Electronic structure of liquid metal alloys
[DE85-000904] 09 p1295 N85-18136
Metal atom diffusion in amorphous silica and at the silica surface
[DE84-017351] 09 p1360 N85-18674
Theoretical studies of atomic transition
[DE85-001325] 09 p1361 N85-18687
Compilation of atomic data for diagnostics of Tokamak
09 p1390 N85-18744
Comparative studies on the electronic structures of W2(O2CH)4 and W2(O2CH)4-(CH3)2 by the relativistic X Alpha-SW method: A d3-d3 metal dimer with a quadruple metal-metal bond?
[AD-A148814] 09 p1397 N85-18793
Microscopic determinations of lattice and electronic structures of solids
[DE84-017323] 09 p1399 N85-18806
Surface physics and crystallography
[DE85-003126] 11 p1735 N85-20910
Electronic structure of silicon superlattices
[NASA-CR-175536] 11 p1736 N85-20916
Structural, morphological and optical characteristics of KGd(WO4)2 crystals 14 p2280 N85-24126
Theory and calculations of the electronic structure of solids having directional bonding
[AD-A151062] 14 p2428 N85-24971
Test of the electronic structure of Fe(100) by absorbed current spectroscopy
[DE85-004942] 15 p2661 N85-26422
Experimental studies of the electronic structure of 1-2 and 1-3 intermetallic compounds
[DE85-006978] 15 p2662 N85-26432
Tilt grain boundaries in NiO
[DE85-006839] 16 p2751 N85-26978
Clusters of transition metal atoms
[AD-A153126] 17 p3030 N85-28740
Age hardening and atomic structure of an aluminum-6 at. % silver alloy
[DE85-009977] 18 p3077 N85-29031
Electronic structure calculations for low coverage adlayers
[DE85-007733] 18 p3179 N85-29709
Theoretical studies on the structures of insulating and metallic glasses
[DE85-010022] 18 p3194 N85-29814
VUV synchrotron light as a technique for studying the interface quality and properties of thin overlayers
[DE85-009822] 19 p3262 N85-30227
Many-body processes in atomic and molecular physics
[DE85-009750] 19 p3354 N85-30791
Proceedings of the 1984 Workshop on High-Energy Excitations in Condensed Matter, volume 2
[DE85-007305] 19 p3357 N85-30809
Theoretical investigation of material characteristics of semiconductor superlattices
[AD-A154126] 19 p3375 N85-30938
New adatom model for Si(11) 7X7 and Si(111)Ge 5X5 reconstructed surfaces 20 p3480 N85-31625
Ab initio calculations of materials properties
[DE85-011167] 20 p3531 N85-31964
Experimental studies of the geometric and electronic structure of chemisorption bonding
[PB85-192250] 22 p3747 N85-33228
Standard value for the radiation length in air
[HE-4.4-4] 24 p4193 N85-36013

ATOMIC THEORY
NT HEISENBERG THEORY

ATOMIC WEIGHTS
The inner granulometric density of the tracks in nuclear emulsions and its application to determine the chemical spectrum of primary cosmic ray nuclidi
[OG-4.3-9] 22 p3879 N85-34034

ATOMIZATION
U ATOMIZING

ATOMIZERS
Measurement of drop-size distributions with the aid of a scattered light particle size counting analyser
[BLL-TRANS-WH-620-(9091.9F)]
09 p1317 N85-18278

ATOMIZING
NT GAS ATOMIZATION
NT LIQUID ATOMIZATION
Influence of temperature on wear resistance of detonation coatings of alloy powders
10 p1447 N85-19116
Study of phase composition of Al-B plasma coatings
11 p1598 N85-20050
Liquid fuel spray processes in high-pressure gas flow
[NASA-TM-86944] 12 p1844 N85-21570
Atomization data requirements for rocket combustor modeling 13 p2003 N85-22555
Specifics of fine structure of pressed aluminum alloys manufactured by plasma atomization
19 p3242 N85-30102
Influence of type of processing of AK4 alloy on its surface state and strength of bonding of plasma coatings
19 p3242 N85-30103
Stable generation of highly monodisperse aerosols
21 p3642 N85-32628
Influence of technology of atomization of naturally alloyed iron on grain-size characteristics of powder material
[BLL-M-35810-(5828.4)] 23 p3914 N85-34257

ATOMS
NT HELIUM ATOMS
NT HOT ATOMS
NT HYDROGEN ATOMS
NT METASTABLE ATOMS
NT NEUTRAL ATOMS
NT OXYGEN ATOMS
Diagnostics of ionization in air produced by infrared radiation from A pulse CO2 laser
[AD-A145376] 02 p0201 N85-11342
Dispersion forces of solids under stress. Chemisorption under stress
[AD-A146171] 03 p0373 N85-12380
Deceleration, cooling, and trapping of atoms
[AD-A146234] 03 p0418 N85-12672
Periodic cluster simulation of a disordered impurity system
[INPE-3453-PRE/705] 16 p2858 N85-27628
Studies of collisional and nonlinear radiative process for development of coherent UV and XUV sources
[AD-A152001] 16 p2865 N85-27670
Atom location by electron channeling analysis
[DE85-007549] 16 p2872 N85-27716
The temperature dependence of diffracted beam intensities in atom-surface scattering
[AD-A152762] 17 p3029 N85-28736
Clusters of transition metal atoms
[AD-A153126] 17 p3030 N85-28740
The effect of ion-bombardment-induced atomic mixing on depth-profiling of interfaces
[AD-A153199] 17 p3044 N85-28834
Cavityless optical bistability in systems of two-level atoms 18 p3186 N85-29764
Alkali atom - SbCl(5) reactions: Blue-green chemiluminescence from an inverted population in SbCl
[AD-A154371] 19 p3276 N85-30315
Production of gallium atoms by excimer laser photolysis of trimethyl gallium
[DE85-010742] 19 p3278 N85-30331
Double photon excitation of high-Rydberg atoms as a long-lived submillimeter detector
[NASA-CASE-NPO-16372-1] 19 p3352 N85-30779
Spontaneous emission by two atoms with different resonance frequencies near a metal surface
[AD-A154115] 19 p3353 N85-30781
Many-body processes in atomic and molecular physics
[DE85-009750] 19 p3354 N85-30791
Resonant-transfer-and-excitation for highly charged ions (16 or = Z or = 23) in collisions with helium
[DE85-010550] 19 p3359 N85-30823
New adatom model for Si(11) 7X7 and Si(111)Ge 5X5 reconstructed surfaces 20 p3480 N85-31625
Overlap integrals for atom-metal surface interactions
[AD-A155038] 21 p3702 N85-32996
High-resolution spectroscopy and dynamics of multiphoton processes in atoms and molecules
[AD-A155862] 24 p4147 N85-35714
Exit channels of autoionization resonances in atoms
[DE85-012299] 24 p4149 N85-35726

ATP
U ADENOSINE TRIPHOSPHATE

ATROPHY
Alterations in skeletal muscle with disuse atrophy
[NASA-CR-174195] 06 p0843 N85-15349
Effect of disuse on sarcoplasmic reticulum in fast and slow skeletal muscle
[NASA-CR-174337] 08 p1191 N85-17506
Acid phosphatase and protease activities in immobilized rat skeletal muscles
[NASA-CR-174340] 08 p1192 N85-17509
A comparison of rat myosin from fast and slow skeletal muscle and the effect of disuse
[NASA-CR-174339] 08 p1192 N85-17510
Nutrition in space flight: Some thoughts
14 p2394 N85-24743
Constant fiber number during skeletal muscle atrophy and modified arachidonate metabolism during hypertrophy 15 p2609 N85-26078
Effects of muscle atrophy on motor control: Cage size effects 15 p2609 N85-26080
Responses of skeletal muscle to unloading, a review
[NASA-CR-176177] 24 p4128 N85-35594

ATROPINE
An atropinized heat-stressed rat model: Dose response effects and pharmacokinetics
[AD-A146651] 07 p1011 N85-16423

ATS
Lack of communication 15 p2686 N85-26591

ATTACHMENT
Advanced life analysis methods. Volume 1: Cracking data survey and NDI (nondestructive inspection) assessment for attachment lugs
[AD-A150419] 13 p2103 N85-23108
Advanced life analysis methods. Volume 2: Crack growth analysis methods for attachment lugs
[AD-A150420] 13 p2103 N85-23109

ATTACK AIRCRAFT
NT A-7 AIRCRAFT
NT A-10 AIRCRAFT
NT B-1 AIRCRAFT
NT B-70 AIRCRAFT
NT BOMBER AIRCRAFT
NT CL-41 AIRCRAFT
NT DH 115 AIRCRAFT
NT F-8 AIRCRAFT
NT F-14 AIRCRAFT
NT F-15 AIRCRAFT
NT F-16 AIRCRAFT
NT F-17 AIRCRAFT
NT F-18 AIRCRAFT
NT F-27 AIRCRAFT
NT F-104 AIRCRAFT
NT F-106 AIRCRAFT
NT F-111 AIRCRAFT
NT FIGHTER AIRCRAFT
NT JAGUAR AIRCRAFT
NT JET PROVOST AIRCRAFT
NT MIG AIRCRAFT
NT MIRAGE AIRCRAFT
NT MIRAGE 3 AIRCRAFT
A-5 supersonic attack aircraft described --- Qiang-5 aircraft 06 p0747 N85-14792
Details of export A-5 close-support aircraft given --- Qiang-5 aircraft 06 p0748 N85-14793
The development of a dynamic model of a generalised combat aircraft with forward wings for the identification of stability and control characteristics
[CAR-84-33] 09 p1280 N85-18050
Details of export A-5 close-support aircraft given
10 p1424 N85-18983
Cost-estimating relationships for tactical combat aircraft
[AD-A151575] 15 p2471 N85-25255
ESP (External-Stores Program): A pilot computer program for determining flutter-critical external-store configurations. Volume 2: Final report on program enhancement and delivery
[AD-A152269] 16 p2711 N85-26726

ATTACKING (ASSAULTING)
NyKINM, a further development of KINM 22 --- simulation of a robot attack on an aircraft
[FOA-C-20559-D8(E3)] 07 p0903 N85-15720
Next generation gunship
[AD-A156361] 24 p4065 N85-35193

ATTENTION
Inhibition of return: Neural basis and function
[AD-A145242] 01 p0098 N85-10652
Visual selective attention
[AD-A146220] 03 p0401 N85-12556
Visual attention to radar displays
05 p0704 N85-14514
Selecting one among the many: A simple network implementing shifts in selective visual attention
[AD-A148969] 10 p1530 N85-19644

ATTENUATION
NT ACOUSTIC ATTENUATION
NT ATMOSPHERIC ATTENUATION
NT MANDELSTAM REPRESENTATION
NT MICROWAVE ATTENUATION
NT RADAR ATTENUATION
NT RADIO ATTENUATION
NT SHOCK WAVE ATTENUATION
NT SIDELOBE REDUCTION
NT WAVE ATTENUATION
Transient attenuation in optical fibers
[DE84-016487] 05 p0729 N85-14687
The impact of propagation effects on the design of high capacity digital microwave links in the 18 GHz frequency band 10 p1470 N85-19278
Investigation of bimodal paramagnetic filter
13 p2083 N85-23007
Influence scattering and Q in the lithosphere
[AD-A150939] 14 p2293 N85-24213
Frequency selective signals-to-noise enhancer/limiter apparatus
[AD-D011583] 15 p2548 N85-25724
Multiple scattering of electromagnetic waves in discrete random media
[AD-A151766] 16 p2772 N85-27112
LIGHT: A ray tracing code to simulate light collection in scintillation spectrometers and light pipes
[DE85-007213] 16 p2865 N85-27673

Experimental and analytic characterization of nonlinear seismic attenuation
[AD-A154760] 21 p3631 N85-32556
Normal modes in an overmoded circular waveguide coated with lossy material
[NASA-CR-176186] 24 p4065 N85-35320
Core structure of EAS in 10(15) to 10(17) eV
24 p4189 N85-35969
ATTENUATION COEFFICIENTS
X-ray absorption in perfect crystals
[DE84-016034] 05 p0732 N85-14706
Recommendation on use of series K157UL1 microcircuits 13 p2071 N85-22936
Change of electrical characteristics of radio-frequency cables under thermal effect 13 p2081 N85-22999
Fine structure of vertical distribution of light attenuation index of sea water 13 p2109 N85-23140
Measurement of the attenuation length of an acrylic scintillator — magnetic monopoles
[NOTA-INTERNA-828] 18 p3097 N85-29175
Precision microwave attenuation measurement by time interval ratio
[RSRE-85005] 22 p3755 N85-33260
ATTENUATORS
NT POTENTIOMETERS (RESISTORS)
NT RESISTORS
NT THERMISTORS
EMC enhanced constant Z modulator
[AD-A147715] 08 p1157 N85-17297
Design of low loss helix circuits for interference fitted and brazed circuits
[NASA-CR-168313] 10 p1478 N85-19328
ATTITUDE (INCLINATION)
NT PITCH (INCLINATION)
NT ROLL
NT SATELLITE ORIENTATION
NT YAW
Theory underlying the peripheral vision horizon device
01 p0008 N85-10048
Stimulus factors in motion perception and spatial orientation 01 p0008 N85-10049
Workload demand and CNS depressant stressor effects on spatial orientation information processing
[AD-A145211] 01 p0098 N85-10651
Maximum normalized rate as a flying qualities parameter 05 p0702 N85-14503
OMEGA: An optronic device to measure the incidence angle of a projectile
[ISL-CO-207/83] 14 p2306 N85-24274
A method of estimating aircraft attitude from fly by wire flight control system data 16 p2697 N85-26653
Space optics
[CNES-84/105/T/CT/DRT/TIT/10]
20 p3533 N85-31985
Typological characteristics of hemodynamic states of healthy subjects in orthostatic position
22 p3821 N85-33673
Cosmic ray intensity and the tilt of the neutral sheet
[SH-4.2-8] 23 p4007 N85-34846
ATTITUDE CONTROL
NT DIRECTIONAL CONTROL
NT LATERAL CONTROL
NT LONGITUDINAL CONTROL
NT SATELLITE ATTITUDE CONTROL
NT THRUST VECTOR CONTROL
Effects of foveal information processing
01 p0009 N85-10052
Peripheral vision horizon display on the single seat night attack A-10 01 p0009 N85-10053
Modular design attitude control system
[NASA-CR-171162] 01 p0016 N85-10096
Autonomous Attitude Determination System (AADS). Volume 1: System description
[NASA-TM-87365] 02 p0240 N85-11559
Analysis and simulation of an intertial system (Strapdown) for auxiliary attitude determination by adaptive drift estimation
[INPE-3257-TDL/177] 04 p0454 N85-12882
Propellant tank resupply system
[AD-D011286] 05 p0603 N85-13848
An Assessment of Integrated Flywheel System Technology
[NASA-CP-2346] 05 p0604 N85-13850
A summary of the 1983 Integrated Flywheel Technology Workshop 05 p0605 N85-13855
Comparative energy storage assessment item
05 p0605 N85-13858
Inertial storage for satellites 05 p0605 N85-13859
Perspectives on energy storage wheels for space station application 05 p0605 N85-13860
Description of a laboratory model Annular Momentum Control Device (AMCD) 05 p0606 N85-13863
Hemispherical antenna pointing mechanism — satellite antennas 05 p0627 N85-14021
Infrared horizon sensor modeling for attitude determination and control: Analysis and mission experience
[NASA-TM-86181] 10 p1429 N85-19016
Emitted vibration measurement device and method
[NASA-CASE-MFS-25981-1] 11 p1635 N85-20299
Summary presentation of the Constellations Panel
11 p1644 N85-20359
Report of the Constellations Panel
11 p1645 N85-20368
Space station systems technology study (add-on task). Volume 1: Executive summary
[NASA-CR-171415] 13 p1986 N85-22459
Large antenna control methods: Current status and future trends 14 p2234 N85-23845
Space station systems technology study (add-on task). Volume 2: Trade study and technology selection
[NASA-CR-171416] 15 p2475 N85-25279
Programming for Pioneer 12 15 p2688 N85-26606
Controller requirements for uncoupled aircraft motion, volume 2
[AD-A153300] 17 p2900 N85-27879
Operating characteristics of a 0.87 kW-hr flywheel energy storage module
[NASA-TM-87038] 17 p2974 N85-28371
Rationale for an experimental test for flexible space structure attitude control 20 p3411 N85-31167
Numerical and experimental evaluation for single-axis control of an LSS laboratory model
20 p3411 N85-31168
Attitude control tradeoff study between the use of a flexible beam and a tether configuration for the connection of two bodies in orbit 20 p3412 N85-31174
A control concept for large flexible spacecraft using order reduction techniques 20 p3415 N85-31193
Deployable-erectable trade study for space station truss structures
[NASA-TM-87573] 22 p3740 N85-33181
Computer simulation of a cruise missile using brushless dc motor fin control
[AD-A155935] 24 p4089 N85-35349
ATTITUDE GYROS
NT GYRO HORIZONS
Extracts from the test plan for in-flight evaluation of the NT-33A peripheral vision display
01 p0009 N85-10055
Some notes on a tangent plane oriented heading reference — stabilized platforms
[RAE-TM-IEE-144] 02 p0136 N85-10928
Selection of optimum corrections torque for vertical gyro according to special-purpose program
14 p2273 N85-24082
Optimum parameters of aerogyroscopic satellite orientation system 16 p2718 N85-26782
ATTITUDE INDICATORS
NT GYRO HORIZONS
Peripheral Vision Horizon Display (PVHD)
[NASA-CP-2306] 01 p0006 N85-10044
Effects of foveal information processing
01 p0009 N85-10052
Peripheral vision horizon display testing in RF-4C aircraft 01 p0009 N85-10054
Extracts from the test plan for in-flight evaluation of the NT-33A peripheral vision display
01 p0009 N85-10055
Peripheral vision displays: The future
01 p0009 N85-10058
A production peripheral vision display system
01 p0010 N85-10059
A preliminary flight evaluation of the peripheral vision display using the NT-33A aircraft
[AD-A145123] 01 p0010 N85-10060
Wind tunnel calibration of a hemispherical head angle of attack and angle of sideslip indicator
[FFA-TN-1984-11] 02 p0136 N85-10923
Data analysis techniques for vehicle attitudinal, positional and experimental measurements
[AD-A147752] 08 p1188 N85-17484
Infrared horizon sensor modeling for attitude determination and control: Analysis and mission experience
[NASA-TM-86181] 10 p1429 N85-19016
Wide-field-of-view, helmet-mounted infinity display system development
[AD-A149641] 12 p1777 N85-21159
Attitude data consistence check of rocket payloads
[BMFT-FB-W-84-049] 12 p1790 N85-21239
Studies of the solar mesosphere explorer: Dynamics and horizon sensor performance. Part A: Spin axis precession and atmospheric drag. Part B: Clouds
[NASA-CR-175308] 24 p4069 N85-35213
ATTITUDE STABILITY
NT DIRECTIONAL STABILITY
NT GYROSCOPIC STABILITY
NT LATERAL STABILITY
NT LONGITUDINAL STABILITY
Some aspects of attitude stability of tethered space stations 11 p1646 N85-20369
The design and development of a constant-speed solar array drive 22 p3706 N85-33519
ATTRITION (MATERIALS)
U COMMINUTION
AUDIO EQUIPMENT
NT EARPHONES
NT LOUDSPEAKERS
NT MICROPHONES
Perceptibility of nonlinear distortions in power amplifier
06 p0789 N85-15041
A miniature urethane molded acoustic transducer
[AD-A146459] 06 p0804 N85-15114
Tubes and transistors in audio amplifiers
12 p1837 N85-21532
Robust detection and classification of regional seismic signals using a two mode/two stage cascaded adaptive arma (CAARMA) model
[AD-A154710] 21 p3630 N85-32554
AUDIO FREQUENCIES
Current and current shear effects in the parabolic approximation for underwater sound channels
[AD-A147833] 07 p1039 N85-16597
Application of K176-series microcircuits
13 p2077 N85-22973
Auditory fatigue caused by exposure to different frequency sounds presented at equivalent intensity
[ISL-R-101/84] 20 p3525 N85-31923
AUDIO SIGNALS
Specifics of dynamics of brain biopotentials under the influence of complex audible communicative signals
07 p1014 N85-16440
Processing speech for analysis using optical Fourier techniques
[AD-A151898] 15 p2544 N85-25704
A method and apparatus for operating on companded PCM voice data
[NASA-CASE-KSC-11285-1] 18 p3089 N85-29120
An approach to digital level compression using the zero-crossing points of programme signals
[NHK-LABS-NOTE-308] 18 p3090 N85-29123
AUDIO VISUAL EQUIPMENT
U TRAINING DEVICES
U VISUAL AIDS
AUDIOLOGY
Auditory impairment and the onset of disability and handicap in noise-induced hearing loss
[ISVR-TR-126] 20 p3507 N85-31801
AUDIOMETRY
Second generation USAFSAM (United States Air Force School of Aerospace Medicine) microprocessor audiometer
[AD-A149936] 12 p1905 N85-21963
The audiomat: An automatic audiometer for use in occupational audiometry
[DRIC-T-7136] 13 p2142 N85-23294
Auditory impairment and the onset of disability and handicap in noise-induced hearing loss
[ISVR-TR-126] 20 p3507 N85-31801
Auditory fatigue caused by exposure to different frequency sounds presented at equivalent intensity
[ISL-R-101/84] 20 p3525 N85-31923
AUDITORY DEFECTS
Auditory impairment and the onset of disability and handicap in noise-induced hearing loss
[ISVR-TR-126] 20 p3507 N85-31801
AUDITORY FATIGUE
Comparative assessment of different treatment modalities in miners with vibration- and noise-induced disease 10 p1524 N85-19610
Auditory fatigue caused by exposure to different frequency sounds presented at equivalent intensity
[ISL-R-101/84] 20 p3525 N85-31923
AUDITORY PERCEPTION
Evidence for multiple areas in the human auditory cortex
[AD-A146086] 03 p0401 N85-12555
Inner ear characteristics during 7 day antiorthostatic bedrest (6 deg head down tilt) 05 p0695 N85-14470
Human engineer's guide to auditory displays. Volume 2: Elements of signal reception and resolution affecting auditory displays
[AD-A146513] 06 p0859 N85-15462
Human engineer's guide to auditory displays. Volume 1. Elements of perception and memory affecting auditory displays
[AD-A146601] 06 p0860 N85-15464
Specifics of dynamics of brain biopotentials under the influence of complex audible communicative signals
07 p1014 N85-16440
Detection of low frequency impulsive noise from large wind turbine generators
[NASA-CR-172511] 07 p1036 N85-16586

Neurocognitive pattern analysis of an auditory and visual numeric motor control task. Part 1: Development of methods
[AD-A148809] 09 p1364 N85-18578
Quantitative measurement of human auditory acuity
10 p1524 N85-19614
The audiomat: An automatic audiometer for use in occupational audiometry
[DRIC-T-7138] 13 p2142 N85-23294
Dissociation of autonomic and sensory vestibular reactions 23 p3953 N85-34501
AUDITORY SIGNALS
Auditory information systems in military aircraft: Current configurations versus the state of the art
[AD-A145469] 02 p0275 N85-11794
Human engineer's guide to auditory displays. Volume 2: Elements of signal reception and resolution affecting auditory displays
[AD-A146513] 06 p0859 N85-15462
Human engineer's guide to auditory displays. Volume 1. Elements of perception and memory affecting auditory displays
[AD-A146601] 06 p0860 N85-15464
High-frequency acoustic variability in the arctic
[AD-A150550] 13 p2155 N85-23383
An overview of stochastic signal modeling
[AD-A152144] 16 p2855 N85-27605
Rotor blade test apparatus
[AD-D011725] 23 p3934 N85-34381
AUDITORY STIMULI
Evidence for multiple areas in the human auditory cortex
[AD-A146066] 03 p0401 N85-12555
The construction of auditive tests of attention and spatial orientation and their factorial structure
[DFVLR-FB-84-21] 05 p0699 N85-14485
AUDITORY TASKS
Communications skills for CRM training
09 p1276 N85-18017
Neurocognitive pattern analysis of an auditory and visual numeric motor control task. Part 1: Development of methods
[AD-A148809] 09 p1364 N85-18578
AUGER EFFECT
Aspects of silicon bulk lifetimes
20 p3479 N85-31617
Recombination phenomena in high efficiency silicon solar cells 20 p3479 N85-31618
Inter-zone auger recombination in GaSb laser structures 21 p3682 N85-32875
Multiple inner shell vacancies in laser-irradiated Au plasma 23 p3981 N85-34687
AUGER SPECTROSCOPY
Stress-driven solute enrichment of crack-tips during low ductility intergranular fracture of low-alloy steel
[AERE-R-11120] 03 p0333 N85-12150
Oxygen diffusion from anodic surface oxide films on titanium subhydride studies by auger electron spectroscopy and electron energy loss spectroscopy
[DE84-016942] 04 p0572 N85-13648
Photoemission, vibrational and stimulated desorption studies of metal-semiconductor interfaces and of chemisorbed atoms and molecules
[AD-A147709] 08 p1225 N85-17717
Fundamental study of catalysts using laser Raman, infrared, auger electron spectroscopy and low energy electron diffraction
[DE85-001813] 11 p1595 N85-20033
Surface physics instrumentation
[AD-A149304] 11 p1728 N85-20889
Studies of silicon-refractory metal interfaces: Photoemission study of interface formation and compound nucleation
[AD-A150075] 12 p1800 N85-21293
HREELS and Auger studies of conducting polymers
[DE85-004541] 13 p2038 N85-22764
Threshold double photoionization of argon with synchrotron radiation
[AD-A150615] 13 p2157 N85-23389
Bonding information from Auger spectroscopy
[AD-A150864] 14 p2251 N85-23948
Chemical and localization effects in Auger lineshapes of transition metal compounds
[AD-A150865] 14 p2251 N85-23949
Charge transfer, polarization and relaxation effects in the Auger lineshapes of Si
[AD-A150938] 14 p2252 N85-23954
Self-sustaining coatings for fusion applications: Copper lithium alloys
[DE85-009740] 18 p3190 N85-29783
Study of solute segregation at interfaces using Auger electron spectroscopy
[DE85-005709] 20 p3423 N85-31247
The effect of metal overlayers of thermionic dispenser cathodes
[AD-A154795] 21 p3701 N85-32995
Size and shape dependence of CO adsorption sites on sapphire supported Fe microcrystals
[NASA-CR-176171] 24 p4160 N85-35794
AUGMENTATION
NT STABILITY AUGMENTATION
NT THRUST AUGMENTATION
Design of a digital ride quality augmentation system for commuter aircraft
[NASA-CR-172419] 01 p0006 N85-10037
Development and flight evaluation of an augmented stability active controls concept: Executive summary
[NASA-CR-166009] 02 p0149 N85-11006
Helicopter human factors programs and plans
06 p0751 N85-14808
An update of the Canada/USA augmentor-wing project 08 p1070 N85-16781
The enhancement of concurrent processing through functional programming languages
[AD-A150771] 14 p2404 N85-24822
A modern control design methodology with application to the CH-47 helicopter
[AD-A151946] 16 p2710 N85-26723
Visual and part-task manipulations for teaching simulated carrier landings
[AD-A153622] 18 p3154 N85-29529
AURIGA CONSTELLATION
Eclipse observations of Epsilon Aurigae
11 p1755 N85-21037
UV observations of epsilon aurigae during ingress and totality 11 p1755 N85-21038
AURORAL ACTIVITY
U AURORAS
AURORAL ARCS
Circuit transients due to negative bias arcs on a high-voltage solar array in low Earth orbit
[NASA-TP-2407] 06 p0760 N85-14858
Distribution of electric field near westward propagating bend in aurora 06 p0823 N85-15222
Sun-aligned polar cap auroral arcs
[AD-A148052] 08 p1185 N85-17472
One-dimensional model of auroral magnetic force with longitudinal current and cyclotron heating of ions
13 p1980 N85-22424
Characteristics of the electrodynamics of auroral arcs as inferred from rocket and ground-base observations during IMS 14 p2363 N85-24601
Field-aligned currents observed in the vicinity of a moving auroral arc 14 p2363 N85-24603
Two-dimensional quasineutral description of particles and fields above discrete auroral arcs
[NASA-CR-176170] 24 p4116 N85-35517
AURORAL ELECTROJETS
A model for the propagation of the westward traveling surge
[TRITA-EPP-84-03] 03 p0393 N85-12515
Distribution of electric field near westward propagating bend in aurora 06 p0823 N85-15222
Polar orbit electrostatic charging of objects in shuttle wake 13 p1992 N85-22487
Altitude of auroral scattering observed along auroral electrojets 14 p2339 N85-24465
Ground-based and near-Earth observations during the IMS 14 p2359 N85-24575
Auroral X-rays and equatorial electrons in the morning sector — substorm 14 p2361 N85-24590
The GEOS-2 E-field behavior during dynamic auroral development near the satellite footpoint
14 p2362 N85-24598
Three-dimensional current systems and electric fields during active aurora 14 p2362 N85-24599
The relationship between auroral electrojet and visual aurora 14 p2363 N85-24602
Field-aligned currents observed in the vicinity of a moving auroral arc 14 p2363 N85-24603
On the dynamics of the westward traveling surge
14 p2364 N85-24607
Ground magnetic observations of high-latitude Pi2 pulsations: Scandinavian magnetometer array results
14 p2370 N85-24649
Pi2 pulsations and the substorm current wedge - ground observations 14 p2370 N85-24650
Ground-satellite observations of substorm related Pi 2 pulsations and current systems
14 p2370 N85-24651
The influence of a turbulent region on the flux of auroral electrons
[KGI-PREPRINT-072] 20 p3494 N85-31723
Magnetospheric response to solar wind variations
[DE85-010762] 20 p3547 N85-32074
AURORAL IONIZATION
Auroral X-rays and equatorial electrons in the morning sector — substorm 14 p2361 N85-24590
Afternoon radar aurora and polar cap convection pattern 14 p2361 N85-24592
Geophysical plasmas and atmospheric modeling
[AD-A152805] 17 p2993 N85-28497
Characteristics and sources of E-region ionization in the continuous aurora
[AD-A155016] 21 p3632 N85-32562
AURORAL IRRADIATION
The temporal evolution of a small auroral substorm as viewed from high altitudes with Dynamics Explorer 1
[NASA-CR-176064] 20 p3493 N85-31716
AURORAL SPECTROSCOPY
Measurements with an auroral spectrometer in the Energy Budget Campaign
[BMFT-FB-W-84-050] 14 p2374 N85-24677
AURORAL ZONES
Rocket and satellite observations of electric fields and ion convection in the dayside auroral ionosphere
[TRITA-EPP-84-05] 02 p0229 N85-11497
Relation between polarization of artificial low frequency radiation and parameters of auroral ionosphere
06 p0785 N85-15016
Longitudinal current before westward propagating auroral bend 06 p0823 N85-15223
Simultaneous observations of electron spectra in the auroral zone and near the equatorial plane by the DMSP-5D-F2 and GEOS-1 Satellites
[KGI-184] 09 p1355 N85-18522
Experiment for measuring electric fields within the sounding rocket project Energy Budget
[BMFT-FB-W-84-048] 12 p1891 N85-21866
Conjugacy of ELF-VHF emissions near L=6 — chorus phenomenon, hiss 14 p2367 N85-24629
Fast ion polarization jet in subauroral F-layer and its manifestation in structure of high latitude ionosphere
15 p2480 N85-25306
Auroral zone electric fields from DE-1 and -2 at magnetic conjunctions
[NASA-CR-175974] 18 p3136 N85-29421
Preliminary documentation for the polar code
[AD-A154125] 19 p3336 N85-30667
AURORAS
NT AURORAL ARCS
NT RADIO AURORAS
Magnetosphere, rings, and moons of Uranus
02 p0301 N85-11951
Charging of the DMSP F-2 spacecraft in the aurora on 10 January 1983
[AD-A146303] 03 p0324 N85-12086
Magnetospheric plasma studies using data from the dynamics high and low altitude plasma instruments
[AD-A145751] 03 p0392 N85-12505
Temporal and spatial variations in the intensity of ultraviolet emissions from Jupiter and the Io torus
03 p0448 N85-12846
Dayside cusp aurora 04 p0521 N85-13333
Longitudinal current before westward propagating auroral bend 06 p0823 N85-15223
Application of Fabry-Perot spectrometers for measurement of upper atmosphere temperatures and winds 08 p1183 N85-17454
X rays from the aurora
[AD-A148628] 08 p1186 N85-17477
The flow of plasma in the solar terrestrial environment
[NASA-CR-174301] 08 p1224 N85-17707
Simultaneous observations of electron spectra in the auroral zone and near the equatorial plane by the DMSP-5D-F2 and GEOS-1 Satellites
[KGI-184] 09 p1355 N85-18522
Pitch angle scattering and particle precipitation in a pulsating aurora: An experimental study
[KGI-185] 09 p1355 N85-18523
Spatial distribution of auroras and its relationship to geological structure of Norilsk region
10 p1497 N85-19447
Solar system studies with the IUE: 1982 - 1984
11 p1744 N85-20984
The spatial dependence of the Jovian auroral emissions 11 p1759 N85-21068
Description of the SSB/A (Special Sensor B/Aerospace X-ray spectrometer
[AD-A150040] 12 p1790 N85-21236
S3-3 ONR-118 data analysis
[AD-A149725] 12 p1869 N85-21855
Plans for Interbol satellite experiment
13 p1977 N85-22407
Observations of auroras and related plasma phenomena by the Kyokko and Jikiken satellite in IMS — EXOS-A and B satellite 14 p2354 N85-24547
Ground-based and near-Earth observations during the IMS 14 p2359 N85-24575
Electrodynamics of magnetosphere-ionosphere coupling 14 p2359 N85-24579
Electron and proton precipitation in magnetic substorms — auroral substorms
14 p2360 N85-24585
Development of an auroral absorption substorm
14 p2360 N85-24586

The magnetospheric convection electric field at ionospheric altitudes: A case study based on STARE and Saint-Santin data 14 p2362 N85-24594
The GEOS-2 E-field behavior during dynamic auroral development near the satellite footpoint
14 p2362 N85-24596
Three-dimensional current systems and electric fields during active aurora 14 p2362 N85-24599
Testing of some substorm features by multiple balloon observations 14 p2363 N85-24600
The relationship between auroral electrojet and visual aurora 14 p2363 N85-24602
On-off characteristics of auroral pulsations
14 p2363 N85-24604
Multiple correlation between auroral and magnetic pulsations 14 p2363 N85-24605
Multiple correlation between auroral and magnetic pulsations. Part 2: Determination of electric currents and electric fields around a pulsating auroral patch
14 p2363 N85-24606
Contribution of the Scandinavian Twin Auroral Radar Experiment (STARE) radar to the understanding of the physical mechanisms associated with Pc5 pulsations
14 p2364 N85-24613
Theory and computer simulation of auroral kilometric radiation 14 p2365 N85-24617
Observations of the MF-HF plasma wave emissions in active auroras by the sounding rocket experiments at Syowa station 14 p2366 N85-24620
Role of equatorial Electron Cyclotron Harmonic (ECH) waves in the generation of diffuse auroras. Contribution of the GEOS IMS spacecraft 14 p2367 N85-24632
Short-period magnetic pulsations during substorms
14 p2368 N85-24636
The IMS contributions to the understanding of auroral precipitation, transport and particle sources
14 p2372 N85-24660
Measurements with an auroral spectrometer in the Energy Budget Campaign
[BMFT-FB-W-84-050] 14 p2374 N85-24677
Observation of polar aurora from the Salyut-6 space station during the great geomagnetic storm of 11-13 Apr. 1981 15 p2477 N85-25291
Study of spatial distribution of auroras
16 p2808 N85-27315
IMS (International Magnetospheric Study) contributions to the understanding of auroral precipitation, transport, and particle sources
[AD-A152320] 17 p2992 N85-28492
EISCAT electron density studies
[AD-A152620] 17 p2993 N85-28498
Electron and ion distributions at high latitudes as measured by the Air Force polar orbiting satellites
[AD-A153242] 17 p2993 N85-28500
Images of the Earth's aurora and geocorona from the Dynamics Explorer Mission
[NASA-CR-175983] 18 p3136 N85-29423
The temporal evolution of a small auroral substorm as viewed from high altitudes with Dynamics Explorer 1
[NASA-CR-176064] 20 p3493 N85-31718
The influence of a turbulent region on the flux of auroral electrons
[KGI-PREPRINT-072] 20 p3494 N85-31723
Atmospheric Emission Photometric Imaging (AEPI)
23 p3902 N85-34170
Vehicle Charging And Potential (VCAP)
23 p3902 N85-34173
Cosmic rays 10Be biennal data and their relationship to aurorae and sunspots
[SH-7.1-1] 23 p4047 N85-35094
Cosmic ray secular variations in terrestrial records and aurorae
[SH-7.1-3] 23 p4047 N85-35096
Two-dimensional quasineutral description of particles and fields above discrete auroral arcs
[NASA-CR-176170] 24 p4116 N85-35517

AUSTENITE
Effects of prior austenite and ferrite grain size on fracture properties of a plain carbon steel
[AD-A146276] 03 p0332 N85-12138
Autenite transformation in powder-compacted chromium-nickel-molybdenum steels during continuous cooling
[BLL-M-35981-(5828.4)] 05 p0615 N85-13933
Influence of preliminary cold deformation on fineness of pearlite
[BLL-BISI-TRANS-22409-(9022.06)]
17 p2927 N85-28054
Textural transformations taking place during heat and mechanical treatment in triplex steels
[BLL-BISI-TRANS-22404-(9022.06)]
17 p2927 N85-28063
Influence of structural state and alloy content of austenite on formation of martensitic phases in steels
[BLL-BISI-TRANS-22385-(9022.06)]
17 p2928 N85-28068
Mechanical stabilization of austenite against epsilon martensite and its effect on deformation behavior in high manganese steels
[DE85-007654] 17 p2932 N85-28097
Vacuum pressure welding of commercial titanium with 2Kh13 and 12Kh18N10T steels
19 p3246 N85-30124
Effects of hot deformation on the kinetics of the pearlite transformation in eutectoid steel
[BLL-M-35644-(5828.4)] 23 p3913 N85-34250
Acoustic emission during transformation of austenite in 38KhN3MF steel
[BLL-M-35825-(5828.4)] 23 p3914 N85-34256
Decomposition of martensite in R6M5 and R6AM5 steels after direct immersion in liquid nitrogen
[BLL-M-36305] 24 p4077 N85-35268
Effect of prior warm rolling on the retained austenite content and hardening response of VIM-VAR (vacuum-induction melted-vacuum-arc remelted) AISI M-50 steel
[AD-A156145] 24 p4079 N85-35281

AUSTENITIC STAINLESS STEELS
Influence of nitrogen on the sensitization, corrosion, mechanical, and microstructural properties of austenitic stainless steels
[DE84-015134] 01 p0028 N85-10177
Electro-spark case-hardening of contoured surfaces
01 p0035 N85-10216
Microstructure and deformation aspects of some specialty steels and hard metals
02 p0176 N85-11182
EDS round-robin evaluation of type 308 austenitic stainless steel
[DE84-014574] 02 p0183 N85-11226
Identification of pulse-echo rays in austenitic steels
[AERE-R-11265] 03 p0369 N85-12356
Fractographic study of stress corrosion cracking of SUS 304 stainless steel in various environments
[BLL-RISLEY-TR-4596-(9091.9F)]
05 p0615 N85-13928
Influence of the mechanical and electrochemical characteristics of austenitic and austenoferritic steels on the propagation rate and morphology of stress corrosion cracking
[BLL-RISLEY-TR-4545-(9091.9F)]
06 p0767 N85-14906
Investigations into the fatigue crack growth behaviour of X8CrNi 18 11 (1.4948) austenitic stainless steel
[BLL-RISLEY-TR-4544-(9091.9F)]
06 p0768 N85-14911
Austenitic stainless steel for high temperature and pressure applications
[BLL-RISLEY-TR-4527-(9091.9F)]
07 p0925 N85-15860
Hydrogen trapping, diffusion, and recombination in austenitic stainless steels
[DE85-001871] 09 p1294 N85-18129
Fracture toughness of austenitic stainless steel weld metal at 4 K
[DE84-016638] 09 p1340 N85-18425
Role of nitrogen in improving resistance to localized corrosion in austenitic stainless steels
11 p1609 N85-20115
Partial replacement of chromium in austenitic stainless steels by molybdenum, copper, and vanadium, report of investigations 1984
[PB85-116508] 12 p1809 N85-21346
Hydrogen effects in austenitic stainless steels based on the Fe-Cr-Mn-N system
[DE85-003617] 13 p2023 N85-22672
Swelling behavior of manganese-bearing AISI 216 steel
[DE85-005712] 15 p2512 N85-25495
Swelling behavior of titanium-modified AISI 316 alloys
[DE85-007470] 16 p2752 N85-26962
Method of investigating accumulations of damage to weld joints in the case of low-cycle creep
[BLL-CE-TRANS-8088-(9022.09)]
16 p2792 N85-27219
Stainless steels: Application and welding
[BLL-BISI-TRANS-22357-(9022.06)]
17 p2927 N85-28059
Technical information: Weldability of stainless steel. Part 1: Austenitic stainless steel
[BLL-BISI-TRANS-22456-(9022.06)]
17 p2973 N85-28362
Relaxation properties and fatigue fracture resistance of austenitic spring steel
[BLL-BISI-TRANS-22300-(9022.06)]
17 p2978 N85-28406
Variations in the structure and in the composition of austentic and carbon steel in spot welds
[BLL-BISI-TRANS-21765-(9022.06)]
18 p3073 N85-29007
Development of reduced activation alloys for fusion service: Draft
[DE85-007464] 18 p3074 N85-29014
Elevated temperature erosion of steels
[DE85-008503] 18 p3075 N85-29018
Corrosion performance of metals and alloys in a tuff geochemical environment
[DE85-009449] 18 p3077 N85-29033
Kinetics of H-induced stress corrosion cracking. Part 1: Important features of cracking in respect of high strength steels
[BLL-BISI-TRANS-(9022.06)] 19 p3282 N85-30350
Hot cracking of austenitic stainless steels: The debut of the Sigmajig
[DE85-010560] 20 p3431 N85-31287
Reactor pressure vessel steels ASME SA533B and SA508 C 1.2
[VTT-340] 22 p3794 N85-33507
Phase transformations taking place in austenitic steel during deformation at different rates
[BLL-M-35875-(5828.4)] 23 p3914 N85-34254
The effect of pre-heating on the structure and properties of chromiun-molybdenum steels
[BLL-M-35897-(5828.4)] 23 p3914 N85-34255
Acoustic emission during transformation of austenite in 38KhN3MF steel
[BLL-M-35825-(5828.4)] 23 p3914 N85-34256
The use of austenitic stainless steel versus monel (Ni-cu) alloy in pressurized Gaseous Oxygen (GOX) life support systems
[AD-A156305] 24 p4134 N85-35625

AUSTRALIA
Mineral nutrients in Mediterranean ecosystems
[REPT-71] 01 p0069 N85-10456
Report of the Division of Atmospheric Physics, 1980-1983 03 p0391 N85-12501
Simple prediction of convergence zone propagation in waters around australia
[AD-A145986] 03 p0416 N85-12659
Evaluation of SIR-B imagery for geologic and geomorphic mapping, hydrology, and oceanography in Australia 08 p1146 N85-17229
MAGSAT anomaly field data of the crustal properties of Australia
[E85-10100] 13 p2122 N85-23215
An investigation of the crustal properties of Australia and surrounding regions derived from interpretation of MAGSAT anomaly field data 13 p2122 N85-23216
Data selection techniques in the interpretation of MAGSAT data over Australia 13 p2123 N85-23218
Report of the Hydrographic Service Royal Australian Navy for the year ended 30th june 1984, issue number 20
[AD-A151460] 15 p2583 N85-25932
Australian seismological report, 1980
[REPT-252] 17 p2989 N85-28473

AUSTRIA
Activities report in space research in Austria
11 p1587 N85-19994

AUTOCATALYSIS
Critical analysis of nitramine decomposition data. Preliminary comments on autoacceleration and autoinhibition in HMX and RDX decomposition
[AD-A146570] 06 p0774 N85-14946

AUTOCLAVES
Study of the kinetics of hydrogenation using aged catalysts
[DE85-004373] 12 p1802 N85-21302

AUTOCLAVING
Chemoviscosity modeling for thermosetting resins - I
[NASA-CR-172443] 03 p0326 N85-12096
Chemoviscosity modeling for thermosetting resins, 2
[NASA-CR-177958] 24 p4073 N85-35243

AUTOCOLLIMATORS
U COLLIMATORS

AUTOCORRELATION
Autoregressive nonsteady methods for the analysis and synthesis of the human voice
[FUB-3-1984] 01 p0041 N85-10266
Measures of distance between speech signals in the frequency domain — speech recognition
[FUB-5-1984] 01 p0041 N85-10267
Autoregressive modeling and the classification of land clutter — radar signatures
[ENST-C-84003] 03 p0356 N85-12292
Distributions of extreme values of sequences of autocorrelated random variables
[PB84-240746] 06 p0858 N85-15456
The analysis of spaced sensor records by correlation techniques 08 p1184 N85-17465
Methods and applications of time series analysis. Part 2: Linear stochastic models
[AD-A147292] 08 p1214 N85-17645
Relative-entropy minimization with uncertain constraints--theory and application to spectrum analysis
[AD-A149192] 10 p1546 N85-19752

Asymptotic distributions of the sample mean, autocovariances and autocorrelations of long-memory time series
[AD-A149409] 10 p1651 N85-19781

Method of multivariant intraclass pattern recognition
[AD-D011546] 12 p1818 N85-21405

Method for approximating autocorrelation functions for describing areal photoimage features
13 p1963 N85-22443

Regular synthesis of pairs of phase-keyed binary minimax signals 13 p2069 N85-22923

Parametric coherence estimation via convolved correlations
[DE85-003946] 14 p2416 N85-24909

Higher order residual analysis for nonlinear time series with autoregressive correlation structures
[AD-A149232] 15 p2636 N85-26257

Fast eigenvector methods for digital signal processing
20 p3439 N85-31341

Verification of theoretically computed spectra for a point rotating in a vertical plane
[DE85-011967] 20 p3520 N85-31893

AUTOIONIZATION

Many-electron effects in electron impact ionization of multiply charged ions
[DE85-005570] 15 p2649 N85-26340

Trends in the electric field enhancement of dielectronic recombination cross sections
[DE85-006920] 16 p2871 N85-27711

Experimental approaches to the measurement of dielectronic recombination
[DE85-006927] 17 p3030 N85-28743

Photoelectron studies of autoionizing Rydberg states in HCl
[DE85-011813] 21 p3702 N85-33001

Exit channels of autoionization resonances in atoms
[DE85-012299] 24 p4149 N85-35726

AUTOMATA THEORY

One queue or two pushdown stores take square time on a one-head tape unit
[CWI-CS-R8406] 05 p0717 N85-14601

Advancing automation and robotics technology for the Space Station and for the US economy. Volume 1: Executive overview
[NASA-TM-87566-VOL-1] 13 p1986 N85-22460

Advancing automation and robotics technology for the Space Station and for the US economy, volume 2
[NASA-TM-87566-VOL-2] 13 p1987 N85-22461

The hierarchical database decomposition approach to database concurrency control
[AD-A150612] 13 p2168 N85-23450

USSR report: Machine tools and metalworking equipment
[JPRS-UMM-85-006] 14 p2283 N85-24146

New CNC turning centers described
14 p2284 N85-24148

Large CNC machining center for turbine production
14 p2284 N85-24149

Minister B. V. Balmont on status of automation drive
14 p2284 N85-24151

West Europe report: Science and technology
[JPRS-WST-85-013] 14 p2289 N85-24183

MBB automates aircraft production in many FRG facilities 14 p2289 N85-24186

Robotic deburring. Part 2: Evaluation of cutters and noncompliant tooling
[DE85-006182] 14 p2311 N85-24306

Reliable computation with cellular automata
[AD-A150656] 14 p2399 N85-24790

Space station systems technology study (add-on task). Volume 2: Trade study and technology selection
[NASA-CR-171416] 15 p2475 N85-25279

New stage in robotics development
16 p2762 N85-27045

West Europe report: Science and technology
[JPRS-WST-84-031] 18 p3066 N85-29089

Multinational program to develop intelligent robots
18 p3066 N85-29094

West Europe report: Science and technology
[JPRS-WST-84-035] 18 p3067 N85-29102

Man-machine tradeoff study 18 p3158 N85-29561

Space station automation study. Volume 1: Executive summary. Autonomous systems and assembly
[NASA-CR-171514] 19 p3226 N85-30002

Some examples of the application of automatically guided vehicle systems
[HSE-TRANS-11134] 19 p3281 N85-30348

Computer science: Key to a space program renaissance. The 1981 NASA/ASEE summer study on the use of computer science and technology in NASA. Volume 2: Appendices
[NASA-CR-175295] 22 p3827 N85-33702

Intermittent motion 23 p3925 N85-34323

TRICCS: A proposed teleoperator/robot integrated command and control system for space applications
[NASA-TM-87577] 24 p4136 N85-35637

AUTOMATED EN ROUTE ATC

Start-2 ATC system installation progresses at Leningrad 03 p0311 N85-12007

AUTOMATED GUIDEWAY TRANSIT VEHICLES

Network management simulation of automated guideway transit systems under vehicle-follower control
[PB85-186233] 24 p4166 N85-35830

AUTOMATED TRANSIT VEHICLES

NT AUTOMATED GUIDEWAY TRANSIT VEHICLES

Metrological support for remote transport vehicle speedometers 13 p2076 N85-22963

AUTOMATIC CONTROL

NT ACTIVE CONTROL
NT ADAPTIVE CONTROL
NT AUTOMATIC FLIGHT CONTROL
NT AUTOMATIC FREQUENCY CONTROL
NT AUTOMATIC GAIN CONTROL
NT AUTOMATIC LANDING CONTROL
NT CASCADE CONTROL
NT DYNAMIC CONTROL
NT FEEDBACK CONTROL
NT FEEDFORWARD CONTROL
NT LEARNING MACHINES
NT NUMERICAL CONTROL
NT OFF-ON CONTROL
NT OPTIMAL CONTROL
NT SELF ADAPTIVE CONTROL SYSTEMS
NT SELF ALIGNMENT
NT SEQUENTIAL CONTROL
NT TIME OPTIMAL CONTROL

Development of the Engineering Test Satellite-3 (ETS-3) ion engine system
[NASA-TM-77536] 01 p0017 N85-10101

East Europe report: Science and technology
[JPRS-ESA-84-030] 01 p0101 N85-10670

Automated apparatus for producing gradient gels
[DE84-014507] 01 p0107 N85-10716

Office of Technology Assessment
01 p0127 N85-10872

Technological approach to automation of specialized processing of survey data 02 p0165 N85-11118

Automation of production of semiconductor power devices 03 p0346 N85-12229

New welding equipment for mechanized welding and trends in further development 03 p0352 N85-12264

Individual differences in automatic and controlled information processing
[AD-A146245] 03 p0401 N85-12559

Test-bed for programmable automation research. Phase 1
[AD-A145872] 03 p0409 N85-12614

Developments in Soviet robot technology viewed
04 p0491 N85-13127

Advances of implementing NC machine tools discussed 04 p0491 N85-13131

Fiber optic, Fabry-Perot high temperature sensor
[NASA-CR-174712] 04 p0564 N85-13594

Automated Library Search System (ALSS) user's manual
[DE84-015952] 04 p0576 N85-13672

Self-tuning controller design and implementation
[OUEL-1535/84] 05 p0621 N85-13975

A generalized LQG approach to self-tuning control. Part 1: Aspects of design. Part 2: Implementation and simulation
[OUEL-1536/84] 05 p0622 N85-13976

Measuring and control tasks in OPTIWA
05 p0669 N85-14304

Critical conditions for the automatic control of landing from decision height in variable winds
[UTIAS-284] 06 p0753 N85-14830

A modified unit commitment and generation control for utilities with large wind generation penetrations
[DE84-015362] 06 p0806 N85-15129

Fiat, Peugeot introduce integrated robotized engine: CAD used 07 p0936 N85-15933

Control technology for integrated circuit fabrication at Micro-Circuit Engineering, Incorporated, West Palm Beach, Florida
[PB85-100717/GAR] 07 p0949 N85-16013

Investigation of semiautomatic aircraft control processes employing time redundancy in on-board digital trajectory control computers 07 p0954 N85-16048

Automatic camera tracking for remote manipulators
[DE85-001897] 07 p0974 N85-16167

Interaction of human cognitive models and computer based models in supervisory control
[AD-A142547] 07 p1020 N85-16474

Human factors characteristics of the Joint Tactical Fusion Test Bed: Field test 467 results
[AD-A146856] 07 p1020 N85-16476

Microcomputer control of a residential photovoltaic power conditioning system
[DE84-014774] 07 p1022 N85-16488

Automatic software for controlling cryogenic systems
08 p1097 N85-16932

Managing computer-controlled operations
08 p1097 N85-16934

The effects of manufacturing automation on the surge and mobilization capabilities of the gas turbine engine industry
[AD-A147295] 08 p1137 N85-17162

USSR report: Machine tools and metalworking equipment
[JPRS-UMM-84-021] 08 p1138 N85-17168

Control systems for robotic production lines
08 p1138 N85-17169

Flexible manufacturing system concept features cache memory 08 p1140 N85-17186

Robotics research, integration overview presented. Application objectives cited 08 p1142 N85-17201

Parallel algorithms for robot dynamics
[DE84-016563] 09 p1369 N85-18605

The planning of flexible manufacturing systems
[PNR-90230] 09 p1371 N85-18613

Robotized blanks loader for new forge press
10 p1461 N85-19216

French panel makes specific proposals for robotics research. Current state of French robotics
11 p1618 N85-20180

Linear magnetic bearings
[NASA-CASE-GSC-12582-2] 11 p1641 N85-20337

Control of large collector arrays: The SSPS experience
[DE85-001461] 11 p1675 N85-20553

Operations concept for the advanced automation system man-machine interface
[AD-A149797] 12 p1774 N85-21139

Program for controlling electrical measuring contact instrument on glow-discharge indicator panel
12 p1842 N85-21558

Control of nonlinear objects 12 p1842 N85-21561

Reliability analysis of automatic systems
[VTT-301] 12 p1863 N85-21682

Guidance and control research flight testing with HFB 320 test aircraft 13 p1967 N85-22355

TASS update on unmanned flight of Salyut-7
13 p1977 N85-22404

Automatic charge control system for satellites
13 p1995 N85-22506

Hydraulic brakes for industrial robots
13 p2046 N85-22806

Controllable movements of elastic manipulator with three degrees of freedom 14 p2266 N85-24040

New equipment complex Kaskad 2 for automatic control 14 p2266 N85-24042

Mechanization and automation of production processes in turbine building 14 p2269 N85-24057

Plans, developments in robotics
14 p2289 N85-24191

Computer controlled acquistion of corrosion rate data from multiple sensors
[PB85-157378] 15 p2524 N85-25559

West Europe report: Science and technology
[JPRS-WST-84-007] 15 p2530 N85-25600

West Europe report: Science and technology
[JPRS-WST-84-014] 15 p2536 N85-25647

Calorimeter for measuring high-energy optical pulses
[PB85-160695] 15 p2561 N85-25799

Automation and robotics in welding
15 p2566 N85-25831

A critical review of selected recent advancements in arc welding equipment and processes
15 p2566 N85-25833

Some aspects of nuclear plant fabrication in Japan and the UK relating to automatic and robotic arc welding
15 p2566 N85-25834

Artificial intelligence based control of a sensor-driven machine
[DE85-006972] 15 p2633 N85-26227

Experience of sheet stamping robotic complexes
16 p2761 N85-27041

Automatic manipulators for forging rollers
16 p2762 N85-27042

Updating model RPD-1.25 industrial robot
16 p2762 N85-27043

Industrial robots and automatic manipulators for forging and pressing operations at Second International Exhibition 16 p2762 N85-27044

Status, prospects of computer-aided design discussed
16 p2767 N85-27073

A robotic system for preparing reagent and dilution vials
[DE85-008262] 16 p2793 N85-27231

A Dictionary-Directory System (DDS) for the SPLICE system
[AD-A152223] 16 p2878 N85-27750

Automation and robotics for the National Space Program
[NASA-CR-175661] 17 p2909 N85-27936

Robots, automatic devices inside VW's Wolfsburg plant 17 p2946 N85-28166

Future directions of robotics, automation in Italy 17 p2946 N85-28187

Applications of robots in machine tool industry reviewed 17 p2946 N85-28189

A programming system for a modular flexible multimicrocomputer system for the automatic control of automated test equipment [JUEL-1962] 17 p3014 N85-28641

West European report: Science and technology [JPRS-WST-84-036] 18 p3066 N85-28960

Jet pump-drive system for heat removal [NASA-CASE-NPO-16494-1-CU] 18 p3099 N85-29182

Technical instructions for a control operating system of the gas flow installation for the solid fuel combustion chamber [VTH-LR-410] 18 p3118 N85-29302

An information theoretical method for automatic noise elimination in digital image processing 18 p3124 N85-29345

Computer program for the control/operating system of the gas flow installation for the solid fuel combustion chamber [VTH-LR-430] 18 p3165 N85-29605

Space station automation study. Volume 2: Technical report. Autonomous systems and assembly [NASA-CR-171515] 19 p3226 N85-30001

BREED: A CDC-7600 computer program for the automation of breeder reactor design analysis (LWBR Development Program) [DE85-010327] 19 p3338 N85-30686

Simulation and operation of the EBR-2 automatic control rod drive system [DE85-010262] 19 p3360 N85-30832

Space Station man-machine automation trade-off analysis [NASA-CR-176046] 20 p3408 N85-31147

Automatic assembly of space stations 20 p3409 N85-31153

Automated testing of developmental satellite communications systems and subsystems [NASA-TM-87070] 20 p3440 N85-31348

Automated FMEA (Failure Modes and Effects Analysis) techniques [AD-A154161] 20 p3484 N85-31518

Simulation of automatic control of MFTF-B neutral beams [DE85-010640] 20 p3530 N85-31960

Importance of automation, robotization in economy 21 p3572 N85-32219

Space station automation study. Automation requirements derived from space manufacturing concepts. Volume 1: Executive summary [NASA-CR-176099] 22 p3738 N85-33170

Space Station automation study. Automation requirements derived from space manufacturing concepts. Volume 2: Technical report [NASA-CR-176100] 22 p3738 N85-33171

Space station automation and robotics study. Operator-systems interface [NASA-CR-176095] 22 p3738 N85-33172

Testimony of Robert A. Frosch before the Subcommittee on HUD and Independent Agencies of the Senate Committee on Appropriations [NASA-TM-87496] 22 p3738 N85-33173

Statement of Aaron Cohen, Director, Research and Engineering, Johnson Space Center and Chairman, Space Station Advanced Technology Advisory Committee, National Aeronautics and Space Administration, before the Subcommittee on Science, Technology, and Space, Committee on Commerce, Science, and Transportation, United States Senate [NASA-TM-87497] 22 p3739 N85-33174

Space station automation study: Autonomous systems and assembly, volume 2 [NASA-CR-176092] 22 p3739 N85-33175

Utilization of microwave measuring systems for the automation of composite materials manufacturing [SNIAS-851-430-102] 22 p3742 N85-33197

Probabilistic analysis of automatic control systems for detection systems 22 p3765 N85-33335

Robotic order picking [AD-D011737] 22 p3792 N85-33493

Automatic rotary valve actuator [DE85-012797] 22 p3794 N85-33505

Centralized surveillance of flexible workshops for the manufacturing of composite materials [SNIAS-851-430-103] 23 p3910 N85-34227

Multi-robot assembly of IC's 23 p3964 N85-34577

Maintenance port system [AD-D011724] 23 p3967 N85-34594

Space Missions for Automation and Robotics Technologies (SMART) Program [NASA-TM-86820] 24 p4068 N85-35210

Matched filtering of visual evoked potentials to detect acceleration (+Gz) induced blackout [AD-A155912] 24 p4131 N85-35609

Spreading the control complexity in decentralized control of interconnected systems [BU-117] 24 p4144 N85-35688

AUTOMATIC CONTROL VALVES

NT PRESSURE REGULATORS

The development of a microprocessor-controlled linearly-actuated valve assembly [NASA-CR-174437] 10 p1491 N85-19415

AUTOMATIC DATA PROCESSING

U DATA PROCESSING

AUTOMATIC FLIGHT CONTROL

NT AUTOMATIC LANDING CONTROL

Accounting for error stochasticity in terminal homing of aircraft 04 p0489 N85-13115

Investigation of pilot behavior in flight tests with a rate command/attitude hold control system [DFVLR-FB-84-25] 05 p0699 N85-14486

Flight test of the Open Loop Gust Alleviation (OLGA) system [BMFT-FB-W-84-038] 08 p1088 N85-16881

Algorithms for automatic four-dimensional aircraft guidance, considering the momentary wind situation [DFVLR-FB-84-40] 12 p1775 N85-21146

Analytically redundant output feedback scheme for reduction of structural loads of a flexible transport aircraft [TT-8303] 12 p1777 N85-21154

Automatic control design procedures for restructurable aircraft control [NASA-CR-172469] 12 p1780 N85-21173

A 320 to have combined automatic pilot, flight control system 14 p2289 N85-24186

Automatic flight control modes for the AFTI/F-111 mission adaptive wing aircraft 17 p2905 N85-27909

Human factors in cockpit automation: A field study of flight crew transition [NASA-CR-177333] 19 p3215 N85-29937

The integrated manual and automatic control of complex flight systems [NASA-CR-176166] 24 p4066 N85-35201

Analogies of control mechanisms in flight guidance and medicine 24 p4129 N85-35597

AUTOMATIC FREQUENCY CONTROL

Carrier acquisition and tracking by a COSTAS loop with automatic frequency control [ESA-TT-838] 04 p0493 N85-13149

High-speed adaptation algorithm for harmonic corrector 22 p3765 N85-33336

AUTOMATIC GAIN CONTROL

Gain restoration after Doppler filtering [AD-D011425] 08 p1154 N85-17267

AUTOMATIC LANDING CONTROL

Flight tests of the Digital Integrated Automatic Landing System (DIALS) [NASA-CR-3859] 04 p0457 N85-12900

Research at automated ATC Scientific-Experimental Center 09 p1278 N85-18037

AUTOMATIC PATTERN RECOGNITION

U PATTERN RECOGNITION

AUTOMATIC PILOTS

Polaris guidance system [AD-D011324] 07 p0900 N85-15704

A digital piloting system for the combat helicopter 08 p1074 N85-16806

A 320 to have combined automatic pilot, flight control system 14 p2289 N85-24186

An approach to planning in the inflight emergency domain [AD-A151869] 15 p2467 N85-25228

Multi-rate digital autopilot modeling methodology [AD-A152044] 15 p2474 N85-25272

Development and evaluation of a Fault-Tolerant Multiprocessor (FTMP) computer. Volume 2: FTMP software [NASA-CR-166072] 19 p3341 N85-30706

Development of control laws for a flight test maneuver autopilot for an F-15 aircraft [NASA-TM-86736] 22 p3730 N85-33122

AUTOMATIC ROCKET IMPACT PREDICTORS

U COMPUTERIZED SIMULATION

U IMPACT PREDICTION

AUTOMATIC TEST EQUIPMENT

Investigation of the application of the marginal tension technique to test electronic devices, phase 3 [ESD-11-301] 02 p0206 N85-11360

Artificial Intelligence in Maintenance: Proceedings of the Joint Services Workshop [AD-A145349] 02 p0244 N85-11592

The need for improvements in weapon system maintenance: What can AI (Artificial Intelligence) contribute? [AD-P003913] 02 p0244 N85-11593

Artificial intelligence applications to maintenance [AD-P003914] 02 p0244 N85-11594

On applying AI (Artificial Intelligence) to maintenance and troubleshooting [AD-P003915] 02 p0244 N85-11595

An overview of the Joint Logistics Commanders Automatic Test Equipment Panel [AD-P003916] 02 p0244 N85-11596

AI (Artificial Intelligence) approaches to troubleshooting [AD-P003918] 02 p0245 N85-11598

An expert system for representing procedural knowledge [AD-P003923] 02 p0245 N85-11603

Depot level problems in the testing of printed circuit boards [AD-P003932] 02 p0247 N85-11612

NAVAIR's (Naval air systems command) AI (Artificial Intelligence) program for ATE (Automated Test Equipment) [AD-P003935] 02 p0247 N85-11615

Artificial intelligence applications to automatic test equipment [AD-P003936] 02 p0247 N85-11616

Application of artificial intelligence to equipment maintenance [AD-P003939] 02 p0248 N85-11619

LES: (Lockheed Expert System): A model-based expert system for electronic maintenance [AD-P003944] 02 p0248 N85-11624

Accelerated stress facility 1976-1983 [AD-A146101] 03 p0359 N85-12303

DYNA-SIM: A nonstationary queuing simulation with application to the automated test equipment problem [AD-A146384] 06 p0857 N85-15450

Diagnostic apparatus for radar pulse repetition frequency control circuit card [AD-D011364] 07 p0937 N85-15936

Design for Tactical Avionics Maintainability [AGARD-CP-361] 08 p1063 N85-16731

Study and realisation of a 3rd level maintenance center based on ATE systems utilization 08 p1063 N85-16735

ATE user's view on design for maintainability 08 p1064 N85-16737

Built-in-test for first line testing 08 p1064 N85-16739

Functional built-in-test in a pipelined image processor 08 p1064 N85-16740

Built-in test and self repair mechanisms in a digital correlator integrated circuit 08 p1064 N85-16741

Design of a bit-sliced processor array with built-in-self-test [AD-A149785] 12 p1835 N85-21513

Automation of servicibility of radio-relay station equipment 15 p2527 N85-25582

A programming system for a modular flexible multimicrocomputer system for the automatic control of automated test equipment [JUEL-1962] 17 p3014 N85-28641

Proceedings of the Electronic Test Equipment Division's Annual Program Review of Electronic Test Equipment Industry Response to Emerging Defense Requirements [AD-A154455] 20 p3436 N85-31320

F-111 automatic test equipment replacement program 20 p3437 N85-31322

Air Force bid sample testing 20 p3437 N85-31323

An overview of measurement solutions for digital systems 20 p3437 N85-31326

Automated testing of developmental satellite communications systems and subsystems [NASA-TM-87070] 20 p3440 N85-31348

AUTOMATIC WEATHER STATIONS

Simple methods in very short-range forecasting based on data from a mesoscale network of automatic stations (ANETZ) and from satellite (Meteosat) and radar --- Swiss Alps 01 p0082 N85-10548

Operational precipitation observation system using digitized radar and rain gages 01 p0082 N85-10549

An automatic weather station network for low-altitude wind shear investigations [AD-A148139] 08 p1189 N85-17493

Project PAPA: The integration of drifting buoy data into an operational meteorological service 14 p2238 N85-23874

Applications of ARGOS data collection systems in Arctic regions 14 p2238 N85-23875

Data collection and winter ice dynamics in the Beaufort Sea 14 p2238 N85-23878

Applications of ARGOS data collection system for automatic meteorological observatories in Arctic regions 14 p2240 N85-23893

Automatic weather stations in Antarctica 14 p2324 N85-24360

The development of an automated marine meteorological data system 14 p2324 N85-24362

Meteorological buoys developed at the EERM laboratory 14 p2326 N85-24974

Hydrology and climatic conditions in Greenland 14 p2327 N85-24387

Drifting buoy studies for weather applications 14 p2329 N85-24396

Antarctic automatic weather stations 14 p2329 N85-24397

Collecting meteorological reports with the ARGOS system 14 p2329 N85-24398

Telemetered meteorological and engineering data from a deep sea moored body in the Long Term Upper Ocean Study (LOTUS) 14 p2329 N85-24402

Practical considerations when using water quality and structure monitoring sensors as applied to portable ARGOS satellite transmitter equipment 14 p2330 N85-24405

Applications of ARGOS measurements in equatorial Pacific Ocean-atmosphere interaction studies 14 p2331 N85-24414

Overview of data processing at AES local user terminals — Canadian Atmospheric Environment Service (AES) 14 p2331 N85-24418

The Data Acquisition Control and Telemetry (DACT) system — meteorological buoys 14 p2332 N85-24419

Tactical deployment of satellite-reporting drifting data buoys for environmental data acquisition 14 p2332 N85-24423

DB2 and DB3: The next generation — buoys 16 p2811 N85-27337

An operational buoy network collecting meteorological data 16 p2813 N85-27351

Operational experiences with the ARGOS system in Greenland 16 p2813 N85-27353

Data from BOC-yachts: A significant input to Southern Hemisphere analysis 16 p2814 N85-27356

Automated Weather Observing System (AWOS) demonstration program [AD-A153463] 18 p3148 N85-29493

AUTOMATION

Automation of coastal engineering modelling facilities [CSIR-T/SEA-8304] 01 p0035 N85-10219

Automated installation methods for photovoltaic arrays 2 [SAND-84-7035] 02 p0222 N85-11453

Depot modernization at the Defense Logistics Agency [AD-P004008] 03 p0308 N85-11988

Future robotics program at San Antonio ALC (Air Logistics Center) [AD-P004011] 03 p0309 N85-11991

Research activities of the Illinois University Coordinated Science Laboratory [AD-A145569] 03 p0449 N85-12856

Development, new application of Soviet robots 04 p0491 N85-13129

DNC, CNC network for robotized machining cells 04 p0491 N85-13130

Human factors in cockpit automation 06 p0752 N85-14819

Situational planning of production processes in a flexible automated production system 06 p0776 N85-14959

Machine tools at 1984 Leipzig Spring Fair 06 p0815 N85-15177

NC programming, machine tool information 06 p0816 N85-15178

West Europe report: Science and technology [JPRS-WST-84-039] 07 p0936 N85-15929

Automation of checkout for the shuttle operations era 08 p1092 N85-16900

Technology planning for flexible manufacturing systems 08 p1139 N85-17170

Automated plant, production management system 08 p1139 N85-17171

Design features, applications of new robots 08 p1139 N85-17174

West Europe report: Science and technology [JPRS-WST-85-001] 08 p1141 N85-17190

Europeans active in magnetic bearing industry 08 p1141 N85-17195

Role of engineering psychology 09 p1361 N85-18561

Problems of psychological support of automated organization control systems 09 p1362 N85-18571

Dialog system of preparation and presentation of visual information 10 p1526 N85-19622

Pilot workload, performance and aircraft control automation 10 p1534 N85-19670

French firm has most advanced continuous-casting machine 11 p1592 N85-20017

East Europe report: Science and technology [JPRS-ESA-85-009] 11 p1616 N85-20165

Robot production lines in operation 11 p1617 N85-20166

Institute director surveys industrial automation drive 11 p1617 N85-20167

Reliability of DNC system examined 11 p1617 N85-20171

Design of tightening device and calculation of forces in manipulator transmissions with base-drive mounted 13 p2046 N85-22804

USSR report: Machine tools and metalworking equipment [JPRS-UMM-85-005] 13 p2051 N85-22839

Advances in cutting tool technology surveyed 13 p2051 N85-22840

Motion planning with six degrees of freedom [AD-A150312] 13 p2165 N85-23432

Mini-Seminar on Non-Destructive Testing [CSIR-TSD-0009/83] 14 p2316 N85-24308

USSR report: Cybernetics, computers, and automation technology [JPRS-UCC-85-002] 14 p2400 N85-24794

The retrieval expert model of information retrieval 14 p2433 N85-25003

Experience in automation of data processing in interpretation and defining of linear elements from space photographs 15 p2486 N85-25349

West Europe report: Science and technology [JPRS-WST-84-012] 15 p2523 N85-25552

French robotics research at Grenoble labs 15 p2523 N85-25555

France develops new continuous vacuum treatment method 15 p2531 N85-25611

USSR report: Cybernetics, computers and automation technology [JPRS-UCC-85-003] 15 p2625 N85-26174

CAD/CAM (Computer-Aided Design/Computer-Aided Manufacturing) highlights [AD-A151532] 15 p2629 N85-26201

System design of automated VLSI (Very Large Scale Integrated) test station and implementation of selected system aspects [AD-A151961] 16 p2778 N85-27147

The introduction of new cockpit technology: A human factors study [NASA-TM-86659] 16 p2843 N85-27528

Efforts at office automation and information systems utilization at Martin Marietta Energy Systems, Incorporated [DE85-008154] 17 p3013 N85-28633

DLA: Data/data base administration analysis [AD-A153031] 17 p3050 N85-28879

West Europe report: Science and technology [JPRS-WST-84-037] 18 p3088 N85-29106

Automated maintenance system test program increment VI production scheduling [AD-A153694] 18 p3198 N85-29838

Automatic ac/dc thermal voltage converter and ac voltage calibration system [PB85-182574] 19 p3274 N85-30304

Implementation of a proposed system for automated microcode generation [AD-A154235] 19 p3336 N85-30671

Survey of Ada (Trademark)-based PDLs (Program Design Language) [AD-A154402] 19 p3338 N85-30680

Galileo battery testing and the impact of test automation 20 p3444 N85-31381

NASA space station automation: AI-based technology review [NASA-CR-176094] 21 p3558 N85-32134

NASA space station automation: AI-based technology review. Executive summary [NASA-CR-176096] 21 p3558 N85-32135

East Europe report: Science and technology [JPRS-ESA-85-023] 21 p3572 N85-32217

Robotic order picking [AD-D011737] 22 p3792 N85-33493

AUTOMOBILE ENGINES

An expert system for representing procedural knowledge [AD-P003923] 02 p0245 N85-11603

Ceramic technology for advanced heat engines program plan [DE84-013567] 04 p0479 N85-13055

Advanced concepts for methanol fuel vehicles [DE84-013612] 04 p0482 N85-13071

Advanced automotive diesel assessment program [NASA-CR-168285] 04 p0507 N85-13235

Advanced Automotive Diesel Assessment Program, executive summary 04 p0507 N85-13236

A study of the Armstrong Whitworth swing beam engine for automotive application 04 p0508 N85-13239

Advanced automotive diesel engine system study 04 p0508 N85-13240

A.A.D. engine noise evaluation 04 p0508 N85-13241

Long term technology development program 04 p0508 N85-13244

Evaluation of heat engine for hybrid vehicle application [NASA-CR-174163] 04 p0508 N85-13245

Vibroacoustic control diagnostics of selected machines based on research on the slide bearing of an automobile engine and the alternator [ISSN-0208-5658] 05 p0641 N85-14112

Fiat, Peugeot introduce integrated robotized engine: CAD used 07 p0936 N85-15933

FRG ceramic engine components (PET) 08 p1141 N85-17193

Development of high temperature ceramic parts for vehicular gas turbines [PNR-90245] 09 p1282 N85-18062

Advanced Gas Turbine (AGT) powertrain system development for automotive applications [NASA-CR-174809] 09 p1403 N85-18831

Knock syndrome: Its cures and its victims [NASA-CR-174395] 10 p1458 N85-19185

West Europe report: Science and technology [JPRS-WST-85-006] 11 p1618 N85-20183

Fiat introduces 1000-CC engine 11 p1618 N85-20185

Numerical simulation of turbulent reacting flows [DE84-016777] 11 p1632 N85-20278

Engine wear and cold startability of methanol fueled engines. [DE85-001208] 11 p1647 N85-20381

Introducing engine innovations: An examination of future markets for Brayton and Stirling automotive engines [DE84-016319] 11 p1647 N85-20382

PSA, Renault work on all fuel automobile engine 15 p2531 N85-25604

Fiat conducts R and D in ceramic parts for diesel engine 15 p2534 N85-25637

Ceramic technology for advanced heat engines project [DE85-004798] 16 p2755 N85-27002

Determination of wear intensity and resource of crankshafts and cylinder liners of ZIL-130 and ZMZ-53 engines [BLL-BISI-TRANS-21393-(9022.06)] 17 p2972 N85-28355

Exhaust systems for passenger vehicles: Test procedure for resistance to internal corrosion of silencers [BLL-BISI-TRANS-22360-(9022.06)] 17 p2973 N85-28361

Advanced Gas Turbine (AGT) technology project [NASA-CR-174798] 19 p3219 N85-29961

Durability of oxygen sensors [PB85-183093] 22 p3789 N85-33477

AUTOMOBILE FUELS

Status of gaseous fuels for use in highway transportation: A 1983 perspective [DE84-015205] 01 p0034 N85-10211

State of knowledge of environmental concerns related to natural gas-fueled vehicles [DE84-015894] 01 p0070 N85-10461

Application of the CSRL language to the design of expert diagnosis systems: The Auto-Mech experience [AD-P003922] 02 p0245 N85-11602

Methane-fueled vehicle RD and D [GPO-37-926] 04 p0481 N85-13064

Dissociated methanol vehicle test results [DE84-004507] 04 p0509 N85-13248

Some characteristics of automotive gasolines and their performance in a light aircraft engine [FAA-CT-84-12] 07 p0934 N85-15919

Dissociated methanol citation [DE85-000505] 10 p1458 N85-19188

Volatility of in-use gasoline and gasoline-methanol blends [PB85-117976] 10 p1459 N85-19189

Engine wear and cold startability of methanol fueled engines. [DE85-001208] 11 p1647 N85-20381

PSA, Renault work on all fuel automobile engine 15 p2531 N85-25604

Low pressure storage of methane on interlayered clays for potential vehicular applications [DE85-006949] 16 p2756 N85-27017

Auto fuel efficiency standards, part 2 [GPO-41-189] 20 p3435 N85-31309

AUTOMOBILES

NT ELECTRIC AUTOMOBILES

Pavement friction measurements on nontangent sections of roadways, vol. 1 [PB84-219732] 01 p0036 N85-10227

Predictor model for seasonal variations in skid resistance. Volume 2: Comprehensive report [PB84-226620] 01 p0037 N85-10230

Study of annoyance due to urban automobile traffic [NASA-TM-77514] 01 p0069 N85-10458

Performance evaluation of automotive wheel bearing greases
[AD-A145948] 03 p0337 N85-12168
Advanced concepts for methanol fuel vehicles
[DE84-013612] 04 p0482 N85-13071
Advanced automotive diesel assessment program
[NASA-CR-168285] 04 p0507 N85-13235
Dissociated methanol vehicle test results
[DE84-004507] 04 p0509 N85-13248
Summary results of the DOE flywheel development effort 05 p0606 N85-13665
ECUT energy data reference series: Lightweight materials for ground transportation
[DE84-015269] 05 p0621 N85-13974
Possibilities of increasing the simulation quality of multiaxial test stands — vehicle testing
05 p0649 N85-14169
Theoretical analysis of the dynamic behavior of structures with a passenger car as example
05 p0649 N85-14170
Evaluation of the crack initiation life behavior of fatigue loaded automotive components made from high strength aluminium alloys
[ESA-TT-739] 05 p0651 N85-14181
West Europe report: Science and technology
[JPRS-WST-84-039] 07 p0936 N85-15929
West Europe report: Science and technology
[JPRS-WST-85-001] 08 p1141 N85-17190
BBC of Switzerland develops electric car
08 p1141 N85-17192
FRG firms jump into market for auto, aircraft ceramics
09 p1309 N85-18225
Evaluation of the particulate levels occurring under 1.0/1.2 g/mi nitrogen oxide standards for light duty diesel vehicles and light duty diesel trucks
[PB85-115939/GAR] 09 p1350 N85-18494
Knock syndrome: Its cures and its victims
[NASA-CR-174395] 10 p1458 N85-19185
Dissociated methanol citation
[DE85-000505] 10 p1458 N85-19188
West Europe report: Science and technology
[JPRS-WST-85-004] 10 p1460 N85-19204
Flexible applications robot used in Moscow training course 10 p1462 N85-19217
Feasibility demonstration of a novel, flat-belt, continuously variable transmission or automotive and electric-hybrid vehicle application
[NASA-CR-174430] 10 p1569 N85-19894
Structural ceramics in transportation: Fuel implications and economic impacts
[DE85-003024] 11 p1611 N85-20130
Robot production lines in operation
11 p1617 N85-20166
Uses of composite materials
13 p2027 N85-22698
Lasers in automobile production
14 p2309 N85-24288
Performance testing and system characterization. DOE hybrid test vehicle, phase 3
[NASA-CR-175668] 14 p2434 N85-25010
Detonation flame spraying extends life of automotive parts 15 p2513 N85-25507
West Europe report: Science and technology
[JPRS-WST-84-007] 15 p2530 N85-25600
Mercedes-Benz auto 2000 achieves low drag coefficient 15 p2530 N85-25602
West Europe report: Science and technology
[JPRS-WST-84-009] 15 p2535 N85-25639
Functional impairment and structureal cervical injuries in human surrogates
[PB85-167436] 15 p2619 N85-26137
Nematic liquid crystals for car dashboards
[BMFT-FB-T-84-298] 16 p2872 N85-27718
Hybrid propulsion technologies for urban bus transit
[PB85-157489] 16 p2880 N85-27773
Robots, automatic devices inside VW's Wolfsburg plant 17 p2946 N85-28186
Exhaust systems for passenger vehicles: Test procedure for resistance to internal corrosion of silencers
[BLL-BISI-TRANS-22360-(9022.06)]
17 p2973 N85-28361
Report to Congress on the Automotive Technology Development Program
[DE85-005640] 17 p3052 N85-28890
West Europe report: Science and technology
[JPRS-WST-84-031] 18 p3066 N85-29089
West Europe report: Science and technology
[JPRS-WST-84-035] 18 p3067 N85-29102
Fuel cell applications literature review
[DE85-011891] 22 p3809 N85-33592

AUTOMORPHISMS
On rotation automorphic functions with descrete rotation groups 10 p1536 N85-19686
On the boundary behaviour of a rotation automorphic function with finite spherical Dirichlet integral
15 p2634 N85-26236

AUTONOMIC NERVOUS SYSTEM
NT SYMPATHETIC NERVOUS SYSTEM
Anatomy of the vestibulo-automatic outflow to the gut
15 p2614 N85-26106
Dissociation of autonomic and sensory vestibular reactions 23 p3953 N85-34501

AUTONOMOUS NAVIGATION
Autonomous navigation of USAF spacecraft
03 p0321 N85-12074
Combinatorial performance/cost analysis of an autonomous navigation system for aircraft
16 p2695 N85-26840
Visual position determination for autonomous vehicle navigation
[AD-A156007] 24 p4063 N85-35181

AUTONOMOUS SPACECRAFT CLOCKS
GPS system field testing 11 p1711 N85-20762
First results of GPS time transfer to Australia
17 p2962 N85-28294
Separating the variances of noise components in the Global Positioning System
[AD-P004578] 17 p2963 N85-28295
On-orbit frequency stability analysis of the GPS NAVSTAR's 3 and 4 rubidium clocks and NAVSTAR's 5 and 6 cesium clocks 17 p2963 N85-28298
Rubidium and cesium frequency standards status and performance on the GPS program
18 p3106 N85-29228

AUTONOMY
Autonomous navigation of USAF spacecraft
03 p0321 N85-12074
Space station systems technology study (add-on task). Volume 1: Executive summary
[NASA-CR-171415] 13 p1966 N85-22459
Autonomous state determination for an Earth orbiting satellite using horizon and star sensors
[AD-A151827] 15 p2493 N85-25379
In orbit infrastructure
[DM-51/CC-FL-044-83] 18 p3066 N85-28966
Standard Generic approach for Spacecraft Autonomy and Automation, phase 2 (SGASA-2). Volume 1: Executive summary
[ESA053-1-VOL-1] 18 p3167 N85-29623
Standard Generic Approach for Spacecraft Autonomy and Automation, phase 2 (SGASA-2). Volume 2: Technical report
[ESA053-1-VOL-2] 18 p3167 N85-29624
Standard Generic Approach for Spacecraft Autonomy and Automation, phase 2 (SGASA-2). Volume 3: Appendices
[ESA053-1-VOL-3] 18 p3167 N85-29625
Development of a temperature-compensated hot-film anemometer system for boundary-layer transition detection on high-performance aircraft
[NASA-TM-86732] 22 p3730 N85-33121

AUTOPILOTS
U AUTOMATIC PILOTS

AUTOPSIES
Head/neck injury: Post mortem procedures, Annex B
12 p1907 N85-21977

AUTORADIOGRAPHY
Electronic autofluorography: Principles, problems and prospects
[DE84-016696] 06 p0630 N85-14097
Development of a recombinant DNA assay system for the detection of genetic change in astronauts cells
[DE85-010103] 20 p3504 N85-31781

AUTOREGRESSIVE PROCESSES
Auto-regressive moving average spectral estimation using modified and least squares modified Yule-Walker estimates
[AD-A145516] 02 p0254 N85-11663
Parametric models for signal processing: Autoregressive (AR), Moving Average (MA) and mixed autoregressive with moving average (ARMA)
[ENST-84D001] 05 p0628 N85-14028
Texture classification using autoregressive filtering
07 p0984 N85-16254
Autoregressive spectral estimation for two dimensional time series 07 p0985 N85-16258
Conditionally heteroscedastic autoregressions
[AD-A147168] 07 p1035 N85-16567
Infinite order autoregressive representations of multivariate stationary stochastic processes
[AD-A147863] 07 p1036 N85-16580
Time series analysis of closed-loop pilot vehicle dynamics 08 p1087 N85-16876
Methods and applications of time series analysis. Part 2: Linear stochastic models
[AD-A147292] 08 p1214 N85-17645
Multivariable Autoregressive Moving Average (ARMA) models: A time approach to antenna processing
[ENST-84E015] 09 p1313 N85-18252
Data-driven choice of a spectrum estimate: Extending the applicability of cross-validation methods
[DE85-001411] 10 p1437 N85-19056
Statistical analysis of autoregressive spectral estimates for noise corrupted autoregressive series
[AD-A149543] 11 p1708 N85-20747
A review of some aspects of robust inference for time series
[AD-A149706] 12 p1923 N85-22082
Higher order residual analysis for nonlinear time series with autoregressive correlation structures
[AD-A149232] 15 p2636 N85-26257
Robust detection and classification of regional seismic signals using a two mode/two stage cascaded adaptive arma (CAARMA) model
[AD-A154710] 21 p3630 N85-32554
Methods and software for cosmic ray scintillation studies
[SH-9.1-17] 23 p4052 N85-35132

AUXILIARY EQUIPMENT (COMPUTERS)
NT PLOTTERS
NT PRINTERS (DATA PROCESSING)

AUXILIARY POWER SOURCES
NT NUCLEAR AUXILIARY POWER UNITS
NT SNAP
NT SOLAR AUXILIARY POWER UNITS
NT SPACE POWER REACTORS
NT SPACE POWER UNIT REACTORS
Ion thruster system (8-cm) cyclic endurance test
[NASA-CR-174745] 04 p0483 N85-12937
SNAP (Space Nuclear Auxiliary Power) reactor overview
[AD-A148831] 07 p1041 N85-16612
Space shuttle orbiter auxiliary power unit development challenges 08 p1099 N85-16945
The solid rocket booster auxiliary power unit: Meeting the challenge 08 p1099 N85-16946
Regenerative fuel cell systems for space station
20 p3443 N85-31372
Multikilowatt hydrogen-nickel oxide battery system
20 p3443 N85-31373

AUXILIARY PROPULSION
Ion thruster system (8-cm) cyclic endurance test
[NASA-CR-174745] 04 p0483 N85-12937

AV-8A AIRCRAFT
U HARRIER AIRCRAFT

AV-8B AIRCRAFT
U HARRIER AIRCRAFT

AVAILABILITY
Availability of transmission systems in continental and intercontinental connections — telecommunication
[FUB-33-1983] 01 p0040 N85-10261
Artificial intelligence approaches to monitoring system integrity
[AD-P003930] 02 p0246 N85-11610
Correlation and reassessment of the OTEC plant power cycle
[DE84-015467] 04 p0529 N85-13382
A practical example of reducing life cycle costs and increased availability 08 p1063 N85-16736
A replication and extension of the inducement of the availability heuristic
[AD-A149755] 12 p1923 N85-22083
Statistical aspects of reliability, maintainability and availability
[AD-A151228] 15 p2640 N85-26282
Solar pond technology for Navy applications
[AD-A155877] 24 p4112 N85-35488

AVALANCHE DIODES
Fine grained hodoscopes based on scintillating optical fibers
[DE84-014849] 01 p0120 N85-10825
The 30 GHz solid state amplifier for low cost low data rate ground terminals
[NASA-CR-174795] 03 p0358 N85-12300
Novel transport and recombination processes in semiconductors
[AD-A145969] 03 p0433 N85-12757
Avalanche photodiode statistics in triggered-avalanche detection mode 05 p0623 N85-13987
The development of a 90 GHz solid state noise source
[CD.6500695] 05 p0733 N85-14715
Millimeter-wave travelling-wave IMPATT diode
[AD-A146545] 06 p0804 N85-15117
Calculations of high-current characteristics of silicon diodes at microwave frequencies
[AD-A147406] 09 p1314 N85-18261
Advanced metal oxide varistor concepts
[DE84-016677] 09 p1316 N85-18276
Image line voltage controlled oscillator with replaceable components
[AD-D011436] 10 p1479 N85-19333
GaAlAs Sb APD optimization
[AD-A149406] 10 p1480 N85-19344

Investigations of the high frequency performance of impact avalanche transit-time diodes
13 p2063 N85-22884
Photon detection with cooled avalanche photodiodes: Theory and preliminary experimental results
16 p2770 N85-27096
Development of photodetectors
[AD-A153773] 18 p3095 N85-29158
Self-detecting optical sensors
[AD-D011657] 18 p3185 N85-29751
Noise characteristics of an avalanche photodiode
[AD-A154096] 19 p3258 N85-30205
Millimetre wave pulse technology — satellite mapping
[ESA-CR(P)-2004] 20 p3478 N85-31611
Sixty GHz IMPATT diode development
[NASA-CR-174969] 22 p3758 N85-33293

AVALANCHES
NT ELECTRON AVALANCHE
Spectral distribution of radiation in n junctions of GaAs during avalanche breakdown 02 p0258 N85-11688
Avalanche photodiode statistics in triggered-avalanche detection mode 05 p0623 N85-13987
Dependence of breakdown voltage for p-n junction on parameters of ion implantation and semiconductor heat treatment 07 p0954 N85-16046
Automated Lavina collects data on snow
07 p0980 N85-16224

AVERAGE
NT MEAN
Limit theory for the sample covariance and correlation functions of moving averages
[AD-A145466] 02 p0251 N85-11642
Auto-regressive moving average spectral estimation using modified and least squares modified Yule-Walker estimates
[AD-A145516] 02 p0254 N85-11663
Model equation for simulating flows in multistage turbomachinery
[NASA-TM-86869] 03 p0315 N85-12036
Distribution of total solar radiation in Spain
04 p0523 N85-13344
Parametric models for signal processing: Autoregressive (AR), Moving Average (MA) and mixed autoregressive with moving average (ARMA)
[ENST-84D001] 05 p0628 N85-14028
Multivariable Autoregressive Moving Average (ARMA) models: A time approach to antenna processing
[ENST-84E015] 09 p1313 N85-18252
The relevance of averaging period to wind power measurements and efficiency of Wind Energy Conversion Systems (WECS)
[GKSS-84-E-35] 11 p1676 N85-20562
Models of the upper atmosphere
12 p1945 N85-22217
Why do noninvertible estimated moving averages occur?
[AD-A150388] 13 p2153 N85-23368
Local likelihood estimation
[DE85-007238] 16 p2857 N85-27620
Method of and apparatus for generating an interstitial point in a data stream having an even number of data points
[NASA-CASE-MFS-25319-1] 22 p3827 N85-33701

AVIATION
U AERONAUTICS

AVIATORS
U AIRCRAFT PILOTS

AVIONICS
The Malcolm horizon: History and future
01 p0008 N85-10046
Avionics integrity program (Avip). Volume 4: Force management. Economic life considerations
[AD-A145592] 02 p0138 N85-10941
Avionics integrity program (Avip). Volume 3: Program cost assessment - environmental stress screening and diagnostic techniques
[AD-A145644] 02 p0139 N85-10942
Avionics integrity program (Avip). Volume 1: Procurement phase issues: Design, manufacturing, and integration
[AD-A145651] 02 p0139 N85-10943
Avionics Integrity Program (Avip). Volume 2: Hardware case studies
[AD-A145689] 02 p0139 N85-10944
Increased joint avionics standardization could result in major economies and operational benefits
[AD-A145730] 02 p0139 N85-10945
Expert systems in maintenance diagnostics for self-repair of digital flight control systems
[AD-P003933] 02 p0247 N85-11613
Army aviation today and tomorrow
06 p0751 N85-14810
HH-65A Dolphin digital integrated avionics
06 p0751 N85-14815
Integrated cockpit design for the Army helicopter improvement program 06 p0751 N85-14816
HH-60D night hawk helicopter
06 p0752 N85-14817
Avionics/crew station integration
06 p0752 N85-14818
Avionics technology - system concepts
06 p0753 N85-14824
Avionics system design for requirements for the United States Coast Guard HH-65A Dolphin
06 p0753 N85-14827
Certification of advanced systems
06 p0753 N85-14829
Integrated Application of Active Controls (IAAC) technology to an advanced subsonic transport project. ACT/Control/Guidance System study, volume 1
[NASA-CR-165963-VOL-1] 06 p0754 N85-14837
The effect of aircraft generated electromagnetic interference (EMI) on future avionics systems: A compendium
[AD-A146380] 06 p0799 N85-15101
Equipment for preflight test of an Electronic Countermeasures (ECM) avionic system
07 p0939 N85-15949
Design for Tactical Avionics Maintainability
[AGARD-CP-361] 08 p1063 N85-16731
Objectives in studying the maintainability of aircraft systems 08 p1063 N85-16732
Joint service design for testability program
08 p1063 N85-16733
The embedded test (BIT): Impact on the total cost of possession 08 p1063 N85-16734
Study and realisation of a 3rd level maintenance center based on ATE systems utilization
08 p1063 N85-16735
ATE user's view on design for maintainability
08 p1064 N85-16737
Built-in-test for first line testing
08 p1064 N85-16739
Maintainability: An ILS effort to manipulate LCC
08 p1064 N85-16743
Documentation and separate test program development is most important for test/maintenance
08 p1065 N85-16745
Effective life cycle software support: A study in discipline and versatility 08 p1065 N85-16746
Experience in using on-aircraft software for testing integrated systems 08 p1065 N85-16747
Investigating version dependence in fault-tolerant software 08 p1065 N85-16749
The effect on software design of testing by symbolic execution 08 p1065 N85-16750
Reliable software design for avionics and space applications 08 p1065 N85-16751
A weapon system design approach to diagnostics
08 p1066 N85-16752
Avionics fault tree analysis and artifical intelligence for future aircraft maintenance 08 p1066 N85-16755
Automatic briefing and mission management systems for battlefield support 08 p1073 N85-16799
Development of a Helicopter integrated navigation system 08 p1073 N85-16802
Standard Attitude Heading Reference System (SAHRS) full scale development program
08 p1073 N85-16804
Evolution toward a multi-bus architecture for Army helicopter avionic systems 08 p1074 N85-16812
Integration of sensor fusion in advanced helicopter cockpit design 08 p1074 N85-16813
Development, production and testing of central control and display unit for helicopters
[BMFT-FB-W-84-039] 08 p1085 N85-16871
Evolution of shuttle avionics redundancy management/fault tolerance 08 p1090 N85-16890
Shuttle avionics software trials, tribulations and success 08 p1090 N85-16891
Shuttle avionics software development trials: Tribulations and successes, the backup flight system
08 p1091 N85-16892
SSME digital control design characteristics
08 p1091 N85-16893
Man-machine interface and control of the shuttle digital flight system 08 p1091 N85-16894
Space shuttle main engine hardware simulation
08 p1091 N85-16895
Development and implementation of the verification process for the shuttle avionics system
08 p1091 N85-16896
Integrated design checkout of shuttle payload avionics interfaces 08 p1092 N85-16899
Automation of checkout for the shuttle operations era
08 p1092 N85-16900
Space Shuttle Technical Conference, part 2
[NASA-CP-2342-PT-2] 08 p1096 N85-16937
Life cycle cost model for very high speed integrated circuits
[AD-A147798] 08 p1157 N85-17298
Human Factors Considerations in High Performance Aircraft
[AGARD-CP-371] 10 p1532 N85-19653
Aircrew and avionics: Friends or Foes?
10 p1532 N85-19654
The evolution of methods of air traffic control
[AD-A149606] 12 p1774 N85-21137
A safety evaluation of the relocation of the ACM (Air Combat Maneuver) panel in the F-14 ( )/AIP (Avionics Integration Program)
[AD-A149596] 12 p1777 N85-21158
Proceedings of the 6th Advanced Aircrew Display Symposium
[AD-A150044] 12 p1778 N85-21160
Development of the F-20 nose radome
[AD-P004374] 12 p1827 N85-21466
Interface specifications for SCR (Software Cost Reduction) (A-7E) extended computer module, revised
[AD-A149948] 12 p1915 N85-22024
Investigation of device and electronic interactions in GaAs device processing
[AD-A149747] 12 p1940 N85-22182
Ground and flight testing for aircraft guidance and control
[AGARD-AG-262] 13 p1966 N85-22350
Civil avionics flight testing with the RAE(B) BAC1-11
13 p1967 N85-22354
Guidance and control research flight testing with HFB 320 test aircraft 13 p1967 N85-22355
Avionics Flight Evaluation System (AFES)
13 p1967 N85-22357
AIRLAB: A laboratory for flight-crucial-electronics system research 13 p1968 N85-22362
Reliability predictions for military avionics. Royal Signals and Radar Establishment reliability prediction method no. 250
[BR89221] 13 p1973 N85-22388
Shuttle flight test of an advanced gamma-ray detection system
[AD-A150316] 13 p1988 N85-22489
Design for tactical avionics maintainability, technical evaluation report
[AGARD-AR-204] 14 p2225 N85-23798
Rotorcraft digital advanced avionics system (RODAAS) functional description
[NASA-CR-166611] 15 p2468 N85-25237
YAV-8B Harrier 15 p2688 N85-26605
Rotorcraft digital advanced avionics system (Rodaas)
15 p2688 N85-26606
Design adequacy: An effectiveness factor
16 p2695 N85-26642
Design-To-Cost (DTC) methodology to achieve affordable avionics 16 p2696 N85-26645
Navigation and flight director guidance for the NASA/FAA helicopter MLS curved approach flight test program
[NASA-CR-177350] 16 p2704 N85-26691
Avionics integrity issues presented during NAECON (National Aerospace and Electronics Convention) 1984
[AD-A151923] 16 p2707 N85-26707
Avionics data base
[AD-A152415] 17 p2897 N85-27863
The Avionics Flight Evaluation System (AFES) of DFVLR
[DFVLR-MITT-85-01] 17 p2897 N85-27864
Air Force technical objective document FY 86
[AD-A152730] 17 p3047 N85-28855
Avionics Data Base users manual
[AD-A153810] 18 p3062 N85-28942
Avionics and civil aircraft systems: The present and the future
[SNIAS-851-111-104] 20 p3392 N85-31038
F-111 automatic test equipment replacement program
20 p3437 N85-31322
Aviation system delays
[S-HRG-98-1241] 21 p3553 N85-32102
HLLM software support
[AD-A154828] 21 p3671 N85-32805

AVOIDANCE
NT COLLISION AVOIDANCE
NT VORTEX AVOIDANCE
Development and certification of a new stall warning and avoidance system 05 p0702 N85-14507

AWARDS
National Science Foundation grants and awards for fiscal year 1983, volume 2
[PB84-212323] 01 p0125 N85-10854
An analysis of production competition and award methodology
[AD-A147775] 08 p1226 N85-17733
1985 Resident research associateships: Postdoctoral and senior research awards
[NASA-TM-87456] 12 p1963 N85-22339

AXAF
U X RAY ASTROPHYSICS FACILITY

AXES (COORDINATES)
U COORDINATES
AXES (REFERENCE LINES)
NT AXES OF ROTATION
NT EARTH AXIS
Acceleration resistant combination of opposite-handed piezoelectric crystals
[AD-D011626] 16 p2778 N85-27143
AXES OF ROTATION
NT EARTH AXIS
Design of two-mirror scanner with axes of rotation not in plane of mirrors 06 p0777 N85-14969
Shoulder and hip joint for hard space suits and the like
[NASA-CASE-ARC-11543-1] 12 p1910 N85-21986
Motion of symmetrical satellite with flexible viscoelastic rods about center of mass in circular orbit
13 p1979 N85-22420
Axial representations of shape
[AD-A150387] 13 p2151 N85-23356
Precise mounting of instruments in universal suspension with skewed axes 14 p2273 N85-24083
Stability of steady modes of motion by axis of rotating wheel in nonlinear bearings 14 p2279 N85-24117
Stability of permanent rotation modes of asymmetric heavy solid body 14 p2279 N85-24118
Structural design of the Sandia 34-meter vertical-axis wind turbine
[DE85-011146] 18 p3118 N85-29300
Wake effects on the aerodynamic performance of horizontal axis wind turbines
[NASA-CR-174820] 18 p3127 N85-29364
Studies of the solar mesosphere explorer: Dynamics and horizon sensor performance. Part A: Spin axis precession and atmospheric drag Part B: Clouds
[NASA-CR-175308] 24 p4069 N85-35213
AXIAL COMPRESSION LOADS
Fatigue in composite materials
04 p0467 N85-12966
Stability of cylindrical shells with one-way constraints
13 p2048 N85-22820
Dynamic shock studies of PZT 95/5 ferroelectric ceramic
[DE85-008137] 14 p2261 N85-24015
An analysis for axially compressed orthotropic shells with a multimode imperfection representation
[VTH-LR-422] 16 p2803 N85-27281
Optimization of axially compressed carbon fiber reinforced plastic (CFRP) cylinders
18 p3121 N85-29318
Polymer matrix and graphite fiber interface study
[NASA-CR-177357] 19 p3232 N85-30036
Mechanical ratcheting behaviors of a steel pipe under combined cyclic axial load and internal pressure
23 p3904 N85-34184
Monotonous stress-strain properties of structural steel subjected to nonstationary repetitive pre-loading
23 p3904 N85-34185
AXIAL COMPRESSORS
U TURBOCOMPRESSORS
AXIAL FLOW
Development of a Navier-Stokes rotor and stator analysis
[AD-A148967] 07 p0958 N85-16070
Axial flow laser cavity
[AD-D011506] 12 p1855 N85-21633
Flow-induced vibrations of a circular cylinder due to turbulent internal flows
[DE85-002766] 13 p2103 N85-23110
Fluid mechanics and heat transfer spirally fluted tubing
[AD-A150774] 14 p2301 N85-24247
On the structure of the turbulent vortex
15 p2463 N85-25213
Monogroove heat pipe design: Insulated liquid channel with bridging wick
[NASA-CASE-MSC-20497-1] 18 p3098 N85-29180
Classical emission of relativistic charged particles during axial channeling 21 p3681 N85-32871
Second order modelling in non-constant density flows
22 p3744 N85-33206
Wingtip vortex propeller
[NASA-CASE-LAR-13019-1] 24 p4065 N85-35194
AXIAL FLOW COMPRESSORS
U TURBOCOMPRESSORS
AXIAL FLOW PUMPS
NT TURBINE PUMPS
AXIAL LOADS
NT AXIAL COMPRESSION LOADS
Post buckling behavior of a circular rod constrained within a circular cylinder 02 p0207 N85-11365
Flywheel containment and safety considerations
05 p0606 N85-13669
Low cycle fatigue strength for multiaxial loading of ductile materials 05 p0649 N85-14167
Stability of hollow shafts under torsion
06 p0780 N85-14966
Life prediction at high temperature under multiaxial loading 07 p0907 N85-15745
Evaluation of the blind hole drilling method for the measurement of residual stress
[AD-A151459] 15 p2579 N85-25905
Calculation of friction at spherical bearing journals in turbomachines 17 p2940 N85-26150
Improvement of conditions for meshing spiral bevel gears
[NASA-TM-77867] 18 p3117 N85-29294
Multiaxial fatigue and fracture: A literature review
[ARL/STRUC-R-410] 19 p3285 N85-30370
On design of off-axis specimens
[AD-A154328] 19 p3286 N85-30379
Experimental study of collapse of thick-walled tube under external pressure and axial force
23 p3904 N85-34186
AXIAL MODES
The axial velocity spread acceptance of free electron lasers
[AD-A149024] 10 p1489 N85-19403
AXIAL STRAIN
Composite laminate optimization program suitable for microcomputers 01 p0059 N85-10389
The effect of overload on three different kinds of steel
02 p0174 N85-11165
Device for measuring relative axial expansion of turbine rotor employing space-vector tracking method
06 p0776 N85-14962
Strain-controlled creep rupture in non-isothermal materials 09 p1332 N85-18368
Dissipation of energy in composite material
13 p2027 N85-22703
Correlation of uniaxial and biaxial fracture strengths of ceramics
[DE85-003779] 14 p2261 N85-24011
Finite axisymmetric deformation of a thin shell of revolution 16 p2796 N85-27251
Transverse periodic boundary conditions in molecular dynamics with uniaxial strain shock waves
[DE85-006497] 16 p2863 N85-27656
Uniaxial angular accelerometers
17 p2944 N85-28173
Multiaxial fatigue low cycle fatigue testing
20 p3468 N85-31544
Results of an interlaboratory fatigue test program conducted on alloy 800H at room and elevated temperatures
[NASA-CR-174940] 21 p3587 N85-32340
AXIAL STRESS
Improved multiaxial creep-rupture strength criterion
[DE84-014273] 01 p0062 N85-10413
Fatigue limit analysis involving biaxial stress components 03 p0370 N85-12363
Improved beam theory for anisotropic materials
04 p0468 N85-12973
Stress concentration due to axial tension of loaded nonsymmetric-shaped grooves
[AD-A149425] 10 p1496 N85-19442
Multiaxial stress response of ceramics
[DE85-004350] 12 p1814 N85-21379
Dynamic crack curving and branching under biaxial loading
[AD-A151451] 15 p2578 N85-25904
Mechanical properties of high performance carbon fibers 16 p2742 N85-26922
Biaxial buckling of specially orthotropic, symmetric composite rectangular plates
[AD-A152958] 17 p2979 N85-28417
Uniaxial stress induced symmetry breaking for muon sites in Fe 17 p3042 N85-28820
Multiaxial fatigue low cycle fatigue testing
20 p3468 N85-31544
Multiaxial stress analysis taking account of penetration depth of X-rays. A solution by means of polynomial approximation 23 p3907 N85-34204
AXISYMMETRIC BODIES
Method for prompt modeling of quasiperiodic movement of solid near-axisymmetrical body in atmosphere
13 p2043 N85-22790
Flight dynamics of axisymmetrical rotating bodies in air medium 13 p2043 N85-22791
Absolute stability of unsteady movement of axisymmetrical rotating flight vehicle
13 p2044 N85-22793
Steady-state reaction of three-layered cylindrical shell to effect of moving load 13 p2047 N85-22811
Comparison of measured and computed boundary layers at the tail-end of an axisymmetric body in an air-jet
[AMTE(N)-TM-83053] 14 p2209 N85-23700
Flow around axisymmetric bodies with uniform-velocity zones 14 p2278 N85-24103
Some problems in optimally designing shells of revolution 14 p2278 N85-24114
An experimental investigation of confined, multiple, turbulent jet mixing with recirculation — flow distribution in combustors with injection plates
15 p2555 N85-25764
Direct transient analysis of a fuze assembly by axisymmetric solid elements 15 p2576 N85-25890
Stress analysis of axisymmetric sandwich shells of variable thickness 24 p4101 N85-35419
AXISYMMETRIC DEFORMATION
U AXIAL STRAIN
AXISYMMETRIC FLOW
NT ANNULAR FLOW
Mass and momentum transport in a turbulent buoyant vertical axisymmetric jet 05 p0635 N85-14070
Design of swirled axisymmetric turbulent jets
05 p0724 N85-14657
Applications of finite and wave envelope element approximations to acoustic radiation from turbofan engine inlets in flight 05 p0726 N85-14664
A three-dimensional axisymmetric calculation procedure for turbulent flows in a radial vaneless diffuser
[NASA-TM-86903] 06 p0749 N85-14796
Variable loading of elastic-plastic shells of revolution
06 p0779 N85-14981
Analytical modeling of circuit aerodynamics in the new NASA Lewis wind tunnel
[NASA-TM-86912] 07 p0897 N85-15688
A computer program for the performance analysis of scarfed nozzles
[AD-A147370] 07 p0905 N85-15730
Aeroacoustic data for high Reynolds number supersonic axisymmetric jets
[NASA-TM-86296] 07 p1038 N85-16587
Thrust chamber performance using Navier-Stokes solution — space shuttle main engine viscous nozzle calculation
[NASA-CR-171346] 10 p1430 N85-19019
Computer studies of baroclinic flow — Atmospheric General Circulation Experiment
[NASA-CR-171338] 10 p1517 N85-19566
The modelling of latitudinal gradients in the solar wind in the outer solar system 12 p1947 N85-22231
The low frequency behaviour of an immersed structure at a standstill in a high density fluid with free surface
[TP-1983-31] 13 p2103 N85-23105
Analysis of combustion oscillations in heterogeneous systems
[AD-A151999] 16 p2745 N85-26942
Studies of structure and modeling in turbulent shear flows
[AD-A151807] 16 p2782 N85-27170
Computation model of turbulent free flow: Application to axisymmetric jets
[ISL-R-126/83] 16 p2785 N85-27185
Characteristics of steady-state hypersonic flow about blunted bodies with discontinuities in generators
17 p2941 N85-28155
Impact starting of plane nozzles with wide divergence angle 17 p2941 N85-28156
Navier-Stokes computational study of axisymmetric transonic turbulent flows with a two-equation model of turbulence
[AD-A152653] 17 p2958 N85-28265
Modifications to SOLA-VOF for flow dynamics in spinning cylinders
[AD-A154093] 19 p3265 N85-30250
On the evaluation of boundary layer measurements on boattailed bodies of revolution in axisymmetric compressible subsonic flow
[ESA-TT-883] 20 p3457 N85-31471
A panel method study of vortex sheets with special emphasis on sheets of axisymmetric geometry
[NASA-CR-177385] 21 p3552 N85-32095
A numerical study of Taylor-Vortex flow
[AD-A154787] 21 p3584 N85-32277
A mixed pseudospectral/finite difference method for a thermally driven fluid in a nonuniform gravitational field
[NASA-TM-87581] 22 p3783 N85-33436
Studies on effects of boundary conditions in confined turbulent flow predictions
[NASA-CR-3929] 24 p4093 N85-35371
AXISYMMETRY
U SYMMETRY
AXLES
U SHAFTS (MACHINE ELEMENTS)
AZIDES (INORGANIC)
Azido nitramino ether containing solid propellants
[AD-D011511] 12 p1816 N85-21392
Spray pyrolysis as a synthetic tool
[AD-A153891] 19 p3234 N85-30047
AZIDES (ORGANIC)
NT TRIAMINOGUANIDINIUM AZIDE
Spray pyrolysis as a synthetic tool
[AD-A153891] 19 p3234 N85-30047

AZIMUTH

Structural investigation of the Grenville Province by radar and other imaging and nonimaging sensors
06 p1147 N85-17237

The effects of internal waves on acoustic normal modes
[AD-A150235] 13 p2155 N85-23379

The access of energetic charged particles to satellite altitudes
[AD-A150799] 14 p2373 N85-24670

Azimuthal variations in Saturn's A ring
15 p2671 N85-26478

Additional possibilities of radiometeor azimuthal method for measuring wind velocity in lower thermosphere
19 p3296 N85-30438

Terrain illumination conditions when taking scanning photographs from space 22 p3736 N85-33159

Calculating solar highlight and shadeless areas for scanning photographs from space and optimizing lighting conditions 22 p3736 N85-33160

Comprehensive fracture diagnostics experiement. Part 2: Comparison of seven fracture azimuth measurements
[DE85-011707] 23 p3948 N85-34470

A star camera aspect system suitable for use in balloon experiments
[OG-9.3-10] 23 p4028 N85-34965

Azimuthal and meridional asymmetries of the solar wind and quasiperiodic variations of intensity of Galactic Cosmic Rays (GCR)
[SH-4.4-20] 23 p4035 N85-35016

Jets in air-jet family
[HE-3.2-1] 24 p4179 N85-35912

A comparative analysis of gamma and hadron families at the superhigh energies recorded in experiment Pamir
[HE-3.7-1] 24 p4185 N85-35960

AZINES

NT METHYLENE BLUE

Effects of triazine components on physicochemical properties of polybutadiene: urethane block copolymers
13 p2014 N85-22635

The electrochemistry of azine, oxazine and thiazine dyes
[AD-A152394] 17 p2918 N85-27990

AZO COMPOUNDS

NT RDX

Substituent effects on the electrical conductivities of the phenazine derivatives
[NASA-TM-77792] 14 p2249 N85-23938

Electrochemistry of Hexanitroazobenzene (HNAB)
[DE85-010807] 21 p3565 N85-32171

Synthesis of energetic materials
[AD-A154887] 21 p3571 N85-32210

AZOLES

NT CARBAZOLES
NT OXAZOLE
NT PYRROLES
NT TRYPTOPHAN

Development of new and improved polymer matrix resin systems, phase 1
[NASA-CR-166595] 01 p0017 N85-10104

A method for obtaining new cyclical imides of derivative benzimidazoles
[AD-A145042] 01 p0017 N85-10106

Chemically modified electrodes and related solution chemistry
[DE84-017110] 05 p0614 N85-13924

Theoretical studies on N-bonded pyrazole derivatives of boron
[AD-A150036] 12 p1813 N85-21374

Ethylenediamine salt of 5-nitrotetrazole and preparation
[DE85-005738] 23 p3923 N85-34306

B

B STARS

The rotation of B-type stars and processes of star formation 03 p0443 N85-12823

The influence of stellar luminosity and temperature calibration on the determination of the initial mass function 05 p0740 N85-14760

The velocity-age relation for B and A stars
05 p0740 N85-14762

Kinematics of B and A stars 05 p0741 N85-14766

Nonradial pulsation and mass loss in early B stars
08 p1232 N85-17759

Light variations of the B-type star HD 160202
08 p1232 N85-17761

The UV extinction laws in two very young clusters, NGC 6530 in the galaxy and NGC 2100 in the LMC
11 p1748 N85-20994

Interstellar extinction in the nucleus of H PER
11 p1749 N85-21001

Superionized species and winds in low luminosity B and Be stars 11 p1749 N85-21003

Main sequence B stars with strong winds
11 p1750 N85-21005

Analysis of high-depression IUE spectra of subdwarf B stars 11 p1751 N85-21011

Ultraviolet spectroscopy of the interacting binary U Sagittae 11 p1755 N85-21042

Strange F + Be binary star systems
11 p1756 N85-21045

Studies of hot B subdwarfs. Part 2: Energy distributions of three bright sdB/sdOB stars in the 950-5500 angstrom range
[NASA-CR-175854] 16 p2981 N85-27775

B-A-W DEVICES

U BULK ACOUSTIC WAVE DEVICES

B-1 AIRCRAFT

Logistics support costs for the B-1B aircraft can be reduced
[AD-A145846] 03 p0309 N85-11996

B-70 AIRCRAFT

Supersonic cruise technology
[NASA-SP-472] 18 p3057 N85-28912

BABOONS

Functional impairment and structureal cervical injuries in human surrogates
[PB85-167436] 15 p2619 N85-26137

BAC AIRCRAFT

NT JET PROVOST AIRCRAFT

BACILLUS

Differences in susceptibility of inbred mice to bacillus anthracis
[AD-A155646] 21 p3662 N85-32750

Genetic and physiological control of protective antigen synthesis by bacillus anthracis
[AD-A156324] 24 p4133 N85-35617

BACKGROUND NOISE

Sources, paths, and concepts for reduction of noise in the test section of the NASA Langley 4x7m wind tunnel
[NASA-CR-172446-VOL-1] 05 p0726 N85-14666

Comparison of options for reduction of noise in the test section of the NASA Langley 4x7m wind tunnel, including reduction of nozzle area
[NASA-CR-172446-VOL-2] 05 p0726 N85-14667

Synthesis of systems for coherent weighted signal processing against background of correlated interference 06 p0790 N85-15045

Synoptic observations of the radio noise background in the frequency range 150-180 kHz to provide design data for the low frequency communications designer
[AD-A147438] 07 p0941 N85-15965

Microseism level, time variations at Turkmen seismic stations studied 07 p0981 N85-16231

Discriminability of signals from noise in a dynamic stereoscopic space
[AD-A148406] 08 p1196 N85-17535

Extraction of signals from background interference with unknown parameters in quantized sample
13 p2084 N85-23013

Approximate rules for signal detection against background of Gaussian correlated interference
13 p2086 N85-23027

Background noise measurements from jet exit vanes designed to reduced flow pulsations in an open-jet wind tunnel
[NASA-TM-86383] 17 p2906 N85-27916

Fiber optic gyroscope with alternating output signal
[AD-D011669] 19 p3271 N85-30284

Application of adaptive noise cancellation to Coast Guard voice communications
[AD-A154796] 21 p3574 N85-32230

Design of a freestanding noise measurement and recording system to predict the intensity and location of electromagnetic radiation from earthquakes
[AD-A155070] 21 p3632 N85-32563

A real time index of geomagnetic background noise for the MAD (Magnetic Anomaly Detection) frequency band
[AD-A155717] 22 p3814 N85-33627

A comparison of calculated and measured background noise rates in hard X-ray telescopes at balloon altitude
[OG-9.3-7] 23 p4028 N85-34962

BACKGROUND RADIATION

The Belikt experiment 02 p0159 N85-11079

On syntheses of the X-ray background with power-law sources
[NASA-TM-82173] 03 p0446 N85-12840

A large scale height galactic component of the diffuse 2-60 keV background
[NASA-TM-83637] 03 p0446 N85-12841

Search for the radiative decay of a cosmic relic particle with IUE
[PREPRINT-410] 04 p0580 N85-13707

New measurements of the spectrum of the cosmic microwave background
[DE84-016055] 05 p0748 N85-14785

The soft X-ray diffuse background: Implications for the nature of the local interstellar medium
06 p0876 N85-15566

Ultrasoft X-ray background observations of the local interstellar medium 06 p0877 N85-15571

Observations of local ISM emission with the Berkeley EUV/FUV shuttle telescope 06 p0880 N85-15594

Cosmology 07 p1056 N85-16701

The HEAO-1 diffuse component spectrum from 15 to above 500 keV — X and gamma rays
08 p1240 N85-17820

The origin of the X-ray background
08 p1243 N85-17841

Background calculations for the measurement of the ion temperature in a deuterium plasma
[DE84-016546] 09 p1393 N85-18768

An electronically controlled array for simulation of passive target/background signatures at millimeter wavelengths
[AD-D011456] 10 p1468 N85-19263

Elimination of sensor artifacts from infrared data
[AD-A149048] 10 p1556 N85-19814

Galaxy formation 12 p1960 N85-22321

Measurement of the large-scale anisotropy of the cosmic background radiation at 3 MM 13 p2206 N85-23680

A measurement of the intensity of the cosmic background radiation at 3.9 cm
13 p2206 N85-23681

Interplanetary plasma turbulence and the Doppler detection of a gravitational background radiation
[IFSI-85-1] 20 p3546 N85-32066

Visibility and vertical structure measurements in southern Germany
[AD-A154714] 21 p3635 N85-32574

Spectrum of the gamma-ray diffuse component observed from HEAO-1
[OG-3.1-12] 22 p3874 N85-34000

The 1984 biotic studies of Yucca Mountain, Nevada test site, Nye County, Nevada
[DE85-011715] 23 p3951 N85-34487

CYLTRAN calculations of electron effects on XD detectors
[LA-10264-MS] 23 p3969 N85-34601

The design of an experiment to detect low energy antiprotons
[OG-9.1-1] 23 p4022 N85-34928

Neutron-induced 2.2 MeV background in gamma ray telescopes
[OG-9.3-6] 23 p4027 N85-34961

Three dimensional calculation of flux of low energy atmospheric neutrinos
[SH-8.1-11] 23 p4050 N85-35116

The muon content of gamme-ray showers
[HE-4.5-7] 24 p4195 N85-36031

The Nagoya cosmic-ray muon spectrometer 3, part 1: Preliminary observations
[HE-5.2-2] 24 p4202 N85-36060

BACKINGS

U BACKUPS

BACKSCATTERING

Active microwave measurements of sea ice under fall conditions: The RADARSAT/FIREX fall experiment — in the Canadian Arctic
[E85-10019] 02 p0217 N85-11432

Development of a global model for atmospheric backscatter at CO2 wavelengths
[NASA-CR-174053] 02 p0228 N85-11489

Scattering from snow backgrounds at 35, 98, and 140 GHz
[AD-A145798] 03 p0355 N85-12280

Dust properties determined from backscattering in the interplanetary and interstellar medium
03 p0446 N85-12838

Anglo-German millimeter wave backscatter measurements on snow, environmental data report
[REPT-7-84] 04 p0492 N85-13136

Scattering from randomly oriented scatterers of arbitrary shape in the low-frequency limit with application to vegetation 04 p0525 N85-13362

Scattering from randomly oriented circular discs with application to vegetation 04 p0525 N85-13363

Materials characterization using ion, electron, and photon probes
[DE84-004518] 04 p0560 N85-13568

Relation between atmospheric scattering and backscattering coefficient
[ESA-TT-837] 05 p0677 N85-14350

Research on acoustical and optical scattering, optics of bubbles, diffraction catastrophes, laser generation of sound, and shock induced cavitation
[AD-A146703] 06 p0860 N85-15468

Intermediate results of radar backscatter measurements from summer sea ice
[AD-A147212] 07 p0940 N85-15960

Method for non contacting gauging of the wall thickness of tubes by backscattering radiation
[OEFZS-4274] 07 p0968 N85-16144

Simultaneous ocean cross-section and rainfall measurements from space with a nadir-pointing radar
[NASA-TM-86167] 07 p0987 N85-16273
Chemical information from ion scattering spectrometry
[AD-A148267] 08 p1121 N85-17069
The interpretation of SIR-B imagery of surface waves and other oceanographic features using in-situ, meteorological satellite, and infrared satellite data
08 p1143 N85-17212
Quantitative use of multiincidence-angle SAR for geologic mapping 08 p1145 N85-17220
Geologic mapping of Indonesian rain forest with analysis of multiple SIR-B incidence angles
08 p1145 N85-17221
German Radar Observation Shuttle Experiment (ROSE) 08 p1148 N85-17245
Evaluation of the radar response to land surfaces and volumes: Examination of theoretical models, target statistics, and applications 08 p1149 N85-17250
Ground truth for SIR-B images obtained by SIR system 8 impulse radar 08 p1149 N85-17251
Remote sensing of soil moisture
08 p1149 N85-17252
Carbon dioxide laser radar for monitoring atmospheric transmittance and atmospheric aerosol
09 p1354 N85-18516
Specifics of backscattering of sound by bottom of bank in open sea 10 p1499 N85-19460
Cyclone diagnostics — rainfall estimation, backscatter, and lidar
[NASA-CR-171337] 10 p1518 N85-19567
Parametric processes in underdense UV laser-produced plasmas
[DE85-002812] 10 p1559 N85-19830
Nonlinear saturation of stimulated Raman scattering in collisional homogeneous plasma
[DE85-002814] 10 p1559 N85-19831
Applications of the Heavy-Iron Rutherford Backscattering Spectrometry (HIRBS) to the analysis of contact structures on GaAs and Ge
[DE85-000671] 10 p1564 N85-19861
Lidar observations of stratospheric aerosol over Mauna Loa Observatory, 1974 - 1981
[PB85-115061] 11 p1682 N85-20597
Quantitative non-destructive evaluation of damage in composite materials using transmitted and reflected ultrasound
[NASA-CR-175550] 12 p1796 N85-21269
Aerosol multiple-scanning code, ASCAT
[LA-10046-MS] 12 p1823 N85-21440
On the inversion of the lidar equation
[AD-A149653] 12 p1856 N85-21641
Oceanographic and meteorological research based on the data products of SEASAT
[E85-10091] 12 p1874 N85-21753
Phase function, backscatter, extinction, and absorption for standard radiation atmosphere and El Chichon aerosol models at visible and near-infrared wavelengths
[NASA-TM-86379] 12 p1892 N85-21874
Effects of scatterer spacing statistics on ultrasonic backscatter signal spectra
[DE85-003259] 12 p1928 N85-22114
Atmospheric transmissometer
[AD-D011540] 12 p1932 N85-22140
Reaction of amorphous NiNb films with crystalline metal overlayers
[DE85-005483] 13 p2024 N85-22680
Optical reflectometer for multimode fiber lightpipes
13 p2075 N85-22961
The microwave propagation and backscattering characteristics of vegetation — wheat, sorghum, soybeans and corn fields in Kansas
[E85-10088] 13 p2122 N85-23213
Microwave remote sensing of soil moisture
13 p2125 N85-23235
Investigations of ultrasonic wave interactions at boundaries separating anisotropic materials
[DE85-003506] 13 p2155 N85-23384
Influence scattering and Q in the lithosphere
[AD-A150939] 14 p2293 N85-24213
Afternoon radar aurora and polar cap convection pattern 14 p2361 N85-24592
Secondary fluorescence effects on X-ray microanalysis
[DE85-005585] 15 p2506 N85-25457
Development of global model for atmospheric backscatter at CO2 wavelengths
[NASA-CR-175679] 15 p2591 N85-25971
Modeling the backscattering and transmission properties of vegetation canopies
[E85-10099] 16 p2809 N85-27320
Test of lidar inversion algorithm sensitivity to atmospheric backscatter and extinction parameters, revision A
[AD-A152082] 16 p2865 N85-27671
An experimental investigation of the angular scattering and backscattering behaviors of the simulated clouds of the outer planets
[NASA-CR-175909] 17 p3052 N85-28896
Amorphous alloys of ion-implanted Fe-Ti-C
[DE85-010658] 19 p3360 N85-30634
Broadside scattering of a tubular cylinder for evaluation of target identification
[AD-A155739] 21 p3577 N85-32248
Plating density standards
[DE85-010014] 21 p3591 N85-32316
Meteorological and aeronomical requirements for MST radar networks (keynote paper), part 1
21 p3615 N85-32467
A modified Fresnel scattering model for the parameterization of Fresnel returns, part 2.3A
21 p3618 N85-32483
Observations of mesospheric turbulence by rocket probe and VHF radar, part 2.4A 21 p3619 N85-32484
Interpretation of radar returns from the mesosphere, part 2.3A 21 p3619 N85-32485
Usefulness of multifrequency MST radar measurements, part 2.6B 21 p3619 N85-32487
Relationship of spaced antenna and Doppler techniques for velocity measurements (keynote paper), part 3
21 p3619 N85-32488
Anisotropy of the permittivity field inferred from aspect-sensitive radar echoes 21 p3620 N85-32492
Visibility and vertical structure measurements in southern Germany
[AD-A154714] 21 p3635 N85-32574
Fluctuations in light intensity during backscattering in turbulent medium 21 p3695 N85-32958
Data on the backscattering coefficients on light ions from solids: A revision
[IPPJ-AM-41-REV] 23 p3982 N85-34689
Quantitative non-destructive evaluation of composite materials based on ultrasonic wave propagation
[NASA-CR-176176] 24 p4074 N85-35244

BACKSHORES
U BEACHES

BACKUPS
Shuttle avionics software development trials: Tribulations and successes, the backup flight system
08 p1091 N85-16892
SSME digital control design characteristics
08 p1091 N85-16893
Autonomous uninterruptable power supply apparatus
[AD-D011571] 14 p2298 N85-24232

BACKWARD FACING STEPS
Heat transfer and fluid mechanics measurements in the turbulent reattaching flow behind a backward-facing step
15 p2553 N85-25753
A finite element, Navier-Stokes study of the confined, laminar flow over a downstream facing step
15 p2553 N85-25754
An experimental study of compressible turbulent reattaching free shear layers 16 p2781 N85-27161
An implicit finite-difference code for a two-equation turbulence model for three-dimensional flows
[NASA-TM-86752] 20 p3454 N85-31448

BACKWARD WAVE TUBES
NT HELITRONS

BACTERIA
NT BACILLUS
NT CLOSTRIDIUM BOTULINUM
NT ESCHERICHIA
NT PSEUDOMONAS
NT STAPHYLOCOCCUS
An electrochemical approach to the prevention of biofouling phenomena
[PB84-202613] 01 p0025 N85-10155
Proton pumping in purple membrane, appendix 1
[DE84-014601] 01 p0118 N85-10811
Phylogenic distribution of the large 5S rRNA from Halococcus morrhuae
[NASA-CR-174019] 02 p0234 N85-11523
Microbiological method for the desiliconization of high-silica bauxites
[BLL-MINTEK-TR-1168-(5610.5759)]
07 p0925 N85-15864
Respiratory chain of alkalophilic bacteria
[DE84-012558] 09 p1360 N85-18556
Investigation of the initial events in biofouling
[AD-A149995] 12 p1900 N85-21927
Production and turnover of suspended organic detritus in the coastal water of the southeastern continental shelf
[DE85-003977] 13 p2140 N85-23290
Studies of photosynthetic Energy Conversion
[DE85-005973] 15 p2586 N85-25944
The effects of simulated weightlessness on susceptibility to viral and bacterial infections using a murine model
15 p2613 N85-26100
Fatty and aromatic acid catabolizing bacteria from methanogenic ecosystems
[DE85-008133] 17 p2996 N85-28537
A basic study to assess the potential usefulness of resonance Raman spectroscopy as a means of rapidly detecting and identifying bacteria and other microorganisms
[AD-A153549] 18 p3152 N85-29613
Survival of microorganisms and bacterial predation in nature
[AD-A153574] 18 p3152 N85-29514
Genetics in methylotrophic bacteria
[DE85-011460] 19 p3327 N85-30615
Investigation of variation in the concentration of bacteria in outdoor testing, with the use of a detector for aerosols of bacteria
[FOA-C-40201-B2] 20 p3504 N85-31784
Ice active bacteria as condensation nuclei
21 p3639 N85-32603
Aerobic sulfur-oxidizing bacteria: Environmental selection and diversification 21 p3656 N85-32712
Protocyanobacteria: Oxygenic and Anoxygenic photosynthesis in mat-forming bacteria
21 p3657 N85-32714
Sulfur transformations at the hydrogen sulfide/oxygen interface in stratified waters and in cyanobacterial mats
21 p3657 N85-32715
Distribution and abundance of organic thiols
21 p3657 N85-32717
Cytochromes and iron sulfur proteins in sulfur metabolism of phototrophic bacteria
21 p3657 N85-32718
Insights into the phylogenetic positions of photosynthetic bacteria obtained from 5S rRNA and 16S rRNA sequence data 21 p3658 N85-32719
Ecophysiology of phototrophic sulfur bacteria in lakes: Vertical distribution of planktonic populations
21 p3658 N85-32722
Chemolithotrophy and physiology of bacterial nutrient limitation 21 p3659 N85-32730
Structure and physiology of Beggiatoa and Thiothrix
21 p3659 N85-32734
Phototrophic bacteria and their role in the biogeochemical sulfur cycle 21 p3660 N85-32735
Sulfur cycling and metabolism of phototrophic and filamentous sulfur bacteria 21 p3660 N85-32737
Enrichments for phototrophic bacteria and characterization by morphology and pigment analysis
21 p3660 N85-32738
Anaerobic reduction of elemental sulfur by Chromatium vinosum and Beggiatoa alba 21 p3660 N85-32739
Buoyant densities of phototrophic sulfur bacteria and cyanobacteria 21 p3660 N85-32740
Interactions among sulfide-oxidizing bacteria
21 p3661 N85-32741
Cyanobacterial mats: Microanalysis of community metabolism 21 p3661 N85-32743
Microanalysis of dissolved iron and phosphate in pore waters of hypersaline sediment
21 p3661 N85-32744
Glutathione in cyanobacteria
21 p3661 N85-32745
Microbial communities and microprofiles of sulfide and oxygen of alum rock sulfur springs
21 p3661 N85-32746
Composition and dynamics of bacteriocenosis associated with algae in human life-support systems
22 p3823 N85-33684
Legionnaires' disease bacteria in power plant cooling systems: Phase 2
[DE85-011546] 22 p3825 N85-33695
Microbiological and biochemical studies towards optimization of substrate utilization by methanogenic bacteria
[PB85-188332] 24 p4084 N85-35310

BACTERIOLOGY
Growth of soil bacteria in presence of Martian soil analog, carbon dioxide and hydrogen peroxide
09 p1361 N85-18560
Structural-functional changes in bacterial cells under spaceflight conditions 16 p2724 N85-26812
Distinctions in formation of microflora on construction materials used in habitable pressurized compartments
22 p3823 N85-33683

BAFFLES
Internal heat transfer and pressure drop measurements in a variously baffled shell and tube heat exchanger
03 p0360 N85-12310
Optimization of combined convective and film cooling of perforated baffle blades in gas turbines
14 p2270 N85-24067
Strutless diffuser for gas turbine engine
[AD-D011662] 18 p3062 N85-28943
Failure analysis of fractured capscrews in centrifugal coolant compressor
[DE85-010029] 19 p3287 N85-30384

BAGS

Air bag restraint system
[AD-D011671] 19 p3215 N85-29936

BAILOUT

Study of several factors affecting crew escape trajectories from the Space Shuttle Orbiter at low-subsonic speeds
[NASA-TM-86303] 10 p1428 N85-19006

BAINITE

Development of a high strength isothermally heat-treated nodular iron road wheel arm
[AD-A155756] 24 p4099 N85-35406

BAJA CALIFORNIA

U LOWER CALIFORNIA (MEXICO)

BAKEOUT

U DEGASSING

BALANCE

Force and moment measurements on a 74 deg delta wing with an apex flap
[NASA-CR-166081] 02 p0134 N85-10918

LFMR definition study
[AD-A153691] 18 p3090 N85-29126

Two-plane balance and slip-ring design
22 p3799 N85-33536

All particle energy spectrum of cosmic rays in 10 to the 15th power - 10 to the 20th power eV region
[OG-5.1-15] 22 p3882 N85-34056

BALANCE EQUATIONS

U EQUATIONS

BALANCING

Laser balancing system for high material removal rates
[NASA-CR-174731] 03 p0365 N85-12341

Development of a multiplane multispeed balancing system for turbine systems
[NASA-CR-174750] 13 p1976 N85-22400

Development and application of a unified balancing approach with multiple constraints
16 p2737 N85-26891

Stressed-strained state of tightening buckles in sectional runners of gas turbines 17 p2940 N85-28149

The balancing of complex linkage mechanisms
23 p3924 N85-34313

A versatile computer package for mechanism analysis, part 2: Dynamics and balance
23 p3924 N85-34315

BALL BEARINGS

An evaluation of grease type ball bearing lubricants operating in various environments
[NASA-TM-86480] 02 p0185 N85-11239

Effect of two inner-ring oil-flow distribution schemes on the operating characteristics of a 35 millimeter bore ball bearing to 2.5 million DN
[NASA-TP-2404] 04 p0507 N85-13233

Development of new materials for turbopump bearings
16 p2735 N85-26877

Bearings working group 16 p2735 N85-26878

Hybrid bearings for LH2 and LO2 turbopumps
16 p2736 N85-26880

Rolling contact fatigue life of chromium ion plated 440C bearing steel 16 p2736 N85-26882

Physio-chemical mechanisms of the processes of the formation of globular inclusions in ball-bearing metal
[BLL-BISI-TRANS-22235-(9022.06)]
17 p2924 N85-28030

Operating characteristics of a 0.87 kW-hr flywheel energy storage module
[NASA-TM-87036] 17 p2974 N85-28371

Mechanics of a gaseous film barrier to lubricant wetting of elastohydrodynamically lubricated conjunctions
[NASA-TP-2500] 21 p3595 N85-32330

Friction and wear of solid-lubricated contact in gas turbine engine bearings
[AD-A155042] 21 p3596 N85-32335

The properties of thin-section, four-point-contact ball bearings in space 22 p3797 N85-33521

The use of perfluoroether lubricants in unprotected space environments 22 p3797 N85-33523

Special features of the fracture of ball-bearing steel close to non-metallic inclusion eutectics
[BLL-M-35809-(5828.4)] 23 p3914 N85-34256

BALLASTS (IMPEDANCES)

Determining lamp/ballast system performance with a temperature-controlled integrating chamber
[DE84-014606] 05 p0631 N85-14049

BALLISTIC CAMERAS

Using synchro-ballistic cameras to determine the velocity and spin rate of high-velocity projectiles
[DE85-010629] 19 p3367 N85-30884

BALLISTIC MISSILES

NT INTERCONTINENTAL BALLISTIC MISSILES
NT MINUTEMAN ICBM
NT POLARIS MISSILES

NORAD operational system 12 p1783 N85-21189

BALLISTIC TRAJECTORIES

Tristatic tracking filter used by the multistatic measurement system
[AD-A146885] 07 p0911 N85-15769

A method of calculating the aim point for an unguided projectile fired at a moving target
[BAE-BT-12717] 15 p2469 N85-25365

AN investigation into the control limitations of a bank to turn missile in the terminal homing phase
[AD-A152193] 16 p2704 N85-26696

OMEGA: Optoelectronic measurement of the incidence angle of a projectile
[ISL-CO-223/84] 23 p3974 N85-34634

BALLISTIC VEHICLES

An air-breathing ballistic space transporter for Europe
[NASA-TM-77645] 12 p1792 N85-21244

BALLISTICS

NT INTERIOR BALLISTICS
NT TERMINAL BALLISTICS

ILIR task of digital recoil travel measurement system
[AD-A147102] 07 p0967 N85-16140

Interferometric velocity measurements in ballistics
[ISL-CO-239/83] 14 p2306 N85-24276

Lasers in the domains of ultrashort-time phenomena physics and ballistics
[ISL-CO-236/83] 14 p2310 N85-24299

Effect of low-velocity or ballistic impact damage on the strength of thin composite and aluminum shear panels
[NASA-TP-2441] 16 p2742 N85-26924

Conceptual design and analysis of high-speed electronic imaging
[LA-10072-MS] 22 p3758 N85-33292

BALLISTOCARDIOGRAPHY

Three-dimensional ballistocardiography in weightlessness (experiment 1ES 028) — Spacelab
05 p0691 N85-14447

Three-dimensional ballistocardiography in microgravity
20 p3510 N85-31818

BALLOON FLIGHT

Space Research in Japan. National report
01 p0013 N85-10082

The de Tifini star pointer characterization and conclusions on the 1982 transmediterranean flight
[CESR-83-1070] 02 p0139 N85-10946

Location and data collection for long stratospheric balloon flights 14 p2326 N85-24377

BALLOON SOUNDING

The BALSAMINE experiment
14 p2238 N85-23676

Coordinated balloon-satellite studies of energetic electron precipitation mechanisms
14 p2360 N85-24587

Testing of some substorm features by multiple balloon observations 14 p2363 N85-24600

The SAMBO-GEOS experiment: A Ps-6 event from ground-satellite observations 14 p2369 N85-24641

Observations of a pulsation event from the ground with balloons and with a geostationary satellite
14 p2369 N85-24643

Upper-air data collection during CAPTEX
[DE85-006300] 16 p2627 N85-27438

Improvement of the basic knowledge of the climatology of the vertical ozone layer by enhanced balloon sounding
[BPT-6/84] 18 p3137 N85-29426

Atmospheric X-rays at 11 deg S geomagnetic latitude
[INPE-3539-PRE/755] 19 p3386 N85-31004

The role of scientific ballooning for exploration of the magnetosphere
[TRITA-EPP-84-07] 20 p3494 N85-31724

Initial results from the Caltech/DRSI balloon-borne isotope experiment
[OG-4.3-8] 22 p3879 N85-34033

Observations of ultraheavy cosmic ray particles at 10 GV cutoff rigidity
[OG-4.4-2] 22 p3879 N85-34035

The dependence of solar modulation on the sign of the cosmic ray particle charge
[SH-4.2-23] 23 p4009 N85-34880

Environmental-physical measurements and determination of atmospheric turbulence with the ASK-16 motor glider 24 p4122 N85-35549

Partitioning of the vertical turbulent energy transport into positive and negative contributions — meteorology
24 p4122 N85-35551

Aircraft measurements during the Bonn Experiment (BONEX 1) — meteorology 24 p4122 N85-35552

BALLOON-BORNE INSTRUMENTS

Balloon observations 01 p0014 N85-10086

Study of a coded mask telescope for astronomical measurements in the hard X-ray domain
[MPE-182] 01 p0129 N85-10889

The de Tifini star pointer characterization and conclusions on the 1982 transmediterranean flight
[CESR-83-1070] 02 p0139 N85-10946

Optical studies of nitrogen oxides in the stratosphere
08 p1163 N85-17455

Instrumental background in balloon-borne gamma-ray spectrometers and techniques for its reduction
[NASA-TM-86162] 09 p1413 N85-18911

The Venus Balloon Project 10 p1465 N85-19243

Measurement of nuclear lines with a dual Ge(Li) telescope aboard a stratospheric balloon
[INPE-3380-TDL/185] 11 p1762 N85-21083

Calibration of solar cells outside the atmosphere
13 p2009 N85-22603

Land mobile satellite transmission measurements at 869 MHz: Selected results from the dedicated stratospheric balloon experiment of November 12 and 13, 1984
[NASA-CR-175734] 15 p2541 N85-25885

Free radicals in the stratosphere: A new observational technique 16 p2624 N85-27415

Stratospheric ClO: In-situ detection with a new approach 16 p2624 N85-27416

Balloon-borne, He-cooled Fourier transform spectrometer for far infrared astronomy
[MPE-IR-41] 17 p3053 N85-28899

Damping of suspension oscillations for stratospheric balloon experiments
[MPE-IR-42] 20 p3463 N85-31517

A Cerenkov-delta E-Cerenkov detector for high energy cosmic ray isotopes and an accelerator study of Ar-40 and Fe-56 fragmentation
[NASA-CR-176028] 20 p3549 N85-32086

A balloon-borne imaging gamma-ray telescope
[OG-9.2-2] 21 p3714 N85-33049

Balloon-borne video cassette recorders for digital data storage
[OG-9.3-11] 21 p3715 N85-33050

Development of an adjustable buoyancy balloon tracer of atmospheric motion. Phase 1: Systems design and demonstration of feasibility
[PB85-185817] 22 p3817 N85-33646

A search for solar neutrons on a long duration balloon flight
[SH-1.4-6] 23 p3995 N85-34766

The design of an experiment to detect low energy antiprotons
[OG-9.1-1] 23 p4022 N85-34928

Cherenkov-dE/dx-range measurements on cosmic ray iron group nuclei
[OG-9.1-12] 23 p4024 N85-34937

A balloon-borne imaging gamma-ray telescope
[OG-9.2-2] 23 p4024 N85-34941

The Gamma-Ray Imaging Spectrometer (GRIS): A new balloon-borne experiment for gamma-ray line astronomy
[OG-9.2-4] 23 p4025 N85-34943

An experimental assessment of the imaging quality of the low energy gamma-ray telescope ZEBRA
[OG-9.2-8] 23 p4025 N85-34947

High energy gamma ray balloon instrument
[OG-9.2-12] 23 p4026 N85-34951

Measured performance of the new University of California gamma ray telescope
[OG-9.2-13] 23 p4026 N85-34952

An improved time of flight gamma-ray telescope to monitor diffuse gamma-ray in the energy range 5 MeV - 50 MeV
[OG-9.3-2] 23 p4027 N85-34957

An approach of reducing the background induced by neutrons
[OG-9.3-5] 23 p4027 N85-34960

A star camera aspect system suitable for use in balloon experiments
[OG-9.3-10] 23 p4028 N85-34965

Balloon-borne video cassette recorders for digital data storage
[OG-9.3-11] 23 p4028 N85-34966

Photometric and spectroscopic gamma-ray observations of solar transient phenomena using long duration balloons
[SH-9.1-5] 23 p4051 N85-35120

Some characteristic cosmic ray events and an attempt at their explanation
[HE-3.1-8] 24 p4178 N85-35906

BALLOONING MODES

Theory of resistive ballooning modes in Tokamaks
[DE84-015626] 04 p0566 N85-13606

Fusion plasma theory. Task 1: Magnetic confinement fusion plasma theory
[DE84-014941] 04 p0566 N85-13608

Limits of possible operation of the R-Tokamak due to ideal MHD instabilities
[IPPJ-694] 06 p0863 N85-15486

Theoretical investigations relevant to magnetic fusion research, April 1, 1983 - March 31, 1984
[DE85-001778] 06 p0865 N85-15498

Shear-Alfven dynamics of toroidally confined plasmas, part A
[DE85-001590] 06 p0866 N85-15502

Shear-Alfven dynamics of toroidally confined plasmas, part B
[DE85-001787]
08 p0866 N85-15504
Comments on the paper by F. Pegoraro, L. Sugiyama: Spatial diffusion of charged high-energy fusion products by shear Alfven perturbations
[INPE-3291-PRE/606]
16 p2866 N85-27675
Ballooning beta limits of dee and bean shaped Tokamaks
[IPPJ-713]
16 p2866 N85-27676

BALLOONS
NT HIGH ALTITUDE BALLOONS
NT JIMSPHERE BALLOONS
NT METEOROLOGICAL BALLOONS
NT MICROBALLOONS
NT SUPERPRESSURE BALLOONS
NT TETHERED BALLOONS
Optical pin apparatus for measuring the arrival time and velocity of shock waves and particles
[DE84-014501]
01 p0120 N85-10824
The use of tracers for the study of atmospheric chemical and physical transformation processes
[DE84-015297]
05 p0671 N85-14313
A new physical Lagrangian tracer
[DE84-016212]
05 p0687 N85-14419
Results of the 1984 NASA/JPL balloon flight solar cell calibration program
[NASA-CR-174270]
07 p0991 N85-16294
Balloon observations of hard X-rays from some galactic X-ray sources
[OG-2.5-11]
22 p3870 N85-33966
Gamma-radiation with E gamma 5 MeV detected from Seyfert galaxy 3C120 and region with 1' = 190 deg and b' = 20 deg
[OG-2.8-8]
22 p3871 N85-33981
Lapex: A Phoswich balloon experiment for hard X-ray astronomy
[OG-9.3-1]
23 p4027 N85-34956
A comparison of calculated and measured background noise rates in hard X-ray telescopes at balloon altitude
[OG-9.3-7]
23 p4028 N85-34962
Structure and properties of polyethylene films used in heavy lift balloons
[NASA-CR-176227]
24 p4083 N85-35306

BALLS
Hubble space telescope: Pointing error effects on nonlinear ball joints
[NASA-TM-86511]
20 p3545 N85-32058

BALMER SERIES
Alignment of high Ryberg states in hydrogen
[DE85-000582]
09 p1380 N85-18677
Broad emission features in active galactic nuclei
11 p1746 N85-20979
A model for eclipsing cataclysmic variables
13 p2171 N85-23467
High resolution geocoronal Balmer alpha observations
20 p3489 N85-31686

BALTIC SEA
Intrusion of radioactive industrially polluted water from North Sea into central Baltic Sea
10 p1498 N85-19454

BALTIC SHIELD (EUROPE)
Study of stratigraphy of the Precambrian Soviet Baltic shield
13 p2110 N85-23148

BANACH SPACE
NT SOBOLEV SPACE
Measure determining classes of balls in Banach space
[CTH-MATH-1984-14]
04 p0556 N85-13541
Loeb Sobolev spaces with applications to variational integrals and differential equations
[CTH-MATH-1984-19]
04 p0556 N85-13544
Stable monotone variational inequalities
[AD-A147123]
07 p1031 N85-16544
Generalization of Beurling algebras
11 p1696 N85-20675
Using semigroups and the Trotter product formula to solve quasi-linear systems
[DE85-002041]
11 p1706 N85-20736
On stochastic integral representation of stable processes with sample paths in Banach spaces
[AD-A152927]
17 p3025 N85-28703

AND STRUCTURE OF SOLIDS
Dispersion forces of solids under stress. Chemisorption under stress
[AD-A146171]
03 p0373 N85-12380
Theory of silicon superlattices: Band structure and mobility enhancement
09 p1396 N85-18789
Fermi surface study of CeSb
[DE85-002532]
10 p1584 N85-19862
A mixed-basis band structure interpolation scheme pplied to the fluorite structure compounds NiSi2, AuAl2, uGa2 and AuIn2
AD-A150131]
12 p1940 N85-22187

Preventing the formation of an anomalous structure in chemically sealed low carbon steel
[BLL-BISI-TRANS-22373-(9022.08)]
17 p2930 N85-28085

BANDGAP
U ENERGY GAPS (SOLID STATE)

BANDPASS FILTERS
NT CRYSTAL FILTERS
NT TRACKING FILTERS
Microstrip directional filters
[INPE-3127-PRE/518]
02 p0194 N85-11293
China report: Science and technology
[JPRS-CST-84-001]
04 p0557 N85-13545
Present status, future prospects of domestic acoustical instruments
04 p0557 N85-13548
Superconducting NbTi and Pb(Cu) bandpass filters
05 p0623 N85-13986
Charge domain filters for enhanced monolithic signal processing
[AD-A147426]
07 p0941 N85-15964
Compensation of skew passband of a SAW filter using predistortion
12 p1821 N85-21422
Detection of angular modulated electromagnetic signals
[AD-D011563]
12 p1823 N85-21437
High-frequency input device for superheterodyne radio receiver with wideband preselector
12 p1839 N85-21540
Method of designing digital band-pass filters with infinite memory
12 p1840 N85-21546
Investigation of bimodal paramagnetic filter
13 p2083 N85-23007
Margin leveling algorithm for fully saturated satellite transponder with CDMA (Code Division Multiple Access) signalling
[AD-A151710]
15 p2543 N85-25699
A short range, high accuracy radar ranging system
[AD-A152195]
16 p2774 N85-27122
Topics in time delay estimation
[AD-A152231]
16 p2855 N85-27607
Reactanceless synthesized impedance bandpass amplifier
[NASA-CASE-GSC-12788-1] 18 p3093 N85-29145
Bandpass filter formed by serial gratings operating in a wood's anomaly region
[AD-D011660]
18 p3093 N85-29148
The seasonal cycle of storminess as measured by band-pass fluctuations
18 p3144 N85-29467
Some studies in filtering of atmospheric turbulence
[AD-A154042]
19 p3316 N85-30557
Optimum filter computation for data transmission
[CNES-83/DRT/TIT/TR/142] 20 p3441 N85-31359
Color evolution in high redshift galaxies
20 p3544 N85-32055
Microwave SAW (Surface Acoustic Wave) monochromator
[AD-D011718]
21 p3590 N85-32311
Design of high-order analog and digital filters with identical sections
22 p3766 N85-33341
Design of digital bandpass filters with finite memory
22 p3775 N85-33392
Miniature two-mode filters 22 p3775 N85-33394
Method of designing digital band-pass filters with pulse response of finite duration 22 p3775 N85-33395
Waveguide dielectric millimeter band filter with enhanced selectivity
22 p3780 N85-33421
A real time index of geomagnetic background noise for the MAD (Magnetic Anomaly Detection) frequency band
[AD-A155717]
22 p3814 N85-33627

BANDWIDTH
NT BROADBAND
NT NARROWBAND
NT SPECTRAL LINE WIDTH
An error analysis for the use of presently available lunar radio flux data in broadbeam antenna-system measurements
[PB84-218361]
01 p0016 N85-10097
Resistance to HF jamming interference in mobile radio networks by an adaptive, distributed reconfiguration technique
[AD-A145117]
01 p0038 N85-10238
Noise jammer discrimination by noise spectral bandwidth
[AD-D011224]
01 p0038 N85-10242
A limbus-sensing eye movement recorder
[AD-A144772]
01 p0049 N85-10323
A high resolution spectroscopic study of the oxygen molecule
[NASA-CR-174061]
02 p0172 N85-11150
Electronic bandwidth compression module
[AD-A145843]
03 p0366 N85-12343
Pulse code modulation telemetry: Properties of various binary modulation types
[AD-A147214]
07 p0913 N85-15780
Array sidelobes, error tolerance, gain, and beamwidth
[AD-A147004]
07 p0940 N85-15956
Multivariable flight control with time-scale separation
[NASA-CR-174320]
08 p1087 N85-16873
An optically coupled sampling system with 4 GHz bandwith
[AD-A148057]
09 p1384 N85-18702
Noise jammer discrimination by noise modulation bandwidth
[AD-D011473]
10 p1468 N85-19264
A technical solution to fadings in tactical satellite digital transmissions
10 p1473 N85-19297
Heterocontact effects in point contact electron-phonon spectroscopy of the alkali metals
[AD-A149760]
12 p1800 N85-21290
Multichannel digital processing of wideband signals
12 p1840 N85-21548
An asymptotically efficient solution to the bandwidth problem of kernel density estimation, revision
[AD-A149800]
12 p1920 N85-22056
Beamwidth control in pyramidal horns
[R-NIAS-27]
13 p2053 N85-22853
Gyrator frequency selectors with bandwidth independent of input signal level
13 p2083 N85-23009
Infrared nonlinear processes in semiconductors
[AD-A150966]
14 p2427 N85-24968
Linewidth and bandwidth measurements of the q-branch of h2 using CW coherent anti-Stokes Raman spectroscopy
[AD-A151868]
15 p2506 N85-25456
Statistical techniques for signal processing
[AD-A151231]
15 p2541 N85-25690
Wideband fiber optic communications link
[AD-A151704]
15 p2542 N85-25697
Feasibility studies of optical processing of image bandwidth compression schemes
[AD-A151254]
15 p2651 N85-26350
The HURRA, a high resolution experimental radar system broadband receiver
[FOA-C-30375-E1]
18 p3091 N85-29132
Multichannel birefringent filter
18 p3206 N85-29688
Study of a limited band signal transmission chain
[CNES-CT/DRT/TIT/TR-83/221]
20 p3442 N85-31361
Experimental evaluation of a new form of M-ary (M = 8) phase shift keying including design of the transmitter and receiver
[AD-A155103]
21 p3576 N85-32239
Controllable companding in low-frequency FM radio communication systems 22 p3776 N85-33402
Necessary bandwidth and spectral properties of digital modulation
[PB85-185367]
24 p4088 N85-35340
Optical synthetic aperture techniques
[AD-A156151]
24 p4154 N85-35752

BANG-BANG CONTROL
U OFF-ON CONTROL

BANGLADESH
The use of digital spaceborne SAR data for the delineation of surface features indicative of malaria vector breeding habitats
08 p1146 N85-17230

BANKING FLIGHT
U TURNING FLIGHT

BARCHANS
U DUNES

BARDEEN APPROXIMATION
U BARRIER LAYERS
U ELECTRICAL PROPERTIES
U SURFACE PROPERTIES

BARENTS SEA
Eddy detection in the Norwegian, Greenland, and Barents Seas with a radar altimeter
03 p0382 N85-12442
Modern sedimentation in the northern Barents Sea: Input, dispersal and deposition of suspended sediments from glacial meltwater
[AD-A152520]
17 p2997 N85-28530

BARIUM
Search for white dwarf companions of cool stars with peculiar element abundances
[NASA-CR-174030]
02 p0297 N85-11923
The Georges Bank monitoring program 1983: Analysis of trace metals in bottom sediments
[CIRC-915]
05 p0688 N85-14423
The role of finite parallel length on the stability of barium clouds
[AD-A146972]
07 p0996 N85-16326
Experimental research on ionospheric disturbance caused by cumulative barium vapor injection
16 p2719 N85-26787
Environmental surveillance at Los Alamos during 1984
[DE85-011886]
22 p3811 N85-33605

BARIUM ALLOYS
Critical evaluation of binary rare earth phase diagrams
[DE84-015057]
05 p0614 N85-13922

BARIUM COMPOUNDS
NT BARIUM OXIDES
NT BARIUM SULFIDES
NT BARIUM TITANATES
Solid phase reactions among manganese, potassium perchlorate and barium chromate [HSE-TRANS-11166] 19 p3237 N85-30071
BARIUM ION CLOUDS
Numberical simulation of the effects of radially injected barium plasma in the ionosphere [NASA-CR-175636] 14 p2354 N85-24542
BARIUM OXIDES
Density and thermal expansion measurements of several mixed oxide glasses in the solid and liquid regions [DE85-006134] 14 p2261 N85-24014
BARIUM SULFIDES
Application of thermoluminescence for detection of cascade shower 1: Hardware and software of reader system [HE-7.1-6] 24 p4213 N85-36160
Spatial distribution read-out system for thermoluminescence sheets [HE-7.1-7] 24 p4213 N85-36161
Application of thermoluminescence for detection of cascade shower 2: Detection of cosmic ray cascade shower at Mount Fuji [HE-7.1-12] 24 p4214 N85-36162
BARIUM TITANATES
Center for dielectric studies [AD-A146183] 03 p0434 N85-12761
Degradation mechanisms in ceramic dielectrics [AD-A149791] 12 p1813 N85-21369
Planar ferroelectric microcapacitors for microwave devices 13 p2087 N85-23032
BARLEY
Multi crop area estimation in Idaho using EDITOR [E85-10064] 06 p0827 N85-15251
BAROCLINIC INSTABILITY
Layered sloping mesoscale structures and rainbands in atmospheric frontal regions and their relation to symmetric instability 01 p0075 N85-10497
Combined effects of baroclinic and barotropic instability in a nonlinear low order model [DM-41] 09 p1358 N85-18544
Three-dimensional baroclinic instability of a Hadley cell for small Richardson number [NASA-TP-2450] 11 p1687 N85-20605
A numerical study of the Pacific polar low [AD-A153777] 18 p3149 N85-29495
BAROCLINIC WAVES
An improved analytical theory of Rossby wave driven Eulerian and Lagrangian mean flows along non-zonal barriers with application to the Hawaiian Ridge [AD-A144951] 01 p0088 N85-10593
Structure and energetics of medium-scale atmospheric waves in the southern hemisphere summer 05 p0685 N85-14403
Experiments on the assimilation of patches of data using a barotropic model 18 p3140 N85-29441
Energy sources of the dominant frequency dependent 3-dimensional atmospheric modes 18 p3143 N85-29462
The seasonal cycle of storminess as measured by band-pass fluctuations 18 p3144 N85-29467
Strongly nonlinear dynamics of baroclinic waves 20 p3486 N85-31681
Structure and energetics of medium-scale atmospheric waves in the Southern Hemisphere 20 p3489 N85-31685
On development mechanisms for polar lows 20 p3495 N85-31727
Subseasonal variability in a two-level atmospheric general circulation model 24 p4114 N85-35504
BAROCLINITY
Fully implicit numerical methods for the baroclinic primitive equations 05 p0679 N85-14365
Computer studies of baroclinic flow — Atmospheric General Circulation Experiment [NASA-CR-171338] 10 p1517 N85-19566
Mountain barrier baroclinity effects on surface winds along the Alaskan Arctic coast 14 p2236 N85-23877
Local mechanism of equatorial countercurrents 14 p2336 N85-24446
Atmospherically forced, coastally trapped, long period gravity waves off the south coast of southern Africa 16 p2832 N85-27461
BAROMETERS
Seismic observation of infrasonic signals [AD-A149574] 12 p1889 N85-21853
On the solar cycle variation in the barometer coefficients of high latitude neutron monitors [SH-6.1-2] 23 p4044 N85-35077
The neutron moderated detector and groundbased cosmic ray modulation studies [SH-9.1-13] 23 p4052 N85-35126
BAROMETRIC PRESSURE
U ATMOSPHERIC PRESSURE
BAROTRAUMA
Hyperbaric physiology (status and prospects) 08 p1194 N85-17521
BAROTROPIC FLOW
Index cycles simulated by a low order forced barotropic model 07 p1002 N85-16384
Spectral modeling of a potential vorticity equation for a barotropic flow on a beta-plane [CWI-AM-R8406] 08 p1186 N85-17478
High-frequency wind wave spectrum in storm basin 14 p2336 N85-24444
Modeling evolution of unstable geostropic eddies in barotropic ocean 14 p2336 N85-24447
Experiments on the assimilation of patches of data using a barotropic model 18 p3140 N85-29441
A factored implicit scheme for numerical weather prediction with small factorization error 18 p3141 N85-29447
Energy sources of the dominant frequency dependent 3-dimensional atmospheric modes 18 p3143 N85-29462
The contrasting Northern Hemisphere winters of 1980-81 and 1981-82 18 p3144 N85-29466
On Fofonoff's mode 18 p3145 N85-29471
Multiple equilibria of the barotropic vorticity equation on a sphere 18 p3146 N85-29475
Moist barotropic instability in the tropics 20 p3489 N85-31683
A study of the adequacy of quasi-geostrophic dynamics for modeling the effect of frontal cyclones on the larger scale flow [NASA-CR-176065] 20 p3495 N85-31731
BAROTROPISM
NT PLANETARY WAVES
A comparison of the bounded derivative and the normal mode initialization methods using real data 18 p3144 N85-29463
BARRED GALAXIES
Gas dynamics of the barred spiral galaxy NGC 3359 13 p2170 N85-23465
BARRELS (CONTAINERS)
Conceptual design report for a remotely operated cask handling system, revision 1 [DE85-000348] 08 p1169 N85-17371
Three-dimensional finite element impact analysis of a nuclear waste truck cask [DE85-010653] 19 p3288 N85-30369
Container for radioactive materials [DE85-005757] 23 p3972 N85-34626
BARRICADES
U BARRIERS
BARRIER LAYERS
Stochasticity and transport in Hamiltonian systems 02 p0282 N85-11836
Diffusion barrier for long wavelength laser diodes [AD-D011390] 07 p0970 N85-16157
Rolls-Royce experience with thermal barrier coatings — in aircraft engines [PNR-90222] 08 p1135 N85-17152
Advanced thermal barrier system bond coatings for use on Ni, Co-, and Fe-base alloy substrates [NASA-TM-87062] 20 p3431 N85-31283
BARRIERS
Classical free-streamline flow over a polygonal obstacle [NASA-CR-172448] 01 p0046 N85-10301
Reversible change in parameters of GaAs-based surface-barrier metal-semiconductor diodes induced by hydrogen absorption-desorption 02 p0258 N85-11690
Analysis of waveguide discontinuities by the method of moments [AD-A151499] 15 p2547 N85-25721
BARRIERS (LANDFORMS)
NT REEFS
Most important geochemical barrier zones in ocean (with example of Atlantic Ocean basin) 14 p2343 N85-24491
BARS
NT ELASTIC BARS
NT PRISMATIC BARS
Thermal-mechanical fatigue crack growth in Inconel X-750 [NASA-CR-174740] 07 p0927 N85-15877
Ultrasonic inspection of alloyed tungsten bars [AD-A148900] 10 p1495 N85-19435
NDE for heat engine ceramics [NASA-TM-86949] 11 p1649 N85-20389
Pyrotechnic shock simulation using the controlled response of a resonating bar fixture [DE85-006537] 16 p2784 N85-27181
Behaviors of stress waves in a conical bar 23 p3904 N85-34182
BARYCENTER
U CENTER OF GRAVITY
BARYON RESONANCE
Proposal for the systematic naming of mesons and baryons [DE85-008453] 17 p3035 N85-28773
BARYONS
NT HYPERONS
On the nature of the baryon asymmetry [NASA-TM-86156] 05 p0746 N85-14784
A 1-2 GeV/c beam line for hypernuclear and kaon research [DE85-007623] 16 p2863 N85-27659
Proposal for the systematic naming of mesons and baryons [DE85-008453] 17 p3035 N85-28773
On mini-cluster observed by Chacaltaya emulsion chamber experiment [HE-3.6-12] 24 p4185 N85-35959
An experiment to detect gut monopoles [HE-6.1-7] 24 p4210 N85-36133
BASALT
The petrology and geochemistry of high cascade volcanics in southern Washington: Mount Saint Helens volcano and the Indian Heaven basalt field 02 p0227 N85-11487
Impact cratering: The process and its effects on planetary evolution — and silicate-carbonate reactions on Venus [NASA-CR-174016] 02 p0228 N85-11488
Nickel-cobalt systematics and their bearing on lunar origin 04 p0582 N85-13719
Moon 09 p1411 N85-18893
Characteristics of basaltic lava flows on Venus 13 p2177 N85-23508
Magmas as selective filters of volatiles between planetary mantles and surfaces 13 p2185 N85-23557
Basaltic pressure ridges: Formation and relationship to flow emplacement 13 p2186 N85-23567
Basalts of Mars: Constraints on volatile evolution 13 p2194 N85-23610
Mechanisms of basalt-plains ridge formation 13 p2199 N85-23643
Parameters of magnetically active layers of Indian Ocean determined from deep drilling data and magnetic surveys 14 p2337 N85-24451
Identification of the youngest meteorites and a discussion of the possibility that they came from Mars 15 p2681 N85-26559
Sodium concrete reaction: Structural considerations [DE85-009031] 18 p3081 N85-29063
Chlorine isotopes as environmental tracers in Columbia River basalt groundwaters [DE85-011392] 19 p3302 N85-30473
The degassing history of the Earth: Noble gas studies of Archaean cherts and zero age glassy submarine basalts 21 p3718 N85-33072
Primordial magmaspheres and their lasting consequences 22 p3857 N85-33862
BASE FLOW
An experimental study of clustered, two-dimensional rocket nozzles [AD-A151889] 15 p2495 N85-25390
BASE PRESSURE
Empirical formulas for the prediction of the base pressure of missile bodies at subsonic velocities [DFVLR-FB-84-23] 03 p0316 N85-12044
An experimental study of clustered, two-dimensional rocket nozzles [AD-A151889] 15 p2495 N85-25390
Empirical formulas for the prediction of the base pressure of missile bodies at subsonic velocities [ESA-TT-893] 20 p3399 N85-31082
BASES (CHEMICAL)
The conversion of smaller borane fragments to larger structures. Systematics of boron hydride reactions [AD-A153443] 18 p3070 N85-28985
BASES (FOUNDATIONS)
U FOUNDATIONS
BASIC (PROGRAMMING LANGUAGE)
Convergent Technologies, mega frame CTIX BASIC interpreter version 1.03 [PB84-227776] 03 p0404 N85-12579
Gould Incorporated, Gould PS-3000, Gould PS-3000 BASIC Interpreter Version 1.00 [PB84-229186] 06 p0851 N85-15404
NCR Corporation, NCR 9300, NCR ITX-BASIC Release 2.0 [PB84-229228] 06 p0852 N85-15414
Sperry Corporation, 1100/80, UBASIC/BBASIC Level 9R1 [PB84-229202] 06 p0852 N85-15415
Compter Sciences Corporation, UNIVAC 1100/80, CSTS BASIC Release BAS160 [PB84-229145] 06 p0852 N85-15418

Control Data Corporation, Cyber 835, BASIC Release 3.5 Level 614
[PB84-227990] 06 p0853 N85-15420
Burroughs Corporation B26-CPU, Burroughs B20 BASIC Rel. 4.0
[PB84-216324] 06 p0855 N85-15436
Convergent Technologies NGEN CP001, CT BASIC Version 9.0
[PB84-216332] 06 p0855 N85-15437
Sperry Univac System 80, Model 6, OS/3 BASIC, Version 10.01
[PB85-108066] 10 p1542 N85-19722
Selection and use of general-purpose programming-language: Program examples, volume 2
[PB85-122000] 12 p1917 N85-22039
Selection and use of general-purpose programming language: Overview, volume 1
[PB85-122018] 12 p1917 N85-22040
How a BASIC program works
[DE85-009142] 22 p3831 N85-33727

BASINS
U STRUCTURAL BASINS

BATCH PROCESSING
Computer center introductory reference manual for CDC CYBER
[AD-A145796] 03 p0406 N85-12593
New YeS 1056 unified system computer model described 04 p0485 N85-13092
Method of production of metals by cathodic solution of their compounds in electrolytic cells
[BLL-OA-TRANS-3207-(6196.300)] 20 p3429 N85-31266
Optimize computer throughput using array processors
[AD-A155843] 24 p4135 N85-35628

BATHOLITHS
Stratigraphy, petrology, and tectonic setting of the Alisitos Group, Baja California, Mexico 03 p0389 N85-12488
Geology of selected migmatite zones within the bitterroot lobe of the Idaho batholith, Idaho and Montana 03 p0389 N85-12489

BATHS
NT SALT BATHS
Comparison of simulation of weightlessness by Head Down Tilt (HDT) and Water Immersion (WI) 05 p0692 N85-14454
Hemodynamics and plasma arginine vasopressin during water immersion in normal men 05 p0693 N85-14458
Trace metal determinations in nickel-plating baths by polarographic methods
[DE85-007064] 15 p2511 N85-25488

BATHYMETERS
The investigation of selected oceanographic applications of spaceborne synthetic-aperture radar 08 p1146 N85-17233
Advanced technology for hydrographic mapping
[FOA-C-30371-E1] 08 p1176 N85-17418
Along-track deflection of the vertical from SEASAT: GEBCO (General Bathymetric Chart of the Oceans) overlays
[PB85-129641] 12 p1876 N85-21767
An assessment of the potential role of multispectral imagery in bathymetric charting
[AD-A152460] 17 p2984 N85-28436

BATHYMETRY
U BATHYMETERS

BATHYTHERMOGRAPHS
ADAPS (Airborne Data Acquisition and Processing System) operation and maintenance manual
[AD-A149297] 11 p1585 N85-19983
Preliminary results of the oceanographic cruise of USCGC NORTHWIND to the Greenland Sea
[AD-A149802] 12 p1898 N85-21919
Report of the Hydrographic Service Royal Australian Navy for the year ended 30th june 1984, issue number 20
[AD-A151460] 15 p2583 N85-25832

BATTERIES
U ELECTRIC BATTERIES

BATTERY CHARGERS
Summary of activities pertaining to utilization of grant purchase of batteries for electric van
[DE84-015793] 02 p0195 N85-11305
Performance characteristics of a battery charger and state-of-charge indicator
[NASA-CR-174273] 07 p0946 N85-15992
Battery control and fault detection method
[AD-D011384] 07 p0993 N85-16307
BBC of Switzerland develops electric car 08 p1141 N85-17192
Battery charger
[AD-D011420] 08 p1178 N85-17425
Autonomous uninterruptable power supply apparatus
[AD-D011571] 14 p2298 N85-24232
INEL electric vehicle laboratory qualification: Transition test results and comparisons with JPL ETV1-2 data
[DE85-008006] 16 p2860 N85-27772
Test and evaluation of the Hoppecke Model E240G144/16 electric vehicle battery charger
[DE85-900573] 17 p2955 N85-28253
LEO life testing with different charge control 20 p3446 N85-31393
Deep reconditioning of batteries during DSCS 3 flight operations 20 p3446 N85-31397
Safety characteristics of non-lithium battery systems
[AD-A155733] 22 p3806 N85-33574
Rechargeable lithium-organic electrolyte battery having overcharge protection and method of providing overcharge protection for a lithium-organic electrolyte battery
[AD-D011738] 22 p3806 N85-33575

BATTERY SEPARATORS
U SEPARATORS

BAUXITE
Microbiological method for the desiliconization of high-silica bauxites
[BLL-MINTEK-TR-1168-(5810.5759)] 07 p0925 N85-15864

BAYES THEOREM
Estimation of the threshold in fatigue crack initiation models: A Bayesian approach
[AD-A144847] 01 p0062 N85-10410
Testing of inequality hypotheses in linear models using the Bayes method
[SER-C-292] 01 p0112 N85-10761
Credibility approximations for Bayesian prediction of second moments
[AD-A144996] 01 p0113 N85-10768
Bayesian analysis of item response curves
[AD-A145627] 02 p0254 N85-11665
Maximum likelihood and Bayesian parameter estimation in item response theory
[AD-A145775] 03 p0413 N85-12644
Performance of Bayes-optimal angle-of-arrival estimators
[AD-A146594] 06 p0858 N85-15454
Bayesian estimation of normal mixture parameters 07 p0985 N85-16255
Spatial estimation from remotely sensed data via empirical Bayes models 07 p0985 N85-16256
Multivariate spline methods in surface fitting 07 p0985 N85-16257
Bayesian estimation of undetected errors
[AD-A147198] 07 p1031 N85-16545
Belief structures
[AD-A147526] 07 p1036 N85-16575
A method for automatic water mass classification
[AD-D011405] 08 p1191 N85-17505
A numerical analysis of sampling plans based on prior distribution and costs
[AD-A147718] 08 p1210 N85-17616
An analysis of robust and efficient priors associated with a finite Bayesian model for compliance testing
[AD-A148497] 08 p1213 N85-17635
Empirical Bayes rules for selecting good binomial populations
[AD-A147614] 08 p1214 N85-17646
Improved estimation procedures for item response functions
[AD-A147677] 08 p1215 N85-17648
Minimax multiple t-tests for comparing k normal populations with a control
[AD-A148306] 08 p1215 N85-17656
W.E. Johnson's Sufficientness postulate
[AD-A149014] 10 p1550 N85-19774
Bayesian analysis of time series 1: Householder transformation analyses
[DE85-004449] 11 p1708 N85-20749
Asymptotically optimum multialternative sequential procedures for discernment of processes minimizing average length of observations 13 p2084 N85-23012
Accuracy of approximation of Bayes estimates in presence of noninformative parameters 13 p2084 N85-23015
Spatial acquisition algorithms and systems for intersatellite optical communication links
[AD-A150794] 14 p2292 N85-24207
Bayesian estimation of one dimensional discrete markov random fields
[AD-A151503] 15 p2640 N85-26284
Estimation of launch vehicle performance parameters
[AD-A151927] 16 p2728 N85-26839
Optimal design and use of retry in fault tolerant real-time computer systems
[NASA-CR-175920] 17 p3015 N85-28643
Studies in quality improvement 2. An analysis for unreplicated fractional factorials
[AD-A153539] 18 p3169 N85-29640
Bayesian full rank marginalization for 2-way contingency tables
[AD-A153841] 18 p3171 N85-29649
Bayesian inference and diagnostics for the 3 parameter logistic model
[AD-A153840] 18 p3175 N85-29681
Bayesian factor analysis
[AD-A154184] 19 p3347 N85-30747
A critique of Deming's discussion of acceptance sampling procedures
[AD-A154305] 19 p3348 N85-30751
Reconciling Bayesian and frequentist evidence in the one-sided testing program
[AD-A155603] 21 p3678 N85-32850
Bayesian vs MAP multiple model adaptive estimation for field of view expansion in tracking airborne targets
[AD-A155466] 21 p3679 N85-32855
Optimal Bayesian estimators for image segmentation and surface reconstruction
[AD-A155732] 22 p3827 N85-33704
Model robust response surface designs: Scaling two-level factorials
[AD-A156218] 24 p4143 N85-35686

BAYESIAN STATISTICS
U BAYES THEOREM

BAYOUS
Microseismic monitoring of Chocolate Bayou, Texas: The Pleasant Bayou no. 2 geopressured/geothermal energy test well program
[DE84-014825] 01 p0072 N85-10477

BAYS (STRUCTURAL UNITS)
Investigation of experimental lightweight firewall materials for A/C engine bay applications
[AD-A155765] 24 p4062 N85-35175

BAYS (TOPOGRAPHIC FEATURES)
NT CHESAPEAKE BAY (US)
NT DELAWARE BAY (US)
NT MONTEREY BAY (CA)
NT SAN FRANCISCO BAY (CA)
Geothermal studies in Alaska: Conditions at Prudhoe Bay 04 p0516 N85-13290
Proceedings of the 1st Glacier Bay Science Symposium
[PB85-115913] 11 p1682 N85-20599

BCC LATTICES
U BODY CENTERED CUBIC LATTICES

BCH CODES
Adaptation of bit error rate by coding — spacecraft transmissions
[ESA-CR(P)-1070] 15 p2545 N85-25711

BEACHES
Field studies of run-up generated by wind waves on dissipative beaches
[AD-A148793] 09 p1359 N85-18548
Hurricane storm surge research
[GPO-40-048] 12 p1893 N85-21880
Coastal erosion along Monterey Bay
[AD-A155610] 21 p3655 N85-32707

BEACONS
NT RADAR BEACONS
NT RADIO BEACONS
NT RADIO DIRECTION FINDERS

BEADS
Method for thermal monitoring subcutaneous tissue
[NASA-CASE-LAR-13028-1] 19 p3328 N85-30618

BEAM CURRENTS
Experimental observation of neoclassical currents
[DE84-015113] 01 p0122 N85-10834
In-line beam current monitor
[DE84-014054] 04 p0580 N85-13567
Macroscopic currents and wind perturbations in the frame of the wind and shock model — galactic nuclei 08 p1242 N85-17836
Experimental investigation of certain beam transport issues in a pulsed transmission line linear accelerator
[DE85-002310] 10 p1555 N85-19805
Survey of initial experiments on ATA beam dynamics
[DE85-004410] 10 p1555 N85-19806
SEM (Scanning Electron Microscope) investigation of silicon diodes using the electron beam induced current method
[AD-A150356] 13 p2064 N85-22894
High energy beam experiment 15 p2654 N85-26376
Generalization of the Child-Langmuir relation for 1-dimensional time-dependent diodes
[DE85-007386] 16 p2779 N85-27152
Accelerator column models for low-current beams
[DE85-010722] 19 p3262 N85-30226
Performance of an RF beam monitor on the NBS-Los Alamos racetrack microtron
[DE85-010725] 19 p3262 N85-30232
Beam dynamics in MABE
[DE85-010670] 19 p3358 N85-30619
Beam current sensor
[DE85-011600] 20 p3459 N85-31482

EBIC characterization and hydrogen passivation in silicon sheet 20 p3481 N85-31634
The cw operation of the FMIT RFQ accelerator [DE85-012667] 22 p3837 N85-33757
RADLAC technolgy review [DE85-011995] 23 p3962 N85-34691
Technology of magnetically driven accelerators [DE85-011857] 23 p3983 N85-34700
ATA upgrade to 150 MeV [DE85-013174] 24 p4098 N85-35404
Robinson instability and beam loading [DE85-013301] 24 p4151 N85-35737
Beam intensity increases at the intense pulsed neutron source accelerator [DE85-012377] 24 p4155 N85-35764
High resolution beam profile monitors in the SLC [DE85-013375] 24 p4157 N85-35774
Recent advances in remote handling at LAMPF [DE85-012725] 24 p4157 N85-35775
Kinetic loss experiments on Mite [DE85-012826] 24 p4158 N85-35780
Numerical studies of high current beam compression in heavy ion fusion [DE85-011874] 24 p4158 N85-35783

BEAM INJECTION
Use of a first-harmonic RF system in the NSLS booster [DE84-016432] 02 p0277 N85-11806
ATA gas propagation: 1 foot tank experiment [DE84-016395] 04 p0561 N85-13575
Mechanism of damping of plasma oscillations in initial stage of injection of electron beams from spacecraft into ionosphere in active experiments 06 p0823 N85-15225
Ion cluster beam deposition research 06 p0831 N85-15283
Sources, densities, and transport of impurities in neutral-beam injected Tokamaks 09 p1388 N85-18731
The plasma assisted modified betatron [AD-A148726] 09 p1390 N85-18748
Long-pulse beamlines for the mirror fusion test facility [DE84-017091] 09 p1392 N85-18760
Numerical model for swirl cooling in high-heat-flux particle beam targets and the design of a swirl-flow-based plasma limiter [DE85-003824] 11 p1732 N85-20894
Neutral beam injector oxygen impurity measurements and concentration reduction via gettering processes [DE85-000861] 12 p1836 N85-21521
Electric potential of satellite in electron emitting experiments in initial stage of electron beam injection in steady-state mode 15 p2480 N85-25309
MHD fluctuations in ISX-B [DE85-004800] 15 p2657 N85-26395
Experiments with light ions at CERN super proton synchrotron [DE85-007625] 17 p3031 N85-28744
Alternating gradient synchrotron [DE85-005950] 17 p3033 N85-28759
Definition of requirements for injection locking of pulsed UV lasers [DE85-010126] 18 p3113 N85-29275
Accelerator technology working group summary [DE85-009547] 18 p3180 N85-29717
Tritium system design for the mirror reactors FPD-1, FPD-2 and FPD-3 [DE85-010490] 19 p3363 N85-30852
Injection of hydrogen macroparticles into T-10 tokamak 21 p3692 N85-32937
The cw operation of the FMIT RFQ accelerator [DE85-012667] 22 p3837 N85-33757
Transverse emittance of a 2.0-MeV RFQ beam with high brightness [DE85-012718] 22 p3837 N85-33758
Rf program for LAMPF 2 [DE85-012693] 22 p3837 N85-33760
Acceleration of polarized H(-) in the BNL 200 MeV linac [DE85-011836] 22 p3840 N85-33777
Ultrahigh vacuum system of the heavy ion transport line at Brookhaven [DE85-011838] 22 p3840 N85-33778
Commissioning the polarized beam in the AGS [DE85-010958] 22 p3841 N85-33788
Design status of heavy ion injector program [DE85-010751] 22 p3842 N85-33793
Considerations on collective ion aceleration as an intense ion injector [DE85-012706] 24 p4155 N85-35757
Ion source development for the Los Alamos heavy ion fusion injector [DE85-012682] 24 p4156 N85-35766

BEAM INTERACTIONS
Considerations regarding the choice of beam parameters and IP configuration for the SSC [DE84-014532] 01 p0118 N85-10803
Neutral beam interactions with materials [AD-A145636] 02 p0285 N85-11857
Survey of initial experiments on ATA beam dynamics [DE85-004410] 10 p1555 N85-19806
Statistical phenomena in particle beams [DE85-001050] 12 p1929 N85-22118
System for forming and focusing high current beam of deuterium ions 13 p2045 N85-22798
Experiments and detectors for high energy heavy ion colliders [DE85-007927] 17 p3031 N85-28748
Report of the Working Group on Other Acceleration Schemes [DE85-008447] 17 p3033 N85-28764
Some comments on SSC physics [DE85-008444] 18 p3179 N85-29712
Phase and amplitude considerations for the 2-beam accelerator [DE85-008455] 18 p3180 N85-29715
Beam dynamics in MABE [DE85-010670] 19 p3358 N85-30819
Quantum effects in linear collider scaling laws [DE85-009846] 19 p3363 N85-30851
Analysis of beam interaction of the electrical thruster RIT 10 (particle emission) with surfaces [ESA-TT-826] 20 p3421 N85-31231
Nonlinear dynamics: A personal perspective [DE85-010982] 20 p3521 N85-31899
Studies in mixed species charged particle beam dynamics [OUEL-1545/84] 20 p3531 N85-31989
Laser beam interactions with vapor plumes during Nd:YAG laser welding on aluminum [DE85-009793] 21 p3593 N85-32328
Report of working group on detectors for hadrons and event parameters at colliders 24 p4146 N85-35705
A survey of multiplicities and rapidity densities from existing emission data on hadron-nucleus nucleus-nucleus collisions 24 p4146 N85-35706

BEAM LEADS
Yield joint condition for three-dimensional I-beams [ILR-MITT-137] 12 p1867 N85-21716
Low capacitance e-beam fabricated beam-lead Schottky barrier diodes [AD-A150238] 13 p2063 N85-22888

BEAM NEUTRALIZATION
Measurement of proton autoneutralization potential [DE85-001752] 06 p0865 N85-15501

BEAM SPLITTERS
Environmentally independent fiber optic rotation sensor [AD-D011219] 01 p0119 N85-10818
Precision electrooptical deflector based on corrugated light guide 07 p0950 N85-16020
Matrix-matrix multiplication using an electrooptical systolic-engagement array processing architecture [AD-D011410] 08 p1223 N85-17704
Multichannel birefringent filter 18 p3206 N85-29888
Applications of holography to X-ray imaging [DE85-010984] 23 p3934 N85-34384
Polarisation insensitive achromatic cube beamsplitter — binocular microscopes [NPL-MOM-72] 23 p3973 N85-34630
Differentiating spatial light modulator [AD-D011727] 23 p3973 N85-34632

BEAM WAVEGUIDES
Improved directional couplers for overmoded waveguide systems [IPF-84-1] 09 p1394 N85-18775
Design of mode converters from TE circular om modes in circular waveguides to TE rectangular mo modes in rectangular waveguides for high power applications in the frequency range 1 to 30 GHz [IPF-84-7] 09 p1395 N85-18781
Heavy ion fusion accelerator research in the US [DE85-008465] 17 p3034 N85-28767
Beam potential measurement of an intense H(-) beam by use of the emissive probe technique [DE85-012671] 24 p4155 N85-35762
Beam intensity increases at the intense pulsed neutron source accelerator [DE85-012377] 24 p4155 N85-35764

BEAMS
Coriolis effects on the vibrations of rotating beams, plates and shells 09 p1331 N85-18366
New concepts in deployable beam structures 14 p2232 N85-23832

BEAMS (RADIATION)
NT ATOMIC BEAMS
NT ELECTRON BEAMS
NT GAMMA RAY BEAMS
NT ION BEAMS
NT LIGHT BEAMS
NT MOLECULAR BEAMS
NT NEUTRAL BEAMS
NT NEUTRINO BEAMS
NT NEUTRON BEAMS
NT PARTICLE BEAMS
NT PHOTON BEAMS
NT PION BEAMS
NT PROTON BEAMS
NT RADAR BEAMS
NT RELATIVISTIC ELECTRON BEAMS
Considerations regarding the choice of beam parameters and IP configuration for the SSC [DE84-014532] 01 p0118 N85-10803
The Berkeley mini-collider [DE84-014594] 01 p0118 N85-10808
Focusing beam of 1-GeV protons with volumetric capture to the mode of channeling by bent single crystal 02 p0268 N85-11750
Positron flux concentrator: An update [DE84-016260] 04 p0561 N85-13578
Focussing and confinement [DE84-016181] 05 p0640 N85-14106
Tracking servo compensator with rate aiding [AD-D011372] 07 p0942 N85-15971
Design and testing of a refractive laser beam homogenizer [AD-A146997] 07 p0970 N85-16162
Longer-scalelength plasma perturbations by an intense laser beam [AD-A147005] 07 p1045 N85-16638
Beam propagation studies at NRL (Naval Research Laboratory) July 1983 to June 1984, volume 2 [AD-A148196] 08 p1152 N85-17270
Beam-foil spectroscopy of highly ionized aluminum atoms 09 p1390 N85-18746
AEM with a convergent beam [DE85-000667] 11 p1714 N85-20784
Transmission and reflection of laser beams propagating through aerosol clouds in space [LA-9998-MS] 12 p1856 N85-21636
Atmospheric transmissometer [AD-D011540] 12 p1932 N85-22140
Beamwidth control in pyramidal horns [R-NIAS-27] 13 p2053 N85-22853
Experimental verification of beam deflection from hybrid reflector antenna within wide-angle sector 13 p2079 N85-22984
Laser beam shaping system with reduced objective diameter 14 p2275 N85-24096
The measurement of laser beam parameters 14 p2308 N85-24263
Atomic physics aspects of a Relativistic Nuclear Collider [DE85-006867] 15 p2650 N85-26342
The 10 MWe solar thermal central receiver pilot plant: Beam safety tests and analyses [SAND-83-8035] 16 p2816 N85-27379
A 1-2 GeV/c beam line for hypernuclear and kaon research [DE85-007623] 16 p2863 N85-27659
High precision materials characterization in the near millimeter wave-length range [AD-A153267] 17 p2968 N85-28331
The temperature dependence of diffracted beam intensities in atom-surface scattering [AD-A152762] 17 p3029 N85-28736
Heavy ion fusion accelerator research in the US [DE85-008465] 17 p3034 N85-28767
Large, energetic cluster impacts on surfaces [DE85-006559] 17 p3034 N85-28769
Beam forming network [NASA-CASE-NPO-15743-1] 18 p3089 N85-29118
Two-degree-of-freedom linear and planar microwave array lenses [AD-A153701] 18 p3095 N85-2915
Physics of High Energy Particle Accelerators. AI Conference Proceedings no. 127 [DE85-008891] 18 p3182 N85-2973
Performance of an RF beam monitor on the NBS-Lo Alamos racetrack microtron [DE85-010725] 19 p3262 N85-3023
Clearing of polydisperse aqueous aerosol by las radiation pulses 19 p3298 N85-3044
Circular-beam ray tracing on a microcomputer [DE85-010754] 19 p3338 N85-306
Moments in particle-in-cell simulations [DE85-010792] 19 p3356 N85-308
Study of a novel shielding principle for protection agai intense gamma-ray beams [AD-A154374] 19 p3357 N85-308
Proposed use of the radio-frequency quadrup structure to funnel high-current ion beams [DE85-010746] 19 p3364 N85-308

Grazing incidence beam expander
[DE85-010784] 19 p3368 N85-30889

Hierarchical beamforming with application to a large aperture array system 20 p3439 N85-31345

ECM multiple-target retrodirective antenna
[AD-D011528] 20 p3439 N85-31346

Method to render second order beam optics programs symplectic
[DE85-010631] 20 p3515 N85-31855

Permanent magnets for production and use of high energy particle beams
[DE85-009934] 20 p3522 N85-31905

Propagation and reflection of a finite amplitude ultrasonic beam including harmonic content: A numeric model
20 p3523 N85-31914

Guide to the Main Ring DO overpass
[DE85-011722] 20 p3531 N85-31963

New approximations and findings of theory of nonlinear acoustic beams 21 p3680 N85-32863

Reflection of acoustic beam from inhomogeneous boundary 21 p3680 N85-32864

The problem of brightness enhancement during laser frequency doubling 21 p3686 N85-32897

Design of electrooptical system with annular cathode and electrostatic compressor 22 p3770 N85-33367

Characteristics of optical information-measurement channels with utilization of scattering effects
22 p3781 N85-33429

Method and apparatus for measuring areas of photoelectric cells and photoelectric cell performance parameters
[DE85-011629] 22 p3810 N85-33599

Solar energy meteorological research and training program: Region 4
[DE85-011783] 22 p3816 N85-33640

Materials characterization with intense positron beams
[DE85-011850] 22 p3839 N85-33769

Iris tilting and RF steering in the SLAC Linac
[DE85-011704] 22 p3841 N85-33783

Commissioning the polarized beam in the AGS
[DE85-010958] 22 p3841 N85-33786

Width of nonlinear difference resonances
[DE85-013026] 24 p4148 N85-35719

Use of a minimum-ellipse criterion in the study of ion-beam extraction systems
[DE85-012670] 24 p4148 N85-35721

Time domain reflectometry for SLC BPM system
[DE85-012389] 24 p4155 N85-35758

High resolution beam profile monitors in the SLC
[DE85-013375] 24 p4157 N85-35774

BEAMS (SUPPORTS)
NT CANTILEVER BEAMS
NT CURVED BEAMS
NT I BEAMS
NT RECTANGULAR BEAMS

Interactive buckling of thin-walled structural components under static and dynamic loads
01 p0059 N85-10392

Deformation measurements of composite multi-span beam shear specimens by Moire interferometry
[NASA-CR-3844] 02 p0169 N85-11135

Approximation methods for inverse problems involving the vibration of beams with tip bodies
[NASA-CR-172468] 02 p0209 N85-11379

Static and dynamic characteristics of materials with beam-microstructure 03 p0370 N85-12361

Complex frequency analysis of damped thin-walled beams with open cross sections
03 p0371 N85-12366

Turbine blade damping study
[NASA-CR-171255] 04 p0456 N85-12890

Forced vibrations of friction-damped beam structures in two dimensions
[UDR-TM-82-08] 04 p0456 N85-12892

Contact behavior, impact response and damage in graphite-epoxy laminates subjected to initial stresses
08 p1171 N85-17386

The response of metallic structures to dynamic loading 08 p1172 N85-17389

Durability and behavior of prestressed concrete beams. Posttensioned concrete beam investigation, supplemental laboratory tests of beams exposed from 1961 to 1982
[AD-A148821] 09 p1304 N85-18191

Optimization of vibrating beams including the effects of coupled bending and torsional modes
09 p1331 N85-18364

Reanalysis of continuous dynamic systems with continuous modifications 09 p1337 N85-18411

Determination of shear coefficient of a general beam cross section by finite element method
09 p1338 N85-18413

Swing-arm beam erector (SABER) concept for single astronaut assembly of space structure
[NASA-TP-2379] 10 p1429 N85-19015

A Galerkin method for the estimation of parameters in hybrid systems governing the vibration of flexible beams with tip bodies
[NASA-CR-172537] 10 p1544 N85-19734

Transverse vibration and buckling of a cantilevered beam with tip body under constant axial base acceleration
[NASA-CR-175567] 12 p1864 N85-21694

Control Of Flexible Structures (COFS) flight experiment background and description 14 p2236 N85-23864

Reflection and transmission of flexural waves at discontinuities 15 p2572 N85-25861

Control of a flexible beam
[DE85-007243] 15 p2580 N85-25914

Adaptation of continuous beams and the method of optimizing the flexibility of their elastic supports. Theorem on maximal adaptation loading, supplement
[REPT-10/1984-SUPPL] 16 p2797 N85-27241

Principles of wave formation along web of H-beams
[BLL-M-36041-(5828.4)] 16 p2798 N85-27253

Nonlinear equations for dynamics of pretwisted beams undergoing small strains and large rotations
[NASA-TP-2470] 16 p2799 N85-27258

Deployable controllable geometry truss beam
[NASA-TM-86366] 17 p2909 N85-27934

Numerical solution of one-dimensional nonlinear problems of statics for elastic beams and shells under rigid constraints 17 p2943 N85-28166

Structural dynamics modification of generalized beams using a local eigenvalue modification procedure
19 p3282 N85-30353

Dynamic response of a flexible space beam
[NASA-TM-86441] 19 p3285 N85-30366

Shear deflection in a three-point bend beam of a solid circular cross-section
[AD-A154458] 19 p3287 N85-30381

Attitude control tradeoff study between the use of a flexible beam and a tether configuration for the connection of two bodies in orbit 20 p3412 N85-31174

Stress distribution of fiberglass reinforced plastic beam with a delamination under three-point bending
23 p3906 N85-34210

Design and behavior of coped beams
24 p4100 N85-35417

User's guide: A computer program for strength analysis of non-hydraulic concrete structural elements. Report 1. Concrete General Strength Investigation (CGSI)
[AD-A156392] 24 p4102 N85-35428

User's guide: A computer program for strength analysis of non-hydraulic concrete structural elements. Report 2. Strength design of reinforced concrete column sections (PCAUC)
[AD-A156393] 24 p4102 N85-35429

Static and cyclic behavior of semi-rigid steel beam-column connections
[PB85-194363] 24 p4103 N85-35433

BEAMSHAPING
U COLLIMATION

BEARING

New ferrous metallurgy technology
01 p0019 N85-10114

BEARING (DIRECTION)

Three position estimation procedures
[AD-A148748] 09 p1278 N85-18042

Helium atoms in interstellar and interplanetary space. II: Determination of direction of interstellar gas motion relative to Sun 13 p1980 N85-22425

Wave directional spectra via ARGOS
16 p2812 N85-27343

UTM (Universal Transverse Mercator) determinations from geographical data
[AD-A152293] 16 p2856 N85-27610

Arrival direction distribution of cosmic rays of energy 10 (18) eV
[OG-5.3-7] 22 p3885 N85-34073

Observation of arrival times of EAS with energies or = 6 x 10 (14) eV
[OG-5.3-8] 22 p3885 N85-34074

Angular resolution of air-shower array-telescopes
[OG-9.5-6] 23 p4030 N85-34983

BEARING ALLOYS

Testing the antifriction properties of alloys for heavily loaded bearings 06 p0780 N85-14990

Powder metallurgy bearings for advanced rocket engines 16 p2736 N85-26881

Conservation and substitution technology for critical metals in bearings and related components for industrial equipment and opportunities for improved bearing performance
[PB85-176246] 18 p3082 N85-29069

BEARINGLESS ROTORS

Integrated technology rotor/flight research rotor hub concept definition
[NASA-CR-166447] 09 p1280 N85-18051

Integrated Technology Rotor/Flight Research Rotor (ITR/FRR) concept definition
[NASA-CR-166443] 10 p1423 N85-18978

Integrated Technology Rotor/Flight Research Rotor (ITR/FRR) concept definition
[NASA-CR-166445] 10 p1423 N85-18979

Integrated technology rotor/flight research rotor concept definition study
[NASA-CR-166446] 10 p1424 N85-18980

Integrated Technology Rotor/Flight Research Rotor (ITR/FRR) concept definition study
[NASA-CR-166444] 10 p1424 N85-18981

Electric motors with elastically mounted rotors
16 p2763 N85-27048

An improved servo-controlled inertial clock for laboratory tests of general relativity 19 p3378 N85-30955

BEARINGS
NT ANTIFRICTION BEARINGS
NT BALL BEARINGS
NT FOIL BEARINGS
NT GAS BEARINGS
NT JOURNAL BEARINGS
NT MAGNETIC BEARINGS
NT ROLLER BEARINGS
NT THRUST BEARINGS

Experimental on-stream elimination of resonant whirl in a large centrifugal compressor 05 p0642 N85-14121

Design of electromagnetic bearing for vibration control of flexible transmission shaft 05 p0645 N85-14136

Squeeze-film dampers for turbomachinery stabilization
05 p0645 N85-14138

Dynamic stiffness characteristics of high eccentricity ratio bearings and seals by perturbation testing
05 p0645 N85-14141

Improvement of the corrosion resistance of turbine engine bearings
[AD-A147430] 07 p0905 N85-15731

Thermally isolated structural support link
[AD-D011349] 07 p0972 N85-16176

Bearing tester fit analysis
[NASA-CR-171282] 07 p0973 N85-16181

Assessment of the operating characteristics of the SSME LOX turbopump pump-end bearing
[NASA-CR-171287] 08 p1167 N85-17362

An evaluation of the 64-meter antenna radial bearing for use on the 70-meter antenna
10 p1464 N85-19238

Elevation bearing maximum load, 70-meter antenna
10 p1464 N85-19239

Hydrostatic bearing pad maximum load and overturning conditions for the 70-meter antenna
10 p1465 N85-19241

Low leakage turbine shaft seals for advanced combined cycle systems
[AD-A149372] 10 p1492 N85-19420

Precise bearing support ditherer
[AD-D011470] 10 p1493 N85-19428

Emitted vibration measurement device and method
[NASA-CASE-MFS-25861-1] 11 p1635 N85-20299

Characterization of lubricated bearing surfaces operated under high loads
[NASA-TM-86964] 12 p1811 N85-21357

Experimental study of heat transfer from shaft in cooled radial bearing of GNT-25 gas turbine
14 p2270 N85-24068

Selection of bearing type for large steam turbines
14 p2271 N85-24069

Design of piping for oil drain from turbine bearings
14 p2271 N85-24073

Stability of turbine runners in sliding bearings under external circulation forces 14 p2272 N85-24074

Stability of steady modes of motion by axis of rotating wheel in nonlinear bearings 14 p2279 N85-24117

Thermal deformation of flexible rotors in friction bearings 14 p2280 N85-24123

Study of axial bearings without oil bath with radial cooling of blocks 14 p2286 N85-24164

Model of friction bearing hydrodynamics
14 p2288 N85-24178

Computations for segmented radial bearings
14 p2288 N85-24180

Advanced rocket engine cryogenic turbopump bearing thermal model 16 p2735 N85-26879

Effects of bearing deadbands on bearing loads and rotor stability 16 p2737 N85-26889

Reusable rocket engine turbopump condition monitoring 16 p2740 N85-26907

Non-contact hydrostatic bearings
16 p2762 N85-27046

Fatigue life analysis of a turboprop reduction gearbox
[NASA-TM-87014] 16 p2793 N85-27226

BEARS

Polar bear telemetry results from the Nimbus-6 system
14 p2325 N85-24365

BEAT
U SYNCHRONISM

BEAT FREQUENCIES
Optical injection locking of solid-state oscillators by frequency-multiplexed injection-locked, laser diodes
[AD-D011695] 19 p3275 N85-30307
BEAUFORT SEA (NORTH AMERICA)
Analysis and interpretation of current measurements from the Beaufort Sea
[AD-A145197] 01 p0069 N85-10600
Geothermal studies in Alaska: Conditions at Prudhoe Bay 04 p0516 N85-13290
Shore ice ride-up and pile-up features. Part 2. Alaska's Beaufort Sea coast, 1983 - 1984
[AD-A148428] 08 p1190 N85-17501
Atlas of the Beaufort Sea
[AD-A149545] 11 p1689 N85-20619
Data collection and winter ice dynamics in the Beaufort Sea 14 p2236 N85-23878
BED REST
Physical performance capacity after a 7 day head-down tilt (-6 deg) 05 p0692 N85-14451
Leg volume changes. Responses to Lower Body Negative Pressure (LBNP) during 7 days of zero-g simulation (6 deg Head-Down Tilt (HDT))
05 p0692 N85-14452
Heart rate variability during 7 day head-down tilt (6 deg) 05 p0692 N85-14453
Comparison of simulation of weightlessness by Head Down Tilt (HDT) and Water Immersion (WI)
05 p0692 N85-14454
Glucose tolerance in trained and untrained subjects during head-down tilt (6 deg) 05 p0693 N85-14461
Alterations/corrections to the BRASS Program
[NASA-CR-171874] 15 p2616 N85-26121
Effect of 120-day antiorthostatic bedrest on gas exchange and pulmonary circulation in man
19 p3323 N85-30589
Regional circulation during testing on isokinetic dynamometer following 14-day bedrest
19 p3323 N85-30590
BEDROCK
NT BALTIC SHIELD (EUROPE)
NT BATHOLITHS
Geophysical investigations of the central part of Niger State, Nigeria 03 p0390 N85-12496
SIR-B analysis of the Precambrian shield of Sudan and Egypt: Penetration studies and subsurface mapping
08 p1145 N85-17219
Saudi Arabian refraction profile: Crustal structure of the Red Sea-Arabian Shield transition
17 p2990 N85-28484
Saudi Arabian refraction profile: A preliminary interpretation for the Red Sea-Arabian Shield transition
17 p2991 N85-28485
A traveltime interpretation of the 1978 seismic refraction profile in the Kingdom of Saudi Arabia
17 p2991 N85-28486
Interpretation of the data of USGS seismic refraction profile across the Arabian Shield in western Saudi Arabia 17 p2991 N85-28488
One-dimensional velocity-depth functions determined for the Arabian Shield and the southwestern Red Sea: A comparison of models 17 p2992 N85-28490
A comparison of crustal sections: Arabian Shield to the Red Sea 17 p2992 N85-28491
Reduced to pole long-wavelength magnetic anomalies of Africa and Europe 20 p3475 N85-31595
Euro-African MAGSAT anomaly-tectonic observations
20 p3475 N85-31596
Bedrock geology of the Brattleboro Quadrangle, Vermont-New Hampshire
[DE85-011027] 22 p3815 N85-33634
BEDS (GEOLOGY)
NT SALT BEDS
BEDS (PROCESS ENGINEERING)
Influence of inter-layer effect on charge gas-permeability
[BLL-M-35919-(5828.4)] 05 p0616 N85-13940
Influence of size grading of sintering ore on the sintering process
[BLL-M-36004-(5828.4)] 07 p0924 N85-15854
Transition to detonation from rapid-compression (ramp-waves) generated in a burning porous bed
[AD-P004345] 10 p1455 N85-19169
BEER LAW
Aerosol multiple-scanning code, ASCAT
[LA-10046-MS] 12 p1823 N85-21440
BEHAVIOR
NT HUMAN BEHAVIOR
Command control group behaviors. Objective 1: A methodology for and identification of command control group behaviors
[AD-A145690] 02 p0191 N85-11279
Decision process models of contractor behavior: The development of effective contract incentives
[AD-A145524] 02 p0292 N85-11898
USSR report: Life sciences. Biomedical and behavioral sciences
[JPRS-UBB-84-027] 07 p1012 N85-16426
Model of team organization and behavior and team description method
[AD-A147540] 07 p1053 N85-16680
USSR report: Life sciences. Biomedical and behavioral sciences
[JPRS-UBB-85-001] 08 p1193 N85-17515
USSR report: Life sciences. Biomedical and behavioral sciences
[JPRS-UBB-85-007] 09 p1362 N85-18566
Behaviour of soil under a lugged wheel
[AD-P004267] 09 p1407 N85-18864
Turning behaviour of articulated frame steering tractor
[AD-P004304] 09 p1409 N85-18881
USSR report: Life sciences. Biomedical and behavioral sciences
[JPRS-UBB-85-009] 10 p1526 N85-19625
Blackbirds and starlings: Population ecology and habits related to airport environments
[AD-P004190] 11 p1560 N85-19953
Cattle Egret hazard assessment
[AD-P004191] 11 p1560 N85-19954
Learning to search. From weak methods to domain-specific heuristics
[AD-A149949] 12 p1918 N85-22045
Analysis of team performance in a programmed environment
[NASA-CR-175634] 14 p2392 N85-24728
Large-time behavior of viscous surface waves
[AD-A154805] 21 p3584 N85-32278
Experimental and analytic characterization of nonlinear seismic attenuation
[AD-A154760] 21 p3631 N85-32556
Sobolev-Poincare's inequality and the Neumann problem for u sub t = divergence of the absolute value of the gradient u to the p-2 power x the gradient u
[AD-A154788] 21 p3676 N85-32839
BELGIUM
Satellite-determined stresses in the crust of Europe with particular consideration to the Liege earthquake of November 8, 1983 20 p3490 N85-31694
150 years of meteorology in Belgium
22 p3817 N85-33642
BELL AIRCRAFT
NT UH-1 HELICOPTER
BENCHES
U SEATS
BEND TESTS
Yield stress determination from miniaturized disk bend test data
[DE85-009495] 18 p3122 N85-29330
BENDING
NT ELASTIC BENDING
Material degradation in heavy steel plates caused by bending with a laser
[AD-A144784] 01 p0052 N85-10343
Initial sailplane project: The RP-1
04 p0468 N85-12976
Second sailplane project: The RP-2
04 p0468 N85-12977
On a general nonlinear theory of plates and shells: Formulation and applications 08 p1172 N85-17387
Modelling and identification of the structural properties of an astromast
[CRC-1374] 09 p1329 N85-18352
NOAA OTEC CWP (National Oceanic and Atmospheric Administration Ocean Thermal Energy Conversion Cold Water Pipe) at-sea test. Volume 3, part 1: Tabulation of the power spectra for selected channels
[PB84-238955] 09 p1346 N85-18467
Turning behaviour of articulated frame steering tractor
[AD-P004304] 09 p1409 N85-18881
Bending two-layer metal-polymer plates
11 p1604 N85-20085
Simple theoretical models for composite rotor blades
[NASA-CR-175620] 13 p1971 N85-22382
Load carrying capacity of double circular arc gears
14 p2221 N85-23776
Thermomechanically induced pre- and postbuckling of general structure 20 p3467 N85-31540
The effect of abrasive blasting on the fatigue and corrosion of an aluminium-copper alloy
[AD-A154954] 21 p3566 N85-32182
User's guide for computer program CGFAG, Concrete General Flexure Analysis with Graphics
[AD-A155555] 21 p3570 N85-32204
Thin-film reliability and engineering overview
21 p3612 N85-32450
Analysis of long bone and vertebral failure patterns
[AD-A154796] 21 p3663 N85-32758
Stress distribution of fiberglass reinforced plastic beam with a delamination under three-point bending
23 p3906 N85-34210
Stress-intensity factors for circumferential surface cracks in pipes and rods under tension and bending loads
[NASA-TM-87594] 24 p4101 N85-35424
Major facility overhauls at LAMPF
[DE85-012724] 24 p4156 N85-35765
BENDING FATIGUE
Effect of internal pressure on flexibility and stress intensification factors for pipe elbows analyzed by the finite element method
[AD-A151161] 15 p2578 N85-25901
Rotating bending fatigue strength of silicon carbide and alumina-fiber reinforced aluminum
23 p3907 N85-34208
BENDING MOMENTS
Optimum design of nonplaner wings: Minimum induced drag for a given lift and wing root bending moment
[NAL-TR-797] 01 p0002 N85-10011
Three programs for evaluating bending moments, deflections and shear forces in simply-supported uniform bridge decks under South African NA loading: NAB, NAD and NAS. NITRR manual P13
[ISBN-0-7988-2263-X] 01 p0102 N85-10681
Helicopter active control with rotor blades relaxation
06 p1075 N85-16819
Negative flexural behavior of precase composite slabs with steel joint 23 p3904 N85-34183
Nonlinear flap-lag-extensional vibrations of rotating, pretwisted, preconed beams including Coriolis effects
[NASA-TM-87102] 23 p3941 N85-34427
BENDING VIBRATION
Optimization of vibrating beams including the effects of coupled bending and torsional modes
09 p1331 N85-18364
BENDS (PHYSIOLOGY)
U DECOMPRESSION SICKNESS
BENEFICIATION
Novel analytical approaches to coal beneficiation
[DE85-010437] 19 p3229 N85-30021
BENZENE
Effect of toluene on the solubility of biohazardous volatile synthetic organic compounds
[AD-A145188] 01 p0018 N85-10109
Multiphoton ionization of benzene in solution
[DE85-000693] 06 p0766 N85-14689
Vibrational spectroscopy of chemisorption phenomena on model catalyst surfaces
[AD-A146753] 07 p0922 N85-15840
Subtractively normalized interfacial Fourier transform infrared spectroscopy of difluorobenzene adsorbed at polycrystalline platinum electrodes
[AD-A148660] 08 p1123 N85-17080
Supersonic molecular jet study of the liquid state
[AD-A147416] 09 p1379 N85-18671
Improved lithium-intercalation cathode material
[AD-A149319] 10 p1435 N85-19043
Laser schlieren, shock tube studies of high temperature hydrocarbon pyrolysis rates
[DE85-003314] 11 p1636 N85-20303
Synthesis, static and reactive characterization of supported organometallics
[DE85-004285] 12 p1808 N85-21340
Formation of high molecular weight products from benzene during boundary lubrication
[NASA-TM-86966] 13 p2017 N85-22644
Collaborative shock tube studies of benzene pyrolysis
[DE85-006347] 14 p2253 N85-23962
The mobile phase in coals: Its nature and modes of release
[DE85-011696] 19 p3230 N85-30026
Flash pyrolysis of biomass with reactive and non-reactive gases
[DE85-010962] 19 p3306 N85-30496
Vibrational energy transfer in benzene-argon collisions
[DE85-009603] 19 p3355 N85-30797
Fuel-rich catalytic combustion: A soot-free technique for in situ hydrogen-like enrichment
[NASA-TP-2498] 20 p3423 N85-31244
Thermal reactions of aromatics with CaO
[DE85-010668] 22 p3742 N85-33193
Ionization detection of stimulated Raman spectra
[DE85-010672] 22 p3746 N85-33218
Carcinogenesis of nitrated toluenes and benzenes skin and lung tumor assays in mice
[AD-A155723] 22 p3818 N85-33655
BENZOIC ACID
Condensation of anhydrides or dicarboxylic acids with compounds containing active methylene groups. Part 19: Condensation of phthalic and substituted phthalic anhydrides with benzoylacetic ester
[NASA-TM-77885] 19 p3227 N85-30008
BERING SEA
Drift characteristics of northeastern Bering Sea ice during 1982
[PB84-213982] 01 p0089 N85-10604

Recent observations of tides and tidal currents from the northeastern Bering Sea shelf
[PB84-241765] 04 p0543 N85-13452
New data on structure of Shirshov Ridge (Bering Sea)
10 p1496 N85-19456
Seafloor seismic measurements in the southern Bering
[DE85-004906] 14 p2374 N85-24675
Regional meteorology of the Bering Sea during MIZEX-West, February and March 1983
[PB85-173699] 18 p3150 N85-29503
Geological-geophysical and gas-biochemical studies in Bering Sea 19 p3291 N85-30404

BERMUDA
AWS (Air Weather Service) climatic briefs: North America
[AD-A152161] 16 p2835 N85-27483

BERNOULLI EQUATION
U BERNOULLI THEOREM

BERNOULLI THEOREM
The distribution of the number of empty cells in a generalized random allocation scheme
[AD-A154806] 21 p3677 N85-32841

BERYL
Spectroscopic investigation of materials for frequency agile laser systems
[AD-A151731] 16 p2790 N85-27208

BERYLLIUM
NT BERYLLIUM ISOTOPES
NT BERYLLIUM 7
NT BERYLLIUM 9
NT BERYLLIUM 10
Dependence of microplasticity of beryllium on grain size and heat treatment 03 p0353 N85-12273
Narrow absorption components in Be star winds
08 p1232 N85-17760
Mechanical properties of Be-Al composite
10 p1443 N85-19094
Structure-phase state and properties of high-durability VAL8 alloy 11 p1597 N85-20046
Weldability of alloy ABM1 to alloy 1201
11 p1603 N85-20080
Conductivity changes in neutron-irradiated commercial copper alloys at approximately 450(O)C
[DE85-003007] 11 p1606 N85-20100
Effect on work-hardening in dynamic deformation of beryllium
[DE85-002691] 11 p1608 N85-20111
Stability of temporal and energy parameters of picosecond lanthanum beryllate laser
11 p1717 N85-20804
Nondestructive method for detecting machine damage in beryllium
[DE85-001074] 12 p1862 N85-21681
TEM/FIM study of modulated microstructures in the Fe-Be system
[DE85-005379] 13 p2023 N85-22678
Gigantic lithium deposit discovered in France
14 p2289 N85-24184
China report: Science and technology
[JPRS-CST-85-007] 15 p2533 N85-25621
Professional Committee on Solid Propulsion hold conference 15 p2533 N85-25623
Radiation damage experiments and lifetime estimates for beryllium components in fusion systems
[DE85-006038] 17 p3040 N85-28811
Preliminary proposal for a beryllium technology program for fusion applications
[DE85-009615] 18 p3183 N85-29737
Machining of beryllium with the LLNL precision engineering research lathe
[DE85-010832] 19 p3250 N85-30146
The production and destruction of metastable negative ions
[DE85-011056] 19 p3364 N85-30858
Design of a helium-cooled molten salt fusion breeder
[DE85-010474] 20 p3528 N85-31943
Investigation of thick-target neutron emission from Be-9(d,n)B-10 at E(d) = 7 MeV for angles other than zero degrees
[DE85-010254] 20 p3528 N85-31947
Beryllium production
[DE85-013360] 24 p4148 N85-35716

BERYLLIUM ALLOYS
Re-evaluation of phase separation in Ti-Zr-Be metallic glasses
[DE84-015803] 03 p0338 N85-12176
The Al-Be system: The effects of RSP on structure and phase relating
[DE84-015804] 04 p0474 N85-13019
Critical evaluation of binary rare earth phase diagrams
[DE84-015057] 05 p0614 N85-13922
Design and use of nonstandard tensile specimens for irradiated materials testing
[DE85-001071] 11 p1652 N85-20408
Temperature variation of resistivity of certain alloys based on transition and simple metals in amorphous and crystalline states 15 p2496 N85-25399

BERYLLIUM COMPOUNDS
NT BERYL
NT BERYLLIUM FLUORIDES
NT BERYLLIUM OXIDES
Determination of the average neutron activation cross section with an annular-shaped 241 Am/Be neutron source and a NaI(T1) detector for the 27 Al (n,p)27 Mg-reaction
[REPT-4/1984] 20 p3532 N85-31975

BERYLLIUM FLUORIDES
Computer simulations of rare earth sites in glass: Experimental tests and applications to laser materials
[DE85-006156] 14 p2261 N85-24013

BERYLLIUM ISOTOPES
NT BERYLLIUM 7
NT BERYLLIUM 9
NT BERYLLIUM 10
Galactic propagation models consistent with the cosmic ray lifetime derived from Be-10 measurements
[OG-4.3-1] 22 p3878 N85-34026

BERYLLIUM OXIDES
Development of the Cascade inertial-confinement-fusion reactor
[DE85-010933] 19 p3357 N85-30812

BERYLLIUM 7
Proposed solar neutrino experiment using (81)Br(nu,e(-e)) (81)Kr
[DE85-004602] 15 p2664 N85-26579

BERYLLIUM 9
Fast-neutron-spectrum measurements for the thick-target (9)Be(d/ = 7 MeV
[DE85-010461] 18 p3183 N85-29735

BERYLLIUM 10
Cosmic rays 10Be biennal data and their relationship to aurorae and sunspots
[SH-7.1-1] 23 p4047 N85-35094

BESSEL FUNCTIONS
Simplified continued fraction calculation of spherical Bessel functions
[AD-A146644] 06 p0858 N85-15455
Some scientific subroutines in LISP
[AD-A147869] 07 p1026 N85-16515
Calculation of roots of transcendental equations in problems of determining thermal conductivity of cylinder with non-uniform boundary conditions
[BLL-M-35788-(5828.4)] 23 p3929 N85-34349

BETA FACTOR
Elimination of stochasticity in stellarators
02 p0282 N85-11839
Limits of possible operation of the R-Tokamak due to ideal MHD instabilities
[IPPJ-694] 06 p0863 N85-15486
Experimental results on Tokamak beta limits from ISX-B
[DE84-015372] 07 p1046 N85-16644
Effects of q and high beta on Tokamak stability
[DE84-016650] 09 p1393 N85-18767
Finite-(beta) optimization of tandem mirrors
[DE85-002658] 10 p1560 N85-19835
Ballooning beta limits of dee and bean shaped Tokamaks
[IPPJ-713] 16 p2866 N85-27676
System and method of operating toroidal magnetic confinement devices
[DE85-011670] 22 p3845 N85-33814
Simulation studies on stability of hot electron plasma
23 p3978 N85-34664
Confinement and heating of high beta plasmas with emphasis on compact toroids
[DE85-011459] 24 p4155 N85-35761
Generalized reduced fluid model with finite ion-gyroradius effects
[DE85-013123] 24 p4157 N85-35777

BETA INTERACTIONS
U WEAK INTERACTIONS (FIELD THEORY)

BETA PARTICLES
Investigation of internal fields and motions, radiation damages and recovery processes using beta and gamma active probe nuclei 03 p0427 N85-12726
High-Beta Tokamak research
[DE84-016470] 04 p0568 N85-13618
Electronic autofluorography: Principles, problems and prospects
[DE84-016698] 05 p0639 N85-14097
Whist code calculations of ignition margin in an ignition Tokamak
[DE85-009507] 18 p3190 N85-29784
Nuclear structure problems in double beta decay
[DE85-010739] 19 p3364 N85-30859
Beta response of selected instruments
[DE85-013278] 22 p3788 N85-33469
Pulsed-neutron-source models for the astrophysical s-process
[DE85-012927] 24 p4151 N85-35740

BETATRONS
Self potentials of an electron ring in a torus for large ring displacement from the minor axis
[AD-A146088] 03 p0421 N85-12691
Non-linear transverse electron beam dynamics in a modified betatron accelerator
[AD-A148106] 08 p1220 N85-17685
Acceleration of an electron ring in a modified betatron with transverse pressure
[AD-A148626] 08 p1221 N85-17688
The plasma assisted modified betatron
[AD-A148728] 09 p1390 N85-18748
Betatron-synchrotron detrapping in a tapered wiggler free electron laser
[AD-A149686] 12 p1856 N85-21642
Resonance between betatron and synchrotron oscillations in a free electron laser: A 3-D numerical study
[AD-A150059] 12 p1857 N85-21645
Modified betatron accelerator studies
[AD-A151420] 15 p2648 N85-26332

BETHE-SALPETER EQUATION
Notes for lectures in China: The Bethe theory of inelastic collisions of fast charged particles with atoms and molecules
[DE84-017487] 09 p1380 N85-18676

BIAS
Fast envelope detector with bias compensation
[AD-D011226] 01 p0038 N85-10243
Aerosol sampling bias from differential electrostatic charge and particle size 02 p0224 N85-11467
Evaluation of thermocouple junction temperature
[DE84-015159] 04 p0502 N85-13206
Blind zones and aspect ratio bias in acquisition of discontinuity orientation data
[DE84-002718] 04 p0533 N85-13410
Treatment and expression of measurement uncertainties 05 p0630 N85-14042
Circuit transients due to negative bias arcs on a high-voltage solar array in low Earth orbit
[NASA-TP-2407] 06 p0760 N85-14858
Coherent array of Josephson oscillators with external bias leads
[AD-D011367] 08 p1156 N85-17293
Improved magnetic bias and delay linearity in a magnetostatic wave delay line
[AD-D011441] 10 p1479 N85-19337
A replication and extension of the inducement of the availability heuristic
[AD-A149755] 12 p1923 N85-22083
Switching mixer
[AD-D011602] 16 p2777 N85-27139

BIBLIOGRAPHIES
Compilation of data sources for existing chemicals
[GSF-A-2/84] 01 p0017 N85-10103
Publications of Center for Manufacturing Engineering (of the National Bureau of Standards), 1978-1983
[PB84-224526] 01 p0036 N85-10228
Bibliography of data on electrical breakdown in gases
[PB84-218049] 01 p0045 N85-10294
Geology and geomorphology of the southern central Blue Ridge: An indexed bibliography
[PB84-225119] 01 p0072 N85-10480
Space medicine and biology, continuing bibliography (supplement 263)
[NASA-SP-7011(263)] 01 p0094 N85-10636
Publications of the exobiology program for 1981: A special bibliography
[NASA-TM-86653] 01 p0099 N85-10657
Publications of the National Bureau of Standards, 1983 catalog
[PB84-218031] 01 p0126 N85-10869
A bibliography of planetary geology and geophysics principal investigators and their associates, 1983 - 1984
[NASA-TM-87361] 01 p0127 N85-10874
The Shock and Vibration Digest, volume 16, no. 8
[AD-A145653] 02 p0208 N85-11372
Bibliography of climate textbooks and studies
[WCP-84] 02 p0231 N85-11505
Aerospace Medicine and Biology, a continuing bibliography with indexes
[NASA-SP-7011(264)] 02 p0234 N85-11525
Engineering Physics Division
[DE84-007778] 02 p0274 N85-11787
Aeronautical Engineering, A Continuing Bibliography With Indexes
[NASA-SP-7037(179)] 03 p0307 N85-11976
Fire research publications, 1983
[PB84-217066] 03 p0343 N85-12208
Spread-spectrum communications
[AD-A148135] 03 p0355 N85-12285
Center for Electronic and Electrical Engineering Technical Progress Bulletin, January - March 1983, no. 2
[PB84-231224] 03 p0360 N85-12308

Bibliography of Soviet laser developments, number 65, May - June 1983
[AD-A146169] 03 p0366 N85-12347

Penetrator/armour interactions: Background to Australian work
[MRL-R-936] 03 p0367 N85-12353

Earth Resources, A Continuing Bibliography with Indexes
[NASA-SP-7041(43)] 03 p0378 N85-12411

Aeronautical Engineering, a continuing bibliography with indexes
[NASA-SP-7037(180)] 04 p0451 N85-12858

A bibliography of publications on corrosion and oxidation from UK government laboratories at Teddington, 1924 - 1983
[NPL-DMA(A)-82] 04 p0472 N85-13004

Bibliography of US patents on augmentation of convective heat and mass transfer, part 2
[DE84-014865] 04 p0496 N85-13178

Aerospace Medicine and Biology, a continuing bibliography with indexes
[NASA-SP-7011(265)] 04 p0545 N85-13467

Space medicine research publications: 1983-1984
[NASA-CR-3860] 04 p0545 N85-13469

FY 1984 scientific and technical reports, articles, papers and presentations
[NASA-TM-86470] 04 p0575 N85-13670

Economic value of consumer information: A selected, annotated bibliography
[PB84-235795] 04 p0576 N85-13673

Carbon dioxide and climate: Summaries of research in FY 1983 and FY 1984
[DE85-001245] 06 p0839 N85-15327

Publications of the Executive Office of the President: January 20, 1981 - June 30, 1984
[PB84-230671] 06 p0871 N85-15533

A summary of the foundation research program
[AD-A146524] 06 p0891 N85-15656

Circulation control: A bibliography of DTNSRDC research and selected outside references: Update
[AD-A146966] 07 p0893 N85-15661

Loads and Aeroelasticity Division research and technology accomplishments for FY 1984 and plans for FY 1985
[NASA-TM-86356] 07 p0898 N85-15691

Optics of solids (surface related) and effect of surface roughness on MOS
[AD-A148883] 07 p0948 N85-15996

Earth science investigations in the United States Antarctic Research Program (USARP)
[PB84-240506] 07 p0990 N85-16268

Aeronautical Engineering: A continuing bibliography with indexes (supplement 182)
[NASA-SP-7037(182)] 08 p1067 N85-16758

Bibliography update on the California current system and related mesoscale ocean modeling
[AD-A148546] 08 p1190 N85-17503

Bibliography of venomous and poisonous marine animals and their toxins
[AD-A148409] 08 p1192 N85-17514

Aerospace medicine and biology: A continuing bibliography with indexes
[NASA-SP-7011(266)] 08 p1194 N85-17525

Aerospace medicine and biology: A continuing bibliography with indexes, supplement 268
[NASA-SP-7011(268)] 08 p1194 N85-17526

Software test handbook: Software test guidebook, volume 2
[AD-A147289] 08 p1204 N85-17578

Bibliography of adaptive control
[OUEL-1544/84] 08 p1209 N85-17602

Scientific and technical information output of the Langley Research Center for calendar year 1984
[NASA-TM-86336] 08 p1229 N85-17740

Aeronautical engineering, a continuing bibliography with indexes
[NASA-SP-7037(181)] 09 p1263 N85-17932

Brief outline of analytic stability studies of magnetically insulated systems — bibliolographies
[DE85-000212] 09 p1393 N85-18765

Bibliography of unclassified reports, FY 1984
[AD-A148836] 09 p1401 N85-18819

Aeronautical engineering: A continuing bibliography with indexes
[NASA-SP-7037(184)] 10 p1419 N85-18949

Bibliography of Soviet laser developments, Number 66, July-August 1983
[AD-A149113] 10 p1490 N85-19406

Laser Hazards Bibliography, October 1984
[AD-A149534] 10 p1490 N85-19408

Earth resources: A continuing bibliography with indexes
[NASA-SP-7041(44)] 10 p1503 N85-19484

Aerospace medicine and biology: A continuing bibliography with indexes
[NASA-SP-7011(269)] 10 p1526 N85-19628

Post-processing of bibliographic citations from DOE/Recon, NASA/Recon, and DOD/DROLS
[DE85-000517] 11 p1739 N85-20938

Sourcebook: Gaining access to US government information on the environment and natural resources
[DE84-017419] 11 p1740 N85-20941

Metrology for Electronic Technology: A bibliography of NBS (National Bureau of Standards)
[PB85-112895] 12 p1830 N85-21486

Choice reaction time and color: An annotated bibliography
[AD-A149722] 12 p1908 N85-21979

Cumulutive reports and publications through December 31, 1984
[NASA-CR-172569] 12 p1911 N85-21991

Bibliography of atomic and molecular processes, 1983
[DE85-000662] 12 p1929 N85-22121

Compiled and thermodynamic data sources for aqueous and biochemical systems: An annotated bibliography, 1930 - 1983
[PB85-137693] 12 p1944 N85-22208

Bibliography of Lewis Research Center technical publications announced in 1983
[NASA-TM-83693] 12 p1951 N85-22255

List of RAE (Royal Aircraft Establishment) translations issued during the period 1 March 1983 - 31 March 1984
[AD-A149787] 12 p1951 N85-22257

Aeronautical Engineering: A continuing bibliography with indexes, supplement 185
[NASA-SP-7037(185)] 13 p1965 N85-22342

Aeronautical Engineering: A cumulative index to the 1984 issues of the continuing bibliography
[NASA-SP-7037(183)] 13 p1965 N85-22343

Cryogenic wind tunnels: A selected annotated bibliography
[NASA-TM-86346] 13 p1976 N85-22401

Small business innovation research: Abstracts of 1984. Phase 1 awards
[NASA-TM-87427] 13 p2165 N85-23431

NASA Patent Abstracts Bibliography. A continuing bibliography. Section 2: Indexes
[NASA-SP-7039(26)] 13 p2167 N85-23445

Aeronautical engineering, a continuing bibliography with indexes
[NASA-SP-7037(186)] 14 p2207 N85-23682

JP-8 and JP-5 as compression ignition engine fuel
[AD-A150796] 14 p2263 N85-24022

Probalistic analysis of combinatorial algorithms: An annotated bibliography
[CWI-OS-R8411] 14 p2411 N85-24864

Technology for large space systems: A bibliography with indexes, supplement 11
[NASA-SP-7046(11)] 15 p2475 N85-25277

Microwave tubes: Literature survey no. 5 comprising year 1983
[FOA-C-30377-E] 15 p2550 N85-25739

Bibliography of Soviet Laser Developments, Number 67, September-October 1983
[AD-A151199] 15 p2562 N85-25805

Aerospace Medicine and Biology: A continuing bibliography with indexes
[NASA-SP-7011(270)] 15 p2615 N85-26114

Human factors department 1981 publications
[BAE-BT-12685] 15 p2620 N85-26147

Management: A bibliography for NASA managers
[NASA-SP-7500(19)] 15 p2664 N85-26439

List of serials indexed for online users, 1985
[PB85-143220] 15 p2666 N85-26455

The biological effects of radiofrequency radiation
16 p2775 N85-27131

A bibliography of reports of the Sandia solar thermal distributed receiver systems project
[SAND-84-0313] 16 p2817 N85-27378

Review and annotated bibliography of benthic studies in coastal and estuarine areas of Florida with a selected compilation of worldwide benthic methodological references and southeastern United States benthic taxonomic references
[PB85-151041] 16 p2822 N85-27405

Aerospace medicine and biology: A continuing bibliography with indexes, supplement 271, May 1985
[NASA-SP-7011(271)] 16 p2840 N85-27514

Compilation of abstracts of theses submitted by candidates for degrees
[AD-A151722] 16 p2875 N85-27739

Documents of the JPL Photovoltaics Program Analysis and Integration Center: An annotated bibliography
[NASA-CR-175873] 17 p2985 N85-28448

COSMIC Software Catalog, 1985 edition
[NASA-CR-174070] 17 p3010 N85-28606

Design issues in video disc map display
[AD-A153531] 18 p3109 N85-29253

Earth Resources: A continuing bibliography with indexes, issue 45
[NASA-SP-7041(45)] 18 p3123 N85-29336

Data base of all known, published data on trace elements in oil shale and its products
[DE85-003399] 18 p3126 N85-29357

SERI photovoltaic advanced research and development project: FY 1984 accomplishments
[DE85-002939] 18 p3128 N85-29368

Fuel cells: A bibliography
[DE85-004585] 18 p3128 N85-29371

Publications of the Jet Propulsion Laboratory 1983
[NASA-CR-175979] 18 p3199 N85-29848

Aeronautical Engineering: A continuing bibliography with indexes (supplement 188)
[NASA-SP-7037(188)] 19 p3211 N85-29910

Aeronautical Engineering: A continuing bibliography with indexes
[NASA-SP-7037(187)] 19 p3211 N85-29911

Multiaxial fatigue and fracture: A literature review
[ARL/STRUC-R-410] 19 p3285 N85-30370

Publications of the NASA CELSS (Controlled Ecological Life Support Systems) program
[NASA-CR-3911] 19 p3326 N85-30608

Aerospace Medicine and Biology: A continuing bibliography with indexes (supplement 272)
[NASA-SP-7011(272)] 19 p3328 N85-30620

A theoretical study of electron capture in ion-ion and ion-atom collisions
[DE85-011154] 19 p3362 N85-30842

Human factors engineering data sources; an overview
[FOA-C-56044-H2] 20 p3513 N85-31637

Atomic, Molecular and Solid-State Theory, and Computational Quantum Chemistry, part 1
[DE85-009401] 20 p3526 N85-31929

Publications from the Department of Plasma Physics and the Unit of Accelerator Technology, index and abstracts, 1984
[TRITA-EPP-84-13] 20 p3534 N85-31991

Aerospace medicine and biology: A continuing bibliography with indexes, supplement 273
[NASA-SP-7011(273)] 21 p3663 N85-32755

Human performance in continuous/sustained operations and the demands of extended work/rest schedules. An annotated bibliography
[AD-A155619] 21 p3666 N85-32771

A short bibliography of recent developments in selection and ranking procedures
[AD-A155648] 21 p3679 N85-32856

Air Force Office of Scientific Research (AFOSR). Technical report summaries: First quarter (CY)
[AD-A154757] 21 p3713 N85-33041

Aeronautical engineering: A continuing bibliography with indexes (supplement 189)
[NASA-SP-7037(189)] 22 p3727 N85-33104

Military hydrology. Report 9: State-of-the-art review and annotated bibliography of dam-breach flood forecasting
[AD-A155383] 22 p3801 N85-33553

Bibliography and index for nuclear reactions among light charged particles, volume 26
[DE85-011482] 22 p3836 N85-33768

NASA patent abstracts bibliography: A continuing bibliography. Section 1: Abstracts (supplement 27)
[NASA-SP-7039(27)-SECTION-1]
22 p3849 N85-33840

Index of laser program publications and related reports, calendar year 1984
[DE85-011863] 23 p3936 N85-34398

Aerospace Medicine and Biology: A continuing bibliography with indexes (supplement 274)
[NASA-SP-7011(274)] 23 p3952 N85-34491

The next assignment: The state of the literature on space 23 p4057 N85-35146

Aeronautical engineering: A continuing bibliography with indexes, supplement 190
[NASA-SP-7037(190)] 24 p4059 N85-35152

Technology for large space systems: A bibliography with indexes
[NASA-SP-7046(12)] 24 p4068 N85-35209

Bibliography on tidal hydraulics. Report 2. Supplement 9: Supplementary material compiled from June 1980 - June 1983. Tidal flows in rivers and harbors
[AD-A155990] 24 p4125 N85-35574

A research program to reduce the interior noise in general aviation aircraft, index and summary
[NASA-CR-176178] 24 p4145 N85-35695

NASA patent abstracts bibliography, a continuing bibliography. Section 2: Indexes (supplement 27)
[NASA-SP-7039(27)-SECTION-2]
24 p4164 N85-35820

Fire research publications, 1984
[PB85-208502] 24 p4166 N85-35827

BICARBONATES

U CARBONATES

BICRYSTALS

Flux-line pinning by the grain boundary in niobium bicrystals
[DE84-016668] 04 p0570 N85-13638

Characterization of bicrystal grain boundary properties using device structures
[DE84-004509] 06 p0869 N85-15523
BIFURCATION (MATHEMATICS)
U BRANCHING (MATHEMATICS)
BIG BANG COSMOLOGY
Cosmology 07 p1056 N85-16701
Cosmology, galactic astronomy and elementary particle physics 12 p1956 N85-22289
Galaxy formation 12 p1960 N85-22321
Integral constraints on stress energy perturbations in general relativity and applications to cosmology
19 p3383 N85-30985
Charge 4/3 leptons in cosmic rays
[HE-6.2-14] 24 p4212 N85-36150
BIGHORN MOUNTAINS (MT-WY)
Chronologic and climatic control on soil development, northern Bighorn Basin, Wyoming and Montana
08 p1181 N85-17443
BIGHTS
U BAYS (TOPOGRAPHIC FEATURES)
BIHARMONIC EQUATIONS
Numerical treatment of corner singularities of the biharmonic equation
[TUM-M8315] 05 p0717 N85-14602
Multinomial form of the solution of problems of the statistics of elastic rectangular disks
[REPT-17/1984] 16 p2797 N85-27244
BILLETS
The effects of radial yarns, 3-dimensionally reinforced carbon-carbon composite
[AD-A144751] 01 p0022 N85-10134
Modelling temperature changes during hot working operations 06 p0798 N85-15095
Continuous casting of quality steels on billet casters
[BMFT-FB-T-84-262] 18 p3078 N85-29041
BIMETALS
Evaluation of residual stress in laminated metallic composites 11 p1598 N85-20052
Method of constructing diagram of bimetal fatigue failure 11 p1599 N85-20058
Microscopic magnetic structure of multiple bilayers of thin films of Fe and Ge
[DE85-004188] 13 p2024 N85-22682
New process for production of bimetal with corrosion-resistant cladding layer
[BLL-BISI-TRANS-22371-(9022.06)]
17 p2927 N85-28056
Effects of the structural state in thermo-bimetals on their resistance to microscopic plastic deformation
[BLL-BISI-TRANS-22403-(9022.06)]
17 p2979 N85-28412
In situ Moessbauer investigation of bimetallic catalysts on a base: FeRu, FeRh, FePd, FeIr, and FePt on SiO2
[B8563200] 20 p3432 N85-31293
Determination of deformation speed during high-speed deformation of cylindrical shells
[BLL-M-36280-(5828.4)] 20 p3465 N85-31527
Chromium-base powder alloys for welding cladding layer of bimetal
[BLL-M-35776-(5828.4)] 23 p3915 N35-34260
BIMETRIC THEORIES
Fake topological Hilbert spaces and characterizations of dimension in terms of negligibility
[CWI-TRACT-2] 14 p2414 N85-24893
BINARY ALLOYS
Wear properties of rapidly solidified surfaces of a pseudo-binary Fe-TiC alloy 02 p0179 N85-11204
Review: The influence of short circuit diffusion on the oxidation of nickel, chromium and nickel/chromium alloys
[AERE-R-11311] 02 p0185 N85-11237
Low temperature properties of Mo/Mi superlattices
[DE84-014729] 02 p0288 N85-11881
NBS (National Bureau of Standards): Materials measurements
[NASA-CR-174038] 03 p0332 N85-12143
Structure of two-phase titanium alloys with different microstructures 03 p0351 N85-12257
Critical evaluation of binary rare earth phase diagrams
[DE84-015057] 05 p0614 N85-13922
Synergestic sputtering properties of binary alloys
06 p0865 N85-15497
Application of the diffraction model to amorphous magnesium zinc alloys
[AD-A147369] 07 p0928 N85-15883
Phase formation and stability in the pseudobinary Ni3Al-Ni3V alloy system
[DE85-001117] 09 p1296 N85-18143
Synergistic sputtering properties of binary alloys
[DE84-017493] 09 p1297 N85-18148
Research on rapidly solidified alloys
[AD-A149380] 10 p1441 N85-19080
1984 model of binary alloy solidification
[DE85-002497] 11 p1608 N85-20110
Experimental determination of systems suitable for study as monotectic binary metallic alloy solidification models
12 p1948 N85-22235
Models of long-period superstructure
[DE85-007659] 16 p2751 N85-26981
Glassy metals: New highly resistant material
[BLL-BISI-TRANS-21764-(9022.06)]
17 p2926 N85-28049
The structure of carbon martensite analyzed with Moessbauer spectra
[BLL-BISI-TRANS-22402-(9022.06)]
17 p2927 N85-28062
Use of principle of local equilibrium for assessing diffusional supersaturation during solidification of alloys
[BLL-BISI-TRANS-22487-(9022.06)]
17 p2929 N85-28077
Electrical conductivity and phase diagram of binary alloys. 21: The system palladium-chromium
[NASA-TM-77883] 18 p3073 N85-29009
Process for the epitaxial deposition of 3-5 compounds utilizing a binary alloy as the metallic source
[AD-D011683] 18 p3193 N85-29801
MPS solidification model. Analysis and calculation of macrosegregation in a casting ingot
[NASA-CR-171589] 21 p3566 N85-32178
Thermodynamic properties of alloys in the Fe-Ti system
[NPL-DMA(A)-96] 22 p3748 N85-33229
Anti wear property of two phasic metal composite
23 p3906 N85-34199
Enthalpies of formation of liquid Fe-Ce-Si and Fe-Ce-Al three-component alloys
[BLL-M-36296-(5828.4)] 23 p3913 N85-34247
Calculation of activities of components in liquid alloys of iron with yttrium
[BLL-M-35868-(5828.4)] 23 p3914 N85-34253
BINARY CODES
Linear intersecting codes — error correction
[ENST-C-84002] 03 p0356 N85-12291
A very efficient transfer function bounding technique on bit error rate for Viterbi decoded, rate 1/N convolutional codes 05 p0624 N85-13991
On the binary weight distribution of some Reed-Solomon codes
[NASA-CR-174375] 09 p1373 N85-18628
Codes with parity conditions on subsets of coordinates 10 p1465 N85-19247
The ambiguity function of random binary-phase-coded waveforms
[AD-A148906] 10 p1466 N85-19249
Error probability during optimal noncoherent reception of binary signals in multibeam channel
13 p2069 N85-22922
BINARY DATA
Noise tolerance of digital demodulator for complex signal system employing binary quantization
13 p2070 N85-22929
CRAYCDC
[NASA-CR-177374] 24 p4137 N85-35639
CDCCRAY
[NASA-CR-177375] 24 p4137 N85-35640
BINARY DIGITS
Development of new circuit symbols for binary logic elements
[MBB-Z-39/85-O] 17 p3014 N85-28640
Basic features of personal computers
22 p3766 N85-33344
BINARY MIXTURES
NT EUTECTIC ALLOYS
NT EUTECTICS
Thermodynamic properties of isobutane-isopentane mixtures from -40 to +600(0)F and up to 1000 psia
[DE84-015137] 01 p0124 N85-10850
Thermodynamic study of CO2-organic compound interaction at high pressures and temperatures
[DE84-015777] 04 p0573 N85-13654
Theoretical thermodynamics of mixtures at high pressures 13 p2183 N85-23550
Convective instability of horizontal layer of binary mixture 14 p2338 N85-24456
Ca-Ga, Sr-Ga and Ba-Ga binary systems
[DE85-006454] 16 p2751 N85-26980
Experimental and theoretical study of condensation in multicomponent vapors
[DE85-009357] 17 p2923 N85-28021
Response of steam-water mixtures to pressure transients
[DE85-010798] 19 p3267 N85-30262
Transport and relaxation processes in supercritical fluids
[DE85-010554] 19 p3358 N85-30816
Burn front velocity as a function of pellet density in iron-potassium perchlorate heat powders
[DE85-011448] 21 p3572 N85-32214
Relaxation lens in inhomogeneous binary mixture
21 p3695 N85-32957
BINARY STARS
NT CATACLYSMIC VARIABLES
NT COMPANION STARS
NT DWARF NOVAE
NT ECLIPSING BINARY STARS
NT SYMBIOTIC STARS
NT X RAY BINARIES
Variations of the H and K emission lines of singly ionized calcium in the eclipsing binary star system AR Lacertae
02 p0296 N85-11921
RS CV sub n binary systems
[NASA-CR-174164] 04 p0580 N85-13704
The behaviour of brighter binaries and yellow giants in open clusters 05 p0737 N85-14736
The fate of globular clusters 05 p0739 N85-14751
Nonthermal radio emission and the HR diagram
08 p1232 N85-17763
High precision measurement of stellar radial velocity variations 08 p1250 N85-17896
Combined ultraviolet studies of astronomical sources
[NASA-CR-174361] 09 p1413 N85-18910
Radio emission from RS CVn binary systems
09 p1417 N85-18939
A spectroscopic study of LMC X-4
[NASA-CR-174414] 10 p1571 N85-19905
Contributions of the X-ray astronomy group — conference
[MPE-PREPRINT-28] 11 p1741 N85-20947
Search for millisecond rotational periods in some low-mass X-ray binaries observed by EXOSAT
11 p1741 N85-20949
Optical and X-ray observations of 4U2129+47/V1727 CYG in a quiescent state 11 p1742 N85-20950
EXOSAT observations of the galactic bulge X-ray source GX17+2 — X ray binary star 11 p1742 N85-20951
Contributions of the X-ray astronomy group — conference
[MPE-PREPRINT-29] 11 p1742 N85-20952
EXOSAT observations of the 35d intensity variations of Her X-1 — X ray binary source
11 p1742 N85-20956
Pulse phase spectroscopy of Her X-1 with EXOSAT — X ray binary source 11 p1743 N85-20957
Simultaneous EXOSAT and optical observations of the pulsing X-ray binary H2252-035 / AO Psc
11 p1743 N85-20958
Spectral studies of low-mass X-ray binaries observed by EXOSAT 11 p1743 N85-20959
EXOSAT observations of 4U1705-44 — X ray binary
11 p1743 N85-20960
Interacting binary systems 11 p1744 N85-20967
White dwarf stars at ultraviolet wavelengths
11 p1744 N85-20971
Three short-period binaries seen at high-dispersion UX ARI, IOTA TRI and HA5110 11 p1756 N85-21047
Physical models for the UV continua of symbiotic stars
11 p1756 N85-21048
IUE and optical observations of LMC X-ray binaries
11 p1757 N85-21050
Circumstellar material in Algols and Serpentids
11 p1757 N85-21051
MU Sagittarii and Beta Lyrae: Combined IUE/Voyager observations 11 p1757 N85-21052
A search for the spectroscopic binary companions of Polaris using IUE spectra 11 p1757 N85-21053
LSS 2018: A double-lined spectroscopic binary central star with an extremely large reflection effect
[NASA-CR-175503] 11 p1762 N85-21062
Theoretical and observational studies of stellar activity
13 p2171 N85-23468
Offerings of the Astronomical Institute of Bonn
15 p2667 N85-26459
Photoelectric observations of contact binary stars
[REPT-96] 15 p2667 N85-26460
Photoelectric observations of the dwarf nova VW Hydri during the November 1977 supermaximum
[REPT-97] 15 p2667 N85-26461
Stellar surface phenomena: A spectroscopic study of the RS canum venaticorum binaries
15 p2669 N85-26467
A study of W Serpentis binaries: SX Cassiopeiae, RX Cassiopeiae, and W Serpentis 20 p3544 N85-32053
On gamma and neutrino radiation from Cyg X-3
[OG-2.1-7] 22 p3863 N85-33924
Constraints on cosmic-ray observation of Cygnus X-3
[OG-2.2-3] 22 p3864 N85-33930
Hercules X-1: Pulsed gamma-rays detected above 150 GeV
[OG-2.2-9] 22 p3865 N85-33935
Search for gamma ray lines from SS433
[OG-2.4-11] 22 p3868 N85-33955
Observation of gamma-rays from LMC X-4 above 10(16) eV
[OG-2.6-10] 22 p3870 N85-33972

The 4U 0115+63: Another energetic gamma ray binary pulsar
[OG-2.6-11] 22 p3670 N85-33973

BINARY SUMMATORS
U ADDING CIRCUITS

BINARY SYSTEMS (DIGITAL)
U DIGITAL SYSTEMS

BINARY SYSTEMS (MATERIALS)
NT BINARY ALLOYS
NT BINARY MIXTURES
NT EUTECTIC ALLOYS
NT EUTECTICS
High pressure cosmochemistry applied to major planetary interiors: Experimental studies
[NASA-CR-174032] 02 p0302 N85-11958
Structure of two-phase titanium alloys with different microstructures 03 p0351 N85-12257
Possibilities of conjugating binary solutions for thermal energy storage
[DE84-016704] 04 p0531 N85-13392
Photochemistry and kinetics of the O*2-HI system
[AD-A147433] 07 p0971 N85-16167
Characterization and selection of polymer materials for binary munitions storage. Part 2: Characterization of LLDPE resins
[AD-A148324] 08 p1133 N85-17144
Investigation of foam flotation and phase partitioning techniques 12 p1945 N85-22216
Microstructural characteristics during the controlled solidification of a binary system
[DE85-005200] 15 p2507 N85-25461

BINAURAL HEARING
Psychological and physiological basis of stereophonic effect 15 p2526 N85-25574

BINDERS (ADHESIVES)
U ADHESIVES

BINDERS (MATERIALS)
NT PROPELLANT BINDERS
NT SOLID ROCKET BINDERS
Effects of surface interactions and mechanical properties of PBXs (plastic bonded explosives) on explosive sensitivity
[AD-A146368] 06 p0773 N85-14944
Structure and property formation mechanism in magnetite alloy-binder composite
10 p1444 N85-19103
Polymer blends as high explosive binders
[DE85-001210] 11 p1611 N85-20131
Development and study of two-matrix glass fiber composite with increased transverse deformation
13 p2027 N85-22700

BINDING
Universal binding energy relations in metallic adhesion
[NASA-TM-86889] 03 p0331 N85-12132
CO adsorption on (111) and (100) surfaces of the Pt sub 3 Ti alloy. Evidence for parallel binding and strong activation of CO
[NASA-CR-176077] 21 p3565 N85-32176
Improved flow cytometer measurement of binding assays
[DE85-006407] 23 p3935 N85-34390

BINOCULAR VISION
Binocular overlap in a fiber optic helmet mounted display
[AD-P004331] 09 p1270 N85-17965

BINOMIAL COEFFICIENTS
On the quadratic mean radius of a polynomial in Cz
[AD-A149189] 10 p1546 N85-19751

BINOMIALS
Empirical Bayes rules for selecting good binomial populations
[AD-A147614] 08 p1214 N85-17646
Statistical analysis techniques for small sample sizes
[NASA-CR-171872] 15 p2639 N85-26279

BIOASSAY
Response of algal populations to changes in stream water quality
[PB84-202464] 01 p0070 N85-10465
Molecular interactions of high energy fuels and jet fuels with oncogenic viruses and endogenous viruses
[AD-A145484] 02 p0188 N85-11255
Alterations in skeletal muscle with disuse atrophy
[NASA-CR-174195] 06 p0843 N85-15349
X-ray holography of biological specimens
[DE85-002437] 10 p1489 N85-19398
New techniques for studying calcium gradients
15 p2609 N85-26076
An in vitro method for the screening of trichothecene mycotoxin cytotoxicity and the study of mycotoxin countermeasures
[AD-A153863] 18 p3152 N85-29517
Flow cytometry for health monitoring in space
[DE85-009572] 19 p3329 N85-30625
Development of a recombinant DNA assay system for the detection of genetic change in astronauts cells
[DE85-010103] 20 p3504 N85-31781
Investigation of variation in the concentration of bacteria in outdoor testing, with the use of a detector for aerosols of bacteria
[FOA-C-40201-B2] 20 p3504 N85-31784
Marine environmental quality assessment program, five-year plan (FY 1984 - 1988)
[AD-A154715] 21 p3613 N85-32459
Current internal-dosimetry practices at US Department of Energy facilities
[DE85-011718] 22 p3787 N85-33486
Applications of holography to X-ray imaging
[DE85-010984] 23 p3934 N85-34384

BIOASTRONAUTICS
USSR report: Space Biology and Aerospace Medicine, volume 18, no. 4, July - August 1984
[JPRS-USB-84-006] 01 p0091 N85-10611
USSR report: Space Biology and Aerospace Medicine, volume 18, no. 6, November - December 1984
[JPRS-USB-85-002] 12 p1900 N85-21931
External respiration, gas exchange and energy expenditures of man in weightlessness
12 p1900 N85-21932
Blood amino acids of cosmonauts before and after 211-day spaceflight 12 p1900 N85-21933
Circadian rhythm of human body temperature during spaceflights 12 p1901 N85-21934
Biochemical status of adrenocortical dysfunction following spaceflight 12 p1901 N85-21935
Comparative analysis of effects of weightlessness and its models on velocity and strength properties and tone of human skeletal muscles 12 p1901 N85-21936
Cosmonauts' blood plasma free amino acid levels during preflight training 12 p1901 N85-21937
Plasmodium of myxomycete as research object in gravitational biology 15 p2483 N85-25327
Aerospace Medicine and Biology: A continuing bibliography with indexes
[NASA-SP-7011(270)] 15 p2615 N85-26114
Research opportunities in loss of red blood cell mass in space flight
[NASA-CR-175808] 16 p2841 N85-27517
The cosmic history of the biogenic elements and compounds
[NASA-SP-476] 17 p3003 N85-28562
Spatial orientation in weightlessness and readaptation to Earth's gravity 20 p3509 N85-31811
Study of the cardiovascular system in microgravity: Results and perspectives 20 p3509 N85-31816
Hydroponics developments for spaceship garden
21 p3663 N85-32754
Aerospace medicine and biology: A continuing bibliography with indexes, supplement 273
[NASA-SP-7011(273)] 21 p3663 N85-32755
USSR report: Space Biology and Aerospace Medicine, vol. 19, no. 3, May - June 1985
[JPRS-USB-85-005] 23 p3952 N85-34494
Proceedings of a Scientic Meeting on the Occasion of the Inauguration of New Buildings for the DFVLR Institute for Aerospace Medicine
[ESA-TT-857] 24 p4129 N85-35595
The research programme of the Institute for Aerospace Medicine 24 p4129 N85-35596

BIOCHEMICAL OXYGEN DEMAND
Results of study of hypoxia problems
04 p0544 N85-13462
The effect of an unphysiological oxygen supply on the organism 24 p4130 N85-35605

BIOCHEMISTRY
NT BACTERIOLOGY
NT BIOGEOCHEMISTRY
NT PHYSIOCHEMISTRY
In vivo dermal absorption method and system for laboratory animals
[AD-D011231] 01 p0094 N85-10635
Lagging development of biotechnology described
01 p0115 N85-10787
East Europe report: Science and technology
[JPRS-ESA-84-038] 03 p0343 N85-12210
Architecture of dermatophyte cell Walls: Electron microscopic and biochemical analysis
[NASA-TM-77441] 03 p0399 N85-12546
USSR report: Chemistry
[JPRS-UCH-84-012] 06 p0761 N85-14865
Structure and functions of fungal cell surfaces
[NASA-TM-77439] 06 p0842 N85-15347
The structure and function of fungal cells
[NASA-TM-77443] 06 p0842 N85-15348
Alterations in skeletal muscle with disuse atrophy
[NASA-CR-174195] 06 p0843 N85-15349
Chemistry and metabolism of delayed neurotoxic organophosphorus esters
[AD-P004023] 06 p0844 N85-15357
Biochemistry and pathogenic hypotheses of organophosphorus-induced delayed neurotoxicity
[AD-P004026] 06 p0844 N85-15360
Biocatalyzed processes for production of commodity chemicals: Assessment of future research advances for N-butanol production
[NASA-CR-174264] 07 p0919 N85-15819
USSR report: Life sciences. Biomedical and behavioral sciences
[JPRS-UBB-84-015] 07 p1010 N85-16416
Biochemical evaluation of bodily influence of high and low temperatures 07 p1014 N85-16441
USSR report: Life sciences. Biomedical and behavioral sciences
[JPRS-UBB-85-002] 09 p1360 N85-18559
Aluminum in biogenic cycle and forms of its occurence in ocean 10 p1499 N85-19463
Bioelectrochemistry 2: Membrane phenomena
[AD-A149132] 10 p1522 N85-19602
USSR report: Life sciences. Biomedical and behavioral sciences
[JPRS-UBB-85-010] 11 p1690 N85-20628
Characteristics of human masseter under conditions of hypokinesia 11 p1691 N85-20630
Effects of hypothermia on brain metabolism
11 p1692 N85-20636
A double blind comparative trial of powdered ginger root, hyosine hydrobromide, and cinnarizine in the prophylaxis of motion sickness induced by cross coupled stimulation
11 p1695 N85-20657
Multiple regression method used to assess animal adaptation to hypoxic hypoxia 12 p1902 N85-21947
Parameters of carbohydrate metabolism and blood serum enzyme activity after short-term spaceflights
12 p1903 N85-21951
Compiled and thermodynamic data sources for aqueous and biochemical systems: An annotated bibliography, 1930 - 1983
[PB85-137693] 12 p1944 N85-22209
International Conference on Coordination Chemistry (23rd) held at Boulder, Colorado on 29 July - 3 August, 1984
[AD-A150960] 14 p2252 N85-23956
NMR imaging and spectroscopy of the mammalian central nervous system after heavy ion radiation
[DE85-004509] 14 p2386 N85-24696
USSR report: Life sciences. Biomedical and behavioral sciences
[JPRS-UBB-85-012] 14 p2386 N85-24697
Abstracts of the 36th Southeastern Regional Meeting of the American Chemical Society
[AD-A151506] 15 p2496 N85-25394
Use and disuse and the control of acetylcholinesterase activity in fast and slow twitch muscle of rat
[NASA-CR-175717] 15 p2614 N85-26109
Experiments in microwave exposure in the rat: Body temperature, serum chemistry and the use of chemical restraint
[PB85-156834] 16 p2840 N85-27512
Academician Ovchinnikov on future of bioorganic chemistry 17 p3049 N85-28874
Diet of first Soviet expedition on Mount Everest
19 p3323 N85-30596
Investigation of biochemical and psychological parameters of air traffic controllers in prestart state before beginning to work 19 p3325 N85-30599
Biocatalysis project
[NASA-CR-176044] 20 p3498 N85-31744
Kidney cell electrophoresis, continuing task
20 p3498 N85-31747
USSR report: Life sciences. Biomedical and behavioral sciences
[JPRS-UBB-85-017] 20 p3504 N85-31785
Marine environmental quality assessment program, five-year plan (FY 1984 - 1988)
[AD-A154715] 21 p3613 N85-32459
Interaction of opiate and phencyclidine derivatives with the acetylcholine receptor
[AD-A155119] 21 p3664 N85-32761
The composition of the primitive atmosphere and the synthesis of organic compounds on the early Earth
21 p3717 N85-33065
USSR report: Life sciences. Biomedical and behavioral sciences
[JPRS-UBB-85-018] 22 p3819 N85-33660
Improved flow cytometer measurement of binding assays
[DE85-006407] 23 p3935 N85-34390
Anaerobic microbial transformations in subsurface environments: Project description
[DE85-012789] 23 p3951 N85-34496
USSR report: Space Biology and Aerospace Medicine, vol. 19, no. 3, May - June 1985
[JPRS-USB-85-005] 23 p3952 N85-34494
Microbiological and biochemical studies towards optimization of substrate utilization by methanogenic bacteria
[PB85-168332] 24 p4084 N85-35310

BIOCLIMATOLOGY
U BIOMETEOROLOGY
BIOCONTROL SYSTEMS
Effects of external loads on human head movement control systems 05 p0707 N85-14534
Factors determining effectiveness of voluntary decrease in ventilation during muscular work using instrumented feedback 08 p1193 N85-17520
Airsickness control using biofeedback to self-regulate psychophysiological responses
[AD-A151167] 15 p2617 N85-26128
BLSS: A contribution to future life support
18 p3155 N85-29534
Advanced regenerative environmental control and life support systems: Air and water regeneration
18 p3155 N85-29535
Atmosphere behavior in gas-closed mouse-algal systems: An experimental and modelling study
18 p3155 N85-29536
CELSS transportation analysis
18 p3156 N85-29538
BIOCONVERSION
Cultivation and conversion of marine macroalgae — biomass energy production
[DE84-004522] 04 p0544 N85-13464
Current alternative energy research and development in Illinois
[PB85-163137] 16 p2820 N85-27397
Screening Prosopis (mesquite) species for biofuel production on semi-arid lands
[DE85-010048] 19 p3302 N85-30471
Biomass thermochemical conversion program
[DE85-011867] 21 p3572 N85-32213
Aerobic sulfur-oxidizing bacteria: Environmental selection and diversification 21 p3656 N85-32712
Distribution and abundance of organic thiols
21 p3657 N85-32717
Cytochromes and iron sulfur proteins in sulfur metabolism of phototrophic bacteria
21 p3657 N85-32718
Seventh Symposium on Biotechnology for Fuels and Chemicals: Program and abstracts
[DE85-011197] 22 p3742 N85-33192
Pacific Northwest and Alaska bioenergy program glossary
[DE85-011740] 22 p3808 N85-33591
Microbiological and biochemical studies towards optimization of substrate utilization by methanogenic bacteria
[PB85-188332] 24 p4084 N85-35310
BIODEGRADATION
Denitrification-efficiencies of alternate carbon sources
[AD-A148029] 08 p1119 N85-17050
Anaerobic microbial transformations in subsurface environments
[DE85-012790] 22 p3819 N85-33659
Two dimensional CO2-ocean model including the biological processes
[DE85-012341] 23 p3950 N85-34463
Biodegradation of jet fuel by aquatic microbial communities
[PB85-191971] 24 p4084 N85-35311
BIODYNAMICS
Multi-property modeling of the marine biosphere in relation to global climate and carbon cycles
05 p0678 N85-14355
Twentieth Annual Conference on Manual Control, volume 1
[NASA-CP-2341-VOL-1] 05 p0699 N85-14487
New uses for sensitivity analysis: How different movement tasks effect limb model parameter sensitivity
05 p0706 N85-14529
Suppression of biodynamic interference by adaptive filtering 05 p0706 N85-14530
Active sticks: A new dimension in controller design
05 p0706 N85-14531
An analysis of kinetic response variability
05 p0707 N85-14533
Effects of external loads on human head movement control systems 05 p0707 N85-14534
Interaction between lung mechanics and gas exchange by low volume high frequency pulmonary ventilation in patients with respiratory failure
[AD-A146604] 06 p0846 N85-15372
Biodynamic resistant control stick
[AD-D011380] 07 p0904 N85-15721
Unsteady separated flows: Generation and use by insects
[AD-P004168] 09 p1266 N85-17953
Biomechanical studies of impact acceleration research
[AD-A149077] 10 p1522 N85-19601
Biomechanics finds practical applications in aerospace research 11 p1621 N85-20205
Biotechnology in Japan
[PB85-169464] 15 p2615 N85-26113
Stabilizing force feedback in bio-actuated control systems
[AD-D011634] 17 p3002 N85-28560
USSR report: Space Biology and Aerospace Medicine, vol. 19, no. 3, May - June 1985
[JPRS-USB-85-005] 23 p3952 N85-34494
Using dynamic analysis to animate articulated bodies such as humans and robots 23 p3959 N85-34537
BIOELECTRIC POTENTIAL
Change in relationship of biopotentials of brain zones for various levels of working capacity
07 p1013 N85-16438
Specifics of dynamics of brain biopotentials under the influence of complex audible communicative signals
07 p1014 N85-16440
BIOELECTRICITY
Interactions between electromagnetic fields
[AD-A153796] 18 p3091 N85-29129
Changes in the impedance and bioelectrical activity of the cerebral cortex of rats under the action of anaesthetic drugs
[HSE-TRANS-10371] 19 p3327 N85-30617
Physical chemical state of water in living cells
[AD-A154566] 21 p3662 N85-32749
BIOENGINEERING
NT ANTHROPOMETRY
NT BALLISTOCARDIOGRAPHY
NT BIOINSTRUMENTATION
NT BIOMETRICS
NT BODY MEASUREMENT (BIOLOGY)
NT CARDIOGRAPHY
NT ECHOCARDIOGRAPHY
NT ELECTROCARDIOGRAPHY
NT ELECTROENCEPHALOGRAPHY
NT ELECTROMYOGRAPHY
NT PLETHYSMOGRAPHY
China report: Science and technology
[JPRS-CST-84-025] 11 p1620 N85-20197
Research in environmental biology reviewed
11 p1622 N85-20211
A communications link for an implantable electrode array
[AD-A152238] 16 p2840 N85-27510
Bioengineering and rehabilitation: Windows of opportunity past, present and future
[NASA-EP-216] 16 p2841 N85-27516
Applications of aerospace technology in biology and medicine
[NASA-CR-166100] 19 p3328 N85-30619
Seventh Symposium on Biotechnology for Fuels and Chemicals: Program and abstracts
[DE85-011197] 22 p3742 N85-33192
BIOFEEDBACK
NT SENSORY FEEDBACK
Factors determining effectiveness of voluntary decrease in ventilation during muscular work using instrumented feedback 08 p1193 N85-17520
Biofeedback treatment of airsickness: A review
11 p1696 N85-20660
Airsickness control using biofeedback to self-regulate psychophysiological responses
[AD-A151167] 15 p2617 N85-26128
Biofeedback and performance: An update
[AD-A153228] 17 p3001 N85-28553
Stabilizing force feedback in bio-actuated control systems
[AD-D011634] 17 p3002 N85-28560
BIOGENESIS
U BIOLOGICAL EVOLUTION
BIOGENY
Aluminum in biogenic cycle and forms of its occurence in ocean 10 p1499 N85-19463
BIOGEOCHEMISTRY
The Interaction of Global Biochemical Cycles
[NASA-CR-174184] 05 p0652 N85-14183
Biogeochemical cycles: Interactions in global metabolism 05 p0652 N85-14184
Global biogeochemical cycles: Studies of interaction and change, some views on the strategy of approach
05 p0652 N85-14185
Assessment of Techniques for Measuring Tropospheric H sub x O sub y: Summary 05 p0675 N85-14337
Deforestation, floodplain dynamics, and carbon biogeochemistry in the Amazon Basin
08 p1144 N85-17216
Environmental Sciences Division report
[DE85-010452] 19 p3308 N85-30506
Biogeochemical cycling and remote sensing
21 p3659 N85-32733
Phototrophic bacteria and their role in the biogeochemical sulfur cycle 21 p3660 N85-32735
Isotopic Biogeochemistry
[NASA-CR-176128] 22 p3741 N85-33189
BIOGRAPHY
For the sacred air space of our motherland; an interview with our country's famous aircraft designer, Lu Hsiao-Peng
[AD-A146291] 03 p0309 N85-11997
East Europe report: Scientific affairs, no. 791
[JPRS-84624] 03 p0341 N85-12195
Fr. Angelo Secchi, a pioneer in the study of solar-terrestrial relationships 04 p0519 N85-13312
Harold Hazen and the theory and design of servomechanism
[RR-270] 22 p3794 N85-33506
BIOINSTRUMENTATION
NT IMPLANTED ELECTRODES (BIOLOGY)
Clinical measurements using fiber optics and optrodes
[DE84-015043] 05 p0696 N85-14481
A biological sensor for the detection of toxicants
[AD-D011304] 07 p0967 N85-16141
Spirolit-2 instrument used to test pulmonary ventilation
12 p1903 N85-21950
The audiomat: An automatic audiometer for use in occupational audiometry
[DRIC-T-7138] 13 p2142 N85-23294
A communications link for an implantable electrode array
[AD-A152238] 16 p2840 N85-27510
Development of an EM-Based lifeform detector
[AD-A153504] 18 p3151 N85-29512
Chemoreception and detection of micropollutants by means of a telemetric bionic detector
[DRIC-T-7460] 22 p3810 N85-33600
BIOLOGICAL ACTIVITY
U ACTIVITY (BIOLOGY)
BIOLOGICAL ANALYSIS
U BIOASSAY
BIOLOGICAL CELLS
U CELLS (BIOLOGY)
BIOLOGICAL CLOCKS
U RHYTHM (BIOLOGY)
BIOLOGICAL EFFECTS
NT JET LAG
Ecology of estuarine channels of the pacific northwest coast: A community profile
[PB84-209709] 01 p0070 N85-10464
A study of fatigue of shiftworkers in air traffic control and weather service groups in JASDF
01 p0090 N85-10610
Effect of spaceflight factors on rat bone marrow cells
01 p0092 N85-10620
Effect of short-term hypokinesia on rat opioid system reaction 01 p0093 N85-10625
Reaction of cerebral ventricles to antiorthostatic position and occlusion of jugular veins 01 p0093 N85-10626
Effect of maximum physical load on oxygen-transport properties of blood 01 p0093 N85-10627
Effect of hyperoxia and increased gas atmosphere density on contractile function of the right ventricle
01 p0093 N85-10628
Change in energetics of muscular contraction as a result of hyperoxia 01 p0093 N85-10629
Hemodynamics and neurodynamics of the human brain during exposure to moderate hypoxic hypoxia
01 p0094 N85-10630
Space medicine and biology, continuing bibliography (supplement 263)
[NASA-SP-7011(263)] 01 p0094 N85-10636
Proton pumping in purple membrane, appendix 1
[DE84-014601] 01 p0118 N85-10811
Aerospace Medicine and Biology, a continuing bibliography with indexes
[NASA-SP-7011(264)] 02 p0234 N85-11525
The case for concern about very low frequency fields from visual display terminals: The need for further research and shielding of VDTs
[CCOHS-P83-2E] 02 p0234 N85-11526
Electrical parameters in 60-Hz biological exposure systems and their measurement: A primer
[PB84-217793] 03 p0400 N85-12548
Field/cell interaction model
[DE84-011914] 04 p0544 N85-13465
A survey of space biology and space medicine
[ESA-BR-17] 04 p0545 N85-13466
Aerospace Medicine and Biology, a continuing bibliography with indexes
[NASA-SP-7011(265)] 04 p0545 N85-13467
Acid rain and tree physiology: Some hypotheses for observed changes in forest productivity
[DE84-016568] 05 p0672 N85-14318
Report of the Meeting of Experts on Climate and Human Health
[WCP-78] 05 p0687 N85-14413
Organization of the session 05 p0687 N85-14414
Introduction to human biometeorology
05 p0687 N85-14415

Difficulties encountered in determining the potential involvement of consultants on health problems in various climatic zones 05 p0687 N85-14416
Epidemiologic methods applied to the study of the relationship between climate and human health
05 p0687 N85-14418
USSR report: Life sciences. Biomedical and behavioral sciences
[JPRS-UBB-84-027] 07 p1012 N85-16426
Distinctions of SPF rats used in experiments aboard biosatellites 07 p1012 N85-16427
Effect of microwave radiation on local blood circulation and oxygenation of brain tissue
07 p1012 N85-16431
Something in the air at Windscale — radioactive contaminants from the Sellafield nuclear Complex for reprocessing and storing irradiated fuel
[BLL-RISLEY-TR-4998-(9091.9F)]
08 p1179 N85-17429
Aerospace medicine and biology: A continuing bibliography with indexes
[NASA-SP-7011(266)] 08 p1194 N85-17525
Aerospace medicine and biology: A continuing bibliography with indexes, supplement 268
[NASA-SP-7011(268)] 08 p1194 N85-17526
Genetic effects of microwave exposure on mammalian cells in vitro, volume 2
[AD-A149347] 10 p1523 N85-19603
USSR report: Life sciences. Biomedical and behavioral sciences
[JPRS-UBB-85-008] 10 p1523 N85-19605
Aerospace medicine and biology: A continuing bibliography with indexes
[NASA-SP-7011(269)] 10 p1526 N85-19628
Effects of electromagnetic fields produced by high voltage transmission lines
[DE85-900034] 11 p1625 N85-20230
Laboratory tests of motion sickness susceptibility
11 p1694 N85-20648
Effects of air pollution and acid rain on forest decline
[GPO-37-459] 12 p1883 N85-21818
Summary report of the Workshop on Structure Activity Concepts in Environmental Sciences
[PB85-137339] 12 p1887 N85-21841
Biological effects on radiofrequency radiation
[PB85-120848] 12 p1900 N85-21930
USSR report: Space Biology and Aerospace Medicine, volume 18, no. 6, November - December 1984
[JPRS-USB-85-002] 12 p1900 N85-21931
Biological effects of blast and impact waves
[FOA-C-52006-H4-D7] 12 p1906 N85-21968
Interaction of metals and metalloids with biomembranes
[DE85-004902] 13 p2141 N85-23293
Nationwide Urban Runoff Project, Champaign, Illinois: The biological impact of urban runoff on the Saline Branch Drainage Ditch and Boneyard Creek
[PB85-150274] 14 p2348 N85-24515
Photoreactivation and other ultraviolet/visible light effects on DNA in human skin
[DE85-005135] 14 p2390 N85-24719
Psychobiology and food perception
14 p2394 N85-24745
The interaction of calcium and auxin in the gravitropic response of roots 15 p2606 N85-26062
The effects of simulated weightlessness on susceptibility to viral and bacterial infections using a murine model
15 p2613 N85-26100
Aerospace Medicine and Biology: A continuing bibliography with indexes
[NASA-SP-7011(270)] 15 p2615 N85-26114
The Impact of Proposed Radio Frequency Radiation Standards on Military Operations
[AGARD-LS-138] 16 p2775 N85-27128
The physical interactions of radiofrequency radiation fields and biological systems 16 p2775 N85-27129
The biological effects of radiofrequency radiation
16 p2775 N85-27131
The cumulative effects of long term exposure to low levels of radiofrequency radiation (RFR)
16 p2776 N85-27132
The medical results of human exposures to radio frequency radiation 16 p2776 N85-27133
Review of epidemiological studies of human exposures to radiofrequency radiation 16 p2776 N85-27134
Evaluation of human exposures to low frequency fields 16 p2776 N85-27135
Development and application of new radiofrequency radiation safety standards 16 p2777 N85-27137
Interactive effects of acid rain and gaseous air pollutants on natural terrestrial vegetation
[DE85-005255] 16 p2821 N85-27401
Aerospace medicine and biology: A continuing bibliography with indexes, supplement 271, May 1985
[NASA-SP-7011(271)] 16 p2840 N85-27514
Biological influences of low-frequency sinusoidal electromagnetic signals alone and superimposed on RF carrier waves
[PB85-161248] 16 p2842 N85-27527
Photosynthetic acclimation of Acer saccharum
[DE85-008247] 17 p2998 N85-28536
Biological and human health effects of extremely low frequency electromagnetic fields. Post-1977 literature review
[AD-A152731] 17 p2999 N85-28539
The cosmic history of the biogenic elements and compounds
[NASA-SP-476] 17 p3003 N85-28562
Investigation of biochemical and psychological parameters of air traffic controllers in prestart state before beginning to work 19 p3325 N85-30599
Metabolic mechanisms of plant growth at low water potentials 19 p3327 N85-30612
Aerospace Medicine and Biology: A continuing bibliography with indexes (supplement 272)
[NASA-SP-7011(272)] 19 p3328 N85-30620
A systems analysis of the erythropoietic responses to weightlessness. Volume 1: Mathematical model simulations of the erythropoietic responses to weightlessness
[NASA-CR-171890] 20 p3506 N85-31794
Zinc: Biological effects. Facts and fiction
[USIP-84-12] 20 p3507 N85-31798
Nordic Association for Aerosol Research (NOSA) Aerosol Symposium: Program and abstracts
[FOA-E-40019] 22 p3812 N85-33616
Antihypertensive neutral lipid
[DE85-011625] 22 p3819 N85-33656
Microdosimetric spectra measurements of JANUS neutrons
[DE85-012108] 22 p3843 N85-33801
Ocean thermal energy conversion
[DE85-012291] 23 p3946 N85-34456
Aerospace Medicine and Biology: A continuing bibliography with indexes (supplement 274)
[NASA-SP-7011(274)] 23 p3952 N85-34491
Effect of seeds of heavy charged particles of galactic cosmic radiation 23 p3954 N85-34505
Electromagnetic compatibility conference features biological interactions
[AD-A155813] 24 p4144 N85-35692

BIOLOGICAL EVOLUTION
NT ABIOGENESIS
Impact phenomena as factors in the evolution of the Earth
[NASA-CR-174015] 01 p0072 N85-10474
Influence of simulated weightlessness on the motility of the acellular slime mold Physarum polycephalum
05 p0689 N85-14430
Observation of the contractile vacuolar system of Paramecium caudatum on the fast running clinostat
05 p0689 N85-14431
Development and maturation of the neuromuscular junciton in cell culture under conditions of simulated zero-gravity 15 p2611 N85-26093
Effects of simulated weightlessness on mammalian development. Part 2: Meiotic maturation of mouse oocytes during clinostat rotation 15 p2612 N85-26094
ONR (Office of Naval Research) Far East Scientific Bulletin, Volume 9, Number 4, October-December 1984
[AD-A151274] 15 p2665 N85-26448
Organization of the R region in maize
[DE85-011273] 20 p3504 N85-31780
Origin of life 21 p3657 N85-32713
Protocyanobacteria: Oxygenic and Anoxygenic photosynthesis in mat-forming bacteria
21 p3657 N85-32714
Insights into the phylogenetic positions of photosynthetic bacteria obtained from 5S rRNA and 16S rRNA sequence data 21 p3658 N85-32719
Search for the universal ancestors
[NASA-SP-477] 21 p3667 N85-32777
Submarine hydrothermal environments as sites for the origin and evolution of life 21 p3719 N85-33074
Biological modulation of planetary atmospheres: The early Earth scenario 22 p3854 N85-33867
NASA Developmental Biology Workshop: A summary
[NASA-TM-86756] 24 p4126 N85-35578
Effects of microgravity and hypergravity on invertebrate development 24 p4126 N85-35579
Vertebrate development in space: Gravity is a drag (and has been for eons and eons) 24 p4126 N85-35580
Report of the NASA Mammalian Developmental Biology Working Group 24 p4126 N85-35581
Report of the Avian Development Working Group
24 p4127 N85-35582
Report of Amphibian Development Group
24 p4127 N85-35583
Report of the Insect Development Group
24 p4127 N85-35584
Aquatic Invertebrate Development Working Group
24 p4127 N85-355
Report of the Microbial Development Working Group
24 p4127 N85-355

BIOLOGICAL MODELS
U BIONICS

BIOLOGICAL MODELS (MATHEMATICS)
Mathematical Models of the Circadian Sleep-Wak Cycle
[AD-A145712] 02 p0235 N85-115
A mathematical model of visual perception regardin peripheral vision and its application to the Hermann' illusion 04 p0483 N85-130
Multi-property modeling of the marine biosphere i relation to global climate and carbon cycles
05 p0678 N85-1435
Inverse modelling to obtain head movement controll signal 05 p0705 N85-1452
A control model: Interpretation of Fitts' law
05 p0706 N85-1452
New uses for sensitivity analysis: How differen movement tasks effect limb model parameter sensitivity
05 p0706 N85-1452
The growth and composition of supercritical branchin populations on general type spaces
[CTH-MATH-1984-18] 05 p0721 N85-1463
Hollings hungry mantid model for the invertebrat functional response considered as a Markov process. Pa 3: Mathematical elaborations
[CWI-AM-R8407-PT-3] 05 p0722 N85-1463
Control and modeling of a CELSS (Controlled Ecologic Life Support System)
[NASA-CR-177324] 07 p1020 N85-164
Close air support mission: Development of a unitar measure of pilot performance
[AD-A149285] 11 p1697 N85-206
Artificial Intelligence and Bionics Workshop held a Stowe, Vermont on 11-15 June 1984
[AD-A150463] 13 p2149 N85-233
The dynamical behavior of the age-size-distribution o a cell population
[CWI-AM-R8414] 17 p2998 N85-285
Stability and feasibility of model ecosystems
[PREPRINT-431] 18 p3134 N85-294
An integrated analysis of the physiological effects o space flight: Executive summary
[NASA-CR-171892] 20 p3506 N85-317
Mathematical analysis of heart rhythm assessment o distinctive features in adaptation to spacefligh conditions 22 p3733 N85-331
Tritium hazard via the ingestion pathway
[DE85-012697] 24 p4133 N85-356

BIOLOGICAL RHYTHM
U RHYTHM (BIOLOGY)

BIOLOGY
Applications of aerospace technology in biology an medicine
[NASA-CR-165872] 02 p0234 N85-115
East Europe report: Science and technology
[JPRS-ESA-84-038] 03 p0343 N85-122
Achievements in biology outlined
03 p0343 N85-122
Abstracts of papers submitted in 1983 for publicatio
[PB84-217579] 03 p0398 N85-125
Overview of German microgravity activities in the fie of life science 05 p0696 N85-144
Aerospace Medicine and Biology: A continuin bibliography with indexes, supplement 267, Januar 1985
[NASA-SP-7011(267)] 12 p1904 N85-219
Biology and Medicine Division
[DE85-010638] 19 p3327 N85-306
USSR Space Life Sciences Digest
[NASA-CR-3922] 21 p3656 N85-327

BIOLUMINESCENCE
Bio-optical variability in the Alboran Sea as assesse by Nimbus-7 coastal zone color scanner
[AD-A147909] 07 p0989 N85-162
Luminescence in the ocean
[AD-B089136L] 13 p2140 N85-232
Seasonal variability and spatial non-uniformity bioluminescence in the Mediterranean Sea
[DRIC-T-7545] 24 p4125 N85-355
Background light measurements at the DUMAND s
[HE-5.2-7] 24 p4203 N85-360
Measurements of light background at large depth in t ocean
[HE-5.2-8] 24 p4203 N85-360

BIOMAGNETISM
Mammalian tissue sensitivity to long-term exposure high-intensity stationary magnetic fields
22 p3823 N85-33

BIOMASS
The Marine Resources Experiment Program (MARE
[NASA-TM-87368] 01 p0086 N85-10

Modeling effects of toxicants on aquatic systems
[DE84-016694] 04 p0531 N85-13396
Biomass thermochemical conversion program
[DE84-017177] 05 p0621 N85-13972
Ethanol production by enzymatic hydrolysis: Parametric analysis of a base-case process
[DE84-013105] 11 p1614 N85-20147
Alternative anodic reactions in water splitting
[DE85-004159] 12 p1802 N85-21300
Anaerobic digestion of biomass: status summary and research development needs, 1983
[PB85-161925] 13 p2040 N85-22772
Remote sensing of coastal wetlands biomass using Thematic Mapper wavebands — Lewes, Delaware
13 p2119 N85-23198
The impact ejection of living organisms into space
15 p2682 N85-26566
Flash pyrolysis of biomass with reactive and non-reactive gases
[DE85-010962] 19 p3306 N85-30496
Chemical composition of Musca domestica L. larval and pupal biomass when developing in organic waste of biological life-support system for man
22 p3824 N85-33691

BIOMASS ENERGY PRODUCTION
Prospectus of the utilization of leafy spurge (Euphorbia Esula L.) as a source of liquid fuel and biomass
[DE84-015203] 01 p0034 N85-10208
Bench-scale research in biomass direct liquefaction
[DE84-011881] 02 p0223 N85-11460
Construction of a bacterium to convert cellulose to ethanol
[TI84-901639] 04 p0481 N85-13068
Cultivation and conversion of marine macroalgae — biomass energy production
[DE84-004522] 04 p0544 N85-13464
Alcohol fuel from Ohio farms: An introduction
[TI-84-901290] 05 p0621 N85-13970
Versatility of peat emphasized
07 p0994 N85-16316
Developments in the production and use of ethanol fuels
[GPO-40-678] 12 p1817 N85-21398
Alcohol Fuels Program technical review, spring 1984
[DE85-002919] 17 p2938 N85-28134
Renewable technologies program summaries
[DE85-001509] 19 p3307 N85-30500
Uniform cost-estimation method for biomass production and conversion technologies
[DE85-011714] 19 p3380 N85-30970
Biomass thermochemical conversion program
[DE85-011867] 21 p3572 N85-32213
Pacific Northwest and Alaska bioenergy program glossary
[DE85-011740] 22 p3808 N85-33591

BIOMECHANICS
U BIODYNAMICS

BIOMEDICAL DATA
An optically isolated amplifier
[CSIR-SR-ELEK-257] 01 p0049 N85-10321
Potential use of dialogue with computers in biomedical research 01 p0091 N85-10614
Applications of aerospace technology in biology and medicine
[NASA-CR-165872] 02 p0234 N85-11521
USSR report: Life Sciences: Biomedical and behavioral sciences
[JPRS-UBB-84-026] 04 p0543 N85-13457
Space adaptation syndrome: Incidence and operational implications for the space transportation system program
11 p1695 N85-20655
Analysis of head motion during simulated, rough water operation of a 2200 ton surface effect ship
11 p1695 N85-20656
Research and technology activities at Ames Research Center's Biomedical Research Division
[NASA-TM-86692] 12 p1899 N85-21925
Introduction: The clinical and biomedical evaluation for trauma and fatalities associated with aircrew ejection and crash 12 p1906 N85-21970
Development and diffusion of automated clinical chemistry analyzers
[PB85-150696] 15 p2561 N85-25798
Chemicals identified in human biological media, a data base. Volume 6, part 2: Records 7586-8694
[DE85-008767] 18 p3154 N85-29528
Zinc: Biological effects. Facts and fiction
[USIP-84-12] 20 p3507 N85-31798
USSR report: Life sciences. Biomedical and behavioral sciences
[JPRS-UBB-85-021] 23 p3951 N85-34489

BIOMETEOROLOGY
Bibliography of climate textbooks and studies
[WCP-84] 02 p0231 N85-11505
Introduction to human biometeorology
05 p0687 N85-14415

Ecological impacts of hydroelectric projects in Amazonia 07 p1003 N85-16374

BIOMETRICS
NT ANTHROPOMETRY
NT BALLISTOCARDIOGRAPHY
NT BODY MEASUREMENT (BIOLOGY)
NT CARDIOGRAPHY
NT ECHOCARDIOGRAPHY
NT ELECTROCARDIOGRAPHY
NT ELECTROENCEPHALOGRAPHY
NT ELECTROMYOGRAPHY
NT PLETHYSMOGRAPHY
Applications of aerospace technology in biology and medicine
[NASA-CR-165872] 02 p0234 N85-11521

BIONICS
USSR report: Life sciences. Biomedical and behavioral sciences
[JPRS-UBB-84-025] 04 p0543 N85-13453
Applications of connectionist modeling techniques to simulations of motor control systems
05 p0717 N85-14598
Eyes for computers 07 p1012 N85-16428
Artificial Intelligence and Bionics Workshop held at Stowe, Vermont on 11-15 June 1984
[AD-A150463] 13 p2149 N85-23339
A detailed analysis of the erythropoietic control system in the human, squirrel, monkey, rat and mouse
[NASA-CR-171879] 15 p2614 N85-26107
Analysis of head-down tilt as an analog of weightlessness using a mathematical simulation model
[NASA-CR-171870] 15 p2616 N85-26118
Simulation of a G-tolerance curve using the pulsatile cardiovascular model
[NASA-CR-171873] 15 p2616 N85-26120
Description, validation, and modification of the Guyton model for space-flight applications. Part A. Guyton model of circulatory, fluid and electrolyte control. Part B. Modification of the Guyton model for circulatory, fluid and electrolyte control
[NASA-CR-171876] 15 p2616 N85-26122
Distributed memory
[AD-A153364] 17 p3001 N85-28554
Numerical estimation of the curvature of biological surfaces 17 p3006 N85-28588
Verbal information processing paradigms: A review of theory and methods
[AD-A153229] 17 p3050 N85-28880
Organization of the R region in maize
[DE85-011273] 20 p3504 N85-31780
USSR report: Life sciences. Biomedical and behavioral sciences
[JPRS-UBB-85-017] 20 p3504 N85-31785
USSR report: Life sciences. Biomedical and behavioral sciences
[JPRS-UBB-85-020] 21 p3663 N85-32752
Tritium hazard via the ingestion pathway
[DE85-012897] 24 p4133 N85-35618

BIOPHYSICS
NT HEALTH PHYSICS
NT PUBLIC HEALTH
Change in relationship of biopotentials of brain zones for various levels of working capacity
07 p1013 N85-16438
Workshop on membrane biophysics
[AD-A148238] 08 p1192 N85-17512
Radiation physics, biophysics, and radiation biology
[DE84-014885] 09 p1360 N85-18557
Bioelectrochemistry 2: Membrane phenomena
[AD-A149132] 10 p1522 N85-19602
Biophysical evaluation of the wet globe temperature index (Botsball) at high air movements and constant dew point temperature
[AD-A151065] 14 p2378 N85-24683
USSR report: Life sciences. Biomedical and behavioral sciences
[JPRS-UBB-85-012] 14 p2386 N85-24697
Current approaches for the biophysical and physiological evaluation of combat clothing for environmental extremes
[AD-A151012] 14 p2395 N85-24752
Plant growth biophysics: The basis for growth asymmetry induced by gravity 15 p2611 N85-26089
Computerized biophysical data acquisition system for motion sickness studies
[AD-A151691] 15 p2618 N85-26131
Evaluation of human exposures to low frequency fields 16 p2776 N85-27135
Biology and Medicine Division
[DE85-010638] 19 p3327 N85-30613
USSR report: Life sciences. Biomedical and behavioral sciences
[JPRS-UBB-85-017] 20 p3504 N85-31785
Zinc: Biological effects. Facts and fiction
[USIP-84-12] 20 p3507 N85-31798

USSR report: Life sciences. Biomedical and behavioral sciences
[JPRS-UBB-85-018] 22 p3819 N85-33660

BIOPROCESSING
Second Symposium on Space Industrialization — space commercialization
[NASA-CP-2313] 02 p0149 N85-11011
Opportunities for space bioprocessing
02 p0150 N85-11018
Bioprocessing in space 05 p0690 N85-14438
Current concepts and future directions of CELSS
18 p3155 N85-29532

BIOREGENERATION
U REGENERATION (PHYSIOLOGY)

BIOREGENERATIVE LIFE SUPPORT SYSTEMS
U CLOSED ECOLOGICAL SYSTEMS

BIOSATELLITES
Plasmodium of myxomycete as research object in gravitational biology 15 p2483 N85-25327
General description of experiment dealing with rat ontogenesis aboard Cosmos-1514 biosatellite
22 p3822 N85-33679

BIOSENSORS
U BIOINSTRUMENTATION

BIOSIMULATION
U BIONICS

BIOSPHERE
International Geosphere/Biosphere Program: 1984
[GPO-39-222] 04 p0578 N85-13691
Multi-property modeling of the marine biosphere in relation to global climate and carbon cycles
05 p0678 N85-14355
Magmas as selective filters of volatiles between planetary mantles and surfaces
13 p2185 N85-23557
Comet showers and Nemesis, the death star
[DE85-003736] 15 p2683 N85-26575
Mathematical model of global processes in the biosphere 19 p3295 N85-30431
Carbon isotope geochemistry and geobiology
21 p3657 N85-32716

BIOSYNTHESIS
Bioprocessing in space 05 p0690 N85-14438
Nitrogen control of photosynthetic protein synthesis
[DE85-003513] 11 p1690 N85-20623
Effects of hypothermia on brain metabolism
11 p1692 N85-20636
The role of sulfur in osmoregulation and salinity tolerance in cyanobacteria, algae, and plants
21 p3660 N85-32736
Isotopic Biogeochemistry
[NASA-CR-176128] 22 p3741 N85-33189
Production of liquid fuels and chemicals by microalgae
[DE85-006780] 22 p3819 N85-33658
Genetic and physiological control of protective antigen synthesis by bacillus anthracis
[AD-A156324] 24 p4133 N85-35617

BIOTECHNOLOGY
East Europe report: Science and technology
[JPRS-ESA-84-029] 01 p0115 N85-10783
Lagging development of biotechnology described
01 p0115 N85-10787
Opportunities for space bioprocessing
02 p0150 N85-11018
Applications of aerospace technology in biology and medicine
[NASA-CR-165872] 02 p0234 N85-11521
USSR report: Life sciences. Biomedical and behavioral sciences
[JPRS-UBB-84-025] 04 p0543 N85-13453
Outlook for expanding the Federal research in progress system
[AD-A148354] 08 p1229 N85-17737
West Europe report: Science and technology
[JPRS-WST-85-004] 10 p1460 N85-19204
Functional system theory in practice
11 p1690 N85-20629
Laser welding in the manufacture of heart pacemakers
14 p2308 N85-24286
USSR report: Life sciences. Biomedical and behavioral sciences
[JPRS-UBB-85-012] 14 p2386 N85-24697
Complex program of ergonomic studies Pilot described 14 p2386 N85-24698
West Europe report: Science and technology
[JPRS-WST-84-007] 15 p2530 N85-25600
Bioenergy, solar biotech research in France, Europe
15 p2536 N85-25646
Biotechnology in Japan
[PB85-169464] 15 p2615 N85-26113
Progress, goals in biotechnology summarized
17 p2945 N85-28182
Applications of aerospace technology in biology and medicine
[NASA-CR-166100] 19 p3328 N85-30619

West Europe report: Science and technology
[JPRS-WST-85-020] 20 p3436 N85-31333
USSR report: Life sciences. Biomedical and behavioral sciences
[JPRS-UBB-85-017] 20 p3504 N85-31785
East Europe report: Science and technology
[JPRS-ESA-85-023] 21 p3572 N85-32217
USSR report: Life sciences. Biomedical and behavioral sciences
[JPRS-UBB-85-020] 21 p3663 N85-32752
Air force technical objective document, Aerospace Medical Division, Fiscal Year 1986
[AD-A155195] 21 p3664 N85-32762
Seventh Symposium on Biotechnology for Fuels and Chemicals: Program and abstracts
[DE85-011197] 22 p3742 N85-33192

BIOTITE
The mineralogy of global magnetic anomalies
[E85-10061] 07 p0987 N85-16272

BIPLANES
Study of winglets applied to biplanes
[NASA-TM-86350] 08 p1083 N85-16862

BIPOLAR TRANSISTORS
Microwave susceptibility experiments
[DE84-016188] 02 p0192 N85-11281
Trends in development of bipolar power transistors
06 p0793 N85-15072
High-speed power devices with field control
06 p0794 N85-15073
Development of a planar heterojunction bipolar transistor for very high speed logic
[AD-A150374] 13 p2064 N85-22895
Improved, cheaper SIPMOS circuits no. 10, 1983 p 370 15 p2534 N85-25630
High voltage lateral power transisters: Theory and design 19 p3257 N85-30194
Evaluation of semiconductor devices for Electric and Hybrid Vehicle (EHV) ac-drive applications, volume 2
[NASA-CR-176103] 22 p3759 N85-33294
Realization and linearization of a hyperfrequency power amplifier implemented with bipolar transistors in class C polarization — microwave amplifiers
[CNES-NT-114] 23 p3928 N85-34346

BIPOLARITY
Advanced nickel-hydrogen cell configuration study
[NASA-CR-174775] 01 p0067 N85-10444
Bipolar molecular outflows: T Tauri stars and Herbig-Haro objects 03 p0446 N85-12637
Quasi-three dimensional modeling of functionally-integrated elements of large-scale integrated circuits 04 p0490 N85-13122
Analysis of dynamic characteristics and ways of development of bipolar main memory with miniaturization of integrated circuit elements 04 p0490 N85-13123
Deer control using 7 strand vertical fence
11 p1581 N85-19958
Drift fields and boundary conditions at grain boundaries in bipolar P/N junction silicon devices
13 p2062 N85-22879
Recent developments 15 p2533 N85-25628
Life cycle test results of a bipolar nickel hydrogen battery
[NASA-TM-87046] 19 p3304 N85-30480
Computer simulation of integrated injection logic
22 p3767 N85-33349
Acoustic detection of air shower cores
[HE-7.1-4] 24 p4213 N85-36158

BIPROPELLANTS
U LIQUID ROCKET PROPELLANTS

BIRD-AIRCRAFT COLLISIONS
A study of bird ingestions into large high bypass ratio turbine aircraft engines
[DOE/FAA/CT-84/13] 01 p0005 N85-10028
A bird strike handbook for base-level managers
[AD-A147928] 07 p0948 N85-16008
Evaluation of the birdstrike threat to the F-15 present fleet, rapid deployment force, and dual role fighter transparencies
[AD-A148954] 10 p1421 N85-18966
Wildlife Hazards to Aircraft Conference and Training Workshop: Proceedings
[AD-A148330] 11 p1578 N85-19938
Birds and aviation
[AD-P004177] 11 p1578 N85-19939
Avoiding serious bird strike incidents
[AD-P004178] 11 p1578 N85-19940
Don't fowl out
[AD-P004179] 11 p1578 N85-19941
Accidents and serious incidents to civil aircraft due to birstrikes
[AD-P004180] 11 p1578 N85-19942
Analysis of bird strikes reported by European airlines, 1976 - 1980
[AD-P004181] 11 p1578 N85-19943
1983 Air Force bird strikes
[AD-P004182] 11 p1579 N85-19944
Worldwide birdstrike statistics of Lufthansa German Airlines
[AD-P004183] 11 p1579 N85-19945
Birds and aircraft engine strike rates
[AD-P004184] 11 p1579 N85-19946
Review of engine ingestions to wide body transport aircraft
[AD-P004185] 11 p1579 N85-19947
Aircraft transparency bird impact analysis using the MAGNA computer program
[AD-P004186] 11 p1579 N85-19948
Bird impact evaluation of the F/RF-4 transparency system 11 p1579 N85-19949
Microscopic identification of feathers in order to improve birdstrike statistics
[AD-P004187] 11 p1579 N85-19950
The use of small mobile radars to detect, monitor, and quantify bird movements
[AD-P004188] 11 p1580 N85-19951
On the altitudinal distribution of birds and bird strikes in the Netherlands
[AD-P004189] 11 p1580 N85-19952
Blackbirds and starlings: Population ecology and habits related to airport environments
[AD-P004190] 11 p1580 N85-19953
Cattle Egret hazard assessment
[AD-P004191] 11 p1580 N85-19954
Birds on airports: The reason for their presence
11 p1580 N85-19955
The use of falconry as mean to persuade the birds to stay out of the airport vicinity 11 p1580 N85-19956
Landscape management on airports for reduction of bird populations
[AD-P004194] 11 p1581 N85-19960
FAA policy regarding solid waste disposal facilities
[AD-P004196] 11 p1581 N85-19963
Airport bird hazards associated with solid waste disposal facilities
[AD-P004197] 11 p1581 N85-19964
Successful control of gulls and other birds at a sanitary landfill
[AD-P004198] 11 p1582 N85-19965
Bird Strike Committee Europe
[AD-P004207] 11 p1583 N85-19974
Birds and airport agriculture in the conterminous United States: A review of literature
[AD-P004208] 11 p1583 N85-19975

BIRDS
A study of bird ingestions into large high bypass ratio turbine aircraft engines
[DOE/FAA/CT-84/13] 01 p0005 N85-10028
Aircraft transparency bird impact analysis using the MAGNA computer program
[AD-P004186] 11 p1579 N85-19948
Bird impact evaluation of the F/RF-4 transparency system 11 p1579 N85-19949
Microscopic identification of feathers in order to improve birdstrike statistics
[AD-P004187] 11 p1579 N85-19950
The use of small mobile radars to detect, monitor, and quantify bird movements
[AD-P004188] 11 p1580 N85-19951
On the altitudinal distribution of birds and bird strikes in the Netherlands
[AD-P004189] 11 p1580 N85-19952
Blackbirds and starlings: Population ecology and habits related to airport environments
[AD-P004190] 11 p1580 N85-19953
Cattle Egret hazard assessment
[AD-P004191] 11 p1580 N85-19954
Birds on airports: The reason for their presence
11 p1580 N85-19955
The use of falconry as mean to persuade the birds to stay out of the airport vicinity 11 p1580 N85-19956
Airport site selection and design
[AD-P004193] 11 p1581 N85-19959
Reducing gull use of some attractions near airports
[AD-P004195] 11 p1581 N85-19962
Effectiveness of an overhead wire barrier in deterring gulls from feeding at a sanitary landfill
[AD-P004199] 11 p1582 N85-19966
Effectiveness of an overhead wire barrier system in reducing gull use at the BFI Jedburg sanitary landfill, Berkeley and Dorchester counties, South Carolina
[AD-P004200] 11 p1582 N85-19967
Evaluation of effectiveness of bird scaring operations at a sanitary landfill site near CFB Trenton, Ontario, Canada
[AD-P004201] 11 p1582 N85-19968
Development of bird hazard reduction for airport operational safety
[AD-P004202] 11 p1582 N85-19969
The bird strike situation and its ecological background in the Copenhagen Airport, Kastrup
[AD-P004203] 11 p1582 N85-19970
Bird control program Orlando International Airport
[AD-P004204] 11 p1583 N85-19971
Staff assistance to bases for bird hazards
[AD-P004205] 11 p1583 N85-19972
Bird strike avoidance system for Dover AFB, Delaware
[AD-P004206] 11 p1583 N85-19973
Birds and airport agriculture in the conterminous United States: A review of literature
[AD-P004208] 11 p1583 N85-19975
The potential of the NEXRAD radar system for warning of bird hazards
[AD-P004210] 11 p1583 N85-19977
Report of the Avian Development Working Group
24 p4127 N85-35582

BIREFRINGENCE
Investigating compression failure mechanisms in composite laminates with a transparent fiberglass-epoxy birefringent materials
[NASA-TM-86306] 02 p0170 N85-11137
Polarization transformation by single-mode fibers — optical fibers
[FI-452-TBR-59] 11 p1729 N85-20876
Incident beam polarization for laser Doppler velocimetry employing a sapphire cylindrical window
[NASA-TM-87064] 17 p3037 N85-28786
An evaluation and preparation of ferromagnetic liquid composites for use at millimeter wavelengths
[AD-A153939] 18 p3069 N85-28980
Fiber optic sensors operating at dc
[AD-D011674] 19 p3271 N85-30283
Combustion control with smart sensors
[DE85-009419] 19 p3274 N85-30303

BIREFRINGENT FILTERS
Stokes parameters modulator for birefringent filters
18 p3205 N85-29684
Multichannel birefringent filter
18 p3206 N85-29688

BISMUTH
The growth of metastable peritectic compounds
[NASA-CR-171290] 07 p0920 N85-15825
SPAR X technical report for experiment 76-22 directional solidification of magnetic composites
[NASA-CR-171271] 07 p0927 N85-15880
Use of alternative solvents for low-temperature LPE growth of CdTe films
[AD-A149418] 10 p1562 N85-19853
Electrical resistance measurements of metals to 40 GPa in the diamond cell
[DE85-001009] 11 p1629 N85-20262
Topics in optical materials and device research, 3: Volume 1
[AD-A149726] 12 p1933 N85-22145

BISMUTH ALLOYS
Directional solidification studies of Pb-Bi peritectic alloys
[DE84-015656] 04 p0474 N85-13016
Atomistic studies of grain boundaries with segregated impurities
[DE85-000063] 11 p1737 N85-20924
Directional solidification of an eutectic Bi-MnBi alloy
[BLL-M-36270-(5828.4)] 20 p3430 N85-31275

BISMUTH COMPOUNDS
NT BISMUTH OXIDES
Shuttle flight test of an advanced gamma-ray detection system
[AD-A150316] 13 p1988 N85-22469
Improvements in the energy resolution and high-count-rate performance of bismuth germanate
[DE85-010763] 19 p3240 N85-30092
Bismuth germanate scintillators: Applications in nuclear safeguards and health physics
[DE85-010730] 19 p3365 N85-30865

BISMUTH OXIDES
Recent progress in BGO development for high resolution calorimetry
[MPI-PAE/EXP-E1-129] 01 p0124 N85-10848

BISTABLE AMPLIFIERS
U FLIP-FLOPS

BISTABLE CIRCUITS
Optically bistable devices using semiconductor materials
[AD-A149551] 11 p1628 N85-20253

BISTATIC RADAR
U MULTISTATIC RADAR

BISTATIC REFLECTIVITY
Influence of refraction effects on informativeness of bistatic acoustical atmospheric sounding systems
06 p0825 N85-15237
The effects of soil moisture on bistatic clutter power
[AD-A147636] 08 p1150 N85-17261

BIT ERROR RATE
A very efficient transfer function bounding technique on bit error rate for Viterbi decoded, rate 1/N convolutional codes 05 p0624 N85-13991
TDRSS S-shuttle unique receiver equipment
08 p1100 N85-16951

Modeling techniques used in the communications link analysis and simulation system (CLASS)
08 p1100 N85-16953
Validation of the communications link analysis and simulation system (CLASS) 08 p1100 N85-16954
Further results on rate 1/N convolutional code constructions with minimum required SNR criterion
10 p1464 N85-19235
The impact of propagation effects on the design of high capacity digital microwave links in the 18 GHz frequency band 10 p1470 N85-19278
An error generator to support the trials of the ZODIAC prototype system — raster links
[PHL-1984-71] 14 p2293 N85-24216
Bit error rate of coherent M-ary PSK
16 p2770 N85-27098
Phase locked loop synchronization for direct detection optical PPM communication systems
[NASA-CR-176026] 19 p3254 N85-30176
Study of a limited band signal transmission chain
[CNES-CT/DRT/TIT/TR-83/221]
20 p3442 N85-31361
Necessary bandwidth and spectral properties of digital modulation
[PB85-185387] 24 p4088 N85-35340

BIT SYNCHRONIZATION
Detection and symbol synchronization for multiple-bit per photon optical communications
10 p1463 N85-19228
Design criteria for limited scan antennas at digital microwave line of sight links 10 p1471 N85-19284
Distributed elections in a ring of processors using Archimedean time
[CWI-CS-R8416] 17 p3016 N85-28653

BITERNARY CODE
Converters of sum/difference of codes to frequency
15 p2526 N85-25578
Construction of complementary code sequence sets, part 7.1D 21 p3625 N85-32523

BITS
Floating-point function generation routines for 16-bit microcomputers
[NASA-TM-83783] 01 p0102 N85-10683
Basic features of personal computers
22 p3766 N85-33344

BITUMENS
A study of bituminous pavements to determine a correlation between pavement structure designs and tripping of asphalt cement
[PB84-217751] 01 p0037 N85-10231
Skid resistance of bituminous surfaces in Ohio
[PB84-234491] 04 p0484 N85-13086
Geology and resources of the Tar Sand Triangle, southeastern Utah
[DE84-012017] 05 p0677 N85-14346
Immobilization of toxic waste by embedding it in bitumen
[OEFZS-4277] 07 p0995 N85-16322
Field validation of statistically-based acceptance plan for bituminous airport pavements. Volume 1: Correlation analysis of Marshall properties of laboratory-compacted specimens
[FAA-PM-84-12-VOL-1] 12 p1781 N85-21180
Field validation of statistically-based acceptance plan for bituminous airport pavements. Volume 2: Statistical analysis of Marshall properties of plant-produced bituminous materials
[FAA-PM-84-12-VOL-2] 12 p1781 N85-21181
Field validation of statistically-based acceptance plan for bituminous airport pavements. Volume 3: Statistical analysis of 3 methods for determining maximum specific gravity of bituminous concrete mixtures
[FAA-PM-84-12-VOL-3] 12 p1781 N85-21182
Field validation of statistically-based acceptance plan for bituminous airport pavements. Volume 5: Summary of validation studies
[FAA-PM-84-12-VOL-5] 12 p1782 N85-21184
Stress-relieving interlayers for bituminous resurfacings
[PB85-136885] 12 p1820 N85-21415
Study of acceptance criteria for joint densities in bituminous airport pavements
[FAA-PM-85-5] 16 p2715 N85-26761

BIVARIATE ANALYSIS
Bayesian analysis of item response curves
[AD-A145627] 02 p0254 N85-11665
A variable span smoother
[AD-A148241] 08 p1215 N85-17655
Exact simultaneous confidence intervals for pairwise comparisons of three normal means
[AD-A148751] 09 p1375 N85-18645
Some qualitative properties of bivariate Euler-Frobenius polynomials
[AD-A149408] 10 p1547 N85-19755
Scrawl plots, and letter and bletter strips
[DE85-001409] 11 p1707 N85-20739
Approximation order from certain spaces of smooth bivariate splines on a 3-direction mesh
[AD-A149633] 12 p1925 N85-22092

BL LACERTAE OBJECTS
Far-infrared photometry of compact extragalactic sources: OJ 187 and BL Lac
[NASA-TM-86022] 04 p0580 N85-13701
X-ray and ultraviolet observations of BL Lacertae objects 05 p0741 N85-14767
X-ray and UV Emission from Active Galactic Nuclei — conference
[MPE-184] 08 p1236 N85-17790
BL Lacertae objects: Multifrequency observations and model applications 08 p1236 N85-17792
The extragalactic nature of H0323+022
08 p1237 N85-17802
Soft X-ray emission from BL Lac objects
08 p1239 N85-17810
X-ray emission from PKS 2155-304 — BL Lac object
08 p1239 N85-17812
One to eight month X-ray light curves for active extragalactic objects 08 p1239 N85-17817
On the surface density of X-ray selected BL Lacertae objects 08 p1240 N85-17822
On the broadband energy spectra of quasars and BL Lac objects 08 p1240 N85-17825
Multifrequency observations of BL LAC objects and violently variable quasars 11 p1746 N85-20981
Very recent IUE observations of 2 BL lacertae objects
11 p1746 N85-20982
Coordinated multifrequency observations of the BL LAC objects MRK 180, MRK 421, and MRK 501
11 p1746 N85-20983
X-ray emission from active galactic nuclei
[NASA-TM-86175] 11 p1763 N85-21088

BLACK AND WHITE PHOTOGRAPHY
Metric camera experiment: Spacelab 1 mission
05 p0658 N85-14229
Some nonatlas work at the European Southern Observatory (ESO) Sky Atlas Laboratory — astronomical photography 07 p0964 N85-16117

BLACK BODY RADIATION
Microwave blackbodies for spaceborne receivers
[NASA-CR-175647] 13 p2094 N85-23068
Measurement of the large-scale anisotropy of the cosmic background radiation at 3 MM 13 p2206 N85-23680
Scaling blackbody laser to high powers
[NASA-TM-86395] 14 p2309 N85-24292
Theoretical studies of solar-pumped lasers
[NASA-CR-175801] 16 p2789 N85-27206
Stable density stratification solar pond
[NASA-CASE-NPO-15419-2] 19 p3303 N85-30474
Self-study manual on optical radiation measurements. Part 1: Concepts. Chapter 12: Blackbodies, blackbody radiation, and temperature scales
[PB85-195303] 24 p4154 N85-35754

BLACK HOLES (ASTRONOMY)
Gravitational vacuum 02 p0265 N85-11734
Topics in black-hole physics: Geometric constraints on noncollapsing, gravitating systems, and tidal distortions of a Schwarzschild black hole 05 p0742 N85-14769
Some aspects of active galactic nuclei
07 p1056 N85-16702
Shock acceleration in active galactic nuclei and quasars 08 p1241 N85-17828
On the hydrodynamical equations of astrophysical jets — active galactic nuclei 08 p1241 N85-17831
Thermal convection and magnetic fields in accretion disks of black holes 12 p1955 N85-22285
Numberical simulation of the effects of radially injected barium plasma in the ionosphere
[NASA-CR-175638] 14 p2354 N85-24542
Gravitational effects in theories with interacting fields: Two studies 15 p2663 N85-26435
A numerical study of nonspherical black hole accretion 16 p2881 N85-27780
Activities report of the Institute of Astronomy
20 p3545 N85-32059
Comments on RS-17 X-ray telescope
22 p3731 N85-33132
Breakdown of helium nuclei in matter processed near black holes
[OG-8.2-20] 23 p4021 N85-34916
High energy cosmic ray signature of quark nuggets
[HE-6.2-11] 24 p4212 N85-36147

BLACK SEA
Black Sea coastal frontogenesis
01 p0075 N85-10500
Manganese in recent sediments of Ukrainian SSR Black Sea shelf 06 p0819 N85-15200
Hydrologic characteristics of the Mediterranean and Black Sea 07 p0981 N85-16228
Electromagnetic field of currents and its use to estimate total conductivity of sedimentary deposits in Western Black Sea 14 p2334 N85-24434
Sea water photoluminescence
19 p3292 N85-30415
Temporal variations of Rn222 concentrations in Black Sea coastal zone 19 p3293 N85-30417

BLACKOUT (PHYSIOLOGY)
Matched filtering of visual evoked potentials to detect acceleration (+Gz) induced blackout
[AD-A155912] 24 p4131 N85-35609
Simulation of high +Gz onset in the dynamic environment simulator
[AD-A155963] 24 p4131 N85-35610

BLACKOUT (PROPAGATION)
NT ATMOSPHERICS
NT DAWN CHORUS
NT ELECTROMAGNETIC NOISE
NT HISS
NT IONOSPHERIC NOISE
NT SHOT NOISE
NT THERMAL NOISE
NT WHISTLERS
NT WHITE NOISE

BLADDER
Spontaneous transitional cell carcinoma in the urinary bladder of a strain 13 guinea pig
[AD-A155645] 21 p3665 N85-32764

BLADDERS (MECHANICS)
U DIAPHRAGMS (MECHANICS)

BLADE SLAP NOISE
Interaction of a turbulent vortex with a lifting surface
15 p2464 N85-25214

BLADE TIPS
Observations from varying the lift and drag inputs to a noise prediction method for supersonic helical tip speed propellers
[NASA-TM-83797] 01 p0115 N85-10786
An experimental investigation and numerical simulation of the thermomechanical phenomena in compressor rotor tip rubbing 03 p0367 N85-12352
Pressure loss due to the tip clearance of impeller blades in centrifugal and axial blowers
05 p0636 N85-14083
Transonic flow of elastic medium past slender solid body 06 p0778 N85-14976
A feasibility study of free-tip rotor application as a passive cyclic control device 09 p1279 N85-18046
Inviscid analysis of unsteady blade tip flow correlation studies
[NASA-CR-172506] 10 p1420 N85-18958
One-piece HPTR blade squealer tip
[AD-D011452] 10 p1425 N85-18989
Cooled turbine blade tip closure
[AD-D011525] 12 p1858 N85-21654
An experimental investigation of the chopping of helicopter main rotor tip vortices by the tail rotor
[NASA-CR-177338] 13 p2154 N85-23376
Unsteady analysis of rotor blade tip flow
[NASA-CR-3868] 15 p2462 N85-25202
Interaction of a turbulent vortex with a lifting surface
15 p2464 N85-25214
Turbine blade-tip clearance excitation forces
[NASA-CR-171534] 19 p3220 N85-29963
Oxidizing seal for a turbine tip gas path
[NASA-CASE-LEW-14053-1] 23 p3937 N85-34402
Optimally designed propellers constrained by noise
24 p4065 N85-35196

BLADES
Post stall airfoil data for wind turbines: Wind tunnel test results
[DE85-004052] 10 p1511 N85-19534

BLADES (CUTTERS)
Device for preventing intrusion of a blade during vibration cutting of intermittent cutting with a lathe
16 p2794 N85-27232

BLANKETS (FISSION REACTORS)
Feasibility study of a fission-suppressed Tokamak fusion breeder
[DE85-009099] 18 p3190 N85-29786

BLANKETS (FUSION REACTORS)
Blanket materials for fusion reactors: Comparisons of thermochemical performance
[DE84-016240] 04 p0568 N85-13622
Special topics reports for the reference tandem mirror fusion breeder: Liquid metal MHD pressure drop effects in the packet bed blanket, volume 1
[DE85-002142] 06 p0865 N85-15500
Magnetic divertor design for the compact reversed-field pinch reactor
[DE85-002031] 09 p1391 N85-18753
Heat transfer and mechanical interactions in fusion nuclear systems
[DE84-016233] 09 p1392 N85-18761
Experimental facility for studying MHD effects in liquid metal cooled blankets
[DE85-000583] 14 p2423 N85-24943

Magneto-fluid-dynamic issues for fusion first wall and
blanket systems
[DE85-004022] 14 p2424 N85-24954
Magnetohydrodynamic considerations for the design of
self-cooled liquid-metal fusion reactor blankets
[DE85-000242] 14 p2425 N85-24957
Fusion-power-core design of a Compact Reversed-Field
Pinch Reactor (CRFPR)
[DE85-007710] 16 p2668 N85-27692
Radiation damage experiments and lifetime estimates
for beryllium components in fusion systems
[DE85-008036] 17 p3040 N85-28811
Two-dimensional TBR calculations for conceptual
compact reversed-field pinch reactor blanket
[DE85-007636] 17 p3040 N85-28812
Preliminary proposal for a beryllium technology program
for fusion applications
[DE85-009815] 18 p3183 N85-29737
Modeling and experiments on tritium permeation in
fusion reactor blankets
[DE85-008439] 18 p3183 N85-29741
US blanket technology programs
[DE85-010505] 19 p3358 N85-30817
Test cell modeling and optimization for FPD-2
[DE85-010836] 19 p3358 N85-30821
Molten salt cooling/17Li-83Pb breeding blanket
concept
[DE85-010522] 19 p3363 N85-30854
Flow characteristics of the Cascade granular blanket
[DE85-010932] 20 p3420 N85-31227
Neutronics activities for next generation devices
[DE85-010488] 20 p3527 N85-31939
Design of a helium-cooled molten salt fusion breeder
[DE85-010474] 20 p3528 N85-31943
Modeling and optimization of a test-cell upgrade for
MFTF-B operating in the high neutron wall loading mode
[DE85-009997] 20 p3528 N85-31946
MFTF-(alpha) + T shield design
[DE85-010496] 20 p3529 N85-31948
Monte Carlo and discrete ordinates calculations of
14-MeV neturons streaming through a stainless-steel duct
(L/D = 4.6): Comparison with experiment
[DE85-011423] 22 p3840 N85-33776
Key issues of fusion nuclear technology development
(FINESSE)
[DE85-012599] 22 p3845 N85-33817
Blanket optimization studies for Cascade
[DE85-010002] 22 p3846 N85-33824

BLANKS
Correction of engraving stamp for forming blanks of gas
turbine engine blades 09 p1307 N85-18213

BLASIUS EQUATION
Existence and non-uniqueness of similarity solutions of
a boundary layer problem
[NASA-CR-172503] 07 p0957 N85-16064

BLASIUS FLOW
A mathematical analysis of the effect of free stream
turbulence on the Blasius boundary layer
20 p3451 N85-31430

BLAST DEFLECTORS
Wind tunnel tests on a tube-launched missile
configuration with a deflectable nose control and a novel
wrap-around fin stabiliser
[AR-003-696] 01 p0001 N85-10003
Results of tests of MTA-2 TPS on the SRB hold-down
bolt blast container
[NASA-CR-170891] 24 p4070 N85-35224

BLAST LOADS
Model study of the interaction of a blast wave with the
superstructure of ships. Part 5: Application of optical
measurement methods to the study of blast interaction
[PML-1984-12-PT-5] 01 p0057 N85-10375
Dynamic shear failure of shallow-buried flat-roofed
reinforced concrete structures subjected to blast loading
[AD-A145974] 03 p0373 N85-12378
A model of the soft X-ray background as a blast wave
viewed from inside 06 p0879 N85-15586
Penetration of short duration airblast into protective
structures 09 p1336 N85-18404
Preliminary design criteria and certification test
specifications for blast resistant windows
09 p1337 N85-18405
The clinical and biomedical evaluation of trauma and
fatalities associated with aircrew ejection and crash. A
Working Group report
[AGARD-AR-194] 12 p1906 N85-21969
Introduction: The clinical and biomedical evaluation for
trauma and fatalities associated with aircrew ejection and
crash 12 p1906 N85-21970
List of head/neck injury on ejection in the German Armed
Forces from 1972-1981 12 p1906 N85-21972
Windblast arm protector assembly
[AD-D011512] 12 p1909 N85-21984
Elastic-workhardening SDF
(Single-Degree-of-Freedom) system subjected to random
blast excitations
[AD-A151886] 15 p2579 N85-25909
The shock desensitization of PBX-9404 and composition
B-3
[DE85-009604] 18 p3084 N85-29077
Constitutive modeling for blast-induced wave
propagation
[AD-A153576] 18 p3099 N85-29187
Environmental airblast around large shock tubes
[DE85-010654] 20 p3463 N85-31512
Development of an NBS (National Bureau of Standards)
polymer gage for dynamic soil stress measurement
[PB85-208494] 24 p4118 N85-35528

BLASTOFF
U ROCKET LAUNCHING

BLASTS
Some of the features of movement of gas through a
layer of free-flowing substances
[BLL-M-35732-(5829.4)] 02 p0196 N85-11312

BLEACHING
Hologram bleaching 06 p0769 N85-15038

BLEED-OFF
U PRESSURE REDUCTION

BLENDS
U MIXTURES

BLINDNESS
NT FLASH BLINDNESS
Baffled eye and confounded brain or using visual illusions
to train blind pilots
[AD-P004332] 09 p1271 N85-17986
Investigation into the use of the TV magnifier in the
Netherlands
[HSE-TRANS-11142] 20 p3533 N85-31986

BLOCH BAND
Electronic bandstructure of an incommensurate crystal
[DE84-016891] 05 p0733 N85-14714
Analysis of solution of Bloch's equations in time
domain 22 p3771 N85-33371

BLOCK DIAGRAMS
Dispersion of phase-shift keyed systems with fixed
number of blocks 13 p2070 N85-22928

BLOCKING
Experiences with a high-blockage model tested in the
NASA Ames 12-foot pressure wind tunnel
03 p0315 N85-12032
Beginner's guide to blocked records on magnetic tape
[DE85-001691] 06 p0855 N85-15433
A simulator for determining the performance of
transaction manager and lock manager combinations in
a database
[AD-A147827] 07 p1055 N85-16696
Navy tactical applications guide. Volume 4. Part 1.
Eastern North Pacific weather analysis and forecast
applications
[AD-A150097] 12 p1896 N85-21900
Maintenance of blocking anticyclones in a general
circulation model
[PB85-190666] 24 p4124 N85-35567

BLOCKS
Detonator block
[AD-D011248] 06 p0773 N85-14941
Phase diagram of polymer blends containing block
copolymers
[AD-A147706] 08 p1132 N85-17134
Lattice actions improved by block-spin renormalisation
group and maximally symmetric lattices
[DE85-007416] 17 p3045 N85-28841
Comparison of TT-F-1098 solvent-thinned block fillers
with water-thinnable block fillers
[AD-A154207] 19 p3249 N85-30142

BLOOD
NT ERYTHROCYTES
NT LYMPHOCYTES
Effect of maximum physical load on oxygen-transport
properties of blood 01 p0093 N85-10627
Measurement of blood and plasma density with the
mechanical oscillator technique
05 p0693 N85-14456
Clinical measurements using fiber optics and optrodes
[DE84-015043] 05 p0696 N85-14481
Fatal hemorrhagic shock and acetate solutions
[AD-A146754] 07 p1014 N85-16444
Aviation-related cardiorespiratory effects of blood
donation in female pilots
[AD-A148045] 08 p1195 N85-17529
Parameters of carbohydrate metabolism and blood
serum enzyme activity after short-term spaceflights
12 p1903 N85-21951
Effect of stationary magnetic field on bleeding time
12 p1904 N85-21956
Blood serum enzyme activity following long term
spaceflights 19 p3326 N85-30604
Rat blood serum and liver carbohydrates and lipids
recovery period after 15-day hypokinesia
19 p3326 N85-3060
A system for the assessment of non-thermal effects
ultrasound on cells at liquid nitrogen temperatures
20 p3523 N85-3191
The effect of +Gx acceleration on platelet activatio
as determined by plasma platelet factor 4 levels
[AD-A155881] 24 p4131 N85-3560

BLOOD CIRCULATION
NT BRAIN CIRCULATION
NT CORONARY CIRCULATION
NT PULMONARY CIRCULATION
Study and realization of a Doppler system with pulse
directional, multiport (128) emission and sequential sign
treatment — ultrasonic echography, blood flow
[ENST-84E008] 05 p0639 N85-1410
Pulmonary blood flow and oxygenation of arterial bloo
in a healthy subject upon 7 days hypokinesia
07 p1014 N85-1643
Biochemical evaluation of bodily influence of high an
low temperatures 07 p1014 N85-1644
Carotid baroreceptor influences on peripheral circulato
and thermal responses during cold exposure
[AD-A146806] 07 p1015 N85-1644
Random pattern tracking acceleration tolerance test
[AD-D011404] 07 p1017 N85-1645
Blood viscosity responses to acute exercise and aerobi
conditioning in women 09 p1363 N85-1857
Hemodynamics responses to upright tilt at sea level an
high altitude
[AD-A148848] 10 p1527 N85-1963
China report: Science and technology
[JPRS-CST-84-008] 13 p1972 N85-2238
Exercise-heat strain during hypohydration: Interactio
with heat acclimation and aerobic fitness
[AD-A151023] 14 p2389 N85-2471
Regional circulation during testing on isokinet
dynamometer following 14-day bedrest
19 p3323 N85-3059
Long term exposure of animals to antiorthostatis (-
deg) as a model of critical homeostatic disturbances
19 p3324 N85-3059
Nature of postural changes in human hemodynamic
with intake of sydnocarb alone and in combination w
obsidan 19 p3325 N85-3059
Effects of blood volume overload on myocardi
ultrastructure in relation to adaptation to high altitud
hypoxia 22 p3820 N85-3366
Typological characteristics of hemodynamic states
healthy subjects in orthostatic position
22 p3821 N85-3367
Vascular mechanisms of adaptation to antiorthostati
position 22 p3822 N85-3367
Cerebral hemodynamics and ventricular function in -1
deg antiorthostatic position 22 p3822 N85-3367
Effect of short-term antiorthostatic hypokinesia o
dynamics of cardiorespiratory parameters during grade
physical exercise 22 p3822 N85-3367
Morphological manifestations of hemodynamic change
in lungs of monkeys submitted to antiorthostati
hypokinesia 22 p3824 N85-3368
Effect of hypokinesia and +Gz accelerations o
transport function of human blood
23 p3952 N85-3449
Oxygenation and regional circulation in gingival mucos
during exposure to lower body negative pressure
23 p3953 N85-3449

BLOOD FLOW
Circulatory orthostatic instability: Role of deconditionin
of resistive vessels 01 p0091 N85-1061
Left heart ventricular function during a 7 day zero-
simulation (6 deg head down tilt)
05 p0691 N85-1444
Distribution of blood flow to brain, kidneys, gut, sple
and posterior extremities in cats in acute hypoxia
07 p1013 N85-1643
Analysis of the transient response of temporal arte
blood flow data relative to various anti-G suit pressu
schedules 10 p1533 N85-196
Simultaneous determination of cerebral blood flow a
partition coefficient with a freely diffusable tracer
[DE85-001226] 11 p1690 N85-206
A two phase flow model at the level of a narrowi
section — blood flow 20 p3507 N85-317
Morphological manifestations of hemodynamic chang
in lungs of monkeys submitted to antiorthosta
hypokinesia 22 p3824 N85-336

BLOOD PLASMA
USSR report: Space Biology and Aerospace Medici
volume 18, no. 6, November - December 1984
[JPRS-USB-85-002] 12 p1900 N85-219
Research opportunities in loss of red blood cell m
in space flight
[NASA-CR-175808] 16 p2841 N85-275

Plasma hormonal responses at graded hypohydration levels during exercise/heat stress
[AD-A153681] 18 p3153 N85-29523
Rat plasma hormone levels following flight aboard Cosmos-1129 biosatellite 22 p3823 N85-33681

BLOOD PRESSURE
NT LOWER BODY NEGATIVE PRESSURE
Hemodynamics and plasma arginine vasopressin during water immersion in normal man
05 p0693 N85-14456
Blood pressure levels of active pilots compared with those of air traffic controllers
[AD-A146645] 06 p0846 N85-15373
Effect of microwave radiation on local blood circulation and oxygenation of brain tissue
07 p1012 N85-16431
Carotid baroreceptor influences on peripheral circulatory and thermal responses during cold exposure
[AD-A146808] 07 p1015 N85-16447
Blood pressure responses and mineral ocorticoid levels in the suspended rat model for weightlessness
15 p2609 N85-26079
Effect of 120-day antiorthostatic bedrest on gas exchange and pulmonary circulation in man
19 p3323 N85-30569
Antihypertensive neutral lipid
[DE85-011625] 22 p3819 N85-33656
Cerebral hemodynamics and ventricular function in -15 deg antiorthostatic position 22 p3822 N85-33676
Effect of short-term antiorthostatic hypokinesia on dynamics of cardiorespiratory parameters during graded physical exercise 22 p3822 N85-33677
Effect of water immersion of parameters of central hemodynamics in individuals over 45 years old
23 p3953 N85-34499

BLOOD VESSELS
NT ARTERIES
NT VEINS
Cerebral hemodynamics and ventricular function in -15 deg antiorthostatic position 22 p3822 N85-33676
Development of the osmium-191 yields iridium-191m radionuclide generator
[DE85-011165] 23 p3970 N85-34611

BLOOD VOLUME
A systems analysis of the erythropoietic responses to weightlessness. Volume 1: Mathematical model simulations of the erythropoietic responses to weightlessness
[NASA-CR-171690] 20 p3506 N85-31794
Effects of blood volume overload on myocardial ultrastructure in relation to adaptation to high altitude hypoxia 22 p3820 N85-33664
Thirst and fluid intake following graded hypohydration levels in humans
[AD-A156201] 24 p4132 N85-35615

BLOWDOWN WIND TUNNELS
Experiences with the use of a side-strut model support system for high angles of attack in the Trinsonik wind tunnel TMK
[DFVLR-MITT-84-09] 07 p0910 N85-15763
Transonic Mach number determination in a blow-down wind tunnel with solid walls and a downstream throat
[VTH-LR-402] 17 p2893 N85-27835
Experiences with the use of a side-strut model support system for high angles for attack in the TMK Trinsonik Wind Tunnel
[ESA-TT-895] 20 p3396 N85-31069

BLOWERS
Pressure loss due to the tip clearance of impellar blades in centrifugal and axial blowers
05 p0636 N85-14083
Low solidity cascade diffusers for wide flow range centrifugal blowers 05 p0637 N85-14086
Strong turbulence chemistry interaction in a piloted turbulent jet diffusion flame 20 p3425 N85-31257

BLOWING
Drag reduction due to boundary-layer control by combined blowing and suction 08 p1070 N85-16785

BLUE GREEN ALGAE
Production of hydrogen by cyanobacteria
[PB85-113421/GAR] 07 p0935 N85-15925

BLUE STARS
NT SYMBIOTIC STARS
Blue companions of Cepheids
11 p1754 N85-21033

BLUFF BODIES
Vorticity amplification in viscous flow around a body
03 p0360 N85-12309
Large structure in the far wakes of two-dimensional bluff bodies 05 p0592 N85-13771
Flow Around Bluff Bodies: Numerical and Experimental Approaches — conferences
[VKI-LS-1984-06] 05 p0593 N85-13778
Flow around bluff bodies 05 p0593 N85-13779
The aerodynamics of bluff bodies in turbulent shear layers 05 p0593 N85-13780
Experimental techniques and instrumentation for bluff body aerodynamics 05 p0593 N85-13781
Numerical methods for bluff body aerodynamics
05 p0593 N85-13782
Wake flow behind bluff bodies
05 p0593 N85-13783
Numerical integrations of the Navier-Stokes equations for flow over surface-mounted obstacles
05 p0593 N85-13784
On the generation of trailing vortices by surface mounted obstacles 05 p0593 N85-13785
Acceleration of bluff bodies through fluids
05 p0593 N85-13786
Numerical calculation of the cold-flow characteristics of a bluff-body flame stabilizer
[CFD/84/14] 08 p1124 N85-17088
Experimental investigation of heat transfer to bluff cylinders and cones in hypersonic rarefied gas flow
11 p1620 N85-20195
The mechanisms of flame holding in the wake of a bluff body
[NASA-CR-3866] 12 p1779 N85-21166
Investigation of the aerodynamic forces on bluff bodies at high Reynolds numbers
[DFVLR-MITT-84-19] 14 p2213 N85-23727
Numerical solutions of 3-dimensional Navier-Stokes equations for closed bluff-bodies
[NASA-CR-175755] 15 p2636 N85-26255
An experimental investigation of a turbulent junction vortex
[NASA-CR-175915] 17 p2957 N85-28259

BLUFFS (LANDFORMS)
U CLIFFS

BLUNT BODIES
Numerical method for computing supersonic flow over wings of flight vehicles 05 p0725 N85-14659
Hypersonic flow of mixture around blunt body
06 p0779 N85-14979
Controllable rotation of system of two solid bodies with elastic elements 06 p0780 N85-14988
On detached shock wave of sphere moving with transonic velocities 11 p1622 N85-20215
A 3-dimensional Navier-Stokes-Euler code for blunt-body flow computations
[NASA-TM-58266] 15 p2463 N85-25211
Navier-Stokes solution of hypersonic blunt-nosed body flowfields 16 p2693 N85-26624
Bypass transition to turbulence and research Desiderata 20 p3453 N85-31442
Laser Doppler Anemometer (LDA) measurements in the turbulent near-wake of blunt bodies
[ISL-CO-212/84] 22 p3785 N85-33450

BLURRING
New image deblurring method described
16 p2806 N85-27305

BMC
U BONE MINERAL CONTENT

BO-105 HELICOPTER
Flight tests with a new helicopter Force Feel System (FFS) 08 p1075 N85-16818
Flight research on visual aids and navigation equipment for helicopter low-level flight at night
08 p1076 N85-16820

BOATS
NT LIFEBOATS
The 1981 transatlantic boat race contribution for marine meteorological measurements 14 p2324 N85-24361
The transpacific experimental sailing by YASEIGO 3
14 p2327 N85-24380
Miscellaneous ARGOS maritime applications — yacht races 14 p2327 N85-24383
The sinking of the Les Mutuelles du Mans trimaran
14 p2327 N85-24384
The ARGOS contribution to the demonstration of the effectiveness of a satellite-based search and rescue system 14 p2330 N85-24404
Data from BOC-yachts: A significant input to Southern Hemisphere analysis 16 p2614 N85-27356
Some applications of aeronautical engineering in the construction of yachts
[NLR-MP-83042-U] 20 p3394 N85-31052

BOATTAILS
On the evaluation of boundary layer measurements on boattailed bodies of revolution in axisymmetric compressible subsonic flow
[ESA-TT-883] 20 p3457 N85-31471
Laser Doppler Anemometer (LDA) measurements in the turbulent near-wake of blunt bodies
[ISL-CO-212/84] 22 p3785 N85-33450

BOD
U BIOCHEMICAL OXYGEN DEMAND

BODIES OF REVOLUTION
NT CELESTIAL SPHERE
NT CONCENTRIC SPHERES
NT CONICAL BODIES
NT CYLINDRICAL BODIES
NT FALLING SPHERES
NT PARABOLIC BODIES
NT POINCARE SPHERES
NT ROTATING CYLINDERS
NT ROTATING SPHERES
NT SLENDER CONES
NT SPHERES
NT TORUSES
Stability of stellar disk and ratio of halo to disk masses in the galaxy 05 p0740 N85-14763
Numerical modeling of complex interaction of shell of revolution and its filler with allowance for friction
06 p0779 N85-14980
Motion of heavy symmetric body with flexible bars about stationary point 06 p0780 N85-14989
Transient currents of ideally conducting body of revolution with transient diffraction
06 p0785 N85-15019
Effects of body shape on the aerodynamics of a body of revolution at Mach numbers from 1.6 to 4.6
[NASA-TM-86345] 07 p0893 N85-15657
A frozen vorticity approach to the axisymmetric strong interaction problem
[AD-A149101] 10 p1484 N85-19369
Average spacing for rings of individual multi-ring basins is 2.0(0.5)D 13 p2182 N85-23541
Method of solving problems of statics for multilayer shells of revolution 17 p2943 N85-28167
Proceedings of the 9th US Air Force and the Federal Republic of Germany Data Exchange Agreement Meeting. Viscous and Interacting Flow Field Effects
[AD-A153020] 17 p2958 N85-28266

BODY CENTERED CUBIC LATTICES
Lattice defects in body centered cubic transition metals 03 p0427 N85-12727

BODY FLUIDS
NT BLOOD
NT CEREBROSPINAL FLUID
NT ENDOLYMPH
NT ERYTHROCYTES
NT LYMPHOCYTES
NT SWEAT
NT URINE
Intraocular fluid dynamics in microgravity
05 p0693 N85-14455
Fluid metabolism of monkeys during two-week antiorthostatic hypokinesia 12 p1902 N85-21943
Exercise-heat strain during hypohydration: Interaction with heat acclimation and aerobic fitness
[AD-A151023] 14 p2389 N85-24717
Structural development and gravity
15 p2608 N85-26071
Computer simulation studies in fluid and calcium regulation and orthostatic intolerance
[NASA-CR-171869] 15 p2616 N85-26117
The behavior of renal-regulating hormones during hypogravic stress
[NASA-CR-171877] 15 p2616 N85-26123
Fluid-electrolyte responses during prolonged space flight: A review and interpretation of significant findings
[NASA-CR-171878] 15 p2617 N85-26124
Chemicals identified in human biological media, a data base. Volume 6, part 2: Records 7588-8694
[DE85-008767] 18 p3154 N85-29528
Investigation of spectrum of human bile acids during 120-day antiorthostatic hypokinesia
22 p3821 N85-33674
Fluid-electrolyte metabolism and renal function in cosmonauts following 185-day spaceflight
23 p3952 N85-34495

BODY KINEMATICS
Acceleration of bluff bodies through fluids
05 p0593 N85-13786
Electromyographic patterns associated with discrete limb movements 05 p0710 N85-14551
Human body dimensions: Body outlines and envelope curves at different normal positions and movements
[HSE-TRANS-10866] 19 p3332 N85-30640
Effect of body position and immobilization on intensity of spatial illusions in weightlessness
22 p3821 N85-33672
The dynamics of articulated rigid bodies for purposes of animation 23 p3965 N85-34579

BODY MEASUREMENT (BIOLOGY)
NT ANTHROPOMETRY
Human body dimensions: Body outlines and envelope curves at different normal positions and movements
[HSE-TRANS-10866] 19 p3332 N85-30640
Physical dimensions of humans, values, envelope curves in different postures
[HSE-TRANS-10869] 20 p3513 N85-31838

BODY SIZE (BIOLOGY)
Prediction of percent body fat for U.S. Navy women from body circumferences and height
[AD-A146456] 06 p0845 N85-15370

BODY SWAY TEST
Typological characteristics of hemodynamic states of healthy subjects in orthostatic position
22 p3821 N85-33673

BODY TEMPERATURE
Biochemical evaluation of bodily influence of high and low temperatures 07 p1014 N85-16441
Comparison of thermal responses between rest and leg exercise in water
[AD-A146818] 07 p1015 N85-16448
Tolerance endpoint for evaluating the effects of heat stress in dogs
[AD-A148104] 08 p1192 N85-17511
Simultaneous determination of radiation and convection heat transfer 08 p1194 N85-17523
Influence of hyperthermia on body temperature and content of catecholamines in white rat hypothalamus
10 p1524 N85-19815
Heat stress and personal protective equipment
[DE85-003552] 10 p1532 N85-19852
China report: Science and technology
[JPRS-CST-84-030] 13 p2041 N85-22777
Study of effective physiological temperature
13 p2042 N85-22780
Peripheral changes in regional sweating responses to exercise in hypobaric environments
[AD-A150757] 14 p2388 N85-24710
Mathematical models relating to human thermoregulation: Basic assumptions, validation, and application. Parts A and B
[AD-A151556] 15 p2618 N85-26130
Thermal consequences of localized SAR from RFR exposures 16 p2775 N85-27130
Experiments in microwave exposure in the rat: Body temperature, serum chemistry and the use of chemical restraint
[PB85-156834] 16 p2840 N85-27512
Investigation of the requirement for auxiliary heating of Canadian forces personnel
[AD-A151950] 16 p2841 N85-27522
Method for thermal monitoring subcutaneous tissue
[NASA-CASE-LAR-13026-1] 19 p3328 N85-30618
Heat injury: Prevention is the key
[AD-A153734] 19 p3328 N85-30622
Electroanesthesia as a means of controlling cold stress of local hypothermia 22 p3823 N85-33687
Thermal stress suffered by tank crews working in summer heat
[DRIC-T-7492] 22 p3826 N85-33698
Weight loss, rectal temperature and heart rates following the 1984 Boston Marathon
[AD-A155964] 24 p4132 N85-35612

BODY TEMPERATURE (NON-BIOLOGICAL)
U TEMPERATURE

BODY TEMPERATURE REGULATION
U THERMOREGULATION

BODY VOLUME (BIOLOGY)
Leg volume changes. Responses to Lower Body Negative Pressure (LBNP) during 7 days of zero-g simulation (6 deg Head-Down Tilt (HDT))
05 p0692 N85-14452
An analysis of aerobic capacity in a large United States population
[AD-A156200] 24 p4132 N85-35614

BODY WEIGHT
Effects of body mass and morphology on thermal responses in water
[AD-A147558] 07 p1016 N85-16455
The effect of occupational exposure and the body weight to height ratio on exhaled methylene chloride breath concentration in females at one, eighteen and sixty-six hours post exposure 14 p2388 N85-24708
Role of glucocorticoids in the response to unloading of muscle protein and amino acid metabolism
15 p2609 N85-26077
Gravity, body mass and composition, and metabolic rate 15 p2610 N85-26084
Weight loss, rectal temperature and heart rates following the 1984 Boston Marathon
[AD-A155964] 24 p4132 N85-35612
Thirst and fluid intake following graded hypohydration levels in humans
[AD-A156201] 24 p4132 N85-35615

BODY-WING AND TAIL CONFIGURATIONS
The aerodynamics of some guided projectiles
[NASA-TM-86334] 06 p0747 N85-14786
Theoretical study of boundary-layer control
08 p1070 N85-16784
Tail behaviour for suprema of empirical processes
[AD-A147629] 08 p1210 N85-17613
Supersonic aerodynamic characteristics of canard, tailless, and aft-tail configurations for 2 wing planforms
[NASA-TP-2434] 17 p2891 N85-27822
Experimental and theoretical determination of the wing-induced lateral wind on the tail surfaces in oscillating rolling motion. Part 1: Application of the Mobile Oscillating Derivatives (MOD) on an experimental part
[IFD-1/84-PT-1] 18 p3061 N85-28939
Experimental and theoretical determination of the wing-induced lateral wind on the tail surfaces in oscillating rolling motion. Part 2: Theoretical investigations for calculation of the lateral wind
[IFD-1/84-PT-2] 18 p3061 N85-28940
Transonic and supersonic wind tunnel tests on control effectiveness on schematic missile configurations
[FFA-TN-1983-20] 20 p3389 N85-31020
Transonic and supersonic wind tunnel tests on control effectiveness on schematic missile configurations: Supplement
[FFA-TN-1983-20-SUPPL] 20 p3389 N85-31021

BODY-WING CONFIGURATIONS
An experimental study of the transonic equivalence rule with lift, part 2
[AR-LR-614-PT-2] 01 p0001 N85-10004
A study of aerodynamic characteristics of wing-body combinations. Part 2: Low-wing airplane
[NAL-TR-796] 01 p0002 N85-10010
Drag reduction due to boundary-layer control by combined blowing and suction 08 p1070 N85-16785
Wing rock flow phenomena
[AD-P004154] 09 p1264 N85-17939
Flight mechanics analysis of dynamic derivatives of the Dornier variable wind tunnel model
[ESA-TT-854] 11 p1577 N85-19937
Comparison of computational results of a few representative three-dimensional transonic potential flow analysis programs 16 p2693 N85-26628
The role of computational fluid dynamics in aeronautical engineering 16 p2694 N85-26629
Experimental and theoretical determination of the wing-induced lateral wind on the tail surfaces in oscillating rolling motion. Part 1: Application of the Mobile Oscillating Derivatives (MOD) on an experimental part
[IFD-1/84-PT-1] 18 p3061 N85-28939
Calculation of transonic flows around an aircraft configuration with motorized nacelle
[SNIAS-851-111-106] 20 p3387 N85-31006
Calculation of flow around the SF 310 airplane using a full potential equation method
[FFA-TN-1984-63] 20 p3389 N85-31022

BOEING AIRCRAFT
NT BOEING 727 AIRCRAFT
NT BOEING 737 AIRCRAFT
NT BOEING 747 AIRCRAFT
NT BOEING 767 AIRCRAFT
NT C-135 AIRCRAFT
NT CH-47 HELICOPTER

BOEING MILITARY AIRCRAFT
U MILITARY AIRCRAFT

BOEING 727 AIRCRAFT
Safety recommendation(s), A-84-65
[REPT-3906] 14 p2216 N85-23743

BOEING 737 AIRCRAFT
Full-scale testing, production and cost analysis data for the advanced composite stabilizer for Boeing 737 aircraft. Volume 1: Technical summary
[NASA-CR-3649] 05 p0612 N85-13912
Design, ancillary testing, analysis and fabrication data for the advanced composite stabilizer for Boeing 737 aircraft. Volume 1: Technical summary
[NASA-CR-3648] 05 p0612 N85-13913
Design, ancillary testing, analysis and fabrication data for the advanced composite stabilizer for Boeing 737 aircraft, volume 2
[NASA-CR-166011] 05 p0612 N85-13914
Full-scale testing, production and cost analysis data for the advanced composite stabilizer for Boeing 737 aircraft, volume 2
[NASA-CR-166012] 05 p0613 N85-13915
A preliminary evaluation of a failure detection filter for detecting and identifying control element failures in a transport aircraft
[NASA-TM-87576] 24 p4067 N85-35204

BOEING 747 AIRCRAFT
The orbiter mate/demate device
08 p1103 N85-16972
Simultaneous cabin and ambient ozone measurements on two Boeing 747 airplanes. Volume 3: October 1978 - July 1979
[NASA-TM-86883] 12 p1802 N85-21872

BOEING 767 AIRCRAFT
What pilots like (and don't like) about the new cockpit technology 05 p0710 N85-14554

BOGS
U MARSHLANDS

BOILERS
The effects of microstructure on the temper embrittlement susceptibility of a Cr-2-1/4 1Mo forging
[AERE-R-11110] 03 p0334 N85-12151
Actual versus design performance of solar systems in the National Solar Data Network
[DE85-001190] 09 p1344 N85-18456
Weldability and mechanical property characterization of weld clad alloy 800H tubesheet forging
[DE85-001737] 11 p1609 N85-20116
Carbon granule probe microphone for leak detection — recovery boilers
[NASA-CASE-NPO-16027-1] 12 p1849 N85-21597
Steam generator tube vibration tests
[DE85-003599] 12 p1867 N85-21712
The use of heat pumps in district heat supply
[BLL-OA-TRANS-2726-(6196.3)]
16 p2761 N85-27163
Erosion of corrosion-resistant surface treatments on alloy steels
[DE85-008446] 17 p2932 N85-28100
Current status of TVA's atmospheric fluidized bed combustion development efforts
[DE85-901209] 19 p3306 N85-30507
Control system for fluid heated steam generator
[DE85-005734] 23 p3939 N85-34417
Calculations on the feasibility of ultrasonic inspection of steam generator tubing in pressurized water reactors
[AERE-R-10960] 23 p3940 N85-34419
Computer code calculations of the TMI-2 accident: Initial and boundary conditions
[DE85-012613] 24 p4140 N85-35666

BOILING
NT FILM BOILING
NT NUCLEATE BOILING
Time resolved calorimetry of 30 nm Te-films during laser annealing
[AD-A145047] 01 p0052 N85-10346
Method for making alloy additions to base metals having higher melting points
[AD-D011403] 07 p0928 N85-15884
Review of anode phenomena in vacuum arcs
[DE85-002736] 12 p1926 N85-22101
Effects of temperature variation among droplets in an evaporating fuel spray 13 p2004 N85-22562
Spacecraft, straight-tube evaporator design
[AD-A154462] 19 p3226 N85-30003
An experimental apparatus to study nucleate pool boiling of R-114 and oil mixtures
[AD-A154077] 19 p3265 N85-30249
Two-phase flow visualization in a transparent, atmospheric pressure, boiling water loop
[DE84-016857] 21 p3586 N85-32286
Effects of ambient pressure on the instability of a liquid boiling explosively at the superheat limit
[DE85-009476] 23 p3932 N85-34370

BOILING WATER REACTORS
Stress corrosion of pressure vessel steel A533-B in high temperature water
[BLL-RISLEY-TR-4600-(9091.9F)]
03 p0330 N85-12125
Deterministic sensitivity analysis of two-phase flow systems: Forward and adjoint methods
[DE84-016276] 04 p0499 N85-13165
Steel containment buckling
[DE85-003744] 13 p2103 N85-23111
Inspection evaluation and repair of the flawed feedwater nozzle of the 50 MWe Dodewaard GKN boiling water reactor
[ISBN-90-353-0017-3] 17 p2977 N85-28394
Graphic display development program, volume 1
[DE85-011076] 19 p3333 N85-30649
Advanced ultrasonic imaging of piping in Dresden and Vermont Yankee reactors
[TI85-010049] 20 p3464 N85-31520
Technical assessment of thermal-hydraulics for high heat flux fusion components
[DE85-013178] 23 p3930 N85-34359
Response of a BWR Mark 2 containment vessel head to loads beyond the design basis
[DE85-010524] 24 p4103 N85-35432

BOLIVIA
A silicic shield volcano in Bolivia
13 p2187 N85-23572

BOLKOW AIRCRAFT
NT BO-105 HELICOPTER

BOLOGRAMS
U BOLOMETERS

BOLOMETERS
Thick film radiation detector
[AD-D011211] 01 p0048 N85-10318
Physics and design of advanced infrared bolometers and photoconductors
[DE84-016683] 04 p0503 N85-13213
Imaging polarimeter-interferometer arrays for Tokamak measurements
[DE84-015916] 05 p0730 N85-14693
Fast granular superconducting bolometer
[AD-D011332] 07 p0961 N85-16093

Infrared technology for satellite power conversion --- antenna arrays and bolometers
[NASA-CR-174266] 07 p0991 N85-16293
The mechanical procedures for the 8 channel bolometer --- United Kingdom Infrared Telescope
[UKIRT-18] 09 p1414 N85-18916
BIG MAC: A bolometer array for mid-infrared astronomy, Center Director's Discretionary Fund
[NASA-TM-86502] 13 p2170 N85-23483

BOLTS
Measurement of the preloading of bolted joints by the ultrasonic method
[CETIM-1-5H-38-6] 04 p0558 N85-13556
Hydraulic locking boltwork system
[AD-D011299] 06 p0815 N85-15174
Corrosion of aircraft Al and Al-Zn ion plated steel fasteners 13 p2021 N85-22666
Three-dimensional finite element failure model for predicting failure in fibre reinforced bolted joints
[BR94778] 23 p3940 N85-34423
Stresses and strains in a plate resulting from two closely-spaced interference-fit fasteners
[ARL/STRUC-TM-409] 23 p3941 N85-34429
Results of tests of MTA-2 TPS on the SRB hold-down bolt blast container
[NASA-CR-170891] 24 p4070 N85-35224

BOLTZMANN DISTRIBUTION
Loeb solutions of the Boltzmann equation with initial boundary values and external forces
[CTH-MATH-1984-23] 05 p0719 N85-14616
Theoretical foundations of turbulent flows
21 p3683 N85-32880
Time-resolved spectroscopic studies of detonating heterogeneous explosives
[DE85-009760] 23 p3921 N85-34297

BOLTZMANN TRANSPORT EQUATION
Solution of the Boltzmann transport equations for a permeable base transistor
[AD-A144969] 01 p0112 N85-10757
The Boltzmann equation: Global existence for a rare gas in an infinite vacuum
[PREPRINT-78] 01 p0124 N85-10851
Equations of plasma transport in a curved magnetic field
[DE84-015625] 05 p0730 N85-14690
A linear characteristic-nodal transport method for the two-dimensional (X,Y)-geometry multigroup discrete ordinates equations over an arbitrary triangle mesh
[LA-10092-T] 12 p1913 N85-22008
User's guide for TWODANT: A code package for two-dimensional, diffusion-accelerated, neutral-particle transport
[LA-10049-M] 12 p1913 N85-22009
User's guide for TWOHEX: A code package for two-dimensional, neutral-particle transport in equilateral triangular meshes
[DE85-004482] 12 p1930 N85-22125
Semiconductor materials for high frequency solid state sources
[AD-A150020] 12 p1940 N85-22186
The transport of neutral H, D, T and He and O in the boundary layers of a Tokamak plasma
[REPT-84-153] 17 p3041 N85-28817
Direct simulation techniques for the Boltzmann equation
[DFVLR-FB-85-13] 20 p3457 N85-31470

BOLTZMANN-VLASOV EQUATION
Covariant Poisson brackets for classical fields
[DE85-010085] 18 p3171 N85-29654

BOMBER AIRCRAFT
NT B-1 AIRCRAFT
NT B-70 AIRCRAFT
Avionics Integrity Program (Avip). Volume 2: Hardware case studies
[AD-A145689] 02 p0139 N85-10944
The effect of load factor on aircraft handling qualities
[AD-A152116] 16 p2710 N85-26724
The introduction of new cockpit technology: A human factors study
[NASA-TM-86659] 16 p2843 N85-27528
Electronic reconnaissance aircraft of the Soviet Union Navy
[AD-A154706] 21 p3551 N85-32091
Maintenance and the military environment
22 p3750 N85-33243

BOMBING EQUIPMENT
System for radio remote control of dropping bombs
[CH-639335-A5] 15 p2491 N85-25371

BOMBS (ORDNANCE)
A two-step bomb to determine the inflammability of propellant charge powders
[ISL-CO-211/83] 14 p2264 N85-24026
Components of the combustion gases of propellant charge powders after reaction in the high pressure bomb in the pressure range up to 1000 MPa. Part 1: Nitroglycerine powder GB Pa 125
[ISL-CO-217/83-PT-1] 14 p2264 N85-24027
Optmizing the specifications for an air-surface laser system 16 p2696 N85-26644

BOMBS (PRESSURE GAGES)
U PRESSURE GAGES

BOMBS (SAMPLERS)
U SAMPLERS

BONDING
NT ADHESIVE BONDING
NT AGGLUTINATION
NT CERAMIC BONDING
NT EXPLOSIVE WELDING
NT METAL BONDING
NT METAL-METAL BONDING
NT REACTION BONDING
Optical contacting for gravity probe star tracker
[NASA-TM-86475] 01 p0120 N85-10819
Growth and magnetic investigations of single crystals of intermetallic compounds of rare earths and uranium --- magnetic properties 03 p0425 N85-12712
Contamination problems during surface cleaning for thermocompression bonding
[DE84-013066] 04 p0475 N85-13023
Method for bonding insulator to insulator
[AD-D011340] 07 p0929 N85-15891
Insulation bonding test system
[NASA-CASE-MFS-25862-1] 11 p1610 N85-20126
Infrared-thermal wave scanner for NDE of naval thermal spray coatings
[DE85-002237] 11 p1650 N85-20391
Amine salts as bonding agents
[AD-D011543] 12 p1817 N85-21396
Activation of Si-N modes in silicon by pulsed laser annealing
[DE85-003988] 13 p2097 N85-23082
Multiple scattering effects in low energy alkali ion scattering: Application to the analysis of adsorbate ordering and bonding geometry
[DE85-007575] 17 p3032 N85-28757
Method for ultrasonic bonding to soft microelectronic substrates
[NASA-CASE-NPO-16087-1] 18 p3094 N85-29151
Ultrasonic test evaluation of the insert bond on hermetic connectors
[DE85-008394] 18 p3120 N85-29310
X-ray photoelectron spectroscopy study of the compatibility of the explosive PETN with candidate plastic bonding materials
[DE85-010804] 19 p3251 N85-30161
STPI/LARC: A 200 deg C polyimide adhesive
[NASA-TM-86447] 20 p3433 N85-31297
EVA-glass interface bond stability
21 p3608 N85-32406
Non-bonded ultrasonic transducer
[DE85-011006] 22 p3794 N85-33504
Dynamic compaction of a monosized spherical tungsten powder
[DE85-014808] 24 p4080 N85-35289
Ionic crystals
[DE85-009482] 24 p4163 N85-35809

BONE DEMINERALIZATION
Bone structure and microgravity
05 p0694 N85-14463
Loss of bone substance in consequence of amputation as a model for the adaptation to microgravity
05 p0694 N85-14464
Structural development and gravity
15 p2608 N85-26071
Evidence that resorption of bone by rat peritonal macrophages occurs in an acidic environment
15 p2612 N85-26098
Changes in bone structure and metabolism during simulated weightlessness: Endocrine and dietary factors
[NASA-CR-175961] 18 p3153 N85-29521
The role of 1,25-dihydroxyvitamin D in the inhibition of bone formation induced by skeletal unloading
[NASA-TM-87480] 18 p3153 N85-29522
Rat bone tissue after flight aboard Cosmos-1129 biosatellite 19 p3324 N85-30593

BONE MARROW
Addendum to the STCAL and LTCAL user's guide
[NASA-CR-171880] 15 p2628 N85-26194
Mammalian tissue sensitivity to long-term exposure to high-intensity stationary magnetic fields
22 p3823 N85-33686

BONE MINERAL CONTENT
Actual and simulated weightlessness inhibit osteogenesis in long bone metaphysis by different mechanisms 15 p2608 N85-26074
Evidence that resorption of bone by rat peritonal macrophages occurs in an acidic environment
15 p2612 N85-26098
Rat bone tissue after flight aboard Cosmos-1129 biosatellite 19 p3324 N85-30593

BONES
NT CEREBRUM
NT FEMUR
NT MARROW
NT PELVIS
NT SCIATIC REGION
NT SKULL
NT VERTEBRAE
Effect of 1,25-dihydroxycholecalciferol and 24,25 dihydroxycholecalciferol on growth and alteration of rat bones during hypokinesa (histomorphometric study)
01 p0092 N85-10622
Vitamin K and the metabolic state of bone
05 p0694 N85-14465
Polyactic-polyglycolic acid copolymer combined with decalcified freeze-dried bone for use as a bone repair material
[AD-D011438] 10 p1451 N85-19142
Distribution of radium and plutonium in human bone
[DE85-005025] 13 p2142 N85-23298
Structural development and gravity
15 p2608 N85-26071
The role of vitamin D in the bone changes associated with simulated weightlessness 15 p2608 N85-26072
The salutary effect of dietary calcium on bone mass in a rat model of simulated weightlessness
15 p2608 N85-26073
Quantitative alterations in the function of bone forming cells due to reduced weight bearing
15 p2609 N85-26075
Evidence that resorption of bone by rat peritonal macrophages occurs in an acidic environment
15 p2612 N85-26098
Addendum to the STCAL and LTCAL user's guide
[NASA-CR-171880] 15 p2628 N85-26194
Histological and compositional responses of bone to immobilization and other experimental conditions
[NASA-CR-175637] 16 p2841 N85-27518
Changes in bone structure and metabolism during simulated weightlessness: Endocrine and dietary factors
[NASA-CR-175961] 18 p3153 N85-29521
Rat bone tissue after flight aboard Cosmos-1129 biosatellite 19 p3324 N85-30593
Mechanisms of osteodystrophy in weightlessness
22 p3733 N85-33143
Report of the NASA Mammalian Developmental Biology Working Group 24 p4126 N85-35581

BOOLEAN ALGEBRA
NT BOOLEAN FUNCTIONS
Boolean approach to zero-one linear programming
[DE84-016654] 04 p0550 N85-13498
Minimal cut-set methodology for artificial intelligence applications
[DE84-016674] 04 p0553 N85-13518
Investigation of three-dimensional mesh generation with precise controls
[AD-A148759] 09 p1374 N85-18636
Synthesis of tests for programmable logic arrays
22 p3777 N85-33406

BOOLEAN FUNCTIONS
Comparison analysis of algorithm for construction of functional tests for combined large-scale integrated circuits 04 p0490 N85-13121
Priority rewrite systems --- computer programming
[CWI-CS-R8407] 05 p0720 N85-14621
Efficient VLSI (Very Large Scale Integration) fault simulation
[AD-A152661] 17 p2953 N85-28233
An analysis and algorithm for filling propagation
23 p3961 N85-34551
EPALIT: A data management system applied to the control and retrieval of technical reports
[PB85-193068] 24 p4166 N85-35828

BOOMS (EQUIPMENT)
F-8 refueling boom ground vibration test
[NASA-TM-84914] 07 p0902 N85-15713
Extended moment arm anti-spin device
[NASA-CASE-LAR-12979-1] 12 p1776 N85-21147
Modeling and analysis of pinhole occulter experiment: Initial study phase
[NASA-CR-175978] 19 p3272 N85-30287
Environmental background measurement program
[AD-A153860] 19 p3319 N85-30577
The Galeleo spacecraft magnetometer boom
22 p3796 N85-33513

BOOST
U ACCELERATION (PHYSICS)

BOOSTER RECOVERY
Structural and mechanical design challenges of space shuttle solid rocket boosters separation and recovery subsystems 08 p1095 N85-16917
Solid rocket booster retrieval operations
08 p1096 N85-16928

BOOSTER ROCKET ENGINES
Structural and mechanical design challenges of space shuttle solid rocket boosters separation and recovery subsystems 08 p1095 N85-16917
External tank processing from barge to pad 08 p1096 N85-16927
Solid rocket booster retrieval operations 08 p1096 N85-16928
Thermal design of the space shuttle solid rocket booster 08 p1103 N85-16976
Verification of the SRB motor case pin retainer band tips [NASA-CR-170682] 24 p4070 N85-35220
Results of tests of MTA-2 TPS on the SRB hold-down bolt blast container [NASA-CR-170691] 24 p4070 N85-35224
Evaluation of SRB phenolic TPS material made by an alternate vendor [NASA-CR-170694] 24 p4073 N85-35240
Space shuttle SRB TPS protective paint test and evaluation in NASA Hot Gas Facility and AEDC Tunnel C [NASA-CR-170684] 24 p4081 N85-35294
Results of tests of Insta-Foam Thermal Protection System (TPS) material for protection of equipment inside the SRB aft skirt [NASA-CR-170692] 24 p4081 N85-35295
BOOTS (FOOTWEAR)
The energy cost of women walking and running in shoes and boots [AD-A151022] 14 p2389 N85-24716
BORANES
NT CARBORANE
New synthetic routes to boron cage compounds [AD-A153554] 18 p3071 N85-28991
BORATES
NT LITHIUM BORATES
Glass corrosion in liquid lithium [DE85-002086] 09 p1299 N85-18162
Luminescence and absorption of indium-activated potassium-borate glasses subjected to high-power excitation 21 p3681 N85-32866
BORAZON (TRADEMARK)
U BORON NITRIDES
BOREDOM
Study of bodily functional status and quality of controlling action of power unit operators with various intensities of labor 09 p1362 N85-18569
BOREHOLES
The Midway Atoll coral cap: Meteoric diagenesis, amplitude of sea-level fluctuation and dolomitization 09 p1351 N85-18499
On the stress analysis of bonded inserts [ARL/STRUC-R-407] 12 p1865 N85-21696
The residual strength of cracked specimens representing a section of the mirage into wing main spar [ARL/STRUC-R-408] 12 p1865 N85-21699
Experimental stiffness of tapered bore seals [NASA-TM-86978] 15 p2568 N85-25847
Analysis of the elastic and strength properties of Yucca Mountain tuff, Nevada [DE85-006975] 19 p3300 N85-30460
Preliminary evaluation of alterant geophysical tomography in welded tuff [DE85-010826] 19 p3302 N85-30469
Physical and chemical changes to rock near electrically heated boreholes at Spent Fuel Test-Climax [DE85-010834] 19 p3302 N85-30472
Shear wave transducer for boreholes [DE85-011662] 22 p3787 N85-33461
Generation of round bores in composite structure railguns [DE85-011872] 22 p3793 N85-33501
Fracture detection and characterization for geothermal reservoir definition [DE85-008677] 22 p3815 N85-33630
Lithology and stratigraphy of drill holes completed during 1984 in LANL use areas of Yucca Flat, Nevada Test Site, volume 6 [DE85-010695] 22 p3815 N85-33631
Design analysis for a repository in crystalline rock [DE85-011802] 22 p3839 N85-33771
Iron and manganese in oxide minerals and in glasses: Preliminary consideration of Eh buffering potential at Yucca Mountain, Nevada [DE85-011892] 23 p3916 N85-34271
BOREL SETS
Measure determining classes of balls in Banach space [CTH-MATH-1984-14] 04 p0556 N85-13541
Schubert varieties are arithmetically Cohen-Macaulay 16 p2853 N85-27592
BORES
U CAVITIES
BORESIGHT ERROR
Electromagnetic analysis of radomes by the moment method [AD-P004351] 12 p1824 N85-21445
Generalized radome BSE (radome boresight error) characterization using superposition techniques [AD-P004354] 12 p1825 N85-21448
A subaperture approach to the calculation of flashlobes introduced by airborne radomes [AD-P004355] 12 p1825 N85-21449
Near-field effects on radome boresight errors [AD-P004356] 12 p1825 N85-21450
Automated radome testing [AD-P004362] 12 p1826 N85-21456
Hot radome boresight error measurements [AD-P004364] 12 p1826 N85-21458
Ziv-Zakai bound applied to an amplitude-comparison monopulse radar [AD-A151937] 16 p2773 N85-27118
BORIDES
NT CHROMIUM BORIDES
NT TITANIUM BORIDES
High temperature thermoelectric energy conversion 05 p0610 N85-13894
Vapor pressure and evaporation rate of certain heat-resistant compounds in a vacuum at high temperatures [NASA-TM-77807] 10 p1434 N85-19036
A program to develop thermite reactions to produce refractory borides and carbides [AD-A148972] 10 p1434 N85-19037
Pressed boride cathodes [NASA-TM-77821] 17 p2918 N85-27984
Consortium program for the study of boron-rich borides [DE85-011378] 22 p3752 N85-33260
Magnitude and range of the RKKy interaction in SmRh4B4 [DE85-012284] 23 p3985 N85-34712
BORING MACHINES
Report on high-precision jig-boring machines 01 p0035 N85-10215
BORN APPROXIMATION
Plane-wave born collision strengths for electron-ion excitation: Comparison with other theoretical methods [DE85-002346] 10 p1555 N85-19802
Vacancy-rearrangement theory in the first Magnus approximation [DE85-004435] 12 p1930 N85-22123
Born inversion with a stratified reference velocity [AD-A149222] 16 p2853 N85-27594
BORN-MAYER EQUATION
U BORN APPROXIMATION
BORON
NT BORON FIBERS
NT BORON 10
Effects of cobalt, boron, and zirconium on the microstructure of Udimet 738 [NASA-CR-174762] 01 p0027 N85-10166
The determination of soluble and insoluble boron in steel by emission spectrometry using an inductively coupled plasma and a scanning monochromator 02 p0180 N85-11211
A study of precipitation and boron distribution in 20 Cr 25Ni base stainless steels [AERE-M-3353] 03 p0334 N85-12154
Boron cosmochemistry 06 p0888 N85-15642
Fuel-rich solid propellant boron combustion [AD-A148522] 08 p1136 N85-17157
CVD boron on calcium chromate powder [DE85-000214] 09 p1299 N85-18158
An infrared study of the hydrogenation of carbon dioxide on supported rhodium catalysts [AD-A149477] 10 p1436 N85-19049
Study of phase composition of Al-B plasma coatings 11 p1596 N85-20050
Research on the basic understanding of high efficiency in silicon solar cells [DE85-000507] 11 p1672 N85-20537
Theoretical studies on N-bonded pyrazole derivatives of boron [AD-A150036] 12 p1813 N85-21374
Status of boron combustion research 13 p1998 N85-22528
Gasification of boron oxide drops and boron slurry agglomerates in combustion gases 13 p1999 N85-22529
Technological process effect on the carrier lifetime degradation of silicon solar cell base layer irradiated by 1 MeV electrons (boron doping case) 13 p2007 N85-22585
Annealing of radiation damage in boron and gallium doped silicon solar cells 13 p2012 N85-22624
Weldability of Ni3Al-type aluminide alloys [DE85-006932] 15 p2512 N85-25496
Effect of nickel addition on the thermal, magnetic and magnetomechanical properties of Fe(80)B(15)Si(5) [AD-A152281] 16 p2749 N85-26967
The influence of melting practice and of microalloying, with rare earth metals and with boron, on the quality of low-carbon steel [BLL-BISI-22467-(9022.06)] 17 p2925 N85-28036
The conversion of smaller borane fragments to larger structures. Systematics of boron hydride reactions [AD-A153443] 18 p3070 N85-28985
Status of boron combustion research [AD-A154762] 21 p3563 N85-32160
Consortium program for the study of boron-rich borides [DE85-011378] 22 p3752 N85-33260
Evaluation of low-temperature geothermal potential in Utah and Goshen Valleys and adjacent areas, Utah. Part 2: Water temperature and chemistry [DE85-009344] 23 p3943 N85-34438
BORON ALLOYS
Copper-boron low alloy high strength steels 02 p0176 N85-11183
Radiation effects in amorphous metallic alloys [DE84-014302] 04 p0475 N85-13025
Structural properties of amorphous metals by Raman scattering [DE84-016947] 04 p0475 N85-13027
Electrical resistivity and structural changes upon relaxation and crystallization of (Mo/sub 0.6/Ru/sub 0.4)sub 100-x/B/sub x/ metallic glasses [DE84-017281] 09 p1299 N85-18160
Kinetics of the formation of a complex alloyed boride coating on iron and its properties [BLL-BISI-TRANS-22303-(9022.06)] 17 p2930 N85-28084
Examples of application of machinability tests [BLL-BISI-TRANS-22346-(9022.06)] 17 p2973 N85-28383
Thermoelectric properties of beta-boron and some boron compounds [DE85-011978] 21 p3582 N85-32270
BORON CARBIDES
Metallographic evaluation of the reactions between boronated graphite and Fe-Ni-Cr alloys [DE84-015374] 06 p0769 N85-14922
Anomalous electronic transport in boron carbides [DE84-015620] 06 p0868 N85-15518
Sintering reactions, structure and properties of a cobalt free nonconventional hard material [DE85-007704] 18 p3076 N85-29025
TFCK shielding optimization [DE85-010503] 19 p3359 N85-30626
Shield design for next-generation, low-neutron-fluence, superconducting tokamaks [DE85-011409] 23 p3962 N85-34695
Elliptical X-ray analyzer spectrograph application to a laser-produced plasma [DE85-013790] 24 p4097 N85-35398
BORON COMPOUNDS
NT BORANES
NT BORATES
NT BORIDES
NT BORON CARBIDES
NT BORON FLUORIDES
NT BORON HYDRIDES
NT BORON NITRIDES
NT BORON OXIDES
NT CARBORANE
NT CHROMIUM BORIDES
NT LITHIUM BORATES
NT TITANIUM BORIDES
The effect of temperature on the radiation induced losses of large diameter GPS (Germanium phosphosilicate) and GBS core optical fibers [AD-A145409] 02 p0280 N85-11823
Boron-nitrogen polymers. 1: Mechanistic studies of borazine pyrolyses [AD-A146470] 06 p0771 N85-14833
Thermoelectric properties of beta-boron and some boron compounds [DE85-011978] 21 p3582 N85-32270
BORON FIBERS
Chemical modification of the surface of high modulus carbon fibers 04 p0467 N85-12967
Damage to boron fibers during thermal cycling and annealing 10 p1445 N85-19107
Effect of surface state on durability of aluminized boron fibers 19 p3244 N85-30115
BORON FLUORIDES
On the origins of structural defects in BF2(+)-implanted and rapid thermally annealed silicon: Conditions for defect free regrowth [DE84-016060] 04 p0572 N85-13659
BORON HYDRIDES
NT BORANES
NT CARBORANE

Closed-bomb combustion of Hivelite-based, Very High Burn Rate (VHBR) propellant
[AD-A155740] 21 p3571 N85-32212

BORON ISOTOPES
NT BORON 10

BORON NITRIDES
The current status of diamond and cubic boron nitride composites 02 p0178 N85-11194
Boron-nitrogen polymers. 1: Mechanistic studies of borazine pyrolyses
[AD-A146470] 06 p0771 N85-14933
Tribological properties of boron nitride synthesized by ion beam deposition
[NASA-TM-86962] 12 p1810 N85-21355
BN coating of ceramic fibers for ceramic fiber composites
[AD-D011700] 19 p3249 N85-30145
Thermodynamics of high temperature materials
[AD-A154269] 19 p3378 N85-30958

BORON OXIDES
Method for removing oxide contamination from silicon carbide powders
[DE85-011648] 23 p3919 N85-34287

BORON REINFORCED MATERIALS
Experiences with implanted Back Surface Field (BSF) solar cells 13 p2005 N85-22571
Use of acoustical emission method to study specifics of fracture of boron reinforced plastic structural elements 13 p2026 N85-22696
Effect of operating medium on cyclic durability of AD33-W composite 13 p2029 N85-22716

BORON TRIFLUORIDE
U BORON FLUORIDES

BORON 10
Fast-neutron-spectrum measurements for the thick-target (9)Be(d/ = 7 MeV
[DE85-010461] 18 p3183 N85-29735
Spin dependence of the lamda-nucleus interaction determined by observation of hypernuclear gamma rays
[DE85-011878] 19 p3364 N85-30863

BOROSILICATE GLASS
Sealing ceramic material in low melting point glass
[NASA-TM-77599] 01 p0031 N85-10190
Structural evolution during the gel to glass conversion
[DE84-014954] 06 p0772 N85-14939
Effect of fatigue and thermal loads on silicon carbide fiber reinforced glass matrix composites
[DE85-006069] 15 p2503 N85-25441
Physical-chemical model for the mechanism of glass corrosion with particular consideration of simulated radioactive waste glasses
[DE85-007713] 17 p2935 N85-28121
Slow crack growth in metal reinforced glass composites
[DE85-010094] 18 p3082 N85-29064
Technical and historical overview of the study at Lawrence of porous antireflection coatings
[DE85-010925] 20 p3434 N85-31302
Thermal expansion of selected graphite reinforced polyimide-, epoxy-, and glass-matrix composite
[NASA-TM-87572] 21 p3561 N85-32149

BOSE-CHAUDHURI-HOCQUENGHEM CODES
U BCH CODES

BOSE-EINSTEIN STATISTICS
U QUANTUM STATISTICS

BOSONS
NT ALPHA PARTICLES
NT KAONS
NT LIGHT BEAMS
NT MESONS
NT MUONS
NT PHOTONS
NT PIONS
NT VECTOR MESONS
Sturmian expansion approximation to three-body scattering
[CSIR-TWISK-309] 01 p0109 N85-10731
Thin end of the wedge
[DE84-016439] 09 p1401 N85-18816
Cosmic axions
[DE85-001330] 09 p1418 N85-18944
Theoretical aspects of electroweak and other interactions in medium-energy nuclear physics
[DE85-003821] 13 p2157 N85-23392
Overview of the physics issues at the SSC
[DE85-007074] 16 p2859 N85-27634
Boson degrees of freedom in Fermion many-body systems
[DE85-006997] 16 p2863 N85-27660
Topics in intermediate vector boson physics
[NOTA-INTERNA-841] 18 p3184 N85-29743
Did bosonic sneutrino stars ever exist
[PREPRINT-421] 18 p3202 N85-29867
Boson-fermion symmetries in the W-Pt region
[DE85-009755] 19 p3362 N85-30845
The standard model and beyond
[DE85-010239] 19 p3362 N85-30847
New O(6) region near A = 130 and the interplay of triaxiality and gamma-softness in the IBA
[DE85-010957] 20 p3530 N85-31981
Exotic events of p bar p-collider: Excited quark or excited color boson? 21 p3691 N85-32930
Interacting Boson approximation
[DE85-003016] 22 p3837 N85-33756
Charge 4/3 leptons in cosmic rays
[HE-6.2-14] 24 p4212 N85-36150

BOTANY
NT GEOBOTANY
Botany facility, phase A study. Part 1: Executive summary — EURECA
[BF-DOC-10-VOL-1] 08 p1110 N85-17015
Botany facility phase A study. Core payload number 6 EURECA carrier, volume 1
[ESA-CR(P)-1978-VOL-1] 17 p2906 N85-27918
Botany facility phase A study. Core payload number 6 for EURECA carrier, volume 2
[BF-TD-DRD-03-VOL-2] 17 p2906 N85-27919

BOTTLES
Ten year environmental test of glass fiber/epoxy pressure vessels
[NASA-TM-87056] 19 p3231 N85-30034

BOUGUER LAW
Reduction to outside the atmosphere and statistical tests used in Geneva photometry 08 p1251 N85-17902
Aerosol multiple-scanning code, ASCAT
[LA-10046-MS] 12 p1823 N85-21440
Bouguer images of the North American craton
13 p2200 N85-23648
Optical stability, atmospheric transparency and aerosol absorption 19 p3297 N85-30442
Earth Albedo and the orbit of LAGEOS
[NASA-TM-86210] 21 p3558 N85-32131

BOULES
Ingot slicing machine and method
[NASA-CASE-NPO-15483-1] 12 p1857 N85-21650

BOUNDARIES
NT FLUID BOUNDARIES
NT FREE BOUNDARIES
NT GAS-SOLID INTERFACES
NT GRAIN BOUNDARIES
NT JET BOUNDARIES
NT LIQUID-LIQUID INTERFACES
NT LIQUID-SOLID INTERFACES
NT LIQUID-VAPOR INTERFACES
Metrological consequences of the hard optical boundary assumption
[PB84-223577] 01 p0121 N85-10827
Analysis of accretion and deletion at boundaries in dynamic scenes
[AD-A145944] 03 p0419 N85-12678
Multiple steady states for characteristic initial value problems
[NASA-CR-172486] 06 p0749 N85-14800
Deer control using 7 strand vertical fence
11 p1581 N85-19958
Numerical methods for tracking interfaces
[LA-9917-MS] 12 p1919 N85-22052
Thermal stability of static coronal loops: Part 1: Effects of boundary conditions
[NASA-CR-175495] 12 p1961 N85-22330
On meromorphic functions continuous on the Stollow boundary 15 p2633 N85-26232
On the boundary behaviour of a rotation automorphic function with finite spherical Dirichlet integral
15 p2634 N85-26238
Remarks of the maximal dilatation of the Beurling-Ahlfors extension 15 p2634 N85-26239
An IKBS approach to image understanding
[AD-A151992] 16 p2854 N85-27599
Transverse periodic boundary conditions in molecular dynamics with uniaxial strain shock waves
[DE85-006497] 16 p2863 N85-27656
Boundary to constructive solid geometry mappings: A focus on 2-D issues 17 p3004 N85-28570
Intermediate boundary conditions for LOD, ADI and approximate factorization methods
[NASA-CR-172591] 18 p3167 N85-29626
Mathematics of oil production
[DE85-011235] 19 p3267 N85-30261
Scaling differences between large interplate and intraplate earthquakes
[NASA-CR-176149] 23 p3948 N85-34467
A user-friendly computer-aided construction of boundaries 23 p3962 N85-34564
Dynamics of the penetration boundaries of solar protons during a strong magnetic storm
[SH-6.1-16] 23 p4046 N85-35089
Absorbing boundary conditions for exterior problems
[NASA-CR-177944] 24 p4142 N85-35676

BOUNDARY ELEMENT METHOD
Analysis of in-plane and out-of-plane ground motions using the boundary element method
[AD-A146229] 03 p0355 N85-12287
Boundary element methods in potential theory: Four lectures
[NPL-DITC-46/84] 05 p0718 N85-14604
Integral equation formulations in two dimensions
05 p0718 N85-14605
Applications of the simple-layer logarithmic potential
05 p0718 N85-14606
Applications of Green's boundary formula
05 p0718 N85-14607
Three-dimensional and axisymmetric problems
05 p0718 N85-14608
Element methods for calculation of sound fields
[RUB-IFM-MITT-41] 05 p0726 N85-14665
Transient dynamic solutions of some half space problems by the boundary element method
19 p3283 N85-30360
On the methods to determine the stress intensity factors in boundary element method 23 p3905 N85-34189

BOUNDARY LAYER CONTROL
NT POROUS BOUNDARY LAYER CONTROL
Hybrid laminar flow control study
[NASA-CR-165930] 02 p0137 N85-10933
Effect of upstream sidewall boundary layer removal on an airfoil test — conducted in Langley 0.3-m transonic cryogenic tunnel 03 p0313 N85-12019
Circulation control: A bibliography of DTNSRDC research and selected outside references: Update
[AD-A146966] 07 p0893 N85-15661
Improvement of Aerodynamic Performance Through Boundary Layer Control and High Lift Systems
[AGARD-CP-365] 08 p1068 N85-16771
An update of the Canada/USA augmentor-wing project 08 p1070 N85-16781
Aircraft drag reduction technology
08 p1070 N85-16782
Theoretical study of boundary-layer control
08 p1070 N85-16784
Drag reduction due to boundary-layer control by combined blowing and suction 08 p1070 N85-16785
Technology developments for laminar boundary layer control on subsonic transport aircraft
08 p1071 N85-16787
Shock/turbulent boundary layer interaction and its control 08 p1071 N85-16792
Active and passive shock/boundary layer interaction control on supercritical airfoils 08 p1072 N85-16795
Transonic shock interaction with a tangentially-injected turbulent boundary layer 08 p1072 N85-16796
Re-design of ARL/HLF (Heated Laminar Flow) body nose region
[AD-A150063] 12 p1846 N85-21585
Boundary layer control by transition fixing — conference
[DFVLR-MITT-84-17] 14 p2211 N85-23712
Boundary layer transition control for takeoff and landing configurations 14 p2211 N85-23714
Experiences with transition fixation in the high-speed regime at NLR 14 p2211 N85-23715
Transition fixing in the high speed range for the development of civil aircraft wings
14 p2211 N85-23716
Transition fixing on wings in industrial wind tunnels and associated problems 14 p2212 N85-23717
Transition fixing and simulation of high Reynolds number flow at transonic velocities 14 p2212 N85-23721
Numerical simulation of boundary layer excitation by surface heating/cooling
[NASA-CR-172575] 15 p2554 N85-25756
Three-Dimensional Boundary Layers
[AGARD-R-719] 15 p2558 N85-25784
Investigation to optimize the passive shock wave/boundary layer control for supercritical airfoil drag reduction
[NASA-CR-175788] 16 p2699 N85-26665
Numerical study of porous airfoils in transonic flow
[NASA-TM-86713] 17 p2892 N85-27826
Experiments on the influence of active walls on the initial amplitudes and growths of instability waves
[AD-A154630] 21 p3583 N85-32275

BOUNDARY LAYER EQUATIONS
Finite difference method for solving turbulent boundary layer equations 11 p1619 N85-20193
Low-dimensional behavior of the pattern formation Cahn-Hilliard equation
[DE85-003727] 12 p1922 N85-22072
Significance of the thin-layer Navier-Stokes approximation
[DE85-002630] 13 p2092 N85-23063
Three-Dimensional Boundary Layers
[AGARD-R-719] 15 p2558 N85-25784
Three-dimensional boundary layers: A report on work in Germany 15 p2559 N85-25786

Three-dimensional boundary layer research at NLR
15 p2559 N85-25787

Problems and opportunities with three-dimensional boundary layers — aircraft, missile, and ship components 15 p2559 N85-25789

Computational aerodynamics in designing aircraft
16 p2693 N85-26622

Boundary layer at moving cylinder surface
16 p2765 N85-27064

Boundary layer and parabolic flows
[DFVLR-FB-84-46] 17 p2960 N85-28285

On spectral multigrid methods for the time-dependent Navier-Stokes equations
[NASA-CR-172613] 19 p3344 N85-30725

BOUNDARY LAYER FLOW
NT BOUNDARY LAYER SEPARATION
NT REATTACHED FLOW
NT SECONDARY FLOW
NT SEPARATED FLOW

Measurement of the development of the boundary layer in the annulus walls of a fourstage compressor
[CUED/A-TURBO-TR-121] 01 p0046 N85-10299

Design and wind tunnel evaluation of a symmetric airfoil series for large wind turbine applications
[NASA-CR-174764] 02 p0135 N85-10919

Stability of heated boundary layers
02 p0196 N85-11311

Development in UK of a method for calculating tunnel wall corrections from flow measurements
03 p0314 N85-12026

Wall effects on the slow steady motion of a particle in a viscous incompressible fluid
[PREPRINT-828] 03 p0363 N85-12327

A local slot boundary condition for transonic flow calculations in slotted-wall test sections of wind tunnels
[FFA-TN-1984-34] 04 p0453 N85-12879

Incorporation of viscous-inviscid interactions in turbomachinery design
[PNR-90219] 04 p0457 N85-12897

Modelling viscous flow in turbomachinery
[PNR-90220] 04 p0457 N85-12898

Progress in the development of a two-fluid model of turbulence for near-wall flows, part 1
[CFD/84/7-PT-1] 04 p0501 N85-13196

Progress in the development of a two-fluid model of turbulence for near-wall flows. Part 3: Preliminary investigation of a stably-stratified boundary layer
[CFD/84/9-PT-3] 04 p0501 N85-13197

The resistance and mobility functions of two equal spheres in low Reynolds number flow
[AD-A147301] 07 p0959 N85-16080

Detailed study of the flow around a multi-element airfoil. Comparison with calculations 08 p1069 N85-16775

Application of two and three-dimensional criteria for calculating transitions and boundary layers over swept wings 08 p1070 N85-16783

Numerical modeling of steady, laminar free-convective boundary layer flow beneath heated or combusting horitzonal surfaces 08 p1160 N85-17318

Simultaneous flow visualization and unsteady lift measurement on an oscillating lifting surface
[AD-P004157] 09 p1264 N85-17942

Can the singularity be removed in time-dependent flows?
[AD-P004165] 09 p1265 N85-17950

Preliminary results from the unsteady airfoil model USTAR2
[AD-P004171] 09 p1266 N85-17956

Leading edge separation criterion for an oscillating airfoil
[AD-P004175] 09 p1267 N85-17960

Natural unsteadiness of a separation bubble behind a backward-facing step
[AD-P004176] 09 p1267 N85-17961

Averaging effects in models of three-dimensional two-phase flows
[AD-A149313] 10 p1484 N85-19371

A three-dimensional spectral algorithm for simulations of transition and turbulence
[NASA-CR-172561] 12 p1845 N85-21575

Wind-tunnel research on the mechanics of plumes in the atmospheric surface layer
[AD-A150019] 12 p1846 N85-21584

Aerodynamic heating rate distributions induced by trailing edge controls on hypersonic aircraft configurations at Mach 8
[NASA-TM-87453] 13 p1969 N85-22370

Preliminary study of inphase gusts and moment force wind loads over the first 150 meters at KSC, Florida
[NASA-TM-86501] 13 p2137 N85-23273

Calculating isothermal flow in wake beyond injection zone 14 p2287 N85-24175

SAMBO-GEOS: Substorm trapped particle particle boundary movements, particle precipitation and acceleration 14 p2361 N85-24589

Wind tunnel wall interference
[AD-A151212] 15 p2474 N85-25273

Comparison of computational results of a few representative three-dimensional transonic potential flow analysis programs 16 p2693 N85-26628

A curved test section for research on transonic shock wave-boundary layer interaction
[VTH-LR-414] 16 p2701 N85-26682

Numerical solution of transonic normal shock wave-boundary layer interaction using the Bohning-Zierop model — wind tunnel flow
[VTH-LR-416] 16 p2701 N85-26683

Numerical analysis of flow non-uniformity in the hot gas manifold of the Space Shuttle main engine
16 p2738 N85-26899

Vortex studies relating to boundary layer turbulence and noise
[NASA-TM-87475] 16 p2782 N85-27169

A Navier-Stokes capillary free boundary in open boat crystal growth
[REPT-84-34] 17 p2960 N85-28283

Tidal rectification in lateral viscous boundary layers of a semienclosed basin
[CWI-AM-R8415] 17 p2960 N85-28284

Boundary layer and parabolic flows
[DFVLR-FB-84-46] 17 p2960 N85-28285

The transport of neutral H, D, T and He and O in the boundary layers of a Tokamak plasma
[REPT-84-153] 17 p3041 N85-28817

Combined riblet and LEBU drag reduction system
[NASA-CASE-LAR-13286-1] 18 p3058 N85-28922

An experimental investigation of curvature and freestream turbulence effects on heat transfer and fluid mechanics in transitional boundary layer flows
19 p3264 N85-30240

The application of laser anemometry to the study of transonic shock boundary-layer interactions
[ISL-CO-204/84] 20 p3396 N85-31067

Transition in a disturbed environment
20 p3452 N85-31436

On the solution for the sound field in a semi-infinite uniform duct with sheared mean flow
20 p3523 N85-31912

An evaluation of four methods of numerical analysis for two-dimensional airfoil flows
[AD-A155202] 21 p3552 N85-32096

A comparison of laser Doppler anemometry and probe measurements within the boundary layer of an airfoil at subsonic flow
[ISL-CO-219/84] 23 p3895 N85-34127

Adverse pressure gradient and separating turbulent boundary-layer flows: The effect of disequilibrium in initial conditions 24 p4059 N85-35155

Studies on effects of boundary conditions in confined turbulent flow predictions
[NASA-CR-3929] 24 p4093 N85-35371

BOUNDARY LAYER NOISE
U AERODYNAMIC NOISE
U BOUNDARY LAYERS

BOUNDARY LAYER PLASMAS

Some contributions to knowledge of the magnetospheric plasma by ISEE-1 investigators
14 p2354 N85-24548

Hot plasma and energetic particles in the Earth's outer magnetosphere: New understandings during the IMS
14 p2355 N85-24552

Satellite-borne electric field measurements with spherical double probes — ISEE satellites
14 p2356 N85-24558

Structure of the boundary layer for steady-state magnetopause reconnection 14 p2356 N85-24561

Electric fields in the plasma sheet and plasma sheet boundary layer 14 p2357 N85-24562

The ionospheric O+ streams in the magnetotail between 22 RE and 6 RE 14 p2360 N85-24582

SAMBO-GEOS: Substorm trapped particle particle boundary movements, particle precipitation and acceleration 14 p2361 N85-24589

Images of the Earth's aurora and geocorona from the Dynamics Explorer Mission
[NASA-CR-175983] 18 p3136 N85-29423

The temporal evolution of a small auroral substorm as viewed from high altitudes with Dynamics Explorer 1
[NASA-CR-176064] 20 p3493 N85-31718

Wave/particle interactions in the plasma sheet
[NASA-CR-171537] 20 p3547 N85-32072

BOUNDARY LAYER SEPARATION

Prediction of aerodynamic characteristics of fighter wings at high angles of attack
[AD-A145107] 01 p0003 N85-10017

An integral method for analyzing incompressible two dimensional turbulent boundary layers with separation
02 p0196 N85-11309

Approximate solution of a laminar flow over a flat plate with suction and pressure gradient
[AD-A145482] 02 p0198 N85-11321

Geometric characteristics of turbulent boundary layer separation upon action with direct shock wave in conical flows 02 p0269 N85-11755

Laminar and turbulent boundary layers in a plane of symmetry
[AD-A146261] 03 p0362 N85-12323

The role of freestream turbulence scale in subsonic flow separation
[NASA-CR-174172] 04 p0452 N85-12870

Surge and stall in centrifugal compressors
05 p0637 N85-14087

Investigation of phase separation models in RELAP 4/MOD 6
[OEFZS-4286] 05 p0638 N85-14093

Unsteady flow characteristics in the near-wake of a two-dimensional obstacle
[NASA-TM-77762] 07 p0897 N85-15684

Some important problems in unsteady boundary layers including separation. 2: Unsteady boundary layers close to the stagnation region of slender bodies
[AD-A146964] 07 p0958 N85-16069

Some important problems in unsteady boundary layers including separation. 1: Nature of singularity on oscillating airfoils
[AD-A147897] 07 p0960 N85-16067

Drag reduction due to boundary-layer control by combined blowing and suction 08 p1070 N85-16785

Pneumatic turbulators: A device for drag reduction at Reynolds numbers below 5 million
08 p1071 N85-16791

Prediction of dynamic stall characteristics using advanced nonlinear panel methods
[AD-P004160] 09 p1264 N85-17945

Some structural features of unsteady separating turbulent shear flows
[AD-P004164] 09 p1265 N85-17949

On the shedding of vorticity at separation
[AD-P004166] 09 p1265 N85-17951

Genesis of unsteady separation
[AD-P004173] 09 p1266 N85-17958

Flow separation induced by periodic aerodynamic interference
[AD-P004174] 09 p1266 N85-17959

Numerical approach for the aerodynamic analysis of airfoils with laminar separation
[NASA-CR-172496] 09 p1273 N85-18001

Laminar separation bubble with transition: Prediction test with local interaction — airfoils
[PNR-90231] 09 p1274 N85-18006

Experimental studies of Quasi-Two-Dimensional and three-dimensional viscous interaction regions induced by skewed-shock and swept-shock boundary layer interactions
[AD-A150060] 12 p1847 N85-21587

Double and inverse Taylor-Hogg vortices in a stratified ocean 13 p2108 N85-23137

The structure of separated flow regions occurring near the leading edge of airfoils, including transition
[NASA-CR-175670] 14 p2209 N85-23703

Application possibilities of laser Doppler anemometry in the investigation of the transonic interaction between shock wave and boundary layer
[ISL-R-131/83] 14 p2304 N85-24285

Low-speed aerodynamic test of an axisymmetric supersonic inlet with variable cowl slot
[NASA-TM-87039] 16 p2708 N85-26710

Structural stability and bifurcation in conical flow fields
[VTH-LR-424] 16 p2803 N85-27282

An experimental investigation of a turbulent junction vortex
[NASA-CR-175915] 17 p2957 N85-28259

Proceedings of the 9th US Air Force and the Federal Republic of Germany Data Exchange Agreement Meeting. Viscous and Interacting Flow Field Effects
[AD-A153020] 17 p2958 N85-2830

Turbulence structure in the boundary layers of an oscillating airfoil
[AD-A153631] 18 p3059 N85-289

A study of aerodynamic control in stalled flight long laminar separation bubble analysis
[AD-A153650] 18 p3059 N85-289

Effect of leading-edge load constraints on the design and performance of supersonic wings
[NASA-TP-2446] 19 p3213 N85-299

Two approaches for the prediction of plume-induced separation
[AD-A154098] 19 p3215 N85-299

SANDRAG: A computer code for predicting drag of bodies of revolution at zero angle of attack in incompressible flow
[DE85-011170] 19 p3338 N85-308

Two-dimensional separation in an incompressible flu — boundary layer separation
[ONERA-RTS-16/3232-RY-060-R]
20 p3456 N85-3145

An evaluation of four methods of numerical analysis for two-dimensional airfoil flows
[AD-A155202] 21 p3552 N85-32098

Experimental investigations on airfoils with different geometries in the domain of high angles of attack-flow separation
[NASA-TM-77802] 22 p3728 N85-33110

Modelling of unsteady, incompressible separation on an aerofoil using an inviscid flow algorithm
[GU-AERO-8412] 23 p3894 N85-34122

Study of boundary layer separation on a supercritical profile with a spoiler by means of a laser Doppler velocimeter
[ISL-CO-225/84] 23 p3895 N85-34128

Computation of three-dimensional shock wave and boundary-layer interactions
[NASA-TM-86760] 24 p4093 N85-35372

BOUNDARY LAYER STABILITY

Stability of heated boundary layers
02 p0196 N85-11311

On the instability of a 3-dimensional attachment line boundary layer: Weakly nonlinear theory and a numerical approach
[NASA-CR-172504] 07 p0957 N85-16063

Perturbation of a multiple eigenvalue in the Benard problem for two fluid layers
[AD-A149068] 10 p1546 N85-19745

The unsteady boundary layer on an elliptic cylinder following the impulsive onset of translational and rotational motion — dynamic stall 14 p2209 N85-23699

Generation and development of small-amplitude disturbances in a laminar boundary layer in the presence of an acoustic field
[NASA-TM-77826] 14 p2299 N85-24237

Stability of an oscillating boundary layer
[NASA-TM-77827] 14 p2299 N85-24238

Convective instability of horizontal layer of binary mixture 14 p2338 N85-24458

Structural stability and bifurcation in conical flow fields
[VTH-LR-424] 16 p2803 N85-27282

Application of the MHD energy principle to magnetostatic atmospheres
[NASA-CR-175967] 18 p3136 N85-29420

A survey of wind and turbulence modeling methods
[AD-A154470] 20 p3496 N85-31733

Mesoscale features and atmospheric refraction conditions of the Arctic marginal ice zone
[AD-A155139] 21 p3636 N85-32584

Development of artificially produced perturbations in supersonic boundary layer 21 p3683 N85-32879

BOUNDARY LAYER TRANSITION

A review and analysis of boundary layer transition data for turbine application
[NASA-TM-86880] 01 p0047 N85-10306

Natural laminar flow airfoil design considerations for winglets on low-speed airplanes
[NASA-CR-3853] 04 p0452 N85-12883

Experiments on the structure of turbulent reattaching flow 05 p0635 N85-14074

Application of two and three-dimensional criteria for calculating transitions and boundary layers over swept wings 08 p1070 N85-16783

Orbiter entry aerothermodynamics
08 p1104 N85-16978

Aerothermal tests of a 12.5 percent cone at Mach 6.7 for various Reynolds numbers, angles of attack and nose shapes — conducted in Langley 8-foot high temperature tunnel
[NASA-TP-2345] 08 p1161 N85-17322

Research done at DERAT (October 1982 through September 1983); summary of principal results obtained
[NASA-TM-77786] 08 p1228 N85-17730

Laminar separation bubble with transition: Prediction test with local interaction — airfoils
[PNR-90231] 09 p1274 N85-18008

Flight-measured laminar boundary-layer transition phenomena including stability theory analysis
[NASA-TP-2417] 12 p1771 N85-21118

Skin friction measurements for 2 relatively thick airfoil sections at high Reynolds number
[AD-A150021] 12 p1772 N85-21125

Re-design of ARL/HLF (Heated Laminar Flow) body nose region
[AD-A150063] 12 p1846 N85-21585

Hydrodynamic stability problem formulated by numerical solutions of the Navier-Stokes equations
12 p1946 N85-22223

Boundary layer control by transition fixing — conference
[DFVLR-MITT-84-17] 14 p2211 N85-23712

Boundary layer transition control for takeoff and landing configurations 14 p2211 N85-23714

Experiences with transition fixation in the high-speed regime at NLR 14 p2211 N85-23715

Transition fixing in the high speed range for the development of civil aircraft wings
14 p2211 N85-23716

Transition fixing on wings in industrial wind tunnels and associated problems 14 p2212 N85-23717

The influence of transition strips on the pressure distribution on transonic profiles
14 p2212 N85-23718

Development of an artificial boundary layer for different outlet flows 14 p2212 N85-23719

Investigation of the conditions for tripping transition with roughness elements and their influence on boundary layer development 14 p2212 N85-23720

Transition fixing and simulation of high Reynolds number flow at transonic velocities 14 p2212 N85-23721

Transition detection using surface pressure holes
14 p2212 N85-23722

Investigations of the experimental detection of boundary layer transitions 14 p2213 N85-23723

Three-dimensional boundary layers and shear flows activities at ONERA/CERT 15 p2558 N85-25785

Brief review of current work in the UK on three dimensional boundary layers 15 p2559 N85-25788

On the effect of wing taper and sweep direction on leading edge transition
[CA-8435] 17 p2892 N85-27827

An experimental investigation of curvature and freestream turbulence effects on heat transfer and fluid mechanics in transitional boundary layer flows
19 p3264 N85-30240

Transition in Turbines
[NASA-CP-2386] 20 p3452 N85-31433

Experimental observation of transition behavior on a flat plate 20 p3452 N85-31437

Flat-plate transition 20 p3452 N85-31438

Heat transfer and fluid mechanics measurements in transitional boundary layer flows
20 p3453 N85-31439

A review and analysis of boundary layer transition data for turbine application 20 p3453 N85-31440

Bypass transition to turbulence and research Desiderata 20 p3453 N85-31442

Slow tearing modes: Transitions to instability
20 p3534 N85-31969

Development of a temperature-compensated hot-film anemometer system for boundary-layer transition detection on high-performance aircraft
[NASA-TM-86732] 22 p3730 N85-33121

Nozzle wall roughness effects on free-stream noise and transition in the pilot low-disturbance tunnel
[NASA-TM-86389] 23 p3930 N85-34355

BOUNDARY LAYERS

NT ATMOSPHERIC BOUNDARY LAYER
NT COMPRESSIBLE BOUNDARY LAYER
NT HYPERSONIC BOUNDARY LAYER
NT INCOMPRESSIBLE BOUNDARY LAYER
NT LAMINAR BOUNDARY LAYER
NT PLANETARY BOUNDARY LAYER
NT SUPERSONIC BOUNDARY LAYERS
NT THERMAL BOUNDARY LAYER
NT THREE DIMENSIONAL BOUNDARY LAYER
NT TURBULENT BOUNDARY LAYER
NT TWO DIMENSIONAL BOUNDARY LAYER

Prediction of aerodynamic characteristics of fighter wings at high angles of attack
[AD-A145107] 01 p0003 N85-10017

The development of a diode laser Doppler velocimeter for boundary layer measurements under ice: A feasibility investigation
[AD-A145076] 01 p0053 N85-10348

Effect of upstream sidewall boundary layer removal on an airfoil test — conducted in Langley 0.3-m transonic cryogenic tunnel 03 p0313 N85-12019

Effect of boundary layers on solid walls in three-dimensional subsonic wind tunnels
03 p0313 N85-12023

Investigations of boundary layers in the Emmen Federal Aircraft works transonic tunnel, Switzerland
[FW-FO-1641] 04 p0453 N85-12877

Meteorological analysis for clusters of wind turbines
[DE84-013164] 04 p0539 N85-13425

Boundary layer simulator improvement
[NASA-CR-174199] 05 p0597 N85-13802

Influence of inter-layer effect on charge gas-permeability
[BLL-M-35919-(5828.4)] 05 p0616 N85-13940

Atmospheric studies in complex terrain
[DE84-006553] 05 p0676 N85-14345

An investigation of the marine boundary layer during cold air outbreak 05 p0680 N85-14368

Structure and growth of the marine boundary layer
05 p0680 N85-14369

Linear problem of harmonic vibrator acting at supercritical frequencies in subsonic boundary layer
06 p0779 N85-14978

Existence and non-uniqueness of similarity solutions of a boundary layer problem
[NASA-CR-172503] 07 p0957 N85-16064

Aero-optics experimental techniques
[AD-A146755] 07 p0957 N85-16067

Some important problems in unsteady boundary layers including separation. 2: Unsteady boundary layers close to the stagnation region of slender bodies
[AD-A146964] 07 p0958 N85-16069

Bulk cavitation caused by a plane shock wave
[AD-A147031] 07 p0958 N85-16072

Free-surface boundary layer and the origin of bow vortices
[AD-A147427] 07 p0960 N85-16083

Shock/turbulent boundary layer interaction and its control 08 p1071 N85-16792

Active and passive shock/boundary layer interaction control on supercritical airfoils 08 p1072 N85-16795

An experimental study on the instability of a mixing-layer with laminar wake as the initial condition
08 p1076 N85-16824

Corrections for attached sidewall boundary-layer effects in 2-dimensional airfoil testing
[NASA-CR-3873] 09 p1272 N85-17997

Heat-transfer enhancement in natural convection enclosure flow
[DE84-013048] 09 p1319 N85-18297

Benthic boundary layer, IOS observational programme: Discovery Gap measurements, March 1984 — Institute of Oceanographic Sciences (IOS)
[ISO-180] 09 p1359 N85-18552

Efficient self-consistent viscous-inviscid solutions for unsteady transonic flow
[NASA-TM-86335] 10 p1420 N85-18959

Evaluation of inviscid/boundary layer and parabolized Navier-Stokes solutions for design of reentry vehicles
[DE84-014329] 10 p1428 N85-19006

A frozen vorticity approach to the axisymmetric strong interaction problem
[AD-A149101] 10 p1484 N85-19369

Perturbation of a multiple eigenvalue in the Benard problem for two fluid layers
[AD-A149068] 10 p1546 N85-19745

Instrumentation for Application Number 1: Mass spectrometric analysis of the boundary layer associated with the tethered satellite 11 p1646 N85-20372

Turbulence parameters impacting dispersion in an urban convection boundary layer
[PB85-116036] 11 p1682 N85-20598

Pre-turbulence: Transitional Laminar-turbulent flows
11 p1716 N85-20793

Numerical study of large-eddy breakup and its effect on the drag characteristics of boundary layers
[NASA-CR-3884] 12 p1797 N85-21272

Investigations of micro-turbulence in the bottom of the boundary layer
[AD-A149823] 12 p1896 N85-21897

Non-precipitating cumulus cloud study
[DE85-002352] 12 p1896 N85-21902

Investigations of reactive and non reactive acoustic boundary layers in porous walled ducts
13 p2000 N85-22535

The relationship between marine aerosol particles and satellite-detected radiance 13 p2131 N85-23263

H-division materials physics progress
[DE85-004990] 13 p2165 N85-23430

Three-layer generic Ganymedes: Structure and evolution 13 p2202 N85-23657

Comparison of measured and computed boundary layers at the tail-end of an axisymmetric body in an air-jet
[AMTE(N)-TM-83053] 14 p2209 N85-23700

Effect of form and clearance of a piston launched in a tube on the boundary layer and the heat transfer
[ISL-CO-216/83] 14 p2302 N85-24255

Low Reynolds number vehicles
[AGARD-AG-288] 16 p2699 N85-26686

Modeling plasma mantle of Earth's magnetosphere
16 p2720 N85-26790

On the effect of wing taper and sweep direction on leading edge transition
[CA-8435] 17 p2892 N85-27827

Free-surface phenomena under low- and zero-gravity conditions
[NASA-CR-175885] 17 p2907 N85-27922

The boundary layers as the primary transport regions of the Earth's magnetotail
[AD-A152714] 17 p2992 N85-28496

Post-stall wind tunnel data for NACA 44XX series airfoil sections
[DE85-002948] 18 p3060 N85-28931

Development and testing of the variable vertical resolution Fourth Order GCM 18 p3142 N85-29453

Parameterization of surface fluxes in the VVR Fourth Order GCM 18 p3142 N85-29454

Specification of surface roughness over oceans in the GLAS Fourth Order GCM 18 p3142 N85-29455

Modifications to SOLA-VOF for flow dynamics in spinning cylinders
[AD-A154093] 19 p3265 N85-30250

Sidewall boundary-layer effects in two-dimensional airfoil testing
[NASA-CR-176034] 20 p3396 N85-31065

Numerical and experimental investigation of turbomachinery rotor flow fields
20 p3451 N85-31429

Benthic boundary layer modelling studies
[IOS-181] 20 p3497 N85-31742

Mean and large-scale turbulence characteristics of the noise-producing region of an acoustically excited round jet 20 p3523 N85-31911

Applicability of surface CCN measurements
21 p3652 N85-32696

Evaluation of source strength and dispersion model predications with data from large nitrogen tetroxide field experiments
[DE85-011855] 23 p3947 N85-34485

Unsteady flow in a supersonic cascade with two in-passage shocks
[NASA-CR-3925] 24 p4060 N85-35158

BOUNDARY LUBRICATION

Formation of high molecular weight products from benzene during boundary lubrication
[NASA-TM-86986] 13 p2017 N85-22644

BOUNDARY VALUE PROBLEMS

NT CAUCHY PROBLEM
NT DIRICHLET PROBLEM
NT NEUMANN PROBLEM

Wave multiple scattering by a finite number of unclosed circular cylinders
[NASA-TM-77593] 01 p0037 N85-10232

The initialization of mesoscale models
01 p0079 N85-10529

The approximation of nonsmooth solutions of hyperbolic partial differential equations
[CSIR-TWISK-297] 01 p0108 N85-10723

Location of several outliers in multiple regression data using elemental data
[CSIR-TWISK-300] 01 p0108 N85-10724

The convergence of Garlerkin approximation schemes for second-order hyperbolic equations with dissipation
[CSIR-TWISK-325] 01 p0109 N85-10736

On wave propagation in linear viscoelasticity
[AD-A144739] 01 p0111 N85-10750

Boundary behavior of analytic functions, analytic wave front sets and the intersection problem of Ehrenpreis
[PREPRINT-809] 01 p0114 N85-10778

Characteristic boundary conditions for three-dimensional transonic unsteady aerodynamics
[NASA-TM-86292] 02 p0134 N85-10915

Boundary conditions in Chebyshev and Legendre methods
[NASA-CR-172469] 02 p0250 N85-11635

Numerical methods for singularly perturbed differential equations with applications
[AD-A145839] 02 p0252 N85-11650

Theory of radio wave propagation over the ocean
02 p0259 N85-11698

Effects of the oceans on polar motion: Continued investigations
[E85-10037] 03 p0379 N85-12416

Dynamic occlusion analysis in optical flow fields
[AD-A145805] 03 p0406 N85-12594

A comparative study of the finite element and boundary element methods as applied to a boundary value problem of a harmonic function
[AD-A146018] 03 p0411 N85-12627

Free-edge failures of composite laminates
04 p0467 N85-12971

Interval mathematics reports
[REPT-84/1] 04 p0556 N85-13536

Interval-mathematical treatment of initial value problems of ordinary differential equations
04 p0556 N85-13538

Applications of the simple-layer logarithmic potential
05 p0718 N85-14606

Loeb solutions of the Boltzmann equation with initial boundary values and external forces
[CTH-MATH-1984-23] 05 p0719 N85-14616

Step-by-step stability in the numerical solution of partial differential equations
[CWI-NW-161/83] 05 p0720 N85-14623

Mixed defect correction (iteration) for the solution of a singular perturbation problem
[MC-NW-162/83] 05 p0720 N85-14624

Convergence of method of lines approximations to partial differential equations
[CWI-NM-R8404] 05 p0720 N85-14627

Multiple steady states for characteristic initial value problems
[NASA-CR-172486] 06 p0749 N85-14800

Free-surface boundary layer and the origin of bow vortices
[AD-A147427] 07 p0980 N85-16063

Multivariate spline methods in surface fitting
07 p0985 N85-16257

Solution of partial differential equations on vector and parallel computers
[NASA-CR-172500] 07 p1028 N85-16525

An operator method for computing the asymptotics of a collision resolution interval
[AD-A146837] 07 p1028 N85-16528

Viscosity solutions of Hamilton-Jacobi equations at the boundary
[AD-A147444] 07 p1032 N85-16553

Nonlinear wave propagation
[AD-A148114] 08 p1152 N85-17269

Weakly-reflective boundary conditions for two-dimensional shallow water flow problems
[PUBL-322] 08 p1163 N85-17341

Numerical solution of elastodynamic problems in fracture mechanics 08 p1171 N85-17385

An invariant measure for the equation u sub tt - u sub xx + u3 = O
[AD-A147300] 08 p1210 N85-17612

A finite difference method for inverse mode calculations of a three-dimensional boundary layer
[ESA-TT-863] 09 p1274 N85-18007

A finite element analysis of viscoelastic materials with varying time scales 09 p1330 N85-18355

Mechanical and transient hygrothermal loading of multilayer orthotropic cylinders 09 p1330 N85-18359

Boundary conditions for artificial dissipation operators — convection
[FFA-TN-1984-53] 09 p1375 N85-18642

Evaluation of inviscid/boundary layer and parabolized Navier-Stokes solutions for design of reentry vehicles
[DE84-014329] 10 p1428 N85-19006

Methodology for stress analysis of heavy metal plate
10 p1460 N85-19203

A program design for an adaptive, non-linear finite element solver
[AD-A148880] 10 p1539 N85-19705

Asymptotic representation of solutions of the basic semiconductor device equations
[AD-A149040] 10 p1545 N85-19741

Recent developments and open problems in the mathematical theory of viscoelasticity
[AD-A149043] 10 p1545 N85-19742

Vectorization and implementation of an efficient multigrid algorithm for the solution of elliptic partial differential equations
[AD-A149049] 10 p1545 N85-19743

Neumann type boundary conditions for Hamilton-Jacobi equations
[AD-A149069] 10 p1546 N85-19746

Numerical solution of semilinear elliptic problems on unbounded domains
[AD-A149559] 10 p1549 N85-19767

Comparison of spherical wave ray tracing and exact boundary value solutions for spherical radomes
[AD-P004353] 12 p1824 N85-21447

A study of coupling the boundary and finite element methods in two-dimensional elastostatics
[AD-A149619] 12 p1865 N85-21702

A convergent series expansion for hyperbolic systems of conservation laws
[NASA-CR-172557] 12 p1910 N85-21990

The performance of a type-insensitive Runge-Kutta code on a personal computer
[TUM-I8410] 12 p1919 N85-22048

Determining conductivity by boundary measurements. Part 2: Interior results
[AD-A148750] 12 p1921 N85-22063

Propagation of three-dimensional turbulent jet from lobar nozzle through surrounding stream
13 p2042 N85-22785

Liquid moment on a filled coning cylinder during spin-up: Ad hoc model
[AD-A150280] 13 p2092 N85-23060

Calculating boundary layer on profile with laminar and turbulent flow zone 14 p2286 N85-24177

On the shift parameter in the backward beam method for parabolic problems for preceding times
[CWI-NM-R8411] 14 p2410 N85-24861

High specific power aircraft turn maneuvers: Tradeoff of time-to-turn versus change in specific energy
[AD-A151701] 15 p2471 N85-25257

Control of a flexible beam
[DE85-007243] 15 p2580 N85-25914

A problem of Burkholder and the existence of harmonic majorants of the absolute value of x sup p in certain domains in R sup d 15 p2634 N85-26236

A new approach to queer differential equations
[AD-A149321] 15 p2636 N85-26272

Propagation of wave packet in a dissipative dielectric medium
[IPPJ-710] 15 p2655 N85-26385

A numerical design method for three-dimensional transonic wings 16 p2694 N85-26631

Three-dimensional wing boundary layer analysis program BLAY and its application
16 p2694 N85-26632

Optimum rotation of solid body with 1 axis of symmetry 16 p2718 N85-26781

Accuracy of the calculated stress field around a craze
[DE85-005520] 16 p2801 N85-27272

An approximation to the problem of a pin-loaded hole in an orthothropic plate
[VTH-LR-386] 16 p2802 N85-27278

Incorporation of an elliptical boundary condition into the program POISSON
[DE85-006820] 16 p2849 N85-27584

The vector potential in a branched Riemann space
[VTH-LR-395] 16 p2856 N85-27614

On the accuracy of the Poincare-Lindstedt method
[REPT-84-37] 17 p3022 N85-28690

On the algebraic equations in implicit Runge-Kutta methods
[CWI-NM-R8413] 17 p3022 N85-28698

Analysis of nonlinear parabolic equations modeling plasma diffusion across a magnetic field
[DE85-007683] 17 p3040 N85-28807

Recent developments in nonlinear normal mode initialization 18 p3142 N85-29451

Singularity solutions for ellipsoids in Low-Reynolds-Number flows: With applications to the calculation of hydrodynamic interactions in suspensions of ellipsoids
[AD-A153503] 18 p3168 N85-29632

Sensitivity analysis of initial value problems with mixed ode's and algebraic equations
[AD-A153528] 18 p3169 N85-29637

On the numerical computation of nonlinear force-free magnetic fields 18 p3203 N85-29871

Numerical methods for the solution of stiff delay differential equations 19 p3334 N85-30653

Well-posedness of one-way wave equations and absorbing boundary conditions
[NASA-CR-172619] 19 p3345 N85-30727

Asymptotic expansions for the finite element approximation of parabolic functions
19 p3345 N85-30731

Superconvergence of finite element approximation for Navier-Stokes equations 19 p3345 N85-30732

On MGR (Upsilon) multigrid methods
[AD-A153667] 19 p3345 N85-30733

Solving Volterra integral equations with ODE codes
[DE85-011216] 19 p3346 N85-30740

Electromagnetic lateral waves in layered media
19 p3369 N85-30894

Approximate solution to the problem of heating massive bodies by radiation
[BLL-M-36272-(5828.4)] 20 p3450 N85-31422

User's manual of the BNDSCO computer program for solving constrained optimal control problems
[DFVLR-MITT-85-05] 20 p3516 N85-31865

Attractors for the Kuramoto-Sivashinsky equations
[DE85-009631] 20 p3520 N85-31892

Scattering from foliage covered terrain
[AD-A154724] 21 p3574 N85-32228

Oscillatory solutions of the Peaceman-Rachford alternating direction implicit method and a comparison of methods for the solution of the two dimensional heat diffusion equation
[AD-A154670] 21 p3675 N85-32833

Sobolev-Poincare's inequality and the Neumann problem for u sub t = divergence of the absolute value of the gradient u to the p-2 power x the gradient u
[AD-A154788] 21 p3676 N85-32839

Exact solutions of singular equations for viscous transonic flows 21 p3683 N85-32882

Comments on two matters related to turbulent combustion 22 p3743 N85-33204

Pressure correlations in turbulent reacting flows
22 p3744 N85-33205

Fundamentals of radio optical theory of resonant and directional quasi-optical devices
22 p3780 N85-33420

Linear boundary detection using pressure buildup tests
[DE85-009926] 22 p3784 N85-33444

A new method for boundary value problems
[AD-A155934] 24 p4143 N85-35683

Some rigorous results concerning spectral theory for ideal MHD
[DE85-013427] 24 p4156 N85-35770

BOUSSINESQ APPROXIMATION

Some approximations of geophysical hydrodynamics
14 p2336 N85-24448

Two-point closure study of covariance budgets for turbulent Rayleigh-Benard convection
[PB85-189106] 24 p4124 N85-35568

BOW SHOCK WAVES
U BOW WAVES
U SHOCK WAVES

BOW WAVES
The propagation and growth of whistler mode waves generated by electron beams in Earth's bow shock
[AD-A145572] 02 p0228 N85-11492
Magnetohydrodynamic and gasdynamic theories for planetary bow waves
[NASA-CR-174132] 03 p0448 N85-12850
Magnetohydrodynamic and gasdynamic theories for planetary bow waves
[NASA-CR-174135] 04 p0589 N85-13760
Waves and instabilities in collisionless shocks
[AD-A146889] 06 p0881 N85-15597
Research study of space plasma boundary processes
[NASA-CR-174351] 10 p1558 N85-19823
Electric field and plasma observations near the magnetopause and bow shock during a rapid compression 14 p2355 N85-24553
The keV electrons and 80 keV protons in the vicinity of the high latitude magnetosphere and at the bow shock 14 p2355 N85-24554
Satellite-borne electric field measurements with spherical double probes — ISEE satellites
14 p2356 N85-24558
Magnetohydrodynamics of Earth's bow shock
15 p2481 N85-25311
Fast and optimal solution to the Rankine-Hugoniot problem
[NASA-TM-86214] 19 p3344 N85-30724
Properties of the reflected beams from the Earth's bow shock: A simple model
[IFSI-84-14] 20 p3549 N85-32088

BOXES (CONTAINERS)
An automatic device for amphibian egg fertilization in space: Technical aspects and biological requirements
05 p0689 N85-14427
Double window viewing chamber assembly
[NASA-CASE-MFS-28057-1] 18 p3063 N85-28951

BRAGG ANGLE
Bragg reflection of surface electroacoustic shear waves 04 p0485 N85-13096
Bragg cell spectrum analyzer specification
[AD-D011320] 07 p1044 N85-16629
Influence of Bragg reflecting lattice groove depth modulation on Rayleigh wave reflection coefficient
10 p1499 N85-19458

BRAGG CURVE
Results from a Bragg curve spectrometer
[DE85-007870] 18 p3176 N85-29691

BRAIN
NT BRAIN STEM
NT CEREBELLUM
NT CEREBRAL CORTEX
NT CEREBRAL VENTRICLES
NT CEREBRUM
Compensatory and adaptive regional hemodynamic reactions to weightlessness during long-term spaceflights 01 p0091 N85-10616
Effect of short-term hypokinesia on rat opioid system reaction 01 p0093 N85-10625
Hemodynamics and neurodynamics of the human brain during exposure to moderate hypoxic hypoxia
01 p0094 N85-10630
Cognitive science program. A framework for relating cognitive to neural systems
[AD-A145185] 01 p0097 N85-10649
Neural control of the direction of covert visual orienting
[AD-A145189] 01 p0097 N85-10650
Mechanisms of oxygen toxicity and methods of protection
[AD-A145830] 03 p0400 N85-12551
Reflection of laterization of sound stimuli in evoked potentials of human brain 04 p0544 N85-13463
ERPS to monitor non-conscious mentation
05 p0707 N85-14536
Performance enhancements under dual-task conditions 05 p0707 N85-14537
Measurement of workload: Physics, psychophysics, and metaphysics 05 p0708 N85-14539
Distribution of blood flow to brain, kidneys, gut, spleen and posterior extremities in cats in acute hypoxia
07 p1013 N85-16434
Lateral specifics of visual perception
07 p1013 N85-16436
Visual evoked potentials with disrupted functioning of nonspecific cerebral systems 07 p1013 N85-16437
Change in relationship of biopotentials of brain zones for various levels of working capacity
07 p1013 N85-16438
Vision by man and machine: How the brain processes visual information may be suggested by studies in computer vision (and vice versa)
[AD-A147890] 07 p1017 N85-16458
Functional inter-hemisphere asymmetry in recognition of visual stimuli of various classes
08 p1193 N85-17517
Cognitive asymmetry and occupation. Computer programmers, students, and bank personnel, part 1 and part 2
[AD-A147125] 08 p1197 N85-17540
Neurocognitive pattern analysis of an auditory and visual numeric motor control task. Part 1: Development of methods
[AD-A148809] 09 p1364 N85-18578
Electrosleep therapy advanced at medical institute
10 p1526 N85-19623
Multiple resources and brain laterality
[AD-A148912] 10 p1530 N85-19643
Effects of hyperthermia on free amino acids in rat brain and in subcellular fractions 11 p1691 N85-20631
Functional significance of some EEG parameters and dominant principle 11 p1691 N85-20634
Effects of hypothermia on brain metabolism
11 p1692 N85-20636
Rat tissue opioid peptide content during long-term hypokinesia 12 p1904 N85-21954
Effect of long-term repeated exposure to high-intensity stationary magnetic field on adrenomedullary activity
12 p1904 N85-21955
Brain mechanisms underlying individual differences in reaction to stress: An animal model
[AD-A150195] 13 p2143 N85-23301
Biological investigations of adaptive networks. Neuronal control of conditioned responding
[AD-A150959] 14 p2385 N85-24695
Space brain research in China reported
15 p2537 N85-25657
Thermoregulatory and vestibular systems in the rat
15 p2610 N85-26062
A comparison of alternative analytic models for event related potential records
[AD-A151977] 15 p2618 N85-26134
Infinite computing
[AD-A151437] 15 p2628 N85-26197
Does a 50-cycle alternating field have central nervous effects?
[BLL-CE-TRANS-8083-(9022.09)]
16 p2839 N85-27507
Biological influences of low-frequency sinusoidal electromagnetic signals alone and superimposed on RF carrier waves
[PB85-161248] 16 p2842 N85-27527
Distributed memory
[AD-A153364] 17 p3001 N85-28554
Language design, computers and brains
[AD-A152819] 17 p3008 N85-28594
Influence of limboreticular complex on some reactions of rabbits 19 p3326 N85-30607
Changes in pentose and glucuronate pathway dehydrogenases in rat brains following single or multiple hypothermic episodes 20 p3505 N85-31790
Sleep and wake physiology in weightlessness
20 p3510 N85-31819
Resource allocation in cerebral specialization of function: Behavioral and electrophysiological studies
[AD-A155092] 21 p3664 N85-32759

BRAIN CIRCULATION
Reaction of cerebral ventricles to antiorthostatic position and occlusion of jugular veins 01 p0093 N85-10626
Hemodynamics and neurodynamics of the human brain during exposure to moderate hypoxic hypoxia
01 p0094 N85-10630
Effect of microwave radiation on local blood circulation and oxygenation of brain tissue
07 p1012 N85-16431

BRAIN STEM
Visual evoked potentials with disrupted functioning of nonspecific cerebral systems 07 p1013 N85-16437

BRAKES (FOR ARRESTING MOTION)
NT AERODYNAMIC BRAKES
NT DRAG CHUTES
NT LEADING EDGE SLATS
NT TRAILING EDGE FLAPS
NT WHEEL BRAKES
NT WING FLAPS
Investigations on the dynamic loading of wind energy converters with vertical axis and problems of control during starting and overload conditions
[BMFT-FB-T-84-155] 03 p0386 N85-12472
Comparison between cycle ergometers with different mechanical braking systems
[FOA-C-54058-H1] 07 p0975 N85-16193
Space shuttle wheels and brakes
08 p1101 N85-16962
Space shuttle rudder/speedbrake actuation subsystem
08 p1102 N85-16965
Use of braking stages for control of turbine speed
09 p1306 N85-18215
Hydraulic brakes for industrial robots
13 p2046 N85-22806

BRAKING
Testing solution for IL-76 braking system problem
08 p1067 N85-16766
Use of braking stages for control of turbine speed
09 p1306 N85-18215
Expedient runway surfacing with post tensioning system for expeditionary airfields
[AD-D011677] 19 p3222 N85-29976

BRANCHING (MATHEMATICS)
A martingale approach to supercritical (C-M-J) branching processes
[CTH-MATH-1984-25] 05 p0722 N85-14643
On the instability of a 3-dimensional attachment line boundary layer: Weakly nonlinear theory and a numerical approach
[NASA-CR-172504] 07 p0957 N85-16063
Study of mathematical models of mutation and selection in multi-locus systems
[DE85-000873] 09 p1376 N85-18648
Research in nonlinear problems of energy: Informal technical report
[DE85-001529] 11 p1595 N85-20031
Bifurcation theory applied to aircraft motions
[NASA-TM-86704] 14 p2210 N85-23705
Nonlinear problems in flight dynamics involving aerodynamic bifurcations
[NASA-TM-86706] 15 p2462 N85-25206
Solving set covering problems using heuristics with branch and bound
[AD-A151905] 15 p2638 N85-26269
The vector potential in a branched Riemann space
[VTH-LR-395] 16 p2856 N85-27614
Flow through finite collapsible tubes: A branching problem
[REPT-84-29] 17 p2960 N85-28281
Analytical shear buckling investigation of curved composite panels
[AD-A153138] 17 p2980 N85-28421
Chaos and order in an optical ring cavity
[CWI-AM-R8416] 17 p3038 N85-28795
Nonlinear problems in continuum mechanics
[AD-A153387] 17 p3046 N85-28846
Nonlinear global stability analysis of compressor stall phenomena
[NASA-CR-174908] 19 p3219 N85-29960
Nonlinear dynamics: A personal perspective
[DE85-010982] 20 p3521 N85-31899
A note on a theorem of R. Duffin
[AD-A154786] 21 p3676 N85-32838
Diakoptic calculation of characteristics for optimization of linear circuits with respect to parameters of individual branches 22 p3767 N85-33346

BRANCHING (PHYSICS)
Selected topics from J/psi decays
[DE85-010537] 18 p3183 N85-29736
Status of the zeta(8.3)
[DE85-013070] 24 p4149 N85-35724

BRASSES
Corrosion of brass in potable water service
[CETIM-100390] 04 p0477 N85-13037
X-ray diffraction study of changes in stress-strain distributions during fatigue of a 2-phase alloy
[AD-A152367] 17 p2930 N85-28087

BRAYTON CYCLE
Dynamic power systems for power generation
05 p0609 N85-13892
Dynamic conversion working group summary
05 p0611 N85-13904
Active cooling requirements for propellant storage
08 p1108 N85-17004
Introducing engine innovations: An examination of future markets for Brayton and Stirling automotive engines
[DE84-016319] 11 p1647 N85-20382
Some solar dish/heat engine design considerations
[DE85-003479] 12 p1881 N85-21802
Small central receiver Brayton cycle study
[DE85-008882] 18 p3128 N85-29369
Reciprocating Brayton cycle motor
[REPT-84-RR-336] 20 p3482 N85-31507
Comparative evaluation of three alternative power cycles for waste heat recovery from the exhaust of adiabatic diesel engines
[NASA-TM-86953] 20 p3542 N85-32043

BRAZIL
Utilization of LANDSAT orbital imagery in the soil survey processes at Rio Grande do Norte state
[E85-10009] 02 p0216 N85-11422
Remote sensing applied to forest resources
[E85-10012] 02 p0216 N85-11425

Mapping land use changes in the carboniferous region of Santa Catarina, report 2
[E85-10017] 02 p0217 N85-11430

Development and testing of a rural credit supervision system at the level of counties and rural properties utilizing remote sensing techniqes
[E85-10018] 02 p0217 N85-11431

Thematic mapping of likely target areas for the occurence of cassiterite in the Serra do Mocambo (GO) granitic massifs using LANDSAT 2 digital imaging
[E85-10027] 02 p0219 N85-11440

Shuttle Experimental Radar for Geological Exploration (SERGE) project: Field work relating to the Shuttle Experimental Radar A (SIR-A) in Brazil (phase 2)
[NASA-CR-174033] 02 p0219 N85-11444

Forecast of the northeastern drought by the method of periodicities: Use and abuses
[INPE-3109-PRE/508] 02 p0230 N85-11502

Evaluation of criteria for selecting the spectral attributes of digital LANDSAT MSS imagery for discriminating lithological units in the lower Curaca River Valley, Bahia — Brazil
[E85-10036] 03 p0379 N85-12415

Contribution to the radiogeology of Sao Roque, SP, granites
[INPE-3079-PRE/492] 03 p0391 N85-12503

Report of the field work performed in the Basins of the Quebra Osso and Tanque Petro Rivers in the Catas Altas quadrangle, Minas Gerais
[INPE-3268-NTE/225] 04 p0525 N85-13359

Heat sources in the tropics and large scale flow anomalies associated with precipitation anomalies in northeast Brazil
[INPE-3211-TDL/175] 04 p0536 N85-13421

Behavior of the ionospheric F region in low latitudes and in the equatorial region of Brazil during strong magnetic storms in the 1978 to 1983 period
[INPE-3231-PRE/581] 05 p0675 N85-14333

Nocturnal increases of ionization in the ionospheric F region in the low latitude of Brazil during magnetic storms
[INPE-3271-PRE/596] 05 p0675 N85-14334

Diagnostics of rainfall anomalies in the nordeste during the global weather experiment 05 p0685 N85-14405

Integrated analysis of remote sensing products from basic geological surveys — Brazil
[E85-10052] 07 p0984 N85-16246

Droughts and floods in South America due to the 1982-83 El Nino-southern oscillation episode
[INPE-3408-PRE/677] 09 p1357 N85-18535

The BRESEX multispectral camera: Preliminary characteristics
[INPE-3357-PRE/635] 10 p1487 N85-19386

Brazilian remote sensing receiving, recording and processing ground systems in the 1980's
[E85-10079] 10 p1504 N85-19493

The sharing of remote sensing techniques in Brazilian geographic research
[INPE-3307-PRE/617] 10 p1506 N85-19502

U, Th, K content, heat production and thermal conductivity of Sao Paulo, Brazil continental shelf sediments: A reconnaissance work
[INPE-3401-PRE/670] 10 p1515 N85-19558

First sodium nightglow results for Natal
[INPE-3397-PRE/666] 10 p1515 N85-19560

Planetary scale circulation anomalies associated with droughts over northeast Brazil
[INPE-3351-PRE/630] 10 p1518 N85-19570

Large scale circulation anomalies and prediction of northeast Brazil droughts
[INPE-3405-PRE/674] 10 p1518 N85-19571

Meridional penetration of frontal systems in South America and its relation to organized convection in the Amazon
[INPE-3407-PRE/676] 10 p1518 N85-19572

Interannual variations of the winter circulation in the Northern Hemisphere and in the southern oscillation (meridian) and their possible connections with the climate of Northeast Brazil
[INPE-3333-TDL/182] 10 p1519 N85-19573

Precursors for Brazilian magnetic anomalies from 1922 to 1969
[INPE-3283-PRE/605] 11 p1681 N85-20590

CNPq/INPE LANDSAT system: Report of activities from October 1, 1983 to September 30, 1984 — Brazil
[E85-10097] 16 p2808 N85-27318

Study of the urban evolution of Brasilia with the use of LANDSAT data
[E85-10101] 16 p2809 N85-27321

The relevance of remote sensing to Brazil
[INPE-3421-PRE/686] 16 p2811 N85-27332

The ARGOS system in Brazil — hydrology
16 p2813 N85-27349

On the 1983 drought in northeast Brazil
[INPE-3412-PRE/678] 16 p2834 N85-27476

An appraisal of the duration of the recent drought in northeast Brazil and a forecast for 1985
[INPE-3477-PRE/720] 16 p2834 N85-27478

BRAZILIAN SPACE PROGRAM

Brazilian Remote Sensing Shuttle Experiment (BRESEX): Characteristics and future utilization on satellites
[INPE-3313-PRE/620] 10 p1487 N85-19385

Remote sensing activities in Latin America
[INPE-3297-PRE/612] 10 p1506 N85-19501

SELPER (Latin American Society of Remote Sensory Specialists)
[INPE-3316-PRE/622] 16 p2810 N85-27328

BRAZING

NT LOW TEMPERATURE BRAZING

Dispersed metal-toughened ceramics and ceramic brazing
[NASA-CR-174284] 07 p0933 N85-15916

Repair welding and brazing procedures for turbine components and investigation of the brazing behavior of thin filler foils
[MTU-TB-908/84] 07 p0974 N85-16190

Design of low loss helix circuits for interference fitted and brazed circuits
[NASA-CR-168313] 10 p1478 N85-19328

Thermodynamics of copper-nickel alloys containing aluminum, silicon, titanium, and chromium relative to their use in ceramic brazing
[DE85-004787] 13 p2023 N85-22674

Indirect brazing of structural ceramics for uncooled diesels
[DE85-005569] 17 p2935 N85-28116

X-ray residual stress analysis on the coarse grain of copper and its application to the brazed copper
23 p3907 N85-34202

BREADBOARD MODELS

Design and analysis report for the RL10-2B breadboard low thrust engine
[NASA-CR-174857] 10 p1430 N85-19020

Firefighters' communication transceiver test plan
[NASA-CR-171419] 13 p2053 N85-22854

Development of a microprocessor controlled communication system for ships
[BMFT-FB-T-84-275] 17 p2950 N85-28216

Research pressure instrumentation for NASA space shuttle main engine
[NASA-CR-176014] 19 p3227 N85-30006

Noiseless coding for the Gamma Ray spectrometer
[NASA-CR-176201] 24 p4069 N85-35219

BREAKAWAY

U BOUNDARY LAYER SEPARATION

BREAKDOWN

Spectral distribution of radiation in n junctions of GaAs during avalanche breakdown 02 p0258 N85-11688

BREAKERS (ELECTRIC)

U CIRCUIT BREAKERS

BREAKING

Electromagnetic braking of a metallic projectile in flight
[AD-A149424] 10 p1480 N85-19345

The investigation of tethered satellite system dynamics
[NASA-CR-176180] 24 p4069 N85-35215

BREATHING

Encephalographic correlates of autogenous change in human functional state 06 p1193 N85-17518

BREATHING APPARATUS

NT UNDERWATER BREATHING APPARATUS

Experiments with hydrox at 1.3 MPa (13 atm) — for divers
[FOA-C-58014-H1] 04 p0545 N85-13471

Operating and maintenance guidelines for the kinergetics (trade name) environmental control system. Carbon dioxide scrubber model DH-10 and heat exchanger model CCU-01
[AD-A148107] 08 p1200 N85-17557

Hazards in welding due to oxygen changes in the workplace atmosphere
[BLL-WI-TRANS-684-(9312.57)]
16 p2792 N85-27224

Ten year environmental test of glass fiber/epoxy pressure vessels
[NASA-TM-87058] 19 p3231 N85-30034

Light-weight oxygen delivery hood assembly for hyperbaric chamber
[AD-D011709] 19 p3331 N85-30634

The use of superoxide mixtures as air-revitalization chemicals in hyperbaric, self-contained, closed-circuit breathing apparatus
[NASA-TM-86709] 20 p3512 N85-31831

Improved oxygen sources for breathing apparatus
[NASA-TM-86671] 24 p4134 N85-35623

The use of austenitic stainless steel versus monel (Ni-cu) alloy in pressurized Gaseous Oxygen (GOX) life support systems
[AD-A156305] 24 p4134 N85-35625

BRECCIA

Mineralogical investigations of lunar samples and meteorites
[NASA-CR-174291] 08 p1258 N85-17916

Moon 09 p1411 N85-18693

BREEDER REACTORS

NT EXPERIMENTAL BREEDER REACTOR 2

NT LIQUID METAL FAST BREEDER REACTORS

Blanket materials for fusion reactors: Comparisons of thermochemical performance
[DE84-016240] 04 p0568 N85-13622

Heat transfer and mechanical interactions in fusion nuclear systems
[DE84-016233] 09 p1392 N85-18761

Radiation damage experiments and lifetime estimates for beryllium components in fusion systems
[DE85-008036] 17 p3040 N85-28811

Two-dimensional TBR calculations for conceptual compact reversed-field pinch reactor blanket
[DE85-007636] 17 p3040 N85-28812

Feasibility study of a fission-suppressed Tokamak fusion breeder
[DE85-009099] 18 p3190 N85-29786

BREED: A CDC-7600 computer program for the automation of breeder reactor design analysis (LWBR Development Program)
[DE85-010327] 19 p3338 N85-30686

Molten salt cooling/17Li-83Pb breeding blanket concept
[DE85-010522] 19 p3363 N85-30654

Consolidated fuel reprocessing program
[DE85-008750] 19 p3366 N85-30671

A review of the SIMMER-2 analyses of liquid-metal-cooled fast breeder reactor core-disruptive accident fuel escape
[DE85-010803] 19 p3366 N85-30676

Tritium technology review
[DE85-010504] 21 p3703 N85-33006

Key issues of fusion nuclear technology development (FINESSE)
[DE85-012599] 22 p3845 N85-33817

BREMSSTRAHLUNG

Bremsstrahlung radiation from longitudinal plasma waves caused by subthermal electrons in plasma
02 p0264 N85-11730

Bremsstrahlung from nuclear scattering at low energy near a resonance
[DE84-014652] 04 p0561 N85-13572

A neutral gas jet in a low velocity shock front at the boundary of the Draco Nebula 06 p0878 N85-15576

Physics of nonmagnetic relativistic thermal plasmas
09 p1386 N85-18715

Lithography radiation effects study
[AD-A149552] 10 p1468 N85-19260

Directivity of Bremsstrahlung radiation from relativistic beams and the Gamma-Rays from solar flares
[NASA-CR-174433] 10 p1572 N85-19913

X-ray intensification at balloon altitudes of the South Atlantic magnetic anomaly in association with geomagnetic activity
[INPE-3469-PRE/712] 16 p2827 N85-27437

Comparison of calculations and measurements of the off-axis radiation dose (SI) in liquid nitrogen as a function of radiation length
[AD-A153676] 18 p3178 N85-29704

Electron temperature measurements from induced toroidal current in ELMO Bumpy Torus scale
[DE85-008549] 18 p3189 N85-2977

Poloidal variations in toroidal fusion reactor wall powe loadings
[DE85-009505] 19 p3362 N85-3064

Study of non-thermal photon production under differen scenarios in solar flares. 2: The Compton inverse an Bremsstrahlung models and fittings
[SH-1.2-3] 23 p3991 N85-3473

Burst size distributions in the digitized data of the io chambers t Mt. Norikura and sea level stations
[SH-9.1-9] 23 p4051 N85-3512

LPM effect and primary energy estimations
[HE-3.6-4] 24 p4185 N85-3595

Result of Monte-Carlo simulation of electron-photo cascades in lead and layers of lead-scintillator
[HE-3.6-11] 24 p4185 N85-3595

BRIDGES

The free electron laser variable bridge coupler
[DE85-009630] 18 p3114 N85-2927

BRIDGES (LANDFORMS)

Structure of Reykjanes Ridge rift zone and Icelandi thermal anomaly 19 p3289 N85-303

BRIDGES (STRUCTURES)

Three programs for evaluating bending moment deflections and shear forces in simply-supported unifor bridge decks under South African NA loading: NAB, NA and NAS. NITRR manual P13
[ISBN-0-7988-2263-X] 01 p0102 N85-10

Exploratory study of shear strength of joints for precast segmental bridges
[PB84-235449] 05 p0651 N85-14182
The Shock and Vibration Digest, volume 16, no. 9
[AD-A146779] 07 p0976 N85-16200
Evaluation of Epoxo 300-C nonskid coating for use on bridge decks
[PB85-108843] 12 p1819 N85-21412
Implementation of polymer impregnation as a bridge deck sealant
[PB85-185718] 22 p3753 N85-33265

BRIDGMAN METHOD
Simulation of solidification in a Bridgman cell
[NASA-CR-3843] 02 p0197 N85-11314
The growth of metastable peritectic compounds
[NASA-CR-171289] 07 p0920 N85-15824
SPAR X technical report for experiment 76-22 directional solidification of magnetic composites
[NASA-CR-171271] 07 p0927 N85-15880
Simulation of solidification in a Bridgman cell
[NASA-CR-175838] 16 p2870 N85-27705

BRIGHTNESS
NT SOLAR GRANULATION
UBV photometry of E region stars: Some intercomparisons 01 p0128 N85-10680
Some statistical characteristics of atmospheric optical thickness in visible spectral range
02 p0164 N85-11109
Holographic subtraction of images by Fourier plane recording and spatial filtration with a narrow beam
02 p0263 N85-11721
Brightness comparison of electroluminescent versus incandescent lighting: A photometric validation
[AD-A145395] 02 p0280 N85-11822
Variability of Neptune 02 p0299 N85-11938
Lyman-Alpha aurora 02 p0302 N85-11953
Infrared images of the Uranian rings
02 p0302 N85-11955
Individual differences in chromatic brightness matching
[AD-A148882] 10 p1529 N85-19641
Brightness limitations in multi-kiloampere electron beam sources
[DE84-017417] 10 p1555 N85-19807
Enhancing the performance of a high-gain free electron laser operating at millimeter wavelengths
[DE85-000662] 12 p1857 N85-21646
The relationship between marine aerosol particles and satellite-detected radiance 13 p2131 N85-23263
Formation of bright terrain bands on Ganymede by unstable lithosphere extension 13 p2173 N85-23485
Remarks on cometary astrometry
14 p2435 N85-25019
Photometric study of Pluto near perihelion. Part 2: Refinement of rotation period: Color indices
15 p2483 N85-25325
The problem of brightness enhancement during laser frequency doubling 21 p3686 N85-32897
Transverse emittance of a 2.0-MeV RFQ beam with high brightness
[DE85-012718] 22 p3837 N85-33758

BRIGHTNESS DISTRIBUTION
Method for interpreting soil cover of flowed fields using spectral brightnesses measured from space photographs
02 p0164 N85-11112
Fiber cable in optical system with brightness amplifier
02 p0263 N85-11724
A review of the millimeter and centimeter observations of Uranus 02 p0299 N85-11935
Brightness distribution in globular clusters derived by the narrow-slit scanning method
05 p0738 N85-14748
Atmospheric limitations in stellar seismology: Should one measure radial velocity or brightness fluctuations?
08 p1251 N85-17899
The physical implications of an isothermal model for the hot intracluster medium
[NASA-TM-86174] 11 p1763 N85-21089
A posteriori increase of resolving power of optical system forming averaged monochromatic images
13 p2082 N85-23003
Relationship between brighiness spectrum of photographic image and spectrum of rises on a water surface with waves 13 p2115 N85-23171
Azimuthal variations in Saturn's A ring
15 p2671 N85-26478
Saturn rings: Divisions, gaps and ringlets from ground-based telescopes 15 p2672 N85-26485
Possible period of Jovian activity and possibility of seasons 16 p2723 N85-26810
Effective brightness of zero-point fluctuations of the electromagnetic vacuum accompanying parametric scattering of light 21 p3694 N85-32951
Clusters and cycles in the cosmic ray age distributions of meteorites
[SH-7.1-11] 23 p4048 N85-35103
Longitudinal trial functions and the cosmic ray energy scale 24 p4193 N85-36014
Muon spectrum in air showers initiated by gamma rays
[HE-4.5-4] 24 p4195 N85-36028

BRIGHTNESS TEMPERATURE
An error analysis for the use of presently available lunar radio flux data in broadbeam antenna-system measurements
[PB84-216361] 01 p0016 N85-10097
Multispectral passive microwave correlations with an antecedent precipitation index using the Nimbus 7 SMMR
[AD-A145419] 02 p0200 N85-11334
A review of the millimeter and centimeter observations of Uranus 02 p0299 N85-11935
Mixed layers and satellite retrievals
05 p0686 N85-14411
Mathematical models for the brightness temperature of object and environment in the microwave region
[ESA-TT-829] 05 p0718 N85-14610
A neutral gas jet in a low velocity shock front at the boundary of the Draco Nebula 06 p0878 N85-15576
The Draco Nebula, a molecular cloud associated with a high velocity cloud? 06 p0878 N85-15577
Microwave emissions from snow
[E85-10065] 08 p1174 N85-17403
An alternative to relativistic beaming in AGN — Active Galactic Nuclei (AGN) 08 p1242 N85-17833
On the error of typhoon intensity estimation by means of IR Dvorak technique occurring when the eye is very small 12 p1894 N85-21886
An analysis of the data obtained by a simultaneous observation of GMS and GMS-2: A study of the difference between the brightness temperatures by GMS and those by GMS-2 12 p1894 N85-21888
VISSR infrared calibration by means of calculated radiances 12 p1894 N85-21889
Calculations of microwave brightness temperature of rough soil surfaces: Bare field
[NASA-TM-86200] 13 p2123 N85-23221
General report of the researches of snowpack properties, snowmelt runoff and evapotranspiration in Japan 13 p2124 N85-23225
Microwave radiometer observations of snowpack properties and comparison of U.S. Japanese results — Hokkaido, Japan and Vermont and North Dakota test sites 13 p2125 N85-23230
Studies on physical properties of snow based on multi channel microwave radiometer
13 p2125 N85-23231
Analysis of NIMBUS-7 SMMR data — Hokkaido, Japan snow cover 13 p2125 N85-23232
Estimation of regional evapotranspiration using remotely sensed land surface temperature. Part 1: Measurement of evapotranspiration at the Environmental Research Center and determination of Priestley-Taylor parameter
13 p2125 N85-23233
Venus surface composition from radio/radar measurements 13 p2177 N85-23509
Determination of total moisture content in cloud-free atmosphere by relative radio emission measurements
14 p2340 N85-24472
Digital processing of passive Ka-band microwave images for sea-ice classification
[AD-A150686] 14 p2347 N85-24511
Severe storm detection with passive 37 GHz observations 15 p2596 N85-25997
The validation of sea surface temperatures determined from AVHRR data using in situ data recovered via system ARGOS 16 p2812 N85-27342
Active and passive remote sensing of ice
[AD-A151741] 16 p2815 N85-27369
Atmospheric frontal zone studies
[NASA-CR-175293] 16 p2833 N85-27489
Electron-cyclotron maser emission during solar and stellar flares
[NASA-CR-175883] 17 p3054 N85-28907
Applications of some artificial intelligence methods to satellite soundings 18 p3141 N85-29446
Sea surface radio emission at wavelengths 0.86 and 1.3 cm near Brewster angle 19 p3293 N85-30418
Variations in the small-scale galactic magnetic field and short time-scale intensity variations of extragalactic radio sources 20 p3540 N85-32084
The use of TOMS data in evaluating and improving the total ozone from TOVS measurements
[NOAA-TR-NESDIS-23] 22 p3814 N85-33626

BRILLOUIN EFFECT
Brillouin scattering in underdense UV laser-produced plasmas
[DE84-015164] 04 p0567 N85-13614
Parametric processes in underdense UV laser-produced plasmas
[DE85-002812] 10 p1559 N85-19830
Experimental investigation of wavefront conjugation during Mandelstam-Brillouin scattering of focused laser beams in condensed media 11 p1716 N85-20796
Stimulated Brillouin scattering reflectivity in the presence of various aberrators
[AD-A151750] 15 p2563 N85-25812
Caviton collapse of SRS by SBS
[DE85-009805] 20 p3535 N85-31999
Stimulated Mandelstam-Brillouin scattering with distributed feedback 21 p3696 N85-32961

BRILLOUIN ZONES
A study of structural phase transitions using light scattering techniques
[AD-A147261] 07 p1048 N85-16654
Conducting a thermal conductivity survey
[NASA-CR-175792] 16 p2782 N85-27166

BRINES
Doubly diffusive linear stability with nonconstant gradients
[DE84-013008] 05 p0670 N85-14310
Towing tank studies of stratified flow over ridges and valleys
[DE84-011418] 06 p0839 N85-15329
An experimental study of brine upward migration in thin sea ice 15 p2582 N85-25923
Offshore oceanographic and environmental monitoring services for the Strategic Petroleum Reserve, volume 3
[DE85-009907] 20 p3497 N85-31741
Microbiology of solar salt ponds
21 p3658 N85-32724
Technology transfer report: Feasibility study for the use of geothermal brine in the Ashdod area, Israel
[DE85-013316] 22 p3810 N85-33596
Proposed resource evaluation plan. Salton Sea scientific drilling program
[DE85-011294] 22 p3815 N85-33633
Chemistry of ore-forming fluids
24 p4103 N85-35436
Heat transfer and brine evolution in magma-hydrothermal systems 24 p4104 N85-35441

BRITISH COLUMBIA
The northern coast plutonic-metamorphic complex, southeastern Alaska and northwestern British Columbia
04 p0518 N85-13305

BRITISH GUINEA
U GUYANA

BRITTLE MATERIALS
Evaluation of machining damage in brittle materials
[DE85-001794] 11 p1612 N85-20136
Simulation of brittle fracture via molecular dynamics
[DE85-001061] 11 p1653 N85-20410
Reliability of structural brittle materials
12 p1946 N85-22222
Correlation of uniaxial and biaxial fracture strengths of ceramics
[DE85-003779] 14 p2261 N85-24011
Statistical fracture theories for brittle materials
[AD-A153530] 18 p3121 N85-29324
The shearing contribution in transformation toughening of brittle materials
[AD-A154656] 21 p3568 N85-32195
Mechanics of near tip microcracking in brittle material
[AD-A154684] 21 p3598 N85-32346

BRITTLENESS
Delayed fracture of high-strength steels in spherical tanks for LP gas
[BLL-RISLEY-TR-4926-(9091.9F)]
01 p0026 N85-10162
Mechanism of brittle heat fracture of inhomogeneous solids by high temperature gas jets
02 p0265 N85-11731
Brittleness of ceramics
[NASA-TM-77504] 03 p0335 N85-12156
Effect of crack-tip region constraint on fracture in the ductile-to-brittle transition
[PB84-237395] 06 p0770 N85-14926
Moving nonlocal crack: Anti-plane shear case
[AD-A149996] 12 p1868 N85-21709
Cast-iron technology: Metallographic and mechanical testing results
[DE85-002684] 14 p2257 N85-23984
Study of oxidized surface coating on titanium after annealing 15 p2498 N85-25412
Frangibility of obstacles at airports
[NLR-MP-84002-U] 17 p2981 N85-28431
Fatigue resistance of homogeneous and heterogeneous welded joints of TS5 titanium alloy
19 p3246 N85-30126
Indentation fractography: A measure of brittleness
[PB85-179059] 20 p3473 N85-31581
Influence of the resin on interlaminar mixed-mode fracture
[NASA-TM-87571] 21 p3561 N85-32150

Metallurgical origins of fracture toughness and microstructure and fracture toughness of an HSLA (High-Strength/Low-Alloy) steel
[AD-A155530] 21 p3567 N85-32187

BROADBAND

Broadband local distribution networks: Problems and prospects in Italy
[FUB-18-1983] 01 p0040 N85-10255

Free electron lasers
[AD-A145109] 01 p0053 N85-10349

Wideband integrated voice/data technology
[AD-A146054] 03 p0356 N85-12283

Distributed reservation-based code division multiple access
[AD-A147007] 07 p0940 N85-15957

Compact wideband multiple conductor monopole antenna
[AD-D011331] 07 p0944 N85-15981

Lightweight, broadband Rayleigh wave transducer
[AD-D011345] 07 p1037 N85-16584

Determination of crustal and upper mantle structure from analysis of broadband teleseismic P-waveforms
08 p1181 N85-17440

A broadband matching network
[AD-D011406] 08 p1219 N85-17675

On the broadband energy spectra of quasars and BL Lac objects 08 p1240 N85-17825

Broad-band UHF dipole array
[NASA-TM-86373] 10 p1462 N85-19222

HF broadband whip antenna evaluation
[AD-A149527] 10 p1467 N85-19258

Propagation of wide bandwidth signals in a tropospheric ducting system 10 p1469 N85-19271

Wideband line-of-sight channel measurements and simulation: Application to digital radio links
10 p1471 N85-19283

A broadband kevlar radome for shipboard
[AD-P004365] 12 p1826 N85-21459

Multichannel digital processing of wideband signals
12 p1840 N85-21548

Method of measuring sea surface water temperature with a satellite including wideband passive synthetic-aperture multichannel receiver
[NASA-CASE-NPO-15651-1] 12 p1869 N85-21723

Efficiency of digital compensator of strong non-Gaussian interference 13 p2072 N85-22942

Programmable filter with fanned interdigital surface acoustic wave transducer 13 p2083 N85-23008

Design and measured performance of a broadband Archimedes spiral antenna
[R-NIAS-22] 14 p2290 N85-24194

A compact, aperture-matched, balanced transmission line antenna
[R-NIAS-26] 14 p2290 N85-24196

Disturbances in structure of lower ionosphere at terminators based on results of winde-band LW sounding 14 p2339 N85-24467

Wideband integrated voice/data technology
[AD-A152329] 17 p2947 N85-28197

AGS broad band neutrino beam
[DE85-010954] 19 p3366 N85-30875

Wideband disturbance accomodation in precision flexible space structures 20 p3415 N85-31194

Investigation of plasma processes in electronic transition lasers
[AD-A155598] 21 p3593 N85-32327

Cylindrical lens-array antenna for wideband electronic scanning
[AD-A156085] 24 p4090 N85-35350

Scale separation closure and Alfven wave turbulence
[DE85-013124] 24 p4095 N85-35385

BROADBAND AMPLIFIERS

Broadband transverse field interaction continuous beam amplifier
[AD-D011229] 01 p0043 N85-10279

Development of a 30 GHz/1 kW broadband traveling wave tube with suppression of band edge oscillations
[BMFT-FB-W-84-035] 07 p0948 N85-16011

New construction principles for oscillator power summing devices 07 p0946 N85-16016

Development of thin film hybrid IC active filter for video band use
[NHK-LABS-NOTE-312] 18 p3094 N85-29153

BROADCASTING

Subliminal communication technology
[GPO-38-833] 05 p0622 N85-13979

US objectives generally achieved at broadcasting satellite international conference: Improvements can help in future conferences
[PB84-235316] 06 p0800 N85-15109

Measurement of signal separation between radio service and air navigation service
[IRT-TB-B-40/82] 08 p1069 N85-16960

Satellite broadcasting: The performance of C-MAC in a hardware simulation of a DBS transmission chain
[BBC-RD-1984/9] 08 p1143 N85-17206

Subjective evaluation of the effect of noise and interference on frequency modulated NTSC television signals
[CRC-1367] 09 p1310 N85-18230

Star on the horizon: The emergence of the direct broadcast satellite in American mass communications
[AD-A148819] 09 p1312 N85-18242

Study of factors affecting an HF/VHF direct broadcasting satellite service
[PB85-120889/GAR] 09 p1313 N85-18255

Travelling wave tube for broadcast satellites
10 p1475 N85-19310

China's future domestic satellite communications systems 10 p1476 N85-19312

Electronic generation of text for television
[BBC-RD-1984/14] 13 p2053 N85-22856

Alternatives for satellite sound broadcast systems at HF and VHF 14 p2229 N85-23815

The distortion of AM broadcast antenna patterns as caused by nearby towers and highrise buildings
[CRC-1379] 15 p2536 N85-25668

Optimal frequencies for broadcast transmitters in the UHF domain: Report
[TUM-M8404] 16 p2769 N85-27088

SESC (Space Environment Services Center) satellite broadcasting 10-year plan
[PB85-163541] 16 p2775 N85-27126

Generalized graph coloring: A frequency assignment method for VHF broadcasting
[TUM-M8405] 16 p2844 N85-27535

Channel multiplexers for broadcast satellite transponders in the 12 GHz band
[NHK-LABS-NOTE-310] 18 p3090 N85-29122

Preliminary investigation of the performance of repeater technology for satellite sound broadcasting
[SSP/017/82] 18 p3092 N85-29137

Predicting the effects of non-Gaussian interference in HF (High-Frequency) broadcasting. Part 1: A methodology for an analytic approach
[PB85-171544] 18 p3092 N85-29140

BROKEN SYMMETRY

Dynamics of symmetry breaking: Phase coherence in finite and random systems
[NOTA-INTERNA-813] 02 p0253 N85-11658

Cosmic axions
[DE85-001330] 09 p1418 N85-18944

Symmetry breaking for a class of semi-linear elliptic problems
[AD-A149093] 10 p1546 N85-19748

Research in theoretical physics
[DE85-004286] 12 p1944 N85-22207

Standard model and beyond
[DE85-004299] 14 p2418 N85-24919

Activities of the Solid State Physics Research Institute
[NASA-CR-175899] 17 p3042 N85-28818

Uniaxial stress induced symmetry breaking for muon sites in Fe 17 p3042 N85-28820

BROMIDES

NT HYDROBROMIC ACID

Comparison study of analytical methods for the determination of fluoride, chloride, and bromide in plastics
[DE84-015008] 04 p0470 N85-12989

Graphite fiber intercalation: Dynamics of the bromine intercalation process
[NASA-TM-87015] 16 p2742 N85-26921

Determination of organobromide compounds in water by gas chromatography-negative ion chemical ionisation mass spectrometry
[DRIC-T-7411] 22 p3743 N85-33199

Rechargeable lithium-organic electrolyte battery having overcharge protection and method of providing overcharge protection for a lithium-organic electrolyte battery
[AD-D011736] 22 p3806 N85-33575

BROMINE

NT BROMINE ISOTOPES

Stability of bromine intercalated graphite fibers
[NASA-TM-86859] 01 p0031 N85-10187

Investigation of bromine complexed hydrogen/bromine regenerative fuel cells for portable electric power
[AD-A146401] 06 p0833 N85-15300

A study of liquid-vapor equilibria of the bromine-hydrobromic acid-water system
[NASA-TM-77748] 14 p2249 N85-23940

Homogeneity of pristine and bromine intercalated graphite fibers
[NASA-TM-87016] 15 p2517 N85-25521

Environmental stability of intercalated graphite fibers
[NASA-TM-87025] 16 p2753 N85-26992

A micrographic and gravimetric study of intercalation and deintercalation of graphite fibers
[NASA-TM-87026] 17 p2934 N85-28110

BROMINE COMPOUNDS

NT BROMIDES

NT HYDROBROMIC ACID

Study of the liquid vapor equilibrium in the bromine-hydrobromic acid-water system
[NASA-TM-77787] 07 p0921 N85-15836

Crossed molecular beam studies of the reactions of oxygen and fluorine atoms
[AD-A153302] 17 p2921 N85-28006

BROMINE ISOTOPES

Proposed solar neutrino experiment using (81)Br(nu,e(-e)) (81)Kr
[DE85-004802] 15 p2684 N85-26579

BROMINE 82

U BROMINE ISOTOPES

BROMINE 87

U BROMINE ISOTOPES

BRONCHI

Deposition in the human lung during respiration of small particles suspended in the air
[BLL-RISLEY-TR-5021-(9091.9F)]
03 p0400 N85-12549

BRONZES

Testing the antifriction properties of alloys for heavily loaded bearings 06 p0780 N85-14990

Effect of form memory in alloys based on Cu-Al systems 11 p1604 N85-20088

Microstructural study on the processing and properties of high-field A15 superconducting materials
[DE85-004652] 13 p2164 N85-23423

Ferroelectric tungsten bronze bulk crystals and epitaxial thin films for electro-optic device applications
[AD-A151044] 14 p2427 N85-24970

The microstructural state of Nb3Sn in a multifilamentary titanium doped bronze-process wire
[DE85-010979] 19 p3240 N85-30089

BROWNIAN MOVEMENTS

Deuteron NMR (Nuclear Magnetic Resonance) in relation to the glass transition in polymers
[AD-P003910] 01 p0032 N85-10196

A perturbation solution for rigid dumbbell suspensions in steady shear flow
[AD-A144876] 01 p0111 N85-10755

Neutron scattering on polysiloxanes
03 p0432 N85-12751

Study of submicron particle size distributions by laser Doppler measurement of Brownian motion
[AD-A149139] 10 p1487 N85-19388

Brownian motion with a parabolic drift and Airy functions
[CWI-MS-R8413] 12 p1925 N85-22097

A diffusion process and its application to detecting a change in the drift of Brownian motion
[AD-A150096] 12 p1926 N85-22100

Beam loss due to the aperture limitation resulting from intrabeam scattering
[DE85-005138] 12 p1930 N85-22124

Boundary crossing probabilities and statistical applications
[AD-A151027] 14 p2411 N85-24869

Brownian motion with quadratic killing and some implications: Revision
[AD-A151323] 15 p2642 N85-26298

Comments on estimating quantiles for Gaussian functionals by simulation
[AD-A154302] 19 p3348 N85-30750

The influence of Brownian coagulation on the size distributions of atmospheric aerosols
21 p3645 N85-32643

Scavenging of submicron aerosol particles by snow crystals: Theory and experiments
21 p3648 N85-32667

Large deviations for the maxima of some random fields
[AD-A155909] 24 p4143 N85-35681

BRUCETON TEST

U STATISTICAL TESTS

BRUSH (BOTANY)

Determination of low chloride values in Rocky Flats scrub alloy solutions and other complex matrices
[DE85-011506] 23 p3911 N85-34234

BRUSHES

NT BRUSHES (ELECTRICAL CONTACTS)

Investigation of electric and wear phenomena of liquid metal wetted copper fiber brushes under conditions of high slip ring eccentricity
[AD-A147634] 08 p1156 N85-17295

BRUSHES (ELECTRICAL CONTACTS)

Thermal and thermoelastic effects in rolling/sliding contacts
[AD-A150435] 13 p2165 N85-23429

Brush and commutator segment torquer motor
[AD-D011726] 23 p3927 N85-34340

BUBBLE CHAMBERS

Multidimensional analysis of data obtained in experiments with X-ray emulsion chambers and extensive air showers
[HE-3.6-2] 24 p4184 N85-35951

Experimental basis for the models of cascade propagation in atmosphere
[HE-3.6-6] 24 p4185 N85-35954

A comparative analysis of gamma and hadron families at the superhigh energies recorded in experiment Pamir
[HE-3.7-1] 24 p4185 N85-35960

Hadrons registration in emulsion chamber with carbon block
[HE-3.7-3] 24 p4186 N85-35962

New analysis of nuclear interaction observed by Mt. Kanbara emulsion chamber experiment
[HE-3.7-4] 24 p4186 N85-35963

Intensities of high-energy cosmic rays at Mount Kanbala
[HE-3.7-5] 24 p4186 N85-35964

Structured events in Pamir carbon X-ray chambers
[HE-3.7-7] 24 p4186 N85-35965

Ultra high energy events in ECHOS series and primary energy spectrum
[HE-3.7-9] 24 p4186 N85-35966

Search for anomalons using plastic nuclear track detectors
[HE-6.2-12] 24 p4212 N85-36148

BUBBLE MEMORY DEVICES

Integrated circuits, MBM's, form focus of work at French LETI 03 p0341 N85-12194

Feasibility of self-structured current accessed bubble devices in spacecraft recording systems
[NASA-CR-172554] 13 p1998 N85-22525

Advanced detectors and signal processing for bubble memories
[NASA-CR-172534] 14 p2297 N85-24219

SSMIR (Solid State Memory Instrumentation Recorder): A new approach to acquiring data during an aircraft seat/sled ejection sequence
[AD-A154780] 21 p3589 N85-32308

Advanced detectors and signal processing
[NASA-CR-176193] 24 p4088 N85-35343

BUBBLES

Soil tilt measurement: First results of the comparative analysis of the response of two different tiltmeters
[NOTA-INTERNA-818] 02 p0228 N85-11494

Collapse of cavitation bubbles between two walls in ultrasonic field 02 p0266 N85-11739

Characterization of ion implanted deuterium traps in nickel by equilibration with deuterium gas
[DE84-014958] 02 p0288 N85-11879

Laminar separation bubble with transition: Prediction test with local interaction
[BLL-PNR-90231-(8019.3153)]
06 p0806 N85-15132

VORT: A computer code for bubbly two-phase flow
[DE84-017076] 06 p0809 N85-15142

Research on acoustical and optical scattering, optics of bubbles, diffraction catastrophes, laser generation of sound, and shock induced cavitation
[AD-A146703] 06 p0860 N85-15466

Non equilibrium ionization in the local hot bubble
06 p0879 N85-15587

Large-scale bubble structure of the interstellar medium (ISM) and properties of the Local Spiral Arm (LSA)
06 p0879 N85-15588

Turbulent bubbles behind airfoils and wings at high angle of attack 08 p1069 N85-16779

Pneumatic turbulators: A device for drag reduction at Reynolds numbers below 5 million
08 p1071 N85-16791

A theoretical method for selecting space craft and space suit atmospheres
[AD-A148219] 08 p1200 N85-17559

Laminar separation bubble with transition: Prediction test with local interaction --- airfoils
[PNR-90231] 09 p1274 N85-18008

Statistical comparison of pooled nitrogen washout data of various altitude decompression response groups
[NASA-TM-58265] 15 p2639 N85-26278

Fluid surface behavior in low gravity. Center discretionary fund no. 83-21
[NASA-TP-2486] 17 p2957 N85-28260

A study of aerodynamic control in stalled flight long laminar separation bubble analysis
[AD-A153850] 18 p3059 N85-28330

Dynamics of thin-film breakup in a constricted pore
[DE85-008442] 18 p3101 N85-29199

The effects of microbubbles on turbulent boundary layer skin friction 20 p3451 N85-31425

Magnetic materials
[AD-A154879] 21 p3580 N85-32256

Experimental studies of glass refining
[NASA-CR-176130] 22 p3751 N85-33248

Features of behavior of gas bubbles in molten oxide films during enamelling: Communication 2
[BLL-M-35781-(5828.4)] 23 p3919 N85-34283

SU(2) x U(1) vacuum and the Centauro events
24 p4175 N85-35885

Exploring results of the possibility on detecting cosmic ray particles by acoustic way
[HE-7.1-3] 24 p4213 N85-36157

BUCKLING

NT CREEP BUCKLING
NT ELASTIC BUCKLING
NT EULER BUCKLING

Design proposals for torsional buckling of stiffeners
[AD-A144783] 01 p0062 N85-10409

A buckling analysis for rectangular orthotropic plates with centrally located cutouts
[NASA-TM-86263] 04 p0513 N85-13268

Formulation and solution methods for classical problems of static buckling
[CETIM-101010] 04 p0514 N85-13280

A review of imperfection sensitivity of stiffened shells
[AD-A147311] 07 p0978 N85-16213

Buckling analysis of cracked, floating ice sheets
[AD-A147330] 07 p0988 N85-16277

Buckling and eccentricity effects on orifice metering accuracy --- gas meters
[ERS-E.350] 09 p1324 N85-18321

Transverse vibration and buckling of a cantilevered beam with tip body under constant axial base acceleration
[NASA-CR-175567] 12 p1864 N85-21694

Steel containment buckling
[DE85-003744] 13 p2103 N85-23111

A model for the compressive buckling of extended chain polymers
[AD-A151025] 14 p2260 N85-24008

Solution to eigenvalue problems of antisymmetric cross-ply and antisymmetric angle-ply laminated plates using affine transformations
[AD-A153040] 17 p2917 N85-27980

Continuum modeling of latticed structures
17 p2977 N85-28399

The Shock and Vibration Digest, volume 17, no. 2
[AD-A153129] 17 p2977 N85-28400

Recent progress in the dynamic plastic behaviour of structures, part 4 17 p2978 N85-28402

Buckling and bracing of cantilevers
[CE-42] 17 p2979 N85-28413

Biaxial buckling of specially orthotropic, symmetric composite rectangular plates
[AD-A152958] 17 p2979 N85-28417

Analytical shear buckling investigation of curved composite panels
[AD-A153138] 17 p2980 N85-28421

Buckling and postbuckling behavior of shallow shells
18 p3120 N85-29317

Measurement and calculation of the mechanical response of a highly fractured rock
[DE85-008421] 18 p3127 N85-29362

Buckling and post-buckling behavior of sparsely connected built-up columns 19 p3283 N85-30358

Stress and buckling analysis 21 p3611 N85-32439

Structural analysis of imperfect three-legged truss columns for large space structures applications
24 p4100 N85-35416

Design and behavior of coped beams
24 p4100 N85-35417

BUDGETING

Managing recoverable aircraft components in the PPB and related processes: Executive summary
[AD-A148806] 07 p1050 N85-16667

Activities report of the aerospace industry in West Germany
[ISSN-0722-3838] 07 p1053 N85-16686

Activities report of the aerospace industry in West Germany
[ISSN-0722-3838] 07 p1054 N85-16687

FRG study looks at participation in ESA, US space station 08 p1141 N85-17191

Criteria for qualifying for FRG federal CAD/CAM subsidies 15 p2536 N85-25651

Manufacturing cost analysis of a parabolic dish concentrator (General Electric design) for solar thermal electric power systems in selected production volumes
[NASA-CR-175772] 16 p2818 N85-27380

New ESA director on Ariane, space station, future trends 18 p3086 N85-29096

FRG weighs ESA participation, budget issues
18 p3088 N85-29110

Thermal Energy Storage Program annual operating plan FY 1985
[DE85-008745] 19 p3307 N85-30499

Pricing options for the space shuttle. Special study
21 p3559 N85-32138

Space research in the United Kingdom: An assessment
[AD-A155334] 21 p3712 N85-33038

The 1986 National Aeronautics and Space Administration authorization
[GPO-47-635] 24 p4166 N85-35829

BUDGETS

Non-US approaches to space commercialization
02 p0150 N85-11012

AGARD bulletin technical programme, 1985
[AGARD-BUL-84-2] 02 p0305 N85-11971

Organizations as information processing systems. Toward a strategic contingencies model of budget related influence in municipal government organizations
[AD-A149364] 10 p1567 N85-19883

FRG's DFVLR ready for participation in space station
11 p1618 N85-20176

Academic science and engineering: R and D funds, fiscal year 1982 (detailed statistical tables)
[PB85-154763] 15 p2664 N85-26443

BUFFER STORAGE

A data collection system
[AD-D011268] 05 p0713 N85-14573

Precision digital sampler
[AD-D011285] 06 p0809 N85-15143

The Multimission Image Processing Laboratory's virtual frame buffer interface
[NASA-CR-175655] 14 p2402 N85-24805

Techniques for operating Charge Coupled Devices (CCD's) in very high speed framing mode
[AD-A152678] 17 p2953 N85-28236

Investigation of cosmic rays in very short time scales
[HE-4.6-7] 24 p4197 N85-36044

BUFFERS (CHEMISTRY)

Kinetics of hydrolysis and products of hydrolysis and photolysis of tetryl
[AD-A153144] 17 p2921 N85-28005

Development anmd testing of electrophoresis solutions. Task I.1: Development of optimal buffer system
20 p3500 N85-31755

Electrophoretic mobilities of erythrocytes in various buffers 20 p3500 N85-31756

Electrophoretic mobilities of cultured human embryonic kidney cells in various buffers 20 p3501 N85-31761

Pre-flight report on cultured human embryonic kidney cell handling and cell electrophoresis. Prepared prior to continuous-flow electrophoretic separation experiments aboard space shuttle flight STS-8
20 p3503 N85-31775

Iron and manganese in oxide minerals and in glasses: Preliminary consideration of Eh buffering potential at Yucca Mountain, Nevada
[DE85-011892] 23 p3916 N85-34271

BUFFETING

La Recherche Aerospatiale Bimonthly Bulletin, Number 1984-4, 221/July-August
[ESA-TT-884] 16 p2695 N85-26637

Wing buffeting active control testing on a transport aircraft configuration in a large sonic tunnel
16 p2714 N85-26750

Wing buffeting active control testing on a transport aircraft configuration in a large sonic windtunnel
17 p2904 N85-27903

BUILDING MATERIALS

U CONSTRUCTION MATERIALS

BUILDING STRUCTURES

U BUILDINGS

BUILDINGS

Patterns of behavior in lodgings exposed to traffic noise
[NASA-TM-77750] 03 p0387 N85-12479

Hurricane Alicia, Galveston and Houston, Texas, 17-18 August 1983
[PB84-237056] 04 p0541 N85-13441

The development of fire evaluation system for detention and correctional occupancies
[NBSIR-84-2976] 10 p1459 N85-19192

The 35 kilowatt peak power photovoltaic system
[DE85-000180] 10 p1511 N85-19537

Research on heat-exchanger corrosion
[PB85-126316] 11 p1616 N85-20164

Thermal stress-dependent dilation of concrete
[DE84-014888] 11 p1653 N85-20412

Phase change thermal energy storage and the model building codes
[PB85-111201] 12 p1883 N85-21813

Multiyear plan for experimental systems research passive and hybrid solar energy program
[PB85-148988] 12 p1883 N85-21815

Preliminary investigation of dispersion of pollutants in model building wake flows using bipolar space charge
[IC-AERO-84-04] 20 p3487 N85-31671

BULGARIA

Achievements in biology outlined
03 p0343 N85-12213

Contribution to space program reviewed
16 p2727 N85-26834

BULK ACOUSTIC WAVE DEVICES

Compensation of acoustic wave devices
[AD-D011582] 16 p2646 N85-26322

BULK MODULUS
Research program on the effect of pressure on the mechanical properties of polymers, part 2
[DE85-000995] 13 p2037 N85-22761
Hydrostatic compression of Fe1-chi 0 wustite.
15 p2508 N85-25472

BUMPY TORUSES
N-frequency quasiperiodicity and chaos in dissipative dynamical systems 02 p0282 N85-11840
EBT electron energy confinement experiments
[DE84-015402] 04 p0567 N85-13613
Proceedings of the US-Japan Theory Workshop on 3-D MHD Studies
[DE84-012019] 04 p0568 N85-13620
Elma Bumpy Torus physics
[DE84-015909] 05 p0730 N85-14694
Theoretical investigations relevant to magnetic fusion research, April 1, 1983 - March 31, 1984
[DE85-001776] 06 p0865 N85-15496
Theoretical investigations relevant to magnetic fusion research
[DE85-001777] 06 p0866 N85-15503
Far-infrared laser diagnostic on EBT and extreme far-forward laser scattering on ISX
[DE85-001788] 07 p1046 N85-16843
Density measurements of atomic hydrogen in NBT-IM by laser-induced fluorescence spectroscopy
09 p1389 N85-18739
Effect of alpha particles on the stability of Elmo Bumpy Torus (EBT) reactor
[DE84-017266] 09 p1392 N85-18759
Electron bounce resonance heating in a bumpy cylinder
[DE85-001732] 10 p1561 N85-19845
Direct reading fast microwave interferometer for EBT
[DE85-000183] 11 p1636 N85-20306
Observations of low frequency plasma fluctuations in ELMC Bumpy Torus
[DE85-003796] 11 p1732 N85-20895
Transient waveform acquisition system for the ELMO Bumpy Torus
[DE85-000154] 11 p1733 N85-20901
Suppression of tilting instability of a compact torus by energetic particle beams
[IPPJ-705] 12 p1935 N85-22157
Electrostatic confinement in a bumpy torus
[DE85-003794] 12 p1936 N85-22164
Nagoya bumpy torus 15 p2655 N85-26377
Heavy ion beam study of potential formation in bumpy torus plasma
[IPPJ-711] 15 p2656 N85-26386
Theoretical studies of Elmo Bumpy Torus
[DE85-007202] 15 p2658 N85-26402
Inherent magnetic field error measurements in ELMO Bumpy Torus
[DE85-005855] 16 p2867 N85-27685
Theoretical and numerical studies of magnetic field line displacements in an Elmo Bumpy Torus
[DE85-006757] 17 p3041 N85-28816
Electron temperature measurements from induced toroidal current in ELMO Bumpy Torus scale
[DE85-008549] 18 p3189 N85-29779
Magnetics calculations for an ELMO Bumpy Square
[DE85-010442] 18 p3191 N85-29792
The effects of alpha particle production on the stability of an Elmo Bumpy Torus (EBT) reactor
19 p3369 N85-30895
Research support for plasma diagnostics on Elmo Bumpy Torus: Diamagnetic measurements and data analysis and development of ring models for realistic representation of fields near the plasma
[DE85-010035] 19 p3371 N85-30912
Thomson scattering on Elmo Bumpy Torus
[DE85-010584] 20 p3527 N85-31941
Magnetics calculations for an ELMO Bumpy Square
[DE85-011438] 21 p3707 N85-33021
Elmo bumpy square plasma confinement device
[DE85-011628] 22 p3845 N85-33816
Assessment of magnetic field asymmetries in ELMO Bumpy square
[DE85-011905] 22 p3846 N85-33819
High-field launch electron cyclotron heating experiments in the ELMO Bumpy Torus
[DE85-012068] 22 p3846 N85-33825
Proceedings of the US-Japan Workshop on Transport in Open-Ended Systems
[IPPJ-727] 23 p3975 N85-34644
Compact DT fusion spherical tori at modest field
[DE85-011568] 23 p3982 N85-34692
Multiple-frequency electron cyclotron heating of hot electron rings in EBT-1
[DE85-011302] 23 p3983 N85-34701
Assessment of magnetic field asymmetries in ELMO Bumpy square
[DE85-011559] 23 p3984 N85-34705

BUNCHING
NT ELECTRON BUNCHING
Considerations regarding the choice of beam parameters and IP configuration for the SSC
[DE84-014532] 01 p0118 N85-10803
Antiproton source beam position system
[DE84-016716] 09 p1380 N85-18679
Bunch coalescing in the main ring to form intense proton and antiproton bunches without RF counterphasing
[DE85-001364] 09 p1382 N85-18692
Adaptive corrector operating in frequency domain
22 p3765 N85-33337
Synchronous timing of multi-energy fast beam extraction during a single AGS cycle
[DE85-011829] 24 p4158 N85-35781

BUNDLES
An efficient algorithm for the computation of the inverse in bundle adjustment systems — photogrammetry
08 p1175 N85-17411
Study of hadron bundles observed in Chacaltaya two-story emulsion chamber
[HE-3.3-4] 24 p4180 N85-35922

BUOYANCY
The properties of plane turbulent buoyant jet
[NAL-TR-798] 01 p0046 N85-10304
Mass and momentum transport in a turbulent buoyant vertical axisymmetric jet 05 p0635 N85-14070
A new physical Lagrangian tracer
[DE84-016212] 05 p0687 N85-14419
The properties of a round turbulent buoyant jet
[NAL-TR-826] 06 p0806 N85-15136
Finite difference calculations of buoyant convection in an enclosure. Part 2: Verification of the nonlinear algorithm
[PB85-104065/GAR] 07 p0961 N85-16089
Primer for mass metrology
[PB85-121424/GAR] 09 p1305 N85-18199
An experimental study of single and multiple turbulent buoyant jets in crossflow 09 p1317 N85-18281
On the flow processes in sharply inclined and stalled airfoils in parallel movement and rotation
[NASA-TM-77509] 10 p1419 N85-18952
Wind-tunnel research on the mechanics of plumes in the atmospheric surface layer
[AD-A150019] 12 p1846 N85-21584
Mechanisms of heat and mass transfer across a double-diffusive interface
[PB85-148468] 12 p1848 N85-21594
Assembly Concept for Construction of Erectible Space Structure (ACCESS) neutral buoyancy testing results
14 p2236 N85-23862
Magnetic buoyancy instabilities in the convective overshoot zone — Sun 14 p2447 N85-25101
Numerical techniques for steady two-dimensional transcritical stratified flow problems, with an application to the intermediate field dynamics of ocean thermal energy conversion plants
[DE85-008347] 18 p3151 N85-29509
Experiences with neutral buoyance testing mockups
18 p3159 N85-29571
Buoyant jet entrainment in stratified fluids
19 p3263 N85-30238
Numerical solutions of turbulent models for flow over a flat plate with angle of attack
[DE85-010380] 21 p3585 N85-32286
Gravity-wave spectra in the atmosphere observed by MST radar, part 4.2B 21 p3622 N85-32502
Buoyant densities of phototrophic sulfur bacteria and cyanobacteria 21 p3660 N85-32740
The calculation of two-dimensional buoyant surface jets with the k-W model of turbulence — kinetic energy-vorticity fluctuations (k-W)
[CFD/84/21] 22 p3785 N85-33448

BUOYS
Sea ice data buoys in the Weddell Sea
[AD-A144953] 01 p0088 N85-10594
High-data-rate wide-angle underwater acoustic telemetry system
[DE84-015696] 02 p0233 N85-11519
Terrestrial locating — of buoys from space
05 p0599 N85-13816
Mariners weather log, volume 28, no. 3, July-August-September 1984
[PB85-107266] 06 p0840 N85-15334
Improvements in linked-spar motion-compensated lifting system
[AD-D011413] 08 p1138 N85-17165
Drifting buoy data from equatorial Pacific Ocean, 31 Aug. 1980 - 30 Apr. 1982
[PB85-120046] 10 p1522 N85-19598
Project PAPA: The integration of drifting buoy data into an operational meteorological service
14 p2238 N85-23874
Automatic buoys to assist the tuna fishery off the Azores 14 p2238 N85-23879
Fourier transform of wave data on ARGOS buoys
14 p2323 N85-24351
The development of Platform Transmitter Terminal (PTT) and its application for drifting buoys
14 p2323 N85-24353
Surface currents in the tropical Pacific during 1979-1980 using drifting buoys 14 p2323 N85-24354
Inferences of future operations drawn from past and present applications of drifting buoys
14 p2323 N85-24356
US program in anchored data buoy and the other fixed observation platforms 14 p2324 N85-24358
One thousand days in the brine — platform transmitter terminals 14 p2324 N85-24359
The development of an automated marine meteorological data system 14 p2324 N85-24362
The ARGOS contribution to the First GARP Global Experiment (FGGE) study of drifting buoys
14 p2325 N85-24371
Meteorological buoys developed at the EERM laboratory 14 p2326 N85-24374
The ARGOS contribution to the successful dredging of a deep moored current meter 14 p2327 N85-24381
Drifting buoy studies for weather applications
14 p2329 N85-24396
Collecting meteorological reports with the ARGOS system 14 p2329 N85-24398
The French Ocean Climate in Equatorial Atlantic (FOCAL) Drifter Program, 1983-1984
14 p2329 N85-24399
The Deep Drifter Program — deep ocean sensors
14 p2329 N85-24400
Telemetered meteorological and engineering data from a deep sea moored body in the Long Term Upper Ocean Study (LOTUS) 14 p2329 N85-24402
Drifting buoy development and future programs — Japanese ARGOS program 14 p2330 N85-24406
Development of a low cost drifting buoy
14 p2330 N85-24408
Arabian gulf circulation — pollution monitoring
14 p2331 N85-24412
A report on the DRIFTERS program — buoys
14 p2331 N85-24413
Drifting buoys on the Labrador shelf
14 p2331 N85-24415
Moored buoy stationkeeping and location system
14 p2331 N85-24416
Overview of data processing at AES local user terminals — Canadian Atmospheric Environment Service (AES) 14 p2331 N85-24418
The Data Acquisition Control and Telemetry (DACT) system — meteorological buoys
14 p2332 N85-24419
An overview of NDBC drifting buoy development programs — NOAA Data Buoy Center (DBC)
14 p2332 N85-24422
Tactical deployment of satellite-reporting drifting data buoys for environmental data acquisition
14 p2332 N85-24423
Studies into location accuracy — ARGOS system
16 p2811 N85-27334
Positioning accuracy of the ARGOS system in operational use 16 p2811 N85-27335
DB2 and DB3: The next generation — buoys
16 p2811 N85-27337
Development of a Lagrangian drifting buoy
16 p2811 N85-27338
Long term drifting float for measuring mean oceanic circulation using ARGOS system
16 p2811 N85-27339
ARGOS-tracked drifters in the Rockall Trough
16 p2812 N85-27340
Monitoring of marine environment
16 p2812 N85-27341
The validation of sea surface temperatures determined from AVHRR data using in situ data recovered via system ARGOS 16 p2812 N85-27342
Wave directional spectra via ARGOS
16 p2812 N85-27343
Routine wave and meteorological measurements in offshore areas using ARGOS data surveillance
16 p2812 N85-27344
Results of an initial trial of a satellite telemetering buoy measuring near surface current
16 p2812 N85-27345
An operational buoy network collecting meteorological data 16 p2813 N85-27351
Checking on the position of navigation marker buoys by the ARGOS system 16 p2813 N85-27354
An inexpensive radar-responding relocation device for drifting oceanographic instruments
[AD-A152170] 16 p2836 N85-27505
A laser slope gauge and a spar buoy wave gauge: Tools for the validation of microwave remote sensors
[AD-A154038] 19 p3272 N85-30290

Free-float Emergency Position Indicating Radio Beacons (EPIRBs) and release mechanism on board Norwegian ships. Main specifications and user experience
20 p3404 N85-31120
Experiments of a LORAN-C aided recovery system and a proposal of its application to rescue system
20 p3404 N85-31121
BURGER EQUATION
On limits of applicability of linear models to dynamics of gas channels in aircraft engines
09 p1308 N85-18219
The stress-strain-time graph of rheological soils and its application
[AD-P004286] 09 p1407 N85-18863
On the relation between upwind-differencing schemes of Godunov, Engquist-Osher and Roe
[NASA-CR-175805] 18 p2852 N85-27583
The Hamiltonian structure of a complex version of the Burgers hierarchy
[PREPRINT-423] 18 p3173 N85-29665
BURNERS
Heat flux sensors for burner liners and turbine blades and vanes 02 p0142 N85-10961
Burner liner thermal/structural load modelling
02 p0143 N85-10970
Burner stabilized flames in fluids
[DE84-017429] 09 p1291 N85-18109
Ribbon burner simulation of T-700 turbine shroud for ceramic lined seals research
[NASA-TM-86940] 10 p1483 N85-19364
Digital temperature and velocity control of mach 0.3 atmospheric pressure durability testing burner rigs in long time, unattended cyclic testing
[NASA-TM-86959] 12 p1805 N85-21321
BURNING
U COMBUSTION
BURNING PROCESS
U COMBUSTION
BURNING RATE
HMX combustion modification
[AD-A145071] 01 p0024 N85-10149
Catalyzed low burning rate propellants for upper-stage solid rocket motor
[NAL-TR-805] 03 p0339 N85-12181
Thrust characterization of very high burning rate propellants
[AD-A145891] 03 p0340 N85-12186
Combustion properties of fuel-rich magnesium propellants with HTPB as binder
[FOA-C-20555-D1] 07 p0935 N85-15924
The pressure deflagration limit of solid rocket propellants 08 p1117 N85-17046
Thermal profiles of thermite reactions
[DE85-003308] 10 p1438 N85-19061
Recovery of damaged solid propellants by interrupting burning and crack-propagation processes
[AD-P004343] 10 p1455 N85-19167
A thermal-mechanical model of deflagration-to-detonation in granular energetic materials
[AD-P004346] 10 p1455 N85-19170
Effects of perforation L/D ratio and slotting on stick propellant combustion
[AD-A148854] 10 p1456 N85-19177
Study of HTPB-based SOFRAM fuels
[FOA-C-20563-D3] 11 p1614 N85-20150
Mechanism of burning rate enhancement by ferric oxide 13 p2002 N85-22546
Effect of variable solid phase thermal properties on propellant combustion 13 p2002 N85-22547
Mutiple reflection theory for microwave measurement of solid propellant burning rates
13 p2002 N85-22549
In-situ burning rate determination using flash radiography 13 p2002 N85-22550
Chemical kinetics of gas phase decomposition products of nitramine propellants 13 p2003 N85-22556
A comprehensive review of black powder
[AD-A150455] 13 p2039 N85-22769
A fundamental study of liquid phase particle breakup. Revision
[AD-A150791] 14 p2301 N85-24249
The overall reaction concept in premixed, laminar, steady-state flames. 2: Initial temperatures and pressures
[AD-A152132] 16 p2746 N85-26944
Burn rates of explosives at high pressures
[DE85-010606] 19 p3251 N85-30159
Radiative augmented combustion
[AD-A154137] 20 p3423 N85-31246
The role of aircraft panel materials in cabin fires and their properties
[FAA-CT-84-30] 21 p3553 N85-32104
Closed-bomb combustion of Hivelite-based, Very High Burn Rate (VHBR) propellant
[AD-A155740] 21 p3571 N85-32212
Investigation of the flame speeds of propane/methanol gas mixtures
[DE85-012817] 23 p3912 N85-34239
Modeling heterogeneous high explosive burn with an explicit hot-spot process
[DE85-009593] 23 p3922 N85-34300
BURNOUT
A review of the physics and response models for burnout of semiconductor devices
[AD-A155031] 21 p3709 N85-33028
BURNS (INJURIES)
Man's physical tolerance to heat. Heat storage, burn injury
[FOA-C-54055-H1] 02 p0235 N85-11533
BURSTS
NT GAMMA RAY BURSTS
NT RADIO BURSTS
NT SOLAR RADIO BURSTS
NT TYPE 3 BURSTS
NT TYPE 4 BURSTS
The vertical structure and stability of alpha model accretion disks 09 p1417 N85-18938
X-ray bursts: Observation versus theory
[NASA-CR-174415] 10 p1573 N85-19916
Hydrodynamic simulations of recurrent novae
11 p1753 N85-21025
X-ray spectra of bursting neutron stars
23 p3961 N85-34686
DMSK: A practical 2400-bps receiver for the mobile satellite service: An MSAT-X Report
[NASA-CR-176194] 24 p4088 N85-35324
BUS CONDUCTORS
Fiber optic data bus using Frequency Division Multiplexing (FDM) and an asymmetric coupler
[NASA-TM-86015] 04 p0492 N85-13139
EMI (electromagnetic interference) filter capacitor unit
[AD-D011392] 07 p0937 N85-15941
Analysis of the performance of multiaccess networks of the bus type
[FUB-47-1983] 09 p1313 N85-18249
Survivable local area network
[AD-D011453] 10 p1488 N85-19262
Development of an integrated control unit for the PDV bus concept
[BMFT-FB-T-84-300] 15 p2551 N85-25745
Design of a microprogram control unit with concurrent error detection
[AD-A156447] 24 p4139 N85-35655
BUSHINGS
Damping seal verification setup
16 p2736 N85-26893
Telescoping low vibration pulling mechanism for Czochralski crystal growth
[AD-D011655] 17 p3044 N85-28836
Further investigations to improve the fatigue life of the Mirage 1110 wing main span
[ARL/STRUC-TM-397] 18 p3061 N85-28938
BUSINESS MANAGEMENT
U INDUSTRIAL MANAGEMENT
BUTADIENE
The effect of pressure on the mechanical properties of polymers. Part 2: Measurement of the time-dependent Poisson's ratio
[DE85-002139] 06 p0772 N85-14938
Reactions of butadiyne. 1: The reaction with hydrogen atoms
[NASA-TM-77805] 07 p0921 N85-15834
Laser schlieren, shock tube studies of high temperature hydrocarbon pyrolysis rates
[DE85-003314] 11 p1636 N85-20303
BUTANES
Thermodynamic properties of isobutane-isopentane mixtures from -40 to +600(0)F and up to 1000 psia
[DE84-015137] 01 p0124 N85-10850
Butene oxidation by molybdenum crystalographic shear compounds
[DE84-013910] 05 p0614 N85-13923
Biocatalyzed processes for production of commodity chemicals: Assessment of future research advances for N-butanol production
[NASA-CR-174264] 07 p0919 N85-15819
Catalytic conversion of C3-C4 paraffins to gasoline
[DE85-004181] 10 p1458 N85-19187
Thermophysical properties of working fluids for binary geothermal cycles
[DE85-000385] 12 p1881 N85-21804
Detailed chemical kinetic study of the effect of molecular structure on autoignition of fuel-air mixtures
[DE85-004424] 17 p2921 N85-28010
On the low temperature chemistry preceding end gas autoignition
[DE85-010471] 19 p3252 N85-30162
Optical waveguide sensor for methane gas
[AD-D011691] 19 p3273 N85-30294
Experimental study of engine knock
[DE85-009851] 22 p3754 N85-33268
Production of butanol by fermentation in the presence of cocultures of clostridium
[NASA-CASE-NPO-16203-1] 24 p4071 N85-35227
BUTENES
Study of vibrational energy transfer at a liquid tin surface
[AD-A145741] 02 p0277 N85-11604
BUTT JOINTS
Radiographic inspection of butt welds described
11 p1620 N85-20198
Evaluation of stress concentration coefficients in butt-welded joints with displaced edges
15 p2501 N85-25425
Differential between crack and pseudo-crack indications by means of objective magnetic flux leakage testing
[BLL-BISI-TRANS-22033-(9022.06)]
17 p2976 N85-28386
Low pressure arc butt welding of dissimilar metals
19 p3246 N85-30126
BUTTERFLY VALVES
NT DAMPERS (VALVES)
BUTYLENE
U BUTENES
BUTYLENE OXIDES
U TETRAHYDROFURAN
BUTYRIC ACID
Production of butanol by fermentation in the presence of cocultures of clostridium
[NASA-CASE-NPO-16203-1] 24 p4071 N85-35227
BY-PRODUCTS
Versatility of peat emphasized
07 p0994 N85-16316
Oil-shale exploration expansion urged
07 p0994 N85-16317
Rockwell Hanford operations defense waste and byproducts management
[DE85-000553] 09 p1382 N85-18694
Current regulatory and licensing status for byproduct sources, facilities and applications
[DE85-010967] 22 p3842 N85-33796
BYPASS RATIO
A study of bird ingestions into large high bypass ratio turbine aircraft engines
[DOE/FAA/CT-84/13] 01 p0005 N85-10028
Effect of combined pressure and temperature distortion orientation on high-bypass-ratio turbofan engine stability
[NASA-TM-83771] 01 p0011 N85-10067
Effect of steady-state temperature distortion on inlet flow to a high-bypass-ration turbofan engine
[NASA-TM-86896] 07 p0904 N85-15725
Planning of air cushion transport vehicles
14 p2285 N85-24160
Energy efficient engine. Fan and quarter-stage component performance report
[NASA-CR-168070] 23 p3897 N85-34141
Energy Efficient Engine Program technology benefit/cost study, volume 1
[NASA-CR-174766-VOL-1] 24 p4066 N85-35197
Energy Efficient Engine Program technology benefit/cost study, volume 2
[NASA-CR-174766-VOL-2] 24 p4066 N85-35198
BYPASSES
Noise isolation system for high-speed circuits
[DE84-014229] 01 p0043 N85-10283
Problems in high temperature thermocouple thermometry
[DE85-000808] 10 p1488 N85-19367
Diodes in photovoltaic modules and arrays
[NASA-CR-175454] 10 p1508 N85-19513
Problems with electrical interference between solar generators and shunt type regulators
13 p2010 N85-22607

C

C BAND
Non-local origin of a substantial portion of the soft X-ray background 06 p0877 N85-15567
The nature of the soft X-ray emitting region in the direction of the North Polar spur
06 p0877 N85-15568
Spectrum resource assessment of the 7125-8500 MHz band
[PB85-127413] 11 p1626 N85-20242
Strongly coupled millimeter-band waveguide directional couplers 22 p3779 N85-33416
C-5 AIRCRAFT
Performance capabilities of the C-5 and C-17 cargo aircraft
[AD-A145618] 02 p0138 N85-10939
Airborne performance measurement system design: C-5 aircraft
[AD-A145436] 02 p0236 N85-11539
The structural finite element model of the C-5A
15 p2576 N85-25665

C-135 AIRCRAFT
Investigation of surface tension phenomena using the KC-135 aircraft
[NASA-TM-82506] 10 p1426 N85-18095
Design of robust controllers for a multiple input-multiple output control system with uncertain parameters application to the lateral and longitudinal modes of the KC-135 transport aircraft
[AD-A153100] 17 p2900 N85-27877
C-141 AIRCRAFT
Far-infrared spectroscopy of interstellar gas
08 p1245 N85-17858
Molecular spectroscopy from the Kuiper Airborne Observatory
[NASA-CR-175748] 16 p2882 N85-27783
CABIN ATMOSPHERES
NT SPACECRAFT CABIN ATMOSPHERES
Airliner cabin air quality
[S-REPT-98-468] 03 p0402 N85-12580
Other challenges in the development of the orbiter environmental control hardware
08 p1096 N85-16924
Simultaneous cabin and ambient ozone measurements on two Boeing 747 airplanes. Volume 3: October 1978 - July 1979
[NASA-TM-86883] 12 p1892 N85-21872
CABLES
Evaluation of the Kerie Cable thermal arc cutting equipment
[AD-A147813] 07 p0974 N85-16186
The dynamics of slack marine cables
[AD-A155022] 21 p3599 N85-32349
Enhanced heat transfer computations for internally cooled cable superconductor
[DE85-011897] 24 p4095 N85-35383
CABLES (ROPES)
Sea water rope batteries
[AD-A144775] 01 p0042 N85-10275
NATFREQ users manual: A FORTRAN 4 program for computing natural frequencies, mode shapes and drag coefficients for taut strumming cables with attached masses and spring-mass combinations
[AD-A146058] 03 p0407 N85-12600
Test methods for cable cars
[CETIM-1-5K-45-1] 04 p0515 N85-13282
Electromagnetic inspection of wire ropes using sensor arrays
[AD-A148317] 08 p1170 N85-17379
Electromagnetic inspection of wire ropes using sensor arrays
[AD-A149016] 10 p1495 N85-19436
Cable-catenary large antenna concept
14 p2231 N85-23829
Apparatus producing constant cable tension for intermittent demand
[DE85-006434] 23 p3938 N85-34412
Study of NSI and related cable performance during tests performed in the NASA Hot Gas Facility
[NASA-CR-170886] 24 p4101 N85-35423
CAD (DESIGN)
U COMPUTER AIDED DESIGN
CADASTRAL MAPPING
Application of the Siemans Computer Aided Computer (Sicad) system to the surveying management in Baden-Wuerttemberg 16 p2814 N85-27361
Automatic engraving of map frames in the revision of the TK 25, 1:25,000 topographical map
16 p2814 N85-27362
The significance of orthophoto maps for developing countries 18 p3124 N85-29341
CADMIUM
Features of laser welding of medium carbon steel through a cadmium coating 01 p0020 N85-10122
Optical bistability in Cd(x)Hg(1-x)Te
18 p3186 N85-29760
Physical and chemical aerosol characteristics in extremely clean air masses at Cape Grim, Tasmania
21 p3646 N85-32855
Environmental surveillance at Los Alamos during 1984
[DE85-011886] 22 p3811 N85-33605
Towards the development of technological processes for the preparation of cadmium plated steel articles
[BLL-M-36315-(5828.4)] 23 p3913 N85-34248
CADMIUM COMPOUNDS
NT CADMIUM FLUORIDES
NT CADMIUM SELENIDES
NT CADMIUM SULFIDES
NT CADMIUM TELLURIDES
An investigation of the role of sintering in gas-solid interactions
[DE84-015481] 02 p0288 N85-11884
The alpha-form of the hydroxides of bivalent metals
[NASA-TM-77508] 04 p0473 N85-13009
CADMIUM FLUORIDES
High temperature laser interferometric studies of solid electrolytes 09 p1396 N85-18785
CADMIUM MERCURY TELLURIDES
U MERCURY CADMIUM TELLURIDES
CADMIUM NICKEL BATTERIES
U NICKEL CADMIUM BATTERIES
CADMIUM SELENIDES
Luminescent properties of graded cadmium sulfoselenide electrodes prepared from cadmium sulfide substrates
[AD-A146710] 06 p0766 N85-14898
Preliminary studies on the low-cost preparation of chalcogenide semiconductors from solution depositions
[DE85-000538] 11 p1736 N85-20918
Development of a CdSe thin film solar cell
12 p1880 N85-21796
The ESFET: Evaporated Sensing Fiald Effect Transistor 19 p3256 N85-30188
CADMIUM SULFIDES
Development of copper sulfide/cadmium sulfide thin-film solar cells
[DE84-004513] 01 p0044 N85-10287
Preparation and properties of evaporated CdTe films compared with single crystal CdTe
[DE85-000502] 02 p0222 N85-11452
Development of the production technology of Cu2S/CdS solar generators
[BMFT-FB-T-84-137] 03 p0386 N85-12469
Development and utilization of CdS/Cu2S
05 p0662 N85-14256
Luminescent properties of graded cadmium sulfoselenide electrodes prepared from cadmium sulfide substrates
[AD-A146710] 06 p0766 N85-14898
Preliminary studies on the low-cost preparation of chalcogenide semiconductors from solution depositions
[DE85-000538] 11 p1736 N85-20918
Testing and optimization of the production technology of large-surface Cu2S/CdS solar generators
12 p1880 N85-21793
Physical-chemical investigations of copper sulfides for use in CdS/Cu2S solar cells 12 p1880 N85-21794
A study of the stability of cadmium sulfide/copper sulfide and cadmium sulfide copper-indium-diselenide solar cells
[DE85-002902] 15 p2587 N85-25947
Zn3P2 as an improved semiconductor for photovoltaic solar cells
[DE85-008772] 18 p3097 N85-29171
SERI photovoltaic advanced research and development project: FY 1984 accomplishments
[DE85-002939] 18 p3128 N85-29368
Post-deposition heat treatments of CdS/CuInSe2 solar cells
[DE85-002943] 18 p3128 N85-29373
Cadmium sulfide/copper ternary heterojunction cell research
[DE85-008778] 19 p3305 N85-30486
Liquid crystal light valve structures
[NASA-CASE-MSC-20036-1] 22 p3847 N85-33826
Vectorial electron transfer on designed surfaces
[PB85-204600] 24 p4076 N85-35263
CADMIUM TELLURIDES
Preparation and properties of evaporated CdTe films compared with single crystal CdTe
[DE85-000502] 02 p0222 N85-11452
DOE/SERI polycrystalline thin-film photovoltaic research
[DE84-004516] 02 p0223 N85-11464
Liquid-phase epitaxial growth of CdTe on HgCdTe
[AD-D011482] 10 p1561 N85-19846
Investigation of the effect of annealing on the dislocation and sub-grain boundary content of solvent-evaporation-grown CdTe
[AD-A144087] 13 p2162 N85-23415
Investigation of the MBE growth of InSb and novel quantum well structures
[AD-A151014] 14 p2427 N85-24969
Thin film cadmium telluride and zinc phosphide solar cells
[DE85-002904] 15 p2587 N85-25950
Applications of CdTe to nuclear medicine
[DE85-011677] 23 p3952 N85-34492
HgCdTe surface and defect study program
[AD-A156079] 24 p4161 N85-35799
Electron irradiation of N type cadmium telluride
[AD-A156117] 24 p4161 N85-35301
CAI
U COMPUTER ASSISTED INSTRUCTION
CAISSONS
Safe decompression schedules for caisson workers
[PB85-103612/GAR] 07 p1017 N85-16463
CALCIFEROL
The role of vitamin D in the bone changes associated with simulated weightlessness 15 p2608 N85-26072
The role of 1,25-dihydroxyvitamin D in the inhibition of bone formation induced by skeletal unloading
[NASA-TM-87480] 18 p3153 N85-29522
CALCINATION
U ROASTING
CALCITE
Impact cratering: The process and its effects on planetary evolution --- and silicate-carbonate reactions on Venus
[NASA-CR-174016] 02 p0228 N85-11468
Shock and release equation of state of calcite
[DE85-013151] 23 p3942 N85-34432
Uranium, thorium isotopic analyses and uranium-series ages of calcite and opal and stable isotopic compositions of calcite from drill cores UE25a no. 1, USR G-2 and USW G-3/GU-3, Yucca Mountain, Nevada
[DE85-013039] 23 p3948 N85-34471
CALCIUM
NT CALCIUM ISOTOPES
Variations of the H and K emission lines of singly ionized calcium in the eclipsing binary star system AR Lacertae
02 p0296 N85-11921
Non-invasive techniques for determining musculoskeleton body composition
[DE84-015718] 04 p0545 N85-13470
Abundancies of Ni, Cr, CO and major elements in the silicate portion of the Moon: Constraints from primary lunar magmas 04 p0582 N85-13720
Effect of disuse on sarcoplasmic reticulum in fast and slow skeletal muscle
[NASA-CR-174337] 08 p1191 N85-17508
Study of superplastic alloys based on Al-Zn-Ca
10 p1442 N85-19092
Evaluation of ettringite and related compounds for use in solar energy storage
[PB85-146876] 12 p1883 N85-21816
Carbonate chemistry of the Weddell Sea
[DOE/EV-110611/4] 12 p1898 N85-21916
Aluminum alloy ATs5K5 (5% Zn + 5% Ca) for superplastic forming 13 p2026 N85-22697
Effect of phase state of TiC-NiTi powder composite materials on nature of failure and mechanical properties
13 p2027 N85-22702
Polyamines as possible modulators of gravity induced calcium transport in plants 15 p2606 N85-26060
Calcium and calmodulin localization in gravitropically-responding plant organs
15 p2606 N85-26061
The interaction of calcium and auxin in the gravitropic response of roots 15 p2606 N85-26062
The role of vitamin D in the bone changes associated with simulated weightlessness 15 p2608 N85-26072
New techniques for studying calcium gradients
15 p2609 N85-26076
Isolation of hybridomas for golgi-associated proteins and a plant calmodulin 15 p2613 N85-26103
Computer simulation studies in fluid and calcium regulation and orthostatic intolerance
[NASA-CR-171869] 15 p2616 N85-26117
Addendum to the STCAL and LTCAL user's guide
[NASA-CR-171880] 15 p2628 N85-26194
The effect of microalloying with calcium and magnesium on the plasticity of Poldi AKN 20 Ni-based alloy
[BLL-BISI-TRANS-2174-(9022.06)]
17 p2929 N85-28075
Examples of application of machinability tests
[BLL-BISI-TRANS-22346-(9022.06)]
17 p2973 N85-28363
Cluster production and entropy
[DE85-007626] 17 p3032 N85-28752
Effect of periodic accelerations on physiochemical properties and Ca2+ reactivity of actomyosin in white ra myocardium and skeletal muscles
19 p3324 N85-30594
Space-flight simulations of calcium metabolism using a mathematical model of calcium regulation
[NASA-CR-171863] 19 p3328 N85-30621
The production and destruction of metastable negative ions
[DE85-011056] 19 p3364 N85-3085
Relative abundances of sub-iron to iron nuclei in lo energy (50-250 MeV/N) cosmic rays as observed in th Skylab experiment
[OG-4.1-4] 22 p3876 N85-3401
A new analysis of cosmic ray isotopes at 3 GeV/n fro HEA03-C2 data
[OG-4.3-6] 22 p3879 N85-3403
Effects of acid rain on forest nutrient status
[DE85-012466] 23 p3947 N85-3446
CALCIUM CARBONATES
NT CALCITE
Shock-induced CO2 loss from CaCO3: Implications fo early planetary atmospheres
[NASA-CR-174197] 05 p0745 N85-1477
Two dimensional CO2-ocean model including th biological processes
[DE85-012341] 23 p3950 N85-3448

CALCIUM CHLORIDES
Salt action on concrete
[AD-A147812] 07 p0933 N85-15912
Binary phase diagram determinations
[DE85-010856] 19 p3235 N85-30058
CALCIUM COMPOUNDS
NT CALCITE
NT CALCIUM CARBONATES
NT CALCIUM CHLORIDES
NT CALCIUM FLUORIDES
NT CALCIUM OXIDES
NT CALCIUM PHOSPHATES
NT CALCIUM SULFIDES
NT FLUORITE
NT PEROVSKITES
Investigation of the dissolution of CaCrO4 in molten LiCl-KCl eutectic
[DE84-016394] 04 p0469 N85-12985
CVD boron on calcium chromate powder
[DE85-000214] 09 p1299 N85-18156
CALCIUM FLUORIDES
The observation of a single thermoluminescence glow peak described by kinetics more general than the usual 1st and 2nd order kinetics
[DE84-014697] 02 p0173 N85-11160
Spectroscopic investigation of materials for frequency agile laser systems
[AD-A151731] 16 p2790 N85-27208
CALCIUM ISOTOPES
Biological influences of low-frequency sinusoidal electromagnetic signals alone and superimposed on RF carrier waves
[PB85-161248] 16 p2842 N85-27527
The isotopic composition of cosmic ray calcium
[OG-4.3-5] 22 p3879 N85-34030
CALCIUM METABOLISM
Alterations in gut transport of minerals and in binding proteins during simulated weightlessness
[NASA-CR-175637] 14 p2388 N85-24709
Mammalian gravity receptors: Structure and metabolism 15 p2605 N85-26055
The salutary effect of dietary calcium on bone mass in a rat model of simulated weightlessness
15 p2608 N85-26073
The role of 1,25-dihydroxyvitamin D in the inhibition of bone formation induced by skeletal unloading
[NASA-TM-87480] 18 p3153 N85-29522
Space-flight simulations of calcium metabolism using a mathematical model of calcium regulation
[NASA-CR-171863] 19 p3328 N85-30621
Mechanisms of osteodystrophy in weightlessness
22 p3733 N85-33143
CALCIUM OXIDES
Sub-eutectic densification and second phase formation in Al2O3 - CaO
[DE85-002065] 09 p1398 N85-18796
Thermal reactions of aromatics with CaO
[DE85-010688] 22 p3742 N85-33193
Improved oxygen sources for breathing apparatus
[NASA-TM-86671] 24 p4134 N85-35623
CALCIUM PHOSPHATES
Ultramicroscopic study of structure of phosphorites from Sea of Japan floor 19 p3290 N85-30400
CALCIUM SULFIDES
Evaluation of ettringite and related compounds for use in solar energy storage
[DE85-003249] 12 p1882 N85-21809
CALCIUM 45
U CALCIUM ISOTOPES
CALCULATION
U COMPUTATION
CALCULATORS
Digital high speed programmable convolver
[AD-D011455] 10 p1481 N85-19348
Fibre composite laminated plate analysis using a card programmable calculator (HP41C/CV)
[MAST-83/86] 13 p2103 N85-23106
Art of programming programmable microcalculators, part 4: errors of calculations 22 p3778 N85-33411
Development of NATOPS performance software for the SH-3D and SH-3H helicopters
[AD-A156140] 24 p4065 N85-35192
CALCULUS
NT ASYMPTOTIC SERIES
NT COLLINEARITY
NT CONTINUITY (MATHEMATICS)
NT COPLANARITY
NT DIFFERENTIAL CALCULUS
NT FOURIER SERIES
NT INTEGRAL CALCULUS
NT LIMITS (MATHEMATICS)
NT PADE APPROXIMATION
NT POWER SERIES
NT SERIES (MATHEMATICS)
NT TAYLOR SERIES
NT VECTOR ANALYSIS
NT VORTICITY
Representation and refinement of visual specifications in PegaSys
[AD-A148733] 09 p1366 N85-18598
Analytical foundations of the theory of quasiconformal mappings in Rn 10 p1536 N85-19679
Computable real analysis
[AD-A149079] 10 p1546 N85-19747
A PASCAL interpreter for the functional programming language ELC (Extended lambda calculus)
[AD-A155218] 21 p3672 N85-32810
CALCULUS OF VARIATIONS
Stable monotone variational inequalities
[AD-A147123] 07 p1031 N85-16544
Schubert varieties are arithmetically Cohen-Macaulay
16 p2853 N85-27592
Generalized formulation of a class of explicit and implicit TVD schemes
[NASA-TM-86775] 21 p3675 N85-32830
Edge detection and geometric methods in computer vision
[AD-A155873] 24 p4135 N85-35630
CALDERAS
High-resolution microseismicity study of possible magmatic intrusion in the Long Valley Caldera
[DE85-001076] 11 p1681 N85-20593
Workshop on Recent Research in the Valles Caldera
[DE85-010569] 23 p3949 N85-34472
CALIBRATING
NT WIND TUNNEL CALIBRATION
Single viewpoint self calibration: A contribution to field calibration of recording chambers
[SER-C-289] 01 p0049 N85-10320
Analysis of highly precise gravity measurements
[SER-C-294] 01 p0071 N85-10472
Calibration of hall probes
[CSIR-NAC-83-04] 01 p0116 N85-10794
Photon and electron dosimetry at the Physikalische-Technische Bundesanstalt in Brunswick
[PTB-DOS-9] 01 p0119 N85-10814
Photoelectric photometry of globular cluster giants
01 p0128 N85-10884
A proof-of-principle getaway special free-flying satellite demonstration 02 p0155 N85-11051
Radar, target and ranging
[AD-A145407] 02 p0190 N85-11272
Some considerations on the capacitive calibration used for the 2.3 ton cryogenic antenna at CERN --- gravitational antennas
[NOTA-INTERNA-809] 02 p0192 N85-11284
The analysis of tank calibration data from several runs
[DE84-015529] 02 p0200 N85-11337
Evaluation of laser profile and deflection measuring system
[FAA-PM-84-24] 02 p0201 N85-11341
Wall interference measurements for three-dimensional models in transonic wind tunnels: Experimental difficulties 03 p0311 N85-12012
Survey of ONERA activities on adaptive-wall applications and computation of residual corrections
03 p0312 N85-12013
Wind tunnel wall interference in closed, ventilated and adaptive test sections 03 p0312 N85-12014
SEASAT altimeter data over the Mediterranean: Implications for ERS-1 03 p0382 N85-12443
Ice sheets as invariant surfaces for radar altimeter calibration and orbit determination
03 p0383 N85-12449
ERS-1 radar altimeter system performance evaluation and calibration 03 p0383 N85-12451
Calibration and validation areas --- satellite altimeters
03 p0384 N85-12456
Self-study manual on optical radiation measurements. Part 1: Concepts. Chapter 11: Linearity considerations and calibrations
[PB84-218346] 03 p0421 N85-12690
Evaluation of thermocouple junction temperature
[DE84-015159] 04 p0502 N85-13206
Special Developments and Methods in High Frequency Measuring Techniques --- conferences
[PTB-E-24] 05 p0629 N85-14030
Realization of noise power in the microwave range by thermal noise standards 05 p0629 N85-14034
Calibration of noise power transfer standards, measurement uncertainties and long term stability
05 p0630 N85-14035
Coaxial noise measurement circuits
05 p0630 N85-14036
A computer controlled measuring system for the calibration of HF components 05 p0630 N85-14037
Calibrating and measuring systems for electromagnetic fields
05 p0630 N85-14041
Evaluation and results of national and international intercomparison measurements --- electromagnetic measurement 05 p0631 N85-14043
LANDSAT instruments characterization
[E85-10030] 05 p0654 N85-14199
Study of the improvement in analyzing passive microwave remote sensing data by integrated use of ground data 05 p0658 N85-14226
Formation of reference signals in laser-type gas analyzers with mechanical switching of optical channels
06 p0787 N85-15027
Experimentation and measurement
[PB84-233659] 06 p0812 N85-15157
Effective use of remote sensing products in litigation
[E85-10046] 06 p0827 N85-15250
Tornado: Structural Usage Monitoring System (SUMS) 07 p0896 N85-15680
Recalibration of the KPNO spot sensitometers --- Kitt Peak National Observatory 07 p0963 N85-16103
Extending magnitude standards to faint stars with a sub-beam prism 07 p0965 N85-16124
Sub-beam prism used at the Bosscha Schmidt telescope 07 p0965 N85-16125
Astronomers' problems with the calibration of Schmidt plates 07 p0965 N85-16126
Stellar photographic photometry using a double wedge technique with a focal reducer system
07 p0966 N85-16133
Six-component strain gage block scale 167-6B. Part 1: Calibration, September 1983
[F+W-FO-1699] 07 p0968 N85-16143
NBS (National Bureau of Standards) switching radiometers
[PB84-235694] 07 p0968 N85-16147
Thematic Mapper. Volume 1: Calibration report flight model, LANDSAT 5
[E85-10059] 07 p0987 N85-16270
Research in geodesy based upon radio interferometric observations of extragalactic radio sources
[AD-A147581] 07 p0988 N85-16280
Results of the 1984 NASA/JPL balloon flight solar cell calibration program
[NASA-CR-174270] 07 p0991 N85-16294
High accuracy Doppler navigation employing optimum integrated position fix information
08 p1073 N85-16803
Numerical analysis of the first static calibration of the RSRA helicopter active-isolator rotor balance system
[NASA-TM-85975] 08 p1083 N85-16863
Amplitude calibration experiment for SIR-B
08 p1146 N85-17227
Evaluation of the L-band scattering characteristics of volcanic terrain in aid of lithologic identification, assessment of SIR-B calibration, and development of planetary geomorphic analogs 08 p1146 N85-17232
Application and calibration of the subsurface mapping capability of SIR-B in desert regions
08 p1146 N85-17244
German Radar Observation Shuttle Experiment (ROSE) 08 p1148 N85-17245
Multicomponent calibration and quantitation methods
[AD-A148252] 08 p1212 N85-17629
Primer for mass metrology
[PB85-121424/GAR] 09 p1305 N85-18199
Calibration of thermocouples based on two state points of water and BS 4937; part 5, 1974
09 p1324 N85-18317
Flux reconstruction and calibration
09 p1412 N85-18904
Historical cost curves for hydrogen masers and cesium beam frequency and timing standards
10 p1465 N85-19245
High-current measurement techniques
[PB85-100444] 11 p1637 N85-20311
Magnetic measurements, calibrations, and standards: Report on a survey
[PB85-127827] 11 p1638 N85-20317
Generalized method for the calibration of 4-terminal-pair type digital impedance meters
[PB85-126122] 11 p1638 N85-20318
Automated TEM (Transverse electromagnetic) cell calibration system
[PB85-134377] 11 p1638 N85-20319
Report on the Workshop on Intercomparison of Solar UV Irradiance Measurements and Related Instrument Calibration 11 p1658 N85-20448
Radiometric calibration and processing procedure for reflective bands on LANDSAT-4 protoflight Thematic Mapper 11 p1668 N85-20510
Prelaunch absolute radiometric calibration of the reflective bands on the LANDSAT-4 protoflight Thematic Mapper 11 p1669 N85-20515
Characterization of radiometric calibration of LANDSAT-4 reflective bands 11 p1669 N85-20516

Instructor's handbook on meteorological instrumentation
[PB85-105930] 11 p1688 N85-20615

State measurement laboratories: Program description (part 1). Directory (part 2)
[PB85-137651] 11 p1739 N85-20935

Self-consistent recalibration of IUE determination of hot DA white dwarf effective temperatures
11 p1751 N85-21016

IUE observations of faint standard stars for calibration of the space telescope 11 p1761 N85-21076

Calibrations of wavelengths in SWP echelle spectra
11 p1761 N85-21077

Radar calibration using direct measurement equipment and oblique photometry
[AD-D011530] 12 p1822 N85-21433

Method and apparatus for self-calibration and phasing of array antenna
[NASA-CASE-NPO-15920-1] 12 p1832 N85-21493

Thermal band characterization of the LANDSAT-4 Thematic Mapper 12 p1869 N85-21727

Preliminary evaluation of the radiometric calibration of LANDSAT-4 Thematic Mapper data by the Canada Centre for Remote Sensing 12 p1870 N85-21729

VISSR infrared calibration by means of calculated radiances 12 p1894 N85-21889

GMS operational calibration procedure and status
12 p1895 N85-21893

Journal of Research of the National Bureau of Standards, volume 89, number 2, March - April 1984
[PB85-115426] 12 p1926 N85-22103

Fast times at high temperatures
[DE85-003306] 12 p1943 N85-22205

Considerations for upgrading modifications to the Marshall Space Flight Center's X-ray calibration facility
12 p1946 N85-22226

Germanium resistance thermometer calibration at superfluid helium temperatures
12 p1947 N85-22228

Determination of angular resolution of coded aperture gamma-ray telescope 13 p1961 N85-22432

Calibration of solar cells outside the atmosphere
13 p2009 N85-22603

Nonlinearity and spectral mismatch problems of solar cells 13 p2010 N85-22605

A standard aircraft diffusion flame: Spectral characteristics and a feasibility study for developing an alternate calibration source for aircraft optical fire detection systems
[AD-A150231] 13 p2039 N85-22768

Metrological support for remote transport vehicle speedometers 13 p2076 N85-22963

Microwave blackbodies for spaceborne receivers
[NASA-CR-175647] 13 p2094 N85-23068

Low temperature calibration fixture
[DE85-003969] 13 p2094 N85-23071

User's guide to calibration of analog electronic controllers in HVAC systems
[AD-A150603] 14 p2298 N85-24229

Calibration loading of a strain-gauged diverless helicopter weapon recovery system
[AD-A151486] 15 p2471 N85-25253

Detection and location of partial discharges in transformer windings using electrical methods
15 p2551 N85-25750

Space radiation studies for the reporting period, June 1983 - July 1984
[NASA-CR-171411] 15 p2685 N85-26583

Qualification of a wall gage for the SIMA wagon, adapted to the test of helt models motorized by compressed air turbines --- SIMA wind tunnel
[ONERA-PV-1/8068-GY] 16 p2701 N85-26677

Management of vacuum leak-detection processes, standards and calibration
[DE85-008705] 16 p2788 N85-27202

NBS physical measurement services
[NBSIR-84-2875] 16 p2859 N85-27633

Calibration methods in millimeter-wave radioastronomy
[INPE-3481-PRE/724] 16 p2861 N85-27778

Transonic Mach number determination in a blow-down wind tunnel with solid walls and a downstream throat
[VTH-LR-402] 17 p2893 N85-27835

Simulation of gyrocompassing alignment and calibration of strapdown inertial navigation system in a swaying vehicle
[DFVLR-MITT-84-20] 17 p2895 N85-27850

Construction 1976-1980: Design, manufacturing, calibration of the German-Dutch wind tunnel (DNW)
17 p2905 N85-27913

Heat flux sensor calibrator 17 p2915 N85-27970

Proceedings of the Fifteenth Annual Precise Time and Time Interval (PTTI) Applications and Planning Meeting
[AD-A149163] 17 p2961 N85-28287

New time and frequency services at the National Bureau of Standards 17 p2961 N85-28289

Separating the variances of noise components in the Global Positioning System
[AD-P004578] 17 p2963 N85-28295

Unattended TV time transfer results
17 p2964 N85-28305

Field theory analysis using the finite element method to determine the deliberation curves of three dimensional fracture mechanics specimens with a semicircular surface crack applying the electrical direct current potential method for crack depth measurement
[GKSS-84-E-53] 17 p2982 N85-28434

Comparison of measurement and simulation results of radiation temperatures applied to the thermal mapping of Munich
[DFVLR-FB-85-06] 17 p2984 N85-28442

Absolute calibrations of SO2 and NO analyzers by photographic methods
[DFVLR-MITT-85-02] 17 p2994 N85-28504

Tone calibrated digital radio communication system
[NASA-CASE-NPO-16414-1-CU]
18 p3089 N85-29121

Automatic volume calibration system
[DE85-006955] 18 p3102 N85-29204

Oscillating pressure device for dynamic calibration of pressure transducers
[NASA-CASE-LAR-13094-1] 18 p3104 N85-29217

State Weights and Measures Laboratories: Program handbook
[PB85-183358] 18 p3111 N85-29263

An operational analysis of system calibration
[AD-A153556] 18 p3170 N85-29644

Carbon foil secondary electron emission during ion passage through the 40 to 500 keV energy field
[MPE-190] 18 p3184 N85-29747

Automatic ac/dc thermal voltage converter and ac voltage calibration system
[PB85-182574] 19 p3274 N85-30304

Using regression analysis for determining air data sensor errors by means of an inertial navigation system
[ESA-TT-886] 20 p3392 N85-31041

The 1982 National Measurement Requirements Survey
[NMRC-83-01-SUMM] 20 p3436 N85-31321

Outline of CCVT (Coupling Capacitor Voltage Transformer) calibration procedure, EPRI-NBS (Electric Power Research Institute/National Bureau of Standards) prototype system. Supplement to EPRI report EL-890 (Field Calibration System for CCVTs, April 1978)
[PB85-182566] 20 p3450 N85-31418

Pycnometer shaker
[PB85-174985] 20 p3460 N85-31491

Spectroradiometric calibration of the Thematic Mapper and Multispectral Scanner system
[E85-10104] 20 p3476 N85-31601

TOPEX error budget 20 p3493 N85-31717

An absolute calibration of the solid state detectors in the narrow band neutrino beam at CERN
[NIKHEF-H/84-10] 20 p3536 N85-32017

The response of ionization chambers to relativistic heavy nuclei 20 p3544 N85-32051

Calibration and use of clutter data for simulation
[AD-A154793] 21 p3574 N85-32229

Background equatorial astronomical measurements focal plane assembly (refurbished HI STAR SOUTH)
[AD-A155215] 21 p3590 N85-32313

Improved coordinate measuring machine calibration and control
[DE85-012053] 21 p3590 N85-32315

Reference-cell calibration activities
21 p3613 N85-32453

The 100 years of Aitken Nuclei (AN) study-reminiscence, current and future problems 21 p3641 N85-32621

On-line temperature sensor
[DE85-011641] 22 p3787 N85-33465

Evaluation of coordinate measuring machines
[DE85-011712] 22 p3788 N85-33467

IEA-SSPS CRS calibration report: Calibration of relevant measuring sensors
[DE85-010174] 22 p3788 N85-33468

Beta response of selected instruments
[DE85-013278] 22 p3788 N85-33469

Development of a microorifice uniform deposit cascade impactor
[DE85-006765] 22 p3812 N85-33614

AMI calibration study. Volume 1: SAR calibration. Volume 2: Ground Targets. Volume 3: Scatterometer calibration --- Active Microwave Instrument (AMI) ERS-1
[C2248/4/4-VOL-1] 23 p3936 N85-34394

Multi-robot assembly of IC's 23 p3964 N85-34577

Measured performance of the new University of California gamma ray telescope
[OG-9.2-13] 23 p4026 N85-34952

The final COS-B database: In-flight calibration of instrumental parameters
[OG-9.3-9] 23 p4028 N85-34964

Detector calibration of the Indian cosmic ray experiment (IONS) in Space-Shuttle Spacelab-13
[SH-9.1-2] 23 p4050 N85-35117

Calibrator for displacement gages used in the rock mechanics laboratory
[DE85-013257] 24 p4096 N85-35380

Calibration of a high-level photon irradiation
[DE85-013044] 24 p4151 N85-35738

CALIFORNIA

Mineral nutrients in Mediterranean ecosystems
[REPT-71] 01 p0069 N85-10458

Vertical crustal movements in southern California, 1974 to 1978
[GS-CIRC-905] 02 p0228 N85-11491

Franciscan and related rocks of southern Humbol County, northern California coast ranges: Analysis of structure, tectonics, sedimentary petrology, paleogeography, depositional histroy, and thermal maturity 03 p0390 N85-12495

Investigation of several aspects of LANDSAT 4/5 data quality
[E85-10036] 04 p0525 N85-13367

Effects of acid rain on plant microbial associations in California
[PB84-242122] 04 p0532 N85-13404

Models for volcanic processes in Long Valley, California: Testing by continental drilling
[DE84-014943] 04 p0534 N85-13414

Characterizing the scientific potential of satellite sensors --- San Francisco, California
[E85-10044] 07 p0983 N85-16244

Characterizing the scientific potential of satellite sensors --- San Francisco, California
[E85-10053] 07 p0984 N85-16249

LANDSAT-4 Thematic Mapper Modulation Transfer Function (MFT) evaluation --- California and New Mexico
[E85-10055] 07 p0984 N85-16250

Image variance and spatial structure in remotely sensed scenes --- South Dakota, California, Missouri, Kentucky, Louisiana, Tennessee, District of Columbia, and Oregon
07 p0986 N85-16265

Image-to-image correspondence: Linear structure matching 07 p0986 N85-16266

Analysis of SIR-B radar illumination of geometry for depth of penetration and surface feature and vegetation detection, Nevada and California
08 p1149 N85-17248

Mesozoic ophiolitic olistostromes and Cenozoic imbricate thrust faulting in the northern California coast ranges: Geology of the Mysterious Valley area, Napa County 08 p1182 N85-17445

Bibliography update on the California current system and related mesoscale ocean modeling
[AD-A148546] 08 p1190 N85-17503

Anaysis of the quality of image data required by the LANDSAT-4 Thematic Mapper and Multispectral Scanner --- agricultural and forest cover types in California
[E85-10074] 10 p1504 N85-19488

Vegetation analysis for arid lands geobotany
[NASA-CR-175455] 10 p1506 N85-19509

The 35 kilowatt peak power photovoltaic system
[DE85-000189] 10 p1511 N85-19537

California coastal erosion and storm damage during the winter 1982 - 1983, a reconnaissance report
[PB85-121705] 10 p1521 N85-19591

Investigation of radiometric properties of LANDSAT-4 MSS --- California, North Carolina, South Carolina, and New England 11 p1666 N85-20500

Geodetic accuracy of LANDSAT 4 Multispectral Scanner and Thematic Mapper data --- Washington, DC, California, Alabama, South Dakota, and Illinois
11 p1667 N85-20504

Impact of LANDSAT MSS sensor differences on change detection analysis --- New Mexico, San Francisco, CA, New Hampshire, and Connecticut
11 p1667 N85-20506

High-resolution microseismicity study of possible magmatic intrusion in the Long Valley Caldera
[DE85-001076] 11 p1681 N85-20593

Analysis of the NASA/MSFC Airborne Doppler Lidar results from San Gorgonio Pass, California
[NASA-CR-171355] 12 p1892 N85-21873

USC (University of Southern California) Sea Grant Program Directory, 1984-1985
[PB85-135051] 12 p1899 N85-21922

The future of lightwave technology
[PB85-109759] 12 p1935 N85-22155

Summary of Meteorological Observations, Surface (SMOS) Camp Pendleton, California
[AD-A150482] 13 p2138 N85-23277

Observations of the California countercurrent
[AD-A150781] 14 p2382 N85-24681

Selection of promising sites for magma energy experiments
[DE85-006832] 16 p2620 N85-27380

Air quality benefit analysis for Los Angeles and San Francisco based on housing values and visibility
[PB85-166049] 16 p2822 N85-27409
Application of hierarchical data structures to geographical information systems
[AD-A152169] 16 p2877 N85-27753
Quality assurance for RESOLVE (Research on Operations-Limiting Visual Extinction). A visibility study in the California desert
[AD-A152383] 17 p2992 N85-28494
Formation and fate of toxic chemicals in California's atmosphere
[PB85-172609] 18 p3134 N85-29414
Application of climatological analysis to minimize air pollution impacts in California
[PB85-172963] 18 p3149 N85-29502
Sand dispersion from an ephemeral river delta on the wave-dominated central California coast
[AD-A154352] 19 p3300 N85-30458
Simulated effects of increased recharge on the ground-water flow system of Yucca Mountain and vicinity, Nevada-California
[DE85-012965] 24 p4106 N85-35469
Geology: Structural history and fluvial geomorphology of the southern Death Valley Fault Zone, Inyo and San Bernardino Counties, California
24 p4114 N85-35506
Carbon fiber strainmeter studies in southern California
[PB85-196889] 24 p4118 N85-35528
Sea surface and remotely sensed temperatures off Cape Mendocino, California
[NASA-TM-86712] 24 p4125 N85-35573

CALIFORNIUM
NT CALIFORNIUM ISOTOPES

CALIFORNIUM ISOTOPES
Magnetism of californium metal
[DE85-001141] 09 p1377 N85-18657
Historical review of californium-252 discovery and development
[DE85-010223] 19 p3362 N85-30844
Effects of space radiation on advanced semiconductor devices. Part 3: Further cosmic ray simulation studies of single event upsets and latch-up in CMOS memories
[AERE-G-3368-PT-3] 22 p3848 N85-33833

CALIFORNIUM 252
U CALIFORNIUM ISOTOPES

CALLISTO
Ripple ring basins on Ganymede and Callisto
13 p2183 N85-23547
Tectonics of the Valhalla structure on Callisto
13 p2202 N85-23662
Ganymede and Callisto: Beauty is only skin deep
15 p2680 N85-26552

CALORIC REQUIREMENTS
Nutritional criteria for military rations and effects of prolonged feeding on acceptability
14 p2394 N85-24742
Nutrition in space flight: Some thoughts
14 p2394 N85-24743

CALORIC STIMULI
Caloric stimulation of the vestibular system in microgravity 05 p0695 N85-14469
Inner ear characteristics during 7 day antiorthostatic bedrest (6 deg head down tilt) 05 p0695 N85-14470

CALORIMETERS
A concept for a hadron calorimeter with photodiode readout
[MPI-PAE/EXP-E1-130] 01 p0050 N85-10332
Electromagnetic shower development and applications to sampling calorimeters
[DE84-016355] 04 p0493 N85-13142
Instruments for characterization of carbon black and polymers
[AD-A146475] 06 p0810 N85-15146
Thermal performance testing of passive solar components in NBS (National Bureau of Standards) calorimeter
[PB85-119345/GAR] 09 p1346 N85-18470
Synthesis and thermomechanical properties of new AT-Phenylene R systems
[AD-A149961] 12 p1813 N85-21372
Applications of high pressure differential scanning calorimetry to aviation fuel thermal stability research
[NASA-TM-87002] 14 p2249 N85-23941
Physical chemistry of exothermic gas-aerosol calorimetry
[AD-A150872] 14 p2251 N85-23950
Calorimeter for measuring high-energy optical pulses
[PB85-160695] 15 p2561 N85-25799
A calorimetric approach for measuring emittance and normal spectral absorptance at elevated temperatures
[AD-A151292] 15 p2651 N85-26351
Thermodynamic systematics of oxides of americium, orium and neighboring elements
[DE85-009704] 18 p3197 N85-29831
Cryogenic laser calorimetry for impurity analysis
[NASA-CR-176102] 22 p3743 N85-33201
A lead glass tubing drift calorimeter
24 p4147 N85-35711
X-ray film chamber with carbon target of Tien-Shan complex array 24 p4179 N85-35916
Peculiarities of gamma-quanta distribution at 20 TeV energy
[HE-3.7-10] 24 p4186 N85-35967
Study of muons near shower cores at sea level using the E594 neutrino detector 24 p4191 N85-36000
Measurement of energy muons in EAS at energy region larger thean 10(17) eV
[HE-4.3-8] 24 p4191 N85-36002
Magnetic monopole search by 130 m(2)sr He gas proportional counter
[HE-6.1-2] 24 p4209 N85-36128
Results of a search for monopoles and tachyons in horizontal cosmic ray flux
[HE-6.1-3] 24 p4209 N85-36129
Search for proton decay in the Frejus experiment
[HE-6.2-2] 24 p4210 N85-36136
Results on nucleon life-time from the Kolar gold field experiment
[HE-6.2-3] 24 p4211 N85-36139
Data acquisition system for phase-2 KGF proton decay experiment
[HE-6.2-4] 24 p4211 N85-36140
Construction of the Soudan 2 detector
[HE-6.2-5] 24 p4211 N85-36141
Tien-Shan effect and charmed particles
[HE-6.2-17] 24 p4212 N85-36153
Search for acoustic signals from high energy cascades
[HE-7.1-1] 24 p4213 N85-36155
Spatial distribution read-out system for thermoluminescence sheets
[HE-7.1-7] 24 p4213 N85-36161
Application of thermoluminescence for detection of cascade shower 2: Detection of cosmic ray cascade shower at Mount Fuji
[HE-7.1-12] 24 p4214 N85-36162

CALORIMETRY
U HEAT MEASUREMENT

CALUTRONS
U CYCLOTRONS

CAM (MANUFACTURING)
U COMPUTER AIDED MANUFACTURING

CAMBER
NT WING CAMBER
Effect of a variable camber and twist wing at transonic Mach numbers
[NASA-TM-86281] 04 p0452 N85-12889
Low-speed characteristics of a circulation control airfoil with AFT camber and a spiral trailing edge
[AD-A150851] 14 p2213 N85-23725

CAMBERED WINGS
Extension of the small perturbations method in three-dimensional transonic, unsteady flow to the case of real wings
[ONERA-NT-17/3064-RY-070-R]
20 p3369 N85-31017

CAMERA SHUTTERS
Initial feasibility ground test of a proposed photogrammetric system for measuring the shapes of ice accretions on helicopter rotor blades during forward flight
[NASA-TM-87391] 04 p0455 N85-12887
High-resolution SIT TV tube for subnanosecond image shuttering
[DE85-005189] 13 p2095 N85-23072
Electronic imaging system and technique
[DE85-005740] 23 p3935 N85-34393

CAMERA TUBES
NT IMAGE DISSECTOR TUBES
NT RETURN BEAM VIDICONS
NT THERMICONS
NT VIDICONS
High-resolution SIT TV tube for subnanosecond image shuttering
[DE85-005189] 13 p2095 N85-23072
A new high-resolution pickup tube for live X-ray topography
[NHK-LABS-NOTE-309] 18 p3193 N85-29802

CAMERAS
NT BALLISTIC CAMERAS
NT FRAMING CAMERAS
NT HIGH SPEED CAMERAS
NT MULTISPECTRAL BAND CAMERAS
NT PANORAMIC CAMERAS
NT PINHOLE CAMERAS
NT SCHMIDT CAMERAS
NT STREAK CAMERAS
NT TELEVISION CAMERAS
NASA thunderstorm overflight program: Atmospheric electricity research. An overview report on the optical lightning detection experiment for spring and summer 1983
[NASA-TM-86468] 03 p0363 N85-12330
Developments of optical fast-gated imaging systems
[DE84-016170] 04 p0502 N85-13204
Positron ring system using Anger-type detectors
[DE84-016788] 04 p0503 N85-13212
Improvements in avalanche-transistor sweep circuitry for electrooptic streak cameras
[DE84-016195] 06 p0811 N85-15155
Searching for impact craters using space shuttle photography 06 p0889 N85-15645
Automatic camera tracking for remote manipulators
[DE85-001897] 07 p0974 N85-16187
Improved radiographic viewing system
[AD-A147587] 07 p1016 N85-16456
The ROSAT XUV wide field camera
08 p1243 N85-17844
Time series photometry with a CCD camera
08 p1252 N85-17906
The BRESEX multispectral camera: Preliminary characteristics
[INPE-3357-PRE/635] 10 p1487 N85-19398
Microstrain analysis in bent single crystal silicon by double crystal X-ray topography technique
[DE85-000422] 10 p1584 N85-19863
Preliminary design of an Earth-based debris detection system using current technology and existing installations 12 p1784 N85-21199
Intensified CCD camera system for plasma diagnostics
[DE85-002252] 12 p1853 N85-21620
Electronics Engineering Department EE Technical Review
[UCRL-50025-84-1] 13 p2063 N85-22887
A normal incidence, high resolution X-ray telescope for solar coronal observations
[NASA-CR-175622] 13 p2169 N85-23461
The astrometry programme at Mt. John Observatory
14 p2436 N85-25026
French firm develops new kind of CTD camera for robots 15 p2523 N85-25556
Experimental investigation of the electric breakdown in SF6
[BLL-CE-TRANS-7987-(9022.09)]
15 p2546 N85-25714
Development of robots and application to industrial processes
[NASA-CR-175754] 15 p2567 N85-25840
Errors in compensating for image oscillation by means of a gyroscopic head 16 p2763 N85-27051
The 8.3 and 12.4 micron imaging of the Galactic Center source complex with the Goddard infrared array camera
[NASA-TM-86225] 19 p3382 N85-30982
Large format camera photographs: A new tool for understanding arid environments
21 p3604 N85-32379
Microcomputer controlled image processor
[AD-D011734] 22 p3833 N85-33735
A star camera aspect system suitable for use in balloon experiments
[OG-9.3-10] 23 p4028 N85-34965
Parametric stability of analytical close-range photogrammetry 24 p4107 N85-35461
Application of thermoluminescence for detection of cascade shower 1: Hardware and software of reader system
[HE-7.1-6] 24 p4213 N85-36160
Application of thermoluminescence for detection of cascade shower 2: Detection of cosmic ray cascade shower at Mount Fuji
[HE-7.1-12] 24 p4214 N85-36162

CAMS
Kinematic synthesis of planar cam-link mechanisms for exact path and exact motion generation
03 p0341 N85-12189
Adjustment structure
[AD-D011461] 10 p1459 N85-19193
A rational approach to cam design
23 p3923 N85-34311

CANADA
NT BRITISH COLUMBIA
A summary of operational developments in nowcasting and short-range forecasting techniques on the Canadian West Coast 01 p0082 N85-10547
Canada report to COSPAR 01 p0131 N85-10906
Active microwave measurements of sea ice under fall conditions: The RADARSAT/FIREX fall experiment --- in the Canadian Arctic
[E85-10019] 02 p0217 N85-11432
Evaluation of the radar response to land surfaces and volumes: Examination of theoretical models, target statistics, and applications 08 p1149 N85-17250
Birds and aviation
[AD-P004177] 11 p1578 N85-19939

Birds and aircraft engine strike rates
[AD-P004184] 11 p1579 N85-19946

PMP-1 report: The fourth winter of PMP-1, 1981 - 1982: A winter with several interesting features
11 p1657 N85-20441

Canadian plans for Thematic Mapper data
11 p1668 N85-20513

Hydrometric telemetry in Canada
14 p2239 N85-23882

Corrosion problems in the Canadian maritime forces
[AD-A151594] 15 p2509 N85-25481

AWS (Air Weather Service) climatic briefs: North America
[AD-A152161] 16 p2835 N85-27483

Investigation of the requirement for auxiliary heating of Canadian forces personnel
[AD-A151950] 16 p2841 N85-27522

Structural analysis of terrane accretions in the eastern Brooks Range and adjacent areas in central Alaska and Canada
[DE85-008279] 17 p2993 N85-28501

Search and rescue in Canada
20 p3401 N85-31098

COSPAS-SARSAT demonstration and evaluation results in Canada 20 p3405 N85-31129

CANADAIR AIRCRAFT
NT CL-41 AIRCRAFT

CANADAIR CF-104 AIRCRAFT
U F-104 AIRCRAFT

CANADAIR CL-41 AIRCRAFT
U CL-41 AIRCRAFT

CANADIAN SHIELD

Structural investigation of the Grenville Province by radar and other imaging and nonimaging sensors
08 p1147 N85-17237

CANADIAN SPACE PROGRAM

Canada report to COSPAR 01 p0131 N85-10906

Non-US approaches to space commercialization
02 p0150 N85-11012

Tactical military communications by satellite relay at high latitudes 11 p1709 N85-20756

CANADIAN SPACECRAFT
NT ANIK SATELLITES

CANARD CONFIGURATIONS

Aerodynamic-structural study of canard wing, dual wing, and conventional wing systems for general aviation applications
[NASA-CR-172529] 08 p1077 N85-16829

Unsteady transonic flow calculations for two-dimensional canard-wing configurations with aeroelastic applications
[NASA-TM-86375] 10 p1420 N85-18960

Space Shuttle orbiter trimmed center-of-gravity extension study
[NASA-TP-2284] 10 p1428 N85-19003

Wind-tunnel investigation of a full-scale canard-configured general aviation airplane
[NASA-TP-2382] 11 p1575 N85-19925

Parametric study of a canard-configured transport using conceptual design optimization
[NASA-TP-2400] 11 p1584 N85-19979

Approximate neutral point of a subsonic canard aircraft
[NASA-TM-86894] 15 p2462 N85-25205

Description of a computer program treating transonic steady state aeroelastic effects for a canard or tail airplane
[FFA-TN-1983-23] 16 p2700 N85-26674

Supersonic aerodynamic characteristics of canard, tailless, and aft-tail configurations for 2 wing planforms
[NASA-TP-2434] 17 p2891 N85-27822

Real scale test of the Petit Canard aircraft in the number 3 section, 47 sqm, of the SIMA wind tunnel, May 1984
[ONERA-PV-1/0772-GY] 20 p3389 N85-31018

Study of an efficient long-range Mach 2.7 supersonic transport configuration concept
[NASA-TM-86414] 21 p3554 N85-32110

The aerodynamic characteristics of a GU25-5(11)8 aerofoil for low Reynolds numbers
[GU-AERO-8410] 23 p3894 N85-34121

Vortex boundary-layer interactions
[NASA-CR-176192] 24 p4093 N85-35373

CANCELLATION

Research on adaptive antenna techniques 6
[AD-A149341] 11 p1624 N85-20228

CANCELLATION CIRCUITS

Self-adaptive echo cancellation for telephony
[ENST-84E013] 20 p3441 N85-31353

CANCER
NT LEUKEMIAS

Radiation physics, biophysics, and radiation biology
[DE84-014885] 09 p1360 N85-18557

Effects of long-term low-level radiofrequency radiation exposure on rats. Volume 8: Evaluation of longevity, cause of death, and histopathological findings
[AD-A154283] 19 p3327 N85-30610

Spontaneous transitional cell carcinoma in the urinary bladder of a strain 13 guinea pig
[AD-A155645] 21 p3665 N85-32764

Carcinogenesis of nitrated toluenes and benzenes skin and lung tumor assays in mice
[AD-A155723] 22 p3818 N85-33656

CANISTERS
U CANS

CANNING

A scanning laser velocimeter for turbulence research
[NASA-CR-172493] 07 p0897 N85-15686

CANNONS
U GUNS (ORDNANCE)

CANONICAL FORMS

Canonical analysis of the fermion sector in higher-derivative supergravity
[DE85-007828] 16 p2859 N85-27635

Method to render second order beam optics programs symplectic
[DE85-010631] 20 p3515 N85-31855

Design of high-order analog and digital filters with identical sections 22 p3766 N85-33341

Diakoptic calculation of characteristics for optimization of linear circuits with respect to parameters of individual branches 22 p3767 N85-33346

CANOPIES

Deciduous forest radiation regimes: Effects of forest structure, phenology and Earth-Sun geometry upon their spatial, temporal and spectral variability
[AD-A146804] 07 p0996 N85-16327

A theoretical view on the stress analysis of fully inflated parachute canopies
[AD-A148387] 08 p1078 N85-16835

Age life prediction of nylon 66 parachute materials. Part 1: Mechanical properties
[AD-A147898] 08 p1170 N85-17378

Aircraft transparency bird impact analysis using the MAGNA computer program
[AD-P004186] 11 p1579 N85-19948

CANOPIES (VEGETATION)

Space observation of latitudinal changes in vegetation cover 02 p0164 N85-11113

Relationships between grass canopy characteristics and LANDSAT Thematic Mapper bands
02 p0213 N85-11402

Botanical sciences team 02 p0214 N85-11407

Biophysical and spectral modeling for crop identification and assessment
[E85-10006] 02 p0215 N85-11419

Development and testing of a rural credit supervision system at the level of counties and rural properties utilizing remote sensing techniqes
[E85-10018] 02 p0217 N85-11431

Remote sensing of plant stress and diseases
05 p0657 N85-14216

Variation in spectral response of soybeans with respect to illumination, view, and canopy geometry
[E85-10040] 07 p0982 N85-16241

Spectral estimators of absorbed photosynthetically active radiation in corn canopies
[E85-10041] 07 p0983 N85-16242

Growth/reflectance model interface for wheat and corresponding model
[E85-10058] 07 p0987 N85-16269

Development and evaluation of techniques for using combined microwave and optical image data for vegetation studies 08 p1148 N85-17240

The extension of an invertible coniferous forest canopy reflectance model using SIR-B and LANDSAT data
08 p1149 N85-17246

Analysis of terrestrial conditions and dynamics
[E85-10063] 08 p1174 N85-17401

Shortwave infrared detection of vegetation
[E85-10064] 08 p1174 N85-17402

Growth and reflectance characteristics of winter wheat canopies
[E85-10080] 10 p1505 N85-19494

Techniques for measuring intercepted and absorbed PAR in corn canopies
[E85-10081] 10 p1505 N85-19495

Influence of the atmosphere on remotely sensed reflection from vegetation surfaces
[DE85-000658] 11 p1670 N85-20521

Investigations of vegetation and soils information contained in LANDSAT Thematic Mapper and Multispectral Scanner data
[E85-10082] 12 p1873 N85-21747

Modeling interception of rainfall by forests and the role of interception in the water balance
[DE85-002822] 12 p1884 N85-21825

Remote sensing of coastal wetlands biomass using Thematic Mapper wavebands — Lewes, Delaware
13 p2119 N85-23198

The microwave propagation and backscattering characteristics of vegetation — wheat, sorghum, soybeans and corn fields in Kansas
[E85-10088] 13 p2122 N85-23213

Testing an energy balance model for estimating actual evapotranspiration using remotely sensed data — Hannover, West Germany barley and wheat fields
13 p2125 N85-23236

Use of space photographic information to map plant cover 15 p2488 N85-25359

Identification of structure of soil-vegetation cover using aerial and space photographs 16 p2726 N85-26826

Radar return from vegetation covered terrains
[INPE-3470-PRE/713] 16 p2770 N85-27093

Modeling the backscattering and transmission properties of vegetation canopies
[E85-10099] 16 p2809 N85-27320

Earth observation modeling based on layer scattering matrices
[NLR-MP-84015-U] 17 p2964 N85-28440

Light scattering by leaf layers with application to canopy reflectance modeling: The Scattering by Arbitrarily Inclined Leaves (SAIL) model
[NLR-MP-84011-U] 17 p3038 N85-28796

Biogeochemical cycling and remote sensing
21 p3659 N85-32733

CANS

Lateral support system for canister-launched missile
[AD-D011369] 08 p1106 N85-16987

CANT
U SLOPES

CANTILEVER BEAMS

Characterization of interlaminar crack growth in composites with the double cantilever beam specimen
04 p0463 N85-12942

Experimental investigation of vibroimpact of two cantilever beams 09 p1336 N85-18386

Comparison of shock-induced displacements with displacements produced by a centrifuge acceleration
[DE85-000467] 12 p1852 N85-21618

Planar dynamics of a uniform beam with rigid bodies affixed to the ends
[NASA-CR-175566] 12 p1864 N85-21693

Stress intensity factor in a tapered specimen
[NASA-CR-175589] 13 p2102 N85-23099

Thermal deformation of flexible rotors in friction bearings 14 p2280 N85-24123

Research and development of subsurface acoustic wave devices for sensor applications
[AD-A152197] 16 p2861 N85-27642

Mathematical modeling and control of a large space structure as applied to a shuttle-antenna configuration
[AD-A153269] 17 p2910 N85-27939

Buckling and bracing of cantilevers
[CE-42] 17 p2979 N85-28413

Large deflections of a cantilever beam under arbitrarily directed tip load
[NASA-TM-86442] 19 p3284 N85-30363

ISAAC (Integrated Structural Analysis and Control) via continuum modeling and distributed frequency domain design techniques 20 p3414 N85-31185

Shear-stress distribution and shear stiffness in the case represented by a non-homogeneous cross-section, of any shape, but composed of an orthotropic material, when subjected to a shear force
[DRIC-T-7430] 20 p3469 N85-31554

Influence of the resin on interlaminar mixed-mode fracture
[NASA-TM-87571] 21 p3561 N85-32150

Nonlinear flap-lag-extensional vibrations of rotating, pretwisted, preconed beams including Coriolis effects
[NASA-TM-87102] 23 p3941 N85-34427

The application of bispectral analyses to aeroelastic phenomena 24 p4060 N85-35157

CANTILEVER MEMBERS
NT CANTILEVER BEAMS
NT CANTILEVER PLATES

Flutter parametric studies of cantilevered twin-engine transport type wing with and without winglet. Volume 2: Transonic and density effect investigations
[NASA-CR-172410-VOL-2] 04 p0513 N85-13270

CANTILEVER PLATES

Deformation of cylindrical shell with cantilevered elastic plates attached 06 p0779 N85-14884

CANTILEVER WINGS
U WINGS

CANYONS

Study of pollutant dispersion in an urban street canyon
[DE85-002646] 11 p1677 N85-20571

Analysis of slope stability, Wilmington to Lindenkohl Canyons, US mid-Atlantic margin
[DE84-012278] 12 p1899 N85-21821

Lithologic and structural control on slope morphology in the Valles Marineris 13 p2201 N85-23651

Valles Marineris basin beds: A complex story
13 p2201 N85-23652

CAP CLOUDS

The physics of the marine stratocumulus-capped mixed layer
15 p2593 N85-25979

CAPACITANCE

Capacitive reactance of compensated semiconductors with deep centers under conditions of transmission of exclusion and double injection currents
02 p0266 N85-11742

Machine computation of delay and capacitance of transistor structures of subnanosecond large integrated circuits
04 p0490 N85-13120

Calculation of transmission line impedances using the ANSYS finite element program
[DE84-016715] 11 p1629 N85-20261

New preamplifier for particle detectors
[DE85-004115] 12 p1836 N85-21524

Low capacitance e-beam fabricated beam-lead Schottky barrier diodes
[AD-A150238] 13 p2063 N85-22888

On filter binary processes
[AD-A150328] 13 p2063 N85-22890

Change of electrical characteristics of radio-frequency cables under thermal effect 13 p2081 N85-22999

New electronic measurement, control devices
14 p2289 N85-24192

Transient voltage oscillations in coils
[DE85-006715] 15 p2550 N85-25736

Studies in electron phenomena in MOS structures: The pulsed C-V method 15 p2659 N85-26407

Germanium detectors with a built-in transverse drift field
[DE85-009944] 18 p3096 N85-29165

A laser slope gauge and a spar buoy wave gauge: Tools for the validation of microwave remote sensors
[AD-A154038] 19 p3272 N85-30290

Sixty GHz IMPATT diode development
[NASA-CR-174969] 22 p3758 N85-33293

Capacitance measuring device
[DE85-011643] 22 p3787 N85-33460

CAPACITANCE SWITCHES

Switched Capacitor (SC) filter and design centering of integrated circuits, part 1
[BMFT-FB-T-84-190-PT-1] 05 p0633 N85-14062

CAPACITORS

Isolated load switching with surge suppression
[AD-D011218] 01 p0042 N85-10274

Some considerations on the capacitive calibration used for the 2.3 ton cryogenic antenna at CERN — gravitational antennas
[NOTA-INTERNA-809] 02 p0192 N85-11284

A high-voltage discharger
[AD-A145659] 02 p0194 N85-11299

Determination of the conservation state of long conservation agricultural products by means of capacitive sensors
[NOTA-INTERNA-799] 02 p0220 N85-11447

Pulse injection on a power cable penetrating a shielding wall by feed-through capacitors
[FOA-C-30372-A3] 04 p0497 N85-13171

Flywheel-powered X-ray generator
05 p0605 N85-13861

Implications of the chiral anomaly for quantum Hall effect devices
[NUB-2662] 05 p0629 N85-14029

EMI (electromagnetic interference) filter capacitor unit
[AD-D011392] 07 p0937 N85-15941

Determination of threshold and maximum operating electric stresses for selected high voltage insulation. Task 3: Investigation of high voltage capacitor insulation
[DE84-017051] 09 p1316 N85-18274

Reliability studies of ceramic capacitors
[AD-A149126] 10 p1479 N85-19338

Technological and economic assessment of advanced ceramic materials. Volume 3: A case study of ceramic capacitors
[PB85-113106] 11 p1613 N85-20141

Rep rated long life capacitor development: Phase 1 and 2
[DE85-000719] 11 p1629 N85-20256

Degradation mechanisms in ceramic dielectrics
[AD-A149791] 12 p1813 N85-21369

Control of cascaded induction generator systems
[AD-A150429] 13 p2065 N85-22897

Planar ferroelectric microcapacitors for microwave devices 13 p2087 N85-23032

Erosion of electrodes due to switching of capacitor-bank discharge circuits
[AD-A151207] 15 p2547 N85-25718

Adjustment of the frequency-temperature characteristics of crystal oscillators
[AD-D011588] 15 p2548 N85-25726

Advanced capacitors
[AD-A151709] 15 p2548 N85-25727

Outline of CCVT (Coupling Capacitor Voltage Transformer) calibration procedure, EPRI-NBS (Electric Power Research Institute/National Bureau of Standards) prototype system. Supplement to EPRI report EL-890 (Field Calibration System for CCVTs, April 1978)
[PB85-182566] 20 p3450 N85-31418

East Europe report: Science and technology
[JPRS-ESA-85-021] 21 p3568 N85-32190

Stress corrosion of ceramic materials
[AD-A155020] 21 p3570 N85-32202

Capacitive energy storage at cryogenic temperatures
[AD-A154506] 21 p3579 N85-32253

A fast discharge excimer laser with symmetric geometry
[AD-A155294] 21 p3592 N85-32322

Batteryless magneto-driven portable radiac
[DE85-011622] 22 p3760 N85-33300

Switching power supply
[DE85-005993] 22 p3761 N85-33312

Capacitance measuring device
[DE85-011643] 22 p3787 N85-33460

Reversing-counterpulse repetitive-pulse inductive storage circuit
[DE85-006409] 23 p3928 N85-34344

Tuning system for capacitively loaded 1/4 accelerating cavity
[DE85-012516] 24 p4091 N85-35358

CAPACITY

Open cycle OTEC thermal-hydraulic systems analysis and parametric studies
[DE84-013011] 04 p0530 N85-13391

CAPE KENNEDY LAUNCH COMPLEX

Chronology of KSC and KSC related events for 1983
[NASA-TM-87400] 08 p1261 N85-17927

Preliminary results of associating cloud-to-ground lightning with surface convergence and radar reflectivity at Kennedy Space Center in 1983
[NASA-CR-175543] 12 p1897 N85-21910

Chronology of KSC and KSC related events for 1983
[NASA-TM-87435] 12 p1963 N85-22339

CAPES (LANDFORMS)

Estuaries of the Cape. Part 2: Synopses of available information on individual systems. Report 12: Buffels (WES) (CSW 1), Elsies (CSW 2), Sir Lowry's Pass (CSW8), Steenbras (CSW 9), and Buffels (OOS) (CSW 11)
[CSIR-RR-411-PT-2] 01 p0086 N85-10581

Estuaries of the Cape. Part 2: Synopses of available information on individual systems. Report 13: Silvermine (CSW 3)
[CSIR-RR-412-PT-2] 01 p0086 N85-10582

Estuaries of the Cape. Part 2: Synopses of available information on individual systems. Report no. 14: Sand (CSW 4)
[CSIR-RR-413-PT-2] 01 p0086 N85-10583

Estuaries of the Cape. Part 2: Synopses of available information on individual systems. Report no. 15: Zeekoe (CSW 5)
[CSIR-RR-414-PT-2] 01 p0087 N85-10584

Estuaries of the Cape. Part 2: Synopses of available information on individual systems. Report no. 16: Eerste (CSW 6)
[CSIR-RR-415-PT-2] 01 p0087 N85-10585

CAPILLARY CIRCULATION

U CAPILLARY FLOW

CAPILLARY FLOW

Capillary Pump Loop (CPL) heat pipe development status report
[NASA-CR-175273] 08 p1161 N85-17323

Special features of the temperature dependence of the capillary constant in the vicinity of the critical point
[BLL-T6436/BG/LRS/LRST750/85] 16 p2659 N85-27632

Generation of capillary instabilities by external disturbances in a liquid jet
[NASA-TM-87041] 19 p3265 N85-30246

Quasi non-intrusive sampling and analysis of gases associated with the boundary layer on the tethered satellite and similar supersonic and hypersonic research vehicles
[NASA-CR-176075] 20 p3407 N85-31140

A two phase flow model at the level of a narrowing section — blood flow 20 p3507 N85-31799

CAPILLARY WAVES

NT BAROCLINIC WAVES
NT GRAVITY WAVES
NT RIPPLES

A laser slope gauge and a spar buoy wave gauge: Tools for the validation of microwave remote sensors
[AD-A154036] 19 p3272 N85-30290

CAPSULES (SPACECRAFT)

U SPACE CAPSULES

CAPTIVE TESTS

NT STATIC FIRING
NT STATIC TESTS

CAPTURE CROSS SECTIONS

U ABSORPTION CROSS SECTIONS

CAPTURE EFFECT

Focusing beam of 1-GeV protons with volumetric capture to the mode of channeling by bent single crystal
02 p0268 N85-11750

Capture of planetesimals into a circumterrestrial swarm 04 p0588 N85-13751

Orbital resonances and planetary accretion in the solar nebula 13 p2179 N85-23523

Capture of liquid hydrogen boiloff with metal hydride absorbers
[NASA-CR-175677] 14 p2249 N85-23939

Computer program for prediction of capture maneuver probability for an on-off reaction controlled upper stage
[NASA-CR-165937] 17 p3010 N85-28611

Capture in the 1.15-keV iron resonance
[DE85-011913] 23 p3970 N85-34612

Electron loss process and cross section of multiply charged ions by neutral atoms 23 p3981 N85-34685

CARBAMATES (TRADENAME)

NT URETHANES

CARBAZOLES

Photophysical studies of triplet exciton processes in pure polymer films
[DE84-016258] 05 p0620 N85-13965

Electrically conducting complexes of poly(3,6-n-methylcarbazolyl methylene)
[AD-A147884] 07 p0933 N85-15914

CARBENES

Transition metal carbene complexes
[AD-A144879] 01 p0028 N85-10173

CARBIDES

NT ALUMINUM CARBIDES
NT BORON CARBIDES
NT CEMENTITE
NT CHROMIUM CARBIDES
NT NIOBIUM CARBIDES
NT SILICON CARBIDES
NT TITANIUM CARBIDES
NT TUNGSTEN CARBIDES
NT URANIUM CARBIDES
NT ZIRCONIUM CARBIDES

Study to optimize Cr-Mo steels to resist hydrogen and temper embrittlement. A study of carbides formed in low alloy Cr-Mo steels
[DE84-015208] 01 p0029 N85-10179

The influence of the carbide distribution on the abrasive wear of ledeburitic chromium steels
01 p0054 N85-10359

Microstructural design and control of sintered hard materials 02 p0176 N85-11180

Some reflections on the competition among different hard materials in industrial applications
02 p0177 N85-11192

Development and performance of CVD-coatings on cutting tools 02 p0178 N85-11193

The adhesion of hard and wear resistant coatings
02 p0179 N85-11203

Wear properties of rapidly solidified surfaces of a pseudo-binary Fe-TiC alloy 02 p0179 N85-11204

Process for producing carbide coatings
[AD-D011295] 06 p0764 N85-14885

The effect of tantalum on the structure/properties of two polycrystalline nickel-base superalloys: B-1900 + Hf MAR-M247
[NASA-CR-174647] 09 p1294 N85-18127

SANS and TEM studies of carbide precipitation and creep damage in type 304 stainless steel
[DE85-000933] 09 p1296 N85-18139

Method of testing carbide inserts for premature fracture by face milling of cylindrical workpieces
09 p1303 N85-18183

Vapor pressure and evaporation rate of certain heat-resistant compounds in a vacuum at high temperatures
[NASA-TM-77807] 10 p1434 N85-19036

A program to develop thermite reactions to produce refractory borides and carbides
[AD-A148972] 10 p1434 N85-19037

Influence of melting conditions on strength of transition zone between steel and composite material
10 p1450 N85-19133

Neutron scattering studies of graphite intercalation compounds
[DE85-003079] 12 p1942 N85-22196

Ordered carbon metal alloys for extraterrestrial power systems
[AD-A150881] 14 p2255 N85-23977

Development of carbon based brake lining materials without asbestos content in the form of carbon-carbon composites and carbon-metal or carbon-carbide composites
[BMFT-FB-T-85-014] 18 p3082 N85-29067

Influence of microstructure on mechanical properties in cemented tungsten-carbides 19 p3230 N85-30029

Method for production of ceramic oxide and carbide bodies by polymer inclusion and decomposition
[DE85-011668] 19 p3250 N85-30152

Thermodynamic data for mineral technology
[PB85-184331] 22 p3603 N85-33560

CARBOHYDRATE METABOLISM

Dynamics of some parameters of carbohydrate and lipid metabolism in recovery period following long-term hypokinesia 01 p0093 N85-10623

Effect of high ammonia content in closed environment on some parameters of human nitrogen and carbohydrate metabolism against background of a controlled diet
12 p1903 N85-21948

Parameters of carbohydrate metabolism and blood serum enzyme activity after short-term spaceflights
12 p1903 N85-21951

Rat blood serum and liver carbohydrates and lipids in recovery period after 15-day hypokinesia
19 p3326 N85-30606

Possible mechanism for changes in glycogen metabolism in unloaded soleus muscle
[NASA-CR-176184] 24 p4127 N85-35588

Muscle protein and glycogen responses to recovery from hypogravity and unloading by tail-cast suspension
[NASA-CR-176181] 24 p4128 N85-35591

CARBOHYDRATES

NT ADENOSINE DIPHOSPHATE
NT ADENOSINE TRIPHOSPHATE
NT ADENOSINES
NT CELLULOSE
NT CHOLINE
NT CITRIC ACID
NT FATS
NT GALACTOSE
NT GLUCOSE
NT GLYCOGENS
NT NUCLEOSIDES
NT PENTOSE
NT RIBOSE
NT STARCHES
NT SUCROSE
NT SUGARS

Pacific Northwest and Alaska bioenergy program glossary
[DE85-011740] 22 p3806 N85-33591

CARBON

NT ACTIVATED CARBON
NT CARBON ISOTOPES
NT CARBON 12
NT CARBON 13
NT CARBON 14
NT CHARCOAL
NT GLASSY CARBON

Electrically conductive rigid polyurethane foam
[DE84-014490] 01 p0033 N85-10203

Plasma deposited diamondlike carbon on GaAs and InP
[NASA-TM-86870] 01 p0123 N85-10844

Microstructural basis of strength and toughness in hardmetals 02 p0177 N85-11185

Magnetic properties of the cobalt matrix in WC-Co compacts 02 p0177 N85-11186

The inter-relation of microstructure, toughness and fatigue crack growth behaviour in WC-Co hardmetals
02 p0177 N85-11188

The effect of tantalum and carbon on the structure/properties of a single crystal nickel-base superalloy
[NASA-CR-174779] 02 p0182 N85-11223

Characterization of amorphous surface layers in Fe implanted with Ti and C
[DE84-014960] 02 p0289 N85-11885

Weld metal solidification cracking in a carbon-manganese steel 03 p0330 N85-12126

Polymer-carbon black interaction in electrically conducting fiber-forming composites
06 p0762 N85-14875

Preparation of polymers of functionalized acetylenes
[AD-D011296] 06 p0771 N85-14935

Instruments for characterization of carbon black and polymers
[AD-A146475] 06 p0810 N85-15146

Arc-evaporated carbon films: Optical properties and electron mean free paths
[DE85-001246] 06 p0867 N85-15510

Reciprocal solubility of phases in multi-component systems
[BLL-M-36003-(5828.4)] 07 p0926 N85-15870

Kinetics of interaction between carbon and iron oxides of metallized materials in solid phase
[BLL-M-36023-(5828.4)] 07 p0926 N85-15873

Electrochemical features of the ferric sulfate leaching of CuFeS2/C aggregates
[AD-A146661] 08 p1123 N85-17081

Deforestation, floodplain dynamics, and carbon biogeochemistry in the Amazon Basin
08 p1144 N85-17216

The 157 micron (C II) luminosity of the galaxy
08 p1248 N85-17877

Far-infrared spectroscopy of galaxies: The 158 micron C(+) line 08 p1249 N85-17882

Implantation of Ti + C for reduced friction and wear of steels
[DE85-001606] 09 p1295 N85-18135

Investigation of vanadium solid solution and zeta phase regions of vanadium-carbon system
[DE85-002678] 11 p1605 N85-20092

Deposition of diamondlike carbon films
[NASA-CASE-LEW-14080-1] 11 p1615 N85-20153

Apparatus for producing diamond-like carbon flakes
[NASA-CASE-LEW-13837-3] 11 p1615 N85-20155

Textured carbon surfaces on copper
[NASA-CASE-LEW-14130-1] 11 p1616 N85-20156

Comments on the origins and variations of carbon and nitrogen in the ISM of galaxies as evident from IUE spectroscopy of H 2 regions 11 p1745 N85-20973

Carbon, silicon, and oxygen in the white dwarf star GD 40 11 p1752 N85-21017

The abundances of the elements -carbon to silicon- in Nova Corona Austrina 1981 11 p1753 N85-21024

Carbon filter plates for aluminum filtration at casting
[BMFT-FB-T-84-242] 12 p1808 N85-21343

Carbon granule probe microphone for leak detection — recovery boilers
[NASA-CASE-NPO-16027-1] 12 p1849 N85-21597

Plasma-edge studies using carbon resistance probes
[DE85-005589] 14 p2424 N85-24955

Studies of metal/carbon surface chemistry
[DE85-005513] 15 p2507 N85-25463

Damage development during low cycle fatigue of carbon-black loaded SBR
[DE85-006234] 15 p2519 N85-25533

Aviation turbine fuels from tar sands bitumen and heavy oils. Part 1: Process analysis
[AD-A151319] 15 p2521 N85-25539

West Europe report: Science and technology
[JPRS-WST-84-012] 15 p2523 N85-25552

Size distributions of elemental carbon in atmospheric aerosols
[PB85-153534] 15 p2580 N85-25963

Optical properties of hydrogenated amorphous carbon films grown from methane plasma
[NASA-TM-86995] 15 p2658 N85-26406

Transitional metal activation and functionalization of C-H bonds
[DE85-006816] 16 p2746 N85-26949

Two-d heat transfer through porous media with heat generation
[AD-A151965] 16 p2783 N85-27173

Multi-phase crystallization of ferrous alloys
[BLL-BISI-TRANS-22441-(9022.06)]
17 p2925 N85-28037

The structure of carbon martensite analyzed with Moessbauer spectra
[BLL-BISI-TRANS-22402-(9022.06)]
17 p2927 N85-28062

Influence of manganese and heat treatment on structure and properties of Fe-0.1 percent-C-14 percent Cr-based steels
[BLL-BISI-TRANS-22299-(9022.06)]
17 p2928 N85-28071

Bifunctional oxygen electrodes
[DE85-006871] 17 p2956 N85-28248

Thermodynamic calculations of equilibrium states in metal-carbon-hydrogen-oxygen system
[BLL-BISI-TRANS-22092-(9022.06)]
17 p3045 N85-28844

Development of carbon based brake lining materials without asbestos content in the form of carbon-carbon composites and carbon-metal or carbon-carbide composites
[BMFT-FB-T-85-014] 18 p3082 N85-29067

Role of natural dissolved organic compounds in determining the concentrations of americium in natural waters
[DE85-010266] 19 p3229 N85-30022

New form of graphite 19 p3243 N85-30111

Mechanical protection of DLC films on fused silica slides
[NASA-TM-87056] 19 p3248 N85-30138

Special materials: Carbons
[SNIAS-851-551-104] 20 p3421 N85-31235

Carbon reduction of mixtures of MnO(2) and Fe(2)O(3)
[BLL-M-36260-(5828.4)] 20 p3422 N85-31241

Laminar diffusion flames, carbon gasification, and laser diagnostics applied to combustion systems. 1: Laminar diffusion flames with cylindrical symmetry. 2: Diffusion-controlled gasification of carbon particles. 3: Laser diagnostics applied to combustion systems
20 p3423 N85-31243

Recent measurements in turbulent jet flames at Sandia Combustion Research Facility 20 p3424 N85-31254

Contribution to the modelling of the gas carburizing process for steels
[BLL-OA-TRANS-3205-(8196.300)]
20 p3428 N85-31283

Computer-controlled carburizing
[BLL-OA-TRANS-3204-(8196.300)]
20 p3429 N85-31288

RAY-O-VAC BR2325 lithium carbon monofluoride cell performance 20 p3444 N85-31362

Oxygen and carbon impurities and related defects in silicon 20 p3481 N85-31631

Excitation of some alkaline Earth-like ions
[DE85-010737] 20 p3529 N85-31951

Thermoelectric properties of beta-boron and some boron compounds
[DE85-011978] 21 p3582 N85-32270

Studies of oxygen- and carbon-related defects in high-efficiency silicon solar cells
21 p3609 N85-32420

Physical and chemical aerosol characteristics in extremely clean air masses at Cape Grim, Tasmania
21 p3646 N85-32655

Carbon and nitrogen in the deep Earth
21 p3721 N85-33085

Stress and efficiency studies in EFG
[NASA-CR-176125] 22 p3751 N85-33251

Biological modulation of planetary atmospheres: The early Earth scenario 22 p3854 N85-33867

A measurement of the cosmic ray elements C to Fe in the two energy intervals 0.5-2.0 GeV/n and 20-60 GeV/n
[OG-4.1-6] 22 p3876 N85-34012

Electron photoejection in carbanions
[DE85-011747] 23 p3911 N85-34230

Electron photoejection in carbanions
[DE85-011748] 23 p3912 N85-34237

Diamondlike carbon protective coatings for IR materials
[NASA-TM-87083] 23 p3973 N85-34631

Pressure measurements in a hydrogen combustion environment: Hydrogen-air combustion test series 1 and 2 in the FITS tank, volume 1
[TI85-000800] 24 p4076 N85-35259

Development and characterization of carbon-bonded carbon fiber insulation for radioisotope space power systems
[DE85-013365] 24 p4082 N85-35298

Excessive production of electron pairs by soft photons in low multiplicity ion interactions
[HE-1.4-6] 24 p4176 N85-35894

The effect of the relative nuclear size on the nucleus-nucleus interactions
[HE-1.4-13] 24 p4177 N85-35900

Japan - USSR joint emulsion chamber experiment at Pamir
[HE-3.1-1] 24 p4177 N85-35901

Hadron intensity and energy spectrum at 4380 m above level
[HE-3.1-7] 24 p4178 N85-35905

Scaling violation in fragmentation region at energies above 10-15 eV based on the data on cosmic ray hadron component
[HE-3.1-11] 24 p4178 N85-35909

Hadrons registration in emulsion chamber with carbon block
[HE-3.7-3] 24 p4186 N85-35982

Structured events in Pamir carbon X-ray chambers
[HE-3.7-7] 24 p4186 N85-35986

CARBON ARCS

Diamondlike flakes
[NASA-CASE-LEW-13837-2] 12 p1796 N85-21267

CARBON COMPOUNDS

NT ALUMINUM CARBIDES
NT BORON CARBIDES
NT CALCITE
NT CALCIUM CARBONATES
NT CARBIDES
NT CARBONATES
NT CEMENTITE
NT CHROMIUM CARBIDES
NT DOLOMITE (MINERAL)
NT FLUOROPOLYMERS
NT HALOCARBONS
NT NIOBIUM CARBIDES
NT POLYCARBONATES
NT SIDERITES
NT SILICON CARBIDES
NT TITANIUM CARBIDES
NT TUNGSTEN CARBIDES
NT URANIUM CARBIDES
NT ZIRCONIUM CARBIDES

Analysis and characterization of organic carbon compounds in atmospheric particulate matter
[PB84-232636] 06 p0766 N85-14

Critical overview of hexacarbons and organophosphates
[AD-P004027] 08 p0844 N85-15361

Gas cooled fuel cell systems technology development
[NASA-CR-174732] 07 p0991 N85-16291

Denitrification-efficiencies of alternate carbon sources
[AD-A148029] 08 p1119 N85-17050

Gas phase ion-molecule chemistry of carbon, nitrogen and oxygen compounds
[AD-A152876] 17 p2919 N85-27996

CARBON CYCLE

The Marine Resources Experiment Program (MAREX)
[NASA-TM-87366] 01 p0086 N85-10580

Some aspects of understanding changes in the global carbon cycle 05 p0652 N85-14186

Carbon cycle: Terrestrial interactions
05 p0652 N85-14187

Global carbon - nitrogen - phosphorus cycle interactions: A key to solving the atmospheric CO2 balance problem?
05 p0652 N85-14188

Interactions of the marine phosphorus and carbon cycles 05 p0653 N85-14190

Recent studies of the ocean nitrogen cycle
05 p0653 N85-14193

Multi-property modeling of the marine biosphere in relation to global climate and carbon cycles
05 p0678 N85-14355

Carbon dioxide and climate: Summaries of research in FY 1983 and FY 1984
[DE85-001245] 06 p0839 N85-15327

Carbon isotope geochemistry and geobiology
21 p3657 N85-32716

Sulfur and carbon cycling in organic-rich marine sediments 21 p3659 N85-32720

Isotopic Biogeochemistry
[NASA-CR-176128] 22 p3741 N85-33189

Two dimensional CO2-ocean model including the biological processes
[DE85-012341] 23 p3950 N85-34483

Carbon dioxide and climate: A working glossary
[DE85-013535] 24 p4124 N85-35562

CARBON DIOXIDE

The oxidation behaviour of a 20 percent Cr/25 percent Ni/Nb stabilized stainless steel in carbon dioxide at high temperatures and its improvement by cerium and yttrium
[AERE-R-11228] 01 p0029 N85-10182

Response of arctic ecosystems to elevated carbon dioxide regimes, volume 2
[DE84-015236] 01 p0069 N85-10460

Future scenarios and ozone change
[DE84-014781] 01 p0085 N85-10573

The changing pattern of fossil fuel CO2 emissions
[DOE/OR-21400/2] 02 p0224 N85-11469

Impact cratering: The process and its effects on planetary evolution — and silicate-carbonate reactions on Venus
[NASA-CR-174016] 02 p0228 N85-11488

Variations with time of the carbon dioxide partial pressure in central and south Atlantic surface waters
[AD-A145825] 03 p0398 N85-12537

Radiation transport in the Earth atmosphere
04 p0522 N85-13341

CO-2-silica geothermometer for low temperature geothermal resource assessment, with application to resources in the Safford Basin, Arizona
[DE84-013958] 04 p0534 N85-13411

Thermodynamic study of CO2-organic compound interaction at high pressures and temperatures
[DE84-015777] 04 p0573 N85-13654

Quality assurance in the Antares Laser Fusion Construction Project
[DE84-015493] 05 p0640 N85-14104

Some aspects of understanding changes in the global carbon cycle 05 p0652 N85-14186

Three dimensional global modeling of atmospheric CO2 05 p0652 N85-14189

Polar regions and climatic change
[PB84-237023] 05 p0688 N85-14421

Simple formula to estimate carbon dioxide gas effect in radiation balance of underlying surface
06 p0823 N85-15226

Carbon dioxide and climate: Summaries of research in FY 1983 and FY 1984
[DE85-001245] 06 p0839 N85-15327

A biological sensor for the detection of toxicants
[AD-D011304] 07 p0967 N85-16141

Noncontact photo-thermal probe-beam deflection measurement of thermal diffusivity in an confined hot gas
[AD-A147481] 07 p0971 N85-16170

Simulating responses to expected climate change in eastern North America: Applications to decision-making in the forest industry
[DE85-001272] 07 p1008 N85-16406

Manned testing of two closed-circuit oxygen underwater breathing apparatus: US Navy Emerson Rig and Fenzy PO.68
[AD-A148300] 08 p1200 N85-17580

Supercritical fluid chromatography/supersonic jet spectroscopy
[DE85-003310] 09 p1292 N85-18115

Transport and relaxation processes in supercritical fluids
[DE85-002079] 09 p1398 N85-18797

The establishment and experience of the Carbon Dioxide Information Center (CDIC)
[DE85-001934] 09 p1402 N85-18825

An infrared study of isotopic exchange during methanation over supported rhodium catalysts; an inverse spillover effect
[AD-A149390] 10 p1435 N85-19046

An infrared study of the oxidation of carbon monoxide over supported rhodium catalysts
[AD-A149478] 10 p1436 N85-19050

Separation of gas mixtures with coordination complexes
[DE85-000363] 10 p1438 N85-19062

Monte Carlo simulation of gas Cerenkov detectors
[DE85-002422] 10 p1488 N85-19394

Photoelectrochemical reduction of carbon dioxide
[PB85-129054] 11 p1596 N85-20036

Lake ice occurrence as a possible detector of atmospheric CO2 effects on climate
[DE85-002951] 11 p1687 N85-20606

An infrared study of the dissociation of carbon dioxide over supported rhodium catalysts
[AD-A149813] 12 p1800 N85-21291

Pseudo-stationary oblique-shock-wave reflections in a polyatomic gas, sulfur hexafluoride
[UTIAS-TN-253] 12 p1845 N85-21577

Response of unmanaged forests to CO2-induced climate change: Available information, initial tests and data requirements
[DOE/NSB-0053] 12 p1883 N85-21817

Carbonate chemistry of the Weddell Sea
[DOE/EV-110611/4] 12 p1898 N85-21916

Modeling of mechanism of positive feedback between mean Earth surface temperature and atmospheric carbon dioxide in geologic time scale 13 p2106 N85-23122

The evolution of CO2 on Mars
13 p2185 N85-23558

Improvement by cerium and yttrium ion implantation of oxidation behaviour of stabilised stainless steel in carbon dioxide
[AERE-R-11523] 14 p2259 N85-23996

Predischarge parameters of SF6-CO2 determined by laser 15 p2564 N85-25821

North Atlantic Deep Water formation: Information from ice cores 15 p2602 N85-26035

Climatic impact of a change in North Atlantic Deep Water formation 15 p2603 N85-26045

Welding of 11 458.1 steel in shielding atmospheres
[BLL-BISI-TRANS-21763-(9022.06)]
17 p2972 N85-28353

Potential climatic impacts of increasing atmospheric CO2 with emphasis on water availability and hydrology in the United States
[NASA-TM-87479] 17 p2995 N85-28517

Time-dependence of CO2-induced climate change
[DE85-007568] 17 p2997 N85-28525

Photosynthetic acclimation of Acer saccharum
[DE85-008247] 17 p2998 N85-28536

Identification and characterization of watershed models for evaluation of impacts of climate change on hydrology
[DE85-008575] 18 p3125 N85-29348

Reconstruction of past atmospheric CO/sub 2/ contents from the chemistry of the contemporary ocean: An evaluation
[DE85-008426] 18 p3133 N85-29401

A new CO2 transmittance parameterization and its impact on the GLA GCM 18 p3146 N85-29476

Program planning using the GMAP procedure in SAS/GRAPH software
[DE85-008356] 18 p3199 N85-29842

The effect of surface reactions in catalytic combustion
[AD-A154217] 19 p3234 N85-30049

Thermodynamic study of CO2-organic compound interaction at high pressures and temperatures
[DE85-010909] 19 p3268 N85-30266

Mathematical model of global processes in the biosphere 19 p3295 N85-30431

Examination of the time and spatial scales appropriate for the carbon dioxide climate change issue
[DE85-009852] 19 p3317 N85-30563

Transport and relaxation processes in supercritical fluids
[DE85-010554] 19 p3358 N85-30816

Carbon dioxide and climate: Potential impacts
[DE85-009473] 20 p3496 N85-31734

Polymer solution-supercritical fluid behavior
[AD-A154514] 21 p3566 N85-32192

Carbon isotope geochemistry and geobiology
21 p3657 N85-32716

Carbon and sulfur cycling through geologic time
21 p3658 N85-32720

Evolution of the atmosphere 21 p3658 N85-32725

Thermophysical properties of fluids for the gas industry
[PB85-188471] 22 p3747 N85-33227

Model projections of time-dependent response to increasing carbon dioxide
[DE85-013326] 22 p3816 N85-33641

Climatic consequences of very high CO2 levels in Earth's early atmosphere 22 p3854 N85-33865

Potential spin-offs of the carbon dioxide observational platform system (CO-OPS) for remote sensing opportunities
[NASA-TP-2510] 23 p3899 N85-34149

Separation of gas mixtures by supported complexes
[DE85-011996] 23 p3912 N85-34236

Climate modeling: A retrospective-prospective view with consideration for the atmospheric carbon dioxide-climate issue
[DE85-011532] 23 p3950 N85-34481

Increase of total CO2 in the World ocean
[DE85-007756] 23 p3950 N85-34484

Solar modulation of cosmic ray intensity and solar flare events inferred from (14)C contents in dated tree rings
[SH-7.1-2] 23 p4047 N85-35095

Thermodynamics of the corrosion of chromium in molten carbonates
[DE85-011407] 24 p4079 N85-35282

Microbiological and biochemical studies towards optimization of substrate utilization by methanogenic bacteria
[PB85-188332] 24 p4084 N85-35310

Time-dependent response of the climate to increasing atmospheric carbon dioxide 24 p4119 N85-35532

Carbon dioxide and climate: A working glossary
[DE85-013535] 24 p4124 N85-35562

Far-infrared emission lines of CO and OH in the Orion-KL molecular shock
[NASA-TM-86721] 24 p4167 N85-35832

CARBON DIOXIDE CONCENTRATION

Measurement of range-resolved water vapor concentration by coherent CO2 differential absorption lidar
[PB84-236692] 04 p0535 N85-13420

Shock-induced CO2 loss from CaCO3: Implications for early planetary atmospheres
[NASA-CR-174197] 05 p0745 N85-14777

The CSIRO (Australia) atmospheric carbon dioxide monitoring program: Surface data
[CSIRO-TP-6] 07 p0996 N85-16324

The problem of climate and climate variation
07 p1001 N85-16353

Proceedings of a Workshop on Environment of West Antarctica: Potential CO2-induced changes
[PB85-110757] 11 p1671 N85-20527

Carbon dioxide and the greenhouse effect
[GPO-39-043] 11 p1677 N85-20569

Effect of elevated atmospheric CO2 on plant communities
[DE85-001810] 11 p1678 N85-20576

Possible role of ocean biota in global carbon balance — phytoplankton production 13 p2107 N85-23129

Changes in the high-latitude ocean as possible causes of atmosphere CO2 variations 15 p2602 N85-26036

The Martian climate: Energy balance models with CO2/H2O atmospheres
[NASA-CR-175722] 15 p2679 N85-26547

Density and confinement effects on mixing characteristics of an axisymmetrical CO(2) jet
[AD-A154468] 19 p3267 N85-30258

Potential spin-offs of the carbon dioxide observational platform system (CO-OPS) for remote sensing opportunities
[NASA-TP-2510] 23 p3899 N85-34149

Current inventory of anthropogenic carbon dioxide in the North Pacific Subarctic Gyre
[PB85-187938] 24 p4125 N85-35570

CARBON DIOXIDE LASERS

Real time sensing and control of out-of-plane distortion due to line heating by laser
[AD-A144773] 01 p0027 N85-10169

Development of the Antares electron gun
[DE84-014043] 01 p0053 N85-10352

Diagnostics of ionization in air produced by infrared radiation from A pulse CO2 laser
[AD-A145376] 02 p0201 N85-11342

Time variability of directionality properties of pulsed EB-EDL (Electron Beam-Electric Discharge Laser) N2-CO2 lasers
[AD-A145546] 02 p0202 N85-11344

Transient optical nutation in CO2 laser
02 p0261 N85-11709

Optical recording of information on paper by CO2 and YAG-lasers 02 p0261 N85-11710

Optimizing CW CO2 lasers with respect to output power in different bands 02 p0271 N85-11786

Investigation of RF excited CW CO2 waveguide lasers
[NASA-CR-174106] 04 p0505 N85-13221

Scattering from multi-scale surface — infrared lasers
[RSRE-MEMO-3656] 04 p0505 N85-13222

Laser for determining the ignition conditions of a pyrotechnic mixture
[FOA-C-20542-D1] 04 p0506 N85-13230

Silent discharge carbon dioxide gas laser machining facility
[BLL-CTO-2267-(9091.9F)] 07 p0969 N85-16150

Remote sensing of atmospheric gases with CO2 lasers. Continuation and conclusion of spectroscopic investigations
[BMFT-FB-W-84-030] 07 p0989 N85-16285

Technology for satellite power conversion
[NASA-CR-174335] 09 p1343 N85-18451

Carbon dioxide laser radar for monitoring atmospheric transmittance and atmospheric aerosol
09 p1354 N85-18516

Electron-hole plasma formation in semiconductors due to the absorption of pulsed CO2 laser light
[DE85-001559] 09 p1392 N85-18757

Experimental investigations of driven Alfven wave resonances in a Tokamak plasma using carbon dioxide laser interferometry
[DE85-001049] 09 p1392 N85-18758

Influence of laser hardening on mechanical properties of type 45 steel with various preliminary heat treatments
10 p1446 N85-19111

Study of microstructure of aluminum and copper alloys after processing with continuous CO2 laser beam
11 p1601 N85-20066

Chemically amplified laser direct-writing of aluminum
[DE85-000306] 11 p1639 N85-20324

Model calculations for a CO2 mixing laser with screen nozzle
[ESA-TT-859] 11 p1640 N85-20336

Absorption of ozone molecules in strong field of tea CO2 injection laser 11 p1718 N85-20806

Life study of RF excited Hg arc lamps and CO2 waveguide lasers
[AD-A149618] 12 p1856 N85-21640

A 50-kW electric-discharge CO2 laser
[AD-A149779] 12 p1857 N85-21644

The effects of atmospheric water vapor on infrared propagation
[AD-A150030] 12 p1934 N85-22150

Near Field/Far Field (NF/FF) energy loss in Electric Discharge Lasers (EDL's): A mode-medium interaction
[AD-A150299] 13 p2096 N85-23075

Feasibility of alpha particle measurement by CO2 laser Thomson scattering
[DE85-004938] 13 p2097 N85-23081

Thresholds of optical breakdown in alkali-halide crystals under pulses from CO2-laser 14 p2282 N85-24134

Laser Welding, Cutting and Surface Treatment
14 p2306 N85-24278

Trends in laser equipment 14 p2306 N85-24280

Laser cutting: A new tool for shipbuilding
14 p2306 N85-24285

Lasers in the nuclear industry
14 p2309 N85-24289

Future trends in the use of lasers in manufacturing
14 p2309 N85-24291

Optimization of the catalytic oxidation of CO for closed-cycle CO2 laser applications
[NASA-TM-86421] 15 p2504 N85-25445

Ground slot waveguide laser
[AD-D011600] 15 p2563 N85-25813

Development of global model for atmospheric backscatter at CO2 wavelengths
[NASA-CR-175679] 15 p2591 N85-25971

Characteristics of laser emission discharge created by pulsed CO2-laser 15 p2643 N85-26305

Theoretical investigation of lasing in 4.3 micron region in CO2 laser 15 p2643 N85-26306

Population inversion in laser-initiated vacuum arcs
[AD-A151958] 16 p2790 N85-27210

Europe's primary producers of industrial lasers surveyed 18 p3087 N85-29101

Technology assessment of high pulse energy CO(2) lasers for remote sensing from satellites
[NASA-TM-86415] 19 p3275 N85-30309

Summary of research for the Inertial Confinement Fusion Program at Los Alamos National Laboratory
[DE85-010330] 19 p3361 N85-30836

Robot, laser tridimensional cutting technology detailed
20 p3438 N85-31335

Simplified analytical model for calculation of population inversion in channels of CW gasdynamic lasers operating at various transitions among levels pertaining to coupled upsilon 1 and upsilon 2 modes of CO2
[STN-2] 20 p3461 N85-31498

Requirements for attaining Treanor's distribution of vibrational energy among CO2 levels in CW gasdynamic laser flows
[STN-3] 20 p3461 N85-31499

Identification of vibrational-rotational transitions of Os-192O4 within frequency tuning limits of high pressure CO2 waveguide laser 21 p3689 N85-32017

The possibility of observing and exploiting the generation of high-energy photons by electrons in the field of an intense electromagnetic wave 21 p3691 N85-32931

Investigation of ion-acoustic plasma turbulence in field of powerful electromagnetic wave by CO2-laser radiation scattering 21 p3691 N85-32935

Sliding discharge in CO2 and excimer lasers
22 p3773 N85-33379

Expansion ratio influence on population inversion in CO2/Ar CW gasdynamic lasers operating at various transitions within coupled upsilon 1 and upsilon 2 modes of CO2
[STN-4] 22 p3790 N85-33485

Hole cutting in building frames by laser
[FOA-C-20569-D9] 22 p3791 N85-33487

CARBON DIOXIDE TENSION
NT HYPERCAPNIA

CARBON DISULFIDE

Measurements of atmospheric carbon disulfide using aircraft platforms and a GC/MS isotopic dilution analysis technique 03 p0391 N85-12500

CARBON FIBER REINFORCED PLASTICS

Flight simulation fatigue crack propagation in metal/carbon-epoxy laminates
[NLR-TR-83006-U] 01 p0063 N85-10416

Thermoplastic-carbon fiber hybrid yarn
[NASA-CR-3849] 03 p0325 N85-12093

Modern structural materials. Present situation and evolution prospects — aircraft materials
[SNIAS-842-551-101] 04 p0455 N85-12886

Optimization of the injection process for thermostatic polyether-ether-ketone (Peek) thermoplastics reinforced with short carbon fibers
[SNIAS-842-422-102] 04 p0460 N85-13062

Mechanical properties of aligned short carbon fiber reinforced PES and PI laminates
[DFVLR-FB-84-24] 05 p0613 N85-13918

Influence of thermal cycling on the behavior of CFRP material for space structures 05 p0626 N85-14013

The fourth LBF colloquium
[ISSN-0721-5320] 05 p0648 N85-14163

Development of damage in fatigue loaded carbon fiber reinforced plastics 05 p0650 N85-14172

Fatigue behavior of bolted joints made of carbon fiber reinforced epoxy resins 05 p0650 N85-14173

A new generation of sub mm telescopes, made of carbon fiber reinforced plastic 08 p1250 N85-17890

FRG radiotelescope made of carbon fiber-reinforced plastic 09 p1309 N85-18226

Studies of structure and mechanical properties of carbon-reinforced plastic based on spirally reinforced filler 10 p1444 N85-19100

Control technology for fiber reinforced plastics industry at AMF Hatteras Yachts, New Bern Division, New Bern, North Carolina
[PB85-109015] 10 p1460 N85-19198

Initial fracture stages of orthogonally reinforced composite material 11 p1599 N85-20055

Strength properties of unidirectionally reinforced hybrid composites 11 p1599 N85-20056

Electrostatic discharge testing on a carbon fiber solar panel structure 13 p2007 N85-22584

Diffusion of water vapor in Carbon Fiber Reinforced Plastics (CFRP). Measurement of the diffusion coefficient under influence of concentration
[DFVLR-FB-84-41] 14 p2262 N85-24018

Ultrasonic testing of carbon fiber reinforced plastics (CFRP) using pattern recognition methods
[MBB-BB-563/84-0] 16 p2873 N85-27726

Development of a fuselage forward section in Carbon Fiber Reinforced Plastic (CFRP) type of construction
[MBB/LFA34/CFK/PUB/008] 17 p2895 N85-27851

Integral profile method for production of carbon fiber sheets
[MBB/LFA34/CFK/PUB/006] 17 p2916 N85-27975

Heat resistant Carbon Fiber Reinforced Plastics (CFRP) hardening equipment
[MBB/LFA33/CFK/PUB/007] 17 p2916 N85-27976

Optimization of axially compressed carbon fiber reinforced plastic (CFRP) cylinders
18 p3121 N85-29318

Mechanical properties of aligned short carbon fiber reinforced PES and PI laminates
[ESA-TT-898] 20 p3422 N85-31240

High reflective surfaces for millimeter RF waves, phas
A — satellite antenna reflectors
[HRS-FR-01] 20 p3442 N85-312

Development of fracture mechanics maps for composi
materials, volume 1
[ESA-CR(P)-2017-VOL-1] 20 p3471 N85-31573

Development of fracture mechanics maps for composi
materials, volume 2
[ESA-CR(P)-2017-VOL-2] 20 p3471 N85-31574

Development of fracture mechanics maps for composi
materials. Volume 3: Appendices A-E
[ESA-CR(P)-2017-VOL-3] 20 p3472 N85-31575

Development of fracture mechanics maps for composi
materials. Volume 4: Appendices F-K
[ESA-CR(P)-2017-VOL-4] 20 p3472 N85-3157

Utilization of microwave measuring systems for th
automation of composite materials manufacturing
[SNIAS-851-430-102] 22 p3742 N85-3319

Filament wound structures in PSP carbon composi
[RV10/84424] 22 p3743 N85-331

Ultrasonic inspection of carbon fiber reinforced plasti
by means of sample-recognition methods
[NASA-TM-77896] 24 p4074 N85-352

Contribution to the properties of carbon fiber reinforc
composites — structural mechanics
[ESA-TT-849] 24 p4074 N85-352

Methods for nondestructive tests of CFRP laminates
24 p4074 N85-352

Damage mechanisms in damaged CFRP laminates
24 p4074 N85-352

CARBON FIBERS

Distributions of fatigue life and fatigue strength i
notched specimens of a carbon 8-harness-satin lamina
[NAL-TR-809T] 01 p0061 N85-1040

Thermoplastic-carbon fiber hybrid yarn
[NASA-CR-3849] 03 p0325 N85-120

The chemical nature of the fiber/resin interface i
composite materials 04 p0465 N85-129

Newer carbon fibers and their properties
04 p0465 N85-129

Composite structural materials
[NASA-CR-174077] 04 p0467 N85-129

Chemical modification of the surface of high modul
carbon fibers 04 p0467 N85-129

Flexible matrix composite laminated disk/ring flywhe
05 p0606 N85-13

Carbon fibre reinforced aluminum matrix composites: A
critical review
[AD-A146367] 06 p0764 N85-14

All-composite Airbus empennage
07 p0936 N85-15

Composite batteries 07 p0936 N85-15

Studies of structure and mechanical properties o
carbon-reinforced plastic based on spirally reinforce
filler 10 p1444 N85-191

Thermoviscoelastic analysis of dimensionally stable fi
composite space structures
[AD-A149275] 11 p1593 N85-20

Composite structural materials
[NASA-CR-175515] 12 p1796 N85-21

Segregation of silicon in silumin-carbon fi
composites 13 p2028 N85-227

Environmental effects on the tensile strength o
chemically vapor deposited silicon carbide fibers
[NASA-TM-86961] 14 p2250 N85-240

High resistance and raised modulus carbon fibers
[NASA-TM-76884] 15 p2502 N85-25

In-plane shear properties of graphite Fibre/Epo
composites for aerospace applications: Evaluation of te
methods by the decision analysis technique
[AD-A151599] 15 p2503 N85-25

MBB uses new CFC form tool for titanium alloy a
intake 15 p2523 N85-25

Glass, carbon fibers made at Fibre et Mica in France
15 p2534 N85-25

Graphite fiber intercalation: Dynamics of the brom
intercalation process
[NASA-TM-87015] 16 p2742 N85-2

Mechanical properties of high performance carb
fibers 16 p2742 N85-2

Environmental stability of intercalated graphite fi
[NASA-TM-87025] 16 p2753 N85-2

Fiber reinforcement of gun propellant
[AD-A152296] 16 p2757 N85-27

Lightning-safe carbon fiber composite for Airbus
unit 18 p3087 N85-29

Mesophase mechanisms in the formation of graph
microstructures
[AD-A154100] 19 p3248 N85-30

Thermal expansion of selected graphite reinfor
polyimide-, epoxy-, and glass-matrix composite
[NASA-TM-87572] 21 p3561 N85-32

Improved materials for composite and adhesive jo
[AD-A155065] 21 p3562 N85-3

Electrical and mechanical properties of intercalated graphite fibers
[AD-A155560] 21 p3570 N85-32205
Crystallization of Polyetheretherketone (PEEK) in carbon fiber composites
[AD-A156316] 24 p4075 N85-35252
Carbon fiber strainmeter studies in southern California
[PB85-196869] 24 p4118 N85-35528

CARBON ISOTOPES
NT CARBON 12
NT CARBON 13
NT CARBON 14
Sixteenth Lunar and Planetary Science Conference. Press abstracts
[NASA-CR-175692] 15 p2660 N85-26548
Carbon isotopes in bulk carbonaceous chondrites
15 p2681 N85-26557
Resonance ionization mass spectrometry of carbon
[DE85-009040] 17 p2923 N85-28018
Isotopic Biogeochemistry
[NASA-CR-176128] 22 p3741 N85-33189
Control technology for radioactive emissions to the atmosphere at US Department of Energy facilities: The Los Alamos Meson Physics Facility
[DE85-011402] 22 p3811 N85-33809
Implications of new measurements of O-16 + p + C-12,13, N-14,15 for the abundances of C, N isotopes at the cosmic ray source
[OG-4.3-2] 22 p3878 N85-34027
Nucleosynthesis in the terrestrial and solar atmospheres
[SH-2.2-2] 23 p4000 N85-34707
Measurements of the fragmentation of (40)Ar, (28)Si and (12)C in CH2C and H targets between 300 and 1500 MeV/nuc at the Bevalac
[OG-7.2-19] 23 p4016 N85-34866

CARBON LASERS
Carbon vaporization/condensation effects
[NASA-TM-87430] 10 p1436 N85-19048

CARBON MONOXIDE
Investigation of the CARS spectrum of carbon monoxide at high pressure and temperature
[AD-A144816] 01 p0024 N85-10146
Mobile source exposure estimation
[PB84-224518] 01 p0095 N85-10643
Review of the NAAQS (National Ambient Air Quality Standards) for carbon monoxide: Reassessment of scientific and technical information
[PB84-231315] 03 p0388 N85-12485
Theoretical studies in molecular fragmentation: Processes, energetics and diagnostics
[AD-A146310] 03 p0418 N85-12673
Carbon monoxide study, Anchorage, Alaska, November 22, 1982 to February 11, 1983
[PB84-236595] 05 p0673 N85-14321
Results of the carbon monoxide study in Washington, D.C. and Denver, Colorado, in the winter of 1982-83
[PB84-230069] 06 p0834 N85-15309
NAAQS (National Ambient Air Quality Standards) Exposure Model (NEM) applied to carbon monoxide
[PB84-242551] 06 p0834 N85-15310
A wide latitude CO survey of molecular clouds in the northern Milky Way 06 p0877 N85-15574
The adsorption of CO and oxygen on Cu layers on a W(110) surface
[AD-A147345] 07 p0923 N85-15847
Bipolar flows and X-ray emission from young stellar object 08 p1234 N85-17779
Far-infrared photometry of low-mass pre-main-sequence stars with broad CO wings 08 p1246 N85-17866
Cation promotion effects in zeolite-supported F-T catalysts
[DE85-001708] 09 p1291 N85-18108
Measurement and analysis of ambient carbon monoxide concentrations for project-level air quality impact studies
[PB85-104602/GAR] 09 p1350 N85-18492
Meteorological factors responsible for high CO (carbon monoxide) levels in Alaskan cities
[PB85-115137/GAR] 09 p1350 N85-18493
New phases and chemical reactions in solid CO under pressure
[DE85-002033] 09 p1377 N85-18655
Experimental determination of the 1 sigma(+) state electron-dipole-moment function of carbon monoxide up to a large internuclear separation
[NASA-TM-85979] 09 p1379 N85-18670
Characterization of CO binding sites on Rh(111) and Rh(331) surfaces by XPS and LEED (Low Energy Electron Diffraction): Comparison to EELS (Electron Energy Loss Spectroscopy) results
[AD-A149331] 10 p1435 N85-19044
An infrared study of the oxidation of carbon monoxide over supported rhodium catalysts
[AD-A149478] 10 p1436 N85-19050
Separation of gas mixtures with coordination complexes
[DE85-000363] 10 p1438 N85-19062
Improved operation of transversely exited N2O lasers
[AD-D011488] 10 p1490 N85-19409
Photoelectrochemical reduction of carbon dioxide
[PB85-129054] 11 p1596 N85-20036
Development of a low cost electrochemical CO monitor based on stripping voltammetry
[PB85-113470] 11 p1637 N85-20312
Development of a low cost electrochemical CO monitor based on anodic scanning voltammetry in nonaqueous electrolyte
[PB85-113488] 11 p1637 N85-20314
Stability evaluation of sulfur dioxide nitric oxide and carbon monoxide gases in cylinders
11 p1648 N85-20387
Carbon monoxide adsorption on a platinum electrode studied by polarization modulated FT-IRRAS (Fourier Transform-IR Reflections Adsorption Spectroscopy). Part 1: CO adsorbed in the double layer potential region and its oxidation in acids
[AD-A149751] 12 p1800 N85-21288
The seasonal cycle of atmospheric CO in the Southern Hemisphere 16 p2630 N85-27447
Hydrogen degradation of pipeline steels
[DE85-008930] 17 p2932 N85-28101
Study of synthesis gas conversion over metal oxides
[DE85-010136] 18 p3072 N85-28999
Heat of mixing experiments for liquified gases
[PB85-183697] 18 p3084 N85-29081
Development of a stationary carbon monoxide detector
[BMFT-FB-T-84-253] 18 p3134 N85-29413
Shock tube measurements of growth constants in the branched-chain ethane-carbon monoxide-oxygen system
[NASA-TM-87068] 21 p3562 N85-32156
Why CO bonds side-on at low coverage and both side-on and upright at high coverage on the Cr(110) surface
[NASA-CR-176071] 21 p3565 N85-32173
CO adsorption on (111) and (100) surfaces of the Pt sub 3 Ti alloy. Evidence for parallel binding and strong activation of CO
[NASA-CR-176077] 21 p3565 N85-32176
The problem of the Earth's CO2 content and the iron core 21 p3718 N85-33080
Effects of low level carbon monoxide (CO) on tracking and monitoring. An attempt to replicate the findings of Putz et al. (1976) protocol 2
[AD-A155722] 22 p3825 N85-33694
Infrared studies of the influence of alkali metals on the C-O bond in chemisorbed carbon monoxide
[DE85-005306] 23 p3911 N85-34232
Separation of gas mixtures by supported complexes
[DE85-011996] 23 p3912 N85-34236
Oxygen analyzer
[DE85-006002] 23 p3935 N85-34392
CO + H2 reaction over nitrogn-modified iron catalysts
[DE85-013791] 24 p4072 N85-35231
Characterization of catalysts with metal-support effects and of the species adsorbed on their surfaces
[DE85-012254] 24 p4096 N85-35394
Size and shape dependence of CO adsorption sites on sapphire supported Fe microcrystals
[NASA-CR-176171] 24 p4160 N85-35794

CARBON MONOXIDE LASERS
Microwave discharge in a supersonic flow for the excitation of a gas dynamic CO laser
[ESA-TT-833] 09 p1326 N85-18337
Developement of a theoretical model to describe the interaction between electric discharge and supersonic flow of a pulsed CO laser
[DFVLR-FB-84-45] 14 p2310 N85-24301
Optically bistable devices using InSb
18 p3186 N85-29758

CARBON MONOXIDE POISONING
Pathophysiological study of poisoning due to thermal degradation of materials — aircraft cabins
[CERMA-84-15] 11 p1692 N85-20640

CARBON STARS
Carbon stars: There is no such thing as a dead leg
08 p1247 N85-17871
Variability of ultraviolet emission lines in the carbon star TX Psc 11 p1753 N85-21027
Neutron-rich nuclei in cosmic rays and Wolf-Rayet stars
[OG-8.2-6] 23 p4019 N85-34906

CARBON STEELS
NT LOW CARBON STEELS
Features of laser welding of medium carbon steel through a cadmium coating 01 p0020 N85-10122
Fretting corrosion and fretting fatigue of medium carbon steels 01 p0054 N85-10356
The effect of overload on three different kinds of steel
02 p0174 N85-11165
Microstructural design in low alloy steels
02 p0176 N85-11179
Effects of prior austenite and ferrite grain size on fracture properties of a plain carbon steel
[AD-A146276] 03 p0332 N85-12136
Study of fatigue fracture in hardened and tempered carbon steel. Report 1: Microscopic observation of the fatigue crack formation process
[BLL-PNR-90242-(8019.3153)]
06 p0767 N85-14909
Ultrahigh carbon steel
[AD-A147762] 08 p1128 N85-17113
Two-dimensional shock response of a mass on energy-absorbing shock mounts
09 p1334 N85-18389
New application possibilities for clad steel by reducing surface treatment expenditure and by using improved welding technology
[BMFT-FB-T-84-236] 12 p1861 N85-21672
Characteristics of polyacrylic acid-complexed zinc phosphate conversion films deposited on metal surfaces
[DE85-004057] 16 p2750 N85-26974
The state of martensite after quenching in a magnetic field
[BLL-BISI-TRANS-22297-(9022.06)]
17 p2926 N85-28051
Variations in the structure and in the composition of austenitic and carbon steel in spot welds
[BLL-BISI-TRANS-21765-(9022.06)]
18 p3073 N85-29007
Corrosion performance of metals and alloys in a tuff geochemical environment
[DE85-009449] 18 p3077 N85-29033
Powder metallurgy forged gear development
[NASA-TM-87483] 18 p3117 N85-29295
Microstructures and mechanical properties of microalloyed medium carbon steels
19 p3236 N85-30074
Corrosion fatigue strength and crack growth in prestrained 0.16% C carbon steel
23 p3905 N85-34192
Effect of microstructure on the fatigue behavior of Fe-C-X alloys
[DE85-011749] 24 p4080 N85-35265

CARBON TETRACHLORIDE
Health assessment document for carbon tetrachloride
[PB85-124196] 10 p1528 N85-19638

CARBON TETRAFLUORIDE
Atomic hydrogen maser measurements with wall surfaces of carbon tetrafluoride
18 p3106 N85-29243

CARBON 12
Spin distributions in heavy ion fusion at and below the Coulomb barrier
[DE85-007817] 17 p3031 N85-28751

CARBON 13
Stable isotope studies
[DE84-016752] 04 p0562 N85-13583
The 13C nuclear magnetic resonance in graphite intercalation compounds
[NASA-CR-174261] 07 p1040 N85-16601
Guest molecules in coal
[DE85-010435] 19 p3228 N85-30016

CARBON 14
Solar modulation of cosmic ray intensity and solar flare events inferred from (14)C contents in dated tree rings
[SH-7.1-2] 23 p4047 N85-35096
High precise measurements of cosmogenic radiocarbon abundance by complex of scintillation equipments
[SH-7.1-14] 23 p4048 N85-35105

CARBON-CARBON COMPOSITES
The effects of radial yarns, 3-dimensionally reinforced carbon-carbon composite
[AD-A144751] 01 p0022 N85-10134
Carbon/carbon rocket motor exit cone reinforcement
[AD-D011360] 07 p0916 N85-15799
Thermophysical property testing using transient techniques
[AD-A147085] 07 p1049 N85-16664
Disclinations in carbon-carbon composites
[AD-A148290] 08 p1119 N85-17052
Glass, carbon fibers made at Fibre et Mica in France
15 p2534 N85-25834
Evaluation of the PSP resin as a precursor of carbon
[ONERA-RT-11/1784-M] 16 p2744 N85-26932
Lightweight piston
[NASA-CASE-LAR-13150-1] 18 p3066 N85-28975
Development of carbon based brake lining materials without asbestos content in the form of carbon-carbon composites and carbon-metal or carbon-carbide composites
[BMFT-FB-T-85-014] 18 p3082 N85-29067
Effects of weak interfaces on thermostructural behavior of carbon-carbon composites
[AD-A155330] 21 p3582 N85-32154

Carbon/carbon combustor external insulation
[AD-D011719] 23 p3910 N85-34224
Oxidation resistant slurry coating for carbon-based materials
[NASA-CASE-LEW-13923-1] 24 p4077 N85-35267

CARBONACEOUS CHONDRITES
NT ALLENDE METEORITE
Bulk compositions of Al-rich chondrules in ordinary and carbonaceous chondrites: Variations and similarities
06 p0881 N85-15601
Hydrothermal alteration of CM carbonaceous chondrites: Implications of the identification of tochilinite as one type of meteoritic PCP 06 p0884 N85-15616
Aqueous alteration of meteorite parent bodies: Possible role of unfrozen water and the Antarctic meteorite analogy 06 p0884 N85-15617
Minor elements and cathodoluminescence of Mg-rich olivines from Murchison and Allende carbonaceous meteorites 06 p0884 N85-15619
Strain analysis of the Leoville chondrite and conditions in asteroidal interiors 06 p0885 N85-15620
Hibonite: Crystal chemistry and origin of blue coloration in meteoritic assemblages 13 p2184 N85-23555
Refractory inclusions in the Ornans C30 chondrite
15 p2680 N85-26553

CARBONACEOUS MATERIALS
NT PEAT
Supercritical solvent extraction of lignite to form carbonaceous chars
[DE85-010159] 19 p3229 N85-30019
Ash contents of Costa Rican peat deposits
[DE85-010734] 19 p3301 N85-30462
Development of wide band recording materials
[AD-A154961] 21 p3589 N85-32309
Method of distributing liquefaction catalysts in solid carbonaceous material
[DE85-005759] 23 p3909 N85-34218
Fluidized bed desulfurization
[NASA-CASE-NPO-15924-1] 24 p4075 N85-35253

CARBONACEOUS METEORITES
Minor elements in relict olivine grains of deep-sea spheres: Match with Mg-rich olivines from C2 meteorites 06 p0883 N85-15610

CARBONACEOUS ROCKS
NT COAL
NT LIGNITE

CARBONATES
NT CALCITE
NT CALCIUM CARBONATES
NT DOLOMITE (MINERAL)
NT POLYCARBONATES
NT SIDERITES
Effects of H2S on molten carbonate fuel cells
[DE84-015166] 02 p0195 N85-11307
Syntheses of polyhedranes and polyhedral carboranes
[AD-A146076] 03 p0340 N85-12187
Dynamic compression and volatile release of carbonates
[NASA-CR-174076] 03 p0391 N85-12504
Molten carbonate fuel cell performance model update, draft
[DE85-005423] 13 p2129 N85-23252
Cathode materials for molten carbonate fuel cells
[DE85-004078] 13 p2130 N85-23254
Analysis of SMIRR data for volcanic and sedimentary terrains of the trans-Pecos region, Texas
13 p2197 N85-23626
Chemical weathering of soils from the dry valleys of Antarctica: A terrestrial analog of Martian weathering processes 13 p2197 N85-23628
Exploratory corrosion tests on alloys in molten salts at 900(0)C
[DE85-000511] 14 p2257 N85-23983
Development of molten carbonate fuel cell power plant technology
[DE84-016839] 14 p2352 N85-24536
Carbon isotopes in bulk carbonaceous chondrites
15 p2681 N85-26557
Molten carbonate fuel cell performance model update
[DE85-003356] 17 p2986 N85-28454
Molten carbonate fuel cell cathode material development
[DE85-010268] 18 p3081 N85-29057
Development of molten carbonate fuel cell power plant, volume 1
[DE85-006743] 18 p3131 N85-29394
Advanced fuel cell development
[DE85-009662] 19 p3306 N85-30497
Integrated current collector and catalyst support
[DE85-011616] 22 p3761 N85-33311
Deep-burial diagenesis in carbonates
[DE85-011224] 22 p3802 N85-33554
Thermodynamic data for mineral technology
[PB85-184331] 22 p3803 N85-33560
Molten carbonate fuel cell separator
[DE85-011615] 22 p3806 N85-33577
Effects of H2S on molten carbonate fuel cells. Literature review on the impact of SO2 in the oxidant supplied to molten carbonate fuel cells
[DE85-011698] 22 p3806 N85-33586
Electrolyte reservoir for carbonate fuel cells
[DE85-005736] 23 p3947 N85-34460
Thermodynamics of the corrosion of chromium in molten carbonates
[DE85-011407] 24 p4079 N85-35282

CARBONYL COMPOUNDS
Method of obtaining polychalcones
[AD-A145051] 01 p0018 N85-10107
Development and application of fluorine-containing reagents in the gas chromatography of carbonyl compounds
[BLL-DRIC-TRANS-7205-(3623.66)]
01 p0023 N85-10140
Method for the preparation of poly(carbonyl fluoride) oligomers
[AD-D011207] 01 p0030 N85-10184
Stratospheric concentration of nitric acid, ozone and carbonyl sulfide: Measurement of nitric acid absorption in the Q branch of the V4 band as a function of temperature
[ESA-TT-864] 09 p1355 N85-18524
An infrared study of the hydrogenation of carbon dioxide on supported rhodium catalysts
[AD-A149477] 10 p1436 N85-19049
Analysis of aldehydes and ketones in the gas phase
[PB85-181865] 20 p3426 N85-31261

CARBORANE
Syntheses of polyhedranes and polyhedral carboranes
[AD-A146076] 03 p0340 N85-12187
The synthesis, structural characterization and reactions of closo-Rhodacarborane Anions containing a formal d8 metal vertex 1,2
[AD-A149640] 12 p1799 N85-21265

CARBOXYLATION
Vitamin K and the metabolic state of bone
05 p0694 N85-14465

CARBOXYLIC ACIDS
NT ALANINE
NT ASPARTIC ACID
NT BENZOIC ACID
NT CITRIC ACID
NT DICARBOXYLIC ACIDS
NT TRYPTOPHAN
Method for making heterocyclic block copolymers
[AD-D011446] 10 p1451 N85-19143
Fatty and aromatic acid catabolizing bacteria from methanogenic ecosystems
[DE85-008133] 17 p2998 N85-28537
Alkaline battery containing a separator of a cross-linked copolymer of vinyl alcohol and unsaturated carboxylic acid
[NASA-CASE-LEW-13102-1] 18 p3093 N85-29144

CARBURIZING
Recent developments on the role of molybdenum in irons and steels 02 p0180 N85-11206
Contribution to the modelling of the gas carburizing process for steels
[BLL-OA-TRANS-3205-(6196.300)]
20 p3428 N85-31263
An investigation of cementation and carbonitriding by means of ionic bombardment
[BLL-OA-TRANS-3203-(6196.300)]
20 p3429 N85-31265
Computer-controlled carburizing
[BLL-OA-TRANS-3204-(6196.300)]
20 p3429 N85-31268

CARCINOGENS
Molecular interactions of high energy fuels and jet fuels with oncogenic viruses and endogenous viruses
[AD-A145484] 02 p0188 N85-11255
Toxicology of natural and man-made toxicants in drinking water
[AD-P004035] 06 p0845 N85-15365
Ambient air contamination: Characterization and detection techniques 18 p3157 N85-29548
Use of environmental health-risk analysis for managing toxic substances
[DE85-008964] 18 p3160 N85-29574
Factor analysis of atmospheric pollution by polycyclic aromatic hydrocarbons
[HSE-TRANS-10968] 19 p3311 N85-30528
Repair of DNA treated with lambda-irradiation and chemical carcinogens
[DE85-010298] 19 p3327 N85-30616
Carcinogenesis of nitrated toluenes and benzenes skin and lung tumor assays in mice
[AD-A155723] 22 p3818 N85-33655

CARCINOMA
U CANCER

CARDIAC VENTRICLES
Left heart ventricular function during a 7 day zero-g simulation (6 deg head down tilt)
05 p0691 N85-14446
Changes in cardiovascular function: Weightlessness and ground-based studies 20 p3509 N85-31815

CARDIOGRAPHY
NT BALLISTOCARDIOGRAPHY
NT ECHOCARDIOGRAPHY
NT ELECTROCARDIOGRAPHY
Mapping of mammalian arrhythmias with the cardiac laser scanner 03 p0399 N85-12545
NDE methods for green ceramics
[DE85-004019] 13 p2038 N85-22766
Changes in cardiovascular function: Weightlessness and ground-based studies 20 p3509 N85-31815
Current status of the Os-191 yields Ir-191m generator
[DE85-008306] 23 p3971 N85-34614

CARDIOLOGY
Gravity perception and cardiac function in the spider
15 p2606 N85-26058

CARDIOVASCULAR SYSTEM
NT ARTERIES
NT BLOOD VESSELS
NT CARDIAC VENTRICLES
NT ERYTHROCYTES
NT HEART
NT HEMATOPOIESIS
NT HEMATOPOIETIC SYSTEM
NT LYMPHOCYTES
NT MYOCARDIUM
NT VEINS
Functional capacities of elderly subjects exposed to simulated spaceflight factors 01 p0091 N85-10617
Frequency and nature of electrocardiographic disturbances in dogs during single and repeated exposure to +G sub z accelerations 01 p0092 N85-10619
Cardiovascular disease among U.S. Navy pilots
[AD-A145871] 03 p0400 N85-12552
Impact of space medicine on Earth-based medicine: Academician Ye. I. Chazov comments on the work in orbit of physician O. Atkov 04 p0543 N85-13458
Ultrasonic study of early cardiovascular adaptation to zero gravity 05 p0691 N85-14445
Biochemical evaluation of bodily influence of high and low temperatures 07 p1014 N85-16441
Influence of geomagnetic disturbances on cardiovascular function of athletes
08 p1193 N85-17516
Health examination findings among active civil airmen
[AD-A148325] 08 p1195 N85-17533
Work capacity of heat and electric power plant operations working 12 hour day and night shifts
09 p1362 N85-18567
Morbidity and mortality associated with exposure to Otto Fuel II in the U.S. Navy 1966-1979
[AD-A148726] 09 p1363 N85-18574
Variability of cardiac rhythm during information loading
10 p1525 N85-19619
Medically disqualified airline pilots
[AD-A149454] 10 p1526 N85-19637
Symposium on Military Aviation Medicine summarized
11 p1696 N85-20880
USSR report: Space Biology and Aerospace Medicine, volume 18, no. 6, November - December 1984
[JPRS-USB-85-002] 12 p1900 N85-21931
LBNP training of crew members on main missions aboard Salyut-6 orbital station 12 p1901 N85-21936
Main component method used to study variations of cardiovascular parameters 12 p1901 N85-21939
Morphological study of monkeys submitted to antiorthostatic hypokinesia 12 p1902 N85-21942
Preventive effect of acute heat factors during hypokinesia 12 p1902 N85-21945
Multiple regression method used to assess animal adaptation to hypoxic hypoxia 12 p1902 N85-21947
Computer simulation studies in fluid and calcium regulation and orthostatic intolerance
[NASA-CR-171869] 15 p2616 N85-26117
Analysis of head-down tilt as an analog of weightlessness using a mathematical simulation model
[NASA-CR-171870] 15 p2616 N85-26118
Predictions of cardiovascular responses during STS reentry using mathematical models
[NASA-CR-171871] 15 p2616 N85-26119
Simulation of a G-tolerance curve using the pulsatile cardiovascular model
[NASA-CR-171873] 15 p2616 N85-26120
Cardiovascular effects of weightlessness
15 p2686 N85-26607
Cosmonauts' postural reactions after long-term missions aboard Salyut-6 orbital station 19 p3323 N85-30595
Nature of postural changes in human hemodynamics with intake of sydnocarb alone and in combination with obsidan 19 p3325 N85-30597

Longitudinal study of cardiovascular disease in US Navy pilots
[AD-A154331] 19 p3326 N85-30823
Study of the cardiovascular system in microgravity: Results and perspectives 20 p3509 N85-31816
Cardiovascular research in space: Problems and results 20 p3510 N85-31817
Studies of circulatory and metabolic changes during ketamine narcosis
[AD-A154512] 21 p3663 N85-32756
Intracardiac hemodynamics and human heart function in simulated weightlessness 22 p3733 N85-33140
Cosmonauts' cardiovascular system function during long-term orbital flights aboard Salyut-6 station
22 p3733 N85-33141
Cardiorespiratory function and work performance during adaptation to industrial labor in midalpine conditions
22 p3820 N85-33665
Cerebral hemodynamics and ventricular function in -15 deg antiorthostatic position 22 p3822 N85-33676
Effect of acute hypoxia on coronary and systemic hemodynamics 23 p3953 N85-34503
Cardiovascular responses to orthostatism and weightlessness 24 p4130 N85-35601

CARDS
Radio frequency probing apparatus for surface acoustic wave devices
[AD-D011230] 01 p0050 N85-10327
Computer center CDC Libraries-PROCFIL (procedures)
[AD-A148633] 08 p1206 N85-17589
Fibre composite laminated plate analysis using a card programmable calculator (HP41C/CV)
[NIAST-83/88] 13 p2103 N85-23106

CARGO
USSR report: Space
[JPRS-USP-84-005] 02 p0156 N85-11060
Features and uses of progress cargo ships
02 p0157 N85-11061
Tass reports launch of Progress-22
02 p0157 N85-11063
Progress-22 docks with Salyut-7
02 p0157 N85-11064
Orbit of Salyut-7 station boosted
02 p0157 N85-11067
Portable pallet weighing apparatus
[NASA-CASE-GSC-12789-1] 11 p1635 N85-20294
Cargo handling system
[AD-D011569] 14 p2219 N85-23762
Mi-8 helicopter cargo loading experiment for Arctic shipping 14 p2332 N85-24425
Air traffic: Instruments, airports, companies, post, cargo and passengers 18 p3060 N85-28932
Laboratory vibration schedules
[AD-A155856] 24 p4064 N85-35188

CARGO AIRCRAFT
NT C-5 AIRCRAFT
NT C-135 AIRCRAFT
NT C-141 AIRCRAFT
NT F-27 AIRCRAFT
Performance capabilities of the C-5 and C-17 cargo aircraft
[AD-A145518] 02 p0138 N85-10939
USSR report: Transportation
[JPRS-UTR-84-025] 17 p2894 N85-27841
Test flight of IL-76TD long-range transport variant
17 p2894 N85-27842
OWEMA report: A project study concerning the possibilities and the desirability of a east-west runway for Maastricht Airport (Netherlands) as a Euro-regional air freight center
[B8476490] 18 p3064 N85-28955

CARGO SHIPS
NT TANKER SHIPS

CARIBBEAN SEA
Review of climate problems in Latin America and the Caribbean 07 p1001 N85-16354
Deep source gas
[DE85-001984] 18 p3126 N85-29358

CARNOT CYCLE
Operating experience with potassium systems — thermal power stations
[DEFZS-4275] 03 p0387 N85-12473

CAROTENE
Enrichments for phototrophic bacteria and characterization by morphology and pigment analysis
21 p3680 N85-32738

CARPATHIAN MOUNTAINS (EUROPE)
Earthquake activity in the Bohemian massif and in the western Carpathians
[REPT-547] 03 p0375 N85-12390

CARRIAGES
Small Payload Flight Systems (SPFS)
02 p0152 N85-11030
Dual optical mechanical position tracker
[AD-D011739] 22 p3844 N85-33611

CARRIER DENSITY (SOLID STATE)
Avalanche photodiode statistics in triggered-avalanche detection mode 05 p0623 N85-13967
GaAs material properties and models
05 p0665 N85-14277
Density of states and recombination in amorphous silicon (a-Si:H)
[BMFT-FB-T-84-216] 08 p1135 N85-17151
Investigations of radiation-induced and carrier-enhanced conductivity 13 p1996 N85-22515
Technological process effect on the carrier lifetime degradation of silicon solar cell base layer irradiated by 1 MeV electrons (boron doping case)
13 p2007 N85-22585
Phenomena simulation for heavy doping and surface recombination velocity 20 p3482 N85-31636

CARRIER FREQUENCIES
Carrier acquisition and tracking by a COSTAS loop with automatic frequency control
[ESA-TT-838] 04 p0493 N85-13149
Design and performance of sampled data loops for subcarrier and carrier tracking 05 p0623 N85-13968
Improved carrier tracking by smoothing estimators
05 p0623 N85-13969
Low noise multiple crystal-controlled oscillator
[AD-D011401] 07 p0948 N85-16010
Method and means for providing frequency agile operation of MTI (Moving Target Indicator) radar
[AD-D011561] 12 p1823 N85-21436
Wideband phase keyers 12 p1839 N85-21544
Experimental results on the application of convolutional coding and Viterbi decoding as a frequency diversity technique in HF data transmission
[CRC-1377] 13 p2052 N85-22850
Global positioning system carrier phase: Description and use
[PB85-174126] 19 p3216 N85-29946

CARRIER INJECTION
Capacitive reactance of compensated semiconductors with deep centers under conditions of transmission of exclusion and double injection currents
02 p0266 N85-11742
Surface and allied studies in silicon solar cells
[NASA-CR-175468] 10 p1508 N85-19516

CARRIER LIFETIME
Method and apparatus for measuring minority carrier lifetime in a direct band-gap semiconductor
[NASA-CASE-NPO-163371-1] 11 p1628 N85-20251
Technological process effect on the carrier lifetime degradation of silicon solar cell base layer irradiated by 1 MeV electrons (boron doping case)
13 p2007 N85-22585
Quantitative analysis of defects in silicon-characterization of UCP, HAMCO, and microcrystalline material
[NASA-CR-175988] 18 p3079 N85-29046
Electrical and structural characterization of web dendrite crystals 20 p3481 N85-31633

CARRIER MOBILITY
NT ELECTRON MOBILITY
NT HOLE MOBILITY
Mobility and trapping time measurements in HgI2
[DE84-015954] 06 p0869 N85-15522
Characterization of high temperature electrically conducting oxides
[DE85-004296] 12 p1803 N85-21307
Heavy doping effects in high efficiency silicon solar cells
[NASA-CR-175687] 15 p2585 N85-25937
Heavy doping effects in high efficiency silicon solar cells
[NASA-CR-175681] 15 p2586 N85-25940
Heavy doping effects in high efficiency silicon solar cells
[NASA-CR-175779] 16 p2818 N85-27383
Quantitative analysis of defects in silicon-characterization of UCP, HAMCO, and microcrystalline material
[NASA-CR-175988] 18 p3079 N85-29046
Quantized Hall conductance as a topological invariant
[DE85-007796] 18 p3193 N85-29806
Drift mobilities by time-of-flight methods and time-dependent phototransport in the nanosecond regime in amorphous semiconductors
[DE85-008729] 18 p3194 N85-29815
Measurement of electrical parameters and current components in the bulk of silicon solar cells
20 p3481 N85-31635
Planar doped barrier semiconductor device
[AD-D011591] 20 p3537 N85-32010

CARRIER MODULATION
U MODULATION

CARRIER ROCKETS
U LAUNCH VEHICLES

CARRIER SYSTEMS
U WIRELESS COMMUNICATION

CARRIER TRANSPORT (SOLID STATE)
Characterization of surface electronic properties of semi-insulating InP
[AD-A146553] 06 p0866 N85-15507
Application of the diffraction model to amorphous magnesium zinc alloys
[AD-A147369] 07 p0928 N85-15883
Development of high efficiency solar cells on silicon web
[NASA-CR-174435] 10 p1509 N85-19521
Heavy doping effects in high efficiency silicon solar cells
[NASA-CR-175681] 15 p2586 N85-25940

CARRIER WAVES
Design and performance of sampled data loops for subcarrier and carrier tracking 05 p0623 N85-13968
Performance of the DSA's subcarrier demodulation digital loop 10 p1465 N85-19242

CARRINGTON ROTATION
U SOLAR ROTATION

CARTESIAN COORDINATES
Development of multigrid algorithms for problems from fluid dynamics
[GMD-111] 09 p1321 N85-18305
Generation of sound by a vortex point in a steady flow of slightly compressible fluid 11 p1715 N85-20789
Location and synchronization — space-time coordinates 14 p2397 N85-24768
Augmented weighted diamond force of the linear nodal scheme for Cartesian coordinate systems
[DE85-005631] 17 p3020 N85-28679
Equations of motion for electromagnetic waves in 4-dimensional Euclidian space 21 p3697 N85-32970
Algorithm for calculation of strain state from measurements of node coordinates of arbitrary curvilinear grid
[BLL-M-38304-(5828.4)] 23 p3940 N85-34422

CARTOGRAPHY
U MAPPING

CARTRIDGE ACTUATED DEVICES
U ACTUATORS
U EXPLOSIVE DEVICES

CARTRIDGES
Flares and photoflash items
[AD-A145442] 02 p0187 N85-11253

CASCADE CONTROL
Multiloop manual control of dynamic systems
05 p0702 N85-14505
FAUST: Introduction and overview — self tuning control
[OUEL-1566/85] 20 p3519 N85-31882

CASCADE FLOW
Characteristics of controlled-oscillating annular cascade test facility with Freon gas
[NAL-TR-812] 01 p0003 N85-10014
Further development of a transonic cascade analysis
[AD-A145410] 02 p0198 N85-11319
Inverse design technique for cascades
[NASA-CR-3836] 03 p0311 N85-12008
Incompressible lifting-surface aerodynamics for a rotor-stator combination
[NASA-TM-83767] 03 p0316 N85-12039
A finite element method for the solution of two-dimensional transonic flows in cascades
[PNR-90216] 03 p0316 N85-12045
Performance deterioration of cascades exposed to solid particles 03 p0319 N85-12057
Unsteady aerodynamic response of cascades and turborotors 03 p0319 N85-12058
Low solidity cascade diffusers for wide flow range centrifugal blowers 05 p0637 N85-14086
Turbine blade test cascade modifications and orations, August 1982 - April 1983
[DE84-009258] 06 p0833 N85-15303
Unsteady pressure measurements on a biconvex airfoil in a transonic oscillating cascade
[NASA-TM-86914] 07 p0898 N85-15689
A method for solving the inverse problem of transonic cascade flow
[AD-A146739] 07 p0899 N85-15696
Results of S5 CH tests with an ARL (Aerospace Research Laboratory) cascade
[NASA-TM-77510] 08 p1089 N85-16882
Secondary flow in cascades
[AD-A148415] 08 p1162 N85-17333
Designing the profile of turbine blades using an iteration technique 09 p1305 N85-18201
Calculating secondary nonviscous gas flows in spatial cascades of turbines 09 p1305 N85-18202
Estimating unsteady aerodynamic forces on a cascade in a three-dimensional turbulence field
[NASA-TM-86701] 14 p2209 N85-23704
An experimental study of aerodynamic damping characteristics of a compressor annular cascade in high speed flow and the visualization of annular cascade flow
[NAL-TR-838] 15 p2554 N85-25758

Gasdynamic evaluation of choking cascade turns
[AD-A151854] 15 p2557 N85-25776
Influence of surface roughness on compressor blades at high reynolds number in a two-dimensional cascade
[AD-A151855] 15 p2557 N85-25777
Proceedings of the NAL Symposium on Aircraft Computational Aerodynamics
[NAL-SP-1] 16 p2691 N85-26611
Two computational methods for cascade flows
16 p2692 N85-26617
Numerical simulation of inviscid compressible flow through three-dimensional cascade
16 p2692 N85-26619
Application of conformal mapping to grid generation
16 p2692 N85-26621
Notes on unsteady transonic cascade flows
[AD-A154829] 21 p3552 N85-32096
Unsteady flow in a supersonic cascade with two in-passage shocks
[NASA-CR-3925] 24 p4060 N85-35158
Analysis of incompressible cascade flows using state-of-the-art computer programs
[AD-A155850] 24 p4062 N85-35173
Experimental basis for the models of cascade propagation in atmosphere
[HE-3.6-6] 24 p4185 N85-35954
A comparative analysis of gamma and hadron families at the superhigh energies recorded in experiment Pamir
[HE-3.7-1] 24 p4185 N85-35960
Hadrons registration in emulsion chamber with carbon block
[HE-3.7-3] 24 p4186 N85-35962
Structured events in Pamir carbon X-ray chambers
[HE-3.7-7] 24 p4186 N85-35965
Peculiarities of gamma-quanta distribution at 20 TeV energy
[HE-3.7-10] 24 p4188 N85-35967

CASCADE RANGE (CA-OR-WA)
The petrology and geochemistry of high cascade volcanics in southern Washington: Mount Saint Helens volcano and the Indian Heaven basalt field
02 p0227 N85-11487
Morphologic evolution of the Mount St. Helens crater area, Washington 13 p2187 N85-23568

CASCADE WIND TUNNELS
Inverse design technique for cascades
[NASA-CR-3836] 03 p0311 N85-12008
Results of S5 CH tests with an ARL (Aerospace Research Laboratory) cascade
[NASA-TM-77510] 08 p1089 N85-16882
Methods for design aerodynamics of modern transport aircraft
[DFVLR-FB-85-05] 17 p2893 N85-27838

CASCADES (FLUID DYNAMICS)
U FLUID DYNAMICS

CASCODE MOSFET
U FIELD EFFECT TRANSISTORS

CASE BONDED PROPELLANTS
Dissected motors-propellants motor number STM-012. Phase 15: Surveillance report, stage 1
[AD-A156068] 24 p4071 N85-35226

CASES (CONTAINERS)
NT ROCKET ENGINE CASES
Gear case vibration isolation in a geared turbine generator 09 p1338 N85-18414
SRB filament wound case material property study
[NASA-CR-171469] 17 p2910 N85-27940
Electrically conductive containment vessel for molten aluminum
[DE85-006518] 23 p3939 N85-34415

CASKS
U BARRELS (CONTAINERS)

CASPIAN SEA
Horizontal coherence of temperature microstructure in upper ocean layer 13 p2109 N85-23139

CASSEGRAIN ANTENNAS
Configuration study for a 30 GHz monolithic receive array: Technical assessment
[NASA-CR-174697] 09 p1311 N85-18238
Configuration study for a 30 GHz monolithic receive array, volume 1
[NASA-CR-174697-VOL-1] 09 p1311 N85-18239
Design procedure for the new 70-meter antenna subreflector positioner 10 p1463 N85-19232
Subreflector focusing techniques applied to new DSS-15 and DSS-45 34-meter antennas
10 p1464 N85-19233
DSN 34-meter antenna optics analysis for wideband SETI investigations 10 p1465 N85-19244

CASSEGRAIN OPTICS
Dual-secondary mirror Cassegrain optical system
[AD-D011273] 06 p0862 N85-15478
Construction of a superheterodyne receiver for 10 micron waves to be put on a Cassegrain optics telescope for spectroscopic research on the Mars and Venus atmospheres
[MPE-183] 06 p0872 N85-15538
Dual mode radio frequency-infrared frequency system
[AD-D011402] 08 p1081 N85-16850
BBC receiving terminal for the European orbital test satellite
[BBC-RD-1984/15] 08 p1142 N85-17205
Innovative solar thermal dish technology development
[DE85-002787] 11 p1673 N85-20539
The astrometry programme at Mt. John Observatory
14 p2436 N85-25026

CASSIOPEIA A
Absolute measurements of radiation intensity from Cassiopeia-A, Cygnus-A and crab nebula in 60-100 cm band 13 p2078 N85-22978

CASSIOPEIA CONSTELLATION
A study of W Serpentis binaries: SX Cassiopeiae, RX Cassiopeiae, and W Serpentis 20 p3544 N85-32053

CAST ALLOYS
Development of rapidly quenched alloys with special physical properties and of processes for their continuous production
[BMFT-FB-T-84-179] 04 p0477 N85-13039
Mechanical properties and microstructure of centrifugally cast alloy 718
[AD-A147800] 08 p1129 N85-17116
Anomalies of aluminum structure and properties
13 p2026 N85-22693
Concept development evaluation for John Deere/UA STS middeck experiment location
[NASA-CR-171541] 20 p3397 N85-31071
Mechanical behavior of Ni-Cr-base superalloys in forms and conditions representative of service
[NPL-DMA(A)-94] 20 p3431 N85-31282

CASTING
NT CENTRIFUGAL CASTING
NT SLIP CASTING
Effect of scandium on the structure and properties of Al-Zn-Mg alloys 01 p0018 N85-10111
New ferrous metallurgy technology
01 p0019 N85-10114
Low-gravity solidification of cast iron and space technology applications 02 p0151 N85-11022
Directional solidification of flake and nodular cast iron during KC-135 low-g maneuvers
02 p0154 N85-11040
Investigation of toughened neat resins and their relations to advanced composite mechanical properties
04 p0464 r:85-12949
Development of rapidly quenched alloys with special physical properties and of processes for their continuous production
[BMFT-FB-T-84-179] 04 p0477 N85-13039
Controlled directionally solidified precision casting for superalloys and steels
[BMFT-FB-T-84-198] 05 p0619 N85-13960
Applicability of fatigue strength data obtained from small separately cast specimens on large cast components
05 p0651 N85-14178
Cyclic endurance testing of the RB211-22B cast HP turbine blade 07 p0908 N85-15747
Making high explosive bodies for shaped charges by casting or pressing. Shaped charge resrarch at Research Institute of National Defence (FOA) in 1972 - 1983, part 1
[FOA-C-20554-D4-PT-1] 07 p0935 N85-15923
New applications for robot loaders, unloaders
08 p1139 N85-17175
The effect of tantalum on the structure/properties of two polycrystalline nickel-base superalloys: B-1900 + Hf MAR-M247
[NASA-CR-174847] 09 p1294 N85-18127
Study of superplastic alloys based on Al-Zn-Ca
10 p1442 N85-19092
Method for continuously casting
[AD-D011481] 10 p1459 N85-19195
French firm has most advanced continuous-casting machine 11 p1592 N85-20017
Comparison of the fatigue resistance (initiation, propagation) of cast TA6V with hot rolled TA6V — titanium alloy
[DGT-25369-PT-1] 12 p1808 N85-21341
Carbon filter plates for aluminum filtration at casting
[BMFT-FB-T-84-242] 12 p1808 N85-21343
Nondestructive testing of stainless steel to improve quality and output efficiency of the processing of ingot and continuous casting
[BMFT-FB-T-84-240] 12 p1808 N85-21345
Steel castings by the electroslag casting technique
[DE85-003812] 12 p1819 N85-21409
Development of silicon nitride materials for the casting of solar cell silicon 12 p1878 N85-21779
The influence of melting practice and of microalloying, with rare earth metals and with boron, on the quality of low-carbon steel
[BLL-BISI-22467-(9022.06)] 17 p2925 N85-29036
Influence of temperature in melting and casting on quality of medium-alloy steel
[BLL-BISI-TRANS-22310-(9902.06)]
17 p2938 N85-28137
Precision die forging of blades or gas turbines
17 p2940 N85-28148
Continuous casting of quality steels on billet casters
[BMFT-FB-T-84-262] 18 p3078 N85-29041
Semicrystalline casting process development and verification
[DE85-007695] 18 p3081 N85-29058
Aluminum pressure die casting process for the production of low porosity castings and new casting alloys
[BMFT-FB-T-84-286] 18 p3123 N85-29335
Feasibility of melt casting strontium fluoride to produce high-density heat sources
[DE85-009429] 18 p3130 N85-29381
MPS solidification model. Analysis and calculation of macrosegregation in a casting ingot
[NASA-CR-171589] 21 p3566 N85-32178
Tape casting as an approach to an all-ceramic turbine shroud seal
[NASA-TM-87078] 21 p3596 N85-32333
Method and apparatus for casting conductive and semi-conductive materials
[DE85-011655] 22 p3792 N85-33494
Characterization of modified 9 r-1 Mo steel sand castings
[DE85-012057] 24 p4080 N85-35287
Development of a high strength isothermally heat-treated noduler iron road wheel arm
[AD-A155755] 24 p4099 N85-35408

CASTING SOLVENTS
U PLASTICIZERS

CASTINGS
NT INGOTS
Materials studies for magnetic fusion energy applications at low temperatures, 7
[DE84-013487] 01 p0122 N85-10837
Adaptation of remelting procedures for the use of recycled metal in nickel-base superalloy castings
[PNR-90232] 09 p1297 N85-18149
Robotized blanks loader for new forge press
10 p1461 N85-19216
Method for refining microstructures of cast titanium articles
[AD-D011518] 12 p1804 N85-21318
Fatigue and corrosion fatigue resistance of aluminum casting alloy VAL10 and forging alloy AK6
13 p2025 N85-22690
Cast-iron technology: Metallographic and mechanical testing results
[DE85-002664] 14 p2257 N85-23984
Robotic deburring. Part 2: Evaluation of cutters and noncompliant tooling
[DE85-006182] 14 p2311 N85-24306
Ultrasonic characterization of porosity: Theory
[DE85-005922] 15 p2646 N85-26325
Detection of pores in hot continuously cast rounds
[BMFT-FB-T-85-007] 18 p3072 N85-29000
Continuous casting of quality steels on billet casters
[BMFT-FB-T-84-262] 18 p3078 N85-29041
Aluminum pressure die casting process for the production of low porosity castings and new casting alloys
[BMFT-FB-T-84-286] 18 p3123 N85-29335
Reliability of welds to repair defects in cast components made from CrMoV steel
[BLL-CE-TRANS-8054-(9022.09)]
20 p3461 N85-31501
Centrifugal castings of stainless steel spiked with radioactive tracers
[DE85-012003] 22 p3748 N85-33234

CASUALTIES
Don't fowl out
[AD-P004179] 11 p1578 N85-19941
The clinical and biomedical evaluation of trauma and fatalities associated with aircrew ejection and crash. A Working Group report
[AGARD-AR-194] 12 p1906 N85-21969
Introduction: The clinical and biomedical evaluation for trauma and fatalities associated with aircrew ejection and crash 12 p1906 N85-21970
Statistics of french Armee de l'air ejections 1970 - 1980 12 p1906 N85-21971
List of head/neck injury on ejection in the German Armed Forces from 1972-1981 12 p1906 N85-21972
A review of neck injury and impaired consciousness associated with US Navy ejections 1 January 1969 - 31 December 1979 12 p1906 N85-21973

A review of fatality, impairment of consciousness, and head/neck injury on USAF ejections 1971 - July 1983
12 p1906 N85-21974

A review of fatality, impairment of consciousness and head and neck injury on Royal Air Force ejections 1968-1981
12 p1907 N85-21975

Head/neck injury: Post mortem procedures, Annex B
12 p1907 N85-21977

CAT SCANNER
U COMPUTER AIDED TOMOGRAPHY

CATACLYSMIC VARIABLES

The vertical structure and stability of alpha model accretion disks 09 p1417 N85-18938

Observations of cataclysmic variable star winds
11 p1755 N85-21041

A survey for galactic plane ultraviolet-excess objects: Space densities for white dwarfs, subdwarfs, and cataclysmic variables 13 p2169 N85-23456

A model for eclipsing cataclysmic variables
13 p2171 N85-23467

X-ray emission and the winds of cataclysmic variables
[DE85-007663] 17 p3053 N85-28902

CATALASE

Toxicity, mutagenesis and aging due to endogenous oxygen radicals
[AD-A150121] 12 p1900 N85-21928

CATALOGS

Computer center CDC Libraries-PROCFIL (procedures)
[AD-A148633] 08 p1206 N85-17589

Catalog of completed studies, US Army health care studies and clinical investigation activity
[AD-A149450] 10 p1568 N85-19885

CATALOGS (PUBLICATIONS)
NT ASTRONOMICAL CATALOGS

Sea-level in the world ocean. Part 5: The North-East Pacific and Arctic Oceans, a catalogue of measurements
[CSIR-T/SEA-8303-5] 01 p0067 N85-10569

FSTC (Federal Software Testing Center) software tool catalog
[PB84-212156] 01 p0105 N85-10703

Depository librarians' views on GPO's administration of the depository library program. Report to the Chairman, Joint Committee on Printing
[PB84-212265] 01 p0126 N85-10867

Criss-cross directory of NASA N numbers and DOD AD numbers, 1962-1978 04 p0575 N85-13669

The SPOT data bank system
05 p0659 N85-14236

Orbital maneuvers with finite thrust. Volume 1: Mathematical formulation, numerical methods, catalog concept
[ESA-CR(P)-1910-VOL-1] 06 p0758 N85-14848

Orbit maneuvers with finite thrust. Volume 2: Reference manual, part 1
[ESA-CR(P)-1910-VOL-2-PT-1]
06 p0758 N85-14849

Orbit maneuvers with finite thrust. Volume 3: User's guide, part 2
[ESA-CR(P)-1910-VOL-3-PT-2]
06 p0758 N85-14850

Orbit maneuvers with finite thrust. Volume 3: Reference catalog, parts 1 and 2
[ESA-CR(P)-1910-VOL-3-PT-1/2]
06 p0758 N85-14851

Orbit maneuvers with finite thrust. Volume 3: Reference catalog, part 3
[ESA-CR(P)-1910-VOL-3-PT-3]
06 p0758 N85-14852

Crustal dynamics project: Catalogue of site information
[NASA-TM-87452] 13 p2131 N85-23258

Catalog of the National Energy Software Center
[TI85-900521] 15 p2630 N85-26209

Glossary of landscape and vegetation ecology for Alaska
[PB85-153831] 16 p2816 N85-27372

Catalog of research projects at Lawrence Berkeley Laboratory, 1985
[DE85-008679] 17 p3049 N85-28869

Combined catalog of ionosphere vertical soundings data
[PB85-166494] 18 p3138 N85-29430

Notes for medical catalogers, 1984
[PB85-180206] 18 p3200 N85-29853

CAE tool catalog
[DE85-011290] 19 p3334 N85-30657

Data base management: MSTRAC (keynote paper), part 8 21 p3626 N85-32530

CATALYSIS
NT AUTOCATALYSIS

Liquid hydrocarbon fuels from syngas
[DE84-015942] 04 p0482 N85-13069

USSR report: Chemistry
[JPRS-UCH-84-012] 06 p0761 N85-14865

Catalytic oxidation by transition metal ions in zeolites
[AD-A146826] 07 p0922 N85-15842

Conference on Singlet Molecular Oxygen (COSMO 84), program and abstracts
[AD-A147281] 07 p1040 N85-16605

Catalytic ignition and combustion of lean mixtures
[AD-A148101] 08 p1121 N85-17067

Research in phase transfer catalysis
[AD-A148266] 08 p1121 N85-17068

Multiplex gas chromatography for use in space craft
[NASA-TM-86868] 09 p1290 N85-18097

Dynamics and mechanisms of catalytic processes and hot chemistry
[DE85-002899] 09 p1292 N85-18114

A metal-catalyzed rearrangement of alkene-alkynes and the stereochemistry of metallacyclobutene ring opening
[AD-A149084] 10 p1435 N85-19042

Adsorption thermodynamics and surface transport of metal catalyst poisons
[DE85-002866] 10 p1441 N85-19084

Photosynthesis of ammonia
[DE85-001482] 11 p1595 N85-20029

Studies of the kinetics and mechanisms of ammonia synthesis and hydrodesulfurization on metal single crystal surfaces
[DE85-001650] 11 p1595 N85-20030

Ozone measurements in the mesosphere during a solar proton event 11 p1665 N85-20490

In situ monitoring of electrochemical reactions by surface enhanced Raman scattering
[PB85-149789] 12 p1803 N85-21312

Solar-assisted hydrogen generation by photoelectrocatalysis
[PB85-149706] 12 p1804 N85-21314

The use of hydrazine as an alternate source of energy
[NASA-CR-175535] 12 p1817 N85-21397

Application of modulated hydrodynamic voltammetry to the study of anodic electrocatalysis
[DE85-004182] 13 p2018 N85-22653

International Conference on Coordination Chemistry (23rd) held at Boulder, Colorado on 29 July - 3 August, 1984
[AD-A150980] 14 p2252 N85-23956

A novel polymeric organosilazane precursor to Si3N4/SiC ceramics
[AD-A150748] 14 p2260 N85-24003

The mechanisms of phenylacetylene polymerization by molybdenum and titanium initiators
[AD-A150993] 14 p2260 N85-24007

Electronic structure calculations for low coverage adlayers
[DE85-007733] 18 p3179 N85-29709

Catalytic hydrotreatment studies with model compounds
[DE85-010187] 19 p3236 N85-30064

Molecular toxicology of chromatin: The role of Poly(ADP-Ribose) in gene control
[AD-A154415] 19 p3327 N85-30611

Highly dispersed metal atoms in zeolites
[DE85-010515] 19 p3354 N85-30792

Fuel-rich catalytic combustion: A soot-free technique for in situ hydrogen-like enrichment
[NASA-TP-2498] 20 p3423 N85-31244

Biocatalysis project
[NASA-CR-176044] 20 p3498 N85-31744

Rigid zeolite containing polyurethane foams
[DE85-006406] 23 p3919 N85-34286

Chemistry division report
[DE85-010586] 24 p4071 N85-35228

Vectorial electron transfer on designed surfaces
[PB85-204600] 24 p4076 N85-35263

Review of US NOx abatement technology
[PB85-193522] 24 p4114 N85-35501

CATALYSTS
NT ELECTROCATALYSTS

Study of catalysts and mechanisms in synthesis reactions
[DE84-015025] 04 p0470 N85-12990

Reactive sintering of SiC 04 p0473 N85-13010

Butene oxidation by molybdenum crystalographic shear compounds
[DE84-013910] 05 p0614 N85-13923

Biocatalyzed processes for production of commodity chemicals: Assessment of future research advances for N-butanol production
[NASA-CR-174264] 07 p0919 N85-15819

Vibrational spectroscopy of chemisorption phenomena on model catalyst surfaces
[AD-A146753] 07 p0922 N85-15840

Imide modified epoxy matrix resins
[NASA-CR-174695] 07 p0930 N85-15892

Optimization of technical catalysts with the help of surface analysis
[BMFT-FB-T-84-225] 08 p1124 N85-17086

Electric utility acid fuel cell stack technology advancement
[NASA-CR-174804] 08 p1178 N85-17422

Advanced NMR characterization of zeolite catalysts
[DE85-000456] 09 p1291 N85-18104

Cation promotion effects in zeolite-supported F-T catalysts
[DE85-001708] 09 p1291 N85-18108

Metal-support interactions: The effect of catalyst preparation on catalytic activity
[DE84-017425] 09 p1293 N85-18118

Liquid phase methanol process development unit: Installation, operation, and support studies
[DE85-001311] 09 p1301 N85-18171

ECUT, Energy Conversion and Utilization Technologies program: Technical and economic assessment of processes for the production of butanol and acetone. Phase 2: Analysis of research advances
[NASA-CR-175471] 10 p1434 N85-19034

An infrared study of isotopic exchange during methanation over supported rhodium catalysts; an inverse spillover effect
[AD-A149390] 10 p1435 N85-19046

An infrared study of the oxidation of carbon monoxide over supported rhodium catalysts
[AD-A149478] 10 p1436 N85-19050

Catalytic conversion of C3-C4 paraffins to gasoline
[DE85-004181] 10 p1458 N85-19187

Fundamental study of catalysts using laser Raman, infrared, auger electron spectroscopy and low energy electron diffraction
[DE85-001813] 11 p1595 N85-20033

An infrared study of the dissociation of carbon dioxide over supported rhodium catalysts
[AD-A149813] 12 p1800 N85-21291

Adsorption thermodynamics and surface transport of metal catalyst poisons
[DE85-003750] 12 p1802 N85-21301

Study of the kinetics of hydrogenation using aged catalysts
[DE85-004373] 12 p1802 N85-21302

Properties of supported metal catalysts
[DE85-003927] 12 p1802 N85-21303

Synthesis, static and reactive characterization of supported organometallics
[DE85-004285] 12 p1808 N85-21340

Fluorinated polyurethanes
[AD-D011526] 12 p1810 N85-21353

Tritium catalyzed deuterium Tokamaks
[DE85-004825] 12 p1936 N85-22166

Workshop report: Catalysis of Burn Rate of Energetic Binder propellants 13 p2001 N85-22545

Mechanism of burning rate enhancement by ferric oxide 13 p2002 N85-22546

USSR report: Chemistry
[JPRS-UCH-85-001] 13 p2013 N85-22629

Trifunctional catalysts for conversion of syngas to alcohols
[DE85-004577] 13 p2040 N85-22771

Diagrams of chemical and electrochemical equilibria in the presence of oxygen and sulphur
[AD-A150929] 14 p2251 N85-23953

Characterization of supported metal catalysts by imaging, microdiffraction and microanalysis techniques
[DE85-005567] 14 p2253 N85-23961

Investigation and optimization of fuel production using dye-based transition metal complexes as charge-transfer intermediates
[PB85-161941] 14 p2264 N85-24029

Optimization of the catalytic oxidation of CO for closed-cycle CO2 laser applications
[NASA-TM-86421] 15 p2504 N85-25445

Improved catalysts for liquid hydrocarbon fuels from syngas
[DE85-006569] 16 p2746 N85-26947

The production of copper phthalocyanine and/or its derivatives
[NASA-TM-77629] 17 p2917 N85-27963

Michelle-derived catalysts for extended Schulz-Flory
[DE85-005656] 17 p2922 N85-28012

Correlation of zeolite ZSM-5 acid strength with catalytic activity and selectivity
[DE85-005415] 17 p2922 N85-28013

Catalyst and reactor development for a liquid phase Fischer-Tropech process
[DE85-005894] 17 p2922 N85-28014

Transition metal catalyzed transformations of unsaturated molecules
[DE85-009531] 18 p3080 N85-29055

Effects of H2S on molten carbonate fuel cells
[DE85-008310] 18 p3130 N85-29386

Liquid hydrocarbon fuels from snygas
[DE85-009613] 19 p3228 N85-30017

Mechanism of the catalytic gasification and reactivity of graphite
[DE85-009932] 19 p3229 N85-30020

Study of the kinetics of hydrogenation using aged catalysts
[DE85-010427] 19 p3230 N85-30025
The mobile phase in coals: Its nature and modes of release
[DE85-011696] 19 p3230 N85-30026
Metallophthalocyanine dimers incorporating five atom covalent bridges
[AD-A154365] 19 p3234 N85-30051
New catalysts and new electrolytes for acid fuel cells
[DE85-009940] 19 p3307 N85-30498
Advanced NMR characterization of zeolite catalysts
[DE85-010143] 19 p3363 N85-30853
Improved catalysts for liquid hydrocarbon fuels from syngas
[DE85-011062] 20 p3421 N85-31234
In situ Moessbauer investigation of bimetallic catalysts on a base: FeRu, FeRh, FePd, FeIr, and FePt on SiO2
[B8563200] 20 p3432 N85-31293
Decomposition of sulfuric acid using solar thermal energy
[DE85-012288] 21 p3564 N85-32170
A safe, high-power-density lithium battery
[AD-A155223] 21 p3613 N85-32454
Experimental studies of the geometric and electronic structure of chemisorption bonding
[PB85-192250] 22 p3747 N85-33228
Integrated current collector and catalyst support
[DE85-011616] 22 p3761 N85-33311
Solids mixing in a three phase fluidized bed containing spherically shaped-porous solid particles
[PB85-187961] 22 p3785 N85-33453
Method of distributing liquefaction catalysts in solid carbonaceous material
[DE85-005759] 23 p3900 N85-34218
FTIR studies of hydrocarbon synthesis on Pd/ZSM5 catalysts
[DE85-012430] 24 p4071 N85-35230
CO + H2 reaction over nitrogn-modified iron catalysts
[DE85-013791] 24 p4072 N85-35231

CATALYTIC ACTIVITY
Radiation/catalytic augmented combustion
[AD-A148758] 09 p1290 N85-18101
Metal-support interactions: The effect of catalyst preparation on catalytic activity
[DE84-017425] 09 p1293 N85-18118
Electrocatalysis research
[NASA-CR-174352] 10 p1437 N85-19054
Catalytic conversion of C3-C4 paraffins to gasoline
[DE85-004181] 10 p1458 N85-19187
Investigation and optimization of fuel production using dye-based transition metal complexes as charge-transfer intermediates
[PB85-161941] 14 p2264 N85-24029
Quantitation of Na+, K+-ATPase enzyme activity in tissues of the mammalian vestibular system
15 p2613 N85-26102
The role of surface generated radicals in catalytic combustion 17 p2898 N85-27869
Oxygen evolution on NiCo2O4 electrodes
17 p2924 N85-28026
Fuel rich catalytic comustion: The first stage of a two-stage combustor
[NASA-TM-87042] 18 p3069 N85-28983
Galactose oxidase in stereospecific oxidation of primary alcohols
[AD-A154059] 19 p3234 N85-30048
Mechanistic and kinetic studies of the elementary processes in catalytic combustion of methane
[PB85-188306] 20 p3435 N85-31314
Elementary processes in the catalytic combustion of methane (mechanism, intermediates, and controlling reactions)
[PB85-188357] 20 p3436 N85-31316
Method for removing chlorine compounds from hydrocarbon mixtures
[DE85-011606] 22 p3742 N85-33191

CATARACTS
Technical support for microwave experiments on the eye lens
[AD-A149702] 12 p1933 N85-22144

CATASTROPHE THEORY
Nonlinear global stability analysis of compressor stall phenomena
[NASA-CR-174908] 19 p3219 N85-29960

CATCHMENT AREAS
U WATERSHEDS

CATECHOLAMINE
NT EPINEPHRINE
Endocrine responses to hypotensive gravitational stress: Catecholamines, pancreatic polypeptide, and vasopressin 05 p0693 N85-14460
Catecholamine excretion and subjective ratings of tension during autogenic training and mental stress
[REPT-172] 05 p0697 N85-14483
Influence of hyperthermia on body temperature and content of catecholamines in white rat hypothalamus
10 p1524 N85-19615

CATENARIES
Cable-catenary large antenna concept
14 p2231 N85-23829
The dynamics of slack marine cables
[AD-A155022] 21 p3599 N85-32349

CATHODE RAY TUBES
NT PICTURE TUBES
Manufacturing Methods and Technology (MM/T) specifications for miniature cathode ray tube
[AD-A145597] 02 p0194 N85-11298
Human engineering data base for design and selection of cathode ray tube and other display systems
[AD-A145704] 02 p0238 N85-11549
Matrix display simulation
[AD-D011371] 07 p1055 N85-16695
Device for controlling operation of lithicon cathode-ray memory tube 12 p1839 N85-21542
A description of the process of elaborating man-machine dialog in an aircraft equipped with cathode tubes: Roles and specifications of piloted simulation methods
16 p2698 N85-26658
Effect of background/foreground color coding on detection in acoustic data displays
[AD-A154105] 19 p3352 N85-30774
Ergonomic problems regarding the interactive touch input via screens in onboard and ground-based flight control
[NASA-TM-77814] 20 p3512 N85-31832
High pressure working mode of hollow cathode arc discharges
[NASA-TM-77880] 20 p3535 N85-31992
The effect of set size on time to recall color coded information
[AD-A155013] 21 p3665 N85-32767
A new large-scale, high-resolution multicolor software display concept
[AD-A155404] 22 p3827 N85-33703
Maintenance port system
[AD-D011724] 23 p3967 N85-34594

CATHODES
NT CELL CATHODES
NT COLD CATHODES
NT HOLLOW CATHODES
NT HOT CATHODES
NT PHOTOCATHODES
NT THERMIONIC CATHODES
NT TUBE CATHODES
Advanced fuel cell development
[DE84-014847] 01 p0044 N85-10289
The driving-force dependence of electrochemical rate parameters: Origins of anodic-cathodic asymmetries for metal aquo redox couples
[AD-A145605] 02 p0172 N85-11153
Method of making a porous carbon cathode: A porous carbon cathode so made, and electrochemical cell including the porous carbon cathode
[AD-D011243] 02 p0195 N85-11301
Properties of cathode materials in alkaline cells
[NASA-CR-174082] 04 p0495 N85-13161
Behaviour of lead-silver anodes in zinc electrodeposition from sulphuric acid baths
[BLL-MINTEK-TR-1160-(5810.5759)]
06 p0764 N85-14887
Synthesis and properties of Hexachloromolybdates(5) and related species
[AD-A139599] 07 p0924 N85-15852
Explosive emission cathode plasmas in intensive relativistic electron beam diodes
[AD-A147917] 07 p1046 N85-16642
Electric utility acid fuel cell stack technology advancement
[NASA-CR-174804] 08 p1178 N85-17422
New liquid cathodes for lithium batteries. Part A: Halocarbons
[AD-A148433] 08 p1178 N85-17423
Improved electron emission by use of a cloth fiber cathode
[AD-A149250] 10 p1480 N85-19340
Virtual cathode oscillator study
[AD-A149268] 10 p1480 N85-19342
Brightness limitations in multi-kiloampere electron beam sources
[DE84-017417] 10 p1555 N85-19807
Approaches to ultrafast neutron detectors
[DE85-001206] 11 p1636 N85-20307
Corrosion and coatings review of specifications and drawings of facilities for the Oman Military Construction Program at Masirah Island, Oman
[AD-A149739] 12 p1812 N85-21366
Molten carbonate fuel cell performance model update, draft
[DE85-005423] 13 p2129 N85-23252
Cathode materials for molten carbonate fuel cells
[DE85-004076] 13 p2130 N85-23254
Diagnostics of a glow discharge used to produce hydrogenated amorphous silicon films
[DE85-002914] 15 p2661 N85-26420
The loss of material from the cathode of metal arcs
[NASA-TM-77845] 17 p2918 N85-27985
Continued development and testing of tungsten controlled porosity dispenser cathodes
[AD-A152595] 17 p2931 N85-28090
Process for making electrodes for discharge tubes
[DE85-008898] 17 p2955 N85-28247
Bifunctional oxygen electrodes
[DE85-008871] 17 p2955 N85-28248
Electrodes for flash discharge lamps
[DE85-008897] 17 p2955 N85-28250
Streak tube characterization
[DE85-009674] 17 p2956 N85-28256
Apparatus for mounting a field emission cathode
[NASA-CASE-LEW-14108-1] 18 p3094 N85-29149
Method for predicting the performance of cathode materials
[AD-D011665] 19 p3257 N85-30198
Advanced fuel cell development
[DE85-009662] 19 p3306 N85-30497
Method of production of metals by cathodic solution of their compounds in electrolytic cells
[BLL-OA-TRANS-3207-(6196.300)]
20 p3429 N85-31266
A safe, high-power-density lithium battery
[AD-A155223] 21 p3613 N85-32454
Electrode erosion in arc discharges at atmospheric pressure
[NASA-TM-87087] 23 p3903 N85-34178
Injector losses on Mite
[DE85-012356] 24 p4090 N85-35355
Considerations on collective ion aceleration as an intense ion injector
[DE85-012706] 24 p4155 N85-35757

CATHODIC COATINGS
Marine corrosion
[AD-A153843] 18 p3074 N85-29012

CATHODOLUMINESCENCE
Minor elements and cathodoluminescence of Mg-rich olivines from Murchison and Allende carbonaceous meteorites 06 p0884 N85-15619
Sedimentary petrology and provenance of the upper Jackforth Sandstone (Morrowan) Quachita Mountains, Arkansas, USA 08 p1182 N85-17447

CATIONS
NT FERRIC IONS
NT METAL IONS
Trivalent ion exchange in beta alumina
[AD-A145373] 02 p0172 N85-11151
Magnetic resonance studies of transient radicals and radical ions
[DE84-011699] 03 p0328 N85-12116
Electronic and redox properties of stacked-ring silicon phthalocyanines from molecular orbital theory
[AD-A147161] 07 p0922 N85-15844
Homogeneous reaction involving components of different redox couples. 1: Theoretical considerations and digital simulation
[AD-A148666] 08 p1124 N85-17084
Homogeneous reaction involving components of different redox couples. 2: Polarographic studies of the interactions of alkali metal cations with anthracene and fluoroanthene dianions in N,N-dimethylformamide and acetonitrile
[AD-A148667] 08 p1124 N85-17085
Cation promotion effects in zeolite-supported F-T catalysts
[DE85-001708] 09 p1291 N85-18106
Ion transporting composite membranes. 1: Nafion impregnated gore-tex
[AD-A151020] 14 p2252 N85-23860
A comparative evaluation of the effects of acid precipitation, natural acid production and harvesting of cation removal from forests
[DE85-005254] 15 p2569 N85-25961
The electronic spectra of phthalocyanine radical anions and cations
[AD-A152328] 17 p2918 N85-27986
The conversion of smaller borane fragments to larger structures. Systematics of boron hydride reactions
[AD-A153443] 18 p3070 N85-28985
Cation promotion effects in zeolite-supported F-T catalysts
[DE85-000969] 19 p3233 N85-30044
Method of reducing impurity and antisite defects in semiconductor crystal materials, and device and apparatus respectively produced from and utilizing same
[AD-D011698] 19 p3260 N85-30216

A comparative evaluation of the effects of acid precipitation, natural acid production and harvesting on cation removal from forests
[DE85-010821] 19 p3309 N85-30511
Low-temperature positron lifetime and Doppler-broadening measurements for single-crystal nickel oxide containing cation vacancies
[DE85-010238] 19 p3376 N85-30944
Throughfall rate and chemistry studies: Whiteface Mountain
[DE85-012407] 23 p3947 N85-34464
Effect of temperature and ionic impurities at very low concentrations on stress corrosion cracking of Type 304 stainless steel
[TI85-003048] 24 p4079 N85-35283

CATS
Susceptibility of cat and squirrel monkey to motion sickness induced by visual stimulation: Correlation with susceptibility to vestibular stimulation
11 p1694 N85-20650
Brain mechanisms underlying individual differences in reaction to stress: An animal model
[AD-A150195] 13 p2143 N85-23301
Percutaneous connectors
[NASA-CR-175627] 16 p2839 N85-27508

CAUCHY PROBLEM
Approximation of discontinuous solutions of hyperbolic partial differential equations
[NRIMS-TWISK-302] 02 p0250 N85-11831
Checking optical-polarization measurements at interfaces 02 p0271 N85-11770
Self similar solutions for a degenerate Cauchy problem
[AD-A147241] 07 p1031 N85-16548
Regularity of the free boundary for the porous medium equation
[AD-A147299] 08 p1210 N85-17611
Multidimensional inverse scattering for first order systems
[AD-A148711] 08 p1214 N85-17642
The Cauchy problem for u sub t = Delta u(m) when O m 1
[AD-A153521] 18 p3169 N85-29635
Art of programming programmable microcalculators: Calculation of response from current values of action
22 p3767 N85-33348
Fundamentals of radio optical theory of resonant and directional quasi-optical devices
22 p3780 N85-33420

CAULKING
Corrosion properties of second-generation conductive materials 07 p1000 N85-16348

CAUSES
Probable cause: A decision making framework
[AD-A147642] 08 p1210 N85-17614

CAUSTIC LINES
The investigation of short wave signal structure in the vicinity of the caustic by means of a high-directed antenna
[PR-194] 03 p0354 N85-12277

CAUSTICS
U ALKALIES

CAVITATION
U CAVITATION FLOW

CAVITATION CORROSION
Characterization of erosion of metallic materials under cavitation attack in a mineral oil
[NASA-TM-86934] 10 p1440 N85-19075
Prediction of the resistance of structural materials to cavitation erosion
[BLL-DRIC-TRANS-7435-(3623.66)]
13 p2020 N85-22659
Marine corrosion
[AD-A153643] 18 p3074 N85-29012

CAVITATION FLOW
Collapse of cavitation bubbles between two walls in ultrasonic field 02 p0266 N85-11739
Diffraction of plane polarized waves by noncircular cylindrical cavity 02 p0269 N85-11754
Potential application of robotics and state-of-the art end effectors at Letterkenny Army Depot
[AD-P004015] 03 p0309 N85-11994
Cavitation phenomenon in superplastic creep
[DE84-015484] 04 p0513 N85-13271
Bulk cavitation caused by a plane shock wave
[AD-A147031] 07 p0958 N85-16072
Study of optical sound generation and amplification
[AD-A147359] 07 p1039 N85-16592
The role of nuclei size in transient cavitation threshold measurements
[AD-A148334] 08 p1162 N85-17332
Cavitation erosion resistant coatings for pumps
[PB85-120210/GAR] 09 p1300 N85-18167
Cavitation phenomenon in superplastic creep
[DE85-001716] 10 p1441 N85-19083
Properties of materials using acoustic waves
[AD-A150465] 13 p2155 N85-23362
Cavitation erosion of plasma sprayed alloys
[DE85-009542] 18 p3077 N85-29036
Effects of annealing treatments on superplasticity in a thermomechanically processed Aluminum-10.2%Mg-0.52%Mn
[AD-A154414] 19 p3239 N85-30060
Bubble dynamics in polymer solutions undergoing shear
[AD-A154575] 21 p3568 N85-32193
Experimental studies of chemical reactivity during shock initiation of hexanitrostilbene
[DE85-011726] 22 p3754 N85-33270

CAVITIES
A finite element method for three dimensional cavity circulation 05 p0635 N85-14071
Analysis of physical-chemical processes governing SSME internal fluid flows
[NASA-CR-174245] 06 p0760 N85-14862
Catalytic oxidation by transition metal ions in zeolites
[AD-A148828] 07 p0922 N85-15842
High Marangoni number convection in a square cavity
[NASA-CR-174283] 07 p0959 N85-16078
Numerical solutions for steady natural convection in a square cavity
[PB84-245752] 07 p0961 N85-16090
Some aspects of the micromechanics of hot spot formation in energetic materials
08 p1116 N85-17036
Effect of air cavity on the vibration analysis of loaded drums 09 p1339 N85-18422
Some aspects of the micromechanics of hot spot formation in energetic materials
[AD-P004348] 10 p1456 N85-19172
An investigation of compressible flows over open cavities including shear layer thickness effects
[AD-A150086] 12 p1847 N85-21588
An investigation of aerowindows for solar receivers
[DE84-010931] 12 p1877 N85-21772
Micromechanical modeling of microstructural damage in creeping alloys
[DE85-003925] 13 p2022 N85-22671
High frequency estimation of 2-dimensional cavity scattering
[AD-A151697] 15 p2542 N85-25696
Transition region for corner cracks at holes
[AD-A151835] 15 p2579 N85-25908
Parametric study of autooscillation upon flow of supersonic jet into cylindrical cavity
16 p2765 N85-27060
The definition and computation of a metric on plane curves. The meaning of a face on a geometric model
17 p3004 N85-28571
Incorporation of Monte Carlo electron interface studies into photon general cavity theory
[DE85-007674] 17 p3034 N85-28772
Maser cavity servo-tuning system
[NASA-CASE-NPO-15890-1-CU]
18 p3093 N85-29143
Hydrogen maser oscillation at 10 K
18 p3108 N85-29241
A collective interaction klystron specification
[AD-D011704] 19 p3255 N85-30186
Fundamentals of radio optical theory of resonant and directional quasi-optical devices
22 p3780 N85-33420
Role of ECRH in potential formation for tandem mirrors
[DE85-011859] 22 p3848 N85-33834
Method of precisely modifying predetermined surface layers of a workpiece by cluster ion impact therewith
[DE85-006519] 23 p3984 N85-34710
Moment-method formulation of the cavity-probe aperture antenna
[DE85-013264] 24 p4088 N85-35338
Experimental study of free and mixed convective flow of air in a heated cavity
[DE85-012538] 24 p4094 N85-35380

CAVITONS
Role of cavitons in laser-plasma interactions
[DE85-001842] 11 p1731 N85-20886

CAVITY RESONATORS
Synchronously pumped mode-locked semiconductor platelet laser
[AD-D011214] 01 p0051 N85-10340
Tunable CW semiconductor platelet laser
[AD-D011215] 01 p0052 N85-10341
Frequency stabilized laser
[AD-D011223] 01 p0053 N85-10351
Time variability of directionality properties of pulsed EB-EDL (Electron Beam-Electric Discharge Laser) N2-CO2 lasers
[AD-A145546] 02 p0202 N85-11344
The S-matrix and acoustic signal structure in simple and compound waveguides
[PP-583] 03 p0415 N85-12652
An 850 J, 150 ns narrow-band krypton fluoride laser
[DE84-013077] 04 p0506 N85-13226
Dual mode directionally coupled band reject filter apparatus
[AD-D011359] 07 p0945 N85-15984
Research relative to the development of a cryogenic microwave cavity gradiometer for orbital use
[NASA-CR-174249] 07 p0962 N85-16095
Halogen mass flow rate detection system
[AD-D011398] 08 p1166 N85-17352
Image line voltage controlled oscillator with replaceable components
[AD-D011436] 10 p1479 N85-19333
A coaxial cavity gunn oscillator using probe coupled microstrip
[AD-D011437] 10 p1479 N85-19334
An integrated varactor tuned coaxial gunn oscillator for 60 GHz operation
[AD-D011439] 10 p1479 N85-19335
Filter reflection image guide oscillator and solid state line scanning device
[AD-D011440] 10 p1479 N85-19336
Integrated circuit tunable cavity oscillator
[AD-D011474] 10 p1481 N85-19351
Single-cavity SLED device
[DE85-002587] 12 p1929 N85-22117
Coupled-cavity gyrotrons with mode conversion
13 p2076 N85-22967
Experimental study of high-stability oscillator with surface-acoustic-wave resonator in feedback loop
13 p2090 N85-23053
Dependence of properties of optical cavity on misalignment 14 p2276 N85-24099
Superconducting traveling wave accelerators
[DE85-005247] 15 p2661 N85-26424
In situ microwave measurements of dielectric properties and moisture in materials
[DE85-003622] 16 p2747 N85-26953
Jinc-trap resonator
[AD-D011650] 17 p2970 N85-28339
Chaos and order in an optical ring cavity
[CWI-AM-R8416] 17 p3038 N85-28795
Maser cavity servo-tuning system
[NASA-CASE-NPO-15890-1-CU]
18 p3093 N85-29143
Atomic hydrogen maser active oscillator cavity and bulb design optimization 18 p3108 N85-29240
Operation of a quasioptical electron cyclotron maser
[DE85-008450] 18 p3113 N85-29276
Cavityless optical bistability in systems of two-level atoms 18 p3186 N85-29764
Performance of an RF beam monitor on the NBS-Los Alamos racetrack microtron
[DE85-010725] 19 p3262 N85-30232
Dye laser traveling wave amplifier
[NASA-CR-175989] 19 p3275 N85-30308
Experimental and theoretical investigations of open resonators --- precipitation measurement
[DFVLR-FB-85-12] 20 p3449 N85-31414
Cryogenic system for the University of Washington Superconducting Booster
[DE85-010604] 22 p3754 N85-33274
High-power solid-state rf source for accelerator cavities
[DE85-012672] 22 p3761 N85-33309
Iris tilting and RF steering in the SLAC Linac
[DE85-011704] 22 p3841 N85-33783
New directional couplers for multimode circular waveguides applied to intense pulsed microwave systems
[DE85-011753] 23 p3926 N85-34330
Tuning system for capacitively loaded 1/4 accelerating cavity
[DE85-012516] 24 p4091 N85-35358

CCD
U CHARGE COUPLED DEVICES

CCD STAR TRACKER
Design, manufacture and testing of a medium accuracy star tracker
[REPT-TR/84-048] 20 p3459 N85-31486

CDC COMPUTERS
NT CDC CYBER 170 SERIES COMPUTERS
NT CDC CYBER 205 COMPUTER
Computer center introductory reference manual for CDC CYBER
[AD-A145796] 03 p0406 N85-12593
U: The universal utility controller, revision 1
[DE84-017077] 04 p0547 N85-13481
The CDC: Facilities on offer from the CNES computing center for space mathematics (a look at the capacities of CDC computers) 05 p0599 N85-13818

Computer center CDC Libraries-PROCFIL (procedures)
[AD-A148633] 08 p1206 N85-17589

CDC CYBER 170 SERIES COMPUTERS
The computing facilities of the Toulouse Space Center 14 p2397 N85-24770

CDC CYBER 205 COMPUTER
Developement of an optimum interpolation analysis method for the CYBER 205 18 p3143 N85-29456

CDMA
U CODE DIVISION MULTIPLE ACCESS

CEILING (AIRCRAFT CAPABILITY)
Effect of ground and/or ceiling planes on thrust of rotors in hover
[NASA-TM-86754] 20 p3388 N85-31014

CEILINGS (METEOROLOGY)
Joint probability of selected cloud and visibility thresholds around Koblenz, Germany
[AD-A145294] 02 p0231 N85-11506
Revised Uniform Summary of Surface Weather Observations (RUSSWO). McChord AFB, Washington, parts A-F
[AD-A146914] 07 p1005 N85-16385
Revised Uniform Summary of Surface Weather Observations (RUSSWO). Dobbins AFB, Georgia, parts A-F
[AD-A146916] 07 p1005 N85-16387
Summary of Meteorological Observations, Surface (SMOS), Beaufort, South Carolina
[AD-A150536] 13 p2138 N85-23279
Comparison of some West German cloud height and visibility data — weapon test sites
[BAE-BT-12734] 15 p2593 N85-25982
An evaluation of discretized conditional probability and linear regression threshold techniques in model output statistics forecasting of cloud amount and ceiling over the North Atlantic Ocean
[AD-A155100] 21 p3636 N85-32581

CEILOMETERS
U CLOUD HEIGHT INDICATORS

CELESTIAL BODIES
NT A STARS
NT ALLENDE METEORITE
NT AMOR ASTEROID
NT ANDROMEDA GALAXIES
NT APOLLO ASTEROIDS
NT ARIETID METEOROIDS
NT ASTEROID BELTS
NT ASTEROIDS
NT B STARS
NT BARRED GALAXIES
NT BINARY STARS
NT BL LACERTAE OBJECTS
NT BLUE STARS
NT CALLISTO
NT CARBON STARS
NT CARBONACEOUS CHONDRITES
NT CARBONACEOUS METEORITES
NT CASSIOPEIA A
NT CATACLYSMIC VARIABLES
NT CEPHEID VARIABLES
NT CHARON
NT CHONDRITES
NT COMET NUCLEI
NT COMET TAILS
NT COMETS
NT COMPANION STARS
NT COOL STARS
NT CRAB NEBULA
NT DEIMOS
NT DISK GALAXIES
NT DWARF NOVAE
NT DWARF STARS
NT EARLY STARS
NT EARTH (PLANET)
NT ECLIPSING BINARY STARS
NT ELLIPTICAL GALAXIES
NT ENCKE COMET
NT EUROPA
NT EXTRAGALACTIC RADIO SOURCES
NT FLARE STARS
NT GALACTIC CLUSTERS
NT GALAXIES
NT GALILEAN SATELLITES
NT GANYMEDE
NT GAS GIANT PLANETS
NT GIACOBINI-ZINNER COMET
NT GIANT STARS
NT GLOBULAR CLUSTERS
NT HALLEY'S COMET
NT HERBIG-HARO OBJECTS
NT HERCULES NOVA
NT HOT STARS
NT INFRARED STARS
NT IO
NT IRAS-ARAKI-ALCOCK COMET
NT IRON METEORITES
NT JUPITER (PLANET)
NT JUPITER RINGS
NT JUPITER SATELLITES
NT LATE STARS
NT M STARS
NT MAGNETIC STARS
NT MAIN SEQUENCE STARS
NT MARS (PLANET)
NT MERCURY (PLANET)
NT METALLIC STARS
NT METEORITES
NT METEOROID SHOWERS
NT METEOROIDS
NT MICROMETEORITES
NT MICROMETEOROIDS
NT MILKY WAY GALAXY
NT MOON
NT NATURAL SATELLITES
NT NEBULAE
NT NEPTUNE (PLANET)
NT NEUTRON STARS
NT NOVAE
NT O STARS
NT ORION NEBULA
NT ORIONID METEOROIDS
NT PANTAR CHONDRITES
NT PECULIAR STARS
NT PHOBOS
NT PLANETARY NEBULAE
NT PLANETARY RINGS
NT PLANETS
NT PLUTO (PLANET)
NT PRAESEPE STAR CLUSTERS
NT PRE-MAIN SEQUENCE STARS
NT PROTOPLANETS
NT PROTOSTARS
NT PULSARS
NT QUASARS
NT RADIO GALAXIES
NT RADIO METEORS
NT RADIO SOURCES (ASTRONOMY)
NT RADIO STARS
NT RED DWARF STARS
NT RED GIANT STARS
NT REFERENCE STARS
NT SATURN (PLANET)
NT SATURN RINGS
NT SEYFERT GALAXIES
NT SOLAR SYSTEM
NT SPIRAL GALAXIES
NT STAR CLUSTERS
NT STARS
NT STONY METEORITES
NT SUBDWARF STARS
NT SUBGIANT STARS
NT SUN
NT SUPERGIANT STARS
NT SUPERMASSIVE STARS
NT SUPERNOVAE
NT SYMBIOTIC STARS
NT T TAURI STARS
NT TEKTITES
NT TERRESTRIAL PLANETS
NT TITAN
NT TRITON
NT URANUS (PLANET)
NT URANUS RINGS
NT VARIABLE STARS
NT VENUS (PLANET)
NT VESTA ASTEROID
NT VIRGO GALACTIC CLUSTER
NT WHITE DWARF STARS
NT WOLF-RAYET STARS
NT X RAY BINARIES
NT ZETA AURIGAE STAR
NT ZODIACAL DUST
Dark matter near the sun: Simulated star counts and the Oort limit 06 p0880 N85-15592
Determination of the observation conditions of celestial bodies with the aid of the DISPO system
[NAS 1.15:77632] 14 p2438 N85-25044
Observation of hard X-rays from the Crab pulsar and A0535 + 26
[OG-2.3-7] 22 p3866 N85-33944
Results of low energy background measurements with the Liquid Scintillation Detector (LSD) of the Mont Blanc Laboratory
[HE-5.3-5] 24 p4205 N85-36099

CELESTIAL GEODESY
Research in geodesy based upon radio interferometric observations of extragalactic radio sources
[AD-A147561] 07 p0988 N85-16280
Recent development in astronomic position determinations
[AD-A148335] 08 p1062 N85-16858
Basic formulae for the computation of the deflection of the vertical from astronomical star observations
[AD-A154912] 21 p3605 N85-32990

CELESTIAL MECHANICS
Some considerations on elliptic heliocentric orbits
[INPE-3217-PRE/570] 02 p0297 N85-11936
Physical properties of Neptune and Triton inferred from the Orbit of Triton 02 p0300 N85-11942
Tidal disruption and the origin of the Moon
04 p0586 N85-13739
Interplanetary trajectories 05 p0600 N85-13827
The restricted problem of 2 + N bodies
09 p1414 N85-18825
Lagrangian solutions in photogravitational restricted circular three-body problem 13 p1979 N85-22416
Computation of elliptical functions in problems of celestial mechanics 13 p1979 N85-22418
Feoktistov argues against U.S. space shuttle design concept 13 p1985 N85-22453
China report: Science and technology
[JPRS-CST-85-005] 13 p2052 N85-22843
Development, prospect of satellite dynamics discussed 13 p2052 N85-22847
Dynamics of gas disks in triaxial galaxies
13 p2171 N85-23469
Elements of celestial mechanics
14 p2396 N85-24762
The solar system: Improving knowledge of the system
14 p2398 N85-24782
Construction of conditionally periodic solutions of problem of reciprocating motion of axially symmetric satellite of triaxial planet 15 p2480 N85-25304
Evolution of collisional systems — planetary disks
15 p2674 N85-26505
The Adiabatic invariant: A tool for the study of the dynamics of the solar system 15 p2676 N85-26519
Instabilities and the fine structure of Saturn's rings
15 p2676 N85-26520
Optimal open loop and nonlinear feedback control for remote orbital capture
[AD-A151967] 16 p2732 N85-26859
The study of the physics of cometary nuclei
[NASA-CR-175917] 17 p3054 N85-28905

CELESTIAL NAVIGATION
NT ASTRONAVIGATION
Optimization of orientation in navigation by two heavenly bodies 07 p0951 N85-16027

CELESTIAL OBSERVATION
U ASTRONOMY

CELESTIAL REFERENCE SYSTEMS
References in space and time
05 p0598 N85-13809
Reference systems — in space mechanics
14 p2399 N85-24784
Materialization of a reference system via a star catalog 14 p2399 N85-24787
Relating the planetary ephemerides and the radio reference frame 16 p2770 N85-27096

CELESTIAL SPHERE
A model of the soft X-ray background as a blast wave viewed from inside 06 p0879 N85-15586
Non equilibrium ionization in the local hot bubble
06 p0879 N85-15587
The stellar wind in the BO V-type eclipsing binary Y Cygni 11 p1755 N85-21040
Investigating statistical characteristics of atmospheric background brightness and star background density in equatorial region of celestial sphere
15 p2478 N85-25298

CELL ANODES
Nickel-cadmium cell design variable program data analysis
[NASA-TM-86198] 19 p3258 N85-30203

CELL CATHODES
Development and testing of TiB2, used as cathode material in Al-electrolysis cells
[BMFT-FB-T-84-176] 05 p0633 N85-14060
The effect of potential on the corrosion fatigue behavior of a precipitation hardened aluminum alloy
[AD-A146537] 06 p0766 N85-14816
Molten carbonate fuel cell cathode material development
[DE85-010266] 18 p3081 N85-29057
Nickel-cadmium cell design variable program data analysis
[NASA-TM-86198] 19 p3258 N85-30203

CELL DIVISION
Chromosome aberrations in Crepis capillaris exposed to gamma radiation and clinostat
19 p3325 N85-30600
Preparative electrophoresis of cultured human cells: Effect of cell cycle phase 20 p3500 N85-31758

CELLS
Lithium battery safety: A fiber-optic application for safe observation of lithium cells under severe tests
[AD-A146646] 06 p0804 N85-15118

Opacity control technique for jet engine test cells
[AD-D011666] 19 p3220 N85-29968
Summary electrophoretic data base on human embryonic kidney cell strain 8514
20 p3501 N85-31766
The Fibrin slide assay for detecting urokinase activity in human fetal kidney cells 20 p3502 N85-31768
CELLS (BIOLOGY)
NT CHROMOSOMES
NT ERYTHROCYTES
NT FIBROBLASTS
NT GAMETOCYTES
NT HEMATOPOIESIS
NT HEMOGLOBIN
NT LYMPHOCYTES
NT MITOCHONDRIA
NT NEURONS
NT OXYHEMOGLOBIN
NT PROTOPLASTS
Effect of spaceflight factors on rat bone marrow cells
01 p0092 N85-10620
Purification of biomaterials by phase partitioning
02 p0154 N85-11043
Architecture of dermatophyte cell Walls: Electron microscopic and biochemical analysis
[NASA-TM-77441] 03 p0399 N85-12546
Field/cell interaction model
[DE84-011614] 04 p0544 N85-13465
Further cell biology experiments with Physarum polycephalum for a reflight of Biorack
05 p0689 N85-14429
Observation of the contractile vacuolar system of Paramecium caudatum on the fast running clinostat
05 p0689 N85-14431
Plant cell cultures in biological space experiments
05 p0690 N85-14434
Structure and functions of fungal cell surfaces
[NASA-TM-77439] 06 p0842 N85-15347
The structure and function of fungal cells
[NASA-TM-77443] 06 p0842 N85-15348
The development of the vestibular apparatus under conditions of weightlessness
[NASA-TM-77517] 07 p1011 N85-16422
Radiation physics, biophysics, and radiation biology
[DE84-014885] 09 p1360 N85-18557
Genetic effects of microwave exposure on mammalian cells in vitro. Volume 2, Appendix A: Cytogenetics and growth kinetics data, 850 MHz
[AD-A148866] 10 p1522 N85-19599
Genetic effects of microwave exposure on mammalian cells in vitro. Volume 2, Appendix B: Cytogenetics and growth kinetics data, 1.2 GHz
[AD-A148867] 10 p1522 N85-19600
Genetic effects of microwave exposure on mammalian cells in vitro, volume 2
[AD-A149347] 10 p1523 N85-19603
Purification and cultivation of human pituitary growth hormone secreting cells
[NASA-CR-171846] 12 p1899 N85-21923
Toxicity, mutagenesis and aging due to endogenous oxygen radicals
[AD-A150121] 12 p1900 N85-21928
Morphological study of monkeys submitted to antiorthostatic hypokinesia 12 p1902 N85-21942
Investigation of foam flotation and phase partitioning techniques 12 p1945 N85-22216
Second Soviet-French Symposium on Space Technology 15 p2483 N85-25326
Actual and simulated weightlessness inhibit osteogenesis in long bone metaphysis by different mechanisms 15 p2608 N85-26074
Quantitative alterations in the function of bone forming cells due to reduced weight bearing
15 p2609 N85-26075
Gravitropism in leafy dicot stems
15 p2610 N85-26086
Development and maturation of the neuromuscular jencition in cell culture under conditions of simulated zero-gravity 15 p2611 N85-26093
Differential wall growth in gravistimulated corn roots: Its timing and regulation 15 p2614 N85-26105
Structural-functional changes in bacterial cells under spaceflight conditions 16 p2724 N85-26812
The dynamical behavior of the age-size-distribution of a cell population
[CWI-AM-R8414] 17 p2966 N85-28538
Interactions between electromagnetic fields
[AD-A153796] 18 p3091 N85-29129
Radiation damage and repair in cells and cell components. Part 2: Physical radiations and biological significance
[DE85-008934] 18 p3152 N85-29518
Radiation damage and repair in cells and cell component, part 1
[DE85-008867] 18 p3152 N85-29519
Controlled Ecological Life Support System. Life Support Systems in Space Travel
[NASA-CP-2378] 18 p3155 N85-29531
Current concepts and future directions of CELSS
18 p3155 N85-29532
Molecular toxicology of chromatin: The role of Poly(ADP-Ribose) in gene control
[AD-A154415] 19 p3327 N85-30611
Metabolic mechanisms of plant growth at low water potentials 19 p3327 N85-30612
Mouse oocyte killing by neutrons: Target considerations
[DE85-011362] 19 p3328 N85-30624
Flow cytometry for health monitoring in space
[DE85-009572] 19 p3329 N85-30625
Kidney cell electrophoresis
[NASA-CR-171889] 20 p3498 N85-31745
Task description for the 1983 catalog of tasks for the materials processing in space program
20 p3498 N85-31746
Kidney cell electrophoresis, continuing task
20 p3498 N85-31747
Asymmetric electroosmotic flow and mobility measurements at nonstationary positions in the rectangular chamber 20 p3499 N85-31749
Theoretical prediction of stationary positions in the rectangular chamber during asymmetric electroosmotic flow 20 p3499 N85-31750
A computer program for determining the electrophoretic mobility of cells in a rectangular chamber during asymmetric electroosmotic flow
20 p3499 N85-31751
Operation of the Zeiss cytopherometer with Zn/ZnSO4 electrode system of Tenforde et al
20 p3499 N85-31752
Electrophoretic mobility of cells in a vertical Ficoll gradient 20 p3499 N85-31753
Free-zone electrophoresis of animal cells. 1: Experiments on cell-cell interactions
20 p3499 N85-31754
Development anmd testing of electrophoresis solutions. Task I.1: Development of optimal buffer system
20 p3500 N85-31755
Effects of method of detachment on electrophoretic mobility of mammalian cells grown in monolayer culture
20 p3500 N85-31757
Preparative electrophoresis of cultured human cells: Effect of cell cycle phase 20 p3500 N85-31758
Size and DNA distributions of electrophoretically separated cultured human kidney cells
20 p3500 N85-31759
The role of cell size in density gradient electrophoretic separation of mouse leukemia cells according to position in the cell cycle 20 p3500 N85-31760
Electrophoretic mobilities of cultured human embryonic kidney cells in various buffers 20 p3501 N85-31761
Effect of passage number on electrophoretic mobility distributions of cultured human embryonic kidney cells
20 p3501 N85-31762
Density gradient electrophoresis of cultured human embryonic kidney cells 20 p3501 N85-31763
Identification and quantitation of morphological cell types in electrophoretically separated human embryonic kidney cell cultures 20 p3501 N85-31764
Urokinase production by electrophoretically separated cultured human embryonic kidney cells
20 p3501 N85-31765
A critical synopsis: Continuous growth of proximal tubular kidney epithelial cells in hormone-supplemented serum-free medium 20 p3501 N85-31767
Results of computer calculations for a simulated distribution of kidney cells 20 p3502 N85-31771
Properties of electrophoretic fractions of human embryonic kidney cells separated on space shuttle flight STS-8 20 p3503 N85-31776
Detection of internal structure by scattered light intensity: Application to kidney cell sorting
20 p3503 N85-31777
Flow cytometry of human embryonic kidney cells: A light scattering approach 20 p3503 N85-31778
A cluster analysis method for identification of subpopulations of cells in flow cytometric list-mode arrays 20 p3503 N85-31779
Development of a recombinant DNA assay system for the detection of genetic change in astronauts cells
[DE85-010103] 20 p3504 N85-31781
A system for the assessment of non-thermal effects of ultrasound on cells at liquid nitrogen temperatures
20 p3523 N85-31915
From microbial communities to cells
21 p3659 N85-32728
Physical chemical state of water in living cells
[AD-A154566] 21 p3662 N85-32749
Microorganisms in space flight
23 p3951 N85-34490
Report of Amphibian Development Group
24 p4127 N85-35583
Are living cells generally sensitive to gravity?
24 p4130 N85-35602
CELLULAR MATERIALS (NON BIOLOGICAL)
U FOAMS
CELLULOSE
Fire retardant cellulosehydrate fibers
06 p0761 N85-14870
Effect of polymer matrix on properties of fibers obtained by caking polymer dispersions 06 p0762 N85-14876
Environmental cycling of cellulosic thermal insulation and its influence on fire performance
[DE85-004295] 13 p2041 N85-22776
Effects of coating rectangular microscopic electrophoresis chamber with methylcellulose
20 p3498 N85-31748
CELLULOSE NITRATE
Oxidation resistant slurry coating for carbon-based materials
[NASA-CASE-LEW-13923-1] 24 p4077 N85-35267
CEMENTATION
Some reflections on the competition among different hard materials in industrial applications
02 p0177 N85-11192
Development and performance of CVD-coatings on cutting tools 02 p0178 N85-11193
An investigation of cementation and carbonitriding by means of ionic bombardment
[BLL-OA-TRANS-3203-(6196.300)]
20 p3429 N85-31265
CEMENTITE
Reciprocal solubility of phases in multi-component systems
[BLL-M-36003-(5828.4)] 07 p0926 N85-15670
CEMENTS
Materials for emergency repair of runways
[AD-A146139] 03 p0320 N85-12068
Development of a rapid test method for asphalt concrete content determination in hot-mix paving mixtures
[PB84-218692] 03 p0342 N85-12204
Development of a preliminary ALRS stabilized material pavement analysis system (SPAS)
[AD-A147116] 07 p0910 N85-15760
Development and evaluation of a procedure for the rapid analysis of fresh concrete
[AD-A149741] 12 p1866 N85-21703
Hazardous air pollutants: Dry-deposition phenomena
[PB85-136279] 12 p1867 N85-21843
Pycnometer shaker
[PB85-174985] 20 p3460 N85-31491
Experimental characterization and stability of salt- and nonsalt-containing grouts and mortars (BCT-1F- and BCT-1FF-related)
[DE85-012339] 22 p3753 N85-33283
High temperature polymer concrete
[DE85-005756] 23 p3920 N85-34290
CENSORED DATA (MATHEMATICS)
The EM algorithm for censored data
[AD-A148136] 08 p1212 N85-17626
A power transformation exponential regression model for censored failure time data
[AD-A148377] 08 p1212 N85-17632
Small-sample properties of kernel density estimators from randomly right-censored data
[AD-A148752] 09 p1374 N85-18634
A kernel type estimator of a quantile function from right-censored data
[AD-A148753] 09 p1374 N85-18635
Inference for censored matched pairs using signed ranks
[MATHEMATICS-RESEARCH-16?]
12 p1923 N85-22078
On the confidence limits for Weibull reliability and quantiles: The case of maximum likelihood estimation from small size censored samples
[REPT-84-RR-345] 20 p3521 N85-31896
CENTAUR LAUNCH VEHICLE
NT ATLAS CENTAUR LAUNCH VEHICLE
Shuttle/Centaur project perspective
08 p1106 N85-16991
Shuttle/Centaur upper stage capability
11 p1712 N85-20773
Linearization of digital derived rate algorithm for use in linear stability analysis
[NASA-TM-87000] 14 p2243 N85-23904
CENTAUR VEHICLE
U CENTAUR LAUNCH VEHICLE
CENTAURUS CONSTELLATION
X-ray emission from Centaurus A — Vela 5B; radio galaxy 08 p1239 N85-17813
X-ray emission from Centaurus A
[DE85-002030] 09 p1417 N85-18943

CENTER OF GRAVITY
Mobility of the small combine (track type) on soft ground-relationship between the position of the center of gravity and the mobility
[AD-P004285] 09 p1407 N85-18902
Space Shuttle Orbiter trimmed center-of-gravity extension study. Volume 9: Effects of configuration modifications on the aerodynamic characteristics of the 140 A/B Orbiter at Mach numbers of 1.5, 2.0, and 2.5 — wind tunnel tests
[NASA-TM-72861-VOL-9] 10 p1420 N85-18956
Space Shuttle orbiter trimmed center-of-gravity extension study
[NASA-TP-2284] 10 p1428 N85-19003
On the quadratic mean radius of a polynomial in Cz
[AD-A149189] 10 p1546 N85-19751

CENTER OF MASS
Spurious center of mass effects in a dynamically determined basis
[CSIR-TWISK-310] 01 p0109 N85-10732
Comment on the validity of an L2 treatment of the center of mass problem
[CSIR-TWISK-324] 01 p0114 N85-10779
Nonlinear oscillations of 2 body system relative to center of mass in elliptical orbit 02 p0159 N85-11082
Motion of symmetrical satellite with flexible viscoelastic rods about center of mass in circular orbit
13 p1979 N85-22420
Rotational motion of a satellite
13 p1981 N85-22428
Evaluating accuracy in determining position of Earth's center of mass and elements of orientation of geodetic coordinate system 13 p1983 N85-22441
Periodic movements of axisymmetrical satellite about center of mass due to gravitational moment
13 p2042 N85-22783
Stability of periodic satellite motions relative to center of mass in circular orbit 16 p2718 N85-26780
Satellite physical and orbital characteristics
16 p2804 N85-27287
Physics of (very) high energy e(+)-e(-) colliders
[DE85-008177] 17 p3036 N85-28780

CENTIMETER WAVES
An Earth-based attempt to detect Saturn Electrostatic Discharge (SED) at 21 centimeters
15 p2674 N85-26501

CENTRAL AMERICA
Climate Conference for Latin America and the Caribbean
[WMO-632] 07 p1000 N85-16352
Review of climate problems in Latin America and the Caribbean 07 p1001 N85-16354
The climate in food production in Latin America
07 p1001 N85-16359
Requirements for training in climate-related subjects
07 p1004 N85-16378
Education and training for the climate related activities in Latin America and the Caribbean
07 p1004 N85-16379

CENTRAL ATLANTIC REGION (US)
East coast snowstorm survey
15 p2598 N85-26013
Model sensitivity studies of major east coast storms
15 p2598 N85-26016
Justification and plan for participation in GALE
15 p2599 N85-26017

CENTRAL EUROPE
Specific phenomena associated with the propagation of seismic waves in central Europe
[REPT-548] 03 p0375 N85-12391
Information relative to cartography and geodesy. Series 2: Translations, Number 42, Volume 2 — maps
[ISSN-0469-4244] 18 p3123 N85-29337
Two satellite image maps of Central Europe
18 p3123 N85-29339

CENTRAL NERVOUS SYSTEM
NT BRAIN
NT BRAIN STEM
NT CEREBELLUM
NT CEREBRAL CORTEX
NT CEREBRAL VENTRICLES
NT CEREBRUM
NT SPINAL CORD
NT SPINE
NT THALAMUS
Nicholet MED-80 (trademark) programs in the Naval Biodynamics Laboratory evoked potential series
[AD-A147105] 07 p1018 N85-16451
Encephalographic correlates of autogenous change in human functional state 08 p1193 N85-17518
Work capacity of heat and electric power plant operations working 12 hour day and night shifts
09 p1362 N85-18567
NMR imaging and spectroscopy of the mammalian central nervous system after heavy ion radiation
[DE85-004509] 14 p2386 N85-24696
Cell death, neuronal plasticity and functional loading in the development of the central nervous system
15 p2612 N85-26096
Circadian rhythm control: Neurophysiological investigations 15 p2612 N85-26099
Does a 50-cycle alternating field have central nervous effects?
[BLL-CE-TRANS-8083-(9022.09)]
16 p2839 N85-27507
Effect of triphthasine and elenium on changes in evoked bioelectrical activity of the brain exposed to stationary magnetic field 19 p3325 N85-30601

CENTRAL PROCESSING UNITS
NT ARITHMETIC AND LOGIC UNITS
Clutter generator for use in radar evaluation
[AD-D011234] 01 p0039 N85-10245
Solution of contaminant transport equations using an orthogonal-upstream finite element scheme
[DE84-014286] 01 p0070 N85-10463
Concurrency in parallel processing systems
05 p0714 N85-14581
Atmospheric Modeling And Sensor Simulation (AMASS) study
[NASA-CR-171283] 07 p0996 N85-16325
Programmable realtime interface between a block floating point processor and memory
[AD-D011431] 08 p1203 N85-17571
Vector computer memory bank contention
[NASA-CR-177342] 09 p1376 N85-18649
Distributing a distributed problem solving network simulator
[AD-A149065] 10 p1537 N85-19693
Relative performance of micro and mainframe computers
[AD-A149281] 10 p1538 N85-19695
Research using a DISCUS based network emulator
[AD-A141294] 13 p2149 N85-23338
Use of function processors in multiprocessor systems
14 p2400 N85-24796
Space-variant optical systems
[AD-A151032] 14 p2421 N85-24939
Use of vector processors in cartographic raster data processing, with special regard to the AP-120B vector processor 16 p2814 N85-27358
A high-accuracy optical linear algebra processor for finite element applications
[NASA-CR-175894] 17 p3017 N85-28658
Optimize computer throughput using array processors
[AD-A155843] 24 p4135 N85-35628

CENTRIFUGAL CASTING
Mechanical properties and microstructure of centrifugally cast alloy 718
[AD-A147800] 08 p1129 N85-17116

CENTRIFUGAL COMPRESSORS
Flow in Centrifugal Compressors — conferences
[VKI-LS-1984-07] 05 p0636 N85-14079
Experimental observation of the flow in impellers and diffusers — centrifugal compressors
05 p0636 N85-14080
Answering thermodynamic questions with three-dimensional viscous flow calculations
05 p0636 N85-14081
Design and off-design performance prediction of high pressure ratio centrifugal compressors
05 p0636 N85-14082
Pressure loss due to the tip clearance of impeller blades in centrifugal and axial blowers
05 p0636 N85-14083
Vaneless diffusers — flow in centrigal compressors
05 p0637 N85-14084
Vaned diffusers — in centrifugal compressors
05 p0637 N85-14085
Low solidity cascade diffusers for wide flow range centrifugal blowers 05 p0637 N85-14086
Surge and stall in centrifugal compressors
05 p0637 N85-14087
Subsynchronous vibrations in a high pressure centrifugal compressor: A case history 05 p0642 N85-14118
Experiences with nonsynchronous forced vibration in centrifugal compressors 05 p0642 N85-14119
Experimental on-stream elimination of resonant whirl in a large centrifugal compressor 05 p0642 N85-14121
Internal hysteresis experienced on a high pressure syn gas compressor 05 p0642 N85-14122
Lateral fluid forces acting on a whirling centrifugal impeller in vaneless and vaned diffuser
05 p0643 N85-14123
Hydraulic forces on a centrifugal impeller undergoing synchronous whirl 05 p0643 N85-14124
Experimental investigation of the oscillation behaviour of a liquid-filled rotor with centrifugal motion
[BLL-DOUNREAY-TR-836-(9091.9F)]
08 p1160 N85-17317
Open-cycle centrifugal vapor-compression heat pump
[PB85-113405/GAR] 09 p1328 N85-18348
Failure analysis of fractured capscrews in centrifuga coolant compressor
[DE85-010029] 18 p3267 N85-3008
R and D activities of the Propulsion Division
20 p3539 N85-320
A 3-D Euler method for internal transonic flow computation with a multi-domain approach
21 p3587 N85-322

CENTRIFUGAL FORCE
Two-dimensional unsteady analysis of fluid forces on a whirling centrifugal impeller in a volute
05 p0643 N85-141
Centrifugally driven magnetohydrodynamic (MHD) wind and the nonthermal emission regions in Active Galactic Nuclei (AGN) 08 p1242 N85-178
Aerodynamic forces developing in channels between vanes in turbine drive wheels 16 p2765 N85-270
Modifications to SOLA-VOF for flow dynamics in spinning cylinders
[AD-A154093] 19 p3265 N85-302
Drying of pulverized material with heated condensable vapor
[DE85-011656] 22 p3783 N85-334

CENTRIFUGAL PUMPS
A study on dynamic characteristics of liquid oxygen pumps for rocket engines
[NAL-TR-808] 03 p0324 N85-120
Analysis and testing for rotordynamic coefficients of turbulent annular seals with different, directionally homogeneous surface-roughness treatment for rotor and stator elements 05 p0644 N85-1413
Influence of stationary components on unsteady flow in industrial centrifugal compressors
05 p0645 N85-141
Effect of apparent fluid masses on natural vibration frequencies of impellers of multistage centrifugal pumps
14 p2277 N85-2410
Two-phase flow in centrifugal pumps
[BLL-CE-TRANS-8065-(9022.09)]
15 p2605 N85-260
Design and operation of solar thermal heat transfer systems
[DE85-009837] 19 p3267 N85-302

CENTRIFUGES
NT HUMAN CENTRIFUGES
Investigations into the improvement of processing of Bolivian tin ores
[BMFT-FB-T-84-184] 07 p0917 N85-1580
Unsymmetrical flow in a centrifuge
[DE85-009021] 18 p3103 N85-292
Method for controlling the viscosity of siloxane oils
[DE85-011586] 23 p3909 N85-3422
Matched filtering of visual evoked potentials to detect acceleration (+Gz) induced blackout
[AD-A155812] 24 p4131 N85-358
Simulation of high +Gz onset in the dynamic environment simulator
[AD-A155863] 24 p4131 N85-358

CENTRIFUGING
China report: Science and technology
[JPRS-CST-84-003] 04 p0491 N85-1313
Magnetohydrodynamic flow of two-component ga analyzed 04 p0491 N85-1313
Solution of the h-equation for a single point sourc excitation of magnitude K
[DE84-017574] 09 p1374 N85-186
Centrifuge tests to provide closure bounds for switche subjected to random vibration
[DE85-002003] 10 p1482 N85-193
Comparison of shock-induced displacements wi displacements produced by a centrifuge accelerati
[DE85-000467] 12 p1852 N85-216
Measurement of uranium enrichment for gaseou uranium at low pressure
[DE85-012697] 24 p4150 N85-357

CENTRIFUGING STRESS
Hydrodynamic impeller stiffness, damping, and iner in the rotordynamics of centrifugal flow pumps
05 p0643 N85-141
Centrifuge impact cratering experiments
13 p2181 N85-235
Positive Gz accelerations tolerance of individuals 41 58 years of age 19 p3323 N85-305

CENTRIPETAL FORCE
Hydraulic forces on a centrifugal impeller undergoi synchronous whirl 05 p0643 N85-141

CENTROIDS
Quantitative non-destructive evaluation of damage composite materials using transmitted and reflect ultrasound
[NASA-CR-175550] 12 p1796 N85-212

CEPHEID VARIABLES
Simultaneous photometry and radial velocities of dw cepheids and Delta Scuti stars
01 p0128 N85-10

Thermal effects in stellar pulsations
02 p0297 N85-11925
Mg 2 emission of Pop. 2 long-period Cepheids
11 p1754 N85-21032
Blue companions of Cepheids
11 p1754 N85-21033
Ultraviolet observations of Population 2 Cepheids
11 p1754 N85-21034
Ultraviolet analysis of the peculiar F supergiant HD 112374 11 p1754 N85-21035
The color excesses of classical cepheids and the structure of our galaxy 13 p2169 N85-23459
The Feinheit method: A phase-independent formulation of the period-luminosity relation for Cephids
[NASA-CR-175708] 14 p2440 N85-25056
CEPSTRAL ANALYSIS
Classification methods for Italian vowels --- speech recognition
[FUB-61-1982] 01 p0039 N85-10248
Autoregressive modeling and the classification of land clutter --- radar signatures
[ENST-C-84003] 03 p0356 N85-12292
Radar measurement of thickness of drifting ocean ice employing cepstral signal processing
15 p2644 N85-26313
A classification vocoder: A very low rate speech transmission by vector quantization of the spectrum
[ENST-84D003] 20 p3441 N85-31356
CERAMAL PROTECTIVE COATINGS
U CERMETS
U PROTECTIVE COATINGS
CERAMALS
U CERMETS
CERAMIC BONDING
Ceramic/ceramic seals by microwave heating
[DE84-007486] 04 p0479 N85-13050
BN coating of ceramic fibers for ceramic fiber composites
[AD-D011700] 19 p3249 N85-30145
CERAMIC COATINGS
FRG ceramic engine components (PET)
08 p1141 N85-17193
An investigation of enhanced capability thermal barrier coating systems for diesel engine components
[NASA-CR-174820] 09 p1298 N85-18154
Improved ceramic anodes for corrosion protection
[AD-A149492] 10 p1452 N85-19149
Thermal barrier coating system
[NASA-CASE-LEW-13324-2] 12 p1796 N85-21266
Tribological properties of boron nitride synthesized by ion beam deposition
[NASA-TM-86962] 12 p1810 N85-21355
Metallic and metalloceramic coating by thermal decomposition
[NASA-TM-86992] 13 p2036 N85-22755
Rocket thrust chamber thermal barrier coatings
16 p2734 N85-26867
Simultaneous chemical vapor deposition of SiC-dispersed phase composites
[DE85-007751] 16 p2744 N85-26931
Method for preparing Pb-(beta)-aluminum ceramic
[DE85-011665] 22 p3752 N85-33256
CERAMIC FIBERS
BN coating of ceramic fibers for ceramic fiber composites
[AD-D011700] 19 p3249 N85-30145
CERAMIC MATRIX COMPOSITES
Factors influencing the ball milling of Si3N4 in water
[NASA-TM-86932] 10 p1450 N85-19136
Fabrication of fiber-reinforced ceramic composites by chemical vapor infiltration
[DE85-003609] 11 p1611 N85-20132
Technological and economic assessment of advanced ceramic materials. Volume 3: A case study of ceramic capacitors
[PB85-113106] 11 p1613 N85-20141
Film and interstitial formation of metals in plasma-sprayed ceramics
[NASA-TM-86993] 13 p2036 N85-22756
Evaluation methods of ceramic fiber reinforced metal matrix composite 23 p3907 N85-34206
CERAMIC NUCLEAR FUELS
Inquiry into disintegration control of irradiated low enrichment uranium for high temperature gas cooled reactors
[OEFZS-7281] 07 p1042 N85-16615
Technological apparatus for laser treatment of materials 17 p2944 N85-28174
CERAMICS
NT CERAMIC NUCLEAR FUELS
Silicon nitride sintered body
[NASA-TM-77602] 01 p0021 N85-10131
Silicon nitride powder
[NASA-TM-77731] 01 p0022 N85-10132
Synthesis and characterization of advanced materials
[PB84-215326] 01 p0025 N85-10156
Powder containing 2H-type silicon carbide produced by reacting silicon dioxide and carbon powder in nitrogen atmosphere in the presence of aluminum
[NASA-TM-77597] 01 p0027 N85-10167
Ceramic microstructure and adhesion
[NASA-TM-83804] 01 p0031 N85-10186
Processing ceramics
[NASA-TM-77603] 01 p0031 N85-10188
Fabrication and characterization of Si3N4 ceramics without additives by high pressure hot pressing
[NASA-TM-77724] 01 p0031 N85-10189
Sealing ceramic material in low melting point glass
[NASA-TM-77599] 01 p0031 N85-10190
Milling of Si3N4 with Si3N4 hardware
[NASA-TM-86864] 01 p0031 N85-10191
Selecting the proper ceramic material for a regenerator experiencing large temperature gradients
[AD-A144796] 01 p0032 N85-10199
Fundamental studies of structure property relationship in transformation toughened ceramics
[DE84-015344] 01 p0033 N85-10204
Silicon carbide ceramic production
[NASA-TM-77596] 01 p0035 N85-10220
Single-drop impact damage prediction for low density, coated ceramic materials — rain erosion
01 p0061 N85-10402
Surface protection overview 02 p0144 N85-10978
Energy efficient engine high pressure turbine ceramic shroud support technology report
[NASA-CR-168036] 02 p0147 N85-10996
Inorganic composites for space applications
02 p0155 N85-11047
International Conference on Recent Developments in Specialty Steels and Hard Materials. Conference abstracts
[CSIR-S-256] 02 p0176 N85-11177
Microstructural design and control of sintered hard materials 02 p0176 N85-11180
Some reflections on the competition among different hard materials in industrial applications
02 p0177 N85-11192
The current status of diamond and cubic boron nitride composites 02 p0178 N85-11194
Non-oxide ceramics: A new class of engineering materials 02 p0179 N85-11199
The constitution as the basis for recent and future developments of wear resistant materials
02 p0179 N85-11205
Ceramic materials for MHD electrodes
[DE84-015580] 02 p0187 N85-11250
ONR (Office of Naval Research) Far east Scientific Bulletin, Volume 9, Number 2, April - June 1984
[AD-A145681] 02 p0305 N85-11974
High performance fibers for structurally reliable metal and ceramic composites — advanced gas turbine engine materials
[NASA-TM-86878] 03 p0325 N85-12095
Microstructure and properties of ceramics
[NASA-TM-77416] 03 p0335 N85-12155
Brittleness of ceramics
[NASA-TM-77504] 03 p0335 N85-12156
Microstructure of ceramics fabricated by unidirectional solidification
[NASA-TM-77423] 03 p0336 N85-12157
Ceramic powder for sintering materials
[NASA-TM-77434] 03 p0336 N85-12160
The colloidal chemistry of ceramic clays
[NASA-TM-77734] 03 p0336 N85-12163
Ceramic microstructure development
[AD-A145753] 03 p0337 N85-12166
Time-temperature dependence of the strength of commercial zirconia ceramics
[AD-A146233] 03 p0338 N85-12173
New coatings for high temperature materials protection
[AERE-R-11367] 03 p0339 N85-12180
Center for dielectric studies
[AD-A146183] 03 p0434 N85-12761
Structural changes during milling of aluminum oxide powders
[NASA-TM-77486] 04 p0472 N85-13008
Reactive sintering of SiC 04 p0473 N85-13010
Zeta potential in ceramic industry
[NASA-TM-77478] 04 p0478 N85-13047
Study of the pore structure of ceramics prepared by the slip casting method
[NASA-TM-77495] 04 p0478 N85-13048
Materials for high-temperature fuel cells
[DE84-016316] 04 p0479 N85-13054
Ceramic technology for advanced heat engines program plan
[DE84-013567] 04 p0479 N85-13055
High temperature mechanical properties of ceramics
[DE84-016492] 04 p0480 N85-13056
A study of the Armstrong Whitworth swing beam engine for automotive application 04 p0508 N85-13239
Long term technology development program
04 p0508 N85-13244
Imaging of surfaces and defects of crystals
[DE84-016449] 04 p0570 N85-13632
Controlled directionally solidified precision casting for superalloys and steels
[BMFT-FB-T-84-198] 05 p0619 N85-13960
High temperature corrosion of ceramics
[DE84-017084] 05 p0620 N85-13967
Fundamental tribological properties of ceramics
[NASA-TM-86915] 07 p0930 N85-15893
Oxidation resistence of silicon ceramics
[NASA-TM-77429] 07 p0931 N85-15898
Moisture absorbing anti-arcing coating and method for applying same
[AD-D011310] 07 p0932 N85-15904
Dispersed metal-toughened ceramics and ceramic brazing
[NASA-CR-174284] 07 p0933 N85-15916
Transformation toughened ceramics for the heavy duty diesel engine technology program
[NASA-CR-174669] 07 p1055 N85-16698
Ceramic fabricatinn process before firing-surface treatment of ceramic powder
[NASA-TM-77437] 08 p1131 N85-17129
Application of computer methods for calculation of multicomponent phase diagrams of high temperature structural ceramics
[AD-A148138] 08 p1133 N85-17140
Experimental and analytical study of ceramic-coated turbine-tip shroud seals for small turbine engines
[NASA-TM-86881] 09 p1281 N85-18057
Development of high temperature ceramic parts for vehicular gas turbines
[PNR-90245] 09 p1282 N85-18062
Fabrication of SiC whiskers and composites
[DE85-002038] 09 p1289 N85-18091
Fabrication of ceramic-ceramic composites by chemical vapor deposition
[DE85-000981] 09 p1298 N85-18155
Mechanisms of elevated temperature rupture in single phase ceramics
[DE85-000697] 09 p1299 N85-18156
High-technology ceramics in Japan
[TI85-900389] 09 p1299 N85-18157
Corrosion of ceramics in heat exchanger applications
[DE84-017459] 09 p1299 N85-18161
Study of charge transport in the thermoelectret state of some ceramics and glasses
[DE85-001763] 09 p1300 N85-18163
Ceramic fabric material testing
[DE84-012014] 09 p1300 N85-18165
West Europe report: Science and technology
[JPRS-WST-85-003] 09 p1309 N85-18224
Advanced latent heat storage media for high-temperature industrial applications
[DE85-000907] 09 p1345 N85-18461
Formation of amorphous layers in Al2O3 by ion implantation
[DE85-001289] 09 p1397 N85-18794
Advanced Gas Turbine (AGT) powertrain system development for automotive applications
[NASA-CR-174809] 09 p1403 N85-18831
Strength and failure of ceramic-metallic material
10 p1446 N85-19112
Effect of powder characteristics on microstructure and properties in alkoxide prepared PZT ceramics
[AD-A149082] 10 p1451 N85-19141
Densification of submicron YSZ (Yttria-Stabilized Zirconia) powders with alumina and borate additives
[AD-A149520] 10 p1452 N85-19150
Hot rolling of ceramics by the use of self propagating synthesis
[AD-D011486] 10 p1453 N85-19154
Evaluating the variability of ceramics with X-ray fluorescence
[DE85-002026] 10 p1453 N85-19155
Amorphization of ceramics by ion beams
[DE85-000936] 10 p1453 N85-19156
Optical studies of dynamical processes in disordered materials
[DE85-002400] 10 p1453 N85-19158
Reliability studies of ceramic capacitors
[AD-A149126] 10 p1479 N85-19336
Experimental study of ceramic coated tip seals for turbojet engines
[NASA-TM-86939] 10 p1483 N85-19363
Ribbon burner simulation of T-700 turbine shroud for ceramic lined seals research
[NASA-TM-86940] 10 p1483 N85-19364
Metals and Ceramics Division Materials Science Program
[DE85-003795] 11 p1592 N85-20012
Kinetics of reaction of metals and non-metals during diffusion welding 11 p1602 N85-20076

Structure of transient zone in diffusion welding of TsTS-19 piezoceramic with AMg6 alloy
11 p1603 N85-20082
Structural ceramics in transportation: Fuel implications and economic impacts
[DE85-003024] 11 p1611 N85-20130
Laser processing of ceramics
[DE85-001184] 11 p1612 N85-20135
Evaluation of machining damage in brittle materials
[DE85-001794] 11 p1612 N85-20136
High temperature corrosion of ceramics
[DE85-002179] 11 p1612 N85-20139
Technological and economic assessment of advanced ceramic materials. Volume 3: A case study of ceramic capacitors
[PB85-113108] 11 p1613 N85-20141
SEP of France manufactures its first silicon carbide fibers 11 p1618 N85-20184
NDE for heat engine ceramics
[NASA-TM-86949] 11 p1649 N85-20369
Slit-ring test for evaluating fracture in tubular cross sections
[DE85-003550] 11 p1654 N85-20416
Oxidation and hot corrosion of hot-pressed Si3N4 at 1000 deg C
[NASA-TM-86977] 12 p1811 N85-21358
Evaluation of corrosion-erosion behavior of various ceramic materials
[AD-A149756] 12 p1812 N85-21367
Degradation mechanisms in ceramic dielectrics
[AD-A149791] 12 p1813 N85-21369
Multiaxial stress response of ceramics
[DE85-004350] 12 p1814 N85-21379
Technological and economic assessment of advanced ceramic materials. Volume 1: Summary and conclusions
[PB85-113082] 12 p1815 N85-21383
Technological and economic assessment of advanced ceramic materials. Volume 2: A case study of ceramics in heat engine applications
[PB85-113090] 12 p1815 N85-21384
Technological and economic assessment of advanced ceramic materials: Volume 4: A case study of integrated optic devices
[PB85-113116] 12 p1815 N85-21385
Technological and economic assessment of advanced ceramic materials. Volume 5: A case study of ceramic toxic and combustible gas sensors
[PB85-113124] 12 p1815 N85-21386
Technological and economic assessment of advanced ceramic materials. Volume 6: A case study of ceramic cutting tools
[PB85-113132] 12 p1815 N85-21387
High-technology ceramics in Japan
[PB85-125029] 12 p1815 N85-21389
Slip casting and nitridation of silicon powder
[NASA-TM-77809] 12 p1818 N85-21406
Silicon carbide-silicon nitride fibers: Preparation and characterization of polycarbosilazane precursors
12 p1945 N85-22214
Thermodynamics of copper-nickel alloys containing aluminum, silicon, titanium, and chromium relative to their use in ceramic brazing
[DE85-004767] 13 p2023 N85-22674
Densification and deformation in the presence of a liquid phase
[DE85-005101] 13 p2038 N85-22763
NDE methods for green ceramics
[DE85-004019] 13 p2038 N85-22766
Cathode materials for molten carbonate fuel cells
[DE85-004078] 13 p2130 N85-23254
Fabrication of ceramic substrate-reinforced and free forms
[NASA-TM-86894] 14 p2247 N85-23926
Exploratory corrosion tests on materials and fluids for advanced high-temperature molten-salt storage
[DE85-002911] 14 p2258 N85-23991
A novel polymeric organosilazane precursor to Si3N4/SiC ceramics
[AD-A150748] 14 p2260 N85-24003
Effect of elevated-temperature neutron irradiation on fracture toughness of ceramics
[DE85-000652] 14 p2261 N85-24010
Correlation of uniaxial and biaxial fracture strengths of ceramics
[DE85-003779] 14 p2261 N85-24011
Pressure-density behavior for AlN, Al2O3, SiO2, TiB2, and TiC powders up to 3.5 GPa
[DE85-006146] 14 p2261 N85-24012
Dynamic shock studies of PZT 95/5 ferroelectric ceramic
[DE85-006137] 14 p2261 N85-24015
Solid state compressor
[AD-A150790] 14 p2311 N85-24302
Special purpose materials for fusion application
[DE85-005346] 14 p2424 N85-24950
Structure and properties of ion-implanted Al sub 2 O sub 3
[DE85-005374] 14 p2430 N85-24987
USSR report: Materials science and metallurgy
[JPRS-UMS-85-001] 15 p2496 N85-25396
Transformation toughened ceramics: A potential material for light diesel engine applications
[AD-A151413] 15 p2518 N85-25525
Transformation toughened ceramics: A potential material for light diesel engine application
[AD-A151421] 15 p2518 N85-25526
Mechanical aspects of interfaces and surfaces in ceramic containing systems
[AD-A151978] 15 p2519 N85-25530
Interfacial and colloidal aspects of aqueous suspension containing oxidic powders
[DE85-005972] 15 p2519 N85-25534
Fabrication of fiber reinforced ceramic composites by chemical vapor infiltration
[DE85-007565] 15 p2520 N85-25536
France develops own aluminum-based composite ceramic 15 p2534 N85-25636
Fiat conducts R and D in ceramic parts for diesel engine 15 p2534 N85-25637
West Europe report: Science and technology
[JPRS-WST-84-010] 15 p2535 N85-25644
Sweden invents new ceramic for more durable cutting tools 15 p2536 N85-25645
Abrasive cutting-off wheel 15 p2568 N85-25843
Nondestructive tests of ceramic components for aircraft turbines 16 p2709 N85-26718
Ceramics for advanced O2/H2 application
16 p2734 N85-26868
Simultaneous chemical vapor deposition of SiC-dispersed phase composites
[DE85-007751] 16 p2744 N85-26931
Material for protection of metal surfaces against corrosion by molten salts
[DE85-007714] 16 p2750 N85-26968
Effects of wear on structure-sensitive magnetic properties of ceramic ferrite in contact with magnetic tape
[NASA-TM-87007] 16 p2753 N85-26991
Breakway friction and dynamic friction/wear measurements of various ceramic materials from 25 C (75 F) to 650 C (1200 F)
[NASA-CR-174803] 16 p2754 N85-26994
Ceramic technology for advanced heat engines project
[DE85-004788] 16 p2755 N85-27002
Screening ceramic materials for intense radiant heat applications
[DE85-006989] 16 p2756 N85-27006
Development of a new faster process for the fabrication of ceramic fiber-reinforced ceramic composites by chemical vapor infiltration
[DE85-007550] 16 p2756 N85-27007
Sintering and properties of metal-ceramic alloys of the Kovar type
[BLL-BISI-TRANS-21822-(9022.06)]
17 p2927 N85-28060
Preparation of silicon carbide-silicon nitride fibers by the pyrolysis of polycarbosilazane precursors
[NASA-TM-86505] 17 p2933 N85-28107
Ceramic applications in turbine engines
[NASA-CR-174715] 17 p2934 N85-28109
Characterization of the fatigue and slow crack growth behavior of partially stabilized zirconia ceramics
[DE85-006240] 17 p2934 N85-28113
Indirect brazing of structural ceramics for uncooled diesels
[DE85-005569] 17 p2935 N85-28116
Microstructure-mechanical property relationships in transformation-toughened ceramics
[DE85-009722] 17 p2935 N85-28117
Ac field-induced order in dense colloidal systems
[DE85-009107] 17 p2935 N85-28119
Investigation of charge transport in the thermoelectret state of some ceramics and glasses
[DE85-009318] 17 p2936 N85-28122
Development of high temperature resistant, noncorrosible, non-metallic ceramic materials, especially silicon nitride in gas turbine application
[BMFT-FB-T-85-015] 17 p2936 N85-28125
Ceramic turbochargers: A case study of a near-term application of high-strength ceramics
[DE85-006495] 17 p2975 N85-28379
Future of ceramic turbochargers: Promises and pitfalls
[DE85-006209] 17 p2975 N85-28380
High temperature composite thermal storage systems
[DE85-005073] 17 p2986 N85-28455
Ceramic Technology for Advanced Heat Engines Project
[DE85-008755] 18 p3080 N85-29052
Ceramic coatings for heat engine materials: Status and future needs
[DE85-008759] 18 p3080 N85-2905
Ceramic coatings for heat engine materials
[DE85-005238] 18 p3080 N85-29054
Predicting microfracture in ceramics via a microcontact model
[DE85-005654] 18 p3081 N85-2908
Synthesis chemistry of ceramics by solid-state combustion processes in micro-gravity
[DE85-009595] 18 p3081 N85-29081
Conservation and substitution technology for critical metals in bearings and related components for industrial equipment and opportunities for improved bearing performance
[PB85-178246] 18 p3082 N85-2908
West Europe report: Science and technology
[JPRS-WST-84-031] 18 p3086 N85-2908
British breakthrough in lightweight lithium batteries
18 p3086 N85-2909
Use of ceramics in internal combustion engines
18 p3088 N85-29114
Burner rig corrosion of SiC at 1000 deg C
[NASA-TM-87061] 19 p3227 N85-30011
USSR report: Materials Science and Metallurgy
[JPRS-UMS-85-005] 19 p3241 N85-3008
Diffusion welding of aluminum with vacuum-tight corundum ceramic 19 p3247 N85-30130
The mechanics of internal stress and microcrack toughening mechanisms in ceramics
[AD-A154049] 19 p3248 N85-30139
BN coating of ceramic fibers for ceramic fiber composites
[AD-D011700] 19 p3249 N85-30145
Study of solute segregation at interfaces using Auger electron spectroscopy
[DE85-005709] 20 p3423 N85-31247
Prediction of lifetime for ceramic materials in the elastic and viscoelastic region by fracture mechanical methods
[ESA-TT-825] 20 p3434 N85-31305
West Europe report: Science and technology
[JPRS-WST-85-020] 20 p3438 N85-31333
Estimation of power-law creep parameters from bend test data
[PB85-183408] 20 p3472 N85-31579
Controlled indentation flaws for the construction of toughness and fatigue master maps
[PB85-179067] 20 p3473 N85-31582
Development of processes for the inclusion of radioactive waste in glass-metal compounds and ceramic materials
[BLL-CE-TRANS-8014-(9022.09)]
20 p3526 N85-31801
The shearing contribution in transformation toughening of brittle materials
[AD-A154656] 21 p3568 N85-32185
Matrix fracture in fiber-reinforced ceramics
[AD-A154704] 21 p3569 N85-32197
Stress corrosion of ceramic materials
[AD-A155020] 21 p3570 N85-32202
Sintering studies project
[AD-A154750] 21 p3572 N85-32218
Capacitive energy storage at cryogenic temperatures
[AD-A154508] 21 p3579 N85-32253
Tape casting as an approach to an all-ceramic turbine shroud seal
[NASA-TM-87078] 21 p3596 N85-32333
Friction and wear of solid-lubricated contact in gas turbine engine bearings
[AD-A155042] 21 p3596 N85-32335
Reliability of void detection in structural ceramics using scanning laser acoustic microscopy
[NASA-TM-87035] 21 p3597 N85-32337
System for electro-optical ceramic recrystallization
21 p3682 N85-32872
Tensile fatigue of glass fibers and composites with conventional and surface compressed fibers
[RR-84-4] 22 p3742 N85-33196
Research study for gel precursors as glass and ceramic starting materials for space processing applications research
[NASA-CR-176113] 22 p3751 N85-33250
Dispersion toughened ceramic composites and method for making same
[DE85-011601] 22 p3751 N85-33252
Sodium nitrate containing mixture for producing ceramic-glass-ceramic seal by microwave heating
[DE85-011610] 22 p3751 N85-33254
Improved process for the preparation of fiber-reinforced ceramic composites by chemical vapor deposition
[DE85-011584] 22 p3752 N85-33255
Microstructure-mechanical property relationships in the transformation-toughened ceramics
[DE85-011946] 22 p3752 N85-3326

Process and device for forming imprints on ceramic tubes
[DE85-013137] 22 p3753 N85-33264
Integrated current collector and catalyst support
[DE85-011616] 22 p3761 N85-33311
Woven heat exchanger
[DE85-011633] 22 p3783 N85-33439
Latch assembly
[DE85-011660] 22 p3792 N85-33492
Technology of off-gas treatment for liquid-fed ceramic melters
[DE85-012467] 22 p3812 N85-33610
Thermal protection systems for reentry vehicles
[CNES-NT-113] 23 p3900 N85-34157
X-ray residual stress analysis on the coarse grain of copper and its application to the brazed copper
23 p3907 N85-34202
High resolution electron microscopic characterization of interfaces in ceramics
[DE85-011207] 23 p3920 N85-34289
High temperature structural insulating material
[DE85-006361] 23 p3920 N85-34291
Synthesis of ultrafine ceramic and metallic powders in a thermal argon rf plasma
[DE85-009634] 23 p3983 N85-34696
Method for measuring surface activity of silicon nitride powder
[NASA-TM-77906] 24 p4073 N85-35242
Noise in silver beta alumina ceramics
[AD-A156135] 24 p4082 N85-35297
Method of preparing thin porous sheets of ceramic material
[DE85-006399] 24 p4082 N85-35300
High temperature corrosion of ceramics
[DE85-013481] 24 p4083 N85-35303
Noise in sodium beta alumina crystals
[AD-A156025] 24 p4161 N85-35798

CEREBELLUM

Visual evoked potentials with disrupted functioning of nonspecific cerebral systems 07 p1013 N85-16437
Specifics of dynamics of brain biopotentials under the influence of complex audible communicative signals
07 p1014 N85-16440
Neurophysiological correlates of motion sickness: Role of vestibulocerebellum and 'vomiting center' reanalyzed
11 p1693 N85-20643
Sensory and motor properties of the cerebellar uvula and modulus 15 p2613 N85-26104

CEREBRAL CORTEX

Visually evoked responses from non-occipital areas of the human cortex
[AD-A146079] 03 p0400 N85-12553
Evidence for multiple areas in the human auditory cortex
[AD-A146086] 03 p0401 N85-12555
Visual selective attention
[AD-A146220] 03 p0401 N85-12558
Electrophysiological correlates of Vernier acuity in human visual cortex
[AD-A146533] 06 p0846 N85-15371
Encephalographic correlates of autogenous change in human functional state 08 p1193 N85-17518
Topography of human brain electric potentials and dominance 11 p1691 N85-20633
Functional significance of some EEG parameters and dominant principle 11 p1691 N85-20634
A communications link for an implantable electrode array
[AD-A152238] 16 p2840 N85-27510
A multipole model of the observed cerebral cortex magnetic field
[AD-A152237] 16 p2842 N85-27526
Encapsulation and packaging of a semiconductor multielectrode array for cortical implantation
[AD-A153180] 17 p2998 N85-28535
Effect of triphthasine and elenium on changes in evoked bioelectrical activity of the brain exposed to stationary magnetic field 19 p3325 N85-30601
Changes in the impedance and bioelectrical activity of the cerebral cortex of rats under the action of anaesthetic drugs
[HSE-TRANS-10371] 19 p3327 N85-30617
Discovery regarding visual neuron adaptation applicable to robot use 20 p3504 N85-31786

CEREBRAL VENTRICLES

Reaction of cerebral ventricles to antiorthostatic position and occlusion of jugular veins 01 p0093 N85-10626

CEREBROSPINAL FLUID

Reaction of cerebral ventricles to antiorthostatic position and occlusion of jugular veins 01 p0093 N85-10626

CEREBRUM

Reaction of cerebral ventricles to antiorthostatic position and occlusion of jugular veins 01 p0093 N85-10626
Pathogenesis and treatment of cerebral air embolism and associated disorders
[AD-A146723] 07 p1014 N85-16443
Simultaneous determination of cerebral blood flow and partition coefficient with a freely diffusable tracer
[DE85-001226] 11 p1690 N85-20625
Resource allocation in cerebral specialization of function: Behavioral and electrophysiological studies
[AD-A155092] 21 p3664 N85-32759
Cerebral hemodynamics and ventricular function in -15 deg antiorthostatic position 22 p3822 N85-33676

CERENKOV COUNTERS

Monte Carlo simulation of gas Cerenkov detectors
[DE85-002422] 10 p1488 N85-19394
Electrons and cosmic ray produced protons in Saturn's inner magnetosphere
[NASA-TM-87469] 15 p2579 N85-26546
A Cerenkov-delta E-Cerenkov detector for high energy cosmic ray isotopes and an accelerator study of Ar-40 and Fe-56 fragmentation
[NASA-CR-176026] 20 p3549 N85-32086
Very high energy gamma rays from the Crab Nebula
[OG-2.3-3] 22 p3866 N85-33940
Search for gamma-rays above 400 GeV from Geminga
[OG-2.4-4] 22 p3867 N85-33951
Energy spectra of elements with 18 or = Z or = 28 between 10 and 300 GeV/amu
[OG-4.1-8] 22 p3876 N85-34014
Results of a search for deuterium at 25-50 GC/c using a magnetic spectrometer
[OG-4.2-4] 22 p3876 N85-34024
EAS spectrum in the primary energy region above 10 to the 15th power eV by the Akeno and Yakutsk array data
[OG-5.1-16] 22 p3882 N85-34057
EAS Cerenkov measurements of the composition of the cosmic ray flux around 10 to the 16th power eV
[OG-5.2-11] 22 p3884 N85-34067
High resolution Cherenkov detectors for cosmic ray isotope experiment
[OG-9.1-4] 23 p4023 N85-34930
Cerenkov counters for high energy nuclei: Some new developments
[OG-9.1-5] 23 p4023 N85-34931
A high resolution gas Cerenkov detector for the superconducting magnet facility
[OG-9.1-6] 23 p4023 N85-34932
Bevalac calibration of the SOFIE range and hodoscope detectors
[OG-9.1-7] 23 p4023 N85-34933
The development of a high energy cosmic ray detector for Spacelab-2
[OG-9.1-8] 23 p4023 N85-34934
Mass resolution optimization in a large isotopic composition experiment
[OG-9.1-9] 23 p4023 N85-34935
Cherenkov-dE/dx-range measurements on cosmic ray iron group nuclei
[OG-9.1-12] 23 p4024 N85-34937
Application of imaging to the atmospheric Cherenkov technique
[OG-9.5-4] 23 p4030 N85-34981
A method to improve observations of gamma-ray sources near 10 (15) eV
[OG-9.5-5] 23 p4030 N85-34982
The response of a scintillation counter below an emulsion chamber to heavy nucleus interactions in the chamber 24 p4175 N85-35889
Study of the energy spectrum of primary cosmic rays: EAS size fluctuations at a fixed primary energy
[HE-4.4-14] 24 p4194 N85-36020
The experimental cascade curves of EAS at E sub 0 10(17) eV obtained by the method of detection of Cherenkov pulse shape
[HE-4.4-18] 24 p4194 N85-36024

CERENKOV EFFECT

U CERENKOV RADIATION

CERENKOV RADIATION

Cerenkov radiation in the neighborhood of the emission threshold, revised
[AD-A145458] 02 p0284 N85-11855
Generation of superpowerful microsecond electromagnetic radiation pulses
03 p0347 N85-12234
Laser-driven particle accelerators
[DE84-015953] 04 p0506 N85-13227
Cerenkov ring imaging detector development at SLAC
[DE84-015883] 04 p0560 N85-13564
Gamma-ray to Cerenkov-light conversion efficiency for pure-silica-core optical fibers
[DE84-015041] 05 p0729 N85-14685
Monte Carlo simulation of gas Cerenkov detectors
[DE85-002422] 10 p1488 N85-19394
Design consideration for the X-ray Cerenkov experiment
[AD-A153636] 18 p3189 N85-29777
Abundances of secondary elements among the ultra heavy cosmic rays: Results from HEAO-3
20 p3543 N85-32047
Lead, platinum, and other heavy elements in the primary cosmic radiation: HEAO-3 results sec wg032961 cb553087 20 p3543 N85-32048
Cerenkov maser and Cerenkov laser devices
[AD-A155443] 21 p3592 N85-32324
Predictive model of electron beam induced flashblindness
[AD-A155260] 21 p3664 N85-32763
Form factor effects on microwave Cerenkov radiation
[AD-A154577] 21 p3701 N85-32993
1000 GeV gamma rays from Cygnus X-3: An update
[OG-2.1-8] 22 p3863 N85-33925
Evidence for long-term variability in the ultra high energy photon flux from Cygnus X-3
[OG-2.1-10] 22 p3863 N85-33926
Pulsed emission of TeV gamma rays from Vela pulsar
22 p3867 N85-33947
Periodic gamma-ray emissions from Geminga at or = 10(12) eV
[OG-2.4-2] 22 p3867 N85-33949
Search for TeV gamma rays from extragalactic sources and the Galactic Center
[OG-2.7-1] 22 p3871 N85-33976
Absolute rigidity spectrum of protons and helium nuclei above 10 GV/c
[OG-4.1-1] 22 p3875 N85-34007
Cosmic ray charge and energy spectrum measurements using a new large area Cerenkov x dE/dx telescope
[OG-4.1-5] 22 p3876 N85-34011
Cosmic ray isotope measurements with a new Cerenkov X total energy telescope
[OG-4.3-4] 22 p3878 N85-34029
Initial results from the Caltech/DRSI balloon-borne isotope experiment
[OG-4.3-8] 22 p3879 N85-34033
Ariel 6 measurements of ultra-heavy cosmic ray fluxes in the region 34 or = Z or = 48
[OG-4.4-3] 22 p3879 N85-34036
Ariel 6 measurements of ultra-heavy cosmic ray fluxes in the region Z or = 48
[OG-4.4-4] 22 p3880 N85-34037
Elemental abundances of cosmic rays with Z 33 as measured on HEAO-3
[OG-4.4-5] 22 p3880 N85-34038
Abundances of secondary elements among the ultra heavy cosmic rays: Results from HEAO-3
[OG-4.4-6] 22 p3880 N85-34039
A new measurement of the cosmic ray energy spectrum between 3 x 10 to the 15th power eV and 3 x 10 to the 16th power eV
[OG-5.1-6] 22 p3881 N85-34048
Fluctuations of development maximum depth and nuclear composition of primary cosmic radiation
[OG-5.1-13] 22 p3882 N85-34054
Estimation of composition of cosmic rays with E sub zero approximately equals 10(17) - 10(18) eV
[OG-5.1-14] 22 p3882 N85-34055
Cosmic ray spectra measurements at the Yakutsk EAS array
[OG-5.1-17] 22 p3882 N85-34058
Observation of cosmic ray positrons from 5 to 25 GeV
[OG-6.2-5] 22 p3889 N85-34104
A high resolution gas Cerenkov detector for the superconducting magnet facility
[OG-9.1-6] 23 p4023 N85-34932
A Cerenkov imaging telescope for high energy gamma rays
[OG-9.3-13] 23 p4029 N85-34968
The University of Durham Mark 3 very high energy gamma ray telescope
[OG-9.4-2] 23 p4029 N85-34969
Cerenkov light images of EAS produced by primary gamma
[OG-9.5-3] 23 p4030 N85-34979
Angular resolution of an EAS array for gamma ray astronomy energies 5 x 10 (13) eV
[OG-9.5-8] 23 p4031 N85-34985
Cerenkov radiation from periodic electron bunches for finite emission length in air
[AD-A156156] 24 p4090 N85-35362
Simulation of EAS properties on the basis of high energy interaction model deduced from the accelerator data
24 p4187 N85-35973
Sensitivity of depth of maximum and absorption depth of EAS to hadron production mechanism
24 p4188 N85-35982
Muon fluctuation studies of EAS 10(17) eV
[HE-4.3-9] 24 p4191 N85-36003
EAS development curve at energy of 10(16) - 10(18) eV measured by optical Cerenkov light
[HE-4.4-7] 24 p4193 N85-36015
On the determination of the depth of EAS development maximum using the lateral distribution of Cerenkov light at distances 150 m from EAS axis
[HE-4.4-13] 24 p4194 N85-36019

Study of the shower maximum depth by the method of detection of the EAS Cerenkov light pulse shape
[HE-4.4-15] 24 p4194 N85-36021
Analysis of Cerenkov pulses recorded simultaneously at two sites
[HE-4.4-16] 24 p4194 N85-36022
Preliminary results of the Cerenkov EAS flashes the Crimean Astrophysical Observatory
[HE-4.4-17] 24 p4194 N85-36023
Lateral-angular and temporal characteristics of EAS optical radiation
[HE-4.4-19] 24 p4194 N85-36025
The hump in the Cerenkov lateral distribution of gamma ray showers
[HE-4.5-9] 24 p4195 N85-36032
A new study on the emission of EM waves from large EAS
[HE-4.6-5] 24 p4197 N85-36042
Radio wave emitted by an extensive air showers in 10KHz to 1MHz region
[HE-4.6-15] 24 p4198 N85-36051
Longitudinal development of muons in large air showers studies from the arrival time distributions measured at 900m above sea level
[HE-4.7-4] 24 p4199 N85-36055
The thickness of the shower disc as observed in showers produced by primaries above 10 (19)eV
[HE-4.7-6] 24 p4199 N85-36057
Measurements of light background at large depth in the ocean
[HE-5.2-6] 24 p4203 N85-36085
Measurement of muon intensity by Cerenkov method
[HE-5.2-15] 24 p4204 N85-36091
A transient digitiser for fast air shower events
[HE-5.2-21] 24 p4204 N85-36097

CERIUM
NT CERIUM 144
Low temperature properties of CeOs2 in the C14 and C15 crystallographic Laves phases
[DE85-003754] 10 p1564 N85-19866
Improvement by cerium and yttrium ion implantation of oxidation behaviour of stabilised stainless steel in carbon dioxide
[AERE-R-11523] 14 p2259 N85-23996
Long range ordered alloys modified by addition of niobium and cerium
[DE85-011661] 20 p3431 N85-31285
Trivalent cerium doped crystals as tunable laser systems: Two bad apples
[DE85-008168] 22 p3790 N85-33462
Enthalpies of formation of liquid Fe-Ce-Si and Fe-Ce-Al three-component alloys
[BLL-M-36296-(5828.4)] 23 p3913 N85-34247

CERIUM COMPOUNDS
NT CERIUM OXIDES
Cerium compounds in the fashion of the light actinides
[DE84-014642] 04 p0475 N85-13024
Supercell band structure calculations of the two peak photo-and inverse photoemission spectra in Ce and Pr compounds
[DE84-017485] 06 p0867 N85-15513
Fermi surface study of CeSb
[DE85-002532] 10 p1564 N85-19862
The UFe4P12 and CeFe4P12: Non-metallic isotopes of superconducting LaFe4P12
[DE85-003724] 12 p1942 N85-22195
Anomalous magnetism of CeRh3B2 under pressure
[DE85-003069] 13 p2164 N85-23425

CERIUM ISOTOPES
NT CERIUM 144

CERIUM OXIDES
Defect interactions at high concentrations in solid oxide electrolytes
[DE85-011824] 22 p3807 N85-33580

CERIUM 144
High altitude sampling program: Radioactivity in the stratosphere
[DE85-005824] 14 p2374 N85-24676

CERMETS
Strength and failure of ceramic-metallic material
10 p1446 N85-19112
Effect of zero-wear in friction pairs operating in abrasive media 13 p2045 N85-22801
Thin film phase transition materials development program
[AD-A154260] 19 p3259 N85-30209

CERTIFICATION
Certification of advanced systems
06 p0753 N85-14829
Orbiter wheel and tire certification
08 p1101 N85-16959
Preliminary design criteria and certification test specifications for blast resistant windows
09 p1337 N85-18405
GPS system field testing 11 p1711 N85-20762
State measurement laboratories: Program description (part 1). Directory (part 2)
[PB85-137661] 11 p1739 N85-20935
Glider Nimbus 3-24.5. Partial certification test results for importation in the U category
[REPT-CEV/IS/SE/AV/84] 14 p2220 N85-23763
Interactive design of specifications for airborne software set (GISELE) 16 p2714 N85-26753
The certification of airborne complex digital systems
16 p2714 N85-26754
Statistical study of the dynamic analysis of the workload in the A310 certification campaign
16 p2844 N85-27531
Certifying complex digital systems on civil aviation aircraft 17 p2904 N85-27907
A systematic determination of skill and simulator requirements for airline transport pilot certification
[AD-A154135] 19 p3330 N85-30830
Standardization of helicopter certification requirements in the western world
[SNIAS-851-210-103] 20 p3393 N85-31046

CESIUM
NT CESIUM ISOTOPES
NT CESIUM 134
NT CESIUM 137
Multiphoton ionization of atomic cesium
[DE85-001286] 09 p1360 N85-18678
Multiphoton ionization of cesium atoms above and below the two-photon ionization threshold
[DE85-000976] 09 p1361 N85-18682
Effects of dc electric fields on multiphoton ionization spectra in cesium
[DE85-001542] 09 p1361 N85-18684
Calorimetric investigation into the possibility of a charge density wave ground state in alkali metals
[DE85-002006] 09 p1397 N85-18795
Historical cost curves for hydrogen masers and cesium beam frequency and timing standards
10 p1465 N85-19245
Frequency and time standards based on stored ions
18 p3105 N85-29223
On the accuracy of Cs beam primary frequency standards 18 p3105 N85-29224
Diode laser 87Rb optical pumping in an evacuated wall-coated cell 18 p3105 N85-29226
On-orbit frequency stability analysis of the GPS NAVSTAR-1 quartz clock and the NAVSTARs-6 and -8 rubidium clocks 18 p3105 N85-29227
The time and frequency comparisons via Loran-C and National TV Network in Yugoslavia
18 p3109 N85-29246
The 1984 environmental monitoring program report for Idaho National Engineering Laboratory site
[DE85-011209] 22 p3812 N85-33611
Infrared generation and wave-mixing studies in cesium
[DE85-012863] 24 p4093 N85-35304

CESIUM ALLOYS
Mossbauer spectrometry: Testing of a new computer based system and its application to a study of an aluminum-iron-cerium alloy
[AD-A151626] 15 p2510 N85-25463

CESIUM COMPOUNDS
NT CESIUM IODIDES

CESIUM HALIDES
NT CESIUM IODIDES

CESIUM IODIDES
Improvements in photodiode readout for small CsI (T1) crystals
[MPI-PAE/EXP-E1-131] 01 p0051 N85-10333
Downstream behavior of volatile fission product species
[DE85-012124] 23 p3971 N85-34617

CESIUM IONS
Intense non-relativistic cesium ion beam
[DE84-012575] 04 p0580 N85-13566
Collision-induced dipole moments
[AD-A147682] 08 p1121 N85-17063

CESIUM ISOTOPES
NT CESIUM 134
NT CESIUM 137
Portable real-time clock
[AD-A146218] 03 p0364 N85-12336

CESIUM 134
Intrusion of radioactive industrially polluted water from North Sea into central Baltic Sea
10 p1498 N85-19454

CESIUM 137
WESF (173)Cs gamma ray sources
[DE85-000676] 11 p1727 N85-20859
High altitude sampling program: Radioactivity in the stratosphere
[DE85-005824] 14 p2374 N85-24676
Environmental surveillance at Los Alamos during 1984
[DE85-011886] 22 p3811 N85-33605
The 1984 environmental monitoring report, Sandia National Laboratories, Albuquerque, New Mexico
[DE85-011175] 22 p3811 N85-33607
Estimation of Sr90 and Cs137 activity introduced and accumulation in the Po basin until 1983
[CISE-2515] 22 p3813 N85-33617

CESSNA AIRCRAFT
NT CESSNA 402B AIRCRAFT

CESSNA MILITARY AIRCRAFT
U MILITARY AIRCRAFT

CESSNA 402B AIRCRAFT
Design of a digital ride quality augmentation system for commuter aircraft
[AD-A148233] 08 p1066 N85-16870

CF-104 AIRCRAFT
U F-104 AIRCRAFT

CFRP
U CARBON FIBER REINFORCED PLASTICS

CH-47 HELICOPTER
A mathematical simulation model of the CH-47B helicopter, volume 1
[NASA-TM-84351-VOL-1] 01 p0006 N85-10033
Noise measurement flight test for Boeing Vertol 234/CH 47-d helicopter: Data/analyses
[AD-A148172] 08 p1218 N85-17670
A modern control design methodology with application to the CH-47 helicopter
[AD-A151946] 16 p2710 N85-26723

CHAFF
An empirical self-protection chaff model
[AD-A151926] 16 p2773 N85-27115

CHAINS
Kinematic synthesis of planar cam-link mechanisms for exact path and exact motion generation
03 p0341 N85-12189
Safing and arming mechanism
[AD-D011261] 05 p0621 N85-13960
Chain dynamics and structure property relation in high impact strength polycarbonate plastic
[AD-A152011] 15 p2519 N85-25531

CHAIRS
U SEATS

CHALCOGENIDES
NT ALKALINE EARTH OXIDES
NT ALUMINUM OXIDES
NT ANHYDRIDES
NT BARIUM OXIDES
NT BARIUM SULFIDES
NT BERYLLIUM OXIDES
NT BISMUTH OXIDES
NT BORON OXIDES
NT CADMIUM SELENIDES
NT CADMIUM SULFIDES
NT CADMIUM TELLURIDES
NT CALCIUM OXIDES
NT CALCIUM SULFIDES
NT CARBON DIOXIDE
NT CARBON DISULFIDE
NT CARBON MONOXIDE
NT CHLORINE OXIDES
NT CHROMITES
NT CHROMIUM OXIDES
NT COBALT OXIDES
NT COPPER OXIDES
NT COPPER SELENIDES
NT COPPER SULFIDES
NT DIOXIDES
NT DISULFIDES
NT ENSTATITE
NT GERMANIUM OXIDES
NT HYDROGEN PEROXIDE
NT HYDROGEN SULFIDE
NT INDIUM TELLURIDES
NT INORGANIC PEROXIDES
NT IRON OXIDES
NT LEAD OXIDES
NT LEAD TELLURIDES
NT LITHIUM OXIDES
NT MAGNESIUM OXIDES
NT MAGNETITE
NT MANGANESE OXIDES
NT MERCURY TELLURIDES
NT METAL OXIDES
NT MOLYBDENUM DISULFIDES
NT MOLYBDENUM OXIDES
NT NICKEL OXIDES
NT NIOBIUM OXIDES
NT NITRIC OXIDE
NT NITROGEN DIOXIDE
NT NITROGEN OXIDES
NT NITROGEN TETROXIDE
NT NITROUS OXIDES
NT ORGANIC PEROXIDES
NT OXIDES
NT PEROXIDES
NT PLUTONIUM OXIDES

NT POLYSULFIDES
NT POTASSIUM OXIDES
NT PYRITES
NT PYROXENES
NT QUARTZ
NT RUTILE
NT SAPPHIRE
NT SELENIDES
NT SILICON DIOXIDE
NT SILICON OXIDES
NT SULFIDES
NT SULFUR DIOXIDES
NT SULFUR OXIDES
NT TIN OXIDES
NT TIN TELLURIDES
NT TITANIUM OXIDES
NT TROILITE
NT VANADIUM OXIDES
NT YTTRIUM OXIDES
NT ZINC OXIDES
NT ZINC SELENIDES
NT ZINC SULFIDES
NT ZIRCONIUM OXIDES
Effect of light pulses on film of chalcogenide vitreous semiconductors 02 p0258 N85-11687
Neutron scattering for the investigation of solid state materials, utilization in chemical structures
03 p0432 N85-12752
High temperature thermoelectric energy conversion
05 p0610 N85-13804
Preliminary studies on the low-cost preparation of chalcogenide semiconductors from solution depositions
[DE85-000538] 11 p1736 N85-20918
Multilayer reflecting systems based on glassy chalcogenides for infrared lasers
14 p2274 N85-24089
CHALLENGER (ORBITER)
National Space Transportation Systems Program mission report
[NASA-TM-87455] 14 p2242 N85-23900
CHAMBERS
Heat exchanger
[DE84-014299] 01 p0047 N85-10309
CHANCE-VOUGHT MILITARY AIRCRAFT
U MILITARY AIRCRAFT
CHANDLER MOTION
U POLAR WANDERING (GEOLOGY)
CHANDRASEKHAR EQUATION
Chandrasekhar equations and computational algorithms for distributed parameter systems
[NASA-CR-172467] 03 p0402 N85-12564
Chandrasekhar equations for infinite dimensional systems
[NASA-CR-172515] 09 p1376 N85-18651
CHANGE DETECTION
An amplitude correlation and differencing method for the monitoring of flaws in repeat ultrasonic inspections
[AERE-R-11416] 15 p2571 N85-25854
CHANNEL CAPACITY
A system for measuring the characteristics of the ionospheric channel by digital transmissions
10 p1472 N85-19287
Serial data transmission with large output on the HF channel 10 p1475 N85-19305
The coding capacity of mismatched Gaussian channels
[AD-A149453] 10 p1551 N85-19782
CHANNEL FLOW
NT OPEN CHANNEL FLOW
The effect of channel convergence on heat transfer in a passage with short pin fins
[NASA-TM-83801] 01 p0046 N85-10303
Vertical channel free convection for a power law fluid with a constant heat flux
[DE84-014551] 01 p0047 N85-10311
Direct numerical simulation of curved turbulent channel flow
[NASA-TM-85974] 02 p0197 N85-11316
The structure of the vorticity field in turbulent channel flow. Part 2: Study of ensemble-averaged fields
[NASA-TM-86657] 03 p0361 N85-12317
Modelling the aerodynamics in a system of continuous channels and experimentation procedure
[BLL-M-35923-(5828.4)] 05 p0634 N85-14067
Direct numerical simulation of curved turbulent channel flow 05 p0635 N85-14072
Channel constructed to provide well defined boundary layers for vorticity optical probe measurements
[AD-A146679] 06 p0809 N85-15140
Shock waves in transonic flows at moderate Reynolds Number 08 p1076 N85-16823
A study of Reynolds-stress closure model
[NASA-CR-174342] 08 p1161 N85-17324
On limits of applicability of linear models to dynamics of gas channels in aircraft engines
09 p1308 N85-18219
Application of large eddy interaction model to channel flow
[NASA-TM-86691] 12 p1844 N85-21572
A three-dimensional spectral algorithm for simulations of transition and turbulence
[NASA-CR-172561] 12 p1846 N85-21575
Turbulent wake of a submerged flat plate
[AD-A153776] 18 p3100 N85-29190
Finite amplitude stability of a Rossby wave in a channel 19 p3314 N85-30543
Finite analytic solutions of supersonic flows in two-dimensional non-symmetrical channels
24 p4069 N85-35154
CHANNEL MULTIPLIERS
Analysis of a coded, M-ary orthogonal input optical channel with random-gain photomultiplier detection
05 p0624 N85-13990
Correlation of intensities of different scattering channels 21 p3694 N85-32962
CHANNEL NOISE
SVKD and SVKM-3 seismographs with a low-sensitivity channel
[REPT-553] 03 p0376 N85-12396
Synthesis of systems for coherent weighted signal processing against background of correlated interference 06 p0790 N85-15045
CHANNELS
Novel applications of the NASA/GSFC Viterbi decoder hardware simulator 08 p1101 N85-16957
The effect of jamming/deception on decision making
[AD-A149740] 12 p1828 N85-21472
Study of fatigue strength of shafts with segmented channels 14 p2282 N85-24138
Receiver optimization for detection in doubly spread communication channels
[AD-A151226] 15 p2541 N85-25689
Current enhancement in a conducting channel
[AD-A155418] 22 p3845 N85-33812
Recombination and ionization in a nitrogen plasma
[AD-A155426] 22 p3845 N85-33813
CHANNELS (DATA TRANSMISSION)
Gaussian Wide Sense Stationary Uncorrelated Scattering (GWSSUS) channel simulation program to be used for mobile radio systems
[FUB-40-1983] 01 p0041 N85-10265
Atmospheric channel performance measurements at 10 to 100 GHz
[PB84-211325] 01 p0042 N85-10271
Evaluation of criteria for selecting the spectral attributes of digital LANDSAT MSS imagery for discriminating lithological units in the lower Curaca River Valley, Bahia --- Brazil
[E85-10036] 03 p0379 N85-12415
Formation of reference signals in laser-type gas analyzers with mechanical switching of optical channels
06 p0787 N85-15027
A perspective on multiaccess channels
[AD-A146606] 06 p0799 N85-15105
Systems study for an Integrated Digital-Electric Aircraft (IDEA)
[NASA-CR-3840] 07 p0902 N85-15714
Evolution toward a multi-bus architecture for Army helicopter avionic systems 08 p1074 N85-16812
Integration of sensor fusion in advanced helicopter cockpit design 08 p1074 N85-16813
Multidimensional digital signal processing
[AD-A148055] 08 p1205 N85-17585
Reed-Solomon code synchronization revisited
10 p1464 N85-19234
Propagation Influences on Digital Transmission Systems: Problems and Solutions
[AGARD-CP-363] 10 p1469 N85-19260
Digital data communications over microwave radio channels 10 p1469 N85-19272
A review of atmospheric multipath measurements and digital system performance 10 p1470 N85-19279
An ionospheric mode detection system for HF communications application 10 p1471 N85-19282
Time and space domain filtering for improved HF communication 10 p1473 N85-19298
Extracting digital data from a bus and multiplexing it with a video signal
[AD-D011491] 11 p1636 N85-20302
Prelaunch absolute radiometric calibration of the reflective bands on the LANDSAT-4 protoflight Thematic Mapper 11 p1669 N85-20515
The 20:16 block code for digital recording and transmission channels
[BBC-RD-1985/1] 12 p1824 N85-21443
Digital channel efficiency model
[AD-A150084] 12 p1829 N85-21479
Data compression for noiseless channels
13 p2053 N85-22851
Horizontal deflection TS-257
13 p2069 N85-22926
Dynamics of adaptive signal corrector
13 p2071 N85-22940
Interactive communication channel
[AD-D011580] 15 p2542 N85-25695
Multi-access fiber optic data bus using FDM/FSK
[NASA-CR-175739] 15 p2621 N85-26152
On the throughput of channel access algorithms with limited sensing
[AD-A151984] 15 p2630 N85-26208
A study of topologies and protocols for fiber optic local area network
[NASA-CR-175771] 16 p2864 N85-27669
Introduction to the IEEE-488 bus
[INPE-3316-NTE/227] 17 p3010 N85-28613
High performance asynchronous limited sensing algorithms for CSMA and CSMA-CD channels
[AD-A153919] 18 p3171 N85-29650
Adaptive corrector operating in frequency domain
22 p3765 N85-33337
Optimum predistortion of digital signals for transmission over parallel channels 22 p3776 N85-33397
Estimate of signal-to-interference energy ratio in discrete-data transmission 22 p3776 N85-33398
Operations considerations in designing a high speed multi-channel data acquisition system
[DE85-012840] 24 p4154 N85-35756
CHANNELTRONS
U CHANNEL MULTIPLIERS
CHAOS
Chaos near the Coulomb Barrier: Nuclear molecules
[DE85-001280] 07 p1041 N85-16606
Synchrotron emission from chaotic stellar winds
08 p1234 N85-17774
Chaotic dynamics of instabilities in solids
[DE85-004909] 14 p2429 N85-24978
Chaos and order in an optical ring cavity
[CWI-AM-R8416] 17 p3038 N85-28795
CHAOTIC CLOUD PATTERNS
U CLOUDS (METEOROLOGY)
CHAPMAN SHEAR LAYER
U SHEAR LAYERS
CHAPMAN-ENSKOG THEORY
Surface-slip equations for multicomponent nonequilibrium air flow
[NASA-TM-85820] 12 p1845 N85-21573
CHAPMAN-JOUGET FLAME
U CHEMICAL EQUILIBRIUM
U DETONATION
U FLAME PROPAGATION
CHARACTER RECOGNITION
Comparative review of single-line and multiline optical character readers used in mail processing
[PB84-234624] 04 p0548 N85-13489
The combinatorics of local constraints in model-based recognition and localization
[AD-A148338] 08 p1230 N85-17746
ONR (Office of Naval Research) Far East Scientific Bulletin, volume 9, number 3, July to September 1984
[AD-A147282] 08 p1262 N85-17930
Character recognition using correlation techniques
[AD-A152006] 16 p2847 N85-27549
CHARACTERISTIC EQUATIONS
U EIGENVALUES
U EIGENVECTORS
CHARACTERISTIC FUNCTIONS
U EIGENVALUES
U EIGENVECTORS
CHARACTERISTIC METHOD
U METHOD OF CHARACTERISTICS
CHARACTERIZATION
Synthesis and characterization of advanced materials
[PB84-215326] 01 p0025 N85-10156
Novel techniques for the fabricating and characterization of GaAs MIS (Metal Insulator Semiconductor) structures
[AD-A145766] 03 p0358 N85-12301
The TA6Zr5D (IMI 685) characterization in strain controlled tests. (Specimens obtained from a forged spinning wheel) no. M4-45670
[M4-45670] 03 p0373 N85-12384
Quality assurance of composite materials, test report no. 45-649/F 04 p0460 N85-12981
Characterization of aluminum alloy 7010 in moderate width plate and T651 and T7651 metallurgical states
[REPT-44-606/F] 05 p0619 N85-13961
The synthesis, structural characterization and reactions of closo-Rhodacarborane Anions containing a formal d6 metal vertex 1,2
[AD-A149640] 12 p1799 N85-21285
Production and characterization of amorphous silicon (a-Si:H) as base material for solar cells
12 p1879 N85-21791
Electrical characterization of analog microprocessors
[AD-A149829] 12 p1911 N85-21996
Crack propation in unidirectional laminates by the stress intensity factors 18 p3121 N85-29320

CHARACTERS

Loss-of-flow transient characterization in carbide-fueled LMFBRs
[DE85-009552] 18 p3269 N85-30270

CHARACTERS
U SYMBOLS

CHARCOAL
NT ACTIVATED CARBON
A comprehensive review of black powder
[AD-A150455] 13 p2039 N85-22769
Remarks on preparation of indandione detection reagents
[NASA-TM-77805] 21 p3560 N85-32146

CHARGE CARRIERS
NT FREE ELECTRONS
NT HOLES (ELECTRON DEFICIENCIES)
NT MINORITY CARRIERS
Lifetime of excess charge carriers in weakly doped epitaxial GaAs layers 04 p0487 N85-13106
Determination of parameters of doped thin semiconductor layers from plasmatic minimum of reflection coefficient for infrared radiation
07 p0954 N85-16047
Current carriers for the field-aligned current system
[NASA-TM-86161] 08 p1280 N85-17925
A picosecond population modulation study of near interband resonances in semiconductors
09 p1386 N85-18787
Determination of the mobility profile in GaAs-MESFETs
[NASA-TM-77818] 11 p1734 N85-20905
Characterization of high purity Si-doped molecular beam epitaxial GaAs
[AD-A149851] 12 p1936 N85-22181
A scanning optical microprobe for infrared detector measurement
[AD-A151748] 15 p2653 N85-26361
Carrier loss in dispersive transport in amorphous semiconductors
[DE85-009122] 18 p3194 N85-29811
Influence of coherent light beams on free carriers in semiconductors 21 p3681 N85-32867
Hermetic chip carrier compliant soldering pads
[AD-D011722] 23 p3936 N85-34410

CHARGE COUPLED DEVICES
Multiple object spectroscopy: The MX spectrometer design 02 p0296 N85-11920
Electronic bandwidth compression module
[AD-A145843] 03 p0366 N85-12343
Characterization of electronic streak tubes including one with internal CCD readout
[DE84-016823] 05 p0639 N85-14098
Electronic satellite imaging system MOMS-ESA
[BMFT-FB-W-84-033] 05 p0661 N85-14248
Electrooptical sensor for automatic detection of objects 06 p0769 N85-15040
Numerical estimation of charge transfer time in charge-coupled device employing latent gallium arsenide channel 06 p0793 N85-15069
Oblique focus ICCD laboratory evaluation
[NASA-CR-174205] 06 p0862 N85-15480
Study of alternate optical and fine guidance sensor designs for the space infrared telescope facility (SIRTF)
[NASA-CR-168614] 07 p0915 N85-15794
Design and fabrication of a CCD camera for use with relay optics in solar X-ray astronomy
[NASA-CR-174334] 08 p1164 N85-17344
A CCD system for photometry of direct and spectroscopic images 08 p1252 N85-17904
CCDs: Their cause and cure
08 p1252 N85-17905
Time series photometry with a CCD camera
08 p1252 N85-17906
Airborne remote sensing CCD imaging system
11 p1623 N85-20220
Intensified CCD camera system for plasma diagnostics
[DE85-002252] 12 p1853 N85-21820
Monolithic short wave infrared (SWIR) detector array
[NASA-CR-175284] 12 p1874 N85-21759
Development of high resolution imaging detectors for X-ray astronomy
[NASA-CR-175505] 12 p1953 N85-22266
French firm develops new kind of CTD camera for robots 15 p2523 N85-25556
Parallel programmable charge domain device
[AD-D011589] 15 p2549 N85-25733
Summary of optical groundbased E ring observations at the University of Arizona 15 p2671 N85-26482
INPE's line imaging camera: Preliminary results
[INPE-3476-PRE/719] 16 p2787 N85-27194
Self-scanning MOS-integrated photosensor strip
17 p2940 N85-28151
Pipelined programmable charge domain device
[AD-D011596] 17 p2951 N85-28225
Techniques for operating Charge Coupled Devices (CCD's) in very high speed framing mode
[AD-A152678] 17 p2953 N85-28236
Energizing arrangement for charge coupled device control electrodes
[AD-D011712] 19 p3261 N85-30220
The Extended Range X-Ray Telescope center director's discretionary fund report
[NASA-TM-86507] 19 p3362 N85-30983
CCD-based X-ray spectrometry for on-line determination of laser plasma electron temperature
21 p3692 N85-32938
Solid state research
[AD-A154783] 21 p3709 N85-33025
Microcomputer controlled image processor
[AD-D011734] 22 p3833 N85-33735
The nature and origin of outer solar system asteroids from reflectance spectrophotometry
24 p4156 N85-35838
Application of thermoluminescence for detection of cascade shower 1: Hardware and software of reader system
[HE-7.1-6] 24 p4213 N85-36160
Spatial distribution read-out system for thermoluminescence sheets
[HE-7.1-7] 24 p4213 N85-36161
Application of thermoluminescence for detection of cascade shower 2: Detection of cosmic ray cascade shower at Mount Fuji
[HE-7.1-12] 24 p4214 N85-36162

CHARGE DISTRIBUTION
Minimizing the energy spread within a single bunch by shaping its charge distribution
[DE84-016172] 05 p0727 N85-14676
Mathematical physics approaches to lightning discharge problems
[NASA-TM-86349] 08 p1187 N85-17492
Accelerator column models for low-current beams
[DE85-010722] 19 p3262 N85-30226
Form factor effects on microwave Cerenkov radiation
[AD-A154577] 21 p3701 N85-32993
Charge composition and energy spectral of cosmic ray primary particles for energies higher than 1 TeV
[OG-4.1-14] 22 p3677 N85-34020
Electron photoejection in carbanions
[DE85-011747] 23 p3911 N85-34230
Electron photoejection in carbanions
[DE85-011748] 23 p3912 N85-34237
Calculations of heavy ion charge state distributions for nonequilibrium conditions
[SH-2.1-12] 23 p3999 N85-34793
On the influence of the heliomagnetospheric periphery on the galactic cosmic rays
[SH-4.2-19] 23 p4009 N85-34856
Lateral distribution on charged particles in EAS
[HE-4.3-15] 24 p4192 N85-36009
Lateral distribution of high energy muons in EAS of sizes Ne approximately equals 10(5) and Ne approximately equals 10(6)
[HE-4.3-16] 24 p4192 N85-36010
Properties of 10 (18)-10 (19)eV EAS at far core distance
[HE-4.7-3] 24 p4198 N85-36054

CHARGE EFFICIENCY
Electrical and thermal performance during charging and discharging a Phase 1 gel cell battery
[PB85-114312] 11 p1677 N85-20565
State-of-charge coulometer
[NASA-CASE-NPO-15759-1] 12 p1849 N85-21596
Kapton charging characteristics: Effects of material thickness and electron-energy distribution
13 p1996 N85-22513
An improved battery state-of-charge indicator
[NASA-CR-175701] 14 p2296 N85-24227
Method for determining the point of zero zeta potential of semiconductor
[NASA-CASE-LAR-12893-1] 19 p3373 N85-30923
Modeling taper charge with a non-linear equation
20 p3445 N85-31390
A 34 ampere-hour nickel-cadmium minimum trickle charge testing 20 p3446 N85-31394
Two-dimensional inversion of resistivity monitoring data from the Cerro Prieto geothermal field
[DE85-012554] 24 p4113 N85-35494

CHARGE EXCHANGE
Twisted domain wall in very thin magnetic films with perpendicular anisotropy 03 p0350 N85-12252
Experimental investigations in particle physics at intermediate energies
[DE85-001481] 11 p1722 N85-20832
Time dependent Hartree-Fock theory of ion-atom collisions: Application to F(9+) + Ne
[DE85-003083] 11 p1723 N85-20836
Atomic processes involving impurities in the plasma edge
[DE85-001277] 11 p1730 N85-20882
Theoretical study of near-threshold electron-molecule scattering
[DE85-004530] 12 p1930 N85-22126
Development of an apparatus for obtaining molecular beams in the energy range from 2 to 200 eV
[NASA-TM-77835] 15 p2647 N85-26328
Germanium detectors with a built-in transverse drift field
[DE85-009944] 18 p3096 N85-29165
Excited state populations and charge-exchange of fast ions in solids
[DE85-009362] 18 p3180 N85-29714
An alpha particle diagnostic beam line system to generate an intense Li(O) beam with an ORNL SITEX source
[DE85-010564] 18 p3182 N85-29730
Resonant-transfer-and-excitation for highly charged ions (16 or = Z or = 23) in collisions with helium
[DE85-010550] 19 p3359 N85-30823
The production and destruction of metastable negative ions
[DE85-011056] 19 p3364 N85-30859
Discussion session: Nucleon- and antinucleon-nucleus inelastic scattering and charge exchange
[DE85-010723] 19 p3364 N85-30860
Evaluated nuclear-data file for niobium
[DE85-012095] 21 p3704 N85-33009
Calculated neutron-induced cross sections for /sup 63,65/Cu/sup 58,60/Ni and (52) Cr from 1 to 20 MeV and comparisons with experiments
[DE85-011928] 22 p3844 N85-33808
Propagation and secondary production of low energy antiprotons in the atmosphere
[OG-6.1-3] 22 p3867 N85-34094
Noble metals as incipient transition metals
[DE85-013263] 24 p4060 N85-35286
Is the inelastic charge-exchange contribution constant at the large X and superhigh energies? Qaut 01Kuchin, I. A. 24 p4173 N85-35871
A study of gamma-families generated in nucleon-nucleus (NA) and pion-nucleus (pi A) interactions
[HE-3.7-2] 24 p4186 N85-36061

CHARGE INJECTION DEVICES
Photometry with Multi-Anode Microchannel Arrays (MAMAs) and Charge Injection Devices (CIDs)
08 p1252 N85-17909
Performance of charge-injection-device infrared detector arrays at low and moderate backgrounds
[NASA-TM-86667] 15 p2560 N85-25788

CHARGE SEPARATION
U POLARIZATION (CHARGE SEPARATION)

CHARGE TRANSFER
Study of application of organic semiconductors to electronic components
[BMFT-FB-T-84-142] 02 p0280 N85-11690
Theoretical studies of highly ionized species
[DE84-016797] 04 p0561 N85-13574
Laboratory studies of atomic collision processes of importance in planetary atmospheres
[NASA-CR-174142] 04 p0589 N85-13758
Numerical estimation of charge transfer time in charge-coupled device employing latent gallium arsenide channel 06 p0793 N85-15069
Recent development in astronomic position determinations
[AD-A148335] 08 p1082 N85-16868
Correlation of electronic charge transfer transitions and electrochemical potentials. The Bipyrazine(Tetracarbonyl)Molybdenum(O) system in various solvents
[AD-A147680] 08 p1120 N85-17062
Study of charge transport in the thermoelectret state of some ceramics and glasses
[DE85-001763] 09 p1300 N85-18163
Battery response to pulse loads: A mathematical model
[DE85-001149] 09 p1316 N85-18277
Process for preparing highly optically transparent-colorless armomatic polyimide film
[NASA-CASE-LAR-13351-1] 12 p1811 N85-21380
Observation of a novel low-lying excited state in zinc complexes
[AD-A150188] 13 p2156 N85-23385
Charge transfer, polarization and relaxation effects in the Auger lineshapes of Si
[AD-A150938] 14 p2252 N85-23954
Charge isolation in a spatial light modulator
[AD-D011581] 15 p2652 N85-26358
Neutralization and excitation in low-energy ion-surface collisions
[AD-A151568] 15 p2660 N85-26414
Theory of electron-impact atomic ionization cross sections
[AD-A151783] 16 p2861 N85-27648
Investigation of charge transport in the thermoelectret state of some ceramics and glasses
[DE85-009316] 17 p2936 N85-28122

The mean trajectory approximation for charge and energy transfer processes at surfaces
[AD-A152708] 17 p3043 N85-28830
Characteristics of charge transfer in the dispersed phase of electrorheological suspensions
[RAE-TRANS-2125] 19 p3233 N85-30040
Photoeffects of semiconductor electrolyte interfaces
[AD-A154163] 20 p3449 N85-31411
Polymer-water interaction studies
21 p3609 N85-32411

CHARGE TRANSFER DEVICES
NT CHARGE COUPLED DEVICES
NT CHARGE INJECTION DEVICES
Charge Injection Device (CID) used as a photodector: implementation and performance. Application to light source tracking (stars, lasers)
[CNES-83/CT/DRT/TIT/OE/146]
20 p3533 N85-31963

CHARGED PARTICLES
NT ALPHA PARTICLES
NT ANIONS
NT ANTIPROTONS
NT ARGON PLASMA
NT BETA PARTICLES
NT BOUNDARY LAYER PLASMAS
NT CATIONS
NT COLD PLASMAS
NT COLLISIONAL PLASMAS
NT COLLISIONLESS PLASMAS
NT CONDUCTION ELECTRONS
NT COSMIC PLASMA
NT CYLINDRICAL PLASMAS
NT DENSE PLASMAS
NT DEUTERIUM PLASMA
NT DEUTERONS
NT ELECTRON PLASMA
NT ELECTRONS
NT ELLIPTICAL PLASMAS
NT ENERGETIC PARTICLES
NT EVEN-EVEN NUCLEI
NT FERRIC IONS
NT FREE ELECTRONS
NT HEAVY NUCLEI
NT HELIUM PLASMA
NT HIGH ENERGY ELECTRONS
NT HIGH TEMPERATURE PLASMAS
NT HOT ELECTRONS
NT HYDROGEN PLASMA
NT HYPERNUCLEI
NT INNER RADIATION BELT
NT LASER PLASMAS
NT MAGNETICALLY TRAPPED PARTICLES
NT METAL IONS
NT METALLIC PLASMAS
NT NEGATIVE IONS
NT NEGATRONS
NT NITROGEN PLASMA
NT NONEQUILIBRIUM PLASMAS
NT NONUNIFORM PLASMAS
NT NUCLEI (NUCLEAR PHYSICS)
NT ODD-EVEN NUCLEI
NT ODD-ODD NUCLEI
NT OUTER RADIATION BELT
NT PHOTOELECTRONS
NT PLASMA CLOUDS
NT PLASMA FOCUS
NT PLASMA LAYERS
NT PLASMA SHEATHS
NT PLASMAS (PHYSICS)
NT POLARONS
NT POSITIVE IONS
NT POSITRONS
NT PROTON BELTS
NT PROTONS
NT RADIATION BELTS
NT RELATIVISTIC ELECTRON BEAMS
NT RELATIVISTIC PLASMAS
NT ROTATING PLASMAS
NT SEMICONDUCTOR PLASMAS
NT SOLAR ELECTRONS
NT SOLAR PROTONS
NT SOLAR WIND
NT SPACE PLASMAS
NT SPHERICAL PLASMAS
NT STELLAR WINDS
NT STRONGLY COUPLED PLASMAS
NT THERMAL PLASMAS
NT TOROIDAL PLASMAS
Behavior of charged particles in lower ionosphere with acoustical effects 02 p0161 N85-11089
Charged particle erosion of icy satellites: Coronal atmospheres and surface redistribution
03 p0448 N85-12845
Cerenkov ring imaging detector development at SLAC
[DE84-015863] 04 p0560 N85-13564
Charge trapping in low temperature MOS (Metal-Oxide-Silicon) oxides
[AD-A148450] 06 p0860 N85-15467
Fermilab research program workbook
[DE84-012568] 06 p0862 N85-15476
Earth's radiation belts
[AD-A147927] 07 p0998 N85-16339
Beam propagation studies at NRL (Naval Research Laboratory) July 1983 to June 1984, volume 2
[AD-A148198] 08 p1152 N85-17270
Force balance limiting current for charged particle beams
[DE84-016976] 09 p1381 N85-18685
One-electron capture processes by highly charged ions from helium: Present status of HICE-IPP
09 p1389 N85-18736
Diffusion of particles in a slowly modulated wave
[DE85-000729] 09 p1391 N85-18756
Ozone measurements in the mesosphere during a solar proton event 11 p1685 N85-20490
Self-Optimized Sector (SOS) model of self-consistent energy loss and scattering for an electron beam propagating in air
[DE85-003161] 11 p1722 N85-20831
Covariant lie-transformed plasma action principle
[DE85-000285] 11 p1732 N85-20891
SCATHA (spacecraft charging at high altitudes) plasma interaction experiment: SC-3 high energy particle spectrometer; SC-8 energetic ion composition experiment
[AD-A149728] 12 p1793 N85-21252
S3-3 ONR-118 data analysis
[AD-A149725] 12 p1869 N85-21855
Characteristics of latitude effect on cosmic ray charged component in atmosphere at altitudes 3-5 KM
13 p1978 N85-22413
Observation of cosmic ray flux variations in stratosphere 13 p1981 N85-22430
Suprathermal plasma observed on STS-3 Mission by plasma diagnostics package 13 p1989 N85-22472
Discharges on a negatively biased solar cell array in a charged-particle environment 13 p1994 N85-22499
EMI characteristics of a potential control system
13 p1994 N85-22502
Spacecraft environmental interactions: A joint Air Force and NASA research and technology program
13 p1997 N85-22517
Variable flexing device for targets in internal beams of charged particle accelerators 13 p2044 N85-22797
Scattering of electromagnetic waves by charged particles 13 p2067 N85-22913
Nonrelativistic Kapitza-Dirac scattering
[AD-A150622] 13 p2159 N85-23405
Local phase transformation in alloys during charged-particle irradiation
[DE85-005012] 14 p2258 N85-23990
The access of energetic charged particles to satellite altitudes
[AD-A150799] 14 p2373 N85-24870
Active Magnetospheric Particle Tracing Explorers (AMPTE)
[AD-A151072] 14 p2374 N85-24874
Nonrelativistic Kapitza-Dirac scattering
[AD-A150649] 14 p2417 N85-24911
First- and second-order charged particle optics
[DE85-006310] 14 p2421 N85-24940
Space radiation monitor observations from Salyut-4 orbital station 15 p2482 N85-25317
Beam trapping in high current cyclic accelerators with strong focusing fields
[AD-A151392] 15 p2648 N85-26331
Gravitational effects in theories with interacting fields: Two studies 15 p2663 N85-26435
Implications for supersymmetry of the CERN monojets
[DE85-008178] 17 p3030 N85-28741
Conversion efficiencies of charged particle beam driven free electron lasers
[AD-A154404] 19 p3276 N85-30316
Circular-beam ray tracing on a microcomputer
[DE85-010754] 19 p3338 N85-30685
LINE: A code which simulates spectral line shapes for fusion reaction products generated by various speed distributions
[DE85-010833] 19 p3341 N85-30702
Present and future directions of atomic physics research with multiply-charged ions at Brookhaven National Laboratory
[DE85-010980] 19 p3354 N85-30788
Surface effects on sputtered atoms and their angular and energy dependence
[DE85-010806] 19 p3364 N85-30790
Radiation interactions for tomography
[DE85-008981] 19 p3365 N85-30799
High-energy particle Monte Carlo at Los Alamos
[DE85-010716] 19 p3383 N85-30856
Energy-advanced nuclear data: Measurements and physical interpretations
[DE85-006198] 19 p3386 N85-30872
Schottky theory of three component plasmas
[AD-A154461] 19 p3371 N85-30907
Monte-Carlo treatment of nonlinear collisional effects in charged-particle transport
[DE85-010755] 20 p3521 N85-31897
Studies in mixed species charged particle beam dynamics
[OUEL-1545/84] 20 p3531 N85-31969
Trapping of ion conics by downward parallel electric fields
[AD-A155306] 21 p3633 N85-32566
Classical emission of relativistic charged particles during axial channeling 21 p3681 N85-32871
Transformation of charged particle beams by concentrating electro-optical systems
21 p3690 N85-32925
Mirror reflection of charged particles from + amorphous and polycrystalline surfaces 21 p3690 N85-32927
Possibility of developing charged-particle energy analyzer based on hyperboloidal axisymmetrical lens
21 p3691 N85-32933
Multistage spent particle collector and a method for making same
[NASA-CASE-LEW-13914-1] 22 p3791 N85-33489
Bibliography and index for nuclear reactions among light charged particles, volume 26
[DE85-011482] 22 p3838 N85-33768
Heavy quarks and CP: Moriond 1985
[DE85-010553] 22 p3841 N85-33790
High-energy multiple muons and heavy primary cosmic-rays
[OG-5.2-9] 22 p3883 N85-34085
Effect of seeds of heavy charged particles of galactic cosmic radiation 23 p3954 N85-34505
Theoretical and computational research on the focused transport of intense charged particle beams
[DE85-012980] 23 p3972 N85-34621
Guiding center distribution function and longitudinal invariant 23 p3978 N85-34663
Acceleration of ions and electrons to near-cosmic ray energies in a perpendicular shock: The January 6, 1978 event
[SH-1.5-4] 23 p3996 N85-34773
The Jovian electron spectrum: 1978-1984
[SH-1.5-19] 23 p3998 N85-34782
Silicon to iron abundances in solar cosmic rays and in the sun
[SH-2.1-6] 23 p3998 N85-34787
The mean ionic charges of N, Ne, MG, Si and S in solar energetic particle events
[SH-2.1-11] 23 p3999 N85-34792
On the connection between the 3HE-enrichment and spectral index of solar energetic particles
[SH-2.2-8] 23 p4001 N85-34804
The dispersive evolution of charged-particle bunches in random magnetic fields
[SH-4.1-2] 23 p4004 N85-34829
Spatial distribution of cosmic rays in magnetic cycles of the Sun
[SH-4.2-20] 23 p4009 N85-34857
The dependence of solar modulation on the sign of the cosmic ray particle charge
[SH-4.2-23] 23 p4009 N85-34860
Observation of energy spectrum of electron albedo in low latitude region at Hyderabad, India
[SH-6.1-7] 23 p4045 N85-35081
The influence of quiet asymmetric magnetosphere on the cutoff rigidities of the main cone
[SH-6.1-10] 23 p4045 N85-35083
A bi-directional charged particle telescope to observe flux, energy spectrum and angular distribution of relativistic and non-relativistic particles
[SH-9.1-4] 23 p4050 N85-35119
Burst size distributions in the digitized data of the ion chambers t Mt. Norikura and sea level stations
[SH-9.1-9] 23 p4051 N85-35124
Plastic scintillators in coincidence for the study of multi-particle production of sea level cosmic rays in dense medium
[SH-9.1-11] 23 p4052 N85-35126
Observation of nuclei with energies 8-30 MeV per nucleon in the Earth's magnetosphere at the altitudes 350 KM
[SH-10.1-5] 23 p4053 N85-35136
The effect of the relative nuclear size on the nucleus-nucleus interactions
[HE-1.4-13] 24 p4177 N85-35900
Experimental basis for the models of cascade propagation in atmosphere
[HE-3.6-6] 24 p4185 N85-35954

The lateral distributions of charged particles of energy greater than 0.3 E sub crit in electron-photon cascades in lead and air
[HE-3.6-10] 24 p4185 N85-35957
A study of gamma-families generated in nucleon-nucleus (NA) and pion-nucleus (pi A) interactions
[HE-3.7-2] 24 p4186 N85-35961
Lateral distribution on charged particles in EAS
[HE-4.3-15] 24 p4192 N85-36009
Muon spectrum in air showers initiated by gamma rays
[HE-4.5-4] 24 p4195 N85-36026
High energy cosmic ray signature of quark nuggets
[HE-6.2-11] 24 p4212 N85-36147
Experimental investigation of radiative-acoustic effects in the water by the thermodynamical conditions of Dumand
[HE-7.1-2] 24 p4213 N85-36156

CHARM (PARTICLE PHYSICS)
Anomalies in cosmic rays: New particles versus charm?
[HE-5.4-9] 24 p4208 N85-36120
Collimated groups of particles as possible manifestation of heavy meson production
[HE-5.4-14] 24 p4208 N85-36124
Tien-Shan effect and charmed particles
[HE-6.2-17] 24 p4212 N85-36153

CHARON
Research in planetary studies and operation of Mauna Kea Observatory
[NASA-CR-175616] 13 p2100 N85-23460

CHARPY IMPACT TEST
The influence of rare Earth elements on the temper embrittlement behaviour and mechanical properties of a low alloy steel 02 p0180 N85-11210
Instrumented impact testing machine with reduced specimen oscillation effects
[VTT-290] 04 p0504 N85-13218
Statistical aspects of shear fracture propagation
[ERS-E.366] 09 p1341 N85-18434
Development of an automated miniature Charpy test method
[DE85-003011] 11 p1652 N85-20405
The Hopkinson pressure bar: An alternative to the instrumented pendulum for Charpy tests
[OUEL-1566/85] 20 p3471 N85-31569
Inertial analysis of the Charpy test
[OUEL-1571/85] 20 p3471 N85-31570

CHARTS
NT FLOW CHARTS
NT GRAPHS (CHARTS)
NT METEOROLOGICAL CHARTS
NT NAUTICAL CHARTS
A program to produce standard shewhart control charts for the statistics X-bar and R or S, P, NP, C, or U
[AD-A146971] 07 p1024 N85-16501
Commercial data base management system for geonames data base
[AD-A150835] 14 p2433 N85-25007
Dialog system with minicomputer for plotting performance charts 22 p3766 N85-33355

CHASSIS
The guidelines to design the lever turning gears in articulated vehicles
[AD-P004301] 09 p1409 N85-18678

CHEBYSHEV APPROXIMATION
Calibration of hall probes
[CSIR-NAC-83-04] 01 p0116 N85-10794
Minimax optimal control in the reentry of a space glider 02 p0167 N85-11124
Boundary conditions in Chebyshev and Legendre methods
[NASA-CR-172469] 02 p0250 N85-11635
Optimized response functions for 2-dimensional observations of solar oscillations
14 p2443 N85-25075
H-sets, convex programming and constrained approximation
[TRITA-NA-8306] 16 p2853 N85-27587
To the theory of approximation of experimental curves by smooth functions
[PREPRINT-436] 18 p3173 N85-29671
Spectral methods for limited area models
20 p3468 N85-31679

CHECKOUT
Debug testing and confidence testing
[AD-A147104] 07 p1025 N85-16504
Joint service design for testability program
08 p1063 N85-16733
Launch processing system concept to reality
08 p1097 N85-16931
Mathematical models for space shuttle ground systems 08 p1097 N85-16933
PASLIB programmer's guide for the finite element machine, revision 2.1-A
[NASA-CR-172281] 11 p1705 N85-20727
Definition of ground test for Large Space Structure (LSS) control verification
[NASA-TM-86495] 12 p1792 N85-21249
Two-phase flow in geothermal systems
[DE85-004692] 12 p1848 N85-21591
Equipment for the ARGOS system from Eidsvoll Electronics A.S. 14 p2239 N85-23865
Automation of development of software for switching units that are implemented in the form of multiprocessor systems on a microcomputer base
14 p2401 N85-24802
Using a logic analyser and trigger unit to de-bug a program
[BAE-881/ELO/1487] 15 p2626 N85-26160
Reentrancy and multitasking on CRAY computers
[DE85-007256] 15 p2630 N85-26211
Debugging distributed computations in a nested atomic action system
[AD-A153617] 18 p3162 N85-29585
International flight planning handbook
[AD-A156330] 24 p4062 N85-35177

CHECKOUT EQUIPMENT
U TEST EQUIPMENT

CHELATE COMPOUNDS
U CHELATES

CHELATES
Polymers and macromolecules
[DE85-003176] 10 p1454 N85-19160
A soluble linear Schiff-base coordination polymer containing eight-coordinate zirconium(4)
[AD-A151446] 15 p2518 N85-25527
Nuclear magnetic resonance study of the intramolecular rearrangement of 2-(5-cyanotetrazolato)pentaammine cobalt (III) perchlorate
[DE85-010810] 22 p3839 N85-33772

CHEMICAL ANALYSIS
NT ELECTROPHOTOMETRY
NT GAS ANALYSIS
NT LASER SPECTROSCOPY
NT MICROANALYSIS
NT NEUTRON ACTIVATION ANALYSIS
NT OZONOMETRY
NT QUALITATIVE ANALYSIS
NT QUANTITATIVE ANALYSIS
NT SPECTROSCOPIC ANALYSIS
NT URINALYSIS
NT VOLUMETRIC ANALYSIS
Development and application of fluorine-containing reagents in the gas chromatography of carbonyl compounds
[BLL-DRIC-TRANS-7205-(3823.66)]
01 p0023 N85-10140
Synthesis and characterization of advanced materials
[PB84-215326] 01 p0025 N85-10156
Water resources data for Michigan, water year 1983
[PB84-225176] 01 p0066 N85-10442
Ecology of estuarine channels of the pacific northwest coast: A community profile
[PB84-209709] 01 p0070 N85-10464
Inorganic composites for space applications
02 p0155 N85-11047
Fluids Experiment Apparatus (FEA)
02 p0156 N85-11048
Surface chemistry of palladium
[DE84-014572] 02 p0173 N85-11163
The oxidation of transition-metal ions by molecular oxygen
[BLL-M-29693-(5828.4)] 02 p0175 N85-11172
EDS round-robin evaluation of type 308 austenitic stainless steel
[DE84-014574] 02 p0183 N85-11226
Optical detection of alkali compounds
[DE84-015505] 03 p0326 N85-12117
The colloidal chemistry of ceramic clays
[NASA-TM-77734] 03 p0336 N85-12163
Compound class quantitation of JP-5 jet fuels by high performance liquid chromatography-differential refractive index detection
[AD-A145754] 03 p0340 N85-12185
Crystal chemistry and real structure of crystals
03 p0423 N85-12703
Matrix resin characterization in cured graphite composites using diffuse reflectance-FTIR
04 p0466 N85-12959
Comparison study of analytical methods for the determination of fluoride, chloride, and bromide in plastics
[DE84-015008] 04 p0470 N85-12989
Official journey to USA, November 1983. Symposium on the Compatibility of Explosives; Mound Laboratory; Naval Surface Weapons Center
[FOA-C-20548-D1] 04 p0482 N85-13072
Measuring system with ion selective electrodes
[BMFT-FB-T-84-170] 05 p0639 N85-14100
Geothermal assessment of a portion of the Escalante Valley, Utah
[DE84-015964] 06 p0826 N85-15257
The toxicity of complex mixtures
[AD-P004033] 06 p0844 N85-15363
The influence of sample collection and methods of analysis on chemical concentrations measured in rainwater
[KNMI-TR-55] 07 p0924 N85-15663
Coso Monitoring Program, January 1981 through December 1983
[AD-A147894] 07 p0996 N85-16339
Analysis of Nonvolatile Residue (NVR) from spacecraft systems
[NASA-TM-86164] 08 p1113 N85-17019
Comparative usefulness of flue gas oxygen and carbon dioxide analysis
[BLL-TRANS-T6358/BG/WH783/84]
08 p1179 N85-17430
Advanced NMR characterization of zeolite catalysts
[DE85-000456] 09 p1291 N85-18104
Geothermal assessment of part of the east shore area, Davis and Weber Counties, Utah
[DE84-016817] 09 p1342 N85-18446
Location of volatile buried wastes by field portable instrumentation
[AD-P004147] 09 p1348 N85-18463
Quality assurance for environmental analytical chemistry, 1983
[DE84-016045] 09 p1349 N85-18469
Correlation and petrological interpretation of abyssal and terrestrial tephra layers 09 p1353 N85-18512
Metal atom diffusion in amorphous silica and at the silica surface
[DE84-017351] 09 p1380 N85-18674
Microstructural analysis of ion containing polymers
[DE85-001594] 10 p1453 N85-19157
SANS studies of polymers
[DE85-002471] 11 p1612 N85-20134
Chemical and photographic evaluation of rigid explosive transfer lines
[AD-A149303] 11 p1613 N85-20145
China report: Science and technology
[JPRS-CST-84-040] 11 p1623 N85-20219
Theta pinch discharges for solids vaporization and elemental chemical analysis
[DE85-002968] 11 p1733 N85-20899
Method and apparatus for mapping the distribution of chemical elements in an extended medium
[NASA-CASE-GSC-12806-1] 12 p1796 N85-21279
Microprocessor-controlled anodic stripping voltammeter for trace metal analysis in tap water
[DE85-002781] 12 p1852 N85-21619
Stability of organic audit materials and results of source test analysis audits
[PB85-116184] 12 p1865 N85-21832
Standard analytical procedures of the NOAA National Analytical Facility, 1984-85: Extractable toxic organic compounds
[PB85-126262] 12 p1867 N85-21840
Characterization of material surfaces exposed to atomic oxygen on space shuttle missions
12 p1946 N85-22220
Analyses via automated mass spectrometry (MS/DS)
12 p1947 N85-22227
Structural distortions of ultra-dispersed titanium nitride powders 13 p2020 N85-22717
Compositional and structural analysis of Air Force materials
[AD-A150992] 14 p2252 N85-23957
Literature review for development of the master analytical scheme for organic compounds in water
[PB85-152874] 15 p2507 N85-25469
Development and diffusion of automated clinical chemistry analyzers
[PB85-150696] 15 p2561 N85-25796
Infinite computing
[AD-A151437] 15 p2628 N85-26197
Development of a persistent chemical agent simulation system
[NASA-CR-175780] 16 p2745 N85-26937
Development of a Persistent Chemical Agent Simulator System (PCASS)
[NASA-CR-175776] 16 p2745 N85-26938
Design of a Mobile Combustion Diagnostic Fixture (MCDF)
[AD-A151614] 16 p2745 N85-26941
Photoionization mass spectrometry with VUV hydrogen laser source
[AD-A153362] 17 p2921 N85-28008
Examination of steels by chemical analysis for quality assurance
[BLL-BISI-TRANS-22068-(9022.06)]
17 p2929 N85-28074
Proton induced X-ray emission method, its application in analytics 17 p2945 N85-28178

Voltammetric analysis of ordnance materials. Part 2: A portable digital voltammeter for use with a silver wire working electrode
[AD-A152480] 17 p2967 N85-28325
Analytical Chemistry Division
[DE85-010585] 18 p3068 N85-28974
Chemical, biological, and physical measurements from the subtropical western North Atlantic Ocean. Summer 1982, USNS Lynch, cruise 710-82
[AD-A153823] 18 p3201 N85-29657
Study of the chemical mechanism in lubrication
[DE85-010766] 19 p3228 N85-30013
Guest molecules in coal
[DE85-010435] 19 p3228 N85-30016
Technical and administrative activities of the Analytical Chemistry Laboratory (ACL)
[DE85-010150] 19 p3236 N85-30063
Advanced NMR characterization of zeolite catalysts
[DE85-010143] 19 p3363 N85-30853
Differential optical absorption techniques for diagnostics of coal gasification
[DE85-010177] 19 p3368 N85-30890
Quasi non-intrusive sampling and analysis of gases associated with the boundary layer on the tethered satellite and similar supersonic and hypersonic research vehicles
[NASA-CR-176075] 20 p3407 N85-31140
Development anmd testing of electrophoresis solutions. Task I.1: Development of optimal buffer system
20 p3500 N85-31755
Toxic hazards tests for vehicles and other equipment
[AD-A149164] 20 p3506 N85-31797
Remarks on preparation of indandione detection reagents
[NASA-TM-77905] 21 p3560 N85-32146
A manual of methods for the continuous flow determination of ammonia, nitrate-nitrite, phosphate and silicate in seawater
[IOS-177] 23 p3913 N85-34243
Uranium, thorium isotopic analyses and uranium-series ages of calcite and opal and stable isotopic compositions of calcite from drill cores UE25a no. 1, USR G-2 and USW G-3/GU-3, Yucca Mountain, Nevada
[DE85-013039] 23 p3948 N85-34471
Aspects of high-resolution gas chromatography as applied to the analysis of hydrocarbon fuels and other complex organic mixtures. Volume 1
[AD-A156154] 24 p4076 N85-35257
Experimental technique for measuring the isentrope of hydrogen to several megabars
[DE85-014332] 24 p4095 N85-35386
Measurement control for plutonium isotopic measurements using gamma-ray spectrometry
[DE85-013394] 24 p4097 N85-35397

CHEMICAL ATTACK
NT INTERGRANULAR CORROSION
The effect of replacing molybdenum with vanadium on the corrosion resistant properties of stainless steels
02 p0178 N85-11197
Hydrogen attack of steel
[DE85-002645] 11 p1608 N85-20113
Study of Kapton under simulated shuttle environment
[NASA-CR-176003] 19 p3225 N85-29997
Burner rig corrosion of SiC at 1000 deg C
[NASA-TM-87061] 19 p3227 N85-30011
On compounding nickel alloys as defense against sulfide-oxide corrosion 19 p3243 N85-30109
Magnetically-localizable, polymerized lipid vesicles and method of disrupting same
[AD-D011686] 19 p3249 N85-30144

CHEMICAL BONDS
NT COVALENT BONDS
NT HYDROGEN BONDS
Chemically modified electrodes and related solution chemistry
[DE84-017110] 05 p0614 N85-13924
Neutron diffraction studies of the hydrogen bonding and water molecules in zeolites
[DE84-016431] 06 p0766 N85-14900
Structure of adsorbed monolayers. The surface chemical bond
[DE84-016879] 06 p0861 N85-15471
(Vinyloxy)fluorocyclotriphosphazenes
[AD-A147446] 07 p0924 N85-15850
Electronic structure, chemical bonding, and superconductivity of silver films on germanium
[AD-A147720] 08 p1128 N85-17112
Electronic structure, chemical bonding, and electron conductivity of thin-film transition-metal silicides
[AD-A147721] 08 p1226 N85-17716
Characterization of CO binding sites on Rh(111) and Rh(331) surfaces by XPS and LEED (Low Energy Electron Diffraction): Comparison to EELS (Electron Energy Loss Spectroscopy) results
[AD-A149331] 10 p1435 N85-19044
(Vinyloxy)chlorocyclotriphosphazenes
[AD-D011471] 10 p1453 N85-19152
Theoretical studies on N-bonded pyrazole derivatives of boron
[AD-A150036] 12 p1813 N85-21374
Bonding information from Auger spectroscopy
[AD-A150864] 14 p2251 N85-23946
Chemical and localization effects in Auger lineshapes of transition metal compounds
[AD-A150865] 14 p2251 N85-23949
C2H(n) fragments on metal surfaces
[AD-A151474] 15 p2505 N85-25449
Nitrolysis of the CN single bond and related chemistry of nitro and nitroso groups
[AD-A151753] 15 p2505 N85-25453
System for NDH of thermal spray coating bonds
[DE85-007463] 15 p2572 N85-25858
Molecular dynamics studies of energy transfer processes in crystal systems
[DE85-007247] 15 p2662 N85-26426
Compensation of dangling bonds in A-Si, Ge:H alloys
[DE85-002905] 15 p2662 N85-26433
Transitional metal activation and functionalization of C-H bonds
[DE85-006816] 16 p2746 N85-26949
New examples of clusters, extended metal-metal bonding and interstitial derivatives
[DE85-005926] 17 p3044 N85-28837
Exploratory study of coal conversion chemistry
[DE85-010393] 19 p3229 N85-30018
Diffusion welding of incompatible materials
19 p3245 N85-30121
Producing titanium-sapphire items by solid-phase bonding through aluminum gasket
19 p3246 N85-30127
Diffusion welding of aluminum with vacuum-tight corundum ceramic 19 p3247 N85-30130
Threshold effects and cellular recognition
[DE85-010816] 19 p3327 N85-30614
Why CO bonds side-on at low coverage and both side-on and upright at high coverage on the Cr(110) surface
[NASA-CR-176071] 21 p3565 N85-32173
Defects in tetrahedrally coordinated amorphous semiconductors
[AD-A155150] 21 p3581 N85-32263
Interfacial bonding stability 21 p3608 N85-32409
Infrared studies of the influence of alkali metals on the C-O bond in chemisorbed carbon monoxide
[DE85-005306] 23 p3911 N85-34232
Separation of gas mixtures by supported complexes
[DE85-011996] 23 p3912 N85-34236
The photodissociation of acetylene at 193.3 NM
[AD-A155775] 24 p4075 N85-35255
Dangling bonds and sub-gap optical absorption in silicon
[DE85-011752] 24 p4082 N85-35302

CHEMICAL CLEANING
NT PICKLING (METALLURGY)
Composition and method for cleaning embedded soil from surfaces having low gloss coatings
[AD-D011465] 10 p1459 N85-19194
Chemical cleaning of 304 and 304-L stainless steel surfaces by the nitradd passivation process
[DE85-003714] 11 p1615 N85-20158

CHEMICAL CLOUDS
NT BARIUM ION CLOUDS

CHEMICAL COMPOSITION
NT CARBON DIOXIDE CONCENTRATION
NT STELLAR COMPOSITION
Compilation of elemental concentration data for NBS (National Bureau of Standards) biological, geological and environmental standard reference materials, 1982
[PB84-218338] 01 p0025 N85-10158
Milling of Si3N4 with Si3N4 hardware
[NASA-TM-86864] 01 p0031 N85-10191
Microtektite discovered in Beijing
[NASA-TM-77765] 01 p0130 N85-10695
Solidification and crystal growth of solid solution semiconducting alloys 02 p0155 N85-11046
Factor analysis applied to a silane coupling agent on E-glass fiber system
[AD-A145637] 02 p0187 N85-11249
Variability of major organic components in aircraft fuels. Volume 3: Sample data package for the reference JP-4 fuel
[AD-A145483] 02 p0188 N85-11254
Variability of major organic components in aircraft fuels. Volume 1: Technical discussion
[AD-A145574] 02 p0188 N85-11256
Mechanical properties of a leaded, resulfurized, rephosphorized steel in various thermo/mechanical conditions
[PB84-216464] 03 p0333 N85-12144
Effect of oxidizing medium and heat treatment on stoichiometry of ZnSe crystal surface
03 p0353 N85-12272
Nutritional models for space travel from chemically defined diets
[NASA-CR-3850] 03 p0402 N85-12561
CVD parameter study using strategy of experimentation
[DE84-015900] 04 p0473 N85-13011
Variability of major organic components in aircraft fuels. Volume 2: Illustrations
[AD-A145831] 04 p0481 N85-13067
Development and evaluation of cloud water collectors
[PB84-232529] 04 p0540 N85-13437
Non-invasive techniques for determining musculoskeleton body composition
[DE84-015718] 04 p0545 N85-13470
Testing of production of silicon-titanium-magnesium alloying composition
[BLL-M-35904-(5828.4)] 05 p0616 N85-13937
In vivo neutron activation analysis: Body composition studies in health and disease
[DE84-014092] 05 p0696 N85-14480
Clinical measurements using fiber optics and optrodes
[DE84-015043] 05 p0696 N85-14481
In situ analysis of corrosive and passive surfaces by laser-excited Raman spectroscopy — lead, galvanized iron, and asbestos-cement pipes
[PB84-229756] 06 p0767 N85-14904
Method for predicting the creep rupture life of nickel-base precipitation-hardened superalloys from their chemical composition
[BLL-PNR-90241-(6019.3153)]
06 p0768 N85-14910
Bulk compositions of Al-rich chondrules in ordinary and carbonaceous chondrites: Variations and similarities
06 p0881 N85-15601
Major element chemical compositions of chondrules in unequilibrated chondrites 06 p0881 N85-15602
Chondrule rims and interchondrule matrix in UOC
06 p0882 N85-15604
The Colony meteorite and the possible existence of a new chemical subgroup of CO3 chondrites
06 p0885 N85-15621
Where is the Earth's missing xenon?
06 p0888 N85-15641
The chemistry of rare earth elements in the solar nebula 06 p0889 N85-15643
Optimization of the NiCrAl-Y/ZrO-Y2O3 thermal barrier system
[NASA-TM-86905] 07 p0927 N85-15878
Gradient polymers
[AD-A146836] 07 p0931 N85-15900
General theory and design considerations for optical waveguide chemical vapor sensors
[AD-A148505] 08 p1223 N85-17702
Variation of oxygen and nitrogen abundances in the galaxy 08 p1248 N85-17878
Aromatics determination in middle distillate petroleum fractions by spectrophotometric titration
[PNR-90239] 09 p1293 N85-18123
CVD boron on calcium chromate powder
[DE85-000214] 09 p1299 N85-18156
Corrosion of ceramics in heat exchanger applications
[DE84-017459] 09 p1299 N85-18161
Compositional, structural, and physical studies of some graphite hexafluoroarsenates and their relatives
[DE85-000855] 10 p1432 N85-19030
Composition and method for cleaning embedded soil from surfaces having low gloss coatings
[AD-D011465] 10 p1459 N85-19194
Interaction of large meteoroids with the atmosphere
11 p1656 N85-20431
Microalgae culture collection, 1984-1985
[DE84-013035] 11 p1690 N85-20626
Carbon, silicon, and oxygen in the white dwarf star GD 40 11 p1752 N85-21017
Plasticizer system for propellant compositions
[AD-D011514] 12 p1817 N85-21393
Summary report of the Workshop on Structure Activity Concepts in Environmental Sciences
[PB85-137339] 12 p1867 N85-21841
Chemical characterization and toxicologic evaluation of airborne mixtures. Inhalation toxicology of diesel fuel obscurant aerosol in Sprague-Dawley rats. Phase 3. Subchronic exposures
[AD-A150100] 12 p1905 N85-21966
Characterization of high purity Si-doped molecular beam epitaxial GaAs
[AD-A149651] 12 p1939 N85-22181
Silicon carbide-silicon nitride fibers: Preparation and characterization of polycarbosilazane precursors
12 p1945 N85-22214
Cosmic ray composition and origin
12 p1955 N85-22287
The influence of fuel quality upon flame-tube temperature and flame radiation in a model gas-turbine primary zone
[K233] 13 p1974 N85-22396

Structural distortions of ultra-dispersed titanium nitride powders 13 p2029 N85-22717

Composition and thickness of oxide coatings on granule surfaces of aluminum alloys 13 p2030 N85-22719

Impurities in Kevlar 49 fibers
[DE85-004996] 13 p2038 N85-22767

Composition and photochemical reactivity of turbine engine exhaust
[AD-A150559] 13 p2130 N85-23256

Chemical composition of coastal haze aerosol
14 p2338 N85-24456

Long-term exposure of pressed plutonium oxide heat sources to aquatic environments
[DE85-007385] 15 p2495 N85-25392

Resonant coherent anti-Stokes Raman scattering
[ESA-TT-876] 15 p2507 N85-25466

Studies of photosynthetic Energy Conversion
[DE85-005973] 15 p2586 N85-25944

A review of radar observations of Saturn's rings
15 p2670 N85-26474

Physical properties of Saturn's rings
15 p2672 N85-26493

Technical and economic analysis of liquid fuel production from microalgae
[DE85-002926] 16 p2758 N85-27018

High resolution spectroscopy of C13O16 in gas mixtures
[AD-A152625] 17 p2919 N85-27991

Influence of structural state and alloy content of austenite on formation of martensitic phases in steels
[BLL-BISI-TRANS-22385-(9022.06)]
17 p2928 N85-28066

The effect of microalloying with calcium and magnesium on the plasticity of Poldi AKN 20 Ni-based alloy
[BLL-BISI-TRANS-2174-(9022.06)]
17 p2929 N85-28075

In situ HVEM studies of electron beam-driven composition changes in thin film alloys: Displacement-rate gradient effects
[DE85-007992] 17 p2931 N85-28092

Application of scattering methods to the studies of the structure of polymer blends
[FPR-13/1984] 17 p2933 N85-28104

Chemicals identified in human biological media, a data base, volume 6, part 1
[DE85-008766] 17 p2999 N85-28542

Adsorption of Hg on lunar samples
[DE85-007948] 17 p3054 N85-28906

The distribution of higher n-alkanes in partially frozen middle distillate fuels
[AD-A153940] 18 p3083 N85-29074

Measurement of radical species concentrations and polycyclic aromatic hydrocarbons in flames by fluorescence and absorption using a tunable dye laser
[DE85-008624] 18 p3113 N85-29274

Chemicals identified in human biological media, a data base. Volume 6, part 2: Records 7588-8694
[DE85-008767] 18 p3154 N85-29526

Combustion characterization of coals for industrial applications
[DE85-010673] 19 p3228 N85-30014

Adherence of ash particles from the combustion of micronized coal
[DE85-008600] 19 p3229 N85-30023

The mobile phase in coals: Its nature and modes of release
[DE85-011696] 19 p3230 N85-30026

Chemical composition and kinetics of libration of gases upon welding of aluminum alloys
19 p3247 N85-30131

The origin and evolution of the Earth's atmosphere and hydrosphere 19 p3312 N85-30533

Debye temperature and static displacements in LuH sub x single crystals from energy dispersive X-ray diffraction
[DE85-010961] 19 p3376 N85-30946

Solar photospheric and coronal abundances from solar energetic particle measurements
[NASA-CR-176029] 20 p3547 N85-32073

The effect of diffusive hydrogen segregation on fracture of polycrystalline nickel
[AD-A155238] 21 p3567 N85-32186

Chemical composition of atmospheric aerosol at Delhi
21 p3646 N85-32653

Investigation of the formation of cloud particle spectrum on natural condensation nuclei
21 p3649 N85-32674

Variations of particulate sulfur concentrations in a coastal atmospheric environment in connection with the change of air masses origin 21 p3652 N85-32692

Liquid-phase compositions from vapor-phase analyses 2: Adaptation of the Prausnitz program to UF6 and some of its potential impurities
[DE85-011521] 21 p3673 N85-32819

Evaluation of pilot ESP used with a spray dryer FGD system at Pittsburgh Energy Technology Center, Bruceton, Pennsylvania
[DE85-011151] 22 p3746 N85-33217

Experimental studies of glass refining
[NASA-CR-176130] 22 p3751 N85-33248

Metallic glass composition
[DE85-011594] 22 p3751 N85-33253

Technology of off-gas treatment for liquid-fed ceramic melters
[DE85-012467] 22 p3812 N85-33610

Venus, Earth and Mars: Present bounds on similarities and differences in bulk composition
22 p3856 N85-33876

A new method to determine the chemical composition of the cosmic rays beyond 10 to the 15th power eV
[OG-5.1-11] 22 p3882 N85-34052

Cosmic ray composition between 10 to the 15th power - 10 to the 17th power eV obtained by air shower experiments
[OG-5.1-12] 22 p3882 N85-34053

The primary composition beyond 10 to the 5th power GeV as deduced from high energy hadrons and muons in air showers
[OG-5.2-6] 22 p3883 N85-34063

Determination of low chloride values in Rocky Flats scrub alloy solutions and other complex matrices
[DE85-011506] 23 p3911 N85-34234

The influence of temperature on the composition density of the transition metals
[BLL-M-35896-(5826.4)] 23 p3915 N85-34262

Throughfall rate and chemistry studies: Whiteface Mountain
[DE85-012407] 23 p3947 N85-34464

Thermally induced chemical migration: A natural analog approach
[DE85-012308] 23 p3949 N85-34474

Energetic particle observations of the solar-gamma ray/neutron flare events of 3 Jun 1982 and 21 June 1980 isotopic and chemical composition
[SH-2.1-3] 23 p3998 N85-34784

Precision measurements of solar energetic particle elemental composition
[SH-2.1-4] 23 p3998 N85-34785

Variations in elemental composition of several MEV/nucleon ions observed in interplanetary space
[SH-2.1-7] 23 p3998 N85-34788

The cosmic ray composition as viewed from the chemical abundances of the solar system
[OG-7.1-8] 23 p4013 N85-34869

The 4He1H ratios in the chemical compositions of solar flare particles and the primordial solar nebula
[SH-7.1-12] 23 p4048 N85-35104

Measurement of low energy cosmic rays aboard Spacelab-1
[SH-10.1-6] 23 p4053 N85-35137

Ion composition measurements of the disturbed and quiet D-region in 1980 - 1981
[AD-A156055] 24 p4117 N85-35521

Energy spectra of proton and nuclei of primary cosmic rays in energy region 10 TeV/particle
[HE-3.1-10] 24 p4178 N85-35908

A comparative analysis of gamma and hadron families at the superhigh energies recorded in experiment Pamir
[HE-3.7-1] 24 p4185 N85-35960

Correlation of high energy muons with primary composition in extensive air shower
[HE-4.3-7] 24 p4191 N85-36001

A large area cosmic muon detector located at Ohya stone mine
[HE-5.1-7] 24 p4201 N85-36072

On muon energy spectrum in muon groups underground
[HE-5.1-14] 24 p4201 N85-36076

Multiple muons in MACRO
[HE-5.2-1] 24 p4202 N85-36079

CHEMICAL COMPOUNDS

Compilation of data sources for existing chemicals
[GSF-A-2/84] 01 p0017 N85-10103

Method for fluorination of actinide fluorides and oxyfluorides using O2F2
[DE85-011646] 22 p3[illegible] N85-33202

CHEMICAL DEFENSE

Anthropometric cockpit compatibility assessment of US Army aircraft for large and small personnel wearing A cold weather, armored vest, chemical defense protective clothing configuration
[AD-A145472] 02 p0238 N85-11547

CHEMICAL EFFECTS

Chemical-mechanical interaction in gears
14 p2223 N85-23785

Detailed chemical kinetic study of the effect of molecular structure on autoignition of fuel-air mixtures
[DE85-004424] 17 p2921 N85-28010

CHEMICAL ELEMENTS

NT ACTINIDE SERIES
NT ACTIVATED CARBON
NT ALKALI METALS
NT ALKALINE EARTH METALS
NT ALUMINUM
NT ALUMINUM ISOTOPES
NT ALUMINUM 26
NT AMERICIUM
NT AMERICIUM ISOTOPES
NT AMERICIUM 241
NT ANTIMONY
NT ARGON
NT ARGON ISOTOPES
NT ARSENIC
NT BARIUM
NT BERYLLIUM
NT BERYLLIUM ISOTOPES
NT BERYLLIUM 7
NT BERYLLIUM 9
NT BERYLLIUM 10
NT BISMUTH
NT BORON
NT BORON 10
NT BROMINE
NT BROMINE ISOTOPES
NT CADMIUM
NT CALCIUM
NT CALCIUM ISOTOPES
NT CALIFORNIUM ISOTOPES
NT CARBON
NT CARBON ISOTOPES
NT CARBON 12
NT CARBON 13
NT CARBON 14
NT CERIUM
NT CERIUM 144
NT CESIUM
NT CESIUM ISOTOPES
NT CESIUM 134
NT CESIUM 137
NT CHARCOAL
NT CHLORINE
NT CHROMIUM
NT CHROMIUM ISOTOPES
NT COBALT
NT COBALT 60
NT COPPER
NT CURIUM
NT CURIUM 244
NT DEUTERIUM
NT DEUTERIUM PLASMA
NT ERBIUM
NT FLUORINE
NT GADOLINIUM
NT GALLIUM
NT GERMANIUM
NT GERMANIUM ISOTOPES
NT GOLD
NT HAFNIUM
NT HALOGENS
NT HELIUM
NT HELIUM ATOMS
NT HELIUM ISOTOPES
NT HOLMIUM
NT HYDROGEN
NT HYDROGEN ATOMS
NT HYDROGEN IONS
NT HYDROGEN ISOTOPES
NT HYDROGEN PLASMA
NT INDIUM
NT IODINE
NT IODINE ISOTOPES
NT IRIDIUM
NT IRON
NT IRON ISOTOPES
NT IRON 59
NT ISOTOPES
NT KRYPTON
NT KRYPTON ISOTOPES
NT KRYPTON 85
NT LANTHANUM
NT LEAD (METAL)
NT LIGHT ELEMENTS
NT LIQUID HELIUM
NT LIQUID HELIUM 2
NT LIQUID HYDROGEN
NT LIQUID LITHIUM
NT LIQUID NITROGEN
NT LIQUID POTASSIUM
NT LIQUID SODIUM
NT LITHIUM
NT LUTETIUM
NT MAGNESIUM
NT MAGNESIUM ISOTOPES
NT MANGANESE

NT MANGANESE ISOTOPES
NT MERCURY (METAL)
NT METALLIC HYDROGEN
NT METALLOIDS
NT MOLYBDENUM
NT NEODYMIUM
NT NEODYMIUM ISOTOPES
NT NEON
NT NEON ISOTOPES
NT NICKEL
NT NICKEL ISOTOPES
NT NIOBIUM
NT NITROGEN
NT NITROGEN IONS
NT NITROGEN ISOTOPES
NT NITROGEN 15
NT NUCLIDES
NT OSMIUM
NT OSMIUM ISOTOPES
NT OXYGEN
NT OXYGEN ATOMS
NT OXYGEN IONS
NT OXYGEN ISOTOPES
NT OXYGEN PLASMA
NT PALLADIUM
NT PHOSPHORUS
NT PLATINUM
NT PLUTONIUM
NT PLUTONIUM ISOTOPES
NT PLUTONIUM 238
NT PLUTONIUM 239
NT POTASSIUM
NT POTASSIUM 40
NT POWDERED ALUMINUM
NT PRASEODYMIUM
NT RADIOACTIVE ISOTOPES
NT RADIUM
NT RADON
NT RADON ISOTOPES
NT RARE EARTH ELEMENTS
NT RARE GASES
NT REFRACTORY METALS
NT RHODIUM
NT RUBIDIUM
NT RUBIDIUM ISOTOPES
NT RUTHENIUM
NT SAMARIUM
NT SCANDIUM
NT SCANDIUM ISOTOPES
NT SELENIUM
NT SILICON
NT SILICON ISOTOPES
NT SILVER
NT SINTERED ALUMINUM POWDER
NT SODIUM
NT SODIUM ISOTOPES
NT SODIUM VAPOR
NT STRONTIUM 90
NT SULFUR
NT TANTALUM
NT TECHNETIUM
NT TELLURIUM
NT THALLIUM
NT THORIUM
NT THORIUM ISOTOPES
NT TIN
NT TITANIUM
NT TRACE ELEMENTS
NT TRANSURANIUM ELEMENTS
NT TRITIUM
NT TUNGSTEN
NT URANIUM
NT URANIUM ISOTOPES
NT URANIUM 235
NT VANADIUM
NT XENON
NT XENON ISOTOPES
NT XENON 129
NT YTTERBIUM
NT YTTRIUM
NT ZINC
NT ZIRCONIUM

User's manual for GRIZZLY
[DE85-001405] 11 p1702 N85-20702

The cosmic ray composition as viewed from the chemical abundances of the solar system
[OG-7.1-8] 23 p4013 N85-34869

CHEMICAL ENERGY
NT ENERGY OF FORMATION

Phase equilibria of stored chemical energy reactants
[AD-A146527] 06 p0765 N85-14896

Sensitization and quenching in the conversion of light energy into chemical energy
[DE85-006301] 14 p2351 N85-24535

Modeling heterogeneous high explosive burn with an explicit hot-spot process
[DE85-009593] 23 p3922 N85-34300

CHEMICAL ENGINEERING

Experimental and theoretical study of a solar thermochemical receiver module
[NASA-CR-174107] 04 p0528 N85-13374

Chemical engineering principles of constant temperature-constant supersaturation growth of potassium dihydrogen phosphate (KDP) crystals
[DE84-017081] 04 p0571 N85-13645

Activities report in technology
[ISBN-951-38-1998-1] 04 p0577 N85-13681

USSR report: Chemistry
[JPRS-UCH-85-001] 13 p2013 N85-22629

Current plans for development of chemical industry
13 p2014 N85-22633

Failure mechanisms in metal-sheathed thermocouples
[DE85-011929] 21 p3590 N85-32317

CHEMICAL EQUILIBRIUM
NT ACID BASE EQUILIBRIUM

Catalyzed low burning rate propellants for upper-stage solid rocket motor
[NAL-TR-805] 03 p0339 N85-12181

Computer calculation of chemical equilibrium in multi-component systems
[BLL-M-35973-(5828.4)] 05 p0614 N85-13919

Effect of water on hydrogen permeability --- Stirling engines
[NASA-TM-86904] 06 p0761 N85-14864

Phase equilibria of stored chemical energy reactants
[AD-A146527] 06 p0765 N85-14896

Vaporization behavior, phase equilibria, and thermodynamic stabilities of nickel phosphides
[AD-A146683] 06 p0765 N85-14897

Computer program for calculation of complex chemical equilibrium compositions and applications. Supplement 1: Transport properties
[NASA-TM-86885] 07 p1049 N85-16663

Carbon vaporization/condensation effects
[NASA-TM-87430] 10 p1436 N85-10048

French activities relevant to middle atmosphere research 11 p1655 N85-20423

Diagrams of chemical and electrochemical equilibria in the presence of oxygen and sulphur
[AD-A150929] 14 p2251 N85-23953

The origin and evolution of the Earth's atmosphere and hydrosphere 19 p3312 N85-30533

Combustion gas properties. Part 3: Hydrogen gas fuel and dry air
[NASA-TP-2477] 20 p3395 N85-31058

Nonequilibrium chemistry in an isothermal turbulent flow 22 p3745 N85-33211

Comparison of experimental data on detonation velocity and Chapman-Jouget pressure vs initial HE density with predictions from Ree's model equation of state
[DE85-007266] 23 p3922 N85-34304

Aqueous volatile weak electrolyte equilibria to 300 C
[DE85-013840] 24 p4076 N85-35261

CHEMICAL EVOLUTION

Chemical evolution of the solar nebula: A new model
06 p0687 N85-15631

Origin of life 21 p3657 N85-32713

Insights into the phylogenetic positions of photosynthetic bacteria obtained from 5S rRNA and 16S rRNA sequence data 21 p3658 N85-32719

Search for the universal ancestors
[NASA-SP-477] 21 p3667 N85-32777

Submarine hydrothermal environments as sites for the origin and evolution of life 21 p3719 N85-33074

CHEMICAL EXPLOSIONS
NT GAS EXPLOSIONS

Measurements of two-phase exhaust flow parameters of a small caliber gun associated with muzzle flash phenomena
[ISL-CO-212/83] 16 p2784 N85-27182

Detonation behavior of LX-14 and PBX-9404: Theoretical aspect
[DE85-010038] 18 p3084 N85-29076

The shock desensitization of PBX-9404 and composition B-3
[DE85-009804] 18 p3084 N85-29077

Explosibility of ammonium nitrate
[HSE-TRANS-11111] 19 p3252 N85-30164

Combustion-deflagration-detonation transition in a confined spherical powder
[ISL-R-108/84] 22 p3747 N85-33223

Behavior of the porous bed in a combustion-deflagration-detonation transition
[ISL-CO-220/84] 22 p3747 N85-33224

Nuclear magnetic resonance study of the intramolecular rearrangement of 2-(5-cyanotetrazolato)pentaammine cobalt (III) perchlorate
[DE85-010810] 22 p3839 N85-33772

Time-resolved spectroscopic studies of detonating heterogeneous explosives
[DE85-009760] 23 p3921 N85-34297

Pressure-shear loading of PBX-9404
[DE85-009962] 23 p3921 N85-34298

Modeling heterogeneous high explosive burn with an explicit hot-spot process
[DE85-009593] 23 p3922 N85-34300

Three-dimensional hydrodynamic hot-spot model
[DE85-009587] 23 p3922 N85-34301

Effect of precipitation variables on the specific surface and explosion characteristics of pentaerythritol tetranitrate
[DE85-009620] 23 p3922 N85-34302

Comparison of experimental data on detonation velocity and Chapman-Jouget pressure vs initial HE density with predictions from Ree's model equation of state
[DE85-007266] 23 p3922 N85-34304

Friction, impact, and electrostatic discharge sensitivities of energetic materials
[DE85-013321] 24 p4083 N85-35309

CHEMICAL EXTINGUISHERS
U FIRE EXTINGUISHERS

CHEMICAL FRACTIONATION

Effects of method of detachment on electrophoretic mobility of mammalian cells grown in monolayer culture
20 p3500 N85-31757

Isotopic Biogeochemistry
[NASA-CR-176128] 22 p3741 N85-33189

CHEMICAL FUELS
NT AIRCRAFT FUELS
NT AUTOMOBILE FUELS
NT DIESEL FUELS
NT GASOHOL (FUEL)
NT GASOLINE
NT HYDROCARBON FUELS
NT HYDROGEN FUELS
NT JET ENGINE FUELS
NT JP-4 JET FUEL
NT JP-5 JET FUEL
NT JP-8 JET FUEL
NT KEROSENE
NT LIQUID FUELS
NT SLURRY PROPELLANTS
NT SYNTHETIC FUELS

Technical instructions for a control operating system of the gas flow installation for the solid fuel combustion chamber
[VTH-LR-410] 18 p3116 N85-29302

CHEMICAL INDICATORS

Electrochromic display device
[AD-D011733] 22 p3759 N85-33299

CHEMICAL KINETICS
U REACTION KINETICS

CHEMICAL LASERS

Influence of translational and hyperfine relaxation on energy characteristics of oxygen-iodine laser
02 p0261 N85-11707

Delta wing nozzle assembly for chemical lasers
[AD-D011396] 07 p0970 N85-16158

Conference on Singlet Molecular Oxygen (COSMO 84), program and abstracts
[AD-A147281] 07 p1040 N85-16605

Halogen mass flow rate detection system
[AD-D011398] 08 p1165 N85-17352

Bibliography of Soviet laser developments, Number 66, July-August 1983
[AD-A149113] 10 p1490 N85-19406

Chemically amplified laser direct-writing of aluminum
[DE85-000308] 11 p1639 N85-20324

Saturation kinetics of active medium of oxygen-iodine laser 11 p1718 N85-20807

Waveguide phenomena in dense relaxing gases and their use in chemical and gas-dynamic lasers
15 p2644 N85-26308

Short Wavelength Chemical Laser (SWCL) Workshop
[AD-A151959] 16 p2790 N85-27211

Rotational relaxation studies of hydrogen fluoride
[AD-A152711] 17 p3029 N85-28734

Review of short wavelength lasers
[DE85-009858] 18 p3114 N85-29277

Chemical lasers
[ISL-R-107/84] 23 p3936 N85-34400

CHEMICAL MACHINING
NT ELECTROCHEMICAL MACHINING

Electropulse chemical machining
[DE84-016693] 04 p0484 N85-13084

CHEMICAL MILLING
U CHEMICAL MACHINING

CHEMICAL PROPERTIES
NT ACIDITY
NT HEAT OF FORMATION
NT HEAT OF FUSION
NT HEAT OF VAPORIZATION
NT SALINITY
NT THERMOCHEMICAL PROPERTIES

Development of new and improved polymer matrix resin systems, phase 1
[NASA-CR-168596] 01 p0017 N85-10104

Synthesis and characterization of advanced materials
[PB84-215326] 01 p0025 N85-10156

Guide to the selection of rubbers
[AMTE(N)-TM-84301] 03 p0336 N85-12164

Online directory of databases for material properties
[DE84-016511] 09 p1402 N85-18824

Monitoring approaches for assessing quality of high altitude lakes: Colorado Flat Tops Wilderness Area
[PB85-117232] 11 p1679 N85-20579

A brief review of the technology of microemulsions and other micellar systems
[AD-A149759] 12 p1800 N85-21289

Sequential excitation preparation of molecular energy levels with special structural and chemical properties
[AD-A150301] 13 p2158 N85-23386

Resistance of optical coatings to alkali solutions and sea water 14 p2261 N85-24129

Water-resistence and some other properties of polyalkali fluorophosphate glasses 14 p2261 N85-24133

Electrochemical behavior of amorphous alloys based on iron, cobalt and nickel in H3PO4 solutions alone and mixed with HF 15 p2513 N85-25505

Liquid propellants for use in guns: A review
[AD-A153051] 17 p2937 N85-28131

Operation guiding light-scientific program and field plan. The pilot field experiment for NORDA project chemical dynamics in ocean frontal areas
[AD-A153765] 18 p3150 N85-29507

Chemical spectroscopy
[DE85-009594] 18 p3191 N85-29790

Chemical, biological, and physical measurements from the subtropical western North Atlantic Ocean. Summer 1982, USNS Lynch, cruise 710-82
[AD-A153823] 18 p3201 N85-29857

Chemical-acoustic interactions in combustion systems
[AD-A153857] 19 p3233 N85-30046

Optical 3-D signature device for detecting chemical agents
[AD-D011669] 19 p3272 N85-30293

Numerical simulation of chemical and physical properties of cumulus clouds
[DE85-009744] 19 p3317 N85-30584

Chromophores with auxochrome-like function
[NASA-TM-77649] 20 p3421 N85-31233

Electrochemistry of Hexanitroazobenzene (HNAB)
[DE85-010807] 21 p3565 N85-32171

Physical chemical state of water in living cells
[AD-A154566] 21 p3662 N85-32749

Experimental studies of chemical reactivity during shock initiation of hexanitrostilbene
[DE85-011726] 22 p3754 N85-33270

Hydrazine nitrate based explosives
[ISL-CO-229/84] 22 p3754 N85-33272

The effect of liquid-liquid phase separation of glass on the properties and crystallization behavior
[NASA-TM-77890] 23 p3919 N85-34285

Chemical lasers
[ISL-R-107/84] 23 p3936 N85-34400

Chemoviscosity modeling for thermosetting resins, 2
[NASA-CR-177958] 24 p4073 N85-35243

CHEMICAL PROPULSION
NT HYBRID PROPULSION

Preliminary assessment of power-generating tethers in space and of propulsion for their orbit maintenance
13 p1997 N85-22520

Primary propulsion of electrothermal, ion and chemical systems for space-based radar orbit transfer
[NASA-TM-87043] 17 p2916 N85-27972

CHEMICAL REACTION CONTROL

China report: Science and technology
[JPRS-CST-85-011] 16 p2551 N85-25746

CHEMICAL REACTIONS
NT ALKYLATION
NT ATOMIC RECOMBINATION
NT CARBOXYLATION
NT CHLORINATION
NT COPOLYMERIZATION
NT CRACKING (CHEMICAL ENGINEERING)
NT DECARBONATION
NT DEHYDROGENATION
NT DENITROGENATION
NT DEOXIDIZING
NT DESULFURIZING
NT DIELS-ALDER REACTIONS
NT ELECTROCHEMICAL OXIDATION
NT EXOTHERMIC REACTIONS
NT FERMENTATION
NT FLUORINATION
NT HALOGENATION
NT HYDROGENATION
NT HYDROGENOLYSIS
NT HYDROLYSIS
NT ION RECOMBINATION
NT METHANATION
NT NITRATION
NT NITRIDING
NT NITROGENATION
NT NITROLYSIS
NT OXIDATION
NT OXIDATION-REDUCTION REACTIONS
NT OXYGEN RECOMBINATION
NT OXYGENATION
NT PHOSPHORYLATION
NT PHOTOCHEMICAL REACTIONS
NT PHOTOCHROMISM
NT PHOTODECOMPOSITION
NT PHOTOLYSIS
NT PHOTOOXIDATION
NT PHOTOSYNTHESIS
NT PYROLYSIS
NT RADIOLYSIS
NT REDUCTION (CHEMISTRY)
NT RUSTING
NT SULFATION
NT SULFIDATION
NT THERMAL DECOMPOSITION
NT THERMAL DISSOCIATION
NT TITRATION

Treating silicon carbide sinter by heating in nitrogen
[NASA-TM-77601] 01 p0021 N85-10130

Lagging development of biotechnology described
01 p0115 N85-10787

Kinetics of simple inner- and outer-sphere electrochemical reactions at rotating silver electrodes as examined using surface-enhanced Raman spectroscopy
[AD-A145606] 02 p0172 N85-11154

Surface environmental effects in electrochemical kinetics: Outer-sphere chromium (3) reductions at mercury, gallium, lead, and thallium surfaces
[AD-A145607] 02 p0172 N85-11155

Alloying effects of reactive elements in ferritic stainless steels 02 p0178 N85-11196

The reactions of cobalt, iron and nickel in SO-2 atmospheres: Similarities and differences
[NASA-TM-86866] 02 p0181 N85-11217

The 7-Amino-4,6-Dinitrobenzofuroxan, an insensitive high explosive
[AD-A145665] 02 p0186 N85-11257

Impact cratering: The process and its effects on planetary evolution — and silicate-carbonate reactions on Venus
[NASA-CR-174016] 02 p0228 N85-11488

Study of singlet oxygen-pentavalent phosphorus reactions
[AD-A145896] 03 p0327 N85-12107

Experimental and theoretical study of a solar thermochemical receiver module
[NASA-CR-174107] 04 p0526 N85-13374

Mononitration of durene
[NASA-TM-77774] 06 p0765 N85-14892

Integrating chemical kinetic rate equations by selective use of stiff and nonstiff methods
[NASA-TM-86923] 07 p0904 N85-15726

Influence of temperatures of reactants on nature of product of solid-phase reactions
[BLL-M-36019-(5828.4)] 07 p0921 N85-15832

Laser spectroscopy of alkali atom-tetrahaloethylene reactions
[AD-A147431] 07 p0923 N85-15846

(Vinyloxy)fluorocyclotriphosphazenes
[AD-A147448] 07 p0924 N85-15850

Thio and seleno compounds of the transition metals with the d (o) configuration
[BLL-MINTEK-TR-1177-(5810.5759)]
07 p0925 N85-15863

Imide modified epoxy matrix resins
[NASA-CR-174695] 07 p0930 N85-15892

Performance and cost of energy transport and storage systems for dish applications using reversible chemical reactions
[NASA-CR-174263] 07 p0992 N85-16298

Method for introducing fluorine into an aromatic ring
[AD-D011397] 08 p1120 N85-17061

Basic instability mechanisms in chemically reacting subsonic and supersonic flows
[AD-A148408] 08 p1122 N85-17071

Homogeneous reaction involving components of different redox couples. 1: Theoretical considerations and digital simulation
[AD-A148666] 08 p1124 N85-17084

Ground-based measurements of mesosphere temperatures by optical means
08 p1163 N85-17453

Effects of heteroatom substituents on the properties of 1,2-dioxetanes
[AD-A148727] 09 p1290 N85-18100

Behavior of pressurized tubes of candidate alloys in a simulated low-Btu environment
[DE85-003403] 09 p1296 N85-18141

Time-resolved studies of free radicals and laser-initiated chain reactions
[DE85-002100] 09 p1326 N85-18332

New phases and chemical reactions in solid CO under pressure
[DE85-002033] 09 p1377 N85-18665

Reactivity of ion implanted silicon carbide
[DE85-001543] 09 p1399 N85-18802

Effects of a periodic disturbance on structure and mixing in turbulent shear layers and wakes
[AD-A149278] 10 p1484 N85-19370

Bibliography of Soviet laser developments, Number 66, July-August 1983
[AD-A149113] 10 p1490 N85-19408

Mixing chemical reaction and flow field development in ducted rockets
[DE85-002710] 11 p1591 N85-20009

Dynamical studies of molecular systems
[DE85-003053] 11 p1594 N85-20028

Analysis of the natural initiation of vapor explosions
[DE85-000188] 11 p1632 N85-20279

A study of organic chemical reactions in microemulsions
[AD-A150083] 12 p1796 N85-21265

Process for producing tris s(n-methylamino) methylsilane
[NASA-CASE-MFS-25721-1] 12 p1799 N85-21280

Ionic mechanisms of soot formation in flames
[AD-A150119] 12 p1801 N85-21297

Electrostatic potentials: A new method for interpreting and predicting molecular reactivities and for designing synthetic pathways. Applications to nitroaromatics, nitramines and nitrated
[AD-A150120] 12 p1801 N85-21298

Alternative anodic reactions in water splitting
[DE85-004159] 12 p1802 N85-21300

Low temperature deposition of nickel films
[AD-D011568] 12 p1805 N85-21319

Chemical approach for controlling nadimide cure temperature and rate
[NASA-CASE-LEW-13770-5] 12 p1810 N85-21352

Amine salts as bonding agents
[AD-D011543] 12 p1817 N85-21386

Sulfur oxygen processes on Io
13 p2173 N85-23481

Evaluation of unimolecular rate constants for some outer-sphere electrochemical reactions
[AD-A150758] 14 p2250 N85-23946

Diagrams of chemical and electrochemical equilibria in the presence of oxygen and sulphur
[AD-A150929] 14 p2251 N85-23953

Spectral methods for modeling supersonic chemically reacting flow fields
[NASA-CR-172578] 14 p2300 N85-24240

Modelling of photodegradation in solar cell modules of substrate and superstrate design made with ethylene-vinyl acetate as pottant material
[NASA-CR-175690] 14 p2350 N85-24527

Shock tube study of the fuel structure effects on the chemical kinetic mechanisms responsible for soot formation, part 2
[NASA-CR-174880] 15 p2504 N85-25444

Scattering properties of a moving dielectric object
[AD-A151974] 15 p2544 N85-25706

Transduction of the root gravitropic stimulus: Can apical calcium regulate auxin distribution?
15 p2606 N85-26063

Development of a persistent chemical agent simulation system
[NASA-CR-175780] 16 p2745 N85-26837

Development of a Persistent Chemical Agent Simulator System (PCASS)
[NASA-CR-175776] 16 p2745 N85-26838

Fluorinated polyesters
[AD-D011611] 16 p2753 N85-26888

Dual electrochemical system
[AD-D011616] 16 p2817 N85-27376

Evaluation of chemical reaction mechanisms for photochemical smog. Part 2: Quantitative evaluation of the mechanisms, revised
[PB85-160080] 16 p2822 N85-27408

Atmospheric chemistry
[INPE-3190-PRE/554] 16 p2826 N85-27430

The production of copper phthalocyanine and/or its derivatives
[NASA-TM-77629] 17 p2917 N85-27963

Investigation of reaction layer formation in high-load capacity lubricating oils
[MPA-83-01] 17 p2975 N85-28381

Average collisional vibrational energy transfer quantities and the inversion temperature
[AD-A152674] 17 p3029 N85-28733

The conversion of smaller borane fragments to larger structures. Systematics of boron hydride reactions
[AD-A153443] 18 p3070 N85-2896

Continous chemical reaction chromatography
[DE85-009812] 18 p3072 N85-28996
Effects of H2S on molten carbonate fuel cells
[DE85-008310] 18 p3130 N85-29386
Expected behavior of plutonium in the IFR fuel cycle
[DE85-008225] 18 p3181 N85-29725
Study of the chemical mechanism in lubrication
[DE85-010766] 19 p3228 N85-30013
Chemical-acoustic interactions in combustion systems
[AD-A153657] 19 p3233 N85-30046
Selective detection of species in complex matrices by SIMS (Secondary Ion Mass Spectrometry)
[AD-D011685] 19 p3235 N85-30053
Determination of the association constant for pertechnetic acid
[DE85-010224] 19 p3235 N85-30057
Variational transition state theory
[DE85-010685] 19 p3235 N85-30059
Thermodynamic study of CO2-organic compound interaction at high pressures and temperatures
[DE85-010969] 19 p3268 N85-30266
Production of gallium atoms by excimer laser photolysis of trimethyl gallium
[DE85-010742] 19 p3278 N85-30331
Lithium cell reactions
[AD-A154429] 19 p3305 N85-30484
KIVA: A computer program for two- and three-dimensional fluid flows with chemical reactions and fuel sprays
[DE85-010334] 19 p3339 N85-30693
Reactions of metal ions and their clusters in the gas phase using laser ionization-ion cyclotron resonance spectroscopy
[DE85-009478] 19 p3361 N85-30838
Slow chemistry effects in a turbulent mixing layer
20 p3424 N85-31252
Strong turbulence chemistry interaction in a piloted turbulent jet diffusion flame 20 p3425 N85-31257
Remarks on preparation of indandione detection reagents
[NASA-TM-77905] 21 p3560 N85-32146
Interface chemistry of Hg(1-x)Cd(x)Te
[AD-A154876] 21 p3563 N85-32161
Design of micelles as dephosphorylating agents
[AD-A155589] 21 p3564 N85-32166
EVA-glass interface bond stability
21 p3606 N85-32408
Experimental studies of the formation of Aitken nuclei in the atmosphere 21 p3644 N85-32641
In-cavity laser IR spectrum analyzer for investigating non-steady-state processes 21 p3685 N85-32894
Prospects for a new kind of synthesis: Assembly of molecular components to achieve functions
[AD-A155023] 21 p3702 N85-32997
Pulsed hydrojet propulsion
[DE85-010771] 22 p3784 N85-33446
Separation of gas mixtures by supported complexes
[DE85-011996] 23 p3912 N85-34236
Experimental evaluation of the thermodynamic properties of concentrated aqueous potassium hydroxide solutions
[DE85-010828] 23 p3912 N85-34238
Metal alkoxides: Models for metal oxides. Alkoxide ligands in early transition metal organometallic chemistry
[DE85-011368] 23 p3916 N85-34269
Fire-resistant phosphorus containing polyimides and copolyimides
[NASA-CASE-ARC-11522-2] 23 p3918 N85-34280
Real time analysis of PETN detonation products
[DE85-009581] 23 p3922 N85-34303
Chemical lasers
[ISL-R-107/84] 23 p3936 N85-34400
Studies in thermo-hydro-chemical transport in porous and fractured media
[DE85-012556] 23 p3949 N85-34473
Thermally induced chemical migration: A natural analog approach
[DE85-012306] 23 p3949 N85-34474
Multi-solute subsurface transfer modeling for energy solid wastes: Highlights FY 1984
[DE85-012786] 23 p3966 N85-34591
CO + H2 reaction over nitrogn-modified iron catalysts
[DE85-013791] 24 p4072 N85-35231

CHEMICAL REACTORS
Development of a polysilicon process based on chemical vapor deposition of dichlorosilane in an advanced Siemen's reactor
[NASA-CR-174148] 04 p0483 N85-13083
Aerosol reactor for silicon processing
06 p0832 N85-15292
Assessment of the need for an advanced high-strength chromium-molybdenum steel for construction of third-generation gasifier pressure vessels
[DE85-002865] 11 p1606 N85-20097
Development of a polysilicon process based on chemical vapor deposition of dichlorosilane in an advanced Siemen's reactor
[NASA-CR-174445] 11 p1672 N85-20532
Monodisperse Latex Reactor (MLR): A materials processing space shuttle mid-deck payload
[NASA-TM-86487] 12 p1782 N85-21187
Apparatus and method to keep the walls of a free-space reactor free from deposits of solid materials
[NASA-CASE-NPO-15851-1] 12 p1858 N85-21652
Preparation of polystryene latex particles in a rotating reactor
[NASA-CR-171475] 17 p2933 N85-28106
Continous chemical reaction chromatography
[DE85-009812] 18 p3072 N85-28996
Comparison of isothermal kerogen decomposition results using reactors with different heat-up rates
[DE85-008563] 19 p3237 N85-30068
Flash pyrolysis of biomass with reactive and non-reactive gases
[DE85-010962] 19 p3306 N85-30496
Decomposition of sulfuric acid using solar thermal energy
[DE85-012288] 21 p3564 N85-32170
Silicon production in an aerosol reactor
21 p3609 N85-32416

CHEMICAL RELAXATION
U MOLECULAR RELAXATION

CHEMICAL RELEASE MODULES
Environmental effects of space activities
11 p1678 N85-20577

CHEMICAL SHIFT
U CHEMICAL EQUILIBRIUM

CHEMICAL TESTS
NT CHEMICAL ANALYSIS
NT ELECTROPHOTOMETRY
NT GAS ANALYSIS
NT MICROANALYSIS
NT NEUTRON ACTIVATION ANALYSIS
NT OZONOMETRY
NT QUALITATIVE ANALYSIS
NT QUANTITATIVE ANALYSIS
NT SALT SPRAY TESTS
NT SPECTROSCOPIC ANALYSIS
NT URINALYSIS
NT VOLUMETRIC ANALYSIS
Chemical approach for controlling nadimide cure temperature and rate
[NASA-CASE-LEW-13770-6] 19 p3232 N85-30039
Soil extraction kit
[AD-D011736] 22 p3742 N85-33190
Quantitative determination of mineral composition by powder X-ray diffraction
[DE85-011654] 22 p3760 N85-33301

CHEMICAL WARFARE
Effects of pyridostigmine on psychomotor and visual performance
[AD-A148553] 08 p1196 N85-17539
Development of a persistent chemical agent simulation system
[NASA-CR-175780] 16 p2745 N85-26937
Development of a Persistent Chemical Agent Simulator System (PCASS)
[NASA-CR-175776] 16 p2745 N85-26938
Design of micelles as dephosphorylating agents
[AD-A155589] 21 p3564 N85-32166
The identification of compounds in mustard hydrolysate
[AD-A156381] 24 p4076 N85-35258

CHEMILUMINESCENCE
Two silicon phthalocyanines and a silicon naphthalocyanine: Synthesis, electrochemistry and electrogenerated chemiluminescence
[AD-A144760] 01 p0023 N85-10145
NaK chemiluminescence
[AD-A146077] 03 p0328 N85-12110
A silicon phthalocyanine and a silicon naphthalocyanine: Synthesis, electrochemistry, and electrogenerated chemiluminescence
[AD-A146441] 06 p0765 N85-14695
Laser spectroscopy of alkali atom-tetrahaloethylene reactions
[AD-A147431] 07 p0923 N85-15848
An investigation of chemiluminescent reactions
[AD-A148460] 08 p1122 N85-17073
Mg 2 emission of Pop. 2 long-period Cepheids
11 p1754 N85-21032
Magnetically-induced luminescence of (Ir(2=phos)(2)C10(4)
[AD-A149659] 12 p1799 N85-21266
Luminescence in the ocean
[AD-B089136L] 13 p2140 N85-23288
Thermolysis of 4-methyl-4-(1-propenyl)malonyl peroxide: Mechanistic limits to chemiluminescence efficiency
[AD-A151567] 15 p2505 N85-25452
Spectroscopic studies of lead oxide in a flow tube
[AD-A151649] 15 p2505 N85-25455
Electrogenerated chemiluminescence
[AD-A153547] 18 p3070 N85-28990
Equipment development for rapid detection of microorganisms in air and water
[FOA-A-40046-B2] 18 p3134 N85-29410
Alkali atom - SbCl(5) reactions: Blue-green chemiluminescence from an inverted population in SbCl
[AD-A154371] 19 p3276 N85-30315
Function of a device for detection of biological aerosols in field testing
[FOA-C-40194-B2] 20 p3504 N85-31782
Investigation of variation in the concentration of bacteria in outdoor testing, with the use of a detector for aerosols of bacteria
[FOA-C-40201-B2] 20 p3504 N85-31784
Calculation of molecular constants potential energy curves and Franck-Condon factors for lead oxide
[AD-A154521] 21 p3562 N85-32158
Nitrogen analysis by chemiluminescence
[AD-A156197] 24 p4083 N85-35308

CHEMISORPTION
Surface chemistry of palladium
[DE84-014572] 02 p0173 N85-11163
Dispersion forces of solids under stress. Chemisorption under stress
[AD-A146171] 03 p0373 N85-12380
Vibrational spectroscopy of chemisorption phenomena on model catalyst surfaces
[AD-A146753] 07 p0922 N85-15840
A study of the chemical interaction of gases with activated carbon
[AD-A147342] 07 p0923 N85-15846
The reaction of oxygen-nitrogen mixtures with granular activated carbons below the spontaneous ignition temperature
[AD-A149041] 10 p1434 N85-19039
Characterization of CO binding sites on Rh(111) and Rh(331) surfaces by XPS and LEED (Low Energy Electron Diffraction): Comparison to EELS (Electron Energy Loss Spectroscopy) results
[AD-A149331] 10 p1435 N85-19044
Adsorption thermodynamics and surface transport of metal catalyst poisons
[DE85-003750] 12 p1802 N85-21301
Chemisorption theory: Adsorption on copper-nickel alloys and titanium surface embrittlement
[DE85-001815] 12 p1807 N85-21334
Dipole active surface vibrational resonances on clean and hydrogen covered Ni(110)
[AD-A150546] 13 p2163 N85-23420
C2H(n) fragments on metal surfaces
[AD-A151474] 15 p2505 N85-25449
Experimental and theoretical study of the infrared reflectance of thin oxide films on metals
[DE85-005799] 15 p2653 N85-26366
Coadsorption studies on transition metals
[PB85-183713] 18 p3072 N85-29003
Pseudopotentials and total energy calculations: Applications to crystal stability, vibrational properties, phase transformations, and surface structures
[DE85-007657] 18 p3194 N85-29810
Cation promotion effects in zeolite-supported F-T catalysts
[DE85-009669] 19 p3233 N85-30044
Why CO bonds side-on at low coverage and both side-on and upright at high coverage on the Cr(110) surface
[NASA-CR-176071] 21 p3565 N85-32173
Experimental studies of the geometric and electronic structure of chemisorption bonding
[PB85-192250] 22 p3747 N85-33228
Infrared studies of the influence of alkali metals on the C-O bond in chemisorbed carbon monoxide
[DE85-005306] 23 p3911 N85-34232

CHEMISTRY
Abstracts of papers submitted in 1983 for publication
[PB84-217579] 03 p0396 N85-12543
Neutron scattering for the investigation of solid state materials, utilization in chemical structures
03 p0432 N85-12752
On the relationship between electronics and chemistry
[DRIC-T-7480] 22 p3743 N85-33200
Solar energy education: Renewable energy activities for chemistry and physics
[DE85-010371] 23 p3946 N85-34455

CHEMONUCLEAR PROPULSION
U CHEMICAL PROPULSION

CHEMORECEPTORS
Chemoreception and detection of micropollutants by means of a telemetric bionic detector
[DRIC-T-7460] 22 p3610 N85-33600

CHEMOTHERAPY
Magnetically-localizable, polymerized lipid vesicles and method of disrupting same
[AD-D011686] 19 p3249 N85-30144

CHESAPEAKE BAY (US)
Spectral model for subtidal variability in the Chesapeake Bay
[PB84-226679] 06 p0842 N85-15345
Comparison of MSS and TM data for landcover classification in the Chesapeake Bay area: A preliminary report — Taylor's Island, Maryland
13 p2121 N85-23210
Reverification of the Chesapeake Bay model
[AD-A155486] 21 p3655 N85-32706

CHEWING
U MASTICATION

CHILD-LANGMUIR LAW
Quenching of the beam-plasma instability by 3-D spectra of large scale density fluctuations
[NASA-CR-175969] 19 p3369 N85-30697

CHILDREN
Respiratory protection for children 3 - 6 years of age
[FOA-C-40197-C2] 02 p0238 N85-11550
Test and evaluation of the 2.4-micron photorefractor ocular screening system
[NASA-TM-86492] 15 p2615 N85-26115
Oral discussion, group-to-individual transfer and achievement in cooperative learning groups
[AD-A153209] 17 p3001 N85-28552

CHILE
Mineral nutrients in Mediterranean ecosystems
[REPT-71] 01 p0069 N85-10456

CHILLING
U COOLING

CHIMES
U AUDITORY SIGNALS

CHIMNEYS
Leakage-flow induced vibrations of a chimney structure suspended in a liquid flow — nuclear reactors
09 p1339 N85-18420

CHINA
Development of nowcasting in China
01 p0083 N85-10554
Microtektite discovered in Beijing
[NASA-TM-77765] 01 p0130 N85-10895
China report: Science and technology
[JPRS-CST-84-003] 04 p0491 N85-13132
Development of robot technology in Shanghai surveyed 04 p0492 N85-13134
China report: Science and technology
[JPRS-CST-84-001] 04 p0557 N85-13545
Present status, future prospects of domestic acoustical instruments 04 p0557 N85-13548
The characteristics of generation and the rate of distribution for science and technology information in our country (China)
[AD-A141037] 04 p0575 N85-13671
China report: Science and technology
[JPRS-CST-84-042] 06 p0747 N85-14789
New fighter aircraft reported — Jian-8 aircraft
06 p0747 N85-14790
F-7 supersonic day fighter viewed — Jian-7 aircraft
06 p0747 N85-14791
A-5 supersonic attack aircraft described — Qiang-5 aircraft 06 p0747 N85-14792
Details of export A-5 close-support aircraft given — Qiang-5 aircraft 06 p0748 N85-14793
China report: Science and technology
[JPRS-CST-84-037] 10 p1424 N85-18982
Details of export A-5 close-support aircraft given
10 p1424 N85-18983
China's future domestic satellite communications systems 10 p1476 N85-19312
China's domestic satellite communications
10 p1476 N85-19313
China report: Science and technology
[JPRS-CST-84-026] 11 p1619 N85-20189
Remote sensing technology now playing practical roles 11 p1619 N85-20190
China report: Science and technology
[JPRS-CST-84-025] 11 p1620 N85-20197
Thermophysical properties of matter
11 p1620 N85-20199
China report: Science and technology
[JPRS-CST-84-032] 11 p1621 N85-20202
China report: Science and technology
[JPRS-CST-84-039] 11 p1621 N85-20206
China report: Science and technology
[JPRS-CST-84-036] 11 p1696 N85-20661
China report: Science and technology
[JPRS-CST-85-008] 12 p1820 N85-21416
Systems research on China in year 2000
12 p1820 N85-21418
Studies of the development of cyclones over Southern China coastal areas and adjacent seas
[AD-A150108] 12 p1896 N85-21901
China report: Science and technology
[JPRS-CST-84-030] 13 p2041 N85-22777
China report: Science and technology
[JPRS-CST-85-003] 13 p2166 N85-23433
The astrometry network of observers in China
14 p2436 N85-25027
China report: Science and technology
[JPRS-CST-85-009] 15 p2530 N85-25596
Future prospects of China's microwave semiconductor technology 15 p2530 N85-25598
China report: Science and technology
[JPRS-CST-85-007] 15 p2533 N85-25621
China report: Science and technology
[JPRS-CST-85-011] 15 p2551 N85-25746
China report: Science and technology
[JPRS-CST-85-010] 15 p2564 N85-25819
China report: Science and Technology
[JPRS-CST-85-012] 16 p2806 N85-27300
China has developed a new version of fighter aircraft
[AD-A155293] 21 p3555 N85-32118
Geology and petroleum resources of basins in western China
[DE85-013036] 23 p3946 N85-34469
Space activities in the Soviet Union, Japan, and the People's Republic of China 23 p4057 N85-35149

CHINA (COMMUNIST) MAINLAND
U CHINA

CHINESE PEOPLES REPUBLIC
U CHINA

CHINOOK HELICOPTER
U CH-47 HELICOPTER

CHIPS (ELECTRONICS)
Routing the power and ground wires on a VLSI chip
[AD-A145356] 02 p0194 N85-11296
NMOS test chip for a course in semiconductor parameter measurements
[PB84-216506] 04 p0497 N85-13174
VLSI architectures for the multiplication of integers modulo a Fermat number 05 p0624 N85-13993
Specialized silicon compilers for language recognition
[AD-A146526] 06 p0853 N85-15425
Charge domain filters for enhanced monolithic signal processing
[AD-A147428] 07 p0941 N85-15964
Built-in test and self repair mechanisms in a digital correlator integrated circuit 08 p1064 N85-16741
Life cycle cost model for very high speed integrated circuits
[AD-A147798] 08 p1157 N85-17298
Design of a bit-sliced processor array with built-in-self-test
[AD-A149785] 12 p1835 N85-21513
Built-in tests for VLSI (Very Large Scale Integration) finite-state machines
[AD-A149784] 12 p1911 N85-21997
UW/NW (University of Washington/Northwest) VLSI Consortium
[AD-A150740] 14 p2404 N85-24818
Developments in microelectronics: Past and future
15 p2530 N85-25597
Improved, cheaper SIPMOS circuits no. 10, 1983 p 370 15 p2534 N85-25630
An integrated UNIX-based CAD system for the design and testing of custom VLSI chips
16 p2771 N85-27102
Goals, achievements of microelectronics program
17 p2945 N85-28179
Modern equipment for manufacture of IC's in Hungary
17 p2945 N85-28181
Measurement methods for accurate microwave characterization and modeling of MESFET chips
[AD-A152360] 17 p2952 N85-28227
Encapsulation and packaging of a semiconductor multielectrode array for cortical implantation
[AD-A153180] 17 p2998 N85-28535
Random access memory technologies
[AD-A153069] 17 p3006 N85-28597
Speed-up techniques for complementary metal oxide semiconductor very large scale integration
[AD-A152466] 17 p3043 N85-28829
Evaluation of VLSI technology — space applications
[CD.6501702] 18 p3096 N85-29177
Basic development of one-chip control circuitry for commutatorless dc motors
[BMFT-FB-T-84-305] 18 p3098 N85-29178
Electro-optic techniques for VLSI interconnect
18 p3188 N85-29774
A single chip VLSI architecture for radar signal processing 19 p3257 N85-30195
Leading-edge microelectronics research at Sweden's Chalmers 20 p3438 N85-31337
Digital integrated circuits 21 p3669 N85-32787
Hermetic chip carrier compliant soldering pads
[AD-D011722] 23 p3938 N85-34410

CHIPS (MEMORY DEVICES)
Compository speech output (KOSA) with a very large scale integration speech synthesis chip
[FI-13-TBR-16] 07 p0942 N85-15974
Vector computer memory bank contention
[NASA-CR-177342] 09 p1376 N85-18649
Siemens, Philips megaproject to yield superchip in 5 years 11 p1592 N85-20018
The design of an adaptive predictive coder using a single-chip digital signal processor
[AD-A152461] 17 p2952 N85-28231
Evaluation of VLSI technology — space applications
[CD.6501702] 18 p3096 N85-29177
Fault-tolerant computing research
[AD-A154082] 19 p3342 N85-30710

CHIRAL DYNAMICS
Skyrmions and vector mesons: A symmetric approach
[DE84-015297] 04 p0563 N85-13584
Implications of the chiral anomaly for quantum Hall effect devices
[NUB-2662] 05 p0629 N85-14029
Comment on quantum effects on 4-dimensional space-time symmetries
[DE85-007780] 16 p2872 N85-27722
Modern test of chiral anomalies
[DE85-005892] 17 p3020 N85-28680
Lattice actions improved by block-spin renormalisation group and maximally symmetric lattices
[DE85-007416] 17 p3045 N85-28841
On the definition of topological susceptibility via lattice anomalous Ward identities and its perturbative tail
[PREPRINT-416] 18 p3184 N85-29744

CHLORIDES
NT ALUMINUM CHLORIDES
NT CALCIUM CHLORIDES
NT CARBON TETRACHLORIDE
NT COPPER CHLORIDES
NT DICHLORIDES
NT HYDROCHLORIC ACID
NT HYDROGEN CHLORIDES
NT IRON CHLORIDES
NT LITHIUM CHLORIDES
NT MAGNESIUM CHLORIDES
NT POTASSIUM CHLORIDES
NT SILVER CHLORIDES
NT SODIUM CHLORIDES
NT TITANIUM CHLORIDES
NT ZINC CHLORIDES
Dynamics of graphite fiber intercalation: In situ resistivity measurements with a four point probe
[NASA-TM-86858] 01 p0017 N85-10105
Comparison study of analytical methods for the determination of fluoride, chloride, and bromide in plastics
[DE84-015008] 04 p0470 N85-12989
Development and evaluation of a procedure for the rapid analysis of fresh concrete
[AD-A149741] 12 p1866 N85-21703
Exploratory corrosion tests on alloys in molten salts at 900(0)C
[DE85-000511] 14 p2257 N85-23983
The effect of occupational exposure and the body weight to height ratio on exhaled methylene chloride breath concentration in females at one, eighteen and sixty-six hours post exposure 14 p2388 N85-24708
Radiation-induced degradation of trichloroethylene and tetrachloroethylene in drinking water
[OEFZS-4296] 18 p3134 N85-29409
Alkali atom - SbCl(5) reactions: Blue-green chemiluminescence from an inverted population in SbCl
[AD-A154371] 19 p3276 N85-30315
Lithium cell reactions
[AD-A154429] 19 p3305 N85-30484
Safety of Li-SOCl2 cells 20 p3444 N85-31383
Environmental surveillance at Los Alamos during 1984
[DE85-011886] 22 p3811 N85-33605

CHLORINATION
Bifouling and corrosion studies at the Seacoast Test Facility in Hawaii
[DE84-014643] 01 p0029 N85-10190
The development of titanium production in the USSR
[BLL-OA-TRANS-3226-(6196.3)]
23 p3913 N85-34244

CHLORINE
Chlorine isotopes as environmental tracers in Columbia River basalt groundwaters
[DE85-011392] 19 p3302 N85-30473
Facility for large-scale hazardous gas testing
[DE85-011852] 21 p3564 N85-32169
Characteristics of aerosol composition in a nonurban area, north China 21 p3646 N85-32651
Precision measurements of solar energetic particle elemental composition
[PAPER-SH-2.1-4] 21 p3715 N85-33052
Method for removing chlorine compounds from hydrocarbon mixtures
[DE85-011606] 22 p3742 N85-33191
The isotopic composition of cosmic ray chlorine
[OG-4.3-3] 22 p3876 N85-34089

Results of ultra-low level 71ge counting for application in the Gallex-solar neutrino experiment at the Gran Sasso Underground Physics Laboratory
[SH-8.1-2] 23 p4049 N85-35108
Correlation between solar neutrino flux and other solar phenomena 23 p4049 N85-35109
Fluidized bed desulfurization
[NASA-CASE-NPO-15924-1] 24 p4075 N85-35253
CHLORINE COMPOUNDS
NT ALUMINUM CHLORIDES
NT AMMONIUM PERCHLORATES
NT CALCIUM CHLORIDES
NT CARBON TETRACHLORIDE
NT CHLORIDES
NT CHLORINE OXIDES
NT CHLOROSILANES
NT COPPER CHLORIDES
NT DDT
NT DICHLORIDES
NT HYDROCHLORIC ACID
NT IRON CHLORIDES
NT LITHIUM CHLORIDES
NT MAGNESIUM CHLORIDES
NT PERCHLORATES
NT POTASSIUM CHLORIDES
NT POTASSIUM PERCHLORATES
NT SILVER CHLORIDES
NT SODIUM CHLORIDES
NT TITANIUM CHLORIDES
NT ZINC CHLORIDES
Study of effectiveness of fire-resistant activity of antipyrenes for fibers of aromatic polyamides
06 p0762 N85-14874
Working medium for sorption heat pumps
[BLL-T6360/BG/WH785/84] 06 p0807 N85-15131
Thermally modulated electron affinity detector for priority pollutant analysis
[PB85-158145] 15 p2508 N85-25469
Atmospheric chloroflurométhanes as tracers of ocean circulation and mixing: Measurement and calibration techniques and studies in the Greenland and Norwegian Seas 19 p3319 N85-30573
Throughfall rate and chemistry studies: Whiteface Mountain
[DE85-012407] 23 p3947 N85-34464
CHLORINE OXIDES
Stratospheric ClO: In-situ detection with a new approach 16 p2824 N85-27416
Investigation of the reaction system NOX/ClOX/HOX under tropospheric and stratospheric conditions
[BPT-11/84] 18 p3137 N85-29427
CHLOROAROMATICS
Sensitization and quenching in the conversion of light energy into chemical energy
[DE85-006301] 14 p2351 N85-24535
CHLOROETHYLENE
Fate and disposition of trichloroethylene in surface soils
[AD-A147918] 07 p0995 N85-16321
Search for acoustic signals from high energy cascades
[HE-7.1-1] 24 p4213 N85-36155
CHLOROFORM
The mobile phase in coals: Its nature and modes of release
[DE85-011696] 19 p3230 N85-30026
CHLOROPHYLLS
Characteristic vector analysis of inflection ratio spectra: New technique for analysis of ocean color data
[NASA-TP-2426] 13 p2126 N85-23237
Eight DOE Solar Photochemistry Research Conference: Proceedings
[DE85-005094] 15 p2587 N85-25948
Chemical, biological, and physical measurements from the subtropical western North Atlantic Ocean. Summer 1982, USNS Lynch, cruise 710-82
[AD-A153823] 18 p3201 N85-29857
CHLOROPRENE RESINS
Design, manufacture, and testing of compliant coatings for reduction of turbulent drag
[AD-A145510] 02 p0198 N85-11323
The effect of pressure on the mechanical properties of polymers. Part 2: Measurement of the time-dependent Poisson's ratio
[DE85-002139] 06 p0772 N85-14938
CHLOROSILANES
Silazane precursors to silicon nitride
[AD-A146791] 07 p0931 N85-15899
A novel polymeric organosilazane precursor to Si3N4/SiC ceramics
[AD-A150748] 14 p2260 N85-24003
An analysis of the feasibility of producing silicon for solar cells by a dichlorosilane/fluidized-bed reactor process
[NASA-CR-176036] 20 p3476 N85-31614
CHOICE
U SELECTION
CHOKES
Investigation of the choking effect of an inert granular bed on an ignition gas jet charged with particles
[ISL-CO-235/83] 14 p2264 N85-24026
CHOLESKY FACTORIZATION
Internal variables in the lattice for cholesky factorization. Kalman filtering and model identification
[AD-A149431] 10 p1547 N85-19757
Parallel Cholesky factorization on a multiprocessor
[DE85-008762] 17 p3021 N85-28682
Parallel Cholesky factorization in message-passing multiprocessor environments
[DE85-012079] 22 p3630 N85-33717
CHOLINE
Induced changes in the cholinergic system of sciatic nerve and slow and fast twitch muscle of rats
15 p2609 N85-26081
Changes in the cholinergic system of rat sciatic nerve and skeletal muscle following suspension induced disuse
[NASA-CR-175718] 15 p2615 N85-26111
CHOLINERGIC BLOCKING AGENTS
U ANTICHOLINERGICS
CHOLINERGICS
NT ANTICHOLINERGICS
CHOLINESTERASE
Effects of pyridostigmine on psychomotor and visual performance
[AD-A148553] 08 p1196 N85-17539
Is fast fiber innervation responsible for increased acetylcholinesterase activity in reinnervating soleus muscles?
[NASA-CR-175716] 15 p2614 N85-26108
Use and disuse and the control of acetylcholinesterase activity in fast and slow twitch muscle of rat
[NASA-CR-175717] 15 p2614 N85-26109
Changes in the cholinergic system of rat sciatic nerve and skeletal muscle following suspension induced disuse
[NASA-CR-175718] 15 p2615 N85-26111
CHONDRITES
NT ALLENDE METEORITE
NT CARBONACEOUS CHONDRITES
NT CARBONACEOUS METEORITES
NT PANTAR CHONDRITES
The asteroidal source region of ordinary chondrites
06 p0881 N85-15600
Major element chemical compositions of chondrules in unequilibrated chondrites 06 p0881 N85-15602
Fine-grained millimeter-sized objects in type 3 ordinary chondrites and their relation to chondrules and matrix
06 p0882 N85-15603
Chondrules in the bishunpur L13 chondrite
06 p0882 N85-15605
Size dependence of chondrule textural types
06 p0882 N85-15606
Neutron activation analysis of stoney spherules from a marine sediment sample 06 p0883 N85-15608
Oxygen isotopes in deep sea spherules
06 p0883 N85-15609
Evolutionary history of CI and CM chondrites
06 p0884 N85-15615
Unexplained Fe, Ni and S anomalies in CV chondrite components 06 p0884 N85-15618
The Colony meteorite and the possible existence of a new chemical subgroup of CO3 chondrites
06 p0885 N85-15621
Meteoritic constraints on processes in the solar nebula 06 p0887 N85-15630
Chemical evolution of the solar nebula: A new model
06 p0887 N85-15631
Where is the Earth's missing xenon?
06 p0888 N85-15641
Boron cosmochemistry 06 p0888 N85-15642
The chemistry of rare earth elements in the solar nebula 06 p0889 N85-15643
Differentiated meteorites and the components of chondrites
[NASA-CR-174201] 06 p0890 N85-15649
Origin and evolution of ordinary chondrite meteorites
15 p2683 N85-26571
A model for core formation in the early Earth
21 p3719 N85-33078
Noble gases in meteorites and terrestrial planets
22 p3851 N85-33850
Relationships between chondritic meteorites and planets 22 p3851 N85-33851
Nebular volatile fractionations associated with chondrule formation 22 p3852 N85-33855
The cosmic ray composition as viewed from the chemical abundances of the solar system
[OG-7.1-8] 23 p4013 N85-34869
Cosmogenic Mn-53 in meteorites
[SH-7.1-17] 23 p4049 N85-35107
CHONDRULE
Dynamic crystallization of silicate melts
[NASA-CR-174103] 05 p0743 N85-14774
Bulk compositions of Al-rich chondrules in ordinary and carbonaceous chondrites: Variations and similarities
06 p0881 N85-15601
Major element chemical compositions of chondrules in unequilibrated chondrites 06 p0881 N85-15602
Fine-grained millimeter-sized objects in type 3 ordinary chondrites and their relation to chondrules and matrix
06 p0882 N85-15603
Chondrule rims and interchondrule matrix in UOC
06 p0882 N85-15604
Chondrules in the bishunpur L13 chondrite
06 p0882 N85-15605
Size dependence of chondrule textural types
06 p0882 N85-15606
The influence of gravitational body force in meteoritic chondrule and lunar glass formation
06 p0884 N85-15614
Meteoritic constraints on processes in the solar nebula 06 p0887 N85-15630
Chemical evolution of the solar nebula: A new model
06 p0887 N85-15631
Chondrule-like particles provide evidence of early Archean meteorite impacts, South Africa and western Australia 15 p2682 N85-26562
CHORUS (DAWN PHENOMENON)
U DAWN CHORUS
CHORUS PHENOMENON
U DAWN CHORUS
CHROMATES
Investigation of the dissolution of CaCrO4 in molten LiCl-KCl eutectic
[DE84-016394] 04 p0469 N85-12985
Determination of Faradaic current through a bipolar electrode in acidic bichromate 04 p0483 N85-13077
CVD boron on calcium chromate powder
[DE85-000214] 09 p1299 N85-18158
Solid phase reactions among manganese, potassium perchlorate and barium chromate
[HSE-TRANS-11166] 19 p3237 N85-30071
CHROMATOGRAPHY
NT GAS CHROMATOGRAPHY
NT LIQUID CHROMATOGRAPHY
Ion chromatographic determination of gold in plating baths
[DE84-016187] 02 p0184 N85-11230
Comparison study of analytical methods for the determination of fluoride, chloride, and bromide in plastics
[DE84-015008] 04 p0470 N85-12989
Determination of halogens and sulfur in organic compounds and polymers by combustion-ion chromatography
[DE84-016186] 05 p0614 N85-13921
ECUT, Energy Conversion and Utilization Technologies program: Isothermal separation processes update
[NASA-CR-175463] 10 p1433 N85-19033
High performance size exclusion chromatography (IX) bulk and component analysis of silanol groups in polydimethylsiloxanes: Process development endeavor
[DE85-006853] 15 p2506 N85-25458
Experiments on sorption characteristics of solid desiccant materials for solar desiccant cooling systems
[DE85-000542] 17 p2923 N85-28019
Continous chemical reaction chromatography
[DE85-009812] 18 p3072 N85-28998
Multidimensional luminescence measurements
[AD-A154950] 21 p3563 N85-32162
Size exclusion chromatography-low angle laser light scattering photometry of lignite macromolecules
[DE85-012017] 22 p3745 N85-33215
Supercritical fluid chromatography/supersonic jet spectroscopy
[DE85-007005] 22 p3746 N85-33221
Electrochromic display device
[AD-D011733] 22 p3759 N85-33299
Modulated voltage metastable ionization detector
[NASA-CASE-ARC-11503-1] 23 p3933 N85-34374
CHROME
U CHROMIUM
CHROMIC ACID
Electrolytic deposition of chromium from aqueous chromium solutions containing foreign anions
[BLL-MINTEK-TR-1170-(5810.5759)]
06 p0764 N85-14889
CHROMITES
Some recent deposit modeling efforts
24 p4106 N85-35453
CHROMIUM
NT CHROMIUM ISOTOPES
An investigation of the solubility and diffusivity of chromium in gallium arsenide
[AD-A144949] 01 p0024 N85-10148

Thermodynamic properties and environmental chemistry of chromium
[DE84-015123] 01 p0025 N85-10152
The oxidation behaviour of a 20 percent Cr/25 percent Ni/Nb stabilized stainless steel in carbon dioxide at high temperatures and its improvement by cerium and yttrium
[AERE-R-11228] 01 p0029 N85-10182
EDS round-robin evaluation of type 308 austenitic stainless steel
[DE84-014574] 02 p0183 N85-11226
Review: The influence of short circuit diffusion on the oxidation of nickel, chromium and nickel/chromium alloys
[AERE-R-11311] 02 p0185 N85-11237
EXAFS and Moessbauer study of small metal clusters isolated in rare-gas solids
[DE84-015976] 04 p0470 N85-12994
Abundancies of Ni, Cr, CO and major elements in the silicate portion of the Moon: Constraints from primary lunar magmas 04 p0582 N85-13720
Studies on copper alloys containing chromium on the copper side phase diagram
[NASA-TM-77752] 07 p0927 N85-15876
Optimization of the NiCrAl-Y/ZrO-Y2O3 thermal barrier system
[NASA-TM-86905] 07 p0927 N85-15878
Influence of plastic deformation on structural stability of nichrome-tungsten composite materials
11 p1509 N85-20060
Transverse microstructure of an oxide scale formed on a 20 % Cr/25 % Ni niobium stabilized stainless steel
[AERE-R-11034] 12 p1804 N85-21315
Effects of chromium and aluminum on mechanical and oxidation properties of iron-nickel-base superalloys based on CG-27
[NASA-TP-2443] 12 p1805 N85-21323
Dispersed-metal-toughened alumina
[NASA-CR-174687] 13 p2037 N85-22758
Microstructure and properties of ferrous alloy weldments
[DE85-005582] 14 p2257 N85-23987
Positron annihilation studies of vacancy formation in tungsten, chromium, and niobium
[DE85-006837] 16 p2671 N85-27710
Influence of manganese and heat treatment on structure and properties of Fe-0.1 percent-C-14 percent Cr-based steels
[BLL-BISI-TRANS-22299-(9022.06)]
17 p2928 N85-28071
Determination of the vacancy formation enthalpy in chromium by positron annihilation
[DE85-010266] 19 p3239 N85-30064
Why CO bonds side-on at low coverage and both side-on and upright at high coverage on the Cr(110) surface
[NASA-CR-176071] 21 p3565 N85-32173
Electrodeposition of chromium and copper in magnetic fields
[AD-A154648] 21 p3566 N85-32180
Microscopic control of semiconductor surface oxidation
[AD-A154799] 21 p3709 N85-33026
Measurements of Fe and Ar fragmentation cross sections
[PAPER-OG-7.2-20] 21 p3714 N85-33047
Environmental surveillance at Los Alamos during 1984
[DE85-011886] 22 p3811 N85-33605
Calculated neutron-induced cross sections for /sup 63,65/Cu/sup 58,60/Ni and (52) Cr from 1 to 20 MeV and comparisons with experiments
[DE85-011928] 22 p3844 N85-33806
The effect of pre-heating on the structure and properties of chromium-molybdenum steels
[BLL-M-35897-(5828.4)] 23 p3914 N85-34255
Special features of the fracture of ball-bearing steel close to non-metallic inclusion eutectics
[BLL-M-35809-(5828.4)] 23 p3914 N85-34258
Process for improving moisture resistance of epoxy resins by addition of chromium ions
[NASA-CASE-LAR-13226-1] 23 p3919 N85-34282
Thermodynamics of the corrosion of chromium in molten carbonates
[DE85-011407] 24 p4079 N85-35282
X-ray fluorescence analysis of 304L stainless steel
[DE85-013254] 24 p4080 N85-35288
Applications of the mineral resources data system and the international strategic minerals inventory in mineral-resource assessments by region and commodity
24 p4105 N85-35451
The Conterminous United States Mineral Assessment Program 24 p4106 N85-35458
The Alaska Mineral Resources Assessment Program
24 p4107 N85-35460
Development of electrodes for the NASA iron/chromium
[NASA-CR-174724] 24 p4109 N85-35471

CHROMIUM ALLOYS
NT CHROMIUM STEELS
NT RENE 95
Thermodynamics of decarburization of niobium-bearing high-alloy melts
[BLL-M-35729-(5828.4)] 02 p0175 N85-11169
Review: The influence of short circuit diffusion on the oxidation of nickel, chromium and nickel/chromium alloys
[AERE-R-11311] 02 p0185 N85-11237
Study of the reactive-element effect in oxidation of Fe-Cr alloys using transverse section analytical electron microscopy
[DE84-016237] 04 p0571 N85-13641
Experimental determination of the critical cavity radius in Fe-10% Cr for ion irradiation
[DE84-016570] 04 p0571 N85-13646
Thermal diffusivity and conductivity of chromium-manganese alloying compositions
[BLL-M-35925-(5828.4)] 05 p0616 N85-13938
The effect of trace elements on the properties at high temperature of a Ni-Cr-base alloy
05 p0617 N85-13944
Metallographic evaluation of the reactions between boronated graphite and Fe-Ni-Cr alloys
[DE84-015374] 06 p0769 N85-14922
The formation of isolated phase precipitates during the decomposition of high-coercive force Fe-Cr-Co alloys
[BLL-M-36028-(5828.4)] 07 p0924 N85-15655
On heat-treatable copper-chromium alloy, 1
[NASA-TM-77753] 07 p0927 N85-15879
On reversion phenomena in Cu-Zr-Cr alloys
[NASA-TM-77791] 08 p1125 N85-17092
Reversion phenomena of Cu-Cr alloys
[NASA-TM-77780] 08 p1125 N85-17094
Recommendations for the use of Ni-Cr-base alloy extensometers for measurement of creep strain
[NPL-DMA(A)-81] 08 p1164 N85-17342
Low and moderate temperature oxidation of atomically clean nickel, chromium and Ni-Cr alloys
[DE84-017350] 09 p1295 N85-18131
Initial aging phenomena in copper-chromium alloys
[NASA-TM-77790] 10 p1436 N85-19070
Influence of volumetric fiber content on some matrix damage factors during thermal cycling of tungsten-El 765 composite 10 p1443 N85-19097
Stress relief of transition zones
[DE85-000234] 11 p1653 N85-20411
Partial replacement of chromium in austenitic stainless steels by molybdenum, copper, and vanadium, report of investigations 1984
[PB85-116508] 12 p1809 N85-21346
Performance of Chromel versus Alumel and Nicrosil versus Nisil thermocouple assemblies in vacuum and argon between 1000 deg C and 1200 deg C
[DE85-000810] 12 p1853 N85-21624
Orientation and temperature dependence of some mechanical properties of the single-crystal nickel-base superalloy Rene N4. 3: Tension-compression anisotropy
[NASA-TM-86982] 13 p2021 N85-22660
Study of the effects of implantation on the high Fe-Ni-Cr and Ni-Cr-Al alloys
[NASA-CR-175625] 13 p2021 N85-22661
Structure and aging of amorphous chromium-germanium alloys 15 p2497 N85-25401
Reduced-chromium stainless steel substitutes containing silicon and aluminum
[PB85-160786] 15 p2513 N85-25502
Electrical conductivity and phase diagram of binary alloys. 21: The system palladium-chromium
[NASA-TM-77863] 18 p3073 N85-29009
Changes of structure of EP648-VI alloy as a result of high-temperature gas corrosion
19 p3243 N85-30110
Optimisation of MCr Al coating compositions for marine gas turbines
[BR91159] 20 p3394 N85-31056
Mechanical behavior of Ni-Cr-base superalloys in forms and conditions representative of service
[NPL-DMA(A)-94] 20 p3431 N85-31282
A systematic plan for the continued study of dimensional stability of metallic alloys considered for the fabrication of cryogenic wind tunnel models
[NASA-CR-172449] 21 p3565 N85-32172
Dynamics of the melting of chromium-manganese alloys in molten steel
[BLL-M-35850-(5828.4)] 23 p3914 N85-34252
Chromium-base powder alloys for welding cladding layer of bimetal
[BLL-M-35776-(5828.4)] 23 p3915 N85-34260
Deposition of nickel-cobalt alloys by controlled-potential electrolysis
[PB85-198562] 24 p4061 N85-35291

CHROMIUM BORIDES
The use of moments of momentum to account for crystal habits
[NASA-CR-3907] 20 p3421 N85-31202
CHROMIUM CARBIDES
Effects of silver and group 2 fluorides addition to plasma sprayed chromium carbide high temperature solid lubricant for foil gas bearing to 650 deg C
[NASA-TM-86895] 06 p0770 N85-14
Antifriction properties of gas thermal coatings of clad carbine powders 10 p1447 N85-19115
CHROMIUM COMPOUNDS
NT CHROMATES
NT CHROMIC ACID
NT CHROMITES
NT CHROMIUM BORIDES
NT CHROMIUM CARBIDES
NT CHROMIUM OXIDES
Vaporization behavior of chromium phosphides. The solid 2-phase regions CrP-Cr12P7, Cr12P7-Cr3P, and Cr3P-Cr
[AD-A145481] 02 p0172 N85-11152
Properties of chromate coatings formed on electrolytic zinc substrates
[BLL-BISI-TRANS-22349-(9022.06)]
17 p2926 N85-28062
Electrical conductivity and phase diagram of binary alloys. 21: The system palladium-chromium
[NASA-TM-77863] 18 p3073 N85-29009
CHROMIUM ISOTOPES
Experimental test for interpreting the increase in sensibility of doped CR-39
[OG-4.4-11] 22 p3880 N85-34042
CHROMIUM OXIDES
NT CHROMITES
Review: The influence of short circuit diffusion on the oxidation of nickel, chromium and nickel/chromium alloys
[AERE-R-11311] 02 p0185 N85-11237
Diffusion of Cr-51 tracer in Cr-2O-3 and the growth of Cr-2O-3 films
[AERE-R-11314] 03 p0333 N85-12146
Interaction between chromium oxide and carbon
[BLL-M-36002-(5828.4)] 07 p0926 N85-15867
Strength and failure of ceramic-metallic material
10 p1446 N85-19112
Test and modeling for sintering theory
[DE85-007761] 16 p2755 N85-27004
CHROMIUM STEELS
Study to optimize Cr-Mo steels to resist hydrogen and temper embrittlement. A study of carbides formed in low alloy Cr-Mo steels
[DE84-015208] 01 p0029 N85-10179
Structure and wear workshop colloquium
01 p0054 N85-10356
The influence of the carbide distribution on the abrasive wear of ledeburitic chromium steels
01 p0054 N85-10359
Metalurgy of a 12 percent chromium stainless steel
02 p0178 N85-11186
Thermal ageing studies of 9%Cr 1%Mo steel
[AERE-R-11109] 03 p0333 N85-12149
The effects of microstructure on the temper embrittlement susceptibility of a Cr-2-1/4 1Mo forging
[AERE-R-11110] 03 p0334 N85-12151
A study of precipitation and boron distribution in 20 Cr 25Ni base stainless steels
[AERE-M-3353] 03 p0334 N85-12154
Stress relief cracking studies of 2 1/4Cr1Mo steel
[AERE-R-11111] 03 p0374 N85-12288
Autenite transformation in powder-compacted chromium-nickel-molybdenum steels during continuous cooling
[BLL-M-35981-(5828.4)] 05 p0615 N85-13933
Susceptibility of 2 1/4 Cr-1Mo steel to liquid metal induced embrittlement by lithium-lead solutions
[DE85-000997] 09 p1294 N85-18130
Effect of tempering on the strength and toughness of 2 1/4 Cr-1 Mo steel weldments
[DE85-003618] 09 p1296 N85-18140
Assessment of the need for an advanced high-strength chromium-molybdenum steel for construction of third-generation gasifier pressure vessels
[DE85-002665] 11 p1606 N85-20087
The role of void nucleation in the swelling resistance of ferritic steel
[AERE-R-11525] 11 p1610 N85-20122
Frictional and structural characterization of ion-nitrided low and high chromium steels
[NASA-TM-86991] 13 p2098 N85-2308
Radiation effects on structural materials
[DE85-007032] 15 p2649 N85-2633
The corrosion resistance of chromium-nickel steel containing rare-earth metals
[BLL-BISI-TRANS-22477-(9022.06)]
17 p2925 N85-2804

Influence of heat treatment parameters on the properties of induction hardened Ni-Cr-Mo steels [BLL-BISI-TRANS-2499-(9022.06)] 17 p2926 N85-28053

Obtaining oxide films on surface of tubes of chromium-nickel steels [BLL-BISI-TRANS-22478-(9022.06)] 17 p2929 N85-28076

Dispersion-strengthened powder-metallurgical chromium steels [BLL-BISI-TRANS-22323-(9022.06)] 17 p2929 N85-28081

Study to optimize Cr-Mo steels to resist hydrogen and temper embrittlement [DE85-005492] 17 p2932 N85-28096

Influence of temperature in melting and casting on quality of medium-alloy steel [BLL-BISI-TRANS-22310-(9902.06)] 17 p2938 N85-28137

Study of a simulated test for assessing the machinability of steels [BLL-BISI-TRANS-22344-(9022.06)] 17 p2972 N85-28357

Fracture mechanics analysis of cold drawn Si-Cr valve steel [BLL-BISI-TRANS-22216-(9022.06)] 17 p2978 N85-28405

Fatigue and chromium-ferritic steels at elevated temperatures [DE85-007735] 18 p3074 N85-29015

Elevated temperature erosion corrosion of 9Cr1Mo steel [DE85-008445] 18 p3074 N85-29016

Surface degradation of ductile metal in elevated temperature gas-particle streams [DE85-008428] 18 p3074 N85-29017

Corrosion-erosion rates/mechanisms of 9Cr1Mo steel [DE85-008506] 18 p3076 N85-29029

The effect of temperature on the corrosion-erosion of 9Cr1Mo steel [DE85-008507] 18 p3076 N85-29030

Conservation and substitution technology for critical metals in bearings and related components for industrial equipment and opportunities for improved bearing performance [PB85-176246] 18 p3082 N85-29069

Effects of heat treatment and tracer element impurities on the impact properties of the 12Cr steels [DE85-010676] 19 p3240 N85-30088

Vacuum pressure welding of commercial titanium with 2Kh13 and 12Kh18N10T steels 19 p3246 N85-30124

Structural transformation of a 9% Cr - 2%Mo steel (type Z10CDNbV 09-02) for use in steam generators for fast neutron reactors [BLL-CE-TRANS-7943-(9022.09)] 20 p3430 N85-31271

Fatigue-crack growth and ductile fracture toughness behavior of ASTM A387 Grade 91 steel [DE85-008495] 20 p3431 N85-31286

Reliability of welds to repair defects in cast components made from CrMoV steel [BLL-CE-TRANS-8054-(9022.09)] 20 p3461 N85-31501

Application of the unloading compliance methods in fracture toughness measurements of a quenched and tempered steel [BLL-CE-TRANS-7953-(9022.09)] 20 p3465 N85-31523

Fatigue behavior of chromium-containing ferritic steels at elevated temperature [DE85-012309] 22 p3748 N85-33231

Characterization of modified 9 Cr Mo steel extruded pipe [DE85-012056] 23 p3941 N85-34430

Characterization of modified 9 r-1 Mo steel sand castings [DE85-012057] 24 p4080 N85-35287

CHROMOSOMES

Chromosome aberrations in Crepis capillaris exposed to gamma radiation and clinostat 19 p3325 N85-30600

Three-dimensional reconstruction and data display of chromosome structure studied by electron microscope tomography [DE85-011562] 22 p3825 N85-33697

CHROMOSPHERE

Vector magnetic field analysis of Lorentz forces acting in the solar atmosphere [AD-A145941] 03 p0449 N85-12852

Time dependent effects at the foot of the chromosphere [NASA-CR-174143] 04 p0589 N85-13762

Theoretical studies of chromospheres and winds in cool stars [NASA-CR-174204] 06 p0880 N85-15596

Spicules and surges [AD-A146785] 07 p1061 N85-16727

Heating in the solar mantle 06 p1233 N85-17769

Extreme limb profiles of the Sun at far infrared and submillimeter wavelengths 06 p1244 N85-17852

Coronal and chromospheric physics — Sun, sunspots, and solar limb [NASA-CR-174290] 06 p1259 N85-17921

The calculation of theoretical chromospheric models and the interpretation of solar spectra from rockets and spacecraft [NASA-CR-174289] 06 p1259 N85-17922

A search for young stellar chromospheres in NGC 2264 11 p1746 N85-20993

Chromospheric activity in M giants 11 p1757 N85-21056

Chromospheric emission lines in high-resolution LWR spectra (220 - 3000 alpha) of gamma CRU (M3 3) and alpha ORI (M2 lab) 11 p1758 N85-21058

Betelgeuse at maximum luminosity 11 p1758 N85-21061

Rotational modulation of chromospheric emission in cool giants and hybrid stars 11 p1759 N85-21064

Thermal stability of static coronal loops: Part 1: Effects of boundary conditions [NASA-CR-175495] 12 p1961 N85-22330

Application of the MHD energy principle to magnetostatic atmospheres [NASA-CR-175967] 18 p3136 N85-29420

Heating of the deep chromosphere during solar flares [AD-A155256] 21 p3723 N85-33100

Study of photon emission by electron capture during solar nuclei acceleration. 3: Photon production evaluations [SH-1.1-10] 23 p3990 N85-34737

Onset of solar flares as predicted by two-dimensional MHD-models of quiescent prominences [SH-1.3-1] 23 p3992 N85-34750

On the detectability of key-MeV solar protons through their nonthermal Lyman-alpha emission [SH-1.3-5] 23 p3993 N85-34752

Diffusion in the chromosphere and the composition of the solar corona and energetic particles [SH-2.1-9] 23 p3999 N85-34790

Sporadic radio emission connected with a definite manifestation of solar activity in the near Earth space [SH-10.1-8] 23 p4053 N85-35139

Near Earth space sporadic radio emission busts occurring during sunrise [SH-10.1-9] 23 p4054 N85-35140

CHRONIC CONDITIONS

Estimating risks of lead-induced hemoglobin decrements under conditions of uncertainty: Methodology, pilot judgments and illustrative calculations [DE85-012293] 23 p3952 N85-34493

CHRONOGRAPHS
U CHRONOMETERS

CHRONOLOGY
NT GEOCHRONOLOGY

Open star clusters and the evolution of the galactic disk 05 p0736 N85-14734

Chronologic and climatic control on soil development, northern Bighorn Basin, Wyoming and Montana 06 p1161 N85-17443

Chronology of KSC and KSC related events for 1983 [NASA-TM-87400] 06 p1261 N85-17927

Chronology of KSC and KSC related events for 1983 [NASA-TM-87435] 12 p1963 N85-22339

Relative time-scale for channeling events within chaotic terrains, Margaritifer Sinus, Mars 13 p2190 N85-23589

Heat flow through ocean floor and its relationship to lithosphere structure and thickness 19 p3294 N85-30422

A new global geomorphology? 21 p3601 N85-32358

Why do leaky-box models work so fine? [OG-7.2-8] 23 p4014 N85-34877

CHRONOMETERS

Timing-system design considerations for a mobile astrolabe 17 p2965 N85-28309

CHRONOTRONS
U PULSE RATE
U TIME LAG

CHUGGING
U COMBUSTION STABILITY

CHUTES

Air carrier overwater emergency equipment and procedures [PB85-917006] 21 p3553 N85-32105

CID
U CHARGE INJECTION DEVICES

CINDER CONES
U CONES (VOLCANOES)

CINEFLUOROGRAPHY
U MOTION PICTURES
U RADIOGRAPHY

CINEMATOGRAPHY

Sub-nanosecond cinematography in laser fusion research: Current techniques and applications at the Lawrence Livermore Laboratory [DE85-007252] 17 p2968 N85-28334

Holographic cinematography with the help of a pulse YAG laser [ISL-CO-213/84] 22 p3788 N85-33472

Cineholography [ISL-CO-214/84] 22 p3788 N85-33473

CINERADIOGRAPHY
U MOTION PICTURES
U RADIOGRAPHY

CIRCADIAN RHYTHMS

Jet lag prevention: Physiological mechanisms and pharmacological therapy [AD-A145444] 02 p0235 N85-11529

Mathematical Models of the Circadian Sleep-Wake Cycle [AD-A145712] 02 p0235 N85-11532

Spontaneous motility of goldfish in absence of terrestrial zeitgebers: Space flight simulation in a mine 05 p0689 N85-14432

Heart rate variability during 7 day head-down tilt (6 deg) 05 p0692 N85-14453

Circadian rhythm of human body temperature during spaceflights 12 p1901 N85-21934

Annals of the New York Academy of Sciences, Volume 423 --- timing and time perception [AD-A150031] 12 p1909 N85-21981

Homeostasis in primates in the hyperdynamic environment --- circadian timekeeping and effects of lower body positive pressure on sleep 15 p2610 N85-26085

Circadian rhythm control: Neurophysiological investigations 15 p2612 N85-26099

Circadian dynamics of potassium excretion in urine as related to working on one and two shifts 19 p3325 N85-30598

Human performance in continuous/sustained operations and the demands of extended work/rest schedules. An annotated bibliography [AD-A155619] 21 p3666 N85-32771

CIRCLES (GEOMETRY)

On the turning lozange of constant side whose vertices alternate between two fixed circles of a ring [AD-A154803] 21 p3677 N85-32840

CIRCUIT BOARDS

Extractor for spring-lock pin connectors [AD-D011235] 01 p0043 N85-10280

Depot level problems in the testing of printed circuit boards [AD-P003932] 02 p0247 N85-11612

Mechanical locking between multi-layer printed wiring board conductors and through-hole plating [AD-D011477] 10 p1481 N85-19352

The state of the art in printed wiring board inspection [AD-A149871] 12 p1862 N85-21679

Applications, specifications of Robotron CAD-CAM work stations 15 p2537 N85-25661

Design and swept-frequency measurement of printed circuit board log-periodic dipole arrays [R-NIAS-23] 15 p2539 N85-25671

Voltammetric analysis of ordnance materials. Part 2: A portable digital voltammeter for use with a silver wire working electrode [AD-A152480] 17 p2967 N85-28325

Beam forming network [NASA-CASE-NPO-15743-1] 18 p3069 N85-29118

A comparison and analysis of Vint's global routing algorithm with the Lee routing algorithm in two-layer printed circuit boards [AD-A155600] 21 p3673 N85-32816

Heat sinking for printed circuitry [DE85-011585] 22 p3783 N85-33440

CIRCUIT BREAKERS

Improvement of lightning arresters energy capability [SNIAS-842-422-104] 04 p0497 N85-13172

High-voltage, high-power, solid-state remote power controllers for aerospace applications [NASA-TP-2437] 12 p1795 N85-21263

Optimization of overall dimensions of enclosures for low-voltage devices and equipment 13 p2087 N85-23033

Derated application of parts for (Electronic Systems Division) systems development. Revision [AD-A153299] 17 p2955 N85-28246

CIRCUIT DIAGRAMS

Measured noise performance of a new method of frequency hopping [AD-A152679] 17 p2953 N85-28234

Development of new circuit symbols for binary logic elements
[MBB-Z-39/85-O] 17 p3014 N85-28640

Recognition and clear representation of handwritten electronic diagrams 23 p3960 N85-34541

CIRCUIT PROTECTION

Improvement of lightning arresters energy capability
[SNIAS-842-422-104] 04 p0497 N85-13172

Circuit transients due to negative bias arcs on a high-voltage solar array in low Earth orbit
[NASA-TP-2407] 06 p0760 N85-14856

The ac power line protection for an IEEE 587 Class B environment 07 p1000 N85-16347

Intermediate load modules for test and evaluation: Flat-Plate Solar Array Project
[NASA-CR-174450] 10 p1508 N85-19512

Electrical overstress protection of submicron devices
[AD-A150334] 13 p2064 N85-22892

Requirements placed on information processing equipment
[BLL-CE-TRANS-7983-(9022.09)] 13 p2144 N85-23307

Aspects of CSSR CMOS integrated circuits discussed 15 p2533 N85-25627

CIRCUIT RELIABILITY

Procedures for precap visual inspection
[NASA-RP-1122] 04 p0495 N85-13156

Qualification of a thick film hybrid
[BMFT-FB-W-84-024] 04 p0497 N85-13170

Design of self-checking N-MOS (H-MOS) integrated circuits 08 p1064 N85-16742

Circuit topology, signal propagation delay and the efficiency of VLSI circuits
[CWI-CS-R8414] 11 p1630 N85-20267

Transistor-transistor logic microcircuit tester 12 p1842 N85-21556

Designing VLSI (Very Large Scale Integrated) circuits for testability
[AD-A151834] 15 p2549 N85-25729

Improved Gonda's circuit described 15 p2551 N85-25748

Efficient VLSI (Very Large Scale Integration) fault simulation
[AD-A152661] 17 p2953 N85-28233

Derated application of parts for (Electronic Systems Division) systems development. Revision
[AD-A153299] 17 p2955 N85-28246

Split-cross-bridge resistor for testing for proper fabrication of integrated circuits
[NASA-CASE-NPO-16021-1] 19 p3256 N85-30187

CIRCUITS
- NT ADDING CIRCUITS
- NT ANALOG CIRCUITS
- NT BISTABLE CIRCUITS
- NT CANCELLATION CIRCUITS
- NT CIRCULATORS (PHASE SHIFT CIRCUITS)
- NT COINCIDENCE CIRCUITS
- NT COMPARATOR CIRCUITS
- NT COUNTING CIRCUITS
- NT COUPLING CIRCUITS
- NT DELAY CIRCUITS
- NT DIGITAL INTEGRATORS
- NT DIPLEXERS
- NT DISCRIMINATORS
- NT ECHO SUPPRESSORS
- NT ELECTRIC BRIDGES
- NT EQUIVALENT CIRCUITS
- NT FEEDBACK CIRCUITS
- NT FLIP-FLOPS
- NT FLUID SWITCHING ELEMENTS
- NT FLUIDIC CIRCUITS
- NT FREQUENCY DISCRIMINATORS
- NT GATES (CIRCUITS)
- NT HYBRID CIRCUITS
- NT INTEGRATED CIRCUITS
- NT ITERATIVE NETWORKS
- NT LARGE SCALE INTEGRATION
- NT LIMITER CIRCUITS
- NT LINEAR CIRCUITS
- NT LOGIC CIRCUITS
- NT MAGNETIC CIRCUITS
- NT MATRICES (CIRCUITS)
- NT MICROWAVE CIRCUITS
- NT MIXING CIRCUITS
- NT OHMS LAW
- NT PHASE DETECTORS
- NT PHASE SHIFT CIRCUITS
- NT POWER SUPPLY CIRCUITS
- NT PRINTED CIRCUITS
- NT RC CIRCUITS
- NT SCALERS
- NT SWEEP CIRCUITS
- NT SWITCHING CIRCUITS
- NT THRESHOLD GATES
- NT TRANSISTOR CIRCUITS
- NT TRANSMISSION CIRCUITS
- NT TRIGGER CIRCUITS
- NT TTL INTEGRATED CIRCUITS
- NT VERY LARGE SCALE INTEGRATION
- NT VHSIC (CIRCUITS)
- NT WHEATSTONE BRIDGES
- NT WIRE BRIDGE CIRCUITS

Electrical system technology Working Group (WG) report 05 p0611 N85-13907

USSR report: Electronics and electrical engineering
[JPRS-UEE-84-011] 06 p0789 N85-15042

The replacement of precious metal thick film inks using conductive polymer technology. Phase 1: Feasibility study
[AD-A147814] 07 p0933 N85-15913

Characterization of CNRS Fizeau wedge laser tuner
[NASA-CR-174357] 09 p1325 N85-18328

Low voltage two wire to four wire telephone circuit converter apparatus
[AD-D011449] 10 p1466 N85-19261

Design of low loss helix circuits for interference fitted and brazed circuits
[NASA-CR-168313] 10 p1476 N85-19328

A circuit grammar for operational amplifier design
[AD-A149566] 10 p1481 N85-19346

Problems in high temperature thermocouple thermometry
[DE85-000608] 10 p1488 N85-19397

Processing circuit with asymmetry corrector and convolutional encoder for digital data
[NASA-CASE-MSC 20187-1] 11 p1626 N85-20249

Digital channel efficiency model
[AD-A150084] 12 p1829 N85-21479

Electromagnetic rail launcher as a circuit element
[AD-A150067] 12 p1835 N85-21516

Summator of radio pulse signals 12 p1839 N85-21539

Problems with electrical interference between solar generators and shunt type regulators 13 p2010 N85-22607

Repetitive energy transfers from an inductive energy store 13 p2062 N85-22881

USSR report: Electronics and electrical engineering
[JPRS-UEE-85-001] 13 p2078 N85-22976

Design, fabrication and testing of a multibeam forming network
[NASA-CR-175695] 14 p2298 N85-24228

Distributed control of circuits in multiuser communication networks with circuit precedence and path suitability criteria using failsafe routing concepts
[AD-A151625] 16 p2772 N85-27113

Numerical methods for stiff ordinary and elliptic partial differential equations
[AD-A153247] 17 p3020 N85-28675

High voltage power supply
[NASA-CASE-GSC-12818-1] 18 p3093 N85-29147

Temperature sensitive oscillator
[NASA-CASE-GSC-12958-1] 19 p3258 N85-30201

Parallel simulation of digital LSI circuits
[AD-A154745] 21 p3560 N85-32258

State of art and development problems in computer-aided design of electronic circuits 22 p3766 N85-33342

Algorithms and organization of software for computer-aided circuit design 22 p3767 N85-33347

System for computer-aided design of analog electronic circuits 22 p3768 N85-33353

Optimization of radioelectronic circuits with software for modeling of integrated circuits on unified system computer 22 p3768 N85-33354

Dialog system with minicomputer for plotting performance charts 22 p3768 N85-33355

Algorithms for constructing models of circuit elements in input language of computer-aided design software 22 p3768 N85-33356

Electronic temperature equalizer
[PB85-181485] 22 p3789 N85-33475

Method and apparatus for transfer function simulator for testing complex systems
[NASA-CASE-NPO-15696-1] 23 p3926 N85-34333

Interfacing interactive circuit simulation with standard graphics facilities 23 p3958 N85-34529

CIRCULAR CYLINDERS

Wave multiple scattering by a finite number of unclosed circular cylinders
[NASA-TM-77593] 01 p0037 N85-10232

An experimental study of jet impingement on a circular cylinder
[AD-A145583] 02 p0198 N85-11326

Post buckling behavior of a circular rod constrained within a circular cylinder 02 p0207 N85-11365

Stress intensity factors for a circular ring with uniform array of radial cracks of unequal depth
[AD-A145893] 03 p0372 N85-12377

Acoustic radiation from single and double ribbed circular cylindrical shells
[AD-A148771] 08 p1219 N85-17676

Numerical predictions for unsteady viscous flow past an array of cylinders 09 p1318 N85-18284

Turbulent bouyant flow and pressure variations around a circular cylinder in a cross uniform flow near the ground 09 p1318 N85-18287

Stability evaluation of sulfur dioxide nitric oxide and carbon monoxide gases in cylinders 11 p1648 N85-20387

Generation of sound by a vortex point in a steady flow of slightly compressible fluid 11 p1715 N85-20789

Electromagnetic analysis of radomes by the moment method
[AD-P004351] 12 p1824 N85-21446

Behavior of buried flexible cylinders under the influence of nonuniform hoop compression
[PB85-116523] 12 p1866 N85-21718

Turbulent flow around circular cylinder uniformly rotating in infinite incompressible fluid 14 p2277 N85-24108

Measurements in the flow field of a cylinder with a laser transit anemometer and a drag rake in the Langley 0.3 m transonic cryogenic tunnel
[NASA-TM-86399] 14 p2305 N85-24270

The influence of jet-grid turbulence on heat transfer from the stagnation region of a cylinder in crossflow
[NASA-TM-87011] 15 p2554 N85-25760

Natural convection in cylindrical containers 15 p2555 N85-25763

Flow around rotating and nonmoving circular cylinder near flat screen. Report 1: Aerodynamic forces in cylinder 16 p2765 N85-2706

Boundary layer at moving cylinder surface 16 p2765 N85-2706

On residual stress in an elastic body 16 p2796 N85-2724

Solution of problem of equilibrium confinement of plasma by magnetic field in an infinite circular cylinder 21 p3692 N85-3293

Vibrations of free hollow circular cylindrical bodies 24 p4100 N85-3541

CIRCULAR ORBITS
- NT STATIONARY ORBITS

Stability of periodic satellite motions relative to cent of mass in circular orbit 16 p2718 N85-267

Maximizing the semi-major axis for a freely coning so sailcraft
[AD-A153175] 17 p2909 N85-279

CIRCULAR PLATES

Large transverse deflections of circular plates load symmetrically
[NPL-DMA(A)-86] 04 p0512 N85-132

CIRCULAR POLARIZATION

Characteristics of circular-polarized printed radiators planar phased antenna array 06 p0790 N85-150

Modern problems in polarimetry of solid surfaces cosmic bodies 13 p1977 N85-22

Design and measured performance of a broadb Archimedes spiral antenna
[R-NIAS-22] 14 p2290 N85-24

Design and performance of etched polaris transformers for microwave frequencies
[R-NIAS-26] 14 p2297 N85-24

Dual sense, circularly polarized helical antenna
[AD-D011680] 19 p3254 N85-30

A special antenna for SARSAT EPIRBs providing circ polarization and hemispheric coverage for reli transmission to satellites — Emergency Position Indic Radio Beacon (EPIRB) 20 p3404 N85-3

CIRCULAR SHELLS

Stability of circular cylindrical shell with piece constant thickness subjected to radial pressure 06 p0779 N85-1

CIRCULAR TUBES

Estimating defectiveness buildup during service in of welded runner in low-pressure cylinder of turbine 14 p2271 N85-2

Steel Tubes
[BLL-BISI-TRANS-22064-(9022.06)] 17 p2973 N85-2

CIRCULAR WAVEGUIDES

Scattering of waves by axisymmetrical edge 13 p2060 N85-

New directional couplers for multimode c waveguides applied to intense pulsed micr systems
[DE85-011753] 23 p3926 N85-

CIRCULATION
- NT ATMOSPHERIC CIRCULATION
- NT BLOOD CIRCULATION
- NT BRAIN CIRCULATION
- NT COASTAL CURRENTS
- NT CORONARY CIRCULATION
- NT EL NINO
- NT GULF STREAM
- NT OCEAN CURRENTS

NT PULMONARY CIRCULATION
NT WATER CIRCULATION
NT WATER CURRENTS
Urban aerosol modeling
[PB84-233469] 04 p0532 N85-13401
Circulation control: A bibliography of DTNSRDC research and selected outside references: Update
[AD-A146966] 07 p0893 N85-15661
Heat and mass exchange in a partially stratified fluid
[DE85-000526] 10 p1486 N85-19364
Some preliminary results concerning deep northern-boundary currents in the North Pacific
[AD-A151021] 14 p2382 N85-24692
Heat management system for aircraft
[AD-D011658] 18 p3061 N85-28936
Lost circulation in geothermal wells: Research and development status
[DE85-009636] 19 p3266 N85-30267

CIRCULATION CONTROL AIRFOILS
Modelling circulation control by blowing — airfoils
08 p1069 N85-16778
Low-speed characteristics of a circulation control airfoil with AFT camber and a spiral trailing edge
[AD-A150851] 14 p2213 N85-23725
Basic consideration of the lifting capability of stoppable rotors
[AD-A150850] 14 p2219 N85-23759
Circulation control propellers for general aviation, including a BASIC computer program
[NASA-CR-165968] 19 p3219 N85-29959
Circulation control lift generation experiment: Hardware development 22 p3799 N85-33535

CIRCULATION DISTRIBUTION
Structure and energetics of medium-scale atmospheric waves in the Southern Hemisphere
20 p3489 N85-31685

CIRCULATORS (PHASE SHIFT CIRCUITS)
Basic development of one-chip control circuitry for commutatorless dc motors
[BMFT-FB-T-84-305] 18 p3096 N85-29178

CIRCULATORY SYSTEM
NT ARTERIES
NT BLOOD VESSELS
NT VASCULAR SYSTEM
NT VEINS
Circulatory orthostatic instability. Role of deconditioning of resistive vessels 01 p0091 N85-10612
Management of microcirculatory disorders in vibration sickness 10 p1524 N85-19611
Cosmonauts' postural reactions after long-term missions aboard Salyut-6 orbital station 19 p3323 N85-30585

CIRCUMFERENCES
Prediction of percent body fat for U.S. Navy women from body circumferences and height
[AD-A146456] 06 p0645 N85-15370
Circumferential cracks in cylindrical shells
09 p1330 N85-18354

CIRCUMSOLAR RADIATION
Neutron and gamma-ray signatures for particle acceleration in solar flares 12 p1954 N85-22278

CIRCUMSTELLAR MATTER
U STELLAR ENVELOPES

CIRRUS CLOUDS
Investigation of cloud feedback in the GLAS model
05 p0685 N85-14404
Ice crystal nucleation on hygroscopic aerosols
21 p3639 N85-32605

CITIES
NT MOSCOW
NT SAN FRANCISCO (CA)
Review of the attributes and performance of six urban diffusion models
[PB84-236850] 04 p0484 N85-13087
Impact of alcohol fuels on urban air pollution: Methanol photochemistry study
[DE84-012950] 04 p0531 N85-13397
Urban aerosol modeling
[PB84-233469] 04 p0532 N85-13401
Transformation processes and wet deposition on the urban scale
[DE84-015294] 04 p0539 N85-13432
Detecting agricultural to urban land use change from multi-temporal MSS digital data — Salt Lake County, Utah
[E85-10049] 07 p0983 N85-16245
Image variance and spatial structure in remotely sensed scenes — South Dakota, California, Missouri, Kentucky, Louisiana, Tennessee, District of Columbia, and Oregon
07 p0986 N85-16265
Meteorological factors responsible for high CO (carbon monoxide) levels in Alaskan cities
[PB85-115137/GAR] 09 p1350 N85-18493
Weather data for simplified energy calculation methods. Volume 4: United States, WYEC data
[DE85-000491] 09 p1357 N85-18539
Measurements of propagation at 900 MHz in an urban zone for establishing a digital radiomobile system
10 p1472 N85-19286
Statistical study of anthropogenic seismic noise with IVK-7 computer system 10 p1503 N85-19483
Nationwide urban runoff program. Relationship of urban runoff to land use and groundwater resources
[PB85-114692] 10 p1506 N85-19505
Organizations as information processing systems. Toward a strategic contingencies model of budget related influence in municipal government organizations
[AD-A149364] 10 p1567 N85-19883
The use of image registration technique in Brasilia's urban growth monitoring
[INPE-3302-PRE/614] 10 p1569 N85-19896
Study of pollutant dispersion in an urban street canyon
[DE85-002648] 11 p1677 N85-20571
Turbulence parameters impacting dispersion in an urban convection boundary layer
[PB85-116036] 11 p1682 N85-20596
A comparison of metropolitan and non-metropolitan employment characteristics: Indications of the size of non-metropolitan mobile communication services user classes
[NASA-CR-175648] 13 p2053 N85-22855
The use of Thematic Mapper data for land cover discrimination: Preliminary results from the UK SATMaP programme 13 p2121 N85-23207
Technology and Economics, Inc. Technology Application Team
[NASA-CR-175630] 13 p2168 N85-23454
Spectroscopic study of gas pollutants in atmosphere over large cities: A review 14 p2341 N85-24478
Nationwide Urban Runoff Project, Champaign, Illinois: The biological impact of urban runoff on the Saline Branch Drainage Ditch and Boneyard Creek
[PB85-150274] 14 p2348 N85-24515
Experience of the Institute of Space Research with the use of remote sensing in urban planning studies
[INPE-3159-PRE/533] 16 p2880 N85-27770
Impact of alcohol fuels on urban air pollution: Methanol photochemistry study
[DE85-009539] 18 p3133 N85-29403
Urban climate and air hygiene before, during, and after the lifework of Hellmut Berg. Overview of a branch of applied meteorology 18 p3147 N85-29487
The timing of noise-sensitive activities in residential areas
[NASA-CR-177937] 20 p3524 N85-31918
On the transformation regularities of time series of solid aerosol concentrations in the surface atmospheric layer
21 p3645 N85-32648
An electron microscopic study of urban aerosol
21 p3651 N85-32689
Helicopter noise survey for selected cities in the contiguous US
[AD-A154893] 21 p3699 N85-32985
Department of Housing and Urban Development Independent Agencies Appropriation Bill, 1986
[S-REPT-99-129] 23 p3987 N85-34720
Motor glider measurements during the Urban Atmosphere Energy Budget Experiment (EESA 1)
24 p4122 N85-35553

CITRIC ACID
Vinyl citrates from citric acid as new monomers
[BMFT-FB-T-83-256] 03 p0338 N85-12178

CIVIL AVIATION
Development trends and requirements of propulsion system technology for civil aircraft
01 p0011 N85-10066
Foreign civil aviation competition: 1976 summary and implications
[NASA-TM-X-73907] 02 p0133 N85-10907
Energy efficient engine. Volume 2. Appendix A: Component development and integration program
[NASA-CR-173085] 02 p0146 N85-10991
USSR report: Transportation
[JPRS-UTR-84-028] 03 p0310 N85-12002
Ministry wants better commo facilities for agroaviation
03 p0310 N85-12003
Editorial urges improved aviation repair work quality
03 p0310 N85-12004
Activities report of the aerospace industry in West Germany
[ISSN-0176-5086] 05 p0734 N85-14718
Design study of technology requirements for high performance single-propeller-driven business airplanes
[NASA-CR-3863] 07 p0898 N85-15692
West Europe report: Science and technology
[JPRS-WST-84-039] 07 p0936 N85-15929
Activities report of the aerospace industry in West Germany
[ISSN-0722-3838] 07 p1053 N85-16686
Activities report of the aerospace industry in West Germany
[ISSN-0722-3838] 07 p1054 N85-16687
FAA (Federal Aviation Administration) statistical handbook of aviation, calendar year 1983
[AD-A148171] 08 p1067 N85-16760
USSR report: Transportation
[JPRS-UTR-85-001] 08 p1067 N85-16763
Director on institute's civil aviation projects
08 p1067 N85-16764
Designer on Aeroflot automated COMMO system development 08 p1067 N85-16765
Testing solution for IL-76 braking system problem
08 p1067 N85-16766
International projects, other work of Aeroproyekt Institute 08 p1068 N85-16767
Designer on civil aircraft design trends in USSR
08 p1068 N85-16768
Improved sprayer for AN-2 cropdusting work
08 p1068 N85-16769
Airport activity statistics of certificated route air carriers
[AD-A148472] 08 p1081 N85-16846
Directions of the West German Ministry of Transport for education and control of airline personnel (section 3, chapters 2 and 12) 08 p1081 N85-16848
Directions of the West German Ministry of Transport for education and control or airline personnel, Report 6; chapters 3/A and 3/B 08 p1081 N85-16849
Satellite navigation
[S-HRG-98-856] 08 p1082 N85-16851
Activities report on West German civil airports. Part 1: Text
[ISBN-3-87977-055-7-PT-1] 08 p1090 N85-16887
Activities report for the West German Civil Airports. Part 2: Tables
[ISBN-3-87977-055-7-PT-2] 08 p1090 N85-16888
West Europe report: Science and technology
[JPRS-WST-85-001] 08 p1141 N85-17190
Flight Training Technology for Regional/Commuter Airline Operations: Regional Airline Association/NASA Workshop Proceedings
[NASA-CP-2348] 09 p1275 N85-18009
Captain development training at US Air
09 p1275 N85-18012
Management training for cockpit crews at Piedmont flight 09 p1276 N85-18013
Integrated approach to flight crew training
09 p1276 N85-18014
Video concepts in CRM training
09 p1276 N85-18015
Use of simplifier scenarios for CRM training
09 p1276 N85-18016
First deputy minister on 1984 civil aviation performance 09 p1277 N85-18033
Collegium on aviation fuel conservation efforts
09 p1278 N85-18034
Finnair, LOT, SAS reps in USSR on present operations, plans 09 p1278 N85-18035
Activities at Mil Experimental Design Bureau
09 p1278 N85-18036
Research at automated ATC Scientific-Experimental Center 09 p1278 N85-18037
Airport ground equipment under development at Riga
09 p1278 N85-18038
Improvements in Kazan airport equipment, facilities
09 p1278 N85-18039
Improvements under way at Gorkiy airport
09 p1278 N85-18040
New discovery in supersonic flight research
09 p1278 N85-18041
Sunset of the Civil Aeronautics Board
[S-HRG-98-940] 09 p1403 N85-18829
Digest of the Deutsche Lufthansa report, 1983
[ISSN-0415-603X] 09 p1418 N85-18948
Semiannual report to Congress on the effectiveness of the civil aviation security program
[AD-A149522] 10 p1421 N85-18967
Medically disqualified airline pilots
[AD-A149454] 10 p1528 N85-19637
Wildlife Hazards to Aircraft Conference and Training Workshop: Proceedings
[AD-A148330] 11 p1578 N85-19938
Accidents and serious incidents to civil aircraft due to birstrikes
[AD-P004180] 11 p1578 N85-19942
Analysis of bird strikes reported by European airlines, 1976 - 1980
[AD-P004181] 11 p1578 N85-19943
West Europe report: Science and technology
[JPRS-WST-85-008] 11 p1617 N85-20174
General aviation activity and avionics survey
[AD-A149572] 12 p1769 N85-21103
Transportation
[JPRS-UTR-85-004] 12 p1769 N85-21105

Aviation repair plant directors on quality control measures 12 p1769 N85-21106
New flight simulators at Vnukovo permit less in-flight training 12 p1769 N85-21107
Annual review of aircraft accident data: US air carrier operations calendar year 1981 [NTSB/ARC-85/01] 12 p1774 N85-21134
Ground and flight testing for aircraft guidance and control [AGARD-AG-262] 13 p1966 N85-22350
Civil avionics flight testing with the RAE(B) BAC1-11 13 p1967 N85-22354
USSR report: Transportation [JPRS-UTR-85-005] 14 p2207 N85-23688
Minister Bugayev on civil aviation in 1984, plans for 1985 14 p2208 N85-23689
1st deputy minister on civil aviation support of economy 14 p2208 N85-23690
Deputy minister on civil aviation fuel conservation efforts 14 p2208 N85-23691
Deputy minister on civil aviation construction projects 14 p2208 N85-23692
Improvements in personnel needed for better flight safety 14 p2208 N85-23693
USSR report: Transportation [JPRS-UTR-84-006] 14 p2208 N85-23694
Minister Bugayev reviews 1983 civil aviation work, sets course for 1984 14 p2208 N85-23695
Bugayev on civil aviation ministry's 1983 achievements 14 p2208 N85-23696
Riga Institute seeking faster introduction of new technology 14 p2208 N85-23698
Safety recommendation(s), A84-111 through -115 [REPT-4011C/27] 14 p2216 N85-23744
Safety recommendation(s), A-84-103 [REPT-3909B/101B] 14 p2216 N85-23745
FAA aviation forecasts: Fiscal years 1985-1996 [AD-A151050] 14 p2216 N85-23747
Safety recommendation(s), A-84-82 through -84 [REPT-3957] 14 p2217 N85-23748
West Europe report: Science and technology [JPRS-WST-85-013] 14 p2289 N85-24183
USSR report: Transportation [JPRS-UTR-85-008] 15 p2460 N85-25189
Roundtable on effective use of flight simulators 15 p2460 N85-25190
Official on Soviet research in deicing techniques 15 p2460 N85-25191
USSR report: Transportation [JPRS-UTR-84-015] 15 p2460 N85-25192
Administration chief on air traffic control improvements 15 p2460 N85-25193
Civil air code international flights section explained 15 p2460 N85-25194
USSR report: Transportation [JPRS-UTR-84-017] 15 p2461 N85-25196
Chronic fuel shortages in Volga civil aviation administration 15 p2461 N85-25198
Safety recommendation(s), A-84-128 through -133 [REPT-3996C/41] 15 p2466 N85-25221
Safety recommendation(s), A-84-123 and -124 [REPT-3894B/93] 15 p2466 N85-25222
USSR report: Transportation [JPRS-UTR-84-014] 15 p2467 N85-25229
Ilyushin bureau designer on fuel conservation research 15 p2467 N85-25231
Calculation and display of stack departure times for aircraft inbound to Heathrow Airport [AD-A151991] 15 p2469 N85-25241
West Europe report: Science and technology [JPRS-WST-84-003] 15 p2534 N85-25635
FRG journal analyzes state, prospects of airbus programs: General analysis 15 p2535 N85-25638
West Europe report: Science and technology [JPRS-WST-84-009] 15 p2535 N85-25639
West Europe report: Science and technology [JPRS-WST-84-014] 15 p2536 N85-25647
Certifying complex digital systems on civil aviation aircraft 17 p2904 N85-27907
Operations research [B8561897] 17 p3026 N85-28712
West Europe report: Science and technology [JPRS-WST-84-037] 18 p3086 N85-29108
A systematic determination of skill and simulator requirements for airline transport pilot certification [AD-A154135] 19 p3330 N85-30630
FAA regulation of 9-seat and under passenger aircraft [GPO-42-703] 20 p3391 N85-31032
Search and rescue services for international civil aviation 20 p3400 N85-31090
West Europe report: Science and technology [JPRS-WST-85-020] 20 p3438 N85-31333
MBB demonstrates new research aircraft ATTAS 20 p3438 N85-31334
NASA authorization, 1986, volume 1 [GPO-46-365] 20 p3541 N85-32039
An error-dependent model of instrument-scanning behavior in commercial airline pilots [NASA-CR-3906] 21 p3665 N85-32765
U.S. Civil airmen statistics for calendar year 1984 [AD-A156326] 24 p4059 N85-35153
The contribution made by flight mechanics to civil aviation 24 p4061 N85-35169
Introduction to European air traffic control [AD-A156328] 24 p4062 N85-35176

CL-41 AIRCRAFT
TUTOR (CL-41A) tail flight load survey 07 p0896 N85-15678

CLADDING
Microfluorescence studies of zirconium oxide [DE84-016116] 03 p0329 N85-12118
Effect of iron on the performance of IN 625 weld deposits [BR91456] 08 p1169 N85-17376
Elevated temperature creep behavior of Inconel alloy 625 [DE84-015636] 09 p1297 N85-18144
Antifriction properties of gas thermal coatings of clad carbine powders 10 p1447 N85-19115
Fracture resistance of surface layer with technological defects under cyclical loading 10 p1448 N85-19126
Lightweight cladding for magnetic circuits [AD-D011469] 10 p1461 N85-19350
New application possibilities for clad steel by reducing surface treatment expenditure and by using improved welding technology [BMFT-FB-T-84-236] 12 p1861 N85-21672
Ring-on-ring tests and load capacity of cladding glass [PB85-106391] 12 p1868 N85-21717
Fatigue of clad aluminum materials D16T and 2024-T3 with stepped loading 15 p2496 N85-25397
Investigation of the influence of some paint systems and water displacing corrosion inhibitors on anodic undermining corrosion of aluminum 2024 clad alloy — aircraft structures [VTH-LR-443] 16 p2756 N85-27009
New process for production of bimetal with corrosion-resistant cladding layer [BLL-BISI-TRANS-22371-(9022.06)] 17 p2927 N85-28056
Fiber optic moisture sensor [DE85-011651] 22 p3787 N85-33462
Chromium-base powder alloys for welding cladding layer of bimetal [BLL-M-35776-(5828.4)] 23 p3915 N85-34260
Manufacturing process to reduce large grain growth in zirconium alloys [DE85-011649] 23 p3915 N85-34267
Effect of stainless steel weld overlay cladding on the structural integrity of flawed steel plates in bending, series 1 [TI85-010349] 23 p3939 N85-34418

CLAMPS
A metallographic investigation of rotating bands for 7.5 cm artillery projectiles [FOA-C-20551-D2] 07 p0929 N85-15888
Reusable thermal cycling clamp [NASA-CASE-LAR-12866-1] 12 p1858 N85-21651
Pneumatic clamping device [AD-D011544] 12 p1858 N85-21656
Effectiveness of use of heat-dissipating clamps to reduce deformation during argon arc welding of thin sheets of AMg6 alloy 15 p2501 N85-25427

CLARK Y AIRFOIL
U AIRFOIL PROFILES

CLASSES
The rate of convergence of a class of block Jacobi schemes [AD-A144736] 01 p0111 N85-10749

CLASSICAL MECHANICS
NT ASTRODYNAMICS
NT CELESTIAL MECHANICS
NT KEPLER LAWS
NT MINIMUM VARIANCE ORBIT DETERMINATION
NT ORBITAL MECHANICS
NT SPACE MECHANICS
Semiclassical theory of resonances [REPT-67] 01 p0114 N85-10777
Study on controllability and stability of high speed tracked vehicles [AD-P004302] 09 p1409 N85-18879
How a swing behaves [DE85-008280] 17 p3027 N85-28720

CLASSIFICATIONS
NT HIERARCHIES
NT INDEXES (DOCUMENTATION)
NT SUBJECTS
Direction dependent radiation behavior in the classification of multispectral aircraft remote sensing data [SER-C-290] 01 p0063 N85-10419
An investigation into fuzzy clustering and classification [AD-A145571] 02 p0251 N85-11645
Interdisciplinary structure of information science 03 p0436 N85-12779
Comparability and accuracy of industry codes in different data systems [PB84-215607] 04 p0548 N85-13482
Documentation for the machine-readable version of the MK classification extension catalogue Morris-Kennedy (1983) [NASA-TM-87372] 04 p0549 N85-13491
Generic composite flywheel designs 05 p0606 N85-13864
Estimating location parameters in a mixture 07 p0984 N85-16252
Texture classification using autoregressive filtering 07 p0984 N85-16254
A method for automatic water mass classification [AD-D011405] 08 p1191 N85-17505
Assessment of LANDSAT for rangeland mapping, Rush Valley, Utah [E85-10072] 10 p1503 N85-19486
An IUE high-resolution atlas of O-type spectra 11 p1760 N85-21074
Multiple resolution representation and probabilistic matching of 2-D gray-scale shape [AD-A149981] 12 p1933 N85-22147
On the morphology of spiral modes — disk galaxies 12 p1955 N85-22283
Impact of Thematic Mapper sensor characteristics on classification accuracy — suburban Washington, D.C., Maryland, and the Chesapeake Bay 13 p2117 N85-2318
Quick look analysis of TM data of the Washington, District of Columbia, area 13 p2119 N85-23197
Microcomputer: Controlled statistics analyzer [BLL-CE-TRANS-7971-(9022.09)] 13 p2144 N85-2330
Geomorphic classification of lava flows on Io 13 p2173 N85-2348
Classification of circular features on Venus 13 p2177 N85-2351
Digital processing of passive Ka-band microwave image for sea-ice classification [AD-A150686] 14 p2347 N85-2451
A structural classification of geomagnetic pulsations 14 p2371 N85-2465
Classification and multiple regression through projectio pursuit [AD-A150797] 14 p2411 N85-2486
Efficient contextual measures for classification o multispectral image data 14 p2433 N85-2500
Low-resolution target classification from a starin infrared sensor [AD-A151690] 15 p2652 N85-2635
Criteria for the classification of hydrographic positionin data [AD-A152283] 16 p2705 N85-2669
Comparative study of the digital analysis of areas the Earth's surface prepared for planting using differe classification algorithms [INPE-3359-PRE/637] 16 p2846 N85-2754
New method of calculating the economic effects corrosion [BLL-BISI-TRANS-22348-(9022.06)] 17 p2929 N85-2807
Air photo analysis, photo interpretation logic, and featu extraction [AD-A153926] 18 p3124 N85-293
Geomorphic classification of Icelandic and Marti volcanoes: Limitations of comparative planetolo research from LANDSAT and Viking orbiter images 21 p3603 N85-323
Source hierarchy list. Volume 1: A through H [AD-A156300] 24 p4165 N85-358

CLASSIFYING
Efficient sorting routines in FORTRAN 77 [OUEL-1529/84] 05 p0716 N85-145
Diamonds and diamond sorting [PB85-128502] 10 p1542 N85-197
Generation and termination of binary decision trees nonparametric multiclass classification [AD-A151361] 15 p2640 N85-262

CLATHRATES
Volatiles in the outer solar system. 1: Thermodynam of clathrate hydrates. 2: Ethane ocean on Titan. Evolution of primordial Titan atmosphere 19 p3382 N85-300

CLAYS
The colloidal chemistry of ceramic clays [NASA-TM-77734] 03 p0336 N85-12
Site-specific research conducted in support of the Sa Sea Solar Pond Project, FY 1982 report [NASA-CR-174182] 05 p0666 N85-14
Laboratory investigations 05 p0666 N85-14

Solar pond research at Argonne National Laboratory
05 p0667 N85-14291
Interactions of hydrazine and of hydrazine derivatives with soil constituents and with soils
[AD-A148475] 08 p1122 N85-17074
Evaluating the variability of ceramics with X-ray fluorescence
[DE85-002028] 10 p1453 N85-19155
Response of earth-covered slabs in clay and sand backfills
[AD-A149296] 11 p1616 N85-20157
First direct detection of clay minerals on Mars
13 p2194 N85-23612
Analysis of SMIRR data for volcanic and sedimentary terrains of the trans-Pecos region, Texas
13 p2197 N85-23626
Chemical weathering of soils from the dry valleys of Antarctica: A terrestrial analog of Martian weathering processes 13 p2197 N85-23628
Low pressure storage of methane on interlayered clays for potential vehicular applications
[DE85-006949] 16 p2758 N85-27017
Clay identification and amount measured by laboratory techniques compared to well log responses: Application to tight gas sands and shales
[DE85-010411] 19 p3362 N85-30843

CLEAN FUELS
NT FUEL OILS

CLEAN ROOMS
Particle size distribution on surfaces in clean rooms
[AD-A146057] 03 p0328 N85-12109
MATRA has Europe's largest white room for satellites
10 p1477 N85-19320
Particulate contamination control in clean rooms by particle fallout (PFO) measurements
[ESA-PSS-01-204-ISSUE-1] 20 p3487 N85-31673

CLEANERS
NT AIR FILTERS
Apparatus and method to keep the walls of a free-space reactor free from deposits of solid materials
[NASA-CASE-NPO-15851-1] 12 p1858 N85-21652

CLEANING
NT ULTRASONIC CLEANING
Hot-gas cleanup for molten carbonate fuel cells-dechlorination and soot formation
[DE84-003072] 01 p0068 N85-10450
Potential application of robotics and state-of-the art end effectors at Letterkenny Army Depot
[AD-P004015] 03 p0309 N85-11994
Contamination problems during surface cleaning for thermocompression bonding
[DE84-013066] 04 p0475 N85-13023
Certain optimal parameters of high-velocity Venturi ejection tubes
[BLL-M-35924-(5828.4)] 05 p0634 N85-14066
Antisoiling technology: Theories of surface soiling and performance of antisoiling surface coatings
[NASA-CR-174274] 07 p0991 N85-16296
Community relations activities at Department of Defense sites
[AD-P004150] 09 p1349 N85-18486
Protocol for aquifer cleanup decision making at military installations
[AD-P004151] 09 p1349 N85-18487
Improved techniques for removal of sediments contaminated with hazardous materials
[PB85-116093] 11 p1679 N85-20580
Control of surface composition and hydrogen recycling by plasma conditioning
[DE85-001859] 11 p1731 N85-20889
Apparatus and method to keep the walls of a free-space reactor free from deposits of solid materials
[NASA-CASE-NPO-15851-1] 12 p1858 N85-21652
Steam generator tube vibration tests
[DE85-003599] 12 p1867 N85-21712
The effect of abrasive blasting on the fatigue and corrosion of an aluminium-copper alloy
[AD-A154954] 21 p3566 N85-32182
Review of hazardous waste cleanup and disposal efforts at Tinker Air Force Base
[GPO-43-294] 21 p3613 N85-32457

CLEAR AIR TURBULENCE
Safety recommendation(s), A84-111 through -115
[REPT-4011C/27] 14 p2216 N85-23744
Millstone Hill radar: Capabilities for S/T observations
21 p3629 N85-32548
Millimeter-wave propagation in moist air: Model versus path data
[AD-A156040] 24 p4087 N85-35331
The physical and empirical basis for a specific clear-air turbulence risk index
[NASA-CR-178522] 24 p4120 N85-35540

CLEARANCES
Pressure loss due to the tip clearance of impeller blades in centrifugal and axial blowers
05 p0636 N85-14083
Effect of form and clearance of a piston launched in a tube on the boundary layer and the heat transfer
[ISL-CO-216/83] 14 p2302 N85-24255
Effects of bearing deadbands on bearing loads and rotor stability 16 p2737 N85-26889

CLEARINGS (OPENINGS)
Relationship between forest clearing and biophysical factors in tropical environments: Implications for the design of a forest change monitoring approach --- Costa Rica
[E85-10051] 07 p0983 N85-16247

CLEBSCH-GORDAN COEFFICIENTS
A packed storage program for angular momentum coupling coefficients
[TWISK-316] 01 p0102 N85-10660
Interacting Boson approximation
[DE85-003016] 22 p3837 N85-33756

CLIFFS
Coastal erosion along Monterey Bay
[AD-A155610] 21 p3655 N85-32707

CLIMATE
Illinois Climate: Trends, Impacts and Issues
[PB84-211986] 01 p0086 N85-10577
Bibliography of climate textbooks and studies
[WCP-84] 02 p0231 N85-11505
The Martian climate: Energy balance models with CO2/H2O atmospheres
[NASA-CR-174073] 03 p0448 N85-12849
Research activities of the Illinois University Coordinated Science Laboratory
[AD-A145580] 03 p0449 N85-12856
Climate of the Northern Hemisphere, 1851 - 1900 compared to contemporary climate
[DE84-016366] 04 p0539 N85-13426
Climate-chamber experiments to improve pilots' work conditions 04 p0543 N85-13454
Massively parallel processor 05 p0680 N85-14366
Spectral energetics diagnoses and FGGE spectral observing periods and energetics analyses of forecast experiments with GLAS GCM 05 p0683 N85-14391
Report of the Meeting of Experts on Climate and Human Health
[WCP-78] 05 p0687 N85-14413
Organization of the session 05 p0687 N85-14414
Difficulties encountered in determining the potential involvement of consultants on health problems in various climatic zones 05 p0687 N85-14416
Review on physiological and medical problems related to climates ranging from altitude to sub-tropics
05 p0687 N85-14417
Epidemiologic methods applied to the study of the relationship between climate and human health
05 p0687 N85-14418
Polar regions and climatic change
[PB84-237023] 05 p0688 N85-14421
Paleoclimatologists use past to predict weather patterns 06 p0819 N85-15197
Monthly and seasonal climatology over the global tropics and subtropics for the decade 1973 to 1983. Volume 1: 200 mb winds
[AD-A146521] 06 p0838 N85-15322
Carbon dioxide and climate: Summaries of research in FY 1983 and FY 1984
[DE85-001245] 06 p0839 N85-15327
Climate Conference for Latin America and the Caribbean
[WMO-632] 07 p1000 N85-16352
The problem of climate and climate variation
07 p1001 N85-16353
Review of climate problems in Latin America and the Caribbean 07 p1001 N85-16354
Climate applications: General
07 p1001 N85-16355
Meteorological aspects of the 1982-83 El Nino/southern oscillation episode 07 p1001 N85-16356
Climate and climate data. Report on the workshop held in Brasilia (Argentina) from 11-15 April 1983
07 p1001 N85-16357
The climate in food production in Latin America
07 p1001 N85-16359
The challenge of food production: The importance of climate 07 p1001 N85-16361
Ocean and climate, an example. The interannual variability of the tropical Pacific Ocean
07 p1002 N85-16365
Climate and water quality 07 p1002 N85-16368
The water balance and climate --- Amazon region
07 p1003 N85-16370
The potential contributions of the World Climate Program (WCP) to the economies of developing countries
07 p1003 N85-16371
Socio-economic impact of climate --- Mexico
07 p1003 N85-16372
Climate and fisheries: A Peruvian case study
07 p1003 N85-16373
Energy and climate: Problems in Latin America
07 p1003 N85-16375
Requirements for training in climate-related subjects
07 p1004 N85-16378
Education and training for the climate related activities in Latin America and the Caribbean
07 p1004 N85-16379
Revised Uniform Summary of Surface Weather Observations (RUSSWO). Alconbury RAF United Kingdom, parts A-F
[AD-A146913] 07 p1004 N85-16384
Revised Uniform Summary of Surface Weather Observations (RUSSWO). Mildenhall RAF, United Kingdom, parts A-F
[AD-A146915] 07 p1005 N85-16386
Revised Uniform Summary of Surface Weather Observations (RUSSWO). Dobbins AFB, Georgia, parts A-F
[AD-A146916] 07 p1005 N85-16387
Limited surface observations climatic summary (LISOCS). Hohenfels, AAF, West Germany
[AD-A147167] 07 p1006 N85-16393
Revised Uniform Summary of Surface Weather Observations (RUSSWO). Offutt AFB, Nebraska, parts A-F
[AD-A147183] 07 p1006 N85-16394
Revised Uniform Summary of Surface Weather Observations (RUSSWO). Hill AFB, Utah, parts A-F
[AD-A147184] 07 p1006 N85-16395
Interrelationship of atmospheric parameters in Honduras
[AD-A147371] 07 p1007 N85-16401
Simulating responses to expected climate change in eastern North America: Applications to decision-making in the forest industry
[DE85-001272] 07 p1008 N85-16406
Chronologic and climatic control on soil development, northern Bighorn Basin, Wyoming and Montana
08 p1181 N85-17443
Revised Uniform Summary of Surface Weather Observations (RUSSWO). Parts A-F Zweibrucken AB, Germany
[AD-A147165] 09 p1357 N85-18536
A model for the climatic behavior of water on Mars
09 p1415 N85-18931
Natural environment analysis
[NASA-CR-171333] 10 p1428 N85-19010
Atlas of snow and ice resources
10 p1497 N85-19449
Climate of Salt Lake City, Utah
[PB85-123875] 10 p1521 N85-19589
Carbon dioxide and the greenhouse effect
[GPO-39-043] 11 p1677 N85-20569
Lake ice occurrence as a possible detector of atmospheric CO2 effects on climate
[DE85-002951] 11 p1687 N85-20606
Oceanic role in terrestrial climate
[DE85-004422] 12 p1896 N85-21904
Impact of aerosols on visibility and climate: A report prepared for Panel 3, Environmental Impact, of the NATO/CCMS Air Pollution Pilot Study on Air Pollution Control Strategies and Impact Modelling
[PB85-106744] 12 p1897 N85-21906
Environmental cycling of cellulosic thermal insulation and its influence on fire performance
[DE85-004295] 13 p2041 N85-22776
Global paleoclimatic data base for 6000 years BP
[DE85-006628] 15 p2600 N85-26024
North Atlantic Deep Water formation: Information from ice cores 15 p2602 N85-26035
Sea ice, climate and Fram Strait
15 p2603 N85-26042
The Martian climate: Energy balance models with CO2/H2O atmospheres
[NASA-CR-175722] 15 p2679 N85-26547
Regularities in recent changes in surface air temperature and atmospheric precipitation fields
16 p2807 N85-27311
Ecology of Pamlico River, North Carolina: An estuarine profile
[PB85-155703] 16 p2822 N85-27404
AWS (Air Weather Service) climatic briefs: Asia
[AD-A151944] 16 p2835 N85-27481
AWS (Air Weather Service) climatic briefs: North America
[AD-A152161] 16 p2835 N85-27483
A climatic data bank for Northern Hemisphere land areas, 1851-1980
[DE85-007863] 16 p2835 N85-27486
Intercomparison of Radiation Codes in Climate Models (ICRCCM)
[DE85-007251] 16 p2835 N85-27487
Preliminary assessment of climatic change during late Wisconsin time, southwest Great Basin and vicinity, Arizona, California and Nevada
[DE85-008343] 16 p2836 N85-27488
Time-dependence of CO2-induced climate change
[DE85-007568] 17 p2997 N85-28525

Identification and characterization of watershed models for evaluation of impacts of climate change on hydrology
[DE85-008575] 18 p3125 N85-29348

Humidity/cloud-radiation feedback on possible climate perturbation due to fossil fuel utilization
[DE85-008886] 18 p3133 N85-29402

Hellmut Berg issue --- meteorology
[MITT-39] 18 p3147 N85-29483

Environmental Research Laboratories (of the National Oceanic and Atmospheric Administration) programs and plans: FY 1984 programs and FY 1985 plans
[PB85-171494] 18 p3149 N85-29501

Summary of archived Atlantic coast wave information study pressure, wind, wave, and water level data
[AD-A153782] 18 p3151 N85-29508

Examination of the time and spatial scales appropriate for the carbon dioxide climate change issue
[DE85-009852] 19 p3317 N85-30563

Carbon dioxide and climate: Potential impacts
[DE85-009473] 20 p3496 N85-31734

Acclimatization to far north 20 p3506 N85-31792

Quantitative analysis in megageomorphology
21 p3603 N85-32376

Meteorological weapons
[AD-A154735] 21 p3635 N85-32575

Model projections of time-dependent response to increasing carbon dioxide
[DE85-013326] 22 p3816 N85-33641

Climatic consequences of very high CO2 levels in Earth's early atmosphere 22 p3854 N85-33865

The polar caps and the climatic evolution of Mars
22 p3854 N85-33866

Simulated effects of increased recharge on the ground-water flow system of Yucca Mountain and vicinity, Nevada-California
[DE85-012985] 24 p4108 N85-35469

Time-dependent response of the climate to increasing atmospheric carbon dioxide 24 p4119 N85-35532

Carbon dioxide and climate: A working glossary
[DE85-013535] 24 p4124 N85-35562

CLIMATOLOGY

NT AGROCLIMATOLOGY

NT MICROCLIMATOLOGY

The climate of Denmark: Summaries of observations from light vessels. 3: Sea temperature
[ISBN-87-7478-215-0] 01 p0073 N85-10481

Report of the First Session of the International Working Group on Data Management for the International Satellite Cloud Climatology Project (ISCCP)
[WCP-42] 01 p0073 N85-10483

Cloud cover sampling capability of various satellite combinations for ISCCP 01 p0073 N85-10484

ISCCP Cloud Algorithm Intercomparison Workshop
01 p0073 N85-10485

ISSCP Cloud Algorithm Intercomparison Workshop
01 p0073 N85-10486

Spatial relationships in stream flow residuals
02 p0212 N85-11397

A study of greenhouse effects using zero, 1 and 2 dimensional climate models 02 p0230 N85-11498

Report of the Third Session of the International Working Group on Data Management for the International Satellite Cloud Climatology Project (ISCCP)
[WCP-82] 02 p0231 N85-11504

Bibliography of climate textbooks and studies
[WCP-84] 02 p0231 N85-11505

A temperature climatology for New York State
03 p0394 N85-12517

Carbon dioxide, the greenhouse effect and climate: A primer
[GPO-33-444] 03 p0395 N85-12519

Plans for the NRL/NORDA (Naval Research Laboratory-Naval Ocean Research and Development Activity) fine-scale variability experiment - 1984 (FVX-84)
[AD-A146041] 03 p0398 N85-12540

Homogeneous macroclimatic zones of the lake states
[PB84-215811] 04 p0540 N85-13436

Global biogeochemical cycles: Scales of interaction and change, some views on the strategy of approach
05 p0652 N85-14185

Modeling long-term changes in forested landscapes and their relation to the Earth's energy balance
05 p0653 N85-14194

Combining Heat Capacity Mapping Mission (HCMM) LANDSAT and thematic map information into a unique high precision merged information system --- climatology 05 p0655 N85-14209

Numerical modeling of the atmosphere
05 p0682 N85-14370

Some new mesoanalysis methods for operational objective analysis 05 p0683 N85-14375

Extended range forecasting 05 p0683 N85-14376

Weather and climate measurements from Tenerife
05 p0683 N85-14377

Monthly and seasonal climatology over the global tropics and subtropics for the decade 1973 to 1983. Volume 1: 200 mb winds
[AD-A146521] 06 p0836 N85-15322

Diurnal and seasonal patterns of temperature and wind flow in the planetary boundary layer for ten locations in complex terrain
[PB85-106698/GAR] 06 p0840 N85-15333

Climatological information and water resources
07 p1002 N85-16367

Water and climate, study of one case
07 p1002 N85-16369

The Amazon and climate 07 p1003 N85-16376

A microprocessor data system for developing countries --- climatology 07 p1003 N85-16377

Revised Uniform Summary of Surface Weather Observations (RUSSWO). Spangdahlem AB, Germany, parts A-F
[AD-A147166] 07 p1006 N85-16392

Polar research in Earth sciences described
08 p1142 N85-17204

Natural environment analysis
[NASA-CR-174330] 08 p1180 N85-17433

Pilot climate data system
[NASA-CR-174321] 08 p1187 N85-17481

The visibility climatology of McMurdo Sound-Williams Field, Antarctica
[AD-A148108] 08 p1189 N85-17492

Consideration of future climatic changes in three geologic settings
[DE85-001704] 09 p1357 N85-18537

The establishment and experience of the Carbon Dioxide Information Center (CDIC)
[DE85-001934] 09 p1402 N85-18825

Optimization of a ground coupled heat pump
[DE85-000273] 10 p1486 N85-19380

Polar regions and climatic change: Appendix
[PB85-122679] 10 p1521 N85-19590

Soviet National Middle Atmosphere Program
11 p1655 N85-20428

Lidar observations of stratospheric aerosol over Mauna Loa Observatory, 1974 - 1981
[PB85-115061] 11 p1682 N85-20537

A study of eddy-mean flow interactions using Eliassen-Palm diagnostics: FGGE SOP-1 data and the NASA GLAS general circulation model compared
[NASA-CR-175506] 11 p1686 N85-20604

Performance evaluation of an active solar cooling system utilizing low cost plastic collectors and an evaporatively-cooled absorption chiller
[DE84-010813] 12 p1880 N85-21798

NBS solar collector durability/reliability test program
[DE85-003489] 12 p1881 N85-21801

Response of unmanaged forests to CO2-induced climate change: Available information, initial tests and data requirements
[DOE/NSB-0053] 12 p1883 N85-21817

Rationale and basic design for experimental acidification of a lake ecosystem in Northern Wisconsin
[PB85-116077] 12 p1885 N85-21829

The effect of stochastic surface heat fluxes on the climatology of the seasonal thermocline
[AD-A149957] 12 p1889 N85-21857

21 Layer troposphere-stratosphere climate model
[NASA-TM-86183] 12 p1892 N85-21871

A new NASA/MSFC mission analysis global cloud cover data base
[NASA-TP-2448] 12 p1893 N85-21878

Los Alamos MINI-Review: Tracking Antarctic winds
[DE85-004597] 12 p1896 N85-21903

Earth radiation budget experiment software development
[NASA-CR-172567] 12 p1912 N85-22002

Relationship of Indian monsoon intensity to time of onset 13 p2106 N85-23120

Numerical experiments with simple model of ocean climate 13 p2106 N85-23123

Summary of Meteorological Observations, Surface (SMOS), Fallon, Nevada
[AD-A150481] 13 p2138 N85-23276

Summary of Meteorological Observations, Surface (SMOS) Camp Pendleton, California
[AD-A150482] 13 p2138 N85-23277

Summary of Meteorological Observations, Surface (SMOS), Alameda, California
[AD-A150609] 13 p2138 N85-23281

Classification of atmospheric aerosol for evaluation of its effect on climate 14 p2333 N85-24428

Absolute movement of Pacific Ocean plate based on paleoclimatic and paleomagnetic data and trajectory of hot spots during last 120 million years
14 p2334 N85-24435

Atlas of archived vegetation, land-use and seasonal Albedo data sets
[NASA-TM-86199] 14 p2346 N85-24508

Geophysical Fluid Dynamics Laboratory activities, FY84, plans, FY85
[PB85-147601] 15 p2558 N85-25783

SAM 2 measurements of the polar stratospheric aerosol, volume 5
[NASA-RP-1140] 15 p2590 N85-25970

An Earth longwave radiation climate model
[NASA-CR-175749] 15 p2594 N85-25984

Characteristics of precipitation regimes during first global atmospheric research project global experiments
[AD-A151572] 15 p2599 N85-26021

Possible sea ice impacts on oceanic deep convection
15 p2603 N85-26041

Climatic impact of a change in North Atlantic Deep Water formation 15 p2603 N85-26045

Origin of the Greenland ice sheet
15 p2604 N85-26046

Real-time enhancement of a climatology or forecast of ocean thermal structure using observed ocean temperatures
[AD-A151116] 15 p2604 N85-26049

Evaluation of the area and severity of last night's frosts
[REPT-109] 16 p2833 N85-27473

Geophysical monitoring for climatic change, number 12
[PB85-172278] 16 p2837 N85-27498

NASA Oceanic Processes Program annual review
[NASA-TM-87565] 16 p2838 N85-27503

Centralized Storm Information System (CSIS)
[NASA-CR-175898] 17 p2994 N85-28506

A report from the Space Science and Engineering Center, the University of Wisconsin-Madison, Madison, Wisconsin 17 p2994 N85-28507

CSIS test and evaluation 17 p2994 N85-28509

Potential climatic impacts of increasing atmospheric CO2 with emphasis on water availability and hydrology in the United States
[NASA-TM-87479] 17 p2995 N85-28517

Air Weather Service (AWS) climatic briefs: Europe
[AD-A152528] 17 p2996 N85-28519

Characteristics of North Indian Ocean tropical cyclone activity
[AD-A153085] 17 p2997 N85-28524

Mathematical modeling and simulation of climate and climatic change
[DE85-008974] 17 p2997 N85-28526

Improvement of the basic knowledge of the climatology of the vertical ozone layer by enhanced balloon sounding
[BPT-6/84] 18 p3137 N85-29426

Research Review, 1983
[NASA-TM-86219] 18 p3139 N85-29433

Analysis of a simulated cloud climatology
18 p3145 N85-29472

Hellmut Berg issue --- meteorology
[MITT-39] 18 p3147 N85-29483

Applied climatology --- regional planning
18 p3147 N85-29486

Climatological data of stations in the Netherlands No. 11: Frequency tables and tables with runs according to measurements at principal climatological stations 1961-1980, sunshine stations 1956-1980, precipitation stations 1951-1980
[KNMI-150-11] 18 p3149 N85-29499

A global low order spectral model designed for climate sensitivity studies
[NASA-CR-175999] 19 p3315 N85-30549

On the dynamical climatology of the Amazon Basin and associated rain producing mechanisms
[INPE-3531-RPE/477] 19 p3315 N85-30552

A modified Fresnel scattering model for the parameterization of Fresnel returns, part 2.3A
21 p3618 N85-32483

Activities report of the Aeronomy Department
[G-774-1984] 21 p3633 N85-32569

Paleoenvironmental investigations at seed cave (Windust cave H-45FR46), Franklin County, Washington
[AD-A154777] 21 p3635 N85-32576

A simulation of weather in 3D space
[AD-A155221] 21 p3636 N85-32586

Airborne measurements of the vertical distribution of Arctic haze 21 p3647 N85-32657

Middle Atmosphere Program. Handbook for MAP, volume 11
[NASA-CR-176107] 22 p3814 N85-33625

Reports from the German Meteorological Service. No. 166: The optimal spectral density of climatological station networks
[ISBN-3-88148-214-8] 23 p3950 N85-34478

Lake ice occurence as a possible detector of atmospheric CO2 effects on climate
[DE85-012987] 23 p3950 N85-34480

Current inventory of anthropogenic carbon dioxide in the North Pacific Subarctic Gyre
[PB85-187938] 24 p4125 N85-35570

CLIMBING FLIGHT
Wind tunnel results of advanced high speed propellers in the takeoff, climb and landing operating regimes
[NASA-TM-87054] 19 p3213 N85-29925
CLINICAL MEDICINE
Review on physiological and medical problems related to climates ranging from altitude to sub-tropics
05 p0687 N85-14417
In vivo neutron activation analysis: Body composition studies in health and disease
[DE84-014092] 05 p0696 N85-14480
Comparative assessment of different treatment modalities in miners with vibration- and noise-induced disease 10 p1524 N85-19610
Management of microcirculatory disorders in vibration sickness 10 p1524 N85-19611
Catalog of completed studies, US Army health care studies and clinical investigation activity
[AD-A149450] 10 p1568 N85-19885
A double blind comparative trial of powdered ginger root, hyosine hydrobromide, and cinnarizine in the prophylaxis of motion sickness induced by cross coupled stimulation
11 p1695 N85-20657
Review of US manual of clinical aviation medicine
12 p1904 N85-21957
The clinical and radiological assessment of cervical injury, Annex A 12 p1907 N85-21976
Oversight review of the five-year outlook report on science and technology
[GPO-41-058] 12 p1949 N85-22243
Medical subject headings, tree structures, 1985
[PB84-216092] 12 p1952 N85-22261
Permuted medical subject headings, 1985
[PB84-216100] 12 p1952 N85-22262
Technology transfer to the Middle East
[PB85-127744] 12 p1952 N85-22264
Medical planning criteria for implementation of clinical hyperbaric facilities
[AD-A151001] 14 p2389 N85-24715
Development and diffusion of automated clinical chemistry analyzers
[PB85-150696] 15 p2561 N85-25798
List of serials indexed for online users, 1985
[PB85-143220] 15 p2666 N85-26455
Thermal consequences of localized SAR from RFR exposures 16 p2775 N85-27130
Diagnostic system
[INPE-3350-PRE/659] 16 p2841 N85-27519
New technologies to improve laboratory testing
[DE85-008151] 18 p3110 N85-29257
Effect of spironolactone on acute mountain sickness
[AD-A153780] 18 p3153 N85-29525
Accepting error to make less error
[AD-A153949] 18 p3171 N85-29651
Test and Evaluation Master Plan (TEMP) for the Navy Occupational Health Information Management System (NOHIMS). Phase 1: Appendix A through appendix U
[AD-A154179] 19 p3380 N85-30967
USSR report: Life sciences. Biomedical and behavioral sciences
[JPRS-UBB-85-018] 22 p3819 N85-33660
Heavy ion medical accelerator options
[DE85-011204] 22 p3841 N85-33784
USSR report: Life sciences. Biomedical and behavioral sciences
[JPRS-UBB-85-021] 23 p3951 N85-34489
Effect of water immersion of parameters of central hemodynamics in individuals over 45 years old
23 p3953 N85-34499
Effect of dibazol on parameters of nonspecific resistance of subjects in pressurized cabins
23 p3954 N85-34504
Analogies of control mechanisms in flight guidance and medicine 24 p4129 N85-35597
LOCKS
NT ATOMIC CLOCKS
NT AUTONOMOUS SPACECRAFT CLOCKS
NT CHRONOMETERS
Portable real-time clock
[AD-A146218] 03 p0364 N85-12336
Precision digital sampler
[AD-D011285] 06 p0809 N85-15143
Laser clock
[AD-D011513] 12 p1855 N85-21634
Application of K176-series microcircuits
13 p2077 N85-22973
Active dispersion control for a Doppler broadened laser
[AD-D011570] 14 p2310 N85-24297
Maintenance of time and frequency in the DSN using the global positioning system 16 p2771 N85-27105
Proceedings of the Fifteenth Annual Precise Time and Time Interval (PTTI) Applications and Planning Meeting
[AD-A149163] 17 p2961 N85-28287
Unattended TV time transfer results
17 p2964 N85-28305
Clock characterization tutorial
17 p2965 N85-28311
A plan for the development of inertial reconstruction of initial state clock (IRIS) 17 p2966 N85-28317
Atmospheric limitations to clock synchronization at microwave frequencies 18 p3107 N85-29236
Development of hydrogen masers for K-3 VLBI system
18 p3108 N85-29239
Numerical optical computing at the Ohio State University 18 p3188 N85-29775
A new fault-tolerant algorithm for clock synchronization
[AD-A154771] 21 p3676 N85-32836
Method of characterizing critical timing paths and analyzing timing related failure modes in very large scale integrated circuits
[AD-D011731] 22 p3759 N85-33298
Recording system for the solar neutron monitoring at Mt. Norikura
[SH-9.1-8] 23 p4051 N85-35123
CLOSED BASINS
U STRUCTURAL BASINS
CLOSED CYCLES
Advanced technology cogeneration system conceptual design study: Closed cycle gas turbines
[NASA-CR-168222] 07 p0992 N85-16300
Manned testing of two closed-circuit oxygen underwater breathing apparatus: US Navy Emerson Rig and Fenzy PO.68
[AD-A148300] 08 p1200 N85-17560
Closed cycle versus open cycle gas turbines. A review of A.D. Little's ICOP report, vol. 3
[DE85-000564] 12 p1861 N85-21671
Solid state compressor
[AD-A150790] 14 p2311 N85-24302
Optimization of the catalytic oxidation of CO for closed-cycle CO2 laser applications
[NASA-TM-86421] 15 p2504 N85-25445
CLOSED ECOLOGICAL SYSTEMS
Problems associated with the utilization of algae in bioregenerative life support systems
[NASA-CR-166615] 07 p1019 N85-16469
Algal culture studies related to a Closed Ecological Life Support System (CELSS)
[NASA-CR-177322] 07 p1019 N85-16470
Controlled ecological life support system higher plant flight experiments
[NASA-CR-177323] 07 p1020 N85-16471
Control and modeling of a CELSS (Controlled Ecological Life Support System)
[NASA-CR-177324] 07 p1020 N85-16472
Feasibility of producing a range of food products from a limited range of undifferenitiated major food components
[NASA-CR-177329] 07 p1020 N85-16473
Effect of high ammonia content in closed environment on some parameters of human nitrogen and carbohydrate metabolism against background of a controlled diet
12 p1903 N85-21948
Controlled Ecological Life Support System. Life Support Systems in Space Travel
[NASA-CP-2378] 18 p3155 N85-29531
Current concepts and future directions of CELSS
18 p3155 N85-29532
Survey of CELSS concepts and preliminary research in Japan 18 p3155 N85-29533
Dynamic considerations for control of closed life support systems 18 p3155 N85-29537
CELSS transportation analysis
18 p3156 N85-29538
Extended mission life support systems
18 p3157 N85-29547
Space shuttle revitalization system
18 p3157 N85-29548
Internal contamination in the space station
18 p3157 N85-29549
Space station trace contaminant control
18 p3157 N85-29550
Publications of the NASA CELSS (Controlled Ecological Life Support Systems) program
[NASA-CR-3911] 19 p3326 N85-30608
CLOSED FAULTS
U GEOLOGICAL FAULTS
CLOSED LOOP SYSTEMS
U FEEDBACK CONTROL
CLOSTRIDIUM BOTULINUM
Production of butanol by fermentation in the presence of cocultures of clostridium
[NASA-CASE-NPO-16203-1] 24 p4071 N85-35227
CLOSURE LAW
A study of Reynolds-stress closure model
[NASA-CR-174342] 08 p1161 N85-17324
A 2-dimensional second order closure model of the upper atmosphere 08 p1182 N85-17450
A turbulent closure model for the free atmosphere
09 p1351 N85-18502
Centrifuge tests to provide closure bounds for switches subjected to random vibration
[DE85-002003] 10 p1482 N85-19357
A study of the second and third order closure models of turbulence for prediction of separated shear flows
[NASA-CR-176127] 23 p3929 N85-34353
Application of a turbulent closure model to the parameterization of the vertical diffusion of heat, momentum, and humidity in the ECMWF model — European Center for Medium Term Weather Forecasting (ECMWF)
[MITT-41] 24 p4095 N85-35387
CLOSURES
Cooled turbine blade tip closure
[AD-D011525] 12 p1858 N85-21654
Synthesis of tree-structured computing systems through use of closures
[AD-A150502] 13 p2147 N85-23326
Scale separation closure and Alfven wave turbulence
[DE85-013124] 24 p4095 N85-35385
CLOTH
U FABRICS
CLOTHING
NT BOOTS (FOOTWEAR)
NT COVERALLS
NT FLIGHT CLOTHING
NT GOGGLES
NT HELMETS
NT PRESSURE SUITS
NT PROTECTIVE CLOTHING
NT SHOES
NT SPACE SUITS
Measurement of stress in clothing: A literature review and methods selected
[AD-A147674] 08 p1132 N85-17132
Current approaches for the biophysical and physiological evaluation of combat clothing for environmental extremes
[AD-A151012] 14 p2395 N85-24752
The location of stress in clothing
[AD-A154423] 19 p3331 N85-30633
Physical dimensions of humans; values; the effect of clothing, working clothes and protective equipment on the design of work places
[HSE-TRANS-10868] 19 p3331 N85-30638
Human body dimensions: Body outlines and envelope curves at different normal positions and movements
[HSE-TRANS-10866] 19 p3332 N85-30640
CLOUD CHAMBERS
An experimental investigation of the angular scattering and backscattering behaviors of the simulated clouds of the outer planets
[NASA-CR-175909] 17 p3052 N85-28896
Construction of University of Missouri, Rolla's full scale cloud simulation chamber and applied research
[AD-A154682] 21 p3557 N85-32128
Missing energies at pair creation
[HE-4.4-8] 24 p4193 N85-36016
Progress report on a new search for free e/3 quarks in the cores of 10(15) - 10(16) eV air showers
[HE-6.2-15] 24 p4212 N85-36151
CLOUD COVER
Shipboard measurement of cloud bases and average surface visibility with an eye-safe lidar
[AD-A144889] 01 p0052 N85-10345
Report of the First Session of the International Working Group on Data Management for the International Satellite Cloud Climatology Project (ISCCP)
[WCP-42] 01 p0073 N85-10483
ISSCP Cloud Algorithm Intercomparison Workshop
01 p0073 N85-10486
Combining radar and satellite data for the localization and identification of summer convection
01 p0077 N85-10509
The possibility of detection and measurement of cloud structure in the atmosphere of Uranus
02 p0299 N85-11937
Investigations of severe/tornadic thunderstorm development and evolution based on satellite and AVE/SESAME/VAS data
[NASA-CR-174154] 04 p0538 N85-13424
Investigation of satellite measurements in the presence of clouds, forcing influences on clouds and feedback to the large scale following convection
05 p0682 N85-14381
NOAA/NASA joint simulation of AMTS and HIRS
05 p0682 N85-14384
Modeling influence of three layer cloud cover on outgoing thermal radiation 06 p0825 N85-15242
Conditions governing the formation of stratocumulus clouds over the western Atlantic during cold air outbreaks
[AD-A146780] 07 p1004 N85-16383
First sodium nightglow results for Natal
[INPE-3397-PRE/666] 10 p1515 N85-19560

Military applications of meteorological satellite (METSAT) data 11 p1711 N85-20767
A new NASA/MSFC mission analysis global cloud cover data base
[NASA-TP-2448] 12 p1893 N85-21878
Summary of Meteorological Observations, Surface (SMOS), Alameda, California
[AD-A150609] 13 p2138 N85-23281
Variation of Arctic cloud cover in summer
[DE85-004507] 13 p2139 N85-23285
Mean free path lenght of photons with broken cloud cover 14 p2338 N85-24455
Methods for cloud cover estimation
14 p2444 N85-25081
ILUM code: Solar and lunar flux calculations for multi-cloud layered atmospheres
[DE85-005578] 15 p2600 N85-26025
Symposium on Atmospheric Sciences in South Africa
[CSIR-S-331] 16 p2829 N85-27442
A modeling analysis program for the JPL table mountain Io sodium cloud
[NASA-CR-175851] 16 p2833 N85-27468
AWS (Air Weather Service) climatic briefs: Asia
[AD-A151944] 16 p2835 N85-27481
Space photographs confirm 40-year-old hydrodynamics discovery 19 p3289 N85-30393
Issue of sky conditions
[DE85-010590] 19 p3317 N85-30562
A simulation of weather in 3D space
[AD-A155221] 21 p3636 N85-32586
Enhancing precision of remote temperature sensing data from satellites under cloudy atmospheric conditions
22 p3734 N85-33148
Determination of altitude of cloud cover top from Meteor satellite data 22 p3734 N85-33150
Repetition of dense cloud cover above Indian Ocean from generalized satellite data 22 p3737 N85-33165
Mean cloudiness over the global tropics from satellite observations
[AD-A156188] 24 p4123 N85-35561

CLOUD DISPERSAL
The effect of the arbitrary level assignment of satellite cloud motion wind vectors on wind analyses in the pre-thunderstorm environment
[NASA-TM-86186] 10 p1517 N85-19565

CLOUD HEIGHT INDICATORS
Shipboard measurement of cloud bases and average surface visibility with an eye-safe lidar
[AD-A144889] 01 p0052 N85-10345
Improved cloud and surface fields derived from HIRS2/MSU 18 p3140 N85-29439

CLOUD PHOTOGRAPHY
Geostationary satellite cloud and precipitation analysis using an interactive computer system
01 p0076 N85-10506
Technique that uses satellite, radar, and conventional data for analyzing and short-range forecasting of precipitation from extratropical cyclones
[PB85-164994] 16 p2837 N85-27499
Radio-frequency radiation of storm clouds
21 p3692 N85-32939
Determination of altitude of cloud cover top from Meteor satellite data 22 p3734 N85-33150

CLOUD PHYSICS
Processing and display of atmospheric phenomenas data
[NASA-CR-171178] 01 p0072 N85-10475
Cloud cover sampling capability of various satellite combinations for ISCCP 01 p0073 N85-10484
A tropical cyclone precipitation estimation technique using geostationary satellite data
[PB84-226703] 01 p0086 N85-10579
Observed rate of tropospheric diffusion
[DE84-016047] 02 p0224 N85-11470
Theoretical development of Monte Carlo codes for modeling cumulus cloud fields
[NASA-CR-174063] 02 p0230 N85-11500
Report of the Third Session of the International Working Group on Data Management for the International Satellite Cloud Climatology Project (ISCCP)
[WCP-82] 02 p0231 N85-11504
Aircraft flow effects on cloud droplet images and concentrations
[AD-A146176] 03 p0396 N85-12529
Operational test of three instruments for measuring liquid water content in laboratory and from aircraft
[DFVLR-MITT-84-08] 03 p0397 N85-12531
International Conference on Physics of Clouds
06 p0819 N85-15198
First stage of equipping a Do 28 as a research aircraft for icing, and first research results
[ESA-TT-855] 11 p1584 N85-19982
Case studies of snow clouds by means of snow crystal sondes 15 p2581 N85-25921
The physics of the marine stratocumulus-capped mixed layer 15 p2593 N85-25979
Convection modeling and application to severe storms
15 p2595 N85-25991
Modeling of cloud systems 15 p2595 N85-25992
Anvil structure of severe thunderstorms
15 p2595 N85-25993
The use of radar in determining precipitation processes in the BEWMEX area 16 p2831 N85-27455
Effects of cloud seeding on precipitation development in cumulus clouds 16 p2831 N85-27456
Cloud physics studies in the SCPP (Sierra Cooperative Pilot Project)
[PB85-163095] 16 p2837 N85-27501
An experimental investigation of the angular scattering and backscattering behaviors of the simulated clouds of the outer planets
[NASA-CR-175909] 17 p3052 N85-28896
Atmospheric probing by active millimeter wave system
[AD-A153550] 18 p3136 N85-29422
Cloud physics 18 p3147 N85-29485
On the state of knowledge on meteorologically caused icing of aircraft in clouds
[ESA-TT-861] 20 p3486 N85-31738
Eleventh International Conference on Atmospheric Aerosols, Condensation and Ice Nuclei, volume 2
[PB85-182418] 21 p3638 N85-32596
Experimental studies of the kinetics of deposition nucleation on an ice nucleant used in weather modification 21 p3638 N85-32598
Inactivation of silver iodide by atmospheric nucleation inhibitors 21 p3638 N85-32599
Ice active bacteria as condensation nuclei
21 p3639 N85-32603
The effect of supersaturation, temperature and particle size on ice-nucleating ability of atmospheric aerosol
21 p3639 N85-32604
On the efficiency of the mechanism of ice particles formation in the vapor supersaturation field around a freezing droplet 21 p3639 N85-32606
The nucleation of ice crystals during the freezing of large supercooled drops 21 p3640 N85-32608
On the problem of possible mechanism of ice nuclei formation in convective clouds 21 p3640 N85-32610
Bacterial ice nuclei of marine origin: Some recent observations 21 p3640 N85-32611
Airborne measurements of atmospheric ice nuclei
21 p3640 N85-32612
Aircraft observations of condensation and ice nuclei at a tropical station 21 p3640 N85-32613
The nucleation of ice at very low temperatures and pressures 21 p3641 N85-32617
The 100 years of Aitken Nuclei (AN) study-reminiscence, current and future problems 21 p3641 N85-32621
A thermal diffusion chamber for the measurement of cloud condensation nuclei 21 p3642 N85-32627
Stable generation of highly monodisperse aerosols
21 p3642 N85-32628
Monte Carlo studies of H2O layers adsorbed on a model basal face of AgI 21 p3643 N85-32633
Eleventh International Conference on Atmospheric Aerosols, Condensation and Ice Nuclei, volume 1
[PB85-182400] 21 p3644 N85-32636
The first condensation nucleus conference
21 p3644 N85-32637
Cloud condensation on insoluble particles
21 p3648 N85-32670
Measurements of the critical supersaturation of 0.029 to 0.035 micron radius particles at Washington, District of Columbia 21 p3649 N85-32676
A relationship between cloud droplet size and CCN critical supersaturation 21 p3649 N85-32677
Fog activation and supersaturation
21 p3650 N85-32678
On the question to the effect of surfactants on the spectrum of cloud drops in the process of their condensation growth 21 p3650 N85-32679
Aircraft observations of cloud condensation nuclei in maritime and continental environments
21 p3650 N85-32680
The distribution of giant salt nuclei inside and outside cloud over the basin of Xin and Jiang
21 p3650 N85-32681
Characterization of insoluble particles associated with cloud droplets 21 p3652 N85-32693
Applicability of surface CCN measurements
21 p3652 N85-32696
Effect of ions on cloud formation and its role in solar terrestrial relationship 21 p3653 N85-32697
on the transport of large condensation nuclei in the atmosphere at various altitudes over the territory of the USSR 21 p3653 N85-32698
Study of the parameters affecting the collapse of a rotating protostellar cloud 24 p4168 N85-35837

CLOUD SEEDING
NOAA/NASA joint simulation of AMTS and HIRS
05 p0682 N85-14384
Ground-based snow and ice crystal observation system used in Sierra Nevada winter orographic storms
[PB85-115343] 10 p1520 N85-19584
Methods for cloud cover estimation
14 p2444 N85-25081
Cloud-seeding for regulating precipitation in Moscow area 16 p2807 N85-27308
Effects of cloud seeding on precipitation development in cumulus clouds 16 p2831 N85-27458
SCPP (Sierra Cooperative Pilot Project) Forecasting Support 16 p2837 N85-27493
Cloud physics studies in the SCPP (Sierra Cooperative Pilot Project)
[PB85-163095] 16 p2837 N85-27501
Observations of cloud droplets, aerosol particles and cloud condensation nuclei in continental air masses
21 p3649 N85-32671
Project Skywater, 1983-84 SCPP (Sierra Cooperative Pilot Project) data inventory
[PB85-187052] 24 p4124 N85-35565

CLOUDS
NT ANVIL CLOUDS
NT ARC CLOUDS
NT BARIUM ION CLOUDS
NT CAP CLOUDS
NT CIRRUS CLOUDS
NT CLOUDS (METEOROLOGY)
NT CONVECTION CLOUDS
NT CUMULUS CLOUDS
NT ELECTRON CLOUDS
NT HYDROGEN CLOUDS
NT MAGELLANIC CLOUDS
NT MOLECULAR CLOUDS
NT NOCTILUCENT CLOUDS
NT PLASMA CLOUDS
NT STRATOCUMULUS CLOUDS
NT STRATUS CLOUDS
NT VENUS CLOUDS
Clouds above the Martin Limb: Viking observations
[NASA-CR-174027] 02 p0296 N85-11922
Aircraft flow effects on cloud droplet images and concentrations
[AD-A146176] 03 p0396 N85-12529
The Jovian atmospheric window at 2.7 microns: A search for H2S
[NASA-TM-86661] 03 p0445 N85-12836
Optical observations of nearby interstellar gas
06 p0875 N85-15557
Distances of local clouds from optical line observations 06 p0875 N85-15558
Dark cloud and globule distribution for galactic longitudes 230 to 360 degrees 06 p0878 N85-15575
The smallest sizes of diffuse interstellar clouds
06 p0878 N85-15578
Polarization of radio molecular lines and mapping of magnetic field direction 06 p0878 N85-15581
Fuel-rich solid propellant boron combustion
[AD-A148522] 08 p1136 N85-17157
The radiation temperature of a cloud of particles
[FOA-C-30367-E4] 08 p1190 N85-17497
A modeling analysis program for the JPL table mountain Io sodium cloud data
[NASA-CR-175474] 10 p1572 N85-19910
Fragmentation and turbulence in collapsing gas clouds
[DE85-003745] 11 p1633 N85-20282
A modeling analysis program for the JPL Table Mountain Io sodium cloud data
[NASA-CR-175493] 11 p1681 N85-20589
Transmission and reflection of laser beams propagating through aerosol clouds in space
[LA-9998-MS] 12 p1856 N85-21638
The orientation distribution of nonspherical aerosol particles within a cloud
[AD-A150600] 13 p2092 N85-23061
Snow reflectance from Thematic Mapper
13 p2120 N85-23205
Water-ice clouds on Mars: Location and seasonal variation 13 p2194 N85-23611
Participation in the Mars Data Analysis Program: Analysis of cloud forms in Viking and Mariner 9 images
[NASA-CR-175604] 13 p2204 N85-23673
PLUVIUS: A generalized 1-dimensional model of reactive pollutant behavior, including dry deposition, precipitation formation, and wet removal, 2nd edition
[DE85-005542] 14 p2353 N85-24538
The structure and angular momentum content of dark clouds 14 p2439 N85-25064
SAM II measurements of the polar stratospheric aerosol. Volume 6: April to October 1981
[NASA-RP-1141] 16 p2825 N85-27422
Evolution of stratospheric aerosol size distribution from ground-based radiometric measurements: A study of El Chichon aerosol
[DE85-007555] 16 p2827 N85-27439

Humidity/cloud-radiation feedback on possible climate perturbation due to fossil fuel utilization
[DE85-008868] 18 p3133 N85-29402
Environmental Research Division report: Atmospheric physics
[DE85-009659] 18 p3133 N85-29404
Stable generation of highly monodisperse aerosols
21 p3642 N85-32626
Cloud droplet nucleation and initial growth derived from lidar depolarization studies 21 p3644 N85-32635
A simple model to investigate the activation process in waterclouds 21 p3649 N85-32675
A relationship between cloud droplet size and CCN critical supersaturation 21 p3649 N85-32677
Properties of forest derived cloud condensation nuclei
21 p3650 N85-32682
Influence on an industrial site on the characteristics of CCN supersaturation with air masses of different origin
21 p3650 N85-32683
Airborne cloud tracking measurements during the Three Mile Island nuclear station accident, Middletown, Pennsylvania. Date of survey: March - June 1979
[DE85-012060] 22 p3816 N85-33638
Electrons and positrons from expanding supernova envelopes in dense clouds
[OG-8.2-9] 22 p3869 N85-34108
Far-infrared observations of young clusters embedded in the R Coronae Austrinae and RHO Ophiuchi dark clouds
[NASA-TM-86681] 24 p4167 N85-35834

CLOUDS (METEOROLOGY)
NT ANVIL CLOUDS
NT ARC CLOUDS
NT BARIUM ION CLOUDS
NT CAP CLOUDS
NT CIRRUS CLOUDS
NT CONVECTION CLOUDS
NT CUMULUS CLOUDS
NT NOCTILUCENT CLOUDS
NT STRATOCUMULUS CLOUDS
NT STRATUS CLOUDS
ISCCP Cloud Algorithm Intercomparison Workshop
01 p0073 N85-10485
Boundary layer-cloud interactions as potential storm predictors 01 p0081 N85-10543
The identification of rain-bearing synoptic systems through principal component analysis
02 p0212 N85-11394
Joint probability of selected cloud and visibility thresholds around Koblenz, Germany
[AD-A145294] 02 p0231 N85-11506
Development and evaluation of cloud water collectors
[PB84-232529] 04 p0540 N85-13437
Planetary scale interactions 05 p0684 N85-14397
Atmospheric environment for Space Shuttle (STS-41G) launch
[NASA-TM-86486] 07 p0995 N85-16320
Radiation parameterization programs for use in general circulation models
[AD-A148015] 08 p1188 N85-17488
The concentration of sulfate in broken cloud layers
[DE85-000228] 11 p1678 N85-20574
Accuracy of typhoon center determined by GMS imagery 12 p1894 N85-21887
A supplement study on the subsynoptic cloud system off the south coast of Japan 12 p1895 N85-21892
Studies of the mechanisms and rates with which nitrogen species are incorporated into cloud water and precipitation
[PB85-144350] 12 p1898 N85-21914
Empirical and modeled synoptic cloud climatology of the Arctic Ocean
[NASA-CR-175628] 13 p2137 N85-23272
Sea surface temperatures from VAS MSI data
[NASA-CR-175706] 14 p2382 N85-24689
Observation of precipitating clouds by a vertically pointing radar at Morino in the Iburi District, Hokkaido, Japan 15 p2582 N85-25922
Mesoscale Atmospheric Processes Research Program Science Review
[NASA-TM-87465] 15 p2594 N85-25987
Hurricane structure and dynamics from stereoscopic and infrared satellite observations and radar data
15 p2594 N85-25988
Modeling of cloud systems 15 p2595 N85-25992
Lidar and radiometer observations of thunderstorm tops 15 p2595 N85-25994
Modeling of midwest severe thunderstorms
15 p2596 N85-25995
Estimation of convective rainfall from visible and infrared satellite data 15 p2596 N85-25999
Studies of electro-optical attenuation in the vicinity of cloud base
[AD-A151745] 15 p2653 N85-26360
The development and application of volume scan and cell tracking capabilities for the analysis of convective cloud systems 16 p2830 N85-27451
Cloud physics studies in the SCPP (Sierra Cooperative Pilot Project)
[PB85-163095] 16 p2837 N85-27501
Presentations at the Tri-Service Cloud Modeling Workshop (2nd), held at the Naval Surface Weapons Center, White Oak, Maryland, 26-27 June 1984, volume 1
[AD-A152735] 17 p2996 N85-28522
Improved cloud and surface fields derived from HIRS2/MSU 18 p3140 N85-29439
Analysis of a simulated cloud climatology
18 p3145 N85-29472
Cloud physics 18 p3147 N85-29485
Satellite measurements of atmospheric aerosols
[AD-A153807] 19 p3316 N85-30556
An evaluation of discretized conditional probability and linear regression threshold techniques in model output statistics forecasting of cloud amount and ceiling over the North Atlantic Ocean
[AD-A155100] 21 p3636 N85-32581
A simulation of weather in 3D space
[AD-A155221] 21 p3636 N85-32586
Circulation analysis of two snowstorms during the SNOW-TWO program
[AD-A155225] 21 p3637 N85-32587
A thermal diffusion chamber for the measurement of cloud condensation nuclei 21 p3642 N85-32627
Measurements of giant salt nuclei from inland in east China 21 p3648 N85-32668
Investigation of the formation of cloud particle spectrum on natural condensation nuclei
21 p3649 N85-32674
The nuclei of cloud formation
21 p3651 N85-32685
The measured rate of condensation nucleation to droplets using the techniques of chemical kinetics
21 p3652 N85-32694
Applicability of surface CCN measurements
21 p3652 N85-32696
Mean cloudiness over the global tropics from satellite observations
[AD-A156188] 24 p4123 N85-35561

CLUMPS
Comparative analysis of the clustering of the LPC coefficients in phoneme recognition
[FUB-39-1983] 01 p0041 N85-10264
Open cluster formation --- stellar evolution
03 p0442 N85-12815
Meteorological analysis for clusters of wind turbines
[DE84-013164] 04 p0539 N85-13425
Large-scale bubble structure of the interstellar medium (ISM) and properties of the Local Spiral Arm (LSA)
06 p0879 N85-15588
Direct assessment of synaptic modification rules
[AD-A148376] 08 p1196 N85-17534
Data reduction 09 p1412 N85-18903
Integrating non-semantic knowledge into image segmentation processes
[AD-A149571] 12 p1851 N85-21612
The chemistry of RDX and HMX cluster ions
13 p2004 N85-22561
Relationship between topological and magnetic order in small metal clusters
[AD-A150547] 13 p2018 N85-22651
Clustering and ordering in 3-5 alloys
[AD-A150604] 13 p2022 N85-22670
Clusters of transition metal atoms
[AD-A153126] 17 p3030 N85-28740
Large, energetic cluster impacts on surfaces
[DE85-006559] 17 p3034 N85-28769
Applications of fuzzy clustering techniques to stratified by tropopause MSU temperature retrievals
18 p3141 N85-29444
Applications of some artificial intelligence methods to satellite soundings 18 p3141 N85-29446
Two-point theory of current-driven ion-cyclotron turbulence
[DE85-010114] 19 p3372 N85-30918
A cluster analysis method for identification of subpopulations of cells in flow cytometric list-mode arrays 20 p3503 N85-31779
Clusters and cycles in the cosmic ray age distributions of meteorites
[SH-7.1-11] 23 p4048 N85-35103
Cluster variation study of coherent ordering in FCC and BCC solid solutions
[AD-A156039] 24 p4079 N85-35280

CLUSTER ANALYSIS
An investigation into fuzzy clustering and classification
[AD-A145571] 02 p0251 N85-11645
Homogeneous macroclimatic zones of the lake states
[PB84-215821] 04 p0540 N85-13436
Calibration or inverse regression: Which is appropriate for crop surveys using LANDSAT data?
07 p0985 N85-16260
Local dependence and point processes of exceedances in stationary sequences
[AD-A147859] 07 p1036 N85-16578
Asteroid taxonomy from cluster analysis of Photometry
09 p1411 N85-18897
Technical support for creating an artificial intelligence system for feature extraction and experimental design
[NASA-CR-175286] 12 p1916 N85-22044
Multi-sample cluster analysis as an alternative to multiple comparison procedures
[AD-A149960] 12 p1923 N85-22084
Decomposing the joint distribution of several linear combinations of uniform spacings
[AD-A155056] 21 p3677 N85-32845

CLUSTERS
U CLUMPS

CLUTCHES
Clutchless mechanism for engagement of forging press 14 p2268 N85-24051
Non-backdriveable free wheeling coupling
[NASA-CASE-MSC-20475-1] 18 p3116 N85-29290

CLUTTER
Clutter generator for use in radar evaluation
[AD-D011234] 01 p0039 N85-10245
A radar sea clutter model for atmospheric ducting conditions
[AD-A145321] 02 p0190 N85-11268
Autoregressive modeling and the classification of land clutter --- radar signatures
[ENST-C-84003] 03 p0356 N85-12292
Rivista Tecnica Selenia, volume 9, number 1
07 p0938 N85-15945
Reference oscillator stability effect on clutter cancellation in a radar system 07 p0938 N85-15946
Support for the Naval Research Laboratory Passive Microwave Clutter Analysis Program
[AD-A146771] 07 p0939 N85-15951
The effects of soil moisture on bistatic clutter power
[AD-A147636] 08 p1150 N85-17261
Loop radiating elements
[AD-D011409] 08 p1158 N85-17308
MTI system simulation and clutter output statistics
[AD-A149193] 10 p1467 N85-19255
A short range, high accuracy radar ranging system
[AD-A152195] 16 p2774 N85-27122
Phase synchronizing large antenna arrays using the spatial correlation properties of radar clutter
20 p3439 N85-31344
The use of the glistening surface concept in rough surface scattering
[AD-A154922] 21 p3575 N85-32234
Most desirable terrain, e.g., flat vs valley location, part 5.1B 21 p3624 N85-32513
Nonlinear filtration of clutter 22 p3777 N85-33404

CMOS
Switched Capacitor (SC) filter and design centering of integrated circuits, part 1
[BMFT-FB-T-84-190-PT-1] 05 p0633 N85-14062
Development of a 2 micrometer silicon-gate-CMOS-technology for microcomputer oriented VLSI circuits with a supply voltage range between 1.5 and 5 V
[BMFT-FB-T-84-203] 07 p0949 N85-16012
High quality super-large circuits developed
11 p1622 N85-20209
Tally cell circuit
[AD-D011492] 11 p1629 N85-20254
Aspects of CSSR CMOS integrated circuits discussed
15 p2533 N85-25627
Recent developments 15 p2533 N85-25628
MHB4046 phase-lock circuit 15 p2533 N85-25629
Phase-locked loop design with MHB4046
15 p2534 N85-25631
Additional PLL designs 15 p2534 N85-25632
Analysis of the capability to effectively design complementary metal oxide semiconductor integrated circuits
[AD-A151832] 15 p2548 N85-25728
Speed-up techniques for complementary metal oxide semiconductor very large scale integration
[AD-A152466] 17 p3043 N85-28829
Silicide conductors reliability research
[AD-A153768] 18 p3095 N85-29157
Design of a sixteen-bit pipelined adder using CMOS bulk P-well technology
[AD-A155043] 21 p3580 N85-32260
East Europe report: Science and technology. Selections on CSSR computer technology
[JPRS-ESA-84-017] 21 p3668 N85-32781
Selections on CSSR computer technology
21 p3668 N85-32782

best copy available

Effects of space radiation on advanced semiconductor devices. Part 3: Further cosmic ray simulation studies of single event upsets and latch-up in CMOS memories
[AERE-G-3368-PT-3] 22 p3848 N85-33833
Transient two-dimensional simulation of SEU in a CMOS SRAM cell
[DE85-008419] 22 p3890 N85-34111
Total integrated dose testing of solid-state scientific CD4011, CD4013, and CD4060 devices by irradiation with CO-60 gamma rays
[NASA-CR-176196] 24 p4161 N85-35795

CN EMISSION
The fluorescence of cometary OH and CN
09 p1411 N85-18896

CNOIDAL WAVES
An analytical model of periodic waves in shallow water
[AD-A147501] 07 p0960 N85-16085
An analytical model of periodic waves in shallow water
[AD-A147502] 07 p0960 N85-16086

COAGULATION
Evolution of grains in a turbulent solar nebula
13 p2179 N85-23525
The influence of Brownian coagulation on the size distributions of atmospheric aerosols
21 p3645 N85-32643
Size spectra for the source-enhanced coagulation with the turbulent mass transfer 21 p3645 N85-32640

COAL
NT LIGNITE
Compilation of elemental concentration data for NBS (National Bureau of Standards) biological, geological and environmental standard reference materials, 1982
[PB84-218338] 01 p0025 N85-10158
The feasibility of satellite remote sensing as a technique for evaluating coal mine surface features
02 p0213 N85-11401
Mapping land use changes in the carboniferous region of Santa Catarina, report 2
[E85-10017] 02 p0217 N85-11430
Interactive system for the interpretation of coal deposit data as a basis of future mine planning systems
[BMFT-FB-T-83-115] 02 p0220 N85-11449
Dynamics of burnout of solid fuel in fluidized bed of finely divided inert particles 02 p0273 N85-11782
The status of synthetic fuels and cost-shared energy R and D facilities
[GPO-36-903] 03 p0339 N85-12162
Fabric filter system study
[PB84-229749] 03 p0342 N85-12206
Estimation of dynamic stresses around the shot point by scale model experiment 04 p0432 N85-13076
US energy for the rest of the century, 1984 edition
[PB84-207406] 04 p0531 N85-13393
Additives for heat engine coal slurry fuels
[DE84-016434] 05 p0621 N85-13971
Ceramic fabric material testing
[DE84-012014] 09 p1300 N85-18165
Combustion characterization of coals for industrial applications
[DE85-010673] 19 p3228 N85-30014
Application of the reference intensity method to coal analysis
[DE85-009528] 19 p3228 N85-30015
Guest molecules in coal
[DE85-010435] 19 p3228 N85-30016
Novel analytical approaches to coal beneficiation
[DE85-010437] 19 p3229 N85-30021
Adherence of ash particles from the combustion of micronized coal
[DE85-008600] 19 p3229 N85-30023
The mobile phase in coals: Its nature and modes of release
[DE85-011696] 19 p3230 N85-30026
Development of a coal-water slurry-fueled diesel engine for industrial cogeneration. Task 1.0 topical report: Thermodynamic analysis
[DE85-010455] 19 p3236 N85-30062
Current status of TVA's atmospheric fluidized bed combustion development efforts
[DE85-901209] 19 p3308 N85-30507
Technical guide for estimating fugitive dust impacts from coal handling operations, volume 2
[DE85-010939] 19 p3309 N85-30514
Coal slurry ignition in a diesel engine simulator
[DE85-010987] 20 p3463 N85-31513
Ames Laboratory measurements of alkali levels in the Curtiss-Wright PFBC gas stream
[DE85-011357] 22 p3745 N85-33214
Drying of pulverized material with heated condensible vapor
[DE85-011656] 22 p3783 N85-33438
Shuttle car loading system
[NASA-CASE-NPO-15949-1] 23 p3987 N85-34722
Fluidized bed desulfurization
[NASA-CASE-NPO-15924-1] 24 p4075 N85-35253
Depositional systems and coal occurrence in the Fort Union Formation (Paleocene), Powder River Basin, Wyoming and Montana 24 p4114 N85-35505

COAL DERIVED LIQUIDS
Superheated fuel injection for combustion of liquid-solid slurries
[DE85-011624] 22 p3753 N85-33266

COAL GASIFICATION
Optical detection of alkali compounds
[DE84-015505] 03 p0328 N85-12117
USSR report: Chemistry
[JPRS-UCH-84-012] 06 p0761 N85-14865
Behavior of pressurized tubes of candidate alloys in a simulated low-Btu environment
[DE85-003403] 09 p1296 N85-18141
Corrosion of ceramics in heat exchanger applications
[DE84-017459] 09 p1299 N85-18161
Assessment of the need for an advanced high-strength chromium-molybdenum steel for construction of third-generation gasifier pressure vessels
[DE85-002865] 11 p1606 N85-20097
USSR report: Chemistry
[JPRS-UCH-85-001] 13 p2013 N85-22629
Electricity production from coal through molten-carbonate fuel cells
[TI85-005072] 14 p2351 N85-24534
Studies of metal/carbon surface chemistry
[DE85-005513] 15 p2507 N85-25463
Commercial feasibility of underground gasification of Texas lignite to produce synthetic gas
[DE85-001996] 18 p3127 N85-29361
Differential optical absorption techniques for diagnostics of coal gasification
[DE85-010177] 19 p3368 N85-30890
Energy and Technology Review
[DE85-011767] 21 p3716 N85-33061
Photofragment fluorescence as a sensitive probe for gas-phase alkali compounds and their photochemistry
[DE85-010707] 22 p3746 N85-33219

COAL LIQUEFACTION
Developing a flowmeter for streams with high solids content
[DE84-016643] 09 p1323 N85-18316
Integration of advanced preparation with coal liquefaction
[DE85-010432] 19 p3228 N85-30012
Exploratory study of coal conversion chemistry
[DE85-010393] 19 p3229 N85-30018
Method of distributing liquefaction catalysts in solid carbonaceous material
[DE85-005759] 23 p3909 N85-34218

COAL UTILIZATION
USSR report: Energy
[JPRS-UEN-84-038] 07 p0994 N85-16312
Closed cycle versus open cycle gas turbines. A review of A.D. Little's ICOP report, vol. 3
[DE85-000564] 12 p1861 N85-21671
Development of molten carbonate fuel cell power plant, volume 1
[DE85-008743] 18 p3131 N85-29394
Magnetohydrodynamics and the National Coal Science, Technology, and Engineering Development Acts
[S-HRG-98-1179] 20 p3535 N85-31994
Superheated fuel injection for combustion of liquid-solid slurries
[DE85-011624] 22 p3753 N85-33266
Chemistry division report
[DE85-010586] 24 p4071 N85-35228

COALESCENCE
U COALESCING

COALESCING
Bunch coalescing in the main ring to form intense proton and antiproton bunches without RF counterphasing
[DE85-001364] 09 p1382 N85-18692
Signatures of the coalescence instability in solar flares
12 p1956 N85-22293

COANDA EFFECT
Circulation control propellers for general aviation, including a BASIC computer program
[NASA-CR-165968] 19 p3219 N85-29959

COARSENESS
X-ray residual stress analysis on the coarse grain of copper and its application to the brazed copper
23 p3907 N85-34202

COASTAL CURRENTS
Satellite definition of the bio-optical and thermal variation of coastal eddies associated with the African current
[AD-A147910] 07 p0969 N85-16282
Studies of coastal mesoscale winds using SIR-B
08 p1147 N85-17238
California coastal erosion and storm damage during the winter 1982 - 1983, a reconnaissance report
[PB85-121705] 10 p1521 N85-19591
Two-cycle mechanism of dissipation of tidal energy in ocean 14 p2335 N85-24438
The sea level response to weather along the coast of southern Africa 16 p2829 N85-27446
Atmospherically forced, coastally trapped, long period gravity waves off the south coast of southern Africa
16 p2832 N85-27461
Comparison of a diffusion model with dye dispersion measurements to study turbulence in coastal waters
[INPE-3492-PRE/729] 16 p2838 N85-27504

COASTAL DUNES
U DUNES

COASTAL ECOLOGY
Environmental geologic atlas of the North Carolina coastal zone: Dare, Hyde, Tyrrell and Washington Counties
[PB84-222975] 01 p0066 N85-10439
The SANCOR programme on coastal processes, April 1982 - March 1988
[REPT-68] 01 p0069 N85-10456
Ecology of estuarine channels of the pacific northwest coast: A community profile
[PB84-209709] 01 p0070 N85-10464
The ecology of tundra ponds of the Arctic coastal plain: A community profile
[TI85-900650] 15 p2589 N85-25958
Review and annotated bibliography of benthic studies in coastal and estuarine areas of Florida with a selected compilation of worldwide benthic methodological references and southeastern United States benthic taxonomic references
[PB85-151041] 16 p2822 N85-27405

COASTAL MARSHLANDS
U MARSHLANDS

COASTAL PLAINS
Potential geological natural landmarks of the East Gulf Coastal Plain
[PB84-230317] 06 p0835 N85-15316
Soil formation on tertiary landsurfaces of the New Jersey coastal plain 08 p1181 N85-17441
The ecology of tundra ponds of the Arctic coastal plain: A community profile
[TI85-900650] 15 p2589 N85-25958

COASTAL RANGES (CA)
Franciscan and related rocks of southern Humbolt County, northern California coast ranges: Analysis of structure, tectonics, sedimentary petrology, paleogeography, depositional histroy, and thermal maturity 03 p0390 N85-12495
Mesozoic ophiolitic olistostromes and Cenozoic imbricate thrust faulting in the northern California coast ranges: Geology of the Mysterious Valley area, Napa County 08 p1182 N85-17445

COASTAL WATER
The SANCOR estuaries programme, 1982-1986
[ISBN-0-7988-2662-2] 01 p0068 N85-10454
The SANCOR programme on coastal processes, April 1982 - March 1988
[REPT-68] 01 p0069 N85-10455
Ecology of estuarine channels of the pacific northwest coast: A community profile
[PB84-209709] 01 p0070 N85-10464
Estuaries of the Cape. Part 2: Synopses of available information on individual systems. Report 12: Buffels (WES) (CSW 1), Elsies (CSW 2), Sir Lowry's Pass (CSW 8), Steenbras (CSW 9), and Buffels (OOS) (CSW 11)
[CSIR-RR-411-PT-2] 01 p0086 N85-10581
Estuaries of the Cape. Part 2: Synopses of available information on individual systems. Report no. 14: Sand (CSW 4)
[CSIR-RR-413-PT-2] 01 p0086 N85-10583
Estuaries of the Cape. Part 2: Synopses of available information on individual systems. Report no. 15: Zeekoe (CSW 5)
[CSIR-RR-414-PT-2] 01 p0087 N85-10584
The altimeter as a support to the scatterometer in the representation of winds and derived wave fields in coastal waters and enclosed seas: A research at its onset
03 p0383 N85-12453
Use of SIR-B multiincidence-angle imagery to study iceberg detectability and offshore ocean feature extraction 08 p1145 N85-17225
Analysis of flow within the coastal boundary layer off Long Island, New York
[DE85-001384] 09 p1359 N85-18550
Mesoscale studies of flow regimes and fluxes of particulate matter in coastal waters
[DE85-003625] 11 p1689 N85-20620
USC (University of Southern California) Sea Grant Program Directory, 1984-1985
[PB85-135051] 12 p1899 N85-21922
Production and turnover of suspended organic detritus in the coastal water of the southeastern continental shelf
[DE85-003977] 13 p2140 N85-23290
Evaluation of wave energy resources on the French Atlantic seaboard 14 p2325 N85-24389

Chemical composition of coastal haze aerosol
14 p2338 N85-24456
Analysis of hydrometeorological conditions in Antarctic coastal waters according to data from hydrological and satellite observations 15 p2487 N85-25354
Analysis of suspended sediment distributions in the surface waters of Delaware Bay using remote sensing of optical properties 15 p2582 N85-25926
Deepwater wind wave growth with fetch and duration
[AD-A151604] 15 p2604 N85-26051
Diffusion coefficients for coastal water determined from aerial photographs
[INPE-3413-PRE/679] 16 p2810 N85-27331
The sea level response to weather along the coast of southern Africa 16 p2829 N85-27446
Comparison of a diffusion model with dye dispersion measurements to study turbulence in coastal waters
[INPE-3492-PRE/729] 16 p2838 N85-27504
Properties of aerosol particles detected by satellites in coastal regions 21 p3641 N85-32622
Coastal erosion along Monterey Bay
[AD-A155610] 21 p3655 N85-32707
Arctic and offshore research
[DE85-001995] 22 p3818 N85-33653
Sea surface and remotely sensed temperatures off Cape Mendocino, California
[NASA-TM-86712] 24 p4125 N85-35573

COASTAL ZONE COLOR SCANNER

Coastal Zone Color Scanner (CZCS): Imagery of near-surface phytoplankton pigment concentrations from the first coastal ocean dynamics experiment (CODE-1), March - July 1981
[NASA-CR-174169] 04 p0542 N85-13447
Bio-optical variability in the Alboran Sea as assessed by Nimbus-7 coastal zone color scanner
[AD-A147909] 07 p0969 N85-16261
The use of principal components analysis techniques Nimbus-7 coastal zone color scanner data to define mesoscale ocean features through a warm humid atmosphere
[AD-A148567] 08 p1176 N85-17416
Nimbus 7 Coastal Zone Color Scanner (CZCS). Level 2 data product users' guide
[NASA-TM-86202] 19 p3299 N85-30452
Nimbus 7 Coastal Zone Color Scanner (CZCS). Level 1 data product users' guide
[NASA-TM-86203] 19 p3299 N85-30453

COASTS

Environmental geologic atlas of the North Carolina coastal zone: Dare, Hyde, Tyrrell and Washington Counties
[PB84-222975] 01 p0066 N85-10439
The SANCOR estuaries programme, 1982-1986
[ISBN-0-7988-2662-2] 01 p0068 N85-10454
The SANCOR programme on coastal processes, April 1982 - March 1988
[REPT-68] 01 p0069 N85-10455
Black Sea coastal frontogenesis
01 p0075 N85-10500
Some aspects of post-frontal convective areas along the west coast of the united states
[AD-A144895] 01 p0085 N85-10572
Estuaries of the Cape. Part 2: Synopses of available information on individual systems. Report 12: Buffels (WES) (CSW 1), Elsies (CSW 2), Sir Lowry's Pass (CSW8), Steenbras (CSW 9), and Buffels (OOS) (CSW 11)
[CSIR-RR-411-PT-2] 01 p0086 N85-10581
Estuaries of the Cape. Part 2: Synopses of available information on individual systems. Report no. 14: Sand (CSW 4)
[CSIR-RR-413-PT-2] 01 p0086 N85-10583
Estuaries of the Cape. Part 2: Synopses of available information on individual systems. Report no. 15: Zeekoe (CSW 5)
[CSIR-RR-414-PT-2] 01 p0087 N85-10584
Evaluation of an aerosol prediction model for coastal regions using marine aerosol generation and transport data
[AD-A145443] 02 p0231 N85-11510
Plotting TDL coastal wind forecasts
[PB84-220789] 03 p0397 N85-12533
Prediction of wave height of wind-generated seas in finite water depth
[AD-A145996] 03 p0398 N85-12539
Numerical prediction of the president's day cyclone
05 p0684 N85-14399
Avionics system design for requirements for the United States Coast Guard HH-65A Dolphin
06 p0753 N85-14827
Conditions governing the formation of stratocumulus clouds over the western Atlantic during cold air outbreaks
[AD-A146780] 07 p1004 N85-16363
On the formation of the nocturnal coastal surface wind speed maximum 09 p1356 N85-18528
Nautical charting with remotely sensed imagery, volume 1
[AD-A149361] 10 p1506 N85-19503
Nautical charting with remotely sensed imagery. Volume 2: Case studies
[AD-A149362] 10 p1506 N85-19504
Hurricane experience levels of coastal county populations: Texas to Maine
[PB85-111383] 10 p1520 N85-19581
Atlantic Coast Unique Regional Atmospheric Tracer Experiment (ACURATE)
[PB85-126460] 12 p1886 N85-21839
Studies of the development of cyclones over Southern China coastal areas and adjacent seas
[AD-A150108] 12 p1896 N85-21901
Observations of the California countercurrent
[AD-A150781] 14 p2382 N85-24691
Research on atmospheric dust formations using satellite observation data 15 p2485 N85-25339
Meso-8 scale numerical simulations of the jet streak adjustments which organized the Carolina tornado outbreak and the subsequent explosive coastal cyclogenesis 15 p2598 N85-26011
Contamination of the fetch-limited directional wave spectrum by waves emanating from an embayment
[NASA-TM-84441] 15 p2604 N85-26048
Review and annotated bibliography of benthic studies in coastal and estuarine areas of Florida with a selected compilation of worldwide benthic methodological references and southeastern United States benthic taxonomic references
[PB85-151041] 16 p2822 N85-27405
Operation guiding light-scientific program and field plan. The pilot field experiment for NORDA project chemical dynamics in ocean frontal areas
[AD-A153765] 18 p3150 N85-29507
Summary of archived Atlantic coast wave information study pressure, wind, wave, and water level data
[AD-A153782] 18 p3151 N85-29508
Geoacoustic models: Washington state continental margin
[AD-A153781] 18 p3177 N85-29699
Temporal variations of Rn222 concentrations in Black Sea coastal zone 19 p3293 N85-30417
Sand dispersion from an ephemeral river delta on the wave-dominated central California coast
[AD-A154352] 19 p3300 N85-30458
Properties of aerosol particles detected by satellites in coastal regions 21 p3641 N85-32622
Aircraft observations of cloud condensation nuclei in maritime and continental environments
21 p3650 N85-32680
Marine phosphorite deposits model for exploration, with emphasis on deposits in the US Atlantic coastal plain
24 p4104 N85-35439
USGS coastal research, studies and maps: A source of information for coastal decision making
[USGS-CIRC-883] 24 p4106 N85-35465
Atlantic coast hindcast. Phase 2: Wave information, additional extremal estimates
[AD-A156137] 24 p4125 N85-35575

COATING

NT ANODIZING
NT ELECTROPLATING
NT ENCAPSULATING
NT METALLIZING

Thermodynamic calculations and the chemical vapour deposition of hard materials 02 p0179 N85-11200
Textured carbon surfaces on copper
[NASA-CASE-LEW-14130-1] 11 p1615 N85-20156
Corrosion resistant coating
[NASA-CASE-NPO-15928-1] 18 p3073 N85-29005
New metal coating method developed
21 p3568 N85-32191

COATINGS

NT ALUMINUM COATINGS
NT ANODIC COATINGS
NT ANTIREFLECTION COATINGS
NT CATHODIC COATINGS
NT CERAMIC COATINGS
NT ELECTROPLATING
NT ENAMELS
NT ENCAPSULATING
NT GLASS COATINGS
NT GLAZES
NT GOLD COATINGS
NT LACQUERS
NT MAGNETIC FILMS
NT METAL COATINGS
NT METALLIZING
NT NICKEL COATINGS
NT PAINTS
NT PLASTIC COATINGS
NT PRIMERS (COATINGS)
NT PROTECTIVE COATINGS
NT REFRACTORY COATINGS
NT RUBBER COATINGS
NT SPRAYED COATINGS
NT THERMAL CONTROL COATINGS
NT ZINC COATINGS

USSR report: Materials science and metallurgy, no. 93
[JPRS-84810] 01 p0018 N85-10110
Aircraft surface coatings
[NASA-CR-3861] 02 p0137 N85-10935
Turbine Engine Hot Section Technology (HOST)
[NASA-TM-83022] 02 p0140 N85-10951
The adhesion of hard and wear resistant coatings
02 p0179 N85-11203
Plasma variables and tribological properties of coatings in low pressure (0.1 - 10.0 torr) plasma systems
[NASA-TM-83798] 02 p0189 N85-11261
Simulation of vibration processes in damped structures with allowance for temperature-frequency characteristics of vibration absorbing materials
02 p0257 N85-11680
The effect of heat treatment on wear resistance of gas-plasma eutectic coatings
[BLL-M-35756-(5828.4)] 03 p0329 N85-12122
Surface coatings for low emittance in the thermal surveillance band
[MRL-R-937] 03 p0336 N85-12158
Effects of monolayer converages on substrate sputtering yields
[DE84-016312] 04 p0476 N85-13033
Effect of oxide coated thickness on thermal ignition of titanium-based pyrotechnics
[DE84-013061] 04 p0481 N85-13065
Effect of water on hydrogen permeability --- Stirling engines
[NASA-TM-86904] 06 p0761 N85-14864
Process for producing carbide coatings
[AD-D011295] 06 p0764 N85-14885
Surface studies of Nb, its compounds, and coatings
[DE84-017353] 06 p0868 N85-15516
Deposition of titanium nitride coatings by reactive evaporation and electrically activated reactive evaporation
[BLL-TRANS-5043-(9091.9F)] 07 p0925 N85-15858
Experimental test program for evaluation of solid lubricant coating as applied to compliant foil gas bearings to 315 deg C
[NASA-CR-174837] 07 p0930 N85-15895
Moisture absorbing anti-arcing coating and method for applying same
[AD-D011310] 07 p0932 N85-15904
Damping capacity of multilayer tube during torsion
[BLL-M-36011-(5828.4)] 07 p0977 N85-16202
Antisoiling technology: Theories of surface soiling and performance of antisoiling surface coatings
[NASA-CR-174274] 07 p0991 N85-16296
Corrosion properties of second-generation conductive materials 07 p1000 N85-16348
Optical fibers with reduced pressure sensitivity to high frequency acoustic field
[AD-D011306] 07 p1043 N85-16627
Construction tolerances for low loss, dielectric coated, metallic waveguide for transmission optical radiation
[DE85-004056] 10 p1558 N85-19822
Study of phase composition of Al-B plasma coatings
11 p1598 N85-20050
Improving operational properties of titanium alloys by diffusion siliciding 11 p1602 N85-20075
Status of specific FRG high tech research funded by BMFT 11 p1618 N85-20181
Time resolved Raman studies of laser induced damage in TiO2 optical coatings
[DE85-003166] 11 p1640 N85-20332
Evaluation of infrared reflectance as a technique for measuring absorber materials degradation
[DE85-002171] 11 p1729 N85-20674
Diamondlike flakes
[NASA-CASE-LEW-13837-2] 12 p1796 N85-21267
Corrosion and coatings review of specifications and drawings of facilities for the Oman Military Construction Program at Masirah Island, Oman
[AD-A149739] 12 p1812 N85-21366
Evaluation of Epoxo 300-C nonskid coating for use on bridge decks
[PB85-108843] 12 p1819 N85-21412
Numerical methods for analyzing electromagnetic scattering
[NASA-CR-175507] 12 p1823 N85-21438
Advanced thin film thermocouples
[NASA-CR-175541] 12 p1850 N85-21607
Experimental studies of low temperature surface interactions of atomic hydrogen using maser technique
[AD-A150216] 13 p2017 N85-22647
USSR report: Materials science and metallurgy
[JPRS-UMS-85-002] 13 p2025 N85-22688

Research directed advanced high temperature coating system beyond current state-of-the art systems
[AD-A150696] 14 p2255 N85-23974
High-temperature X-ray diffraction study of coating-substrate compatibility in yttria-coated graphite
[DE85-005916] 14 p2262 N85-24016
Multilayer reflecting systems based on glassy chalcogenides for infrared lasers
14 p2274 N85-24089
Color-selective coating for viewfinder in optical instruments 14 p2276 N85-24098
Selective coatings for solar-to-thermal energy converters 14 p2280 N85-24127
Corrosion control through a better understanding of the metallic substrate-organic coating-interface
[AD-A151238] 15 p2509 N85-25479
USSR report: Materials science and metallurgy
[JPRS-UMS-85-004] 15 p2513 N85-25503
Surface composition, properties and thermal stability of massive and fine metallic glasses
15 p2513 N85-25506
Procedure for certifying quantity of volatile organic compounds emitted by paint, ink and other coatings
[PB85-159044] 15 p2520 N85-25537
Investigation of silicon surface passivation by silicon nitride film deposition
[NASA-CR-175693] 15 p2585 N85-25936
Performance of a copper-lithium alloy as an impurity control system surface material for a fusion reactor
[DE85-006494] 15 p2657 N85-26398
In situ thin film measurement
[AD-A151365] 15 p2659 N85-26411
Tooth wear in worm gears in vacuum
16 p2766 N85-27070
Development of a polystyrene insulation system
[DE85-006950] 16 p2784 N85-27180
High-altitude testing of selective optical coatings for solar radiators and collectors 17 p2939 N85-28143
Heat pipe and method of making same
[AD-D011654] 17 p2959 N85-28273
Raman studies of laser damaged single and multi-layer optical coatings
[DE85-009431] 17 p2971 N85-28351
Absorber coatings degradation
[DE85-008628] 18 p3128 N85-29367
Self-sustaining coatings for fusion applications: Copper lithium alloys
[DE85-009740] 18 p3190 N85-29783
Influence of type of processing of AK4 alloy on its surface state and strength of bonding of plasma coatings
19 p3242 N85-30103
Effect of protective method on cyclic durability and nature of failure of titanium alloy welded joints
19 p3245 N85-30122
Effect of heating temperature in a vacuum on state of surface layers of welded OT4 titanium alloy
19 p3245 N85-30123
BN coating of ceramic fibers for ceramic fiber composites
[AD-D011700] 19 p3249 N85-30145
Mutual coupling analysis for conformal microstrip antennas
[AD-A154292] 19 p3259 N85-30210
Stress concentration in the elastoplastic state and residual stress after unloading
[AD-A155628] 21 p3600 N85-32356
Dielectric mirror with ferromagnetic substrate
21 p3696 N85-32966
Management of Corrosion
[AGARD-LS-141] 22 p3749 N85-33238
Land vehicle corrosion management
22 p3750 N85-33246
Electrically conductive containment vessel for molten aluminum
[DE85-006518] 23 p3939 N85-34415

COAXIAL CABLES
Microminiature coaxial cable and methods of manufacture
[DE84-014228] 01 p0044 N85-10284
Coaxial noise measurement circuits
05 p0630 N85-14036
A coaxial probe for measuring the current density profile of intense electron beams
[AD-D011407] 08 p1164 N85-17347
High voltage RF coaxial cable
[AD-D011493] 11 p1629 N85-20255
A moment solution for an arbitrary configuration of partly shielded wires above a ground plane
[AD-A149762] 12 p1828 N85-21473
Change of electrical characteristics of radio-frequency cables under thermal effect 13 p2081 N85-22999
Spectral evaluation of irregularity of superconducting coaxial cables 13 p2082 N85-23000
Basic EMC technology advancement for C3 systems. Volume 4F: Prediction of crosstalk in flatpack coaxial cables
[AD-A153111] 17 p2954 N85-28242
Predicting electrical performance parameters of underwater cables 22 p3775 N85-33391

COAXIAL FLOW
Stability of fluid flow in a cylindrical annulus
[NASA-TM-77720] 01 p0046 N85-10300
Turbulent transport and length scale measurement experiments with confined coaxial jets
[NASA-CR-174831] 19 p3265 N85-30245

COAXIAL PLASMA ACCELERATORS
Steady-state spheromak reactor studies
[DE85-009585] 19 p3372 N85-30916
Intercomparison of the calculated absolute efficiency values between true coaxial and true closed-end coaxial Ge (Li) and NaI detectors
[REPT-5-1984] 20 p3532 N85-31976

COAXIAL TRANSMISSION
U COAXIAL CABLES
U TRANSMISSION

COBALT
NT COBALT 60
Effects of cobalt, boron, and zirconium on the microstructure of Udimet 736
[NASA-CR-174762] 01 p0027 N85-10166
Microstructural basis of strength and toughness in hardmetals 02 p0177 N85-11185
Magnetic properties of the cobalt matrix in WC-Co compacts 02 p0177 N85-11186
The inter-relation of microstructure, toughness and fatigue crack growth behaviour in WC-Co hardmetals
02 p0177 N85-11188
Erosion of sintered WC-Co alloys
02 p0179 N85-11201
The reactions of cobalt, iron and nickel in SO-2 atmospheres: Similarities and differences
[NASA-TM-86868] 02 p0181 N85-11217
Nickel-cobalt systematics and their bearing on lunar origin 04 p0582 N85-13719
Abundancies of Ni, Cr, CO and major elements in the silicate portion of the Moon: Constraints from primary lunar magmas 04 p0582 N85-13720
Anisotropy and relaxation effects of Co2+ ions in LiTi ferrite
[AD-A146550] 06 p0861 N85-15469
Preparation and electronic properties of MoS(2) and WS(2) single crystals grown in the presence of cobalt
[AD-A146508] 06 p0866 N85-15506
The growth of metastable peritectic compounds
[NASA-CR-171289] 07 p0920 N85-15824
Metal-support interactions: Their effects upon adsorption, electronics, and activity/selectivity properties of cobalt in hydrogenation
[DE85-003316] 09 p1292 N85-18113
Improved lithium-intercalation cathode material
[AD-A149319] 10 p1435 N85-19043
Antifriction properties of gas thermal coatings of clad carbine powders 10 p1447 N85-19115
The response of cobalt-free Udimet 700 type alloy to modified heat treatments
[NASA-TM-86942] 11 p1597 N85-20043
Ligand structural influences upon electrochemical reactivity: Organic substituent effects upon Carboxylatopentaamminecobalt(3) reductions at mercury and gold electrodes
[AD-A150685] 14 p2250 N85-23944
Neutron scattering and reactions on 59Co from 1 to 20 MeV
[AERE-R-11439] 17 p3028 N85-28729
Improved catalysts for liquid hydrocarbon fuels from syngas
[DE85-011062] 20 p3421 N85-31234
Analysis of ferrates and ferrites of three transition metals using Moessbauer effects
[BLL-CE-TRANS-8019-(9022.09)]
20 p3430 N85-31273
Measurements of Fe and Ar fragmentation cross sections
[PAPER-OG-7.2-20] 21 p3714 N85-33047
Metal (2) 4,4',4',4'' phthalocyanine tetraamines as curing agents for epoxy resins
[NASA-CASE-ARC-11424-1] 23 p3919 N85-34281
Cobalt-rich ferromanganese crusts in the oceans
24 p4104 N85-35444
Applications of the mineral resources data system and the international strategic minerals inventory in mineral-resource assessments by region and commodity
24 p4105 N85-35451
The Conterminous United States Mineral Assessment Program 24 p4106 N85-35458
The Alaska Mineral Resources Assessment Program
24 p4107 N85-35460

COBALT ALLOYS
NT RENE 95
The Palmqvist test and its applications in WC-Co alloys 02 p0177 N85-11187
Erosion of multiphase materials
[DE84-015816] 04 p0474 N85-13018
Laser-initiated combustion studies on metallic alloys in pressurized oxygen
[PB85-128114] 10 p1438 N85-19066
Production method of nickel electrode
[NASA-TM-76946] 10 p1439 N85-19069
Method of producing nickel electrode
[NASA-TM-76944] 10 p1440 N85-19077
Creep-rupture behavior of iron superalloys in high-pressure hydrogen
[NASA-CR-174411] 10 p1441 N85-19078
Proton NMR and susceptibility measurements in TiCoH/sub x
[DE85-003309] 12 p1807 N85-21336
Corrosion-resistant amorphous alloys
13 p2035 N85-22748
Determination of symmetry of immediate surroundings in amorphous Co-P alloys 15 p2496 N85-25398
Erosion of multiphase materials
[DE85-008895] 18 p3068 N85-28978
Slow crack growth in metal reinforced glass composites
[DE85-010094] 18 p3082 N85-29064
Long range ordered alloys modified by addition of niobium and cerium
[DE85-011661] 20 p3431 N85-31285
Nonequilibrium kinetics of growth of oxide layer grains during laser heating of metals in air
21 p3689 N85-32919
Deposition of nickel-cobalt alloys by controlled-potential electrolysis
[PB85-198562] 24 p4081 N85-35291

COBALT COMPOUNDS
NT COBALT OXIDES
The alpha-form of the hydroxides of bivalent metals
[NASA-TM-77508] 04 p0473 N85-13009
Chemically modified electrodes and related solution chemistry
[DE84-017110] 05 p0614 N85-13924
Phase size distribution in WC/Co hardmetal
[NPL-DMA(A)-93] 20 p3431 N85-31281
Nuclear magnetic resonance study of the intramolecular rearrangement of 2-(5-cyanotetrazolato)pentaammine cobalt (III) perchlorate
[DE85-010810] 22 p3839 N85-33772

COBALT ISOTOPES
NT COBALT 60

COBALT OXIDES
Mechanisms of elevated temperature rupture in single phase ceramics
[DE85-000697] 09 p1299 N85-18158

COBALT 60
Mechanisms of impurity diffusion in rutile
[DE84-014741] 06 p0766 N85-14902

COBOL
Digital equipment Corporation, professional 350, COBOL-81 Version 2.1
[PB84-227602] 03 p0403 N85-12572
Digital Equipment Corporation, Professional 350, COBOL-81 Version 2.1 (COBOL technical report)
[PB84-227719] 03 p0403 N85-12573
Northern Telecom, Incorporated, NTI-585/565, ACOBOL/3 Release 4.1 Version H(01)
[PB84-228022] 03 p0404 N85-12574
Northern Telecom, Incorporated NTI-585/565, ACOBOL/3 Release 4.1 Version H(01) (COBOL technical report)
[PB84-228030] 03 p0404 N85-12575
Digital Equipment Corporation, DECSYSTEM-10, model 1090-SMP, COBOL-74 V12B
[PB84-227941] 03 p0404 N85-12576
Data General Corporation, Eclipse C350, AOS COBOL Release 3.51
[PB84-227883] 03 p0404 N85-12577
Convergent Technologies, NGEN CP001, CT COBOL version 9.0
[PB84-227784] 03 p0404 N85-12578
Digital Equipment Corp., VAX/750, VAX COBOL version 3.0
[PB84-227693] 03 p0405 N85-12583
IBM Corporation, IBM 5381 model 5, system/38 COBOL release 6
[PB84-227677] 03 p0405 N85-12584
Gould Incorporated, GOULD Concept 32/87, COBOL release 1.4
[PB84-227669] 04 p0548 N85-13484
Digital Equipment Corp., VAX/750, VAX COBOL version 3.0
[PB84-227651] 04 p0548 N85-13485
Digital Equipment Corp., MICRO/PDF-11, COBOL-81 version 2.2
[PB84-227644] 04 p0548 N85-13486

C3, Incorporated, C50 System, C3 COBOL/75 version 2.00
[PB84-228006] 04 p0548 N85-13488
Burroughs Corporation B26-CPU, B20 COBOL, Release 4.0
[PB84-216241] 04 p0551 N85-13505
Burroughs Corporation B26-CPU, B20 COBOL Version 4.0 (COBOL technical report)
[PB84-216258] 04 p0551 N85-13506
Convergent technologies NGEN CP001, CT COBOL Version 9.0
[PB84-216266] 04 p0551 N85-13507
Convergent Technologies, Incorporated, NGEN CP001, CT COBOL Version 9.0 (COBOL technical report)
[PB84-216274] 04 p0551 N85-13508
Computer Sciences Corporation UNIVAC 1100/80, CSTS COBOL Release COB250
[PB84-216282] 04 p0551 N85-13509
C3, Incorporated NGEN CP001, COBOL Version 9.0
[PB84-216308] 04 p0552 N85-13511
NECIS Incorporated, NEC ASTRA model 270, COBOL 74 version 8.3 (COBOL technical report)
[PB84-227933] 06 p0848 N85-15381
Data general Corporation, Eclipse C150, interactive COBOL Revision 1.30 (COBOL technical report)
[PB84-227834] 06 p0849 N85-15391
Data General Corporation, Eclipse C150, interactive COBOL Revision 1.30
[PB84-227891] 06 p0849 N85-15392
IBM Corporation, IBM Series/1 4955, IBM Series/1 host COBOL Release 1.1 EDX (COBOL technical report)
[PB84-227909] 06 p0849 N85-15393
IBM Corporation, IBM Series/1 4955, IBM Series/1 host COBOL Release 1.1 EDX
[PB84-227818] 06 p0849 N85-15394
IBM Corporation, IBM Series/1 4955, IBM Series/1 host COBOL Release 1.1 RPS
[PB84-227917] 06 p0850 N85-15395
IBM Corporation, IBM Series/1 4955, IBM Series/1 host COBOL Release 1.1 RPS (COBOL technical report)
[PB84-227925] 06 p0850 N85-15396
NECIS, Incorporated, NEC ASTRA model 270 COBOL 74 Version 8.3
[PB84-227636] 06 p0850 N85-15397
Digital Equipment Corporation, DECSYSTEM-20, model 2060, COBOL V13
[PB84-227958] 06 p0850 N85-15398
Digital Equipment Corporation, DECSYSTEM-20, model 2060, COBOL V13 (COBOL technical report)
[PB84-227966] 06 p0850 N85-15399
Northern Telecom, Incorporated, IBM 3033 (compilation), NTI-585/565 (execution), XCOBOL Release 4.1 Version H(01)
[PB84-227875] 06 p0850 N85-15400
NCR Corporation, NCR I9300, NCR ITX Cobol Release 3.0
[PB84-228055] 06 p0850 N85-15401
NCR Corporation, NCR I9300, NCR ITX COBOL Release 3.0 (COBOL technical report)
[PB84-228063] 06 p0850 N85-15402
Gould Incorporated, Gould PS-3000, Gould PS-3000 COBOL V2.0
[PB84-229160] 06 p0850 N85-15403
Control Data Corporation, CYBER 835, COBOL Release 5.3 Level 614
[PB84-227842] 06 p0851 N85-15408
Prime Computer, Inc., PRIME 750, COBOL-74 Revision 19.3.2
[PB84-227826] 06 p0851 N85-15409
Sperry Univac, System 80 Model 6, OS/3 COBOL, Version 08.00/06
[PB84-227800] 06 p0851 N85-15410
Digital Equipment Corporation, MICRO/PDP-11, COBOL-81 Version 2.2
[PB84-229236] 06 p0852 N85-15413
Computer Sciences Corporation, UNIVAC 1100/80, CSTS COBOL Release COB250
[PB84-229154] 06 p0852 N85-15417
Data General Corporation, Eclipse C350, AOS COBOL Release 3.51
[PB84-227982] 06 p0853 N85-15421
C3, Incorporated NGEN CP001, C3 COBOL Version 9.0 (COBOL Technical Report)
[PB84-216316] 06 p0855 N85-15435
Microsoft Corporation, Sun Microsystems, Microsoft COBOL Version 2.0
[PB84-243401] 06 p0856 N85-15443
Microsoft Corporation, IBM PC XT, Microsoft COBOL, Version 2.0
[PB84-243419] 06 p0856 N85-15444
Four Phase Systems, Incorporated, Four Phase Series 5000, COBOL 1974 version BE08.8
[PB85-108017] 10 p1541 N85-19717
Four Phase Systems, Incorporated, Mini-Frame Series 6000, COBOL Series 6000
[PB85-108025] 10 p1541 N85-19718
Micro focus DEC Rainbow 100 + compact level 2 COBOL; V2.5
[PB85-108975] 10 p1542 N85-19719
Micro focus DEC Rainbow 100 + high performance level 2 COBOL; V2.5
[PB85-108983] 10 p1542 N85-19720
DTSS, Incorporated, DPS 8/44, DTSS COBOL Release 12
[PB85-108058] 10 p1542 N85-19721
Micro Focus, Intel Microprocessor Development System MDS221 CIS COBOL; V4.5
[PB85-110823] 11 p1699 N85-20682
Validation Summary Report (VSR), Ryan-McFarland Corporation, AT and T 385, RM/COBOL Version 2.0
[PB85-102093] 11 p1703 N85-20709
Micro focus Cifer 2887 high performance level 2 COBOL; V2.5
[PB85-108959] 11 p1703 N85-20714
Micro focus Cifer 2887 compact level 2 COBOL; V2.5
[PB85-108967] 11 p1703 N85-20715
Micro focus Fortune 32:16 compact level 2 COBOL; V2.5
[PB85-108884] 11 p1704 N85-20718
Micro focus Fortune 32:16 high performance level 2 COBOL; V2.5
[PB85-108892] 11 p1704 N85-20719
Micro Focus IBM personal computer XT CIS COBOL; V4.5
[PB85-108868] 11 p1704 N85-20720
ICL, ICL 2988 COBOL C2COB. 1321
[PB85-108876] 11 p1704 N85-20721
MICRO FOCUS Intel Microprocessor Development System MDS221 Compact Level 2 COBOL; V2.5
[PB85-108900] 11 p1704 N85-20722
Selection and use of general-purpose programming-language: Program examples, volume 2
[PB85-122000] 12 p1917 N85-22039
Selection and use of general-purpose programming language: Overview, volume 1
[PB85-122018] 12 p1917 N85-22040

COCHLEA
Measurement of cochlear acoustic pressure in guinea pigs
[ISL-CO-234/83] 16 p2861 N85-27644
Design of a physical model of the cochlea. Displacement sensor for small amplitudes in a highly viscous liquid
[STN-6] 20 p3507 N85-31802

COCKPIT SIMULATORS
Psychophysical research in development of a fiber-optic helmet mounted display 05 p0701 N85-14501
Predictions of cockpit simulator experimental outcome using system models 05 p0702 N85-14504
Advanced flight simulation for helicopter development
08 p1075 N85-16815
Dynamic training devices in CRM training
09 p1276 N85-18018
Cockpit resources management and the theory of the situation 09 p1276 N85-18022
Cockpit resource management training
09 p1276 N85-18023
Research Flight Simulator for Helicopters (RFSH): Description and application to fire control system design
[SNIAS-851-210-106] 20 p3393 N85-31050

COCKPITS
Effects of foveal information processing
01 p0009 N85-10052
LED multifunction keyboard engineering study
[AD-A145199] 01 p0010 N85-10061
Training effectiveness evaluation and utilization demonstration of a low cost cockpit procedures trainer
[AD-A145179] 01 p0013 N85-10078
Anthropometric cockpit compatibility assessment of US Army aircraft for large and small personnel wearing a training, warm-weather clothing configuration
[AD-A145206] 01 p0099 N85-10656
Anthropometric cockpit compatibility assessment of US Army aircraft for large and small personnel wearing A cold weather, armored vest, chemical defense protective clothing configuration
[AD-A145472] 02 p0238 N85-11547
Psychophysical research in development of a fiber-optic helmet mounted display 05 p0701 N85-14501
Cockpit window edge proximity effects on judgements of horizon vertical displacement
05 p0704 N85-14518
What pilots like (and don't like) about the new cockpit technology 05 p0710 N85-14554
Technical Workshop: Advanced Helicopter Cockpit Design
[NASA-CP-2351] 06 p0750 N85-14806
Superaugmented rotorcraft program
06 p0750 N85-14807
Helicopter human factors programs and plans
06 p0751 N85-14808
Civil law enforcement missions
06 p0751 N85-14812
HH-65A Dolphin digital integrated avionics
06 p0751 N85-14815
Integrated cockpit design for the Army helicopter improvement program 06 p0751 N85-14816
HH-60D night hawk helicopter
06 p0752 N85-14817
Avionics/crew station integration
06 p0752 N85-14818
Human factors in cockpit automation
06 p0752 N85-14819
Human factors of visual displays
06 p0752 N85-14821
Operational requirements - system concepts
06 p0752 N85-14823
Avionics technology - system concepts
06 p0753 N85-14824
Attack helicopter (AH-1T) cockpit systems integration
06 p0753 N85-14826
Integration of sensor fusion in advanced helicopter cockpit design 08 p1074 N85-16813
A cockpit-display concept for executing a multiple glide-slope approach for wake-vortex avoidance
[NASA-TP-2386] 08 p1085 N85-16869
Simulation 09 p1277 N85-18024
Crewstation assessment of reach as applied to the OH-58A helicopter
[AD-A149413] 10 p1531 N85-19650
Impact of future aircombat characteristics on pilot performance and cockpit design
10 p1533 N85-19661
Electronic displays: Their strengths and weaknesses for advanced high performance aircraft
10 p1533 N85-19664
Changing system and display concepts and their impact on aircrew performance 10 p1533 N85-19665
The cockpit of the year 2000: How big a step?
10 p1534 N85-19667
Influence of a perspective cockpit traffic display format on pilot avoidance maneuvers 10 p1534 N85-19668
The F-18: A new era for human factors
10 p1534 N85-19671
Aviation medicine's role in modern airforce discussed
11 p1696 N85-20662
A safety evaluation of the relocation of the ACM (Air Combat Maneuver) panel in the F-14 ( )/AIP (Avionics Integration Program)
[AD-A149596] 12 p1777 N85-21158
Analysis of estimation algorithms for CDTI and CAS applications
[NASA-CR-172444] 13 p1973 N85-22387
Dual-task timesharing using a projected attitude display (Malcolm horizon)
[AD-A150789] 14 p2395 N85-24750
YAV-8B Harrier 15 p2688 N85-26605
A comparison of pictorial and speech warning messages in the modern cockpit
[AD-A151917] 16 p2707 N85-26706
The introduction of new cockpit technology: A human factors study
[NASA-TM-86659] 16 p2843 N85-27528
Trends shaping advanced aircrew training capabilities through the 1990s
[AD-A152277] 16 p2843 N85-27530
Human factors in cockpit automation: A field study of flight crew transition
[NASA-CR-177333] 19 p3215 N85-29937
Crew systems and flight station concepts for a 1995 transport aircraft
[NASA-CR-166068] 19 p3221 N85-29973

COCKS
Tap noise-pressure fluctuations. Study of the acoustic behavior of hydraulic equipment in buildings as a function of the temperature
[CETIM-11-H-337] 04 p0502 N85-13201

CODE DIVISION MULTIPLE ACCESS
Distributed reservation-based code division multiple access
[AD-A147007] 07 p0940 N85-15957
Margin leveling algorithm for fully saturated satellite transponder with CDMA (Code Division Multiple Access) signalling
[AD-A151710] 15 p2543 N85-25699

CODERS
Improvement of the narrowband linear predictive coder. Part 2: Synthesis improvements
[AD-A145031] 01 p0038 N85-10237
Digital raster timing encoder-decoder
[AD-D011279] 06 p0804 N85-15120
ILIR task of digital recoil travel measurement system
[AD-A147102] 07 p0967 N85-16140
The removal, mechanical handling and installation procedures for declination tachometer and ltek encoder — United Kingdom Infrared Telescope
[UKIRT-17] 09 p1414 N85-18915

The removal, mechanical handling and installation procedures for the RA Itek encoder
[UKIRT-21] 09 p1414 N85-18919
Extracting digital data from a bus and multiplexing it with a video signal
[AD-D011491] 11 p1636 N85-20302
Low-bit rate speech encoders based on Line-Spectrum Frequencies (LSF)
[AD-A150518] 13 p2056 N85-22671
A software simulation study of a (255,223) Reed-Solomon encoder-decoder
[NASA-CR-175872] 17 p2947 N85-28192
Filtration of higher harmonic components in two-level digital computing synthesizers 22 p3778 N85-33410
Noiseless coding for the Gamma Ray spectrometer
[NASA-CR-176201] 24 p4069 N85-35219

CODES
The POK project; studies of information handling problems with a new kind of communication device — precoded signals
[FOA-A-53001-H2] 18 p3091 N85-29131

CODING
NT DECODING
NT REDUNDANCY ENCODING
NT SIGNAL ENCODING
Digital correlator speed improvement by multiplexing
[AD-A145207] 01 p0100 N85-10662
A comparative evaluation of algorithms for generalized network problems
[TWISK-289] 01 p0107 N85-10721
Study of a coded mask telescope for astronomical measurements in the hard X-ray domain
[MPE-182] 01 p0129 N85-10889
Gas flow environment and heat transfer nonrotating 3D program 02 p0142 N85-10966
Dynamical models for radio jets
03 p0449 N85-12854
Comparability and accuracy of industry codes in different data systems
[PB84-215607] 04 p0546 N85-13482
Electrooptical matrix multiplication using the twos complement arithmetic for improved accuracy
[AD-D011252] 05 p0728 N85-14682
Wavelength coded image transmission and holographic optical elements
[AD-A146490] 06 p0810 N85-15147
Techniques for vector quantization
[AD-A147052] 07 p1030 N85-16539
Data stimulated on-line-checking (IROLD)
08 p1066 N85-16754
The ambiguity function of random binary-phase-coded waveforms
[AD-A148906] 10 p1466 N85-19249
A modem with pseudo-orthoganal codes: Experimental results 10 p1474 N85-19302
The coding capacity of mismatched Gaussian channels
[AD-A149453] 10 p1551 N85-19782
Extracting digital data from a bus and multiplexing it with a video signal
[AD-D011491] 11 p1636 N85-20302
Object-oriented algebraic specification: Proposal for a notation and 12 examples
[CWI-CS-R8411] 11 p1707 N85-20744
ITS: The Integrated TIGER Series of coupled electron/photon Monte Carlo transport codes
[DE85-003719] 11 p1725 N85-20847
Integrated control system engineering support
[AD-A149742] 12 p1780 N85-21177
Automatic multi-banking of memory for microprocessors
[NASA-CASE-NPO-15295-1] 12 p1911 N85-21992
Determination of angular resolution of coded aperture gamma-ray telescope 13 p1981 N85-22432
Experimental results on the application of convolutional coding and Viterbi decoding as a frequency diversity technique in HF data transmission
[CRC-1377] 13 p2052 N85-22850
Code lock with microcircuit 13 p2071 N85-22935
A perspective on multiaccess channels
[AD-A150183] 13 p2146 N85-23322
ANTENA user guide
[DE85-004961] 14 p2424 N85-24953
Recent trends in software technology for vector processors 16 p2691 N85-26615
DOD manual for standard data elements, part 1
[AD-A152201] 16 p2878 N85-27754
Alphabet-constrained data compression
[AD-A152887] 17 p3019 N85-28667
Fourier coding and reconstruction of complicated contours
[REPT-84-39] 17 p3022 N85-28691
System of white-light density pseudocolor encoding with three primary colors
[AD-D011651] 17 p3037 N85-28791
ZOG-Vinson technology demonstration project. Volume 2: System description
[AD-A153671] 19 p3333 N85-30645
Comparison of 8 to 12 micrometer and 3 to 5 micrometer CVF transmissometer data with LOWTRAN calculations
[AD-A154218] 19 p3350 N85-30763
Construction of complementary code sequence sets, part 7.1D 21 p3625 N85-32523
Colour coding scales and computer graphics
23 p3963 N85-34568
Hexagonal uniformly redundant arrays for coded-aperture imaging
[OG-9.2-1] 23 p4024 N85-34940
A coded aperture imaging system optimized for hard X-ray and gamma ray astronomy
[OG-9.2-3] 23 p4024 N85-34942
SONTRAC: A solar neutron track chamber detector
[SH-9.1-12] 23 p4052 N85-35127
X-ray fluorescence analysis of 304L stainless steel
[DE85-013254] 24 p4060 N85-35286

COEFFICIENT OF FRICTION
Proposal for wall function for friction and heat transfer in the presence of roughness and mass transfer
[CFD/84/12] 04 p0501 N85-13198
Effects of B, Ti and Ta implantation on the wear resistance of Fe and Ni-plated Fe
[AD-A149947] 12 p1806 N85-21330
Interaction of cylindrical shell with concentrated mass moving along its inner surface 13 p2047 N85-22810
Experimental study of heat transfer from shaft in cooled radial bearing of GNT-25 gas turbine
14 p2270 N85-24068
Studies on surface processes during friction and wear
[AD-A153509] 18 p3117 N85-29296
Friction and wear of solid-lubricated contact in gas turbine engine bearings
[AD-A155042] 21 p3596 N85-32335
Kinetic friction coefficient of ice
[AD-A155035] 21 p3680 N85-32859
Action of wear-inhibiting Al2O3-coatings when applied to hard metal cutting tools
[BLL-RISLEY-TR-5041-(9091.9F)]
24 p4061 N85-35292

COEFFICIENTS
NT AERODYNAMIC COEFFICIENTS
NT ATTENUATION COEFFICIENTS
NT BINOMIAL COEFFICIENTS
NT CLEBSCH-GORDAN COEFFICIENTS
NT COEFFICIENT OF FRICTION
NT COHERENCE COEFFICIENT
NT CORRELATION COEFFICIENTS
NT COUPLING COEFFICIENTS
NT DIFFUSION COEFFICIENT
NT FLOW COEFFICIENTS
NT HEAT TRANSFER COEFFICIENTS
NT INFLUENCE COEFFICIENT
NT IONIZATION COEFFICIENTS
NT NOZZLE THRUST COEFFICIENTS
NT RECOMBINATION COEFFICIENT
NT REGRESSION COEFFICIENTS
NT SCATTERING COEFFICIENTS
NT VIRIAL COEFFICIENTS
NT WIGNER COEFFICIENT
Some statistical characteristics of atmospheric optical thickness in visible spectral range
02 p0164 N85-11109
Individual geopotential coefficients of order 15 and 30, from resonant satellite orbits
[AD-A146667] 06 p0828 N85-15256
Determination of shear coefficient of a general beam cross section by finite element method
09 p1338 N85-18413
On the local behaviour of solutions of degenerate parabolic equations with measurable coefficients
[AD-A147412] 09 p1373 N85-18631
Fourier-Stieltjes coefficients and continuation of functions 15 p2633 N85-26231
An incremental multigrid strategy for the fluid dynamics equations
[AD-A151953] 16 p2783 N85-27172
GAMPHI: A database of activity and osmotic coefficients for aqueous electrolyte solutions
[PB85-183390] 18 p3072 N85-29002
Evaluation of densities and distributions via hermite and generalized laguerre series employing high-order expansion coefficients determined recursively via moments or cumulants
[AD-A153950] 18 p3175 N85-29682
Thermal expansion coefficients of a 30% glass fiber filled PEEK pyrotechnic charge holder
[DE85-010605] 19 p3251 N85-30155
Visibility and vertical structure measurements in southern Germany
[AD-A154714] 21 p3635 N85-32574
Hardware realization of digital filters without multipliers
22 p3766 N85-33340

COENZYMES
NT CYTOCHROMES
NT GLUTATHIONE

COERCIVITY
Cobalt-free permanent magnet alloys
[AD-A149272] 10 p1441 N85-19079
Investigation for low-cost permanent magnets
[AD-A154387] 19 p3260 N85-30212

COGENERATION
Free-piston Stirling engine development
[PB84-237767] 01 p0056 N85-10369
Control and performance of a photovoltaic-thermal energy system 03 p0387 N85-12475
Advanced technology cogeneration system conceptual design study: Closed cycle gas turbines
[NASA-CR-168222] 07 p0992 N85-16300
Closed cycle versus open cycle gas turbines. A review of A.D. Little's ICOP report, vol. 3
[DE85-000564] 12 p1861 N85-21671
Development of a coal-water slurry-fueled diesel engine for industrial cogeneration. Task 1.0 topical report: Thermodynamic analysis
[DE85-010455] 19 p3236 N85-30062

COGNITION
Cognitive science program. A framework for relating cognitive to neural systems
[AD-A145185] 01 p0097 N85-10649
Inhibition of return: Neural basis and function
[AD-A145242] 01 p0098 N85-10652
Cognitive coordinate systems: Accounts of mental rotation and individual differences in spatial ability
[AD-A146149] 03 p0401 N85-12557
The impact of pictorial display on operator learning and performance 05 p0706 N85-14527
ERPS to monitor non-conscious mentation
05 p0707 N85-14536
Performance enhancements under dual-task conditions 05 p0707 N85-14537
Interaction of human cognitive models and computer based models in supervisory control
[AD-A142547] 07 p1020 N85-16474
Cognitive performance during successive sustained physical work episodes
[AD-A148061] 08 p1200 N85-17556
Neurocognitive pattern analysis of an auditory and visual numeric motor control task. Part 1: Development of methods
[AD-A148809] 09 p1364 N85-18578
Study of cognitive styles of students in automated teaching system 10 p1525 N85-19620
Military pilot ergonomics 10 p1532 N85-19655
Some effects of display format variables on the perception of aircraft spatial orientation
10 p1534 N85-19666
Research needs on the interaction between information systems and their users: Report of a workshop
[PB85-121523] 10 p1568 N85-19891
Human cognition and intelligence: Towards an integrated theoretical perspective
[CSIR-SR-PERS-350] 13 p2143 N85-23300
Stereotype traits can be processed automatically
[AD-A150947] 14 p2391 N85-24725
The acquisition of procedures from text. A production-system analysis of transfer of training
[AD-A151029] 14 p2392 N85-24732
Mental workload measurement: Event-related potentials and ratings of workload and fatigue
[NASA-CR-177354] 15 p2619 N85-26139
Effects of dehydration or cold exposure and restricted fluid intake upon cognitive performance
[AD-A151973] 16 p2942 N85-27525
Verbal information processing paradigms: A review of theory and methods
[AD-A153229] 17 p3050 N85-28880
Individual differences in online search behavior: The effect of learning styles and cognitive abilities on process and outcome 20 p3541 N85-32037
Resource allocation in cerebral specialization of function: Behavioral and electrophysiological studies
[AD-A155092] 21 p3664 N85-32759
Review of the psychological issues relating to the effectiveness of structured programming
[AD-A154593] 21 p3665 N85-32766

COGNITIVE PSYCHOLOGY
Cognitive science program. A framework for relating cognitive to neural systems
[AD-A145185] 01 p0097 N85-10649
Toward a computational neuropsychology of high-level vision
[AD-A145711] 02 p0236 N85-11540
The psychology of technical devices and technical discourse
[AD-P003929] 02 p0246 N85-11609
The construction of auditive tests of attention and spatial orientation and their factorial structure
[DFVLR-FB-84-21] 05 p0699 N85-14485

On looking into the black box: Prospects and limits in the search for mental models 05 p0709 N85-14546

Issues in developing a normative descriptive model for dyadic decision making 05 p0709 N85-14547

The design and use of subtasks in part training and their relationship to the whole task
05 p0711 N85-14559

Human cognition and intelligence: Towards an integrated theoretical perspective
[CSIR-SR-PERS-350] 13 p2143 N85-23300

Stereotype traits can be processed automatically
[AD-A150947] 14 p2391 N85-24725

Skilled memory
[AD-A152063] 15 p2620 N85-26143

The levels of processing conceptualization of human memory: Some empirical and theoretical issues
[AD-A152321] 17 p3000 N85-28544

Identifying solution paths in cognitive diagnosis
[AD-A152463] 17 p3000 N85-28549

Conceptualizing in assembly tasks
[AD-A155564] 21 p3665 N85-32770

COHERENCE

Singular perturbations, coherency and aggregation of dynamic systems
[DE84-014166] 01 p0114 N85-10772

Field coherence function in layerwise nonhomogeneous troposphere 06 p0784 N85-15012

COHERENCE COEFFICIENT

Proust radar: Decoding hardware and coherent integration, part 7.2A 21 p3626 N85-32524

COHERENT ACOUSTIC RADIATION

LANDSAT-4/5 image data quality analysis
[E85-10105] 24 p4107 N85-35463

COHERENT ANTI-STOKES RAMAN SPECTROSCOPY
U RAMAN SPECTROSCOPY

COHERENT ELECTROMAGNETIC RADIATION
NT COHERENT LIGHT

Device for measuring average power of laser radiation
06 p0786 N85-15026

Transmission line biased coherent array of Josephson oscillators
[AD-D011323] 07 p0944 N85-15979

A new free electron laser using a relativistic beam with spiralling electron
[AD-D011318] 07 p0971 N85-16165

High energy particle acceleration by coherent electromagnetic waves propagating across the magnetic field
[IPPJ-717] 16 p2866 N85-27679

Solvability of some inverse problems in laser radiation focusing 21 p3696 N85-32963

The 2nd European Conference on Atomic and Molecular Physics
[AD-A155863] 24 p4148 N85-35715

COHERENT LIGHT

Effect of aberration in optical system on illuminance distribution over image of strip in semicoherent light
06 p0777 N85-14970

Two-photon coherent state light - its generation and potential applications
[AD-A148245] 08 p1166 N85-17356

A posteriori increase of resolving power of optical system forming averaged monochromatic images
13 p2082 N85-23003

Influence of coherent light beams on free carriers in semiconductors 21 p3681 N85-32867

COHERENT RADAR

Test and evaluation of a coherent 35 gigahertz radar repeater
[AD-A145714] 02 p0191 N85-11280

Test signal generator for coherent air-to-ground radars
[AD-D011278] 05 p0628 N85-14025

Activities report in Earth and planetary environments physics
[CRPE-NT-134] 05 p0734 N85-14720

The MST radar technique 08 p1185 N85-17466

Bistatic coherent radar receiving system
[AD-D011447] 10 p1466 N85-19252

Digital coherent detector
[AD-D011560] 12 p1833 N85-21501

The magnetospheric convection electric field at ionospheric altitudes: A case study based on STARE and Saint-Santin data 14 p2362 N85-24594

A brief summary of results derived from Scandinavian Twin Auroral Radar Experiment (STARE) observations during IMS — ionospheric electric fields
14 p2362 N85-24595

Contribution of the Scandinavian Twin Auroral Radar Experiment (STARE) radar to the understanding of the physical mechanisms associated with Pc5 pulsations
14 p2364 N85-24613

Satellite, auroral radar and ground magnometer observations of transient ULF pulsations
14 p2369 N85-24645

Forth system for coherent-scatter radar data acquisition and processing
[NASA-CR-176055] 20 p3494 N85-31720

Observations of frontal zone structures with a VHF Doppler radar and radiosondes, part 1.2A
21 p3616 N85-32469

Potential advantages of the spaced antenna method for operational wind profiling, part 3.1B
21 p3620 N85-32490

Proust radar: Decoding hardware and coherent integration, part 7.2A 21 p3626 N85-32524

Potential coordinate estimate accuracy estimation accuracy by multiposition radar systems
22 p3763 N85-33322

Detection of signals from coherent pulsed radars with random variation in parameters of sounding signals from pulse to pulse against background of worst-case Gaussian noise 22 p3763 N85-33324

COHERENT RADIATION
NT COHERENT ACOUSTIC RADIATION
NT COHERENT ELECTROMAGNETIC RADIATION
NT COHERENT LIGHT

Diffusion and intermittency in an extended one-dimensional maps 02 p0282 N85-11834

Influence of propagation in digital wireless beam, microwave links 10 p1470 N85-19277

Exploration of new methods to produce efficient sources of coherent near millimeter wave radiation
[AD-A150094] 12 p1829 N85-21481

A spatially incoherent and temporally coherent source
[AD-A151281] 13 p2157 N85-23390

Parametric coherence estimation via convolved correlations
[DE85-003946] 14 p2416 N85-24909

Principle and design of a medium-enhanced free-electron laser 15 p2561 N85-25802

Studies of collisional and nonlinear radiative process for development of coherent UV and XUV sources
[AD-A152001] 16 p2865 N85-27670

Coherent X-rays and vacuum-ultraviolet radiation from storage-ring-based undulators and free electron lasers
[DE85-009968] 18 p3183 N85-29738

Method of reducing impurity and antisite defects in semiconductor crystal materials, and device and apparatus respectively produced from and utilizing same
[AD-D011698] 19 p3260 N85-30216

Laser radiation propagation in inertialess nonlinear medium 21 p3686 N85-32898

Mean intensity of wave reflected by wavefront reversing mirror in turbulent medium 22 p3782 N85-33432

A theoretical and empirical analysis of coherent ray-tracing 23 p3957 N85-34524

COHERENT SCATTERING

Measurement of scattering cross sections of liquid and solid hydrogen deuterium and deuterium hydride for thermal neutrons
[DE84-014814] 05 p0727 N85-14671

A spatially incoherent and temporally coherent source
[AD-A151281] 13 p2157 N85-23390

The Hanle effect applied to magnetic field measurements 18 p3204 N85-29878

Grain structure identification by ultrasound frequency averaging and deconvolution
[AD-A154332] 19 p3352 N85-30777

Forth system for coherent-scatter radar data acquisition and processing
[NASA-CR-176055] 20 p3494 N85-31720

Morphology of the scattering targets: Fresnel and turbulent mechanisms, part 2.1A
21 p3618 N85-32481

Numerical and analytic descriptions of cosmic-ray transport
[SH-4.1-4] 23 p4005 N85-34830

COHERENT SOURCES
U COHERENT RADIATION
U RADIATION SOURCES

COHERENT TRANSMISSION
U COHERENT RADIATION

COHESION

Experimental AC (Asphalt Concrete) overlays of PCC pavement
[PB84-218171] 03 p0342 N85-12203

COHOMOLOGY
U HOMOLOGY

COILS

Induction voidmeter
[DE84-014321] 01 p0050 N85-10329

COINCIDENCE CIRCUITS

A theoretical basis for the analysis of redundant software subject to coincident errors
[NASA-TM-86369] 13 p2145 N85-23317

COLD ACCLIMATIZATION

Effects of restricted water intake on performance in a cold environment
[AD-A146904] 07 p1015 N85-16450

Predictors of cold weather health behaviors
[AD-A151910] 16 p2843 N85-27529

Acclimatization to far north 20 p3506 N85-31792

COLD CATHODE TUBES
NT PHOTOMULTIPLIER TUBES

Process for making electrodes for discharge tubes
[DE85-008698] 17 p2955 N85-28247

COLD CATHODES

High power pulsed accelerators with potential industrial applications
[DE85-001710] 11 p1720 N85-20821

COLD DRAWING

Impact toughness of wire after cold deformation and annealing
[BLL-M-35941-(5828.4)] 05 p0615 N85-13930

Uniaxial orientation of linear low density polyethylene
[AD-A151037] 14 p2261 N85-24009

Fracture mechanics analysis of cold drawn Si-Cr valve steel
[BLL-BISI-TRANS-22216-(9022.06)]
17 p2978 N85-28405

A new drawing technique for nylon 6 by reversible plasticization with iodine
[AD-A156272] 24 p4162 N85-35803

COLD FLOW TESTS

An experimental study of clustered, two-dimensional rocket nozzles
[AD-A151889] 15 p2495 N85-25390

Contribution to the study of equivalent noise source identification in fast cold jets
[ISL-R-114/83] 16 p2861 N85-27645

COLD FORMING
U COLD WORKING

COLD FRONTS

Frontal motion in mountainous terrain: Analysis and implications for 0 to 12 hour forecasts
01 p0076 N85-10502

The extremeness of the cold front of December 31, 1978 over the CSR
[REPT-566] 03 p0377 N85-12409

Conditions governing the formation of stratocumulus clouds over the western Atlantic during cold air outbreaks
[AD-A146780] 07 p1004 N85-16383

The structure and dynamics of an observed moist front 18 p3146 N85-29480

The kinematic structure of cold frontal rainbands
24 p4119 N85-35531

COLD GAS

Study of the velocity-acoustic pressure correlation in a cold jet, centered on the sign and the amplitude of the velocity fluctuations
[ISL-R-124/83] 04 p0501 N85-13193

Experiment on triggered fragmentation on a molten copper droplet in water
[BLL-WH-602-(9091.9F)] 08 p1125 N85-17091

Localization of sources of equivalent noise in fast cold jets, excited and nonexcited
[ISL-CO-201/83] 14 p2416 N85-24910

Preliminary wind tunnel experiments to investigate the effect of heat transfer on the dispersion of cold dense gases
[OUEL-1546/84] 20 p3456 N85-31467

COLD NEUTRONS

Construction of a cold neutron source at FRM, Munich
03 p0427 N85-12722

Breakthrough in container confinement of ultracold neutrons 15 p2644 N85-26311

COLD PLASMAS

Direct measurements of severe spacecraft charging in auroral ionosphere 13 p1991 N85-22480

Charging of DMSP/F6 spacecraft in aurora on 10 January 1983 13 p1991 N85-22481

Double layer formation due to contact of different temperature plasmas
[IPPJ-722] 19 p3370 N85-30900

COLD PRESSING

Fatigue resistance of VT3-1 titanium alloy related to surface cold working 19 p3245 N85-30120

Establishment of a Computer-Aided Design (CAD)-Computer-Aided Manufacturing (CAM) process for the production of cold forged gears
[AD-A155756] 24 p4137 N85-35644

COLD ROLLING

Effect of texture in steel on the susceptibility of hydrogen embrittlement
[BLL-BISI-TRANS-22026-(9022.06)]
17 p2926 N85-28046

Influence of preliminary thermomechanical treatment on depth and hardness of nitrided layers
[BLL-BISI-TRANS-22488-(9022.06)]
17 p2929 N85-28078

Fatigue resistance of VT3-1 titanium alloy related to surface cold working 19 p3245 N85-30120

COLD SURFACES
Low temperature deposition of nickol films
[AD-D011568] 12 p1805 N85-21319
Experimental aerodynamic heating to simulated space shuttle tiles in laminar and turbulent boundary layers with variable flow angles at a nominal Mach number of 7
[NASA-TP-2307] 23 p3929 N85-34351
COLD TOLERANCE
Advances in study of cold injury in Army
14 p2263 N85-24145

COLD WALLS
U COLD SURFACES
U WALLS
COLD WATER
Comparison of thermal responses between rest and leg exercise in water
[AD-A146818] 07 p1015 N85-16448
NOAA OTEC CWP (National Oceanic and Atmospheric Administration Ocean Thermal Energy Conversion Cold Water Pipe) at-sea test. Volume 3: Additional tabulation of the power spectra, part 2
[PB84-238997] 09 p1346 N85-18468
SCPP (Sierra Cooperative Pilot Project) data collection and analysis. Volume 1: Executive summary
[PB85-156065] 16 p2637 N85-27494
COLD WEATHER
Anthropometric cockpit compatibility assessment of US Army aircraft for large and small personnel wearing A cold weather, armored vest, chemical defense protective clothing configuration
[AD-A145472] 02 p0238 N85-11547
Behavior and characteristics of storm cold outflows
09 p1356 N85-18529
A systems analysis of alternative concepts for aircrew cold weather clothing
[AD-A148605] 09 p1365 N85-18580
Investigation of the requirement for auxiliary heating of Canadian forces personnel
[AD-A151950] 16 p2841 N85-27522
Predictors of cold weather health behaviors
[AD-A151910] 16 p2843 N85-275∠9
Land vehicle corrosion management
22 p3750 N85-33246

COLD WELDING
Method of calculating strength of joint produced by cold welding of aluminum under discrete loading
13 p2034 N85-22743
Diffusion vacuum welding 15 p2499 N85-25416
COLD WORKING
NT COLD ROLLING
NT ELECTROHYDRAULIC FORMING
NT EXPLOSIVE FORMING
Mechanical properties of a leaded, resulfurized, rephosphorized steel in various thermo/mechanical conditions
[PB84-216464] 03 p0333 N85-12144
Defining effect of hardening on mean yield strength in deformation zone
[BLL-M-35934-(5826.4)] 05 p0647 N85-14154
On heat-treatable copper-chromium alloy, 1
[NASA-TM-77753] 07 p0927 N85-15879
Role of residual stresses in stress corrosion cracking in alloy 600 tubes. Part 1: Determination of throughwall residual stresses and their modification by transient heat treatment
[DE85-004646] 14 p2257 N85-23988
Modular design, versatility of robots viewed
14 p2284 N85-24155
Calculating reliability and productivity of cold stamping robot complex as queuing system
16 p2761 N85-27039
Preparation of metal for cold upsetting
[BLL-BISI-TRANS-22383-(9022.06)]
17 p2926 N85-28043
The fabrication, microstructure, and strengthening behavior of heavily cold-worked in situ composites
19 p3231 N85-30031
The effect of prior parent phase cold work on martensite transformation in Cu-Zn-Al shape memory alloys
[AD-A155140] 21 p3566 N85-32183
Wear-resistant coatings for tools intended for cold working
[BLL-RISLEY-TR-5040-(9091.9F)]
24 p4061 N85-35293

COLLAPSE
Collapse of cavitation bubbles between two walls in ultrasonic field 02 p0266 N85-11739
Some aspects of the micromechanics of hot spot formation in energetic materials
[AD-P004348] 10 p1456 N85-19172
Neutrino-antineutrino annihilation around collapsing star
[OG-1.1-10] 22 p3861 N85-33911
Experimental study of collapse of thick-walled tube under external pressure and axial force
23 p3904 N85-34186

The capability of the existing network of installations for detecting the antineutrino burst from collapsing stars
[HE-5.3-13] 24 p4206 N85-36107
COLLATING
Design of a scientific information collation and dissemination system, volumes 1 thru 3
[AD-A146002] 03 p0438 N85-12791
COLLECTION
Acid rain: Towards automated monitoring
16 p2629 N85-27444
Evaluation of a field expedient technique for sweat sample collection
[AD-A151916] 16 p2841 N85-27521
COLLECTORS
U ACCUMULATORS
COLLEGES
U UNIVERSITIES
COLLIMATION
Collimation techniques for dense object flash radiography
[DE84-016461] 05 p0647 N85-14152
On the hydrodynamical equations of astrophysical jets — active galactic nuclei 06 p1241 N85-17831
Collimated winds from active galactic nuclei
06 p1241 N85-17832
Intensity fluctuations of focused laser beam during reflection in turbulent atmosphere
13 p2076 N85-22975
Distortion functions
[DE85-007511] 16 p2862 N85-27655
Laser Schlieren crystal monitor
[NASA-CASE-MFS-28060-1] 19 p3374 N85-30932
COLLIMATORS
Study of a coded mask telescope for astronomical measurements in the hard X-ray domain
[MPE-182] 01 p0129 N85-10889
Collimation techniques for dense object flash radiography
[DE84-016461] 05 p0647 N85-14152
Apparatus for determining the liquid water content of a gas
[AD-D011297] 07 p0922 N85-15839
A cometary ion mass spectrometer
[NASA-CR-174328] 06 p1164 N85-17343
Measurement of sensitivity of shadowgraphic instruments with spherical autocollimating mirror
14 p2274 N85-24087
Muon spin rotation studies 17 p3042 N85-28819
Soft X-ray polychromator for the Solar Maximum Mission
[NASA-CR-175297] 21 p3723 N85-33096
COLLINEARITY
The information in the minor principal components
[CSIR-TWISK-320] 01 p0109 N85-10735
COLLISION AVOIDANCE
Enhanced TCAS 2/CDTI traffic Sensor digital simulation model and program description
[NASA-CR-172445] 02 p0136 N85-10927
Air-to-air visual acquisition performance with TCAS 2
[FAA-PM-84-17] 02 p0236 N85-11537
TCAS 2 logic performance during phase one operational evaluation
[DOT/FAA/PM-84/20] 05 p0595 N85-13793
A bird strike handbook for base-level managers
[AD-A147928] 07 p0948 N85-16008
Influence of a perspective cockpit traffic display format on pilot avoidance maneuvers 10 p1534 N85-19668
Collision avoidance for Naval training aircraft
[FAA-PM-84-4] 12 p1774 N85-21136
TCAS II: Design and validation of the high-traffic-density surveillance subsystem
[DOT/FAA/PM-84/5] 13 p1970 N85-22375
Analysis of estimation algorithms for CDTI and CAS applications
[NASA-CR-172444] 13 p1973 N85-22387
An analysis of the impacts of the Airport Radar Service Area (ARSA)
[AD-A150954] 14 p2217 N85-23749
Helicopter user survey: Traffic alert and collision avoidance system (TCAS)
[FAA-PM-85-6] 15 p2468 N85-25236
Aircraft accident report: United Airlines Flight 663, Boeing 727-222, N7647U, Denver, Colorado, May 31, 1984
[PB85-910405] 16 p2703 N85-26686
Traffic alert and collision avoidance system: Operational simulation
[FAA-PM-85-10] 19 p3216 N85-29941
System safety study of minimum TCAS 2 for instrument weather conditions
[FAA-PM-85-12] 22 p3728 N85-33113
COLLISION PARAMETERS
NT COLLISION RATES
The coordinated research program at IAEA on atomic collision data for plasma diagnostics
09 p1390 N85-18747

Collision detection for moving polyhedra
[AD-A148961] 10 p1544 N85-19735
Plane-wave born collision strengths for electron-ion excitation: Comparison with other theoretical methods
[DE85-002348] 10 p1555 N85-19802
Beam loss due to the aperture limitation resulting from intrabeam scattering
[DE85-005138] 12 p1930 N85-22124
Workshop on Nuclear Dynamics 3
[INC-40007-24] 12 p1931 N85-22130
Statistical theory of planet growth
15 p2678 N85-26534
Experiments and detectors for high energy heavy ion colliders
[DE85-007927] 17 p3031 N85-28748
Polarization of fast particle beams by collisional pumping
[DE85-011621] 22 p3838 N85-33784
Fokker-Planck calculation of hot electron formation in the thermal barrier region of tandem mirror Gamma-10
[IPPJ-726] 23 p3979 N85-34669
Electron loss process and cross section of multiply charged ions by neutral atoms 23 p3981 N85-34685
Observations of accelerated high current low emittance beams in the SLC Linac
[DE85-013073] 24 p4068 N85-35211
Relation between gamma-ray family and EAS core: Monte-Carlo simulation of EAS core
[HE-3.6-7] 24 p4185 N85-35903
On mini-cluster observed by Chacaltaya emulsion chamber experiment
[HE-3.6-12] 24 p4185 N85-35909
Observation of genetic relation among new phenomena Geminion, Chiron and mini-Centauro
[HE-6.2-16] 24 p4212 N85-36152
COLLISION RATES
Dense but collisionless orbiting rings — Saturn rings
15 p2675 N85-26517
Multiple collision solutions for time-dependent neutron transport in slabs of finite thickness
[OEFZS-4312] 22 p3836 N85-33762
Breakdown of intrinsic ambipolarity for the radial diffusion due to a rotating RF field 23 p3977 N85-34660
COLLISION WARNING DEVICES
U COLLISION AVOIDANCE
U WARNING SYSTEMS
COLLISIONAL PLASMAS
NT STRONGLY COUPLED PLASMAS
Report of the reference designs study group on the superconducting super collider
[DE84-015567] 04 p0569 N85-13830
Equations of plasma transport in a curved magnetic field
[DE84-015625] 05 p0730 N85-14680
A propagator expansion method for solving linearized plasma kinetic equations with collisions
[AD-A147524] 07 p1045 N85-16640
Hydrodynamic response of a radiating Al plasma excited by a proton beam
[AD-A148904] 10 p1558 N85-19824
Nonlinear saturation of stimulated Raman scattering in collisional homogeneous plasma
[DE85-002814] 10 p1559 N85-19831
Atomic processes involving impurities in the plasma edge
[DE85-001277] 11 p1730 N85-20682
Analysis and computations of microwave-atmospheric interactions
[AD-A149666] 12 p1889 N85-21854
Fluid modeling of magnetized plasmas
[DE85-007679] 17 p3039 N85-28804
Time-implicit Monte-Carlo collision algorithm for particle-in-cell electron transport models
[DE85-010758] 20 p3521 N85-31900
Investigation of space-time structure of glow of laser plasma colliding with flat screen
21 p3693 N85-32947
Recombination and ionization in a nitrogen plasma
[AD-A155426] 22 p3845 N85-33013
Collisional transport for a superthermal ion species in a plasma
[DE85-011943] 22 p3845 N85-33018
COLLISIONLESS PLASMAS
Review of simulation of quasiparallel collisionless shocks
[DE84-015489] 02 p0304 N85-11967
Preliminary user's guide for BIGONE on the Cray
[DE84-017075] 04 p0568 N85-13623
Collective processes and formation of star clusters
05 p0738 N85-14743
Strong iron accelerating by collisionless magnetosonic shock wave propagating perpendicular to a magnetic field
[IPPJ-709] 12 p1935 N85-22181

Resonant ion acceleration by oblique magnetosonic shock wave in a collisionless plasma
[IPPJ-736] 23 p3975 N85-34643
Numerical solutions of the Vlasov equation
23 p3979 N85-34672
Current interruption by density depression
[DE85-013120] 24 p4169 N85-35846

COLLISIONS
NT ATOMIC COLLISIONS
NT BIRD-AIRCRAFT COLLISIONS
NT COULOMB COLLISIONS
NT INELASTIC COLLISIONS
NT IONIC COLLISIONS
NT METECRITE COLLISIONS
NT MIDAIR COLLISIONS
NT MOLECULAR COLLISIONS
NT PARTICLE COLLISIONS
Throughput characteristics of Carrier Sense Multiple Access (CSMA) networks
[FUB-25-1983] 01 p0106 N85-10713
Mechanical models of close approaches and collisions of large protoplanets 04 p0588 N85-13756
Aircraft accident report, Scandinavian Airlines System, Flight 901, McDonnell Douglas DC-10-30, John F. Kennedy International Airport, Jamaica, New York, February 28, 1984
[PB84-910415] 05 p0594 N85-13788
An operator method for computing the asymptotics of a collision resolution interval
[AD-A146837] 07 p1028 N85-16528
Orbital Debris
[NASA-CP-2360] 12 p1783 N85-21188
NASA/JSC orbital debris study: Debris model
12 p1783 N85-21193
Assessment of satellite collision hazards by simulated sampling in space 12 p1784 N85-21195
A model for the evolution of on-orbit manmade debris environment 12 p1784 N85-21196
Geosynchronous satellite collision avoidance
12 p1784 N85-21197
Preliminary design of an Earth-based debris detection system using current technology and existing installations 12 p1784 N85-21199
Debris impact on Earth-orbiting spacecraft
12 p1948 N85-22234
Experimental studies of low temperature surface interactions of atomic hydrogen using maser technique
[AD-A150216] 13 p2017 N85-22647
Asteroid collisional evolution studies
13 p2178 N85-23501
A circum-terrestrial compositional filter
13 p2179 N85-23520
Neutralization and excitation in low-energy ion-surface collisions
[AD-A151568] 15 p2660 N85-26414
Collisional outcomes in the asteroid belt
15 p2678 N85-26538
Comet showers and Nemesis, the death star
[DE85-003736] 15 p2683 N85-26575
Refinements in the computation of collision probabilities
[DE85-006118] 16 p2864 N85-27663
Average collisional vibrational energy transfer quantities and the inversion temperature
[AD-A152674] 17 p3029 N85-28733
Theory of high energy collision processes
[DE85-010183] 19 p3362 N85-30846

COLLOIDING
The colloidal chemistry of ceramic clays
[NASA-TM-77734] 03 p0336 N85-12163

COLLOIDS
NT AEROSOLS
NT FOG
Electrokinetic potential and stability of SiC suspensions in electrolyte solutions
[NASA-TM-77492] 04 p0469 N85-12984
Combustion waves in dispersed-2-phase mixtures
[CFD/84/13] 04 p0472 N85-13003
Zeta potential in ceramic industry
[NASA-TM-77478] 04 p0478 N85-13047
Light scattering studies of lower dimensional colloidal particle and critical fluid systems
[DE85-002087] 09 p1377 N85-18654
Solar fuel synthesis based on colloidal and particulate semiconductors
[PB85-129104] 11 p1614 N85-20152
Ac field-induced order in dense colloidal systems
[DE85-009107] 17 p2935 N85-28119
An evaluation and preparation of ferromagnetic liquid composites for use at millimeter wavelengths
[AD-A153939] 18 p3069 N85-28980
Collodial particle transport with simultaneous birth, growth and capture
[DE85-010388] 19 p3235 N85-30055

COLOMBIA
Characteristics of a recent Columbian earthquake, December 12, 1979 04 p0523 N85-13347
Use of minicomputers for the formation of hydrological data banks 07 p1001 N85-16358

COLONIES
Cyanobacterial mats: Microanalysis of community metabolism 21 p3661 N85-32743
Microbial communities and microprofiles of sulfide and oxygen of alum rock sulfur springs
21 p3661 N85-32746
Microbial colonization and growth on metal sulfides and other mineral surfaces 21 p3662 N85-32747

COLOR
NT WATER COLOR
Peripheral vision displays: The future
01 p0009 N85-10056
Effects of alternative chromatic mixed graphics displays in decision support systems
[AD-A145561] 02 p0242 N85-11578
Visibility of various target-background color combinations under different chromatic ambient illuminations
[AD-A146348] 03 p0420 N85-12684
Analysis of data entry performance: Chromatic versus monochromatic
[AD-A145568] 03 p0438 N85-12789
Coastal Zone Color Scanner (CZCS): Imagery of near-surface phytoplankton pigment concentrations from the first coastal ocean dynamics experiment (CODE-1), March - July 1981
[NASA-CR-174169] 04 p0542 N85-13447
Color and grey scale in sonar displays
05 p0710 N85-14552
Human factors of visual displays
06 p0752 N85-14821
Local interstellar extinction with an emphasis on uvby beta results 06 p0875 N85-15559
Do the arching HI filaments show in local reddening data? 06 p0876 N85-15561
Inverse relations between 0.25 keV counts and local interstellar dust 06 p0877 N85-15572
New technology high efficiency and high stability color motion video compression system
[AD-A147523] 07 p0941 N85-15968
A comparative study of dust and young stars in three small galaxies 09 p1415 N85-18928
Pictorial format display evaluation
[AD-A149252] 10 p1425 N85-18986
Individual differences in chromatic brightness matching
[AD-A148882] 10 p1529 N85-19641
The relative effectiveness of red and white light for subsequent dark-adaptation
[AD-A148883] 10 p1530 N85-19642
Electronic displays: Their strengths and weaknesses for advanced high performance aircraft
10 p1533 N85-19664
Proceedings of the 6th Advanced Aircrew Display Symposium
[AD-A150044] 12 p1778 N85-21160
Television animation store: Digital chroma, key and mixer units
[BBC-RD-1984/16] 12 p1824 N85-21442
A concept for the processing and display of Thematic Mapper data 13 p2119 N85-23196
Color-selective coating for viewfinder in optical instruments 14 p2276 N85-24096
Using color to separate reflection components
[AD-A150999] 14 p2405 N85-24828
The Feinheit method: A phase-independent formulation of the period-luminosity relation for Cephids
[NASA-CR-175708] 14 p2440 N85-25056
The Mars ancient cratered terrain, smooth plains boundary: Implications of Viking color data for evolution of the Amenthes Region 15 p2682 N85-26564
System of white-light density pseudocolor encoding with three primary colors
[AD-D011651] 17 p3037 N85-28791
A general area air traffic controller simulation using colour graphics
[AD-A153634] 18 p3060 N85-28933
Effect of background/foreground color coding on detection in acoustic data displays
[AD-A154105] 19 p3352 N85-30774
Chromophores with auxochrome-like function
[NASA-TM-77849] 20 p3421 N85-31233
Color evolution in high redshift galaxies
20 p3544 N85-32055
Passive Q-modulation of optical cavities by KCl crystals containing OH(-) -ions 21 p3688 N85-32915
Pulsed lasers for filming color holographic film images
22 p3781 N85-33426
The development and evaluation of color display systems for airborne applications. Phase 1: Fundamental visual, perceptual, and display system considerations
[FAA/PM-85-19] 22 p3826 N85-33700
Electrolytic synthesis of colored eta alumina film
23 p3906 N85-34201
Theoretical and experimental analyses of the performance of two-color laser ranging systems
[NASA-CR-176159] 23 p3936 N85-34397
Graph-theoretical exorcism
[DE85-011916] 23 p3955 N85-34512
An analysis and algorithm for filling propagation
23 p3961 N85-34551
Design and implementation of an interactive route editor 23 p3962 N85-34559
Colour spaces and colour contrast
23 p3963 N85-34567
Colour coding scales and computer graphics
23 p3963 N85-34568
Low cost geometric modelling system for CAM
23 p3964 N85-34578
Radiation measurements on magnesium flames
[BLL-CE-TRANS-8110-(9022.09)]
24 p4075 N85-35254
Edge information in color images based on histograms of differences
[AD-A156002] 24 p4154 N85-35751

COLOR (PARTICLE PHYSICS)
U QUANTUM CHROMODYNAMICS

COLOR CENTERS
Polarimetric image recorder
[AD-D011605] 16 p2787 N85-27192

COLOR CODING
Choice reaction time and color: An annotated bibliography
[AD-A149722] 12 p1908 N85-21979
The effect of set size on color matching
[AD-A150899] 14 p2388 N85-24713
Effect of background/foreground color coding on detection in acoustic data displays
[AD-A154105] 19 p3352 N85-30774
The effect of set size on time to recall color coded information
[AD-A155013] 21 p3665 N85-32767

COLOR INFRARED PHOTOGRAPHY
Metric camera experiment: Spacelab 1 mission
05 p0658 N85-14229

COLOR PERCEPTION
U COLOR VISION

COLOR PHOTOGRAPHY
Some nonatlas work at the European Southern Observatory (ESO) Sky Atlas Laboratory --- astronomical photography 07 p0964 N85-16117
Bio-optical variability in the Alboran Sea as assessed by Nimbus-7 coastal zone color scanner
[AD-A147909] 07 p0989 N85-16281

COLOR TELEVISION
Problems relevant to town incoming radio TV links
[NASA-TM-77623] 08 p1150 N85-17255
Electronic detection and concealment of film dirt
[BBC-RD-1985/4] 15 p2538 N85-25667
LI481 and LI482 vidicons for two-tube color TV cameras with improved image quality 22 p3764 N85-33333
Theoretical principles of vertical subsampling of color difference signals at half the sampling rate --- television
[FI-447-TBR-18] 23 p3926 N85-34332

COLOR VISION
Color visual simulation applications at the Defense Mapping Agency
[AD-P004315] 09 p1268 N85-17969
Color measurement and discrimination
[NASA-CR-3824] 09 p1365 N85-18579
Individual observer data for the 1955 Stiles-Burch 2 deg pilot investigation --- color vision
[NPL-QU-68] 20 p3512 N85-31830
Theoretical principles of vertical subsampling of color difference signals at half the sampling rate --- television
[FI-447-TBR-18] 23 p3926 N85-34332
Edge information in color images based on histograms of differences
[AD-A156002] 24 p4154 N85-35751

COLORADO
Green River air quality model development: Meteorological and tracer data, July/August 1982. Field study in Brush Valley, Colorado
[DE84-014975] 02 p0225 N85-11474
Atmospheric tracer experiments in a deep narrow valley
[PB84-234590] 04 p0532 N85-13402
Effect of lithology and climate on the morphology of drainage basins in northwestern Colorado
[PB84-228238] 06 p0828 N85-15258
Results of the carbon monoxide study in Washington, D.C. and Denver, Colorado, in the winter of 1982-83
[PB84-230069] 06 p0834 N85-15309

Water resources data for Colorado, water year 1983. Volume 1: Missouri River Basin, Arkansas River Basin and Rio Grande Basin
[PB85-123659] 11 p1671 N85-20528
Water resources data for Colorado, water year 1983. Volume 2: River Basin above Dolores River
[PB85-123667] 11 p1671 N85-20529
Monitoring approaches for assessing quality of high altitude lakes: Colorado Flat Tops Wilderness Area
[PB85-117232] 11 p1679 N85-20579
Measurements of the surface energy budget in the southern Gobi Desert of China, and in the Rocky Mountains of Colorado
[NASA-CR-175506] 12 p1888 N85-21847
Volcanism of the Colorado Plateau (basin and range transition): Implications for crustal processes
13 p2187 N85-23569
Evaluation of the PROFS (Program for Regional Observing and Forecasting Services) 1982, real-time forecast experiment
[PB85-159747] 16 p2837 N85-27495
Categorization of nocturnal drainage flows within the Brush Creek valley in western Colorado and the variability of sigma theta in complex terrain
[DE85-011291] 19 p3300 N85-30461
Aeromagnetic and gravity models of the pluton below the Lake City caldera, Colorado
24 p4104 N85-35442

COLORADO RIVER (NORTH AMERICA)
Water resources data for Colorado, water year 1983. Volume 2: River Basin above Dolores River
[PB85-123667] 11 p1671 N85-20529

COLORATION
U COLOR

COLORIMETRY
NUTSATSEA: An on line data reduction program linking a Chemlab continuous flow analyser to a Commodore PET microcomputer
[IOS-176] 03 p0403 N85-12570
Comparison study of analytical methods for the determination of fluoride, chloride, and bromide in plastics
[DE84-015008] 04 p0470 N85-12989
A comparison of some photometric parameters of active and normal spiral galaxies 08 p1236 N85-17806
Photometric study of Pluto near perihelion. Part 2: Refinement of rotation period: Color indices
15 p2483 N85-25325
System of white-light density pseudocolor encoding with three primary colors
[AD-D011651] 17 p3037 N85-28791
Chromophores with auxochrome-like function
[NASA-TM-77849] 20 p3421 N85-31233
A manual of methods for the continuous flow determination of ammonia, nitrate-nitrite, phosphate and silicate in seawater
[IOS-177] 23 p3913 N85-34243

COLS
U GAPS (GEOLOGY)

COLUMBIA (ORBITER)
National Space Transportation Systems Program mission report
[NASA-TM-87456] 14 p2241 N85-23898
Correlation of predicted and measured sonic boom characteristics from the reentry of STS-1 orbiter
[NASA-TP-2475] 18 p3177 N85-29694

COLUMBIUM
U NIOBIUM

COLUMNS (PROCESS ENGINEERING)
Free zone electrophoresis simulation of static column electrophoresis in microgravity on shuttle flight STS-3
20 p3502 N85-31773

COLUMNS (SUPPORTS)
Interactive buckling of thin-walled structural components under static and dynamic loads
01 p0059 N85-10392
Refined modeling of reinforced concrete columns of seismic analysis
[PB84-234384] 04 p0484 N85-13089
Support structures for optical components in the Laser Demonstration Facility
[DE85-008879] 17 p2971 N85-28349
Buckling and post-buckling behavior of sparsely connected built-up columns 19 p3283 N85-30358
Structural analysis of imperfect three-legged truss columns for large space structures applications
24 p4100 N85-35416
User's guide: A computer program for strength analysis of non-hydraulic concrete structural elements. Report 1. Concrete General Strength Investigation (CGSI)
[AD-A156392] 24 p4102 N85-35428
Static and cyclic behavior of semi-rigid steel beam-column connections
[PB85-194363] 24 p4103 N85-35433

COMBAT
Air Force Human Resources Laboratory report: Fiscal year, 1983
[AD-A145647] 02 p0236 N85-11548
Quantification of cross-coupling and motion feedthrough for multiaxis controllers used in an air combat flying task
05 p0700 N85-14491
HH-60D night hawk helicopter
06 p0752 N85-14817
Computer sizing of fighter aircraft
[NASA-TM-86351] 08 p1067 N85-16759
Evaluation of nose, roof, and mast mounted sensor platforms for piloting and sighting, integrated in future combat helicopters 08 p1074 N85-16806
The design and development of an integrated core system for battlefield helicopters
08 p1074 N85-16811
Air combat visual simulation using a head slaved projector
[AD-P004327] 09 p1270 N85-17981
Binocular overlap in a fiber optic helmet mounted display
[AD-P004331] 09 p1270 N85-17985
Combat capable space systems for tactical support
11 p1713 N85-20775
Air combat simulation: Methods, models, trends
13 p1967 N85-22359
Equilibrium solutions, stabilities and dynamics of Lanchester's equations with optimization of initial force commitments
[AD-A151510] 15 p2637 N85-26266
Piloted simulation of one-on-one helicopter air combat at NOE flight levels
[NASA-TM-86686] 16 p2710 N85-26720
The STOL and maneuver technology program integrated control system 16 p2715 N85-26757
An extended two-target differential game model for medium-range air combat game analysis
[NASA-CR-175968] 18 p3175 N85-29687
Design and implementation of input signals for identification of pilot/aircraft models
[ESA-TT-880] 20 p3394 N85-31055
A formulation and analysis of combat games
[NASA-TP-2487] 22 p3835 N85-33745
Air university commander's and supervisor's guide on substance abuse
[AD-A156336] 24 p4133 N85-35622

COMBINATIONS (MATHEMATICS)
Some facets of the tri-index assignment polytope
[AD-A149195] 10 p1547 N85-19753
On large matchings and cycles in sparse random graphs
[AD-A149194] 10 p1550 N85-19778

COMBINATORIAL ANALYSIS
NT BINOMIAL COEFFICIENTS
NT COMBINATIONS (MATHEMATICS)
NT FACTORIALS
NT PARTITIONS (MATHEMATICS)
COM-GEOM Interactive Display Debugger (CIDD)
[AD-A145001] 01 p0104 N85-10692
Heuristics based on spacefilling curves for combinatorial problems in the plane
[AD-A149320] 10 p1552 N85-19788
Multi-sample cluster analysis as an alternative to multiple comparison procedures
[AD-A149960] 12 p1923 N85-22084
Introduction to combinatorial geometry
[DE85-003266] 13 p2152 N85-23364
Probalistic analysis of combinatorial algorithms: An annotated bibliography
[CWI-OS-R8411] 14 p2411 N85-24864
Signal flow model for sequential logic built from combinational logic elements and its implementation in Prolog
[DE85-005792] 15 p2549 N85-25734
Combinatorial performance/cost analysis of an autonomous navigation system for aircraft
16 p2695 N85-26640
Routing algorithms and stochastic analysis for large communications networks
[AD-A154654] 21 p3573 N85-32225

COMBINED CYCLE POWER GENERATION
High pressure combustion test facility for gas turbine research
[NAL-TR-801] 06 p0757 N85-14845
Low leakage turbine shaft seals for advanced combined cycle systems
[AD-A149372] 10 p1492 N85-19420

COMBINED STRESS
Fatigue strength of alpha-titanium alloys under cophasal action of variable normal and tangential stresses
15 p2498 N85-25407

COMBUSTIBILITY
U FLAMMABILITY

COMBUSTIBLE FLOW
Combustion hot section technology
02 p0145 N85-10981
Aerothermal modeling 02 p0145 N85-10982
Aerothermal modeling program
02 p0145 N85-10983
Dilution zone mixing studies 02 p0145 N85-10984
Linear long-wave stability of cylindrical steady laminar flame in rotating medium 02 p0268 N85-11752
Fundamental study of three dimensional two phase flow in combustion systems
[AD-A142886] 04 p0498 N85-13177
Basic instability mechanisms in chemically reacting subsonic and supersonic flows
[AD-A148408] 08 p1122 N85-17071
Burner stabilized flames in fluids
[DE84-017429] 09 p1291 N85-18109
1984 AFOSR Research Meeting on Diagnostics of Reacting Flow held at New Haven, Connecticut on 21-22 March 1984
[AD-A149023] 10 p1484 N85-19387
Mixing chemical reaction and flow field development in ducted rockets
[DE85-002710] 11 p1591 N85-20009
The mechanisms of flame holding in the wake of a bluff body
[NASA-CR-3868] 12 p1779 N85-21186
Investigation of flowfields found in typical combustor geometries
[NASA-CR-3869] 12 p1779 N85-21187
Development of a three-phrase combustion code for modeling liquid rocket engines 13 p2003 N85-22554
Fundamental study of three dimensional two phase flow in combustion systems
[AD-A150739] 14 p2250 N85-23945
Investigation of the choking effect of an inert granular bed on an ignition gas jet charged with particles
[ISL-CO-235/83] 14 p2264 N85-24028
Unsteady flows in a tube with combustion reaction
[ISL-R-118/83] 14 p2303 N85-24261
Error reduction program — combustor performance evaluation codes
[NASA-CR-174776] 16 p2852 N85-27584
Mechanisms of exhaust pollutants and plume formation in continuous combustion
[AD-A154169] 20 p3435 N85-31310
Sandia Cooperative Group on the Aerothermochemistry of Turbulent Combustion. Discussion record of the second meeting
[DE85-007493] 22 p3743 N85-33203
Pressure correlations in turbulent reacting flows
22 p3744 N85-33205
Nonequilibrium chemistry in an isothermal turbulent flow 22 p3745 N85-33211
Modeling of turbulent recirculating combusting flows
22 p3745 N85-33212

COMBUSTION
NT AFTERBURNING
NT DEFLAGRATION
NT EROSIVE BURNING
NT FUEL COMBUSTION
NT HYDROCARBON COMBUSTION
NT METAL COMBUSTION
NT PROPELLANT COMBUSTION
NT SOLID PROPELLANT COMBUSTION
NT SOLID PROPELLANT IGNITION
NT SPONTANEOUS COMBUSTION
Variable inlet vane assembly for a gas turbine combustion
[AD-D011220] 01 p0010 N85-10063
CREKID: A computer code for transient, gas-phase combustion of kinetics
[NASA-TM-83806] 01 p0011 N85-10068
Investigation of the CARS spectrum of carbon monoxide at high pressure and temperature
[AD-A144816] 01 p0024 N85-10146
Turbine Engine Hot Section Technology (HOST)
[NASA-TM-83022] 02 p0140 N85-10951
Laser spectroscopy of combustion intermediates
[DE84-016101] 02 p0173 N85-11161
Gas dynamics of combustion of gas-air mixture in semi-closed space with relief of pressure into gasless adjacent space 02 p0260 N85-11699
Analysis and simulation of the I C engine Otto cycle using the second law of thermodynamics
02 p0291 N85-11891
Thrust characterization of very high burning rate propellants
[AD-A145891] 03 p0340 N85-12186
Studies of ignition and combustion wave propagation in exothermic systems using high-speed photography
[DE84-016482] 04 p0471 N85-12995
Study of combustion and flame processes initiated by laser-induced multiple-photon absorption
[DE84-017095] 04 p0471 N85-12996

New integration techniques for chemical kinetic rate equations. 2: Accuracy comparison
[NASA-TM-86893] 05 p0596 N85-13798

Biomass thermochemical conversion program
[DE84-017177] 05 p0621 N85-13972

Procedural aspects of testing aerodynamic models with combustion in high-enthalpy transient-mode installations
05 p0725 N85-14658

High pressure combustion test facility for gas turbine research
[NAL-TR-801] 06 p0757 N85-14845

Analysis of physical-chemical processes governing SSME internal fluid flows
[NASA-CR-174245] 06 p0760 N85-14862

USSR report: Chemistry
[JPRS-UCH-84-012] 06 p0761 N85-14865

Integrating chemical kinetic rate equations by selective use of stiff and nonstiff methods
[NASA-TM-86923] 07 p0904 N85-15726

The structure of dilute combusting sprays
[NASA-CR-174838] 07 p0905 N85-15728

The two-fluid model of turbulence applied to combustion phenomena
[CFD/84/15] 08 p1124 N85-17089

Closed vessel combustion of stick propellant
[AD-A147802] 08 p1135 N85-17154

Comparative usefulness of flue gas oxygen and carbon dioxide analysis
[BLL-TRANS-T6358/BG/WH783/84]
08 p1179 N85-17430

High pressure combustion test facility for gas turbine research
[NAL-TR-801] 09 p1283 N85-18065

Combustion driven oscillation of ducted diffusion flame
09 p1289 N85-18094

Swirling turbulent spray group combustion
08 p1289 N85-18095

Pressure measurements in a hydrogen combustion environment: An evaluation of 3 pressure transducers
[TI85-003645] 09 p1323 N85-18312

Theoretical studies of the ignition and combustion of silane-hydrogen-air mixtures
[NASA-CR-3876] 10 p1433 N85-19032

Investigation on the burning of unpulverized coal in a self excited acoustic field
[INPE-3295-PRE/610] 10 p1434 N85-19035

Infrared thermography of burn front propagation in heat powders
[DE85-003307] 10 p1438 N85-19060

Thermal profiles of thermite reactions
[DE85-003308] 10 p1438 N85-19061

Capabilities of laser diagnostics for combustion and flow fields
[DE85-002661] 10 p1438 N85-19064

Laser-intiated combustion studies on metallic alloys in pressurized oxygen
[PB85-128114] 10 p1438 N85-19066

Recovery of damaged solid propellants by interrupting burning and crack-propagation processes
[AD-P004343] 10 p1455 N85-19167

Dynamical studies of molecular systems
[DE85-003053] 11 p1594 N85-20028

Research in nonlinear problems of energy: Informal technical report
[DE85-001529] 11 p1595 N85-20031

Combustion gas properties. 2: Natural gas fuel and dry air
[NASA-TP-2435] 12 p1779 N85-21168

Atmospheric dispersion of hypergolic liquid rocket fuels, volume 1
[AD-A149597] 12 p1817 N85-21399

Size and velocity distributions of particles and droplets in spray combustion systems
[AD-A150355] 13 p2017 N85-22648

A comprehensive review of black powder
[AD-A150455] 13 p2039 N85-22769

Fundamental study of three dimensional two phase flow in combustion systems
[AD-A150739] 14 p2250 N85-23945

Non-steady combustion of composite solid propellants
[AD-A150827] 14 p2250 N85-23947

Model of normal and erosive burning of composite propellants
[ONERA-NT-1984-3] 14 p2263 N85-24024

Ignition of metals in high pressure oxygen
16 p2735 N85-26874

Ignition/combustion processes
16 p2740 N85-26909

Laser Schlieren and ultraviolet diagnostics of rocket combustion 16 p2740 N85-26911

Combustion and micro-explosion of water/oil emulsions in high pressure environments
[AD-A152960] 17 p2919 N85-27997

Photochemical ignition studies. 1: Laser ignition of flowing premixed gases
[AD-A153048] 17 p2920 N85-28002

Elementary reactions of importance in oxidation, combustion ignition and flame inhibitions
[AD-A153139] 17 p2921 N85-28004

Fuel rich catalytic comustion: The first stage of a two-stage combustor
[NASA-TM-87042] 18 p3069 N85-28983

Synthesis chemistry of ceramics by solid-state combustion processes in micro-gravity
[DE85-009595] 18 p3081 N85-29061

Measurement of radical species concentrations and polycyclic aromatic hydrocarbons in flames by fluorescence and absorption using a tunable dye laser
[DE85-008624] 18 p3113 N85-29274

Chemical-acoustic interactions in combustion systems
[AD-A153857] 19 p3233 N85-30046

Measurement of combustion species by electron impact fluorescence
[DE85-011163] 19 p3236 N85-30065

The acoustic mode in numerical calculations of subsonic combustion
[DE85-010788] 19 p3237 N85-30066

Theoretical studies of combustion chemistry
[DE85-010284] 19 p3237 N85-30069

Study of the explosive combustion of drops of sulphur at high temperatures
[HSE-TRANS-11182] 19 p3252 N85-30163

Explosibility of ammonium nitrate
[HSE-TRANS-11111] 19 p3252 N85-30164

LDA study of the unburned gas motion induced by nonsteady flame propagation in a constant volume duct
[DE85-009938] 19 p3270 N85-30277

Experimental determination of the mixing frequency parameter for coalescence/dispersion modeling of turbulent combustion
[DE85-011468] 19 p3270 N85-30280

Applied Science Division's Environmental Research Program
[DE85-010637] 19 p3308 N85-30510

Combustion gas properties. Part 3: Hydrogen gas fuel and dry air
[NASA-TP-2477] 20 p3395 N85-31056

Laminar diffusion flames, carbon gasification, and laser diagnostics applied to combustion systems. 1: Laminar diffusion flames with cylindrical symmetry. 2: Diffusion-controlled gasification of carbon particles. 3: Laser diagnostics applied to combustion systems
20 p3423 N85-31243

Radiative augmented combustion
[AD-A154137] 20 p3423 N85-31246

Sandia Cooperative Group on the Aerothermochemistry of Turbulent Combustion. Discussion record of fourth meeting
[DE85-004720] 20 p3423 N85-31248

Intermittency, conditional sampling and turbulent combustion 20 p3424 N85-31249

Mechanisms of exhaust pollutants and plume formation in continuous combustion
[AD-A154169] 20 p3435 N85-31310

Mechanistic and kinetic studies of the elementary processes in catalytic combustion of methane
[PB85-188308] 20 p3435 N85-31314

Elementary processes in the catalytic combustion of methane (mechanism, intermediates, and controlling reactions)
[PB85-188357] 20 p3436 N85-31316

Sandia Cooperative Group on the Aerothermochemistry of Turbulent Combustion
[DE85-004720] 20 p3455 N85-31453

Sandia Cooperative Group on the Aerothermochemistry of Turbulent Combustion
[DE85-007493] 20 p3455 N85-31454

PHOENICS 84: A multi-dimensional multi-phase general-purpose computer simulator for fluid flow, heat transfer and combustion: 36 lecture panels
[CFD/84/18] 20 p3457 N85-31468

Aerosol analysis and emission spectrometry with free jets
[DE85-010576] 21 p3564 N85-32168

Biomass thermochemical conversion program
[DE85-011867] 21 p3572 N85-32213

In-cavity laser IR spectrum analyzer for investigating non-steady-state processes 21 p3685 N85-32894

Comments on two matters related to turbulent combustion 22 p3743 N85-33204

Turbulent mixing and combustion
22 p3744 N85-33207

Jet flows: Modelling and experiments
22 p3744 N85-33208

Simultaneous measurement of velocity and density in a turbulent nonpremixed flame 22 p3744 N85-33209

Vortex dynamics simulation of conserved scalar dissipation 22 p3745 N85-33210

Combustion-deflagration-detonation transition in a confined spherical powder
[ISL-R-108/84] 22 p3747 N85-33223

Superheated fuel injection for combustion of liquid-solid slurries
[DE85-011624] 22 p3753 N85-33266

Development of a prototype energy meter
[PB85-198430] 22 p3789 N85-33476

Multiparameter conditionally sampled laser velocimetry measurements during flame propagation in a spark ignition engine
[DE85-009850] 22 p3793 N85-33502

Description of a test site for large-scale heavy gas dispersion and combustion experiments
[DE85-004987] 23 p3911 N85-34231

The application of models to the assessment of fire hazard from consumer products
[NBSIR-85-3219] 23 p3925 N85-34325

Upgrading auxiliary facility outleakage and combustion detection
[DE85-012796] 23 p3934 N85-34386

Pressure measurements in a hydrogen combustion environment: Hydrogen-air combustion test series 1 and 2 in the FITS tank, volume 1
[TI85-009899] 24 p4076 N85-35259

Laser probes of natural gas ignition chemistry
[PB85-200210] 24 p4077 N85-35264

An analytical and numerical model of radiation heat transfer in direct injection-type diesel combustion
24 p4092 N85-35368

Review of US NOx abatement technology
[PB85-193522] 24 p4114 N85-35501

COMBUSTION CHAMBERS

Variable inlet vane assembly for a gas turbine combustion
[AD-D011220] 01 p0010 N85-10063

Columbium chamber fabrication study
[AD-A145230] 01 p0017 N85-10102

Turbine Engine Hot Section Technology (HOST)
[NASA-TM-83022] 02 p0140 N85-10951

Nonlinear structural and life analyses of a combustor liner 02 p0141 N85-10955

Dynamic gas temperature measurement system
02 p0141 N85-10958

Effects of surface chemistry on hot corrosion life: Overview 02 p0145 N85-10980

Combustion hot section technology
02 p0145 N85-10981

Aerothermal modeling 02 p0145 N85-10982

Aerothermal modeling program
02 p0145 N85-10983

Dilution zone mixing studies 02 p0145 N85-10984

Combustion system for radiation investigations
02 p0145 N85-10986

Validation of structural analysis methods using the in-house liner cyclic rigs 02 p0146 N85-10987

Energy efficient engine component development and integration program
[NASA-CR-170034] 02 p0146 N85-10990

Alternate fuels combustion research
[AD-A145691] 02 p0188 N85-11258

Methane heat transfer investigation
[NASA-CR-171199] 03 p0362 N85-12318

Back end valves: History and modifications
[DE84-009272] 05 p0646 N85-14145

Design of swirled axisymmetric turbulent jets
05 p0724 N85-14657

Combined cycle ramjet engine
[AD-D011247] 06 p0760 N85-14859

The structure of dilute combusting sprays
[NASA-CR-174838] 07 p0905 N85-15728

Verification of life prediction through component testing 07 p0906 N85-15748

Integral boost, heat protection, port covers and transition 07 p0918 N85-15813

Combustion chamber floatwall panel attachment arrangement
[AD-D011358] 07 p1047 N85-16647

Design evolution of the orbiter reaction control subsystem 08 p1099 N85-16944

Advanced OTV engine concepts
08 p1108 N85-17001

Rayleigh and Raman scattering for density in a swirling flow combustor 08 p1120 N85-17060

A study of air breathing rockets. Part 4: Direct fuel injection into a secondary combustor
[NAL-TR-832] 09 p1287 N85-18083

Analysis of sudden expansion flow in a two-dimensional duct with and without side-wall injection using the k-epsilon turbulence model 09 p1317 N85-18282

SSME thrust chamber simulation using Navier-Stokes equations
[NASA-CR-171349] 10 p1430 N85-19017

Investigation on the burning of unpulverized coal in a self excited acoustic field
[INPE-3295-PRE/610] 10 p1434 N85-19035

Analytical fuel property effects: Small combustors, phase 2
[NASA-CR-174848] 10 p1456 N85-19175

Preliminary analysis of selected gas dynamic problems — space shuttle main engine main combustion transients and IUS nozzle flow
[NASA-CR-171343] 10 p1483 N85-19361

Low loss injector for liquid propellant rocket engines
[NASA-CASE-MFG-25989-1] 11 p1591 N85-20008

A new method for calculating the flow field in a dump combustor
[AD-A149305] 11 p1631 N85-20271

Experimental investigation of a pulse combustor: Flow visualization by Schlieren photography
[DE85-002862] 11 p1636 N85-20304

Advanced liner-cooling techniques for gas turbine combustors
[NASA-TM-86952] 12 p1770 N85-21115

Combustion research for gas turbine engines
[NASA-TM-86963] 12 p1778 N85-21164

Investigation of flowfields found in typical combustor geometries
[NASA-CR-3869] 12 p1779 N85-21167

On the coupling of an anchored flame with an acoustic field
[COLL-AERON-8434] 12 p1799 N85-21282

Deflected jet experiments in a turbulent combustor flowfield
[NASA-CR-174863] 13 p1973 N85-22390

Dilution jet configurations in a reverse flow combustor
[NASA-CR-174888] 13 p1974 N85-22392

Nonlinear interactions between vortices and acoustic waves in a rocket combustion chamber
13 p1999 N85-22533

Exergetical analysis of turbojet engine cycle
13 p2049 N85-22825

Fundamental study of three dimensional two phase flow in combustion systems
[AD-A150739] 14 p2250 N85-23945

Application of laser anemometry to jets in combustion chambers
[ISL-CO-210/83] 14 p2302 N85-24253

Hypergolic combustion demonstration in a reciprocating internal combustion engine
[AD-A150846] 14 p2311 N85-24303

Small gas turbine combustor study: Fuel injector performance in a transpiration-cooled liner
[NASA-TM-86989] 15 p2473 N85-25264

Experiments in dilution jet mixing effects of multiple rows and non-circular orifices
[NASA-TM-86996] 15 p2473 N85-25266

The effect of air holes on combustor liner wall temperature profile: Experiments
[NAL-TR-840] 15 p2504 N85-25443

An experimental investigation of confined, multiple, turbulent jet mixing with recirculation -- flow distribution in combustors with injection plates
15 p2555 N85-25764

Large-scale commercial combustion systems for producing energy from municipal solid waste
[DE85-007097] 15 p2587 N85-25946

Analytical fuel property effects--small combustors
[NASA-CR-174738] 16 p2708 N85-26709

Turbulence characteristics of swirling flowfields
[NASA-CR-174918] 16 p2709 N85-26717

Study of the primary zone of gas turbine hearths
[ONERA-RTS-22/3256-EY] 16 p2709 N85-26719

Advanced High Pressure O2/H2 Technology
[NASA-CP-2372] 16 p2733 N85-26862

Thrust chamber life prediction
16 p2733 N85-26865

Rocket thrust chamber thermal barrier coatings
16 p2734 N85-26867

Liquid rocket combustor computer code development
16 p2740 N85-26910

Laser Schlieren and ultraviolet diagnostics of rocket combustion 16 p2740 N85-26911

Solid fuel combustion chamber
[VTH-LR-415] 16 p2741 N85-26918

Solid fuel combustion chamber
[VTH-LR-438] 16 p2741 N85-26919

Solid fuel combustion chamber research in the Netherlands
[VTH-LR-444] 16 p2742 N85-26920

Design of a Mobile Combustion Diagnostic Fixture (MCDF)
[AD-A151814] 16 p2745 N85-26941

Error reduction program — combustor performance evaluation codes
[NASA-CR-174776] 16 p2852 N85-27584

Segmented zoned fuel injection system for use with a combustor
[AD-D011640] 17 p2897 N85-27865

Predictions and measurements of isothermal flowfields in axisymmetric combustor geometries
[NASA-CR-174916] 17 p2898 N85-27867

The role of surface generated radicals in catalytic combustion 17 p2898 N85-27869

Future fundamental combustion research for aeropropulsion systems
[NASA-TM-87049] 17 p2898 N85-27870

Reaction-bonded and fiber-reinforced SiC static and dynamic gas turbine components
[BMFT-FB-T-84-302] 17 p2899 N85-27874

Polynomial approaches for the characteristic velocity and flame temperature as a function of mixing compounding and pressure for the systems PMMA/O2, PMMA/air, PE/O2, PE/air, PS/O2 and PS/air
[VTH-LR-421] 17 p2924 N85-28024

Multi-ducted inlet combustor research and development
[AD-A153753] 18 p3063 N85-28946

Fuel rich catalytic comustion: The first stage of a two-stage combustor
[NASA-TM-87042] 18 p3069 N85-28983

Research test facility for evaporation and combustion of alternative jet fuels at high air temperatures
[AD-A153830] 18 p3083 N85-29073

Time-averaged and time-dependent computations of isothermal flowfields in a centerbody combustor
[AD-A153682] 18 p3100 N85-29169

Technical instructions for a control operating system of the gas flow installation for the solid fuel combustion chamber
[VTH-LR-410] 18 p3118 N85-29302

Computer program for the control/operating system of the gas flow installation for the solid fuel combustion chamber
[VTH-LR-430] 18 p3165 N85-29605

A model for the combustion of polymethyl methacrylate in air in a laminar diffusion flame
[VTH-LR-439] 18 p3165 N85-29606

The effect of surface reactions in catalytic combustion
[AD-A154217] 19 p3234 N85-30049

Radiative augmented combustion
[AD-A154137] 20 p3423 N85-31246

Application of the Diffusion Raman Anti-Stokes Coherent (DRASC) method to a SNECMA combustion chamber
[YKC-3086/84] 20 p3425 N85-31260

Mechanisms of exhaust pollutants and plume formation in continuous combustion
[AD-A154169] 20 p3435 N85-31310

An experimental investigation of confined, multiple, turbulent jet mixing with recirculation
20 p3451 N85-31426

Combustor turbulence 20 p3452 N85-31434

R and D activities of the Propulsion Division
20 p3539 N85-32025

Carbon/carbon combustor external insulation
[AD-D011719] 23 p3910 N85-34224

Numerical model of a pulse combustor
[DE85-011717] 23 p3912 N85-34240

Investigation of non-intrusive radiometers for entrained gasifier temperature measurement, revision 3
[DE85-011795] 23 p3934 N85-34385

Flow modifying device
[NASA-CASE-LEW-13562-2] 24 p4065 N85-35195

Basic research on pulse-combustion phenomena
[PB85-200228] 24 p4077 N85-35265

Development of advanced high-temperature heat flux sensors. Phase 2: Verification testing
[NASA-CR-174973] 24 p4098 N85-35391

COMBUSTION CONTROL

Energy efficient engine combustor test hardware detailed design report
[NASA-CR-167945] 02 p0140 N85-10950

The mechanisms of flame holding in the wake of a bluff body
[NASA-CR-174058] 02 p0172 N85-11149

The detonation of aerosols and vapors of combustible substances under controlled conditions. Part 1: Construction of a test installation
[ISL-R-109/83-PT-1] 14 p2254 N85-23966

Nonintrusive shaft speed sensor
16 p2740 N85-26908

On the low temperature chemistry preceding end gas autoignition
[DE85-010471] 19 p3252 N85-30162

Combustion control with smart sensors
[DE85-009419] 19 p3274 N85-30303

Reduction of pollutant formation in combustion processes
[DE85-010181] 19 p3309 N85-30512

COMBUSTION EFFICIENCY

Comparison of numerical techniques for integration of stiff ordinary differential equations arising in combustion chemistry
[NASA-TP-2372] 01 p0011 N85-10065

Combustion modeling of a 2 cylinder cycle reciprocating engine
[AD-A144782] 01 p0055 N85-10364

An interactive computer code for calculation of gas-phase chemical equilibrium (EQLBRM)
[NASA-CR-168337] 02 p0140 N85-10948

The mechanisms of flame holding in the wake of a bluff body
[NASA-CR-174058] 02 p0172 N85-11149

Speed governor for diesel engine
09 p1307 N85-18214

Investigation on the burning of unpulverized coal in a self excited acoustic field
[INPE-3295-PRE/610] 10 p1434 N85-19035

Study of HTPB-based SOFRAM fuels
[FOA-C-20563-D3] 11 p1614 N85-20150

The influence of fuel quality upon flame-tube temperature and flame radiation in a model gas-turbine primary zone
[K233] 13 p1974 N85-22396

Dependence of combustion of homogeneous kerosene-air mixtures on humidity of air
13 p2051 N85-22835

A fundamental study of liquid phase particle breakup. Revision
[AD-A150791] 14 p2301 N85-24249

Shock tube study of the fuel structure effects on the chemical kinetic mechanisms responsible for soot formation, part 2
[NASA-CR-174860] 15 p2504 N85-25444

Influence of fuel properties on gas turbine combustion performance
[AD-A151464] 15 p2504 N85-25448

PSA, Renault work on all fuel automobile engine
15 p2531 N85-25604

The role of surface generated radicals in catalytic combustion 17 p2898 N85-27869

SSME fuel preburner two-dimensional analysis
17 p2911 N85-27943

Coal-Fired MHD Combustor Development Project, Phase 3D
[DE85-008822] 18 p3192 N85-29795

Combustion characterization of coals for industrial applications
[DE85-010673] 19 p3228 N85-30014

A mathematical model of reciprocating combustion engine dynamics for the diagnosis of deficient energy conversion 19 p3280 N85-30339

Closed-bomb combustion of Hivelite-based, Very High Burn Rate (VHBR) propellant
[AD-A155740] 21 p3571 N85-32212

Effect of precipitation variables on the specific surface and explosion characteristics of pentaerythritol tetranitrate
[DE85-009620] 23 p3922 N85-34302

COMBUSTION INSTABILITY
U COMBUSTION STABILITY

COMBUSTION PHYSICS

Combustion hot section technology
02 p0145 N85-10981

Aerothermal modeling 02 p0145 N85-10982

Aerothermal modeling program
02 p0145 N85-10983

Gravitational effects on premixed particle cloud flames
02 p0171 N85-11144

The mechanisms of flame holding in the wake of a bluff body
[NASA-CR-174058] 02 p0172 N85-11149

Dynamics of burnout of solid fuel in fluidized bed of finely divided inert particles 02 p0273 N85-11782

Combustion and detonation of hydrogen-air mixture in free spaces 02 p0274 N85-11783

Limiting effects during turbulent combustion
02 p0274 N85-11784

Diffusive combustion of fluids with free surface
02 p0274 N85-11785

Combustion kinetics of metal oxide and halide radicals
[AD-A148521] 08 p1122 N85-17076

The two-fluid model of turbulence applied to combustion phenomena
[CFD/84/15] 08 p1124 N85-17089

Investigation on the burning of unpulverized coal in a self excited acoustic field
[INPE-3295-PRE/610] 10 p1434 N85-19035

Mixing chemical reaction and flow field development in ducted rockets
[DE85-002710] 11 p1591 N85-20009

A comparison of the efficiency of numerical methods for integrating chemical kinetic rate equations
[NASA-TM-83590] 12 p1778 N85-21182

Gasification of boron oxide drops and boron slurry agglomerates in combustion gases
13 p1999 N85-22529

Comprehensive mechanisms for combustion chemistry. An experimental and numerical study with emphasis on applied sensitivity analysis
[DE85-000173] 13 p2018 N85-22656

Combustion kinetics of metal oxide and halide radicals
[AD-A150924] 14 p2251 N85-23952

Asymptotic methods especially in combustion
[AD-A151505] 15 p2505 N85-25450

Solid fuel combustion chamber
[VTH-LR-415] 16 p2741 N85-26918
Solid fuel combustion chamber
[VTH-LR-438] 16 p2741 N85-26919
A model for the combustion of polymethyl methacrylate in air in a laminar diffusion flame
[VTH-LR-439] 18 p3165 N85-29606
Measurement of combustion species by electron impact fluorescence
[DE85-011163] 19 p3236 N85-30065
Sandia Cooperative Group on the Aerothermochemistry of Turbulent Combustion. Discussion record of the second meeting
[DE85-007493] 22 p3743 N85-33203
Second order modelling in non-constant density flows
22 p3744 N85-33206
Behavior of the porous bed in a combustion-deflagration-detonation transition
[ISL-CO-220/84] 22 p3747 N85-33224
Combustion-deflagration-detonation transition
[ISL-CO-221/84] 22 p3747 N85-33225

COMBUSTION PRODUCTS
Combustion gas properties I-ASTM jet A fuel and dry air
[NASA-TP-2359] 01 p0010 N85-10064
HMX combustion modification
[AD-A145071] 01 p0024 N85-10149
Size specific total particulate emission factors for mobile sources
[PB84-226653] 01 p0071 N85-10471
Clean-burning diesel engines
[AD-A145515] 02 p0205 N85-11349
Dissociated methanol vehicle test results
[DE84-004507] 04 p0509 N85-13248
Mechanism of soot formation
[AD-A146817] 07 p0922 N85-15841
Heater block assembly for use in thermal oxidation testing of jet fuel
[AD-D011430] 08 p1123 N85-17077
Ceramic fabric material testing
[DE84-012014] 09 p1300 N85-18165
Atmospheric science and power production
[DE84-005177] 09 p1354 N85-18521
Study of deposition control using transpiration
[DE85-002339] 10 p1465 N85-19378
Study of deposition control using transpiration
[DE85-003463] 11 p1585 N85-19984
Combustion gas properties. 2: Natural gas fuel and dry air
[NASA-TP-2435] 12 p1779 N85-21168
Kinetics of nitric oxide formation in laminar and turbulent methane combustion
[PB85-149698] 12 p1804 N85-21313
Digital temperature and velocity control of mach 0.3 atmospheric pressure durability testing burner rigs in long time, unattended cyclic testing
[NASA-TM-86959] 12 p1805 N85-21321
Determination of toxicity of combustion products of habitability foams concurrently with flammability studies of these materials
[AD-A149647] 12 p1905 N85-21961
Experimental investigations of thermal radiation from potassium atoms in magnetohydrodynamic system: Preliminary report
[DE85-003715] 12 p1936 N85-22169
Solid propellant combustion diagnostics and automated data retrieval from holograms 13 p1996 N85-22527
Picosecond lidar techniques in laboratory and field diagnostics
[AD-A150755] 14 p2309 N85-24294
Transformation of nitrogen oxides while sampling combustion products
[AD-A152184] 16 p2746 N85-26945
Analytical methods for determination of POHC (Principal Organic Hazardous Constituents) in combustion products
[PB85-161578] 16 p2747 N85-26955
The remote detection of polynuclear aromatic hydrocarbons using laser-induced fluorescence
[AD-A152294] 16 p2757 N85-27013
Jet fuel instability mechanisms
[NASA-CR-175856] 17 p2936 N85-28127
Equation of state for detonation products
[DE85-009608] 18 p3084 N85-29079
Changes of structure of EP648-VI alloy as a result of high-temperature gas corrosion
19 p3243 N85-30110
Flow field effects on nucleation in a reacting mixing layer
[ARL/AERO-R-165] 19 p3263 N85-30237
Fuel-rich catalytic combustion: A soot-free technique for in situ hydrogen-like enrichment
[NASA-TP-2496] 20 p3423 N85-31244
Polyesters: A review of the literature on products of combustion and toxicity
[NBSIR-85-3139] 20 p3433 N85-31298
Toxic hazards tests for vehicles and other equipment
[AD-A149164] 20 p3506 N85-31797
Ice nucleating characteristics of Capparis Aphylla, an Indian herb 21 p3641 N85-32619
System for the continuous generation of phosphorous aerosols from red phosphorus-butyl rubber
[DE85-013527] 24 p4072 N85-35232
Proceedings of the 7th Joint Panel Meeting of the UJNR Panel on Fire Research and Safety
[PB85-199545] 24 p4085 N85-35317
Fire research publications, 1984
[PB85-208502] 24 p4166 N85-35827

COMBUSTION STABILITY
NT FLAME STABILITY
An experimental investigation of combustion pressure oscillations in solid fuel ramjets
[AD-A144870] 01 p0024 N85-10147
Chemistry of fuel deposits and sediments and their predursors
[NASA-CR-174778] 01 p0034 N85-10209
Combustion dynamics in rockets
[AD-A148478] 08 p1114 N85-17024
Basic instability mechanisms in chemically reacting subsonic and supersonic flows
[AD-A148408] 08 p1122 N85-17071
Proceedings of the AFOSR/AFRPL Rocket Propulsion Research Meeting: Abstracts and Agenda
[AD-A148818] 09 p1288 N85-18085
Radiation/catalytic augmented combustion
[AD-A148758] 09 p1290 N85-18101
Burner stabilized flames in fluids
[DE84-017429] 09 p1291 N85-18109
Numerical simulations of liquid propellant combustion instability: Onset and growth
[DE85-000743] 10 p1458 N85-19186
An investigation of space shuttle main engine shutdown chugging instability 12 p1946 N85-22221
Twenty-first JANNAF Combustion Meeting, volume 1
[AD-A150981] 13 p1998 N85-22526
Coupling between velocity oscillations and solid propellant combustion 13 p2000 N85-22536
Acoustic energy balance method
13 p2000 N85-22537
Coupled acoustic and hydrodynamic wave instabilities
13 p2000 N85-22538
Characterization of heterogeneity of composite propellants and its effects on combustion behavior
13 p2000 N85-22539
Investigation of the characteristics of the velocity-coupled response functions of solid propellants
13 p2001 N85-22540
Comparisons of solid propellant with instability predictions and motor firing experience
13 p2001 N85-22541
Measurements of distributed combustion
13 p2001 N85-22542
Distributed combustion: A mechanism of acoustic suppression 13 p2001 N85-22543
Workshop report: Catalysis of Burn Rate of Energetic Binder propellants 13 p2001 N85-22545
An integral closed loop combustion stability model-status and review 13 p2003 N85-22553
Transient combustion dynamics
[AD-A154430] 19 p3235 N85-30052
The acoustic mode in numerical calculations of subsonic combustion
[DE85-010788] 19 p3237 N85-30066
Combustor turbulence 20 p3452 N85-31434
Status of boron combustion research
[AD-A154762] 21 p3563 N85-32160
Closed-bomb combustion of Hivelite-based, Very High Burn Rate (VHBR) propellant
[AD-A155740] 21 p3571 N85-32212

COMBUSTION TEMPERATURE
Application of atomic fluorescence to measurement of combustion temperature in solid propellants
[AD-A150733] 14 p2263 N85-24021
Nonintrusive shaft speed sensor
16 p2740 N85-26906
Combustion characterization of coals for industrial applications
[DE85-010673] 19 p3228 N85-30014

COMBUSTION VIBRATION
An investigation of space shuttle main engine shutdown chugging instability 12 p1946 N85-22221

COMBUSTION WAVES
U FLAME PROPAGATION

COMBUSTORS
U COMBUSTION CHAMBERS

COMET NUCLEI
Giacobini-Zinner comet: Polarimetric and physical observations
[NASA-TM-77771] 01 p0130 N85-10894
Implications of the presence of S2 in cometary ice
11 p1760 N85-21072
The international VEGA 'Venus-Halley' (1984-1986 experiment: Description and scientific objectives
[NASA-TM-77536] 12 p1960 N85-22324
Studies of icy bodies: Uranian satellites and cometary nuclei 13 p2175 N85-23496
Surfaces of asteroids and cometary nuclei
13 p2176 N85-23503
An idealized short period comet model: Surface insolation, H2O flux, dust flux and mantle evolution
13 p2176 N85-23504
Comet thermal modeling 13 p2176 N85-23505
Dynamics of long-period comets
13 p2176 N85-23506
Halley's Comet, a bibliography
[LC-84-600109] 13 p2204 N85-23674
Current ideas on the nature of comets
14 p2435 N85-25017
Dust emission of Comet Halley at large heliocentric distances 15 p2681 N85-26556

COMET TAILS
Halley's Comet, a bibliography
[LC-84-600109] 13 p2204 N85-23674
Current ideas on the nature of comets
14 p2435 N85-25017
Occultations of stars and radio sources by comets: Predictions and observing prospects
14 p2437 N85-25034
Dust emission of Comet Halley at large heliocentric distances 15 p2681 N85-26556
Comet Halley returns: A teachers' guide 1985-1986
[NASA-EP-197] 24 p4168 N85-35839

COMETARY ATMOSPHERES
Outer satellite atmospheres: Their nature and planetary interactions
[NASA-CR-174146] 04 p0569 N85-13759
Studies of radiative transfer in planetary atmospheres
[NASA-CR-174194] 05 p0745 N85-14778
Extended atmospheres of outer planet satellites and comets
[NASA-CR-174336] 06 p1258 N85-17916
The fluorescence of cometary OH and CN
09 p1411 N85-18896
Extended atmospheres of outer planet satellites and comets
[NASA-CR-174398] 09 p1416 N85-18933
The essence of binary star coalescence: A coordinated ground-based photometric and IUE ultraviolet study of FK Comae 11 p1756 N85-21044
Observations of comets: Radio and otherwise — conference
[TB-64] 11 p1762 N85-21086
Cometary atmospheres: Modeling the spatial distribution of observed neutral radicals
[NASA-CR-175491] 11 p1765 N85-21097
Cometary atmospheres: Modeling the spatial distribution of observed neutral radicals
[NASA-CR-175485] 11 p1765 N85-21098
Averaging of equations of cometary orbital motion with allowance for nongravitational effects
13 p1978 N85-22411
An idealized short period comet model: Surface insolation, H2O flux, dust flux and mantle evolution
13 p2176 N85-23504
Comet thermal modeling 13 p2176 N85-23505
Dynamics of long-period comets
13 p2176 N85-23506
Halley's Comet, a bibliography
[LC-84-600109] 13 p2204 N85-23674
Current ideas on the nature of comets
14 p2435 N85-25017
Occultations of stars and radio sources by comets: Predictions and observing prospects
14 p2437 N85-25034
Astrometric needs for the ISEE-3/ICE mission to Comet Giocobini-Zinner 14 p2438 N85-25043
Extended atmospheres of outer planet satellites and comets
[NASA-CR-175673] 14 p2440 N85-25058
Magnetic field penetration into cometary ionosphere
15 p2477 N85-25290
Development of a global 3-D magnetohydrodynamic computational model for solar wind/cometary and planetary studies
[NASA-CR-175724] 15 p2684 N85-26577
Cometary atmospheres: Modeling the spatial distribution of observed neutral radicals
[NASA-CR-175852] 16 p2882 N85-27781
Cometary atmospheres: Modeling the spatial distribution of observed neutral radicals
[NASA-CR-175882] 17 p3054 N85-28904
The study of the physics of cometary nuclei
[NASA-CR-175917] 17 p3054 N85-28905
Extended atmospheres of outer planet satellites and comets
[NASA-CR-176137] 22 p3851 N85-33848

Comet Halley returns: A teachers' guide 1985-1986 [NASA-EP-197] 24 p4168 N85-35839

COMETS
NT COMET NUCLEI
NT COMET TAILS
NT ENCKE COMET
NT GIACOBINI-ZINNER COMET
NT HALLEY'S COMET
NT IRAS-ARAKI-ALCOCK COMET
Forbidden lines of oxygen in comet spectra 02 p0163 N85-11105
The significance of comets for star formation 03 p0443 N85-12824
Dust properties determined from backscattering in the interplanetary and interstellar medium 03 p0446 N85-12836
Sample return from a comet flyby 06 p0889 N85-15646
Airborne observations of comets 08 p1244 N85-17853
The geology of the terrestrial planets [NASA-SP-469] 09 p1410 N85-18888
Asteroids, comets and planet formation 09 p1410 N85-18889
Solar system studies with the IUE: 1982 - 1984 11 p1744 N85-20964
Observations of comets: Radio and otherwise — conference [TB-64] 11 p1762 N85-21086
Magnetospheres in the solar system 12 p1954 N85-22274
Study and estimation of planet-crossing asteroid populations: Discoveries and analysis 13 p2175 N85-23498
Cometary Astrometry [NASA-CR-175880] 14 p2435 N85-25015
Remarks on cometary astrometry 14 p2435 N85-25019
Cometary astrometry with Schmidt cameras 14 p2435 N85-25020
Astrometry of comets using hypersensitized type 2415 film 14 p2435 N85-25021
Astrometric plates obtained at the primary focus of large aperture reflectors 14 p2436 N85-25022
Problems and procedures of cometary astometry 14 p2436 N85-25024
Astometry at La Silla 14 p2436 N85-25025
Desired characteristics of catalogs for cometary astrometry 14 p2436 N85-25030
Comets and nongravitational forces 14 p2437 N85-25038
On the orbit improvement results obtained by referring old cometary observations to the SAO Star Catalog 14 p2438 N85-25042
Systematic and random deformations of orbits of long-period comets 15 p2479 N85-25299
Periodic cometary showers: Real or imaginary? 15 p2680 N85-26555
Mining cosmic dust from the blue ice lakes of Greenland 15 p2682 N85-26563
A search for evidence of large body Earth impacts associated with biological crisis zones in the fossil record 15 p2682 N85-26567
Comet showers and Nemesis, the death star [DE85-003736] 15 p2683 N85-26575
Radio observations of comet P/Crommelin [INPE-3480-PRE/723] 16 p2881 N85-27777
Study of the accuracy of astrometric observations of comets [ESA-CR(P)-1964] 17 p3054 N85-28903
Cometary atmospheres: Modeling the spatial distribution of observed neutral radicals [NASA-CR-175882] 17 p3054 N85-28904
The study of the physics of cometary nuclei [NASA-CR-175917] 17 p3054 N85-28905

COMFORT
Ride comfort of off-road vehicles [AD-P004279] 09 p1406 N85-18855
Comparison of measured and simulated ride comfort for an agricultural tractor and influence of travel speed and tyre-inflation pressure on dynamic response [AD-P004281] 09 p1407 N85-18857
Operator's functional comfort zone when controlling moving object 22 p3621 N85-33670

COMMAND AND CONTROL
Command control group behaviors. Objective 1: A methodology for and identification of command control group behaviors [AD-A145690] 02 p0191 N85-11279
Air Force Human Resources Laboratory report: Fiscal year, 1983 [AD-A145647] 02 p0238 N85-11548
A mathematical theory of command and control structures [AD-A145608] 02 p0256 N85-11675
An approach to interfacing data bases in WWMCCS ADP [AD-A146350] 03 p0439 N85-12793
A framework for research on adaptive decision aids [AD-A138331] 05 p0734 N85-14719
Human factors characteristics of the Joint Tactical Fusion Test Bed: Field test 467 results [AD-A146856] 07 p1020 N85-16476
Acquisition planning at the Defense Communications Agency [AD-A146877] 07 p1051 N85-16639
A simulator for determining the performance of transaction manager and lock manager combinations in a database [AD-A147827] 07 p1055 N85-16696
Defense Meteorological Satellite Program (DMSP) 11 p1711 N85-20766
Optimization of guidance and control using function minimization and NAVSTAR/GPS [AD-A149956] 12 p1775 N85-21141
The effect of jamming/deception on decision making [AD-A149740] 12 p1828 N85-21472
Space station systems technology study (add-on task). Volume 1: Executive summary [NASA-CR-171415] 13 p1986 N85-22459
Basic EMC (electromagnetic interference) technology advancement for c3 systems. Volume 3A: Probabilistic analysis of combinational circuits with random delays [AD-A150349] 13 p2055 N85-22866
Remote control of an impact demonstration vehicle [NASA-TM-85925] 14 p2225 N85-23797
Interference effects of vocalization on dual task performance [AD-A150687] 14 p2291 N85-24203
Basic EMC (Electromagnetic Compatibility) technology advancement for C3 systems: Model revision for IEMCAP (Intrasystem Electromagnetic Compatibility Analysis Program) [AD-A150795] 14 p2292 N85-24208
Research needs for artificial intelligence applications in support of C3 (Command, Control, and Communication) [AD-A150867] 14 p2292 N85-24210
Automated CPX support system preliminary design phase [NASA-CR-175784] 16 p2769 N85-27091
A study of error rates in voice recognition [AD-A153282] 17 p2949 N85-28211
Rome Development Center Air Force technical objective document C3I FY-86 [AD-A152476] 17 p3047 N85-28851
LAN (Local Area Network) interoperability study of protocols needed for distributed command and control [AD-A154033] 19 p3255 N85-30182
Study and realization of a command system adapted to space robotics [SNIAS-851-440-106] 22 p3740 N85-33183
Assured information flow capping architecture [AD-A155392] 22 p3756 N85-33283
TRICCS: A proposed teleoperator/robot integrated command and control system for space applications [NASA-TM-87577] 24 p4136 N85-35637

COMMAND GUIDANCE
Determining functional requirements for NASA Goddard's command management system software design using expert systems 20 p3539 N85-32020

COMMAND LANGUAGES
NT QUERY LANGUAGES
Construction of a menu-based system [NASA-CR-172560] 13 p2146 N85-23321

COMMAND SYSTEMS
U COMMAND GUIDANCE

COMMAND-CONTROL
U COMMAND AND CONTROL

COMMERCE
Foreign civil aviation competition: 1976 summary and implications [NASA-TM-X-73907] 02 p0133 N85-10907
Commercial space services 02 p0153 N85-11039
The Expendable Launch Vehicle Commercialization Act [GPO-30-838] 04 p0460 N85-12919
Power for commercial space applications 05 p0608 N85-13884
International airport study: How to improve the effect of airports on trade and on export-related industries [PB85-124923] 11 p1586 N85-19992
The 1981 transatlantic boat race contribution for marine meteorological measurements 14 p2324 N85-24361
Miscellaneous ARGOS maritime applications — yacht races 14 p2327 N85-24383
RESO: Expert system applied to company computer networks [ENST-84E016] 20 p3518 N85-31874
Spin-offs from technical commercial infrastructures, no. 2 20 p3540 N85-32035
New innovative businesses from industry. Experiences in the Netherlands in the successful transfer of technology from university to industry 22 p3849 N85-33843

COMMERCE LAB
Commerce Lab: Mission analysis payload integration study. Appendix A: Data bases [NASA-CR-176016] 19 p3224 N85-29988

COMMERCIAL AIRCRAFT
NT A-310 AIRCRAFT
NT A-320 AIRCRAFT
NT BOEING 727 AIRCRAFT
NT BOEING 737 AIRCRAFT
NT BOEING 747 AIRCRAFT
NT BOEING 767 AIRCRAFT
NT CV-990 AIRCRAFT
NT DC 8 AIRCRAFT
NT DC 9 AIRCRAFT
NT DC 10 AIRCRAFT
NT EUROPEAN AIRBUS
NT L-1011 AIRCRAFT
NT LEAR JET AIRCRAFT
Energy efficient engine component development and integration program [NASA-CR-170034] 02 p0146 N85-10990
USSR report: Transportation [JPRS-UTR-84-028] 03 p0310 N85-12002
Commercial aircraft noise [PNR-90206] 03 p0417 N85-12965
Aircraft navigation and landing technology: Status of implementation [GPO-38-615] 04 p0454 N85-12993
Airport activity statistics of certificated route air carriers [AD-A148472] 08 p1081 N85-16846
Design of a digital ride quality augmentation system for commuter aircraft [AD-A148233] 08 p1088 N85-16879
Use of airplanes for loft training 09 p1276 N85-18019
Study of advanced fuel system concepts for commercial aircraft and engines [NASA-CR-174752] 10 p1456 N85-19176
Study of advanced fuel system concepts for commercial aircraft [NASA-CR-174751] 11 p1584 N85-19978
Minister Bugayev on civil aviation in 1984, plans for 1985 14 p2208 N85-23689
Minister Bugayev reviews 1983 civil aviation work, sets course for 1984 14 p2208 N85-23695
Bugayev on civil aviation ministry's 1983 achievements 14 p2208 N85-23696
Ilyushin bureau designer on fuel conservation research 15 p2467 N85-25231
Calculation and display of stack departure times for aircraft inbound to Heathrow Airport [AD-A151991] 15 p2469 N85-25241
Demonstration of relaxed stability on a commercial transport 16 p2713 N85-26745
Realisation of relaxed static stability on a commercial transport 16 p2713 N85-26746
Demonstration of relaxed static stability on a commercial transport 17 p2903 N85-27888
Realisation of relaxed static stability on a commercial transport 17 p2903 N85-27889
Aircraft accident report: World Airways Inc., Flight 30H, McDonnell Douglas DC-10-30CF, N113WA, Boston-Logan International Airport, Boston, Massachusetts, January 23, 1982 [PB85-910406] 22 p3728 N85-33114
U.S. Civil airmen statistics for calendar year 1984 [AD-A156326] 24 p4059 N85-35153

COMMERCIAL AVIATION
U CIVIL AVIATION
U COMMERCIAL AIRCRAFT

COMMERCIAL ENERGY
Solar-gas systems impact analysis study [PB85-129088] 11 p1616 N85-20163

COMMERCIAL SPACECRAFT
The Ariane launch vehicle is the key of the Europeans to the space market 17 p2908 N85-27931
Commerce Lab: Mission analysis payload integration study. Appendix A: Data bases [NASA-CR-176016] 19 p3224 N85-29988
Insurance and the commercialization of space [S-PRT-99-16] 20 p3397 N85-31074

COMMINUTION
NT CRUSHING
NT GRINDING (COMMINUTION)
Grainsize evolution and differential comminution in an experimental regolith 06 p0888 N85-15638

COMMITTEE ON SPACE RESEARCH
Space research in Spain 08 p1231 N85-17751
Space research in Denmark 08 p1231 N85-17753
Space activities in Finland 08 p1231 N85-17754
Space research in the Federal Republic of Germany 09 p1265 N85-18074

Activities report in space research in Austria
11 p1587 N85-19994
The French space program 22 p3731 N85-33127
COMMODITIES
Biocatalyzed processes for production of commodity chemicals: Assessment of future research advances for N-butanol production
[NASA-CR-174264] 07 p0919 N85-15819
Intermediate term forecasting techniques for management
[AD-A151370] 15 p2637 N85-26262
COMMUNICATING
NT AIRCRAFT COMMUNICATION
NT CONVERSATION
NT GROUND-AIR-GROUND COMMUNICATION
NT INFORMATION DISSEMINATION
NT INTERSTELLAR COMMUNICATION
NT MESSAGES
NT SELECTIVE DISSEMINATION OF INFORMATION
NT VERBAL COMMUNICATION
Communications skills for CRM training
09 p1276 N85-18017
The multiple resources model of human performance: Implications for display design 10 p1534 N95-19669
Lack of communication 15 p2686 N85-26591
COMMUNICATION
NT FACSIMILE COMMUNICATION
NT INFORMATION DISSEMINATION
NT LINE OF SIGHT COMMUNICATION
NT OPTICAL COMMUNICATION
NT SHIP TO SHORE COMMUNICATION
NT VERBAL COMMUNICATION
Second Symposium on Space Industrialization --- space commercialization
[NASA-CP-2313] 02 p0149 N85-11011
The real world: The user 02 p0150 N85-11017
Inclusion of audiovisual media in information services for the special subjects journalism and communication science (pilot study)
[BMFT-FB-ID-83-004] 02 p0294 N85-11909
Research activities of the Illinois University Coordinated Science Laboratory
[AD-A145589] 03 p0449 N85-12856
Equivocation limits in Gaussian additive channels
[INPE-2828-PRE/380] 04 p0492 N85-13137
Scientific communications and national security
[GPO-36-093] 04 p0492 N85-13138
Subliminal communication technology
[GPO-38-833] 05 p0622 N85-13979
A comparative study of alternative controls and displays for by the severely physically handicapped
05 p0709 N85-14549
USSR report: Electronics and electrical engineering
[JPRS-UEE-84-012] 06 p0781 N85-14991
Space infrastructure 07 p0914 N85-15783
An analysis of constraints to coordinated tactical crew interaction in the P-3C aircraft
[AD-A147220] 07 p1021 N85-16478
Space Shuttle Technical Conference, part 2
[NASA-CP-2342-PT-2] 08 p1098 N85-16937
Commission operation. National Low-Level Radioactive Waste Management Program
[DOE/LLW-33T] 09 p1383 N85-18699
Space System Applications to Tactical Operations
[AGARD-CP-344] 11 p1709 N85-20751
Civil weather satellite systems
11 p1711 N85-20768
Application of the Hardman methodology to the Single Channel Ground-Airborne Radio System (SINCGARS)
[NASA-CR-175694] 14 p2218 N85-23756
China report: Science and technology
[JPRS-CST-85-013] 15 p2536 N85-25652
Management communication and financial modeling
15 p2627 N85-26190
White paper on new international satellite systems
[PB85-162501] 16 p2775 N85-27127
Numerical modeling of subsurface communication
[DE85-012818] 21 p3577 N85-32249
Adaptive corrector operating in frequency domain
22 p3765 N85-33337
A new description of combined trellis coding with asymmetric modulation
[NASA-CR-176197] 24 p4086 N85-35323
DMSK: A practical 2400-bps receiver for the mobile satellite service: An MSAT-X Report
[NASA-CR-176194] 24 p4086 N85-35324
COMMUNICATION CABLES
NT BEAM WAVEGUIDES
NT CIRCULAR WAVEGUIDES
NT COAXIAL CABLES
NT OPTICAL WAVEGUIDES
NT PLASMAGUIDES
NT RECTANGULAR WAVEGUIDES
NT WAVEGUIDES
Regenerators of binary pulses for optical communication systems 04 p0485 N85-13099
Metallized synthetic cable
[AD-D011263] 05 p0628 N85-14023
Characterization of fiber optic cables under large tensile loads
[DE84-016816] 05 p0651 N85-14180
Siemens-Corning plant to manufacture optical fibers
11 p1617 N85-20175
Optical fiber communications link design in compliance with systems performance standards
[PB85-111037] 12 p1830 N85-21489
Surge strength of symmetric cable with monolithic polyethylene insulation of quads
13 p2082 N85-23001
Frequency selection for dispersion signal in satellite communication lines 15 p2526 N85-25584
Instrument for measuring dispersional distortions in optical fibers and cables 15 p2530 N85-25595
COMMUNICATION EQUIPMENT
NT DIPLEXERS
NT RADIO RECEIVERS
NT SATELLITE TELEVISION
NT SPACECRAFT TELEVISION
NT SUPERHETERODYNE RECEIVERS
NT TRANSMITTER RECEIVERS
The ACE (Automated Cable Expert) experiment: Initial evaluation of an expert system for preventive maintenance
[AD-P003943] 02 p0248 N85-11623
Spread-spectrum communications
[AD-A146135] 03 p0355 N85-12285
Problems of development of space communication
06 p0793 N85-15067
The Western Aeronautical Test Range of NASA Ames Research Center
[NASA-TM-85924] 07 p0909 N85-15756
Electronics systems test laboratory testing of shuttle communications systems 08 p1101 N85-16958
NTT unveils satellite communications equipment
10 p1478 N85-19315
Automation of servicibility of radio-relay station equipment 15 p2527 N85-25582
System of light protection of antenna-mast structures of radio-relay lines 15 p2527 N85-25583
Survey of developments in tropospheric communication apparatus 15 p2528 N85-25587
Quality control of radioelectronic apparatus components on basis of external characteristics in frequency domain
15 p2529 N85-25590
ADCCP (Advanced Data Communication Control Procedure) communication processor
[AD-D011595] 15 p2544 N85-25709
The POK project; studies of information handling problems with a new kind of communication device --- precoded signals
[FOA-A-53001-H2] 18 p3091 N85-29131
US Coast Guard High Frequency Emergency Network (HFEN) implementation plan
[PB85-174167] 18 p3092 N85-29141
Time transfer techniques: Historical overview, current practices and future capabilities
18 p3108 N85-29245
Transmission Monitoring and Control (TRAMCON) segmentation plan for the DCS (Defense Communications System) digital transmission network
[AD-A154175] 20 p3440 N85-31351
Design of a jamming simulator for a binary communication system
[AD-A154617] 21 p3573 N85-32221
Globally-asynchronous locally-synchronous systems
[AD-A154624] 21 p3573 N85-32222
COMMUNICATION NETWORKS
Broadband local distribution networks: Problems and prospects in Italy
[FUB-18-1983] 01 p0040 N85-10255
Voice communication handling in X 25 packet switching networks
[FUB-30-1983] 01 p0040 N85-10260
Availability of transmission systems in continental and intercontinental connections --- telecommunication
[FUB-33-1983] 01 p0040 N85-10261
Reserve and authentication in Integrated Services Distributed Networks (ISDN) networks
[FUB-37-1983] 01 p0041 N85-10262
Communications protocols for a fault tolerant, integrated local area network for Space Station applications
[NASA-TM-86304] 01 p0106 N85-10711
Agribusiness and space: No limits to growth
02 p0152 N85-11029
Pluribus satellite IMP (Interface Message Provision) development mobile access terminal network
[AD-A145348] 02 p0190 N85-11269
Distributed hypothesis testing in distributed sensor networks
[AD-A145434] 02 p0294 N85-11905
Wideband integrated voice/data technology
[AD-A146054] 03 p0355 N85-12283
Distributed sensor networks
[AD-A146209] 03 p0355 N85-12286
DCS (Defense Communications System) network synchronization design criteria
[AD-A146251] 03 p0356 N85-12289
The design and performance analysis of an arbiter for a multi-processor shared-memory system
[AD-A146074] 03 p0403 N85-12566
Computer center introductory reference manual for CDC CYBER
[AD-A145796] 03 p0406 N85-12593
Ongoing activities in the field of communication at DFVLR 04 p0459 N85-12913
The application of queueing theory to communications networks: A review
[AD-A146680] 04 p0492 N85-13140
The Telecom 1 satellite telecommunication system
04 p0493 N85-13147
APOLLO system requirements specification --- electronic document delivery
[ESA-SP-1068] 04 p0494 N85-13150
Test experience on an ultrareliable computer communication network
[NASA-TM-85915] 04 p0552 N85-13514
Implementation assessment of a network service. The test responder exerciser specification
[NPL-DITC-44/84] 05 p0716 N85-14594
The transient behavior of networks with infinite server nodes
[CWI-OS-R8408] 05 p0722 N85-14640
Problems of development of space communication
06 p0793 N85-15067
Hardwire missile receiver coupler
[AD-D011350] 07 p0937 N85-15936
Distributed reservation-based code division multiple access
[AD-A147007] 07 p0940 N85-15957
Synoptic observations of the radio noise background in the frequency range 150-180 kHz to provide design data for the low frequency communications designer
[AD-A147438] 07 p0941 N85-15965
Shuttle S-band communications technical concepts
08 p1099 N85-16948
The Communications link analysis and simulation system (CLASS) 08 p1100 N85-16952
Architecture for a demonstration radar-communication link
[AD-A147635] 08 p1150 N85-17260
Distributed sensor networks
[AD-A147638] 08 p1151 N85-17262
Extremely Low Frequency (ELF) Communications System Ecological Monitoring Program: Summary of 1983 progress
[AD-A147704] 08 p1151 N85-17265
Transmission scheduling to reduce convex delay costs in packet networks
[AD-A148451] 08 p1153 N85-17278
Performance evaluation and control of distributed computer communication networks
[AD-A148103] 08 p1208 N85-17598
DDN directory
[AD-A148213] 08 p1230 N85-17744
Voice data processing in packet switching modes
[FUB-44-1983] 09 p1312 N85-18248
Analysis of the performance of multiaccess networks of the bus type
[FUB-47-1983] 09 p1313 N85-18249
Dissemination of ERS-1 low bit rate data and the use of L-band receiving stations
[NLR-TR-83049-U] 09 p1358 N85-18542
Asymptotic analysis of Markovian access control computer communication networks
09 p1372 N85-18619
An ultra reliable computer communication network: The dispersed sensor processing mesh
09 p1372 N85-18620
Survivable local area network
[AD-D011453] 10 p1468 N85-19262
Commentary on start of scientific data transmissions with USSR 10 p1476 N85-19319
Selected NBSNET software
[PB85-109148] 10 p1542 N85-19723
Process algebra with asynchronous communication mechanisms
[CWI-CS-R8410] 11 p1625 N85-20235
Communications software for Olympics Micromation Computer System
[PB85-109510] 11 p1704 N85-20723
Minimization of system vulnerability in Naval satellite communication networks 11 p1710 N85-20758
Defense Meteorological Satellite Program (DMSP)
11 p1711 N85-20766
Base communications issues for the 1980s
[AD-A149764] 12 p1828 N85-21474

Space Shuttle interactive meteorological data system study
[NASA-CR-171418] 12 p1892 N85-21876
System dynamics and network control
[AD-A149420] 13 p2054 N85-22863
Integrated digital networks
[AD-A150605] 13 p2056 N85-22873
Satellite channels in packet-switching networks
13 p2067 N85-22909
Satellite bridges in communications networks
13 p2067 N85-22910
Introduction to the Space Physics Analysis Network (SPAN)
[NASA-TM-86499] 14 p2290 N85-24196
Research needs for artificial intelligence applications in support of C3 (Command, Control, and Communication)
[AD-A150867] 14 p2292 N85-24210
Data-link alternatives for the NASA pilot data systems
[NASA-TM-85999] 14 p2412 N85-24873
Survey of developments in tropospheric communication apparatus 15 p2528 N85-25587
Pluribus Satellite IMP (Interface Message Provision) development mobile access terminal network
[AD-A151312] 15 p2542 N85-25692
Evaluating computer-communication networks with simulation techniques
[AD-A151852] 15 p2632 N85-26222
Thin Route Project 15 p2687 N85-26598
Communications 15 p2687 N85-26600
Design and specification of a local area network architecture for use in real-time flight simulation
[AD-A152242] 16 p2716 N85-26762
Distributed control of circuits in multiuser communication networks with circuit precedence and path suitability criteria using failsafe routing concepts
[AD-A151825] 16 p2772 N85-27113
Evaluation of Ada (trademark) as a communications programming language, volume 1
[AD-A152314] 16 p2848 N85-27559
Evaluation of Ada (trademark) as a communications programming language. Volume 2: Communications protocols application
[AD-A152315] 16 p2848 N85-27560
Evaluation of Ada (trademark) as a communications programming language. Volume 3: Trusted software application
[AD-A152316] 16 p2848 N85-27561
A study of topologies and protocols for fiber optic local area network
[NASA-CR-175771] 16 p2864 N85-27669
Future information technology, 1984: Telecommunications
[NBS/SP-500/119] 16 p2878 N85-27762
Wideband integrated voice/data technology
[AD-A152329] 17 p2947 N85-28197
Logical design of a decision support system to forecast technology, prices and costs for the national communications system
[AD-A152330] 17 p2948 N85-28198
A real-time executive for multiple-computer clusters
[AD-A152961] 17 p3015 N85-28646
Reliability report for communication networks
[AD-A153764] 18 p3090 N85-29127
US Coast Guard High Frequency Emergency Network (HFEN) implementation plan
[PB85-174167] 18 p3092 N85-29141
Maser and secondary clock in telecommunications networks 18 p3108 N85-29246
High performance asynchronous limited sensing algorithms for CSMA and CSMA-CD channels
[AD-A153919] 18 p3171 N85-29650
LAN (Local Area Network) interoperability study of protocols needed for distributed command and control
[AD-A154033] 19 p3255 N85-30182
INMARSAT: An overview 20 p3400 N85-31091
Existing and potential INMARSAT capabilities for the Future Global Maritime Distress and Safety System
20 p3402 N85-31110
INMARSAT distress and safety communication
20 p3406 N85-31134
Future prospects for a combined INMARSAT polar communication and search and rescue satellite system
20 p3406 N85-31137
Scientific report of the Department of Systems and Communications
[ENST-84D002] 20 p3441 N85-31355
A comparison of millimeter wave, direct detect and heterodyne laser intersatellite links
[AD-A151964] 20 p3461 N85-31496
Routing algorithms and stochastic analysis for large communications networks
[AD-A154654] 21 p3573 N85-32225
Broadcasting topology and routing information in computer networks
[AD-A155668] 21 p3674 N85-32827
Assured information flow capping architecture
[AD-A155392] 22 p3756 N85-33283
Petcom: A software instrument for the analysis of Petri networks, oriented towards communication protocols
[FUB-50-1983] 22 p3756 N85-33286
Research on distributed artificial intelligence
[AD-A155356] 22 p3833 N85-33733
Performance interface document for the S-band diplexer for space users of NASA networks
[NASA-TM-86224] 23 p3900 N85-34155
A graphics interface for interactive simulation of packet-switched networks 23 p3962 N85-34556
Communication complexity of distributed shortest path algorithms
[AD-A156049] 24 p4087 N85-35332
A ray trace program for line-of-sight microwave communication links
[AD-A156168] 24 p4087 N85-35336

COMMUNICATION SATELLITES
NT AERONAUTICAL SATELLITES
NT COMMUNICATIONS TECHNOLOGY SATELLITE
NT EUROPEAN COMMUNICATIONS SATELLITE
NT INTELSAT SATELLITES
NT L-SAT
NT SYMPHONIE SATELLITES
The Telecom 1 satellite telecommunication system
04 p0493 N85-13147
Space power for communication satellites beyond 1995 05 p0606 N85-13883
Evaluating NASA technology programs in terms of private sector impacts 05 p0608 N85-13885
Offset unfurlable antenna concepts
05 p0625 N85-14002
Technology and performances of structural thermal mechanical equipment used for antenna of TV.SAT-TDF 1 program 05 p0626 N85-14012
Demand for satellite-provided domestic communications services up to the year 2000
[NASA-TM-86894] 06 p0798 N85-15099
US objectives generally achieved at broadcasting satellite international conference. Improvements can help in future conferences
[PB84-235316] 06 p0800 N85-15109
NOAA (National Oceanic and Atmospheric Administration) Aircraft Satellite Data Link (ASDL)
[PB84-243773] 07 p0942 N85-15976
A modified Monte-Carlo technique for the simulation of satellite communication systems
[AD-A148689] 08 p1214 N85-17641
Propagation measurements for land-mobile satellite services in the 800 MHz band
[CRC-TN-724] 09 p1310 N85-18231
Propagation measurements for land-mobile satellite systems at 1541 MHz
[CRC-TN-723] 09 p1310 N85-18232
Star on the horizon: The emergence of the direct broadcast satellite in American mass communications
[AD-A148819] 09 p1312 N85-18242
Technical evaluation report on the 46th Symposium of the Avionics Panel on Space System Applications to Tactical Operations
[AGARD-AR-203] 10 p1425 N85-18988
Commercial space: Europe should have independent strategy 10 p1460 N85-19205
Worldwide report: Telecommunications policy, research and development
[JPRS-TTP-85-002] 10 p1475 N85-19309
Traveling wave tube for broadcast satellites
10 p1475 N85-19310
Worldwide report: Telecommunications policy, research and development
[JPRS-TTP-85-006] 10 p1476 N85-19314
NTT unveils satellite communications equipment
10 p1476 N85-19315
Ex-minister urges communications satellite development 10 p1476 N85-19316
Communications satellite needs examined
10 p1476 N85-19317
MATRA has Europe's largest white room for satellites
10 p1477 N85-19320
US MILSATCOM: Present and future
11 p1709 N85-20753
Tactical military communications by satellite relay at high latitudes 11 p1709 N85-20756
The Ferranti Tactical SHF SATCOM station (MANSAT) 11 p1710 N85-20759
The international environment UNISPACE '82 and the ITU: A relationship between orbit-spectrum resource allocation and orbital debris 12 p1787 N85-21215
Transmission and orbital constraints in space-related programs: Briefing summary 12 p1787 N85-21216
Engineering calculations for communications satellite systems planning
[NASA-CR-175552] 12 p1789 N85-21233
Radioelectronics and space exploration
12 p1838 N85-21533
Satellite communications and amateur radio
12 p1838 N85-21534
NASA mobile satellite program
14 p2229 N85-23814
Alternatives for satellite sound broadcast systems at HF and VHF 14 p2229 N85-23815
Damping models for flexible communications satellites by substructural damping synthesis
[UTIAS-267] 14 p2237 N85-23868
Spatial acquisition algorithms and systems for intersatellite optical communication links
[AD-A150794] 14 p2292 N85-24207
Satellite reception of reentry vehicle telemetry
[AD-A151651] 15 p2492 N85-25372
Frequency selection for dispersion signal in satellite communication lines 15 p2528 N85-25584
Preliminary estimation of mutual interference between fixed satellite service systems 15 p2528 N85-25586
Trade-off between land vehicle antenna cost and gain for satellite mobile communications
[NASA-CR-175732] 15 p2540 N85-25681
Measurement results from a balloon experiment simulating land mobile satellite transmissions
[NASA-CR-175740] 15 p2540 N85-25683
Pluribus Satellite IMP (Interface Message Provision) development mobile access terminal network
[AD-A151201] 15 p2541 N85-25686
Pluribus Satellite IMP (Interface Message Provision) development mobile access terminal network
[AD-A151312] 15 p2542 N85-25692
Lack of communication 15 p2686 N85-26591
Thin Route Project 15 p2687 N85-26598
Communications 15 p2687 N85-26600
Satellite provided customer promises services, a forecast of potential domestic demand through the year 2000. Volume 4: Sensitivity analysis
[NASA-CR-174662] 16 p2769 N85-27092
FAA (Federal aviation administration) assessment of satellite concepts and aviation spectrum requirements
[AD-A152338] 17 p2948 N85-28199
Spread spectrum time transfer experiment via INTELSAT 17 p2964 N85-28304
Channel multiplexers for broadcast satellite transponders in the 12 GHz band
[NHK-LABS-NOTE-310] 18 p3090 N85-29122
International space research perspectives of commercialization for German industry
[NASA-TM-77657] 19 p3222 N85-29979
Design and evaluation of control systems for large communications satellites 20 p3409 N85-31157
Analysis of beam interaction of the electrical thruster RIT 10 (particle emission) with surfaces
[ESA-TT-826] 20 p3421 N85-31231
Combined trellis coding with asymmetric MPSK modulation: An MSAT-X report
[NASA-CR-176039] 20 p3440 N85-31347
A comparison of millimeter wave, direct detect and heterodyne laser intersatellite links
[AD-A151964] 20 p3461 N85-31496
A model for predicting propagation-related DSCS (Defense Communications Engineering Center) margin requirements
[AD-A155355] 22 p3756 N85-33281
International prototype network in Dubna experimental satellite communications system
22 p3773 N85-33380
Telecommunications forecast for ITU Region 2 to the year 1995
[NASA-TM-87077] 23 p3899 N85-34150
Spacecraft (Mobile Satellite) configuration design study
[NASA-CR-176153] 23 p3899 N85-34152
Satellites and politics: Weather, communications, and earth resources 23 p4057 N85-35144
Second-generation mobile satellite system. A conceptual design and trade-off study
[NASA-CR-176195] 24 p4086 N85-35325

COMMUNICATION SYSTEMS
U TELECOMMUNICATION

COMMUNICATION THEORY
NT WORDS (LANGUAGE)
Research activities of the Illinois University Coordinated Science Laboratory
[AD-A145569] 03 p0449 N85-12856
Knowledge-based communication and management support in a system development environment
05 p0717 N85-14596
Process algebra for communication and mutual excitation
[CWI-CS-R8409] 05 p0720 N85-14622
Process algebra with asynchronous communication mechanisms
[CWI-CS-R8410] 11 p1625 N85-20225
The study of certain aspects of probability with applications in communications theory
[AD-A149620] 12 p1829 N85-21478

Algebra of communicating processes
[CWI-CS-R8421] 17 p2950 N85-28214
Expressiveness and language choice
[AD-A153280] 17 p3012 N85-28623

COMMUNICATIONS TECHNOLOGY SATELLITE
Damping synthesis for a spacecraft using substructure and component data
[CRC-1365] 03 p0323 N85-12062

COMMUNITIES
Test of dispersal of turbojet aircraft departure tracks at washington National Airport (1983-84), volume 1 report
[AD-A146111] 08 p1218 N85-17669
Air quality benefit analysis for Los Angeles and San Francisco based on housing values and visibility
[PB85-166049] 16 p2822 N85-27409

COMMUTATION
Finite products of commutators in C* algebras
11 p1698 N85-20678
Positioning errors of commutating lenses and their influence on characteristics of high speed movie cameras 14 p2273 N85-24065

COMMUTATORS
Summator of radio pulse signals
12 p1839 N85-21539
Brush and commutator segment torquer motor
[AD-D011726] 23 p3927 N85-34340

COMPACTING
Solid-phase sintering of tantalum carbide
[BLL-M-36013-(5828.4)] 07 p0926 N85-15872
No-slump Roller-Compacted Concrete (RCC) for use in mass concrete construction
[AD-A148564] 08 p1138 N85-17164
Traction forces of drive tyre on the compacted soil
[AD-P004264] 09 p1404 N85-18840
Quality control in soil compaction by behaviours of exciter
[AD-P004295] 09 p1408 N85-18872
Compaction of sand using ordinary off-road vehicles
[AD-P004297] 09 p1409 N85-18874
Flotation tires and subsurface compaction
[AD-P004299] 09 p1409 N85-18876
Tractor power selection with compaction constraints
[AD-P004300] 09 p1409 N85-18877
Dynamic compaction of powders
[DE85-001062] 11 p1612 N85-20137
Pressure-density behavior for AlN, Al2O3, SiO2, TiB2, and TiC powders up to 3.5 GPa
[DE85-006146] 14 p2261 N85-24012
Rapid solidification of candidate ferritic steels
[DE85-006596] 16 p2750 N85-26971
Ac field-induced order in dense colloidal systems
[DE85-009107] 17 p2935 N85-28119
Hot Isostatic Pressing (HIP): Techniques, applications and economical use
[JUEL-SPEZ-288] 17 p2939 N85-28141
Feasibility of melt casting strontium fluoride to produce high-density heat sources
[DE85-009429] 18 p3130 N85-29381
Deep-burial diagenesis in carbonates
[DE85-011224] 22 p3802 N85-33554
Dynamic compaction of a monosized spherical tungsten powder
[DE85-014808] 24 p4080 N85-35289
Computational methods for the explosive and impact compaction of powders
[AD-A156219] 24 p4139 N85-35653

COMPACTNESS
U VOID RATIO

COMPANDING
Digital sound: Programme-modulated noise levels in sound signals subjected to a number of digital companding processes
[BBC-RD-1984/11] 09 p1310 N85-18233
Controllable companding in low-frequency FM radio communication systems 22 p3776 N85-33402

COMPANION STARS
Search for white dwarf companions of cool stars with peculiar element abundances
[NASA-CR-174030] 02 p0297 N85-11923
Evidence for a solar companion star
[DE85-002069] 10 p1571 N85-19907
A search for white-dwarf companions of subgiant CH stars 11 p1752 N85-21019
The white dwarf companion of the mild BA star Xi1 Cet 11 p1752 N85-21020
The outburst and long term behavior of the triple period cataclysmic variable TV Col 11 p1752 N85-21021
Blue companions of Cepheids
11 p1754 N85-21033
Comet showers and Nemesis, the death star
[DE85-003736] 15 p2683 N85-26575

COMPARATOR CIRCUITS
Qualification of a thick film hybrid
[BMFT-FB-W-84-024] 04 p0497 N85-13170

COMPARATORS
Comparator with noise suppression
[NASA-CASE-LAR-13151-1] 11 p1627 N85-20247
MHB4046 phase-lock circuit 15 p2533 N85-25629

COMPARISON
Observations of four Beta Cephei stars in NGC6231
01 p0128 N85-10877
Atmospheric and pressurized low speed wind tunnel performance and cost comparisons
[ARL/AERO-R-160] 02 p0149 N85-11008
Comparison of the multigrid and ICCG methods in solving the diffusion equation
[DE84-014409] 02 p0253 N85-11657
A comparison of methods for predicting ductile crack growth instability
[AERE-R-11199] 03 p0374 N85-12387
Comparative energy storage assessment item
05 p0605 N85-13858
Evaluation and results of national and international intercomparison measurements — electromagnetic measurement 05 p0631 N85-14043
Comparison of optimum interpolation and Cressman analyses 05 p0680 N85-14371
Comparison of uniform perturbation solutions and numerical solutions for some potential flows past slender bodies
[NASA-CR-172485] 06 p0749 N85-14799
Analysis of the flow field about a T-45 using PANAIR
[AD-A146811] 07 p0899 N85-15699
Comparison measurements on optical particle counters
[BLL-DOUNREAY-TR-934-(9091.9F)]
07 p0961 N85-16092
Comparative investigation of three commercial radiosonde systems
[KNMI-TR-53] 07 p1009 N85-16409
Can the Aggressors continue to be effective in the F-5E?
[AD-A146861] 07 p1019 N85-16465
A computer package for ranking, selection and multiple comparisons with the best
[AD-A147617] 08 p1204 N85-17579
Models for mixture experiments when the response depends on the total amount
[DE85-000370] 09 p1374 N85-18637
Comparison of methods for predicting fiber stresses in a cracked Kevlar/epoxy monolayer
[DE84-016118] 11 p1593 N85-20022
Cost comparison of small gas turbines versus electric motors in a variable load industrial application
[PB85-149763] 12 p1837 N85-21530
A diffusion process and its application to detecting a change in the drift of Brownian motion
[AD-A150096] 12 p1926 N85-22100
Optimal designs for comparisons between two sets of treatments
[AD-A150621] 13 p2152 N85-23360
Costs, payload of Ariane, US Space Shuttle compared
15 p2530 N85-25601
Self-scanning MDS-integrated photosensor strip
17 p2940 N85-28151
Generic data entry quality assurance tool
[DE85-008359] 18 p3200 N85-29852
Inherent angular tracking error in an amplitude comparison monopulse radar
[AD-A154212] 19 p3255 N85-30185
Comparison of 8 to 12 micrometer and 3 to 5 micrometer CVF transmissometer data with LOWTRAN calculations
[AD-A154218] 19 p3350 N85-30763
Multiaxial fatigue low cycle fatigue testing
20 p3468 N85-31544
Fuel cell applications literature review
[DE85-011891] 22 p3809 N85-33592
Large-scale sea surface temperature variability from satellite and shipboard measurements
[NASA-CR-176123] 22 p3818 N85-33651
Comparison of experimental data on detonation velocity and Chapman-Jouget pressure vs initial HE density with predictions from Ree's model equation of state
[DE85-007266] 23 p3922 N85-34304

COMPARTMENTATION
U COMPARTMENTS

COMPARTMENTS
NT AIR LOCKS
NT AIRCRAFT COMPARTMENTS
NT ANECHOIC CHAMBERS
NT HYPERBARIC CHAMBERS
NT PRESSURE CHAMBERS
NT PRESSURIZED CABINS
NT SPACECRAFT CABINS
NT TEST CHAMBERS
NT VACUUM CHAMBERS
The distribution of the number of empty cells in a generalized random allocation scheme
[AD-A154806] 21 p3677 N85-32841

COMPASSES
NT GYROCOMPASSES
NT MAGNETIC COMPASSES
Determining an azimuth with a north seeking gyro
[AD-A155880] 24 p4063 N85-35180

COMPATIBILITY
NT ELECTROMAGNETIC COMPATIBILITY
NT SYSTEMS COMPATIBILITY
Anthropometric cockpit compatibility assessment of US Army aircraft for large and small personnel wearing A cold weather, armored vest, chemical defense protective clothing configuration
[AD-A145472] 02 p0238 N85-11547
Official journey to USA, November 1983. Symposium on the Compatibility of Explosives; Mound Laboratory; Naval Surface Weapons Center
[FOA-C-20548-D1] 04 p0482 N85-13072
Metallographic evaluation of the reactions between boronated graphite and Fe-Ni-Cr alloys
[DE84-015374] 06 p0769 N85-14922
Deuterium isotope effect on the compatibility between polystyrene and polybutadiene
[AD-A148551] 08 p1134 N85-17145
Implementation of an Intel 8086 microprocessor-based realization library for the control system design language
[AD-A148506] 08 p1202 N85-17569
Quantitative estimate of compatibility of fiber composite material components 10 p1444 N85-19099
High-temperature X-ray diffraction study of coating-substrate compatibility in yttria-coated graphite
[DE85-005916] 14 p2262 N85-24016
Deployable Core Automated Maintenance System (DCAMS)
[AD-A153695] 18 p3198 N85-29839
Compatibility, contamination and IR microspectrophotometry
[DE85-010809] 19 p3273 N85-30297
A study of the effect of a mismatch in gamma and gamma prime phase lattice spacings on the high temperature strength characteristics of dispersion-hardened nickel alloys
[BLL-CE-TRANS-8048-(9022.09)]
20 p3430 N85-31279
Determination of instrument errors by compatibility checking: Results from dynamic flight test data
[ARL/AERO-R-162] 23 p3896 N85-34137
Parallel processing on the Livermore VAX 11/780-4 parallel processor system with compatability to Cray Research, Inc. (CRI) multitasking, version 1
[DE85-011856] 23 p3967 N85-34595

COMPENSATORS
Robust rate control system designs for a submersible
[AD-A144792] 01 p0111 N85-10753
Tracking servo compensator with rate aiding
[AD-D011372] 07 p0942 N85-15971
Dynamic polymer pressure transducer with temperature compensation
[AD-D011373] 07 p0967 N85-16142
Multivariable flight control with time-scale separation
[NASA-CR-174320] 08 p1087 N85-16873
Compensator development and examination of performance and robustness
[NASA-CR-175470] 11 p1627 N85-20244
Dynamic visual servo control of robots: An adaptive image-based approach
[AD-A150057] 12 p1860 N85-21667
Efficiency of digital compensator of strong non-Gaussian interference 13 p2072 N85-22942
Aberration characteristics of plane-parallel compensator plate 14 p2276 N85-24100
Compensator development and examination of performance and robustness
[NASA-CR-175703] 15 p2540 N85-25678
Flight control system reconfiguration design using quantitative feedback theory
[AD-A151771] 16 p2710 N85-26722
Principles of designing digital compensating accelerometers 17 p2944 N85-28172
Interactive computer program for the analysis and design of linear time invariant systems
[AD-A154076] 19 p3335 N85-30664
Approximation of optimal infinite dimensional compensators for flexible structures
20 p3413 N85-31181
Control of a flexible space antenna: A finite dimensional perspective based on distributed parameter theory
20 p3413 N85-31182
Selectivity of weight compensator of passive interference to unknown velocities of detectable targets
22 p3762 N85-33317
Magnetic field and equivalent circuit of induction motors with shielded poles 22 p3772 N85-33378
Design of dynamic compensators of prescribed pattern
[BU-109] 24 p4142 N85-35674

COMPETITION
An analysis of production competition and award methodology
[AD-A147775] 08 p1228 N85-17733
International cooperation and competition in civilian space activities
[OTA-ISC-240] 08 p1231 N85-17750
Competitive assessment of the US manufacturing automation equipment industries
[PB85-103927] 10 p1569 N85-19893
COMPILATION (COMPUTERS)
U COMPILERS
COMPILER PROGRAMS
U COMPILERS
COMPILERS
THLL (TRIDENT Higher Level Language) reference manual
[AD-A145116] 01 p0104 N85-10696
PASCAL-MP algebraic and numerical manipulator for polynomials
[INPE-3229-TDL/176] 02 p0240 N85-11562
SMILE user's guide: A macro preprocessor for extending FORTRAN
[DE84-015984] 02 p0243 N85-11584
Application of a silicon compiler to VLSI (Very Large Scale Integrated circuits) design of digital pipelined multipliers
[AD-A146328] 03 p0403 N85-12569
Digital equipment Corporation, professional 350, COBOL-81 Version 2.1
[PB84-227602] 03 p0403 N85-12572
Digital Equipment Corporation, Professional 350, COBOL-81 Version 2.1 (COBOL technical report)
[PB84-227719] 03 p0403 N85-12573
Northern Telecom, Incorporated, NTI-585/565, ACOBOL/3 Release 4.1 Version H(01)
[PB84-228022] 03 p0404 N85-12574
Northern Telecom, Incorporated NTI-585/565, ACOBOL/3 Release 4.1 Version H(01) (COBOL technical report)
[PB84-228030] 03 p0404 N85-12575
Digital Equipment Corporation, DECSYSTEM-10, model 1090-SMP, COBOL-74 V12B
[PB84-227941] 03 p0404 N85-12576
Data General Corporation, Eclipse C350, AOS COBOL Release 3.51
[PB84-227883] 03 p0404 N85-12577
Convergent Technologies, NGEN CP001, CT COBOL version 9.0
[PB84-227784] 03 p0404 N85-12578
Convergent Technologies, mega frame CTIX BASIC interpreter version 1.03
[PB84-227776] 03 p0404 N85-12579
Convergent Technologies, mega frame, CTIX FORTRAN 77 version 2.1
[PB84-227768] 03 p0404 N85-12580
Convergent Technologies, mega frame, CTIX COBOL version 2.0
[PB84-227750] 03 p0404 N85-12581
Digital Equipment Corp., VAX-11/782, VAX FORTRAN version 4.0
[PB84-227701] 03 p0405 N85-12582
Digital Equipment Corp., VAX/750, VAX COBOL version 3.0
[PB84-227693] 03 p0405 N85-12583
IBM Corporation, IBM 5381 model 5, system/38 COBOL release 6
[PB84-227677] 03 p0405 N85-12584
Gould Incorporated, GOULD Concept 32/87, COBOL release 1.4
[PB84-227669] 04 p0548 N85-13484
Digital Equipment Corp., VAX/750, VAX COBOL version 3.0
[PB84-227651] 04 p0548 N85-13485
Digital Equipment Corp., MICRO/PDP-11, COBOL-81 version 2.2
[PB84-227644] 04 p0548 N85-13486
Prime Computer, Inc., PRIME 750, FORTRAN-77 revision 19.4
[PB84-227628] 04 p0548 N85-13487
C3, Incorporated, C50 System, C3 COBOL/75 version 2.00
[PB84-228006] 04 p0548 N85-13488
Burroughs Corporation B26-CPU, B20 COBOL, Release 4.0
[PB84-216241] 04 p0551 N85-13505
Burroughs Corporation B26-CPU, B20 COBOL Version 4.0 (COBOL technical report)
[PB84-216258] 04 p0551 N85-13506
Convergent technologies NGEN CP001, CT COBOL Version 9.0
[PB84-216266] 04 p0551 N85-13507
Convergent Technologies, Incorporated, NGEN CP001, CT COBOL Version 9.0 (COBOL technical report)
[PB84-216274] 04 p0551 N85-13508
Computer Sciences Corporation UNIVAC 1100/80, CSTS COBOL Release COB250
[PB84-216282] 04 p0551 N85-13509
Control Data Corporation CYBER 205 model 442, FORTRAN 200 (G201-25)
[PB84-216290] 04 p0551 N85-13510
C3, Incorporated NGEN CP001, COBOL Version 9.0
[PB84-216308] 04 p0552 N85-13511
United Information Services, Inc., CRAY 1-S/2000, FORTRAN CFT 1.10
[PB84-227685] 04 p0552 N85-13512
Datapoint Corporation Datapoint 6600, 8600, DOS COBOL Version 3.6
[PB84-242973] 04 p0552 N85-13513
Northern Telecom, Inc., IBM 3033 (compilation), NTI-585/565 (execution), XCOBOL, release 4.1, version H(01) (COBOL technical report)
[PB84-228048] 05 p0714 N85-14578
NECIS Incorporated, NEC ASTRA model 270, COBOL 74 version 8.3 (COBOL technical report)
[PB84-227933] 06 p0848 N85-15381
Digital Research Incorporated, IBM PC XT, FORTRAN-77 V4.0
[PB84-243633] 06 p0849 N85-15388
Perkin-Elmer, Perkin-Elmer 3230, FORTRAN 7 D R00-00
[PB84-243682] 06 p0849 N85-15389
Gould Incorporated, Gould PS-3000, Gould PS-3000 FORTRAN 77 V2.1
[PB84-229178] 06 p0849 N85-15390
Data general Corporation, Eclipse C150, interactive COBOL Revision 1.30 (COBOL technical report)
[PB84-227834] 06 p0849 N85-15391
Data General Corporation, Eclipse C150, interactive COBOL Revision 1.30
[PB84-227891] 06 p0849 N85-15392
IBM Corporation, IBM Series/1 4955, IBM Series/1 host COBOL Release 1.1 EDX (COBOL technical report)
[PB84-227909] 06 p0849 N85-15393
IBM Corporation, IBM Series/1 4955, IBM Series/1 host COBOL Release 1.1 EDX
[PB84-227818] 06 p0849 N85-15394
IBM Corporation, IBM Series/1 4955, IBM Series/1 host COBOL Release 1.1 RPS
[PB84-227917] 06 p0850 N85-15395
IBM Corporation, IBM Series/1 4955, IBM Series/1 host COBOL Release 1.1 RPS (COBOL technical report)
[PB84-227925] 06 p0850 N85-15396
NECIS, Incorporated, NEC ASTRA model 270 COBOL 74 Version 8.3
[PB84-227636] 06 p0850 N85-15397
Digital Equipment Corporation, DECSYSTEM-20, model 2060, COBOL V13
[PB84-227958] 06 p0850 N85-15398
Digital Equipment Corporation, DECSYSTEM-20, model 2060, COBOL V13 (COBOL technical report)
[PB84-227966] 06 p0850 N85-15399
Northern Telecom, Incorporated, IBM 3033 (compilation), NTI-585/565 (execution), XCOBOL Release 4.1 Version H(01)
[PB84-227875] 06 p0850 N85-15400
NCR Corporation, NCR I9300, NCR ITX Cobol Release 3.0
[PB84-228055] 06 p0850 N85-15401
NCR Corporation, NCR I9300, NCR ITX COBOL Release 3.0 (COBOL technical report)
[PB84-228063] 06 p0850 N85-15402
Gould Incorporated, Gould PS-3000, Gould PS-3000 COBOL V2.0
[PB84-229160] 06 p0850 N85-15403
Gould Incorporated, Gould PS-3000, Gould PS-3000 BASIC Interpreter Version 1.00
[PB84-229186] 06 p0851 N85-15404
Digital Equipment Corporation, PDP-11/23-PLUS PDP-11 FORTRAN-77 V5.0
[PB84-227610] 06 p0851 N85-15405
Computervision Corporation, CDS-4000 32-Bit processor, CV FORTRAN Version 2.84
[PB84-227867] 06 p0851 N85-15406
Plexus Computers, Inc., Plexus P/60, Plexus FORTRAN 77 Version 1.1
[PB84-227859] 06 p0851 N85-15407
Control Data Corporation, CYBER 835, COBOL Release 5.3 Level 614
[PB84-227842] 06 p0851 N85-15408
Prime Computer, Inc., PRIME 750, COBOL-74 Revision 19.3.2
[PB84-227826] 06 p0851 N85-15409
Sperry Univac, System 80 Model 6, OS/3 COBOL, Version 08.00/08
[PB84-227800] 06 p0851 N85-15410
Modular Computer Systems, Incorporated, MODCOMP CLASSIC 7860, MODCOMP FORTRAN 77/16 Version A.0
[PB84-230556] 06 p0852 N85-15411
Modular Computer Systems, Incorporated, MODCOMP CLASSIC 7860, MODCOMP NASA EXTENDED FORTRAN 78 Version A.40
[PB84-230549] 06 p0852 N85-15412
Digital Equipment Corporation, MICRO/PDP-11, COBOL-81 Version 2.2
[PB84-229236] 06 p0852 N85-15413
NCR Corporation, NCR 9300, NCR ITX-BASIC Release 2.0
[PB84-229228] 06 p0852 N85-15414
Sperry Corporation, 1100/80, UBASIC/BBASIC Level 9R1
[PB84-229202] 06 p0852 N85-15415
Sperry Corporation, 1100/80 ASC2 FORTRAN Level 11R1
[PB84-229194] 06 p0852 N85-15416
Computer Sciences Corporation, UNIVAC 1100/80, CSTS COBOL Release COB250
[PB84-229154] 06 p0852 N85-15417
Compter Sciences Corporation, UNIVAC 1100/80, CSTS BASIC Release BAS180
[PB84-229145] 06 p0852 N85-15418
Wang Laboratories, Incorporated, Wang VS100, FORTRAN 77 Version 01.00.02
[PB84-228014] 06 p0852 N85-15419
Control Data Corporation, Cyber 835, BASIC Release 3.5 Level 614
[PB84-227990] 06 p0853 N85-15420
Data General Corporation, Eclipse C350, AOS COBOL Release 3.51
[PB84-227982] 06 p0853 N85-15421
Digital Equipment Corporation, DECSYSTEM-20 2060 Model B, FORTRAN-20 Version 10
[PB84-227974] 06 p0853 N85-15422
Specialized silicon compilers for languege recognition
[AD-A146526] 06 p0853 N85-15425
C3, Incorporated NGEN CP001, C3 COBOL Version 9.0 (COBOL Technical Report)
[PB84-216316] 06 p0855 N85-15435
Burroughs Corporation B26-CPU, Burroughs B20 BASIC Rel. 4.0
[PB84-216324] 06 p0855 N85-15436
Convergent Technologies NGEN CP001, CT BASIC Version 9.0
[PB84-216332] 06 p0855 N85-15437
Convergent Technologies, NGEN CP001, CT FORTRAN Version 9.0
[PB84-229210] 06 p0856 N85-15442
Microsoft Corporation, Sun Microsystems, Microsoft COBOL Version 2.0
[PB84-243401] 06 p0856 N85-15443
Microsoft Corporation, IBM PC XT, Microsoft COBOL, Version 2.0
[PB84-243419] 06 p0856 N85-15444
Research on introspective systems
[AD-A146406] 06 p0870 N85-15530
Ada compiler validation summary report: New York University (NYU Ada/Ed) compiler, version 1.4 for VAX 11/780, using VMS 3.5
[AD-A146924] 07 p1022 N85-16483
Ada compiler validation summary report: TeleSoft (TeleSoft Ada) compiler, version 2.0a for Sun 120 Motorola M68010, using 4.2 BSD UNIX-Sun Version 1.1
[AD-A146925] 07 p1022 N85-16484
NYU Ada/Ed user's guide: Version 1.4 for VAX/VMS systems
[AD-A146759] 07 p1024 N85-16495
Ada compiler validation summary report: TeleSoft (TeleSoft Ada) compiler, version 2.0a2 for Callan Unistar 300, using System V, version 4.1a
[AD-A147115] 07 p1025 N85-16505
The production of maintainable, trustworthy, and portable software 08 p1064 N85-16744
FLAD user's manual: FLAD file contents
[AD-A148700] 09 p1368 N85-18594
Digital Equipment Corporation VAX Ada Compiler Version T0.6-2 VAX-11/785, 11/750, 11/730, using VMS, Version 4.0 and MicroVAX 1, using MicroVMS Version 1.0
[AD-A149375] 10 p1538 N85-19696
Ada in mission critical system acquisition: A guidebook
[AD-A149271] 10 p1540 N85-19710
Four Phase Systems, Incorporated, Four Phase Series 5000, COBOL 1974 version BE08.8
[PB85-108017] 10 p1541 N85-19717
Four Phase Systems, Incorporated, Mini-Frame Series 6300, COBOL Series 6000
[PB85-108025] 10 p1541 N85-19718
Micro focus DEC Rainbow 100 + compact level 2 COBOL; V2.5
[PB85-108975] 10 p1542 N85-19719
Micro focus DEC Rainbow 100 + high performance level 2 COBOL; V2.5
[PB85-108983] 10 p1542 N85-19720

DTSS, Incorporated, DPS 8/44, DTSS COBOL Release 12
[PB85-108058] 10 p1542 N85-19721
Sperry Univac System 80, Model 6, OS/3 BASIC, Version 10.01
[PB85-108066] 10 p1542 N85-19722
Ada compiler validation summary report, Dansk Datamatik Center, VAX 11 compiler version 1.1
[AD-A149340] 11 p1699 N85-20681
Micro Focus, Intel Microprocessor Development System MDS221 CIS COBOL; V4.5
[PB85-110823] 11 p1699 N85-20682
Prime Computer, Incorporated, PRIME 750, BASICV revision 19.4
[PB85-108074] 11 p1699 N85-20683
Validation Summary Report (VSR), Ryan-McFarland Corporation, AT and T 385, RM/COBOL Version 2.0
[PB85-102093] 11 p1703 N85-20709
Burroughs Corporation, Burroughs B3955 COBOL9 Version 6.8
[PB85-103110] 11 p1703 N85-20710
Burroughs Corporation, Burroughs B3955 FORT77 Version 6.8
[PB85-110328] 11 p1703 N85-20711
Micro Focus Plessy Micro Systems 68/50 Compact Level 2 COBOL; V2.5
[PB85-108934] 11 p1703 N85-20712
Micro Focus Plessy Micro Systems 68/50 High Performance Level 2 Cobol; V2.5
[PB85-108942] 11 p1703 N85-20713
Micro focus Cifer 2887 high performance level 2 COBOL; V2.5
[PB85-108959] 11 p1703 N85-20714
Micro focus Cifer 2887 compact level 2 COBOL; V2.5
[PB85-108967] 11 p1703 N85-20715
Micro Focus IBM personal computer XT Compact Level 2 COBOL; V2.5
[PB85-108918] 11 p1703 N85-20716
Micro Focus IBM personal computer XT High Performance Level 2 COBOL; V2.5
[PB85-108926] 11 p1704 N85-20717
Micro focus Fortune 32:16 compact level 2 COBOL; V2.5
[PB85-108884] 11 p1704 N85-20718
Micro focus Fortune 32:16 high performance level 2 COBOL; V2.5
[PB85-108892] 11 p1704 N85-20719
Micro Focus IBM personal computer XT CIS COBOL; V4.5
[PB85-108868] 11 p1704 N85-20720
ICL, ICL 2988 COBOL C2COB. 1321
[PB85-108876] 11 p1704 N85-20721
MICRO FOCUS Intel Microprocessor Development System MDS221 Compact Level 2 COBOL; V2.5
[PB85-108900] 11 p1704 N85-20722
Micro focus IBM personal computer XT, high performance level, 2 COBOL, IBM PC tailored; V2.6
[PB85-110815] 11 p1705 N85-20725
An algorithm for generating abstract syntax trees
[NASA-CR-172541] 12 p1912 N85-22003
A Gypsy-to-Ada program compiler
[TR-39] 12 p1913 N85-22005
Programs for dynamic loading of precompiled subroutine packages, especially for applications with the Watfiv compiler
[DFVLR-MITT-84-18] 12 p1917 N85-22035
Ryan-McFarland Corporation, IBM PC model XT, RM/FORTRAN, version 2.0.0
[PB85-107993] 12 p1917 N85-22037
Ryan-McFarland Corporation, sun microsystem with sky fast floating point processor, RM/FORTRAN version 1.5.0
[PB85-108009] 12 p1917 N85-22038
Validation summary report, Burroughs Corporation, 820 FORTRAN release 4.0
[PB84-227792] 13 p2145 N85-23316
Praxis language environment: Distribution package description, revision 1
[DE85-006699] 15 p2630 N85-26212
Ada validation summary report. ALS AdaVAX version 1.1 VAX-11/780 using VAX/VMS release 3.6
[AD-A153684] 18 p3162 N85-29588
Ada (trademark) compiler validation summary report. Honeywell information systems GCOS6 Ada version 1.1
[AD-A153746] 18 p3162 N85-29590
Ada compiler validation summary report, University of Karlsruhe-GMD/German MOD Siemens - BS 2000 version 7.30
[AD-A153747] 18 p3163 N85-29591
Ada (trademark) compiler validation summary report: ALSYS ALSYCOMP-0001
[AD-A153750] 18 p3163 N85-29592
Development and analysis of a global compaction technique of microprograms 19 p3334 N85-30654
BP (Basic Processor) TRICOMP user's guide
[AD-A154340] 19 p3337 N85-30674
VAX TRICOMP user's guide
[AD-A154341] 19 p3337 N85-30675
Ada compiler validation summary report: University of Karlsruhe-GMD/German MOD VAX 11 compiler, version v1.0
[AD-A154370] 19 p3337 N85-30678
Resource management for the tagged token dataflow architecture
[AD-A154773] 21 p3667 N85-32779
Integrated Support Software System (ISSS)
[AD-A155715] 22 p3829 N85-33710
The parser generator as a general purpose tool
[NASA-CR-177955] 23 p3957 N85-34521

COMPLEMENTARY METAL OXIDE SEMICONDUCTORS
U CMOS

COMPLETENESS
Sky coverage, confusion, completeness and reliability
09 p1412 N85-18906

COMPLEX COMPOUNDS
Transition metal carbene complexes
[AD-A144879] 01 p0028 N85-10173
Surface environmental effects in electrochemical kinetics: Outer-sphere chromium (3) reductions at mercury, gallium, lead, and thallium surfaces
[AD-A145607] 02 p0172 N85-11155
Macrocyclic poly(tertiary) phosphines for the attachment of metals to surfaces of photodevices
[DE84-015552] 05 p0617 N85-13946
Polyphosphazene solid electrolytes
[AD-A147008] 07 p0931 N85-15902
Separation of gas mixtures with coordination complexes
[DE85-000383] 10 p1438 N85-19062
Observation of a novel low-lying excited state in zinc complexes
[AD-A150188] 13 p2156 N85-23385
Selective detection of species in complex matrices by SIMS (Secondary Ion Mass Spectrometry)
[AD-D011685] 19 p3235 N85-30053

COMPLEX SYSTEMS
Grasp of information by the pilot in future combat aircraft 10 p1533 N85-19662
Improving engineering system design by formal decomposition, sensitivity analysis, and optimization
[NASA-TM-86377] 10 p1551 N85-19785
Mean flow and turbulence in complex terrain NPS (Naval Postgraduate School)/Vandenberg measurement system
[AD-A150184] 13 p2138 N85-23274
Automatic symbolic solution of Markov chains
[AD-A150476] 13 p2153 N85-23369

COMPLEX VARIABLES
NT AIRY FUNCTION
NT ANALYTIC FUNCTIONS
NT BESSEL FUNCTIONS
NT CONFORMAL MAPPING
NT CONJUGATE POINTS
NT ELLIPTIC FUNCTIONS
NT ENTIRE FUNCTIONS
NT EXPONENTIAL FUNCTIONS
NT GAMMA FUNCTION
NT HARMONIC FUNCTIONS
NT HYPERBOLIC FUNCTIONS
NT HYPERGEOMETRIC FUNCTIONS
NT LAGUERRE FUNCTIONS
NT LEGENDRE FUNCTIONS
NT LOGARITHMS
NT MEROMORPHIC FUNCTIONS
NT ORTHOGONAL FUNCTIONS
NT SINGULARITY (MATHEMATICS)
NT SPHERICAL HARMONICS
Simultaneous rational approximation of a function and its derivatives in the complex plane
[CSIR-TWISK-311] 01 p0109 N85-10733
Existence and non-uniqueness of similarity solutions of a boundary layer problem
[NASA-CR-172503] 07 p0957 N85-16064
Bootstrap confidence intervals
[AD-A147572] 07 p1033 N85-16559
Complex symmetric matrices with strongly stable iterates
[NASA-CR-172542] 11 p1706 N85-20731
Computation of elliptical functions in problems of celestial mechanics 13 p1979 N85-22418
Applicability of log-normal model to probabilitistic description of quasi-pulse interference
13 p2084 N85-23014
Pade tables of a class of entire functions
[CSIR-TWISK-337] 14 p2413 N85-24877
Fourier-Stieltjes coefficients and continuation of functions 15 p2633 N85-26231

COMPLEXITY
NT TASK COMPLEXITY
Atmospheric studies in complex terrain
[DE84-008553] 05 p0676 N85-14345
Recognition of complex 3-dimensional objects using 3-dimensional moment invariants
[AD-A148119] 08 p1212 N85-17625
Categorization of nocturnal drainage flows within the Brush Creek valley in western Colorado and the variability of sigma theta in complex terrain
[DE85-011291] 19 p3300 N85-30461
Determination of low chloride values in Rocky Flats scrub alloy solutions and other complex matrices
[DE85-011506] 23 p3911 N85-34234
Communication complexity of distributed shortest path algorithms
[AD-A156049] 24 p4087 N85-35332

COMPLIANCE (ELASTICITY)
U MODULUS OF ELASTICITY

COMPLICATION
U COMPLEXITY

COMPONENT RELIABILITY
Procedures for precap visual inspection
[NASA-RP-1122] 04 p0495 N85-13156
Electronic components for space applications
[CNES-NT-109] 04 p0496 N85-13169
Component reliability and assembling technologies
[CNES-NT-108] 04 p0511 N85-13258
Evaluation of the crack initiation life behavior of fatigue loaded automotive components made from high strength aluminium alloys
[ESA-TT-733] 05 p0651 N85-14181
Engine cyclic durability by analysis and material testing 07 p0907 N85-15744
Bearing tester fit analysis
[NASA-CR-171282] 07 p0973 N85-16181
A practical example of reducing life cycle costs and increased availability 08 p1063 N85-16736
Investigation of accelerated stress factors and failure/degradation mechanisms in terrestrial solar cells
[NASA-CR-175469] 10 p1510 N85-19524
Reliability predictions for military avionics. Royal Signals and Radar Establishment reliability prediction method no. 250
[BR69221] 13 p1973 N85-22388
Reliability bounds for fault-tolerant systems with competing responses to component failures
[NASA-TP-2409] 13 p2100 N85-23090
Automatic symbolic solution of Markov chains
[AD-A150476] 13 p2153 N85-23369
Current transmission systems
14 p2220 N85-23767
The observation and interpretation of gear tooth failures 14 p2224 N85-23792
Establishment and maintenance of certification standards for helicopter and turboprop power transmission systems 14 p2224 N85-23796
Experimental development of a failure detection scheme for large space structures 14 p2234 N85-23846
Estimate of fatigue stability of gas-turbine engine compressor vanes in probabilistic aspect
14 p2287 N85-24169
Detonation flame spraying extends life of automotive parts 15 p2513 N85-25507
Creep ratcheting simplified methods experience from structural design of elevated temperature components
[DE85-007433] 15 p2580 N85-25915
Cost prediction model for various payloads and instruments for the Space Shuttle Orbiter
[NASA-CR-175781] 16 p2729 N85-26842
Component-specific modeling
[NASA-CR-174765] 16 p2799 N85-27261
Experimental measurements and analysis of heat transfer and gas dynamics in a rotating turbine stage
17 p2911 N85-27949
Flow-induced vibration of SSME main injector liquid-oxygen posts 17 p2912 N85-27951
Composite loads spectra for select space propulsion structural components 17 p2912 N85-27953
Development of high temperature resistant, noncorrosible, non-metallic ceramic materials, especially silicon nitride in gas turbine application
[BMFT-FB-T-85-015] 17 p2936 N85-28125
Atomic hydrogen maser active oscillator cavity and bulb design optimization 18 p3108 N85-29240
High level radioactive waste vitrification process equipment component testing
[DE85-011143] 19 p3273 N85-30296
A modular docking mechanism for in-orbit assembly and spacecraft servicing 22 p3796 N85-33516
Failure testing of active solar energy system components
[DE84-013024] 22 p3804 N85-33561
High pressure compressor component performance report
[NASA-CR-168245] 23 p3897 N85-34138

COMPOSITE FUNCTIONS
The nonlinear analysis of thick composite plates using a cubic spline function
[AD-A152115] 16 p2801 N85-27268

COMPOSITE MATERIALS
NT ALUMINUM BORON COMPOSITES
NT ALUMINUM GRAPHITE COMPOSITES
NT BORON REINFORCED MATERIALS
NT CARBON FIBER REINFORCED PLASTICS
NT CARBON-CARBON COMPOSITES
NT CERAMIC MATRIX COMPOSITES
NT CERMETS
NT COMPOSITE PROPELLANTS
NT EPOXY MATRIX COMPOSITES
NT FIBER COMPOSITES
NT FIBER REINFORCED COMPOSITES
NT GLASS FIBER REINFORCED PLASTICS
NT GLASSY CARBON
NT GRAPHITE-EPOXY COMPOSITES
NT GRAPHITE-POLYIMIDE COMPOSITES
NT LAMINATES
NT METAL MATRIX COMPOSITES
NT PLYWOOD
NT POLYMER MATRIX COMPOSITES
NT REINFORCED PLASTICS
NT RESIN MATRIX COMPOSITES
NT SUPERHYBRID MATERIALS
NT WHISKER COMPOSITES
Development of powder metallurgy in various sections of USSR 01 p0019 N85-10116
The theory of elastic modulus of fabric composites and its examination by experiments
[NAL-TR-808] 01 p0022 N85-10133
Piezoelectric and electrostrictive materials for transducer applications
[AD-A145115] 01 p0043 N85-10277
Development of advanced constitutive model for reinforced concrete
[AD-A145050] 01 p0062 N85-10411
Materials studies for magnetic fusion energy applications at low temperatures, 7
[DE84-013487] 01 p0122 N85-10837
Advanced blade tip seal system, volume 2
[NASA-CR-167851] 02 p0147 N85-10999
Advanced manufacturing development of a composite empennage component for L-1011 aircraft
[NASA-CR-165885] 02 p0170 N85-11141
Cumulative damage model for advanced composite materials
[AD-A145441] 02 p0171 N85-11142
Determination of nonlinear viscoelasticity parameters for polymeric and composite materials by numerical methods
[AD-A145311] 02 p0185 N85-11240
Metallography of Kovar/glass/thermite interfaces
[DE84-015247] 02 p0195 N85-11302
Thermal deformation measurements of heat-resistant structural materials for aircraft by electro optical displacement transducer
[NAL-TR-810] 03 p0325 N85-12092
Fatigue-impact studies in laminated composites
[AD-A142841] 03 p0326 N85-12097
A digital algorithm for composite laminate analysis: FORTRAN, Revised
[AD-A145833] 03 p0326 N85-12098
General studies on composite materials. Evaluation of auxiliary products of national origin
[SNIAS-2500/DCI-PR/84] 03 p0326 N85-12101
Modeling the stress field in laminated composite plates near discontinuities
[PB84-219237] 03 p0327 N85-12103
Research in quantitative NDE techniques
[AD-A145990] 03 p0369 N85-12358
Matrix synthesis and characterization
04 p0467 N85-12965
Numerical investigation of the micromechanics of composite fracture 04 p0467 N85-12970
Work hardening of simple two phase composites
[DE84-014629] 04 p0468 N85-12978
Quality assurance of composite materials, test report no. 45-649/F 04 p0469 N85-12981
Erosion of multiphase materials
[DE84-015816] 04 p0474 N85-13018
Insulating polymer concrete
[DE84-017239] 04 p0480 N85-13057
Rotating assembly working group summary
05 p0604 N85-13851
Investigation of the relations between neat resin and advanced composite mechanical properties. Volume 1: Results
[NASA-CR-172303] 05 p0612 N85-13911
Synthesis of reinforced composite threads based on polymer mixtures 06 p0761 N85-14869
Carbon fibre reinforced aluminum matrix composites: A critical review
[AD-A146367] 06 p0764 N85-14883
Optical properties of composite materials
[AD-A146768] 07 p0920 N85-15828
All-composite Airbus empennage
07 p0936 N85-15931
Composite batteries 07 p0936 N85-15932
Advances in composites technology
[NASA-TM-86353] 08 p1118 N85-17048
Model for prediction of the elastic response of composite materials over wide ranges of concentration
[AD-A148186] 08 p1119 N85-17051
Composites with a periodic structure, mathematical analysis and numerical treatment
[AD-A148301] 08 p1119 N85-17053
Composite structure repair, addendum
[AGARD-R-716-ADD] 08 p1120 N85-17057
Repair of composites 08 p1120 N85-17058
Composite repair of aircraft structures
08 p1120 N85-17059
High pressure physics research focusing on composite materials 08 p1140 N85-17186
Nonlinear analysis of composite laminates
09 p1288 N85-18087
Fabrication of ceramic-ceramic composites by chemical vapor deposition
[DE85-000981] 09 p1298 N85-18155
West Europe report: Science and technology
[JPRS-WST-85-003] 09 p1309 N85-18224
Electromagnetic processing of materials
[AD-A148804] 09 p1311 N85-18241
European Scientific Notes, volume 38, number 12
[AD-A148713] 09 p1418 N85-18946
Resistance fail strain gage technology as applied to composite materials
[NASA-CR-3872] 10 p1431 N85-19024
Mechanics of composite materials
[DE85-003611] 10 p1432 N85-19031
Mechanical properties of Be-Al composite
10 p1443 N85-19094
Influence of volumetric fiber content on some matrix damage factors during thermal cycling of tungsten-EI 765 composite 10 p1443 N85-19097
Study of surface damage in cathode composite materials in a high flux CO2 laser 10 p1444 N85-19098
Laser rupture of composite materials
10 p1444 N85-19102
Influence of melting conditions on strength of transition zone between steel and composite material
10 p1450 N85-19133
Ultrasonic analysis of Kevlar-epoxy filament wound spherical test specimens
[DE85-005198] 11 p1593 N85-20024
USSR report: Materials science and metallurgy
[JPRS-UMS-84-005] 11 p1597 N85-20044
Evaluation of residual stress in laminated metallic composites 11 p1598 N85-20052
Predicting stability of full-scale composite constructions of the basis of stiffness 11 p1599 N85-20054
High-strength composite materials for aircraft, body armor 11 p1599 N85-20057
Influence of plastic deformation on structural stability of nichrome-tungsten composite materials
11 p1599 N85-20060
Structure and properties of copper-titanium-aluminum composites obtained by thermoreactive sintering
11 p1600 N85-20061
Stability of superconducting composites in a magnetic field
[DE85-002731] 11 p1734 N85-20907
Magnetization measurements on multifilamentary Nb3Sn and NbTi conductors
[DE85-001237] 11 p1737 N85-20923
Composite structural materials
[NASA-CR-175515] 12 p1796 N85-21268
Temperature responses of composite panels
[AD-A150053] 12 p1798 N85-21277
Chemical approach for controlling nadimide cure temperature and rate with maleimide
[NASA-CASE-LEW-13770-3] 12 p1809 N85-21350
Chemical approach for controlling nadimide cure temperature and rate with maleimide
[NASA-CASE-LEW-13770-4] 12 p1810 N85-21351
Finger materials for air cushion vehicles. Volume 2: Base fabrics for finger materials
[AD-A149701] 12 p1819 N85-21408
Fiber reinforced fused silica for hypersonic radome applications
[AD-P004366] 12 p1826 N85-21460
Proceedings of the 9th Biennial Army Symposium on Solid Mechanics. Advances in Solid Mechanics for Design and Analysis
[AD-A150042] 12 p1867 N85-21710
Nonlinear analysis of layered composite plates and shells
[PB85-127181] 12 p1868 N85-21719
Research Reports: 1984 NASA/ASEE Summer Faculty Fellowship Program
[NASA-CR-171317] 12 p1944 N85-22210
Investigation of the effects of NaOH dopant level on the physical and mechanical properties of carbon/phenolic composite material 12 p1945 N85-22213
Silicon carbide-silicon nitride fibers: Preparation and characterization of polycarbosilazane precursors
12 p1945 N85-22214
Solid Rocket Motor Case (SRMC) dynamic sensitivity to changes in composite properties
12 p1948 N85-22238
Simple theoretical models for composite rotor blades
[NASA-CR-175620] 13 p1971 N85-22282
Mechanism of strengthening plastics with rubbers
13 p2014 N85-22636
USSR report: Materials science and metallurgy
[JPRS-UMS-85-002] 13 p2025 N85-22688
Uses of composite materials
13 p2027 N85-22696
Dissipation of energy in composite material
13 p2027 N85-22703
Possibility of producing monolithic composite materials based on niobium carbide 13 p2028 N85-22707
Theoretical and experimental investigation of mechanically fastened composites
[AD-A150961] 14 p2248 N85-23935
Some optimization problems in static aeroelasticity for wings made of composite materials
14 p2277 N85-24104
Recent developments in the dynamics of advanced rotor systems
[NASA-TM-86669] 14 p2317 N85-24320
USSR report: Materials science and metallurgy
[JPRS-UMS-85-001] 15 p2496 N85-25285
West Europe report: Science and technology
[JPRS-WST-84-012] 15 p2523 N85-25552
MBB uses new CFC form tool for titanium alloy air intake 15 p2523 N85-25553
West Europe report: Science and technology
[JPRS-WST-84-008] 15 p2531 N85-25606
Pechiney strategy includes development of new materials 15 p2531 N85-25607
Glass, carbon fibers made at Fibre et Mica in France
15 p2534 N85-25634
West Europe report: Science and technology
[JPRS-WST-84-003] 15 p2534 N85-25635
France develops own aluminum-based composite ceramic 15 p2534 N85-25636
A study of the time dependence in fracture processes relating to service prediction of adhesive joints and advanced composites
[AD-A152064] 15 p2579 N85-25910
Simultaneous chemical vapor deposition of SiC-dispersed phase composites
[DE85-007751] 16 p2744 N85-26831
The nonlinear analysis of thick composite plates using a cubic spline function 16 p2798 N85-27252
The nonlinear analysis of thick composite plates using a cubic spline function
[AD-A152115] 16 p2801 N85-27268
Friction and wear behavior of aluminum and composite I-beam stiffened airplane skins
[NASA-TM-86418] 17 p2895 N85-27852
Gordon Research Conference on Composites
[AD-A152886] 17 p2917 N85-27979
Solution to eigenvalue problems of antisymmetric cross-ply and antisymmetric angle-ply laminated plates using affine transformations
[AD-A153040] 17 p2917 N85-27980
Interaction among inhomogeneities and inclusions
[AD-A153114] 17 p2979 N85-28419
Analytical shear buckling investigation of curved composite panels
[AD-A153138] 17 p2980 N85-28421
High temperature composite thermal storage systems
[DE85-005073] 17 p2986 N85-28455
Erosion of multiphase materials
[DE85-008895] 18 p3068 N85-28978
An evaluation and preparation of ferromagnetic liquid composites for use at millimeter wavelengths
[AD-A153939] 18 p3069 N85-28980
Application of lightweight composite materials to naval weapons systems
[PB85-173607] 18 p3069 N85-28981
British breakthrough in lightweight lithium batteries
18 p3086 N85-29092
West Europe report: Science and technology
[JPRS-WST-84-032] 18 p3086 N85-29095
West Europe report: Science and technology
[JPRS-WST-84-037] 18 p3088 N85-29108
Structural Analysis
[DFVLR-MITT-84-21] 18 p3120 N85-29313
Mechanics of composite materials, theory and application
[VTH-LR-431] 18 p3123 N85-29334
Influence of microstructure on mechanical properties in cemented tungsten-carbides 19 p3230 N85-30020
The fabrication, microstructure, and strengthening behavior of heavily cold-worked in situ composites
19 p3231 N85-30031

A study of the stress wave factor technique for the characterization of composite materials
[NASA-CR-174870] 19 p3231 N85-30035
USSR report: Materials Science and Metallurgy
[JPRS-UMS-85-005] 19 p3241 N85-30095
Thermo-mechanical and thermal behavior of high-temperature structural materials
[AD-A154154] 19 p3266 N85-30251
Impact dynamics research on composite transport structures
[NASA-TM-86391] 19 p3284 N85-30367
Some asymptotic problems in the optimal control of distributed systems 20 p3412 N85-31175
Long-term thermal aging of Celion/V378A composite materials
[NASA-TM-86362] 20 p3421 N85-31236
Design and fabrication of durable owner-built wind turbine blades
[DE85-009200] 20 p3484 N85-31650
R and D programmes at the National Aeronautical Laboratory
[AR-22] 20 p3539 N85-32022
R and D activities of the Materials Science Division
20 p3539 N85-32024
A cracked orthotropic sheet stiffened by a semi-infinite orthotropic sheet
[NASA-TP-2455] 21 p3597 N85-32339
New materials needs in aeronautics
[SNIAS-851-502-101] 22 p3729 N85-33120
Dispersion toughened ceramic composites and method for making same
[DE85-011601] 22 p3751 N85-33252
Proceedings of the Twentyseventh Japan Congress on Materials Research
[ISSN-0368-3141] 23 p3903 N85-34180
Negative flexural behavior of precase composite slabs with steel joint 23 p3904 N85-34183
Composite desiccant structure
[DE85-006400] 23 p3910 N85-34226
Centralized surveillance of flexible workshops for the manufacturing of composite materials
[SNIAS-851-430-103] 23 p3910 N85-34227
Product definition: Technical specification of needs
[SNIAS-851-430-104] 23 p3910 N85-34228
Process for improving moisture resistance of epoxy resins by addition of chromium ions
[NASA-CASE-LAR-13226-1] 23 p3919 N85-34282
Development and demonstration of a spiral-wound thin-film composite membrane system for the economical production of oxygen-enriched air, phase 4
[DE85-012380] 23 p3920 N85-34288
SRB TFS closeout materials characterization
[NASA-CR-170885] 24 p4070 N85-35222

COMPOSITE PROPELLANTS
Catalyzed low burning rate propellants for upper-stage solid rocket motor
[NAL-TR-805] 03 p0339 N85-12181
Study of the transition from deflagration to detonation of previously fragmented propellants
08 p1115 N85-17032
The heat sensitivity of solid propellants
08 p1117 N85-17043
Plasticizer system for propellant compositions
[AD-D011502] 12 p1816 N85-21390
Characterization of heterogeneity of composite propellants and its effects on combustion behavior
13 p2000 N85-22539
Mechanism of burning rate enhancement by ferric oxide 13 p2002 N85-22546
Non-steady combustion of composite solid propellants
[AD-A150627] 14 p2250 N85-23947
Model of normal and erosive burning of composite propellants
[ONERA-NT-1984-3] 14 p2263 N85-24024
PSA, Renault work on all fuel automobile engine
15 p2531 N85-25604
Propellant plasticizer
[AD-D011501] 20 p3434 N85-31306

COMPOSITE STRUCTURES
NT LAMINATES
NT PLYWOOD
Lightweight composite launcher pod
[AD-D011238] 01 p0015 N85-10092
Effect of stress concentrations in composite structures
[NASA-CR-173976] 02 p0170 N85-11140
Solvent resistant thermoplastic composite matrices
04 p0466 N85-12960
Composite fracture toughness and impact characterization 04 p0466 N85-12963
Full-scale testing, production and cost analysis data for the advanced composite stabilizer for Boeing 737 aircraft. Volume 1: Technical summary
[NASA-CR-3649] 05 p0612 N85-13912
Design, ancillary testing, analysis and fabrication data for the advanced composite stabilizer for Boeing 737 aircraft. Volume 1: Technical summary
[NASA-CR-3648] 05 p0612 N85-13913
Design, ancillary testing, analysis and fabrication data for the advanced composite stabilizer for Boeing 737 aircraft, volume 2
[NASA-CR-166011] 05 p0612 N85-13914
Full-scale testing, production and cost analysis data for the advanced composite stabilizer for Boeing 737 aircraft, volume 2
[NASA-CR-166012] 05 p0613 N85-13915
Verification of a computer program for vibration analysis of composite wing cores
[NAL-TR-825] 06 p0817 N85-15187
Evaluation of the alkaline peroxide pre-bond surface treatment for titanium
[AD-A147352] 07 p0928 N85-15881
Modeling localized stress fields in composite laminates
[AD-A148630] 08 p1120 N85-17056
Composite structure repair, addendum
[AGARD-R-716-ADD] 08 p1120 N85-17057
Wave propagation in periodic, composite structures
09 p1332 N85-18370
Proceedings of Colloquium/Workshop on Composite Materials and Structures, Standardization, Qualification, Certification held at washington, D.C. on 8-10 May 1984
[AD-A149039] 10 p1432 N85-19029
Thermoviscoelastic analysis of dimensionally stable fiber composite space structures
[AD-A149275] 11 p1593 N85-20021
Ultrasonic characterization of advanced composite flywheels
[DE85-000158] 11 p1593 N85-20026
Characterization of mode 1 and mixed-mode failure of adhesive bonds between composite adherends
[NASA-TM-86355] 12 p1797 N85-21270
Temperature responses of composite panels
[AD-A150053] 12 p1798 N85-21277
Use of acoustical emission method to study specifics of fracture of boron reinforced plastic structural elements 13 p2026 N85-22696
Axisymmetrical oscillations of shell systems subjected to impulse loads 13 p2047 N85-22814
Finite element model for creep in composite masonry
[PB85-150324] 14 p2322 N85-24347
Design, fabrication and test of composite curved frames for helicopter fuselage structure
[NASA-CR-172438] 15 p2470 N85-25247
A preliminary investigation into transverse fracture of unidirectional fiber composites
[AERE-R-11494] 15 p2503 N85-25438
Directional thermal conductivities of graphite-epoxy composites: 0/90 and 0/ + or - 45/90
[AD-A152209] 16 p2743 N85-26929
Effects of the phase compositions of cast low-pearlite steels micro-alloyed with vanadium and titanium of their structure and properties
[BLL-BISI-TRANS-22301-(9022.06)]
17 p2926 N85-28067
Initial imperfection surveys on conical shells at Hoechst AG
[VTH-LR-407] 17 p2981 N85-28429
Light weight fire resistant graphite composites
[NASA-CASE-ARC-11615-1-SB]
18 p3068 N85-28976
The effect of center delamination on the instability of composite cylindrical panels
[AD-A153494] 18 p3069 N85-28979
Expedient runway surfacing with post tensioning system for expeditionary airfields
[AD-D011677] 19 p3222 N85-29976
Thermo-mechanical and thermal behavior of high-temperature structural materials
[AD-A154154] 19 p3266 N85-30251
Automated fabrication of composite structures for helicopters
[SNIAS-851-210-104] 20 p3393 N85-31049
Generation of round bores in composite structure railguns
[DE85-011672] 22 p3793 N85-33501

COMPOSITE WRAPPING
Testing of wound materials for strength with loading in the reinforcement plane 13 p2027 N85-22701

COMPOSITES
U COMPOSITE MATERIALS

COMPOSITION (PROPERTY)
NT ATMOSPHERIC COMPOSITION
NT ATMOSPHERIC MOISTURE
NT ATOM CONCENTRATION
NT CARBON DIOXIDE CONCENTRATION
NT CHEMICAL COMPOSITION
NT CONCENTRATION (COMPOSITION)
NT GAS COMPOSITION
NT IONOSPHERIC COMPOSITION
NT LOW CONCENTRATIONS
NT LUNAR COMPOSITION
NT MASCONS
NT METEORITIC COMPOSITION
NT MOISTURE CONTENT
NT PLANETARY COMPOSITION
NT PLASMA COMPOSITION
NT STELLAR COMPOSITION
The constitution as the basis for recent and future developments of wear resistant materials
02 p0179 N85-11205
The effects of Cr, Co, Al, Mo and Ta on the cyclic oxidation behavior of a prototype cast Ni-base superalloy based on a 2(5) composite statistically designed experiment
[NASA-TM-83784] 03 p0331 N85-12131
The influence of inert particulate material on the properties of RDX/polyethylene wax compositions
[MRL-R-929] 03 p0336 N85-12159
Compound class quantitation of JP-5 jet fuels by high performance liquid chromatography-differential refractive index detection
[AD-A145754] 03 p0340 N85-12185
The growth of metastable peritectic compounds
[NASA-CR-171289] 07 p0920 N85-15824
Properties of miscible polymer blends
[AD-A147090] 07 p0931 N85-15903
Clustering and ordering in 3-5 alloys
[AD-A150604] 13 p2022 N85-22670
Synthesis and properties of elevated temperature P/M aluminum alloys
[AD-A151031] 14 p2256 N85-23981
Ion kinetics, small neutral and excited components in D-region with elevated ionization level. Part 2: Variations in small neutral and excited components
15 p2480 N85-25307
Self-sustaining coatings for fusion applications: Copper lithium alloys
[DE85-009740] 18 p3190 N85-29783
Application of the Diffusion Raman Anti-Stokes Coherent (DRASC) method to a SNECMA combustion chamber
[YKC-3086/84] 20 p3425 N85-31260
Chemical structure of interfaces
20 p3480 N85-31629
Quantitative determination of mineral composition by powder X-ray diffraction
[DE85-011654] 22 p3760 N85-33301
Energy dependence of cosmic ray composition above 10(15) GeV/nucleus
[OG-5.4-4] 22 p3886 N85-34081
The primary cosmic ray mass composition at energies above 10(14) eV
[OG-5.4-6] 22 p3886 N85-34083
Uranium, thorium isotopic analyses and uranium-series ages of calcite and opal and stable isotopic compositions of calcite from drill cores UE25a no. 1, USR G-2 and USW G-3/GU-3, Yucca Mountain, Nevada
[DE85-013039] 23 p3948 N85-34471
Screening and characterizing oleaginous microalgal species from the southeastern United States
[DE85-006787] 23 p3951 N85-34488

COMPOUNDING
Milling of Si3N4 with Si3N4 hardware
[NASA-TM-86864] 01 p0031 N85-10191

COMPRESSED AIR
Dynamic and other secondary benefits of compressed air energy storage
[DE84-015571] 03 p0386 N85-12468
Qualification of a wall gage for the SIMA wagon, adapted to the test of half models motorized by compressed air turbines — SIMA wind tunnel
[ONERA-PV-1/8068-GY] 16 p2701 N85-26677

COMPRESSED GAS
Experiments with phase transitions at very high pressure
[NASA-CR-174029] 02 p0172 N85-11148
Internal hysteresis experienced on a high pressure syn gas compressor 05 p0642 N85-14122
Development of improved capabilities for computation of gas supercompressibility factors and other properties
[PB85-188316] 20 p3436 N85-31315

COMPRESSIBILITY
Design proposals for torsional buckling of stiffeners
[AD-A144783] 01 p0062 N85-10409
Methods to increase linac efficiency
[DE84-014692] 01 p0118 N85-10809
Volume compressibilities of transuranium elements compounds, especially of neptunium compounds
03 p0431 N85-12744
Influence of pressure on compaction during compression of powders of iron and 40Kh and 10R6MS steels
[BLL-M-35995-(5828.4)] 07 p0926 N85-15866
Investigations into the effects of scale and compressibility on lift and drag in the RAE 5m pressurized low-speed wind tunnel 08 p1066 N85-16773

New discovery in supersonic flight research
09 p1278 N85-18041

Measurement of gas compressibility factor data for natural gas and synthetic gas components and their mixtures
[PB85-129047] 11 p1614 N85-20151

Development and evaluation of a procedure for the rapid analysis of fresh concrete
[AD-A149741] 12 p1866 N85-21703

Pion production and the nuclear equation of state
[DE85-009941] 19 p3365 N85-30870

Development of improved capabilities for computation of gas supercompressibility factors and other properties
[PB85-188316] 20 p3436 N85-31315

Analysis of long bone and vertebral failure patterns
[AD-A154796] 21 p3663 N85-32758

Characteristics of central collision events in Fe-nucleus interactions for 20 - 60 GeV/nucleon
[HE-1.4-3] 24 p4176 N85-35891

COMPRESSIBILITY EFFECTS

Flutter parametric studies of cantilevered twin-engine-transport type wing with and without winglet. Volume 1: Low-speed investigations
[NASA-CR-172410-VOL-1] 04 p0513 N85-13269

Investigations into the effects of scale and compressibility on lift and drag in the RAE 5m pressurised low-speed wind tunnel
[RAE-TM-AERO-2006] 13 p1969 N85-22372

Deceleration of a supersonic flow behind a curved shock wave with isentropic precompression
[NASA-TM-77920] 24 p4061 N85-35164

COMPRESSIBLE BOUNDARY LAYER

Measurement of the development of the boundary layer in the annulus walls of a fourstage compressor
[CUED/A-TURBO-TR-121] 01 p0046 N85-10299

COMPRESSIBLE FLOW

NT TRANSONIC FLOW

Measurement of the development of the boundary layer in the annulus walls of a fourstage compressor
[CUED/A-TURBO-TR-121] 01 p0046 N85-10299

Review of some vortex relations
[NASA-CR-172452] 01 p0046 N85-10302

Particle entrainment in a compressible vortex
[ISL-CO-230/83] 04 p0500 N85-13192

An iwatsubo-based solution for labyrinth seals - comparison with experimental results
05 p0644 N85-14131

A simple extension to multidimensional problems of the artificial viscosity due to Lapidus
06 p0808 N85-15134

Inviscid compressible flow past a multi-element aerofoil 08 p1069 N85-16776

A Van Leer shock capturing algorithm for the Euler equations
[AD-A148761] 08 p1163 N85-17335

Front tracking for gac dynamics
[DE85-000571] 08 p1163 N85-17336

Notes on compressible flow equations for thermodynamics of hot jets
[BAE-KRS-N-GEN-273] 09 p1318 N85-18289

Development of multigrid algorithms for problems from fluid dynamics
[GMD-111] 09 p1321 N85-18305

A 3-dimensional mass conserving element for compressible flows
[NASA-CR-172513] 09 p1373 N85-18626

Efficient self-consistent viscous-inviscid solutions for unsteady transonic flow
[NASA-TM-86335] 10 p1420 N85-18959

SSME thrust chamber simulation using Navier-Stokes equations
[NASA-CR-171349] 10 p1430 N85-19017

Algorithms for the Euler and Navier-Stokes equations for supercomputers
[NASA-CR-172543] 10 p1539 N85-19701

Modeling turbulent flow in compressible fluids: Metrological aspects — conferences
11 p1575 N85-19926

An investigation of compressible flows over open cavities including shear layer thickness effects
[AD-A150086] 12 p1847 N85-21588

Computations of two-dimensional airfoil-vortex interactions — helicopter rotor flowfields
[NASA-CR-3885] 14 p2210 N85-23709

Experimental and theoretical investigation of the motion of particles in a compressible vortex
[ISL-R-129/83] 14 p2303 N85-24264

Gasdynamic evaluation of choking cascade turns
[AD-A151854] 15 p2557 N85-25776

Pseudo-unsteady systems for steady inviscid flows
[ESA-TT-877] 15 p2558 N85-25782

Waveguide phenomena in dense relaxing gases and their use in chemical and gas-dynamic lasers
15 p2644 N85-26308

Numerical simulation of inviscid compressible flow through three-dimensional cascade
16 p2692 N85-26619

Recent progress in computational aerodynamics
16 p2693 N85-26626

LU methods for the compressible Navier-Stokes equations 16 p2781 N85-27160

An experimental study of compressible turbulent reattaching free shear layers 16 p2781 N85-27161

Solution of Onsager's equation for a rotating compressible fluid in a multiply-connected domain
[DE85-007048] 16 p2784 N85-27178

A four-field model for Tokamak plasma dynamics
[DE85-007111] 16 p2866 N85-27694

Calculation of viscous compressible flows in small gas turbines 17 p2912 N85-27950

Supersonic flow around blunt wedge
17 p2942 N85-28158

The method of residual minimization in compressible steady flows
[AD-A153924] 18 p3100 N85-29193

Application of computational fluid dynamics to complex inlet ducts
[NASA-TM-87060] 19 p3265 N85-30247

An implicit finite-difference code for a two-equation turbulence model for three-dimensional flows
[NASA-TM-86752] 20 p3454 N85-31446

On the evaluation of boundary layer measurements on boattailed bodies of revolution in axisymmetric compressible subsonic flow
[ESA-TT-883] 20 p3457 N85-31471

Two-dimensional simulation of instability growth due to shocks
[DE85-011869] 22 p3784 N85-33442

Scalar/Vector potential formulation for compressible viscous unsteady flows
[NASA-CR-3921] 23 p3893 N85-34113

Compressible two-phase flow instabilities simulated with a hybrid Lagrange-Euler pseudospectral method
[DE85-009904] 23 p3931 N85-34361

Calculation of compressible flow about three-dimensional inlets with auxiliary inlets, slats and vanes by means of a panel method
[NASA-CR-174975] 24 p4060 N85-35162

Acoustic resonances in cylinder bundles oscillating in a compressible fluid
[DE85-004066] 24 p4145 N85-35699

COMPRESSIBLE FLUIDS

Rayleigh-Taylor instability in compressible media
[AD-A145491] 02 p0198 N85-11322

Nonsteady motion of solid sphere in compressible viscous fluid 02 p0269 N85-11753

Analysis of the surface load and radiated sound of a vibrating airfoil with application to the experiment of Brooks
[NASA-CR-3864] 07 p1038 N85-16590

Generation of sound by a vortex point in a steady flow of slightly compressible fluid 11 p1715 N85-20789

Some approximations of geophysical hydrodynamics
14 p2336 N85-24448

An analysis of flow models: From Navier-Stokes to potential flow equations 21 p3587 N85-32295

COMPRESSING

NT PLASMA COMPRESSION

Light scattering studies of lower dimensional colloidal particle and critical fluid systems
[DE85-002087] 09 p1377 N85-18654

Simplified theory for the behaviour of buried flexible cylinders under the influence of uniform hoop compression
[PB85-116531] 11 p1654 N85-20419

Thermocompression welding of parts made from AMts and VT1 alloys 15 p2501 N85-25430

Design of electrooptical system with annular cathode and electrostatic compressor 22 p3770 N85-33367

Preliminary considerations for the gasdynamic precompression of solid molecular hydrogen
[DE85-013256] 22 p3784 N85-33445

COMPRESSION LOADS

NT AXIAL COMPRESSION LOADS

NT IMPACT LOADS

Method and apparatus for determining pressure-induced frequency-shifts in shock-compressed materials
[DE84-014313] 01 p0024 N85-10151

Force standard machines of the National Institutes for Metrology, vol. 2
[PTB-ME-62-VOL-2] 01 p0036 N85-10224

Interactive buckling of thin-walled structural components under static and dynamic loads
01 p0059 N85-10392

Locomotion research for the analysis of the human gait and for the determination of the maximum loads of the pelvis-leg skeleton. Volume 2: Three-dimensional analysis
[BMFT-FB-T-83-188-VOL-2] 02 p0236 N85-11536

A buckling analysis for rectangular orthotropic plates with centrally located cutouts
[NASA-TM-86263] 04 p0513 N85-13268

Fatigue life improvement due to mechanically induced compressive residual stresses 05 p0650 N85-14175

Computer program for determining induced stresses and consolidation settlements (CSETT)
[AD-A146730] 07 p1023 N85-16493

Delamination growth in graphite epoxy laminates under compressive loads 09 p1266 N85-18088

Slit-ring test for evaluating fracture in tubular cross sections
[DE85-003550] 11 p1654 N85-20418

Simplified theory for the behaviour of buried flexible cylinders under the influence of uniform hoop compression
[PB85-116531] 11 p1654 N85-20419

Stability of viscoelastic constructions subjected to steady random compressing loads 11 p1720 N85-20819

Behavior of buried flexible cylinders under the influence of nonuniform hoop compression
[PB85-116523] 12 p1868 N85-21718

Orientation and temperature dependence of some mechanical properties of the single-crystal nickel-base superalloy Rene N4. 3: Tension-compression anisotropy
[NASA-TM-86982] 13 p2021 N85-22680

Testing of wound materials for strength with loading in the reinforcement plane 13 p2027 N85-22701

Impacts in ice: Commissions of solar system crater population 13 p2181 N85-23538

Design of transversely stiffenend FRP panels under compressive load — fiber reinforced plastic (FRP) ships
[AMTE(S)-R-84104] 23 p3940 N85-34424

User's guide: A computer program for strength analysis of non-hydraulic concrete structural elements. Report 2. Strength design of reinforced concrete column sections (PCAUC)
[AD-A156393] 24 p4102 N85-35429

COMPRESSION RATIO

Converting gasoline farm tractors to run efficiently on farm-produced alcohol
[DE84-015796] 02 p0205 N85-11350

COMPRESSION TESTERS

U COMPRESSION TESTS

COMPRESSION TESTS

Effects of constituent properties on compression failure mechanisms 04 p0464 N85-12946

Compression of a band made of elastic, ideally Coulomb plastic material
[ISSN-0208-5658] 05 p0648 N85-14157

Strength properties of unidirectionally reinforced hybrid composites 11 p1599 N85-20058

Experimental investigation of crippling strength of Chinese aluminum alloy (LY12CZ) sections
13 p2041 N85-22779

Hydrostatic compression of Fe1-chi 0 wustite.
15 p2508 N85-25472

System expectations for Pioneer 1 foil implosion experiments
[DE85-014129] 24 p4091 N85-35359

COMPRESSION WAVES

Dynamic compression and volatile release of carbonates
[NASA-CR-174076] 03 p0391 N85-12504

Shock compression of liquid helium to 56 GPa (560) kbar 13 p2184 N85-23551

Compression waves in front of and behind a piston launched in a shock tube
[ISL-R-101/83] 14 p2303 N85-24260

Crosswell acoustic surveying in gas sands: Travel-time pattern recognition, seismic Q and channel waves
[DE85-010777] 19 p3352 N85-30778

COMPRESSIVE STRENGTH

Effect of impact damage and open holes on the compression strength of tough resin/high strain fiber laminates 04 p0464 N85-12945

Effects of constituent properties on compression failure mechanisms 04 p0464 N85-12946

Mechanical property data 7050-t736511 alloy
[AD-A147365] 07 p0928 N85-15882

Laboratory investigation on adhesives for Naval facilities construction
[AD-A147453] 07 p0932 N85-15900

Compressive strength-maturity relationships of mortar containing fly ash
[AD-A148705] 09 p1339 N85-18423

Studies of structure and mechanical properties of carbon-reinforced plastic based on spirally reinforced filler 10 p1444 N85-19100

A model for the compressive buckling of extended chain polymers
[AD-A151025] 14 p2260 N85-24008

Compressive strength of epoxy resin chocks subjected to elevated temperatures
[AD-A152018] 15 p2519 N85-25532

Experimental study of the effect of moist environments on epoxy resin chocks
[AD-A152052] 15 p2566 N85-25849

User's guide for concrete strength investigation and design (CSTR)
[AD-A151617] 15 p2579 N85-25906

Buckling and post-buckling behavior of sparsely connected built-up columns 19 p3283 N85-30358

Analysis of the elastic and strength properties of Yucca Mountain tuff, Nevada
[DE85-006975] 19 p3300 N85-30460

Geothermal COMPAX drill hit development
[DE85-011353] 20 p3469 N85-31556

The effect of mould size on the exothermic reaction and compressive strength of epoxy resin chocks
[AD-A155102] 21 p3570 N85-32203

COMPRESSOR BLADES

Jet engine blade repair at the Oklahoma Air Logistics Center, Propulsion Division
[AD-P004003] 03 p0307 N85-11983

An experimental investigation and numerical simulation of the thermomechanical phenomena in compressor rotor tip rubbing 03 p0367 N85-12352

Users manual for a computer program for dynamic response analysis of bladed systems
[UDR-TR-84-38] 04 p0456 N85-12893

Vaned diffusers --- in centrifugal compressors
05 p0637 N85-14085

Annular groove in compressor casing as device for control of air stream 13 p2050 N85-22832

Influence of surface roughness on compressor blades at high reynolds number in a two-dimensional cascade
[AD-A151855] 15 p2557 N85-25777

Precision die forging of blades or gas turbines
17 p2940 N85-28148

Design, development and operation of a high simultaneous capacity digital telemetry system --- turbomachine blade flutter
[PNR-90261] 23 p3899 N85-34151

Unsteady flow in a supersonic cascade with two in-passage shocks
[NASA-CR-3925] 24 p4060 N85-35158

COMPRESSOR EFFICIENCY

Vaneless diffusers --- flow in centrigal compressors
05 p0637 N85-14084

Experimental study of influence of size of upper and lower laps on operational efficiency of centripetal full-inlet air driven microturbines 09 p1307 N85-18211

COMPRESSOR ROTORS

Energy efficient engine component development and integration program
[NASA-CR-170034] 02 p0146 N85-10990

An experimental investigation and numerical simulation of the thermomechanical phenomena in compressor rotor tip rubbing 03 p0367 N85-12352

Experimental on-stream elimination of resonant whirl in a large centrifugal compressor 05 p0642 N85-14121

Problems and possibilities for life extension in gas turbine components 07 p0907 N85-15742

Study of dynamic characteristics of prefabricated gas turbine compressor rotor 14 p2272 N85-24078

Investigation of gas-turbine engine blower impeller vibrations with change in engine intake conditions
14 p2287 N85-24170

Ceramic turbochargers: A case study of a near-term application of high-strength ceramics
[DE85-006495] 17 p2975 N85-28379

Numerical and experimental investigation of turbomachinery rotor flow fields
20 p3451 N85-31429

COMPRESSORS

NT CENTRIFUGAL COMPRESSORS
NT SUPERCHARGERS
NT TRANSONIC COMPRESSORS
NT TURBOCOMPRESSORS

Measurement of the development of the boundary layer in the annulus walls of a fourstage compressor
[CUED/A-TURBO-TR-121] 01 p0046 N85-10299

Energy efficient engine. High pressure compressor detail design report
[NASA-CR-165558] 02 p0147 N85-10998

Development of a Braun linear engine-driven, heat-actuated heat pump
[DE84-016647] 04 p0500 N85-13188

Screw expander for light duty diesel engines
04 p0506 N85-13242

Noise in small portable motocompressors. Experiments on limited-cost acoustic treatments to obtain progressive improvements
[CETIM-11-H-445] 04 p0558 N85-13557

Measurements of satellite refrigeration compressor power consumption and efficiency
[DE84-016724] 05 p0632 N85-14056

Open-cycle vapor compression heat pump
[PB85-101475/GAR] 06 p0775 N85-14951

Verification of life prediction through component testing 07 p0908 N85-15748

Turbo fluid machinery and diffusers
[NASA-TM-77467] 08 p1167 N85-17383

On one design principle of surge protector for gas turbine engine compressor 09 p1306 N85-18206

New air supply-prime mover facility for engine tests detailed 11 p1621 N85-20204

Magentically actuatnd compressor
[NASA-CASE-GSC-12799-1] 12 p1818 N85-21404

Annular groove in compressor casing as device for control of air stream 13 p2050 N85-22832

Automating the study of error in discrete aerodynamic fairing design 14 p2288 N85-24176

Solid state compressor
[AD-A150790] 14 p2311 N85-24302

An experimental study of aerodynamic damping characteristics of a compressor annular cascade in high speed flow and the visualization of annular cascade flow
[NAL-TR-838] 15 p2554 N85-25759

Testing of materials and coatings for jet engine components under simulated operational conditions
[B8580073] 17 p2899 N85-27873

Strutless diffuser for gas turbine engine
[AD-D011682] 18 p3062 N85-28943

Compressor and turbine models - numerical stability and other aspects
[AD-A153811] 18 p3063 N85-28948

Nonlinear global stability analysis of compressor stall phenomena
[NASA-CR-174908] 19 p3219 N85-29960

High pressure compressor component performance report
[NASA-CR-168245] 23 p3897 N85-34138

Combined cold compressor/ejector helium refrigerator
[DE85-006408] 23 p3925 N85-34326

COMPTON EFFECT

Neutron activation analysis of stoney spherules from a marine sediment sample 06 p0883 N85-15608

An inverse Compton model of the X-ray emission in Seyfert galaxies 08 p1241 N85-17827

Power law X- and gamma-ray emission from relativistic thermal plasmas 08 p1241 N85-17829

Consequences of hot gas in the broad line region of active galactic nuclei
[NASA-TM-86176] 11 p1763 N85-21090

X-ray polarimetry: The measurement of the polarization of solar flare X-rays and the design of a Compton polarimeter 14 p2441 N85-25059

A synchrotron/inverse Compton interpretation of a solar burst producing fast pulses at lambda 3 mm and hard X-rays 16 p2887 N85-27815

Angle averaged Compton cross sections for degenerate electron gases
[AD-A154464] 19 p3371 N85-30908

Variations in the small-scale galactic magnetic field and short time-scale intensity variations of extragalactic radio sources 20 p3549 N85-32084

The possibility of observing and exploiting the generation of high-energy photons by electrons in the field of an intense electromagnetic wave 21 p3691 N85-32931

Inverse-Compton gamma rays in the galaxy
[OG-3.1-2] 22 p3873 N85-33990

Multicomponent analysis of total COS-B gamma-ray data at intermediate lattitudes
[OG-3.1-3] 22 p3873 N85-33991

X-ray spectra of bursting neutron stars
23 p3981 N85-34686

Study of non-thermal photon production under different scenarios in solar flares. 2: The Compton inverse and Bremsstrahlung models and fittings
[SH-1.2-3] 23 p3991 N85-34739

Solar flare gamma-ray line spectroscopy
[SH-2.1-14] 23 p3999 N85-34795

Breeding new light into old machines (and new)
[DE85-013055] 24 p4155 N85-35763

Result of Monte-Carlo simulation of electron-photon cascades in lead and layers of lead-scintillator
[HE-3.6-11] 24 p4185 N85-35958

COMPUTATION

NT MINIMUM VARIANCE ORBIT DETERMINATION
NT ORBIT CALCULATION

Interpolation formulas for viscosity of six gases: Air, nitrogen, carbon dioxide, helium, argon and oxygen
[PB84-217801] 01 p0026 N85-10161

Research in Structures and Dynamics, 1984
[NASA-CP-2335] 01 p0057 N85-10377

Numerical algorithms and parallel tasking
[AD-A145090] 01 p0104 N85-10693

Fast Fourier transform for unequally spaced data
01 p0128 N85-10876

Calculations of optical properties of transition metals
[BLL-M-35744-(5828.4)] 02 p0175 N85-11175

Criteria for the optimization of processing flow in a model of an incremental computer with multiprocessing resources
[INPE-3046-TDL/158] 02 p0240 N85-11560

Parallel triangularization of substructured finite element problems
[NASA-CR-172466] 02 p0241 N85-11569

Concurrent processing and the decomposition of problems
[DE84-015285] 02 p0242 N85-11581

Research topics: Multiprocessing algorithms for computational logic
[DE84-015500] 02 p0242 N85-11583

Shuffle-exchanges on augmented meshes
[NASA-CR-172476] 02 p0243 N85-11587

Comparison of the multigrid and ICCG methods in solving the diffusion equation
[DE84-014409] 02 p0253 N85-11657

Survey of ONERA activities on adaptive-wall applications and computation of residual corrections
03 p0312 N85-12013

An inviscid computational method for supersonic inlets
[AD-A145997] 03 p0316 N85-12042

Verification of a class of deadlock-free, self-timed, computational arrays
[AD-A146272] 03 p0412 N85-12638

Computational models of crystals
[DE84-016631] 04 p0572 N85-13647

Numerical method for computing supersonic flow over wings of flight vehicles 05 p0725 N85-14659

Advanced cube processor
[AD-D011262] 05 p0729 N85-14663

Current status of blast wave theory and computations. Volume 2: The quasi-similar solution
[AD-A146538] 06 p0808 N85-15138

Progress in numerical calculations of ion-atom collisions
[DE84-016598] 06 p0861 N85-15474

Research in applied mathematics, numerical analysis, and computer science
[NASA-CR-172505] 07 p1021 N85-16480

Sequential and parallel matrix computations
[AD-A147871] 07 p1034 N85-16562

Structural optimization and other large-scale processes
[AD-A147895] 07 p1034 N85-16564

Efficient computation of optimal time for transaction processing in a database system
[AD-A147568] 07 p1054 N85-16693

Automated plant, production management system
08 p1139 N85-17171

Computing worldwide sunrise, sunset, moonrise, moonset and twilight times using 5 WWPs 105-3 and 105-4
[AD-A148049] 08 p1189 N85-17490

Resistivity of alloys
[DE85-000906] 09 p1296 N85-18138

Computing environments for data analysis. Part 1. Introduction
[AD-A148677] 09 p1373 N85-18632

Computing environments for data analysis. Part 2. Hardware
[AD-A148678] 09 p1374 N85-18633

Computation of thermal shock-free straightening conditions for aluminum-magnesium alloy welded structures 10 p1449 N85-19131

A circuit grammar for operational amplifier design
[AD-A149566] 10 p1481 N85-19346

Digital high speed programmable convolver
[AD-D011455] 10 p1481 N85-19348

Domain decomposition techniques for solving elliptic partial differential equations on multiprocessors
[DE85-004448] 10 p1549 N85-19769

Application of Monte Carlo and molecular dynamics methods to the calculation of thermodynamic properties of molten salts
[AD-A148897] 10 p1565 N85-19869

Applied mathematics of transport theory
[DE85-000848] 11 p1633 N85-20283

Parallel processing experiences on the Denelcor HEP computer
[DE85-000653] 11 p1702 N85-20703

Polylith and environments for mathematical computation
[DE85-002967] 11 p1702 N85-20704

Solving partial differential equations on multiprocessors
[DE85-000745] 11 p1706 N85-20734

Numerical model for swirl cooling in high-heat-flux particle beam targets and the design of a swirl-flow-based plasma limiter
[DE85-003824] 11 p1732 N85-20894

Instrumentation award
[AD-A150081] 12 p1912 N85-21999

PISCES: An environment for parallel scientific computation
[NASA-CR-172544] 12 p1913 N85-22004
Surface forward scattering and reflection
[AD-A150115] 12 p1928 N85-22112
Development of a Global 3-D magnetohydrodynamic computational model for solar wind-cometary and planetary studies
[NASA-CR-175490] 12 p1962 N85-22331
Rejection of anomalous observations when determining spacecraft trajectories 13 p1979 N85-22421
Second thoughts on the mathematical software effort: A perspective
[DE85-004831] 13 p2148 N85-23333
Sparse matrix computations
[DE85-004780] 13 p2152 N85-23362
Some recent developments in systems reliability
[AD-A150661] 14 p2317 N85-24318
Perceptual organization and vis: al recognition
[AD-A150626] 14 p2391 N85-24723
Propagation of numerical errors in computers and numerical quality 14 p2396 N85-24760
Arithmetic and elementary functions on mini and microcomputers 14 p2396 N85-24761
Practical methods for the compensation and control of multivariable systems
[AD-A151047] 14 p2407 N85-24841
Properties of systems which lead to efficient computation of reliability
[AD-A151033] 14 p2409 N85-24853
Mathematical modeling of the AEDC (Arnold Engineering Development Center) propulsion wind tunnel (16T)
[AD-A151293] 15 p2475 N85-25275
Infinite computing
[AD-A151437] 15 p2628 N85-26197
BLAS (Basic Linear Algebra Subroutines), linear algebra modules and supercomputers
[AD-A151504] 15 p2628 N85-26199
Recent progress in computational aerodynamics
16 p2693 N85-26626
Techniques for computing the DFT using the residue Fermat number systems and VLSI
16 p2770 N85-27097
Management of vacuum leak-detection processes, standards and calibration
[DE85-006705] 16 p2788 N85-27202
Error reduction program — combustor performance evaluation codes
[NASA-CR-174776] 16 p2852 N85-27584
Nonlinear DSA difference schemes for radiative transfer applications
[DE85-005729] 16 p2856 N85-27611
Optimizing computational efficiency and user convenience in plasma simulation codes
[DE85-007661] 16 p2866 N85-27682
Heating parameter estimation using coaxial thermocouple gages in wind tunnel test articles
[AD-A153039] 17 p2968 N85-28328
The definition and computation of a metric on plane curves. The meaning of a face on a geometric model
17 p3004 N85-28571
Software environment for conducting interactive statistical analysis
[AD-A153378] 17 p3012 N85-28626
Projected discrete ordinates methods for numerical transport problems
[DE85-005632] 17 p3020 N85-28678
Augmented weighted diamond force of the linear nodal scheme for Cartesian coordinate systems
[DE85-005631] 17 p3020 N85-28679
An examination of the use of wave packets for the calculation of atom diffraction by surface
[AD-A152760] 17 p3029 N85-28735
Debugging distributed computations in a nested atomic action system
[AD-A153617] 18 p3162 N85-29585
Computable numerical bounds for Lagrange multipliers of stationary points of nonconvex differentiable nonlinear programs
[AD-A153513] 18 p3169 N85-29633
A comparison of methods of least squares adjustment of traverses
[AD-A153612] 18 p3170 N85-29645
Electronic structure calculations for low coverage adlayers
[DE85-007733] 18 p3179 N85-29709
Numerical optical computing at the Ohio State University 18 p3188 N85-29775
A method for computing the core flow in three-dimensional leading-edge vortices
[NASA-TM-87489] 19 p3214 N85-29932
Research on optimal control, stabilization and computational algorithms for aerospace applications
[NASA-CR-172528] 19 p3221 N85-29970
Approximate factorization method for computation of nonhydrostatic mesoscale flows
[DE85-007259] 19 p3313 N85-30537
SHAPS-2: A three-dimensional computer program for linear/non-linear, static/dynamic analyses of piping systems
[DE85-010500] 19 p3335 N85-30658
An algorithm to test for confluence in a system of left to right rewrite rules
[AD-A154066] 19 p3335 N85-30662
MCNP variance reduction overview
[DE85-010765] 19 p3348 N85-30741
Development of improved capabilities for computation of gas supercompressibility factors and other properties
[PB85-188316] 20 p3436 N85-31315
Optimum filter computation for data transmission
[CNES-83/DRT/TIT/TR/142] 20 p3441 N85-31359
Global mean sea surface based upon a combination of the GEOS-3 and SEASAT altimeter data
20 p3492 N85-31710
Symposium on Computational Mathematics-State-of-the-Art: Informal Proceedings
[DE85-008122] 20 p3516 N85-31858
Intersatellite optical links: The point ahead angle
[CNES-83/DRT/TIT/TR/150] 20 p3533 N85-31984
Survival function of hypo-exponential distributions
[AD-A155518] 21 p3672 N85-32814
On the dependence of the convergence of Gummel's algorithm on the regularity of the solution
[AD-A154628] 21 p3675 N85-32832
Ice fog as an electro-optical obscurant
[AD-A155059] 21 p3705 N85-33015
Magnetics calculations for an ELMO Bumpy Square
[DE85-011438] 21 p3707 N85-33021
System of microprocessor instructions
22 p3770 N85-33362
Finite element methods for viscoelastic flow
[AD-A154877] 22 p3783 N85-33437
Report of Workshop on Computational Geometry and summary of related research
[AD-A155399] 22 p3833 N85-33734
Calculated neutron-induced cross sections for /sup 63,65/Cu/sup 58,60/Ni and (52) Cr from 1 to 20 MeV and comparisons with experiments
[DE85-011928] 22 p3844 N85-33808
Reordering computations for parallel execution
[NASA-CR-177961] 23 p3957 N85-34522
On the statistical significance of excess events: Remarks of caution and the need for a standard method of calculation
[OG-9.5-10] 23 p4031 N85-34987
Adaptive rezoner in a two-dimensional Lagrangian hydrodynamic code
[DE85-010108] 24 p4094 N85-35381
DEPTH-CHARGE static and time-dependent perturbation/sensitivity system for nuclear reactor core analysis, revision 1
[DE85-013103] 24 p4139 N85-35659
COMPUTATIONAL ASTROPHYSICS
Development of a global 3-D magnetohydrodynamic computational model for solar wind/cometary and planetary studies
[NASA-CR-175724] 15 p2684 N85-26577
COMPUTATIONAL CHEMISTRY
Computer calculation of chemical equilibrium in multi-component systems
[BLL-M-35973-(5828.4)] 05 p0614 N85-13919
Integrating chemical kinetic rate equations by selective use of stiff and nonstiff methods
[NASA-TM-86923] 07 p0904 N85-15726
COMPUTATIONAL FLUID DYNAMICS
Computational methods for complex flowfields
[AD-A145219] 01 p0004 N85-10019
Experimental data base for computers program assessment. Report of the Fluid Dynamics Panel Working Group 04: Addendum
[AGARD-AR-138-ADD] 01 p0004 N85-10020
Transonic wing and far field test data on a high aspect ratio transport wing for three dimensional computational method evaluation 01 p0004 N85-10021
Transonic wing and far field test data on a moderate aspect ratio wing for three dimensional computational method evaluation 01 p0004 N85-10022
Computational thermo-fluid dynamics contributions to advanced gas turbine engine design
[NASA-TM-86865] 01 p0011 N85-10069
Aerothermal modeling 02 p0145 N85-10982
Aerothermal modeling program
02 p0145 N85-10983
Numerical simulation of natural convection in porous media — heat transfer
[CFD/84/10] 02 p0199 N85-11330
Computer simulation techniques for turbulent flows
[CFD/84/11] 02 p0199 N85-11331
Inverse design technique for cascades
[NASA-CR-3836] 03 p0311 N85-12006
Model equation for simulating flows in multistage turbomachinery
[NASA-TM-86869] 03 p0315 N85-12036
Status and prospects of computational fluid dynamics for unsteady transonic viscous flows
[NASA-TM-86018] 03 p0315 N85-12037
Vorticity amplification in viscous flow around a body
03 p0360 N85-12309
Second order modeling of scalar turbulent flows
03 p0360 N85-12311
Numerical studies of unsteady transonic flow over an oscillating airfoil
[NASA-TM-86011] 03 p0361 N85-12318
Study of the structure of turbulent shear flows at supersonic speeds and high Reynolds number
[NASA-CR-174144] 04 p0452 N85-12865
Development of computational fluid dynamics at NASA Ames Research Center
[NASA-TM-86021] 04 p0452 N85-12866
Fundamental study of three dimensional two phase flow in combustion systems
[AD-A142886] 04 p0498 N85-13177
Numerical calculations of stratified Ekman layer flow over ridges with a finite element model
[DE84-014482] 04 p0499 N85-13179
Numerical calculation of steady turbulent flows in adverse pressure gradients
[CFD/83/9] 04 p0501 N85-13185
Simulation of seperated transonic airfoil flow by finite-difference viscous-inviscid interaction
05 p0591 N85-13768
Transition and mixing in axisymmetric jets and vortex rings 05 p0591 N85-13769
The numerical simulation of steady transonic rotational flow using a dual potential formulation
05 p0591 N85-13770
Transonic jets: A numerical approach in the hodograph plane 05 p0592 N85-13774
Flow calculation on a thin wing, with specific attention to separation point at the trailing edge
[FTW-FO-1721] 05 p0594 N85-13787
A finite element method for three dimensional cavity circulation 05 p0635 N85-14071
Numerical investigations into the parabolized Navier-Stokes equations 05 p0635 N85-14075
Theoretical description of film boiling in a two phase flow calculation
[IKE-2-66] 05 p0638 N85-14082
Review of requirements and status of simulation and scaling of transonic, viscous flows
[AD-A146357] 06 p0808 N85-15137
Supersonic nonlinear potential analysis
[NASA-CR-172456] 07 p0897 N85-15685
Analysis of the flow field about a T-45 using PANAIR
[AD-A148811] 07 p0899 N85-15689
Current problems in turbomachinery fluid dynamics
[AD-A147127] 07 p0958 N85-16074
Detailed study of the flow around a multi-element airfoil. Comparison with calculations 08 p1069 N85-16775
Vectorizable multigrid algorithms for transonic flow calculations
[NASA-CR-174326] 08 p1077 N85-16827
The NYU inverse swept wing code
[NASA-CR-3662] 08 p1077 N85-16830
Numerical calculation of the cold-flow characteristics of a bluff-body flame stabilizer
[CFD/84/14] 08 p1124 N85-17088
Analysis of a penalty finite element approximation of the Navier Stokes equations 08 p1161 N85-17321
Computational fluid mechanics utilizing the variational principle of modeling damping seals
[NASA-CR-174332] 08 p1161 N85-17325
Front tracking for gas dynamics
[DE85-000571] 08 p1163 N85-17336
Numerical experiments and theoretical analysis of the flow of an elastic liquid of the Maxwell-Oldroyd type in the presence of geometrical singularities
[WTHD-164] 08 p1163 N85-17340
A numerical study of several supersonic flows
09 p1272 N85-17985
Numerical approach for the aerodynamic analysis of airfoils with laminar separation
[NASA-CR-172496] 09 p1273 N85-18001
Calculating heat transfer coefficients for turbine profiles taking surface curvature and elevated flow turbulence into account 09 p1307 N85-18212
Turbulent jet flow in a channel with a circulation region
09 p1308 N85-18218
Long range effect of turbulent pressure pulsations in plane-parallel flows at different velocities with various flame fronts 09 p1308 N85-18220
Microscopic study of fluid flow
09 p1317 N85-18280
Numerical predictions for unsteady viscous flow past an array of cylinders 09 p1318 N85-18284

An implicit, conservative, zonal-boundary scheme for Euler equation calculations
[NASA-CR-3865] 09 p1318 N85-18290

Researched applied to transonic compressors in numerical fluid mechanics of inviscid flow and viscous flow
[NASA-CR-174353] 09 p1319 N85-18291

Three-dimensional vortex methods
[DE85-000391] 09 p1320 N85-18299

Accuracy of the finite analytic method for scalar transport calculations
[DE85-001474] 09 p1320 N85-18300

Development of multigrid algorithms for problems from fluid dynamics
[GMD-111] 09 p1321 N85-18305

Large deformations of a nonlinear elastic solid and the diffusion of an ideal fluid treated as interacting continua
09 p1330 N85-18356

NASA Lewis Research Center/University Graduate Research Program on Engine Structures
[NASA-TM-86916] 09 p1333 N85-18375

Verification of a model of the Eastern Scheldt
[RAND/R-3108-NETH] 09 p1354 N85-18518

Effects of airfoil shape, thickness, camber, and angle of attack on calculated transonic unsteady airloads
[NASA-TM-86320] 10 p1420 N85-18957

Unsteady transonic flow calculations for two-dimensional canard-wing configurations with aeroelastic applications
[NASA-TM-86375] 10 p1420 N85-18960

Viscous effects on transonic airfoil stability and response
[NASA-TM-86374] 10 p1421 N85-18961

Thrust chamber performance using Navier-Stokes solution — space shuttle main engine viscous nozzle calculation
[NASA-CR-171346] 10 p1430 N85-19019

Preliminary analysis of selected gas dynamic problems — space shuttle main engine main combustion transients and IUS nozzle flow
[NASA-CR-171343] 10 p1483 N85-19361

Calculation of flow about posts and powerhead model — space shuttle main engine
[NASA-CR-171344] 10 p1483 N85-19362

Computer studies of baroclinic flow — Atmospheric General Circulation Experiment
[NASA-CR-171338] 10 p1517 N85-19566

Contribution to the study of a numerical implicit method for solving the Euler equations
[ESA-TT-872] 10 p1549 N85-19771

Developments in the simulation of compressible inviscid and viscous flow on supercomputers
[NASA-TM-86674] 11 p1575 N85-19924

A fast algorithm of the finite difference method for computation of the transonic flow past an arbitrary airfoil with the conservative full-potential equation
11 p1619 N85-20191

A mixed finite difference analysis of the internal and external transonic flow fields of inlets with centerbody
11 p1619 N85-20192

Finite difference method for solving turbulent boundary layer equations 11 p1619 N85-20193

A study for calculating rotor loads using free vortex concept 11 p1620 N85-20194

Triple layer system for numerical integration of equations of gas dynamics and nonlinear heat conduction equation
[DE85-000297] 11 p1632 N85-20277

Three-dimensional unsteady lifting surface theory in the subsonic range
[NASA-TM-77812] 12 p1770 N85-21111

Transonic interactions of unsteady vortical flows
[NASA-TM-86658] 12 p1770 N85-21113

Combustion research for gas turbine engines
[NASA-TM-86963] 12 p1778 N85-21164

China report: Science and technology
[JPRS-CST-85-008] 12 p1820 N85-21416

Application of large eddy interaction model to channel flow
[NASA-TM-86691] 12 p1844 N85-21572

Algorithm for the simulation of transient viscoelastic flows with free surfaces
[DE85-002713] 12 p1848 N85-21590

Robust calculation of three-dimensional transonic potential flow based on the nonlinear gas multigrid method and a mixed incomplete lower upper decomposition/strongly implicit procedure (ILU/SIP) algorithm
[NLR-MP-84003-U] 12 p1848 N85-21593

High-pressure rocket engine turnaround duct computational fluid dynamics analysis
13 p2003 N85-22556

Grid generation for a pump collector
[AD-A150217] 13 p2092 N85-23059

F-14A aircraft high-speed flow simulations
[NASA-CR-172559] 14 p2209 N85-23702

Calculating isothermal flow in wake beyond injection zone 14 p2287 N85-24175

Discrete models for the numerical analysis of time-dependent multidimensional gas dynamics
[NASA-CR-172574] 14 p2300 N85-24239

Spectral methods for modeling supersonic chemically reacting flow fields
[NASA-CR-172578] 14 p2300 N85-24240

Transonic Unsteady Aerodynamics and its Aeroelastic Applications
[AGARD-CP-374] 15 p2457 N85-25171

Trends in computational capabilities for fluid dynamics
15 p2457 N85-25172

Numerical studies of unsteady transonic flow over oscillating airfoil 15 p2458 N85-25174

Calculation of harmonic aerodynamic forces of aerofoils and wings from the Euler equations
15 p2458 N85-25177

Calculation of unsteady transonic separated flows by viscous-inviscid interaction 15 p2458 N85-25178

A semi-empirical unsteady transonic method with supersonic free stream 15 p2458 N85-25179

Status and prospects of computational fluid dynamics for unsteady transonic flow 15 p2459 N85-25180

Improvement and extension of a numerical procedure for the three dimensional unsteady transonic flows
15 p2459 N85-25181

Application of time-linearized methods to oscillating wings in transonic flow and flutter
15 p2459 N85-25182

Computation of unsteady transonic flows about two-dimensional and three-dimensional AGARD standard configurations 15 p2459 N85-25183

Calculation of unsteady transonic flow around a high swept wing 15 p2459 N85-25184

Unsteady transonic aerodynamic and aeroelastic calculations about airfoils and wings
15 p2459 N85-25185

The application of transonic unsteady methods for calculation of flutter airloads 15 p2460 N85-25186

The development of unsteady transonic 3-D full potential code and its aeroelastic applications
15 p2460 N85-25187

Transonic aerodynamic and aeroelastic characteristics of a variable sweep wing
[NASA-TM-86677] 15 p2462 N85-25203

A critical evaluation of various turbulence models as applied to internal fluid flows
[NASA-TP-2474] 15 p2554 N85-25757

Flow over a biconic configuration with an afterbody compression flap
[AD-A151882] 15 p2557 N85-25778

Application of the Van Leer method to the solution of one-dimensional volume fraction equations
[CFD/84/17] 15 p2558 N85-25781

Three-dimensional boundary layers and shear flows activities at ONERA/CERT 15 p2558 N85-25785

Three-dimensional boundary layers: A report on work in Germany 15 p2559 N85-25786

Three-dimensional boundary layer research at NLR
15 p2559 N85-25787

Brief review of current work in the UK on three dimensional boundary layers 15 p2559 N85-25788

Problems and opportunities with three-dimensional boundary layers — aircraft, missile, and ship components 15 p2559 N85-25789

Inviscid upwind finite difference model for two dimensional vertical axis wind turbines
15 p2585 N85-25933

Stream dynamics between 1 AU and 2 AU: A detailed comparison of observations and theory
[NASA-TM-86086] 15 p2684 N85-26578

Proceedings of the NAL Symposium on Aircraft Computational Aerodynamics
[NAL-SP-1] 16 p2691 N85-26611

Some numerical analyses of flows with separation
16 p2692 N85-26616

Two computational methods for cascade flows
16 p2692 N85-26617

The role of computational fluid dynamics in aeronautical engineering 16 p2694 N85-26629

A method for simulating 3-D aircraft flow fields with jet plume effects
[NASA-CR-175802] 16 p2699 N85-26664

Low Reynolds number vehicles
[AGARD-AG-288] 16 p2699 N85-26666

Application of CFD techniques toward the validation of nonlinear aerodynamic models
[NASA-TM-86715] 16 p2700 N85-26671

A numerical simulation of the NFAC (National Full-scale Aerodynamics Complex) open-return wind tunnel inlet flow
[NASA-TM-86724] 16 p2700 N85-26672

Numerical solution of transonic normal shock wave-boundary layer interaction using the Bohning-Zierop model — wind tunnel flow
[VTH-LR-416] 16 p2701 N85-26683

Solid fuel combustion chamber
[VTH-LR-415] 16 p2741 N85-26918

Solid fuel combustion chamber
[VTH-LR-438] 16 p2741 N85-26919

Turbulent flow of fluid near trailing edge of plate in stream at zero angle of attack 16 p2764 N85-27057

LU methods for the compressible Navier-Stokes equations 16 p2781 N85-27160

Theoretical investigation of three-dimensional shock wave turbulent boundary layer interactions. Part 3
[AD-A152251] 16 p2783 N85-27177

The development of a computational model for a two-dimensional turbulent flow. Part 1: Mathematical background — solid fuel combustion
[VTH-LR-436-PT-1] 16 p2785 N85-27188

Adaptive grid generation for numerical solution of Burger's equation
[AD-A152217] 16 p2855 N85-27606

Future fundamental combustion research for aeropropulsion systems
[NASA-TM-87049] 17 p2898 N85-27870

CALTECH-DOE program on numerical analysis, computing and fundamental studies of motion, energy and mass transfer in fluids
[DE85-008106] 17 p2959 N85-28274

A second-order pressure-correction method for viscous incompressible flow
[REPT-84-15] 17 p2960 N85-28280

Numerical simulation of unsteady motion in a turbulent mixing layer
[NAL-TR-849T] 18 p3099 N85-29183

Two approaches for the prediction of plume-induced separation
[AD-A154098] 19 p3215 N85-29935

Study of second order upwind differencing in a recirculating flow
[NASA-CR-174939] 19 p3264 N85-30243

Decay of a coherent scalar disturbance in a turbulent flow
[NASA-TM-86700] 19 p3264 N85-30244

Application of computational fluid dynamics to complex inlet ducts
[NASA-TM-87060] 19 p3265 N85-30247

On spectral multigrid methods for the time-dependent Navier-Stokes equations
[NASA-CR-172613] 19 p3344 N85-30725

Calculation of transonic flows around an aircraft configuration with motorized nacelle
[SNIAS-851-111-106] 20 p3387 N85-31008

Transonic calculations for a flexible supercritical wing and comparison with experiment
[NASA-TM-86439] 20 p3388 N85-31012

Calculation of flow around the SF 310 airplane using a full potential equation method
[FFA-TN-1984-63] 20 p3389 N85-31022

A theory of quasi-conical solutions of noninteger degree — flow fields on supersonic wings
[UTH-LR-420] 20 p3390 N85-31024

A supersonic potential gradient method for the calculation of unsteady aerodynamic pressures on harmonically oscillating wings
[DFVLR-FB-85-11] 20 p3390 N85-31026

Verification of calculation methods for unsteady airloads in the precipitation of transonic flutter
[NLR-MP-84016-U] 20 p3390 N85-31027

Numerical and experimental investigation of turbomachinery rotor flow fields
20 p3451 N85-31429

A new finite element approach: Progress in inviscid flow computations
[NASA-TM-86434] 20 p3454 N85-31450

Three-Dimensional Techniques Applied to Internal Flows in Propulsion Systems
[AGARD-LS-140] 21 p3586 N85-32293

The calculation of fully three dimensional flow through any type of turbomachine blade row
21 p3587 N85-32294

An analysis of flow models: From Navier-Stokes to potential flow equations 21 p3587 N85-32295

Computation of three-dimensional, inviscid, rotational flows 21 p3587 N85-32296

An elliptic calculation procedure for 3-D viscous flow
21 p3587 N85-32297

A 3-D Euler method for internal transonic flows computation with a multi-domain approach
21 p3587 N85-32298

Performance evaluation of flow in turbomachinery blade rows 21 p3587 N85-32299

Numerical solution of the Navier-Stokes equations for 3-D internal flows: An emerging capability
21 p3588 N85-32300

Calculation of 3-D flow without numerical mixing
21 p3586 N85-32301

Gradient scaling for nonuniform meshes
[DE85-009625] 22 p3784 N85-33443

Tabular and graphical solutions of regular and Mach reflections in pseudo-stationary frozen and vibrational-equilibrium flows, part 1
[UTIAS-283-PT-1] 23 p3893 N85-34117

Tabular and graphical solutions of regular and Mach reflections in pseudo-stationary frozen and vibrational-equilibrium flows, part 2
[UTIAS-283-PT-2] 23 p3894 N85-34118

A study of the second and third order closure models of turbulence for prediction of separated shear flows
[NASA-CR-176127] 23 p3929 N85-34353

Studies on effects of boundary conditions in confined turbulent flow predictions
[NASA-CR-3929] 24 p4093 N85-35371

COMPUTATIONAL GRIDS

Embedded-grid generation with complete continuity across interfaces for multi-element airfoils
02 p0133 N85-10911

Discretization formulas on an arbitrary grid
[FFA-MEMO-127] 02 p0253 N85-11659

Comprehensive silicon solar cell computer modeling
[NASA-CR-174151] 04 p0530 N85-13386

Analytical construction of flight vehicle surfaces
06 p0775 N85-14957

Vectorizable multigrid algorithms for transonic flow calculations
[NASA-CR-174326] 06 p1077 N85-16827

Front tracking for gas dynamics
[DE85-000571] 06 p1163 N85-17336

Numerical generation of orthogonal and nonorthogonal coordinates in two dimensional simply and doubly connected regions
[VKI-TN-151] 08 p1216 N85-17662

An implicit, conservative, zonal-boundary scheme for Euler equation calculations
[NASA-CR-3865] 09 p1318 N85-18290

Development of multigrid algorithms for problems from fluid dynamics
[GMD-111] 09 p1321 N85-18305

On the connection between multigrid and cyclic reduction
[NASA-TM-86020] 09 p1373 N85-18629

The implementation of irregular grid systems for the finite difference solution of partial differential equations
[LU-MATH-RES-181] 09 p1373 N85-18630

Experimental approach to terms within grids --- turbulent flow calculations 11 p1576 N85-19930

Computation of the inviscid velocity potential for general ellipsoids on a nearly quadratic surface grid
[REPT-25/84] 11 p1633 N85-20287

Solution of the three-dimensional Navier-Stokes equations for a steady laminar horseshoe vortex flow
[AD-A149851] 12 p1846 N85-21582

Robust calculation of three-dimensional transonic potential flow based on the nonlinear gas multigrid method and a mixed incomplete lower upper decomposition/strongly implicit procedure (ILU/SIP) algorithm
[NLR-MP-84003-U] 12 p1848 N85-21593

Mesh effects on the computation of non-linear gravity waves of arbitrary discharge
[COLL-AERON-8501] 12 p1888 N85-21848

Differentiating matrices for arbitrarily spaced grid points
[NASA-CR-172556] 12 p1919 N85-22051

Numerical methods for tracking interfaces
[LA-9917-MS] 12 p1919 N85-22052

Approximation order from certain spaces of smooth bivariate splines on a 3-direction mesh
[AD-A149633] 12 p1925 N85-22092

Correcting depth line on nonlongitudinal seismic profile 13 p2117 N85-23184

The complexity of reliability computations in planar and acyclic graphs
[AD-A150759] 14 p2408 N85-24845

A fast ray tracing routine for laterally inhomogeneous media
[AD-A150984] 14 p2421 N85-24938

Communication complexity of the Gaussian elimination algorithm on multiprocessors
[AD-A151891] 15 p2638 N85-26267

Mathematical software for hyperbolic equations and two point boundary value problems
[AD-A151982] 15 p2638 N85-26270

Solution of coupled system of PDE by the transistorized multigrid method
[DE85-006377] 15 p2639 N85-26276

Application of conformal mapping to grid generation
16 p2692 N85-26621

Local uniform mesh refinement on loosely-coupled parallel processors
[AD-A152199] 16 p2850 N85-27571

Adaptive grid generation for numerical solution of Burger's equation
[AD-A152217] 16 p2855 N85-27606

Computational Geometry and Computer-Aided Design
[NASA-CP-2379] 17 p3003 N85-28563

Examination of the circle spline routine
17 p3004 N85-28573

Parameterization in grid generation
17 p3005 N85-28581

Contouring trivariate data 17 p3005 N85-28582

Generation of surface coordinates by elliptic partial differential equations 17 p3006 N85-28583

A survey of composite grid generation for general three-dimensional sections 17 p3006 N85-28584

A discussion of adaptive grids and their applicability in numerical hydrodynamic modeling
[AD-A151843] 17 p3017 N85-28650

Developement of an optimum interpolation analysis method for the CYBER 205 18 p3143 N85-29456

Response of winter forecasts made with the GLA Fourth Order GCM to Changes in the horizontal grid resolution
18 p3143 N85-29458

Tradeoffs among portability, complexity, and efficiency in multiprocessing environments
[DE85-007899] 18 p3161 N85-29580

Embedding graphs in lines, trees and grids
19 p3334 N85-30652

On spectral multigrid methods for the time-dependent Navier-Stokes equations
[NASA-CR-172613] 19 p3344 N85-30725

On MGR (Upsilon) multigrid methods
[AD-A153887] 19 p3345 N85-30733

Computer program for plotting and fairing wind-tunnel data
[NASA-TM-85648] 20 p3387 N85-31009

Application of closed-form solutions to a mesh point field in silicon solar cells 20 p3482 N85-31637

Generation of three-dimensional body-fitted coordinates using hyperbolic partial differential equations
[NASA-TM-86753] 20 p3519 N85-31887

Calculation of transonic steady and oscillatory pressures on a low aspect ratio model and comparison with experiment
[NASA-TM-86449] 21 p3551 N85-32092

Simulation of complex three-dimensional flows
[NASA-TM-86773] 21 p3675 N85-32831

A vectorized nearest-neighbors algorithm of order N using a monotonic logical grid
[AD-A155169] 21 p3679 N85-32853

Generation by conformal mappings of aerofoil sections and of certain other simple shapes suitable for both aerodynamic and stress-concentration problems
[AD-A154901] 22 p3728 N85-33112

Use of a hyperbolic grid generation scheme in simulating supersonic viscous flow about three-dimensional winged configuration
[NASA-TM-85344] 23 p3893 N85-34116

Box truss analysis and technology development. Task 1: Mesh analysis and control
[NASA-CR-172570] 23 p3900 N85-34156

COMPUTER AIDED DESIGN

Applications of numerical optimization methods to helicopter design problems: A survey
[NASA-TM-86010] 01 p0006 N85-10036

The Influence of Large Scale Computing on Aircraft Structural Design
[AGARD-R-706] 01 p0007 N85-10040

Aerospatiale's experimentations of vectorization on supercomputers for aircraft structural problems
01 p0007 N85-10041

Large scale computing in aeronautical design
01 p0007 N85-10043

AGS-880 menu system user guide
[DE84-014338] 01 p0104 N85-10699

Interactive system for the interpretation of coal deposit data as a basis of future mine planning systems
[BMFT-FB-T-83-115] 02 p0220 N85-11449

Air Force Human Resources Laboratory report: Fiscal year, 1983
[AD-A145647] 02 p0236 N85-11548

Air Force honeycomb shaping at SM-ALC (Sacramento Air Logistics Center)
[AD-P004005] 03 p0308 N85-11985

Kinematic synthesis of planar cam-link mechanisms for exact path and exact motion generation
03 p0341 N85-12189

VLSI (Very Large Scale Integration) design tools reference manual, release 1.0
[AD-A146273] 03 p0408 N85-12604

An input translator for a computer-aided design system
[AD-A146337] 03 p0408 N85-12605

CONTROL: A suite of interactive transfer-function analysis programs
[OUEL-1527/84] 03 p0408 N85-12609

Turbomachinery blade design using advanced calculation methods
[PNR-90218] 04 p0456 N85-12896

Conceptual design for scaled truss antenna flight experiment
[NASA-TM-85804] 04 p0462 N85-12932

High-temperature steam electrolysis: Technical and economic evaluation of alternative process designs
[DE84-015702] 04 p0469 N85-12986

Computerized circuit designs: Realization of masks to manufacture microwave circuits
[CNES-NT-107] 04 p0496 N85-13166

Standard cell initial placement strategy
[DE84-016921] 05 p0632 N85-14051

User-oriented development and production of integrated circuits in small and medium quantities
[BMFT-FB-T-84-171] 05 p0633 N85-14059

Increase in the economy of design and process planning by integrated and graphic data processing, phase 2 -- aircraft design
[BMFT-FB-W-84-028] 05 p0716 N85-14599

Computer-aided design of extrusion dies by metal-flow simulation 06 p0797 N85-15094

VLSI design tools, reference manual, release 2.0
[AD-A146444] 06 p0803 N85-15112

Specialized silicon compilers for language recognition
[AD-A146526] 06 p0853 N85-15425

Recent advances in data compression
[DE85-001133] 06 p0854 N85-15432

Control system design language implementation of a gas turbine starting controller
[AD-A147896] 07 p0905 N85-15732

The design of high order active RC-filters
[DRIC-T-7147] 07 p0945 N85-15987

Trends in development of software for computer-aided analysis of large-scale integrated circuits
07 p0955 N85-16056

Program visualization: Graphics support for software development
[AD-A146887] 07 p1024 N85-16480

The reactor dynamic code RETRANS: Structure and users guide
[OEFZS-4287] 07 p1041 N85-16614

Hardware/software codesign for maintainable systems
08 p1066 N85-16753

Design of an airfoil leading edge slat using an inverse aerodynamic calculation method
08 p1069 N85-16777

Design of a digital ride quality augmentation system for commuter aircraft
[AD-A148233] 08 p1088 N85-16879

Challenges of developing an electro-optical system for measuring man's operational envelope
08 p1095 N85-16921

East Europe report: Science and technology
[JPRS-ESA-84-047] 08 p1140 N85-17180

A computer aided Multi-Man-Machine Work Area Design and Evaluation System (MAWADES)
[AD-A147950] 08 p1199 N85-17554

Adapting logistics models to a microcomputer for interface with computer-aided design systems
[AD-A147666] 08 p1202 N85-17566

Extraction of feature information from 3-dimensional CAD data 08 p1203 N85-17573

COPES/ADS (Control Program for Engineering Synthesis) (Automated Design Synthesis) using the ADS optimization program
[AD-A148576] 08 p1206 N85-17588

Correction of engraving stamp for forming blanks of gas turbine engine blades 09 p1307 N85-18213

Generation of radiation transport geometry from computer-generated design data --- monte carlo solution of the neutron transport equation
[DE84-017380] 09 p1370 N85-18606

Siemens' CAD system designs VLSI circuits
10 p1461 N85-19209

Productivity gains through CAD of CNC programs
10 p1462 N85-19219

Research into self-timed VLSI circuits
[AD-A149140] 10 p1479 N85-19339

SUBOPT: A CAD program for suboptimal linear regulators
[NASA-CR-172536] 10 p1539 N85-19702

Graphics translators for computer-aided drafting and design: Interface alternatives for the A/E community
[AD-A148892] 10 p1540 N85-19706

Management challenges encountered in CAD implementation
[DE85-002072] 10 p1541 N85-19716

Design of explosive logic elements
[DE84-009611] 11 p1614 N85-20146

Overview of leading-edge research at French CNRS lab 11 p1618 N85-20179

CAD/CAM systems for printed circuit design, manufacture 11 p1619 N85-20188

Console I/O routines
[DE85-002644] 11 p1702 N85-20700

Computer aided of maintainability design: A feasibility study
[AD-A149293] 11 p1738 N85-20932

ACOSS 17 (Active Control of Space Structures)
[AD-A150007] 12 p1793 N85-21253

Computer integration of engineering design and production: A national opportunity
[NASA-CR-175483] 12 p1820 N85-21414

Structural sensitivity analysis: Methods, applications and needs
[NASA-TM-85827] 12 p1865 N85-21695

A survey of the project CIP: Computer aided, intuition-guided programming. Wide spectrum language and program transformations
[TUM-I8406] 12 p1912 N85-22000

Evaluation of PHOENICS as a design analysis tool for SSME 12 p1949 N85-22240

Study for the optimization of a transport aircraft wing for maximum fuel efficiency. Volume 1: Methodology, criteria, aeroelastic model definition and results
[NASA-CR-172551] 13 p1971 N85-22378

A description of the Langley wireframe geometry standard (LaWGS) format
[NASA-TM-85767] 13 p1971 N85-22380

Preliminary development of an approximation procedure for supercritical wing design optimization applications
[AD-A150177] 13 p1972 N85-22383

Computer aided engineering applied to the design and verification of the generic Advanced Rigid Array (ARA) — solar array 13 p2008 N85-22593

Redesign of fuselage compartments by method of special contours 13 p2042 N85-22784

Computer aided antenna design and frequency selection for HF communications
[AD-A150485] 13 p2055 N85-22869

Optimum design of electrical motors for multilink manipulators and automated manufacturing systems
13 p2062 N85-22880

Algorithm in Walsh function basis for analysis of integrated microcircuits on MOS-structures
13 p2083 N85-23006

Grid generation for a pump collector
[AD-A150217] 13 p2092 N85-23059

Development of a single-family absorption chiller for use in a solar heating and cooling system, phase 3, volume 2
[DE85-003218] 13 p2130 N85-23253

Motion planning with six degrees of freedom
[AD-A150312] 13 p2165 N85-23432

Software for designing teeth for reduction gears and transmissions 14 p2221 N85-23773

Cable-catenary large antenna concept
14 p2231 N85-23829

Construction of profiles of intermediate blade sections from master profiles given on conical surfaces
14 p2272 N85-24075

French work toward flexible software workshops
14 p2289 N85-24187

East Europe report: Science and technology
[JPRS-ESA-85-015] 14 p2289 N85-24189

Research on CAD/CAM support for microprocessor development surveyed 14 p2290 N85-24193

Integration of solid modeling and database management for CAD/CAM 14 p2402 N85-24804

An expert system for choosing the best combination of options in a general-purpose program for automated design synthesis
[NASA-TM-86329] 14 p2402 N85-24807

Mini-Seminar on CAD/CAM
[CSIR-TSD-0007/83] 14 p2402 N85-24809

Selection criteria for a CAD/CM system
14 p2402 N85-24810

The use of a 3-D system for a civil engineering project
14 p2402 N85-24811

EDIPAS: A multidiscipline and integrated facility for management and evaluation of engineering data
[NLR-MP-83062-U] 14 p2405 N85-24832

Selection criteria and computer aided design (CAD) systems
[NLR-MP-84037-U] 14 p2406 N85-24834

Executive control systems in the engineering design environment
[NASA-CR-172582] 14 p2406 N85-24835

Preliminary helicopter design decision making based on flight performance factors
[AD-A151486] 15 p2471 N85-25254

Resources for robotics research in Europe, by country
15 p2489 N85-25364

An analysis of grid-based line drawing quantization methods
[AD-A151847] 15 p2522 N85-25547

French firm plans recapture of domestic CAD/CAM market 15 p2535 N85-25641

Criteria for qualifying for FRG federal CAD/CAM subsidies 15 p2536 N85-25651

East Europe report: Science and technology
[JPRS-ESA-85-016] 15 p2537 N85-25658

Process control systems for largely automated manufacturing 15 p2537 N85-25659

CaD systems for electronic component design reviewed 15 p2537 N85-25660

Applications, specifications of Robotron CAD-CAM work stations 15 p2537 N85-25661

Mathematical aspect of welding technology research discussed 15 p2538 N85-25663

Conversion of algorithms to custom integrated circuit devices
[AD-A151268] 15 p2547 N85-25720

Analysis of the capability to effectively design complementary metal oxide semiconductor integrated circuits
[AD-A151832] 15 p2548 N85-25728

Use of computer-aided design in large-computer development described 15 p2564 N85-25822

Isoparametric 3-D finite element mesh generation using interactive computer graphics 15 p2574 N85-25873

CADS: A Computer Aided Design System
15 p2574 N85-25876

Use of COSMIC NASTRAN in a design department
15 p2575 N85-25881

The structural finite element model of the C-5A
15 p2576 N85-25885

User's guide for concrete strength investigation and design (CSTR)
[AD-A151617] 15 p2579 N85-25906

Symposium on Computers in Civil Engineering 1983
[CSIR-S-298] 15 p2626 N85-26182

Future directions in computers
15 p2626 N85-26183

Computers and the consulting engineer
15 p2626 N85-26184

Programme development: A state of the art
15 p2626 N85-26185

CAD/CAM (Computer-Aided Design/Computer-Aided Manufacturing) highlights
[AD-A151532] 15 p2629 N85-26201

A microcomputer-based program for printing check plots of integrated circuits specified in Caltech intermediate form
[AD-A151715] 15 p2629 N85-26205

SPRING: Helical spring design software for microcomputers
[DE85-006200] 15 p2631 N85-26217

IPAD: Integrated Programs for Aerospace-vehicle Design
[NASA-CR-3890] 15 p2632 N85-26221

Design of a variable-focal-length optical system
[NASA-CR-175710] 15 p2651 N85-26349

Computational aerodynamics for aircraft wing design
16 p2693 N85-26627

A numerical design method for three-dimensional transonic wings 16 p2694 N85-26631

Three-dimensional wing boundary layer analysis program BLAY and its application
16 p2694 N85-26632

Design-To-Cost (DTC) methodology to achieve affordable avionics 16 p2696 N85-26645

A modern control design methodology with application to the CH-47 helicopter
[AD-A151946] 16 p2710 N85-26723

Status, prospects of computer-aided design discussed
16 p2767 N85-27073

An integrated UNIX-based CAD system for the design and testing of custom VLSI chips
16 p2771 N85-27102

Development and application of optimum sensitivity analysis of structures
[NASA-CR-175857] 16 p2799 N85-27257

China report: Science and Technology
[JPRS-CST-85-012] 16 p2806 N85-27300

Fujian forges ahead in electronic production
16 p2806 N85-27301

The systematic integration of very large scale integrated circuit computer-aided design tools into a toolkit optimized for academic applications
[AD-A151813] 16 p2845 N85-27538

Further development of an Interactive Control Engineering Computer Analysis Package (ICECAP) for discrete and continuous systems
[AD-A151783] 16 p2846 N85-27546

Manufacturing methods and technology CAD/CAM (Computer-Aided Design/Computer-Aided Manufacturing) related efforts (FY 1980 - 1986)
[AD-A151817] 16 p2846 N85-27547

Numerical optimization algorithm for engineering problems using microcomputer
[AD-A152135] 16 p2847 N85-27554

Mathematical programming in computer network design
[AD-A152275] 16 p2848 N85-27558

Mapping principles for the standards interface for computer aided design
[PB85-177905] 16 p2849 N85-27566

The application of computer aided structural optimization to the design of aircraft components
[MBB-UT-21/84-O] 16 p2873 N85-27728

NBS (National Bureau of Standards) research reports
[PB85-127421] 16 p2879 N85-27764

Aerodynamic research in preparation for a new Dutch transport aircraft with supercritical wings
[B8580077] 17 p2893 N85-27836

Methods for design aerodynamics of modern transport aircraft
[DFVLR-FB-85-05] 17 p2893 N85-27838

USAF damage tolerant design handbook: Guidelines for the analysis and design of damage tolerant aircraft structures, revision B
[AD-A153161] 17 p2896 N85-27858

Engineering robot actions in a computer integrated manufacturing environment
[CWI-CS-R8415] 17 p2936 N85-28139

Future directions of robotics, automation in Italy
17 p2946 N85-28187

Report on high intensity solar cells
[DE85-006396] 17 p2987 N85-28462

Computational Geometry and Computer-Aided Design
[NASA-CP-2379] 17 p3003 N85-28563

Multivariate spline algorithms for CAGD
17 p3003 N85-28566

A survey of patch methods 17 p3003 N85-28567

Boundary to constructive solid geometry mappings: A focus on 2-D issues 17 p3004 N85-28570

Adapting shape parameters for cubic Bezier curves
17 p3004 N85-28576

Triangular Berstein-Bezier patches, a survey and new results 17 p3005 N85-28577

A uniform subdivision method for triangular Bezier patches 17 p3005 N85-28578

An intuitive approach to geometric continuity for parametric curves and surfaces ‘extended abstract)
17 p3005 N85-28579

Urn models and beta-splines
17 p3005 N85-28580

A unified representation scheme for solid geometric objects using B-splines (extended abstract)
17 p3006 N85-28585

Improving the effectiveness of integral property calculation in a CSG solid modeling system by exploiting predictability 17 p3006 N85-28586

Spline curves, wire frames and B-value
17 p3006 N85-28587

A new technique for system-to-system transfer of surface data 17 p3007 N85-28589

Curved finite elements and curve approximation
17 p3007 N85-28590

Comparison of two algebraic methods for curve/curve intersection 17 p3007 N85-28591

Manufacturing information system
[AD-A152715] 17 p3011 N85-28616

A modern control theory enhancement to an Interactive Control Engineering Computer Analysis Package (ICECAP)
[AD-A153249] 17 p3012 N85-28622

Advanced secondary power system for transport aircraft
[NASA-TP-2463] 18 p3062 N85-28944

West Europe report: Science and technology
[JPRS-WST-84-032] 18 p3086 N85-29095

MBB expands CADAM system for a 320 program
18 p3087 N85-29099

An interactive computer aid for the design and analysis of linear, single input/single output digital and continuous control systems
[AD-A153704] 18 p3162 N85-29589

Two-dimensional/speed/couple/data base management system
[A-1] 18 p3165 N85-29608

Three-dimensional/integration two and three dimensional/numerical control/communication
[A-2] 18 p3165 N85-29609

The CEADS-CADD system
[A-4] 18 p3165 N85-29610

System test CALMA DDM (Design Drafting Manufacturing)
[A-5] 18 p3165 N85-29611

The International Computers Limited (ICL) PERQ 1/Engineering Architectural Graphics Language Environment (EAGLE) Computer Aided Design system (CAD)
[A-7] 18 p3165 N85-29612

System test: Hewlett-Packard draft
[A-9] 18 p3166 N85-29613

Test Drawing Office Graphics System (DOGS)/APOLLO
[A-10] 16 p3166 N85-29614
Some examples of the application of automatically guided vehicle systems
[HSE-TRANS-11134] 19 p3281 N85-30348
CAE tool catalog
[DE85-011290] 19 p3334 N85-30657
Demonstration project: Putting the bioastronautics data book on line
[NASA-CR-178424] 19 p3335 N85-30659
Interactive computer program for the analysis and design of linear time invariant systems
[AD-A154076] 19 p3335 N85-30684
Design of the nacelle for the A-320 aircraft
[SNIAS-851-111-111] 20 p3393 N85-31046
Design and evaluation of control systems for large communications satellites 20 p3409 N85-31157
Intersection of three-dimensional geometric surfaces
[NASA-TP-2454] 20 p3513 N85-31839
System test Oce 5200
[A-3] 20 p3515 N85-31850
The General Drafting System (GDS) design system
[A-6] 20 p3517 N85-31869
The IGOS design system
[A-8] 20 p3517 N85-31870
FAUST: Introduction and overview --- self tuning control
[OUEL-1568/85] 20 p3519 N85-31882
R and D activities of the Aerodynamics Division
20 p3539 N85-32023
R and D activities of the Propulsion Division
20 p3539 N85-32025
NASA space station automation: AI-based technology review. Executive summary
[NASA-CR-176096] 21 p3556 N85-32135
Importance of automation, robotization in economy
21 p3572 N85-32219
Design of a sixteen-bit pipelined adder using CMOS bulk P-well technology
[AD-A155043] 21 p3580 N85-32260
Design of a generator for near-tangential transonic swirling outflow
[AD-A155163] 21 p3584 N85-32280
Research and development activities in unified control-structure modeling and design
[NASA-CR-176129] 22 p3740 N85-33179
State of art and development problems in computer-aided design of electronic circuits
22 p3766 N85-33342
Modeling of electronic circuits with high degree of component integration 22 p3766 N85-33343
Adaptive modeling of electronic circuits
22 p3766 N85-33345
Algorithms and organization of software for computer-aided circuit design 22 p3767 N85-33347
System for computer-aided design of analog electronic circuits 22 p3768 N85-33353
Algorithms for constructing models of circuit elements in input language of computer-aided design software
22 p3768 N85-33356
IGES/RIM Parser/Converter users guide
[DE85-011965] 22 p3829 N85-33716
User commands for product design and system management
[DE85-011708] 22 p3830 N85-33721
A strategy planner for NASA robotics applications
[NASA-CR-175319] 22 p3834 N85-33736
Proceedings of the Mechanisms Conference, volume 1 23 p3923 N85-34309
Proceedings of the Mechanisms Conference, volume 2 23 p3924 N85-34318
Optimisation in the computer aided design of mechanisms 23 p3924 N85-34321
Design and lubrication of high-speed rolling-element bearings
[NASA-TM-87107] 23 p3938 N85-34409
A model for graphics interface tool development
23 p3960 N85-34545
An analysis and algorithm for filling propagation
23 p3961 N85-34551
The CADME approach to the interface of solid modellers 23 p3961 N85-34554
An innovative user interface for microcomputer-based computer-aided design 23 p3961 N85-34555
A geometric modeller for turbomachinery applications
23 p3962 N85-34556
Architecture of languages for large CAD systems development 23 p3962 N85-34557
Design and implementation of an interactive route editor 23 p3962 N85-34559
A user-friendly computer-aided construction of boundaries 23 p3962 N85-34564
A simple but systematic CSG system
23 p3963 N85-34569
Geometric continuity with interpolating Bezier curves
23 p3963 N85-34570
An intuitive approach to geometric continuity for parametric curves and surfaces
23 p3963 N85-34571
Developing graphical tools with minimal GKS
23 p3964 N85-34573
Designing a graphics application interface
23 p3964 N85-34574
Low cost geometric modelling system for CAM
23 p3964 N85-34578
Computer animation in distance teaching
23 p3965 N85-34581
Generative design in architecture using an expert system 23 p3965 N85-34582
Design and construction of an advanced power conditioning subsystem for small photovoltaic applications
[DE85-013940] 24 p4113 N85-35495
VLSI (Very Large Scale Integrated) tutorials through the video-computer courseware implementation system
[AD-A155889] 24 p4135 N85-35631
Establishment of a Computer-Aided Design (CAD)-Computer-Aided Manufacturing (CAM) process for the production of cold forged gears
[AD-A155756] 24 p4137 N85-35644
Software maintenance relating to the input translator and z-80 realization volume of the computer systems design environment
[AD-A155849] 24 p4138 N85-35646
Computer Aided Design (CAD) methods for very large scale integration systems
[BMFT-FB-T-85-029] 24 p4141 N85-35668

COMPUTER AIDED MANUFACTURING

ICAM (Integrated Computer Aided Manufacturing) conceptual design for computer-integrated manufacturing. Volume 4, part 6: Task d. Quality assurance/quality control/technical requirement/tasks, quality assurance modeling and analysis, quality assurance program management standard recommendations (ISP)
[AD-A144891] 01 p0056 N85-10372
Integrated computer-aided manufacturing (ICAM) architecture. Part 3, volume 8: Technology transfer
[AD-A144732] 01 p0103 N85-10689
Computer aided process planning of machined metal parts
[AD-A145628] 02 p0189 N85-11263
DoD Robotics Application Workshop Proceedings
[AD-A145867] 03 p0307 N85-11978
Sensor technology for second, third generation industrial robots. Optical sensor applications
03 p0342 N85-12198
East Europe report: Science and technology
[JPRS-ESA-84-041] 04 p0484 N85-13090
Use of robotics in heavy machinery, equipment construction industry 04 p0485 N85-13093
Robotics technology application assessed, statistics
04 p0485 N85-13094
Computerized circuit designs: Realization of masks to manufacture microwave circuits
[CNES-NT-107] 04 p0496 N85-13168
Manufacturing Sciences and Robotics Research and Development Act of 1984
[H-REPT-98-1078] 04 p0578 N85-13688
Design and construction of a mode converter from rectangular TE 10 to circular TE 11
[REPT-84-158] 05 p0633 N85-14064
Specialized silicon compilers for language recognition
[AD-A146526] 06 p0853 N85-15425
Manufacturing methods and technology project summary reports
[AD-A148209] 08 p1138 N85-17163
Automated plant, production management system
08 p1139 N85-17171
Coordinated research in robotics and integrated manufacturing
[AD-A148204] 08 p1168 N85-17365
Cognitive asymmetry and occupation. Computer programmers, students, and bank personnel, part 1 and part 2
[AD-A147125] 08 p1197 N85-17540
Extraction of feature information from 3-dimensional CAD data 08 p1203 N85-17573
Flexible manufacturing system for machining axially symmetric workpieces
[PNR-90229] 09 p1305 N85-18196
The planning of flexible manufacturing systems
[PNR-90230] 09 p1371 N85-18613
The use of simulation for the technical and economic evaluation of flexible manufacturing systems. Part 2: Results of the simulation
[PNR-90233-PT-2] 09 p1371 N85-18614
Control of the manufacturing process and material flow in flexible manufacturing systems
[PNR-90234] 09 p1371 N85-18615
The control of manufacturing systems for varying medium-batch production
[PNR-90235] 09 p1371 N85-18616
State and development of the machine-tool industry in Japan. Part 2: Flexible manufacturing systems
[PNR-90236-PT-2] 09 p1371 N85-18617
Material flow in the manufacturing system: Fault-diagnosis systems as support for the maintenance of highly automated manufacturing systems
[PNR-90238] 09 p1371 N85-18618
European Scientific Notes, volume 38, number 12
[AD-A148713] 09 p1418 N85-18946
Competitive assessment of the US manufacturing automation equipment industries
[PB85-103927] 10 p1569 N85-19893
West Europe report: Science and technology
[JPRS-WST-85-006] 11 p1618 N85-20183
CAD/CAM systems for printed circuit design, manufacture 11 p1619 N85-20188
Computer integration of engineering design and production: A national opportunity
[NASA-CR-175483] 12 p1820 N85-21414
Impacts of robotic and flexible manufacturing technologies on manufacturing costs and employment
[AD-A150060] 12 p1860 N85-21668
The EEC's information technology program: An update
[AD-A150022] 12 p1951 N85-22258
Flexible manufacturing system for the production of aircraft parts
[PNR-90237] 14 p2207 N85-23667
MBB automates aircraft production in many FRG facilities 14 p2289 N85-24168
East Europe report: Science and technology
[JPRS-ESA-85-015] 14 p2289 N85-24169
Research on CAD/CAM support for microprocessor development surveyed 14 p2290 N85-24193
Integration of solid modeling and database management for CAD/CAM 14 p2402 N85-24804
Mini-Seminar on CAD/CAM
[CSIR-TSD-0007/83] 14 p2402 N85-24809
EDIPAS: A multidiscipline and integrated facility for management and evaluation of engineering data
[NLR-MP-83062-U] 14 p2405 N85-24832
Executive control systems in the engineering design environment
[NASA-CR-172582] 14 p2406 N85-24835
Resources for robotics research in Europe, by country
15 p2489 N85-25364
East European report: Science and technology
[JPRS-ESA-85-010] 15 p2524 N85-25560
Electrical features of new DNC, CNC system viewed --- direct numerical control 15 p2524 N85-25562
Flexible machining systems described
15 p2524 N85-25563
Operation of Prisma flexible manufacturing system
15 p2524 N85-25564
West Europe report: Science and technology
[JPRS-WST-84-009] 15 p2535 N85-25639
French firm plans recapture of domestic CAD/CAM market 15 p2535 N85-25641
French consulting firm develops own robotics
15 p2535 N85-25642
Italy invents robot to compete with Asea, Hitachi
15 p2535 N85-25643
Criteria for qualifying for FRG federal CAD/CAM subsidies 15 p2536 N85-25651
East Europe report: Science and technology
[JPRS-ESA-85-018] 15 p2537 N85-25658
Process control systems for largely automated manufacturing 15 p2537 N85-25659
Applications, specifications of Robotron CAD-CAM work stations 15 p2537 N85-25661
Automation and robotics in welding
15 p2566 N85-25831
Recent advances in arc welding equipment and their application 15 p2566 N85-25832
A critical review of selected recent advancements in arc welding equipment and processes
15 p2566 N85-25833
Some aspects of nuclear plant fabrication in Japan and the UK relating to automatic and robotic arc welding
15 p2566 N85-25834
Welding techniques in pressure part technology
15 p2566 N85-25835
SHAFT: Interactive shaft design program
[DE85-007333] 15 p2568 N85-25850
CAD/CAM (Computer-Aided Design/Computer-Aided Manufacturing) highlights
[AD-A151532] 15 p2629 N85-26201
IPAD: Integrated Programs for Aerospace-vehicle Design
[NASA-CR-3890] 15 p2632 N85-26221
Method of selecting robotized system design for pressing process 16 p2761 N85-27040

Experience of sheet stamping robotic complexes
16 p2761 N85-27041
Robotic thermal battery pellet fabrication
[DE85-007755] 16 p2779 N85-27154
Fujian forges ahead in electronic production
16 p2806 N85-27301
Manufacturing methods and technology CAD/CAM (Computer-Aided Design/Computer-Aided Manufacturing) related efforts (FY 1980 - 1986)
[AD-A151817] 16 p2846 N85-27547
Engineering robot actions in a computer integrated manufacturing environment
[CWI-CS-R8415] 17 p2938 N85-28139
The application of numerical control (NC) in manufacturing wind tunnel models
[B8580078] 17 p2939 N85-28140
A new technique for system-to-system transfer of surface data 17 p3007 N85-28589
Comparison of two algebraic methods for curve/curve intersection 17 p3007 N85-28591
Manufacturing information system
[AD-A152715] 17 p3011 N85-28616
Automated fabrication of composite structures for helicopters
[SNIAS-851-210-104] 20 p3393 N85-31049
Robot, laser tridimensional cutting technology detailed
20 p3438 N85-31335
NASA space station automation: AI-based technology review
[NASA-CR-176094] 21 p3558 N85-32134
Importance of automation, robotization in economy
21 p3572 N85-32219
IGES/RIM Parser/Converter users guide
[DE85-011965] 22 p3829 N85-33716
Low cost geometric modelling system for CAM
23 p3964 N85-34578
Establishment of a Computer-Aided Design (CAD)-Computer-Aided Manufacturing (CAM) process for the production of cold forged gears
[AD-A155756] 24 p4137 N85-35644

COMPUTER AIDED MAPPING
Specification and preliminary design of the CARTA system for satellite cartography
[E85-10035] 03 p0378 N85-12414
The integrated use of digital cartographic data and remotely sensed imagery 05 p0655 N85-14206
Statistics and mapping of land uses by means of LANDSAT MSS imagery 05 p0657 N85-14219
A geoinformation expert system for synergetic use of map and image data 05 p0659 N85-14233
A methodology for an integrated spatial data model and its application tc image classification
05 p0659 N85-14234
Contour line generalization using digital image processing methods
[SER-C-291] 11 p1700 N85-20688
Assessment of computer based geologic mapping of rock units in the LANDSAT-4 scene of northern Death Valley, California 13 p2119 N85-23195
An investigation of the crustal properties of Australia and surrounding regions derived from interpretation of MAGSAT anomaly field data 13 p2122 N85-23216
Data structure considerations in automatic cartography
15 p2583 N85-25930
Reports on cartography and geodesy. Series 1: Original reports, no. 94
[ISSN-0469-4236] 16 p2814 N85-27357
Use of vector processors in cartographic raster data processing, with special regard to the AP-120B vector processor 16 p2814 N85-27358
Testing of scanner-assisted revision of the topographic map 1:25,000 (TK 25) 16 p2814 N85-27359
Realization of cartographic tasks on the multiprocessor system EGPA — image processing
16 p2814 N85-27360
Application of the Siemens Computer Aided Computer (Sicad) system to the surveying management in Baden-Wuerttemborg 16 p2814 N85-27361
Automatic engraving of map frames in the revision of the TK 25, 1:25,000 topographical map
16 p2814 N85-27362
Application of interactive graphic systems in land consolidation. Processing of planning maps
16 p2815 N85-27363
A concept for map updating using digital image processing methods 16 p2815 N85-27364
Raster or vector processing. Experience with the application of programs for the construction of thematic maps with boundary design in the Lower Saxony (West Germany) Land Administration for ground research
16 p2815 N85-27365
Status of computer aided mapping in hydrographic services 16 p2815 N85-27366
Contour line generalization using digital image processing methods 16 p2815 N85-27367
What does digital image processing perform in the production of orthophotomaps 16 p2815 N85-27368
A graphic system for drawing synoptic maps by computer
[INPE-3215-PRE/568] 16 p2834 N85-27474
Information relative to cartography and geodesy. Series 2: Translations, number 42, volume 1
[ISSN-0469-4244] 18 p3123 N85-29338
Two satellite image maps of Central Europe
18 p3123 N85-29339
Digital image mapping of Antarctica using NOAA-7 AVHRR imagery 18 p3124 N85-29340
Interactive procedures for discriminating and restoring contour line networks 22 p3736 N85-33158
A model for graphics interface tool development
23 p3960 N85-34545
The scientific and technical issues in integrating remotely sensed imagery with geocoded data bases
23 p3960 N85-34547
A new approach to linear quadtrees
23 p3961 N85-34550
The automatic labeling of geographic maps: A problem in computer aesthetics 23 p3962 N85-34561
How map designers can represent their ideas in thematic maps: Effective user interfaces for thematic map design
23 p3962 N85-34562
Applied computer graphics in a geographic information system: Problems and successes
23 p3962 N85-34563

COMPUTER AIDED TOMOGRAPHY
Three-dimensional reconstruction and data display of chromosome structure studied by electron microscope tomography
[DE85-011562] 22 p3825 N85-33697

COMPUTER ASSISTED INSTRUCTION
Self-paced instruction. Factors critical to implementation in Air Force technical training: A preliminary inquiry
[AD-A145098] 01 p0097 N85-10647
Factors critical to the implementation of self-paced instruction: A background review
[AD-A145143] 01 p0097 N85-10648
Command control group behaviors. Objective 1: A methodology for and identification of command control group behaviors
[AD-A145690] 02 p0191 N85-11279
GUIDON
[AD-P003925] 02 p0246 N85-11605
Air Force honeycomb shaping at SM-ALC (Sacramento Air Logistics Center)
[AD-P004005] 03 p0308 N85-11985
Training capabilities test of Electronics Equipment Maintenance Trainer (EEMT): Findings and conclusions
[AD-A146075] 03 p0359 N85-12302
Experience with a sophisticated computer based authoring system
[DE84-014644] 05 p0713 N85-14575
Computer-managed instruction: Theory, application, and some key implementation issues
[AD-A146564] 06 p0854 N85-15426
Producing high scene content with perspective validity
[AD-P004314] 09 p1268 N85-17968
Study of cognitive styles of students in automated teaching system 10 p1525 N85-19620
Micro-CAE mechanical engineering software development at Lawrence Livermore National Laboratory and participating universities and technology transfer
[DE85-006880] 18 p3163 N85-29597
Air Force Human Resources Laboratory research and development summary
[AD-A154310] 19 p3331 N85-30632
Engineering education based on computer simulation
[CFD/85/1] 20 p3512 N85-31829
The Naval Postgraduate School Flight Mechanics Laboratory: A feasibility study
[AD-A154578] 21 p3557 N85-32127
A microcomputer tutorial on spreadsheets and databases with a simulated budget preparation
[AD-A155516] 21 p3672 N85-32813
Designing a graphics application interface
23 p3964 N85-34574
VLSI (Very Large Scale Integrated) tutorials through the video-computer courseware implementation system
[AD-A155889] 24 p4135 N85-35631

COMPUTER COMPATIBLE TAPES
Standardization of data formats for radar altimeter data 03 p0384 N85-12455
TM digital image products for applications
11 p1668 N85-20512
Cabauw (Netherlands) meteorological data tapes 1973-1984: Description of instrumentation and data processing for continuous measurements
[KNMI-WR-84-6] 14 p2379 N85-24685

COMPUTER COMPONENTS
Hardware multiplier processor
[DE84-006174] 05 p0713 N85-14574
Distributed database components in a DBMS (Database Management System) component architecture
[PB84-217546] 06 p0848 N85-15382
Microcomputers in transit: A hardware handbook
[PB85-113660] 10 p1538 N85-19700
Image processing instrumentation for speckle interferometry and imaging
[AD-A149308] 11 p1762 N85-21084
Bipolar nonswitching logic arrays: Universal components of function expanders for computation of elementary functions 14 p2400 N85-24797
Preliminary assessment of the Heuristics H2000 speechlink - speech recognition device --- voice data input for Apple 2 computer
[BAE-BT-12276] 15 p2539 N85-25674

COMPUTER DESIGN
Description of MBB computerized design techniques for A320 08 p1141 N85-17194
Design and analysis of an access control system for a multi-backend database system
[AD-A148750] 09 p1367 N85-18586
Automatic multi-banking of memory for microprocessors
[NASA-CASE-NPO-15295-1] 12 p1911 N85-21992
UW/NW (University of Washington/Northwest) VLSI Consortium
[AD-A150740] 14 p2404 N85-24818
Czech institute develops microcomputer for satellites
15 p2484 N85-25331
Use of computer-aided design in large-computer development described 15 p2564 N85-25822
Recent advances in supercomputers
16 p2693 N85-26625
East Europe report: Science and technology
[JPRS-ESA-85-021] 21 p3568 N85-32190
Globally-asynchronous locally-synchronous systems
[AD-A154624] 21 p3573 N85-32222
A methodology for the design of testable custom large-scale integrated circuits
[AD-A156098] 24 p4090 N85-35351

COMPUTER GRAPHICS
Analysis of on-board CIG (Computer Image Generator) applications for aircrew training
[AD-A145214] 01 p0013 N85-10079
Interactive graphics nonlinear constrained optimization
01 p0058 N85-10387
FRONTIERS: Progress with a system for nowcasting rain — Forecasting Rain Optimized using New Techniques of Interactively Enhanced Radar and Satellite (FRONTIERS) 01 p0082 N85-10552
A subjective evaluation of the PROFS operational workstation based upon a real-time forecasting experiment in summer 1983 --- Program for Regional Observing and Forecasting Services (PROFS) 01 p0083 N85-10556
Interactive computer display systems in nowcasting
01 p0083 N35-10557
COM-GEOM Interactive Display Debugger (CIDD)
[AD-A145001] 01 p0104 N85-10692
RSCORS graphics system
[DE84-015693] 01 p0104 N85-10698
Halfspace representations of extrusions, solids of revolution and pyramids
[DE84-015005] 01 p0104 N85-10700
DATAPLOT: Introduction and overview
[PB84-214055] 01 p0105 N85-10708
A modular data acquisition and display software system for a laboratory environment
[PB84-217892] 01 p0105 N85-10709
EG and G idaho's response to a request for a graphic data base support package
[DE84-015171] 01 p0126 N85-10862
Interactive system for the interpretation of coal deposit data as a basis of future mine planning systems
[BMFT-FB-T-83-115] 02 p0220 N85-11449
Effects of alternative chromatic mixed graphics displays in decision support systems
[AD-A145561] 02 p0242 N85-11578
An effective graphics user interface for rules and inference mechanisms
[AD-P003942] 02 p0246 N85-11622
Use of prototyping for man-machine interface requirements definition on the AWDS (Automated Weather Distribution System) program
[AD-A146033] 03 p0396 N85-12526
Plotting TDL coastal wind forecasts
[PB84-220789] 03 p0397 N85-12533
CONTROL: A suite of interactive transfer-function analysis programs
[OUEL-1527/84] 03 p0408 N85-12609
DATAPLOT: Implementation tapes guide
[PB84-214063] 03 p0408 N85-12610
Graphics software for the display of body deformation motion
[FW-FO-1640] 04 p0455 N85-12888

Computerized circuit designs: Realization of masks to manufacture microwave circuits
[CNES-NT-107] 04 p0496 N85-13168

Documentation for DIGLIB: Device independent graphics library
[DE84-017385] 04 p0550 N85-13500

International information networks for material properties
[DE84-013836] 04 p0576 N85-13676

A method for measuring the effective throughput time delay in simulated displays involving manual control
05 p0701 N85-14497

The impact of pictorial display on operator learning and performance 05 p0706 N85-14527

Increase in the economy of design and process planning by integrated and graphic data processing, phase 2 — aircraft design
[BMFT-FB-W-84-028] 05 p0716 N85-14589

AFOS (Automation of Field Operations and Services) display of MDR (Manually Digitized Radar) data on local map backgrounds
[PB84-220797] 06 p0840 N85-15338

Nonparametric analysis of Minnesota spruce and aspen tree data and LANDSAT data 07 p0984 N85-16253

Research activities of the Norwegian seismic array (NORSAR)
[AD-A146778] 07 p0996 N85-16326

Interactive Signal Analysis Software (ISAS). User's manual
[AD-A146999] 07 p1022 N85-16485

Program visualization: Graphics support for software development
[AD-A146887] 07 p1024 N85-16499

A program to produce standard shewhart control charts for the statistics X-bar and R or S, P, NP, C, or U
[AD-A146971] 07 p1024 N85-16501

Interactive color-graphics interface for energy monitoring and control systems
[AD-A147538] 07 p1025 N85-16509

PLOT3D: An interactive graphics code for 3-dimensional plots
[AD-A147887] 07 p1026 N85-16514

Local area network evaluation by MICROSS extensions
[AD-A146773] 07 p1027 N85-16521

A Computer-generated topographic display system for navigation and mission planning in helicopters
08 p1073 N85-16800

Computer aided processing using laser measurements
08 p1103 N85-16973

Description of MBB computerized design techniques for A320 08 p1141 N85-17194

Two-dimensional modeling for lineal and areal probabilities of weather conditions
[AD-A147970] 08 p1188 N85-17486

A FORTRAN plotting package for graphic VDUs
[AD-A148489] 08 p1204 N85-17577

The IMAGE 3 Conference Proceedings
[AD-A148836] 09 p1267 N85-17962

Color visual simulation applications at the Defense Mapping Agency
[AD-P004315] 09 p1268 N85-17969

Raster graphics extensions to the core system
[NASA-CR-174348] 09 p1367 N85-18590

SPADE: Series-parallel directed acyclic graph evaluator
[AD-A148458] 09 p1368 N85-18592

Representation and refinement of visual specifications in PegaSys
[AD-A148733] 09 p1368 N85-18596

Introduction to LBL graphics
[DE85-000389] 09 p1369 N85-18600

Organizational tools for data analysis environments
[DE85-000396] 09 p1369 N85-18601

Role of environments in managing data analysis
[DE85-000397] 09 p1369 N85-18602

User/programmer guide for UCMD 108 multi-vertex polyarc/path integrity verifier
[DE84-017173] 09 p1369 N85-18604

User's manual: Menu-driven data graphing program for the Tektronix 7912AD and 7612D transient digitizer system
[DE85-002151] 09 p1370 N85-18610

Computing environments for data analysis. Part 1. Introduction
[AD-A148677] 09 p1373 N85-18632

Computing environments for data analysis. Part 2. Hardware
[AD-A148678] 09 p1374 N85-18633

Application of SIMCA (Soft Independent Modeling of Class Analogy) pattern recognition to air pollutant analytical data
[PB85-124683] 10 p1513 N85-19549

Hurricane plotting program
[PB85-121432] 10 p1521 N85-19592

Graphics translators for computer-aided drafting and design: Interface alternatives for the A/E community
[AD-A148892] 10 p1540 N85-19706

Design of a pictorial program reference language
[AD-A149323] 10 p1540 N85-19711

Interactive Graphics Simulator: Design, development and effectiveness/cost evaluation
[AD-A149417] 10 p1540 N85-19712

Research study of space plasma boundary processes
[NASA-CR-174351] 10 p1558 N85-19823

Digital and color energy maps for graphic display of hourly data
[DE85-000526] 11 p1673 N85-20543

Computer-generated display system guidelines. Volume 1: Display design
[DE85-000679] 11 p1701 N85-20699

Looking at multivariate data through fuzzy sets
[DE85-000684] 11 p1702 N85-20706

Data and information systems and decision making in large public organizations: Research agenda
[DE85-003639] 11 p1738 N85-20931

Tests of low-frequency geometric distortions in LANDSAT 4 images 12 p1872 N85-21744

Review of computer mapping and display techniques applicable to regional analysis
[DE85-003545] 12 p1875 N85-21764

HGRAPH: A subroutine package for the IBM personal computer to support the Hercules Graphic Card
[LA-10144-MS] 12 p1914 N85-22013

Tekedit: An enhanced editor for Direct View Storage Tube (DVST) graphics display devices
[AD-A149715] 12 p1915 N85-22021

Design of graphic displays in computerized systems
[AD-A150071] 12 p1916 N85-22027

EZPIX: A tablet entry method for computer-generated slides, drawings, and graphs
[DE85-005234] 12 p1916 N85-22030

A description of the Langley wireframe geometry standard (LaWGS) format
[NASA-TM-85767] 13 p1971 N85-22380

MAGSAT anomaly field data of the crustal properties of Australia
[E85-10100] 13 p2122 N85-23215

Data selection techniques in the interpretation of MAGSAT data over Australia 13 p2123 N85-23218

Low altitude texture comparison data base and smooth shaded texture
[AD-A150342] 13 p2146 N85-23323

ROSS: An object-oriented language for constructing simulations
[AD-A150556] 13 p2147 N85-23330

Introduction to CHART: A graphic analysis and display system, revision
[DE85-004612] 13 p2148 N85-23335

An error generator to support the trials of the ZODIAC prototype system — raster links
[PHL-1984-71] 14 p2293 N85-24216

The use of a 3-D system for a civil engineering project
14 p2402 N85-24811

The integration of information from an analog-visual display: The role of dimensional integrality
[AD-A150756] 14 p2404 N85-24820

Easyplot: An interactive, user-friendly graphics program
[AD-A150779] 14 p2404 N85-24824

Video animation system
[DE85-005494] 14 p2405 N85-24831

EDIPAS: A multidiscipline and integrated facility for management and evaluation of engineering data
[NLR-MP-83062-U] 14 p2405 N85-24832

Computer Visual System (CVS) reference manual
[DE85-006328] 14 p2407 N85-24837

Determination of the observation conditions of celestial bodies with the aid of the DISPO system
[NAS 1.15:77632] 14 p2438 N85-25044

Using SM-4 Omega system in checking and editing digital terrain information 15 p2487 N85-25350

NPLOT: An interactive plotting program for NASTRAN finite element models 15 p2573 N85-25869

COSMIC/NASTRAN-PATRAN interface
15 p2574 N85-25870

Two interactive graphics postprocessors for NASTRAN 15 p2574 N85-25871

An unusual application of NASTRAN contour plotting capability 15 p2574 N85-25872

Isoparametric 3-D finite element mesh generation using interactive computer graphics 15 p2574 N85-25873

CADS: A Computer Aided Design System
15 p2574 N85-25876

An experimental investigation into the dynamic response of a stiffened flat plate loaded impulsively by an underwater shockwave
[AD-A151321] 15 p2578 N85-25903

Three-dimensional/perspective display techniques for meteorological data sets 15 p2599 N85-26016

Activities report for FOA 53: Laboratory for man and information systems
[FOA-C-53019-H] 15 p2621 N85-26150

The interactive plotting program: GRAPH
[AD-A151371] 15 p2623 N85-26166

An extension of a microcomputer based system for analysis of line drawing quantization schemes
[AD-A152008] 15 p2624 N85-26171

Programme development: A state of the art
15 p2626 N85-2618

Computer aided draughting in a civil engineering consulting practice 15 p2627 N85-2618

A microcomputer-based program for printing check plots of integrated circuits specified in Caltech intermediate form
[AD-A151715] 15 p2629 N85-26205

VAX-based graphics mail system
[DE85-007231] 15 p2630 N85-26214

Interactive graphical data analysis
[DE85-005946] 15 p2631 N85-26215

Graphic simulation of a machine-repairman model
[AD-A151761] 16 p2694 N85-26633

Criteria for the classification of hydrographic positioning data
[AD-A152283] 16 p2705 N85-266

Development of a graphic system: Example using the outline of synoptic charts
[INPE-3296-PRE/611] 16 p2810 N85-27327

Application of interactive graphic systems in land consolidation. Processing of planning maps
16 p2815 N85-273

SINOGRAFO: A system for influencing and forecasting weather
[INPE-3349-PRE/628] 16 p2834 N85-27475

Development of computer aided database design and maintenance tools
[AD-A151782] 16 p2845 N85-27537

Span graphics display utilities handbook, first edition
[NASA-TM-86500] 16 p2849 N85-27567

A fast hidden line algorithm with contour option
[NASA-CR-175803] 16 p2852 N85-27582

An interpolation method with the possibility of first derivative correction
[INPE-3352-PRE/631] 16 p2853 N85-27590

Surface interpolation using weighted splines
[INPE-3387-PRE/656] 16 p2853 N85-27591

The interactive generation of specifications for an onboard software series (GISELE)
17 p2904 N85-27906

FLOWPLOT 2: A fluid dynamics and heat transfer plotting package
[DE85-009802] 17 p2959 N85-28277

Free-form design in solid modelling
17 p3004 N85-28569

Boundary to constructive solid geometry mappings: A focus on 2-D issues 17 p3004 N85-28570

Examination of the circle spline routine
17 p3004 N85-28573

A natural bias approach to cardinal spline curves
17 p3004 N85-28575

Adapting shape parameters for cubic Bezier curves
17 p3004 N85-28576

Triangular Berstein-Bezier patches, a survey and new results 17 p3005 N85-28577

A uniform subdivision method for triangular Bezier patches 17 p3005 N85-28578

An intuitive approach to geometric continuity for parametric curves and surfaces (extended abstract)
17 p3005 N85-28579

Urn models and beta-splines
17 p3005 N85-28580

Parameterization in grid generation
17 p3005 N85-28581

Contouring trivariate data 17 p3005 N85-28582

Generation of surface coordinates by elliptic partial differential equations 17 p3006 N85-28583

A survey of composite grid generation for general three-dimensional sections 17 p3006 N85-28584

A unified representation scheme for solid geometric objects using B-splines (extended abstract)
17 p3006 N85-28585

Improving the effectiveness of integral property calculation in a CSG solid modeling system by exploiting predictability 17 p3006 N85-2858

Looking at more than three dimensions
[DE85-007764] 17 p3009 N85-2860

Tracking algorithm performance analysis program (TRAPP)
[DE85-007304] 17 p3009 N85-2860

Computing environments for data analysis. Part 1. Introduction
[DE85-007919] 17 p3009 N85-2860

Computing environments for data analysis. Part 2. Hardware
[DE85-008320] 17 p3009 N85-2860

Research in computer science
[NASA-CR-175922] 17 p3010 N85-28612

AFIT GKS: A GKS implementation in the Ada programming language
[AD-A152964] 17 p3012 N85-28620

Study of raster metafile formats
[AD-A153322] 17 p3012 N85-28624

The addition of advanced scene rendering techniques to a general purpose graphics package
[AD-A153323] 17 p3012 N85-28625

Software environment for conducting interactive statistical analysis
[AD-A153378] 17 p3012 N85-28626

Introduction to LINE: A Feynman diagram graphic operator
[DE85-009299] 17 p3013 N85-28632

Ray tracing general sweep defined objects
[REPT-84-36] 17 p3014 N85-28636

Fourier coding and reconstruction of complicated contours
[REPT-84-39] 17 p3022 N85-28691

Visual simulation of radiographs
[DE85-010213] 18 p3110 N85-29255

Two satellite image maps of Central Europe
18 p3123 N85-29339

The use of VLSI technology for the real-time generation of graphics displays: A proposal
[AD-A153766] 18 p3160 N85-29578

Program DISAS: A computer program to obtain hard-copy plots of an image displayed on a vector graphics device in a local-area-network
[AD-A153643] 18 p3162 N85-29586

Graphics package, version 4: User reference manual
[DE85-007894] 18 p3163 N85-29596

Two-dimensional/speed/couple/data base management system
[A-1] 18 p3165 N85-29608

Three-dimensional/integration two and three dimensional/numerical control/communication
[A-2] 18 p3165 N85-29609

The CEADS-CADD system
[A-4] 18 p3165 N85-29610

System test CALMA DDM (Design Drafting Manufacturing)
[A-5] 18 p3165 N85-29611

System test: Hewlett-Packard draft
[A-9] 18 p3166 N85-29613

Test Drawing Office Graphics System (DOGS)/APOLLO
[A-10] 18 p3166 N85-29614

Solar physics applications of computer graphics and image processing 18 p3208 N85-29903

Graphic displays of vector magnetograph data
18 p3209 N85-29904

AEV local verification for aviation, precipitation, and temperature programs: AV, REL, TEM
[PB85-179125] 19 p3318 N85-30568

Cultural data base implementation study and computer-aided scene modeling system users manual
[AD-A154232] 19 p3333 N85-30646

Graphic display development program. Volume 2, revision 0: Appendices
[DE85-011078] 19 p3333 N85-30648

Interactive graphics for a data analysis management system
[DE85-010977] 19 p3334 N85-30651

Demonstration project: Putting the bioastronautics data book on line
[NASA-CR-178424] 19 p3335 N85-30659

Defense Mapping Agency (DMA) raster-to-Vector analysis
[AD-A154153] 19 p3336 N85-30668

Defense Mapping Agency (DMA) raster-to-Vector benchmark testing
[AD-A154152] 19 p3338 N85-30683

A Lotus 1-2-3 based system reliability program
[DE85-010533] 19 p3340 N85-30701

MANHIST user's guide
[DE85-010684] 19 p3348 N85-30754

Radiation interactions for tomography
[DE85-008961] 19 p3355 N85-30799

User's guide for the Mk-3 D-coronameter data system
[PB85-181204] 19 p3385 N85-31002

A feasibility study for the use of electronic flight strips in ATC controller workstations
[DFVLR-FB-85-08] 20 p3392 N85-31039

The application of computer imaging techniques to ocean topography and geophysical data
20 p3492 N85-31711

Intersection of three-dimensional geometric surfaces
[NASA-TP-2454] 20 p3513 N85-31839

Visualization of computation results. Definition of a graphics satellite computer
[ONERA-RT-2/3587-CY] 20 p3514 N85-31845

A set of subroutines for masked three-dimensional plotting with rotations
[MEAH-33] 20 p3514 N85-31846

System test Oce 5200
[A-3] 20 p3515 N85-31850

The General Drafting System (GDS) design system
[A-6] 20 p3517 N85-31869

The IGOS design system
[A-8] 20 p3517 N85-31870

R and D activities of the Computer Centre
20 p3540 N85-32029

User's guide for computer program CGFAG, Concrete General Flexure Analysis with Graphics
[AD-A155555] 21 p3570 N85-32204

Flexible satellite communications systems simulator, phase 3
[AD-A155647] 21 p3577 N85-32247

Realizing the full potential of the video disc for mapping applications
[AD-A154966] 21 p3606 N85-32391

Real-time contour surface display generation
[AD-A155232] 21 p3668 N85-32780

DYNA3D, INGRID, and TAURUS: An integrated, interactive software system for crashworthiness engineering
[DE85-010928] 21 p3677 N85-32846

Interactive procedures for discriminating and restoring contour line networks 22 p3736 N85-33156

Dialog system with minicomputer for plotting performance charts 22 p3768 N85-33355

A new large-scale, high-resolution multicolor software display concept
[AD-A155404] 22 p3827 N85-33703

QKPLT users guide, version 2.0
[L-10094-M] 22 p3828 N85-33707

IGES/RIM Parser/Converter users guide
[DE85-011965] 22 p3829 N85-33716

MORSE-CGA: A Monte Carlo radiation transport code with array geometry capability
[DE85-012063] 22 p3830 N85-33718

An introduction to finite elements
23 p3924 N85-34319

A device-independent 2D plotting package written in FORTRAN
[RSRE-MEMO-3776] 23 p3956 N85-34514

Graphics Interface 1985: Proceedings
[ISSN-0713-5424] 23 p3957 N85-34523

A theoretical and empirical analysis of coherent ray-tracing 23 p3957 N85-34524

Frame buffer algorithms for stochastic models
23 p3957 N85-34525

Specifying stochastic objects in a hierarchical graphics system 23 p3957 N85-34526

The interactive planning work station: A graphics-based UNIX (trademark) tool for application users and developers 23 p3957 N85-34527

Computer graphics for multivariate data
23 p3958 N85-34528

Interfacing interactive circuit simulation with standard graphics facilities 23 p3958 N85-34529

Computer analysis techniques for the temporal evaluation of cardiac wall motion
23 p3958 N85-34530

A computerized system for spot detection and analysis of two-dimensional electrophoresis images
23 p3958 N85-34531

An image management kernel for the design of relational and pictorial data bases 23 p3958 N85-34532

Spatial trees: A fast access method for unstructured graphical data 23 p3958 N85-34533

Graphics Interaction in databases
23 p3958 N85-34534

Animengine: An engineering animation system
23 p3959 N85-34535

3D computer animation: More an evolution problem than a motion problem 23 p3959 N85-34536

Using dynamic analysis to animate articulated bodies such as humans and robots 23 p3959 N85-34537

Towards an integrated view of 3-D computer character animation 23 p3959 N85-34538

Research issues in generating graphical explanations
23 p3959 N85-34539

An integrated system for printing and publishing applications 23 p3959 N85-34540

Recognition and clear representation of handwritten electronic diagrams 23 p3960 N85-34541

A model for a document maintenance system
23 p3960 N85-34542

Efficient recovery and reversal in graphical user interfaces generated by the Higgens system
23 p3960 N85-34544

A model for graphics interface tool development
23 p3960 N85-34545

Using percent-done program indicators to enhance user interfaces 23 p3960 N85-34546

Selection of segment similarity measures for hierarchical picture segmentation 23 p3960 N85-34548

A general purpose image processing package
23 p3961 N85-34549

A new approach to linear quadtrees
23 p3961 N85-34550

An analysis and algorithm for filling propagation
23 p3961 N85-34551

The CADME approach to the interface of solid modellers 23 p3961 N85-34554

A graphics interface for interactive simulation of packet-switched networks 23 p3962 N85-34558

Design and implementation of an interactive route editor 23 p3962 N85-34559

Project management using graphics
23 p3962 N85-34560

The automatic labeling of geographic maps: A problem in computer aesthetics 23 p3962 N85-34561

How map designers can represent their ideas in thematic maps: Effective user interfaces for thematic map design
23 p3962 N85-34562

Applied computer graphics in a geographic information system: Problems and successes
23 p3962 N85-34563

Image synthesis: Optical identity or pictorial communication? 23 p3963 N85-34565

Strategic use of business graphics: A stakeholder approach 23 p3963 N85-34566

Colour spaces and colour contrast
23 p3963 N85-34567

Colour coding scales and computer graphics
23 p3963 N85-34568

Geometric continuity with interpolating Bezier curves
23 p3963 N85-34570

An intuitive approach to geometric continuity for parametric curves and surfaces
23 p3963 N85-34571

Building an octree from a set of parallelepipeds
23 p3964 N85-34572

Developing graphical tools with minimal GKS
23 p3964 N85-34573

Designing a graphics application interface
23 p3964 N85-34574

NAPGEN: Automatic NAPLPS page generator
23 p3964 N85-34575

Low cost geometric modelling system for CAM
23 p3964 N85-34578

The dynamics of articulated rigid bodies for purposes of animation 23 p3965 N85-34579

Shadow volumes for non-planar polygons
23 p3965 N85-34580

Computer animation in distance teaching
23 p3965 N85-34581

Generative design in architecture using an expert system 23 p3965 N85-34582

Heuristic rules for visualization
23 p3965 N85-34584

Using LINE as an interactive graphics package. Interfacing line and Topdraw in 43 and 24 VM
[DE85-012007] 23 p3965 N85-34585

Raster functionality for a VDI
[DE85-006734] 24 p4097 N85-35396

Edge detection and geometric methods in computer vision
[AD-A155873] 24 p4135 N85-35630

An exploratory study of the effect of screen size and resolution on the legibility of graphics in automated job performance aids
[AD-A155969] 24 p4136 N85-35632

Selected publications in image understanding and computer vision from 1974 to 1983
[AD-A156196] 24 p4136 N85-35634

Master Fit users' guide, version 1.0
[DE85-014199] 24 p4140 N85-35667

COMPUTER INFORMATION SECURITY

Reserve and authentication in Integrated Services Distributed Networks (ISDN) networks
[FUB-37-1983] 01 p0041 N85-10262

Computer science and technology: Overview of computer security certification and accreditation
[PB84-217819] 06 p0848 N85-15384

Digital signatures: An update
[NPL-DITC-51/84] 09 p1367 N85-18589

French commentary on Soviet industrial espionage
10 p1461 N85-19210

Computer crime
[GPO-30-544] 10 p1537 N85-19691

Computer and communications security and privacy
[GPO-39-741] 12 p1911 N85-21994

Security of personal computer systems: A management guide
[PB85-161040] 14 p2400 N85-24793

Commercial data base management system for geonames data base
[AD-A150835] 14 p2433 N85-25007

COMPUTER METHODS

Future information technology, 1984 telecommunications
[PB85-165850] 15 p2624 N85-26173

Future information technology, 1984: Telecommunications
[NBS/SP-500/119] 16 p2678 N85-27762

NASA guidelines for assuring the adequacy and appropriateness of security safeguards in sensitive applications
[NASA-CR-175489] 17 p3007 N85-28593

A secure high-speed transaction protocol
[CWI-CS-R8417] 17 p3009 N85-28605

Computer center policy
[AD-A154416] 19 p3336 N85-30661

Security controls in the Stockpoint Logistics Integrated Communications Environment (SPLICE)
[AD-A155536] 21 p3576 N85-32244

Design guidelines for user-system interface software
[AD-A154907] 21 p3671 N85-32807

An approach to determining computer security requirements for Navy systems
[AD-A155750] 24 p4135 N85-35627

COMPUTER METHODS
U COMPUTER PROGRAMS

COMPUTER NETWORKS

Tendencies in the development of utilization protocols, seminar report — communication networks
[FUB-11-1983] 01 p0039 N85-10252

Interactive graphics nonlinear constrained optimization
01 p0058 N85-10387

Nowcasting with Doppler radar: The forecaster-computer relationship
01 p0077 N85-10514

Evaluating a scientific workstation computer
[DE84-014764] 01 p0100 N85-10663

REMOTE: Modem Communicator Program for the IBM personal computer
[DE84-015047] 01 p0100 N85-10665

Assessing the reliability of computer software and computing networks: An opportunity for partnership with computer scientists
[AD-A145131] 01 p0104 N85-10697

Storage in the LLNL Octopus network: An overview and reflections
[DE84-014711] 01 p0106 N85-10712

Throughput characteristics of Carrier Sense Multiple Access (CSMA) networks
[FUB-25-1983] 01 p0106 N85-10713

End-to-end performance in local area networks of interconnected token rings
[FUB-42-1983] 01 p0107 N85-10714

Proceedings of the 5th LAN-Transport Workshop
[PB84-232667] 01 p0107 N85-10715

The computer-communication link for the innovative use of Space Station 02 p0150 N85-11016

Shuffle-exchanges on augmented meshes
[NASA-CR-172476] 02 p0243 N85-11587

Fault tolerant computing research
[AD-A145640] 02 p0244 N85-11590

Study on the conversion and test of protocols
[ENST-84E005] 03 p0356 N85-12293

On a program for solution of BCMP queueing network model
[NAL-TR-813] 03 p0405 N85-12585

Regenerative simulation methods for local area computer networks
[AD-A146197] 03 p0409 N85-12612

Verification of a class of deadlock-free, self-timed, computational arrays
[AD-A146272] 03 p0412 N85-12638

Test experience on an ultrareliable computer communication network
[NASA-TM-85915] 04 p0552 N85-13514

User behavior upon introduction of a network help system
[DE84-016466] 04 p0552 N85-13515

International information networks for material properties
[DE84-013836] 04 p0576 N85-13676

Development of the NLTSS operating system
[DE84-013702] 05 p0714 N85-14576

Requirements and overview of the LINCS distributed operating system architecture
[DE84-013721] 05 p0714 N85-14577

Contribution to the study and realization of the CARTHAGE multiservice local network
[ENST-84E006] 05 p0716 N85-14595

Specification of a transport protocol for computer communications. Volume 1: Overview and Services. Volume 2: Class 2 protocol. Volume 3: Class 4 protocol
[PB84-222650] 06 p0848 N85-15380

Distributed database components in a DBMS (Database Management System) component architecture
[PB84-217546] 06 p0848 N85-15382

Specification of a transport protocol for computer communications. Volume 4: Service specifications. Volume 5: Guidance for the implementor. Volume 6: Guidance for implementation selection
[PB84-222668] 06 p0848 N85-15385

Specification of a transport protocol for computer communications. Volume 7: Testing OSL protocols, a compendium of papers. Volume 8: User's guide to the testing system for implementations of the ICST transport protocol. Volume 9: A test suite for implementations of the ICST transport protocol. Volume 10: Specification of a remote scenario interpreter for implementations of the ICST transport protocol
[PB84-222676] 06 p0848 N85-15386

Selecting a leader in a clique in O(N log N) messages
[AD-A146561] 06 p0857 N85-15453

Stuttgart Interconnection Network Project from PIX to NICS
[NASA-TM-77802] 06 p0870 N85-15528

Upper Atmosphere Research Satellite (UARS) trade analysis
[NASA-CR-175269] 07 p0912 N85-15774

Support for distributed transactions in the TABS (Transaction based systems) prototype
[AD-A147213] 07 p1022 N85-16486

NSW (National Software Works) lessons learned
[AD-A146737] 07 p1023 N85-16494

Reliability analysis of local area networks, intermediate report
[BLL-WH-610-(9091.9F)] 07 p1027 N85-16520

Local area network evaluation by MICROSS extensions
[AD-A146773] 07 p1027 N85-16521

NSWC-NADC interactive communication links for AN/UYS-1 loadtape creation and retrieval
[AD-A148418] 08 p1153 N85-17277

Performance evaluation and control of distributed computer communication networks
[AD-A148103] 08 p1208 N85-17598

DDN directory
[AD-A148213] 08 p1230 N85-17744

Identification of emerging designer needs and high payoff CAE tools
[DE85-000755] 09 p1369 N85-18599

Software for event oriented processing on multiprocessor systems
[DE84-016720] 09 p1370 N85-18607

Asymptotic analysis of Markovian access control computer communication networks
09 p1372 N85-18619

Gateway testing techniques — computer system interconnection
[NPL-DITC-49/84] 09 p1372 N85-18621

Concepts and tools for the software life cycle
10 p1464 N85-19236

A validated methodology for determination of laboratory instrument computer interface efficacy
[AD-A149338] 10 p1487 N85-19391

Distributing a distributed problem solving network simulator
[AD-A149065] 10 p1537 N85-19693

Guidepost routing algorithm for distributed computer networks 11 p1622 N85-20210

Development of computer centers, equipment described: Problems of computer centers
11 p1700 N85-20686

Personal desktop computing in a research and development laboratory
[DE85-002765] 11 p1705 N85-20728

Post-processing of bibliographic citations from DOE/Recon, NASA/Recon, and DOD/DROLS
[DE85-000617] 11 p1739 N85-20936

Multicomputer communication system
[NASA-CASE-NPO-15433-1] 12 p1822 N85-21428

Collection and use of lightning strike data in the western US during summer 1983
[PB85-110534] 12 p1897 N85-21907

Computing Division two-year operational plan, FY 1984 - 1985
[LA-9978-MS] 12 p1913 N85-22006

Satellite channels in packet-switching networks
13 p2067 N85-22909

Exploiting parallel computing with limited program changes using a network of microcomputers
[NASA-TM-86387] 13 p2146 N85-23318

Introduction to CHART: A graphic analysis and display system, revision
[DE85-004612] 13 p2148 N85-23335

Research using a DISCUS based network emulator
[AD-A141294] 13 p2149 N85-23338

Introduction to the Space Physics Analysis Network (SPAN)
[NASA-TM-86499] 14 p2290 N85-24198

The problem of creating a standardized series of personal computers 14 p2400 N85-24795

LINCS
[DE85-006151] 14 p2407 N85-2480

Pluribus Satellite IMP (Interface Message Provision) development mobile access terminal network
[AD-A151201] 15 p2541 N85-2568

Pluribus Satellite IMP (Interface Message Provision) development mobile access terminal network
[AD-A151312] 15 p2542 N85-2569

Standards in process: Foundation and profiles of ISDN (Integrated Services Digital Network) and OSI (Open Systems Interconnection) studies
[PB85-165041/GAR] 15 p2545 N85-25712

Mini- and microcomputer local control network architecture and design principles
15 p2625 N85-26179

Backbone network simulations: A comparative study
[DE85-006974] 15 p2632 N85-26224

Maintaining consistency and accommodating network repair in a self-regenerative distributed database management system (a discussion of the means and cost) 16 p2696 N85-2660

East Europe report: Science and technology
[JPRS-ESA-84-032] 16 p2727 N85-2693

Network information management subsystem
16 p2771 N85-27108

Standards and specifications for geodetic control networks
[PB85-166476] 16 p2816 N85-27374

Mathematical programming in computer network design
[AD-A152275] 16 p2848 N85-27558

Span graphics display utilities handbook, first edition
[NASA-TM-86500] 16 p2849 N85-27567

Continued development and implementation of the Universal Network Interface Device (UNID) 2, Digital Engineering Laboratory Network (DELNET), volume 1
[AD-A151935] 16 p2850 N85-27569

Continued development and implementation of the Universal Network Interface Device (UNID) 2 in the Digital Engineering Laboratory Network (DELNET), volume 2
[AD-A151947] 16 p2850 N85-27570

Internation information networks for material properties. Revision 1
[DE85-007412] 16 p2850 N85-27572

Access path optimization for network database retrieval 16 p2877 N85-27749

Design of an interface to an information retrieval network 16 p2877 N85-27750

There is no I/O like no I/O
[DE85-009115] 17 p3014 N85-28634

System Analysis for the Huntsville Operation Support Center, Distributed Computer System
[NASA-CR-171506] 17 p3015 N85-28642

Interfacing the VAX 11/780 using Berkeley Unix 4.2BSD and Ethernet based Xerox network systems, volume 1
[AD-A152953] 17 p3015 N85-28645

Distributed systems management in wide area networks
[CWI-CS-R8419] 17 p3016 N85-28651

Distributed matchmaking for processes in computer networks
[CWI-CS-R8421] 17 p3016 N85-28652

Distributed elections in a ring of processors using Archimedean time
[CWI-CS-R8416] 17 p3016 N85-28653

Performance measurement of OSI (Open System Interconnection) class 4 transport implementations
[PB85-177657] 18 p3161 N85-29582

INEL User Network Exchange, volume 1-85, Jan./Feb. 1985
[DE85-006108] 18 p3166 N85-29615

Distribution of mathematical software via electronic mail
[DE85-009664] 18 p3166 N85-29617

Graceful fault tolerance in large networks of microcomputers 19 p3332 N85-30643

A new taxonomy for distributed computer systems based upon operating system structure
[NASA-TM-86438] 19 p3342 N85-30709

ZOG/VINSON technology demonstration project system description. Volume 1
[AD-A154211] 19 p3342 N85-30713

Apollo multiplexer operations manual
[DE85-011293] 19 p3343 N85-30719

The application of artificial intelligence techniques to large distributed networks
[NASA-CR-177346] 19 p3344 N85-30721

Computerized Laboratory Analytical and Diagnostic Services (CLADS)
[DE85-010854] 20 p3518 N85-31871

RESO: Expert system applied to company computer networks
[ENST-84E016] 20 p3518 N85-31874

Interactive on-line conferences
[AD-A154723] 21 p3574 N85-3222

A high-speed digital signal processor for atmospheric radar, part 7.3A
21 p3626 N85-32525

Microcomputer network: investigation and implementation
[AD-A155631] 21 p3674 N85-32826

Broadcasting topology and routing information in computer networks
[AD-A155666] 21 p3674 N85-32827

Some plant location problems — computer networks
[FUB-14-1984] 22 p3835 N85-33746

An innovative user interface for microcomputer-based computer-aided design 23 p3961 N85-34555

COMPUTER PROGRAM INTEGRITY

Assessing the reliability of computer software and computing networks: An opportunity for partnership with computer scientists
[AD-A145131] 01 p0104 N85-10697

NECIS Incorporated, NEC ASTRA model 270, COBOL 74 version 8.3 (COBOL technical report)
[PB84-227933] 06 p0848 N85-15381

Computer science and technology: Overview of computer security certification and accreditation
[PB84-217819] 06 p0848 N85-15384

Digital Research Incorporated, IBM PC XT, FORTRAN-77 V4.0
[PB84-243633] 06 p0849 N85-15388

Perkin-Elmer, Perkin-Elmer 3230, FORTRAN 7 D R00-00
[PB84-243682] 06 p0849 N85-15389

Gould Incorporated, Gould PS-3000, Gould PS-3000 FORTRAN 77 V2.1
[PB84-229178] 06 p0849 N85-15390

NECIS, Incorporated, NEC ASTRA model 270 COBOL 74 Version 8.3
[PB84-227636] 06 p0850 N85-15397

Digital Equipment Corporation, DECSYSTEM-20, model 2060, COBOL V13
[PB84-227958] 06 p0850 N85-15398

Digital Equipment Corporation, DECSYSTEM-20, model 2060, COBOL V13 (COBOL technical report)
[PB84-227966] 06 p0850 N85-15399

Northern Telecom, Incorporated, IBM 3033 (compilation), NTI-585/565 (execution), XCOBOL Release 4.1 Version H(01)
[PB84-227875] 06 p0850 N85-15400

NCR Corporation, NCR I9300, NCR ITX Cobol Release 3.0
[PB84-228055] 06 p0850 N85-15401

NCR Corporation, NCR I9300, NCR ITX COBOL Release 3.0 (COBOL technical report)
[PB84-228063] 06 p0850 N85-15402

Computervision Corporation, CDS-4000 32-Bit processor, CV FORTRAN Version 2.84
[PB84-227867] 06 p0851 N85-15406

Sperry Univac, System 80 Model 6, OS/3 COBOL, Version 08.00/08
[PB84-227800] 06 p0851 N85-15410

Modular Computer Systems, Incorporated, MODCOMP CLASSIC 7860, MODCOMP FORTRAN 77/16 Version A.0
[PB84-230556] 06 p0852 N85-15411

Modular Computer Systems, Incorporated, MODCOMP CLASSIC 7860, MODCOMP NASA EXTENDED FORTRAN 78 Version A.40
[PB84-230549] 06 p0852 N85-15412

Digital Equipment Corporation, MICRO/PDP-11, COBOL-81 Version 2.2
[PB84-229236] 06 p0852 N85-15413

NCR Corporation, NCR 9300, NCR ITX-BASIC Release 2.0
[PB84-229228] 06 p0852 N85-15414

Sperry Corporation, 1100/80, UBASIC/BBASIC Level 9R1
[PB84-229202] 06 p0852 N85-15415

Sperry Corporation, 1100/80 ASC2 FORTRAN Level 11R1
[PB84-229194] 06 p0852 N85-15416

Computer Sciences Corporation, UNIVAC 1100/80, CSTS COBOL Release COB250
[PB84-229154] 06 p0852 N85-15417

Computer Sciences Corporation, UNIVAC 1100/80, CSTS BASIC Release BAS180
[PB84-229145] 06 p0852 N85-15418

Wang Laboratories, Incorporated, Wang VS100, FORTRAN 77 Version 01.00.02
[PB84-228014] 06 p0852 N85-15419

Control Data Corporation, Cyber 835, BASIC Release 3.5 Level 614
[PB84-227990] 06 p0853 N85-15420

Data General Corporation, Eclipse C350, AOS COBOL Release 3.51
[PB84-227982] 06 p0853 N85-15421

Digital Equipment Corporation, DECSYSTEM-20 2060 Model B, FORTRAN-20 Version 10
[PB84-227974] 06 p0853 N85-15422

Convergent Technologies, NGEN CP001, CT FORTRAN Version 9.0
[PB84-229210] 06 p0856 N85-15442

Formal verification of mathematical software
[NASA-CR-172407] 07 p1023 N85-16489

Completely monotone regression estimates of software failure rates
[NASA-CR-174319] 08 p1204 N85-17575

Ada (trademark) Joint Program Office objectives and progress through 1983
[AD-A149436] 10 p1541 N85-19713

Sperry Univac System 80, Model 6, OS/3 BASIC, Version 10.01
[PB85-108066] 10 p1542 N85-19722

FORTRAN 66 analyser: User's manual
[PB85-111748] 10 p1542 N85-19724

Ada compiler validation summary report, Dansk Datamatik Center, VAX 11 compiler version 1.1
[AD-A149340] 11 p1699 N85-20681

Micro Focus IBM personal computer XT Compact Level 2 COBOL; V2.5
[PB85-108918] 11 p1703 N85-20716

Micro Focus IBM personal computer XT High Performance Level 2 COBOL; V2.5
[PB85-108926] 11 p1704 N85-20717

Micro focus IBM personal computer XT, high performance level, 2 COBOL, IBM PC tailored; V2.6
[PB85-110815] 11 p1705 N85-20725

A theoretical basis for the analysis of redundant software subject to coincident errors
[NASA-TM-86369] 13 p2145 N85-23317

Security of personal computer systems: A management guide
[PB85-161040] 14 p2400 N85-24793

Management aspects of software maintenance
[AD-A152035] 16 p2847 N85-27550

Integrated software engineering system (SIGL)
[DT/GL/7254/Z462/G-C./MJ]
20 p3516 N85-31863

COMPUTER PROGRAMMING

NT ASSEMBLER ROUTINES
NT LANGUAGE PROGRAMMING
NT LOGIC PROGRAMMING
NT MICROPROGRAMMING
NT MULTIPROGRAMMING
NT PARALLEL PROGRAMMING
NT SYMBOLIC PROGRAMMING

Applications of numerical optimization methods to helicopter design problems: A survey
[NASA-TM-86010] 01 p0006 N85-10036

Research in Structures and Dynamics, 1984
[NASA-CP-2335] 01 p0057 N85-10377

Digital correlator speed improvement by multiplexing
[AD-A145207] 01 p0100 N85-10662

Ada (trademark) training curriculum. Basic Ada programming I202 teacher's guide. Laboratory manual and exercises
[AD-A143583] 01 p0103 N85-10687

THLL (TRIDENT Higher Level Language) reference manual
[AD-A145116] 01 p0104 N85-10696

Mathmatics and Computer Science Division activities
[DE84-014842] 01 p0104 N85-10701

Establishing a Software Engineering Technology (SET)
[PB84-212141] 01 p0105 N85-10702

FSTC (Federal Software Testing Center) software tool catalog
[PB84-212158] 01 p0105 N85-10703

DATAPLOT: Introduction and overview
[PB84-214055] 01 p0105 N85-10708

Software engineering environments for mission critical applications: STARS alternative programmatic approaches
[AD-A145285] 02 p0241 N85-11571

DOD related software technology requirements, practices, and prospects for the future
[AD-A145493] 02 p0242 N85-11575

Yearly report for programming productivity enhancement by the use of application generators
[AD-A145623] 02 p0242 N85-11579

Research on distributed languages and algorithms
[AD-A145661] 02 p0242 N85-11580

GUIDON
[AD-P003925] 02 p0246 N85-11605

Artificial intelligence applications to automatic test equipment
[AD-P003936] 02 p0247 N85-11616

Memory-based expert systems
[AD-A145612] 02 p0249 N85-11628

Pointwise iterations of finite element modeling of advection-diffusion equations
[DE84-015284] 02 p0253 N85-11656

Programmable optical sensor
[AD-D011244] 02 p0281 N85-11829

Air Force Materials Laboratory plans/projects
[AD-P004010] 03 p0306 N85-11990

An inviscid computational method for supersonic inlets
[AD-A145997] 03 p0316 N85-12042

Power subsystem automation study
[NASA-CR-171213] 03 p0358 N85-12299

A methodology for the analysis of programmer productivity and effort estimation within the framework of software conversion
[AD-A145757] 03 p0406 N85-12592

Computer center introductory reference manual for CDC CYBER
[AD-A145796] 03 p0406 N85-12593

Programming effort estimation
[AD-A145839] 03 p0406 N85-12595

Configuration management for mission-critical software: The Los Alamos solution
[DE84-015515] 03 p0408 N85-12606

Experimenting with the Rolm Ada language workshop for specifying and designing 03 p0408 N85-12607

Definition of technology development missions for early Space Station satellite servicing. Volume 1: Executive summary
[NASA-CR-171228] 04 p0460 N85-12922

DNC, CNC network for robotized machining cells
04 p0491 N85-13130

Concentrator optical characterization using computer mathematical modelling and point source testing
[NASA-CR-174109] 04 p0528 N85-13375

Minimal cut-set methodology for artificial intelligence applications
[DE84-016674] 04 p0553 N85-13518

An electronic documentation system
[SNIAS-842-111-101] 04 p0577 N85-13683

Research in computer science
[NASA-CR-174088] 05 p0713 N85-14572

Experience with a sophisticated computer based authoring system
[DE84-014644] 05 p0713 N85-14575

Control of walking: Local control and real time systems 05 p0715 N85-14583

A proposal for standard basic functions in Ada
[NPL-DITC-45/84] 05 p0715 N85-14584

How to implement the welcome program in compatible microcomputers such as Apple 2
[INPE-3114-PRE/511] 05 p0715 N85-14586

Use of monitors in FORTRAN: A tutorial on the barrier, self-scheduling DO-loop and Askfor monitors
[DE84-016506] 05 p0715 N85-14587

Experimental techniques of formal specifications for the design of tested and reliable computer programs
[ENST-84E007] 05 p0716 N85-14591

Towards a specification of the B programming environment
[CWI-CS-R8408] 05 p0716 N85-14593

Programming and application of numerical controlled measuring machines (NCMES)
[BMFT-FB-T-84-153] 05 p0717 N85-14599

Priority rewrite systems — computer programming
[CWI-CS-R8407] 05 p0720 N85-14621

Setting time standards at NISTARS (Naval Integrated Storage and Retrieval System)
[AD-A146371] 06 p0870 N85-15529

Art of programming programmable microcalculators. Part 12: Solution of differential equations
07 p0953 N85-16043

RATFOR user's guide version 2.0
[NASA-CR-166601] 07 p1023 N85-16490

Program visualization: Graphics support for software development
[AD-A146887] 07 p1024 N85-16499

Functional semantics of modules
[AD-A146923] 07 p1024 N85-16500

The electronic typesetting program programmer's manual
[AD-A147500] 07 p1025 N85-16508

Implementation of a constraint machine for prism - A parallel problem solver
[AD-A147844] 07 p1026 N85-16512

Operating system versus programming environment, for example the UNIX
[SWA-84/037] 07 p1027 N85-16516

Trust region methods for minimization
[AD-A147073] 07 p1030 N85-16540

The production of maintainable, trustworthy, and portable software 08 p1064 N85-16744

On the validation of computer science theories
[AD-A148637] 08 p1203 N85-17572

Fundamentals of computer programming for engineers
[AD-A147964] 08 p1205 N85-17583

Computer center CDC Libraries-PROCFIL (procedures)
[AD-A148633] 08 p1206 N85-17589

Concept paper for the development of a DOD Ada (trademark) software engineering education and training plan
[AD-A148774] 08 p1206 N85-17592

Computer center CDC libraries/NSRD (subprograms)
[AD-A148782] 08 p1206 N85-17593

Solutions to structural dynamics problems
09 p1334 N85-18384

Automatic map name placement system
09 p1341 N85-18438

Computer center CDC libraries/utility (programs)
[AD-A148680] 09 p1368 N85-18593

FLAD user's manual: FLAD file contents
[AD-A148700] 09 p1368 N85-18594

Partial evaluation as a means of language extensibility
[AD-A148730] 09 p1368 N85-18596

Organizational tools for data analysis environments
[DE85-000396] 09 p1369 N85-18601

Role of environments in managing data analysis
[DE85-000397] 09 p1369 N85-18602

Software for event oriented processing on multiprocessor systems
[DE84-016720] 09 p1370 N85-18607

Multitasking kernel for the C and FORTRAN programming languages
[DE85-001799] 09 p1370 N85-18609

Computing environments for data analysis. Part 2. Hardware
[AD-A148678] 09 p1374 N85-18633

MACSYMA usage at Langley
[NASA-CR-172518] 10 p1537 N85-19688

Managing permanent objects
[AD-A149007] 10 p1540 N85-19708

SOLIDGEN: A solid finite element data generator. User's manual
[AD-A149490] 10 p1541 N85-19715

East Europe report: Science and technology
[JPRS-ESA-85-009] 11 p1616 N85-20165

Space Station Software issues
[NASA-CP-2361] 11 p1700 N85-20689

Software development environment issues — space station software development 11 p1700 N85-20691

Software technology within NASA
11 p1701 N85-20695

A computer system for generating single and double sampling plans for attributes data
[AD-A149548] 11 p1701 N85-20698

Polylith and environments for mathematical computation
[DE85-002967] 11 p1702 N85-20704

User's guide for the computer program response factor (REFAC)
[PB85-138600] 11 p1705 N85-20726

Integrated control system engineering support
[AD-A149742] 12 p1780 N85-21177

Universal file processing program for field programmable integrated circuits
[DE85-004384] 12 p1837 N85-21526

A survey of the project CIP: Computer aided, intuition-guided programming. Wide spectrum language and program transformations
[TUM-I8406] 12 p1912 N85-22000

PISCES: An environment for parallel scientific computation
[NASA-CR-172544] 12 p1913 N85-22004

Towards the generation of efficient code from verified programs
[TR-40] 12 p1914 N85-22017

Very-high level concurrent programming
[AD-A150009] 12 p1916 N85-22026

METC VAX-IBM guide to ASPEN
[DE85-001974] 12 p1916 N85-22031

VAX-ASPEN installation guide
[DE85-001973] 12 p1916 N85-22032

Programs for dynamic loading of precompiled subroutine packages, especially for applications with the Watfiv compiler
[DFVLR-MITT-84-18] 12 p1917 N85-22035

A formal method for specifying computer resources in an implementation independent manner
[AD-A149955] 12 p1918 N85-22043

Research Reports: 1984 NASA/ASEE Summer Faculty Fellowship Program
[NASA-CR-171317] 12 p1944 N85-22210

Requirements for a database management system
[DE85-004661] 12 p1951 N85-22259

Optimal allocation of components in parallel-series and series-parallel systems
[AD-A150169] 13 p2144 N85-23309

FORTRAN in the 90's
[DE85-006154] 13 p2148 N85-23332

The hierarchical database decomposition approach to database concurrency control
[AD-A150612] 13 p2168 N85-23450

Design for tactical avionics maintainability, technical evaluation report
[AGARD-AR-204] 14 p2225 N85-23796

Ground-up-to-Space (GUTS) laser propagation code description and manual
[AD-A150783] 14 p2309 N85-24295

Propagation of numerical errors in computers and numerical quality 14 p2396 N85-24780

Flowcharting with D-charts
[NASA-CR-175641] 14 p2402 N85-24806

Guidelines for development structured FORTRAN programs
[NASA-TM-86407] 14 p2402 N85-24808

Functional analysis of programs
[AD-A150742] 14 p2404 N85-24819

The HORNE reasoning system, revision
[AD-A150983] 14 p2405 N85-24827

Software and its relationship to methods
[DE85-004784] 14 p2405 N85-24829

Unsteady transonic aerodynamic and aeroelastic calculations about airfoils and wings
15 p2459 N85-25185

Study of experimental robotized system for arc welding based on Universal-15 manipulator
15 p2500 N85-25423

The design and implementation of a syntax directed editor for a space constrained microcomputer
[AD-A151313] 15 p2623 N85-26163

Continued development of a data base management system performance monitor, volume 2
[AD-A151714] 15 p2623 N85-26167

Computer program TRAMP: Inclusion of state space facilities and the analysis of non-linear elements
[BAE-BT-12643] 15 p2626 N85-26181

Efficient implementation of real-time programs under the VAX/VMS operating system
[NASA-TM-86354] 15 p2627 N85-26193

GRID: A FORTRAN program for using a digitizing table to enter a finite element GRID
[AD-A151317] 15 p2628 N85-26196

A learning strategy approach for teaching novice computer programmers
[AD-A151523] 15 p2628 N85-26200

The development of a programming support system for rapid prototyping. Tasks 2 and 3
[AD-A151549] 15 p2629 N85-26202

Preliminary design of the Ada programming support environment configuration manager
[AD-A151845] 15 p2629 N85-26206

Extension of the software development workbench to include microcomputer workstations
[AD-A151903] 15 p2630 N85-26207

Praxis language environment: Distribution package description, revision 1
[DE85-006699] 15 p2630 N85-26212

Harnessing computional power: Distributed combinator reduction
[DE85-005967] 15 p2631 N85-26216

Numerical solutions of 3-dimensional Navier-Stokes equations for closed bluff-bodies
[NASA-CR-175755] 15 p2636 N85-26255

Programming for Pioneer 12 15 p2688 N85-26606

Rotorcraft digital advanced avionics system (Rodaas)
15 p2688 N85-26608

Automatic manipulators for forging rollers
16 p2762 N85-27042

A heuristic solution to the spacing problem: Maximizing the minimum Euclidean distance among N points in a convex region
[AD-A152116] 16 p2855 N85-27603

Management considerations for an information center
[AD-A151774] 16 p2875 N85-27742

A method to calculate the parameters of wings of arbitrary planform
[AD-A152689] 17 p2892 N85-27831

Investigation and implementation of a tree transformation system for user friendly programming
[AD-A152716] 17 p3011 N85-28617

Sample problems for STAGSC-1
[AD-A153142] 17 p3012 N85-28621

A modern control theory enhancement to an interactive Control Engineering Computer Analysis Package (ICECAP)
[AD-A153249] 17 p3012 N85-28622

Software for estimating sparse Hessian matrices
[DE85-008121] 17 p3013 N85-28629

Introduction to LINE: A Feynman diagram graphic operator
[DE85-009299] 17 p3013 N85-28632

Towards a uniform topological treatment of streams and functions on streams
[CWI-CS-R8422] 17 p3014 N85-28639

Parallel Cholesky factorization on a multiprocessor
[DE85-008762] 17 p3021 N85-28682

Evaluation and Validation (E/V) team public report, volume 1
[AD-A153609] 18 p3161 N85-29584

Graphics package, version 4: User reference manual
[DE85-007894] 18 p3163 N85-29596

Ada developments
[REPT-84-28] 18 p3164 N85-29604

Hybrid uncertainty theory
[DE85-008357] 18 p3167 N85-29622

Activities of the Institute for Computer Applications in Science and Engineering (ICASE)
[NASA-CR-172610] 19 p3332 N85-30641

Proceedings of the Argonne Workshop on Programming the Next Generation of Supercomputers
[DE85-008348] 19 p3343 N85-30718

Perspectives of nonlinear dynamics
[IPPJ-723] 19 p3370 N85-30902

Modified dynamic hashing
[DE85-011166] 19 p3381 N85-30974

Synthetic aperture radar data processing — satellite-borne radar
[CNES-196-T-CT/DRT/TIT/RL]
20 p3442 N85-31369

Informatics Division 20 p3449 N85-31416

Study of new computing algorithms for supercomputers. Application to parallel processing computation
[SNIAS-440-070/84] 20 p3516 N85-31860

Coordinate transformations and programming for small revolute coordinate robots
[RR-273] 20 p3519 N85-31881

Determining functional requirements for NASA Goddard's command management system software design using expert systems 20 p3539 N85-32020

Review of the psychological issues relating to the effectiveness of structured programming
[AD-A154593] 21 p3665 N85-32763

Ada (trademark) training curricuium. Advanced Ada topics L305 teacher's guide exercises
[AD-A154621] 21 p3670 N85-32798

SIGMA - A stochastic-integration global minimization algorithm
[AD-A154876] 21 p3671 N85-32806

Design guidelines for user-system interface software
[AD-A154907] 21 p3671 N85-32807

Experience with omega: Implementation of a prototype programming environment: Part 1
[AD-A155438] 21 p3672 N85-32811

Evaluation of a software design approach: Develop a threat resolution module in Ada (trademark)
[AD-A155599] 21 p3672 N85-32815

A simple software environment based on objects and relations
[AD-A155704] 21 p3673 N85-32817

Microcomputer network: Investigation and implementation
[AD-A155631] 21 p3674 N85-32828

New developments on the core function for efficient implementation of the difficult residue number system operations
[AD-A154678] 21 p3676 N85-32834

Continued development of a data base management system performance monitor: Volume 1
[AD-A154635] 21 p3713 N85-33040

Art of programming programmable microcalculators: Calculation of response from current values of action
22 p3767 N85-33348

Method of estimating convergence of Haar coefficients in message compression problems
22 p3769 N85-33350

USSR report: Electronics and electrical engineering
[JPRS-UEE-84-003] 22 p3773 N85-33361

Art of programming programmable microcalculators, part 4: errors of calculations 22 p3778 N85-33411

Use of monitors in Pascal on the Lemur: A tutorial on the barrier, self-scheduling FOR-loop, and askfor monitors
[ANL-84-53] 22 p3828 N85-33706

Integrated Support Software System (ISSS)
[AD-A155715] 22 p3829 N85-33710

AUTSKED: An addendum
[DE85-010410] 22 p3829 N85-33712

Portable database driven control system for SPEAR
[DE85-010465] 22 p3830 N85-33720

Flat is not necessarily good
[DE85-012819] 22 p3830 N85-33723

How a BASIC program works
[DE85-009142] 22 p3831 N85-33727

Microcomputer controlled image processor
[AD-D011734] 22 p3833 N85-33735

Logical and physical modeling and design of scientific and statistical databases for energy research
[DE85-006081] 22 p3833 N85-33737

The interactive planning work station: A graphics-based UNIX (trademark) tool for application users and developers 23 p3957 N85-34527

Graphics Interaction in databases
23 p3958 N85-34534

Parallel processing on the Livermore VAX 11/784 parallel processor system with compatability to Cray Research, Inc. (CRI) multitasking, version 1
[DE85-011856] 23 p3967 N85-34596

Development of NATOPS (Naval Air Training and Operating Procedure Standardization) performance software for the H-46D helicopter
[AD-A156069] 24 p4064 N85-35190

AUTOSIM: An automated repetitive software testing tool
[NASA-CR-177930] 24 p4137 N85-35643

Polylith: The early goals
[DE85-012534] 24 p4139 N85-35658

COMPUTER PROGRAMS
NT APPLICATIONS PROGRAMS (COMPUTERS)
NT ASSEMBLER ROUTINES
NT COMPILERS
NT COMPUTER SYSTEMS PROGRAMS
NT EDITING ROUTINES (COMPUTERS)
NT INPUT/OUTPUT ROUTINES
NT MACHINE-INDEPENDENT PROGRAMS
NT NASTRAN
NT OPERATING SYSTEMS (COMPUTERS)
NT SUBROUTINE LIBRARIES (COMPUTERS)
NT SUBROUTINES

Three degree of freedom steady state point performance program: Updated version 1
[CSIR-NIAST-83/48] 01 p0001 N85-10005

Implementation of the supersonic triplet singularity into the USTORE computer code
[CSIR-NIAST-83/47] 01 p0001 N85-10006

Experimental data base for computers program assessment. Report of the Fluid Dynamics Panel Working Group 04: Addendum
[AGARD-AR-138-ADD] 01 p0004 N85-10020

Impact of new computing systems on computational mechanics and flight-vehicle structures technology
01 p0007 N85-10042

CREKID: A computer code for transient, gas-phase combustion of kinetics
[NASA-TM-83806] 01 p0011 N85-10068

High frequency radar software reference manual for Product Two
[PB84-210079] 01 p0041 N85-10270

Battery optimization considerations
[DE84-014759] 01 p0044 N85-10288

ICARUS: A general one-dimensional heat conduction code
[DE84-016125] 01 p0047 N85-10310

Combustion modeling of a 2 cylinder cycle reciprocating engine
[AD-A144782] 01 p0055 N85-10364

Application guide for Hydrological Simulation Program FORTRAN (HSPF)
[PB84-215783] 01 p0064 N85-10427

Manual of phosphoric acid fuel cell stack three-dimensional model and computer program
[NASA-CR-174722] 01 p0067 N85-10447

Processing and display of atmospheric phenomenaa data
[NASA-CR-171178] 01 p0072 N85-10475

Severe weather statistics STADTS decoder (SXW) and plotter (SWY)
[PB84-213893] 01 p0086 N85-10576

Psychological testing on the computer
[R/PERS-618] 01 p0097 N85-10645

REMOTE: Modem Communicator Program for the IBM personal computer
[DE84-015047] 01 p0100 N85-10665

IAC user manual
[NASA-CR-175300] 01 p0102 N85-10677

A packed storage program for angular momentum coupling coefficients
[TWISK-316] 01 p0102 N85-10680

Three programs for evaluating bending moments, deflections and shear forces in simply-supported uniform bridge decks under South African NA loading: NAB, NAD and NAS. NITRR manual P13
[ISBN-0-7988-2283-X] 01 p0102 N85-10681

Floating-point function generation routines for 16-bit microcomputers
[NASA-TM-83783] 01 p0102 N85-10683

RSCORS graphics system
[DE84-015693] 01 p0104 N85-10698

A modular data acquisition and display software system for a laboratory environment
[PB84-217892] 01 p0105 N85-10709

Methods, applications of image processing
01 p0115 N85-10785

SANDYL radiation transport code at the Naval Research Laboratory
[AD-A144890] 01 p0117 N85-10799

Automated Data Systems (ADS) documentation standards
[AD-A144867] 01 p0125 N85-10857

Fast Fourier transform for unequally spaced data
01 p0128 N85-10876

Transonic flow analysis for rotors. Part 1: Three-dimensional quasi-steady, full-potential calculation
[NASA-TP-2375-PT-1] 02 p0134 N85-10914

VORCOR: A computer program for calculating characteristics of wings with edge vortex separation by using a vortex-filament and-core model
[NASA-CR-165902] 02 p0135 N85-10921

PAN AIR: A computer program for predicting subsonic or supersonic linear potential flows about arbitrary configurations using a higher order panel method. Volume 3: Case manual (version 1.0)
[NASA-CR-3253] 02 p0135 N85-10922

Enhanced TCAS 2/CDTI traffic Sensor digital simulation model and program description
[NASA-CR-172445] 02 p0136 N85-10927

An interactive computer code for calculation of gas-phase chemical equilibrium (EQLBRM)
[NASA-CR-168337] 02 p0140 N85-10948

Burner liner thermal/structural load modelling
02 p0143 N85-10970

Computations for the 16-foot transonic tunnel, NASA, Langley Research Center
[NASA-TM-86319] 02 p0149 N85-11009

Resistance and inductance calculations for helical flux compression generators
[DE84-015068] 02 p0195 N85-11306

The CMC/3DPNS computer program for prediction of three-dimensional, subsonic, turbulent aerodynamic juncture region flow. Volume 3: Programmers' manual
[NASA-CR-165998] 02 p0197 N85-11318

Efficient methods for mechanical and structural reliability analysis and design 02 p0205 N85-11355

STARS: A general-purpose finite element computer program for analysis of engineering structures
[NASA-RP-1129] 02 p0209 N85-11378

Phosphoric acid fuel cell power plant system performance model and computer program
[NASA-CR-174638] 02 p0222 N85-11456

Generalized linear inversion of 2.5 - dimensional gravity and magnetic anomalies 02 p0226 N85-11480

Proposal for a semiautomatic program testing system
[INPE-3262-TDL/178] 02 p0240 N85-11561

Description of the logical support for an image processing system
[INPE-2783-PRE/349] 02 p0240 N85-11563

SITIM system: Object manager module
[INPE-3284-NTE/226] 02 p0240 N85-11564

SITIM system: Supervisor utilization
[INPE-3267-NTE/224] 02 p0240 N85-11565

Contracting for computer software development: Serious problems require management attention to avoid wasting additional millions
[FGMSD-80-4] 02 p0241 N85-11567

SMP: A solid modeling program
[NASA-CR-172473] 02 p0241 N85-11570

Program flow analyzer, volume 1
[AD-A145320] 02 p0241 N85-11572

DOD related software technology requirements, practices, and prospects for the future
[AD-A145493] 02 p0242 N85-11575

Parametric analysis for generalized network flow problems
[AD-A145558] 02 p0243 N85-11589

GUIDON
[AD-P003925] 02 p0246 N85-11605

Modeling holographic recognition system by using number-theory convolution transformation
02 p0272 N85-11774

Turbofan noise generation. Volume 2: Computer programs
[NASA-CR-167952] 02 p0275 N85-11791

Archiving and exchange of a computerized marine seismic database: The ROSE (Rivera Ocean Seismic Experiment) data archive system
[AD-A145658] 02 p0294 N85-11908

A data base for three-dimensional all-interference code evaluation 03 p0312 N85-12017

An inerference assessment approach for a three-dimensional slotted tunnel with sparse wall pressure data 03 p0314 N85-12030

Estimation of helicopter performance using a program based on blade element analysis
[AD-A146341] 03 p0318 N85-12055

A digital algorithm for composite laminate analysis: FORTRAN, Revised
[AD-A145833] 03 p0326 N85-12098

Ballpark reliability estimation techniques
[AD-A145971] 03 p0369 N85-12357

A research program in computer technology
[AD-A145776] 03 p0402 N85-12565

On line digitizer software
[AD-A146249] 03 p0403 N85-12568

NUTSATSEA: An on line data reduction program linking a Chemlab continuous flow analyser to a Commodore PET microcomputer
[IOS-176] 03 p0403 N85-12570

On a program for solution of BCMP queueing network model
[NAL-TR-813] 03 p0405 N85-12585

A user's guide to the Flexible Spacecraft Dynamics and Control Program
[NASA-TM-87389] 03 p0405 N85-12586

Conversion of FEB (Fast and Easy Binary) utilities to ASCII FORTRAN
[AD-A145840] 03 p0406 N85-12596

A sequential quadratic programming algorithm for solving large, sparse nonlinear programs
[AD-A145854] 03 p0407 N85-12597

Automating software design metrics
[AD-A145869] 03 p0407 N85-12598

An input translator for a computer-aided design system
[AD-A146337] 03 p0408 N85-12605

Designing optimal AOQL sampling plans a computerized approach
[AD-A146288] 03 p0413 N85-12639

Analysis of piezoelectric disks and cylinders using finite element method
[AD-A146323] 03 p0414 N85-12650

Free-space propagation of light pulses
[PB84-217108] 03 p0421 N85-12689

Information Center handbook
[PB84-211341] 03 p0439 N85-12795

Development of gas-lubricated pistons for heavy duty diesel engine technology program
[NASA-CR-174746] 03 p0441 N85-12808

Algorithm for astronomical, extended source, signal-to-noise radio calculations
[NASA-TP-2396] 03 p0445 N85-12833

Algorithm for astronomical, point source, signal to noise ratio calculations
[NASA-TP-2397] 03 p0445 N85-12834

NIKE3D: An Implicit, finite-deformation, finite element code for analyzing the static and dynamic response of three-dimensional solids, revision 1
[DE84-017161] 04 p0514 N85-13277

Concentrator optical characterization using computer mathematical modelling and point source testing
[NASA-CR-174109] 04 p0528 N85-13375

Software used with the flux mapper at the solar parabolic dish test site
[NASA-CR-174108] 04 p0528 N85-13376

Open cycle OTEC thermal-hydraulic systems analysis and parametric studies
[DE84-013011] 04 p0530 N85-13391

WXR (hydrologic weather wire and PLT product software package)
[PB84-237221] 04 p0541 N85-13442

U: The universal utility controller, revision 1
[DE84-017077] 04 p0547 N85-13481

Expert systems in design and manufacture
[DE84-005522] 04 p0550 N85-13496

Design and implementation of a modular program system for statistical analyses
[IKE-4-114] 04 p0551 N85-13503

Multigrid iteration solution procedure for solving two-dimensional sets of coupled equations
[DE84-016554] 04 p0555 N85-13533

Preliminary user's guide for BIGONE on the Cray
[DE84-017075] 04 p0568 N85-13623

Real space solution to the phase problem in X-ray crystallography: ALCAMPS (Ames Laboratory Computer-aided Analysis of Multi-solution Patterson Superpositions)
[DE84-015476] 04 p0572 N85-13651

Archiving and exchange of a computerized marine seismic database: The ROSE data archive system
[DE84-901453] 04 p0576 N85-13677

Certain optimal parameters of high-velocity Venturi ejection tubes
[BLL-M-35824-(5828.4)] 05 p0634 N85-14066

Navier-Stokes computational study of axisymmetric transonic turbulent flows with a two-equation model of turbulence 05 p0634 N85-14068

Comparison of SCAPID/GaAs to experiment
05 p0665 N85-14279

A summary description of a computer program concept for the design and simulation of solar pond electric power generation systems 05 p0666 N85-14285

Implicit numerical methods in meteorology
05 p0686 N85-14408

Improving the Spacelab mass memory unit tape layout with a simulation model
[NASA-TM-86483] 05 p0713 N85-14571

How to implement the welcome program in compatible microcomputers such as Apple 2
[INPE-3114-PRE/511] 05 p0715 N85-14586

Use of monitors in FORTRAN: A tutorial on the barrier, self-scheduling DO-loop and Askfor monitors
[DE84-016506] 05 p0715 N85-14587

Maximum likelihood estimation of parameters in linear systems from flight test data: A FORTRAN program
[AD-B087198L] 05 p0715 N85-14588

Knowledge-based communication and management support in a system development environment
05 p0717 N85-14596
Use of artificial intelligence and simple mathematics to analyze a physiological model 05 p0717 N85-14597
Development of the code NSFOIL for analyzing high Reynolds number transonic flow around an airfoil
[NAL-TR-816] 06 p0749 N85-14801
PROGRAM VSAERO: A computer program for calculating the non-linear aerodynamic characteristics of arbitrary configurations: User's manual
[NASA-CR-166476] 06 p0749 N85-14802
HH-60D night hawk helicopter
06 p0752 N85-14817
Certification of advanced systems
06 p0753 N85-14829
Software for Crimea-Pushchino radiointerferometer
06 p0783 N85-15007
Computer-aided design of extrusion dies by metal-flow simulation 06 p0797 N85-15094
Summary of photovoltaic performance models
06 p0832 N85-15298
Probable maximum flood estimation - Eastern United States
[AD-A146536] 06 p0839 N85-15324
AFOS (Automation of Field Operations and Services) display of MDR (Manually Digitized Radar) data on local map backgrounds
[PB84-220797] 06 p0840 N85-15336
Two-dimensional lake wave prediction system
[PB84-231034] 06 p0841 N85-15342
Reusable software
[AD-A146575] 06 p0854 N85-15427
Time series analysis programs for stratigraphic data
[AD-A146627] 06 p0854 N85-15429
Two programs for the HP9836C computer to acquire frequency or voltage data from a source
[AD-A146632] 06 p0854 N85-15430
Introduction to software packages
[PB84-217843] 06 p0856 N85-15441
Intercomparison between West Germany and US thermodynamic codes
[AD-A146622] 06 p0869 N85-15525
Research on introspective systems
[AD-A146406] 06 p0870 N85-15530
Analysis of the flow field about a T-45 using PANAIR
[AD-A146811] 07 p0899 N85-15699
NyKINM, a further development of KINM 22 — simulation of a robot attack on an aircraft
[FOA-C-20559-D6(E3)] 07 p0903 N85-15720
Integrating chemical kinetic rate equations by selective use of stiff and nonstiff methods
[NASA-TM-86923] 07 p0904 N85-15726
A computer program for the performance analysis of scarfed nozzles
[AD-A147370] 07 p0905 N85-15730
High altitude chemically reacting gas particle mixtures. Volume 3: Computer code user's and applications manual — rocket nozzle and orbital plume flow fields
[NASA-CR-171828] 07 p0917 N85-15803
A study of interply layer effects on the free-edge stress field of angleplied laminates
[NASA-TM-86924] 07 p0919 N85-15822
Bearing tester fit analysis
[NASA-CR-171282] 07 p0973 N85-16181
Research activities of the Norwegian seismic array (NORSAR)
[AD-A146778] 07 p0996 N85-16326
Computer program to compute soil thermal conductivity from transient temperature measurements
[PB85-100550] 07 p0998 N85-16341
Upset susceptibility study employing circuit analysis and digital simulation — digital systems and electromagnetic interference 07 p0999 N85-16344
Random pattern tracking acceleration tolerance tester
[AD-D011404] 07 p1017 N85-16459
Formal verification of mathematical software
[NASA-CR-172407] 07 p1023 N85-16489
Computer program for determining induced stresses and consolidation settlements (CSETT)
[AD-A146730] 07 p1023 N85-16493
A program to produce standard shewhart control charts for the statistics X-bar and R or S, P, NP, C, or U
[AD-A146971] 07 p1024 N85-16501
The effects of software quality control and baseline management on the acquisition of computer programs
[AD-A147051] 07 p1024 N85-16502
NOISEMAP 4.4 computer program update, operator's manual, addendum 1
[AD-A147091] 07 p1025 N85-16503
Debug testing and confidence testing
[AD-A147104] 07 p1025 N85-16504
A virial equation of state option for the TIGER computer program
[AD-A147490] 07 p1025 N85-16507
A survey and evaluation of software quality assurance
[AD-A147552] 07 p1026 N85-16510
On the structure of information in software
[AD-A147580] 07 p1026 N85-16511
PLOT3D: An interactive graphics code for 3-dimensional plots
[AD-A147887] 07 p1026 N85-16514
FORTRAN version of the quantitative energy-dispersive electron beam X-ray analysis program FRAME C
[PB84-240936] 07 p1027 N85-16519
Extracting embedded generalized networks from linear programming problems
[AD-A147565] 07 p1033 N85-16558
Arctic marine acoustics
[AD-A147492] 07 p1039 N85-16594
Computer program for calculation of complex chemical equilibrium compositions and applications. Supplement 1: Transport properties
[NASA-TM-86885] 07 p1049 N85-16663
Data base support for SIO (System Integration Office)
[AD-A147487] 07 p1054 N85-16692
ATE user's view on design for maintainability
08 p1064 N85-16737
Built-in-test for first line testing
08 p1064 N85-16739
Development of a Helicopter integrated navigation system 08 p1073 N85-16802
A Generalized Escape System Simulation (GESS) computer program. Volume 2: GESS programmer's manual, version 2
[AD-A148363] 08 p1081 N85-16845
Shuttle avionics software trials, tribulations and success 08 p1090 N85-16891
Shuttle avionics software development trials: Tribulations and successes, the backup flight system
08 p1091 N85-16892
SSME digital control design characteristics
08 p1091 N85-16893
Automatic software for controlling cryogenic systems
08 p1097 N85-16932
Managing computer-controlled operations
08 p1097 N85-16934
The Communications link analysis and simulation system (CLASS) 08 p1100 N85-16952
Modeling techniques used in the communications link analysis and simulation system (CLASS)
08 p1100 N85-16953
Validation of the communications link analysis and simulation system (CLASS) 08 p1100 N85-16954
Performance assessment of aero-assisted orbital transfer vehicles 08 p1106 N85-16993
Computer subroutines for estimation of human exposure to radiation in low Earth orbit
[NASA-TM-86324] 08 p1199 N85-17550
Performance management system enhancement and maintenance
[NASA-CR-175271] 08 p1202 N85-17564
On the validation of computer science theories
[AD-A148637] 08 p1203 N85-17572
A FORTRAN plotting package for graphic VDUs
[AD-A148489] 08 p1204 N85-17577
A computer package for ranking, selection and multiple comparisons with the best
[AD-A147617] 08 p1204 N85-17579
Developing double sampling plans for attributes to meet sample size criteria
[AD-A148144] 08 p1205 N85-17587
COPES/ADS (Control Program for Engineering Synthesis) (Automated Design Synthesis) using the ADS optimization program
[AD-A148576] 08 p1206 N85-17588
Algorithm for space-time analysis of data on geomagnetic field
[NASA-TM-77804] 08 p1209 N85-17609
Numerical generation of orthogonal and nonorthogonal coordinates in two dimensional simply and doubly connected regions
[VKI-TN-151] 08 p1216 N85-17662
SIMM1: A linearized particle code
[AD-A148627] 08 p1221 N85-17669
A voice-actuated wind tunnel model leak checking system
[NASA-TM-86359] 09 p1263 N85-17936
Preliminary results from the unsteady airfoil model USTAR2
[AD-P004171] 09 p1266 N85-17956
Automatic land vehicle navigation using road map data
[DE84-017176] 09 p1278 N85-18043
FORTRAN 77 computer program for test procedure calculations of vented heaters
[PB85-109627/GAR] 09 p1305 N85-18198
Mesoscale storm and dry period parameters from hourly precipitation data: Program documentation
[DE85-001366] 09 p1357 N85-18538
JOVIAL J73 automated verification system: Implementation phase
[AD-A148732] 09 p1368 N85-18597
Introduction to LBL graphics
[DE85-000389] 09 p1369 N85-18605
User/programmer guide for UCMD 106 multi-vertex polyarc/path integrity verifier
[DE84-017173] 09 p1369 N85-18604
Beyond fault trees to fault graphs
[DE84-017022] 09 p1370 N85-18608
User's manual: Menu-driven data graphing program for the Tektronix 7912AD and 7612D transient digitizer system
[DE85-002151] 09 p1370 N85-18610
Computer programs for the adjustment of indirect observation with condition equations between the unknowns
[SER-B-266-MITT-170] 09 p1370 N85-18612
System software for the finite element machine
[NASA-CR-3870] 09 p1372 N85-18622
Fixed vs. variable order Runge-Kutta
[DE85-001320] 09 p1374 N85-18639
Theoretical studies of atomic transition
[DE85-001325] 09 p1381 N85-18687
Documentation for an instrument database system
[DE84-017392] 09 p1402 N85-18828
UKIRT spectro-photometry system — United Kingdom Infrared Telescope (UKIRT)
[UKIRT-23] 09 p1414 N85-18921
Analysis of inviscid transonic flow around an airfoil by diagonal form of IAF scheme
[NAL-TR-831] 10 p1420 N85-18955
Inviscid analysis of unsteady blade tip flow correlation studies
[NASA-CR-172506] 10 p1420 N85-18958
Efficient self-consistent viscous-inviscid solutions for unsteady transonic flow
[NASA-TM-86335] 10 p1420 N85-18959
Directory of range data conversion and processing systems
[AD-A148996] 10 p1427 N85-19001
A shock wave capability for the improved Two-Dimensional Kinetics (TDK) computer program
[NASA-CR-171302] 10 p1483 N85-19360
PATHFINDER: A trajectory prediction system for the Great Lakes
[PB85-115335] 10 p1506 N85-19508
Application of SIMCA (Soft Independent Modeling of Class Analogy) pattern recognition to air pollutant analytical data
[PB85-124683] 10 p1513 N85-19549
OBLOG: Designed to create and maintain a 48 hour observation log file
[PB85-109528] 10 p1519 N85-19579
Hurricane plotting program
[PB85-121432] 10 p1521 N85-19592
Crewstation assessment of reach as applied to the OH-58A helicopter
[AD-A149413] 10 p1531 N85-19659
Microprocessor-based monitoring and control project, phase 1
[DE84-901974] 10 p1536 N85-19699
A program design for an adaptive, non-linear finite element solver
[AD-A148880] 10 p1539 N85-19705
RELTIM: A library of routines used in real time machine control applications
[PB85-116507] 10 p1542 N85-19725
Modeling the internal combustion engine
[NASA-RP-1094] 10 p1544 N85-19733
LOVEL-84: A LOw-VELocity aerodynamic heating code for flat plates, wedges, and cones
[DE85-002604] 11 p1576 N85-19933
Aircraft transparency bird impact analysis using the MAGNA computer program
[AD-P004186] 11 p1579 N85-19948
Reliability of DNC system examined
11 p1617 N85-20171
CAD/CAM systems for printed circuit design, manufacture 11 p1619 N85-20189
Computation of the inviscid velocity potential for general ellipsoids on a nearly quadratic surface grid
[REPT-25/84] 11 p1633 N85-20287
Vertical solar louver project
[DE84-017335] 11 p1676 N85-20558
Plotfile appender
[PB85-109502] 11 p1688 N85-20616
Isentropic objective analysis
[PB85-112167] 11 p1688 N85-20617
User's manual for GRIZZLY
[DE85-001405] 11 p1702 N85-20702
MCNP code
[DE85-002565] 11 p1702 N85-20705
Standardized format for computer series
[PB85-109668] 11 p1705 N85-20724

Needs, opportunities, and options for large scale systems research
[DE85-002884] 11 p1709 N85-20750

GPS system field testing 11 p1711 N85-20762

Self-Optimized Sector (SOS) model of self-consistent energy loss and scattering for an electron beam propagating in air
[DE85-003161] 11 p1722 N85-20831

AID: Access to Informal Documentation
[DE85-000418] 11 p1740 N85-20939

Sample size and precision in communication performance measurements
[PB85-1143270] 12 p1830 N85-21486

Program for controlling electrical measuring contact instrument on glow-discharge indicator panel
12 p1842 N85-21558

Method of calculating cooldown process in cryostat of cryogenic electric machine 12 p1843 N85-21567

TRACR3D: A model of flow and transport in porous/fractured media
[LA-9867-MS] 12 p1845 N85-21576

3-D inelastic analysis methods for hot section components (base program) — turbine blades, turbine vanes, and combustor liners
[NASA-CR-174700] 12 p1863 N85-21686

Time marching numerical solution of the dynamic response of nonlinear systems
[NAF-AN-25] 12 p1865 N85-21696

An analysis of the high frequency vibrations in early Thematic Mapper scenes 12 p1872 N85-21742

User's manual for the University of Houston individual heliostat layout and performance code
[DE85-004643] 12 p1882 N85-21808

Investigations of micro-turbulence in the bottom of the boundary layer
[AD-A149823] 12 p1896 N85-21897

FTASUM: Aviation forecast summaries
[PB85-112977] 12 p1897 N85-21906

SAOSUM: A short summary of observations
[PB85-120384] 12 p1897 N85-21909

TRAJ: Single station trajectory plot
[PB85-135002] 12 p1897 N85-21911

AFOS (Automation of Field Operations and Service) surface observation decoding
[PB85-137586] 12 p1898 N85-21913

Topics in optical materials and device research, 3. Volume 2
[AD-A149727] 12 p1911 N85-21996

Computing Division two-year operational plan, FY 1984 - 1985
[LA-9978-MS] 12 p1913 N85-22006

The liner package: An incipient MHD capability for CCUBE
[LA-9969-MS] 12 p1913 N85-22007

User's guide for TWODANT: A code package for two-dimensional, diffusion-accelerated, neutral-particle transport
[LA-10049-M] 12 p1913 N85-22009

Adaptive meshes in the 2DL code
[LA-9938-MS] 12 p1914 N85-22011

The automated reasoning system ITP
[ANL-84-27] 12 p1914 N85-22016

A user's guide to sensitivity testing on computer models at Los Alamos National Laboratory
[LA-10104-M] 12 p1914 N85-22018

The portable LISP translation tool
[AD-A149765] 12 p1915 N85-22023

Interface specifications for SCR (Software Cost Reduction) (A-7E) extended computer module, revised
[AD-A149948] 12 p1915 N85-22024

MFTF sensor verification computer program
[DE85-004452] 12 p1916 N85-22029

EZPIX: A tablet entry method for computer-generated slides, drawings, and graphs
[DE85-005234] 12 p1916 N85-22030

VAX-ASPEN installation guide
[DE85-001973] 12 p1916 N85-22032

Software for special functions
[DE85-004684] 12 p1917 N85-22033

Parallel linear algebra library for the Denelcor HEP
[DE85-004685] 12 p1917 N85-22034

SIMULA: Digital controller simulation package
[PB85-134492] 12 p1917 N85-22041

Experimental mathematics
[CWI-PM-R8411] 12 p1925 N85-22096

User's guide for TWOHEX: A code package for two-dimensional, neutral-particle transport in equilateral triangular meshes
[DE85-004482] 12 p1930 N85-22125

Strong iron accelerating by collisionless magnetosonic shock wave propagating perpendicular to a magnetic field
[IPPJ-709] 12 p1935 N85-22161

Models of the upper atmosphere
12 p1945 N85-22217

A study of the compatibility of an existing CFD package with a broader class of material constitutions
12 p1945 N85-22219

Analyses via automated mass spectrometry (MS/DS)
12 p1947 N85-22227

Evaluation of expert systems
12 p1947 N85-22229

Method for the prediction of the installation aerodynamics of a propfan at subsonic speeds
[NASA-CR-3887] 13 p1969 N85-22369

Two degree-of-freedom flutter solution for a personal computer
[NASA-TM-86381] 13 p1971 N85-22379

Three-dimensional calculation of shuttle charging in polar orbit 13 p1992 N85-22486

NASCAP simulation of PIX 2 experiments
13 p1993 N85-22497

Investigations of radiation-induced and carrier-enhanced conductivity 13 p1996 N85-22515

Development of a three-phrase combustion code for modeling liquid rocket engines 13 p2003 N85-22554

Numerical/Electromagnetics Code (NEC)
[DE85-004999] 13 p2056 N85-22874

Pre- and post-processing for stream-function eddy current calculations
[AD-A150417] 13 p2065 N85-22896

New atmospheric sensor analysis study
[NASA-CR-171426] 13 p2094 N85-23069

Use of three omega radionavigation system position lines for solving problems in marine geodesy
13 p2107 N85-23131

ROSA: A computer model for optical power ratio calculations
[DE85-005174] 13 p2129 N85-23251

A design analysis and implementation of a user-friendly interface for the UNIX operating system
[AD-A150558] 13 p2145 N85-23312

Principles of software engineering environment design
[AD-A150352] 13 p2147 N85-23324

ROSS: An object-oriented language for constructing simulations
[AD-A150556] 13 p2147 N85-23330

Second thoughts on the mathematical software effort: A perspective
[DE85-004831] 13 p2148 N85-23333

On a mathematical structure for an image algebra
[AD-A150226] 13 p2150 N85-23348

Hexagonal data base study
[AD-A150176] 13 p2167 N85-23448

Copyright law, computer software, and government acquisition
[AD-A150347] 13 p2168 N85-23453

Comet thermal modeling 13 p2176 N85-23505

Model for high rate gas flows in deformable and reactive porous beds
[DE85-006140] 14 p2253 N85-23964

Analysis of slabs-on-grade for a variety of loading and support conditions
[AD-A150965] 14 p2264 N85-24030

Investigation of doubly-fed machine in variable speed application
[DE85-004378] 14 p2299 N85-24234

Effect of flight sequences in complex load histories on crack front marking 14 p2318 N85-24326

Observation model and parameter partials for the JPL VLBI parameter estimation software MASTERFIT-F 2.0
[NASA-CR-175640] 14 p2347 N85-24509

Modelling of photodegradation in solar cell modules of substrate and superstrate design made with ethylene-vinyl acetate as pottant material
[NASA-CR-175690] 14 p2350 N85-24527

Streamlined Test Reporting And Planning (STRAP): Computerized human factors questionnaire
[AD-A150811] 14 p2395 N85-24751

Security of personal computer systems: A management guide
[PB85-161040] 14 p2400 N85-24793

GRAFIT language for simulating two-dimensional geometric entities and sketches
14 p2401 N85-24801

Automation of development of software for switching units that are implemented in the form of multiprocessor systems on a microcomputer base
14 p2401 N85-24802

The Multimission Image Processing Laboratory's virtual frame buffer interface
[NASA-CR-175655] 14 p2402 N85-24805

The use of a 3-D system for a civil engineering project
14 p2402 N85-24811

Runstreams for using ASKA
[NIAST-84/27] 14 p2403 N85-24812

An experiment in software reliability
[NASA-CR-172553] 14 p2403 N85-24813

TAPTRN: A tape utility program
[AD-A150644] 14 p2403 N85-24814

Software library: A reusable software issue
[AD-A150722] 14 p2403 N85-24816

Functional analysis of programs
[AD-A150742] 14 p2404 N85-24819

The enhancement of concurrent processing through functional programming languages
[AD-A150771] 14 p2404 N85-24822

Integration of an Apple 2 Plus computer into an existing dual axis sun tracker system
[AD-A150778] 14 p2404 N85-24823

Implementation of a C1 triangular element based on the p-version of the finite element method
[AD-A150904] 14 p2404 N85-24825

Dataflow computation
[CWI-TRACT-6] 14 p2406 N85-24833

LINCS
[DE85-006151] 14 p2407 N85-24836

Computer Visual System (CVS) reference manual
[DE85-006326] 14 p2407 N85-24837

A fast ray tracing routine for laterally inhomogeneous media
[AD-A150984] 14 p2421 N85-24936

Thermodynamic calculations and the chemical vapour deposition of hard materials 14 p2431 N85-24991

Documentation for the machine-readable version of the Revised S210 Catalog of Far-Ultraviolet Objects (Page, Carruthers and Heckathorn 1982)
[NASA-TM-87439] 14 p2438 N85-25047

Cosmic ray environment model for Earth orbit
[NASA-CR-175666] 14 p2455 N85-25165

Trends in computational capabilities for fluid dynamics
15 p2457 N85-25172

Unsteady analysis of rotor blade tip flow
[NASA-CR-3868] 15 p2462 N85-25202

A computer program to calculate the supersonic flow over a solid cone in air or water
[AD-A151102] 15 p2464 N85-25217

Global positioning system: A modification to the baseline satellite constellation for improved geometric performance
[AD-A151692] 15 p2469 N85-25239

The development of a performance and mission planning program for the A-7E aircraft
[AD-A151717] 15 p2471 N85-25258

A user's manual for AMEER flight path trajectory simulation code
[DE85-006580] 15 p2472 N85-25260

Mathematical modeling of the AEDC (Arnold Engineering Development Center) propulsion wind tunnel (16T)
[AD-A151293] 15 p2475 N85-25275

A decision support methodology for space technology advocacy
[AD-A151695] 15 p2476 N85-25283

Selection of optimal control program for solar cell panels of Earth satellites 15 p2484 N85-25335

Computing parameters characterizing possibility of planets falling in star camera field of view during space survey 15 p2487 N85-25351

A FORTRAN program for deep space sensor analysis
[AD-A151700] 15 p2489 N85-25366

The investigation of tethered satellite system dynamics
[NASA-CR-171433] 15 p2492 N85-25375

Computer-assisted Gran titration procedure for strong acid determination
[DE85-006801] 15 p2507 N85-25462

CON1D: A computer program for calculating spherically symmetric droplet combustion
[DE85-005604] 15 p2507 N85-25464

The design and validation of software for dimensional metrology
[NPL-DITC-50/84] 15 p2521 N85-25542

An analysis of grid-based line drawing quantization methods
[AD-A151847] 15 p2522 N85-25547

Computer-aided identification of complete constitution model of transistor structure for design of subnanosecond large-scale-integrated circuits 15 p2529 N85-25594

West Europe report: Science and technology
[JPRS-WST-84-026] 15 p2532 N85-25617

Applications, specifications of Robotron CAD-CAM work stations 15 p2537 N85-25661

New sensor for industrial metrology developed
15 p2538 N85-25665

Design and swept-frequency measurement of printed circuit board log-periodic dipole arrays
[R-NIAS-23] 15 p2539 N85-25671

Null generation using discs on a reflector
[AD-A151897] 15 p2544 N85-25703

On the interconnection of incompatible solid finite element meshes using multipoint constraints
15 p2575 N85-25879

Use of COSMIC NASTRAN in a design department
15 p2575 N85-25881

An elastic analysis of a plated bone to determine fracture gap motion 15 p2575 N85-25882

An experimental investigation into the dynamic response of a stiffened flat plate loaded impulsively by an underwater shockwave
[AD-A151321] 15 p2578 N85-25903

Crack closure characteristics considering center cracked and compact tension specimens
[AD-A151702] 15 p2579 N85-25907

Elastic-workhardening SDF (Single-Degree-of-Freedom) system subjected to random blast excitations
[AD-A151866] 15 p2579 N85-25909

Technical development to improve satellite sounding over radiatively complex terrain
[NASA-CR-175746] 15 p2583 N85-25929

Plasma and magnetospheric research
[NASA-CR-171447] 15 p2591 N85-25976

ILUM code: Solar and lunar flux calculations for multi-cloud layered atmospheres
[DE85-005578] 15 p2600 N85-26025

Alterations/corrections to the BRASS Program
[NASA-CR-171874] 15 p2616 N85-26121

Interactive data analysis. Development of an interactive data manipulation system
[AD-A151359] 15 p2623 N85-26164

Development of a user support package for CPESIM 2 (a computer simulation for CPE (Computer Performance Evaluation) use
[AD-A151899] 15 p2624 N85-26170

Role of supercomputers in energy research programs
[DE85-006865] 15 p2624 N85-26172

USSR report: Cybernetics, computers and automation technology
[JPRS-UCC-85-003] 15 p2625 N85-26174

Computer technology advances exhibited
15 p2625 N85-26175

Effective microinstruction pipeline organization in a high-capacity microprocessor 15 p2625 N85-26176

Principles of organizing a real-time control system
15 p2625 N85-26177

Care 3 model overview and user's guide, first revision
[NASA-TM-86404] 15 p2627 N85-26192

Efficient implementation of real-time programs under the VAX/VMS operating system
[NASA-TM-86354] 15 p2627 N85-26193

GRID: A FORTRAN program for using a digitizing table to enter a finite element GRID
[AD-A151317] 15 p2628 N85-26196

A microcomputer-based program for printing check plots of integrated circuits specified in Caltech intermediate form
[AD-A151715] 15 p2629 N85-26205

Preliminary design of the Ada programming support environment configuration manager
[AD-A151845] 15 p2629 N85-26206

Catalog of the National Energy Software Center
[TI85-900521] 15 p2630 N85-26209

MATRIX: A program that shows how row and column orderings affect matrix fill-in
[DE85-007522] 15 p2630 N85-26213

VAX-based graphics mail system
[DE85-007231] 15 p2630 N85-26214

SPRING: Helical spring design software for microcomputers
[DE85-006200] 15 p2631 N85-26217

GEMINI: A computer program for two and three dimensional linear static and seismic structural analysis, CDC 7600 version
[DE85-007496] 15 p2631 N85-26218

Mathematical software for hyperbolic equations and two point boundary value problems
[AD-A151982] 15 p2638 N85-26270

SPLOT: A plot program for finite element data, function versus distance
[DE85-007129] 15 p2638 N85-26273

Implementation of Weeks' method for the inverse Laplace transform problem
[DE85-005919] 15 p2639 N85-26275

Time dependent and steady-state solutions of the electron energy distribution in a weakly ionized gas subject to an ac or dc electric field
[AD-A151829] 15 p2656 N85-26391

A database design for the Brazilian Air Force Flying Unit Operational Control System
[AD-A151848] 15 p2666 N85-26452

The controlled ecological life support system
15 p2688 N85-26603

Proceedings of the NAL Symposium on Aircraft Computational Aerodynamics
[NAL-SP-1] 16 p2691 N85-26611

Computer software for aerodynamic design of aircraft developed within the National Aerospace Laboratory
16 p2691 N85-26613

Recent trends in software technology for vector processors 16 p2691 N85-26615

A computer program for the drag prediction of subsonic, turbine powered aircraft in the en-route configuration
[VTH-LR-412] 16 p2701 N85-26681

Generation of flight paths using heuristic search
[AD-A151949] 16 p2704 N85-26694

ESP (External-Stores Program): A pilot computer program for determining flutter-critical external-store configurations. Volume 3, part 2. Program compilation
[AD-A152271] 16 p2706 N85-26703

Confined turbulent swirling recirculating flow predictions
[NASA-CR-174917] 16 p2709 N85-26716

The effect of load factor on aircraft handling qualities
[AD-A152118] 16 p2710 N85-26724

ESP (External-Stores Program): A pilot computer program for determining flutter-critical external-store configurations. Volume 3, part 1: Program compilation
[AD-A152270] 16 p2711 N85-26727

A modular dissimilar redundant computer designed for high integrity control 16 p2714 N85-26751

Interactive design of specifications for airborne software set (GISELE) 16 p2714 N85-26753

The flight control system for the Experimental Aircraft Programme (EAP) demonstrator aircraft
16 p2714 N85-26755

Flight Experiment Demonstration System (FEDS) functional description and interface document
[NASA-CR-175290] 16 p2717 N85-26769

The effect of inaccuracies in structural models on the control of large space structures
[AD-A151794] 16 p2732 N85-26858

Application of the hydraulic system frequency response program to propellant feed systems
[AD-A151824] 16 p2741 N85-26914

Paramagnetic form factors from itinerant electron theory
[DE85-005272] 16 p2750 N85-26973

The design of an English word-processor for scientific and technical use in which superscripts, subscripts and Greek characters are operated by screen-edit. 3
16 p2759 N85-27025

East Europe report: Science and technology
[JPRS-ESA-85-019] 16 p2767 N85-27077

Evaluating syntactic constraints to speech recognition in a fighter aircraft environment
[AD-A152117] 16 p2773 N85-27119

An analysis of data dictionaries and their role in information resource management
[AD-A152134] 16 p2774 N85-27121

A study of computational techniques for noncanonical microstrip antennas and arrays
[AD-A152216] 16 p2774 N85-27123

Computer program for the calculation of multicomponent convective diffusion deposition rates from chemically frozen boundary layer theory
[NASA-CR-168329] 16 p2781 N85-27164

A general simulation program for robot manipulator arm dynamics
[AD-A152121] 16 p2793 N85-27230

Automatic tracking of crack growth via finite elements
16 p2797 N85-27246

Development and application of optimum sensitivity analysis of structures
[NASA-CR-175857] 16 p2799 N85-27257

Component-specific modeling
[NASA-CR-174765] 16 p2799 N85-27261

Stress analysis of the space telescope focal plane structure joint
[NASA-CR-175797] 16 p2803 N85-27284

Gravity model development software status
16 p2804 N85-27289

Development of computer aided database design and maintenance tools
[AD-A151782] 16 p2845 N85-27537

The systematic integration of very large scale integrated circuit computer-aided design tools into a toolkit optimized for academic applications
[AD-A151813] 16 p2845 N85-27538

Forward library searching of previously-quantitated peaks, using a scan list created from a quantitation list by a novel FORTRAN program for the INCOS data system
[PB85-165835] 16 p2845 N85-27541

Further development of an Interactive Control Engineering Computer Analysis Package (ICECAP) for discrete and continuous systems
[AD-A151783] 16 p2846 N85-27546

Numerical optimization algorithm for engineering problems using microcomputer
[AD-A152135] 16 p2847 N85-27554

Development of graphical pole-zero, root-locus, Bode, Nyquist, and Nichols responses using the OPTSYSX program
[AD-A152148] 16 p2847 N85-27555

Development of graphical time response using the OPTSYSX program
[AD-A152221] 16 p2848 N85-27557

Evaluation of Ada (trademark) as a communications programming language, volume 1
[AD-A152314] 16 p2848 N85-27559

Evaluation of Ada (trademark) as a communications programming language. Volume 2: Communications protocols application
[AD-A152315] 16 p2848 N85-27560

Evaluation of Ada (trademark) as a communications programming language. Volume 3: Trusted software application
[AD-A152316] 16 p2848 N85-27561

Incorporation of an elliptical boundary condition into the program POISSON
[DE85-006820] 16 p2849 N85-27564

Continued development and implementation of the Universal Network Interface Device (UNID) 2 in the Digital Engineering Laboratory Network (DELNET), volume 2
[AD-A151947] 16 p2850 N85-27570

Error reduction program — combustor performance evaluation codes
[NASA-CR-174776] 16 p2852 N85-27584

A decomposition procedure for convex quadratic programs
[AD-A151732] 16 p2854 N85-27596

UTM (Universal Transverse Mercator) determinations from geographical data
[AD-A152293] 16 p2856 N85-27610

Computer assisted flight schedule optimization
[AD-A151689] 16 p2858 N85-27623

Optimizing computational efficiency and user convenience in plasma simulation codes
[DE85-007661] 16 p2866 N85-27682

Tokamak systems code
[DE85-008147] 16 p2869 N85-27696

Management considerations for an information center
[AD-A151774] 16 p2875 N85-27742

Users manual for coordinate generation code CRDSRA
[NASA-CR-172584] 17 p2891 N85-27824

User's manual for airfoil flow field computer code SRAIR
[NASA-CR-172585] 17 p2891 N85-27825

Addition of flexible body option to the TOLA computer program, part 1
[NASA-CR-132732-1] 17 p2896 N85-27855

Addition of flexible body option to the TOLA computer program. Part 2: User and programmer documentation
[NASA-CR-132732-2] 17 p2896 N85-27856

Predictions and measurements of isothermal flowfields in axisymmetric combustor geometries
[NASA-CR-174916] 17 p2898 N85-27867

Operational and developmental experience with the F/A-18A digital flight control system
17 p2902 N85-27895

Certifying complex digital systems on civil aviation aircraft 17 p2904 N85-27907

SRB filament wound case material property study
[NASA-CR-171469] 17 p2910 N85-27940

Composite loads spectra for select space propulsion structural components: Probabilistic load model development 17 p2912 N85-27954

Probabilistic finite element development
17 p2913 N85-27956

Structural tailoring of SSME blades (vanes)
17 p2913 N85-27960

Electromagnetic transmission through a slot in a perfectly conducting plane
[AD-A153224] 17 p2949 N85-28210

Restructurable VLSI (Very large scale integration) program
[AD-A152340] 17 p2951 N85-28226

Analysis of physical-chemical processes governing SSME internal fluid flows
[NASA-CR-175893] 17 p2957 N85-28261

FLOWPLOT 2: A fluid dynamics and heat transfer plotting package
[DE85-009602] 17 p2959 N85-28277

Voltammetric analysis of ordnance materials. Part 2: A portable digital voltammeter for use with a silver wire working electrode
[AD-A152480] 17 p2967 N85-28325

Documentation of PHOTO: A user's manual for the analysis of photographic and X-ray negatives
[AD-A152988] 17 p2967 N85-28327

Heating parameter estimation using coaxial thermocouple gages in wind tunnel test articles
[AD-A153039] 17 p2968 N85-28329

Multi-mesh gear dynamics program evaluation and enhancements
[NASA-CR-174747] 17 p2974 N85-28372

System analysis of a field Army Topographic Support System
[AD-A153318] 17 p2984 N85-28439

A program for the calculation of paraboloidal-dish solar thermal power plant performance
[NASA-CR-175874] 17 p2985 N85-28449

Report on high intensity solar cells
[DE85-008396] 17 p2987 N85-28462

Two-dimensional inverse kinematic problem: Application to the Saudi Arabian refraction profile
17 p2990 N85-28478

Crustal structure of the Red Sea-Arabian Shield transition 17 p2990 N85-28479

Centralized Storm Information System (CSIS)
[NASA-CR-175896] 17 p2994 N85-28506

A survey of composite grid generation for general three-dimensional sections 17 p3006 N85-28584

A new technique for system-to-system transfer of surface data 17 p3007 N85-28589

Language design, computers and brains
[AD-A152819] 17 p3008 N85-28594

Optical phenomena in computer vision
[AD-A152970] 17 p3008 N85-28595

Tracking algorithm performance analysis program (TRAPP)
[DE85-007304] 17 p3009 N85-28601

COSMIC Software Catalog, 1985 edition
[NASA-CR-174070] 17 p3010 N85-28608

Automatic distribution of programs in MASCOT and Ada (trademark) environments: A feasibility study
[AD-A152665] 17 p3010 N85-28614

Implementation of a general finite element code on an IBM PC compatible microcomputer
[AD-A152661] 17 p3011 N85-28615

CLEANROOM software development: An empirical evaluation
[AD-A152924] 17 p3011 N85-28619

The addition of advanced scene rendering techniques to a general purpose graphics package
[AD-A153323] 17 p3012 N85-28625

Evidential reasoning in expert systems for image analysis
[AD-A153379] 17 p3013 N85-28627

TRINITY: A pre- and post-processing program for 2-dimensional finite element data
[DE85-008029] 17 p3013 N85-28628

Numerical benchmark study for the finite element computer code NEPTUNE
[DE85-008400] 17 p3013 N85-28630

VULTURE manual
[DE85-008873] 17 p3013 N85-28631

CAMAC 488 module: 68000 based GPIB interface module
[DE85-009367] 17 p3014 N85-28635

Analytical generation of satellite orbits at the RAE (Royal Aircraft Establishment)
[AD-A152655] 17 p3053 N85-28901

Flight testing for performance and flying qualities
18 p3058 N85-28920

DEAN: A program for dynamic engine analysis
[NASA-TM-87033] 18 p3062 N85-28945

Computer-aided thermohydraulic design of TEMA type E shell and tube heat exchangers for use in low pressure, liquid-to-liquid, single phase applications
[AD-A153779] 18 p3100 N85-29191

KIVA: A comprehensive model for 2D and 3D engine simulations
[DE85-005562] 18 p3118 N85-29298

Buckling and postbuckling behavior of shallow shells
18 p3120 N85-29317

Description and illustration of the use of CRACKS IV
[AD-A153543] 18 p3121 N85-29325

Program RNTHR/2: An HP-41 C program for the calculation of RaA, RaB, and RaC concentrations in air based on three measurements of an air-dust sample
[IRI-190-83-10] 18 p3134 N85-29412

Comparison of two orographical data sets for the GLAS Fourth Order GCM 18 p3142 N85-29452

Model development highlight for 1984: The GLA Fourth Order GCM 18 p3143 N85-29457

Isotropic plotter
[PB85-175651] 18 p3150 N85-29504

A task battery for applied human performance assessment research
[AD-A153677] 18 p3154 N85-29530

Program DISAS: A computer program to obtain hard-copy plots of an image displayed on a vector graphics device in a local-area-network
[AD-A153643] 18 p3162 N85-29586

Specification of software quality attributes, volume 1
[AD-A153988] 18 p3163 N85-29593

Specification of software quality attributes. Volume 2: Software quality specification guidebook
[AD-A153989] 18 p3163 N85-29594

Specification of software quality attributes. Volume 3: Software quality evaluation guidebook
[AD-A153990] 18 p3163 N85-29595

Graphics package, version 4: User reference manual
[DE85-007894] 18 p3163 N85-29596

Micro-CAE mechanical engineering software development at Lawrence Livermore National Laboratory and participating universities and technology transfer
[DE85-008880] 18 p3163 N85-29597

Scattered data interpolation codes
[DE85-007337] 18 p3164 N85-29601

Computer program for the control/operating system of the gas flow installation for the solid fuel combustion chamber
[VTH-LR-430] 18 p3165 N85-29605

Annotated bibliography of recent papers on software engineering environments
[PB85-191385] 18 p3165 N85-29607

Distribution of mathematical software via electronic mail
[DE85-009664] 18 p3166 N85-29617

A quadratic programming algorithm
[AD-A153476] 18 p3168 N85-29631

A comparison of methods of least squares adjustment of traverses
[AD-A153612] 18 p3170 N85-29645

Further studies of the NRL collective particle accelerator via numerical modeling with the MAGIC code
[AD-A153583] 18 p3178 N85-29703

Comparison of calculations and measurements of the off-axis radiation dose (SI) in liquid nitrogen as a function of radiation length
[AD-A153676] 18 p3178 N85-29704

Program planning using the GMAP procedure in SAS/GRAPH software
[DE85-008356] 18 p3199 N85-29842

Distributed database design tool
[AD-A153760] 18 p3200 N85-29850

Generic data entry quality assurance tool
[DE85-008359] 18 p3200 N85-29852

Solar physics applications of computer graphics and image processing 18 p3208 N85-29903

Application of two-dimensional unsteady aerodynamic to a free-tip rotor response analysis
[NASA-CR-177348] 19 p3215 N85-29933

A computation of fin-line impedance
[AD-A154080] 19 p3258 N85-30204

Fast approach for calculating film thicknesses and pressures in elastohydrodynamically lubricated contacts at high loads
[NASA-TM-87032] 19 p3264 N85-30242

Modifications to SOLA-VOF for flow dynamics in spinning cylinders
[AD-A154093] 19 p3265 N85-30250

Structural dynamics modification of generalized beams using a local eigenvalue modification procedure
19 p3282 N85-30353

Large deflections of a cantilever beam under arbitrarily directed tip load
[NASA-TM-86442] 19 p3284 N85-30363

Application of the ADAMS program to deployable space truss structures
[NASA-CR-177927] 19 p3284 N85-30366

Nimbus 7 Coastal Zone Color Scanner (CZCS). Level 2 data product users' guide
[NASA-TM-86202] 19 p3299 N85-30452

Flood-runoff forecasting with HEC1F
[AD-A154286] 19 p3300 N85-30456

Modeling water resources systems for water quality
[AD-A154288] 19 p3300 N85-30457

MELSAR: A mesoscale air quality model for complex terrain. Volume 2: Appendices
[DE85-010991] 19 p3310 N85-30519

VIDTEX
[PB85-175669] 19 p3318 N85-30567

AEV local verification for aviation, precipitation, and temperature programs: AV, REL, TEM
[PB85-179125] 19 p3318 N85-30568

An interim user's manual for the advanced scavenging module version 1.2
[PB85-173904] 19 p3318 N85-30572

Environmental background measurement program
[AD-A153860] 19 p3319 N85-30577

Activities of the Institute for Computer Applications in Science and Engineering (ICASE)
[NASA-CR-172610] 19 p3332 N85-30641

CAE tool catalog
[DE85-011290] 19 p3334 N85-30657

SHAPS-2: A three-dimensional computer program for linear/non-linear, static/dynamic analyses of piping systems
[DE85-010500] 19 p3335 N85-30658

Demonstration project: Putting the bioastronautics data book on line
[NASA-CR-178424] 19 p3335 N85-30659

Interactive computer program for the analysis and design of linear time invariant systems
[AD-A154078] 19 p3335 N85-30664

Defense Mapping Agency (DMA) raster-to-Vector analysis
[AD-A154153] 19 p3336 N85-30668

The design, implementation and application of a table-driven syntax-directed editor
[AD-A154234] 19 p3336 N85-30670

Implementation of a proposed system for automated microcode generation
[AD-A154235] 19 p3336 N85-30671

The origin of the binary-search paradigm
[AD-A154367] 19 p3337 N85-30677

A parallelized point successive over-relaxation method on a multiple instruction multiple data stream computer
[AD-A154377] 19 p3337 N85-30679

Survey of Ada (Trademark)-based PDLs (Program Design Language)
[AD-A154402] 19 p3338 N85-30680

Computer center policy
[AD-A154416] 19 p3338 N85-30681

Computer Performance Modeling Tool (CPMT)
[AD-A154436] 19 p3338 N85-30682

Defense Mapping Agency (DMA) raster-to-Vector benchmark testing
[AD-A154152] 19 p3338 N85-30683

SANDRAG: A computer code for predicting drag of bodies of revolution at zero angle of attack in incompressible flow
[DE85-011170] 19 p3338 N85-30684

Circular-beam ray tracing on a microcomputer
[DE85-010754] 19 p3338 N85-30685

BREED: A CDC-7600 computer program for the automation of breeder reactor design analysis (LWBR Development Program)
[DE85-010327] 19 p3338 N85-30686

MELCOR Accident Consequence Code System (MACCS)
[DE85-009712] 19 p3339 N85-30689

Performance and library issues for mathematical software on high performance computers
[DE85-010263] 19 p3339 N85-30690

Touch-off: A method to determine the position of an object by means of a sensor-driven robot
[DE85-011176] 19 p3339 N85-30691

SABRINA: An interactive solid geometry modeling program for Monte Carlo
[DE85-010796] 19 p3339 N85-30692

Energy accounting software
[DE85-010612] 19 p3340 N85-30694

Using MATHLIB on the IBM computer and sundry plotting examples with a taste of IMSL
[DE85-011395] 19 p3340 N85-30695

Combined finite element meshing techniques using SUPERTAB
[DE85-011393] 19 p3340 N85-30696

CMP: Code Maintenance Package reference manual, version 2.0
[DE85-011396] 19 p3340 N85-30697

EDS operator and control software
[DE85-010470] 19 p3340 N85-30698

A dynamic programming approach to time-staged convex programs
[DE85-010616] 19 p3340 N85-30700

A Lotus 1-2-3 based system reliability program
[DE85-010533] 19 p3340 N85-30701

System enhancements of Mesoscale Analysis and Space Sensor (MASS) computer system
[NASA-CR-171463] 19 p3342 N85-30706

MCNP: A general Monte Carlo code for neutron and photon transport
[DE85-010764] 19 p3348 N85-30753

MANHIST user's guide
[DE85-010684] 19 p3348 N85-30754

Nonequilibrium air radiation (Nequair) program: User's manual
[NASA-TM-86707] 19 p3353 N85-30780

Surface effects on sputtered atoms and their angular and energy dependence
[DE85-010506] 19 p3354 N85-30790

Measurement problem in PROGRAM UNIVERSE
[DE85-008179] 19 p3378 N85-30959

Description and operation of CHISQMO, INVRTS, VOIGEN, VOIGTV, SMEAR, RUFF, AND POSCAR in the Stokes Analysis Program
[PB85-180628] 19 p3384 N85-30991

Computer program for plotting and fairing wind-tunnel data
[NASA-TM-85648] 20 p3387 N85-31009

Computer programs for smoothing and scaling airfoil coordinates
[NASA-TM-84666] 20 p3388 N85-31011

Combustion gas properties. Part 3: Hydrogen gas fuel and dry air
[NASA-TP-2477] 20 p3395 N85-31056

Design of multivariable controllers using the Integrated Analysis Capability (IAC) 20 p3412 N85-31172

A structural dynamics approach to the simulation of spacecraft control/structure interaction
20 p3412 N85-31173

SPAR improved structural-fluid dynamic analysis capability
[NASA-CR-171549] 20 p3454 N85-31449

A comparison of smooth specimen and analytical simulation techniques for notched members at elevated temperatures 20 p3466 N85-31546

Nonlinear analysis of an axisymmetric structure subjected to non-axisymmetric loading
20 p3466 N85-31549

Geodyn systems development
20 p3492 N85-31706

The application of computer imaging techniques to ocean topography and geophysical data
20 p3492 N85-31711

A computer program for determining the electrophoretic mobility of cells in a rectangular chamber during asymmetric electroosmotic flow
20 p3499 N85-31751

A cluster analysis method for identification of subpopulations of cells in flow cytometric list-mode arrays 20 p3503 N85-31779

Distributed implementation of functional program evaluation
[DE85-009573] 20 p3514 N85-31844

PIPE-1000: An implementation of piping on an HP-1000 minicomputer
[PB85-191955] 20 p3514 N85-31847

Methods for design and evaluation of integrated hardware-software systems for concurrent computation
[NASA-CR-176066] 20 p3515 N85-31851

Exponential order statistic models of software reliability growth
[NASA-CR-3909] 20 p3515 N85-31852

Proceedings of the 1st Workshop for the Design of Expert System Partial Differential Equation Solvers
[AD-A154192] 20 p3515 N85-31853

SCAP: A Shaped Charge Analysis Program. User's manual for SCAP 1.0
[DE85-011182] 20 p3515 N85-31854

Model documentation of the gas analysis modeling system. Volume 1: Model overview
[DE85-010952] 20 p3515 N85-31856

Microcomputers in transportation: Software and source book, February 1985
[PB85-181022] 20 p3517 N85-31868

Monte Carlo: In the beginning and some great expectations
[DE85-010789] 20 p3518 N85-31872

Nonlinear dynamics: A personal perspective
[DE85-010982] 20 p3521 N85-31899

Calculation of transonic steady and oscillatory pressures on a low aspect ratio model and comparison with experiment
[NASA-TM-86449] 21 p3551 N85-32092

Tip vortex computer code SRATIP. User's guide
[NASA-CR-172603] 21 p3551 N85-32093

Preliminary sizing and performance of aircraft
[NASA-TM-86357] 21 p3554 N85-32111

Component-specific modeling
[NASA-CR-174925] 21 p3556 N85-32119

Microprocessor control design for a low-head crossflow turbine
[AD-A155477] 21 p3556 N85-32121

Development and validation of a general purpose linearization program for rigid aircraft models
[NASA-TM-86737] 21 p3556 N85-32122

Development of reduced order models for control system design using the OPTSYSX program
[AD-A154552] 21 p3556 N85-32124

Myoelectric control of a computer based expert system for flight control
[AD-A154981] 21 p3557 N85-32126

MPS solidification model. Analysis and calculation of macrosegregation in a casting ingot
[NASA-CR-171589] 21 p3566 N85-32178

User's guide for computer program CGFAG, Concrete General Flexure Analysis with Graphics
[AD-A155555] 21 p3570 N85-32204

Fin line filters technology and electronic warfare
[AD-A154975] 21 p3576 N85-32237

Calculation of 3-D flow without numerical mixing
21 p3586 N85-32301

SSMIR (Solid State Memory Instrumentation Recorder): A new approach to acquiring data during an aircraft seat/sled ejection sequence
[AD-A154780] 21 p3589 N85-32308

Plating density standards
[DE85-010014] 21 p3591 N85-32318

An investigation into the comparisons of the underwater shock effects on a stiffened flat plate to the predictive nature of a computer model
[AD-A155612] 21 p3600 N85-32355

Analysis of inclined growth of silicon sheet
21 p3612 N85-32442

Assessment of the performance of an in-field Gaussian plume/puff model for overwater use
[AD-A155435] 21 p3614 N85-32460

Nuclear thermal transmittance in the atmosphere using LOWTRAN-6 computer code
[AD-A154669] 21 p3630 N85-32553

An evaluation of discretized conditional probability and linear regression threshold techniques in model output statistics forecasting of cloud amount and ceiling over the North Atlantic Ocean
[AD-A155100] 21 p3636 N85-32581

Analysis of spacecraft data
[NASA-CR-171587] 21 p3666 N85-32789

Analysis of spacecraft data
[NASA-CR-171597] 21 p3669 N85-32790

CARE 3 user friendly interface user's guide
[NASA-CR-172606] 21 p3669 N85-32791

Design of an expert-system flight status monitor
[NASA-TM-86739] 21 p3669 N85-32794

The NAS kernel benchmark program
[NASA-TM-86711] 21 p3670 N85-32795

Development of computer programs using the method of images to predict the sound field in a wedge overlaying a fast fluid and comparison with laboratory experiments
[AD-A154580] 21 p3670 N85-32797

An automated quality assurance surveillance plan for ADP (Automated Data Processing) operations under the Navy's commercial activities program
[AD-A154767] 21 p3671 N85-32802

The design and implementation of an object-oriented, production-rule interpreter
[AD-A154769] 21 p3671 N85-32803

Qualitative analysis of sign-bit processing
[AD-A154776] 21 p3671 N85-32804

The formal specification of an abstract machine: Design and implementation
[AD-A155167] 21 p3672 N85-32808

A comprehensive study of the AFIT (Air Force Institute of Technology) software development environment
[AD-A155450] 21 p3672 N85-32812

Survival function of hypo-exponential distributions
[AD-A155518] 21 p3672 N85-32814

A practical approach to Karmarkar's algorithm
[AD-A155714] 21 p3673 N85-32818

Praxis release notes, version 7.3
[DE85-011882] 21 p3673 N85-32820

Discrete-element acoustic analysis of submerged structures using doubly asymptotic approximations
[AD-A154959] 21 p3700 N85-32987

Speech understanding research
[AD-A155462] 21 p3700 N85-32990

An EPR (Electron-Paramagnetic-Resonance) and ENDOR (Electron-Nuclear-Double-Resonance) study of ferroelectric ammonium sulfate
[AD-A155560] 21 p3710 N85-33033

Continued development of a data base management system performance monitor: Volume 1
[AD-A154635] 21 p3713 N85-33040

Use of the computer programs PARA 80 to study results from firing the railgun ERGS-1M
[MRL-R-900] 22 p3738 N85-33167

SHELTER: Description of a program code — indoor climate
[FOA-C-56002-H1] 22 p3755 N85-33278

Petcom: A software instrument for the analysis of Petri networks, oriented towards communication protocols
[FUB-50-1983] 22 p3756 N85-33286

Introduction to adaptive techniques for voice signal processing
[FUB-52-1983] 22 p3756 N85-33287

Algorithms and organization of software for computer-aided circuit design 22 p3767 N85-33347

Software for frequency analysis of microwave circuits
22 p3768 N85-33352

Optimization of radioelectronic circuits with software for modeling of integrated circuits on unified system computer 22 p3768 N85-33354

Dialog system with minicomputer for plotting performance charts 22 p3768 N85-33355

Algorithms for constructing models of circuit elements in input language of computer-aided design software
22 p3768 N85-33356

Algorithm for determination of isomorphic graphs
22 p3769 N85-33357

Analysis of crosstalk in nonhomogeneous multiconductor lines 22 p3769 N85-33360

Developmental trends in radio receiver design
22 p3777 N85-33407

KRAK: A computer program for two-phase two-component porous flow and fracture
[LA-9703] 22 p3782 N85-33434

Machine intelligence for robotics applications
[DE85-011430] 22 p3793 N85-33503

Electromagnetic inspection of wire ropes using sensor arrays
[AD-A155412] 22 p3795 N85-33509

A new large-scale, high-resolution multicolor software display concept
[AD-A155404] 22 p3827 N85-33703

Electronic file system on an SM 90 minicomputer: The SARDE project
[ENST-84E018] 22 p3828 N85-33706

QKPLT users guide, version 2.0
[L-10094-M] 22 p3828 N85-33707

DECODE: A software manual for use with the Serial ASCII Instrumentation Loop (SAIL) system
[AD-A155358] 22 p3828 N85-33709

AUTSKED: An addendum
[DE85-010410] 22 p3829 N85-33712

Data Base Workshop: Availability-Reliability Modeling
[DE85-011570] 22 p3829 N85-33713

SANCHO: A finite element computer program for the quasistatic, large deformation, inelastic response of two-dimensional solids
[DE85-011456] 22 p3829 N85-33714

MORSE-CGA: A Monte Carlo radiation transport code with array geometry capability
[DE85-012083] 22 p3830 N85-33718

KIVA computer program for multidimensional chemically reactive fluid flows with fuel sprays
[DE85-012730] 22 p3830 N85-33722

PMEXA: Diagnostic filtering program for the PBFA-1 performance monitoring and evaluation system
[DE85-013179] 22 p3831 N85-33725

How a BASIC program works
[DE85-009142] 22 p3831 N85-33727

Search of the VAXintosh customizing VMS V4.0 for DCL windows
[DE85-011306] 22 p3831 N85-33729

A strategy planner for NASA robotics applications
[NASA-CR-175319] 22 p3834 N85-33738

Electron and ion cyclotron heating calculations in the tandem-mirror
[DE85-011658] 22 p3842 N85-33797

A hierarchy of knowledge levels implemented in a rule-based production system to calculate bounds on the size of intersections and unions of simple sets
[AD-A155291] 22 p3848 N85-33836

Component-specific modeling
[NASA-CR-174765] 23 p3897 N85-34140

Box truss analysis and technology development. Task 1: Mesh analysis and control
[NASA-CR-172570] 23 p3900 N85-34156

An introduction to finite elements
23 p3924 N85-34319

Detailed validation of a liquid and heat flow code against field performance
[DE85-009901] 23 p3932 N85-34366

Modular digital holographic fringe data processing system
[NASA-CR-177952] 23 p3933 N85-34376

Hardware math for the 6502 microprocessor
[NASA-TM-86517] 23 p3955 N85-34511

DISPL1: A software package for one and two spatially dimensioned kinetics-diffusion problems
[ANL-84-56] 23 p3956 N85-34516

User's operating procedures. Volume 3: Projects directorate information programs
[NASA-CR-177950] 23 p3956 N85-34520

Computer graphics for multivariate data
23 p3958 N85-34528

Interfacing interactive circuit simulation with standard graphics facilities 23 p3958 N85-34529

Research issues in generating graphical explanations
23 p3959 N85-34539

An integrated system for printing and publishing applications 23 p3959 N85-34540

Using percent-done program indicators to enhance user interfaces 23 p3960 N85-34546

Knowledge engineering application in image processing 23 p3965 N85-34583

Using LINE as an interactive graphics package. Interfacing line and Topdraw in 43 and 24 VM
[DE85-012007] 23 p3965 N85-34585

Analysis of transient radiation upset in a 16K SRAM
[DE85-009442] 23 p3965 N85-34586

Real-time multiparameter pulse processing with decision tables
[DE85-011683] 23 p3966 N85-34589

User's manual for the FLORA equilibrium and stability code
[DE85-013182] 23 p3966 N85-34590

Maintenance port system
[AD-D011724] 23 p3967 N85-34594

CYLTRAN calculations of electron effects on XD detectors
[LA-10264-MS] 23 p3969 N85-34601

Modeling a high energy gamma-ray telescope
[OG-9.2-5] 23 p4025 N85-34944

The final COS-B database now publicly available
[OG-9.3-8] 23 p4026 N85-34980

General design method for 3-dimensional potential flow fields. Part 2: Computer program DIN3D1 for simple, unbranched ducts
[NASA-CR-3926] 24 p4060 N85-35159

Analysis of incompressible cascade flows using state-of-the-art computer programs
[AD-A155850] 24 p4062 N85-35173

Development of NATOPS performance software for the SH-3D and SH-3H helicopters
[AD-A156140] 24 p4065 N85-35192

The investigation of tethered satellite system dynamics
[NASA-CR-176160] 24 p4069 N85-35215

Cluster variation study of coherent ordering in FCC and BCC solid solutions
[AD-A156039] 24 p4079 N85-35280

X-ray fluorescence analysis of 304L stainless steel
[DE85-013254] 24 p4080 N85-35288

Millimeter-wave propagation in moist air: Model versus path data
[AD-A156040] 24 p4087 N85-35331

Solid state high power amplifier for driving the SLC injector klystron
[DE85-013063] 24 p4090 N85-35356

Studies on effects of boundary conditions in confined turbulent flow predictions
[NASA-CR-3929] 24 p4093 N85-35371

Design and behavior of coped beams
24 p4100 N85-35417

Justified generalization: Acquiring procedures from examples
[AD-A156406] 24 p4135 N85-35626

DSS/MIS (Decision Support Systems/Management Information Systems) design and implementation for LAMPS Mk 3 utilizing a microcomputer and a maintenance personnel assignment program
[AD-A155852] 24 p4135 N85-35629

Users guide for optimum interpolation method of global data assimilation
[AD-A155929] 24 p4138 N85-35648

Specifying and verifying concurrent programs
[AD-A156190] 24 p4138 N85-35652

Using an LSI-11/23 and RT-11 to digitize analog tapes
[DE85-012736] 24 p4139 N85-35656

SASSYS-1 computer code verification with EBR-2 test data
[DE85-012119] 24 p4139 N85-35657

DEPTH-CHARGE static and time-dependent perturbation/sensitivity system for nuclear reactor core analysis, revision 1
[DE85-013103] 24 p4139 N85-35659

RFC modeling computer program
[DE85-012665] 24 p4140 N85-35661

Error message recording and reporting in the SLC control system
[DE85-013057] 24 p4140 N85-35664

Toolpack
[DE85-013135] 24 p4140 N85-35665

Computer code calculations of the TMI-2 accident: Initial and boundary conditions
[DE85-012613] 24 p4140 N85-35666

Master Fit users' guide, version 1.0
[DE85-014199] 24 p4140 N85-35667

COMPUTER SIMULATION

U COMPUTERIZED SIMULATION

COMPUTER STORAGE DEVICES

NT BUBBLE MEMORY DEVICES
NT BUFFER STORAGE
NT COMPUTER COMPATIBLE TAPES
NT FLIP-FLOPS
NT MAGNETIC DISKS
NT MAGNETIC TAPES
NT OPTICAL DISKS
NT RANDOM ACCESS MEMORY
NT READ-ONLY MEMORY DEVICES
NT REGISTERS (COMPUTERS)

Storage in the LLNL Octopus network: An overview and reflections
[DE84-014711] 01 p0106 N85-10712

Reducing spectral dimension of remotely sensed data using principal components analysis and a Peano scanning 02 p0212 N85-11399

Parallel searching and merging on ZMOB
[AD-A145424] 02 p0241 N85-11574

The design and performance analysis of an arbiter for a multi-processor shared-memory system
[AD-A146074] 03 p0403 N85-12566

Electromechanical switch
[AD-D011400] 07 p0948 N85-16009

An algorithm for assembly of stiffness matrices into a compacted data structure
[AD-A146727] 07 p1023 N85-16492

Vector computer memory bank contention
[NASA-CR-177342] 09 p1376 N85-18649

Redundancy of codes for detection and correction of unidirectional errors 12 p1842 N85-21557

Variable data base generator apparatus
[AD-D011515] 12 p1911 N85-21993

Problems in decentralized decision making and computation
[AD-A150025] 12 p1950 N85-22251

Fibre composite laminated plate analysis using a card programmable calculator (HP41C/CV)
[NIAST-83/66] 13 p2103 N85-23106

A general purpose scatter storage subsystem and a comparison of hashing methods
[NASA-CR-175614] 16 p2845 N85-27542

A stored data acquisition system: Update
[DE85-010534] 18 p3166 N85-29616

Memory effects in dynamical many-body systems: The isomnesic (constant-memory) approximation
[AD-A154160] 20 p3520 N85-31889

SSMIR (Solid State Memory Instrumentation Recorder): A new approach to acquiring data during an aircraft seat/sled ejection sequence
[AD-A154780] 21 p3589 N85-32308

Development of a dedicated speech work station
[AD-A155465] 21 p3674 N85-32824

Method of and apparatus for generating an interstitial point in a data stream having an even number of data points
[NASA-CASE-MFS-25319-1] 22 p3827 N85-33701

Spatial trees: A fast access method for unstructured graphical data 23 p3956 N85-34533

L-step sequential decoding
[AD-A156121] 24 p4138 N85-35649

COMPUTER SYSTEMS DESIGN

TEQUEL: The query language of SADDLE
01 p0058 N85-10382

SAGA: A project to automate the management of software production systems
[NASA-CR-174017] 01 p0103 N85-10665

Microcomputer management guidelines
[PB84-212174] 01 p0105 N85-10704

Logical database processor interface specifications
[PB84-216456] 01 p0105 N85-10705

The development of an optoelectronic assembly applied to computer systems
[AD-A145028] 01 p0120 N85-10821

The computer-communication link for the innovative use of Space Station 02 p0150 N85-11016

DISCUS multiprocessor enhancements — Distributed Control Microprocessor System (DISCUS)
[RSRE-MEMO-3591] 02 p0239 N85-11554

Systems analysis for microcomputer acquisitions
[AD-A145447] 02 p0239 N85-11556

Design and descriptive tools for systolic architectures
[DE84-015521] 02 p0239 N85-11557

East Europe report, science and technology. Czechoslovakia: System of small electronic computers
[JPRS-ESA-84-040] 02 p0239 N85-11558

Autonomous Attitude Determination System (AADS). Volume 1: System description
[NASA-TM-87385] 02 p0240 N85-11559

Concurrent processing and the decomposition of problems
[DE84-015285] 02 p0242 N85-11581

Telemetry (TM)/telecommand (TC) processor study
[ESA-CR(P)-1915] 03 p0323 N85-12081

An introduction to the MIAS conversion system
[IOS-184] 03 p0403 N85-12571

A control scheme for microcomputers being used in multiprocessor arrays
[DE84-014590] 04 p0547 N85-13479

The facilities of the Calculation Center and Real Time Room for satellite positioning 05 p0599 N85-13819

A geoinformation expert system for synergetic use of map and image data 05 p0659 N85-14233

Integrated resource management algorithms for computer systems 05 p0715 N85-14582

S-MICRO: A system for simulating a microprogrammed control unit
[INPE-3224-PRE/575] 05 p0715 N85-14585

Heterogeneous data base access
06 p0735 N85-14724

Role of DESIGNMANAGER in information engineering
[DE84-016807] 06 p0736 N85-14730

NC programming, machine tool information
06 p0816 N85-15178

Implementation of a Zilog Z-80 base realization library for the computer systems design environment
[AD-A146359] 06 p0853 N85-15423

The Torun measuring system for astronomical spectra
07 p0966 N85-16130

Support for distributed transactions in the TABS (Transaction based systems) prototype
[AD-A147213] 07 p1022 N85-16486

Integration of ground and on-board system for terminal count 08 p1092 N85-16896

Kernel Ada Programming Support Environment (KAPSE) interface team public report, volume 4
[AD-A147648] 08 p1205 N85-17581

Computer equipment at 1984 Leipzig Spring Fair
09 p1378 N85-18662

Dialog system of preparation and presentation of visual information 10 p1526 N85-19622

ESOP expert system model described
11 p1619 N85-20187

Needs, opportunities, and options for large scale systems research
[DE85-002664] 11 p1709 N85-20750

AID: Access to Informal Documentation
[DE85-000418] 11 p1740 N85-20939

A survey of the project CIP: Computer aided, intuition-guided programming. Wide spectrum language and program transformations
[TUM-I8406] 12 p1912 N85-22000

Construction of a menu-based system
[NASA-CR-172560] 13 p2146 N85-23321

Measurement of SIFT operating system overhead
[NASA-TM-86322] 13 p2149 N85-23337

The hierarchical database decomposition approach to database concurrency control
[AD-A150612] 13 p2166 N85-23450

Design for tactical avionics maintainability, technical evaluation report
[AGARD-AR-204] 14 p2225 N85-23798

The Edmonton data collection platform processing and locating facility 14 p2323 N85-24352

Systems design and application of computers with flexible architecture 14 p2401 N85-24800

Integration of solid modeling and database management for CAD/CAM 14 p2402 N85-24804

LINCS
[DE85-006151] 14 p2407 N85-24836

Properties of systems which lead to efficient computation of reliability
[AD-A151033] 14 p2409 N85-24853

Design and analysis of ordering and join for a multi-backed database system
[AD-A150711] 14 p2433 N85-25006

Microprocessor controlled storage sampling oscilloscope 15 p2533 N85-25622

CaD systems for electronic component design reviewed 15 p2537 N85-25660

A review of speech systems
[BAE-BT-12265] 15 p2539 N85-25676

General meteorological package (GEMPAK)
15 p2599 N85-26019

Activities report for FOA 53: Laboratory for man and information systems
[FOA-C-53019-H] 15 p2621 N85-26150

Logic analyzer survey and reviews
[BAE-881/ELO/1645] 15 p2621 N85-26151

Research in the design of high-performance reconfigurable systems
[NASA-CR-175705] 15 p2621 N85-26153

Workshop on Parallel Computer Architectures in Pattern Recognition and Image Processing
[BMFT-FB-DV-84-006] 15 p2622 N85-26154

High-capacity real-time computer system for processing hydrophysical data 15 p2625 N85-26178

Mini- and microcomputer local control network architecture and design principles
15 p2625 N85-26179

Design and analysis of a complete relational interface for a multi-backend database system
[AD-A151501] 15 p2626 N85-26198

The development of a programming support system for rapid prototyping. Tasks 2 and 3
[AD-A151549] 15 p2629 N85-26202

Procedures for use in compiling requirements specifications for computerized library systems
[CSTI-76] 1[illegible] p2666 N85-26446

Reusable software: A concept for cost reduction
16 p2697 N85-26655

Active control technology: Past, present, future
16 p2711 N85-26731

Automated CPX support system preliminary design phase
[NASA-CR-175784] 16 p2769 N85-27091

Use of vector processors in cartographic raster data processing, with special regard to the AP-120B vector processor 16 p2814 N85-27358

Detailed design of an object oriented, multiprogramming, multitasking operating system for sixteen-bit microcomputers
[AD-A152086] 16 p2847 N85-27552

Continued development and implementation of the Universal Network Interface Device (UNID) 2, Digital Engineering Laboratory Network (DELNET), volume 1
[AD-A151935] 16 p2850 N85-27569

Development of a microprocessor controlled communication system for ships
[BMFT-FB-T-84-275] 17 p2960 N85-28216

VLSI workshop and project: February - November 1982
[WSRL-0374-TR] 17 p2951 N85-28223
CAMAC 488 module: 68000 based GPIB interface module
[DE85-009367] 17 p3014 N85-28635
A programming system for a modular flexible multimicrocomputer system for the automatic control of automated test equipment
[JUEL-1962] 17 p3014 N85-28641
System Analysis for the Huntsville Operation Support Center, Distributed Computer System
[NASA-CR-171506] 17 p3015 N85-28642
The design of a capability-based distributed operating system
[CWI-CS-R8416] 17 p3016 N85-28650
The IRAS end-to-end data system
[NLR-MP-83056-U] 17 p3051 N85-28883
The development of information systems at NLR
[B8580079] 17 p3051 N85-28884
An interactive computer aid for the design and analysis of linear, single input/single output digital and continuous control systems
[AD-A153704] 18 p3162 N85-29589
The multiple processor machine for image processing, volume 5
[ESA-CR(P)-1976-VOL-5] 18 p3164 N85-29603
Investigation and construction of the Mini Remote Terminal Unit (mRTU-M) Analog Processor Module (AP-M), volume 1
[MR-DS-01-VOL-1] 18 p3166 N85-29619
Investigation and construction of the Mini Remote Terminal Unit (mRTU-M), Analog Processor Module (AP-M), volume 2
[MR-DS-01-VOL-2] 18 p3166 N85-29620
Statistical estimation of software reliability
[AD-A154097] 19 p3335 N85-30665
A micro/PDP-11 system for 406 MHz COSPAS/SARSAT processing 20 p3403 N85-31117
Fault tolerant multiprocessor SARSAT-COSPAS 406 MHz local user terminal 20 p3404 N85-31123
Visualization of computation results. Definition of a graphics satellite computer
[ONERA-RT-2/3587-CY] 20 p3514 N85-31845
Work in Amsterdam on local intelligence — artificial intelligence
[NIKHEF-H/84-9] 20 p3518 N85-31877
Determining functional requirements for NASA Goddard's command management system software design using expert systems 20 p3539 N85-32020
A high-speed digital signal processor for atmospheric radar, part 7.3A 21 p3626 N85-32525
Comparative study on data system architectures --- spacecraft data processing
[ESA-CR(P)-2015] 21 p3675 N85-32828
Hardware realization of digital filters without multipliers 22 p3766 N85-33340
Basic features of personal computers 22 p3766 N85-33344
Algorithms and organization of software for computer-aided circuit design 22 p3767 N85-33347
Software for frequency analysis of microwave circuits 22 p3768 N85-33352
Re-designing a mechanism for higher speed: A case history from textile machinery 23 p3923 N85-34310
An integrated system for printing and publishing applications 23 p3959 N85-34540
Efficient recovery and reversal in graphical user interfaces generated by the Higgens system 23 p3960 N85-34544
A model for graphics interface tool development 23 p3960 N85-34545
Using percent-done program indicators to enhance user interfaces 23 p3960 N85-34546
Selection of segment similarity measures for hierarchical picture segmentation 23 p3960 N85-34548
A graphics interface for interactive simulation of packet-switched networks 23 p3962 N85-34558
A Programmable Automatic Noise Data and Other Related parameter Acquisition system (PANDORA) --- wind energy converters 24 p4111 N85-35479
Software maintenance relating to the input translator and z-80 realization volume of the computer systems design environment
[AD-A155849] 24 p4138 N85-35646
Toolpack
[DE85-013135] 24 p4140 N85-35665

COMPUTER SYSTEMS PERFORMANCE
Finite element computation on nearest neighbor connected machines 01 p0057 N85-10379
Application of concurrent processing to structural dynamic response computations 01 p0057 N85-10380
Performance evaluation of database systems: A benchmark methodology
[PB84-217504] 01 p0105 N85-10707
Throughput characteristics of Carrier Sense Multiple Access (CSMA) networks
[FUB-25-1983] 01 p0106 N85-10713
Systems analysis for microcomputer acquisitions
[AD-A145447] 02 p0239 N85-11556
Autonomous Attitude Determination System (AADS). Volume 1: System description
[NASA-TM-87385] 02 p0240 N85-11559
A unified method for evaluating real-time computer controllers: A case study --- aircraft control
[NASA-CR-174166] 04 p0547 N85-13478
Integrated resource management algorithms for computer systems 05 p0715 N85-14562
Human factors characteristics of the Joint Tactical Fusion Test Bed: Field test 467 results
[AD-A146856] 07 p1020 N85-16476
Performance evaluation and control of distributed computer communication networks
[AD-A148103] 08 p1208 N85-17598
A unified model for performance and reliability of Fault-Tolerant/Multi-Mode systems
[AD-A148789] 08 p1208 N85-17601
Results of data base management system parameterized performance testing related to GSFC scientific applications
[NASA-CR-170615] 08 p1229 N85-17741
Vector computer memory bank contention
[NASA-CR-177342] 09 p1376 N85-18649
Man-machine interaction: Operator
[AD-A149075] 10 p1531 N85-19648
Bottleneckology: Evaluating supercomputers
[DE85-005574] 13 p2145 N85-23315
Service ARGOS technical report and improvement 14 p2328 N85-24395
Plasma and magnetospheric research
[NASA-CR-175675] 14 p2354 N85-24543
Selection criteria for a CAD/CM system 14 p2402 N85-24810
Continued development of a data base management system performance monitor, volume 2
[AD-A151714] 15 p2623 N85-26167
Development of a user support package for CPESIM 2 (a computer simulation for CPE (Computer Performance Evaluation) use
[AD-A151899] 15 p2624 N85-26170
Future information technology, 1984 telecommunications
[PB85-165850] 15 p2624 N85-26173
There is no I/O like no I/O
[DE85-009115] 17 p3014 N85-28634
Tradeoffs among portability, complexity, and efficiency in multiprocessing environments
[DE85-007899] 18 p3161 N85-29580
Two-dimensional/speed/couple/data base management system
[A-1] 18 p3165 N85-29608
Three-dimensional/integration two and three dimensional/numerical control/communication
[A-2] 18 p3165 N85-29609
The CEADS-CADD system
[A-4] 18 p3165 N85-29610
System test CALMA DDM (Design Drafting Manufacturing)
[A-5] 18 p3165 N85-29611
The International Computers Limited (ICL) PERQ 1/Engineering Architectural Graphics Language Environment (EAGLE) Computer Aided Design system (CAD)
[A-7] 18 p3165 N85-29612
Test Drawing Office Graphics System (DOGS)/APOLLO
[A-10] 18 p3166 N85-29614
INEL User Network Exchange, volume 1-85, Jan./Feb. 1985
[DE85-006108] 18 p3166 N85-29615
Instrument Systems Analysis and Verification Facility (ISAVF) users guide
[NASA-TM-86226] 19 p3223 N85-29982
An approach to modeling database activity 19 p3332 N85-30642
Development and analysis of a global compaction technique of microprograms 19 p3334 N85-30654
The completion time of a job on multi-mode systems
[AD-A154113] 19 p3336 N85-30666
Computer Performance Modeling Tool (CPMT)
[AD-A154438] 19 p3338 N85-30682
Performance and library issues for mathematical software on high performance computers
[DE85-010263] 19 p3339 N85-30690
Development and evaluation of a Fault-Tolerant Multiprocessor (FTMP) computer. Volume 3: FTMP test and evaluation
[NASA-CR-166073] 19 p3341 N85-30707
SPAR improved structural-fluid dynamic analysis capability
[NASA-CR-171549] 20 p3454 N85-31449
System test Oce 5200
[A-3] 20 p3515 N85-31860
The General Drafting System (GDS) design system
[A-6] 20 p3517 N85-31869
The IGOS design system
[A-8] 20 p3517 N85-31870
The 8080 emulator 21 p3668 N85-32783
The NAS kernel benchmark program
[NASA-TM-86711] 21 p3670 N85-32796
An image compression survey and algorithm switching based on scene activity
[NASA-TP-2458] 22 p3727 N85-33106
Some ideas for decomposing the domain of elliptic partial differential equations in the Schwarz process
[DE85-011844] 22 p3834 N85-33739
Raster functionality for a VDI
[DE85-006734] 24 p4097 N85-35396

COMPUTER SYSTEMS PROGRAMS
NT ASSEMBLER ROUTINES
NT INPUT/OUTPUT ROUTINES
NT OPERATING SYSTEMS (COMPUTERS)
NT SUBROUTINE LIBRARIES (COMPUTERS)
DYNKIN: A computer program for the description of detailed gas reactions in interaction with gas dynamics
[AD-B085364] 01 p0046 N85-10298
Three-dimensional mesoscale analysis of serial soundings 01 p0074 N85-10493
Geostationary satellite cloud and precipitation analysis using an interactive computer system 01 p0076 N85-10506
Operational use of shipboard numerical aid programs 01 p0082 N85-10546
East Europe report: Science and technology
[JPRS-ESA-84-030] 01 p0101 N85-10670
Remote data processing system software in Hungary 01 p0101 N85-10673
SAGA: A project to automate the management of software production systems
[NASA-CR-174017] 01 p0103 N85-10685
MICROSCOPE: A software system for multivariate analysis
[AD-A144720] 01 p0103 N85-10688
Normal approximation for response time in a processor-shared computer system model
[AD-A144997] 01 p0103 N85-10690
Autonomous Attitude Determination System (AADS). Volume 1: System description
[NASA-TM-87385] 02 p0240 N85-11559
Software engineering environments for mission critical applications: STARS alternative programmatic approaches
[AD-A145285] 02 p0241 N85-11571
ADAM: An abstract database machine
[RSRE-84007] 02 p0293 N85-11904
Specification and preliminary design of the CARTA system for satellite cartography
[E85-10035] 03 p0378 N85-12414
Simulation of wavefronts returned by realistic surfaces 03 p0383 N85-12448
CONTROL: A suite of interactive transfer-function analysis programs
[OUEL-1527/84] 03 p0408 N85-12609
PRIAMUS, a computer program for the calculation of thermophysical properties of gas mixtures containing O2, N2, CO, CO2, He, H2O, H2, CH4
[JUEL-1916] 04 p0472 N85-13062
Simulation of a transmission circuit composed of slightly nonlinear elements. Computation of the intermodulation on signals composed of N carriers
[CNES-NT-105] 04 p0496 N85-13167
An organ-pipe oscillation --- PHOENICS code
[PDR/CFDU-IC/14] 04 p0501 N85-13199
Laminar jet issuing into stagnant surroundings --- PHOENICS code
[PDR/CFDU-IC/15] 04 p0501 N85-13200
New directions in software for advanced computer architectures
[DE84-017435] 04 p0550 N85-13502
The CDC: Facilities on offer from the CNES computing center for space mathematics (a look at the capacities of CDC computers) 05 p0599 N85-13618
The Search And Rescue Satellite Aided Tracking (SARSAT) experiment. Presentation of CNES processing for the SARGOS project: Context and orbit processing 05 p0600 N85-13630
Loss of bone substance in consequence of amputation as a model for the adaptation to microgravity 05 p0694 N85-14464
SENSIT.FOR: A program for sensitometric reduction 07 p0963 N85-16105
Characterizing the scientific potential of satellite sensors --- San Francisco, California
[E85-10044] 07 p0983 N85-16244
On the structure of information in software
[AD-A147580] 07 p1026 N85-16511

Operating system versus programming environment, for example the UNIX
[SWA-84/037] 07 p1027 N85-16516

Austrian contributions to fuel rod failure models shown at the International Standard Problem (ISP)-14
[OEFZS-4276] 07 p1041 N85-16613

Investigating version dependence in fault-tolerant software 08 p1065 N85-16749

The effect on software design of testing by symbolic execution 08 p1065 N85-16750

Reliable software design for avionics and space applications 08 p1065 N85-16751

Hardware/software codesign for maintainable systems
08 p1066 N85-16753

Sensor-atmosphere-target simulation. Computer program SENSAT
[DFVLR-FB-84-32] 08 p1176 N85-17419

MINDS: A microcomputer interactive data system for 8086-based controllers
[NASA-TP-2378] 08 p1204 N85-17576

Software test handbook: Software test guidebook, volume 2
[AD-A147289] 08 p1204 N85-17578

An application of discriminant analysis to the selection of software cost estimating models
[AD-A147632] 08 p1204 N85-17580

Approaches to structuring the software development process
[AD-A147694] 08 p1205 N85-17582

The description of large systems
[AD-A148072] 08 p1205 N85-17586

Results of data base management system parameterized performance testing related to GSFC scientific applications
[NASA-CR-170615] 08 p1229 N85-17741

Four-fluid description of turbulent plasma focus dynamics
[IPF-84-4] 09 p1395 N85-18778

Computer-assisted data processing and analysis system for ground-based meteorological data collection, report on the Sierra Cooperative Pilot Project
[PB85-115350] 10 p1520 N85-19587

Digital Equipment Corporation VAX Ada Compiler Version T0.6-2 VAX-11/785, 11/750, 11/730, using VMS, Version 4.0 and MicroVAX 1, using MicroVMS Version 1.0
[AD-A149375] 10 p1538 N85-19696

SUBOPT: A CAD program for suboptimal linear regulators
[NASA-CR-172536] 10 p1539 N85-19702

Methodology investigation software testing of multiprocessor systems
[AD-A149446] 10 p1541 N85-19714

SOLIDGEN: A solid finite element data generator. User's manual
[AD-A149490] 10 p1541 N85-19715

French work toward flexible software workshops
11 p1592 N85-20015

Crack growth geometry in aluminum alloy sheet material under flight simulation loading. 1: A comparison between TWIST and miniTWIST FALSTAFF and short FALSTAFF. 2: Effect of truncating high loads
[VTH-LR-441] 11 p1609 N85-20119

Application of model following control and estimation techniques to attitude control of maneuvering spacecraft. Part 2: Simulation software description
[NLR-TR-82116-U-PT-2] 12 p1793 N85-21254

Interface specifications for SCR (Software Cost Reduction) (A-7E) extended computer module, revised
[AD-A149948] 12 p1915 N85-22024

Computer aided engineering applied to the design and verification of the generic Advanced Rigid Array (ARA) — solar array 13 p2006 N85-22593

Contribution of instrumentation and control software to system reliability
[DE85-004693] 13 p2149 N85-23340

Numerical algorithms and software for matrix Riccati equations
[AD-A150148] 13 p2150 N85-23344

French work toward flexible software workshops
14 p2289 N85-24187

Plasma and magnetospheric research
[NASA-CR-175675] 14 p2354 N85-24543

Finite element methods in space mathematics
14 p2396 N85-24757

The computing facilities of the Toulouse Space Center
14 p2397 N85-24770

Organization of conveyor processing of vector commands in multiprocessor computer systems with a reorganizable structure 14 p2401 N85-24799

ESABASE extension to spacecraft charging analysis. Phase 1: NASCAP software (VAX version)
[ESA-CR(P)-1968] 15 p2493 N85-25381

The design and validation of software for dimensional metrology
[NPL-DITC-50/84] 15 p2521 N85-25542

Computer program TRAMP: Inclusion of state space facilities and the analysis of non-linear elements
[BAE-BT-12643] 15 p2626 N85-26181

Design and analysis of a complete relational interface for a multi-backend database system
[AD-A151501] 15 p2628 N85-26198

Mathematical software for hyperbolic equations and two point boundary value problems
[AD-A151982] 15 p2636 N85-26270

Reusable software: A concept for cost reduction
16 p2697 N85-26655

Description of a computer program treating transonic steady state aeroelastic effects for a canard or tail airplane
[FFA-TN-1983-23] 16 p2700 N85-26674

Computation model of turbulent free flow: Application to axisymmetric jets
[ISL-R-126/83] 16 p2785 N85-27185

Raster or vector processing. Experience with the application of programs for the construction of thematic maps with boundary design in the Lower Saxony (West Germany) Land Administration for ground research
16 p2815 N85-27365

Generalized graph coloring: A frequency assignment method for VHF broadcasting
[TUM-M8405] 16 p2844 N85-27535

Management aspects of software maintenance
[AD-A152035] 16 p2847 N85-27550

Proposal for an extended set of FORTRAN Basic Linear Algebra subprograms
[DE85-007241] 16 p2848 N85-27562

Formulation of a coherent light-sheet by means of a cylindrical-spherical optical system
[ISL-R-116/83] 16 p2865 N85-27674

Software for reflectivity calculations of X-ray mirrors, revision 1
[DE85-006642] 16 p2867 N85-27688

A secure high-speed transaction protocol
[CWI-CS-R8417] 17 p3009 N85-28605

Research in computer science
[NASA-CR-175922] 17 p3010 N85-28612

CLEANROOM software development: An empirical evaluation
[AD-A152924] 17 p3011 N85-28619

Software environment for conducting interactive statistical analysis
[AD-A153376] 17 p3012 N85-28626

Software for estimating sparse Hessian matrices
[DE85-008121] 17 p3013 N85-28629

Optimal design and use of retry in fault tolerant real-time computer systems
[NASA-CR-175920] 17 p3015 N85-28643

A program for solving first kind Fredholm integral equations by means of regularization
[CWI-NM-R8416] 17 p3022 N85-28697

Specification of software quality attributes, volume 1
[AD-A153988] 18 p3163 N85-29593

Specification of software quality attributes. Volume 2: Software quality specification guidebook
[AD-A153989] 18 p3163 N85-29594

Specification of software quality attributes. Volume 3: Software quality evaluation guidebook
[AD-A153990] 18 p3163 N85-29595

ODIN: An extensible software environment. Report and user's reference manual
[DE85-008459] 18 p3164 N85-29600

A computer code IB-KB for interior ballistics of recoiling and recoilless guns
[FOA-C-20566-D2] 18 p3164 N85-29602

Fracture mechanics formulas on microcomputers
[NASA-TM-77850] 19 p3284 N85-30362

ZOG-Vinson technology demonstration project. Volume 2: System description
[AD-A153871] 19 p3333 N85-30645

Local automation model software benchmarking: Test plan
[AD-A154349] 19 p3337 N85-30676

Development and evaluation of a Fault-Tolerant Multiprocessor (FTMP) computer. Volume 2: FTMP software
[NASA-CR-166072] 19 p3341 N85-30706

Definition and layout of a traffic generator for an air traffic control simulation
[ESA-TT-888] 20 p3391 N85-31034

PHOENICS 84: A multi-dimensional multi-phase general-purpose computer simulator for fluid flow, heat transfer and combustion: 36 lecture panels
[CFD/84/18] 20 p3457 N85-31468

Visualization of computation results. Definition of a graphics satellite computer
[ONERA-RT-2/3587-CY] 20 p3514 N85-31845

Evaluative report on the Institute for Computer Sciences and Technology, National Bureau of Standards, fiscal year 1984
[PB85-176097] 20 p3514 N85-31846

A system identification package for VAX and LSI 11
[OUEL-1569/85] 20 p3516 N85-31862

Monte Carlo: In the beginning and some great expectations
[DE85-010789] 20 p3518 N85-31872

FAUST: Introduction and overview — self tuning control
[OUEL-1568/85] 20 p3519 N85-31882

A guide to the statistical analysis of the results of linear and nonlinear least-squares data fitting
[NPL-DITC-53/84] 20 p3521 N85-31895

HLLM software support
[AD-A154828] 21 p3671 N85-32805

Design guidelines for user-system interface software
[AD-A154907] 21 p3671 N85-32807

The effect of communication-language designs on software specifications
[AD-A155173] 21 p3672 N85-32809

Evaluation of a software design approach: Develop a threat resolution module in Ada (trademark)
[AD-A155599] 21 p3672 N85-32815

A simple software environment based on objects and relations
[AD-A155704] 21 p3673 N85-32817

DYNA3D, INGRID, and TAURUS: An integrated, interactive software system for crashworthiness engineering
[DE85-010928] 21 p3677 N85-32846

SHELTER: Description of a program code — indoor climate
[FOA-C-58002-H1] 22 p3755 N85-33278

State of art and development problems in computer-aided design of electronic circuits
22 p3766 N85-33342

Integrated Support Software System (ISSS)
[AD-A155715] 22 p3829 N85-33710

Proceedings of the Mechanisms Conference, volume 1 23 p3923 N85-34309

A versatile computer package for mechanism analysis, part 2: Dynamics and balance
23 p3924 N85-34315

Proceedings of the Mechanisms Conference, volume 2 23 p3924 N85-34318

Software for mechanism design
23 p3925 N85-34324

An innovative user interface for microcomputer-based computer-aided design 23 p3961 N85-34555

A geometric modeller for turbomachinery applications
23 p3962 N85-34556

Architecture of languages for large CAD systems development 23 p3962 N85-34557

The automatic labeling of geographic maps: A problem in computer aesthetics 23 p3962 N85-34561

Calculation of the diffusion of light by aerosols: Description of the MIELOR software and results obtained
[REPT-80] 24 p4137 N85-35638

AUTOSIM: An automated repetitive software testing tool
[NASA-CR-177930] 24 p4137 N85-35643

Attacking software crisis: A macro approach
[AD-A155846] 24 p4138 N85-35645

Software maintenance relating to the input translator and z-80 realization volume of the computer systems design environment
[AD-A155849] 24 p4138 N85-35646

COMPUTER SYSTEMS SIMULATION

Hardware for a real-time multiprocessor simulator
[NASA-TM-83805] 01 p0099 N85-10659

S-MICRO: A system for simulating a microprogrammed control unit
[INPE-3224-PRE/575] 05 p0715 N85-14585

Research using a DISCUS based network emulator
[AD-A141294] 13 p2149 N85-23338

Use of computer-aided design in large-computer development described 15 p2564 N85-25822

Distributed database design tool
[AD-A153760] 18 p3200 N85-29850

Development and evaluation of a Fault-Tolerant Multiprocessor (FTMP) computer. Volume 3: FTMP test and evaluation
[NASA-CR-166073] 19 p3341 N85-30707

Comments on estimating quantiles for Gaussian functionals by simulation
[AD-A154302] 19 p3348 N85-30750

Construction of University of Missouri, Rolla's full scale cloud simulation chamber and applied research
[AD-A154682] 21 p3557 N85-32126

COMPUTER TECHNIQUES

NT COMPUTER AIDED DESIGN
NT COMPUTER AIDED MANUFACTURING
NT COMPUTER AIDED MAPPING
NT COMPUTER AIDED TOMOGRAPHY
NT COMPUTER ASSISTED INSTRUCTION

COMPUTER TECHNIQUES

The Influence of Large Scale Computing on Aircraft Structural Design
[AGARD-R-706] 01 p0007 N85-10040

Impact of new computing systems on computational mechanics and flight-vehicle structures technology
01 p0007 N85-10042

Large scale computing in aeronautical design
01 p0007 N85-10043

Analysis of on-board CIG (Computer Image Generator) applications for aircrew training
[AD-A145214] 01 p0013 N85-10079

A thermodynamic surface for the critical region of ethylene
[PB84-217650] 01 p0025 N85-10159

A review of selected studies of computerized speech recognition conducted at the Naval Postgraduate School
[AD-A144841] 01 p0037 N85-10235

Electronics Engineering Department: EE technical review
[DE84-016124] 01 p0044 N85-10286

Research in Structures and Dynamics, 1984
[NASA-CP-2335] 01 p0057 N85-10377

Finite element computation on nearest neighbor connected machines 01 p0057 N85-10379

Application of concurrent processing to structural dynamic response computations
01 p0057 N85-10380

USSR report: Space Biology and Aerospace Medicine, volume 18, no. 4, July - August 1984
[JPRS-USB-84-006] 01 p0091 N85-10611

Potential use of dialogue with computers in biomedical research 01 p0091 N85-10614

Analysis of computer and communication information processing and system development
[AD-A144966] 01 p0100 N85-10660

Activities of the MIT Laboratory for Computer Science
[AD-A145134] 01 p0100 N85-10661

REMOTE: Modem Communicator Program for the IBM personal computer
[DE84-015047] 01 p0100 N85-10665

On the formal description and derivation of temporal proof rules for program properties
[TUM-I8405] 01 p0101 N85-10675

Construction of approximate confidence intervals for probability-of-kill via the bootstrap
[AD-A144761] 01 p0113 N85-10764

Microcomputers in Hungary 01 p0115 N85-10786

LANDSAT data and interactive computer mapping
02 p0152 N85-11026

Computer aided process planning of machined metal parts
[AD-A145626] 02 p0189 N85-11263

Hardware and software selection for experimental modal analysis 02 p0208 N85-11373

A system for the management of requests at an image data bank
[E85-10014] 02 p0216 N85-11427

Visual representations subserving texture perception
[AD-A145412] 02 p0236 N85-11538

East Europe report, science and technology. Czechoslovakia: System of small electronic computers
[JPRS-ESA-84-040] 02 p0239 N85-11556

Criteria for the optimization of processing flow in a model of an incremental computer with multiprocessing resources
[INPE-3046-TDL/158] 02 p0240 N85-11560

Software engineering environments for mission critical applications: STARS alternative programmatic approaches
[AD-A145285] 02 p0241 N85-11571

Description of the software acquisition process (SWAP) model
[AD-A145413] 02 p0241 N85-11573

Yearly report for programming productivity enhancement by the use of application generators
[AD-A145623] 02 p0242 N85-11579

Concurrent processing and the decomposition of problems
[DE84-015285] 02 p0242 N85-11581

Shuffle-exchanges on augmented meshes
[NASA-CR-172476] 02 p0243 N85-11587

AI (Artificial Intelligence) approaches to troubleshooting
[AD-P003918] 02 p0245 N85-11596

Diagnosis based on description of structure and function
[AD-P003919] 02 p0245 N85-11599

Artificial intelligence approaches to monitoring system integrity
[AD-P003930] 02 p0246 N85-11610

NAVAIR's (Naval air systems command) AI (Artificial Intelligence) program for ATE (Automated Test Equipment)
[AD-P003935] 02 p0247 N85-11615

DELTA: An expert system for diesel electric locomotive repair
[AD-P003941] 02 p0248 N85-11621

On the requirements of expert systems for fault isolation
[AD-P003947] 02 p0249 N85-11627

Memory-based expert systems
[AD-A145612] 02 p0249 N85-11628

Tomographic reconstruction of neutron radiograph images
[AD-A145682] 02 p0280 N85-11826

Decision Support System (DSS): A survey
[NRIMS-TWISK-317] 02 p0292 N85-11896

An operational system for subject switching between controlled vocabularies: A computational linguistics approach
[NASA-CR-3838] 02 p0293 N85-11903

A management workstation concept
[AD-A145617] 02 p0294 N85-11906

AGARD Highlights
[AGARD-HIGHLIGHTS-84/2] 02 p0305 N85-11972

ONR (Office of Naval Research) Far east Scientific Bulletin, Volume 9, Number 2, April - June 1984
[AD-A145681] 02 p0305 N85-11974

European Scientific Notes, Number 38-9
[AD-A145683] 02 p0306 N85-11975

DoD Robotics Application Workshop Proceedings
[AD-A145867] 03 p0307 N85-11978

Air force plasma spray at SA-ALC (San Antonio Air Logistics Center)
[AD-P004004] 03 p0308 N85-11984

NEO robotic application development at Letterkenny Army Depot: The application of robotics to agricultural blast cleaning
[AD-P004007] 03 p0308 N85-11987

Expert systems: The application of new computer methods to corrosion problems
[AERE-M-3395] 03 p0334 N85-12153

Assessment of computer techniques for processing digital LANDSAT MSS data for lithological discrimination of Serra do Ramalho, State of Bahia
[E85-10033] 03 p0378 N85-12412

A research program in computer technology
[AD-A145776] 03 p0402 N85-12565

Computer equipment for research in statistics
[AD-A145755] 03 p0406 N85-12591

Test-bed for programmable automation research. Phase 1
[AD-A145872] 03 p0409 N85-12614

Psychological issues in the design of expert systems
[AD-A146061] 03 p0436 N85-12792

USSR report: Electronics and electrical engineering
[JPRS-UEE-84-010] 04 p0485 N85-13095

Architecture of adaptive space-frequency-time signal processing system 04 p0486 N85-13103

Microprocessor implementation of algorithms of nonlinear filtration 04 p0486 N85-13104

Revision of signal and interference space-time processing algorithms for implementation by microprocessors 04 p0487 N85-13105

Efficiency of computer system digital processing of signals 04 p0487 N85-13106

Computer-generated latitude and longitude templates for rapid determination of geographic positions in Alaska
04 p0516 N85-13288

The 1984 ASEE-NASA summer faculty fellowship program (aeronautics and research)
[NASA-TM-87393] 04 p0575 N85-13664

A refined computer program for the transient simulation of ground coupled heat pump systems
[DE84-014096] 05 p0637 N85-14088

Simulation experiments on the relative accuracy of inferred atmospheric states from idealized wind and temperature profiling systems 05 p0682 N85-14386

Integrated navigation systems: Where are we headed?
[AD-A146425] 06 p0753 N85-14832

Computer investigation of effects of high injection in transistor large integrated circuit structures
06 p0793 N85-15068

Computer vision research and its applications to automated cartography
[AD-A146668] 06 p0828 N85-15255

Standard SHEF (Standard Hydrometeorologic Exchange Format) decoder Version 1.1
[PB85-106508/GAR] 06 p0840 N85-15332

Architecture, design, and system; performance assessment and development methodology for computer-based systems. Volume 1: Methodology description, discussion, and assessment
[AD-A146577] 06 p0847 N85-15379

A framework for the development of Navy computer-based systems: Combat system architecture and combat system engineering put into perspective
[AD-A146460] 06 p0856 N85-15445

Methodology investigation. Streamlined Test Reporting and Planning (STRAP): Data flow procedures
[AD-A146463] 06 p0871 N85-15531

Automated Lavina collects data on snow
07 p0960 N85-16224

Alabama Tin Belt: Metallogenesis and mineral resource evaluation. Year-end report
[DE84-901335] 07 p0989 N85-16283

Research in applied mathematics, numerical analysis, and computer science
[NASA-CR-172505] 07 p1021 N85-16480

NSW (National Software Works) lessons learned
[AD-A146737] 07 p1023 N85-16484

Ada training curriculum. Real-time systems in Ada L401 teacher's guide, volume 1
[AD-A146782] 07 p1024 N85-16486

Ada training curriculum. Real-time systems in Ada L401 teacher's guide, volume 2
[AD-A146783] 07 p1024 N85-16487

Local area network evaluation by MICROSS extensions
[AD-A146773] 07 p1027 N85-16521

Ion microscopy of metals and semiconductors
[AD-A147118] 07 p1043 N85-16626

Manual and automated line generalization and feature displacement: Appendixes
[AD-A143251] 07 p1054 N85-16689

Distributed knowledge base systems for diagnosis and information retrieval
[AD-A146690] 07 p1054 N85-16690

Computer sizing of fighter aircraft
[NASA-TM-86351] 08 p1067 N85-16759

Automation of checkout for the shuttle operations era
08 p1092 N85-16900

Modeling techniques used in the communications link analysis and simulation system (CLASS)
08 p1100 N85-16953

Validation of the communications link analysis and simulation system (CLASS) 08 p1100 N85-16954

Computer aided processing using laser measurements
08 p1103 N85-16973

Application of computer methods for calculation of multicomponent phase diagrams of high temperature structural ceramics
[AD-A148138] 08 p1133 N85-17140

Description of MBB computerized design techniques for A320 08 p1141 N85-17184

Beam propagation studies at NRL (Naval Research Laboratory) July 1983 to June 1984, volume 2
[AD-A148198] 08 p1152 N85-17270

Performance management system enhancement and maintenance
[NASA-CR-175271] 08 p1202 N85-17504

Steps towards parsing of query sequences to a database
[AD-A148769] 08 p1206 N85-17580

Guide to personal desktop computing at ANL
[DE85-001436] 08 p1206 N85-17584

A unified model for performance and reliability of Fault-Tolerant/Multi-Mode systems
[AD-A148789] 08 p1206 N85-17601

Reduction to outside the atmosphere and statistical tests used in Geneva photometry 08 p1251 N85-17902

Integrated approach to flight crew training
09 p1276 N85-18014

Electrical resistivity technique to assess the integrity of geomembrane liners
[PB85-122414/GAR] 09 p1325 N85-18327

Shock response analysis by personal computer using the extended IFT algorithm 09 p1335 N85-18387

SPADE: Series-parallel directed acyclic graph evaluator
[AD-A148456] 09 p1366 N85-18582

An object-oriented signal processing environment: The knowledge-based signal processing package
[AD-A148963] 10 p1466 N85-19251

A circuit grammar for operational amplifier design
[AD-A149566] 10 p1481 N85-19346

Electromagnetic inspection of wire ropes using sensor arrays
[AD-A149016] 10 p1495 N85-19436

Equations and algorithms for meteorological applications in air weather service
[AD-A148894] 10 p1519 N85-19675

Methods of computer-aided analysis of non-Gaussian noise and application to robust adaptive detection, part 2
[AD-A148879] 10 p1539 N85-19704

Ada in mission critical system acquisition: A guidebook
[AD-A149271] 10 p1540 N85-19710

French plans for fifth generation computer systems
[AD-A149435] 10 p1544 N85-19732

Computable real analysis
[AD-A149079] 10 p1546 N85-19747

Image Understanding: Proceedings of the 15th Workshop
[AD-A149496] 10 p1557 N85-19816
Optical implementation of the synthetic discriminant function
[AD-A149562] 10 p1557 N85-19817
The integrated library system design concepts for a complete serials control subsystem
[AD-A149379] 10 p1566 N85-19884
East Europe report: Science and technology
[JPRS-ESA-85-009] 11 p1616 N85-20165
ESOP expert system model described
11 p1619 N85-20187
Computer aided of maintainability design: A feasibility study
[AD-A149293] 11 p1736 N85-20932
A computer analysis of the RF performance of a ground-mounted, air-supported radome
[AD-P004352] 12 p1824 N85-21446
Radioelectronics and space exploration
12 p1838 N85-21533
The man-machine interface
[AD-A149971] 12 p1910 N85-21989
A computer-based gaming system for assessing recognition performance (RECOG)
[AD-A149752] 12 p1915 N85-22022
Very-high level concurrent programming
[AD-A150009] 12 p1916 N85-22026
Experimental mathematics
[CWI-PM-R8411] 12 p1925 N85-22096
Evaluation of PHOENICS as a design analysis tool for SSME 12 p1949 N85-22240
Theoretical interpretation of thermal arrest data from differential thermal analysis measurements
12 p1949 N85-22241
The EEC's information technology program: An update
[AD-A150022] 12 p1951 N85-22258
Aviation maintenance computerized management information systems: Perspective for the future
[AD-A150637] 13 p1966 N85-22349
Avionics Flight Evaluation System (AFES)
13 p1967 N85-22357
The potential for advanced computerized aids for comprehensible writing of technical documents
[AD-A150501] 13 p2055 N85-22870
Orphan detection in the Argus system
[AD-A150562] 13 p2148 N85-23331
Map design for computer processing: Literature review and DMA product critique
[AD-A151061] 14 p2347 N85-24513
Evaluating the appropriateness of microcomputers for litigation document management using the analytic hierarchy process 14 p2399 N85-24788
A two-cycle shift register with error detection
[AD-A150768] 14 p2400 N85-24791
The problem of creating a standardized series of personal computers 14 p2400 N85-24795
ANTENA user guide
[DE85-004961] 14 p2424 N85-24953
Microcomputer application of aerospace asset surface search planning
[AD-A151833] 15 p2467 N85-25227
Calculation and display of stack departure times for aircraft inbound to Heathrow Airport
[AD-A151991] 15 p2469 N85-25241
Microcomputer controlled automatic peak locking of laser circuit 15 p2537 N85-25655
Applicability of modular versus universal robots discussed 15 p2538 N85-25664
Using a single-board computer to maintain constant voltage, current sources 15 p2551 N85-25749
Calorimeter for measuring high-energy optical pulses
[PB85-160695] 15 p2561 N85-25799
Eye movement in response to single and multiple targets
[AD-A151115] 15 p2617 N85-26126
USSR report: Cybernetics, computers and automation technology
[JPRS-UCC-85-003] 15 p2625 N85-26174
Progress through cooperation and exchange of ideas and experiences 15 p2626 N85-26186
Computers in the determination of rainfall depth-duration-frequencies in Natal
15 p2627 N85-26188
Computer aided draughting in a civil engineering consulting practice 15 p2627 N85-26189
Interactive graphical data analysis
[DE85-005946] 15 p2631 N85-26215
Developing an automated technique for translating a relational database into an equivalent network one
[AD-A151844] 15 p2666 N85-26451
Information technology applications in voluntary sector transport operations. SP1: Objectives and programme of work
[TT-8501] 15 p2667 N85-26457
Computer software for aerodynamic design of aircraft developed within the National Aerospace Laboratory
16 p2691 N85-26613
Planning fuel-conservative descents in an airline environmental using a small programmable calculator: Algorithm development and flight test results
[NASA-TP-2393] 16 p2707 N85-26705
The design of an English word-processor for scientific and technical use in which superscripts, subscripts and Greek characters are operated by screen-edit. 3
16 p2759 N85-27025
China report: Science and Technology
[JPRS-CST-85-012] 16 p2806 N85-27300
New image deblurring method described
16 p2806 N85-27305
A wind-bivane/microprocessor system for on-line prediction and display of pollutant distributions
16 p2830 N85-27449
The development and application of volume scan and cell tracking capabilities for the analysis of convective cloud systems 16 p2830 N85-27451
Incorporation of an elliptical boundary condition into the program POISSON
[DE85-006820] 16 p2849 N85-27564
Finite elements and the method of conjugate gradients on a concurrent processor
[NASA-CR-175812] 16 p2853 N85-27588
Adaptive grid generation for numerical solution of Burger's equation
[AD-A152217] 16 p2855 N85-27606
ACT applied to helicopter flight control
17 p2902 N85-27891
Some flight test results with redundant digital flight control systems 17 p2902 N85-27892
Evaluation of used crankcase oils using computerized infrared spectrometry
[AD-A152993] 17 p2920 N85-27999
Evaluation of used crankcase oils using computerized infrared spectrometry. Appendices
[AD-A152994] 17 p2920 N85-28000
Automation of Precise Time Reference Stations (PTRS) 17 p2962 N85-28291
US Naval Observatory collection and utilization of time comparison data 17 p2962 N85-28292
Documentation of PHOTO: A user's manual for the analysis of photographic and X-ray negatives
[AD-A152988] 17 p2967 N85-28327
Generation and display apparatus
[AD-D011639] 17 p3008 N85-28599
Microprocessor controlled temperature chassis
[DE85-008392] 17 p3009 N85-28602
Computer program for prediction of capture maneuver probability for an on-off reaction controlled upper stage
[NASA-CR-165937] 17 p3010 N85-28611
Interfacing the VAX 11/780 using Berkeley Unix 4.2.BSD and Ethernet based Xerox network systems, volume 1
[AD-A152953] 17 p3015 N85-28645
Computing in the Soviet general economy: An introductory overview
[AD-P004563] 17 p3047 N85-28858
Turbulence structure in the boundary layers of an oscillating airfoil
[AD-A153631] 18 p3058 N85-28926
MBB expands CADAM system for a 320 program
18 p3087 N85-29099
Automatic volume calibration system
[DE85-008955] 18 p3102 N85-29204
Improved model for fluid-driven cracks in jointed rock
[DE85-008963] 18 p3125 N85-29349
Deployable Core Automated Maintenance System (DCAMS)
[AD-A153695] 18 p3198 N85-29839
Projects of the Computer Center of the academy's Siberian branch 19 p3295 N85-30425
Activities of the Institute for Computer Applications in Science and Engineering (ICASE)
[NASA-CR-172610] 19 p3332 N85-30641
Multigrid method for multiprocessors
[DE85-007929] 19 p3333 N85-30647
Local automation model software benchmarking: Test plan
[AD-A154349] 19 p3337 N85-30676
Survey of Ada (Trademark)-based PDLs (Program Design Language)
[AD-A154402] 19 p3338 N85-30680
T sub EX font tables
[DE85-011394] 19 p3339 N85-30687
Identification of a mathematical model 1: Goodness of fit criterion
[HSE-TRANS-11109] 19 p3341 N85-30703
Development and evaluation of a fault-tolerant multiprocessor (FTMP) computer. Volume 1: FTMP principles of operation
[NASA-CR-166071] 19 p3341 N85-30705
Computer studies of the quench behavior of an SSC model-dipole
[DE85-010633] 19 p3360 N85-30829
Galileo battery testing and the impact of test automation 20 p3444 N85-31381
Computer methods in manipulator kinematics, dynamics and control: A comparative study
20 p3462 N85-31506
Electrophoretic mobility of cells in a vertical Ficoll gradient 20 p3499 N85-31753
Activities report of the Laboratory for Computer Science (FOA 32)
[FOA-C-30384-E1] 20 p3516 N85-31861
Mathematical programming in the Netherlands
[REPT-ARW-03-THE-BDK/ORS/83/10]
20 p3517 N85-31866
USAFSAM review and analysis of radiofrequency radiation bioeffects literature
[AD-A155113] 21 p3664 N85-32760
Design guidelines for user-system interface software
[AD-A154907] 21 p3671 N85-32807
New developments on the core function for efficient implementation of the difficult residue number system operations
[AD-A154676] 21 p3676 N85-32834
Distributed name management
[AD-A154785] 21 p3712 N85-33037
Interactive procedures for discriminating and restoring contour line networks 22 p3736 N85-33156
Discrimination of linear contour elements of space photographs based on visual perception model
22 p3736 N85-33161
Signal processing in quasi-holographic system as an inverse problem 22 p3762 N85-33315
Synthesis of tests for programmable logic arrays
22 p3777 N85-33408
Detection of and search for faults in programmable logic arrays 22 p3778 N85-33409
Computer science: Key to a space program renaissance. The 1981 NASA/ASEE summer study on the use of computer science and technology in NASA. Volume 2: Appendices
[NASA-CR-175295] 22 p3827 N85-33702
Microcomputer controlled image processor
[AD-D011734] 22 p3833 N85-33735
Proceedings of the Mechanisms Conference, volume 1 23 p3923 N85-34309
A versatile computer package for mechanism analysis
23 p3924 N85-34314
A versatile computer package for mechanism analysis, part 2: Dynamics and balance
23 p3924 N85-34315
Optimisation in the computer aided design of mechanisms 23 p3924 N85-34321
Method and apparatus for transfer function simulator for testing complex systems
[NASA-CASE-NPO-15696-1] 23 p3926 N85-34333
Animengine: An engineering animation system
23 p3959 N85-34535
Efficient recovery and reversal in graphical user interfaces generated by the Higgens system
23 p3960 N85-34544
Numerical and analytic descriptions of cosmic-ray transport
[SH-4.1-4] 23 p4005 N85-34830
Computational techniques for fiber reinforced components 24 p4075 N85-35250
Wholebody radiation counting system
[AD-A155842] 24 p4131 N85-35607
TRICCS: A proposed teleoperator/robot integrated command and control system for space applications
[NASA-TM-87577] 24 p4136 N85-35637
Design of a microprogram control unit with concurrent error detection
[AD-A156447] 24 p4139 N85-35656
Toolpack
[DE85-013135] 24 p4140 N85-35665
Edge information in color images based on histograms of differences
[AD-A156002] 24 p4154 N85-35751

COMPUTER VISION

Computer vision research and its applications to automated cartography
[AD-A146668] 06 p0828 N85-15255
Vision by man and machine: How the brain processes visual information may be suggested by studies in computer vision (and vice versa)
[AD-A147880] 07 p1017 N85-16456
JPL Robotics Laboratory computer vision software library
[NASA-CR-174272] 07 p1023 N85-16491
Dutch institutes do research in tactile visual robot sensors 09 p1310 N85-18226
French firm develops 2D, 3D computer vision system
10 p1461 N85-19206

Fourth International Conference on Robot Vision and Sensory Controls
[AD-A149524] 10 p1492 N85-19422
A method for reduction of ambiguity in segmentation of images
[INPE-3394-TDL/186] 11 p1697 N85-20664
3D (Three-Dimensional) sensor for adaptive suspension vehicle
[AD-A150921] 14 p2311 N85-24305
Positioning of a robotic manipulator through the use of visual feedback
[AD-A151933] 16 p2851 N85-27577
Optical phenomena in computer vision
[AD-A152970] 17 p3008 N85-28595
Activities report of the Laboratory for Computer Science (FOA 32)
[FOA-C-30384-E1] 20 p3516 N85-31861
Edge detection and geometric methods in computer vision
[AD-A155873] 24 p4135 N85-35630
Selected publications in image understanding and computer vision from 1974 to 1983
[AD-A156196] 24 p4136 N85-35634

COMPUTERIZED CONTROL
U NUMERICAL CONTROL

COMPUTERIZED DESIGN
U COMPUTER AIDED DESIGN

COMPUTERIZED SIMULATION
NT ANALOG SIMULATION
NT DIGITAL SIMULATION
Computer simulation of the shock initiation of detonation in solid explosives
[PML-1984-23] 01 p0033 N85-10207
Clutter generator for use in radar evaluation
[AD-D011234] 01 p0039 N85-10245
Availability of transmission systems in continental and intercontinental connections --- telecommunication
[FUB-33-1983] 01 p0040 N85-10261
Gaussian Wide Sense Stationary Uncorrelated Scattering (GWSSUS) channel simulation program to be used for mobile radio systems
[FUB-40-1983] 01 p0041 N85-10265
DYNKIN: A computer program for the description of detailed gas reactions in interaction with gas dynamics
[AD-B085364] 01 p0046 N85-10298
Application guide for Hydrological Simulation Program FORTRAN (HSPF)
[PB84-215763] 01 p0064 N85-10427
Variable geometry Darrieus wind machine
[PB84-207281] 01 p0068 N85-10453
Processing and display of atmospheric phenomenaa data
[NASA-CR-171178] 01 p0072 N85-10475
Feature discovery by competitive learning
[AD-A145052] 01 p0097 N85-10646
A relational approach to the development of expert diagnostic systems
[NASA-TM-86288] 01 p0099 N85-10658
Three programs for evaluating bending moments, deflections and shear forces in simply-supported uniform bridge decks under South African NA loading: NAB, NAD and NAS. NITRR manual P13
[ISBN-0-7988-2283-X] 01 p0102 N85-10681
PDSS/IMC CIS user's guide
[NASA-CR-171179] 01 p0102 N85-10682
Robust rate control system designs for a submersible
[AD-A144792] 01 p0111 N85-10753
KrCl lasers for fusion
[DE84-012210] 01 p0122 N85-10835
VORCOR: A computer program for calculating characteristics of wings with edge vortex separation by using a vortex-filament and-core model
[NASA-CR-165902] 02 p0135 N85-10921
Enhanced TCAS 2/CDTI traffic Sensor digital simulation model and program description
[NASA-CR-172445] 02 p0136 N85-10927
Command control group behaviors. Objective 1: A methodology for and identification of command control group behaviors
[AD-A145690] 02 p0191 N85-11279
Simulation study of a new inverse-pinch high Coulomb transfer switch
[NASA-CR-172420] 02 p0194 N85-11294
Robotics investment decision model user's manual
[AD-A145467] 02 p0204 N85-11347
A constitutive modeling technique based on a generalized rheological model to predict the response of materials 02 p0207 N85-11368
Computer models and output, Spartan REM: Appendix B
[NASA-CR-171093] 02 p0208 N85-11376
Basic research for the geodynamics program
[NASA-CR-174055] 02 p0228 N85-11490
Description of the software acquisition process (SWAP) model
[AD-A145413] 02 p0241 N85-11573
Parallel searching and merging on ZMOB
[AD-A145424] 02 p0241 N85-11574
Diagnosis via causal reasoning: Paths of interaction and the locality principle
[AD-P003920] 02 p0245 N85-11600
A generalized model of fault-isolation performance
[AD-P003928] 02 p0246 N85-11608
Experimental study with parameter variations on a hydraulic positioning servo with computer implemented observer
[FOA-C-20545-E3] 02 p0256 N85-11673
Modeling holographic recognition system by using number-theory convolution transformation
02 p0272 N85-11774
Decision process models of contractor behavior: The development of effective contract incentives
[AD-A145524] 02 p0292 N85-11898
Review of simulation of quasiparallel collisionless shocks
[DE84-015489] 02 p0304 N85-11967
Numerical simulation of the subsonic wing-rock phenomenon 03 p0320 N85-12064
Liquid payload moment equations
[AD-A145977] 03 p0362 N85-12319
Numerical simulations of fuel droplet flows using a Lagrangian triangular mesh
[AD-A146067] 03 p0362 N85-12320
Simulation of wavefronts returned by realistic surfaces
03 p0383 N85-12448
A user's guide to the Flexible Spacecraft Dynamics and Control Program
[NASA-TM-87369] 03 p0405 N85-12586
Regenerative simulation methods for local area computer networks
[AD-A146197] 03 p0409 N85-12612
Rotary-wing aircraft noise measurements: Analysis of variations and proposed measurement standard
[AD-A146207] 03 p0416 N85-12662
Ways to improve management of Federal funded computerized models
[LCD-75-111] 03 p0435 N85-12771
A comparison of Wortmann airfoil computer-generated lift and drag polars with flight and wind tunnel results
[NASA-TM-86035] 04 p0452 N85-12868
A transmission analysis for the use of 2-4 PSK modulation in satellite broadcasting
[ESA-STM-231] 04 p0494 N85-13151
Simulation of a transmission circuit composed of slightly nonlinear elements. Computation of the intermodulation on signals composed of N carriers
[CNES-NT-105] 04 p0496 N85-13167
Comprehensive silicon solar cell computer modeling
[NASA-CR-174151] 04 p0530 N85-13386
Regional-scale (1000 KM) model of photochemical air pollution. Part 2: Input processor network design
[PB84-232651] 04 p0532 N85-13400
Measurement of range-resolved water vapor concentration by coherent CO2 differential absorption lidar
[PB84-236892] 04 p0535 N85-13420
Development and verification of MCD-2 and MOD-OA simulation models
[DE84-017389] 04 p0550 N85-13499
Evaluation of automated decisionmaking methodologies and development of an integrated robotic system simulation
[NASA-CR-172401] 04 p0552 N85-13516
Preliminary user's guide for BIGONE on the Cray
[DE84-017075] 04 p0566 N85-13623
Dynamic decision making --- and programming
[FOA-C-53015-H2] 04 p0575 N85-13668
Numerical simulations of fission
04 p0585 N85-13737
Simulation of separated transonic airfoil flow by finite-difference viscous-inviscid interaction
05 p0591 N85-13768
Boundary layer simulator improvement
[NASA-CR-174199] 05 p0597 N85-13802
Level of effort 05 p0602 N85-13839
Elimination of uncontrollable rigid body mode, appendix C 05 p0603 N85-13842
Simulation of the interaction of single-pulsed optical lasers with targets in a vacuum
[DE84-016476] 05 p0640 N85-14107
MC2969 escapement study
[DE84-014542] 05 p0645 N85-14143
Improving the Spacelab mass memory unit tape layout with a simulation model
[NASA-TM-86483] 05 p0713 N85-14571
High-efficiency solar-cell design modeling
06 p0829 N85-15262
Probable maximum flood estimation - Eastern United States
[AD-A146536] 06 p0839 N85-15324
Sigma code testing
[AD-A146548] 06 p0841 N85-15340
Translational control of a graphically simulated robot arm by kinematic rate equations that overcome elbow joint singularity
[NASA-TP-2376] 06 p0856 N85-15448
Large-eddy simulation. Guidelines for its application to planetary boundary layer research
[AD-A146381] 06 p0890 N85-15651
A Q-GERT network simulation model for examining pipeline time in the Navy's J-52 intermediate level jet engine repair cycle
[AD-A147269] 07 p0894 N85-15663
On the generation of random variables for radar simulation purposes 07 p0936 N85-15947
An interactive FORTRAN program for determining reliability of pseudo-range geodetic point positioning using the global positioning system
[AD-A147133] 07 p0966 N85-16275
Experiments in forecasting atmospheric marine horizontal visibility using model output statistics with conditional probabilities of discretized parameters
[AD-A147574] 07 p1008 N85-16404
Interaction of human cognitive models and computer based models in supervisory control
[AD-A142547] 07 p1020 N85-16474
Convection schemes for use with curvilinear coordinate systems: A survey
[AD-A147093] 07 p1031 N85-16543
A simulation model for Air Launched Cruise Missile engine management
[AD-A147018] 07 p1051 N85-16672
Computer sizing of fighter aircraft
[NASA-TM-86351] 08 p1067 N85-16759
Development of a Helicopter integrated navigation system 08 p1073 N85-16802
A Generalized Escape System Simulation (GESS) computer program. Volume 2: GESS programmer's manual, version 2
[AD-A148363] 08 p1081 N85-16845
Space shuttle main engine hardware simulation
08 p1091 N85-16886
Managing computer-controlled operations
08 p1097 N85-16934
The Communications link analysis and simulation system (CLASS) 08 p1100 N85-16952
Modeling techniques used in the communications link analysis and simulation system (CLASS)
08 p1100 N85-16953
Numerical simulation of the shock detonation transition 08 p1116 N85-17039
Satellite broadcasting: The performance of C-MAC in a hardware simulation of a DBS transmission chain
[BBC-RD-1984/9] 08 p1143 N85-17206
The extension of an invertible coniferous forest canopy reflectance model using SIR-B and LANDSAT data
08 p1149 N85-17246
Characterization of jet-contaminant interaction flow in chemical decontamination
[AD-A147298] 08 p1161 N85-17327
The value and utility of inflight onboard simulation
[AD-A148033] 08 p1196 N85-17543
Exposure modelling of particle beam lithography
[AD-A147849] 08 p1219 N85-17678
SIMM1: A linearized particle code
[AD-A148627] 08 p1221 N85-17689
Supermaneuverability
[AD-P004153] 09 p1263 N85-17938
The IMAGE 3 Conference Proceedings
[AD-A148636] 09 p1267 N85-17962
Geographic subdivision and top level data structures, Columbus, Magellan, and expanding CIG (Computer Image Generation) horizons
[AD-P004317] 09 p1268 N85-17971
CIG (Computer image generation) data bases in an instance: Bits and pieces
[AD-P004318] 09 p1269 N85-17972
The generation of three-dimensional data bases using a building block approach
[AD-P004319] 09 p1269 N85-17973
Control systems analysis program: A tool for analysis of the GE-VSCDP (General Electric-Visual System Component Display Program) image display system
[AD-P004325] 09 p1270 N85-17979
Air combat visual simulation using a head slaved projector
[AD-P004327] 09 p1270 N85-17981
The fiber-optic helmet-mounted display
[AD-P004330] 09 p1270 N85-17984
Baffled eye and confounded brain or using visual illusions to train blind pilots
[AD-P004332] 09 p1271 N85-17986
On-board Computer Image Generator (CIG) applications
[AD-P004335] 09 p1271 N85-17989
CIG (Computer Image Generator) goes to war: The tactical illusion
[AD-P004336] 09 p1271 N85-17990

AVTS (Advanced Visual Technology System): A high fidelity visual simulator
[AD-P004338] 09 p1271 N85-17992

An analytic model of gas turbine engine installations
[AD-A148708] 09 p1281 N85-18059

Study of bridgewire size and pyrotechnic density relationships on all-fire levels
[DE84-016946] 09 p1302 N85-18177

Simulation in the design of gas pressure control equipment
[ERS-E.352] 09 p1324 N85-18322

Simulation of repetitively-pulsed laser irradiation of graphite-epoxy composite
[AD-A148698] 09 p1325 N85-18329

Comparing computing formulas for estimating concentration ratios
[DE84-008644] 09 p1349 N85-18490

Identification of emerging designer needs and high payoff CAE tools
[DE85-000755] 09 p1369 N85-18599

The use of simulation for the technical and economic evaluation of flexible manufacturing systems. Part 2: Results of the simulation
[PNR-90233-PT-2] 09 p1371 N85-18614

Issues in sensitivity and statistical analysis of large-scale, computer-based models
[PB85-116317/GAR] 09 p1376 N85-18650

Calculation and computer simulation of the Paraboloidal Mirror Analyzer (PMA)
[DE85-001417] 09 p1384 N85-18705

Simulation of bent crystal spectrometers
[DE85-002042] 09 p1385 N85-18709

Computational plasma physics and supercomputers
[DE85-001739] 09 p1393 N85-18766

Computer simulation of multiple stability regions in an internally cooled superconducting conductor and of helium replenishment in a bath-cooled conductor
[DE85-002112] 09 p1399 N85-18805

Dynamic simulation of track laying vehicles
[AD-P004266] 09 p1405 N85-18842

Numerical simulations of liquid propellant combustion instability: Onset and growth
[DE85-000743] 10 p1458 N85-19186

Simulation of the performance of adaptively controlled Navstar antennas in battlefield scenarios
10 p1472 N85-19292

A shock wave capability for the improved Two-Dimensional Kinetics (TDK) computer program
[NASA-CR-171302] 10 p1483 N85-19360

Mechanical interactions of rough surfaces
[DE85-000814] 10 p1494 N85-19434

Distributing a distributed problem solving network simulator
[AD-A149065] 10 p1537 N85-19693

Microprocessor-based monitoring and control project, phase 1
[DE84-901974] 10 p1538 N85-19699

Interactive Graphics Simulator: Design, development and effectiveness/cost evaluation
[AD-A149417] 10 p1540 N85-19712

Regenerative structure of Markov chains simulated via common random numbers
[AD-A149082] 10 p1550 N85-19777

Optical implementation of the synthetic discriminant function
[AD-A148562] 10 p1557 N85-19817

Some investigations of molecular beam epitaxial growth of 3-5 semiconductor films via Monte-Carlo computer simulations, carrier tunneling and spectroscopic ellipsometry
[AD-A149465] 10 p1563 N85-19854

Application of Monte Carlo and molecular dynamics methods to the calculation of thermodynamic properties of molten salts
[AD-A148897] 10 p1565 N85-19869

Wildlife Hazards to Aircraft Conference and Training Workshop: Proceedings
[AD-A148330] 11 p1578 N85-19938

Shock propagation in the exhaust gas handling system of the proposed large altitude rocket cell: Methods and preliminary analysis
[DE85-003055] 11 p1591 N85-20010

Distribution of hydrogen in multi-layer welded joints of alloyed steels 11 p1603 N85-20079

Effect on work-hardening in dynamic deformation of beryllium
[DE85-002691] 11 p1608 N85-20111

Acta Electronica Sinica (selected articles)
[AD-A148829] 11 p1628 N85-20252

Three-dimensional analysis of heat transfer and gas flow in a radiant furnace
[DE84-011732] 11 p1633 N85-20284

Neutron streak camera electron gun design
[DE85-000620] 11 p1637 N85-20315

A computerized study of rigid cones penetrating aluminum targets
[FOA-C-20561-D4] 11 p1648 N85-20384

Simulation of brittle fracture via molecular dynamics
[DE85-001061] 11 p1653 N85-20410

Influence of the atmosphere on remotely sensed reflection from vegetation surfaces
[DE85-000658] 11 p1670 N85-20521

Performance of the SERI parallel-passage dehumidifier
[DE85-000509] 11 p1672 N85-20536

Digital and color energy maps for graphic display of hourly data
[DE85-000526] 11 p1673 N85-20543

Envelope thermal test unit: Technical description
[DE84-012254] 11 p1674 N85-20548

Continued research in mesoscale air pollution simulation modeling. Volume 5: Refinements in numerical analysis, transport, chemistry, and pollutant removal
[PB85-137362] 11 p1680 N85-20585

Evaluation of two numerical integrator schemes
[PB85-138196] 11 p1683 N85-20603

BIT/BITE tradeoff analysis model
[AD-A149345] 11 p1701 N85-20697

Advanced concepts in systems analysis and simulation
[DE85-002728] 11 p1702 N85-20701

Computerized study of several electrostatic, surface-ionization ion-source configurations
[DE85-001512] 11 p1721 N85-20823

Self-Optimized Sector (SOS) model of self-consistent energy loss and scattering for an electron beam propagating in air
[DE85-003161] 11 p1722 N85-20831

Aperture studies with PATRICIA and RACETRACK on simple attices containing SSC dipoles
[DE85-004163] 11 p1724 N85-20842

Computer simulation of grain-boundary properties in ionic crystals and metals
[DE85-000577] 11 p1734 N85-20906

Simulating supersymmetry at the SSC
[DE85-000699] 11 p1736 N85-20917

Hydrodynamic simulations of recurrent novas
11 p1753 N85-21025

Deflection model of a CT4-A undercarriage
[AD-A149778] 12 p1777 N85-21156

A safety evaluation of the relocation of the ACM (Air Combat Maneuver) panel in the F-14 ( )/AIP (Avionics Integration Program)
[AD-A149596] 12 p1777 N85-21158

Field validation of statistically-based acceptance plan for bituminous airport pavements. Volume 4: Computer simulation of multiple acceptance criteria
[FAA-PM-84-12-VOL-4] 12 p1782 N85-21183

Field validation of statistically-based acceptance plan for bituminous airport pavements. Volume 5: Summary of validation studies
[FAA-PM-84-12-VOL-5] 12 p1782 N85-21184

Impacts of Space Shuttle thermal protection system tile on F-15 aircraft vertical tile
[NASA-TM-85904] 12 p1792 N85-21245

A computer simulation of thin film nucleation and growth: The Volmer-Weber case
[NASA-TM-86968] 12 p1796 N85-21264

Near-field effects on radome boresight errors
[AD-P004356] 12 p1825 N85-21450

Nickel-cadmium battery cell reversal from resistive network effects
[AD-A149626] 12 p1834 N85-21505

Concurrent simulation techniques exploiting hierarchy
[AD-A149783] 12 p1835 N85-21512

Distributed Gunn effect devices; a numerical analysis of microstrip circuits on thin active GaAs substrates
[FOA-C-30383-E] 12 p1837 N85-21527

Computer simulation of equipment and processes involved in high-frequency heating of dielectrics
12 p1841 N85-21555

Modeling of transient heat pipe operation
[NASA-CR-175496] 12 p1844 N85-21571

Experimental test of the three subaperture method for estimating target elevation angle
[AD-A149687] 12 p1851 N85-21614

On local total strain redistribution using a simplified cyclic inelastic analysis based on an elastic solution
[NASA-TM-86913] 12 p1864 N85-21690

Computer analysis of wind turbine blade dynamic loads
[DE85-000530] 12 p1867 N85-21714

Numerical simulation of static and dynamic shadow patterns using an atomistic description of crack initiation and propagation
[DE85-003226] 12 p1867 N85-21715

A linear characteristic-nodal transport method for the two-dimensional (X,Y)-geometry multigroup discrete ordinates equations over an arbitrary triangle mesh
[LA-10092-T] 12 p1913 N85-22008

The automated reasoning system ITP
[ANL-84-27] 12 p1914 N85-22016

A user's guide to sensitivity testing on computer models at Los Alamos National Laboratory
[LA-10104-M] 12 p1914 N85-22018

SIMULA: Digital controller simulation package
[PB85-134492] 12 p1917 N85-22041

Theoretical study of collective ion acceleration in the Luce diode
[AD-A150107] 12 p1929 N85-22116

Simulation of space charge effects in particle accelerators
[DE85-001828] 12 p1929 N85-22120

Electron image simulation: A complementary processing technique
[DE85-000685] 12 p1941 N85-22190

Computational mechanics: A perspective on problems and opportunities for increasing productivity and quality of engineering
[PB85-128106] 12 p1950 N85-22252

Space shuttle pilot-induced-oscillation research testing
13 p1966 N85-22351

Dynamic wind tunnel testing for active control research 13 p1966 N85-22352

Algorithm for determining optimal three impulse point-to-orbit transfer with limited transfer time
13 p1979 N85-22419

Three-dimensional calculation of shuttle charging in polar orbit 13 p1992 N85-22486

Self-consistent simulation of plasma interactions with secondary-emitting insulators 13 p1993 N85-22492

NASCAP simulation of PIX 2 experiments
13 p1993 N85-22497

Development of a three-phrase combustion code for modeling liquid rocket engines 13 p2003 N85-22554

Method for prompt modeling of quasiperiodic movement of solid near-axisymmetrical body in atmosphere
13 p2043 N85-22790

Research efforts in support of resonance extraction studies. Volume 1: Improvement and validation of TWFD (Thin-Wire Frequency-Domain): A thin-wire frequency-domain scattering code
[AD-A150296] 13 p2054 N85-22864

Advanced mixed-mode simulation techniques
13 p2062 N85-22883

Investigations of the high frequency performance of impact avalanche transit-time diodes
13 p2063 N85-22884

Numerical simulation of inverters with I2L elements including effects of high doping level
13 p2088 N85-23039

T700 cutter life improvement program
[AD-A150450] 13 p2099 N85-23069

Effects of assuming independent component failure times, if they are actually dependent, in a series system
[AD-A150582] 13 p2101 N85-23092

Structural design of the Sandia 34-M Vertical Axis Wind Turbine
[DE85-002631] 13 p2129 N85-23247

ROSA: A computer model for optical power ratio calculations
[DE85-005174] 13 p2129 N85-23251

Molten carbonate fuel cell performance model update, draft
[DE85-005423] 13 p2129 N85-23252

ROSS: An object-oriented language for constructing simulations
[AD-A150556] 13 p2147 N85-23330

SIGPI: A user's manual for the fast computation of the probabilistic performance of a complex system
[DE85-005447] 13 p2148 N85-23336

Regenerative simulation of non-Markovian stochastic systems
[AD-A150344] 13 p2153 N85-23367

Accumulation of the terrestrial planets
13 p2179 N85-23524

A parmetric study of crater-saturation simulation
13 p2182 N85-23540

Load capacity of cages of roller bearings for planet wheels 14 p2221 N85-23775

Shuttle attached antenna Flight Experiment Definition Study (FEDS) 14 p2237 N85-23865

Diesel combustion: Advances in analysis and simulation 14 p2253 N85-23965

Computer simulations of rare earth sites in glass: Experimental tests and applications to laser materials
[DE85-006156] 14 p2261 N85-24013

Multidimensional digital signal processing
[AD-A150833] 14 p2292 N85-24209

Ground-up-to-Space (GUTS) laser propagation code description and manual
[AD-A150783] 14 p2309 N85-24295

Modelling of photodegradation in solar cell modules of substrate and superstrate design made with ethylene-vinyl acetate as pottant material
[NASA-CR-175690] 14 p2350 N85-24527

Theory and computer simulation of auroral kilometric radiation 14 p2365 N85-24617

Characteristics and behavior of atmospheric aerosols; application to prediction of infrared extinction
[AD-A150691] 14 p2372 N85-24665

GRAFIT language for simulating two-dimensional geometric entities and sketches
14 p2401 N85-24801

A numerical simulation of the formation of solar prominences 14 p2448 N85-25112

Automatic Dynamic Aircraft Modeler (ADAM), volume 1
[AD-A151410] 15 p2471 N85-25252

A user's manual for AMEER flight path trajectory simulation code
[DE85-006580] 15 p2472 N85-25260

Shuttle fleet operations: A simulation analysis
[AD-A151383] 15 p2491 N85-25370

The investigation of tethered satellite system dynamics
[NASA-CR-171433] 15 p2492 N85-25375

Analysis of space station operations in the space debris environment
[AD-A151872] 15 p2493 N85-25380

Numerical experiments on flexible spacecraft with the aid of the Dynamic Control and Analysis Package (DCAP)
[ESA-STM-229] 15 p2493 N85-25382

The effects of atmospheric turbulence on an air-to-air optical communication link
[AD-A151840] 15 p2543 N85-25700

CSMP (Continuous System Modeling Program) modeling of brushless DC motors
[AD-A152043] 15 p2549 N85-25731

Development of simulation procedures for VLSI systems (timing simulation)
[BMFT-FB-T-84-297] 15 p2550 N85-25743

Modeling and optimization of a multiple-cell photovoltaic converter system 15 p2585 N85-25934

Impact of soil moisture in organizing a severe storm outbreak 15 p2597 N85-26009

General meteorological package (GEMPAK)
15 p2599 N85-26019

Computer simulation studies in fluid and calcium regulation and orthostatic intolerance
[NASA-CR-171669] 15 p2616 N85-26117

Analysis of head-down tilt as an analog of weightlessness using a mathematical simulation model
[NASA-CR-171670] 15 p2616 N85-26118

Simulation of a G-tolerance curve using the pulsatile cardiovascular model
[NASA-CR-171673] 15 p2616 N85-26120

Mathematical models relating to human thermoregulation: Basic assumptions, validation, and application. Parts A and B
[AD-A151556] 15 p2618 N85-26130

Research in the design of high-performance reconfigurable systems
[NASA-CR-175705] 15 p2621 N85-26153

Development of a user support package for CPESIM 2 (a computer simulation for CPE (Computer Performance Evaluation) use
[AD-A151699] 15 p2624 N85-26170

CAD/CAM (Computer-Aided Design/Computer-Aided Manufacturing) highlights
[AD-A151532] 15 p2629 N85-26201

Catalog of the National Energy Software Center
[TI85-900521] 15 p2630 N85-26209

Backbone network simulations: A comparative study
[DE85-006874] 15 p2632 N85-26224

The modeling and simulation of feedback control systems
[NASA-CR-171675] 15 p2632 N85-26225

High current beam hollowing instability study
[AD-A151301] 15 p2648 N85-26329

Low-resolution target classification from a staring infrared sensor
[AD-A151690] 15 p2652 N85-26358

Lattice overview
[DE85-007282] 15 p2662 N85-26427

The formation of the terrestrial planets from lunar sized planetesimals 15 p2678 N85-26533

Galileo 15 p2688 N85-26601

Numerical simulation of inviscid compressible flow through three-dimensional cascade
16 p2692 N85-26619

Numerical simulation of transonic flutter of a high-aspect ratio transport wing 16 p2694 N85-26630

Graphic simulation of a machine-repairman model
[AD-A151761] 16 p2694 N85-26633

Simulation: A tool for cost-effective systems design and live test reduction 16 p2698 N85-26657

Generalized escape system simulation: Its purpose, recent modifications and potential
[DE85-005571] 16 p2703 N85-26689

Study of the primary zone of gas turbine hearths
[ONERA-RTS-22/3256-EY] 16 p2709 N85-26719

The effect of load factor on aircraft handling qualities
[AD-A152118] 16 p2710 N85-26724

Probabilistic computer model of optimal runway turnoffs
[NASA-CR-172549] 16 p2715 N85-26760

A SLAM II simulation model for analyzing space station mission processing requirements
[NASA-CR-175664] 16 p2731 N85-26853

Ignition/combustion processes
16 p2740 N85-26909

Liquid rocket combustor computer code development
16 p2740 N85-26910

Laser Schlieren and ultraviolet diagnostics of rocket combustion 16 p2740 N85-26911

Influence of behavior laws in the explosive deformation of metal plates
[ISL-R-122/83] 16 p2760 N85-27032

Automated CPX support system preliminary design phase
[NASA-CR-175784] 16 p2769 N85-27091

A software simulation study of a sequential decoder using the Fano algorithm 16 p2771 N85-27100

An empirical self-protection chaff model
[AD-A151928] 16 p2773 N85-27115

Radiation and scattering of spiral antennas
[AD-A151829] 16 p2773 N85-27116

Pulsewidth modulated speed control of brushless dc motors
[AD-A151966] 16 p2778 N85-27148

Electrical resistivity in amorphous metals: Consequences of phonon ineffectiveness in the diffraction model
[AD-A152130] 16 p2779 N85-27150

Computer modeling of vibrational energy levels of potential laser candidates (diatomic molecules)
[AD-A151765] 16 p2790 N85-27209

A general simulation program for robot manipulator arm dynamics
[AD-A152121] 16 p2793 N85-27230

Numerical resolution calculation for elastic-plastic impact problems
[AD-A152292] 16 p2801 N85-27270

Hopkinson bar simulation using DYNA2D
[DE85-006766] 16 p2802 N85-27275

Diagnostic system
[INPE-3350-PRE/659] 16 p2841 N85-27519

A multipole model of the observed cerebral cortex magnetic field
[AD-A152237] 16 p2842 N85-27526

Parallel time 0(log N) acceptance of deterministic CFLs
[AD-A152255] 16 p2845 N85-27539

An interactive computer package for use with simulation models which performs multidimensional sensitivity analysis by employing the techniques of response surface methodology
[AD-A151956] 16 p2846 N85-27548

Development of graphical pole-zero, root-locus, Bode, Nyquist, and Nichols responses using the OPTSYSX program
[AD-A152146] 16 p2847 N85-27555

Kinematic rate control of simulated robot hand at or near wrist singularity
[NASA-TP-2440] 16 p2851 N85-27575

The NAVTAG (Naval Tactical Game) system and its modification to include the SH-60B helicopter
[AD-A152004] 16 p2858 N85-27624

LIGHT: A ray tracing code to simulate light collection in scintillation spectrometers and light pipes
[DE85-007213] 16 p2865 N85-27673

Optimizing computational efficiency and user convenience in plasma simulation codes
[DE85-007661] 16 p2866 N85-27682

Fundamentals of plasma simulation
[DE85-007699] 16 p2867 N85-27683

Tokamak systems code
[DE85-008147] 16 p2869 N85-27696

Electronic density of states for the double donor system Si:P, As
[INPE-3447-PRE/700] 16 p2869 N85-27700

Addition of flexible body option to the TOLA computer program. Part 2: User and programmer documentation
[NASA-CR-132732-2] 17 p2896 N85-27856

OLGA: An open loop gust alleviation system
17 p2903 N85-27897

Simulation of multistage turbine flows
17 p2911 N85-27945

Calculation of viscous compressible flows in small gas turbines 17 p2912 N85-27950

Stressed-strained state of tightening buckles in sectional runners of gas turbines 17 p2940 N85-28149

Performance evaluation of fiber-optic converters
17 p2941 N85-28154

A software simulation study of a (255,223) Reed-Solomon encoder-decoder
[NASA-CR-175672] 17 p2947 N85-28182

Analysis and modeling for thermal focal plane arrays
[AD-A153156] 17 p2966 N85-28328

System analysis of a field Army Topographic Support System
[AD-A153318] 17 p2984 N85-28439

Comparison of measurement and simulation results of radiation temperatures applied to the thermal mapping of Munich
[DFVLR-FB-85-06] 17 p2984 N85-28442

Simplified analysis of Stirling engines and heat pumps
[DE85-008753] 17 p2986 N85-28457

Comprehensive silicon solar cell computer modeling
[NASA-CR-175959] 17 p2987 N85-28461

Performance of an active/passive hybrid solar system utilizing vapor transport
[DE85-008627] 17 p2988 N85-28468

A crustal section for the Arabian Shield and adjacent Red Sea margin derived from first-arrival data
17 p2990 N85-28480

A seismic refraction profile across the Arabian Shield
17 p2990 N85-28481

Technical evaluation of the Naval Automated Pilot Aptitude Measurement System (NAPAMS)
[AD-A152361] 17 p3000 N85-28547

Computer program for prediction of capture maneuver probability for an on-off reaction controlled upper stage
[NASA-CR-165937] 17 p3010 N85-28611

Manufacturing information system
[AD-A152715] 17 p3011 N85-28618

VULTURE manual
[DE85-008873] 17 p3013 N85-28631

Adding computationally efficient realism to Monte Carlo turbulence simulation
[NASA-TP-2469] 17 p3025 N85-28708

Operations research
[B8561897] 17 p3026 N85-28712

Theoretical studies of heavy ion scattering processes
[DE85-008823] 17 p3032 N85-28753

Multiple time-scale methods in particle simulations of plasmas
[DE85-007519] 17 p3040 N85-28808

Experimental and theoretical determination of the wing-induced lateral wind on the tail surfaces in oscillating rolling motion. Part 2: Theoretical investigations for calculation of the lateral wind
[IFD-1/84-PT-2] 18 p3061 N85-28940

DEAN: A program for dynamic engine analysis
[NASA-TM-87033] 18 p3062 N85-28945

Compressor and turbine models - numerical stability and other aspects
[AD-A153811] 18 p3063 N85-28948

Piloted simulation of an algorithm for onboard control of time-optimal intercept
[NASA-TP-2445] 18 p3063 N85-28949

An approach to digital level compression using the zero-crossing points of programme signals
[NHK-LABS-NOTE-308] 18 p3090 N85-29123

A simulation study of jammer nulling trade-offs in a reactively steered adaptive array
[AD-A153461] 18 p3090 N85-29124

Electrical line source and point source interactions with anomalies in the ground
[DE85-009777] 18 p3095 N85-29161

Visual simulation of radiographs
[DE85-010213] 18 p3110 N85-29255

KIVA: A comprehensive model for 2D and 3D engine simulations
[DE85-005562] 18 p3118 N85-29298

Establishment of a methodology for predicting lifetimes in active solar systems
[DE85-008629] 18 p3130 N85-29383

F-cell: The Aspen fuel cell model
[DE85-001975] 18 p3131 N85-29393

Materials research for passive solar systems: Solid-state phase-change materials
[DE85-008779] 18 p3132 N85-29396

On the improvement of satellite temperature retrievals by means of boundary layer models
18 p3140 N85-29443

Transient eddies in the UCLA GCM
18 p3145 N85-29470

Analysis of a simulated cloud climatology
18 p3145 N85-29472

An operational analysis of system calibration
[AD-A153556] 18 p3170 N85-29644

Fast electromagnetic (EM) shower simulation
[NOTA-INTERNA-631] 18 p3175 N85-29683

An experimental study of the pressure in a fast bottom beneath the apex of an overlying fluid wedge
[AD-A153618] 18 p3177 N85-29696

Calculations of beam dynamics in Sandia linear electron accelerators, 1984
[DE85-010417] 18 p3180 N85-29719

Circulation control propellers for general aviation, including a BASIC computer program
[NASA-CR-165968] 19 p3219 N85-29959

Computer simulation of the effects of a distributed array antenna on synthetic aperture radar images
[NASA-CR-171888] 19 p3254 N85-30176

Approaches to digital image registration and recognition 19 p3257 N85-30197

Dynamic simulation of dispersed, grid-connected photovoltaic power systems: System studies
[DE85-011179] 19 p3262 N85-30231

An investigation of hydraulic transients in combination free surface and pressurized flows
19 p3264 N85-30239

Seismic analysis of liquid-filled tanks with an eccentric core barrel
[DE85-010249] 19 p3269 N85-30272

Modeling and analysis of pinhole occulter experiment: Initial study phase
[NASA-CR-175976] 19 p3272 N85-30287

Flood-runoff forecasting with HEC1F
[AD-A154286] 19 p3300 N85-30456

Modeling water resources systems for water quality
[AD-A154288] 19 p3300 N85-30457

A multiphase continuum model to describe dynamic loading effects in nonlinear porous media
[DE85-010102] 19 p3301 N85-30463

Reference data source documentation for performance assessment studies, Basalt Waste Isolation Project, Hanford Site, Washington
[DE85-010543] 19 p3301 N85-30468

Using PVFORM, a systems performance model, to determine optimum mounting configurations for flat-plate photovoltaic modules
[DE85-011191] 19 p3306 N85-30495

F-CAP documentation
[DE85-003369] 19 p3307 N85-30503

Qualitative and quantitative examination of the performance of regional air quality models representing different modeling approaches
[DE85-010506] 19 p3310 N85-30518

Synthetic rainfall and its use in hydrologic modeling
19 p3314 N85-30542

Arctic acoustic tomography MIZEX 84
[AD-A154426] 19 p3320 N85-30580

Activities of the Institute for Computer Applications in Science and Engineering (ICASE)
[NASA-CR-172610] 19 p3332 N85-30641

CAE tool catalog
[DE85-011290] 19 p3334 N85-30657

Preliminary documentation for the polar code
[AD-A154125] 19 p3336 N85-30667

Computer Performance Modeling Tool (CPMT)
[AD-A154438] 19 p3338 N85-30682

Circular-beam ray tracing on a microcomputer
[DE85-010754] 19 p3338 N85-30685

SABRINA: An interactive solid geometry modeling program for Monte Carlo
[DE85-010796] 19 p3339 N85-30692

A Lotus 1-2-3 based system reliability program
[DE85-010533] 19 p3340 N85-30701

LINE: A code which simulates spectral line shapes for fusion reaction products generated by various speed distributions
[DE85-010833] 19 p3341 N85-30702

Development and evaluation of a Fault-Tolerant Multiprocessor (FTMP) computer. Volume 3: FTMP test and evaluation
[NASA-CR-166073] 19 p3341 N85-30707

Expanding expertise by use of an expert system
[DE85-010759] 19 p3344 N85-30723

Comparison of simulation with experiment in an RFQ
[DE85-010770] 19 p3349 N85-30757

Comparison of 8 to 12 micrometer and 3 to 5 micrometer CVF transmissometer data with LOWTRAN calculations
[AD-A154218] 19 p3350 N85-30763

Moments in particle-in-cell simulations
[DE85-010792] 19 p3356 N85-30803

A model for the economic assessment of solar power plants
[DE85-009355] 19 p3381 N85-30977

Description and operation of CHISQMO, INVRTS, VOIGEN, VOIGTV, SMEAR, RUFF, AND POSCAR in the Stokes Analysis Program
[PB85-180628] 19 p3384 N85-30991

Numerical simulation of potential flow in transonic steady regimes 20 p3369 N85-31016

Analysis of rotorcraft crash dynamics for development of improved crashworthiness design criteria
[FAA-CT-85-11] 20 p3391 N85-31031

Definition and layout of a traffic generator for an air traffic control simulation
[ESA-TT-888] 20 p3391 N85-31034

Search and rescue satellite (SARSAT) error analysis of the 406 MHz system 20 p3403 N85-31118

Docking simulation analysis of range data requirements for the orbital maneuvering vehicle
[NASA-TM-86510] 20 p3407 N85-31143

Large space structure flight experiment
20 p3410 N85-31163

A structural dynamics approach to the simulation of spacecraft control/structure interaction
20 p3412 N85-31173

Solid state altimeter model: Simulation description; analysis of first results (narrow band filters, weighting) — satellite-borne instruments
[CNES-DRT/TIT/RL-160-T] 20 p3419 N85-31220

Comparison of ERS-1 scatterometer Monte Carlo performance simulations using a weighted nonlinear least squares and a maximum likelihood estimation method
20 p3420 N85-31224

Flow modeling at the base region of missiles
[SNIAS-851-320-101] 20 p3420 N85-31226

The use of moments of momentum to account for crystal habits
[NASA-CR-3907] 20 p3421 N85-31232

Fundamental algorithms of the Goddard battery model
20 p3445 N85-31389

Nickel-cadmium battery cell reversal from resistive network effects 20 p3446 N85-31392

High Re separated flow solutions using the Navier-Stokes and approximate equations
[AD-A152252] 20 p3454 N85-31451

Environmental airblast around large shock tubes
[DE85-010654] 20 p3463 N85-31512

Investigation of dynamic noise affecting geodynamics information in a tethered subsatellite
[NASA-CR-176031] 20 p3476 N85-31602

Comparative study of fracture planes computed from topography and lineaments from imagery with structures and mineralization in the magnetic belt of Washington State
[DE85-010972] 20 p3477 N85-31608

Application of closed-form solutions to a mesh point field in silicon solar cells 20 p3482 N85-31637

Phenomena simulation for heavy doping and surface recombination velocity 20 p3482 N85-31638

Design and fabrication of durable owner-built wind turbine blades
[DE85-009200] 20 p3484 N85-31650

Results of computer calculations for a simulated distribution of kidney cells 20 p3502 N85-31771

A systems analysis of the erythropoietic responses to weightlessness. Volume 2: Description of the model of erythropoiesis regulation. Part A: Model for regulation of erythropoiesis. Part B: Detailed description of the model for regulation of erythropoiesis
[NASA-CR-171891] 20 p3506 N85-31795

An integrated analysis of the physiological effects of space flight: Executive summary
[NASA-CR-171892] 20 p3506 N85-31796

Learning and self adaptation applied to the simulation of a human pilot
[ONERA-RT-24/5122-SY] 20 p3511 N85-31826

SCAP: A Shaped Charge Analysis Program. User's manual for SCAP 1.0
[DE85-011182] 20 p3515 N85-31854

Model documentation of the gas analysis modeling system. Volume 1: Model overview
[DE85-010952] 20 p3515 N85-31856

MIG: MCNP Input Generator for EFFI magnet geometrics
[DE85-010494] 20 p3515 N85-31857

Monte Carlo: In the beginning and some great expectations
[DE85-010789] 20 p3518 N85-31872

FAUST: Introduction and overview — self tuning control
[OUEL-1568/85] 20 p3519 N85-31882

Methods of Monte Carlo electron transport in particle-in-cell codes
[DE85-010702] 20 p3521 N85-31896

Simulation studies of time-control procedures for the advanced air traffic control system
[NASA-TP-2493] 21 p3553 N85-32101

Development and validation of a general purpose linearization program for rigid aircraft models
[NASA-TM-86737] 21 p3556 N85-32122

Numerical modeling of subsurface communication
[DE85-012818] 21 p3577 N85-32249

Parallel simulation of digital LSI circuits
[AD-A154745] 21 p3580 N85-32256

BLAF: A blast field reconstruction program from pressure histories
[AD-A155300] 21 p3585 N85-32263

Characteristics of a numerical fluid dynamics simulator
[DE85-009602] 21 p3586 N85-32290

An investigation into the comparisons of the underwater shock effects on a stiffened flat plate to the predictive nature of a computer model
[AD-A155612] 21 p3600 N85-32355

Micromolecular modeling 21 p3608 N85-32405

Comprehensive silicon solar-cell computer modeling
21 p3609 N85-32421

Emergency modeling of hazardous air pollutants
[AD-A155441] 21 p3614 N85-32461

Simulation of complex three-dimensional flows
[NASA-TM-86773] 21 p3675 N85-32831

SHELTER: Description of a program code — indoor climate
[FOA-C-58002-H1] 22 p3755 N85-33276

Modeling of electronic circuits with high degree of component integration 22 p3766 N85-33343

Adaptive modeling of electronic circuits
22 p3766 N85-33345

Computer simulation of integrated injection logic
22 p3767 N85-33349

Numerical simulation of nonisothermal transient processes in GaAs diode structures
22 p3767 N85-33350

Determination of sensitivity functions for discrete dynamic systems from results of function modeling on digital computer 22 p3769 N85-33359

Analysis of crosstalk in nonhomogeneous multiconductor lines 22 p3769 N85-33360

Calculation of external magnetic field of a shielded transformer 22 p3771 N85-33373

Computer and water-model simulation of flow through poppet valves
[CFD/85/2] 22 p3785 N85-33449

Lasertron simulation with a two-gap output cavity
[DE85-011213] 22 p3790 N85-33480

Development of a chemical kinetic mechanism for the US EPA (Environmental Protection Agency) regional oxidant model
[PB85-185858] 22 p3813 N85-33618

Surface wave modes of a multilayered medium backed by a perfectly conducting ground plane: Computation of propagation constants
[DE85-011454] 22 p3829 N85-33715

Determination of DTL configurations
[DE85-010714] 22 p3830 N85-33719

PMEXA: Diagnostic filtering program for the PBFA-1 performance monitoring and evaluation system
[DE85-013179] 22 p3831 N85-33725

Numerical simulation of interior and terminal ballistics phenomena. Investigation of the effects of the parameters and application examples
[ISL-R-112/84] 22 p3831 N85-33731

Some ideas for decomposing the domain of elliptic partial differential equations in the Schwarz process
[DE85-011844] 22 p3834 N85-33739

Presentation of numerical simulation work in terminal ballistics using a few examples. Applications of the calculation model Program for Elastoplastic Simulation of Impacts (PEPSI) of the Franco-German Research Institute Saint Louis (ISL)
[ISL-CO-209/84] 22 p3834 N85-33741

Transverse emittance of a 2.0-MeV RFQ beam with high brightness
[DE85-012718] 22 p3837 N85-33758

Long term variability of the cosmic ray intensity
[OG-3.1-11] 22 p3874 N85-33999

Transient two-dimensional simulation of SEU in a CMOS SRAM cell
[DE85-008419] 22 p3890 N85-34111

Time-resolved spectroscopic studies of detonating heterogeneous explosives
[DE85-009760] 23 p3921 N85-34297

Method and apparatus for transfer function simulator for testing complex systems
[NASA-CASE-NPO-15696-1] 23 p3926 N85-34333

Compressible two-phase flow instabilities simulated with a hybrid Lagrange-Euler pseudospectral method
[DE85-009904] 23 p3931 N85-34361

The impact of supercomputers on experimentation: A view from a national laboratory
[NASA-TM-86822] 23 p3955 N85-34510

System maintenance manual for master modeling of aerodynamic surfaces by three-dimensional explicit representation
[NASA-CR-178224] 23 p3956 N85-34517

Frame buffer algorithms for stochastic models
23 p3957 N85-34525

Specifying stochastic objects in a hierarchical graphics system 23 p3957 N85-34526

Interfacing interactive circuit simulation with standard graphics facilities 23 p3958 N85-34529

A computerized system for spot detection and analysis of two-dimensional electrophoresis images
23 p3958 N85-34531

Animengine: An engineering animation system
23 p3959 N85-34535

3D computer animation: More an evolution problem than a motion problem 23 p3959 N85-34536

Using dynamic analysis to animate articulated bodies such as humans and robots 23 p3959 N85-34537

Towards an integrated view of 3-D computer character animation 23 p3959 N85-34538

The CADME approach to the interface of solid modellers 23 p3961 N85-34554

An innovative user interface for microcomputer-based computer-aided design 23 p3961 N85-34555

Analysis of transient radiation upset in a 16K SRAM
[DE85-009442] 23 p3965 N85-34586

Circuit approaches to increasing SRAM performance in total dose environments
[DE85-009441] 23 p3966 N85-34588

Workshop report on Simulation Techniques for Shock Wave Phenomena and Characteristics of Plasmas in Inertial Confinement Fusion
[IPPJ-725] 23 p3979 N85-34670

Vector calculation of particle code
23 p3981 N85-34688

Data on the backscattering coefficients on light ions from solids: A revision
[IPPJ-AM-41-REV] 23 p3982 N85-34689

Perspective on the next ten years in plasma physics
[DE85-011849] 23 p3984 N85-34706

Acceleration of ions and electrons to near-cosmic ray energies in a perpendicular shock: The January 6, 1978 event
[SH-1.5-4] 23 p3996 N85-34773

Particle acceleration due to shocks in the interplanetary field: High time resolution data and simulation results
[SH-1.5-5] 23 p3996 N85-34774

Energy management of three-dimensional minimum-time intercept
[NASA-CR-176174] 24 p4064 N85-35186

The investigation of tethered satellite system dynamics
[NASA-CR-176180] 24 p4069 N85-35215

Actuator rigging test set electromagnetic interference test (CE03)
[AD-A155819] 24 p4086 N85-35327

Investment justification of robotic technology in aerospace manufacturing. User's manual
[AD-A156193] 24 p4099 N85-35410

Expert systems research in regional resource evaluation: Experiences in the application of microcomputer technologies 24 p4105 N85-35450

The NORDA/FNOC (Naval Ocean Research and Development Activity's/Fleet Numerical Oceanography Center) Polar Ice Prediction System (PIPS)-Arctic: A technical description
[AD-A156332] 24 p4126 N85-35577

Enhancement of the flexible spacecraft dynamics program for open spacecraft
[NASA-CR-175309] 24 p4137 N85-35641

Benchmark evaluation of PC simscript
[AD-A156133] 24 p4138 N85-35651

Computational methods for the explosive and impact compaction of powders
[AD-A156219] 24 p4139 N85-35653

SASSYS-1 computer code verification with EBR-2 test data
[DE85-012119] 24 p4139 N85-35657

RFQ modeling computer program
[DE85-012665] 24 p4140 N85-35661

TOSCA calculations and measurements for the SLAC SLC damping ring dipole magnet
[DE85-014366] 24 p4160 N85-35793

Investigations of the molecular beam epitaxial growth and characteristics of external excitation induced non-equilibrium phases of immiscible 3-5 compound semiconductors
[AD-A156325] 24 p4162 N85-35804

Simulation of lattice damage due to dynamic loading
[DE85-006468] 24 p4162 N85-35808

Network management simulation of automated guideway transit systems under vehicle-follower control
[PB85-188233] 24 p4166 N85-35830

Preliminary results on underground muon bundles observed in the Frejus proton-decay detector
[HE-5.1-1] 24 p4200 N85-36067

A transient digitiser for fast air shower events
[HE-5.2-21] 24 p4204 N85-36097

COMPUTERS
NT AIRBORNE/SPACEBORNE COMPUTERS
NT ANALOG COMPUTERS
NT CDC COMPUTERS
NT CDC CYBER 170 SERIES COMPUTERS
NT CDC CYBER 205 COMPUTER
NT DIGITAL COMPUTERS
NT EMBEDDED COMPUTER SYSTEMS
NT HEWLETT-PACKARD COMPUTERS
NT HYBRID COMPUTERS
NT IBM COMPUTERS
NT MICROCOMPUTERS
NT MINICOMPUTERS
NT OPTICAL COMPUTERS
NT PARALLEL COMPUTERS
NT PDP 11 COMPUTER
NT PDP 11/70 COMPUTER
NT PERSONAL COMPUTERS
NT SEQUENTIAL COMPUTERS
NT UNIVAC COMPUTERS
NT UNIVAC 1100 SERIES COMPUTERS
NT VAX COMPUTERS
NT VAX-11 SERIES COMPUTERS
NT VAX-11/780 COMPUTER

Storage in the LLNL Octopus network: An overview and reflections
[DE84-014711] 01 p0106 N85-10712

Diagnosis via causal reasoning: Paths of interaction and the locality principle
[AD-P003920] 02 p0245 N85-11600

Technological institute director views artificial intelligence 03 p0341 N85-12197

A research program in computer technology
[AD-A145776] 03 p0402 N85-12565

Research activities of the Illinois University Coordinated Science Laboratory
[AD-A145589] 03 p0449 N85-12856

Computer Literacy Act of 1983, part 2
[H-REPT-98-752-PT-2] 04 p0578 N85-13687

USSR report: Electronics and electrical engineering
[JPRS-UEE-84-011] 06 p0789 N85-15042

FCC (Federal Communication Commission) methods of measurement of radio noise emissions from computing devices
[PB84-243591] 06 p0849 N85-15387

A summary of the foundation research program
[AD-A146524] 06 p0891 N85-15656

West Europe report: Science and technology
[JPRS-WST-84-039] 07 p0936 N85-15929

Eyes for computers 07 p1012 N85-16428

Computer science research in Europe
[AD-A146905] 07 p1022 N85-16482

Research and technology, 1984 report
[NASA-TM-83096] 07 p1061 N85-16730

Hardware/software codesign for maintainable systems
08 p1066 N85-16753

East Europe report: Science and technology
[JPRS-ESA-84-047] 08 p1140 N85-17183

ES devices at fair 08 p1141 N85-17187

MOM peripherals 08 p1141 N85-17189

West Europe report: Science and technology
[JPRS-WST-85-001] 08 p1141 N85-17190

Performance management system enhancement and maintenance
[NASA-CR-175271] 08 p1202 N85-17564

On the validation of computer science theories
[AD-A148637] 08 p1203 N85-17572

Technology development for unmanned untethered submersible vehicle systems
[AD-A148794] 09 p1304 N85-18190

East Europe report: Science and technology
[JPRS-ESA-85-005] 09 p1377 N85-18659

Computer equipment at 1984 Leipzig Spring Fair
09 p1378 N85-18662

West Europe report: Science and technology
[JPRS-WST-85-004] 10 p1460 N85-19204

Computers and education
[GPO-28-378] 10 p1537 N85-19689

Computer crime
[GPO-30-544] 10 p1537 N85-19691

Computer center CDC libraries
[AD-A149005] 10 p1540 N85-19707

China report: Science and technology
[JPRS-CST-84-025] 11 p1620 N85-20197

Development of computer centers, equipment described: Problems of computer centers
11 p1700 N85-20686

Long-range electronics program outlined
11 p1700 N85-20687

USSR report: Electronics and electrical engineering
[JPRS-UEE-85-004] 12 p1837 N85-21531

Cumulative reports and publications through December 31, 1984
[NASA-CR-172569] 12 p1911 N85-21991

Computing Division two-year operational plan, FY 1984 - 1985
[LA-9978-MS] 12 p1913 N85-22006

Oversight review of the five-year outlook report on science and technology
[GPO-41-058] 12 p1949 N85-22243

Research and Modeling of Supervisory Control Behavior, report of a workshop
[AD-A149621] 12 p1950 N85-22246

Liquid mass flow rate computer
13 p2075 N85-22962

China report: Science and technology
[JPRS-CST-85-003] 13 p2166 N85-23433

West Europe report: Science and technology
[JPRS-WST-85-013] 14 p2289 N85-24183

The Effect of Computers on the Generation and Use of Technical Data
[NBSIR-84-2907] 14 p2400 N85-24792

Integration of an Apple 2 Plus computer into an existing dual axis sun tracker system
[AD-A150778] 14 p2404 N85-24823

Gordon Conference on Fundamentals of Cybernetics
[AD-A151074] 14 p2408 N85-24842

Our future in the cosmos: Computers
14 p2432 N85-24997

Computer controlled acquistion of corrosion rate data from multiple sensors
[PB85-157378] 15 p2524 N85-25559

East Europe report: Science and technology
[JPRS-ESA-84-016] 15 p2533 N85-25624

West Europe report: Science and technology
[JPRS-WST-84-009] 15 p2535 N85-25639

West Europe report: Science and technology
[JPRS-WST-84-014] 15 p2536 N85-25647

China report: Science and technology
[JPRS-CST-85-013] 15 p2536 N85-25652

Microcomputer controlled image acquisition system
15 p2537 N85-25654

China report: Science and technology
[JPRS-CST-85-011] 15 p2551 N85-25748

Computerized biophysical data acquisition system for motion sickness studies
[AD-A151691] 15 p2618 N85-26131

Future directions in computers
15 p2626 N85-26183

Computers and the consulting engineer
15 p2626 N85-26184

Physics, Computer Science and Mathematics Div.
[DE85-006868] 15 p2642 N85-26298

Computer software for aerodynamic design of aircraft developed within the National Aerospace Laboratory
16 p2691 N85-26613

Design of computer-related workstations in relation to job functions and productivity
[AD-A151938] 16 p2844 N85-27534

Squeezing the most out of Eigenvalue solvers on high-performance computers
[DE85-007569] 16 p2849 N85-27565

East Europe report: Science and technology
[JPRS-ESA-85-017] 17 p2945 N85-28177

The touch panel system: Design and development
[AD-A153014] 17 p3008 N85-28596

Efforts at office automation and information systems utilization at Martin Marietta Energy Systems, Incorporated
[DE85-008154] 17 p3013 N85-28633

Synchronization and fault-masking in redundant real-time systems
[NASA-TM-87478] 17 p3015 N85-28644

European Science Notes, Volume 39, Number 3
[AD-A152446] 17 p3027 N85-28717

Computing in the Soviet general economy: An introductory overview
[AD-P004563] 17 p3047 N85-28858

A study of user-defined searching requirements for the on-line version of the directory of DOD-sponsored R and D data bases on the Defense Gateway computer system
[AD-A153000] 17 p3050 N85-28878

West Europe report: Science and technology
[JPRS-WST-84-031] 18 p3086 N85-29089

France's use of Cray 1, plans for national supercomputer 18 p3086 N85-29093

West Europe report: Science and technology
[JPRS-WST-84-035] 18 p3087 N85-29102

West Europe report: Science and technology
[JPRS-WST-84-037] 18 p3088 N85-29108

Coping with computer terminology
[DE85-006076] 18 p3161 N85-29579

Projects of the Computer Center of the academy's Siberian branch 19 p3295 N85-30425

A parallelized point successive over-relaxation method on a multiple instruction multiple data stream computer
[AD-A154377] 19 p3337 N85-30678

High accuracy digital acousto-optic matrix computer
[AD-D011692] 19 p3343 N85-30718

Simulation and operation of the EBR-2 automatic control rod drive system
[DE85-010262] 19 p3360 N85-30832

Proust radar: Decoding hardware and coherent integration, part 7.2A 21 p3625 N85-32524

East Europe report: Science and technology. Selections on CSSR computer technology
[JPRS-ESA-84-017] 21 p3658 N85-32781

Machine intelligence for robotics applications
[DE85-011430] 22 p3793 N85-33503

Computer science: Key to a space program renaissance. The 1981 NASA/ASEE summer study on the use of computer science and technology in NASA. Volume 2: Appendices
[NASA-CR-175295] 22 p3827 N85-33702

Integration of office automation within computing
[DE85-010021] 22 p3833 N85-33736

Issues and techniques in touch-sensitive tablet input (executive summary) 23 p3960 N85-34543

Ranging system which compares an object reflected component of a light beam to a reference component of the light beam
[NASA-CASE-NPO-15665-1] 23 p3973 N85-34629

CONCATENATED CODES
Reed-Solomon code synchronization revisited
10 p1484 N85-19234
A concatenated coding scheme for error control
[NASA-CR-175504] 12 p1912 N85-22001
A concatenated coding scheme for error control
[NASA-CR-176006] 19 p3334 N85-30655

CONCAVITY
Equivocation limits in Gaussian additive channels
[INPE-2828-PRE/380] 04 p0492 N85-13137
Measurement of the configuration of a concave surface by the interference of reflected light
[NASA-TM-77796] 11 p1728 N85-20867

CONCENTRATION
Measuring methods of atmospheric electric elements at the Earth's surface during snowfall and investigation of these relationships 15 p2581 N85-25920

CONCENTRATION (COMPOSITION)
NT ATMOSPHERIC MOISTURE
NT ATOM CONCENTRATION
NT CARBON DIOXIDE CONCENTRATION
NT LOW CONCENTRATIONS
NT MASCONS
NT MOISTURE CONTENT
Factor analysis applied to a silane coupling agent on E-glass fiber system
[AD-A145687] 02 p0187 N85-11249
Evaluation of an aerosol prediction model for coastal regions using marine aerosol generation and transport data
[AD-A145443] 02 p0231 N85-11510
Effect of liquid phase composition on thickness of epitaxial Ga sub (1-x) Al sub x As films
02 p0257 N85-11683
The influence of aluminum on the qualities of low and medium carbon steel
[BLL-M-35754-(5828.4)] 03 p0330 N85-12123
Feasibility of the electrochemical method of determining nitrogen content in metallic melts
[BLL-M-35730-(5828.4)] 03 p0330 N85-12124
Development of a rapid test method for asphalt concrete content determination in hot-mix paving mixtures
[PB84-218692] 03 p0342 N85-12204
Aircraft flow effects on cloud droplet images and concentrations
[AD-A146176] 03 p0396 N85-12529
The effect of temperature and pressure on the composition density of alkaline metals
[BLL-M-35940-(5828.4)] 05 p0616 N85-13934
Reproducibility of readings from oxygen concentration elements
[BLL-M-35920-(5828.4)] 05 p0616 N85-13941
Fundamental equations of the LIF hydroxyl measurements, appendix A 05 p0676 N85-14338
Detailed performance calculations: Harvard Group, appendix G
05 p0676 N85-14344
Meteorite concentrations in Antarctica: How complete is the picture? 06 p0889 N85-15644
The influence of sample collection and methods of analysis on chemical concentrations measured in rainwater
[KNMI-TR-55] 07 p0924 N85-15853
Fluid temperature and concentration gradient measurement study — for spaceborne experiments
[CISE-R/FL/1/04] 11 p1637 N85-20309
Saturation kinetics of active medium of oxygen-iodine laser
11 p1718 N85-20807
Simultaneous cabin and ambient ozone measurements on two Boeing 747 airplanes. Volume 3: October 1978 - July 1979
[NASA-TM-86883] 12 p1892 N85-21872
The body burden of organic vapors in artificial air trial measurements aboard a moored submarine
[AD-A149696] 12 p1910 N85-21966
Spectroscopic study of sources and control of impurities in TMX-U: Revision 1
[DE85-004423] 12 p1937 N85-22170
Characterization of high purity Si-doped molecular beam epitaxial GaAs
[AD-A149651] 12 p1939 N85-22181
Progress on studies of early intense cratering
13 p2181 N85-23535
A parametric study of crater-saturation simulation
13 p2182 N85-23540
Influence of phosphorus content and heat treatment on the machinability of electroless nickel deposits
[DE85-007250] 15 p2522 N85-25548
Compositional control of plate steels
15 p2565 N85-25826
On the analytic calculation of premixed flames
[VTH-LR-417] 16 p2747 N85-26954
Comparison of observed and predicted short-term tracer-gas concentrations in the atmosphere
[DE85-007566] 16 p2821 N85-27399
Evaluation of chemical reaction mechanisms for photochemical smog. Part 2: Quantitative evaluation of the mechanisms, revised
[PB85-166060] 16 p2822 N85-27408
Radon concentration inversion in the troposphere: Still unexplained
[INPE-3360-PRE/638] 16 p2826 N85-27431
The distribution of higher n-alkanes in partially frozen middle distillate fuels
[AD-A153940] 18 p3083 N85-29074
Compact L-edge densitometer for uranium concentration assay
[DE85-010344] 18 p3110 N85-29261
The effect of surface reactions in catalytic combustion
[AD-A154217] 19 p3234 N85-30049
concentration variation of work function of alloys in the system nickel-titanium-aluminum
19 p3247 N85-30134
Temporal variations of Rn222 concentrations in Black Sea coastal zone 19 p3293 N85-30417
Toxic hazards tests for vehicles and other equipment
[AD-A149164] 20 p3506 N85-31797
Concentrations of ice nuclei of different modes of activities 21 p3641 N85-32616
Observations of the atmospheric ice nucleus at northwest China 21 p3641 N85-32618
Concentration and source areas of ice nuclei in the Alaskan atmosphere 21 p3643 N85-32634
Human activity and production rate of secondary nuclei 21 p3645 N85-32645
On the transformation regularities of time series of solid aerosol concentrations in the surface atmospheric layer
21 p3645 N85-32648
Variability of rural aerosols under stable weather conditions 21 p3647 N85-32663
Marine aerosols at the Dutch North Sea coast: Size distributions and fractionation of trace elements
21 p3648 N85-32664
A statistical study of CCN concentration in subequatorial climate: The particular case of the tropical wet forest
21 p3649 N85-32673
Sulfur Cycle 21 p3662 N85-32748
Measurement of velocity and concentration in free jets
[ISL-CO-215/84] 22 p3785 N85-33451
The heavy ion composition in 3HE-rich solar flares
[SH-2.2-7] 23 p4000 N85-34802
The effect of +Gx acceleration on platelet activation as determined by plasma platelet factor 4 levels
[AD-A155881] 24 p4131 N85-35608

CONCENTRATORS
Liquid cooled, linear focus solar cell receiver
[DE84-014446] 01 p0067 N85-10448
Evaluation of some photovoltaic concentrator solar cell-heat sink coupling materials
[DE84-016027] 04 p0529 N85-13378
Positron flux concentrator: An update
[DE84-016260] 04 p0561 N85-13576
Trends in concentrator, receiver, and storage development for terrestrial applications
05 p0609 N85-13891
Joint Indo-German program on solar energy: Parabolic dish program, step 1
[BMFT-FB-T-84-175] 05 p0670 N85-14312
Advanced high-efficiency concentrator cells
[DE84-013020] 09 p1344 N85-18459
Nebulization reflux concentrator
[NASA-CASE-LAR-13254-1] 11 p1615 N85-20154
Innovative solar thermal dish technology development
[DE85-002787] 11 p1673 N85-20539
Photovoltaic Systems Development and Evaluation Projects Integration Meeting
[DE84-008530] 11 p1673 N85-20542
Phase 2 fabrication and construction of the Sky Harbor Airport, solar photovoltaic concentrator project
[DE85-000019] 11 p1676 N85-20561
Concentrator technologies evaluation for large solar arrays and their application for space stations/platforms
13 p2010 N85-22609
Study of concentration for space photovoltaic generators 13 p2011 N85-22618
Power plants of modular construction with quasi-paraboloidal concentrators of solar energy
14 p2266 N85-24036
Development and testing of Parabolic Dish Concentrator No. 1
[NASA-CR-175651] 14 p2350 N85-24522
Development of an Organic Rankine-Cycle power module for a small community solar thermal power experiment
[NASA-CR-175650] 14 p2350 N85-24523
Development of mass-producible line-focus tracking concentrating solar collectors. Category 2: Control systems
[DE85-007873] 17 p2987 N85-28459
Development of a second-generation linear Fresnel Photovoltaic and Thermal (PVT) concentrator array, including fabrication and installation of a 200 square meter collector field
[DE85-008473] 17 p2988 N85-28465
DOE/Sandia point-focus concentrator program, draft
[DE85-008209] 17 p3038 N85-28793
Airport solar photovoltaic concentrator phase 3
[DE85-006773] 18 p3128 N85-29370
Nomographs for estimating the levelized cost of energy from flat-plate and concentrator photovoltaic systems
[NASA-CR-176048] 20 p3483 N85-31645
Photovoltaic concentrator research status
[DE85-010110] 20 p3483 N85-31647
Study of concentration for space photovoltaic generators
[SNIAS-851-440-105] 20 p3485 N85-31658
Photovoltaics technology program summary
[DE85-013098] 24 p4112 N85-35493

CONCENTRIC CYLINDERS
Stability of fluid flow in a cylindrical annulus
[NASA-TM-77720] 01 p0046 N85-10300
Unsteady free-convection heat transfer inside an annular cavity
[CFD/84/16] 08 p1163 N85-17339
On spectral multigrid methods for the time-dependent Navier-Stokes equations
[NASA-CR-172613] 19 p3344 N85-30725
Acoustic radiation from concentric shells containing an inner fluid
[AD-A155476] 21 p3700 N85-32991
Couette flow of two fluids between concentric cylinders
[AD-A155827] 24 p4093 N85-35376

CONCENTRIC SPHERES
Average spacing for rings of individual multi-ring basins is 2.0(0.5)D 13 p2182 N85-23541
Ring-diameter ratios for multi-ring basins average 2.0(0.5)D 13 p2182 N85-23542

CONCORDE AIRCRAFT
Avionics and civil aircraft systems: The present and the future
[SNIAS-851-111-104] 20 p3392 N85-31038

CONCRETE STRUCTURES
A rigid body mechanism in structural dynamics
02 p0206 N85-11361
Related studies to cathodic protection of reinforced concrete structures
[PB84-218114] 03 p0333 N85-12145
Dynamic shear failure of shallow-buried flat-roofed reinforced concrete structures subjected to blast loading
[AD-A145974] 03 p0373 N85-12378
Refined modeling of reinforced concrete columns of seismic analysis
[PB84-234384] 04 p0484 N85-13089
Measuring the corrosion rate of reinforcing steel in concrete
[PB84-244532] 06 p0770 N85-14925
Finite element procedures applicable to nonlinear analysis of reinforced concrete shell structures
[AD-A146796] 07 p0978 N85-16209
User's guide for concrete strength investigation and design (CSTR)
[AD-A151617] 15 p2579 N85-25906
An approach for user controlled reinforced concrete design optimization 15 p2627 N85-26187
In-service supervision of a pressurized concrete pressure vessel
[OEFZS-4306] 20 p3470 N85-31564
Implementation of polymer impregnation as a bridge deck sealant
[PB85-185718] 22 p3753 N85-33265
Prestressed concrete vessel according to the hot liner concept: A critical evaluation of experimental results with a prototype vessel
[OEFZS-4313] 22 p3801 N85-33550
Negative flexural behavior of precase composite slabs with steel joint 23 p3904 N85-34183
Membrane reinforcement in concrete shells: Design versus nonlinear behavior 24 p4084 N85-35312

CONCRETES
Development of advanced constitutive model for reinforced concrete
[AD-A145050] 01 p0062 N85-10411
Experimental AC (Asphalt Concrete) overlays of PCC pavement
[PB84-218171] 03 p0342 N85-12203
Evaluation of moduli and thicknesses of pavement systems by spectral-analysis-of-surface-waves method
[PB84-219112] 03 p0342 N85-12205
Improved reinforcement metal
03 p0353 N85-12271

Insulating polymer concrete
[DE84-017239] 04 p0480 N85-13057
Underground engineering (selected articles)
[AD-A141053] 04 p0483 N85-13082
Pulse-echo method for flaw detection in concrete
[PB84-234509] 06 p0775 N85-14953
Tests of the load-bearing and deformation behaviour of reinforced concrete spherical shells under point loading
[BLL-RISLEY-TR-4550-9091.9F)]
06 p0816 N85-15182
Salt action on concrete
[AD-A147812] 07 p0933 N85-15912
Thermal and mechanical properties of polyurethane foams and a survey of insulating concretes at cryogenic temperatures
[PB85-100949/GAR] 07 p0934 N85-15918
No-slump Roller-Compacted Concrete (RCC) for use in mass concrete construction
[AD-A146564] 08 p1138 N85-17164
Durability and behavior of prestressed concrete beams. Posttensioned concrete beam investigation, supplemental laboratory tests of beams exposed from 1961 to 1982
[AD-A148821] 09 p1304 N85-18191
Fracture toughness of fiber reinforced concrete
[AD-A149403] 10 p1496 N85-19441
Response of earth-covered slabs in clay and sand backfills
[AD-A149296] 11 p1615 N85-20157
Thermal stress-dependent dilation of concrete
[DE84-014686] 11 p1653 N85-20412
A new rheological model for concrete structural analysis
[DE84-014743] 11 p1653 N85-20413
Field validation of statistically-based acceptance plan for bituminous airport pavements. Volume 3: Statistical analysis of 3 methods for determining maximum specific gravity of bituminous concrete mixtures
[FAA-PM-84-12-VOL-3] 12 p1781 N85-21182
Development and evaluation of a procedure for the rapid analysis of fresh concrete
[AD-A149741] 12 p1866 N85-21703
Electrically conductive polymer concrete overlays
[DE85-006728] 15 p2522 N85-25549
Overlays for plain jointed concrete pavements
[PB85-156297] 15 p2523 N85-25557
Repair of the DSS-14 pedestal concrete
16 p2772 N85-27108
Hopkinson bar simulation using DYNA2D
[DE85-006766] 16 p2802 N85-27275
Development of concrete polymer materials
[DE85-005957] 17 p2934 N85-28114
Sodium concrete reaction: Structural considerations
[DE85-009031] 18 p3081 N85-29063
Behavior of reinforced concrete at elevated temperatures
[DE85-009032] 18 p3123 N85-29332
Effect of matrix composition on steel fiber reinforced concrete properties 19 p3230 N85-30028
Effects of humidity cycles on the corrosion of galvanised reinforcements in carbonated and uncarbonated mortars
[BLL-CE-TRANS-8039-(9022.09)]
20 p3430 N85-31272
Pycnometer shaker
[PB85-174985] 20 p3460 N85-31491
User's guide for computer program CGFAG, Concrete General Flexure Analysis with Graphics
[AD-A155555] 21 p3570 N85-32204
Dynamic fracture of concrete and other heterogeneous materials
[AD-A154513] 21 p3598 N85-32343
Hole cutting in building frames by laser
[FOA-C-20569-D9] 22 p3791 N85-33487
Monte Carlo and discrete ordinates calculations of 14-MeV neturons streaming through a stainless-steel duct (L/D = 4.6): Comparison with experiment
[DE85-011423] 22 p3840 N85-33776
High temperature polymer concrete
[DE85-005756] 23 p3920 N85-34290
User's guide: A computer program for strength analysis of non-hydraulic concrete structural elements. Report 1. Concrete General Strength Investigation (CGSI)
[AD-A156392] 24 p4102 N85-35428
User's guide: A computer program for strength analysis of non-hydraulic concrete structural elements. Report 2. Strength design of reinforced concrete column sections (PCAUC)
[AD-A156393] 24 p4102 N85-35429

CONCURRENT PROCESSING
Concurrent processing and the decomposition of problems
[DE84-015265] 02 p0242 N85-11581
Concurrency in parallel processing systems
05 p0714 N85-14581
Concurrency in a data flow database machine
09 p1366 N85-18582
The enhancement of concurrent processing through functional programming languages
[AD-A150771] 14 p2404 N85-24822
Performance evaluation of stochastic timed decision-free Petri Nets
[AD-A153987] 18 p3171 N85-29652
Methods for design and evaluation of integrated hardware-software systems for concurrent computation
[NASA-CR-176066] 20 p3515 N85-31851
Concurrent implementation of the Crank-Nicolson method for heat transfer analysis
[NASA-TM-86448] 21 p3674 N85-32822
Simulation of complex three-dimensional flows
[NASA-TM-86773] 21 p3675 N85-32831
Specifying and verifying concurrent programs
[AD-A156190] 24 p4136 N85-35652

CONDENSATES
Neutron interferometry and double diffractometer for condensed matter 03 p0424 N85-12705
Experimental and theoretical study of condensation in multicomponent vapors
[DE85-000843] 10 p1485 N85-19376
Continued research in mesoscale air pollution simulation modeling. Volume 7. Mathematical modeling of urban aerosol dynamics
[PB85-137388] 11 p1679 N85-20584
Proper quality of anticorrosion work no matter how bad the atmospheric conditions
[BLL-BISI-TRANS-22080-(9022.06)]
17 p2975 N85-28383
Aitken particle size distribution in Antarctica
21 p3646 N85-32656
Properties of forest derived cloud condensation nuclei
21 p3650 N85-32682
Influence on an industrial site on the characteristics of CCN supersaturation with air masses of different origin
21 p3650 N85-32683

CONDENSATION
The lifting condensation level and its relation to convective cloud base
[AD-A145654] 02 p0232 N85-11513
Chemical evolution of the solar nebula: A new model
06 p0887 N85-15631
Homogeneous condensation of gaseous mixtures of Si, Fe, O, N, and C in relative cosmic abundance and implications for astronomical condensation
06 p0887 N85-15632
Theoretical analysis of condensation in the presence of noncondensable gases as applied to open cycle OTEC condensers
[DE84-015809] 11 p1675 N85-20556
An examination of the Southern Oscillation in the upper troposheric tropical and subtopical wind field
20 p3488 N85-31680
Remarks on preparation of indandione detection reagents
[NASA-TM-77905] 21 p3560 N85-32146
Eleventh International Conference on Atmospheric Aerosols, Condensation and Ice Nuclei, volume 2
[PB85-182418] 21 p3638 N85-32596
Ice active bacteria as condensation nuclei
21 p3639 N85-32603
Generation of lead, lead iodide and iodide aerosols and their ice nucleation 21 p3639 N85-32607
Ice nucleus measurements 21 p3640 N85-32609
Airborne measurements of atmospheric ice nuclei
21 p3640 N85-32612
Aircraft observations of condensation and ice nuclei at a tropical station 21 p3640 N85-32613
Supersaturation spect A of Ice Nuclei at different locations in Europe and over the North-Atlantic
21 p3640 N85-32615
The nuclei of cloud formation
21 p3651 N85-32685
Transport and formation of summertime cloud condensation nuclei over the Arctic Ocean
21 p3651 N85-32686
A review on the formation of aerosol particles in the atmosphere 21 p3651 N85-32687
The measured rate of condensation nucleation to droplets using the techniques of chemical kinetics
21 p3652 N85-32694
The interaction of polynuclear aromatic hydrocarbons PAH's with water vapor and their role as condensation nuclei in the formation of haze and fog
21 p3652 N85-32695
Applicability of surface CCN measurements
21 p3652 N85-32696
on the transport of large condensation nuclei in the atmosphere at various altitudes over the territory of the USSR 21 p3653 N85-32698

CONDENSATION NUCLEI
NT AITKEN NUCLEI
Condensational transformation of atmospheric aerosol particle distribution functions 10 p1500 N85-19468
Test results from a comparative evaluation of a condensation nuclei fire detector
[NASA-CR-3874] 12 p1862 N85-21675
Measurements of giant salt nuclei from inland in east China 21 p3648 N85-32669
Cloud condensation on insoluble particles
21 p3648 N85-32670
Observations of cloud droplets, aerosol particles and cloud condensation nuclei in continental air masses
21 p3649 N85-32671
A statistical study of CCN concentration in subequatorial climate: The particular case of the tropical wet forest
21 p3649 N85-32673
Investigation of the formation of cloud particle spectrum on natural condensation nuclei
21 p3649 N85-32674
A simple model to investigate the activation process in waterclouds 21 p3649 N85-32675
A relationship between cloud droplet size and CCN critical supersaturation 21 p3649 N85-32677
On the question to the effect of surfactants on the spectrum of cloud drops in the process of their condensation growth 21 p3650 N85-32679
Aircraft observations of cloud condensation nuclei in maritime and continental environments
21 p3650 N85-32680
The distribution of giant salt nuclei inside and outside cloud over the basin of Xin and Jiang
21 p3650 N85-32681

CONDENSER RADIATORS
U CONDENSERS (LIQUEFIERS)
U HEAT RADIATORS

CONDENSERS
Modeling of a second-generation solar-driven Rankine air conditioner
[DE84-015132] 01 p0036 N85-10020

CONDENSERS (LIQUEFIERS)
Heat transfer due to film condensation on vertical fluted tubes
[AD-A147258] 07 p0959 N85-16079
Theoretical analysis of condensation in the presence of noncondensable gases as applied to open cycle OTEC condensers
[DE84-015809] 11 p1675 N85-20556
Direct-contact condensers for solar pond power production
[DE84-004510] 12 p1876 N85-21771
Mass and heat transfer in reflux condensers of absorption heat pumps
[DFVLR-FB-83-43] 14 p2304 N85-24286
Filmwise condensation of steam on low integral-finned tubes
[AD-A152220] 16 p2783 N85-27176

CONDENSING
NT FILM CONDENSATION
Method of obtaining polychalcones
[AD-A145051] 01 p0018 N85-10107
Experimental and theoretical study of condensation in multicomponent vapors
[DE84-015610] 02 p0174 N85-11164
Carbon vaporization/condensation effects
[NASA-TM-87430] 10 p1436 N85-19048
Isentropic objective analysis
[PB85-112167] 11 p1688 N85-20817
Experimental and theoretical study of condensation in multicomponent vapors
[DE85-009357] 17 p2923 N85-28021
Condensation of anhydrides or dicarboxylic acids with compounds containing active methylene groups. Part 19: Condensation of phthalic and substituted phthalic anhydrides with benzoylacetic ester
[NASA-TM-77885] 19 p3227 N85-30009
Condensation of anhydrides or dicarboxylic acids with compounds containing active methylene groups. Part 1: Condensation of phthalic anhydride with acetoacetic and malonic ester
[NASA-TM-77886] 19 p3227 N85-30010
Flow field effects on nucleation in a reacting mixing layer
[ARL/AERO-R-165] 19 p3263 N85-30237
Construction of University of Missouri, Rolla's full scale cloud simulation chamber and applied research
[AD-A154682] 21 p3557 N85-32128
The 100 years of Aitken Nuclei (AN) study-reminiscence, current and future problems 21 p3641 N85-32621
Supersaturation obtained in a condensation nucleus counter 21 p3642 N85-32624
Analysis of performance of dynamic thermal diffusion chamber 21 p3642 N85-32625
A thermal diffusion chamber for the measurement of cloud condensation nuclei 21 p3642 N85-32627
Critical supersaturations with respect to water for fast condensation-freezing ice nucleation
21 p3643 N85-32632

Eleventh International Conference on Atmospheric Aerosols, Condensation and Ice Nuclei, volume 1
[PB85-182400] 21 p3644 N85-32636
The first condensation nucleus conference
21 p3644 N85-32637
Cloud condensation on insoluble particles
21 p3648 N85-32670
Condensation properties of atmospheric aerosol
21 p3649 N85-32672

CONDITIONED RESPONSES
U CONDITIONING (LEARNING)

CONDITIONING (LEARNING)
Control of mammals at airports
[AD-P004192] 11 p1580 N85-19957
Psychological components in the development and prevention of air sickness 11 p1695 N85-20659
Biofeedback treatment of airsickness: A review
11 p1696 N85-20660
M-BLASER: A device to study pursuit tracking in the rhesus monkey
[AD-A152986] 17 p2996 N85-28534

CONDITIONS
NT ADIABATIC CONDITIONS
NT CHRONIC CONDITIONS
NT FLIGHT CONDITIONS
NT LIPSCHITZ CONDITION
NT NONEQUILIBRIUM CONDITIONS
NT RUNWAY CONDITIONS
Setting hurricane conditions of readiness with high confidence
[AD-A144785] 01 p0085 N85-10570
Computer programs for the adjustment of indirect observation with condition equations between the unknowns
[SER-B-268-MITT-170] 09 p1370 N85-18612
Estimating risks of lead-induced hemoglobin decrements under conditions of uncertainty: Methodology, pilot judgments and illustrative calculations
[DE85-012293] 23 p3952 N85-34493

CONDUCTANCE
U RESISTANCE

CONDUCTING FLUIDS
Magnetic inductive flowmeter for low conducting liquids
[BMFT-FB-T-84-136] 04 p0504 N85-13216

CONDUCTING MEDIA
U CONDUCTORS

CONDUCTION BANDS
Electron and hole effective masses for two-dimensional transport in strained-layer superlattices
[DE84-016222] 04 p0570 N85-13637
The Valence- and conduction-band structure of the sapphire (1102) surface
[AD-A150001] 12 p1940 N85-22184
Modulation doped GaAs/Al(x)Ga(1-x)As layered structures with applications to field effect transistors
[AD-A155360] 22 p3759 N85-33296

CONDUCTION ELECTRONS
Very low temperature studies of hyperfine effects in metals
[DE85-013367] 22 p3749 N85-33236

CONDUCTIVE HEAT TRANSFER
Self-similar expansion of dense matter due to heat transfer by nonlinear conduction
[MPQ-81] 01 p0046 N85-10297
ICARUS: A general one-dimensional heat conduction code
[DE84-016125] 01 p0047 N85-10310
A similarity analysis of phase change heat conduction in corners 05 p0634 N85-14069
Wave propagation in compliant tubes containing a heat-conducting viscous fluid
[WTHD-163] 05 p0638 N85-14094
Intensification of convective heat transfer by means of artificial surface roughness 06 p0778 N85-14975
New aspects of thermoelastic contact
[AD-A147554] 07 p0979 N85-16217
Two-dimensional modeling of conduction-mode laser welding
[DE85-001804] 09 p1327 N85-18341
Measurements of sediment temperatures, conductivity and heat flow in the North Atlantic and their relevance to radioactive waste disposal
[IOS-172] 09 p1359 N85-18551
Triple layer system for numerical integration of equations of gas dynamics and nonlinear heat conduction equation
[DE85-000297] 11 p1632 N85-20277
Temperature responses of composite panels
[AD-A150053] 12 p1798 N85-21277
Models of the upper atmosphere
12 p1845 N85-22217
Conducting a thermal conductivity survey
[NASA-CR-175792] 16 p2782 N85-27166
Evaluation of the eigenvalue method in the solution of transient heat conduction problems
[AD-A154434] 19 p3266 N85-30256
Sequential regularization solution of the inverse heat conduction problem
[DE85-010657] 23 p3931 N85-34362
Analytic solutions of inverse heat conduction problems
24 p4092 N85-35367

CONDUCTIVITY
Conductivity changes in neutron-irradiated commercial copper alloys at approximately 450(O)C
[DE85-003007] 11 p1606 N85-20100
The replacement of precious metal thick film inks using conductive polymer technology
[AD-A152002] 16 p2749 N85-26965
Gyrotron traveling-wave device including quarter wavelength anti-reflective dielectric layer to enhance microwave absorption
[AD-D011690] 19 p3271 N85-30285

CONDUCTIVITY METERS
NT ELECTRICAL CONDUCTIVITY METERS

CONDUCTORS
NT BUS CONDUCTORS
NT ELECTRIC CONDUCTORS
NT ELECTRIC WIRE
NT ELECTROLYTES
NT ION EXCHANGE MEMBRANE ELECTROLYTES
NT MOLTEN SALT ELECTROLYTES
NT NONAQUEOUS ELECTROLYTES
NT PHOTOCONDUCTORS
NT SOLID ELECTROLYTES
NT SUPERCONDUCTORS
Diffraction of plane electromagnetic waves on semiinfinite grid of parallel conductors arranged at angle to its edge 03 p0344 N85-12217
Magnetic field calculation for ideal conductors by method of equivalent currents 06 p0788 N85-15035
Corrosion properties of second-generation conductive materials 07 p1000 N85-16348
Control of electronic, magnetic and optical properties of doped polyacetylene conductors
[AD-A150117] 12 p1814 N85-21375
Performance ranges of helical antenna made of conductor with extra bends 12 p1838 N85-21536
Study of amorphous strips and microconductors by ferromagnetic resonance method
15 p2497 N85-25402
Electronic properties of new organic conductors
[DE85-005590] 15 p2549 N85-25736
Nuclear responses in INTOR plasma stabilization elements
[DE85-010489] 20 p3535 N85-31995
Method for determining depth and shape of a sub-surface conductive object
[DE85-006502] 23 p3935 N85-34389

CONES
NT CONICAL BODIES
NT NOSE CONES
NT SLENDER CONES
Aerothermal tests of a 12.5 percent cone at Mach 6.7 for various Reynolds numbers, angles of attack and nose shapes — conducted in Langley 8-foot high temperature tunnel
[NASA-TP-2345] 08 p1161 N85-17322
LOVEL-84: A LOw-VELocity aerodynamic heating code for flat plates, wedges, and cones
[DE85-002604] 11 p1576 N85-19933
Experimental investigation of heat transfer to bluff cylinders and cones in hypersonic rarefied gas flow
11 p1620 N85-20195

CONES (VOLCANOES)
The geology of Mt. Hope, a silicic volcanic center in West Central Arizona 13 p2167 N85-23571

CONFERENCES
Aeronautics Technology Possibilities for 2000: Report of a workshop
[NASA-CR-174018] 01 p0001 N85-10001
Experimental data base for computers program assessment. Report of the Fluid Dynamics Panel Working Group 04: Addendum
[AGARD-AR-138-ADD] 01 p0004 N85-10020
Proceedings of the Aviation Accident Investigation Symposium
[PB84-917004] 01 p0005 N85-10029
Peripheral Vision Horizon Display (PVHD)
[NASA-CP-2306] 01 p0008 N85-10044
Nuclear Magnetic Resonance of Polymeric Materials
[AD-A145078] 01 p0032 N85-10192
Tendencies in the development of utilization protocols, seminar report — communication networks
[FUB-11-1983] 01 p0039 N85-10252
Voice phonetic coding and decoding processes
[FUB-29-1983] 01 p0040 N85-10259
Second All-Union Seminar on Hydromechanics and Heat and Mass Exchange in Weightlessness, summaries of reports
[NASA-TM-77590] 01 p0047 N85-10305
Structure and wear workshop colloquium
01 p0054 N85-10356
NASA Geodynamics Program
[NASA-TM-87359] 01 p0063 N85-10418
Technical Review of the Solid Particle Receiver Program
[DE84-015181] 01 p0068 N85-10451
Report of the First Session of the International Working Group on Data Management for the International Satellite Cloud Climatology Project (ISCCP)
[WCP-42] 01 p0073 N85-10483
Nowcasting 2. Mesoscale Observations and Very-Short-Range Weather Forecasting — conferences
[ESA-SP-208] 01 p0073 N85-10487
Illinois Climate: Trends, Impacts and Issues
[PB84-211986] 01 p0086 N85-10577
Office of Technology Assessment
01 p0127 N85-10872
Workshop on Automated Space Station
01 p0127 N85-10873
Turbine Engine Hot Section Technology (HOST)
[NASA-TM-83022] 02 p0140 N85-10951
Second Symposium on Space Industrialization — space commercialization
[NASA-CP-2313] 02 p0149 N85-11011
Seminar on Principal Components Analysis in the Atmospheric and Earth Sciences
[CSIR-S-334] 02 p0211 N85-11366
The Multispectral Imaging Science Working Group. Volume 2: Working group reports
[E85-10002] 02 p0213 N85-11405
MIZEX. A program for mesoscale air-ice-ocean interaction experiments in arctic marginal ice zones. III: Modeling the marginal ice zone
[AD-A145351] 02 p0233 N85-11517
Mathematical Models of the Circadian Sleep-Wake Cycle
[AD-A145712] 02 p0235 N85-11532
Statistical Plasma Physics. Proceedings of the Workshop of the US-Japan Joint Institute for Fusion Theory Program
[IPPJ-689] 02 p0282 N85-11832
Gauge Theory on a Lattice, 1984: Proceedings
[DE84-014856] 02 p0291 N85-11892
Uranus and Neptune
[NASA-CP-2330] 02 p0298 N85-11927
Wind Tunnel Wall Interference Assessment and Correction, 1983
[NASA-CP-2319] 03 p0311 N85-12011
Proceedings of a Workshop on Applications of Tethers in Space, Executive Summary
[NASA-CR-171195] 03 p0322 N85-12075
Proceedings of a Workshop on the Applications of Tethers in Space, Volume 1
[NASA-CR-171196] 03 p0322 N85-12076
Proceedings of a Workshop on Applications of Tethers in Space, Volume 2
[NASA-CR-171197] 03 p0322 N85-12077
ERS-1 radar altimeter data products — conferences
[ESA-SP-221] 03 p0379 N85-12419
Star Formation Workshop
[ROE-OR-13] 03 p0441 N85-12809
Colloquium about Joint Projects within DFVLR/ISRO Cooperation
[DFVLR-MITT-84-12] 04 p0458 N85-12907
Tough Composite Materials
[NASA-CP-2334] 04 p0463 N85-12941
Official journey to USA, November 1983. Symposium on the Compatibility of Explosives; Mound Laboratory; Naval Surface Weapons Center
[FOA-C-20548-D1] 04 p0482 N85-13072
Digital image processing; report from a conference and study trip to the USA and Canada, summer 1984
[FOA-C-30369-E1] 04 p0494 N85-13153
Scientific contributions in commemoration of Ebro Observatory's 75th anniversary — conference
[ISBN-84-00-05380-X] 04 p0518 N85-13306
National Photovoltaics Program Annual Review Meeting, abstracts
[DE84-013003] 04 p0530 N85-13390
Proceedings of a Workshop on Atmospheric Research Needs for the Western United States
[DE84-015069] 04 p0534 N85-13412
Proceedings of the US-Japan Theory Workshop on 3-D MHD Studies
[DE84-012019] 04 p0568 N85-13620
The 1984 ASEE-NASA summer faculty fellowship program (aeronautics and research)
[NASA-TM-87393] 04 p0575 N85-13664
FY 1984 scientific and technical reports, articles, papers and presentations
[NASA-TM-86470] 04 p0575 N85-13670
Energy information exchange, 1983
[DE84-901446] 04 p0577 N85-13680
Conference on the Origin of the Moon
[NASA-CR-174066] 04 p0581 N85-13709

Flow Around Bluff Bodies: Numerical and Experimental Approaches — conferences
[VKI-LS-1984-06] 05 p0593 N85-13778

An Assessment of Integrated Flywheel System Technology
[NASA-CP-2346] 05 p0604 N85-13850

Space Power
[NASA-CP-2352] 05 p0608 N85-13860

Workshop on Mechanical Technology for Antennas — conferences; satellite antennas
[ESA-SP-225] 05 p0625 N85-13999

Special Developments and Methods in High Frequency Measuring Techniques — conferences
[PTB-E-24] 05 p0629 N85-14030

Flow in Centrifugal Compressors — conferences
[VKI-LS-1984-07] 05 p0636 N85-14079

Rotordynamic Instability Problems in High-Performance Turbomachinery
[NASA-CP-2338] 05 p0642 N85-14116

The fourth LBF colloquium
[ISSN-0721-5320] 05 p0648 N85-14163

The Interaction of Global Biochemical Cycles
[NASA-CR-174184] 05 p0652 N85-14183

EARSeL/ESA Symposium on Integrative Approaches in Remote Sensing
[ESA-SP-214] 05 p0655 N85-14202

Assessment of Techniques for Measuring Tropospheric H sub x O sub y
[NASA-CP-2332] 05 p0675 N85-14336

Report of the Meeting of Experts on Climate and Human Health
[WCP-78] 05 p0687 N85-14413

Life Sciences Research in Space — conference
[ESA-SP-212] 05 p0689 N85-14425

Twentieth Annual Conference on Manual Control, volume 1
[NASA-CP-2341-VOL-1] 05 p0699 N85-14487

Twentieth Annual Conference on Manual Control, volume 2
[NASA-CP-2341-VOL-2] 06 p0707 N85-14535

Fifth Conference on Star Clusters and Associations and Their Relation to the Evolution of the Galaxy
[PUBL-58] 06 p0736 N85-14732

Technical Workshop: Advanced Helicopter Cockpit Design
[NASA-CP-2351] 06 p0750 N85-14806

US objectives generally achieved at broadcasting satellite international conference. Improvements can help in future conferences
[PB84-235316] 06 p0800 N85-15109

International Conference on Physics of Clouds
06 p0819 N85-15198

Proceedings of the 23rd Project Integration Meeting
[NASA-CR-174186] 06 p0829 N85-15260

Miniworkshop on effects of stress and strain in high-speed-growth silicon ribbons
06 p0831 N85-15284

Proceedings of the 22nd Project Integration Meeting
[DE85-000334] 06 p0833 N85-15302

Recent developments in photovoltaics
[DE84-004528] 06 p0833 N85-15305

Proceedings of the 14th Conference on Environmental Toxicology
[AD-A146400] 06 p0843 N85-15350

Proceedings of the National Bureau of Standards and National Security Agency Workshop on Standardization Issues for Optical Data Disk (OD3) Technology
[PB84-217785] 06 p0848 N85-15383

Proceedings of Workshop on Synergistic Effects in Surface Phenomena Related to Plasma-Wall Interactions
[IPPJ-AM-35] 06 p0864 N85-15488

ASC 1984 Applied Superconductivity Conference
[DE84-016204] 06 p0866 N85-15521

Local Interstellar Medium. International Astronomical Union Colloquium No. 81
[NASA-CP-2345] 06 p0872 N85-15539

The 47th Annual Meteoritical Society Meeting
[NASA-CR-174071] 06 p0881 N85-15599

Proceedings of the International Conference and Exposition on Structural Impact and Crashworthiness
[AD-A147845] 07 p0900 N85-15703

Engine Cyclic Durability by Analysis and Testing
[AGARD-CP-368] 07 p0905 N85-15733

Modern signal processing and reconnaissance — conferences
[FOA-C-30374-E1] 07 p0942 N85-15975

Astronomical photography 1984 — conferences
[ROE-OR-14] 07 p0962 N85-16102

Proceedings of the Second Annual Symposium on Mathematical Pattern Recognition and Image Analysis Program
[E85-10056] 07 p0984 N85-16251

International Aerospace and Ground Conference on Lightning and Static Electricity. 1984 technical papers. Supplement
[NASA-CP-2356] 07 p0999 N85-16343

Climate Conference for Latin America and the Caribbean
[WMO-632] 07 p1000 N85-16352

QUASAT: A VLBI observatory in space — conferences
[ESA-SP-213] 07 p1056 N85-16700

Helicopter Guidance and Control Systems for Battlefield Support
[AGARD-CP-359] 08 p1072 N85-16797

Space Shuttle Technical Conference, part 2
[NASA-CP-2342-PT-2] 08 p1098 N85-16937

OTV Propulsion Issues
[NASA-CP-2347] 08 p1106 N85-16989

Hazard Studies for Solid Propellant Rocket Motors
[AGARD-CP-367] 08 p1114 N85-17025

Proceedings of the 2nd Workshop on Nondestructive Evaluation (NDE) of Titanium Alloys
[AD-A147626] 08 p1125 N85-17095

Papers of the 15th International Society for Photogrammetry and Remote Sensing (ISPRS) Congress — conferences
[TRITA-FMI-9] 08 p1175 N85-17406

Proceedings of a Workshop on Research Issues in Simulator Sickness
[AD-A148543] 08 p1198 N85-17538

International Conference on Luminescence
[AD-A148470] 08 p1223 N85-17701

The Origin of Nonradiative Heating/Momentum in Hot Stars
[NASA-CP-2358] 08 p1231 N85-17755

X-ray and UV Emission from Active Galactic Nuclei — conference
[MPE-184] 08 p1236 N85-17790

Airborne Astronomy Symposium. A symposium commemorating the tenth anniversary of operations of the Kuiper Airborne Observatory
[NASA-CP-2353] 08 p1244 N85-17848

Proceedings of the Workshop on Improvements to Photometry
[NASA-CP-2350] 08 p1250 N85-17892

Proceedings of the workshop on unsteady separated flow held at the United States Air Force Academy on August 10-11, 1983
[AD-A148249] 09 p1263 N85-17937

The IMAGE 3 Conference Proceedings
[AD-A148636] 09 p1267 N85-17962

Simulating speed and height cues in the C-130 weapon system trainer
[AD-P004313] 09 p1268 N85-17967

Producing high scene content with perspective validity
[AD-P004314] 09 p1268 N85-17968

Geographic subdivision and top level data structures, Columbus, Magellan, and expanding CIG (Computer Image Generation) horizons
[AD-P004317] 09 p1268 N85-17971

An overview of the research program at the visual technology research simulator
[AD-P004321] 09 p1269 N85-17975

Considerations in an optical variable acuity display system
[AD-P004323] 09 p1269 N85-17977

Control systems analysis program: A tool for analysis of the GE-VSCDP (General Electric-Visual System Component Display Program) image display system
[AD-P004325] 09 p1270 N85-17979

The effects of time delay in man-machine control systems: Implications for design of flight simulator Visual-Display-Delay compensation
[AD-P004329] 09 p1270 N85-17983

The fiber-optic helmet-mounted display
[AD-P004330] 09 p1270 N85-17984

Binocular overlap in a fiber optic helmet mounted display
[AD-P004331] 09 p1270 N85-17985

Baffled eye and confounded brain or using visual illusions to train blind pilots
[AD-P004332] 09 p1271 N85-17986

Simulator sickness: Sensorimotor disturbances induced in flight simulators
[AD-P004334] 09 p1271 N85-17988

On-board Computer Image Generator (CIG) applications
[AD-P004335] 09 p1271 N85-17989

CIG (Computer Image Generator) goes to war: The tactical illusion
[AD-P004336] 09 p1271 N85-17990

Military applications of the Singer Link-Miles IMAGE visual system
[AD-P004337] 09 p1271 N85-17991

Flight Training Technology for Regional/Commuter Airline Operations: Regional Airline Association/NASA Workshop Proceedings
[NASA-CP-2348] 09 p1275 N85-18009

Proceedings of the AFOSR/AFRPL Rocket Propulsion Research Meeting: Abstracts and Agenda
[AD-A148818] 09 p1286 N85-18065

The Shock and Vibration Bulletin 54. Part 1: Welcome, keynote address, invited papers MIL-STD-810D, MIL-STD-810D panel session
[AD-A148131] 09 p1333 N85-18377

Proceedings of the Environmental Systems Symposium (13th) held at Bethesda, Md., 20-22 March 1984
[AD-A148194] 09 p1346 N85-18471

Proceedings of the International Conference on the Performance of Off-Road Vehicles and Machines, (8th), volume 1
[AD-A148634] 09 p1403 N85-18823

Proceedings of the 8th International Conference on the Performance of Off-Road Vehicles and Machines, volume 2
[AD-A148635] 09 p1407 N85-18859

Proceedings of Colloquium/Workshop on Composite Materials and Structures, Standardization, Qualification, Certification held at washington, D.C. on 8-10 May 1984
[AD-A149039] 10 p1432 N85-19029

The 1984 JANNAF Propulsion Systems Hazards Subcommittee Meeting, volume 1
[AD-A148865] 10 p1454 N85-19162

Report on AGARD Meeting: Hazards Studies for Solid Propellant Rocket Motors
[AD-P004340] 10 p1454 N85-19164

National Machine Tools Conference slated for 1985: Conference agenda, papers 10 p1460 N85-19202

Proceedings of the 17th Symposium on Electromagnetic Windows, part 1
[AD-A149185] 10 p1466 N85-19253

Propagation Influences on Digital Transmission Systems: Problems and Solutions
[AGARD-CP-363] 10 p1469 N85-19269

1984 AFOSR Research Meeting on Diagnostics of Reacting Flow held at New Haven, Connecticut on 21-22 March 1984
[AD-A149023] 10 p1484 N85-19367

Fourth International Conference on Robot Vision and Sensory Controls
[AD-A149524] 10 p1492 N85-19422

Summer study program in geophysical fluid dynamics, the Woods Hole Oceanographic Institution, dynamic differentiation
[AD-A149386] 10 p1521 N85-19585

Image Understanding: Proceedings of the 15th Workshop
[AD-A149496] 10 p1557 N85-19816

Calendar of selected aeronautical and space meetings
[AGARD-CAL-84/2] 10 p1573 N85-19917

Proceedings of the 14th Army Science Conference. Volume 1: Principal Authors A through H
[AD-A149200] 10 p1573 N85-19920

Modeling turbulent flow in compressible fluids: Metrological aspects — conferences
11 p1575 N85-19926

Wildlife Hazards to Aircraft Conference and Training Workshop: Proceedings
[AD-A148330] 11 p1578 N85-19939

Applications of Tethers in Space, volume 1
[NASA-CP-2364] 11 p1642 N85-20339

Applications of Tethers in Space, volume 2
[NASA-CP-2365] 11 p1644 N85-20361

Middle Atmosphere Program. Handbook for MAP, volume 4
[NASA-CR-175482] 11 p1654 N85-20420

Middle Atmosphere Program. Handbook for MAP, volume 10
[NASA-CR-175477] 11 p1658 N85-20450

LANDSAT-4 Science Characterization Early Results. Volume 2, part 1: Thematic Mapper (TM)
[E85-10068] 11 p1668 N85-20508

Proceedings of a Workshop on Environment of West Antarctica: Potential CO2-induced changes
[PB85-110757] 11 p1671 N85-20527

Photovoltaic Systems Development and Evaluation Projects Integration Meeting
[DE84-008530] 11 p1673 N85-20542

Proceedings of the 1st Glacier Bay Science Symposium
[PB85-115913] 11 p1682 N85-20599

Symposium on Military Aviation Medicine summarized
11 p1696 N85-20683

Contributions of the X-ray astronomy group — conference
[MPE-PREPRINT-28] 11 p1741 N85-20947

Contributions of the X-ray astronomy group — conference
[MPE-PREPRINT-29] 11 p1742 N85-20952

Observations of comets: Radio and otherwise — conference
[TB-64] 11 p1762 N85-21086

Proceedings of the 6th Advanced Aircrew Display Symposium
[AD-A150044] 12 p1778 N85-21180

Orbital Debris
[NASA-CP-2360] 12 p1783 N85-21188

Proceedings of the Symposium on Electromagnetic Windows (17th) held at Georgia Inst. of Technology, Engineering Experiment Station, Atlanta, Georgia on 25-27 July 1984. Part 2
[AD-A149125] 12 p1824 N85-21444

International Congress Centrum Berlin report on photovoltaics 12 p1877 N85-21773

Gas-liquid chemistry of natural waters, volume 2
[DE85-002457] 12 p1884 N85-21823

Biological effects of blast and impact waves
[FOA-C-52006-H4-D7] 12 p1906 N85-21968

Proceedings of the 1984 DOE Nuclear Reactor and Facility Safety Conference, volume 1
[DE84-012130] 12 p1931 N85-22132

Proceedings of the DOE Nuclear Reactor and Facility Safety Conference, volume 2
[DE84-012694] 12 p1931 N85-22133

The future of lightwave technology
[PB85-109759] 12 p1935 N85-22155

International Conference on Defects in Insulating Crystals
[AD-A149611] 12 p1939 N85-22180

Research and Modeling of Supervisory Control Behavior, report of a workshop
[AD-A149621] 12 p1950 N85-22248

Plasma Astrophysics — conference
[ESA-SP-207] 12 p1953 N85-22270

All-Union conference of radio astronomers
13 p1977 N85-22408

Spacecraft Environmental Interactions Technology, 1983
[NASA-CP-2359] 13 p1989 N85-22470

Twenty-first JANNAF Combustion Meeting, volume 1
[AD-A150981] 13 p1998 N85-22526

Workshop report: Swirl Enhanced Combustion
13 p2005 N85-22564

Photovoltaic Generators in Space — conferences
[ESA-SP-210] 13 p2005 N85-22565

LANDSAT-4 Science Characterization Early Results. Volume 4: Applications — agriculture, soils land use, geology, hydrology, wetlands, water quality, biomass identification, and snow mapping
[E85-10070] 13 p2117 N85-23186

Remote Sensing of Snow and Evapotranspiration
[NASA-CP-2363] 13 p2123 N85-23223

Abstracts of 6th Annual Review Meeting on Photovoltaic Advanced Research and Development
[DE84-013047] 13 p2128 N85-23246

Proceedings of the Geoscience Instrumentation Workshop
[DE85-004359] 13 p2132 N85-23268

The ASCOT Data Analysis Workshop
[DE85-004407] 13 p2139 N85-23283

Modulation of light energy transduction in photosynthesis
[DE85-004711] 13 p2141 N85-23292

Technical Digest: Symposium on Optical Fiber measurements, 1984
[PB85-114700] 13 p2160 N85-23407

Gears and Power Transmission Systems for Helicopters and Turboprops
[AGARD-CP-369] 14 p2220 N85-23765

Large Space Antenna Systems Technology, 1984
[NASA-CP-2368-PT-1] 14 p2229 N85-23813

Large Space Antenna Systems Technology, 1984
[NASA-CP-2368-PT-2] 14 p2233 N85-23840

Data Collection and Platform Location by Satellite: ARGOS Users' Conference 14 p2237 N85-23869

Report on the panel discussion of the Workshop on Data Collection Platform Networks
14 p2239 N85-23880

Data Collection and Platform Location by Satellite: ARGOS Users' Conference 14 p2239 N85-23883

The Giotto spacecraft impact-induced plasma environment
[ESA-SP-224] 14 p2243 N85-23905

Proceedings of the ARGOS Users Conference on Data Collection and Location by Satellite
14 p2322 N85-24348

Data Collection and Platform Location by Satellite: ARGOS Users' Conference 14 p2325 N85-24366

Data Collection and Platform Location by Satellite: ARGOS users' Conference 14 p2328 N85-24391

Data Collection and Platform Location by Satellite: ARGOS Users' Conference 14 p2330 N85-24409

Achievements of the International Magnetospheric Study (IMS) — conference
[ESA-SP-217] 14 p2354 N85-24544

Second Soviet-French Symposium on Space Cytology
14 p2386 N85-24699

Mini-Seminar on CAD/CAM
[CSIR-TSD-0007/83] 14 p2402 N85-24809

Finite Element Methods in South Africa 1983 — conference
[S-332] 14 p2410 N85-24863

Investigations carried out under the Director's Discretionary Fund
[NASA-CR-175676] 14 p2432 N85-24999

Cometary Astrometry
[NASA-CR-175660] 14 p2435 N85-25015

The hydromagnetics of the Sun — conferences
[ESA-SP-220] 14 p2445 N85-25091

Solar magnetohydrodynamics: Symposium review
14 p2455 N85-25162

Transonic Unsteady Aerodynamics and its Aeroelastic Applications
[AGARD-CP-374] 15 p2457 N85-25171

Roundtable on effective use of flight simulators
15 p2460 N85-25190

NASA R and T aerospace plane vehicles: Progress and plans
[NASA-TM-86429] 15 p2491 N85-25368

Three-Dimensional Boundary Layers
[AGARD-R-719] 15 p2558 N85-25784

Welding technology: Japan — Conference
[ISBN-0-85300177-4] 15 p2565 N85-25823

Thirteenth NASTRAN Users' Colloquium
[NASA-CP-2373] 15 p2573 N85-25863

Eight DOE Solar Photochemistry Research Conference: Proceedings
[DE85-005094] 15 p2587 N85-25948

Papers from the Symposium on Emissions: The Value of Incentives and Guidelines for Control
[S-336] 15 p2590 N85-25967

NASA Space Biology Program: 9th Annual Symposium
[NASA-CP-2336] 15 p2605 N85-26054

Proceedings of the BAe human factors seminar
[BAE-BT-11873] 15 p2620 N85-26145

Workshop on Parallel Computer Architectures in Pattern Recognition and Image Processing
[BMFT-FB-DV-84-006] 15 p2622 N85-26154

Very large least squares problems and supercomputers
[AD-A151270] 15 p2623 N85-26162

Supercomputers and symbolic computation
[AD-A151376] 15 p2623 N85-26166

Symposium on Computers in Civil Engineering 1983
[CSIR-S-298] 15 p2626 N85-26182

ONR (Office of Naval Research) Far East Scientific Bulletin, Volume 9, Number 4, October-December 1984
[AD-A151274] 15 p2665 N85-26448

Planetary Rings. Colloquium 75 — conferences
[ISBN-2-85428-100-4] 15 p2670 N85-26473

Proceedings of the NAL Symposium on Aircraft Computational Aerodynamics
[NAL-SP-1] 16 p2691 N85-26611

Technical evaluation report on the Flight Mechanics Symposium on Active Control Systems: Review, Evaluation and Projections
[AGARD-AR-220] 16 p2711 N85-26730

Tenth Conference of Working Group of Socialist Countries on Remote Sensing of Earth under Intercosmos Program 16 p2725 N85-26820

Advanced High Pressure O2/H2 Technology
[NASA-CP-2372] 16 p2733 N85-26862

Sixth DOE Electrochemical Contractor's Review. Extended abstracts
[DE84-013679] 16 p2779 N85-27151

Short Wavelength Chemical Laser (SWCL) Workshop
[AD-A151959] 16 p2790 N85-27211

Data Collection and Platform Location by Satellite: ARGOS Users' Conference 16 p2811 N85-27333

Proceedings of the Workshop on Polarized Targets in Storage Rings
[DE85-002704] 16 p2862 N85-27653

Active Control Systems: Review, Evaluation and Projections
[AGARD-CP-364] 17 p2901 N85-27883

Adaptive wall wind tunnels and wall interference correction methods
[DFVLR-IB-222-84-A-37] 17 p2905 N85-27912

Structural Integrity and Durability of Reusable Space Propulsion Systems
[NASA-CP-2381] 17 p2910 N85-27941

Systematic nomenclature of the nitrogen, oxygen and sulfur functional polycyclic aromatic hydrocarbons
[DE85-007426] 17 p2916 N85-27974

Gordon Research Conference on Composites
[AD-A152888] 17 p2917 N85-27979

Proceedings of the 9th US Air Force and the Federal Republic of Germany Data Exchange Agreement Meeting. Viscous and Interacting Flow Field Effects
[AD-A153020] 17 p2958 N85-28266

Airphoto interpretation of vegetation and landforms for soil mapping 17 p2983 N85-28436

Presentations at the Tri-Service Cloud Modeling Workshop (2nd), held at the Naval Surface Weapons Center, White Oak, Maryland, 26-27 June 1984, volume 1
[AD-A152735] 17 p2996 N85-28522

Peer Review of a Formal Verification/Design Proof Methodology
[NASA-CP-2377] 17 p3010 N85-28609

Science and Technology in the Soviet Union
[AD-A152828] 17 p3047 N85-28856

Proceedings of the Sixteenth Annual Precise Time and Time Interval (PTTI) Applications and Planning Meeting
[NASA-TM-87581] 18 p3105 N85-29221

Environmental management needs
[DE85-007859] 18 p3133 N85-29405

Controlled Ecological Life Support System. Life Support Systems in Space Travel
[NASA-CP-2378] 18 p3155 N85-29531

Proceedings of the Seminar on Space Station Human Productivity
[NASA-TM-86673] 18 p3156 N85-29539

Report of the 11th Regional IRPA Congress on Recent Developments and New Trends in Radiation Protection
[IRI-190-83-13] 18 p3160 N85-29575

Proceedings of the 14th European Solid State Device Research Conference Including Solid State Device Technology, ESSDERC 84
[AD-A153409] 18 p3193 N85-29804

Space methods for geological research
19 p3295 N85-30429

Symposium on Luminescent Radiation Receivers and Converters 19 p3295 N85-30430

Proceedings of the Distributed Receiver Solar Thermal Technology Conference
[DE85-010551] 19 p3306 N85-30493

Third US/USSR Symposium on Particulate Control
[PB85-190890] 19 p3310 N85-30522

Proceedings of the Argonne Workshop on Programming the Next Generation of Supercomputers
[DE85-008348] 19 p3343 N85-30718

MCNP variance reduction overview
[DE85-010765] 19 p3346 N85-30741

Proceedings of the 1984 Workshop on High-Energy Excitations in Condensed Matter, volume 2
[DE85-007395] 19 p3357 N85-30809

Possibilities for studying short-lived nuclei produced at LAMPF
[DE85-010740] 19 p3365 N85-30864

U.S.-China conference on science policy
[PB85-176345] 19 p3380 N85-30971

Satellite aided search and rescue. Experimental results and operational prospects — conference
[ISBN-2-85428-120-9] 20 p3400 N85-31068

Proceedings of the Workshop on Identification and Control of Flexible Space Structures, volume 1
[NASA-CR-176051] 20 p3408 N85-31148

Sandia Cooperative Group on the Aerothermochemistry of Turbulent Combustion. Discussion record of fourth meeting
[DE85-004720] 20 p3423 N85-31248

Cryogenics for the Superconducting Super Collider: Workshop Proceedings
[DE85-010951] 20 p3437 N85-31327

The 1984 Goddard Space Flight Center Battery Workshop
[NASA-CP-2382] 20 p3443 N85-31371

Nonlinear Constitutive Relations for High Temperature Application, 1984
[NASA-CP-2369] 20 p3465 N85-31530

Remote Sensing Technology: Symposium Proceedings
[DE85-010212] 20 p3477 N85-31606

Proceedings of the Flat-Plate Solar Array Project Research Forum on High-Efficiency Crystalline Silicon Solar Cells
[NASA-CR-176047] 20 p3478 N85-31615

Commission for Marine Meteorology
[WMO-640] 20 p3496 N85-31735

Results of Space Experiments in Physiology and Medicine and Informal Briefings by the F-16 Medical Working Group
[AGARD-CP-377] 20 p3507 N85-31805

Spectral Theory of Sturm-Liouville Differential Operators: Proceedings of the 1984 Workshop
[DE85-009893] 20 p3520 N85-31890

Proceedings of the 19th Annual Conference of the Finnish Physical Society
[REPT-104] 20 p3532 N85-31974

VLF (Very low frequency) workshop held at San Diego California, 24-25 January 1985
[AD-A154652] 21 p3573 N85-32224

Middle Atmosphere Program. Handbook for MAP. Volume 14: URSI/SCOSTEP Workshop on Technical Aspects of MST Radar
[NASA-CR-176085] 21 p3615 N85-32466

Data base management: MSTRAC (keynote paper), part 8 21 p3626 N85-32530

Eleventh international Conference on Atmospheric Aerosols, Condensation and Ice Nuclei, volume 2
[PB85-182418] 21 p3638 N85-32596

Eleventh International Conference on Atmospheric Aerosols, Condensation and Ice Nuclei, volume 1
[PB85-182400] 21 p3644 N85-32636
Software for interactive on-line conferences
[AD-A154742] 21 p3670 N85-32801
Workshop on the Early Earth: The Interval from Accretion to the Older Archean
[NASA-CR-176037] 21 p3717 N85-33062
Management of Corrosion
[AGARD-LS-141] 22 p3749 N85-33236
Ninteenth Aerospace Mechanisms Symposium
[NASA-CP-2371] 22 p3795 N85-33512
Nordic Association for Aerosol Research (NOSA) Aerosol Symposium: Program and abstracts
[FOA-E-40019] 22 p3812 N85-33616
Proceedings of the 18th LAMPF Users Group Meeting
[DE85-011886] 22 p3839 N85-33773
Terrestrial Planets: Comparative Planetology
[NASA-CR-176093] 22 p3851 N85-33849
Ninteenth International Cosmic Ray Conference. Conference program and author index
[NASA-CP-2376] 22 p3860 N85-33901
Ninteenth International Cosmic Ray Conference. OG sessions, volume 1
[NASA-CP-2376-VOL-1] 22 p3860 N85-33902
Ninteenth International Cosmic Ray Conference. OG sessions, volume 2
[NASA-CP-2376-VOL-2] 22 p3875 N85-34006
Space Station Engineering and Technology Development: Proceedings of the Panel on In-Space Engineering Research and Technology Development
[NASA-CR-176110] 23 p3899 N85-34153
Coordinated study of solar-terrestrial payloads on space station
[NASA-CR-176160] 23 p3900 N85-34158
Proceedings of the Twentyseventh Japan Congress on Materials Research
[ISSN-0368-3141] 23 p3903 N85-34180
Proceedings of the Mechanisms Conference, volume 1 23 p3923 N85-34309
Proceedings of the Mechanisms Conference, volume 2 23 p3924 N85-34318
Problems of aviation and space medicine and psychology discussed at 14th Gagarin lectures
23 p3954 N85-34509
Graphics Interface 1985: Proceedings
[ISSN-0713-5424] 23 p3957 N85-34523
Nintoenth International Cosmic Ray Conference. SH sessions, volume 4
[NASA-CP-2376-VOL-4] 23 p3969 N85-34729
Ninteenth International Cosmic Ray Conference. OG sessions, volume 3
[NASA-CP-2376-VOL-3] 23 p4012 N85-34862
Ninteenth International Cosmic Ray Conference. SH sessions, volume 5
[NASA-CP-2376-VOL-5] 23 p4031 N85-34991
Lectures of a Flight Mechanics Conference — conferences
[ESA-TT-831] 24 p4061 N85-35165
Proceedings of the 7th Joint Panel Meeting of the UJNR Panel on Fire Research and Safety
[PB85-199545] 24 p4085 N85-35317
USGS research on mineral resources, 1985
[CIRC-949] 24 p4103 N85-35435
Implementing agreement for cooperation in the development of large scale wind energy conversion systems
[JUEL-SPEZ-278] 24 p4110 N85-35473
Land Disposal of Hazardous Waste
[PB85-196376] 24 p4113 N85-35500
Workshop Proceedings: Interpretation of Seismic Wave Propagation in Laterally Heterogeneous Structures
[BMR-258] 24 p4118 N85-35530
Proceedings of Meteorological Motor Glider (MEMO) Workshop '84
[DFVLR-MITT-85-04] 24 p4121 N85-35542
Proceedings of a Scientic Meeting on the Occasion of the Inauguration of New Buildings for the DFVLR Institute for Aerospace Medicine
[ESA-TT-857] 24 p4129 N85-35595
Proceedings of the 14th Army Science Conference. Volume 2: Principal authors ! through O
[AD-A149201] 24 p4144 N85-35690
Proceedings of the 14th Army Science Conference. Volume 3: Principal authors P through Z
[AD-A149202] 24 p4144 N85-35691
Proceedings of the Workshop on Detectors for Relativistic Nuclear Collisions
[LBL-18225] 24 p4146 N85-35700
The 2nd European Conference on Atomic and Molecular Physics
[AD-A155863] 24 p4148 N85-35715
Nineteenth International Cosmic Ray Conference. HE Sessions, volume 6
[NASA-CP-2376-VOL-6] 24 p4170 N85-35848
Nineteenth International Cosmic Ray Conference. HE Sessions, volume 7
[NASA-CP-2376-VOL-7] 24 p4186 N85-35968
Nineteenth International Cosmic Ray Conference. HE sessions, volume 8
[NASA-CP-2376-VOL-8] 24 p4200 N85-36068

CONFIDENCE
Setting hurricane conditions of readiness with high confidence
[AD-A144785] 01 p0085 N85-10570
Bootstrap confidence intervals
[AD-A147572] 07 p1033 N85-16559
Exact simultaneous confidence intervals for pairwise comparisons of three normal means
[AD-A146751] 09 p1375 N85-18645

CONFIDENCE LIMITS
Construction of approximate confidence intervals for probability-of-kill via the bootstrap
[AD-A144761] 01 p0113 N85-10764
Construction of a confidence region for linear functions with unknown parameters
[CTH-MATH-1984-17] 05 p0721 N85-14630
The theory of optimal confidence limits for systems reliability with counterexamples for results on optimal confidence limits for series systems
[AD-A147236] 07 p1031 N85-16546
Bootstrap confidence intervals
[AD-A147572] 07 p1033 N85-16559
Exact simultaneous confidence intervals for pairwise comparisons of three normal means
[AD-A146751] 09 p1375 N85-18645
An asymptotically optimal subclass of BTIB designs for comparisons with a control
[AD-A149819] 12 p1921 N85-22066
Confidence intervals using the regenerative method for simulation output analysis
[AD-A150147] 13 p2149 N85-23343
Better bootstrap confidence intervals
[AD-A150798] 14 p2406 N85-24846
Shuttle fleet operations: A simulation analysis
[AD-A151383] 15 p2491 N85-25370
Criteria for the classification of hydrographic positioning data
[AD-A152283] 16 p2705 N85-26697
Confidence intervals based on interpolated order statistics
[AD-A152607] 17 p3025 N85-28701
Limit theorems for the method of replication
[AD-A153541] 18 p3170 N85-29642
On the confidence limits for Weibull reliability and quantiles: The case of maximum likelihood estimation from small size censored samples
[REPT-84-RR-345] 20 p3521 N85-31896
The optimality of lower confidence limits for the reliability of series systems obtained by the method of key test results or other related techniques
[AD-A154880] 21 p3597 N85-32338

CONFIGURATION MANAGEMENT
Configuration management for mission-critical software: The Los Alamos solution
[DE84-015515] 03 p0408 N85-12606
Software configuration management across project boundaries and in distributed development environments
[RSRE-MEMO-3704] 04 p0549 N85-13494
Managing computer-controlled operations
08 p1097 N85-16934
Space Station Software Issues
[NASA-CP-2361] 11 p1700 N85-20689
Space Station reference configuration description
[NASA-TM-87493] 20 p3408 N85-31146
Integrated Support Software System (ISSS)
[AD-A155715] 22 p3829 N85-33710

CONFIGURATIONS
Changes in spectral properties of detached leaves
[E85-10042] 07 p0983 N85-16243

CONFINEMENT
Focussing and confinement
[DE84-016181] 05 p0640 N85-14106
Confinement of low-energy electrons near metallic surfaces for plasmon generation
[DE85-001119] 09 p1381 N85-18688
Efficient heating and confinement of ions in an axisymmetric magnetic mirror supplemented with dc electric field
[IPPJ-707] 12 p1935 N85-22160
Behavior of turbulent gas jets in an axisymmetric confinement
[NASA-CR-174829] 15 p2473 N85-25265
Effects of muscle atrophy on motor control: Cage size effects 15 p2609 N85-26080
Breakthrough in container confinement of ultracold neutrons 15 p2644 N85-26311
Effect of confinement on failure in 95 TATB/5 KEL-F
[DE85-010790] 19 p3251 N85-30158
Density and confinement effects on mixing characteristics of an axisymmetrical CO(2) jet
[AD-A154468] 19 p3267 N85-30258
Los Alamos Spheromak Program
[DE85-010748] 20 p3398 N85-31077
Magnetics calculations for an ELMO Bumpy Square
[DE85-011438] 21 p3707 N85-33021
Behavior of the porous bed in a combustion-deflagration-detonation transition
[ISL-CO-220/84] 22 p3747 N85-33224
Combustion-deflagration-detonation transition
[ISL-CO-221/84] 22 p3747 N85-33225

CONFIRMATION
U PROVING

CONFLUENCE
U CONVERGENCE

CONFORMAL MAPPING
Deformations of two-dimensional dissipative maps – orbit perturbation
[REPT-89] 01 p0129 N85-10891
What formulas are good for representing dipole and generalized oscillator-strength spectra
[DE84-014641] 02 p0278 N85-11809
Nicolai maps and stochastic observables from a coupling constant flow
[BONN-HE-84-26] 09 p1376 N85-18653
Annuals of the Finnish Academy of Sciences, series A. 1: Mathematics, volume 8, part 2
[ISSN-0066-1953] 10 p1535 N85-19673
Domains with Lipschitz mapping functions
10 p1535 N85-19675
Simplified proofs of some basic theorems for quasiregular mappings 10 p1535 N85-19677
Diffeomorphic approximation of quasiconformal and quasisymmetric homeomorphisms
10 p1536 N85-19678
Analytical foundations of the theory of quasiconformal mappings in Rn 10 p1536 N85-19679
A conformal mapping suitable for problems involving interaction between given geometries and known far fields
[AD-A149050] 10 p1545 N85-19744
Applications of the conformal mapping method to the solution of mechanical vibrations problems
13 p2102 N85-23103
Investigation of potential and viscous flow effects contributing to dynamic stall
[AD-A151696] 15 p2557 N85-25773
Annals of the Scientific Academy of Finland, series A. 1: Mathematics, volume 9
[ISSN-0066-1953] 15 p2633 N85-26228
Harmonic univalent functions
15 p2633 N85-26230
Old and new in Moebius groups
15 p2634 N85-26236
Remarks of the maximal dilatation of the Beurling-Ahlfors extension 15 p2634 N85-26239
A remark on the conformal capacity of Groetzsch's condenser in space 15 p2634 N85-26240
Extension of embeddings close to isometries or similarities 15 p2634 N85-26242
Application of conformal mapping to grid generation
16 p2692 N85-26921
Conditions for the possibility of conformal sewing
[ST-AASF-IMD-58] 16 p2858 N85-27625
Chaos and order in an optical ring cavity
[CWI-AM-R8416] 17 p3038 N85-28795
Generation by conformal mappings of aerofoil sections and of certain other simple shapes suitable for both aerodynamic and stress-concentration problems
[AD-A154901] 22 p3728 N85-33112
Adaptive rezoner in a two-dimensional Lagrangian hydrodynamic code
[DE85-010108] 24 p4094 N85-35381

CONFORMAL TRANSFORMATIONS
U CONFORMAL MAPPING

CONGRESSIONAL REPORTS
Soviet space programs, 1976-1980, with supplementary data through 1983. Part 2: Manned space programs and space life sciences
[S-REPT-98-235-PT-2] 01 p0014 N85-10068
Department of Housing and Urban Development, and certain independent agencies appropriations for fiscal year 1985, part 2
[S-REPT-98-888-PT-2] 01 p0127 N85-10870
National Aeronautics and Space Administration
01 p0127 N85-10871
Office of Technology Assessment
01 p0127 N85-10872
Workshop on Automated Space Station
01 p0127 N85-10873
Initiatives to promote space commercialization
[GPO-37-551] 02 p0156 N85-11068
Statement of Hon. James M. Beggs, Administrator, NASA, Washington, DC 02 p0156 N85-11069

Civilian space stations and the US future in space: Summary
[OTA-STI-242] 03 p0323 N85-12083
The status of synthetic fuels and cost-shared energy R and D facilities
[GPO-36-903] 03 p0339 N85-12182
Carbon dioxide, the greenhouse effect and climate: A primer
[GPO-33-444] 03 p0395 N85-12519
Airliner cabin air quality
[S-REPT-98-488] 03 p0402 N85-12560
Emergency Mathematics and Science Education Act
[GPO-29-561] 03 p0435 N85-12770
Ways to improve management of Federal funded computerized models
[LCD-75-111] 03 p0435 N85-12771
Federal Telecommunications Privacy Act of 1984
[H-REPT-98-815] 03 p0441 N85-12807
Aircraft navigation and landing technology: Status of implementation
[GPO-38-615] 04 p0454 N85-12883
The Expendable Launch Vehicle Commercialization Act
[GPO-30-838] 04 p0460 N85-12919
Review of Space Shuttle requirements, operations, and future plans
[GPO-39-101] 04 p0461 N85-12927
Results of Space Shuttle Flight 41-C
[GPO-36-092] 04 p0461 N85-12928
Statement of Captain Robert L. Crippen, USN, Commander of Space Shuttle Flight 41-C; Francis R. Scobee, pilot; Doctor George D. Nelson, Mission Specialist; Terry J. Hart, Mission Specialist; and Doctor James D. Van Hoften, Mission Specialist; accompanied by Frank Cepollina, Solar Maximum Repair Mission Project Manager, Goddard Space Flight Center
04 p0461 N85-12929
Guayule research
[GPO-29-562] 04 p0477 N85-13042
Methane-fueled vehicle RD and D
[GPO-37-926] 04 p0481 N85-13064
Fire prevention and control
[GPO-30-743] 04 p0482 N85-13074
Scientific communications and national security
[GPO-36-093] 04 p0492 N85-13138
Summary and analysis of hearing on improving the research infrastructure at US universities and colleges
[GPO-36-854] 04 p0574 N85-13660
Improving the research infrastructure at US universities and colleges
[GPO-35-290] 04 p0574 N85-13661
The Uniform Science and Technology Research and Development Utilization Act
[GPO-36-327] 04 p0577 N85-13685
Uniform Science and Technology Research and Development Utilization Act
[H-REPT-98-983-PT-1] 04 p0577 N85-13686
Computer Literacy Act of 1983, part 2
[H-REPT-98-752-PT-2] 04 p0578 N85-13687
Manufacturing Sciences and Robotics Research and Development Act of 1984
[H-REPT-98-1078] 04 p0578 N85-13688
Commercial Space Launch Act
[GPO-39-613] 04 p0578 N85-13690
International Geosphere/Biosphere Program: 1984
[GPO-39-222] 04 p0578 N85-13691
Space telescope cost, schedule, and performance review, 1984
[GPO-39-065] 04 p0579 N85-13696
Vandenberg space shuttle launch complex
[S-HRG-98-1075] 05 p0601 N85-13833
Statement of Edward C. Aldridge, Jr., Under Secretary of the Air Force, Department of the Air Force, accompanied by Lieutenant General Robert W. Bazley, Inspector General and Brigadier General Donald J. Kutyna, Director of Space Systems and Command, Control and Communications, Deputy Chief of Staff, Research, Development and Acquisition
05 p0601 N85-13834
Statement of Honorable James M. Beggs, Administrator, National Aeronautics and Space Administration
05 p0601 N85-13835
Subliminal communication technology
[GPO-38-833] 05 p0622 N85-13979
Land Remote-Sensing Commercialization Act
[S-REPT-98-458] 05 p0654 N85-14201
The availability of Japanese scientific and technical information in the United States
[GPO-35-241] 05 p0735 N85-14726
Man in Space: National Historic Landmark Theme Study
[PB85-107233/GAR] 07 p0911 N85-15768
Civilian space stations and the US future in space
[OTA-STI-241] 07 p0914 N85-15781
Satellite navigation
[S-HRG-98-656] 08 p1082 N85-16651
International cooperation and competition in civilian space activites
[OTA-ISC-240] 08 p1231 N85-17750
Sunset of the Civil Aeronautics Board
[S-HRG-98-940] 09 p1403 N85-18829
Semiannual report to Congress on the effectiveness of the civil aviation security program
[AD-A149522] 10 p1421 N85-18967
Computers and education
[GPO-28-378] 10 p1537 N85-19689
Computer crime
[GPO-30-544] 10 p1537 N85-19691
Department of defense, office of inspector general semiannual report to the Congress, 1 April - 30 September 1984
[AD-A149580] 10 p1567 N85-19879
Provision of Federal government publication in electronic format to depository libraries
[S-PRT-98-260] 10 p1567 N85-19880
High-speed intercity rail passenger service
[GPO-35-896] 10 p1570 N85-19897
Synthetic fuels policy
[GPO-34-227] 11 p1613 N85-20143
Environmental Monitoring Improvement Act
[GPO-39-742] 11 p1677 N85-20568
Carbon dioxide and the greenhouse effect
[GPO-39-043] 11 p1677 N85-20569
National Acid Precipitation Assessment Program. Report to the President and Congress (1983)
[PB85-116713] 11 p1679 N85-20581
Ultralight aircraft technology and public safety
[GPO-38-948] 12 p1773 N85-21131
Legislation to improve airline safety
[GPO-38-222] 12 p1773 N85-21132
Commercial space launches
[S-REPT-98-656] 12 p1788 N85-21225
Brussels Satellite Convention
[S-EXEC-REPT-98-52] 12 p1790 N85-21234
Results of Space Shuttle flight 41-D
[GPO-39-481] 12 p1791 N85-21243
Developments in the production and use of ethanol fuels
[GPO-40-678] 12 p1817 N85-21398
Effects of air pollution and acid rain on forest decline
[GPO-37-459] 12 p1883 N85-21818
Wind shear detection technology
[GPO-38-920] 12 p1893 N85-21879
Hurricane storm surge research
[GPO-40-048] 12 p1893 N85-21880
Computer and communications security and privacy
[GPO-39-741] 12 p1911 N85-21994
Oversight review of the five-year outlook report on science and technology
[GPO-41-058] 12 p1949 N85-22243
1984 science and technology posture hearing with the director of the Office of Science and Technology Policy
[GPO-41-060] 12 p1949 N85-22244
An agenda for a study of government science policy
[GPO-40-860] 12 p1949 N85-22245
Transfer of technology
[S-REPT-98-684] 12 p1949 N85-22246
Transfer of technology
[S-HRG-98-986] 12 p1949 N85-22247
The availability of Japanese scientific and technical information in the United States
[GPO-39-478] 12 p1951 N85-22254
Summary of activities of the Committee on Science and Technology
[H-REPT-98-1189] 12 p1964 N85-22341
The impact of weather on aviation safety
[GPO-35-520] 16 p2703 N85-26685
Recent failures of weather satellites
[S-HRG-98-1070] 16 p2731 N85-26855
Soviet space programs, 1976-1980 (with supplementary data through 1983). Part 3: Unmanned space activities
[S-PRT-98-235-PT-3] 16 p2879 N85-27765
National Telecommunications and Information Administration authorization
[GPO-38-660] 16 p2879 N85-27766
East-West cooperation in outer space
[S-HRG-98-1064] 16 p2879 N85-27767
Department of Housing and Urban Development-independent agencies appropriations for 1986. Part 6: National Aeronautics and Space Administration
[GPO-47-235] 16 p2879 N85-27768
The Department of Defense statement on the Science and Technology Program by Colonel Donald I. Carter, USAF Acting Deputy Under Secretary of Defense for Research and Advanced Technology before the Subcommittee on Research and Development of the Committee on Armed Services of the United States House of Representatives, 99th Congress, first session
[AD-A152467] 17 p3046 N85-26850
National Aeronautics and Space Administration Authorization Act, 1986
[S-REPT-99-91] 17 p3051 N85-28885
Report to Congress on the Automotive Technology Development Program
[DE85-005640] 17 p3052 N85-28890
Electric and hybrid vehicle program
[DE85-010025] 19 p3262 N85-30230
National Aeronautics and Space Administration Authorization Act, 1986
[S-REPT-99-91] 19 p3381 N85-30978
Department of Housing and Urban Development-Independent Agencies Appropriation Bill, 1986
[H-REPT-99-212] 19 p3382 N85-30979
National Aeronautics and Space Administration
19 p3382 N85-30980
FAA regulation of 9-seat and under passenger aircraft
[GPO-42-703] 20 p3391 N85-31032
Status of air traffic control system
[S-HRG-98-1197] 20 p3391 N85-31036
Insurance and the commercialization of space
[S-PRT-99-16] 20 p3397 N85-31074
Auto fuel efficiency standards, part 2
[GPO-41-189] 20 p3435 N85-31309
Antarctica
[S-HRG-98-1181] 20 p3473 N85-31584
Magnetohydrodynamics and the National Coal Science, Technology, and Engineering Development Acts
[S-HRG-98-1179] 20 p3535 N85-31994
NASA authorization, 1986, volume 1
[GPO-46-385] 20 p3541 N85-32039
United States-Soviet satellite accord: SARSAT/Cospas search-and-rescue program
[GPO-41-113] 20 p3541 N85-32040
Department of Housing and Urban Development-Independent Agencies Appropriation Act, 1986
20 p3542 N85-32041
National Aeronautics and Space Administration research and development 20 p3542 N85-32042
Aviation system delays
[S-HRG-98-1241] 21 p3553 N85-32102
Status of the air traffic control system
[GPO-40-343] 21 p3554 N85-32107
Review of hazardous waste cleanup and disposal efforts at Tinker Air Force Base
[GPO-43-294] 21 p3613 N85-32457
Hazardous air pollutants
[GPO-43-064] 21 p3613 N85-32458
Acid rain in Europe
[COMMITTEE-PRINT-99-F] 22 p3810 N85-33601
Aviation safety (aircraft passenger survivability and cabin safety)
[GPO-39-847] 23 p3895 N85-34130
Department of Housing and Urban Development Independent Agencies Appropriation Bill, 1986
[S-REPT-99-129] 23 p3987 N85-34720
National Aeronautics and Space Administration research and development: Program description
23 p3987 N85-34721
The 1986 National Aeronautics and Space Administration authorization
[GPO-47-635] 24 p4166 N85-35829

CONGRUENCES
Algebra of communicating processes
[CWI-CS-R8421] 17 p2950 N85-28214
A complete inference system for regular processes with silent moves
[CWI-CS-R8420] 17 p3014 N85-28638

CONICAL BODIES
NT SLENDER CONES
An algorithm for least squares projections onto the intersection of shifted, convex cones
[AD-A145428] 02 p0251 N85-11640
Experimental and predicted heating distributions for biconics at incidence in air at Mach 10
[NASA-TP-2334] 03 p0361 N85-12313
A computer program to calculate the supersonic flow over a solid cone in air or water
[AD-A151102] 15 p2464 N85-25217
Flow over a biconic configuration with an afterbody compression flap
[AD-A151882] 15 p2557 N85-25778
Cone drag in the transition from continuum to free molecular flow
[OUEL-1538/84] 20 p3390 N85-31023
Aerodynamic characteristics of the standard dynamics model in coning motion at Mach 0.6
[NASA-TM-86717] 21 p3552 N85-32094
Behaviors of stress waves in a conical bar
23 p3904 N85-34182

CONICAL FLARE
U CONES

CONICAL FLOW
Geometric characteristics of turbulent boundary layer separation upon action with direct shock wave in conical flows 02 p0269 N85-11755
Conical stagnation points in the flow around an external corner --- delta wings
[VTH-LR-396] 16 p2701 N85-26880
CONICAL NOZZLES
Density distribution in supersonic jet discharged into vacuum from nozzle with bevel tip
02 p0269 N85-11757
Carbon/carbon rocket motor exit cone reinforcement
[AD-D011360] 07 p0916 N85-15799
Nozzle wall roughness effects on free-stream noise and transition in the pilot low-disturbance tunnel
[NASA-TM-86389] 23 p3930 N85-34355
CONICAL SCANNING
Integrated dual beam line scanning antenna and negative resistance diode oscillator
[AD-D011717] 19 p3261 N85-30223
CONICAL SHELLS
Determination of stresses and deformations in linearly elastic conical shell subjected to aerodynamic loading and heating 13 p2047 N85-22812
Initial imperfection surveys on conical shells at Hoechst AG
[VTH-LR-407] 17 p2981 N85-28429
CONICS
NT ELLIPSES
NT HYPERBOLAS
NT PARABOLAS
Precursors for Brazilian magnetic anomalies from 1922 to 1969
[INPE-3283-PRE/605] 11 p1681 N85-20590
Trapping of ion conics by downward parallel electric fields
[AD-A155306] 21 p3633 N85-32568
CONIFERS
The 1984 NASA/ASEE summer faculty fellowship program
[NASA-CR-174138] 04 p0574 N85-13663
Microwave model prediction and verifications for vegetated terrain
[E85-10102] 16 p2809 N85-27322
Study of the formation of particles from natural hydrocarbons released by vegetation
21 p3644 N85-32640
CONJUGATE GRADIENT METHOD
Comparison of the multigrid and ICCG methods in solving the diffusion equation
[DE84-014409] 02 p0253 N85-11657
Solution of finite element problems by preconditioned conjugate gradient and Lanczos methods
[AD-A146921] 07 p1029 N85-16532
Solving large linear systems 14 p2396 N85-24759
CONJUGATE POINTS
Conjugacy of ELF-VHF emissions near L=6 --- chorus phenomenon, hiss 14 p2367 N85-24629
Conjugated symmetrical coupler curves, produced by 4-bar linkages having the same transmission angles
23 p3924 N85-34322
CONJUGATES
NT CONJUGATE POINTS
CONJUGATION
NT PHASE CONJUGATION
Experimental investigation of wavefront conjugation during Mandelstam-Brillouin scattering of focused laser beams in condensed media 11 p1716 N85-20796
Four-wave hypersonic reversing mirrors in saturated mode 11 p1719 N85-20812
CONNECTICUT
Impact of LANDSAT MSS sensor differences on change detection analysis --- New Mexico, San Francisco, CA, New Hampshire, and Connecticut
11 p1667 N85-20506
CONNECTIONS
U JOINTS (JUNCTIONS)
CONNECTIVE TISSUE
NT MARROW
CONNECTORS
NT ELECTRIC CONNECTORS
Extractor for spring-lock pin connectors
[AD-D011235] 01 p0043 N85-10260
Vehicle-to-vehicle connection mechanism
[AD-D011267] 05 p0645 N85-14142
Safety requirements for wiring systems and connectors for photovoltaic systems
[NASA-CR-174211] 06 p0803 N85-15110
Connection system --- insuring against loss of a tool component without using multiple tethers
[NASA-CASE-MSC-20319-1] 12 p1857 N85-21649
Releasable cable connector assembly for use between a mobile and stationary object
[AD-D011536] 12 p1858 N85-21655
Fiber optics applications for MIL-STD-1760
[AD-A151113] 15 p2470 N85-25251
Wideband fiber optic communications link
[AD-A151704] 15 p2542 N85-25697
Ultrasonic test evaluation of the insert bond on hermetic connectors
[DE85-008394] 18 p3120 N85-29310
Fiber optic expanded beam connector
[AD-A154057] 19 p3367 N85-30880
Attitude control tradeoff study between the use of a flexible beam and a tether configuration for the connection of two bodies in orbit 20 p3412 N85-31174
Static and cyclic behavior of semi-rigid steel beam-column connections
[PB85-194363] 24 p4103 N85-35433
CONNECTORS (ELECTRIC)
U ELECTRIC CONNECTORS
CONOIDS
U CONICAL BODIES
CONSCIOUSNESS
G-induced Loss of Consciousness (GLC)
20 p3510 N85-31823
Centrifuge operations and training in the Royal Netherlands Air Force 20 p3511 N85-31825
CONSERVATION
NT ENERGY CONSERVATION
Research and development requirements for ion implantation
[AD-P003951] 02 p0286 N85-11867
Use of ion implantation to modify the corrosion behavior of metals
[AD-P003953] 02 p0286 N85-11869
Closed-loop concepts for the Army: Water conservation, recycle, and reuse
[AD-A146839] 09 p1365 N85-18581
Basic cryogenics and materials. Phase 1
[NASA-CR-177932] 21 p3572 N85-32215
CONSERVATION EQUATIONS
Further developments of a nongradient theory of premixed turbulent flames
[NAL-TR-802T] 01 p0023 N85-10143
Numerical analysis of flow and heat transfer in the VAFB LOX storage Dewar tank
[NASA-CR-171203] 02 p0197 N85-11315
Statistical Plasma Physics. Proceedings of the Workshop of the US-Japan Joint Institute for Fusion Theory Program
[IPPJ-689] 02 p0282 N85-11832
Conservative and nonconservative schemes for the solution of the nonlinear Schroedinger equation
[CWI-NM-R8405] 05 p0720 N85-14628
High altitude chemically reacting gas particle mixtures. Volume 1: A theoretical analysis and development of the numerical solution --- rocket nozzle and orbital plume flow fields
[NASA-CR-171826] 07 p0916 N85-15801
The omni-transform in single-channel queues
[AD-A151019] 14 p2409 N85-24852
On coupling factors of explosion
15 p2551 N85-25747
Progress of computational fluid dynamics in the world
16 p2691 N85-26612
Approximate factorization method for computation of nonhydrostatic mesoscale flows
[DE85-007259] 19 p3313 N85-30537
On the convergence of difference approximations to scalar conservation laws
[NASA-CR-172614] 19 p3344 N85-30726
CONSERVATION LAWS
Conservation laws and the numerical solution of ODEs
[DE84-016206] 04 p0555 N85-13531
Parity and time-reversal non-conversation in atoms
[DE84-016924] 04 p0562 N85-13581
A geometric approach to high resolution TVD schemes
[NASA-CR-172484] 06 p0857 N85-15449
Isolated systems in general relativity
09 p1400 N85-18813
A convergent series expansion for hyperbolic systems of conservation laws
[NASA-CR-172557] 12 p1910 N85-21990
An approximation theory for nonlinear evolution equations and single conservation laws
16 p2691 N85-26614
New semi-implicit method for solving the time-dependent conservation equations for incompressible flow
[DE85-010926] 23 p3931 N85-34367
Generalized reduced fluid model with finite ion-gyroradius effects
[DE85-013123] 24 p4157 N85-35777
Phase space factors in multiparticle processes
24 p4175 N85-35888
CONSISTENCY
Precedency control and other semantic integrity issues in a workbench database 13 p2123 N85-23220
Consistency of smoothing with running linear fits
[AD-A150232] 13 p2150 N85-23349
CONSOLIDATION
Computer program for determining induced stresses and consolidation settlements (CSETT)
[AD-A146730] 07 p1023 N85-16493
Consolidation of thermites by pressing and sintering
[DE84-016943] 09 p1297 N85-18146
Consolidation around a point heat source
[PB85-116549] 11 p1682 N85-20601
Metallurgical characterization of aluminum powder consolidation
[AD-A151990] 15 p2510 N85-25484
CONSTANT SPEED PROPELLERS
U VARIABLE PITCH PROPELLERS
CONSTANT VOLUME BALLOONS
U SUPERPRESSURE BALLOONS
CONSTANTS
NT GRUNEISEN CONSTANT
NT HUBBLE CONSTANT
NT PLANCKS CONSTANT
NT SOLAR CONSTANT
NT TIME CONSTANT
One-dimensional two-phase constant lag flow in combustion chamber of solid propellant rocket motors
[AD-A145679] 02 p0173 N85-11157
Quark models of hadronic interactions
[DE84-013787] 04 p0561 N85-13570
Chemical kinetics and photochemical data for use in stratospheric modeling. Evaluation number 6
[NASA-CR-175564] 12 p1888 N85-21846
Conserved quantities and radiative aspects of asymptotically anti-de Sitter space-times
12 p1958 N85-22303
An integral representation of the generalized Euler-Mascheroni constants
[NASA-TP-2456] 13 p2144 N85-23305
Attenuated total reflection method for obtaining optical constants of powders
[AD-A154094] 19 p3367 N85-30881
Large-time behavior of viscous surface waves
[AD-A154805] 21 p3584 N85-32276
On the turning lozange of constant side whose vertices alternate between two fixed circles of a ring
[AD-A154803] 21 p3677 N85-32840
CONSTELLATIONS
NT AURIGA CONSTELLATION
NT CASSIOPEIA CONSTELLATION
NT CENTAURUS CONSTELLATION
NT CORONA BOREALIS CONSTELLATION
NT CYGNUS CONSTELLATION
NT LYRA CONSTELLATION
NT ORION CONSTELLATION
Proceedings of a Workshop on Applications of Tethers in Space, Executive Summary
[NASA-CR-171195] 03 p0322 N85-12075
Proceedings of a Workshop on Applications of Tethers in Space, Volume 2
[NASA-CR-171197] 03 p0322 N85-12077
CONSTITUTIONAL DIAGRAMS
U PHASE DIAGRAMS
CONSTITUTIVE EQUATIONS
Biaxial constitutive equation development for single crystals
[NASA-CR-174056] 02 p0286 N85-11862
Dynamics of coupled ice-ocean system in the marginal ice zone: Study of the mesoscale processes and of constitutive equations for sea ice
[NASA-CR-174171] 04 p0542 N85-13448
Single integral constitutive equations for viscoelastic fluids
[AD-A149410] 10 p1547 N85-19756
Viscoplastic constitutive relationships with dependence on thermomechanical history
[NASA-CR-174836] 12 p1864 N85-21691
Unified constitutive material models for nonlinear finite-element structural analysis --- gas turbine engine blades and vanes
[NASA-TM-86985] 14 p2320 N85-24338
On thermomechanical testing in support of constitutive equation development for high temperature alloys
[NASA-CR-174879] 15 p2577 N85-25694
Some remarks on the constitutive equations of stratified gas-liquid flow
[EME-137] 20 p3456 N85-31489
Nonlinear Constitutive Relations for High Temperature Application, 1984
[NASA-CP-2369] 20 p3465 N85-31530
A survey of unified constitutive theories
20 p3466 N85-31531
Physical concepts in the development of constitutive equations 20 p3467 N85-31537
Numerical considerations in the development and implementation of constitutive models
20 p3467 N85-31541
On numerical integration and computer implementation of viscoplastic models 20 p3467 N85-31542

Finite element analysis of notch behavior using a state variable constitutive equation 20 p3468 N85-31548
Analytical simulation of weld effects in creep range 20 p3468 N85-31550
Creep crack growth predictions in INCO 718 using a continuum damage model 20 p3469 N85-31551

CONSTRAINTS
NT METEOROLOGICAL PARAMETERS
Simple nonrestrictive arm restraint system [AD-D011216] 01 p0005 N85-10026
Aircraft chocks [AD-A145135] 01 p0012 N85-10077
Resistance to HF jamming interference in mobile radio networks by an adaptive, distributed reconfiguration technique [AD-A145117] 01 p0038 N85-10238
Constraint-based scheduling in an intelligent logistics support system: An artificial intelligence approach [AD-A145613] 02 p0293 N85-11900
Barriers to achieving high efficiency 06 p0829 N85-15264
Implementation of a constraint machine for prism - A parallel problem solver [AD-A147844] 07 p1026 N85-16512
Trust region methods for minimization [AD-A147073] 07 p1030 N85-16540
The analysis of kinematic restraint and freedom using point contacts [RR-154/03/75/02] 08 p1169 N85-17372
The synthesis of kinematic restraint and freedom using point contacts [RR-154/03/75/03] 08 p1169 N85-17373
The combinatorics of local constraints in model-based recognition and localization [AD-A148338] 08 p1230 N85-17746
The IRAS mission 09 p1412 N85-18901
A generalized ordering constraint for stereo correspondence [AD-A149182] 10 p1487 N85-19390
Brightness limitations in multi-kiloampere electron beam sources [DE84-017417] 10 p1555 N85-19807
A FORTRAN program for deep space sensor analysis [AD-A151700] 15 p2489 N85-25366
Orbiter middeck/payload standard interfaces control document [NASA-TM-87473] 16 p2729 N85-26840
On the exceedance point process for a stationary sequence [AD-A152827] 17 p3018 N85-28665
Construction of constraint equation for stresses and strains [BLL-M-36239-(5828.4)] 20 p3465 N85-31524
On the limiting configuration of interfacial gravity waves [AD-A154821] 21 p3631 N85-32557
Detector problems at the SSC [DE85-010217] 21 p3703 N85-33007
Design and testing of an energy-absorbing crewseat for the F/FB-111 aircraft. Volume 2: Data from seat testing [NASA-CR-3917] 24 p4084 N85-35184

CONSTRICTIONS
Test your contacts by measuring their constriction resistance [BLL-WH-611-(9091.9F)] 07 p0944 N85-15978
A two phase flow model at the level of a narrowing section — blood flow 20 p3507 N85-31799

CONSTRUCTION
Modelling the demand for construction [CSIR-TWISK-322] 01 p0035 N85-10218
Copper-boron low alloy high strength steels 02 p0176 N85-11183
Construction of a cold neutron source at FRM, Munich 03 p0427 N85-12722
Construction of a neutron single crystal diffractometer 03 p0427 N85-12723
Field testing of a lightweight relocatable structure in a desert environment [AD-A148841] 09 p1304 N85-18192
Increase in performance and improvement of ride comfort of self-propelled construction machinery by reducing pitch and vertical vibration [AD-P004269] 09 p1405 N85-18845
Airport site selection and design [AD-P004193] 11 p1581 N85-19959
Landscape management on airports for reduction of bird populations [AD-P004194] 11 p1581 N85-19960
Inexpensive multipurpose landscaping 11 p1581 N85-19961
Institute director surveys industrial automation drive 11 p1617 N85-20167
Laser-Electron-Gamma-Source (LEGS) [DE85-003204] 11 p1636 N85-20322
New runway enables IL-76 flights to Tenkeli in far north 12 p1769 N85-21108
Stress-relieving interlayers for bituminous resurfacings [PB85-136885] 12 p1820 N85-21415
Phase change thermal energy storage and the model building codes [PB85-111201] 12 p1883 N85-21813
The space station as a construction base for large space structures 14 p2235 N85-23856
Microwave methods for paving [DE85-004194] 14 p2265 N85-24032
Construction in space 15 p2484 N85-25328
Evidential reasoning in expert systems for image analysis [AD-A153379] 17 p3013 N85-28627
A bilaterally deterministic rho-mixing stationary random sequence [AD-A152856] 17 p3019 N85-28666
US restrictions on technology transfer reviewed 18 p3086 N85-29115
Fire performance of interstitial space construction system [NBSIR-85-3158] 20 p3436 N85-31318
Airborne sound transmission loss characteristics of wood-frame construction [AD-A154174] 20 p3524 N85-31919
Construction of University of Missouri, Rolla's full scale cloud simulation chamber and applied research [AD-A154682] 21 p3557 N85-32128
Field testing of a lightweight relocatable structure in a temperate environment [AD-A155171] 21 p3599 N85-32350
Literature survey of underground construction methods for application to hardened facilities [AD-A155212] 21 p3599 N85-32351
Deployable-erectable trade study for space station truss structures [NASA-TM-87573] 22 p3740 N85-33181
Low-head hydroelectric power demonstration project: City of Gonzales, Texas [DE85-010403] 22 p3809 N85-33595
A 1984 environmental summary: Sandia National Laboratories Tonopah Test Range, Tonopah, Nevada [DE85-011145] 22 p3812 N85-33612
Nuclear physics in the 10 to 300 MeV energy range using a pulsed white neutron source [DE85-003713] 22 p3839 N85-33775
Space Station Engineering and Technology Development: Proceedings of the Panel on In-Space Engineering Research and Technology Development [NASA-CR-176110] 23 p3899 N85-34153
Small Hydroelectric Power Plan Demonstration Project [DE85-011343] 23 p3946 N85-34454
Design and construction of an advanced power conditioning subsystem for small photovoltaic applications [DE85-013940] 24 p4113 N85-35495
Reachable grasps on a polygon: The convex rope algorithm [AD-A155913] 24 p4138 N85-35647
The 1986 National Aeronautics and Space Administration authorization [GPO-47-635] 24 p4166 N85-35829

CONSTRUCTION IN SPACE
U ORBITAL ASSEMBLY

CONSTRUCTION INDUSTRY
Use of short-range weather forecasts at construction sites: Some results from a user and a market test 01 p0084 N85-10563
Activities report in technology [ISBN-951-38-1998-1] 04 p0577 N85-13681
Robotics application in construction industry assessed 08 p1139 N85-17178
Deputy minister on civil aviation construction projects 14 p2208 N85-23692

CONSTRUCTION MATERIALS
Models for shock damage to marine structural materials 09 p1336 N85-18400
Hazardous air pollutants: Dry-deposition phenomena [PB85-138279] 12 p1887 N85-21843
Expedient runway surfacing with post tensioning system for expeditionary airfields [AD-D011677] 19 p3222 N85-29976
Field testing of a lightweight relocatable structure in a temperate environment [AD-A155171] 21 p3599 N85-32350

CONSUMABLES (SPACECRAFT)
NT CONSUMABLES (SPACECREW SUPPLIES)
NT PROPELLANT STORAGE
NT SPACE LOGISTICS
NT SPACE RATIONS
NT STORABLE PROPELLANTS
NT WORKING FLUIDS

CONSUMABLES (SPACECREW SUPPLIES)
NT POTABLE WATER
NT SPACE RATIONS
Food Service and Nutrition for the Space Station [NASA-CP-2370] 14 p2393 N85-24733
Food acquisition: Food ingredients, raw materials and supply 14 p2393 N85-24737
Preparation methods: Past and potential methods of food preparation for space 14 p2393 N85-24738
Alternative food preservation techniques, new technology in food preparation and appropriateness of food supply for the permanently manned space station 14 p2393 N85-24739
Use of irradiated foods 14 p2393 N85-24740
Equipment for hot-to-serve foods 14 p2393 N85-24741
Food service and nutritional needs 14 p2394 N85-24744
Packaging's contribution for the effectiveness of the space station's food service operation 14 p2394 N85-24746
Packaging for food service 14 p2394 N85-24747
A life-saving device for ships [NASA-TM-77670] 23 p3895 N85-34129

CONSUMERS
Economic value of consumer information: A selected, annotated bibliography [PB84-235795] 04 p0576 N85-13673
Sunset of the Civil Aeronautics Board [S-HRG-98-940] 09 p1403 N85-18829

CONSUMPTION
NT ENERGY CONSUMPTION
NT FUEL CONSUMPTION
NT OXYGEN CONSUMPTION
NT WATER CONSUMPTION
Cosmonauts' blood plasma free amino acid levels during preflight training 12 p1901 N85-21937

CONTACT RESISTANCE
Test your contacts by measuring their constriction resistance [BLL-WH-611-(9091.9F)] 07 p0944 N85-15978
Oil resistant silicone elastomers [AD-131523] 16 p2753 N85-26987

CONTACTORS
Free-surface phenomena under low- and zero-gravity conditions [NASA-CR-175835] 16 p2782 N85-27168

CONTACTS (ELECTRIC)
U ELECTRIC CONTACTS

CONTACTS (GEOLOGY)
Contact properties of rare-earth silicides and germanides on Si and Ge 19 p3374 N85-30931
The 3.5 b.y. old Onverwacht Group: A remnant of ancient oceanic crust 21 p3718 N85-33073

CONTAINERLESS MELTS
Microgravity containerless processing in long drop tubes 02 p0153 N85-11037
Containerless drop tube solidification and grain refinement of NiAl3 02 p0154 N85-11042
NBS (National Bureau of Standards): Materials measurements [NASA-CR-174038] 03 p0332 N85-12143

CONTAINERS
Inert atmosphere transfer vessel [AD-D011433] 08 p1169 N85-17370
Vibrational loading mechanism of unitized corrugated containers with cushions and non-load-bearing contents 09 p1339 N85-18419
Single crystal silicon as a low-temperature structural material [DE84-017469] 09 p1400 N85-18810
Latch assembly [DE85-011660] 22 p3792 N85-33492

CONTAINMENT
Flywheel containment and safety considerations 05 p0606 N85-13869
Polymeric liner selection for military waste impoundments [AD-P004143] 09 p1348 N85-18479
Thermal stress-dependent dilation of concrete [DE84-014688] 11 p1653 N85-20412
Hemispherical latching apparatus [NASA-CASE-MFS-25837-1] 19 p3224 N85-29991
Counter current extraction system for tritium recovery from 17Li-83Pb [DE85-010519] 19 p3240 N85-30090
Explosive containment study [DE85-011719] 22 p3753 N85-33267
Corrosion resistant storage container for radioactive material [DE85-011666] 22 p3838 N85-33765
Measurement of radionuclides in waste packages [DE85-011674] 22 p3838 N85-33766
MATADOR (Methods for the Analysis of Transport And Deposition Of Radionuclides) code description and user's manual [TI85-901402] 23 p3966 N85-34592

Fuel containment and damage tolerance for large composite primary aircraft structures. Phase 1: Testing
[NASA-CR-166091] 24 p4073 N85-35241
Response of a BWR Mark 2 containment vessel head to loads beyond the design basis
[DE85-010524] 24 p4103 N85-35432
CONTAMINANTS
NT RADIOACTIVE CONTAMINANTS
NT TRACE CONTAMINANTS
The use of fixed-bed adsorber models to predict the fluxes of toxic substances in groundwaters and soil environments
[PB84-202563] 01 p0C71 N85-10468
Reverse osmosis treatment to control inorganic and volatile organic contamination
[PB84-223526] 01 p0071 N85-10470
Toxicological evaluation of Columbia spacecraft
01 p0094 N85-10631
Clean-burning diesel engines
[AD-A145515] 02 p0205 N85-11349
VOC emissions from volatile organic liquid storage tanks: Background information for proposed standards
[PB84-237320] 04 p0532 N85-13403
Climatological variability in modeling of long-term regional transport and deposition of air pollutants
[DE84-014726] 04 p0539 N85-13430
Portable instrument for the detection and identification of air pollutants
[DE84-014767] 05 p0672 N85-14316
Fate and disposition of trichloroethylene in surface soils
[AD-A147918] 07 p0995 N85-16321
Evaluation of test equipment for the detection of contamination on electronic circuits — spacecraft electronics
[ESA-STM-234] 08 p1159 N85-17316
A new fast response probe for diffusion studies in atmospheric air — pollution modeling
[IC-AERO-84-01] 08 p1180 N85-17437
Applying an innovative approach to field investigations at a remedial action site
[AD-P004145] 09 p1348 N85-18481
Measurement and analysis of ambient carbon monoxide concentrations for project-level air quality impact studies
[PB85-104602/GAR] 09 p1350 N85-18492
Meteorological factors responsible for high CO (carbon monoxide) levels in Alaskan cities
[PB85-115137/GAR] 09 p1350 N85-18493
Improved techniques for removal of sediments contaminated with hazardous materials
[PB85-116093] 11 p1679 N85-20580
Method and apparatus for mapping the distribution of chemical elements in an extended medium
[NASA-CASE-GSC-12808-1] 12 p1798 N85-21279
The body burden of organic vapors in artificial air trial measurements aboard a moored submarine
[AD-A149698] 12 p1910 N85-21988
Spectroscopic study of gas pollutants in atmosphere over large cities: A review 14 p2341 N85-24478
Thermally modulated electron affinity detector for priority pollutant analysis
[PB85-158145] 15 p2508 N85-25469
Density of impurity states associated to inversion layers
[INPE-3406-PRE/675] 16 p2869 N85-27702
A study of gas solid reactions using coated piezoelectric detectors
[AD-A153047] 17 p2920 N85-28001
Elemental tracers of source regions of contaminants in precipitation
[DE85-007366] 18 p3133 N85-29407
Internal contamination issues
18 p3156 N85-29543
Reduction of pollutant formation in combustion processes
[DE85-010181] 19 p3309 N85-30512
Mechanisms of exhaust pollutants and plume formation in continuous combustion
[AD-A154169] 20 p3435 N85-31310
Toxic hazards tests for vehicles and other equipment
[AD-A149164] 20 p3506 N85-31797
New estimating procedures for surface runoff, sediment yield, and contaminant transport in Los Alamos County, New Mexico
[DE85-011890] 21 p3606 N85-32393
Atmospheric modeling of organics for risk assessment: A Chemist's view
[DE85-009770] 23 p3909 N85-34217
CONTAMINATION
NT FUEL CONTAMINATION
NT SPACECRAFT CONTAMINATION
Contamination problems during surface cleaning for thermocompression bonding
[DE84-013066] 04 p0475 N85-13023
Gas contamination detection device
[AD-D011386] 07 p0921 N85-15833
Contamination and distortion of steady flow field induced by discrete frequency in aircraft gas turbines
[AD-A147092] 07 p0958 N85-16073
Assessment of radiation dosages obtained by intake of radioactive fallout contaminated food
[VTT-292] 07 p1017 N85-16460
Other challenges in the development of the orbiter environmental control hardware
08 p1096 N85-16924
Proceedings of the 2nd Workshop on Nondestructive Evaluation (NDE) of Titanium Alloys
[AD-A147626] 08 p1125 N85-17095
Acoustical characterization of Ti-6211 weldments and oxygen contamination Ti-6211 plate
[AD-P004125] 08 p1126 N85-17100
Ultrasonic evaluation of titanium contamination with correlation techniques
[AD-P004126] 08 p1126 N85-17101
Photoacoustic microscopy of oxygen contaminated titanium alloys
[AD-P004127] 08 p1127 N85-17102
High resolution acoustic microstructural characterization of titanium with interstitial contamination
[AD-P004128] 08 p1127 N85-17103
Feasibility study to demonstrate detection of low levels of oxygen contaminant in titanium using eddy current and ultrasonic NDE (Nondestructive Evaluation) techniques
[AD-P004129] 08 p1127 N85-17104
Evaluation of interstitial gas contamination in titanium alloys using induced magnetic field analysis
[AD-P004130] 08 p1127 N85-17105
Neutron activation analysis of titanium with oxygen contamination
[AD-P004134] 08 p1128 N85-17109
Location of volatile buried wastes by field portable instrumentation
[AD-P004147] 09 p1348 N85-18483
Practical application of earth resistivity methods in phase 2 of the installation restoration program
[AD-P004148] 09 p1348 N85-18484
Ventilation flow: Submerged
18 p3156 N85-29545
Compatibility, contamination and IR microspectrophotometry
[DE85-010809] 19 p3273 N85-30297
Occurrence of uranium in ground water in the vicinity of the US Department of Energy Feed Materials Production Center, Fernald, Ohio
[DE85-010340] 19 p3364 N85-30862
The influence of oil contamination on the nucleate pool-boiling behavior of R-114 from a structured surface
[AD-A155609] 21 p3585 N85-32284
JPL in-house fluidized-bed reactor research
21 p3609 N85-32414
Soil extraction kit
[AD-D011736] 22 p3742 N85-33190
The 1984 environmental monitoring report, Sandia National Laboratories, Albuquerque, New Mexico
[DE85-011175] 22 p3811 N85-33607
Method for removing oxide contamination from silicon carbide powders
[DE85-011648] 23 p3919 N85-34287
Radiation safety problems in handling highly active tritium targets
[DE85-014268] 24 p4151 N85-35742
CONTENT
NT BONE MINERAL CONTENT
CONTEXT
Efficient contextual measures for classification of multispectral image data 14 p2433 N85-25005
CONTINENTAL DRIFT
Antarctic glaciation, or what are catastrophes in Earth's history 13 p2105 N85-23118
CONTINENTAL MARGINS
U CONTINENTAL SHELVES
CONTINENTAL SHELVES
Marine geological and geophysical investigations of the Antarctic Continental Margin, 1984
[GS-CIRC-935] 02 p0212 N85-11400
Submarine sand ridges: Geology and development, New Jersey, USA 02 p0227 N85-11482
Recent observations of tides and tidal currents from the northeastern Bering Sea shelf
[PB84-241785] 04 p0543 N85-13452
Maritime prospecting, mining discussed
07 p0980 N85-16226
Types of placer formation of eastern Arctic shelf
10 p1496 N85-19452
Calculation of optical characteristics of shelf ecological system based on its mathematical model
10 p1496 N85-19453
U, Th, K content, heat production and thermal conductivity of Sao Paulo, Brazil continental shelf sediments: A reconnaissance work
[INPE-3401-PRE/670] 10 p1515 N85-19556
Preliminary results of the oceanographic cruise of USCGC NORTHWIND to the Greenland Sea
[AD-A149802] 12 p1896 N85-21919
Biological processes in the water column of the South Atlantic Bight. Volume 1: Published manuscripts
[DE85-004610] 12 p1900 N85-21929
Twenty-five sound propagation tests on the continental shelf between Long Island, New York and Cape Canaveral, Florida
[AD-A149669] 12 p1928 N85-22111
A tectonic model of an incipient spreading center and its margins: The Northern Red Sea and the Dead Sea rift 13 p2140 N85-23286
Two-cycle mechanism of dissipation of tidal energy in ocean 14 p2335 N85-24438
MARMAP survey of the continental shelf from Cape Hatteras, North Carolina to Cape Sable, Nova Scotia (1977 - 1983). Atlas 1: Summary of operations
[PB85-150985] 16 p2839 N85-27508
An assessment of the potential role of multispectral imagery in bathymetric charting
[AD-A152460] 17 p2984 N85-28438
Geoacoustic models: Washington state continental margin
[AD-A153781] 18 p3177 N85-29869
Pacific index, April 1983 - October 1984
[TI85-901335] 19 p3320 N85-30582
CONTINENTS
NT AFRICA
NT ASIA
NT AUSTRALIA
NT EUROPE
NT NORTH AMERICA
NT SOUTH AMERICA
Some methodological aspects of study of layer associations in continents and oceans
06 p0820 N85-15205
Continental and oceanic magnetic anomalies: Enhancement through GRM 20 p3476 N85-31598
Continental magnetic anomaly constraints on continental reconstruction 20 p3476 N85-31599
Regional magnetic anomaly constraints on continental rifting 20 p3476 N85-31600
The origin of continental crust: Outlines of a general theory 21 p3720 N85-33083
Crustal radiogenic heat production and the selective survival of ancient continental crust
21 p3721 N85-33086
CONTINGENCY
Log linear model applications
[AD-A146620] 06 p0858 N85-15457
A model for large sparse contingency tables
[AD-A150320] 13 p2151 N85-23880
An examination of alternative forms of fit in contingency theory
[AD-A152602] 17 p3047 N85-28853
The concept of fit in contingency theory
[AD-A152603] 17 p3047 N85-28854
Bayesian full rank marginalization for 2-way contingency tables
[AD-A153841] 18 p3171 N85-29849
CONTINUITY
Viscosity solutions of Hamilton-Jacobi equations at the boundary
[AD-A147444] 07 p1032 N85-16553
On existence and uniqueness of solutions of Hamilton-Jacobi equations
[AD-A147597] 07 p1033 N85-16560
CONTINUITY (MATHEMATICS)
Shear deformation plate continua of large double-layered space structures
01 p0059 N85-10391
Continuity of the null space basis and constrained optimization
[AD-A147038] 07 p1030 N85-16538
Domains with Lipschitz mapping functions
10 p1535 N85-19675
Topology and Order Structures, part 2
[MCT-169-PT-2] 14 p2413 N85-24879
Twenty questions on ordered spaces
14 p2413 N85-24880
A note on perfect normality in generalized ordered spaces 14 p2413 N85-24881
Metrization theorems for continuous images of compact ordered spaces 14 p2413 N85-24882
A pathological homogeneous subspace of the real line
14 p2413 N85-24883
A note on topological groups with dense orderable subspaces 14 p2413 N85-24884
The Kappa sub n property in small Omega sub 1 trees
14 p2413 N85-24885
On compactifications of generalized order GO-spaces
14 p2413 N85-24886
The orderability of compact scattered spaces
14 p2413 N85-24887

Submetrizable topologies on the ordinals 14 p2414 N85-24888
When is a GO-space JO(2)? 14 p2414 N85-24889
Local bases and product partial order II 14 p2414 N85-24890
Mappings of finite oscillations at local separating points 14 p2414 N85-24891
Orderable subspaces of compact F-spaces 14 p2414 N85-24892
Extension of embeddings close to isometries or similarities 15 p2634 N85-26242
On functions with a finite or locally bounded Dirichlet integral 15 p2635 N85-26243

CONTINUITY EQUATION
New approach for solving large residual nonlinear least squares problems [DE85-002555] 11 p1707 N85-20742
Theory of oriented nucleation with asymmetric single elements. 2: Effects of rotational diffusion [IFTR-32/1984] 12 p1939 N85-22179

CONTINUOUS RADIATION
NT MODULATED CONTINUOUS RADIATION
The IMS advances in understanding terrestrial myriametric radiation 14 p2365 N85-24618
Terrestrial continuum radiation study during the IMS 14 p2365 N85-24619
A sampling phasemeter design for pulsed continuous wave signals [AD-A155237] 21 p3581 N85-32264
Optimal complex nonlinear processing of continuous and pulsed signals 22 p3763 N85-33323
The cw operation of the FMIT RFQ accelerator [DE85-012867] 22 p3837 N85-33757
Search for positron annihilation line and continuum radiation from the Galactic Center [OG-2.5-5] 22 p3869 N85-33962

CONTINUOUS SPECTRA
The continuous spectrum of an axisymmetric, self-gravitating equilibrium in the presence of a poloidal magnetic field 12 p1959 N85-22315
The continuous spectrum of an axisymmetric equilibrium with a mixed poloidal and toroidal magnetic field with gravity included 14 p2450 N85-25128

CONTINUOUS WAVE LASERS
Tunable CW semiconductor platelet laser [AD-D011215] 01 p0052 N85-10341
Study of CW injection laser with a dispersive external cavity 02 p0270 N85-11780
Optimizing CW CO2 lasers with respect to output power in different bands 02 p0271 N85-11786
Transformation of energy spread of laser pumping via phase conjugation 05 p0725 N85-14661
Instrumentation for particle-beams research using laser excited merging beams [AD-A147968] 08 p1220 N85-17681
A 50-kW electric-discharge CO2 laser [AD-A149779] 12 p1857 N85-21644
Laser Welding, Cutting and Surface Treatment 14 p2308 N85-24278
The measurement of laser beam parameters 14 p2308 N85-24283
A plasma initiation-flow chamber to study CW laser beamed energy absorption in light gases [AD-A151225] 15 p2562 N85-25806
Design and construction of a CW ND:YAG laser using a single elliptical cavity and water cooled krypton arc lamp pumping [AD-A152657] 17 p2970 N85-28340
Simplified analytical model for calculation of population inversion in channels of CW gasdynamic lasers operating at various transitions among levels pertaining to coupled upsilon 1 and upsilon 2 modes of CO2 [STN-2] 20 p3461 N85-31496
High-power two-frequency CW dye laser 21 p3686 N85-32900
Expansion ratio influence on population inversion in CO2/Ar CW gasdynamic lasers operating at various transitions within coupled upsilon 1 and upsilon 2 modes of CO2 [STN-4] 22 p3790 N85-33485
Laser and electron beam processing of semiconductors [AD-A155914] 24 p4161 N85-35796

CONTINUOUS WAVE RADAR
Design of an analog spectrum analyzer for probing experiments [AD-A147364] 07 p0941 N85-15863
Signal processing and range spreading in the FM-CW radar [PB85-108256] 11 p1626 N85-20239
Use of radar with frequency modulation for studying atmospheric boundary layer 19 p3296 N85-30437

CONTINUOUS WAVES
U CONTINUOUS RADIATION

CONTINUUM FLOW
Modeling of transient heat pipe operation [NASA-CR-175496] 12 p1844 N85-21571

CONTINUUM MECHANICS
Acceleration waves 02 p0207 N85-11367
Free-edge failures of composite laminates 04 p0467 N85-12971
Continuum distributions of active galactic nuclei 05 p0742 N85-14770
Physical conditions in low-luminosity active galactic nuclei 05 p0742 N85-14771
Theoretical studies relating to the interaction of radiation with matter: Atomic collision processes occurring in the presence of radiation fields [AD-A146854] 07 p1040 N85-16602
Computational methods for nonlinear dynamics problems in solid and structural mechanics [AD-A148352] 08 p1172 N85-17392
The principle of virtual work and associated variational principles [ESA-TT-873] 09 p1340 N85-18426
Axiomatic characterizations of continuum structure functions [AD-A149817] 12 p1866 N85-21706
A solution method for nonlinear dynamic analysis of shell structures [AD-A149846] 12 p1866 N85-21708
Adaptive meshes in the 2DL code [LA-9936-MS] 12 p1914 N85-22011
Parallel processing for computational continuum dynamics [AD-A150513] 13 p2147 N85-23327
The Shock and Vibration Digest, volume 17, no. 1 [AD-A151051] 17 p2977 N85-28397
Continuum modeling of latticed structures 17 p2977 N85-28399
Nonlinear problems in continuum mechanics [AD-A153367] 17 p3046 N85-28846
A high energy X-ray study of the galactic center [AD-A153852] 18 p3202 N85-29862
Efficient solution methods for nonlinear finite element analysis 20 p3519 N85-31886
Mechanics of near tip microcracking in brittle material [AD-A154664] 21 p3596 N85-32346

CONTINUUM MODELING
Spline-based Rayleigh-Ritz methods for the approximation of the natural modes of vibration for flexible beams with tip bodies [NASA-CR-172566] 13 p2102 N85-23100

CONTINUUMS
Modules of continuum structures, revised [AD-A148620] 08 p1213 N85-17639
Bounding the stochastic performance of continuum structure functions 1 [AD-A148621] 08 p1213 N85-17640
An extension of the multiconfiguration Hartree-Fock program for continuum functions [DE85-002080] 09 p1379 N85-18672
Bounding the stochastic performance of continuum structure functions 2 [AD-A149458] 10 p1548 N85-19762
Mappings of finite oscillations at local separating points 14 p2414 N85-24891
On the definition of topological susceptibility via lattice anomalous Ward identities and its perturbative tail [PREPRINT-416] 18 p3184 N85-29744
Low-excitation Herbig-Haro objects and interstellar extinction [NASA-CR-176142] 23 p3988 N85-34726

CONTOUR SENSORS
A digital contour-corrector for a high-definition TV camera [NHK-LABS-NOTE-311] 19 p3254 N85-30179
LANDSAT-4/5 image data quality analysis [E85-10105] 24 p4107 N85-35463

CONTOURS
Detection and coding techniques of contours in image signals [FUB-8-1983] 01 p0039 N85-10251
Image signals encoding techniques oriented towards the reduction of perceptive redundance [FUB-23-1983] 01 p0040 N85-10256
A human visual system investigation applicable to image contour coding [FUB-36-1983] 01 p0095 N85-10640
Detection and estimation of image contours [FUB-35-1983] 01 p0112 N85-10760
A decomposable algorithm for contour surface display generation [AD-A145783] 03 p0410 N85-12619
Free-surface boundary layer and the origin of bow vortices [AD-A147427] 07 p0960 N85-16083
Transonic shock interaction with a tangentially-injected turbulent boundary layer 08 p1072 N85-16796
Critical flashing flow of subcooled fluids in nozzles with contour discontinuities [DE84-017229] 09 p1319 N85-18296
The feasibility of a multiprocessor architecture for real-time contour surface display generation [AD-A149427] 10 p1536 N85-19697
Experimental investigation of a turbulent incompressible boundary layer on a curved wall 11 p1577 N85-19936
Contour line generalization using digital image processing methods [SER-C-291] 11 p1700 N85-20688
An unusual application of NASTRAN contour plotting capability 15 p2574 N85-25872
Contamination of the fetch-limited directional wave spectrum by waves emanating from an embayment [NASA-TM-84441] 15 p2604 N85-26048
Acceleration sensitivity reduction method [AD-D011631] 16 p2778 N85-27146
Contour line generalization using digital image processing methods 16 p2815 N85-27367
A fast hidden line algorithm with contour option [NASA-CR-175803] 16 p2852 N85-27582
Application of hierarchical data structures to geographical information systems [AD-A152169] 16 p2877 N85-27753
Contouring trivariate data 17 p3005 N85-28582
Fourier coding and reconstruction of complicated contours [REPT-84-39] 17 p3022 N85-28691
SEASAT altimetry for surface height of inland seas 20 p3493 N85-31714
Real-time contour surface display generation [AD-A155232] 21 p3668 N85-32780
Interactive procedures for discriminating and restoring contour line networks 22 p3736 N85-33156
Discrimination of linear contour elements of space photographs based on visual perception model 22 p3736 N85-33161
Block-implicit calculations of three-dimensional laminar flow in strongly curved ducts [DE85-003047] 23 p3931 N85-34363
Evaluation: Close-range photogrammetry for slope inventory and monitoring [PB85-192755] 24 p4108 N85-35470
Invariant tests and likelihood ratio tests for multivariate elliptically contoured distributions [AD-A155844] 24 p4142 N85-35679

CONTRACT INCENTIVES
Decision process models of contractor behavior: The development of effective contract incentives [AD-A145524] 02 p0292 N85-11898
Using incentives to improve maintainability [AD-A153792] 18 p3199 N85-29841

CONTRACT MANAGEMENT
Contracting for computer software development: Serious problems require management attention to avoid wasting additional millions [FGMSD-80-4] 02 p0241 N85-11567
Benefit value to the Air Force of the GIDEP (Government Industry Data Exchange Program) alert [AD-A145470] 02 p0292 N85-11897
Decision process models of contractor behavior: The development of effective contract incentives [AD-A145524] 02 p0292 N85-11898
The application of artificial intelligence to contract management [AD-A146881] 06 p0857 N85-15448
Technical performance measurement handbook [AD-A147314] 07 p1052 N85-16675
An appraisal of the USAF Technology Modernization Program [AD-A147344] 07 p1052 N85-16677
Evaluation of the effectiveness of the weighted guidelines to induce contractor's investment in cost reducing facilities equipment [AD-A147586] 07 p1053 N85-16681
Government contract contingent liabilities. The anti-deficiency act, and the hobgoblin of little minds [AD-A147919] 07 p1053 N85-16684
Ground test article for deployable space structure systems [NASA-CR-171301] 10 p1429 N85-19011
Expert systems in contract management: A pilot study [AD-A149363] 10 p1566 N85-19873
Department of defense, office of inspector general semiannual report to the Congress, 1 April - 30 September 1984 [AD-A149560] 10 p1567 N85-19879
Program manager: The Journal of the Defense Systems Management College. Volume 13, Number 6, November-December 1984 [AD-A149546] 11 p1739 N85-20933
Life cycle costing in government procurement [AD-A151878] 15 p2666 N85-26456

Automation of the reporting and tracking requirements of architect-engineering type contracts
[AD-A152216] 16 p2876 N85-27745
R/D contracts in the Soviet Union
[AD-P004569] 17 p3048 N85-28865
Cost savings from multiyear contracting
[AD-A153564] 18 p3197 N85-29834
Capital investment motivational techniques used by prime contractors on subcontractors
[AD-A153660] 18 p3196 N85-29837
Using incentives to improve maintainability
[AD-A153792] 18 p3199 N85-29841
Analyzing performance of small projects using URS and PMAS, information pamphlet
[DE85-011964] 23 p3966 N85-34718
DoD Value Engineering conference report. Value Engineering (VE): A tool that benefits line management. Part 4, Workshop B: VE on spare parts
[AD-A156070] 24 p4163 N85-35813
DoD Value Engineering conference report. Value Engineering (VE): A tool that benefits line management. Part 7, Workshop E: VE in construction and architect engineer contracts
[AD-A156073] 24 p4164 N85-35816

CONTRACT NEGOTIATION
Using incentives to improve maintainability
[AD-A153792] 18 p3199 N85-29841

CONTRACTION
Effect of hyperoxia and increased gas atmosphere density on contractile function of the right ventricle
01 p0093 N85-10628
Change in energetics of muscular contraction as a result of hyperoxia 01 p0093 N85-10629
On the convergence of an iterative formulation of the electromagnetic scattering from an infinite grating of thin wires 24 p4085 N85-35319

CONTRACTORS
Decision process models of contractor behavior: The development of effective contract incentives
[AD-A145524] 02 p0292 N85-11898
Contractor productivity measurement
[AD-A146756] 07 p1050 N85-16666
An appraisal of the USAF Technology Modernization Program
[AD-A147344] 07 p1052 N85-16677
Evaluation of the effectiveness of the weighted guidelines to induce contractor's investment in cost reducing facilities equipment
[AD-A147586] 07 p1053 N85-16681
Integrated control system engineering support
[AD-A149742] 12 p1780 N85-21177
Capital investment motivational techniques used by prime contractors on subcontractors
[AD-A153660] 18 p3196 N85-29837
The evolution of the U.S. helicopter industry
[AD-A154290] 19 p3211 N85-29913
The flow of scientific and technical information in the US Army Research Laboratories
[AD-A155050] 21 p3713 N85-33043

CONTRACTS
Contracting for computer software development: Serious problems require management attention to avoid wasting additional millions
[FGMSD-80-4] 02 p0241 N85-11567
Companies participating in the Department of Defense Subcontracting Program, first three quarters fiscal year 1984
[AD-A146137] 03 p0436 N85-12775
Contractor productivity measurement
[AD-A146756] 07 p1050 N85-16666
Government contract contingent liabilities. The anti-deficiency act, and the hobgoblin of little minds
[AD-A147919] 07 p1053 N85-16684
Cost-plus-percentage-of-costs in government contracts
[AD-A147779] 08 p1228 N85-17735
R/D contracts in the Soviet Union
[AD-P004569] 17 p3048 N85-28865
Cost savings from multiyear contracting
[AD-A153564] 18 p3197 N85-29834
The evolution of the U.S. helicopter industry
[AD-A154290] 19 p3211 N85-29913
Progress report on implementing the recommendations of the White House Science Council's Federal Laboratory Review Panel, volume 1
[PB85-185072] 24 p4164 N85-35819

CONTRAST
NT IMAGE CONTRAST
NT PHASE CONTRAST
Reconciling Bayesian and frequentist evidence in the one-sided testing program
[AD-A155603] 21 p3678 N85-32850

CONTROL
Real time sensing and control of out-of-plane distortion due to line heating by laser
[AD-A144773] 01 p0027 N85-10169
Turnaround control for mechanically scanned radar antennas
[AD-D011238] 01 p0039 N85-10246
Research activities of the Illinois University Coordinated Science Laboratory
[AD-A145589] 03 p0449 N85-12856
A control model: Interpretation of Fitts' law
05 p0706 N85-14526
Decentralized control of scheduling in distributed systems
[AD-A147446] 07 p1022 N85-16487
NASA three-laser airborne differential absorption lidar system electronics
[NASA-CR-174293] 08 p1166 N85-17353
Problems of psychological support of automated organization control systems 09 p1362 N85-18571
Operational effectiveness of a Multiple Aquila Control System (MACS)
[NASA-CR-174436] 10 p1427 N85-19000
Active control of large space structures: An introduction and overview
[NASA-TM-86490] 10 p1429 N85-19014
Successful control of gulls and other birds at a sanitary landfill
[AD-P004198] 11 p1582 N85-19965
Control technology for integrated circuit fabrication at Honeywell Optoelectronics Division, Richardson, Texas
[PB85-109023] 11 p1616 N85-20162
Design of a semi-custom integrated circuit for the SLAC SLC timing control system
[DE85-003091] 11 p1629 N85-20258
Television camera video level control system
[NASA-CASE-MSC-18578-1] 12 p1821 N85-21427
Transfer of technology
[S-REPT-98-664] 12 p1949 N85-22246
The performance of an alternating-current thyristor-controlled motor 15 p2546 N85-25716
Airsickness control using biofeedback to self-regulate psychophysiological responses
[AD-A151167] 15 p2617 N85-26126
Ultrareliable, fault-tolerant control systems: A conceptual description
[NASA-TM-86017] 19 p3221 N85-29972
Control and regulation of generalized linear systems
19 p3257 N85-30193
Frequency domain control design of large space structures: A practical approach
20 p3415 N85-31192
Solid state high power amplifier for driving the SLC injector klystron
[DE85-013063] 24 p4090 N85-35356

CONTROL BOARDS
LED multifunction keyboard engineering study
[AD-A145199] 01 p0010 N85-10061
New control design principles based on measured performance and energy analysis of HVAC (Heating, Ventilating, and Air-Conditioning) systems
[AD-A151708] 15 p2522 N85-25546
Information presentation in power plant control rooms
[VTT-320] 16 p2864 N85-27668
The touch panel system: Design and development
[AD-A153014] 17 p3006 N85-28596
Crew systems and flight station concepts for a 1995 transport aircraft
[NASA-CR-166068] 19 p3221 N85-29973

CONTROL CONFIGURED VEHICLES
A 320 to have combined automatic pilot, flight control system 14 p2289 N85-24186
Multivariable control of a soft coupled space station
20 p3408 N85-31151

CONTROL DATA (COMPUTERS)
Design and analysis of an access control system for a multi-backend database system
[AD-A148750] 09 p1367 N85-18586
Meta-level control through fault detection and diagnosis
[AD-A149064] 10 p1540 N85-19709

CONTROL DEVICES
U CONTROL EQUIPMENT

CONTROL EQUIPMENT
NT CONTROL STICKS
NT CRYOSTATS
NT PRESSURE REGULATORS
NT SPEED REGULATORS
NT TELEOPERATORS
NT THERMOSTATS
Potential application of robotics and state-of-the art end effectors at Letterkenny Army Depot
[AD-P004015] 03 p0309 N85-11994
Torque sensor
[AD-D011276] 05 p0639 N85-14086
Back end valves: History and modifications
[DE84-009272] 05 p0646 N85-14145
S-MICRO: A system for simulating a microprogrammed control unit
[INPE-3224-PRE/575] 06 p0715 N85-14585
Lighting controls: The role of advanced technology: past, present and future
[DE84-015977] 09 p1384 N85-1
Electromagnetic compatibility of measurement and control equipment in nuclear installations
[BLL-WH-607-(9091.9F)] 11 p1623 N85-20
Electronics Engineering Department EE Technical Review
[UCRL-50025-84-1] 13 p2063 N85-22
Experimental development of a failure detection scheme for large space structures 14 p2234 N85-2
Controllable movements of elastic manipulator with three degrees of freedom 14 p2266 N85-24
New equipment complex Kaskad 2 for automatic control 14 p2268 N85-240
Investigation of transport operations of ergatic robot
14 p2286 N85-241
New electronic measurement, control devices
14 p2289 N85-241
New control design principles based on measured performance and energy analysis of HVAC (Heating, Ventilating, and Air-Conditioning) systems
[AD-A151708] 15 p2522 N85-2554
Italy's Fiat uses Sweden's Asea seeing robot
15 p2536 N85-25
Development of an integrated control unit for the PDV bus concept
[BMFT-FB-T-84-300] 15 p2551 N85-2574
Superfine laser position control using statistically enhanced resolution in real time
[DE85-005643] 15 p2564 N85-25817
Development of a multiprocessor system, using the MOTORLA microprocessor 6809, with the aim of providing maximum flexibility in the design of individual control devices
[BMFT-FB-T-84-270] 17 p3010 N85-2860
Control system design for lightly coupled large space structures 20 p3399 N85-310
Computer methods in manipulator kinematics, dynamics and control: A comparative study
20 p3462 N85-3150
Improved coordinate measuring machine calibration and control
[DE85-012053] 21 p3590 N85-32315
Robots, Manipulators 21 p3668 N85-3278
Dual optical mechanical position tracker
[AD-D011739] 22 p3844 N85-33811
Method for controlling the viscosity of siloxane oils
[DE85-011586] 23 p3909 N85-34221
The compliance of end effector force sensors for robot manipulator control 24 p4096 N85-3540
On-line model driven control of the SLC electron Damping Ring
[DE85-013377] 24 p4157 N85-3677

CONTROL MOMENT GYROSCOPES
Torque command steering law for double-gimbaled control moment gyros applied to rotor energy storage
05 p0606 N85-13
Active nutation control of spacecraft using a magnetic bearing momentum wheel with Vernier gimbaling capability
[NAL-TR-8201] 06 p0759 N85-14
A Gimbal sizing analysis for an IPACS rotating assembly
[NASA-CR-172524] 16 p2741 N85-2
Space station automation and robotics study. Operator-systems interface
[NASA-CR-176095] 22 p3736 N85-33172
Application of traction drives as servo mechanisms
22 p3797 N85-33

CONTROL PANELS
U CONTROL BOARDS

CONTROL RODS
Simulation and operation of the EBR-2 automatic control rod drive system
[DE85-010262] 19 p3360 N85-30
Source Term Experiments Project (STEP): Aerosol characterization system
[DE85-010248] 19 p3361 N85-30

CONTROL SIMULATION
Control aspects of the Schuchuli Village stand-alone photovoltaic power system
[NASA-TM-83790] 04 p0495 N85-13157
Elimination of uncontrollable rigid body mode, appendix C 05 p0603 N85-13
Application of model following control and estimation techniques to attitude control of maneuvering spacecraft. Part 2: Simulation software description
[NLR-TR-82116-U-PT-2] 12 p1793 N85-21
Construction of high speed guaranteed regulators
14 p2270 N85-24
Modal synthesis of multidimensional PI-regulators for objects with inertial sections 14 p2270 N85-24
The modeling and simulation of feedback control systems
[NASA-CR-171875] 15 p2832 N85-2

In-flight investigation of the influence of pitch damping and pitch control effectiveness on landing approach flying qualities of statically unstable transport aircraft
[DFVLR-FB-84-12] 17 p2900 N85-27880
Application of model following control and estimation techniques to attitude control of maneuvering spacecraft. Part 1: Theory and simulation results
[NLR-TR-82116-U-PT-1] 18 p3065 N85-28957
Adaptive filtering for large space structures: A closed-form solution 20 p3417 N85-31208
Reduced order models and simulation data in control systems design
[RR-267] 20 p3463 N85-31516
Learning and self adaptation applied to the simulation of a human pilot
[ONERA-RT-24/5122-SY] 20 p3511 N85-31828
Power density and threshold control strategies for radar track initiation
[AD-A155357] 22 p3756 N85-33282
A preliminary evaluation of a failure detection filter for detecting and identifying control element failures in a transport aircraft
[NASA-TM-87576] 24 p4067 N85-35204
Enhancement of the flexible spacecraft dynamics program for open spacecraft
[NASA-CR-175309] 24 p4137 N85-35641
Network management simulation of automated guideway transit systems under vehicle-follower control
[PB85-186233] 24 p4166 N85-35830

CONTROL STABILITY
The numerical range: A tool for robust stability studies — multivariable feedback systems
[RR-255] 02 p0253 N85-11680
On the relationship between Lehtomaki's robustness test and an inverse Nyquist based test
[OUEL-1526/84] 03 p0409 N85-12616
Space Shuttle Orbiter trimmed center-of-gravity extension study. Volume 8: Effects of configuration modifications on the aerodynamic characteristics of the 140 A/B Orbiter at a Mach number of 5.97
[NASA-TM-72661-VOL-8] 04 p0452 N85-12887
Self-tuning control of offset: A unified approach
[OUEL-1539/84] 04 p0553 N85-13520
An H-infinity-minimax approach to the design of robust control systems
[OUEL-1537/84] 05 p0717 N85-14600
On the global asymptotic stabilization of nonlinear systems
[PREPRINT-838] 08 p1209 N85-17604
Improved stability and performance bounds using approximate models — control system design
[RR-260] 08 p1209 N85-17606
Some stability and control problems with trailed farm tankers on slopes
[AD-P004291] 09 p1408 N85-18868
Control of tractors on sloping ground
[AD-P004292] 09 p1408 N85-18869
Wind-tunnel investigation of a full-scale canard-configured general aviation airplane
[NASA-TP-2382] 11 p1575 N85-19925
Contribution to the study of perturbational stabilization
[ONERA-NT-1984-1] 11 p1714 N85-20781
Structural dynamics analysis 14 p2233 N85-23838
Static longitudinal stability and control characteristics of the Fokker F27 Friendship calculated by simple handbook methods
[VTH-LR-394] 16 p2711 N85-26728
Matrix transfer function design for flexible structures: An application 20 p3416 N85-31199
Maximum likelihood estimation with emphasis on aircraft flight data 20 p3417 N85-31208
Extensions of the small-mu test for robust stability — control stability
[OUEL-1573/85-REV] 20 p3519 N85-31884
Decentralized control of dynamically interconnected systems
[BU-111] 22 p3835 N85-33744

CONTROL STICKS
Level of effort 05 p0602 N85-13839
Effects of control stick parameters on human controller response 05 p0701 N85-14496
Active sticks: A new dimension in controller design
05 p0706 N85-14531
Biodynamic resistant control stick
[AD-D011380] 07 p0904 N85-15721

CONTROL SURFACES
NT AERIAL RUDDERS
NT AILERONS
NT ELEVATORS (CONTROL SURFACES)
NT ELEVONS
NT FLAPERONS
NT FLAPS (CONTROL SURFACES)
NT GUIDE VANES
NT HORIZONTAL TAIL SURFACES
NT JET FLAPS
NT JET VANES
NT LEADING EDGE FLAPS
NT LEADING EDGE SLATS
NT RUDDERS
NT SPOILERS
NT TABS (CONTROL SURFACES)
NT TRAILING EDGE FLAPS
NT WING FLAPS
Integral equation of lifting surfaces in Laplace domain and analytic continuation of its pressure kernel
[NAL-TR-795T] 01 p0002 N85-10009
Advanced composite stabilizer for Boeing 737 aircraft
[NASA-CR-166451] 02 p0137 N85-10934
Improvement of Aerodynamic Performance Through Boundary Layer Control and High Lift Systems
[AGARD-CP-365] 06 p1068 N85-16771
Steady- and unsteady-pressure measurements on a supercritical-wing model with oscillating control surfaces at subsonic and transonic speeds
[NASA-TM-84543] 06 p1077 N85-16831
Transonic steady- and unsteady-pressure measurements on a high-aspect-ratio supercritical-wing model with oscillating control surfaces
[NASA-TM-81888] 09 p1273 N85-18003
Subsonic and transonic pressure measurements on a high-aspect-ratio supercritical-wing model with oscillating control surfaces
[NASA-TM-83201] 09 p1273 N85-18004
Wind-tunnel investigation of a full-scale canard-configured general aviation airplane
[NASA-TP-2382] 11 p1575 N85-19925
Multivariable control law design for the AFTI/F-16 with a failed control surface
[AD-A151908] 15 p2474 N85-25271
Harrier 15 p2687 N85-26595
Flight control system reconfiguration design using quantitative feedback theory
[AD-A151771] 16 p2710 N85-26722
The aerodynamics of controls
16 p2713 N85-26748
X-29 digital flight control system design
17 p2901 N85-27889
The aerodynamics of control
17 p2903 N85-27901
Method of calculating separation flow of subsonic gas stream around wings 17 p2942 N85-28161
A study of aerodynamic control in stalled flight leading-edge vortex formation analysis
[AD-A153758] 18 p3059 N85-28928
Gust load alleviation of a cantilevered rectangular elastic wing. Wind tunnel experiment and analysis
[NAK-TR-86] 18 p3063 N85-28950
Mathematics of surfaces
[DE85-010439] 19 p3346 N85-30742

CONTROL SYSTEMS
U CONTROL

CONTROL SYSTEMS DESIGN
Return difference feedback design for robust uncertainty tolerance in stochastic multivariable control systems
[AD-A145861] 03 p0411 N85-12624
Development and demonstration of a vertical axis wind turbine POWERHOUSE
[DE84-901449] 04 p0527 N85-13369
Frequency response design methods for large scale systems
[DE84-01416'] 04 p0553 N85-13517
Model reduction for control system design
05 p0596 N85-13799
Level of effort 05 p0602 N85-13839
Oral presentation of first year final report, appendix A
05 p0602 N85-13840
An apparatus for and a method of controlling multiple time-varying processes
[AD-D011253] 05 p0631 N85-14045
Using the control system design environment in the design of a data link receiver unit for the Coast Guard HH-65A helicopter
[AD-A148624] 06 p1088 N85-16880
Man-machine interface and control of the shuttle digital flight system 06 p1091 N85-16894
Implementation of an Intel 8086 microprocessor-based realization library for the control system design language
[AD-A148506] 08 p1202 N85-17569
Improved stability and performance bounds using approximate models — control system design
[RR-260] 08 p1209 N85-17606
Design of mismatched Smith predictors using plant step data
[RR-263] 08 p1217 N85-17664
Simulation in the design of gas pressure control equipment
[ERS-E.352] 09 p1324 N85-18322
The influence of modern control techniques on the gas industry
[ERS-E.395] 09 p1325 N85-18326
NASA-VCOSS dynamic test facility
[NASA-TM-864[illegible]1] 10 p1427 N85-18998
Development of mass-producible line-focus tracking concentrating solar collectors. Category 2: Trackers
[DE85-002673] 10 p1512 N85-19543
Personnel protection concepts for advance escape system design 10 p1532 N85-19658
Microprocessor-based monitoring and control project, phase 1
[DE84-901074] 10 p1538 N85-19699
Robustness of continuous multivariable flight controls
[ONERA-RT-12/7224-SY] 11 p1586 N85-19987
Robustness of continuous multivariable flight controls
[ONERA-RT-11/7224-SY] 11 p1586 N85-19988
Compensator development and examination of performance and robustness
[NASA-CR-175470] 11 p1627 N85-20244
Automatic control design procedures for restructurable aircraft control
[NASA-CR-172489] 12 p1780 N85-21173
Some aspects of the design of a fly-by-wire flying control system for a supersonic V/STOL fighter aircraft
[COLL-AERON-8413] 12 p1780 N85-21175
Application of model following control and estimation techniques to attitude control of maneuvering spacecraft. Part 2: Simulation software description
[NLR-TR-82116-U-PT-2] 12 p1793 N85-21254
System dynamics and network control
[AD-A149420] 13 p2054 N85-22863
Activities in flight mechanics and flight control
[ISSN-0720-7808] 14 p2227 N85-23803
Application of the maximum entropy/optimal projection control design approach for large space structures
14 p2234 N85-23849
Synthesis of hyperstable control system with adaptive model 14 p2273 N85-24084
Modeling needed for the design and definition of spacecraft attitude and orbit control systems
14 p2397 N85-24766
Modeling and control of large flexible structures, phase 1
[AD-A150736] 14 p2403 N85-24817
Multivariable control law design for the AFTI/F-16 with a failed control surface
[AD-A151908] 15 p2474 N85-25271
Definition of ground test for verification of large space structure control
[NASA-CR-171438] 15 p2492 N85-25377
Process control systems for largely automated manufacturing 15 p2537 N85-25659
Cost Effective and Affordable Guidance and Control Systems
[AGARD-CP-360] 16 p2695 N85-26638
Some aspects of how to design cost-effective flight control systems 16 p2695 N85-26639
Design adequacy: An effectiveness factor
16 p2695 N85-26642
A modern control design methodology with application to the CH-47 helicopter
[AD-A151946] 16 p2710 N85-26723
Application of linear optimal control theory to the design of the elevator control system of the DHC-2 Beaver experimental aircraft
[VTH-LR-411] 16 p2711 N85-26729
The flight control system for the Experimental Aircraft Programme (EAP) demonstrator aircraft
16 p2714 N85-26755
The STOL and maneuver technology program integrated control system 16 p2715 N85-26757
Corrective-predictive systems
[BLL-M-36063-(5828.4)] 16 p2851 N85-27573
Some aspects of how to design cost-effective flight control systems
[MBB-LKE-32/S/PUB/143] 16 p2873 N85-27729
The state-of-the-art and future of flight control systems 17 p2901 N85-27885
Aspects of application of ACT systems for pilot workload alleviation 17 p2901 N85-27887
Application of AFTI/F-16 task-tailored control modes in advanced multirole fighters 17 p2901 N85-27888
X-29 digital flight control system design
17 p2901 N85-27889
The evolution of ACS for helicopters: Conceptual simulation studies to preliminary design
17 p2902 N85-27890
ACT applied to helicopter flight control
17 p2902 N85-27891
An update of experience on the fly by wire Jaguar equipped with a full-time digital flight control system
17 p2902 N85-27893
ACT flight research experience
17 p2902 N85-27894
Operational and developmental experience with the F/A-18A digital flight control system
17 p2902 N85-27895
Flight testing and development of the F/A-18A digital flight control system 17 p2902 N85-27896

OLGA: An open loop gust alleviation system
17 p2903 N85-27897
A modular dissimilar redundant computer designed for high integrity control 17 p2904 N85-27904
The flight control system for the Experimental Aircraft Programme (EAP) demonstration aircraft
17 p2904 N85-27906
Automatic flight control modes for the AFTI/F-111 mission adaptive wing aircraft 17 p2905 N85-27909
The STOL and maneuver technology program integrated control system development 17 p2905 N85-27910
Development of a multiprocessor system, using the MOTORLA microprocessor 6809, with the aim of providing maximum flexibility in the design of individual control devices
[BMFT-FB-T-84-270] 17 p3010 N85-28607
A modern control theory enhancement to an interactive Control Engineering Computer Analysis Package (ICECAP)
[AD-A153249] 17 p3012 N85-28622
Technical instructions for a control operating system of the gas flow installation for the solid fuel combustion chamber
[VTH-LR-410] 18 p3118 N85-29302
Research Flight Simulator for Helicopters (RFSH): Description and application to fire control system design
[SNIAS-851-210-106] 20 p3393 N85-31050
A study of the ESA-NAVSAT control segment
[ESA-CR(P)-2000] 20 p3396 N85-31079
Control system design for lightly coupled large space structures 20 p3399 N85-31086
Multivariable control of a soft coupled space station
20 p3408 N85-31151
A hardware demonstration of distributed control for a flexible offset-feed antenna 20 p3410 N85-31160
Control of flexible structures 20 p3410 N85-31161
Time-optimal bang-bang slew of rigidized SCOLE configuration 20 p3410 N85-31164
Numerical and experimental evaluation for single-axis control of an LSS laboratory model
20 p3411 N85-31168
Self-tuning adaptive-controller using online frequency identification 20 p3417 N85-31205
Robust adaptive control 20 p3417 N85-31207
Experimental verification of identification algorithms for control of flexible structures 20 p3418 N85-31211
Feedforward-feedback control logic for robust target-tracking 20 p3436 N85-31317
Control system for parabolic dish concentrator No. 1
[NASA-CR-176045] 20 p3463 N85-31510
Reduced order models and simulation data in control systems design
[RR-267] 20 p3463 N85-31516
On the equivalent bilinearization of nonlinear controlled delay systems
[RR-272] 20 p3519 N85-31880
FAUST: Introduction and overview — self tuning control
[OUEL-1568/85] 20 p3519 N85-31882
Models for describing active noise control in ducts
[ISVR-TR-127] 20 p3525 N85-31922
Performance improvements of a highly integrated digital electronic control system for an F-15 airplane
[NASA-TM-86748] 21 p3556 N85-32120
A preliminary investigation of handling qualities requirements for helicopter instrument flight during decelerating approach maneuvers and overshoot
[AD-A154850] 21 p3557 N85-32125
Research on an expert system for database operation of simulation-emulation math models. Volume 1, Phase 1: Results
[NASA-CR-176087] 21 p3669 N85-32792
Flight test experience and controlled impact of a large, four-engine, remotely piloted airplane
[NASA-TM-86738] 22 p3730 N85-33123
Application of frequency domain handling qualities criteria to the longitudinal landing task
[NASA-TM-86728] 22 p3730 N85-33124
The interpretation of flying qualities requirements for flight control system design
[NASA-CR-177942] 22 p3730 N85-33125
Research and development activities in unified control-structure modeling and design
[NASA-CR-176129] 22 p3740 N85-33179
Portable database driven control system for SPEAR
[DE85-010465] 22 p3830 N85-33720
Reactant pressure differential control for fuel cell gases
[NASA-CASE-MSC-20127-2] 23 p3937 N85-34403
Robot environment expert system
[NASA-CR-3915] 23 p3967 N85-34593
Discrete simulation models - their role in the design, development and management of inventory control systems
[PNR-90249] 23 p3986 N85-34719

Report on the SLC control system
[DE85-013076] 24 p4148 N85-35722
CONTROL THEORY
Research in Structures and Dynamics, 1984
[NASA-CP-2335] 01 p0057 N85-10377
Control of the dynamic response of a damped membrane by distributed forces
[CSIR-TWISK-312] 01 p0061 N85-10406
Markovian control problems: Functional equations and algorithms
[MCTH-97] 01 p0107 N85-10717
Robust rate control system designs for a submersible
[AD-A144792] 01 p0111 N85-10753
Model simplification of flight control systems
02 p0147 N85-11000
A research program in active control/aeroelasticity in the JIAFS at NASA Langley Research Center
[NASA-CR-174052] 02 p0148 N85-11001
Application of modern guidance control theory to a bank-to-turn missile
[AD-A145646] 02 p0186 N85-11123
Asynchronous discrete control of continuous processes
[AD-A145570] 02 p0189 N85-11262
Asymptotically optimal adaptive control
[AD-A145666] 02 p0249 N85-11629
On a class of suboptimal controls for infinite-dimensional bilinear systems
[RR-258] 02 p0249 N85-11630
The numerical range: A tool for robust stability studies — multivariable feedback systems
[RR-255] 02 p0253 N85-11660
Linear and bilinear infinite-dimensional representations of finite-dimensional nonlinear systems
[RR-259] 02 p0254 N85-11661
Gain-phase structures for linear multivariable systems
[RR-256] 02 p0256 N85-11674
Theory of information, automation in Czechoslovakia
04 p0485 N85-13091
Self-tuning control of offset: A unified approach
[OUEL-1539/84] 04 p0553 N85-13520
Dynamic decision making — and programming
[FOA-C-53015-H2] 04 p0575 N85-13668
Definition of ground test for verification of large space structure control
[NASA-CR-171206] 05 p0602 N85-13838
Definition of ground test for Large Space Structure (LSS) control verification, appendix G
05 p0603 N85-13845
Review of technical papers, appendix H
05 p0603 N85-13846
Ground test experiment for large space structures, appendix I 05 p0603 N85-13847
Self-tuning controller design and implementation
[OUEL-1535/84] 05 p0621 N85-13975
A generalized LQG approach to self-tuning control. Part 1: Aspects of design. Part 2: Implementation and simulation
[OUEL-1536/84] 05 p0622 N85-13976
Getting mental models and computer models to cooperate 05 p0709 N85-14548
Manual-control analysis applied to the money-supply control task 05 p0710 N85-14553
Determination of row-and-column control principle of phase antenna array from amplitude-phase distribution of field in aperture 07 p0952 N85-16033
Precise control of flexible manipulators
[NASA-CR-174210] 07 p0973 N85-16178
Control and modeling of a CELSS (Controlled Ecological Life Support System)
[NASA-CR-177324] 07 p1020 N85-16472
Numerical methods and approximation and modelling problems in stochastic control theory
[AD-A146927] 07 p1029 N85-16533
Bibliography of adaptive control
[OUEL-1544/84] 08 p1209 N85-17602
Research on optimal control, stabilization and computational algorithms for aerospace applications
[NASA-CR-174318] 08 p1209 N85-17603
On the global asymptotic stabilization of nonlinear systems
[PREPRINT-838] 08 p1209 N85-17604
Optimal stochastic LQ control with measurements displaced in time
[OUEL-1547/84] 08 p1209 N85-17605
Improved stability and performance bounds using approximate models — control system design
[RR-260] 08 p1209 N85-17606
The practical identification of systems with nonlinearities
[RR-264] 08 p1209 N85-17607
Approximate models in multivariable process control: An inverse Nyquist array and robust tuning regulator interpretation
[RR-261] 08 p1216 N85-17663

Design of mismatched Smith predictors using plant
data
[RR-263] 08 p1217 N85-17
Ground test experiment for large space structures
[NASA-TM-86480] 10 p1429 N85-18
A note on the disturbance decoupling problem
retarded systems
[AD-A149045] 10 p1543 N85-197
Advanced industrial robot control systems
[PB85-110773] 11 p1646 N85-20
Advanced industrial robot control systems
[PB85-110781] 11 p1648 N85-20
Needs, opportunities, and options for large
systems research
[DE85-004642] 12 p1925 N85-22
Testing of the digital flight control system of the Ger
CCV fighter experimental aircraft
13 p1968 N85-22
Model reduction for control system design
[NASA-CR-170417] 13 p1975 N85-22
AFWAL space control technology program
14 p2233 N85-23
Large antenna control methods: Current status and
future trends 14 p2234 N85-23
A mathematical formulation of the Scole control problem,
part 1
[NASA-CR-172581] 14 p2243 N85-23
Adaptive techniques for control of large spa
structures
[AD-A150957] 14 p2246 N85-23
Construction of high speed guaranteed regulators
14 p2270 N85-24
Modal synthesis of multidimensional PI-regulators
objects with inertial sections 14 p2270 N85-24
Synthesis of hyperstable control system with adaptive
model 14 p2273 N85-24
Optimal control and optimization
14 p2395 N85-247
High specific power aircraft turn maneuvers: Tradeof
of time-to-turn versus change in specific energy
[AD-A151701] 15 p2471 N85-25
Multivariable control law design for the AFTI/F-16 with
a failed control surface
[AD-A151908] 15 p2474 N85-25
Frequency/period estimation and adaptive rejection
periodic disturbances
[AD-A149229] 15 p2632 N85-26
Fundamental equivalence of generalised state spa
systems
[MATHEMATICS-RESEARCH-182]
15 p2642 N85-26
Optimal control theory applied to fusion plasma thermal
stabilization
[DE85-007599] 15 p2658 N85-26
AN investigation into the control limitations of a ban
to turn missile in the terminal homing phase
[AD-A152193] 16 p2704 N85-26
Flight control system reconfiguration design using
quantitative feedback theory
[AD-A151771] 16 p2710 N85-26
Application of linear optimal control theory to the design
of the elevator control system of the DHC-2 Beaver
experimental aircraft
[VTH-LR-411] 16 p2711 N85-26
Technical evaluation report on the Flight Mechanics
Symposium on Active Control Systems: Review,
Evaluation and Projections
[AGARD-AR-220] 16 p2711 N85-26
ACT applied to helicopter flight control
16 p2712 N85-26
The flight control system for the Experimental Aircraft
Programme (EAP) demonstrator aircraft
16 p2714 N85-26
The investigation of tethered satellite system
dynamics
[NASA-CR-175855] 16 p2731 N85-26
Optimal open loop and nonlinear feedback control
remote orbital capture
[AD-A151967] 16 p2732 N85-26
Control of motion of manipulator robots on basis
first-order kinematic algorithms
16 p2762 N85-27
Design of robust controllers for a multiple input-multiple
output control system with uncertain parameters
application to the lateral and longitudinal modes of the
KC-135 transport aircraft
[AD-A153100] 17 p2900 N85-27
Controller requirements for uncoupled aircraft motion,
volume 1
[AD-A153173] 17 p2900 N85-27
Controller requirements for uncoupled aircraft motion,
volume 2
[AD-A153300] 17 p2900 N85-27
Active Control Systems: Review, Evaluation and
Projections
[AGARD-CP-384] 17 p2901 N85-27

Hand controllers for teleoperation. A state-of-the-art technology survey and evaluation
[NASA-CR-175890] 17 p3002 N85-28559

A modern control theory enhancement to an interactive Control Engineering Computer Analysis Package (ICECAP)
[AD-A153249] 17 p3012 N85-28622

Scalar model control of a nonlinear system using time varying gain
[AD-A153252] 17 p3020 N85-28676

Nonlinear global stability analysis of compressor stall phenomena
[NASA-CR-174906] 19 p3219 N85-29960

Research on optimal control, stabilization and computational algorithms for aerospace applications
[NASA-CR-172526] 19 p3221 N85-29970

Proceedings of the Workshop on Identification and Control of Flexible Space Structures, volume 1
[NASA-CR-176051] 20 p3408 N85-31148

AFWAL control technology programs
20 p3408 N85-31150

Time-optimal bang-bang slew of rigidized SCOLE configuration 20 p3410 N85-31164

Experiments in structural dynamics and control using a grid 20 p3410 N85-31165

Rationale for an experimental test for flexible space structure attitude control 20 p3411 N85-31167

Proceedings of the Workshop on Identification and Control of Flexible Space Structures, volume 2
[NASA-CR-176052] 20 p3411 N85-31170

Finite control in underdamped distributed parameter systems 20 p3412 N85-31176

Control of a flexible space antenna: A finite dimensional perspective based on distributed parameter theory
20 p3413 N85-31182

Sensor/actuator selection for the constrained variance control problem 20 p3415 N85-31197

Decentralized control synthesis method for large-scale interconnected systems
[DE85-000746] 20 p3518 N85-31878

Linear system structure and cone containment for bilinear systems
[RR-268] 20 p3519 N85-31879

Multivariable model-following self-tuning control with offset rejection
[OUEL-1572/85] 20 p3519 N85-31883

Extensions of the small-mu test for robust stability — control stability
[OUEL-1573/85-REV] 20 p3519 N85-31884

Robust control of multivariable and large space systems
[AD-A155117] 21 p3559 N85-32140

Development of control laws for a flight test maneuver autopilot for an F-15 aircraft
[NASA-TM-86736] 22 p3730 N85-33122

Research and development activities in unified control-structure modeling and design
[NASA-CR-176129] 22 p3740 N85-33179

Decentralized control of dynamically interconnected systems
[BU-111] 22 p3835 N85-33744

Analogies of control mechanisms in flight guidance and medicine 24 p4129 N85-35597

Network management simulation of automated guideway transit systems under vehicle-follower control
[PB85-188233] 24 p4166 N85-35830

CONTROL UNITS (COMPUTERS)

Direct digital control study
[AD-A153685] 18 p3167 N85-29621

CONTROL VALVES

Slow opening valve — valve design for shuttle portable oxygen system
[NASA-CASE-MSC-20112-1] 11 p1642 N85-20338

Voyager 0.2-lbf thruster valve assembly short pulse test report
[NASA-CR-176121] 22 p3741 N85-33185

Computer and water-model simulation of flow through poppet valves
[CFD/85/2] 22 p3785 N85-33449

CONTROLLABILITY

Integrated Application of Active Controls (IAAC) technology to an advanced subsonic transport project-longitudinal handling qualities study of a relaxed-stability airplane
[NASA-CR-3660] 02 p0148 N85-11005

Simulation evaluation of two VTOL control/display systems in IMC approach and shipboard landing
[NASA-TM-85896] 06 p0756 N85-14841

Controllable rotation of system of two solid bodies with elastic elements 06 p0780 N85-14988

Electric and hybrid vehicle demonstration project
[DE84-014622] 06 p0871 N85-15535

Operational requirements versus technological capabilities 08 p1072 N85-16798

Space shuttle handling qualities
08 p1092 N85-16904

The development of a dynamic model of a generalised combat aircraft with forward wings for the identification of stability and control characteristics
[CAR-84-33] 09 p1280 N85-18050

Dynamics and control of general linear lumped-parameter systems 09 p1372 N85-18623

Study on controllability and stability of high speed tracked vehicles
[AD-P004302] 09 p1409 N85-18679

A functional vehicle for autonomous mobile robot research
[AD-A150052] 12 p1860 N85-21666

Simulation of aircraft behaviour on and close to the ground
[NASA-TM-87480] 14 p2218 N85-23754

A preliminary investigation of handling qualities requirements for helicopter instrument flight during decelerating approach maneuvers and overshoot
[NRC-24173] 17 p2896 N85-27857

ACT flight research experience
17 p2902 N85-27894

How to handle failures in advanced flight control systems of future transport aircraft 17 p2904 N85-27905

Mission requirements and handling qualities
18 p3057 N85-28918

Development of control laws for a flight test maneuver autopilot for an F-15 aircraft
[NASA-TM-86736] 22 p3730 N85-33122

Application of frequency domain handling qualities criteria to the longitudinal landing task
[NASA-TM-86728] 22 p3730 N85-33124

Ground-based and in-flight simulator studies of flight characteristics of a twin-fuselage passenger transport airplane during approach and landing
[NASA-TP-2451] 23 p3898 N85-34144

Analysis of flexible aircraft longitudinal dynamics and handling qualities. Volume 1: Analysis methods
[NASA-CR-177943-VOL-1] 24 p4066 N85-35202

Analysis of flexible aircraft longitudinal dynamics and handling qualities. Volume 2: Data
[NASA-CR-177943-VOL-2] 24 p4067 N85-35203

CONTROLLED ATMOSPHERES
NT CABIN ATMOSPHERES
NT INERT ATMOSPHERE
NT SPACECRAFT CABIN ATMOSPHERES

Stability of several substituted ferrites in a reducing atmosphere
[AD-A146108] 03 p0328 N85-12112

Inert atmosphere transfer vessel
[AD-D011433] 08 p1169 N85-17370

A theoretical method for selecting space craft and space suit atmospheres
[AD-A148219] 08 p1200 N85-17559

The body burden of organic vapors in artificial air trial measurements aboard a moored submarine
[AD-A149698] 12 p1910 N85-21988

Effect of protective atmosphere composition on durability of welded joints of niobium alloys
15 p2502 N85-25432

Preparation of heavy metal fluoride glasses in the bulk form
[AD-A153784] 18 p3079 N85-29049

Controlled Ecological Life Support System. Life Support Systems in Space Travel
[NASA-CP-2378] 18 p3155 N85-29531

Survey of CELSS concepts and preliminary research in Japan 18 p3155 N85-29533

Advanced regenerative environmental control and life support systems: Air and water regeneration
18 p3155 N85-29535

Atmosphere behavior in gas-closed mouse-algal systems: An experimental and modelling study
18 p3155 N85-29536

Ventilation flow: Submerged
18 p3156 N85-29545

An environmentally-controlled extended-use small animal hypobaric chamber
[AD-A153735] 19 p3221 N85-29974

Development of growth techniques for electromagnetic crystals
[AD-A154089] 19 p3375 N85-30937

Hydroponics developments for spaceship garden
21 p3683 N85-32754

CONTROLLED FUSION

Progress in inertial confinement fusion at Lawrence Livermore National Laboratory
[DE84-016227] 04 p0566 N85-13621

Lider-Thomson scattering — nuclear fusion
[IPP-1/299] 08 p1221 N85-17693

Atomic data for controlled fusion research. Volume 4: Spectroscopic data for iron
[DE85-009658] 19 p3354 N85-30787

Research activities of the Physics Division
[DE85-006958] 19 p3357 N85-30811

Report to the Working Group on Technology, Growth and Employment
[DE85-010320] 19 p3372 N85-30920

CONTROLLED STABILITY
U CONTROL

CONTROLLERS
NT POWER FACTOR CONTROLLERS
NT SERVOMECHANISMS
NT SERVOMOTORS

Aircraft cabin pressurization control system tester
[AD-D011225] 01 p0013 N85-10081

Programmable digital temperature controller apparatus
[AD-D011221] 01 p0049 N85-10319

Robust rate control system designs for a submersible
[AD-A144792] 01 p0111 N85-10753

An input translator for a computer-aided design system
[AD-A146337] 03 p0408 N85-12605

A unified method for evaluating real-time computer controllers: A case study — aircraft control
[NASA-CR-174168] 04 p0547 N85-13478

Microcomputer control of a residential photovoltaic power conditioning system
[DE84-013867] 04 p0547 N85-13480

Level of effort 05 p0602 N85-13839

Speed test results and hardware/software study of computational speed problem, appendix D
05 p0603 N85-13843

Self-tuning controller design and implementation
[OUEL-1535/84] 05 p0621 N85-13975

Quantification of cross-coupling and motion feedthrough for multiaxis controllers used in an air combat flying task
05 p0700 N85-14491

Model estimation and identification of manual controller objectives in complex tracking tasks
05 p0700 N85-14494

Effects of control stick parameters on human controller response 05 p0701 N85-14496

Measurements of pilot time delay as influenced by controller characteristics and vehicles time delays
05 p0701 N85-14500

Active sticks: A new dimension in controller design
05 p0706 N85-14531

Implementation of a Zilog Z-80 base realization library for the computer systems design environment
[AD-A146359] 06 p0853 N85-15423

Control system design language implementation of a gas turbine starting controller
[AD-A147896] 07 p0905 N85-15732

Flutter control with unsteady aerodynamic models
[AD-A147858] 07 p0909 N85-15753

Battery control and fault detection method
[AD-D011384] 07 p0993 N85-16307

Interactive color-graphics interface for energy monitoring and control systems
[AD-A147538] 07 p1025 N85-16509

Mirror actuator control system
[AD-D011383] 07 p1042 N85-16619

Experience of one UK electronic equipment supplier with bite on engine/flight control systems over the past ten years 08 p1064 N85-16738

Mission-oriented requirements for updating MIL-H-8501. Volume 1: STI proposed structure — military rotorcraft
[NASA-CR-177331-VOL-1] 08 p1088 N85-16877

Implementation of an Intel 8086 microprocessor-based realization library for the control system design language
[AD-A148506] 08 p1202 N85-17569

Dual arm master controller concept
[DE85-001901] 09 p1327 N85-18344

An ultra reliable computer communication network: The dispersed sensor processing mesh
09 p1372 N85-18620

Dynamics and control of general linear lumped-parameter systems 09 p1372 N85-18623

RELTIM: A library of routines used in real time machine control applications
[PB85-116507] 10 p1542 N85-19725

Solar optical telescope primary mirror controller
[NASA-CR-174416] 10 p1570 N85-19903

Digital controller for the Wave Propagation Laboratory's VHF and UHF wind-profiling radars
[PB85-112142] 11 p1626 N85-20238

Microprocessor-controlled rotating shadowband radiometer
[DE85-003633] 12 p1854 N85-21630

Model reduction for control system design
[NASA-CR-170417] 13 p1975 N85-22396

Large antenna control methods: Current status and future trends 14 p2234 N85-23845

Model and controller reduction of uncertain systems using covariance equivalent realizations
14 p2243 N85-23902

Modal synthesis of multidimensional PI-regulators for objects with inertial sections 14 p2270 N85-24064

Some problems in improving reliability and accuracy of regulators with hydraulic amplifiers in main channel of power turbine 14 p2271 N85-24071

Investigation of transport operations of ergatic robot 14 p2286 N85-24166

User's guide to calibration of analog electronic controllers in HVAC systems
[AD-A150803] 14 p2298 N85-24229

Effects of side-stick controllers on rotorcraft handling qualities for terrain flight
[NASA-TM-86688] 15 p2473 N85-25267

Space station systems technology study (add-on task). Volume 3: Technology advancement program plan
[NASA-CR-171417] 15 p2475 N85-25260

Czech institute develops microcomputer for satellites 15 p2484 N85-25331

Development of robots and application to industrial processes
[NASA-CR-175754] 15 p2567 N85-25840

Feasibility analysis of moving bank multiple model adaptive estimation and control algorithms
[AD-A152015] 15 p2641 N85-26292

Model reduction techniques applied to the control of large space structures
[AD-A151784] 16 p2731 N85-26857

Further development of an Interactive Control Engineering Computer Analysis Package (ICECAP) for discrete and continuous systems
[AD-A151783] 16 p2846 N85-27546

Design of robust controllers for a multiple input-multiple output control system with uncertain parameters application to the lateral and longitudinal modes of the KC-135 transport aircraft
[AD-A153100] 17 p2900 N85-27877

Controller requirements for uncoupled aircraft motion, volume 2
[AD-A153300] 17 p2900 N85-27879

ACT applied to helicopter flight control 17 p2902 N85-27891

A ten channel temperature controller
[AD-A152664] 17 p2967 N85-28326

Scalar modal control of a nonlinear system using time varying gain
[AD-A153252] 17 p3020 N85-28676

A proportional-plus-integral controller for a particle beam weapon
[AD-A153213] 17 p3035 N85-28778

Ultrareliable, fault-tolerant control systems: A conceptual description
[NASA-TM-86017] 19 p3221 N85-29972

Thrust vectoring apparatus for maneuvering missile in flight
[AD-D011693] 19 p3226 N85-30004

A variable frequency control for three-phase induction motors 19 p3256 N85-30190

Spillover minimization: An approach for actuators and sensors placement in distributed parameter study
[INPE-3525-PRE/746] 19 p3272 N85-30289

Physiochemically controlled scour jet array system
[AD-D011686] 19 p3308 N85-30505

The experimental computer control of a two-dimensional hyperbolic system 20 p3411 N85-31166

Rationale for an experimental test for flexible space structure attitude control 20 p3411 N85-31167

Proceedings of the Workshop on Identification and Control of Flexible Space Structures, volume 2
[NASA-CR-176052] 20 p3411 N85-31170

Design of multivariable controllers using the Integrated Analysis Capability (IAC) 20 p3412 N85-31172

ISAAC (Integrated Structural Analysis and Control) via continuum modeling and distributed frequency domain design techniques 20 p3414 N85-31185

Frequency domain control design of large space structures: A practical approach 20 p3415 N85-31192

A control concept for large flexible spacecraft using order reduction techniques 20 p3415 N85-31193

Wideband disturbance accomodation in precision flexible space structures 20 p3415 N85-31194

Proceedings of the Workshop on Identification and Control of Flexible Space Structures, volume 3
[NASA-CR-176053] 20 p3415 N85-31195

Sensor/actuator selection for the constrained variance control problem 20 p3415 N85-31197

Eigenvalue placement and stabilization by constrained optimization 20 p3416 N85-31198

Adaptive control: Actual status and trends 20 p3416 N85-31202

Stable direct adaptive control of linear infinite-dimensional systems using a command generator tracker approach 20 p3416 N85-31204

Multivariable model-following self-tuning control with offset rejection
[OUEL-1572/85] 20 p3519 N85-31883

Microprocessor control design for a low-head crossflow turbine
[AD-A155477] 21 p3556 N85-32121

Secure digital voice communications in the Defense Data Network (DDN)
[AD-A154677] 21 p3574 N85-32226

An analysis of the effects of active solar energy system control sensor degradation on system performance
[DE84-013023] 22 p3804 N85-33562

Feedback regulated induction heater for a flowing fluid
[DE85-006508] 23 p3939 N85-34414

Neutral particle beam intensity controller
[DE85-006411] 23 p3969 N85-34604

State-of-the-art of solid-state motor controllers
[TI85-008674] 24 p4162 N85-35806

CONVAIR MILITARY AIRCRAFT
U MILITARY AIRCRAFT

CONVAIR 990 AIRCRAFT
U CV-990 AIRCRAFT

CONVECTION
NT FORCED CONVECTION
NT FREE CONVECTION
NT MARANGONI CONVECTION

Second All-Union Seminar on Hydromechanics and Heat and Mass Exchange in Weightlessness, summaries of reports
[NASA-TM-77590] 01 p0047 N85-10305

Preparation steps for the use of one-dimensional interpretation models for nowcasting purposes in the German weather net 01 p0081 N85-10540

Some aspects of post-frontal convective areas along the west coast of the united states
[AD-A144895] 01 p0085 N85-10572

Investigation of summertime convection over the upper Current River valley of southeast Missouri
[PB84-222389] 01 p0086 N85-10578

Analytical modeling of random thermal fluctuations in the NORDA high-frequency sound scattering facility
[AD-A145024] 01 p0116 N85-10790

The absence of convective stability in incongruent crystal growth on Earth 02 p0150 N85-11019

Finite element analysis of thermoelasticity problems 02 p0208 N85-11369

The arc cloud complex: A case study
[AD-A145384] 02 p0231 N85-11507

NBS (National Bureau of Standards): Materials measurements
[NASA-CR-174038] 03 p0332 N85-12143

Mesoscale and convective-scale characteristics of mature hurricanes 03 p0394 N85-12516

On the cause of X-line formation in the near-Earth plasma sheet: Results of adiabatic convection of Plasma-Sheet-Plasma
[AD-A145835] 03 p0396 N85-12525

Study of plasma convection and wall interactions in magnetic confinement systems
[DE84-013959] 03 p0421 N85-12692

A preliminary study of numerical simulation of thermosolutal convection of interest to crystal growth
[NASA-TP-2394] 04 p0498 N85-13175

Planetary scale interactions 05 p0684 N85-14397

Stresses and strains in lithosphere caused by Earth's thermoconvective oscillations 06 p0822 N85-15217

Convective scale weather analysis and forecasting
[NASA-CR-174185] 06 p0838 N85-15320

Precipitation characteristics of a dual mesoscale convective complex
[PB84-226711] 06 p0840 N85-15337

Studies of the ocean surface and the coupling between the sea and the atmosphere
[AD-A146546] 06 p0841 N85-15339

The growth of metastable peritectic compounds
[NASA-CR-171290] 07 p0920 N85-15825

Finite difference calculations of buoyant convection in an enclosure. Part 2: Verification of the nonlinear algorithm
[PB85-104065/GAR] 07 p0961 N85-16089

Numerical solutions for steady natural convection in a square cavity
[PB84-245752] 07 p0961 N85-16090

Convection schemes for use with curvilinear coordinate systems: A survey
[AD-A147093] 07 p1031 N85-16543

Sea breeze-induced mesoscale systems and severe weather
[NASA-CR-174317] 08 p1187 N85-17480

Heat-transfer enhancement in natural convection enclosure flow
[DE84-013048] 09 p1319 N85-18297

The influence of deep cumulus convection on large-scale flow during AVE/SESAME 1, 10-11 April 1979 09 p1355 N85-18526

Behavior and characteristics of storm cold outflows 09 p1356 N85-18529

Meridional penetration of frontal systems in South America and its relation to organized convection in the Amazon
[INPE-3407-PRE/676] 10 p1518 N85-19572

Stochastic convective-dispersive transport model for wastes disposed at the 106-mile ocean disposal site
[PB85-116176] 12 p1865 N85-21801

Observational study of transport in the free troposphere
[PB85-144145] 12 p1887 N85-21846

Thermal convection and magnetic fields in accretion disks of black holes 12 p1955 N85-22285

The role of convective perturbations in supercritical inter oscillations 13 p2004 N85-22583

Contribution to theory of ocean-atmosphere gas exchange 13 p2108 N85-23134

Cumulus effects on the large-scale vorticity and momentum fields in the tropical atmosphere 13 p2137 N85-23270

Implications of convection in the Moon and the terrestrial planets 13 p2183 N85-23548

Solar wind control of magnetospheric convection 14 p2365 N85-24615

Implications of observed frequencies of solar P modes 14 p2443 N85-25073

Numerical simulations of convectively excited gravity waves 14 p2444 N85-25082

On the influence of turbulent motions on non-radial oscillations 14 p2444 N85-25091

Magnetoconvection: The interaction of convection and small scale magnetic fields — photosphere 14 p2446 N85-25098

Oscillatory convection in sunspots 14 p2446 N85-25099

Amplification and maintenance of thin magnetic flux tubes by compressible convection — solar magnetism 14 p2447 N85-25104

Nonlinear time-evolution of kink-unstable magnetic flux tubes in the convection zone of the Sun 14 p2447 N85-25105

Linear incompressible magnetoconvection in a plane layer with a nonuniform horizontal magnetic field 14 p2450 N85-25127

Convective collapse and overstable oscillations in solar flux tubes 14 p2452 N85-25139

Modeling longitudinal motions of thermal O+ and H+ ions in magnetic field tube convective through daytime polar cusp 15 p2481 N85-25314

Natural convection in cylindrical containers 15 p2555 N85-25783

VAS/model impact study 15 p2597 N85-26006

Role of jet streaks and boundary layer processes in organizing a pre-convective environment 15 p2597 N85-26009

Possible sea ice impacts on oceanic deep convection 15 p2603 N85-26041

Optimum convection conditions for Czochralski growth of semiconductors
[INPE-3395-PRE/665] 16 p2870 N85-27703

Centralized Storm Information System (CSIS)
[NASA-CR-175898] 17 p2994 N85-28506

Natural convection in square partitioned enclosures
[AD-A153707] 18 p3197 N85-29639

Coolant mixing in LMFBR rod bundles and outlet plenum mixing transients
[DE85-010336] 19 p3268 N85-30288

Diagnosis of vertical motions from VAS retrievals during a convective outbreak
[NASA-CR-171569] 19 p3316 N85-30554

Natural convection experiments in a stratified liquid-saturated porous medium
[DE85-009003] 20 p3455 N85-31457

Automated cell detection as a mesocyclone precursor tool
[AD-A154952] 21 p3635 N85-32577

On the problem of possible mechanism of ice nuclei formation in convective clouds 21 p3640 N85-32610

Magnetic fields in laser heated plasmas
[DE85-010715] 21 p3707 N85-33082

Solar convection
[AD-A155214] 21 p3723 N85-33099

Forced convective, nonequilibrium, post-CHF heat transfer experiment data and correlation comparison report
[TI85-009331] 23 p3932 N85-34371

Diffusion-convection function of cosmic rays
[SH-3.2-10] 23 p4004 N85-34605

IMF-sense-dependent cosmic ray anisotropy produced from diffusion-convection in heliosphere
[SH-4.3-9] 23 p4032 N85-34684

Diurnal anisotropy during solar activity cycle twenty and diffusion-convection model
[SH-4.5-7] 23 p4036 N85-35055

Experimental study of free and mixed convective flow of air in a heated cavity
[DE85-012536] 24 p4094 N85-35380

Airborne Investigations of Mesoscale Convective Systems (AIMCS), 1984: Operational summary and data inventory
[PB86-187904] 24 p4125 N85-35571

CONVECTION CLOUDS
NT ARC CLOUDS
NT CIRRUS CLOUDS
NT STRATOCUMULUS CLOUDS
NT STRATUS CLOUDS

Generation of deep convective clouds along mesoscale storm outflow boundaries 01 p0074 N85-10480

Automated analysis and nowcasting of mesoscale convective systems 01 p0074 N85-10482

Combining radar and satellite data for the localization and identification of summer convection
01 p0077 N85-10509

The use of dual polarisation radar for observing and predicting convective activity 01 p0077 N85-10512

Doppler radar analysis of a frontal zone prior to convective development 01 p0077 N85-10515

The lifting condensation level and its relation to convective cloud base
[AD-A145854] 02 p0232 N85-11513

Experimental study of anisotropy of scattering of radar signals by clouds and precipitation
14 p2340 N85-24473

Case studies of snow clouds by means of snow crystal sondes 15 p2561 N85-25921

Assessment of VAS soundings in the analysis of a preconvective environment
[NASA-TM-86205] 16 p2825 N85-27427

Statistical comparison of radar echoes of convective precipitation between the northern Alps and its foreland
[DFVLR-FB-85-07] 17 p2950 N85-28215

Vertical redistribution of a pollutant tracer due to cumulus convection
[PB85-172971] 18 p3134 N85-29415

Mesoscale features and atmospheric refraction conditions of the Arctic marginal ice zone
[AD-A155139] 21 p3636 N85-32584

CONVECTION CURRENTS

Theoretical and observational studies of stellar activity
13 p2171 N85-23468

Atmosphere ice-ocean interactions in the Antarctic (IAGO) 14 p2326 N85-24375

Afternoon radar aurora and polar cap convection pattern 14 p2361 N85-24592

Disturbance of midlatitude electrodynamic parameters due to the magnetospheric convection
14 p2362 N85-24593

The magnetospheric convection electric field at ionospheric altitudes: A case study based on STARE and Saint-Santin data 14 p2362 N85-24594

Ionosphere-magnetosphere coupling and convection
14 p2364 N85-24609

On the structure of magnetic fields in the solar convection zone 14 p2447 N85-25103

Convection modeling and application to severe storms
15 p2595 N85-25991

Modeling of cloud systems 15 p2595 N85-25992

The sensitivity of mesoscale cyclogenesis forecasts to detailed three-dimensional isentropic initial analyses and varied vertical model resolution
15 p2598 N85-26015

Assessment of VAS soundings in the analysis of a preconvective environment
[NASA-TM-86205] 16 p2825 N85-27427

Diagnostics of severe convection and subsynoptic scale ageostrophic circulations
[NASA-CR-171581] 21 p3634 N85-32571

Dynamics of Mesoscale Weather Systems: 1984 Summer Colloquium
[PB85-186266] 22 p3817 N85-33649

Measurements for the determination of the vertical structure of the convective boundary layer — atmospheric boundary layer 24 p4122 N85-35550

Two-point closure study of covariance budgets for turbulent Rayleigh-Benard convection
[PB86-189108] 24 p4124 N85-35568

CONVECTIVE FLOW

Vertical channel free convection for a power law fluid with a constant heat flux
[DE84-014561] 01 p0047 N85-10311

The mesoscale-beta-scale evolution of mid-latitude meso-alpha-scale convective complexes
01 p0073 N85-10488

Convection of plasma in polar ionosphere, comparison of measurements from Cosmos-184 with model dependent on interplanetary magnetic field vector
02 p0160 N85-11086

Stresses and strains in lithosphere caused by Earth's thermoconvective oscillations 06 p0822 N85-15217

High Marangoni number convection in a square cavity
[NASA-CR-174283] 07 p0959 N85-16078

Numerical investigation of phase change heat transfer in a horizontal cylinder including effects of natural convection 09 p1318 N85-18286

A 3-D treatment of convective flow in the Earth's mantle
[DE85-003734] 12 p1890 N85-21863

Convective instability of horizontal layer of binary mixture 14 p2338 N85-24458

What would a dynamo theorist like to know about the dynamics of the solar convection zone?
14 p2441 N85-25062

North Atlantic Deep Water Formation
[NASA-CP-2367] 15 p2601 N85-26026

Deep water formation 15 p2601 N85-26030

Temporal and spatial scales of Labrador Sea water formation 15 p2601 N85-26031

Possible sea ice impacts on oceanic deep convection
15 p2603 N85-26041

Large-eddy simulation in planetary boundary-layer research 18 p3147 N85-29482

Spacecraft, straight-tube evaporator design
[AD-A154462] 19 p3226 N85-30003

Development of thermoconvective instabilities in porous media. Influence of boundary conditions
20 p3456 N85-31461

Effects of solar magnetic field on cosmic rays
[SH-4.2-12] 23 p4008 N85-34850

Difference between even and odd 11-year cycles in cosmic ray intensity
[SH-4.2-22] 23 p4009 N85-34859

CONVECTIVE HEAT TRANSFER

About the influence of nonadiabatic processes on frontogenesis near the ground 01 p0075 N85-10498

Investigation of crisis phenomena in thermosyphons with internal heat-dissipation
[BLL-M-35765-(5828.4)] 02 p0197 N85-11313

Numerical simulation of natural convection in porous media — heat transfer
[CFD/84/10] 02 p0199 N85-11330

Methane heat transfer investigation
[NASA-CR-171199] 03 p0362 N85-12318

Bibliography of US patents on augmentation of convective heat and mass transfer, part 2
[DE84-014865] 04 p0498 N85-13178

Influence of Prandtl number on natural convection heat transfer correlations
[DE84-013006] 05 p0637 N85-14089

Convection heat transfer in the critical region of fluid mixtures
[DE85-002118] 07 p0961 N85-16088

Methods for heat transfer and temperature field analysis of the insulated diesel
[NASA-CR-174783] 07 p1056 N85-16899

Numerical modeling of steady, laminar free-convective boundary layer flow beneath heated or combusting horizonal surfaces 08 p1160 N85-17318

Unsteady free-convection heat transfer inside an annular cavity
[CFD/84/16] 08 p1163 N85-17339

Simultaneous determination of radiation and convection heat transfer 08 p1194 N85-17523

Natural convection experiments about a finite-length cylindrical heat source in a liquid-saturated porous medium
[DE84-012657] 09 p1320 N85-18298

Natural convection heat transfer between arrays of horizontal cylinders and their enclosure
[DE85-003773] 11 p1632 N85-20280

Convection heat transfer in the critical region of fluid mixtures
[DE85-001282] 11 p1633 N85-20285

Theoretical and empirical studies of the basic structure of turbulent shear flows, including separated flows and effects of wall curvature
[AD-A149657] 12 p1846 N85-21580

Turbulent convecting flow in a square duct with a 180 deg bend: An experimental and numerical study
[AD-A149969] 12 p1846 N85-21583

A 3-D treatment of convective flow in the Earth's mantle
[DE85-003734] 12 p1890 N85-21863

Theory of relaxation processes in decomposing polymer materials during high-intensity convective heating
13 p2028 N85-22710

Natural convection during heat accumulation by substances with change of aggregate state
13 p2043 N85-22787

A theoretical analysis of solar-driven natural convection energy conversion systems
[DE84-004431] 13 p2128 N85-23245

Cumulus cloud venting of mixed layer ozone
[NASA-TM-87429] 13 p2132 N85-23269

Optimization of combined convective and film cooling of perforated baffle blades in gas turbines
14 p2270 N85-24067

Convective instability of horizontal layer of binary mixture 14 p2338 N85-24458

Models of solar differential rotation
14 p2446 N85-25097

North Atlantic Deep Water and the world ocean
15 p2602 N85-26033

Unsteady heat transfer due to time-dependent free stream velocity 17 p2911 N85-27947

Effects of the corona wind on the cooling of a horizontal cylinder
[AD-A153101] 17 p2954 N85-28241

Heat transfer in pipes
[NASA-TM-77838] 17 p2957 N85-28262

Solar pond research at the Los Alamos National Laboratory
[DE85-008631] 18 p3128 N85-29366

Natural convection in square partitioned enclosures
[AD-A153707] 18 p3197 N85-29828

Spacecraft, straight-tube evaporator design
[AD-A154462] 19 p3226 N85-30003

Selective radiative cooling with MgO and/or LiF layers
[DE85-011595] 19 p3262 N85-30228

Experimental investigation of turbulent heat transfer in straight and curved rectangular ducts
[AD-A154413] 19 p3266 N85-30255

A numerical solution of a nonisothermal wall using the two-dimensional Navier-Stokes equations
[AD-A154467] 19 p3266 N85-30257

Enhanced thermal coupling by a repetitively pulsed laser
[AD-A154435] 19 p3276 N85-30317

Parametric description of cold film on ocean surface
19 p3292 N85-30410

Natural convection experiments in a stratified liquid-saturated porous medium
[DE85-009003] 20 p3455 N85-31457

Evaluation of the effects of roll angle on the natural convection heat transfer from an array of cylindrical spines
[AD-A154594] 21 p3583 N85-32273

CONVERGENCE

The effect of channel convergence on heat transfer in a passage with short pin fins
[NASA-TM-83801] 01 p0046 N85-10303

The convergence of Garlerkin approximation schemes for second-order hyperbolic equations with dissipation
[CSIR-TWISK-325] 01 p0109 N85-10736

Legendre-Tau approximation for functional differential equations. Part 3: Eigenvalue approximations and uniform stability
[NASA-CR-172447] 01 p0110 N85-10744

The rate of convergence of a class of block Jacobi schemes
[AD-A144738] 01 p0111 N85-10749

Accelerated convergence for incompressible flow calculations
[NASA-TM-86863] 02 p0140 N85-10949

Qualitative results for distributed systems with discrete damping and stiffness with application to control
[AD-A145525] 02 p0209 N85-11382

An iterative procedure for obtaining i-projections onto the intersection of convex sets
[AD-A145402] 02 p0251 N85-11639

Rapidly convergent algorithms for nonsmooth optimization
[AD-A145556] 02 p0251 N85-11643

Comparison of the multigrid and ICCG methods in solving the diffusion equation
[DE84-014409] 02 p0253 N85-11657

On the rate of mean convergence of finite linear predictors of multivariate stationary stochastic processes
[AD-A145603] 02 p0254 N85-11664

Convergence of SIP (Strongly Implicit Procedure)
[AD-A145810] 03 p0410 N85-12621

Sinc method of solution of singular integral equations
[AD-A146155] 03 p0411 N85-12631

Oceanic plateaus, anomalous subduction, and the accretion of buoyant features at convergent margins
05 p0688 N85-14422

On an algorithm for Pythagorean sums and its connection with continued fractions
[NPL-DITC-42/84] 05 p0718 N85-14603

Random equations in aerodynamics
[NASA-CR-174279] 06 p1077 N85-16825

Convergence of quasi-stationary to stationary distributions for stochastically monotone Markov processes
[AD-A146041] 08 p1215 N85-17652

New methods for numerical solution of one class of strongly nonlinear partial differential equations with applications in hydrodynamics
[AD-A149026] 10 p1545 N85-19730

On the modified likelihood for density estimation
[AD-A149437] 10 p1547 N85-19758

A method of calculating periodic solutions of second order dynamical systems
[AD-A149634] 12 p1920 N85-22058

Determining conductivity by boundary measurements. Part 2: Interior results
[AD-A149750] 12 p1921 N85-22063

Distributed asynchronous deterministic and stochastic gradient optimization algorithms: Revision
[AD-A149997] 12 p1921 N85-22066

Convergence rates in the strong law for bounded mixing sequences
[CWI-MS-R8412] 12 p1922 N85-22076

Rates of convergence of semistochastic approximation procedures for solving stochastic optimization problems
12 p1924 N85-22088

A note about the strong convergence of the nonparametric estimation of a regression function
[AD-A150325] 13 p2151 N85-23353

Attainable rates of convergence of maxima
[AD-A150638] 14 p2408 N85-24847

Weak convergence of a sequence of queueing and storage processes to a singular diffusion
[AD-A150655] 14 p2411 N85-24866

The South Pacafic convergence zone and energy balance of the southern hemisphere
15 p2593 N85-25980

An incremental multigrid strategy for the fluid dynamics equations
[AD-A151953] 16 p2783 N85-27172

Analysis of the convergance of mixed finite element methods
[HTKK-MAT-A227] 16 p2856 N85-27613

Convergence of Newton's method for a single real equation
[NASA-TP-2489] 17 p3017 N85-28656

About product formulas with variable step-size
[AD-A153527] 18 p3169 N85-29636

Control of a flexible space antenna: A finite dimensional perspective based on distributed parameter theory
20 p3413 N85-31182

On the dependence of the convergence of Gummel's algorithm on the regularity of the solution
[AD-A154628] 21 p3675 N85-32832

Method of estimating convergence of Haar coefficients in message compression problems
22 p3769 N85-33356

Design of electrooptical system with annular cathode and electrostatic compressor 22 p3770 N85-33367

Admissible convergence of Poisson integrals in symmetric spaces
[CTH-MATH-1985-04] 22 p3836 N85-33750

Reordering computations for parallel execution
[NASA-CR-177961] 23 p3957 N85-34522

On the convergence of an iterative formulation of the electromagnetic scattering from an infinite grating of thin wires 24 p4085 N85-35319

Characterizations of generalized hyperexponential distributions
[AD-A155855] 24 p4142 N85-35680

CONVERGENT NOZZLES

Experimental investigation of shock-cell noise reduction for dual-stream nozzles in simulated flight
[NASA-CR-3846] 04 p0557 N85-13549

Experimental investigation of shock-cell noise reduction for single stream nozzles in simulated flight
[NASA-CR-3845] 04 p0557 N85-13550

Static internal performance of a two-dimensional convergent nozzle with thrust-vectoring capability up to 60 deg
[NASA-TP-2391] 10 p1419 N85-18951

Modifications to the nozzle test chamber to extend nozzle static-test capability
[NASA-TM-86368] 15 p2464 N85-25216

CONVERGENT-DIVERGENT NOZZLES

Experimental investigation of shock-cell noise reduction for dual-stream nozzles in simulated flight
[NASA-CR-3846] 04 p0557 N85-13549

Experimental investigation of shock-cell noise reduction for single stream nozzles in simulated flight
[NASA-CR-3845] 04 p0557 N85-13550

A computer program for the performance analysis of scarfed nozzles
[AD-A147370] 07 p0905 N85-15730

Vacuum chamber pressure effects on thrust measurements of low Reynolds number nozzles
[NASA-TM-86955] 12 p1794 N85-21259

An experimental study of clustered, two-dimensional rocket nozzles
[AD-A151869] 15 p2495 N85-25390

Characteristics of heat exchange in the region of injection into a supersonic high-temperature flow
[NASA-TM-77833] 15 p2555 N85-25762

Static investigation of several yaw vectoring concepts on nonaxisymmetric nozzles
[NASA-TP-2432] 18 p3058 N85-28924

CONVERSATION

Communications skills for CRM training
09 p1276 N85-18017

CONVERSION

Conversion of FEB (Fast and Easy Binary) utilities to ASCII FORTRAN
[AD-A145640] 03 p0406 N85-12596

Conversion efficiencies of charged particle beam driven free electron lasers
[AD-A154404] 19 p3276 N85-30316

CONVERTAPLANES

U V/STOL AIRCRAFT

CONVERTERS

Symposium on Luminescent Radiation Receivers and Converters 19 p3295 N85-30430

CONVEXITY

Generalized convex functions: Properties, optimality and duality
[DE85-001553] 09 p1376 N85-18652

Close-to-convex functions and linear-invariant families
10 p1536 N85-19683

An extension of the Gleason problem in pseudoconvex domains 11 p1698 N85-20671

Intertwining functions on compact Lie groups
[CWI-TRACT-5] 14 p2414 N85-24895

On positive vectors, positive matrices and the specialization ordering
[CWI-PM-R8407] 14 p2414 N85-24899

A convexity theorem for semisimple symmetric spaces
[CWI-PM-R8414] 14 p2415 N85-24900

An experimental investigation of the interaction between a shock wave and a turbulent boundary layer on a convex wall
[VTH-LR-428] 16 p2785 N85-27187

The essence of invexity
[CSIR-TWISK-321] 16 p2858 N85-27626

Convex interpolating splines of arbitrary degree
17 p3004 N85-28574

A quadratic programming algorithm
[AD-A153476] 18 p3168 N85-29631

An experimental investigation of curvature and freestream turbulence effects on heat transfer and fluid mechanics in transitional boundary layer flows
19 p3264 N85-30240

A dynamic programming approach to time-staged convex programs
[DE85-010616] 19 p3340 N85-30700

Reachable grasps on a polygon: The convex rope algorithm
[AD-A155913] 24 p4138 N85-35647

CONVEYORS

Automated parts storage and retrieval system positioning device and method
[AD-D011494] 11 p1647 N85-20379

Shuttle car loading system
[NASA-CASE-NPO-15949-1] 23 p3987 N85-34722

CONVOLUTION INTEGRALS

Modeling holographic recognition system by using number-theory convolution transformation
02 p0272 N85-11774

A very efficient transfer function bounding technique on bit error rate for Viterbi decoded, rate 1/N convolutional codes 05 p0624 N85-13991

Sequential syndrome decoding of convolutional codes
05 p0624 N85-13992

Linear autonomous retarded functional differential equations; a sharp version of Henry's theorem
[CWI-AM-R8405] 05 p0720 N85-14625

FLAD user's manual: FLAD file contents
[AD-A148700] 09 p1368 N85-18594

Digital high speed programmable convolver
[AD-D011455] 10 p1481 N85-19348

A remark on regularization in Hilbert spaces
[AD-A149046] 10 p1552 N85-19787

Generalization of Beurling algebras
11 p1698 N85-20675

New convolution and discrete Fourier transformation algorithms based on rectangular transformations over field of roots of unity 13 p2085 N85-23022

Convolution of the IFRA (Increasing Failure Rate Average) scaled-mins class
[AD-A151070] 14 p2411 N85-24870

Generalised translation invariance and systems theory
[CRM-8501] 17 p3017 N85-28657

Deconvolution methods for multi-sensors
[AD-A152351] 17 p3018 N85-28660

A convolution integral equation solved by Laplace transformation
[CWI-AM-R8409] 17 p3022 N85-28692

Convoluted nozzle design for the RL10 derivative 2B engine
[NASA-CR-174953] 19 p3220 N85-29965

CONVOLUTIONS (MATHEMATICS)

U CONVOLUTION INTEGRALS

CONVULSIONS

Mechanisms of oxygen toxicity and methods of protection
[AD-A145830] 03 p0400 N85-12551

COOL STARS

Search for white dwarf companions of cool stars with peculiar element abundances
[NASA-CR-174030] 02 p0297 N85-11923

Theoretical studies of chromospheres and winds in cool stars
[NASA-CR-174204] 06 p0880 N85-15598

Spectrophotometry of cool stars from objective prism spectra 07 p0966 N85-18134

COOLANTS

NT ENGINE COOLANTS

Coolant passage heat transfer with rotation
02 p0143 N85-10968

Electrochemical pitting evaluation of aluminum alloy 7075 in machining coolant
[DE84-016844] 04 p0475 N85-13026

Drop of coolant temperature in individual components of solar heating system 14 p2265 N85-24035

Role of fluid lubricant-coolant in fine grinding of optical glass by diamond tool 14 p2280 N85-24125

Jet pump-drive system for heat removal
[NASA-CASE-NPO-16494-1-CU]
18 p3099 N85-29182

Modeling and experiments on tritium permeation in fusion reactor blankets
[DE85-008439] 18 p3183 N85-29741

Coolant mixing in LMFBR rod bundles and outlet plenum mixing transients
[DE85-010336] 19 p3268 N85-30258

Resolution of thermal striping issue downstream of a horizontal pipe elbow in stratified pipe flow
[DE85-006195] 21 p3586 N85-32292

Drying of pulverized material with heated condensible vapor
[DE85-011656] 22 p3783 N85-33438

Reaction of uranium and the fluorocarbon FC-75
[DE85-012322] 22 p3843 N85-33862

Computer code calculations of the TMI-2 accident: Initial and boundary conditions
[DE85-012613] 24 p4140 N85-35066

COOLERS

Modeling of a second-generation solar-driven Rankine air conditioner
[DE84-015132] 01 p0036 N85-10223

COOLING

NT ABSORPTION COOLING
NT AIR COOLING
NT CRYOGENIC COOLING
NT EVAPORATIVE COOLING
NT FILM COOLING
NT GAS COOLING
NT LIQUID COOLING
NT MAGNETIC COOLING
NT QUENCHING (COOLING)
NT RADIANT COOLING
NT SOLAR COOLING
NT SPACE COOLING (BUILDINGS)
NT SUPERCOOLING
NT SURFACE COOLING
NT SWEAT COOLING

The effect of channel convergence on heat transfer in a passage with short pin fins
[NASA-TM-83801] 01 p0046 N85-10303

Investigation of crisis phenomena in thermosyphons with internal heat-dissipation
[BLL-M-35765-(5828.4)] 02 p0197 N85-11313

Producing semiconductor materials by superfast cooling of melt 03 p0354 N85-12274

Heat transfer and pressure drop in blade cooling channels with turbulence promoters
[NASA-CR-3837] 03 p0361 N85-12315

Autenite transformation in powder-compacted chromium-nickel-molybdenum steels during continuous cooling
[BLL-M-35981-(5828.4)] 05 p0615 N85-13693

Thermal characterization of photovoltaic modules in natural environments 06 p0832 N85-15298

Low temperature diffusion coefficients in the Fe-Ni and FeNiP systems: Application to meteorite cooling rates
06 p0886 N85-15928

Dynamic thermal episodes in the protosolar nebula: Development of models from observations on CAI's
06 p0887 N85-15933

The feasibility of low-G grey solidification of nodular iron in the F-104 experimental furnace package
[NASA-TM-82527] 10 p1426 N85-18996

Vibration isolated cold plate assembly
[AD-D011444] 10 p1484 N85-19368

An evaluation of liquid and two-phase cooling techniques for use in electrical machinery
[AD-A149528] 10 p1484 N85-19372

Evaluation of residual stress in laminated metallic composites 11 p1598 N85-20052

Residual stress after laser processing 11 p1600 N85-20065

Proposal for hollow cathode electron gun for electron cooling
[DE85-002721] 11 p1630 N85-20263

The Middle Atmosphere Program: Winter in Northern Europe (MAP/WINE) 11 p1655 N85-20429

Numerical model for swirl cooling in high-heat-flux particle beam targets and the design of a swirl-flow-based plasma limiter
[DE85-003824] 11 p1732 N85-20694

Improvements in glazings: SERI materials research in progress
[DE84-013049] 12 p1814 N85-21378

Heat pipe cooled probe
[NASA-CASE-LAR-12588-1] 12 p1844 N85-21568

Cooled turbine blade tip closure
[AD-D011525] 12 p1858 N85-21654

Energy losses at leading edge of turbine blade during multirow jet cooling 13 p2049 N85-22826

Pressure drop and coefficients of internal heat transfer necessary for transpiration cooling 13 p2050 N85-22831

Cooling performance improvement of a horizontal ground coupled heat pump
[DE85-002470] 13 p2093 N85-23065

Cooling of neutron stars with hyperons
[DE85-004641] 13 p2171 N85-23472

A measurement of the intensity of the cosmic background radiation at 3.9 cm 13 p2206 N85-23661

Fabrication of ceramic substrate-reinforced and free forms
[NASA-TM-86994] 14 p2247 N85-23926

Experimental study of heat transfer from shaft in cooled radial bearing of GNT-25 gas turbine 14 p2270 N85-24068

Computations for segmented radial bearings 14 p2288 N85-24180

The effects of cooling on delay-time limits in IC's 14 p2297 N85-24224

Experimental facility for studying MHD effects in liquid metal cooled blankets
[DE85-000582] 14 p2423 N85-24943

Small gas turbine combustor study: Fuel injector performance in a transpiration-cooled liner
[NASA-TM-86989] 15 p2473 N85-25264

Effectiveness of use of heat-dissipating clamps to reduce deformation during argon arc welding of thin sheets of AMg6 alloy 15 p2501 N85-25427

Sweden develops new rapid solidification process 15 p2531 N85-25610

Numerical simulation of boundary layer excitation by surface heating/cooling
[NASA-CR-172575] 15 p2554 N85-25756

Experimental and theoretical studies of laser cooling and emittance control of neutral beams
[AD-A149215] 15 p2562 N85-25804

Development of high strength ship hull steel for high heat input welding --- controlled rolling and accelerated cooling 15 p2565 N85-25827

Mechanism of formation of low temperatures in nighttime Venusian thermosphere 16 p2723 N85-26807

The use of heat pumps in district heat supply
[BLL-OA-TRANS-2728-(6196.3)] 16 p2781 N85-27163

Multi-phase crystallization of ferrous alloys
[BLL-BISI-TRANS-22441-(9022.06)] 17 p2925 N85-28037

Production and compaction of amorphous metal powders
[BLL-BISI-TRANS-22387-(9022.06)] 17 p2929 N85-28080

Performance analysis of radiation cooled dc transmission lines for high power space systems
[NASA-TM-87040] 17 p2951 N85-28222

Effects of the corona wind on the cooling of a horizontal cylinder
[AD-A153101] 17 p2954 N85-28241

Opacity control technique for jet engine test cells
[AD-D011668] 19 p3220 N85-29968

Heat injury: Prevention is the key
[AD-A153734] 19 p3328 N85-30622

Experiments with stored heavy ions
[DE85-009976] 19 p3356 N85-30802

Molten salt cooling/17Li-83Pb breeding blanket concept
[DE85-010522] 19 p3363 N85-30854

Design of aggressive superconducting TFCX magnet systems
[DE85-010003] 19 p3376 N85-30943

The nature of the anomalies on the polytherms of the properties of molten metallic alloys
[BLL-M-36265-(5828.4)] 20 p3430 N85-31277

Design principles for nickel-hydrogen cells and batteries
[NASA-TM-87037] 20 p3483 N85-31646

Design of a helium-cooled molten salt fusion breeder
[DE85-010474] 20 p3528 N85-31943

Temperature field around a spherical, cylindrical, and needle-shaped crystal, growing in a pre-cooled melt
[NASA-TM-77889] 20 p3537 N85-32011

Observations of the use of the setapoint detector
[AD-A154533] 21 p3571 N85-32208

Design and lubrication of high-speed rolling-element bearings
[NASA-TM-87107] 23 p3938 N85-34409

Enhanced heat transfer computations for internally cooled cable superconductor
[DE85-011897] 24 p4095 N85-35383

COOLING FINS

Optimization of combined convective and film cooling of perforated baffle blades in gas turbines 14 p2270 N85-24067

Welding of steel-aluminum cooling panels for the holds of refrigerator vessels 19 p3246 N85-30129

COOLING SYSTEMS

Heat rejection working group synopsis 05 p0611 N85-13906

Phosphoric and electric utility fuel cell technology development
[NASA-CR-174215] 06 p0805 N85-15124

Cooling system investigation of the 3-kW MEP models 016A, 021A, and 026A (60Hz, 400-Hz and 28-V dc) gasoline-engine-driven generator sets
[AD-A147571] 07 p0974 N85-16185

Hybrid system for producing and storing ice
[DE84-017474] 09 p1304 N85-18195

Thermal energy storage
[DE85-001492] 09 p1344 N85-18454

15KW power supply development
[DE85-001057] 11 p1629 N85-20260

Performance of the SERI parallel-passage dehumidifier
[DE85-000509] 11 p1672 N85-20536

Transmissive Dewar cooling chamber for optically pumped semiconductor ring lasers
[AD-D011550] 12 p1855 N85-21636

Latent heat storage in cooling systems
[DE85-005355] 13 p2129 N85-23248

Thermal state of cooled thin-walled nozzle blade 14 p2270 N85-24066

High thermal power density heat transfer apparatus providing electrical isolation at high temperature using heat pipes
[NASA-CASE-LEW-12950-2] 18 p3098 N85-29179

Jet pump-drive system for heat removal
[NASA-CASE-NPO-16494-1-CU] 18 p3099 N85-29182

Precision manipulator heating and cooling apparatus for use in UHV systems with sample transfer capability
[NASA-CASE-LAR-13040-1] 18 p3116 N85-29286

Spacecraft, straight-tube evaporator design
[AD-A154462] 19 p3226 N85-30003

Vortex generating flow passage design for increased film cooling effectiveness
[NASA-CASE-LEW-14039-1] 22 p3782 N85-33433

On-line temperature sensor
[DE85-011641] 22 p3787 N85-33465

Legionnaires' disease bacteria in power plant cooling systems: Phase 2
[DE85-011546] 22 p3825 N85-33695

Mathematical modeling of ultimate heat sink cooling ponds
[TI85-009747] 23 p3932 N85-34369

A two-phase flow and heat transfer model for zero gravity
[AD-A156097] 24 p4094 N85-35377

Transient three-phase three-component systems. Part 1: Formulation of the system of differential equations
[DE85-013267] 24 p4095 N85-35384

COOPERATION

The effects of controversy and concurrence seeking on effective decision making
[AD-A153370] 17 p3002 N85-28555

COORDINATE SYSTEMS

U COORDINATES

COORDINATE TRANSFORMATIONS

Automatic camera tracking for remote manipulators
[DE85-001897] 07 p0974 N85-16187

The Gauss-Krueger projection of the Earth ellipsoid with direct calculation of elliptic integrals through Landen transformations
[SER-C-298] 11 p1686 N85-20495

Distance-inertial guidance of launch vehicle described 12 p1820 N85-21417

Reduction of astrographic catalogues 14 p2437 N85-25033

Least squares reduction technique 14 p2437 N85-25036

Reduction of astrometric plates 14 p2437 N85-25037

Allowance for differences in ellipsoids and geodetic control coordinate systems in determining ship's position using radio navigation systems 19 p3292 N85-30413

Coordinate transformations and programming for small revolute coordinate robots
[RR-273] 20 p3519 N85-31881

Second-order Compton-Getting effect on arbitrary intensity distribution
[SH-3.1-10] 23 p4002 N85-34814

COORDINATES

NT ASTRONOMICAL COORDINATES
NT CARTESIAN COORDINATES
NT GEOCENTRIC COORDINATES
NT GEODETIC COORDINATES
NT HYPERBOLIC COORDINATES
NT LAGRANGE COORDINATES
NT SPHERICAL COORDINATES

Cognitive coordinate systems: Accounts of mental rotation and individual differences in spatial ability
[AD-A146149] 03 p0401 N85-12557

Development of a modular multicoordinate measuring system with continuous-path microprocessor control
[BMFT-FB-T-84-158] 03 p0406 N85-12608

Analysis of frequency-selective integrated circuits in system of normal coordinates 04 p0489 N85-13119

References in space and time 05 p0598 N85-13809

Use of coordinate functions to calculate deformation fields
[BLL-M-36010-(5828.4)] 07 p1028 N85-16524

Numerical generation of orthogonal and nonorthogonal coordinates in two dimensional simply and doubly connected regions
[VKI-TN-151] 08 p1216 N85-17662

Generation of 3-dimensional body fitted coordinates using hyperbolic partial differential equations
[AD-A148059] 09 p1274 N85-18006

Codes with parity conditions on subsets of coordinates 10 p1465 N85-19247

Geodetic accuracy of LANDSAT 4 Multispectral Scanner and Thematic Mapper data 12 p1873 N85-21746

Motion of symmetrical satellite with flexible viscoelastic rods about center of mass in circular orbit 13 p1979 N85-22420

Analysis of systematic errors in systems of selenodetic coordinates 13 p1982 N85-22435

Coordinate determination errors in measuring characteristics of radiation field of airborne antennas 13 p2068 N85-22919

Zero-crossings on lines of curvature
[AD-A150171] 13 p2150 N85-23345

A unified lunar control network 13 p2203 N85-23669

The control network of Mars: October 1984 13 p2203 N85-23670

The control networks of the satellites of Jupiter and Saturn 13 p2204 N85-23671

Shape of Io 13 p2204 N85-23672

An analysis of grid-based line drawing quantization methods
[AD-A151847] 15 p2522 N85-25547

Electromagnetic scattering by arbitrarily shaped reflectors: Subreflector efficiency
[AD-A149224] 15 p2541 N85-25687

Analysis of elastoplastic grids under conditions of variable loads
[REPT-16/1984] 16 p2797 N85-27242

When is a Bernstein-Bezier curve the graph of a function? 17 p3003 N85-28568

Generation of surface coordinates by elliptic partial differential equations 17 p3006 N85-28583

A survey of composite grid generation for general three-dimensional sections 17 p3006 N85-28584

A discussion of adaptive grids and their applicability in numerical hydrodynamic modeling
[AD-A151843] 17 p3017 N85-28659

Montonicity preserving bicubic interpolation, revision 1
[DE85-007976] 17 p3021 N85-28683

Derivation of model topography 18 p3141 N85-29449

Three-dimensional data display on the two-dimensional screen
[AD-A153699] 18 p3160 N85-29577

A comparison of methods of least squares adjustment of traverses
[AD-A153612] 18 p3170 N85-29645

Computer programs for smoothing and scaling airfoil coordinates
[NASA-TM-84666] 20 p3388 N85-31011

A note on a theorem of R. Duffin
[AD-A154786] 21 p3676 N85-32838

Potential coordinate estimate accuracy estimation accuracy by multiposition radar systems
22 p3763 N85-33322
Production of initial estimates of photogrammetric variables
[NPL-MOM-66] 23 p3943 N85-34434
Second-order Compton-Getting effect on arbitrary intensity distribution
[SH-3.1-10] 23 p4002 N85-34814

COORDINATION
Collection overlap and coordinated collection development 02 p0293 N85-11902
A full mission simulator study of aircrew performances: The measurement of crew coordination and decisionmaking factors and their relationships to flight task performances 05 p0710 N85-14556
Communication on the flight deck
05 p0711 N85-14557
Instrument for determining spatial coordination of hand movements 14 p2387 N85-24702
Photochemistry of coordination complexes: The phthalocyanines
[DE85-007693] 17 p2923 N85-28022
Improved coordinate measuring machine calibration and control
[DE85-012053] 21 p3590 N85-32315
United States Army welding research and development topical and coordination meeting
[AD-A155634] 24 p4099 N85-35409

COORDINATION POLYMERS
A soluble linear Schiff-base coordination polymer containing eight-coordinate zirconium(4)
[AD-A151446] 15 p2518 N85-25527

COPERNICUS SPACECRAFT
U OAO 3

COPILOTS
U AIRCRAFT PILOTS

COPLANARITY
Experiment Pamir-3. Coplanar emission of high energy gamma-quanta at interaction of hadrons with nuclei of air atoms at energies above 10 to the 7th power GeV
[HE-1.4-12] 24 p4177 N85-35899

COPOLYMERIZATION
Vinyl citrates from citric acid as new monomers
[BMFT-FB-T-83-256] 03 p0338 N85-12176
Chemical control of nadimide cure temperature and rate
[NASA-CASE-LEW-13770-2] 18 p3069 N85-28982
Transition metal catalyzed transformations of unsaturated molecules
[DE85-009531] 18 p3080 N85-29055
High performance mixed bisimide resins and composites based thereon
[NASA-CASE-ARC-11538-1-SB]
19 p3231 N85-30033

COPOLYMERS
Nuclear Magnetic Resonance of Polymeric Materials
[AD-A145078] 01 p0032 N85-10192
13C and 1H NMR (Nuclear Magnetic Resonance) studies of solid polyolefines
[AD-P003909] 01 p0032 N85-10195
Diblock copolymers of polystyrene/1,2 polybutadiene and polystyrene/polybutene-1: Molecular structure, morphology and mechanical properties
[AD-A144980] 01 p0033 N85-10201
Physical-chemical properties of articulated rodlike polymers
[AD-A145549] 02 p0186 N85-11244
Low temperature synthesis of polycaproamide copolymers grafted with polydimethylaminothylmethacrylate
06 p0761 N85-14868
Forming fluorine-containing threads from vinylidene fluoride-tetrafluoroethylene copolymer by dry method
06 p0762 N85-14873
Polymer-carbon black interaction in electrically conducting fiber-forming composites
06 p0762 N85-14875
Properties of miscible polymer blends
[AD-A147090] 07 p0931 N85-15903
Synthesis and characterization of unique liquid crystalline block copolyesters. A proposal for a polymer research center at the Atlanta University
[AD-A147280] 07 p0932 N85-15907
New synthesis of phosphazene polymers
[AD-A147567] 07 p0933 N85-15910
Phase diagram of polymer blends containing block copolymers
[AD-A147706] 08 p1132 N85-17134
Synthesis and characterization of a 1,4 Polybutadiene/Isotactic polypropylene block copolymer
[AD-A148199] 08 p1133 N85-17142
The synthesis and characterization of Poly(Oxy(2-Methyl-1,3-Phenylene) Methyl-1,3 -Phenylene) Oxyterephthaloyl)Oxy
[AD-A148269] 08 p1133 N85-17143
Poly(dimethylsiloxane)-polyurethane elastomers: Synthesis and properties of segmented copolymers and related zwitterionomers
[AD-A148571] 08 p1134 N85-17147
GC-FTIR (Fourier Transform Infrared Spectrometry) of jet fuels
[AD-A148272] 08 p1135 N85-17155
Crystallization behavior of poly(3,3-bis(Ethoxymethyl) oxeniane) and poly(3,3-bis(Azidomethyl) oxetane)
[AD-A148271] 08 p1226 N85-17720
Characterization of novel binders based on energetic thermoplastic elastomers
[AD-A148993] 10 p1451 N85-19139
Polyactic-polyglycolic acid copolymer combined with decalcified freeze-dried bone for use as a bone repair material
[AD-D011436] 10 p1451 N85-19142
Method for making heterocyclic block copolymers
[AD-D011446] 10 p1451 N85-19143
Chemical approach for controlling nadimide cure temperature and rate with maleimide
[NASA-CASE-LEW-13770-3] 12 p1809 N85-21350
Chemical approach for controlling nadimide cure temperature and rate with maleimide
[NASA-CASE-LEW-13770-4] 12 p1810 N85-21351
Effects of triazine components on physicochemical properties of polybutadiene: urethane block copolymers
13 p2014 N85-22635
Influence of hydrogen bonding in block copolymers and their blends 13 p2036 N85-22752
Exploratory development of foams from liquid crystal polymers
[NASA-CR-172510] 13 p2036 N85-22754
Chiral polymers
[AD-A150366] 13 p2037 N85-22760
An investigation of molecular structure of copolymers using positron annihilation spectroscopy
[NASA-TM-86431] 17 p2916 N85-27977
Thermally stable elastomers: Review of silarylene-siloxane polymers and polysilmethylenes
[AD-A152323] 17 p2934 N85-28111
Alkaline battery containing a seperator of a cross-linked copolymer of vinyl alcohol and unsaturated carboxylic acid
[NASA-CASE-LEW-13102-1] 18 p3093 N85-29144
High performance mixed bisimide resins and composites based thereon
[NASA-CASE-ARC-11538-1-SB]
19 p3231 N85-30033
Self-developing polysilane deep-UV resists: Photochemistry, photophysics and submicron lithography
[DE85-007608] 19 p3237 N85-30067
STPI/LARC: A 200 deg C polyimide adhesive
[NASA-TM-86447] 20 p3433 N85-31297
Structure-property relationships in thermoplastic elastomers. Part 3: Segmented polyacetal-polyurethanes
[AD-A154897] 21 p3569 N85-32200
Electrically conductive doped block copolymer of polyacetylene and polyisoprene
[DE85-006500] 24 p4082 N85-35301

COPPER
Numerical analysis of parameters of self-heating copper vapor lasers 02 p0260 N85-11704
Polycyclic aromatic hydrocarbons on the inner surfaces of copper tubing
[AD-A145979] 03 p0337 N85-12169
Fast and precise processing of material by means of an intensive electron beam
[BMFT-FB-T-84-123] 03 p0342 N85-12201
The metallurgical processes during the soft soldering of copper and copper alloys and the strength characteristics of soldered joints
[BLL-T6388/BG/WH603/84] 06 p0767 N85-14908
Thermal conductivity of aluminum, copper, iron and tungsten for temperature from 1 K to the melting point
[PB84-235878] 06 p0770 N85-14924
The adsorption of CO and oxygen on Cu layers on a W(110) surface
[AD-A147345] 07 p0923 N85-15847
Investigation of electric and wear phenomena of liquid metal wetted copper fiber brushes under conditions of high slip ring eccentricity
[AD-A147634] 08 p1156 N85-17295
Antifriction properties of gas thermal coatings of clad carbine powders 10 p1447 N85-19115
Behavior and specifics of fracture of porous fiber materials in extension 10 p1447 N85-19118
Magnetization of very thin Ni films in epitaxial metal film sandwiches of Cu
[DE85-001840] 10 p1563 N85-19860
Structure and properties of copper-titanium-aluminum composites obtained by thermoreactive sintering
11 p1600 N85-20061
Effect of temperature and deformation rate on hardness of copper 11 p1605 N85-20090
Effect of rhodamine-B on the electrodeposition of lead on copper, revision
[DE85-000674] 11 p1606 N85-20101
Effect of interfacial characteristics of metal clad polymeric substrates on electrical high frequency interconnection performance
[NASA-TM-86948] 11 p1624 N85-20223
Mechanical properties of electrodeposited nickel and copper
[DE85-005321] 13 p2023 N85-22677
Effects of neutron irradiation at 450(0)C and 16 dpa on the properties of various commercial copper alloys
[DE85-005716] 13 p2024 N85-22684
Structural strenght of strip D16T aluminum alloy with low copper and magnesium content
13 p2025 N85-22691
New deformable secondary aluminum alloys
13 p2026 N85-22694
Possibility of producing monolithic composite materials based on niobium carbide 13 p2028 N85-22707
Observation of surface vibrational resonances on (110) surfaces of FCC metals
[AD-A150469] 13 p2163 N85-23419
Nd-isotopic evidence for the origin of the Sudbury complex by meteoritic impact 15 p2680 N85-26554
Measurement of elements in the stratosphere
[NASA-CR-175891] 16 p2823 N85-27414
The production of copper phthalocyanine and/or its derivatives
[NASA-TM-77629] 17 p2917 N85-27983
The loss of material from the cathode of metal arcs
[NASA-TM-77845] 17 p2918 N85-27985
Improving the properties of copper and copper alloys through heat treatment and alloying
[BLL-BISI-TRANS-21939-(9022.06)]
17 p2926 N85-28047
Localized ionic currents from a corroding iron-copper galvanic couple
[AD-A153627] 18 p3074 N85-29011
Establishment of a methodology for predicting lifetimes in active solar systems
[DE85-008629] 18 p3130 N85-29383
Preliminary results on open accelerating structures
[DE85-010231] 18 p3191 N85-29793
Effect of confinement on failure in 95 TATB/5 KEL-F
[DE85-010790] 19 p3251 N85-30158
Investigation for low-cost permanent magnets
[AD-A154387] 19 p3260 N85-30212
Sources of copper air emissions
[PB85-191138] 19 p3310 N85-30623
Defect production and recovery in FCC metals irradiated at 4.2 K
[DE85-010477] 20 p3538 N85-32014
Electrodeposition of chromium and copper in magnetic fields
[AD-A154648] 21 p3566 N85-32180
The effect of abrasive blasting on the fatigue and corrosion of an aluminium-copper alloy
[AD-A154954] 21 p3566 N85-32182
Modification of the grain size of sputtered copper with additions of oxygen, krypton, silver, or yttrium
[DE85-010975] 21 p3567 N85-32189
Plasma mass and effective inductance in a small railgun
[AD-A154644] 21 p3589 N85-32304
Management of Corrosion
[AGARD-LS-141] 22 p3749 N85-33238
Corrosion management strategies for aircraft and related systems 22 p3749 N85-33239
Metal vapor lasers and their applications
[ISL-CO-218/84] 22 p3791 N85-33486
Environmental surveillance at Los Alamos during 1984
[DE85-011886] 22 p3811 N85-33605
Calculated neutron-induced cross sections for /sup 63,65/Cu/sup 58,60/Ni and (52) Cr from 1 to 20 MeV and comparisons with experiments
[DE85-011928] 22 p3844 N85-33806
X-ray residual stress analysis on the coarse grain of copper and its application to the brazed copper
23 p3907 N85-34202
Metal (2) 4,4',4',4'' phthalocyanine tetraamines as curing agents for epoxy resins
[NASA-CASE-ARC-11424-1] 23 p3919 N85-34281
Some recent deposit modeling efforts
24 p4106 N85-35453
The Conterminous United States Mineral Assessment Program 24 p4106 N85-35458
The Alaska Mineral Resources Assessment Program
24 p4107 N85-35480
Ore genesis at the Monterrosas deposit in the Coastal Batholith, Ica, Peru 24 p4115 N85-35510
Few-particles generation channels in inelastic hadron-nuclear interactions at energy approximately equals 400 GeV
[HE-3.2-9] 24 p4179 N85-35917

COPPER ALLOYS
NT BRASSES
NT BRONZES
Copper-boron low alloy high strength steels
02 p0176 N85-11183
Calculation of critical temperature for Nb-Cu multilayer film superconductor
[AD-A144321] 02 p0274 N85-11786
The metallurgical processes during the soft soldering of copper and copper alloys and the strength characteristics of soldered joints
[BLL-T6388/BG/WH803/84] 06 p0767 N85-14908
Application of solidification theory to rapid solidification processing
[AD-A148619] 06 p0769 N85-14917
Studies on copper alloys containing chromium on the copper side phase diagram
[NASA-TM-77752] 07 p0927 N85-15876
On heat-treatable copper-chromium alloy, 1
[NASA-TM-77753] 07 p0927 N85-15879
On reversion phenomena in Cu-Zr-Cr alloys
[NASA-TM-77791] 08 p1125 N85-17092
Reversion phenomena of Cu-Cr alloys
[NASA-TM-77780] 08 p1125 N85-17094
Synergistic sputtering properties of binary alloys
[DE84-017493] 09 p1297 N85-18148
Initial aging phenomena in copper-chromium alloys
[NASA-TM-77790] 10 p1439 N85-19070
Magnetic excitation in CuMn spin glass alloy
[DE85-002584] 10 p1453 N85-19159
Study of microstructure of aluminum and copper alloys after processing with continuous CO2 laser beam
11 p1601 N85-20066
Conductivity changes in neutron-irradiated commercial copper alloys at approximately 450(O)C
[DE85-003007] 11 p1606 N85-20100
Surface physics and crystallography
[DE85-003128] 11 p1735 N85-20910
Chemisorption theory: Adsorption on copper-nickel alloys and titanium surface embrittlement
[DE85-001815] 12 p1807 N85-21334
Partial replacement of chromium in austenitic stainless steels by molybdenum, copper, and vanadium, report of investigations 1984
[PB85-116508] 12 p1809 N85-21346
Structures of ordered linear dislocation multipoles in Cu-Al alloys
[ISSN-0379-6906] 13 p2021 N85-22664
Thermodynamics of copper-nickel alloys containing aluminum, silicon, titanium, and chromium relative to their use in ceramic brazing
[DE85-004787] 13 p2023 N85-22674
First principles theory of Fermi-surface driven concentration waves in Cu/sub c/Pd/sub 1-c/ alloys
[DE85-005367] 13 p2024 N85-22681
Effects of neutron irradiation at 450(0)C and 16 dpa on the properties of various commercial copper alloys
[DE85-005716] 13 p2024 N85-22684
Application of solidification theory to rapid solidification processing
[AD-A151251] 15 p2509 N85-25480
Performance of a copper-lithium alloy as an impurity control system surface material for a fusion reactor
[DE85-006494] 15 p2657 N85-26398
Self-sustaining low-Z coatings for fusion applications 2 - copper-lithium
[DE85-002553] 15 p2658 N85-26403
Improving the properties of copper and copper alloys through heat treatment and alloying
[BLL-BISI-TRANS-21939-(9022.06)]
17 p2926 N85-28047
Aging study of copper alloy 172
[DE85-009848] 18 p3075 N85-29023
The precipitation mechanism in a metallic solid solution crystal: Case of the aluminum-copper and aluminum-silver systems
[DE85-009981] 18 p3077 N85-29032
Self-sustaining coatings for fusion applications: Copper lithium alloys
[DE85-009740] 18 p3190 N85-29783
Current state of development and expected performance of copper-lithium alloys as an impurity control system in fusion applications
[DE85-009673] 19 p3372 N85-30917
Critical current density and microstructural state of an internal tin multifilamentary superconducting wire
[DE85-009966] 22 p3761 N85-33306

COPPER CHLORIDES
Environmental stability of intercalated graphite fibers
[NASA-TM-87025] 16 p2753 N85-26992
Stationary properties and switching characteristics of dispersive optical bistability in CuCl
18 p3186 N85-29763

COPPER COMPOUNDS
NT COPPER CHLORIDES
NT COPPER OXIDES
NT COPPER SELENIDES
NT COPPER SULFIDES
The X-ray Absorption Coefficient Fine Structure (EXAFS) study on precipitates in AlCu
[DESY-SR-84-15] 01 p0025 N85-10153
Electrochemical features of the ferric sulfate leaching of CuFeS2/C aggregates
[AD-A148661] 08 p1123 N85-17061
Sources of copper air emissions
[PB85-191136] 19 p3310 N85-30523

COPPER OXIDES
Textured carbon surfaces on copper
[NASA-CASE-LEW-14130-1] 11 p1615 N85-20156
Time-resolved and infrared spectroscopy of excitons
[DE85-011879] 23 p3912 N85-34235

COPPER SELENIDES
CuInSe2-based photoelectrochemical cells: Their use in characterization of thin CuInSe2 films, and as photovoltaic cells per se
[DE84-004514] 04 p0529 N85-13379
Preliminary studies on the low-cost preparation of chalcogenide semiconductors from solution depositions
[DE85-000538] 11 p1736 N85-20918
Low cost, sprayed CuInSe2 solar cell research
[DE85-003467] 12 p1881 N85-21799
A study of the stability of cadmium sulfide/copper sulfide and cadmium sulfide copper-indium-diselenide solar cells
[DE85-002902] 15 p2587 N85-25947
Post-deposition heat treatments of CdS/CuInSe2 solar cells
[DE85-002943] 18 p3128 N85-29373
Cadmium sulfide/copper ternary heterojunction cell research
[DE85-008778] 19 p3305 N85-30486
Stable n-CuInSe/sub 2/iodide-iodine photoelectrochemical cell
[DE85-011597] 22 p3806 N85-33576

COPPER SULFIDES
Development of copper sulfide/cadmium sulfide thin-film solar cells
[DE84-004513] 01 p0044 N85-10287
Development of the production technology of Cu2S/CdS solar generators
[BMFT-FB-T-84-137] 03 p0386 N85-12469
Development and utilization of CdS/Cu2S
05 p0662 N85-14256
Testing and optimization of the production technology of large-surface Cu2S/CdS solar generators
12 p1880 N85-21793
Physical-chemical investigations of copper sulfides for use in CdS/Cu2S solar cells 12 p1880 N85-21794
A study of the stability of cadmium sulfide/copper sulfide and cadmium sulfide copper-indium-diselenide solar cells
[DE85-002902] 15 p2587 N85-25947

COPYRIGHTS
Copyright law, computer software, and government acquisition
[AD-A150347] 13 p2168 N85-23453

CORAL HEADS
U CORAL REEFS

CORAL REEFS
The Midway Atoll coral cap: Meteoric diagenesis, amplitude of sea-level fluctuation and dolomitization
09 p1351 N85-18499

CORDITE
U DOUBLE BASE PROPELLANTS

CORE FLOW
Transports studies of ECH and ICRH-heated bumpy torus plasma in NBT-1M 23 p3978 N85-34662
Simulation studies on stability of hot electron plasma
23 p3978 N85-34664

CORE SAMPLING
Cosmogenic Na-22 and Al-26 in Luna-24 lunar drill core soil samples 13 p1981 N85-22427
Characteristics of fast sea ice collected near Barrow, Alaska 15 p2582 N85-25925
Deep-burial diagenesis in carbonates
[DE85-011224] 22 p3802 N85-33554
Uranium, thorium isotopic analyses and uranium-series ages of calcite and opal and stable isotopic compositions of calcite from drill cores UE25a no. 1, USR G-2 and USW G-3/GU-3, Yucca Mountain, Nevada
[DE85-013039] 23 p3948 N85-34471

CORES
NT EARTH CORE
NT HONEYCOMB CORES
NT LUNAR CORE
NT PLANETARY CORES
NT REACTOR CORES
NT STELLAR CORES
Iron core collapse models of Type 2 supernovae
[DE84-013909] 05 p0743 N85-14775
Induction motors with minimum waste of magnetic iron
22 p3772 N85-33377
Monte Carlo simulations of electron lateral distributions in the core region of 10(13) - 10(16) eV air showers
24 p4190 N85-35992
A new study of shower age distribution in near vertical showers by EAS air shower array
24 p4190 N85-35996
Lateral distribution of electrons of air showers
24 p4191 N85-35998
Properties of 10 (18)-10 (19)eV EAS at far core distance
[HE-4.7-3] 24 p4198 N85-36054
Longitudinal development of muons in large air showers studies from the arrival time distributions measured at 900m above sea level
[HE-4.7-4] 24 p4199 N85-36055
Arrival time distributions of electrons in air showers with primary energies above 10 (18)eV observed at 900m above sea level
[HE-4.7-5] 24 p4199 N85-36056
The thickness of the shower disc as observed in showers produced by primaries above 10 (19)eV
[HE-4.7-6] 24 p4199 N85-36057
Sub-luminal pulses from cosmic ray air showers
[HE-4.7-13] 24 p4200 N85-36063
Progress report on a new search for free e/3 quarks in the cores of 10(15) - 10(16) eV air showers
[HE-6.2-15] 24 p4212 N85-36151
Acoustic detection of air shower cores
[HE-7.1-4] 24 p4213 N85-36158

CORIOLIS EFFECT
Effects of the oceans on polar motion: Continued investigations
[E85-10037] 03 p0379 N85-12416
Hydraulic forces on a centrifugal impeller undergoing synchronous whirl 05 p0643 N85-14124
Coriolis effects on the vibrations of rotating beams, plates and shells 09 p1331 N85-18366
Influence of gravitoinertial force level on apparent magnitude of coriolis cross-coupled angular accelerations and motion sickness 11 p1693 N85-20644
Susceptability to kinetoses and the amplitude perceived from sensory illusions 11 p1694 N85-20651
Space adaptation syndrome: Incidence and operational implications for the space transportation system program
11 p1695 N85-20655
Biofeedback treatment of airsickness: A review
11 p1696 N85-20660
Vibration and buckling of rotating, pretwisted, preconed beams including Cooriolis effects
[NASA-TM-87004] 15 p2577 N85-25893
What is being done to control motion sickness?
15 p2687 N85-26599
Elastic wave gyrometer
[REPT-26/4924/HF] 20 p3459 N85-31484
Nonlinear flap-lag-extensional vibrations of rotating, pretwisted, preconed beams including Coriolis effects
[NASA-TM-87102] 23 p3941 N85-34427
Applications of the Galerkin formalism in the coupling of the earth's free oscillations 24 p4116 N85-35514

CORK (MATERIALS)
Verification of the SRB motor case pin retainer band tips
[NASA-CR-170882] 24 p4070 N85-35220
SRB TPS closeout materials characterization
[NASA-CR-170885] 24 p4070 N85-35222

CORN
Multi crop area estimation in Idaho using EDITOR
[E85-10054] 06 p0827 N85-15251
Spectral estimators of absorbed photosynthetically active radiation in corn canopies
[E85-10041] 07 p0983 N85-16242
Shortwave infrared detection of vegetation
[E85-10064] 08 p1174 N85-17402
Comparative effects of auxin and abscisic acid on growth, hydrogen ion efflux and gravitropism in primary roots of maize
[NASA-CR-174355] 09 p1342 N85-18444
Techniques for measuring intercepted and absorbed PAR in corn canopies
[E85-10081] 10 p1505 N85-19495
NOAA-AISC user's guide for implementing CERES maize model for large area yield estimation
[E85-10083] 12 p1873 N85-21748
Amyloplast sedimentation kinetics in corn roots
15 p2606 N85-26059
Calcium and calmodulin localization in gravitropically-responding plant organs
15 p2606 N85-26061
Gravistimulus production in roots of corn
15 p2607 N85-26066
Differential wall growth in gravistimulated corn roots: Its timing and regulation 15 p2614 N85-26105

Modeling the backscattering and transmission properties of vegetation canopies
[E85-10099] 16 p2809 N85-27320
Organization of the R region in maize
[DE85-011273] 20 p3504 N85-31780

CORNER FLOW
First derivatives of flow quantities behind two-dimensional, nonuniform supersonic flow over a convex corner
[NASA-TM-86272] 08 p1077 N85-16628
Three-dimensional boundary layers and shear flows activities at ONERA/CERT 15 p2558 N85-25785
Conical stagnation points in the flow around an external corner — delta wings
[VTH-LR-396] 16 p2701 N85-26680

CORNERS
Stress intensity factors for corner cracks at holes located near an edge
[FFA-TN-1984-20] 04 p0514 N85-13279
A similarity analysis of phase change heat conduction in corners 05 p0634 N85-14069
On the corner singularity of a 3-D Griffith crack
[AD-A150989] 14 p2321 N85-24342
Transition region for corner cracks at holes
[AD-A151835] 15 p2579 N85-25908
Free-surface phenomena under low- and zero-gravity conditions
[NASA-CR-175835] 16 p2782 N85-27168

CORONA BOREALIS CONSTELLATION
The fading of R coronae borealis
11 p1753 N85-21029

CORONA DISCHARGES
U ELECTRIC CORONA

CORONAGRAPHS
Lyman alpha coronagraph research sounding rocket program
[NASA-CR-174376] 09 p1354 N85-18517
User's guide for the Mk-3 D-coronameter data system
[PB85-181204] 19 p3385 N85-31002

CORONAL HOLES
A leaky waveguide model for MHD wave driven winds from coronal holes 08 p1235 N85-17781
Correlation of interplanetary medium parameters in transition region of high-velocity solar wind streams
13 p1978 N85-22412
Solar cycle variation of ephemeral regions
[AD-A154967] 21 p3723 N85-33097
A study of the cyclical variations of coronal holes and their relation to open magnetic fields
[AD-A155251] 21 p3723 N85-33099
White Light Coronograph (WLC) and Ultra-Violet Coronal Spectrometer (UVCS) 23 p3901 N85-34161
The expected cosmic ray density and stream distributions at the heliolatitudinal asymmetry of solar wind
[SH-4.2-14] 23 p4008 N85-34852
Study of dominating parameters of high speed solar plasma streams in relation to cosmic ray and geomagnetic storms
[SH-5.1-11] 23 p4042 N85-35064

CORONAL LOOPS
Studies of solar flares and coronal loops
[AD-A145009] 01 p0130 N85-10896
Active late-type stars and the applicability of coronal loop models 11 p1758 N85-21059
Thermal stability of static coronal loops: Part 1: Effects of boundary conditions
[NASA-CR-175495] 12 p1961 N85-22330
Heating of coronal loops by tearing turbulence
14 p2448 N85-25114
Axisymmetric magnetofluidistatic (MFS) equilibria of solar coronal loops: An integral equation approach
14 p2449 N85-25116
Prominences, two-ribbon flares and coronal transients
14 p2454 N85-25158
Very large array observations of coronal loops and related observations of solar type stars
[AD-A152027] 16 p2688 N85-27817
Simultaneous Solar Maximum Mission and Very Large Array (VLA) observations of solar active regions
[NASA-CR-176090] 22 p3859 N85-33697
The propagation of solar flare particles in a turbulent coronal loop
[SH-1.1-3] 23 p3989 N85-34730
Ion energy storage for post-flare loops
[SH-1.2-10] 23 p3992 N85-34745
Helios 1 energetic particle observations of the solar gamma ray flare events of 7, 21 June 1980 and 3 June 1982
[SH-1.3-8] 23 p3993 N85-34755

CORONARY ARTERY DISEASE
The effect of propranolol on the training response to endurance exercise in normal human adults
05 p0696 N85-14479

CORONARY CIRCULATION
Natural electrical activity of human sympathetic nerve fibers, recorded from body surface
07 p1013 N85-16433
Effect of acute hypoxia on coronary and systemic hemodynamics 23 p3953 N85-34503

CORONAS
NT CORONAL HOLES
NT CORONAL LOOPS
NT ELECTRIC CORONA
NT SOLAR CORONA
NT STELLAR CORONAS
Coronal spectroscopy in laser plasmas
[DE85-002617] 11 p1730 N85-20880
Images of the Earth's aurora and geocorona from the Dynamics Explorer Mission
[NASA-CR-175983] 18 p3136 N85-29423
Magnetic probing of the solar interior
[NASA-CR-176025] 19 p3385 N85-30998
Helios 1 energetic particle observations of the solar gamma ray flare events of 7, 21 June 1980 and 3 June 1982
[SH-1.3-8] 23 p3993 N85-34755
Source energy spectra from demodulation of solar particle data by interplanetary and coronal transport
[SH-1.3-13] 23 p3994 N85-34758
Far-infrared observations of young clusters embeddad in the R Coronae Austrinae and RHO Ophiuchi dark clouds
[NASA-TM-86881] 24 p4167 N85-35834

CORPUSCULAR RADIATION
NT BETA PARTICLES
NT CYCLOTRON RADIATION
NT ELECTRON BEAMS
NT ELECTRON PRECIPITATION
NT ELECTRON RADIATION
NT ENERGETIC PARTICLES
NT ION CYCLOTRON RADIATION
NT PRIMARY COSMIC RAYS
NT RADIATION BELTS
NT RELATIVISTIC ELECTRON BEAMS
NT SOLAR CORPUSCULAR RADIATION
NT SOLAR COSMIC RAYS
NT SOLAR ELECTRONS
NT SOLAR PROTONS
Search for neutral, penetrating, metastable particles produced in the SLAC beam dump
[DE84-012468] 04 p0560 N85-13569
Standing of industrial radiography in South Africa
14 p2316 N85-24311
Limits on deeply penetrating particles in the 10(17) eV cosmic ray flux
[HE-5.3-1] 24 p4205 N85-36096

CORRECTION
NT ATMOSPHERIC CORRECTION
NT OPTICAL CORRECTION PROCEDURE
Wall influence corrections in wind tunnels: Blockage correction according to the wall pressure signature method
[FW-FO-1613] 04 p0453 N85-12875
Automatic correction of static characteristics of measurement channel of digital oscillograph
06 p0795 N85-15083
Wind sheltering correction — anemometry
[KNMI-TR-52] 07 p1009 N85-16406
Determination of corrections to flow direction measurements obtained with a wing-tip mounted sensor
[NASA-CR-174412] 10 p1421 N85-18962
Dynamics of adaptive signal corrector
13 p2071 N85-22940
Design of single-wheel gyrocompass with correction
14 p2272 N85-24079
Selection of optimum corrections torque for vertical gyro according to special-purpose program
14 p2273 N85-24082
A digital contour-corrector for a high-definition TV camera
[NHK-LABS-NOTE-311] 19 p3254 N85-30179
Computation of three-dimensional, inviscid, rotational flows 21 p3587 N85-32296
Microcomputer controlled image processor
[AD-D011734] 22 p3833 N85-33735

CORRELATION
NT ANGULAR CORRELATION
NT AUTOCORRELATION
NT CORRELATION COEFFICIENTS
NT CORRELATION DETECTION
NT CROSS CORRELATION
NT DATA CORRELATION
NT SIGNAL ANALYSIS
NT STATISTICAL CORRELATION
An investigation of the effect of correlated abilities on observed test characteristics
[AD-A144869] 01 p0113 N85-10765
Limit theory for the sample covariance and correlation functions of moving averages
[AD-A145488] 02 p0251 N85-11842
Many-body correlations in strongly-coupled plasmas
02 p0264 N85-11850
Study of the velocity-acoustic pressure correlation in a cold jet, centered on the sign and the amplitude of the velocity fluctuations
[ISL-R-124/83] 04 p0501 N85-13130
Correlation and reassessment of the OTEC plant power cycle
[DE84-015467] 04 p0529 N85-13382
Variability of short-term eddy-correlation estimates of mass exchange
[DE84-007271] 05 p0677 N85-14349
Advanced cube processor
[AD-D011262] 05 p0729 N85-14883
Energy correlation between natural extra-low-frequency noises at various frequencies 06 p0784 N85-15010
Correlation radius of gravitational and magnetic anomalies and methods of its determination
06 p0821 N85-15213
Correlations of solar irradiance and daylight illuminance for building energy analysis
[DE85-001736] 06 p0839 N85-15328
Non-local origin of a substantial portion of the soft X-ray background 06 p0877 N85-15587
Analysis of subpixel registration
07 p0986 N85-16267
Built-in test and self repair mechanisms in a digital correlator integrated circuit 08 p1064 N85-16741
Analysis of pressure gradient-velocity correlation in turbulent, premixed flames 09 p1272 N85-17984
Inviscid analysis of unsteady blade tip flow correlation studies
[NASA-CR-172506] 10 p1420 N85-18958
Internal forced convection to low Prandtl number gas mixtures
[AD-A148932] 10 p1464 N85-19386
Estimating deformability upon pressing of aluminum alloys based on results of mechanical testing
11 p1598 N85-20049
Double pinhole spatial phase correlator apparatus
[AD-D011495] 11 p1729 N85-20872
Response time correlations for platinum resistance thermometers in flowing fluids
[NASA-CR-172523] 12 p1850 N85-21808
Method for determining the number of correlative measurements required to validate the SBUV/2 ozone retrievals 13 p2105 N85-23114
Calculations of microwave brightness temperature of rough soil surfaces: Bare field
[NASA-TM-86200] 13 p2123 N85-23221
Surface units on Venus derived from Pioneer-Venus altimetry, roughness, and reflectivity measurements
13 p2177 N85-23510
Venus gravity: Global field results
13 p2177 N85-23512
Localization of sources of equivalent noise in fast cold jets, excited and nonexcited
[ISL-CO-201/83] 14 p2416 N85-24810
The Feinheit method: A phase-independent formulation of the period-luminosity relation for Cephids
[NASA-CR-175706] 14 p2440 N85-25058
An amplitude correlation and differencing method for the monitoring of flaws in repeat ultrasonic inspections
[AERE-R-11416] 15 p2571 N85-25854
Analysis of motions of Jupiter's great red spot and white ovals 15 p2670 N85-26472
Elevated temperature biaxial fatigue
[NASA-CR-175795] 16 p2800 N85-27283
Correlation of zeolite ZSM-5 acid strength with catalytic activity and selectivity
[DE85-005415] 17 p2922 N85-28013
A bilaterally deterministic rho-mixing stationary random sequence
[AD-A152856] 17 p3019 N85-28086
Study of the equilibrium vacancy ensemble in aluminum using 1D- and 2D-angular correlation of annihilation radiation
[DE85-006967] 18 p3194 N85-29813
Thermophysical properties correlations and pseudocomponent characterization parameter estimation for fossil fluids
[DE85-009297] 19 p3230 N85-30024
Orthogonalizer for inphase and quadrature digital data
[AD-D011679] 19 p3254 N85-30174
A comparison of four Monte Carlo methods for estimating the probability OF S=T connectedness
[AD-A154264] 19 p3348 N85-30749
Development of improved capabilities for computation of gas supercompressibility factors and other properties
[PB85-188316] 20 p3436 N85-31315
Bivariate Rayleigh distribution: Formulas and curves for correlation computing using the distribution function
[FOA-C-30380-E2] 20 p3521 N85-31901

Correlation analysis of 1 to 30 MeV celestial gamma rays 20 p3549 N85-32083
Effect of ions on cloud formation and its role in solar terrestrial relationship 21 p3653 N85-32697
Digital matched filter 22 p3765 N85-33339
Comparison of experimental data on detonation velocity and Chapman-Jouget pressure vs initial HE density with predictions from Ree's model equation of state
[DE85-007266] 23 p3922 N85-34304
An update on the correlation between the cosmic radiation intensity and the geomagnetic AA index
[SH-4.2-24] 23 p4009 N85-34861
Implications of source abundances of ultraheavy cosmic rays
[OG-7.1-4] 23 p4013 N85-34886
On the solar cycle variation in the barometer coefficients of high latitude neutron monitors
[SH-6.1-2] 23 p4044 N85-35077
Correlation between solar neutrino flux and other solar phenomena 23 p4049 N85-35109
A search for mini-clusters in Japan-USSR Joint Experiment at Pamir
[HE-3.5-2] 24 p4183 N85-35941
Tskhra-Tskaro complex intended for the investigations of EAS spatial characteristics near axis
24 p4190 N85-35995
Correlation of high energy muons with primary composition in extensive air shower
[HE-4.3-7] 24 p4191 N85-36001

CORRELATION COEFFICIENTS
Flame propagation and stabilization studies using Rayleigh scattering and laser Doppler velocimetry
[AD-A148602] 09 p1290 N85-18102
An HF communications frequency-management procedure for forecasting the frequency of optimum transmission
[AD-A149191] 10 p1467 N85-19254
Formation of galaxies
[DE85-009537] 18 p3202 N85-29863
The corotating variation of the north-south anisotropy of cosmic rays
[SH-4.3-15] 23 p4033 N85-34999

CORRELATION DETECTION
The ambiguity function of random binary-phase-coded waveforms
[AD-A148906] 10 p1466 N85-19249
Theory of optimum M-filtration of signals against background of correlated interference
13 p2069 N85-22927
On the 1983 drought in northeast Brazil
[INPE-3412-PRE/676] 16 p2834 N85-27476
On the probability density of signal-to-noise ratio in an improved detector
[AD-A152529] 17 p2952 N85-28232

CORRELATION FUNCTIONS
U CORRELATION

CORRELATORS
NT IMAGE CORRELATORS
Digital correlator speed improvement by multiplexing
[AD-A145207] 01 p0100 N85-10662
An automatic pattern recognition apparatus
[AD-D011319] 07 p1043 N85-16628
Correlator and data processing requirements for QUASAT 07 p1057 N85-16709
Processing system for space VLBI
07 p1057 N85-16711
Built-in test and self repair mechanisms in a digital correlator integrated circuit 08 p1064 N85-16741
Double pinhole spatial phase correlator apparatus
[AD-D011495] 11 p1729 N85-20872
Study of phase radiogeodetic systems with phase-locked loops 13 p2115 N85-23172
Fatigue damage detection in steels by optical correlation
[AD-A155830] 24 p4079 N85-35277

CORRIDORS
NT GREAT PLAINS CORRIDOR (NORTH AMERICA)

CORROSION
NT CAVITATION CORROSION
NT ELECTROCHEMICAL CORROSION
NT FRETTING CORROSION
NT HOT CORROSION
NT INTERGRANULAR CORROSION
NT RUSTING
NT SCALE (CORROSION)
NT STRESS CORROSION
USSR report: Materials science and metallurgy, no. 93
[JPRS-84810] 01 p0018 N85-10110
Biofouling and corrosion studies at the Seacoast Test Facility in Hawaii
[DE84-014643] 01 p0029 N85-10180
User experience of existing corrosion monitoring techniques and the development of Thin Layer Activation (TLA) for corrosion monitoring
[AERE-R-11248] 01 p0029 N85-10183
Sea water rope batteries
[AD-A144775] 01 p0042 N85-10275
The reactions of cobalt, iron and nickel in SO-2 atmospheres: Similarities and differences
[NASA-TM-86868] 02 p0181 N85-11217
Investigation of chemical durability mechanisms in fluoride glasses
[AD-A145420] 02 p0186 N85-11241
Proceedings of the Ion Implantation for Army Needs Workshop
[AD-A145474] 02 p0286 N85-11863
Expert systems: The application of new computer methods to corrosion problems
[AERE-M-3395] 03 p0334 N85-12153
Wear and corrosion of components under stress and subjected to motion
[AD-A145781] 03 p0372 N85-12372
A bibliography of publications on corrosion and oxidation from UK government laboratories at Teddington, 1924 - 1983
[NPL-DMA(A)-82] 04 p0472 N85-13004
Materials characterization using ion, electron, and photon probes
[DE84-004518] 04 p0560 N85-13568
Current and potential transients during localized corrosion of stainless steel
[DE84-014100] 05 p0618 N85-13954
High temperature corrosion of ceramics
[DE84-017084] 05 p0620 N85-13967
Titanium-potassium heat pipe corrosion studies
[DE84-015526] 05 p0637 N85-14090
Rack end valves: History and modifications
[DE84-009272] 05 p0646 N85-14145
In situ analysis of corrosive and passive surfaces by laser-excited Raman spectroscopy — lead, galvanized iron, and asbestos-cement pipes
[PB84-229756] 06 p0767 N85-14904
The effect of potential on the corrosion fatigue behavior of a precipitation hardened aluminum alloy
[AD-A146537] 06 p0768 N85-14916
Measuring the corrosion rate of reinforcing steel in concrete
[PB84-244532] 06 p0770 N85-14925
Encapsulation materials and processing
06 p0830 N85-15269
Turbine blade test cascade modifications and orations, August 1982 - April 1983
[DE84-009268] 06 p0833 N85-15303
Mechanical aspects of high temperature coatings
07 p0906 N85-15749
Corrosion study on zirconium refractory coatings. 1: Oxidation of zirconium nitride coatings by oxygen
[BLL-RISLEY-TR-5044-(9091.9F)]
07 p0925 N85-15857
Surface effects of corrosive media on hardness, friction, and wear of materials
[NASA-TM-83711] 07 p0930 N85-15896
Salt action on concrete
[AD-A147812] 07 p0933 N85-15912
Application of electrochemical engineering methods and theory to solving corrosion and adhesion problems with organic coatings
[AD-A147799] 08 p1129 N85-17115
Fluctuation phenomena studies in chemically sensitive field effect transistor. Part 1: Corrosion of aluminum
[AD-A148240] 08 p1129 N85-17118
Fluctuation phenomena studies in chemically sensitive field effect transistors. Part 2: Corrosion of silicon oxynitride
[AD-A148227] 08 p1157 N85-17302
Photoacoustic spectroscopy at electrode-solution interface
[DE85-001872] 09 p1292 N85-18111
Replaceable blade turbine and stationary specimen corrosion testing facility
[NASA-TM-86931] 09 p1294 N85-18126
Behavior of pressurized tubes of candidate alloys in a simulated low-Btu environment
[DE85-003403] 09 p1296 N85-18141
Corrosion of ceramics in heat exchanger applications
[DE84-017459] 09 p1299 N85-18161
Glass corrosion in liquid lithium
[DE85-002086] 09 p1299 N85-18162
Study of surface damage in cathode composite materials in a high flux CO2 laser 10 p1444 N85-19096
USSR report: Materials science and metallurgy
[JPRS-UMS-84-005] 11 p1597 N85-20044
Application of Raman, TEM and other ion based techniques to oxidation problems
[AERE-R-11447] 11 p1610 N85-20121
Research on heat-exchanger corrosion
[PB85-126316] 11 p1616 N85-20164
The application of expert systems to corrosion problems
[AERE-M-3445] 12 p1804 N85-21316
Electrochemical cell to measure corrosion rates in noncondensing environments
[DE85-003148] 12 p1807 N85-21336
Corrosion and coatings review of specifications and drawings of facilities for the Oman Military Construction Program at Masirah Island, Oman
[AD-A149739] 12 p1812 N85-21366
Evaluation of corrosion-erosion behavior of various ceramic materials
[AD-A149756] 12 p1812 N85-21367
Steam generator tube vibration tests
[DE85-003599] 12 p1867 N85-21712
Local electrochemistry of pitting corrosion in stainless steels
[DE85-005207] 13 p2023 N85-22673
Applications of the vibration probe to localized current measurements
[DE85-004702] 13 p2023 N85-22675
The effect of water chemistry on the rates of hydrogen generation for galvanized steel corrosion at post-loca conditions
[NUREG/CR-3361] 14 p2253 N85-23963
Studies of the initiation of pitting corrosion on stainless steels
[AERE-M-3400] 14 p2254 N85-23967
Role of passive surface films on corrosion fatigue crack initiation
[DE85-000438] 14 p2257 N85-23985
Corrosion problems in the Canadian maritime forces
[AD-A151594] 15 p2509 N85-25481
Corrosion inhibitor formulation for molybdenum, tungsten and other metals
[AD-D011593] 15 p2510 N85-25486
Computer controlled acquistion of corrosion rate data from multiple sensors
[PB85-157378] 15 p2524 N85-25559
Sodium and lithium corrosion in molybedenum heat pipes
[DE85-005561] 16 p2784 N85-27179
NBS (National Bureau of Standards) research reports
[PB85-127421] 16 p2879 N85-27764
Thermomechanical treatment aimed at the protection of type 316 stainless steel from IGC and IGSCC
[BLL-BISI-TRANS-22498-(9022.06)]
17 p2925 N85-28040
Effect of the agressive action of soil on metallic pipelines. New possibilities for the passive and active corrosion protection
[BLL-BISI-TRANS-21630-(9022.06)]
17 p2928 N85-28070
New method of calculating the economic effects of corrosion
[BLL-BISI-TRANS-22348-(9022.06)]
17 p2929 N85-28079
Metallurgical means of preventing the corrosion of metal
[BLL-BISI-TRANS-22320-(9022.06)]
17 p2929 N85-28082
Physical-chemical model for the mechanism of glass corrosion with particular consideration of simulated radioactive waste glasses
[DE85-007713] 17 p2935 N85-28121
Exhaust systems for passenger vehicles: Test procedure for resistance to internal corrosion of silencers
[BLL-BISI-TRANS-22360-(9022.06)]
17 p2973 N85-28361
Surface degradation of ductile metal in elevated temperature gas-particle streams
[DE85-008428] 18 p3074 N85-29017
Long-Term Materials Test Program
[DE85-003248] 18 p3077 N85-29034
High-temperature oxidation of alloys in mixed oxidants
[DE85-009706] 18 p3077 N85-29035
Protection products for the conductors of high voltage overhead lines
[BLL-OA-TRANS-3219-(6196.300)]
20 p3429 N85-31269
Effects of humidity cycles on the corrosion of galvanised reinforcements in carbonated and uncarbonated mortars
[BLL-CE-TRANS-8039-(9022.09)]
20 p3430 N85-31272
Corrosion in civil aircraft structures
[SNIAS-851-111-105] 20 p3432 N85-31291
Decomposition of sulfuric acid using solar thermal energy
[DE85-012288] 21 p3564 N85-32170
Understanding and laboratory prediction of the atmospheric corrosion behavior of steels and of non-ferrous metals and alloys
[AD-A154842] 21 p3586 N85-32179
The effect of abrasive blasting on the fatigue and corrosion of an aluminium-copper alloy
[AD-A154954] 21 p3586 N85-32182
Polymer-water interaction studies
21 p3609 N85-32411

Theoretical aspects of corrosion and practical implications for aircraft and related systems
22 p3749 N85-33240

Maintenance and the military environment
22 p3750 N85-33243

Current requirements for the design and maintenance against corrosion of UK military aircraft
22 p3750 N85-33244

Ocean thermal energy conversion
[DE85-012291] 23 p3946 N85-34456

Thermodynamics of the corrosion of chromium in molten carbonates
[DE85-011407] 24 p4079 N85-35282

Experimental lithium system
[DE85-013252] 24 p4094 N85-35382

CORROSION PREVENTION

Implantation of ionized monomer into aluminum alloy 6061 for marine corrosion protection
[AD-A144874] 01 p0028 N85-10172

Aircraft surface coatings
[NASA-CR-3661] 02 p0137 N85-10935

Research and development requirements for ion implantation
[AD-P003951] 02 p0286 N85-11867

Use of ion implantation to modify the corrosion behavior of metals
[AD-P003953] 02 p0286 N85-11869

The modification of metallic corrosion by ion implantation: Engineering applications and fundamentals studies
[AD-P003954] 02 p0286 N85-11870

Effects of introduction of alkyl groups into aluminium anodized coatings
[DRIC-T-7244] 03 p0331 N85-12133

Related studies to cathodic protection of reinforced concrete structures
[PB84-218114] 03 p0333 N85-12145

Improved reinforcement metal
03 p0353 N85-12271

A review of metallic surface treatments for corrosion mitigation
[AD-A146701] 06 p0769 N85-14918

Improved ceramic anodes for corrosion protection
[AD-A149492] 10 p1452 N85-19149

Oxidation protection coatings for polymers
[NASA-CASE-LEW-14072-1] 11 p1611 N85-20129

Formation of alumina layers on iron-base alloys
[BLL-T6418/BG/LRS/LRST737/84]
13 p2020 N85-22657

Chemical-mechanical interaction in gears
14 p2223 N85-23785

Corrosion control through a better understanding of the metallic substrate-organic coating-interface
[AD-A151238] 15 p2509 N85-25479

Corrosion inhibitor formulation for molybdenum, tungsten and other metals
[AD-D011593] 15 p2510 N85-25486

Electrical research on solar cells and photovoltaic materials
[NASA-CR-175699] 15 p2585 N85-25935

Protective coatings for aircraft structures: A review
[VTH-LR-413] 16 p2706 N85-26704

Material for protection of metal surfaces against corrosion by molten salts
[DE85-007714] 16 p2750 N85-26968

Forming of coating protection system: Mechanism of paint-coating anti-corrosion protection of steel
[BLL-BISI-TRANS-22081-(9022.06)]
17 p2925 N85-28033

Anticorrosion protection of reinforcing steel in prestressed gypsum and anhydrite concrete
[BLL-BISI-TRANS-22079-(9022.06)]
17 p2926 N85-28044

Properties of chromate coatings formed on electrolytic zinc substrates
[BLL-BISI-TRANS-22349-(9022.06)]
17 p2926 N85-28052

Effect of the agressive action of soil on metallic pipelines. New possibilities for the passive and active corrosion protection
[BLL-BISI-TRANS-21630-(9022.06)]
17 p2928 N85-28070

Marine corrosion
[AD-A153843] 18 p3074 N85-29012

Effect of multi-functional inhibitors on the electrochemistry within corrosion crack
19 p3238 N85-30075

On compounding nickel alloys as defense against sulfide-oxide corrosion 19 p3243 N85-30109

Atomized magnesium-aluminum protective coatings
19 p3244 N85-30116

Concretization of high level radioactive source in marine sediment
[AD-D011703] 19 p3249 N85-30146

Protection products for the conductors of high voltage overhead lines
[BLL-OA-TRANS-3219-(6196.300)]
20 p3429 N85-31269

New corrosion protection concept for very high voltage line towers
[BLL-OA-TRANS-2691-(6196.300)]
20 p3429 N85-31270

Inhibited anticorrosion protection of automotive steel strip in the NLMK
[BLL-M-36250-(5828.4)] 20 p3430 N85-31274

Corrosion in civil aircraft structures
[SNIAS-851-111-105] 20 p3432 N85-31291

Management of Corrosion
[AGARD-LS-141] 22 p3749 N85-33238

Corrosion management strategies for aircraft and related systems 22 p3749 N85-33239

Environmental factors in corrosion and deterioration of materials 22 p3750 N85-33241

Rationale in the selection of corrosion protective coating systems 22 p3750 N85-33242

Maintenance and the military environment
22 p3750 N85-33243

Current requirements for the design and maintenance against corrosion of UK military aircraft
22 p3750 N85-33244

Protective systems and maintenance policies for marine environments 22 p3750 N85-33245

Land vehicle corrosion management
22 p3750 N85-33246

Relating corrosion maintenance to environmental factors 22 p3750 N85-33247

CORROSION RESISTANCE
NT OXIDATION RESISTANCE

Effect of scandium on the structure and properties of Al-Zn-Mg alloys 01 p0018 N85-10111

Effect of welding method on corrosion resistance of welded compositions made of 1201 alloy
01 p0020 N85-10124

Methods for producing platinum-group metal coatings from molten alkali cyanides
[PB84-225994] 01 p0029 N85-10181

International Conference on Recent Developments in Specialty Steels and Hard Materials. Conference abstracts
[CSIR-S-256] 02 p0176 N85-11177

Metalurgy of a 12 percent chromium stainless steel
02 p0178 N85-11195

The effect of replacing molybdenum with vanadium on the corrosion resistant properties of stainless steels
02 p0178 N85-11197

Non-oxide ceramics: A new class of engineering materials 02 p0179 N85-11199

The influence of metallurgical aspects on the pitting corrosion behaviour of high alloy stainless steels
02 p0179 N85-11202

Recent developments on the role of molybdenum in irons and steels 02 p0180 N85-11206

The transient oxidation of single crystal NiAl + Zr
[NASA-CR-174756] 02 p0182 N85-11221

Optimization of mechanical/corrosion properties of Ticode-12 plate and sheet. Part 1: Compositional effects, stage 1
[DE84-015935] 02 p0184 N85-11231

Corrosion in alkali metal/molybdenum heat pipes
[DE84-014039] 02 p0184 N85-11233

Investigation of chemical durability mechanisms in fluoride glasses
[AD-A145420] 02 p0186 N85-11241

Localized corrosion and stress corrosion cracking behavior of stainless steel weldments
[DE84-016095] 04 p0474 N85-13017

Corrosion of brass in potable water service
[CETIM-100390] 04 p0477 N85-13037

Corrosion resistance of nitrided low-alloy steels
[PB84-235027] 04 p0477 N85-13040

Galvanized wire protected against corrosion by chromate passivization
[BLL-M-35908-(5828.4)] 05 p0616 N85-13936

Material selection consideration for solar ponds
05 p0666 N85-14284

Characterization of newly developed conductive composites
[AD-A146652] 06 p0764 N85-14884

A review of metallic surface treatments for corrosion mitigation
[AD-A146701] 06 p0769 N85-14918

Copper-nickel sheathing study, phase 2. Two-year service performance of test panels on the ARCO TEXAS
[PB84-242411] 06 p0775 N85-14952

Improvement of the corrosion resistance of turbine engine bearings
[AD-A147430] 07 p0905 N85-15731

Corrosion properties of second-generation conductive materials 07 p1000 N85-16346

Effect of iron on the performance of IN 625 weld deposits
[BR91456] 08 p1169 N85-17376

Development of materials for open-cycle MHD
[DE84-017293] 09 p1393 N85-18770

Evaluation of 7010 aluminium alloy extruded tube in the T76 condition
[BR92019] 11 p1596 N85-20[illegible]

Initial development of nickel and nickel-iron aluminides for structural uses
[DE84-016641] 11 p1608 N85-2010[illegible]

Role of nitrogen in improving resistance to localized corrosion in austenitic stainless steels
11 p1609 N85-20115

Research on heat-exchanger corrosion
[PB85-126316] 11 p1616 N85-20184

Progress on transparent yttria
[AD-P004370] 12 p1827 N85-2148[illegible]

Carbon granule probe microphone for leak detection — recovery boilers
[NASA-CASE-NPO-16027-1] 12 p1849 N85-2159[illegible]

Delayed cracking strength of experimental grades of 42 CD 4 steel in aqueous H2S surroundings
[BLL-T6419/BG/LRS/LRST738/84]
13 p2020 N85-22[illegible]

Study of the effects of implantation on the high Fe-Ni-Cr and Ni-Cr-Al alloys
[NASA-CR-175625] 13 p2021 N85-22[illegible]

Corrosion of aircraft Al and Al-Zn ion plated steel fasteners 13 p2021 N85-22[illegible]

Influence of 3% NaCl solution on rate of accumulation of damage and residual strength of aluminum-boron composite 13 p2027 N85-22[illegible]

Corrosion-resistant amorphous alloys
13 p2035 N85-2274[illegible]

Exploratory corrosion tests on materials and fluids for advanced high-temperature molten-salt storage
[DE85-002911] 14 p2256 N85-23[illegible]

Conservation of turbines by inhibited air
14 p2268 N85-2403[illegible]

Development of molten carbonate fuel cell power plant technology
[DE84-016839] 14 p2352 N85-245[illegible]

Resistance of hydrogenated alpha-titanium alloys to corrosion-fatigue fracture 15 p2499 N85-25413

Mechanisms of corrosion fatigue in high strength I/M (Ingot Metallurgy) and P/M (Powder Metallurgy) aluminum alloys
[AD-A151177] 15 p2509 N85-25478

Corrosion control through a better understanding of the metallic substrate-organic coating-interface
[AD-A151238] 15 p2509 N85-25479

The corrosion resistance of zinc coatings on depleted uranium and uranium alloys
[DE85-007216] 15 p2510 N85-25487

Oxidation of nickel-aluminum and iron-aluminum alloys
[DE85-006930] 15 p2512 N85-25497

Surface composition, properties and thermal stability of massive and fine metallic glasses
15 p2513 N85-25508

Modified aluminosilicide coating for heat-resistant nickel alloys 15 p2514 N85-25509

Titanium diffusion method prevents metal corrosion
15 p2514 N85-25510

Inhibiting titanium corrosion in hot nitrogen [illegible] solutions using sulfate ions 15 p2514 N85-25511

Corrosion behavior of Al4 aluminum alloy hardened by CO2 laser radiation 15 p2514 N85-25512

The influence of abrasive blast cleaning and corrosion inhibitors on protective paint coatings
15 p2517 N85-25[illegible]

Electrically conductive polymer concrete overlays
[DE85-006728] 15 p2522 N85-25[illegible]

Powder metallurgy bearings for advanced rocket engines 16 p2736 N85-26[illegible]

Evaluation of the corrosion properties of aluminum alloy 5083 weldments
[DE85-007729] 16 p2751 N85-26977

Investigation of the pitting potential of rapidly solidified aluminum-lithium alloys
[VTH-LR-434] 16 p2752 N85-26[illegible]

Investigation of the influence of some paint systems and water displacing corrosion inhibitors on anodic undermining corrosion of aluminum 2024 clad alloy — aircraft structures
[VTH-LR-443] 16 p2756 N85-2700[illegible]

Material for electrodes of pulsed and arc sources of light
[DE85-007453] 16 p2760 N85-2715[illegible]

Properties of corrosion resistant stabilized ferritic steels
[BLL-BISI-TRANS-22519-(9022.06)]
17 p2925 N85-28[illegible]

The corrosion resistance of chromium-nickel steel containing rare-earth metals
[BLL-BISI-TRANS-22477-(9022.06)] 17 p2925 N85-28041

Anticorrosion protection of reinforcing steel in prestressed gypsum and anhydrite concrete
[BLL-BISI-TRANS-22079-(9022.06)] 17 p2926 N85-28044

Properties of chromate coatings formed on electrolytic zinc substrates
[BLL-BISI-TRANS-22349-(9022.06)] 17 p2926 N85-28052

New process for production of bimetal with corrosion-resistant cladding layer
[BLL-BISI-TRANS-22371-(9022.06)] 17 p2927 N85-28056

Obtaining oxide films on surface of tubes of chromium-nickel steels
[BLL-BISI-TRANS-22476-(9022.06)] 17 p2929 N85-28076

Dispersion-strengthened powder-metallurgical chromium steels
[BLL-BISI-TRANS-22323-(9022.06)] 17 p2929 N85-28081

Metallurgical means of preventing the corrosion of metal
[BLL-BISI-TRANS-22320-(9022.06)] 17 p2929 N85-28082

Properties of nitrogen containing stainless alloy designed for high resistance to pitting
[DE85-008282] 17 p2931 N85-28095

Development of high temperature resistant, noncorrosible, non-metallic ceramic materials, especially silicon nitride in gas turbine application
[BMFT-FB-T-85-015] 17 p2936 N85-28125

Development of high temperature resistant noncorrodible silicon carbide components for gas turbine applications, follow-up report
[BMFT-FB-T-85-016] 17 p2936 N85-28126

Exhaust systems for passenger vehicles: Test procedure for resistance to internal corrosion of silencers
[BLL-BISI-TRANS-22360-(9022.06)] 17 p2973 N85-28361

Proper quality of anticorrosion work no matter how bad the atmospheric conditions
[BLL-BISI-TRANS-22080-(9022.06)] 17 p2975 N85-28383

Corrosion resistant coating
[NASA-CASE-NPO-15928-1] 18 p3073 N85-29005

Variations in the structure and in the composition of austenitic and carbon steel in spot welds
[BLL-BISI-TRANS-21765-(9022.06)] 18 p3073 N85-29007

Development of reduced activation alloys for fusion service: Draft
[DE85-007464] 18 p3074 N85-29014

Long-Term Materials Test Program
[DE85-003248] 18 p3077 N85-29034

Development of corrosion resistant heat exchangers for flue gas desulfurization
[BMFT-FB-T-84-281] 18 p3103 N85-29211

SERI Solar Energy Storage Program: FY 1984
[DE85-002936] 18 p3130 N85-29385

USSR report: Materials Science and Metallurgy
[JPRS-UMS-85-005] 19 p3241 N85-30095

On compounding nickel alloys as defense against sulfide-oxide corrosion 19 p3243 N85-30109

Vacuum pressure welding of commercial titanium with 2Kh13 and 12Kh18N10T steels 19 p3246 N85-30124

Mechanism of strength degradation for hot corrosion of alpha-SiC
[NASA-TM-87052] 19 p3248 N85-30135

Concretization of high level radioactive source in marine sediment
[AD-D011703] 19 p3249 N85-30146

Optimisation of MCr Al coating compositions for marine gas turbines
[BR91159] 20 p3394 N85-31056

Corrosion in civil aircraft structures
[SNIAS-851-111-105] 20 p3432 N85-31291

Management of Corrosion
[AGARD-LS-141] 22 p3749 N85-33236

Theoretical aspects of corrosion and practical implications for aircraft and related systems 22 p3749 N85-33240

Rationale in the selection of corrosion protective coating systems 22 p3750 N85-33242

Current requirements for the design and maintenance against corrosion of UK military aircraft 22 p3750 N85-33244

Corrosion resistant storage container for radioactive material
[DE85-011666] 22 p3838 N85-33765

Nitriding of super alloys for enhancing physical properties
[DE85-005762] 23 p3917 N85-34275

The development and evaluation of the creep and corrosion resistant alloy IN6201
[PNR-90253] 23 p3917 N85-34278

Electrically conductive containment vessel for molten aluminum
[DE85-006518] 23 p3939 N85-34415

Electrochemical method for investigation of the susceptibility of corrosion-resistant steels to intercrystalline corrosion
[BLL-CE-TRANS-8082-(9022.09)] 24 p4077 N85-35269

X-ray fluorescence analysis of 304L stainless steel
[DE85-013254] 24 p4080 N85-35288

Development of a mathematical model for predicting the percentage fatigue life increase resulting from shot peened components
[AD-A155774] 24 p4101 N85-35425

CORROSION TESTS
NT SALT SPRAY TESTS

Interactions between corrosion and creep of uncoated and coated superalloys in sulfate melts 04 p0477 N85-13038

Method for evaluating petrol products corrosivity using piezoelectric crystals. Part 2: Instruction manual --- jet engine corrosion tests
[FOA-C-40198-B4] 04 p0482 N85-13073

A simple, low cost potentiostat for corrosion studies
[NPL-DMA(A)-47] 04 p0502 N85-13203

Testing of non-alloyed and low-alloyed steels for their behaviour with respect to intercrystalline stress corrosion cracking
[BLL-RISLEY-TR-4546-(9091.9F)] 07 p0925 N85-15861

Replaceable blade turbine and stationary specimen corrosion testing facility
[NASA-TM-86931] 09 p1294 N85-18126

Forced corrosion tests of construction components of passenger aircraft fuselages 11 p1600 N85-20062

Compatibility experiments of facilities, materials, and propellants for electrothermal thrusters
[NASA-TM-86956] 12 p1795 N85-21260

An electrochemical study of the corrosion behavior of primer coated 2219-T87 aluminum
[NASA-TP-2459] 13 p2021 N85-22662

Change in microstructure of heat-resistant nickel alloys upon thermal cycling in a current of gas 13 p2031 N85-22725

Variability in constant-load-amplitude fatigue crack growth rates in marine environments
[AD-A150786] 14 p2255 N85-23975

Exploratory corrosion tests on alloys in molten salts at 900(0)C
[DE85-000511] 14 p2257 N85-23983

Exploratory corrosion tests on materials and fluids for advanced high-temperature molten-salt storage
[DE85-002911] 14 p2258 N85-23991

The design and construction of a flow channel and rig for corrosion studies
[AERE-M-3455] 15 p2508 N85-25474

Influence of pretreatment, environment and strain rate on stress corrosion cracking of the aluminum alloy 7075-T6
[VTH-LR-433] 16 p2752 N85-26985

Corrosion characteristics of some steels produced through a self-cleaning rotating electrode
[BLL-BISI-TRANS-22046-(9022.06)] 17 p2925 N85-28034

Corrosion test on high-alloy steels
[BLL-BISI-TRANS-21627-(9022.06)] 17 p2926 N85-28046

Exhaust systems for passenger vehicles: Test procedure for resistance to internal corrosion of silencers
[BLL-BISI-TRANS-22360-(9022.06)] 17 p2973 N85-28361

Tendency of selected low-carbon steels to corrosion cracking in nitrates
[BLL-BISI-TRANS-22262-(9022.06)] 18 p3073 N85-29006

Burner rig corrosion of SiC at 1000 deg C
[NASA-TM-87061] 19 p3227 N85-30011

Corrosion fatigue cooperative testing program statistical analysis
[AD-A153886] 19 p3236 N85-30077

Management of Corrosion
[AGARD-LS-141] 22 p3749 N85-33236

Protective systems and maintenance policies for marine environments 22 p3750 N85-33245

Corrosion fatigue strength and crack growth in prestrained 0.16% C carbon steel 23 p3905 N85-34192

CORRUGATED SHELLS

Vibrational loading mechanism of unitized corrugated containers with cushions and non-load-bearing contents 09 p1339 N85-18419

Stressed state of multilayer thick-walled longitudinally corrugated cylinders 16 p2766 N85-27069

CORRUGATING

Microwave SAW (Surface Acoustic Wave) monochromator
[AD-D011718] 21 p3590 N85-32311

CORSAIR AIRCRAFT
U A-7 AIRCRAFT

CORTICOSTEROIDS
NT ALDOSTERONE
NT CORTISONE
NT HYDROXYCORTICOSTEROID

Role of glucocorticoids in the response to unloading of muscle protein and amino acid metabolism 15 p2609 N85-26077

Blood pressure responses and mineral ocorticoid levels in the suspended rat model for weightlessness 15 p2609 N85-26079

CORTISONE

Skeletal muscle metabolism in hypokinetic rats
[NASA-CR-174059] 02 p0233 N85-11520

CORUNDUM
U ALUMINUM OXIDES

COS-B SATELLITE

The galactic gamma-ray distribution: Implications for galactic structure and the radial cosmic ray gradient
[NASA-TM-86173] 07 p1061 N85-16729

Multicomponent analysis of total COS-B gamma-ray data at intermediate lattitudes
[OG-3.1-3] 22 p3873 N85-33991

COSMIC DUST
NT INTERPLANETARY DUST
NT ZODIACAL DUST

The distribution of dust in the region of the Rosette Nebula and MON OB2 association 05 p0739 N85-14753

Local interstellar extinction with an emphasis on uvby beta results 06 p0875 N85-15559

The unidentified emission features: A study of the Orion Bar and planetary nebulae 08 p1246 N85-17862

Circumstellar dust disks around young stars 08 p1247 N85-17870

Spectral characteristics of dust in planetary nebulae 08 p1247 N85-17873

Interstellar grain mantles 08 p1247 N85-17874

Dust reradiation from NGC 6946 08 p1248 N85-17880

A comparative study of dust and young stars in three small galaxies 09 p1415 N85-18928

Dust in the region of Herbig-Haro objects: The case of NGC 1999 11 p1747 N85-20991

Survey of probable micrometer-sized Earth-orbital debris fragments in the NASA-JSC cosmic dust sample collection 12 p1785 N85-21203

In-situ detection of micron-sized dust particles in near-Earth space 12 p1785 N85-21205

Research in planetary studies and operation of Mauna Kea Observatory
[NASA-CR-175818] 13 p2169 N85-23460

Sixteenth Lunar and Planetary Science Conference. Press abstracts
[NASA-CR-175692] 15 p2680 N85-26548

Dust emission of Comet Halley at large heliocentric distances 15 p2681 N85-26556

Mining cosmic dust from the blue ice lakes of Greenland 15 p2682 N85-26563

A comprehensive investigation of the dynamics of micron and submicron lunar ejecta in heliocentric space 19 p3364 N85-30994

COSMIC GAMMA RAY BURSTS
U GAMMA RAY BURSTS

COSMIC GASES
NT INTERSTELLAR GAS
NT NEUTRAL GASES

Measuring EUV line emission from the hot interstellar medium 06 p0860 N85-15595

Constraints on the galactic distribution of cosmic rays from the COS-B gamma-ray data
[OG-3.1-6] 22 p3873 N85-33994

Relevance of cosmic gamma rays to the mass of gas in the galaxy
[OG-3.1-8] 22 p3874 N85-33996

COS-B gamma-ray sources and interstellar gas
[OG-3.1-9] 22 p3874 N85-33997

Excess gamma rays from the Loop I supernova remnant
[OG-3.1-10] 22 p3874 N85-33998

Breakdown of helium nuclei in matter processed near black holes
[OG-8.2-20] 23 p4021 N85-34916

COSMIC PLASMA
Space research and the new approach to the mechanics of fluid media in cosmos [TRITA-EPP-84-04] 03 p0447 N85-12844
Physical processes in relativistic plasmas — active galactic nuclei 08 p1240 N85-17824
Plasma Astrophysics -- conference [ESA-SP-207] 12 p1953 N85-22270
Space research and the new approach to the mechanics of fluid media in cosmos 12 p1953 N85-22271
X-ray astronomy and plasma astrophysics 12 p1956 N85-22288
Explosive transverse electric field and particle acceleration during magnetic collapse — cosmic plasma 12 p1956 N85-22292
Nonlinear evolution of astrophysical Alfven waves 12 p1956 N85-22294
Plasma in the clusters of galaxies 12 p1957 N85-22299
Plasma processes in Herbig-Haro objects 12 p1957 N85-22301
Hydromagnetic precursors of interplanetary plasma burst 13 p1978 N85-22414
Solar wind and cosmic rain 15 p2644 N85-26312
On planetary rings as sources and sinks of magnetospheric plasmas 15 p2677 N85-26526
Prognoz-10 intercosmos' station launched to study shock waves 19 p3296 N85-30434
Implications of source abundances of ultraheavy cosmic rays 20 p3543 N85-32049
Interstellar turbulence, random density variations, and scintillation measurements [OG-7.2-13] 23 p4015 N85-34880
The role of cosmic rays in magnetic hydrodynamics of interstellar medium [OG-7.2-15] 23 p4015 N85-34882

COSMIC RADIATION
U COSMIC RAYS

COSMIC RADIO WAVES
U EXTRATERRESTRIAL RADIO WAVES

COSMIC RAY ALBEDO
Longitude and pitch-angle distributions of streams of high-energy electrons under Earth's radiation belts 13 p1978 N85-22415

COSMIC RAY SHOWERS
Electromagnetic shower development and applications to sampling calorimeters [DE84-016355] 04 p0493 N85-13142
Characteristics of latitude effect on cosmic ray charged component in atmosphere at altitudes 3-5 KM 13 p1978 N85-22413
Longitude and pitch-angle distributions of streams of high-energy electrons under Earth's radiation belts 13 p1978 N85-22415
Solar wind and cosmic rain 15 p2644 N85-26312
Yakutsk Institute's cosmic ray research facility 22 p3732 N85-33135
Search for gamma rays of energy 10(15) eV from Cygnus X-3 [OG-2.1-1] 22 p3862 N85-33919
Observation of an excess of cosmic ray muons of energies 2 TeV from the direction of Cygnus X-3 [OG-2.1-3] 22 p3863 N85-33920
Muon content of gamma ray induced EAS from Cygnus X-3 [OG-2.1-4] 22 p3863 N85-33921
Gamma rays of energy or = 10(15) eV from Cyg X-3 [OG-2.1-5] 22 p3863 N85-33922
1000 GeV gamma rays from Cygnus X-3: An update [OG-2.1-6] 22 p3863 N85-33925
Evidence for long-term variability in the ultra high energy photon flux from Cygnus X-3 [OG-2.1-10] 22 p3863 N85-33926
Variability in the high energy gamma ray emission from Cyg X-3 over a two-year period (1983 - 1984) at E 4 x 10(11) eV [OG-2.1-11] 22 p3864 N85-33927
A search for gamma-ray point sources with the Carpet shower array [OG-2.1-12] 22 p3864 N85-33928
Cyg X-3: Not seen in high-energy gamma rays by COS-B [OG-2.2-2] 22 p3864 N85-33929
Constraints on cosmic-ray observation of Cygnus X-3 [OG-2.2-3] 22 p3864 N85-33930
Ultra high energy gamma rays, cosmic rays and neutrinos from accreting degenerate stars [OG-2.2-5] 22 p3864 N85-33931
Relevance of the observation of UHE gammas to hard X-ray astronomy [OG-2.2-6] 22 p3865 N85-33932
500 TeV gamma rays from Hercules X-1 [OG-2.2-7] 22 p3865 N85-33933
A model for the UHE gamma-rays from Hercules X-1 [OG-2.2-8] 22 p3865 N85-33934
Hercules X-1: Pulsed gamma-rays detected above 150 GeV [OG-2.2-9] 22 p3865 N85-33935
Experimental results on gamma-ray sources at E sub 0 = 10(13) - 10(14) eV [OG-2.2-12] 22 p3865 N85-33937
Search for excess showers from Crab Nebula [OG-2.3-2] 22 p3866 N85-33939
All sky Northern Hemisphere 10(15) EV gamma-ray survey [OG-2.6-3] 22 p3870 N85-33968
Search for ultra high energy gamma-rays from various sources [OG-2.6-7] 22 p3870 N85-33969
A search for sources of ultra high energy gamma rays at air shower energies with Ooty EAS array [OG-2.6-8] 22 p3870 N85-33970
Observations of potential ultra high energy gamma-ray sources above 10(15) eV [OG-2.6-9] 22 p3870 N85-33971
Observation of gamma-rays from LMC X-4 above 10(16) eV [OG-2.6-10] 22 p3870 N85-33972
The 4U 0115+63: Another energetic gamma ray binary pulsar [OG-2.6-11] 22 p3870 N85-33973
Primary gamma-rays with E gamma or = to 10(15) eV: Evidence for ultrahigh energy particle acceleration in galactic sources [OG-2.6-13] 22 p3871 N85-33974
Search for the gamma-ray fluxes with energies above 10915) eV from various objects [OG-2.6-14] 22 p3871 N85-33975
Search for gamma-rays from M31 and other extragalactic objects [OG-2.7-3] 22 p3871 N85-33977
Some evidence for high energy gamma-ray sources at large galactic latitudes [OG-2.7-5] 22 p3871 N85-33978
Energy spectrum and arrival direction of primary cosmic rays of energy above 10 to the 18th power eV [OG-5.1-1] 22 p3880 N85-34043
Ultra high energy cosmic ray spectrum [OG-5.1-2] 22 p3881 N85-34044
The primary cosmic ray spectrum above 10 to the 19th power eV [OG-5.1-3] 22 p3881 N85-34045
New calorimetric all-particle energy spectrum [OG-5.1-4] 22 p3881 N85-34046
The muon content of EAS as a function of primary energy [OG-5.1-8] 22 p3881 N85-34050
On the possibility of the determining the average mass composition near 10 to the 14th power eV through the solar magnetic field [OG-5.1-9] 22 p3882 N85-34051
Cosmic ray composition between 10 to the 15th power - 10 to the 17th power eV obtained by air shower experiments [OG-5.1-12] 22 p3882 N85-34053
Estimation of composition of cosmic rays with E sub zero approximately equals 10(17) - 10(18) eV [OG-5.1-14] 22 p3882 N85-34055
All particle energy spectrum of cosmic rays in 10 to the 15th power - 10 to the 20th power eV region [OG-5.1-15] 22 p3882 N85-34056
Cosmic ray spectra measurements at the Yakutsk EAS array [OG-5.1-17] 22 p3882 N85-34058
Composition of primary cosmic rays near the bend from a study of hadrons in air showers at sea level [OG-5.2-2] 22 p3883 N85-34059
The composition of cosmic rays near the Bend (10 to the 15th power eV) from a study of muons in air showers at sea level [OG-5.2-3] 22 p3883 N85-34060
Composition of primary cosmic rays at energies 10(15) to approximately 10(16) eV [OG-5.2-4] 22 p3883 N85-34061
EAS fluctuation approach to primary mass composition investigation [OG-5.2-5] 22 p3883 N85-34062
The primary composition beyond 10 to the 5th power GeV as deduced from high energy hadrons and muons in air showers [OG-5.2-6] 22 p3883 N85-34063
Implication of EAS data for the study of primary cosmic rays above 10 to the 5th power GeV [OG-5.2-7] 22 p3883 N85-34064
Composition of primary cosmic rays near the knee [OG-5.2-10] 22 p3884 N85-34066
EAS Cerenkov measurements of the composition of the cosmic ray flux around 10 to the 16th power eV [OG-5.2-11] 22 p3884 N85-34067
Electron and muon parameters of EAS and the composition of primary cosmic rays in 10(15) to approximately 10(16) eV [OG-5.2-12] 22 p3884 N85-34
Arrival directions of large air showers, low-mu showers and old-age low-mu air showers observed at Chacaltaya [OG-5.3-2] 22 p3884 N85-34
Anisotropy of cosmic rays of energy 10 (15) eV to 10 (17) eV observed at Akeno [OG-5.3-3] 22 p3884 N85-34
Arrival directions of cosmic rays of E .4 EeV [OG-5.3-4] 22 p3884 N85-34
The sidereal anisotropy of cosmic rays around 3 x 10 (15) eV observed at a middle north latitude [OG-5.3-6] 22 p3884 N85-34
Arrival direction distribution of cosmic rays of energy 10 (18) eV [OG-5.3-7] 22 p3885 N85-34
Observation of arrival times of EAS with energies or = 6 x 10 (14) eV [OG-5.3-8] 22 p3885 N85-34
Cosmic ray intensity variations at primary rigidities near 1900 GV [OG-5.3-9] 22 p3885 N85-34
Search for bursts in air shower data [OG-5.3-10] 22 p3885 N85-34
Air shower arrival directions measured at Buckland Park [OG-5.3-11] 22 p3885 N85-34
A simulation of high energy cosmic ray propagation 1 [OG-5.4-1] 22 p3885 N85-34
A simulation of high energy cosmic ray propagation 2 [OG-5.4-2] 22 p3885 N85-34
Cosmic rays in the 10(16) to 10(19) eV range from pulsars [OG-5.4-3] 22 p3886 N85-34
Energy dependence of cosmic ray composition above 10(15) GeV/nucleus [OG-5.4-4] 22 p3886 N85-34
Implications of the experimental results on high energy cosmic rays with regard to their origin [OG-5.4-5] 22 p3886 N85-34
The primary cosmic ray mass composition at energies above 10(14) eV [OG-5.4-6] 22 p3886 N85-34
UHE particle production in close binary systems [OG-5.4-7] 22 p3886 N85-34
Virgo cluster as a high energy cosmic rays source [OG-5.4-8] 22 p3886 N85-34
Modeling cosmic ray anisotropies near 10(18) eV [OG-5.4-9] 22 p3886 N85-34
Anisotropy and the knee of the energy spectrum [OG-5.4-10] 22 p3887 N85-34
Anisotropy of cosmic rays above 10(14) eV [OG-5.4-11] 22 p3887 N85-34
A model for the proton spectrum and cosmic ray anisotropy [OG-5.4-12] 22 p3887 N85-34
Interpretation of cosmic-ray anisotropy below 10(14) eV [OG-5.4-13] 22 p3887 N85-34
Injection of energetic particles following the gamma-ray flares on June 7, 1980, as observed on Helios 1 [SH-1.3-9] 23 p3993 N85-347
Spectra of solar proton ground level events using neutron monitor and neutron moderated detector recordings [SH-1.3-14] 23 p3994 N85-347
Ground increase of cosmic ray intensity on February 16, 1984 [SH-1.3-15] 23 p3994 N85-347
The SCR flare of 16 February 1984 as recorded by the Sayan spectrograph [SH-1.3-17] 23 p3994 N85-347
Energetic solar particle events [SH-3.2-2] 23 p4003 N85-34
Cosmic ray intensity and the tilt of the neutral sheet [SH-4.2-8] 23 p4007 N85-34
Differential measurement of cosmic-ray gradient with respect to interplanetary current sheet [SH-4.2-9] 23 p4007 N85-34
Effects of a wavy neutral sheet on cosmic ray anisotropies [SH-4.2-11] 23 p4008 N85-34
Implications of cross section errors for cosmic ray propagation [OG-7.2-3] 23 p4014 N85-34
Cosmic ray secondary nuclei and the structure of the galaxy [OG-7.2-4] 23 p4014 N85-34
Why do leaky-box models work so fine? [OG-7.2-8] 23 p4014 N85-34
Alfven wave scattering and the secondary to primary ratio [OG-7.2-9] 23 p4015 N85-34

On the cosmic ray diffusion in a violent interstellar medium
[OG-7.2-14] 23 p4015 N85-34881

The role of cosmic rays in magnetic hydrodynamics of interstellar medium
[OG-7.2-15] 23 p4015 N85-34882

A new ultra high energy gamma ray telescope at Ohya mine
[OG-9.4-3] 23 p4029 N85-34970

The Buckland Park air shower array
[OG-9.4-4] 23 p4029 N85-34971

An EAS experiment at mountain altitude for the detection of gamma-ray sources
[OG-9.4-5] 23 p4029 N85-34972

An observatory to study 10 (10) to 10 (17) by EV gamma rays
[OG-9.4-6] 23 p4029 N85-34973

A new array for the study of ultra high energy gamma-ray sources
[OG-9.4-7] 23 p4029 N85-34974

Akeno 20 km (2) air shower array (Akeno Branch)
[OG-9.4-8] 23 p4029 N85-34975

Mini and super mini arrays for the study of highest energy cosmic rays
[OG-9.4-9] 23 p4029 N85-34976

Detection of 10 (1) GeV cosmic neutrinos with a space station
[OG-9.4-10] 23 p4030 N85-34977

The longitudinal thickness of air-shower fronts
[OG-9.5-1] 23 p4030 N85-34978

Cerenkov light images of EAS produced by primary gamma
[OG-9.5-3] 23 p4030 N85-34979

Shower disc sampling and the angular resolution of gamma-ray shower detectors
[OG-9.5-2] 23 p4030 N85-34980

A method to improve observations of gamma-ray sources near 10 (15) eV
[OG-9.5-5] 23 p4030 N85-34982

Angular resolution of air-shower array-telescopes
[OG-9.5-6] 23 p4030 N85-34983

Astrophysical applications of high angular resolution array-telescopes
[OG-9.5-7] 23 p4031 N85-34984

Angular resolution of an EAS array for gamma ray astronomy energies 5 x 10 (13) eV
[OG-9.5-8] 23 p4031 N85-34985

Note on the detection of high energy primary cosmic gamma rays by air shower observation
[OG-9.5-9] 23 p4031 N85-34986

On the statistical significance of excess events: Remarks of caution and the need for a standard method of calculation
[OG-9.5-10] 23 p4031 N85-34987

A new statistic for the analysis of circular data in gamma-ray astronomy
[OG-9.5-13] 23 p4031 N85-34989

The angular resolution of air shower gamma ray telescopes
[OG-9.5-14] 23 p4031 N85-34990

Accelerator experiments on the contribution of secondary particles to the production of cosmogenic nuclides in meteorites
[SH-7.1-8] 23 p4048 N85-35100

Depth and size effects on cosmogenic nuclide production in meteorites
[SH-7.1-9] 23 p4048 N85-35101

A suggested standardized format for cosmic ray ground-level event data
[SH-8.1-15] 23 p4052 N85-35130

Using the information of cosmic rays to predict influence epidemic
[SH-10.1-2] 23 p4053 N85-35134

Strong earthquakes, novae and cosmic ray environment
[SH-10.1-3] 23 p4053 N85-35135

Proton-air and proton-proton cross sections from air shower data
[HE-1.1-1] 24 p4170 N85-35849

Proton-air inelastic cross section at S(1/2) = 30 TeV
[HE-1.1-2] 24 p4170 N85-35850

Hadron cross sections at ultra high energies and unitarity bounds on diffraction dissociation
[HE-1.1-3] 24 p4170 N85-35851

PP bar)P elastic scattering and cosmic ray data
[HE-1.1-6] 24 p4170 N85-35854

Estimation of the total inelasticity coefficient in interaction of greater than or equal to 20 TeV hadrons with lead
[HE-1.1-9] 24 p4171 N85-35857

The method for the study of the inelastic cross-section for high energy protons by means of shower arrays with the large calorimetric area
[HE-1.1-11] 24 p4171 N85-35858

Multiplicity distributions in interaction models used for cascade simulations
[HE-1.2-5] 24 p4172 N85-35863

Some remarks about simulation of cosmic ray phenomena with use of nuclear interaction models based on the current SPS proton-antiproton data
[HE-1.2-6] 24 p4172 N85-35864

Anugler distribution of shower particles produced in the collisions of 20-GeV/c and 300-GeV negative pions with emulsion nuclei 24 p4172 N85-35866

Scaling violation in the fragmentation region of inclusive nucleon spektrum 24 p4173 N85-35874

The response of a scintillation counter below an emulsion chamber to heavy nucleus interactions in the chamber 24 p4175 N85-35889

Japan - USSR joint emulsion chamber experiment at Pamir
[HE-3.1-1] 24 p4177 N85-35901

Energy spectra of proton and nuclei of primary cosmic rays in energy region 10 TeV/particle
[HE-3.1-10] 24 p4178 N85-35908

Scaling violation in fragmentation region at energies above 10-15 eV based on the data on cosmic ray hadron component
[HE-3.1-11] 24 p4178 N85-35909

High sensitive X-ray films to detect electron showers in 100 GeV region
[HE-3.1-13] 24 p4178 N85-35911

Exotic interactions among C-jets and Pb-jets
[HE-3.2-6] 24 p4179 N85-35914

X-ray film chamber with carbon target of Tien-Shan complex array 24 p4179 N85-35915

Penetrative nature of high energy showers observed in Chacaltaya emulsion chamber
[HE-3.3-5] 24 p4180 N85-35923

Anomalous correlation between hadron and electromagnetic particles in hadron and gamma-ray families
[HE-3.3-6] 24 p4180 N85-35924

Atmospheric interactions detected in both the upper and the lower chambers at Chacaltaya
[HE-3.3-7] 24 p4180 N85-35925

Lateral distribution of high energy hadrons and gamma ray in air shower cores observed with emulsion chambers
[HE-3.3-8] 24 p4180 N85-35926

Size distributions of air showers accompanied with high energy gamma ray bundles observed at Mt. Chacaltaya
[HE-3.3-9] 24 p4181 N85-35927

EAS accompanied by gamma-families at Mt. Norikura and comparison with Monte Carlo simulation
[HE-3.3-10] 24 p4181 N85-35928

Comparison of absolute intensity between EAS with gamma-families and general EAS at Mount Norikura
[HE-3.3-11] 24 p4181 N85-35929

Analytical-numerical methods of calculations of energy and three-dimensional particle distributions in electromagnetic cascades
[HE-3.5-13] 24 p4184 N85-35950

Multidimensional analysis of data obtained in experiments with X-ray emulsion chambers and extensive air showers
[HE-3.6-2] 24 p4184 N85-35951

LPM effect and primary energy estimations
[HE-3.6-4] 24 p4185 N85-35953

Experimental basis for the models of cascade propagation in atmosphere
[HE-3.6-6] 24 p4185 N85-35954

Relation between gamma-ray family and EAS core: Monte-Carlo simulation of EAS core
[HE-3.6-7] 24 p4185 N85-35955

Comparison of big event with calculations of the air shower development
[HE-3.6-8] 24 p4185 N85-35956

The lateral distributions of charged particles of energy greater than 0.3 E sub crit in electron-photon cascades in lead and air
[HE-3.6-10] 24 p4185 N85-35957

Result of Monte-Carlo simulation of electron-photon cascades in lead and layers of lead-scintillator
[HE-3.6-11] 24 p4185 N85-35958

On mini-cluster observed by Chacaltaya emulsion chamber experiment
[HE-3.6-12] 24 p4185 N85-35959

A comparative analysis of gamma and hadron families at the superhigh energies recorded in experiment Pamir
[HE-3.7-1] 24 p4185 N85-35960

A study of gamma-families generated in nucleon-nucleus (NA) and pion-nucleus (pi A) interactions
[HE-3.7-2] 24 p4186 N85-35961

New analysis of nuclear interaction observed by Mt. Kanbara emulsion chamber experiment
[HE-3.7-4] 24 p4186 N85-35963

Intensities of high-energy cosmic rays at Mount Kanbala
[HE-3.7-5] 24 p4186 N85-35964

Structured events in Pamir carbon X-ray chambers
[HE-3.7-7] 24 p4186 N85-35965

Ultra high energy events in ECHOS series and primary energy spectrum
[HE-3.7-9] 24 p4186 N85-35966

Peculiarities of gamma-quanta distribution at 20 TeV energy
[HE-3.7-10] 24 p4186 N85-35967

Nineteenth International Cosmic Ray Conference. HE Sessions, volume 7
[NASA-CP-2376-VOL-7] 24 p4186 N85-35968

Electrons, muons and hadrons in extensive air showers and how do they depend on nuclear interaction model, part 2 24 p4187 N85-35969

Analysis of equi-intensity curves and NU distribution of EAS 24 p4187 N85-35970

Analysis of the hadron component in E.A.S.
24 p4187 N85-35971

Electrons, muons and hadrons in extensive air showers and how do they depend on nuclear interaction model, part 1 24 p4187 N85-35972

Simulation of EAS properties on the basis of high energy interaction model deduced from the accelerator data
24 p4187 N85-35973

New aspects in nucleon-nucleus collisions and EAS properties around 10(6) GeV 24 p4187 N85-35974

Small air showers and collider physics
[HE-4.1-9] 24 p4137 N85-35975

High energy hadrons in extensive air showers
24 p4187 N85-35976

Dependence of the average spatial and energy characteristics of the hadron-lepton cascade on the strong interaction parameters at superhigh energies
24 p4188 N85-35977

Hadronic components of EAS by rigorous saddle point method in the energy range between 10(5) and 10(8) GeV 24 p4188 N85-35978

About increase of the large transvere momentum processes fraction in hA interactions at energies 5.10(14) - 10(16) eV according to the data on E.A.S. hadrons
24 p4188 N85-35979

Phenomenology of soft hadron interactions and the relevant EAS data 24 p4188 N85-35980

The maximum depth of shower with E sub 0 larger then 10(17) eV on average characteristics of EAS different components 24 p4188 N85-35981

Sensitivity of depth of maximum and absorption depth of EAS to hadron production mechanism
24 p4188 N85-35982

A critical analysis of air shower structure functions and size spectrum measurements with the NBU air shower array 24 p4188 N85-35983

Character of energy flow in air shower core
24 p4189 N85-35985

Observation of EAS using a large water tank
24 p4189 N85-35986

The development of air shower in the iron absorber
24 p4189 N85-35987

Application of photodiodes to the detection of electromagnetic bursts 24 p4189 N85-35988

Core structure of EAS in 10(15) to 10(17) eV
24 p4189 N85-35989

Particle distributions in approximately 10(14) 10(16) eV air shower cores at sea level 24 p4189 N85-35990

Theoretical study of EAS hadronic structure
24 p4189 N85-35991

Monte Carlo simulations of electron lateral distributions in the core region of 10(13) - 10(16) eV air showers
24 p4190 N85-35992

Comparison of simulation results with sea-level experimental data on 10(14) - 10(16) air shower cores
24 p4190 N85-35993

Particle distributions in approximately 10(13) - 10(16) eV air shower cores at mountain altitude and comparison with Monte Carlo simulations
[HE-4.2-18] 24 p4190 N85-35994

Tskhra-Tskaro complex intended for the investigations of EAS spatial characteristics near axis
24 p4190 N85-35995

A new study of shower age distribution in near vertical showers by EAS air shower array
24 p4190 N85-35996

A new study of muons in air showers by NBU air shower array 24 p4190 N85-35997

Lateral distribution of electrons of air showers
24 p4191 N85-35998

Detailed studies of the electron lateral distribution in extensive air showers with energies around 10(16) eV
24 p4191 N85-35999

Study of muons near shower cores at sea level using the E594 neutrino detector 24 p4191 N85-36000

Correlation of high energy muons with primary composition in extensive air shower
[HE-4.3-7] 24 p4191 N85-36001

COSMIC RAYS

Measurement of energy muons in EAS at energy region larger thean 10(17) eV [HE-4.3-8] 24 p4191 N85-36002

Muon fluctuation studies of EAS 10(17) eV [HE-4.3-9] 24 p4191 N85-36003

Average features of the muon component of EAS or = 10(17) eV [HE-4.3-10] 24 p4191 N85-36004

Measurement of shower electrons and muons using a small air shower array [HE-4.3-11] 24 p4192 N85-36005

The longitudinal development of muons in cosmic ray air showers at energies 10(15) - 10(17) eV [HE-4.3-12] 24 p4192 N85-36006

Topological aspects of age parameter [HE-4.3-13] 24 p4192 N85-36007

Monte Carlo simulation of EAS generated by 10(14) - 10(16) eV protons [HE-4.3-14] 24 p4192 N85-36008

Lateral distribution on charged particles in EAS [HE-4.3-15] 24 p4192 N85-36009

Lateral distribution of high energy muons in EAS of sizes Ne approximately equals 10(5) and Ne approximately equals 10(6) [HE-4.3-16] 24 p4192 N85-36010

Energy calibration of the fly's eye detector [HE-4.4-1] 24 p4192 N85-36011

The structure of EAS at E 0.1 EeV [HE-4.4-2] 24 p4193 N85-36012

Standard value for the radiation length in air [HE-4.4-4] 24 p4193 N85-36013

Longitudinal trial functions and the cosmic ray energy scale 24 p4193 N85-36014

EAS development curve at energy of 10(16) - 10(18) eV measured by optical Cerenkov light [HE-4.4-7] 24 p4193 N85-36015

Transition effect of air shower particles in plastic scintillators [HE-4.4-9] 24 p4193 N85-36017

The system of EAS time analysis [HE-4.4-10] 24 p4193 N85-36018

On the determination of the depth of EAS development maximum using the lateral distribution of Cerenkov light at distances 150 m from EAS axis [HE-4.4-13] 24 p4194 N85-36019

Study of the energy spectrum of primary cosmic rays: EAS size fluctuations at a fixed primary energy [HE-4.4-14] 24 p4194 N85-36020

Study of the shower maximum depth by the method of detection of the EAS Cerenkov light pulse shape [HE-4.4-15] 24 p4194 N85-36021

Analysis of Cerenkov pulses recorded simultaneously at two sites [HE-4.4-16] 24 p4194 N85-36022

Preliminary results of the Cerenkov EAS flashes the Crimean Astrophysical Observatory [HE-4.4-17] 24 p4194 N85-36023

The experimental cascade curves of EAS at E sub 0 10(17) eV obtained by the method of detection of Cherenkov pulse shape [HE-4.4-18] 24 p4194 N85-36024

Lateral-angular and temporal characteristics of EAS optical radiation [HE-4.4-19] 24 p4194 N85-36025

The identification of gamma ray induced EAS [HE-4.5-1] 24 p4195 N85-36026

Muons in gamma showers [HE-4.5-3] 24 p4195 N85-36027

Muon spectrum in air showers initiated by gamma rays [HE-4.5-4] 24 p4195 N85-36028

Electromagnetic and muonic structure of showers initiated by gamma-rays and by hadrons [HE-4.5-6] 24 p4195 N85-36030

The muon content of gamma-ray showers [HE-4.5-7] 24 p4195 N85-36031

Simulation of gamma-initiated showers [HE-4.5-10] 24 p4195 N85-36033

Phenomenological characteristic of the electron component in gamma-quanta initiated showers [HE-4.5-11] 24 p4196 N85-36034

A three-dimensional Monte Carlo calculation of the photon initiated showers and Kiel result [HE-4.5-13] 24 p4196 N85-36035

Construction of a cosmic ray air shower telescope [HE-4.5-14] 24 p4196 N85-36036

On the possibilities of large-scale radio and fiber optics detectors in cosmic rays [HE-4.6-2] 24 p4196 N85-36039

Radio signals from very large showers [HE-4.6-3] 24 p4196 N85-36040

On the production mechanism of radio-pulses from large extensive air showers [HE-4.6-4] 24 p4196 N85-36041

A new study on the emission of EM waves from large EAS [HE-4.6-5] 24 p4197 N85-36042

Air fluorescence detection of large air showers below the horizon [HE-4.6-6] 24 p4197 N85-36043

A facility for investigation of multiple hadrons at cosmic-ray energies [HE-4.6-8] 24 p4197 N85-36045

A possible EAS array above the Soudan 2 detector [HE-4.6-9] 24 p4197 N85-36046

Fast scintillation counter system and performance [HE-4.6-10] 24 p4197 N85-36047

Performance of a local electron density trigger to select extensive air showers at sea level [HE-4.6-11] 24 p4198 N85-36048

Microprocessor-based single particle calibration of scintillation counter [HE-4.6-13] 24 p4198 N85-36049

Samarkand complex setup for investigation of cosmic ray variation in the energy range of 7 10 (9) - 10 (15) eV [HE-4.6-14] 24 p4198 N85-36050

Radio wave emitted by an extensive air showers in 10KHz to 1MHz region [HE-4.6-15] 24 p4198 N85-36051

The structure of the shower disk observed at Mt. Norikura [HE-4.7-1] 24 p4198 N85-36052

Structure of air shower disc near the core [HE-4.7-2] 24 p4198 N85-36053

Properties of 10 (18)-10 (19)eV EAS at far core distance [HE-4.7-3] 24 p4198 N85-36054

Longitudinal development of muons in large air showers studies from the arrival time distributions measured at 900m above sea level [HE-4.7-4] 24 p4199 N85-36055

Arrival time distributions of electrons in air showers with primary energies above 10 (18)eV observed at 900m above sea level [HE-4.7-5] 24 p4199 N85-36056

The thickness of the shower disc as observed in showers produced by primaries above 10 (19)eV [HE-4.7-6] 24 p4199 N85-36057

Methods for roof-top mini-arrays [HE-4.7-7] 24 p4199 N85-36058

Expected rates with mini-arrays for air showers [HE-4.7-8] 24 p4199 N85-36059

Fast scintillation counter preamplifier for the observation of Linsley effect [HE-4.7-9] 24 p4199 N85-36060

A mini-array for large air showers [HE-4.7-10] 24 p4199 N85-36061

A note on some statistical properties of rise time parameters used in muon arrival time measurements [HE-4.7-12] 24 p4199 N85-36062

Sub-luminal pulses from cosmic ray air showers [HE-4.7-13] 24 p4200 N85-36063

Thickness of the particle swarm in cosmic ray air showers [HE-4.7-14] 24 p4200 N85-36064

Study of the time-differentiated particle flux density at various distances from EAS axis [HE-4.7-15] 24 p4200 N85-36065

Muon and neutrino results from KGF experiment at a depth of 7000 hg/square cm [HE-5.1-2] 24 p4200 N85-36066

A large area cosmic muon detector located at Ohya stone mine [HE-5.1-7] 24 p4201 N85-36072

The Nagoya cosmic-ray muon spectrometer 3, part 2: Track detector [HE-5.2-3] 24 p4202 N85-36081

An upper limit of muon flux of energies above 100 TeV determined from horizontal air showers observed at Akeno [HE-5.2-12] 24 p4203 N85-36088

Comments on the measurements of multiple muon phenomena [HE-5.2-13] 24 p4203 N85-36089

Energy spectrum of cascade showers induced by cosmic ray muons in the range from 50 GeV to 5 TeV [HE-5.2-14] 24 p4203 N85-36090

Measurement of muon intensity by Cerenkov method [HE-5.2-15] 24 p4204 N85-36091

Photo nuclear energy loss term for muon-nucleus interactions based on xi scaling model of QCD [HE-5.2-17] 24 p4204 N85-36093

On method of muon spectrum measurements by the scintillation detectors of a large thickness T4t sub o [HE-5.2-18] 24 p4204 N85-36094

A transient digitiser for fast air shower events [HE-5.2-21] 24 p4204 N85-36097

A study of atmospheric neutrinos with the IMB detector [HE-5.3-7] 24 p4205 N85-36101

Atmospheric neutrinos observed in underground detectors [HE-5.3-8] 24 p4205 N85-36102

Analysis of the electron component of EAS a observational level 700 g x cm(-2) with a scale breaking interaction model and gammaisation hypothesis [HE-5.4-8] 24 p4208 N85-361

Calculation of intensity of high energy muon grou observed deep underground [HE-5.4-13] 24 p4208 N85-361

A search for heavy long lived particles in high energ cosmic rays [HE-6.2-7] 24 p4211 N85-3614

Delayed particles in EAS at Akeno [HE-6.2-8] 24 p4211 N85-3614

Energetic delayed hadrons in large air showers observed at 5200m above sea level [HE-6.2-9] 24 p4211 N85-3614

Search for long-lived massive particles in extensive a showers [HE-6.2-10] 24 p4212 N85-3614

High energy cosmic ray signature of quark nugget [HE-6.2-11] 24 p4212 N85-3614

Search for tachyons associated with extensive a showers in the ground level cosmic radiation [HE-6.2-13] 24 p4212 N85-3614

Charge 4/3 leptons in cosmic rays [HE-6.2-14] 24 p4212 N85-3615

Progress report on a new search for free e/3 quarks in the cores of 10(15) - 10(16) eV air showers [HE-6.2-15] 24 p4212 N85-3615

Observation of genetic relation among new phenomena Geminion, Chiron and mini-Centauro [HE-6.2-16] 24 p4212 N85-3615

Tien-Shan effect and charmed particles [HE-6.2-17] 24 p4212 N85-3615

Search for acoustic signals from high energ cascades [HE-7.1-1] 24 p4213 N85-3615

Experimental investigation of radiative-acoustic effects in the water by the thermodynamical conditions o Dumand [HE-7.1-2] 24 p4213 N85-3615

Exploring results of the possibility on detecting cosmi ray particles by acoustic way [HE-7.1-3] 24 p4213 N85-3615

Acoustic detection of air shower cores [HE-7.1-4] 24 p4213 N85-3615

Detection threshold energy of high energy cascade showers using thermoluminescence PTFE-sheet and hot-gas reader [HE-7.1-5] 24 p4213 N85-3615

Application of thermoluminescence for detection o cascade shower 1: Hardware and software of reader system [HE-7.1-6] 24 p4213 N85-361

Spatial distribution read-out system fo thermoluminescence sheets [HE-7.1-7] 24 p4213 N85-361

Application of thermoluminescence for detection o cascade shower 2: Detection of cosmic ray cascade shower at Mount Fuji [HE-7.1-12] 24 p4214 N85-361

COSMIC RAYS

- NT COSMIC RAY SHOWERS
- NT GALACTIC COSMIC RAYS
- NT GAMMA RAY BURSTS
- NT PRIMARY COSMIC RAYS
- NT SECONDARY COSMIC RAYS
- NT SOLAR COSMIC RAYS

Cosmic ray effects on microelectronics. Part 3: Propagation of cosmic rays in the atmosphere [AD-A145026] 01 p0131 N85-10

Interplanetary cosmic ray intensity: 1972-1984 and ou to 32 AU [AD-A145130] 01 p0131 N85-10

Cosmic ray propagation in the local superbubble [NASA-TM-85030] 03 p0449 N85-12

Supernova envelope shock origin of cosmic rays: A review [DE84-016479] 04 p0590 N85-13

New measurements of the spectrum of the cosmic microwave background [DE84-016055] 05 p0746 N85-14

Nature of short-period variations of cosmic rays in stratosphere 06 p0823 N85-15

Diurnal variation harmonics and spatial change in cosmic ray flux 06 p0824 N85-15

On the record of galactic cosmic ray flux and traffic break-ups in iron meteorites 06 p0867 N85-15

The low-energy secondary cosmic ray flux: Detection in iron meteorites 06 p0867 N85-15

Solar wind and cosmic ray irradiation of grains and ice - application to erosion and synthesis of organic compounds in the solar system 06 p0868 N85-15

Solar-geophysical data number 478, June 1984. Part 1 (prompt reports): Data for May 1984, Apr. 1984, and late data
[PB84-243153] 06 p0890 N85-15653

The calibration of photographic and spectroscopic films: A densitometric analysis of IIaO film flown aboard the Space Shuttle 3
[NASA-CR-174278] 07 p0962 N85-16101

The galactic gamma-ray distribution: Implications for galactic structure and the radial cosmic ray gradient
[NASA-TM-86173] 07 p1061 N85-16729

A T-matrix theory of galactic heavy-ion fragmentation
[NASA-TP-2363] 08 p1221 N85-17690

Extragalactic cosmic rays from active galaxies
08 p1238 N85-17805

SU(2) x U(1) vacuum and the Centauro events
[NASA-TM-86082] 08 p1260 N85-17926

High energy physics study
[DE84-015803] 09 p1383 N85-18700

Radiation safety of crew and passengers of air transportation in civil aviation. Provisional standards
[NASA-TM-77610] 11 p1692 N85-20638

Charge-to-mass dispersion methods for abrasion-ablation fragmentation models
[NASA-TM-86340] 11 p1726 N85-20857

Cosmic ray generation by plasma turbulence: Development of a new paradigm in physics
12 p1955 N85-22286

Cosmic ray composition and origin
12 p1955 N85-22287

Self-similar modified shock structures — cosmic rays
12 p1956 N85-22290

Solar-geophysical data number 483. November 1984. Part 1: (Prompt reports). Data for October 1984, September 1984 and late data
[PB85-147692] 12 p1962 N85-22335

Research in particles and fields
[NASA-CR-175472] 12 p1963 N85-22337

Correlation of interplanetary medium parameters in transition region of high-velocity solar wind streams
13 p1978 N85-22412

Observation of cosmic ray flux variations in stratosphere 13 p1981 N85-22430

Dielectric detector device for registering heavy cosmic radiation particles 13 p2045 N85-22799

Measurement of the large-scale anisotropy of the cosmic background radiation at 3 MM 13 p2206 N85-23680

A measurement of the intensity of the cosmic background radiation at 3.9 cm
13 p2206 N85-23681

The access of energetic charged particles to satellite altitudes
[AD-A150799] 14 p2373 N85-24670

Cosmic ray environment model for Earth orbit
[NASA-CR-175666] 14 p2455 N85-25165

Pulsations of cosmic ray intensities before increasing flux of relativistic particles from solar flares
15 p2477 N85-25292

Cyclic changes in barometric coefficient of cosmic ray neutron component 15 p2478 N85-25293

Space-time features of solar cosmic ray penetration into high latitude regions of Earth's magnetosphere based on Intercosmos-19 satellite data 15 p2481 N85-25310

Electron flux with electron energies above 40 MeV at altitudes of about 500 km in region where capture is possible and outside it when L is 3 or greater
15 p2481 N85-25315

Professional Committee on Solid Propulsion hold conference 15 p2533 N85-25623

Interstellar Al-26 and excess Mg-26
15 p2680 N85-26551

Identification of the youngest meteorites and a discussion of the possibility that they came from Mars
15 p2681 N85-26550

The propagation of ultraheavy cosmic rays
15 p2685 N85-26582

Measurements of fluxes of high-energy protons and electrons by 2 oppositely oriented spectrometers aboard Cosmos-366 artificial Earth satellite
16 p2722 N85-26800

The fast individualists in the solar system: Cosmic rays 16 p2886 N85-27806

Results from the Helios galactic and solar cosmic ray experiment (E7) 16 p2886 N85-27807

Cosmic ray modulation and turbulent interaction regions near 11 AU
[NASA-TM-86193] 18 p3209 N85-29909

A comparison of the radiation hardness of various VLSI technologies for defense applications
[DE85-006973] 19 p3263 N85-30236

Biostack experiments on STS-flights and the impact for man in space 20 p3510 N85-31621

Contributions to the 19th International Cosmic Ray Conference
[NASA-CR-176049] 20 p3543 N85-32044

Abundances of secondary elements among the ultra heavy cosmic rays: Results from HEAO-3
20 p3543 N85-32047

Lead, platinum, and other heavy elements in the primary cosmic radiation: HEAO-3 results sec wg032961 cb553097 20 p3543 N85-32048

Implications of source abundances of ultraheavy cosmic rays 20 p3543 N85-32049

Interactions of heavy nuclei, Kr, Xe and Ho, in light targets 20 p3544 N85-32050

Solar-geophysical data no. 485, January 1985. Part 1 (prompt reports): Data for December 1984, November 1984 and late data
[PB85-181360] 20 p3548 N85-32079

A Cerenkov-delta E-Cerenkov detector for high energy cosmic ray isotopes and an accelerator study of Ar-40 and Fe-56 fragmentation
[NASA-CR-176028] 20 p3549 N85-32086

Contributions to the 19th International Cosmic Ray Conference
[NASA-CR-176060] 21 p3714 N85-33044

Cosmic ray He3 measurements
[OG-4.2-3] 21 p3714 N85-33045

Initial results from the Caltech/DSRI balloon-borne isotope experiment
[OG-4.3-8] 21 p3714 N85-33046

Measurements of Fe and Ar fragmentation cross sections
[PAPER-OG-7.2-20] 21 p3714 N85-33047

Precision measurements of solar energetic particle elemental composition
[PAPER-SH-2.1-4] 21 p3715 N85-33052

Research in extreme ultraviolet and far ultraviolet astronomy
[NASA-CR-176068] 21 p3716 N85-33080

Research in particles and fields
[NASA-CR-176069] 21 p3724 N85-33103

Effects of space radiation on advanced semiconductor devices. Part 3: Further cosmic ray simulation studies of single event upsets and latch-up in CMOS memories
[AERE-G-3368-PT-3] 22 p3848 N85-33833

Ninteenth International Cosmic Ray Conference. Conference program and author index
[NASA-CP-2376] 22 p3860 N85-33901

Ninteenth International Cosmic Ray Conference. OG sessions, volume 1
[NASA-CP-2376-VOL-1] 22 p3860 N85-33902

Excess gamma-rays in the direction of the rho Ophiuchi cloud: An exotic object?
[OG-2.5-1] 22 p3868 N85-33958

Spectral evolution of gamma-rays from adiabatically expanding sources in dense clouds
[OG-2.5-2] 22 p3869 N85-33959

Search for positron annihilation line and continuum radiation from the Galactic Center
[OG-2.5-5] 22 p3869 N85-33962

Cosmic gamma rays from quasars
[OG-2.7-10] 22 p3872 N85-33983

Ultrahigh energy gamma rays: Carriers of cosmological information
[OG-2.7-14] 22 p3872 N85-33987

Local interstellar medium and gamma-ray astronomy
[OG-3.1-1] 22 p3873 N85-33989

The galactic gamma-ray distribution and the radial cosmic ray gradient
[OG-3.1-4] 22 p3873 N85-33992

Radial distribution of cosmic ray intensity in the galaxy from gamma-ray data
[OG-3.1-5] 22 p3873 N85-33993

Constraints on the galactic distribution of cosmic rays from the COS-B gamma-ray data
[OG-3.1-6] 22 p3873 N85-33994

Relevance of cosmic gamma rays to the mass of gas in the galaxy
[OG-3.1-8] 22 p3874 N85-33996

Excess gamma rays from the Loop I supernova remnant
[OG-3.1-10] 22 p3874 N85-33998

Long term variability of the cosmic ray intensity
[OG-3.1-11] 22 p3874 N85-33999

SMM detection of interstellar Al-26 gamma radiation
[OG-3.2-1] 22 p3874 N85-34001

Galactic distribution of interstellar Al-26
[OG-3.2-3] 22 p3874 N85-34002

Gamma ray line production from cosmic ray spallation reactions 22 p3875 N85-34005

Ninteenth International Cosmic Ray Conference. OG sessions, volume 2
[NASA-CP-2376-VOL-2] 22 p3875 N85-34006

Source spectral index of heavy cosmic ray nuclei
[OG-4.1-2] 22 p3875 N85-34008

Charge and energy dependence of the residence time of cosmic ray nuclei below 15 GeV/nucleon
[OG-4.1-3] 22 p3876 N85-34009

Relative abundances of sub-iron to iron nuclei in low energy (50-250 MeV/N) cosmic rays as observed in the Skylab experiment
[OG-4.1-4] 22 p3876 N85-34010

Cosmic ray charge and energy spectrum measurements using a new large area Cerenkov x dE/dx telescope
[OG-4.1-5] 22 p3876 N85-34011

A measurement of the cosmic ray elements C to Fe in the two energy intervals 0.5-2.0 GeV/n and 20-60 GeV/n
[OG-4.1-6] 22 p3876 N85-34012

Relative abundances of elements (20 or = Z or = 28) at energies up to 70 GeV/amu using relativistic rise in ion chambers
[OG-4.1-7] 22 p3876 N85-34013

Primary cosmic ray spectra in the range 20-60 GeV/n
[OG-4.1-9] 22 p3877 N85-34015

Energy spectrum of cosmic-ray iron nucleus observed with emulsion chamber
[OG-4.1-10] 22 p3877 N85-34016

Measurement of the iron spectrum from 60 to 200 GeV per nucleon
[OG-4.1-11] 22 p3877 N85-34017

Cosmic ray nuclei of energy 50 GeV/NUC
[OG-4.1-12] 22 p3877 N85-34018

Composition and energy spectra of cosmic ray nuclei above 500 GeV/nucleon from the JACEE emulsion chambers
[OG-4.1-13] 22 p3877 N85-34019

Charge composition and energy spectral of cosmic ray primary particles for energies higher than 1 TeV
[OG-4.1-14] 22 p3877 N85-34020

Interstellar propagation and the isotopic composition of hydrogen in the galactic cosmic rays
[OG-4.2-1] 22 p3877 N85-34021

Measurements of galactic hydrogen and helium isotopes from 1978 through 1983
[OG-4.2-2] 22 p3877 N85-34022

Cosmic ray He-3 measurements
[OG-4.2-3] 22 p3878 N85-34023

Parametrized energy spectrum of cosmic-ray protons with kinetic energies down to 1 GeV
[OG-4.2-11] 22 p3878 N85-34025

Galactic propagation models consistent with the cosmic ray lifetime derived from Be-10 measurements
[OG-4.3-1] 22 p3878 N85-34026

Implications of new measurements of O-16 + p + C-12,13, N-14,15 for the abundances of C, N isotopes at the cosmic ray source
[OG-4.3-2] 22 p3878 N85-34027

Cosmic ray isotope measurements with a new Cerenkov X total energy telescope
[OG-4.3-4] 22 p3878 N85-34029

The isotopic composition of cosmic ray calcium
[OG-4.3-5] 22 p3879 N85-34030

A new analysis of cosmic ray isotopes at 3 GeV/n from HEAO3-C2 data
[OG-4.3-6] 22 p3879 N85-34031

The energy dependence of the neon-22 excess in the cosmic radiation
[OG-4.3-7] 22 p3879 N85-34032

Initial results from the Caltech/DRSI balloon-borne isotope experiment
[OG-4.3-8] 22 p3879 N85-34033

Ariel 6 measurements of ultra-heavy cosmic ray fluxes in the region 34 or = Z or = 48
[OG-4.4-3] 22 p3879 N85-34036

Ariel 6 measurements of ultra-heavy cosmic ray fluxes in the region Z or = 48
[OG-4.4-4] 22 p3880 N85-34037

Elemental abundances of cosmic rays with Z 33 as measured on HEAO-3
[OG-4.4-5] 22 p3880 N85-34038

Abundances of secondary elements among the ultra heavy cosmic rays: Results from HEAO-3
[OG-4.4-6] 22 p3880 N85-34039

Capabilities of the LDEF-2 heavy nuclei collection
[OG-4.4-8] 22 p3880 N85-34040

Ultraheavy cosmic ray tracks in meteorites: A reappraisal, based on calibrations with relativistic ions
[OG-4.4-10] 22 p3880 N85-34041

Energy spectrum and arrival direction of primary cosmic rays of energy above 10 to the 18th power eV
[OG-5.1-1] 22 p3880 N85-34043

Ultra high energy cosmic ray spectrum
[OG-5.1-2] 22 p3881 N85-34044

The primary cosmic ray spectrum above 10 to the 19th power eV
[OG-5.1-3] 22 p3881 N85-34045

A new measurement of the cosmic ray energy spectrum between 3 x 10 to the 15th power eV and 3 x 10 to the 16th power eV
[OG-5.1-6] 22 p3881 N85-34048

Study of composition of cosmic rays with energy .7 E 3 Ee
[OG-5.1-7] 22 p3881 N85-34049

The muon content of EAS as a function of primary energy
[OG-5.1-8] 22 p3881 N85-34050

EAS fluctuation approach to primary mass composition investigation
[OG-5.2-5] 22 p3883 N85-34062

On galactic origin of cosmic rays with energy up to 10(19) eV
[OG-5.4-15] 22 p3887 N85-34091

Abundance of low energy (50-150 MeV) antiprotons in cosmic rays
[OG-6.1-1] 22 p3887 N85-34092

Search for heavy antinuclei in the cosmic radiation
[OG-6.1-2] 22 p3887 N85-34093

The flux of secondary anti-deuterons and antihelium produced in the interstellar medium
[OG-6.1-5] 22 p3888 N85-34096

Observed antiprotons and energy dependent confinement of cosmic rays: A conflict?
[OG-6.1-7] 22 p3888 N85-34098

Antiparticles in the extragalactic cosmic radiation
[OG-6.1-8] 22 p3888 N85-34099

Galactic cosmic ray antiprotons and supersymmetry
[OG-6.1-9] 22 p3888 N85-34100

Galactic antiprotons of 0.2-2 GeV energy
[OG-6.1-11] 22 p3888 N85-34101

Evidence for a dynamical halo around the edge-on galaxy NGC 4631
[OG-6.2-1] 22 p3889 N85-34102

Halo of NGC 4631 and models of cosmic-ray transport
[OG-6.2-3] 22 p3889 N85-34103

Observation of cosmic ray positrons from 5 to 25 GeV
[OG-6.2-5] 22 p3889 N85-34104

An observation of cosmic ray positrons from 10-20 GeV
[OG-6.2-6] 22 p3889 N85-34105

Electrons and positrons from expanding supernova envelopes in dense clouds
[OG-6.2-9] 22 p3889 N85-34108

The electron spectra in the synchrotron nebula of the supernova remnant G 29.7-0.3
[OG-6.2-10] 22 p3889 N85-34109

Relativistic electron in curved magnetic fields
[OG-6.2-11] 22 p3890 N85-34110

Transient two-dimensional simulation of SEU in a CMOS SRAM cell
[DE85-008419] 22 p3890 N85-34111

Effect of seeds of heavy charged particles of galactic cosmic radiation 23 p3954 N85-34505

Ninteenth International Cosmic Ray Conference. SH sessions, volume 4
[NASA-CP-2376-VOL-4] 23 p3989 N85-34729

Acceleration of ions and electrons to near-cosmic ray energies in a perpendicular shock: The January 6, 1978 event
[SH-1.5-4] 23 p3996 N85-34773

Cosmic ray acceleration by stellar wind. Simulation for heliosphere
[SH-1.5-17] 23 p3997 N85-34780

The energy spectrum of Jovian electrons in interplanetary space
[SH-1.5-18] 23 p3997 N85-34781

Observation of the fluxes of nuclei with energies 10-20 MEV per nucleon during the solar flare of April 28, 1984
[SH-2.1-1] 23 p3998 N85-34783

On the retention of high-energy protons and nuclei with charges Z or equal to 2 in large solar flares after the process of their acceleration
[SH-2.1-8] 23 p3998 N85-34789

Type 3 solar radio bursts and 3HE-rich events
[SH-2.2-3] 23 p4000 N85-34798

Numerical descriptions of cosmic-ray transport
[SH-4.1-3] 23 p4004 N85-34829

Numerical and analytic descriptions of cosmic-ray transport
[SH-4.1-4] 23 p4005 N85-34830

the role of shock waves in modulation of galactic cosmic rays
[SH-4.1-7] 23 p4005 N85-34831

The intensity recovery of Forbush-type decreases as a function of heliocentric distance and its relationship to the 11-year variation
[SH-4.1-9] 23 p4005 N85-34832

Cumulative effect of Forbush decreases in the heliospheric modulation during the present solar cycle
[SH-4.1-10] 23 p4005 N85-34833

Cosmic ray modulatin and merged interaction regions
[SH-4.1-11] 23 p4005 N85-34834

Longitudinal distribution of cosmic rays in the heliosphere
[SH-4.1-14] 23 p4006 N85-34837

The 1973-1984 solar modulation of cosmic ray nuclei
[SH-4.1-16] 23 p4006 N85-34838

Cosmic ray modulation in a random anisotropic magnetic field
[SH-4.1-20] 23 p4006 N85-34839

Evidence for regions of negligible cosmic-ray modulation in the inner heliosphere (10 AU)
[SH-4.1-21] 23 p4006 N85-34840

Notes on drift theory
[SH-4.2-3] 23 p4006 N85-34841

Drift and observations in cosmic-ray modulation, 1
[SH-4.2-4] 23 p4007 N85-34842

Drift and observations in cosmic-ray modulation, 2
[SH-4.2-5] 23 p4007 N85-34843

Cosmic ray north-south anisotropy 1961 - 1983
[SH-4.2-6] 23 p4007 N85-34844

Ninteenth International Cosmic Ray Conference. OG sessions, volume 3
[NASA-CP-2376-VOL-3] 23 p4012 N85-34862

Germanium and lead: Significant differences between meteoritic and photospheric abundances?
[OG-7.1-2] 23 p4012 N85-34864

Lead and uranium group abundances in cosmic rays
[OG-7.1-3] 23 p4013 N85-34865

Implications of source abundances of ultraheavy cosmic rays
[OG-7.1-4] 23 p4013 N85-34866

Propagation and nucleosynthesis of ultraheavy cosmic rays
[OG-7.1-5] 23 p4013 N85-34867

Sources of the ultraheavy cosmic rays
[OG-7.1-7] 23 p4013 N85-34868

The cosmic ray composition as viewed from the chemical abundances of the solar system
[OG-7.1-8] 23 p40.3 N85-34869

Elemental technetium as a cosmic-ray clock
[OG-7.1-9] 23 p4013 N85-34870

Electron capture decay of cosmic rays: A model of the inhomogeneous interstellar medium
[OG-7.1-10] 23 p4014 N85-34871

The model-independence of cosmic ray source determinations
[OG-7.2-1] 23 p4014 N85-34873

Interstellar turbulence, random density variations, and scintillation measurements
[OG-7.2-13] 23 p4015 N85-34880

Diffusion of strongly magnetized cosmic ray particles in a turbulent medium
[OG-7.2-16] 23 p4015 N85-34883

Cosmic-ray transport in the galactic magnetosphere
[OG-7.2-17] 23 p4016 N85-34884

The role of cosmic rays and Alfven waves in the structure of the galactic halo
[OG-7.2-18] 23 p4016 N85-34885

Measurements of Fe and Ar fragmentation cross sections
[OG-7.2-20] 23 p4016 N85-34887

Interactions of heavy nuclei, Kr, Xe and Ho, in light targets
[OG-7.2-21] 23 p4016 N85-34888

The cosmic-ray shock structure problem for relativistic shocks
[OG-8.1-1] 23 p4017 N85-34891

Instabilities in decelerating supersonic flows with applications to cosmic ray shocks
[OG-8.1-2] 23 p4017 N85-34892

Time-dependent nonlinear cosmic ray shocks confirming abstract
[OG-8.1-3] 23 p4017 N85-34893

A cosmic ray driven instability
[OG-8.1-5] 23 p4018 N85-34895

Relativistic cosmic ray spectra in the full non-linear theory of shock acceleration
[OG-8.1-6] 23 p4018 N85-34896

Acceleration of cosmic rays in supernova-remnants
[OG-8.1-9] 23 p4018 N85-34899

Onion-shell model for cosmic ray electrons and radio synchrotron emission in supernova remnants
[OG-8.1-10] 23 p4018 N85-34900

Approximate supernova remnant dynamics with cosmic ray production
[OG-8.1-12] 23 p4019 N85-34901

A numerical study of diffusive shock acceleration of cosmic rays in supernova shocks
[OG-8.2-2] 23 p4019 N85-34903

Scaling from Jupiter to pulsars and the acceleration of cosmic ray particles by pulsars, 3
[OG-8.2-3] 23 p4019 N85-34904

Do supernovae of type 1 paly a role in cosmic-ray production?
[OG-8.2-5] 23 p4019 N85-34905

Neutron-rich nuclei in cosmic rays and Wolf-Rayet stars
[OG-8.2-6] 23 p4019 N85-34906

Interstellar (Ne-22) as a possible source of the excess (Ne-22) in the galactic cosmic ray
[OG-8.2-12] 23 p4020 N85-34908

The electromagnetic ram action of the plasma focus as a paradigm for the generation of cosmic rays and the gigantic jets in active galaxies
[OG-8.2-14] 23 p4020 N85-34910

The origins of cosmic rays and quantum effects on gravity
[OG-8.2-15] 23 p4020 N85-34911

Evaluation of parameters for particles acceleration by the zero-point field of quantum electrodynamics
[OG-8.2-16] 23 p4020 N85-34912

Giant molecular clouds as regions of particle acceleration 23 p4020 N85-34913

The nucleosynthesis of deterium and helium-3
[OG-8.2-18] 23 p4020 N85-34914

Pulsars as cosmic ray particle accelerators: Proton orbits
[OG-8.2-21] 23 p4021 N85-34917

Pulsars as cosmic ray accelerators: Energy development of protons
[OG-8.2-22] 23 p4021 N85-34918

Pulsars as cosmic ray particle accelerators: Dynamics of electrons
[OG-8.2-23] 23 p4021 N85-34919

Propagation of injected cosmic rays under distributed reacceleration
[OG-8.3-3] 23 p4021 N85-34922

Propagation of cosmic rays and new evidence for distributed acceleration
[OG-8.3-5] 23 p4022 N85-34924

Exact solutions for sporadic acceleration of cosmic rays
[OG-8.3-7] 23 p4022 N85-34925

Relativistic transport theory for cosmic-rays
[OG-8.3-8] 23 p4022 N85-34926

The design of an experiment to detect low energy antiprotons
[OG-9.1-1] 23 p4022 N85-34928

An experiment to measure the energy spectrum of cosmic ray antiprotons from 100 to 1000 MeV
[OG-9.1-3] 23 p4022 N85-34929

High resolution Cherenkov detectors for cosmic ray isotope experiment
[OG-9.1-4] 23 p4023 N85-34930

A high resolution gas Cerenkov detector for the superconducting magnet facility
[OG-9.1-6] 23 p4023 N85-34932

Bevalac calibration of the SOFIE range and hodoscope detectors
[OG-9.1-7] 23 p4023 N85-34933

The development of a high energy cosmic ray detector for Spacelab-2
[OG-9.1-8] 23 p4023 N85-34934

Mass resolution optimization in a large isotopic composition experiment
[OG-9.1-9] 23 p4023 N85-34935

The heavy ions in space experiment
[OG-9.1-10] 23 p4023 N85-34936

Cherenkov-dE/dx-range measurements on cosmic ray iron group nuclei
[OG-9.1-12] 23 p4024 N85-34937

The response of ionization chambers to relativistic heavy nuclei
[OG-9.1-13] 23 p4024 N85-34939

A balloon-borne imaging gamma-ray telescope
[OG-9.2-2] 23 p4024 N85-34941

A coded aperture imaging system optimized for hard X-ray and gamma ray astronomy
[OG-9.2-3] 23 p4024 N85-34942

The final COS-B database: In-flight calibration of instrumental parameters
[OG-9.3-9] 23 p4026 N85-34984

Nintenth International Cosmic Ray Conference. SH sessions, volume 5
[NASA-CP-2376-VOL-5] 23 p4031 N85-34991

Isotropic intensity waves and features of their occurrence
[SH-4.3-8] 23 p4032 N85-34999

Cosmic ray sidereal diurnal variation of galactic origin observed by neutron monitors
[SH-4.4-2] 23 p4033 N85-35000

Sidereal anisotropies in the median rigidity range 60-600GV in 1978-1983
[SH-4.4-3] 23 p4033 N85-35001

Sidereal variations deep underground in Tasmania
[SH-4.4-4] 23 p4033 N85-35002

The effect of the interplanetary magnetic field on sidereal variations observed at medium depth underground detectors
[SH-4.4-5] 23 p4033 N85-35003

Corrected sidereal anisotropy for underground muons
[SH-4.4-7] 23 p4033 N85-35005

A study of periodicities and recurrences in solar activity and cosmic ray modulation
[SH-4.4-14] 23 p4034 N85-35010

Cosmic ray biannual variation
[SH-4.4-15] 23 p4034 N85-35011

Cosmic ray power spectral variations. 3: Solar rotation periodicities
[SH-4.4-16] 23 p4034 N85-35012

Variations of the cosmic ray general component in Antarctica
[SH-4.4-17] 23 p4035 N85-35013

The difference in the energy spectra of galactic cosmic rays at the minima of the 19th and 20th solar activity cycles
[SH-4.4-18] 23 p4035 N85-35014

Cosmic ray variations with the period close to 27 days and their connection with solar activity longitudinal distribution
[SH-4.4-19] 23 p4035 N85-35015

Long-term modulation of galactic cosmic rays in high-energy region
[SH-4.4-22] 23 p4035 N85-35018

The first three harmonics of solar daily variation caused by the diffusive propagation of galactic cosmic rays through the heliosphere
[SH-4.5-1] 23 p4035 N85-35019

Formulation of cosmic-ray solar daily variation and its seasonal variation, produced from generalized stationary anisotropy of solar origin
[SH-4.5-2] 23 p4036 N85-35020

Diurnal effect in cosmic rays at middle latitudes according to stratospheric measurements
[SH-4.5-8] 23 p4036 N85-35026

Comparative study of the phase of diurnal anisotropy on quiet and disturbed days on a long term basis up to recent period
[SH-4.5-9] 23 p4037 N85-35027

Study of spectral exponent on quiet and disturbed days
[SH-4.5-10] 23 p4037 N85-35028

Diurnal variation of galactic cosmic ray intensity on quiet days
[SH-4.5-11] 23 p4037 N85-35029

Diurnal variations from muon data at Takeyama underground station
[SH-4.5-13] 23 p4037 N85-35030

Long term changes in cosmic ray diurnal variations observed by ion chambers in Hong Kong and Japan
[SH-4.5-14] 23 p4037 N85-35031

The modulation features of the long-period cosmic ray variations in connection with the sign change of the general magnetic field of the Sun
[SH-4.5-15] 23 p4037 N85-35032

The cosmic ray differential diurnal variation dependences on the zenith angle and the geomagnetic disturbance
[SH-4.5-16] 23 p4038 N85-35033

Cosmic ray density gradient and its dependence on the north-south asymmetry in solar activity
[SH-4.5-17] 23 p4038 N85-35034

Anomalous increase of solar anisotropy above 150GV in 1981-1983
[SH-4.5-18] 23 p4038 N85-35035

Diagnostic of electromagnetic conditions in space using cosmic rays
[SH-4.5-19] 23 p4038 N85-35036

Change of cosmic ray anisotropy with solar activity
[SH-4.5-20] 23 p4038 N85-35037

Magnetic fluctuation and cosmic ray diurnal variations
[SH-4.5-21] 23 p4038 N85-35038

Changes in the energy spectrum of anomalous oxygen and helium during 1977-1985
[SH-4.6-1] 23 p4039 N85-35039

Solar cycle variations of the anaomalous cosmic ray component
[SH-4.6-2] 23 p4039 N85-35040

Radial and latitudinal gradients of anomalous oxygen during 1977 - 1985
[SH-4.6-4] 23 p4039 N85-35042

Observation of pick-up ions in the solar wind: Evidence for the source of the anomalous cosmic ray component?
[SH-4.6-5] 23 p4039 N85-35043

On the anomalous component
[SH-4.6-6] 23 p4039 N85-35044

Possible origin of the anomalous component of cosmic rays
[SH-4.6-7] 23 p4039 N85-35045

The cosmic ray interplanetary radial gradient from 1972 - 1985
[SH-4.7-1] 23 p4040 N85-35046

The large scale dynamics of the outer heliosphere and the long-term modulation of galactic cosmic rays
[SH-4.7-3] 23 p4040 N85-35048

Solar modulation and interplanetary gradients of the galactic electrons flux, 1977 - 1984
[SH-4.7-4] 23 p4040 N85-35049

Galactic cosmic ray radial gradients and the anomalous He component near maximum solar modulation and to radii beyond 34 AU from the Sun
[SH-4.7-5] 23 p4040 N85-35050

Voyager 1 and 2 measurements of radial and latitudinal cosmic ray gradients during 1981 - 1984
[SH-4.7-6] 23 p4041 N85-35051

The recovery of the cosmic ray flux from maximum solar modulation at IMP-8 (1 AU) and at Pioneer (R 30 AU)
[SH-4.7-7] 23 p4041 N85-35052

The large-scale modulation of cosmic rays in mid-1982: Its dependence on heliospheric longitude and radius
[SH-4.7-9] 23 p4041 N85-35053

Nonstationary modulation of galactic cosmic rays in a nonlinear model
[SH-4.7-10] 23 p4041 N85-35054

Dimensions of the solar wind cavity and of the region of interplanetary cosmic ray modulation
[SH-4.7-11] 23 p4041 N85-35055

Drift and Forbush decreases
[SH-5.1-2] 23 p4041 N85-35056

Anomalous short-term increases in the galactic cosmic ray intensity: Are they related to the interplanetary magnetic cloud-like structures?
[SH-5.1-3] 23 p4041 N85-35057

The flare origin of Forbush decreases not associated with solar flares on the visible hemisphere of the Sun
[SH-5.1-4] 23 p4041 N85-35058

Longitudinal dependence of the interplanetary perturbation produced by energetic type 4 solar flares and of the associated cosmic ray modulation
[SH-5.1-5] 23 p4042 N85-35059

Rigidity spectrum of Forbush decrease
[SH-5.1-6] 23 p4042 N85-35060

Spectral analysis of the Forbush decrease of 13 July 1982
[SH-5.1-7] 23 p4042 N85-35061

Transient cosmic ray increase associated with a geomagnetic storm
[SH-5.1-8] 23 p4042 N85-35062

Galactic cosmic ray currents and magnetic field irregularity degree in high-speed solar wind streams
[SH-5.1-9] 23 p4042 N85-35063

Study of dominating parameters of high speed solar plasma streams in relation to cosmic ray and geomagnetic storms
[SH-5.1-11] 23 p4042 N85-35064

Influence of magnetic clouds on cosmic ray intensity variations
[SH-5.1-12] 23 p4042 N85-35065

The solar wind effect on cosmic rays and solar activity
[SH-5.1-13] 23 p4043 N85-35066

A relation between the short time variations of cosmic rays and geomagnetic field change
[SH-5.1-14] 23 p4043 N85-35067

Anomalous low level of cosmic ray intensity decreases observed during 1980
[SH-5.1-15] 23 p4043 N85-35068

Observations of cosmic-ray modulations in the fall, 1984
[SH-5.1-16] 23 p4043 N85-35069

Study of cosmic ray scintillations from 5-minute data of the scintillations telescope Izmran and world-wide network stations
[SH-5.1-18] 23 p4043 N85-35071

The theoretical and experimental investigation of cosmic ray Forbush-effects
[SH-5.1-20] 23 p4044 N85-35072

Peculiarities of Galactic Cosmic Ray (GCR) anisotropy variation in connection with the recurrent and sporadic Forbush effects
[SH-5.1-21] 23 p4044 N85-35073

Cosmic ray modulation by high-speed solar wind fluxes
[SH-5.1-22] 23 p4044 N85-35074

Solar activity beyond the disk and variations of the cosmic ray gradient
[SH-5.1-23] 23 p4044 N85-35075

Coupling functions for lead and lead-free neutron monitors from the latitudinal measurements performed in 1982 in the research station Academician Kurchatov
[SH-6.1-1] 23 p4044 N85-35076

On the solar cycle variation in the barometer coefficients of high latitude neutron monitors
[SH-6.1-2] 23 p4044 N85-35077

Altitude variations of cosmic-ray soft and hard components observed by airborne detectors
[SH-6.1-5] 23 p4045 N85-35079

Additional flux of particles and albedo-electrons in upper atmosphere
[SH-6.1-6] 23 p4045 N85-35080

Observation of energy spectrum of electron albedo in low latitude region at Hyderabad, India
[SH-6.1-7] 23 p4045 N85-35081

Proton albedo spectrum observation in low latitude region at Hyderabad, India
[SH-6.1-8] 23 p4045 N85-35082

The influence of quiet asymmetric magnetosphere on the cutoff rigidities of the main cone
[SH-6.1-10] 23 p4045 N85-35083

Re-evaluation of cosmic ray cutoff terminology
[SH-6.1-11] 23 p4045 N85-35084

The use of the McIlwain L-parameter to estimate cosmic ray vertical cutoff rigidities for different epochs of the geomagnetic field
[SH-6.1-12] 23 p4045 N85-35085

Estimating the change in asymptotic direction due to secular changes in the geomagnetic field
[SH-6.1-13] 23 p4045 N85-35086

Short perturbations of cosmic ray intensity and electric field in atmosphere
[SH-6.1-18] 23 p4046 N85-35090

Long-period cosmic ray variations and their altitude dependence
[SH-6.1-19] 23 p4046 N85-35091

Diurnal variations of cosmic ray geomagnetic cut-off threshold rigidities
[SH-6.1-21] 23 p4046 N85-35092

The influence of the Earth's magnetosphere on the high-energy solar protons
[SH-6.1-22] 23 p4046 N85-35093

Cosmic rays 10Be biennal data and their relationship to aurorae and sunspots
[SH-7.1-1] 23 p4047 N85-35094

Solar modulation of cosmic ray intensity and solar flare events inferred from (14)C contents in dated tree rings
[SH-7.1-2] 23 p4047 N85-35095

Cosmic ray secular variations in terrestrial records and aurorae
[SH-7.1-3] 23 p4047 N85-35096

When did the average cosmic ray flux increase?
[SH-7.1-4] 23 p4047 N85-35097

Cosmic-ray exposure records and origins of meteorites
[SH-7.1-7] 23 p4047 N85-35099

Accelerator experiments on the contribution of secondary particles to the production of cosmogenic nuclides in meteorites
[SH-7.1-8] 23 p4048 N85-35100

Depth and size effects on cosmogenic nuclide production in meteorites
[SH-7.1-9] 23 p4048 N85-35101

Spallogenic origin of nuclei in meteorites
[SH-7.1-10] 23 p4048 N85-35102

Clusters and cycles in the cosmic ray age distributions of meteorites
[SH-7.1-11] 23 p4048 N85-35103

High precise measurements of cosmogenic radiocarbon abundance by complex of scintillation equipments
[SH-7.1-14] 23 p4048 N85-35105

Radiocarbon content in the annual tree rings during last 150 years and time variation of cosmic rays
[SH-7.1-15] 23 p4048 N85-35106

Cosmogenic Mn-53 in meteorites
[SH-7.1-17] 23 p4049 N85-35107

Solar neutrinos, solar flares, solar activity cycle and the proton decay
[SH-8.1-8] 23 p4049 N85-35113

Neutrino production from the solar atmosphere
[SH-8.1-9] 23 p4050 N85-35114

Three dimensional calculation of flux of low energy atmospheric neutrinos
[SH-8.1-11] 23 p4050 N85-35116

Detector calibration of the Indian cosmic ray experiment (IONS) in Space-Shuttle Spacelab-13
[SH-9.1-2] 23 p4050 N85-35117

Biophysical research in space — radiation effects
24 p4130 N85-35603

Gamma-ray production cross sections for alpha-particle induced reactions on F-19 and Na-23
[DE85-012603] 24 p4150 N85-35732

Nineteenth International Cosmic Ray Conference. HE Sessions, volume 6
[NASA-CP-2376-VOL-6] 24 p4170 N85-35848

Measurement of interaction cross section of cosmic ray Fe nuclei (E4 GeV/N) with Al target
[HE-1.1-7] 24 p4170 N85-35855

QCD-motivated description of very high energy particle interactions
[HE-1.2-2] 24 p4171 N85-35861

Nucleon-nucleus interactions from JACEE
24 p4173 N85-35869

General consequences of the violated Feynman scaling 24 p4173 N85-35872

Propagation of cosmic rays through the atmosphere in the quark-gluon strings model 24 p4173 N85-35873

Determination of primary energy in nucleus-nucleus collisions and the high P(sub)T tail of alpha-particles
24 p4173 N85-35875

SU(2) x U(1) vacuum and the Centauro events
24 p4175 N85-35885

Ringlike inelastic events in cosmic rays and accelerators 24 p4175 N85-35887

Heavy nucleus collisions between 20 and 60 GeV/nucleon
[HE-1.4-2] 24 p4175 N85-35890

Characteristics of central collision events in Fe-nucleus interactions for 20 - 60 GeV/nucleon
[HE-1.4-3] 24 p4176 N85-35891

Nucleus-nucleus interaction above several hundred GeV/n
[HE-1.4-4] 24 p4176 N85-35892

Excessive production of electron pairs by soft photons in low multiplicity ion interactions
[HE-1.4-6] 24 p4176 N85-35894

Forward particle production in inelastic Ne-22 inteVractions in emulsion at 4.1 A Ge/c
[HE-1.4-7] 24 p4176 N85-35895

On the mechanism of anomalous nucleus-nucleus interactions at energies above 1 TeV/nucleon
[HE-1.4-8] 24 p4177 N85-35896

Meson multiplicity in nucleus-nucleus collisions above 4 GeV/amu
[HE-1.4-10] 24 p4177 N85-35897

Inclusive angular distribution of alpha and Li fragments produced in the Fe-C and Fe-Pb collisions at 1.88 GeV/u
[HE-1.4-11] 24 p4177 N85-35898

The effect of the relative nuclear size on the nucleus-nucleus interactions
[HE-1.4-13] 24 p4177 N85-35900

Intensities of high-energy cosmic rays at Mount Kanbala
[HE-3.1-2] 24 p4177 N85-35902

On the characteristics of emulsion chamber family events produced in low heights
[HE-3.1-6] 24 p4178 N85-35904

Hadron intensity and energy spectrum at 4380 m above level
[HE-3.1-7] 24 p4178 N85-35905

The nucleon intensity in the atmosphere and the Pt distribution
[HE-3.1-9] 24 p4178 N85-35907

Conn ction between variations of the atmosphere temperature profile and variations of the meson component intensity
[HE-3.1-12] 24 p4178 N85-35910

Search for anomalous C-jets in Chacaltaya emulsion chamber experiment
[HE-3.2-5] 24 p4179 N85-35913

Scaling violation in hadron-nucleus interaction
[HE-3.2-8] 24 p4179 N85-35916

Few-particles generation channels in inelastic hadron-nuclear interactions at energy approximately equals 400 GeV
[HE-3.2-9] 24 p4179 N85-35917

A cosmic ray super high multicore family event. 1: Experiment and general features
[HE-3.4-1] 24 p4181 N85-35930

A cosmic ray super high energy multicore family event. 2: Structure and fragmentation characteristics of the jets
[HE-3.4-2] 24 p4181 N85-35931

Observation of super high energy big family with large scale Fe emulsion chambers
[HE-3.4-3] 24 p4182 N85-35932

A halo event created at 200 m above the Chacaltaya emulsion chamber
[HE-3.4-5] 24 p4182 N85-35933

A binocular-type atmospheric interaction generating sequential exotic features
[HE-3.4-6] 24 p4182 N85-35934

Gamma-hadron families and scaling violation
[HE-3.4-7] 24 p4182 N85-35935

Super-family P2 C-96-125 observed by Japan-URSS Joint Emulsion Chamber Experiment
[HE-3.4-8] 24 p4182 N85-35936

On the halo events observed by Mount Fuji and Mount Kanbala Emulsion Chamber Experiments
[HE-3.4-9] 24 p4182 N85-35937

Experiment Pamir-2. Fianit: A giant super-family with halo (Epsilon sub 0 at approximately 10(17) eV)
[HE-3.4-10] 24 p4182 N85-35938

Experiment Pamir-4. Analysis of superfamily with halo of electromagnetic nature detected in deep XEC
[HE-3.4-11] 24 p4183 N85-35939

Particle interactions at energies over 1000 TeV inferred from gamma-families observed at Mount Fuji
[HE-3.5-1] 24 p4183 N85-35940

A search for mini-clusters in Japan-USSR Joint Experiment at Pamir
[HE-3.5-2] 24 p4183 N85-35941

Mini-clusters
[HE-3.5-3] 24 p4183 N85-35942

Giant mini-clusters as possible origin of halo phenomena observed in super-families
[HE-3.5-4] 24 p4183 N85-35943

Structure of super-families
[HE-3.5-7] 24 p4183 N85-35944

Extremely high energy hadron and gamma-ray families(3). Core structure of the halo of superfamily
[HE-3.5-8] 24 p4183 N85-35945

Numerical analysis of electromagnetic cascades in emulsion chambers
[HE-3.5-9] 24 p4184 N85-35946

An experimental study of correlations in the development of the electron-photon cascades
[HE-3.5-10] 24 p4184 N85-35947

The electromagnetic component of albedo from superhigh energy cascades in dense media
[HE-3.5-11] 24 p4184 N85-35948

Integral functions of electron lateral distribution and their fluctuations in electron-photon cascades
[HE-3.5-12] 24 p4184 N85-35949

Nineteenth International Cosmic Ray Conference. HE Sessions, volume 7
[NASA-CP-2376-VOL-7] 24 p4186 N85-35968

Measurement of the local density spectrum
24 p4189 N85-35984

An underground cosmic ray muon telescope for observation of cosmic ray anisotropy
24 p4196 N85-36037

Investigation of cosmic rays in very short time scales
[HE-4.6-7] 24 p4197 N85-36044

Nineteenth International Cosmic Ray Conference. HE sessions, volume 8
[NASA-CP-2376-VOL-8] 24 p4200 N85-36066

Preliminary results on underground muon bundles observed in the Frejus proton-decay detector
[HE-5.1-1] 24 p4200 N85-36067

The spectrum of cosmic ray muons obtained with 100-ton scintillation detector underground and the analysis of recent experimental data
[HE-5.1-6] 24 p4201 N85-36071

A new world survey expression for cosmic ray vertical intensity vs. depth in standard rock
[HE-5.1-10] 24 p4201 N85-36073

On muon energy spectrum in muon groups underground
[HE-5.1-14] 24 p4201 N85-36076

Energy spectrum of cascades generated by muons in Baksan underground scintillation telescope
[HE-5.1-15] 24 p4202 N85-36077

Underwater measurements of muon intensity
[HE-5.1-16] 24 p4202 N85-36078

The Nagoya cosmic-ray muon spectrometer 3, part 1: Preliminary observations
[HE-5.2-2] 24 p4202 N85-36080

The Nagoya cosmic-ray muon spectrometer 3, part 3: Automatic film scanning equipment
[HE-5.2-4] 24 p4202 N85-36082

The Nagoya cosmic-ray muon spectrometer 3, part 4: Track reconstruction method
[HE-5.2-5] 24 p4202 N85-36083

Background light measurements at the DUMAND site
[HE-5.2-7] 24 p4203 N85-36084

Measurements of light background at large depth in the ocean
[HE-5.2-8] 24 p4203 N85-36085

Hybrid TLC-pair meter for the Sphinx Project
[HE-5.2-10] 24 p4203 N85-36086

Proportional drift tubes for large area muon detectors
[HE-5.2-11] 24 p4203 N85-36087

Analytical calculation of muon intensities under deep sea-water
[HE-5.2-16] 24 p4204 N85-36092

The spectrum of neutrons at 60 hg m(-2)
[HE-5.2-20] 24 p4204 N85-36096

Limits on deeply penetrating particles in the 10(17) eV cosmic ray flux
[HE-5.3-1] 24 p4205 N85-36098

Results of low energy background measurements with the Liquid Scintillation Detector (LSD) of the Mont Blanc Laboratory
[HE-5.3-5] 24 p4205 N85-36099

Geophysical searches for three-neutrino oscillations
[HE-5.3-9] 24 p4205 N85-36103

Measurement of neutrino oscillations in MACRO experiment
[HE-5.3-10] 24 p4206 N85-36104

Energy spectra of high energy atmospheric neutrinos
[HE-5.3-14] 24 p4206 N85-36108

A search for cosmic sources of high energy neutrinos with small underground detectors
[HE-5.3-16] 24 p4206 N85-36110

Neutrino astronomy and the atmospheric background
[HE-5.3-17] 24 p4207 N85-36111

High-energy neutrinos from a lunar observatory
[HE-5.3-21] 24 p4207 N85-36112

Angular distribution of muons produced by cosmic ray neutrinos in rock
[HE-5.3-24] 24 p4207 N85-36115

Underground measurements on secondary cosmic rays
[HE-5.4-1] 24 p4207 N85-36116

Atmospheric muons and neutrinos, and the neutrino-induced muon flux underground
[HE-5.4-7] 24 p4207 N85-36118

Anomalies in cosmic rays: New particles versus charm?
[HE-5.4-9] 24 p4208 N85-36120

Results of investigation of muon fluxes of superhigh energy cosmic rays with X-ray emulsion chambers
[HE-5.4-16] 24 p4208 N85-36126

Search for magnetic monopoles using proportional counters filled with helium gas
[HE-6.1-1] 24 p4209 N85-36127

Magnetic monopole search by 130 m(2)sr He gas proportional counter
[HE-6.1-2] 24 p4209 N85-36128

Results of a search for monopoles and tachyons in horizontal cosmic ray flux
[HE-6.1-3] 24 p4209 N85-36129

Monopole, astrophysics and cosmic ray observatory at Gran Sasso
[HE-6.1-4] 24 p4209 N85-3613

COSMIC X RAYS

The HEAO-1 diffuse component spectrum from 15 to above 500 keV — X and gamma rays
08 p1240 N85-17820

The origin of the X-ray background
08 p1243 N85-17841

X-ray emission from Centaurus A
[DE85-002030] 09 p1417 N85-18843

High resolution hard X-ray spectra of solar and cosmic sources 14 p2455 N85-25183

Long-term observations of Cyg X-3 with Vela 5B
[DE85-005556] 15 p2686 N85-26586

Observation of the Crab nebula in the hard X-ray
[MPE-186] 17 p3053 N85-28897

Cosmic X-ray physics
[NASA-CR-175908] 17 p3055 N85-28910

Atmospheric X-rays at 11 deg S geomagnetic latitude
[INPE-3539-PRE/755] 19 p3386 N85-31004

Balloon observations of hard X rays from NGC 4151 and an X-ray transient source
[OG-2.7-6] 22 p3871 N85-33979

CEN A observation at MeV-energies
[OG-2.7-7] 22 p3871 N85-33980

COSMOCHEMISTRY

High pressure cosmochemistry applied to major planetary interiors: Experimental studies
[NASA-CR-174032] 02 p0302 N85-11958

Decaying particles do not heat up the Universe
[DE85-002191] 11 p1763 N85-21081

Implications of convection in the Moon and the terrestrial planets 13 p2183 N85-23548

High pressure cosmochemistry of major planetary interiors: Laboratory studies of the water-rich region of the system ammonia-water 13 p2183 N85-23549

High pressure cosmochemistry applied to major planetary interiors: Experimental studies
[NASA-CR-175715] 15 p2679 N85-26544

The cosmic ray composition as viewed from the chemical abundances of the solar system
[OG-7.1-8] 23 p4013 N85-34989

COSMOGONY

U COSMOLOGY

COSMOLOGY

NT BIG BANG COSMOLOGY
NT HUBBLE DIAGRAM

The origin and evolution of Uranus and Neptune
02 p0296 N85-11928

Future theoretical needs in studies of star formation
03 p0444 N85-12829

Space research and the new approach to the mechanics of fluid media in cosmos
[TRITA-EPP-84-04] 03 p0447 N85-12844

Toward unification of elementary particle physics and cosmology in 10-dimensions
[DE84-013950] 05 p0727 N85-14674

On collective effects in the rotation of stars in clusters and associations 05 p0737 N85-14739

On the nature of the baryon asymmetry
[NASA-TM-86156] 05 p0746 N85-14784

Local Interstellar Medium. International Astronomical Union Colloquium No. 81
[NASA-CP-2345] 06 p0872 N85-15539

Supersymmetric inflationary cosmology
[DE85-001331] 06 p0881 N85-15586

Supersymmetric inflationary cosmology
[DE85-001332] 09 p1415 N85-18929

Axions in astrophysics and cosmology
[DE85-002720] 11 p1763 N85-21084

Recent heavy particle decay in a matter dominated universe
[NASA-CR-175501] 11 p1764 N85-21085

Space research and the new approach to the mechanics of fluid media in cosmos 12 p1953 N85-22271

University of Cambridge Institute of Astronomy report of activities 13 p2170 N85-23484

Measurement of the large-scale anisotropy of the cosmic background radiation at 3 MM 13 p2206 N85-23680

Formation of the solar system
15 p2677 N85-26532

Superheavy magnetic monopoles and the standard cosmology
[DE85-003922] 15 p2686 N85-26587

Dark matter, galaxies, and large scale structure in the universe
[DE85-006053] 16 p2882 N85-27786

Inflation from extra dimensions
[DE85-007834] 16 p2883 N85-27787

Formation of galaxies
[DE85-009537] 18 p3202 N85-29863

Cosmology in theories with extra dimensions
18 p3202 N85-29864

Did bosonic sneutrino stars ever exist
[PREPRINT-421] 18 p3202 N85-29867

Primordial inflation and supergravity
[DE85-009538] 19 p3383 N85-30989

The dimensional reduction transition
[DE85-003948] 19 p3383 N85-30990

Activities report of the Institute of Astronomy
20 p3545 N85-32059

Activities report of the Department of Astrophysics
20 p3546 N85-32064

Cosmogenic-nuclide production by primary cosmic-ray protons
[SH-7.1-6] 23 p4047 N85-35096

COSMONAUTS

Vitamin metabolism in cosmonauts following short-term flights 01 p0091 N85-10615

Compensatory and adaptive regional hemodynamic reactions to weightlessness during long-term spaceflights 01 p0091 N85-10616

Cosmonauts complete 4th month aboard Salyut-7
02 p0157 N85-11065

Orbit of Salyut-7 station boosted
02 p0157 N85-11067

Commentary on cosmonauts geological mapping, photography 02 p0158 N85-11069

Tass reports launch of Soyuz T-12
02 p0158 N85-11070

25th anniversary of the Gagarin Cosmonaut Training Center
[NASA-TM-77644] 09 p1286 N85-18076

Feoktistov recalls period leading to Gagarin spaceflight 13 p1965 N85-22451

Feoktistov says manned lunar, Mars flights lack justification 13 p1965 N85-22452

Cosmonaut Savitskaya says many women in cosmonaut training 16 p2717 N85-26774

Cosmonauts' postural reactions after long-term missions aboard Salyut-6 orbital station 19 p3323 N85-30585

USSR report: Space
[JPRS-USP-84-006] 22 p3731 N85-33128

Results and prospects of physiological research during spaceflights 22 p3732 N85-33139

COSMOS SATELLITES

NT COSMOS 1129 SATELLITE
NT INTERCOSMOS SATELLITES

Hemopoiesis in rats submitted to weightlessness
01 p0091 N85-10613

Geopotential harmonics of order 15 and 30, from analysis of the orbit of satellite 1971-10B
[RAE-TR-84006] 02 p0165 N85-11121

Plasmodium of myxomycete as research object in gravitational biology 15 p2483 N85-25327

International conference on COSPAS-SARSAT system
15 p2484 N85-25336

The COSPAS-SARSAT space segment: Present status and evolution 20 p3401 N85-31102

Rescue satellite COSPAS 20 p3401 N85-31103

The 406 MHz ELT/EPIRBs --- Emergency Locator Transmitters/Emergency Position Indicating Radio Beacons (ELT/EPIRB) 20 p3402 N85-31106

Soviet Emergency Locator Transmitter/Emergency Position Indicating Radio Beacon (ELT/EPIRBs) at 121.5 and 406 MHz 20 p3402 N85-31107

Ground segment of COSPAS system
20 p3402 N85-31108

The COSPAS system tests. Technical results
20 p3404 N85-31125

COSPAS-SARSAT demonstration and evaluation phase: COSPAS tests in the USSR and their results
20 p3405 N85-31130

General description of experiment dealing with rat ontogenesis aboard Cosmos-1514 biosatellite
22 p3622 N85-33679

Charge composition and energy spectral of cosmic ray primary particles for energies higher than 1 TeV
[OG-4.1-14] 22 p3677 N85-34020

COSMOS 936 SATELLITE

Results of sanitary-microbiological studies aboard Cosmos-1129 biosatellites 12 p1903 N85-21952

COSMOS 1129 SATELLITE

Results of sanitary-microbiological studies aboard Cosmos-1129 biosatellites 12 p1903 N85-21952

Lipogenesis in rat liver after flight aboard Cosmos-1129 biosatellite 23 p3954 N85-34508

COSPAR (COMMITTEE)

U COMMITTEE ON SPACE RESEARCH

COSPAS

COSPAS-SARSAT satellite orbit predictor, volume 5
[NASA-TM-85015-VOL-5] 14 p2439 N85-25052

United States-Soviet satellite accord: SARSAT/Cospas search-and-rescue program
[GPO-41-113] 20 p3541 N85-32040

COST ANALYSIS

Battery optimization considerations
[DE84-014759] 01 p0044 N85-10288

Standards for commercially emerging technologies: A preliminary cost-benefit assessment for the Optical Digital data disk (OD3) technology for mass data storage applications
[PB84-223593] 01 p0101 N85-10669

Shuffle-exchanges on augmented meshes
[NASA-CR-172476] 02 p0243 N85-11587

Artificial intelligence applications to maintenance
[AD-P003914] 02 p0244 N85-11594

Use and value of a geodetic reference system
[PB84-216167] 03 p0379 N85-12418

A methodology for comparing the variable costs of the continuous and periodic review models
[AD-A146351] 03 p0436 N85-12776

Economic analysis handbook
[AD-A146263] 03 p0441 N85-12805

Full-scale testing, production and cost analysis data for the advanced composite stabilizer for Boeing 737 aircraft. Volume 1: Technical summary
[NASA-CR-3649] 05 p0612 N85-13912

Full-scale testing, production and cost analysis data for the advanced composite stabilizer for Boeing 737 aircraft, volume 2
[NASA-CR-166012] 05 p0613 N85-13915

Integrated technology wing study (oral presentation)
[NASA-CR-169497] 07 p0902 N85-15718

More than you want to know about maximum likelihood estimation
[NASA-TM-85905] 07 p0909 N85-15752

The effect of assumptions about cost element probability distributions on operating and support cost risk analysis
[AD-A147553] 07 p1036 N85-16576

Evaluation of the effectiveness of the weighted guidelines to induce contractor's investment in cost reducing facilities equipment
[AD-A147586] 07 p1053 N85-16681

On estimating the cost growth of weapon systems
[AD-A147297] 08 p1230 N85-17749

Assessment of environmental costs at ordnance activities
[AD-P004140] 09 p1347 N85-18476

Electrocatalysis research
[NASA-CR-174352] 10 p1437 N85-19054

Interactive Graphics Simulator: Design, development and effectiveness/cost evaluation
[AD-A149417] 10 p1540 N85-19712

Space Transportatioin System (STS) propellant scavenging system study. Volume 3: Cost and work breakdown structure-dictionary
[NASA-CR-171850-VOL-3] 11 p1590 N85-20002

Impacts of robotic and flexible manufacturing technologies on manufacturing costs and employment
[AD-A150080] 12 p1860 N85-21668

An analysis of a dynamic project cost problem
[CSIR-TWISK-336] 13 p2149 N85-23341

Sensitivities of projected 1980 photovoltaic system costs to major system cost drivers
[NASA-CR-175669] 14 p2349 N85-24519

Investigations carried out under the Director's Discretionary Fund
[NASA-CR-175676] 14 p2432 N85-24999

Minimal cost flow in processing networks: A primal approach
[CWI-TRACT-4] 14 p2432 N85-25001

Space station propulsion: The advanced development program at Lewis
[NASA-TM-86999] 15 p2494 N85-25386

Pavement-marking materials: New York's experience
[PB85-153294] 15 p2523 N85-25558

An application of the Rayleigh distribution to contract cost data
[AD-A151551] 15 p2664 N85-26441

Combinatorial performance/cost analysis of an autonomous navigation system for aircraft
16 p2695 N85-26640

Design-To-Cost (DTC) methodology to achieve affordable avionics 16 p2696 N85-26645

Cost prediction model for various payloads and instruments for the Space Shuttle Orbiter
[NASA-CR-175781] 16 p2729 N85-26842

Model reduction techniques applied to the control of large space structures
[AD-A151784] 16 p2731 N85-26857

Manufacturing cost analysis of a parabolic dish concentrator (General Electric design) for solar thermal electric power systems in selected production volumes
[NASA-CR-175772] 16 p2818 N85-27360

Logical design of a decision support system to forecast technology, prices and costs for the national communications system
[AD-A152330] 17 p2948 N85-28198

Space insurance firms view shuttle, Ariane reliability
18 p3066 N85-29090

Conceptual design of a fixed-pitch wind turbine generator system rated at 400 kilowatts
[NASA-CR-174677] 18 p3127 N85-29363

Plastic heliostat enclosure analysis
[DE85-009112] 18 p3130 N85-29387

Solar Thermal Research Program
[DE85-000514] 18 p3131 N85-29388

10 MWe Solar Thermal Central Receiver Pilot Plant total capitol costs
[DE85-009113] 18 p3131 N85-29390

KrF laser cost/performance model for ICF commercial applications
[DE85-009589] 18 p3182 N85-29728

Megajoule-class single-pulse KrF laser test facility as a logical step toward inertial fusion commercialization
[DE85-009590] 18 p3191 N85-29794

Cost savings from multiyear contracting
[AD-A153564] 18 p3197 N85-29834

Overhead management guide for aerospace procurements
[AD-A153626] 18 p3198 N85-29835

Advanced evacuated tube collectors
[DE85-010271] 19 p3274 N85-30302

Steady-state spheromak reactor studies
[DE85-009585] 19 p3372 N85-30916

Test and Evaluation Master Plan (TEMP) for the Navy Occupational Health Information Management System (NOHIMS). Phase 1: Appendix A through appendix U
[AD-A154179] 19 p3380 N85-30967

Cost and schedule implications of multinational coproduction
[AD-A154358] 19 p3380 N85-30969

An overview of latest model reduction and control methods of large flexible space structures
20 p3414 N85-31191

Hidden costs of robotized production systems revealed 20 p3438 N85-31332

Pricing options for the space shuttle. Special study
21 p3559 N85-32136

High-efficiency crystalline silicon technology development 21 p3607 N85-32395

Flat-plate module efficiency versus cost tradeoffs
21 p3607 N85-32398

Los Alamos optical materials reliability, maintainability, and exposure testing program
[DE85-011894] 21 p3613 N85-32456

Tritium technology review
[DE85-010504] 21 p3703 N85-33006

Feasibility of applications of Competition Decision Assist Package (CDAP) to spare parts
[AD-A154716] 21 p3712 N85-33036

The Human Resource Management Information Network (HRMIN): A cost comparison in accordance with Office of Management and Budget (OMB) Circular no. A-76, 5 April 1979
[AD-A154583] 21 p3713 N85-33039

Spacecraft (Mobile Satellite) configuration design study
[NASA-CR-176153] 23 p3899 N85-34152

Energy Efficient Engine Program technology benefit/cost study, volume 1
[NASA-CR-174766-VOL-1] 24 p4066 N85-35197

Energy Efficient Engine Program technology benefit/cost study, volume 2
[NASA-CR-174766-VOL-2] 24 p4066 N85-35198

Assessment of metal heating technologies for ferrous forging: A pilot study of the form value of natural gas
[PB85-204394] 24 p4084 N85-35314

Investment justification of robotic technology in aerospace manufacturing. User's manual
[AD-A156193] 24 p4099 N85-35410

DoD Value Engineering conference report. Value Engineering (VE): A tool that benefits line management. Part 3, Workshop A: VE in the program office
[AD-A156069] 24 p4163 N85-35812

DoD Value Engineering conference report. Value Engineering (VE): A tool that benefits line management. Part 5, Workshop C: VEP/VECP administration, negotiation, and implementation
[AD-A156071] 24 p4163 N85-35814

DoD Value Engineering conference report. Value Engineering (VE): A tool that benefits line management. Part 6, Workshop D: VE training-orientation
[AD-A156072] 24 p4164 N85-35815

COST EFFECTIVENESS

Increased joint avionics standardization could result in major economies and operational benefits
[AD-A145730] 02 p0139 N85-10945

Atmospheric and pressurized low speed wind tunnel performance and cost comparisons
[ARL/AERO-R-160] 02 p0149 N85-11008

Economic evaluation of space survey materials use in land improvement engineering field work
02 p0165 N85-11115

Modular photovoltaic array field
[SAND-83-7028] 02 p0222 N85-11454

Benefit value to the Air Force of the GIDEP (Government Industry Data Exchange Program) alert
[AD-A145470] 02 p0292 N85-11897

Continuing issues (FY 1983) concerning military use of the space transportation system
[AD-A146091] 03 p0323 N85-12080

The human role in space. Volume 3: Generalizations on human roles in space
[NASA-CR-171225] 04 p0546 N85-13475

Toward an improved FIPS cost-benefit methodology. Phase 2: Descriptive models, general purpose application software development and maintenance
[PB84-226943] 06 p0870 N85-15527

Integrated technology wing study (oral presentation)
[NASA-CR-169497] 07 p0902 N85-15718

Europeans active in magnetic bearing industry
08 p1141 N85-17195

Low cost training aids and devices
09 p1277 N85-18025

A validated methodology for determination of laboratory instrument computer interface efficacy
[AD-A149338] 10 p1487 N85-19391

A low-cost, general purpose image processing system
[INPE-3292-PRE/607] 10 p1537 N85-19690

Department of defense, office of inspector general semiannual report to the Congress, 1 April - 30 September 1984
[AD-A149560] 10 p1567 N85-19879

Polymer intermediates from limonene (follow-up project)
[BMFT-FB-T-84-243] 12 p1814 N85-21380

RAPIDbus: Design of an extensible multiprocessor structure
[AD-A150061] 12 p1912 N85-21998

Comprehensive evaluation of cost effectiveness of solar electric power plants 14 p2265 N85-24036

Pulsed excimer laser processing for cost-effective solar cells
[NASA-CR-175700] 14 p2351 N85-24530

Electricity production from coal through molten-carbonate fuel cells
[TI85-005072] 14 p2351 N85-24534

Artificial intelligence applications to testability
[AD-A150694] 14 p2407 N85-24839

Financial, economic commentary on Airbus, European aviation 15 p2536 N85-25649

Cost Effective and Affordable Guidance and Control Systems
[AGARD-CP-360] 16 p2695 N85-26638

The series 2000: A miniature gas bearing DTG for low cost strapdown guidance and control
16 p2696 N85-26648

A cost-efficient control procedure for the benefit of all airspace users 16 p2697 N85-26651

Simulation: A tool for cost-effective systems design and live test reduction 16 p2698 N85-26657

New stage in robotics development
16 p2762 N85-27045

Paton Institute expert on GDR-USSR welding research
16 p2768 N85-27078

Parametric study of potential early commercial power plants Task 3-A MHD cost analysis
[NASA-CR-175839] 16 p2817 N85-27377

Trends shaping advanced aircrew training capabilities through the 1990s
[AD-A152277] 16 p2843 N85-27530

Some aspects of how to design cost-effective flight control systems
[MBB-LKE-32/S/PUB/143] 16 p2873 N85-27729

Plasma processing of materials
[AD-A152396] 17 p3039 N85-28800

Some Europeans voice opposition to space station participation 18 p3066 N85-28961

Space insurance firms view shuttle, Ariane reliability
18 p3086 N85-29090

Time transfer techniques: Historical overview, current practices and future capabilities
18 p3106 N85-29245

The human role in space (THURIS)
18 p3158 N85-29557

Energy efficient engine component development and integration program
[NASA-CR-172846] 19 p3219 N85-29958

Operational results for the experimental DOE/NASA Mod-OA wind turbine project
[NASA-TM-83517] 19 p3304 N85-30479

EOQ (Economic Order Quantity) range model
[AD-A153709] 19 p3379 N85-30965

Multi-kW solar arrays for Earth orbit applications
[NASA-CR-171536] 20 p3406 N85-31139

Historical perspective of barriers to achieving high-efficiency silicon solar cells
20 p3479 N85-31616

The future of crystalline silicon technology in the US Department of Energy program
21 p3607 N85-32399

Advanced module development overview
21 p3612 N85-32445

The effect of communication-language designs on software specifications
[AD-A155173] 21 p3672 N85-32809

Feasibility of applications of Competition Decision Assist Package (CDAP) to spare parts
[AD-A154716] 21 p3712 N85-33036

The Human Resource Management Information Network (HRMIN): A cost comparison in accordance with Office of Management and Budget (OMB) Circular no. A-76, 5 April 1979
[AD-A154583] 21 p3713 N85-33039

Estimating optimum technical and economic indicators of data transmission systems 22 p3777 N85-33406

A modular docking mechanism for in-orbit assembly and spacecraft servicing 22 p3796 N85-33516

Development of an adjustable buoyancy balloon tracer of atmospheric motion. Phase 1: Systems design and demonstration of feasibility
[PB85-185817] 22 p3817 N85-33648

Cost effective single crystals: The Rolls Royce approach --- gas turbine components
[PNR-90262] 23 p3985 N85-34717

Solar pond technology for Navy applications
[AD-A155877] 24 p4112 N85-35488

Design for MISP: A multiple instruction stream shared pipeline processor
[AD-A156314] 24 p4136 N85-35635

COST ESTIMATES

Microcomputers in Hungary 01 p0115 N85-10786

Atmospheric and pressurized low speed wind tunnel performance and cost comparisons
[ARL/AERO-R-160] 02 p0149 N85-11008

Description of the software acquisition process (SWAP) model
[AD-A145413] 02 p0241 N85-11573

Economic analysis handbook
[AD-A146263] 03 p0441 N85-12805

Parametric estimates of propulsion system maintenance manhours
[AD-A147120] 07 p0894 N85-15662

A buyer's guide to space infrastructure
07 p0914 N85-15784

Performance and cost of energy transport and storage systems for dish applications using reversible chemical reactions
[NASA-CR-174263] 07 p0992 N85-16298

The effect of assumptions about cost element probability distributions on operating and support cost risk analysis
[AD-A147553] 07 p1036 N85-16576

The application of a technology index to aircraft turbine engine cost estimating relationships
[AD-A147701] 08 p1067 N85-16874

An application of discriminant analysis to the selection of software cost estimating models
[AD-A147632] 08 p1204 N85-17580

On estimating the cost growth of weapon systems
[AD-A147297] 08 p1230 N85-17749

An agenda for a study of government science policy
[GPO-40-860] 12 p1949 N85-22245

Feasibility study for an AFGL fiber optic data link at WSMR sounding rocket launch area
[AD-A150852] 14 p2240 N85-23894

Sensitivities of projected 1980 photovoltaic system costs to major system cost drivers
[NASA-CR-175669] 14 p2349 N85-24519

Cost-estimating relationships for tactical combat aircraft
[AD-A151575] 15 p2471 N85-25255

Intermediate term forecasting techniques for management
[AD-A151370] 15 p2637 N85-26262

Cost prediction model for various payloads and instruments for the Space Shuttle Orbiter
[NASA-CR-175781] 16 p2729 N85-26842

Manufacturing cost analysis of a parabolic dish concentrator (General Electric design) for solar thermal electric power systems in selected production volumes
[NASA-CR-175772] 16 p2818 N85-27380

Airport and airway system cost allocation model. Volume 7: User's manual
[AD-A152877] 17 p2906 N85-27917

Structural analysis and cost estimate of an eight-leg space frame as a support structure for horizontal axis wind turbines
[NASA-TM-83470] 19 p3264 N85-30061

Regression diagnostics in practice: Experiences from modelling jet engine costs
[AD-A154199] 19 p3347 N85-30749

Uniform cost-estimation method for biomass production and conversion technologies
[DE85-011714] 19 p3360 N85-30970

Methodology for assessing benefits and costs of government information collection
[DE85-010594] 19 p3361 N85-30975

Wind energy in the north Netherlands region
20 p3485 N85-31661

Pricing options for the space shuttle. Special study
21 p3559 N85-32138

Clarke Stations and mercurian mass-drivers: Energy for large-scale transportation systems
[DE85-009607] 21 p3560 N85-32145

Low-head hydroelectric power demonstration project: City of Gonzales, Texas
[DE85-010403] 22 p3809 N85-33596

Control technology for radioactive emissions to the atmosphere at US Department of Energy facilities: The Los Alamos Meson Physics Facility
[DE85-011402] 22 p3811 N85-33600

Attacking software crisis: A macro approach
[AD-A155846] 24 p4138 N85-35645

Progress report on implementing the recommendations of the White House Science Council's Federal Laboratory Review Panel, volume 1
[PB85-185072] 24 p4164 N85-35819

COST INCENTIVES

DoD Value Engineering conference report. Value Engineering (VE): A tool that benefits line management. Part 3, Workshop A: VE in the program office
[AD-A156069] 24 p4163 N85-35812

COST REDUCTION

Energy efficient engine. Volume 1: Component development and integration program
[NASA-CR-173084] 02 p0146 N85-10992

Energy-saving technological methods of obtaining controlled atmospheres
[BLL-M-35724-(5828.4)] 02 p0171 N85-11145

Logistics support costs for the B-1B aircraft can be reduced
[AD-A145846] 03 p0309 N85-11996

Modern structural materials. Present situation and evolution prospects --- aircraft materials
[SNIAS-842-551-101] 04 p0455 N85-12886

A practical example of reducing life cycle costs and increased availability 08 p1063 N85-16736

Conceptual design of a 10 MW shore-based OTEC plant
[DE84-015808] 10 p1511 N85-19532

MBB uses superplastic forming, diffusion bonding for alloys 11 p1618 N85-20177

Photovoltaic solar components
12 p1878 N85-21782

President's private sector survey on cost control, report on research and development
[PB84-173269] 12 p1951 N85-22253

A low cost approach with larger diameter silicon wafer --- solar cells 13 p2006 N85-22572

MBB cost-reduction plan for Airbus construction described 15 p2532 N85-25616

Reusable software: A concept for cost reduction
16 p2697 N85-28655

A simplified GPS C/A reciever front end with low noise performance 18 p3109 N85-28851

Cost savings from multiyear contracting
[AD-A153584] 18 p3197 N85-29854

Evaluation of radio navigation systems and their configuration with respect to minimum cost
[ESA-TT-847] 20 p3392 N85-31043

High-efficiency cell concepts on low-cost silicon sheets 20 p3479 N85-31621

Design improvements and cost reductions for a 5000 MWh superconducting Magnetic Energy Storage plant
[DE85-010572] 22 p3847 N85-33630

DoD Value Engineering conference report. Value Engineering (VE): A tool that benefits line management. Part 3, Workshop A: VE in the program office
[AD-A156069] 24 p4163 N85-35812

DoD Value Engineering conference report. Value Engineering (VE): A tool that benefits line management. Part 5, Workshop C: VEP/VECP administration, negotiation, and implementation
[AD-A156071] 24 p4163 N85-35814

DoD Value Engineering conference report. Value Engineering (VE): A tool that benefits line management. Part 6, Workshop D: VE training-orientation
[AD-A156072] 24 p4164 N85-35815

DoD Value Engineering conference report. Value Engineering (VE): A tool that benefits line management. Part 7, Workshop E: VE in construction and architect engineer contracts
[AD-A156073] 24 p4164 N85-35816
COSTA RICA
Relationship between forest clearing and biophysical factors in tropical environments: Implications for the design of a forest change monitoring approach --- Costa Rica
[E85-10051] 07 p0983 N85-16247
Ash contents of Costa Rican peat deposits
[DE85-010734] 19 p3301 N85-30462
COSTS
NT AIRCRAFT PRODUCTION COSTS
NT LIFE CYCLE COSTS
NT LOW COST
NT OPERATING COSTS
A methodology for comparing the variable costs of the continuous and periodic review models
[AD-A146351] 03 p0436 N85-12776
Space telescope cost, schedule, and performance review, 1984
[GPO-39-065] 04 p0579 N85-13696
Determining training device requirements in Army aviation systems 05 p0711 N85-14558
Analyses to develop models to project failure rates and repair costs of electronic modules and subassemblies
[AD-A146509] 06 p0816 N85-15180
Synopsis of the OTA Workshop on Cost Containment of Civilian Infrastructure (Civilian Space Station) Elements 07 p0915 N85-15790
An analysis of the effect of process controls on productivity and weapon system costs in DoD procurement
[AD-A147496] 07 p1052 N85-16678
The embedded test (BIT): Impact on the total cost of possession 08 p1063 N85-16734
Transmission scheduling to reduce convex delay costs in packet networks
[AD-A148451] 08 p1153 N85-17278
A numerical analysis of sampling plans based on prior distribution and costs
[AD-A147718] 08 p1210 N85-17616
Cost-plus-percentage-of-costs in government contracts
[AD-A147779] 08 p1228 N85-17735
Assessment of environmental costs at ordnance activities
[AD-P004140] 09 p1347 N85-18476
Historical cost curves for hydrogen masers and cesium beam frequency and timing standards
10 p1465 N85-19245
Electric-Hybrid Vehicle (E-HV) demonstration-test project
[DE85-002370] 10 p1570 N85-19899
Worldwide birdstrike statistics of Lufthansa German Airlines
[AD-P004183] 11 p1579 N85-19945
Inexpensive multipurpose landscaping
11 p1581 N85-19961
Advanced mixed-mode simulation techniques
13 p2062 N85-22883
Status of the U.K. N.D.T. industry today
14 p2316 N85-24309
The energy cost of women walking and running in shoes and boots
[AD-A151022] 14 p2369 N85-24716
Costs, payload of Ariane, US Space Shuttle compared
15 p2530 N85-25601
Jet fuel property changes and their effect on producibility and cost in the U.S., Canada, and Europe
[NASA-CR-174840] 16 p2757 N85-27012
Flying in spite of the weather
[NLR-MP-84021-U] 17 p2885 N85-27847
10 MWe Solar Thermal Central Receiver Pilot Plant total capital costs
[DE85-009113] 18 p3131 N85-29390
Cost savings from multiyear contracting
[AD-A153564] 18 p3197 N85-29834
Overhead management guide for aerospace procurements
[AD-A153626] 18 p3198 N85-29835
Hidden costs of robotized production systems revealed 20 p3438 N85-31332
Nomographs for estimating the levelized cost of energy from flat-plate and concentrator photovoltaic systems
[NASA-CR-176048] 20 p3483 N85-31645
COUETTE FLOW
Couette flow of two fluids between concentric cylinders
[AD-A155627] 24 p4093 N85-35376
COULEES
U CANYONS
COULOMB COLLISIONS
Chaos near the Coulomb Barrier: Nuclear molecules
[DE85-001280] 07 p1041 N85-16608
Plane-wave born collision strengths for electron-ion excitation: Comparison with other theoretical methods
[DE85-002348] 10 p1555 N85-19802
Monte-Carlo treatment of nonlinear collisional effects in charged-particle transport
[DE85-010755] 20 p3521 N85-31897
Collisional relaxation of electron tail distribution
[IPPJ-729] 23 p3974 N85-34635
LPM effect and primary energy estimations
[HE-3.6-4] 24 p4185 N85-35953
Result of Monte-Carlo simulation of electron-photon cascades in lead and layers of lead-scintillator
[HE-3.6-11] 24 p4185 N85-35956
Structure of air shower disc near the core
[HE-4.7-2] 24 p4198 N85-36053
COULOMB POTENTIAL
Memory function for cyclotron resonance of two-dimensional electron systems
[AD-A152632] 17 p3029 N85-28731
Spin distributions in heavy ion fusion at and below the Coulomb barrier
[DE85-007817] 17 p3031 N85-28751
Screening phase transitions in two-dimensional Coulomb gas
[NOTA-INTERNA-830] 18 p3192 N85-29796
K(-) hydrogen bound and continuum states in momentum space
[DE85-010429] 22 p3841 N85-33789
Electron loss process and cross section of multiply charged ions by neutral atoms 23 p3981 N85-34685
Anomalous abundances of solar energetic particles and coronal gas: Coulomb effects and First Ionization Potential (FIP) ordering
[SH-2.1-10] 23 p3999 N85-34791
COULOMETERS
State-of-charge coulometer
[NASA-CASE-NPO-15759-1] 12 p1849 N85-21596
Portable electrochemical cell interrogator
[DE85-005186] 13 p2065 N85-22901
COULOMETRY
Voltammetry and coulometry with immersed thin layer electrodes. Part 1: Model for effects of solution resistivity in linear sweep voltammetry
[AD-A148655] 08 p1159 N85-17313
Voltammetry and coulometry with immersed thin layer electrodes. Part 2: Practical considerations and experimental results
[AD-A148656] 08 p1159 N85-17314
Computer-assisted Gran titration procedure for strong acid determination
[DE85-006801] 15 p2507 N85-25462
Electrochemistry of Hexanitroazobenzene (HNAB)
[DE85-010807] 21 p3565 N85-32171
COUNTDOWN
West Europe report: Science and technology
[JPRS-WST-84-004] 03 p0309 N85-11996
View of Ariane countdown procedures, Kourou launch facilities 03 p0310 N85-12001
COUNTER-ROTATING WHEELS
Perspectives on energy storage wheels for space station application 05 p0605 N85-13860
An improved servo-controlled inertial clock for laboratory tests of general relativity 19 p3378 N85-30955
COUNTERFLOW
Local mechanism of equatorial countercurrents
14 p2336 N85-24446
COUNTERMEASURES
NT CHAFF
NT ELECTRONIC COUNTERMEASURES
NT JAMMING
Resistance to HF jamming interference in mobile radio networks by an adaptive, distributed reconfiguration technique
[AD-A145117] 01 p0038 N85-10238
Minimization of system vulnerability in Naval satellite communication networks 11 p1710 N85-20758
Dual band radome wall design
[AD-P004357] 12 p1825 N85-21451
COUNTERS
NT CERENKOV COUNTERS
NT NEUTRON COUNTERS
NT NEUTRON SPECTROMETERS
NT PARTICLE TELESCOPES
NT PROPORTIONAL COUNTERS
NT QUANTUM COUNTERS
NT RADIATION COUNTERS
NT SCINTILLATION COUNTERS
NT SPARK CHAMBERS
Methods for the design of quantizers for image signals
[FUB-38-1983] 01 p0041 N85-10263
Safety evaluation of an electronic totalizer containing a Li/(CF)x cell
[AD-A147306] 07 p0993 N85-16305
Charge depletion meter
[AD-D011484] 10 p1488 N85-19393
Extraction of signals from background interference with unknown parameters in quantized sample
13 p2084 N85-23013
The 100 years of Aitken Nuclei (AN) study-reminiscence, current and future problems 21 p3641 N85-32621
Supersaturation obtained in a condensation nucleus counter 21 p3642 N85-32624
Observations on (3)He neutron spectrometry
[DE85-010731] 23 p3970 N85-34606
COUNTING
Estimating number, time and length; a baseline study
05 p0695 N85-14473
Counting is easy --- Turing machines
[CWI-CS-R8423] 17 p3009 N85-28606
COUNTING CIRCUITS
NT SCALERS
Tally cell circuit
[AD-D011492] 11 p1629 N85-20254
COUPLED MODES
Behavior orbits of two coupled oscillators
02 p0282 N85-11833
Quark models of hadronic interactions
[DE84-013787] 04 p0561 N85-13570
Coupled-cavity gyrotrons with mode conversion
13 p2076 N85-22967
Techniques for operating Charge Coupled Devices (CCD's) in very high speed framing mode
[AD-A152878] 17 p2953 N85-28236
Simplified analytical model for calculation of population inversion in channels of CW gasdynamic lasers operating at various transitions among levels pertaining to coupled upsilon 1 and upsilon 2 modes of CO2
[STN-2] 20 p3461 N85-31498
Expansion ratio influence on population inversion in CO2/Ar CW gasdynamic lasers operating at various transitions within coupled upsilon 1 and upsilon 2 modes of CO2
[STN-4] 22 p3790 N85-33485
Mechanical ratcheting behaviors of a steel pipe under combined cyclic axial load and internal pressure
23 p3904 N85-34184
Nonlinear flap-lag-extensional vibrations of rotating, pretwisted, preconed beams including Coriolis effects
[NASA-TM-87102] 23 p3941 N85-34427
COUPLERS
NT ANTENNA COUPLERS
NT COUPLING CIRCUITS
NT DIPLEXERS
NT DIRECTIONAL COUPLERS
Fiber optic data bus using Frequency Division Multiplexing (FDM) and an asymmetric coupler
[NASA-TM-86015] 04 p0492 N85-13139
Application of commercial star couplers to increase signal dynamic range
[DE84-014769] 04 p0565 N85-13600
Vehicle-to-vehicle connection mechanism
[AD-D011267] 05 p0645 N85-14142
Multihole couplers for overmoded waveguide systems
[IPF-83-8] 09 p1394 N85-18773
Short mode selective directional couplers
[IPF-83-9] 09 p1394 N85-18774
Improved directional couplers for overmoded waveguide systems
[IPF-84-1] 09 p1394 N85-18775
A coaxial cavity gunn oscillator using probe coupled microstrip
[AD-D011437] 10 p1479 N85-19334
Multi-access fiber optic data bus using FDM/FSK
[NASA-CR-175739] 15 p2621 N85-26152
The free electron laser variable bridge coupler
[DE85-009630] 18 p3114 N85-29278
The 3lembda/4 post coupler for drift-tube linacs
[DE85-010753] 20 p3531 N85-31962
Conjugated symmetrical coupler curves, produced by 4-bar linkages having the same transmission angles
23 p3924 N85-34322
COUPLES
Localized ionic currents from a corroding iron-copper galvanic couple
[AD-A153627] 18 p3074 N85-29011
Additional experiments relative to the shelf life of Li(Si)/FeS2 thermal batteries
[DE85-008482] 18 p3095 N85-29162
COUPLING
NT COUPLES
NT CROSS COUPLING
NT MICROWAVE COUPLING
NT OPTICAL COUPLING
NT SPIN-SPIN COUPLING
NT THERMODYNAMIC COUPLING
Factor analysis applied to a silane coupling agent on E-glass fiber system
[AD-A145687] 02 p0187 N85-11249
Using fiber-optics light guides in diagnosing intense shock waves 02 p0272 N85-11773

Structure of silane coupling agents adsorbed on silicon powder
[AD-A145803] 03 p0327 N85-12105
Evaluation of some photovoltaic concentrator solar cell-heat sink coupling materials
[DE84-016027] 04 p0529 N85-13378
Coupling of multidirectional diffusions by reflection
[CTH-MATH-1984-20] 05 p0719 N85-14613
Wavelength scaling of laser plasma coupling
[DE84-014637] 06 p0866 N85-15505
Application of quantum chemistry of atmospheric chemistry
[AD-A147035] 07 p0922 N85-15843
Photoacoustic spectroscopy at electrode-solution interface
[DE85-001872] 09 p1292 N85-18111
Electromagnetic processing of materials
[AD-A148804] 09 p1311 N85-18241
Modal analysis of structural systems involving nonlinear coupling 09 p1337 N85-18409
Effect of coupled torsional-flexural vibration of a geared shaft system on the dynamic tooth load
09 p1338 N85-18415
Nicolai maps and stochastic observables from a coupling constant flow
[BONN-HE-84-26] 09 p1376 N85-18653
An optically coupled sampling system with 4 GHz bandwith
[AD-A148057] 09 p1384 N85-18702
Nonlocal and nonlinear effects on solar oscillations
09 p1416 N85-18934
A coaxial cavity gunn oscillator using probe coupled microstrip
[AD-D011437] 10 p1479 N85-19334
Parametric processes in underdense UV laser-produced plasmas
[DE85-002812] 10 p1559 N85-19830
Nonlinear saturation of stimulated Raman scattering in collisional homogeneous plasma
[DE85-002814] 10 p1559 N85-19831
Comparison of measured and calculated mutual coupling in the near field between microwave antennas
[PB85-105963] 11 p1625 N85-20237
Coupling between the thermosphere and the stratosphere: The role of nitric oxide
11 p1662 N85-20472
Application of dimensional analysis to the problem of solar wind-magnetosphere energy coupling
[DE85-002414] 11 p1674 N85-20551
Magnetically-induced luminescence of (Ir(2=phos)(2)C10(4)
[AD-A149659] 12 p1799 N85-21266
A study of coupling the boundary and finite element methods in two-dimensional elastostatics
[AD-A149619] 12 p1865 N85-21702
Coupling between velocity oscillations and solid propellant combustion 13 p2000 N85-22536
Characterization of heterogeneity of composite propellants and its effects on combustion behavior
13 p2000 N85-22539
Impacts in ice: Commissions of solar system crater population 13 p2181 N85-23536
ICRF antenna coupling theory for a cylindrically stratified plasma
[DE85-004960] 14 p2424 N85-24952
Effect of nickel addition on the thermal, magnetic and magnetomechanical properties of Fe(80)B(15)Si(5)
[AD-A152281] 16 p2749 N85-26967
Study of the coupling between average, coherent and turbulent fields in a circular excited free jet
[ISL-R-115/83] 16 p2765 N85-27184
An analytical investigation of dynamic coupling in nonlinear, geared rotor systems
16 p2792 N85-27218
Laser plasma LINAC
[DE85-008294] 17 p2971 N85-28348
Basic EMC (Electromagnetic compatibility) technology advancement for C3 systems. Volume 4D: Modeling crosstalk in balanced twisted pairs
[AD-A153678] 18 p3090 N85-29125
The free electron laser variable bridge coupler
[DE85-009630] 18 p3114 N85-29278
Torsion-tension coupling in rods
18 p3120 N85-29315
Chemical-acoustic interactions in combustion systems
[AD-A153657] 19 p3233 N85-30046
Mutual coupling analysis for conformal microstrip antennas
[AD-A154292] 19 p3259 N85-30210
Seismic analysis of liquid-filled tanks with an eccentric core barrel
[DE85-010249] 19 p3269 N85-30272
Progress in inertial fusion at LLNL
[DE85-010931] 19 p3277 N85-30321
Strong-coupling approximations
[DE85-007829] 19 p3353 N85-30785
ICRF antenna coupling and wave propagation in a tokamak plasma 19 p3369 N85-30893
Control system design for lightly coupled large space structures 20 p3396 N85-31086
The 3lambda/4 post coupler for drift-tube linacs
[DE85-010753] 20 p3531 N85-31962
Ab initio calculations of materials properties
[DE85-011167] 20 p3531 N85-31964
A substructure coupling procedure applicable to general linear time-invariant dynamic systems
[NASA-CR-176144] 22 p3800 N85-33542
Substructure coupling in the frequency domain
[NASA-CR-176140] 22 p3800 N85-33543
Experimental measurements of the ion cyclotron antennas' coupling and RF characteristics
[DE85-011569] 23 p3962 N85-34694
Generation of stimulated emission in the soft X-ray range by nonlinear processes with excimer lasers
[DE85-012465] 24 p4098 N85-35403
Applications of the Galerkin formalism in the coupling of the earth's free oscillations 24 p4116 N85-35514
Study to assess the effects of magnetohydrodynamic electromagnetic pulse on electric power systems, phase 1, volume 3
[DE85-011301] 24 p4156 N85-35771

COUPLING CIRCUITS
Cascode and differential amplifier using field-effect transistors 15 p2529 N85-25591
Outline of CCVT (Coupling Capacitor Voltage Transformer) calibration procedure, EPRI-NBS (Electric Power Research Institute/National Bureau of Standards) prototype system. Supplement to EPRI report EL-890 (Field Calibration System for CCVTs, April 1978)
[PB85-182566] 20 p3450 N85-31418

COUPLING COEFFICIENTS
A packed storage program for angular momentum coupling coefficients
[TWISK-316] 01 p0102 N85-10880
The application of dimensional analysis to the problem of solar wind-magnetosphere energy coupling
14 p2357 N85-24564
Coupling of the solar wind to measures of magnetic activity 14 p2357 N85-24565
On coupling factors of explosion
15 p2551 N85-25747
Finite-perturbation intermediate neglect of differential overlap molecular orbital calculations of nuclear magnetic resonance spin-spin coupling constants for polycyclic aromatic hydrocarbons and aromatic nitrogen heterocyclics
[NASA-TM-87486] 20 p3525 N85-31927
Noise in stages and in interstage couplings of various transistor circuits 22 p3765 N85-33334
Statistical analyses in the study of solar wind-magnetosphere coupling
[DE85-009596] 22 p3859 N85-33896

COUPLINGS
Nonlinear oscillations of 2 body system relative to center of mass in elliptical orbit 02 p0159 N85-11062
Stress analysis of pin-loaded orthotropic plates using orthotropic photoelasticity 02 p0207 N85-11366
Improvement of gas-tightness of OTTG and TBO-5 threaded pipe couplings
[BLL-M-35093-(5828.4)] 07 p0972 N85-16175
Flexible line support assembly
[AD-D011391] 07 p0972 N85-16177
Tube coupling device
[NASA-CASE-MFS-25964-1] 11 p1647 N85-20378
Connection system — insuring against loss of a tool component without using multiple tethers
[NASA-CASE-MSC-20319-1] 12 p1857 N85-21649
Normal coordinate monolithic crystal filter
[AD-D011486] 12 p1941 N85-22186
Cooling performance improvement of a horizontal ground coupled heat pump
[DE85-002470] 13 p2093 N85-23065
Clutchless mechanism for engagement of forging press 14 p2268 N85-24051
Vibrations of rotors connected through couplings with backlash 17 p2940 N85-28147
Non-backdriveable free wheeling coupling
[NASA-CASE-MSC-20475-1] 18 p3116 N85-29290
Mechanical ratcheting behaviors of a steel pipe under combined cyclic axial load and internal pressure
23 p3904 N85-34184
The balancing of complex linkage mechanisms
23 p3924 N85-34313

COVALENT BONDS
Metallophthalocyanine dimers incorporating five atom covalent bridges
[AD-A154365] 19 p3234 N85-30051

COVARIANCE
Principal components: A review
02 p0211 N85-11390
Limit theory for the sample covariance and correlatio functions of moving averages
[AD-A145486] 02 p0251 N85-1164
Filtering and prediction performance for a class o systems with uncertain parameters
[AD-A146145] 03 p0411 N85-12
Construction of a confidence region for linear functions with unknown parameters
[CTH-MATH-1984-17] 05 p0721 N85-146
Methodology for economic evaluation of proces technologies in the early research and developme stages
[DE84-015863] 05 p0736 N85-14731
An interactive FORTRAN program for determining reliability of pseudo-range geodetic point positioning using the global positioning system
[AD-A147133] 07 p0988 N85-16275
Estimation for a semimartingale rugression model using the method of sieves
[AD-A146809] 07 p1028 N85-16527
Local likelihood estimation
[AD-A147317] 07 p1035 N85-16571
A factor analysis for time series
[AD-A147495] 07 p1036 N85-16574
Generating positively correlated random variables from a sequence of independent random variables with symmetric logarithmically concave densities
[AD-A148438] 08 p1216 N85-1703
Initialization of Thompson-Pisarenko's algorithm – sinusoidal signal parameter estimation
[FUB-46-1983] 09 p1375 N85-18641
Data-driven choice of a spectrum estimate: Extending the applicability of cross-validation methods
[DE85-001411] 10 p1437 N85-1906
On the probability density of signal-to-noise ratio in an improved adaptive detector, part 1
[AD-A148856] 10 p1550 N85-19772
Asymptotic distributions of the sample mean, autocovariances and autocorrelations of long-memory time series
[AD-A149409] 10 p1551 N85-19781
Tests of fit based on normalized spacings
[AD-A149749] 12 p1921 N85-22092
Asymptotics for configural estimators
[AD-A150106] 12 p1924 N85-22097
On limit of the largest eigenvalue of the large dimensional sample covariance matrix
[AD-A150589] 13 p2151 N85-2335
Model and controller reduction of uncertain systems using covariance equivalent realizations
14 p2243 N85-23902
Local covariance functions and density distributions
[AD-A150792] 14 p2373 N85-2466
Statistical analysis techniques for small sample size
[NASA-CR-171872] 15 p2639 N85-2627
Optimal relative data weights
16 p2805 N85-2728
Robust regression through robust covariances
[AD-A153301] 17 p3020 N85-2867
Hybrid uncertainty theory
[DE85-008357] 18 p3167 N85-2982
Two-point closure study of covariance budgets fo turbulent Rayleigh-Benard convection
[PB85-189108] 24 p4124 N85-3558

COVERALLS
The new Navy flier's fire-resistant blue coverall
[AD-A146611] 06 p0846 N85-1637
Fire pit tests of blue flight coverall program
[AD-A151884] 15 p2620 N85-2614

COVERINGS
Protective coverings for fiber reinforced epo composites
[PB84-231059] 04 p0480 N85-1308
Solar cell coverslide extraction method and appara
[AD-D011275] 05 p0669 N85-143
Integral boost, heat protection, port covers a transition 07 p0918 N85-1591
NBS solar collector durability/reliability test progra
[DE85-003489] 12 p1881 N85-218
Analysis of optimum front cover thickness for lightweig solar arrays 13 p2010 N85-22

COVES
U BAYS (TOPOGRAPHIC FEATURES)

COWELL METHOD
U NUMERICAL INTEGRATION

COWLINGS
Low-speed aerodynamic test of an axisymme supersonic inlet with variable cowl slot
[NASA-TM-87039] 16 p2708 N85-2671

CRAB NEBULA
Observation of gamma radiation from crab nebula 5-100 MeV range 02 p0162 N85-110
The X-ray structure of the Crab Nebula
11 p1741 N85-20
The X-ray structure of the Crab Nebula
11 p1742 N85-20

Recent results on the Crab Pulsar X-ray light curve
11 p1742 N85-20955
Old and new neutron stars
[DE85-002716] 11 p1782 N85-21085
Absolute measurements of radiation intensity from Cassiopeia-A, Cygnus-A and crab nebula in 60-100 cm band 13 p2078 N85-22978
High resolution hard X-ray spectra of solar and cosmic sources 14 p2455 N85-25163
Optical pulsar in the Large Magellanic Cloud remnant 0540-69.3
[DE85-006707] 16 p2883 N85-27788
Observation of the Crab nebula in the hard X-ray
[MPE-186] 17 p3053 N85-28897
Salyut-7 cosmonauts work with RS-17 and GSPS X-ray telescopes 22 p3731 N85-33131
Observations of the Crab Nebula at energies 4.10(11)
[OG-2.3-1] 22 p3865 N85-33938
Search for excess showers from Crab Nebula
[OG-2.3-2] 22 p3866 N85-33939
Very high energy gamma rays from the Crab Nebula
[OG-2.3-3] 22 p3866 N85-33940
Detection of gamma-ray lines from the direction of the Crab Nebula 22 p3866 N85-33943
Observation of hard X-rays from the Crab pulsar and A0535+26
[OG-2.3-7] 22 p3866 N85-33944
Gamma rays of 0.3 to 30 MeV from PSR 0531+21
[OG-2.3-8] 22 p3866 N85-33945
The 1000 GeV gamma ray emission from radio pulsars 22 p3867 N85-33946
High energy radiation from neutron stars
[DE85-014353] 24 p4169 N85-35843

CRACK ARREST
Retardation analytical model to extend service life
[NASA-CR-171177] 01 p0057 N85-10376

CRACK CLOSURE
Near-threshold fatigue crack growth and crack closure in 17-4 precipitation hardening steel and 2043-T3 aluminum alloy
[FFA-TN-1984-16] 02 p0210 N85-11385
Short cracks and crack closure in AL 2024-T3
[FFA-TN-1984-40] 02 p0210 N85-11387
Ultrasound interaction with partially closed fatigue cracks
[DE84-016360] 04 p0514 N85-13276
The effect of overload cycles on fatigue crack propagation in structural steels
15 p2577 N85-25897
Crack closure characteristics considering center cracked and compact tension specimens
[AD-A151702] 15 p2579 N85-25907
Fatigue crack retardation phenomenon caused by single-multiple overloads in 2017-T3 aluminum allow
23 p3906 N85-34196

CRACK FORMATION
U CRACK INITIATION

CRACK GEOMETRY
NT CRACK TIPS
Short cracks and crack closure in AL 2024-T3
[FFA-TN-1984-40] 02 p0210 N85-11387
The effect of orientation on fatigue growth in a nickel-based single crystal superalloy
[PNR-90207] 03 p0332 N85-12141
Correlation of stable crack growth with the J-integral and the crack tip opening displacement, effects of geometry, size and material: Report on an investigation of the elastic-plastic R-curve methodology
[GKSS-84-E-37] 08 p1173 N85-17395
Measurement of fracture macro-geometry in evaluating fracture toughness
[BLL-BISI-TRANS-22241-(9022.06)]
17 p2978 N85-28403
A clamped rectangular plate containing a crack
[NASA-CR-177925] 20 p3469 N85-31552

CRACK INITIATION
Estimation of the threshold in fatigue crack initiation models: A Bayesian approach
[AD-A144847] 01 p0062 N85-10410
Nonlinear structural and life analyses of a combustor liner
02 p0141 N85-10955
Pre-HOST high temperature crack propagation
02 p0141 N85-10956
Life prediction and constitutive behavior: Overview
02 p0143 N85-10973
Creep-fatigue life prediction for engine hot section materials (isotropic) 02 p0144 N85-10974
Constitutive model development for isotropic materials
02 p0144 N85-10975
Life prediction and constitutive models for anisotropic materials
02 p0144 N85-10976
The inter-relation of microstructure, toughness and fatigue crack growth behaviour in WC-Co hardmetals
02 p0177 - N85-11188
Detection of hydrogen assisted crack growth by measurement of modulus changes and acoustic emission
[DE84-015752] 02 p0184 N85-11236
The influence of sublaminate cracks on the tension fatigue behavior of a graphite epoxy laminate
[FFA-TN-1984-32] 02 p0210 N85-11386
Stress-driven solute enrichment of crack-tips during low ductility intergranular fracture of low-alloy steel
[AERE-R-11120] 03 p0333 N85-12150
Sequence of effects in the crack initiation and crack propagation phase 05 p0649 N85-14168
Evaluation of the crack initiation life behavior of fatigue loaded automotive components made from high strength aluminium alloys
[ESA-TT-733] 05 p0651 N85-14181
Study of fatigue fracture in hardened and tempered carbon steel. Report 1: Microscopic observation of the fatigue crack formation process
[BLL-PNR-90242-(8019.3153)]
06 p0767 N85-14909
Comparative investigation of testing methods to determine hot crack susceptibility during welding
[BAM-ERP-2415] 07 n0979 N85-16218
Influence of constant amplitude and variable amplitude loading on crack initiation and micro crack propagation in Al 2024-T3
[DFVLR-FB-84-29] 07 p0979 N85-16220
The effect of the test atmosphere on the formation and propagation of creep cracks in commercial high temperature alloys
[JUEL-1939] 07 p0980 N85-16221
Hydrogen induced cracking in pipeline steels
[ERS-E.327] 09 p1340 N85-18429
Mechanism of hydrogen induced cracking in pipeline steels
[ERS-E.349] 09 p1340 N85-18430
Fracture resistance of surface layer with technological defects under cyclical loading 10 p1448 N85-19126
Mechanism and pattern of fatigue crack growth in aluminum alloys 11 p1597 N85-20047
New method for studying surface crack growth in laminated polymer composite materials
11 p1598 N85-20051
Theoretical and experimental study of crack resistance and macrocrack growth rate in organic fiber reinforced plastic under pure shear condition
11 p1598 N85-20053
Initial fracture stages of orthogonally reinforced composite material 11 p1599 N85-20055
Distribution of hydrogen in multi-layer welded joints of alloyed steels 11 p1603 N85-20079
Comparison of the fatigue resistance (initiation, propagation) of cast TA6V with hot rolled TA6V — titanium alloy
[DGT-25369-PT-1] 12 p1808 N85-21341
Fatigue life, crack initiation, and propagation of 304 stainless steel with non-proportional axialtorsional strain-paths 13 p2101 N85-23094
An investigation of elevated temperature fatigue crack initiation in 2 and 1/4 cR-1 MO low alloy steel
[AD-A150670] 14 p2255 N85-23973
Role of passive surface films on corrosion fatigue crack initiation
[DE85-000438] 14 p2257 N85-23985
On the use of marker loads and replicas for measuring growth rates for small cracks 14 p2319 N85-24331
Study of oxidized surface coating on titanium after annealing 15 p2498 N85-25412
Fatigue damage and small crack growth during biaxial loading 16 p2797 N85-27247
The practical and theoretical significance of small cracks: An evaluation
[VTH-LR-432] 16 p2803 N85-27263
Engineering significance of fatigue thresholds and short fatigue cracks for structural design
[NLR-MP-84001-U] 17 p2981 N85-28430
High temperature fracture mechanics of silicon nitride
[BMFT-FB-T-84-265] 17 p2981 N85-28433
Method of assessment of start of slow crack growth by acoustic emission technique
[BLL-BISI-TRANS-21762-(9022.06)]
17 p3027 N85-28722
An effective substructure technique applied to crack problems 18 p3121 N85-29319
Experimental and theoretical study of fatigue crack initiation in metals 19 p3283 N85-30357
Creep fatigue life prediction for engine hot section materials (isotropic)
[NASA-CR-168226] 20 p3394 N85-31057
Long-term thermal aging of Celion/V378A composite materials
[NASA-TM-86362] 20 p3421 N85-31236
Finite element modeling of cracked bodies using the Bodner-Partom flow law 20 p3468 N85-31547
Creep crack growth predictions in INCO 718 using a continuum damage model 20 p3469 N85-31551
The three-dimensional J-integral. An investigation into its use for post-yield fracture safety assessment
[WTHD-167] 20 p3472 N85-31578
A cracked orthotropic sheet stiffened by a semi-infinite orthotropic sheet
[NASA-TP-2455] 21 p3597 N85-32339
Short-time creep of ice
[NRC/CNR-TT-2111] 23 p3941 N85-34428
Computational techniques for fiber reinforced components 24 p4075 N85-35250
Evaluation of the crack plane equilibrium model for predicting plastic fractures
[DE85-005558] 24 p4102 N85-35431

CRACK PROPAGATION
Influence of annealing on properties of AT3 alloy welded joints 01 p0019 N85-10118
Cumulative damage model for advanced composite materials
[AD-A144840] 01 p0022 N85-10135
Acoustic emission linear pulse holography
[DE84-014519] 01 p0050 N85-10330
Fracture, failure, and fragmentation
01 p0059 N85-10390
Crack tip opening displacement for work hardening materials
[GKSS-34-E-26] 01 p0063 N85-10415
Flight simulation fatigue crack propagation in metal/carbon-epoxy laminates
[NLR-TR-83006-U] 01 p0063 N85-10416
Pre-HOST high temperature crack propagation
02 p0141 N85-10956
HOST high temperature crack propagation
02 p0144 N85-10977
Tensile strength of composite sheets with unidirectional stringers and crack-like damage: A brief report
[NASA-TM-86310] 02 p0170 N85-11139
The inter-relation of microstructure, toughness and fatigue crack growth behaviour in WC-Co hardmetals
02 p0177 N85-11188
Detection of hydrogen assisted crack growth
[DE84-015920] 02 p0183 N85-11228
Environment-induced embrittlement: Effect of impurity segregation and state of stress
[DE84-015436] 02 p0184 N85-11235
Detection of hydrogen assisted crack growth by measurement of modulus changes and acoustic emission
[DE84-015752] 02 p0184 N85-11236
Model for non-linear crack growth prediction, taking load sequence (LOSEQ) effects into consideration
[BLL-RAE-TRANS-2114-(5207)]
02 p0208 N85-11371
Near-threshold fatigue crack growth and crack closure in 17-4 precipitation hardening steel and 2043-T3 aluminum alloy
[FFA-TN-1984-16] 02 p0210 N85-11385
Short cracks and crack closure in AL 2024-T3
[FFA-TN-1984-40] 02 p0210 N85-11387
Wedge with crack in bielastic medium
02 p0273 N85-11780
Weld metal solidification cracking in a carbon-manganese steel 03 p0330 N85-12126
The effect of orientation on fatigue growth in a nickel-based single crystal superalloy
[PNR-90207] 03 p0332 N85-12141
Sour-gas cracking in ferritic steels
[AERE-R-10906] 03 p0333 N85-12146
Acoustic emission monitoring of fatigue in 7010 aluminum alloys
[AERE-R-11167] 03 p0334 N85-12152
Crack resistance of pressed and rolled semifinished goods of aluminum alloys used in load-bearing aircraft wing structures 03 p0348 N85-12245
Kinetics of fatigue factor of AT3 titanium alloys in air, distilled water and 3.5% aqueous NaCl solution
03 p0350 N85-12255
Viscoplastic finite element analysis of rapid fracture
03 p0370 N85-12365
Applications of integral equations with strong singularities in fracture mechanics
03 p0371 N85-12367
Bending strength studies on hot-pressed silicon carbide
[NASA-TM-77512] 03 p0371 N85-12369
Fatigue crack propagation in metastable titanium alloys
[AD-A145824] 03 p0372 N85-12376
Influence of cyclic tangential loading on indentation fracture
[DE84-015969] 03 p0373 N85-12382
Tensile and crack propagation tests on aluminum alloys of the 2000 and 7000 series in laminated plate and forged products
[M2-678300] 03 p0373 N85-12383

A comparison of methods for predicting ductile crack growth instability
[AERE-R-11199] 03 p0374 N85-12387

Stress relief cracking studies of 2 1/4Cr1Mo steel
[AERE-R-11111] 03 p0374 N85-12388

Characterization of interlaminar crack growth in composites with the double cantilever beam specimen
04 p0463 N85-12942

Numerical investigation of the micromechanics of composite fracture 04 p0467 N85-12970

Ultrasound interaction with partially closed fatigue cracks
[DE84-016360] 04 p0514 N85-13276

Mechanical properties of aligned short carbon fiber reinforced PES and PI laminates
[DFVLR-FB-84-24] 05 p0613 N85-13918

Fractographic study of stress corrosion cracking of SUS 304 stainless steel in various environments
[BLL-RISLEY-TR-4598-(9091.9F)]
05 p0615 N85-13928

The fourth LBF colloquium
[ISSN-0721-5320] 05 p0648 N85-14163

Sequence of effects in the crack initiation and crack propagation phase 05 p0649 N85-14168

Processes to increase the fatigue life of constructions with already initiated cracks 05 p0650 N85-14176

Influence of the mechanical and electrochemical characteristics of austenitic and austenoferritic steels on the propagation rate and morphology of stress corrosion cracking
[BLL-RISLEY-TR-4545-(9091.9F)]
06 p0767 N85-14906

Study of fatigue fracture in hardened and tempered carbon steel. Report 1: Microscopic observation of the fatigue crack formation process
[BLL-PNR-90242-(8019.3153)]
06 p0767 N85-14909

Investigations into the fatigue crack growth behaviour of X6CrNi 18 11 (1.4948) austenitic stainless steel
[BLL-RISLEY-TR-4544-(9091.9F)]
06 p0768 N85-14911

Fractographic observation and estimation of crack growth curve of aluminum alloy under ramdom flight simulation loading
[NAL-TR-824] 06 p0768 N85-14913

Development and characterization of ductile Long-Range-Ordered (LRO) alloys (Fe,Co, Ni)3V for high-temperature structural use
[DE84-016750] 06 p0769 N85-14921

Constitutive modeling of engine materials
[AD-A146630] 06 p0817 N85-15189

Inclined dislocation emission at a shielded crack tip
[DE84-016703] 06 p0818 N85-15192

Inconel 718 alloy resistance to crack propagation
07 p0907 N85-15740

Cumulative damage modeling of fatigue crack growth
07 p0907 N85-15741

Thermal-mechanical fatigue crack growth in Inconel X-750
[NASA-CR-174740] 07 p0927 N85-15877

Possibilities for a more accurate life prediction of components — gas turbine disks
07 p0976 N85-16198

Investigation of the HPFTP first stage impeller crack
[NASA-CR-171281] 07 p0977 N85-16208

A hydrogen partitioning model for hydrogen assisted crack growth
[AD-A147385] 07 p0978 N85-16214

Influence of constant amplitude and variable amplitude loading on crack initiation and micro crack propagation in Al 2024-T3
[DFVLR-FB-84-29] 07 p0979 N85-16220

The effect of the test atmosphere on the formation and propagation of creep cracks in commercial high temperature alloys
[JUEL-1939] 07 p0980 N85-16221

Crack growth in propellants 08 p1116 N85-17034

Mechanical properties of adhesively bonded aluminum structures protected with hydration inhibitors
[AD-A148123] 08 p1133 N85-17139

Electrodes for repairing power engineering equipment made from creep resisting steel
[BLL-CE-TRANS-8064-(9022.09)]
08 p1167 N85-17360

Correlation of stable crack growth with the J-integral and the crack tip opening displacement, effects of geometry, size and material: Report on an investigation of the elastic-plastic R-curve methodology
[GKSS-84-E-37] 08 p1173 N85-17395

A simple engineering treatment of center cracked tension panels in the regime of nonlinear fracture mechanics under plane stress conditions
[GKSS-84-E-38] 08 p1173 N85-17396

Engineering property comparisons of PM and IM aluminum alloy forgings
[AD-B088146L] 08 p1173 N85-17398

Delamination growth in graphite epoxy laminates under compressive loads 09 p1286 N85-18086

A study of spectrum fatigue crack propagation in two aluminum alloys. 1: Spectrum simplification
[NASA-TM-86929] 09 p1293 N85-18124

A study of spectrum fatigue crack propagation in two aluminum alloys. 2: Influence of microstructures
[NASA-TM-86930] 09 p1294 N85-18125

Applicability of linear elastic fracture mechanics to fatigue in polymers and short-fiber composites
09 p1296 N85-18152

Circumferential cracks in cylindrical shells
09 p1330 N85-18354

Assessing expired fatigue life in large turbine shafts
[DE84-016676] 09 p1340 N85-18427

Statistical aspects of shear fracture propagation
[ERS-E.366] 09 p1341 N85-18434

A comprehensive study on sublaminate crack growth stability and its effects on the load-carrying capacity
[AD-A149037] 10 p1432 N85-19028

Development of surface cracks in AMg6 alloy under low-cycle loading conditions 10 p1442 N85-19089

K sub 1° -n diagram of cyclical crack resistance of aluminum alloys 10 p1442 N85-19090

Impact toughness of composites with layered microstructure of OT4 titanium alloy
10 p1445 N85-19104

Fracture resistance of surface layer with technological defects under cyclical loading 10 p1448 N85-19126

Recovery of damaged solid propellants by interrupting burning and crack-propagation processes
[AD-P004343] 10 p1455 N85-19167

Antiplane cracks in solid propellants
[AD-P004344] 10 p1455 N85-19168

Interaction between a crack and a soft inclusion
[NASA-CR-172533] 10 p1495 N85-19439

Fracture toughness of fiber reinforced concrete
[AD-A149403] 10 p1496 N85-19441

Rock mechanics: Issues and research needs in the disposal of wastes in hydraulic fractures
[DE85-001399] 10 p1556 N85-19809

Fracture analysis of notched composites
[NASA-CR-172563] 11 p1593 N85-20020

Mechanism and pattern of fatigue crack growth in aluminum alloys 11 p1597 N85-20047

Estimating deformability upon pressing of aluminum alloys based on results of mechanical testing
11 p1598 N85-20049

Theoretical and experimental study of crack resistance and macrocrack growth rate in organic fiber reinforced plastic under pure shear condition
11 p1598 N85-20053

Contributions of segregated phosphorus to the intergranular stress corrosion cracking of nickel
[DE85-003112] 11 p1606 N85-20099

Fatigue crack growth in Aramid Reinforced Aluminum Laminates (ARALL): Mechanisms and predictions
[DFVLR-FB-84-37] 11 p1609 N85-20118

Crack growth geometry in aluminum alloy sheet material under flight simulation loading. 1: A comparison between TWIST and miniTWIST FALSTAFF and short FALSTAFF. 2: Effect of truncating high loads
[VTH-LR-441] 11 p1609 N85-20119

Direct comparison of unloading compliance and potential drop techniques in J-integral testing
[DE85-001550] 11 p1650 N85-20392

Statistical theory of fragmentation processes
[DE85-002206] 11 p1653 N85-20414

Fatigue crack propagation in mirage 1110 wing main spar specimens and the effects of spectrum truncation on life
[ARL/STRUC-R-405] 12 p1776 N85-21152

Defect characterisation and monitoring by acoustic emission
[AERE-R-11409] 12 p1863 N85-21683

Translational and extensional energy release rates (the J- and M-integrals) for a crack layer in thermoelasticity
[NASA-CR-174872] 12 p1863 N85-21685

Interaction of part-through cracks in a flat plate
[NASA-CR-175588] 12 p1864 N85-21692

The residual strength of cracked specimens representing a section of the mirage into wing main spar
[ARL/STRUC-R-406] 12 p1865 N85-21699

Fracture analysis of cracks in complete cylindrical shells
[AD-A150091] 12 p1867 N85-21711

Fracture toughness of materials
[DE85-004306] 12 p1867 N85-21713

Numerical simulation of static and dynamic shadow patterns using an atomistic description of crack initiation and propagation
[DE85-003226] 12 p1867 N85-21715

Characterisation of fatigue crack extension by quantitative acoustic emission
[AERE-R-11289] 12 p1868 N85-21721

Longitudinal splitting in unidirectional composites, analysis and experiments
[NASA-CR-3881] 13 p2015 N85-22[illegible]

Delayed cracking strength of experimental grades of 42 CD 4 steel in aqueous H2S surroundings
[BLL-T8419/BG/LRS/LRST738/84]
13 p2020 N85-22[illegible]

Micromechanical modeling of microstructural damage in creeping alloys
[DE85-003925] 13 p2022 N85-22871

Creep crack growth in ductile alloys
[DE85-003937] 13 p2023 N85-2287[illegible]

Characteristics of surface crack development in AMg6 aluminum alloy during slow-cycle loading
13 p2034 N85-2276[illegible]

Fatigue life, crack initiation, and propagation of 304 stainless steel with non-proportional axial-torsional strain-paths 13 p2101 N85-23094

Elastic wave scattering from an interface crack in a layered half space 13 p2101 N85-23096

Fracture mechanics evaluation of GaAs
[NASA-CR-175657] 13 p2102 N85-23101

Advanced life analysis methods. Volume 1: Cracking data survey and NDI (nondestructive inspection) assessment for attachment lugs
[AD-A150419] 13 p2103 N85-23108

Advanced life analysis methods. Volume 2: Crack growth analysis methods for attachment lugs
[AD-A150420] 13 p2103 N85-23109

Advanced life analysis methods. Volume 5: Executive summary and damage tolerance criteria recommendations for attachment lugs
[AD-A151017] 14 p2219 N85-23781

Variability in constant-load-amplitude fatigue crack growth rates in marine environments
[AD-A150786] 14 p2255 N85-23975

Role of passive surface films on corrosion fatigue crack initiation
[DE85-000438] 14 p2257 N85-239[illegible]

A study of fatigue crack growth in 2 1/4 Cr1Mo steel. Part 1: The influences of environment and material condition
[AERE-R-11472] 14 p2258 N85-239[illegible]

Effect of elevated-temperature neutron irradiation on fracture toughness of ceramics
[DE85-000652] 14 p2261 N85-24010

Advanced life analysis methods. Volume 3: Experimental evaluation of crack growth analysis methods for attachment lugs
[AD-A151058] 14 p2317 N85-24310

Fatigue Crack Topography
[AGARD-CP-376] 14 p2318 N85-24321

Essential features in fatigue fractures and remarkable phenomena in fatigue crack growth
14 p2318 N85-24322

Fatigue crack propagation and fracture in 7050 and 7091 aluminum alloy forgings 14 p2318 N85-24324

Two recent cases of marker load applications on cargo/fighter aircraft fatigue tests
14 p2318 N85-24325

Effect of flight sequences in complex load histories on crack front marking 14 p2318 N85-24326

Periodic loading sequences for the systematic marking of fatigue crack fracture surfaces
14 p2319 N85-24329

On the use of marker loads and replicas for measuring growth rates for small cracks 14 p2319 N85-24331

On the use of marker loads for fatigue crack growth measurements 14 p2319 N85-24332

Fatigue crack topography and crack growth analysis – wrought and cast aluminum 14 p2319 N85-24333

Application of optical and electron microscopic techniques in the fractographic determination of fatigue crack growth rates 14 p2320 N85-24334

New analysis aspects of the fatigue crack propagation behavior by SEM in situ microscopy
14 p2320 N85-24335

Crack propagation under constant and variable stress amplitudes: A comparison of calculations based on the Striation spacing and tests 14 p2320 N85-24336

Crack growth direction in unidirectional off-axis graphite epoxy
[NASA-CR-175752] 15 p2502 N85-25433

Finger materials for air cushion vehicles. Volume 1: Flexible coatings for finger materials
[AD-A151438] 15 p2522 N85-25545

On Rayleigh waves and Rayleigh wave extension of surface micro-cracks 15 p2572 N85-25880

Fatigue life, fatigue crack propagation and fracture toughness study of 7075 aluminum alloy subjected to thermomechanical processing 15 p2573 N85-25882

The effect of overload cycles on fatigue crack propagation in structural steels
15 p2577 N85-25897

The effect of frictional forces on fatigue crack growth in lugs
[AD-A151994] 15 p2578 N85-25898

Fracture problems in power law viscoelastic materials
[AD-A149221] 15 p2578 N85-25900

Entropy production during fatigue as a criterion for failure. A local theory of fracture in engineering materials
[AD-A151289] 15 p2578 N85-25902

Dynamic crack curving and branching under biaxial loading
[AD-A151451] 15 p2578 N85-25904

Transition region for corner cracks at holes
[AD-A151835] 15 p2579 N85-25908

A study of the time dependence in fracture processes relating to service prediction of adhesive joints and advanced composites
[AD-A152064] 15 p2579 N85-25910

Degradation phenomena in solid electrolytes
[DE85-007066] 15 p2587 N85-25949

Advanced life analysis methods. Volume 6: User's manual for LUGRO computer program to predict crack growth in attachment lugs
[AD-A151235] 15 p2628 N85-26195

A review of fracture mechanics life technology
16 p2733 N85-26863

Hydrogen induced crack growth in Grade-12 Titanium
[BNL-NUREG-35598] 16 p2751 N85-26976

Initial quality of advanced joining concepts
[AD-A152241] 16 p2759 N85-27027

Automatic tracking of crack growth via finite elements
16 p2797 N85-27246

Predicting fully plastic mode 2 crack growth from an asymmetric defect
[AD-A152227] 16 p2801 N85-27269

On the use of marker loads for fatigue crack growth measurements
[FFA-TN-1984-52] 16 p2802 N85-27277

The practical and theoretical significance of small cracks: An evaluation
[VTH-LR-432] 16 p2803 N85-27283

USAF damage tolerant design handbook: Guidelines for the analysis and design of damage tolerant aircraft structures, revision B
[AD-A153161] 17 p2896 N85-27858

The synergistic actions of stress corrosion cracking and corrosion fatigue
[BLL-BISI-TRANS-22334-(9022.06)]
17 p2926 N85-28045

Study on mechanism of surface deformation induced by stress corrosion cracking
[BLL-BISI-TRANS-21896-(9022.06)]
17 p2928 N85-28066

Overload effects on sustained load crack growth at elevated temperature
[AD-A153223] 17 p2931 N85-28091

Hydrogen degradation of pipeline steels
[DE85-008930] 17 p2932 N85-28101

Characterization of the fatigue and slow crack growth behavior of partially stabilized zirconia ceramics
[DE85-005240] 17 p2934 N85-28113

Differential between crack and pseudo-crack indications by means of objective magnetic flux leakage testing
[BLL-BISI-TRANS-22033-(9022.06)]
17 p2976 N85-28386

On validity of threshold values of fatigue strength of steel structures
[BLL-BISI-TRANS-22192-(9022.06)]
17 p2978 N85-28408

The fatigue properties of welds at low temperature, according to the type of steel
[BLL-BISI-TRANS-22455-(9022.06)]
17 p2978 N85-28410

Fatigue crack propagation characteristics and fatigue fracture toughness in 780 MPa grade high strength steel weldments at low temperature
[BLL-BISI-TRANS-22369-(9022.06)]
17 p2979 N85-28411

Interaction among inhomogeneities and inclusions
[AD-A153114] 17 p2979 N85-28419

Evaluation of interpolative modeling concepts for fatigue crack growth at elevated temperature
[AD-A153222] 17 p2980 N85-28422

Method of assessment of start of slow crack growth by acoustic emission technique
[BLL-BISI-TRANS-21762-(9022.06)]
17 p3027 N85-28722

Fatigue and chromium-ferritic steels at elevated temperatures
[DE85-007735] 18 p3074 N85-29015

Slow crack growth in metal reinforced glass composites
[DE85-010094] 18 p3082 N85-29064

Ultrasonic testing of plates containing edge cracks
[NASA-CR-3904] 18 p3119 N85-29307

Structural Analysis
[DFVLR-MITT-84-21] 18 p3120 N85-29313

An effective substructure technique applied to crack problems 18 p3121 N85-29319

Crack propation in unidirectional laminates by the stress intensity factors 18 p3121 N85-29320

Description and illustration of the use of CRACKS IV
[AD-A153543] 18 p3121 N85-29325

Study of the influence of metallurgical factors on fatigue and fracture of aerospace structural materials
[AD-A153913] 18 p3122 N85-29328

Fracture of laminated composite materials
19 p3230 N85-30030

Effect of multi-functional inhibitors on the electrochemistry within corrosion crack
19 p3238 N85-30075

Thermo-mechanical and thermal behavior of high-temperature structural materials
[AD-A154154] 19 p3266 N85-30251

Kinetics of H-induced stress corrosion cracking. Part 1: Important features of cracking in respect of high strength steels
[BLL-BISI-TRANS-(9022.06)] 19 p3282 N85-30350

Acoustic emission study of fatigue crack extension position in a stress cycle 19 p3283 N85-30355

Hold-time effects in elevated temperature fatigue crack propagation
[AD-A154146] 19 p3286 N85-30376

Micromechanism of fracture for stage 1 hydrogen-induced crack growth
[DE85-010027] 19 p3288 N85-30390

Fatigue-crack propagation behavior of alloy A-286
[DE85-007460] 19 p3288 N85-30391

Fatigue-crack growth and ductile fracture toughness behavior of ASTM A387 Grade 91 steel
[DE85-008495] 20 p3431 N85-31286

Hot cracking of austenitic stainless steels: The debut of the Sigmajig
[DE85-010560] 20 p3431 N85-31287

Crack growth data for two aluminum alloys 7050-T73651 and 2024-T3
[FFA-TN-1984-51] 20 p3432 N85-31290

Finite element modeling of cracked bodies using the Bodner-Partom flow law 20 p3468 N85-31547

Creep crack growth predictions in INCO 718 using a continuum damage model 20 p3469 N85-31551

A clamped rectangular plate containing a crack
[NASA-CR-177925] 20 p3469 N85-31552

R and D activities of the Materials Science Division
20 p3539 N85-32024

Metallurgical origins of fracture toughness and microstructure and fracture toughness of an HSLA (High-Strength/Low-Alloy) steel
[AD-A155530] 21 p3567 N85-32187

Stress corrosion of ceramic materials
[AD-A155020] 21 p3570 N85-32202

A cracked orthotropic sheet stiffened by a semi-infinite orthotropic sheet
[NASA-TP-2455] 21 p3597 N85-32339

Measurement and analysis of critical crack tip processes during fatigue crack growth
[NASA-CR-172597] 21 p3598 N85-32342

KRAK: A computer program for two-phase two-component porous flow and fracture
[LA-9703] 22 p3782 N85-33434

The influence of temperature on static and dynamic SCC crack growth behavior in aluminum alloy
23 p3905 N85-34190

A fractographic study on mode 2 and mode 3 SCC crack growth in an Al-Zn-Mg alloy 23 p3905 N85-34191

Corrosion fatigue strength and crack growth in prestrained 0.16% C carbon steel
23 p3905 N85-34192

Experimental study on time and temperature dependent behavior of crack growth in viscoelastic strip
23 p3905 N85-34193

Fractographic analysis for nonpropagating conditions of fatigue crack at high stress ratios in mild steel
23 p3905 N85-34194

Crystallographic orientation dependence of fatigue crack propagation in extremely low carbon steel
23 p3906 N85-34195

Influence of cyclic thermal loading on internal stress in casted epoxy resin 23 p3908 N85-34211

Near-threshold fatigue: An overview of the role of microstructure and environment
[DE85-009903] 23 p3941 N85-34431

Fatigue lives of specimens representing critical locations in Mirage 3 spars under Australian and Swiss test spectra
[ARL-STRUC-R-415] 24 p4064 N85-35187

Effect of microstructure on the fatigue behavior of Fe-C-X alloys
[DE85-011749] 24 p4080 N85-35265

Stress-intensity factors for circumferential surface cracks in pipes and rods under tension and bending loads
[NASA-TM-87594] 24 p4101 N85-35424

On size effects in plane stress crack-growth resistance
[AD-A155926] 24 p4102 N85-35426

Evaluation of the crack plane equilibrium model for predicting plastic fractures
[DE85-005558] 24 p4102 N85-35431

Subcritical fracture propagation in rocks: An examination using the methods of fracture mechanics and non-destructive testing 24 p4116 N85-35516

CRACK TIPS

Stress-driven solute enrichment of crack-tips during low ductility intergranular fracture of low-alloy steel
[AERE-R-11120] 03 p0333 N85-12150

Viscoplastic finite element analysis of rapid fracture
03 p0370 N85-12365

Stress intensity factors for corner cracks at holes located near an edge
[FFA-TN-1984-20] 04 p0514 N85-13279

Correlation of stable crack growth with the J-integral and the crack tip opening displacement, effects of geometry, size and material: Report on an investigation of the elastic-plastic R-curve methodology
[GKSS-84-E-37] 08 p1173 N85-17395

The fracture mechanics of a slit crack with crack-tip dual zones 09 p1332 N85-18371

Creep crack growth in ductile alloys
[DE85-003937] 13 p2023 N85-22676

Detecting and analyzing crack defects
[BLL-BISI-TRANS-22062-(9022.06)]
17 p3027 N85-28723

Ultrasonic crack tip method for the determination of crack depth 17 p3028 N85-28725

Crack tip chemistry modeling of intergranular stress corrosion cracks of nickel containing segregated phosphorus and sulphur
[DE85-010059] 18 p3076 N85-29026

A cracked orthotropic sheet stiffened by a semi-infinite orthotropic sheet
[NASA-TP-2455] 21 p3597 N85-32339

CRACKING (CHEMICAL ENGINEERING)

NT PYROLYSIS

Jet fuel property changes and their effect on producibility and cost in the U.S., Canada, and Europe
[NASA-CR-174840] 16 p2757 N85-27012

Crack tip chemistry modeling of intergranular stress corrosion cracks of nickel containing segregated phosphorus and sulphur
[DE85-010059] 18 p3076 N85-29026

The effect of surface reactions in catalytic combustion
[AD-A154217] 19 p3234 N85-30049

CRACKING (FRACTURING)

NT STRESS CORROSION CRACKING

Delayed fracture of high-strength steels in spherical tanks for LP gas
[BLL-RISLEY-TR-4926-(9091.9F)]
01 p0026 N85-10162

Research on high-strength steels with an improved resistance against weld cracking
[AD-A144830] 01 p0027 N85-10170

Thermomechanical cracking due to moving frictional loads
[AD-A146271] 03 p0373 N85-12381

Effect of crack-tip region constraint on fracture in the ductile-to-brittle transition
[PB84-237395] 06 p0770 N85-14926

Research on nondestructive testing
[AD-A148375] 08 p1171 N85-17380

Stress-relieving interlayers for bituminous resurfacings
[PB85-136885] 12 p1820 N85-21415

Advanced life analysis methods. Volume 2: Crack growth analysis methods for attachment lugs
[AD-A150420] 13 p2103 N85-23109

Terrestrial analog studies for Martian patterned ground
13 p2190 N85-23590

An investigation of elevated temperature fatigue crack initiation in 2 and 1/4 cR-1 MO low alloy steel
[AD-A150670] 14 p2255 N85-23973

Fracture toughness of HY-130 steel weld metals
[AD-A150841] 14 p2255 N85-23976

Periodic loading sequences for the systematic marking of fatigue crack fracture surfaces
14 p2319 N85-24329

Mechanical aspects of interfaces and surfaces in ceramic containing systems
[AD-A151976] 15 p2519 N85-25530

Creep ratcheting simplified methods experience from structural design of elevated temperature components
[DE85-007433] 15 p2580 N85-25915

Echo-response from crack-like two-dimensional reflectors in focused ultrasonic fields. Ultrasonic crack tip method for the determination of crack depth
[BLL-BISI-22062-(9022.06)] 16 p2798 N85-27236

Initiation, growth and coalescence of small fatigue cracks
[AD-A151799] 16 p2800 N85-27265

Technical information: Weldability of stainless steel. Part 1: Austenitic stainless steel
[BLL-BISI-TRANS-22456-(9022.06)]
17 p2973 N85-28362

On validity of threshold values of fatigue strength of steel structures
[BLL-BISI-TRANS-22192-(9022.06)]
17 p2978 N85-28406

Interaction among inhomogeneities and inclusions
[AD-A153114] 17 p2979 N85-28419

Detecting and analyzing crack defects
[BLL-BISI-TRANS-22062-(9022.06)]
17 p3027 N85-28723

Echo-response from crack-like two-dimensional reflectors in focused ultrasonic fields
17 p3027 N85-28724

Fatigue and chromium-ferritic steels at elevated temperatures
[DE85-007735] 18 p3074 N85-29015

Fatigue characterization of fabricated ship details for design
[SSC-318] 19 p3285 N85-30371

Study on fracture behavior of epoxy resin
23 p3909 N85-34216

CRACKS
NT CRACK TIPS
NT MICROCRACKS
NT SURFACE CRACKS

Cumulative damage model for advanced composite materials
[AD-A144840] 01 p0022 N85-10135

Wedge with crack in bielastic medium
02 p0273 N85-11780

Study of delamination cracking under static and cyclic loads of carbon-epoxy composite materials
[REPT-42-727/F] 03 p0327 N85-12102

Stress intensity factors for a circular ring with uniform array of radial cracks of unequal depth
[AD-A145893] 03 p0372 N85-12377

Ultrasound interaction with partially closed fatigue cracks
[DE84-016360] 04 p0514 N85-13276

Stress intensity factors for corner cracks at holes located near an edge
[FFA-TN-1984-20] 04 p0514 N85-13279

Processes to increase the fatigue life of constructions with already initiated cracks 05 p0650 N85-14176

Pulse-echo method for flaw detection in concrete
[PB84-234509] 06 p0775 N85-14953

Elastodynamic stress intensity factors of an interface finite-width crack
[DE84-016906] 06 p0817 N85-15190

Cumulative damage modeling of fatigue crack growth
07 p0907 N85-15741

Problems and possibilities for life extension in gas turbine components 07 p0907 N85-15742

Disc fatigue life predictions for gas turbine engines
07 p0907 N85-15743

A general theory of circuit analogy in fracture diagnosis
[AD-A147177] 07 p0978 N85-16212

Buckling analysis of cracked, floating ice sheets
[AD-A147330] 07 p0988 N85-16277

Modeling of real UT transducer field/flaw interactions
[DE85-000341] 09 p1329 N85-18351

The fracture mechanics of a slit crack with crack-tip dual zones 09 p1332 N85-18371

Antiplane cracks in solid propellants
[AD-P004344] 10 p1455 N85-19166

Statistical theory of fragmentation processes
[DE85-002206] 11 p1653 N85-20414

Finger materials for air cushion vehicles. Volume 2: Base fabrics for finger materials
[AD-A149701] 12 p1819 N85-21406

Eddy current test probe with circumferential segments and method of testing material surrounding fastener holes
[AD-D011554] 12 p1850 N85-21603

Defect characterisation and monitoring by acoustic emission
[AERE-R-11409] 12 p1863 N85-21683

Interaction of part-through cracks in a flat plate
[NASA-CR-175586] 12 p1864 N85-21692

Moving nonlocal crack: Anti-plane shear case
[AD-A149996] 12 p1866 N85-21709

Characterisation of fatigue crack extension by quantitative acoustic emission
[AERE-R-11289] 12 p1868 N85-21721

Experimental and numerical analysis of electric currents and electromagnetic blunting of cracks in thin plates
[AD-A150418] 13 p2022 N85-22669

Effects of fracture roughness on fluid flow through a single deformable fracture
[DE85-004593] 13 p2092 N85-23062

Stress intensity factor in a tapered specimen
[NASA-CR-175569] 13 p2102 N85-23099

Fatigue fracture topography 14 p2318 N85-24323

On the corner singularity of a 3-D Griffith crack
[AD-A150989] 14 p2321 N85-24342

Weldability of Ni3Al-type aluminide alloys
[DE85-006932] 15 p2512 N85-25496

Crack elements for COSMIC/NASTRAN
15 p2573 N85-25866

Fracture problems in power law viscoelastic materials
[AD-A149221] 15 p2578 N85-25900

Dynamic crack curving and branching under biaxial loading
[AD-A151451] 15 p2578 N85-25904

Fatigue life extension 16 p2733 N85-26864

The practical and theoretical significance of small cracks: An evaluation
[VTH-LR-432] 16 p2803 N85-27283

Measurement of fracture macro-geometry in evaluating fracture toughness
[BLL-BISI-TRANS-22241-(9022.06)]
17 p2978 N85-28403

On validity of threshold values of fatigue strength of steel structures
[BLL-BISI-TRANS-22192-(9022.06)]
17 p2978 N85-28406

Ultrasonic testing of plates containing edge cracks
[NASA-CR-3904] 18 p3119 N85-29307

Study of the influence of metallurgical factors on fatigue and fracture of aerospace structural materials
[AD-A153913] 18 p3122 N85-29328

Improved model for fluid-driven cracks in jointed rock
[DE85-006963] 18 p3125 N85-29340

Hold-time effects in elevated temperature fatigue crack propagation
[AD-A154146] 19 p3286 N85-30376

Physical and chemical changes to rock near electrically heated boreholes at Spent Fuel Test-Climax
[DE85-010834] 19 p3302 N85-30472

Reliability of welds to repair defects in cast components made from CrMoV steel
[BLL-CE-TRANS-8054-(9022.09)]
20 p3461 N85-31501

Source characterization of point-like and distributed sources of acoustic emission 20 p3523 N85-31910

Automatic capability to store and retrieve component data and to calculate structural integrity of these components
[DE85-012429] 22 p3631 N85-33728

Damage induced stress redistribution in composite laminates 24 p4072 N85-35235

On size effects in plane stress crack-growth resistance
[AD-A155926] 24 p4102 N85-35426

CRANES
NT GANTRY CRANES

Increase in performance and improvement of ride comfort of self-propelled construction machinery by reducing pitch and vertical vibration
[AD-P004289] 09 p1405 N85-18845

Modernization of running gear of crane
14 p2286 N85-24163

CRANKED WINGS
U SWEPT WINGS

CRASH INJURIES

Functional impairment and structureal cervical injuries in human surrogates
[PB85-167436] 15 p2619 N85-26137

Design and testing of an energy-absorbing crewseat for the F/FB-111 aircraft. Volume 3: Data from crew module testing
[NASA-CR-3918] 23 p3896 N85-34134

CRASH LANDING
NT DITCHING (LANDING)

Safety recommendation(s), A-84-65
[REPT-3908] 14 p2216 N85-23743

Safety recommendation(s), A-84-93 through -95
[REPT-3983/33] 14 p2216 N85-23746

Air carrier overwater emergency equipment and procedures
[PB85-917006] 21 p3553 N85-32105

Aircraft accident report: World Airways Inc., Flight 30H, McDonnell Douglas DC-10-30CF, N113WA, Boston-Logan International Airport, Boston, Massachusetts, January 23, 1982
[PB85-910406] 22 p3726 N85-33114

CRASHES
NT CRASH LANDING
NT DITCHING (LANDING)

Establishment of posture and working movements of pilot in air crash enquiries 07 p1010 N85-16417

Annual review of aircraft accident data: US air carrier operations calendar year 1981
[NTSB/ARC-85/01] 12 p1774 N85-21134

The clinical and biomedical evaluation of trauma and fatalities associated with aircrew ejection and crash. A Working Group report
[AGARD-AR-194] 12 p1906 N85-21969

Introduction: The clinical and biomedical evaluation fo trauma and fatalities associated with aircrew ejection and crash 12 p1906 N85-21

Safety recommendation(s), A-84-93 through -95
[REPT-3983/33] 14 p2216 N85-237

Structures and Dynamics Division research and technology plans for FY 1985 and accomplishments fo FY 1984
[NASA-TM-86417] 15 p2577 N85-25

General Aviation Crashworthiness Project. Phase 2: Impact severity and potential injury prevention in general aviation accidents
[PB85-917002] 19 p3215 N85-2

Analysis of rotorcraft crash dynamics for development of improved crashworthiness design criteria
[FAA-CT-85-11] 20 p3391 N85-31

CRASHWORTHINESS

Crashworthiness of light aircraft fuselage structures: A numerical and experimental investigation
01 p0060 N85-10

Full-scale crash-test evaluation of two load-limiting subfloors for general aviation airframes
[NASA-TP-2380] 04 p0512 N85-13

A study of crashworthiness of light aircraft fuselage structures: A numerical and experimental investigatio
[UTIAS-286] 06 p0750 N85-14

Proceedings of the International Conference and Exposition on Structural Impact and Crashworthiness
[AD-A147645] 07 p0900 N85-157

Recommended improvements for second generatio 121.5/243 MHz ELT's
[NASA-CR-175274] 08 p1060 N85-16

The Shock and Vibration Digest, volume 17, no. 2
[AD-A153129] 17 p2977 N85-2

Recent progress in the dynamic plastic behavior of structures, part 4 17 p2978 N85-2

General Aviation Crashworthiness Project. Phase 2: Impact severity and potential injury prevention in general aviation accidents
[PB85-917002] 19 p3215 N85-2

Impact dynamics research on composite transport structures
[NASA-TM-86391] 19 p3284 N85-30

The role of aircraft panel materials in cabin fires and their properties
[FAA-CT-84-30] 21 p3553 N85-32

Seat experiments for the full-scale transport aircraft controlled impact demonstration
[AD-A155024] 21 p3553 N85-32

DYNA3D, INGRID, and TAURUS: An integrated interactive software system for crashworthiness engineering
[DE85-010928] 21 p3677 N85-32

Flight test experience and controlled impact of a large, four-engine, remotely piloted airplane
[NASA-TM-86738] 22 p3730 N85-33

Aviation safety (aircraft passenger survivability and cabin safety)
[GPO-39-647] 23 p3895 N85-341

Design and testing of an energy-absorbing crewseat for the F/FB-111 aircraft. Volume 3: Data from crew module testing
[NASA-CR-3918] 23 p3896 N85-3413

Design and testing of an energy-absorbing crewseat for the F/FB-111 aircraft. Volume 2: Data from seat testing
[NASA-CR-3917] 24 p4064 N85-35

CRATERING
NT PROJECTILE CRATERING

Impact cratering: The process and its effects on planetary evolution — and silicate-carbonate reactions on Venus
[NASA-CR-174016] 02 p0228 N85-11

Impact and collisional processes in the solar system
[NASA-CR-174297] 08 p1255 N85-17

Reports of the Planetary Geology and Geophysics Program, 1984
[NASA-TM-87563] 13 p2172 N85-23

Study and estimation of planet-crossing asteroid populations: Discoveries and analysis
13 p2175 N85-2

Impact and collisional processes in the solar system
13 p2180 N85-2

Centrifuge impact cratering experiments
13 p2181 N85-2

Progress on Experimental impact studies
13 p2181 N85-2

Progress on studies of early intense cratering
13 p2181 N85-2

Martian terrain ages 13 p2181 N85-2

Impacts in ice: Commissions of solar system crater population 13 p2181 N85-2

Problems in recovering crater production functions
13 p2182 N85-2

A parmetric study of crater-saturation simulation
13 p2182 N85-2

Ring-diameter ratios for multi-ring basins average 2.0(0.5)D 13 p2182 N85-23542
Morphology and mechanics of terraces in lunar craters 13 p2182 N85-23543
The nature of Martian flow ejecta craters 13 p2183 N85-23545
Periodic cometary showers: Real or imaginery? 15 p2680 N85-26555
Planetary surface processes: A review 22 p3855 N85-33860

CRATERS
NT LUNAR CRATERS
NT MARS CRATERS
NT METEORITE CRATERS
NT PLANETARY CRATERS
NASA-Ames vertical gun 04 p0579 N85-13606
Searching for impact craters using space shuttle photography 06 p0869 N85-15645
Shuttle navigation status 06 p1092 N85-16901
Dark halo craters and the thickness of grooved terrain on Ganymede 13 p2173 N85-23484
Average spacing for rings of individual multi-ring basins is 2.0(0.5)D 13 p2182 N85-23541
Ring-diameter ratios for multi-ring basins average 2.0(0.5)D 13 p2182 N85-23542
Ridged plains of Lunae Planum: Thickness distribution revised 13 p2185 N85-23559
Planetary analogs in Antarctica: Icy satellites 13 p2193 N85-23605
Analyses of radar images of small craters 13 p2199 N85-23642
Impact processes and their implications for planetary formation and early evolution 22 p3853 N85-33860

CRATONS
The mineralogy of global magnetic anomalies [E85-10061] 07 p0987 N85-16272
Synthesis of proterozoic data as a prerequisite for tectonic and thermal modeling [NASA-CR-174252] 07 p0995 N85-16323

CRAY COMPUTERS
U: The universal utility controller, revision 1 [DE84-017077] 04 p0547 N85-13481
Preliminary user's guide for BIGONE on the Cray [DE84-017075] 04 p0568 N85-13623
Reentrancy and multitasking on CRAY computers [DE85-007256] 15 p2630 N85-26211
Introduction to programming multiple-processor computers [DE85-010274] 18 p3164 N85-29599
Performance and library issues for mathematical software on high performance computers [DE85-010263] 19 p3339 N85-30690
Experiments and improvements of the ordinary differential equation solvers DEPAC on the CRAY computer [DE85-013260] 22 p3831 N85-33726
Parallel processing on the Livermore VAX 11/780-4 parallel processor system with compatability to Cray Research, Inc. (CRI) multitasking, version 1 [DE85-011856] 23 p3967 N85-34595

CRAZING
U SURFACE CRACKS

CREATION
U CREATIVITY

CREATIVITY
Central problems in the management of innovation [AD-A152598] 17 p3047 N85-28852

CREEP ANALYSIS
Strength analysis of fan-shaped wing considering temperature deformation and creep deformations 06 p0779 N85-14983
Recommendations for the use of Ni-Cr-base alloy extensometers for measurement of creep strain [NPL-DMA(A)-81] 08 p1164 N85-17342
Stress studies in EFG [NASA-CR-175464] 10 p1509 N85-19522
Low dose irradiation creep of pure nickel [DE85-006320] 16 p2751 N85-26975
Interferometric creep testing [AD-A154249] 19 p3286 N85-30378

CREEP BUCKLING
A new rheological model for concrete structural analysis [DE84-014743] 11 p1653 N85-20413
Dynamic creep buckling: Analysis of shell structures subjected to time-dependent mechanical and thermal loading 17 p2913 N85-27959
A state variable approach to transient creep deformation in stress reduction experiments [DE85-009492] 18 p3122 N85-29331

CREEP PROPERTIES
NT SHEAR CREEP
NT STEADY STATE CREEP
NT TENSILE CREEP
Evaluation of the role of diffusion creep in superplastic deformation 01 p0021 N85-10127
Nonlinear structural and life analyses of a combustor liner 02 p0141 N85-10955
Creep-fatigue life prediction for engine hot section materials (isotropic) 02 p0144 N85-10974
Life prediction and constitutive models for anisotropic materials 02 p0144 N85-10976
Swaged Mo-5 percent W alloy and recrystallized commercially pure molybdenum 02 p0180 N85-11208
Microstructure and creep behaviour at elevated temperature of unidirectionally solidified eutectic nickel base superalloys 02 p0181 N85-11216
Critical assessment of low fluence irradiation creep mechanisms [DE84-015578] 02 p0184 N85-11232
Determination of nonlinear viscoelasticity parameters for polymeric and composite materials by numerical methods [AD-A145311] 02 p0185 N85-11240
Reliability considerations for the total strain range version of strainrange partitioning [NASA-CR-174757] 02 p0209 N85-11380
High temperature deformation of hot-pressed polycrystalline orthoenstatite [NASA-CR-174026] 02 p0285 N85-11861
The rheology of icy satellites [NASA-CR-174024] 02 p0302 N85-11959
Accelerated viscoelastic characterization of T300/5208 graphite-epoxy laminates 03 p0325 N85-12091
Evaluation of ferritic alloy Fe-2 1/4Cr-1Mo after neutron irradiation: Irradiation creep and swelling [DE84-014647] 04 p0474 N85-13022
Cavitation phenomenon in superplastic creep [DE84-015484] 04 p0513 N85-13271
The effect of trace elements on the properties at high temperature of a Ni-Cr-base alloy 05 p0617 N85-13944
Influence of the mechanical and electrochemical characteristics of austenitic and austenoferritic steels on the propagation rate and morphology of stress corrosion cracking [BLL-RISLEY-TR-4545-(9091.9F)] 06 p0767 N85-14906
Longevity of thin-walled engine parts subjected to transient stresses under creep conditions 06 p0777 N85-14966
Irradiation creep induced anisotropy in a/2110 dislocation populations [DE84-016623] 06 p0868 N85-15520
Study of residual stresses introduced into TA6ZrD (685) cylinders by quenching [BLL-PNR-90240-(8019.3153)] 07 p0925 N85-15859
Investigation of the creep behaviour of soft soldered joints with solder L-SnAg5 at ambient temperature [BLL-T6383/BG/WH798/84] 07 p0926 N85-15865
Back stress in dislocation creep. Part 1: Basic concepts and measuring techniques [NASA-TM-77773] 07 p0977 N85-16206
Electrodes for repairing power engineering equipment made from creep resisting steel [BLL-CE-TRANS-8064-(9022.09)] 08 p1167 N85-17360
Elevated temperature creep behavior of Inconel alloy 625 [DE84-015836] 09 p1297 N85-18144
Creep deformation of compacted decomposed granite soils 09 p1303 N85-18187
Comparison of property regeneration techniques and life prediction procedures applied to laboratory tested and service exposed Ni-Cr alloys [NPL-DMA(A)-91] 09 p1333 N85-18374
Cavitation phenomenon in superplastic creep [DE85-001716] 10 p1441 N85-19083
Stress studies in EFG [NASA-CR-175488] 10 p1563 N85-19856
Non-isothermal irradiation creep of nickel alloys Inconel 706 and PE-16 [DE85-000842] 11 p1607 N85-20102
Accelerated viscoelastic characterization of T300-5208 graphite-epoxy laminates [NASA-CR-3871] 12 p1797 N85-21271
Multiaxial stress response of ceramics [DE85-004350] 12 p1814 N85-21379
Steel castings by the electroslag casting technique [DE85-003812] 12 p1819 N85-21409
Creep crack growth in ductile alloys [DE85-003937] 13 p2023 N85-22676
Some specifics of development of fatigue and creep in heat-resistant alloys with asymmetrical multicycle loading 13 p2031 N85-22724
Densification and deformation in the presence of a liquid phase [DE85-005101] 13 p2038 N85-22763
Microstructure and properties of ferrous alloy weldments [DE85-005582] 14 p2257 N85-23987
Variation in the spacing of dislocations in subgrain boundaries with creep strain in Type 304 stainless steel [DE85-006184] 15 p2511 N85-25493
Creep ratcheting simplified methods experience from structural design of elevated temperature components [DE85-007433] 15 p2580 N85-25915
Method of investigating accumulations of damage to weld joints in the case of low-cycle creep [BLL-CE-TRANS-8088-(9022.09)] 16 p2792 N85-27219
Liquid-metal transducers for strain measurement during in-pile materials testing 17 p2945 N85-28176
Influence of materials creep on rotor dynamics [DE85-008545] 17 p2981 N85-28426
Interferometric creep testing [AD-A154249] 19 p3286 N85-30378
Creep fatigue life prediction for engine hot section materials (isotropic) [NASA-CR-168228] 20 p3394 N85-31057
Long range ordered alloys modified by addition of niobium and cerium [DE85-011661] 20 p3431 N85-31285
A comparison of two contemporary creep-fatigue life prediction methods 20 p3467 N85-31538
Estimation of power-law creep parameters from bend test data [PB85-183408] 20 p3472 N85-31579
The effect of stress and hot corrosion on nickel-base superalloys [AD-A154722] 21 p3566 N85-32181
SANCHO: A finite element computer program for the quasistatic, large deformation, inelastic response of two-dimensional solids [DE85-011456] 22 p3829 N85-33714
Short-time creep of ice [NRC/CNR-TT-2111] 23 p3941 N85-34428

CREEP RESISTANCE
U CREEP STRENGTH

CREEP RUPTURE STRENGTH
The effects of seven alloying elements on the microstructure and stress-rupture behavior of nickle-base superalloys [NASA-TM-83791] 01 p0027 N85-10188
Improved multiaxial creep-rupture strength criterion [DE84-014273] 01 p0062 N85-10413
Effects of tin on microstructure and mechanical behavior of Inconel 718 [NASA-TM-86866] 03 p0330 N85-12129
Stirling material technology [NASA-TM-86888] 04 p0472 N85-13007
Non-linear data fitting for the analyses of creep rupture data on GRP materials in aggressive environments --- glass reinforced plastics (GRP) [NPL-DMA(A)-79] 04 p0512 N85-13261
The effect of trace elements on the properties at high temperature of a Ni-Cr-base alloy 05 p0617 N85-13944
Method for predicting the creep rupture life of nickel-base precipitation-hardened superalloys from their chemical composition [BLL-PNR-90241-(8019.3153)] 06 p0768 N85-14910
Inconel 718 alloy resistance to crack propagation 07 p0907 N85-15740
Strain-controlled creep rupture in non-isothermal materials 09 p1332 N85-18368
Creep-rupture behavior of iron superalloys in high-pressure hydrogen [NASA-CR-174411] 10 p1441 N85-19078
High-thermal-gradient superalloy crystal growth 17 p2914 N85-27966
Experiments and micromechanical models for creep-rupture in polymer matrix composites [DE85-009533] 17 p2935 N85-28118
Fatigue behavior of synthetic fibers, yarns and ropes 17 p2979 N85-28415
Long-term strength of glass fibre/phenolic resin composites [NPL-DMA(A)-98] 22 p3742 N85-33195

CREEP STRENGTH
The metallurgical processes during the soft soldering of copper and copper alloys and the strength characteristics of soldered joints [BLL-T6388/BG/WH803/84] 06 p0767 N85-14908
Advanced stress analysis methods applicable to turbine engine structures [NASA-CR-175573] 12 p1778 N85-21165
Alloys based on NiAl for high temperature applications [NASA-TM-86976] 12 p1805 N85-21322
Investigation of the development possibilities of a ferritic creep and oxidation-resistant steel for application under creep conditions above 650 deg C [BMFT-FB-T-84-244] 12 p1808 N85-21344

Finite element model for creep in composite masonry
[PB85-150324] 14 p2322 N85-24347
An investigation of the structure and high temperature mechanical properties of oxide dispersion strengthened alloys
[AD-A151107] 15 p2509 N85-25477
Mechanical properties of polycrystalline alpa titanium
[BLL-BISI-TRANS-21923-(9022.08)]
17 p2924 N85-28029
Load-carrying capabilities of refractory alloys for space reactor power applications
[DE85-010566] 19 p3240 N85-30087
The effect of stress and hot corrosion on nickel-base superalloys
[AD-A154722] 21 p3566 N85-32181
The development and evaluation of the creep and corrosion resistant alloy IN6201
[PNR-90253] 23 p3917 N85-34278

CREEP TESTS
Interactions between corrosion and creep of uncoated and coated superalloys in sulfate melts
04 p0477 N85-13038
The creep and creep rupture of SMC-R50 under different thermomechanical conditions 05 p0648 N85-14160
The effect of the test atmosphere on the formation and propagation of creep cracks in commercial high temperature alloys
[JUEL-1939] 07 p0960 N85-16221
Creep-fatigue interaction of notched 304 stainless steel bars 16 p2798 N85-27249
Design and fabrication of durable owner-built wind turbine blades
[DE85-009200] 20 p3484 N85-31650
The effect of stress and hot corrosion on nickel-base superalloys
[AD-A154722] 21 p3566 N85-32181
A continuous damage model based on stepwise-stress creep rupture tests
[NASA-CR-174941] 21 p3597 N85-32341
Tensile testing apparatus
[NASA-CASE-LAR-13243-1] 23 p3933 N85-34375

CRESTATRONS
U TRAVELING WAVE TUBES

CRESTS
U WAVES

CREVASSES
NT GLACIERS

CREVICES
U CRACKS

CREW PROCEDURES (INFLIGHT)
A comparative evaluation of EMADS (Engine Monitoring and Display System) and conventional engine instruments
[AD-A145901] 03 p0319 N85-12060
Aircraft accident report, Scandinavian Airlines System, Flight 901, McDonnell Douglas DC-10-30, John F. Kennedy International Airport, Jamaica, New York, February 28, 1984
[PB84-910415] 05 p0594 N85-13768
A full mission simulator study of aircrew performances: The measurement of crew coordination and decisionmaking factors and their relationships to flight task performances 05 p0710 N85-14556
Multi-crew model analytic assessment of landing performance and decision-making demands
05 p0712 N85-14567
Influence of a perspective cockpit traffic display format on pilot avoidance maneuvers 10 p1534 N85-19668
Contamination control for increased crew productivity
18 p3158 N85-29555

CREW STATIONS
NT CREW WORKSTATIONS
The human role in space. Volume 3: Generalizations on human roles in space
[NASA-CR-171225] 04 p0546 N85-13475
Avionics/crew station integration
06 p0752 N85-14816
Crewstation design and validation
06 p0752 N85-14822
Display Techniques for Advanced Crew Stations (DTACS). Phase 1: Display techniques study
[AD-A146922] 07 p0904 N85-15722
Proceedings of the 6th Advanced Aircrew Display Symposium
[AD-A150044] 12 p1778 N85-21160
Habitability sleep accommodations
18 p3150 N85-29566
Crew systems and flight station concepts for a 1995 transport aircraft
[NASA-CR-166068] 19 p3221 N85-29973

CREW WORKSTATIONS
An analysis of constraints to coordinated tactical crew interaction in the P-3C aircraft
[AD-A147220] 07 p1021 N85-16478
A computer aided Multi-Man-Machine Work Area Design and Evaluation System (MAWADES)
[AD-A147960] 08 p1199 N85-17554

CREWS
NT FLIGHT CREWS
NT SPACECREWS
The human role in space. Volume 2: Research analysis and technology report
[NASA-CR-171224] 04 p0546 N85-13474
Crew communication as a factor in aviation accidents
05 p0710 N85-14555
Communication on the flight deck
05 p0711 N85-14557
A crew exposure study. Volume 1: Offshore
[AD-A146804] 07 p1015 N85-16449
The sinking of the Les Mutuelles du Mans trimaran
14 p2327 N85-24384
The ARGOS contribution to the demonstration of the effectiveness of a satellite-based search and rescue system 14 p2330 N85-24404
Space station crew safety alternatives study, volume 1
[NASA-CR-3854] 19 p3223 N85-29985
A crew exposure study. Phase II. Volume 2. At sea. Part A
[AD-A155233] 21 p3686 N85-32774
Design and testing of an energy-absorbing crewseat for the F/FB-111 aircraft. Volume 3: Data from crew module testing
[NASA-CR-3918] 23 p3896 N85-34134

CRIME
Computer crime
[GPO-30-544] 10 p1537 N85-19691

CRITERIA
NT STRUCTURAL DESIGN CRITERIA
The identification of the scientific community's choice criteria in the history of scientific research: The case of quantum mechanics
[NOTA-INTERNA-797] 02 p0291 N85-11693
Measurement procedures for the radar spectrum engineering criteria
[PB85-119022/GAR] 09 p1313 N85-18254
Transient vibration test criteria for spacecraft hardware — galileo spacecraft 09 p1338 N85-18418
Experimental investigation of a breakdown criterion for a vortex in an incompressible flow — delta wing
[ONERA-RT-27/1147-AY] 11 p1577 N85-19935
Stability results for discrete Volterra equations: Numerical experiments
[CWI-NM-R8409] 11 p1707 N85-20743
Stochastic runaway of dynamical systems
[IPP-6/244] 11 p1708 N85-20745
Air quality criteria for ozone and other photochemical oxidants. External review draft, volume 4
[PB85-126068] 12 p1886 N85-21838
Personal decision making: The influence of perceived locus of control and degree of rationality on information seeking strategies 13 p2167 N85-23446
Discovery refutation and verification refutation: The proposals of Von Neumann and Wiener in the development of 20th century physics
[NOTA-INTERNA-840] 14 p2431 N85-24993
Selection of promising sites for magma energy experiments
[DE85-006832] 16 p2820 N85-27393

CRITICAL EXPERIMENTS
Drag-free satellite simulator
[REPT-615] 12 p1789 N85-21229

CRITICAL FLOW
Investigation of phase separation models in RELAP 4/MOD 6
[OEFZS-4286] 05 p0638 N85-14093
Critical flashing flow of subcooled fluids in nozzles with contour discontinuities
[DE84-017229] 09 p1319 N85-18296
Flow-induced vibration of the SSME LOX posts: Additional issues
[DE85-007339] 16 p2741 N85-26916

CRITICAL FREQUENCIES
Global maps of foF2 derived from observations and theoretical values
[AD-A145866] 03 p0392 N85-12509
Dispersion curves for normal waves in cylindrical shell and conditions for spatial coincidence in vicinity of critical frequencies 06 p0776 N85-14973
Linear problem of harmonic vibrator acting at supercritical frequencies in subsonic boundary layer
06 p0779 N85-14978
Domain of applicability of asymptotic description of radio pulse fields near critical frequency
13 p2073 N85-22949

CRITICAL LOADING
Design oriented identification of critical points in transient response 09 p1330 N85-18357
An evaluation of the 64-meter antenna radial bearing for use on the 70-meter antenna
10 p1464 N85-19238
Spectral frequency of eigenvalues in optimal problems of stability of cylindrical shells of variable thickness
13 p2047 N85-22815

CRITICAL MACH NUMBER
U CRITICAL VELOCITY
U MACH NUMBER

CRITICAL MASS
A very important process of nucleosynthesis in stars
[OG-7.1-11] 23 p4014 N85-34872

CRITICAL PATH METHOD
On stochastic integral representation of stable processes with sample paths in Banach spaces
[AD-A152927] 17 p3025 N85-28700
Method of characterizing critical timing paths and analyzing timing related failure modes in very large scale integrated circuits
[AD-D011731] 22 p3750 N85-33298

CRITICAL POINT
Critical point wetting drop tower experiment
02 p0155 N85-11046
The isochoric heat capacity of fluid substances in the critical region. Pre-examinations for a Spacelab experiment
[BMFT-FB-W-84-034] 05 p0723 N85-14680
A study of degenerate and nondegenerate critical points in three-dimensional flow fields
[DFVLR-FB-84-36] 11 p1633 N85-20288
Explorations into thermodynamics analogies and critical points in reference to gas-solid transport
[DE85-000816] 11 p1738 N85-20829
Special features of the temperature dependence of the capillary constant in the vicinity of the critical point
[BLL-T6438/BG/LRS/LRST750/85]
16 p2859 N85-27682

CRITICAL PRESSURE
Liquid-phase compositions from vapor-phase analyses 2: Adaptation of the Prausnitz program to UF6 and some of its potential impurities
[DE85-011521] 21 p3673 N85-32819

CRITICAL REYNOLDS NUMBER
U CRITICAL VELOCITY
U REYNOLDS NUMBER

CRITICAL SPEED
U CRITICAL VELOCITY

CRITICAL STRESS
U CRITICAL LOADING

CRITICAL TEMPERATURE
Critical point wetting drop tower experiment
02 p0155 N85-11046
External fuel vaporization study, phase 2
[NASA-CR-174079] 02 p0187 N85-11252
Calculation of critical temperature for Nb-Cu multilayer film superconductor
[AD-A144321] 02 p0274 N85-11786
Storage life of thermal detents
[DE84-016934] 04 p0476 N85-13030
Modelling the thermal explosion phenomenon in solid propellants: The case of fixed and variable temperatures 08 p1117 N85-17044
Convection heat transfer in the critical region of fluid mixtures
[DE85-001282] 11 p1633 N85-20285
Examination of the contact wetting angle in the vicinity of critical temperature
[BLL-T6416/BG/CRS/LR-ST735/84]
13 p2091 N85-23054
Lattice Monte Carlo calculations of finite temperature QCD
[DE85-004035] 14 p2431 N85-24982
Self-heating to ignition measurements and computation of critical size for solar energy collector materials
[PB85-183374] 20 p3485 N85-31663

CRITICAL VELOCITY
Critical velocities in He II for independently varied superfluid and normal fluid velocities
09 p1396 N85-18784
Shuttle Molecular Gun: Smog. Potential experiment for the electrodynamic Tethered Satellite System (TSS) mission
[IFSI-84-17] 20 p3419 N85-31221
Improved turbopump dynamics
[NASA-TM-86514] 20 p3462 N85-31509
On the role of the magnetic field strength in critical ionization velocity interaction
[TRITA-EPP-85-01] 20 p3536 N85-32003

CROCCO METHOD
Existence and non-uniqueness of similarity solutions of a boundary layer problem
[NASA-CR-172503] 07 p0957 N85-16064

CROP DUSTING
Effectiveness of agricultural aviation
04 p0544 N85-13460
Operation of aviation support bases
04 p0544 N85-13461
Director on institute's civil aviation projects
08 p1067 N85-16764

Improved sprayer for AN-2 cropdusting work
06 p1066 N85-16760

CROP GROWTH

Remote sensing of plant stress and diseases
05 p0657 N85-14216

Timing in dry seeds 05 p0690 N85-14437

Spectral estimators of absorbed photosynthetically active radiation in corn canopies
[E85-10041] 07 p0983 N85-16242

Growth/reflectance model interface for wheat and corresponding model
[E85-10058] 07 p0987 N85-16269

Controlled ecological life support system higher plant flight experiments
[NASA-CR-177323] 07 p1020 N85-16471

Growth and reflectance characteristics of winter wheat canopies
[E85-10080] 10 p1505 N85-19494

NOAA-AISC user's guide for implementing CERES maize model for large area yield estimation
[E85-10083] 12 p1873 N85-21746

Research on zero-gravity botany apparatus
16 p2723 N85-26811

Evaluation of the area and severity of last night's frosts
[REPT-109] 16 p2833 N85-27473

Publications of the NASA CELSS (Controlled Ecological Life Support Systems) program
[NASA-CR-3911] 19 p3326 N85-30606

Deficit irrigation feasibility study and demonstration project
[DE85-011531] 22 p3802 N85-33555

CROP IDENTIFICATION

Biophysical and spectral modeling for crop identification and assessment
[E85-10006] 02 p0215 N85-11419

Basic principles, methodology, and applications of remote sensing in agriculture
[E85-10016] 02 p0217 N85-11429

Application of digital analysis of MSS to agro-environmental studies
[E85-10024] 02 p0218 N85-11437

Characterization of LANDSAT-4 TM and MSS image quality for the interpretation of California's agricultural resources --- Central Valley 13 p2116 N85-23190

An initial analysis of LANDSAT-4 Thematic Mapper data for the discrimination of agricultural, forested wetlands, and urban land cover --- Poinsett County, Arkansas; and Reelfoot Lake and Union City, Tennessee
13 p2116 N85-23193

Preliminary evaluation of Thematic Mapper image data quality 13 p2118 N85-23194

Interpretation of multiband photographs made during Teleloto-80 experiment for the purpose of discriminating agricultural crops 22 p3735 N85-33152

Direct regression analysis of remote sensing data (using example of grass cover) 22 p3736 N85-33157

CROP INVENTORIES

Executive report: Results of the IRGA-CNPq/INPE experimental project
[E85-10011] 02 p0216 N85-11424

Basic principles, methodology, and applications of remote sensing in agriculture
[E85-10016] 02 p0217 N85-11429

Multispectral (X and C band) crop classification with synthetic aperture radar (SAR-580) optical data
05 p0657 N85-14217

Multi crop area estimation in Idaho using EDITOR
[E85-10054] 06 p0827 N85-15251

Calibration or inverse regression: Which is appropriate for crop surveys using LANDSAT data?
07 p0965 N85-16260

Remote sensing research for agricultural applications -- San Joaquin County, California and Snake River Plain and Twin Falls area, Idaho
[E85-10090] 12 p1873 N85-21752

Thematic Mapper data quality and performance assessment in renewable resources/agriculture/remote sensing 13 p2120 N85-23201

CROP INVENTORIES BY REMOTE SENSING

U AGRISTARS PROJECT

CROPLANDS

U FARMLANDS

CROPS

Research activities of the Illinois University Coordinated Science Laboratory
[AD-A145589] 03 p0449 N85-12856

Thematic Mapper spectral dimensionality and data structure 12 p1871 N85-21736

CROSS CORRELATION

Optimum parameters for determining the motion of radar field by cross-correlation method
01 p0079 N85-10524

Electrostatic wave observation during a space simulation Beam-Plasma-Discharge (BPD)
[NASA-CR-174286] 07 p1045 N85-16639

The analysis of spaced sensor records by correlation techniques 08 p1184 N85-17465

Method and apparatus for calibrating the ionosphere and application to surveillance of geophysical events
[NASA-CASE-NPO-15430-1] 12 p1887 N85-21846

Regular synthesis of pairs of phase-keyed binary minimax signals 13 p2069 N85-22923

Parametric coherence estimation via convolved correlations
[DE85-003946] 14 p2416 N85-24909

Higher order residual analysis for nonlinear time series with autoregressive correlation structures
[AD-A149232] 15 p2636 N85-26257

Scene analysis using recursive frequency domain correlation with energy normalization
[AD-A151777] 16 p2654 N85-27596

Optical 3-D signature device for detecting chemical agents
[AD-D011669] 19 p3272 N85-30293

CROSS COUPLING

Quantification of cross-coupling and motion feedthrough for multiaxis controllers used in an air combat flying task
05 p0700 N85-14491

Particle sources, transport, storage and precipitation --- magnetosphere 14 p2359 N85-24576

Electrodynamics of magnetosphere-ionosphere coupling 14 p2359 N85-24579

Ionosphere-magnetosphere coupling and convection
14 p2364 N85-24609

Magnetosphere-ionosphere interaction through hydromagnetic waves 14 p2364 N85-24610

CROSS FAULTS

U GEOLOGICAL FAULTS

CROSS FLOW

Jet array impingement flow distributions and heat transfer characteristics: Effects of initial crossflow and nonuniform array geometry 02 p0142 N85-10967

Dilution zone mixing studies 02 p0145 N85-10984

Dilution jet mixing 02 p0145 N85-10985

Tunnel constraint for a jet in crossflow
03 p0314 N85-12027

A study of flow past an airfoil with a jet issuing from its lower surface
[NASA-CR-166610] 04 p0451 N85-12860

Computer programs to predict induced effects of jets exhausting into a crossflow
[NASA-CR-166591] 05 p0592 N85-13776

An experimental study of single and multiple turbulent buoyant jets in crossflow 09 p1317 N85-18281

Turbulent bouyant flow and pressure variations around a circular cylinder in a cross uniform flow near the ground 09 p1318 N85-18287

Effect of inclination, transverse intertip spacing, and logitudinal pitch on crossflow heat transfer from an array of finned tubes 10 p1482 N85-19359

Flow visualization study of the effect of injection hole geometry on an inclined jet in crossflow
[NASA-TM-86936] 11 p1631 N85-20269

Non-steady combustion of composite solid propellants
[AD-A150827] 14 p2250 N85-23947

Development of a temperature measurement system with application to a jet in a cross flow experiment
[NASA-CR-174896] 15 p2472 N85-25262

Numerical calculation of subsonic jets in crossflow with reduced numerical diffusion
[NASA-TM-87003] 15 p2472 N85-25263

The influence of jet-grid turbulence on heat transfer from the stagnation region of a cylinder in crossflow
[NASA-TM-87011] 15 p2554 N85-25760

Design and construction of a computer controlled mirothermocouple probe for the study of buoyant jets
[AD-A152224] 16 p2788 N85-27199

A study of aerodynamic control in stalled flight leading-edge vortex formation analysis
[AD-A153758] 18 p3059 N85-28928

Acrosswind response of towers and stacks of circular cross-section 19 p3282 N85-30354

Microprocessor control design for a low-head crossflow turbine
[AD-A155477] 21 p3556 N85-32121

Wingtip vortex propeller
[NASA-CASE-LAR-13019-1] 24 p4085 N85-35194

CROSS POLARIZATION

Environmentally independent fiber optic rotation sensor
[AD-D011219] 01 p0119 N85-10818

Scattering from snow backgrounds at 35, 98, and 140 GHz
[AD-A145798] 03 p0355 N85-12280

Mechanical/thermal design of a polarization sensitive reflector --- communication satellites
05 p0626 N85-14009

The impact of propagation effects on the design of high capacity digital microwave links in the 18 GHz frequency band 10 p1470 N85-19278

CROSS RELAXATION

Contribution of relaxation sounding experiments to the understanding of magnetospheric processes
14 p2371 N85-24655

CROSS SECTIONS

Experimental studies of atomic inner shell ionization phenomena
[DE84-013448] 01 p0118 N85-10805

Stark broadening of H(-) resonances in large electric fields
[DE84-016974] 04 p0496 N85-13164

Focusing effects of a laser beam in the nonresonant multiphoton ionization (MPI) of gases
[LP-207] 04 p0506 N85-13231

Theoretical studies of highly ionized species
[DE84-016797] 04 p0561 N85-13574

On the importance of interstellar helium for the propagation of heavy cosmic rays
[OG-7.2-11] 23 p4015 N85-34879

CROSSBEDDING (GEOLOGY)

The U.S. Geological Survey in Alaska: Accomplishments during 1982
[US-GEOL-SURV-CIRC-939] 20 p3493 N85-31719

CROSSED FIELDS

Improved negative ion source
[DE85-006445] 23 p3912 N85-34241

CROSSINGS

Some studies in filtering of atmospheric turbulence
[AD-A154042] 19 p3316 N85-30557

CROSSLINKING

Method of obtaining heterocyclic polymers
[AD-A145127] 01 p0033 N85-10202

The effect of cross-link density on the toughening mechanism of elastomer-modified epoxies
04 p0465 N85-12951

Gradient polymers
[AD-A146836] 07 p0931 N85-15900

Thermoset-thermoplastic aromatic polyamide containing N-propargyl groups
[NASA-CASE-LAR-12723-1] 11 p1610 N85-20123

Status of specific FRG high tech research funded by BMFT 11 p1618 N85-20181

Chemical approach for controlling nadimide cure temperature and rate
[NASA-CASE-LEW-13770-5] 12 p1810 N85-21352

Synthesis of hydrophobic, crosslinkable resins
[AD-A150658] 14 p2260 N85-24002

Polyaromatic ether-sulfone-keytones with fluoro-substituted-p-cyclophane units as cross-linking sites
[AD-D011649] 17 p2933 N85-28105

Chemical control of nadimide cure temperature and rate
[NASA-CASE-LEW-13770-2] 18 p3069 N85-28982

Orientation and strength of semi-crystalline polymers
20 p3432 N85-31294

Development of a lithium secondary battery separator
20 p3444 N85-31378

CROSSOVERS

Interference immunity of fiber-optic communication lines with spectral multiplexing of channels
13 p2069 N85-22924

CROSSTALK

A gyro sensor block suspension
[AD-D011411] 08 p1154 N85-17284

In-flight tests 09 p1412 N85-18902

Basic EMC technology advancement for C3 systems. Volume 4F: Prediction of crosstalk in flatpack coaxial cables
[AD-A153111] 17 p2954 N85-28242

Basic EMC (Electromagnetic compatibility) technology advancement for C3 systems. Volume 4D: Modeling crosstalk in balanced twisted pairs
[AD-A153678] 18 p3090 N85-29125

Analysis of crosstalk in nonhomogeneous multiconductor lines 22 p3769 N85-33360

On the principle of uniformity of satellite communications systems 22 p3773 N85-33382

CRUCIBLES

High-temperature X-ray diffraction study of coating-substrate compatibility in yttria-coated graphite
[DE85-005916] 14 p2262 N85-24016

Power control of induction equipment for founding optical glass in array of platinum crucibles
14 p2267 N85-24044

Structure and properties of VT20L titanium alloy with 0.1-0.3 percent content 15 p2515 N85-25517

CRUDE OIL

USSR report: Chemistry
[JPRS-UCH-84-012] 06 p0761 N85-14865

Aromatics determination in middle distillate petroleum fractions by spectrophotometric titration
[PNR-90239] 09 p1293 N85-18123

Diesel fuel alternatives for engines in civil works prime movers
[AD-A149738] 12 p1817 N85-21400

Hydrocarbon pool and vapor fire data analysis
[DE85-005857] 15 p2523 N85-25550
Analysis of mesofissuring on space photographs: New technique for study of petroleum and gas deposits
16 p2726 N85-26626
Fracture detection and mapping for geothermal reservoir definition: An assessment of current technology, research, and research needs
[DE85-010627] 19 p3301 N85-30464
Subsurface petroleum geology of Santa Rosa sandstone (Triassic), northeast New Mexico
[TI85-901364] 19 p3313 N85-30536
Petroleum and mineral resources of Antarctica
[US-GEOL-SURV-CIRC-909] 20 p3477 N85-31605
A crew exposure study. Phase II. Volume 2. At sea. Part A
[AD-A155233] 21 p3666 N85-32774
AUTSKED: An addendum
[DE85-010410] 22 p3629 N85-33712
Preliminary SPR thermal model description and results for WH-11 and BM-4
[DE85-013171] 23 p3931 N85-34360
Geology and petroleum resources of basins in western China
[DE85-013036] 23 p3948 N85-34469

CRUISE MISSILES
A simulation model for Air Launched Cruise Missile engine management
[AD-A147016] 07 p1051 N85-16672
Evaluation of air and ground launched cruise missile navigational element containers
[AD-A149654] 12 p1774 N85-21136
AN investigation into the control limitations of a bank to turn missile in the terminal homing phase
[AD-A152193] 16 p2704 N85-26696
An artificial intelligence based framework for planning air launched cruise missile missions
[AD-A154466] 19 p3344 N85-30722
Computer simulation of a cruise missile using brushless dc motor fin control
[AD-A155935] 24 p4089 N85-35349
Application of pulsed power in the simulation of severe natural lightning
[DE85-012666] 24 p4124 N85-35564

CRUISING FLIGHT
Insight. Background information for multipurpose pilots: Flight phenomena 02 p0136 N85-10940

CRUSADER AIRCRAFT
U F-8 AIRCRAFT

CRUSHING
Single-point diamond crushing of Zerodur with in-situ polishing and metrology on a diamond turning machine
[DE85-012918] 24 p4083 N85-35305

CRUSTAL FRACTURES
Localization of destruction process
10 p1500 N85-19470
On the absence of strike-slip faults from the planets and satellites 13 p2200 N85-23645
Lunar mascon loading: An example of the importance of fault initiation depth on fault type predictions from stresses on planetary surfaces
13 p2200 N85-23646
Fault offsets and lateral crustal movement on Europa
13 p2201 N85-23656
Basic research for the geodynamics program
[NASA-CR-175751] 16 p2825 N85-27424
Fracture detection and mapping for geothermal reservoir definition: An assessment of current technology, research, and research needs
[DE85-010627] 19 p3301 N85-30464
Geodynamics Branch research program
[NASA-TM-86223] 20 p3489 N85-31688
The global VLBI fiducial network
20 p3490 N85-31690
First epoch measurements by Mark III VLBI of the San Andreas Fault experiment baseline
20 p3490 N85-31691
Geophysical interpretation of satellite laser ranging measurements 20 p3490 N85-31692
Satellite-determined stresses in the crust of Europe with particular consideration to the Liege earthquake of November 8, 1983 20 p3490 N85-31694
Mega-geomorphology and neotectonics
21 p3602 N85-32366
Use of space photographs for analysis of structural and dynamic conditions of formation of ancient phlogopite and apatite deposits 22 p3735 N85-33153
Subcritical fracture propagation in rocks: An examination using the methods of fracture mechanics and non-destructive testing 24 p4116 N85-35516
Groundwater radon studies for earthquake precursors in southern California
[PB85-196871] 24 p4118 N85-35529

CRUSTS
NT EARTH CRUST
NT LUNAR CRUST
More precise curve of dependence between density and velocity of longitudinal waves in consolidated crust and top of mantle in oceanic structures
13 p2110 N85-23143
Crustal and upper mantle density model of Owen fault zone 13 p2110 N85-23144
Interrelationship of earthquake magnitude and lithospheric-asthenospheric thermodynamic parameters in seismically active zones 13 p2116 N85-23183
Crustal development in the terrestrial planets
22 p3856 N85-33879
Cobalt-rich ferromanganese crusts in the oceans
24 p4104 N85-35444

CRYOGENIC COOLING
Active cooling requirements for propellant storage
08 p1108 N85-17004
Computer simulation of multiple stability regions in an internally cooled superconducting conductor and of helium replenishment in a bath-cooled conductor
[DE85-002112] 09 p1399 N85-18805
Experimental studies of low temperature surface interactions of atomic hydrogen using maser technique
[AD-A150216] 13 p2017 N85-22647
Effect of deep cooling on crack resistance and low-temperature hardening of aluminum alloys
15 p2496 N85-25396
A liquid nitrogen cooled composite wall hollow cathode --- molecular spectroscopy
[USIP-85-07] 20 p3526 N85-31930

CRYOGENIC EQUIPMENT
Exothermic processes in solids under low temperatures, their physics and their cryogenic implications
[JUEL-1919] 03 p0414 N85-12651
Passive Orbital Disconnect Strut (PODS 3) structural test program
[NASA-CR-177325] 08 p1113 N85-17020
Magentically actuated compressor
[NASA-CASE-GSC-12799-1] 12 p1818 N85-21404
Transmissive Dewar cooling chamber for optically pumped semiconductor ring lasers
[AD-D011550] 12 p1855 N85-21636
France officially proposes development of Ariane 5 to ESA 15 p2532 N85-25613
SEP of France to make Ariane HM-60 cryogenic engine 15 p2532 N85-25614
Infrared telescope
[NASA-CR-171392] 15 p2668 N85-26465
Cryogenic test technology, 1984
[AGARD-AR-212] 18 p3088 N85-29116
Vapor-liquid phase separator studies
[NASA-CR-168545] 21 p3583 N85-32272
Results of variable enthalpy tests of CPR-488 TIP panels in MSFC Hot Gas Facility
[NASA-CR-170889] 24 p4072 N85-35237

CRYOGENIC FLUID STORAGE
Shock testing of a nitrogen tank (Cryo diffusion type 220 VLR) on the middle weight shock stand
[NASA-TM-77747] 06 p0817 N85-15183
Risks in the transport and storage of liquefied natural gas. Sub-project 5-2: Investigation into building damage
[BLL-RISLEY-TR-4608-(9091.9F)]
07 p0935 N85-15926
Space shuttle electrical power generation and reactant supply system 08 p1099 N85-16947
Passive storage technologies
08 p1108 N85-17003
Propellant transfer: Attached depot
08 p1108 N85-17005
OTV fluid mangement systems
08 p1108 N85-17007
Passive Orbital Disconnect Strut (PODS 3) structural test program
[NASA-CR-177325] 08 p1113 N85-17020
Technology requirements to be addressed by the NASA Lewis Research Center Cryogenic Fluid Management Facility program
[NASA-TM-87048] 19 p3224 N85-29987
Vapor-liquid phase separator studies
[NASA-CR-168545] 21 p3583 N85-32272

CRYOGENIC FLUIDS
NT FERMI LIQUIDS
NT LIQUID HELIUM
NT LIQUID HELIUM 2
NT LIQUID HYDROGEN
NT LIQUID NITROGEN
NT LIQUID OXYGEN
NT SOLIDIFIED GASES
OTV Propulsion Issues
[NASA-CP-2347] 08 p1106 N85-16989
Ignition characterization of LOX/hydrocarbon propellants
[NASA-CR-171884] 18 p3083 N85-29070
Ignition characterization of LOX/hydrocarbon propellants
[NASA-CR-171882] 18 p3083 N85-29071
Technology requirements to be addressed by the NASA Lewis Research Center Cryogenic Fluid Management Facility program
[NASA-TM-87048] 19 p3224 N85-29987
Basic cryogenics and materials. Phase 1
[NASA-CR-177932] 21 p3572 N85-32215

CRYOGENIC MAGNETS
MFTF sensor verification computer program
[DE85-004452] 12 p1916 N85-22039

CRYOGENIC ROCKET PROPELLANTS
History, design and performance of the space shuttle hazardous gas detection system
08 p1098 N85-16938
Earth-to-orbit propellant transportation overview
08 p1108 N85-17002
Assessment study of liquid content measurement methods applicable to space missions --- Infrared Space Observatory
[TU-HH-TRI-ESA-84-2] 17 p2936 N85-28125
Investigation, development, and certification of a burst disk for cryogenic fuel tanks
[GCP-3/MT-CM-21-2546] 18 p3067 N85-28972

CRYOGENIC WIND TUNNELS
Review of the advanced technology airfoil test program in the 0.3-meter transonic cryogenic tunnel
03 p0315 N85-12033
Some experience with Barnwell-Sewall type correction to two-dimensional airfoil data 03 p0315 N85-12034
Adaptation of a four-wall interference assessment/correction procedure for airfoil tests in the 0.3-m TCT 03 p0315 N85-12035
First cryogenic test of the CAST 7 profile in the T2 wind tunnel. Comparison with calculations --- airfoils
[ONERA-RTS-56/1685-AY-035-D]
04 p0577 N85-13882
Description of the insulation system for the Langley 0.3-Meter Transonic Cryogenic Tunnel
[NASA-TM-86274] 07 p0909 N85-15755
Initial investigation of cryogenic wind tunnel model filler materials
[NASA-TM-86363] 09 p1283 N85-18089
Exploratory flutter test in a cryogenic wind tunnel
[NASA-TM-86380] 12 p1863 N85-21688
Cryogenic wind tunnels: A selected annotated bibliography
[NASA-TM-86346] 13 p1976 N85-22401
Qualification of the T2 wind tunnel in cryogenic operation. A: Thermal field, preliminary study of a schematic model
[NASA-TM-77781] 14 p2227 N85-23805
Qualification of the T2 wind tunnel in cryogenic operation. B: Flow fluctuations, particle detection and qualification
[NASA-TM-77782] 14 p2227 N85-23806
Measurements in the flow field of a cylinder with a laser transit anemometer and a drag rake in the Langley 0.3 m transonic cryogenic tunnel
[NASA-TM-86399] 14 p2305 N85-24270
Cryogenic test technology, 1984
[AGARD-AR-212] 18 p3088 N85-29116
High Reynolds number tests of a NASA SC(3)-0712(B) airfoil in the Langley 0.3-meter transonic cryogenic tunnel
[NASA-TM-86371] 19 p3213 N85-29826
Pressure distribution from high Reynolds number tests of a NASA SC(3)-0712(B) airfoil in the Langley 0.3-meter transonic cryogenic tunnel
[NASA-TM-86370] 19 p3213 N85-29827
Sidewall boundary-layer effects in two-dimensional airfoil testing
[NASA-CR-176034] 20 p3396 N85-31085
Materials and techniques for model construction
[NASA-CR-172620] 20 p3396 N85-31086
A systematic plan for the continued study of dimensional stability of metallic alloys considered for the fabrication of cryogenic wind tunnel models
[NASA-CR-172449] 21 p3565 N85-32172
A theoretical study of non-adiabatic surface effects for a model in the NTF cryogenic wind tunnel
[NASA-CR-3924] 23 p3929 N85-34352

CRYOGENICS
Conversion of microwave signals by superconducting films in the resistive state
[NASA-TM-77595] 01 p0123 N85-10843
Formation of superconductive Al(GeSi) alloys by low temperature laser quenching methods
[DE84-016667] 04 p0474 N85-13021
Thermal and cryogenic design study for space infrared telescope facility (SIRTF)
[NASA-CR-166613] 07 p0915 N85-15783
Cryogenic glass-to-metal seal
[AD-D011370] 07 p0933 N85-15911
Study of infrared atmospheric emission
[AD-A147517] 07 p0998 N85-16336
Research and technology, 1984 report
[NASA-TM-83096] 07 p1061 N85-16730

Automatic software for controlling cryogenic systems 08 p1097 N85-16932
Cryogenic propellant management: Integration of design, performance and operational requirements 08 p1098 N85-16939
Advanced OTV engines and issues 08 p1108 N85-17000
Acoustic microscopy at cryogenic temperatures [AD-A148755] 09 p1384 N85-18704
Analysis of compact heat exchanger performance [DE84-012624] 10 p1485 N85-19377
Emergency Locator Transmitter (ELT) batteries guidance and recommendations [NASA-TM-87436] 11 p1624 N85-20225
Method of calculating cooldown process in cryostat of cryogenic electric machine 12 p1843 N85-21567
Electrical performance of semiconductor devices at cryogenic temperatures 12 p1948 N85-22239
Survey of the state-of-the-art of miniature cryocoolers for superconductive devices [AD-A150319] 13 p2041 N85-22774
Manrating orbital transfer vehicle propulsion [NASA-TM-87019] 15 p2494 N85-25385
Electronic transport in Mo/Ni superlattice [DE85-008835] 15 p2661 N85-26425
Bearings working group 16 p2735 N85-26878
Advanced rocket engine cryogenic turbopump bearing thermal model 16 p2735 N85-26879
Hybrid bearings for LH2 and LO2 turbopumps 16 p2736 N85-26880
Rolling contact fatigue life of chromium ion plated 440C bearing steel 16 p2736 N85-26882
Research on design of cryotransformers and its prospects for the future [AD-A152400] 17 p2952 N85-28230
Experience with oepration of a large magnet system in the international fusion superconducting magnet test facility [DE85-009288] 17 p3027 N85-28721
Technique to reduce scattered light in optical systems [AD-D011597] 18 p3185 N85-29752
E-beam-induced fluorescence of excimers in cryogenic solutions [DE85-010703] 19 p3278 N85-30328
Cryogenics for the Superconducting Super Collider: Workshop Proceedings [DE85-010051] 20 p3437 N85-31327
Capacitive energy storage at cryogenic temperatures [AD-A154508] 21 p3579 N85-32253
SCRIBE data of October 23, 1983 flight [AD-A154884] 21 p3705 N85-33012
Cryogenic system for the University of Washington Superconducting Booster [DE85-010604] 22 p3754 N85-33274
Evaluation study of mechanical refrigeration systems for application to space missions — infrared astronomy [SNIAS-1029ACA/LL/V] 22 p3755 N85-33277
Partial discharges in and electric strength of high-voltage polymer insulation at cryogenic temperatures 22 p3770 N85-33364
Separation of gas mixtures by supported complexes [DE85-011996] 23 p3912 N85-34236
Cryogenic laser calorimetry for impurity analysis [NASA-CR-176179] 24 p4097 N85-35395
Solid neon sources for plasma and X-ray lasers [DE85-011347] 24 p4098 N85-35402

CRYOSORPTION
U SORPTION

CRYOSTATS
Method of calculating cooldown process in cryostat of cryogenic electric machine 12 p1843 N85-21567
Superconducting magnet technology for accelerators [DE85-004192] 12 p1926 N85-22102
Germanium resistance thermometer calibration at superfluid helium temperatures 12 p1947 N85-22228
Infrared telescope [NASA-CR-171392] 15 p2668 N85-26465
Cryostat and electronic development associated with multi-detector spectrometer systems [DE85-007624] 16 p2788 N85-27203
Operation of HFTF to test the MIT 12 T coil [DE85-010409] 18 p3195 N85-29821
Cryogenic system for the University of Washington Superconducting Booster [DE85-010604] 22 p3754 N85-33274

CRYPTOGRAPHY
Reserve and authentication in Integrated Services Distributed Networks (ISDN) networks [FUB-37-1983] 01 p0041 N85-10262
Most wanted factorizations using the quadratic sieve [DE84-016208] 05 p0718 N85-14609
A public key cryptographic algorithm based on a generalization of the knapsack problem [FUB-7-1984] 09 p1313 , N85-18250
Digital signatures: An update [NPL-DITC-51/84] 09 p1367 N85-18589
Security controls in the Stockpoint Logistics Integrated Communications Environment (SPLICE) [AD-A155536] 21 p3576 N85-32244
An algorithm for the generation of primitive polynomials [FUB-17-1984] 22 p3831 N85-33730

CRYSTAL DEFECTS
NT CRYSTAL DISLOCATIONS
NT EDGE DISLOCATIONS
NT POINT DEFECTS
NT SCREW DISLOCATIONS
NT VACANCIES (CRYSTAL DEFECTS)
Process Research of Polycrystalline Silicon Material (PROPSM) [NASA-CR-173838] 01 p0067 N85-10446
Toughness in high speed steels and hard metals 02 p0176 N85-11181
Formation of lattice defects by nitrogen laser exposure in A2B6 semiconductors with wide forbidden band 02 p0258 N85-11692
Internal friction, microstructure and radiation effects [DE84-013905] 02 p0288 N85-11860
Annealing of implanted Al-2O-3 in a reducing environment [DE84-015370] 03 p0332 N85-12140
Microstructure of ceramics fabricated by unidirectional solidification [NASA-TM-77423] 03 p0336 N85-12157
Study of structure of sponge titanium varieties 03 p0350 N85-12256
Energy of stacking fault and dislocation structure of titanium alloys 03 p0351 N85-12259
Lattice defects in body centered cubic transition metals 03 p0427 N85-12727
Neutron irradiation of semiconductors — lattice defects, electron irradiation 03 p0428 N85-12732
Radiation induced defects in superconductors of type 2 03 p0429 N85-12734
Determination of depth profiles and lattice positions with (n, p)- and (n, alpha) reactions (n, alpha) and channeling-blocking method) 03 p0429 N85-12735
Mossbauer spectroscopic investigations of the diffusion and correlation of lattice defects (complementary to neutron spectroscopic investigations) 03 p0429 N85-12736
Investigation of the production and properties of lattice defects induced by low temperature reactor irradiation 03 p0430 N85-12739
X-ray and neutron scattering and X-ray spectroscopy for the study of defects in solid state materials 03 p0430 N85-12741
Spectroscopic investigations on neutron induced impurity atoms and radiation defects 03 p0430 N85-12742
Studies of grown-in defects versus growth parameters in 3-4 compound semiconductors [AD-A145864] 03 p0433 N85-12755
Interaction of hydrogen with defects in metals [DE84-016781] 04 p0476 N85-13032
Imaging of surfaces and defects of crystals [DE84-016449] 04 p0570 N85-13632
EPR linewidth studies of unpaired electrons at the Si-SiO2 [DE84-016727] 05 p0733 N85-14712
Investigation of structural and electrical properties of low-angle silicon sheet 06 p0831 N85-15288
Semicrystalline casting process development and verification 06 p0832 N85-15289
Defective nature of the crystalline lattice of nickel ferrite-based solid solutions [BLL-WH-595-(9091.9F)] 07 p1046 N85-16645
Ferromagnetism in metals at finite temperatures [DE85-000898] 09 p1377 N85-18656
Fundamental aspects on ion-beam surface modification: Defect production and migration processes [DE85-000093] 09 p1399 N85-18804
Stress studies in EFG [NASA-CR-175488] 10 p1563 N85-19856
International Conference on Defects in Insulating Crystals [AD-A149611] 12 p1939 N85-22180
Fracture mechanics evaluation of GaAs [NASA-CR-175657] 13 p2102 N85-23101
Recent developments in semiconductor research 14 p2297 N85-24222
Influences of thermal spikes in ion beam mixing [DE85-006130] 14 p2419 N85-24924
Energy trapping, release, and transport in three-dimensional energetic solids and molecular crystals: Theory of defects and impurities [AD-A151071] 14 p2428 N85-24973
High resolution Z-contrast imaging and lattice location analysis of dopants in ion-implanted silicon [DE85-005261] 14 p2429 N85-24980
Electrochemical behavior of amorphous alloys based on iron, cobalt and nickel in H3PO4 solutions alone and mixed with HF 15 p2513 N85-25505
Process Research on Polycrystalline Silicon Material (PROPSM) [NASA-CR-175761] 15 p2587 N85-25951
Compensation of dangling bonds in A-Si, Ge:H alloys [DE85-002905] 15 p2602 N85-26433
Simulation of solidification in a Bridgman cell [NASA-CR-175838] 16 p2670 N85-27705
TEM investigation of polar-on-nonpolar epitaxy: GaAs-AlGaAs on (100) Ge [DE85-007613] 16 p2871 N85-27714
Quantitative analysis of defects in silicon-characterization of UCP, HAMCO, and microcrystalline material [NASA-CR-175988] 18 p3079 N85-29046
Method of reducing impurity and antisite defects in semiconductor crystal materials, and device and apparatus respectively produced from and utilizing same [AD-D011698] 19 p3260 N85-30216
Method for growing low defect, high purity crystalline layers [NASA-CASE-NPO-15813-2] 19 p3374 N85-30933
Solid State Division report on its mission-oriented basic research [DE85-008766] 19 p3376 N85-30941
Surface passivation and junction formation using low energy hydrogen implants 20 p3480 N85-31628
Structural defects in crystalline silicon 20 p3481 N85-31630
Oxygen and carbon impurities and related defects in silicon 20 p3481 N85-31631
EBIC characterization and hydrogen passivation in silicon sheet 20 p3481 N85-31634
Defect production and recovery in FCC metals irradiated at 4.2 K [DE85-010477] 20 p3538 N85-32014
Studies of oxygen- and carbon-related defects in high-efficiency silicon solar cells 21 p3609 N85-32420
High-purity silicon crystal growth 21 p3612 N85-32444
Defect formation in amorphous hydrated silicon subjected to laser radiation 21 p3682 N85-32873
An EPR (Electron-Paramagnetic-Resonance) and ENDOR (Electron-Nuclear-Double-Resonance) study of ferroelectric ammonium sulfate [AD-A155580] 21 p3710 N85-33033
Solid-melt interface studies of high-speed silicon sheet growth [NASA-CR-176112] 22 p3751 N85-33249
Simulation of lattice damage due to dynamic loading [DE85-008468] 24 p4162 N85-35808

CRYSTAL DISLOCATIONS
NT EDGE DISLOCATIONS
NT SCREW DISLOCATIONS
Plastic deformation and microstructural transformations of metals under shock waves 02 p0272 N85-11775
Energy of stacking fault and dislocation structure of titanium alloys 03 p0351 N85-12259
Irradiation creep induced anisotropy in a/2110 dislocation populations [DE84-016623] 06 p0868 N85-15520
Strain analysis of the Leoville chondrite and conditions in asteroidal interiors 06 p0885 N85-15620
Back stress in dislocation creep. Part 1: Basic concepts and measuring techniques [NASA-TM-77773] 07 p0977 N85-16206
The fundamentals of dislocation transport of hydrogen in bcc iron [AD-A148143] 08 p1129 N85-17117
Influence of the amorphous-crystalline interface morphology on dislocation nucleation in pre-amorphized silicon [DE85-002068] 09 p1398 N85-18800
Comparisons between computed and observed grain boundary structures and properties in metals [DE85-002596] 10 p1442 N85-19085
Role of hydrogen in processes of deformation and fracture of metals 10 p1449 N85-19132
Stress studies in EFG [NASA-CR-175464] 10 p1509 N85-19522
The role of dislocations in ultrasonic attenuation [AERE-R-11364] 12 p1804 N85-21317
Investigation of the effect of annealing on the dislocation and sub-grain boundary content of solvent-evaporation-grown CdTe [AD-A144087] 13 p2162 N85-23415
Solid/melt interface studies of high-speed silicon sheet growth [NASA-CR-175698] 14 p2350 N85-24525
Stress and efficiency studies [NASA-CR-175688] 14 p2351 N85-24531

Studies of deformation in niobium by X-ray topographic methods
[AD-A150726] 14 p2427 N85-24965

Structural unit/grain boundary dislocation model for twist boundaries in cubic crystals
[DE85-000425] 14 p2430 N85-24965

Effects of gamma-ray irradiation on dislocations in sodium nitrate single crystals
[DE85-008291] 18 p3195 N85-29818

Electrical and structural characterization of web dendrite crystals 20 p3481 N85-31633

Solid-melt interface studies of high-speed silicon sheet growth
[NASA-CR-176112] 22 p3751 N85-33249

An enhanced photoresponse at dislocation subgrain boundaries revealed by X-ray topography of polysilicon solar cells 22 p3806 N85-33572

CRYSTAL FILTERS

Single crystal semiconductor multilayers for electrically active optical interference filters
[DE84-015614] 04 p0571 N85-13640

Quartz filter transceiver 12 p1838 N85-21538

Normal coordinate monolithic crystal filter
[AD-D011496] 12 p1941 N85-22188

CRYSTAL GROWTH

NT CZOCHRALSKI METHOD
NT DIRECTIONAL SOLIDIFICATION (CRYSTALS)
NT ELECTROEPITAXY
NT EPITAXY
NT HYDROTHERMAL CRYSTAL GROWTH
NT LIQUID PHASE EPITAXY
NT MOLECULAR BEAM EPITAXY
NT TRAVELING SOLVENT METHOD
NT VAPOR PHASE EPITAXY

Critical conditions for the growth of SiC, Si3N4, and SiO2
[DE84-014824] 01 p0030 N85-10185

The absence of convective stability in incongruent crystal growth on Earth 02 p0150 N85-11019

Solidification and crystal growth of solid solution semiconducting alloys 02 p0155 N85-11046

Microstructural design in low alloy steels
02 p0176 N85-11179

The growth of twins and twin lamellae in synthetic diamond crystals 02 p0181 N85-11213

Simulation of solidification in a Bridgman cell
[NASA-CR-3843] 02 p0197 N85-11314

Silicon sheet with molecular beam epitaxy for high efficiency solar cells
[NASA-CR-174022] 02 p0222 N85-11459

Large-area sheet task advanced dendritic web growth development
[NASA-CR-174021] 02 p0223 N85-11463

Low-threshold injection lasers on grown GaInPAs/InP heterostructures (1.2-1.6 micrometers wavelengths)
02 p0258 N85-11693

Transport phenomena in the boundary layer during solution solidification under microgravity. Ice growth from a water-salt solution
[BMFT-FB-W-84-031] 03 p0329 N85-12121

Bibliography of Soviet laser developments, number 65, May - June 1983
[AD-A146189] 03 p0366 N85-12347

Measurements on the triple axis spectrometer UNIDAS for the investigation of dynamic processes in crystals using inelastic neutron scattering 03 p0426 N85-12716

Structure and kinetics of physisorption, properties of helium during reduction of the dimension
03 p0432 N85-12749

Studies of grown-in defects versus growth parameters in 3-4 compound semiconductors
[AD-A145864] 03 p0433 N85-12755

The effect of thin-film growth mode on XPS/UPS/AES intensities
[AD-A146284] 03 p0434 N85-12763

A preliminary study of numerical simulation of thermosolutal convection of interest to crystal growth
[NASA-TP-2394] 04 p0498 N85-13175

Silicon for solar cells
[DE84-004503] 04 p0529 N85-13381

Chemical engineering principles of constant temperature-constant supersaturation growth of potassium dihydrogen phosphate (KDP) crystals
[DE84-017081] 04 p0571 N85-13645

Electron channeling and EBIC studies of polycrystalline silicon sheets
[DE84-004515] 05 p0670 N85-14309

Miniworkshop on effects of stress and strain in high-speed-growth silicon ribbons
06 p0831 N85-15284

Advanced dendritic web growth development
06 p0831 N85-15286

Preparation and electronic properties of MoS(2) and WS(2) single crystals grown in the presence of cobalt
[AD-A146508] 06 p0866 N85-15506

Research on submicrometer structures
[AD-A146578] 06 p0867 N85-15508

The growth and properties of semiconductor strained-layer superlattices
[DE84-012979] 06 p0868 N85-15515

Float zone experiments in space
[NASA-CR-171284] 07 p0911 N85-15786

Crystal growth and characterization of BaMgF4
[AD-A146805] 07 p1047 N85-16650

Improved solid-state laser sources, volume 2
[DE85-000759] 09 p1325 N85-18330

Advanced high-efficiency concentrator cells
[DE84-013020] 09 p1344 N85-18459

The growth of large diameter single crystals by vertical solidification of the melt
[AD-A148756] 09 p1397 N85-18792

Silicon film solar cell process
[NASA-CR-174446] 10 p1506 N85-19514

Material growth and characterization for solid state devices
[NASA-CR-174410] 10 p1561 N85-19847

Quaternary narrow-band semiconductors (HgTe)x (InSb)1-x for far-infrared detectors
[AD-A149350] 10 p1562 N85-19852

Development of a polysilicon process based on chemical vapor deposition of dichlorosilane in an advanced Siemen's reactor
[NASA-CR-174445] 11 p1672 N85-20532

A computer simulation of thin film nucleation and growth: The Volmer-Weber case
[NASA-TM-86968] 12 p1796 N85-21264

Topics in optical materials and device research, 3: Volume 1
[AD-A149726] 12 p1933 N85-22145

Nucleation of phase transitions in the vicinity of phase boundary. Part 1: Comparison of various idolated mechanisms. Part 2: Coupled cluster growth processes
[N-0208-5658] 12 p1936 N85-22174

Method for the preparation of epitaxial films of mercury cadmium telluride
[AD-D011532] 12 p1938 N85-22175

Total immersion crystal growth
[NASA-CASE-NPO-15800-2] 12 p1939 N85-22178

Basis and pyramidal slipping in single crystals of alpha-alloy Ti-Al-Sn 13 p2032 N85-22730

Hibonite: Crystal chemistry and origin of blue coloration in meteoritic assemblages 13 p2184 N85-23555

Material research in microgravity
[NASA-TM-77628] 14 p2228 N85-23811

Proceedings of the Cold Electronics Workshop
[NASA-CR-175662] 14 p2297 N85-24220

Recent developments in semiconductor research
14 p2297 N85-24222

Stress and efficiency studies
[NASA-CR-175688] 14 p2351 N85-24531

Development of solid state infrared emitters for gas detection applications
[PB85-148450] 15 p2561 N85-25800

Fundamental studies of growth, doping and transformation in beta silicon carbide
[AD-A152047] 15 p2660 N85-26416

Optimum convection conditions for Czochralski growth of semiconductors
[INPE-3395-PRE/665] 16 p2870 N85-27703

Simulation of solidification in a Bridgman cell
[NASA-CR-175838] 16 p2870 N85-27705

Dendritic growth from amorphous matrix
[DE85-007630] 16 p2871 N85-27712

High-thermal-gradient superalloy crystal growth
17 p2914 N85-27966

Research on the kinetics of phase changes in solids
[AD-A152387] 17 p2918 N85-27989

Model for the growth of fractal silica polymers
[DE85-007884] 17 p2935 N85-28115

Heat pipe and method of making same
[AD-D011654] 17 p2959 N85-28273

InP materials
[AD-A152341] 17 p3043 N85-28828

Telescoping low vibration pulling mechanism for Czochralski crystal growth
[AD-D011655] 17 p3044 N85-28836

Rapid growth of potassium dihydrogen phosphate crystals
[DE85-007261] 17 p3045 N85-28839

Morphology of GaAs/sub 1-x/P/sub x/ superlattices grown by MOCVD and chloride VPE
[DE85-002944] 17 p3045 N85-28842

Method for growth of crystals by pressure reduction of supercritical or subcritical solution
[NASA-CASE-NPO-15772-1] 18 p3192 N85-29800

Growth mechanism and properties of the thermal and anodic oxides of the 3-5 compound semiconductors
[AD-A153406] 18 p3193 N85-29803

TEM combined with Al/sub x/Ga/sub 1-x/ as marker layers as a technique for the study of GaAs MBE growth
[DE85-008451] 18 p3194 N85-29809

Crystal growth from the vapor in low gravity environments
[DE85-009628] 18 p3195 N85-29816

Method of reducing impurity and antisite defects in semiconductor crystal materials, and device and apparatus respectively produced from and utilizing same
[AD-D011698] 19 p3260 N85-30216

Electrohydrodynamic process for the production of large area polycrystalline silicon sheet
[DE85-008781] 19 p3261 N85-30225

Method for the preparation of photochromic insulating crystals
[DE85-011606] 19 p3262 N85-30229

Spectroscopic investigation of materials for tunable infrared lasers
[AD-A154124] 19 p3272 N85-30281

Low defect, high purity crystalline layers grown by selective deposition
[NASA-CASE-NPO-15813-1] 19 p3373 N85-30922

Method for growing low defect, high purity crystalline layers
[NASA-CASE-NPO-15813-2] 19 p3374 N85-30933

Crystal growth of device quality GaAs in space
[NASA-CR-176024] 19 p3375 N85-30935

Development of growth techniques for electromagnetic crystals
[AD-A154089] 19 p3375 N85-30937

The use of moments of momentum to account for crystal habits
[NASA-CR-3907] 20 p3421 N85-31232

High-efficiency cell concepts on low-cost silicon sheets 20 p3479 N85-31621

Temperature field around a spherical, cylindrical, and needle-shaped crystal, growing in a pre-cooled melt
[NASA-TM-77869] 20 p3537 N85-32011

The EURECA solution growth facility conceptual design study. Executive summary
[ESA-CR(P)-2007] 20 p3538 N85-32016

High-frequency furnace
[DE85-011210] 21 p3586 N85-32291

Silicon production in an aerosol reactor
21 p3609 N85-32416

Silicon dendritic web growth 21 p3611 N85-32435

Temperature-stress modeling
21 p3611 N85-32436

Silicon ribbon stress-strain activities
21 p3611 N85-32437

Analysis of stress-strain relationships in silicon ribbon
21 p3611 N85-32438

Stress and buckling analysis 21 p3611 N85-32439

Stress and efficiency studies in EFG
21 p3611 N85-32440

Silicon sheet surface studies
21 p3611 N85-32441

Analysis of inclined growth of silicon sheet
21 p3612 N85-32442

Edge-defined film-fed growth of thin silicon sheets
21 p3612 N85-32443

High-purity silicon crystal growth
21 p3612 N85-32444

Failure analysis of thin-film amorphous-silicon solar-cell modules 21 p3613 N85-32452

Ice crystal nucleation on hygroscopic aerosols
21 p3639 N85-32805

The nucleation of ice crystals during the freezing of large supercooled drops 21 p3640 N85-32808

X-ray diffractometric measurements and calculations of limiting values of discrepancy between lattices and layer thicknesses, preventing generation of dislocations during growth of multilayer heterostructures
21 p3681 N85-32866

Nonequilibrium kinetics of growth of oxide layer grains during laser heating of metals in air
21 p3689 N85-32919

The development and evaluation of point defect models for the growth of passive films on single crystal, polycrystalline, and amorphous metal surfaces
[AD-A154685] 21 p3709 N85-33023

Chemical constraints on the evolution of Archean continental crust 21 p3722 N85-33093

New and revised methods of purifying mercuric iodide
[DE85-011684] 22 p3749 N85-33237

Solid-melt interface studies of high-speed silicon sheet growth
[NASA-CR-176112] 22 p3751 N85-33249

Stress and efficiency studies in EFG
[NASA-CR-176125] 22 p3751 N85-33251

Striation free doped silicon
[AD-A155730] 22 p3847 N85-33827

Apparatus and method for the horizontal, crucible-free growth of silicon sheet crystals
[DE85-011588] 22 p3847 N85-33829

Manufacturing process to reduce large grain growth in zirconium alloys
[DE85-011649] 23 p3915 N85-34267

Crystallization of Polyetheretherketone (PEEK) in carbon fiber composites [AD-A156316] 24 p4075 N85-35252
Investigations of the molecular beam epitaxial growth and characteristics of external excitation induced non-equilibrium phases of immiscible 3-5 compound semiconductors [AD-A156325] 24 p4162 N85-35804

CRYSTAL LATTICES
NT BODY CENTERED CUBIC LATTICES
NT CUBIC LATTICES
NT FACE CENTERED CUBIC LATTICES
NT SUPERLATTICES
Structure and wear workshop colloquium 01 p0054 N85-10356
Structure and abrasive resistance of iron based alloys rich in hardening components 01 p0054 N85-10360
Friction, wear and structure of heterogeneous materials 01 p0055 N85-10362
Kinetics of short-range ordering in metallic glasses: Analysis of the crossover effect [DE84-015524] 02 p0187 N85-11251
Microfluorescence studies of zirconium oxide [DE84-016116] 03 p0329 N85-12116
Annealing of implanted Al-2O-3 in a reducing environment [DE84-015370] 03 p0332 N85-12140
Neutron scattering on the FRM double crystal spectrometer 03 p0423 N85-12704
Anharmonic lattice effects in molecular crystals 03 p0424 N85-12709
Phonon anomalies in superconducting transition metal compounds --- lanthanum and niobium compounds 03 p0426 N85-12718
Electronic structure and lattice dynamics of solid state substances from gamma nuclear resonance absorption and angular correlation measurements 03 p0427 N85-12728
Determination of depth profiles and lattice positions with (n, p)- and (n, alpha) reactions (n, alpha) and channeling-blocking method) 03 p0429 N85-12735
Reaction mechanisms in the formation of intercalation complexes, and properties of intercalated molecules 03 p0431 N85-12745
Structural changes during milling of aluminum oxide powders [NASA-TM-77488] 04 p0472 N85-13008
The alpha-form of the hydroxides of bivalent metals [NASA-TM-77508] 04 p0473 N85-13009
The disordering process in an L1sub2 ordered alloy [DE84-016599] 04 p0475 N85-13028
Interaction of hydrogen with defects in metals [DE84-016781] 04 p0476 N85-13032
Coherent amplification of ultrasonic pulses in activated crystals 05 p0724 N85-14653
The atomic structure of Si-SiO2 interfaces suggesting a ledge mechanism of silicon oxidation [DE84-016057] 05 p0731 N85-14703
Electronic bandstructure of an incommensurate crystal [DE84-016891] 05 p0733 N85-14714
Theoretical investigation of device aspects of semiconductor superlattices [AD-A146641] 06 p0867 N85-15509
Superlattice ultrasonic wave generator [AD-D011363] 07 p1038 N85-16585
Defective nature of the crystalline lattice of nickel ferrite-based solid solutions [BLL-WH-595-(9091.9F)] 07 p1046 N85-16645
Microscopic determinations of lattice and electronic structures of solids [DE84-017323] 09 p1399 N85-18806
Defective nature of the crystalline lattice of nickel ferrite-based solid solutions [BLL-TRANS-WH-595-(9091.9F)] 10 p1439 N85-19068
Comparisons between computed and observed grain boundary structures and properties in metals [DE85-002596] 10 p1442 N85-19085
Study of influence of cold plastic deformation on aging of VT30 alloy 10 p1448 N85-19124
Solid electrolytes. Mechanisms for achieving optimal conductivity [AD-A150116] 12 p1801 N85-21296
The crystal and molecular structure of a new propellant compound: Triaminoguanidium Azide Nitrate (TAZN) 13 p2002 N85-22551
Molecular dynamics studies of energy transfer processes in crystal systems [AD-A150161] 13 p2163 N85-23416
Peculiarities of MgF2 film formation and optimization of MgF2 film deposition process 14 p2281 N85-24132
Recent developments in semiconductor research 14 p2297 N85-24222
Monte Carlo lattice models for adsorbed polymer conformation [NASA-TP-2453] 14 p2426 N85-24961
Interaction of low energy electrons with surface lattice vibrations [DE85-005475] 14 p2428 N85-24975
Relationship between symmetrical tilt, twist, special, and favored grain boundaries [DE85-004024] 14 p2429 N85-24982
Novel materials properties of strained-layer superlattices [DE85-003676] 14 p2430 N85-24989
Raman scattering of light in epitaxial films of solid phosphide-gallium arsenide solutions 15 p2643 N85-26301
Electronic transport in Mo/Ni superlattice [DE85-006835] 15 p2661 N85-26425
Molecular dynamics studies of energy transfer processes in crystal systems [DE85-007247] 15 p2662 N85-26426
On the feasibility of Ab Initio calculations of ordering alloy phase diagrams [DE85-007073] 16 p2751 N85-26979
Thermal annealing of Fe implanted Al2O3 in oxidizing and reducing environment: Revised version [DE85-007546] 16 p2752 N85-26983
Atom location by electron channeling analysis [DE85-007549] 16 p2872 N85-27716
Investigation of superlattice device structures [NASA-CR-3903] 18 p3094 N85-29152
Structural and physical studies on a new class of low-dimensional conducting material: FeOCl intercalated with TTF and related molecules [DE85-009701] 18 p3196 N85-29824
Quasiparticle excitations in valence-fluctuation materials: Effects of band structure and crystal fields [DE85-010783] 19 p3359 N85-30824
Solid State Division report on its mission-oriented basic research [DE85-008766] 19 p3376 N85-30941
A study of the effect of a mismatch in gamma and gamma prime phase lattice spacings on the high temperature strength characteristics of dispersion-hardened nickel alloys [BLL-CE-TRANS-8048-(9022.09)] 20 p3430 N85-31279
Structural defects in crystalline silicon 20 p3481 N85-31630
Interfacial bonding stability 21 p3608 N85-32409
Raman scattering studies in solids [AD-A155528] 21 p3710 N85-33032
On the potential link equation of a spot centre with relative deformation for a semi-infinite molecular crystal [BLL-M-35795-(5828.4)] 23 p3985 N85-34711
Flux-line lattice anisotropy in V3Si: Observation and interpretation [DE85-011935] 23 p3985 N85-34713
Simulation of lattice damage due to dynamic loading [DE85-008468] 24 p4162 N85-35808

CRYSTAL OPTICS
Coherent amplification of ultrasonic pulses in activated crystals 05 p0724 N85-14653
Research progress on laser crystals in China 13 p2166 N85-23440
Lidar ER2 (ozone). Crystal characterization for harmonic conversion --- laser systems [CERT-2/6129-00] 16 p2872 N85-27717
Generation and amplification of radiation during stimulated Raman scattering in crystals 21 p3681 N85-32869

CRYSTAL OSCILLATORS
NT PIEZOELECTRIC CRYSTALS
Method of heating quartz resonators [AD-D011454] 10 p1481 N85-19347
SAW oscillator with digital compensation for the temperature related frequency changes [AD-D011537] 12 p1833 N85-21500
Externally compensated crystal oscillator (ECXO) study [AD-A150335] 13 p2064 N85-22693
Adjustment of the frequency-temperature characteristics of crystal oscillators [AD-D011586] 15 p2548 N85-25726
Development of a Digitally Compensated SAW Oscillator (DCSO) to provide temperature stable frequency [AD-A151907] 15 p2549 N85-25730
Cut angles for quartz crystal resonators [AD-D011652] 17 p2951 N85-28220
Acceleration insensitive oscillator [AD-D011621] 17 p2953 N85-28236
Proceedings of the Fifteenth Annual Precise Time and Time Interval (PTTI) Applications and Planning Meeting [AD-A149163] 17 p2961 N85-28287
A new precision time and frequency source for stationary PTTI applications 17 p2963 N85-28297
A plan for the development of inertial reconstruction of initial state clock (IRIS) 17 p2966 N85-28317
High performances from a new design of crystal oscillator 17 p2966 N85-28318
Design of SC cut 10 MHZ H.Q. crystals with G. sensitivity better than 2.10(-10)/G 17 p2966 N85-28319
Crystal resonator/oscillator test facility and test results 17 p2967 N85-28322
The Rubidium-Crystal Oscillator Hybrid Development Program 18 p3106 N85-29230
New features of different frequency generating systems due to the use of electrodeless rigidly mounted VBA quartz crystal resonator 18 p3106 N85-29231

CRYSTAL STRUCTURE
13C and 1H NMR (Nuclear Magnetic Resonance) studies of solid polyolefines [AD-P003909] 01 p0032 N85-10195
Fundamental studies of structure property relationship in transformation toughened ceramics [DE84-015344] 01 p0033 N85-10204
Rapid solidification processing and the control of structure/property relationships 02 p0176 N85-11178
Photoelectric effect in liquid crystals 02 p0259 N85-11695
Determining composition in surface region of semiconductor crystals by method of sudden changes in X-ray photoelectric effect 02 p0267 N85-11746
Low temperature properties of Mo/Mi superlattices [DE84-014729] 02 p0288 N85-11881
Fundamental electronic properties of donor-type graphite intercalated compounds [AD-A146148] 03 p0326 N85-12099
Effect of heat treatment on phase composition and crystal structure of thin WSi2 films on silicon substrates 03 p0350 N85-12253
One-dimensional model of thin films. Analysis of aluminum surface 03 p0350 N85-12254
Report on research results in solid state nuclear physics, 1980-1982 [JUEL-SPEZ-250] 03 p0422 N85-12696
Fine structure analysis with thermal neutrons and development and construction of a multidetector system 03 p0422 N85-12698
Crystal chemistry and real structure of crystals 03 p0423 N85-12703
Diffuse elastic and inelastic neutron scattering of disorder transitions and boundaries. Phase determination of structure factors 03 p0424 N85-12708
Anharmonic lattice effects in molecular crystals 03 p0424 N85-12709
Phase transformations of AlPO4 with SiO2 structures 03 p0425 N85-12713
Inelastic neutron scattering on crystals for the clarification of structure and semiconductor properties 03 p0425 N85-12714
Magnetic interaction in low-dimensional systems 03 p0426 N85-12717
Investigations on low-dimensional solid state substances --- solitons 03 p0426 N85-12720
Structural phase transitions in doped hexahalogen metallates 03 p0426 N85-12721
Structure and kinetics of physisorption, properties of helium during reduction of the dimension 03 p0432 N85-12749
Neutron scattering for the investigation of solid state materials, utilization in chemical structures 03 p0432 N85-12752
Static and quasielastic neutron scattering for the investigation of structure, dynamics and transport properties of lipid layers and lipid/protein compounds 03 p0432 N85-12753
A physical interpretation of the structure and electron-optical data for spinel (MgAl2O4) [AERE-R-11278] 03 p0434 N85-12767
Critical evaluation of binary rare Earth diagrams [DE84-014880] 04 p0470 N85-12991
Structural changes during milling of aluminum oxide powders [NASA-TM-77488] 04 p0472 N85-13008
Cerium compounds in the fashion of the light actinides [DE84-014642] 04 p0475 N85-13024
Nonthermal mechanism for laser annealing of semiconductors and formation of super structure 04 p0487 N85-13109
Improved apparatus and techniques for high temperature and pressure deformation of crystalline materials [DE84-016049] 04 p0569 N85-13629
Computational models of crystals [DE84-016631] 04 p0572 N85-13647
Real space solution to the phase problem in X-ray crystallography: ALCAMPS (Ames Laboratory Computer-aided Analysis of Multi-solution Patterson Superpositions) [DE84-015476] 04 p0572 N85-13651
Critical evaluation of binary rare earth phase diagrams [DE84-015057] 05 p0614 N85-13922
Structural studies on lead dioxides [DE84-015837] 06 p0805 N85-15127

Structural development in the Santa Catharina meteorite 06 p0886 N85-15625
Snow characterization measurements from SNOW-TWO/Smoke Week 6
[AD-A147423] 07 p1008 N85-16402
Clusters of defects in semiconductors
[AD-A147426] 07 p1048 N85-16655
Temperature dependence of the crystal structures of Nylon 11
[AD-A147563] 07 p1049 N85-16661
Depositional modeling of tetrahedrite in the Coeur d'Alene district, Idaho 08 p1182 N85-17448
Structure-property relationships in intercalated graphite
[AD-A147949] 08 p1219 N85-17680
Crystalline structure of urea ice sheets used in modeling experiments in the CRREL test basin
[AD-A148434] 08 p1226 N85-17722
The growth of large diameter single crystals by vertical solidification of the melt
[AD-A148756] 09 p1397 N85-18792
Characterization of erosion of metallic materials under cavitation attack in a mineral oil
[NASA-TM-86934] 10 p1440 N85-19075
Characterization of novel binders based on energetic thermoplastic elastomers
[AD-A148993] 10 p1451 N85-19139
Fundamental studies of growth, doping and transformation in beta silicon carbide
[AD-A149339] 10 p1562 N85-19851
Electronic structure of silicon superlattices
[NASA-CR-175536] 11 p1736 N85-20916
A mixed-basis band structure interpolation scheme applied to the fluorite structure compounds NiSi2, AuAl2, AuGa2 and AuIn2
[AD-A150131] 12 p1940 N85-22187
Specifics of structure and mechanical properties of metastable beta-titanium alloys after deformation and aging 13 p2032 N85-22731
H-division materials physics progress
[DE85-004990] 13 p2165 N85-23430
Solid/melt interface studies of high-speed silicon sheet growth
[NASA-CR-175698] 14 p2350 N85-24525
Structural unit/grain boundary dislocation model for twist boundaries in cubic crystals
[DE85-000425] 14 p2430 N85-24985
Determination of symmetry of immediate surroundings in amorphous Co-P alloys 15 p2496 N85-25398
Structure and aging of amorphous chromium-germanium alloys 15 p2497 N85-25401
Study of structural changes of dual-phase titanium alloy during shock wave loading 15 p2498 N85-25408
Superplasticity in a thermo-mechanically processed Aluminum-10.2%Mg-0.52%Mn alloy
[AD-A152016] 15 p2510 N85-25485
Influence of solidification parameters on the formation of the gamma-M7C3 eutectic structure of 2% C-12%Cr steel 15 p2512 N85-25500
Crystallinity determination by curvefit procedure for a semi-crystalline polymer
[NASA-TM-86412] 15 p2517 N85-25520
Applications of piezoelectric and pyroelectric thin films: Opportunities for Langmuir-Blodgett technology
[AD-A149239] 15 p2659 N85-26408
On the feasibility of Ab Initio calculations of ordering alloy phase diagrams
[DE85-007073] 16 p2751 N85-26979
Conducting a thermal conductivity survey
[NASA-CR-175792] 16 p2782 N85-27166
Simulation studies for surfaces and materials strength
[NASA-CR-175766] 16 p2800 N85-27262
Effects of the cooling rate on the structure of the graphite in inoculated irons
[BLL-BISI-TRANS-22305-(9022.06)] 17 p2930 N85-28063
Pseudopotentials and total energy calculations: Applications to crystal stability, vibrational properties, phase transformations, and surface structures
[DE85-007657] 18 p3194 N85-29810
Fundamental studies of beta phase decomposition modes in titanium alloys
[AD-A154122] 19 p3236 N85-30078
Effects of annealing treatments on superplasticity in a thermomechanically processed Aluminum-10.2%Mg-0.52%Mn
[AD-A154414] 19 p3239 N85-30080
Grain structure identification by ultrasound frequency averaging and deconvolution
[AD-A154332] 19 p3352 N85-30777
Journal of Research of the National Bureau of Standards, volume 89, no. 6, November - December 1984
[PB85-179042] 20 p3472 N85-31580
The interactions of composition and stress in crystalline solids
[PB85-179075] 20 p3473 N85-31583
Proceedings of the Flat-Plate Solar Array Project Research Forum on High-Efficiency Crystalline Silicon Solar Cells
[NASA-CR-176047] 20 p3478 N85-31615
Aspects of silicon bulk lifetimes 20 p3479 N85-31617
Structural defects in crystalline silicon 20 p3481 N85-31630
NBS (National Bureau of Standards) reactor: Summary of activities Jul. 1983 through Jun. 1984
[PB85-184836] 20 p3522 N85-31907
Z-contrast imaging and electron channeling analysis of dopants in semiconductors
[DE85-011410] 21 p3582 N85-32269
Silicon dendritic web growth 21 p3611 N85-32435
Temperature-stress modeling 21 p3611 N85-32436
Silicon ribbon stress-strain activities 21 p3611 N85-32437
Analysis of stress-strain relationships in silicon ribbon 21 p3611 N85-32438
Stress and buckling analysis 21 p3611 N85-32439
Stress and efficiency studies in EFG 21 p3611 N85-32440
Silicon sheet surface studies 21 p3611 N85-32441
Analysis of inclined growth of silicon sheet 21 p3612 N85-32442
Edge-defined film-fed growth of thin silicon sheets 21 p3612 N85-32443
High-purity silicon crystal growth 21 p3612 N85-32444
Influence on bi-phonon states on Raman scattering of light in molecular crystals 21 p3680 N85-32865
X-ray diffractometric measurements and calculations of limiting values of discrepancy between lattices and layer thicknesses, preventing generation of dislocations during growth of multilayer heterostructures 21 p3681 N85-32866
Classical emission of relativistic charged particles during axial channeling 21 p3681 N85-32871
Influence of background electrically neutral argon admixture on mechanical strength of silicon crystals 21 p3683 N85-32878
Low-threshold injection InGaAsP/GaAs double heterostructure lasers with separate limiting obtained by liquid-phase epitaxy (lambda = 0.78 divided by 0.87 microns, I sub thr = 460 A/cm 2, T = 300 K) 21 p3687 N85-32908
An EPR (Electron-Paramagnetic-Resonance) and ENDOR (Electron-Nuclear-Double-Resonance) study of ferroelectric ammonium sulfate
[AD-A155580] 21 p3710 N85-33033
Striation free doped silicon
[AD-A155730] 22 p3847 N85-33827
Electrolytic synthesis of colored eta alumina film 23 p3906 N85-34201
High resolution electron microscopic characterization of interfaces in ceramics
[DE85-011207] 23 p3920 N85-34289
On the potential link equation of a spot centre with relative deformation for a semi-infinite molecular crystal
[BLL-M-35795-(5828.4)] 23 p3985 N85-34711
Cluster variation study of coherent ordering in FCC and BCC solid solutions
[AD-A156039] 24 p4079 N85-35280
Ionic crystals
[DE85-009482] 24 p4163 N85-35809

CRYSTAL SURFACES
Effect of oxidizing medium and heat treatment on stoichiometry of ZnSe crystal surface 03 p0353 N85-12272
Dispersion forces of solids under stress. Chemisorption under stress
[AD-A146171] 03 p0373 N85-12380
USSR report: Physics and mathematics
[JPRS-UPM-84-007] 05 p0723 N85-14651
Laser excitation of coupled surface electromagnetic and acoustic waves and of static structures in solids 05 p0723 N85-14652
Amorphization of ceramics by ion beams
[DE85-000936] 10 p1453 N85-19156
Studies of the kinetics and mechanisms of ammonia synthesis and hydrodesulfurization on metal single crystal surfaces
[DE85-001650] 11 p1595 N85-20030
Low-energy, high-intensity positron beam experiments with a linac
[DE85-001048] 11 p1723 N85-20835
The use of moments of momentum to account for crystal habits
[NASA-CR-3907] 20 p3421 N85-31232
The development and evaluation of point defect models for the growth of passive films on single crystal, polycrystalline, and amorphous metal surfaces
[AD-A154685] 21 p3709 N85-33023
Characterization of catalysts with metal-support effects and of the species adsorbed on their surfaces
[DE85-012254] 24 p4096 N85-35304

CRYSTALLINITY
Symmetry of exchange interaction in crystalline magnetic films 02 p0259 N85-11084
Newer carbon fibers and their properties 04 p0465 N85-12865
Study of the physical properties of crystalline rocks in the southeast Voronezh anteclise
[NASA-TM-77823] 10 p1514 N85-19861
Characterization and adhesive bonding of poly(etheretherketone) resins and composites
[DE85-002526] 11 p1593 N85-20023
Development of AK18 alloy production technology based on electrothermic silumin 11 p1598 N85-20048
Theory of oriented nucleation with asymmetric single elements. 2: Effects of rotational diffusion
[IFTR-32/1984] 12 p1939 N85-22179
Influence of substrate heating and thermal annealing on the surface crystallinity in single Si crystals implanted with high doses of (16)O
[DE85-005264] 13 p2164 N85-23428
Silicon-sheet and thin-film cell and module technology potential: Issue study
[NASA-CR-175654] 14 p2349 N85-24520
Excimer laser annealing to fabricate low cost solar cells
[NASA-CR-175702] 14 p2351 N85-24529
Crystallinity determination by curvefit procedure for a semi-crystalline polymer
[NASA-TM-86412] 15 p2517 N85-25520
Application of the reference intensity method to coal analysis
[DE85-009528] 19 p3228 N85-30015
NMR investigation of crystalline electric field effect on spin-spin relaxation in (Y(1-x)RE(x))Rh4B4
[DE85-010512] 19 p3357 N85-30814
Method for growing low defect, high purity crystalline layers
[NASA-CASE-NPO-15813-2] 19 p3374 N85-30933
Use of low energy hydrogen ion implants in high efficiency crystalline silicon solar cells
[NASA-CR-176109] 22 p3806 N85-33571
Investigation of the microstructure and photovoltaic properties of semicrystalline silicon 22 p3806 N85-33573

CRYSTALLITES
Structural changes during milling of aluminum oxide powders
[NASA-TM-77468] 04 p0472 N85-13006
Study of energy versus misorientation for grain boundaries in gold by crystallite rotation method. 1: 001 twist boundaries
[DE85-004598] 12 p1943 N85-22201
Plastic deformation of crystalline polymers
[AD-A152090] 16 p2755 N85-26999

CRYSTALLIZATION
NT DIRECTIONAL SOLIDIFICATION (CRYSTALS)
NT MELT SPINNING
NT RECRYSTALLIZATION
New metallurgical processes based on high-speed crystallization and diffusion of metals 01 p0021 N85-10125
Second All-Union Seminar on Hydromechanics and Heat and Mass Exchange in Weightlessness, summaries of reports
[NASA-TM-77590] 01 p0047 N85-10305
International Conference on Recent Developments in Specialty Steels and Hard Materials. Conference abstracts
[CSIR-S-256] 02 p0176 N85-11177
Rapid solidification processing and the control of structure/property relationships 02 p0176 N85-11178
Microstructural design in low alloy steels 02 p0176 N85-11179
Transport phenomena in the boundary layer during solution solidification under microgravity. Ice growth from a water-salt solution
[BMFT-FB-W-84-031] 03 p0329 N85-12121
Microstructure development in polymers
[AD-A145980] 03 p0337 N85-12170
Magnetic properties of and superfine interactions in amorphous Fe-Cr-Co-Si-B alloys 03 p0349 N85-12248
Producing semiconductor materials by superfast cooling of melt 03 p0354 N85-12274
Nickel-cobalt systematics and their bearing on lunar origin 04 p0582 N85-13719
Ge abundances in the lunar mantle and implications for the origin of the Moon 04 p0582 N85-13721
Dynamic crystallization of silicate melts
[NASA-CR-174103] 05 p0743 N85-14774

Low temperature diffusion coefficients in the Fe-Ni and FeNiP systems: Application to meteorite cooling rates
06 p0686 N85-15626

Extreme incompatibility of Pb during the crystallization of magmatic iron meteorites 06 p0686 N85-15627

Experimental and theoretical study of the formation of the 2AB, 3AB, and 9A meteorite chemical groups from the parent liquid 06 p0686 N85-15628

Method of preparing single crystalline cubic silicon carbide layers
[AD-D011305] 07 p1048 N85-16653

Temperature dependence of the crystal structures of Nylon 11
[AD-A147583] 07 p1049 N85-16661

Crystallization behavior of poly(3,3-bis(Ethoxymethyl) oxetane) and poly(3,3-bis(Azidomethyl) oxetane)
[AD-A148271] 08 p1226 N85-17720

Electrical resistivity and structural changes upon relaxation and crystallization of (Mo/sub 0.6/Ru/sub 0.4)sub 100-x/B/sub x/ metallic glasses
[DE84-017281] 09 p1299 N85-18160

Light scattering studies of lower dimensional colloidal particle and critical fluid systems
[DE85-002087] 09 p1377 N85-18654

Influence of excess phases on fracture toughness of cast alumium-magnesium-zinc alloy
10 p1442 N85-19091

Conduction in polymerized polyfunctional diacetylenes
[AD-A149104] 10 p1451 N85-19145

Heavy ion induced crystallization in amorphous phases
[DE85-003114] 11 p1606 N85-20098

Total immersion crystal growth
[NASA-CASE-NPO-15800-2] 12 p1939 N85-22178

Reaction of amorphous NiNb films with crystalline metal overlayers
[DE85-005483] 13 p2024 N85-22680

Study of processes of modification of Al-Si alloys
13 p2026 N85-22695

Composition and thickness of oxide coatings on granule surfaces of aluminum alloys 13 p2030 N85-22719

Thermodynamic and kinetic studies of pulsed laser annealing from transient conductivity measurements
[DE85-003677] 13 p2096 N85-23078

Modelling equilibrium and fractional crystallization in the system MgO-FeO-CaO-Al2O3-SiO2
13 p2184 N85-23552

Effect of zirconium on forming ultrafine-grained structure in Al-Mg-Zr alloy 15 p2513 N85-25504

Development of solid state infrared emitters for gas detection applications
[PB85-148450] 15 p2561 N85-25800

An analysis of the economics of turning titanium alloys with polycrystalline diamond tools
15 p2567 N85-25841

Plastic deformation of crystalline polymers
[AD-A152090] 16 p2755 N85-26999

Dendritic growth from amorphous matrix
[DE85-007630] 16 p2871 N85-27712

Multi-phase crystallization of ferrous alloys
[BLL-BISI-TRANS-22441-(9022.06)]
17 p2925 N85-28037

The synthesis and structure of polyphosphazenes
[AD-A153134] 17 p2934 N85-28112

Microstructure-mechanical property relationships in transformation-toughened ceramics
[DE85-009722] 17 p2935 N85-28117

The distribution of higher n-alkanes in partially frozen middle distillate fuels
[AD-A153940] 18 p3083 N85-29074

Aluminum-air power cell: The M3-3 experiment
[DE85-008678] 18 p3096 N85-29168

Study of phase equilibria and crystallization processes in Al-Zn-Mg alloy systems 19 p3241 N85-30098

Crystallization of aluminum-based alloys in weightlessness 19 p3242 N85-30101

The use of moments of momentum to account for crystal habits
[NASA-CR-3907] 20 p3421 N85-31232

Interaction of solutes with stretched polymers
[AD-A154662] 21 p3569 N85-32196

Introduction of structural variations into oxide polymers and their effect on sintering and crystallization
[AD-A155507] 21 p3570 N85-32206

A fluidized-bed reactor for silane pyrolysis
21 p3609 N85-32413

The effect of liquid-liquid phase separation of glass on the properties and crystallization behavior
[NASA-TM-77890] 23 p3919 N85-34265

Crystallization of Polyetheretherketone (PEEK) in carbon fiber composites
[AD-A156316] 24 p4075 N85-35252

High temperature corrosion of ceramics
[DE85-013481] 24 p4083 N85-35303

A new drawing technique for nylon 6 by reversible plasticization with iodine
[AD-A156272] 24 p4162 N85-35803

CRYSTALLOGRAPHY

Report on research results in solid state nuclear physics, 1980-1982
[JUEL-SPEZ-250] 03 p0422 N85-12696

Investigation of solid state problems using the hyperfine interaction between static and dynamic internal fields with short live excited probe nuclei 03 p0428 N85-12729

Measurement of state and dynamic solid state properties in nonmetals using excited probe nuclei on the Erlanger 12 MeV tandem accelerator 03 p0428 N85-12730

Solid state investigations with nuclear physics methods 03 p0428 N85-12731

Utilization of a tandem accelerator for the investigation of solid state properties by means of heavy ions
03 p0429 N85-12733

Investigation of the interaction of atoms with lattice defects using probe methods 03 p0429 N85-12737

Fast ions as probes in solid state research
03 p0430 N85-12740

X-ray and neutron scattering and X-ray spectroscopy for the study of defects in solid state materials
03 p0430 N85-12741

Real space solution to the phase problem in X-ray crystallography: ALCAMPS (Ames Laboratory Computer-aided Analysis of Multi-solution Patterson Superpositions)
[DE84-015476] 04 p0572 N85-13851

Butene oxidation by molybdenum crystalographic shear compounds
[DE84-013910] 05 p0614 N85-13923

Investigation of structural and electrical properties of low-angle silicon sheet 06 p0831 N85-15288

Semicrystalline casting process development and verification 06 p0832 N85-15289

AEM with a convergent beam
[DE85-000667] 11 p1714 N85-20784

Influence of individual reflections on the precision of parameter estimates in least squares refinement
[DE85-000830] 11 p1735 N85-20909

Surface physics and crystallography
[DE85-003126] 11 p1735 N85-20910

New high resolution scanning ion microprobe and focused ion beam applications
[AD-A149992] 12 p1852 N85-21616

Crystal chemistry of meteoritic hibonites
13 p2185 N85-23556

Structural, morphological and optical characteristics of KGd(WO4)2 crystals 14 p2280 N85-24126

Case studies of snow clouds by means of snow crystal sondes 15 p2581 N85-25921

Characteristics of fast sea ice collected near Barrow, Alaska 15 p2582 N85-25925

Atom location by electron channeling analysis
[DE85-007549] 16 p2872 N85-27716

X-ray crystallography of steel U8 after pulsed laser hardening
[BLL-BISI-22444-(9022.06)] 17 p2925 N85-28038

A new high-resolution pickup tube for live X-ray topography
[NHK-LABS-NOTE-309] 18 p3193 N85-29602

Low-energy electron diffraction experiment and theory
[DE85-009967] 18 p3195 N85-29620

X-ray diffractometric measurements and calculations of limiting values of discrepancy between lattices and layer thicknesses, preventing generation of dislocations during growth of multilayer heterostructures
21 p3681 N85-32866

Crystallographic orientation dependence of fatigue crack propagation in extremely low carbon steel
23 p3906 N85-34195

CRYSTALS
NT BICRYSTALS
NT BOULES
NT CRYSTAL OSCILLATORS
NT CRYSTALLITES
NT DENDRITIC CRYSTALS
NT DOPED CRYSTALS
NT IONIC CRYSTALS
NT LIQUID CRYSTALS
NT METAL CRYSTALS
NT MICROCRYSTALS
NT MIXED CRYSTALS
NT PIEZOELECTRIC CRYSTALS
NT POLYCRYSTALS
NT QUARTZ CRYSTALS
NT SINGLE CRYSTALS
NT WHISKERS (CRYSTALS)

Current controlled LPE (Liquid Phase Epitaxy) growth of semiconductors
[AD-A145536] 02 p0287 N85-11875

Static and dynamic disordering in amorphous magnets and crystals 03 p0422 N85-12699

Computational models of crystals
[DE84-016631] 04 p0572 N85-13847

X-ray absorption in perfect crystals
[DE84-016034] 05 p0732 N85-14708

Theoretical methods for the study of transition metals in crystals
[DE84-015606] 05 p0732 N85-14709

Microstructural origins of hot spots in RDX explosive and a reference inert material
[AD-A146685] 06 p0774 N85-14947

Semicrystalline casting process development and verification 06 p0832 N85-15289

Simulation of bent crystal spectrometers
[DE85-002042] 09 p1365 N85-18709

International Conference on Defects in Insulating Crystals
[AD-A149611] 12 p1939 N85-22180

Electron image simulation: A complementary processing technique
[DE85-000685] 12 p1941 N85-22190

Molecular dynamics studies of energy transfer processes in crystal systems
[AD-A150161] 13 p2163 N85-23416

Thresholds of optical breakdown in alkali-halide crystals under pulses from CO2-laser 14 p2282 N85-24134

Energy trapping, release, and transport in three-dimensional energetic solids and molecular crystals: Theory of defects and impurities
[AD-A151071] 14 p2426 N85-24073

Method of fabricating acceleration resistant crystal resonators and acceleration resistant crystal resonators so formed
[AD-D011630] 16 p2778 N85-27145

Ac field-induced order in dense colloidal systems
[DE85-009107] 17 p2935 N85-28119

Central limit theorems in the area of large deviations for some dependent random variables
[AD-A153125] 17 p3043 N85-28831

Method of reducing impurity and antisite defects in semiconductor crystal materials, and device and apparatus respectively produced from and utilizing same
[AD-D011698] 19 p3260 N85-30216

A method to estimate the self-consistency effects on electronic structure calculations
[INPE-3536-PRE/752] 19 p3375 N85-30936

Leading-edge microelectronics research at Sweden's Chalmers 20 p3438 N85-31337

High temperature electronics technology: Life test report
[AD-A154681] 21 p3560 N85-32257

Monte Carlo studies of H2O layers adsorbed on a model basal face of AgI 21 p3643 N85-32633

USSR report: Physics and mathematics
[JPRS-UPM-85-004] 21 p3680 N85-32860

Lasing on LiF:F(-)2 - dye centers with transverse pumping 21 p3684 N85-32890

The problem of brightness enhancement during laser frequency doubling 21 p3686 N85-32897

Transparent electrode for optical switch
[DE85-011618] 22 p3761 N85-33310

Striation free doped silicon
[AD-A155730] 22 p3847 N85-33827

Refractive indices and thermo-optic coefficients of nonlinear crystals isomorphic to KH2PO4
[DE85-012968] 22 p3847 N85-33831

Lead and uranium group abundances in cosmic rays
[OG-7.1-3] 23 p4013 N85-34865

Characterization of catalysts with metal-support effects and of the species adsorbed on their surfaces
[DE85-012254] 24 p4096 N85-35394

Search for supermassive magnetic monopoles using mica crystals
[HE-6.1-8] 24 p4210 N85-36134

CT-114 AIRCRAFT
U CL-41 AIRCRAFT

CTD
U CHARGE TRANSFER DEVICES

CUBA

Evaluation of the climatic resources of Cuba applied to agricultural work 07 p1004 N85-16380

CUBIC LATTICES
NT BODY CENTERED CUBIC LATTICES
NT FACE CENTERED CUBIC LATTICES

Monotonicity preserving bicubic interpolation
[DE85-004206] 18 p3172 N85-29657

On the group-theoretical approach to the energy spectra problem of charge carriers in cubic solids
[PREPRINT-435] 18 p3196 N85-29827

CUES

An in-flight investigation of a twin fuselage configuration in approach and landing
[NASA-CR-172366] 05 p0596 N85-13801

Use of linear perspective scene cues in a simulated height regulation task 05 p0704 N85-14517

best copy available

Cockpit window edge proximity effects on judgements of horizon vertical displacement
05 p0704 N85-14518
Mean and random errors of visual roll rate perception from central and peripheral visual displays
05 p0704 N85-14519
Direction judgement errors in perspective displays
05 p0705 N85-14520
The interaction of focused attention with flow-field sensitivity 05 p0705 N85-14521
Accuracy of system step response roll magnitude estimation from central and peripheral visual displays and simulator cockpit motion 05 p0705 N85-14522
Models for the effects of G-seat cuing on roll-axis tracking performance 05 p0707 N85-14532
Low altitude texture comparison data base and smooth shaded texture
[AD-A150342] 13 p2146 N85-23323

CUESTAS
U RIDGES

CULTIVATION
NT PLOWING
Assessing erosion on US cropland: Land management and physical features
[PB84-219252] 04 p0526 N85-13386
Cultivation and conversion of marine macroalgae --- biomass energy production
[DE84-004522] 04 p0544 N85-13464
Screening Prosopis (mesquite) species for biofuel production on semi-arid lands
[DE85-010048] 19 p3302 N85-30471

CULTURE (SOCIAL SCIENCES)
The legacy of science 14 p2432 N85-24995

CULTURE TECHNIQUES
Bioprocessing in space 05 p0690 N85-14439
Problems associated with the utilization of algae in bioregenerative life support systems
[NASA-CR-166615] 07 p1019 N85-16469
Algal culture studies related to a Closed Ecological Life Support System (CELSS)
[NASA-CR-177322] 07 p1019 N85-16470
Research and development of shallow algal mass culture systems for the production of oils
[DE85-000518] 11 p1690 N85-20624
Microalgae culture collection, 1984-1985
[DE84-013035] 11 p1690 N85-20626
Flow through bacteria detection system
[NASA-CASE-LAR-12871-1] 18 p3104 N85-29218
Effects of method of detachment on electrophoretic mobility of mammalian cells grown in monolayer culture
20 p3500 N85-31757
Preparative electrophoresis of cultured human cells: Effect of cell cycle phase 20 p3500 N85-31758
Size and DNA distributions of electrophoretically separated cultured human kidney cells
20 p3500 N85-31759
The role of cell size in density gradient electrophoretic separation of mouse leukemia cells according to position in the cell cycle 20 p3500 N85-31760
Electrophoretic mobilities of cultured human embryonic kidney cells in various buffers 20 p3501 N85-31761
Flow cytometry of human embryonic kidney cells: A light scattering approach 20 p3503 N85-31776
Chemolithotrophy and physiology of bacterial nutrient limitation 21 p3659 N85-32730
Microbial colonization and growth on metal sulfides and other mineral surfaces 21 p3662 N85-32747
Production of liquid fuels and chemicals by microalgae
[DE85-008780] 22 p3819 N85-33658
Production of butanol by fermentation in the presence of cocultures of clostridium
[NASA-CASE-NPO-16203-1] 24 p4071 N85-35227

CUMULATIVE DAMAGE
Cumulative damage model for advanced composite materials
[AD-A144840] 01 p0022 N85-10135
Equivalent damage: A critical assessment
02 p0140 N85-10952
Cumulative damage model for advanced composite materials
[AD-A145441] 02 p0171 N85-11142
The influence of mechanical damage on transmission pipeline integrity
[ERS-E.351] 09 p1340 N85-18431
Recent studies of the significance of mechanical damage in pipelines
[ERS-E.367] 09 p1341 N85-18433
Influence of 3% NaCl solution on rate of accumulation of damage and residual strength of aluminum-boron composite 13 p2027 N85-22699
The cumulative effects of long term exposure to low levels of radiofrequency radiation (RFR)
16 p2776 N85-27132
Modifications of flight-by-flight load sequences to provide for good fracture surface readability
[NLR-MP-84012-U] 20 p3472 N85-31577
Damage mechanisms in damaged CFRP laminates
24 p4074 N85-35249

CUMULONIMBUS CLOUDS
NT ANVIL CLOUDS
NT ARC CLOUDS

CUMULUS CLOUDS
NT ANVIL CLOUDS
Theoretical development of Monte Carlo codes for modeling cumulus cloud fields
[NASA-CR-174063] 02 p0230 N85-11500
Non-precipitating cumulus cloud study
[DE85-002352] 12 p1896 N85-21902
Cumulus cloud venting of mixed layer ozone
[NASA-TM-87429] 13 p2132 N85-23269
Cumulus effects on the large-scale vorticity and momentum fields in the tropical atmosphere
13 p2137 N85-23270
Convection modeling and application to severe storms
15 p2595 N85-25991
Ice multiplication in summertime cumulus clouds in the BEWMEX area 16 p2829 N85-27445
The use of radar in determining precipitation processes in the BEWMEX area 16 p2831 N85-27455
Effects of cloud seeding on precipitation development in cumulus clouds 16 p2831 N85-27456
Vertical redistribution of a pollutant tracer due to cumulus convection
[PB85-172971] 18 p3134 N85-29415
Numerical simulation of chemical and physical properties of cumulus clouds
[DE85-009744] 19 p3317 N85-30564
Aircraft investigations of the distribution of aerosols in the lower troposphere 21 p3647 N85-32659

CURIE TEMPERATURE
Determination of optimum Curie point as a function of source and sink temperatures for magnetic heat pumps
[DE84-016995] 04 p0499 N85-13182
Magnetic studies of Ni3Al(Fe) compounds
[DE85-005262] 13 p2025 N85-22686

CURIE-WEISS LAW
Magnetism of californium metal
[DE85-001141] 09 p1377 N85-18657

CURING
Development of new and improved polymer matrix resin systems, phase 1
[NASA-CR-166595] 01 p0017 N85-10104
Infrared spectroscopy study of the SP-250 epoxy resin system
[AD-A145660] 03 p0337 N85-12167
Morphology and dynamic mechanical properties of diglycidyl ether of bisphenol-A toughened with carboxyl-terminated butadiene-acrylonitrile
04 p0466 N85-12958
Matrix resin characterization in cured graphite composites using diffuse reflectance-FTIR
04 p0466 N85-12959
Solvent resistant thermoplastic composite matrices
04 p0466 N85-12960
Aliphatic-aromatic heterocyclics as potential thermoplastics for composite matrices
04 p0466 N85-12962
Variation of resin properties through the thickness of cured samples 04 p0468 N85-12974
Rubber-modified epoxies. 1: Cure, transitions, and morphology
[AD-A147377] 07 p0932 N85-15906
Monitoring cure of epoxy resins using a microdielectrometer
[AD-A148618] 08 p1119 N85-17054
The use of microdielectrometry in monitoring the cure of resins and composites
[AD-A148619] 08 p1119 N85-17055
Characterization of a thermoplastic polyimidesulfone
[NASA-TM-86358] 10 p1450 N85-19135
Characterization of acetylene-terminated resin cure states
[AD-A149463] 10 p1452 N85-19148
Chemical approach for controlling nadimide cure temperature and rate with maleimide
[NASA-CASE-LEW-13770-3] 12 p1809 N85-21350
Chemical approach for controlling nadimide cure temperature and rate with maleimide
[NASA-CASE-LEW-13770-4] 12 p1810 N85-21351
SRM filament wound case resin characterization studies 12 p1944 N85-22212
Monitoring of laminate cure with microdielectrometry
[AD-A150663] 14 p2248 N85-23934
Chemical interpretation of the relaxed permittivity during epoxy resin cure
[AD-A150955] 14 p2260 N85-24006
Characterization-curing-property studies of HBRF 55A resin formulations
[NASA-CR-175836] 16 p2753 N85-26989
Formulation/cure technology for ultrahigh molecular weight silphenylene-siloxane polymers
[NASA-TP-2476] 16 p2753 N85-26990
Evaluation of experimental epoxy monomers
[NASA-TM-87476] 16 p2754 N85-2
Chemical control of nadimide cure temperature and rate
[NASA-CASE-LEW-13770-2] 18 p3069 N85-2
Metal (2) 4,4',4',4'' phthalocyanine tetraamines as curing agents for epoxy resins
[NASA-CASE-ARC-11424-1] 23 p3919 N85-34
Chemoviscosity modeling for thermosetting resins, 2
[NASA-CR-177056] 24 p4073 N85-352

CURIUM
NT CURIUM 244
Thermodynamic systematics of oxides of americium, curium and neighboring elements
[DE85-009704] 18 p3197 N85-29

CURIUM ISOTOPES
NT CURIUM 244

CURIUM 244
Historical review of californium-252 discovery and development
[DE85-010223] 19 p3362 N85-30844

CURL (VECTORS)
NT VORTICITY

CURRENT ALGEBRA
Modern test of chiral anomalies
[DE85-005892] 17 p3020 N85-2

CURRENT AMPLIFIERS
NT PHOTOMULTIPLIER TUBES
Multi-channel pulser for the SLC thermionic electron source
[DE85-014222] 24 p4160 N85-35792

CURRENT CONVERTERS (AC TO DC)
Design and operating experience of an ac-dc power converter for a superconducting magnetic energy storage unit
[DE84-014041] 09 p1316 N85-18275

CURRENT DENSITY
Manual of phosphoric acid fuel cell stack three-dimensional model and computer program
[NASA-CR-174722] 01 p0067 N85-10447
Theory of the double critical state in type-2 superconductors
[DE84-015461] 02 p0269 N85-11
Westinghouse programs in pulsed homopolar power supplies 05 p0606 N85-13
Transient currents of ideally conducting body of revolution with transient diffraction
06 p0785 N85-15
Current-voltage characteristics of semiconductor power devices operating at high current densities
06 p0795 N85-150
Semiconductor submicrosecond power commutator switches 06 p0795 N85-15081
A coaxial probe for measuring the current density profile of intense electron beams
[AD-D011407] 08 p1164 N85-17347
A superconducting quantum current standard
[NPL-QU-67] 08 p1224 N85-17710
Contributions of segregated phosphorus to the intergranular stress corrosion cracking of nickel
[DE85-003112] 11 p1606 N85-20
Hydrogen vibrational population distributions and negative ion generation in tandem high density hydrogen discharges
[DE85-001207] 11 p1722 N85-20634
Pre- and post-processing for stream-function eddy current calculations
[AD-A150417] 13 p2065 N85-22
New high-efficiency silicon solar cells
[NASA-CR-175643] 13 p2128 N85-23
Degradation phenomena in solid electrolytes
[DE85-007066] 15 p2587 N85-25
Investigation of pseudo bi-polar nickel cadmium batteries as filter elements for pulsed power loads
[AD-A152112] 16 p2819 N85-27
Maximum current densities from tandem high density systems
[DE85-008966] 18 p3180 N85-29
Development of power system measurements
[PB85-182582] 20 p3450 N85-314
The electric current densities beneath thunderstorms
20 p3494 N85-317
Superconducting toroidal field coil current densities for the TFCX
[DE85-010285] 20 p3530 N85-319
Detection of excited states by laser-induced fluorescence
[AD-A155558] 21 p3592 N85-323
Influence of technological factors on luminescence characteristics of InGaAsP/InP heterolasers (lambda = 1.55 microns) 21 p3688 N85-329
Critical current density and microstructural state of an internal tin multifilamentary superconducting wire
[DE85-009066] 22 p3761 N85-33

Electrochemical method for investigation of the susceptibility of corrosion-resistant steels to intercrystalline corrosion
[BLL-CE-TRANS-8062-(9022.09)] 24 p4077 N85-35269
Effect of Cu4Ti compound formation on the characteristics of NbTi accelerator magnet wire
[DE85-014226] 24 p4159 N85-35786
Current interruption by density depression
[DE85-013120] 24 p4169 N85-35846
CURRENT DISTRIBUTION
A generalized solution to a class of printed circuit antennas
[AD-A145626] 02 p0191 N85-11278
Magnetic field calculation for ideal conductors by method of equivalent currents 06 p0766 N85-15035
Radiation patterns of a pyramidal horn antenna
09 p1311 N85-18236
Mathematical simulation of thermal prrocesses involved in electron-beam treatment 12 p1843 N85-21565
Solar cells with distributed parameters: Current-voltage characteristics under uniform and nonuniform illumination 14 p2275 N85-24093
IMS advances in studies of field-aligned currents and their related electrodynamics 14 p2359 N85-24578
Current distribution in a plasma erosion opening switch
[AD-A150987] 14 p2424 N85-24949
Acoustic emission of semiconductor devices
15 p2529 N85-25593
CURRENT REGULATORS
Optimization of design parameters for alternating current stabilizer based on magnetic suspension
22 p3772 N85-33374
CURRENT SHEETS
Solar flares and laboratory experiments on magnetic reconnection in current sheaths
02 p0162 N85-11099
Structure and evolution of the large scale solar and heliospheric magnetic fields 05 p0746 N85-14782
Birkeland currents correlated with dc-electric fields observed during the CENTAUR BBX rocket experiments
[DRI-6-84] 06 p0834 N85-15311
Partial penetration of IMF B(sub y) into the magnetosphere
[DRI-5-84] 10 p1514 N85-19554
Magnetotail current sheet and energetic particles observed on ISEE-1 14 p2357 N85-24566
Entry of solar energetic protons into the distant plasma sheet dependencience on distance from the neutral sheet
14 p2357 N85-24567
Estimate of the amplitude of transient electric fields in the magnetotail 14 p2358 N85-24568
Plasma sheet dynamics deduced from ISEE-1 and -2 energetic particle flux data 14 p2358 N85-24570
Plasma waves at and near the neutral sheet
14 p2358 N85-24572
The near Earth current sheet: ISEE-1 and -2 case studies 14 p2358 N85-24573
Ring current dynamics and plasma sheet sources — magnetic storms 14 p2359 N85-24577
Pi2 pulsations and the substorm current wedge - ground observations 14 p2370 N85-24650
Ground-satellite observations of substorm related Pi 2 pulsations and current systems
14 p2370 N85-24651
The influence of the heliospheric current sheet and angular separation on flare accelerated solar wind
[NASA-CR-175962] 18 p3209 N85-29907
Contributions to the 19th International Cosmic Ray Conference
[NASA-CR-176060] 21 p3714 N85-33044
Differential measurement of cosmic-ray gradient with respect to interplanetary current sheet
[PAPER-SH-4.2-9] 21 p3715 N85-33055
Cosmic ray intensity and the tilt of the neutral sheet
[SH-4.2-8] 23 p4007 N85-34846
Differential measurement of cosmic-ray gradient with respect to interplanetary current sheet
[SH-4.2-9] 23 p4007 N85-34847
Spatial variation of cosmic rays near the heliospheric current sheet
[SH-4.2-10] 23 p4007 N85-34848
Determination of galactic cosmic ray latitudinal gradient using Earth based detectors
[SH-4.2-13] 23 p4008 N85-34851
Latitudinal gradients of cosmic rays and the polarity reversal of the heliospheric magnetic field: A preliminary evaluation
[SH-4.2-16] 23 p4008 N85-34853
The effect of the neutral sheet structure of the interplanetary magnetic field on cosmic ray distribution in space
[SH-4.2-18] 23 p4008 N85-34855
Difference between even and odd 11-year cycles in cosmic ray intensity
[SH-4.2-22] 23 p4009 N85-34859
The dependence of solar modulation on the sign of the cosmic ray particle charge
[SH-4.2-23] 23 p4009 N85-34860
CURRENT STABILIZERS
U CURRENT REGULATORS
CURRENTS
An optically isolated amplifier
[CSIR-SR-ELEK-257] 01 p0049 N85-10321
CURRENTS (OCEANOGRAPHY)
U WATER CURRENTS
CURTAINS
Experimental investigation of annular air curtain domes
[UTIAS-288] 15 p2521 N85-25543
Particle curtain generator for optical property measurements of solid particles
[DE85-005784] 15 p2560 N85-25797
Results of tests on a specimen of the SRB aft skirt heat shield curtain in the MSFC LRLF
[NASA-CR-170883] 24 p4070 N85-35221
Results of tests of the SRB aft skirt heat shield curtain in the MSFC Hot Gas Facility
[NASA-CR-170888] 24 p4070 N85-35223
CURTISS-WRIGHT MILITARY AIRCRAFT
U MILITARY AIRCRAFT
CURVATURE
Direct numerical simulation of curved turbulent channel flow
[NASA-TM-85974] 02 p0197 N85-11316
First derivatives of flow quantities behind two-dimensional, nonuniform supersonic flow over a convex corner
[NASA-TM-86272] 06 p1077 N85-16828
Convective heat transfer coefficients for pipe flow with curvature induced secondary motion
09 p1318 N85-18285
Theoretical and empirical studies of the basic structure of turbulent shear flows, including separated flows and effects of wall curvature
[AD-A149657] 12 p1846 N85-21580
Zero-crossings on lines of curvature
[AD-A150171] 13 p2150 N85-23345
Gravity perception and response in shoot of cereal grasses 15 p2611 N85-26091
Temperature: Curvature relationships for unsymmetric graphite-epoxy laminates
[VPI-E-85-08] 16 p2743 N85-26926
Formulas for updating the generalized inverse of a symmetric matrix perturbed by a symmetric rank 2 matrix composed of 2 nonsymmetric DYADS
[AD-A151736] 16 p2858 N85-27629
Examination of the circle spline routine
17 p3004 N85-28573
Convex interpolating splines of arbitrary degree
17 p3004 N85-28574
Effects of solar magnetic field on cosmic rays
[SH-4.2-12] 23 p4008 N85-34850
The effect of the neutral sheet structure of the interplanetary magnetic field on cosmic ray distribution in space
[SH-4.2-18] 23 p4008 N85-34855
The dependence of solar modulation on the sign of the cosmic ray particle charge
[SH-4.2-23] 23 p4009 N85-34860
RF stabilization of interchange-ballooning modes
[DE85-012080] 24 p4090 N85-35353
CURVE FITTING
A method for evaluating the contamination of steel in relation to the solidification curve
[BLL-M-35735-(5828.4)] 02 p0175 N85-11171
Non-linear data fitting for the analysis of creep rupture data on GRP materials in aggressive environments — glass reinforced plastics (GRP)
[NPL-DMA(A)-79] 04 p0512 N85-13261
Response surface designs
[AD-A147202] 07 p1035 N85-16569
A variable span smoother
[AD-A148241] 08 p1215 N85-17655
Smoothing with split linear fits
[AD-A149032] 10 p1545 N85-19740
Determination of quantitative relationships between selected critical helicopter design parameters
[AD-A152034] 16 p2706 N85-26700
Locally-weighted-regression scatter-plot smoothing (LOWESS): A graphical exploratory data analysis technique
[AD-A152239] 16 p2855 N85-27609
A new world survey expression for cosmic ray vertical intensity vs. depth in standard rock
[HE-5.1-10] 24 p4201 N85-36073
CURVED BEAMS
Design, fabrication and test of composite curved frames for helicopter fuselage structure
[NASA-CR-172438] 15 p2470 N85-25247
CURVED PANELS
Vortex sheet modeling with higher order curved panels
20 p3451 N85-31428
CURVED SURFACES
U CONTOURS
U SHAPES
U SURFACES
CURVES
Principal curves and surfaces
[AD-A148833] 09 p1375 N85-18646
CURVES (GEOMETRY)
NT CATENARIES
NT EPICYCLOIDS
An integral equation formulation for a boundary value problem of elasticity in the domain exterior to an arc
[PREPRINT-833] 03 p0413 N85-12643
Spacefilling curves and the planer travelling salesman problem
[AD-A149337] 10 p1551 N85-19766
Reflected wave travel-time curves in stratified media with vertically heterogeneous layers and slightly sloping curved boundaries 13 p2114 N85-23167
Constrained parabolic approximation of curves in the finite element method
[CSIR-TWISK-340] 14 p2408 N85-24843
Entire functions with spiral limits
15 p2634 N85-26241
On the role of mother-planet magnetic field in spiral structure explanation of formation of spokes — Saturn rings 15 p2676 N85-26525
Shape preserving spline interpolation
17 p3003 N85-28564
The construction of curves and surfaces using numerical optimization techniques 17 p3003 N85-28565
A survey of patch methods 17 p3003 N85-28567
When is a Bernstein-Bezier curve the graph of a function? 17 p3003 N85-28568
Boundary to constructive solid geometry mappings: A focus on 2-D issues 17 p3004 N85-28570
The definition and computation of a metric on plane curves. The meaning of a face on a geometric model
17 p3004 N85-28571
A natural bias approach to cardinal spline curves
17 p3004 N85-28575
Adapting shape parameters for cubic Bezier curves
17 p3004 N85-28576
A uniform subdivision method for triangular Bezier patches 17 p3005 N85-28578
An intuitive approach to geometric continuity for parametric curves and surfaces (extended abstract)
17 p3005 N85-28579
Spline curves, wire frames and B-value
17 p3006 N85-28587
Numerical estimation of the curvature of biological surfaces 17 p3006 N85-28588
Curved finite elements and curve approximation
17 p3007 N85-28590
Comparison of two algebraic methods for curve/curve intersection 17 p3007 N85-28591
A comparison of three curve intersection algorithms
17 p3007 N85-28592
Some relations among directions of curves at an invariant point on a thermodynamic phase diagram
19 p3312 N85-30530
Conjugated symmetrical coupler curves, produced by 4-bar linkages having the same transmission angles
23 p3924 N85-34322
Geometric continuity with interpolating Bezier curves
23 p3963 N85-34570
An intuitive approach to geometric continuity for parametric curves and surfaces
23 p3963 N85-34571
The dynamics of articulated rigid bodies for purposes of animation 23 p3965 N85-34579
CURVILINEAR COORDINATES
U SPHERICAL COORDINATES
CUSHIONCRAFT GROUND EFFECT MACHINE
Planning of air cushion transport vehicles
14 p2285 N85-24160
CUSHIONS
Vibrational loading mechanism of unitized corrugated containers with cushions and non-load-bearing contents
09 p1339 N85-18419
Blanket integrated cushioning of foldable and retractable solar arrays 13 p2011 N85-22612
CUSPS
Dayside cusp aurora 04 p0521 N85-13333
CUT-OUTS
U OPENINGS
CUTANEOUS PERCEPTION
U TOUCH

CUTTERS
NT BLADES (CUTTERS)
NT DRILL BITS
NT DRILLS
NT SAWS
Portable slotting device
[AD-D011213] 01 p0033 N85-10206
Development and performance of CVD-coatings on cutting tools 02 p0178 N85-11183
Evaluation of the Kerie Cable thermal arc cutting equipment
[AD-A147813] 07 p0974 N85-16186
Technological and economic assessment of advanced ceramic materials: Volume 4: A case study of integrated optic devices
[PB85-113116] 12 p1815 N85-21385
Technological and economic assessment of advanced ceramic materials. Volume 6: A case study of ceramic cutting tools
[PB85-113132] 12 p1815 N85-21387
Diamond cutters' grinders 13 p2051 N85-22841
T700 cutter life improvement program
[AD-A150450] 13 p2099 N85-23089
New technology of finish cutting teeth in large gear blanks 14 p2267 N85-24047
Milling machine with numerical programmed control for cutting teeth 14 p2268 N85-24052
Cutting structural materials in vacuum
14 p2286 N85-24165
An analysis of machine tool systems suitable for laser profiling 14 p2308 N85-24282
Sweden invents new ceramic for more durable cutting tools 15 p2536 N85-25645
Classification and types of diamond wear in honing
15 p2567 N85-25842
Abrasive cutting-off wheel 15 p2568 N85-25843
Removal of longitudinal internal flash from electrically welded tubes
[BLL-BISI-TRANS-22380-(9022.06)]
17 p2938 N85-28136
Portable cutting apparatus
[DE85-011635] 22 p3792 N85-33496
Properties of tungsten-free steel for cutting tools
[BLL-M-35806-(5828.4)] 23 p3915 N85-34259
Action of wear-inhibiting Al2O3-coatings when applied to hard metal cutting tools
[BLL-RISLEY-TR-5041-(9091.9F)]
24 p4081 N85-35292

CUTTING
NT LASER CUTTING
NT METAL CUTTING
NT MILLING (MACHINING)
NT SCARFING
NT SHEARING
NT SLICING
NT SPARK MACHINING
Portable slotting device
[AD-D011213] 01 p0033 N85-10206
Thermal shock as a carbide grade development tool
[DE84-016839] 04 p0506 N85-13251
Evaluation of the Kerie Cable thermal arc cutting equipment
[AD-A147813] 07 p0974 N85-16186
New method for heat treatment of metals
10 p1446 N85-19110
Specifics of laser heat treatment of high steel tools
13 p2029 N85-22714
USSR report: Machine tools and metalworking equipment
[JPRS-UMM-85-005] 13 p2051 N85-22839
T700 cutter life improvement program
[AD-A150450] 13 p2099 N85-23089
Cutting structural materials in vacuum
14 p2286 N85-24165
Device for preventing intrusion of a blade during vibration cutting of intermittent cutting with a lathe
16 p2794 N85-27232
Semicrystalline casting process development and verification
[DE85-007695] 18 p3081 N85-29058
Geothermal COMPAX drill bit development
[DE85-011353] 20 p3469 N85-31556
Hole cutting in building frames by laser
[FOA-C-20569-D9] 22 p3791 N85-33487
Portable cutting apparatus
[DE85-011635] 22 p3792 N85-33496

CV-990 AIRCRAFT
MIZEX, 1984, NASA CV-990 flight report
[NASA-TM-86216] 19 p3299 N85-30451

CW RADAR
U CONTINUOUS WAVE RADAR

CYANIDE EMISSION
U CN EMISSION

CYANIDES
NT CYANOGEN
NT IRON CYANIDES
Ion chromatographic determination of gold in plating baths
[DE84-016187] 02 p0184 N85-11230
Acetonitrile in the Earth's atmosphere: An upper limit deduced from infrared solar spectra
[AERONOMICA-ACTA-A-285-1985]
22 p3813 N85-33623

CYANO COMPOUNDS
NT DIISOCYANATES
NT ISOCYANATES
Protocyanobacteria: Oxygenic and Anoxygenic photosynthesis in mat-forming bacteria
21 p3657 N85-32714
Sulfur transformations at the hydrogen sulfide/oxygen interface in stratified waters and in cyanobacterial mats
21 p3657 N85-32715

CYANOGEN
Adiabatic approach in the theory of polyatomic photodissociation: Application to C2N2
[DE85-008515] 18 p3071 N85-28996
Cyanobacterial mats: Microanalysis of community metabolism 21 p3661 N85-32743
Microanalysis of dissolved iron and phosphate in pore waters of hypersaline sediment
21 p3661 N85-32744
Glutathione in cyanobacteria
21 p3661 N85-32745

CYANOPHYTA
U BLUE GREEN ALGAE

CYBERNETICS
Asynchronous discrete control of continuous processes
[AD-A145570] 02 p0189 N85-11262
The application of basic control laws to human medicine
[DFVLR-MITT-84-13] 05 p0697 N85-14482
Applications of connectionist modeling techniques to simulations of motor control systems
05 p0717 N85-14598
Functional system theory in practice
11 p1690 N85-20629
USSR report: Cybernetics, computers, and automation technology
[JPRS-UCC-85-002] 14 p2400 N85-24794
Gordon Conference on Fundamentals of Cybernetics
[AD-A151074] 14 p2408 N85-24842
Development of robots, robotics discussed
15 p2530 N85-25599
New sensor for industrial metrology developed
15 p2538 N85-25665
USSR report: Cybernetics, computers and automation technology
[JPRS-UCC-85-003] 15 p2625 N85-26174
Mathematical analysis of heart rhythm assessment of distinctive features in adaptation to spaceflight conditions 22 p3733 N85-33142

CYCLES
NT ACTIVITY CYCLES (BIOLOGY)
NT BRAYTON CYCLE
NT CARBON CYCLE
NT CARNOT CYCLE
NT OTTO CYCLE
NT RANKINE CYCLE
NT SOLAR CYCLES
NT STIRLING CYCLE
NT STRESS CYCLES
NT SUNSPOT CYCLE
NT THERMODYNAMIC CYCLES
NT WORK-REST CYCLE
The nitrogen cycle: Atmosphere interactions
05 p0653 N85-14191
Terrestrial nitrogen cycles: Some unanswered questions 05 p0653 N85-14192
Recent studies of the ocean nitrogen cycle
05 p0653 N85-14193
Cyclic endurance testing of the RB211-22B cast HP turbine blade 07 p0906 N85-15747
View of future requirements for engine cyclic durability by analysis and testing 07 p0906 N85-15751
Investigation of welded interconnection of large area wraparound contacted silicon solar cells
[NASA-CR-174436] 10 p1509 N85-19519
Exergetical analysis of turbojet engine cycle
13 p2049 N85-22825
Mathematical model of the nitrogen cycle in a nonsaturated area of cultivated soil
20 p3478 N85-31610
Possible roles of manganese redox chemistry in the sulfur cycle 21 p3659 N85-32731
Biogeochemical cycling and remote sensing
21 p3659 N85-32733
Phototrophic bacteria and their role in the biogeochemical sulfur cycle 21 p3660 N85-32735
Sulfur cycling and metabolism of phototrophic and filamentous sulfur bacteria 21 p3660 N85-32737

CYCLIC ACCELERATORS
NT BETATRONS
NT STORAGE RINGS (PARTICLE ACCELERATORS)
NT SYNCHROTRONS
A low perturbation electron injector for cyclic accelerators
[AD-D011312] 07 p1040 N85-1680
Stability in dynamical systems
[DE85-006698] 17 p3034 N85-287
Physics of High Energy Particle Accelerators. AIP Conference Proceedings no. 127
[DE85-006891] 18 p3162 N85-297
High-power solid-state rf source for accelerator cavities
[DE85-012672] 22 p3761 N85-33

CYCLIC COMPOUNDS
NT CYCLIC HYDROCARBONS
A method for obtaining new cyclical imides of derivative benzimidazoles
[AD-A145042] 01 p0017 N85-101
Infrared spectroscopy study of the SP-250 epoxy resin system
[AD-A145860] 03 p0337 N85-121
Pseudo-p-1,2,2,9,9,10,10-octofluoro (2,2)-p-cyclophane bis-acid chloride
[AD-D011393] 07 p0919 N85-152
Research on microemulsions for storage and conversion of solar energy
[DE85-000181] 12 p1882 N85-218
Polyaromatic ether-sulfone-keytones with fluoro-substituted-p-cyclophane units as cross-linking sites
[AD-D011649] 17 p2933 N85-281
Synthesis of energetic materials
[AD-A154887] 21 p3571 N85-322
Influence of particle arrangement on sintering
[AD-A155337] 21 p3599 N85-32

CYCLIC HYDROCARBONS
NT ANTHRACENE
NT CYCLOPROPANE
Study of vibrational energy transfer at a liquid surface
[AD-A145741] 02 p0277 N85-118
A metal-catalyzed rearrangement of alkene-alkynes and the stereochemistry of metallacyclobutene ring opening
[AD-A149084] 10 p1435 N85-190
Synthesis of energetic materials
[AD-A154887] 21 p3571 N85-322
Synthesis of 2,4,8,10-tetroxaspiro5,5undecane
[NASA-CASE-ARC-11243-2] 22 p3741 N85-301

CYCLIC LOADS
Benchmark notch test for life prediction
02 p0140 N85-109
Nonlinear structural and life analyses of a combustor liner 02 p0141 N85-109
Strain distribution in a type 316/16-8-2 stainless steel weldment during cyclic loading
[DE84-015644] 02 p0210 N85-113
Study of delamination cracking under static and cyclic loads of carbon-epoxy composite materials
[REPT-42-727/F] 03 p0327 N85-121
Structure of two-phase titanium alloys with different microstructures 03 p0351 N85-122
Influence of cyclic tangential loading on indentation fracture
[DE84-015969] 03 p0373 N85-122
Autonomous momentum management for space station
[NASA-CR-174065] 04 p0462 N85-125
Possibilities of fatigue life estimation in the higher cycle range 05 p0649 N85-141
Low cycle fatigue strength for multiaxial loading of ductile materials 05 p0649 N85-141
Design procedures for fiber composite structural components: Panels subjected to combined in-plane loads
[NASA-TM-86909] 07 p0919 N85-158
Low cycle fatigue of MAR-M 200 single crystals at 760 and 870 deg C
[NASA-TM-86933] 10 p1440 N85-190
Mechanisms of damage accumulation in time-dependent cyclic deformation
[DE85-001004] 10 p1496 N85-194
Effect of stress concentration fatigue resistance of refractory nickel alloys under asymmetrical multicycle loading, communication 1 11 p1604 N85-200
Local strain redistribution corrections for a simplified inelastic analysis procedure based on an elastic finite-element analysis
[NASA-TP-2421] 11 p1651 N85-20
On local total strain redistribution using a simplified cyclic inelastic analysis based on an elastic solution
[NASA-TM-86913] 12 p1864 N85-21
Fatigue and corrosion fatigue resistance of aluminum casting alloy VAL10 and forging alloy AK6
13 p2025 N85-22

Dissipation of energy in composite material
13 p2027 N85-22703
Effect of operating medium on cyclic durability of AD95-W composite 13 p2029 N85-22716
Cyclic industrial robots with mechanical energy storing devices: Multipositional system with one or several degrees of freedom 13 p2045 N85-22803
Cyclic industrial robots with mechanical energy storing devices: Principles of drive design
13 p2046 N85-22807
Cyclic structural analyses of anisotropic turbine blades for reusable space propulsion systems — ssme fuel turbopump
[NASA-TM-86990] 14 p2320 N85-24339
Elastic-plastic analysis for cyclic loading using a linearized yield condition
[PB85-149607] 14 p2322 N85-24346
Long-life high performance fuel cell program
[NASA-CR-174874] 15 p2494 N85-25384
Effect of fatigue and thermal loads on silicon carbide fiber reinforced glass matrix composites
[DE85-006069] 15 p2503 N85-25441
Analysis of shell type structures subjected to time dependent mechanical and thermal loading
[NASA-CR-175747] 15 p2577 N85-25896
A review of fracture mechanics life technology
16 p2733 N85-26883
Analysis of elastoplastic grids under conditions of variable loads
[REPT-16/1984] 16 p2797 N85-27242
On the use of marker loads for fatigue crack growth measurements
[FFA-TN-1984-52] 16 p2802 N85-27277
Structural tailoring of SSME blades (vanes)
17 p2913 N85-27960
Interaction of high-cycle and low-cycle fatigue of Haynes 188 alloy at 1400 F deg 17 p2913 N85-27961
Effects of high mean stress on high-cycle fatigue behavior of PWA 1480 17 p2914 N85-27964
Constitutive cyclic deformation behavior in single-crystal and directionally solidified SSME high-pressure fuel turbopump airfoil materials 17 p2914 N85-27965
Fatigue behavior of synthetic fibers, yarns and ropes
17 p2979 N85-28415
Effect of protective method on cyclic durability and nature of failure of titanium alloy welded joints
19 p3245 N85-30122
Thermomechanical deformation in the presence of metallurgical changes 20 p3466 N85-31533
Micromechanics of high temperature deformation and failure 20 p3466 N85-31534
Results of an interlaboratory fatigue test program conducted on alloy 800H at room and elevated temperatures
[NASA-CR-174940] 21 p3597 N85-32340
Influence of cyclic thermal loading on internal stress in casted epoxy resin 23 p3906 N85-34211
Static and cyclic behavior of semi-rigid steel beam-column connections
[PB85-194383] 24 p4103 N85-35433

CYCLING
U CYCLES

CYCLOGENESIS
NT ARC CLOUDS
A simulation experiment of a rapidly developed medium scale cyclone 01 p0079 N85-10530
Mesoscale lee cyclogenesis 09 p1355 N85-18527
Meso-8 scale numerical simulations of the jet streak adjustments which organized the Carolina tornado outbreak and the subsequent explosive coastal cyclogenesis 15 p2598 N85-26011
The sensitivity of mesoscale cyclogenesis forecasts to detailed three-dimensional isentropic initial analyses and varied vertical model resolution
15 p2598 N85-26015
Justification and plan for participation in GALE
15 p2599 N85-26017
A survey of major east coast snowstorms, 1960-1983. Part 2. Summary of surface and upperlevel characteristics
[NASA-TM-86195] 16 p2833 N85-27471
A survey of major east coast snowstorms, 1960-1983. Part 2: Case studies of eighteen storms
[NASA-TM-86196] 16 p2833 N85-27472
Diagnostic verification of the GLAS (Goddard Laboratory for Atmospheric Sciences) general circulation model as applied to a case of extratropical maritime explosive cyclogenesis
[AD-A153686] 18 p3148 N85-29494
A numerical and analytical investigation of lee cyclogenesis
[AD-A156607] 21 p3638 N85-32594
Surface cyclogenesis as indicated by satellite imagery
[PB85-191815] 24 p4124 N85-35566

CYCLOHEXANE
Influence of pressure on speed of sound in single-phase region of stratifying mixtures 11 p1715 N85-20768

CYCLONES
NT CYCLOGENESIS
NT HURRICANES
NT TYPHOONS
Statistical tropical cyclone forecasting techniques for the Southern Hemisphere
[AD-A144752] 01 p0086 N85-10569
Summary of 1984 Atlantic seasonal tropical cyclone activity and verification of author's forecast
03 p0385 N85-12520
Energy diagnostics and impact studies of FGGE global data sets and GLAS GCM simulations
05 p0683 N85-14390
A study of the adequacy of quasi-geostrophic dynamics for modeling the effect of frontal cyclones on the larger scale flow 05 p0684 N85-14398
Numerical prediction of the president's day cyclone
05 p0684 N85-14399
Observational-numerical study of maritime extratropical cyclones using FGGE data 05 p0685 N85-14400
Frequency and motion of western North Pacific tropical cyclones
[PB85-106466/GAR] 06 p0839 N85-15331
Estimations of diabatic heating for an explosively-developing maritime cyclone
[AD-A147678] 08 p1188 N85-17483
A possible mechanism for the diurnal oscillations of tropical cyclones 09 p1356 N85-18530
Annual data and verification tabulation for Eastern North Pacific tropical storms and hurricanes, 1983
[PB85-109635] 10 p1520 N85-19580
Tropical cyclone data tape for the Eastern and Central North Pacific Basins, 1949-1983: Contents, limitations and uses
[PB85-110054] 10 p1520 N85-19585
Varying structure and intensity change characteristics of 4 Western North Pacific tropical cyclones
[AD-A149628] 12 p1895 N85-21895
Studies of the development of cyclones over Southern China coastal areas and adjacent seas
[AD-A150108] 12 p1896 N85-21901
Influence of interaction between ocean and atmosphere on intensity of moving tropical cyclone
14 p2333 N85-24431
Mesoscale Atmospheric Processes Research Program Science Review
[NASA-TM-87465] 15 p2594 N85-25987
Monitoring tropical cyclone growth using GOES VISSR/VAS and Nimbus-7 TOMS data
15 p2595 N85-25989
Model sensitivity studies of major east coast storms
15 p2598 N85-26016
Technique that uses satellite, radar, and conventional data for analyzing and short-range forecasting of precipitation from extratropical cyclones
[PB85-164994] 16 p2837 N85-27499
Kinetic energy and vorticity of lee cyclones
[MITT-40] 17 p2993 N85-28502
Characteristics of North Indian Ocean tropical cyclone activity
[AD-A153085] 17 p2997 N85-28524
A study of the adequacy of quasi-geostrophic dynamics for modeling the effect of frontal cyclones on the larger scale flow
[NASA-CR-176065] 20 p3495 N85-31731
Real-time automated detection of mesocyclones and tornado vortex signatures
[AD-A154968] 21 p3635 N85-32578
Forecasting of tropical cyclone motion using an EOF (Empirical Orthogonal Function) representation of wind forcing
[AD-A155034] 21 p3636 N85-32580

CYCLONES (EQUIPMENT)
U CENTRIFUGES

CYCLOPROPANE
Cation promotion effects in zeolite-supported F-T catalysts
[DE85-001708] 09 p1291 N85-18108

CYCLOTETRAMETHYLENE TETRANITRAMINE
U HMX

CYCLOTRIMETHYLENE TRINITRAMINE
U RDX

CYCLOTRON FREQUENCY
Two-point theory of current-driven ion-cyclotron turbulence
[DE85-010114] 19 p3372 N85-30918
Analysis of Jovian decametric data: Study of radio emission mechanisms
[NASA-CR-176057] 22 p3851 N85-33846
Generalized reduced fluid model with finite ion-gyroradius effects
[DE85-013123] 24 p4157 N85-35777
Proposed FRX-D experiment
[DE85-012766] 24 p4158 N85-35778

CYCLOTRON RADIATION
NT ION CYCLOTRON RADIATION
Polarized electron cyclotron emission in the Tokapole 2 Tokamak
[DE84-014953] 01 p0122 N85-10839
Generation and propagation of electron cyclotron harmonic waves 14 p2367 N85-24630
Theoretical studies of electric cyclotron harmonic (ECH) waves based on experimental data from GEOS 1
14 p2367 N85-24631
Role of equatorial Electron Cyclotron Harmonic (ECH) waves in the generation of diffuse auroras. Contribution of the GEOS IMS spacecraft 14 p2367 N85-24632
Heating of electrons in a high density tokamak by a micro-wave near second harmonic frequency
[DE85-010682] 19 p3359 N85-30822
Poloidal variations in toroidal fusion reactor wall power loadings
[DE85-009505] 19 p3362 N85-30846
Activation analysis of natural water using neutrons of various energies 21 p3690 N85-32924
Diamagnetic instability of cyclotron waves in plasma
21 p3693 N85-32948
Electrostatic ion cyclotron instability due to a nonuniform electric field perpendicular to the external magnetic field
[AD-A155474] 21 p3707 N85-33019
Research on gyrotrons
[AD-A154032] 23 p3934 N85-34380
Multiple-frequency electron cyclotron heating of hot electron rings in EBT-1
[DE85-011302] 23 p3983 N85-34701

CYCLOTRON RESONANCE
Fine structure of Alfven maser radiation
06 p0824 N85-15232
Effect of resonant microwave power on a PIG ion source
[DE85-001396] 09 p1379 N85-18673
ORNL ECR multicharged ion source
[DE85-001283] 09 p1380 N85-18681
Recent activities on JIPP T-IIU Tokamak
09 p1387 N85-18724
Memory function for cyclotron resonance of two-dimensional electron systems
[AD-A152632] 17 p3029 N85-28731
Millimeter wave generation by relativistic electron beams
[AD-A153980] 18 p3179 N85-29708
Reactions of metal ions and their clusters in the gas phase using laser ionization-ion cyclotron resonance spectroscopy
[DE85-009478] 19 p3361 N85-30838
Electromagnetic wave amplification during cyclotron resonance in a medium 21 p3693 N85-32942
Influence of ECR-heating on MHD activity of plasma in tokamak-10 installation 21 p3694 N85-32949
Cyclotron resonance in a nonneutral plasma
[AD-A155248] 21 p3707 N85-33017
Investigations of the cyclotron resonance effects in the X ray spectrum of the neutron star Hercules X-1
[MPE-191] 22 p3890 N85-34112
Transport issues in Phaedrus-type plasmas
23 p3976 N85-34853

CYCLOTRON RESONANCE DEVICES
A nonlinear theory for gyro-devices
[AD-A145297] 02 p0200 N85-11333
Harmonic emission from high power gyrotron oscillators
[AD-A145621] 02 p0200 N85-11335
Gyrotron beam generation with helical magnetic fields
[AD-A145987] 03 p0417 N85-12670
Buildup of oscillations in two-mode gyrotron
06 p0788 N85-15037
Quasi-optical harmonic gyrotron and gyroklystron
[AD-D011308] 07 p0947 N85-16001
Analytical and numerical modeling of gyrotrons
[AD-A148100] 08 p1157 N85-17300
Electron cyclotron resonance heating system for the stellarator W 7-AS
[IPF-84-5] 09 p1395 N85-18779
High power millimeter-wave mode converters in overmoded circular waveguides using periodic wall perturbations
[IPF-84-6] 09 p1395 N85-18780
The use of synthesis method in the design of gyrotron electron guns
[INPE-3305-PRE/616] 10 p1478 N85-19329
Activities report of the Institute of Plasma Research
11 p1733 N85-20903
Millimeter wave dielectric property measurement of gyrotron window materials
[DE85-004430] 12 p1802 N85-21304
The 60 GHz gyrotron development program
[DE85-000599] 12 p1836 N85-21522

Design considerations for a 100 kW CW, 140 GHz gyrotron oscillator
[DE85-005282] 13 p2066 N85-22904
A 60 GHz 200 kW CW gyrotron with high output mode purity
[DE85-005283] 13 p2066 N85-22905
Coupled-cavity gyrotrons with mode conversion
13 p2076 N85-22967
Design and testing of gyroklystron amplifiers
[AD-A151026] 14 p2298 N85-24231
Design and testing of a high power quasi-optical gyrotron
[AD-A153212] 17 p2968 N85-28330
The design of megawatt gyrotrons
[DE85-007892] 17 p3032 N85-28754
Proposal for continuation of research on megawatt gyrotrons for the period January 1, 1985 through December 31, 1986
[DE85-009962] 18 p3110 N85-29260
Operation of a quasioptical electron cyclotron maser
[DE85-008450] 18 p3113 N85-29276
High harmonic rectangular gyrotron
19 p3256 N85-30189
140 GHz gyrotron development program
[DE85-010346] 20 p3537 N85-32013
Research on gyrotrons
[AD-A154032] 23 p3934 N85-34380

CYCLOTRONS
NT MICROTRONS
Notes on NAC report NAC-83-05: Beam Pulse Length Determination by Spectral Analysis
[CSIR-NAC-83-06] 01 p0119 N85-10616
Operation of a quasioptical electron cyclotron maser
[DE85-008450] 18 p3113 N85-29276
Summary of the discussion of the theory of radiative processes
[DE85-007812] 19 p3371 N85-30914
Cyclotron absorption of fast magnetosonic wave in stellarator 21 p3693 N85-32945
Low frequency instabilities driven by an ion temperature anisotropy
[AD-A154902] 21 p3707 N85-33016
Experimental measurements of the ion cyclotron antennas' coupling and RF characteristics
[DE85-011569] 23 p3982 N85-34694

CYGNUS CONSTELLATION
Optical and X-ray observations of 4U2129+47/V1727 CYG in a quiescent state 11 p1742 N85-20950
Accretion in the zeta Aurigae and 32 Cygni shock cones 11 p1754 N85-21036
Long-term observations of Cyg X-3 with Vela 5B
[DE85-005556] 15 p2686 N85-26566
Salyut-7 cosmonauts work with RS-17 and GSPS X-ray telescopes 22 p3731 N85-33131
Search for gamma rays of energy 10(15) eV from Cygnus X-3
[OG-2.1-1] 22 p3862 N85-33919
1000 GeV gamma rays from Cygnus X-3: An update
[OG-2.1-6] 22 p3863 N85-33925
Variability in the high energy gamma ray emission from Cyg X-3 over a two-year period (1983 - 1984) at E 4 x 10(11) eV
[OG-2.1-11] 22 p3864 N85-33927
A search for gamma-ray point sources with the Carpet shower array
[OG-2.1-12] 22 p3864 N85-33928
Cyg X-3: Not seen in high-energy gamma rays by COS-B
[OG-2.2-2] 22 p3864 N85-33929
Constraints on cosmic-ray observation of Cygnus X-3
[OG-2.2-3] 22 p3864 N85-33930
Ultra high energy gamma rays, cosmic rays and neutrinos from accreting degenerate stars
[OG-2.2-5] 22 p3864 N85-33931
Relevance of the observation of UHE gammas to hard X-ray astronomy
[OG-2.2-6] 22 p3865 N85-33932
Low-energy gamma rays from Cygnus X-1
[OG-2.4-13] 22 p3868 N85-33957
UHE particle production in close binary systems
[OG-5.4-7] 22 p3836 N85-34084
The identification of gamma ray induced EAS
[HE-4.5-1] 24 p4195 N85-36026

CYLINDERS
Experimental study on the glow plug aided alcohol driven diesel engine 04 p0483 N85-13078
Electromagnetic resonances of cylinders and aircraft model with resistive wires
[NASA-CR-174203] 06 p0838 N85-15319
Temperature prediction in mechanical components, an analytical approach 09 p1327 N85-18339
Large deformations of a nonlinear elastic solid and the diffusion of an ideal fluid treated as interacting continua
09 p1330 N85-18356
A remote source system for measuring relative positron annihilation line widths in individual slab cylindrical samples
[AERE-R-10549] 12 p1936 N85-22173
Alignment and assembly tool for very large diameter cylinders
[NASA-CASE-MFS-26001-1] 18 p3116 N85-29289

CYLINDRICAL AFTERBODIES
U AFTERBODIES
U CYLINDRICAL BODIES

CYLINDRICAL ANTENNAS
Transient analysis of loaded thin-wire antennas and transmission lines 13 p2053 N85-22852
Experimental verification of beam deflection from hybrid reflector antenna within wide-angle sector
13 p2079 N85-22984
Digital holographic sythesis of pattern-forming transparencies for ring antenna arrays
22 p3783 N85-33326
Cylindrical lens-array antenna for wideband electronic scanning
[AD-A156065] 24 p4090 N85-35350

CYLINDRICAL BODIES
NT ROTATING CYLINDERS
Influence of aluminum metallization coatings on corrosion fatigue properties of steel
01 p0018 N85-10112
Overall heat transfer coefficients for a horizontal cylinder in a fluidized bed
[AD-A144876] 01 p0124 N85-10649
Scattering by a parabolic cylinder: A uniform asymptotic expansion
[AD-A145686] 02 p0252 N85-11652
Analysis of piezoelectric disks and cylinders using finite element method
[AD-A146323] 03 p0414 N85-12650
Allowing for the temperature field in the wall thickness of checkerwork in thermal calculation
[BLL-M-36015-(5828.4)] 07 p0956 N85-16058
Stability of rigid motions and rollers in bicomponent flows of immiscible liquids
[AD-A147302] 07 p0960 N85-16081
Shock and impact response of solid rocket propellants: Experimental and theoretical 08 p1116 N85-17040
Method of testing carbide inserts for premature fracture by face milling of cylindrical workpieces
09 p1303 N85-18183
Numerical investigation of phase change heat transfer in a horizontal cylinder including effects of natural convection 09 p1318 N85-18286
Natural convection experiments about a finite-length cylindrical heat source in a liquid-saturated porous medium
[DE84-012657] 09 p1320 N85-18298
Study of residual stresses introduced into TA6ZrD (685) cylinders by quenching — compressor disk alloy
[PNR-90240] 09 p1341 N85-18435
Experimental investigation of heat transfer to bluff cylinders and cones in hypersonic rarefied gas flow
11 p1620 N85-20195
Natural convection heat transfer between arrays of horizontal cylinders and their enclosure
[DE85-003773] 11 p1632 N85-20280
Determining distribution of complex dielectric permittivity over cylindrical body of intricate cross section from electromagnetic field measurement
12 p1842 N85-21559
Pneumatic clamping device
[AD-D011544] 12 p1858 N85-21656
Transonic merging separated flows
[AD-A150667] 14 p2213 N85-23724
Measurement of damping of graphite epoxy materials
[NASA-CR-175663] 14 p2248 N85-23931
One physical mechanism of formation of fine structure of ocean waters 14 p2334 N85-24436
Investigation of potential and viscous flow effects contributing to dynamic stall
[AD-A151696] 15 p2557 N85-25773
Measurements of the symmetric aerodynamic coefficients for flat faced cylinders in the angle of attack regime 0 to 90 deg for transonic and supersonic speeds
[FFA-TN-1984-04] 16 p2700 N85-26675
Buildup of oscillation of bodies in stratified fluid
17 p2941 N85-28157
Effects of the corona wind on the cooling of a horizontal cylinder
[AD-A153101] 17 p2954 N85-28241
Unsymmetrical flow in a centrifuge
[DE85-009021] 18 p3103 N85-29208
Mutual coupling analysis for conformal microstrip antennas
[AD-A154292] 19 p3259 N85-30210
Seismic analysis of liquid-filled tanks with an eccentric core barrel
[DE85-010249] 19 p3269 N85-30272
Solid-state resistance welding cylinders and spheres
[DE85-010064] 20 p3469 N85-315
The effect of stress and hot corrosion on nickel-base superalloys
[AD-A154722] 21 p3566 N85-321
TNT equivalency of EAK explosive
[AD-A155737] 21 p3571 N85-321
Evaluation of the effects of roll angle on the natural convection heat transfer from an array of cylindrical spines
[AD-A154594] 21 p3583 N85-327
Nonlinear response and failure characteristics of internally pressurized composite cylindrical panels
[NASA-CR-176148] 22 p3800 N85-338
Calculation of roots of transcendental equations in problems of determining thermal conductivity of cylinders with non-uniform boundary conditions
[BLL-M-35786-(5828.4)] 23 p3929 N85-340
Vibrations of free hollow circular cylindrical bodies
24 p4100 N85-354
A towed instrument vehicle for deep ocean sampling
[AD-A156322] 24 p4125 N85-352
Acoustic resonances in cylinder bundles oscillating in a compressible fluid
[DE85-004066] 24 p4145 N85-355

CYLINDRICAL PLASMAS
ICRF antenna coupling theory for a cylindrically stratified plasma
[DE85-004960] 14 p2424 N85-248

CYLINDRICAL SHELLS
Oil flow patterns of separated flow on a hemispherical cylinder at incidence
[DFVLR-FB-84-20] 01 p0048 N85-103
Initial postbuckling analysis of elastoplastic thin-shell structures 01 p0059 N85-103
Resonant frequencies and mode shapes for single and double cylindrical shells
[AD-A144778] 01 p0062 N85-104
Three dimensional separation and vortex formation
02 p0196 N85-113
Scattering of plane wave on cylindrical shell in low-frequency region 02 p0256 N85-116
Dispersion curves for normal waves in cylindrical shell and conditions for spatial coincidence in vicinity of critical frequencies 06 p0778 N85-147
Stability of circular cylindrical shell with piecewise constant thickness subjected to radial pressure
06 p0779 N85-148
Deformation of cylindrical shell with cantilevered elastic plates attached 06 p0779 N85-148
Stability of hollow shafts under torsion
06 p0780 N85-148
Saint Venant conditions in theory of piezoelastic shells
06 p0780 N85-148
Acoustic radiation from single and double ribbed circular cylindrical shells
[AD-A148771] 08 p1219 N85-176
Circumferential cracks in cylindrical shells
09 p1330 N85-183
Direct energy minimization approach to whipping analysis of pressure hulls 09 p1335 N85-183
Simplified theory for the behaviour of buried flexible cylinders under the influence of uniform hoop compression
[PB85-116531] 11 p1654 N85-204
Fracture analysis of cracks in complete cylindrical shells
[AD-A150091] 12 p1867 N85-21711
Behavior of buried flexible cylinders under the influence of nonuniform hoop compression
[PB85-116523] 12 p1868 N85-2171
Solid Rocket Motor Case (SRMC) dynamic sensitivity to changes in composite properties
12 p1948 N85-222
Automatic multi-layer welding of thick cylindrical structures under flux 13 p2035 N85-227
Interaction of cylindrical shell with concentrated mass moving along its inner surface 13 p2047 N85-228
Steady-state reaction of three-layered cylindrical shell to effect of moving load 13 p2047 N85-228
Spectral frequency of eigenvalues in optimal problems of stability of cylindrical shells of variable thickness
13 p2047 N85-228
Stability of cylindrical shells with one-way constraints
13 p2048 N85-229
Parametric study of autooscillation upon flow of supersonic jet into cylindrical cavity
16 p2765 N85-270
Stability of anisotropic cylindrical sandwich shells
16 p2766 N85-270
Study of oscillations of composite cylindrical shells using a dynamic stiffness technique 16 p2766 N85-270
Stressed state of multilayer thick-walled longitudinally corrugated cylinders 16 p2766 N85-270

An analysis for axially compressed orthotropic shells with a multimode imperfection representation
[VTH-LR-422] 16 p2803 N85-27281

Stability of cylindrical shells with variable thickness under external pressure 17 p2943 N85-28164

Scattering of sounds by piezoceramic cylindrical shell near rigid surface 17 p2943 N85-28168

The effect of center delamination on the instability of composite cylindrical panels
[AD-A153494] 18 p3069 N85-28979

Optimization of axially compressed carbon fiber reinforced plastic (CFRP) cylinders
18 p3121 N85-29318

Determination of deformation speed during high-speed deformation of cylindrical shells
[BLL-M-36280-(5828.4)] 20 p3465 N85-31527

Finite elastic deformations of cylindrical and spherical shells under pressure
[OUEL-1549/84] 20 p3470 N85-31559

Acoustic wave scattering by round cylindrical shell reinforced with stringers 21 p3688 N85-32916

Iteration solution for a submerged force-driven finite cylinder
[AD-A154587] 21 p3699 N85-32982

Acoustic radiation from concentric shells containing an inner fluid
[AD-A155476] 21 p3700 N85-32991

CYLINDRICAL TANKS

SRB filament wound case material property study
[NASA-CR-171469] 17 p2910 N85-27940

Local heat treatment of welded joints of pipes and rotary vessels 17 p2924 N85-28028

CYLINDRICAL WAVES

Parameters of detonation waves excited in gas during concentrated release of energy
02 p0268 N85-11751

Propagation of non-axisymmetric elastic waves through shell with filler under radial load at one end
17 p2943 N85-28169

A dual spin space station design
20 p3408 N85-31152

CYLINDROIDS

U CYLINDRICAL BODIES

CYTOCHROMES

Respiratory chain of alkalophilic bacteria
[DE84-012558] 09 p1360 N85-18556

Cytochromes and iron sulfur proteins in sulfur metabolism of phototrophic bacteria
21 p3657 N85-32718

CYTOLOGY

Second Soviet-French Symposium on Space Cytology
14 p2386 N85-24699

Second Soviet-French Symposium on Space Technology 15 p2483 N85-25326

Flow cytometry for health monitoring in space
[DE85-009572] 19 p3329 N85-30625

Operation of the Zeiss cytopherometer with Zn/ZnSO4 electrode system of Tenforde et al
20 p3499 N85-31752

Detection of internal structure by scattered light intensity: Application to kidney cell sorting
20 p3503 N85-31777

Flow cytometry of human embryonic kidney cells: A light scattering approach 20 p3503 N85-31778

A cluster analysis method for identification of subpopulations of cells in flow cytometric list-mode arrays 20 p3503 N85-31779

Improved flow cytometer measurement of binding assays
[DE85-006407] 23 p3935 N85-34390

CYTOPLASM

Further cell biology experiments with Physarum polycephalum for a reflight of Biorack
05 p0689 N85-14429

Influence of simulated weightlessness on the motility of the acellular slime mold Physarum polycephalum
05 p0689 N85-14430

Physical chemical state of water in living cells
[AD-A154566] 21 p3662 N85-32749

CZECHOSLOVAKIA

Earthquake activity in the Bohemian massif and in the western Carpathians
[REPT-547] 03 p0375 N85-12390

Hole shots along refraction profile R4/78 recorded at the temporary seismic station near Stary Plzenec (west Bohemia)
[REPT-549] 03 p0375 N85-12392

Catalogue of earthquakes for the territory of Czechoslovakia for the period 1957 - 1980
[REPT-555] 03 p0376 N85-12398

The extremeness of the cold front of December 31, 1978 over the CSR
[REPT-566] 03 p0377 N85-12409

Aspects of CSSR CMOS integrated circuits discussed
15 p2533 N85-25627

Recent developments 15 p2533 N85-25628

MHB4046 phase-lock circuit 15 p2533 N85-25629

Improved, cheaper SIPMOS circuits no. 10, 1983 p 370 15 p2534 N85-25630

Phase-locked loop design with MHB4046
15 p2534 N85-25631

Additional PLL designs 15 p2534 N85-25632

CZOCHRALSKI METHOD

Recent progress in BGO development for high resolution calorimetry
[MPI-PAE/EXP-E1-129] 01 p0124 N85-10848

Research on gallium arsenide diffused junction solar cells
[NASA-CR-174057] 02 p0222 N85-11457

Investigation of liquid encapsulation Chochralski growth of InP
[AD-A146096] 03 p0433 N85-12760

Stress studies of EFG
[NASA-CR-174078] 05 p0651 N85-14179

Crystal growth and characterization of BaMgF4
[AD-A146805] 07 p1047 N85-16650

Clusters of defects in semiconductors
[AD-A147426] 07 p1048 N85-16655

Stress studies in EFG
[NASA-CR-175488] 10 p1563 N85-19856

Research on the basic understanding of high efficiency in silicon solar cells
[DE85-000507] 11 p1672 N85-20537

Thermally stimulated conductivity in semi-insulating gallium arsenide 13 p2068 N85-23036

InP materials
[AD-A152341] 17 p3043 N85-28828

Telescoping low vibration pulling mechanism for Czochralski crystal growth
[AD-D011655] 17 p3044 N85-28836

Current status of silicon materials research for photovoltaic applications
[DE85-008799] 19 p3304 N85-30482

Oxygen and carbon impurities and related defects in silicon 20 p3481 N85-31631

D

D LAYER

U D REGION

D LINES

Distances of local clouds from optical line observations 06 p0875 N85-15558

D REGION

Experience with proposed improvements of the International Reference Ionosphere (IRI)
[PB84-235870] 05 p0678 N85-14353

Analysis of ionization sources in D region based on theoretical models 06 p0825 N85-15240

Partial reflection D-region electron densities
08 p1184 N85-17461

D1 LF wind measurements in the 90 to 100 km height range 08 p1185 N85-17468

Middle Atmosphere Program. Handbook for MAP, volume 10
[NASA-CR-175477] 11 p1658 N85-20450

Neutral atmosphere properties determining D-region electron densities 11 p1658 N85-20451

Variation of derived mesospheric nitric oxide in relation to wind and temperature in winter
11 p1658 N85-20452

Middle atmosphere temperature and dynamics as revealed from D-region observations
11 p1659 N85-20453

Indirect phase height measurements in central and eastern Europe for monitoring D region plasma
11 p1659 N85-20456

Abnormal circulation changes in the winter stratosphere, detected through variations of D region ionospheric absorption 11 p1659 N85-20458

A model of the influence of neutral air dynamics on the seasonal variation in the low ionosphere
11 p1660 N85-20462

Seasonal characteristics of mesospheric plasma and their transitions 11 p1660 N85-20464

The dynamics of ionospheric D region over East Siberia 11 p1662 N85-20477

Stratwarm effects in the ionospheric D region wind field 11 p1663 N85-20479

The high latitude D region during electron precipitation events 11 p1664 N85-20484

High energy particle effects in the D region during and after geomagnetic storms 11 p1664 N85-20485

Solar terrestrial influences on the D region as shown by the level of atmospheric radio noise
11 p1664 N85-20488

Ion kinetics, small neutral and excited components in D-region with elevated ionization level. Part 2: Variations in small neutral and excited components
15 p2480 N85-25307

Ion composition measurements of the disturbed and quiet D-region in 1980 - 1981
[AD-A158055] 24 p4117 N85-35521

DAEMO (DATA ANALYSIS)

U DATA PROCESSING
U DATA REDUCTION
U DATA TRANSMISSION

DAMA

U DEMAND ASSIGNMENT MULTIPLE ACCESS

DAMAGE

NT CUMULATIVE DAMAGE
NT EARTHQUAKE DAMAGE
NT FIRE DAMAGE
NT FROST DAMAGE
NT IMPACT DAMAGE
NT LASER DAMAGE
NT METEORITIC DAMAGE
NT RADIATION DAMAGE
NT STORM DAMAGE

Material degradation in heavy steel plates caused by bending with a laser
[AD-A144784] 01 p0052 N85-10343

Deformation measurements of composite multi-span beam shear specimens by Moire interferometry
[NASA-CR-3844] 02 p0169 N85-11135

Development of powder metallurgy 2XXX series Al alloys for high temperature aircraft structural applications
[NASA-CR-172408] 02 p0182 N85-11220

Influence of cyclic tangential loading on indentation fracture
[DE84-015969] 03 p0373 N85-12382

Selection, procurement and description of Salem Limestone samples used to study the effects of acid rain
[PB84-231067] 04 p0484 N85-13068

Development of damage in fatigue loaded carbon fiber reinforced plastics 05 p0650 N85-14172

The F-15 flight loads tracking program
07 p0894 N85-15666

Cumulative damage modeling of fatigue crack growth
07 p0907 N85-15741

Advances in composites technology
[NASA-TM-86353] 08 p1118 N85-17048

Repair of composites 08 p1120 N85-17058

Life assessment and damage tolerance of wind turbines
[AD-B088148L] 08 p1179 N85-17427

Models for shock damage to marine structural materials 09 p1336 N85-18400

Influence of volumetric fiber content on some matrix damage factors during thermal cycling of tungsten-EI 765 composite 10 p1443 N85-19097

Applications of vibration analysis to the condition monitoring of rolling element bearings
[ARL/AERO-R-163] 12 p1859 N85-21663

Nondestructive method for detecting machine damage in beryllium
[DE85-001074] 12 p1862 N85-21681

Advanced life analysis methods. Volume 1: Cracking data survey and NDI (nondestructive inspection) assessment for attachment lugs
[AD-A150419] 13 p2103 N85-23108

Advanced life analysis methods. Volume 2: Crack growth analysis methods for attachment lugs
[AD-A150420] 13 p2103 N85-23109

Advanced life analysis methods. Volume 5: Executive summary and damage tolerance criteria recommendations for attachment lugs
[AD-A151017] 14 p2219 N85-23761

Significant parameters of the behavior and of the surface damage of the lubricated Hertzian contact: An application to gears 14 p2222 N85-23783

Estimating defectiveness buildup during service in metal of welded runner in low-pressure cylinder of turbine
14 p2271 N85-24070

Experimental report on a fiber optic light guide made by Galileo Electro-Optics Corporation
[DE85-006161] 14 p2421 N85-24941

Damage development during low cycle fatigue of carbon-black loaded SBR
[DE85-006234] 15 p2519 N85-25533

Differential effect of denervation on free radical scavenging enzymes in slow and fast muscle of rat
[NASA-CR-175719] 15 p2614 N85-26110

Thermal annealing of Fe implanted Al2O3 in oxidizing and reducing environment: Revised version
[DE85-007546] 16 p2752 N85-26983

Damage caused to polyurethane foams by aging, simulated sunlight exposure, heat and fire
[AD-A152040] 16 p2754 N85-26996

Method of investigating accumulations of damage to weld joints in the case of low-cycle creep
[BLL-CE-TRANS-8088-(9022.09)]
16 p2792 N85-27219

Impact of ozone on vegetation
[PB85-159937] 16 p2821 N85-27403

Reexamination of cumulative fatigue damage laws
17 p2914 N85-27962

Laboratory investigation of formation damage of an artificial fracture at simulated geothermal conditions
[DE85-010301] 18 p3102 N85-29201

Description and illustration of the use of CRACKS IV
[AD-A153543] 18 p3121 N85-29325

Fuel containment and damage tolerance in large composite primary aircraft structures
[NASA-CR-166083] 19 p3231 N85-30032

Temperature and surface damage under lubricated sliding-rolling contacts 19 p3260 N85-30336

A continuous damage model based on stepwise-stress creep rupture tests
[NASA-CR-174941] 21 p3597 N85-32341

Damage induced stress redistribution in composite laminates 24 p4072 N85-35235

Fuel containment and damage tolerance for large composite primary aircraft structures. Phase 1: Testing
[NASA-CR-166091] 24 p4073 N85-35241

Fatigue damage detection in steels by optical correlation
[AD-A155830] 24 p4079 N85-35277

Static and cyclic behavior of semi-rigid steel beam-column connections
[PB85-194363] 24 p4103 N85-35433

Three-dimensional finite deformation viscoelastic model accounting for damage effects
[DE85-012951] 24 p4139 N85-35660

Thermal hydraulic features of the TMI accident
[DE85-014569] 24 p4152 N85-35747

DAMAGE ASSESSMENT

Review of aircraft accident data: US General Aviation
[PB84-230960] 01 p0005 N85-10027

Results of tests of advanced flexible insulation vortex and flow environments in the North American Aerodynamics Laboratory lowspeed wind tunnel using 0.0405-scale Space Shuttle Orbiter model 16-0 (test OA-309)
[NASA-CR-167692] 01 p0015 N85-10096

Construction of approximate confidence intervals for probability-of-kill via the bootstrap
[AD-A144761] 01 p0113 N85-10764

Integrative investigation on forest damage detection based on airborne Multispectral Scanner data
05 p0656 N85-14215

Mechanisms of damage accumulation in time-dependent cyclic deformation
[DE85-001004] 10 p1496 N85-19443

History of satellite break-ups in space
12 p1783 N85-21190

Systems vulnerability and lethality in the development phase
[AD-A149737] 12 p1924 N85-22089

USAF damage tolerant design handbook: Guidelines for the analysis and design of damage tolerant aircraft structures, revision B
[AD-A153161] 17 p2896 N85-27858

Theoretical modeling of laser induced optical degradation
[AD-A155302] 21 p3592 N85-32323

Maintenance and the military environment
22 p3750 N85-33243

Protective systems and maintenance policies for marine environments 22 p3750 N85-33245

Relating corrosion maintenance to environmental factors 22 p3750 N85-33247

DAMAGE THRESHOLD
U YIELD POINT

DAMKOHLER NUMBER

Flow field effects on nucleation in a reacting mixing layer
[ARL/AERO-R-165] 19 p3263 N85-30237

DAMPERS (VALVES)

Multiple rate shock isolator damping valve
[AD-D011429] 08 p1168 N85-17368

Dual clearance squeeze film damper
[NASA-CASE-LEW-13506-1] 22 p3791 N85-33490

DAMPING
NT ELASTIC DAMPING
NT LANDAU DAMPING
NT VIBRATION DAMPING
NT VISCOELASTIC DAMPING
NT VISCOUS DAMPING

Review of some vortex relations
[NASA-CR-172452] 01 p0046 N85-10302

Power flow between non-conservatively coupled oscillators
[ISVR-TR-125] 02 p0209 N85-11377

Dynamics of the Uranian rings
02 p0302 N85-11956

Damping synthesis for a spacecraft using substructure and component data
[CRC-1365] 03 p0323 N85-12082

Complex frequency analysis of damped thin-walled beams with open cross sections
03 p0371 N85-12366

Experimental on-stream elimination of resonant whirl in a large centrifugal compressor 05 p0642 N85-14121

Hydrodynamic impeller stiffness, damping, and inertia in the rotordynamics of centrifugal flow pumps
05 p0643 N85-14125

Effects of fluid inertia and turbulence on force coefficients for squeeze film dampers
05 p0645 N85-14137

Squeeze-film dampers for turbomachinery stabilization
05 p0645 N85-14138

Status of beam transport with the ETA and ATA accelerators
[DE84-013205] 05 p0726 N85-14670

Mechanism of damping of plasma oscillations in initial stage of injection of electron beams from spacecraft into ionosphere in active experiments
06 p0823 N85-15225

Computational fluid mechanics utilizing the variational principle of modeling damping seals
[NASA-CR-174332] 08 p1161 N85-17325

Identification of vibration parameters of flexible structures 09 p1331 N85-18360

Integrated Technology Rotor/Flight Research Rotor (ITR/FRR) concept definition
[NASA-CR-166445] 10 p1423 N85-18979

Modal testing and analysis of NOVA laser structures
[DE84-017569] 11 p1638 N85-20321

A study of transonic flutter of a two-dimensional airfoil using the U-g and p-k methods
[LR-615] 12 p1771 N85-21121

Stability analysis of flexible spacecraft with PID controller
[CRC-1372] 12 p1792 N85-21247

Workshop on Nuclear Dynamics 3
[INC-40007-24] 12 p1931 N85-22130

Distributed combustion: A mechanism of acoustic suppression 13 p2001 N85-22543

Damping models for flexible communications satellites by substructural damping synthesis
[UTIAS-267] 14 p2237 N85-23868

An experimental study of aerodynamic damping characteristics of a compressor annular cascade in high speed flow and the visualization of annular cascade flow
[NAL-TR-838] 15 p2554 N85-25759

Energy dependence of the emittance of damping ring beams
[DE85-007080] 15 p2649 N85-26341

Model reduction techniques applied to the control of large space structures
[AD-A151784] 16 p2731 N85-26857

Turbine blade friction damping study
16 p2736 N85-26886

Measurement of damping of graphite expoxy materials
[NASA-CR-175793] 16 p2743 N85-26925

Non-contact hydrostatic bearings
16 p2762 N85-27046

Influence of materials creep on rotor dynamics
[DE85-006545] 17 p2981 N85-28426

Hyperbolic phenomena in the flow of viscoelastic fluids
[AD-A153533] 18 p3099 N85-29186

The effect of line damping, magneto-optics and parasitic light on the derivation of sunspot vector magnetic fields
18 p3207 N85-29895

Arrangement for damping the resonance in a laser diode
[NASA-CASE-NPO-15980-1] 19 p3274 N85-30305

Damping seal for turbomachinery
[NASA-CASE-MFS-25842-2] 19 p3280 N85-30341

SSME seal test program: Test results for hole-pattern damper seals
[NASA-CR-171595] 20 p3395 N85-31059

Measurement of material damping in a simulated space environment 20 p3397 N85-31070

On the measurement of material damping in a simulated space environment 20 p3411 N85-31169

Finite control in underdamped distributed parameter systems 20 p3412 N85-31176

An overview of latest model reduction and control methods of large flexible space structures
20 p3414 N85-31191

Report of near field group
[DE85-010536] 20 p3527 N85-31940

Measurement of damping of graphite epoxy materials
[NASA-CR-176073] 21 p3596 N85-32334

Nonradiative damping of molecular electronic excited states by metal surfaces
[AD-A154619] 21 p3701 N85-32994

A research program to reduce the interior noise in general aviation aircraft, index and summary
[NASA-CR-176178] 24 p4145 N85-35695

Accelerator physics measurements at the damping ring
[DE85-013373] 24 p4159 N85-3678

TOSCA calculations and measurements for the SLAC SLC damping ring dipole magnet
[DE85-014366] 24 p4160 N85-3679

DAMPING FACTOR
U DAMPING

DAMPING IN PITCH
U DAMPING
U PITCH (INCLINATION)

DAMPING IN ROLL
U DAMPING
U ROLL

DAMPING IN YAW
U DAMPING
U YAW

DAMPING TESTS

Measurement of damping of graphite epoxy materials
[NASA-CR-176073] 21 p3596 N85-3233

DAMPNESS
U MOISTURE CONTENT

DAMS

Military hydrology. Report 9: State-of-the-art review and annotated bibliography of dam-breach flood forecasting
[AD-A155383] 22 p3801 N85-3355

National program for inspection of non-federal dams. Woodward reservoir dam (VT 00209), Connecticut River Basin, Plymouth, Vermont. Phase 1 inspection report
[AD-A156256] 24 p4144 N85-356

DANGER
U HAZARDS

DARK ADAPTATION

Effect of extreme peripheral light on dark adaptation
[AD-A148923] 10 p1528 N85-1963

The relative effectiveness of red and white light for subsequent dark-adaptation
[AD-A148883] 10 p1530 N85-19642

Glutathione in cyanobacteria
21 p3661 N85-32745

DARKNESS

Dark focus: Intersubject variation, intrasubject stability, and relationship to near retinoscopy
[AD-A145489] 02 p0235 N85-11530

Long-term light induced changes in dark conductivity of kapton
[AD-A148791] 08 p1224 N85-17706

DART TURBOPROP ENGINES
U TURBOPROP ENGINES

DASSAULT AIRCRAFT
NT MIRAGE AIRCRAFT
NT MIRAGE 3 AIRCRAFT

DASSAULT MIRAGE 3 AIRCRAFT
U MIRAGE 3 AIRCRAFT

DATA

Quality of scientific and engineering data
[DE85-000294] 11 p1739 N85-2093

A study of frequency effects and damage accumulation during the fatigue of graphite/epoxy and glass/epoxy composite materials 14 p2247 N85-2393

DATA ACQUISITION

User experience of existing corrosion monitoring techniques and the development of Thin Layer Activation (TLA) for corrosion monitoring
[AERE-R-11248] 01 p0029 N85-1018

Automation of coastal engineering modelling facilities
[CSIR-T/SEA-8304] 01 p0035 N85-1021

Flight demonstration of new NRL real-time data acquisition system and laser video waveform sampler
[AD-A145126] 01 p0053 N85-1035

Analysis strategies for field dependent estimation and network design — mesoscale modeling
01 p0078 N85-1052

East Europe report: Science and technology
[JPRS-ESA-84-030] 01 p0101 N85-1067

Decentralized data acquisition to remedy EDP bottleneck 01 p0101 N85-10671

A modular data acquisition and display software system for a laboratory environment
[PB84-217892] 01 p0105 N85-10709

Field tests of the real-data acquisition system for the NASA-LaRC differential absorption lidar
[NASA-CR-174020] 01 p0106 N85-10710

Data input, processing and presentation — helicopter rotor balance measurement
[NASA-TM-77739] 01 p0125 N85-1085

EG and G Idaho's response to a request for a graphic data base support package
[DE84-015171] 01 p0126 N85-1086

Airborne performance measurement system design: C-5 aircraft
[AD-A145436] 02 p0236 N85-1153

NESDIS international activities, appendix 2
02 p0295 N85-11917

Satellite, airborne remote sensing development outlined 03 p0342 N85-12199
The current formal status of the ERS-1 ground segment 03 p0380 N85-12423
An inexpensive microcomputer for laboratory data acquisition and test equipment control
[AD-A146095] 03 p0403 N85-12567
Noise analysis of the Coarse Optical Power Spectrum Estimator (COPSE) data acquisition system
[AD-A145918] 03 p0419 N85-12677
Heavy duty precision pan and tilt head
[AD-A146669] 04 p0509 N85-13246
Solar energy resource assessment in Eastern New Mexico and solar and wind energy resource assessment in Eastern New Mexico
[DE84-901511] 04 p0527 N85-13370
FSA field test
[NASA-CR-174114] 04 p0528 N85-13373
Testing of production of silicon-titanium-magnesium alloying composition
[BLL-M-35904-(5828.4)] 05 p0616 N85-13937
ECUT energy data reference series: Lightweight materials for ground transportation
[DE84-015269] 05 p0621 N85-13974
The Telecommunications and Data Acquisition Report
[NASA-CR-174149] 05 p0622 N85-13980
Programmable digital baud integrators for the radar high-speed data acquisition system
05 p0624 N85-13994
The acquisition, processing, and use of tactile sensor data in robot control 05 p0641 N85-14114
Measurement data acquisition and processing system for wind rotor measurements in the wind channel of Bremen University 05 p0668 N85-14298
Measuring-technical investigation of wind energy units from the control-technical, electrical and energetic point of view 05 p0668 N85-14301
Measuring techniques in the measuring program for the windpowered unit GROWIAN 05 p0669 N85-14303
Water vapor profile retrievals from the HIRS/MSU satellite sounder 05 p0681 N85-14378
Miniature personal physiological tape recorder (experiment 1ES 30) — Spacelab
05 p0692 N85-14448
A data collection system
[AD-D011266] 05 p0713 N85-14573
Statistical analysis of visual wave observations and gage/radar measurements
[AD-A146358] 06 p0798 N85-15100
Spring program summary, 1983
[PB84-222223] 06 p0839 N85-15330
The chemistry of rare earth elements in the solar nebula 06 p0889 N85-15643
Operational Loads Data
[AGARD-CP-375] 07 p0894 N85-15664
Operational loads measurement: A philosophy and its implementation 07 p0894 N85-15665
Navy operational loads data sources and systems
07 p0635 N85-15668
Advanced fatigue monitoring on service aircraft
07 p0895 N85-15671
Helicopter data acquisition in WHL
07 p0896 N85-15676
USAF approach to airborne structural data recording: Airborne Data Acquisition Multifunction System (ADAMS)
07 p0897 N85-15683
Support for the Naval Research Laboratory Passive Microwave Clutter Analysis Program
[AD-A146771] 07 p0939 N85-15951
National Bureau of Standards passive solar test facility: Instrumentation and site handbook
[PB85-100451/GAR] 07 p0968 N85-16148
Rule-based evidence accrual system for image understanding
[AD-A147635] 07 p1044 N85-16634
Data acquisition channel apparatus
[AD-D011428] 08 p1159 N85-17311
Sequential data processing for photogrammetric acquisition of digital elevation models
08 p1176 N85-17413
Guidelines for atmospheric measurements in support of electro-optical systems testing
[AD-A148090] 08 p1186 N85-17474
Noise measurement flight test: Data-analyses, Sikorsky S-76A helicopter
[AD-A148525] 08 p1218 N85-17673
Survey of remote data monitoring systems
[DE85-001385] 09 p1323 N85-18313
Medium speed computer interface (digitizer) for general purpose data acquisition
[DE85-001585] 09 p1367 N85-18587
East Europe report: Science and technology
[JPRS-ESA-85-005] 09 p1377 N85-18659
Data acquisition, measurement devices at 1984 Leipzig Spring Fair 09 p1378 N85-18661
The Telecommunications and Data Acquisition Report
[NASA-CR-174366] 10 p1462 N85-19224
Nationwide urban runoff program. Relationship of urban runoff to land use and groundwater resources
[PB85-114692] 10 p1506 N85-19505
OBLOG: Designed to create and maintain a 49 hour observation log file
[PB85-109528] 10 p1519 N85-19579
Tropical cyclone data tape for the Eastern and Central North Pacific Basins, 1949-1983: Contents, limitations and uses
[PB85-110054] 10 p1520 N85-19585
Computer-assisted data processing and analysis system for ground-based meteorological data collection, report on the Sierra Cooperative Pilot Project
[PB85-115350] 10 p1520 N85-19587
Drifting buoy data from equatorial Pacific Ocean, 31 Aug. 1980 - 30 Apr. 1982
[PB85-120046] 10 p1522 N85-19598
Characteristics of quality data
[DE85-001203] 10 p1568 N85-19889
Research needs on the interaction between information systems and their users: Report of a workshop
[PB85-121523] 10 p1568 N85-19891
ADAPS (Airborne Data Acquisition and Processing System) operation and maintenance manual
[AD-A149297] 11 p1585 N85-19983
Extracting digital data from a bus and multiplexing it with a video signal
[AD-D011491] 11 p1636 N85-20302
An overview of LANDSAT-4 and the Thematic Mapper
11 p1666 N85-20509
Image processing instrumentation for speckle interferometry and imaging
[AD-A149308] 11 p1762 N85-21084
In-situ detection of micron-sized dust particles in near-Earth space 12 p1785 N85-21205
Research in image understanding as applied to 3-D tomographic imaging with near optical resolution
[AD-A150098] 12 p1829 N85-21483
Building a functional, integrated GIS/remote sensing resource analysis and planning system — Utah
[E85-10092] 12 p1874 N85-21754
Atmospheric handbook: Atmospheric data tables available on computer tape
[PB85-108512] 12 p1891 N85-21867
Catalog of submarine volcanoes and hydrological phenomena associated with volcanic events: 1500 BC to 31 Dec. 1899
[PB85-117964] 12 p1891 N85-21869
Collection and use of lightning strike data in the western US during summer 1983
[PB85-110534] 12 p1897 N85-21907
Topics in optical materials and device research, 3: Volume 1
[AD-A149726] 12 p1933 N85-22145
Analyses via automated mass spectrometry (MS/DS)
12 p1947 N85-22227
Development of a multiplane multispeed balancing system for turbine systems
[NASA-CR-174750] 13 p1976 N85-22400
Measurement requirements for the detection of ozone trends 13 p2105 N85-23115
Analysis of the inflow layer and air-sea interactions in Hurricane Frederic (1979)
[NASA-CR-175616] 13 p2137 N85-23271
Mean flow and turbulence in complex terrain NPS (Naval Postgraduate School)/Vandenberg measurement system
[AD-A150184] 13 p2138 N85-23274
Operational loads measurement: A philosophy and its implementation — aircraft structures
[AD-A149445] 13 p2144 N85-23308
The experience of the Swedish Meteorological and Hydrological Institute (SMHI) with the ARGOS system
[PM-U1/81] 14 p2240 N85-23892
Fatigue crack topography and crack growth analysis — wrought and cast aluminum 14 p2319 N85-24333
Automatic hydrological data collection facility using ARGOS 14 p2324 N85-24363
Hydrological data collection from Swedish mountain areas 14 p2327 N85-24386
Geostationary Operational Environmental Satellite Data Collection System 14 p2328 N85-24393
The Data Acquisition Control and Telemetry (DACT) system — meteorological buoys
14 p2332 N85-24419
Seafloor seismic measurements in the southern Bering
[DE85-004908] 14 p2374 N85-24675
Variational mesoscale satellite data assimilation and initialization
[NASA-CR-175704] 14 p2378 N85-24680
Kitt Peak measurements of P/Halley positions
14 p2436 N85-25023
Shuttle imaging radar-B (SIR-B) data analysis for identifying rainfall event occurrence and intensity
[NASA-CR-175712] 15 p2594 N85-25986
Space methods in oceanology
[NASA-TM-77652] 15 p2604 N85-26047
Computerized biophysical data acquisition system for motion sickness studies
[AD-A151691] 15 p2618 N85-26131
A practical system for collecting reliable data on the space-time behavior of people
[AD-A151174] 15 p2619 N85-26140
The human engineering of laboratory data acquisition and control systems
[AD-A151576] 15 p2620 N85-26148
Computer use in research for data analysis
[PB85-153567] 15 p2631 N85-26220
The Telecommunications and Data Acquisition Report
[NASA-CR-175842] 16 p2770 N85-27094
Infrared presensitization photography
16 p2786 N85-27189
Design and construction of a computer controlled mirothermocouple probe for the study of buoyant jets
[AD-A152224] 16 p2788 N85-27199
CNPq/INPE LANDSAT system: Report of activities from October 1, 1983 to September 30, 1984 — Brazil
[E85-10097] 16 p2808 N85-27318
Present stage of utilization of the ARGOS system by the ORSTOM hydrological service for hydrometric data collection 16 p2813 N85-27348
Use of a network of telemetered meteorological stations for prediction of the distribution of an atmospheric tracer
16 p2831 N85-27458
A climatic data bank for Northern Hemisphere land areas, 1851-1980
[DE85-007863] 16 p2835 N85-27486
Data processing on the rotor test stand at DFVLR in Brunswick: Microprogrammable interfaces and array processor as key components in a PDP 11 real time data acquisition and processing system
[DFVLR-MITT-85-03] 17 p2906 N85-27921
Automation of Precise Time Reference Stations (PTRS) 17 p2962 N85-28291
US Naval Observatory collection and utilization of time comparison data 17 p2962 N85-28292
Laser measurement techniques: Laser spectroscopy in semiconductors
[DE85-007887] 17 p2971 N85-28350
DOE/ANL/HTRI heat exchanger tube vibration data bank: Addendum 5
[DE85-007730] 17 p2980 N85-28425
Microcomputer-controlled system for measuring atmospheric particle fluxes
[DE85-007910] 17 p2988 N85-28469
Centralized Storm Information System (CSIS)
[NASA-CR-175898] 17 p2994 N85-28506
Test and evaluation plan for the Centralized Storm Information System 17 p2994 N85-28508
CSIS test and evaluation 17 p2994 N85-28509
Functional and performance requirements of the next NOAA-Kasas City computer system
17 p2994 N85-28510
Axial topography from digitized real time radiography
[DE85-006767] 18 p3091 N85-29130
Some further aspects of the influence of raindrop-size distributions on millimeter-wave propagation
[PB85-168334] 18 p3092 N85-29138
Reliability derating procedures
[AD-A153744] 18 p3119 N85-29309
Revised draft: Southeastern regional geologic characterization report
[DE85-008295] 18 p3125 N85-29351
Pacific Northwest solar radiation data
[DE85-009773] 18 p3149 N85-29496
A stored data acquisition system: Update
[DE85-010534] 18 p3166 N85-29616
Deployment of a regional array in Norway
[AD-A154120] 19 p3313 N85-30536
Workshop on objective analysis: Analysis strategies for field-dependent estimation
[PB85-179901] 19 p3318 N85-30569
EDS operator and control software
[DE85-010470] 19 p3340 N85-30698
ASME performance test on TVA Sequoyah unit 1
[DE85-901316] 19 p3358 N85-30815
TMI-2 technical information and examination program
[DE85-010614] 19 p3359 N85-30827
Methodology for assessing benefits and costs of government information collection
[DE85-010594] 19 p3381 N85-30975
Remote Sensing Technology: Symposium Proceedings
[DE85-010212] 20 p3477 N85-31606
New stations supporting crustal dynamics project VLBI measurements 20 p3491 N85-31701
New VLBI technology developments
20 p3491 N85-31702

Forth system for coherent-scatter radar data acquisition and processing
[NASA-CR-176055] 20 p3494 N85-31720

Tropical Ocean and Global Atmosphere (TOGA) heat exchange project: A summary report
[NASA-CR-176038] 20 p3496 N85-31738

A cluster analysis method for identification of subpopulations of cells in flow cytometric list-mode arrays 20 p3503 N85-31779

Microprocessor AirborneData Acquisition and Replay (MADAR) system
[AD-A151728] 20 p3514 N85-31843

A miroprocessor based multiscaling data acquisition system for Mossbauer spectroscopy
[USIP-85-01] 20 p3518 N85-31875

SSMIR (Solid State Memory Instrumentation Recorder): A new approach to acquiring data during an aircraft seat/sled ejection sequence
[AD-A154780] 21 p3589 N85-32306

Microcomputer processing of LANDSAT Thematic Mapper data for the acquisition of military tactical terrain data
[AD-A154781] 21 p3605 N85-32389

Problems and solutions in analyzing partial-reflection drift data by correlation techniques
21 p3626 N85-32529

Continued development of a data base management system performance monitor: Volume 1
[AD-A154635] 21 p3713 N85-33040

Sensitivity and performance characterization of DINGU
[DE85-010750] 22 p3754 N85-33269

Conceptual design and analysis of high-speed electronic imaging
[LA-10072-MS] 22 p3758 N85-33292

Control technology for radioactive emissions to the atmosphere at US Department of Energy facilities: The Los Alamos Meson Physics Facility
[DE85-011402] 22 p3811 N85-33609

Technology of off-gas treatment for liquid-fed ceramic melters
[DE85-012467] 22 p3812 N85-33610

The 1984 environmental monitoring program report for Idaho National Engineering Laboratory site
[DE85-011209] 22 p3812 N85-33611

Hit-size effectiveness theory applied to high doses of low LET radiation for pink mutations in Tradescantia
[DE85-011835] 22 p3819 N85-33657

Determination of instrument errors by compatibility checking: Results from dynamic flight test data
[ARL/AERO-R-162] 23 p3896 N85-34137

Separation of gas mixtures by supported complexes
[DE85-011996] 23 p3912 N85-34236

Throughfall rate and chemistry studies: Whiteface Mountain
[DE85-012407] 23 p3947 N85-34464

The 1984 biotic studies of Yucca Mountain, Nevada test site, Nye County, Nevada
[DE85-011715] 23 p3951 N85-34487

Akeno 20 km (2) air shower array (Akeno Branch)
[OG-9.4-8] 23 p4029 N85-34975

Miniature infra-red data acquisition and telemetry system
[NASA-CR-177953] 24 p4096 N85-35390

Federal Mineral Land Information System
24 p4106 N85-35459

A Programmable Automatic Noise Data and Other Related parameter Acquisition system (PANDORA) — wind energy converters 24 p4111 N85-35479

Incorporating meteorological data into receptor analysis: RAPS (Regional Air Pollution Study) revisited
[PB85-186944] 24 p4114 N85-35503

Development and operation of a measuring data acquisition system for use in light airplanes
24 p4123 N85-35556

Airborne Investigations of Mesoscale Convective Systems (AIMCS), 1984: Operational summary and data inventory
[PB85-187904] 24 p4125 N85-35571

Users guide for optimum interpolation method of global data assimilation
[AD-A155929] 24 p4138 N85-35648

Operations considerations in designing a high speed multi-channel data acquisition system
[DE85-012840] 24 p4154 N85-35756

Data acquisition system for phase-2 KGF proton decay experiment
[HE-6.2-4] 24 p4211 N85-36140

DATA ADAPTIVE EVALUATOR/MONITOR
U DATA PROCESSING
U DATA REDUCTION
U DATA TRANSMISSION

DATA ANALYSIS
U DATA PROCESSING
U DATA REDUCTION

DATA BASE MANAGEMENT SYSTEMS

TEQUEL: The query language of SADDLE
01 p0056 N85-10382

Logical database processor interface specifications
[PB84-216456] 01 p0105 N85-10705

Analysis of three database system architectures using benchmarks
[PB84-217512] 01 p0105 N85-10706

Performance evaluation of database systems: A benchmark methodology
[PB84-217504] 01 p0105 N85-10707

EG and G Idaho's response to a request for a graphic data base support package
[DE84-015171] 01 p0126 N85-10862

A technique to model and design physical database systems
[DE84-015337] 01 p0126 N85-10863

Vertical compression algorithms
[DE84-015040] 01 p0126 N85-10864

Attenuation experimental data bank in the COST 205 project. Structure and management of the final supports
[FUB-5-1983] 01 p0126 N85-10865

Information Science Panel joint meeting with Imaging Science Panel 02 p0214 N85-11415

ADAM: An abstract database machine
[RSRE-84007] 02 p0293 N85-11904

On update semantics and relational views
[AD-A145622] 02 p0294 N85-11907

Business planning for information services under special consideration of German management information systems
[BMFT-FB-ID-83-007] 02 p0294 N85-11910

A building blocks approach to statistical databases
03 p0437 N85-12782

A methodology for supporting views in relational databases 03 p0437 N85-12783

Preserving the time dimension in information systems
03 p0437 N85-12784

Competitive assessment of the US information services industry
[PB84-174804] 03 p0440 N85-12803

Climate of the Northern Hemisphere, 1851 - 1900 compared to contemporary climate
[DE84-016368] 04 p0539 N85-13426

NODC/1983: National Oceanographic Data Center report
[PB84-222231] 04 p0542 N85-13449

The human role in space. Volume 3: Generalizations on human roles in space
[NASA-CR-171225] 04 p0546 N85-13475

Archiving and exchange of a computerized marine seismic database: The ROSE data archive system
[DE84-901453] 04 p0576 N85-13677

Nuclear criticality information system: Database examples
[DE84-014462] 04 p0576 N85-13678

Research in computer science
[NASA-CR-174088] 05 p0713 N85-14572

Optimal query processing in distributed data base management systems with data redundancy
05 p0734 N85-14722

Lower level inference control in statistical database systems
[DE84-016005] 05 p0735 N85-14729

Role of DESIGNMANAGER in information engineering
[DE84-016807] 05 p0736 N85-14730

Distributed database components in a DBMS (Database Management System) component architecture
[PB84-217546] 06 p0848 N85-15382

Design and analysis of an SQL (Structured Query Language) interface for a multi-backend database system
[AD-A146534] 06 p0856 N85-15447

Future database machine architectures
[AD-A146786] 07 p1022 N85-16481

The effects of software quality control and baseline management on the acquisition of computer programs
[AD-A147051] 07 p1024 N85-16502

Model-model mappings and conversion in a family of data model specifications
[PB84-217124] 07 p1027 N85-16518

Data base support for SIO (System Integration Office)
[AD-A147487] 07 p1054 N85-16692

A simulator for determining the performance of transaction manager and lock manager combinations in a database
[AD-A147827] 07 p1055 N85-16696

The space shuttle ascent vehicle aerodynamic challenges configuration design and data base development 08 p1093 N85-16906

Flexible manufacturing system for the production of aircraft parts
[BLL-PNR-90237-(8019.3153)]
08 p1137 N85-17159

Data user's manual 08 p1150 N85-17254

Kernel Ada Programming Support Environment (KAPSE) interface team public report, volume 4
[AD-A147648] 08 p1205 N85-17581

Steps towards parsing of query sequences to a database
[AD-A148769] 08 p1206 N85-17590

Results of data base management system parameterized performance testing related to GSFC scientific applications
[NASA-CR-170615] 08 p1229 N85-17741

Towards an ideal database server for office automation environments
[AD-A148184] 08 p1229 N85-17742

Boring information and subsurface data base package user's guide
[AD-A148623] 08 p1230 N85-17747

Automated and interactive data base generation
[AD-P004316] 09 p1268 N85-17970

Geographic subdivision and top level data structure, Columbus, Magellan, and expanding CIG (Computer Image Generation) horizons
[AD-P004317] 09 p1268 N85-17971

CIG (Computer image generation) data bases in an instance: Bits and pieces
[AD-P004318] 09 p1269 N85-17972

Design and analysis of an access control system for a multi-backend database system
[AD-A146750] 09 p1367 N85-18586

Integrating heterogeneous non-geometric information systems using RIM
[DE84-017600] 09 p1402 N85-18823

Online directory of databases for material properties
[DE84-016511] 09 p1402 N85-18824

Sector suite man-machine functional capabilities and performance requirements
[AD-A148881] 10 p1531 N85-19647

Managing permanent objects
[AD-A149007] 10 p1540 N85-19706

Structure and application of extremely large geophysical data bases
[DE85-003527] 10 p1566 N85-19888

Data and information systems and decision making in large public organizations: Research agenda
[DE85-003639] 11 p1738 N85-20931

Requirements formulation subtask 1.A of the Major Item System Mapping (MISM) project
[DE85-000978] 11 p1740 N85-20940

Use of the ORACLE DEMS in determining the response of complex scientific instrumentation
[DE85-001742] 12 p1853 N85-21621

Computer and communications security and privacy
[GPO-39-741] 12 p1911 N85-21984

Research Reports: 1984 NASA/ASEE Summer Faculty Fellowship Program
[NASA-CR-171317] 12 p1944 N85-22210

Using a data base management system for modeling SSME test history data 12 p1944 N85-22211

The intelligent database machine
12 p1949 N85-22242

Requirements for a database management system
[DE85-004661] 12 p1951 N85-22259

New atmospheric sensor analysis study
[NASA-CR-171426] 13 p2094 N85-23089

GADB: A database facility for modelling naturally occurring geophysical fields 13 p2122 N85-23217

Precedency control and other semantic integrity issues in a workbench database 13 p2123 N85-23220

Presentation based user interfaces
[AD-A150311] 13 p2144 N85-23311

Digital processing of mesoscale analysis and space sensor data
[NASA-CR-171429] 13 p2146 N85-23319

Hexagonal data base study
[AD-A150176] 13 p2167 N85-23448

The hierarchical database decomposition approach to database concurrency control
[AD-A150612] 13 p2168 N85-23450

Integration of solid modeling and database management for CAD/CAM 14 p2402 N85-24804

EDIPAS: A multidiscipline and integrated facility for management and evaluation of engineering data
[NLR-MP-83062-U] 14 p2405 N85-24832

Design and analysis of ordering and join for a multi-backed database system
[AD-A150711] 14 p2433 N85-25006

Commercial data base management system for geonames data base
[AD-A150835] 14 p2433 N85-25007

Continued development of a data base management system performance monitor, volume 2
[AD-A151714] 15 p2623 N85-26167

Backend control processor for a multi-processor relational database computer system
[AD-A151692] 15 p2624 N85-26169

Symposium on Computers in Civil Engineering 1983
[CSIR-S-298] 15 p2626 N85-26182

Design and analysis of a complete relational interface for a multi-backend database system
[AD-A151501] 15 p2628 N85-26198

CAD/CAM (Computer-Aided Design/Computer-Aided Manufacturing) highlights
[AD-A151532] 15 p2629 N85-26201

The design and analysis of a complete hierarchical interface for the multi-backend database system
[AD-A151580] 15 p2629 N85-26203

Document retrieval from a relational database management system: An investigation of multiple-line query formulation using SEQUEL
15 p2665 N85-26447

Design and implementation of the digital engineering laboratory distributed database management system
[AD-A151694] 15 p2665 N85-26450

Developing an automated technique for translating a relational database into an equivalent network one
[AD-A151844] 15 p2666 N85-26451

A database design for the Brazilian Air Force Flying Unit Operational Control System
[AD-A151848] 15 p2666 N85-26452

Analysis and specification of a universal data model for distributed data base systems
[AD-A151856] 15 p2666 N85-26453

Maintaining consistency and accommodating network repair in a self-regenerative distributed database management system (a discussion of the means and cost) 16 p2698 N85-26656

Flow dynamic environment data base development for the SSME 16 p2736 N85-26885

Network information management subsystem
16 p2771 N85-27106

Implementation and analysis of a microcomputer based relational database system
[AD-A151770] 16 p2845 N85-27536

An adaptive technique and its application in database design 16 p2877 N85-27748

Internal and external performance measurement methodologies for database systems
[AD-A152025] 16 p2877 N85-27751

Data dictionary design as a stepping-stone to DBMS (Data Base Management System) implementation in the Indonesian Army Data Collecting and Processing Service
[AD-A152101] 16 p2877 N85-27752

Application of hierarchical data structures to geographical information systems
[AD-A152169] 16 p2877 N85-27753

DOD manual for standard data elements, part 1
[AD-A152201] 16 p2878 N85-27754

Scientific data bases on a VAX-11/780 running VMS
[DE85-007925] 16 p2878 N85-27760

Data management issues of statistical databases
[DE85-007616] 16 p2679 N85-27763

Defense data network support concept analysis
[AD-A153214] 17 p3016 N85-28649

Complete development and implement AFIT/ENG database management system, volume 1
[AD-A153043] 17 p3048 N85-28866

DLA: Data/data base administration analysis
[AD-A153031] 17 p3050 N85-28879

Avionics Data Base users manual
[AD-A153810] 18 p3062 N85-28942

Distributed database design tool
[AD-A153760] 18 p3200 N85-29850

Generic data entry quality assurance tool
[DE85-008359] 18 p3200 N85-29852

Cultural data base implementation study and computer-aided scene modeling system users manual
[AD-A154232] 19 p3333 N85-30646

System enhancements of Mesoscale Analysis and Space Sensor (MASS) computer system
[NASA-CR-171463] 19 p3342 N85-30708

CODA: A concept organization and development aid for the research environment
[AD-A154240] 19 p3343 N85-30715

Test and Evaluation Master Plan (TEMP) for the Navy Occupational Health Information Management System (NOHIMS). Phase 1: Appendix A through appendix U
[AD-A154179] 19 p3360 N85-30967

Design and implementation of an intelligence database
[AD-A154095] 19 p3381 N85-30973

Guide on logical database design
[PB85-177970] 19 p3381 N85-30976

Data base management: MSTRAC (keynote paper), part 8 21 p3626 N85-32530

Analysis of spacecraft data
[NASA-CR-171587] 21 p3669 N85-32789

The architectural requirements and integration analysis of a database server for office automation
[AD-A155517] 21 p3674 N85-32825

Continued development of a data base management system performance monitor: Volume 1
[AD-A154635] 21 p3713 N85-33040

Investigation of DBMS (Data Base Management Systems) for use in a research environment
[AD-A154862] 21 p3713 N85-33042

IGES/RIM Parser/Converter users guide
[DE85-011965] 22 p3829 N85-33716

Automatic capability to store and retrieve component data and to calculate structural integrity of these components
[DE85-012429] 22 p3831 N85-33728

Technology transfer system automation implementation
[PB85-177335] 22 p3849 N85-33838

User's operating procedures. Volume 1: Scout project financial analysis program
[NASA-CR-177949] 23 p3956 N85-34519

The interactive planning work station: A graphics-based UNIX (trademark) tool for application users and developers 23 p3957 N85-34527

An image management kernel for the design of relational and pictorial data bases 23 p3958 N85-34532

DSS/MIS (Decision Support Systems/Management Information Systems) design and implementation for LAMPS Mk 3 utilizing a microcomputer and a maintenance personnel assignment program
[AD-A155852] 24 p4135 N85-35629

Prototyping with data dictionaries for requirements analysis
[AD-A156303] 24 p4139 N85-35654

EPALIT: A data management system applied to the control and retrieval of technical reports
[PB85-193068] 24 p4166 N85-35826

DATA BASES

Pressure distribution on a swept wing aircraft in flight
01 p0004 N85-10025

TEQUEL: The query language of SADDLE
01 p0058 N85-10382

A relational approach to the development of expert diagnostic systems
[NASA-TM-86288] 01 p0089 N85-10658

Logical database processor interface specifications
[PB84-216456] 01 p0105 N85-10705

Performance evaluation of database systems: A benchmark methodology
[PB84-217504] 01 p0105 N85-10707

Updating logical databases
[AD-A144937] 01 p0125 N85-10860

Set-theoretic problems of null completion in relational databases
[AD-A145045] 01 p0125 N85-10861

EG and G Idaho's response to a request for a graphic data base support package
[DE84-015171] 01 p0126 N85-10862

EPA (Environmental Protection Agency) environmental data base and model directory, volume 1
[PB84-207562] 01 p0126 N85-10868

Royal Signals and Radar Establishment speech database recordings 1983: Part 2: Recordings made for automatic speech recognition assessment and research
[RSRE-84008-PT-2] 02 p0190 N85-11267

A system for the management of requests at an image data bank
[E85-10014] 02 p0216 N85-11427

Human engineering data base for design and selection of cathode ray tube and other display systems
[AD-A145704] 02 p0238 N85-11549

Research on distributed languages and algorithms
[AD-A145661] 02 p0242 N85-11580

Failure detection processes by pattern recognition and expert systems
[AD-P003924] 02 p0246 N85-11604

On update semantics and relational views
[AD-A145622] 02 p0294 N85-11907

Archiving and exchange of a computerized marine seismic database: The ROSE (Rivera Ocean Seismic Experiment) data archive system
[AD-A145658] 02 p0294 N85-11906

Inclusion of audiovisual media in information services for the special subjects journalism and communication science (pilot study)
[BMFT-FB-ID-83-004] 02 p0294 N85-11909

A data base for three-dimensional all-interference code evaluation 03 p0312 N85-12017

Expert systems: The application of new computer methods to corrosion problems
[AERE-M-3395] 03 p0334 N85-12153

International banking of satellite and in-situ wave data by the Marine Information and Advisory Services (MIAS)
03 p0381 N85-12434

An introduction to the MIAS conversion system
[IOS-184] 03 p0403 N85-12571

Knowledge representation and natural-language semantics
[AD-A146025] 03 p0409 N85-12615

A topological approach to database theory
03 p0437 N85-12781

On complementary and independent mappings on databases
[AD-A145557] 03 p0438 N85-12788

An approach to interfacing data bases in WWMCCS ADP
[AD-A146350] 03 p0439 N85-12793

Evaluation of the National Library of Medicine's programs in the medical behavior sciences. Coverage of the Medical Behavioral Sciences (MBS) literature in monographic databases, study 5
[PB84-230531] 03 p0439 N85-12797

Evaluation of the National Library of Medicine's programs in the medical behavior sciences. Online searchers' reactions to database and vendor capabilities in the Medical Behavioral Sciences (MBS), study 4
[PB84-230523] 03 p0439 N85-12798

Evaluation of the National Library of Medicine's programs in the medical behavior sciences. Quality of indexing: The development and testing of a methodology comparing databases covering the Medical Behavioral Sciences (MBS) literature, study 3
[PB84-230515] 03 p0439 N85-12799

Evaluation of the National Library of Medicine's programs in the medical behavior sciences. Test retrievals in five major databases covering the Medical Behavioral Sciences (MBS) literature, study 2
[PB84-230507] 03 p0440 N85-12800

Evaluation of the National Library of Medicine's programs in the medical behavior sciences. Coverage, overlaps and gaps in bibliographic databases dealing with the Medical Behavioral Sciences (MBS) literature, study 1
[PB84-230499] 03 p0440 N85-12801

Evaluation of the National Library of Medicine's program in the medical behavior sciences. An analysis of the National Library of Medicine's (NLM) handling of Medical Behavioral Sciences (MBS) literatures: Some research tests of methods for evaluating bibliographic databases, executive summary
[PB84-230481] 03 p0440 N85-12802

Experimental and theoretical study of a solar thermochemical receiver module
[NASA-CR-174107] 04 p0528 N85-13374

Relationship between model complexity and data base quality for complex terrain tracer experiments
[DE84-015022] 04 p0539 N85-13429

Comparability and accuracy of industry codes in different data systems
[PB84-215607] 04 p0548 N85-13482

Physical database processor preliminary interface specifications
[PB84-217561] 04 p0548 N85-13483

The 1984 NASA/ASEE summer faculty fellowship program
[NASA-CR-174138] 04 p0574 N85-13663

Energy information exchange, 1983
[DE84-901446] 04 p0577 N85-13680

The SPOT data bank system
05 p0659 N85-14236

Combinations of remote sensing data with a digital map data base — regional planning 05 p0660 N85-14240

Helicopter pilot performance for discrete-maneuver flight tasks 05 p0702 N85-14502

Optimal query processing in distributed data base management systems with data redundancy
05 p0734 N85-14722

Interpretation of natural language database queries using optimization methods 05 p0735 N85-14723

Heterogeneous data base access
05 p0735 N85-14724

A self-organizing database system: A different approach to query optimization 05 p0735 N85-14725

Integrated data base program: A status report
[DE84-013604] 05 p0735 N85-14727

Spring program summary, 1983
[PB84-222223] 06 p0839 N85-15330

Tree Query Language Flat (TQLF) specifications
[PB84-217116] 06 p0855 N85-15438

Relational Query Language Flat (RQLF) specifications
[PB84-217405] 06 p0855 N85-15439

Network Query Language Flat (NQLF) specifications
[PB84-217538] 06 p0855 N85-15440

Commerce Laboratory: Mission analysis payload integration study
[NASA-CR-171298] 07 p0911 N85-15764

Climatological information and water resources
07 p1002 N85-16367

Water and climate, study of one case
07 p1002 N85-16369

The potential contributions of the World Climate Program (WCP) to the economies of developing countries
07 p1003 N85-16371

An algorithm for assembly of stiffness matrices into a compacted data structure
[AD-A146727] 07 p1023 N85-16492

DATA BASES

Model-model mappings and conversion in a family of data model specifications
[PB84-217124] 07 p1027 N85-16518

Managing recoverable aircraft components in the PPB and related processes: Executive summary
[AD-A146806] 07 p1050 N85-16667

NBS (National Bureau of Standards) daylight availability database
[PB84-245745] 07 p1054 N85-16688

Distributed knowledge base systems for diagnosis and information retrieval
[AD-A146890] 07 p1054 N85-16690

Efficient computation of optimal time for transaction processing in a database system
[AD-A147568] 07 p1054 N85-16693

Mission-oriented requirements for updating MIL-H-8501. Volume 2: STI background and rationale --- military rotorcraft
[NASA-CR-177331-VOL-2] 08 p1068 N85-16878

The orbiter air data system 08 p1094 N85-16912

Managing computer-controlled operations
08 p1097 N85-16934

Computer aided processing using laser measurements
08 p1103 N85-16973

Commerce Lab: Mission analysis. Payload integration study
[NASA-CR-171285] 08 p1104 N85-16982

Distributed sensor networks
[AD-A147638] 08 p1151 N85-17262

Hierarchical data structures and algorithms for digital stereoscopical mensuration 08 p1175 N85-17410

Pilot climate data system
[NASA-CR-174321] 08 p1187 N85-17481

Benchmarking database systems in multiple backend configurations
[AD-A148191] 08 p1202 N85-17568

A single server queue with mixed types of interruptions
[AD-A148538] 08 p1213 N85-17637

Antisampling for estimation: An overview
[AD-A148545] 08 p1216 N85-17659

Performance evaluation of a database system in multiple backend configurations
[AD-A148192] 08 p1229 N85-17743

The combinatorics of local constraints in model-based recognition and localization
[AD-A148338] 08 p1230 N85-17746

A description of the NRL oblique-incidence-ionogram data base
[AD-A148625] 08 p1230 N85-17748

Color visual simulation applications at the Defense Mapping Agency
[AD-P004315] 09 p1268 N85-17969

The generation of three-dimensional data bases using a building block approach
[AD-P004319] 09 p1269 N85-17973

Calculation of the area covered by mobile radio systems using geographic data stored in a computer
[FUB-43-1983] 09 p1312 N85-18247

Organizational tools for data analysis environments
[DE85-000396] 09 p1369 N85-18601

Methodology for evaluating related databases and a computerized algorithm for merging their output
09 p1401 N85-18821

Online database search strategies and thesaural relationship models 09 p1402 N85-18822

Documentation for an instrument database system
[DE84-017392] 09 p1402 N85-18826

Automation of information services furnished by documentation centers and specialized libraries
[FUB-6-1984] 09 p1402 N85-18827

Guide to human factors information sources
[AD-A149102] 10 p1531 N85-19649

SOLIDGEN: A solid finite element data generator. User's manual
[AD-A149490] 10 p1541 N85-19715

Air quality criteria for ozone and other photochemical oxidants. External review draft, volume 5
[PB85-126076-VOL-5] 11 p1679 N85-20583

A DOE directory of databases for material properties
[UCAR-10124] 11 p1739 N85-20937

Sourcebook: Gaining access to US government information on the environment and natural resources
[DE84-017419] 11 p1740 N85-20941

Conclusion of Viking Lander Imaging Investigation: Picture catalog of experiment data record
[NASA-RP-1137] 11 p1765 N85-21099

Transmission and orbital constraints in space-related programs: Briefing summary 12 p1787 N85-21216

Base communications issues for the 1980s
[AD-A149764] 12 p1828 N85-21474

Theoretical and empirical studies of the basic structure of turbulent shear flows, including separated flows and effects of wall curvature
[AD-A149657] 12 p1846 N85-21580

An analysis of short-to-medium-range seismic attenuation tests using a multilayered viscoelastic seismic propagation model
[AD-A149771] 12 p1869 N85-21856

Atlas of relectance patterns for uniform earth and cloud surfaces (NIMBUS-7ERB-61 days)
[PB85-116382] 12 p1891 N85-21870

A new NASA/MSFC mission analysis global cloud cover data base
[NASA-TP-2448] 12 p1893 N85-21878

A review of fatality, impairment of consciousness, and head/neck injury on USAF ejections 1971 - July 1983
12 p1906 N85-21974

Variable data base generator apparatus
[AD-D011515] 12 p1911 N85-21993

Evaluation of the vocabulary switching systems
[PB85-127157] 12 p1951 N85-22260

Precedency control and other semantic integrity issues in a workbench database 13 p2123 N85-23220

Low altitude texture comparison data base and smooth shaded texture
[AD-A150342] 13 p2146 N85-23323

General design considerations of an Air Force information system
[AD-A150611] 13 p2168 N85-23449

The hierarchical database decomposition approach to database concurrency control
[AD-A150612] 13 p2168 N85-23450

Intel IDIS evaluation
[DE85-003748] 13 p2168 N85-23451

Unsupervised classification of global radar units on Venus 13 p2198 N85-23632

Space Shuttle aerothermodynamic data report, phase C
[NASA-CR-171858] 14 p2241 N85-23897

An introduction to USAFETAC (USAF Environmental Technical Applications Center)
[AD-A150971] 14 p2378 N85-24682

Programmer/analyst workstation evaluation report
[NASA-CR-175269] 14 p2394 N85-24749

The Effect of Computers on the Generation and Use of Technical Data
[NBSIR-84-2907] 14 p2400 N85-24792

The identification of semantics for the file/database problem domain and their use in a template-based software environment 14 p2401 N85-24803

Integration of solid modeling and database management for CAD/CAM 14 p2402 N85-24804

Design and analysis of ordering and join for a multi-backed database system
[AD-A150711] 14 p2433 N85-25006

CADS: A Computer Aided Design System
15 p2574 N85-25876

Global paleoclimatic data base for 6000 years BP
[DE85-006628] 15 p2600 N85-26024

Alterations/corrections to the BRASS Program
[NASA-CR-171874] 15 p2616 N85-26121

Backend control processor for a multi-processor relational database computer system
[AD-A151892] 15 p2624 N85-26169

Computers in the determination of rainfall septh-duration-frequencies in Natal
15 p2627 N85-26188

Computer science and technology: A guide to performance evaluation of database systems
[PB85-155794] 15 p2631 N85-26219

Computer use in research for data analysis
[PB85-153567] 15 p2631 N85-26220

Procedures for use in compiling requirements specifications for computerized library systems
[CSTI-76] 15 p2665 N85-26446

Developing an automated technique for translating a relational database into an equivalent network one
[AD-A151844] 15 p2666 N85-26451

A database design for the Brazilian Air Force Flying Unit Operational Control System
[AD-A151848] 15 p2666 N85-26452

Analysis and specification of a universal data model for distributed data base systems
[AD-A151856] 15 p2666 N85-26453

List of serials indexed for online users, 1985
[PB85-143220] 15 p2666 N85-26455

Flow dynamic environment data base development for the SSME 16 p2736 N85-26865

An analysis of data dictionaries and their role in information resource management
[AD-A152134] 16 p2774 N85-27121

Status of the observational data sets — TOPEX
16 p2804 N85-27286

Acid precipitation in North America: 1980, 1981 and 1982 annual data summaries from acid deposition system data base
[PB85-162477] 16 p2822 N85-27410

Implementation and analysis of a microcomputer based relational database system
[AD-A151770] 16 p2845 N85-27536

Diagnosis: Using automatic test equipment and a artificial intelligence expert system
[AD-A151918] 16 p2851 N85-27578

Software for reflectivity calculations of X-ray mirrors, revision 1
[DE85-006642] 16 p2867 N85-27688

Retrieval performance in a full text journal article database 16 p2877 N85-27747

Access path optimization for network database retrieval 16 p2877 N85-27749

Design of an interface to an information retrieval network 16 p2877 N85-27750

Internal and external performance measurement methodologies for database systems
[AD-A152025] 16 p2877 N85-27751

Data management issues of statistical databases
[DE85-007616] 16 p2879 N85-27763

Evaluation of Defense Mapping Agency level 1 second edition digital data for training simulator applications
[AD-A152444] 17 p2983 N85-28437

Chemicals identified in human biological media, a data base, volume 6, part 1
[DE85-008768] 17 p2999 N85-28542

A test methodology for an automated and interactive software development environment
[AD-A152857] 17 p3011 N85-28618

Distributed systems management in wide area networks
[CWI-CS-R8419] 17 p3016 N85-28651

Experimental philosophy leading to a small scale digital data base of the conterminous United States for designing experiments with remotely sensed data
[NASA-TM-85009] 17 p3049 N85-28877

A study of user-defined searching requirements for the on-line version of the directory of DOD-sponsored R and D data bases on the Defense Gateway computer system
[AD-A153000] 17 p3050 N85-28878

Energy data base: Subject categories and scope
[DE84-017376] 17 p3050 N85-28881

Avionics Data Base users manual.
[AD-A153810] 18 p3062 N85-28942

GAMPHI: A database of activity and osmotic coefficients for aqueous electrolyte solutions
[PB85-183390] 18 p3072 N85-29002

Data base of all known, published data on trace elements in oil shale and its products
[DE85-003399] 18 p3126 N85-29357

Error growth in operational 10-day forecasts
18 p3143 N85-29480

Summary of archived Atlantic coast wave information study pressure, wind, wave, and water level data
[AD-A153782] 18 p3151 N85-29508

Chemicals identified in human biological media, a data base. Volume 6, part 2: Records 7588-8694
[DE85-006767] 18 p3154 N85-29528

Bayesian full rank marginalization for 2-way contingency tables
[AD-A153641] 18 p3171 N85-29649

Notes for medical catalogers, 1984
[PB85-180206] 18 p3200 N85-29853

CSIN (Chemical Substances Information Network) workbook: US Geological Survey training course for Chemical Substances Information Network
[PB85-170058] 18 p3200 N85-29855

North American acid deposition data base system (ADS and its use in spatial analysis
[PB85-173235] 18 p3201 N85-2985

Analysis of the elastic and strength properties of Yucc Mountain tuff, Nevada
[DE85-006975] 19 p3300 N85-304

VIDTEX
[PB85-175669] 19 p3318 N85-305

An approach to modeling database activity
19 p3332 N85-306

Cultural data base implementation study a computer-aided scene modeling system users manu
[AD-A154232] 19 p3333 N85-306

EDS operator and control software
[DE85-010470] 19 p3340 N85-30

CODA: A concept organization and development for the research environment
[AD-A154240] 19 p3343 N85-307

SAFEORD: Safety of explosive ordnance databa
[AD-A154058] 19 p3380 N85-30

Design and implementation of an intelligen database
[AD-A154095] 19 p3381 N85-30

Transmission Monitoring and Control (TRAMCO segmentation plan for the DCS (Defense Communicati System) digital transmission network
[AD-A154175] 20 p3440 N85-31

An industry and government survey: A nickel-hydro testing data base 20 p3448 N85-31

Remote Sensing Technology: Sympo Proceedings
[DE85-010212] 20 p3477 N85-31

Human factors engineering data sources; an overview
[FOA-C-56044-H2] 20 p3513 N85-31837
Inference in hierarchic classification — data bases
[ENST-84E014] 20 p3518 N85-31873
Realizing the full potential of the video disc for mapping applications
[AD-A154966] 21 p3606 N85-32391
A transportable, machine oriented library of european sky and terrain radiance distributions with contemporary radiometric and meteorological profiles
[AD-A155254] 21 p3637 N85-32590
USAFSAM review and analysis of radiofrequency radiation bioeffects literature
[AD-A155113] 21 p3664 N85-32760
Research on an expert system for database operation of simulation-emulation math models. Volume 1, Phase 1: Results
[NASA-CR-176087] 21 p3669 N85-32792
The architectural requirements and integration analysis of a database server for office automation
[AD-A155517] 21 p3674 N85-32825
Investigation of DBMS (Data Base Management Systems) for use in a research environment
[AD-A154862] 21 p3713 N85-33042
Evaluation of the 2DFLOW and hybrid complex-terrain dispersion models with the 1980 ASCOT data base from the Geysers
[DE85-012960] 22 p3812 N85-33613
Portable database driven control system for SPEAR
[DE85-010465] 22 p3830 N85-33720
Logical and physical modeling and design of scientific and statistical databases for energy research
[DE85-006081] 22 p3833 N85-33737
A hierarchy of knowledge levels implemented in a rule-based production system to calculate bounds on the size of intersections and unions of simple sets
[AD-A155291] 22 p3848 N85-33838
Novette diagnostic support
[DE85-012837] 23 p3934 N85-34383
User's operating procedures. Volume 3: Projects directorate information programs
[NASA-CR-177950] 23 p3956 N85-34520
Graphics interaction in databases
23 p3958 N85-34534
NAPGEN: Automatic NAPLPS page generator
23 p3964 N85-34575
The final COS-B database now publicly available
[OG-9.3-8] 23 p4028 N85-34963
The final COS-B database: In-flight calibration of instrumental parameters
[OG-9.3-9] 23 p4028 N85-34964
Applications of the mineral resources data system and the international strategic minerals inventory in mineral-resource assessments by region and commodity
24 p4105 N85-35451
The NORDA/FNOC (Naval Ocean Research and Development Activity's/Fleet Numerical Oceanography Center) Polar Ice Prediction System (PIPS)-Arctic: A technical description
[AD-A156332] 24 p4126 N85-35577
LOCAT: A data retrieval program
[AD-A156004] 24 p4165 N85-35822
Source header list, supplement 3
[AD-A156100] 24 p4165 N85-35824

DATA BUSSES
U CHANNELS (DATA TRANSMISSION)

DATA COLLECTION PLATFORMS
Data Collection and Platform Location by Satellite: ARGOS Users' Conference 14 p2237 N85-23869
The ARGOS Platform Transmitter Terminals (PTTs)
14 p2237 N85-23872
The ARGOS VHF direct readout mini-station and CML-80-MP data collection Platform Transmitter Terminals (PTTs) 14 p2238 N85-23873
Project PAPA: The integration of drifting buoy data into an operational meteorological service
14 p2236 N85-23874
Applications of ARGOS data collection systems in Arctic regions 14 p2238 N85-23875
Data collection and winter ice dynamics in the Beaufort Sea 14 p2238 N85-23878
Report on the panel discussion of the Workshop on Data Collection Platform Networks
14 p2239 N85-23880
Data Collection and Platform Location by Satellite: ARGOS Users' Conference 14 p2239 N85-23883
Equipment for the ARGOS system from Eidsvoll Electronics A.S. 14 p2239 N85-23885
ARGOS VHF direct readout mini-station
14 p2239 N85-23886
Applications of ARGOS data collection system for automatic meteorological observatories in Arctic regions
14 p2240 N85-23893
Proceedings of the ARGOS Users Conference on Data Collection and Location by Satellite
14 p2322 N85-24348
Improvements brought about to the system since 1978 and statements on future development
14 p2323 N85-24349
New directions in ARGOS instrumentation at Polar Research Lab (PRL) 14 p2323 N85-24350
The Edmonton data collection platform processing and locating facility 14 p2323 N85-24352
The development of Platform Transmitter Terminal (PTT) and its application for drifting buoys
14 p2323 N85-24353
US programs using the ARGOS data collection and platform location system 14 p2323 N85-24355
US program in anchored data buoy and the other fixed observation platforms 14 p2324 N85-24358
One thousand days in the brine — platform transmitter terminals 14 p2324 N85-24359
Data Collection and Platform Location by Satellite: ARGOS Users' Conference 14 p2325 N85-24368
Data Collection and Platform Location by Satellite: ARGOS users' Conference 14 p2328 N85-24391
Collecting meteorological reports with the ARGOS system 14 p2329 N85-24398
US programs using the ARGOS data collection and platform location system 14 p2329 N85-24401
Data Collection and Platform Location by Satellite: ARGOS Users' Conference 14 p2330 N85-24409
US program using the ARGOS data collection and platform location system 14 p2330 N85-24410
A new versatile ARGOS PTT for oceanographic applications — Platform Transmit Terminal (PTT)
14 p2331 N85-24417
Data Collection and Platform Location by Satellite: ARGOS Users' Conferance 16 p2811 N85-27333
DB2 and DB3: The next generation — buoys
16 p2811 N85-27337
A seismic ARGOS data collection platform
16 p2813 N85-27350
An operational buoy network collecting meteorological data 16 p2813 N85-27351
Operational experiences with the ARGOS system in Greenland 16 p2813 N85-27353

DATA COMPACTION
U DATA COMPRESSION

DATA COMPRESSION
Vertical compression algorithms
[DE84-015040] 01 p0126 N85-10864
Utilization of interpolation and transformation for the compression of digital image data
[INPE-3061-PRE/479] 02 p0240 N85-11566
Electronic bandwidth compression module
[AD-A145843] 03 p0366 N85-12343
Vector quantization of digital images
05 p0714 N85-14580
Recent advances in data compression
[DE85-001133] 06 p0854 N85-15432
Information extraction and transmission techniques for spaceborne synthetic aperture radar images
[NASA-CR-174341] 08 p1150 N85-17256
Data compression for noiseless channels
13 p2053 N85-22851
Image data compression using uneven knots selection
[AD-A150602] 13 p2152 N85-23359
Feasibility studies of optical processing of image bandwidth compression schemes
[AD-A151254] 15 p2651 N85-26350
Alphabet-constrained data compression
[AD-A152887] 17 p3019 N85-28667
Research on signal detection and block truncation cooling for image compression
[AD-A153444] 18 p3168 N85-29628
Development and analysis of a global compaction technique of microprograms 19 p3334 N85-30654
An image compression survey and algorithm switching based on scene activity
[NASA-TP-2458] 22 p3727 N85-33106
Electronic file system on an SM 90 minicomputer: The SARDE project
[ENST-84E018] 22 p3828 N85-33705
Noiseless coding for the Gamma Ray spectrometer
[NASA-CR-176201] 24 p4069 N85-35219
Raster functionality for a VDI
[DE85-006734] 24 p4097 N85-35396

DATA CONVERSION ROUTINES
NT SUBROUTINES
An introduction to the MIAS conversion system
[IOS-184] 03 p0403 N85-12571
A methodology for the analysis of programmer productivity and effort estimation within the framework of software conversion
[AD-A145757] 03 p0406 N85-12592
Data handling for the Spectral Radiometer (SPERAD)
[FOA-C-30368-E1,E4] 07 p0968 N85-16145
Defense Mapping Agency (DMA) raster-to-Vector analysis
[AD-A154153] 19 p3336 N85-30668
CRAYCDC
[NASA-CR-177374] 24 p4137 N85-35639
CDCCRAY
[NASA-CR-177375] 24 p4137 N85-35640
Two methods of global data assimilation
[AD-A155981] 24 p4143 N85-35684

DATA CONVERTERS
NT ANALOG TO DIGITAL CONVERTERS
NT DIGITAL TO ANALOG CONVERTERS

DATA CORRELATION
NT SIGNAL ANALYSIS
Numerical studies of mesoscale eddies using quasigeostrophic and primitive equation ocean models
[PB84-214048] 01 p0069 N85-10602
KrCl lasers for fusion
[DE84-012210] 01 p0122 N85-10835
Simulator study of flight characteristics of several large, dissimilar, cargo transport airplanes during approach and landing
[NASA-TP-2357] 02 p0148 N85-11002
Multispectral passive microwave correlations with an antecedent precipitation index using the Nimbus 7 SMMR
[AD-A145419] 02 p0200 N85-11334
A constitutive modeling technique based on a generalized rheological model to predict the response of materials 02 p0207 N85-11368
A principal component analysis of eastern Transvaal seasonal rainfall, 1950 to 1981
02 p0212 N85-11395
Study on spectral/radiometric characteristics of the Thematic Mapper for land use applications
[E85-10021] 02 p0218 N85-11434
Report of the Third Session of the International Working Group on Data Management for the International Satellite Cloud Climatology Project (ISCCP)
[WCP-82] 02 p0231 N85-11504
A study of highly energetic near-bottom ocean flow at the base of the Scotian Rise 02 p0233 N85-11515
Fluctuations in parameters of light beam along path with reflection in turbulent atmosphere
02 p0263 N85-11722
Optical constant determination of thin polymer films in the infrared
[AD-A145669] 02 p0287 N85-11877
Laboratory evaluation of microwave absorption properties under simulated conditions for planetary atmospheres
[NASA-CR-174080] 02 p0303 N85-11960
Methods for correlating geological, geochemical and geophysical data with satellite imagery in central Ireland
05 p0655 N85-14208
Selection of spacing of modular and gradient measurement surveys based on statistical characteristics of measured geomagnetic field
06 p0821 N85-15214
Characterization of radiometric calibration of LANDSAT-4 reflective bands 11 p1669 N85-20516
Looking at multivariate data through fuzzy sets
[DE85-000684] 11 p1702 N85-20706
TM geometric performance: Line to Line Displacement Analysis (LLDA) — New Mexico
12 p1870 N85-21732
Investigation of TM band-to-band registration using the JSC registration processor 12 p1872 N85-21745
Ozone Correlative Measurements Workshop
[NASA-CP-2362] 13 p2105 N85-23112
Lectures on probability and statistics
[DE85-007079] 15 p2641 N85-26291
A suggested standardized format for cosmic ray ground-level event data
[SH-9.1-15] 23 p4052 N85-35130

DATA FLOW ANALYSIS
Innovative image processing architectures
15 p2622 N85-26159

DATA HANDLING SYSTEMS
U DATA SYSTEMS

DATA INTEGRATION
Use and value of a geodetic reference system
[PB84-216167] 03 p0379 N85-12418
An integrated remote sensing approach for identifying ecological range sites — parker mountain
[E85-10050] 07 p0983 N85-16246
Global scale diagnoses of FGGE data
[NASA-CR-174356] 09 p1356 N85-18533
LANDSAT 4 investigation of Thematic Mapper and Multispectral Scanner applications
[E85-10076] 10 p1504 N85-19490
Spectroradiometric calibration of the Thematic Mapper and Multispectral Scanner system
[E85-10077] 10 p1504 N85-19491

DATA LINKS

Hardware implementation of a support system for the 2501 Western digital LSI, complete controller of the second level, first version of the CCITT 25 (CAP) recommendations
[FUB-60-1982] 01 p0100 N85-10666

Photo-reconnaissance system
[AD-D011287] 06 p0826 N85-15245

National airspace system configuration management interface control document. Maintenance processor subsystem to remote monitoring subsystems and remote monitoring subsystem concentrators
[NAS-MD-790] 07 p0900 N85-15705

NOAA (National Oceanic and Atmospheric Administration) Aircraft Satellite Data Link (ASDL)
[PB84-243773] 07 p0942 N85-15976

Using the control system design environment in the design of a data link receiver unit for the Coast Guard HH-65A helicopter
[AD-A148624] 08 p1088 N85-16880

TDRSS S-shuttle unique receiver equipment
08 p1100 N85-16951

The Communications link analysis and simulation system (CLASS) 08 p1100 N85-16952

Modeling techniques used in the communications link analysis and simulation system (CLASS)
08 p1100 N85-16953

Validation of the communications link analysis and simulation system (CLASS) 08 p1100 N85-16954

Digital scrambling for shuttle communication links: Do drawbacks outweigh advantages?
08 p1101 N85-16956

Novel applications of the NASA/GSFC Viterbi decoder hardware simulator 08 p1101 N85-16957

NSWC-NADC interactive communication links for AN/UYS-1 loadtape creation and retrieval
[AD-A148418] 08 p1153 N85-17277

The impact of propagation effects on the design of high capacity digital microwave links in the 18 GHz frequency band 10 p1470 N85-19278

Graphics translators for computer-aided drafting and design: Interface alternatives for the A/E community
[AD-A148892] 10 p1540 N85-19706

The evolution of methods of air traffic control
[AD-A149606] 12 p1774 N85-21137

Satellite bridges in communications networks
13 p2067 N85-22910

Optimum path selection in automated radio relay link design 13 p2073 N85-22947

Investigation of influence of communications link and synchronization error on noise tolerence of group transmission of binary information based on orthogonal Walsh function 13 p2086 N85-23026

Feasibility study for an AFGL fiber optic data link at WSMR sounding rocket launch area
[AD-A150852] 14 p2240 N85-23894

Geostationary Operational Environmental Satellite Data Collection System 14 p2328 N85-24393

NOAA'S role in support of service ARGOS
14 p2328 N85-24394

Data-link alternatives for the NASA pilot data systems
[NASA-TM-85999] 14 p2412 N85-24879

Satellite reception of reentry vehicle telemetry
[AD-A151851] 15 p2492 N85-25372

Consultative Committee for Space Data Systems. Panel 1: Support
[NASA-CR-175786] 16 p2769 N85-27090

Continued development and implementation of the Universal Network Interface Device (UNID) 2 in the Digital Engineering Laboratory Network (DELNET), volume 2
[AD-A151947] 16 p2850 N85-27570

Performance measurement of OSI (Open System Interconnection) class 4 transport implementations
[PB85-177657] 18 p3161 N85-29582

Phase-locked loops for optical homodyne detection, volume 1 — spaceborne receivers
[ESA-CR(P)-2029-VOL-1] 20 p3442 N85-31367

Phase locked loops for optical homodyne detection, volume 2 — spaceborne receivers
[ESA-CR(P)-2029-VOL-2] 20 p3442 N85-31368

Space optics
[CNES-84/105/T/CT/DRT/TIT/10]
20 p3533 N85-31985

Broadcasting topology and routing information in computer networks
[AD-A155688] 21 p3674 N85-32827

Satellite links in the ISO architecture: Models and performance evaluation
[ENST-84E017] 22 p3756 N85-33284

Performance interface document for the S-band diplexer for space users of NASA networks
[NASA-TM-86224] 23 p3900 N85-34155

DATA MANAGEMENT

Facsimile transmission of microforms
[AD-A144855] 01 p0038 N85-10236

MERIT: A man/computer data management and enhancement system for upper air nowcasting/forecasting in the United States — Minimum Energy Routes using Interactive Techniques (MERIT)
01 p0083 N85-10558

Hardware implementation of a support system for the 2501 Western digital LSI, complete controller of the second level, first version of the CCITT 25 (CAP) recommendations
[FUB-60-1982] 01 p0100 N85-10666

Telemetry (TM)/telecommand (TC) processor study
[ESA-CR(P)-1915] 03 p0323 N85-12081

The current formal status of the ERS-1 ground segment 03 p0380 N85-12423

International banking of satellite and in-situ wave data by the Marine Information and Advisory Services (MIAS)
03 p0381 N85-12434

Lessons from the SEASAT and GEOS-3 altimeters data projects 03 p0384 N85-12457

Research in data management and system reliability
[AD-A145498] 03 p0436 N85-12773

Primer on the registration of technical information in industry 03 p0438 N85-12786

Archiving and exchange of a computerized marine seismic database: The ROSE data archive system
[DE84-901453] 04 p0576 N85-13677

Integrated resource management algorithms for computer systems 05 p0715 N85-14582

Recent advances in data compression
[DE85-001133] 06 p0854 N85-15432

Methodology investigation. Streamlined Test Reporting and Planning (STRAP): Data flow procedures
[AD-A146463] 06 p0871 N85-15531

Climate and climate data. Report on the workshop held in Brasilia (Argentina) from 11-15 April 1983
07 p1001 N85-16357

Decentralized control of scheduling in distributed systems
[AD-A147446] 07 p1022 N85-16487

Pilot climate data system
[NASA-CR-174321] 08 p1187 N85-17481

DDN directory
[AD-A148213] 08 p1230 N85-17744

Concurrency in a data flow database machine
09 p1366 N85-18582

Role of environments in managing data analysis
[DE85-000397] 09 p1369 N85-18602

Elimination of sensor artifacts from infrared data
[AD-A149048] 10 p1556 N85-19814

A proposed integration among organizational information requirements, media richness and structural design
[AD-A149317] 10 p1567 N85-19881

Some data manipulation requirements for the exploratory analysis of large data sets
[DE85-002541] 10 p1568 N85-19887

A DOE directory of databases for material properties
[UCAR-10124] 11 p1739 N85-20937

A GC/MS (Gas Chromatograph/Mass Spectrometer) data management process. Part 1: User's guide, version 1.0
[PB85-116051] 12 p1803 N85-21309

A GC/MS (Gas Chromatograph/Mass Spectrometer) data management process. Part 2: Program documentation, version 1.0
[PB85-116069] 12 p1803 N85-21310

Introduction to the Space Physics Analysis Network (SPAN)
[NASA-TM-86499] 14 p2290 N85-24198

Integration of solid modeling and database management for CAD/CAM 14 p2402 N85-24804

Interactive data analysis. Development of an interactive data manipulation system
[AD-A151359] 15 p2623 N85-26164

Implementation and analysis of a microcomputer based relational database system
[AD-A151770] 16 p2845 N85-27536

Data dictionary design as a stepping-stone to DBMS (Data Base Management System) implementation in the Indonesian Army Data Collecting and Processing Service
[AD-A152101] 16 p2877 N85-27752

Replication methods for abstract data types
[AD-A153648] 18 p3162 N85-29587

CSIN (Chemical Substances Information Network) workbook: US Geological Survey training course for Chemical Substances Information Network
[PB85-170058] 18 p3200 N85-29855

The international scope of data evaluation
[DE85-005953] 19 p3349 N85-30760

Guide on logical database design
[PB85-177970] 19 p3381 N85-30976

Distributed name management
[AD-A154785] 21 p3712 N85-33037

Report of Workshop on Computational Geometry and summary of related research
[AD-A155399] 22 p3833 N85-33734

DATA PROCESSING
- NT ASSOCIATIVE PROCESSING (COMPUTERS)
- NT ATMOSPHERIC & OCEANOGRAPHIC INFORM SYS
- NT BATCH PROCESSING
- NT CENSORED DATA (MATHEMATICS)
- NT CONCURRENT PROCESSING
- NT DATA CORRELATION
- NT DATA REDUCTION
- NT DATA RETRIEVAL
- NT DATA SMOOTHING
- NT DATA STORAGE
- NT DISTRIBUTED PROCESSING
- NT KARHUNEN-LOEVE EXPANSION
- NT MULTIPROCESSING (COMPUTERS)
- NT OPTICAL DATA PROCESSING
- NT PARALLEL PROCESSING (COMPUTERS)
- NT PIPELINING (COMPUTERS)
- NT SCENE ANALYSIS
- NT SIGNAL ANALYSIS
- NT SIGNAL PROCESSING
- NT VOICE DATA PROCESSING

The data processing system of the NAL 2m x 2m transonic wind tunnel
[NAL-TR-811] 01 p0012 N85-10075

TEQUEL: The query language of SADDLE
01 p0058 N85-10382

Seismic discrimination of a geothermal field: Cerro Prieto
[DE84-014581] 01 p0064 N85-10425

Analysis of highly precise gravity measurements
[SER-C-294] 01 p0071 N85-10472

Data flow computer architecture
[DE84-014362] 01 p0100 N85-10664

East Europe report: Science and technology
[JPRS-ESA-84-030] 01 p0101 N85-10670

Decentralized data acquisition to remedy EDP bottleneck 01 p0101 N85-10671

Remote data processing system software in Hungary
01 p0101 N85-10673

Normal approximation for response time in a processor-shared computer system model
[AD-A144997] 01 p0103 N85-10680

A modular data acquisition and display software system for a laboratory environment
[PB84-217892] 01 p0105 N85-10708

Construction of approximate confidence intervals for probability-of-kill via the bootstrap
[AD-A144761] 01 p0113 N85-10764

Hardware and software selection for experimental modal analysis 02 p0208 N85-11373

A mathematical theory of command and control structures
[AD-A145606] 02 p0256 N85-11675

On update semantics and relational views
[AD-A145622] 02 p0294 N85-11907

Nonlinear system identification methodology development based on F-4S flight test data analysis
[AD-A146289] 03 p0318 N85-12063

Satellite, airborne remote sensing development outlined 03 p0342 N85-12199

The current formal status of the ERS-1 ground segment 03 p0380 N85-12423

Factors affecting the archiving, processing and dissemination of ERS-1 altimeter data
03 p0381 N85-12435

Individual differences in automatic and controlled information processing
[AD-A146245] 03 p0401 N85-12559

On line digitizer software
[AD-A146249] 03 p0403 N85-12568

Vibration data analysis system for SNLA area 3 reference manual
[DE84-016207] 04 p0514 N85-13275

Advantages and limitations of spherical harmonic analyses of geomagnetic data 04 p0519 N85-13318

Human reliability data bank: Feasibility study
[DE84-015215] 04 p0546 N85-13476

Toward a non-bureaucratic approach to quality assurance in data processing
[DE84-007484] 04 p0550 N85-13487

Formats for numerical and textual data in data processing
[DFVLR-MITT-84-07] 04 p0551 N85-13504

Measurement of infrasonic waves from remotely detonated artificial explosion 04 p0557 N85-13546

Nuclear criticality information system: Database examples
[DE84-014462] 04 p0576 N85-13678

Speed test results and hardware/software study of computational speed problem, appendix D
05 p0603 N85-13843

Treatment and expression of measurement uncertainties 05 p0630 N85-14042

The acquisition, processing, and use of tactile sensor data in robot control 05 p0641 N85-14114

LANDSAT instruments characterization
[E85-10030] 05 p0654 N85-14199

Measurement data acquisition and processing system for wind rotor measurements in the wind channel of Bremen University 05 p0668 N85-14298

Measuring techniques in the measuring program for the windpowered unit GROWIAN 05 p0669 N85-14303

Weather and climate parameters from Tiros-N
05 p0681 N85-14377

Global scale diagnosis of FGGE data
05 p0683 N85-14394

Application of the bounded derivative initialization method 05 p0686 N85-14407

Increase in the economy of design and process planning by integrated and graphic data processing, phase 2 — aircraft design
[BMFT-FB-W-84-028] 05 p0716 N85-14589

Integrated navigation systems: Where are we headed?
[AD-A146425] 06 p0753 N85-14832

Geological effectiveness of automated processing of highly precise aeromagnetic surveys in Caspian region
06 p0821 N85-15216

Standard SHEF (Standard Hydrometeorologic Exchange Format) decoder Version 1.1
[PB85-106508/GAR] 06 p0840 N85-15332

Investigative findings of image enhancement techniques
[AD-A146392] 06 p0853 N85-15424

Recent advances in data compression
[DE85-001133] 06 p0854 N85-15432

Beginner's guide to blocked records on magnetic tape
[DE85-001691] 06 p0855 N85-15433

Recommended documentation for computer users at ANL
[DE84-016285] 06 p0855 N85-15434

Research on introspective systems
[AD-A146406] 06 p0870 N85-15530

Methodology investigation. Streamlined Test Reporting and Planning (STRAP): Data flow procedures
[AD-A146463] 06 p0871 N85-15531

Adaptive preprocessing system
[AD-D011327] 07 p0937 N85-15935

Literature review of voice recognition and generation technology for Army helicopter applications
[AD-A146878] 07 p0939 N85 15954

Efficient computation of optimal time for transaction processing in a database system
[AD-A147568] 07 p1054 N85-16693

Correlator and data processing requirements for QUASAT 07 p1057 N85-16709

TDRSS S-shuttle unique receiver equipment
08 p1100 N85-16951

EDP computer tapes described
08 p1142 N85-17203

A scanning alarm electronic processor
[AD-D011419] 08 p1158 N85-17309

An efficient algorithm for the computation of the inverse in bundle adjustment systems — photogrammetry
08 p1175 N85-17411

Plasma and magnetospheric research
[NASA-CR-171293] 08 p1183 N85-17451

Data analysis techniques for vehicle attitudinal, positional and experimental measurements
[AD-A147752] 08 p1188 N85-17484

Hybrid data processing research facility
[AD-A148092] 08 p1202 N85-17567

A nonlinear technique for high-resolution data processing
[AD-D011415] 08 p1203 N85-17570

Approaches to structuring the software development process
[AD-A147694] 08 p1205 N85-17582

On edge detection
[AD-A148573] 08 p1223 N85-17703

Survey of remote data monitoring systems
[DE85-001385] 09 p1323 N85-18313

Data report on variations in the composition of sea ice during MIZEX/East'83 with the Nimbus-7 SMMR
[NASA-TM-86170] 09 p1342 N85-18443

NOAA OTEC CWP (National Oceanic and Atmospheric Administration Ocean Thermal Energy Conversion Cold Water Pipe) at-sea test. Volume 3: Additional tabulation of the power spectra, part 2
[PB84-236997] 09 p1346 N85-18468

Analysis of geohydrologic data by kriging
[AD-P004152] 09 p1349 N85-18486

Velocity stack and slant stack inversion methods
09 p1351 N85-18497

Proposal for a small scheme implementation
[AD-A148707] 09 p1368 N85-18595

JOVIAL J73 automated verification system: Implementation phase
[AD-A148732] 09 p1368 N85-18597

Organizational tools for data analysis environments
[DE85-000396] 09 p1369 N85-18601

Role of environments in managing data analysis
[DE85-000397] 09 p1369 N85-18602

Software for event oriented processing on multiprocessor systems
[DE84-016720] 09 p1370 N85-18607

User's manual: Menu-driven data graphing program for the Tektronix 7912AD and 7612D transient digitizer system
[DE85-002151] 09 p1370 N85-18610

Computing environments for data analysis. Part 1. Introduction
[AD-A148677] 09 p1373 N85-18632

Computing environments for data analysis. Part 2. Hardware
[AD-A148678] 09 p1374 N85-18633

Principal curves and surfaces
[AD-A148833] 09 p1375 N85-18646

Data reduction 09 p1412 N85-18903

Analysis of processing 09 p1412 N85-18905

Prospects and means for development of theory and practice of interpretation of gravitational and magnetic anomalies 10 p1501 N85-19474

Brazilian remote sensing receiving, recording and processing ground systems in the 1980's
[E85-10079] 10 p1504 N85-19493

Processing of Global Area Coverage (GAC) data of the TIROS-N/NOAA series polar orbiters
[AD-A148992] 10 p1519 N85-19576

Computer-assisted data processing and analysis system for ground-based meteorological data collection, report on the Sierra Cooperative Pilot Project
[PB85-115350] 10 p1520 N85-19587

Ada (trademark) primer
[AD-A148855] 10 p1539 N85-19703

Diamonds and diamond sorting
[PB85-128502] 10 p1542 N85-19726

The evolution from data processing to information resource management
[AD-A149429] 10 p1567 N85-19878

Some data manipulation requirements for the exploratory analysis of large data sets
[DE85-002541] 10 p1568 N85-19887

Characteristics of quality data
[DE85-001203] 10 p1568 N85-19889

A modeling analysis program for the JPL table mountain Io sodium cloud data
[NASA-CR-175474] 10 p1572 N85-19910

European Scientific Notes. Volume 39, number 2
[AD-A148994] 10 p1573 N85-19919

Comparative evaluation of GC/MS (Gas Chromatography/Mass Spectrometry) data analysis processing
[PB85-125664] 11 p1596 N85-20037

Processing circuit with asymmetry corrector and convolutional encoder for digital data
[NASA-CASE-MSC-20187-1] 11 p1628 N85-20249

Photonic methods of high speed analog data recording
[DE84-016723] 11 p1637 N85-20306

Middle Atmosphere Program. Handbook for MAP. Volume 12: Coordinated Study of the Behavior of the Middle Atmosphere in Winter (PMP-1) Workshops
[NASA-CR-175475] 11 p1665 N85-20492

An overview of the Thematic Mapper geometric correction system 11 p1668 N85-20511

Canadian plans for Thematic Mapper data
11 p1668 N85-20513

A DOE directory of databases for material properties
[UCAR-10124] 11 p1739 N85-20937

Post-processing of bibliographic citations from DOE/Recon, NASA/Recon, and DOD/DROLS
[DE85-000617] 11 p1739 N85-20938

Base communications issues for the 1980s
[AD-A149764] 12 p1828 N85-21474

Universal file processing program for field programmable integrated circuits
[DE85-004384] 12 p1837 N85-21526

GSFC specification electronic data processing magnetic recording tape
[NASA-TM-60599] 12 p1851 N85-21609

Use of the ORACLE DEMS in determining the response of complex scientific instrumentation
[DE85-001742] 12 p1853 N85-21621

An analysis of the high frequency vibrations in early Thematic Mapper scenes 12 p1872 N85-21742

Draftsman displays: A graphical technique for exploratory data analysis
[AD-A150515] 13 p2041 N85-22775

Laser applications in last 10 years reviewed
13 p2052 N85-22844

Liquid mass flow rate computer
13 p2075 N85-22962

Efficiency of multitarget signal detection by digital radar data processing devices 13 p2080 N85-22991

Application of field X-ray: Radiometric analysis in exploratory geology and means for its improvement
13 p2115 N85-23176

Analysis and evaluation of the LANDSAT-4 MSS and TM sensors and ground data processing systems: Early results 13 p2117 N85-23189

Geologic utility of LANSDAT-4 TM data — Death Valley, California and the Silver Bell area of southern Arizona
13 p2118 N85-23192

Microcomputer: Controlled statistics analyzer
[BLL-CE-TRANS-7971-(9022.09)]
13 p2144 N85-23306

Presentation based user interfaces
[AD-A150311] 13 p2144 N85-23311

Measurement of SIFT operating system overhead
[NASA-TM-86322] 13 p2149 N85-23337

Map design for computer processing: Literature review and DMA product critique
[AD-A151061] 14 p2347 N85-24513

Evaluation of carrying capacity and landscape damage in northern Kenya by multistage remote sensing
[DFVLR-FB-84-47] 14 p2347 N85-24514

Cabauw (Netherlands) meteorological data tapes 1973-1984: Description of instrumentation and data processing for continuous measurements
[KNMI-WR-84-6] 14 p2379 N85-24685

Scientific experiments. Preprocessing of scientific data — spaceborne experiments
14 p2398 N85-24779

The problem of creating a standardized series of personal computers 14 p2400 N85-24795

TAPTRN: A tape utility program
[AD-A150644] 14 p2403 N85-24814

CHIL: A comprehensive histogramming language
[DE85-005356] 14 p2405 N85-24830

Dataflow computation
[CWI-TRACT-6] 14 p2406 N85-24833

Experience in automation of data processing in interpretation and defining of linear elements from space photographs 15 p2486 N85-25349

Data structure considerations in automatic cartography
15 p2583 N85-25930

General meteorological package (GEMPAK)
15 p2599 N85-26019

Interactive data analysis. Development of an interactive data manipulation system
[AD-A151359] 15 p2623 N85-26164

USSR report: Cybernetics, computers and automation technology
[JPRS-UCC-85-003] 15 p2625 N85-26174

GRID: A FORTRAN program for using a digitizing table to enter a finite element GRID
[AD-A151317] 15 p2628 N85-26196

Constructing unifying frameworks for the study of distributed system and algorithms
[AD-A151287] 15 p2637 N85-26261

Scattered data interpolation and approximation
[DE85-007495] 15 p2641 N85-26290

An application of the Rayleigh distribution to contract cost data
[AD-A151551] 15 p2664 N85-26441

Space radiation studies — Spacelab 2 Payload
[NASA-CR-171410] 15 p2685 N85-26584

Consultative Committee for Space Data Systems. Panel 1: Support
[NASA-CR-175786] 16 p2769 N85-27090

Gravity model development software status
16 p2804 N85-27269

The relevance of remote sensing to Brazil
[INPE-3421-PRE/686] 16 p2811 N85-27332

Comparison of circulation statistics based on FGGE (First GARP Global Experiment) level 3-B analyses produced by GFDL (Geophysics Fluid Dynamics Laboratory) and ECMWF (European Centre for Medium Range Weather Forecasts) for special observing periods
[PB85-153948] 16 p2836 N85-27492

Algorithms for determining the relative complexity of dynamic signals
[BLL-M-36111-(5828.4)] 16 p2851 N85-27574

Management considerations for an information center
[AD-A151774] 16 p2875 N85-27742

DOD manual for standard data elements, part 1
[AD-A152201] 16 p2878 N85-27754

A Dictionary-Directory System (DDS) for the SPLICE system
[AD-A152223] 16 p2878 N85-27759

A study of error rates in voice recognition
[AD-A153282] 17 p2949 N85-28211

Restructurable VLSI (Very large scale integration) program
[AD-A152340] 17 p2951 N85-28226

Developments in remote sensing
[B8580069] 17 p2984 N85-28441
A comparison of numeric data entry with touch-sensitive and conventional numeric keypads
[AD-A153276] 17 p3008 N85-28598
Computing environments for data analysis. Part 1: Introduction
[DE85-007919] 17 p3009 N85-28603
Computing environments for data analysis. Part 2: Hardware
[DE85-008320] 17 p3009 N85-28604
Interfacing the VAX 11/780 using Berkeley Unix 4.2.BSD and Ethernet based Xerox network systems, volume 1
[AD-A152953] 17 p3015 N85-28645
Estimating random integrals from noisy observations: Sampling designs and their performance
[AD-A152926] 17 p3025 N85-28702
Complete development and implement AFIT/ENG database management system, volume 1
[AD-A153043] 17 p3048 N85-28866
Processing methods of rawinsonde measurements at the descent by parachute
[KNMI-WR-84-7] 18 p3149 N85-29498
Scattered data interpolation codes
[DE85-007337] 18 p3164 N85-29601
Annotated bibliography of recent papers on software engineering environments
[PB85-191365] 18 p3165 N85-29607
Transform domain adaptive filtering using a recursive DFT
[DE85-008965] 18 p3172 N85-29656
Activities report in energy technology
[OEFZS-4302] 18 p3199 N85-29846
LDV multiplexer interface
[NASA-CASE-ARC-11536-1] 19 p3258 N85-30202
An approach to modeling database activity
19 p3332 N85-30642
Cultural data base implementation study and computer-aided scene modeling system users manual
[AD-A154232] 19 p3333 N85-30646
Recovery of lost files from VAX/WMS disk structures: A case study
[DE85-010652] 19 p3333 N85-30650
Interactive graphics for a data analysis management system
[DE85-010977] 19 p3334 N85-30651
Local automation model software benchmarking: Test plan
[AD-A154349] 19 p3337 N85-30676
Ada compiler validation summary report: University of Karlsruhe-GMD/German MOD VAX 11 compiler, version v1.0
[AD-A154370] 19 p3337 N85-30678
Computer Performance Modeling Tool (CPMT)
[AD-A154438] 19 p3338 N85-30682
Defense Mapping Agency (DMA) raster-to-Vector benchmark testing
[AD-A154152] 19 p3338 N85-30683
CMP: Code Maintenance Package reference manual, version 2.0
[DE85-011396] 19 p3340 N85-30697
EDS operator and control software
[DE85-010470] 19 p3340 N85-30698
Guide on workload forecasting
[PB85-177632] 19 p3341 N85-30704
System enhancements of Mesoscale Analysis and Space Sensor (MASS) computer system
[NASA-CR-171463] 19 p3342 N85-30706
TMI-2 technical information and examination program
[DE85-010614] 19 p3359 N85-30827
Modified dynamic hashing
[DE85-011166] 19 p3381 N85-30974
France's LETI reports 1983 electronic components research 20 p3436 N85-31336
Scientific report of the Department of Systems and Communications
[ENST-84D002] 20 p3441 N85-31355
Informatics Division 20 p3449 N85-31416
Microprocessor AirborneData Acquisition and Replay (MADAR) system
[AD-A151728] 20 p3514 N85-31843
Symposium on Computational Mathematics-State-of-the-Art: Informal Proceedings
[DE85-008122] 20 p3516 N85-31858
Overview of on-line data processing for MST radars (keynote paper), part 7 21 p3625 N85-32519
The Norwegian seismic array (NORSAR)
[AD-A154751] 21 p3631 N85-32555
Analysis of spacecraft data
[NASA-CR-171597] 21 p3669 N85-32790
An automated quality assurance surveillance plan for ADP (Automated Data Processing) operations under the Navy's commercial activities program
[AD-A154767] 21 p3671 N85-32802
Design guidelines for user-system interface software
[AD-A154907] 21 p3671 N85-32807
Environmental surveillance at Los Alamos during 1984
[DE85-011886] 22 p3811 N85-33605
Solar energy meteorological research and training program: Region 4
[DE85-011783] 22 p3816 N85-33640
DECODE: A software manual for use with the Serial ASCII Instrumentation Loop (SAIL) system
[AD-A155358] 22 p3828 N85-33709
Automatic capability to store and retrieve component data and to calculate structural integrity of these components
[DE85-012429] 22 p3831 N85-33728
Report of Workshop on Computational Geometry and summary of related research
[AD-A155399] 22 p3833 N85-33734
Comparison of experimental data on detonation velocity and Chapman-Jouget pressure vs initial HE density with predictions from Ree's model equation of state
[DE85-007266] 23 p3922 N85-34304
Modular digital holographic fringe data processing system
[NASA-CR-177952] 23 p3933 N85-34376
Evaluation of low-temperature geothermal potential in Utah and Goshen Valleys and adjacent areas, Utah. Part 2: Water temperature and chemistry
[DE85-009344] 23 p3943 N85-34438
Real-time multiparameter pulse processing with decision tables
[DE85-011683] 23 p3966 N85-34569
Vector calculation of particle code
23 p3981 N85-34668
On the statistical significance of excess events: Remarks of caution and the need for a standard method of calculation
[OG-9.5-10] 23 p4031 N85-34967
Aspects of input signal design for order and parameter estimation in linear dynamical systems
[ER-83/05] 24 p4091 N85-35362
Adaptive rezoner in a two-dimensional Lagrangian hydrodynamic code
[DE85-010108] 24 p4094 N85-35381
Federal Mineral Land Information System
24 p4106 N85-35459
Gravity gradiometer survey data processing
[AD-A156165] 24 p4117 N85-35522
An approach to determining computer security requirements for Navy systems
[AD-A155750] 24 p4135 N85-35627
Optimize computer throughput using array processors
[AD-A155843] 24 p4135 N85-35628
Using an LSI-11/23 and RT-11 to digitize analog tapes
[DE85-012736] 24 p4139 N85-35656
Analysis of two-parameter constant background born inversion for acoustic synthetic data
[AD-A156394] 24 p4145 N85-35698
Data processing professionals and DP application users' perceptions and expectations of operational roles of persons working in a DP/application user interface group 24 p4165 N85-35821
Investigation of cosmic rays in very short time scales
[HE-4.6-7] 24 p4197 N85-36044

DATA PROCESSING EQUIPMENT
NT AIRBORNE/SPACEBORNE COMPUTERS
NT ANALOG COMPUTERS
NT CDC COMPUTERS
NT CDC CYBER 170 SERIES COMPUTERS
NT CDC CYBER 205 COMPUTER
NT COMPUTERS
NT DATA PROCESSING TERMINALS
NT DIGITAL COMPUTERS
NT EMBEDDED COMPUTER SYSTEMS
NT HEWLETT-PACKARD COMPUTERS
NT HYBRID COMPUTERS
NT IBM COMPUTERS
NT MICROCOMPUTERS
NT MICROPROCESSORS
NT MINICOMPUTERS
NT OPTICAL COMPUTERS
NT PARALLEL COMPUTERS
NT PDP 11 COMPUTER
NT PDP 11/70 COMPUTER
NT PERSONAL COMPUTERS
NT PRINTERS (DATA PROCESSING)
NT SEQUENTIAL COMPUTERS
NT UNIVAC COMPUTERS
NT UNIVAC 1100 SERIES COMPUTERS
NT VAX COMPUTERS
NT VAX-11 SERIES COMPUTERS
NT VAX-11/780 COMPUTER
The FLEX/32 multicomputing environment
01 p0057 N85-10378
On line digitizer software
[AD-A146249] 03 p0403 N85-12568
Intelligent interfaces for tactical airborne platforms
06 p0752 N85-14820
Papers of the 15th International Society for Photogrammetry and Remote Sensing (ISPRS) Congress — conferences
[TRITA-FMI-9] 08 p1175 N85-17408
Hybrid data processing research facility
[AD-A148092] 08 p1202 N85-17587
Dual adaptive control based upon sensitivity functions
[NASA-CR-169331] 10 p1543 N85-19727
New types of power supplies for ultrasonic processing equipment 12 p1843 N85-21596
RAPIDbus: Design of an extensible multiprocessor structure
[AD-A150061] 12 p1912 N85-21998
Instrumentation award
[AD-A150081] 12 p1912 N85-21999
Requirements placed on information processing equipment
[BLL-CE-TRANS-7983-(9022.09)]
13 p2144 N85-23007
Parallel test method for LSI (Large Scale Integration) microprocessors
[AD-A150237] 13 p2144 N85-23010
Research on CAD/CAM support for microprocessor development surveyed 14 p2290 N85-24193
Microprocessor controlled storage sampling oscilloscope 15 p2533 N85-25622
ADCCP (Advanced Data Communication Control Procedure) communication processor
[AD-D011595] 15 p2544 N85-25739
Computer use in research for data analysis
[PB85-153567] 15 p2631 N85-26220
A procedure for communications with PDP-10 and PDP-11 (IS/1 UNIX) type computers through use of CPT word processing equipment, revision 1
[DE85-007596] 16 p2845 N85-27540
The touch panel system: Design and development
[AD-A153014] 17 p3008 N85-28596
A study of user-defined searching requirements for the on-line version of the directory of DOD-sponsored R and D data bases on the Defense Gateway computer system
[AD-A153000] 17 p3050 N85-28878
User's guide for the Mk-3 D-coronameter data system
[PB85-181204] 19 p3385 N85-31002

DATA PROCESSING TERMINALS
Analysis of data entry performance: Chromatic versus monochromatic
[AD-A145568] 03 p0438 N85-12769
Selected NBSNET software
[PB85-109148] 10 p1542 N85-19723
Optical processor for synthetic aperture radar
11 p1621 N85-20203
The ARGOS Platform Transmitter Terminals (PTTs)
14 p2237 N85-23872
The ARGOS VHF direct readout mini-station and CML-80-MP data collection Platform Transmitter Terminals (PTTs) 14 p2238 N85-23873
Direct readout and dissemination of results using ARGOS keypad terminals 14 p2328 N85-24390
Data transmission using ARGOS keypad platform transmitter terminals (PTT) 14 p2330 N85-24407
A new versatile ARGOS PTT for oceanographic applications — Platform Transmit Terminal (PTT)
14 p2331 N85-24417
Overview of data processing at AES local user terminals — Canadian Atmospheric Environment Service (AES) 14 p2331 N85-24418
Investigation and construction of the Mini Remote Terminal Unit (mRTU-M) Analog Processor Module (AP-M), volume 1
[MR-DS-01-VOL-1] 18 p3166 N85-29619
Investigation and construction of the Mini Remote Terminal Unit (mRTU-M), Analog Processor Module (AP-M), volume 2
[MR-DS-01-VOL-2] 18 p3166 N85-29620
Canadian Astronautics Limited's SARSAT ground stations 20 p3401 N85-31104
A 406 MHz ELT processor for geostationary satellites — Emergency Locator Transmitter (ELT)
20 p3403 N85-31114
Evolution of 406 MHz Search and Rescue (SAR) processor 20 p3403 N85-31116
A micro/PDP-11 system for 406 MHz COSPAS/SARSAT processing 20 p3403 N85-31117
Fault tolerant multiprocessor SARSAT-COSPAS 406 MHz local user terminal 20 p3404 N85-31123
Secure digital voice communications in the Defense Data Network (DDN)
[AD-A154677] 21 p3574 N85-32226

DATA PROCESSORS
U DATA PROCESSING EQUIPMENT

DATA READOUT SYSTEMS
U DATA SYSTEMS
U DISPLAY DEVICES

DATA RECORDERS

Analog disc recorder system: Operator's reference manual
[DE84-016926] 04 p0503 N85-13209

System for automatic recording of vibration parameters 14 p2282 N85-24135

Balloon-borne video cassette recorders for digital data storage
[OG-9.3-11] 23 p4028 N85-34966

Mini and super mini arrays for the study of highest energy cosmic rays
[OG-9.4-9] 23 p4029 N85-34976

DATA RECORDING

Requirements and specifications for cartographic video discs
[AD-A144906] 01 p0049 N85-10325

Existing measuring systems for wind energy units
05 p0669 N85-14302

Operational loads measurement: A philosophy and its implementation 07 p0894 N85-15665

The F-15 flight loads tracking program
07 p0894 N85-15666

Flight parameters recording for structure fatigue life monitoring 07 p0896 N85-15682

USAF approach to airborne structural data recording: Airborne Data Acquisition Multifunction System (ADAMS)
07 p0897 N85-15683

Extracting digital data from a bus and multiplexing it with a video signal
[AD-D011491] 11 p1636 N85-20302

Quarter-inch streaming tape drive application with the Serial ASCII Instrumentation Loop (SAIL) system
[AD-A155354] 22 p3759 N85-33295

Error message recording and reporting in the SLC control system
[DE85-013057] 24 p4140 N85-35664

DATA REDUCTION

NT DATA SMOOTHING

Analysis of highly precise gravity measurements
[SER-C-294] 01 p0071 N85-10472

Computations for the 16-foot transonic tunnel, NASA, Langley Research Center
[NASA-TM-86319] 02 p0149 N85-11009

Reducing spectral dimension of remotely sensed data using principal components analysis and a Peano scanning 02 p0212 N85-11399

Command flight path display. Phase I and II: Appendix F
[AD-A145858] 03 p0318 N85-12056

Physical oceanography report. Helicopter-based STD data from MIZEX 83 (Marginal ice zone experiment)
[AD-A145848] 03 p0398 N85-12536

NUTSATSEA: An on line data reduction program linking a Chemlab continuous flow analyser to a Commodore PET microcomputer
[IOS-176] 03 p0403 N85-12570

Reduction and analysis of data from the plasma wave instruments on the IMP-6 and IMP-8 spacecraft
[NASA-CR-175127] 04 p0460 N85-12918

The human role in space. Volume 2: Research analysis and technology report
[NASA-CR-171224] 04 p0546 N85-13474

TCAS 2 logic performance during phase one operational evaluation
[DOT/FAA/PM-84/20] 05 p0595 N85-13793

Measuring system and data evaluation methods of the test field for wind energy units at Pellworm
05 p0668 N85-14296

Utilization of SAGE aerosol profiles in the analysis of Mauna Loa stratospheric lidar data
[NASA-CR-174198] 05 p0675 N85-14332

Forecast impact of components of the FGGE observing system 05 p0681 N85-14373

Some new mathematical methods for variational objective analysis 05 p0681 N85-14375

The use of available potential energy to evaluate two GLAS FGGE data sets 05 p0682 N85-14387

Keeping up with operational loads in the French Air Force: Defining new equipment
07 p0896 N85-15681

Support for the Naval Research Laboratory Passive Microwave Clutter Analysis Program
[AD-A146771] 07 p0939 N85-15951

Results of the 1984 NASA/JPL balloon flight solar cell calibration program
[NASA-CR-174270] 07 p0991 N85-16294

Human factors characteristics of the Joint Tactical Fusion Test Bed: Field test 467 results
[AD-A146858] 07 p1020 N85-16476

Processing system for space VLBI
07 p1057 N85-16711

Reduction to outside the atmosphere and statistical tests used in Geneva photometry 08 p1251 N85-17902

Flux reconstruction and calibration
09 p1412 N85-18904

Analysis of a visual performance experiment
[DE85-000710] 10 p1530 N85-19645

Looking at multivariate data through fuzzy sets
[DE85-000684] 11 p1702 N85-20706

Image processing instrumentation for speckle interferometry and imaging
[AD-A149306] 11 p1762 N85-21084

A GC/MS (Gas Chromatograph/Mass Spectrometer) data management process. Part 1: User's guide, version 1.0
[PB85-116051] 12 p1803 N85-21309

Main component method used to study variations of cardiovascular parameters 12 p1901 N85-21939

Draftsman displays: A graphical technique for exploratory data analysis
[AD-A150515] 13 p2041 N85-22775

MAGSAT anomaly field data of the crustal properties of Australia
[E85-10100] 13 p2122 N85-23215

An investigation of the crustal properties of Australia and surrounding regions derived from interpretation of MAGSAT anomaly field data 13 p2122 N85-23216

Data selection techniques in the interpretation of MAGSAT data over Australia 13 p2123 N85-23218

Variational mesoscale satellite data assimilation and initialization
[NASA-CR-175704] 14 p2378 N85-24680

Scientific experiments. Preprocessing of scientific data — spaceborne experiments
14 p2398 N85-24779

Nonparametric estimation of density and hazard rate functions when samples are censored
[AD-A150946] 14 p2411 N85-24868

Kitt Peak measurements of P/Halley positions
14 p2436 N85-25023

On the orbit improvement results obtained by referring old cometary observations to the SAO Star Catalog
14 p2438 N85-25042

A new NASTRAN capability for data reduction
15 p2574 N85-25874

Plasma and magnetospheric research
[NASA-CR-171447] 15 p2591 N85-25976

VAS/model impact study 15 p2597 N85-26006

Interactive graphical data analysis
[DE85-005946] 15 p2631 N85-26215

Computer use in research for data analysis
[PB85-153567] 15 p2631 N85-26220

Jupiter/Voyager data analysis
[NASA-CR-175723] 15 p2679 N85-26545

Status of the observational data sets — TOPEX
16 p2804 N85-27286

Shuttle imaging radar-A (SIR-A) data analysis — geology of the Ozark Plateau of southern Missouri, land use in western Illinois, and vegetation types at Koonamore Station, Australia
[NASA-CR-175785] 16 p2809 N85-27324

Digital filters for application to data analysis in electron energy loss spectroscopy
[DE85-007932] 17 p2923 N85-28020

US Naval Observatory collection and utilization of time comparison data 17 p2962 N85-28292

Heating parameter estimation using coaxial thermocouple gages in wind tunnel test articles
[AD-A153039] 17 p2968 N85-28328

Flight testing for performance and flying qualities
18 p3058 N85-28920

Measurements of Solar Vector Magnetic Fields
[NASA-CP-2374] 18 p3203 N85-29869

Interactive graphics for a data analysis management system
[DE85-010977] 19 p3334 N85-30651

The application of artificial intelligence techniques to large distributed networks
[NASA-CR-177346] 19 p3344 N85-30721

Foundations of data envelopment analysis for Pareto-Koopmans efficient empirical productions functions
[AD-A154244] 19 p3346 N85-30735

User's guide for the Mk-3 D-coronameter data system
[PB85-181204] 19 p3385 N85-31002

Use of MMLE3 to determine lower order equivalent systems in the time domain
[AD-A154700] 21 p3554 N85-32112

In-situ measurement of wall thermal performance: Data interpretation and apparatus design recommendations
[DE85-011979] 21 p3586 N85-32289

SSMIR (Solid State Memory Instrumentation Recorder): A new approach to acquiring data during an aircraft seat/sled ejection sequence
[AD-A154780] 21 p3589 N85-32308

A modified Fresnel scattering model for the parameterization of Fresnel returns, part 2.3A
21 p3618 N85-32483

Overview of on-line data processing for MST radars (keynote paper), part 7 21 p3625 N85-32519

Analysis of spacecraft data
[NASA-CR-171597] 21 p3669 N85-32790

Search for bursts in air shower data
[OG-5.3-10] 22 p3885 N85-34076

Time-resolved spectroscopic studies of detonating heterogeneous explosives
[DE85-009760] 23 p3921 N85-34297

Computer graphics for multivariate data
23 p3958 N85-34528

An image management kernel for the design of relational and pictorial data bases 23 p3958 N85-34532

Spatial trees: A fast access method for unstructured graphical data 23 p3958 N85-34533

New Matsushiro underground cosmic ray station (220 M.W.E. in depth)
[SH-9.1-14] 23 p4052 N85-35129

A suggested standardized format for cosmic ray ground-level event data
[SH-9.1-15] 23 p4052 N85-35130

Three-dimensional gravity ideal body studies in rough terrain
[DE85-014097] 24 p4118 N85-35525

Users guide for optimum interpolation method of global data assimilation
[AD-A155929] 24 p4138 N85-35648

DATA RETRIEVAL

Facsimile transmission of microforms
[AD-A144855] 01 p0038 N85-10236

SITIM system: Object manager module
[INPE-3284-NTE/226] 02 p0240 N85-11564

NSSDC and WDC-A-R and S document availability and distribution services
[NASA-TM-87374] 03 p0438 N85-12787

Human reliability data bank: Feasibility study
[DE84-015215] 04 p0546 N85-13476

International information networks for material properties
[DE84-013636] 04 p0576 N85-13676

Optimal query processing in distributed data base management systems with data redundancy
05 p0734 N85-14722

Retrieval procedures for hydrologic data from ARS (Agricultural Research Service) experimental watersheds in the US (REPHLEX)
[PB85-111326/GAR] 09 p1402 N85-18828

Solid propellant combustion diagnostics and automated data retrieval from holograms 13 p1998 N85-22527

Notes for medical catalogers, 1984
[PB85-180206] 18 p3200 N85-29853

CODA: A concept organization and development aid for the research environment
[AD-A154240] 19 p3343 N85-30715

MANHIST user's guide
[DE85-010684] 19 p3348 N85-30754

The international scope of data evaluation
[DE85-005953] 19 p3349 N85-30760

Sample interchange of MST radar data from the Urbana radar 21 p3627 N85-32531

Technology transfer system automation implementation
[PB85-177335] 22 p3849 N85-33838

NAPGEN: Automatic NAPLPS page generator
23 p3964 N85-34575

Federal Mineral Land Information System
24 p4106 N85-35459

EPALIT: A data management system applied to the control and retrieval of technical reports
[PB85-193068] 24 p4166 N85-35828

DATA SAMPLING

Adaptive preprocessing system
[AD-D011327] 07 p0937 N85-15935

Diamonds and diamond sorting
[PB85-128502] 10 p1542 N85-19726

Main component method used to study variations of cardiovascular parameters 12 p1901 N85-21939

Measurement requirements for the detection of ozone trends 13 p2105 N85-23115

Application of model following control and estimation techniques to attitude control of maneuvering spacecraft. Part 1: Theory and simulation results
[NLR-TR-82116-U-PT-1] 18 p3065 N85-28957

The HURRA high resolution experimental radar system sampling unit
[FOA-C-30376-E1] 18 p3091 N85-29133

The Mk.1 NPL digital sampling ac wattmeter
[NPL-DES-82] 22 p3758 N85-33290

Theoretical principles of vertical subsampling of color difference signals at half the sampling rate — television
[FI-447-TBR-18] 23 p3926 N85-34332

DATA SIMULATION

Comparison of land cover information from LANDSAT Multispectral Scanner (MSS) and airborne Thematic Mapper simulator (TMS) data for hydrologic applications — Clinton River Basin, Michigan
13 p2122 N85-23211

Calibration and use of clutter data for simulation
[AD-A154793] 21 p3574 N85-32229
DATA SMOOTHING
The approximation of nonsmooth solutions of hyperbolic partial differential equations
[CSIR-TWISK-297] 01 p0108 N85-10723
A variable span smoother
[AD-A148241] 08 p1215 N85-17655
Smoothing with split linear fits
[AD-A149032] 10 p1545 N85-19740
Locally-weighted-regression scatter-plot smoothing (LOWESS): A graphical exploratory data analysis technique
[AD-A152239] 16 p2855 N85-27609
Fast moving average recursive least mean square fit
[DE85-010036] 19 p3348 N85-30752
Smoothing surface data by spline functions
[AD-A155829] 24 p4142 N85-35678
Two methods of global data assimilation
[AD-A155961] 24 p4143 N85-35684
DATA STORAGE
Requirements and specifications for cartographic video discs
[AD-A144906] 01 p0049 N85-10325
A modular data acquisition and display software system for a laboratory environment
[PB84-217892] 01 p0105 N85-10709
Storage in the LLNL Octopus network: An overview and reflections
[DE84-014711] 01 p0106 N85-10712
SITIM system: Object manager module
[INPE-3284-NTE/226] 02 p0240 N85-11584
ADAM: An abstract database machine
[RSRE-84007] 02 p0293 N85-11904
Archiving and exchange of a computerized marine seismic database: The ROSE (Rivera Ocean Seismic Experiment) data archive system
[AD-A145658] 02 p0294 N85-11908
Factors affecting the archiving, processing and dissemination of ERS-1 altimeter data
03 p0381 N85-12435
Standardization of data formats for radar altimeter data 03 p0384 N85-12455
Human reliability data bank: Feasibility study
[DE84-015215] 04 p0546 N85-13476
Multichannel electrooptical modulators for digital information storage and processing systems
07 p0950 N85-16021
Data handling for the Spectral Radiometer (SPERAD)
[FOA-C-30368-E1,E4] 07 p0968 N85-16145
Data stimulated on-line-checking (IROLD)
08 p1066 N85-16754
Benchmarking database systems in multiple backend configurations
[AD-A148191] 08 p1202 N85-17566
Computer center: CDC Libraries-PROCFIL (procedures)
[AD-A148633] 08 p1206 N85-17589
Performance evaluation of a database system in multiple backend configurations
[AD-A148192] 08 p1229 N85-17743
Boring information and subsurface data base package user's guide
[AD-A148623] 08 p1230 N85-17747
Computer center CDC libraries/utility (programs)
[AD-A148680] 09 p1366 N85-18593
FLAD user's manual: FLAD file contents
[AD-A148700] 09 p1368 N85-18594
Satellite-computer interface 10 p1476 N85-19318
Computer center CDC libraries
[AD-A149005] 10 p1540 N85-19707
ADAPS (Airborne Data Acquisition and Processing System) operation and maintenance manual
[AD-A149297] 11 p1585 N85-19983
RAPIDbus: Design of an extensible multiprocessor structure
[AD-A150061] 12 p1912 N85-21998
The intelligent database machine
12 p1949 N85-22242
Role of optical disk at computing centers
[DE85-005124] 13 p2145 N85-23314
Performance evaluation of distributed systems with unbalanced flows: An analysis of the INFOPLEX data storage hierarchy
[AD-A150528] 13 p2147 N85-23328
General design considerations of an Air Force information system
[AD-A150611] 13 p2168 N85-23449
West Europe report: Science and technology
[JPRS-WST-84-026] 15 p2532 N85-25617
Philips tested new materials for optical data storage
15 p2532 N85-25620
China report: Science and technology
[JPRS-CST-85-007] 15 p2533 N85-25621
Microprocessor controlled storage sampling oscilloscope 15 p2533 N85-25622
Use of a network of telemetered meteorological stations for prediction of the distribution of an atmospheric tracer
16 p2831 N85-27458
A climatic data bank for Northern Hemisphere land areas, 1851-1980
[DE85-007863] 16 p2835 N85-27486
Study of raster metafile formats
[AD-A153322] 17 p3012 N85-28824
Replication methods for abstract data types
[AD-A153648] 18 p3162 N85-29587
A stored data acquisition system: Update
[DE85-010534] 18 p3166 N85-29616
ZOG-Vinson technology demonstration project. Volume 2: System description
[AD-A153871] 19 p3333 N85-30645
ZOG/VINSON technology demonstration project system description. Volume 1
[AD-A154211] 19 p3342 N85-30713
CODA: A concept organization and development aid for the research environment
[AD-A154240] 19 p3343 N85-30715
Characteristics of a numerical fluid dynamics simulator
[DE85-009602] 21 p3586 N85-32290
Problems and solutions in analyzing partial-reflection drift data by correlation techniques
21 p3626 N85-32529
Sample interchange of MST radar data from the Urbana radar 21 p3627 N85-32531
Development of a dedicated speech work station
[AD-A155465] 21 p3674 N85-32824
The automatic labeling of geographic maps: A problem in computer aesthetics 23 p3962 N85-34561
Building an octree from a set of parallelepipeds
23 p3964 N85-34572
Balloon-borne video cassette recorders for digital data storage
[OG-9.3-11] 23 p4028 N85-34966
A suggested standardized format for cosmic ray ground-level event data
[SH-9.1-15] 23 p4052 N85-35130
DATA STRUCTURES
An algorithm for assembly of stiffness matrices into a compacted data structure
[AD-A146727] 07 p1023 N85-16492
GADB: A database facility for modelling naturally occurring geophysical fields 13 p2122 N85-23217
Synthesis of tree-structured computing systems through use of closures
[AD-A150502] 13 p2147 N85-23326
Invariant system of technological preparation of production 14 p2268 N85-24056
Data structure considerations in automatic cartography
15 p2583 N85-25930
DATA SYSTEMS
Field tests of the real-data acquisiton system for the NASA-LaRC differential absorption lidar
[NASA-CR-174020] 01 p0106 N85-10710
Time invariant memoryless nonlinear systems identification method
[FUB-9-1983] 01 p0114 N85-10773
Automated Data Systems (ADS) documentation standards
[AD-A144867] 01 p0125 N85-10857
Data dictionary systems and their role in information resource management
[AD-A144905] 01 p0125 N85-10859
Business planning for information services under special consideration of German management information systems
[BMFT-FB-ID-83-007] 02 p0294 N85-11910
Factors affecting the archiving, processing and dissemination of ERS-1 altimeter data
03 p0381 N85-12435
A microprocessor data system for developing countries — climatology 07 p1003 N85-16377
Shuttle payload S-band communications system
08 p1100 N85-16950
Survey of remote data monitoring systems
[DE85-001385] 09 p1323 N85-18313
General design considerations of an Air Force information system
[AD-A150611] 13 p2168 N85-23449
Applications of ARGOS data collection systems in Arctic regions 14 p2236 N85-23875
Applications of ARGOS data collection system for automatic meteorological observatories in Arctic regions
14 p2240 N85-23893
Geostationary Operational Environmental Satellite Data Collection System 14 p2328 N85-24393
NOAA'S role in support of service ARGOS
14 p2328 N85-24394
Service ARGOS technical report and improvement
14 p2328 N85-24395
Data-link alternatives for the NASA pilot data systems
[NASA-TM-85999] 14 p2412 N85-24873
NOAA satellite operations: Programs briefing – Environmental satellites, LANDSAT, and space station polar platform 15 p2599 N85-
Computer use in research for data analysis
[PB85-153567] 15 p2631 N85-
Determining availability characteristics of DSN data systems using discrepancy report data
16 p2772 N85-
US Naval Observatory collection and utilization of time comparison data 17 p2962 N85-
A comparison of numeric data entry with touch-sensitive and conventional numeric keypads
[AD-A153276] 17 p3008 N85-
The IRAS end-to-end data system
[NLR-MP-83056-U] 17 p3051 N85-
CSIN (Chemical Substances Information Network) workbook: US Geological Survey training course for Chemical Substances Information Network
[PB85-170058] 18 p3200 N85-
The international scope of data evaluation
[DE85-005953] 19 p3340 N85-
DATA TRANSMISSION
NT CODE DIVISION MULTIPLE ACCESS
NT FREQUENCY DIVISION MULTIPLE ACCESS
NT MULTIPLE ACCESS
NT SINGLE CHANNEL PER CARRIER TRANSMISSION
Facsimile transmission of microforms
[AD-A144855] 01 p0038 N85-10
Interaction of voice and data traffic in a packet switching communication network and virtual circuit
[FUB-63-1982] 01 p0039 N85-10
The average power density spectra of additive scrambler signals and their versions in AMI code
[FUB-27-1983] 01 p0040 N85-10
Center for Electronics and Electrical Engineering Technical Bulletin covering center programs
[PB84-219716] 01 p0045 N85-10
REMOTE: Modem Communicator Program for the IBM personal computer
[DE84-015047] 01 p0100 N85-10
High-data-rate wide-angle underwater acoustic telemetry system
[DE84-015696] 02 p0233 N85-11
Shuffle-exchanges on augmented meshes
[NASA-CR-172476] 02 p0243 N85-11
Mission science value-cost savings from the Advanced Imaging Communication System (AICS)
[NASA-CR-174170] 04 p0458 N85-12
Regenerators of binary pulses for optical communication systems 04 p0485 N85-13
Digital raster timing encoder-decoder
[AD-D011279] 06 p0804 N85-15
Wavelength coded image transmission and holographic optical elements
[AD-A146490] 06 p0810 N85-15
Recent advances in data compression
[DE85-001133] 06 p0854 N85-15
Methodology investigation. Streamlined Test Reporting and Planning (STRAP): Data flow procedures
[AD-A146463] 06 p0871 N85-15
National airspace system configuration management interface control document. Maintenance processor subsystem to remote monitoring subsystems and remote monitoring subsystem concentrators
[NAS-MD-790] 07 p0900 N85-1
A modified Monte-Carlo technique for the simulation of satellite communication systems
[AD-A148889] 08 p1214 N85-17
Dissemination of ERS-1 low bit rate data and the use of L-band receiving stations
[NLR-TR-83049-U] 09 p1358 N85-18
Directory of range data conversion and processing systems
[AD-A148996] 10 p1427 N85-19
An ionospheric mode detection system for HF communications application 10 p1471 N85-19
Time and space domain filtering for improved HF communication 10 p1473 N85-19
Serial data transmission with large output on the HF channel 10 p1475 N85-19
Worldwide report: Telecommunications policy, research and development
[JPRS-TTP-85-006] 10 p1476 N85-19
Commentary on start of scientific data transmissions with USSR 10 p1476 N85-19
L.F. RADIO-DATA: Specification of BBC phase-modulated transmissions on long-wave
[BBC-RD-1984/19] 12 p1822 N85-21
The 20:16 block code for digital recording and transmission channels
[BBC-RD-1985/1] 12 p1824 N85-21
The intelligent database machine
12 p1949 N85-22

Experimental results on the application of convolutional coding and Viterbi decoding as a frequency diversity technique in HF data transmission
[CRC-1377] 13 p2052 N85-22850

Data compression for noiseless channels
13 p2053 N85-22851

Integrated digital networks
[AD-A150605] 13 p2056 N85-22873

Noise immunity of information transmission system with pseudorandom frequency switching under worst-case interference conditions 13 p2086 N85-23029

Authorizing appropriations to the National Aeronautics and Space Administration for fiscal year 1986
[H-REPT-99-32] 13 p2168 N85-23452

The ARGOS system and hydrology. Results obtained by ORSTROM and benefits of a degree of standardization 14 p2239 N85-23681

Accurate baseline determination by radio interferometry on NAVSTAR GPS satellite transmissions
[AD-A150861] 14 p2291 N85-24202

The ARGOS communications performance trials
14 p2326 N85-24376

Location and data collection for long stratospheric balloon flights 14 p2326 N85-24377

Measurement of water equivalent of mountain snow cover — ARGOS system 14 p2327 N85-24386

Hydrology and climatic conditions in Greenland
14 p2327 N85-24387

The ARGOS system and hydrology: The use of Platform Terminal Transmitter (PTT) with built-in memory and direct reception by the Seine basin hydrology service
14 p2328 N85-24389

Direct readout and dissemination of results using ARGOS keypad terminals 14 p2328 N85-24390

NOAA'S role in support of service ARGOS
14 p2328 N85-24394

Data transmission using ARGOS keypad platform transmitter terminals (PTT) 14 p2330 N85-24407

Analysis of atmospheric interferometer data
[AD-A150692] 14 p2372 N85-24663

ADCCP (Advanced Data Communication Control Procedure) communication processor
[AD-D011595] 15 p2544 N85-25709

Computer use in research for data analysis
[PB85-153567] 15 p2631 N85-26220

A method of estimating aircraft attitude from fly by wire flight control system data 16 p2697 N85-26653

The Record of Electrical and Communication Engineering Conversazione, volume 53, no. 2, November 1984
[ISSN-0385-7719] 16 p2758 N85-27022

Historical perspectives on information transmission engineering 16 p2759 N85-27023

Optical non-line-of-sight covert, secure high data communication system
[AD-D011607] 16 p2769 N85-27087

Meteorological factors in Earth-Satellite propagation
[NASA-CR-175764] 16 p2769 N85-27089

Evaluation of Ada (trademark) as a communications programming language, volume 1
[AD-A152314] 16 p2848 N85-27559

Evaluation of Ada (trademark) as a communications programming language. Volume 2: Communications protocols application
[AD-A152315] 16 p2848 N85-27560

Rational pulse-shaping filters for almost MSK-like modulation
[AD-A153065] 17 p2949 N85-28206

Automation of Precise Time Reference Stations (PTRS) 17 p2962 N85-28291

UHF IRIG G distribution system
17 p2965 N85-28308

A new technique for system-to-system transfer of surface data 17 p3007 N85-28589

Interfacing the VAX 11/780 using berkeley UNIX 4.2BSD and Ethernet based Xerox Network Systems
[AD-A153174] 17 p3016 N85-28647

Torus data flow for parallel computation of missized matrix problems
[DE85-008761] 17 p3026 N85-28715

A concatenated coding scheme for error control
[NASA-CR-176006] 19 p3334 N85-30655

The application of artificial intelligence techniques to large distributed networks
[NASA-CR-177346] 19 p3344 N85-30721

Fiber optics in transient radiation fields
[DE85-010721] 19 p3368 N85-30886

Navigation data for Emergency Position Indicating Radio Beacons (EPIRBs) 20 p3403 N85-31115

Transmission Monitoring and Control (TRAMCON) segmentation plan for the DCS (Defense Communications System) digital transmission network
[AD-A154175] 20 p3440 N85-31351

Microprocessor AirborneData Acquisition and Replay (MADAR) system
[AD-A151728] 20 p3514 N85-31843

Determining functional requirements for NASA Goddard's command management system software design using expert systems 20 p3539 N85-32020

Proust radar: Decoding hardware and coherent integration, part 7.2A 21 p3626 N85-32524

Design guidelines for user-system interface software
[AD-A154907] 21 p3671 N85-32807

An image compression survey and algorithm switching based on scene activity
[NASA-TP-2456] 22 p3727 N85-33106

Telemetry system for the transmission of data from projectiles during the acceleration phase in the gun barrel
[ISL-CO-207/84] 22 p3739 N85-33178

A model for predicting propagation-related DSCS (Defense Communications Engineering Center) margin requirements
[AD-A155365] 22 p3756 N85-33281

Estimating optimum technical and economic indicators of data transmission systems 22 p3777 N85-33406

Developmental trends in radio receiver design
22 p3777 N85-33407

Characteristics of optical information-measurement channels with utilization of scattering effects
22 p3781 N85-33429

IGES/RIM Parser/Converter users guide
[DE85-011965] 22 p3829 N85-33716

Optimizing data access in the LAMPF control system
[DE85-012653] 24 p4140 N85-35863

Investigation of cosmic rays in very short time scales
[HE-4.6-7] 24 p4197 N85-36044

DATING
U CHRONOLOGY
U TIME MEASUREMENT

DAWN CHORUS

ELF chorus in the Earth's outer magnetosphere
14 p2366 N85-24624

Conjugacy of ELF-VHF emissions near L=6 — chorus phenomenon, hiss 14 p2367 N85-24629

DAYTIME

On some new features of semiannual variation of the geomagnetic field 04 p0520 N85-13327

Dayside cusp aurora 04 p0521 N85-13333

Correlations of solar irradiance and daylight illuminance for building energy analysis
[DE85-001738] 06 p0839 N85-15326

DC (CURRENT)
U DIRECT CURRENT

DC 8 AIRCRAFT

Aircraft accident report: Flying Tigers, Inc., Flight 2468, McDonell Douglas DC8-63, N797FT, Chambers Field, Naval Air Station, Norfolk, Virginia, October 25, 1983
[PB84-910408] 02 p0136 N85-10925

DC 9 AIRCRAFT

Safety recommendation(s), A-84-76 through -78
[REPT-3751E] 15 p2466 N85-25224

DC 10 AIRCRAFT

Results of winglet development studies for DC-10 derivatives
[NASA-CR-3677] 02 p0138 N85-10936

Safety recommendation(s), A-84-123 and -124
[REPT-3894B/93] 15 p2466 N85-25222

DC-10 winglet flight evaluation
[NASA-CR-3704] 19 p3217 N85-29949

Flight-service program for advanced composite rudders on transport aircraft
[NASA-CR-174537] 19 p3217 N85-29950

Aircraft accident report: World Airways Inc., Flight 30H, McDonnell Douglas DC-10-30CF, N113WA, Boston-Logan International Airport, Boston, Massachusetts, January 23, 1982
[PB85-910406] 22 p3728 N85-33114

DDT

Development of a PETN DDT detonator
[DE84-016944] 09 p1302 N85-18178

CP DDT detonators. Part 1: Design sensitivity study
[DE84-017255] 09 p1302 N85-18180

DE HAVILLAND AIRCRAFT
NT DH 115 AIRCRAFT
NT DHC 2 AIRCRAFT

DE HAVILLAND DH 115 AIRCRAFT
U DH 115 AIRCRAFT

DE LAVAL NOZZLES
U CONVERGENT-DIVERGENT NOZZLES

DEACCLIMATIZATION
U ACCLIMATIZATION

DEACTIVATION

Adsorption thermodynamics and surface transport of metal catalyst poisons
[DE85-002868] 10 p1441 N85-19084

Elementary processes of electronically excited particles. Part 5: Deactivation of CHF (A1a' (O, V'2, O) after excitation by a pulsed dye laser
[MPIS-13/1984] 14 p2420 N85-24930

DEAD RECKONING

Reference systems for the evaluation of dead-reckoning navigation equipment 13 p1967 N85-22358

DEADWEIGHT
U STATIC LOADS

DEAFNESS
U AUDITORY DEFECTS

DEATH

Fatal hemorrhagic shock and acetate solutions
[AD-A146754] 07 p1014 N85-16444

Effects of long-term low-level radiofrequency radiation exposure on rats. Volume 8: Evaluation of longevity, cause of death, and histopathological findings
[AD-A154283] 19 p3327 N85-30610

DEATH VALLEY (CA)

Assessment of computer based geologic mapping of rock units in the LANDSAT-4 scene of northern Death Valley, California 13 p2119 N85-23195

Geology: Structural history and fluvial geomorphology of the southern Death Valley Fault Zone, Inyo and San Bernardino Counties, California
24 p4114 N85-35506

DEBRIS
NT SPACE DEBRIS

Microfluorescence studies of zirconium oxide
[DE84-016116] 03 p0329 N85-12118

Debris control design achievements of the booster separation motors 06 p1096 N85-16942

On the latitudinal distribution of debris in the Northern Hemisphere of Mars 13 p2188 N85-23579

Marine Sample Exploitation Project: Estimates regarding the sensitivity and technology for the detection of nuclear explosion debris in the marine environment
[DE85-013176] 23 p3947 N85-34462

DEBUGGING
U CHECKOUT

DEBYE TEMPERATURE
U SPECIFIC HEAT

DECAMETRIC WAVES

The catalogue of the discrete sources in the declination range from -13 deg to -2 deg
[NASA-TM-77594] 01 p0129 N85-10887

Interferometry with decametric waves (review)
06 p0781 N85-14996

Analysis of Jovian decametric data: Study of radio emission mechanisms
[NASA-CR-174206] 08 p1258 N85-17917

Standing wave pattern of HF radio waves in the ionospheric reflection region. Part 1: General formulas
[UIO-SR-84-05-PT-1] 09 p1313 N85-18253

Three dimensional ray tracing of the Jovian magnetosphere in the low frequency range
[NASA-CR-175462] 10 p1571 N85-19909

Analysis of Jovian decametric data: Study of radio emission mechanisms
[NASA-CR-176057] 22 p3851 N85-33846

DECARBONATION

Shock-induced CO2 loss from CaCO3: Implications for early planetary atmospheres
[NASA-CR-174197] 05 p0745 N85-14777

DECARBURIZATION

Thermodynamics of decarburization of niobium-bearing high-alloy melts
[BLL-M-35728-(5828.4)] 02 p0175 N85-11169

Production process for steel with decarburized surface adapted for single coating enamelling
[BMFT-FB-T-85-022] 20 p3432 N85-31292

DECAY
NT ACOUSTIC EMISSION
NT ALPHA DECAY
NT BIOLUMINESCENCE
NT CATHODOLUMINESCENCE
NT CHEMILUMINESCENCE
NT CN EMISSION
NT ELECTROLUMINESCENCE
NT ELECTRON EMISSION
NT EMISSION
NT EXHAUST EMISSION
NT FIELD EMISSION
NT FLUORESCENCE
NT HALF LIFE
NT HYDROXYL EMISSION
NT INCANDESCENCE
NT ION EMISSION
NT LIGHT EMISSION
NT LUMINESCENCE
NT MICROWAVE EMISSION
NT NEUTRON DECAY
NT NEUTRON EMISSION
NT NUCLEAR FISSION
NT OPTICAL RESONANCE
NT PARTICLE EMISSION
NT PHOSPHORESCENCE
NT PHOTOELECTRIC EFFECT
NT PHOTOELECTRIC EMISSION
NT PHOTOIONIZATION

NT PHOTOLUMINESCENCE
NT PHOTOPRODUCTION
NT RADIO EMISSION
NT RADIOACTIVE DECAY
NT RESONANCE FLUORESCENCE
NT SECONDARY EMISSION
NT SHOCK WAVE LUMINESCENCE
NT SOLAR RADIO BURSTS
NT SOLAR RADIO EMISSION
NT SPECTRAL EMISSION
NT SPONTANEOUS EMISSION
NT STIMULATED EMISSION
NT STRANGENESS
NT THERMAL EMISSION
NT THERMIONIC EMISSION
NT THERMOLUMINESCENCE
NT TYPE 3 BURSTS
NT TYPE 4 BURSTS
NT WATER MASERS
NT WEAK ENERGY INTERACTIONS
NT X RAY FLUORESCENCE

Searching for top, Higgs, and supersymmetry: The minimum invariant mass technique
[DE84-014539] 01 p0119 N85-10813

The search for proton decay: Introduction
[DE84-014349] 01 p0131 N85-10904

Experimental medium energy physics
[DE84-014625] 02 p0278 N85-11807

Irregularity decay in an isolated plasma bubble
[AD-A145782] 03 p0392 N85-12506

Surface and allied studies in silicon solar cells
[NASA-CR-174447] 11 p1671 N85-20531

Simulating supersymmetry at the SSC
[DE85-000699] 11 p1736 N85-20917

Decaying particles do not heat up the Universe
[DE85-002191] 11 p1763 N85-21091

Nuclear structure problems in double beta decay
[DE85-010739] 19 p3364 N85-30659

Aircraft investigations of the distribution of aerosols in the lower troposphere 21 p3647 N85-32659

Application of evaluated fission-product delayed-neutron precursor data in reactor kinetics calculations
[DE85-012728] 23 p3972 N85-34624

Pulsed-neutron-source models for the astrophysical s-process
[DE85-012927] 24 p4151 N85-35740

High energy physics at Tufts University
[DOE/ER-40085/7] 24 p4152 N85-35744

On mini-cluster observed by Chacaltaya emulsion chamber experiment
[HE-3.6-12] 24 p4185 N85-35959

A study of atmospheric neutrinos with the IMB detector
[HE-5.3-7] 24 p4205 N85-36101

Energy spectra of high energy atmospheric neutrinos
[HE-5.3-14] 24 p4206 N85-36106

A standard source for high energy neutrino astronomy
[HE-5.3-15] 24 p4206 N85-36109

DECAY RATES

Velocity-changing collisional effects in nonlinear atomic spectroscopy and photon echo decay in gases
[NASA-CR-174159] 04 p0559 N85-13559

The stability of the low-degree 5-minute solar oscillations 14 p2444 N85-25084

Some nuclear data needs in astrophysics
[DE85-012916] 24 p4188 N85-35842

DECELERATION

NT SPIN REDUCTION

Laser cooling and trapping of neutral atoms
[AD-A146048] 03 p0366 N85-12345

Deceleration, cooling, and trapping of atoms
[AD-A146234] 03 p0418 N85-12672

Nondestructive deceleration of a rocket sled — target penetration tests
[FOA-C-20549-D3] 07 p0912 N85-15771

Optical flow and texture variables useful in detecting decelerating and accelerating self-motion
[AD-A148718] 09 p1384 N85-18703

Improving inflight negative Gz restraint for aircrewmen
[AD-A151909] 16 p2703 N85-26888

Why do leaky-box models work so fine?
[OG-7.2-8] 23 p4014 N85-34877

Instabilities in decelerating supersonic flows with applications to cosmic ray shocks
[OG-8.1-2] 23 p4017 N85-34892

Deceleration of a supersonic flow behind a curved shock wave with isentropic precompression
[NASA-TM-77920] 24 p4081 N85-35164

Applications of decelerated ions
[DE85-011832] 24 p4156 N85-35767

DECELERATORS

U BRAKES (FOR ARRESTING MOTION)

DECIDUOUS TREES

Changes in spectral properties of detached leaves
[E85-10042] 07 p0983 N85-16243

Effect of elevated atmospheric CO2 on plant communities
[DE85-001810] 11 p1678 N85-20576

Microwave model prediction and verifications for vegetated terrain
[E85-10102] 16 p2809 N85-27322

DECIMETER WAVES

Metric-wave and decimetric-wave aperture synthesis systems (review) 06 p0782 N85-14998

Decimetric-wave aperture synthesis system at Scientific Research Institute of Radiophysics
06 p0782 N85-15000

DECISION ELEMENTS

U LOGICAL ELEMENTS

DECISION MAKING

Hydrologic and economic models for watershed evaluation and research
[PB84-222371] 01 p0066 N85-10438

Some concepts in multi-criteria optimization
[CSIR-TWISK-299] 01 p0108 N85-10722

The inferring of preferences from indifferences in multicriteria decision analysis
[CSIR-TWISK-306] 01 p0108 N85-10729

Command control group behaviors. Objective 1: A methodology for and identification of command control group behaviors
[AD-A145690] 02 p0191 N85-11279

Robotics investment decision model user's manual
[AD-A145467] 02 p0204 N85-11347

Eyelid motion sequences predictive of decision errors
[AD-A145702] 02 p0235 N85-11531

Effects of alternative chromatic mixed graphics displays in decision support systems
[AD-A145561] 02 p0242 N85-11578

Artificial intelligence applications to automatic test equipment
[AD-P003936] 02 p0247 N85-11616

A mathematical theory of command and control structures
[AD-A145608] 02 p0256 N85-11675

Decision Support System (DSS): A survey
[NRIMS-TWISK-317] 02 p0292 N85-11896

Decision process models of contractor behavior: The development of effective contract incentives
[AD-A145524] 02 p0292 N85-11898

Research in knowledge representation for natural language understanding
[AD-A145807] 03 p0409 N85-12613

Psychological issues in the design of expert systems
[AD-A146081] 03 p0436 N85-12792

System status display information
[NASA-CR-172347] 04 p0455 N85-12889

Ocean services user needs assessment. Volume 1: Survey results, conclusions and recommendations
[NASA-CR-174104] 04 p0541 N85-13445

Analysis of the impact of error detection on computer performance
[NASA-CR-174167] 04 p0547 N85-13477

Evaluation of automated decisionmaking methodologies and development of an integrated robotic system simulation
[NASA-CR-172401] 04 p0552 N85-13516

Real-time planning by an intelligent robot
[DE84-016689] 04 p0553 N85-13519

Induction of fuzzy decision rules
[INPE-3053-PRE/474] 04 p0554 N85-13525

R and D project selection with nonnumerical returns
[INPE-2760-PRE/335] 04 p0575 N85-13665

Dynamic decision making — and programming
[FOA-C-53015-H2] 04 p0575 N85-13666

Utilization of historic information in an optimisation task 05 p0700 N85-14490

A model for the effectiveness of aircraft alerting and warning systems 05 p0702 N85-14506

On looking into the black box: Prospects and limits in the search for mental models 05 p0709 N85-14546

Issues in developing a normative descriptive model for dyadic decision making 05 p0709 N85-14547

Getting mental models and computer models to cooperate 05 p0709 N85-14548

A full mission simulator study of aircrew performances: The measurement of crew coordination and decisionmaking factors and their relationships to flight task performances 05 p0710 N85-14558

Communication on the flight deck
05 p0711 N85-14557

On choosing between two probabilistic choice sub-models in a dynamic multitask environment
05 p0711 N85-14563

Multi-crew model analytic assessment of landing performance and decision-making demands
05 p0712 N85-14567

A framework for research on adaptive decision aids
[AD-A138331] 05 p0734 N85-14719

Man-machine interface requirements - advanced technology 06 p0753 N85-14825

Critical conditions for the automatic control of landing from decision height in variable winds
[UTIAS-284] 06 p0753 N85-14

The application of artificial intelligence to contract management
[AD-A146881] 06 p0857 N85-1544

Survey relating to the implementation of cost/schedule control systems criteria within the Department of Defense and industry
[AD-A146864] 06 p0870 N85-15

Performance evaluation of A-10 aircraft maintenance units and aircraft using constrained facet analysis
[AD-A146955] 07 p0893 N85-15

Broadening the debate 07 p0914 N85-157

Distribution and storage of aviation turbine fuel for military operations in northern Australia
[AD-A147180] 07 p0935 N85-15

Ambiguity and uncertainty in probabilistic inference
[AD-A147378] 07 p1035 N85-165

Development of a mixed scanning interactive system for decision support
[AD-A146895] 07 p1051 N85-16

On the complexity of distributed decision problems
[AD-A147174] 07 p1052 N85-16

Principles of multiobjective optimization
[AD-A147520] 07 p1052 N85-16

Compatibility effects and preference reversals
[AD-A148399] 08 p1196 N85-1754

An application of discriminant analysis to the selection of software cost estimating models
[AD-A147632] 08 p1204 N85-175

Probable cause: A decision making framework
[AD-A147642] 08 p1210 N85-1761

A theory of preference reversals
[AD-A147952] 08 p1216 N85-17

An analysis of production competition and award methodology
[AD-A147775] 08 p1228 N85-177

Decision making in stressful conditions: A model based on the coping perspective
[FOA-C-55064-H3] 08 p1229 N85-177

Protocol for aquifer cleanup decision making at military installations
[AD-P004151] 09 p1349 N85-184

Communications satellite needs examined
10 p1476 N85-1931

A validated methodology for determination of laboratory instrument computer interface efficacy
[AD-A149338] 10 p1487 N85-19

Some effects of display format variables on the perception of aircraft spatial orientation
10 p1534 N85-19

A decision model for selection of microcomputers and operating systems
[AD-A149076] 10 p1536 N85-19

Efficient algorithm for fuzzy linear programming with multiple objectives
[AD-A149012] 10 p1544 N85-197

The R and D project selection problem with fuzzy coefficients
[INPE-3329-PRE/626] 10 p1565 N85-1987

Research needs on the interaction between information systems and their users: Report of a workshop
[PB85-121523] 10 p1566 N85-19

Development of computer centers, equipment described: Problems of computer centers
11 p1700 N85-20

Meteorological and oceanographic support during the Falklands conflict 11 p1712 N85-207

Data and information systems and decision making in large public organizations: Research agenda
[DE85-003639] 11 p1736 N85-20

Computer aided of maintainability design: A feasibility study
[AD-A149293] 11 p1738 N85-20

The effect of jamming/deception on decision making
[AD-A149740] 12 p1826 N85-2147

Automatic pickup of trajectory by method of sequential analysis taking into account deviation of radar markers from center of strobe 12 p1838 N85-215

Report on the Second Annual Review Meeting of the National Acid Precipitation Assessment Program. Research to assist decisionmaking: Summary
[DE85-003003] 12 p1864 N85-21

Choice reaction time and color: An annotated bibliography
[AD-A149722] 12 p1906 N85-21

A replication and extension of the inducement of the availability heuristic
[AD-A149755] 12 p1923 N85-22

A statistical approach to vendor selection
[AD-A149781] 12 p1950 N85-22

Task influences in the analytic-intuitive approach to decision making
[AD-A149870] 12 p1950 N85-22

Problems in decentralized decision making and computation
[AD-A150025] 12 p1950 N85-22251
Rejection of anomalous observations when determining spacecraft trajectories 13 p1979 N85-22421
Personal decision making: The influence of perceived locus of control and degree of rationality on information seeking strategies 13 p2167 N85-23446
Spaceborne power systems preference analyses. Volume 1: Summary
[NASA-CR-175644] 14 p2349 N85-24517
Spaceborne power systems preference analyses. Volume 2: Decision analysis
[NASA-CR-175645] 14 p2349 N85-24518
The integration of information from an analog-visual display: The role of dimensional integrality
[AD-A150756] 14 p2404 N85-24820
Gordon Conference on Fundamentals of Cybernetics
[AD-A151074] 14 p2406 N85-24842
Some applications of fuzzy sets and the analytical hierarchy process to decision making
[AD-A150720] 14 p2412 N85-24876
Preliminary helicopter design decision making based on flight performance factors
[AD-A151486] 15 p2471 N85-25254
A decision support methodology for space technology advocacy
[AD-A151695] 15 p2476 N85-25283
Computers and the consulting engineer
15 p2626 N85-26184
Equilibrium solutions, stabilities and dynamics of Lanchester's equations with optimization of initial force commitments
[AD-A151510] 15 p2637 N85-26286
Feasibility analysis of moving bank multiple model adaptive estimation and control algorithms
[AD-A152015] 15 p2641 N85-26292
Management: A bibliography for NASA managers
[NASA-SP-7500(19)] 15 p2664 N85-26439
Design adequacy: An effectiveness factor
16 p2695 N85-26642
Method of selecting robotized system design for pressing process 16 p2761 N85-27040
Diagnostic system
[INPE-3350-PRE/659] 16 p2841 N85-27519
Research in knowledge representation for natural language understanding
[AD-A152260] 16 p2851 N85-27579
Personal computer aided decision analysis
[AD-A151911] 16 p2875 N85-27743
Logical design of a decision support system to forecast technology, prices and costs for the national communications system
[AD-A152330] 17 p2948 N85-28198
The effects of controversy and concurrence seeking on effective decision making
[AD-A153370] 17 p3002 N85-28555
The interface with decision makers in interactive multiobjective linear programming
[REPT-84-38] 17 p3014 N85-28637
On estimating transition intensities of a Markov process with aggregate data of a certain type
[CWI-MS-R8411] 17 p3025 N85-28707
Multicriteria decision analysis as an aid to strategic planning of energy research and development
[REPT-84-02] 17 p3049 N85-28870
Hybrid uncertainty theory
[DE85-008357] 18 p3167 N85-29622
Accepting error to make less error
[AD-A153949] 18 p3171 N85-29651
The economics of private sector R and D decisionmaking in aeronautics
[NASA-CR-176007] 19 p3379 N85-30962
Interactive on-line conferences
[AD-A154723] 21 p3574 N85-32227
Search of the VAXintosh customizing VMS V4.0 for DCL windows
[DE85-011306] 22 p3831 N85-33729
Real-time multiparameter pulse processing with decision tables
[DE85-011683] 23 p3966 N85-34589
Opportunities for policy historians: The evolution of the US civilian space program 23 p4057 N85-35147
Manual and computer-aided sequential diagnostic inference
[AD-A156229] 24 p4133 N85-35620
DSS/MIS (Decision Support Systems/Management Information Systems) design and implementation for LAMPS Mk 3 utilizing a microcomputer and a maintenance personnel assignment program
[AD-A156252] 24 p4135 N85-35629

DECISION THEORY
NT STATISTICAL DECISION THEORY
A combined logistic regression and Zionts-Wallenius methodology for multiple criteria linear programming
[[illegible]-314] 01 p0102 N85-10679

Research activities of the Illinois University Coordinated Science Laboratory
[AD-A145589] 03 p0449 N85-12656
Theory of information, automation in Czechoslovakia
04 p0485 N85-13091
Interaction of human cognitive models and computer based models in supervisory control
[AD-A142547] 07 p1020 N85-16474
Principles of multiobjective optimization
[AD-A147520] 07 p1052 N85-16679
A method for automatic water mass classification
[AD-D011405] 08 p1191 N85-17505
Compatibility effects and preference reversals
[AD-A148399] 08 p1198 N85-17544
Decentralized control of scheduling in distributed systems
[AD-A147688] 08 p1228 N85-17731
Strategic use of business graphics: A stakeholder approach 23 p3963 N85-34566

DECISIONS
Eyelid motion sequences predictive of decision errors
[AD-A145702] 02 p0235 N85-11531

DECKS (FLOORS)
U FLOORS

DECLINATION
The catalogue of the discrete sources in the declination range from -13 deg to -2 deg
[NASA-TM-77594] 01 p0129 N85-10887
Absolute measurement of Declination (D) by means of a proton magnetometer
[DMI-GEOPHYS-PAPERS-R-68]
22 p3836 N85-33751

DECODERS
Digital raster timing encoder-decoder
[AD-D011279] 06 p0804 N85-15120
Precision digital sampler
[AD-D011285] 06 p0809 N85-15143
Novel applications of the NASA/GSFC Viterbi decoder hardware simulator 08 p1101 N85-16957
Reed-Solomon decoder — applicable to Galileo Project requirements
[NASA-CASE-NPO-15982-1] 11 p1699 N85-20680
Stereo decoder without subcarrier restoration
13 p2068 N85-22921
A software simulation study of a sequential decoder using the Fano algorithm 16 p2771 N85-27100
A software simulation study of a (255,223) Reed-Solomon encoder-decoder
[NASA-CR-175872] 17 p2947 N85-28192
Noiseless coding for the Gamma Ray spectrometer
[NASA-CR-176201] 24 p4069 N85-35219

DECODING
Severe weather statistics STADTS decoder (SXW) and plotter (SWY)
[PB84-213693] 01 p0086 N85-10576
Sequential syndrome decoding of convolutional codes
05 p0624 N85-13992
Standard SHEF (Standard Hydrometeorologic Exchange Format) decoder Version 1.1
[PB85-106508/GAR] 06 p0840 N85-15332
Coding for reliable satellite communications
[NASA-CR-174315] 08 p1150 N85-17257
The algebraic structure of convolutional codes with application to code construction and decoding
[AD-A148770] 08 p1206 N85-17591
FLAD user's manual: FLAD file contents
[AD-A148700] 09 p1368 N85-18594
Further results on rate 1/N convolutional code constructions with minimum required SNR criterion
10 p1464 N85-19235
Fundamental limits to synchronization and tracking
[AD-A149623] 12 p1833 N85-21504
Experimental results on the application of convolutional coding and Viterbi decoding as a frequency diversity technique in HF data transmission
[CRC-1377] 13 p2052 N85-22850
A perspective on multiaccess channels
[AD-A150183] 13 p2146 N85-23322
Symbol stream combining in a convolutionally coded system 16 p2771 N85-27101
Proust radar: Decoding hardware and coherent integration, part 7.2A 21 p3626 N85-32524
L-step sequential decoding
[AD-A156121] 24 p4138 N85-35649
Pruned error-trellis decoding of certain non-systematic convolutional codes
[AD-A156122] 24 p4138 N85-35650

DECOMPOSITION
NT CRACKING (CHEMICAL ENGINEERING)
NT HYDROGENOLYSIS
NT NITROLYSIS
NT PHOTODECOMPOSITION
NT PHOTODISSOCIATION
NT PHOTOLYSIS
NT RADIOLYSIS
NT THERMAL DECOMPOSITION
HMX combustion modification
[AD-A145071] 01 p0024 N85-10149
Theoretical studies in molecular fragmentation: Processes, energetics and diagnostics
[AD-A146310] 03 p0418 N85-12673
Deformation, fracture and explosive properties of reactive materials
[AD-A146396] 06 p0774 N85-14945
Metallo-Organic Decomposition (MOD) silver metallization for photovoltaics 06 p0830 N85-15278
Electrochemical production of silicon
06 p0832 N85-15290
The formation of isolated phase precipitates during the decomposition of high-coercive force Fe-Cr-Co alloys
[BLL-M-36028-(5828.4)] 07 p0924 N85-15855
Multiplex gas chromatography for use in space craft
[NASA-TM-86668] 09 p1290 N85-18097
Development of a polysilicon process based on chemical vapor deposition of dichlorosilane in an advanced Siemen's reactor
[NASA-CR-174445] 11 p1672 N85-20532
TEM/FIM study of modulated microstructures in the Fe-Be system
[DE85-005379] 13 p2023 N85-22678
Decomposition of VTAN alloy solid solution upon irradiation and thermal aging 13 p2029 N85-22712
Algorithm for singular decomposition
[DE85-016488] 13 p2152 N85-23361
Decomposition in problem of correcting inertial navigation systems 14 p2287 N85-24172
Solving large linear systems 14 p2396 N85-24759
Photovoltaic cell reliability research: Investigation of accelerated stress factors and failure-degradation mechanisms in terrestrial solar cells
[NASA-CR-175815] 16 p2819 N85-27388
A decomposition procedure for convex quadratic programs
[AD-A151732] 16 p2854 N85-27595
The decomposition of gas phase formaldehyde by plasma discharge
[AD-A153202] 17 p2921 N85-28007
Methanol adsorption on Pt(111)
[DE85-006802] 17 p2923 N85-28017
Powder-metallurgy alloys and steels
[BLL-BISI-TRANS-22239-(9022.06)]
17 p2926 N85-28050
Comparison of isothermal kerogen decomposition results using reactors with different heat-up rates
[DE85-008563] 19 p3237 N85-30068
Fundamental studies of beta phase decomposition modes in titanium alloys
[AD-A154122] 19 p3238 N85-30078
Method for production of ceramic oxide and carbide bodies by polymer inclusion and decomposition
[DE85-011668] 19 p3250 N85-30152
Decomposition of sulfuric acid using solar thermal energy
[DE85-012268] 21 p3564 N85-32170
Decomposing the joint distribution of several linear combinations of uniform spacings
[AD-A155056] 21 p3677 N85-32845

DECOMPRESSION
U PRESSURE REDUCTION

DECOMPRESSION SICKNESS
Hyperbaric physiology (status and prospects)
08 p1194 N85-17521
A theoretical method for selecting space craft and space suit atmospheres
[AD-A148219] 08 p1200 N85-17559
Assessing the short- and long-term health effects of decompression sickness among US Navy divers
[AD-A151887] 15 p2616 N85-26132

DECONTAMINATION
Characterization of jet-contaminant interaction flow in chemical decontamination
[AD-A147298] 08 p1161 N85-17327
Remedial action of hazardous waste US Army Corps of Engineers, Anniston, Alabama
[AD-P004141] 09 p1347 N85-18477
Incineration of explosives contaminated soils
[AD-P004142] 09 p1347 N85-18478
Stabilization of contaminated soils by in situ vitrification
[AD-P004144] 09 p1348 N85-18480
Community relations activities at Department of Defense sites
[AD-P004150] 09 p1349 N85-18486
Protocol for aquifer cleanup decision making at military installations
[AD-P004151] 09 p1349 N85-18487
Development of a Persistent Chemical Agent Simulator System (PCASS)
[NASA-CR-175776] 16 p2745 N85-26938
Ventilation flow: Submerged
18 p3156 N85-29545

TRU decontamination of high-level PUREX waste by solvent extraction using a mixed octyl(phenyl)-N,N-diisobutyl-carbamoyl methylphosphine oxide/TBP/NPH (TRUEX) solvent
[DE85-010251] 19 p3235 N85-30054
Method for removing chlorine compounds from hydrocarbon mixtures
[DE85-011606] 22 p3742 N85-33191

DECOUPLING
Practical considerations for noninteracting control synthesis
[AD-A150130] 12 p1918 N85-22046
Frequency/period estimation and adaptive rejection of periodic disturbances
[AD-A149229] 15 p2632 N85-26226
A modern control design methodology with application to the CH-47 helicopter
[AD-A151946] 16 p2710 N85-26723
On the choice of coordinates for semiconductor simulation
[AD-A152214] 16 p2670 N85-27708
On the dependence of the convergence of Gummel's algorithm on the regularity of the solution
[AD-A154628] 21 p3675 N85-32632

DECOYS
Pyrophoric alkylaluminum compounds in decoy flares
[FOA-C-20562-E4] 18 p3076 N85-29039

DECREMENTING
U REDUCTION

DEEP SPACE
NT INTERPLANETARY SPACE
NT INTERSTELLAR SPACE
A FORTRAN program for deep space sensor analysis
[AD-A151700] 15 p2489 N85-25366

DEEP SPACE NETWORK
The Telecommunications and Data Acquisition Report
[NASA-CR-174149] 05 p0622 N85-13980
Submilliarcsecond VLBI using compact close pairs of radio sources: Error analysis 05 p0622 N85-13981
VLBI solutions for the time variation of DSN baselines: 1978 - 1983 05 p0623 N85-13983
The performance of differential VLBI delay during interplanetary cruise 05 p0623 N85-13984
Development and testing of a 20-kW X-band transmitter with high phase stability 05 p0623 N85-13985
Superconducting NbTi and Pb(Cu) bandpass filters 05 p0623 N85-13986
Mark IVA DSN 26-meter subnet 05 p0624 N85-13995
64-meter to 70-meter antenna extension 05 p0624 N85-13996
Antenna microwave subsystem 05 p0625 N85-13997
VLBI system (BLK I) IF-video down conversion design 05 p0625 N85-13998
The Telecommunications and Data Acquisition Report
[NASA-CR-174366] 10 p1462 N85-19224
Arcsecond positions for milliarcsecond VLBI nuclei of extragalactic radio sources. Part 3: 74 sources 10 p1463 N85-19225
Microwave surface resistivity of several materials at ambient temperature 10 p1463 N85-19226
Subreflector focusing techniques applied to new DSS-15 and DSS-45 34-meter antennas 10 p1464 N85-19233
The Venus Balloon Project 10 p1465 N85-19243
DSN 34-meter antenna optics analysis for wideband SETI investigations 10 p1465 N85-19244
Activities of the Jet Propulsion Laboratory, 1 January - 31 December 1983
[NASA-CR-175555] 13 p2167 N85-23447
Consultative Committee for Space Data Systems. Panel 1: Support
[NASA-CR-175786] 16 p2769 N85-27090
The Telecommunications and Data Acquisition Report
[NASA-CR-175842] 16 p2770 N85-27094
Maintenance of time and frequency in the DSN using the global positioning system 16 p2771 N85-27105
Network information management subsystem 16 p2771 N85-27106
Determining availability characteristics of DSN data systems using discrepancy report data 16 p2772 N85-27109
Performance analysis of the DSN baseband assembly (Bba) Real-Time Combiner (RTC)
[NASA-CR-175876] 17 p2946 N85-28190
Performance analysis of the DSN baseband assembly (Bba) Real-Time Combiner (RTC)
[NASA-CR-175877] 17 p2947 N85-28193
Maintenance of time and frequency in the Jet Propulsion Laboratory's Deep Space Network using the Global Positioning System 18 p3109 N85-29249
Using GPS and VLBI technology to maintain 14 digit synchronization 18 p3109 N85-29250
Publications of the Jet Propulsion Laboratory 1983
[NASA-CR-175979] 18 p3199 N85-29848

DEEP WELL INJECTION (WASTES)
Rock mechanics: Issues and research needs in the disposal of wastes in hydraulic fractures
[DE85-001399] 10 p1556 N85-19609
Office of Civilian Radioactive Waste Management
[DE85-012585] 22 p3639 N85-33774

DEER
Deer control using 7 strand vertical fence 11 p1581 N85-19958

DEFECTS
NT AUDITORY DEFECTS
NT CRYSTAL DEFECTS
NT CRYSTAL DISLOCATIONS
NT EDGE DISLOCATIONS
NT INCLUSIONS
NT POINT DEFECTS
NT SCREW DISLOCATIONS
NT SURFACE DEFECTS
NT VACANCIES (CRYSTAL DEFECTS)
Effects of member imperfections on the behavior of space trusses 02 p0207 N85-11363
Hydrogen passivation of electrically active defects in crystalline silicon solar cells
[DE84-004590] 02 p0223 N85-11461
Application of positron annihilation in materials science
[DE84-014733] 02 p0288 N85-11883
Weld metal solidification cracking in a carbon-manganese steel 03 p0330 N85-12126
Identification of pulse-echo rays in austenitic steels
[AERE-R-11265] 03 p0369 N85-12356
A comparison of methods for predicting ductile crack growth instability
[AERE-R-11199] 03 p0374 N85-12387
Newer carbon fibers and their properties 04 p0465 N85-12955
On the origins of structural defects in BF2(+)-implanted and rapid thermally annealed silicon: Conditions for defect free regrowth
[DE84-016060] 04 p0572 N85-13650
Vandenberg space shuttle launch complex
[S-HRG-98-1075] 05 p0601 N85-13833
Statement of Edward C. Aldridge, Jr., Under Secretary of the Air Force, Department of the Air Force, accompanied by Lieutenant General Robert W. Bazley, Inspector General and Brigadier General Donald J. Kutyna, Director of Space Systems and Command, Control and Communications, Deputy Chief of Staff, Research, Development and Acquisition 05 p0601 N85-13834
The detection and assessment of defects in automatic ultrasonic inspection
[BLL-RISLEY-TR-4597-(9091.9F)] 05 p0647 N85-14150
Impact of NDE unreliability on pressure vessel fracture predictions
[DE84-015586] 05 p0647 N85-14151
A review of imperfection sensitivity of stiffened shells
[AD-A147311] 07 p0978 N85-16213
Ultrasonic measurements, X-ray photographs and image processing
[BLL-RISLEY-TR-4586-(9091.9F)] 07 p1037 N85-16583
Built-in-test for first line testing 08 p1064 N85-16739
Holographic FLI for detection of defects
[AD-A148339] 08 p1164 N85-17345
Experimental verification of eddy-current flaw theory
[DE85-001288] 09 p1329 N85-18350
Modeling of real UT transducer field/flaw interactions
[DE85-000341] 09 p1329 N85-18351
Interaction between a crack and a soft inclusion
[NASA-CR-172533] 10 p1495 N85-19439
Stress studies in EFG
[NASA-CR-174441] 10 p1508 N85-19515
Estimating deformability upon pressing of aluminum alloys based on results of mechanical testing 11 p1598 N85-20049
Collapse and removal of discontinuities in joint zone during diffusion welding 11 p1602 N85-20077
Effect of macrostructure on durability of polycrystalline graphite 11 p1605 N85-20091
Infrared-thermal wave scanner for NDE of naval thermal spray coatings
[DE85-002237] 11 p1650 N85-20391
Effect of input distributions on the probabilistic fracture mechanics analysis of reactor pressure vessels
[DE85-000632] 11 p1652 N85-20403
Requirements of quantitative NDE in developing fracture control plans
[DE85-003147] 11 p1654 N85-20415
Aerostructure nondestructive evaluation by thermal field detection. Phase 2: Technique refinement and quantitative determination of flaw detection capabilities
[AD-A149622] 12 p1777 N85-21155
Reliability of structural brittle materials 12 p1946 N85-22222
Influence of welding defects at melting boundary on static strength of welded joint in large-diameter pipe 13 p2033 N85-2278
NDE methods for green ceramics
[DE85-004019] 13 p2036 N85-2278
Shape optimization for minimal stress concentration 13 p2101 N85-2280
Estimating defectiveness buildup during service in metal of welded runner in low-pressure cylinder of turbine 14 p2271 N85-2407
Effects of primary recoil energy on the production rate of mobile defects during elevated temperature irradiation
[DE85-006218] 15 p2511 N85-2548
Echo-response from crack-like two-dimensional reflectors in focused ultrasonic fields. Ultrasonic crack tip method for the determination of crack depth
[BLL-BISI-22062-(9022.06)] 16 p2796 N85-2723
Predicting fully plastic mode 2 crack growth from an asymmetric defect
[AD-A152227] 16 p2801 N85-2729
An analysis for axially compressed orthotropic shells with a multimode imperfection representation
[VTH-LR-422] 16 p2803 N85-2723
The statistical analysis of initial imperfection measurements — shell profiles
[VTH-LR-442] 16 p2857 N85-2762
Interaction among inhomogeneities and inclusions
[AD-A153114] 17 p2979 N85-2841
Specifics of fine structure of pressed aluminum alloys, manufactured by plasma atomization 19 p3242 N85-30102
Reliability of welds to repair defects in cast components made from CrMoV steel
[BLL-CE-TRANS-8054-(9022.09)] 20 p3461 N85-31501
Experimental and theoretical assessment of a new technique for the non-destructive evaluation of laminated panels
[AD-A155622] 21 p3562 N85-32155
Defects in tetrahedrally coordinated amorphous semiconductors
[AD-A155150] 21 p3581 N85-3225
Reliability of void detection in structural ceramics using scanning laser accustic microscopy
[NASA-TM-87035] 21 p3597 N85-32337

DEFENSE COMMUNICATIONS SATELLITE SYSTEM
US MILSATCOM: Present and future 11 p1709 N85-20753
Integrated support of tactical operations by satellite communications 11 p1709 N85-20754
EHF MILSATCOM systems for tactical users 11 p1709 N85-20755

DEFENSE COMMUNICATIONS SYSTEM (DCS)
DCS (Defense Communications System) network synchronization design criteria
[AD-A146251] 03 p0356 N85-1228
Integrated defense communications system antijamming antenna system
[AD-D011423] 08 p1154 N85-1728
Transmission Monitoring and Control (TRAMCON) segmentation plan for the DCS (Defense Communications System) digital transmission network
[AD-A154175] 20 p3440 N85-31351
Deep reconditioning of batteries during DSCS 3 flight operations 20 p3446 N85-31357

DEFENSE INDUSTRY
The US machine tool industry and the defense industrial base
[PB84-216928] 01 p0036 N85-1022
Companies participating in the Department of Defense Subcontracting Program, first three quarters fiscal year 1984
[AD-A146137] 03 p0436 N85-12775
Survey relating to the implementation of cost/schedule control systems criteria within the Department of Defense and industry
[AD-A146664] 06 p0670 N85-1535
The evolution of the U.S. helicopter industry
[AD-A154290] 19 p3211 N85-2981

DEFENSE METEOROLOGICAL SATELLITE PROGRAM
U DMSP SATELLITES

DEFENSE PROGRAM
DOD related software technology requirements, practices, and prospects for the future
[AD-A145493] 02 p0242 N85-1157
Companies participating in the Department of Defense Subcontracting Program, first three quarters fiscal year 1984
[AD-A146137] 03 p0436 N85-12775
On estimating the cost growth of weapon systems
[AD-A147297] 08 p1230 N85-1774
Proceedings of the Environmental Systems Symposium (13th) held at Bethesda, Md., 20-22 March 1984
[AD-A148194] 09 p1346 N85-1847

Community relations activities at Department of Defense sites
[AD-P004150] 09 p1349 N85-18486

Department of defense, office of inspector general semiannual report to the Congress, 1 April - 30 September 1984
[AD-A149560] 10 p1567 N85-19679

Air Force Office of Scientific Research (AFOSR) technical report summaries. Third quarter (CY)
[AD-A149965] 10 p1573 N85-19916

PRC journal discusses 'Star Wars' space program
11 p1621 N85-20207

Military applications of meteorological satellite (METSAT) data 11 p1711 N85-20767

Program manager: The Journal of the Defense Systems Management College. Volume 13, Number 6, November-December 1984
[AD-A149546] 11 p1739 N85-20933

Fiscal year 1986 technical objective document
[AD-A151039] 14 p2432 N85-25000

Militarization of space activity in United States
15 p2488 N85-25360

Defense data network support concept analysis
[AD-A153214] 17 p3016 N85-28649

The Department of Defense statement on the Science and Technology Program by Colonel Donald I. Carter, USAF Acting Deputy Under Secretary of Defense for Research and Advanced Technology before the Subcommittee on Research and Development of the Committee on Armed Services of the United States House of Representatives, 99th Congress, first session
[AD-A152467] 17 p3046 N85-28850

Rome Development Center Air Force technical objective document C3I FY-86
[AD-A152476] 17 p3047 N85-28851

The revolution in military affairs and the Soviet system
[AD-P004568] 17 p3048 N85-28863

Selected university laboratory needs in support of national security
[AD-A153511] 18 p3197 N85-29633

Improving the defense energy information system (DEIS)
[AD-A153524] 18 p3200 N85-29649

Proceedings of the Electronic Test Equipment Division's Annual Program Review of Electronic Test Equipment Industry Response to Emerging Defense Requirements
[AD-A154455] 20 p3436 N85-31320

Evaluation of a software design approach: Develop a threat resolution module in Ada (trademark)
[AD-A155599] 21 p3672 N85-32815

The flow of scientific and technical information in the US Army Research Laboratories
[AD-A155050] 21 p3713 N85-33043

DoD Value Engineering conference report. Value Engineering (VE): A tool that benefits line management. Part 4, Workshop B: VE on spare parts
[AD-A156070] 24 p4163 N85-35813

DoD Value Engineering conference report. Value Engineering (VE): A tool that benefits line management. Part 7, Workshop E: VE in construction and architect engineer contracts
[AD-A156073] 24 p4164 N85-35816

DEFINITION

Fracture detection and characterization for geothermal reservoir definition
[DE85-008677] 22 p3815 N85-33630

DEFLAGRATION

Hazard Studies for Solid Propellant Rocket Motors
[AGARD-CP-367] 08 p1114 N85-17025

Review of USAF treatment of solid propellant rocket motor hazards 08 p1114 N85-17027

Analysis of Deflagration to Shock to Detonation Transition (DSDT) in porous energetic solid propellants
08 p1115 N85-17030

Penguin warhead safety tests
08 p1115 N85-17031

Study of the transition from deflagration to detonation of previously fragmented propellants
08 p1115 N85-17032

Transient combustion: An important consideration in deflagration-to-detonation transition
08 p1116 N85-17037

The DDT process for high energy propellants
08 p1116 N85-17038

Shock and impact response of solid rocket propellants: Experimental and theoretical 08 p1116 N85-17040

The pressure deflagration limit of solid rocket propellants 08 p1117 N85-17046

Analysis of deflagration to detonation transition in high-energy solid propellants
[AD-A148302] 08 p1135 N85-17156

Transition to detonation from rapid-compression (ramp-waves) generated in a burning porous bed
[AD-P004345] 10 p1455 N85-19169

A thermal-mechanical model of deflagration-to-detonation in granular energetic materials
[AD-P004346] 10 p1455 N85-19170

A summary of the mechanism of delayed detonation
[AD-P004347] 10 p1455 N85-19171

Analysis of Shock to Detonation Transition (SDT) of porous high energy propellant from ramp-wave compression loading
[AD-A149333] 10 p1457 N85-19180

Analysis of deflagration to detonation transition in high-energy solid propellants 16 p2757 N85-27010

Combustion-deflagration-detonation transition in a confined spherical powder
[ISL-R-108/84] 22 p3747 N85-33223

Behavior of the porous bed in a combustion-deflagration-detonation transition
[ISL-CO-220/84] 22 p3747 N85-33224

Combustion-deflagration-detonation transition
[ISL-CO-221/84] 22 p3747 N85-33225

DEFLATING

U INFLATABLE STRUCTURES
U PRESSURE REDUCTION

DEFLECTION

Three programs for evaluating bending moments, deflections and shear forces in simply-supported uniform bridge decks under South African NA loading: NAB, NAD and NAS. NITRR manual P13
[ISBN-0-7988-2263-X] 01 p0102 N85-10681

Initial sailplane project: The RP-1
04 p0468 N85-12976

Second sailplane project: The RP-2
04 p0468 N85-12977

Influence of relaxation on the mechanical characteristics of a carbon-epoxy composite. Report no. 45.427/1
04 p0468 N85-12980

Large transverse deflections of circular plates loaded symmetrically
[NPL-DMA(A)-86] 04 p0512 N85-13262

Encapsulation design analysis
06 p0829 N85-15268

Determination of shear coefficient of a general beam cross section by finite element method
09 p1338 N85-18413

Advanced ion thruster research
[NASA-CR-174862] 10 p1430 N85-19021

Deflection model of a CT4-A undercarriage
[AD-A149778] 12 p1777 N85-21156

Photo-thermal detection of the onset of photo-chemical nucleation (laser-snow) in vapor
[AD-A150111] 12 p1801 N85-21295

Along-track deflection of the vertical from SEASAT: GEBCO (General Bathymetric Chart of the Oceans) overlays
[PB85-129641] 12 p1876 N85-21767

Horizontal deflection TS-257
13 p2069 N85-22926

Load carrying capacity of double circular arc gears
14 p2221 N85-23776

A feasibility study for using low boiling point fluids to change aircraft tire deflection
[AD-A152096] 16 p2706 N85-26701

Analysis of elastoplastic grids under conditions of variable loads
[REPT-16/1984] 16 p2797 N85-27242

Quasi-steady vibrations of a rotating shaft grazing an obstacle: Spiral vibration
[BLL-CE-TRANS-7962-(9022.09)]
16 p2799 N85-27256

Finite element thermal-structural analysis of cable-stiffened space structures
[AD-A153822] 18 p3066 N85-28963

Yield stress determination from miniaturized disk bend test data
[DE85-009495] 18 p3122 N85-29330

Large deflections of a cantilever beam under arbitrarily directed tip load
[NASA-TM-86442] 19 p3284 N85-30363

Shear deflection in a three-point bend beam of a solid circular cross-section
[AD-A154458] 19 p3287 N85-30381

Optical beam deflection detection of thermal waves in opaque solids 19 p3374 N85-30927

A comparison of electronic heterodyne moire deflectometry and electronic heterodyne holographic interferometry for flow measurements
[NASA-TM-87071] 21 p3588 N85-32302

Basic formulas for the computation of the deflection of the vertical from astronomical star observations
[AD-A154912] 21 p3605 N85-32390

Galactic antiprotons of 0.2-2 GeV energy
[OG-6.1-11] 22 p3888 N85-34101

DEFLECTORS

NT BLAST DEFLECTORS

Precision electrooptical deflector based on corrugated light guide 07 p0950 N85-16020

Optimization of piezoceramic optical deflector
11 p1719 N85-20813

Flameholder with integrated air mixer
[AD-D011549] 12 p1776 N85-21161

DEFOCUSING

Artificial defocusing lens in ionosphere
05 p0724 N85-14654

Defocusing losses in a log periodic-fed reflector
[AD-A151616] 15 p2547 N85-25722

DEFORESTATION

Relationship between forest clearing and biophysical factors in tropical environments: Implications for the design of a forest change monitoring approach — Costa Rica
[E85-10051] 07 p0963 N85-16247

The water balance and climate — Amazon region
07 p1003 N85-16370

The Amazon and climate 07 p1003 N85-16376

Deforestation, floodplain dynamics, and carbon biogeochemistry in the Amazon Basin
08 p1144 N85-17216

DEFORMATION

NT AXIAL STRAIN
NT ELASTIC BENDING
NT ELASTIC BUCKLING
NT ELASTIC DEFORMATION
NT NUCLEAR DEFORMATION
NT PLASTIC DEFORMATION
NT STATIC DEFORMATION
NT TENSILE DEFORMATION
NT WAVE FRONT DEFORMATION

Deformation measurements of composite multi-span beam shear specimens by Moire interferometry
[NASA-CR-3844] 02 p0169 N85-11135

Microstructure and deformation aspects of some specialty steels and hard metals
02 p0176 N85-11182

Deformations and strains in adhesive joints by moire interferometry
[NASA-CR-172474] 02 p0185 N85-11238

Vertical crustal movements in southern California, 1974 to 1978
[GS-CIRC-905] 02 p0228 N85-11491

High temperature deformation of hot-pressed polycrystalline orthoenstatite
[NASA-CR-174026] 02 p0285 N85-11861

Study of deformation and fracture of AMg6N weldable aluminum alloy by method of acoustic emission
03 p0352 N85-12266

Penetrator/armour interactions: Background to Australian work
[MRL-R-936] 03 p0367 N85-12353

Deformation mechanisms associated with mesoscopic kinkbands, Jura Mountains (Switzerland) and Chaines Subalpines (France) 03 p0389 N85-12492

Cavitation phenomenon in superplastic creep
[DE84-015484] 04 p0513 N85-13271

Structural observations in the Circle quadrangle, Yukon-Tanana Upland, Alaska 04 p0517 N85-13298

Improved apparatus and techniques for high temperature and pressure deformation of crystalline materials
[DE84-016049] 04 p0569 N85-13629

Multiaxial yield behavior of 1100 aluminum following various magnitudes of prestrain
[DE84-013904] 05 p0617 N85-13949

Experimental investigation and analysis of oscillations of thin-walled spherical shell during pulse loading
05 p0725 N85-14662

Creep of chemically vapor deposited SiC fibers
[NASA-TM-86897] 06 p0763 N85-14878

Deformation, fracture and explosive properties of reactive materials
[AD-A146396] 06 p0774 N85-14945

Process Modeling Applied to Metal Forming and Thermomechanical Processing
[AGARD-LS-137] 06 p0796 N85-15086

Flow-based analyses of metal deformation processes: An overview 06 p0796 N85-15087

Prediction of forming limit diagrams for deep drawing
06 p0796 N85-15089

The role of microstructure in the modelling of plastic flow in P/M superalloys at forging temperatures and strain rate 06 p0796 N85-15090

Control of microstructure during hot working of Ti-6242 06 p0797 N85-15091

Numerical methods in metalforming
06 p0797 N85-15092

Modeling microstructural changes during hot rolling of steels 06 p0798 N85-15096

Tests of the load-bearing and deformation behaviour of reinforced concrete spherical shells under point loading
[BLL-RISLEY-TR-4550-9091.9F)]
06 p0816 N85-15182

Modelling of deformation and fracture in high-temperature structural materials
[DE84-016906] 06 p0818 N85-15191

Analysis of the impact of a deformable missile model on a deformable obstruction
[BLL-RISLEY-TR-8534-(9091.9F)]
06 p0859 N85-15459
Strain analysis of the Leoville chondrite and conditions in asteroidal interiors 06 p0885 N85-15620
Special features of the deformation of molybdenum at high temperatures
[BLL-M-36027-(5828.4)] 07 p0924 N85-15856
Stereo Electro-optical Tracking System (SETS)
[NASA-CR-172471] 07 p0962 N85-16098
The influence of strain rate and porosity on the deformation and fracture of titanium and nickel
[AD-A148670] 08 p1130 N85-17123
On a general nonlinear theory of plates and shells: Formulation and applications 08 p1172 N85-17387
The response of metallic structures to dynamic loading 08 p1172 N85-17389
Modeling of large-scale accretionary wedge and thin-skinned trust-and-fold belt mechanics
08 p1181 N85-17442
Nonlinear analysis of composite laminates
09 p1268 N85-18067
Deformation and fracture of P/M (Powder/Metallurgy) titanium alloys
[AD-A148672] 09 p1294 N85-18126
Large deformations of a nonlinear elastic solid and the diffusion of an ideal fluid treated as interacting continua
09 p1330 N85-18356
Direct energy minimization approach to whipping analysis of pressure hulls 09 p1335 N85-18393
Light scattering studies of lower dimensional colloidal particle and critical fluid systems
[DE85-002087] 09 p1377 N85-18654
Cavitation phenomenon in superplastic creep
[DE85-001716] 10 p1441 N85-19083
Study of superplastic alloys based on Al-Zn-Ca
10 p1442 N85-19092
Mechanical properties of Be-Al composite
10 p1443 N85-19094
Spreading upon compacting of fiber composite materials with porous metal matrix 10 p1443 N85-19096
Behavior and specifics of fracture of porous fiber materials in extension 10 p1447 N85-19118
Influence of extension rate on strength and deformation characteristics of titanium alloys over a broad temperature range 10 p1448 N85-19121
Mechanisms of damage accumulation in time-dependent cyclic deformation
[DE85-001004] 10 p1496 N85-19443
Simple higher-order theory for laminated composite plates
[NASA-CR-174421] 10 p1496 N85-19445
Study of tectonic earthquake precursors by geodetic methods 10 p1502 N85-19479
Estimating deformability upon pressing of aluminum alloys based on results of mechanical testing
11 p1598 N85-20049
Evaluation of features of reinforcing fibers by testing bundles 11 p1599 N85-20059
Effect on work-hardening in dynamic deformation of beryllium
[DE85-002691] 11 p1608 N85-20111
China report: Science and technology
[JPRS-CST-84-025] 11 p1620 N85-20197
Micro-deformation of quartz under dynamic action and its applications 11 p1620 N85-20201
A new rheological model for concrete structural analysis
[DE84-014743] 11 p1653 N85-20413
A three-dimensional geometric-physical model for conventional geodetic observations-observables, parameter estimation, and deformation analysis
[SER-C-298] 11 p1665 N85-20493
Advanced stress analysis methods applicable to turbine engine structures
[NASA-CR-175573] 12 p1778 N85-21165
Algorithm for the simulation of transient viscoelastic flows with free surfaces
[DE85-002713] 12 p1848 N85-21590
An orthogonal grid technique for studying internal deformation and energy absorption in target penetration
[AD-A149989] 12 p1860 N85-21665
Fracture toughness of materials
[DE85-004306] 12 p1867 N85-21713
Summary of recent research on mechanical behavior of polycrystalline solids
[DE85-004801] 12 p1942 N85-22199
Structures of ordered linear dislocation multipoles in Cu-Al alloys
[ISSN-0379-6906] 13 p2021 N85-22664
Temperature effects of heterogenizated annealing on structure and properties of V95 aluminum alloy
13 p2025 N85-22692
High temperature antifriction properties of Ti sub 1-sub xNb sub x C sub 0.5N sub 0.5 alloys
13 p2029 N85-22715
Specifics of structure and mechanical properties of metastable beta-titanium alloys after deformation and aging 13 p2032 N85-22731
Densification and deformation in the presence of a liquid phase
[DE85-005101] 13 p2038 N85-22763
On Hybrid and mixed finite element methods
[NASA-CR-175551] 13 p2101 N85-23096
Normal-fault and fold development in sedimentary rocks above a pre-existing basement normal fault
13 p2131 N85-23259
Theoretical and experimental investigation of mechanically fastened composites
[AD-A150961] 14 p2248 N85-23935
Cast-iron technology: Metallographic and mechanical testing results
[DE85-002684] 14 p2257 N85-23984
Influence of short-range order on deformation mechanisms in solid solutions
[DE85-006374] 14 p2258 N85-23989
Thermal deformation of flexible rotors in friction bearings 14 p2260 N85-24123
Cutting structural materials in vacuum
14 p2286 N85-24165
Systematic and random deformations of orbits of long-period comets 15 p2479 N85-25299
Study of structural changes of dual-phase titanium alloy during shock wave loading 15 p2498 N85-25408
Possible use of rapid heating for improving mechanical properties of titanium alloys 15 p2498 N85-25409
Effect of aluminum on nature of titanium alloy failure
15 p2498 N85-25411
Structure and mechanical properties of dispersion-hardened nickel alloy joints welded by diffusion 15 p2500 N85-25422
Effectiveness of use of heat-dissipating clamps to reduce deformation during argon arc welding of thin sheets of AMg6 alloy 15 p2501 N85-25427
Summary of recent investigations of the mechanical properties of polycrystalline solids
[DE85-006776] 15 p2511 N85-25492
Reflection and transmission of flexural waves at discontinuities 15 p2572 N85-25861
Design of shear deformable antisymmetric angle-ply laminates to maximize the fundamental frenquency and frequency separation
[CSIR-TWISK-333] 15 p2577 N85-25892
Estimation of the depth of a spherical cap in an hydraulic drawing test for some simple conditions of loss of stability
[REPT-4/1984] 16 p2748 N85-26956
Tooth wear in worm gears in vacuum
16 p2766 N85-27070
Optimal modeling with a minimum of local distortion
[REPT-18/1984] 16 p2797 N85-27243
Finite axisymmetric deformation of a thin shell of revolution 16 p2798 N85-27251
Principles of wave formation along web of H-beams
[BLL-M-36041-(5828.4)] 16 p2798 N85-27253
Full statistical characteristics of microdeformation
[BLL-M-36076-(5828.4)] 16 p2798 N85-27254
Nonlinear equations for dynamics of pretwisted beams undergoing small strains and large rotations
[NASA-TP-2470] 16 p2799 N85-27256
Constitutive cyclic deformation behavior in single-crystal and directionally solidified SSME high-pressure fuel turbopump airfoil materials 17 p2914 N85-27965
Preparation of metal for cold upsetting
[BLL-BISI-TRANS-22383-(9022.06)]
17 p2926 N85-28043
Study on mechanism of surface deformation induced by stress corrosion cracking
[BLL-BISI-TRANS-21896-(9022.06)]
17 p2928 N85-28066
Temperature and manganese content dependences of tensile deformation in iron-high manganese binary alloys
[DE85-007656] 17 p2932 N85-28098
Investigations of the material factors in the adiabatic shearing of steels
[AD-A153084] 17 p2979 N85-28418
Interfacial segregation and fracture
[DE85-009779] 18 p3075 N85-29019
Studies of strain rate effects in the deformation of solids by means of stress pulses and ultrasonic methods
[DE85-009463] 18 p3122 N85-29329
A state variable approach to transient creep deformation in stress reduction experiments
[DE85-009492] 18 p3122 N85-29331
Measurement and calculation of the mechanical response of a highly fractured rock
[DE85-008421] 18 p3127 N85-29362
Deformable mirror nearest neighbor optical computer
18 p3166 N85-29772
Effect of matrix composition on steel fiber reinforced concrete properties 19 p3230 N85-30
Deformation, fracture and explosive properties of reactive materials
[AD-A154073] 19 p3251 N85-30
Residual stress distributions in (plastically) surface deformed two-phase materials 19 p3263 N85-30
Fundamental studies related to failure of adhesively bonded structures
[AD-A154072] 19 p3265 N85-30
Interferometric creep testing
[AD-A154249] 19 p3266 N85-30
Influence of error of determination of moire [illegible] orders on the stability of their approximation
[BLL-M-36277-(5828.4)] 20 p3450 N85-314
Determination of local deformation during explosive welding
[BLL-M-36279-(5828.4)] 20 p3462 N85-315
Determination of deformation speed during high-speed deformation of cylindrical shells
[BLL-M-36280-(5828.4)] 20 p3465 N85-315
Indentation fractography: A measure of brittleness
[PB85-179059] 20 p3473 N85-315
Machining-induced deformation in stepped specimens of PH 13-8 Mo, 18 nickel maraging steel grade [illegible] and grain-refined HP 9-4-20
[NASA-CR-172450] 21 p3565 N85-3217
Bubble dynamics in polymer solutions undergoing shear
[AD-A154575] 21 p3568 N85-321
The effect of mould size on the exothermic reaction and compressive strength of epoxy resin chocks
[AD-A155102] 21 p3570 N85-322
A comparison of electronic heterodyne moire deflectometry and electronic heterodyne holographic interferometry for flow measurements
[NASA-TM-87071] 21 p3588 N85-32
Development of improved dynamic failure models
[AD-A155586] 21 p3600 N85-32
Local epi-continuity and local optimization
[AD-A154812] 21 p3677 N85-32
Microstructure-mechanical property relationships in the transformation-toughened ceramics
[DE85-011946] 22 p3752 N85-33
Stresses and deformations in cross-ply composite tubes subjected to a uniform temperature change: Elasticity and Approximate Solutions
[NASA-CR-176147] 22 p3800 N85-33
Crustal Dynamics Project: Catalogue of site information
[NASA-TM-86218] 22 p3801 N85-33
Deep-burial diagenesis in carbonates
[DE85-011224] 22 p3802 N85-33
Discontinuous deformation analysis
[DE85-011208] 22 p3814 N85-33
SANCHO: A finite element computer program for the quasistatic, large deformation, inelastic response of two-dimensional solids
[DE85-011456] 22 p3829 N85-3371
Effects of hot deformation on the kinetics of the pearlite transformation in eutectoid steel
[BLL-M-35844-(5828.4)] 23 p3913 N85-34
Phase transformations taking place in austenitic steel during deformation at different rates
[BLL-M-35875-(5828.4)] 23 p3914 N85-34
Inertial stresses and deformations in mechanisms
23 p3924 N85-34
Scaling differences between large interplate and intraplate earthquakes
[NASA-CR-176149] 23 p3948 N85-344
On the potential link equation of a spot centre with relative deformation for a semi-infinite molecular crystal
[BLL-M-35795-(5828.4)] 23 p3985 N85-3471
Solid-state co-extrusion of nylon 6 gel
[AD-A156187] 24 p4082 N85-35
Strain measurement using point recognition picture processing
[DRIC-T-7407] 24 p4101 N85-354
Response of a BWR Mark 2 containment vessel head to loads beyond the design basis
[DE85-010524] 24 p4103 N85-354
Geology: Structural history and fluvial geomorphology of the southern Death Valley Fault Zone, Inyo and San Bernardino Counties, California
24 p4114 N85-35
Structural development of the west-central Grant Range, Nye County, Nevada 24 p4115 N85-35
Three-dimensional finite deformation viscoelastic model accounting for damage effects
[DE85-012951] 24 p4139 N85-35

DEGASSING
NT DEOXYGENATION
Working medium for sorption heat pumps
[BLL-T6360/BG/WH785/84] 06 p0807 N85-151
Degassification of silicon nitride powders of various origins 13 p2030 N85-227

Chemical composition and kinetics of libration of gases upon welding of aluminum alloys
19 p3247 N85-30131
The degassing history of the Earth: Noble gas studies of Archaean cherts and zero age glassy submarine basalts 21 p3718 N85-33072
Terrestrial Xe isotopic contraints on the early history of the Earth 22 p3652 N85-33652
Evacuate and backfill apparatus and method
[DE85-006018] 23 p3938 N85-34411
DEGENERATION
A study of degenerate and nondegenerate critical points in three-dimensional flow fields
[DFVLR-FB-84-36] 11 p1633 N85-20288
On some physical impurity properties of doped-indirect gap semiconductors at low and intermediate concentrations
[INPE-3452-PRE/704] 16 p2869 N85-27701
DEGENERATIVE FEEDBACK
U NEGATIVE FEEDBACK
DEGRADATION
NT BIODEGRADATION
NT THERMAL DEGRADATION
Mechanisms of syncrude-synfuel degradation
[DE84-015206] 01 p0034 N85-10212
Material degradation in heavy steel plates caused by bending with a laser
[AD-A144784] 01 p0052 N85-10343
Theoretical analysis of physical processes of lasing medium degradation in semiconductor lasers
02 p0269 N85-11759
Boron-nitrogen polymers. 1: Mechanistic studies of borazine pyrolyses
[AD-A146470] 06 p0771 N85-14933
Storage stability of jet fuels
[AD-A146360] 06 p0773 N85-14943
Investigation of accelerated stress factors and failure/degradation mechanisms
06 p0832 N85-15295
Interactions of hydrazine and of hydrazine derivatives with soil constituents and with soils
[AD-A148475] 08 p1122 N85-17074
Design of an evaluation system to measure performance degradation due to continuous operations
[AD-A148188] 08 p1200 N85-17558
Reliability studies of ceramic capacitors
[AD-A149126] 10 p1479 N85-19338
Investigation of accelerated stress factors and failure/degradation mechanisms in terrestrial solar cells
[NASA-CR-175469] 10 p1510 N85-19524
Evaluation of infrared reflectance as a technique for measuring absorber materials degradation
[PB85-108486] 11 p1677 N85-20567
Degradation mechanisms in ceramic dielectrics
[AD-A149791] 12 p1813 N85-21369
Radiation effects induced in pin photodiodes by 40- and 85-MeV protons
[NASA-CR-175678] 14 p2426 N85-24960
Surface degradation of ductile metal in elevated temperature gas-particle streams
[DE85-008428] 18 p3074 N85-29017
Study of Kapton under simulated shuttle environment
[NASA-CR-176003] 19 p3225 N85-29997
Theoretical modeling of laser induced optical degradation
[AD-A155302] 21 p3592 N85-32323
Topics in electrochemical degradation of photovoltaic modules 21 p3608 N85-32410
Accelerated stress factors and failure/degradation mechanisms in terrestrial solar cells
21 p3613 N85-32451
Induction motors with minimum waste of magnetic iron
22 p3772 N85-33377
Solar maximum: Solar array degradation
[NASA-TM-86194] 23 p3903 N85-34175
Degradation mechanisms and accelerated aging test design
[TI85-003251] 23 p3940 N85-34420
DEGREES OF FREEDOM
Three degree of freedom steady state point performance program: Updated version 1
[CSIR-NIAST-83/48] 01 p0001 N85-10005
Direct numerical simulation of curved turbulent channel flow
[NASA-TM-85974] 02 p0197 N85-11316
Autonomous momentum management for space station
[NASA-CR-174065] 04 p0462 N85-12931
Direct numerical simulation of curved turbulent channel flow 05 p0635 N85-14072
Effect of aerodynamic and angle-of-attack uncertainties on the May 1979 entry flight control system of the Space Shuttle from Mach 8 to 1.5
[NASA-TP-2365] 07 p0913 N85-15776
Optimum design for nonlinear shock mounts for transient inputs
09 p1334 N85-18390
Modal analysis of structural systems involving nonlinear coupling 09 p1337 N85-18409
Discrete modifications to continuous dynamic structural systems 09 p1337 N85-18410
An alignment fixture for a 2-Degree-of-Freedom (TDF) gyroscope
[AD-A148885] 10 p1422 N85-18969
Condensed antenna structural models for dynamics analysis 10 p1463 N85-19230
A numerical approach for the vibration analysis of an axisymmetric shell structure with a nonuniform edge constraint
[AD-A149288] 11 p1651 N85-20402
Time marching numerical solution of the dynamic response of nonlinear systems
[NAF-AN-25] 12 p1865 N85-21696
Two degree-of-freedom flutter solution for a personal computer
[NASA-TM-86381] 13 p1971 N85-22379
Cyclic industrial robots with mechanical energy storing devices: Multipositional system with one or several degrees of freedom 13 p2045 N85-22803
Design of tightening device and calculation of forces in manipulator transmissions with base-drive mounted
13 p2046 N85-22804
Approximate rules for signal detection against background of Gaussian correlated interference
13 p2086 N85-23027
Motion planning with six degrees of freedom
[AD-A150312] 13 p2165 N85-23432
Controllable movements of elastic manipulator with three degrees of freedom 14 p2266 N85-24040
Investigation of the time history and model responses of some simple linear and nonlinear systems
[DE85-002027] 14 p2321 N85-24344
Simulator study of the stall departure characteristics of a light general aviation airplane with and without a wing-leading-edge modification
[NASA-TM-86309] 15 p2470 N85-25250
Manipulation and simulation of general robots using the zero-position description 15 p2567 N85-25838
Ritz procedure for COSMIC/NASTRAN
15 p2575 N85-25877
On the interconnection of incompatible solid finite element meshes using multipoint constraints
15 p2575 N85-25879
Elastic-workhardening SDF (Single-Degree-of-Freedom) system subjected to random blast excitations
[AD-A151866] 15 p2579 N85-25909
Dispersion sensitivity of the eight inch advanced ramjet munitions technology projectile due to wind and minor thrust errors
[AD-A152145] 16 p2727 N85-26835
Boson degrees of freedom in Fermion many-body systems
[DE85-006997] 16 p2863 N85-27660
Electroweak interactions in nuclei
[DE85-007811] 17 p3033 N85-28762
Quantum model of dephasing-enhanced laser desorption: Master equation approach
[AD-A153769] 18 p3112 N85-29269
Ground-based and in-flight simulator studies of flight characteristics of a twin-fuselage passenger transport airplane during approach and landing
[NASA-TP-2451] 23 p3898 N85-34144
Identification and control of structures in space
[NASA-CR-176175] 24 p4069 N85-35214
On mini-cluster observed by Chacaltaya emulsion chamber experiment
[HE-3.6-12] 24 p4185 N85-35959
DEHUMIDIFICATION
Performance of the SERI parallel-passage dehumidifier
[DE85-000509] 11 p1672 N85-20536
High performance solar desiccant cooling system: Performance evaluation and research recommendations
[DE85-000508] 11 p1676 N85-20559
Solid desiccant dehumidification systems for residential applications
[PB85-198489] 22 p3755 N85-33279
DEHYDRATION
Voluntary dehydration and electrolyte losses during prolonged exercise in the heat
[AD-A145157] 01 p0095 N85-10639
Effects of restricted water intake on performance in a cold environment
[AD-A146904] 07 p1015 N85-16450
Thermoregulatory responses during exercise at graded hypohydration levels
[AD-A147733] 08 p1195 N85-17528
Preparing Alberto Salazar for the heat of the 1984 Olympic Marathon
[AD-A150942] 14 p2389 N85-24714
Exercise-heat strain during hypohydration: Interaction with heat acclimation and aerobic fitness
[AD-A151023] 14 p2389 N85-24717
Effects of dehydration or cold exposure and restricted fluid intake upon cognitive performance
[AD-A151973] 16 p2842 N85-27525
Plasma hormonal responses at graded hypohydration levels during exercise/heat stress
[AD-A153681] 18 p3153 N85-29523
Transport properties of Topopah Spring tuff
[DE85-010448] 19 p3270 N85-30276
Heat injury: Prevention is the key
[AD-A153734] 1[illegible] p3328 N85-30622
Thirst and fluid intake following graded hypohydration levels in humans
[AD-A156201] 24 p4132 N85-35615
DEHYDROGENATION
Biochemical evaluation of bodily influence of high and low temperatures 07 p1014 N85-16441
Catalytic conversion of C3-C4 paraffins to gasoline
[DE85-004181] 10 p1458 N85-19187
Mechanistic and kinetic studies of the elementary processes in catalytic combustion of methane
[PB85-186308] 20 p3435 N85-31314
DEICERS
To take off and to land safely, Hoechst 1678 for ice and snow free runways 05 p0595 N85-13791
Salt action on concrete
[AD-A147812] 07 p0933 N85-15912
Electro-expulsive separation system
[NASA-CASE-ARC-11613-1] 18 p3094 N85-29150
Land vehicle corrosion management
22 p3750 N85-33246
DEICING
To take off and to land safely, Hoechst 1678 for ice and snow free runways 05 p0595 N85-13791
Analytical and physical modeling program for the NASA Lewis Research Center's Altitude Wind Tunnel (AWT)
[NASA-TM-86919] 07 p0909 N85-15757
Official on Soviet research in deicing techniques
15 p2460 N85-25191
DEICING SYSTEMS
U DEICERS
DEIMOS
Structure and origin of Martian satellites
15 p2463 N85-25323
DEKATRONS
U COUNTERS
DELAMINATING
Study of delamination cracking under static and cyclic loads of carbon-epoxy composite materials
[REPT-42-727/F] 03 p0327 N85-12102
Characterization of interlaminar crack growth in composites with the double cantilever beam specimen
04 p0463 N85-12942
Characterizing delamination resistance of toughened resin composites 04 p0464 N85-12943
Composite materials characterization and development at AFWAL 04 p0464 N85-12944
Free-edge failures of composite laminates
04 p0467 N85-12971
On the effects of delamination damage in fibre composite laminates
[ARL/STRUC-R-403] 06 p0763 N85-14881
Delamination growth in graphite epoxy laminates under compressive loads 09 p1288 N85-18088
Fracture mechanics analysis and prediction of delamination growth in composite structures
[FFA-TN-1984-45] 09 p1289 N85-18092
Forced corrosion tests of construction components of passenger aircraft fuselages 11 p1600 N85-20062
Stress distribution of fiberglass reinforced plastic beam with a delamination under three-point bending
23 p33[illegible] N85-34210
Damage induced stress redistribution in composite laminates 24 p4072 N85-35235
Damage mechanisms in damaged CFRP laminates
24 p4074 N85-35249
Computational techniques for fiber reinforced components 24 p4075 N85-35250
DELAWARE
Contamination of the fetch-limited directional wave spectrum by waves emanating from an embayment
[NASA-TM-84441] 15 p2604 N85-26048
DELAWARE BAY (US)
Analysis of suspended sediment distributions in the surface waters of Delaware Bay using remote sensing of optical properties 15 p2582 N85-25926
DELAY
One-dimensional two-phase constant lag flow in combustion chamber of solid propellant rocket motors
[AD-A145679] 02 p0173 N85-11157
Machine computation of delay and capacitance of transistor structures of subnanosecond large integrated circuits 04 p0490 N85-13120

A group delay standard for the MHz frequency range 05 p0630 N85-14040

Measurements of pilot time delay as influenced by controller characteristics and vehicles time delays 05 p0701 N85-14500

Transmission scheduling to reduce convex delay costs in packet networks [AD-A148451] 08 p1153 N85-17278

Analysis of the performance of multiaccess networks of the bus type [FUB-47-1983] 09 p1313 N85-18249

The effects of cooling on delay-time limits in IC's 14 p2297 N85-24224

On the equivalent bilinearization of nonlinear controlled delay systems [RR-272] 20 p3519 N85-31880

Aviation system delays [S-HRG-98-1241] 21 p3553 N85-32102

FAA requirements for model to support capacity, delay, noise and energy programs [AD-A155815] 24 p4063 N85-35179

DELAY CIRCUITS

Programmable synchronous digital delay line [AD-D011382] 07 p0945 N85-15985

Probabilistic analysis of combinational circuits with random delays 19 p3257 N85-30192

DELAY LINES

Radio frequency probing apparatus for surface acoustic wave devices [AD-D011230] 01 p0050 N85-10327

Magnetostatic wave frequency analyzer apparatus [AD-D011249] 05 p0631 N85-14044

Analog to digital converter [AD-D011338] 07 p0945 N85-15983

Programmable synchronous digital delay line [AD-D011382] 07 p0945 N85-15985

Improved magnetic bias and delay linearity in a magnetostatic wave delay line [AD-D011441] 10 p1479 N85-19337

Dynamics of adaptive signal corrector 13 p2071 N85-22940

Diffraction of periodic grounding system of finite length 13 p2081 N85-22994

A digital contour-corrector for a high-definition TV camera [NHK-LABS-NOTE-311] 19 p3254 N85-30179

Energizing arrangement for charge coupled device control electrodes [AD-D011712] 19 p3261 N85-30220

Optical 3-D signature device for detecting chemical agents [AD-D011669] 19 p3272 N85-30293

DELETION

Analysis of accretion and deletion at boundaries in dynamic scenes [AD-A145944] 03 p0419 N85-12678

DELIVERY

NT PAYLOAD DELIVERY (STS)
NT WEAPONS DELIVERY

Research on knowledge delivery [AD-A149565] 10 p1538 N85-19698

DELPHI METHOD (FORECASTING)

A description of a logistically ideal aircraft [AD-A148425] 08 p1084 N85-16866

DELTA DART AIRCRAFT

U F-106 AIRCRAFT

DELTA FUNCTION

Wake fields and wake field acceleration [DE85-008054] 17 p3031 N85-28750

DELTA WINGS

On vortex bursting [NASA-TM-77587] 01 p0002 N85-10008

Prediction of aerodynamic characteristics of fighter wings at high angles of attack [AD-A145107] 01 p0003 N85-10017

Force and moment measurements on a 74 deg delta wing with an apex flap [NASA-CR-166081] 02 p0134 N85-10918

The lateral-directional characteristics of a 74-degree Delta wing employing gothic planform vortex flaps [NASA-CR-3848] 03 p0311 N85-12009

Flow calculation on a thin wing, with specific attention to separation point at the trailing edge [FTW-FO-1721] 05 p0594 N85-13787

Exploratory investigation of the aerodynamic characteristics of a biwing vehicle at Mach 20.3 [NASA-TM-86314] 08 p1113 N85-17021

A visual study of a delta wing in steady and unsteady motion [AD-P004158] 09 p1264 N85-17943

Experimental investigation of a breakdown criterion for a vortex in an incompressible flow — delta wing [ONERA-RT-27/1147-AY] 11 p1577 N85-19035

Unsteady flows around 3-dimensional wings [AD-A149993] 12 p1772 N85-21124

A calculation of slender delta wing with leading-edge separation by quasi-vortex-lattice method 12 p1821 N85-21423

Stability of vortex structures during separation flow past array of wings 14 p2278 N85-24110

An exploratory study of apex fence flaps on a 74 deg delta wing [NASA-CR-172463] 15 p2463 N85-25208

Investigation of the Vortex Tab [NASA-CR-172586] 15 p2463 N85-25209

Flow past a flat plat with a vortex/sink combination [JIAA-TR-58] 15 p2464 N85-25215

Conical stagnation points in the flow around an external corner --- delta wings [VTH-LR-396] 16 p2701 N85-26680

Lee-side flow over delta wings at supersonic speeds [NASA-TP-2430] 19 p3212 N85-29921

Experimental and theoretical study of the longitudinal aerodynamic characteristics of delta and double-delta wings at Mach numbers of 1.60, 1.90, and 2.16 [NASA-TP-2433] 19 p3213 N85-29922

China has developed a new version of fighter aircraft [AD-A155293] 21 p3555 N85-32118

Vortex boundary-layer interactions [NASA-CR-176192] 24 p4093 N85-35373

DELTAS

NT MISSISSIPPI DELTA (LA)

Study of Volga river delta using space photosurvey materials 15 p2485 N85-25340

Sand dispersion from an ephemeral river delta on the wave-dominated central California coast [AD-A154352] 19 p3300 N85-30458

Mapping of dynamics of deltas by space photography 22 p3737 N85-33163

Depositional systems and coal occurrence in the Fort Union Formation (Paleocene), Powder River Basin, Wyoming and Montana 24 p4114 N85-35505

DEMAGNETIZATION

Magnetic method of inspecting mechanical properties of general purpose tubes [BLL-M-36084-(5828.4)] 16 p2796 N85-27235

DEMAND (ECONOMICS)

Demand for satellite-provided domestic communications services up to the year 2000 [NASA-TM-86894] 06 p0798 N85-15009

Satellite provided customer promises services, a forecast of potential domestic demand through the year 2000. Volume 4: Sensitivity analysis [NASA-CR-174662] 16 p2769 N85-27092

DEMAND ASSIGNMENT MULTIPLE ACCESS

Integrated support of tactical operations by satellite communications 11 p1709 N85-20754

DEMINERALIZING

NT BONE DEMINERALIZATION

DEMODULATION

Carrier acquisition and tracking by a COSTAS loop with automatic frequency control [ESA-TT-838] 04 p0493 N85-13149

Acoustooptic demodulation of frequency-modulated signals 13 p2090 N85-23050

Source energy spectra from demodulation of solar particle data by interplanetary and coronal transport [SH-1.3-13] 23 p3994 N85-34756

DEMODULATORS

NT MODEMS
NT PHASE DEMODULATORS
NT PHASE LOCK DEMODULATORS

Digital signal demodulators with single-sideband 07 p0950 N85-16019

Performance of the DSA's subcarrier demodulation digital loop 10 p1465 N85-19242

Noise tolerance of digital demodulator for complex signal system employing binary quantization 13 p2070 N85-22929

Digital Optical Circuit Technology [AGARD-CP-362] 18 p3185 N85-29757

DEMOGRAPHY

Characteristics of recent science/engineering graduates, 1982: Detailed statistical tables [PB85-149060] 15 p2663 N85-26437

Experience of the Institute of Space Research with the use of remote sensing in urban planning studies [INPE-3159-PRE/533] 16 p2880 N85-27770

An empirical comparison of the accuracy of univariate and multivariate corrections for range restriction [AD-A153071] 17 p3019 N85-28670

On estimating transition intensities of a Markov process with aggregate data of a certain type [CWI-MS-R8411] 17 p3025 N85-28707

DEMONSTRATION

U PROVING

DEMULTIPLEXING

Interference immunity of fiber-optic communication lines with spectral multiplexing of channels 13 p2069 N85-22924

DENDRITIC CRYSTALS

New metallurgical processes based on high-spee crystallization and diffusion of metals 01 p0021 N85-101

Hydrogen passivation of electrically active defects i crystalline silicon solar cells [DE84-004590] 02 p0223 N85-11461

Large-area sheet task advanced dendritic web growt development [NASA-CR-174021] 02 p0223 N85-11463

Microstructure development in polymers [AD-A145960] 03 p0337 N85-12170

Dynamic crystallization of silicate melts [NASA-CR-174103] 05 p0743 N85-14774

Development of high-efficiency solar cells on silico web [NASA-CR-174212] 06 p0628 N85-1525

Advanced dendritic web growth development 06 p0631 N85-1528

The growth of metastable peritectic compounds [NASA-CR-171289] 07 p0920 N85-1582

Characterization of terrestrial solar cells for spac applications: Electrical characteristics of thi Westinghouse dendritic web cells as a function of sol intensity, temperature, and incidence angle [NASA-CR-175642] 14 p2349 N85-2451

Solid/melt interface studies of high-speed silicon shee growth [NASA-CR-175698] 14 p2350 N85-2452

Influence of solidification parameters on the formatio of the gamma-M7C3 eutectic structure of 2% C-12%C steel 15 p2512 N85-2550

Dendritic growth from amorphous matrix [DE85-007630] 16 p2871 N85-2771

Role of hydrogen and structure on CMSX-2 17 p2915 N85-2796

Electrical and structural characterization of web dendrit crystals 20 p3481 N85-3163

Silicon dendritic web growth 21 p3611 N85-3243

Temperature-stress modeling 21 p3611 N85-3243

Silicon ribbon stress-strain activities 21 p3611 N85-3243

Analysis of stress-strain relationships in silicon ribbon 21 p3611 N85-3243

Advanced module development overview 21 p3612 N85-3244

DENDRITIC DRAINAGE

U DRAINAGE PATTERNS

DENDROCHRONOLOGY

Solar modulation of cosmic ray intensity and solar fla events inferred from (14)C contents in dated tree ring [SH-7.1-2] 23 p4047 N85-350

High precise measurements of cosmogenic radiocarbon abundance by complex of scintillation equipments [SH-7.1-14] 23 p4048 N85-3510

Radiocarbon content in the annual tree rings during la 150 years and time variation of cosmic rays [SH-7.1-15] 23 p4048 N85-3510

DENITROGENATION

Denitrification-efficiencies of alternate carbon source [AD-A148029] 08 p1119 N85-1705

DENMARK

The climate of Denmark. Summaries of observation from light vessels. 3: Sea temperature [ISBN-87-7478-215-0] 01 p0073 N85-1048

Space research in Denmark 08 p1231 N85-1775

Finnair, LOT, SAS reps in USSR on present operation plans 09 p1278 N85-180

Siting of large scale wind turbines in Denmark 24 p4111 N85-3548

DENSE PLASMAS

NT PLASMA FOCUS
NT STRONGLY COUPLED PLASMAS

Ion-density correlations and enhancement o thermonuclear reaction rate in dense, inertially confine fusion plasmas 02 p0284 N85-1184

Many-body correlations in strongly-coupled plasmas 02 p0284 N85-118

Compact toroid development, activity plan fo spheromaks [DE84-016736] 04 p0567 N85-1361

A research proposal for the theoretical study of th thermodynamic and transport properties of dens plasmas [AD-A148040] 08 p1224 N85-1770

X-ray spectroscopy of high-Z and high-dens plasmas 09 p1387 N85-1872

Extended abstract: Ergodic magnetic limi experiments on TEXT with a 7/3 resonance [DE85-001390] 09 p1391 N85-187

X-ray line broadening of a diagnostic in laser produ plasma [DE85-001179] 10 p1560 N85-198

Numerical analysis of thermonuclear detonation in den plasma 11 p1719 N85-208

Adequacy of metal ablation process with laser radiation and a shock-compressed plasma
13 p2028 N85-22706
Basic studies. 1: Basic experiments in plasma physics 15 p2655 N85-26378
Basic experiments in plasma physics (TPL)
15 p2655 N85-26379
Direct electron and ion fluid computation of high electrostatic fields in dense inhomogeneous plasma with subsequent nonlinear optical and dynamical laser interaction 15 p2656 N85-26386
Restrike particle beam experiments on a dense plasma focus. Opening switch research on a dense plasma focus
[AD-A152991] 17 p3039 N85-28802
Slow tearing modes: Transitions to instability
20 p3534 N85-31989

DENSIFICATION
A strategy for the adjustment and analysis of densification networks — geodetic networks
[SER-C-295] 01 p0063 N85-10420
Sub-eutectic densification and second phase formation in Al2O3 - CaO
[DE85-002065] 09 p1398 N85-18796
Densification of submicron YSZ (Yttria-Stabilized Zirconia) powders with alumina and borate additives
[AD-A149520] 10 p1452 N85-19150
Densification and deformation in the presence of a liquid phase
[DE85-005101] 13 p2038 N85-22763
Computational methods for the explosive and impact compaction of powders
[AD-A156219] 24 p4139 N85-35653

DENSIMETERS
X-ray gauge measures areal density variations as small as 0.1%
[DE85-003774] 12 p1854 N85-21629

DENSITOMETERS
NT MICRODENSITOMETERS
Compact L-edge densitometer for uranium concentration assay
[DE85-010344] 18 p3110 N85-29261
Applied research and development for falling-sphere air density measuring systems
[AD-A155227] 21 p3552 N85-32099

DENSITY
On the modified likelihood for density estimation
[AD-A149437] 10 p1547 N85-19758
Profile of a relativistic electron beam propagated through a linear wiggler and an axial guide field
[AD-A154403] 19 p3353 N85-30783

DENSITY (MASS/VOLUME)
NT ATMOSPHERIC DENSITY
NT GAS DENSITY
NT SPACE DENSITY
Study of bridgewire size and pyrotechnic density relationships on all-fire levels
[DE84-016946] 09 p1302 N85-18177
Compaction of sand using ordinary off-road vehicles
[AD-P004297] 09 p1409 N85-18874
Investigation of structure-permeability relationships of silicone polymer membranes
[PB85-148476] 11 p1596 N85-20036
Field validation of statistically-based acceptance plan for bituminous airport pavements. Volume 3: Statistical analysis of 3 methods for determining maximum specific gravity of bituminous concrete mixtures
[FAA-PM-84-12-VOL-3] 12 p1781 N85-21182
Field validation of statistically-based acceptance plan for bituminous airport pavements. Volume 4: Computer simulation of multiple acceptance criteria
[FAA-PM-84-12-VOL-4] 12 p1782 N85-21183
Simple EOS for the silicone rubber Sylgard 184
[DE85-001394] 12 p1814 N85-21376
Models of the upper atmosphere
12 p1945 N85-22217
More precise curve of dependence between density and velocity of longitudinal waves in consolidated crust and top of mantle in oceanic structures
13 p2110 N85-23143
Crustal and upper mantle density model of Owen fault zone 13 p2110 N85-23144
Determination of density of the crust and upper mantle from deep seismic sounding and gravimetry, 2
13 p2111 N85-23153
The effect of particle density on aeolian transport
13 p2189 N85-23581
Pressure-density behavior for AlN, Al2O3, SiO2, TiB2, and TiC powders up to 3.5 GPa
[DE85-006146] 14 p2261 N85-24012
Density and thermal expansion measurements of several mixed oxide glasses in the solid and liquid regions
[DE85-006134] 14 p2261 N85-24014
Trends of petroleum fuels
[DE85-000116] 14 p2263 N85-24023
Characterization-curing-property studies of HBRF 55A resin formulations
[NASA-CR-175836] 16 p2753 N85-26989
Distribution of density in closed-impression die forging of axisymmetrical products from metal powders
19 p3245 N85-30118
Density characteristics of asthenosphere in Atlantic Ocean 19 p3294 N85-30423
Haze over eastern North America. Part 1: Haze properties
[PB85-181857] 19 p3311 N85-30526
Pycnometer shaker
[PB85-174985] 20 p3460 N85-31491
An investigation into the fluidization and heat transfer of low density particles in a fluidized bed with applications
[AD-A155259] 21 p3584 N85-32282
A safe, high-power-density lithium battery
[AD-A155223] 21 p3613 N85-32454
Buoyant densities of phototrophic sulfur bacteria and cyanobacteria 21 p3660 N85-32740
Optimization of design parameters for alternating current stabilizer based on magnetic suspension
22 p3772 N85-33374
The influence of temperature on the composition density of the transition metals
[BLL-M-35896-(5826.4)] 23 p3915 N85-34262
Comparison of experimental data on detonation velocity and Chapman-Jouget pressure vs initial HE density with predictions from Ree's model equation of state
[DE85-007266] 23 p3922 N85-34304
Transports studies of ECH and ICRH-heated bumpy torus plasma in NBT-1M 23 p3978 N85-34662

DENSITY (NUMBER/VOLUME)
NT CARRIER DENSITY (SOLID STATE)
NT ELECTRON DENSITY (CONCENTRATION)
NT ELECTRON DENSITY PROFILES
NT ELECTRON DISTRIBUTION
NT ION DENSITY (CONCENTRATION)
NT IONOSPHERIC ELECTRON DENSITY
NT IONOSPHERIC ION DENSITY
NT MAGNETOSPHERIC ELECTRON DENSITY
NT MAGNETOSPHERIC ION DENSITY
NT MAGNETOSPHERIC PROTON DENSITY
NT PACKING DENSITY
NT PARTICLE DENSITY (CONCENTRATION)
NT PLASMA DENSITY
NT PROTON DENSITY (CONCENTRATION)
NT SPACE DENSITY
SIMM1: A linearized particle code
[AD-A148627] 08 p1221 N85-17689
Electronic structure of liquid metal alloys
[DE85-000904] 09 p1295 N85-18136
An equation of profile of snow drift density during snowfall 15 p2581 N85-25919
Rayleigh scattering for density measurements in premixed flames: One point, time series data
20 p3424 N85-31253
Solar flare gamma-ray line spectroscopy
[SH-2.1-14] 23 p3999 N85-34795
Gradients and anisotropies of high energy cosmic rays in the outer heliosphere
[SH-4.3-7] 23 p4032 N85-34992

DENSITY (RATE/AREA)
U FLUX DENSITY

DENSITY DISTRIBUTION
Estimating a monotone density
[CWI-MS-R8403] 05 p0721 N85-14633
Dark matter near the sun: Simulated star counts and the Oort limit 06 p0880 N85-15592
The Malin effect in stellar photography
07 p0966 N85-16131
Feasibility of alpha particle measurement by CO2 laser Thomson scattering
[DE85-001764] 09 p1326 N85-18334
Small-sample properties of kernel density estimators from randomly right-censored data
[AD-A148752] 09 p1374 N85-18634
Gas dynamics of the barred spiral galaxy NGC 3359
13 p2170 N85-23465
Problems in recovering crater production functions
13 p2182 N85-23539
A parmetric study of crater-saturation simulation
13 p2182 N85-23540
Local covariance functions and density distributions
[AD-A150792] 14 p2373 N85-24669
Research on thermionic plasmas
[AD-A150663] 14 p2423 N85-24944
A model containing blobs for the A ring of Saturn
15 p2671 N85-26479
Measurements in low pressure flow using an electronic beam detector — wind tunnel tests
16 p2701 N85-26676
Altimetry data and the elastic stress tensor of subduction zones
[NASA-CR-175796] 16 p2825 N85-27425
The transport of neutral H, D, T and He and O in the boundary layers of a Tokamak plasma
[REPT-84-153] 17 p3041 N85-28817
Anisotropic electron-impurity scattering in dilute AlLi: (Small) corrections to the local density approximation
[DE85-002946] 19 p3238 N85-30076
The electric current densities beneath thunderstorms
20 p3494 N85-31726
Electron density distribution analysis for nitroguanidine
[DE85-009598] 23 p3969 N85-34603
Breakdown of intrinsic ambipolarity for the radial diffusion due to a rotating RF field 23 p3977 N85-34660
Transports studies of ECH and ICRH-heated bumpy torus plasma in NBT-1M 23 p3978 N85-34662
Guiding center distribution function and longitudinal invariant 23 p3978 N85-34663
Cosmic ray density gradient and its dependence on the north-south asymmetry in solar activity
[SH-4.5-17] 23 p4038 N85-35034
Observation of pick-up ions in the solar wind: Evidence for the source of the anomalous cosmic ray component?
[SH-4.6-5] 23 p4039 N85-35043
Average features of the muon component of EAS or = 10(17) eV
[HE-4.3-10] 24 p4191 N85-36004
Transition effect of air shower particles in plastic scintillators
[HE-4.4-9] 24 p4193 N85-36017

DENSITY MEASUREMENT
NT GAMMA RAY ABSORPTIOMETRY
NT PHOTON ABSORPTIOMETRY
NT X RAY DENSITY MEASUREMENT
Measurement of blood and plasma density with the mechanical oscillator technique
05 p0693 N85-14456
A wind-tunnel study of the saltation of heterogeneous (size, density) sands 08 p1182 N85-17449
Density measurements of atomic hydrogen in NBT-IM by laser-induced fluorescence spectroscopy
09 p1389 N85-18739
Fourier densitometry: A new optical method for measuring density fluctuations by Rayleigh scattering — turbulent jets 11 p1576 N85-19932
Field validation of statistically-based acceptance plan for bituminous airport pavements. Volume 3: Statistical analysis of 3 methods for determining maximum specific gravity of bituminous concrete mixtures
[FAA-PM-84-12-VOL-3] 12 p1781 N85-21182
Field validation of statistically-based acceptance plan for bituminous airport pavements. Volume 4: Computer simulation of multiple acceptance criteria
[FAA-PM-84-12-VOL-4] 12 p1782 N85-21183
Determination of permissible heating rate of metal
[BLL-M-36107-(5828.4)] 16 p2748 N85-26957
A study of freezing and melting with eutectic interactions 19 p3378 N85-30956
Applied research and development for falling-sphere air density measuring systems
[AD-A155227] 21 p3552 N85-32099
Application of satellite accelerometer data to improve density models
[AD-A154904] 21 p3631 N85-32558
Second order modelling in non-constant density flows
22 p3744 N85-33206
Simultaneous measurement of velocity and density in a turbulent nonpremixed flame 22 p3744 N85-33209
Calculation of flow kinetics of composite media
[BLL-M-35819-(5828.4)] 23 p3929 N85-34348
The lateral distributions of charged particles of energy greater than 0.3 E sub crit in electron-photon cascades in lead and air
[HE-3.6-10] 24 p4185 N85-35957
Properties of 10 (18)-10 (19)eV EAS at far core distance
[HE-4.7-3] 24 p4196 N85-36054

DENSITY WAVE MODEL
The lunar angular momentum problem
04 p0568 N85-13752
Excitation of spiral patterns in responsible density wave theory 05 p0740 N85-14764
Studies of planetary rings 13 p2174 N85-23488
Structure and dynamics of Saturn's rings as seen by the Voyager stellar occultation 15 p2673 N85-26494
Excitation of turbulence by density waves
[NASA-CR-3905] 19 p3314 N85-30546

DENTISTRY
Catalog of completed studies, US Army health care studies and clinical investigation activity
[AD-A149450] 10 p1568 N85-19885
Applications of CdTe to nuclear medicine
[DE85-011877] 23 p3952 N85-34492
Dental multi-purpose slowspeed handpieces test and evaluation
[AD-A155764] 24 p4130 N85-35606

DEOXIDIZING
Thermodynamics of reactions of deoxidation of nickel melts
[BLL-M-35729-(5828.4)] 02 p0175 N85-11168
Metallurgy Institute's developments for alloy and aircraft producers 03 p0353 N85-12268
The electrochemical deoxidation of molten oxide substances
[BLL-M-35982-(5828.4)] 05 p0614 N85-13920
Improvement of the ladle deoxidizing of Al-killed steel
[BMFT-FB-T-84-172] 06 p0769 N85-14923
DEOXYGENATION
Primary light harvesting system: The relationship of phycobilisomes to photosystem 1 and 2
[DE85-003075] 11 p1689 N85-20622
Noble gases and the early history of the Earth: Inappropriate paradigms and assumptions inhibit research and communication 21 p3719 N85-33075
DEOXYRIBONUCLEIC ACID
Genetic effects of microwave exposure on mammalian cells in vitro. Volume 2, Appendix A: Cytogenetics and growth kinetics data, 850 MHz
[AD-A148866] 10 p1522 N85-19599
Genetic effects of microwave exposure on mammalian cells in vitro. Volume 2, Appendix B: Cytogenetics and growth kinetics data, 1.2 GHz
[AD-A148867] 10 p1522 N85-19600
Genetic effects of microwave exposure on mammalian cells in vitro, volume 2
[AD-A149347] 10 p1523 N85-19603
Photoreactivation and other ultraviolet/visible light effects on DNA in human skin
[DE85-005135] 14 p2390 N85-24719
Molecular toxicology of chromatin: The role of Poly(ADP-Ribose) in gene control
[AD-A154415] 19 p3327 N85-30611
Repair of DNA treated with lambda-irradiation and chemical carcinogens
[DE85-010298] 19 p3327 N85-30616
Size and DNA distributions of electrophoretically separated cultured human kidney cells
20 p3500 N85-31759
Development of a recombinant DNA assay system for the detection of genetic change in astronauts cells
[DE85-010103] 20 p3504 N85-31781
The DNA metabolism and poly-(ADP-ribose) synthesis in lymphocytes of persons exposed to low doses of ionizing radiation
[OEFZS-4307] 20 p3507 N85-31800
Molecular biology of environmental aromatic hydrocarbons
[DE85-015036] 24 p4128 N85-35593
DEPENDENCE
NT SPATIAL DEPENDENCIES
NT TEMPERATURE DEPENDENCE
NT TIME DEPENDENCE
Potential dependence of electrical conductivity and chemical charge storage of poly(pyrrole) films on electrodes
[AD-A148513] 08 p1122 N85-17075
A modified Fresnel scattering model for the parameterization of Fresnel returns, part 2.3A
21 p3618 N85-32483
Observations of mesospheric turbulence by rocket probe and VHF radar, part 2.4A 21 p3619 N85-32484
On the dependence of the convergence of Gummel's algorithm on the regularity of the solution
[AD-A154628] 21 p3675 N85-32832
DEPENDENCY
U DEPENDENCE
DEPENDENT VARIABLES
Development factors and field dependence-independence
[AD-A152337] 17 p3000 N85-28545
On the interpretation of variables — simulation and regression models
[FEW-136] 20 p3522 N85-31903
DEPLETION
The dependence of interstellar element depletions on mean space density 11 p1749 N85-20998
Depletion modeling of liquid dominated geothermal reservoirs
[DE85-009923] 23 p3943 N85-34437
DEPLOYMENT
In-orbit performance of INTELSAT V communications antennae deployment systems 05 p0627 N85-14018
ARABSAT spacecraft: Rx and Tx antenna mechanisms 05 p0628 N85-14022
Deployment of a regional array in Norway
[AD-A147032] 07 p0997 N85-16330
Deployment sequence mode selection system for aircraft ejection seat
[AD-D011464] 10 p1422 N85-18968
Integrated paratroop door
[AD-D011507] 12 p1776 N85-21148
Concept for controlled fold by fold deployment and retraction of flexible, foldable solar generators
13 p2011 N85-22613
Deployment analysis of the Olympus Astromast and comparison with test measurements — solar arrays
13 p2011 N85-22616
Developments in deployable masts to support flexible solar arrays 13 p2012 N85-22620
New concepts in deployable beam structures
14 p2232 N85-23832
Utilization of space station by the large deployment reflector 14 p2235 N85-23857
Deployable controllable geometry truss beam
[NASA-TM-86366] 17 p2909 N85-27934
Solar array flight experiment
[NASA-TM-86506] 17 p2909 N85-27935
Deployable Core Automated Maintenance System (DCAMS)
[AD-A153695] 18 p3198 N85-29838
Application of the ADAMS program to deployable space truss structures
[NASA-CR-177927] 19 p3284 N85-30366
Vibration/libration interaction dynamics during the orbiter based deployment of flexible members
20 p3411 N85-31171
The Galeleo spacecraft magnetometer boom
22 p3796 N85-33513
Hoop/column antenna deployment mechanism overview 22 p3796 N85-33514
Structural dynamics model and response of the deployable reference configuration space station
[NASA-TM-86386] 22 p3799 N85-33539
DEPOLARIZATION
Alternative anodic reactions in water splitting
[DE85-004159] 12 p1802 N85-21300
Using fuel cells or anode depolarization to reduce electrowinning energy consumption
[DE85-006187] 13 p2129 N85-23250
Influence of depolarization of linear polarized radiation on the heterodyne detection in laser range finders
[ESA-TT-903] 20 p3461 N85-31500
DEPOLARIZERS
U DEPOLARIZATION
DEPOSITION
NT ANODIZING
NT ELECTRODEPOSITION
NT ELECTROLESS DEPOSITION
NT ELECTROPLATING
NT VACUUM DEPOSITION
NT VAPOR DEPOSITION
Analysis of glow discharges for understanding the process of film formation
[NASA-TM-83750] 01 p0022 N85-10138
MOD silver metallization for photovoltaics
[NASA-CR-174011] 01 p0026 N85-10163
Acoustic resonator and method of making same
[DE84-014655] 01 p0116 N85-10792
Plasma deposited diamondlike carbon on GaAs and InP
[NASA-TM-86870] 01 p0123 N85-10844
Energy deposition in microvolumes of silicon from high energy proton reactions
[AD-A144713] 01 p0123 N85-10845
Estimation of the potential and probable source regions for acid precipitation
[DE84-015119] 02 p0225 N85-11472
Interaction of UV-laser radiation with molecular surface-films
[AD-A146311] 03 p0366 N85-12349
Analysis of accretion and deletion at boundaries in dynamic scenes
[AD-A145944] 03 p0419 N85-12678
Structural studies of sputtered MOS(2) films by angle-resolved photoelectron spectroscopy
[AD-A146052] 03 p0433 N85-12759
The effect of thin-film growth mode on XPS/UPS/AES intensities
[AD-A146284] 03 p0434 N85-12763
Initial feasibility ground test of a proposed photogrammetric system for measuring the shapes of ice accretions on helicopter rotor blades during forward flight
[NASA-TM-87391] 04 p0455 N85-12867
Liquid phase products and solid deposit formation from thermally stressed model jet fuels
[NASA-TM-86874] 04 p0481 N85-13066
Newly recognized sedimentary environments in the Shelikof Formation, Alaska 04 p0516 N85-13292
Climatological variability in modeling of long-term regional transport and deposition of air pollutants
[DE84-014726] 04 p0539 N85-13430
Transformation processes and wet deposition on the urban scale
[DE84-015294] 04 p0539 N85-13432
Lunar magma ocean and its implication for origin of the Moon 04 p0581 N85-13711
The initial thermal state of the Moon
04 p0581 N85-13712
Origin of the Moon 04 p0587 N85-13745
Lunar origin: role of giant impacts
04 p0587 N85-13749
Oceanic plateaus, anomalous subduction, and the accretion of buoyant features at convergent margins
05 p0686 N85-14422
LPE (Liquid phase epitaxy) semiconductor material transfer method
[AD-D011250] 05 p0731 N85-14
Contamination analysis of Ti-O2 thin films deposited using ion assisted deposition
[DE84-014944] 05 p0732 N85-1472
Substrate preparation for thin film deposition: A survey
[DE84-016119] 06 p0868 N85-15214
Meteoritic constraints on processes in the solar nebula 06 p0887 N85-15930
The adsorption of CO and oxygen on Cu layers on a .W(110) surface
[AD-A147345] 07 p0923 N85-15947
Evaluation of jet fuel deposit kinetics. Lot 4
[AD-A147196] 07 p0935 N85-15982
French research on gallium arsenide devices
08 p1141 N85-171
Impact and collisional processes in the solar system
[NASA-CR-174297] 08 p1255 N85-17914
Plasma deposition of amorphous metal alloys
[DE85-000768] 09 p1295 N85-18132
Quaternary stratigraphy of the lower Iowa and Cedar River Valleys, southeast Iowa 09 p1352 N85-18504
Non-photochemical interactions of sulfur and nitrogen compounds in acid deposition
[DE84-016141] 10 p1513 N85-19546
Study of deposition control using transpiration
[DE85-003463] 11 p1585 N85-19984
Deposition of diamondlike carbon films
[NASA-CASE-LEW-14060-1] 11 p1615 N85-20153
Laser-plasma interactions for the deposition and etching of semiconductor materials
[DE85-000458] 11 p1731 N85-20
Low temperature deposition of nickel films
[AD-D011568] 12 p1805 N85-21319
Combined effects of atmospheric deposition, internal acid production, and harvesting on nutrient gains and losses from forest ecosystems
[DE85-002325] 12 p1884 N85-21821
Hazardous air pollutants: Wet removal rates and mechanisms
[PB85-138626] 12 p1887 N85-21842
Hazardous air pollutants: Dry-deposition phenomena
[PB85-138279] 12 p1887 N85-21843
A simple model of electron beam initiated dielectric breakdown 13 p1996 N85-22516
Diffusion deposition in fibrous filters for parallel and transverse flow models
[DE85-006149] 13 p2093 N85-230
Non-linear optical techniques for visible and UV lasers and thin film deposition
[AD-A150489] 13 p2096 N85-23077
Electronic transport in hydrogenated amorphous silicon films
[DE85 002901] 13 p2164 N85-234
Lunar origin: Role of giant impacts
13 p2179 N85-23519
Impact and collisional processes in the solar system
13 p2180 N85-23530
Eolian erosion on Mars: Three scales
13 p2188 N85-23577
The origin of regional dust deposits on Mars
13 p2188 N85-23578
On the latitudinal distribution of debris in the Northern Hemisphere of Mars 13 p2188 N85-23579
PLUVIUS: A generalized 1-dimensional model of reactive pollutant behavior, including dry deposition, precipitation formation, and wet removal, 2nd edition
[DE85-005542] 14 p2353 N85-245
Aerosol deposition along the respiratory tract at zero gravity: A theoretical study
[DE85-006703] 15 p2619 N85-261
Optical properties of hydrogenated amorphous carbon films grown from methane plasma
[NASA-TM-86995] 15 p2658 N85-264
In situ thin film measurement
[AD-A151365] 15 p2659 N85-26411
LPCVD tungsten deposition on Si-Ge alloy
[DE85-005588] 16 p2750 N85-269
Emission inventory applications to regional acid deposition modeling
[PB85-157386] 16 p2760 N85-27
Energy deposition from particle beams
[DE85-007382] 16 p2862 N85-276
Jet fuel instability mechanisms
[NASA-CR-175856] 17 p2936 N85-281

Heat pipe and method of making same
[AD-D011654] 17 p2959 N85-28273
The structure of ion plated films in relation to coating properties
[NASA-TM-87055] 18 p3085 N85-29085
Energy deposition and its effects on the E+ capture section at Sector 20
[DE85-010964] 18 p3182 N85-29727
Process for the epitaxial deposition of 3-5 compounds utilizing a binary alloy as the metallic source
[AD-D011663] 18 p3193 N85-29801
Micro-reactions of metal contacts on various types of GaAs surfaces
[AD-A153650] 18 p3193 N85-29806
A comparative evaluation of the effects of acid precipitation, natural acid production and harvesting on cation removal from forests
[DE85-010821] 19 p3309 N85-30511
Technical guide for estimating fugitive dust impacts from coal handling operations. Volume 1: Project summary
[DE85-010948] 19 p3309 N85-30515
An interim user's manual for the advanced scavenging module version 1.2
[PB85-173904] 19 p3318 N85-30572
Droplet deposition in vertical two-phase flow
[CFD/84/22] 20 p3456 N85-31460
Design of the National Trends Network for monitoring the chemistry of atmospheric precipitation
[GS-CIRC-964] 20 p3486 N85-31664
Experimental method for measuring positronium reflection from surfaces
[DE85-010949] 20 p3531 N85-31967
Modification of the grain size of sputtered copper with additions of oxygen, krypton, silver, or yttrium
[DE85-010975] 21 p3567 N85-32189
Laser-assisted solar-cell metallization processing
21 p3610 N85-32429
Microwave-enhanced thin-film deposition
21 p3611 N85-32431
Experimental studies of the kinetics of deposition nucleation on an ice nucleant used in weather modification 21 p3638 N85-32598
Ice nucleus measurements 21 p3640 N85-32609
Geology and geochemistry of sulfide and sulfate deposition 21 p3658 N85-32723
Archean sedimentary systems and crustal evolution
21 p3720 N85-33082
Method of bonding silver to glass and mirrors produced according to this method
[DE85-011642] 22 p3792 N85-33495
1985 Amorphous Silicon Review Meeting
[DE85-008794] 22 p3807 N85-33582
Development of a microorifice uniform deposit cascade impactor
[DE85-006765] 22 p3812 N85-33614
Liquid crystal light valve structures
[NASA-CASE-MSC-20036-1] 22 p3847 N85-33826
Oxidation states of iron in the terrestrial planets: Evidence and implications for accretion models
22 p3852 N85-33854
Late-stage planetesimals: How big?
22 p3852 N85-33857
Dual-chamber plasma deposition of A-Si:H solar cells at high rates using disilane
[DE85-011828] 23 p3946 N85-34451
Throughfall rate and chemistry studies: Whiteface Mountain
[DE85-012407] 23 p3947 N85-34464
User's guide to the MATHEW/ADPIC models
[DE85-012952] 23 p3966 N85-34587
MATADOR (Methods for the Analysis of Transport And Deposition Of Radionuclides) code description and user's manual
[TI85-901402] 23 p3966 N85-34592
Diamondlike carbon protective coatings for IR materials
[NASA-TM-87083] 23 p3973 N85-34631
Depositional systems and coal occurrence in the Fort Union Formation (Paleocene), Powder River Basin, Wyoming and Montana 24 p4114 N85-35505
DEPOSITS
Evaluation of jet fuel deposit kinetics. Lot 4
[AD-A147196] 07 p0935 N85-15922
Study of deposition control using transpiration
[DE85-002330] 10 p1485 N85-19378
Study of deposition control using transpiration
[DE85-003463] 11 p1585 N85-19964
Apparatus and method to keep the walls of a free-space reactor free from deposits of solid materials
[NASA-CASE-NPO-15851-1] 12 p1858 N85-21652
Fracture detection and mapping for geothermal reservoir definition: An assessment of current technology, research, and research needs
[DE85-010627] 19 p3301 N85-30484
DEPRESSANTS
Workload demand and CNS depressant stressor effects on spatial orientation information processing
[AD-A145211] 01 p0098 N85-10651
DEPRESSIONS (TOPOGRAPHY)
U STRUCTURAL BASINS
DEPRESSURIZATION
U PRESSURE REDUCTION
DEPRIVATION
NT SENSORY DEPRIVATION
NT SLEEP DEPRIVATION
DEPTH
Nonlinear propagation in a depth-dependent ocean
[AD-A145079] 01 p0116 N85-10791
Active remote sensing of ocean parameters, an engineering study 02 p0213 N85-11403
Determination of depth profiles and lattice positions with (n, p)- and (n, alpha) reactions (n, alpha) and channeling-blocking method) 03 p0429 N85-12735
Subsurface temperatures in northeastern Wyoming measured by bottom hole temperature records
[TI84-901610] 04 p0534 N85-13413
An extension of the Born inversion method to a depth dependent reference profile
[AD-A146469] 06 p0859 N85-15461
Microwave radiometer observations of snowpack properties and comparison of U.S. Japanese results — Hokkaido, Japan and Vermont and North Dakota test sites 13 p2125 N85-23230
Studies on physical properties of snow based on multi channel microwave radiometer
13 p2125 N85-23231
Analysis of NIMBUS-7 SMMR data — Hokkaido, Japan snow cover 13 p2125 N85-23232
The effects of internal waves on acoustic normal modes
[AD-A150235] 13 p2155 N85-23379
Regional seismic wave propagation
[AD-A150801] 14 p2373 N85-24671
Estimation of the depth of a spherical cap in an hydraulic drawing test for some simple conditions of loss of stability
[REPT-4/1984] 16 p2748 N85-26956
The effect of ion-bombardment-induced atomic mixing on depth-profiling of interfaces
[AD-A153199] 17 p3044 N85-28834
Altitude variations of cosmic-ray soft and hard components observed by airborne detectors
[SH-6.1-5] 23 p4045 N85-35079
DEPTH MEASUREMENT
Variations in resistivity of upper crustal layer
13 p2113 N85-23164
An assessment of the potential role of multispectral imagery in bathymetric charting
[AD-A152460] 17 p2984 N85-28438
Detecting and analyzing crack defects
[BLL-BISI-TRANS-22062-(9022.06)]
17 p3027 N85-28723
Ultrasonic crack tip method for the determination of crack depth 17 p3028 N85-28725
Fluctuations of development maximum depth and nuclear composition of primary cosmic radiation
[OG-5.1-13] 22 p3882 N85-34054
Estimation of composition of cosmic rays with E sub zero approximately equals 10(17) - 10(18) eV
[OG-5.1-14] 22 p3882 N85-34055
Method for determining depth and shape of a sub-surface conductive object
[DE85-006502] 23 p3935 N85-34389
The transient electromagnetic depth sounding technique applied to hydrocarbons and geothermal exploration
[MITT-42] 23 p3949 N85-34476
Analysis of Cerenkov pulses recorded simultaneously at two sites
[HE-4.4-16] 24 p4194 N85-36022
DEPTH PERCEPTION
U SPACE PERCEPTION
DERIVATION CALCULUS
U DIFFERENTIAL CALCULUS
DESALINIZATION
An evaluation of the electrodialysis reversal process (Edr) for the desalination of brackish water from the Omaruru delta (SWA/Namibia)
01 p0023 N85-10141
Evaluation of hollow fiber ultrafiltration as a pretreatment for reverse osmosis desalinaton of seawater
[PB84-212406] 01 p0026 N85-10160
Feasibility study for small group water desalination equipment
[AD-A155106] 21 p3563 N85-32164
Oxidation of formaldehyde solutions used for the preservation of reverse osmosis membranes
[PB85-185585] 22 p3742 N85-33194
DESCENT
NT PARACHUTE DESCENT
Error analysis of wind determined using a VLF Omega sonde
[WSRL-0361-TM] 06 p0838 N85-15321
Effects of aircraft and flight parameters on energy-efficient profile descents in time-based metered traffic
[NASA-CR-172338-ADD] 07 p0901 N85-15706
Reference energy-altitude descent guidance: Simulator evaluation — aircraft descent and fuel conservation
[NASA-TP-2383] 08 p1085 N85-16866
Planning fuel-conservative descents in an airline environmental using a small programmable calculator: Algorithm development and flight test results
[NASA-TP-2393] 16 p2707 N85-26705
DESCENT PROPULSION SYSTEMS
Descent vehicles
[NASA-TM-77654] 17 p2909 N85-27933
DESCENT TRAJECTORIES
NT REENTRY TRAJECTORIES
Descent guidance and mission planning for space shuttle 08 p1092 N85-16902
Some effects of digital sampling on orbiter flight control system operation 08 p1092 N85-16903
Descent vehicles
[NASA-TM-77654] 17 p2909 N85-27933
DESCRIPTIONS
Glossary of landscape and vegetation ecology for Alaska
[PB85-153831] 16 p2816 N85-27372
DoD manual for standard data elements, part 2
[AD-A152202] 16 p2878 N85-27755
DoD manual for standard data elements, part 3
[AD-A152203] 16 p2878 N85-27756
Systematic nomenclature of the nitrogen, oxygen and sulfur functional polycyclic aromatic hydrocarbons
[DE85-007426] 17 p2916 N85-27974
DESCRIPTIVE GEOMETRY
Generation of radiation transport geometry from computer-generated design data — monte carlo solution of the neutron transport equation
[DE84-017380] 09 p1370 N85-18606
X-ray satellite
[NASA-TM-77898] 20 p3407 N85-31144
DESENSITIZING
The current status of the RAF programme of densensitisation for motion sick aircrew
11 p1695 N85-20658
The shock desensitization of PBX-9404 and composition B-3
[DE85-009604] 18 p3084 N85-29077
Manufacturing process to reduce large grain growth in zirconium alloys
[DE85-011649] 23 p3915 N85-34267
DESERTS
NT GOBI DESERT
NT MOJAVE DESERT (CA)
NT SAHARA DESERT (AFRICA)
An integrated LANDSAT/ancillary data classification of desert rangeland
[E85-10046] 06 p0826 N85-15248
Application of SIR-B data for groundwater exploration in the Arabian shield and sand-drift monitoring in the AN Nafud and Al Jafurah fringe areas, Kingdom of Saudi Arabia 08 p1144 N85-17214
Application and calibration of the subsurface mapping capability of SIR-B in desert regions
08 p1148 N85-17244
Field testing of a lightweight relocatable structure in a desert environment
[AD-A148841] 09 p1304 N85-18192
Analysis of SMIRR data for volcanic and sedimentary terrains of the trans-Pecos region, Texas
13 p2197 N85-23626
Meteorological conditions affecting electromagnetic propagation on the Arabian Peninsula
[AD-A152019] 15 p2544 N85-25708
The behavior of the atmosphere in the desert planetary boundary layer
[AD-A151286] 15 p2592 N85-25977
Utilization of remote sensing data in the evaluation of air pollution characteristics in the south coast/Southeast Desert Air Basin
[PB85-162063] 16 p2822 N85-27407
Quality assurance for RESOLVE (Research on Operations-Limiting Visual Extinction). A visibility study in the California desert
[AD-A152383] 17 p2992 N85-28494
Microbial ecology of extreme environments: Antarctic yeasts and growth in substrate-limited habitats
[NASA-CR-176005] 19 p3326 N85-30609
DESICCANTS
High performance solar desiccant cooling system: Performance evaluation and research recommendations
[DE85-000508] 11 p1676 N85-20559

Investigation of manganese dioxide as an improved solid desiccant
[DE85-004034] 13 p2018 N85-22654

Experiments on sorption characteristics of solid desiccant materials for solar desiccant cooling systems
[DE85-000542] 17 p2923 N85-28019

Solid desiccant dehumidification systems for residential applications
[PB85-199489] 22 p3755 N85-33279

Advances in open-cycle solid desiccant cooling
[DE85-006797] 22 p3808 N85-33590

Rigid zeolite containing polyurethane foams
[DE85-006406] 23 p3919 N85-34286

DESICCATION
U DRYING

DESIGN

CCDs: Their cause and cure
08 p1252 N85-17905

Ultrareliable, fault-tolerant control systems: A conceptual description
[NASA-TM-86017] 19 p3221 N85-29972

DESIGN ANALYSIS

Applications of numerical optimization methods to helicopter design problems: A survey
[NASA-TM-86010] 01 p0006 N85-10036

Development trends and requirements of propulsion system technology for civil aircraft
01 p0011 N85-10066

Natural environment design criteria for the Advanced X-ray Astrophysics Facility (AXAF) definition and preliminary design
[NASA-TM-86481] 01 p0014 N85-10089

Design sensitivity analysis of an antisymmetric angle-ply laminate
[CSIR-TWISK-318] 01 p0021 N85-10128

Methods for the design of quantizers for image signals
[FUB-38-1983] 01 p0041 N85-10263

Development of the Antares electron gun
[DE84-014043] 01 p0053 N85-10352

Achievements in laser development
01 p0115 N85-10784

Means of varying conditions in the expanded boundary divertor without affecting energy confinement
[DE84-013840] 01 p0122 N85-10836

Energy efficient engine flight propulsion system preliminary analysis and design report
[NASA-CR-174701] 02 p0140 N85-10947

Energy efficient engine high pressure turbine test hardware detailed design report
[NASA-CR-167955] 02 p0147 N85-10995

Conceptual design and evaluation of selected Space Station concepts: Executive summary
[NASA-TM-87382] 02 p0167 N85-11128

Conceptual design and evaluation of selected Space Station concepts, volume 1
[NASA-TM-87383] 02 p0168 N85-11129

Conceptual design and evaluation of selected Space Station concepts, volume 2
[NASA-TM-87384] 02 p0168 N85-11130

Simulation study of a new inverse-pinch high Coulomb transfer switch
[NASA-CR-172420] 02 p0194 N85-11294

Laser source of neutral atoms for collective-field particle accelerator 02 p0263 N85-11719

Optical waveguide spatial filters
[AD-A145674] 02 p0280 N85-11825

Inverse design technique for cascades
[NASA-CR-3836] 03 p0311 N85-12006

Modular electromechanical industrial robots
03 p0345 N85-12223

Burmester theory for 4 precision positions: An extended discourse with application to the dimensional synthesis of arbitrary planar linkages 03 p0367 N85-12351

Accelerator development in support of the NRL (Naval research laboratory) beam dynamic program
[AD-A145976] 03 p0417 N85-12669

A topological approach to database theory
03 p0437 N85-12781

Design, construction, and operational results of an 800-A, 10-kV hot deck amplifier
[DE84-014044] 04 p0496 N85-13162

Westinghouse programs in pulsed homopolar power supplies 05 p0606 N85-13862

Generic composite flywheel designs
05 p0606 N85-13864

Design, ancillary testing, analysis and fabrication data for the advanced composite stabilizer for Boeing 737 aircraft, volume 2
[NASA-CR-166011] 05 p0612 N85-13914

A summary description of a computer program concept for the design and simulation of solar pond electric power generation systems 05 p0666 N85-14285

Salt-gradient solar ponds: Summary of US Department of Energy sponsored research
[NASA-CR-174183] 05 p0667 N85-14286

Salton Sea solar pond power plant design study and regional applicability 05 p0667 N85-14290

Crewstation design and validation
06 p0752 N85-14822

Avionics technology - system concepts
06 p0753 N85-14824

Avionics system design for requirements for the United States Coast Guard HH-65A Dolphin
06 p0753 N85-14827

The need for a dedicated public service helicopter design 06 p0753 N85-14828

A theoretical design method for 3-dimensional transonic wings
[NAL-TR-830] 06 p0754 N85-14834

Efficiency estimation and sensitivity modeling
06 p0829 N85-15263

Computational analysis of scramjet dual mode operation
[NASA-CR-174250] 07 p0956 N85-16060

Development of large wind energy power generation system
[NASA-TM-77779] 07 p0992 N85-16301

Development of a preprototype times wastewater recovery subsystem, addendum
[NASA-CR-171823] 07 p1019 N85-16468

Design of self-checking N-MOS (H-MOS) integrated circuits 08 p1064 N85-16742

A description of a logistically ideal aircraft
[AD-A148425] 08 p1084 N85-16866

Design concept definition study for an improved shuttle waste collection subsystem
[NASA-CR-171834] 08 p1198 N85-17546

MHD performance demonstration experiment, FY 1974 to FY 1984
[DE85-000654] 08 p1224 N85-17709

Finite element computation of structural design sensitivity analysis 09 p1330 N85-18353

Treatment of general boundary conditions and point-wise state variable constraints in optimum design for static and dynamic response
09 p1330 N85-18358

DDL system: Design systhesis of digital systems
[NASA-CR-170759] 09 p1366 N85-18584

Design and analysis of an access control system for a multi-backend database system
[AD-A148750] 09 p1367 N85-18586

Antiproton source beam position system
[DE84-016716] 09 p1380 N85-18679

Cookbook for determining essential transmission characteristics of spherical section electrostatic analyzers
[DE85-001404] 09 p1391 N85-18751

Hybrid vehicle program
[DE85-000326] 09 p1410 N85-18886

Integrated Technology Rotor/Flight Research Rotor (ITR/FRR) concept definition study
[NASA-CR-166444] 10 p1424 N85-18981

Control system of complex CNC machining cell
10 p1462 N85-19218

Proceedings of the 17th Symposium on Electromagnetic Windows, part 1
[AD-A149185] 10 p1466 N85-19253

The use of synthesis method in the design of gyrotron electron guns
[INPE-3305-PRE/616] 10 p1478 N85-19329

Experience highlights from the design and manufacture of US LCT coils
[DE84-017504] 10 p1482 N85-19354

Performance of the 10 KSI Wilson valve breech
[DE85-000258] 10 p1493 N85-19430

Intermediate load modules for test and evaluation: Flat-Plate Solar Array Project
[NASA-CR-174450] 10 p1508 N85-19512

Conceptual design of a 10 MW shore-based OTEC plant
[DE84-015808] 10 p1511 N85-19532

Microstrain analysis in bent single crystal silicon by double crystal X-ray topography technique
[DE85-000422] 10 p1564 N85-19883

Design and analysis of airborne scanning optical systems 11 p1623 N85-20218

Mini-modal testing of wind turbines using novel excitation
[DE85-000666] 11 p1654 N85-20417

Computerized study of several electrostatic, surface-ionization ion-source configurations
[DE85-001512] 11 p1721 N85-20823

Stability analysis of flexible spacecraft with PID controller
[CRC-1372] 12 p1792 N85-21247

A radome for air traffic control SSR radar systems
[AD-P004373] 12 p1827 N85-21467

The 13.9 GHz radiometer design
[AD-A149637] 12 p1851 N85-21613

Reliability of structural brittle materials
12 p1946 N85-22222

Dynamic wind-tunnel testing of active controls by the NASA Langley Research Center
13 p1966 N85-22[illegible]

Rational use of tatanium in nonferrous metallurgy
13 p2031 N85-22778

Experimental determination of optimum ratio of runner blade height at exit to runner blade height at entrance of radial inward-flow microturbines
13 p2049 N85-22827

Reluctance and doubly-excited reluctance motors
[DE85-003585] 13 p2065 N85-22900

A 60 GHz 200 kW CW gyrotron with high output mode purity
[DE85-005263] 13 p2066 N85-22906

Analysis and design of linear microwave transistor amplifiers 13 p2088 N85-23028

Magnetic refrigeration and heat pumping design options
[DE85-003405] 13 p2092 N85-23064

Optimum design and automated dynamic analysis of flexible mechanisms
[AD-A150152] 13 p2099 N85-23088

A design analysis and implementation of a user-friendly interface for the UNIX operating system
[AD-A150558] 13 p2145 N85-23312

Manufacturing perspective in the design of bevel gearing 14 p2221 N85-23777

Manufacturing considerations related to aircraft gearboxes 14 p2222 N85-23778

Possible technological answers to new design requirements for power transmission systems
14 p2222 N85-23779

Design of single-wheel gyrocompass with correction
14 p2272 N85-24078

Determining optimum service conditions for concentrator mirrors by methods of mathematically planned experiment 14 p2274 N85-24080

Module performance and failure analysis area: Flat-plate solar array project
[NASA-CR-175689] 15 p2585 N85-25936

SPRING: Helical spring design software for microcomputers
[DE85-006200] 15 p2631 N85-26217

Outline of alternative design of R-Tokamak
15 p2654 N85-26371

Metal armatures for railguns
[AD-A152129] 16 p2728 N85-26[illegible]

Fuel and oxidizer turbine loss analysis
16 p2739 N85-26[illegible]

Cryostat and electronic development associated with multi-detector spectrometer systems
[DE85-007624] 16 p2788 N85-27200

Numerical optimization algorithm for engineering problems using microcomputer
[AD-A152135] 16 p2847 N85-27554

Radiometer integrated into a communication terminal
[AD-A151746] 17 p2947 N85-28185

SC filters and design centering of integrated circuits. Part 2: Design centering of integrated circuits
[BMFT-FB-T-84-265-PT-2] 17 p2956 N85-28257

A ten channel temperature controller
[AD-A152684] 17 p2967 N85-28[illegible]

Design and construction of a CW ND:YAG laser using a single elliptical cavity and water cooled krypton arc lamp pumping
[AD-A152657] 17 p2970 N85-28340

Resonator optical designs for free electron lasers
[DE85-007678] 17 p2971 N85-28347

Silica problem in the design of geothermal power plants
[DE85-008245] 17 p2986 N85-28453

Peer Review of a Formal Verification/Design Proof Methodology
[NASA-CP-2377] 17 p3010 N85-28[illegible]

Optimum dimensions of power solenoids for magnetic suspension
[NASA-TM-77864] 17 p3026 N85-28716

Impurity control and vacuum pumping system design and analysis for next-generation Tokamaks
[DE85-009291] 17 p3041 N85-28816

A simulation study of jammer nulling trade-offs in a reactively steered adaptive array
[AD-A153461] 18 p3090 N85-29124

Development of hydrogen masers for K-3 VLBI system
18 p3106 N85-29239

Atomic hydrogen maser active oscillator cavity and bulb design optimization 18 p3106 N85-29240

High temperature sensible heat storage options
[DE85-000534] 18 p3129 N85-29375

Atmosphere monitoring requirements
18 p3158 N85-29553

Analysis of remote operating systems for space-based servicing operations, volume 1
[NASA-CR-171885] 19 p3225 N85-29[illegible]

Analysis of remote operating systems for space-based servicing operations. Volume 2: Study results
[NASA-CR-171886] 19 p3225 N85-29994

Space station automation study-satellite servicing, volume 2
[NASA-CR-171513] 19 p3226 N85-30000

Liquid sampling system
[DE85-011673] 19 p3265 N85-30248

A numerical method for the solution of the inverse problem in external aerodynamics
[STN-7] 20 p3390 N85-31025

Design of a basic airfoil for a slightly swept wing. Part 1: Theoretical transonic airfoil design
[ESA-TT-892] 20 p3394 N85-31054

Proceedings of the Workshop on Identification and Control of Flexible Space Structures, volume 3
[NASA-CR-176053] 20 p3415 N85-31195

Optimum filter computation for data transmission
[CNES-89/DRT/TIT/TR/142] 20 p3441 N85-31359

Nickel cadmium cell design variable program data analysis 20 p3445 N85-31367

A small-scale self-excited rotor electrostatic generator
[AD-A155264] 21 p3581 N85-32265

Sensitivity analysis of high-efficiency silicon solar-cell design parameters 21 p3610 N85-32422

Land vehicle corrosion management
22 p3750 N85-33246

Optimization of radioelectronic circuits with software for modeling of integrated circuits on unified system computer 22 p3766 N85-33354

Design of inductive shift transducers
22 p3771 N85-33368

Design analysis for a repository in crystalline rock
[DE85-011802] 22 p3839 N85-33771

Optimisation in the computer aided design of mechanisms 23 p3924 N85-34321

Realization and linearization of a hyperfrequency power amplifier implemented with bipolar transistors in class C polarization — microwave amplifiers
[CNES-NT-114] 23 p3928 N85-34346

SLC arc transport system: Magnet design and construction
[DE85-014289] 24 p4159 N85-35789

SLC Energy Upgrade Program at SLAC
[DE85-014290] 24 p4160 N85-35790

DESIGN OF EXPERIMENTS
U EXPERIMENT DESIGN

DESIGN TO COST

Evaluation of the measured energy performance of four solar systems
[AD-A147912] 07 p0993 N85-16306

Manufacturing considerations related to aircraft gearboxes 14 p2222 N85-23778

Design-To-Cost (DTC) methodology to achieve affordable avionics 16 p2696 N85-26645

The series 2000: A miniature gas bearing DTG for low cost strapdown guidance and control
16 p2696 N85-26648

Reusable software: A concept for cost reduction
16 p2697 N85-26655

A towed instrument vehicle for deep ocean sampling
[AD-A156322] 24 p4125 N85-35576

DESORPTION

Reversible change in parameters of GaAs-based surface-barrier metal-semiconductor diodes induced by hydrogen absorption-desorption
02 p0258 N85-11690

Synergistic effects related to surface composition, session summary 06 p0865 N85-15495

The adsorption of CO and oxygen on Cu layers on a W(110) surface
[AD-A147345] 07 p0923 N85-15847

Phase-dissipative mechanisms for laser-induced surface desorption-dissociation processes
[AD-A147961] 08 p1121 N85-17065

Modulated surface vibrational spectroscopies at electrode/electrolyte interfaces
[AD-A148665] 08 p1123 N85-17083

Photoemission, vibrational and stimulated desorption studies of metal-semiconductor interfaces and of chemisorbed atoms and molecules
[AD-A147709] 08 p1225 N85-17717

Multiplex gas chromatography for use in space craft
[NASA-TM-86668] 09 p1290 N85-18097

Characterization of CO binding sites on Rh(111) and Rh(331) surfaces by XPS and LEED (Low Energy Electron Diffraction): Comparison to EELS (Electron Energy Loss Spectroscopy) results
[AD-A149331] 10 p1435 N85-19044

Desorption efficiencies of vapor phase polynuclear aromatic compounds on solid adsorbents
[DE85-001303] 10 p1436 N85-19052

Separation of gas mixtures with coordination complexes
[DE85-000363] 10 p1438 N85-19062

Quasi-thermodynamic prediction of hydrogen reemission behavior from titanium films
[DE85-003667] 10 p1564 N85-19864

Laser studies of chemical dynamics at the gas-solid interface
[DE84-017590] 11 p1736 N85-20920

Study of outgassing and decomposition of space shuttle heat protection tiles, fillers and adhesive
[NASA-CR-175565] 12 p1791 N85-21242

Electron stimulated desorption and the role of secondary electrons
[AD-A150974] 14 p2252 N85-23955

Studies of metal/carbon surface chemistry
[DE85-006513] 15 p2507 N85-25463

The physical effects of different stress situations on graphite/epoxy compounds 15 p2687 N85-26594

Quantum statistical theory of vibrational dynamics in a laser-driven admolecule-surface system
[AD-A152022] 16 p2872 N85-27719

The development of laser analytical methods for the characterization of solid-liquid and solid-high pressure gas interfaces
[AD-A152382] 17 p2918 N85-27988

Theory of laser-stimulated surface process. 2: A generalized-master-equation approach to energy transfer between an IR laser, an aspecties and phonons
[AD-A153083] 17 p2970 N85-28344

Quantum model of dephasing-enhanced laser desorption: Master equation approach
[AD-A153769] 18 p3112 N85-29269

Selective detection of species in complex matrices by SIMS (Secondary Ion Mass Spectrometry)
[AD-D011685] 19 p3235 N85-30053

Method for measuring surface activity of silicon nitride powder
[NASA-TM-77906] 24 p4073 N85-35242

Evaluation: Close-range photogrammetry for slope inventory and monitoring
[PB85-192755] 24 p4106 N85-35470

DESPINNING
U SPIN REDUCTION

DESTRUCTION

Interaction among inhomogeneities and inclusions
[AD-A153114] 17 p2979 N85-28419

DESTRUCTIVE TESTS

The adhesion of hard and wear resistant coatings
02 p0179 N85-11203

Lithium battery safety: A fiber-optic application for safe observation of lithium cells under severe tests
[AD-A146646] 06 p0804 N85-15119

Comparison of the sensitivities of ultrasonic, radiographic and acoustic emission test methods for the examination of a thick weld
[BLL-RISLEY-TR-4547-(9091.9F)]
07 p0975 N85-16194

Nondestructive tests and fracture mechanics investigations in the Component Integrity Research Programme
[BLL-RISLEY-TR-4541-(9091.9F)]
07 p0976 N85-16199

Quantitative acoustic emission techniques
[AERE-R-11262] 07 p0977 N85-16203

Evaluation of laterally loaded laminated glass units by theory and experiment
[PB85-111532/GAR] 09 p1300 N85-18166

Laser induced damage of zinc sulphide
[BAE-BT-13363] 15 p2562 N85-25803

An improved torsional method for determining the fracture toughness of stiff materials and of adhesive joints
[AD-A152091] 16 p2800 N85-27267

Qualitative and quantitative determination of aging by mechanical tests --- plastics 17 p2977 N85-28393

Seat experiments for the full-scale transport aircraft controlled impact demonstration
[AD-A155024] 21 p3553 N85-32106

DESULFURIZING

Studies of the kinetics and mechanisms of ammonia synthesis and hydrodesulfurization on metal single crystal surfaces
[DE85-001650] 11 p1595 N85-20030

Development of corrosion resistant heat exchangers for flue gas desulfurization
[BMFT-FB-T-84-281] 18 p3103 N85-29211

Evaluation of the Santee limestone for use in flue-gas desulfurization systems
[DE85-901277] 19 p3249 N85-30148

Fluidized bed desulfurization
[NASA-CASE-NPO-15924-1] 24 p4075 N85-35253

DESYNCHRONIZED SLEEP
U RAPID EYE MOVEMENT STATE

DETECTION
NT AIRCRAFT DETECTION
NT CHANGE DETECTION
NT CORRELATION DETECTION
NT FOREST FIRE DETECTION
NT HAZE DETECTION
NT RADAR DETECTION
NT REMOTE SENSING
NT SIGNAL DETECTION
NT TARGET RECOGNITION
NT ULTRASONIC FLAW DETECTION

The perceptual quality of smoke screens: An analysis of the Oldebroek 2 trials, May 1981
[IZF-1984-20] 01 p0095 N85-10641

Visual representations subserving texture perception
[AD-A145412] 02 p0236 N85-11538

Failure detection processes by pattern recognition and expert systems
[AD-P003924] 02 p0246 N85-11604

Compound class quantitation of JP-5 jet fuels by high performance liquid chromatography-differential refractive index detection
[AD-A145754] 03 p0340 N85-12185

Visibility of various target-background color combinations under different chromatic ambient illuminations
[AD-A146348] 03 p0420 N85-12684

Early detection of environmental exposure
[AD-P004039] 06 p0845 N85-15369

Performance of Bayes-optimal angle-of-arrival estimators
[AD-A146594] 06 p0858 N85-15454

Detection of narrow C 4 and Si 4 absorption features in spectra of stars within 200 pc f the Sun
06 p0876 N85-15564

Electronics research at the University of Texas at Austin
[AD-A146900] 07 p0947 N85-15998

A biological sensor for the detection of toxicants
[AD-D011304] 07 p0967 N85-16141

Battery control and fault detection method
[AD-D011384] 07 p0993 N85-16307

Electro-optical target detection
[AD-D011366] 07 p1042 N85-16617

Holographic FLI for detection of defects
[AD-A148339] 08 p1164 N85-17345

Halogen mass flow rate detection system
[AD-D011398] 08 p1166 N85-17352

Spatiotemporal characteristics of visual localization
[AD-A148013] 08 p1200 N85-17555

Background detection and correction in multicomponent analysis
[AD-A148251] 08 p1212 N85-17626

Calculation of cumulative distributions and detection probabilities in communications and optics
[AD-A147781] 08 p1215 N85-17650

On edge detection
[AD-A148573] 08 p1223 N85-17703

Photometric precision needed for planetary detection
08 p1250 N85-17894

Mass spectrometry/mass spectrometry as a screening method for detecting explosive vapors
[DE85-001276] 09 p1292 N85-18110

The use of synthetic aperture radar imagery to detect hazards to navigation
[AD-A149324] 10 p1422 N85-18971

Detection and symbol synchronization for multiple-bit per photon optical communications
10 p1463 N85-19228

Calculation of Si(Li) X-ray detector efficiencies
[DE85-002732] 10 p1489 N85-19400

Infrared-thermal wave scanner for NDE of naval thermal spray coatings
[DE85-002237] 11 p1650 N85-20391

Lake ice occurrence as a possible detector of atmospheric CO2 effects on climate
[DE85-002951] 11 p1687 N85-20606

Double pinhole spatial phase correlator apparatus
[AD-D011495] 11 p1729 N85-20872

In-situ detection of micron-sized dust particles in near-Earth space 12 p1785 N85-21205

Photo-thermal detection of the onset of photo-chemical nucleation (laser-snow) in vapor
[AD-A150111] 12 p1801 N85-21295

Detection of angular modulated electromagnetic signals
[AD-D011563] 12 p1823 N85-21437

Inelastic scattering in condensed matter with high intensity Moessbauer radiation
[DE85-003531] 12 p1854 N85-21627

Radiographic detectability limits for seeded voids in sintered silicon carbide and silicon nitride
[NASA-TM-86945] 12 p1861 N85-21674

Characterisation of fatigue crack extension by quantitative acoustic emission
[AERE-R-11269] 12 p1868 N85-21721

A diffusion process and its application to detecting a change in the drift of Brownian motion
[AD-A150096] 12 p1926 N85-22100

Focal plane array optical proximity sensor
[NASA-CASE-NPO-15155-1] 12 p1932 N85-22139

Operational experience with ion concentration sensors in orientation systems 13 p1980 N85-22422
Optimization of number of pulses in detection of fluctuating optical signals 13 p2081 N85-22993
Orphan detection in the Argus system [AD-A150562] 13 p2148 N85-23331
Sample introduction methods for improving the particle detection capability of the spectrometric oil analysis program [AD-A150139] 13 p2158 N85-23399
Electronic detection and concealment of film dirt [BBC-RD-1985/4] 15 p2536 N85-25667
Receiver optimization for detection in doubly spread communication channels [AD-A151226] 15 p2541 N85-25689
Skywave radar detectability of volcanic aerosols [AD-A151448] 15 p2542 N85-25694
Attempts to localize and identify the gravity sensing device of plant seedlings 15 p2607 N85-26064
Ion sensor signal fluctuations during operation of spacecraft reaction engines 16 p2724 N85-26815
New focal plane detector system for the broad range spectrometer [DE85-005370] 16 p2788 N85-27201
A mathematical model for calculating detection probability of a diffusion target [AD-A152026] 16 p2854 N85-27601
Optimally robust redundancy relations for failure in uncertain systems [NASA-CR-175953] 17 p2976 N85-28391
Automatic detection of gust fronts [FAA-PM-85-11] 17 p2995 N85-28516
Evaluation of a fault tolerant system for an integrated avionics sensor configuration with TSRV flight data [NASA-CR-172589] 18 p3062 N85-28941
Resonant CARS detection of OH radicals [AD-A153842] 18 p3071 N85-28995
Visual simulation of radiographs [DE85-010213] 18 p3110 N85-29255
Dual differential interferometer [NASA-CASE-LAR-12966-1] 19 p3271 N85-30282
Evaluation of a high pressure proportional counter for the detection of radioactive noble gases [AD-A154436] 19 p3272 N85-30292
Optical 3-D signature device for detecting chemical agents [AD-D011669] 19 p3272 N85-30293
Optical waveguide sensor for methane gas [AD-D011691] 19 p3273 N85-30294
Development of a technique for in situ detection of stratospheric nitrogen dioxide 19 p3312 N85-30534
An empirical technique to measure X-ray production and detection efficiencies in the analytical electron microscope [DE85-010270] 19 p3361 N85-30637
Detection of internal structure by scattered light intensity: Application to kidney cell sorting 20 p3503 N85-31777
A cluster analysis method for identification of subpopulations of cells in flow cytometric list-mode arrays 20 p3503 N85-31779
Function of a device for detection of biological aerosols in field testing [FOA-C-40194-B2] 20 p3504 N85-31782
Investigation of variation in the concentration of bacteria in outdoor testing, with the use of a detector for aerosols of bacteria [FOA-C-40201-B2] 20 p3504 N85-31784
Gas sensing with surface acoustic wave devices [DE85-009125] 20 p3524 N85-31921
Experimental and theoretical assessment of a new technique for the non-destructive evaluation of laminated panels [AD-A155622] 21 p3562 N85-32155
A microprocessor-controlled, multichannel fluorimeter for analysis of sea water [AD-A154986] 21 p3590 N85-32310
Detection of excited states by laser-induced fluorescence [AD-A155558] 21 p3592 N85-32326
Automated cell detection as a mesocyclone precursor tool [AD-A154952] 21 p3635 N85-32577
Real-time automated detection of mesocyclones and tornado vortex signatures [AD-A154968] 21 p3635 N85-32578
Resource management for the tagged token dataflow architecture [AD-A154773] 21 p3667 N85-32779
Analysis of unreplicated factorials allowing for possibly faulty observations [AD-A154813] 21 p3678 N85-32848
An attempt to detect induced neutron capture in laser radiation field 21 p3690 N85-32928
Fire protection review revisit no. 2, Argonne National Laboratory, Argonne, Illinois [DE85-013245] 22 p3755 N85-33276
Probabilistic analysis of automatic control systems for detection systems 22 p3765 N85-33335
Linear boundary detection using pressure buildup tests [DE85-009826] 22 p3784 N85-33444
Fiber optic moisture sensor [DE85-011651] 22 p3787 N85-33462
Fracture detection and characterization for geothermal reservoir definition [DE85-008677] 22 p3815 N85-33630
Effects of low level carbon monoxide (CO) on tracking and monitoring. An attempt to replicate the findings of Putz et al. (1976) protocol 2 [AD-A155722] 22 p3825 N85-33694
Dual optical mechanical position tracker [AD-D011739] 22 p3844 N85-33811
Search for infrared counterparts of gamma-ray bursters [OG-1.1-9] 22 p3861 N85-33910
Gamma ray burst size-frequency distributions: Spectral selection effects [OG-1.2-3] 22 p3862 N85-33913
Direct determination of metals in organic matrices by Inductively Coupled Plasma-Atomic Emission Spectrometry (ICP-AES) [DE85-012015] 23 p3911 N85-34233
Instrumentation for sensing moisture content of material using a transient thermal pulse [NASA-CASE-NPO-15493-2] 23 p3933 N85-34373
Modulated voltage metastable ionization detector [NASA-CASE-ARC-11503-1] 23 p3933 N85-34374
Upgrading auxiliary facility outleakage and combustion detection [DE85-012796] 23 p3934 N85-34386
Solar system fault detection [DE85-005987] 23 p3946 N85-34458
Marine Sample Exploitation Project: Estimates regarding the sensitivity and technology for the detection of nuclear explosion debris in the marine environment [DE85-013176] 23 p3947 N85-34462
Magnetic search system [PB85-185108] 23 p3949 N85-34477
Applications of CdTe to nuclear medicine [DE85-011877] 23 p3952 N85-34492
Issues and techniques in touch-sensitive tablet input (executive summary) 23 p3960 N85-34543
On the detectability of key-MeV solar protons through their nonthermal Lyman-alpha emission [SH-1.3-5] 23 p3993 N85-34752
Measurement of low energy cosmic rays aboard Spacelab-1 [SH-10.1-6] 23 p4053 N85-35137
Heavy cosmic ray measurement aboard Spacelab-1 [SH-10.1-7] 23 p4053 N85-35138
A preliminary evaluation of a failure detection filter for detecting and identifying control element failures in a transport aircraft [NASA-TM-87576] 24 p4067 N85-35204
The detection and study of molecular species using time resolved laser spectroscopy [AD-A155910] 24 p4075 N85-35256
Fatigue damage detection in steels by optical correlation [AD-A155830] 24 p4079 N85-35277
LANDSAT-4/5 image data quality analysis [E85-10105] 24 p4107 N85-35463
Literature search for new physical methods for biological aerosol detection [AD-A155683] 24 p4128 N85-35592
Edge detection and geometric methods in computer vision [AD-A155873] 24 p4135 N85-35630
Proceedings of the Workshop on Detectors for Relativistic Nuclear Collisions [LBL-18225] 24 p4146 N85-35700
Detectors for relativistic nuclear collisions (report from the Fixed-Target Hadron Group) 24 p4146 N85-35701
Event parameters: Fixed targets 24 p4146 N85-35702
Working group on penetrating probes at fixed target facilities 24 p4146 N85-35703
Summary of the working group on penetrating probes in collider experiments. 1: The collider environment 24 p4146 N85-35704
Report of working group on detectors for hadrons and event parameters at colliders 24 p4146 N85-35705
Detector requirements for intensity interferometry measurements 24 p4147 N85-35709
A holographic streamer chamber for relativistic nucleus-nucleus collision experiments 24 p4147 N85-35710
A lead glass tubing drift calorimeter 24 p4147 N85-35711
X-ray fluorescence analysis of uranium conce [DE85-013189] 24 p4148 N85-3
Observation of super high energy big family with large scale Fe emulsion chambers [HE-3.4-3] 24 p4182 N85-3
A halo event created at 200 m above the Cha emulsion chamber [HE-3.4-5] 24 p4182 N85-3
A critical analysis of air shower structure functions and size spectrum measurements with the NBU air shower array 24 p4188 N85-3
Measurement of the local density spectrum 24 p4189 N85-3
Character of energy flow in air shower core 24 p4189 N85-3
Observation of EAS using a large water tank 24 p4189 N85-3
The development of air shower in the iron absorber 24 p4189 N85-3
Application of photodiodes to the detection of electromagnetic bursts 24 p4189 N85-3
High-energy neutrinos from a lunar observatory [HE-5.3-21] 24 p4207 N85-3611
Underground measurements on secondary cosmic rays [HE-5.4-1] 24 p4207 N85-3611
Modular detector for deep underwater registration of muons and muon groups [HE-5.4-15] 24 p4208 N85-3612
Application of thermoluminescence for detection of cascade shower 2: Detection of cosmic ray cascade shower at Mount Fuji [HE-7.1-12] 24 p4214 N85-361
DETECTORS
A limbus-sensing eye movement recorder [AD-A144772] 01 p0049 N85-103
Induction voidmeter [DE84-014321] 01 p0050 N85-103
The development and test of ultra-large-format multi-anode microchannel array detector systems [NASA-CR-174247] 07 p1043 N85-16
Leak detectors for organic Rankine cycle power plants: On-line and manual methods [DE85-002792] 12 p1852 N85-2161
Development of high resolution imaging detectors for X-ray astronomy [NASA-CR-175505] 12 p1953 N85-22
Estimation of optimum scores for partition detectors using stochastic approximation techniques 14 p2411 N85-24
Germanium detectors with a built-in transverse drift field [DE85-009944] 18 p3096 N85-291
New concept for a wall detector for alpha particles [DE85-009037] 18 p3183 N85-297
Kalman filter time series analysis of gamma-ray data from NaI(T1) detectors for the ND6620 computer [AD-A154995] 21 p3705 N85-33014
The sidereal anisotropy of cosmic rays around 3 x 10 (15) eV observed at a middle north latitude [OG-5.3-6] 22 p3884 N85-340
The ISAVF opto-mechanical test bed [NASA-TM-87505] 24 p4067 N85-35
Preliminary results on underground muon bundles observed in the Frejus proton-decay detector [HE-5.1-1] 24 p4200 N85-360
DETERIORATION
Life distribution properties of devices subject to deterioration [AD-A145554] 02 p0206 N85-113
Design of alternate launch and recovery surfaces for environmental effects [AD-A145800] 03 p0320 N85-120
Bridge erosion in electrical contacts 04 p0486 N85-1310
Microspots on spectroscopic plates — astronomical photography 07 p0964 N85-16113
Applications of vibration analysis to the condition monitoring of rolling element bearings [ARL/AERO-R-163] 12 p1859 N85-216
Management of Corrosion [AGARD-LS-141] 22 p3749 N85-332
Environmental factors in corrosion and deterioration of materials 22 p3750 N85-33241
Current requirements for the design and maintenance against corrosion of UK military aircraft 22 p3750 N85-3324
Dissected motors-propellants motor number STM-612 Phase 15: Surveillance report, stage 1 [AD-A156066] 24 p4071 N85-352
DETERMINANTS
Computing the Kac determinant using dual mod techniques and more about the No-ghost theorem [DE85-001329] 09 p1375 N85-18
DETERMINATION
U MEASUREMENT

DETONATION

Computer simulation of the shock initiation of detonation in solid explosives
[PML-1984-23] 01 p0033 N85-10207

Combustion and detonation of hydrogen-air mixture in free spaces 02 p0274 N85-11763

The influence of inert particulate material on the properties of RDX/polyethylene wax compositions
[MRL-R-929] 03 p0336 N85-12159

Detonator block
[AD-D011248] 06 p0773 N85-14941

Hazard Studies for Solid Propellant Rocket Motors
[AGARD-CP-367] 08 p1114 N85-17025

Review of USAF treatment of solid propellant rocket motor hazards 08 p1114 N85-17027

Analysis of Deflagration to Shock to Detonation Transition (DSDT) in porous energetic solid propellants
08 p1115 N85-17030

Penguin warhead safety tests
08 p1115 N85-17031

Study of the transition from deflagration to detonation of previously fragmented propellants
08 p1115 N85-17032

Transient combustion: An important consideration in deflagration-to-detonation transition
08 p1116 N85-17037

The DDT process for high energy propellants
08 p1116 N85-17038

Numerical simulation of the shock detonation transition 08 p1116 N85-17039

Influence of temperature on wear resistance of detonation coatings of alloy powders
10 p1447 N85-19116

Transition to detonation from rapid-compression (ramp-waves) generated in a burning porous bed
[AD-P004345] 10 p1455 N85-19169

A thermal-mechanical model of deflagration-to-detonation in granular energetic materials
[AD-P004346] 10 p1455 N85-19170

A summary of the mechanism of delayed detonation
[AD-P004347] 10 p1455 N85-19171

Analysis of Shock to Detonation Transition (SDT) of porous high energy propellant from ramp-wave compression loading
[AD-A148333] 10 p1457 N85-19180

Shock propagation in the exhaust gas handling system of the proposed large altitude rocket cell: Methods and preliminary analysis
[DE85-003055] 11 p1591 N85-20010

Numerical analysis of thermonuclear detonation in dense plasma 11 p1719 N85-20814

Hydrogen flame acceleration and transition to detonation
[DE85-000811] 12 p1802 N85-21299

The detonation of aerosols and vapors of combustible substances under controlled conditions. Part 1: Construction of a test installation
[ISL-R-109/83-PT-1] 14 p2254 N85-23966

Stress in axially symmetrical heavy metal projectiles during discharge — numerical simulation
[ISL-CO-219/83] 14 p2321 N85-24345

Vapor explosions in superheated liquids and fundamental studies of the physics of detonation
[AD-A151362] 15 p2504 N85-25447

Detonations of solid explosives
[AD-A152012] 15 p2521 N85-25540

Analysis of deflagration to detonation transition in high-energy solid propellants 16 p2757 N85-27010

Model for computing late detonations initiated in propellants by impact (XDT reactions)
[DE85-007377] 16 p2758 N85-27019

Generation of detonation waves of given spatial and temporal characteristics
[ISL-R-103/83] 16 p2758 N85-27021

Detonation behavior of LX-14 and PBX-9404: Theoretical aspect
[DE85-010038] 18 p3084 N85-29076

Equation of state for detonation products
[DE85-009608] 18 p3084 N85-29079

Chemical-acoustic interactions in combustion systems
[AD-A153657] 19 p3233 N85-30046

Effect of confinement on failure in 95 TATB/5 KEL-F
[DE85-010790] 19 p3251 N85-30158

Static high pressure study of nitric oxide chemistry: Proposed mechanism for nitric oxide detonation
[DE85-010795] 22 p3746 N85-33220

Combustion-deflagration-detonation transition in a confined spherical powder
[ISL-R-108/84] 22 p3747 N85-33223

Behavior of the porous bed in a combustion-deflagration-detonation transition
[ISL-CO-220/84] 22 p3747 N85-33224

Combustion-deflagration-detonation transition
[ISL-CO-221/84] 22 p3747 N85-33225

Gas composition and molecule velocity in the detonation products of pentaerythritol tetranitrate (PETN) in expansion in a high vacuum container. Analysis by mass spectroscopy and time of flight spectrometry
[ISL-R-109/84] 22 p3747 N85-33226

Explosive containment study
[DE85-011719] 22 p3753 N85-33267

A model of hypersonic two-dimensional oblique detonation wave ramjet
[UTIAS-TN-257] 23 p3897 N85-34139

Intermolecular explosives
[DE85-009609] 23 p3921 N85-34296

Time-resolved spectroscopic studies of detonating heterogeneous explosives
[DE85-009760] 23 p3921 N85-34297

Pressure-shear loading of PBX-9404
[DE85-009982] 23 p3921 N85-34298

Detonation in tungsten-loaded HMX
[DE85-009606] 23 p3922 N85-34299

Modeling heterogeneous high explosive burn with an explicit hot-spot process
[DE85-009593] 23 p3922 N85-34300

Three-dimensional hydrodynamic hot-spot model
[DE85-009587] 23 p3922 N85-34301

Real time analysis of PETN detonation products
[DE85-009581] 23 p3922 N85-34303

Comparison of experimental data on detonation velocity and Chapman-Jouget pressure vs initial HE density with predictions from Ree's model equation of state
[DE85-007266] 23 p3922 N85-34304

Detonation of condensed explosives: Evolution of knowledge in the last 40 years
[ISL-CO-228/84] 23 p3923 N85-34307

Investigation of the lightning vulnerability of nuclear explosive test systems at the Nevada Test Site
[DE85-011761] 24 p4124 N85-35563

Evaluation of nuclear detonation location capability under high attack scenario
[AD-A155761] 24 p4149 N85-35729

DETONATION WAVES

Model study of the interaction of a blast wave with the superstructure of ships. Part 5: Application of optical measurement methods to the study of blast interaction
[PML-1984-12-PT-5] 01 p0057 N85-10375

Parameters of detonation waves excited in gas during concentrated release of energy
02 p0268 N85-11751

Flash radiography as a quantitative tool
[DE84-016465] 04 p0503 N85-13211

Current status of blast wave theory and computations. Volume 2: The quasi-similar solution
[AD-A146538] 06 p0808 N85-15138

Thermal evaporation in blast waves: A model for aneurism formation in the NRL (Naval Research Laboratory) LASER-HANE simulation experiment
[AD-A147006] 07 p0978 N85-16210

Analysis of deflagration to detonation transition in high-energy solid propellants
[AD-A148302] 08 p1135 N85-17156

Dynamic compaction of powders
[DE85-001062] 11 p1612 N85-20137

Waveform control and application of detonation wave in explosives 12 p1820 N85-21420

The behaviour of detonation waves in single phase heterogeneous systems
[AD-A149825] 12 p1846 N85-21581

Vapor explosions in superheated liquids and fundamental studies of the physics of detonation
[AD-A151362] 15 p2504 N85-25447

Viscous effects on blast wave flowfields
[AD-A152013] 15 p2558 N85-25779

NASTRAN analysis comparison to shock tube tests used to simulate nuclear overpressures
15 p2576 N85-25888

The 2-D simulations of the NRL (Naval Research Laboratory) laser experiment
[AD-A154915] 21 p3592 N85-32321

A model of hypersonic two-dimensional oblique detonation wave ramjet
[UTIAS-TN-257] 23 p3897 N85-34139

DETONATORS

Modular detonator device
[AD-D011232] 03 p0340 N85-12184

Detonator block
[AD-D011248] 06 p0773 N85-14941

Parameters affecting hot wire ignition of thermite mixtures
[DE84-016941] 09 p1301 N85-18176

Development of a PETN DDT detonator
[DE84-016944] 09 p1302 N85-18178

CP DDT detonators. Part 1: Design sensitivity study
[DE84-017255] 09 p1302 N85-18180

High-temperature-stable detonators
[DE85-005188] 12 p1818 N85-21402

Nonprimary-explosive, hot-wire detonator
[DE85-005195] 12 p1818 N85-21403

Surveillance program for the dissection and analysis of explosive and pyrotechnic components
[DE85-006105] 16 p2757 N85-27016

CP DDT detonators. 4: Thermal aging
[DE85-011172] 19 p3251 N85-30160

DEUTERIUM

Characterization of ion implanted deuterium traps in nickel by equilibration with deuterium gas
[DE84-014958] 02 p0288 N85-11879

Measurement of scattering cross sections of liquid and solid hydrogen deuterium and deuterium hydride for thermal neutrons
[DE84-014814] 05 p0727 N85-14671

Deuterium abundance in the local interstellar medium
06 p0874 N85-15552

The abundance of deuterium in the outer solar system from ground-based measurements of monodeuterated methane 07 p1060 N85-16725

Deuterium isotope effect on the compatibility between polystyrene and polybutadiene
[AD-A148551] 08 p1134 N85-17145

Deuterium diffusion in a soil-water-ice mixture
[AD-A148457] 08 p1176 N85-17415

NMR study on rotational fluctuation in solid hydrogen and deuterium 09 p1289 N85-18093

Direct measurement of the temperature dependence of the velocity of the reaction of deuterium atoms with vibration-excited hydrogen molecules
[MPIS-12/1984] 11 p1726 N85-20656

Neutral beam injector oxygen impurity measurements and concentration reduction via gettering processes
[DE85-000861] 12 p1836 N85-21521

Tritium catalyzed deuterium Tokamaks
[DE85-004825] 12 p1936 N85-22166

System for forming and focusing high current beam of deuterium ions 13 p2045 N85-22798

Calculations of collision-induced optical gain in high-density mixtures of D2 or HD with a buffer gas
[AD-A151372] 15 p2648 N85-26330

Monodeurated methane in the outer solar system. 2. Its detection on Uranus at 1.6 microns
[NASA-CR-175762] 16 p2882 N85-27782

Possible indication of an A-dependence of R in deep-inelastic electron scattering from nuclei
[DE85-008174] 17 p3033 N85-28763

Trajectories of charged particles traversing a plasma sheath in an oblique magnetic field
[DE85-011070] 19 p3371 N85-30911

Tables of generalized hydrogen diffusion profiles and permeating fluxes for fusion applications
[DE85-008876] 19 p3372 N85-30919

Preparation and use of very pure o-D2
[DE85-009415] 22 p3843 N85-33800

Ultraviolet radiation-damage absorption peak in solid deuterium-tritium, revision 1
[DE85-012969] 22 p3844 N85-33806

Results of a search for deuterium at 25-50 GC/c using a magnetic spectrometer
[OG-4.2-4] 22 p3878 N85-34024

Measuring method and confirmation of H- (D-) ion current by sheet plasma 1
[IPPJ-730] 23 p3974 N85-34638

Size effects of vacuum chamber for H- (D-) ion volume production by sheet plasma 1
[IPPJ-731] 23 p3974 N85-34639

Data on the backscattering coefficients on light ions from solids: A revision
[IPPJ-AM-41-REV] 23 p3982 N85-34689

DEUTERIUM COMPOUNDS

NT DEUTERIUM FLUORIDES

Monodeurated methane in the outer solar system. 2. Its detection on Uranus at 1.6 microns
[NASA-CR-175762] 16 p2882 N85-27782

Nuclear magnetic resonance study of the intramolecular rearrangement of 2-(5-cyanotetrazolato)pentaammine cobalt (III) perchlorate
[DE85-010810] 22 p3839 N85-33772

DEUTERIUM FLUORIDE LASERS

U DF LASERS

DEUTERIUM FLUORIDES

Rotational energy transfer in highly vibrationally excited hydrogen fluoride and deuterium fluoride
[AD-A152003] 16 p2862 N85-27650

DEUTERIUM PLASMA

Background calculations for the measurement of the ion temperature in a deuterium plasma
[DE84-016546] 09 p1393 N85-18768

Scientific activities. A: Reacting plasma physics. 1: Introduction and overview 15 p2654 N85-26370

Plasma heating 15 p2654 N85-26372

Measuring method and confirmation of H- (D-) ion current by sheet plasma 1
[IPPJ-730] 23 p3974 N85-34638

DEUTERON IRRADIATION
Investigation of thick-target neutron emission from Be-9(d,n)B-10 at E(d) = 7 MeV for angles other than zero degrees
[DE85-010254] 20 p3528 N85-31947
DEUTERONS
Performing (p vector, }lc}n), (d vector, n) and (n vector, n) measurements with a rotating magnet beam swinger
[DE84-017003] 04 p0562 N85-13582
Deuteron whistlers at low latitudes in the low altitude topside ionosphere 14 p2366 N85-24625
Cluster production and entropy
[DE85-007626] 17 p3032 N85-28752
Time-resolved energy spectrum of the ion beam generated in the plasma focus 19 p3369 N85-30892
The flux of secondary anti-deuterons and antihelium produced in the interstellar medium
[OG-6.1-5] 22 p3888 N85-34096
The electromagnetic ram action of the plasma focus as a paradigm for the generation of cosmic rays and the gigantic jets in active galaxies
[OG-8.2-14] 23 p4020 N85-34910
DEVELOPING NATIONS
The changing pattern of fossil fuel CO2 emissions
[DOE/OR-21400/2] 02 p0224 N85-11469
Solar energy supplied mobile water purification unit
05 p0664 N85-14270
Realized field tests — solar generators
05 p0664 N85-14271
The potential contributions of the World Climate Program (WCP) to the economies of developing countries
07 p1003 N85-16371
A microprocessor data system for developing countries — climatology 07 p1003 N85-16377
Competitive assessment of the US manufacturing automation equipment industries
[PB85-103927] 10 p1569 N85-19893
The significance of orthophoto maps for developing countries 18 p3124 N85-29341
DEVELOPMENT
Achievements in laser development
01 p0115 N85-10784
Global aspects of stream evolution in the solar wind
[DE85-002207] 11 p1766 N85-21101
DEVIATION
Large deviations for processes with independent increments
[AD-A147293] 08 p1210 N85-17610
Design of single-wheel gyrocompass with correction
14 p2272 N85-24079
DEVICES
Topics in optical materials and device research, 3. Volume 2
[AD-A149727] 12 p1911 N85-21996
DEVITRIFICATION
U CRYSTALLIZATION
DEW POINT
Climate at CRREL (Cold Regions Research and Engineering Laboratory) Hanover, New Hampshire
[AD-A148400] 08 p1189 N85-17495
Precipitable water in the atmosphere, determined from surface dewpoint values 16 p2831 N85-27457
AWS (Air Weather Service) climatic briefs: Asia
[AD-A151944] 16 p2835 N85-27481
Instrumentation for sensing moisture content of mater'al using a transient thermal pulse
[NASA-CASE-NPO-15493-2] 23 p3933 N85-34373
DEWAR SYSTEMS
U CRYOGENIC EQUIPMENT
DEWETTING
U DRYING
DF
U DEUTERIUM FLUORIDES
DF LASERS
Operating characteristics, absorptivity/reflectivity measurements, and pulse system design of the NPS (Naval Postgraduate School) hydrogen fluoride/deuterium fluoride laser
[AD-A152712] 17 p2970 N85-28341
Ship-to-ship propagation: Maritime data analyses
[AD-A155484] 21 p3592 N85-32325
Chemical lasers
[ISL-R-107/84] 23 p3936 N85-34400
DH 115 AIRCRAFT
Long term durability of urea formaldehyde glued joints removed from Vampire aircraft
[AD-A149053] 10 p1424 N85-18965
DHC BEAVER AIRCRAFT
U DHC 2 AIRCRAFT
DHC 2 AIRCRAFT
Application of linear optimal control theory to the design of the elevator control system of the DHC-2 Beaver experimental aircraft
[VTH-LR-411] 16 p2711 N85-26729
DIAGNOSIS
Atmospheric channel performance measurements at 10 to 100 GHz
[PB84-211325] 01 p0042 N85-10271
Application of the CSRL language to the design of expert diagnosis systems: The Auto-Mech experience
[AD-P003922] 02 p0245 N85-11602
Models of natural intelligence in fault diagnosis tasks: Implications for training and aiding of maintenance personnel
[AD-P003927] 02 p0246 N85-11607
Artificial intelligence approaches to monitoring system integrity
[AD-P003930] 02 p0246 N85-11610
The application of basic control laws to human medicine
[DFVLR-MITT-84-13] 05 p0697 N85-14482
A general theory of circuit analogy in fracture diagnosis
[AD-A147177] 07 p0978 N85-16212
Distributed knowledge base systems for diagnosis and information retrieval
[AD-A146890] 07 p1054 N85-16690
Electromagnetic inspection of wire ropes using sensor arrays
[AD-A149016] 10 p1495 N85-19436
Meta-level control through fault detection and diagnosis
[AD-A149064] 10 p1540 N85-19709
Diagnostic system
[INPE-3350-PRE/659] 16 p2841 N85-27519
H1-NMR studies on lymphocyte membranes in human lymphoproliferative diseases 20 p3505 N85-31787
Remote medical diagnosis 21 p3663 N85-32753
Applications of CdTe to nuclear medicine
[DE85-011677] 23 p3952 N85-34492
DIAGRAMS
NT BLOCK DIAGRAMS
NT CIRCUIT DIAGRAMS
NT FEYNMAN DIAGRAMS
NT HERTZSPRUNG-RUSSELL DIAGRAM
NT NYQUIST DIAGRAM
NT PHASE DIAGRAMS
NT S-N DIAGRAMS
NT STRESS-STRAIN DIAGRAMS
The resonant count diagram and solar g mode oscillations 14 p2445 N85-25086
A model for a document maintenance system
23 p3960 N85-34542
DIALYSIS
NT ELECTRODIALYSIS
Synthesis and characterization of novel polymers from non-petroleum sources for use in enhanced oil recovery
[DE85-010922] 19 p3250 N85-30151
DIAMAGNETISM
The plasma assisted modified betatron
[AD-A148728] 09 p1390 N85-18748
Finite-(beta) optimization of tandem mirrors
[DE85-002658] 10 p1560 N85-19635
Diamagnetic instability of cyclotron waves in plasma
21 p3693 N85-32948
DIAMETERS
A low cost approach with larger diameter silicon wafer — solar cells 13 p2006 N85-22572
Spectral evaluation of irregularity of superconducting coaxial cables 13 p2082 N85-23000
Alignment and assembly tool for very large diameter cylinders
[NASA-CASE-MFS-28001-1] 18 p3116 N85-29289
A gel-halo sample pellet: The best of both worlds? Stubby zones without a constricted sample gate
20 p3502 N85-31770
DIAMINES
NT ETHYLENEDIAMINE
NT TRIAMINOGUANIDINIUM AZIDE
A new heat-resistant polymer from dimer diamine bismaleimide. Part 1: Preparation and free radical cure of dimer diamine bismaleimide
[AD-A145664] 02 p0186 N85-11247
Process for preparing highly optically transparent-colorless armomatic polyimide film
[NASA-CASE-LAR-13351-1] 12 p1811 N85-21360
Fire resistant polymers based on 1-(diorgano oxyphosphonyl)methyl-2,4- and 2,6-diamino benzenes
[NASA-CASE-ARC-11512-2] 12 p1811 N85-21362
Polymer intermediates from limonene (follow-up project)
[BMFT-FB-T-84-243] 12 p1814 N85-21380
Remarks on preparation of indandione detection reagents
[NASA-TM-77905] 21 p3560 N85-32146
Preparation of ethylenediamine dinitrate
[DE85-006423] 23 p3922 N85-34305
DIAMOND WINGS
U LOW ASPECT RATIO WINGS
U SWEPT WINGS
DIAMONDS
Fluorinated diamond particles bonded in a filled fluorocarbon resin matrix
[DE84-014444] 01 p0022 N85-1013
The current status of diamond and cubic boron nitride composites 02 p0178 N85-1118
The growth of twins and twin lamellae in synthetic diamond crystals 02 p0181 N85-1121
Process development for the production of technically high quality monocrystalline diamond grits
[BMFT-FB-T-84-204] 08 p1138 N85-1718
Optimization of production of composite diamond-containing materials using titanium carbide-steel alloys 10 p1446 N85-1911
Apparatus for producing diamond-like carbon films
[NASA-CASE-LEW-13837-3] 11 p1615 N85-2015
Electrical resistance measurements of metals to 40 GPa in the diamond cell
[DE85-001009] 11 p1629 N85-2028
Diamondlike flakes
[NASA-CASE-LEW-13837-2] 12 p1796 N85-2125
Sound velocity of carbon at high pressures
[DE85-002016] 12 p1928 N85-2211
Diamond cutters' grinders 13 p2051 N85-2284
Role of fluid lubricant-coolant in fine grinding of optical glass by diamond tool 14 p2280 N85-2412
An analysis of the economics of turning titanium alloys with polycrystalline diamond tools
15 p2567 N85-2584
Classification and types of diamond wear in honing
15 p2567 N85-2584
Geothermal COMPAX drill hit development
[DE85-011353] 20 p3469 N85-3155
Ab initio calculations of materials properties
[DE85-011167] 20 p3531 N85-3198
Single-point diamond crushing of Zerodur with in-situ polishing and metrology on a diamond turning machine
[DE85-012918] 24 p4083 N85-3530
DIAPHRAGM (ANATOMY)
Change in energetics of muscular contraction as a result of hyperoxia 01 p0093 N85-1002
Effects of posture and water immersion on diaphragmatic function 16 p2840 N85-2751
DIAPHRAGMS (MECHANICS)
Scattering of electromagnetic waves in flat waveguide with bilateral diaphragms 03 p0347 N85-1223
Variable friction secondary seal for face seals
[NASA-CASE-LEW-14170-1] 11 p1647 N85-2037
Experimentally determined characteristics of vortex heaters 13 p2050 N85-2283
Theory of diaphragm light modulators with electrical input signal 13 p2082 N85-2300
Effect of diaphragm leakage on turbine stage characteristics 14 p2286 N85-2418
Tuning system for capacitively loaded 1/4 accelerating cavity
[DE85-012516] 24 p4091 N85-3535
Hadrons registration in emulsion chamber with carbon block
[HE-3.7-3] 24 p4186 N85-3598
DIATOMIC GASES
Molecular hydrogen and thermal phases in astrophysics 09 p1414 N85-1882
DIATOMIC MOLECULES
Polarization of radio molecular lines and mapping of magnetic field direction 06 p0878 N85-1558
Spectroscopic studies of lasing transitions in the diatomic mercury halides
[AD-A151553] 15 p2563 N85-2590
Equation of state and two-body correlations for fluids of non-spherical molecules
[AD-A151969] 16 p2783 N85-2717
Computer modeling of vibrational energy levels of potential laser candidates (diatomic molecules)
[AD-A151765] 16 p2790 N85-2720
Calculation of Franck-Condon factors for diatomic molecules
[AD-A154463] 19 p3353 N85-3078
A liquid nitrogen cooled composite wall hollow cathode — molecular spectroscopy
[USIP-85-07] 20 p3526 N85-3193
Vibrationally enhanced dissociation of diatomic molecules
[AD-A154827] 21 p3701 N85-3289
DICARBOXYLIC ACIDS
Condensation of anhydrides or dicarboxylic acids with compounds containing active methylene groups. Part 1: Condensation of phthalic anhydride with acetoacetic and malonic ester
[NASA-TM-77886] 19 p3227 N85-3001
DICHLORIDES
Development of a polysilicon process based on chemical vapor deposition of dichlorosilane in an advanced Siemen's reactor
[NASA-CR-174445] 11 p1672 N85-2052

DICHLORODIPHENYLTRICHLOROETHANE
U DDT
DICHROISM
Multidimensional luminescence measurements
[AD-A154950] 21 p3583 N85-32162
DICHROMATES
U CHROMATES
DICTIONARIES
An operational system for subject switching between controlled vocabularies: A computational linguistics approach
[NASA-CR-3838] 02 p0293 N85-11903
Space Transportation System and associated payloads: Glossary, acronyms, and abbreviations
[NASA-RP-1059-REV] 10 p1428 N85-19007
Glossary of the soil sciences
[PB85-133452] 12 p1952 N85-22263
Glossary of fusion energy
[DE84-017180] 14 p2425 N85-24956
An analysis of data dictionaries and their role in information resource management
[AD-A152134] 16 p2774 N85-27121
Spanish language equivalents for a glossary of terms used in the field of space exploration
[NASA-TM-86211] 19 p3379 N85-30961
Pacific Northwest and Alaska bioenergy program glossary
[DE85-011740] 22 p3808 N85-33591
DIELECTRIC CONSTANT
U PERMITTIVITY
DIELECTRIC MATERIALS
U DIELECTRICS
DIELECTRIC PERMEABILITY
Dielectric measurements in infralow-frequency band
13 p2087 N85-23034
DIELECTRIC POLARIZATION
Center for dielectric studies
[AD-A146183] 03 p0434 N85-12761
Interaction of solutes with stretched polymers
[AD-A154662] 21 p3589 N85-32196
Transient analysis of electromagnetic reflection from dispersive materials
[PB85-200186] 24 p4154 N85-35753
DIELECTRIC PROPERTIES
NT PERMITTIVITY
Recent advances in gaseous dielectrics
[DE84-014279] 02 p0195 N85-11304
Determination of bound water in biological tissue and energy dissipated in bound water by low level microwaves
[AD-A143101] 03 p0399 N85-12547
Extinction by dielectric particles at optical and infrared wavelengths
[AD-A146305] 03 p0413 N85-12640
Dielectric and optical properties of sputtered thin films
[AD-A146210] 03 p0420 N85-12681
Theory of non-linear index of refraction of compound semiconductors
[DE84-013660] 04 p0569 N85-13626
Low frequency electrical properties of selected dielectrics
[DE84-016220] 05 p0632 N85-14052
The HEMP (High-altitude Electromagnetic Pulse) response of a long transmission line buried in the earth
[AD-A146517] 06 p0800 N85-15106
Pulse transmission through frozen silt
[AD-A147106] 07 p0940 N85-15958
A quasi-optical method for measuring the complex permittivity of materials
[AD-A147483] 07 p0941 N85-15966
Monitoring cure of epoxy resins using a microdielectrometer
[AD-A148618] 08 p1119 N85-17054
The use of microdielectrometry in monitoring the cure of resins and composites
[AD-A148619] 08 p1119 N85-17055
Characterization of III-V compound semiconductor device materials
[AD-A148203] 08 p1226 N85-17719
Advanced artificial dielectric materials for millimeter wavelength applications
[AD-A148860] 10 p1431 N85-19027
UHF radiowave propagation through forests
[AD-A149518] 10 p1467 N85-19256
Millimeter wave dielectric property measurement of gyrotron window materials
[DE85-004430] 12 p1802 N85-21304
Method for the fabrication of dielectric isolated junction field effect transistor and PNP transistor
[AD-D011500] 12 p1832 N85-21494
Investigations of radiation-induced and carrier-enhanced conductivity 13 p1996 N85-22515
A simple model of electron beam initiated dielectric breakdown 13 p1996 N85-22516
Monitoring of laminate cure with microdielectrometry
[AD-A150883] 14 p2248 N85-23934
Proceedings of the Cold Electronics Workshop
[NASA-CR-175682] 14 p2297 N85-24220
Design and swept-frequency measurement of printed circuit board log-periodic dipole arrays
[R-NIAS-23] 15 p2539 N85-25671
Scattering properties of a moving dielectric object
[AD-A151974] 15 p2544 N85-25706
In situ microwave measurements of dielectric properties and moisture in materials
[DE85-003622] 16 p2747 N85-26953
Design of the waveguide for microwave heating of solid lithium ceramic blankets
[DE85-009776] 17 p2935 N85-28120
Application of single and multiple scattering techniques to optical properties of dielectric media
19 p3366 N85-30677
Strong coupling effects on bound states in plasmas
[AD-A154353] 19 p3370 N85-30905
Vibrational properties of disordered solids: Far infrared studies
[DE85-010400] 19 p3377 N85-30951
Buildup of electric charge in foil dielectrics during gamma irradiation 22 p3770 N85-33363
Application of field similitude theory to calculation of stripline heating 22 p3780 N85-33419
Waveguide dielectric millimeter band filter with enhanced selectivity 22 p3780 N85-33421
Multidiode integrated-circuit protective device
22 p3781 N85-33425
DIELECTRICS
NT LOSSLESS MATERIALS
NT RADOME MATERIALS
Interaction of a stream of dielectric spheres in an electric field in a high vacuum
[DE84-014714] 01 p0115 N85-10782
Recent advances in gaseous dielectrics
[DE84-014279] 02 p0195 N85-11304
Transformation of heterogeneous surface waves by skewed streams 02 p0259 N85-11697
Center for dielectric studies
[AD-A146183] 03 p0434 N85-12761
Investigation of effect of photocurrent amplification in meta-dielectric-semiconductor structures based on silicon 04 p0486 N85-13110
Microwave measurement of the complex dielectric tensor at anisotropic slab materials
[DE84-017050] 04 p0493 N85-13144
Scattering from thin dielectric disks
[NASA-TM-86155] 06 p0798 N85-15098
Low-loss flexible dielectric waveguide for millimeter-wave transmission and its application to devices
[AD-A147848] 07 p0948 N85-16006
Method of producing a buried long period grating
[AD-D011351] 07 p0969 N85-16153
High specific heat dielectrics and Kapitza resistance at dielectric boundaries
[AD-A148476] 08 p1217 N85-17666
Surface and interfacial properties of Ga(0.47) In(0.53)As alloys
[AD-A148891] 10 p1562 N85-19849
A 10/sup 11/W high current pulse electron beam accelerator described 11 p1620 N85-20200
Adaptation of an air-dielectric RF cable for use as an oil-filled high voltage pulse transmission line
[DE84-017414] 11 p1630 N85-20265
Degradation mechanisms in ceramic dielectrics
[AD-A149791] 12 p1813 N85-21369
Design and calibration of a 35GHz dielectrometer
[AD-P004363] 12 p1826 N85-21457
Program plan for research and development of dielectric materials for electric power systems
[DE85-001327] 12 p1836 N85-21520
Evaluation of resonant modes in isolated dielectric resonators using a surface integral equation formulation
[PB85-110831] 12 p1837 N85-21526
Computer simulation of equipment and processes involved in high-frequency heating of dielectrics
12 p1841 N85-21555
Determining distribution of complex dielectric permittivity over cylindrical body of intricate cross section from electromagnetic field measurement
12 p1842 N85-21559
Electric field effects on ion currents in satellite wakes
13 p1991 N85-22485
Self-consistent simulation of plasma interactions with secondary-emitting insulators 13 p1993 N85-22492
An investigation of arc discharging on negatively biased dielectric conductor samples in a plasma
13 p1994 N85-22498
Characteristics of EMI generated by negative metal-positive dielectric voltage stresses due to spacecraft charging 13 p1995 N85-22506
Discharge pulse phenomenology
13 p1995 N85-22509
Discharge characteristics of dielectric materials examined in mono-, dual-, and spectral energy electron charging environments 13 p1995 N85-22510
Electrical conduction in polymer dielectrics
13 p1996 N85-22514
A simple model of electron beam initiated dielectric breakdown 13 p1996 N85-22516
Dielectric detector device for registering heavy cosmic radiation particles 13 p2045 N85-22799
Scattering of electromagnetic waves by charged particles 13 p2067 N85-22913
Surge strength of symmetric cable with monolithic polyethylene insulation of quads
13 p2082 N85-23001
Chemical interpretation of the relaxed permittivity during epoxy resin cure
[AD-A150955] 14 p2260 N85-24005
Dielectric resonator
[AD-D011573] 14 p2299 N85-24233
Special purpose materials for fusion application
[DE85-005346] 14 p2424 N85-24950
Field-induced phenomena in electrical insulation
[AD-A151234] 15 p2547 N85-25719
Monolithic planar doped barrier limiter
[AD-D011578] 15 p2548 N85-25723
Advanced capacitors
[AD-A151709] 15 p2548 N85-25727
Trends in the electric field enhancement of dielectronic recombination cross sections
[DE85-006920] 16 p2871 N85-27711
Completely consumed carbide: A new process for dielectric isolation
[AD-A152379] 17 p2918 N85-27987
Self-scanning MDS-integrated photosensor strip
17 p2940 N85-28151
Analysis of time dependent dielectric failures
[AD-A153200] 17 p2954 N85-28243
Experimental approaches to the measurement of dielectronic recombination
[DE85-006927] 17 p3030 N85-28743
Integrated electrooptical components using dielectric substrates 18 p3187 N85-29767
Separation of Drude and band-to-band spectra in polyvalent metals
[DE85-010247] 19 p3240 N85-30093
Guided and radiation wave interactions in periodic dielectric waveguides 19 p3253 N85-30173
Dielectric resonator oscillators with digital temperature compensation
[AD-D011715] 19 p3261 N85-30221
High temperature Raman studies of phase transitions in thin film dielectrics
[DE85-010973] 19 p3263 N85-30234
Gyrotron traveling-wave device including quarter wavelength anti-reflective dielectric layer to enhance microwave absorption
[AD-D011690] 19 p3271 N85-30285
A concept for the intrinsic dielectric strength of electrical insulation materials
[NASA-CR-176040] 20 p3448 N85-31410
Chemical structure of interfaces
20 p3480 N85-31629
Guided-mode launching in a slab waveguide by way of diffraction at the edge of a conducting screen residing on one surface of the slab
[AD-A154886] 21 p3575 N85-32232
Radiation-hardened polymeric films
[DE85-011636] 22 p3752 N85-33259
Effect of polymer additives on characteristics of direct-current motor with liquid dielectric filler
22 p3772 N85-33376
Effects of laser radiation on surfaces and coatings
[DE85-010475] 22 p3790 N85-33484
Supermite vacuum interface design
[DE85-012861] 22 p3837 N85-33759
An experimental study of dielectric rod antennas for millimeter-wave imaging applications
[AD-A155832] 24 p4086 N85-35326
DIELECTRONIC SATELLITE LINES
U RESONANCE LINES
DIELS-ALDER REACTIONS
Chemical approach for controlling nadimide cure temperature and rate
[NASA-CASE-LEW-13770-6] 19 p3232 N85-30039
DIENES
NT BUTADIENE
Structural and synthetic organosilicon chemistry
[AD-A147101] 07 p0919 N85-15820
Field test results of experimental EPDM (Ethylene Propylene Diene Monomer) and PUF (Polyurethane Foam) roofing
[AD-A147697] 08 p1132 N85-17133
DIES
Radio frequency probing apparatus for surface acoustic wave devices
[AD-D011230] 01 p0050 N85-10327

Conditions for assembling dies for drawing under hydrodynamic friction conditions
[BLL-M-35954-(5828.4)] 05 p0647 N85-14153
Optimization of the die entrance shape for polymeric extrusion
[DE85-001588] 06 p0772 N85-14937
Computer-aided design of extrusion dies by metal-flow simulation 06 p0797 N85-15094
Correction of engraving stamp for forming blanks of gas turbine engine blades 09 p1307 N85-18213
Precision die forging of blades or gas turbines
17 p2940 N85-28148

DIESEL ENGINES
Cylinder power fault diagnosis in military diesel engines
[TT-8405] 01 p0053 N85-10354
Combustion modeling of a 2 cylinder cycle reciprocating engine
[AD-A144782] 01 p0055 N85-10364
Clean-burning diesel engines
[AD-A145515] 02 p0205 N85-11349
Cooperative program evaluation of NATO multigraded diesel engine oils
[AD-A146072] 03 p0337 N85-12171
Time-temperature dependence of the strength of commercial zirconia ceramics
[AD-A146233] 03 p0338 N85-12173
Development of gas-lubricated pistons for heavy duty diesel engine technology program
[NASA-CR-174746] 03 p0441 N85-12808
Ceramic technology for advanced heat engines program plan
[DE84-013567] 04 p0479 N85-13055
Bulletin of the Faculty of Engineering, Hokkaido University, no. 123
[ISSN-0385-602-X] 04 p0482 N85-13075
Experimental study on the glow plug aided alcohol driven diesel engine 04 p0483 N85-13078
Advanced automotive diesel assessment program
[NASA-CR-168285] 04 p0507 N85-13235
Advanced Automotive Diesel Assessment Program, executive summary 04 p0507 N85-13236
Advanced automotive diesel engine system study
04 p0508 N85-13240
Screw expander for light duty diesel engines
04 p0508 N85-13242
Thermal and mechanical analysis of major components for the advanced adiabatic diesel engine
04 p0508 N85-13243
Overview of waste heat utilization systems
[NASA-TM-86901] 04 p0578 N85-13692
Transformation toughened ceramics for the heavy duty diesel engine technology program
[NASA-CR-174889] 07 p1055 N85-16696
Methods for heat transfer and temperature field analysis of the insulated diesel
[NASA-CR-174783] 07 p1056 N85-16699
FRG ceramic engine components (PET)
08 p1141 N85-17193
An investigation of enhanced capability thermal barrier coating systems for diesel engine components
[NASA-CR-174820] 09 p1298 N85-18154
Natural gas the new locomotive fuel
[DE84-901824] 09 p1302 N85-18179
Speed governor for diesel engine
09 p1307 N85-18214
Structural ceramics in transportation: Fuel implications and economic impacts
[DE85-003024] 11 p1611 N85-20130
Diesel fuel alternatives for engines in civil works prime movers
[AD-A149738] 12 p1817 N85-21400
Sliding seal materials for adiabatic engines
[NASA-CR-174893] 13 p2037 N85-22757
Diesel combustion: Advances in analysis and simulation 14 p2253 N85-23965
JP-8 and JP-5 as compression ignition engine fuel
[AD-A150796] 14 p2263 N85-24022
Transformation toughened ceramics: A potential material for light diesel engine applications
[AD-A151413] 15 p2518 N85-25525
Transformation toughened ceramics: A potential material for light diesel engine application
[AD-A151421] 15 p2518 N85-25526
Fiat conducts R and D in ceramic parts for diesel engine 15 p2534 N85-25637
Diesel engine emissions of particulates and associated organic matter
[PB85-154425] 15 p2590 N85-25964
Breakaway friction and dynamic friction/wear measurements of various ceramic materials from 25 C (75 F) to 650 C (1200 F)
[NASA-CR-174803] 16 p2754 N85-26994
Effect of traffic and meteorology on air pollution
16 p2830 N85-27452
Clean-burning diesel engines
[AD-A152606] 17 p2974 N85-28374
Future of ceramic turbochargers: Promises and pitfalls
[DE85-006209] 17 p2975 N85-28380
Ceramic Technology for Advanced Heat Engines Project
[DE85-008755] 18 p3080 N85-29052
Ceramic coatings for heat engine materials: Status and future needs
[DE85-008759] 18 p3080 N85-29053
Ceramic coatings for heat engine materials
[DE85-005238] 18 p3080 N85-29054
Development of a high-temperature coolant for advanced diesel engines
[AD-A153660] 18 p3117 N85-29297
Development of a coal-water slurry-fueled diesel engine for industrial cogeneration. Task 1.0 topical report: Thermodynamic analysis
[DE85-010455] 19 p3236 N85-30062
A device to detect Top Dead Center (TDC) position in motored engines
[REPT-84-RR-347] 20 p3458 N85-31475
The design of Direct Injection (DI) diesel engines. Injection system by a numerical optimization technique
[REPT-84-RR-346] 20 p3462 N85-31506
Coal slurry ignition in a diesel engine simulator
[DE85-010967] 20 p3463 N85-31513
Noise reduction in the automotive test cell of the Motor Institute of Naples
[REPT-85-RR-361] 20 p3524 N85-31917
An analytical and numerical model of radiation heat transfer in direct injection-type diesel combustion
24 p4092 N85-35368

DIESEL FUELS
Synthesis of transit practice: Diesel fuel quality and effects of fuel additives
[PB84-235688] 05 p0621 N85-13973
Diesel fuel alternatives for engines in civil works prime movers
[AD-A149738] 12 p1817 N85-21400
Chemical characterization and toxicologic evaluation of airborne mixtures. Inhalation toxicology of diesel fuel obscurant aerosol in Sprague-Dawley rats. Phase 3. Subchronic exposures
[AD-A150100] 12 p1905 N85-21966
JP-8 and JP-5 as compression ignition engine fuel
[AD-A150796] 14 p2263 N85-24022
Trends of petroleum fuels
[DE85-000116] 14 p2263 N85-24023
Catalyst and reactor development for a liquid phase Fischer-Tropsch process
[DE85-005894] 17 p2922 N85-28014
The distribution of higher n-alkanes in partially frozen middle distillate fuels
[AD-A153940] 18 p3083 N85-29074
Particle sizing from forward scattered light at two angles using a Variable-Focal-Length optical system
[AD-A154164] 20 p3533 N85-31980

DIETS
Effect of fluid and salt supplements to food allowance on endurance of head-to-pelvis accelerations following 7-day dry immersion and under ordinary motor activity conditions 01 p0092 N85-10618
Nutritional models for space travel from chemically defined diets
[NASA-CR-3850] 03 p0402 N85-12561
Food acquisition: Food ingredients, raw materials and supply 14 p2393 N85-24737
Diet of first Soviet expedition on Mount Everest
19 p3323 N85-30586

DIFFERENCE EQUATIONS
On explicit difference schemes for hyperbolic systems with variable coefficient 2
[PREPRINT-606] 03 p0413 N85-12641
Numerical treatment of corner singularities of the biharmonic equation
[TUM-M8315] 05 p0717 N85-14602
On a random difference equation for matrices and a characterization of the gamma distribution
[AD-A146858] 07 p1029 N85-16529
High order difference schemes with reduced dispersion for hyperbolic differential equations
[CWI-NM-R8406] 11 p1634 N85-20293
Upwind-difference methods for aerodynamic problems governed by the Euler equations
[REPT-84-23] 17 p2893 N85-27834
Intermediate boundary conditions for LOD, ADI and approximate factorization methods
[NASA-CR-172591] 18 p3167 N85-29626
Study of second order upwind differencing in a recirculating flow
[NASA-CR-174939] 19 p3264 N85-30243
Non-model based estimation with applications to sensor calibration using multiple sensors
[AD-A154736] 21 p3589 N85-32306

DIFFERENCES
Individual differences in chromatic brightness matching
[AD-A146882] 10 p1529 N85-19641
An amplitude correlation and differencing method for the monitoring of flaws in repeat ultrasonic inspections
[AERE-R-11416] 15 p2571 N85-25854
Basic research for the geodynamics program
[NASA-CR-175751] 16 p2825 N85-27424
On the relation between upwind-differencing schemes of Godunov, Engquist-Osher and Roe
[NASA-CR-175805] 16 p2852 N85-27580
Retinally stabilized differential resolution television display
[NASA-CASE-NPO-15432-1] 18 p3089 N85-29117
Width of nonlinear difference resonances
[DE85-013026] 24 p4148 N85-35719

DIFFERENTIAL ALGEBRA
U DIFFERENTIAL CALCULUS
U MATRICES (MATHEMATICS)

DIFFERENTIAL AMPLIFIERS
Cascode and differential amplifier using field-effect transistors 15 p2529 N85-25591
High temperature position sensors based on monolithic GaAs Hall IC
[BMFT-FB-T-84-266] 17 p2969 N85-28337

DIFFERENTIAL CALCULUS
A comment on Rosen's comments on activation and inhibition
[CTH-MATH-1984-24] 05 p0719 N85-14617
A geometric approach to high resolution TVD schemes
[NASA-CR-172484] 06 p0857 N85-15446

DIFFERENTIAL EQUATIONS
NT BIHARMONIC EQUATIONS
NT BLASIUS EQUATION
NT BURGER EQUATION
NT CHANDRASEKHAR EQUATION
NT ELLIPTIC DIFFERENTIAL EQUATIONS
NT EULER-CAUCHY EQUATIONS
NT FALKNER-SKAN EQUATION
NT FOKKER-PLANCK EQUATION
NT GAUSS EQUATION
NT HELMHOLTZ VORTICITY EQUATION
NT HYPERBOLIC DIFFERENTIAL EQUATIONS
NT LAME WAVE EQUATIONS
NT LIOUVILLE EQUATIONS
NT MONGE-AMPERE EQUATION
NT PARABOLIC DIFFERENTIAL EQUATIONS
NT PARTIAL DIFFERENTIAL EQUATIONS
NT POISSON EQUATION
NT VLASOV EQUATIONS
NT VORTICITY EQUATIONS
Singular asymptotic expansions in nonlinear rotordynamics
[NASA-CR-174012] 01 p0017 N85-10100
HULL users' manual
[AD-A145000] 01 p0103 N85-10691
Legendre-Tau approximation for functional differential equations. Part 3: Eigenvalue approximations and uniform stability
[NASA-CR-172447] 01 p0110 N85-10744
Quasi-Newton algorithms for large scale nonlinear systems 02 p0208 N85-11370
Boundary conditions in Chebyshev and Legendre methods
[NASA-CR-172469] 02 p0250 N85-11635
Inverse problems, optimization and algorithms
[AD-A145397] 02 p0250 N85-11638
Numerical methods for singularly perturbed differential equations with applications
[AD-A145639] 02 p0252 N85-11650
United States Air Force on research on algebraic manipulation
[AD-A145737] 02 p0253 N85-11655
Discretization formulas on an arbitrary grid
[FFA-MEMO-127] 02 p0253 N85-11659
Forced oscillations theory for resonant extended interaction electron devices
[PR-206] 03 p0358 N85-12298
Control of linear stationary objects subject to external actions by means of various types of feedback
04 p0488 N85-13114
Quasi-three dimensional modeling of functionally-integrated elements of large-scale integrated circuits 04 p0490 N85-13122
Conservation laws and the numerical solution of ODEs
[DE84-016206] 04 p0555 N85-13531
Interval mathematics reports
[REPT-84/1] 04 p0556 N85-13534
Interval-mathematical treatment of initial value problems of ordinary differential equations
04 p0556 N85-13536
Supersymmetric Yang-Mills fields as an integrable system and connections with other non-linear systems
[DE84-013231] 04 p0556 N85-13539

New integration techniques for chemical kinetic rate equations. 2: Accuracy comparison
[NASA-TM-86863] 05 p0596 N85-13798
USSR report: Physics and mathematics
[JPRS-UPM-84-007] 05 p0723 N85-14651
Design of swirled axisymmetric turbulent jets
05 p0724 N85-14657
Iterative method of calculating strength of airframe members using finite element method
06 p0775 N85-14955
Controllable rotation of system of two solid bodies with elastic elements 06 p0780 N85-14986
Integrating chemical kinetic rate equations by selective use of stiff and nonstiff methods
[NASA-TM-86923] 07 p0904 N85-15726
An asymptotic analysis of a transient p-n junction model
[AD-A147270] 07 p0947 N85-16004
Art of programming programmable microcalculators. Part 12: Solution of differential equations
07 p0953 N85-16043
Dynamical characteristics of weak turbulence
[AD-A147186] 07 p0959 N85-16075
Strain-controlled creep rupture in non-isothermal materials 09 p1332 N85-18368
Fixed vs. variable order Runge-Kutta
[DE85-001320] 09 p1374 N85-18639
Magnetostatic problems in nonlinear media with hysteresis
[DE85-003701] 10 p1482 N85-19358
Locally univalent functions in the unit disk
10 p1536 N85-19680
A note on the disturbance decoupling problem for retarded systems
[AD-A149045] 10 p1543 N85-19730
Modeling the internal combustion engine
[NASA-RP-1094] 10 p1544 N85-19733
Asymptotic representation of solutions of the basic semiconductor device equations
[AD-A149040] 10 p1545 N85-19741
Periodic solutions of prescribed energy for a class of Hamiltonian systems
[AD-A149487] 10 p1548 N85-19764
Numerical solution of semilinear elliptic problems on unbounded domains
[AD-A149559] 10 p1549 N85-19767
Using semigroups and the Trotter product formula to solve quasi-linear systems
[DE85-002041] 11 p1706 N85-20736
Solution of structured non-stiff ODEs
[DE85-004137] 11 p1707 N85-20741
A comparison of the efficiency of numerical methods for integrating chemical kinetic rate equations
[NASA-TM-83590] 12 p1778 N85-21162
The performance of a type-insensitive Runge-Kutta code on a personal computer
[TUM-8410] 12 p1919 N85-22048
Differentiating matrices for arbitrarily spaced grid points
[NASA-CR-172556] 12 p1919 N85-22051
Nonlinear partial differential equations and related problems of Pade approximations
[AD-A149650] 12 p1920 N85-22059
Low-dimensional behavior of the pattern formation Cahn-Hilliard equation
[DE85-003727] 12 p1922 N85-22072
Singular asymptotic expansions in nonlinear rotordynamics 12 p1945 N85-22218
New results on the PLL false lock phenomenon
12 p1948 N85-22236
Nonlinear rotordynamics analysis
[NASA-CR-171425] 13 p1966 N85-22364
Controlled movement of elastic manipulator with distributed parameters 13 p2048 N85-22818
Mathematical modeling of transient performance of gas turbine engine 13 p2050 N85-22834
Flow around axisymmetric bodies with uniform-velocity zones 14 p2276 N85-24103
Solving large linear systems 14 p2396 N85-24759
Maintaining soluation invariants in the numerical solution of ODEs
[DE85-005918] 14 p2410 N85-24857
Simple-motion pursuit-evasion differential games in the plane
[CSIR-TWISK-336] 14 p2412 N85-24874
Kinematic dynamo theory for an arbitrary mean flow
14 p2448 N85-25106
One method for constructing model of point masses of planetary gravity field 15 p2479 N85-25300
Resonant rotations of satellite in polar orbit in magnetic and gravitational fields 15 p2479 N85-25302
Equilibrium solutions, stabilities and dynamics of Lanchester's equations with optimization of initial force commitments
[AD-A151510] 15 p2637 · N85-26266
A new approach to queer differential equations
[AD-A149321] 15 p2638 N85-26272
Fundamental equivalence of generalised state space systems
[MATHEMATICS-RESEARCH-182]
15 p2642 N85-26293
Finite axisymmetric deformation of a thin shell of revolution 16 p2798 N85-27251
Use of REDUCE 2 for symbolic programming
[INPE-3355-PRE/633] 16 p2846 N85-27544
Explicit construction of contractivity matrices
[TRITA-NA-8309] 16 p2852 N85-27586
Evaluation of an algorithm for the solution of the time-dependent Euler equations
[AD-A151993] 16 p2854 N85-27600
Projected discrete ordinates methods for numerical transport problems
[DE85-005632] 17 p3020 N85-28678
Spatial differencing for finite difference codes
[DE85-006902] 17 p3021 N85-28684
Dynamical systems and numerical integration
[CWI-AM-R8413] 17 p3022 N85-28695
Symmetric linear multistep methods for second-order differential equations with periodic solutions
[CWI-NM-R8501] 17 p3022 N85-28698
Unsymmetrical flow in a centrifuge
[DE85-009021] 18 p3103 N85-29208
A global optimization algorithm using stochastic differential equations
[AD-A153526] 18 p3161 N85-29583
Shock capturing
[NASA-CR-172592] 18 p3168 N85-29627
Sensitivity analysis of initial value problems with mixed ode's and algebraic equations
[AD-A153528] 18 p3169 N85-29637
Determinal representations of polynomials satisfying linear Ordinary Differential Equations (ODEs) or linear recurrence relations
[PREPRINT-417] 18 p3172 N85-29660
Some applications of a convenient finite-dimensional matrix representation of the differential operator
[PREPRINT-418] 18 p3172 N85-29661
Interpolation and differentiation for periodic functions
[PREPRINT-419] 18 p3172 N85-29662
An introductory view of Raman-Nath type equations
[PREPRINT-422] 18 p3172 N85-29664
Numerical tests of a novel technique to compute the eigenvalues of differential operators
[PREPRINT-427] 18 p3173 N85-29667
Application of Floquet theory to helicopter blade flapping stability
[AD-A154460] 19 p3218 N85-29952
Control and regulation of generalized linear systems
19 p3257 N85-30193
Quantized Hall effect in two-dimensional electron systems
[AD-A154347] 19 p3259 N85-30211
Multigrid method for multiprocessors
[DE85-007929] 19 p3333 N85-30647
Numerical methods for the solution of stiff delay differential equations 19 p3334 N85-30653
MECA: A multiprocessor concept specialized to Monte Carlo
[DE85-010791] 19 p3346 N85-30737
Solving Volterra integral equations with ODE codes
[DE85-011216] 19 p3346 N85-30740
Computer-controlled carburizing
[BLL-OA-TRANS-3204-(6196.300)]
20 p3429 N85-31268
An analysis of multi-fingered hands
20 p3462 N85-31504
A theoretical model for the study of nonlinear dynamics of magnetic bearings 20 p3462 N85-31505
Spectral Theory of Sturm-Liouville Differential Operators: Proceedings of the 1984 Workshop
[DE85-009693] 20 p3520 N85-31890
Attractors for the Kuramoto-Sivashinsky equations
[DE85-009631] 20 p3520 N85-31892
Development of reduced order models for control system design using the OPTSYSX program
[AD-A154552] 21 p3556 N85-32124
Size spectra for the source-enhanced coagulation with the turbulent mass transfer 21 p3645 N85-32649
SIGMA - A stochastic-integration global minimization algorithm
[AD-A154876] 21 p3671 N85-32806
Identification of unsteady aerodynamics and aeroelastic integro-differential systems
[NASA-TM-86749] 21 p3676 N85-32851
Exact solutions of singular equations for viscous transsonic flows 21 p3683 N85-32882
One method of solving the problem of unsteady heat exchange of a body and its ablation
22 p3733 N85-33146
Gradient scaling for nonuniform meshes
[DE85-009625] 22 p3784 N85-33443
Stochastic groundwater flow modeling using the second-order method
[DE85-011250] 22 p3802 N85-33556
Experiments and improvements of the ordinary differential equation solvers DEPAC on the CRAY computer
[DE85-013260] 22 p3831 N85-33726
Implementing linear multistep formulas for solving DAES
[DE85-012400] 22 p3834 N85-33740
Nonlinear flap-lag-extensional vibrations of rotating, pretwisted, preconed beams including Coriolis effects
[NASA-TM-87102] 23 p3941 N85-34427
DISPL1: A software package for one and two spatially dimensioned kinetics-diffusion problems
[ANL-84-56] 23 p3956 N85-34516
A geometric modeller for turbomachinery applications
23 p3962 N85-34556
Second-order Compton-Getting effect on arbitrary intensity distribution
[SH-3.1-10] 23 p4002 N85-34814
The application of bispectral analyses to aeroelastic phenomena 24 p4060 N85-35157
Identification and control of structures in space
[NASA-CR-176175] 24 p4069 N85-35214
Noise-sustained structure, intermittency and the Ginzburg-Landau equation
[DE85-009626] 24 p4094 N85-35379
A new theory for multistep discretizations of stiff ordinary differential equations: Stability with large step sizes
[NASA-CR-177941] 24 p4142 N85-35675
A new method for boundary value problems
[AD-A155934] 24 p4143 N85-35683

DIFFERENTIAL GEOMETRY
NT LIE GROUPS
NT RIEMANN MANIFOLD
NT SPINOR GROUPS
NT TENSOR ANALYSIS
Analytical foundations of the theory of quasiconformal mappings in Rn 10 p1536 N85-19679
On rotation automorphic functions with descrete rotation groups 10 p1536 N85-19686
Supermanifolds and Berezin's new integral
[DE85-001833] 11 p1706 N85-20732
A deformation analysis of flat flexible gear and its equation of original curved surfaces
[NASA-TM-77493] 12 p1859 N85-21660
Zero-crossings on lines of curvature
[AD-A150171] 13 p2150 N85-23345

DIFFERENTIAL INTERFEROMETRY
Measurement of ultrasonic fields in transparent media using a scanning differential interferometer
[NASA-CR-175921] 17 p3028 N85-28726

DIFFERENTIAL OPERATORS
U DIFFERENTIAL EQUATIONS
U OPERATORS (MATHEMATICS)

DIFFERENTIAL THERMAL ANALYSIS
U THERMAL ANALYSIS

DIFFERENTIATION
Differentiating spatial light modulator
[AD-D011727] 23 p3973 N85-34632

DIFFERENTIATION (BIOLOGY)
Gravity and cell differentiation in lentil roots
05 p0690 N85-14433

DIFFRACTION
NT ELECTRON DIFFRACTION
NT FRESNEL DIFFRACTION
NT NEUTRON DIFFRACTION
NT WAVE DIFFRACTION
NT X RAY DIFFRACTION
A determination of the photochemical quantum yields from 2 excited triplet states of biacetyl using holography
[AD-A145091] 01 p0050 N85-10326
Cerenkov radiation in the neighborhood of the emission threshold, revised
[AD-A145458] 02 p0264 N85-11655
Characteristics of light diffraction by two acoustic waves, one with complex frequency composition
03 p0348 N85-12243
DRG theory on the basis of a discrete interaction model
[PR-215] 03 p0358 N85-12297
Transient currents of ideally conducting body of revolution with transient diffraction
06 p0785 N85-15019
Unstable optical resonator with cancelling edge waves
[AD-D011379] 07 p1042 N85-16618
Switchable zero order diffraction gratings as light valves
[AD-A147575] 07 p1044 N85-16633
The evaluation of a deformable diffraction grating for a stigmatic EUV spectroheliometer
[NASA-CR-174350] 09 p1322 N85-18309
Field implementation of geophysical diffraction tomography
[DE84-017594] 09 p1343 N85-18449

Diffraction diffusion screen with holographically-suppressed zero-order beam
[AD-D011445] 10 p1487 N85-19387

Diffraction-limited imaging of space objects 2
[AD-A149344] 11 p1728 N85-20670

High resolution diffraction grating
[AD-D011541] 12 p1933 N85-22141

Switchable zero order diffraction gratings as light valves
[AD-A150129] 12 p1934 N85-22153

Reflex attachment for line alignment in spectral diffraction devices 13 p2044 N85-22794

Integrated optical components utilizing acoustooptic and electrooptic diffraction in micro-waveguides
13 p2089 N85-23044

Acoustooptic cell as space-frequency filter
13 p2090 N85-23051

Application of modern Aperture Integration (AI) and Geometrical Theory of Diffraction (GTD) techniques for analysis of large reflector antennas
14 p2234 N85-23851

Millimeter-wave diffraction devices and materials
[AD-A150676] 14 p2418 N85-24917

Sizing capability of automated ultrasonic time-of-flight diffraction in thick section steel and aspects of reliable inspection in practice
[AERE-R-11548] 15 p2571 N85-25855

An X-ray study of residual stresses in narrow groove TIG weldments
[DE85-006465] 16 p2802 N85-27274

The problem of atmospheric turbulence
[NASA-CR-175783] 16 p2832 N85-27464

Experimental studies of diffractive phenomena
[DE85-006812] 17 p3031 N85-28749

Investigation of superlattice device structures
[NASA-CR-3903] 18 p3094 N85-29152

NBS (National Bureau of Standards) reactor: Summary of activities Jul. 1983 through Jun. 1984
[PB85-184836] 20 p3522 N85-31907

Switchable zero order diffraction gratings as light valves
[AD-A154471] 20 p3533 N85-31961

Guided-mode launching in a slab waveguide by way of diffraction at the edge of a conducting screen residing on one surface of the slab
[AD-A154886] 21 p3575 N85-32232

Optical image of bounded objects
21 p3697 N85-32966

Picosecond-pulse damage studies of diffraction gratings
[DE85-010785] 22 p3790 N85-33481

Optical receivers using rough reflectors
[NASA-CR-176200] 24 p4154 N85-35750

DIFFRACTION GRATINGS
U GRATINGS (SPECTRA)

DIFFRACTION PATTERNS
NT RAINBOWS

A physical interpretation of the structure and electron-optical data for spinel (MgAl2O4)
[AERE-R-11276] 03 p0434 N85-12767

A short note on the high precision navigation of QUASAT 07 p1059 N85-16722

Structural characterization by intensity measurements of electron diffraction patterns
[DE85-004803] 13 p2164 N85-23427

Diffraction analysis of mesh deployable reflector antennas 14 p2235 N85-23854

Image formation in terms of the transport equation
[DE85-004993] 15 p2653 N85-26365

The development and implementation of an optical communications laboratory
[AD-A151682] 16 p2772 N85-27111

DIFFRACTION PROPAGATION

Problems on the diffraction and propagation of waves (selected articles)
[AD-A145139] 01 p0038 N85-10240

Intensity fluctuations of focused laser beam during reflection in turbulent atmosphere
13 p2078 N85-22975

DIFFRACTION TELESCOPES
U SPECTROSCOPIC TELESCOPES

DIFFRACTOMETERS

Neutron interferometry and double diffractometer for condensed matter 03 p0424 N85-12705

Construction of a neutron single crystal diffractometer
03 p0427 N85-12723

DIFFUSE RADIATION

The soft X-ray diffuse background: Implications for the nature of the local interstellar medium
06 p0876 N85-15566

Local contributions to the 0.6 keV diffuse X-ray background 06 p0877 N85-15569

HEAO-1 diffuse soft X-ray sky maps
06 p0877 N85-15570

Observations of local ISM emission with the Berkeley EUV/FUV shuttle telescope 06 p0880 N85-15594

The HEAO-1 diffuse component spectrum from 15 to above 500 keV — X and gamma rays
08 p1240 N85-17820

Weather data for simplified energy calculation methods. Volume 1. Eastern United States: TRY data
[DE85-000493] 09 p1358 N85-18541

Diffuse reflection of light from turbid conservative medium of finite thickness with incidence of beam on surface of scattering glancing 14 p2342 N85-24481

Nineteenth International Cosmic Ray Conference. OG sessions, volume 1
[NASA-CP-2376-VOL-1] 22 p3860 N85-33902

Cosmic gamma rays from quasars
[OG-2.7-10] 22 p3872 N85-33983

Relevance of cosmic gamma rays to the mass of gas in the galaxy
[OG-3.1-8] 22 p3874 N85-33996

COS-B gamma-ray sources and interstellar gas
[OG-3.1-9] 22 p3874 N85-33997

Spectrum of the gamma-ray diffuse component observed from HEAO-1
[OG-3.1-12] 22 p3874 N85-34000

Diffuse galactic annihilation radiation from supernova nucleosynthesis
[OG-3.2-8] 22 p3875 N85-34004

Literature search for new physical methods for biological aerosol detection
[AD-A155883] 24 p4128 N85-35592

DIFFUSERS

Turbo fluid machinery and diffusers
[NASA-TM-77467] 08 p1167 N85-17363

Determination of total pressure losses in stepped annular diffusors with curvilinear outer walls and uniform velocity field at inlet 09 p1306 N85-18203

A diffuser heat transfer code
[AD-A149270] 10 p1430 N85-19022

Mathematical modeling of the AEDC (Arnold Engineering Development Center) propulsion wind tunnel (16T)
[AD-A151293] 15 p2475 N85-25275

DIFFUSION
NT AMBIPOLAR DIFFUSION
NT ATMOSPHERIC DIFFUSION
NT ELECTRON DIFFUSION
NT GASEOUS DIFFUSION
NT GASEOUS SELF-DIFFUSION
NT IONIC DIFFUSION
NT MOLECULAR DIFFUSION
NT PARTICLE DIFFUSION
NT PLASMA DIFFUSION
NT SELF DIFFUSION (SOLID STATE)
NT SELF PROPAGATION
NT SURFACE DIFFUSION
NT THERMAL DIFFUSION
NT TURBULENT DIFFUSION

An investigation of the solubility and diffusivity of chromium in gallium arsenide
[AD-A144949] 01 p0024 N85-10148

Nuclear Magnetic Resonance of Polymeric Materials
[AD-A145078] 01 p0032 N85-10192

NMR (Nuclear Magnetic Resonance) and macromolecular migration in a melt or in concentrated solutions
[AD-P003908] 01 p0032 N85-10194

Sea water rope batteries
[AD-A144775] 01 p0042 N85-10275

Solution of the Boltzmann transport equations for a permeable base transistor
[AD-A144969] 01 p0112 N85-10757

Trapping for Newtonian diffusion processes
[REPT-73] 01 p0130 N85-10893

Review: The influence of short circuit diffusion on the oxidation of nickel, chromium and nickel/chromium alloys
[AERE-R-11311] 02 p0185 N85-11237

A dispersion model for airborne particulates inside a building
[DE84-014961] 02 p0225 N85-11473

Green River air quality model development: Meteorological and tracer data, July/August 1982. Field study in Brush Valley, Colorado
[DE84-014975] 02 p0225 N85-11474

Pointwise iterations of finite element modeling of advection-diffusion equations
[DE84-015284] 02 p0253 N85-11656

Comparison of the multigrid and ICCG methods in solving the diffusion equation
[DE84-014409] 02 p0253 N85-11657

Method of splitting for solution of problems in semiconductor physics 02 p0265 N85-11736

Problems in theory of diffusion under shock wave
02 p0272 N85-11776

Transport phenomena in the boundary layer during solution solidification under microgravity. Ice growth from a water-salt solution
[BMFT-FB-W-84-031] 03 p0329 N85-12121

Diffusion of Cr-51 tracer in Cr-2O-3 and the growth of Cr-2O-3 films
[AERE-R-11314] 03 p0333 N85-121

Analysis techniques for tracer studies of oxidation
[NASA-CR-174796] 03 p0336 N85-121

Effects of core mixing on solar oscillation frequencies
[DE84-015540] 03 p0449 N85-12

Diffusion of gases in porous solids: Simulation and measurements
[DE84-016292] 04 p0500 N85-131

Diffusion mechanisms and point defects in transition-metal oxides
[DE84-016236] 04 p0571 N85-13

Oxygen diffusion from anodic surface oxide films on titanium subhydride studies by auger electron spectroscopy and electron energy loss spectroscopy
[DE84-016942] 04 p0572 N85-13

Zero-flux planes and flux reversals in multicomponent diffusion
[DE84-015212] 05 p0618 N85-13

Parallel flow diffusion battery
[DE84-005964] 05 p0631 N85-1404

Coupling of multidirectional diffusions by reflection
[CTH-MATH-1984-20] 05 p0719 N85-14

Transport and relaxation processes in supercritical fluids
[DE84-006591] 05 p0731 N85-14

Reducing numerical diffusion for incompressible flow calculations
[NASA-TM-83621] 06 p0756 N85-14

Mechanisms of impurity diffusion in rutile
[DE84-014741] 06 p0766 N85-14

The structure of dilute combusting sprays
[NASA-CR-174636] 07 p0905 N85-157

Diffusion in metals under high mechanical strain and acceleration
[JUEL-1913] 07 p0928 N85-15

Dependence of breakdown voltage for p-n junction on parameters of ion implantation and semiconductor heat treatment 07 p0954 N85-160

Hydrologic characteristics of the Mediterranean and Black Sea 07 p0961 N85-16

Estimation for a semimartingale regression model using the method of sieves
[AD-A146809] 07 p1028 N85-1652

Hydrogen embrittlement of nickel
[AD-A148322] 08 p1129 N85-1711

Deuterium diffusion in a soil-water-ice mixture
[AD-A148457] 08 p1176 N85-1741

Study of controlled diffusion stator blading
[NASA-CR-167995] 09 p1281 N85-18

Hydrogen trapping, diffusion, and recombination in austenitic stainless steels
[DE85-001871] 09 p1294 N85-181

Stability of amorphous metals on semiconductor substrates
[DE84-017256] 09 p1295 N85-1813

Battery response to pulse loads: A mathematical model
[DE85-001149] 09 p1316 N85-182

Large deformations of a nonlinear elastic solid and the diffusion of an ideal fluid treated as interacting continua
09 p1330 N85-18

Metal atom diffusion in amorphous silica and at the silica surface
[DE84-017351] 09 p1380 N85-18

Cavitation phenomenon in superplastic creep
[DE85-001716] 10 p1441 N85-190

Diffraction diffusion screen with holographically-suppressed zero-order beam
[AD-D011445] 10 p1487 N85-193

A study of interdiffusion in beta + gamma/gamma + gamma prime Ni-Cr-Al
[NASA-CR-174852] 11 p1597 N85-204

Improving operational properties of titanium alloys by diffusion siliciding 11 p1602 N85-20

Distribution of hydrogen in multi-layer welded joints of alloyed steels 11 p1603 N85-20

Analysis of diffusion in an ion-implanted alloy using a phenomenological model
[AERE-R-11527] 11 p1609 N85-20

Comparison of MESOI atmospheric dispersion estimates with data and estimates from other models
[DE85-002372] 11 p1678 N85-20

Evaluation of two numerical integrator schemes
[PB85-138196] 11 p1683 N85-20

Solid electrolytes: Mechanisms for achieving optimal conductivity
[AD-A150116] 12 p1801 N85-21

The behaviour of detonation waves in single phase heterogeneous systems
[AD-A149825] 12 p1846 N85-21

Time and space variability of turbulent concentration fluctuations
[AD-A149963] 12 p1896 N85-21

A diffusion process and its application to detecting a change in the drift of Brownian motion
[AD-A150096] 12 p1926 N85-22100
Enhanced diffusion from interstitial trapping during solid-phase-epitaxial growth of silicon alloys
[DE85-001285] 12 p1941 N85-22193
Diffusion deposition in fibrous filters for parallel and transverse flow models
[DE85-006149] 13 p2093 N85-23066
Cathode materials for molten carbonate fuel cells
[DE85-004078] 13 p2130 N85-23254
The ASCOT Data Analysis Workshop
[DE85-004407] 13 p2139 N85-23283
Material research in microgravity
[NASA-TM-77628] 14 p2228 N85-23811
The effect of water chemistry on the rates of hydrogen generation for galvanized steel corrosion at post-loca conditions
[NUREG/CR-3361] 14 p2253 N85-23963
Tracer diffusion in an ordered alloy: Application of the path probability and Monte Carlo methods
[DE85-002766] 14 p2257 N85-23986
Synthetic acceleration of coarse-mesh S/sub n/ transport calculations
[DE84-014721] 14 p2409 N85-24855
Weak convergence of a sequence of queueing and storage processes to a singular diffusion
[AD-A150855] 14 p2411 N85-24866
Steady state solution of the Fokker-Planck equation combined with unidirectional quasilinear diffusion under detailed balance conditions
[DE85-004917] 14 p2425 N85-24959
Experimental check of ion transport mechanism in Earth's radiation belt with exposure to nonsteady-state electric fields 15 p2480 N85-25306
Ways of improving level and stability of mechanical characteristics of diffusion-welded joints of OT4 titanium alloy 15 p2499 N85-25417
Structure and mechanical properties of dispersion-hardened nickel alloy joints welded by diffusion 15 p2500 N85-25422
Titanium diffusion method prevents metal corrosion
15 p2514 N85-25510
Development and diffusion of automated clinical chemistry analyzers
[PB85-150696] 15 p2561 N85-25798
Ionic conduction and water diffusion in Li (BETA)-alumina
[DE85-007548] 16 p2755 N85-27005
The seasonal cycle of atmospheric CO in the Southern Hemisphere 16 p2830 N85-27447
Comparison of a diffusion model with dye dispersion measurements to study turbulence in coastal waters
[INPE-3492-PRE/729] 16 p2838 N85-27504
A mathematical model for calculating detection probability of a diffusion target
[AD-A152026] 16 p2854 N85-27601
Polycrystalline semiconductor heterojunction modelling (CdS/CuInSe(sub)2)
[DE85-002913] 16 p2871 N85-27713
The development of laser analytical methods for the characterization of solid-liquid and solid-high pressure gas interfaces
[AD-A152382] 17 p2918 N85-27988
Use of principle of local equilibrium for assessing diffusional supersaturation during solidification of alloys
[BLL-BISI-TRANS-22487-(9022.06)]
17 p2929 N85-28077
Metallurgical means of preventing the corrosion of metal
[BLL-BISI-TRANS-22320-(9022.06)]
17 p2929 N85-28082
The effect of ion-bombardment-induced atomic mixing on depth-profiling of interfaces
[AD-A153199] 17 p3044 N85-28834
Strutless diffuser for gas turbine engine
[AD-D011662] 18 p3062 N85-28943
In situ Tuff water migration/heater experiment
[DE85-010415] 18 p3101 N85-29200
Analysis and model/data comparisons of large-scale releases of nitrogen tetroxide
[DE85-009069] 18 p3133 N85-29406
International space research perspectives of commercialization for German industry
[NASA-TM-77657] 19 p3222 N85-29979
Study of phase equilibria and crystallization processes in Al-Zn-Mg alloy systems 19 p3241 N85-30098
Technical guide for estimating fugitive dust impacts from coal handling operations. Volume 1: Project summary
[DE85-010948] 19 p3309 N85-30515
On MGR (Upsilon) multigrid methods
[AD-A153887] 19 p3345 N85-30733
Tables of generalized hydrogen diffusion profiles and permeating fluxes for fusion applications
[DE85-006676] 19 p3372 N85-30919
Application of the Diffusion Raman Anti-Stokes Coherent (DRASC) method to a SNECMA combustion chamber
[YKC-3086/84] 20 p3425 N85-31260
Measurement of electrical parameters and current components in the bulk of silicon solar cells
20 p3461 N85-31635
High efficiency large area polysilicon solar cells
20 p3482 N85-31639
A positron annihilation Doppler broadening study of niobium
[DE85-010287] 20 p3527 N85-31936
Permeation of mixed penetrants through glassy polymer membranes
[AD-A155605] 21 p3570 N85-32207
A multilevel-multigrid method for recirculating flows
21 p3583 N85-32271
Simultaneous junction formation
21 p3610 N85-32426
Notes on atmospheric stability, turbulence, and its measurements
[AD-A155230] 21 p3637 N85-32588
Scavenging of submicron aerosol particles by snow crystals: Theory and experiments
21 p3648 N85-32667
Evaluation of the 2DFLOW and hybrid complex-terrain dispersion models with the 1980 ASCOT data base from the Geysers
[DE85-012960] 22 p3812 N85-33613
Airborne cloud tracking measurements during the Three Mile Island nuclear station accident, Middletown, Pennsylvania. Date of survey: March - June 1979
[DE85-012060] 22 p3816 N85-33638
A model for the proton spectrum and cosmic ray anisotropy
[OG-5.4-12] 22 p3887 N85-34089
New semi-implicit method for solving the time-dependent conservation equations for incompressible flow
[DE85-010926] 23 p3931 N85-34367
Evaluation of source strength and dispersion model predications with data from large nitrogen tetroxide field experiments
[DE85-011855] 23 p3947 N85-34465
User's guide to the MATHEW/ADPIC models
[DE85-012952] 23 p3966 N85-34587
Grain boundary and surface diffusion in oxide systems
[DE85-007291] 23 p3985 N85-34715
The model-independence of cosmic ray source determinations
[OG-7.2-1] 23 p4014 N85-34873
The role of cosmic rays in magnetic hydrodynamics of interstellar medium
[OG-7.2-15] 23 p4015 N85-34882
IMF-sense-dependent cosmic ray anisotropy produced from diffusion-convection in heliosphere
[SH-4.3-9] 23 p4032 N85-34994
Diurnal anisotropy during solar activity cycle twenty and diffusion-convection model
[SH-4.5-7] 23 p4036 N85-35025
Noise in sodium beta alumina crystals
[AD-A156025] 24 p4161 N85-35798
The nucleon intensity in the atmosphere and the Pt distribution
[HE-3.1-9] 24 p4178 N85-35907
Development of electromagnetic cascades in the atmosphere including the Landau-Pomeranchuk-Migdal effect
[HE-4.5-5] 24 p4195 N85-36029
Search for tachyons associated with extensive air showers in the ground level cosmic radiation
[HE-6.2-13] 24 p4212 N85-36149

DIFFUSION BONDING
U DIFFUSION WELDING

DIFFUSION COEFFICIENT
Definition of global dispersion coefficients — aquifers
[PSE-83/4-B] 01 p0064 N85-10426
Radiotracer studies of the dispersion of solid pollutants in marine and estuarial environment: Measurement of diffusion coefficients and the phenomenon of dispersion by currents
[BLL-DRIC-TRANS-7104-(3623.66)]
02 p0224 N85-11468
Diffusion and intermittency in an extended one-dimensional maps 02 p0282 N85-11834
Long time correlation and stochastic diffusion in the standard map 02 p0282 N85-11835
Diffusion of Fe-55 in Fe-2O-3 single crystals
[AERE-R-11266] 03 p0333 N85-12147
Monte Carlo studies of transport in stellarators
[DE84-017633] 04 p0568 N85-13625
Low temperature diffusion coefficients in the Fe-Ni and FeNiP systems: Application to meteorite cooling rates
06 p0886 N85-15626
Diffusion in metals under high mechanical strain and acceleration
[JUEL-1913] 07 p0928 N85-15887
Adsorption thermodynamics and surface transport of metal catalyst poisons
[DE85-003750] 12 p1802 N85-21301
Measurements of radiation-induced segregation and diffusion in ion irradiated alloy using implanted manganese
[AERE-R-11528] 14 p2258 N85-23994
Diffusion of water vapor in Carbon Fiber Reinforced Plastics (CFRP). Measurement of the diffusion coefficient under influence of concentration
[DFVLR-FB-84-41] 14 p2262 N85-24018
Diffusion coefficients for coastal water determined from aerial photographs
[INPE-3413-PRE/679] 16 p2810 N85-27331
Transport in aqueous battery systems
[DE85-007246] 17 p2955 N85-28251
Computer-controlled carburizing
[BLL-OA-TRANS-3204-(6196.300)]
20 p3429 N85-31268
Relaxation lens in inhomogeneous binary mixture
21 p3695 N85-32957
Breakdown of intrinsic ambipolarity for the radial diffusion due to a rotating RF field 23 p3977 N85-34660
Effect of ECH and ICH on ambipolar potential in NBT-1M 23 p3978 N85-34661
Neoclassical diffusion including ellipticity in a heliotron-like configuration 23 p3978 N85-34667
Spatial dependence of the local diffusion coefficient measured upstream of the November 12, 1978 interplanetary traveling shock
[SH-1.5-12] 23 p3996 N85-34776
The Jovian electron spectrum: 1978-1984
[SH-1.5-19] 23 p3998 N85-34782
Cosmic ray modulatin and merged interaction regions
[SH-4.1-11] 23 p4005 N85-34834
Cosmic ray modulation in a random anisotropic magnetic field
[SH-4.1-20] 23 p4006 N85-34839
Spatial variation of cosmic rays near the heliospheric current sheet
[SH-4.2-10] 23 p4007 N85-34848
Effects of a wavy neutral sheet on cosmic ray anisotropies
[SH-4.2-11] 23 p4008 N85-34849
Effects of solar magnetic field on cosmic rays
[SH-4.2-12] 23 p4008 N85-34850
The expected cosmic ray density and stream distributions at the heliolatitudinal asymmetry of solar wind
[SH-4.2-14] 23 p4008 N85-34852
The influence of nonstationarity of the solar activity and general solar field on modulation of cosmic rays
[SH-4.2-17] 23 p4008 N85-34854
The effect of the neutral sheet structure of the interplanetary magnetic field on cosmic ray distribution in space
[SH-4.2-18] 23 p4008 N85-34855
Spatial distribution of cosmic rays in magnetic cycles of the Sun
[SH-4.2-20] 23 p4009 N85-34857
Difference between even and odd 11-year cycles in cosmic ray intensity
[SH-4.2-22] 23 p4009 N85-34859
Nonstationary modulation of galactic cosmic rays in a nonlinear model
[SH-4.7-10] 23 p4041 N85-35054

DIFFUSION EFFECT
U DIFFUSION

DIFFUSION FLAMES
Engineering method of calculating a turbulent diffusion flame
[BLL-M-35761-(5828.4)] 02 p0171 N85-11147
Ionization and time structure of flames
[LE-484/1-2] 05 p0614 N85-13925
Combustion driven oscillation of ducted diffusion flame
09 p1289 N85-18094
Cars temperature measurements in sooting, laminar diffusion flames
[AD-A148801] 09 p1319 N85-18294
Fuels combustion research
[AD-A149106] 10 p1457 N85-19178
Investigation of fuel additive effects on sooting flames
[AD-A149154] 10 p1457 N85-19179
Laser diagnostic analyses of sooting flames
[AD-A150478] 13 p2017 N85-22649
A standard aircraft diffusion flame: Spectral characteristics and a feasibility study for developing an alternate calibration source for aircraft optical fire detection systems
[AD-A150231] 13 p2039 N85-22766
Asymptotic methods especially in combustion
[AD-A151505] 15 p2505 N85-25450

Laminar diffusion flames, carbon gasification, and laser diagnostics applied to combustion systems. 1: Laminar diffusion flames with cylindrical symmetry. 2: Diffusion-controlled gasification of carbon particles. 3: Laser diagnostics applied to combustion systems
20 p3423 N85-31243
Assessment of superlayer contribution to the conserved scalar PDF in a hydrogen turbulent jet diffusion flame
20 p3425 N85-31255
Blowout of turbulent diffusion flames
20 p3425 N85-31256
Strong turbulence chemistry interaction in a piloted turbulent jet diffusion flame 20 p3425 N85-31257
Non-equilibrium effects in turbulent diffusion flames
20 p3425 N85-31258
Sandia Cooperative Group on the Aerothermochemistry of Turbulent Combustion. Discussion record of the second meeting
[DE85-007493] 22 p3743 N85-33203
Pressure correlations in turbulent reacting flows
22 p3744 N85-33205
Vortex dynamics simulation of conserved scalar dissipation 22 p3745 N85-33210

DIFFUSION THEORY
Definition of global dispersion coefficients — aquifers
[PSE-83/4-B] 01 p0064 N85-10426
Problems in theory of diffusion under shock wave
02 p0272 N85-11776
Beam loss due to the aperture limitation resulting from intrabeam scattering
[DE85-005138] 12 p1930 N85-22124
Projected discrete ordinates methods for numerical transport problems
[DE85-005632] 17 p3020 N85-28678
Augmented weighted diamond force of the linear nodal scheme for Cartesian coordinate systems
[DE85-005631] 17 p3020 N85-28679
Nonlinear problems in continuum mechanics
[AD-A153387] 17 p3046 N85-28846
The Cauchy problem for u sub t = Delta u(m) when O m 1
[AD-A153521] 18 p3169 N85-29635
Oscillatory solutions of the Peaceman-Rachford alternating direction implicit method and a comparison of methods for the solution of the two dimensional heat diffusion equation
[AD-A154670] 21 p3675 N85-32833

DIFFUSION WAVES
Diffusion of particles in a slowly modulated wave
[DE85-000729] 09 p1391 N85-16756

DIFFUSION WELDING
New metallurgical processes based on high-speed crystallization and diffusion of metals
01 p0021 N85-10126
Causes of strength reduction in welded titanium-steel joints 03 p0352 N85-12262
Laser and diffusion welding equipment R and D
03 p0352 N85-12265
Residual stresses at small diffusion welds
[DE84-014982] 07 p0974 N85-16189
Application of diffusion welding of nickel based metals and application of electron beam welding of hot isostatically pressed nickel based powdered metals
08 p1169 N85-17375
Kinetics of joint formation during diffusion welding of VT5 titanium alloys 10 p1448 N85-19125
Diffusion welding with forced deformation of heat-resistant nickel-based dispersion hardened alloy
10 p1449 N85-19130
Kinetics of reaction of metals and non-metals during diffusion welding 11 p1602 N85-20076
Collapse and removal of discontinuities in joint zone during diffusion welding 11 p1602 N85-20077
Structure of transient zone in diffusion welding of TsTS-19 piezoceramic with AMg6 alloy
11 p1603 N85-20082
MBB uses superplastic forming, diffusion bonding for alloys 11 p1618 N85-20177
Mechanical properties and brittle fracture resistance of welded multilayer elements for high pressure vessels
13 p2033 N85-22736
Effect of protective medium on durability and fracture structure on seam zones of thin-walled titanium articles produced by diffusion welding 13 p2033 N85-22738
Technological parameters of diffusion welding processes in honeycomb titanium alloy structures
13 p2033 N85-22739
Durability of VT16 alloy compounds obtained by diffusion welding 13 p2034 N85-22740
Diffusion vacuum welding 15 p2499 N85-25416
Residual oxygen pressure in contact gap upon diffusion welding of titanium 15 p2498 N85-25418
Durability of joints of 30KhGSA and 12Kh18N10T steels made by diffusion welding 15 p2501 N85-25428
Diffusion welding of incompatible materials
19 p3245 N85-30121
Effect of heating temperature in a vacuum on state of surface layers of welded OT4 titanium alloy
19 p3245 N85-30123
Producing titanium-sapphire items by solid-phase bonding through aluminum gasket
19 p3246 N85-30127
Diffusion welding of aluminum with vacuum-tight corundum ceramic 19 p3247 N85-30130
Prospective uses for diffusion welding in vacuum
22 p3733 N85-33145
Welding methods for high melting metals
22 p3794 N85-33508
Joint design for improved fatigue life of diffusion-bonded box-stiffened panels
[NASA-TP-2480] 22 p3799 N85-33537
Diffusion welding of Cassegrainian concentrator cell stack assemblies
[NASA-CR-176104] 22 p3805 N85-33566

DIFFUSIVITY
The reactions of cobalt, iron and nickel in SO-2 atmospheres: Similarities and differences
[NASA-TM-86866] 02 p0181 N85-11217
Mixing in the solar interior 14 p2446 N85-25095
Heavy doping effects in high efficiency silicon solar cells
[NASA-CR-175687] 15 p2585 N85-25937
Diffusely reflecting paints including polytetrafluoroethylene and method of manufacture
[NASA-CASE-GSC-12883-1] 18 p3079 N85-29044
Turbulent wake of a submerged flat plate
[AD-A153776] 18 p3100 N85-29190
Study of molecular diffusivity influence on mass transfer rate at a water-atmosphere interface
22 p3747 N85-33222

DIFLUORIDES
NT CALCIUM FLUORIDES
Method for fluorination of actinide fluorides and oxyfluorides using O2F2
[DE85-011646] 22 p3743 N85-33202

DIFLUORO COMPOUNDS
NT PERFLUOROALKANE
NT POLYTETRAFLUOROETHYLENE
Subtractively normalized interfacial Fourier transform infrared spectroscopy of difluorobenzene adsorbed at polycrystalline platinum electrodes
[AD-A148660] 08 p1123 N85-17060

DIGESTING
Anaerobic digestion of biomass: status summary and research development needs, 1983
[PB85-161925] 13 p2040 N85-22772
Lipid hydrolysis in man during antiorthostatic hypokinesia 23 p3953 N85-34500

DIGESTIVE SYSTEM
NT GASTROINTESTINAL SYSTEM
NT INTESTINES
NT PANCREAS
NT RECTUM
NT TEETH

DIGITAL COMMAND SYSTEMS
Basic EMC (Electromagnetic Compatibility) technology advancement for C3 systems, macromodeling of digital circuits, volume 2B
[AD-A146333] 03 p0359 N85-12306
Speed test results and hardware/software study of computational speed problem, appendix D
05 p0603 N85-13843
Closing the design loop on HiMAT (highly maneuverable aircraft technology)
[NASA-TM-85923] 06 p0754 N85-14836
Some effects of digital sampling on orbiter flight control system operation 08 p1092 N85-16903
Robustness of discrete-time dynamical systems: Application to the multivariable digital control of combat aircraft
[ONERA-NT-1984-2] 11 p1585 N85-19986
Application of AFTI/F-16 task-tailored control modes in advanced multirole fighters 17 p2901 N85-27888
X-29 digital flight control system design
17 p2901 N85-27889
Some flight test results with redundant digital flight control systems 17 p2902 N85-27892

DIGITAL COMMUNICATION
U PULSE COMMUNICATION

DIGITAL COMPUTERS
NT CDC CYBER 170 SERIES COMPUTERS
NT CDC CYBER 205 COMPUTER
NT HEWLETT-PACKARD COMPUTERS
NT MICROCOMPUTERS
NT MINICOMPUTERS
NT PARALLEL COMPUTERS
NT PDP 11 COMPUTER
NT PDP 11/70 COMPUTER
NT PERSONAL COMPUTERS
NT SEQUENTIAL COMPUTERS
NT UNIVAC 1100 SERIES COMPUTERS
NT VAX COMPUTERS
NT VAX-11 SERIES COMPUTERS
NT VAX-11/780 COMPUTER
Data flow computer architecture
[DE84-014362] 01 p0100 N85-10[illegible]
THLL (TRIDENT Higher Level Language) reference manual
[AD-A145116] 01 p0104 N85-10[illegible]
Development and flight evaluation of an augmented stability active controls concept: Executive summary
[NASA-CR-166009] 02 p0149 N85-11[illegible]
International exhibition: Industrial Robots, 1982
03 p0345 N85-122[illegible]
Digital equipment Corporation, professional 350, COBOL-81 Version 2.1
[PB84-227602] 03 p0403 N85-1257[illegible]
Digital Equipment Corporation, Professional 350, COBOL-81 Version 2.1 (COBOL technical report)
[PB84-227719] 03 p0403 N85-1257[illegible]
Digital Equipment Corporation, DECSYSTEM-10, model 1090-SMP, COBOL-74 V12B
[PB84-227941] 03 p0404 N85-1257[illegible]
Data General Corporation, Eclipse C350, AOS COBOL Release 3.51
[PB84-227883] 03 p0404 N85-1257[illegible]
Convergent Technologies, mega frame, CTIX COBOL version 2.0
[PB84-227750] 03 p0404 N85-1258[illegible]
Digital Equipment Corp., VAX/750, VAX COBOL version 3.0
[PB84-227693] 03 p0405 N85-1258[illegible]
Turbine blade damping study, introduction
04 p0456 N85-12[illegible]
New directions in software for advanced computer architectures
[DE84-017435] 04 p0550 N85-135[illegible]
Psychological issues in online adaptive task allocation
05 p0704 N85-145[illegible]
Experience with a sophisticated computer based authoring system
[DE84-014644] 05 p0713 N85-1457[illegible]
Investigation of semiautomatic aircraft control processes employing time redundancy in on-board digital trajectory control computers 07 p0954 N85-160[illegible]
Reliability analysis of local area networks, intermediate report
[BLL-WH-610-(9091.9F)] 07 p1027 N85-165[illegible]
Automatic land vehicle navigation using road map data
[DE84-017178] 09 p1278 N85-180[illegible]
Digital high speed programmable convolver
[AD-D011455] 10 p1481 N85-19[illegible]
Man-machine interaction: Operator
[AD-A149075] 10 p1531 N85-19[illegible]
New CNC systems described
11 p1617 N85-2017[illegible]
A modern approach of a synthetic aperture radar processor and its technological aspects
11 p1713 N85-207[illegible]
Multicomputer communication system
[NASA-CASE-NPO-15433-1] 12 p1822 N85-214[illegible]
Interface specifications for SCR (Software Cost Reduction) (A-7E) extended computer module, revised
[AD-A149948] 12 p1915 N85-220[illegible]
Signal flow model for sequential logic built from combinational logic elements and its implementation in Prolog
[DE85-005792] 15 p2549 N85-257[illegible]
Programming the digital computer ODRA-1204 in MOST-2 language
[NASA-TM-87462] 15 p2627 N85-261[illegible]
GRID: A FORTRAN program for using a digitizing table to enter a finite element GRID
[AD-A151317] 15 p2628 N85-261[illegible]
A concept for map updating using digital image processing methods 16 p2815 N85-27[illegible]
Contour line generalization using digital image processing methods 16 p2815 N85-27[illegible]
An update of experience on the fly by wire Jaguar equipped with a full-time digital flight control system
17 p2902 N85-27[illegible]
Operational and developmental experience with the F/A-18A digital flight control system
17 p2902 N85-27[illegible]
Flight testing and development of the F/A-18A digital flight control system 17 p2902 N85-27[illegible]
Language design, computers and brains
[AD-A152819] 17 p3006 N85-28[illegible]
An approach to digital level compression using the zero-crossing points of programme signals
[NHK-LABS-NOTE-308] 18 p3090 N85-291[illegible]
Tenth-order expansion formulae for the orbital eccentricity function K (sub lpq)(e) obtained using a symbolic algebraic manipulation system
[AD-A153754] 18 p3170 N85-29[illegible]

The prospects of the digital optical computer 18 p3188 N85-29771

A single chip VLSI architecture for radar signal processing 19 p3257 N85-30195

BP (Basic Processor) TRICOMP user's guide [AD-A154340] 19 p3337 N85-30674

Filtration of higher harmonic components in two-level digital computing synthesizers 22 p3778 N85-33410

CARE 3 MENU maintenance manual [NASA-CR-172609] 22 p3828 N85-33708

Re-designing a mechanism for higher speed: A case history from textile machinery 23 p3923 N85-34310

Method and apparatus for transfer function simulator for testing complex systems [NASA-CASE-NPO-15696-1] 23 p3926 N85-34333

DIGITAL DATA

Ultrasonic synthetic aperture focusing using unfocused pulse-echo transducers [AERE-R-11230] 01 p0057 N85-10374

A preliminary study of the feasibility of detecting the floating macrophytes by means of digital processing of MSS/LANDSAT data [E85-10005] 02 p0215 N85-11418

Digital Terrain Elevation Data (DTED) anomaly removal through the use of an interactive Fourier frequency filtering process [AD-A145433] 02 p0219 N85-11445

Description of the logical support for an image processing system [INPE-2783-PRE/349] 02 p0240 N85-11563

Utilization of interpolation and transformation for the compression of digital image data [INPE-3061-PRE/479] 02 p0240 N85-11566

Assessment of computer techniques for processing digital LANDSAT MSS data for lithological discrimination of Serra do Ramalho, State of Bahia [E85-10033] 03 p0378 N85-12412

Digital image processing; report from a conference and study trip to the USA and Canada, summer 1984 [FOA-C-30369-E1] 04 p0494 N85-13153

Digital elevation models improve processing of Alaskan gravity data 04 p0515 N85-13265

Automatic correction of static characteristics of measurement channel of digital oscillograph 06 p0795 N85-15063

Classification of vegetation communities in the Battle Mountain SE quadrangle, Nevada with MSS digital data [E85-10043] 06 p0826 N85-15246

Multi crop area estimation in Idaho using EDITOR [E85-10054] 06 p0827 N85-15251

Characterizing the scientific potential of satellite sensors — San Francisco, California [E85-10044] 07 p0983 N85-16244

Detecting agricultural to urban land use change from multi-temporal MSS digital data --- Salt Lake County, Utah [E85-10049] 07 p0983 N85-16245

Image variance and spatial structure in remotely sensed scenes — South Dakota, California, Missouri, Kentucky, Louisiana, Tennessee, District of Columbia, and Oregon 07 p0986 N85-16265

Analysis of subpixel registration 07 p0986 N85-16267

Interactive digital image processing for terrain data extraction [AD-A148580] 08 p1176 N85-17417

A system for measuring the characteristics of the ionospheric channel by digital transmissions 10 p1472 N85-19287

Satellite-computer interface 10 p1476 N85-19318

Satellite support to the Sierra Cooperative Pilot Project: 1979/80 and 1980/81 [PB85-115079] 10 p1520 N85-19563

Application of SLF (Standard Linear Format) to digital hydrographic products [AD-A149509] 10 p1522 N85-19596

Extracting digital data from a bus and multiplexing it with a video signal [AD-D011491] 11 p1636 N85-20302

Radiometric accuracy assessment of LANDSAT 4 Multispectral Scanner data 11 p1666 N85-20498

LANDSAT scene-to-scene registration accuracy assessment 11 p1667 N85-20502

Geometric accuarcy assessment of LANDSAT-4 Multispectral Scanner (MSS) data 11 p1667 N85-20505

TM digital image products for applications 11 p1668 N85-20512

Digital and color energy maps for graphic display of hourly data [DE85-000526] 11 p1673 N85-20543

Digital channel efficiency model [AD-A150084] 12 p1829 N85-21479

A preliminary assessment of LANDSAT-4 Thematic Mapper data — Windsor, Ontario and Medicine Hat areas, Canada 12 p1869 N85-21728

Preliminary evaluation of the radiometric calibration of LANDSAT-4 Thematic Mapper data by the Canada Centre for Remote Sensing 12 p1870 N85-21729

A preliminary analysis of LANDSAT-4 Thematic Mapper radiometric performance 12 p1870 N85-21730

Dynamics of adaptive signal corrector 13 p2071 N85-22940

Ionospheric distortions of digital signals with wideband modulation 13 p2072 N85-22945

Synthesis of quasi-optimum two-level signal discriminator with level changing at unknown point 13 p2083 N85-23010

LANDSAT-4 Science Characterization Early Results. Volume 4: Applications — agriculture, soils land use, geology, hydrology, wetlands, water quality, biomass identification, and snow mapping [E85-10070] 13 p2117 N85-23186

Overview of TM applications research reports 13 p2117 N85-23187

A preliminary comparison of the information content of data from the LANDSAT 4 Thematic Mapper and Multispectral Scanner --- Arkansas 13 p2119 N85-23199

Early results of investigations of LANDSAT 4 Thematic Mapper and Multispectral Scanner applications --- Washington, D.C. 13 p2119 N85-23200

Relative accuracy assessment of LANDSAT-4 MSS and TM data for level 1 land cover inventory — Washington, D.C. 13 p2122 N85-23212

Using SM-4 Omega system in checking and editing digital terrain information 15 p2487 N85-25350

An amplitude correlation and differencing method for the monitoring of flaws in repeat ultrasonic inspections [AERE-R-11416] 15 p2571 N85-25854

Shuttle imaging radar-B (SIR-B) data analysis for identifying rainfall event occurrence and intensity [NASA-CR-175712] 15 p2594 N85-25986

Three-dimensional/perspective display techniques for meteorological data sets 15 p2599 N85-26018

CNPq/INPE LANDSAT system: Report of activities from October 1, 1983 to September 30, 1984 — Brazil [E85-10097] 16 p2808 N85-27318

A concept for map updating using digital image processing methods 16 p2815 N85-27364

Contour line generalization using digital image processing methods 16 p2815 N85-27367

What does digital image processing perform in the production of orthophotomaps 16 p2815 N85-27368

Evaluation of Defense Mapping Agency level 1 second edition digital data for training simulator applications [AD-A152444] 17 p2983 N85-28437

Experimental philosophy leading to a small scale digital data base of the conterminous United States for designing experiments with remotely sensed data [NASA-TM-85009] 17 p3049 N85-28877

Defense Mapping Agency (DMA) raster-to-Vector benchmark testing [AD-A154152] 19 p3338 N85-30683

A high-speed digital signal processor for atmospheric radar, part 7.3A 21 p3626 N85-32525

Estimate of signal-to-interference energy ratio in discrete-data transmission 22 p3776 N85-33398

Digital tachometer 22 p3779 N85-33416

DIGITAL FILTERS

NT FIR FILTERS

Nonlinear regression with emphasis on spline methods [AD-A146192] 03 p0412 N85-12633

Application of high frequency 2-D digital filtering to remote sensing image processing 05 p0660 N85-14242

Derivation of recursive digital filters by the step-invariant and the ramp-invariant transformations [AD-A146500] 06 p0857 N85-15452

Enhancement of multispectral scanner images by digital filtering [ESA-TT-624] 07 p0989 N85-16284

Digital coherent detector [AD-D011560] 12 p1833 N85-21501

Estimating algorithmic error of digital recursive filters 12 p1839 N85-21543

Synthesis of digital nonrecursive band-elimination filters for moving-target selectors 12 p1840 N85-21545

Method of designing digital band-pass filters with infinite memory 12 p1840 N85-21546

Digital detector of harmonic signals 12 p1840 N85-21549

Optimal design efforts in Shanghai described 13 p1972 N85-22386

Two-dimensional signal processing and storage and theory and applications of electromagnetic measurements [AD-A150590] 13 p2065 N85-22899

Optimal synthesis of surface acoustic wave filters 13 p2070 N85-22933

Efficiency of digital compensator of strong non-Gaussian interference 13 p2072 N85-22942

Methods of digital correction for channels of multichannel radar receivers 13 p2082 N85-23005

Use of Walsh functions for calculating characteristics of digital filters with impulse response of finite duration 13 p2083 N85-23011

Linearization of digital derived rate algorithm for use in linear stability analysis [NASA-TM-87000] 14 p2243 N85-23904

Digital computer applications of Kalman filter in target tracking [AD-A150770] 14 p2404 N85-24821

Correlating and adaptive digital filters [BMFT-FB-T-84-299] 15 p2551 N85-25744

High-speed digital baseband mixer 16 p2771 N85-27103

Digital filters for digital phase-locked loops 16 p2771 N85-27104

Digital filters for application to data analysis in electron energy loss spectroscopy [DE85-007932] 17 p2923 N85-28020

Application of adaptive noise cancellation to Coast Guard voice communications [AD-A154798] 21 p3574 N85-32230

Digital matched filter 22 p3765 N85-33339

Hardware realization of digital filters without multipliers 22 p3766 N85-33340

Design of high-order analog and digital filters with identical sections 22 p3766 N85-33341

Design of digital bandpass filters with finite memory 22 p3775 N85-33392

Maximally flat approximation of attenuation characteristics of coupled-line filters 22 p3775 N85-33393

Miniature two-mode filters 22 p3775 N85-33394

Method of designing digital band-pass filters with pulse response of finite duration 22 p3775 N85-33395

DIGITAL INTEGRATORS

Programmable digital baud integrators for the radar high-speed data acquisition system 05 p0624 N85-13994

Rotorcraft digital advanced avionics system (RODAAS) functional description [NASA-CR-166611] 15 p2468 N85-25237

Digital filters for digital phase-locked loops 16 p2771 N85-27104

Probabilistic analysis of combinational circuits with random delays 19 p3257 N85-30192

DIGITAL NAVIGATION

Implementation of the SITAN algorithm in the digital terrain management and display system [DE85-010659] 22 p3729 N85-33115

DIGITAL RADAR SYSTEMS

Digital radar data as an aid in nowcasting in Hong Kong 01 p0079 N85-10525

AFOS (Automation of Field Operations and Services) display of MDR (Manually Digitized Radar) data on local map backgrounds [PB84-220797] 06 p0840 N85-15338

Digital controller for the Wave Propagation Laboratory's VHF and UHF wind-profiling radars [PB85-112142] 11 p1626 N85-20238

Mathematical model of discriminator for signals with fluctuations and thermal noise 13 p2072 N85-22943

Efficiency of multitarget signal detection by digital radar data processing devices 13 p2080 N85-22991

Factorized algorithms for combined spatial and temporal processing of radar signals 13 p2081 N85-22997

Digital signal processing for spaceborne synthetic aperture radar [FOA-C-30381-E1] 20 p3442 N85-31364

DIGITAL SIMULATION

A simulation experiment of a rapidly developed medium scale cyclone 01 p0079 N85-10530

Numerical simulation of natural convection in porous media — heat transfer [CFD/84/10] 02 p0199 N85-11330

Computer simulation techniques for turbulent flows [CFD/84/11] 02 p0199 N85-11331

Operational behavior of wind energy converters. Control and dynamic and types of generators, volume 1 [BMFT-FB-T-84-154-VOL-1] 03 p0386 N85-12470

Operational behavior of wind energy converters: Control and dynamic and types of generators, volume 2 [BMFT-FB-T-84-154-VOL-2] 03 p0386 N85-12471

Geographic subdivision and top level data structures, Columbus, Magellan, and expanding CIG (Computer Image Generation) horizons [AD-P004317] 09 p1268 N85-17971

Digital simulation of communications channels: An overview 10 p1472 N85-19290

Application of model following control and estimation techniques to attitude control of maneuvering spacecraft. Part 2: Simulation software description [NLR-TR-82116-U-PT-2] 12 p1793 N85-21254

Evolution of collisional systems --- planetary disks 15 p2674 N85-26505

A numerical simulation of the NFAC (National Full-scale Aerodynamics Complex) open-return wind tunnel inlet flow
[NASA-TM-86724] 16 p2700 N85-26672

Dispersion sensitivity of the eight inch advanced ramjet munitions technology projectile due to wind and minor thrust errors
[AD-A152145] 16 p2727 N85-26835

Digital image mapping of Antarctica using NOAA-7 AVHRR imagery 18 p3124 N85-29340

Computer simulation of elastic waves by a new mass-point system with potentials
[DRIC-T-7274] 20 p3469 N85-31553

Flexible satellite communications systems simulator, phase 3
[AD-A155647] 21 p3577 N85-32247

Research on an expert system for database operation of simulation-emulation math models. Volume 1, Phase 1: Results
[NASA-CR-176087] 21 p3669 N85-32792

Research on an expert system for database operation of simulation-emulation math models. Volume 2, Phase 1: Results
[NASA-CR-176088] 21 p3669 N85-32793

A preliminary evaluation of a failure detection filter for detecting and identifying control element failures in a transport aircraft
[NASA-TM-87576] 24 p4067 N85-35204

Computer simulation of a cruise missile using brushless dc motor fin control
[AD-A155935] 24 p4069 N85-35349

DIGITAL SYSTEMS

NT DIGITAL NAVIGATION

NT DIGITAL RADAR SYSTEMS

Design of a digital ride quality augmentation system for commuter aircraft
[NASA-CR-172419] 01 p0006 N85-10037

Clutter generator for use in radar evaluation
[AD-D011234] 01 p0039 N85-10245

Digital correlator speed improvement by multiplexing
[AD-A145207] 01 p0100 N85-10602

Expert systems in maintenance diagnostics for self-repair of digital flight control systems
[AD-P003933] 02 p0247 N85-11613

Minimization of anomalous errors in measuring systems employing search and testing devices
03 p0344 N85-12219

On line digitizer software
[AD-A146249] 03 p0403 N85-12568

Application of a silicon compiler to VLSI (Very Large Scale Integrated circuits) design of digital pipelined multipliers
[AD-A146326] 03 p0403 N85-12569

High-temperature optically activated GaAs power switching for aircraft digital electronic control
[NASA-CR-174711] 04 p0457 N85-12901

Interference immunity of digital equipment for coherent processing of wideband signals
04 p0486 N85-13100

Digital radio receivers and problems of analog-to-digital conversion of narrow-band signals
04 p0486 N85-13101

Architecture of adaptive space-frequency-time signal processing system 04 p0486 N85-13103

Efficiency of computer system digital processing of signals 04 p0487 N85-13106

Test experience on an ultrareliable computer communication network
[NASA-TM-85915] 04 p0552 N85-13514

Primary data processing in very long baseline radiointerferometer 06 p0783 N85-15008

Infralow-frequency digital phase meter
06 p0787 N85-15031

A noise-suppressing digital frequency meter
06 p0796 N85-15084

The effect of aircraft generated electromagnetic interference (EMI) on future avionics systems: A compendium
[AD-A146380] 06 p0799 N85-15101

Digital raster timing encoder-decoder
[AD-D011279] 06 p0804 N85-15120

Precision digital sampler
[AD-D011285] 06 p0809 N85-15143

Systems study for an Integrated Digital-Electric Aircraft (IDEA)
[NASA-CR-3840] 07 p0902 N85-15714

Predicted performance benefits of an adaptive digital engine control system of an F-15 airplane
[NASA-TM-85916] 07 p0905 N85-15729

Programmable synchronous digital delay line
[AD-D011382] 07 p0945 N85-15985

Digital signal demodulators with single-sideband
07 p0950 N85-16019

Digital thermometer with linearizer on slide wire
07 p0954 N85-16049

ILIR task of digital recoil travel measurement system
[AD-A147102] 07 p0967 N85-16140

Metric aspects of digital images and digital image processing
[AD-A147211] 07 p0988 N85-16276

Upset susceptibility study employing circuit analysis and digital simulation — digital systems and electromagnetic interference 07 p0999 N85-16344

Data and results of a laboratory investigation of microprocessor upset caused by simulated lightning-induced analog transients
07 p0999 N85-16345

Experience of one UK electronic equipment supplier with bite on engine/flight control systems over the past ten years 08 p1064 N85-16736

Built-in test and self repair mechanisms in a digital correlator integrated circuit 08 p1064 N85-16741

A digital piloting system for the combat helicopter
08 p1074 N85-16806

Integrated digital/electric aircraft concepts study
[NASA-CR-3841] 08 p1083 N85-16861

Design of a digital ride quality augmentation system for commuter aircraft
[AD-A148233] 08 p1086 N85-16879

Interactive digital image processing for terrain data extraction
[AD-A148580] 08 p1176 N85-17417

VICOM technical description
[REPT-611-0012-REV-A] 08 p1202 N85-17563

Multidimensional digital signal processing
[AD-A148055] 08 p1205 N85-17585

Complexity, testability, and fault analysis of digital, analog and hybrid systems
[AD-A148465] 08 p1213 N85-17634

A modified Monte-Carlo technique for the simulation of satellite communication systems
[AD-A148689] 08 p1214 N85-17641

A description of the NRL oblique-incidence-ionogram data base
[AD-A148625] 08 p1230 N85-17748

Transdigitizer for relaying signals from Global Positioning System (GPS) satellites
[AD-D011442] 10 p1422 N85-18970

French firm develops 2D, 3D computer vision system
10 p1461 N85-19208

Television animation store: Recording pictures on a parallel transfer magnetic disc
[BBC-RD-1984/17] 10 p1462 N85-19220

Limits of the propagation medium with respect to digital signal transmission 10 p1469 N85-19270

Propagation influences on the performance of a reduced bandwidth quadrature phase shift keyed digital radio system 10 p1470 N85-19274

Equatorial transionospheric propagation conditions affecting digital communications
10 p1470 N85-19275

The impact of propagation effects on the design of high capacity digital microwave links in the 18 GHz frequency band 10 p1470 N85-19278

A review of atmospheric multipath measurements and digital system performance 10 p1470 N85-19279

Wideband line-of-sight channel measurements and simulation: Application to digital radio links
10 p1471 N85-19283

Some propagation experimental results on protection techniques for line-of-sight digital systems
10 p1472 N85-19286

LOS microwave channel simulation: A survey of models, realizations and new concepts 10 p1472 N85-19291

A review of transmission and channel evaluation techniques for digital communication systems
10 p1474 N85-19301

Application of SLF (Standard Linear Format) to digital hydrographic products
[AD-A149509] 10 p1522 N85-19596

Telemetry systems of Interkosmos satellites
11 p1617 N85-20173

Extracting digital data from a bus and multiplexing it with a video signal
[AD-D011491] 11 p1636 N85-20302

Digital imaging processing
[INPE-3325-PRE/624] 11 p1701 N85-20696

Integrated support of tactical operations by satellite communications 11 p1709 N85-20754

Integrated control system engineering support
[AD-A149742] 12 p1780 N85-21177

Low sidelobe phased array antenna system
[AD-D011558] 12 p1823 N85-21435

Television animation store: Digital chroma, key and mixer units
[BBC-RD-1984/16] 12 p1824 N85-21442

The study of certain aspects of probability with applications in communications theory
[AD-A149820] 12 p1829 N85-21476

Digital coherent detector
[AD-D011560] 12 p1833 N85-21501

Digital detector of harmonic signals
12 p1840 N85-21540

Synthesis of digital control for object with lag
12 p1843 N85-21582

SIMULA: Digital controller simulation package
[PB85-134492] 12 p1917 N85-22041

Testing of the digital flight control system of the German CCV fighter experimental aircraft
13 p1968 N85-22281

The use of a high-speed 12-bit A/D converter for digital sampling of communication signal carriers
[AD-A150578] 13 p2056 N85-22872

Noise tolerance of digital demodulator for complex signal system employing binary quantization
13 p2070 N85-22929

Analysis of characteristics of digital discriminators for phase-shift keyed signals 13 p2070 N85-22930

Interference immunity of binary systems with second-order phase-difference modulation in various reception modes 13 p2072 N85-22944

Noise tolerance of diversity reception in frequency-adaptive digital transmission systems
13 p2086 N85-23024

Use of importance sampling to investigate signal detection systems by simulated method
13 p2086 N85-23029

Digital laser platemaker modifications
[AD-A150190] 13 p2096 N85-23074

Optical memory research and its application to digital optical processing 13 p2158 N85-23397

Synthesis of optimal controls for real-time linear digital systems 14 p2270 N85-24082

Digital processing of passive Ka-band microwave images for sea-ice classification
[AD-A150686] 14 p2347 N85-24511

Map design for computer processing: Literature review and DMA product critique
[AD-A151061] 14 p2347 N85-24513

Factors affecting dwell times on digital displaying
[NASA-TM-86406] 14 p2390 N85-24722

Multi-rate digital autopilot modeling methodology
[AD-A152044] 15 p2474 N85-25272

Converters of sum/differnce of codes to frequency
15 p2526 N85-25576

Analysis of spectral characteristics of multilevel digital computing synthesis 15 p2527 N85-25579

Interactive communication channel
[AD-D011580] 15 p2542 N85-25695

Standards in process: Foundation and profiles of ISDN (Integrated Services Digital Network) and OSI (Open Systems Interconnection) studies
[PB85-165041/GAR] 15 p2545 N85-25712

Superfine laser position control using statistically enhanced resolution in real time
[DE85-005643] 15 p2564 N85-25817

Data structure considerations in automatic cartography
15 p2583 N85-25930

Design specifications for IMAGER: The DREO (Defence Research Establishment Ottawa) image processing system
[AD-A151752] 15 p2624 N85-26168

User manual for IMAGER: The DREO (Defence Research Establishment Ottawa) image processing system
[AD-A151754] 15 p2653 N85-26362

Technical evaluation report on Avionics Panel Specialists' Meeting on Digital Optical Circuit Technology
[AGARD-AR-202] 15 p2653 N85-26367

Design and implementation of the digital engineering laboratory distributed database management system
[AD-A151694] 15 p2665 N85-26450

Rotorcraft digital advanced avionics system (Rodaas)
15 p2688 N85-26606

Application of AFTI/F-16 task-tailored control modes in advanced multirole fighters 16 p2712 N85-26735

X-29A digital flight control system design
16 p2712 N85-26736

Some flight test results with redundant digital flight control systems 16 p2712 N85-26739

An update on experience on the fly by wire Jaguar equipped with a full-time digital flight control system
16 p2712 N85-26740

Operational and developmental experience with the F/A-18A digital flight control system
16 p2713 N85-26742

Flight testing and development of the F/A-18A digital flight control system 16 p2713 N85-26743

The certification of airborne complex digital systems
16 p2714 N85-26754

Automatic flight control modes for the AFTI/F-111 mission adaptive wing aircraft 16 p2714 N85-26756

High-speed digital baseband mixer
16 p2771 N85-27100

Certifying complex digital systems on civil aviation aircraft 17 p2904 N85-27907

The design of an adaptive predictive coder using a single-chip digital signal processor
[AD-A152461] 17 p2952 N85-28231

Evaluation of Defense Mapping Agency level 1 second edition digital data for training simulator applications
[AD-A152444] 17 p2983 N85-28437

Further study of digital matching of dissimilar images
[AD-A153112] 17 p3019 N85-28672

Tone calibrated digital radio communication system
[NASA-CASE-NPO-16414-1-CU] 18 p3089 N85-29121

A possible digital circuit able to recognize magnetic monopoles crossing a thick scintillator counter
[NOTA-INTERNA-826] 18 p3097 N85-29173

Experimental performance of a digital circuit able to recognize magnetic monopole events
[NOTA-INTERNA-838] 18 p3097 N85-29176

Maser and secondary clock in telecommunications networks 18 p3108 N85-29246

Digital control of diode laser for atmospheric spectroscopy
[NASA-CASE-NPO-16000-1] 18 p3112 N85-29264

An interactive computer aid for the design and analysis of linear, single input/single output digital and continuous control systems
[AD-A153704] 18 p3162 N85-29589

Direct digital control study
[AD-A153685] 18 p3167 N85-29621

Energy Efficient Engine (E3) controls and accessories detail design report
[NASA-CR-168017] 19 p3218 N85-29957

Dielectric resonator oscillators with digital temperature compensation
[AD-D011715] 19 p3261 N85-30221

Environmental background measurement program
[AD-A153860] 19 p3319 N85-30577

Defense Mapping Agency (DMA) raster-to-Vector analysis
[AD-A154153] 19 p3336 N85-30668

High accuracy digital acousto-optic matrix computer
[AD-D011692] 19 p3343 N85-30716

An overview of measurement solutions for digital systems 20 p3437 N85-31326

Performance improvements of a highly integrated digital electronic control system for an F-15 airplane
[NASA-TM-86748] 21 p3556 N85-32120

Myoelectric control of a computer based expert system for flight control
[AD-A154981] 21 p3557 N85-32126

Design of a jamming simulator for a binary communication system
[AD-A154617] 21 p3573 N85-32221

Globally-asynchronous locally-synchronous systems
[AD-A154624] 21 p3573 N85-32222

Secure digital voice communications in the Defense Data Network (DDN)
[AD-A154677] 21 p3574 N85-32226

Experimental evaluation of a new form of M-ary (M = 8) phase shift keying including design of the transmitter and receiver
[AD-A155103] 21 p3576 N85-32239

Microcomputer processing of LANDSAT Thematic Mapper data for the acquisition of military tactical terrain data
[AD-A154781] 21 p3605 N85-32389

Realizing the full potential of the video disc for mapping applications
[AD-A154966] 21 p3606 N85-32391

Bayesian vs MAP multiple model adaptive estimation for field of view expansion in tracking airborne targets
[AD-A155486] 21 p3679 N85-32855

Implementation of the SITAN algorithm in the digital terrain management and display system
[DE85-010659] 22 p3729 N85-33115

Quarter-inch streaming tape drive application with the Serial ASCII Instrumentation Loop (SAIL) system
[AD-A155354] 22 p3759 N85-33295

Characteristics of digital range finder with stroboscopic discretization 22 p3762 N85-33319

Amplitude stabilization of pulse signals
22 p3762 N85-33320

Digital holographic sythesis of pattern-forming transparencies for ring antenna arrays
22 p3763 N85-33326

Design of digital bandpass filters with finite memory
22 p3775 N85-33392

Binary signal detection in acoustooptic receivers
22 p3782 N85-33430

Transceiver test device
[AD-D011726] 22 p3786 N85-33456

Digital characterization of particle tracks for microdosimetry
[DE85-012896] 22 p3846 N85-33822

Modular digital holographic fringe data processing system
[NASA-CR-177952] 23 p3933 N85-34376

Balloon-borne video cassette recorders for digital data storage
[OG-9.3-11] 23 p4028 N85-34986

Burst size distributions in the digitized data of the ion chambers t Mt. Norikura and sea level stations
[SH-9.1-9] 23 p4051 N85-35124

Microprocessor-based single particle calibration of scintillation counter
[HE-4.6-13] 24 p4198 N85-36049

DIGITAL TECHNIQUES

Range-residuated mappings
[AD-A145148] 01 p0112 N85-10759

Research activities of the Illinois University Coordinated Science Laboratory
[AD-A145589] 03 p0449 N85-12856

Interference immunity of digital equipment for coherent processing of wideband signals
04 p0486 N85-13100

Digital radio link: Wave propagation measurements using narrow band technique
[FOA-C-30364-E2] 04 p0494 N85-13152

Digital image processing; report from a conference and study trip to the USA and Canada, summer 1984
[FOA-C-30369-E1] 04 p0494 N85-13153

Digital comparison and correlation techniques of remote sensing images with differing spatial resolutions
05 p0655 N85-14204

Multi-disciplinary techniques for understanding time-varying space-based imagery
[AD-A144357] 05 p0728 N85-14681

Infralow-frequency digital phase meter
06 p0787 N85-15031

Teletrack: A special effect
[BBC-RD-1984/10] 06 p0798 N85-15097

Experiences with digital processing of images at INPE
[E85-10045] 06 p0826 N85-15247

Detecting agricultural to urban land use change from multi-temporal MSS digital data — Salt Lake County, Utah
[E85-10049] 07 p0963 N85-16245

Some effects of digital sampling on orbiter flight control system operation 08 p1092 N85-16903

Information extraction and transmission techniques for spaceborne synthetic aperture radar images
[NASA-CR-174341] 08 p1150 N85-17256

Data acquisition channel apparatus
[AD-D011428] 08 p1159 N85-17311

Mathematical aspects of digital terrain information; Report from International Society for Photogrammetry and Remote Sensing (ISPRS) working group 3:3, 1980 - 1984 — photogrammetry 08 p1175 N85-17407

A comparative test of photogrammetrically sampled digital elevation models 08 p1175 N85-17408

Digital elevation model computation using fast Poisson solutions 08 p1175 N85-17412

Digital sound: Programme-modulated noise levels in sound signals subjected to a number of digital companding processes
[BBC-RD-1984/11] 09 p1310 N85-18233

Multipath and Doppler observations during transatlantic digital HF propagation experiments
10 p1471 N85-19281

Fast synchronization model for UHF spread-spectrum communication system 10 p1473 N85-19296

A technical solution to fadings in tactical satellite digital transmissions 10 p1473 N85-19297

Overview of RADC adaptive antenna developments for communications 10 p1474 N85-19299

The development of a microprocessor-controlled linearly-actuated valve assembly
[NASA-CR-174437] 10 p1491 N85-19415

Solar optical telescope primary mirror controller
[NASA-CR-174416] 10 p1570 N85-19903

Telemetry systems of Interkosmos satellites
11 p1617 N85-20173

Contour line generalization using digital image processing methods
[SER-C-291] 11 p1700 N85-20666

Conclusion of Viking Lander Imaging Investigation: Picture catalog of experiment data record
[NASA-RP-1137] 11 p1765 N85-21099

Semianalytic modeling of aerodynamic shapes
[NASA-TP-2413] 12 p1771 N85-21120

Estimation of the impulse response of television channels from digitized waveforms
[CRC-1376] 12 p1822 N85-21429

Fundamental limits to synchronization and tracking
[AD-A149623] 12 p1833 N85-21504

GSFC specification electronic data processing magnetic recording tape
[NASA-TM-80599] 12 p1851 N85-21609

Assessment of computer based geologic mapping of rock units in the LANDSAT-4 scene of northern Death Valley, California 13 p2119 N85-23195

Comparative techniques used to evaluate Thematic Mapper data for land cover classification in Logan County, West Virginia 13 p2121 N85-23209

Bouguer images of the North American craton
13 p2200 N85-23648

Near-nucleus studies of Comet Halley
14 p2435 N85-25018

Microcomputer controlled image acquisition system
15 p2537 N85-25654

Scene analysis using recursive frequency domain correlation with energy normalization
[AD-A151777] 16 p2854 N85-27596

Digital methods of the optimum processing of radar signals
[AD-A152489] 17 p2948 N85-28202

Image processing: Mathematics, engineering or art
[DE85-007666] 18 p3154 N85-29527

Approaches to digital image registration and recognition 19 p3257 N85-30197

Spectral reflectances of natural targets for use in remote sensing studies
[NASA-RP-1139] 19 p3299 N85-30450

Fast eigenvector methods for digital signal processing
20 p3439 N85-31341

Electron lithography STAR design guidelines. Part 1: The STAR user design manual
[NASA-CR-170765] 20 p3513 N85-31840

Electron lithography STAR design guidelines. Part 2: The design of a STAR for space applications
[NASA-CR-170766] 20 p3513 N85-31841

Electron lithography STAR design guidelines. Part 3: The mosaic transistor array applied to custom microprocessors. Part 4: Stores logic arrays, SLAs implemented with clocked CMOS
[NASA-CR-170767] 20 p3514 N85-31842

Interactive procedures for discriminating and restoring contour line networks 22 p3736 N85-33158

The Mk.1 NPL digital sampling ac wattmeter
[NPL-DES-82] 22 p3758 N85-33290

Design of digital bandpass filters with finite memory
22 p3775 N85-33392

Hierarchical chamfer matching
[FOA-C-30387-E1] 22 p3802 N85-33558

Design, development and operation of a high simultaneous capacity digital telemetry system — turbomachine blade flutter
[PNR-90261] 23 p3899 N85-34151

Computer analysis techniques for the temporal evaluation of cardiac wall motion
23 p3958 N85-34530

The scientific and technical issues in integrating remotely sensed imagery with geocoded data bases
23 p3960 N85-34547

A general purpose image processing package
23 p3961 N85-34549

Hologram-like transmission of pictures
23 p3961 N85-34552

Processing of LANDSAT imagery to map surface mineral alteration on the Alaska Peninsula, Alaska
24 p4106 N85-35455

Remote sensing of hydrologic transport processes using spot simulation data
[DE85-012412] 24 p4108 N85-35467

DIGITAL TO ANALOG CONVERTERS

Clutter generator for use in radar evaluation
[AD-D011234] 01 p0039 N85-10245

Programmable digital temperature controller apparatus
[AD-D011221] 01 p0049 N85-10319

Optical waveguide spatial filters
[AD-A145674] 02 p0280 N85-11825

Formation of reference signals in laser-type gas analyzers with mechanical switching of optical channels
06 p0787 N85-15027

RELTIM: A library of routines used in real time machine control applications
[PB85-116507] 10 p1542 N85-19725

Electrical characterization of analog microprocessors
[AD-A149629] 12 p1911 N85-21995

A method and apparatus for operating on companded PCM voice data
[NASA-CASE-KSC-11285-1] 18 p3089 N85-29120

DIGITIZERS

U ANALOG TO DIGITAL CONVERTERS

DIGITS

NT BINARY DIGITS

DIHEDRAL EFFECT

U LATERAL STABILITY

DIISOCYANATES

Structure-property relationships in thermoplastic elastomers. Part 1: Segmented polyether-polyurethanes
[AD-A148043] 08 p1133 N85-17138

Polymer intermediates from limonene (follow-up project)
[BMFT-FB-T-84-243] 12 p1814 N85-21360

DIKES (GEOLOGY)
U ROCK INTRUSIONS
DILATATION
U STRETCHING
DILATOMETERS
U EXTENSOMETERS
DILUENTS
New air-curing lacquer systems with high solids content
[BMFT-FB-T-85-005] 17 p2936 N85-28124
DILUTION
Dilution zone mixing studies 02 p0145 N85-10984
Dilution jet mixing 02 p0145 N85-10985
Measurements of atmospheric carbon disulfide using aircraft platforms and a GC/MS isotopic dilution analysis technique 03 p0391 N85-12500
Development of a temperature measurement system with application to a jet in a cross flow experiment
[NASA-CR-174896] 15 p2472 N85-25262
Dual electrochemical system
[AD-D011616] 16 p2817 N85-27376
DIMENSIONAL ANALYSIS
Development of structured regression hypotheses/interactive descriptive geometry through five dimensions
[INT-324] 04 p0554 N85 13524
Application of dimensional analysis to the problem of solar wind-magnetosphere energy coupling
[DE85-002414] 11 p1674 N85-20551
The application of dimensional analysis to the problem of solar wind-magnetosphere energy coupling
14 p2357 N85-24564
Applications of fuzzy set theory to satellite soundings
18 p3141 N85-29445
Diffusion-convection function of cosmic rays
[SH-3.2-10] 23 p4004 N85-34825
Computation of three-dimensional shock wave and boundary-layer interactions
[NASA-TM-86780] 24 p4093 N85-35372
DIMENSIONAL MEASUREMENT
Publications of Center for Manufacturing Engineering (of the National Bureau of Standards), 1978-1983
[PB84-224526] 01 p0036 N85-10228
Development of a measuring procedure for the automatic evaluation of the flatness of reflective surfaces
[BMFT-FB-T-84-166] 03 p0421 N85-12688
Programming and application of numerical controlled measuring machines (NCMES)
[BMFT-FB-T-84-153] 05 p0717 N85-14599
Method for non contacting gauging of the wall thickness of tubes by backscattering radiation
[OEFZS-4274] 07 p0988 N85-16144
The design and validation of software for dimensional metrology
[NPL-DITC-50/84] 15 p2521 N85-25542
Interferometric creep testing
[AD-A154249] 19 p3286 N85-30378
A simple optical extensometer achieving high accuracy
[NPL-DMA(A)-95] 20 p3458 N85-31474
DIMENSIONAL STABILITY
NT SHELL STABILITY
NT STRUCTURAL STABILITY
Parameters of geometric stability of laser mirror optical surface 02 p0273 N85-11777
Interferometric creep testing
[AD-A154249] 19 p3286 N85-30378
Materials and techniques for model construction
[NASA-CR-172620] 20 p3396 N85-31066
A systematic plan for the continued study of dimensional stability of metallic alloys considered for the fabrication of cryogenic wind tunnel models
[NASA-CR-172449] 21 p3565 N85-32172
DIMENSIONLESS NUMBERS
NT GRASHOF NUMBER
NT HIGH REYNOLDS NUMBER
NT LOW REYNOLDS NUMBER
NT MACH NUMBER
NT NUSSELT NUMBER
NT PRANDTL NUMBER
NT RAYLEIGH NUMBER
NT REYNOLDS NUMBER
NT RICHARDSON NUMBER
NT SIMILARITY NUMBERS
NT STROUHAL NUMBER
Ohmic potential drop and gas bubble radius distribution in alkaline water electrolysis 17 p2924 N85-28025
Linear boundary detection using pressure buildup tests
[DE85-009926] 22 p3784 N85-33444
DIMENSIONS
NT DEPTH
NT DIAMETERS
NT FILM THICKNESS
NT FRACTALS
NT HEIGHT
NT LARMOR RADIUS
NT LENGTH
NT RADII
NT TARGET THICKNESS
Shift-variant multidimensional systems
[AD-A144756] 01 p0111 N85-10752
Fractals: From snow flakes to galactic clusters
[NOTA-INTERNA-796] 02 p0296 N85-11918
Thermomechanical cracking in layered media from moving friction load
[AD-A146022] 03 p0373 N85-12379
Optimum dimensions of power solenoids for magnetic suspension 04 p0489 N85-13118
Considerations on the dimensioning of photovoltaic supply systems in the low power range
05 p0665 N85-14273
Coupling of multidirectional diffusions by reflection
[CTH-MATH-1984-20] 05 p0719 N85-14613
Challenges in the development of the shuttle extravehicular mobility unit 08 p1095 N85-16922
Cosmology in theories with extra dimensions
18 p3202 N85-29864
Physical dimensions of humans; values; the effect of clothing, working clothes and protective equipment on the design of work places
[HSE-TRANS-10868] 19 p3331 N85-30638
Physical dimensions of humans, values, envelope curves in different postures
[HSE-TRANS-10869] 20 p3513 N85-31836
A simulation study of Sylvester's problem in three dimensions
[AD-A155266] 21 p3679 N85-32854
Photo-acoustic effect in finite-dimensional semiconductors 21 p3682 N85-32876
DIMERS
A new heat-resistant polymer from dimer diamine bismaleimide. Part 1: Preparation and free radical cure of dimer diamine bismaleimide
[AD-A145664] 02 p0186 N85-11247
Theoretical research program to study transition metal trimers and embedded clusters
[NASA-CR-174296] 08 p1125 N85-17093
Comparative studies on the electronic structures of W2(O2CH)4 and W2(O2CH)4-(CH3)2 by the relativistic X Alpha-SW method: A d3-d3 metal dimer with a quadruple metal-metal bond?
[AD-A148814] 09 p1397 N85-18793
Conduction in polymerized polyfunctional diacetylenes
[AD-A149104] 10 p1451 N85-19145
Below-room-temperature water-vapor continuum absorption within the 8- to 10 micron atmospheric transmission window
[TR-0084(4945-09)-1] 13 p2132 N85-23266
Photoreactivation and other ultraviolet/visible light effects on DNA in human skin
[DE85-005135] 14 p2390 N85-24719
Investigation of the structure and dynamics of electrolytes in solvents used for primary and secondary Li-batteries
[AD-A153099] 17 p2954 N85-28240
Metallophthalocyanine dimers incorporating five atom covalent bridges
[AD-A154365] 19 p3234 N85-30051
Method of reducing impurity and antisite defects in semiconductor crystal materials, and device and apparatus respectively produced from and utilizing same
[AD-D011698] 19 p3260 N85-30216
DIMINUTION
U REDUCTION
DINITRATES
Preparation of ethylenediamine dinitrate
[DE85-006423] 23 p3922 N85-34305
DIODES
NT AVALANCHE DIODES
NT GERMANIUM DIODES
NT GUNN DIODES
NT JUNCTION DIODES
NT LIGHT EMITTING DIODES
NT MIM DIODES
NT PHOTODIODES
NT PLASMA DIODES
NT SCHOTTKY DIODES
NT SEMICONDUCTOR DIODES
NT TUNNEL DIODES
NT VARACTOR DIODES
The development of a diode laser Doppler velocimeter for boundary layer measurements under ice: A feasibility investigation
[AD-A145076] 01 p0053 N85-10348
Reversible change in parameters of GaAs-based surface-barrier metal-semiconductor diodes induced by hydrogen absorption-desorption
02 p0258 N85-11690
Gallium-arsenide power devices
06 p0794 N85-15076
Current-voltage characteristics of semiconductor powe devices operating at high current densities
06 p0795 N85-15079
External cavity diode laser sensor
[AD-D011341] 07 p0969 N85-16152
Diffusion barrier for long wavelength laser diodes
[AD-D011390] 07 p0970 N85-16157
EMC enhanced constant Z modulator
[AD-A147715] 08 p1157 N85-17297
Effect of neutron irradiation on the high temperatu operation of injection laser diodes
[DE85-000068] 09 p1326 N85-18035
Radiation effects induced in pin photodiodes by 40- and 85-MeV protons
[NASA-CR-175678] 14 p2426 N85-24880
Development of solid state infrared emitters for gas detection applications
[PB85-148450] 15 p2561 N85-25800
Generalization of the Child-Langmuir relation fo 1-dimensional time-dependent diodes
[DE85-007386] 16 p2779 N85-27182
Diode laser 87Rb optical pumping in an evacuated wall-coated cell 18 p3105 N85-29228
Digital control of diode laser for atmospheric spectroscopy
[NASA-CASE-NPO-16000-1] 18 p3112 N85-29264
Intense ion beam diode diagnostics using a tunable dye laser
[DE85-006079] 18 p3113 N85-29272
Measurements of vector fields with diode array
18 p3204 N85-29880
Integrated dual beam line scanning antenna and negative resistance diode oscillator
[AD-D011717] 19 p3261 N85-30223
Arrangement for damping the resonance in a laser diode
[NASA-CASE-NPO-15980-1] 19 p3274 N85-30306
Optical injection locking of solid-state oscillators by frequency-multiplexed injection-locked, laser diodes
[AD-D011695] 19 p3275 N85-30307
Resistance of polyaniline films as a function of electrochemical potential and the fabrication of polyaniline-based microelectronic devices
[AD-A154999] 21 p3569 N85-32201
A microprocessor-controlled, multichannel fluorimeter for analysis of sea water
[AD-A154986] 21 p3590 N85-32310
T/R switch design for short-range measurements, part 6.1A 21 p3624 N85-32515
Magnetically insulated diode for generating pulsed neutron and gamma ray emissions
[DE85-011658] 22 p3760 N85-33306
Multidiode integrated-circuit protective device
22 p3781 N85-33425
Power flow evaluations for HERMES 3
[DE85-013116] 24 p4156 N85-35780
Surface discharges as intense photon sources in the extreme ultraviolet
[DE85-012593] 24 p4158 N85-35782
DIOXIDES
NT CARBON DIOXIDE
NT HYDROGEN PEROXIDE
NT QUARTZ
NT SILICON DIOXIDE
NT SULFUR DIOXIDES
Structural studies on lead dioxides
[DE84-015837] 06 p0805 N85-15127
Investigation of manganese dioxide as an improved solid desiccant
[DE85-004034] 13 p2018 N85-22654
DIPHOSPHATES
NT ADENOSINE DIPHOSPHATE
DIPLEXERS
Performance interface document for the S-band diplexer for space users of NASA networks
[NASA-TM-86224] 23 p3900 N85-34155
DIPOLE ANTENNAS
Characteristics of two-frequency combined dipole antenna arrays 06 p0791 N85-15053
Infrared technology for satellite power conversion -- antenna arrays and bolometers
[NASA-CR-174266] 07 p0991 N85-16280
Tactical HF communication for military helicopters using the NVIS mode 08 p1074 N85-16807
Broad-band UHF dipole array
[NASA-TM-86373] 10 p1462 N85-19223
Printed circuit balun with a dipole antenna
[AD-D011534] 12 p1833 N85-21498
Surface wave excitation study
[DE85-005301] 13 p2056 N85-22875
Exact design formulas for field intensity of dipole deployed above flat homogeneous Earth with finite conductivity 13 p2081 N85-22898

A special antenna for SARSAT EPIRBs providing circular polarization and hemispheric coverage for reliable transmission to satellites --- Emergency Position Indicating Radio Beacon (EPIRB) 20 p3404 N85-31122
Artificial and natural icing tests YEH-60A quick fix helicopter
[AD-A155147] 21 p3555 N85-32116
Minimizing field scattered by slender dipoles
22 p3774 N85-33388

DIPOLE MOMENTS
NT ELECTRIC MOMENTS
NT MAGNETIC MOMENTS
Studies of the chemistry of vibrationally and electronically excited species in planetary upper atmospheres
[NASA-CR-174134] 03 p0449 N85-12851
Collision-induced dipole moments
[AD-A147682] 08 p1121 N85-17063
Experimental determination of the 1 sigma(+) state electron-dipole-moment function of carbon monoxide up to a large internuclear separation
[NASA-TM-85979] 09 p1379 N85-18670
Development of high field Nb-Ti accelerator dipoles
[DE85-000621] 11 p1714 N85-20782
Charge-to-mass dispersion methods for abrasion-ablation fragmentation models
[NASA-TM-86340] 11 p1726 N85-20857
Applications of piezoelectric and pyroelectric thin films: Opportunities for Langmuir-Blodgett technology
[AD-A149239] 15 p2659 N85-26406
Electroweak interactions in nuclei
[DE85-007611] 17 p3033 N85-28762
Scattering by distributions of small thin particles
19 p3253 N85-30172
Mutual coupling analysis for conformal microstrip antennas
[AD-A154282] 19 p3259 N85-30210
Effects of CP violation in SU(2) sub L x SU(2) sub R x U(1) electroweak models
[DE85-010801] 20 p3531 N85-31965

DIPOLES
Theory of nuclear magnetic relaxation
[AD-P003911] 01 p0032 N85-10197
A generalized solution to a class of printed circuit antennas
[AD-A145626] 02 p0191 N85-11278
Computer studies of the quench behavior of an SSC model-dipole
[DE85-010633] 19 p3360 N85-30629
Testing and optimizing MST coaxial collinear arrays, part 6.4A 21 p3625 N85-32518
The magnetic field of planets
22 p3858 N85-33891
What we have learned about the magnetic field of Mars 22 p3858 N85-33892
Magnetic field generation in the cores of terrestrial bodies 22 p3859 N85-33894

DIRAC EQUATION
Scattering theory by Enss' method for operator valued matrices. Dirac operator in an electric field
[REPT-84] 01 p0045 N85-10290
Solutions of field equations in General Relativity with spinor connection 15 p2663 N85-26436
Interpretation of 119 Sn isomer shifts and 3d 5/2-core-level shifts based on Dirac-Slater calculations on a number of ionic states
[USIP-85-06] 20 p3532 N85-31973

DIRECT CURRENT
Isolated load switching with surge suppression
[AD-D011218] 01 p0042 N85-10274
DC switching regulated power supply for driving an inductive load
[DE84-014236] 01 p0044 N85-10285
Nitriding of titanium and its alloys by N2, NH3 or mixtures of N2 + H2 in a dc arc plasma at low pressures (or = to torr)
[NASA-TM-83803] 06 p0814 N85-15166
Calculations of high-current characteristics of silicon diodes at microwave frequencies
[AD-A147406] 09 p1314 N85-18261
Variable speed generator technology options for wind turbine generators
[RR-84-4] 10 p1478 N85-19331
Study of electric field and ion effects on HVDC lines
[DE85-002975] 12 p1833 N85-21503
Ultrasensitive measuring devices
[DE85-000672] 12 p1853 N85-21622
Efficient heating and confinement of ions in an axisymmetric magnetic mirror supplemented with dc electric field
[IPPJ-707] 12 p1935 N85-22160
Outlook for realization of proximity effect and Josephson direct current in helium-2 13 p2074 N85-22956
Method of improving dynamic characteristics of DC voltage stabilizers with compound regulation
15 p2528 N85-25589
CSMP (Continuous System Modeling Program) modeling of brushless DC motors
[AD-A152043] 15 p2549 N85-25731
Pulsewidth modulated speed control of brushless dc motors
[AD-A151966] 16 p2778 N85-27148
Performance analysis of radiation cooled dc transmission lines for high power space systems
[NASA-TM-87040] 17 p2951 N85-28222
A small-scale self-excited rotor electrostatic generator
[AD-A155264] 21 p3681 N85-32265
Optical output stabilization method for direct current arc lamps
[AD-A154667] 21 p3705 N85-33013
Standard series of direct-current motors for regulated electric drives 22 p3772 N85-33375
Effect of polymer additives on characteristics of direct-current motor with liquid dielectric filler
22 p3772 N85-33376
Computer simulation of a cruise missile using brushless dc motor fin control
[AD-A155935] 24 p4089 N85-35349

DIRECT LIFT CONTROLS
Low-speed characteristics of a circulation control airfoil with AFT camber and a spiral trailing edge
[AD-A150651] 14 p2213 N85-23725
Basic consideration of the lifting capability of stoppable rotors
[AD-A150650] 14 p2219 N85-23759

DIRECT POWER GENERATORS
NT ALKALINE BATTERIES
NT ELECTROSTATIC GENERATORS
NT FUEL CELLS
NT HOMOJUNCTIONS
NT MAGNETOHYDRODYNAMIC GENERATORS
NT NICKEL ZINC BATTERIES
NT PHOSPHORIC ACID FUEL CELLS
NT PHOTOELECTRIC GENERATORS
NT PRIMARY BATTERIES
NT RADIOISOTOPE BATTERIES
NT REGENERATIVE FUEL CELLS
NT SOLAR BLANKETS
NT SOLAR CELLS
NT SOLAR SEA POWER PLANTS
NT THERMAL BATTERIES
NT THERMIONIC CONVERTERS
NT THERMOELECTRIC GENERATORS
NT VERTICAL JUNCTION SOLAR CELLS
Measurement-Technical Investigations of Wind Energy Units
[JUEL-SPEZ-244] 05 p0667 N85-14293
Measuring methods to determine the static and dynamic behavior of wind energy converters
05 p0668 N85-14297
VOITH: Wind energy converter WEC 520
05 p0668 N85-14299
Measuring and control tasks in OPTIWA
05 p0669 N85-14304
Operational performance of the photovoltaic-powered grain mill and water pump at Tangaye, Burkina Faso (formerly Upper Volta)
[NASA-TM-86970] 13 p2128 N85-23243
Space power plants 16 p2724 N85-26813

DIRECTION FINDERS (RADIO)
U RADIO DIRECTION FINDERS

DIRECTION FINDING
Radiation and scattering of spiral antennas
[AD-A151929] 16 p2773 N85-27116
The moving thermoacoustic array: A theoretical feasibility study
[AD-A154510] 21 p3699 N85-32980

DIRECTIONAL ANTENNAS
NT DIPOLE ANTENNAS
NT HELICAL ANTENNAS
NT HORN ANTENNAS
NT LENS ANTENNAS
NT LOG PERIODIC ANTENNAS
NT LOOP ANTENNAS
NT PARABOLIC ANTENNAS
NT RADAR ANTENNAS
NT RHOMBIC ANTENNAS
NT SLOT ANTENNAS
NT STEERABLE ANTENNAS
NT TWO REFLECTOR ANTENNAS
Reflector antenna having sidelobe suppression elements
[AD-D011227] 01 p0039 N85-10244
Possibility of realization of highly-directional antenna arrays 03 p0344 N85-12220
A sphere-scanning radiometer for rapid directional measurements of sky and ground radiance: The PARABOLA field instrument
[NASA-TM-86171] 03 p0363 N85-12329
System of equations for finding antenna radiation pattern from near-field samples 06 p0791 N85-15054
Dual band, low sidelobe, high efficiency mirror antenna
[AD-D011329] 07 p0944 N85-15980
Contamination of the fetch-limited directional wave spectrum by waves emanating from an embayment
[NASA-TM-84441] 15 p2604 N85-26046

DIRECTIONAL CONTROL
NT THRUST VECTOR CONTROL
Relative control effectiveness technique with application to airplane control coordination
[NASA-TP-2416] 14 p2218 N85-23753
Controller requirements for uncoupled aircraft motion, volume 1
[AD-A153173] 17 p2900 N85-27678
New Matsushiro underground cosmic ray station (220 M.W.E. in depth)
[SH-9.1-14] 23 p4052 N85-35129

DIRECTIONAL COUPLERS
Synthesis of multistep directional couplers with nonminimum-phase characteristics
13 p2079 N85-22986
Strongly coupled millimeter-band waveguide directional couplers 22 p3779 N85-33418
New directional couplers for multimode circular waveguides applied to intense pulsed microwave systems
[DE85-011753] 23 p3926 N85-34330

DIRECTIONAL SOLIDIFICATION (CRYSTALS)
Materials for advanced turbine engines. Project 2: Rene 150 directionally solidified superalloy turbine blades, volume 2
[NASA-CR-167993] 03 p0319 N85-12059
Directional solidification studies of Pb-Bi pertectic alloys
[DE84-015656] 04 p0474 N85-13016
Controlled directionally solidified precision casting for superalloys and steels
[BMFT-FB-T-84-196] 05 p0619 N85-13960
Crystallization methods for solar cell silicon
12 p1877 N85-21774
Influence of solidification parameters on the formation of the gamma-M7C3 eutectic structure of 2% C-12%Cr steel 15 p2512 N85-25500
Properties of heat resistant Ni-Al-Nb alloys with unidirectional eutectic structure
19 p3247 N85-30133
Mechanical behavior of Ni-Cr-base superalloys in forms and conditions representative of service
[NPL-DMA(A)-94] 20 p3431 N85-31282
MPS solidification model. Analysis and calculation of macrosegregation in a casting ingot
[NASA-CR-171589] 21 p3586 N85-32178
Directionally solidified gas turbine alloys
[PNR-90264] 23 p3917 N85-34279

DIRECTIONAL STABILITY
NT GYROSCOPIC STABILITY
Determining characteristics of optical radiation reflectors based on results of remote sensing
15 p2488 N85-25358

DIRECTIVITY
Direction dependent radiation behavior in the classification of multispectral aircraft remote sensing data
[SER-C-290] 01 p0063 N85-10419
Short mode selective directional couplers
[IPF-83-9] 09 p1394 N85-18774
Improved directional couplers for overmoded waveguide systems
[IPF-84-1] 09 p1394 N85-18775
Directivity of Bremsstrahlung radiation from relativistic beams and the Gamma-Rays from solar flares
[NASA-CR-174433] 10 p1572 N85-19913
Effect of axisymmetric vibration modes on sensitivity and di rectivity characteristics of piezoceramic sphere --- hydrophones 15 p2525 N85-25569
Study on the correlation between grinding conditions and residual stresses in ground surface of steel by the X-ray method 23 p3907 N85-34203
Properties of 10 (18)-10 (19)eV EAS at far core distance
[HE-4.7-3] 24 p4198 N85-36054
Fast scintillation counter preamplifier for the observation of Linsley effect
[HE-4.7-9] 24 p4199 N85-36060
Acoustic detection of air shower cores
[HE-7.1-4] 24 p4213 N85-36158

DIRECTORIES
EPA (Environmental Protection Agency) environmental data base and model directory, volume 1
[PB84-207562] 01 p0126 N85-10868
DDN directory
[AD-A148213] 08 p1230 N85-17744
Middle Atmosphere Program. Handbook for MAP, volume 6
[NASA-CR-175460] 11 p1656 N85-20436

State measurement laboratories: Program description (part 1). Directory (part 2)
[PB85-137651] 11 p1739 N85-20935
A DOE directory of databases fur material properties
[UCAR-10124] 11 p1739 N85-20937
Current alternative energy research and development in Illinois
[PB85-163137] 16 p2820 N85-27397
A study of user-defined searching requirements for the on-line version of the directory of DOD-sponsored R and D data bases on the Defense Gateway computer system
[AD-A153000] 17 p3050 N85-28678
Worldwide directory of national Earth-science agencies and related international organizations
[GS-CIRC-934] 21 p3605 N85-32386

DIRICHLET PROBLEM
An integral equation formulation for a boundary value problem of elasticity in the domain exterior to an arc
[PREPRINT-833] 03 p0413 N85-12643
Integral equation formulations in two dimensions
05 p0718 N85-14605
Three-dimensional and axisymmetric problems
05 p0718 N85-14608
Lectures on generalized solutions to the minimal surface equation
[DE84-016882] 05 p0722 N85-14642
Orthogonal polynomials and a Dirichlet problem related to the Hilbert transform
[CWI-PM-R8406] 05 p0723 N85-14647
Three-dimensional, direct and vectorized elliptic solvers for various boundary conditions
[AD-B088266L] 08 p1206 N85-17595
A non-hypoelliptic Dirichlet problem from stochastics
10 p1537 N85-19687
W.E. Johnson's Sufficientness postulate
[AD-A149014] 10 p1550 N85-19774
Some estimates of harmonic majorants
15 p2634 N85-26237
On functions with a finite or locally bounded Dirichlet integral 15 p2635 N85-26243

DIRIGIBLES
U AIRSHIPS

DIRT
Antisoiling technology: Theories of surface soiling and performance of antisoiling surface coatings
[NASA-CR-174274] 07 p0991 N85-16296
Electronic detection and concealment of film dirt
[BBC-RD-1985/4] 15 p2538 N85-25667

DISARMAMENT
The structures and the role of an international agency for the control of satellites
[NASA-TM-76765] 03 p0441 N85-12606
Arms control and The President's Strategic Defense Initiative
[AD-A156334] 24 p4068 N85-35212

DISASTERS
Meteorological aspects of the 1982-83 El Nino/southern oscillation episode 07 p1001 N85-16356
Climate and fisheries: A Peruvian case study
07 p1003 N85-16373
The El Nino phenomenon and its agrometeorological implications 07 p1004 N85-16382
Hurricane experience levels of coastal county populations: Texas to Maine
[PB85-111363] 10 p1520 N85-19561
Large natural geophysical events: Planetary planning
[DE85-000859] 11 p1763 N85-21092
Hurricane storm surge research
[GPO-40-048] 12 p1893 N85-21880
Comet showers and Nemesis, the death star
[DE85-003736] 15 p2663 N85-26575
Hazardous air pollutants
[GPO-43-064] 21 p3613 N85-32456

DISCHARGE
Statistical analysis of partial discharge inception in high voltage 15 p2546 N85-25715
Detection and location of partial discharges in transformer windings using electrical methods
15 p2551 N85-25750

DISCHARGE TUBES
U GAS DISCHARGE TUBES

DISCHARGERS
A high-voltage discharger
[AD-A145659] 02 p0194 N85-11299
Extended performance technology study 30-cm thruster
[NASA-CR-168259] 07 p0917 N85-15806

DISCIPLINING
Rapid determination of cadet discipline by projective tests 22 p3821 N85-33671

DISCONNECT DEVICES
High voltage disconnect protection
[AD-D011480] 10 p1481 N85-19353
Releasable cable connector assembly for use between a mobile and stationary object
[AD-D011536] 12 p1858 N85-21655
Torso restraint system
[AD-D011609] 16 p2702 N85-26884
Slide release mechanism — for space shuttle orbiter/external tank connection device
[NASA-CASE-MSC-20080-1] 19 p3279 N85-30334

DISCONNECTORS
U DISCONNECT DEVICES

DISCONTINUITY
NT SHOCK DISCONTINUITY
Visual representations subserving texture perception
[AD-A145412] 02 p0236 N85-11538
Blind zones and aspect ratio bias in acquisition of discontinuity orientation data
[DE84-002718] 04 p0533 N85-13410
MMIC devices for active phased array antennas
[NASA-CR-174281] 07 p0938 N85-15943
Deep structure of Western Siberia
07 p0981 N85-16235
Surface reconstruction preserving discontinuities
[AD-A146741] 07 p1028 N85-16526
Critical flashing flow of subcooled fluids in nozzles with contour discontinuities
[DE84-017229] 09 p1319 N85-18296
Recovering pointwise values of discontinuous data within spectral accuracy
[NASA-CR-172535] 12 p1919 N85-22049
Lateral inhomogeneity of mantle surface in western Eurasia 14 p2344 N85-24497
The GEOS-2 electric field observations at times of solar wind discontinuities 14 p2360 N85-24584
Studies on the interference of wings and propeller slipstreams
[NASA-CR-175753] 15 p2483 N85-25210
Reflection and transmission of flexural waves at discontinuities 15 p2572 N85-25861
Analysis of systems of waveguide discontinuities by the method of moments 19 p3253 N85-30171
MMIC devices for active phased array antennas
[NASA-CR-176015] 19 p3254 N85-30177
Characterization of microstrip discontinuities in the time and frequency domains
[NASA-CR-176190] 24 p4068 N85-35342

DISCOVERING
U EXPLORATION

DISCOVERY (ORBITER)
Results of Space Shuttle flight 41-D
[GPO-39-481] 12 p1791 N85-21243

DISCRETE FUNCTIONS
Long time correlation and stochastic diffusion in the standard map 02 p0282 N85-11835
Some scientific subroutines in LISP
[AD-A147889] 07 p1026 N85-16515
Discrete modifications to continuous dynamic structural systems 09 p1337 N85-18410
Computing convolution of multifrequency signal employing truncated fast Fourier transform algorithms
13 p2085 N85-23019
An incremental multigrid strategy for the fluid dynamics equations
[AD-A151953] 16 p2783 N85-27172
Quadratic spaces over discrete Hodge algebras
16 p2853 N85-27593
On the choice of coordinates for semiconductor simulation
[AD-A152214] 16 p2870 N85-27706
Discrete mathematics for communications systems
[AD-A152614] 17 p3018 N85-28664
Modeling of discrete devices with use of multivalued logic and nomograms 22 p3768 N85-33351
Generalization of discrete Fourier transform for interpolation in time domain 22 p3775 N85-33396
Generalization of discrete Fourier transformation for interpolation in time domain 22 p3776 N85-33400
Monte Carlo techniques for analyzing deep penetration problems
[DE85-011426] 23 p3968 N85-34596

DISCRIMINANT ANALYSIS (STATISTICS)
Statistical tropical cyclone forecasting techniques for the Southern Hemisphere
[AD-A144752] 01 p0065 N85-10569
Asymptotic distributions of estimators for posterior probabilities in a classification model with both continuous and discrete variables
[CWI-MS-R8409] 05 p0722 N85-14637
Discriminant analysis of pulsar groups in the diagram P versus P 12 p1960 N85-22319
Forecasting atmospheric visibility over the summer north Atlantic using the principal discriminant method
[AD-A155537] 21 p3837 N85-32593
Efficiency of discrimination in some invariant signal transformations 22 p3776 N85-33399

DISCRIMINANT FUNCTIONS
U DISCRIMINANT ANALYSIS (STATISTICS)

DISCRIMINATION
NT SENSORY DISCRIMINATION
NT TACTILE DISCRIMINATION
NT VISUAL DISCRIMINATION
Noise jammer discrimination by noise modulation bandwidth
[AD-D011473] 10 p1468 N85-192
Performance of time-position discriminator of composite signal 13 p2072 N85-2294
Vertical discrimination in the sound channel
[AD-A150254] 13 p2155 N85-233
Psychophysiological studies. 1: Performance and physiological response in learning, short-term memory and discrimination tasks
[AD-A151018] 14 p2392 N85-2473
Rayleigh criteria resolution of optical correlations
[AD-A151711] 15 p2652 N85-26
Seismic discrimination
[AD-A154167] 20 p3494 N85-3172
Mass-discrimination during prolonged weightlessness
20 p3509 N85-3181
Efficiency of discrimination in some invariant signal transformations 22 p3776 N85-333

DISCRIMINATORS
NT FREQUENCY DISCRIMINATORS
Mathematical model of discriminator for signals with fluctuations and thermal noise 13 p2072 N85-2294

DISEASES
NT ANEMIAS
NT ARTERIOSCLEROSIS
NT ASTHMA
NT BONE DEMINERALIZATION
NT CANCER
NT CARBON MONOXIDE POISONING
NT CATARACTS
NT CORONARY ARTERY DISEASE
NT EYE DISEASES
NT HEART DISEASES
NT INFECTIOUS DISEASES
NT INFLUENZA
NT LEAD POISONING
NT LEUKEMIAS
NT MYOCARDIAL INFARCTION
NT OSTEOPOROSIS
NT PARKINSON DISEASE
NT PULMONARY LESIONS
NT RESPIRATORY DISEASES
NT TOXIC DISEASES
NT TUMORS
Evaluation of the musculoskeletal diseases program
[PB84-230646] 07 p1017 N85-1648
The physiology of ultradian rhythms and their role in affecting disease resistance
[AD-A148842] 09 p1363 N85-1857
Review of US manual of clinical aviation medicine
12 p1904 N85-2196

DISHES
U PARABOLIC REFLECTORS

DISILICIDES
Reinforcement of molybdenum disilicide with nematic crystals of aluminum oxide 03 p0353 N85-122

DISINFECTANTS
U ANTISEPTICS

DISINTEGRATION
Inquiry into disintegration control of irradiated low enrichment uranium for high temperature gas cooled reactors
[OEFZS-7281] 07 p1042 N85-1661

DISK GALAXIES
Excitation of spiral patterns in responsible density wave theory 05 p0740 N85-1478
Dark matter near the sun: Simulated star counts and the Oort limit 06 p0880 N85-155
On the morphology of spiral modes — disk galaxies
12 p1955 N85-222
Drift-accretion theory of the spiral structure of galaxies
12 p1957 N85-222
Dynamics of gas disks in triaxial galaxies
13 p2171 N85-234
The Formation of preplanetary disks from the collapse of rotating molecular cloud cores
13 p2180 N85-235
Limits on the Doppler factor in relativistic jets by means of gamma-ray observations
[OG-2.7-12] 22 p3872 N85-339
Interpretation of cosmic-ray anisotropy below 10(14) eV
[OG-5.4-13] 22 p3887 N85-340
Evidence for a dynamical halo around the edge-on galaxy NGC 4631
[OG-6.2-1] 22 p3888 N85-341
Solar activity beyond the disk and variations of the cosmic ray gradient
[SH-5.1-23] 23 p4044 N85-350

DISKS

Flexible matrix composite laminated disk/ring flywheel
05 p0806 N85-13866

Proceedings of the National Bureau of Standards and National Security Agency Workshop on Standardization Issues for Optical Data Disk (ODD) Technology
[PB84-217785] 06 p0848 N85-15383

Yield stress determination from miniaturized disk bend test data
[DE85-009495] 18 p3122 N85-29330

DISKS (SHAPES)
NT ACTUATOR DISKS
NT ROTATING DISKS

Hot isostatically pressed manufacture of high strength MERL 76 disk and seal shapes
[NASA-CR-165550] 02 p0183 N85-11225

Basic study of bladed disk structural response
[AD-A146226] 03 p0319 N85-12061

Analysis of piezoelectric disks and cylinders using finite element method
[AD-A146323] 03 p0414 N85-12650

Scattering from thin dielectric disks
[NASA-TM-86155] 06 p0798 N85-15098

Locally univalent functions in the unit disk
10 p1536 N85-19680

The definition and computation of a metric on plane curves. The meaning of a face on a geometric model
17 p3004 N85-28571

DISLOCATIONS (MATERIALS)
NT CRYSTAL DISLOCATIONS
NT EDGE DISLOCATIONS
NT SCREW DISLOCATIONS

Subgrains, dislocations and the elevated-temperature strength of type 304 stainless steel
[DE84-001233] 04 p0473 N85-13014

Inclined dislocation emission at a shielded crack tip
[DE84-016703] 06 p0818 N85-15192

Stress-strain analysis of silicon ribbon
[NASA-CR-175459] 10 p1510 N85-19525

Electron-plastic effect in metals
11 p1605 N85-20089

Structures of ordered linear dislocation multipoles in Cu-Al alloys
[ISSN-0379-6906] 13 p2021 N85-22664

Influence of short-range order on deformation mechanisms in solid solutions
[DE85-006374] 14 p2258 N85-23989

Hydrogen embrittlement testing
[DE85-007352] 23 p3916 N85-34273

HgCdTe surface and defect study program
[AD-A156079] 24 p4161 N85-35799

DISORDERS

Interactions in localization
[NOTA-INTERNA-815] 02 p0279 N85-11818

Comparative analysis of effects of weightlessness and its models on velocity and strength properties and tone of human skeletal muscles 12 p1901 N85-21936

DISORIENTATION
NT DISORDERS
NT JET LAG

Theory underlying the peripheral vision horizon device
01 p0008 N85-10048

DISPENSERS

Improved materials and processes of dispenser cathodes
[AD-A148810] 09 p1314 N85-18262

Continued development and testing of tungsten controlled porosity dispenser cathodes
[AD-A152596] 17 p2931 N85-28090

The effect of metal overlayers of thermionic dispenser cathodes
[AD-A154795] 21 p3701 N85-32995

DISPERSING

Urban aerosol modeling
[PB84-233469] 04 p0532 N85-13401

Determination of the laws governing the changes in the standard deviations of the distribution of pollution based on observations of the atmospheric turbulence spectrum and the possibility of simulating it in the laboratory
[BLL-TR-T6373/BG/MRS14883/84]
08 p1179 N85-17431

Analyzing two-level fractional factorial experiments for possible dispersion effects
[AD-A149455] 10 p1548 N85-19760

Atmospheric dispersion of hypergolic liquid rocket fuels, volume 1
[AD-A149597] 12 p1817 N85-21399

Effect of ScAl3 phase dispersion on hardening of alloy Al-6.3 percent Mg-0.21 percent Sc
19 p3241 N85-30096

Preliminary wind tunnel experiments to investigate the effect of heat transfer on the dispersion of cold dense gases
[DUEL-1546/84] 20 p3456 N85-31467

Benthic boundary layer modelling studies
[IOS-181] 20 p3497 N85-31742

Assessment of the performance of an in-field Gaussian plume/puff model for overwater use
[AD-A155435] 21 p3614 N85-32460

Investigation of the formation of cloud particle spectrum on natural condensation nuclei
21 p3649 N85-32674

DISPERSION

An experimental investigation of microstrip properties on soft substrates from 2 to 40 GHz
[NASA-TM-86961] 11 p1624 N85-20224

Dispersion characteristics of small-mode gradient optical fibers 13 p2082 N85-23004

An investigation of the structure and high temperature mechanical properties of oxide dispersion strengthened alloys
[AD-A151107] 15 p2509 N85-25477

Results of recent large-scale NH3 and N2O4 dispersion experiments
[DE85-004988] 15 p2589 N85-25960

Evaluation of source strength and dispersion model predications with data from large nitrogen tetroxide field experiments
[DE85-011855] 23 p3947 N85-34465

DISPERSION PRECIPITATION HARDENING
U PRECIPITATION HARDENING

DISPERSIONS
NT AEROSOLS
NT COLLOIDS
NT EMULSIONS
NT FOG
NT LIQUID-GAS MIXTURES
NT NUCLEAR EMULSIONS
NT PHOTOGRAPHIC EMULSIONS
NT SMOKE

A perturbation solution for rigid dumbbell suspensions in steady shear flow
[AD-A144876] 01 p0111 N85-10755

Transport properties of multiphase systems
[DE84-015560] 02 p0173 N85-11159

Radiotracer studies of the dispersion of solid pollutants in marine and estuarial environment: Measurement of diffusion coefficients and the phenomenon of dispersion by currents
[BLL-DRIC-TRANS-7104-(3623.66)]
02 p0224 N85-11468

A dispersion model for airborne particulates inside a building
[DE84-014961] 02 p0225 N85-11473

Carbon monoxide study, Anchorage, Alaska, November 22, 1982 to February 11, 1983
[PB84-236595] 05 p0673 N85-14321

Turbulent shear fields for dispersion of aqueous drops in organic liquids and application to gel-sphere processes
[DE84-016562] 06 p0809 N85-15141

Influence of turbulence on erosion by a particle-laden fluid jet
[DE84-014365] 09 p1320 N85-18301

Dispersion of phase-shift keyed systems with fixed number of blocks 13 p2070 N85-22928

Ultrasonic dispersion of soils for routine particle size analysis: Recommended procedures
[DE85-005530] 16 p2861 N85-27843

Transmission of light by disperse medium of densely packed optically soft particles 21 p3697 N85-32969

Calculating dominant (quasi-t) mode group velocity in shielded microstrip line 22 p3780 N85-33422

DISPLACEMENT

Metrological consequences of the hard optical boundary assumption
[PB84-223577] 01 p0121 N85-10827

Predicting optical image displacement velocity in survey of Earth's surface 02 p0165 N85-11116

Deformation measurements of composite multi-span beam shear specimens by Moire interferometry
[NASA-CR-3844] 02 p0169 N85-11135

Deformations and strains in adhesive joints by moire interferometry
[NASA-CR-172474] 02 p0185 N85-11236

An experimental evaluation of the J integral in 50% sidegrooved compact geometry specimens
[AERE-R-11202] 03 p0374 N85-12386

Holographic displacement analysis with fiber optics
[AD-A146185] 03 p0420 N85-12680

Quantification of Saint-Venant's principle for a general prismatic member 04 p0467 N85-12972

Improved beam theory for anisotropic materials
04 p0468 N85-12973

A study of crashworthiness of light aircraft fuselage structures: A numerical and experimental investigation
[UTIAS-286] 06 p0750 N85-14803

Bearing tester fit analysis
[NASA-CR-171282] 07 p0973 N85-16181

Experimental compliance calibration of the NASA Lewis Research Center Mode 2 fatigue specimen
[NASA-TM-86908] 07 p0977 N85-16205

Use of coordinate functions to calculate deformation fields
[BLL-M-36010-(5828.4)] 07 p1028 N85-16524

On some exact solutions in elastostatics in terms of harmonic functions 09 p1332 N85-18367

The fracture mechanics of a slit crack with crack-tip dual zones 09 p1332 N85-18371

Ground shock effect on soil field inclusions
09 p1336 N85-18403

NOAA OTEC CWP (National Oceanic and Atmospheric Administration Ocean Thermal Energy Conversion Cold Water Pipe) at-sea test. Volume 3, part 1: Tabulation of the power spectra for selected channels
[PB84-238955] 09 p1346 N85-18467

Nonlocal and nonlinear effects on solar oscillations
09 p1416 N85-18934

Ice segregation and frost heaving
[PB85-122430] 10 p1460 N85-19199

The likelihood displacement: A unifying principle for influence measures
[AD-A149456] 10 p1551 N85-19783

Elastic compliance of imperfect interfaces: Review and relationship to ultrasonic scattering
[DE85-003068] 11 p1652 N85-20404

Comparison of shock-induced displacements with displacements produced by a centrifuge acceleration
[DE85-000467] 12 p1852 N85-21618

Recent advances in hybrid/mixed finite elements
[NASA-CR-175574] 12 p1863 N85-21687

Elastic response of a half-plane to a bonded interference-fit disc of the same material
[ARL/STRUC-R-406] 12 p1865 N85-21701

On the relative motion of typhoons: In the case of Typhoon 8305 and Typhoons 8306 and 8307
12 p1894 N85-21985

Fault offsets and lateral crustal movement on Europa
13 p2201 N85-23656

Importance of the tectonic motions on Ganymede
13 p2202 N85-23661

Transducer of linear displacements
14 p2281 N85-24130

Evaluation of stress concentration coefficients in butt-welded joints with displaced edges
15 p2501 N85-25425

On the interconnection of incompatible solid finite element meshes using multipoint constraints
15 p2575 N85-25879

Empirical development of ground acceleration, velocity and displacement for accidental explosions at J5 or the proposed large altitude rocket cell at Arnold Engineering Development Center
[DE85-008324] 16 p2758 N85-27020

The nonlinear analysis of thick composite plates using a cubic spline function 16 p2798 N85-27252

Improvement of conditions for meshing spiral bevel gears
[NASA-TM-77867] 18 p3117 N85-29294

Debye temperature and static displacements in LuH sub x single crystals from energy dispersive X-ray diffraction
[DE85-010961] 19 p3376 N85-30946

Finite element modeling of cracked bodies using the Bodner-Partom flow law 20 p3468 N85-31547

Estimation of power-law creep parameters from bend test data
[PB85-183408] 20 p3472 N85-31579

Efficient solution methods for nonlinear finite element analysis 20 p3519 N85-31886

Effects of contact area of an interface on acoustic wave transmission characteristics
[DE85-009935] 20 p3524 N85-31920

Hubble space telescope: Pointing error effects on nonlinear ball joints
[NASA-TM-86511] 20 p3545 N85-32058

The collected data for ramp function tests on a NACA 23012 aerofoil. Volume 1: Description and pressure data
[GU-AERO-8413-VOL-1] 23 p3894 N85-34123

Calibrator for displacement gages used in the rock mechanics laboratory
[DE85-013257] 24 p4096 N85-35393

DISPLACEMENT MEASUREMENT

Development of a modular multicoordinate measuring system with continuous-path microprocessor control
[BMFT-FB-T-84-158] 03 p0408 N85-12606

Instantaneous kinematics and joint displacement analysis of fully-parallel robotic devices
05 p0641 N85-14113

High speed electric field and voltage measurements with field coupled sensors
[DE85-006637] 15 p2642 N85-26299

Improved coordinate measuring machine calibration and control
[DE85-012053] 21 p3580 N85-32315

Possibility of measurement of small displacements by ring laser 21 p3687 N85-32904

New method for compensating and measuring any motion of three-dimensional objects in holographic interferometry
[ISL-CO-216/84] 22 p3789 N85-33474

DISPLAY DEVICES
NT ANEMOMETERS
NT APPROACH INDICATORS
NT FLOW DIRECTION INDICATORS
NT GYRO HORIZONS
NT HEAD-UP DISPLAYS
NT HELMET MOUNTED DISPLAYS
NT HOT-FILM ANEMOMETERS
NT HOT-WIRE ANEMOMETERS
NT PLAN POSITION INDICATORS
NT PLASMA DISPLAY DEVICES
NT POSITION INDICATORS
NT RADARSCOPES
NT RADIO DIRECTION FINDERS
NT SPACECRAFT POSITION INDICATORS
NT SPEED INDICATORS
NT TACHOMETERS
NT WIND VANES

Peripheral Vision Horizon Display (PVHD)
[NASA-CP-2306] 01 p0008 N85-10044
Personal experience with the PVHD and opinion of situations in which a wide Field Of View (FOV) PVHD might be helpful 01 p0008 N85-10045
Effects of foveal information processing
01 p0009 N85-10052
Peripheral vision horizon display on the single seat night attack A-10 01 p0009 N85-10053
Extracts from the test plan for in-flight evaluation of the NT-33A peripheral vision display
01 p0009 N85-10055
NASA Ames-Dryden T-37 demonstration comments
01 p0009 N85-10056
Early Air Force Flight Test Center (AFFTC) experience with Peripheral Vision Horizon Displays (PVHD)
01 p0009 N85-10057
Peripheral vision displays: The future
01 p0009 N85-10058
A production peripheral vision display system
01 p0010 N85-10059
A preliminary flight evaluation of the peripheral vision display using the NT-33A aircraft
[AD-A145123] 01 p0010 N85-10060
LED multifunction keyboard engineering study
[AD-A145199] 01 p0010 N85-10061
Content, variety, and augmentation of simulated visual scenes for teaching air-to-ground attack
[AD-A145218] 01 p0013 N85-10080
A subjective evaluation of the PROFS operational workstation based upon a real-time forecasting experiment in summer 1983 --- Program for Regional Observing and Forecasting Services (PROFS) 01 p0083 N85-10556
Interactive computer display systems in nowcasting
01 p0083 N85-10557
Field tests of the real-data acquisition system for the NASA-LaRC differential absorption lidar
[NASA-CR-174020] 01 p0106 N85-10710
The case for concern about very low frequency fields from visual display terminals: The need for further research and shielding of VDTs
[CCOHS-P83-2E] 02 p0234 N85-11526
Human engineering data base for design and selection of cathode ray tube and other display systems
[AD-A145704] 02 p0238 N85-11549
Implications of artificial intelligence for a user defined technical information system
[AD-P003938] 02 p0248 N85-11618
Command flight path display. Phase I and II: Appendix F
[AD-A145858] 03 p0318 N85-12056
A comparative evaluation of EMADS (Engine Monitoring and Display System) and conventional engine instruments
[AD-A145901] 03 p0319 N85-12060
Analysis of data entry performance: Chromatic versus monochromatic
[AD-A145568] 03 p0438 N85-12780
System status display information
[NASA-CR-172347] 04 p0455 N85-12889
Vibration data analysis system for SNLA area 3 reference manual
[DE84-016207] 04 p0514 N85-13275
Investigation and development of multicolored liquid crystal display systems for automotive dashboard application and large format information boards
[BMFT-FB-T-84-187] 04 p0572 N85-13652
Visual systems for remotely controlled vehicles
05 p0703 N85-14512
A comparative study of alternative controls and displays for by the severely physically handicapped
05 p0709 N85-14549
Color and grey scale in sonar displays
05 p0710 N85-14552
Representing multidimensional systems using visual displays 05 p0711 N85-14560
Experience with a sophisticated computer based authoring system
[DE84-014644] 05 p0713 N85-14575
Human factors of visual displays
06 p0752 N85-14821
Crewstation design and validation
06 p0752 N85-14822
Avionics technology - system concepts
06 p0753 N85-14824
Weather satellite products in the Flight Service Automation System (FSAS)
[AD-A146520] 06 p0759 N85-14855
Human engineer's guide to auditory displays. Volume 2: Elements of signal reception and resolution affecting auditory displays
[AD-A146513] 06 p0859 N85-15462
Human engineer's guide to auditory displays. Volume 1. Elements of perception and memory affecting auditory displays
[AD-A146601] 06 p0860 N85-15464
Display Techniques for Advanced Crew Stations (DTACS). Phase 1: Display techniques study
[AD-A146822] 07 p0904 N85-15722
Interactive Signal Analysis Software (ISAS). User's manual
[AD-A146999] 07 p1022 N85-16485
Program visualization: Graphics support for software development
[AD-A146887] 07 p1024 N85-16499
Matrix display simulation
[AD-D011371] 07 p1055 N85-16695
Built-in-test for first line testing
08 p1064 N85-16739
A Computer-generated topographic display system for navigation and mission planning in helicopters
08 p1073 N85-16800
Map display for helicopters 08 p1073 N85-16801
Integration of sensor fusion in advanced helicopter cockpit design 08 p1074 N85-16813
Flight research on visual aids and navigation equipment for helicopter low-level flight at night
08 p1076 N85-16820
A cockpit-display concept for executing a multiple glide-slope approach for wake-vortex avoidance
[NASA-TP-2366] 08 p1085 N85-16869
Realization and testing of an experimental color display system for general aviation helicopters and aircraft
[BMFT-FB-W-84-042] 08 p1086 N85-16872
Pilot climate data system
[NASA-CR-174321] 08 p1187 N85-17481
A FORTRAN plotting package for graphic VDUs
[AD-A148489] 08 p1204 N85-17577
Improved real-time ultra-high resolution image projection display using laser-addressed liquid crystal light valve
[AD-D011414] 08 p1223 N85-17705
Thin film transistors for addressing flat panel displays
[BMFT-FB-T-84-210] 08 p1227 N85-17726
Producing high scene content with perspective validity
[AD-P004314] 09 p1268 N85-17968
Geographic subdivision and top level data structures, Columbus, Magellan, and expanding CIG (Computer Image Generation) horizons
[AD-P004317] 09 p1268 N85-17971
The use of lasers in wide-angle visual systems
[AD-P004322] 09 p1269 N85-17976
Considerations in an optical variable acuity display system
[AD-P004323] 09 p1269 N85-17977
Design considerations for an eye tracked AOI (Area of Interest) display system
[AD-P004324] 09 p1269 N85-17978
Control systems analysis program: A tool for analysis of the GE-VSCDP (General Electric-Visual System Component Display Program) image display system
[AD-P004325] 09 p1270 N85-17979
Progress report on an eye-slaved area-of-interest visual display
[AD-P004326] 09 p1270 N85-17980
Air combat visual simulation using a head slaved projector
[AD-P004327] 09 p1270 N85-17981
A second generation WAVIDS (Wide Angle Virtual Image Display System)
[AD-P004328] 09 p1270 N85-17982
The effects of time delay in man-machine control systems: Implications for design of flight simulator Visual-Display-Delay compensation
[AD-P004329] 09 p1270 N85-17983
Baffled eye and confounded brain or using visual illusions to train blind pilots
[AD-P004332] 09 p1271 N85-17986
Pictorial format display evaluation
[AD-A149252] 10 p1425 N85-18986
Dialog system of preparation and presentation of visual information 10 p1526 N85-19622
Sector suite man-machine functional capabilities and performance requirements
[AD-A148881] 10 p1531 N85-19647
Human Factors Considerations in High Performance Aircraft
[AGARD-CP-371] 10 p1532 N85-19653
Aircrew and avionics: Friends or Foes?
10 p1532 N85-19654
Observations of physiological and psychological effects of terrain following flight based on in-flight test experience 10 p1532 N85-19657
Electronic displays: Their strengths and weaknesses for advanced high performance aircraft
10 p1533 N85-19664
Changing system and display concepts and their impact on aircrew performance 10 p1533 N85-19666
The cockpit of the year 2000: How big a step?
10 p1534 N85-19667
Influence of a perspective cockpit traffic display format on pilot avoidance maneuvers 10 p1534 N85-19668
The multiple resources model of human performance: Implications for display design 10 p1534 N85-19669
The F-18: A new era for human factors
10 p1534 N85-19671
Aircrew-aircraft integration issues in future US Army helicopters 10 p1535 N85-19672
A low-cost, general purpose image processing system
[INPE-3292-PRE/807] 10 p1537 N85-19690
Digital and color energy maps for graphic display of hourly data
[DE85-000526] 11 p1673 N85-20543
Computer-generated display system guidelines. Volume 1: Display design
[DE85-000679] 11 p1701 N85-20689
Proceedings of the 6th Advanced Aircrew Display Symposium
[AD-A150044] 12 p1778 N85-21160
Program for controlling electrical measuring contact instrument on glow-discharge indicator panel
12 p1842 N85-21558
Choice reaction time and color: An annotated bibliography
[AD-A149722] 12 p1908 N85-21979
Implementation of the computer program-system MOSS (Map Overlay and Statistical System) on a VAX-11 series computer under VMS
[AD-A149612] 12 p1914 N85-22019
Design of graphic displays in computerized systems
[AD-A150071] 12 p1916 N85-22027
An airborne infrared thermal scanning system for easy use on Navy P-3 aircraft
[AD-A149690] 12 p1933 N85-22143
Analysis of estimation algorithms for CDTI and CAS applications
[NASA-CR-172444] 13 p1973 N85-22387
Draftsman displays: A graphical technique for exploratory data analysis
[AD-A150515] 13 p2041 N85-22775
Introduction to CHART: A graphic analysis and display system, revision
[DE85-004612] 13 p2148 N85-23335
Multiple resources and display formatting: The implications of task integration in a simulated air traffic control task
[AD-A150713] 14 p2292 N85-24205
The effect of set size on color matching
[AD-A150899] 14 p2388 N85-24713
Factors affecting dwell times on digital displaying
[NASA-TM-86406] 14 p2390 N85-24722
Dual-task timesharing using a projected attitude display (Malcolm horizon)
[AD-A150789] 14 p2395 N85-24750
Investigation of absorptive electrochemical systems for display applications
[BMFT-FB-T-84-301] 15 p2507 N85-25467
Three-dimensional/perspective display techniques for meteorological data sets 15 p2599 N85-25918
Eye movement in response to single and multiple targets
[AD-A151115] 15 p2617 N85-26126
The measurement of human time estimating ability using a modified jerison device
[AD-A151870] 15 p2620 N85-26141
Infinite computing
[AD-A151437] 15 p2628 N85-26197
A comparison of pictorial and speech warning messages in the modern cockpit
[AD-A151917] 16 p2707 N85-26708
Spatial and temporal visual masking and visibility
[AD-A151968] 16 p2842 N85-27524
Trends shaping advanced aircrew training capabilities through the 1990s
[AD-A152277] 16 p2843 N85-27530

A heuristic solution to the spacing problem: Maximizing the minimum Euclidean distance among N points in a convex region
[AD-A152116] 16 p2855 N85-27803

Nematic liquid crystals for car dashboards
[BMFT-FB-T-84-298] 16 p2872 N85-27718

Centralized Storm Information System (CSIS)
[NASA-CR-175696] 17 p2994 N85-28506

A report from the Space Science and Engineering Center, the University of Wisconsin-Madison, Madison, Wisconsin 17 p2994 N85-28507

CSIS test and evaluation 17 p2994 N85-28509

Generation and display apparatus
[AD-D011639] 17 p3008 N85-28599

Study of raster metafile formats
[AD-A153322] 17 p3012 N85-28624

Spatial light modulator having a capacitively coupled photoconductor
[AD-D011646] 17 p3037 N85-28790

A general area air traffic controller simulation using colour graphics
[AD-A153634] 18 p3060 N85-28933

Retinally stabilized differential resolution television display
[NASA-CASE-NPO-15432-1] 18 p3069 N85-29117

Beam tests of phosphorescent screens
[DE85-009843] 18 p3097 N85-29170

Design issues in video disc map display
[AD-A153531] 18 p3109 N85-29253

Three-dimensional data display on the two-dimensional screen
[AD-A153699] 18 p3160 N85-29577

The use of VLSI technology for the real-time generation of graphics displays: A proposal
[AD-A153766] 18 p3160 N85-29578

Measurements of Solar Vector Magnetic Fields
[NASA-CP-2374] 18 p3203 N85-29869

Solar physics applications of computer graphics and image processing 18 p3208 N85-29903

Graphic displays of vector magnetograph data
18 p3209 N85-29904

Graphic display development program. Volume 2, revision 0: Appendices
[DE85-011078] 19 p3333 N85-30648

Graphic display development program, volume 1
[DE85-011076] 19 p3333 N85-30649

ZOG/VINSON technology demonstration project system description. Volume 1
[AD-A154211] 19 p3342 N85-30713

Effect of background/foreground color coding on detection in acoustic data displays
[AD-A154105] 19 p3352 N85-30774

Avionics and civil aircraft systems: The present and the future
[SNIAS-851-111-104] 20 p3392 N85-31038

Ergonomic problems regarding the interactive touch input via screens in onboard and ground-based flight control
[NASA-TM-77814] 20 p3512 N85-31832

Microprocessor AirborneData Acquisition and Replay (MADAR) system
[AD-A151728] 20 p3514 N85-31843

Switchable zero order diffraction gratings as light valves
[AD-A154471] 20 p3533 N85-31981

Advanced simulator for pilot training and helmet-mounted visual display configuration comparisons
[AD-A155326] 21 p3667 N85-32776

Design guidelines for user-system interface software
[AD-A154907] 21 p3671 N85-32807

Implementation of the SITAN algorithm in the digital terrain management and display system
[DE85-010659] 22 p3729 N85-33115

Electrochromic display device
[AD-D011733] 22 p3759 N85-33299

Batteryless magneto-driven portable radiac
[DE85-011622] 22 p3760 N85-33300

Basic features of personal computers
22 p3766 N85-33344

The development and evaluation of color display systems for airborne applications. Phase 1: Fundamental visual, perceptual, and display system considerations
[FAA/PM-85-19] 22 p3826 N85-33700

A new large-scale, high-resolution multicolor software display concept
[AD-A155404] 22 p3827 N85-33703

The improved display of 625-line television pictures: Adaptive interpolation
[BBC-RD-1985/5] 23 p3925 N85-34326

Instrumentation for sensing moisture content of material using a transient thermal pulse
[NASA-CASE-NPO-15493-2] 23 p3933 N85-34373

An integrated system for printing and publishing applications 23 p3959 N85-34540

Colour coding scales and computer graphics
23 p3963 N85-34566

Developing graphical tools with minimal GKS
23 p3964 N85-34573

NAPGEN: Automatic NAPLPS page generator
23 p3964 N85-34575

Using LINE as an interactive graphics package. Interfacing line and Topdraw in 43 and 24 VM
[DE85-012007] 23 p3965 N85-34585

Maintenance port system
[AD-D011724] 23 p3967 N85-34594

Raster functionality for a VDI
[DE85-006734] 24 p4097 N85-35396

The human engineering eye movement measurement research facility
[AD-A156099] 24 p4132 N85-35613

An exploratory study of the effect of screen size and resolution on the legibility of graphics in automated job performance aids
[AD-A155969] 24 p4136 N85-35632

DISPLAY SYSTEMS
U DISPLAY DEVICES

DISPOSAL
NT HAZARDOUS MATERIAL DISPOSAL (IN SPACE)
NT WASTE DISPOSAL

Records Disposal: A guidebook for laboratory offices
[AD-A156064] 24 p4165 N85-35823

DISRUPTING

Simulating the effects of plasma disruption with a 1 MA current pulse in a coaxial test fixture
[DE85-010491] 20 p3535 N85-31996

DISSIPATION
NT ENERGY DISSIPATION
NT OHMIC DISSIPATION

Deformations of two-dimensional dissipative maps — orbit perturbation
[REPT-69] 01 p0129 N85-10891

Statistical Plasma Physics. Proceedings of the Workshop of the US-Japan Joint Institute for Fusion Theory Program
[IPPJ-689] 02 p0282 N85-11832

Tidal dissipation in the Earth and Moon from lunar laser ranging 04 p0585 N85-13733

Phase-dissipative mechanisms for laser-induced surface desorption-dissociation processes
[AD-A147961] 06 p1121 N85-17065

Generation and evolution of diabatic planetary waves in continuously stratified atmosphere with Ekman dissipation 09 p1354 N85-18515

Analysis of the dissipation mechanism within an instationary cathode spot of metal vapor arcs
[AD-A149256] 10 p1558 N85-19825

Mixing, chemical reaction and flow field development in ducted rockets
[DE85-004083] 14 p2247 N85-23928

Evaluation of the effects of roll angle on the natural convection heat transfer from an array of cylindrical spines
[AD-A154594] 21 p3583 N85-32273

Vortex dynamics simulation of conserved scalar dissipation 22 p3745 N85-33210

On the importance of viscous dissipation in Io
22 p3855 N85-33873

DISSIPATORS
U DISSIPATION

DISSOCIATION
NT AUTOIONIZATION
NT GAS DISSOCIATION
NT PHOTODISSOCIATION
NT THERMAL DISSOCIATION

Effect of maximum physical load on oxygen-transport properties of blood 01 p0093 N85-10627

Computer molecular dynamics of 2-D water (ice) structures under shock
[AD-A145818] 03 p0372 N85-12375

Detailed performance calculations: Wayne State University and Ford Motor Company, appendix C
05 p0676 N85-14340

Ionic reactions of atmospheric importance
[AD-A147354] 07 p0997 N85-16333

Phase-dissipative mechanisms for laser-induced surface desorption-dissociation processes
[AD-A147961] 06 p1121 N85-17065

Time-of-flight spectroscopy of ionic and metastable fragments from dissociating molecules
[AD-A148068] 08 p1220 N85-17683

An infrared study of the hydrogenation of carbon dioxide on supported rhodium catalysts
[AD-A149477] 10 p1436 N85-19049

An infrared study of the dissociation of carbon dioxide over supported rhodium catalysts
[AD-A149813] 12 p1800 N85-21291

Kinetic energies of fragment ions produced by dissociative photoionization of NO
[NASA-CR-175721] 15 p2647 N85-26327

Identification and properties of molecular systems of potential use in solar-pumped lasers
[NASA-CR-175804] 16 p2789 N85-27207

Experimental study of dissociative attachment in optically-pumped lithium molecules
[AD-A152800] 17 p3030 N85-28738

Experimental studies of diffractive phenomena
[DE85-006812] 17 p3031 N85-28749

Vibrationally enhanced dissociation of diatomic molecules
[AD-A154827] 21 p3701 N85-32996

DISSOLUTION
U DISSOLVING

DISSOLVED GASES

North Atlantic Deep Water Formation
[NASA-CP-2367] 15 p2601 N85-26028

Chemical signatures associated with the freshening of Northern Atlantic waters between 1972 and 1981
15 p2601 N85-26032

DISSOLVING

Effects of additives and KOH electrolyte concentration on dissolution of iron electrodes
[DE84-014840] 02 p0173 N85-11162

Investigation of the dissolution of CaCrO4 in molten LiCl-KCl eutectic
[DE84-016394] 04 p0469 N85-12985

Effect of host-rock dissolution and precipitation on permeability in a nuclear waste repository in tuff
[DE85-000675] 11 p1727 N85-20660

Dissolution of solid solutions in absence of internal mass transfer
[BLL-M-36092-(5828.4)] 16 p2748 N85-26959

Sol-gel processing of lead zirconate titanate films
[ATR-85(8343)-2] 18 p3073 N85-29010

DISSYMMETRY
U ASYMMETRY

DISTANCE
NT MISS DISTANCE
NT RADAR RANGE
NT RANGE AND RANGE RATE TRACKING

Distances of local clouds from optical line observations 06 p0875 N85-15558

Long range effect of turbulent pressure pulsations in plane-parallel flows at different velocities with various flame fronts 09 p1308 N85-18220

FAA policy regarding solid waste disposal facilities
[AD-P004196] 11 p1581 N85-19963

Distance-inertial guidance of launch vehicle described
12 p1820 N85-21417

Visual simulation requirements for aircraft aspect recognition at real world distances
[AD-A151040] 14 p2228 N85-23610

Laser measurements of distances from the ORELA neutron target to experiment stations along flight paths 1 and 6
[DE85-009457] 17 p2971 N85-28352

Particle distributions in approximately 10(14) 10(16) eV air shower cores at sea level 24 p4189 N85-35990

DISTANCE MEASURING EQUIPMENT
NT ALTIMETERS
NT LASER RANGE FINDERS
NT OPTICAL RANGE FINDERS
NT RADIO ALTIMETERS
NT RANGE FINDERS

Modular laser distance measurement system for multiaxis machine tools
[BMFT-FB-T-84-166] 05 p0641 N85-14110

Development of a capacitive sensor system for high temperature application
[BMFT-FB-HA-84-027] 05 p0646 N85-14147

Water masers and distance measurements: The impact of QUASAT 07 p1059 N85-16721

Error of distance measurement by phase-type optical range finders with photoreceivers of various types
14 p2276 N85-24101

The integration of information from an analog-visual display. The role of dimensional integrality
[AD-A150756] 14 p2404 N85-24820

Distance Measuring Equipment (DME), general
[AD-A152585] 17 p2895 N85-27846

Evaluation of radio navigation systems and their configuration with respect to minimum cost
[ESA-TT-847] 20 p3392 N85-31043

Comparison of survey and photogrammetry methods to position gravity data, Yucca Mountain, Nevada
[DE85-011685] 21 p3590 N85-32316

Analysis of Cerenkov pulses recorded simultaneously at two sites
[HE-4.4-16] 24 p4194 N85-36022

DISTANCE PERCEPTION
U SPACE PERCEPTION

DISTILLATION

DOE supported research in alcohol fuel technology development
[DE84-007686] 06 p0774 N85-14948

Analysis of middle distillate fuels by high resolution field ionization mass spectrometry
[AD-A147724] 08 p1135 N85-17153
Ethanol production by enzymatic hydrolysis: Parametric analysis of a base-case process
[DE84-013105] 11 p1614 N85-20147
Trends of petroleum fuels
[DE85-000116] 14 p2263 N85-24023
Nitrogen analysis by chemiluminescence
[AD-A156197] 24 p4083 N85-35308

DISTILLATION EQUIPMENT
Alcohol: An alternate energy resource for community use
[DE85-007731] 18 p3084 N85-29075

DISTORTION
NT FLOW DISTORTION
NT SIGNAL DISTORTION
NT SURFACE DISTORTION
Effect of combined pressure and temperature distortion orientation on high-bypass-ratio turbofan engine stability
[NASA-TM-83771] 01 p0011 N85-10067
Real time sensing and control of out-of-plane distortion due to line heating by laser
[AD-A144773] 01 p0027 N85-10169
Iterative method for determining the distortion of elastic-plastic frames
[ISSN-0208-5658] 05 p0647 N85-14156
Effect of aberration in optical system on illuminance distribution over image of strip in semicoherent light
06 p0777 N85-14970
Perceptibility of nonlinear distortions in power amplifier
06 p0789 N85-15041
Characteristics of two-frequency combined dipole antenna arrays 06 p0791 N85-15055
Temperature distortion generator for turboshaft engine testing
[NASA-TM-83748] 07 p0893 N85-15658
Effect of steady-state temperature distortion on inlet flow to a high-bypass-ration turbofan engine
[NASA-TM-86896] 07 p0904 N85-15725
Contamination and distortion of steady flow field induced by discrete frequency in aircraft gas turbines
[AD-A147092] 07 p0958 N85-16073
New aspects of thermoelastic contact
[AD-A147554] 07 p0979 N85-16217
Real-time estimation of amplitude and group delay distortion in a PSK line-of-sight communications channel
[AD-A147735] 08 p1151 N[illegible]266
Distortion of temporal characteristics during [illegible]rametric up-conversion of ultrashort laser pulses
11 p1717 N85-20803
Tests of low-frequency geometric distortions in LANDSAT 4 images 12 p1872 N85-21744
Reflex attachment for line alignment in spectral diffraction devices 13 p2044 N85-22794
Optimal modeling with a minimum of local distortion
[REPT-16/1984] 16 p2797 N85-27243
Distortion functions
[DE85-007511] 16 p2862 N85-27655
Improved statistical analysis method for prediction of maximum inlet distortion
[AD-A153767] 18 p3063 N85-28947
One mechanism for generation of wave disturbances in spectra of turbulent flows near ocean surface
19 p3289 N85-30397
Method of measuring spherical aberration and apparatus therefor
[AD-D011706] 19 p3367 N85-30882
Effects of residual stresses and distortion on the nickel 200 and stainless steel 304 weldments
[DE85-011866] 22 p3748 N85-33233
On the importance of viscous dissipation in Io
22 p3855 N85-33873

DISTRIBUTED PARAMETER SYSTEMS
Qualitative results for distributed systems with discrete damping and stiffness with application to control
[AD-A145525] 02 p0209 N85-11382
Chandrasekhar equations and computational algorithms for distributed parameter systems
[NASA-CR-172467] 03 p0402 N85-12564
Non-linear systems in infinite dimensional state spaces
[AD-A145828] 03 p0410 N85-12623
Effect of space-charge field on output characteristics of O-type oscillators with distributed interaction
13 p2089 N85-23043
LINCS
[DE85-006151] 14 p2407 N85-24836
Proceedings of the Workshop on Identification and Control of Flexible Space Structures, volume 2
[NASA-CR-176052] 20 p3411 N85-31170
Some asymptotic problems in the optimal control of distributed systems 20 p3412 N85-31175
Finite control in underdamped distributed parameter systems 20 p3412 N85-31176
New directions in asymptotically stable finite-dimensional adaptive control of linear distributed parameter systems 20 p3412 N85-31177
Space station parametric models
20 p3413 N85-31180
Approximation of optimal infinite dimensional compensators for flexible structures
20 p3413 N85-31181
Control of a flexible space antenna: A finite dimensional perspective based on distributed parameter theory
20 p3413 N85-31182
Sub-optimal control of nonlinear flexible space structures 20 p3414 N85-31190
A residuals approach to filtering, smoothing and identification for static distributed systems
20 p3418 N85-31213
Numerical experimentation with maximum likelihood identification in static distributed systems
20 p3418 N85-31214

DISTRIBUTED PROCESSING
Research on distributed languages and algorithms
[AD-A145661] 02 p0242 N85-11560
Distributed sensor networks
[AD-A146209] 03 p0355 N85-12286
Advanced Ada (trademark)
[AD-A146257] 03 p0407 N85-12602
Requirements and overview of the LINCS distributed operating system architecture
[DE84-013721] 05 p0714 N85-14577
Distributed database components in a DBMS (Database Management System) component architecture
[PB84-217546] 06 p0848 N85-15382
Logic elements for systems with variable structure
07 p0955 N85-16054
Support for distributed transactions in the TABS (Transaction based systems) prototype
[AD-A147213] 07 p1022 N85-16486
Decentralized control of scheduling in distributed systems
[AD-A147446] 07 p1022 N65-16487
On modeling the performance and reliability of multi-mode computer systems
[AD-A148444] 08 p1208 N85-17599
Decentralized control of scheduling in distributed systems
[AD-A147686] 08 p1226 N85-17731
SPADE: Series-parallel directed acyclic graph evaluator
[AD-A148456] 09 p1368 N85-18592
Distributed data processing design methodology
[AD-A148868] 10 p1537 N85-19692
Distributing a distributed problem solving network simulator
[AD-A149065] 10 p1537 N85-19693
Predicting the performance of distributed knowledge-based systems: A modeling approach
[AD-A149021] 10 p1545 N85-19738
Guidepost routing algorithm for distributed computer networks 11 p1622 N85-20210
Distributed asynchronous deterministic and stochastic gradient optimization algorithms: Revision
[AD-A149967] 12 p1921 N85-22068
Orphan detection in the Argus system
[AD-A150562] 13 p2148 N85-23331
Constructing unifying frameworks for the study of distributed system and algorithms
[AD-A151267] 15 p2637 N85-26261
Analysis and specification of a universal data model for distributed data base systems
[AD-A151856] 15 p2666 N85-26453
Real-Time Multiprocessor Programming Language (RTMPL) user's manual
[NASA-TP-2422] 17 p3010 N85-28610
Automatic distribution of programs in MASCOT and Ada (trademark) environments: A feasibility study
[AD-A152865] 17 p3010 N85-28614
Investigation and implementation of a tree transformation system for user friendly programming
[AD-A152716] 17 p3011 N85-28617
CLEANROOM software development: An empirical evaluation
[AD-A152924] 17 p3011 N85-28619
System Analysis for the Huntsville Operation Support Center, Distributed Computer System
[NASA-CR-171506] 17 p3015 N85-28642
A real-time executive for multiple-computer clusters
[AD-A152961] 17 p3015 N85-28646
Multicomputer operating systems and applications
[AD-A153205] 17 p3016 N85-28648
The design of a capability-based distributed operating system
[CWI-CS-R8418] 17 p3016 N85-28650
Distributed systems management in wide area networks
[CWI-CS-R8419] 17 p3016 N85-28651
Distributed matchmaking for processes in computer networks
[CWI-CS-R8421] 17 p3016 N85-28652
Distributed elections in a ring of processors using Archimedean time
[CWI-CS-R8416] 17 p3016 N85-28653
Debugging distributed computations in a nested atomic action system
[AD-A153617] 18 p3162 N85-29596
Replication methods for abstract data types
[AD-A153648] 18 p3162 N85-29597
LAN (Local Area Network) interoperability study of protocols needed for distributed command and control
[AD-A154033] 19 p3255 N85-30182
Graceful fault tolerance in large networks of microcomputers 19 p3332 N86-30843
A new taxonomy for distributed computer systems based upon operating system structure
[NASA-TM-86436] 19 p3342 N85-30709
Distributed implementation of functional program evaluation
[DE85-009573] 20 p3514 N85-31844
A distributed real-time operating system
[NIKHEF-H/84-8] 20 p3518 N85-31878
Consensus in the presence of partial synchrony (Preliminary version)
[AD-A154705] 21 p3670 N85-32789
Comparative study on data system architectures – spacecraft data processing
[ESA-CR(P)-2015] 21 p3675 N85-32828
A new fault-tolerant algorithm for clock synchronization
[AD-A154771] 21 p3676 N85-32836

DISTRIBUTION
Manganese in recent sediments of Ukrainian SSR Black Sea shelf 06 p0619 N85-15200
Decentralized control of scheduling in distributed systems
[AD-A147445] 07 p1026 N85-16523
On the altitudinal distribution of birds and bird strikes in the Netherlands
[AD-P004189] 11 p1580 N85-19992
Classic Fourier microdistributions in the real analytic case 11 p1696 N85-20673
Consistency of smoothing with running linear fits
[AD-A150232] 13 p2150 N85-23349
Limits on deeply penetrating particles in the 10(17) eV cosmic ray flux
[HE-5.3-1] 24 p4205 N85-36098

DISTRIBUTION (PROPERTY)
NT ANGULAR DISTRIBUTION
NT ANTENNA RADIATION PATTERNS
NT BOLTZMANN DISTRIBUTION
NT BRIGHTNESS DISTRIBUTION
NT CHARGE DISTRIBUTION
NT CURRENT DISTRIBUTION
NT DIFFRACTION PATTERNS
NT ELECTRON DENSITY PROFILES
NT ELECTRON DISTRIBUTION
NT ENERGY DISTRIBUTION
NT FLOW DISTRIBUTION
NT FORCE DISTRIBUTION
NT FREQUENCY DISTRIBUTION
NT HOLE DISTRIBUTION (ELECTRONICS)
NT HOLE DISTRIBUTION (MECHANICS)
NT INTERFERENCE LIFT
NT ION DISTRIBUTION
NT LOAD DISTRIBUTION (FORCES)
NT MASS DISTRIBUTION
NT MOMENT DISTRIBUTION
NT PRESSURE DISTRIBUTION
NT RADIAL DISTRIBUTION
NT RADIATION DISTRIBUTION
NT RAINBOWS
NT SIDELOBES
NT SPATIAL DISTRIBUTION
NT SPECTRAL ENERGY DISTRIBUTION
NT STAR DISTRIBUTION
NT STRESS CONCENTRATION
NT TEMPERATURE DISTRIBUTION
NT VELOCITY DISTRIBUTION
NT VERTICAL DISTRIBUTION
Determination of depth profiles and lattice positions with (n, p)- and (n, alpha) reactions (n, alpha) and channeling-blocking method) 03 p0429 N85-12755
Studies of the chemistry of vibrationally and electronically excited species in planetary upper atmospheres
[NASA-CR-174134] 03 p0446 N85-12861
Determining distribution of complex dielectric permittivity over cylindrical body of intricate cross section from electromagnetic field measurement
12 p1842 N85-21560
Distribution of radium and plutonium in human bone
[DE85-005025] 13 p2142 N85-23096

On the latitudinal distribution of debris in the Northern Hemisphere of Mars 13 p2186 N85-23579

Maintaining consistency and accommodating network repair in a self-regenerative distributed database management system (a discussion of the means and cost) 16 p2666 N85-26656

Hydrogen vibrational population distributions and negative ion generation in tandem high-density hydrogen discharges
[DE85-006764] 16 p2863 N85-27657

Influence of underwater volcanic mountains of Atlantic on microplankton distribution 19 p3294 N85-30424

NASA Space controls research and technology program 20 p3406 N85-31149

Results of computer calculations for a simulated distribution of kidney cells 20 p3502 N85-31771

Subduction zone tectonic studies to develop concepts for the occurrence of sediment subduction
[DE85-011794] 22 p3615 N85-33632

The distribution of compositional classes in the asteroid belt: A cosmochemical fingerprint? 22 p3852 N85-33856

Relationships between log N-log S and celestial distribution of gamma-ray bursts
[OG-1.2-10] 22 p3862 N85-33918

A simulation of high energy cosmic ray propagation 2
[OG-5.4-2] 22 p3885 N85-34079

Pitch angle distributions of solar energetic particles and the local scattering properties of the interplanetary magnetic field
[SH-3.1-13] 23 p4002 N85-34816

Cosmic ray intensity distribution perpendicular to solar equatorial plane at 1 A.U. during 1978-83
[SH-4.3-14] 23 p4032 N85-34998

Cosmogenic Mn-53 in meteorites
[SH-7.1-17] 23 p4049 N85-35107

Distribution of computer functionality for accelerator control at the Brookhaven AGS
[DE85-012520] 24 p4141 N85-35669

Resonance localization in tokamaks excited with ICRF waves
[DE85-014559] 24 p4160 N85-35791

Integral functions of electron lateral distribution and their fluctuations in electron-photon cascades
[HE-3.5-12] 24 p4184 N85-35949

Analysis of equi-intensity curves and NU distribution of EAS 24 p4187 N85-35970

About increase of the large transvere momentum processes fraction in hA interactions at energies 5.10(14) - 10(16) eV according to the data on E.A.S. hadrons 24 p4188 N85-35979

DISTRIBUTION FUNCTIONS

Approximating hierarchical normal priors using a vague component
[CSIR-TWISK-284] 01 p0107 N85-10720

An integral inequality with applications to order statistics
[AD-A145061] 01 p0113 N85-10770

Weighted distributions arising out of methods of ascertainment
[AD-A145615] 02 p0252 N85-11648

Likelihood estimation for generalized mixed exponential distributions
[AD-A145675] 02 p0252 N85-11651

Equations of plasma transport in a curved magnetic field
[DE84-015625] 05 p0730 N85-14690

Limiting distributions of functionals of Markov chains
[AD-A147632] 07 p1036 N85-16577

Electron distribution function and mobility in 3-5 compounds for high and low fields
[AD-A147447] 07 p1048 N85-16658

Transport properties and distribution functions in 3-5 semiconductors
[AD-A147525] 07 p1049 N85-16660

Tail behaviour for suprema of empirical processes
[AD-A147629] 08 p1210 N85-17613

Convergence of quasi-stationary to stationary distributions for stochastically monotone Markov processes
[AD-A148041] 08 p1215 N85-17652

Optical frequency domain reflectometry 08 p1222 N85-17695

User's guide to MIX: A computer code for fitting mixture distributions to data
[DE85-001451] 09 p1369 N85-18603

Estimating the scale parameter of an exponential distribution from a sample of time-censored r-th order statistics
[AD-A148060] 09 p1375 N85-18644

Condensational transformation of atmospheric aerosol particle distribution functions 10 p1500 N85-19468

Inequalities for the M/G/Infinity queue and related shot noise processes
[AD-A148015] 10 p1545 N85-19737

More limit theory for the sample correlation function of moving averages
[AD-A148975] 10 p1550 N85-19773

Asymptotic distributions of the sample mean, autocovariances and autocorrelations of long-memory time series
[AD-A149409] 10 p1551 N85-19781

Checking the shape of discrete distributions
[DE85-000177] 11 p1706 N85-20733

Scrawl plots, and letter and blotter strips
[DE85-001409] 11 p1707 N85-20739

The ambiguity function and the Wigner distribution
[AD-A150095] 12 p1829 N85-21482

On the limiting empirical distribution function of the eigenvalues of a multivariate F matrix
[AD-A149618] 12 p1921 N85-22065

The orientation distribution of nonspherical aerosol particles within a cloud
[AD-A150600] 13 p2092 N85-23061

Attainable rates of convergence of maxima
[AD-A150638] 14 p2403 N85-24847

On limiting empirical distribution function of the eigenvalues of a multivariate F matrix, revised
[AD-A151885] 15 p2641 N85-26288

Asymptotic expansions of the distribution of test statistics associated with several two parameter exponential distributions
[AD-A151906] 15 p2641 N85-26289

Nonsmooth analysis and Frechet differentiability of M-functionals
[AD-A152932] 17 p3019 N85-28668

Determination of the association constant for pertechnetic acid
[DE85-010224] 19 p3235 N85-30057

Acoustic emission study of fatigue crack extension position in a stress cycle 19 p3283 N85-30355

Comments on estimating quantiles for Gaussian functionals by simulation
[AD-A154302] 19 p3348 N85-30750

Bivariate Rayleigh distribution: Formulas and curves, for correlation computing using the distribution function
[FOA-C-30380-E2] 20 p3521 N85-31901

Antistarshapedness, dispersiveness and mixtures
[AD-A155583] 21 p3678 N85-32849

A graphics interface for interactive simulation of packet-switched networks 23 p3962 N85-34558

Numerical solutions of the Vlasov equation 23 p3979 N85-34672

Pitch angle distributions of 35-1000 keV protons at quasi-perpendicular interplanetary shocks
[SH-1.5-6] 23 p3996 N85-34775

The dispersive evolution of charged-particle bunches in random magnetic fields
[SH-4.1-2] 23 p4004 N85-34826

On the determination of the depth of EAS development maximum using the lateral distribution of Cerenkov light at distances 150 m from EAS axis
[HE-4.4-13] 24 p4194 N85-36019

DISTRIBUTION MOMENTS
NT MEAN
NT ORTHOGONALITY
NT STANDARD DEVIATION

Long time correlation and stochastic diffusion in the standard map 02 p0282 N85-11835

A martingale approach to supercritical (C-M-J) branching processes
[CTH-MATH-1984-25] 05 p0722 N85-14643

Annual cycle. Part 2: The annual variation of precipitation over the United States and Canada
[PB85-147684] 15 p2600 N85-26027

Derivation of model topography 18 p3141 N85-29449

Evaluation of densities and distributions via hermite and generalized laguerre series employing high-order expansion coefficients determined recursively via moments or cumulants
[AD-A153950] 18 p3175 N85-29682

DISTRICT OF COLUMBIA

Results of the carbon monoxide study in Washington, D.C. and Denver, Colorado, in the winter of 1982-83
[PB84-230069] 06 p0834 N85-15309

Image variance and spatial structure in remotely sensed scenes — South Dakota, California, Missouri, Kentucky, Louisiana, Tennessee, District of Columbia, and Oregon 07 p0986 N85-16265

Test of dispersal of turbojet aircraft departure tracks at washington National Airport (1983-84), volume 1 report
[AD-A148111] 08 p1218 N85-17669

Geodetic accuracy of LANDSAT 4 Multispectral Scanner and Thematic Mapper data — Washington, DC, California, Alabama, South Dakota, and Illinois 11 p1667 N85-20504

Geometric accuarcy assessment of LANDSAT-4 Multispectral Scanner (MSS) data 11 p1667 N85-20505

Intraband radiometric performance of the LANDSAT 4 Thematic Mapper — Washington, DC, Arkansas, Massachusetts, Virginia, and Arizona 12 p1871 N85-21738

DISTURBANCE THEORY
U PERTURBATION THEORY

DISTURBANCES

Wideband disturbance accomodation in precision flexible space structures 20 p3415 N85-31194

DISULFIDES
NT CARBON DISULFIDE

The violet absorber on Io: Disulfur monoxide derivatives 13 p2173 N85-23482

Geosynchronous performance of a lithium-titanium disulfide battery 20 p3444 N85-31377

DITCHING (EXCAVATION)
U EXCAVATION

DITCHING (LANDING)

Air carrier overwater emergency equipment and procedures
[PB85-917006] 21 p3553 N85-32105

DITHERS

Precise bearing support ditherer
[AD-D011470] 10 p1493 N85-19426

DITHIOLS
U THIOLS

DIURNAL RHYTHMS
U CIRCADIAN RHYTHMS

DIURNAL VARIATIONS

Green River air quality model development: Meteorological and tracer data, July/August 1982. Field study in Brush Valley, Colorado
[DE84-014975] 02 p0225 N85-11474

Analysis of the daily geomagnetic variation with the use of MAGSAT data — MAGSAT satellites 04 p0520 N85-13319

Daily magnetic variations at Ebro, Spain 04 p0520 N85-13325

The need for integrating ground thermal measurements with thermal aircraft imagery 05 p0680 N85-14243

Diurnal variation harmonics and spatial change in cosmic ray flux 06 p0824 N85-15230

Diurnal freeze-thaw frequencies in selected regions of the high latitudes
[AD-A147276] 07 p1007 N85-16400

Interrelationship of atmospheric parameters in Honduras
[AD-A147371] 07 p1007 N85-16401

A possible mechanism for the diurnal oscillations of tropical cyclones 09 p1356 N85-18530

Considering zonal wind in semidiurnal tide problem 14 p2335 N85-24440

Ionospheric effects of seasonal and diurnal variations of electric fields in equatorial F-region 14 p2338 N85-24459

The dawn-dusk asymmetry of particles near the neutral sheet of geomagnetotail 14 p2358 N85-24574

Afternoon radar aurora and polar cap convection pattern 14 p2361 N85-24592

Spectral analysis of diurnal nonuniformity of Earth's rotation 15 p2477 N85-25289

Spectral characteristics of protons at low and high altitudes during geomagnetic storm of 29 July 1977 16 p2719 N85-26786

Precipitation and snow cover data, 1977
[ISBN-951-697-215-2] 17 p2995 N85-28514

Measurements of VHF/UHF radio propagation in a maritime temperate climate
[CRC-1360] 18 p3089 N85-29119

The determination of daily usage or occupancy in the land-mobile band 138-174 MHz at Montreal
[CRC-1383] 19 p3253 N85-30167

Qualitative and quantitative examination of the performance of regional air quality models representing different modeling approaches
[DE85-010508] 19 p3310 N85-30518

Soil temperature extrema recovery rates after precipitation cooling 20 p3491 N85-31697

The diurnal variation of the neutral sodium species in the upper atmosphere: A model study
[AD-A154988] 21 p3631 N85-32561

A study of time transformation of natural photochemical aerosols 21 p3645 N85-32644

Drift and observations in cosmic-ray modulation, 2
[SH-4.2-5] 23 p4007 N85-34843

Cosmic ray sidereal diurnal variation of galactic origin observed by neutron monitors
[SH-4.4-2] 23 p4033 N85-35000

Sidereal anisotropies in the median rigidity range 60-600GV in 1978-1983
[SH-4.4-3] 23 p4033 N85-35001

The sidereal semi-diurnal variation observed at high zenith angles at Mawson, 1968-1984, and the polarity of the solar main field
[SH-4.4-6] 23 p4033 N85-35004

Cosmic ray intensity variations observed at Matsushiro (220 M.W.E. in depth)
[SH-4.4-9] 23 p4034 N85-35007
Solar tri-diurnal variation of cosmic rays in a wide range of rigidity
[SH-4.5-3] 23 p4036 N85-35021
Upper cut-off rigidity for corotation anisotropy during solar activity cycles 20 and 21
[SH-4.5-4] 23 p4036 N85-35022
Twenty-two-year cycle of the upper limiting rigidity of Daily waves
[SH-4.5-5] 23 p4036 N85-35023
Solar wind velocity and daily variation of cosmic rays
[SH-4.5-6] 23 p4036 N85-35024
Diurnal anisotropy during solar activity cycle twenty and diffusion-convection model
[SH-4.5-7] 23 p4036 N85-35025
Diurnal effect in cosmic rays at middle latitudes according to stratospheric measurements
[SH-4.5-8] 23 p4036 N85-35026
Comparative study of the phase of diurnal anisotropy on quiet and disturbed days on a long term basis up to recent period
[SH-4.5-9] 23 p4037 N85-35027
Study of spectral exponent on quiet and disturbed days
[SH-4.5-10] 23 p4037 N85-35028
Diurnal variation of galactic cosmic ray intensity on quiet days
[SH-4.5-11] 23 p4037 N85-35029
Diurnal variations from muon data at Takeyama underground station
[SH-4.5-13] 23 p4037 N85-35030
Long term changes in cosmic ray diurnal variations observed by ion chambers in Hong Kong and Japan
[SH-4.5-14] 23 p4037 N85-35031
The cosmic ray differential diurnal variation dependences on the zenith angle and the geomagnetic disturbance
[SH-4.5-16] 23 p4038 N85-35033
Anomalous increase of solar anisotropy above 150GV in 1981-1983
[SH-4.5-18] 23 p4038 N85-35035
Magnetic fluctuation and cosmic ray diurnal variations
[SH-4.5-21] 23 p4038 N85-35038
Transient cosmic ray increase associated with a geomagnetic storm
[SH-5.1-8] 23 p4042 N85-35062
Long-period cosmic ray variations and their altitude dependence
[SH-6.1-19] 23 p4046 N85-35091
Diurnal variations of cosmic ray geomagnetic cut-off threshold rigidities
[SH-6.1-21] 23 p4046 N85-35092

DIVERGENCE
NT MAGNETIC CHARGE DENSITY
Spatial and temporal interpolation of NEROS radiosonde winds
[PB84-232545] 04 p0540 N85-13438
Active control of forward swept wings with divergence and flutter aeroelastic instabilities
09 p1282 N85-18063
An analysis of the seasonal variations in the water vapor transport fields over the Southern Hemisphere
09 p1356 N85-18531
Advanced ion thruster research
[NASA-CR-174862] 10 p1430 N85-19021
Determining geometrical divergence using seismic observation data 14 p2343 N85-24489

DIVERTERS
A nonnoble front metallization process
06 p0830 N85-15279
Versator divertor experiment: Preliminary designs
[DE84-017159] 09 p1393 N85-18769
HPFTP flow diverter analysis
[NASA-CR-171424] 13 p2091 N85-23057
Coupled plasma-neutral transport model for the scrape-off region
[DE85-007559] 16 p2868 N85-27695
Electrolytic cell
[DE85-011598] 22 p3807 N85-33578
Neutral pumping rates for a next step tokamak ignition device
[DE85-012780] 24 p4157 N85-35776

DIVIDES (LANDFORMS)
Physiography of the Martian west equatorial uplift
12 p1961 N85-22325

DIVIDING (MATHEMATICS)
On the distribution of integral and prime divisors with equal norms 11 p1698 N85-20669

DIVING (UNDERWATER)
Experiments with hydrox at 1.3 MPa (13 atm) — for divers
[FOA-C-58014-H1] 04 p0545 N85-13471
Evaluation of the Kerie Cable thermal arc cutting equipment
[AD-A147813] 07 p0974 N85-16186
Vityaz specialists study human adaptability to ocean depths 07 p0980 N85-16225
Manned testing of two closed-circuit oxygen underwater breathing apparatus: US Navy Emerson Rig and Fenzy PO.68
[AD-A146300] 08 p1200 N85-17560
Hydrogen-oxygen (hydrox) breathing at 1.3MPa
[FOA-C-58015-H1] 09 p1364 N85-18577
High pressure environmental conditioning systems and chamber rehabilitation
[AD-A150039] 12 p1905 N85-21964
Assessing the short- and long-term health effects of decompression sickness among US Navy divers
[AD-A151887] 15 p2618 N85-26132
A comprehensive strategy for saturation decompression with nitrogen-oxygen
[AD-A151800] 16 p2841 N85-27520
Pressure chamber simulation of 450-meter dive
20 p3505 N85-31788
Diving simulation experiment with pressure chambers
20 p3506 N85-31793
Preliminary results of an ALVIN dive program on active hydrothermal vents at the southern Juan de Fuca Ridge
24 p4106 N85-35454
The research programme of the Institute for Aerospace Medicine 24 p4129 N85-35596
The deep diving simulator TITAN: Physiological problems associated with staying in great depths of water 24 p4130 N85-35604

DMSP SATELLITES
Fluxgate magnetometer (SSM) for the defense meteorological satellite program (DMSP) block 5D-2, flight 7
[AD-A155229] 21 p3560 N85-32143

DNA
U DEOXYRIBONUCLEIC ACID

DO-28 AIRCRAFT
First stage of equipping a Do 28 as a research aircraft for icing, and first research results
[ESA-TT-855] 11 p1584 N85-19982
Identification of gust input and gust response characteristics from Do 28 TNT flight test data
[DFVLR-FB-84-48] 17 p2900 N85-27881

DOCKING
U SPACECRAFT DOCKING

DOCUMENT STORAGE
Depository librarians' views on GPO's administration of the depository library program. Report to the Chairman, Joint Committee on Printing
[PB84-212265] 01 p0126 N85-10867
An electronic documentation system
[SNIAS-842-111-101] 04 p0577 N85-13683
Managing permanent objects
[AD-A149007] 10 p1540 N85-19708
Tekedit: An enhanced editor for Direct View Storage Tube (DVST) graphics display devices
[AD-A149715] 12 p1915 N85-22021
The conservation and utilization of scientific research documents: Practical aspects and organization
[NOTA-INTERNA-834] 14 p2433 N85-25008
ZOG-Vinson technology demonstration project. Volume 2: System description
[AD-A153871] 19 p3333 N85-30645
Electronic file system on an SM 90 minicomputer: The SARDE project
[ENST-84E018] 22 p3828 N85-33705
Records Disposal: A guidebook for laboratory offices
[AD-A156064] 24 p4165 N85-35823

DOCUMENTATION
Water resources data for Maine, water year 1983
[PB84-225143] 01 p0066 N85-10440
Water resources data for Ohio, water year 1983. Volume 1: Ohio River basin
[PB84-224690] 01 p0066 N85-10441
AGS-880 menu system user guide
[DE84-014338] 01 p0104 N85-10699
Automated Data Systems (ADS) documentation standards
[AD-A144867] 01 p0125 N85-10857
Improving technical documents
[AD-B084855] 01 p0126 N85-10866
Publications of the National Bureau of Standards, 1983 catalog
[PB84-218031] 01 p0126 N85-10869
Inclusion of audiovisual media in information services for the special subjects journalism and communication science (pilot study)
[BMFT-FB-ID-83-004] 02 p0294 N85-11909
Effective date (E-DATE) model documentation. Changes to reflect model enhancement
[AD-A146050] 03 p0407 N85-12599
NSSDC and WDC-A-R and S document availability and distribution services
[NASA-TM-87374] 03 p0436 N85-127
Criss-cross directory of NASA N numbers and DOD AD numbers, 1962-1976 04 p0575 N85-13
FY 1984 scientific and technical reports, articles, papers and presentations
[NASA-TM-86470] 04 p0575 N85-13
An electronic documentation system
[SNIAS-842-111-101] 04 p0577 N85-13
Recommended documentation for computer users at ANL
[DE84-016285] 06 p0855 N85-15
Built-in-test for first line testing
08 p1064 N85-16
Computer center CDC libraries/NSRD (subprograms)
[AD-A148792] 08 p1206 N85-17
Documentation for an instrument database system
[DE84-017392] 09 p1402 N85-18
Preserve the sense of Earth from space — achieve of remote sensing data
[PB85-124121] 11 p1740 N85-20
Integrated control system engineering support
[AD-A149742] 12 p1780 N85-21177
The availability of Japanese scientific and technical information in the United States
[GPO-39-478] 12 p1951 N85-2225
The conservation and utilization of scientific research documents: Practical aspects and organization
[NOTA-INTERNA-834] 14 p2433 N85-2500
Documentation for the machine-readable version of A Library of Stellar Spectra (Jacoby, Hunter and Christian 1984)
[NASA-TM-87438] 14 p2438 N85-25046
Documentation for the machine-readable version of the Revised S210 Catalog of Far-Ultraviolet Objects (Page, Carruthers and Heckathorn 1982)
[NASA-TM-87439] 14 p2438 N85-25047
Documentation for the machine-readable version of A Finding List for the Multiplet Tables of NSRDS-NBS 3, Sections 1-10 (Adelman, Adelman, Fischel and Warren 1984)
[NASA-TM-87440] 14 p2438 N85-25048
Documentation for the machine-readable version of the Cordoba Durchmusterung (CD)
[NASA-TM-87441] 14 p2439 N85-25049
A modern control theory enhancement to an Interactive Control Engineering Computer Analysis Package (ICECAP)
[AD-A153249] 17 p3012 N85-2862
Bibliography of Lewis Research Center technical publications announced in 1984
[NASA-TM-87012] 17 p3049 N85-2887
National Archives and Records Service (NARS) twenty year preservation plan
[PB85-177640] 18 p3200 N85-2965
Guide on logical database design
[PB85-177970] 19 p3381 N85-3067
The documentation assistant: An intelligent system for documentation
[AD-A154709] 21 p3670 N85-3260
EPALIT: A data management system applied to the control and retrieval of technical reports
[PB85-193068] 24 p4166 N85-3582

DOCUMENTS
NT ABSTRACTS
NT ASTRONOMICAL CATALOGS
NT BIBLIOGRAPHIES
NT CATALOGS (PUBLICATIONS)
NT ENGINEERING DRAWINGS
NT HANDBOOKS
NT INSTALLATION MANUALS
NT MANUALS
NT PERIODICALS
NT PRESIDENTIAL REPORTS
NT RECORDS
NT SUPPLEMENTS
NT TEXTS
NT USER MANUALS (COMPUTER PROGRAMS)
NT VIDEO DISKS
Improving technical documents
[AD-B084855] 01 p0126 N85-108
AGARD bulletin technical programme, 1985
[AGARD-BUL-84-2] 02 p0305 N85-11971
Energy information exchange, 1983
[DE84-901446] 04 p0577 N85-136
Document interchange format
[PB84-217033] 07 p1027 N85-16517
Technical order managers handbook: Utilization assessment
[AD-A147579] 07 p1055 N85-166
Provision of Federal government publication in electronic format to depository libraries
[S-PRT-98-260] 10 p1567 N85-19
M68000 RNF text formatter user's manual
[NASA-TM-86327] 13 p2146 N85-23

Recent Naval Postgraduate School publications
[AD-A151723] 16 p2875 N85-27740
Electrochemical Energy Storage Branch
[DE85-007592] 18 p3131 N85-29391
Technology transfer [illegible]omation implementation
[PB85-177335] 22 p3849 N85-33836
Recognition and clear representation of handwritten electronic diagrams 23 p3960 N85-34541
A model for a document maintenance system
23 p3960 N85-34542

DOGS
Tolerance endpoint for evaluating the effects of heat stress in dogs
[AD-A148104] 08 p1192 N85-17511
Long term exposure of animals to antiorthostatis (-90 deg) as a model of critical homeostatic disturbances
19 p3324 N85-30592

DOLOMITE (MINERAL)
The Midway Atoll coral cap: Meteoric diagenesis, amplitude of sea-level fluctuation and dolomitization
09 p1351 N85-18499
Diagenesis of niagaran (middle silurian) pinnacle reefs, northwest Michigan 09 p1352 N85-18508
Deep-burial diagenesis in carbonates
[DE85-011224] 22 p3802 N85-33554

DOLPHINS
Tracking pelagic dolphins by satellite
14 p2324 N85-24364

DOMAIN WALL
Twisted domain wall in very thin magnetic films with perpendicular anisotropy 03 p0350 N85-12252
Investigation of domain structures and walls using neutron diffraction 03 p0423 N85-12702
Monitoring the execution of plans in SIPE (System for Interactive Planning and Execution) monitoring
[AD-A149138] 10 p1544 N85-19731

DOMAINS
NT MAGNETIC DOMAINS
On Bezout domains, elementary divisor rings, and pole assignability
[CSIR-TWISK-330] 01 p0110 N85-10740
The disordering process in an L1sub2 ordered alloy
[DE84-016599] 04 p0475 N85-13028
Domains with Lipschitz mapping functions
10 p1535 N85-19675
Domain decomposition techniques for solving elliptic partial differential equations on multiprocessors
[DE85-004448] 10 p1549 N85-19769
An extension of the Gleason problem in pseudoconvex domains 11 p1698 N85-20671
On the solution for the sound field in a semi-infinite uniform duct with sheared mean flow
20 p3523 N85-31912
Use of MMLE3 to determine lower order equivalent systems in the time domain
[AD-A154700] 21 p3554 N85-32112

DOMES
Wide angle phased array dome lens antenna with a reflection/transmission switch
[AD-D011562] 12 p1833 N85-21502

DOMES (GEOLOGY)
New data on presence of ores in salt dome structures of Dnieper-Donets Basin 07 p0961 N85-16234
Ridged plains of Lunae Planum: Thickness distribution revised 13 p2185 N85-23559
Preliminary SPR thermal model description and results for WH-11 and BM-4
[DE85-013171] 23 p3931 N85-34360

DOMES (STRUCTURAL FORMS)
NT RADOMES

DOMESTIC ENERGY
Solar house, Freiburg
[BMFT-FB-T-84-249] 15 p2588 N85-25953
Solar energy for highway uses
[DE84-015653] 18 p3130 N85-29382
Operational results for the experimental DOE/NASA Mod-OA wind turbine project
[NASA-TM-83517] 19 p3304 N85-30479

DOMESTIC SATELLITE COMMUNICATIONS SYSTEMS
Methodology for the implementation of a domestic satellite communications network
04 p0493 N85-13148
China's future domestic satellite communications systems 10 p1476 N85-19312
China's domestic satellite communications
10 p1476 N85-19313

DOMINANCE
Functional significance of some EEG parameters and dominant principle 11 p1691 N85-20634

DONOR MATERIALS
Fundamental electronic properties of donor-type graphite intercalated compounds
[AD-A146148] 03 p0326 N85-12099
Electronic density of states for the double donor system Si:P, As
[INPE-3447-PRE/700] 16 p2869 N85-27700
Electron-donor dopant, method of improving conductivity of polymers by doping therewith, and a polymer so treated
[DE85-011640] 22 p3752 N85-33257

DOORS
Hydraulic locking boltwork system
[AD-D011299] 06 p0815 N85-15174
Challenges in the development of the orbiter radiator system 08 p1096 N85-16925
Integrated paratroop door
[AD-D011507] 12 p1776 N85-21148
Get Away Special (GAS) thermal design summary
[X-732-83-8] 15 p2475 N85-25278
Application of lightweight composite materials to naval weapons systems
[PB85-173607] 18 p3069 N85-28981
Airborne sound transmission loss characteristics of wood-frame construction
[AD-A154174] 20 p3524 N85-31919

DOPED CRYSTALS
The transient oxidation of single crystal NiAl+Zr
[NASA-CR-174756] 02 p0182 N85-11221
Silicon sheet with molecular beam epitaxy for high efficiency solar cells
[NASA-CR-174022] 02 p0222 N85-11459
Structural phase transitions in doped hexahalogen metallates 03 p0426 N85-12721
Effect of doping on the voltage holdoff performance of alumina insulators in vacuum
[DE84-017163] 04 p0480 N85-13060
Lifetime of excess charge carriers in weakly doped epitaxial GaAs layers 04 p0487 N85-13108
Development of high responsitivity Ge:Ga photoconductors
[DE84-016902] 04 p0571 N85-13643
Gallium arsenide/AlGaAs multilayer structures with special doping profiles for microwave and optoelectronic devices
[BMFT-FB-T-84-207] 08 p1227 N85-17725
Optical studies of dynamical processes in disordered materials
[DE85-002400] 10 p1453 N85-19158
Modern solid state laser materials
[DE85-003665] 10 p1490 N85-19410
Metal-nonmetal transitions in N-doped many-valley Si and Ge
[INPE-3358-PRE/636] 10 p1562 N85-19848
Use of alternative solvents for low-temperature LPE growth of CdTe films
[AD-A149418] 10 p1562 N85-19853
Research on the basic understanding of high efficiency in silicon solar cells
[DE85-000507] 11 p1672 N85-20537
Preparation of crystal growth experiments in Spacelab: Si (FSLP), CdTe (D1), ZnS (D1)
[BMFT-FB-W-84-045] 12 p1788 N85-21227
Enhanced diffusion from interstitial trapping during solid-phase-epitaxial growth of silicon alloys
[DE85-001285] 12 p1941 N85-22193
Technological process effect on the carrier lifetime degradation of silicon solar cell base layer irradiated by 1 MeV electrons (boron doping case)
13 p2007 N85-22585
Annealing of radiation damage in boron and gallium doped silicon solar cells 13 p2012 N85-22624
High sheet resistance, arsenic implanted polycrystalline silicon for integrated circuit resistors
[DE85-004355] 13 p2065 N85-22902
Noise characteristics of sulfur-doped silicon diodes
13 p2073 N85-22952
Numerical simulation of inverters with I2L elements including effects of high doping level
13 p2088 N85-23039
Structural, morphological and optical characteristics of KGd(WO4)2 crystals 14 p2280 N85-24126
High resolution Z-contrast imaging and lattice location analysis of dopants in ion-implanted silicon
[DE85-005261] 14 p2429 N85-24980
Heavy doping effects in high efficiency silicon solar cells
[NASA-CR-175687] 15 p2585 N85-25937
Fundamental studies of growth, doping and transformation in beta silicon carbide
[AD-A152047] 15 p2660 N85-26416
Flat-plate solar array project process development area: Process research of non-CZ silicon material
[NASA-CR-175777] 16 p2818 N85-27382
Heavy doping effects in high efficiency silicon solar cells
[NASA-CR-175779] 16 p2818 N85-27383
On some physical impurity properties of doped-indirect gap semiconductors at low and intermediate concentrations
[INPE-3452-PRE/704] 16 p2869 N85-27701
Effect of dislocations on gallium arsenide FETs
[AD-A152249] 16 p2870 N85-27709
TEM investigation of polar-on-nonpolar epitaxy: GaAs-AlGaAs on (100) Ge
[DE85-007613] 16 p2871 N85-27714
GaAs MESFET with lateral non-uniform doping
17 p3043 N85-28827
Zn3P2 as an improved semiconductor for photovoltaic solar cells
[DE85-008772] 18 p3097 N85-29171
Chemistry and physics of silicon-based amorphous semiconductors
[DE85-001931] 19 p3377 N85-30949
Aspects of silicon bulk lifetimes
20 p3479 N85-31617
Z-contrast imaging and electron channeling analysis of dopants in semiconductors
[DE85-011410] 21 p3582 N85-32269
Physics of heavily doped silicon and solar-cell parameter measurement 21 p3609 N85-32418
Influence of background electrically neutral argon admixture on mechanical strength of silicon crystals
21 p3683 N85-32878
Doping superlattices in organometallic VPE InP
[AD-A155151] 21 p3710 N85-33029
Modulation doped GaAs/Al(x)Ga(1-x)As layered structures with applications to field effect transistors
[AD-A155360] 22 p3759 N85-33296
Trivalent cerium doped crystals as tunable laser systems: Two bad apples
[DE85-006168] 22 p3790 N85-33482

DOPES
Polarization in chemically doped hydrogen-rich glasses
[DE84-017486] 06 p0771 N85-14936
Lithium counterdoped silicon solar cell
[NASA-CASE-LEW-14177-1] 11 p1672 N85-20535
Status of French research in plastic batteries
15 p2530 N85-25603
Flat-plate solar array project process development area: Process research of non-CZ silicon material
[NASA-CR-175777] 16 p2818 N85-27382
Molecular orbital studies in oxidation: Sulfate formation and metal-metal oxide adhesion
[NASA-CR-176070] 21 p3565 N85-32174
Electron-donor dopant, method of improving conductivity of polymers by doping therewith, and a polymer so treated
[DE85-011640] 22 p3752 N85-33257
Radiation-hardened polymeric films
[DE85-011636] 22 p3752 N85-33259
Experimental test for interpreting the increase in sensibility of doped CR-39
[OG-4.4-11] 22 p3880 N85-34042
Flat-plate solar array project process development area process research of non-CZ silicon material
[NASA-CR-176117] 23 p3945 N85-34445

DOPING (ADDITIVES)
U ADDITIVES

DOPPLER EFFECT
NT DOPPLER-FIZEAU EFFECT
The development of a diode laser Doppler velocimeter for boundary layer measurements under ice: A feasibility investigation
[AD-A145078] 01 p0053 N85-10348
The investigation of short wave signal structure in the vicinity of the caustic by means of a high-directed antenna
[PR-194] 03 p0354 N85-12277
Using measured variance of skywave radar sea-echo power spectra to estimate ionospheric Doppler broadening of mean spectra
[PB84-214071] 03 p0399 N85-12544
Methodology improvement program for the second generation miss distance radar (MIDI 2)
[AD-A148467] 08 p1153 N85-17261
Tropospheric and ionospheric phase perturbations and Doppler frequency shift effects
[AD-A148579] 08 p1154 N85-17263
Five-minute P modes detected in Doppler shift measurement on Alpha Centauri
08 p1250 N85-17895
Atmospheric limitations in stellar seismology: Should one measure radial velocity or brightness fluctuations?
08 p1251 N85-17899
Propagation effects on the Doppler frequency shift of satellite transmissions 10 p1470 N85-19276
Multipath and Doppler observations during transatlantic digital HF propagation experiments
10 p1471 N85-19281
Study of submicron particle size distributions by laser Doppler measurement of Brownian motion
[AD-A149139] 10 p1487 N85-19388

An evaluation of wind measurements by four Doppler sodars
[PB85-115301] 10 p1520 N85-19586

Flow measurement by laser Doppler anemometry in a nuclear fuel assembly
[DE85-003260] 12 p1648 N85-21592

Investigation of generation of oscillations using anomalous Doppler effect 13 p2078 N85-22980

Synthetic aperture radar simulation study
[AD-A151000] 14 p2293 N85-24214

Establishment of hydrographic shore control by Doppler satellite techniques
[AD-A150709] 14 p2347 N85-24512

Optimized response functions for 2-dimensional observations of solar oscillations
14 p2443 N85-25075

Resonance generation of inertial waves (in the atmosphere) by Doppler-shift of inertio-gravity modes
15 p2590 N85-25968

Simulation of a low orbit restitution. Covariance analysis of the position-velocity by Doppler and accelerometer measurements
[CNES-CT/DTI/MS/AE/166] 16 p2728 N85-26836

DORIS: Prediction in Doppler measurement — satellite onboard measurement
[CNES-CT/DTI/MS/AE/170] 16 p2729 N85-26843

LDA study of non-steady flame propagation in a constant volume duct
[DE85-007233] 16 p2746 N85-26948

Thermospheric winds observed by OI6300A Doppler shifts at 23 deg S in the Brazilian sector
[INPE-3384-RPE/470] 16 p2834 N85-27479

A comprehensive strategy for saturation decompression with nitrogen-oxygen
[AD-A151600] 16 p2841 N85-27520

Positron annihilation studies of vacancy formation in tungsten, chromium, and niobium
[DE85-006837] 16 p2871 N85-27710

Vibration-free Raman Doppler velocimeter
[NASA-CASE-LAR-13268-1] 18 p3104 N85-29216

On the accuracy of Cs beam primary frequency standards 18 p3105 N85-29224

Determination of the vacancy formation enthalpy in chromium by positron annihilation
[DE85-010266] 19 p3239 N85-30084

LDA study of the unburned gas motion induced by nonsteady flame propagation in a constant volume duct
[DE85-009938] 19 p3270 N85-30277

Filter induced errors in laser anemometer measurements using counter processors
[NASA-TM-87047] 19 p3272 N85-30288

Accuracy in determining velocity of fluid movement by Doppler method 19 p3293 N85-30419

Velocity visualization in gaseous flows
[NASA-CR-174954] 20 p3453 N85-31445

A derivation of relativistic effects in satellite tracking
[AD-A154620] 21 p3558 N85-32132

Accuracy of velocity and power determination by the Doppler method 21 p3620 N85-32493

Coding schemes for improving MST radar performance, part 7.1A 21 p3625 N85-32520

The moving thermoacoustic array: A theoretical feasibility study
[AD-A154510] 21 p3699 N85-32960

HEAO 3 upper limits to the expected 1634 KeV line from SS 483
[OG-2.4-9] 22 p3868 N85-33954

Search for gamma ray lines from SS433
[OG-2.4-11] 22 p3868 N85-33955

Limits on the Doppler factor in relativistic jets by means of gamma-ray observations
[OG-2.7-12] 22 p3872 N85-33985

Wide Angle Michelson Doppler Imaging Interferometer (WAMDII) 23 p3902 N85-34172

On the detectability of key-MeV solar protons through their nonthermal Lyman-alpha emission
[SH-1.3-5] 23 p3993 N85-34752

DMSK: A practical 2400-bps receiver for the mobile satellite service: An MSAT-X Report
[NASA-CR-176194] 24 p4086 N85-35324

DOPPLER NAVIGATION

Use of microprocessor techniques and new antenna systems to improve the navigation aids very high frequency omnidirectional radar (VOR), Doppler VOR and Instrument Landing System (ILS)
[BMFT-FB-W-84-026] 02 p0137 N85-10930

Observations of lightweight Doppler system accuracy
[AD-A145968] 03 p0317 N85-12049

Flight research on visual aids and navigation equipment for helicopter low-level flight at night
08 p1076 N85-16820

Interplanetary navigation 14 p2396 N85-24781

DOPPLER RADAR

NT MULTISTATIC RADAR

Diagnosis and therapy of geodetic satellite networks of Doppler type — error analysis
[SER-C-293] 01 p0015 N85-10090

Operational evaluation of 5 cm Doppler radar. Two contributions: Review of WSR-74C Doppler radar operations at WSO Montgomery, Alabama (April 1982 - August 1983). The Johnson-Effect resolving ambiguous Doppler velocities
[PB84-207521] 01 p0041 N85-10269

High frequency radar software reference manual for Product Two
[PB84-210079] 01 p0041 N85-10270

The PROMIS Doppler radar system; design and operational experience 01 p0077 N85-10513

Nowcasting with Doppler radar: The forecaster-computer relationship
01 p0077 N85-10514

Doppler radar analysis of a frontal zone prior to convective development 01 p0077 N85-10515

The potential use of atmospheric profilers in short-range prediction 01 p0078 N85-10518

Microburst wind structure and evaluation of Doppler radar for wind shear detection
[DOT/FAA/PM-84/29] 02 p0230 N85-11501

Terrestrial locating — of buoys from space
05 p0599 N85-13816

The motion of the Earth by Doppler observing campaign (MEDOC) 05 p0601 N85-13831

Spring program summary, 1983
[PB84-222223] 06 p0839 N85-15330

High accuracy Doppler navigation employing optimum integrated position fix information
08 p1073 N85-16803

The MST radar technique 08 p1165 N85-17486

Multiple channel adaptive filtering using a fast orthogonalization network: An application to efficient pulsed Doppler radar processing
[AD-A147929] 08 p1211 N85-17619

The potential of the NEXRAD radar system for warning of bird hazards
[AD-P004210] 11 p1583 N85-19977

Analysis of the NASA/MSFC Airborne Doppler Lidar results from San Gorgonio Pass, California
[NASA-CR-171355] 12 p1692 N85-21873

Geophysical interpretation of Venus gravity data
13 p2176 N85-23513

A brief summary of results derived from Scandinavian Twin Auroral Radar Experiment (STARE) observations during IMS — Ionospheric electric fields
14 p2362 N85-24595

Interplanetary navigation 14 p2396 N85-24781

Injection controlled laser transmitter with twin local oscillators
[AD-D011577] 15 p2563 N85-25810

Radar turbulence estimates. Effects of wind shear and reflectivity factor gradients
[AD-A151676] 15 p2590 N85-26023

Comparison of wind velocity in thunderstorms determined from measurements by a ground-based Doppler radar and an F-106B airplane
[NASA-TM-86348] 16 p2703 N85-26687

Analysis of the NASA/MSFC airborne Doppler lidar results from San Gorgonio Pass, California
[NASA-CR-3901] 16 p2832 N85-27463

Influence of coherent mesoscale structures on satellite-based Doppler lidar wind measurements
[NASA-CR-175853] 16 p2833 N85-27467

Weather radar studies
[AD-A152563] 17 p2996 N85-28521

Atmospheric probing by active millimeter wave system
[AD-A153550] 18 p3136 N85-29422

Use of radar with frequency modulation for studying atmospheric boundary layer 19 p3296 N85-30437

Comparison of wind and turbulence measurements from Doppler lidar and instrumented aircraft
[NASA-CR-171535] 20 p3495 N85-31729

Middle Atmosphere Program. Handbook for MAP. Volume 14: URSI/SCOSTEP Workshop on Technical Aspects of MST Radar
[NASA-CR-176065] 21 p3615 N85-32466

Observations of frontal zone structures with a VHF Doppler radar and radiosondes, part 1.2A
21 p3616 N85-32469

Performance of the Colorado wind-profiling network, part 1.5A 21 p3617 N85-32475

Relationship of spaced antenna and Doppler techniques for velocity measurements (keynote paper), part 3
21 p3619 N85-32488

On the spectrum of atmospheric velocity fluctuations seen by MST/ST radar and their interpretation
21 p3622 N85-32504

Coding schemes for improving MST radar performance, part 7.1A 21 p3625 N85-32520

Real-time automated detection of mesocyclones and tornado vortex signatures
[AD-A154968] 21 p3635 N85-32578

A multi-channel radar receiver
[AD-A156058] 24 p4087 N85-35329

Polarization diversity addition to the 10 centimeter Doppler weather radar
[AD-A156062] 24 p4087 N85-35334

DOPPLER-FIZEAU EFFECT

The solar vector magnetograph of the Okayama Astrophysical Observatory 18 p3205 N85-29882

DORNIER AIRCRAFT

NT DO-28 AIRCRAFT

DORNIER DO-28 AIRCRAFT

U DO-28 AIRCRAFT

DOSAGE

NT RADIATION DOSAGE

SANDYL radiation transport code at the Naval Research Laboratory
[AD-A144890] 01 p0117 N85-10798

Acute oral toxicity (LD50) of 4-nitrophenyl monochloromethyl (Phenyl) phosphinate (TA009) in male rats
[AD-A148337] 08 p1192 N85-17513

Study of a novel shielding principle for protection against intense gamma-ray beams
[AD-A154374] 19 p3357 N85-30666

Beta response of selected instruments
[DE85-013278] 22 p3788 N85-33489

Environmental surveillance at Los Alamos during 1984
[DE85-011886] 22 p3811 N85-33805

The 1984 environmental monitoring report, Sandia National Laboratories, Albuquerque, New Mexico
[DE85-011175] 22 p3811 N85-33807

The 1984 environmental monitoring program report for Idaho National Engineering Laboratory site
[DE85-011209] 22 p3812 N85-33811

Hit-size effectiveness theory applied to high doses of low LET radiation for pink mutations in Tradescantia
[DE85-011835] 22 p3819 N85-33857

The 1983 international intercomparison of nuclear accident dosimetry systems at Oak Ridge National Laboratory
[DE85-011303] 23 p3934 N85-34362

The 1984 biotic studies of Yucca Mountain, Nevada test site, Nye County, Nevada
[DE85-011715] 23 p3951 N85-34487

Estimating risks of lead-induced hemoglobin decrements under conditions of uncertainty: Methodology, pilot judgments and illustrative calculations
[DE85-012293] 23 p3952 N85-34490

Analysis of transient radiation upset in a 16K SRAM
[DE85-009442] 23 p3965 N85-34598

DOSE

U DOSAGE

DOSIMETERS

NT THRESHOLD DETECTORS (DOSIMETERS)

Radiation measuring system using transistor flux sensors
[AD-D011239] 01 p0050 N85-10328

Photon and electron dosimetry at the Physikalische-Technische Bundesanstalt in Brunswick
[PTB-DOS-9] 01 p0119 N85-10814

Specific absorption rate in a sitting rhesus model at 225, 1290, and 5950 MHz for E, H, and K polarizations
[AD-A145435] 02 p0234 N85-11524

The effect of the choice or response matrix on unfolded bonner sphere spectra
[AD-A150462] 13 p2159 N85-23404

The physical interactions of radiofrequency radiation fields and biological systems 16 p2775 N85-27129

Radio Frequency Radiation (RFR) measurements in operational settings 16 p2777 N85-27138

Results from radiation monitoring equipment experiment on STS-11
[AD-A152531] 17 p2908 N85-27932

Energy and Technology Review
[DE85-004358] 17 p3049 N85-28660

Results from radiation monitoring equipment experiment on STS-8
[AD-A153241] 17 p3055 N85-28811

Dosimeasurements with thermoluminescence dosimeters at a Febetron 701, 600 kV in room 022 of the Interuniversity Reactor Institute (IRI)
[IRI-190-84-02] 18 p3111 N85-29282

Safety system with microcomputer
[OEFZS-4294] 18 p3166 N85-29618

Comparison of calculations and measurements of the off-axis radiation dose (SI) in liquid nitrogen as a function of radiation length
[AD-A153676] 18 p3176 N85-29704

Safety report, 1982 18 p3184 N85-29746

Symposium on Luminescent Radiation Receivers and Converters 19 p3295 N85-30460

Research on the experimental verification of dosimetry calculations
[DE85-011282] 19 p3331 N85-30637

MELCOR Accident Consequence Code System (MACCS)
[DE85-009712] 19 p3339 N85-30689
Dosimetry and limit values for internal contamination with radionuclides: From (International Commission on Radioactive Protection) ICRP-2 to ICRP-30
[IRI-190-84-03] 20 p3507 N85-31804
Solid-state track recorder neutron dosimetry in the Three-Mile Island Unit-2 reactor cavity
[DE85-011360] 20 p3531 N85-31966
Results from radiation monitoring equipment experiments on STS-41C, 41D, 41G and 51A
[AD-A154676] 21 p3550 N85-32142
A crew exposure study. Phase II. Volume 2. At sea. Part A
[AD-A155233] 21 p3666 N85-32774
Paired ion chamber constants for fission gamma-neutron fields
[AD-A155069] 21 p3702 N85-32999
A practical guide to ionization chamber dosimetry at the AFRRI reactor
[AD-A155185] 21 p3703 N85-33003
Current internal-dosimetry practices at US Department of Energy facilities
[DE85-011718] 22 p3787 N85-33466
Error evaluation in measurements with thermoluminescent dosimeters
[ISS-T-84/6] 22 p3788 N85-33471
Hit-size effectiveness theory applied to high doses of low LET radiation for pink mutations in Tradescantia
[DE85-011835] 22 p3819 N85-33657
Digital characterization of particle tracks for microdosimetry
[DE85-012898] 22 p3846 N85-33822
The 1983 international intercomparison of nuclear accident dosimetry systems at Oak Ridge National Laboratory
[DE85-011303] 23 p3934 N85-34382

DOSIMETRY
U DOSIMETERS

DOUBLE BASE PROPELLANTS
NT DOUBLE BASE ROCKET PROPELLANTS
Study of the transition from deflagration to detonation of previously fragmented propellants
08 p1115 N85-17032
Effects of perforation L/D ratio and slotting on stick propellant combustion
[AD-A148854] 10 p1456 N85-19177

DOUBLE BASE ROCKET PROPELLANTS
Embedment system for ultrahigh-burning rate propellants of solid propulsion subsystems
[AD-D011257] 06 p0773 N85-14942
The vulnerability of cast double base rocket motors to thermomechanical attack 08 p1115 N85-17033
Crack growth in propellants 08 p1116 N85-17034
Determination of the decomposition behavior of double base propellants at low temperatures
08 p1117 N85-17045

DOUBLE STARS
NT BINARY STARS
NT COMPANION STARS
NT DWARF NOVAE
NT ECLIPSING BINARY STARS

DOUGLAS AIRCRAFT
NT DC 8 AIRCRAFT
NT DC 9 AIRCRAFT
NT DC 10 AIRCRAFT

DOUGLAS DC-8 AIRCRAFT
U DC 8 AIRCRAFT

DOUGLAS DC-9 AIRCRAFT
U DC 9 AIRCRAFT

DOUGLAS MILITARY AIRCRAFT
U MILITARY AIRCRAFT

DOVAP
U DOPPLER EFFECT

DOWN-CONVERTERS
Optical RF downconverter
[AD-D011336] 07 p1042 N85-16616

DOWNLINKING
BBC receiving terminal for the European orbital test satellite
[BBC-RD-1984/15] 08 p1142 N85-17205
Polarization angles of linearly polarized antennas and radio waves in satellite communications
[PB85-131613] 11 p1626 N85-20240
Remote control of an impact demonstration vehicle
[NASA-TM-85925] 14 p2225 N85-23797
Analysis of space diversity techniques for EHF (Extremely High Frequency) satellite downlinks
[AD-A151900] 15 p2544 N85-25705
The IRAS end-to-end data system
[NLR-MP-83056-U] 17 p3051 N85-28883

DOWNWASH
Downwash in the plane of symmetry of an elliptically loaded wing
[NASA-TP-2414] 07 p0898 N85-15693

DRAFTING (DRAWING)
Accomplishments of Institute of Cartography summarized 13 p2166 N85-23435
Computer aided draughting in a civil engineering consulting practice 15 p2627 N85-26189

DRAFTING MACHINES
Two-dimensional/speed/couple/data base management system
[A-1] 18 p3165 N85-29608
The CEADS-CADD system
[A-4] 18 p3165 N85-29610
System test CALMA DDM (Design Drafting Manufacturing)
[A-5] 18 p3165 N85-29611
The International Computers Limited (ICL) PERQ 1/Engineering Architectural Graphics Language Environment (EAGLE) Computer Aided Design system (CAD)
[A-7] 18 p3165 N85-29612
System test: Hewlett-Packard draft
[A-9] 18 p3166 N85-29613
Test Drawing Office Graphics System (DOGS)/APOLLO
[A-10] 18 p3166 N85-29614
System test Oce 5200
[A-3] 20 p3515 N85-31850
The General Drafting System (GDS) design system
[A-6] 20 p3517 N85-31869
The IGOS design system
[A-8] 20 p3517 N85-31870

DRAG
NT AERODYNAMIC DRAG
NT FRICTION DRAG
NT INTERFERENCE DRAG
NT SATELLITE DRAG
NT VISCOUS DRAG
NT WAVE DRAG
Observations from varying the lift and drag inputs to a noise prediction method for supersonic helical tip speed propellers
[NASA-TM-83797] 01 p0115 N85-10788
UH-60A external stores support system fixed provision fairings drag determination
[AD-A147188] 07 p0902 N85-15719
The NYU inverse swept wing code
[NASA-CR-3662] 08 p1077 N85-16830
Icing flight research: Aerodynamic effects of ice and ice shape documentation with stereo photography
[NASA-TM-86906] 09 p1279 N85-18049
Report of the Constellations Panel
11 p1645 N85-20368
Evaluating wind flow around buildings on heliport placement
[FAA-PM-84-25] 12 p1893 N85-21881
Effect of drag behind nozzle array on its force and energy characteristics 14 p2277 N85-24107
Hydraulic drag of rod with artificial microroughness in longitudinal flow 14 p2278 N85-24111

DRAG BALANCE
U AERODYNAMIC BALANCE
U LIFT DRAG RATIO

DRAG CHUTES
Extended moment arm anti-spin device
[NASA-CASE-LAR-12979-1] 12 p1776 N85-21147
Parachute extraction device for ultralight gliders
[CH-643499-A5] 16 p2689 N85-26663

DRAG DEVICES
NT AERODYNAMIC BRAKES
NT DRAG CHUTES
NT LEADING EDGE SLATS
NT SPOILERS
NT TRAILING EDGE FLAPS
NT WING FLAPS
Measurements in the flow field of a cylinder with a laser transit anemometer and a drag rake in the Langley 0.3 m transonic cryogenic tunnel
[NASA-TM-86399] 14 p2305 N85-24270

DRAG EFFECT
U DRAG

DRAG MEASUREMENT
Flow through very porous screens
[NASA-TP-2436] 11 p1631 N85-20270
Determination of the drag of free flying particles in supersonic flow with a pulsed laser
12 p1773 N85-21129
Cone drag in the transition from continuum to free molecular flow
[OUEL-1536/84] 20 p3390 N85-31023

DRAG REDUCTION
Force and moment measurements on a 74 deg delta wing with an apex flap
[NASA-CR-166081] 02 p0134 N85-10918
Aircraft surface coatings
[NASA-CR-3661] 02 p0137 N85-10935
Design, manufacture, and testing of compliant coatings for reduction of turbulent drag
[AD-A145510] 02 p0198 N85-11323
Numerical simulations of compliant material response to turbulent flow, revision 1
[AD-A145801] 03 p0372 N85-12373
Installed nacelle drag-improvement tests of an M = 0.8 turboprop transport configuration
[NASA-TM-84302] 07 p0902 N85-15716
Aircraft drag reduction technology
08 p1070 N85-16782
Drag reduction due to boundary-layer control by combined blowing and suction 08 p1070 N85-16785
Turbulent drag reduction research
08 p1071 N85-16788
On the relaxation of a turbulent boundary layer after an encounter with a forward facing step
08 p1071 N85-16789
Full scale experiments into the use of large eddy breakup devices for drag reduction on aircraft
08 p1071 N85-16790
Pneumatic turbulators: A device for drag reduction at Reynolds numbers below 5 million
08 p1071 N85-16791
Study of winglets applied to biplanes
[NASA-TM-86350] 08 p1083 N85-16882
A survey of the turbulent drag reduction using passive devices
[NMI-R-193] 11 p1630 N85-20268
Drag-free satellite simulator
[REPT-615] 12 p1789 N85-21229
Numerical study of large-eddy breakup and its effect on the drag characteristics of boundary layers
[NASA-CR-3884] 12 p1797 N85-21272
Investigation of the initial events in biofouling
[AD-A149995] 12 p1900 N85-21927
Mercedes-Benz auto 2000 achieves low drag coefficient 15 p2530 N85-25602
Exploratory wind-tunnel investigation of a wingtip-mounted vortex turbine for vortex energy recovery
[NASA-TP-2468] 16 p2699 N85-26667
Demonstration of relaxed stability on a commercial transport 16 p2713 N85-26745
Realisation of relaxed static stability on a commercial transport 16 p2713 N85-26746
Numerical study of porous airfoils in transonic flow
[NASA-TM-86713] 17 p2892 N85-27828
Combined riblet and LEBU drag reduction system
[NASA-CASE-LAR-13286-1] 18 p3058 N85-28922
A method for predicting additive drag reduction from small-diameter pipe flows
[AD-A154411] 19 p3266 N85-30254
Injection of drag reducing additives into turbulent water flows: Two-component velocity measurements and mixing length model predictions
[AD-A154604] 21 p3583 N85-32274
Experiments on the influence of active walls on the initial amplitudes and growths of instability waves
[AD-A154630] 21 p3583 N85-32275
An automated technique for encasing specific payloads with low-drag fairings 24 p4063 N85-35183
Wingtip vortex propeller
[NASA-CASE-LAR-13019-1] 24 p4065 N85-35194

DRAGULATORS
U BRAKES (FOR ARRESTING MOTION)
U DRAG DEVICES

DRAINAGE
Systematic data interpretation of remote sensing in the reception of hydrocarbons, volume 1
[E85-10008] 02 p0215 N85-11421
Geothermal assessment of the lower Bear River drainage and northern East Shore ground-water areas, Box Elder County, Utah
[DE84-017358] 04 p0526 N85-13368
Comparison between tracer measurements and model calculations for nighttime drainage flows in complex terrain
[DE84-014709] 04 p0539 N85-13431
Effect of lithology and climate on the morphology of drainage basins in northwestern Colorado
[PB84-228238] 06 p0828 N85-15258
Statistical relationships between meteorological data stations and implications to diagnostic models in complex terrain
[DE84-014380] 06 p0839 N85-15328
Retrieval procedures for hydrologic data from ARS (Agricultural Research Service) experimental watersheds in the US (REPHLEX)
[PB85-111326/GAR] 09 p1402 N85-18828
Nationwide urban runoff program. Relationship of urban runoff to land use and groundwater resources
[PB85-114692] 10 p1506 N85-19505
The ASCOT Data Analysis Workshop
[DE85-004407] 13 p2139 N85-23283

A comparison of terrestrial saltation flux in the laboratory and the field
13 p2189 N85-23582
Fluvial drainage basins and valley networks: Eastern Margaritifer Sinus, Mars
13 p2190 N85-23586
Surface hydrologic characteristics of proposed repository locations in the Palo Duro Basin of the Texas Panhandle
[DE85-010530] 18 p3126 N85-29355
Flood-runoff forecasting with HEC1F
[AD-A154286] 19 p3300 N85-30456
Categorization of nocturnal drainage flows within the Brush Creek valley in western Colorado and the variability of sigma theta in complex terrain
[DE85-011291] 19 p3300 N85-30461
Synthetic rainfall and its use in hydrologic modeling
19 p3314 N85-30542
Geomorphic analyses from space imagery
21 p3603 N85-32374
New estimating procedures for surface runoff, sediment yield, and contaminant transport in Los Alamos County, New Mexico
[DE85-011890] 21 p3606 N85-32393
Long-term exposure of (238) PuO2 to a terrestrial environment, volume 3
[DE85-011896] 22 p3840 N85-33781
Hydrology
[PB85-182954] 23 p3944 N85-34440

DRAINAGE PATTERNS
Utilization of LANDSAT orbital imagery in the soil survey processes at Rio Grande do Norte state
[E85-10009] 02 p0216 N85-11422
Geologic utility of LANSDAT-4 TM data — Death Valley, California and the Silver Bell area of southern Arizona
13 p2118 N85-23192
Nationwide Urban Runoff Project, Champaign, Illinois: The biological impact of urban runoff on the Saline Branch Drainage Ditch and Boneyard Creek
[PB85-150274] 14 p2348 N85-24515
Example of joint use of data from surface studies and space photographs in investigating dynamics of zone of North Zeravshan seismogenic faults
15 p2485 N85-25342

DRAINING
U DRAINAGE
DRAWINGS
NT ENGINEERING DRAWINGS
Intersection of three-dimensional geometric surfaces
[NASA-TP-2454] 20 p3513 N85-31839
DREDGED MATERIALS
Improved techniques for removal of sediments contaminated with hazardous materials
[PB85-116093] 11 p1679 N85-20580
DRIFT
Drift characteristics of northeastern Bering Sea ice during 1982
[PB84-213962] 01 p0089 N85-10604
Acceleration of an electron ring in a modified betatron with transverse pressure
[AD-A148626] 08 p1221 N85-17688
Simulation of the ion-beam-driven drift instability in a magnetic trap, 1
[AD-A149451] 10 p1452 N85-19147
Simulation of the ion-beam-driven drift instability in a magnetic trap, 2
[AD-A149452] 10 p1554 N85-19798
A diffusion process and its application to detecting a change in the drift of Brownian motion
[AD-A150096] 12 p1926 N85-22100
Interpreting refracted waves method data on basis of automated determination of seismic drift
14 p2343 N85-24486

DRIFT (INSTRUMENTATION)
Evaluation of the stochastic drift of rate-integrating gyros as preparation for the analysis of laser gyro drift measurements
[ESA-TT-827] 05 p0639 N85-14099
ATA probe beam experiment
[DE84-016017] 06 p0862 N85-15477
First tests on the astrometric performance of the new PDS1010G at Hamburg Observatory — granite microdensitometer
07 p0966 N85-16135
Drift fields and boundary conditions at grain boundaries in bipolar P/N junction silicon devices
13 p2062 N85-22879
An investigation of tropospheric ions
16 p2823 N85-27412
An inexpensive radar-responding relocation device for drifting oceanographic instruments
[AD-A152170] 16 p2838 N85-27505
Measurements of laser gyro errors as a function of the beam path
[DFVLR-FB-85-02] 17 p2969 N85-28336
Technology development for thin-film-trace humidity sensors
[BMFT-FB-T-84-268] 17 p2969 N85-28338
Relationship between Allan variances and Kalman Filter parameters
18 p3107 N85-29238
Performance data of US Naval Observatory VLG-11 hydrogen masers since September, 1983
18 p3108 N85-29244
Criteria for optimum spacing of spaced antenna, part 3.2A
21 p3620 N85-32491
Problems and solutions in analyzing partial-reflection drift data by correlation techniques
21 p3626 N85-32529
Recording small frequency drifts of microwave oscillators
22 p3771 N85-33372
Improved method for the stabilization of NaI-photomultiplier gamma detectors against thermal and other drift
[DE85-011830] 23 p3970 N85-34613
DRIFT RATE
Evaluation of the stochastic drift of rate-integrating gyros as preparation for the analysis of laser gyro drift measurements
[ESA-TT-827] 05 p0639 N85-14099
Transport properties and distribution functions in 3-5 semiconductors
[AD-A147525] 07 p1049 N85-16660
MIZEX. A program for mesoscale Air-Ice-Ocean interaction experiments in arctic marginal ice zones. 4: Initial results and analysis from MIZEX 83
[AD-A148255] 08 p1173 N85-17399
The analysis of spaced sensor records by correlation techniques
08 p1184 N85-17465
New instabilities in line driven winds
08 p1235 N85-17785
Suspension torques on a gimballed electrostatically supported gyroscope and requirements on the gyroscope and spacecraft for the relativity gyroscope experiment
12 p1851 N85-21608
The use of the ARGOS system for the study of the drift of Antarctic icebergs
14 p2240 N85-23690
Drift mobilities by time-of-flight methods and time-dependent phototransport in the nanosecond regime in amorphous semiconductors
[DE85-008729] 18 p3194 N85-29815
Moving random surfaces and correlation analysis
[CRC-1384] 19 p3253 N85-30168
Test evaluation of the Honeywell GG1111 Single-Degree-of-Freedom (SDF) strapdown gyroscope
[AD-A154768] 21 p3589 N85-32307
Guiding center distribution function and longitudinal invariant
23 p3978 N85-34663
Notes on drift theory
[SH-4.2-3] 23 p4006 N85-34841
Drift and observations in cosmic-ray modulation, 1
[SH-4.2-4] 23 p4007 N85-34842
Drift and observations in cosmic-ray modulation, 2
[SH-4.2-5] 23 p4007 N85-34843
The influence of nonstationarity of the solar activity and general solar field on modulation of cosmic rays
[SH-4.2-17] 23 p4008 N85-34854
Changes in the energy spectrum of anomalous oxygen and helium during 1977-1985
[SH-4.6-1] 23 p4039 N85-35039
On the anomalous component
[SH-4.6-6] 23 p4039 N85-35044
Fractional charge resolution in music
24 p4147 N85-35712
Proportional drift tubes for large area muon detectors
[HE-5.2-11] 24 p4203 N85-36087
DRILL BITS
Geothermal COMPAX drill hit development
[DE85-011353] 20 p3489 N85-31556
DRILLING
NT LASER DRILLING
Priorities for a national program of continental drilling for scientific purposes
04 p0534 N85-13418
The Georges Bank monitoring program 1983: Analysis of trace metals in bottom sediments
[CIRC-915] 05 p0688 N85-14423
Organogenic structures (submerged reefs) in Silhetian limestone of west Bengal basin
10 p1500 N85-19464
Shallow magma targets in the western US
[DE85-003274] 12 p1881 N85-21803
Evaluation of the blind hole drilling method for the measurement of residual stress
[AD-A151459] 15 p2579 N85-25905
Lost circulation in geothermal wells: Research and development status
[DE85-009836] 19 p3268 N85-30267
Geologic, technical, and economic sensitivity analysis in support of the GRI (Gase Research Institute) tight gas reservoirs project area
[PB85-192276] 22 p3802 N85-33559
Lithology and stratigraphy of drill holes completed during 1984 in LANL use areas of Yucca Flat, Nevada Test Site, volume 6
[DE85-010695] 22 p3815 N85-33631
Proposed resource evaluation plan. Salton Sea scientific drilling program
[DE85-011294] 22 p3615 N85-33
DRILLS
Novel drives for machine tools
14 p2266 N85-24

DROGUE PARACHUTES
U DRAG CHUTES
DROGUES
U TOWED BODIES
DRONE HELICOPTERS
U HELICOPTERS
DROP SIZE
Atmospheric extinction in critical environments
[AD-A146102] 03 p0396 N85-12527
Liquid fuel spray processes in high-pressure gas flow
[NASA-TM-86944] 12 p1844 N85-21570
Research study of droplet sizing technology leading to the development of an advanced droplet sizing system
[NASA-CR-174839] 12 p1850 N85-21604
Effects of temperature variation among droplets in an evaporating fuel spray
13 p2004 N85-2258
Experimental study of anisotropy of scattering of radar signals by clouds and precipitation
14 p2340 N85-24473
Limiting factor of flame propagation in mono-sized sprays of low-volatility fuels
[NAL-TR-839T] 15 p2521 N85-2553
Some further aspects of the influence of raindrop-size distributions on millimeter-wave propagation
[PB85-168334] 18 p3092 N85-2913
Particle sizing from forward scattered light at two angles using a Variable-Focal-Length optical system
[AD-A154164] 20 p3533 N85-319
A relationship between cloud droplet size and CCN critical supersaturation
21 p3649 N85-32677
Fog activation and supersaturation
21 p3650 N85-3267
On the question to the effect of surfactants on the spectrum of cloud drops in the process of the condensation growth
21 p3650 N85-3267
The distribution of giant salt nuclei inside and outside cloud over the basin of Xin and Jiang
21 p3650 N85-3268

DROP TESTS
Analysis of a transport fuselage section drop test
01 p0060 N85-1040
Research relative to the development of a cryogen microwave cavity gradiometer for orbital use
[NASA-CR-174249] 07 p0962 N85-160
Results of an EPRG round robin test programme w DWTT specimens — drop weight test (DWTT);pl steels
[ERS-E.365] 09 p1341 N85-164
Direct comparison of unloading compliance and potent drop techniques in J-integral testing
[DE85-001550] 11 p1650 N85-203
Impact studies of a 1/3-scale model of an air cushi vehicle
[NASA-TM-86360] 14 p2218 N85-237
B-52B/DTV (Drop Test Vehicle) flight test results: D test missions
[NASA-CR-171530] 19 p3215 N85-290
Graphite/PMR polyimide composites with impro toughness
[NASA-TM-87081] 21 p3561 N85-32
DROP TOWERS
Results of the technical exchange agreement betw NASA and DuPont on the containerless drop t solidification of NiAl3
[NASA-TM-86472] 01 p0014 N85-10
Microgravity containerless processing in long tubes
02 p0153 N85-11
Containerless drop tube solidification and refinement of NiAl3
02 p0154 N85-1
Critical point wetting drop tower experiment
02 p0156 N85-1

DROP TUBES
U DROP TOWERS
DROP WEIGHT TESTS
U DROP TESTS
DROPS (LIQUIDS)
Single-drop impact damage prediction for low de coated ceramic materials — rain erosion
01 p0061 N85-1
Interaction of a stream of dielectric spheres in an el field in a high vacuum
[DE84-014714] 01 p0115 N85-
Numerical simulations of fuel droplet flows u Lagrangian triangular mesh
[AD-A146087] 03 p0362 N85-
Aircraft flow effects on cloud droplet image concentrations
[AD-A146176] 03 p0396 N85-

Turbulent shear fields for dispersion of aqueous drops in organic liquids and application to gel-sphere processes
[DE84-016562] 06 p0809 N85-15141
Experimental study of the spray characteristics of a research airblast atomizer
[NASA-TM-86911] 07 p0904 N85-15727
The structure of dilute combusting sprays
[NASA-CR-174838] 07 p0905 N85-15728
Swirling turbulent spray group combustion
09 p1289 N85-18095
Measurement of drop-size distributions with the aid of a scattered light particle size counting analyser
[BLL-TRANS-WH-620-(9091.9F)]
09 p1317 N85-18278
Application of scattered light particle size counting analysis to the determination of wide drop size distributions
[BLL-TRANS-WH-619-(9091.9F)]
09 p1317 N85-18279
Effect of water vapor and water droplets on the RAM-1 (Real-Time Aerosol Monitor): Preliminary results
[PB85-109429] 11 p1637 N85-20313
Gasification of boron oxide drops and boron slurry agglomerates in combustion gases
13 p1999 N85-22529
Effects of temperature variation among droplets in an evaporating fuel spray 13 p2004 N85-22562
Size and velocity distributions of particles and droplets in spray combustion systems
[AD-A150355] 13 p2017 N85-22648
Advanced radiator concepts
[NASA-TM-87008] 14 p2300 N85-24245
CON1D: A computer program for calculating spherically symmetric droplet combustion
[DE85-005604] 15 p2507 N85-25464
Experimental investigation of annular air curtain domes
[UTIAS-288] 15 p2521 N85-25543
Study of the explosive combustion of drops of sulphur at high temperatures
[HSE-TRANS-11172] 19 p3252 N85-30163
Laser-induced fluorescence measurement of vapor concentration surrounding evaporating droplets
[DE85-009409] 19 p3277 N85-30320
Droplet deposition in vertical two-phase flow
[CFD/84/22] 20 p3456 N85-31480
Instability and chaotic behavior in a free-surface flow
[AD-A154879] 21 p3584 N85-32279
Ice nucleation of single water droplet by silver iodide: A laboratory observation 21 p3643 N85-32630
Cloud droplet nucleation and initial growth derived from lidar depolarization studies 21 p3644 N85-32635
Characterization of insoluble particles associated with cloud droplets 21 p3652 N85-32693
The measured rate of condensation nucleation to droplets using the techniques of chemical kinetics
21 p3652 N85-32694

DROUGHT
Forecast of the northeastern drought by the method of periodicities: Use and abuses
[INPE-3109-PRE/508] 02 p0230 N85-11502
Droughts and floods in South America due to the 1982-83 El Nino-southern oscillation episode
[INPE-3408-PRE/677] 09 p1357 N85-18535
Planetary scale circulation anomalies associated with droughts over northeast Brazil
[INPE-3351-PRE/630] 10 p1518 N85-19570
Large scale circulation anomalies and prediction of northeast Brazil droughts
[INPE-3405-PRE/674] 10 p1518 N85-19571
On the 1983 drought in northeast Brazil
[INPE-3412-PRE/678] 16 p2834 N85-27476
An appraisal of the duration of the recent drought in northeast Brazil and a forecast for 1985
[INPE-3477-PRE/720] 16 p2834 N85-27478
Preliminary results from numerical experiments on the summer 1980 heat wave and drought
18 p3140 N85-29438
Northeast Brazil droughts and Atlantic SST anomalies
[INPE-3538-PRE/754] 19 p3316 N85-30553

DROUGHT CONDITIONS
U DROUGHT

DROWSINESS
U SLEEP

DRUG THERAPY
U CHEMOTHERAPY

DRUGS
NT ADRENERGICS
NT ANESTHETICS
NT ANTIADRENERGICS
NT ANTICHOLINERGICS
NT ANTIEMETICS AND ANTINAUSEANTS
NT ANTIRADIATION DRUGS
NT ATROPINE
NT CHLOROFORM
NT CORTISONE
NT CYCLOPROPANE
NT EPINEPHRINE
NT INSULIN
NT METHYL CHLORIDE
NT MOTION SICKNESS DRUGS
NT MUSCLE RELAXANTS
NT NOREPINEPHRINE
NT TRANQUILIZERS
China report: Science and technology
[JPRS-CST-84-025] 11 p1620 N85-20197
Review of US guide on medication and flying
12 p1904 N85-21958
Progress, goals in biotechnology summarized
17 p2945 N85-28182
Chemicals identified in human biological media, a data base, volume 6, part 1
[DE85-008768] 17 p2999 N85-28542
Effect of spironolactone on acute mountain sickness
[AD-A153780] 18 p3153 N85-29525
Interaction of opiate and phencyclidine derivatives with the acetylcholine receptor
[AD-A155119] 21 p3664 N85-32761
Effect of dibazol on parameters of nonspecific resistance of subjects in pressurized cabins
23 p3954 N85-34504

DRUMLINS
U GLACIAL DRIFT

DRUMS
Effect of air cavity on the vibration analysis of loaded drums 09 p1339 N85-18422

DRUMS (CONTAINERS)
Centrifugal castings of stainless steel spiked with radioactive tracers
[DE85-012003] 22 p3748 N85-33234
Drying of pulverized material with heated condensible vapor
[DE85-011656] 22 p3783 N85-33438

DRY CELLS
NT NICKEL ZINC BATTERIES

DRY FRICTION
Interactions among system stiffness, wear and vibrations 03 p0370 N85-12364
Thermomechanical cracking due to moving frictional loads
[AD-A146271] 03 p0373 N85-12381

DRYERS (EQUIPMENT)
U DRYING APPARATUS

DRYING
NT DEHUMIDIFICATION
NT DEHYDRATION
NT FREEZE DRYING
Numerical modelling of the drying of porous materials
[DE84-013056] 04 p0499 N85-13181
Improved uniformity of viscous textile fibers obtained by altering drying procedures 06 p0762 N85-14871
Modeling of transient heat pipe operation
[NASA-CR-175496] 12 p1844 N85-21571
New air-curing lacquer systems with high solids content
[BMFT-FB-T-85-005] 17 p2936 N85-28124
Thermomigration in porous media. Study of the development of a drying zone 20 p3456 N85-31462
The design and development of a spacecraft appendage tie down mechanism 22 p3797 N85-33522
Composite desiccant structure
[DE85-006400] 23 p3910 N85-34226
Nonsaturable microdryer
[DE85-005760] 23 p3946 N85-34457
Method of preparing thin porous sheets of ceramic material
[DE85-006399] 24 p4082 N85-35300

DRYING APPARATUS
Performance of the SERI parallel-passage dehumidifier
[DE85-000509] 11 p1672 N85-20536
Evaluation of pilot ESP used with a spray dryer FGD system at Pittsburgh Energy Technology Center, Bruceton, Pennsylvania
[DE85-011151] 22 p3746 N85-33217
Drying of pulverized material with heated condensible vapor
[DE85-011656] 22 p3783 N85-33438

DTA (ANALYSIS)
U THERMAL ANALYSIS

DTMB-111 GROUND EFFECT MACHINE
U GROUND EFFECT MACHINES

DTMB-430 GROUND EFFECT MACHINE
U GROUND EFFECT MACHINES

DUAL MODE PROPULSION
U HYBRID PROPULSION

DUAL SPIN SPACECRAFT
A dual spin space station design
20 p3408 N85-31152

DUALITY THEOREM
The role of duality in optimization problems involving entropy functionals, with applications to information theory
[AD-A152336] 17 p3026 N85-28713

DUCT GEOMETRY
Calculation of flow about posts and powerhead model — space shuttle main engine
[NASA-CR-171344] 10 p1483 N85-19362
Determination of boundary line between reverse jet and surrounding stream 13 p2043 N85-22789
An analytical and numerical study of the interaction of rarefaction waves with area changes in ducts. Part 2: Area enlargements
[UTIAS-273] 14 p2300 N85-24242
Analytical study of flow phenomena in SSME turnaround duct geometries 16 p2739 N85-26902

DUCTED BODIES
Time-averaged and time-dependent computations of isothermal flowfields in a centerbody combustor
[AD-A153682] 18 p3100 N85-29189

DUCTED FANS
Numerical analyses in aerodynamic design of aero-engine fan 16 p2692 N85-26618

DUCTED FLOW
NT KNUDSEN FLOW
Vertical channel free convection for a power law fluid with a constant heat flux
[DE84-014551] 01 p0047 N85-10311
A comparison of evaporation duct models for IREPS (Integrated Refractive Effects Prediction System)
[AD-A146471] 06 p0799 N85-15103
Shock waves in transonic flows at moderate Reynolds Number 08 p1076 N85-16823
Computation of flow and heat transfer in flow around a 180 deg bend
[AD-A148065] 08 p1162 N85-17330
Secondary flow in cascades
[AD-A148415] 08 p1162 N85-17333
Combustion driven oscillation of ducted diffusion flame
09 p1289 N85-18094
Turbulent jet flow in a channel with a circulation region
09 p1308 N85-18218
An experimental investigation of confined, multiple, turbulent jet mixing with recirculation — flow distribution in combustors with injection plates
15 p2555 N85-25764
Application of computational fluid dynamics to complex inlet ducts
[NASA-TM-87060] 19 p3265 N85-30247

DUCTED ROCKET ENGINES
Integral boost, heat protection, port covers and transition 07 p0918 N85-15813
Mixing chemical reaction and flow field development in ducted rockets
[DE85-002710] 11 p1591 N85-20009

DUCTILITY
Material degradation in heavy steel plates caused by bending with a laser
[AD-A144784] 01 p0052 N85-10343
Design of strong, ductile, duplex low alloy steels
02 p0177 N85-11189
Structural uses for ductile ordered alloys. Report of the committee on application potential for ductile ordered alloys
[AD-A146313] 03 p0332 N85-12139
Stress-driven solute enrichment of crack-tips during low ductility intergranular fracture of low-alloy steel
[AERE-R-11120] 03 p0333 N85-12150
Structure and ductility of fracture of joints produced by electron-beam welding of VT6ch titanium alloy parts
03 p0351 N85-12261
A comparison of methods for predicting ductile crack growth instability
[AERE-R-11199] 03 p0374 N85-12387
The effect of cross-link density on the toughening mechanism of elastomer-modified epoxies
04 p0465 N85-12951
Toughening mechanism in elastomer-modified epoxy resins, part 2
[NASA-CR-3852] 04 p0478 N85-13046
Tensile properties and swelling of 20%-cold-worked Type 316 stainless steel irradiated in HFIR
[DE84-014080] 05 p0617 N85-13948
Low cycle fatigue strength for multiaxial loading of ductile materials 05 p0649 N85-14167
Development and characterization of ductile Long-Range-Ordered (LRO) alloys (Fe,Co, Ni)3V for high-temperature structural use
[DE84-016750] 06 p0769 N85-14921
Effect of crack-tip region constraint on fracture in the ductile-to-brittle transition
[PB84-237395] 06 p0770 N85-14926
Effect of input distributions on the probabilistic fracture mechanics analysis of reactor pressure vessels
[DE85-000832] 11 p1652 N85-20403

Creep crack growth in ductile alloys
[DE85-003937] 13 p2023 N85-22676
Analysis of strength and ductility of welded joints in AMtsS and AMg5 aluminum alloys
13 p2033 N85-22737
Effect of oxygen on mechanical properties of Nb-V alloy
[DE85-002681] 14 p2256 N85-23982
Mechanical properties of welded joints of 1201 aluminum alloy 15 p2502 N85-25431
Design of ductile polycrystaline Ni3Al alloys
[DE85-005572] 15 p2511 N85-25491
Weldability of Ni3Al-type aluminide alloys
[DE85-006932] 15 p2512 N85-25496
Ductility equation for porous metals and its linearization
[BLL-M-36118-(5828.4)] 16 p2748 N85-26958
On the accurate representation of large strain non-proportional plastic flow in ductile materials
[DE85-007106] 16 p2801 N85-27273
High-strength weldable steel 03G4N2MAF Sh with improved ductility
[BLL-BISI-TRANS-22233-(9022.06)]
17 p2924 N85-28031
Preparation of metal for cold upsetting
[BLL-BISI-TRANS-22383-(9022.06)]
17 p2926 N85-28043
Assessing the machinability of gearwheel steels during manufacture
[BLL-BISI-TRANS-22343-(9902.06)]
17 p2973 N85-28365
Surface degradation of ductile metal in elevated temperature gas-particle streams
[DE85-008428] 18 p3074 N85-29017
Load-carrying capabilities of refractory alloys for space reactor power applications
[DE85-010566] 19 p3240 N85-30087
Comparative analysis of laboratory and fullscale experimental data for metal flow displacements and speeds
[BLL-M-36266-(5828.4)] 20 p3430 N85-31276
Fatigue-crack growth and ductile fracture toughness behavior of ASTM A387 Grade 91 steel
[DE85-008495] 20 p3431 N85-31286
Numerical study of ductile rupture in plane deformations
[ONERA-RT-23/7169-RY-072-R]
20 p3469 N85-31557
Numerical study of tensile fracture in plane stress
[ONERA-RT-22/7169-RY-070-R]
20 p3470 N85-31563
Metallurgical origins of fracture toughness and microstructure and fracture toughness of an HSLA (High-Strength/Low-Alloy) steel
[AD-A155530] 21 p3567 N85-32187
Development of improved dynamic failure models
[AD-A155586] 21 p3600 N85-32354
Metallic glass composition
[DE85-011594] 22 p3751 N85-33253

DUCTS
NT ACOUSTIC DUCTS
NT AIR DUCTS
NT ANNULAR DUCTS
Vortex-generating coolant-flow-passage design for increased film-cooling effectiveness and surface coverage
[NASA-TP-2388] 03 p0361 N85-12314
Laminar flame propagation/quench for a parallel-wall duct
[DE84-009773] 04 p0470 N85-12993
Modelling the aerodynamics in a system of continuous channels and experimentation procedure
[BLL-M-35923-(5828.4)] 05 p0634 N85-14067
The Shock and Vibration Digest, volume 16, no. 10
[AD-A147588] 09 p1331 N85-18361
Sound transmission in ducts 09 p1331 N85-18362
Basic studies of multiple free and confined jets
[AD-A149556] 10 p1485 N85-19374
An experimental investigation of an underexpanded rectangular jet ejector
[AD-A149656] 12 p1779 N85-21170
Turbulent convecting flow in a square duct with a 180 deg bend: An experimental and numerical study
[AD-A149969] 12 p1846 N85-21583
High frequency estimation of 2-dimensional cavity scattering
[AD-A151697] 15 p2542 N85-25896
Vortex shedding flowmeters for liquids at high flow velocities 16 p2740 N85-26906
LDA study of non-steady flame propagation in a constant volume duct
[DE85-007233] 16 p2746 N85-26948
The hydrosynclastic infundibulum
[AD-A153849] 18 p3100 N85-29192
Experimental investigation of turbulent heat transfer in straight and curved rectangular ducts
[AD-A154413] 19 p3266 N85-30255
Mechanical connection for a tubular assembly
[DE85-011590] 22 p3792 N85-33497
Monte Carlo and discrete ordinates calculations of 14-MeV neturons streaming through a stainless-steel duct (L/D = 4.6): Comparison with experiment
[DE85-011423] 22 p3840 N85-33776
Block-implicit calculations of three-dimensional laminar flow in strongly curved ducts
[DE85-003047] 23 p3931 N85-34363

DUMMY LOADS
U IMPEDANCE
U LOADING
U OUTPUT

DUNES
Surface soil moisture measurements of the White Sands, New Mexico
[NOAA-TM-NESDIS-7] 02 p0219 N85-11441
Application of SIR-B data for groundwater exploration in the Arabian shield and sand-drift monitoring in the AN Nafud and Al Jafurah fringe areas, Kingdom of Saudi Arabia 08 p1144 N85-17214
Microdunes and other aeolian bedforms on Venus: Wind tunnel simulations 13 p2189 N85-23584
Planetary analogs in Antarctica: Mars
13 p2193 N85-23604

DUNGEYS WIND SHEAR MECHANISM
U WIND SHEAR

DUPLEX OPERATION
Design of strong, ductile, duplex low alloy steels
02 p0177 N85-11189
Evaluation of 7010 aluminium alloy extruded tube in the T76 condition
[BR92019] 11 p1596 N85-20039
Combined processing method and matched filter for discrete composite frequency phase-shift keyed signal
13 p2070 N85-22931

DUPLICATING
U REPRODUCTION (COPYING)

DURABILITY
Investigation of chemical durability mechanisms in fluoride glasses
[AD-A145420] 02 p0186 N85-11241
F-16 force management, yesterday, today and tomorrow 07 p0895 N85-15674
Design and test requirements for development of today's engines 07 p0906 N85-15737
Overview of the AGARD SMP activities on turbine engine materials technology in the 1972 - 1982 period
07 p0906 N85-15738
Cyclic endurance testing of the RB211-22B cast HP turbine blade 07 p0908 N85-15747
Experimental test program for evaluation of solid lubricant coating as applied to compliant foil gas bearings to 315 deg C
[NASA-CR-174837] 07 p0930 N85-15895
NBS (National Bureau of Standards) solar collector durability-reliability test program
[PB85-113603/GAR] 09 p1346 N85-18469
Long term durability of urea formaldehyde glued joints removed from Vampire aircraft
[AD-A149053] 10 p1424 N85-18965
Influence of volumetric fiber content on some matrix damage factors during thermal cycling of tungsten-EI 765 composite 10 p1443 N85-19097
USSR report: Materials science and metallurgy
[JPRS-UMS-84-005] 11 p1597 N85-20044
Structure-phase state and properties of high-durability VAL8 alloy 11 p1597 N85-20046
New method for studying surface crack growth in laminated polymer composite materials
11 p1598 N85-20051
Predicting stability of full-scale composite constructions of the basis of stiffness 11 p1599 N85-20054
Evaluation of features of reinforcing fibers by testing bundles 11 p1599 N85-20059
Kinetics of reaction of metals and non-metals during diffusion welding 11 p1602 N85-20076
Effect of macrostructure on durability of polycrystalline graphite 11 p1605 N85-20091
Prediction of the resistance of structural materials to cavitation erosion
[BLL-DRIC-TRANS-7435-(3623.66)]
13 p2020 N85-22659
Temperature effects of heterogenizated annealing on structure and properties of V95 aluminum alloy
13 p2025 N85-22692
Estimate of fatigue stability of gas-turbine engine compressor vanes in probabilistic aspect
14 p2287 N85-24169
Generation of marker lines on fatigue fracture surfaces 14 p2319 N85-24328
Possible use of rapid heating for improving mechanical properties of titanium alloys 15 p2496 N85-25409
Effect of annealing procedures on structure and properties of VT6 alloy with initial large-grained structure
15 p2496 N85-25410
Effect of aluminum on nature of titanium alloy failure
15 p2496 N85-25411
Effect of protective atmosphere composition on durability of welded joints of niobium alloys
15 p2502 N85-25432
Durability of Aramid reinforced aluminum laminate (ARALL)
[VTH-LR-423] 16 p2744 N85-26933
Documentation and solar cell modules
[NASA-CR-175769] 16 p2818 N85-27384
Properties of polyethylene gas piping materials
[PB85-187045] 18 p3082 N85-29088
Effect of thermochemical processing on fatigue resistance of titanium alloys 19 p3244 N85-30112
Effect of heating temperature in a vacuum on state of surface layers of welded OT4 titanium alloy
19 p3245 N85-30123
Vacuum pressure welding of commercial titanium with 2Kh13 and 12Kh18N10T steels
19 p3246 N85-30124
Computational methods in advanced stress and durability analyses
[AD-A154119] 19 p3286 N85-30375
Durability of reinforced hard-alloy draw plates
[BLL-M-36278-(5828.4)] 20 p3465 N85-31528
Thin-film reliability and engineering overview
21 p3612 N85-32450
Durability of oxygen sensors
[PB85-183093] 22 p3789 N85-33477

DURATION
U TIME

DURENE
Mononitration of durene
[NASA-TM-77774] 06 p0765 N85-14892

DUST
NT COSMIC DUST
NT INTERPLANETARY DUST
NT ZODIACAL DUST
Dust properties determined from backscattering in the interplanetary and interstellar medium
03 p0446 N85-12638
A method of making the gas-electric removal of highly dispersed particles more effective
[BLL-M-36030-(5828.4)] 06 p0765 N85-14880
Antisoiling technology: Theories of surface soiling and performance of antisoiling surface coatings
[NASA-CR-174274] 07 p0991 N85-16258
Interaction of large meteoroids with the atmosphere
11 p1656 N85-20431
Theoretical and experimental investigations of dust loaded flow fields in industrial halls
[BMFT-FB-HA-84-044] 12 p1819 N85-21411
Seasonal and secular variation of the Solis Lacus albedo feature: Relation to the Martian dust-transport cycle
13 p2186 N85-23576
Transformation of polar ice sublimate residue into Martian circumpolar sand 13 p2189 N85-23580
Near-nucleus studies of Comet Halley
14 p2436 N85-25018
Research on atmospheric dust formations using satellite observation data 15 p2485 N85-25329
Skywave radar detectability of volcanic aerosols
[AD-A151448] 15 p2542 N85-25894
The behavior of the atmosphere in the desert planetary boundary layer
[AD-A151286] 15 p2592 N85-25977
Multivalued electrostatic potentials; chance or necessity for the charge of solid particles near Saturn?
15 p2677 N85-26629
The gravito-electrodynamics of charged dust in planetary ring systems 15 p2677 N85-26631
Program RNTHR/2: An HP-41 C program for the calculation of RaA, RaB, and RaC concentrations in air based on three measurements of an air-dust sample
[IRI-190-83-10] 18 p3134 N85-29412
Technical guide for estimating fugitive dust impacts from coal handling operations, volume 2
[DE85-010939] 19 p3309 N85-30514
Technical guide for estimating fugitive dust impacts from coal handling operations. Volume 1: Project summary
[DE85-010948] 19 p3309 N85-30515
Ice-forming efficiency of the soluble and insoluble portions of dust contained in snow
21 p3643 N85-32831
Sahara Desert dust transport to the south
21 p3648 N85-32866
Distinctions in formation of microflora on construction materials used in habitable pressurized compartments
22 p3823 N85-33683

DUST COLLECTORS
A Mars dust sample return mission
[CNES-CT/PMF/APS/EMS-177]
04 p0459 N85-12915

Acoustic agglomeration methods and apparatus
[NASA-CASE-NPO-15466-1] 12 p1927 N85-22104
DUST STORMS
A Mars dust sample return mission
[CNES-CT/PMF/APS/EMS-177] 04 p0459 N85-12915
Observed changes at Viking Lander 1
13 p2186 N85-23575
Seasonal and secular variation of the Solis Lacus albedo feature: Relation to the Martian dust-transport cycle
13 p2188 N85-23576
The origin of regional dust deposits on Mars
13 p2188 N85-23578
Dust devils on Mars 15 p2663 N85-26573
The influence of global dust storms on the mean seasonal daily insolations at the Martian surface
[AERONOMICA-ACTA-A-289-1984] 18 p3203 N85-29868
Hadley circulation in planetary atmospheres
20 p3546 N85-32067
DWARF NOVAE
Combined ultraviolet studies of astronomical sources
[NASA-CR-174361] 09 p1413 N85-18910
FP Cygni profiles in HL CMa
11 p1752 N85-21022
Photoelectric observations of the dwarf nova VW Hydri during the November 1977 supermaximum
[REPT-97] 15 p2667 N85-26461
Winds in cataclysmic variable stars
[DE85-006706] 15 p2669 N85-26470
DWARF STARS
NT DWARF NOVAE
NT FLARE STARS
NT RED DWARF STARS
NT SUBDWARF STARS
NT WHITE DWARF STARS
Simultaneous photometry and radial velocities of dwarf cepheids and Delta Scuti stars
01 p0126 N85-10678
A spectroscopic survey of 113 nearby red dwarf stars
01 p0129 N85-10686
Detection of narrow C 4 and Si 4 absorption features in spectra of stars within 200 pc f the Sun
06 p0676 N85-15564
Theoretical studies of chromospheres and winds in cool stars
[NASA-CR-174204] 06 p0680 N85-15596
Evidence for non-radiative activity in stars with T sub eff 10000 K 08 p1231 N85-17757
Theory tested by means of the stars — viability of the alpha-omega dynamo model 08 p1233 N85-17770
Stellar granulation 14 p2451 N85-25132
DWELL
An investigation of elevated temperature fatigue crack initiation in 2 and 1/4 cR-1 MO low alloy steel
[AD-A150670] 14 p2255 N85-23973
DYE LASERS
Manual for Raman cells
[NASA-TM-77756] 01 p0052 N85-10342
A high resolution spectroscopic study of the oxygen molecule
[NASA-CR-174061] 02 p0172 N85-11150
Multifrequency lidar based on dye laser
02 p0262 N85-11715
Narrowband tunable dye laser with amplifier pumped by powerful nitrogen laser 02 p0262 N85-11716
Study in molecular lasers
[AD-A148246] 08 p1166 N85-17357
Influence of structure of thiopyrilocyanic dyes on output characteristics of passive mode-locked laser
11 p1717 N85-20801
Investigation of dye lasers pumped by high-power KrF laser radiation 11 p1718 N85-20806
Chemical stabilization of laser dyes
[AD-A150451] 13 p2096 N85-23076
Elementary processes of electronically excited particles. Part 8: Deactivation of CHF (A1a' (O, V'2, O) after excitation by a pulsed dye laser
[MPIS-13/1984] 14 p2420 N85-24930
Experimental report on a fiber optic light guide made by Galileo Electro-Optics Corporation
[DE85-008161] 14 p2421 N85-24941
Linewidth and bandwidth measurements of the q-branch of H2 using CW coherent anti-Stokes Raman spectroscopy
[AD-A151668] 15 p2506 N85-25456
Electric discharge excitation and energy source integration
[AD-A151502] 15 p2562 N85-25808
Raman studies of surface temperature in laser-heated semiconductors
[AD-A151377] 15 p2650 N85-26412
A study of mode-locked argon ion-dye laser systems
16 p2769 N85-27205
Study on a prismatic dye vat — laser systems
[CERT-2/6124-04-RO] 16 p2791 N85-27217
Intense excitation source for high power laser
[AD-A153424] 18 p3112 N85-29267
Intense ion beam diode diagnostics using a tunable dye laser
[DE85-008079] 18 p3113 N85-29272
Measurement of radical species concentrations and polycyclic aromatic hydrocarbons in flames by fluorescence and absorption using a tunable dye laser
[DE85-008624] 18 p3113 N85-29274
Dye laser traveling wave amplifier
[NASA-CR-175989] 19 p3275 N85-30308
Instrumentation for particle-beams research using excited merging beams
[AD-A154155] 19 p3356 N85-30807
Spectral evolution of the pulse of a dual frequency dye laser
[CNES-83/168/T/CT/DRT/TIT/10]
20 p3461 N85-31497
Lasing on LiF:F(-)2 - dye centers with transverse pumping 21 p3684 N85-32890
Dynamics of emission from dye lasers employing synchronous pumping by limited picosecond pulse train
21 p3686 N85-32899
High-power two-frequency CW dye laser
21 p3686 N85-32900
Self Q-modulation and generation of short pulses in distributed-feedback lasers 21 p3687 N85-32907
Doppler spectrometer for measuring narrow photochemical gaps in inhomogeneously broadened spectra 21 p3689 N85-32921
Pulsed lasers for filming color holographic film images
22 p3781 N85-33426
Picosecond-pulse damage studies of diffraction gratings
[DE85-010785] 22 p3790 N85-33481
Fiber optics interface for a dye laser oscillator and method
[DE85-005765] 23 p3973 N85-34633
Infrared generation and wave-mixing studies in cesium
[DE85-012883] 24 p4083 N85-35304
DYES
NT METHYLENE BLUE
NT THIAZINE (TRADEMARK)
Efficiency of lasing dye media in pumping high-power radiation with nanosecond pulses
02 p0270 N85-11763
Fluorescent dyes for luminescent solar concentrators
[BMFT-FB-T-84-164] 04 p0480 N85-13061
Influence of structure of thiopyrilocyanic dyes on output characteristics of passive mode-locked laser
11 p1717 N85-20801
Investigation of dye lasers pumped by high-power KrF laser radiation 11 p1718 N85-20806
Spontaneous diffraction of sequence of supershort light pulses in dye solution 11 p1718 N85-20811
Practical surface methods 14 p2316 N85-24314
Comparison of a diffusion model with dye dispersion measurements to study turbulence in coastal waters
[INPE-3492-PRE/729] 16 p2838 N85-27504
The production of copper phthalocyanine and/or its derivatives
[NASA-TM-77629] 17 p2917 N85-27983
Chromophores with auxochrome-like function
[NASA-TM-77849] 20 p3421 N85-31233
Lasing on LiF:F(-)2 - dye centers with transverse pumping 21 p3684 N85-32890
Choice of optimum saturating absorber for YAG passive mode-locking laser 21 p3685 N85-32893
DYNAMIC CHARACTERISTICS
NT AERODYNAMIC DRAG
NT AERODYNAMIC STABILITY
NT AIRCRAFT STABILITY
NT ATTITUDE STABILITY
NT BOUNDARY LAYER STABILITY
NT COMBUSTION STABILITY
NT CONTROL STABILITY
NT DIRECTIONAL STABILITY
NT DRAG
NT DYNAMIC PRESSURE
NT DYNAMIC STABILITY
NT FLAME STABILITY
NT FLOW CHARACTERISTICS
NT FLOW DISTRIBUTION
NT FLOW STABILITY
NT FLOW VELOCITY
NT FREQUENCY STABILITY
NT FRICTION DRAG
NT GYROSCOPIC STABILITY
NT INTERFERENCE DRAG
NT INTERFERENCE LIFT
NT LATERAL STABILITY
NT LIFT
NT LONGITUDINAL STABILITY
NT LOW SPEED STABILITY
NT MAGNETOHYDRODYNAMIC STABILITY
NT MOTION STABILITY
NT ROTARY STABILITY
NT SATELLITE DRAG
NT SPACECRAFT STABILITY
NT TRANSIENT RESPONSE
NT VISCOUS DRAG
NT WAVE DRAG
NT WEIBEL INSTABILITY
NT ZERO LIFT
Structural analysis of the Space Shuttle Orbiter
01 p0061 N85-10401
Determination of the input-output characteristics of time-invarient memoryless nonlinear devices
[FUB-41-1983] 01 p0100 N85-10667
Singular perturbations, coherency and aggregation of dynamic systems
[DE84-014166] 01 p0114 N85-10772
High temperature static strain sensor development program 02 p0141 N85-10959
Control of lateral conjectory motion of spacecraft in atmosphere 02 p0160 N85-11085
Transfer function of multilayered magnetooptical space-time modulator 02 p0264 N85-11726
Static and dynamic characteristics of materials with beam-microstructure 03 p0370 N85-12361
Dynamic shear failure of shallow-buried flat-roofed reinforced concrete structures subjected to blast loading
[AD-A145974] 03 p0373 N85-12378
Analysis of dynamic characteristics and ways of development of bipolar main memory with miniaturization of integrated circuit elements 04 p0490 N85-13123
Hydrodynamic impeller stiffness, damping, and inertia in the rotordynamics of centrifugal flow pumps
05 p0643 N85-14125
Does McKuer's law hold for heart rate control via biofeedback display? 05 p0706 N85-14528
Power of deterministic thinking in machine tool accuracy
[DE85-001751] 07 p0974 N85-16188
Ice dynamics
[AD-A147376] 07 p0986 N85-16278
Prediction of dynamic stall characteristics using advanced non-linear panel methods
[AD-A148453] 08 p1078 N85-16836
Low cost gyrocompass
[AD-A148295] 08 p1082 N85-16857
Applications of molecular dynamics to the study of shock-induced chemistry
[AD-A148017] 08 p1121 N85-17066
International Conference on Luminescence
[AD-A148470] 08 p1223 N85-17701
The dynamic interaction between track and soil
[AD-P004274] 09 p1406 N85-18850
The research of driving wheel with movable lugs of the paddy field floating tractor
[AD-P004283] 09 p1407 N85-18860
The analysis on the dynamic performance of a single lug
[AD-P004289] 09 p1408 N85-18866
A tracked vehicle test plant for the simulation of dynamic operation
[AD-P004305] 09 p1410 N85-18882
Integrated Technology Rotor/Flight Research Rotor (ITR/FRR) concept definition
[NASA-CR-166445] 10 p1423 N85-18979
Oscillator development
[AD-A149699] 12 p1834 N85-21509
State-selected ion-molecule reaction dynamics
[AD-A150068] 12 p1926 N85-22115
Dynamics of space charge waves in the laser beat wave accelerator
[AD-A149688] 12 p1936 N85-22163
Dynamics of elliptical galaxies and the r sup 1/4 luminosity law 12 p1955 N85-22282
Comparison of dynamic-tension and constant-load strength characteristics of heat-resistant materials
13 p2030 N85-22722
A parmetric study of crater-saturation simulation
13 p2182 N85-23540
Solar Array Experiment (SAE) flight experience
14 p2236 N85-23861
Determining characteristics of optical radiation reflectors based on results of remote sensing
15 p2483 N85-25358
Dynamic characteristics of ac arc in welding aluminum alloys 15 p2500 N85-25424
Investigation of potential and viscous flow effects contributing to dynamic stall
[AD-A151696] 15 p2557 N85-25773
Ritz procedure for COSMIC/NASTRAN
15 p2575 N85-25877
Active control landing gear for ground loads alleviation
16 p2714 N85-26749
Rotordynamics 16 p2737 N85-26886
LFMR definition study
[AD-A153691] 18 p3090 N85-29126

Operation guiding light-scientific program and field plan. The pilot field experiment for NORDA project chemical dynamics in ocean frontal areas
[AD-A153765] 18 p3150 N85-29507
One- and two-electron transfer processes in ion-surface scattering
[AD-A154208] 19 p3353 N85-30782
Design of helicopter rotor blades for optimum dynamic characteristics
[NASA-CR-176076] 20 p3393 N85-31044
Flight-mechanics test with a restricted flying aircraft model in a wind tunnel
[ESA-TT-865] 20 p3394 N85-31053
Dynamic performance of several large antenna concepts 20 p3409 N85-31155
Space station configuration and flight dynamics identification 20 p3410 N85-31162
Sub-optimal control of nonlinear flexible space structures 20 p3414 N85-31190
Frequency domain control design of large space structures: A practical approach
20 p3415 N85-31192
Design of a physical model of the cochlea. Displacement sensor for small amplitudes in a highly viscous liquid
[STN-6] 20 p3507 N85-31802
Dynamic fracture behavior of structural materials
[AD-A154566] 21 p3598 N85-32345
The dynamics of slack marine cables
[AD-A155022] 21 p3599 N85-32349
Ductile fracture of dynamically loaded naval structures-compact tension specimen tests and analyses
[AD-A155472] 21 p3600 N85-32353
Hydrographic data from the OPTOMA (Ocean Prediction Through Observations, Modeling and Analysis) program: OPTOMA15, 24 January to 23 February 1985
[AD-A155012] 21 p3655 N85-32703
Analysis of flexible aircraft longitudinal dynamics and handling qualities. Volume 1: Analysis methods
[NASA-CR-177943-VOL-1] 24 p4066 N85-35202
Analysis of flexible aircraft longitudinal dynamics and handling qualities. Volume 2: Data
[NASA-CR-177943-VOL-2] 24 p4067 N85-35203
A new drawing technique for nylon 6 by reversible plasticization with iodine
[AD-A156272] 24 p4162 N85-35803

DYNAMIC CONTROL
Qualitative results for distributed systems with discrete damping and stiffness with application to control
[AD-A145525] 02 p0209 N85-11362
Experiments in control of flexible structures with uncertain parameters 05 p0602 N85-13837
Review of technical papers, appendix H
05 p0603 N85-13846
Dynamics and controls working group summary
05 p0604 N85-13854
Efficiency of programmed motion control systems
06 p0776 N85-14961
Aileron effectiveness for a subsonic transport model with a high-aspect-ratio supercritical wing
[NASA-TM-85674] 07 p0888 N85-15695
Power of deterministic thinking in machine tool accuracy
[DE85-001751] 07 p0974 N85-16186
The development of a microprocessor-controlled linearly-actuated valve assembly
[NASA-CR-174437] 10 p1491 N85-19415
Automatic speech recognition in severe environments
[PB85-121697] 12 p1830 N85-21480
Alternatives for jet engine control
[NASA-CR-175831] 16 p2709 N85-26713
Alternatives for jet engine control
[NASA-CR-175832] 16 p2709 N85-26714
Alternatives for jet engine control
[NASA-CR-175833] 16 p2709 N85-26715
A perspective on superaugmented flight control advantages and problems 16 p2712 N85-26733
The investigation of tethered satellite system dynamics
[NASA-CR-175866] 16 p2731 N85-26854
Dynamic considerations for control of closed life support systems 18 p3156 N85-29537
Dynamics and control of tethers in elliptical orbits
20 p3399 N85-31087
Experimental verification of identification algorithms for control of flexible structures 20 p3418 N85-31211
Numerical experimentation with maximum likelihood identification in static distributed systems
20 p3418 N85-31214
Bayesian vs MAP multiple model adaptive estimation for field of view expansion in tracking airborne targets
[AD-A155466] 21 p3679 N85-32855
Design of dynamic compensators of prescribed pattern
[BU-109] 24 p4142 N85-35674
Spreading the control complexity in decentralized control of interconnected systems
[BU-117] 24 p4144 N85-35688
Decentralized stabilization by high gain feedback
[BU-115] 24 p4144 N85-35689

DYNAMIC LOADS
NT AERODYNAMIC LOADS
NT BLAST LOADS
NT CYCLIC LOADS
NT GUST LOADS
NT IMPACT LOADS
NT LANDING LOADS
NT ROLLING CONTACT LOADS
NT SHOCK LOADS
NT THRUST LOADS
NT TRANSIENT LOADS
NT VIBRATORY LOADS
NT WING LOADING
Theoretical analysis of the dynamic behavior of structures with a passenger car as example
05 p0649 N85-14170
Characterization of fiber optic cables under large tensile loads
[DE84-016816] 05 p0651 N85-14180
Evaluation of operational loads to verify structural design 07 p0896 N85-15677
TUTOR (CL-41A) tail flight load survey
07 p0896 N85-15678
Tornado: Structural Usage Monitoring System (SUMS) 07 p0896 N85-15680
Flight parameters recording for structure fatigue life monitoring 07 p0896 N85-15682
USAF approach to airborne structural data recording: Airborne Data Acquisition Multifunction System (ADAMS)
07 p0897 N85-15683
Bearing tester fit analysis
[NASA-CR-171282] 07 p0973 N85-16181
Improvements in linked-spar motion-compensated lifting system
[AD-D011413] 08 p1138 N85-17165
The response of metallic structures to dynamic loading 08 p1172 N85-17389
Response of saturated porous nonlinear materials to dynamic loadings
[AD-A148528] 08 p1173 N85-17394
A discussion of problems encountered in the dynamic fracture toughness testing of materials
[OUEL-1524/84] 08 p1173 N85-17397
Some dynamical aspects of Army missile systems
09 p1333 N85-18380
Effect of coupled torsional-flexural vibration of a geared shaft system on the dynamic tooth load
09 p1338 N85-18415
Vibrational loading mechanism of unitized corrugated containers with cushions and non-load-bearing contents
09 p1339 N85-18419
A tracked vehicle test plant for the simulation of dynamic operation
[AD-P004305] 09 p1410 N85-18882
Analytically redundant output feedback scheme for reduction of structural loads of a flexible transport aircraft
[TT-8303] 12 p1777 N85-21154
Wavecode constitutive models: Nonhomogeneous mixtures
[DE85-000836] 12 p1796 N85-21278
Computer analysis of wind turbine blade dynamic loads
[DE85-000530] 12 p1867 N85-21714
Using NASTRAN to model missile inertia loads
15 p2576 N85-25886
Dynamic crack curving and branching under biaxial loading
[AD-A151451] 15 p2578 N85-25904
An assessment of the suitability of the BHGA structural test rig for aerodynamic testing of hang gliders
[CA-8506] 17 p2896 N85-27853
Critical conditions for failure in materials subjected to high rates of loading
[AD-A153135] 17 p2960 N85-28420
Expedient runway surfacing with post tensioning system for expeditionary airfields
[AD-D011677] 19 p3222 N85-29976
SHAPS-2: A three-dimensional computer program for linear/non-linear, static/dynamic analyses of piping systems
[DE85-010500] 19 p3395 N85-30656
Load transfer by analytical methods
[SNIAS-851-111-109] 20 p3470 N85-31561
In-situ measurement of wall thermal performance: Data interpretation and apparatus design recommendations
[DE85-011979] 21 p3586 N85-32269
The dynamics of slack marine cables
[AD-A155022] 21 p3599 N85-32349
Shock and release equation of state of calcite
[DE85-013151] 23 p3942 N85-34432

DYNAMIC MODELS
Analysis strategies for field dependent estimation and network design — mesoscale modeling
01 p0078 N85-105
Application of automatic pattern methods in very-short-range forecasting 01 p0078 N85-105
The development of objective forecast techniques based on advection of surface weather parameters
01 p0078 N85-105
Predicability of mesoscale phenomena
01 p0079 N85-105
The initialization of mesoscale models
01 p0079 N85-105
Applications of a finite-element regional model to very-short-range forecasting 01 p0080 N85-105
Application of mesoscale numerical model to local weather prediction 01 p0080 N85-105
The United Kingdom Meteorological Office mesoscale forecasting system 01 p0080 N85-105
A local dynamical interpretation method of numerical weather forecasting 01 p0080 N85-105
An operational numerical model for prediction of fog and stratus 01 p0080 N85-105
A 1-dimensional model with a sub-grid scale condensation scheme for stratiform clouds and fog
01 p0080 N85-105
A one-level mesoscale model suitable for nowcasting and short-term forecasting in regions of complex terrain
01 p0081 N85-10541
Development of an operational system for Very-Short-Range Forecasting (VSRF) at Swedish Meteorological and Hydrological Institute (SMHI)
01 p0083 N85-105
The structure of the Uranian rings and the search for rings around Neptune 02 p0302 N85-119
Dynamics of the Uranian rings
02 p0302 N85-119
A model for the propagation of the westward traveling surge
[TRITA-EPP-84-03] 03 p0393 N85-12515
Modeling of aircraft cabin fires
[NBS-GCR-84-473] 04 p0454 N85-12
Users manual for a computer program for dynamic response analysis of bladed systems
[UDR-TR-84-38] 04 p0456 N85-12
Superconducting magnet for probing eddy currents in dynamic models 04 p0489 N85-13117
Quark models of hadronic interactions
[DE84-013787] 04 p0561 N85-135
Satellite attitude determination
05 p0599 N85-138
Analytical modeling of circuit aerodynamics in the new NASA Lewis wind tunnel
[NASA-TM-86912] 07 p0897 N85-15
Dynamical characteristics of weak turbulence
[AD-A147186] 07 p0959 N85-16
Combustion dynamics in rockets
[AD-A148478] 08 p1114 N85-170
Rapid solidification processing and powder metallurgy of Al alloys
[AD-A148427] 08 p1130 N85-171
The development of a dynamic model of a generalized combat aircraft with forward wings for the identification of stability and control characteristics
[CAR-84-33] 09 p1280 N85-18
The optimal control and design of a flexible manipulator arm 09 p1327 N85-18
Reanalysis of continuous dynamic systems with continuous modifications 09 p1337 N85-18411
A one dimensional dynamical model of ocean/atmosphere interactions
09 p1358 N85-18
Condensed antenna structural models for dynamics analysis 10 p1463 N85-19
Experimental determination of systems suitable for study as monotectic binary metallic alloy solidification models
12 p1948 N85-22
Dynamic stochastic model of long-period variability of ocean surface temperature 14 p2334 N85-24
Considering zonal wind in semidiurnal tide problem
14 p2335 N85-24
Electrodynamics of magnetosphere-ionosphere coupling 14 p2359 N85-24
On the dynamics of the westward traveling surge
14 p2364 N85-24
Observations, theoretical ideas and modeling of turbulent flows: Past, present and future
[NASA-TM-86679] 16 p2782 N85-27
Dynamic models of flux tubes in the interpretation of polarization measurements 16 p3206 N85-28
Three-dimensional finite element impact analysis of a nuclear waste truck cask
[DE85-010653] 19 p3286 N85-
Use of adjoint equations in problems of evaluating state of random hydrodynamic fields
19 p3289 N85-

Space station dynamic modeling, disturbance accommodation, and adaptive control
20 p3409 N85-31154
Antenna pointing of large flexible telecommunications spacecraft 20 p3409 N85-31156
An overview of latest model reduction and control methods of large flexible space structures
20 p3414 N85-31191
An examination of the Southern Oscillation in the upper tropospheric tropical and subtropical wind field
20 p3486 N85-31680
Mechanics of a gaseous film barrier to lubricant wetting of elastohydrodynamically lubricated conjunctions
[NASA-TP-2500] 21 p3595 N85-32330
Development of improved dynamic failure models
[AD-A155586] 21 p3600 N85-32354
Numerical modeling of sea ice dynamics and ice thickness characteristics
[AD-A154800] 21 p3654 N85-32700
Space robot simulator vehicle
[NASA-CR-176133] 22 p3739 N85-33176

DYNAMIC MODULUS OF ELASTICITY
Elastic dispersion effects on dynamics and control of large modular antennas — spacecraft antennas
05 p0627 N85-14019

DYNAMIC PRESSURE
The gulf stream deflection and meander energetics experiment. Current meter and bottom pressure gauge data report for the September, 1981 to April, 1982 mooring period
[AD-A144977] 01 p0088 N85-10595
One-year records of current and bottom pressure in the strait between Nordaustlandet and Kvitoeya and Svalbard, 1980 - 1981
[AD-A145594] 02 p0233 N85-11518
A study of wear characteristics due to pressure for hydraulic fixed displacement vane pumps
[AD-A146023] 06 p0814 N85-15169
Dynamic pressure test unit-ratio method
[AD-D011466] 10 p1488 N85-19392
TMX-U neutral pressure measurement diagnostic systems
[DE85-000746] 11 p1730 N85-20881
Strain rate sensitivity estimation from high velocity impact data
[AD-A154703] 21 p3599 N85-32347
Development of a temperature-compensated hot-film anemometer system for boundary-layer transition detection on high-performance aircraft
[NASA-TM-86732] 22 p3730 N85-33121
Pressure-shear loading of PBX-9404
[DE85-009982] 23 p3921 N85-34298

DYNAMIC PROGRAMMING
Dynamic decision making — and programming
[FOA-C-53015-H2] 04 p0575 N85-13668
Programs for dynamic loading of precompiled subroutine packages, especially for applications with the Watfiv compiler
[DFVLR-MITT-84-18] 12 p1917 N85-22035
Normal mode calculations for fuselage type intricate structures by regarding them as systems with superposed constraints 13 p2048 N85-22817
A dynamic programming approach to time-staged convex programs
[DE85-010616] 19 p3340 N85-30700

DYNAMIC PROPERTIES
U DYNAMIC CHARACTERISTICS

DYNAMIC RESPONSE
NT TRANSIENT RESPONSE
Rotordynamic analysis of the SSME turbopumps using reduced models
[NASA-CR-171170] 01 p0054 N85-10355
Nonlinear dynamic analysis of sandwich panels
01 p0060 N85-10394
Non-Gaussian approach for parametric random vibration of non-linear structures 01 p0060 N85-10395
Response and characteristics of structures subjected to SH waves 01 p0060 N85-10396
The Shock and Vibration Digest, volume 16, no. 8
[AD-A145653] 02 p0208 N85-11372
Hardware and software selection for experimental modal analysis 02 p0208 N85-11373
Analysis of turbomachine blades: A review
02 p0208 N85-11374
Basic study of bladed disk structural response
[AD-A146226] 03 p0319 N85-12061
Users manual for a computer program for dynamic response analysis of bladed systems
[UDR-TR-84-39] 04 p0456 N85-12893
Bulletin of the Faculty of Engineering, Hokkaido University, no. 123
[ISSN-0385-602-X] 04 p0482 N85-13075
Estimation of dynamic stresses around the shot point in scale model experiment 04 p0482 N85-13076
Mathematical modeling of assembly processes involving use of sensitized robots 04 p0488 N85-13111
NIKE3D: An implicit, finite-deformation, finite element code for analyzing the static and dynamic response of three-dimensional solids, revision 1
[DE84-017161] 04 p0614 N85-13277
Dynamic stiffness characteristics of high eccentricity ratio bearings and seals by perturbation testing
05 p0645 N85-14141
Effects of control stick parameters on human controller response 05 p0701 N85-14496
Does McKuer's law hold for heart rate control via biofeedback display? 05 p0706 N85-14526
An analysis of kinetic response variability
05 p0707 N85-14533
Dynamic response of electromagnetic current meters
[PB84-229731] 06 p0842 N85-15344
Flutter control with unsteady aerodynamic models
[AD-A147858] 07 p0909 N85-15753
The investigation of tethered satellite system dynamics
[NASA-CR-171278] 07 p0912 N85-15772
Sensitivity tests for solid propellants in Germany
08 p1115 N85-17028
Transient combustion: An important consideration in deflagration-to-detonation transition
08 p1116 N85-17037
Computational methods for nonlinear dynamics problems in solid and structural mechanics
[AD-A148352] 08 p1172 N85-17392
An investigation of spinal injury potential from the use of the ACES 2 ejection seat by lower weight female pilots
[AD-A148449] 08 p1196 N85-17537
Theoretical investigation of dynamic stall using a momentum integral method
[AD-P004170] 09 p1266 N85-17955
Nonlinear analysis of composite laminates
09 p1288 N85-18087
Investigation of the pressure-and velocity-coupled responses of solid propellants using impedance tube method 09 p1300 N85-18168
Pressure measurements in a hydrogen combustion environment: An evaluation of 3 pressure transducers
[TI85-003645] 09 p1323 N85-18312
Modelling and identification of the structural properties of an astromast
[CRC-1374] 09 p1329 N85-18352
Design oriented identification of critical points in transient response 09 p1330 N85-18357
Treatment of general boundary conditions and point-wise state variable constraints in optimum design for static and dynamic response
09 p1330 N85-18358
Keynote address 09 p1333 N85-18378
Elias Klein memorial lecture: Modal testing, a critical review 09 p1334 N85-18383
Least favorable response of inelastic structures
09 p1336 N85-18398
Models for shock damage to marine structural materials 09 p1336 N85-18400
The Shock and Vibration Bulletin 54. Part 3: Structural dynamics, machinery dynamics and vibration problems
[AD-A148133] 09 p1337 N85-18406
Modal analysis of structural systems involving nonlinear coupling 09 p1337 N85-18409
Reanalysis of continuous dynamic systems with continuous modifications 09 p1337 N85-18411
Precision measurement of torsional oscillations induced by gear errors 09 p1338 N85-18416
Dynamic simulation of track laying vehicles
[AD-P004266] 09 p1405 N85-18842
Designing off-road vehicles with good ride behaviour
[AD-P004267] 09 p1405 N85-18843
Operational fitness of box truss antennas in response to dynamic slewing
[NASA-CR-172470] 10 p1429 N85-19012
Response of earth-covered slabs in clay and sand backfills
[AD-A149296] 11 p1615 N85-20157
Multiaxial stress response of ceramics
[DE85-004350] 12 p1814 N85-21379
Method of designing digital band-pass filters with infinite memory 12 p1840 N85-21546
Symmetric primal-dual variational formulations of coupled dynamic systems: Three-dimensional elasticity, shells, fluid-structure interaction
[ONERA-1983-91] 12 p1863 N85-21684
The effect of an elastic foundation and of dissipative forces on the stability of fluid conveying pipes
[TAE-563] 12 p1863 N85-21688
Structural sensitivity analysis: Methods, applications and needs
[NASA-TM-86827] 12 p1865 N85-21695
Time marching numerical solution of the dynamic response of nonlinear systems
[NAF-AN-25] 12 p1866 N85-21698
A solution method for nonlinear dynamic analysis of shell structures
[AD-A149846] 12 p1868 N85-21708
Intraband radiometric performance of the LANDSAT 4 Thematic Mapper — Washington, DC, Arkansas, Massachusetts, Virginia, and Arizona
12 p1871 N85-21738
Vibroacoustic study of the NASA Goddard Space Flight Center OSS-1 payload
[NASA-CR-175320] 13 p1968 N85-22485
Use of importance sampling to investigate signal detection systems by simulated method
13 p2086 N85-23028
Noise immunity of information transmission system with pseudorandom frequency switching under worst-case interference conditions 13 p2086 N85-23029
A research program in active control/aeroelasticity
[NASA-CR-175674] 14 p2218 N85-23752
Dynamic verification of large space structures
14 p2234 N85-23847
Control Of Flexible Structures (COFS) flight experiment background and description 14 p2236 N85-23864
Shuttle payload bay dynamic environments: Summary and conclusion report for STS flights 1-5 and 9
[NASA-CR-175656] 14 p2241 N85-23896
Study of dynamic characteristics of prefabricated gas turbine compressor rotor 14 p2272 N85-24076
Acoustic radiation from bilaminar plates
14 p2415 N85-24903
An experimental investigation into the dynamic response of a stiffened flat plate loaded impulsively by an underwater shockwave
[AD-A151321] 15 p2578 N85-25903
NASTRAN-based software for the structural dynamic analysis of vertical and horizontal axis wind turbines
[DE85-001712] 15 p2580 N85-25911
Mechanical stress regulation of plant growth and development 15 p2610 N85-26087
Ion sensor signal fluctuations during operation of spacecraft reaction engines 16 p2724 N85-26815
Proposal of a method for evaluating accuracy of estimated impulse response of a system
16 p2759 N85-27024
Dynamic response of fluid transmission lines
[AD-A151926] 16 p2782 N85-27171
An analytical investigation of dynamic coupling in nonlinear, geared rotor systems
16 p2792 N85-27218
Dynamic response of shells and plates subjected to variable magnitude traveling loads
16 p2796 N85-27250
Hopkinson bar simulation using DYNA2D
[DE85-006766] 16 p2802 N85-27275
Controller requirements for uncoupled aircraft motion, volume 1
[AD-A153173] 17 p2900 N85-27878
On the accuracy of modelling the dynamics of large space structures 19 p3225 N85-29995
The dynamics and control of large flexible space structures, 8
[NASA-CR-175986] 19 p3225 N85-29996
Underwater shock-induced responses of stiffened flat plates: An investigation into the predictive capabilities of the USA-STAGS code
[AD-A154245] 19 p3286 N85-30377
Forced structural response using component mode synthesis
[DE85-008479] 19 p3287 N85-30383
Flight-mechanics test with a restricted flying aircraft model in a wind tunnel
[ESA-TT-885] 20 p3394 N85-31053
A modal parameter extraction procedure applicable to linear time-invariant dynamic systems
[NASA-CR-176120] 22 p3835 N85-33747
Automated dynamic analytical model improvement for damped structures
[NASA-CR-177945] 23 p3941 N85-34425
A multi-touch three dimensional touch-sensitive tablet (executive summary) 23 p3961 N85-34553
The investigation of tethered satellite system dynamics
[NASA-CR-176180] 24 p4069 N85-35215

DYNAMIC STABILITY
NT AERODYNAMIC STABILITY
NT AIRCRAFT STABILITY
NT ATTITUDE STABILITY
NT BOUNDARY LAYER STABILITY
NT COMBUSTION STABILITY
NT CONTROL STABILITY
NT DIRECTIONAL STABILITY
NT FLAME STABILITY
NT FLOW STABILITY
NT FREQUENCY STABILITY
NT GYROSCOPIC STABILITY
NT LATERAL STABILITY
NT LONGITUDINAL STABILITY

NT LOW SPEED STABILITY
NT MAGNETOHYDRODYNAMIC STABILITY
NT MOTION STABILITY
NT ROTARY STABILITY
NT SPACECRAFT STABILITY
NT WEIBEL INSTABILITY

Index cycles simulated by a low order forced barotropic model 07 p1002 N85-16364

Effect of scattering on instabilities in line-driven stellar winds 08 p1235 N85-17784

Optimum design and automated dynamic analysis of flexible mechanisms
[AD-A150152] 13 p2099 N85-23068

Bifurcation theory applied to aircraft motions
[NASA-TM-86704] 14 p2210 N85-23705

Adaptive techniques for control of large space structures
[AD-A150957] 14 p2246 N85-23923

Method of improving dynamic characteristics of DC voltage stabilizers with compound regulation
15 p2526 N85-25589

Effects of bearing deadbands on bearing loads and rotor stability 16 p2737 N85-26889

Solar array flight experiment
[NASA-TM-86506] 17 p2909 N85-27935

Dynamic stability of a spinning tube conveying a flowing fluid
[DE85-007583] 18 p3102 N85-29207

Newton's method as a dynamical system: Global convergence and predictability
[AD-A155170] 21 p3632 N85-32504

Experimental characterization and stability of salt- and nonsalt-containing grouts and mortars (BCT-1F- and BCT-1FF-related)
[DE85-012339] 22 p3753 N85-33263

DYNAMIC STRUCTURAL ANALYSIS

Helicopter rotor blade design for minimum vibration
[NASA-CR-3825] 01 p0006 N85-10032

The NBS tri-directional test facility
[PB84-217462] 01 p0051 N85-10334

Rotordynamic analysis of the SSME turbopumps using reduced models
[NASA-CR-171170] 01 p0054 N85-10355

Effect of penetrant on fatigue of aluminum alloy lap joints
[NLR-TR-82104-U] 01 p0056 N85-10373

Research in Structures and Dynamics, 1984
[NASA-CP-2335] 01 p0057 N85-10377

Augmented weak forms and element-by-element preconditioners: Efficient iterative strategies for structural finite elements. A preliminary study
01 p0058 N85-10384

Stress-derivative control of keystoning deformation in finite element codes 01 p0058 N85-10385

Interactive buckling of thin-walled structural components under static and dynamic loads
01 p0059 N85-10392

Initial postbuckling analysis of elastoplastic thin-shear structures 01 p0059 N85-10393

Nonlinear dynamic analysis of sandwich panels
01 p0060 N85-10394

Non-Gaussian approach for parametric random vibration of non-linear structures 01 p0060 N85-10395

Response and characteristics of structures subjected to S-H waves 01 p0060 N85-10396

Crashworthiness of light aircraft fuselage structures: A numerical and experimental investigation
01 p0060 N85-10399

Analysis of a transport fuselage section drop test
01 p0060 N85-10400

IAC user manual
[NASA-CR-175300] 01 p0102 N85-10677

A rigid body mechanism in structural dynamics
02 p0206 N85-11361

Aeroelastic stability analysis with interacting structural nonlinearities 02 p0207 N85-11364

Post buckling behavior of a circular rod constrained within a circular cylinder 02 p0207 N85-11365

A constitutive modeling technique based on a generalized rheological model to predict the response of materials 02 p0207 N85-11368

The Shock and Vibration Digest, volume 16, no. 8
[AD-A145653] 02 p0208 N85-11372

STARS: A general-purpose finite element computer program for analysis of engineering structures
[NASA-RP-1129] 02 p0209 N85-11376

Status and prospects of computational fluid dynamics for unsteady transonic viscous flows
[NASA-TM-86018] 03 p0315 N85-12037

Complex frequency analysis of damped thin-walled beams with open cross sections
03 p0371 N85-12366

Theoretical and experimental modal analysis of a rotor test rig — shipboard equipment
[AMTE(N)-TM-83079] 03 p0371 N85-12370

Refined modeling of reinforced concrete columns of seismic analysis
[PB84-234384] 04 p0484 N85-13089

Spacecraft structural acoustic studies: Development of structural acoustic design guides
[ESA-CR(P)-1916] 05 p0604 N85-13649

Elastic dispersion effects on dynamics and control of large modular antennas — spacecraft antennas
05 p0627 N85-14019

Study of structure control dynamic interaction for radio frequency antenna control systems — satellite antennas
05 p0627 N85-14020

Aeroelastic analysis and the identification of flight loads — Mirage 2000 aircraft 07 p0896 N85-15679

Shuttle structural dynamics characteristics: The analysis and verification 08 p1094 N85-16913

Keynote address 09 p1333 N85-18378

Some dynamical aspects of Army missile systems
09 p1333 N85-18380

Elias Klein memorial lecture: Modal testing, a critical review 09 p1334 N85-18383

Solutions to structural dynamics problems
09 p1334 N85-18384

Least favorable response of inelastic structures
09 p1336 N85-18398

The Shock and Vibration Bulletin 54. Part 3: Structural dynamics, machinery dynamics and vibration problems
[AD-A148133] 09 p1337 N85-18406

Discrete modifications to continuous dynamic structural systems 09 p1337 N85-18410

Reanalysis of continuous dynamic systems with continuous modifications 09 p1337 N85-18411

The UKIRT centre section structural investigation — United Kingdom Infrared Telescope (UKIRT)
[UKIRT-22] 09 p1414 N85-18920

The use of analytical models to interpret data properly
[ERS-E.341] 11 p1651 N85-20399

The use of analytical models to interpret measured data properly. 2. The application to modal analysis of structures 11 p1651 N85-20401

Dynamic investigations of a spherical tank structure filled with liquid using ANSYS three-dimensional fluid elements
[MBB-UR-E-737-83-O] 11 p1654 N85-20418

The effect of an elastic foundation and of dissipative forces on the stability of fluid conveying pipes
[TAE-563] 12 p1863 N85-21686

Structural sensitivity analysis: Methods, applications and needs
[NASA-TM-85827] 12 p1865 N85-21695

Deployment analysis of the Olympus Astromast and comparison with test measurements -- solar arrays
13 p2011 N85-22616

Investigation of dynamics of manipulator with elastic sections 13 p2046 N85-22819

Large Space Antenna Systems Technology, 1984
[NASA-CP-2368-PT-1] 14 p2229 N85-23813

Structural dynamics analysis 14 p2233 N85-23838

AFWAL space control technology program
14 p2233 N85-23839

Large Space Antenna Systems Technology, 1984
[NASA-CP-2368-PT-2] 14 p2233 N85-23840

On-orbit systems identification of flexible spacecraft Technol., 1984, Pt. 2 p 465-481
14 p2233 N85-23841

Dynamic verification of large space structures
14 p2234 N85-23847

Space Technology Experiments Platform (STEP) status: An in-space test facility 14 p2236 N85-23863

Seismic analysis of rotating mechanical systems
[PB85-149599] 14 p2311 N85-24307

Runstreams for using ASKA
[NIAST-84/27] 14 p2403 N85-24812

Modeling and control of large flexible structures, phase 1
[AD-A150736] 14 p2403 N85-24817

Experience with transonic unsteady aerodynamic calculations 15 p2458 N85-25176

Status and prospects of computational fluid dynamics for unsteady transonic flow 15 p2459 N85-25180

Numerical experiments on flexible spacecraft with the aid of the Dynamic Control and Analysis Package (DCAP)
[ESA-STM-229] 15 p2493 N85-25382

NASTRAN-based software for the structural dynamic analysis of vertical and horizontal axis wind turbines
[DE85-001712] 15 p2580 N85-25911

Estimation theory applied to improving dynamic structural models
[DE85-004148] 15 p2630 N85-26210

Impact of magnetic isolation on pointing system performance in the presence of structural flexibility
[NASA-CR-172481] 16 p2732 N85-26861

Technical overview structural dynamics
16 p2736 N85-26883

USSR report: Engineering and equipment
[JPRS-UEQ-84-006] 16 p2760 N85-27

Nonlinear equations for dynamics of pretwisted beams undergoing small strains and large rotations
[NASA-TP-2470] 16 p2799 N85-272

Wind energy technology program summary
[DE85-007349] 16 p2820 N85-278

On various Fourier series utilized for solution of structural mechanics problems
[VTH-LR-429] 16 p2856 N85-27815

Overview of structural response: Probabilistic structural analysis 17 p2912 N85-279

Probabilistic finite element development
17 p2913 N85-279

Dynamic creep buckling: Analysis of shell structures subjected to time-dependent mechanical and thermal loading 17 p2913 N85-279

Turbulence structure in the boundary layers of an oscillating airfoil
[AD-A153631] 18 p3059 N85-28

A natural modes formulation and modal identities for structures with linear viscous damping
[CRC-1382] 18 p3120 N85-2931

Spillover minimization: An approach for actuators and sensors placement in distributed parameter study
[INPE-3525-PRE/746] 19 p3272 N85-30

Structural dynamics modification of generalized beams using a local eigenvalue modification procedure
19 p3282 N85-30

Adaptive identification and control of structural dynamics systems using recursive lattice filters
[NASA-TP-2371] 20 p3407 N85-31142

AFWAL control technology programs
20 p3408 N85-31150

Proceedings of the Workshop on Identification and Control of Flexible Space Structures, volume 2
[NASA-CR-176052] 20 p3411 N85-31170

Vibration/libration interaction dynamics during the orbiter based deployment of flexible members
20 p3411 N85-31171

Design of multivariable controllers using the Integrated Analysis Capability (IAC) 20 p3412 N85-31172

A structural dynamics approach to the simulation of spacecraft control/structure interaction
20 p3412 N85-31173

Finite control in underdamped distributed parameter systems 20 p3412 N85-31176

An integrated control and minimum mass structural optimization algorithm for large space structures
20 p3413 N85-31183

ISAAC (Integrated Structural Analysis and Control) via continuum modeling and distributed frequency domain design techniques 20 p3414 N85-31185

Optimization of controlled structures
20 p3414 N85-31186

Parametric stiffness control of flexible structures
20 p3414 N85-31187

Vibrational stabilization of flexible structures
20 p3414 N85-31188

Optimal sensor locations for structural identification
20 p3417 N85-31209

SPAR improved structural-fluid dynamic analysis capability
[NASA-CR-171549] 20 p3454 N85-31449

Load transfer by analytical methods
[SNIAS-851-111-109] 20 p3470 N85-31561

Inertial analysis of the Charpy test
[OUEL-1571/85] 20 p3471 N85-31570

Dynamical study of flat plates by nonlinear elasticity theory
[STN-8] 20 p3471 N85-31572

User's guide for computer program CGFAG, Concrete General Flexure Analysis with Graphics
[AD-A155555] 21 p3570 N85-3220

Dynamic fracture behavior of structural materials
[AD-A154568] 21 p3598 N85-322

Structural dynamics model and response of the deployable reference configuration space station
[NASA-TM-86386] 22 p3799 N85-33

A substructure coupling procedure applicable to general linear time-invariant dynamic systems
[NASA-CR-176144] 22 p3800 N85-3354

Substructure coupling in the frequency domain
[NASA-CR-176140] 22 p3800 N85-3354

Negative flexural behavior of precase composite slabs with steel joint 23 p3904 N85-3418

Mechanical ratcheting behaviors of a steel pipe under combined cyclic axial load and internal pressure
23 p3904 N85-3418

Automated dynamic analytical model improvement for damped structures
[NASA-CR-177945] 23 p3941 N85-344

Structural analysis of imperfect three-legged truss columns for large space structures applications
24 p4100 N85-35

An evaluation of a class of practical optimization techniques for structural dynamics applications
[PB85-186708] 24 p4103 N85-35434
DYNAMIC TESTS
Measuring methods to determine the static and dynamic behavior of wind energy converters
05 p0668 N85-14297
Response of earth-covered slabs in clay and sand backfills
[AD-A149296] 11 p1615 N85-20157
Assessment of dynamic test methods for the measurement of fracture toughness --- steels
[OUEL-1561/85] 20 p3470 N85-31565
The Hopkinson pressure bar: An alternative to the instrumented pendulum for Charpy tests
[OUEL-1596/85] 20 p3471 N85-31569
Seat experiments for the full-scale transport aircraft controlled impact demonstration
[AD-A155024] 21 p3553 N85-32106
DYNAMICAL SYSTEMS
Control of rotordynamic instability in a typical gas turbine's power system 05 p0642 N85-14120
Multiloop manual control of dynamic systems
05 p0702 N85-14505
Four-fluid description of turbulent plasma focus dynamics
[IPF-84-4] 09 p1395 N85-18778
Robustness of discrete-time dynamical systems: Application to the multivariable digital control of combat aircraft
[ONERA-NT-1984-2] 11 p1585 N85-19986
Dynamical studies of molecular systems
[DE85-003053] 11 p1594 N85-20028
Stochastic runaway of dynamical systems
[IPP-6/244] 11 p1708 N85-20745
Solar array dynamical simulation for illumination and temperature variation 13 p2011 N85-22611
Parameter estimation in stochastic dynamic systems
14 p2395 N85-24754
Optimal control and optimization
14 p2395 N85-24755
System theoretic description of physical systems
[CWI-TRACT-3] 14 p2414 N85-24894
The dynamical behavior of the age-size-distribution of a cell population
[CWI-AM-R8414] 17 p2998 N85-28536
Dynamical systems and numerical integration
[CWI-AM-R8413] 17 p3022 N85-28695
Stability in dynamical systems
[DE85-006698] 17 p3034 N85-28766
Characterization of intermittency in chaotic systems
[PREPRINT-429] 18 p3173 N85-29669
Stochastic resonance in the Landau-Ginzburg equation
[PREPRINT-430] 18 p3175 N85-29685
Solar dynamic systems 20 p3443 N85-31374
On the multifractal nature of fully developed turbulence and chaotic systems
[PREPRINT-413] 20 p3455 N85-31458
Decentralized control of dynamically interconnected systems
[BU-111] 22 p3835 N85-33744
The investigation of tethered satellite system dynamics
[NASA-CR-176160] 24 p4069 N85-35215
Aspects of input signal design for order and parameter estimation in linear dynamical systems
[ER-83/05] 24 p4091 N85-35362
DYNAMICS
A mathematical simulation model of the CH-47B helicopter, volume 1
[NASA-TM-84351-VOL-1] 01 p0006 N85-10033
Images of the Earth's aurora and geocorona from the Dynamics Explorer Mission
[NASA-CR-175963] 18 p3136 N85-29423
DYNAMICS EXPLORER SATELLITES
NT DYNAMICS EXPLORER 1 SATELLITE
DYNAMICS EXPLORER 1 SATELLITE
A retarding ion mass spectrometer for the Dynamics Explorer-1
[NASA-CR-171568] 21 p3589 N85-32303
DYNAMO THEORY
Models of nonkeplerian accretion disks based on dynamo magnetic field: Application to Active Galactic Nuclei (AGN) 08 p1242 N85-17834
Nonlinear dynamos --- solar activity
14 p2447 N85-25106
The solar dynamo and the complex Lorenz equations
14 p2447 N85-25107
Kinematic dynamo theory for an arbitrary mean flow
14 p2448 N85-25108
The generation of magnetic fields by a flow with chaotic streamlines 14 p2451 N85-25135
Dynamo action of magnetostrophic waves --- solar atmosphere 14 p2451 N85-25136
Cyclic flows in the solar convection zone due to the dynamo reaction 14 p2451 N85-25137
Modeling 22-year solar activity cycle within framework of dynamo theory with allowance for primary field
15 p2477 N85-25288
Planetary Dynamos
[NASA-CR-176001] 21 p3679 N85-32857
Magnetic field generation in the cores of terrestrial bodies 22 p3859 N85-33894
DYNAMOMETERS
Water brake convertor: A simple device to convert mechanical energy into heat energy
[DE85-006021] 16 p2716 N85-26766
Regional circulation during testing on isokinetic dynamometer following 14-day bedrest
19 p3323 N85-30590
Durability of oxygen sensors
[PB85-183093] 22 p3789 N85-33477
DYNAMOS
U ROTATING GENERATORS

E

E GLASS
NT S GLASS
E LAYERS
U E REGION
E REGION
NT SPORADIC E LAYER
UBV photometry of E region standard stars of intermediate brightness 01 p0128 N85-10879
UBV photometry of E region stars: Some intercomparisons 01 p0128 N85-10880
Occurrences of the polar slant E condition (SEC) at Narssarssuaq, Godhavn, Thule 1982
03 p0393 N85-12514
Experience with proposed improvements of the International Reference Ionosphere (IRI)
[PB84-235670] 05 p0678 N85-14353
Dynamics of the low-latitude thermosphere and ionosphere 09 p1351 N85-18501
Seasonal characteristics of mesospheric plasma and their transitions 11 p1660 N85-20464
Investigation of aeronomic processes on the basis of ionospheric sporadic E 11 p1663 N85-20482
Space and time variations and turbopause dynamical structure 11 p1663 N85-20483
Protons with energies above 30 KeV in Earth's radiation belt at low altitudes during magnetically quiet time close to geomagnetic equator 13 p1980 N85-22423
A brief summary of results derived from Scandinavian Twin Auroral Radar Experiment (STARE) observations during IMS -- ionospheric electric fields
14 p2362 N85-24595
Characteristics and sources of E-region ionization in the continuous aurora
[AD-A155018] 21 p3632 N85-32562
EAR
NT COCHLEA
NT LABYRINTH
NT VESTIBULES
The European vestibular experiments of the Spacelab-1 mission 20 p3506 N85-31808
EARLY STARS
NT PROTOSTARS
NT T TAURI STARS
The Origin of Nonradiative Heating/Momentum in Hot Stars
[NASA-CP-2358] 08 p1231 N85-17755
Evidence for non-radiative activity in hot stars
08 p1231 N85-17756
Observations of nonthermal radio emission from early-type stars 08 p1232 N85-17758
Nonradial pulsation and mass loss in early B stars
08 p1232 N85-17759
Is the ratio of observed X-ray luminosity to bolometric luminosity in early-type stars really a constant?
08 p1234 N85-17777
Multi-spectral observations of the star formation: The role of far infrared photometry 08 p1245 N85-17859
Circumstellar dust disks around young stars
08 p1247 N85-17870
The variation of galactic interstellar extenction in the ultraviolet 11 p1749 N85-21000
Interstellar extinction in the nucleus of H PER
11 p1749 N85-21001
Coronal effects of the winds of early-type stars
11 p1749 N85-21002
The spectroscopic antics of S 18/SMC
11 p1750 N85-21008
EARPHONES
Hearing protection and speech intelligibility of two nonstandard inflight communication headsets
[AD-A148110] 03 p0355 N85-12284
EARTH (PLANET)
Impact phenomena as factors in the evolution of the Earth
[NASA-CR-174015] 01 p0072 N85-10474
Orbit of Salyut-7 station boosted
02 p0157 N85-11067
Lithospheric structure in the Pacific geoid
[NASA-CR-174155] 04 p0526 N85-13365
The problem of iron partition between Earth and Moon during simultaneous formation as a double planet system 04 p0587 N85-13744
Formation of the prelunar accretion disk
04 p0588 N85-13755
Lunar origin from impact on the Earth
04 p0588 N85-13757
Biogeochemical cycles: Interactions in global metabolism 05 p0652 N85-14184
Global biogeochemical cycles: Studies of interaction and change, some views on the strategy of approach
05 p0652 N85-14185
Some aspects of understanding changes in the global carbon cycle 05 p0652 N85-14186
Investigating phase structure of electromagnetic field in local inhomogeneities by modeling method
06 p0822 N85-15220
Where is the Earth's missing xenon?
06 p0888 N85-15641
Sample return from a comet flyby
06 p0889 N85-15646
Research of inverse methods to describe the structure of the earth and ocean bottom
[AD-A147082] 07 p1030 N85-16541
Algorithm for space-time analysis of data on geomagnetic field
[NASA-TM-77804] 08 p1209 N85-17609
The discovery circumstances of Earth-approaching asteroids
[NASA-CR-174327] 08 p1258 N85-17920
The geology of the terrestrial planets
[NASA-SP-469] 09 p1410 N85-18888
Earth 09 p1411 N85-18892
Evolution of sedimentation basins in Earth's history
10 p1497 N85-19451
Recent investigations at INPE in magnetospheric physics and geomagnetism
[INPE-3280-PRE/603] 10 p1514 N85-19555
Multiple parallel wires above a finitely conducting plane earth in the presence of a plane wave (EMP)
[DE85-001116] 11 p1625 N85-20231
Large natural geophysical events: Planetary planning
[DE85-000859] 11 p1763 N85-21092
Evaluating accuracy in determining position of Earth's center of mass and elements of orientation of geodetic coordinate system 13 p1983 N85-22441
Nature of seismic images with amplitude and time fluctuations of recorded oscillations
13 p2112 N85-23156
Gravity field of Venus and comparison with Earth
13 p2178 N85-23514
A circum-terrestrial compositional filter
13 p2179 N85-23520
Models of angular momentum input to a circum-terrestrial swarm from encounters with heliocentric planetesimals 13 p2179 N85-23521
Terrestrial analogs for planetary wrinkle ridges
13 p2199 N85-23644
Motion of satellite with total dynamic symmetry around rotating aspherical Earth 14 p2287 N85-24174
Relationship between seismic status of Earth and relative position of bodies in sun-earth-moon system
14 p2345 N85-24499
Local covariance functions and density distributions
[AD-A150792] 14 p2373 N85-24669
Resonant rotations of satellite in polar orbit in magnetic and gravitational fields 15 p2479 N85-25302
Space-time features of solar cosmic ray penetration into high latitude regions of Earth's magnetosphere based on Intercosmos-19 satellite data 15 p2481 N85-25310
Magnetohydrodynamics of Earth's bow shock
15 p2481 N85-25311
Selection of a model of Earth's albedo radiation, practical calculation of its effect on the trajectory of a satellite
[NASA-TM-77870] 15 p2591 N85-25972
Apparent thichness of Saturn's rings from the observations of the ring plane crossing
15 p2671 N85-26477
Comet showers and Nemesis, the death star
[DE85-003736] 15 p2683 N85-26575
Studies related to the deep Earth gas: 1983
[PB85-171114] 16 p2816 N85-27373
General continuous formulations of atmospheric energy laws 16 p2830 N85-27448
Moon bounce communications to small terminals
[AD-A153297] 17 p2950 N85-28212
Parameterization of surface fluxes in the VVR Fourth Order GCM 18 p3142 N85-29454

Analysis and modeling of variations in length of day
19 p3349 N85-30761

Properties of the reflected beams from the Earth's bow shock: A simple model
[IFSI-84-14] 20 p3549 N85-32088

Earth Albedo and the orbit of LAGEOS
[NASA-TM-86210] 21 p3556 N85-32131

Mega-geomorphology: Mars vis a vis Earth
21 p3601 N85-32360

Workshop on the Early Earth: The Interval from Accretion to the Older Archean
[NASA-CR-176037] 21 p3717 N85-33062

Permafrost features on Earth and Mars: Similarities, differences 22 p3855 N85-33870

Venus, Earth and Mars: Present bounds on similarities and differences in bulk composition
22 p3856 N85-33876

Mineralogy and chemistry of the Earth
22 p3856 N85-33877

Contrasts in evolution of Venus and Earth
22 p3857 N85-33880

Planning for VRM: Radar and sonar studies of volcanic terrains on Earth, Venus and Mars
22 p3857 N85-33884

Comparisons of the North Polar Cap of Mars and the Earth's Northern Hemisphere snow cover
[NASA-TM-86191] 23 p3989 N85-34728

Applications of the Galerkin formalism in the coupling of the earth's free oscillations 24 p4116 N85-35514

EARTH ALBEDO

Modeling influence of three layer cloud cover on outgoing thermal radiation 06 p0825 N85-15242

The effects of long-periodic forcing in a zero-dimensional climate model 07 p1002 N85-16363

Bifacial light sensitive space solar cell
13 p2006 N85-22573

Effect of diffusely-reflected sunlight on the orbit of LAGEOS 20 p3491 N85-31700

The electromagnetic component of albedo from superhigh energy cascades in dense media
[HE-3.5-11] 24 p4184 N85-35948

EARTH ATMOSPHERE
NT BIOSPHERE
NT D REGION
NT E REGION
NT EXOSPHERE
NT F REGION
NT F 2 REGION
NT FREE ATMOSPHERE
NT GEOMAGNETIC TAIL
NT INNER RADIATION BELT
NT IONOSPHERE
NT LOWER ATMOSPHERE
NT LOWER IONOSPHERE
NT MAGNETOPAUSE
NT MAGNETOSPHERE
NT MESOPAUSE
NT MESOSPHERE
NT MIDDLE ATMOSPHERE
NT MIDLATITUDE ATMOSPHERE
NT OUTER RADIATION BELT
NT OZONOSPHERE
NT PRIMITIVE EARTH ATMOSPHERE
NT PROTON BELTS
NT RADIATION BELTS
NT SPORADIC E LAYER
NT STRATOPAUSE
NT STRATOSPHERE
NT THERMOSPHERE
NT TROPOPAUSE
NT TROPOSPHERE
NT TURBOPAUSE
NT UPPER ATMOSPHERE
NT UPPER IONOSPHERE

Alpine meteorology: Translations of classic contributions by Wagner, A., Ekhart, E. and Defant, F.
[DE84-014929] 01 p0065 N85-10574

Green River air quality model development: Meteorological and tracer data, July/August 1982. Field study in Brush Valley, Colorado
[DE84-014975] 02 p0225 N85-11474

Achievements in development of space meteorology
03 p0343 N85-12212

A proposed reference set of scenarios for radiatively active atmospheric constituents
[DOE/NBB-0066] 03 p0386 N85-12483

Millimeter-wave propagation and remote sensing of the atmosphere
[AD-A146339] 03 p0393 N85-12512

Atmospheric extinction in critical environments
[AD-A146102] 03 p0396 N85-12527

Atlas of polar cap energetic particle observations. Volume 1: TIROS-N, 1 January 1979 - 28 February 1981
[PB84-233402] 04 p0535 N85-13419

Atmospheric studies in complex terrain
[DE84-008553] 05 p0676 N85-14345

Chemical kinetics and Earth's atmosphere
06 p0822 N85-15218

Attempted measurement of gaseous H-2O-2 in the ambient atmosphere
[DE85-001937] 06 p0834 N85-15306

Fractionation of siderophiles in cosmic spherules and its implications 06 p0864 N85-15613

Fluctuations during observations of extraterrestrial sources from outer space through Earth's atmosphere
07 p0953 N85-16040

Research in geodesy based upon radio interferometric observations of extragalactic radio sources
[AD-A147581] 07 p0988 N85-16280

Remote sensing of atmospheric gases with CO2 lasers. Continuation and conclusion of spectroscopic investigations
[BMFT-FB-W-84-030] 07 p0989 N85-16285

Development of an airborne measuring system for remote sensing of Earth surface and atmosphere, spectroscopic investigations
[BMFT-FB-W-84-029] 08 p1176 N85-17420

Earth 09 p1411 N85-18892

Study proposal for the possible use of ISS as an aerodynamic facility for aerospace applications
11 p1646 N85-20374

Environmental effects of space activities
11 p1678 N85-20577

Substorms in the Earth's atmosphere
[DE85-000654] 12 p1890 N85-21861

Atmospheric handbook: Atmospheric data tables available on computer tape
[PB85-108512] 12 p1891 N85-21867

Characterization of material surfaces exposed to atomic oxygen on space shuttle missions
12 p1946 N85-22220

Response of Earth's atmosphere to increases in solar flux and implications for loss of water from Venus
13 p2178 N85-23518

The Earth's magnetopause — International Magnetospheric Study 14 p2355 N85-24549

Hot plasma and energetic particles in the Earth's outer magnetosphere: New understandings during the IMS
14 p2355 N85-24552

Magnetic field in the Earth's outer magnetosphere: Prognoz-6, -7 data 14 p2356 N85-24556

Analysis of atmospheric interferometer data
[AD-A150682] 14 p2372 N85-24663

The behavior of the atmosphere in the desert planetary boundary layer
[AD-A151286] 15 p2592 N85-25977

ILUM code: Solar and lunar flux calculations for multi-cloud layered atmospheres
[DE85-005578] 15 p2600 N85-26025

Modeling plasma mantle of Earth's magnetosphere
16 p2720 N85-26790

The problem of atmospheric turbulence
[NASA-CR-175783] 16 p2832 N85-27464

Intercomparison of Radiation Codes in Climate Models (ICRCCM)
[DE85-007251] 16 p2835 N85-27487

The role of thermal motions of air particles for fireballs
[PUBL-59] 17 p3053 N85-28900

Identification and characterization of watershed models for evaluation of impacts of climate change on hydrology
[DE85-008575] 18 p3125 N85-29348

Formation and fate of toxic chemicals in California's atmosphere
[PB85-172609] 18 p3134 N85-29414

The moist available energy of a conditionally unstable atmosphere 18 p3145 N85-29473

Preliminary GCM results with a new radiation parameterization 18 p3145 N85-29474

Environmental Research Laboratories (of the National Oceanic and Atmospheric Administration) programs and plans: FY 1984 programs and FY 1985 plans
[PB85-171494] 18 p3149 N85-29501

Study of Kapton under simulated shuttle environment
[NASA-CR-176003] 19 p3225 N85-29997

Density characteristics of asthenosphere in Atlantic Ocean 19 p3294 N85-30423

Optical stability, atmospheric transparency and aerosol absorption 19 p3297 N85-30442

Approximate method for computing wind velocity in atmosphere 19 p3298 N85-30444

The origin and evolution of the Earth's atmosphere and hydrosphere 19 p3312 N85-30533

Effects of relative humidity gradients on the evaluation of submicron aerosol flux measurements in the atmospheric surface layer
[DE85-010510] 19 p3316 N85-30555

Intraplate crustal deformation due to continental collisions 20 p3490 N85-31693

A survey of wind and turbulence modeling methods
[AD-A154470] 20 p3496 N85-31733

Medium range atmospheric forecast system: Evaluation plan
[AD-A155623] 21 p3638 N85-325[illegible]

Production of stable embryo particles in dense ion tracks of alpha particle emissions in the atmosphere
21 p3644 N85-32[illegible]

Photochemical aerosol formation in polluted atmosphere 21 p3644 N85-32[illegible]

Evolution of the atmosphere 21 p3658 N85-327[illegible]

Constraints on early atmosphere from planetary accretion processes 21 p3717 N85-3306[illegible]

The composition of the primitive atmosphere and the synthesis of organic compounds on the early Earth
21 p3717 N85-3306[illegible]

The degassing history of the Earth: Noble gas studies of Archaean cherts and zero age glassy submarine basalts 21 p3718 N85-33072

Water loss from Venus: Implications for the Earth's early atmosphere 21 p3721 N85-3308[illegible]

Impact of fluctuations in optical properties of atmosphere on the ratio of spectral brighiness from remote sensing of agricultural land 22 p3734 N85-3314[illegible]

Determination of altitude of cloud cover top from Meteor satellite data 22 p3734 N85-331[illegible]

A review of shock waves around aeroassisted orbital transfer vehicles
[NASA-TM-86769] 22 p3739 N85-33177

Evaluation of the 2DFLOW and hybrid complex-terrain dispersion models with the 1980 ASCOT data base from the Geysers
[DE85-012960] 22 p3812 N85-33813

Terrestrial Planets: Comparative Planetology
[NASA-CR-176093] 22 p3851 N85-338[illegible]

Terrestrial Xe isotopic contraints on the early history of the Earth 22 p3852 N85-33862

Noble gas patterns in the atmospheres of Mars and Earth: A comparison via the SNC meteorites
22 p3852 N85-33863

Biological modulation of planetary atmospheres: The early Earth scenario 22 p3854 N85-33867

Imaging Spectrometric Observatory (ISO)
23 p3902 N85-341[illegible]

Evaluation of source strength and dispersion model predications with data from large nitrogen tetroxide field experiments
[DE85-011855] 23 p3947 N85-344[illegible]

Nucleosynthesis in the terrestrial and solar atmospheres
[SH-2.2-2] 23 p4000 N85-347[illegible]

The influences of the galactic cosmic ray on the atmospheric ozone
[SH-10.1-1] 23 p4053 N85-351[illegible]

Propagation of cosmic rays through the atmosphere in the quark-gluon strings model 24 p4173 N85-358[illegible]

Experimental basis for the models of cascade propagation in atmosphere
[HE-3.6-6] 24 p4185 N85-359[illegible]

The lateral distributions of charged particles of energy greater than 0.3 E sub crit in electron-photon cascades in lead and air
[HE-3.6-10] 24 p4185 N85-35957

Longitudinal trial functions and the cosmic ray energy scale 24 p4193 N85-36014

Nuclear cascades in electromagnetic showers produced by primary gamma-quanta in the atmosphere
[HE-4.5-16] 24 p4196 N85-360[illegible]

Air fluorescence detection of large air showers below the horizon
[HE-4.6-6] 24 p4197 N85-360[illegible]

EARTH AXIS

The MEDOC 2: Experimental Doppler measurement of Earth kinematics 14 p2309 N85-247[illegible]

Global coordinate system
[AD-A153878] 19 p3299 N85-304[illegible]

EARTH CORE

Is phosphorus predictably incompatible in igneous processes? 04 p0583 N85-13722

Magnetic location of Earth's core-mantle boundary and estimates of the adjacent fluid motion
13 p2131 N85-2[illegible]

Origin of life 21 p3657 N85-32713

Was core formation violent enough to homogenize the early mantle? 21 p3718 N85-330[illegible]

The problem of the Earth's CO2 content and the iron core 21 p3718 N85-330[illegible]

A model for core formation in the early Earth
21 p3719 N85-33078

Implications for the Earth of the early dynamical environment 21 p3719 N85-33079

Chemical evolution of the Earth: Equilibrium or disequilibrium process? 21 p3721 N85-330[illegible]

Thermal, dynamic and compositional aspects of the core-forming Earth 21 p3722 N85-330[illegible]

EARTH CRUST
Marine geological and geophysical investigations of the Antarctic Continental Margin, 1984
[GS-CIRC-935] 02 p0212 N85-11400
The south-central United States magnetic anomaly
[E85-10025] 02 p0218 N85-11436
A comparison of seismic properties of young and mature oceanic crust 02 p0226 N85-11479
Heat flow map of Europe: Brief summary of the geophysical implications
[REPT-582] 03 p0377 N85-12405
Continental and oceanic crustal magnetization modeling
[E85-10034] 03 p0378 N85-12413
Horizontal-strain observations in the Shumagin island and Yakataga seismic gaps, Alaska
04 p0515 N85-13287
Structure of the crust and upper mantle of the Iberian continental platform 04 p0523 N85-13350
Deep structure and seismicity in the Catalonia-Pyrenees region 04 p0524 N85-13352
Priorities for a national program of continental drilling for scientific purposes 04 p0534 N85-13418
Geophysical investigation of precambrian crustal structure and Laramide effects across a precambrian suture in southeastern Wyoming
05 p0674 N85-14328
Oceanic plateaus, anomalous subduction, and the accretion of buoyant features at convergent margins
05 p0688 N85-14422
Some trends in the modern Earth sciences --- plate tectonics and Earth's crust 06 p0820 N85-15207
Deep structure of terrestrial crust and upper mantle in southeastern Siberia and Far East according geological-geophysical data 06 p0821 N85-15212
Deep structure of Western Siberia
07 p0981 N85-16235
Model of earthquake mechanism
07 p0982 N85-16236
Statistical filtering as method for detecting transcrustal acoustic anomalies 07 p0982 N85-16237
The mineralogy of global magnetic anomalies
[E85-10061] 07 p0987 N85-16272
Analysis of gases in the Earth's crust
[PB85-113397/GAR] 07 p0990 N85-16287
High pressure physics research focusing on composite materials 08 p1140 N85-17185
Determination of crustal and upper mantle structure from analysis of broadband teleseismic P-waveforms
08 p1181 N85-17440
Detailed oceanic crustal modeling
[AD-A148589] 08 p1191 N85-17507
Utilization of mobile VLBI for geodetic measurements
10 p1466 N85-19248
New data on structure of Shirshov Ridge (Bering Sea)
10 p1498 N85-19456
Crustal stretching and subsidence in sedimentary eastern Switzerland and permo-carboniferous basins in the continental United States
[DE85-000622] 11 p1661 N85-20592
Determination of density of the crust and upper mantle from deep seismic sounding and gravimetry, 2
13 p2111 N85-23153
Induction excitation of deep conducting zones
13 p2111 N85-23154
Study of resolution of deep MT soundings by means of physical model 13 p2112 N85-23155
Structure of Iceland and ocean floor spreading
13 p2112 N85-23159
Variations in resistivity of upper crustal layer
13 p2113 N85-23164
Boundary velocities of longitudinal seismic waves and lateral inhomogeneities of upper ocean mantle
13 p2113 N85-23165
Solution of direct magnetometric problem on spherical Earth 13 p2116 N85-23179
MAGSAT anomaly field data of the crustal properties of Australia
[E85-10100] 13 p2122 N85-23215
An investigation of the crustal properties of Australia and surrounding regions derived from interpretation of MAGSAT anomaly field data 13 p2122 N85-23216
Remanent magnetization model for the broken ridge satellite magnetic anomaly 13 p2123 N85-23219
Crustal dynamics project: Catalogue of site information
[NASA-TM-87452] 13 p2131 N85-23258
Volcanism of the Colorado Plateau (basin and range transition): Implications for crustal processes
13 p2187 N85-23569
Bouguer images of the North American craton
13 p2200 N85-23648
Determination of crust and upper mantle density based on deep seismic sounding and gravimetry data, part 1
14 p2345 N85-24498
Polar motions measurement study
[AD-A150690] 14 p2372 N85-24664
Study of spatial distribution of auroras
16 p2808 N85-27315
Altimetry data and the elastic stress tensor of subduction zones
[NASA-CR-175796] 16 p2825 N85-27425
Proceedings of the 1980 Workshop of the International Association of Seismology and Physics of the Earth's Interior on the Seismic Modeling of Laterally Varying Structures: Contributions based on data from the 1978 Saudi Arabian refraction profile
[GS-CIRC-937] 17 p2989 N85-28476
A crustal section for the Arabian Shield and adjacent Red Sea margin derived from first-arrival data
17 p2990 N85-28480
The rifted margin of Saudi Arabia
17 p2990 N85-28483
Density characteristics of asthenosphere in Atlantic Ocean 19 p3294 N85-30423
Discovery in earthquake forecasting and seismic zoning recorded 19 p3295 N85-30426
Improving the geological interpretation of magnetic and gravity satellite anomalies
[E85-10103] 20 p3473 N85-31585
The south-central United States magnetic anomaly
20 p3474 N85-31591
The south-central United States magnetic anomaly
20 p3475 N85-31592
Continental and oceanic magnetic anomalies: Enhancement through GRM 20 p3476 N85-31598
Continental magnetic anomaly constraints on continental reconstruction 20 p3476 N85-31599
Regional magnetic anomaly constraints on continental rifting 20 p3476 N85-31600
The global VLBI fiducial network
20 p3490 N85-31690
Mega-geomorphology: Mars vis a vis Earth
21 p3601 N85-32360
Crustal dynamics project data analysis fixed station VLBI geodetic results
[NASA-TM-86229] 21 p3615 N85-32465
Development of ultrasonic modeling techniques for the study of crustal inhomogeneities
[AD-A155206] 21 p3632 N85-32565
Origin of life 21 p3657 N85-32713
Workshop on the Early Earth: The Interval from Accretion to the Older Archean
[NASA-CR-176037] 21 p3717 N85-33062
Early evolution of the crust-mantle system
21 p3717 N85-33067
Considerations of large scale impact and the early Earth 21 p3718 N85-33070
The 3.5 b.y. old Onverwacht Group: A remnant of ancient oceanic crust 21 p3718 N85-33073
Constraints on the development of the early continental crust from isotopic data 21 p3719 N85-33076
Anorthositic oceanic crust in the Archean Earth
21 p3719 N85-33077
Archean sedimentary systems and crustal evolution
21 p3720 N85-33082
The origin of continental crust: Outlines of a general theory 21 p3720 N85-33083
Crustal radiogenic heat production and the selective survival of ancient continental crust
21 p3721 N85-33086
Large arcuate scars: A geological legacy of the Earth's accretionary past 21 p3721 N85-33089
Spacecraft-aided research discussed at geology Congress 22 p3734 N85-33147
Noble gases in meteorites and terrestrial planets
22 p3851 N85-33850
Crustal structure in southern California from array data
24 p4115 N85-35512
Groundwater radon studies for earthquake precursors in southern California
[PB85-196871] 24 p4116 N85-35529
EARTH CURRENTS
U TELLURIC CURRENTS
EARTH ENVIRONMENT
International Geosphere/Biosphere Program: 1984
[GPO-39-222] 04 p0578 N85-13691
Sourcebook: Gaining access to US government information on the environment and natural resources
[DE84-017419] 11 p1740 N85-20941
EARTH FIGURE
U GEODESY
EARTH HYDROSPHERE
Earth 09 p1411 N85-18892
Drifting ice as mechanical factor in purifying and polluting hydrosphere 13 p2108 N85-23132
World ocean level oscillations and their relationship to change in inflow of continental waters
13 p2108 N85-23133
The origin and evolution of the Earth's atmosphere and hydrosphere 19 p3312 N85-30533
Origin of the atmosphere and hydrosphere of the terrestrial planets 22 p3853 N85-33863
EARTH MANTLE
Structure of the crust and upper mantle of the Iberian continental platform 04 p0523 N85-13350
Constraints on the origin of the Moon from molybdenum and other siderophile elements
04 p0582 N85-13718
Origin of the Moon 04 p0587 N85-13745
Earthquakes and tectonics of Pacific Ocean margins
06 p0820 N85-15206
Boundary velocities of mohorovicic discontinuity and upper mantle structure of Pacific Ocean bed
06 p0821 N85-15211
Deep structure of terrestrial crust and upper mantle in southeastern Siberia and Far East according geological-geophysical data 06 p0821 N85-15212
The mineralogy of global magnetic anomalies
[E85-10061] 07 p0987 N85-16272
Determination of crustal and upper mantle structure from analysis of broadband teleseismic P-waveforms
08 p1181 N85-17440
Detailed oceanic crustal modeling
[AD-A148589] 08 p1191 N85-17507
Vertical movements and structure formation within island systems of northeast Asia 10 p1501 N85-19471
A 3-D treatment of convective flow in the Earth's mantle
[DE85-003734] 12 p1890 N85-21863
Determining degree of partial melting of asthenosphere from seismic data 13 p2107 N85-23127
Determination of density of the crust and upper mantle from deep seismic sounding and gravimetry, 2
13 p2111 N85-23153
Induction excitation of deep conducting zones
13 p2111 N85-23154
Study of resolution of deep MT soundings by means of physical model 13 p2112 N85-23155
Boundary velocities of longitudinal seismic waves and lateral inhomogeneities of upper ocean mantle
13 p2113 N85-23165
Magnetic location of Earth's core-mantle boundary and estimates of the adjacent fluid motion
13 p2131 N85-23260
Bouguer images of the North American craton
13 p2200 N85-23648
Lateral inhomogeneity of mantle surface in western Eurasia 14 p2344 N85-24497
Determination of crust and upper mantle density based on deep seismic sounding and gravimetry data, part 1
14 p2345 N85-24498
Frequency dependence of Q in the mantle underlying the shield areas of eurasia
[AD-A151367] 15 p2592 N85-25978
Internal waves in layers of Earth's upper mantle
16 p2807 N85-27312
Proceedings of the 1980 Workshop of the International Association of Seismology and Physics of the Earth's Interior on the Seismic Modeling of Laterally Varying Structures: Contributions based on data from the 1978 Saudi Arabian refraction profile
[GS-CIRC-937] 17 p2989 N85-28476
Density characteristics of asthenosphere in Atlantic Ocean 19 p3294 N85-30423
Evolution of the oceanic upper mantle and effects on sea floor subsidence geoid height and heat flow
19 p3319 N85-30575
Origin of life 21 p3657 N85-32713
Workshop on the Early Earth: The Interval from Accretion to the Older Archean
[NASA-CR-176037] 21 p3717 N85-33062
The relation between the age of the subconducting slab and the recycling of sediments into the mantle
21 p3717 N85-33063
Constraints on early atmosphere from planetary accretion processes 21 p3717 N85-33064
Early evolution of the crust-mantle system
21 p3717 N85-33067
Was core formation violent enough to homogenize the early mantle? 21 p3718 N85-33068
Constraints on the development of the early continental crust from isotopic data 21 p3719 N85-33076
A model for core formation in the early Earth
21 p3719 N85-33078
Carbon and nitrogen in the deep Earth
21 p3721 N85-33085
Chemical evolution of the Earth: Equilibrium or disequilibrium process? 21 p3721 N85-33088
Thermal, dynamic and compositional aspects of the core-forming Earth 21 p3722 N85-33091
Landscape interpretation capabilities using space photographs of regions of a multistage platform mantle structure 22 p3734 N85-33151
Noble gases in meteorites and terrestrial planets
22 p3851 N85-33850

Terrestrial Xe isotopic contraints on the early history of the Earth 22 p3852 N85-33852
A dynamic model of Venus's gravity field
[NASA-CR-176173] 24 p4169 N85-35845

EARTH MOVEMENTS
NT EARTHQUAKES
Vertical crustal movements in southern California, 1974 to 1978
[GS-CIRC-905] 02 p0228 N85-11491
Soil tilt measurement: First results of the comparative analysis of the response of two different tiltmeters
[NOTA-INTERNA-818] 02 p0228 N85-11494
Analysis of in-plane and out-of-plane ground motions using the boundary element method
[AD-A146229] 03 p0355 N85-12287
The motion of the Earth by Doppler observing campaign (MEDOC) 05 p0601 N85-13831
On seismic waves 08 p1171 N85-17383
Absolute movement of Pacific Ocean plate during last 120 million years 13 p2107 N85-23126
Numerical modeling of plane stick-slip fault
13 p2111 N85-23150
Crustal dynamics project: Catalogue of site information
[NASA-TM-87452] 13 p2131 N85-23258
Inversion of Rayleigh wave group velocities from high-explosive tests
[AD-A152172] 16 p2783 N85-27175
The effects of seismic waves
17 p2978 N85-28401
The global VLBI fiducial network
20 p3490 N85-31690
New stations supporting crustal dynamics project VLBI measurements 20 p3491 N85-31701
Mapping of dynamics of deltas by space photography
22 p3737 N85-33163
Crustal Dynamics Project: Catalogue of site information
[NASA-TM-86218] 22 p3801 N85-33552
Seismic stratigraphic analysis of the Mississippi Fan
24 p4115 N85-35507

EARTH OBSERVATIONS (FROM SPACE)
NT PHOTORECONNAISSANCE
NT SATELLITE OBSERVATION
NT SPOT (FRENCH SATELLITE)
Satellite reconnaissance
[AD-B085034] 01 p0015 N85-10094
NASA's SESAC report on research and analysis in space and Earth sciences 04 p0579 N85-13697
Basic investigation concerning the applicability of multispectral radiation data from microwave radiometry measurements to geoscientific objectives of remote sensing
[ESA-TT-846] 05 p0628 N85-14027
EARSeL/ESA Symposium on Integrative Approaches in Remote Sensing
[ESA-SP-214] 05 p0655 N85-14202
Perspectives of remote sensing at the end of the decade 05 p0659 N85-14236
Electronic satellite imaging system MOMS-ESA
[BMFT-FB-W-84-033] 05 p0661 N85-14248
Simulation experiments on the relative accuracy of inferred atmospheric states from idealized wind and temperature profiling systems 05 p0682 N85-14386
Upper Atmosphere Research Satellite (UARS) trade analysis
[NASA-CR-175269] 07 p0912 N85-15774
Brazilian Remote Sensing Shuttle Experiment (BRESEX): Characteristics and future utilization on satellites
[INPE-3313-PRE/620] 10 p1487 N85-19395
Summary presentation of the Science Applications Panel 11 p1644 N85-20355
Solar flare and IMF sector structure effects in the lower ionosphere 11 p1664 N85-20486
The spot operational remote sensing satellite system: Current status and perspectives
11 p1713 N85-20776
The ESA remote sensing satellite system (ERS-1)
11 p1713 N85-20777
Earth resources research using the Shuttle Imaging Radar system 11 p1713 N85-20779
JPL highlights
[NASA-CR-175517] 11 p1767 N85-21102
NASA's land remote sensing plans for the 1980's
13 p2124 N85-23224
A silicic shield volcano in Bolivia
13 p2187 N85-23572
Utilization of the polar platform of NASA's Space Station Program for operational Earth observations
[PB85-152502] 14 p2240 N85-23896
Environmental satellites 14 p2326 N85-24392
Observation of polar aurora from the Salyut-6 space station during the great geomagnetic storm of 11-13 Apr. 1981 15 p2477 N85-25291
Determining characteristics of optical radiation reflectors based on results of remote sensing
15 p2488 N85-25358
Use of space photographic information to map plant cover 15 p2488 N85-25359
Selection of a model of Earth's albedo radiation, practical calculation of its effect on the trajectory of a satellite
[NASA-TM-77870] 15 p2591 N85-25972
Satellite detection of severe thunderstorms
15 p2596 N85-25996
NOAA satellite operations: Programs briefing — Environmental satellites, LANDSAT, and space station polar platform 15 p2599 N85-26020
Space methods in oceanology
[NASA-TM-77652] 15 p2604 N85-26047
Application of space methods in geodesy
16 p2724 N85-26817
Tenth Conference of Working Group of Socialist Countries on Remote Sensing of Earth under Intercosmos Program 16 p2725 N85-26820
Contribution to space program reviewed
16 p2727 N85-26834
Status of the observational data sets — TOPEX
16 p2804 N85-27296
Shuttle imaging radar-A (SIR-A) data analysis — geology of the Ozark Plateau of southern Missouri, land use in western Illinois, and vegetation types at Koonamore Station, Australia
[NASA-CR-175785] 16 p2809 N85-27324
Modular Optoelectronic Multispectral Scanner (MOMS) for Earth observation. First results of STS-7 mission
[MBB-UR-717/83-O] 16 p2874 N85-27732
Experimental philosophy leading to a small scale digital data base of the conterminous United States for designing experiments with remotely sensed data
[NASA-TM-85009] 17 p3049 N85-28877
Looking down looking forward: Earth observation, sciences and applications, a perspective
[ESA-SP-1073] 18 p3149 N85-29497
Space optics
[CNES-84/105/T/CT/DRT/TIT/10]
20 p3533 N85-31985
Large format camera photographs: A new tool for understanding arid environments
21 p3604 N85-32379
Quantitative geomorphologic studies from spaceborne platforms 21 p3604 N85-32381
Process thresholds: Report of Working Group Number 3 21 p3604 N85-32384
Planetary perspective. Report of Working Group Number 4 21 p3605 N85-32385
Properties of aerosol particles detected by satellites in coastal regions 21 p3641 N85-32622
Cosmonauts participate in multilevel remote sensing experiment 22 p3731 N85-33130
Physico-geographical regionalization of Caspian lowland based on space survey materials
22 p3736 N85-33162

EARTH ORBITING SPACE STATIONS
U EOSS

EARTH ORBITS
NT PERIGEES
Study of proton and neutron activation of metal samples in low Earth orbit
[NASA-CR-171183] 01 p0026 N85-10164
Winged first stages of space transport appliances
[TUM-RT-TB-84/3] 02 p0167 N85-11125
Capture of planetesimals into a circumterrestrial swarm 04 p0588 N85-13751
Contributions to the error analysis in the relativity gyroscope experiment 05 p0636 N85-14095
Theory of the orbital motion of an artificial Earth satellite
[NAL-TR-807] 06 p0758 N85-14847
Electric fields in Earth orbital space
[AD-A146448] 06 p0835 N85-15313
Broadening the debate 07 p0914 N85-15785
OTV propulsion tecnology programmatic overview
08 p1107 N85-16997
Computer subroutines for estimation of human exposure to radiation in low Earth orbit
[NASA-TM-86324] 08 p1199 N85-17550
Report of the Constellations Panel
11 p1645 N85-20368
A model for the evolution of on-orbit manmade debris environment 12 p1784 N85-21196
Debris in the geostationary orbit ring, the endless shooting gallery: The necessity for a disposal policy
12 p1786 N85-21214
Considerations for policy on man-made debris propagation control 12 p1787 N85-21219
Environment definition, large particles
12 p1787 N85-21220
Modeling 12 p1787 N85-21221
Measurements 12 p1787 N85-21222
Environment definition, small particles, diameter less than or equal to 1 MM 12 p1788 N85-21223
Spacecraft hazard and shielding requirements
12 p1788 N85-21224
Radiation exposure and performance of multiple burn LEO-GEO orbit transfer trajectories
[NASA-TM-86946] 12 p1788 N85-21228
Characterization of material surfaces exposed to atomic oxygen on space shuttle missions
12 p1946 N85-22229
Nontraditional method for determining unperturbed orbits of unknown space objects using incomplete optical observational data 13 p1979 N85-22417
Spacecraft Environmental Interactions Technology, 1983
[NASA-CP-2359] 13 p1989 N85-22470
Argon ion pollution of the magnetosphere
13 p1996 N85-22520
Nation said to rank high with 15 satellites
13 p2041 N85-22778
Mission analysis and orbit control of the heliosynchronous satellite SPOT
14 p2397 N85-24773
Cosmic ray environment model for Earth orbit
[NASA-CR-175866] 14 p2455 N85-25186
Some numerical estimates of perturbation of orbital elements of artificial Earth satellite with total dynamic symmetry about rotating aspherical Earth
15 p2478 N85-25294
Autonomous state determination for an Earth orbiting satellite using horizon and star sensors
[AD-A151827] 15 p2493 N85-25379
Nondestructive equipment study
[NASA-CR-171865] 15 p2571 N85-25859
Examination of returned solar-max surfaces for impacting orbital debris and meteoroids
15 p2681 N85-26580
Simultaneous Earth observations from 2 satellites
[NASA-TM-86204] 16 p2810 N85-27325
Maximizing the semi-major axis for a freely coning solar sailcraft
[AD-A153175] 17 p2909 N85-27898
Study of Kapton under simulated shuttle environment
[NASA-CR-176003] 19 p3225 N85-29897
LEO life testing with different charge control
20 p3446 N85-31388
Flight experience of Solar Mesosphere Explorer's two nickel-cadmium batteries 20 p3446 N85-31396
Design principles for nickel hydrogen cells and batteries 20 p3447 N85-31398
Life cycle test results of a bipolar nickel hydrogen battery 20 p3448 N85-31406
Procedure for estimating orbital debris risks
[NASA-TP-2507] 22 p3736 N85-33169

EARTH PLANETARY STRUCTURE
Stratigraphy, sedimentology and tectonic significance of the Upper Cretaceous Virginian Ridge formation, Methow Basin, Washington: Implications for tectonic history of the North Cascades 03 p0390 N85-12494
Individual geopotential coefficients of order 15 and 30, from resonant satellite orbits
[AD-A146687] 06 p0828 N85-15256
Khibiny experiment described
07 p0961 N85-16230
Earth 09 p1411 N85-18882
Crustal dynamics studies in China
[NASA-CR-175617] 13 p2132 N85-23265
Submarine volcanic eruptions and potential analogs for Venus 13 p2187 N85-23573
Altimetry data and the elastic stress tensor of subduction zones
[NASA-CR-175796] 16 p2825 N85-27425
Highly important features of regional tectonics of Earth's Arctic sector 19 p3298 N85-30449
Development of ultrasonic modeling techniques for the study of crustal inhomogeneities
[AD-A155206] 21 p3632 N85-32595
Conditions during formation of the Earth
21 p3717 N85-33066
Constraints on the development of the early continental crust from isotopic data 21 p3719 N85-33076
Anorthositic oceanic crust in the Archean Earth
21 p3719 N85-33077
A model for core formation in the early Earth
21 p3719 N85-33078
Implications for the Earth of the early dynamical environment 21 p3719 N85-33079
Chemical evolution of the Earth: Equilibrium or disequilibrium process? 21 p3721 N85-33086
Earth's primordial differentiation, and its after-effects
21 p3722 N85-33092
Landscape interpretation capabilities using space photographs of regions of a multistage platform mantle structure 22 p3734 N85-33151

EARTH RADIATION
U TERRESTRIAL RADIATION

EARTH RADIATION BUDGET EXPERIMENT

Earth radiation budget experiment software development [NASA-CR-172567] 12 p1912 N85-22002

An Earth longwave radiation climate model [NASA-CR-175749] 15 p2594 N85-25984

Origin of the Greenland ice sheet 15 p2604 N85-26046

Year-to-year variability of components of Earth's radiation budget according to satellite measurement data 16 p2725 N85-26821

Validation of the ERBE scanner scene identification methodology: Analysis with Nimbus-7 ERB data [NASA-CR-172596] 16 p2832 N85-27466

Solar radiance models for determination of ERBE scanner filter factor [NASA-CR-172595] 17 p2995 N85-28513

Space Station Polar Platform: Integrating research and operational missions [PB85-195279] 24 p4069 N85-35218

The 1986 National Aeronautics and Space Administration authorization [GPO-47-635] 24 p4166 N85-35829

EARTH RESOURCES

NT AQUIFERS
NT COAL
NT CRUDE OIL
NT FORESTS
NT FOSSIL FUELS
NT GEOTHERMAL RESOURCES
NT GEYSERS
NT GLACIERS
NT ICEBERGS
NT LAND ICE
NT LIGNITE
NT MARINE RESOURCES
NT OIL FIELDS
NT PEAT
NT RAIN FORESTS
NT SPRINGS (WATER)
NT TAR SANDS
NT THERMAL RESOURCES
NT UNDERWATER RESOURCES
NT WATER RESOURCES

Geophysical experiments, photography aboard Salyut-7 02 p0157 N85-11066

Salyut-7 crew in orbit 150 days 02 p0157 N85-11068

Choice of cartographic projection for space system data bank used in studying natural resources 02 p0165 N85-11119

Seismology 1983: Nuclear test ban verification, earthquake and Earth resource investigation [FOA-C-20537-T1] 02 p0229 N85-11495

Satellite, airborne remote sensing development outlined 03 p0342 N85-12199

Corporate use of information regarding natural resources and environmental quality [PB84-222736] 03 p0439 N85-12794

Deep seabed stable reference areas [PB84-241470] 09 p1360 N85-18555

Reducing gull use of some attractions near airports [AD-P004195] 11 p1581 N85-19962

Remote sensing technology now playing practical roles 11 p1619 N85-20190

Monitoring approaches for assessing quality of high altitude lakes: Colorado Flat Tops Wilderness Area [PB85-117232] 11 p1679 N85-20579

Sourcebook: Gaining access to US government information on the environment and natural resources [DE84-017419] 11 p1740 N85-20941

Process development for commercial production of natural rubber from Guayule [PB85-124956] 12 p1815 N85-21388

Remote sensing used for study of forest resources 13 p1963 N85-22440

Characteristics of alumyte deposits discussed 13 p2166 N85-23438

An analysis of issues concerning acid rain, report to the Congress of the United States [T85-801070] 15 p2589 N85-25959

Comparative study of the digital analysis of areas of the Earth's surface prepared for planting using different classification algorithms [INPE-3350-PRE/637] 16 p2846 N85-27545

Thermal Infrared Multispectral Scanner (TIMS): An investigator's guide to TIMS data [NASA-CR-175875] 17 p2961 N85-28286

Yearbook of the Bureau of Mineral Resources, Geology and Physics: Geoscientific research, resource assessment, and database development, 1 Jul. 1983 to 30 Jun. 1984 [BMR-84] 17 p2989 N85-28474

Earth Resources: A continuing bibliography with indexes, issue 45 [NASA-SP-7041(45)] 18 p3123 N85-29336

Remote Sensing Technology: Symposium Proceedings [DE85-010212] 20 p3477 N85-31606

Gas hydrates [DE85-001986] 20 p3477 N85-31607

The U.S. Geological Survey in Alaska: Accomplishments during 1982 [US-GEOL-SURV-CIRC-939] 20 p3493 N85-31719

Geologic and hydrologic characterization and evaluation of the basin and range province relative to the disposal of high-level radioactive waste. Part 1: Introduction and guidelines [GS-CIRC-904-A] 20 p3526 N85-31932

Handbook for obtaining and using aerial photography to map aquatic plant distribution [AD-A154584] 21 p3605 N85-32388

Cosmonauts participate in multilevel remote sensing experiment 22 p3731 N85-33130

Indications of mineral zoning in a fossil hydrothermal system at the Meager Creek geothermal prospect, British Columbia, Canada from induced polarization studies [DE85-011962] 22 p3815 N85-33636

Geology and petroleum resources of basins in western China [DE85-013038] 23 p3948 N85-34469

The scientific and technical issues in integrating remotely sensed imagery with geocoded data bases 23 p3960 N85-34547

Selection of segment similarity measures for hierarchical picture segmentation 23 p3960 N85-34548

Satellites and politics: Weather, communications, and earth resources 23 p4057 N85-35144

Microwave properties of a quiet sea [NASA-CR-176199] 24 p4085 N85-35322

USGS coastal research, studies and maps: A source of information for coastal decision making [USGS-CIRC-883] 24 p4108 N85-35465

Remote sensing of hydrologic transport processes using spot simulation data [DE85-012412] 24 p4108 N85-35467

EARTH RESOURCES PROGRAM

Earth Resources, A Continuing Bibliography with Indexes [NASA-SP-7041(43)] 03 p0378 N85-12411

Earth resources: A continuing bibliography with indexes [NASA-SP-7041(44)] 10 p1503 N85-19484

EARTH RESOURCES SHUTTLE IMAGING RADAR

Earth resources research using the Shuttle Imaging Radar system 11 p1713 N85-20779

EARTH RESOURCES TECHNOLOGY SATELLITE D

U LANDSAT 4

EARTH RESOURCES TECHNOLOGY SATELLITE 1

U LANDSAT 1

EARTH RESOURCES TECHNOLOGY SATELLITES

U LANDSAT SATELLITES

EARTH ROTATION

Basic research for the geodynamics program [NASA-CR-174055] 02 p0226 N85-11490

Development of optical techniques for Earth rotational measurements [AD-A145850] 03 p0364 N85-12333

The Moon's orbit history and inferences on its origin 04 p0585 N85-13735

A reappraisal of Darwin's fission hypothesis and a possible limit to the primordial angular momentum of the Earth 04 p0585 N85-13736

The motion of the Earth by Doppler observing campaign (MEDOC) 05 p0601 N85-13831

Research in geodesy based upon radio interferometric observations of extragalactic radio sources [AD-A147581] 07 p0968 N85-16260

The wobble of the Earth and the low frequency dynamics of the ocean 09 p1358 N85-18546

The accuracy of radio interferometric measurements of Earth rotation 10 p1465 N85-19246

Earth rotation and polar wandering 14 p2399 N85-24785

The MEDOC 2: Experimental Doppler measurement of Earth kinematics 14 p2399 N85-24786

Spectral analysis of diurnal nonuniformity of Earth's rotation 15 p2477 N85-25289

Some numerical estimates of perturbation of orbital elements of artificial Earth satellite with total dynamic symmetry about rotating aspherical Earth 15 p2478 N85-25294

Full shadow phenomenon in Earth's upper atmosphere 16 p2808 N85-27316

New stations supporting crustal dynamics project VLBI measurements 20 p3491 N85-31701

Crustal dynamics project data analysis fixed station VLBI geodetic results [NASA-TM-86229] 21 p3615 N85-32465

EARTH SHAPE

U GEODESY

EARTH SURFACE

The development of objective forecast techniques based on advection of surface weather parameters 01 p0078 N85-10522

Evaluation of surface sensible heat flux effects on the generation and modification of mesoscale circulations 01 p0079 N85-10527

Predicting optical image displacement velocity in survey of Earth's surface 02 p0165 N85-11116

Plane wave (EMP) incidence on a finitely conducting plane Earth with the magnetic field intensity parallel to the Earth's surface [DE84-015364] 02 p0228 N85-11493

Mars-Earth geographical comparisons: A pictorial view [NASA-TM-86166] 02 p0302 N85-11957

Long-distance propagation of infrasound in atmosphere near Earth's surface 06 p0825 N85-15238

Sensor-atmosphere-target simulation. Computer program SENSAT [DFVLR-FB-84-32] 08 p1176 N85-17419

Earth 09 p1411 N85-18892

Polar regions and climatic change: Appendix [PB85-122679] 10 p1521 N85-19590

Evaluation of the radiometric quality of the TM data using clustering, linear transformations and multispectral distance measures — Illinois 12 p1870 N85-21731

The origin and evolution of terrestrial and Martian rock labyrinths [NASA-CR-175511] 12 p1961 N85-22326

Choice of optimum pairs of spectral intervals for IR-range survey of Earth's surface 15 p2486 N85-25344

Evaluating radiation distortions of optical image of Earth's surface in horizontally inhomogeneous atmosphere 15 p2486 N85-25345

Measuring methods of atmospheric electric elements at the Earth's surface during snowfall and investigation of these relationships 15 p2581 N85-25920

Selection of a model of Earth's albedo radiation, practical calculation of its effect on the trajectory of a satellite [NASA-TM-77870] 15 p2591 N85-25972

Preliminary interpretation of Saudi Arabian seismic refraction data 17 p2989 N85-28477

Expedient runway surfacing with post tensioning system for expeditionary airfields [AD-D011677] 19 p3222 N85-29976

HANDTC: A FORTRAN program to calculate inner-zone terrain corrections [DE85-011196] 19 p3340 N85-30699

Geomorphological similarity and uniqueness 21 p3601 N85-32361

Quantitative analysis of geomorphic processes using satellite image data at different scales 21 p3604 N85-32380

Quantitative geomorphologic studies from spaceborne platforms 21 p3604 N85-32381

Global geomorphology: Report of Working Group Number 1 21 p3604 N85-32382

Landscape inheritance: Report of Working Group Number 2 21 p3604 N85-32383

Planetary perspective. Report of Working Group Number 4 21 p3605 N85-32385

Upward continuation of surface gravity anomalies [AD-A154973] 21 p3631 N85-32560

Large arcuate scars: A geological legacy of the Earth's accretionary past 21 p3721 N85-33069

Landscape interpretation capabilities using space photographs of regions of a multistage platform mantle structure 22 p3734 N85-33151

Cataloging the spectral brightness coefficients of the forested region of the European territory of the USSR 22 p3735 N85-33155

Gravity gradiometer survey data processing [AD-A156165] 24 p4117 N85-35522

EARTH TERMINALS

The Ferranti Tactical SHF SATCOM station (MANSAT) 11 p1710 N85-20759

Tactical satellite terminals for land and airborne C3 applications 11 p1710 N85-20760

Moon bounce communications to small terminals [AD-A153297] 17 p2950 N85-28212

EARTH TIDES

Effects of the oceans on polar motion: Continued investigations [E85-10037] 03 p0379 N85-12416

Constraints on the origin of viscoelastic bodies 04 p0584 N85-13732

Tidal dissipation in the Earth and Moon from lunar laser ranging 04 p0585 N85-13733

Ocean tide models for Topex analysis 16 p2805 N85-27291

Analysis and modeling of variations in length of day 19 p3349 N85-30761

Interpolation problems in meteor radar analysis, part 7.6A 21 p3626 N85-32526

EARTH-MOON SYSTEM
Two lunar global asymmetries 04 p0585 N85-13734
The Moon's orbit history and inferences on its origin 04 p0585 N85-13735
A reappraisal of Darwin's fission hypothesis and a possible limit to the primordial angular momentum of the Earth 04 p0585 N85-13736
Numerical simulations of fission 04 p0585 N85-13737
The dynamic fission instability and the origin of the Moon 04 p0586 N85-13738
A testable gravitational capture model for the origin of the Earth's Moon 04 p0586 N85-13742
The problem of iron partition between Earth and Moon during simultaneous formation as a double planet system 04 p0587 N85-13744
The evolution of complex and higher organisms [NASA-SP-478] 21 p3656 N85-32708
The coorbital hypothesis 22 p3858 N85-33890
The magnetic field of planets 22 p3858 N85-33891

EARTH-VENUS TRAJECTORIES
Kovtunenko discusses Vega Project 16 p2722 N85-26804

EARTHQUAKE DAMAGE
Characteristics of a recent Columbian earthquake, December 12, 1979 04 p0523 N85-13347

EARTHQUAKE RESISTANCE
Refined modeling of reinforced concrete columns of seismic analysis [PB84-234384] 04 p0484 N85-13069
Assessment of seismic survivability 09 p1336 N85-18402

EARTHQUAKE RESISTANT STRUCTURES
Earthquake engineering facilities and instrumentation [PB84-231661] 04 p0504 N85-13220
Assessment of seismic survivability 09 p1336 N85-18402
Seismic analysis of rotating mechanical systems [PB85-149599] 14 p2311 N85-24307

EARTHQUAKES
NASA Geodynamics Program [NASA-TM-87359] 01 p0063 N85-10418
Seismology 1983: Nuclear test ban verification, earthquake and Earth resource investigation [FOA-C-20537-T1] 02 p0229 N85-11495
Earthquake activity in the Bohemian massif and in the western Carpathians [REPT-547] 03 p0375 N85-12390
Specific phenomena associated with the propagation of seismic waves in central Europe [REPT-548] 03 p0375 N85-12391
Catalogue of earthquakes for the territory of Czechoslovakia for the period 1957 - 1980 [REPT-555] 03 p0376 N85-12398
Finite-difference synthetic seismograms for SH waves [AD-A145834] 03 p0392 N85-12508
Horizontal-strain observations in the Shumagin Island and Yakataga seismic gaps, Alaska 04 p0515 N85-13287
Seismology today 04 p0523 N85-13346
Characteristics of a recent Columbian earthquake, December 12, 1979 04 p0523 N85-13347
A review of seismicity in peninsular Spain 04 p0523 N85-13349
Models for volcanic processes in Long Valley, California: Testing by continental drilling [DE84-014943] 04 p0534 N85-13414
Earthquake catalog for northern New Mexico [DE84-016984] 04 p0534 N85-13416
A computational study of two possible intraplate earthquake triggering mechanisms 05 p0674 N85-14329
Documentation of earthquake algorithms [PB84-235324] 05 p0677 N85-14351
Earthquakes and tectonics of Pacific Ocean margins 06 p0820 N85-15206
Statistical relationship of strong earthquakes with planetary geomagnetic field activity 06 p0820 N85-15209
Possible effects of interaction of electric seismic fields with the ionosphere 06 p0823 N85-15228
Evaluation of the RSTN (Regional Seismic Test Network) network and further improvement to automatic association [AD-A146395] 06 p0835 N85-15312
General model of earthquakes and the place of warnings in it 07 p0961 N85-16232
Earthquake forecasting research in the Ukraine 07 p0961 N85-16233
Model of earthquake mechanism 07 p0962 N85-16236
Research activities of the Norwegian seismic array (NORSAR) [AD-A14?778] 07 p0996 N85-16326
Seismicity of southern Sweden [FOA-C-20543-T1] 07 p0998 N85-16340
The Shock and Vibration Digest, volume 16, no. 11 [AD-A148466] 08 p1171 N85-17382
Seismic performance of low-rise light-framed wood buildings 08 p1171 N85-17384
Earthquake-modeling experiment using unique press 10 p1500 N85-19469
Localization of destruction process 10 p1500 N85-19470
Study of tectonic earthquake precursors by geodetic methods 10 p1502 N85-19479
Influence of scattering on Q in the lithosphere [AD-A149318] 10 p1515 N85-19563
High-resolution microseismicity study of possible magmatic intrusion in the Long Valley Caldera [DE85-001078] 11 p1681 N85-20593
Catalog of submarine volcanoes and hydrological phenomena associated with volcanic events: 1500 BC to 31 Dec. 1899 [PB85-117984] 12 p1891 N85-21869
Observation of long-period oscillations of Earth 13 p2110 N85-23149
Space and time distribtuion of aftershocks 13 p2112 N85-23157
Magmatism in continent-ocean transition zone (development of ideas of A. N. Zavaritskiy) 13 p2113 N85-23161
Study of geological media based on scattered earthquake waves 13 p2114 N85-23166
Geomagnetic precursors of intensive earthquakes in the 1-0.-2 Hz frequency range of geomagnetic pulsations 13 p2116 N85-23178
Attenuation of seismic waves at regional distances [AD-A150198] 13 p2132 N85-23267
Study of earthquake preparation processes from distribution of weak tremor epicenters 14 p2345 N85-24501
Seafloor seismic measurements in the southern Bering [DE85-004908] 14 p2374 N85-24675
Innovation in earthquake and natural hazards research: Determining soil liquefaction potential [PB85-149573] 14 p2374 N85-24678
A seismic ARGOS data collection platform 16 p2813 N85-27350
Response of a wind turbine blade to seismic and turbulent wind excitations 16 p2817 N85-27375
The Shock and Vibration Digest, volume 17, no. 2 [AD-A153129] 17 p2977 N85-28400
The effects of seismic waves 17 p2978 N85-28401
Australian seismological report, 1980 [REPT-252] 17 p2989 N85-28473
Revised draft: Southeastern regional geologic characterization report [DE85-008265] 18 p3125 N85-29351
Kuril-Aleutian subduction 19 p3290 N85-30402
Discovery in earthquake forecasting and seismic zoning recorded 19 p3295 N85-30426
Satellite-determined stresses in the crust of Europe with particular consideration to the Liege earthquake of November 8, 1983 20 p3490 N85-31694
Seismic discrimination [AD-A154167] 20 p3494 N85-31722
Design of a freestanding noise measurement and recording system to predict the intensity and location of electromagnetic radiation from earthquakes [AD-A155070] 21 p3632 N85-32563
Tectonic stability and expected ground motion at Yucca Mountain [DE85-012004] 22 p3814 N85-33629
Compressional environment in the location and orientation of planetary dorsa and terrestrial earthquake fault structures 22 p3857 N85-33885
Scaling differences between large interplate and intraplate earthquakes [NASA-CR-176149] 23 p3948 N85-34467
Geophysical-geological studies of possible extensions of the New Madrid fault zone [TI85-901341] 23 p3949 N85-34475
Crustal structure in southern California from array data 24 p4115 N85-35512
Attenuation properties of the Petatlan region, Mexico, and a local magnitude scale for microearthquakes in this area 24 p4116 N85-35513
Simplified procedures for the evaluation of settlements in sands due to earthquake shaking [PB85-197887] 24 p4118 N85-35527
Carbon fiber strainmeter studies in southern California [PB85-196689] 24 p4118 N85-35528
Groundwater radon studies for earthquake precursors in southern California [PB85-196671] 24 p4118 N85-35529

EAST GERMANY
Limited surface observations climatic summary (LISOCS). Hohenfels, AAF, West Germany [AD-A147167] 07 p1006 N85-163
Revised Uniform Summary of Surface Weather Observations (RUSSWO). Parts A-F Zweibrucken AB, Germany [AD-A147165] 09 p1357 N85-18
East Europe report: Science and technology [JPRS-ESA-85-005] 09 p1377 N85-18
East European report: Science and technology [JPRS-ESA-85-010] 15 p2524 N85-25

EATING
Characteristics of human masseter under conditions of hypokinesia 11 p1691 N85-20
Psychobiology and food perception 14 p2394 N85-2474
The effects of prolonged feeding meal, ready-to-eat (MRE) operational rations [AD-A154763] 21 p3686 N85-327

EBR-2 REACTOR
U EXPERIMENTAL BREEDER REACTOR 2

EBULLITION
U BOILING

ECCENTRIC ORBITS
Galactic orbits of globular clusters 05 p0739 N85-14750
Stability of the Galilean satellites in deep orbital resonance 13 p2172 N85-23477
Studies of planetary rings 13 p2174 N85-234
Dynamical studies of Saturn's rings 13 p2174 N85-234
The eccentric ringlet at 1.29 R sub S — Saturn radius (RS) 15 p2673 N85-264

ECCENTRICITY
The structure of the Uranian rings and the search for rings around Neptune 02 p0302 N85-11954
Buckling and eccentricity effects on orifice metering accuracy --- gas meters [ERS-E.350] 09 p1324 N85-18321
An experimental investigation into the effects of plate eccentricity and elastic deformation on orifice meter accuracy [ERS-E.391] 09 p1325 N85-18325
Studies of icy bodies: Uranian satellites and cometary nuclei 13 p2175 N85-234
Global positioning system: A modification to the baseline satellite constellation for improved geometric performance [AD-A151692] 15 p2469 N85-252

ECHELETTE GRATINGS
Calibrations of wavelengths in SWP echelle spectra 11 p1761 N85-21077
A new generation of spectrometer designs for ultraviolet astronomy 11 p1761 N85-21079

ECHELON FAULTS
U GEOLOGICAL FAULTS

ECHO SOUNDING
High-frequency asymptotic behavior of reflected and transmitted waves during scattering of sound by hollow elastic sphere filled with fluid 02 p0266 N85-1173
Technical data on new engineering products 10 p1460 N85-192
Acoustooptic pulse-echo tranaducer system [NASA-CR-175919] 17 p2951 N85-28224

ECHO SUPPRESSORS
Interference suppressor for radar MTI [AD-D011606] 16 p2769 N85-270

ECHOCARDIOGRAPHY
Study and realization of a Doppler system with pulsed, directional, multiport (128) emission and sequential signal treatment --- ultrasonic echography, blood flow [ENST-84E008] 05 p0639 N85-14102

ECHOES
NT CLUTTER
NT LUNAR RADAR ECHOES
NT RADAR ECHOES
NT RADIO ECHOES
NT SIGNAL REFLECTION
NT VENUS RADAR ECHOES
Resonant scattering of acoustic waves by elastic spherical shell in fluid 06 p0778 N85-14972
Self-adaptive echo cancellation for telephony [ENST-84E013] 20 p3441 N85-31

ECLIPSES
NT SOLAR ECLIPSES
A model for eclipsing cataclysmic variables 13 p2171 N85-23487

ECLIPSING BINARY STARS
NT DWARF NOVAE
Observations of the O-type subdwarf eclipsing binary system LB 3459 (AA Dor) 01 p0128 N85-10
Accretion in the zeta Aurigae and 32 Cygni shock cones 11 p1754 N85-210
Eclipse observations of Epsilon Aurigae 11 p1755 N85-21007

UV observations of epsilon aurigae during ingress and totality 11 p1755 N85-21036
Egress spectra of the new eclipsing supergiant 22 Vulleculae 11 p1755 N85-21039
The stellar wind in the BO V-type eclipsing binary Y Cygni 11 p1755 N85-21040
Ultraviolet spectroscopy of the interacting binary U Sagittae 11 p1755 N85-21042
The eclipsing binary U Sagittae: Evidence for CNO processing and mass exchange in the past
11 p1757 N85-21049
Tasks for observations of close binary systems in the extreme ultraviolet 11 p1757 N85-21054
Photoelectric observations of the eclipsing binary V 836 Cygni
[REPT-98] 15 p2668 N85-26462

ECLIPTIC
Electric field in plasma layer of magnetosphere during preliminary substorm phase 06 p0824 N85-15231
An update on the correlation between the cosmic radiation intensity and the geomagnetic AA index
[SH-4.2-24] 23 p4009 N85-34861

ECLOGITE
Anorthositic oceanic crust in the Archean Earth
21 p3719 N85-33077

ECOLOGICAL SYSTEMS
U ECOLOGY

ECOLOGY
NT COASTAL ECOLOGY
Mineral nutrients in Mediterranean ecosystems
[REPT-71] 01 p0069 N85-10456
Future scenarios and ozone change
[DE84-014781] 01 p0085 N85-10573
Fungi of Mt. Babia Gora. 2: Indicative value of macromycetes in forest associations. A: Initial considerations
[NASA-TM-77485] 01 p0094 N85-10632
Fungi of Mount Babia Gora. 3: The indicating value of macromycetes in the forest associations
[NASA-TM-77486] 01 p0094 N85-10633
East Europe report: Science and technology
[JPRS-ESA-84-030] 01 p0101 N85-10670
East Europe report: Science and technology
[JPRS-ESA-84-038] 03 p0343 N85-12210
An integrated remote sensing approach for identifying ecological range sites — parker mountain
[E85-10050] 07 p0983 N85-16246
Relationship between forest clearing and biophysical factors in tropical environments: Implications for the design of a forest change monitoring approach — Costa Rica
[E85-10051] 07 p0983 N85-16247
Ecological impacts of hydroelectric projects in Amazonia 07 p1003 N85-16374
Analysis of terrestrial conditions and dynamics
[E85-10063] 08 p1174 N85-17401
Comparing computing formulas for estimating concentration ratios
[DE84-008644] 09 p1349 N85-18490
Calculation of optical characteristics of shelf ecological system based on its mathematical model
10 p1498 N85-19453
Blackbirds and starlings: Population ecology and habits related to airport environments
[AD-P004190] 11 p1580 N85-19953
The bird strike situation and its ecological background in the Copenhagen Airport, Kastrup
[AD-P004203] 11 p1582 N85-19970
Effect of elevated atmospheric CO2 on plant communities
[DE85-001810] 11 p1678 N85-20576
Large natural geophysical events: Planetary planning
[DE85-000659] 11 p1763 N85-21092
Rationale and basic design for experimental acidification of a lake ecosystem in Northern Wisconsin
[PB85-116077] 12 p1885 N85-21829
Evaluation of carrying capacity and landscape damage in northern Kenya by multistage remote sensing
[DFVLR-FB-84-47] 14 p2347 N85-24514
Controlled Ecological Life Support Systems (CELSS)
15 p2686 N85-26604
ELF (Extremely Low Frequency) communications system ecological monitoring program: Measurements of ELF electromagnetic fields for site selection and characterization, 1983
[AD-A153120] 17 p2949 N85-28209
USSR report: Life sciences. Biomedical and behavioral sciences
[JPRS-UBS-85-017] 20 p3504 N85-31765
The global sulfur cycle
[NASA-TM-87570] 21 p3656 N85-32710
Sulfur cycling and metabolism of phototrophic and filamentous sulfur bacteria 21 p3660 N85-32737
Environmental summary for calendar year 1984
[DE85-012020] 22 p3810 N85-33604
Environmental surveillance at Los Alamos during 1984
[DE85-011880] 22 p3811 N85-33605
A 1984 environmental summary: Sandia National Laboratories Tonopah Test Range, Tonopah, Nevada
[DE85-011145] 22 p3812 N85-33612
Model projections of time-dependent response to increasing carbon dioxide
[DE85-013326] 22 p3816 N85-33641
USSR report: Life sciences. Biomedical and behavioral sciences
[JPRS-UBB-85-018] 22 p3819 N85-33660
Climate modeling: A retrospective-prospective view with consideration for the atmospheric carbon dioxide-climate issue
[DE85-011532] 23 p3950 N85-34481
The 1984 biotic studies of Yucca Mountain, Nevada test site, Nye County, Nevada
[DE85-011715] 23 p3951 N85-34487

ECONOMETRICS
Hydrologic and economic models for watershed evaluation and research
[PB84-222371] 01 p0066 N85-10438
A stochastic model for optimizing the consumption and exploration of nonrenewable natural resources
[INPE-2770-PRE/343] 03 p0440 N85-12804
Scientific, technical progress as factor of intensification of economy 13 p2167 N85-23444

ECONOMIC ANALYSIS
Economic model of calibration improvements for automatic test equipment
[PB84-217827] 01 p0051 N85-10335
Uncertainty in water resource planning: An economic evaluation of a water use reduction alternative
[PB84-202605] 01 p0065 N85-10430
Benefits resulting from tailored very-short-range forecasts in Sweden 01 p0084 N85-10564
Foreign civil aviation competition: 1976 summary and implications
[NASA-TM-X-73907] 02 p0133 N85-10907
Satellite servicing: A business opportunity?
02 p0156 N85-11056
Doing business in space: How to get there from here
02 p0156 N85-11057
Space research benefits national economy
02 p0163 N85-11107
Evaluating effectiveness of using space information in specialized hydrogeological research
02 p0164 N85-11114
Robotics investment decision model user's manual
[AD-A145467] 02 p0204 N85-11347
Economic analysis handbook
[AD-A146263] 03 p0441 N85-12805
Report of the reference designs study group on the superconducting super collider
[DE84-015567] 04 p0569 N85-13630
Evaluating NASA technology programs in terms of private sector impacts 05 p0606 N85-13885
Manual-control analysis applied to the money-supply control task 05 p0710 N85-14553
cost and benefits optimization model for fault-tolerant aircraft electronic systems
[NASA-CR-166043] 07 p0946 N85-15993
Development of design and economic parameters for passive solar systems
[AD-A147181] 07 p0993 N85-16303
Life cycle cost management master plan for the Defense Communications Agency
[AD-A146876] 07 p1050 N85-16668
Planning for the on-orbit servicing of military spacecraft
[AD-A148447] 08 p1104 N85-16983
The use of simulation for the technical and economic evaluation of flexible manufacturing systems. Part 2: Results of the simulation
[PNR-90233-PT-2] 09 p1371 N85-18614
Digest of the Deutsche Lufthansa report, 1983
[ISSN-0415-603X] 09 p1418 N85-18948
An assessment of ground-coil heat-pump technology
[DE85-002567] 10 p1486 N85-19382
A decision model for selection of microcomputers and operating systems
[AD-A149076] 10 p1536 N85-19694
Technological and economic assessment of advanced ceramic materials. Volume 3: A case study of ceramic capacitors
[PB85-113108] 11 p1613 N85-20141
Ethanol production by enzymatic hydrolysis: Parametric analysis of a base-case process
[DE84-013105] 11 p1614 N85-20147
Transportation
[JPRS-UTR-85-004] 12 p1769 N85-21105
Current development, applications of airships in USSR
12 p1769 N85-21109
Feasibility of producing commodities and electricity for space shuttle operations at Vandenberg Air Force Base
[DCN-84-203-001-80-21] 12 p1789 N85-21230
Polymer intermediates from limonene (follow-up project)
[BMFT-FB-T-84-243] 12 p1814 N85-21380
Technological and economic assessment of advanced ceramic materials. Volume 1: Summary and conclusions
[PB85-113082] 12 p1815 N85-21383
Closed cycle versus open cycle gas turbines. A review of A.D. Little's ICOP report, vol. 3
[DE85-000564] 12 p1861 N85-21671
FAA aviation forecasts: Fiscal years 1985-1996
[AD-A151050] 14 p2216 N85-23747
MBB/Erno's views, future plans in aerospace activities
15 p2531 N85-25609
Financial, economic commentary on Airbus, European aviation 15 p2536 N85-25649
Kalman filtering and exponential smoothing in economics 15 p2635 N85-26248
Intermediate term forecasting techniques for management
[AD-A151370] 15 p2637 N85-26262
Technical and economic analysis of liquid fuel production from microalgae
[DE85-002926] 16 p2758 N85-27018
New method of calculating the economic effects of corrosion
[BLL-BISI-TRANS-22348-(9022.06)]
17 p2929 N85-28079
An analysis of the economic impact of the AN/APS-134 FLAR (Forward Looking Airborne Radar) retrofit on Coast Guard HC-130 aircraft
[AD-A152619] 17 p2949 N85-28204
Technology and technical efficiency in the Soviet Union: Dominant patterns of constrained optimization in a noncompetitive economic regime
[AD-P004567] 17 p3048 N85-28862
Semicrystalline casting process development and verification
[DE85-007695] 18 p3081 N85-29058
ERS economic impece study
[ESA-CR(P)-1979] 18 p3199 N85-29847
A model for the economic assessment of solar power plants
[DE85-009355] 19 p3381 N85-30977
The helicopter, instrument of choice for health evacuation
[SNIAS-851-220-101] 20 p3393 N85-31051
Improved catalysts for liquid hydrocarbon fuels from syngas
[DE85-011062] 20 p3421 N85-31234
Hidden costs of robotized production systems revealed 20 p3438 N85-31332
Renewable energy research and development outlook, volume 1
[DE85-011577] 20 p3540 N85-32033
Quality analysis 21 p3668 N85-32785
New materials needs in aeronautics
[SNIAS-851-502-101] 22 p3729 N85-33120
Geologic, technical, and economic sensitivity analysis in support of the GRI (Gase Research Institute) tight gas reservoirs project area
[PB85-192276] 22 p3802 N85-33559
Small-hydropower development: The process, pitfalls, and experience. Volume 1: Feasibility studies summary and analysis
[DE85-010839] 22 p3808 N85-33589
Investment justification of robotic technology in aerospace manufacturing. User's manual
[AD-A156193] 24 p4099 N85-35410
Solar pond technology for Navy applications
[AD-A156877] 24 p4112 N85-35486

ECONOMIC DEVELOPMENT
Fusion and its future in Illinois
[DE84-014686] 01 p0122 N85-10833
Methodology for economic evaluation of process technologies in the early research and development stages
[DE84-015863] 05 p0736 N85-14731
Systems research on China in year 2000
12 p1820 N85-21418
China report: Science and technology
[JPRS-CST-85-011] 15 p2551 N85-25746
Spin-offs from technical scientific infrastructures, no. 1
20 p3540 N85-32034
Spin-offs from technical commercial infrastructures, no. 2 20 p3540 N85-32035
Spin-offs from technical scientific research organizations, no. 5 20 p3540 N85-32036
Testimony of Robert A. Frosch before the Subcommittee on HUD and Independant Agencies of the Senate Committee on Appropriations
[NASA-TM-87496] 22 p3736 N85-33173
Federal export assistance programs applicable to the US photovoltaic industry
[NASA-CR-176114] 22 p3849 N85-33841

ECONOMIC FACTORS
Second Symposium on Space Industrialization — space commercialization
[NASA-CP-2313] 02 p0149 N85-11011
Satellite servicing: A business opportunity?
02 p0156 N85-11056
ERS-1 and its potential for industrial utilization
05 p0659 N85-14235
Area handbook series. Honduras: A country study
[AD-A146510] 06 p0827 N85-15253
Socio-economic impact of climate — Mexico
07 p1003 N85-16372
The El Nino phenomenon and its agrometeorological implications 07 p1004 N85-16382
Development of high-efficiency economic systems for photovoltaics 12 p1860 N85-21795
USSR report: Science and technology policy
[JPRS-UST-85-002] 13 p2167 N85-23442
Economic mechanism of integration of science, production 13 p2167 N85-23443
Ecology of Pamlico River, North Carolina: An estuarine profile
[PB85-155703] 16 p2822 N85-27404
Foundations of data envelopment analysis for Pareto-Koopmans efficient empirical productions functions
[AD-A154244] 19 p3346 N85-30735
A model for the economic assessment of solar power plants
[DE85-009355] 19 p3381 N85-30977
Nomographs for estimating the levelized cost of energy from flat-plate and concentrator photovoltaic systems
[NASA-CR-176048] 20 p3483 N85-31645

ECONOMIC IMPACT
Increased joint avionics standardization could result in major economies and operational benefits
[AD-A145730] 02 p0139 N85-10945
The embedded test (BIT): Impact on the total cost of possession 06 p1063 N85-16734
International airport study: How to improve the effect of airports on trade and on export-related industries
[PB85-124923] 11 p1586 N85-19992
Technological and economic assessment of advanced ceramic materials. Volume 2: A case study of ceramics in heat engine applications
[PB85-113090] 12 p1815 N85-21384
Technological and economic assessment of advanced ceramic materials. Volume 5: A case study of ceramic toxic and combustible gas sensors
[PB85-113124] 12 p1815 N85-21386
Industrial laser use expanding in the USSR
15 p2644 N85-26310
New method of calculating the economic effects of corrosion
[BLL-BISI-TRANS-22348-(9022.06)]
17 p2929 N85-28079
An analysis of the economic impact of the AN/APS-134 FLAR (Forward Looking Airborne Radar) retrofit on Coast Guard HC-130 aircraft
[AD-A152619] 17 p2949 N85-28204
ERS economic impace study
[ESA-CR(P)-1979] 18 p3199 N85-29847
Foundations of data envelopment analysis for Pareto-Koopmans efficient empirical productions functions
[AD-A154244] 19 p3346 N85-30735
Aviation nuise effects
[AD-A154319] 19 p3352 N85-30776

ECONOMICS
NT DEMAND (ECONOMICS)
International cooperation and competition in space. Introduction 02 p0295 N85-11912
Problems in CEMA microelectronic cooperation noted
03 p0341 N85-12196
High-temperature steam electrolysis: Technical and economic evaluation of alternative process designs
[DE84-015702] 04 p0469 N85-12986
USSR report: Machine tools and metalworking equipment
[JPRS-UMM-84-020] 04 p0491 N85-13126
Economic value of consumer information: A selected, annotated bibliography
[PB84-235795] 04 p0576 N85-13673
Manual-control analysis applied to the money-supply control task 05 p0710 N85-14553
Review of climate problems in Latin America and the Caribbean 07 p1001 N85-16354
Oceanographic data for development of the US exclusive economic zone
[PB85-106458/GAR] 07 p1010 N85-16415
An evaluation of the effect of establishing a minimum Economic Order Quantity (EOQ) on the Air Force EOQ item management system
[AD-A147121] 07 p1051 N85-16673
USSR report: Machine tools and metalworking equipment
[JPRS-UMM-85-001] 08 p1139 N85-17172
Summaries of press automation conference presented
08 p1139 N85-17173
FRG study locks at participation in ESA, US space station 08 p1141 N85-17191
Safety awareness, pilot education, and incident reporting programs 09 p1276 N85-18020
Issues in air transport
[PB85-121374/GAR] 09 p1277 N85-18030
National Machine Tools Conference slated for 1985: Conference agenda, papers 10 p1460 N85-19202
USSR report: Machine tools and metalworking equipment
[JPRS-UMM-85-003] 10 p1461 N85-19211
Long-range electronics program outlined
11 p1700 N85-20687
Latent heat storage technology and application workshop. Summary report: Session 5
[DE85-001097] 12 p1882 N85-21806
USSR report: Science and technology policy
[JPRS-UST-85-002] 13 p2167 N85-23442
Scientific, technical progress as factor of intensification of economy 13 p2167 N85-23444
Clutchless mechanism for engagement of forging press 14 p2268 N85-24051
Liquid membranes for the production of oxygen-enriched air
[DE85-006056] 15 p2506 N85-25460
Prospects for developing attractive magnetic fusion concepts
[DE85-006925] 16 p2867 N85-27684
USSR report: Machine tools and metalworking equipment
[JPRS-UMM-84-014] 17 p2946 N85-28188
Foundations of data envelopment analysis for Pareto-Koopmans efficient empirical productions functions
[AD-A154244] 19 p3346 N85-30735
EOQ (Economic Order Quantity) range model
[AD-A153709] 19 p3379 N85-30965
CEMA venture to develop FMS, robot technology
20 p3438 N85-31330
Photovoltaics technical information guide
[DE85-002924] 22 p3808 N85-33585

ECONOMY
1st deputy minister on civil aviation support of economy 14 p2208 N85-23690
Minister Bugayev reviews 1983 civil aviation work, sets course for 1984 14 p2208 N85-23695
Computing in the Soviet general economy: An introductory overview
[AD-P004563] 17 p3047 N85-28858
Quality analysis 21 p3668 N85-32785

ECOSYSTEMS
Response of arctic ecosystems to elevated carbon dioxide regimes, volume 2
[DE84-015236] 01 p0069 N85-10460
The 1984 NASA/ASEE summer faculty fellowship program
[NASA-CR-174138] 04 p0574 N85-13663
Terrestrial nitrogen cycles: Some unanswered questions 05 p0653 N85-14192
Classification of vegetation communities in the Battle Mountain SE quadrangle, Nevada with MSS digital data
[E85-10043] 06 p0826 N85-15246
Ecological impacts of hydroelectric projects in Amazonia 07 p1003 N85-16374
Extremely Low Frequency (ELF) Communications System Ecological Monitoring Program: Summary of 1983 progress
[AD-A147704] 08 p1151 N85-17265
Compilation of annual reports of the Navy ELF (Extremely Low Frequency) communications system ecological monitoring program. Volume 1: Tabs A-E
[AD-A148326] 08 p1152 N85-17272
Compilation of annual reports of the Navy ELF (Extremely Low Frequency) communications system ecological monitoring program (1983). Volume 2: Tabs F-J
[AD-A148327] 08 p1152 N85-17273
Comparing computing formulas for estimating concentration ratios
[DE84-008644] 09 p1349 N85-18490
Air quality criteria for ozone and other photochemical oxidants. External review draft, volume 5
[PB85-126076-VOL-5] 11 p1679 N85-20583
Proceedings of the 1st Glacier Bay Science Symposium
[PB85-115913] 11 p1682 N95-20599
Combined effects of atmospheric deposition, internal acid production, and harvesting on nutrient gains and losses from forest ecosystems
[DE85-002325] 12 p1864 N85-21821
Ecological observations at the site of the 10 MWe solar thermal power system (1976-1984)
[DE85-004572] 12 p1885 N85-21
Rationale and basic design for experimental acidification of a lake ecosystem in Northern Wisconsin
[PB85-116077] 12 p1886 N85-21
Air quality criteria for ozone and other photochemical oxidants. External review draft, volume 2
[PB85-126043] 12 p1886 N85-21
Combined analysis of the dynamics of complex ecosystems based on repeated remote measurements
13 p1985 N85-22
Technologies to sustain tropical forest resources
[TI85-901085] 13 p2126 N85-22
Areas with forest soils sensitive to acidic deposition under alternative damage hypotheses
[DE85-005257] 13 p2130 N85-22
The ecology of tundra ponds of the Arctic coastal plain: A community profile
[TI85-900650] 15 p2589 N85-25
An analysis of issues concerning acid rain, report to the Congress of the United States
[TI85-901070] 15 p2589 N85-25
Ecology of Pamlico River, North Carolina: An estuarine profile
[PB85-155703] 16 p2822 N85-27404
MARMAP survey of the continental shelf from Cape Hatteras, North Carolina to Cape Sable, Nova Scotia (1977 - 1983). Atlas 1: Summary of operations
[PB85-150985] 16 p2839 N85-27
ELF (Extremely Low Frequency) communications system ecological monitoring program: Measurements of ELF electromagnetic fields for site selection and characterization, 1983
[AD-A153120] 17 p2949 N85-28
Fatty and aromatic acid catabolizing bacteria from methanogenic ecosystems
[DE85-008133] 17 p2996 N85-28
Stability and feasibility of model ecosystems
[PREPRINT-431] 18 p3134 N85-29
Use of a two-dimensional flow model to quantify aquatic habitat
[AD-A154287] 19 p3266 N85-30
Microbial ecology of extreme environments: Antarctic yeasts and growth in substrate-limited habitats
[NASA-CR-176005] 19 p3326 N85-30
Global geomorphology 21 p3601 N85-32
Biogeochemical cycling and remote sensing
21 p3659 N85-32

ECS
U EUROPEAN COMMUNICATIONS SATELLITE

EDDIES
U VORTICES

EDDINGTON APPROXIMATION
Energy relations on the small oscillations excitation in the stars 14 p2450 N85-25125
Ultra high energy gamma rays, cosmic rays and neutrinos from accreting degenerate stars
[OG-2.2-5] 22 p3864 N85-33
X-ray spectra of bursting neutron stars
23 p3961 N85-34

EDDY CURRENTS
Technical activities 1983, Office of Nondestructive Evaluation
[PB84-217074] 03 p0370 N85-12360
Superconducting magnet for probing eddy currents in dynamic models 04 p0489 N85-13117
The determination of eddy current losses in electrical equipment
[DE84-016340] 05 p0632 N85-14050
A narrow band pulsed eddy current instrument for materials testing
[AERE-R-11229] 07 p0968 N85-16149
Feasibility study to demonstrate detection of low levels of oxygen contaminant in titanium using eddy current and ultrasonic NDE (Nondestructive Evaluation) techniques
[AD-P004129] 08 p1127 N85-17104
Experimental verification of eddy-current flaw theory
[DE85-001288] 09 p1329 N85-18350
Behavior of small ferromagnetic particles in traveling magnetic field 12 p1843 N85-21584
Eddy current test probe with circumferential segments and method of testing material surrounding fastener holes
[AD-D011554] 12 p1850 N85-2160
Pre- and post-processing for stream-function eddy current calculations
[AD-A150417] 13 p2065 N85-22
Magnetic field interactions with material discontinuities
[AD-A150197] 13 p2154 N85-2337
Applications of eddy currents
14 p2316 N85-2431
Preliminary results on passive eddy current damper technology for SSME turbomachinery
16 p2737 N85-2

Investigation on the application of the pulsed eddy current method of non-destructive testing using controlled signals (CS-technique)
[BLL-BISI-TRANS-22249-(9022.06)] 18 p3119 N85-29303
Plating density standards
[DE85-010014] 21 p3591 N85-32318
Development of contactless sensors for industrial and automotive applications
[BMFT-FB-T-85-031] 24 p4097 N85-35400

EDDY DIFFUSION
U TURBULENT DIFFUSION

EDDY VISCOSITY
Model equations describing unsteady fluid motion
[ESA-TT-850] 04 p0501 N85-13194
Application of large eddy interaction model to channel flow
[NASA-TM-86691] 12 p1844 N85-21572
Modeling evolution of unstable geostropic eddies in barotropic ocean 14 p2336 N85-24447
SSME fuel preburner two-dimensional analysis 17 p2911 N85-27943
SSME turbopump turbine computations 17 p2911 N85-27944
MST radar data management 21 p3627 N85-32532

EDGE DISLOCATIONS
Fracture toughness of materials
[DE85-004306] 12 p1667 N85-21713
Determination of edge and screw dislocation density in single crystals of high-purity iron
[DE85-010237] 20 p3537 N85-32012
Stress and efficiency studies in EFG
[NASA-CR-176125] 22 p3751 N85-33251
Influence of edge effects on performance of electrooptical lens 22 p3770 N85-33366
Crystallographic orientation dependence of fatigue crack propagation in extremely low carbon steel 23 p3906 N85-34195

EDGE LOADING
Checking optical-polarization measurements at interfaces 02 p0271 N85-11770
Large transverse deflections of circular plates loaded symmetrically
[NPL-DMA(A)-86] 04 p0512 N85-13262
Stress intensity factors for corner cracks at holes located near an edge
[FFA-TN-1984-20] 04 p0514 N85-13279
Effect of edge distance on yield initiation in a remotely loaded half-plane containing interference-fit disc of the same material
[ARL/STRUC-R-413] 19 p3285 N85-30369

EDGES
NT LEADING EDGES
NT TRAILING EDGES
Design of edge detectors for reduced images
[AD-A145700] 02 p0252 N85-11653
Analysis of accretion and deletion at boundaries in dynamic scenes
[AD-A145944] 03 p0419 N85-12678
A study of interply layer effects on the free-edge stress field of angleplied laminates
[NASA-TM-86924] 07 p0919 N85-15822
On edge detection
[AD-A148573] 08 p1223 N85-17703
On large matchings and cycles in sparse random graphs
[AD-A149194] 10 p1550 N85-19778
Edge diagnostics for tandem mirror machines
[DE85-001209] 11 p1733 N85-20902
Edge detection in SAR imagery using gradient operators -- synthetic aperture radar (SAR)
[AD-A149411] 13 p2054 N85-22862
Stress intensity factor in a tapered specimen
[NASA-CR-175589] 13 p2102 N85-23099
Feasibility of optical instruments based on multiaperture optics
[AD-A150868] 14 p2421 N85-24936
Evaluation of stress concentration coefficients in butt-welded joints with displaced edges 15 p2501 N85-25425
Mechanical aspects of interfaces and surfaces in ceramic containing systems
[AD-A151978] 15 p2519 N85-25530
Chemical applications of topology and group theory. 17: An information theoretical approach to polyhedral symmetry
[AD-A152821] 17 p2919 N85-27995
Ultrasonic testing of plates containing edge cracks
[NASA-CR-3904] 18 p3119 N85-29307
Experimental and theoretical assessment of a new technique for the non-destructive evaluation of laminated panels
[AD-A155622] 21 p3562 N85-32155
Hierarchical chamfer matching
[FOA-C-30387-E1] 22 p3802 N85-33558
Mechanical properties of plasma arc cut steel 23 p3905 N85-34188
Anti wear property of two phasic metal composite 23 p3906 N85-34190
Edge detection and geometric methods in computer vision
[AD-A155873] 24 p4135 N85-35630
Edge information in color images based on histograms of differences
[AD-A156002] 24 p4154 N85-35751

EDITING
Ada (trademark) training curriculum. Basic Ada programming I202 teacher's guide. Laboratory manual and exercises
[AD-A143583] 01 p0103 N85-10687
Tekedit: An enhanced editor for Direct View Storage Tube (DVST) graphics display devices
[AD-A149715] 12 p1915 N85-22021
The potential for advanced computerized aids for comprehensible writing of technical documents
[AD-A150501] 13 p2055 N85-22870
Computer program for plotting and fairing wind-tunnel data
[NASA-TM-85648] 20 p3387 N85-31009
An integrated system for printing and publishing applications 23 p3959 N85-34540
A model for a document maintenance system 23 p3960 N85-34542

EDITING ROUTINES (COMPUTERS)
SAGA: A project to automate the management of software production systems
[NASA-CR-174017] 01 p0103 N85-10685
PROGEN: An incremental programming environment
[NRIMS-TWISK-315] 02 p0241 N85-11568
SMILE user's guide: A macro preprocessor for extending FORTRAN
[DE84-015984] 02 p0243 N85-11584
DATAPLOT: Implementation tapes guide
[PB84-214063] 03 p0406 N85-12610
MACSYMA usage at Langley
[NASA-CR-172518] 10 p1537 N85-19688
The design and implementation of a syntax directed editor for a space constrained microcomputer
[AD-A151313] 15 p2623 N85-26163
The design, implementation and application of a table-driven syntax-directed editor
[AD-A1542[illegible]4] 19 p3336 N85-30670
Experience with omega: Implementation of a prototype programming environment: Part 1
[AD-A155436] 21 p3672 N85-32611
Design and implementation of an interactive route editor 23 p3962 N85-34559
Procedure for editing the fluxgate magnetometer data of the AFGL (Air Force Geophysics Laboratory) magnetometer network
[AD-A156331] 24 p4117 N85-35523

EDUCATION
NT ASTRONAUT TRAINING
NT FLIGHT TRAINING
NT MAINTENANCE TRAINING
NT PILOT TRAINING
NT SPACE FLIGHT TRAINING
Self-paced instruction. Factors critical to implementation in Air Force technical training: A preliminary inquiry
[AD-A145098] 01 p0097 N85-10647
Comprehension of instructions for operating devices
[AD-A145263] 01 p0098 N85-10653
IAC user manual
[NASA-CR-175300] 01 p0102 N85-10677
Ada (trademark) training curriculum. Using the Ada language reference manual I402 teacher's guide
[AD-A143582] 01 p0103 N85-10686
Ada (trademark) training curriculum. Basic Ada programming I202 teacher's guide. Laboratory manual and exercises
[AD-A143583] 01 p0103 N85-10687
Integrated computer-aided manufacturing (ICAM) architecture. Part 3, volume 8: Technology transfer
[AD-A144732] 01 p0103 N85-10689
National Science Foundation grants and awards for fiscal year 1983, volume 2
[PB84-212323] 01 p0125 N85-10854
A report on the training course at Fortaleza (Ceara)
[E85-10013] 02 p0216 N85-11426
Designing an expert system for training automotive electrical troubleshooting
[AD-P003926] 02 p0246 N85-11606
Emergency Mathematics and Science Education Act
[GPO-29-561] 03 p0435 N85-12770
The 1984 ASEE-NASA summer faculty fellowship program (aeronautics and research)
[NASA-TM-87393] 04 p0575 N85-13664
Computer Literacy Act of 1983, part 2
[H-REPT-98-752-PT-2] 04 p0578 N85-13687
East Europe report: Science and technology
[JPRS-ESA-84-045] 06 p0815 N85-15175
Computer-managed instruction: Theory, application, and some key implementation issues
[AD-A146564] 06 p0854 N85-15426
Requirements for training in climate-related subjects 07 p1004 N85-16378
Education and training for the climate related activities in Latin America and the Caribbean 07 p1004 N85-16379
Human factors and training research in military organizations and systems
[AD-A146832] 07 p1020 N85-16475
Ada training curriculum. Real-time systems in Ada I401 teacher's guide, volume 1
[AD-A146782] 07 p1024 N85-16496
Ada training curriculum. Real-time systems in Ada I401 teacher's guide, volume 2
[AD-A146783] 07 p1024 N85-16497
A study of Air Force Quality Circle program effectiveness as viewed through facilitator's perceptions
[AD-A147633] 08 p1170 N85-17377
Efforts to improve aviation medical examiner performance through continuing medical education and annual performance reports
[AD-A148078] 08 p1195 N85-17531
Training guide for scientific and engineering trainees 1984
[AD-A147963] 08 p1196 N85-17542
Training high performance skills: Fallacies and guidelines
[AD-A148574] 08 p1198 N85-17545
Concept paper for the development of a DOD Ada (trademark) software engineering education and training plan
[AD-A148774] 08 p1206 N85-17592
Pilot education and safety awareness programs 09 p1277 N85-18026
Innovative approaches to recurrent training 09 p1277 N85-18028
NASA Lewis Research Center/University Graduate Research Program on Engine Structures
[NASA-TM-86916] 09 p1333 N85-18375
Bibliography of unclassified reports, FY 1984
[AD-A148838] 09 p1401 N85-18819
Application of the HARDMAN methodology to the single channel ground-airborne radio system (SINCGARS)
[NASA-CR-175486] 10 p1487 N85-19259
USSR report: Life sciences. Biomedical and behavioral sciences
[JPRS-UBB-85-011] 10 p1525 N85-19616
Study of cognitive styles of students in automated teaching system 10 p1525 N85-19620
Computers and education
[GPO-28-378] 10 p1537 N85-19689
Topics in optical materials and device research, 3. Volume 2
[AD-A149727] 12 p1911 N85-21996
Application of the Hardman methodology to the Single Channel Ground-Airborne Radio System (SINCGARS)
[NASA-CR-175694] 14 p2218 N85-23756
The role of prior knowledge in operating equipment from written instructions
[AD-A151007] 14 p2392 N85-24730
The acquisition of procedures from text. A production-system analysis of transfer of training
[AD-A151029] 14 p2392 N85-24732
Administration chief on air traffic control improvements 15 p2460 N85-25193
China report: Science and technology
[JPRS-CST-85-011] 15 p2551 N85-25746
A learning strategy approach for teaching novice computer programmers
[AD-A151523] 15 p2628 N85-26200
Academic science and engineering: Graduate enrollment and support, fall 1982 (detailed statistical tables)
[PB85-154730] 15 p2664 N85-26438
Programming for Pioneer 12 15 p2688 N85-26606
Rotorcraft digital advanced avionics system (Rodaas) 15 p2688 N85-26608
The search for extraterrestrial intelligence 15 p2689 N85-26609
A review of safety practices and safety training for the explosives field
[AD-A152295] 16 p2759 N85-27028
Automated CPX support system preliminary design phase
[NASA-CR-175784] 16 p2769 N85-27091
The impact of group processing on achievement in cooperative learning groups
[AD-A153166] 17 p3001 N85-28551
Oral discussion, group-to-individual transfer and achievement in cooperative learning groups
[AD-A153209] 17 p3001 N85-28552

Summer High School Apprenticeship Research Program (SHARP) of the National Aeronautics and Space Administration
[NASA-CR-175791] 17 p3046 N85-28849
Engineering education based on computer simulation
[CFD/85/1] 20 p3512 N85-31829
The Naval Postgraduate School Flight Mechanics Laboratory: A feasibility study
[AD-A154578] 21 p3557 N85-32127
One application of mega-geomorphology in education
21 p3602 N85-32370
Ada (trademark) training curriculum. Advanced Ada topics L305 teacher's guide exercises
[AD-A154621] 21 p3670 N85-32796
Solar energy meteorological research and training program: Region 4
[DE85-011783] 22 p3816 N85-33640
Solar energy education. Renewable energy: A background text
[DE85-010385] 23 p3946 N85-34452
Development of NATOPS (Naval Air Training and Operating Procedure Standardization) performance software for the H-46D helicopter
[AD-A156089] 24 p4064 N85-35190
Benchmark evaluation of PC simscript
[AD-A156133] 24 p4136 N85-35651
Comet Halley returns: A teachers' guide 1985-1986
[NASA-EP-197] 24 p4168 N85-35839

EEG (ELECTROENCEPHALOGRAMS)
U ELECTROENCEPHALOGRAPHY

EFFECTIVE PERCEIVED NOISE LEVELS
Contribution of tonal components to the overall loudness, annoyance and noisiness of noise: Relation between single tones and noise spectral shape
[NASA-CR-3892] 15 p2645 N85-26317
Noise reduction in the automotive test cell of the Motor Institute of Naples
[REPT-85-RR-361] 20 p3524 N85-31917
The timing of noise-sensitive activities in residential areas
[NASA-CR-177937] 20 p3524 N85-31918

EFFECTIVENESS
NT COST EFFECTIVENESS
NT SYSTEM EFFECTIVENESS

EFFECTORS
U CONTROL EQUIPMENT

EFFECTS
The effect of modified spectacles on the field of view of the helmet display unit of the integrated helmet and display sighting system
[AD-A148693] 09 p1281 N85-18055
Analyzing two-level fractional factorial experiments for possible dispersion effects
[AD-A149455] 10 p1548 N85-19760
The effects of internal waves on acoustic normal modes
[AD-A150235] 13 p2155 N85-23379
The effects of controversy and concurrence seeking on effective decision making
[AD-A153370] 17 p3002 N85-28555

EFFERENT NERVOUS SYSTEMS
Development and evaluation of a performance-based test of saccadic and vestibulo-ocular control
[AD-A145367] 02 p0237 N85-11545
Applications of connectionist modeling techniques to simulations of motor control systems
05 p0717 N85-14598
Advanced development of an active neuromusculature response to mechanical stress
[AD-A148436] 08 p1196 N85-17536
Effects of tasks on responses of human skin mechanoreceptors 11 p1691 N85-20635
Comparative analysis of effects of weightlessness and its models on velocity and strength properties and tone of human skeletal muscles 12 p1901 N85-21936
Effects of muscle atrophy on motor control: Cage size effects 15 p2609 N85-26080
Eye movement in response to single and multiple targets
[AD-A151115] 15 p2617 N85-26126

EFFICIENCY
NT CHARGE EFFICIENCY
NT COMBUSTION EFFICIENCY
NT COMPRESSOR EFFICIENCY
NT ENERGY CONVERSION EFFICIENCY
NT NOZZLE EFFICIENCY
NT POWER EFFICIENCY
NT PROPELLER EFFICIENCY
NT PROPULSIVE EFFICIENCY
NT THERMODYNAMIC EFFICIENCY
NT TRANSMISSION EFFICIENCY
A determination of the photochemical quantum yields from 2 excited triplet states of biacetyl using holography
[AD-A145091] 01 p0050 N85-10326
Oscillatory integrals by Hermite interpolatory rules
[CSIR-TWISK-301] 01 p0108 N85-10725
Fuel efficiency through new airframe technology
[NASA-TM-84548] 02 p0133 N85-10909
Component-specific modeling
02 p0143 N85-10971
Energy efficient engine. High pressure compressor detail design report
[NASA-CR-165558] 02 p0147 N85-10998
Standardized efficiency terms: Comparison of some Stirling engine performance figures
[DE84-015407] 02 p0205 N85-11352
Efficiency of lasing dye media in pumping high-power radiation with nanosecond pulses
02 p0270 N85-11763
Maintenance Management Information and Control System (MMICS): Administrative boon or burden
[AD-A145762] 03 p0438 N85-12790
Comparability and accuracy of industry codes in different data systems
[PB84-215607] 04 p0548 N85-13482
Analyses of energy extraction efficiency of unstable resonators
[AD-A146391] 06 p0813 N85-15161
Recent developments in photovoltaics
[DE84-004528] 06 p0833 N85-15305
Comparison measurements on optical particle counters
[BLL-DOUNREAY-TR-934-(9091.9F)]
07 p0961 N85-16092
Overview od STS ground operations/orbiter turnaround STS-1 through STS-7 08 p1096 N85-16926
USSR report: Machine tools and metalworking equipment
[JPRS-UMM-84-021] 08 p1138 N85-17168
Control systems for robotic production lines
08 p1136 N85-17169
Metallographic grinding efficiency
[DE85-001520] 09 p1304 N85-18194
Available energy method for evaluating thermodynamic performance of heat pump systems
[DE84-017223] 09 p1400 N85-18814
Calculation of Si(Li) X-ray detector efficiencies
[DE85-002732] 10 p1489 N85-19400
Electric-Hybrid Vehicle (E-HV) demonstration-test project
[DE85-002370] 10 p1570 N85-19899
Assessment of effectiveness of electron beam welding of titanium alloys up to 40 mm in thickness by vertical or horizontal beam 11 p1603 N85-20078
Some solar dish/heat engine design considerations
[DE85-003479] 12 p1881 N85-21802
Characterizing the parallelism in rule-based expert systems
[DE85-002432] 12 p1919 N85-22047
Methods of digital correction for channels of multichannel radar receivers 13 p2082 N85-23005
Proceedings of the Cold Electronics Workshop
[NASA-CR-175662] 14 p2297 N85-24220
Cold electronics: An overview
14 p2297 N85-24221
Electromagnetic scattering by arbitrarily shaped reflectors: Subreflector efficiency
[AD-A149224] 15 p2541 N85-25687
Efficiency analysis of the electronic mail system (INFOMAIL) on the defense data network
[AD-A151894] 15 p2632 N85-26223
Optimal control of electric drive with simultaneous control inputs for motor current and flux
16 p2763 N85-27049
High efficiency ionizer using a hollow cathode discharge plasma
[DE85-006690] 16 p2868 N85-27693
Flow characteristics of a partially submerged liquid pickup
[DE85-006744] 17 p2959 N85-28276
Small central receiver Brayton cycle study
[DE85-008882] 18 p3128 N85-29369
Megajoule-class single-pulse KrF laser test facility as a logical step toward inertial fusion commercialization
[DE85-009590] 18 p3191 N85-29794
Receiver loss study of optimized solar central receiver systems as a function of receiver thermal loss per unit area
[DE85-010831] 19 p3268 N85-30265
Design and operation of epitaxial reactor
[DE85-011089] 19 p3306 N85-30491
Foundations of data envelopment analysis for Pareto-Koopmans efficient empirical productions functions
[AD-A154244] 19 p3346 N85-30735
An empirical technique to measure X-ray production and detection efficiencies in the analytical electron microscope
[DE85-010270] 19 p3361 N85-30637
Auto fuel efficiency standards, part 2
[GPO-41-189] 20 p3435 N85-31309
High efficiency large area polysilicon solar cells
20 p3482 N85-31
High efficiency solar cell processing
20 p3482 N85-31
Efficiency tests of samplers for microbiological aerosols, a review
[FOA-C-40199-B1] 20 p3504 N85-31
The use of superoxide mixtures as air-revitalization chemicals in hyperbaric, self-contained, closed-circuit breathing apperatus
[NASA-TM-86709] 20 p3512 N85-31
Application of adaptive noise cancellation to Coast Guard voice communications
[AD-A154796] 21 p3574 N85-32
Physics of heavily doped silicon and solar-cell parameter measurement 21 p3609 N85-32
Sensitivity analysis of high-efficiency silicon solar-cell design parameters 21 p3610 N85-32
Silicon surface passivation by silicon nitride deposition
21 p3610 N85-32
Important loss mechanisms in high-efficiency solar cells 21 p3610 N85-32
Stress and efficiency studies in EFG
21 p3611 N85-32
Sixty GHz IMPATT diode development
[NASA-CR-174969] 22 p3758 N85-33
Experiments and improvements of the ordinary differential equation solvers DEPAC on the CRAY computer
[DE85-013260] 22 p3831 N85-33
Lubrication and cooling for high speed gears
[NASA-TM-87096] 23 p3938 N85-34
Development of a high-efficiency, gas-fired, heat pipe, warm-air heating system
[PB65-199636] 24 p4085 N85-35
The NORDA/FNOC (Naval Ocean Research and Development Activity's/Fleet Numerical Oceanography Center) Polar Ice Prediction System (PIPS)-Arctic: A technical description
[AD-A156332] 24 p4126 N85-35

EFFLUENTS
Supercritical fluid chromatography/supersonic jet spectroscopy
[DE84-016199] 04 p0471 N85-12
The Georges Bank monitoring program 1983: Analysis of trace metals in bottom sediments
[CIRC-915] 05 p0688 N85-14
Investigation of internal friction of free-flowing material during discharge
[BLL-M-36141-(5828.4)] 15 p2553 N85-25
Influence on an industrial site on the characteristics of CCN supersaturation with air masses of different origin
21 p3650 N85-32
The 1984 effluent and environmental monitoring report for the Bettis Atomic Power Laboratory
[DE85-011533] 22 p3810 N85-33
Environmental summary for calendar year 1984
[DE85-012020] 22 p3810 N85-33
Environmental monitoring at Lawrence Livermore National Laboratory: 1984 report
[DE85-011593] 22 p3811 N85-33
The 1984 environmental monitoring report, Sandia National Laboratories, Albuquerque, New Mexico
[DE85-011175] 22 p3811 N85-33
Control technology for radioactive emissions to the atmosphere at US Department of Energy facilities: The Los Alamos Meson Physics Facility
[DE85-011402] 22 p3811 N85-33

EFFORT
A theorem on the optimal allocation of effort
[AD-A148028] 08 p1211 N85-17

EFFUSIVES
NT LAVA
Changes in the organic material in lakes in the blast zone of Mount St. Helens, Washington: Hydrologic effects of the eruptions
[GS-CIRC-850-1] 21 p3630 N85-32

EGGS
An automatic device for amphibian egg fertilization in space: Technical aspects and biological requirements
05 p0689 N85-14
Radiobiological studies on egg systems exposed to heavy nuclei of cosmic galactic radiation — Insects
05 p0690 N85-14
Simulated microgravity as a probe for understanding the mechanisms of early pattern specification
15 p2611 N85-26
Report of Amphibian Development Group
24 p4127 N85-35

EGRESS
Egress spectra of the new eclipsing supergiant 2 Vulleculae 11 p1755 N85-21
Fire research publications, 1984
[PB85-208502] 24 p4166 N85-35

EGYPT
SIR-B analysis of the Precambrian shield of Sudan and Egypt: Penetration studies and subsurface mapping
08 p1145 N85-17219
A brief comparison of Egyptian with West German atmospheric transmission data in the 8 to 11.5 micron waveband
[BAE-BT-12829] 15 p2594 N85-25983
EIGENFUNCTIONS
U EIGENVECTORS
EIGENSTATES
U EIGENVECTORS
EIGENVALUES
Problems on the diffraction and propagation of waves (selected articles)
[AD-A145139] 01 p0036 N85-10240
Rotordynamic analysis of the SSME turbopumps using reduced models
[NASA-CR-171170] 01 p0054 N85-10355
Legendre-Tau approximation for functional differential equations. Part 3: Eigenvalue approximations and uniform stability
[NASA-CR-172447] 01 p0110 N85-10744
Moment induced by liquid payload during spin-up without a critical layer
[AD-A145716] 02 p0199 N85-11327
The application of principal components analysis to LANDSAT MSS data 02 p0212 N85-11398
Gain-phase structures for linear multivariable systems
[RR-256] 02 p0256 N85-11674
A study of the critical layer in a rotating liquid payload
[AD-A146094] 03 p0362 N85-12321
Effects of changing the signs of rows and columns of a matrix and the hyperbolic transpose
[DE84-014851] 04 p0555 N85-13530
A routine to find the lowest few eigenvalues and vectors for the generalised sparse symmetric eigenproblem
[NPL-DITC-43/84] 05 p0722 N85-14641
Splitting methods for the numerical solution of the incompressible Navier-Stokes equations
[AD-A147463] 07 p1032 N85-16554
Eigenvalues of rotating machinery
08 p1167 N85-17361
Experimental investigations of driven Alfven wave resonances in a Tokamak plasma using carbon dioxide laser interferometry
[DE85-001049] 09 p1392 N85-18758
Perturbation of a multiple eigenvalue in the Benard problem for two fluid layers
[AD-A149068] 10 p1546 N85-19745
Applied mathematics of transport theory
[DE85-000848] 11 p1633 N85-20263
A numerical approach for the vibration analysis of an axisymmetric shell structure with a nonuniform edge constraint
[AD-A149286] 11 p1651 N85-20402
The eigenvalues of the pseudospectral Fourier approximation to the operator sin (2x) d/dx
[NASA-CR-172538] 11 p1706 N85-20729
Optical eigenvector
[AD-A149550] 11 p1729 N85-20871
Normal mode analysis for linear resistive magnetohydrodynamics
[IPP-6/235] 11 p1730 N85-20878
Role of cavitons in laser-plasma interactions
[DE85-001842] 11 p1731 N85-20886
Modal control of structural systems
[AD-A149734] 12 p1790 N85-21235
Planar dynamics of a uniform beam with rigid bodies affixed to the ends
[NASA-CR-175566] 12 p1864 N85-21693
Practical considerations for noninteracting control synthesis
[AD-A150130] 12 p1918 N85-22046
On the limiting empirical distribution function of the eigenvalues of a multivariate F matrix
[AD-A149818] 12 p1921 N85-22065
Spectral frequency of eigenvalues in optimal problems of stability of cylindrical shells of variable thickness
13 p2047 N85-22815
On limit of the largest eigenvalue of the large dimensional sample covariance matrix
[AD-A150589] 13 p2151 N85-23358
Design of multivariable feedback control systems via spectral assignment using reduced-order models and reduced-order observers
[NASA-CR-3889] 14 p2226 N85-23800
Representation of temperature and salinity fields using statisticallyt orthogonal functions (in example of polymode data)
14 p2337 N85-24449
On limiting empirical distribution function of the eigenvalues of a multivariate F matrix, revised
[AD-A151865] 15 p2641 N85-26288
On asymptotic joint distribution of the eigenvalues of the noncentral manova matrix for nonnormal populations
[AD-A151866] 15 p2642 N85-26294
Squeezing the most out of Eigenvalue solvers on high-performance computers
[DE85-007569] 16 p2849 N85-27565
Eigenvalue approximation methods for quantum lattice Hamiltonians 16 p2858 N85-27627
Incorporating control into the optimal structural design of large flexible space structures
[AD-A152858] 17 p2909 N85-27937
Solution to eigenvalue problems of antisymmetric cross-ply and antisymmetric angle-ply laminated plates using affine transformations
[AD-A153040] 17 p2917 N85-27980
Continuum modeling of latticed structures
17 p2977 N85-28309
Some applications of a convenient finite-dimensional matrix representation of the differential operator
[PREPRINT-418] 18 p3172 N85-29661
Numerical tests of a novel technique to compute the eigenvalues of differential operators
[PREPRINT-427] 18 p3173 N85-29667
Evaluation of the eigenvalue method in the solution of transient heat conduction problems
[AD-A154434] 19 p3266 N85-30256
Structural dynamics modification of generalized beams using a local eigenvalue modification procedure
19 p3282 N85-30353
Asymptotic expansions for finite element eigenvalues and finite element solution 19 p3345 N85-30730
Monte Carlo alpha calculation
[DE85-010720] 19 p3349 N85-30758
Eigenvalue placement and stabilization by constrained optimization 20 p3416 N85-31198
An Eigensystem Realization Algorithm (ERA) for modal parameter identification and model reduction
20 p3418 N85-31212
Spectral Theory of Sturm-Liouville Differential Operators: Proceedings of the 1984 Workshop
[DE85-009893] 20 p3520 N85-31890
On the solution for the sound field in a semi-infinite uniform duct with sheared mean flow
20 p3523 N85-31912
Systematics of quark mass matrices in the Standard Electroweak Model
[USIP-85-05] 20 p3532 N85-31972
Finding the roots of the transcendental equations in problems in determining the thermal conductivity of spheres with heterogeneous boundary conditions
[BLL-M-35878-(5828.4)] 23 p3929 N85-34347
Vibrations of free hollow circular cylindrical bodies
24 p4100 N85-35418
EIGENVECTORS
A subspace iteration method for determining a dominant span of eigenvectors
[TWISK-329] 01 p0109 N85-10739
The application of principal components analysis to LANDSAT MSS data 02 p0212 N85-11398
Linear autonomous retarded functional differential equations; a sharp version of Henry's theorem
[CWI-AM-R8405] 05 p0720 N85-14625
A routine to find the lowest few eigenvalues and vectors for the generalised sparse symmetric eigenproblem
[NPL-DITC-43/84] 05 p0722 N85-14641
Lax-pair operators for squared-sum and squared-difference eigenfunctions
[AD-B089083L] 09 p1386 N85-18718
A numerical approach for the vibration analysis of an axisymmetric shell structure with a nonuniform edge constraint
[AD-A149286] 11 p1651 N85-20402
The eigenstructure assignment of deadbeat control systems
[AD-A149761] 12 p1834 N85-21510
Practical considerations for noninteracting control synthesis
[AD-A150130] 12 p1918 N85-22046
Analysis of interaction of dynamically adjustable gyroscopes on elastic platform by finite-element method
13 p2048 N85-22822
Design of multivariable feedback control systems via spectral assignment using reduced-order models and reduced-order observers
[NASA-CR-3889] 14 p2226 N85-23800
Observed spatial properties of the solar eigenfunctions and the implications for the existence of resolved multiflets 14 p2443 N85-25074
Squeezing the most out of Eigenvalue solvers on high-performance computers
[DE85-007569] 16 p2849 N85-27565
Mutual coupling analysis for conformal microstrip antennas
[AD-A154282] 19 p3259 N85-30210
Spectral Theory of Sturm-Liouville Differential Operators: Proceedings of the 1984 Workshop
[DE85-009893] 20 p3520 N85-31890
Interacting Boson approximation
[DE85-003016] 22 p3837 N85-33756
EIKONAL EQUATION
A theoretical study of electron capture in ion-ion and ion-atom collisions
[DE85-011154] 19 p3362 N85-30842
EINSTEIN EQUATIONS
Solution generating technique for the Einstein equations 03 p0435 N85-12768
Conserved quantities and radiative aspects of asymptotically anti-de Sitter space-times
12 p1958 N85-22303
Solutions of field equations in General Relativity with spinor connection 15 p2663 N85-26436
EINSTEIN OBSERVATORY
U HEAO 2
EJECTA
Capture of planetesimals into a circumterrestrial swarm 13 p2179 N85-23522
Impact cratering calculation 13 p2180 N85-23531
Progress on Experimental impact studies
13 p2181 N85-23534
The nature of Martian flow ejecta craters
13 p2183 N85-23545
Interaction of Martian flow ejecta blankets with pre-existing impact craters: Morphological observations
13 p2183 N85-23546
Geomorphology and geology of the Southwestern Margaritifer Sinus and Argyre regions of Mars. Part 4: Flow ejecta crater distribution 13 p2193 N85-23603
Magnetic instabilities in solar filaments: Models of twisting motions and ejecta 14 p2454 N85-25156
Identification of the youngest meteorites and a discussion of the possibility that they came from Mars
15 p2681 N85-26559
Examination of returned solar-max surfaces for impacting orbital debris and meteoroids
15 p2681 N85-26560
A comprehensive investigation of the dynamics of micron and submicron lunar ejecta in heliocentric space
19 p3384 N85-30994
EJECTION
NT STELLAR MASS EJECTION
Low-profile fastener
[AD-D011667] 19 p3280 N85-30343
EJECTION INJURIES
The clinical and biomedical evaluation of trauma and fatalities associated with aircrew ejection and crash. A Working Group report
[AGARD-AR-194] 12 p1906 N85-21969
Introduction: The clinical and biomedical evaluation for trauma and fatalities associated with aircrew ejection and crash 12 p1906 N85-21970
Statistics of french Armee de l'air ejections 1970 - 1980 12 p1906 N85-21971
List of head/neck injury on ejection in the German Armed Forces from 1972-1981 12 p1906 N85-21972
A review of neck injury and impaired consciousness associated with US Navy ejections 1 January 1969 - 31 December 1979 12 p1906 N85-21973
A review of fatality, impairment of consciousness, and head/neck injury on USAF ejections 1971 - July 1983
12 p1906 N85-21974
A review of fatality, impairment of consciousness and head and neck injury on Royal Air Force ejections 1968-1981 12 p1907 N85-21975
The clinical and radiological assessment of cervical injury, Annex A 12 p1907 N85-21976
Head/neck injury: Post mortem procedures, Annex B
12 p1907 N85-21977
Tight Ribbon Arm Protection (TRAP) for aircrewman ejection
[AD-A150464] 13 p2143 N85-23303
EJECTION SEATS
Simple nonrestrictive arm restraint system
[AD-D011216] 01 p0005 N85-10026
Windblast leg protector assembly
[AD-D011376] 07 p0899 N85-15700
Powered articulated headrest system
[AD-D011353] 07 p0901 N85-15710
S-3A ballast block final design and engineering tests
[AD-A147685] 08 p1080 N85-16842
A Generalized Escape System Simulation (GESS) computer program. Volume 2: GESS programmer's manual, version 2
[AD-A148363] 08 p1081 N85-16845
An investigation of spinal injury potential from the use of the ACES 2 ejection seat by lower weight female pilots
[AD-A148449] 08 p1196 N85-17537
Deployment sequence mode selection system for aircraft ejection seat
[AD-D011464] 10 p1422 N85-18966
Airspeed sensing pressure valve system
[AD-D011472] 10 p1425 N85-18967
Personnel protection concepts for advance escape system design 10 p1532 N85-19656

A safety evaluation of the relocation of the ACM (Air Combat Maneuver) panel in the F-14 ( )/AIP (Avionics Integration Program)
[AD-A149586] 12 p1777 N85-21158
The clinical and biomedical evaluation of trauma and fatalities associated with aircrew ejection and crash. A Working Group report
[AGARD-AR-194] 12 p1906 N85-21969
Introduction: The clinical and biomedical evaluation for trauma and fatalities associated with aircrew ejection and crash 12 p1906 N85-21970
Statistics of french Armee de l'air ejections 1970 - 1980 12 p1906 N85-21971
List of head/neck injury on ejection in the German Armed Forces from 1972-1981 12 p1906 N85-21972
Windblast arm protector assembly
[AD-D011512] 12 p1909 N85-21984
Tight Ribbon Arm Protection (TRAP) for aircrewman ejection
[AD-A150464] 13 p2143 N85-23303
Preliminary design of a limb restraint evaluator
[AD-A151749] 15 p2486 N85-25226
Air bag restraint system
[AD-D011671] 19 p3215 N85-29936
SSMIR (Solid State Memory Instrumentation Recorder): A new approach to acquiring data during an aircraft seat/sled ejection sequence
[AD-A154780] 21 p3589 N85-32308
Design and testing of an energy-absorbing crewseat for the F/FB-111 aircraft. Volume 2: Data from seat testing
[NASA-CR-3917] 24 p4064 N85-35184

EJECTORS
An engine trade study for a supersonic STOVL fighter-attack aircraft, volume 1
[NASA-CR-166304] 02 p0133 N85-10910
Viscous-inviscid aerodynamic analysis of two-dimensional thrust augmentors
[NASA-CR-177321] 04 p0451 N85-12861
An experimental investigation of two-dimensional thrust augmenting ejectors, part 1
[NASA-CR-174111] 04 p0456 N85-12894
An experimental investigation of two-dimensional thrust augmenting ejectors, part 2
[NASA-CR-174110] 04 p0456 N85-12895
Basic studies of multiple free and confined jets
[AD-A149556] 10 p1485 N85-19374
Mixing characteristics of an underexpanded multiple jet ejector
[AD-A149557] 10 p1485 N85-19375
An experimental investigation of an underexpanded rectangular jet ejector
[AD-A149656] 12 p1779 N85-21170
A theoretical study of two stage thrust augmenting ejectors
[ARL/AERO-R-166] 19 p3218 N85-29954
Applied research and development for falling-sphere air density measuring systems
[AD-A155227] 21 p3552 N85-32099
Combined cold compressor/ejector helium refrigerator
[DE85-006406] 23 p3925 N85-34326

EKMAN LAYER
Numerical calculations of stratified Ekman layer flow over ridges with a finite element model
[DE84-014482] 04 p0499 N85-13179
Strongly nonlinear dynamics of baroclinic waves
20 p3488 N85-31681

EL NINO
Meteorological aspects of the 1982-83 El Nino/southern oscillation episode 07 p1001 N85-16356
Ocean and climate, an example. The interannual variability of the tropical Pacific Ocean
07 p1002 N85-16365
Climate and fisheries: A Peruvian case study
07 p1003 N85-16373
The El Nino phenomenon and its agrometeorological implications 07 p1004 N85-16382
Droughts and floods in South America due to the 1982-83 El Nino-southern oscillation episode
[INPE-3408-PRE/677] 09 p1357 N85-18535
El Nino, the capricious child 13 p2106 N85-23121
Forecast of Atlantic seasonal hurricane activity for 1985 16 p2833 N85-27470
Southern oscillation/El Nino excitation of the Earth's Chandler wobble 20 p3490 N85-31695

ELASTIC BARS
On the asymptotic analysis of travelling shocks and phase boundaries in elastic bars
[AD-A147239] 07 p0959 N85-16076
Hopkinson bar simulation using DYNA2D
[DE85-006766] 16 p2802 N85-27275

ELASTIC BENDING
A model for the compressive buckling of extended chain polymers
[AD-A151025] 14 p2260 N85-24006
An experimental study of the magnetoelastic bending of thin plates made of soft ferromagnetic material
19 p3282 N85-30352
A refinement of the transverse shear deformation theory for multilayered anisotropic plates
[STN-5] 20 p3471 N85-31571

ELASTIC BODIES
Controlling rotation of elastic manipulator link
04 p0488 N85-13113
A compact finite element method for elastic bodies
[NASA-CR-172487] 06 p0817 N85-15185
Stability of viscoelastic constructions subjected to steady random compressing loads 11 p1720 N85-20819
Experience with free bodies 15 p2576 N85-25867
Finite element prediction of loss factors for structures with frequency-dependent damping treatments
15 p2576 N85-25869
A natural modes formulation and modal identities for structures with linear viscous damping
[CRC-1382] 18 p3120 N85-29312
The role of ellipticity and normality assumptions in formulating live-boundary conditions in elasticity
[AD-A153475] 18 p3166 N85-29630
Application of deformable body mean-axis to dynamics of flexible mechanical systems 19 p3283 N85-30359
Approximation techniques for parameter estimation and feedback control for distributed models of large flexible structures 20 p3413 N85-31179
Characteristic elastic systems of time-limited optimal maneuvers 20 p3413 N85-31184

ELASTIC BUCKLING
Initial postbuckling analysis of elastoplastic thin-shear structures 01 p0059 N85-10393
Thermomechanically induced pre- and postbuckling of general structure 20 p3487 N85-31540

ELASTIC COLLISIONS
U ELASTIC SCATTERING

ELASTIC CONSTANTS
U ELASTIC PROPERTIES

ELASTIC CYLINDERS
Second Colloquim on the Scattering of Ultrasonic Waves
[AD-A156298] 24 p4145 N85-35697

ELASTIC DAMPING
NT VISCOELASTIC DAMPING
Controlled movement of elastic manipulator with distributed parameters 13 p2048 N85-22818
Stability of steady modes of motion by axis of rotating wheel in nonlinear bearings 14 p2279 N85-24117

ELASTIC DEFORMATION
NT ELASTIC BENDING
NT ELASTIC BUCKLING
Weak shocks and steady waves in a nonlinear elastic rod or granular material
[AD-A145715] 02 p0209 N85-11383
Symmetry of exchange interaction in crystalline magnetic films 02 p0259 N85-11694
Seismology in rockburst research
[REPT-551] 03 p0375 N85-12394
Iterative method for determining the distortion of elastic-plastic frames
[ISSN-0208-5658] 05 p0647 N85-14156
Deformation of cylindrical shell with cantilevered elastic plates attached 06 p0779 N85-14984
Fundamental tribological properties of ceramics
[NASA-TM-86915] 07 p0930 N85-15893
An experimental investigation into the effects of plate eccentricity and elastic deformation on orifice meter accuracy
[ERS-E.391] 09 p1325 N85-18325
Existence, uniqueness and stability conditions for general finite element methods in linear elasticity
09 p1332 N85-18372
Model analysis of structural systems involving nonlinear coupling 09 p1337 N85-18409
Localization of destruction process
10 p1500 N85-19470
A deformation analysis of flat flexible gear and its equation of original curved surfaces
[NASA-TM-77493] 12 p1850 N85-21660
On local total strain redistribution using a simplified cyclic inelastic analysis based on an elastic solution
[NASA-TM-86913] 12 p1864 N85-21690
Planar dynamics of a uniform beam with rigid bodies affixed to the ends
[NASA-CR-175566] 12 p1864 N85-21693
Deployment analysis of the Olympus Astromast and comparison with test measurements — solar arrays
13 p2011 N85-22616
Time dependent interaction of internal pressure wave with system of two spherical shells
13 p2046 N85-22809
Determination of stresses and deformations in linearly elastic conical shell subjected to aerodynamic loading and heating 13 p2047 N85-22812
Gear noise origins 14 p2224 N85-23791
Determination of parameters of elastically strained facets of rapidly rotating prisms
14 p2262 N85-241
Development of a dynamic finite element model for unrestrained flexible structures
[AD-A151176] 15 p2636 N85-
Identification and control of structures in space
[NASA-CR-175790] 16 p2731 N85-
Simulation studies for surfaces and materials strength
[NASA-CR-175766] 16 p2900 N85-27
Influence of preliminary cold deformation on fineness of pearlite
[BLL-BISI-TRANS-22409-(9022.06)]
17 p2927 N85-
The role of ellipticity and normality assumptions in formulating live-boundary conditions in elasticity
[AD-A153475] 18 p3166 N85-
Application of deformable body mean-axis to dynamics of flexible mechanical systems 19 p3283 N85-
Shear deflection in a three-point bend beam of a solid circular cross-section
[AD-A154458] 19 p3287 N85-
On elastic-plastic fracture criterion
20 p3465 N85-315
Finite elastic deformations of cylindrical and spherical shells under pressure
[OUEL-1549/84] 20 p3470 N85-315
Hertzian contact in two and three dimensions
[NASA-TP-2473] 21 p3596 N85-
Identification and control of structures in space
[NASA-CR-176175] 24 p4069 N85-362

ELASTIC MEDIA
Propagation of longitudinal elastic waves in multilayered half-space 02 p0273 N85-1177
Wedge with crack in bielastic medium
02 p0273 N85-1178
An inverse source problem for elastic waves
03 p0371 N85-12
Transonic flow of elastic medium past slender solid body 06 p0776 N85-14
Numerical experiments and theoretical analysis of the flow of an elastic liquid of the Maxwell-Oldroyd type in the presence of geometrical singularities
[WTHD-164] 08 p1163 N85-17
Numerical evaluation of low frequency sound propagation in layered media
[AD-A152690] 17 p3028 N85-2

ELASTIC MODULUS
U MODULUS OF ELASTICITY

ELASTIC PLATES
Stress intensity factors for corner cracks at holes located near an edge
[FFA-TN-1984-20] 04 p0514 N85-12
Numerical treatment of corner singularities of the biharmonic equation
[TUM-M8315] 05 p0717 N85-14
Investigation of dynamics of manipulator with elastic sections 13 p2048 N85-22
Load transfer by analytical methods
[SNIAS-851-111-109] 20 p3470 N85-315
Generation by conformal mappings of aerofoil sections and of certain other simple shapes suitable for both aerodynamic and stress-concentration problems
[AD-A154901] 22 p3728 N85-3

ELASTIC PROPERTIES
NT AEROELASTICITY
NT DYNAMIC MODULUS OF ELASTICITY
NT ELASTOPLASTICITY
NT HYDROELASTICITY
NT MAGNETOSTRICTION
NT MODULUS OF ELASTICITY
NT PHOTOELASTICITY
NT PHOTOVISCOELASTICITY
NT PROPORTIONAL LIMIT
NT THERMOELASTICITY
NT THERMOVISCOELASTICITY
NT VISCOELASTICITY
Theory of nonlocal elasticity and some applications
[AD-A145201] 01 p0062 N85-104
Wedge with crack in bielastic medium
02 p0273 N85-117
Eta values for compact geometry specimens to calculate the J integral
[AERE-R-11126] 03 p0374 N85-12
In situ experiment on shear waves generation and determination of elastic properties of soils
[REPT-550] 03 p0375 N85-12
An integral equation formulation for a boundary value problem of elasticity in the domain exterior to an arc
[PREPRINT-833] 03 p0413 N85-12
Nondestructive evaluation of residual stress in low-carbon steel
[NASA-CR-174157] 04 p0512 N85-13
Nondestructive determination of mechanical properties — aluminum alloys 04 p0512 N85-13

Influence of the mechanical and electrochemical characteristics of austenitic and austenoferritic steels on the propagation rate and morphology of stress corrosion cracking
[BLL-RISLEY-TR-4545-(9091.9F)]
06 p0767 N85-14906

Saint Venant conditions in theory of piezoelastic shells
06 p0780 N85-14967

Controllable rotation of system of two solid bodies with elastic elements 06 p0780 N85-14968

Elastic fields under a spherical indenter
[AD-A146519] 06 p0817 N85-15188

Theoretical and experimental study of hydro-elastic instability on the line of shafting of a rotating machine
[BLL-DOUNREAY-TR-937-(9091.9F)]
07 p0872 N85-16174

Nonlinear waves in a rod. Results for incompressible elastic materials
[AD-A147485] 07 p0979 N85-16216

Model for prediction of the elastic response of composite materials over wide ranges of concentration
[AD-A148186] 08 p1119 N85-17051

Study of reaction kinetics and development of elastic properties in network polymerization systems by the impulse technique
[AD-A148187] 08 p1133 N85-17141

Determination of the elastic constants of inhomogeneous materials with X-ray diffraction
[AD-A148480] 08 p1173 N85-17393

Nonlinear finite element analysis of elastic and elastic-plastic buckling of cylinders under complex combined loads 09 p1332 N85-18373

Earthquake-modeling experiment using unique press
10 p1500 N85-19469

Simplified theory for the behaviour of buried flexible cylinders under the influence of uniform hoop compression
[PB85-116531] 11 p1654 N85-20419

Parachute inflation dynamics
11 p1715 N85-20792

Rheology of dissemination
[AD-A150006] 12 p1813 N85-21373

Elastic response of a half-plane to a bonded interference-fit disc of the same material
[ARL/STRUC-R-406] 12 p1865 N85-21701

Moving nonlocal crack: Anti-plane shear case
[AD-A149996] 12 p1866 N85-21709

Elasticity formulas for thin-walled shells with piezoceramic layers 13 p2047 N85-22816

Controlled movement of elastic manipulator with distributed parameters 13 p2048 N85-22818

Attenuation of seismic waves at regional distances
[AD-A150198] 13 p2132 N85-23267

Influence of short-range order on deformation mechanisms in solid solutions
[DE85-006374] 14 p2258 N85-23989

Research on composite materials for structural design
[AD-A150802] 14 p2260 N85-24004

Uniaxial orientation of linear low density polyethylene
[AD-A151037] 14 p2261 N85-24009

Analysis of slabs-on-grade for a variety of loading and support conditions
[AD-A150965] 14 p2264 N85-24030

The application of transonic unsteady methods for calculation of flutter airloads 15 p2460 N85-25186

An experimental investigation into the dynamic response of a stiffened flat plate loaded impulsively by an underwater shockwave
[AD-A151321] 15 p2578 N85-25903

Control of a flexible beam
[DE85-007243] 15 p2580 N85-25914

Mechanical properties of high performance carbon fibers 16 p2742 N85-26922

The effects of pin elasticity, clearance, and friction on the stresses in a pin-loaded orthotropic plate
[NASA-CR-175816] 16 p2743 N85-26927

Solution softening in molybdenum-rhenium alloys
[DE85-006706] 16 p2750 N85-26972

On residual stress in an elastic body
16 p2798 N85-27248

Numerical solution of one-dimensional nonlinear problems of statics for elastic beams and shells under rigid constraints 17 p2943 N85-28166

Electronically excited alkaline earth oxides: Chemical production and collisional energy transfer processes
[AD-A153172] 17 p3044 N85-28833

Gust load alleviation of a cantilevered rectangular elastic wing. Wind tunnel experiment and analysis
[NAK-TR-86] 18 p3063 N85-28950

Interaction of large amplitude stress waves in layered elastic-plastic materials
[AD-A153519] 18 p3121 N85-29323

Mechanics of composite materials, theory and application
[VTH-LR-431] 18 p3123 N85-29334

Shear deflection in a three-point bend beam of a solid circular cross-section
[AD-A154458] 19 p3287 N85-30381

Analysis of the elastic and strength properties of Yucca Mountain tuff, Nevada
[DE85-008975] 19 p3300 N85-30460

A survey of unified constitutive theories
20 p3466 N85-31531

Viscoplasticity based on overstress with a differential growth law for the equilibrium stress
20 p3466 N85-31532

On the use of internal state variables in thermoviscoplastic constitutive equations
20 p3466 N85-31536

Dynamical study of flat plates by nonlinear elasticity theory
[STN-8] 20 p3471 N85-31572

Stresses and deformations in cross-ply composite tubes subjected to a uniform temperature change: Elasticity and Approximate Solutions
[NASA-CR-176147] 22 p3800 N85-33545

SANCHO: A finite element computer program for the quasistatic, large deformation, inelastic response of two-dimensional solids
[DE85-011456] 22 p3829 N85-33714

Viscoelastic behavior of short-fiber composite materials
[DE85-011233] 23 p3910 N85-34225

The study of the effect of residual microimpurities on the fatigue strength of 55S2 steel
[BLL-M-36317-(5828.4)] 23 p3913 N85-34246

An introduction to finite elements
23 p3924 N85-34319

Stresses and strains in a plate resulting from two closely-spaced interference-fit fasteners
[ARL/STRUC-TM-409] 23 p3941 N85-34429

Analysis of the nonlinear equations describing the elastic, thermal, and electromagnetic behavior of solids: Existence of solutions of semi-inverse problems
24 p4100 N85-35415

Vibrations of free hollow circular cylindrical bodies
24 p4100 N85-35418

(NAT)Fe(n,n'x) spectra at 65.5 MeV
[AD-A155776] 24 p4150 N85-35730

Ionic crystals
[DE85-009482] 24 p4163 N85-35809

ELASTIC SCATTERING

Sturmian expansion approximation to three-body scattering
[CSIR-TWISK-309] 01 p0109 N85-10731

Monte Carlo simulation of thermalization of subexcitation electrons in molecular hydrogen
[NAL-TR-815T] 01 p0117 N85-10798

Study of structure of nuclei with neutrons and nuclear data measurements for MFE
[DE84-015128] 01 p0117 N85-10802

Molecular beam scattering 03 p0417 N85-12666

Diffuse elastic and inelastic neutron scattering of disorder transitions and boundaries. Phase determination of structure factors 03 p0424 N85-12706

Quasielastic neutron scattering on single crystals of solid ionic conductor 03 p0426 N85-12719

Fundamentals of microcrack nucleation mechanics
[NASA-CR-3851] 07 p0975 N85-16195

High energy physics study
[DE84-015803] 09 p1383 N85-18700

Instrumental background in balloon-borne gamma-ray spectrometers and techniques for its reduction
[NASA-TM-86162] 09 p1413 N85-18911

Low energy antiproton interaction studies at Brookhaven
[DE85-001228] 11 p1720 N85-20820

Recent progress in electron scattering at SLAC
[DE85-002718] 11 p1723 N85-20840

Cometary atmospheres: Modeling the spatial distribution of observed neutral radicals
[NASA-CR-175485] 11 p1765 N85-21098

A remote source system for measuring relative positron annihilation line widths in individual slab cylindrical samples
[AERE-R-10549] 12 p1938 N85-22173

Elastic wave scattering from an interface crack in a layered half space 13 p2101 N85-23095

Intensity vectors of sound scattering by a spherical shell
[AD-A147847] 13 p2103 N85-23107

Elastic wave scattering from cavities and sound inclusions analyzed by the resonance method
[AD-A150315] 13 p2155 N85-23381

Theoretical aspects of the nucleon-nucleon workshop
[DE85-003740] 14 p2420 N85-24933

Interaction of low energy electrons with surface lattice vibrations
[DE85-005475] 14 p2428 N85-24975

Energy deposition from particle beams
[DE85-007382] 16 p2862 N85-27654

Stefan-Maxwell relations for plasma diffusion currents in magnetic field 17 p2942 N85-28160

Experimental studies of diffractive phenomena
[DE85-006812] 17 p3031 N85-28749

Development of the relativistic impulse approximation
[DE85-006505] 18 p3179 N85-29711

Intermediate energy nuclear theory
[DE85-010440] 18 p3182 N85-29731

Theory of high energy collision processes
[DE85-010183] 19 p3362 N85-30846

Energy-advanced nuclear data: Measurements and physical interpretations
[DE85-006196] 19 p3366 N85-30872

Methods of Monte Carlo electron transport in particle-in-cell codes
[DE85-010702] 20 p3521 N85-31898

Spin physics at BNL
[DE85-009768] 20 p3529 N85-31955

Remarks on nucleon-nucleon hard scattering
[NIKHEF-H/84-14] 20 p3532 N85-31979

Spatial parity violation in elastic neutron-nuclei interaction channel 21 p3691 N85-32932

Evaluated nuclear-data file for niobium
[DE85-012095] 21 p3704 N85-33009

P(P bar)P elastic scattering and cosmic ray data
[HE-1.1-6] 24 p4170 N85-35854

General consequences of the violated Feynman scaling 24 p4173 N85-35872

ELASTIC SHELLS

High-frequency asymptotic behavior of reflected and transmitted waves during scattering of sound by hollow elastic sphere filled with fluid 02 p0266 N85-11736

Selective observation of elastic-body resonances via their ringing in transient acoustic scattering
[AD-A145868] 03 p0416 N85-12658

Resonant scattering of acoustic waves by elastic spherical shell in fluid 06 p0778 N85-14972

Some problems in optimally designing shells of revolution 14 p2278 N85-24114

Elastic equilibrium of composite shells with finite shear rigidity 17 p2942 N85-28163

Numerical solution of one-dimensional nonlinear problems of statics for elastic beams and shells under rigid constraints 17 p2943 N85-28166

Scattering of sounds by piezoceramic cylindrical shell near rigid surface 17 p2943 N85-28168

ELASTIC STABILITY
U DAMPING

ELASTIC STRENGTH
U PROPORTIONAL LIMIT

ELASTIC WAVES
NT AERODYNAMIC NOISE
NT AIRCRAFT NOISE
NT BAROCLINIC WAVES
NT CAPILLARY WAVES
NT COHERENT ACOUSTIC RADIATION
NT COMPRESSION WAVES
NT DETONATION WAVES
NT ELECTROACOUSTIC WAVES
NT ELECTROSTATIC WAVES
NT ENGINE NOISE
NT GRAVITY WAVES
NT ION ACOUSTIC WAVES
NT IONIC WAVES
NT JET AIRCRAFT NOISE
NT LAMB WAVES
NT LOVE WAVES
NT MAGNETOACOUSTIC WAVES
NT MAGNETOELASTIC WAVES
NT MAGNETOHYDRODYNAMIC WAVES
NT MICROSEISMS
NT NOISE (SOUND)
NT NORMAL SHOCK WAVES
NT OBLIQUE SHOCK WAVES
NT P WAVES
NT PHONONS
NT PLASMA WAVES
NT RAYLEIGH WAVES
NT RIPPLES
NT S WAVES
NT SEISMIC WAVES
NT SHOCK WAVES
NT SONIC BOOMS
NT SOUND WAVES
NT STRESS WAVES
NT THERMAL NOISE
NT TOLLMEIN-SCHLICHTING WAVES
NT ULTRASONIC RADIATION

Influence of radiation wavelength on elastic pulse shape during laser excitation 02 p0257 N85-11681

Propagation of longitudinal elastic waves in multilayered half-space 02 p0273 N85-11779

Elastic wave propagation through polycrystals
[DE84-016772] 04 p0558 N85-13554

A geometric approach to high resolution TVD schemes
[NASA-CR-172484] 06 p0857 N85-15449
Fundamentals of microcrack nucleation mechanics
[NASA-CR-3851] 07 p0975 N85-16195
Quantitative acoustic emission techniques
[AERE-R-11262] 07 p0977 N85-16203
On seismic waves 08 p1171 N85-17383
Characterisation of fatigue crack extension by quantitative acoustic emission
[AERE-R-11289] 12 p1868 N85-21721
Scattering of elastic waves on fractures randomly distributed in a three-dimensional medium
13 p2111 N85-23151
Elastic wave scattering from cavities and sound inclusions analyzed by the resonance method
[AD-A150315] 13 p2155 N85-23381
An analytical and numerical study of the interaction of rarefaction waves with area changes in ducts. Part 2: Area enlargements
[UTIAS-273] 14 p2300 N85-24242
Propagation of non-axisymmetric elastic waves through shell with filler under radial load at one end
17 p2943 N85-28169
Theoretical and experimental studies of the mechanics of viscoelastic liquids
[AD-A153505] 18 p3070 N85-28987
Computer simulation of elastic waves by a new mass-point system with potentials
[DRIC-T-7274] 20 p3469 N85-31553
Source characterization of point-like and distributed sources of acoustic emission 20 p3523 N85-31910
Numerical experiment of elastic wave propagation by framework model
[DRIC-T-7462] 22 p3795 N85-33511
ELASTICITY
U ELASTIC PROPERTIES
ELASTICIZERS
U PLASTICIZERS
ELASTODYNAMICS
NT ELASTIC DAMPING
NT ELASTOHYDRODYNAMICS
Acoustic emission waveforms in a half space
[AD-A146322] 03 p0417 N85-12664
Transonic flow of elastic medium past slender solid body 06 p0778 N85-14976
Numerical modeling of complex interaction of shell of revolution and its filler with allowance for friction
06 p0779 N85-14980
Deformation of cylindrical shell with cantilevered elastic plates attached 06 p0779 N85-14984
Numerical solution of elastodynamic problems in fracture mechanics 08 p1171 N85-17385
A numerical method for interface problems in elastodynamics
[NASA-TM-86488] 08 p1172 N85-17391
Symmetric primal-dual variational formulations of coupled dynamic systems: Three-dimensional elasticity, shells, fluid-structure interaction
[ONERA-1983-91] 12 p1863 N85-21684
Controllable movements of elastic manipulator with three degrees of freedom 14 p2266 N85-24040
Application of deformable body mean-axis to dynamics of flexible mechanical systems 19 p3283 N85-30359
Transient dynamic solutions of some half space problems by the boundary element method
19 p3283 N85-30360
ELASTOHYDRODYNAMICS
Normal mode method of solving problem forced oscillations of rib-reinforced shell of revolution in liquid
02 p0273 N85-11781
Fluidelastic instability in shell and tube heat exchangers: A framework for a prediction method
[DE84-006518] 10 p1496 N85-19444
Problems of elastic hydrodynamic lubrication of helicopter transmission gears 14 p2222 N85-23784
Wear reduction by lubricants in confined contacts
14 p2223 N85-23786
Fast approach for calculating film thicknesses and pressures in elastohydrodynamically lubricated contacts at high loads
[NASA-TM-87032] 19 p3264 N85-30242
Surface roughness effects in elastohydrodynamic contacts
[NASA-TP-2488] 21 p3595 N85-32329
Mechanics of a gaseous film barrier to lubricant wetting of elastohydrodynamically lubricated conjunctions
[NASA-TP-2500] 21 p3595 N85-32330
ELASTOMERS
NT CHLOROPRENE RESINS
NT VULCANIZED ELASTOMERS
Electrically conductive rigid polyurethane foam
[DE84-014490] 01 p0033 N85-10203
Aircraft surface coatings
[NASA-CR-3661] 02 p0137 N85-10935
The role of molecular diffusion in the adhesion of elastomers
[AD-A145576] 02 p0186 N85-11245
Mechanochemical reactions of elastomers with metals
[AD-A145657] 02 p0186 N85-11246
Description and characterization of deuterated polymers for the analysis with neutron scattering
03 p0431 N85-12748
The effect of cross-link density on the toughening mechanism of elastomer-modified epoxies
04 p0465 N85-12951
Toughening mechanism in elastomer-modified epoxy resins, part 2
[NASA-CR-3852] 04 p0478 N85-13046
Flexible matrix composite laminated disk/ring flywheel
05 p0606 N85-13886
Structure-property relationships in thermoplastic elastomers. Part 1: Segmented polyether-polyurethanes
[AD-A148043] 08 p1133 N85-17136
Poly(dimethylsiloxane)-polyurethane elastomers: Synthesis and properties of segmented copolymers and related zwitterionomers
[AD-A148571] 08 p1134 N85-17147
Development of a heterogeneous laminating resin system
[NASA-CR-172459] 09 p1288 N85-18069
Mechanisms of gas permeation through polymer membranes
[DE84-017423] 09 p1293 N85-18117
Characterization of novel binders based on energetic thermoplastic elastomers
[AD-A148993] 10 p1451 N85-19139
Elastomer toughened polyimide adhesives — bonding metal and composite material structures for aircraft and spacecraft
[NASA-CASE-LAR-12775-2] 12 p1809 N85-21349
Effect of alternative aging and accident simulations on polymer properties
[DE85-002642] 13 p2037 N85-22762
Oil resistant silicone elastomers
[AD-131523] 16 p2753 N85-26987
Formulation/cure technology for ultrahigh molecular weight silphenylene-siloxane polymers
[NASA-TP-2476] 16 p2753 N85-26990
Thermally stable elastomers: Review of silarylene-siloxane polymers and polysilmethylenes
[AD-A152323] 17 p2934 N85-28111
Electro-expulsive separation system
[NASA-CASE-ARC-11613-1] 18 p3094 N85-29150
Elastomers used in aeronautics industry
[SNIAS-851-551-103] 20 p3434 N85-31304
Structure-property relationships in thermoplastic elastomers. Part 3: Segmented polyacetal-polyurethanes
[AD-A154897] 21 p3569 N85-32200
ELASTOPLASTICITY
Initial postbuckling analysis of elastoplastic thin-shear structures 01 p0059 N85-10393
HOST high temperature crack propagation
02 p0144 N85-10977
Acceleration waves 02 p0207 N85-11367
Analysis based on Reissner theory for rectangular plates with all edges built-in 04 p0483 N85-13081
Compression of a band made of elastic, ideally Coulomb plastic material
[ISSN-0208-5658] 05 p0646 N85-14157
Variable loading of elastic-plastic shells of revolution
06 p0779 N85-14981
Correlation of stable crack growth with the J-integral and the crack tip opening displacement, effects of geometry, size and material: Report on an investigation of the elastic-plastic R-curve methodology
[GKSS-84-E-37] 08 p1173 N85-17395
Elastic-plastic analysis for cyclic loading using a linearized yield condition
[PB85-149607] 14 p2322 N85-24346
Local elastoplastic fracture of fibrous composite materials 15 p2497 N85-25405
Influence of behavior laws in the explosive deformation of metal plates
[ISL-R-122/83] 16 p2760 N85-27032
Consolidation theory with consideration of frame plasticity
[REPT-9/1984] 16 p2796 N85-27240
Adaptation of continuous beams and the method of optimizing the flexibility of their elastic supports. Theorem on maximal adaptation loading, supplement
[REPT-10/1984-SUPPL] 16 p2797 N85-27241
Analysis of elastoplastic grids under conditions of variable loads
[REPT-16/1984] 16 p2797 N85-27242
Multinomial form of the solution of problems of the statistics of elastic rectangular disks
[REPT-17/1984] 16 p2797 N85-27244
Specimen thickness effects for elastic-plastic CTO toughness of A36 steel
[DE85-006992] 18 p3077 N85-
Micromechanics of high temperature deformation an failure 20 p3466 N85-31
Numerical study of ductile rupture in pla deformations
[ONERA-RT-23/7169-RY-072-R]
20 p3469 N85-31
A review of path-independent integrals in elastic-plas fracture mechanics, task 4
[NASA-CR-174956] 22 p3799 N85-33
ELASTOSTATICS
On some exact solutions in elastostatics in terms o harmonic functions 09 p1332 N85-18
A study of coupling the boundary and finite elem methods in two-dimensional elastostatics
[AD-A149619] 12 p1865 N85-21
Numerical solution of one-dimensional nonlin problems of statics for elastic beams and shells unde rigid constraints 17 p2943 N85-28
The role of ellipticity and normality assumptions i formulating live-boundary conditions in elasticity
[AD-A153475] 18 p3168 N85-29
Ductile fracture of dynamically loaded stee structures-compact tension specimen tests and analyse
[AD-A155472] 21 p3600 N85-32
ELBOW (ANATOMY)
Elbow and knee joint for hard space suits and the li
[NASA-CASE-ARC-11610-1] 11 p1697 N85-20
ELECTRETS
Study of charge transport in the thermoelectret sta of some ceramics and glasses
[DE85-001763] 09 p1300 N85-18
Investigation of charge transport in the thermoelectre state of some ceramics and glasses
[DE85-009318] 17 p2936 N85-28
ELECTRIC AIRCRAFT
U FLY BY WIRE CONTROL
ELECTRIC APPLIANCES
U ELECTRIC EQUIPMENT
ELECTRIC ARCS
NT CARBON ARCS
NT MERCURY ARCS
The anode mechanism of a thermal argon arc
[NASA-TM-77754] 07 p0921 N85-15
The discharge mechanism of the high-temperature ar
[NASA-TM-77794] 07 p0922 N85-15
Arc erosion of metal in current interval of 1-1 amperes 07 p0953 N85-16
Evaluation of the Kerie Cable thermal arc cutti equipment
[AD-A147813] 07 p0974 N85-16
Metal vapor arc switch electromagnetic accelerat technology
[NASA-CR-174380] 09 p1314 N85-18
Flashover failures from wet-wire arcing and tracking
[AD-A149055] 10 p1478 N85-19
Improved operation of transversely exited N2O lase
[AD-D011468] 10 p1490 N85-19
Analysis of the dissipation mechanism within a instationary cathode spot of metal vapor arcs
[AD-A149258] 10 p1558 N85-19
Apparatus for producing diamond-like carbon film
[NASA-CASE-LEW-13837-3] 11 p1615 N85-20
Thermal investigation of an electrical high-current ar with porous gas-cooled anode
[NASA-TM-77759] 11 p1627 N85-20
Neutral beam injector oxygen impurity measurements and concentration reduction via gettering processes
[DE85-000661] 12 p1836 N85-215
Characteristics of multiarc plasma devices
12 p1841 N85-215
Review of anode phenomena in vacuum arcs
[DE85-002736] 12 p1926 N85-22
Study of a constricted electric arc cooled by transpiration
[NASA-TM-77846] 17 p3038 N85-28
Examination of a method for predicting the properties of railgun plasmas
[AR-004-322] 17 p3039 N85-28
Experimental research on electrical propulsion
[NASA-TM-77876] 18 p3067 N85-29
An alpha particle diagnostic beam line system to generate an intense Li(O) beam with an ORNL SITEX source
[DE85-010564] 18 p3182 N85-29
ELECTRIC AUTOMOBILES
Summary of activities pertaining to utilization of gra purchase of batteries for electric van
[DE84-015793] 02 p0195 N85-11
ElectriFleet Project
[DE85-001596] 10 p1570 N85-19
Electric vehicle demonstration project
[DE85-003124] 11 p1741 N85-20

West Europe report: Science and technology
[JPRS-WST-84-027] 15 p2532 N85-25612
Nickel-iron battery to be used in Peugeot electric car
15 p2532 N85-25615
AC powertrain for an electric vehicle, phase 2 and phase 3
[NASA-CR-175760] 16 p2880 N85-27771
Advanced vehicle systems assessment. Volume 1: Executive summary
[NASA-CR-175876] 17 p3051 N85-28887
West Europe report: Science and technology
[JPRS-WST-84-002] 18 p3086 N85-29095
Electric Peugeot to have new nickel-iron batteries
18 p3086 N85-29096
Electric and hybrid vehicle program: FY 1985 program plan
[DE85-008933] 18 p3201 N85-29858
Test plan for performance testing of the Eaton AC-3 electric vehicle
[DE85-011954] 23 p3927 N85-34341

ELECTRIC BATTERIES
NT ALKALINE BATTERIES
NT LEAD ACID BATTERIES
NT NICKEL CADMIUM BATTERIES
NT NICKEL HYDROGEN BATTERIES
NT NICKEL ZINC BATTERIES
NT PRIMARY BATTERIES
NT REDOX CELLS
NT SILVER HYDROGEN BATTERIES
NT SODIUM SULFUR BATTERIES
NT STORAGE BATTERIES
NT THERMAL BATTERIES
NT ZINC-BROMIDE BATTERIES
NT ZINC-CHLORINE BATTERIES
Sea water rope batteries
[AD-A144775] 01 p0042 N85-10275
Battery optimization considerations
[DE84-014759] 01 p0044 N85-10298
Summary of activities pertaining to utilization of grant purchase of batteries for electric van
[DE84-015793] 02 p0195 N85-11305
Properties of cathode materials in alkaline cells
[NASA-CR-174082] 04 p0495 N85-13161
Lithium battery safety: A fiber-optic application for safe observation of lithium cells under severe tests
[AD-A148646] 06 p0804 N85-15119
Composite batteries 07 p0936 N85-15932
Safety evaluation of an electronic totalizer containing a Li/(CF)x cell
[AD-A147306] 07 p0993 N85-16305
Battery control and fault detection method
[AD-D011364] 07 p0993 N85-16307
New liquid cathodes for lithium batteries. Part A: Halocarbons
[AD-A148433] 08 p1176 N85-17423
Status of the Li-Al/FeS battery manufacturing technology. An evaluation for the US Army, Belvoir R and D Center
[DE85-000776] 09 p1315 N85-18264
Battery response to pulse loads: A mathematical model
[DE85-001149] 09 p1316 N85-18277
The development of a method for the shock-resistant securing of large batteries in submarines
09 p1335 N85-18301
Hybrid vehicle program
[DE85-000326] 09 p1410 N85-18886
Electric vehicle battery test plan and results
[DE84-001972] 09 p1410 N85-18887
Polymer electrolytes: An investigation of some poly (N-propylaziridine)/lithium salt compositions
[AD-A149444] 10 p1452 N85-19146
Charge depletion meter
[AD-D011484] 10 p1488 N85-19393
Emergency Locator Transmitter (ELT) batteries guidance and recommendations
[NASA-TM-87436] 11 p1624 N85-20225
Emergency Locator Transmitter (ELT) batteries guidance and recommendations
[NASA-TM-87415] 11 p1672 N85-20533
Electric vehicle demonstration project
[DE85-002167] 11 p1741 N85-20943
Nickel-cadmium battery cell reversal from resistive network effects
[AD-A149626] 12 p1834 N85-21505
Polymeric electrolytes for ambient temperature lithium batteries
[DE85-001032] 12 p1835 N85-21518
Research to explore the feasibility of sulfolanes as electrolytic solvents for rechargeable lithium batteries
[DE85-004345] 12 p1837 N85-21525
State-of-charge coulometer
[NASA-CASE-NPO-15759-1] 12 p1849 N85-21596
An improved battery state-of-charge indicator
[NASA-CR-175701] 14 p2296 N85-24227
Status of French research in plastic batteries
15 p2530 N85-25803
A portable battery for objective, non-obstrusive measures of human performances
[NASA-CR-171868] 15 p2586 N85-25942
Calcium/thionyl chloride battery technology
[AD-A151875] 15 p2586 N85-25945
INEL electric vehicle laboratory qualification: Transition test results and comparisons with JPL ETV1-2 data
[DE85-008006] 16 p2880 N85-27772
Investigation of the structure and dynamics of electrolytes in solvents used for primary and secondary Li-batteries
[AD-A153099] 17 p2954 N85-28240
Aluminum-air power cell research and development
[DE85-008117] 17 p2986 N85-28458
British breakthrough in lightweight lithium batteries
18 p3086 N85-29092
West Europe report: Science and technology
[JPRS-WST-84-035] 18 p3087 N85-29102
Low-rate discharge of various electrochemical batteries for use with oceanographic instruments
[AD-A153865] 18 p3095 N85-29159
Lithium-alloy/iron sulfide battery design studies
[DE85-007991] 18 p3131 N85-29389
Electric and hybrid vehicle program
[DE85-010025] 19 p3282 N85-30230
Lithium cell reactions
[AD-A154429] 19 p3305 N85-30484
Polyethylene imine-metal salt solid electrolyte
[AD-D011678] 19 p3305 N85-30485
Galileo battery testing and the impact of test automation 20 p3444 N85-31381
An update of the JPL program to develop Li-SOCl2 cells 20 p3445 N85-31384
Nickel-cadmium battery cell reversal from resistive network effects 20 p3446 N85-31392
A 34 ampere-hour nickel-cadmium minimum trickle charge testing 20 p3446 N85-31394
A safe, high-power-density lithium battery
[AD-A155223] 21 p3613 N85-32454
Rechargeable lithium-organic electrolyte battery having overcharge protection and method of providing overcharge protection for a lithium-organic electrolyte battery
[AD-D011738] 22 p3806 N85-33575
Transfer of battery technology developed by the US Department of Energy
[DE85-009868] 22 p3808 N85-33589
Electric vehicle operations by the City of Huntsville, Alabama, March 1983 - May 1984
[DE85-005913] 22 p3849 N85-33842
Test plan for performance testing of the Eaton AC-3 electric vehicle
[DE85-011954] 23 p3927 N85-34341
Wind energy battery storage, phase 2
[DE85-009753] 23 p3945 N85-34450
Development and evaluation of sulfonated polysulfone membranes for the zinc-ferricyanide battery
[DE85-009104] 24 p4090 N85-35357
Cationic exchange membrane for the zinc-ferricyanide battery
[DE85-013152] 24 p4112 N85-35489

ELECTRIC BRIDGES
NT WHEATSTONE BRIDGES
NT WIRE BRIDGE CIRCUITS
Bridge erosion in electrical contacts
04 p0486 N85-13102
Piezoelectric filter with low-Q inductances
13 p2070 N85-22932
Adjustment of the frequency-temperature characteristics of crystal oscillators
[AD-D011586] 15 p2548 N85-25726
Simultaneous phase and frequency control of a three-phase inductor-convertor bridge
[DE85-006197] 18 p3096 N85-29164
Temperature sensors for OTEC applications
[DE85-009807] 18 p3110 N85-29254
R, L, C, G measurement 21 p3668 N85-32784
State of art and development problems in computer-aided design of electronic circuits
22 p3766 N85-33342
Modeling of electronic circuits with high degree of component integration 22 p3766 N85-33343
System for computer-aided design of analog electronic circuits 22 p3768 N85-33353

ELECTRIC CHARGE
NT ELECTRIC DIPOLES
NT ELECTROSTATIC CHARGE
NT ION CHARGE
NT SPACE CHARGE
Performance characteristics of a battery charger and state-of-charge indicator
[NASA-CR-174273] 07 p0946 N85-15982
A comparison of lightning and nuclear electromagnetic pulse response of a helicopter 07 p1000 N85-16349
Potential dependence of electrical conductivity and chemical charge storage of poly(pyrrole) films on electrodes
[AD-A148513] 08 p1122 N85-17075
SIMM1: A linearized particle code
[AD-A148627] 08 p1221 N85-17689
Charge depletion meter
[AD-D011484] 10 p1488 N85-19393
Atmospheric research aircraft — conductivity/charge measurements
[ONERA-RS-87/7154/PY] 11 p1662 N85-20596
Interfacial and colloidal aspects of aqueous suspension containing oxidic powders
[DE85-005972] 15 p2519 N85-25534
Investigation of charge transport in the thermoelectret state of some ceramics and glasses
[DE85-009318] 17 p2936 N85-28122
Preliminary documentation for the polar code
[AD-A154125] 19 p3336 N85-30867
Buildup of electric charge in foil dielectrics during gamma irradiation 22 p3770 N85-33363
Friction, impact, and electrostatic discharge sensitivities of energetic materials
[DE85-013321] 24 p4083 N85-35309

ELECTRIC CIRCUITS
U CIRCUITS

ELECTRIC COILS
NT MAGNETIC COILS
Superconducting rotor dynamics
[AD-A147176] 07 p0947 N85-16000
Fast switching driver for inductive load, such as a phase shifter
[AD-D011388] 08 p1143 N85-17207
High-current measurement techniques
[PB85-100444] 11 p1637 N85-20311
Eddy current test probe with circumferential segments and method of testing material surrounding fastener holes
[AD-D011554] 12 p1850 N85-21603
Detection and location of partial discharges in transformer windings using electrical methods
15 p2551 N85-25750
Outline of alternative design of R-Tokamak
15 p2654 N85-26371

ELECTRIC CONDUCTORS
Conductor structure for thick film electrical device
[AD-D011240] 01 p0043 N85-10281
Resistance and inductance calculations for helical flux compression generators
[DE84-015068] 02 p0195 N85-11306
Plasma drift towards a plane equipotential surface
[TRITA-EPP-84-01] 02 p0285 N85-11860
Mechanical locking between multi-layer printed wiring board conductors and through-hole plating
[AD-D011477] 10 p1481 N85-19352
Characterization of high temperature electrically conducting oxides
[DE85-004296] 12 p1803 N85-21307
The liner package: An incipient MHD capability for CCUBE
[LA-9969-MS] 12 p1913 N85-22007
Properties of Ti alloyed multifilamentary Nb3Sn wires by internal tin process
[DE85-003212] 12 p1941 N85-22191
An investigation of arc discharging on negatively biased dielectric conductor samples in a plasma
13 p1994 N85-22498
Electrical conduction in polymer dielectrics
13 p1996 N85-22514
Transport studies of several novel organic conductors
[DE85-003950] 14 p2429 N85-24979
Heat resistant sheathed insulated electrical conductors
[AD-D011644] 17 p2951 N85-28219
Silicide conductors reliability research
[AD-A153766] 18 p3095 N85-29157
Quantized Hall conductance as a topological invariant
[DE85-007796] 18 p3193 N85-29808
Structural and physical studies on a new class of low-dimensional conducting material: FeOCl intercalated with TTF and related molecules
[DE85-009701] 18 p3196 N85-29824
Tailored vacuum chambers for ac magnets
[DE85-010767] 21 p3591 N85-32319
Method and apparatus for casting conductive and semi-conductive materials
[DE85-011655] 22 p3792 N85-33494
Feasibility study of radar-transmitting materials
[AD-A155839] 24 p4087 N85-35329

ELECTRIC CONNECTORS
Advanced high-power transfer through rotary interfaces 05 p0807 N85-13875
Power quality and protection of electric distribution systems with small, dispersed generation devices
[DE85-000990] 09 p1344 N85-18453

Safety requirements for wiring systems and connectors for photovoltaic systems
[NASA-CR-174431] 10 p1477 N85-19324
Connector/nitinol delta contact force device
[AD-D011467] 10 p1481 N85-19349
Magnetic field interactions with material discontinuities
[AD-A150197] 13 p2154 N85-23373
Characterization of solderless miniwrapping connections
[CNES-NT-112] 16 p2796 N85-27238
Derated application of parts for (Electronic Systems Division) systems development. Revision
[AD-A153299] 17 p2955 N85-28246

ELECTRIC CONTACTS
MOD silver metallization for photovoltaics
[NASA-CR-174011] 01 p0026 N85-10163
Surface segregation of sulfur during oscillatory pin-on-plate wear studies of precious metal electrical contact alloys. 1: Friction and electrical contact resistance
[DE84-006952] 02 p0195 N85-11303
Bridge erosion in electrical contacts
04 p0486 N85-13102
Advanced high-power transfer through rotary interfaces 05 p0607 N85-13875
Thermal contact conductance measurements on Doublet 3 armor tile traphite
[DE84-013554] 05 p0613 N85-13916
Laser-assisted solar cell metallization processing
[NASA-CR-174213] 06 p0813 N85-15160
Electromechanical switch
[AD-D011400] 07 p0948 N85-16009
Arc erosion of metal in current interval of 1-10 amperes 07 p0953 N85-16042
Screen printed interdigitated back contact solar cell
[NASA-CASE-LEW-13414-1] 11 p1671 N85-20530
A solution method for large deformation contact problems
[AD-A149842] 12 p1866 N85-21707
Control of cascaded induction generator systems
[AD-A150429] 13 p2065 N85-22697
Thermal and thermoelastic effects in rolling/sliding contacts
[AD-A150435] 13 p2165 N85-23429
Some observations of heated gallium arsenide heteroface solar cells
[NASA-TM-86388] 14 p2246 N85-23925
Erosion of electrodes due to switching of capacitor-bank discharge circuits
[AD-A151207] 15 p2547 N85-25718
Thin-film polycrystalline silicon research
[DE85-002908] 15 p2683 N85-26434
LPCVD tungsten deposition on Si-Ge alloy
[DE85-005588] 16 p2750 N85-26970
Comprehensive silicon solar cell computer modeling
[NASA-CR-175959] 17 p2987 N85-28461
Temperature and surface damage under lubricated sliding-rolling contacts 19 p3280 N85-30336
Design and operation of epitaxial reactor
[DE85-011089] 19 p3306 N85-30491
Ink jet printing of silver metallization for photovoltaics
[NASA-CR-176019] 19 p3343 N85-30720
Silicon MINP solar cells 20 p3480 N85-31623
A rotating electrical transfer device
22 p3798 N85-33529
Noise in silver beta alumina ceramics
[AD-A156135] 24 p4082 N85-35297
Computer simulation of a cruise missile using brushless dc motor fin control
[AD-A155935] 24 p4089 N85-35349
Development of contactless sensors for industrial and automotive applications
[BMFT-FB-T-85-031] 24 p4097 N85-35400

ELECTRIC CONTROL
Adjustable indicating device for load position
[NASA-CASE-MFS-26008-1] 11 p1635 N85-20300
Robotized system for treating gear wheels
14 p2285 N85-24162

ELECTRIC CORONA
Bibliography of data on electrical breakdown in gases
[PB84-216049] 01 p0045 N85-10294
Electrical parameters in 60-Hz biological exposure systems and their measurement: A primer
[PB84-217793] 03 p0400 N85-12548
Development of power system management
[PB84-216530] 04 p0497 N85-13173
Effects of the corona wind on the cooling of a horizontal cylinder
[AD-A153101] 17 p2954 N85-28241
Third US/USSR Symposium on Particulate Control
[PB85-190890] 19 p3310 N85-30522
Development of power system measurements
[PB85-182582] 20 p3450 N85-31420

ELECTRIC CURRENT
NT ALTERNATING CURRENT
NT ARC DISCHARGES
NT AURORAL ELECTROJETS
NT BEAM CURRENTS
NT CARBON ARCS
NT DIRECT CURRENT
NT EDDY CURRENTS
NT ELECTRIC ARCS
NT ELECTRIC CORONA
NT ELECTRIC DISCHARGES
NT ELECTRIC SPARKS
NT ELECTRODELESS DISCHARGES
NT ELECTROJETS
NT EQUATORIAL ELECTROJET
NT FLASHOVER
NT GAS DISCHARGES
NT GLOW DISCHARGES
NT HIGH CURRENT
NT IONOSPHERIC CURRENTS
NT LIGHTNING
NT MERCURY ARCS
NT PLASMA CURRENTS
NT RADIO FREQUENCY DISCHARGE
NT RING CURRENTS
NT SHORT CIRCUIT CURRENTS
NT TELLURIC CURRENTS
NT THRESHOLD CURRENTS
Excitation of quasi-static magnetic fields with axial structure 02 p0259 N85-11696
Photocurrent oscillations in Bi12GeO20 metal-semiconductor-metal structures
02 p0266 N85-11741
Theory of the double critical state in type-2 superconductors
[DE84-015461] 02 p0289 N85-11886
Related studies to cathodic protection of reinforced concrete structures
[PB84-218114] 03 p0333 N85-12145
Bulletin of the Faculty of Engineering, Hokkaido University, no. 123
[ISSN-0385-602-X] 04 p0482 N85-13075
Determination of Faradaic current through a bipolar electrode in acidic bichromate 04 p0483 N85-13077
Electropulse chemical machining
[DE84-016693] 04 p0484 N85-13084
Investigation of effect of photocurrent amplification in meta-dielectric-semiconductor structures based on silicon 04 p0488 N85-13110
Preliminary evaluation of RCA C83036E prototype photomultiplier
[DE84-016894] 04 p0496 N85-13165
Experimental observation of plasma neoclassical currents
[DE84-015706] 04 p0566 N85-13605
Oscillating field current drive for reversed field pinch discharges
[DE84-015090] 04 p0567 N85-13610
Current and potential transients during localized corrosion of stainless steel
[DE84-014100] 05 p0618 N85-13954
Behaviour of lead-silver anodes in zinc electrodeposition from sulphuric acid baths
[BLL-MINTEK-TR-1180-(5810.5759)]
06 p0764 N85-14867
Transient currents of ideally conducting body of revolution with transient diffraction
06 p0765 N85-15019
Current-voltage characteristics of semiconductor power devices operating at high current densities
06 p0795 N85-15079
Human reactions to transient electric currents, volume 12
[PB84-231463] 06 p0846 N85-15374
Arc erosion of metal in current interval of 1-10 amperes 07 p0953 N85-16042
Region 1 birkeland currents from a global MHD simulation of the magnetosphere
[AD-A147435] 07 p0997 N85-16335
Data and results of a laboratory investigation of microprocessor upset caused by simulated lightning-induced analog transients
07 p0999 N85-16345
A comparison of lightning and nuclear electromagnetic pulse responce of a helicopter 07 p1000 N85-16349
Electromagnetic fields from the generation and absorption of discontinuous linear current fronts
[AD-A148076] 08 p1151 N85-17266
Fluctuation phenomena studies in chemically sensitive field effect transistors. Part 2: Corrosion of silicon oxynitride
[AD-A148227] 08 p1157 N85-17302
Studies on organic semiconductors. 15: Effects of the substituents on the photoconductivities of substituted anthracenes
[NASA-TM-77788] 08 p1225 N85-17712
Exploratory development of advanced surface fla detection methods
[AD-A148757] 09 p1281 N85-1
IREB (Intense Relativistic Electron Beam) converter t ac pulses
[AD-D011479] 10 p1554 N85-1
Thermal investigation of an electrical high-current ar with porous gas-cooled anode
[NASA-TM-77789] 11 p1627 N85-20
The liner package: An incipient MHD capability fo CCUBE
[LA-9969-MS] 12 p1913 N85-2
Calculation of secondary-electron escape currents fro inclined-spacecraft surfaces in a magnetic field
13 p1992 N85-2
Experimental and numerical analysis of electric curren and electromagnetic blunting of cracks in thin plates
[AD-A150418] 13 p2022 N85-2
Critical current measurements on an NbTi superconducting wire standard reference material
[PB85-118594] 13 p2066 N85-2
Noise characteristics of sulfur-doped silicon diodes
13 p2073 N85-2
Localized corrosion currents from graphite/aluminum and welded SiC/Al metal matrix composites
[AD-A150986] 14 p2256 N85-2
New electronic measurement, control devices
14 p2269 N85-241
Investigation of electron attachment and dissociatio rates in C2F6/CH4 electric gas discharges
[AD-A151796] 16 p2862 N85-27
Electro-expulsive separation system
[NASA-CASE-ARC-11613-1] 18 p3094 N85-29
Development of photodetectors
[AD-A153773] 18 p3095 N85-29
Trace water sensor
[NASA-CASE-NPO-15722-1] 18 p3103 N85-2
Theoretical approach to evolution of solar magnetic field 18 p3204 N85-2
Inferred flows of electric currents in solar active regions 18 p3208 N85-2
Design and testing of a pulsed current transformer
[AD-A154228] 19 p3259 N85-30
The electric current densities beneath thunderstorms
20 p3494 N85-317
Runaway electrons and plasma turbulence in current ramping by lower hybrid waves in tokamak plasmas
[DE85-011390] 20 p3535 N85-31
Method of characterizing critical timing paths and analyzing timing related failure modes in very large scale integrated circuits
[AD-D011731] 22 p3759 N85-3
Photothyristor optrons and optron microcircuits, part 1
22 p3781 N85-33
Current enhancement in a conducting channel
[AD-A155418] 22 p3845 N85-33
System expectations for Pioneer 1 foil implosion experiments
[DE85-014129] 24 p4091 N85-3
Current interruption by density depression
[DE85-013120] 24 p4169 N85-35

ELECTRIC DIPOLES
Image theory for a vertical electric dipole above a wire grid with square cells
[REPT-S-150] 02 p0192 N85-112
Impedance of vertical dipoles above a dissipative ground
[REPT-S-152] 02 p0192 N85-112
General image theory for the Sommerfeld problem
[REPT-S-154] 02 p0193 N85-112
Experimental determination of the 1 sigma(+) state electron-dipole-moment function of carbon monoxide up to a large internuclear separation
[NASA-TM-85979] 09 p1379 N85-1
The ULF/ELF/VLF electromagnetic fields generated in a sea of finite depth by elevated dipole sources
[AD-A149636] 12 p1828 N85-21470
Piezoelectric transducer using electrically poled gamma-phase Nylon 11
[AD-D011552] 12 p1850 N85-21
High-field dipoles for future accelerators
[DE85-002315] 13 p2157 N85-2
Ac field-induced order in dense colloidal systems
[DE85-009107] 17 p2935 N85-28
Atomic data for controlled fusion research. Volume 4: Spectroscopic data for iron
[DE85-009656] 19 p3354 N85-30
Effects of CP violation in SU(2) sub L x SU(2) sub R x U(1) electroweak models
[DE85-010801] 20 p3531 N85-31
Numerical modeling of subsurface communication
[DE85-012818] 21 p3577 N85-32

ELECTRIC DISCHARGES
NT ARC DISCHARGES
NT CARBON ARCS
NT ELECTRIC ARCS

NT ELECTRIC CORONA
NT ELECTRIC SPARKS
NT ELECTRODELESS DISCHARGES
NT FLASHOVER
NT GAS DISCHARGES
NT GLOW DISCHARGES
NT LIGHTNING
NT MERCURY ARCS
NT RADIO FREQUENCY DISCHARGE
A high-voltage discharger
[AD-A145659] 02 p0194 N85-11299
Time variability of directionality properties of pulsed EB-EDL (Electron Beam-Electric Discharge Laser) N2-CO2 lasers
[AD-A145546] 02 p0202 N85-11344
Electron collision processes in molecular gases
[AD-A146078] 03 p0416 N85-12671
Glow spots and breakdown in GaAs transistor structure 04 p0487 N85-13107
Physico-chemical investigations on the electronic partial conductivity of molten electrolytes, especially of the eutectic mixture LiCl-KCl
[BMFT-FB-T-84-205] 05 p0633 N85-14063
Pulsed electric discharge laser technology. Electron beam window foil material
[AD-A146420] 06 p0813 N85-15162
Galileo internal electrostatic discharge program
13 p1995 N85-22504
Laboratory studies of spacecraft response to transient discharge pulses 13 p1995 N85-22506
Discharge pulse phenomenology
13 p1995 N85-22509
Discharge characteristics of dielectric materials examined in mono-, dual-, and spectral energy electron charging environments 13 p1995 N85-22510
Mass spectra of neutral particles released during electrical breakdown of thin polymer films
13 p1996 N85-22511
EOS (electrical overstress) protection for VLSI (Very Large Scale Integration) devices
[AD-A150333] 13 p2064 N85-22891
Non-self-maintained high-voltage low-pressure discharge 13 p2088 N85-23037
Near Field/Far Field (NF/FF) energy loss in Electric Discharge Lasers (EDL's): A mode-medium interaction
[AD-A150299] 13 p2096 N85-23075
Developement of a theoretical model to describe the interaction between electric discharge and supersonic flow of a pulsed CO laser
[DFVLR-FB-84-45] 14 p2310 N85-24301
Experimental investigation of the electric breakdown in SF6
[BLL-CE-TRANS-7987-(9022.09)]
15 p2546 N85-25714
Erosion of electrodes due to switching of capacitor-bank discharge circuits
[AD-A151207] 15 p2547 N85-25718
Field-induced phenomena in electrical insulation
[AD-A151234] 15 p2547 N85-25719
On the electric charge carried by dust grain excitation of violent discharge --- planetary rings
15 p2677 N85-26530
Investigation of electron attachment and dissociation rates in C2F6/CH4 electric gas discharges
[AD-A151796] 16 p2862 N85-27649
Electrode for flash discharge lamps
[DE85-008896] 17 p2955 N85-28252
Design and testing of a pulsed current transformer
[AD-A154228] 19 p3259 N85-30206
Coordinated research program in pulsed power physics
[AD-A154629] 21 p3679 N85-32856
Powerful XeCl excimer electric discharge laser with good temporal stability and fast response time
21 p3686 N85-32911
Model that predicts pulse charged gas switching breakdown phenomena
[DE85-013119] 22 p3761 N85-33313
Safety characteristics of non-lithium battery systems
[AD-A155733] 22 p3806 N85-33574
Surface discharges as intense photon sources in the extreme ultraviolet
[DE85-012593] 24 p4158 N85-35782

ELECTRIC ENERGY STORAGE
Battery optimization considerations
[DE84-014759] 01 p0044 N85-10288
Trends in concentrator, receiver, and storage development for terrestrial applications
05 p0609 N85-13891
Electrodynamic tethers. 1: Power generator in LEO. 2: Thrust for propulsion and power storage
05 p0611 N85-13901
Energy storage with lead acid batteries in photovoltaic systems
05 p0663 N85-14260
Energy storage for stationary and mobile operation as a buffer of power supply from additive energy sources
05 p0663 N85-14261
Design and operating experience of an ac-dc power converter for a superconducting magnetic energy storage unit
[DE84-014041] 09 p1316 N85-18275
Thermal design requirements of a 50-kW zinc/redox flow battery for solar electrical energy storage
[DE84-017088] 09 p1345 N85-18463
Cycling performance of the iron-chromium redox energy storage system
[NASA-TM-87034] 16 p2819 N85-27387

ELECTRIC EQUIPMENT
Electrical/electronics working group summary
05 p0804 N85-13853
The determination of eddy current losses in electrical equipment
[DE84-016340] 05 p0832 N85-14050
DOE/ORNL electric systems program overview
[DE85-003334] 10 p1459 N85-19197
The touch panel system: Design and development
[AD-A153014] 17 p3008 N85-28596
High Temperature Heating System (HTHS)
[PB85-188340] 24 p4064 N85-35316

ELECTRIC EQUIPMENT TESTS
Choice of criteria for rejection of insulating components in high-voltage surge equipment
06 p0785 N85-15021
Evaluation of adequacy pf JP54 protection level for large electric machines 15 p2528 N85-25588
Module Hipot and ground continuity test results
21 p3612 N85-32447

ELECTRIC FIELD STRENGTH
Choice of criteria for rejection of insulating components in high-voltage surge equipment
06 p0785 N85-15021
Electric field in plasma layer of magnetosphere during preliminary substorm phase 06 p0824 N85-15231
Method of separately determining electrophysical properties of bulky conductor 13 p2073 N85-22951
Measuring intensity of electric field produced by electromagnetic pulse with aid of active probes
13 p2075 N85-22958
Satellite-borne electric field measurements with spherical double probes --- ISEE satellites
14 p2356 N85-24558
Estimate of the amplitude of transient electric fields in the magnetotail 14 p2358 N85-24568
The GEOS-2 electric field observations at times of solar wind discontinuities 14 p2360 N85-24584
Multiple correlation between auroral and magnetic pulsations. Part 2: Determination of electric currents and electric fields around a pulsating auroral patch
14 p2363 N85-24606
Measuring electrical field fluctuations by Langmuir Double Probe Method 16 p2720 N85-26789
Measurement of RF fields associated with ISM equipment as it relates to aeronautical services
[FAA-ES-84-2] 19 p3254 N85-30180
Experimental and theoretical investigations of open resonators --- precipitation measurement
[DFVLR-FB-85-12] 20 p3449 N85-31414
Development of power system measurements
[PB85-182582] 20 p3450 N85-31420

ELECTRIC FIELDS
NT EXTERNAL SURFACE CURRENTS
Scattering theory by Enss' method for operator valued matrices: Dirac operator in an electric field
[REPT-64] 01 p0045 N85-10290
Interaction of a stream of dielectric spheres in an electric field in a high vacuum
[DE84-014714] 01 p0115 N85-10782
Methods to increase linac efficiency
[DE84-014692] 01 p0118 N85-10809
Rocket and satellite observations of electric fields and ion convection in the dayside auroral ionosphere
[TRITA-EPP-84-05] 02 p0229 N85-11497
Method of splitting for solution of problems in semiconductor physics 02 p0265 N85-11736
Electric field and plasma energization in computer simulations of magnetotail reconnection
[DE84-014023] 02 p0285 N85-11859
Electrical parameters in 60-Hz biological exposure systems and their measurement: A primer
[PB84-217793] 03 p0400 N85-12548
Investigation of solid state problems using the hyperfine interaction between static and dynamic internal fields with short live excited probe nuclei 03 p0428 N85-12729
Stark broadening of H(-) resonances in large electric fields
[DE84-016974] 04 p0496 N85-13164
Development of power system management
[PB84-216530] 04 p0497 N85-13173
Human reactions to ELF (Extremely Low Frequency) electric and magnetic fields. An annotated bibliography of current literature, fourth edition
[PB84-230358] 04 p0545 N85-13472
Local fields in strongly coupled plasmas
[DE84-013375] 04 p0567 N85-13611
Monte Carlo studies of transport in stellarators
[DE84-017633] 04 p0568 N85-13625
Measurements of electric fields obtained by stratospheric balloons in the region of the South Atlantic anomaly
[INPE-3218-PRE/571] 05 p0675 N85-14335
Motion of electrons in non polar classical liquids
[DE84-013609] 05 p0727 N85-14672
Stabilization of the hot electron precessional mode in a symmetric tandem mirror by the axial variation of radial electric field
[DE84-016369] 05 p0730 N85-14692
Optimization of energy conversion during locking of electron bunches by electromagnetic wave in longitudinal electrostatic field 06 p0786 N85-15025
An indirect measure of below-ground electric field, conductivity, and dielectric constant
[AD-A146518] 06 p0804 N85-15115
Distribution of electric field near westward propagating band in aurora 06 p0823 N85-15222
Electric fields in Earth orbital space
[AD-A146448] 06 p0835 N85-15313
High voltage effects measured on dummy mannequin
07 p1012 N85-16432
Research relative to plasma transport across the magnetopause
[NASA-CR-174300] 07 p1045 N85-16836
Electron distribution function and mobility in 3-5 compounds for high and low fields
[AD-A147447] 07 p1048 N85-16858
Transport properties and distribution functions in 3-5 semiconductors
[AD-A147525] 07 p1049 N85-16860
In-situ formation of a grain boundary in field ion microscopy using a laser
[AD-A148225] 08 p1166 N85-17355
Plasma and magnetospheric research
[NASA-CR-171293] 08 p1183 N85-17451
Theoretical studies of Rydberg atom collisions
[AD-A148558] 08 p1220 N85-17687
The flow of plasma in the solar terrestrial environment
[NASA-CR-174301] 08 p1224 N85-17707
Development of photoconductive power switch technology
[DE85-001514] 09 p1315 N85-18270
Multimode harmonic power measurement of 40 MW pulsed S-band klystrons
[DE85-001560] 09 p1316 N85-18272
Effects of dc electric fields on multiphoton ionization spectra in cesium
[DE85-001542] 09 p1381 N85-18684
Calculation and computer simulation of the Paraboloidal Mirror Analyzer (PMA)
[DE85-001417] 09 p1384 N85-18705
Measurements of electric fields in plasmas by using beam probe and laser fluorescence techniques
09 p1389 N85-18737
Ionospheric research at INPE
[INPE-3279-PRE/602] 10 p1514 N85-19556
Electron acceleration by laser fields in a gas
[DE85-000575] 11 p1639 N85-20323
Study of electric field and ion effects on HVDC lines
[DE85-002975] 12 p1833 N85-21503
An improved rocket-borne electric field meter for the middle atmosphere
[NASA-CR-175510] 12 p1888 N85-21851
Reconsideration of sheath related to negative ion extraction
[IPPJ-706] 12 p1935 N85-22159
Efficient heating and confinement of ions in an axisymmetric magnetic mirror supplemented with dc electric field
[IPPJ-707] 12 p1935 N85-22160
Dynamics of space charge waves in the laser beat wave accelerator
[AD-A149688] 12 p1936 N85-22163
Explosive transverse electric field and particle acceleration during magnetic collapse --- cosmic plasma
12 p1956 N85-22292
Galileo internal electrostatic discharge program
13 p1995 N85-22504
Influence of external electric field on structural-mechanical properties of powdered materials
13 p2013 N85-22630
Elasticity formulas for thin-walled shells with piezoceramic layers 13 p2047 N85-22816
Analysis and optimization of parameters of fanned surface acoustic wave transducers
13 p2070 N85-22934

Measuring intensity of electric field produced by electromagnetic pulse with aid of active probes
13 p2075 N85-22958

Theory of diaphragm light modulators with electrical input signal 13 p2082 N85-23002

Discrimination of normal and anomalous magnetic and electric fields in geoelectromagnetic variations
13 p2114 N85-23166

1981 wC-130 airborne lightning characterization program data review
[AD-A150230] 13 p2138 N85-23275

Electric field and plasma observations near the magnetopause and bow shock during a rapid compression 14 p2355 N85-24553

Efficiency of electric field transfer at Earth's magnetopause and flow amplitudes related to reconnection 14 p2356 N85-24557

Electric fields in the plasma sheet and plasma sheet boundary layer 14 p2357 N85-24562

The magnetospheric convection electric field at ionospheric altitudes: A case study based on STARE and Saint-Santin data 14 p2362 N85-24594

A brief summary of results derived from Scandinavian Twin Auroral Radar Experiment (STARE) observations during IMS --- ionospheric electric fields
14 p2362 N85-24595

Comparison of magnetospheric and ionospheric electric fields using different empirical mapping factors
14 p2362 N85-24597

The GEOS-2 E-field behavior during dynamic auroral development near the satellite footpoint
14 p2362 N85-24598

Three-dimensional current systems and electric fields during active aurora 14 p2362 N85-24599

Solar wind control of electric fields and currents in the magnetosphere and ionosphere
14 p2364 N85-24608

Long-period magnetospheric pulsations observed with an electric field experiment in the magnetosphere
14 p2369 N85-24639

Electroreflectance spectroscopy as a probe of the electronic structure at the metal-electronic interface
[DE85-003541] 14 p2428 N85-24976

Experimental check of ion transport mechanism in Earth's radiation belt with exposure to nonsteady-state electric fields 15 p2480 N85-25306

Measuring methods of atmospheric electric elements at the Earth's surface during snowfall and investigation of these relationships 15 p2581 N85-25920

High speed electric field and voltage measurements with field coupled sensors
[DE85-006637] 15 p2642 N85-26299

Compensation of acoustic wave devices
[AD-D011582] 15 p2646 N85-26322

Time dependent and steady-state solutions of the electron energy distribution in a weakly ionized gas subject to an ac or dc electric field
[AD-A151829] 15 p2656 N85-26391

The physical interactions of radiofrequency radiation fields and biological systems 16 p2775 N85-27129

Evaluation of human exposures to low frequency fields 16 p2776 N85-27135

Theoretical and experimental comparisons of nearfield electrogalvanic fields due to nonlinear polarization layers
[AD-A152085] 16 p2779 N85-27149

Equatorial F-region irregularity latitudinal extension and dynamo electric field
[INPE-3494-PRE/731] 16 p2826 N85-27433

Trends in the electric field enhancement of dielectronic recombination cross sections
[DE85-006920] 16 p2871 N85-27711

Ac field-induced order in dense colloidal systems
[DE85-009107] 17 p2935 N85-28119

Dependence of characteristics of centrifugal magnetohydrodynamic conduction pump on electrical conductance of end walls. Part 1: Experiment
17 p2939 N85-28146

Electromagnetic transmission through a slot in a perfectly conducting plane
[AD-A153224] 17 p2949 N85-28210

Laser plasma LINAC
[DE85-008294] 17 p2971 N85-28348

Wake fields and wake field acceleration
[DE85-008054] 17 p3031 N85-28750

Maser cavity servo-tuning system
[NASA-CASE-NPO-15890-1-CU]
18 p3093 N85-29143

Germanium detectors with a built-in transverse drift field
[DE85-009944] 18 p3096 N85-29165

Upgrade of the LLNL EM transient range monocone antenna
[DE85-008639] 18 p3097 N85-29172

Intense ion beam diode diagnostics using a tunable dye laser
[DE85-008079] 18 p3113 N85-29272

Auroral zone electric fields from DE-1 and -2 at magnetic conjunctions
[NASA-CR-175974] 18 p3136 N85-29421

Preliminary results on open accelerating structures
[DE85-010231] 18 p3191 N85-29793

Characteristics of charge transfer in the dispersed phase of electrorheological suspensions
[RAE-TRANS-2125] 19 p3233 N85-30040

Accelerator column models for low-current beams
[DE85-010722] 19 p3262 N85-30226

Many-body processes in atomic and molecular physics
[DE85-009750] 19 p3354 N85-30791

Toroidal viscosity and ambipolarity in the neoclassical transport theory of axisymmetric ion
[DE85-010622] 19 p3356 N85-30820

Emittance growth caused by current variation in a beam-transport channel
[DE85-010743] 19 p3363 N85-30849

Effects of a radial electric field on tokamak edge turbulence
[DE85-010401] 19 p3371 N85-30910

Development of power system measurements
[PB85-182582] 20 p3450 N85-31420

Performance and electric field limitations in inflow disk MHD generators 20 p3534 N85-31987

A theory of electromagnetic shielding with applications to MIL-STD-285, IEEE-299, and EMP simulation
[AD-A154905] 21 p3575 N85-32233

Trapping of ion conics by downward parallel electric fields
[AD-A155306] 21 p3633 N85-32568

Electrostatic ion cyclotron instability due to a nonuniform electric field perpendicular to the external magnetic field
[AD-A155474] 21 p3707 N85-33019

Vacuum interface flashover with bipolar electric fields
[DE85-012027] 22 p3755 N85-33275

New formulation for linear accelerator design
[DE85-011171] 22 p3842 N85-33792

Role of ECRH in potential formation for tandem mirrors
[DE85-011859] 22 p3846 N85-33834

Interplanetary magnetic field control of high-latitude electric fields and currents determined from Greenland magnetometer data
[DMI-GEOPHYS-PAPERS-R-69]
22 p3850 N85-33845

Theoretical and Experimental Beam Plasma Physics (TEBPP) 23 p3901 N85-34166

Improved negative ion source
[DE85-006445] 23 p3912 N85-34241

Negative ion sources equipped with continuous annular and spherical geometry surface ionizers
[DE85-011939] 23 p3971 N85-34619

Potential effect in transport due to non-axisymmetric confining field 23 p3975 N85-34645

Activities of the RF Section 23 p3975 N85-34646

Radial transport phenomena for TMX-upgrade
23 p3976 N85-34647

RF induced radial diffusion in tandem mirrors
23 p3976 N85-34649

Induced azimuthal electric field effects on tandem transport and ambipolarity 23 p3976 N85-34650

Breakdown of intrinsic ambipolarity for the radial diffusion due to a rotating RF field 23 p3977 N85-34660

Transports studies of ECH and ICRH-heated bumpy torus plasma in NBT-1M 23 p3978 N85-34662

Guiding center distribution function and longitudinal invariant 23 p3978 N85-34663

Analytic and numerical calculations of the ambipolar electric field in a stellarator 23 p3978 N85-34665

Confinement experiments on ISX-B
[DE85-012346] 23 p3984 N85-34709

The role of cosmic rays in magnetic hydrodynamics of interstellar medium
[OG-7.2-15] 23 p4015 N85-34882

Short perturbations of cosmic ray intensity and electric field in atmosphere
[SH-6.1-18] 23 p4046 N85-35090

Moment-method formulation of the cavity-probe aperture antenna
[DE85-013264] 24 p4086 N85-35338

Injector losses on Mite
[DE85-012356] 24 p4090 N85-35355

A lead glass tubing drift calorimeter
24 p4147 N85-35711

High energy plasma accelerators
[DE85-013121] 24 p4156 N85-35760

ELECTRIC FILTERS

NT CRYSTAL FILTERS
NT DIGITAL FILTERS
NT FIR FILTERS
NT MICROWAVE FILTERS
NT RADAR FILTERS
NT RADIO FILTERS
NT TRACKING FILTERS
NT WAVEGUIDE FILTERS

Microstrip directional filters
[INPE-3127-PRE/518] 02 p0194 N85-11289

EMI (electromagnetic interference) filter capacitor unit
[AD-D011392] 07 p0937 N85-15941

Analog to digital converter
[AD-D011336] 07 p0945 N85-15986

The design of high order active RC-filters
[DRIC-T-7147] 07 p0945 N85-15987

Optimal discrete filtration of intricate phase-keyed signals 12 p1840 N85-21980

On filter binary processes
[AD-A150328] 13 p2063 N85-22880

Dynamics of adaptive signal corrector
13 p2071 N85-22949

Synthesis of optimum single-channel discrete signals and filters 13 p2080 N85-22990

Pseudo bipolar nickel-cadmium batteries used as filter elements to pulsed current loads
[AD-A151192] 15 p2547 N85-25717

Length dependent, optical time delay/filter device for electrical signals
[AD-D011594] 15 p2549 N85-25732

Development of thin film hybrid IC active filter for video band use
[NHK-LABS-NOTE-312] 18 p3094 N85-29153

High discharge rate characteristics of nickel-cadmium batteries for pulse load filtering
20 p3446 N85-31391

Stripe filters on multispectral linear arrays
[NASA-CR-175305] 21 p3579 N85-32252

ELECTRIC FURNACES

New ferrous metallurgy technology
01 p0019 N85-10114

High Temperature Heating System (HTHS)
[PB85-188340] 24 p4084 N85-35316

ELECTRIC FUSES

Fuse status indicator system
[AD-D011294] 06 p0804 N85-15121

ELECTRIC GENERATORS

NT AC GENERATORS
NT ALKALINE BATTERIES
NT DIRECT POWER GENERATORS
NT DYNAMOMETERS
NT ELECTROSTATIC GENERATORS
NT FUEL CELLS
NT HOMOJUNCTIONS
NT HOMOPOLAR GENERATORS
NT MAGNETOHYDRODYNAMIC GENERATORS
NT NICKEL ZINC BATTERIES
NT PHOSPHORIC ACID FUEL CELLS
NT PHOTOELECTRIC GENERATORS
NT PRIMARY BATTERIES
NT RADIOISOTOPE BATTERIES
NT REGENERATIVE FUEL CELLS
NT ROTATING GENERATORS
NT SOLAR AUXILIARY POWER UNITS
NT SOLAR BLANKETS
NT SOLAR CELLS
NT SOLAR GENERATORS
NT SOLAR SEA POWER PLANTS
NT THERMAL BATTERIES
NT THERMIONIC CONVERTERS
NT THERMOELECTRIC GENERATORS
NT TURBOGENERATORS
NT VERTICAL JUNCTION SOLAR CELLS

Motor/generator and electronic control considerations for energy storage flywheels 06 p0808 N85-13878

Superconducting rotor dynamics
[AD-A147176] 07 p0947 N85-16000

Power quality and protection of electric distribution systems with small, dispersed generation devices
[DE85-000990] 09 p1344 N85-18463

Variable speed generator technology options for wind turbine generators
[RR-84-4] 10 p1478 N85-19331

Rocky Flats Wind Energy Research Center FY 1983 report
[DE85-004500] 10 p1511 N85-19636

15KW power supply development
[DE85-001057] 11 p1629 N85-20280

Solar powered actuator with continuously variable auxiliary power control
[NASA-CASE-MFS-25637-1] 12 p1876 N85-21769

Preliminary assessment of power-generating tethers in space and of propulsion for their orbit maintenance
13 p1997 N85-22528

Control of cascaded induction generator systems
[AD-A150429] 13 p2085 N85-22897

Basic research on inertial confinement fusion by LIMAY-I 15 p2655 N85-26380

Test flight of IL-76TD long-range transport variant
17 p2894 N85-27842

Principles of designing digital compensating accelerometers 17 p2944 N85-28172

Activity and accomplishments of dish/Stirling electric power system development
[NASA-CR-175841] 17 p2985 N85-28445
Control of acid deposition precursors through dry scrubbing
[DE85-010881] 19 p3235 N85-30056
Free-piston Stirling engine/linear alternator 1000-hour endurance test
[NASA-CR-174771] 19 p3304 N85-30461
Experimental investigation of a variable speed constant frequency electric generating system from a utility perspective
[NASA-CR-174950] 21 p3579 N85-32251
Operational window for a plasma erosion opening switch used for voltage multiplication on pulsed power generators
[AD-A155482] 21 p3707 N85-33020
Long-term research in Japan: Amorphous metals, metal oxide varistors, high-power semiconductors and superconducting generators
[DE85-010827] 22 p3748 N85-33230
Study to assess the effects of magnetohydrodynamic electromagnetic pulse on electric power systems, phase 1, volume 3
[DE85-011301] 24 p4156 N85-35771

ELECTRIC HYBRID VEHICLES
Evaluation of heat engine for hybrid vehicle application
[NASA-CR-174163] 04 p0506 N85-13245
Electric and hybrid vehicle demonstration project
[DE84-014822] 06 p0871 N85-15535
Feasibility demonstration of a novel, flat-belt, continuously variable transmission or automotive and electric-hybrid vehicle application
[NASA-CR-174430] 10 p1569 N85-19894
ElectriFleet Project
[DE85-001598] 10 p1570 N85-19898
Electric vehicle demonstration project
[DE85-002167] 11 p1741 N85-20943
Electric and hybrid vehicle demonstration project
[DE85-003839] 13 p2169 N85-23455
A system-level mathematical model for evaluation of power train performance of load-leveled electric-vehicles
[NASA-CR-175652] 14 p2434 N85-25009
Performance testing and system characterization. DOE hybrid test vehicle, phase 3
[NASA-CR-175888] 14 p2434 N85-25010
Advanced vehicle systems assessment. Volume 1: Executive summary
[NASA-CR-175876] 17 p3051 N85-28887
Urban vehicle research project
[DE85-005444] 17 p3052 N85-28889
Electric and hybrid vehicle program
[DE85-010025] 19 p3262 N85-30230
Evaluation of semiconductor devices for Electric and Hybrid Vehicle (EHV) ac-drive applications, volume 1
[NASA-CR-176118] 23 p3927 N85-34335

ELECTRIC IMPULSES
U ELECTRIC PULSES

ELECTRIC MOMENTS
Particle physics
[DE84-013834] 05 p0727 N85-14673

ELECTRIC MOTOR VEHICLES
Performance of improved lead acid batteries for electric vehicles
[DE84-015845] 04 p0495 N85-13160
Electric vehicle maintenance
[PB84-233352] 04 p0579 N85-13693
Research, development, and demonstration of nickel-iron batteries for electric vehicle propulsion
[DE84-017430] 05 p0632 N85-14054
Research, development, and demonstration of lead-acid batteries for electric vehicle propulsion
[DE84-017442] 05 p0632 N85-14055
Performance characteristics of a battery charger and state-of-charge indicator
[NASA-CR-174273] 07 p0946 N85-15992
BBC of Switzerland develops electric car
08 p1141 N85-17192
Hybrid vehicle program
[DE85-000326] 09 p1410 N85-18686
Electric vehicle battery test plan and results
[DE84-901972] 09 p1410 N85-18687
Electric-Hybrid Vehicle (E-HV) demonstration-test project
[DE85-002370] 10 p1570 N85-19899
High-strength composite materials for aircraft, body armor
11 p1599 N85-20057
Electric vehicle demonstration project
[DE85-000124] 11 p1741 N85-20944
Electric vehicle test program: INEL transition qualification test plan
[DE85-005171] 13 p2169 N85-23456
In-vehicle evaluation of the Globe EV 2300 lead-acid, Delco Remy 150 nickel-zinc, and Eagle-Picher NIF 270 nickel-iron battery systems
[NASA-CR-175653] 14 p2349 N85-24521
Field use of electric vehicles compared to prototype tests
[DE85-006887] 15 p2667 N85-26458
INEL electric vehicle laboratory qualification: Transition test results and comparisons with JPL ETV1-2 data
[DE85-008006] 16 p2880 N85-27772
Test and evaluation of the Hoppecke Model E240G144/16 electric vehicle battery charger
[DE85-900573] 17 p2955 N85-28253
Test plan for acceptance, verification and performance testing of the Bedford Lucas Chloride Electric Van. Part 1: Acceptance and verification testing at EG and G Automotive Research. Part 2: INEL performance testing, revision 1
[DE85-005157] 17 p3051 N85-28888
Environmental concerns related to natural gas vehicles
[DE85-010246] 20 p3486 N85-31666
State of knowledge of environmental concerns related to natural-gas-fueled vehicles
[DE85-009746] 20 p3486 N85-31667
Electric vehicle operations by the City of Huntsville, Alabama, March 1983 - May 1984
[DE85-005913] 22 p3849 N85-33842
Evaluation of half wave induction motor drive for use in passenger vehicles
[NASA-CR-176119] 23 p3926 N85-34334
Evaluation of semiconductor devices for Electric and Hybrid Vehicle (EHV) ac-drive applications, volume 1
[NASA-CR-176118] 23 p3927 N85-34335
Test plan for performance testing of the Eaton AC-3 electric vehicle
[DE85-011954] 23 p3927 N85-34341

ELECTRIC MOTORS
NT ASYNCHRONOUS MOTORS
NT INDUCTION MOTORS
NT MICROMOTORS
NT SYNCHRONOUS MOTORS
NT TORQUE MOTORS
Vibrational power transmission of an idealised gearbox
[ISVR-TR-124] 02 p0204 N85-11346
Description of a laboratory model Annular Momentum Control Device (AMCD) 05 p0606 N85-13863
Motor/generator and electronic control considerations for energy storage flywheels 05 p0608 N85-13878
Measurements of satellite refrigeration compressor power consumption and efficiency
[DE84-016724] 05 p0632 N85-14056
Design and test of a four channel motor for electromechanical flight control actuation
[NASA-CR-171838] 08 p1156 N85-17294
Armenia markets new drive motors for machine tools
10 p1461 N85-19212
Permanent magnet motors
[DE85-000660] 10 p1482 N85-19355
An evaluation of liquid and two-phase cooling techniques for use in electrical machinery
[AD-A149526] 10 p1484 N85-19372
Cost comparison of small gas turbines versus electric motors in a variable load industrial application
[PB85-149763] 12 p1837 N85-21530
Optimum design of electrical motors for multilink manipulators and automated manufacturing systems
13 p2062 N85-22880
Reluctance and doubly-excited reluctance motors
[DE85-003585] 13 p2065 N85-22900
Nickel-iron battery to be used in Peugeot electric car
15 p2532 N85-25615
CSMP (Continuous System Modeling Program) modeling of brushless DC motors
[AD-A152043] 15 p2549 N85-25731
Electric motors with elastically mounted rotors
16 p2763 N85-27048
Optimal control of electric drive with simultaneous control inputs for motor current and flux
16 p2763 N85-27049
AC powertrain for an electric vehicle, phase 2 and phase 3
[NASA-CR-175760] 16 p2880 N85-27771
Standard series of direct-current motors for regulated electric drives 22 p3772 N85-33375
Evaluation of half wave induction motor drive for use in passenger vehicles
[NASA-CR-176119] 23 p3926 N85-34334
Computer simulation of a cruise missile using brushless dc motor fin control
[AD-A155935] 24 p4089 N85-35349

ELECTRIC NETWORKS
Diagnosis of insulation defects in 1000 + V distribution networks with insulated neutral
07 p0954 N85-16044
A Monte Carlo sampling plan for estimating network reliability
[AD-A150511] 13 p2065 N85-22898
Numerical methods for stiff ordinary and elliptic partial differential equations
[AD-A153247] 17 p3020 N85-28675
Microcomputer network: investigation and implementation
[AD-A155631] 21 p3674 N85-32826

ELECTRIC POTENTIAL
NT BIOELECTRIC POTENTIAL
NT COULOMB POTENTIAL
NT LOW VOLTAGE
NT OPEN CIRCUIT VOLTAGE
NT PHOTOVOLTAGES
NT QUANTUM WELLS
Effects of H2S on molten carbonate fuel cells
[DE84-015166] 02 p0195 N85-11307
Method of splitting for solution of problems in semiconductor physics 02 p0265 N85-11736
Efficiency of photoelectric conversion of short radiation pulses 03 p0348 N85-12240
Electrokinetic potential and stability of SiC suspensions in electrolyte solutions
[NASA-TM-77492] 04 p0460 N85-12984
Zeta potential in ceramic industry
[NASA-TM-77478] 04 p0478 N85-13047
Study program for encapsulation materials interface for Flat-plate Solar Array (FSA) project
[NASA-CR-174152] 04 p0530 N85-13385
Flywheel-powered X-ray generator
05 p0605 N85-13861
Westinghouse programs in pulsed homopolar power supplies 05 p0606 N85-13862
Potential of flywheels for spacecraft energy storage
05 p0609 N85-13890
Behaviour of lead-silver anodes in zinc electrodeposition from sulphuric acid baths
[BLL-MINTEK-TR-1180-(5810.5759)]
06 p0764 N85-14867
Device for measuring average power of laser radiation
06 p0786 N85-15026
High-speed power thyristors with excellent switching and load characteristics 06 p0793 N85-15070
Gallium-arsenide power devices
06 p0794 N85-15076
Current-voltage characteristics of semiconductor power devices operating at high current densities
06 p0795 N85-15079
Two programs for the HP9836C computer to acquire frequency or voltage data from a source
[AD-A146832] 06 p0854 N85-15430
Measurement of proton autoneutralization potential
[DE85-001752] 06 p0865 N85-15501
The anode mechanism of a thermal argon arc
[NASA-TM-77754] 07 p0921 N85-15835
Studies on copper alloys containing chromium on the copper side phase diagram
[NASA-TM-77752] 07 p0927 N85-15876
Transmission line biased coherent array of Josephson oscillators
[AD-D011323] 07 p0944 N85-15979
Analog to digital converter
[AD-D011336] 07 p0945 N85-15983
Dependence of breakdown voltage for p-n junction on parameters of ion implantation and semiconductor heat treatment 07 p0964 N85-16046
Battery control and fault detection method
[AD-D011384] 07 p0983 N85-16307
Data and results of a laboratory investigation of microprocessor upset caused by simulated lightning-induced analog transients
07 p0999 N85-16345
The ac power line protection for an IEEE 587 Class B environment 07 p1000 N85-16347
Natural electrical activity of human sympathetic nerve fibers, recorded from body surface
07 p1013 N85-16433
Potential dependence of electrical conductivity and chemical charge storage of poly(pyrrole) films on electrodes
[AD-A148513] 08 p1122 N85-17075
Calculations of high-current characteristics of silicon diodes at microwave frequencies
[AD-A147406] 09 p1314 N85-18261
Development of photoconductive power switch technology
[DE85-001514] 09 p1315 N85-18270
Electrical resistivity technique to assess the integrity of geomembrane liners
[PB85-122414/GAR] 09 p1325 N85-18327
Large electrostatic accelerators
[DE85-001120] 09 p1382 N85-18889
High energy pulsed particle accelerator
[AD-A149247] 10 p1554 N85-19797

Thermal investigation of an electrical high-current arc with porous gas-cooled anode
[NASA-TM-77789] 11 p1627 N85-20245
Angular measurement system
[NASA-CASE-MFS-25825-1] 11 p1635 N85-20298
Electrical and thermal performance during charging and discharging a Phase 1 gel cell battery
[PB85-114312] 11 p1677 N85-20565
Topography of human brain electric potentials and dominance 11 p1691 N85-20633
Review of anode phenomena in vacuum arcs
[DE85-002736] 12 p1926 N85-22101
Electrical performance of semiconductor devices at cryogenic temperatures 12 p1948 N85-22239
Discharges on a negatively biased solar cell array in a charged-particle environment 13 p1994 N85-22499
EMI characteristics of a potential control system
13 p1994 N85-22502
Characteristics of EMI generated by negative metal-positive dielectric voltage stresses due to spacecraft charging 13 p1995 N85-22505
Space test program of high-voltage solar array-space plasma interactions 13 p1997 N85-22519
Stability of highly nonlinear oxide-zinc resistors under continuous voltage of industrial frequency
13 p2087 N85-23030
Comparison of flame photometer data with total particle volume calculated from laser spectrometer particle count data
[AD-A151008] 14 p2252 N85-23958
An improved battery state-of-charge indicator
[NASA-CR-175701] 14 p2298 N85-24227
Thermocouple modeling
[DE85-005172] 14 p2306 N85-24273
Electric potential of satellite in electron emitting experiments in initial stage of electron beam injection in steady-state mode 15 p2480 N85-25309
Transient voltage oscillations in coils
[DE85-006715] 15 p2590 N85-25738
High speed electric field and voltage measurements with field coupled sensors
[DE85-006637] 15 p2642 N85-26299
Studies in electron phenomena in MOS structures: The pulsed C-V method 15 p2659 N85-26407
Sources of improvement in quality of contact butt welding of wire
[BLL-M-36085-(5828.4)] 16 p2793 N85-27225
Investigation of pseudo bi-polar nickel cadmium batteries as filter elements for pulsed power loads
[AD-A152112] 16 p2819 N85-27389
Streak tube characterization
[DE85-009874] 17 p2956 N85-28255
Crack tip chemistry modeling of intergranular stress corrosion cracks of nickel containing segregated phosphorus and sulphur
[DE85-010059] 18 p3076 N85-29028
High voltage power supply
[NASA-CASE-GSC-12818-1] 18 p3093 N85-29147
Magnetically switched power supply systems for lasers
[NASA-CASE-NPO-16402-1] 18 p3112 N85-29265
A collective interaction klystron specification
[AD-D011704] 19 p3255 N85-30186
High efficiency large area polysilicon solar cells
20 p3482 N85-31639
Density gradient electrophoresis of cultured human embryonic kidney cells 20 p3501 N85-31763
Plasma erosion opening switch
[DE85-011384] 20 p3535 N85-31996
Module Hipot and ground continuity test results
21 p3612 N85-32447
R, L, C, G measurement 21 p3668 N85-32784
Recent advances in d-c relaxation techniques for the measurement of kinetics of fast electrode reactions
[DE85-005029] 22 p3745 N85-33216
Transparent electrode for optical switch
[DE85-011618] 22 p3761 N85-33310
IEA-SSPS CRS calibration report: Calibration of relevant measuring sensors
[DE85-010174] 22 p3788 N85-33468
Surface voltage gradient role in high voltage solar array-plasma interaction: Center Director's discretionary fund
[NASA-TM-86516] 22 p3805 N85-33567
Experimental evaluation of the thermodynamic properties of concentrated aqueous potassium hydroxide solutions
[DE85-010628] 23 p3912 N85-34236
Reversing-counterpulse repetitive-pulse inductive storage circuit
[DE85-006409] 23 p3928 N85-34344
Modulated voltage metastable ionization detector
[NASA-CASE-ARC-11503-1] 23 p3933 N85-34374
Rapid annealing of temperature-compensated, precision voltage references following fast-neutron irradiation
[DE85-009821] 23 p3970 N85-34609
Statistical distribution of breakdown voltages in rep-rate spark gaps
[DE85-012813] 24 p4090 N85-35354
System expectations for Pioneer 1 foil implosion experiments
[DE85-014129] 24 p4091 N85-35359
ELECTRIC POWER
Survey of remote data monitoring systems
[DE85-001385] 09 p1323 N85-18313
ELECTRIC POWER CONVERSION
U ELECTRIC GENERATORS
ELECTRIC POWER PLANTS
NT FUEL CELL POWER PLANTS
NT NUCLEAR POWER PLANTS
NT SOLAR THERMAL ELECTRIC POWER PLANTS
Manual of phosphoric acid fuel cell power plant optimization model and computer program
[NASA-CR-174721] 01 p0067 N85-10445
Phosphoric acid fuel cell power plant system performance model and computer program
[NASA-CR-174638] 02 p0222 N85-11456
Fabric filter system study
[PB84-229749] 03 p0342 N85-12206
Electrostatic augmentation of fabric filtration: Reverse-air pilot unit experience
[PB84-230002] 03 p0343 N85-12207
Analytical models 05 p0666 N85-14282
A summary description of a computer program concept for the design and simulation of solar pond electric power generation systems 05 p0666 N85-14285
Salton Sea solar pond power plant design study and regional applicability 05 p0667 N85-14290
The upwind power plant Manzanares
05 p0669 N85-14305
Progress in developing tidal electric power plants reported 07 p0994 N85-16314
Geothermal wells drilled in Transcarpathians
07 p0994 N85-16315
On-line monitoring of the true corrosion rate in problems related to power plants
[CISE-2335] 08 p1131 N85-17126
Advancement of remote technology: Past perspectives and future plans
[DE85-000934] 09 p1327 N85-18342
Conceptual design of a 10 MW shore-based OTEC plant
[DE84-015808] 10 p1511 N85-19532
Work physiology of operating personnel at power plants in arid regions 10 p1523 N85-19606
Leak monitoring in high pressure preheaters by a noninvasive ultrasonic method
[CISE-2373] 11 p1650 N85-20394
Leak detection by acoustic emission monitoring in power plant high pressure preheaters
[CISE-2392] 11 p1650 N85-20395
Underground pumped hydroelectric storage
[DE85-000288] 11 p1676 N85-20560
Program plan for research and development of dielectric materials for electric power systems
[DE85-001327] 12 p1838 N85-21520
Heat Cycle Research Experimental Program report, FY-84
[DE85-003558] 12 p1882 N85-21811
Comprehensive evaluation of cost effectiveness of solar electric power plants 14 p2265 N85-24036
Tribological sinks: Money down the drain
[DE85-010019] 17 p2974 N85-28376
A program for the calculation of paraboloidal-dish solar thermal power plant performance
[NASA-CR-175874] 17 p2985 N85-28449
Silica problem in the design of geothermal power plants
[DE85-008245] 17 p2986 N85-28453
Fuel cell applications literature review
[DE85-011891] 22 p3809 N85-33592
Fusion facility siting considerations
[DE85-012894] 22 p3843 N85-33805
ELECTRIC POWER SUPPLIES
NT AIRCRAFT POWER SUPPLIES
NT SPACECRAFT POWER SUPPLIES
Power subsystem automation study
[NASA-CR-171213] 03 p0358 N85-12299
Comparative energy storage assessment item
05 p0605 N85-13858
Westinghouse programs in pulsed homopolar power supplies 05 p0606 N85-13862
High-efficiency power conversion options for flywheel energy storage systems 05 p0607 N85-13876
A historical overview of the electrical power systems in the US manned and some US unmanned spacecraft
[NASA-CR-174806] 05 p0612 N85-13910
Energy supply problems for emergency telephones
05 p0663 N85-14265
Project Pellworm: Solar electric energy supply for a health center 05 p0664 N85-14266
High-speed power thyristors with excellent switching and load characteristics 06 p0793 N85-15070
Evaluation of miniature vacuum ultraviolet lamps for stability and operating characteristics, Lyman-Alpha lamp
[NASA-CR-171345] 10 p1477 N85-19923
The 35 kilowatt peak power photovoltaic system
[DE85-000189] 10 p1511 N85-19537
Microprocessor-based monitoring and control project, phase 1
[DE84-901974] 10 p1538 N85-19869
15KW power supply development
[DE85-001057] 11 p1629 N85-20269
Feasibility of producing commodities and electricity for space shuttle operations at Vandenberg Air Force Base
[DCN-84-203-001-80-21] 12 p1789 N85-21230
New types of power supplies for ultrasonic processing equipment 12 p1843 N85-21586
Autonomous uninterruptable power supply apparatus
[AD-D011571] 14 p2298 N85-24222
Basic research on inertial confinement fusion by LIMAY-I 15 p2655 N85-26393
Maintenance of photovoltaic power systems
[AD-A152299] 16 p2819 N85-27390
Large scale electricity production scheduling via nonlinear optimization
[REPT-84-07] 17 p3017 N85-28665
High voltage power supply
[NASA-CASE-GSC-12818-1] 18 p3093 N85-29147
Dynamic simulation of dispersed, grid-connected photovoltaic power systems: System studies
[DE85-011179] 19 p3262 N85-30231
Experimental investigation of a variable speed constant frequency electric generating system from a utility perspective
[NASA-CR-174950] 21 p3579 N85-32251
Applicability of 100kWe-class of space reactor power systems to NASA manned space station missions
[NASA-CR-174696] 24 p4149 N85-35729
ELECTRIC POWER TRANSMISSION
Laboratory evaluation of Electromagnetic Pulse (EMP) hardness testing concepts for electrical conduit systems
[AD-A145466] 02 p0190 N85-11273
Power subsystem automation study
[NASA-CR-171213] 03 p0358 N85-12299
Electromagnetic pulse and the electric power network
[DE84-015403] 04 p0493 N85-13140
Electrical/electronics working group summary
05 p0604 N85-13850
Effects of Formvar coating and copper-nickel outer sheath on the ac losses of multi-strand subsize cables
[DE85-010413] 18 p3096 N85-29166
Protection products for the conductors of high voltage overhead lines
[BLL-OA-TRANS-3219-(6196.300)]
20 p3429 N85-31269
ELECTRIC PROPULSION
NT ELECTROMAGNETIC PROPULSION
NT ELECTROSTATIC PROPULSION
NT ION PROPULSION
NT PLASMA PROPULSION
Development of the Engineering Test Satellite-3 (ETS-3) ion engine system
[NASA-TM-77538] 01 p0017 N85-10101
Research, development, and demonstration of nickel-iron batteries for electric vehicle propulsion
[DE84-017430] 05 p0632 N85-14054
Experimental research on electric propulsion. Note 7: Analysis of the performance of an arc-jet driven by means of hydrogen and nitrogen
[NASA-TM-77473] 06 p0760 N85-14661
Extended performance technology study 30-cm thruster
[NASA-CR-168259] 07 p0917 N85-15906
High frequency plasma generator for ion thrusters
[NASA-CR-174772] 08 p1114 N85-17023
Proceedings of the AFOSR/AFRPL Rocket Propulsion Research Meeting: Abstracts and Agenda
[AD-A148818] 09 p1288 N85-18086
Preliminary assessment of power-generating tethers in space and of propulsion for their orbit maintenance
13 p1997 N85-22520
Station keeping of geostationary satellites by electric propulsion
[NASA-TM-77820] 14 p2320 N85-24337
Analysis of orbit transfer vehicles for GPS Block 3 satellites
[AD-A152021] 16 p2732 N85-26980
Primary propulsion of electrothermal, ion and chemical systems for space-based radar orbit transfer
[NASA-TM-87043] 17 p2916 N85-27972
Experimental research on electrical propulsion. Note 2: Experimental research on a plasma jet with vortex type stabilization for propulsion
[NASA-TM-77874] 18 p3067 N85-28968
Experimental research on electrical propulsion
[NASA-TM-77876] 18 p3067 N85-28969

Experiments in plasma initiation and laser absorption in flowing gases
[AD-A154303] 19 p3276 N85-30313

ELECTRIC PULSES
Influence of radiation wavelength on elastic pulse shape during laser excitation 02 p0257 N85-11661
Pulsed-power system diagnostics: Electromagnetic data interpretation along pulse lines
[AD-A146607] 06 p0810 N85-15148
Basic research on inertial confinement fusion by LIMAY-I 15 p2655 N85-26383

ELECTRIC RELAYS
Isolated load switching with surge suppression
[AD-D011218] 01 p0042 N85-10274
High or low-side solid state relay with current limiting and operational testing
[AD-D011260] 05 p0631 N85-14046

ELECTRIC ROCKET ENGINES
NT ARC JET ENGINES
NT ELECTROSTATIC ENGINES
NT ELECTROTHERMAL ENGINES
NT ION ENGINES
NT MERCURY ION ENGINES
NT PLASMA ENGINES
NT RESISTOJET ENGINES
NT RIT ENGINES

ELECTRIC SPARKS
Bibliography of data on electrical breakdown in gases
[PB84-218049] 01 p0045 N85-10294
Evaluation of minimum ignition energy measurement techniques used at P.E.R.M.E.
[SG83/A258] 09 p1301 N85-18169
A new theory aiming to define the mechanisms of material removal in electroerosion
[NASA-TM-77875] 18 p3176 N85-29689
Apparatus and method for the spectrochemical analysis of liquids using the laser spark
[DE85-005749] 23 p3935 N85-34387

ELECTRIC SWITCHES
NT THERMOSTATS
Automation of assembly of electrical products
03 p0346 N85-12228
Semiconductor submicrosecond power commutator switches 06 p0795 N85-15081
Electromechanical switch
[AD-D011400] 07 p0946 N85-16009
Metal vapor arc switch electromagnetic accelerator technology
[NASA-CR-174380] 09 p1314 N85-18259
High voltage disconnect protection
[AD-D011480] 10 p1481 N85-19353
High-voltage, high-power, solid-state remote power controllers for aerospace applications
[NASA-TP-2437] 12 p1795 N85-21263
Basic studies of gases for fast switches
[AD-A149828] 12 p1835 N85-21514
Comparison of shock-induced displacements with displacements produced by a centrifuge acceleration
[DE85-000467] 12 p1852 N85-21618
Current distribution in a plasma erosion opening switch
[AD-A150987] 14 p2424 N85-24949
System of light protection of antenna-mast structures of radio-relay lines 15 p2527 N85-25583
Erosion of electrodes due to switching of capacitor-bank discharge circuits
[AD-A151207] 15 p2547 N85-25718
A study of reflex optoelectronic switching matrices and their derivatives
[CRC-TN-720] 19 p3253 N85-30169
Fast transient behavior of thyristor switches
[AD-A154109] 19 p3259 N85-30206

ELECTRIC WELDING
NT ARC WELDING
NT ELECTRON BEAM WELDING
NT ELECTROSLAG WELDING
NT GAS TUNGSTEN ARC WELDING
NT PLASMA ARC WELDING
International exhibition: Industrial Robots, 1982
03 p0345 N85-12224
Robotization of electric welding processes
03 p0345 N85-12225
Robotization of technological processes in high-frequency heating and welding
03 p0345 N85-12226
Electric Welding Institute's space-technology test results 03 p0352 N85-12287
Cosmonauts report on space welding at conference
15 p2484 N85-25329
Contact point and seam welding of heat-resistant alloys 15 p2501 N85-25429
Sources of improvement in quality of contact butt welding of wire
[BLL-M-36085-(5828.4)] 16 p2793 N85-27225

Removal of longitudinal internal flash from electrically welded tubes
[BLL-BISI-TRANS-22360-(9022.06)]
17 p2938 N85-28136
Production of thin-walled electricity welded tubes with reduced internal flash
[BLL-BISI-TRANS-22361-(9022.06)]
17 p2973 N85-28364
Production of electrically welded tubes with removed internal flash
[BLL-BISI-TRANS-22382-(9022.06)]
17 p2973 N85-28367

ELECTRIC WIRE
NT BEAM LEADS
The HEMP (High-altitude Electromagnetic Pulse) response of a long transmission line buried in the earth
[AD-A146517] 06 p0800 N85-15108
Safety requirements for wiring systems and connectors for photovoltaic systems
[NASA-CR-174211] 06 p0803 N85-15110
Hardwire missile receiver coupler
[AD-D011350] 07 p0937 N85-15936
Flashover failures from wet-wire arcing and tracking
[AD-A149055] 10 p1478 N85-19332
Signal propagation delay, wire length distribution and the efficiency of VLSI circuits
[CWI-CS-R8412] 11 p1630 N85-20266
Liquid thickness gage
[NASA-CASE-LAR-13342-1] 11 p1635 N85-20297
Releasable cable connector assembly for use between a mobile and stationary object
[AD-D011538] 12 p1858 N85-21655
Properties of Ti alloyed multifilamentary Nb3Sn wires by internal tin process
[DE85-003212] 12 p1941 N85-22191
Multiconductor flat cable
[AD-D011635] 17 p2950 N85-28218
Unalloyed and alloyed line wires of improved properties
[BLL-BISI-TRANS-21930-(9022.06)]
18 p3073 N85-29008
Critical current density and microstructural state of an internal tin multifilamentary superconducting wire
[DE85-009966] 22 p3761 N85-33306

ELECTRIC WIRING
U ELECTRIC WIRE
U WIRING

ELECTRICAL BREAKDOWN
U ELECTRICAL FAULTS

ELECTRICAL CONDUCTIVITY
U ELECTRICAL RESISTIVITY

ELECTRICAL CONDUCTIVITY METERS
Atmospheric research aircraft — conductivity/charge measurements
[ONERA-RS-87/7154/PY] 11 p1682 N85-20596
Method of separately determining electrophysical properties of bulky conductor 13 p2073 N85-22951

ELECTRICAL ENERGY
U ELECTRIC POWER

ELECTRICAL ENGINEERING
Center for Electronics and Electrical Engineering Technical Bulletin covering center programs with 1984 CEEE events calendar
[PB84-222785] 01 p0045 N85-10292
Center for Electronics and Electrical Engineering Technical Bulletin covering center programs with 1984 CEEE events calendar
[PB84-223684] 01 p0045 N85-10293
Center for Electronics and Electrical Engineering Technical Bulletin covering center programs
[PB84-219716] 01 p0045 N85-10295
Center for Electronics and Electrical Engineering Technical Bulletin covering center programs
[PB84-216056] 01 p0045 N85-10296
Singular perturbations, coherency and aggregation of dynamic systems
[DE84-014166] 01 p0114 N85-10772
Activities report of the Department of Engineering
03 p0342 N85-12202
USSR report: Electronics and electrical engineering
[JPRS-UEE-84-014] 03 p0344 N85-12215
International exhibition: Industrial Robots, 1982
03 p0345 N85-12224
Center for Electronic and Electrical Engineering Technical Progress Bulletin, January - March 1983, no. 2
[PB84-231224] 03 p0360 N85-12306
USSR report: Electronics and electrical engineering
[JPRS-UEE-84-010] 04 p0485 N85-13095
NMOS test chip for a course in semiconductor parameter measurements
[PB84-216506] 04 p0497 N85-13174
USSR report: Electronics and electrical engineering
[JPRS-UEE-84-012] 06 p0781 N85-14991
USSR report: Electronics and electrical engineering
[JPRS-UEE-84-011] 06 p0789 N85-15042

A summary of the foundation research program
[AD-A146524] 06 p0891 N85-15656
Target detection using microwave irradiances from natural sources: A passive, local and global surveillance system
[NASA-CR-174260] 07 p0946 N85-15991
Basic research in electronic (JSEP): Joint Services Electronics Program
[AD-A147891] 07 p0948 N85-16007
USSR report: Electronics and electrical engineering
[JPRS-UEE-84-018] 07 p0949 N85-16014
USSR report: Electronics and electrical engineering
[JPRS-UEE-84-017] 07 p0951 N85-16025
Chemical, material electronics studies established
08 p1142 N85-17200
Flexible applications robot used in Moscow training course 10 p1462 N85-19217
China report: Science and technology
[JPRS-CST-84-025] 11 p1620 N85-20197
Electronics Engineering Department: EE technical review
[DE85-004360] 11 p1629 N85-20259
East Europe report: Scientific affairs
[JPRS-ESA-84-006] 11 p1700 N85-20684
USSR report: Electronics and electrical engineering
[JPRS-UEE-85-004] 12 p1837 N85-21531
The DFS-Kopernikus solar generator electrical design
13 p2008 N85-22590
The DFS-Kopernikus solar generator
13 p2008 N85-22591
Electrical design of the Intelsat 6 solar generator
13 p2008 N85-22592
Development and qualification of the electrical part of the Advanced Rigid Array (ARA) — solar array
13 p2008 N85-22594
Design and qualification testing of the Olympus solar array blanket 13 p2009 N85-22600
Electronics Engineering Department EE Technical Review
[UCRL-50025-84-1] 13 p2063 N85-22887
USSR report: Electronics and electrical engineering
[JPRS-UEE-85-002] 13 p2066 N85-22907
USSR report: Electronics and electrical engineering
[JPRS-UEE-85-001] 13 p2076 N85-22976
Microcomputers and the electrical engineer
[AD-A150499] 13 p2147 N85-23325
China report: Science and technology
[JPRS-CST-85-003] 13 p2166 N85-23433
Basic research in electronics (JSEP)
[AD-A151002] 14 p2296 N85-24230
USSR report: Electronics and electrical engineering
[JPRS-UEE-85-005] 15 p2524 N85-25565
China report: Science and technology
[JPRS-CST-85-011] 15 p2551 N85-25746
A concept for the intrinsic dielectric strength of electrical insulation materials
[NASA-CR-176040] 20 p3448 N85-31410
Failure mechanisms in metal-sheathed thermocouples
[DE85-011929] 21 p3590 N85-32317
USSR report: Electronics and electrical engineering
[JPRS-UEE-84-015] 22 p3762 N85-33314
USSR report: Electronics and electrical engineering
[JPRS-UEE-84-003] 22 p3773 N85-33381
Joint services electronics program
[AD-A154748] 23 p3927 N85-34336
Center for Electronics and Electrical Engineering technical progress bulletin covering center programs, July-September with 1985 CEEE events calendar
[PB85-191393] 24 p4091 N85-35363

ELECTRICAL FAULTS
NT SHORT CIRCUITS
Bibliography of data on electrical breakdown in gases
[PB84-218049] 01 p0045 N85-10294
Luminous points and breakdown in structure of GaAs transistors 02 p0257 N85-11684
Glow spots and breakdown in GaAs transistor structure 04 p0487 N85-13107
Determination of threshold and maximum operating electric stresses for selected high voltage insulation. Task 3: Investigation of high voltage capacitor insulation
[DE84-017051] 09 p1316 N85-18274
Flashover failures from wet-wire arcing and tracking
[AD-A149055] 10 p1478 N85-19332
Mass analysis of neutral particles and ions released during electrical breakdowns on spacecraft surfaces
[NASA-CR-175585] 12 p1793 N85-21250
Concurrent simulation techniques exploiting hierarchy
[AD-A149783] 12 p1835 N85-21512
Basic studies of gases for fast switches
[AD-A149828] 12 p1835 N85-21514
Galileo internal electrostatic discharge program
13 p1995 N85-22504
Mass spectra of neutral particles released during electrical breakdown of thin polymer films
13 p1996 N85-22511

Electrical conduction in polymer dielectrics
13 p1996 N85-22514

Breakdown of thin plates by radiation
13 p2026 N85-22709

High field RF superconductivity: To pulse or not to pulse
[DE85-004381] 14 p2429 N85-24977

Experimental investigation of the electric breakdown in SF6
[BLL-CE-TRANS-7987-(9022.09)]
15 p2546 N85-25714

Field-induced phenomena in electrical insulation
[AD-A151234] 15 p2547 N85-25719

Energy considerations in second breakdown
[AD-A152389] 17 p2952 N85-28229

Analysis of time dependent dielectric failures
[AD-A153200] 17 p2954 N85-28243

Performance and electric field limitations in inflow disk MHD generators 20 p3534 N85-31987

Vacuum interface flashover with bipolar electric fields
[DE85-012027] 22 p3755 N85-33275

Model that predicts pulse charged gas switching breakdown phenomena
[DE85-013119] 22 p3761 N85-33313

Method and apparatus for transfer function simulator for testing complex systems
[NASA-CASE-NPO-15696-1] 23 p3926 N85-34333

Solar system fault detection
[DE85-005987] 23 p3946 N85-34458

Statistical distribution of breakdown voltages in rep-rate spark gaps
[DE85-012813] 24 p4090 N85-35354

ELECTRICAL GROUNDING

Human engineering laboratory grounding analysis: Project Helga
[AD-A145728] 02 p0195 N85-11300

Exact design formulas for field intensity of dipole deployed above flat homogeneous Earth with finite conductivity 13 p2081 N85-22998

ELECTRICAL IMPEDANCE
NT CONTACT RESISTANCE
NT ELECTRICAL RESISTANCE

Impedance of vertical dipoles above a dissipative ground
[REPT-S-152] 02 p0192 N85-11287

An automated immittance measuring system for electroacoustic transducers
[AD-A145701] 02 p0200 N85-11336

Determination of the pressure sensitivity of 1 inch condenser microphones
[PTB-AK-26] 05 p0633 N85-14058

Deer control using 7 strand vertical fence
11 p1581 N85-19958

Effectiveness of an overhead wire barrier system in reducing gull use at the BFI Jedburg sanitary landfill, Berkeley and Dorchester counties, South Carolina
[AD-P004200] 11 p1582 N85-19967

Semiconductor electrochemistry approach to the study of oxide films on nickel electrodes
[DE85-003042] 11 p1630 N85-20264

Change of electrical characteristics of radio-frequency cables under thermal effect 13 p2081 N85-22999

Quality control of radioelectronic apparatus components on basis of external characteristics in frequency domain
15 p2529 N85-25590

A computation of fin-line impedance
[AD-A154080] 19 p3258 N85-30204

Changes in the impedance and bioelectrical activity of the cerebral cortex of rats under the action of anaesthetic drugs
[HSE-TRANS-10371] 19 p3327 N85-30617

Measurement of electrical parameters and current components in the bulk of silicon solar cells
20 p3481 N85-31635

R, L, C, G measurement 21 p3668 N85-32784

ELECTRICAL INSULATION

Development of power system management
[PB84-216530] 04 p0497 N85-13173

USSR report: Electronics and electrical engineering
[JPRS-UEE-84-012] 06 p0781 N85-14991

Choice of criteria for rejection of insulating components in high-voltage surge equipment
06 p0785 N85-15021

Diagnosis of insulation defects in 1000+ V distribution networks with insulated neutral
07 p0954 N85-16044

Determination of threshold and maximum operating electric stresses for selected high voltage insulation. Task 3: Investigation of high voltage capacitor insulation
[DE84-017051] 09 p1316 N85-18274

Transients during the switching of SF6-insulated isolating switches
[BLL-CE-TRANS-7986-(9022.09)]
15 p2546 N85-25713

Statistical analysis of partial discharge inception in high voltage 15 p2546 N85-25715

Field-induced phenomena in electrical insulation
[AD-A151234] 15 p2547 N85-25719

The ESFET: Evaporated Sensing Field Effect Transistor 19 p3256 N85-30188

A concept for the intrinsic dielectric strength of electrical insulation materials
[NASA-CR-176040] 20 p3448 N85-31410

Failure mechanisms in metal-sheathed thermocouples
[DE85-011929] 21 p3590 N85-32317

Partial discharges in and electric strength of high-voltage polymer insulation at cryogenic temperatures
22 p3770 N85-33364

ELECTRICAL LEADS
U ELECTRIC CONDUCTORS

ELECTRICAL MEASUREMENT
NT COULOMETRY
NT POLAROGRAPHY

Electrical parameters in 60-Hz biological exposure systems and their measurement: A primer
[PB84-217793] 03 p0400 N85-12548

Development of power system management
[PB84-216530] 04 p0497 N85-13173

Electrochemistry in near-critical and supercritical fluids. I. Ammonia
[AD-A146429] 06 p0765 N85-14894

Apparatus for measuring dielectric characteristics of polymer materials in millimetric range of wavelengths at 4.2-300 K temperatures 06 p0788 N85-15032

An indirect measure of below-ground electric field, conductivity, and dielectric constant
[AD-A146518] 06 p0804 N85-15115

Electronic and redox properties of stacked-ring silicon phthalocyanines from molecular orbital theory
[AD-A147161] 07 p0922 N85-15844

A narrow band pulsed eddy current instrument for materials testing
[AERE-R-11229] 07 p0968 N85-16149

Monitoring cure of epoxy resins using a microdielectrometer
[AD-A148618] 08 p1119 N85-17054

The use of microdielectrometry in monitoring the cure of resins and composites
[AD-A148619] 08 p1119 N85-17055

Voltammetry and coulometry with immersed thin layer electrodes. Part 1: Model for effects of solution resistivity in linear sweep voltammetry
[AD-A148655] 08 p1159 N85-17313

Voltammetry and coulometry with immersed thin layer electrodes. Part 2: Practical considerations and experimental results
[AD-A148656] 08 p1159 N85-17314

Multimode harmonic power measurement of 40 MW pulsed S-band klystrons
[DE85-001560] 09 p1316 N85-18272

Charge depletion meter
[AD-D011484] 10 p1488 N85-19393

High-current measurement techniques
[PB85-100444] 11 p1637 N85-20311

Development of a low cost electrochemical CO monitor based on anodic scanning voltammetry in nonaqueous electrolyte
[PB85-113488] 11 p1637 N85-20314

Electromagnetic pulse (EMP) injection on cable entries, type ERA; EMP memo no. 10
[FOA-E-30003-A3] 12 p1830 N85-21484

Program for controlling electrical measuring contact instrument on glow-discharge indicator panel
12 p1842 N85-21558

MFTF sensor verification computer program
[DE85-004452] 12 p1916 N85-22029

The high voltage silicon cell: A comparative analysis
13 p2005 N85-22569

Inverse behavior of silicon photovoltaic cells
13 p2010 N85-22604

Comparing different theoretical designs of six-port reflectometer junctions
[AD-A149419] 13 p2054 N85-22861

Portable electrochemical cell interrogator
[DE85-005186] 13 p2065 N85-22901

Measuring intensity of electric field produced by electromagnetic pulse with aid of active probes
13 p2075 N85-22958

Contactless determination of the conductivity of the white paint PCB-Z — Giotto spacecraft thermal control coating 14 p2243 N85-23907

Thermocouple modeling
[DE85-005172] 14 p2306 N85-24273

Instrument for measuring dispersional distortions in optical fibers and cables 15 p2530 N85-25595

A comparison of alternative analytic models for event related potential records
[AD-A151977] 15 p2618 N85-26134

Measurement methods for accurate microwave characterization and modeling of MESFET chips
[AD-A152360] 17 p2952 N85-28227

Voltammetric analysis of ordnance materials. Part 2: A portable digital voltammeter for use with a silver wi working electrode
[AD-A152480] 17 p2967 N85-288

Electrical and structural characterization of web dendritic crystals 20 p3481 N85-3163

Measurement of electrical parameters and current components in the bulk of silicon solar cells
20 p3481 N85-31635

Modelling and parameter estimation for distributed vibratory systems
[AD-A154518] 21 p3598 N85-32344

East Europe report: Science and technology. Selections on CSSR computer technology
[JPRS-ESA-84-017] 21 p3668 N85-32781

R, L, C, G measurement 21 p3668 N85-32784

The measurement of high value resistances at the NPL — electrical resistance
[NPL-DES-81] 22 p3758 N85-33291

ELECTRICAL PROPERTIES
NT CAPACITANCE
NT CARRIER MOBILITY
NT CHARGE DISTRIBUTION
NT CONTACT RESISTANCE
NT DIELECTRIC PROPERTIES
NT ELECTRIC MOMENTS
NT ELECTRICAL IMPEDANCE
NT ELECTRICAL RESISTANCE
NT ELECTRICAL RESISTIVITY
NT ELECTRON MOBILITY
NT ELECTROSTRICTION
NT FERROELECTRICITY
NT HOLE MOBILITY
NT INDUCTANCE
NT IONOSPHERIC CONDUCTIVITY
NT KONDO EFFECT
NT MAGNETORESISTIVITY
NT PERMITTIVITY
NT PHOTOCONDUCTIVITY
NT PHOTOVOLTAIC EFFECT
NT PIEZOELECTRICITY
NT PLASMA CONDUCTIVITY
NT POLARIZATION CHARACTERISTICS
NT PROXIMITY EFFECT (ELECTRICITY)
NT PYROELECTRICITY
NT SUPERCONDUCTIVITY

Solution of the Boltzmann transport equations for a permeable base transistor
[AD-A144969] 01 p0112 N85-10757

A high-voltage discharger
[AD-A145659] 02 p0194 N85-1129

Use of magnetic compression based on amorphous alloys as a drive for induction linacs
[DE84-014524] 02 p0277 N85-11805

Materials modification by ion beam mixing
[AD-P003948] 02 p0266 N85-11864

Characteristics of ion implanters for fabrication of electronic devices
[AD-P003949] 02 p0266 N85-11865

Review of the University of Manchester Ion Implantation Conference
[AD P003950] 02 p0266 N85-11866

Relationships between electronic structure and stability of metallic glasses
[AD-A145506] 02 p0287 N85-11874

Electric properties of neovolcanic rocks of central and east Slovakia
[REPT-558] 03 p0376 N85-12481

Electron channeling and EBIC studies of polycrystalline silicon sheets
[DE84-004515] 05 p0670 N85-1450

Electrical properties of 10-50 nm TEOS (Tetraethoxysilane) LPCVD (Low Pressure Chemical Vapo Deposition) films
[AD-A146416] 06 p0803 N85-15111

Investigation of structural and electrical properties of low-angle silicon sheet 06 p0831 N85-152

Analysis of optical and electrical performance of a TCP-coated solar cell 06 p0832 N85-152

The growth and properties of semiconducto strained-layer superlattices
[DE84-012979] 06 p0868 N85-1551

Characterization of bicrystal grain boundary properties using device structures
[DE84-004509] 06 p0869 N85-1552

Optical properties of composite materials
[AD-A146768] 07 p0920 N85-1582

Thermally induced quasiparticle branch imbalance in thin film superconductors 09 p1396 N85-1878

Robotic safety
[DE85-002314] 10 p1493 N85-19431

Stress studies in EFG
[NASA-CR-174441] 10 p1506 N85-1951

High energy pulsed particle accelerator
[AD-A149247] 10 p1554 N85-1979

Material growth and characterization for solid state devices
[NASA-CR-174410] 10 p1561 N85-19847

Investigation of electric and magnetic properties of intercalated graphite
[AD-A149801] 12 p1797 N85-21274

Electric and magnetic properties of intercalated graphite
[AD-A149848] 12 p1798 N85-21276

Proceedings of the Symposium on Electromagnetic Windows (17th) held at Georgia Inst. of Technology, Engineering Experiment Station, Atlanta, Georgia on 25-27 July 1984. Part 2
[AD-A149125] 12 p1824 N85-21444

Dual band radome wall design
[AD-P004357] 12 p1825 N85-21451

Broadband thermoplastic radomes
[AD-P004369] 12 p1827 N85-21463

Development of the F-20 nose radome
[AD-P004374] 12 p1827 N85-21468

Studies of electrical properties of surface films and localization during electrochemical dimensional working of titanium 13 p2032 N85-22729

High sheet resistance, arsenic implanted polycrystalline silicon for integrated circuit resistors
[DE85-004355] 13 p2065 N85-22902

Electrical and thermal transport property studies of high-temperature thermoelectric materials
[AD-A150167] 13 p2163 N85-23417

AlN insulator for 3-5 MIS applications
[AD-A150674] 14 p2426 N85-24962

Structure and properties of ion-implanted Al sub 2 O sub 3
[DE85-005374] 14 p2430 N85-24987

The structural and electronic properties of amorphous silicon based alloy materials
[DE85-002909] 15 p2660 N85-26419

A transduction path method of solid state sensor analysis and investigation
[AD-A152123] 16 p2870 N85-27707

Completely consumed carbide: A new process for dielectric isolation
[AD-A152379] 17 p2918 N85-27987

Effects of processing chemistry on electrical properties of high field ZnO varistors
[DE85-007688] 17 p2956 N85-28254

GaAs MESFET with lateral non-uniform doping
17 p3043 N85-28827

Materials-process interactions in ternary alloy semiconductors
[AD-A153133] 17 p3043 N85-28832

Properties of defects in Hg(1-x)Cd(x)Te
[AD-A153243] 17 p3044 N85-28835

Growth mechanism and properties of the thermal and anodic oxides of the 3-5 compound semiconductors
[AD-A153406] 18 p3193 N85-29803

Photoelectronic properties of zinc phosphide crystals and heterojunctions
[DE85-008777] 19 p3307 N85-30601

Special materials: Carbons
[SNIAS-851-551-104] 20 p3421 N85-31235

Electrochemistry of Hexanitroazobenzene (HNAB)
[DE85-010807] 21 p3566 N85-32171

Electrical properties of bulk grown nitrogen doped silicon
[AD-A155471] 21 p3581 N85-32266

Failure analysis of thin-film amorphous-silicon solar-cell modules 21 p3613 N85-32452

Electronic phenomena near semiconductor grain boundaries
[DE85-011543] 21 p3711 N85-33036

Grain boundary and surface diffusion in oxide systems
[DE85-007291] 23 p3985 N85-34715

Electronic structure and lattice dynamics of dimensionally constrained and disordered solids
[AD-A156627] 24 p4161 N85-35797

ELECTRICAL RESISTANCE

NT CONTACT RESISTANCE

Human engineering laboratory grounding analysis: Project Helga
[AD-A145728] 02 p0195 N85-11300

Instrumentation techniques for measuring large, high rate strains with foil resistance strain gages
[AD-A146248] 03 p0364 N85-12337

Zeta potential in ceramic industry
[NASA-TM-77478] 04 p0478 N85-13047

Electrical resistance measurements of metals to 40 GPa in the diamond cell
[DE85-001009] 11 p1629 N85-20262

Liquid thickness gage
[NASA-CASE-LAR-13342-1] 11 p1635 N85-20297

On filter binary processes
[AD-A150328] 13 p2063 N85-22890

Plasma-edge studies using carbon resistance probes
[DE85-005569] 14 p2424 N85-24955

Temperature variation of resistivity of certain alloys based on transition and simple metals in amorphous and crystalline states 15 p2496 N85-25399

A strain gauge manual
[AD-A151802] 16 p2787 N85-27197

Ohmic potential drop and gas bubble radius distribution in alkaline water electrolysis 17 p2924 N85-28025

Thin films properties of sputtered niobium silicide on SiO2, Si3N4 and on n+ poly-Si
[AD-A152378] 17 p2952 N85-28228

Effects of the structural state in thermo-bimetals on their resistance to microscopic plastic deformation
[BLL-BISI-TRANS-22403-(9022.06)]
17 p2979 N85-28412

Leakage effects in n-GaAs MESFET with n-GaAs buffer layer 17 p3043 N85-28826

Studies on surface processes during friction and wear
[AD-A153509] 18 p3117 N85-29296

Quantized Hall effect in two dimensional electron systems
[AD-A154347] 19 p3259 N85-30211

Cells for measuring thermoelectromotive force and electrical resistance of metals in temperature range of 20-950 degrees Celsius
[BLL-M-36240-(5828.4)] 20 p3457 N85-31473

Resistance of polyaniline films as a function of electrochemical potential and the fabrication of polyaniline-based microelectronic devices
[AD-A154999] 21 p3569 N85-32201

The measurement of high value resistances at the NPL — electrical resistance
[NPL-DES-81] 22 p3758 N85-33291

Tensile testing apparatus
[NASA-CASE-LAR-13243-1] 23 p3933 N85-34375

ELECTRICAL RESISTIVITY

NT IONOSPHERIC CONDUCTIVITY

NT KONDO EFFECT

NT MAGNETORESISTIVITY

NT PHOTOCONDUCTIVITY

NT PLASMA CONDUCTIVITY

NT SUPERCONDUCTIVITY

Dynamics of graphite fiber intercalation: In situ resistivity measurements with a four point probe
[NASA-TM-86858] 01 p0017 N85-10105

Electrically conductive rigid polyurethane foam
[DE84-014490] 01 p0033 N85-10203

Platinum thin film resistors as accurate and stable temperature sensors
[NASA-TM-77728] 01 p0049 N85-10322

Preparation and properties of single crystals of hydrogen bis(phthalocyaninato) neodymium(3)
[AD-A144933] 01 p0123 N85-10846

Trivalent ion exchange in beta alumina
[AD-A145373] 02 p0172 N85-11151

P-doping of (CH)x to the metallic regime with gaseous oxygen. Application to oxygen fuel cell type electrodes
[AD-A145477] 02 p0186 N85-11242

The concept of doping of conducting polymers. The role of reduction potentials
[AD-A145480] 02 p0186 N85-11243

Ceramic materials for MHD electrodes
[DE84-015580] 02 p0187 N85-11250

Resistance and inductance calculations for helical flux compression generators
[DE84-015068] 02 p0195 N85-11306

Mechanisms of electrical conductivity in olivine
[DE84-014333] 04 p0495 N85-13159

Magnetic susceptibility, electrical resistivity, and specific heat of single crystal LaFe-4P-12
[DE84-009979] 04 p0570 N85-13633

Evidence for d-band conduction in metallic glasses containing transition metal elements
[DE84-014822] 04 p0570 N85-13635

Diffusion mechanisms and point defects in transition-metal oxides
[DE84-016236] 04 p0571 N85-13639

On the Apollo subsatellite evidence for a lunar core
04 p0581 N85-13714

Low frequency electrical properties of selected dielectrics
[DE84-016220] 05 p0632 N85-14052

Polymer-carbon black interaction in electrically conducting fiber-forming composites
06 p0762 N85-14875

Semiconductor high-voltage power devices: State of art and outlook 06 p0794 N85-15074

An indirect measure of below-ground electric field, conductivity, and dielectric constant
[AD-A146518] 06 p0804 N85-15115

An investigation of the electrical conductivity in highly oriented graphite intercalation compounds
[AD-A146539] 06 p0804 N85-15116

Studies on copper alloys containing chromium on the copper side phase diagram
[NASA-TM-77752] 07 p0927 N85-15876

Polyphosphazene solid electrolytes
[AD-A147008] 07 p0931 N85-15902

The relationship between radiation sensitivity and redox equilibria — glass processing variables
[AD-A147216] 07 p0932 N85-15906

Electrically conducting complexes of poly(3,6-n-methylcarbazolyl methylene)
[AD-A147684] 07 p0933 N85-15914

The constant current strain gauge bridge
[ARL/STRUC-TM-385] 07 p0962 N85-16097

On reversion phenomena in Cu-Zr-Cr alloys
[NASA-TM-77791] 08 p1125 N85-17092

Reversion phenomena of Cu-Cr alloys
[NASA-TM-77780] 08 p1125 N85-17094

EDP computer tapes described
08 p1142 N85-17203

An experimental and theoretical investigation of optogalvanic effects
[AD-A148089] 08 p1157 N85-17299

Voltammetry and coulometry with immersed thin layer electrodes. Part 1: Model for effects of solution resistivity in linear sweep voltammetry
[AD-A148655] 08 p1159 N85-17313

Electronic structure, chemical bonding, and electron conductivity of thin-film transition-metal silicides
[AD-A147721] 08 p1226 N85-17718

Characterization of III-V compound semiconductor device materials
[AD-A148203] 08 p1226 N85-17719

Resistivity of alloys
[DE85-000906] 09 p1296 N85-18138

Electrical resistivity and structural changes upon relaxation and crystallization of (Mo/sub 0.6/Ru/sub 0.4)sub 100-x/B/sub x/ metallic glasses
[DE84-017281] 09 p1299 N85-18160

Electrical resistivity technique to assess the integrity of geomembrane liners
[PB85-122414/GAR] 09 p1325 N85-18327

Practical application of earth resistivity methods in phase 2 of the installation restoration program
[AD-P004148] 09 p1348 N85-18484

Compositional, structural, and physical studies of some graphite hexafluoroarsenates and their relatives
[DE85-000855] 10 p1432 N85-19030

Initial aging phenomena in copper-chromium alloys
[NASA-TM-77790] 10 p1439 N85-19070

Water absorption and conductivity in poly(ethylene oxide)-lithium tetrafluoroborate films
[AD-A147989] 10 p1450 N85-19138

Polymer electrolytes: An investigation of some poly (N-propylaziridine)/lithium salt compositions
[AD-A149444] 10 p1452 N85-19146

Microwave surface resistivity of several materials at ambient temperature 10 p1463 N85-19226

Generation of Alfven waves due to thermal modulation of the electrical conductivity
[AD-A149389] 10 p1558 N85-19826

Vacuum ultraviolet electronic properties of liquids
[DE85-000305] 10 p1563 N85-19858

Conductivity changes in neutron-irradiated commercial copper alloys at approximately 450(O)C
[DE85-003007] 11 p1606 N85-20100

Liquid thickness gage
[NASA-CASE-LAR-13342-1] 11 p1635 N85-20297

Normal mode analysis for linear resistive magnetohydrodynamics
[IPP-6/235] 11 p1730 N85-20878

Theory of resistivity-gradient-driven turbulence
[DE85-002175] 11 p1733 N85-20898

Solid electrolytes: Mechanisms for achieving optimal conductivity
[AD-A150116] 12 p1801 N85-21296

Characterization of high temperature electrically conducting oxides
[DE85-004296] 12 p1803 N85-21307

Update of thermal conductivity and electrical resistivity of electrolytic iron, tungsten and stainless steel
[PB85-115614] 12 p1803 N85-21311

Control of electronic, magnetic and optical properties of doped polyacetylene conductors
[AD-A150117] 12 p1814 N85-21375

Fine-grained, isotropic graphite for use as NBS (National Bureau of Standards) thermophysical property RM's from 5 to 2500 K
[PB85-112686] 12 p1814 N85-21381

Research on separators for alkaline zinc batteries
[DE85-003062] 12 p1836 N85-21523

Distribution of atmospheric electric current in the global circuit
[CONTRIB-87] 12 p1888 N85-21852

The liner package: An incipient MHD capability for CCUBE
[LA-9969-MS] 12 p1913 N85-22007

Preliminary investigation of the electrodynamics of a conducting tether 13 p1997 N85-22521

HREELS and Auger studies of conducting polymers
[DE85-004541] 13 p2036 N85-22764
Exact design formulas for field intensity of dipole deployed above flat homogeneous Earth with finite conductivity 13 p2061 N85-22998
Induction excitation of deep conducting zones
13 p2111 N85-23154
Variations in resistivity of upper crustal layer
13 p2113 N85-23164
Contactless determination of the conductivity of the white paint PCB-Z — Giotto spacecraft thermal control coating 14 p2243 N85-23907
Applications of eddy currents
14 p2316 N85-24315
Tunneling in magnetic superconducting systems
[AD-A150677] 14 p2426 N85-24963
Electrically conductive polymer concrete overlays
[DE85-008728] 15 p2522 N85-25549
Status of French research in plastic batteries
15 p2530 N85-25603
Graphite fiber intercalation: Dynamics of the bromine intercalation process
[NASA-TM-87015] 16 p2742 N85-26921
Electrical resistivity in amorphous metals: Consequences of phonon ineffectiveness in the diffraction model
[AD-A152130] 16 p2779 N85-27150
Impurity bands associated with MOS inversion layers
[INPE-3463-PRE/726] 16 p2870 N85-27704
Electrochemistry of polymer films not immersed in solution: Electron transfer on an ion budget
[AD-A152969] 17 p2920 N85-27986
Electrical conductivity and phase diagram of binary alloys. 21: The system palladium-chromium
[NASA-TM-77863] 18 p3073 N85-29009
Molten carbonate fuel cell cathode material development
[DE85-010266] 18 p3081 N85-29057
Zn3P2 as an improved semiconductor for photovoltaic solar cells
[DE85-008772] 18 p3097 N85-29171
Processable and stable conductive polymers
[AD-D011684] 19 p3249 N85-30143
Transport properties of Topopah Spring tuff
[DE85-010448] 19 p3270 N85-30278
Fractional statistics and fractional quantized Hall effect
[DE85-007833] 19 p3375 N85-30940
Electrical and mechanical properties of intercalated graphite fibers
[AD-A155560] 21 p3570 N85-32206
Electron-donor dopant, method of improving conductivity of polymers by doping therewith, and a polymer so treated
[DE85-011640] 22 p3752 N85-33257
Radiation-hardened polymeric films
[DE85-011636] 22 p3752 N85-33259
Optimization of design parameters for alternating current stabilizer based on magnetic suspension
22 p3772 N85-33374
Molten carbonate fuel cell separator
[DE85-011615] 22 p3806 N85-33577
Electrical resistivity and hysteresis of the equiatomic nickel-titanium alloy near the martensitic transformation temperature 23 p3904 N85-34181
Instrumentation for sensing moisture content of material using a transient thermal pulse
[NASA-CASE-NPO-15493-2] 23 p3933 N85-34373
Electrically conductive containment vessel for molten aluminum
[DE85-006516] 23 p3936 N85-34415
Electrically conductive doped block copolymer of polyacetylene and polyisoprene
[DE85-008500] 24 p4062 N85-35301
Conduction and aging of piezoelectric PZT ceramics
24 p4069 N85-35346
Two-dimensional inversion of resistivity monitoring data from the Cerro Prieto geothermal field
[DE85-012554] 24 p4113 N85-36494

ELECTRICALLY SUSPENDED GYROSCOPES
U ELECTROSTATIC GYROSCOPES

ELECTRICITY
NT ALTERNATING CURRENT
NT ATMOSPHERIC ELECTRICITY
NT AURORAL ELECTROJETS
NT ELECTROJETS
NT EQUATORIAL ELECTROJET
NT GEOELECTRICITY
NT HYDROELECTRICITY
NT IONOSPHERIC CURRENTS
NT STATIC ELECTRICITY
NT TELLURIC CURRENTS
Designing an expert system for training automotive electrical troubleshooting
[AD-P003926] 02 p0246 N85-11606
US energy for the rest of the century, 1984 edition
[PB84-207406] 04 p0531 N85-13393
Electromagnetic pulse (EMP) interaction with electric power systems. Power Systems Technology Program
[DE85-000166] 09 p1312 N85-18244
Light your runways and taxiways without electricity
[DE85-000269] 11 p1586 N85-19991
Electricity production from coal through molten-carbonate fuel cells
[TI85-005072] 14 p2351 N85-24534
Electricity from sunlight: The emergence of photovoltaics, revised edition
[DE85-002920] 19 p3307 N85-30502
Superconducting magnetic energy storage for asynchronous electrical systems
[DE85-005966] 22 p3847 N85-33832

ELECTRIFICATION
Electronic information management and productivity
[DE85-013362] 24 p4164 N85-35818

ELECTRO-OPTICAL EFFECT
Integrated optical components utilizing acoustooptic and electrooptic diffraction in micro-waveguides
13 p2069 N85-23044
Modular Optoelectronic Multispectral Scanner (MOMS) for Earth observation. First results of STS-7 mission
[MBB-UR-717/83-O] 16 p2674 N85-27732
Transparent electrode for optical switch
[DE85-011618] 22 p3761 N85-33310
OMEGA: Optoelectronic measurement of the incidence angle of a projectile
[ISL-CO-223/84] 23 p3974 N85-34634

ELECTRO-OPTICAL PHOTOGRAPHY
Investigations of the accuracy of the Digital Photogrammetry System (DPS), a rigorous three-dimensional compilation process for pushbroom imagery
[MBB-UA-753/83-O] 16 p2674 N85-27734
Magnetic materials
[AD-A154679] 21 p3560 N85-32256

ELECTRO-OPTICS
The development of an optoelectronic assembly applied to computer systems
[AD-A145028] 01 p0120 N85-10821
Visible wavelength interferometer for high speed electron density diagnostics
[AD-A145686] 02 p0277 N85-11603
Optical waveguide spatial filters
[AD-A145674] 02 p0280 N85-11625
Thermal deformation measurements of heat-resistant structural materials for aircraft by electro optical displacement transducer
[NAL-TR-810] 03 p0325 N85-12092
USSR report: Electronics and electrical engineering
[JPRS-UEE-84-014] 03 p0344 N85-12215
Dielectric and optical properties of sputtered thin films
[AD-A146210] 03 p0420 N85-12681
Research on materials and components for opto-electronic signal processing
[AD-A145809] 03 p0433 N85-12754
A physical interpretation of the structure and electron-optical data for spinel (MgAl2O4)
[AERE-R-11278] 03 p0434 N85-12767
An overview of Multispectral Electro-Optical Stereo Scanner (MEOSS) mission 04 p0458 N85-12908
The Monocular Electro-Optical Stereo Scanner Experiment (MEOSS) 04 p0459 N85-12910
Heavy duty precision pan and tilt head
[AD-A146669] 04 p0509 N85-13246
Imaging of surfaces and defects of crystals
[DE84-016449] 04 p0570 N85-13632
Electrooptical matrix multiplication using the twos complement arithmetic for improved accuracy
[AD-D011252] 05 p0728 N85-14682
Advanced cube processor
[AD-D011262] 05 p0729 N85-14683
Measurement of parameters defining orientation of liquid crystals in electrooptic cells 06 p0777 N85-14971
USSR report: Electronics and electrical engineering
[JPRS-UEE-84-012] 06 p0781 N85-14991
Electrooptical sensor for automatic detection of objects 06 p0789 N85-15040
Improvements in avalanche-transistor sweep circuitry for electrooptic streak cameras
[DE84-016195] 06 p0811 N85-15155
The growth and properties of semiconductor strained-layer superlattices
[DE84-012979] 06 p0888 N85-15515
USSR report: Electronics and electrical engineering
[JPRS-UEE-84-016] 07 p0949 N85-16014
Precision electrooptical deflector based on corrugated light guide 07 p0950 N85-16020
Multichannel electrooptical modulators for digital information storage and processing systems
07 p0950 N85-16021
Stereo Electro-optical Tracking System (SETS)
[NASA-CR-172471] 07 p0962 N85-16098
Measurement of high temperature strain by the laser-speckle strain gauge
[NASA-TM-77751] 07 p0977 N85-1
Electro-optical target detection
[AD-D011386] 07 p1042 N85-1
The development and test of ultra-large-format multi-anode microchannel array detector systems
[NASA-CR-174247] 07 p1043 N85-1
Optics and opto-electronic systems
[AD-A147277] 07 p1044 N85-1
Crystal growth and characterization of BaMgF4
[AD-A146605] 07 p1047 N85-1
Evaluation of nose, roof, and mast mounted sensor platforms for piloting and sighting, integrated in future combat helicopters 08 p1074 N85-1
Recent development in astronomic position determinations
[AD-A148335] 08 p1082 N85-1
Challenges of developing an electro-optical system for measuring man's operational envelope
08 p1095 N85-1
Telecommunications equipment at 1984 Leipzig Spring Fair 08 p1140 N85-17170
Chemical, material electronics studies established
08 p1142 N85-172
General assessment of GDR microelectronics industry, applications 08 p1142 N85-172
Study in spurious sensitivity of electronics in space
[AD-A148386] 08 p1158 N85-17305
Guidelines for atmospheric measurements in support of electro-optical systems testing
[AD-A148090] 08 p1186 N85-17474
Matrix-matrix multiplication using an electrooptical systolic-engagement array processing architecture
[AD-D011410] 08 p1223 N85-17704
High-speed, eight-frame electro-optic camera with multipulsed ruby laser illuminator
[DE85-001748] 09 p1323 N85-18014
Data acquisition, measurement devices at 1984 Leipzig Spring Fair 09 p1378 N85-18
A methodology for the determination of rotary wing aircraft vulnerabilities in air-to-air combat simulation
[AD-A148964] 10 p1424 N85-18
The cockpit of the year 2000: How big a step?
10 p1534 N85-19
An electro-optic spatial light modulator for thermo-elastic generation of programmably focused ultrasound
[AD-A149078] 10 p1553 N85-19794
Modulation Transfer Function (MTF) measurement techniques for lenses and linear detector arrays
[NASA-TM-86166] 10 p1556 N85-19812
Control technology for integrated circuit fabrication at Honeywell Optoelectronics Division, Richardson, Texas
[PB85-109023] 11 p1616 N85-20182
Status of specific FRG high tech research funded by BMFT 11 p1618 N85-20181
Miniature electrooptical air flow sensor
[NASA-CASE-LAR-13065-1] 11 p1635 N85-20
Photorefractor ocular screening system
[NASA-CASE-MFS-26011-1SB]
11 p1692 N85-20
Imaging apparatus for transverse electrode electro-optic tunable filter
[AD-D011524] 12 p1832 N85-21497
USSR report: Electronics and electrical engineering
[JPRS-UEE-85-004] 12 p1837 N85-21591
Topics in optical materials and device research, 3: Volume 1
[AD-A149726] 12 p1933 N85-22145
USSR report: Engineering and equipment
[JPRS-UEQ-85-003] 13 p2042 N85-22782
Optoelectronic safety system for robotized technological complex 13 p2046 N85-22805
Mathematical modeling of two-frequency laser sounding of scattering media 13 p2069 N85-23045
Accuracy of random signal spectral parameter estimation against interference background in acoustooptical spectrum analyzers
13 p2090 N85-23032
OMEGA: An optronic device to measure the incidence angle of a projectile
[ISL-CO-207/83] 14 p2306 N85-24274
Feasibility of optical instruments based on multiaperture optics
[AD-A150668] 14 p2421 N85-24
Ferroelectric tungsten bronze bulk crystals and epitaxial thin films for electro-optic device applications
[AD-A151044] 14 p2427 N85-24
InGaAs/GaAs, Strained-Layer Superlattice (SLS), junction photodetectors, LED's, injection LASER's and FET's for optoelectronic IC applications
[DE85-001940] 14 p2430 N85-24
An electro-optic spatial light modulator for thermoelastic generation of programmably focused ultrasound
[AD-A152066] 15 p2646 N85-26

Electron-bombarded silicon spatial light modulator
[AD-D011579] 15 p2652 N85-26355
Charge isolation in a spatial light modulator
[AD-D011581] 15 p2652 N85-26356
Studies of electro-optical attenuation in the vicinity of cloud base
[AD-A151745] 15 p2653 N85-26360
Technical evaluation report on Avionics Panel Specialists' Meeting on Digital Optical Circuit Technology
[AGARD-AR-202] 15 p2653 N85-26367
Interaction of liquid crystals with inhomogeneous surfaces
[AD-A151557] 15 p2660 N85-26413
ACT applied to helicopter flight control
16 p2712 N85-26738
INPE's line imaging camera: Preliminary results
[INPE-3476-PRE/719] 16 p2787 N85-27194
Construction and analysis of a PRIZ spatial light modulator exhibiting dynamic image selection
[AD-A152318] 17 p3037 N85-28787
Spatial light modulator having a capacitively coupled photoconductor
[AD-D011646] 17 p3037 N85-28790
InP materials
[AD-A152341] 17 p3043 N85-28826
Mass spectrometry technology at the Jet Propulsion Laboratory (JPL) 18 p3157 N85-29552
Digital Optical Circuit Technology
[AGARD-CP-362] 18 p3185 N85-29757
Optical modulators and bistable devices using molecular gases 18 p3186 N85-29761
Integrated electrooptical components using dielectric substrates 18 p3187 N85-29767
The potential of semiconductors for optical integrated circuits 18 p3187 N85-29768
Picosecond photoconductive devices for 10 Gbit/s optoelectronic switching 18 p3187 N85-29770
Electro-optic techniques for VLSI interconnect
18 p3188 N85-29774
The vector magnetograph of the Sayan Solar Observatory 18 p3206 N85-29887
A study of reflex optoelectronic switching matrices and their derivatives
[CRC-TN-720] 19 p3253 N85-30169
Experimental demonstration of an optoelectronic switch matrix for satellite-switched TDMA signals in the 0.3-4.0 GHz band
[CRC-TN-717] 19 p3253 N85-30170
Strained-layer-superlattice optoelectronic devices
[DE85-009146] 19 p3377 N85-30953
Advanced simulator for pilot training and helmet-mounted visual display configuration comparisons
[AD-A155326] 21 p3667 N85-32776
System for electro-optical ceramic recrystallization
21 p3682 N85-32872
Transformation of charged particle beams by concentrating electro-optical systems
21 p3690 N85-32925
Conceptual design and analysis of high-speed electronic imaging
[LA-10072-MS] 22 p3758 N85-33292
Influence of edge effects on performance of electrooptical lens 22 p3770 N85-33366
Design of electrooptical system with annular cathode and electrostatic compressor 22 p3770 N85-33367
USSR report: Electronics and electrical engineering
[JPRS-UEE-84-003] 22 p3773 N85-33381
Electro-optic harmonic conversion to switch a laser beam out of a cavity
[DE85-011610] 22 p3790 N85-33483
Differentiating spatial light modulator
[AD-D011727] 23 p3973 N85-34632
ELECTROACOUSTIC TRANSDUCERS
NT HYDROPHONES
NT LOUDSPEAKERS
NT MICROPHONES
Electromagnetic-acoustic-transducer
system for thick-weld inspection
[PB84-219402] 01 p0051 N85-10336
An automated immittance measuring system for electroacoustic transducers
[AD-A145701] 02 p0200 N85-11336
Acoustic transducers for fast reactor instrumentation
[BLL-RISLEY-TR-4979-(9091.9F)]
07 p0961 N85-16091
Lightweight, broadband Rayleigh wave transducer
[AD-D011345] 07 p1037 N85-16584
Method and apparatus for detecting acoustic emissions from metal matrix wire
[AD-D011556] 12 p1927 N85-22107
Electroacoustical imaging technique for encoding incoherent radiance fields as Gabor elementary signals
[NASA-TM-86372] 13 p2094 N85-23067
High-frequency acoustic variability in the arctic
[AD-A150550] 13 p2155 N85-23383
Piezoelectric and electrostatic polymeric transducers for acoustic emission detection
[AD-A150883] 14 p2306 N85-24272
System of phase-lock automatic frequency control with acoustoelectronic convolver 15 p2526 N85-25573
Acoustic imaging systems (for robotic object acquisition)
[AD-A154043] 19 p3351 N85-30772
The moving thermoacoustic array: A theoretical feasibility study
[AD-A154510] 21 p3699 N85-32980
ELECTROACOUSTIC WAVES
Bragg reflection of surface electroacoustic shear waves 04 p0485 N85-13096
Electroacoustical imaging technique for encoding incoherent radiance fields as Gabor elementary signals
[NASA-TM-86372] 13 p2094 N85-23067
ELECTROANESTHESIA
Electroanesthesia as a means of controlling cold stress of local hypothermia 22 p3823 N85-33687
ELECTROCARDIOGRAMS
U ELECTROCARDIOGRAPHY
ELECTROCARDIOGRAPHY
Frequency and nature of electrocardiographic disturbances in dogs during single and repeated exposure to +G sub z accelerations 01 p0092 N85-10619
Changes in the impedance and bioelectrical activity of the cerebral cortex of rats under the action of anaesthetic drugs
[HSE-TRANS-10371] 19 p3327 N85-30617
Three-dimensional ballistocardiography in microgravity
20 p3510 N85-31818
ELECTROCATALYSTS
Phosphoric and electric utility fuel cell technology development
[NASA-CR-174215] 06 p0805 N85-15124
Electrocatalysis research
[NASA-CR-174352] 10 p1437 N85-19054
Preparation and evaluation of advanced catalysts for phosphoric acid fuel cells
[NASA-CR-168223] 10 p1508 N85-19511
Oxygen evolution on NiCo2O4 electrodes
17 p2924 N85-28026
Molten carbonate fuel cell cathode material development
[DE85-010268] 18 p3061 N85-29057
Regenerative fuel cell systems for space station
20 p3443 N85-31372
Method of preparing thin porous sheets of ceramic material
[DE85-006399] 24 p4082 N85-35300
ELECTROCHEMICAL CELLS
NT ALKALINE BATTERIES
NT ELECTRIC BATTERIES
NT FUEL CELLS
NT LEAD ACID BATTERIES
NT LITHIUM SULFUR BATTERIES
NT NICKEL CADMIUM BATTERIES
NT NICKEL HYDROGEN BATTERIES
NT NICKEL ZINC BATTERIES
NT PHOSPHORIC ACID FUEL CELLS
NT PRIMARY BATTERIES
NT REDOX CELLS
NT REGENERATIVE FUEL CELLS
NT SILVER HYDROGEN BATTERIES
NT SODIUM SULFUR BATTERIES
NT STORAGE BATTERIES
NT THERMAL BATTERIES
NT ZINC-BROMIDE BATTERIES
NT ZINC-CHLORINE BATTERIES
Advanced nickel-hydrogen cell configuration study
[NASA-CR-174775] 01 p0067 N85-10444
Effects of additives and KOH electrolyte concentration on dissolution of iron electrodes
[DE84-014840] 02 p0173 N85-11162
Method of making a porous carbon cathode: A porous carbon cathode so made, and electrochemical cell including the porous carbon cathode
[AD-D011243] 02 p0196 N85-11301
Research on photoelectrochemical cells based on CdSe, CdSe/sub 1-x/te/sub x and other photoelectrode materials
[DE84-004527] 02 p0224 N85-11466
Investigation of materials for inert electrodes in aluminum electrodeposition cells
[DE84-015036] 05 p0617 N85-13947
High capacity inorganic oxyhalide electrochemical cell
[AD-D011321] 07 p0923 N85-15845
Voltammetry and coulometry with immersed thin layer electrodes. Part 2: Practical considerations and experimental results
[AD-A148656] 08 p1159 N85-17314
Continuous organic electrochemical synthesis
[DE85-001400] 10 p1437 N85-19057
Development of a low cost electrochemical CO monitor based on anodic scanning voltammetry in nonaqueous electrolyte
[PB85-113469] 11 p1637 N85-20314
Electrochemical cell to measure corrosion rates in noncondensing environments
[DE85-003148] 12 p1807 N85-21338
Portable electrochemical cell interrogator
[DE85-005186] 13 p2065 N85-22901
Influence of uncompensated solution resistance upon the evaluation of rate constants for rapid electrochemical reactions
[AD-A150657] 14 p2250 N85-23942
Cycling performance of the iron-chromium redox energy storage system
[NASA-TM-87034] 16 p2619 N85-27387
Research on electrochemical photovoltaic cells
[DE85-008775] 18 p3131 N85-29392
Consolidated fuel reprocessing program
[DE85-010591] 19 p3358 N85-30818
Method for determining the point of zero zeta potential of semiconductor
[NASA-CASE-LAR-12893-1] 19 p3373 N85-30923
Multikilowatt hydrogen-nickel oxide battery system
20 p3443 N85-31373
Improvements in safety testing of lithium cells
20 p3444 N85-31379
Design evaluation of high reliability lithium batteries
20 p3444 N85-31380
RAY-O-VAC BR2325 lithium carbon monofluoride cell performance 20 p3444 N85-31382
Safety of Li-SOCl2 cells 20 p3444 N85-31383
Polymer blends for use in photoelectrochemical cells for conversion of solar energy to electricity
[DE85-011602] 22 p3752 N85-33256
Electrochemical methane sensor
[DE85-011663] 22 p3787 N85-33464
Stable n-CuInSe/sub 2/iodide-iodine photoelectrochemical cell
[DE85-011597] 22 p3806 N85-33576
Experimental evaluation of the thermodynamic properties of concentrated aqueous potassium hydroxide solutions
[DE85-010628] 23 p3912 N85-34238
ELECTROCHEMICAL CORROSION
The modification of metallic corrosion by ion implantation: Engineering applications and fundamentals studies
[AD-P003954] 02 p0266 N85-11870
Corrosion of a zinc rotating disk in one molar hydrochloric acid
[DE84-015974] 04 p0474 N85-13015
Electrochemical pitting evaluation of aluminum alloy 7075 in machining coolant
[DE84-016844] 04 p0475 N85-13026
Research approaches to qualify aluminum for Ocean Thermal Energy Conversion (OTEC) systems
[DE84-013007] 04 p0476 N85-13034
Interactions between corrosion and creep of uncoated and coated superalloys in sulfate melts
04 p0477 N85-13038
Predicting electrochemical breakdown in terrestrial photovoltaic modules 06 p0830 N85-15273
On-line monitoring of the true corrosion rate in problems related to power plants
[CISE-2335] 08 p1131 N85-17126
An electrochemical study of the corrosion behavior of primer coated 2219-T87 aluminum
[NASA-TP-2459] 13 p2021 N85-22662
Localized corrosion currents from graphite/aluminum and welded SiC/Al metal matrix composites
[AD-A150986] 14 p2256 N85-23980
Theoretical and experimental comparisons of nearfield electrogalvanic fields due to nonlinear polarization layers
[AD-A152085] 16 p2779 N85-27149
Electrical research on solar cells and photovoltaic materials
[NASA-CR-175897] 17 p2986 N85-28452
Marine corrosion
[AD-A153843] 18 p3074 N85-29012
Theoretical modelling of the electro-chemistry in a corrosion fatigue crack. Part 2: Mathematical aspects of associated unsteady reaction equations
[NPL-DMA(A)-100-PT-2] 20 p3485 N85-31529
Theoretical aspects of corrosion and practical implications for aircraft and related systems
22 p3749 N85-33240
Corrosion fatigue strength and crack growth in prestrained 0.16% C carbon steel
23 p3905 N85-34192
ELECTROCHEMICAL MACHINING
Simulation of the electrochemical machining process
[DE85-003797] 11 p1616 N85-20159

Role of residual stresses in stress corrosion cracking in alloy 600 tubes. Part 1: Determination of throughwall residual stresses and their modification by transient heat treatment
[DE85-004648] 14 p2257 N85-23966
Electrolytic cell
[DE85-011598] 22 p3807 N85-33578
ELECTROCHEMICAL OXIDATION
Two silicon phthalocyanines and a silicon naphthalocyanine: Synthesis, electrochemistry and electrogenerated chemiluminescence
[AD-A144760] 01 p0023 N85-10145
The concept of doping of conducting polymers. The role of reduction potentials
[AD-A145480] 02 p0186 N85-11243
Electrochemistry at very high potentials: The use of ultramicroelectrodes in the anodic oxidation of short chain alkanes
[AD-A148654] 08 p1123 N85-17078
Homogeneous reaction involving components of different redox couples. 1: Theoretical considerations and digital simulation
[AD-A148666] 08 p1124 N85-17084
Polymeric electrolytes for ambient temperature lithium batteries
[DE85-001032] 12 p1835 N85-21518
Diagrams of chemical and electrochemical equilibria in the presence of oxygen and sulphur
[AD-A150929] 14 p2251 N85-23953
Resistance of polyaniline films as a function of electrochemical potential and the fabrication of polyaniline-based microelectronic devices
[AD-A154999] 21 p3569 N85-32201
ELECTROCHEMISTRY
NT COULOMETRY
NT ELECTROLYSIS
NT PHOTOELECTROCHEMISTRY
An electrochemical approach to the prevention of biofouling phenomena
[PB84-202613] 01 p0025 N85-10155
Preparation and properties of single crystals of hydrogen bis(phthalocyaninato) neodymium(3)
[AD-A144933] 01 p0123 N85-10846
The driving-force dependence of electrochemical rate parameters: Origins of anodic-cathodic asymmetries for metal aquo redox couples
[AD-A145605] 02 p0172 N85-11153
Kinetics of simple Inner- and outer-sphere electrochemical reactions at rotating silver electrodes as examined using surface-enhanced Raman spectroscopy
[AD-A145606] 02 p0172 N85-11154
Surface environmental effects in electrochemical kinetics: Outer-sphere chromium (3) reductions at mercury, gallium, lead, and thallium surfaces
[AD-A145607] 02 p0172 N85-11155
Solvent effects upon electrochemical kinetics: Influences of interfacial solvation and solvent relaxation dynamics
[AD-A145624] 02 p0173 N85-11156
An electrochemical study of hydrogen uptake and elimination by bare and gold-plated waspaloy
[NASA-TM-86479] 02 p0182 N85-11222
Method of making a porous carbon cathode: A porous carbon cathode so made, and electrochemical cell including the porous carbon cathode
[AD-D011243] 02 p0195 N85-11301
Electrochemistry of rare-earth diphthalocyanines
[AD-A145613] 03 p0327 N85-12106
Feasibility of the electrochemical method of determining nitrogen content in metallic melts
[BLL-M-35730-(5828.4)] 03 p0330 N85-12124
Related studies to cathodic protection of reinforced concrete structures
[PB84-218114] 03 p0333 N85-12145
Electrochemical and surface science research on fuel cells
[DE84-015982] 03 p0359 N85-12307
NASA Redox Storage System Development Project
[NASA-TM-83677] 03 p0385 N85-12465
Electrochemical investigations of novel electrode materials
[DE84-014352] 04 p0495 N85-13158
Electrochemistry and storage
05 p0609 N85-13889
The electrochemical deoxidation of molten oxide substances
[BLL-M-35982-(5828.4)] 05 p0614 N85-13920
Chemically modified electrodes and related solution chemistry
[DE84-017110] 05 p0614 N85-13924
USSR report: Chemistry
[JPRS-UCH-84-012] 06 p0761 N85-14865
Electrochemical behaviour of TiCl4 solutions in low melting point organic media
[BLL-OA-TRANS-3174-(6196.3)]
06 p0764 N85-14888
Space charge, interfacial kinetics, and electrical response of condensed matter
[AD-A146364] 06 p0765 N85-14893
Electrochemistry in near-critical and supercritical fluids. I. Ammonia
[AD-A146429] 06 p0765 N85-14894
A silicon phthalocyanine and a silicon naphthalocyanine: Synthesis, electrochemistry, and electrogenerated chemiluminescence
[AD-A146441] 06 p0765 N85-14895
Proceedings of the 23rd Project Integration Meeting
[NASA-CR-174186] 06 p0829 N85-15260
Electrochemical production of silicon
06 p0832 N85-15290
High capacity inorganic oxyhalide electrochemical cell
[AD-D011321] 07 p0923 N85-15845
Correlation of electronic charge transfer transitions and electrochemical potentials. The Bipyrazine(Tetracarbonyl)Molybdenum(O) system in various solvents
[AD-A147660] 08 p1120 N85-17062
Estimation of the rate of electron transfers between 2 contacting polymer surfaces
[AD-A148416] 08 p1122 N85-17072
Electrochemistry at very high potentials: The use of ultramicroelectrodes in the anodic oxidation of short chain alkanes
[AD-A148654] 08 p1123 N85-17078
The construction and behaviour of ultramicroelectrodes: Investigations of novel electrochemical systems
[AD-A148658] 08 p1123 N85-17079
Subtractively normalized interfacial Fourier transform infrared spectroscopy of difluorobenzene adsorbed at polycrystalline platinum electrodes
[AD-A148660] 08 p1123 N85-17080
Electrochemical features of the ferric sulfate leaching of CuFeS2/C aggregates
[AD-A148661] 08 p1123 N85-17081
The adsorption of acrylonitrile at a gold electrode: An EMIRS measurement of the electrochemical stark effect
[AD-A148664] 08 p1123 N85-17082
Modulated surface vibrational spectroscopies at electrode/electrolyte interfaces
[AD-A148665] 08 p1123 N85-17083
Homogeneous reaction involving components of different redox couples. 2: Polarographic studies of the interactions of alkali metal cations with anthracene and fluoroanthene dianions in N,N-dimethylformamide and acetonitrile
[AD-A148667] 08 p1124 N85-17085
Application of electrochemical engineering methods and theory to solving corrosion and adhesion problems with organic coatings
[AD-A147799] 08 p1129 N85-17115
Electrochemistry of polymer films. Applications to chemical analysis and energy conversion
[AD-A147737] 08 p1132 N85-17136
The kinetics of electron transfer reactions in and at films of electroactive polymers
[AD-A148597] 08 p1134 N85-17149
Voltammetry and coulometry with immersed thin layer electrodes. Part 1: Model for effects of solution resistivity in linear sweep voltammetry
[AD-A148655] 08 p1159 N85-17313
Voltammetry and coulometry with immersed thin layer electrodes. Part 2: Practical considerations and experimental results
[AD-A148656] 08 p1159 N85-17314
Electrochemical interfaces and electrode processes
[AD-A147414] 09 p1290 N85-18098
Electrocatalysis research
[NASA-CR-174352] 10 p1437 N85-19054
Continuous organic electrochemical synthesis
[DE85-001400] 10 p1437 N85-19057
Positive electrodes of nickel-cadmium batteries
[NASA-TM-77806] 10 p1478 N85-19330
Bioelectrochemistry 2: Membrane phenomena
[AD-A149132] 10 p1522 N85-19602
Semiconductor electrochemistry approach to the study of oxide films on nickel electrodes
[DE85-003042] 11 p1630 N85-20264
Development of a low cost electrochemical CO monitor based on stripping voltammetry
[PB85-113470] 11 p1637 N85-20312
Electrochemistry and electrochemical methodology in molten salts
[AD-A149613] 12 p1799 N85-21284
Electrochemical processes at the sodium (BETA)" alumina interface
[DE85-004653] 12 p1802 N85-21305
In situ monitoring of electrochemical reactions by surface enhanced Raman scattering
[PB85-149789] 12 p1803 N85-21312
Hydrogen embrittlement of cadmium-plated ultra-high strength steels in paint strippers
[ARL/MAT-R-117] 12 p1806 N85-21326
Stress corrosion cracking behavior of tungsten heavy alloys
[AD-A149843] 12 p1806 N85-21[illegible]
Application of modulated hydrodynamic voltammetry to the study of anodic electrocatalysis
[DE85-004182] 13 p2018 N85-22[illegible]
Local electrochemistry of pitting corrosion in stainless steels
[DE85-006207] 13 p2023 N85-22[illegible]
Studies of electrical properties of surface films and localization during electrochemical dimensional working of titanium 13 p2032 N85-22729
Raman structural studies of the nickel electrode
[NASA-CR-175619] 13 p2162 N85-22414
Ligand structural influences upon electrochemical reactivity: Organic substituent effects upon Carboxylatopentaamminecobalt(3) reductions at mercury and gold electrodes
[AD-A150685] 14 p2250 N85-23[illegible]
Evaluation of unimolecular rate constants for some outer-sphere electrochemical reactions
[AD-A150758] 14 p2250 N85-23[illegible]
USSR report: Materials science and metallurgy
[JPRS-UMS-85-004] 15 p2513 N85-25[illegible]
Electrochemical behavior of amorphous alloys based on iron, cobalt and nickel in H3PO4 solutions alone and mixed with HF 15 p2513 N85-25[illegible]
Status of French research in plastic batteries
15 p2530 N85-25[illegible]
Calcium/thionyl chloride battery technology
[AD-A151975] 15 p2586 N85-25[illegible]
Sixth DOE Electrochemical Contractor's Review. Extended abstracts
[DE84-013679] 16 p2779 N85-27151
Dual electrochemical system
[AD-D011616] 16 p2817 N85-27376
Electrochemistry of polymer films not immersed in solution: Electron transfer on an ion budget
[AD-A152989] 17 p2920 N85-27[illegible]
Localized ionic currents from a corroding iron-copper galvanic couple
[AD-A153627] 18 p3074 N85-28011
Effects of H2S on molten carbonate fuel cells
[DE85-008310] 18 p3130 N85-28[illegible]
Improved acid electrolytes for fuel cells
[PB85-178053] 18 p3132 N85-28087
Electrochemical studies in liquid crystals
[AD-A154317] 19 p3234 N85-30050
Effect of multi-functional inhibitors on the electrochemistry within corrosion crack
19 p3238 N85-30075
Lithium cell reactions
[AD-A154429] 19 p3305 N85-30484
Electrochemical reduction of titanium in dimethyl sulphoxide
[BLL-OA-TRANS-3225-(6196.300)]
20 p3429 N85-31267
Regenerative fuel cell systems for space station
20 p3443 N85-31372
System level electrochemical principles
20 p3443 N85-31375
Electrochemistry of Hexanitroazobenzene (HNAB)
[DE85-010807] 21 p3565 N85-32171
Topics in electrochemical degradation of photovoltaic modules 21 p3608 N85-32410
Characteristics of optogalvanic effect in media with inverse populations 21 p3693 N85-32944
Chemistry division report
[DE85-010586] 24 p4071 N85-35228
Electrochemical method for investigation of the susceptibility of corrosion-resistant steels to intercrystalline corrosion
[BLL-CE-TRANS-8082-(9022.09)]
24 p4077 N85-35[illegible]
ELECTROCHROMISM
Investigation of absorptive electrochemical systems for display applications
[BMFT-FB-T-84-301] 15 p2507 N85-25487
Electrochromic display device
[AD-D011733] 22 p3759 N85-33[illegible]
ELECTROCONDUCTIVITY
U ELECTRICAL RESISTIVITY
ELECTRODE FILM BARRIERS
Studies of electrical properties of surface films and localization during electrochemical dimensional working of titanium 13 p2032 N85-22729
ELECTRODE MATERIALS
Behaviour of lead-silver anodes in zinc electrodeposition from sulphuric acid baths
[BLL-MINTEK-TR-1180-(5810.5759)]
06 p0764 N85-14887
Structural studies on lead dioxides
[DE84-015837] 06 p0805 N85-15127
Preparation and evaluation of advanced catalysts for phosphoric acid fuel cells
[NASA-CR-168223] 10 p1508 N85-19511

Conductor-polymer composite electrode materials
[DE85-005766] 23 p3920 N85-34293

ELECTRODELESS DISCHARGES
Neodymium YAG laser pumped with radiation from high frequency electrodeless discharge
13 p2044 N85-22796

ELECTRODEPOSITION
NT ELECTROPLATING
Methods for producing platinum-group metal coatings from molten alkali cyanides
[PB84-225994] 01 p0029 N85-10181
Electroforming of nickel
[SNIAS-841-501-101] 04 p0484 N85-13085
Investigation of materials for inert electrodes in aluminum electrodeposition cells
[DE84-015036] 05 p0617 N85-13947
Behaviour of lead-silver anodes in zinc electrodeposition from sulphuric acid baths
[BLL-MINTEK-TR-1180-(5810.5759)]
06 p0764 N85-14867
Laser-assisted solar-cell metallization processing
06 p0831 N85-15282
The kinetics of electron transfer reactions in and at films of electroactive polymers
[AD-A148597] 08 p1134 N85-17149
Effect of rhodamine-B on the electrodeposition of lead on copper, revision
[DE85-000674] 11 p1606 N85-20101
Mechanical properties of electrodeposited nickel and copper
[DE85-005321] 13 p2023 N85-22677
Film and interstitial formation of metals in plasma-sprayed ceramics
[NASA-TM-86993] 13 p2036 N85-22756
Demonstration of feasibility of depositing semiconductor layers using microwave enhanced plasma techniques
[NASA-CR-174392] 13 p2163 N85-23421
Pulsed electrodeposition
[DE85-007057] 16 p2747 N85-26950
Electrohydrodynamic process for the production of large area polycrystalline silicon sheet
[DE85-006781] 19 p3261 N85-30225
Development of low-melting fused salts 8: Formation of molybdenum film from molten ammonium formate bath
[BLL-OA-TRANS-3185-(6196.300)]
20 p3429 N85-31264
Electrodeposition of chromium and copper in magnetic fields
[AD-A154648] 21 p3566 N85-32180

ELECTRODERMAL RESPONSE
U GALVANIC SKIN RESPONSE

ELECTRODES
NT ANODES
NT CATHODES
NT CELL ANODES
NT CELL CATHODES
NT COLD CATHODES
NT HOLLOW CATHODES
NT HOT CATHODES
NT IMPLANTED ELECTRODES (BIOLOGY)
NT ION SELECTIVE ELECTRODES
NT PHOTOCATHODES
NT PLASMA ELECTRODES
NT SHELL ANODES
NT THERMIONIC CATHODES
NT TUBE ANODES
NT TUBE CATHODES
P-doping of (CH)x to the metallic regime with gaseous oxygen. Application to oxygen fuel cell type electrodes
[AD-A145477] 02 p0186 N85-11242
The concept of doping of conducting polymers. The role of reduction potentials
[AD-A145480] 02 p0186 N85-11243
Chemical derivatization of an array of three gold microelectrodes with polypyrrole: Fabrication of a molecule-based transistor
[AD-A146221] 03 p0359 N85-12304
Photoelectrochemistry with chemically modified electrodes
[DE84-016796] 04 p0471 N85-12997
Bulletin of the Faculty of Engineering, Hokkaido University, no. 123
[ISSN-0385-602-X] 04 p0482 N85-13075
Determination of Faradaic current through a bipolar electrode in acidic bichromate 04 p0483 N85-13077
Electrochemical investigations of novel electrode materials
[DE84-014352] 04 p0495 N85-13156
Chemically modified electrodes and related solution chemistry
[DE84-017110] 05 p0614 N85-13924
Investigation of materials for inert electrodes in aluminum electrodeposition cells
[DE84-015036] 05 p0617 N85-13947
Optimization of toughness properties of HSCA shielded metal arc welding electrodes
[BMFT-FB-T-84-186] 05 p0646 N85-14148
Photoluminescent and electroluminescent properties of Cd sub 0.95 Mn sub 0.05 Se electrodes
[AD-A146775] 07 p0946 N85-15995
Microwave resonator using lateral excitation
[AD-D011374] 07 p1039 N85-16596
Potential dependence of electrical conductivity and chemical charge storage of poly(pyrrole) films on electrodes
[AD-A148513] 08 p1122 N85-17075
The construction and behaviour of ultramicroelectrodes: Investigations of novel electrochemical systems
[AD-A148658] 08 p1123 N85-17079
Subtractively normalized interfacial Fourier transform infrared spectroscopy of difluorobenzene adsorbed at polycrystalline platinum electrodes
[AD-A148660] 08 p1123 N85-17080
The adsorption of acrylonitrile at a gold electrode: An EMIRS measurement of the electrochemical stark effect
[AD-A148664] 08 p1123 N85-17082
Modulated surface vibrational spectroscopies at electrode/electrolyte interfaces
[AD-A148665] 08 p1123 N85-17083
Voltammetry and coulometry with immersed thin layer electrodes. Part 1: Model for effects of solution resistivity in linear sweep voltammetry
[AD-A148655] 08 p1159 N85-17313
Voltammetry and coulometry with immersed thin layer electrodes. Part 2: Practical considerations and experimental results
[AD-A148656] 08 p1159 N85-17314
Electrodes for repairing power engineering equipment made from creep resisting steel
[BLL-CE-TRANS-8064-(9022.09)]
08 p1167 N85-17360
Electric utility acid fuel cell stack technology advancement
[NASA-CR-174804] 08 p1178 N85-17422
Electrochemical interfaces and electrode processes
[AD-A147414] 09 p1290 N85-18098
A two photoelectrode solid-state photoelectrochemical cell
[AD-A148962] 10 p1434 N85-19038
Production method of nickel electrode
[NASA-TM-76946] 10 p1439 N85-19069
Method of producing nickel electrode
[NASA-TM-76944] 10 p1440 N85-19077
Study of surface damage in cathode composite materials in a high flux CO2 laser 10 p1444 N85-19098
Positive electrodes of nickel-cadmium batteries
[NASA-TM-77808] 10 p1478 N85-19330
Thermionic converter for space reactor described
11 p1621 N85-20208
Semiconductor electrochemistry approach to the study of oxide films on nickel electrodes
[DE85-003042] 11 p1630 N85-20264
High-temperature, solid oxide electrolyte fuel cell power generation system
[DE85-002978] 11 p1675 N85-20552
Carbon monoxide adsorption on a platinum electrode studied by polarization modulated FT-IRRAS (Fourier Transform-IR Reflections Adsorption Spectroscopy). Part 1: CO adsorbed in the double layer potential region and its oxidation in acids
[AD-A149751] 12 p1800 N85-21288
Electrochemical processes at the sodium (BETA)'' alumina interface
[DE85-004653] 12 p1802 N85-21305
Solar-assisted hydrogen generation by photoelectrocatalysis
[PB85-149706] 12 p1804 N85-21314
Suspension torques on a gimballed electrostatically supported gyroscope and requirements on the gyroscope and spacecraft for the relativity gyroscope experiment
12 p1851 N85-21606
EXAFS of monolayers on silver electrodes: SSRL proposal number 717M
[AD-A150623] 13 p2018 N85-22652
Applications of the vibration probe to localized current measurements
[DE85-004702] 13 p2023 N85-22675
Electrodynamic stability of composite liquid-metal contacts 13 p2087 N85-23031
Molten carbonate fuel cell performance model update, draft
[DE85-005423] 13 p2129 N85-23252
Raman structural studies of the nickel electrode
[NASA-CR-175619] 13 p2162 N85-23414
Erosion of electrodes due to switching of capacitor-bank discharge circuits
[AD-A151207] 15 p2547 N85-25718
Numerical modeling of gas dynamic phenomena during supersonic flow of viscous gas in channel with electrical flow discharge 15 p2643 N85-26304
Material for electrodes of pulsed and arc sources of light
[DE85-007453] 16 p2780 N85-27156
Method of fabricating material for the electrodes of gas discharge devices
[DE85-007452] 16 p2780 N85-27157
Investigation of pseudo bi-polar nickel cadmium batteries as filter elements for pulsed power loads
[AD-A152112] 16 p2819 N85-27380
Electrochemistry of polymer films not immersed in solution: Electron transfer on an ion budget
[AD-A152969] 17 p2920 N85-27998
The behaviour of nitride inclusions in nickel-base alloys
[BLL-BISI-TRANS-22396-(9022.06)]
17 p2927 N85-28058
Spark gap electrode erosion
[AD-A152802] 17 p2953 N85-28237
Electrodes for flash discharge lamps
[DE85-008897] 17 p2955 N85-28250
Electrode for flash discharge lamps
[DE85-008896] 17 p2955 N85-28252
Electrogenerated chemiluminescence
[AD-A153547] 18 p3070 N85-28990
Localized ionic currents from a corroding iron-copper galvanic couple
[AD-A153627] 18 p3074 N85-29011
Electrical line source and point source interactions with anomalies in the ground
[DE85-009777] 18 p3095 N85-29161
Trace water sensor
[NASA-CASE-NPO-15722-1] 18 p3103 N85-29212
Electrochemical and morphological study of the effect of temperature on the restructuring and loss of capacity of alkaline battery electrodes
[DE85-006869] 18 p3129 N85-29378
Energizing arrangement for charge coupled device control electrodes
[AD-D011712] 19 p3261 N85-30220
Gyrotron traveling-wave device including quarter wavelength anti-reflective dielectric layer to enhance microwave absorption
[AD-D011690] 19 p3271 N85-30285
High discharge rate characteristics of nickel-cadmium batteries for pulse load filtering
20 p3446 N85-31391
Nickel hydrogen bipolar battery electrode design
20 p3447 N85-31402
The failure mechanism of a nickel electrode in a nickel-hydrogen cell 20 p3448 N85-31408
Operation of the Zeiss cytopherometer with Zn/ZnSO4 electrode system of Tenforde et al
20 p3499 N85-31752
Thermal contraction of current flow through electrode turbulent boundary layer 21 p3690 N85-32926
Recent advances in d-c relaxation techniques for the measurement of kinetics of fast electrode reactions
[DE85-005029] 22 p3745 N85-33216
Transparent electrode for optical switch
[DE85-011618] 22 p3761 N85-33310
Integrated current collector and catalyst support
[DE85-011616] 22 p3761 N85-33311
Model that predicts pulse charged gas switching breakdown phenomena
[DE85-013119] 22 p3761 N85-33313
Electrochemical methane sensor
[DE85-011663] 22 p3787 N85-33464
Stable n-CuInSe/sub 2/iodide-iodine photoelectrochemical cell
[DE85-011597] 22 p3806 N85-33576
Accelerator vibration issues
[DE85-010766] 22 p3842 N85-33791
Electrode erosion in arc discharges at atmospheric pressure
[NASA-TM-87087] 23 p3903 N85-34178
Experimental evaluation of the thermodynamic properties of concentrated aqueous potassium hydroxide solutions
[DE85-010628] 23 p3912 N85-34238
Conductor-polymer composite electrode materials
[DE85-005766] 23 p3920 N85-34293
Nonsaturable microdryer
[DE85-005760] 23 p3946 N85-34457
Negative ion sources equipped with continuous annular and spherical geometry surface ionizers
[DE85-011939] 23 p3971 N85-34619
Thermodynamics of the corrosion of chromium in molten carbonates
[DE85-011407] 24 p4079 N85-35282
Method of preparing thin porous sheets of ceramic material
[DE85-006399] 24 p4082 N85-35300
Development of electrodes for the NASA iron/chromium
[NASA-CR-174724] 24 p4109 N85-35471

ELECTRODIALYSIS
An evaluation of the electrodialysis reversal process (Edr) for the desalination of brackish water from the Omaruru delta (SWA/Namibia) 01 p0023 N85-10141
Research and development work on a single cation specific membrane for the recovery of raw materials with electrodialysis [BMFT-FB-T-84-163] 03 p0329 N85-12120
ELECTRODYNAMICS
NT ELECTROHYDRODYNAMICS
NT ELECTROMECHANICS
NT QUANTUM ELECTRODYNAMICS
Proceedings of a Workshop on the Applications of Tethers in Space, Volume 1 [NASA-CR-171196] 03 p0322 N85-12076
Proceedings of a Workshop on Applications of Tethers in Space, Volume 2 [NASA-CR-171197] 03 p0322 N85-12077
Short-period seismograph SVSN-6 [REPT-554] 03 p0376 N85-12397
Laboratory electron beam simulation of cosmic radio jets [DE84-016179] 04 p0590 N85-13764
Electrodynamic tethers. 1: Power generator in LEO. 2: Thrust for propulsion and power storage 05 p0611 N85-13901
Analysis of flat finite antenna consisting of waveguide radiators 06 p0790 N85-15048
The investigation of tethered satellite system dynamics [NASA-CR-171278] 07 p0912 N85-15772
Science Applications, part 1 11 p1643 N85-20346
Electrodynamic interactions 11 p1643 N85-20348
Transportation applications, part 1 11 p1643 N85-20349
Summary presentation of the Science Applications Panel 11 p1644 N85-20355
Summary presentation of the Electrodynamics Interactions Panel 11 p1644 N85-20356
Applications of Tethers in Space, volume 2 [NASA-CP-2365] 11 p1644 N85-20361
Report of the Electrodynamic interactions Panel 11 p1645 N85-20363
Report of the Transportation Panel 11 p1645 N85-20364
Report of the Technology and Test Panel 11 p1646 N85-20370
MAP activities in Hungary 11 p1657 N85-20440
Spacecraft Environmental Interactions Technology, 1983 [NASA-CP-2359] 13 p1989 N85-22470
Preliminary investigation of the electrodynamics of a conducting tether 13 p1997 N85-22521
Elasticity formulas for thin-walled shells with piezoceramic layers 13 p2047 N85-22816
Electrodynamic stability of composite liquid-metal contacts 13 p2087 N85-23031
Synthesis of optimum smooth transition in microstrip through line on microwave integrated circuit 13 p2089 N85-23041
Particle shape characterization [AD-A151981] 15 p2544 N85-25707
The gravito-electrodynamics of charged dust in planetary ring systems 15 p2677 N85-26531
Ultrasonic testing of tubes [BLL-BISI-TRANS-22337-(9022.06)] 18 p3119 N85-29304
Electrodynamic transducers for ultrasonic reception 18 p3119 N85-29306
ELECTRODYNAMOMETERS
U DYNAMOMETERS
ELECTROENCEPHALOGRAM
U ELECTROENCEPHALOGRAPHY
ELECTROENCEPHALOGRAPHY
Kolmogorov-Smirnov goodness-of-fit test: Corrected for use with EEG-like data [AD-A144711] 01 p0110 N85-10745
Evidence for multiple areas in the human auditory cortex [AD-A146086] 03 p0401 N85-12555
In search of a visual-cortical describing function: A summary of work in progress 05 p0707 N85-14536
Visual evoked potentials with disrupted functioning of nonspecific cerebral systems 07 p1013 N85-16437
Neurocognitive pattern analysis of an auditory and visual numeric motor control task. Part 1: Development of methods [AD-A148809] 09 p1364 N85-18576
Effects of partial deprivation of slow-wave sleep on sleep-wakefulness cycles 10 p1524 N85-19613
Psychological aspects of phenomenon of spatial synchronization of EEG potential 11 p1691 N85-20632
Functional significance of some EEG parameters and dominant principle 11 p1691 N85-20634
Thermoregulatory and vestibular systems in the rat 15 p2610 N85-26082
Measurement and modification of sensory system EEG (electroencephalographic) characteristics during visual-motor performance [AD-A151901] 15 p2618 N85-26133
A communications link for an implantable electrode array [AD-A152236] 16 p2840 N85-27510
The origin of brain potentials associated with selective visual attention [AD-A152291] 16 p2840 N85-27511
Changes in the impedance and bioelectrical activity of the cerebral cortex of rats under the action of anaesthetic drugs [HSE-TRANS-10371] 19 p3327 N85-30617
Resource allocation in cerebral specialization of function: Behavioral and electrophysiological studies [AD-A155062] 21 p3664 N85-32759
ELECTROEPITAXY
Producing gallium arsenide crystals in space 02 p0151 N85-11023
ELECTROEROSION
U SPARK MACHINING
ELECTROEXPLOSIVE DEVICES
U INITIATORS (EXPLOSIVES)
ELECTROFORMING
Electroforming of nickel [SNIAS-841-501-101] 04 p0484 N85-13065
Study of high performance alloy electroforming [NASA-CR-174276] 07 p0927 N85-15875
Study of high performance alloy electroforming [NASA-CR-175494] 11 p1596 N85-20040
Study of high performance alloy electroforming [NASA-CR-175741] 15 p2508 N85-25473
ELECTROGENERATORS
U ELECTRIC GENERATORS
ELECTROHYDRAULIC CONTROL
U ELECTRIC CONTROL
U HYDRAULIC CONTROL
ELECTROHYDRAULIC FORMING
Results of an interlaboratory fatigue test program conducted on alloy 800H at room and elevated temperatures [NASA-CR-174940] 21 p3597 N85-32340
ELECTROHYDRODYNAMICS
IMS advances in studies of field-aligned currents and their related electrodynamics 14 p2359 N85-24578
Electrodynamics of magnetosphere-ionosphere coupling 14 p2359 N85-24579
Characteristics of the electrodynamics of auroral arcs as inferred from rocket and ground-base observations during IMS 14 p2363 N85-24601
Ac field-induced order in dense colloidal systems [DE85-009107] 17 p2935 N85-28119
A new theory aiming to define the mechanisms of material removal in electroerosion [NASA-TM-77875] 18 p3176 N85-29689
Electrohydrodynamic process for the production of large area polycrystalline silicon sheet [DE85-006781] 19 p3261 N85-30225
Electrodynamic tether 23 p3902 N85-34168
Elastohydrodynamic lubrication calculations used as a tool to study scuffing [NASA-TM-87097] 23 p3936 N85-34406
ELECTROJETS
NT AURORAL ELECTROJETS
NT EQUATORIAL ELECTROJET
Periodic substorm activity in the geomagnetic tail [NASA-CR-175629] 13 p2161 N85-23409
ELECTROKINETICS
Electrokinetic potential and stability of SiC suspensions in electrolyte solutions [NASA-TM-77492] 04 p0469 N85-12984
Zeta potential in ceramic industry [NASA-TM-77478] 04 p0478 N85-13047
Circulation and internal waves in a cold Gulf Stream waves [AD-A149704] 12 p1898 N85-21918
Pre-flight report on cultured human embryonic kidney cell handling and cell electrophoresis. Prepared prior to continuous-flow electrophoretic separation experiments aboard space shuttle flight STS-8 20 p3503 N85-31775
ELECTROLESS DEPOSITION
Low temperature deposition of nickel films [AD-D011568] 12 p1805 N85-21319
ELECTROLUMINESCENCE
Brightness comparison of electroluminescent versus incandescent lighting: A photometric validation [AD-A145395] 02 p0260 N85-11822
Luminescent properties of graded cadmium sulfoselenide electrodes prepared from cadmium sulfide substrates [AD-A146710] 06 p0766 N85-14898
Photoluminescent and electroluminescent properties of Cd sub 0.95 Mn sub 0.05 Se electrodes [AD-A146775] 07 p0946 N85-1[illegible]
Research on electroluminescence in thin film yttrium oxysulfide [AD-A146909] 07 p1037 N85-1[illegible]
ELECTROLUMINESCENT LAMPS
U ELECTROLUMINESCENCE
U LUMINAIRES
ELECTROLYSIS
NT COULOMETRY
Solid electrolytes for medium temperature steam electrolysis [DE84-014384] 04 p0463 N85-12[illegible]
High-temperature steam electrolysis: Technical and economic evaluation of alternative process designs [DE84-015702] 04 p0469 N85-12[illegible]
Photoelectrochemistry with chemically modified electrodes [DE84-016796] 04 p0471 N85-12[illegible]
Measurement of oxide ion concentration in NaCl-ZnCl2 molten salt and several applications [BLL-AWRE-TRANS-74-(9091.9F)] 06 p0764 N85-14[illegible]
Electrolytic deposition of chromium from aqueous chromium solutions containing foreign anions [BLL-MINTEK-TR-1170-(5810.5759)] 06 p0764 N85-14[illegible]
Study of the liquid vapor equilibrium in the bromine-hydrobromic acid-water system [NASA-TM-77787] 07 p0921 N85-15[illegible]
Engineering model system study for a regenerative fuel cell: Study report [NASA-CR-174801] 07 p0991 N85-1[illegible]
Hydrogen from solar energy [DE85-001914] 10 p1437 N85-1[illegible]
Electrolysis of simulated lunar melts 15 p2681 N85-2[illegible]
Ohmic potential drop and gas bubble radius distribution in alkaline water electrolysis 17 p2924 N85-2[illegible]
Oxygen evolution on NiCo2O4 electrodes 17 p2924 N85-2[illegible]
Corrosion characteristics of some steels produced through a self-cleaning rotating electrode [BLL-BISI-TRANS-22046-(9022.06)] 17 p2925 N85-2[illegible]
Feasibility of electrolytic hydrogen production in the Pacific Northwest [DE85-009856] 18 p3084 N85-2[illegible]
Photoeffects of semiconductor electrolyte interfaces [AD-A154163] 20 p3440 N85-31411
High temperature solar electrothermal processing 2. Zinc from zinc oxide [AD-A154747] 21 p3562 N85-32[illegible]
Electrolytic cell [DE85-011596] 22 p3807 N85-32[illegible]
Electrolytic synthesis of colored eta alumina film 23 p3906 N85-34[illegible]
Deposition of nickel-cobalt alloys by controlled-potential electrolysis [PB85-196562] 24 p4061 N85-35[illegible]
ELECTROLYTE METABOLISM
Voluntary dehydration and electrolyte losses during prolonged exercise in the heat [AD-A145157] 01 p0095 N85-10[illegible]
Analysis of head-down tilt as an analog of weightlessness using a mathematical simulation model [NASA-CR-171870] 15 p2616 N85-26[illegible]
The behavior of renal-regulating hormones during hypogravic stress [NASA-CR-171877] 15 p2616 N85-26123
Fluid-electrolyte responses during prolonged space flight: A review and interpretation of significant findings [NASA-CR-171878] 15 p2617 N85-26124
Mathematical modeling of fluid-electrolyte alterations during weightlessness [NASA-CR-171881] 15 p2617 N85-26125
Evaluation of a field expedient technique for sweat sample collection [AD-A151916] 16 p2841 N85-27521
Fluid-electrolyte metabolism and renal function in cosmonauts following 185-day spaceflight 23 p3952 N85-34[illegible]
ELECTROLYTES
NT ION EXCHANGE MEMBRANE ELECTROLYTES
NT MOLTEN SALT ELECTROLYTES
NT NONAQUEOUS ELECTROLYTES
NT SOLID ELECTROLYTES
Influence of parameters of alumimun alloy anodizing process on oxide coating thickness 01 p0018 N85-10113
Methods for producing platinum-group metal coatings from molten alkali cyanides [PB84-225994] 01 p0029 N85-101[illegible]
Advanced fuel cell development [DE84-014847] 01 p0044 N85-10[illegible]

Voluntary dehydration and electrolyte losses during prolonged exercise in the heat
[AD-A145157] 01 p0095 N85-10839
Effects of additives and KOH electrolyte concentration on dissolution of iron electrodes
[DE84-014840] 02 p0173 N85-11162
Electrochemical and surface science research on fuel cells
[DE84-015982] 03 p0359 N85-12307
Electrokinetic potential and stability of SiC suspensions in electrolyte solutions
[NASA-TM-77492] 04 p0469 N85-12864
Materials for high-temperature fuel cells
[DE84-016316] 04 p0479 N85-13054
Phosphoric and electric utility fuel cell technology development
[NASA-CR-174215] 06 p0805 N85-15124
Modulated surface vibrational spectroscopies at electrode/electrolyte interfaces
[AD-A148665] 08 p1123 N85-17063
Polymeric electrolytes for ambient temperature lithium batteries
[DE85-001032] 12 p1835 N85-21518
Research to explore the feasibility of sulfolanes as electrolytic solvents for rechargeable lithium batteries
[DE85-004345] 12 p1837 N85-21525
Development of molten carbonate fuel cell power plant technology
[DE84-016839] 14 p2352 N85-24536
Calcium/thionyl chloride battery technology
[AD-A151975] 15 p2586 N85-25945
Quantitation of Na+, K+-ATPase enzyme activity in tissues of the mammalian vestibular system
15 p2613 N85-26102
Process for clarification of water
[DE85-007664] 17 p2923 N85-28023
Investigation of the structure and dynamics of electrolytes in solvents used for primary and secondary Li-batteries
[AD-A153096] 17 p2954 N85-28240
Bifunctional oxygen electrodes
[DE85-006871] 17 p2955 N85-28248
GAMPHI: A database of activity and osmotic coefficients for aqueous electrolyte solutions
[PB85-183390] 18 p3072 N85-29002
Corrosion Research Center of the University of Minnesota
[DE85-009418] 18 p3075 N85-29022
Aluminum-air power cell: The M3-3 experiment
[DE85-008878] 18 p3096 N85-29169
Trace water sensor
[NASA-CASE-NPO-15722-1] 18 p3103 N85-29212
Improved acid electrolytes for fuel cells
[PB85-176053] 18 p3132 N85-29397
The ESFET: Evaporated Sensing Field Effect Transistor 19 p3256 N85-30188
Develop and test fuel cell powered on-site integrated total energy systems. Phase 3: Full-scale power plant development
[NASA-CR-168336] 19 p3304 N85-30483
New catalysts and new electrolytes for acid fuel cells
[DE85-009940] 19 p3307 N85-30496
Photoeffects of semiconductor electrolyte interfaces
[AD-A154163] 20 p3449 N85-31411
A gel-halo sample pellet: The best of both worlds? Bubby zones without a constricted sample gate
20 p3502 N85-31770
Electrodeposition of chromium and copper in magnetic fields
[AD-A154649] 21 p3566 N85-32180
Rechargeable lithium-organic electrolyte battery having overcharge protection and method of providing overcharge protection for a lithium-organic electrolyte battery
[AD-D011738] 22 p3806 N85-33575
Stable n-CuInSe/sub 2/iodide-iodine photoelectrochemical cell
[DE85-011597] 22 p3806 N85-33576
Nonsaturable microdryer
[DE85-005760] 23 p3946 N85-34457
Aqueous volatile weak electrolyte equilibria to 300 C
[DE85-013840] 24 p4076 N85-35261
ELECTROLYTIC CELLS
Development and testing of thin film cells for high temperature water vapor electrolysis
[BMFT-FB-T-84-146] 04 p0471 N85-13001
Development and testing of TiB2, used as cathode material in Al-electrolysis cells
[BMFT-FB-T-84-176] 05 p0633 N85-14060
Physico-chemical investigations on the electronic partial conductivity of molten electrolytes, especially of the eutectic mixture LiCl-KCl
[BMFT-FB-T-84-205] 05 p0633 N85-14063
Hydrogen production employing high-temperature solid oxide cells
[DE84-014559] 06 p0766 N85-14901
High capacity inorganic oxyhalide electrochemical cell
[AD-D011321] 07 p0923 N85-15845
Engineering model system study for a regenerative fuel cell: Study report
[NASA-CR-174801] 07 p0991 N85-16292
Method for increasing linearity of load cell
11 p1623 N85-20221
State-of-charge coulometer
[NASA-CASE-NPO-15759-1] 12 p1849 N85-21596
New electronic measurement, control devices
14 p2269 N85-24192
Method of production of metals by cathodic solution of their compounds in electrolytic cells
[BLL-OA-TRANS-3207-(6196.300)]
20 p3429 N85-31266
An update of the JPL program to develop Li-SOCl2 cells 20 p3445 N85-31384
Electrolytic cell
[DE85-011598] 22 p3807 N85-33578
ELECTROLYTIC GRINDING
U ELECTROCHEMICAL MACHINING
ELECTROLYTIC POLARIZATION
Indications of mineral zoning in a fossil hydrothermal system at the Meager Creek geothermal prospect, British Columbia, Canada from induced polarization studies
[DE85-011962] 22 p3815 N85-33636
ELECTROLYTIC POLISHING
U ELECTROPOLISHING
ELECTROMAGNETIC ABSORPTION
NT GAMMA RAY ABSORPTION
NT INFRARED ABSORPTION
NT MULTIPHOTON ABSORPTION
NT PHOTOABSORPTION
NT ULTRAVIOLET ABSORPTION
NT X RAY ABSORPTION
Magnetoabsorption of weak light wave in presence of intense light wave in semiconductor with narrow forbidden band 02 p0267 N85-11743
The winter anomaly in ionospheric absorption (with special reference to the results obtained in Spain)
04 p0522 N85-13338
Possible anomaly prediction system for the middle atmosphere — ionospheric absorption
04 p0522 N85-13339
Direct measurements of nitrous acid, nitrogen dioxide and formaldehyde in auto exhaust by differential optical absorption spectroscopy
[PB84-229269] 06 p0767 N85-14905
Optical properties of composite materials
[AD-A146768] 07 p0920 N85-15826
Study of optical sound generation and amplification
[AD-A147359] 07 p1039 N85-16592
An experimental and theoretical investigation of optogalvanic effects
[AD-A148089] 08 p1157 N85-17299
An experimental and theoretical investigation of optogalvanic effects
[AD-A148456] 08 p1223 N85-17700
Development of photoconductive power switch technology
[DE85-001514] 09 p1315 N85-18270
Synopsis of mid-latitude radio wave absorption in Europe 11 p1659 N85-20454
Ionospheric absorption on 1539 kHz in relation to solar ionizing radiation 11 p1659 N85-20455
Measurements of partial reflections at 3.18 MHz using the CW radar technique 11 p1659 N85-20457
Abnormal circulation changes in the winter stratosphere, detected through variations of D region ionospheric absorption 11 p1659 N85-20458
Autumn and winter anomalies in ionospheric absorption as measured by riometers 11 p1660 N85-20460
Winter anomaly 1982/83 in comparison with earlier winters (1960-82) 11 p1660 N85-20461
Explanation of the normal winter anomaly from the seasonal variation of short wave absorption
11 p1660 N85-20463
Millimeter wave dielectric property measurement of gyrotron window materials
[DE85-004430] 12 p1802 N85-21304
Aerosol multiple-scanning code, ASCAT
[LA-10046-MS] 12 p1823 N85-21440
Inelastic scattering in condensed matter with high intensity Moessbauer radiation
[DE85-003531] 12 p1854 N85-21627
Anisoptropy of Alfven wave absorption in ionosphere
14 p2339 N85-24464
Electroreflectance spectroscopy as a probe of the electronic structure at the metal-electronic interface
[DE85-003541] 14 p2428 N85-24976
Study on a prismatic dye vat — laser systems
[CERT-2/6124-04-RO] 16 p2791 N85-27217
Upgrade of the LLNL EM transient range monocone antenna
[DE85-006639] 18 p3097 N85-29172
Optical 3-D signature device for detecting chemical agents
[AD-D011669] 19 p3272 N85-30293
Differential optical absorption techniques for diagnostics of coal gasification
[DE85-010177] 19 p3368 N85-30890
Cyclotron absorption of fast magnetosonic wave in stellarator 21 p3693 N85-32945
Dangling bonds and sub-gap optical absorption in silicon
[DE85-011752] 24 p4082 N85-35302
Muons in gamma showers
[HE-4.5-3] 24 p4195 N85-36027
ELECTROMAGNETIC ACCELERATION
Possibilities and limits of electromagnetic acceleration in space applications
[ILR-MITT-136] 02 p0193 N85-11292
Electromagnetic acceleration of macroparticles to hypervelocities in axisymmetric geometry
[IPPJ-696] 06 p0863 N85-15484
Distributed energy store railguns experiment and analysis 09 p1313 N85-18256
Plasma mass and effective inductance in a small rainbow
[MRL-R-947] 12 p1936 N85-22162
High energy particle acceleration by coherent electromagnetic waves propagating across the magnetic field
[IPPJ-717] 16 p2866 N85-27679
Pulsars as cosmic ray accelerators: Energy development of protons
[OG-8.2-22] 23 p4021 N85-34918
Pulsars as cosmic ray particle accelerators: Dynamics of electrons
[OG-8.2-23] 23 p4021 N85-34919
ELECTROMAGNETIC COMPATIBILITY
Planning guide for the review of telecommunications systems for frequency availability and electromagnetic compatibility
[PB84-210238] 01 p0041 N85-10268
Basic EMC (Electromagnetic Compatibility) technology advancement for C3 systems, macromodeling of digital circuits, volume 2B
[AD-A146333] 03 p0359 N85-12306
EMC (Electromagnetic compatibility) spec criteria in Volterra systems
[AD-A147659] 08 p1151 N85-17263
EMC enhanced constant Z modulator
[AD-A147715] 08 p1157 N85-17297
Assessment of satellite power flux-density limits in the 2025-2300 MHz frequency range, part 2
[PB85-101244] 11 p1625 N85-20236
Algorithm for statistical simulation of electromagnetic compatibility characteristics of high-frequency transmission channels in radioelectronic facilities
12 p1842 N85-21560
Design guidelines for assessing and controlling spacecraft charging effects 13 p1994 N85-22500
Basic EMC (Electromagnetic Compatibility) technology advancement for C3 systems. Volume 4E: Modeling of transmission lines. A comparison of lumped-circuit iterative models and the transmission line model
[AD-A150652] 14 p2291 N85-24201
Basic EMC (Electromagnetic Compatibility) technology advancement for C3 systems: Model revision for IEMCAP (Intrasystem Electromagnetic Compatibility Analysis Program)
[AD-A150795] 14 p2292 N85-24208
Basic EMC (Electromagnetic compatibility) technology advancement for C3 systems. Volume 4D: Modeling crosstalk in balanced twisted pairs
[AD-A153678] 18 p3090 N85-29125
Basic EMC (Electromagnetic Compatibility) technology advancement for C3 systems. Volume 1B: Demodulation radio frequency interference effects in operational amplifier circuits
[AD-A154121] 20 p3440 N85-31350
Electromagnetic compatibility conference features biological interactions
[AD-A155813] 24 p4144 N85-35692
ELECTROMAGNETIC CONTROL
U ELECTROMAGNETS
U REMOTE CONTROL
ELECTROMAGNETIC DEDUCTION
U MAGNETIC INDUCTION
ELECTROMAGNETIC FIELDS
NT FAR FIELDS
NT NEAR FIELDS
NT SYSTEM GENERATED ELECTROMAGNETIC PULSES
The case for concern about very low frequency fields from visual display terminals: The need for further research and shielding of VDTs
[CCOHS-P83-2E] 02 p0234 N85-11526
Transformation of heterogeneous surface waves by skewed streams 02 p0259 N85-11697

ELECTROMAGNETIC INTERACTIONS

On generating function of Weber parabolic cylinder functions with a negative integer index and radio pulse deformation by a medium
[PR-213] 03 p0354 N85-12276

Free-space propagation of light pulses
[PB84-217106] 03 p0421 N85-12669

Nonthermal mechanism for laser annealing of semiconductors and formation of super structure
04 p0487 N85-13109

Calibrating and measuring systems for electromagnetic fields
05 p0630 N85-14041

Invariance of mean-square effective area of synthesized apertures
06 p0784 N85-15009

Measurement of electromagnetic field components from arbitrarily oriented gyro platforms
06 p0787 N85-15030

Investigating phase structure of electromagnetic field in local inhomogeneities by modeling method
06 p0822 N85-15220

Khibiny experiment described
07 p0961 N85-16230

A comparison of lightning and nuclear electromagnetic pulse response of a helicopter 07 p1000 N85-16349

A comparison of lightning and nuclear electromagnetic pulse response of tactical shelters
07 p1000 N85-16350

Forces on neutral atoms due to electromagnetic fields
[AD-A146984] 07 p1040 N85-16603

Electromagnetic fields from the generation and absorption of discontinuous linear current fronts
[AD-A148076] 08 p1151 N85-17268

Theoretical issues involving traps for neutral spin-polarized atoms
[AD-A148035] 08 p1220 N85-17682

European Scientific Notes, volume 38, number 12
[AD-A148713] 09 p1418 N85-18946

Propagation of electromagnetic fields along the sea/sea-bed interface
[AD-A149523] 10 p1467 N85-19257

Effects of electromagnetic fields produced by high voltage transmission lines
[DE85-900034] 11 p1625 N85-20230

The ULF/ELF/VLF electromagnetic fields generated in a sea of finite depth by elevated dipole sources
[AD-A149638] 12 p1828 N85-21470

Determining distribution of complex dielectric permittivity over cylindrical body of intricate cross section from electromagnetic field measurement
12 p1842 N85-21559

Characteristics of the boat inductor for keeping liquid metal in the suspended state
[NASA-TM-77816] 12 p1851 N85-21611

Non-contacting electromagnetic de-spin system for Earth orbiting satellites 12 p1946 N85-22225

Models of discontinous random fields
13 p2079 N85-22983

Problem of diffraction by wavy surface: Comparison of numerical methods of solution
13 p2079 N85-22985

Observation of pure resonance and threshold effects in electron impact experiments in high intensity laser fields
[AD-A150725] 14 p2309 N85-24293

Electromagnetic field of currents and its use to estimate total conductivity of sedimentary deposits in Western Black Sea
14 p2334 N85-24434

Electromagnetic fields migration method
14 p2343 N85-24487

Hygienic standardization of electromagnetic fields of radar systems 14 p2367 N85-24703

High field RF superconductivity: To pulse or not to pulse
[DE85-004381] 14 p2429 N85-24977

Solutions of field equations in General Relativity with spinor connection 15 p2663 N85-26436

The Impact of Proposed Radio Frequency Radiation Standards on Military Operations
[AGARD-LS-138] 16 p2775 N85-27128

Hazards of VLF electromagnetic fields
16 p2776 N85-27136

ELF (Extremely Low Frequency) communications system ecological monitoring program: Measurements of ELF electromagnetic fields for site selection and characterization, 1983
[AD-A153120] 17 p2949 N85-28209

Biological and human health effects of extremely low frequency electromagnetic fields. Post-1977 literature review
[AD-A152731] 17 p2999 N85-28539

Plasma engineering models of tandem mirror devices with high-field test-cell inserts
[DE85-010046] 18 p3192 N85-29797

Hybrid two-dimensional Monte-Carlo electron transport in self-consistent electromagnetic fields
[DE85-010757] 19 p3348 N85-30756

Profile of a relativistic electron beam propagated through a linear wiggler and an axial guide field
[AD-A154403] 19 p3353 N85-30783

Guided-mode launching in a slab waveguide by way of diffraction at the edge of a conducting screen residing on one surface of the slab
[AD-A154886] 21 p3575 N85-32232

Calculation of the propagation constant in a rectangular waveguide containing an inhomogeneous longitudinally magnetized plasma
[DE85-012072] 21 p3577 N85-32250

Lower bounds of propagation velocity of steady ionizing waves in field of strong electromagnetic wave
21 p3692 N85-32940

Equations of motion for electromagnetic waves in 4-dimensional Euclidien space 21 p3697 N85-32970

Research in particles and fields
[NASA-CR-176069] 21 p3724 N85-33103

Pulsars as cosmic ray accelerators: Energy development of protons
[OG-8.2-22] 23 p4021 N85-34918

Theory of mutual impedances and multiple reflections in an N-element array environment
[PB85-191419] 24 p4092 N85-35364

Electromagnetic compatibility conference features biological interactions
[AD-A155813] 24 p4144 N85-35692

ELECTROMAGNETIC INTERACTIONS
NT LASER PLASMA INTERACTIONS
NT PLASMA-ELECTROMAGNETIC INTERACTION

Electromagnetic shower development and applications to sampling calorimeters
[DE84-016355] 04 p0493 N85-13142

Metal-support interactions: Their effects upon adsorption, electronics, and activity/selectivity properties of cobalt in hydrogenation
[DE85-003316] 09 p1292 N85-18113

Applications of Tethers in Space, volume 2
[NASA-CP-2365] 11 p1644 N85-20361

Report of the Electrodynamic Interactions Panel
11 p1645 N85-20363

Investigations of the structure and electromagnetic interactions of few-body systems
[DE85-002854] 11 p1721 N85-20824

Theoretical aspects of electroweak and other interactions in medium-energy nuclear physics
[DE85-003821] 13 p2157 N85-23392

Velocity space diffusion of high energy ions induced by a lower hybrid wave in a nonuniform magnetic field
[IPPJ-714] 16 p2866 N85-27681

Modern test of chiral anomalies
[DE85-005892] 17 p3020 N85-28680

Electroweak interactions in nuclei
[DE85-007811] 17 p3033 N85-28762

Energy and Technology Review
[DE85-004358] 17 p3049 N85-28868

Basic EMC (Electromagnetic compatibility) technology advancement for C3 systems. Volume 4D: Modeling crosstalk in balanced twisted pairs
[AD-A153678] 18 p3090 N85-29125

Interactions between electromagnetic fields
[AD-A153796] 18 p3091 N85-29129

Theoretical investigations of the propagation and interactions of surface waves
[AD-A153548] 18 p3185 N85-29753

Effects of CP violation in SU(2) sub L x SU(2) sub R x U(1) electroweak models
[DE85-010801] 20 p3531 N85-31965

ELECTROMAGNETIC INTERFERENCE
NT ATMOSPHERICS
NT CROSSTALK
NT DAWN CHORUS
NT ELECTROMAGNETIC NOISE
NT HISS
NT IONOSPHERIC NOISE
NT JAMMING
NT RADIO FREQUENCY INTERFERENCE
NT SHOT NOISE
NT THERMAL NOISE
NT WHISTLERS
NT WHITE NOISE

Center for Electronics and Electrical Engineering Technical Bulletin covering center programs with 1984 CEEE events calendar
[PB84-223684] 01 p0045 N85-10293

Center for Electronic and Electrical Engineering Technical Progress Bulletin, January - March 1983, no. 2
[PB84-231224] 03 p0360 N85-12308

Interference immunity of digital equipment for coherent processing of wideband signals
04 p0486 N85-13100

Adaptive mutual interference suppression method
[AD-D011268] 05 p0628 N85-14024

Characterization of newly developed conductive composites
[AD-A146652] 06 p0764 N85-14884

Measurement of external antenna characteristics with allowance for distorting factors (review)
06 p0790 N85-15046

The effect of aircraft generated electromagnetic interference (EMI) on future avionics systems: A compendium
[AD-A146380] 06 p0799 N85-15101

Natural interference phenomena affecting spaceborne receivers
[NASA-CR-174256] 07 p0916 N85-15798

EMI (electromagnetic interference) filter capacitor unit
[AD-D011392] 07 p0937 N85-15941

Upset susceptibility study employing circuit analysis and digital simulation — digital systems and electromagnetic interference
07 p0999 N85-16344

Data and results of a laboratory investigation of microprocessor upset caused by simulated lightning-induced analog transients
07 p0999 N85-16346

Adaptive antenna arrays for weak interfering signals
[NASA-CR-174336] 08 p1150 N85-17259

Subjective evaluation of the effect of noise and interference on frequency modulated NTSC television signals
[CRC-1367] 09 p1310 N85-18230

Electromagnetic compatibility of measurement and control equipment in nuclear installations
[BLL-WH-607-(9091.9F)] 11 p1623 N85-20222

Shuttle electrical environment
13 p1990 N85-22475

EMI characteristics of a potential control system
13 p1994 N85-22502

Characteristics of EMI generated by negative metal-positive dielectric voltage stresses due to spacecraft charging
13 p1995 N85-22505

Basic EMC (electromagnetic interference) technology advancement for c3 systems. Volume 3A: Probabilistic analysis of combinational circuits with random delays
[AD-A150349] 13 p2055 N85-22866

Efficiency of digital compensator of strong non-Gaussian interference
13 p2072 N85-22942

Interference immunity of binary systems with second order phase-difference modulation in various reception modes
13 p2072 N85-22944

Spectra of incidental interference resulting from nonlinear conversion of signals from transmitters
13 p2073 N85-22950

Interference flux during reflection of heterogeneous waves
13 p2078 N85-22977

Models of discontinous random fields
13 p2079 N85-22983

Applicability of log-normal model to probabilistic description of quasi-pulse interference
13 p2084 N85-23014

Frequency selection for dispersion signal in satellite communication lines
15 p2526 N85-25584

Preliminary estimation of mutual interference between fixed satellite service systems 15 p2528 N85-25586

An update on experience on the fly by wire Jaguar equipped with a full-time digital flight control system
16 p2712 N85-26740

Thin layered interference mirrors to reduce radiation damage
[DE85-009763] 18 p3185 N85-29756

Theoretical investigation of single-frequency 8-element localizer signal scattering for critical area determination
[FAA-PM-85-4] 20 p3391 N85-31037

Basic EMC (Electromagnetic Compatibility) technology advancement for C3 systems. Volume 1B: Demodulation radio frequency interference effects in operational amplifier circuits
[AD-A154121] 20 p3440 N85-31350

Study of the interferences of 2 GHz radio beams with a DORIS system — precise low orbit determination system (DORIS)
[CNES-CT/DRT/TIT/RL-84/140-T]
20 p3442 N85-31382

Center for Electronics and Electrical Engineering technical progress bulletin covering center programs, April-June 1984 with 1984 CEEE (Center for Electronics and Electrical Engineering) events calendar, issue 7
[PB85-187540] 20 p3450 N85-31410

Stripe filters on multispectral linear arrays
[NASA-CR-175305] 21 p3579 N85-32252

Effect of interference on the performance of a minimum TCAS 2
[FAA-PM-84-33] 23 p3895 N85-34131

Actuator rigging test set electromagnetic interference test (CE03)
[AD-A155819] 24 p4086 N85-35327

Center for Electronics and Electrical Engineering technical progress bulletin covering center programs July-September with 1985 CEEE events calendar
[PB85-191393] 24 p4091 N85-35383

ELECTROMAGNETIC MEASUREMENT
NT ELECTROMAGNETIC NOISE MEASUREMENT

Special Developments and Methods in High Frequency Measuring Techniques --- conferences
[PTB-E-24] 05 p0629 N85-14030

Present status and development tendencies in the field of high frequency measuring techniques
05 p0629 N85-14031

Improvement of the accuracy of reflection factor measurements by a computer 05 p0629 N85-14033

A computer controlled measuring system for the calibration of HF components 05 p0630 N85-14037

Fundamentals and applications of the six port measuring technique --- reflectometer 05 p0630 N85-14039

Calibrating and measuring systems for electromagnetic fields 05 p0630 N85-14041

Evaluation and results of national and international intercomparison measurements --- electromagnetic measurement 05 p0631 N85-14043

Measurement of electromagnetic field components from arbitrarily oriented gyro platforms
06 p0787 N85-15030

Measurement of external antenna characteristics with allowance for distorting factors (review)
06 p0790 N85-15046

Structure of temperature field based on observations of refraction from high meteorological mast
06 p0819 N85-15199

Two-dimensional signal processing and storage and theory and applications of electromagnetic measurements. Supplemental appendix
[AD-A146848] 07 p0939 N85-15953

Khibiny experiment described
07 p0961 N85-16230

Determining distribution of complex dielectric permittivity over cylindrical body of intricate cross section from electromagnetic field measurement
12 p1842 N85-21559

Two-dimensional signal processing and storage and theory and applications of electromagnetic measurements
[AD-A150590] 13 p2065 N85-22899

Discrimination of normal and anomalous magnetic and electric fields in geoelectromagnetic variations
13 p2114 N85-23166

Analytical studies and experimental measurements of amplitude and phase of near-field range antenna probes
[AD-A150922] 14 p2293 N85-24212

Lightning strikes on aircraft. The TRIP 82 experiment and 3-dimensional electromagnetic interferometry
[ONERA-RF-88/7154-PY] 16 p2703 N85-26690

Magnetoconductance in aluminum films, wires, and cylinders 19 p3374 N85-30928

ELECTROMAGNETIC NOISE
NT ATMOSPHERICS
NT DAWN CHORUS
NT HISS
NT IONOSPHERIC NOISE
NT SHOT NOISE
NT THERMAL NOISE
NT WHISTLERS
NT WHITE NOISE

A coaxial noise standard for the 1 GHz to 12.4 GHz frequency range
[PB84-217984] 01 p0042 N85-10272

High frequency phase-noise in semiconductor lasers
[FUB-20-1983] 01 p0053 N85-10353

Energy correlation between natural extra-low-frequency noises at various frequencies 06 p0784 N85-15010

Low frequency noise in oscillator with limited space-charge accumulation 06 p0786 N85-15024

Peculiarities of microprocessor implementation of algorithms for processing radio signals and noise in large antenna arrays 06 p0792 N85-15059

Observation of natural noise near upper hybrid resonance in terrestrial magnetosphere by Prognoz-5 satellite
06 p0822 N85-15221

Estimation of requirements for acceptable noise radiation level of communication transmitters
07 p0949 N85-16017

NBS (National Bureau of Standards) switching radiometers
[PB84-235694] 07 p0968 N85-16147

Noise jammer discrimination by noise modulation bandwidth
[AD-D011473] 10 p1468 N85-19264

Fundamental limits to synchronization and tracking
[AD-A149623] 12 p1833 N85-21504

Research on ocean floor electrical surveys
[AD-A149831] 12 p1899 N85-21920

Statistical phenomena in particle beams
[DE85-001050] 12 p1929 N85-22118

Prefiltration in Kalman filter with a priori indeterminacy
13 p2071 N85-22939

Comparative analysis of noise tolerance of quasi-coherent phase shift keying signal demodulators
13 p2072 N85-22946

Magnetic noise in single-machine rotating frequency converters 13 p2077 N85-22969

Playback amplifier with high interference immunity
13 p2077 N85-22970

An examination of signal-to-noise enhancement at the Edzell CDAA (Circular Disposed Antenna Array)
[AD-A150708] 14 p2291 N85-24204

Study of 1/f noise in solids
[AD-A151069] 14 p2428 N85-24972

The effects of seeing on noise
14 p2443 N85-25077

Analysis and interpretation of synthetic time strings of oscillation data 14 p2444 N85-25079

Adaptive detection of noise signal according to Neumann-Pearson criterion 15 p2527 N85-25580

Noise characteristics of an avalanche photodiode
[AD-A154096] 19 p3258 N85-30205

Overview of applications of SQUIDS
[DE85-009942] 20 p3458 N85-31460

The role of long term lamp fluctuations in the random walk of frequency behavior of the rubidium frequency standard: A case study
[AD-A155338] 21 p3590 N85-32314

Design of a freestanding noise measurement and recording system to predict the intensity and location of electromagnetic radiation from earthquakes
[AD-A155070] 21 p3632 N85-32563

A real time index of geomagnetic background noise for the MAD (Magnetic Anomaly Detection) frequency band
[AD-A155717] 22 p3814 N85-33627

Noise in silver beta alumina ceramics
[AD-A156135] 24 p4082 N85-35297

ELECTROMAGNETIC NOISE MEASUREMENT

FCC (Federal Communication Commission) methods of measurement of radio noise emissions from computing devices
[PB84-243591] 06 p0849 N85-15387

ELECTROMAGNETIC PROPAGATION
U ELECTROMAGNETIC WAVE TRANSMISSION

ELECTROMAGNETIC PROPERTIES
NT ABSORPTANCE
NT ABSORPTIVITY
NT BIREFRINGENCE
NT BRIGHTNESS
NT BRIGHTNESS DISTRIBUTION
NT CAPACITANCE
NT CARRIER MOBILITY
NT COLOR
NT DICHROISM
NT DIELECTRIC PROPERTIES
NT ELECTRICAL PROPERTIES
NT ELECTROMAGNETIC ABSORPTION
NT ELECTRON MOBILITY
NT FARADAY EFFECT
NT FERROELECTRICITY
NT HOLE MOBILITY
NT INDUCTANCE
NT INFRARED ABSORPTION
NT LUMINOSITY
NT OPACITY
NT OPTICAL BISTABILITY
NT OPTICAL PROPERTIES
NT OPTICAL REFLECTION
NT PERMITTIVITY
NT PHOSPHORESCENCE
NT PHOTOCONDUCTIVITY
NT PHOTOELASTICITY
NT PHOTOELECTRIC EFFECT
NT PHOTOELECTRIC EMISSION
NT PHOTOIONIZATION
NT PHOTOVISCOELASTICITY
NT PHOTOVOLTAIC EFFECT
NT PROXIMITY EFFECT (ELECTRICITY)
NT RADIANCE
NT REFLECTANCE
NT REFRACTIVITY
NT SKY BRIGHTNESS
NT SOLAR GRANULATION
NT STELLAR LUMINOSITY
NT STIGMATISM
NT TRANSLUCENCE
NT TRANSMISSIVITY
NT TRANSMITTANCE
NT TRANSPARENCE
NT TURBIDITY
NT WATER COLOR

The effect of aircraft generated electromagnetic interference (EMI) on future avionics systems: A compendium
[AD-A146360] 06 p0799 N85-15101

Shielded enclosures for experimental studies of shielding topology
[AD-A149292] 11 p1624 N85-20227

Electromagnetic analysis of radomes by the moment method
[AD-P004351] 12 p1824 N85-21445

A radome for air traffic control SSR radar systems
[AD-P004373] 12 p1827 N85-21467

Simulation of thermal and electromagnetic processes in induction plasmatrons 12 p1841 N85-21552

Research on ocean floor electrical surveys
[AD-A149831] 12 p1899 N85-21920

Determination of electromagnetic properties of mesh material using advanced radiometer techniques
14 p2235 N85-23855

Design, and testing of a pulsed current transformer
[AD-A154228] 19 p3259 N85-30208

Comparison of the electromagnetic properties of lightning and EMP (Electromagnetic pulse): Results of recent lightning studies
[AD-A154325] 19 p3317 N85-30560

Possibilities for studying short-lived nuclei produced at LAMPF
[DE85-010740] 19 p3365 N85-30864

SAPIENS Memo 8: Electromagnetic properties of the EMP simulator SAPIENS
[FOA-C-30382-A3] 20 p3442 N85-31365

A review of the physics and response models for burnout of semiconductor devices
[AD-A155031] 21 p3709 N85-33028

Analysis of the nonlinear equations describing the elastic, thermal, and electromagnetic behavior of solids: Existence of solutions of semi-inverse problems
24 p4100 N85-35415

ELECTROMAGNETIC PROPULSION
NT MASS DRIVERS (PAYLOAD DELIVERY)

Preliminary analysis of space mission applications for electromagnetic launchers
[NASA-CR-174067] 03 p0321 N85-12071

Plasma mass and effective inductance in a small railgun
[AD-A154644] 21 p3589 N85-32304

ELECTROMAGNETIC PULSES
NT SYSTEM GENERATED ELECTROMAGNETIC PULSES

Laboratory evaluation of Electromagnetic Pulse (EMP) hardness testing concepts for electrical conduit systems
[AD-A145466] 02 p0190 N85-11273

Microwave susceptibility experiments
[DE84-016188] 02 p0192 N85-11281

EMP injection on conduit entries, type Brattberg --- electromagnetic pulse (EMP) injection
[FOA-E-30001-A3] 02 p0193 N85-11290

The case for concern about very low frequency fields from visual display terminals: The need for further research and shielding of VDTs
[CCOHS-P83-2E] 02 p0234 N85-11526

Generation of superpowerful microsecond electromagnetic radiation pulses
03 p0347 N85-12234

Free-space propagation of light pulses
[PB84-217108] 03 p0421 N85-12689

Electromagnetic pulse and the electric power network
[DE84-015403] 04 p0493 N85-13143

Tests for susceptibility to electromagnetic attack
[SNIAS-842-422-101] 04 p0494 N85-13154

Pulse injection on a power cable penetrating a shielding wall by feed-through capacitors
[FOA-C-30372-A3] 04 p0497 N85-13171

The HEMP (High-altitude Electromagnetic Pulse) response of a long transmission line buried in the earth
[AD-A146517] 06 p0800 N85-15108

Dynamic response of electromagnetic current meters
[PB84-229731] 06 p0842 N85-15344

Multiple scattering effects on transmission through the atmosphere
[AD-A147527] 07 p0941 N85-15969

Real-time analysis of space characteristics of microwave electromagnetic pulse fields by means of controllable layer structures 07 p0955 N85-16052

A comparison of lightning and nuclear electromagnetic pulse response of a helicopter 07 p1000 N85-16349

A comparison of lightning and nuclear electromagnetic pulse response of tactical shelters
07 p1000 N85-16350

Nonradial pulsation and mass loss in early B stars
08 p1232 N85-17759

Electromagnetic pulse (EMP) interaction with electric power systems. Power Systems Technology Program
[DE85-000166] 09 p1312 N85-18244

Multiple parallel wires above a finitely conducting plane earth in the presence of a plane wave (EMP)
[DE85-001116] 11 p1625 N85-20231

Distortion of temporal characteristics during parametric up-conversion of ultrashort laser pulses
11 p1717 N85-20803

Numerical investigation of propagation of radiation pulse at xxx 11 p1718 N85-20809

Four-wave hypersonic reversing mirrors in saturated mode 11 p1719 N85-20812

Electromagnetic pulse (EMP) injection on cable entries, type ERA; EMP memo no. 10
[FOA-E-30003-A3] 12 p1830 N85-21484

Intense, broadband, pulsed I-R source at the National Synchrotron Light Source
[DE84-010542] 12 p1935 N85-22154

Design guidelines for assessing and controlling spacecraft charging effects 13 p1994 N85-22500

Processing of signals in experiments with scattering of short radio pulses by conducting sphere
13 p2068 N85-22917

Measuring intensity of electric field produced by electromagnetic pulse with aid of active probes
13 p2075 N85-22958

Use of electronic coding-frequency meters to measure parameters of pulsed radio signals
13 p2076 N85-22964

Pulsations of cosmic ray intensities before increasing flux of relativistic particles from solar flares
15 p2477 N85-25292

Signal processing for the analysis of transient electromagnetic data
[DE85-007244] 16 p2774 N85-27125

Optically triggered transferred-electron device microwave burst and single pulse generators
[AD-D011614] 16 p2778 N85-27141

A synchrotron/inverse Compton interpretation of a solar burst producing fast pulses at lambda 3 mm and hard X-rays 16 p2867 N85-27815

Energy and Technology Review
[DE85-004358] 17 p3049 N85-28868

Comparison of the electromagnetic properties of lightning and EMP (Electromagnetic pulse): Results of recent lightning studies
[AD-A154325] 19 p3317 N85-30560

SAPIENS Memo 8: Electromagnetic properties of the EMP simulator SAPIENS
[FOA-C-30382-A3] 20 p3442 N85-31365

A theory of electromagnetic shielding with applications to MIL-STD-285, IEEE-299, and EMP simulation
[AD-A154905] 21 p3575 N85-32233

Plasmodynamic methods for generating powerful light puses 21 p3693 N85-32943

Methods for measuring and analyzing dispersion properties of multimode fiber optic lightpipes (a review)
21 p3695 N85-32960

Study to assess the effects of magnetohydrodynamic electromagnetic pulse on electric power systems, phase 1, volume 3
[DE85-011301] 24 p4156 N85-35771

ELECTROMAGNETIC RADIATION
NT AIRGLOW
NT BLACK BODY RADIATION
NT BREMSSTRAHLUNG
NT CENTIMETER WAVES
NT CERENKOV RADIATION
NT CN EMISSION
NT COHERENT ELECTROMAGNETIC RADIATION
NT COHERENT LIGHT
NT COMET TAILS
NT COSMIC X RAYS
NT CYCLOTRON RADIATION
NT DECAMETRIC WAVES
NT DECIMETER WAVES
NT ELECTROMAGNETIC PULSES
NT ELECTROMAGNETIC SURFACE WAVES
NT EXTRATERRESTRIAL RADIO WAVES
NT EXTREME ULTRAVIOLET RADIATION
NT FAR INFRARED RADIATION
NT FAR ULTRAVIOLET RADIATION
NT GALACTIC RADIO WAVES
NT GAMMA RAY BEAMS
NT GAMMA RAY BURSTS
NT GAMMA RAYS
NT GEOCORONAL EMISSIONS
NT HYDROXYL EMISSION
NT INFRARED RADIATION
NT KILOMETRIC WAVES
NT LIGHT (VISIBLE RADIATION)
NT LIGHT BEAMS
NT LONG WAVE RADIATION
NT LYMAN ALPHA RADIATION
NT MICROWAVE EMISSION
NT MICROWAVES
NT MILLIMETER WAVES
NT MODULATED CONTINUOUS RADIATION
NT MONOCHROMATIC RADIATION
NT NEAR INFRARED RADIATION
NT NIGHTGLOW
NT NONEQUILIBRIUM RADIATION
NT NORTH POLAR SPUR (ASTRONOMY)
NT PHOTON BEAMS
NT PLANETARY RADIATION
NT PLASMONS
NT POLARIZED ELECTROMAGNETIC RADIATION
NT POLARIZED LIGHT
NT RADIO BURSTS
NT RADIO EMISSION
NT RADIO WAVES
NT SHORT WAVE RADIATION
NT SKY RADIATION
NT SKY WAVES
NT SOLAR RADIO BURSTS
NT SOLAR RADIO EMISSION
NT SOLAR X-RAYS
NT SOMMERFELD WAVES
NT SUBMILLIMETER WAVES
NT SUNLIGHT
NT SYNCHROTRON RADIATION
NT SYSTEM GENERATED ELECTROMAGNETIC PULSES
NT TERRESTRIAL RADIATION
NT THERMAL RADIATION
NT TWILIGHT GLOW
NT TYPE 3 BURSTS
NT TYPE 4 BURSTS
NT ULTRAVIOLET RADIATION
NT X RAYS
NT ZODIACAL LIGHT

Theory of near-field phased arrays for electromagnetic susceptibility testing
[PB84-217836] 01 p0042 N85-10273

Activities report of the Radio Laboratory
[REPT-S-153] 02 p0192 N85-11266

Scattering of electromagnetic waves by plasma half-space after initiation of motion
02 p0264 N85-11729

Diffraction of electromagnetic wave by screen of arbitrary shape 02 p0273 N85-11778

Diffraction of plane electromagnetic waves on semiinfinite grid of parallel conductors arranged at angle to its edge 03 p0344 N85-12217

Scattering of electromagnetic waves in flat waveguide with bilateral diaphragms 03 p0347 N85-12235

Characteristics of absorption and frequency filtration of ULF electromagnetic waves in the ionosphere
03 p0376 N85-12402

Research activities of the Illinois University Coordinated Science Laboratory
[AD-A145589] 03 p0449 N85-12856

Field/cell interaction model
[DE84-011914] 04 p0544 N85-13465

Aharonov-Bohm effect in absorption of electromagnetic wave 06 p0786 N85-15022

Optimization of energy conversion during locking of electron bunches by electromagnetic wave in longitudinal electrostatic field 06 p0786 N85-15025

Diurnal variation harmonics and spatial change in cosmic ray flux 06 p0824 N85-15230

Method for forming electromagnetic-wave-screening composite 07 p0936 N85-15930

Two-dimensional signal processing and storage and theory and applications of electromagnetic measurements. Supplemental appendix
[AD-A146848] 07 p0939 N85-15953

Transformation of electromagnetic waves in plasma with randomly-heterogeneous magnetic field
07 p0953 N85-16039

Tolerance synthesis of multilayer radome walls
07 p0953 N85-16041

Methodical approaches to determination of sanitation protective zone dimensions around TV centers and TV retransmitters 09 p1361 N85-18563

Current measurements by Faraday rotation in single mode optical fibers
[DE85-002025] 09 p1384 N85-18707

Proceedings of the 17th Symposium on Electromagnetic Windows, part 1
[AD-A149185] 10 p1466 N85-19253

Nonlinear saturation of stimulated Raman scattering in collisional homogeneous plasma
[DE85-002814] 10 p1559 N85-19831

Multiple parallel wires above a finitely conducting plane earth in the presence of a plane wave (EMP)
[DE85-001116] 11 p1625 N85-20231

Coronal spectroscopy in laser plasmas
[DE85-002817] 11 p1730 N85-20880

Covariant lie-transformed plasma action principle
[DE85-000285] 11 p1732 N85-20891

Detection of angular modulated electromagnetic signals
[AD-D011563] 12 p1823 N85-21437

Proceedings of the Symposium on Electromagnetic Windows (17th) held at Georgia Inst. of Technology, Engineering Experiment Station, Atlanta, Georgia on 25-27 July 1984. Part 2
[AD-A149125] 12 p1824 N85-21444

Arguments for fundamental emission by the parametric process L yields T + S in interplanetary type III bursts --- langmuir, electromagnetic, ion acoustic waves (L, T, S) 12 p1958 N85-22311

Small scale structure and the Spinar model for acti galactic nuclei 12 p1959 N85-2231

Numerical/Electromagnetics Code (NEC)
[DE85-004999] 13 p2056 N85-2287

Natural electromagnetic radiation in seismically activ regions 13 p2111 N85-2315

Disturbances in structure of lower ionosphere a terminators based on results of winde-band LF sounding 14 p2339 N85-2447

Rain rate determinations from electronic weigh measurements: Instrument description and data reduction techniques
[AD-A150765] 14 p2378 N85-2481

Particle shape characterization
[AD-A151981] 15 p2544 N85-2570

A plasma initiation-flow chamber to study CW lase beamed energy absorption in light gases
[AD-A151225] 15 p2562 N85-2588

Amplification of scattered induced radiation flux i high-gain laser rods 15 p2644 N85-2639

Characteristic functionals of stochastic wav processes
[REPT-14/1984] 16 p2766 N85-2709

Multiple scattering of electromagnetic waves in discre random media
[AD-A151766] 16 p2772 N85-27112

Biological influences of low-frequency sinusoida electromagnetic signals alone and superimposed on RF carrier waves
[PB85-161248] 16 p2842 N85-27527

DARPA/TTO program IR binary optics
[AD-A152196] 16 p2865 N85-27672

Study of the degradation of short-circuit current and the open-circuit tension of spatial solar cells as a function of the fluency of 1MeV electrons
[INPE-3356-PRE/634] 16 p2887 N85-27814

Solar-Geophysical Data Number 484, December 1984 Part 1 (prompt reports): Data for November 1984, October 1984 and late data
[NASA-CR-175829] 16 p2888 N85-27819

X-ray emission and the winds of cataclysmic variables
[DE85-007663] 17 p3053 N85-2892

Upgrade of the LLNL EM transient range monocone antenna
[DE85-006639] 18 p3097 N85-29172

All-optical logic gates with external switching by laser and incoherent radiation 18 p3187 N85-29766

Electromagnetic solitary waves in magnetized plasma
[DE85-010084] 18 p3190 N85-29780

Scattering by distributions of small thin particles
19 p3253 N85-30172

Heating of electrons in a high density tokamak by a micro-wave near second harmonic frequency
[DE85-010682] 19 p3359 N85-3082

Electromagnetic lateral waves in layered media
19 p3369 N85-3089

Localization of waves in a disordered medium
19 p3373 N85-3092

Theoretical investigation of single-frequency 8-element localizer signal scattering for critical area determination
[FAA-PM-85-4] 20 p3391 N85-31037

Simulation and analysis of airborne antenna radiation patterns 20 p3439 N85-31342

Numerical modeling of subsurface communication
[DE85-012818] 21 p3577 N85-3224

Some recent developments in the interpretation of MST radar returns from clear air (keynote paper), part 2
21 p3618 N85-3248

Design of a freestanding noise measurement and recording system to predict the intensity and location of electromagnetic radiation from earthquakes
[AD-A155070] 21 p3632 N85-32583

USAFSAM review and analysis of radiofrequency radiation bioeffects literature
[AD-A155113] 21 p3664 N85-32760

Investigation of ion-acoustic plasma turbulence in fiel of powerful electromagnetic wave by CO2-laser radiation scattering 21 p3691 N85-32935

Lower bounds of propagation velocity of steady ionizing waves in field of strong electromagnetic wave
21 p3692 N85-3294

Amplification of electromagnetic wave by electro stream with negative velocity differences
21 p3692 N85-3294

Electromagnetic wave amplification during cyclotro resonance in a medium 21 p3693 N85-3294

Effective brightness of zero-point fluctuations of th electromagnetic vacuum accompanying paramet scattering of light 21 p3694 N85-3295

Existence of smooth solutions in problems electromagnetic radiation focusing
21 p3697 N85-3297

Ice fog as an electro-optical obscurant
[AD-A155059] 21 p3705 N85-3301

Method of characterizing critical timing paths and analyzing timing related failure modes in very large scale integrated circuits
[AD-D011731] 22 p3759 N85-33298

Surface wave modes of a multilayered medium backed by a perfectly conducting ground plane: Computation of propagation constants
[DE85-011454] 22 p3829 N85-33715

Recoverable Plasma Diagnostics Package (RPDP)
23 p3902 N85-34167

Simulation studies on stability of hot electron plasma
23 p3978 N85-34664

Pulse effect in a light ion beam propagation through a Z-discharge plasma channel 23 p3981 N85-34684

Source energy spectra from demodulation of solar particle data by interplanetary and coronal transport
[SH-1.3-13] 23 p3994 N85-34758

Solar source regions of 3HE-rich particle events
[SH-2.2-4] 23 p4000 N85-34799

RF stabilization of interchange-ballooning modes
[DE85-012080] 24 p4090 N85-35353

Theory of mutual impedances and multiple reflections in an N-element array environment
[PB85-191419] 24 p4092 N85-35364

High energy radiation from neutron stars
[DE85-014353] 24 p4169 N85-35843

Analytical-numerical methods of calculations of energy and three-dimensional particle distributions in electromagnetic cascades
[HE-3.5-13] 24 p4184 N85-35950

The lateral distributions of charged particles of energy greater than 0.3 E sub crit in electron-photon cascades in lead and air
[HE-3.6-10] 24 p4185 N85-35957

Result of Monte-Carlo simulation of electron-photon cascades in lead and layers of lead-scintillator
[HE-3.6-11] 24 p4185 N85-35958

On mini-cluster observed by Chacaltaya emulsion chamber experiment
[HE-3.6-12] 24 p4185 N85-35959

A comparative analysis of gamma and hadron families at the superhigh energies recorded in experiment Pamir
[HE-3.7-1] 24 p4185 N85-35960

Structured events in Pamir carbon X-ray chambers
[HE-3.7-7] 24 p4186 N85-35965

Peculiarities of gamma-quanta distribution at 20 TeV energy
[HE-3.7-10] 24 p4186 N85-35967

ELECTROMAGNETIC SCATTERING

NT HALOS
NT LIGHT SCATTERING
NT MICROWAVE SCATTERING
NT MIE SCATTERING
NT RAMAN SPECTRA
NT RAYLEIGH SCATTERING
NT THOMSON SCATTERING
NT X RAY SCATTERING

Planarity criteria in electromagnetic topology
[AD-A145279] 01 p0038 N85-10241

Gaussian Wide Sense Stationary Uncorrelated Scattering (GWSSUS) channel simulation program to be used for mobile radio systems
[FUB-40-1983] 01 p0041 N85-10265

Theory of near-field phased arrays for electromagnetic susceptibility testing
[PB84-217836] 01 p0042 N85-10273

Scattering of electromagnetic waves by plasma half-space after initiation of motion
02 p0264 N85-11729

Scattering of radio waves on magnitized meteor trail
03 p0344 N85-12221

Scattering of electromagnetic waves in flat waveguide with bilateral diaphragms 03 p0347 N85-12235

Research activities of the Illinois University Coordinated Science Laboratory
[AD-A145589] 03 p0449 N85-12856

Scattering from randomly oriented scatterers of arbitrary shape in the low-frequency limit with application to vegetation 04 p0525 N85-13362

Scattering from randomly oriented circular discs with application to vegetation 04 p0525 N85-13363

A comparison between active and passive sensing of soil moisture from vegetated terrains
04 p0526 N85-13364

Scattering of electromagnetic waves by surface with small asperities 06 p0784 N85-15013

Approach to solution of diffraction problem for waves at rough surface 06 p0784 N85-15014

Scattering from thin dielectric disks
[NASA-TM-86155] 06 p0798 N85-15098

Far-infrared laser diagnostic on EBT and extreme far-forward laser scattering on ISX
[DE85-001788] 07 p1046 N85-16643

Second order Bragg scattering in a SAR
[AD-A148395] 08 p1152 N85-17275

Scattering of electromagnetic waves by human body and its applications 09 p1363 N85-18572

Numerical methods for analyzing electromagnetic scattering
[NASA-CR-175507] 12 p1823 N85-21438

Inelastic scattering in condensed matter with high intensity Moessbauer radiation
[DE85-003531] 12 p1854 N85-21627

Research efforts in support of resonance extraction studies. Volume 1: Improvement and validation of TWFD (Thin-Wire Frequency-Domain): A thin-wire frequency-domain scattering code
[AD-A150296] 13 p2054 N85-22864

Scattering of electromagnetic waves by charged particles 13 p2067 N85-22913

Diffraction of plane TM-wave on continuously irregular elliptical plasma 13 p2067 N85-22914

Extraction of surface-wave energy from plasma waveguide 13 p2077 N85-22974

Scattering of waves by axisymmetrical edge
13 p2080 N85-22987

Analysis of the electromagnetic scattering from an inlet geometry with lossy walls
[NASA-CR-175743] 15 p2541 N85-25686

Electromagnetic scattering by arbitrarily shaped reflectors: Subreflector efficiency
[AD-A149224] 15 p2541 N85-25687

Scattering center analysis for radar cross section modification 16 p2769 N85-27085

Optical non-line-of-sight covert, secure high data communication system
[AD-D011607] 16 p2769 N85-27087

Application of forward scattering renormalization to scattering in turbid media
[AD-A153232] 17 p2959 N85-28271

The stability and dynamics of elastic structures and fluid flows
[AD-A154188] 19 p3266 N85-30252

Active and passive remote sensing of ice
[AD-A154408] 19 p3300 N85-30459

Radar target identification through electromagnetic scattering studies
[AD-A154596] 21 p3573 N85-32220

Scattering from foliage covered terrain
[AD-A154724] 21 p3574 N85-32228

Head-on scattering of a tubular cylinder of finite length for radar target identification purposes
[AD-A155608] 21 p3577 N85-32246

Broadside scattering of a tubular cylinder for evaluation of target identification
[AD-A155739] 21 p3577 N85-32248

Minimizing field scattered by slender dipoles
22 p3774 N85-33388

On the convergence of an iterative formulation of the electromagnetic scattering from an infinite grating of thin wires 24 p4085 N85-35319

Penetrative nature of high energy showers observed in Chacaltaya emulsion chamber
[HE-3.3-5] 24 p4180 N85-35923

Anomalous correlation between hadron and electromagnetic particles in hadron and gamma-ray families
[HE-3.3-6] 24 p4180 N85-35924

ELECTROMAGNETIC SHIELDING

Laboratory evaluation of Electromagnetic Pulse (EMP) hardness testing concepts for electrical conduit systems
[AD-A145466] 02 p0190 N85-11273

Pulse injection on a power cable penetrating a shielding wall by feed-through capacitors
[FOA-C-30372-A3] 04 p0497 N85-13171

A comparison of lightning and nuclear electromagnetic pulse response of tactical shelters
07 p1000 N85-16350

Shielded enclosures for experimental studies of shielding topology
[AD-A149292] 11 p1624 N85-20227

Model calculations for a CO2 mixing laser with screen nozzle
[ESA-TT-859] 11 p1640 N85-20336

Electromagnetic pulse (EMP) injection on cable entries, type ERA; EMP memo no. 10
[FOA-E-30003-A3] 12 p1830 N85-21484

A theory of electromagnetic shielding with applications to MIL-STD-285, IEEE-299, and EMP simulation
[AD-A154905] 21 p3575 N85-32233

Actuator rigging test set electromagnetic interference test (CE03)
[AD-A155819] 24 p4086 N85-35327

ELECTROMAGNETIC SPECTRA

NT BALMER SERIES
NT D LINES
NT ELECTRONIC SPECTRA
NT FRAUNHOFER LINES
NT GAMMA RAY SPECTRA
NT H ALPHA LINE
NT H LINES
NT INFRARED SPECTRA
NT K LINES
NT LINE SPECTRA
NT LYMAN SPECTRA
NT MICROWAVE SPECTRA
NT RADIO SPECTRA
NT RAMAN SPECTRA
NT RYDBERG SERIES
NT SOLAR SPECTRA
NT STELLAR SPECTRA
NT UBV SPECTRA
NT ULTRAVIOLET SPECTRA
NT VIBRATIONAL SPECTRA
NT VISIBLE SPECTRUM
NT X RAY SPECTRA

Summary of the origin of nonradiative heating/momentum in hot stars
08 p1236 N85-17789

Basic principles of industrial radiography
14 p2316 N85-24310

Analytical techniques used to calculate the fields due to refraction and diffraction of electromagnetic waves
[AD-A151705] 15 p2543 N85-25698

A position sensitive phoswich hard X-ray detector system
[OG-9.3-12] 23 p4028 N85-34967

The ISAVF opto-mechanical test bed
[NASA-TM-87505] 24 p4067 N85-35206

ELECTROMAGNETIC SURFACE WAVES

Image theory for a vertical electric dipole above a wire grid with square cells
[REPT-S-150] 02 p0192 N85-11286

Extraction of surface-wave energy from plasma waveguide 13 p2077 N85-22974

ELECTROMAGNETIC WAVE FILTERS

NT BANDPASS FILTERS
NT BIREFRINGENT FILTERS
NT CRYSTAL FILTERS
NT DIGITAL FILTERS
NT ELECTRIC FILTERS
NT FIR FILTERS
NT MATCHED FILTERS
NT MICROWAVE FILTERS
NT OPTICAL FILTERS
NT RADAR FILTERS
NT RADIO FILTERS
NT TRACKING FILTERS
NT WAVEGUIDE FILTERS

Environmentally independent fiber optic rotation sensor
[AD-D011219] 01 p0119 N85-10818

Method for forming electromagnetic-wave-screening composite 07 p0936 N85-15930

Filter and passband problems
08 p1252 N85-17910

Space-time response characteristics of acoustooptic filter for compression of linearly frequency-modulated signal 13 p2071 N85-22937

Some design considerations for a satellite-borne magnetograph 18 p3204 N85-29679

The inference of vector magnetic fields from polarization measurements with limited spectral resolution
18 p3207 N85-29896

ELECTROMAGNETIC WAVE TRANSMISSION

NT HALOS
NT IONOSPHERIC PROPAGATION
NT LIGHT SCATTERING
NT LIGHT TRANSMISSION
NT MANDELSTAM REPRESENTATION
NT MICROWAVE ATTENUATION
NT MICROWAVE TRANSMISSION
NT MULTIPATH TRANSMISSION
NT RADAR TRANSMISSION
NT RADIO TRANSMISSION
NT SCATTER PROPAGATION
NT SHORT WAVE RADIO TRANSMISSION
NT SINGLE SIDEBAND TRANSMISSION
NT SPREAD SPECTRUM TRANSMISSION
NT TELEVISION TRANSMISSION
NT TRANSEQUATORIAL PROPAGATION

Activities report of the Radio Laboratory
[REPT-S-153] 02 p0192 N85-11288

Effects of atmospheric water vapor and clouds on NOAA (National Oceanic and Atmospheric Administration) AVHRR (Advanced Very High Resolution Radiometer) satellite data
[AD-A145425] 02 p0260 N85-11824

Nonlinear electromagnetic waves in ferromagnetic conducting media 03 p0346 N85-12232

The development of new methods for solving the target identification or inverse scattering problem for time-harmonic acoustic and electromagnetic waves
[AD-A145821] 03 p0415 N85-12657

A comparison of evaporation duct models for IREPS (Integrated Refractive Effects Prediction System)
[AD-A146471] 06 p0799 N85-15103

Beam propagation studies at NRL (Naval Research Laboratory) July 1983 to June 1984, volume 2
[AD-A148198] 08 p1152 N85-17270
Methodical approaches to determination of sanitation protective zone dimensions around TV centers and TV retransmitters 09 p1361 N85-18563
Propagation of electromagnetic fields along the sea/sea-bed interface
[AD-A149523] 10 p1467 N85-19257
Generation of Alfven waves due to thermal modulation of the electrical conductivity
[AD-A149389] 10 p1558 N85-19826
Survivable propagation
[AD-A150070] 12 p1829 N85-21478
Analysis and computations of microwave-atmospheric interactions
[AD-A149686] 12 p1889 N85-21854
The use of the spectral matrix in analyzing the propagation characteristics of electromagnetic emissions — magnetosphere 14 p2371 N85-24658
Statistical/Trend analysis of the marine atmospheric boundary layer model
[AD-A151053] 14 p2374 N85-24673
Meteorological conditions affecting electromagnetic propagation on the Arabian Peninsula
[AD-A152019] 15 p2544 N85-25708
The weighting function for scintillation on a folded path
[AD-A152659] 17 p2949 N85-28206
Electromagnetic transmission through a slot in a perfectly conducting plane
[AD-A153224] 17 p2949 N85-28210
Electromagnetic lateral waves in layered media
19 p3369 N85-30894
Control of large antennas based on electromagnetic performance criteria 20 p3409 N85-31158
Effects of hydrometeors on electromagnetic wave propagation
[AD-A155379] 22 p3750 N85-33297
Injection of energetic particles following the gamma-ray flares on June 7, 1980, as observed on Helios 1
[SH-1.3-9] 23 p3993 N85-34756

ELECTROMAGNETIC WAVES
U ELECTROMAGNETIC RADIATION

ELECTROMAGNETICS
U ELECTROMAGNETISM

ELECTROMAGNETISM
NT MAGNETOSTATICS
Joint services electronics program
[AD-A145085] 01 p0042 N85-10276
ASP: A new PEP experiment to measure single photons
[DE84-015732] 04 p0560 N85-13563
Electromechanical/electromagnetics working group summary 05 p0604 N85-13852
Experimental research on electric propulsion. Note 7: Analysis of the performance of an arc-jet driven by means of hydrogen and nitrogen
[NASA-TM-77473] 06 p0760 N85-14861
Two-dimensional signal processing and storage and theory and applications of electromagnetic measurements. Supplemental appendix
[AD-A146848] 07 p0939 N85-15953
USSR report: Electronics and electrical engineering
[JPRS-UEE-84-017] 07 p0951 N85-16025
Electromagnetic inspection of wire ropes using sensor arrays
[AD-A148317] 08 p1170 N85-17379
Electromagnetic braking of a metallic projectile in flight
[AD-A149424] 10 p1480 N85-19345
Electromagnetic inspection of wire ropes using sensor arrays
[AD-A149016] 10 p1495 N85-19436
Linear magnetic bearings
[NASA-CASE-GSC-12582-2] 11 p1641 N85-20337
Magnetic location of Earth's core-mantle boundary and estimates of the adjacent fluid motion
13 p2131 N85-23260
Magnetic field interactions with material discontinuities
[AD-A150197] 13 p2154 N85-23373
Electro-science requirements for shuttle-attached antenna flight experiments 14 p2237 N85-23866
Basic research in electronics (JSEP)
[AD-A151002] 14 p2298 N85-24230
Small aperture analysis of the dual TEM (transverse electromagnetic) cell and an investigation of test object scattering in a single TEM cell
[PB85-159952] 14 p2306 N85-24277
Annual report on electronics research at the University of Texas at Austin
[AD-A150836] 14 p2415 N85-24901
Los Alamos Science, Number 11, Summer-Fall, 1984
[DE85-004634] 14 p2419 N85-24926
A literature review of EMATs, with stress calculations for simple EMAT geometries
[AERE-R-11415] 15 p2642 N85-26295
Joint services electronics program
[AD-A154348] 19 p3375 N85-30939
Electromagnetic inspection of wire ropes using sensor arrays
[AD-A155412] 22 p3795 N85-33509
Diagnostic of electromagnetic conditions in space using cosmic rays
[SH-4.5-19] 23 p4038 N85-35036
Moment-method formulation of the cavity-probe aperture antenna
[DE85-013264] 24 p4088 N85-35338

ELECTROMAGNETS
NT SUPERCONDUCTING MAGNETS
Magnetic spin reduction system for free spinning objects
[NASA-CASE-MFS-25966-1] 02 p0166 N85-11122
Design of electromagnetic bearing for vibration control of flexible transmission shaft 05 p0645 N85-14136
Code lock with microcircuit 13 p2071 N85-22935
The development of a transducer system for the accurate measurement of ultrasonic phase delay of SH plate waves
[AERE-R-11598] 15 p2550 N85-25790
Major facility overhauls at LAMPF
[DE85-012724] 24 p4156 N85-35765

ELECTROMECHANICAL DEVICES
Shock electromechanical energy converter with permanent magnet
[AD-D011228] 01 p0115 N85-10781
Electromechanical/electromagnetics working group summary 05 p0604 N85-13852
Systems study for an Integrated Digital-Electric Aircraft (IDEA)
[NASA-CR-3840] 07 p0902 N85-15714
Electromechanical switch
[AD-D011400] 07 p0948 N85-16009
Improvement of electromechanical systems by utilization of microelectronic technology 07 p0955 N85-16053
Design and test of a four channel motor for electromechanical flight control actuation
[NASA-CR-171838] 08 p1156 N85-17294
The development of a microprocessor-controlled linearly-actuated valve assembly
[NASA-CR-174437] 10 p1491 N85-19415
Design and fabrication of a unique electromechanical machine for long-term fatigue testing
[DE85-006524] 15 p2580 N85-25912
Optimum dimensions of power solenoids for magnetic suspension
[NASA-TM-77864] 17 p3026 N85-28716
Electro-expulsive separation system
[NASA-CASE-ARC-11613-1] 18 p3094 N85-29150
Reliability derating procedures
[AD-A153744] 18 p3119 N85-29309
Experiments on the influence of active walls on the initial amplitudes and growths of instability waves
[AD-A154630] 21 p3583 N85-32275

ELECTROMECHANICS
Modular electromechanical industrial robots
03 p0345 N85-12223
Characterization of CNRS Fizeau wedge laser tuner
[NASA-CR-174357] 09 p1325 N85-18328
Activities of Istituto Elettrotecnico Nazionale Galileo Ferraris 18 p3199 N85-29845
Supersonic flow with feeding of energy
[NASA-TM-77912] 24 p4061 N85-35163

ELECTROMETERS
An improved rocket-borne electric field meter for the middle atmosphere
[NASA-CR-175510] 12 p1888 N85-21851
Dielectric measurements in infralow-frequency band
13 p2087 N85-23034

ELECTROMOTIVE FORCES
NT PONDEROMOTIVE FORCES
Measurement of oxide ion concentration in NaCl-ZnCl2 molten salt and several applications
[BLL-AWRE-TRANS-74-(9091.9F)]
06 p0764 N85-14886
Studies on copper alloys containing chromium on the copper side phase diagram
[NASA-TM-77752] 07 p0927 N85-15876
Cells for measuring thermoelectromotive force and electrical resistance of metals in temperature range of 20-950 degrees Celsius
[BLL-M-36240-(5826.4)] 20 p3457 N85-31473

ELECTROMYOGRAMS
U ELECTROMYOGRAPHY

ELECTROMYOGRAPHS
U ELECTROMYOGRAPHY

ELECTROMYOGRAPHY
Electromyographic patterns associated with discrete limb movements 06 p0710 N85-14551

ELECTRON ACCELERATION
Electron acceleration by laser fields in a gas
[DE85-000575] 11 p1639 N85-208
Electron acceleration
[DE85-002337] 11 p1725 N85-2085
Average and worst-case specifications of precipitating auroral electron environment 13 p1991 N85-2248
Polar plasmas as observed by Dynamics Explorer 1 and 2 13 p1991 N85-2248
Two-dimensional beat wave acceleration simulation
[DE85-005961] 16 p2791 N85-27214
The temporal evolution of a small auroral substorm as viewed from high altitudes with Dynamics Explorer 1
[NASA-CR-176064] 20 p3493 N85-31718
Possibility of potential generation by lower hybrid wave 23 p3977 N85-34654

ELECTRON ACCELERATORS
NT BETATRONS
Accelerator development in support of the NRL (Naval research laboratory) beam dynamic program
[AD-A145976] 03 p0417 N85-128
Self potentials of an electron ring in a torus for large ring displacement from the minor axis
[AD-A146086] 03 p0421 N85-128
Survey of initial experiments on ATA beam dynamics
[DE85-004410] 10 p1555 N85-198
China report: Science and technology
[JPRS-CST-84-025] 11 p1620 N85-20197
A 10/sup 11/W high current pulse electron beam accelerator described 11 p1620 N85-20200
Adaptation of an air-dielectric RF cable for use as an oil-filled high voltage pulse transmission line
[DE84-017414] 11 p1630 N85-20285
Calculations pertaining to the design of a prebuncher for a 150-MeV electron linear accelerator 3. Comparisons with experimental data
[DE85-002866] 11 p1724 N85-20844
High-field dipoles for future accelerators
[DE85-002315] 13 p2157 N85-23391
Transverse electron resonance accelerator
[DE85-006289] 17 p3032 N85-28758
Rapid Electron Beam Accelerators (REBA-TRONS)
[AD-A153835] 18 p3170 N85-29707
Plasma wake field accelerator
[DE85-010538] 18 p3191 N85-29791
High-brightness photoemitter development for electron accelerator injectors
[DE85-009548] 19 p3355 N85-30796
Beam dynamics in MABE
[DE85-010670] 19 p3358 N85-30816
Requirements for very high energy accelerators
[DE85-011173] 20 p3529 N85-31952
Space Experiments with Particle Accelerators (SEPAC) 23 p3901 N85-34165
Vehicle Charging And Potential (VCAP)
23 p3902 N85-34173
Four stage HELIA experiment
[DE85-012026] 24 p4156 N85-3576
Power flow evaluations for HERMES 3
[DE85-013116] 24 p4156 N85-3576

ELECTRON ATTACHMENT
Electron production, electron attachment, and charge recombination process in high pressure gas discharges
[AD-A149535] 10 p1564 N85-1979
Density of impurity states associated to inversion layers
[INPE-3406-PRE/675] 16 p2869 N85-27702

ELECTRON AVALANCHE
LPM effect and primary energy estimations
[HE-3.6-4] 24 p4185 N85-359

ELECTRON BEAM WELDING
Structure and ductility of fracture of joints produced by electron-beam welding of VT6ch titanium alloy parts
03 p0351 N85-1228
Welding of PM-superalloys
[MTU-TB-910/84] 07 p0975 N85-16191
Application of diffusion welding of nickel based metals and application of electron beam welding of hot isostatically pressed nickel based powdered metals
08 p1169 N85-1737
Fatigue resistance of welded joints of high strength steels produced by electron beam welding
10 p1449 N85-1912
Calculation of mode field in electron beam welding o VT6 titanium alloy 10 p1449 N85-1912
Assessment of effectiveness of electron beam weldin of titanium alloys up to 40 mm in thickness by vertical horizontal beam 11 p1603 N85-2007
Mathematical simulation of thermal prroceses involve in electron-beam treatment 12 p1843 N85-215
Structure and mechanical characteristics heterogeneous joints produced by laser welding
13 p2034 N85-227
Softening of metal near seam during welding heat-resistant nickel alloys 13 p2035 N85-227

Paton comments on results of space welding tests
15 p2484 N85-25330
Brittle fracture resistance of electron beam-welded joints in titanium Alpha alloys 15 p2500 N85-25419
Increasing seam formation stability in electron beam welding of very thick titanium alloys
15 p2500 N85-25420
Some aspects of nuclear plant fabrication in Japan and the UK relating to automatic and robotic arc welding
15 p2566 N85-25834
Institute's contribution to Soviet welding technology noted 16 p2767 N85-27072
Paton Institute expert on GDR-USSR welding research
16 p2768 N85-27078
Underwater pipeline: Welding by high frequency induction
[BLL-WI-TRANS-882-(9312.57)]
16 p2792 N85-27221
Welding methods for high melting metals
22 p3794 N85-33508
Laser welding of 6Al-4V titanium alloy
[DE85-012019] 23 p3938 N85-34413

ELECTRON BEAMS
NT RELATIVISTIC ELECTRON BEAMS
Transverse field interaction multibeam amplifier
[AD-D011241] 01 p0043 N85-10282
Time variability of directionality properties of pulsed EB-EDL (Electron Beam-Electric Discharge Laser) N2-CO2 lasers
[AD-A145546] 02 p0202 N85-11344
The propagation and growth of whistler mode waves generated by electron beams in Earth's bow shock
[AD-A145572] 02 p0228 N85-11492
Theory of free-electron lasers with focusing pumping field 02 p0262 N85-11714
Strong Langmuir turbulence 02 p0284 N85-11851
Fast and precise processing of material by means of an intensive electron beam
[BMFT-FB-T-84-123] 03 p0342 N85-12201
Generation of superpowerful microsecond electromagnetic radiation pulses
03 p0347 N85-12234
Accelerator development in support of the NRL (Naval research laboratory) beam dynamic program
[AD-A145976] 03 p0417 N85-12669
ATA gas propagation: 1 foot tank experiment
[DE84-016395] 04 p0561 N85-13575
Ion beam and laser induced surface modifications
[DE84-016569] 04 p0571 N85-13642
Laboratory electron beam simulation of cosmic radio jets
[DE84-016179] 04 p0590 N85-13764
Practical application of electron beam testing in LSI and VLSI circuits
[BMFT-FB-T-84-185] 05 p0633 N85-14061
Status of beam transport with the ETA and ATA accelerators
[DE84-013205] 05 p0726 N85-14670
Minimizing the energy spread within a single bunch by shaping its charge distribution
[DE84-016172] 05 p0727 N85-14676
Transient attenuation in optical fibers
[DE84-016487] 05 p0729 N85-14687
Pulsed electric discharge laser technology. Electron beam window foil material
[AD-A146420] 06 p0813 N85-15162
Processes of smooth increase and dropoff in intensity of glow line lambda' = 5577 A with exposure of ionosphere to electron beam 06 p0822 N85-15219
Mechanism of damping of plasma oscillations in initial stage of injection of electron beams from spacecraft into ionosphere in active experiments
06 p0823 N85-15225
Electron beam propagation along charged foils
[DE85-002137] 06 p0861 N85-15472
ATA probe beam experiment
[DE84-016017] 06 p0862 N85-15477
FORTRAN version of the quantitative energy-dispersive electron beam X-ray analysis program FRAME C
[PB84-240936] 07 p1027 N85-16519
A low perturbation electron injector for cyclic accelerators
[AD-D011312] 07 p1040 N85-16604
Electrostatic wave observation during a space simulation Beam-Plasma-Discharge (BPD)
[NASA-CR-174286] 07 p1045 N85-16639
A coaxial probe for measuring the current density profile of intense electron beams
[AD-D011407] 08 p1164 N85-17347
Exposure modelling of particle beam lithography
[AD-A147849] 08 p1219 N85-17678
Beam propagation study: Stabilization of the resistive hose instability in intense electron beams
[AD-A146071] 08 p1220 N85-17684
Non-linear transverse electron beam dynamics in a modified betatron accelerator
[AD-A148106] 08 p1220 N85-17685
Virtual cathode oscillator study
[AD-A149268] 10 p1480 N85-19342
Two-stage free electron laser research
[AD-A148951] 10 p1489 N85-19402
A free electron laser with a rotating quadrupole wiggler
[AD-A149052] 10 p1489 N85-19404
Facilities for studing radiation damage in nonmetals during irradiation
[DE85-000590] 10 p1554 N85-19801
Experimental investigation of certain beam transport issues in a pulsed transmission line linear accelerator
[DE85-002310] 10 p1555 N85-19805
Brightness limitations in multi-kiloampere electron beam sources
[DE84-017417] 10 p1555 N85-19807
China report: Science and technology
[JPRS-CST-84-025] 11 p1620 N85-20197
A 10/sup 11/W high current pulse electron beam accelerator described 11 p1620 N85-20200
Electron acceleration by laser fields in a gas
[DE85-000575] 11 p1639 N85-20323
Optical guiding in a free electron laser
[DE85-003141] 11 p1639 N85-20327
High power pulsed accelerators with potential industrial applications
[DE85-001710] 11 p1720 N85-20821
Self-Optimized Sector (SOS) model of self-consistent energy loss and scattering for an electron beam propagating in air
[DE85-003161] 11 p1722 N85-20831
Experiments on ETA comparing wire-conditioned and non-wire-conditioned beam propagation
[DE85-004451] 11 p1725 N85-20848
Electron acceleration
[DE85-002337] 11 p1725 N85-20850
Si-on-insulator formation using a line-source electron beam
[DE85-003449] 11 p1737 N85-20925
S3-3 ONR-118 data analysis
[AD-A149725] 12 p1889 N85-21855
Electron beam charging of Space Shuttle thermal protection system tiles 13 p1990 N85-22478
Sheath ionization model of beam emissions from large spacecraft 13 p1992 N85-22489
Electron yields from spacecraft materials
13 p1996 N85-22512
A simple model of electron beam initiated dielectric breakdown 13 p1996 N85-22516
SEM (Scanning Electron Microscope) investigation of silicon diodes using the electron beam induced current method
[AD-A150356] 13 p2064 N85-22894
Design considerations for a 100 kW CW, 140 GHz gyrotron oscillator
[DE85-005282] 13 p2066 N85-22904
Investigation of generation of oscillations using anomalous Doppler effect 13 p2078 N85-22980
Temperature dependence of propagation of high-current electron beam through drift space
13 p2079 N85-22982
Effect of space-charge field on output characteristics of O-type oscillators with distributed interaction
13 p2089 N85-23043
Los Alamos free electron laser: Accelerator performance
[DE85-005722] 13 p2097 N85-23084
Electric potential of satellite in electron emitting experiments in initial stage of electron beam injection in steady-state mode 15 p2480 N85-25309
High current beam hollowing instability study
[AD-A151301] 15 p2648 N85-26329
Two-beam accelerator
[DE85-004662] 15 p2649 N85-26335
Annual Review, April 1983 - March 1984
[ISSN-0547-1567] 15 p2654 N85-26369
High energy beam experiment
15 p2654 N85-26376
Basic studies. 1: Basic experiments in plasma physics 15 p2655 N85-26378
Experimental studies of the electronic structure of 1-2 and 1-3 intermetallic compounds
[DE85-006978] 15 p2662 N85-26432
Measurements in low pressure flow using an electronic beam detector — wind tunnel tests
16 p2701 N85-26676
Investigation of electron attachment and dissociation rates in C2F6/CH4 electric gas discharges
[AD-A151796] 16 p2862 N85-27649
High efficiency transverse dc electron beams
[AD-A152036] 16 p2862 N85-27651
Energy deposition from particle beams
[DE85-007382] 16 p2862 N85-27654
Survey of experimental and theoretical electron-impact ionization cross sections for transition metal ions in low stages of ionization
[DE85-007605] 16 p2863 N85-27658
In situ HVEM studies of electron beam-driven composition changes in thin film alloys: Displacement-rate gradient effects
[DE85-007992] 17 p2931 N85-28092
Uniaxial angular accelerometers
17 p2944 N85-28173
VULTURE manual
[DE85-008873] 17 p3013 N85-28631
Wake fields and wake field acceleration
[DE85-008054] 17 p3031 N85-28750
Measurement and interpretation of electron angle at MABE beam stop
[DE85-008583] 17 p3032 N85-28755
Transverse electron resonance accelerator
[DE85-008289] 17 p3032 N85-28758
Restrike particle beam experiments on a dense plasma focus. Opening switch research on a dense plasma focus
[AD-A152991] 17 p3039 N85-28802
Beam tests of phosphorescent screens
[DE85-009843] 18 p3097 N85-29170
Operation of a quasioptical electron cyclotron maser
[DE85-008450] 18 p3113 N85-29276
The free electron laser variable bridge coupler
[DE85-009830] 18 p3114 N85-29278
Further studies of the NRL collective particle accelerator via numerical modeling with the MAGIC code
[AD-A153583] 18 p3178 N85-29703
Experimental and theoretical investigation of microwave and millimeter wave radiation from hollow, rotating electron beams
[AD-A153827] 18 p3179 N85-29706
Rapid Electron Beam Accelerators (REBA-TRONS)
[AD-A153835] 18 p3179 N85-29707
Phase and amplitude considerations for the 2-beam accelerator
[DE85-008455] 18 p3180 N85-29715
Accelerator technology working group summary
[DE85-009547] 18 p3180 N85-29717
Calculations of beam dynamics in Sandia linear electron accelerators, 1984
[DE85-010417] 18 p3180 N85-29719
Electron multiple, plural and single scattering
[DE85-010325] 18 p3181 N85-29721
Energy deposition and its effects on the E+ capture section at Sector 20
[DE85-010964] 18 p3182 N85-29727
Experience with a high-brightness storage ring: The NSLS 750 MeV VUV ring
[DE85-010547] 18 p3190 N85-29787
Plasma wake field accelerator
[DE85-010536] 18 p3191 N85-29791
A collective interaction klystron specification
[AD-D011704] 19 p3255 N85-30186
Superconducting electronic film structures
[AD-A154196] 19 p3259 N85-30207
Conversion efficiencies of charged particle beam driven free electron lasers
[AD-A154404] 19 p3276 N85-30316
High-brightness photoemitter development for electron accelerator injectors
[DE85-009548] 19 p3355 N85-30796
Interaction of slow electrons with high-pressure gases (quasi-liquids): Synthesis of our knowledge on slow electron-molecule interactions
[DE85-010061] 19 p3355 N85-30800
Beam dynamics in MABE
[DE85-010670] 19 p3358 N85-30819
Quantum effects in linear collider scaling laws
[DE85-009846] 19 p3363 N85-30851
EBIC characterization and hydrogen passivation in silicon sheet 20 p3481 N85-31634
Methods of Monte Carlo electron transport in particle-in-cell codes
[DE85-010702] 20 p3521 N85-31898
Practicality of electronic beam steering for MST/ST radars, part 6.2A 21 p3624 N85-32516
Trapping of ion conics by downward parallel electric fields
[AD-A155306] 21 p3633 N85-32568
Operation of solid state lasers exposed to electron beam 21 p3685 N85-32895
Amplification of electromagnetic wave by electron stream with negative velocity differences
21 p3692 N85-32941
Electron beam enhanced surface modification for making highly resolved structures
[DE85-011609] 22 p3760 N85-33305
Electron trajectories in a combined wiggler and alternating gradient quadrupole field
[DE85-010727] 22 p3842 N85-33794

Theoretical and Experimental Beam Plasma Physics (TEBPP) 23 p3901 N85-34166

RADLAC technolgy review
[DE85-011995] 23 p3962 N85-34691

Measurement and interpretation of electron angle at MABE beam stop
[DE85-011918] 23 p3983 N85-34698

Technology of magnetically driven accelerators
[DE85-011657] 23 p3983 N85-34700

Note on the detection of high energy primary cosmic gamma rays by air shower observation
[OG-9.5-9] 23 p4031 N85-34986

Observations of accelerated high current low emittance beams in the SLC Linac
[DE85-013073] 24 p4068 N85-35211

Four stage HELIA experiment
[DE85-012026] 24 p4156 N85-35768

Power flow evaluations for HERMES 3
[DE85-013116] 24 p4156 N85-35769

Kinetic loss experiments on Mite
[DE85-012826] 24 p4158 N85-35780

Laser and electron beam processing of semiconductors
[AD-A155914] 24 p4161 N85-35796

ELECTRON BOMBARDMENT

Development of the Engineering Test Satellite-3 (ETS-3) ion engine system
[NASA-TM-77538] 01 p0017 N85-10101

Radiation-induced compositional redistribution and local phase transformation in irradiated alloys
[DE85-000080] 10 p1441 N85-19082

Aluminum work function: Effect of oxidation, mechanical scraping and ion bombardment
[NASA-TM-87079] 23 p3915 N85-34265

ELECTRON BUNCHING

Minimizing the energy spread within a single bunch by shaping its charge distribution
[DE84-016172] 05 p0727 N85-14676

Optimization of energy conversion during locking of electron bunches by electromagnetic wave in longitudinal electrostatic field 06 p0786 N85-15025

Calculated parameters for the initial part of an accelerator with high-frequency quadrupole focusing
[RAE-TRANS-2122] 07 p1040 N85-16600

Los Alamos free electron laser: Accelerator performance
[DE85-005722] 13 p2097 N85-23084

Form factor effects on microwave Cerenkov radiation
[AD-A154577] 21 p3701 N85-32993

Cerenkov radiation from periodic electron bunches for finite emission length in air
[AD-A156156] 24 p4090 N85-35352

ELECTRON CAPTURE

Precipitation of protons with E sub p approximately 1 MeV near plasmopause 02 p0161 N85-11093

Theoretical analysis of physical processes of lasing medium degradation in semiconductor lasers
02 p0269 N85-11759

Electron capture by multiply charged ions from hydrogen atoms at low energies
[DE84-016560] 06 p0861 N85-15475

Theoretical studies of Rydberg atom collisions
[AD-A148558] 08 p1220 N85-17687

One-electron capture processes by highly charged ions from helium: Present status of HICE-IPP
09 p1389 N85-18736

Negative lithium emission from a tungsten surface in a plasma
[DE85-003456] 12 p1936 N85-22167

Electron flux with electron energies above 40 MeV at altitudes of about 500 km in region where capture is possible and outside it when L is 3 or greater
15 p2481 N85-25315

Convoy electron production by heavy ions in solids
[DE85-005256] 15 p2660 N85-26418

Excited state populations and charge-exchange of fast ions in solids
[DE85-009362] 18 p3180 N85-29714

Electron capture to the continuum from atomic hydrogen
[DE85-005269] 18 p3181 N85-29722

Atmospheric chlorofluromethanes as tracers of ocean circulation and mixing: Measurement and calibration techniques and studies in the Greenland and Norwegian Seas 19 p3319 N85-30573

A theoretical study of electron capture in ion-ion and ion-atom collisions
[DE85-011154] 19 p3362 N85-30842

Study of photon emission by electron capture during solar nuclei acceleration, 1: Temperature-dependent cross section for charge changing processes
[SH-1.1-8] 23 p3990 N85-34735

Study of photon emission by electron capture during solar nuclei acceleration. 2: Delimitation of conditions for charge transfert establishment
[SH-1.1-9] 23 p3990 N85-34736

Study of photon emission by electron capture during solar nuclei acceleration. 3: Photon production evaluations
[SH-1.1-10] 23 p3990 N85-34737

Electron capture decay of cosmic rays: A model of the inhomogeneous interstellar medium
[OG-7.1-10] 23 p4014 N85-34871

Search for stellar collapse with the MACRO detector at Gran Sasso
[HE-5.3-11] 24 p4206 N85-36105

ELECTRON CLOUDS

Excess gamma-rays in the direction of the rho Ophiuchi cloud: An exotic object?
[OG-2.5-1] 22 p3868 N85-33956

ELECTRON COLLISIONS

U ELECTRON SCATTERING

ELECTRON COMPOUNDS

U INTERMETALLICS

ELECTRON CYCLOTRON HEATING

Theoretical studies in tandem mirror physics
[DE84-015634] 04 p0566 N85-13604

Fusion plasma theory. Task 3: ECRH and transport modeling in tandem mirrors and divertor physics
[DE84-014939] 04 p0567 N85-13612

EBT electron energy confinement experiments
[DE84-015402] 04 p0567 N85-13613

High frequency plasma generator for ion thrusters
[NASA-CR-174772] 08 p1114 N85-17023

ORNL ECR multicharged ion source
[DE85-001283] 09 p1380 N85-18681

Present status of Heliotron E experiment
09 p1387 N85-18721

Discharge initiation experiments in the Tokapole II Tokamak
[DE84-017345] 09 p1391 N85-18755

Electron cyclotron resonance heating system for the stellarator W 7-AS
[IPF-84-5] 09 p1395 N85-18779

High power millimeter-wave mode converters in overmoded circular waveguides using periodic wall perturbations
[IPF-84-6] 09 p1395 N85-18780

Wave absorption and transport studies on Electron Cyclotron Resonance (ECR) heated stellarator plasmas in W 7-A
[IPF-84-9] 09 p1395 N85-18782

Activities report of the Institute of Plasma Research
11 p1733 N85-20903

The 60 GHz gyrotron development program
[DE85-000599] 12 p1836 N85-21522

A 60 GHz 200 kW CW gyrotron with high output mode purity
[DE85-005283] 13 p2066 N85-22905

Investigation of generation of oscillations using anomalous Doppler effect 13 p2078 N85-22980

System for lower hybrid current startup
15 p2654 N85-26373

Basic experiments in plasma physics (TPL)
15 p2655 N85-26379

140 GHz gyrotron development program
[DE85-010348] 20 p3537 N85-32013

Influence of ECR-heating on MHD activity of plasma in tokamak-10 installation 21 p3694 N85-32949

Electron and ion cyclotron heating calculations in the tandem-mirror
[DE85-011858] 22 p3842 N85-33797

High-field launch electron cyclotron heating experiments in the ELMO Bumpy Torus
[DE85-012068] 22 p3846 N85-33825

Role of ECRH in potential formation for tandem mirrors
[DE85-011859] 22 p3848 N85-33834

Plug and thermal barrier potential formation in Gamma 10 23 p3976 N85-34648

Effect of ECH and ICH on ambipolar potential in NBT-1M 23 p3978 N85-34661

Transports studies of ECH and ICRH-heated bumpy torus plasma in NBT-1M 23 p3978 N85-34662

Multiple-frequency electron cyclotron heating of hot electron rings in EBT-1
[DE85-011302] 23 p3983 N85-34701

ECH tokamak
[DE85-012074] 23 p3984 N85-34707

ELECTRON DENSITY (CONCENTRATION)

NT CARRIER DENSITY (SOLID STATE)
NT ELECTRON DENSITY PROFILES
NT IONOSPHERIC ELECTRON DENSITY
NT MAGNETOSPHERIC ELECTRON DENSITY

Visible wavelength interferometer for high speed electron density diagnostics
[AD-A145686] 02 p0277 N85-11803

Gas pressure and electron density at the level of the active zone of hollow cathode arc discharges
[NASA-TM-77477] 03 p0414 N85-12648

Behavior of the ionospheric F region in low latitudes and in the equatorial region of Brazil during strong magnetic storms in the 1978 to 1983 period
[INPE-3231-PRE/581] 05 p0675 N85-14333

Nocturnal increases of ionization in the ionospheric F region in the low latitude of Brazil during magnetic storms
[INPE-3271-PRE/596] 05 p0675 N85-14334

The parallax of pulsar 0950+08 and the local free electron density 06 p0879 N85-15584

Gas pressure and electron density in the active zone level of hollow cathode arc discharges
[NASA-TM-77468] 07 p0945 N85-15869

Electronic structure, chemical bonding, and superconductivity of silver films on germanium
[AD-A147720] 08 p1128 N85-17112

Photoionization structure of the Orion Nebula
08 p1246 N85-17869

Imploding plasma X-ray laser research
[DE85-000057] 09 p1326 N85-18331

Basic studies of atomic dynamics
[DE84-015661] 09 p1380 N85-18675

Calorimetric investigation into the possibility of a charge density wave ground state in alkali metals
[DE85-002006] 09 p1397 N85-18795

Hartree-Fock interaction between a helium atom and lithium-metal: A test for the effective medium theory
[AD-A150468] 13 p2156 N85-23387

Structural inhomogeneities in amorphous nickel-phosphorus alloy
[BLL-M-36103-(5828.4)] 16 p2748 N85-26960

EISCAT electron density studies
[AD-A152820] 17 p2993 N85-28489

Electron and ion distributions at high latitudes as measured by the Air Force polar orbiting satellites
[AD-A153242] 17 p2993 N85-28500

Memory function for cyclotron resonance of two-dimensional electron systems
[AD-A152632] 17 p3029 N85-28731

Quantized Hall effect in two-dimensional electron systems
[AD-A154347] 19 p3259 N85-30211

Shifts and widths of hydrogenic ion lines
[DE85-011375] 19 p3277 N85-30323

Hard X-ray measurements of the hot electron rings in Nagoya BUMPY TORUS (NBT-1M)
[IPPJ-720] 19 p3370 N85-30899

Effect of inner subshell ionization on emission lines OIV ions
[IPPJ-719] 19 p3370 N85-30903

Characteristics and sources of E-region ionization in the continuous aurora
[AD-A155018] 21 p3632 N85-32582

Soft X-ray polychromator for the Solar Maximum Mission
[NASA-CR-175297] 21 p3723 N85-33096

Lithology and stratigraphy of drill holes completed during 1984 in LANL use areas of Yucca Flat, Nevada Test Site, volume 6
[DE85-010695] 22 p3815 N85-33631

Digital characterization of particle tracks for microdosimetry
[DE85-012898] 22 p3846 N85-33822

Role of ECRH in potential formation for tandem mirrors
[DE85-011859] 22 p3848 N85-33834

Simultaneous Solar Maximum Mission and Very Large Array (VLA) observations of solar active regions
[NASA-CR-176090] 22 p3859 N85-33887

Electron density distribution analysis for nitroguanidine
[DE85-009598] 23 p3969 N85-34603

Helios 1 energetic particle observations of the solar gamma ray flare events of 7, 21 June 1980 and 3 June 1982
[SH-1.3-8] 23 p3993 N85-34755

Akeno 20 km (2) air shower array (Akeno Branch)
[OG-9.4-8] 23 p4029 N85-34975

Cerenkov radiation from periodic electron bunches for finite emission length in air
[AD-A156156] 24 p4090 N85-35352

Los Alamos free-electron laser
[DE85-012686] 24 p4098 N85-35405

Structured events in Pamir carbon X-ray chambers
[HE-3.7-7] 24 p4186 N85-35965

Performance of a local electron density trigger to select extensive air showers at sea level
[HE-4.6-11] 24 p4198 N85-36048

ELECTRON DENSITY PROFILES

Irregularity decay in an isolated plasma bubble
[AD-A145782] 03 p0392 N85-12506

CO2 laser interferometer array for Big Dee
[DE85-001718] 10 p1490 N85-19411

Winter anomaly of the lower ionosphere and its possible causes 11 p1660 N85-20459

Light diffraction with collective, thermal electron density fluctuation in plasmas with several ionic components
[IPF-84-5] 11 p1733 N85-20904

Rocket observations of the ionosphere during the eclipse of 26 February 1979
[NASA-CR-175613] 12 p1888 N85-21850

Calculation of ionospheric profiles by inverting VLF/LF reflection data. 2. Anisotropic propagation
[AD-A150105] 12 p1890 N85-21859

Contribution of relaxation sounding experiments to the understanding of magnetospheric processes
14 p2371 N85-24655

Determination of ionospheric electron density profiles from satellite UV (ultraviolet) emission measurements
[AD-A150734] 14 p2373 N85-24667

Heavy ion beam study of potential formation in bumpy torus plasma
[IPPJ-711] 15 p2656 N85-26386

Electrons and cosmic ray produced protons in Saturn's inner magnetosphere
[NASA-TM-87469] 15 p2679 N85-26546

Electrons and grain boundary energies in metals
[DE85-009530] 17 p2932 N85-28099

Rocket measurements of mesospheric ionization irregularities
[NASA-CR-176056] 20 p3494 N85-31721

Interstellar turbulence, random density variations, and scintillation measurements
[OG-7.2-13] 23 p4015 N85-34880

Relation between gamma-ray family and EAS core: Monte-Carlo simulation of EAS core
[HE-3.6-7] 24 p4185 N85-35955

Hadrons registration in emulsion chamber with carbon block
[HE-3.7-3] 24 p4186 N85-35962

ELECTRON DIFFRACTION

Electron spin polarization effects in low energy electron diffraction, ion neutralization and metastable atom deexcitation at solid surfaces
[DE84-016550] 04 p0572 N85-13649

Structure determination of molecular adsorbates with dynamical LEED and HREELS
[DE85-002007] 06 p0861 N85-15473

Characterization of CO binding sites on Rh(111) and Rh(331) surfaces by XPS and LEED (Low Energy Electron Diffraction): Comparison to EELS (Electron Energy Loss Spectroscopy) results
[AD-A149331] 10 p1435 N85-19044

Conduction in polymerized polyfunctional diacetylenes
[AD-A149104] 10 p1451 N85-19145

Fundamental study of catalysts using laser Raman, infrared, auger electron spectroscopy and low energy electron diffraction
[DE85-001813] 11 p1595 N85-20033

Electron-diffraction structural examination of amorphous iron-tin alloys 11 p1604 N85-20084

AEM with a convergent beam
[DE85-000667] 11 p1714 N85-20784

HREELS and Auger studies of conducting polymers
[DE85-004541] 13 p2038 N85-22764

Structural characterization by intensity measurements of electron diffraction patterns
[DE85-004803] 13 p2164 N85-23427

Test of the electronic structure of Fe(100) by absorbed current spectroscopy
[DE85-004942] 15 p2661 N85-26422

Low-energy electron diffraction experiment and theory
[DE85-009967] 18 p3195 N85-29820

Determination of kinetic parameters of molecular beam epitaxy
[AD-A155222] 21 p3710 N85-33030

Size and shape dependence of CO adsorption sites on sapphire supported Fe microcrystals
[NASA-CR-176171] 24 p4160 N85-35794

ELECTRON DIFFUSION

Two-level model for formation of night ionosphere of Venus from radio occulation experiments
02 p0162 N85-11100

Estimation of the rate of electron transfers between 2 contacting polymer surfaces
[AD-A148416] 08 p1122 N85-17072

Energetic electron anisotropy and ELF waves onboard GEOS. How does quasi-linear diffusion work
14 p2366 N85-24623

Time-implicit Monte-Carlo collision algorithm for particle-in-cell electron transport models
[DE85-010756] 20 p3521 N85-31900

Onion-shell model for cosmic ray electrons and radio synchrotron emission in supernova remnants
[OG-8.1-10] 23 p4018 N85-34900

ELECTRON DISTRIBUTION

NT ELECTRON DENSITY PROFILES

Electrons in a disordered medium
[NOTA-INTERNA-818] 02 p0279 N85-11819

Extended X-ray absorption fine structure (Exafs) studies of the actinides
[DE84-015833] 04 p0559 N85-13561

Electron distribution function and mobility in 3-5 compounds for high and low fields
[AD-A147447] 07 p1048 N85-16658

Data analysis of electron measurements of the plasma experiment aboard the HELIOS probes
[MPE-185] 09 p1416 N85-18935

Potential at atomic boundaries in the TF (or TFD) model and equations of states 12 p1820 N85-21419

Kapton charging characteristics: Effects of material thickness and electron-energy distribution
13 p1996 N85-22513

Observations of energetic electron and ion distributions near the magnetopause at geosynchronous orbit and related ground effects 14 p2356 N85-24560

Electron and ion distributions at high latitudes as measured by the Air Force polar orbiting satellites
[AD-A153242] 17 p2993 N85-28500

The universal spectrum of AGNs and QSOs
[OG-2.7-9] 22 p3872 N85-33962

EAS fluctuation approach to primary mass composition investigation
[OG-5.2-5] 22 p3883 N85-34062

Electron density distribution analysis for nitroguanidine
[DE85-009598] 23 p3969 N85-34603

The lateral distributions of charged particles of energy greater than 0.3 E sub crit in electron-photon cascades in lead and air
[HE-3.6-10] 24 p4185 N85-35957

Structured events in Pamir carbon X-ray chambers
[HE-3.7-7] 24 p4186 N85-35965

A new study of shower age distribution in near vertical showers by EAS air shower array
24 p4190 N85-35986

Lateral distribution of electrons of air showers
24 p4191 N85-35998

Detailed studies of the electron lateral distribution in extensive air showers with energies around 10(16) eV
24 p4191 N85-35999

Study of muons near shower cores at sea level using the E594 neutrino detector 24 p4191 N85-36000

Measurement of shower electrons and muons using a small air shower array
[HE-4.3-11] 24 p4192 N85-36005

Monte Carlo simulation of EAS generated by 10(14) - 10(16) eV protons
[HE-4.3-14] 24 p4192 N85-36008

Properties of 10 (18)-10 (19)eV EAS at far core distance
[HE-4.7-3] 24 p4198 N85-36054

ELECTRON EMISSION

NT FIELD EMISSION
NT PHOTOELECTRIC EMISSION
NT SECONDARY EMISSION

Polarized electron cyclotron emission in the Tokapole 2 Tokamak
[DE84-014953] 01 p0122 N85-10836

Plasma variables and tribological properties of coatings in low pressure (0.1 - 10.0 torr) plasma systems
[NASA-TM-83798] 02 p0189 N85-11261

Forward electron production in heavy ion-atom and ion-solid collisions
[DE85-001256] 09 p1381 N85-18683

Improved electron emission by use of a cloth fiber cathode
[AD-A149250] 10 p1480 N85-19340

Textured carbon surfaces on copper
[NASA-CASE-LEW-14130-1] 11 p1615 N85-20156

Coincidence techniques to study electron emission in ion-atom collisions
[DE85-003635] 11 p1724 N85-20846

Recent advances in forward electron production studies in ion-atom and ion-solid collisions
[DE85-001255] 11 p1726 N85-20853

The influence of the local solar wind structures on the propagation of low energy particles
12 p1959 N85-22314

Electron yields from spacecraft materials
13 p1996 N85-22512

Non-self-maintained high-voltage low-pressure discharge 13 p2088 N85-23037

Mean delta-ray energies in ion molecule collisions
[DE85-005524] 13 p2157 N85-23395

Impact ionization from gold, aluminum and PCB-Z — Giotto spacecraft paint PCB-Z 14 p2244 N85-23910

A model of plasma cloud expansion generated by a dust particle impact — Giotto mission
14 p2245 N85-23914

Electrodes for flash discharge lamps
[DE85-008897] 17 p2955 N85-28250

Electrode for flash discharge lamps
[DE85-008896] 17 p2955 N85-28252

VULTURE manual
[DE85-008873] 17 p3013 N85-28631

Electron spin resonance study of interface states induced by electron injection in metal-oxide-semiconductor devices
[DE85-009502] 18 p3195 N85-29817

Resolvability of defect ensembles with positron annihilation studies
[DE85-010041] 18 p3196 N85-29823

Method for predicting the performance of cathode materials
[AD-D011665] 19 p3257 N85-30196

Quantitative passive technique for assay of near-surface tritium in materials
[DE85-010661] 19 p3360 N85-30833

Predamage threshold electron emission from insulator and semiconductor surfaces
[DE85-008968] 19 p3377 N85-30954

Hollow cathodes in high pressure arc discharges
[NASA-TM-87098] 23 p3903 N85-34179

Electron photoejection in carbanions
[DE85-011748] 23 p3912 N85-34237

Improved negative ion source
[DE85-006445] 23 p3912 N85-34241

Workshop report on Simulation Techniques for Shock Wave Phenomena and Characteristics of Plasmas in Inertial Confinement Fusion
[IPPJ-725] 23 p3979 N85-34670

ELECTRON ENERGY

NT ELECTRON STATES

Electron energy loss rates in N-2, O-2 and air
[AD-A145158] 01 p0072 N85-10476

Monte Carlo simulation of thermalization of subexcitation electrons in molecular hydrogen
[NAL-TR-815T] 01 p0117 N85-10798

Electronic-to-vibrational energy transfer studies of singlet molecular oxygen and hydrogen halides
[AD-A145587] 02 p0277 N85-11802

Boundary condition effects in the energy loss spectrum of layered systems
[NOTA-INTERNA-802] 02 p0289 N85-11887

Electron energy loss investigation of the electronic and structural properties of palladium
[NOTA-INTERNA-803] 02 p0289 N85-11888

Reflection electron energy loss investigation of the H-GaAs(110) surface
[NOTA-INTERNA-811] 02 p0289 N85-11889

Ion thruster performance model
[NASA-CR-174810] 04 p0462 N85-12935

EBT electron energy confinement experiments
[DE84-015402] 04 p0567 N85-13613

Departures from LTE populations versus anomalous abundances: The effects of heating
08 p1234 N85-17776

Monte Carlo simulation of electron thermalization in rare gases
[NAL-TR-834T] 09 p1375 N85-18643

Effect of inner subshell ionization for emission lines of OIV ion 09 p1388 N85-18729

Spectra of highly-ionized atoms for the diagnostics of the new generation of Tokamaks
09 p1388 N85-18730

Discharge initiation experiments in the Tokapole II Tokamak
[DE84-017345] 09 p1391 N85-18755

Some unique aspects of fouling on copper as compared to titanium or nickel
[AD-A150072] 12 p1806 N85-21332

Observations of bulk electron heating due to return current in a tokamak discharge started up by lower hybrid waves
[IPPJ-708] 12 p1937 N85-22172

Kapton charging characteristics: Effects of material thickness and electron-energy distribution
13 p1996 N85-22513

Research on thermionic plasmas
[AD-A150663] 14 p2423 N85-24944

High current beam hollowing instability study
[AD-A151301] 15 p2648 N85-26329

Time dependent and steady-state solutions of the electron energy distribution in a weakly ionized gas subject to an ac or dc electric field
[AD-A151829] 15 p2656 N85-26391

Time-resolving electron temperature diagnostic for ALCATOR C
[DE85-004916] 16 p2868 N85-27690

Digital filters for application to data analysis in electron energy loss spectroscopy
[DE85-007932] 17 p2923 N85-28020

The mean trajectory approximation for charge and energy transfer processes at surfaces
[AD-A152706] 17 p3043 N85-28830

Hard X-ray measurements of the hot electron rings in Nagoya BUMPY TORUS (NBT-1M)
[IPPJ-720] 19 p3370 N85-30899

Thermal ion heating in the vicinity of the plasmapause
[NASA-CR-176030] 20 p3535 N85-31993

best copy available

Metal-insulator-metal models of tunneling
20 p3536 N85-32006

CCD-based X-ray spectrometry for on-line determination of laser plasma electron temperature
21 p3692 N85-32938

Contributions to the 19th International Cosmic Ray Conference
[NASA-CR-176080] 21 p3714 N85-33044

The energy spectrum of Jovian electrons in interplanetary space
[SH-1.5-18] 21 p3715 N85-33051

Solar modulation and interplanetary gradients of the galactic electron flux, 1977 - 1984
[PAPER-SH-4.7-4] 21 p3716 N85-33059

Simultaneous Solar Maximum Mission and Very Large Array (VLA) observations of solar active regions
[NASA-CR-176090] 22 p3859 N85-33897

Improved negative ion source
[DE85-006445] 23 p3912 N85-34241

Electron impact ionization of multicharged ions at ORNL: 1980-1984
[DE85-013104] 23 p3972 N85-34622

Recent experiments in Gamma-10
23 p3976 N85-34651

Bounce resonance heating and radial transport of electrons 23 p3977 N85-34655

Transports studies of ECH and ICRH-heated bumpy torus plasma in NBT-1M 23 p3978 N85-34662

Stochastic particle acceleration in flaring stars
[OG-8.3-9] 23 p4022 N85-34927

High-resolution spectroscopy and dynamics of multiphoton processes in atoms and molecules
[AD-A155862] 24 p4147 N85-35714

Proposed FRX-D experiment
[DE85-012766] 24 p4158 N85-35778

ELECTRON FLUX
U ELECTRONS
U FLUX (RATE)

ELECTRON FLUX DENSITY

Ion thruster performance model
[NASA-CR-174810] 04 p0462 N85-12935

Average and worst-case specifications of precipitating auroral electron environment 13 p1991 N85-22482

Three-dimensional calculation of shuttle charging in polar orbit 13 p1992 N85-22486

Polar orbit electrostatic charging of objects in shuttle wake 13 p1992 N85-22487

Electron flux with electron energies above 40 MeV at altitudes of about 500 km in region where capture is possible and outside it when L is 3 or greater
15 p2481 N85-25315

Carbon foil secondary electron emission during ion passage through the 40 to 500 keV energy field
[MPE-190] 18 p3184 N85-29747

EAS fluctuation approach to primary mass composition investigation
[OG-5.2-5] 22 p3883 N85-34062

Spectral shape variation of interstellar electrons at high energies
[OG-8.2-7] 22 p3889 N85-34106

ELECTRON GAS

Stopping powers of solids for low-energy protons
[DE85-001123] 09 p1382 N85-18693

Angle averaged Compton cross sections for degenerate electron gases
[AD-A154464] 19 p3371 N85-30908

Fractional statistics and fractional quantized Hall effect
[DE85-007633] 19 p3375 N85-30940

Breakdown of helium nuclei in matter processed near black holes
[OG-8.2-20] 23 p4021 N85-34916

ELECTRON GUNS

Development of the Antares electron gun
[DE84-014043] 01 p0053 N85-10352

Gyrotron beam generation with helical magnetic fields
[AD-A145987] 03 p0417 N85-12670

High efficiency electron beam gun foil support
[AD-D011434] 08 p1159 N85-17312

The use of synthesis method in the design of gyrotron electron guns
[INPE-3305-PRE/616] 10 p1476 N85-19329

Brightness limitations in multi-kiloampere electron beam sources
[DE84-017417] 10 p1555 N85-19807

Proposal for hollow cathode electron gun for electron cooling
[DE85-002721] 11 p1630 N85-20263

Neutron streak camera electron gun design
[DE85-000620] 11 p1637 N85-20315

Enhancing the performance of a high-gain free electron laser operating at millimeter wavelengths
[DE85-000862] 12 p1857 N85-21646

High efficiency transverse dc electron beams
[AD-A152038] 16 p2862 N85-27651

Design and testing of a high power quasi-optical gyrotron
[AD-A153212] 17 p2968 N85-28330

Induction heating gun
[NASA-CASE-LAR-13181-1] 18 p3065 N85-29083

Generation of intense negative ion beams
[NASA-CASE-NPO-16061-1-CU]
18 p3178 N85-29701

Phase and amplitude feedback control system for the Los Alamos free-electron laser
[DE85-010787] 19 p3277 N85-30325

140 GHz gyrotron development program
[DE85-010348] 20 p3537 N85-32013

Multi-channel pulser for the SLC thermionic electron source
[DE85-014222] 24 p4160 N85-35792

ELECTRON IMPACT

Synergism in materials erosion due to multispecies impact 06 p0864 N85-15494

The coordinated research program at IAEA on atomic collision data for plasma diagnostics
09 p1390 N85-18747

Observation of pure resonance and threshold effects in electron impact experiments in high intensity laser fields
[AD-A150725] 14 p2309 N85-24293

Indirect processes in electron-impact ionization of multiply-charged ions
[DE85-005237] 14 p2419 N85-24925

Many-electron effects in electron impact ionization of multiply charged ions
[DE85-005570] 15 p2649 N85-26340

Theory of electron-impact atomic ionization cross sections
[AD-A151763] 16 p2861 N85-27648

Survey of experimental and theoretical electron-impact ionization cross sections for transition metal ions in low stages of ionization
[DE85-007605] 16 p2863 N85-27658

Measurement of combustion species by electron impact fluorescence
[DE85-011163] 19 p3236 N85-30065

Vibrationally enhanced dissociation of diatomic molecules
[AD-A154827] 21 p3701 N85-32996

Electron impact ionization of multicharged ions at ORNL: 1980-1984
[DE85-013104] 23 p3972 N85-34622

ELECTRON INTENSITY
U ELECTRON FLUX DENSITY

ELECTRON INTERACTIONS
U ELECTRON SCATTERING

ELECTRON IONIZATION
U IONIZATION

ELECTRON IRRADIATION

Neutron irradiation of semiconductors — lattice defects, electron irradiation 03 p0428 N85-12732

Time-of-flight spectroscopy of ionic and metastable fragments from dissociating molecules
[AD-A148068] 08 p1220 N85-17683

Evaluation and prediction of long-term environmental effects of nonmetallic materials
[NASA-CR-171353] 10 p1450 N85-19137

The role of void nucleation in the swelling resistance of ferritic steel
[AERE-R-11525] 11 p1610 N85-20122

Discharge pulse phenomenology
13 p1995 N85-22509

Technological process effect on the carrier lifetime degradation of silicon solar cell base layer irradiated by 1 MeV electrons (boron doping case)
13 p2007 N85-22585

The effects of lithium counterdoping on radiation damage and annealing in n(+)p silicon solar cells
13 p2007 N85-22586

Investigation of the degradation of GaAs photovoltaic cells by proton and electron irradiation
13 p2008 N85-22587

Electron-bombarded silicon spatial light modulator
[AD-D011579] 15 p2652 N85-26355

Electron irradiation of light emitting diodes
[AD-A154441] 19 p3260 N85-30213

Infrared absorption of oxygen complexes in electron-irradiated silicon
[FOA-C-30379-E1,E2,E3,E4] 20 p3538 N85-32015

The degradation of pollutants in water and waste water by means of electron or gamma irradiation
[OEFZS-4317] 22 p3812 N85-33615

Electron irradiation of N type cadmium telluride
[AD-A156117] 24 p4161 N85-35801

ELECTRON MASS

Incorporation of Monte Carlo electron interface studies into photon general cavity theory
[DE85-007674] 17 p3034 N85-28772

ELECTRON MICROSCOPES

Scanning electron microscope facility for examination of radioactive materials
[DE85-008127] 17 p2960 N85-[illegible]

Resolution at its current limit: Applications of the Berkeley ARM
[DE85-009959] 19 p3274 N85-30[illegible]

An empirical technique to measure X-ray production and detection efficiencies in the analytical electron microscope
[DE85-010270] 19 p3381 N85-30[illegible]

ELECTRON MICROSCOPY

EDS round-robin evaluation of type 308 austenitic stainless steel
[DE84-014574] 02 p0183 N85-112[illegible]

Architecture of dermatophyte cell Walls: Electron microscopic and biochemical analysis
[NASA-TM-77441] 03 p0399 N85-12[illegible]

Application of extraction replicas and analytical electron microscopy to precipitate phase studies
[DE85-001253] 06 p0769 N85-14[illegible]

The structure and function of fungal cells
[NASA-TM-77443] 06 p0842 N85-15[illegible]

Comments on the image contrast from inelastically scattered electrons
[DE85-000899] 07 p1041 N85-16[illegible]

Transmission electron microscopy of inorganic materials
[DE85-000706] 09 p1291 N85-18107

SANS and TEM studies of carbide precipitation and creep damage in type 304 stainless steel
[DE85-000933] 09 p1296 N85-18139

Metals and Ceramics Division Materials Science Program
[DE85-003795] 11 p1592 N85-20012

Analytical electron microscopy: A potential new tool in the study of materials compatibility
[DE85-003271] 11 p1606 N85-20086

Application of Raman, TEM and other ion based techniques to oxidation problems
[AERE-R-11447] 11 p1610 N85-20121

K and L-shell cross-sections for X-ray microanalysis in an AEM
[DE85-002733] 11 p1721 N85-20822

Research in surface sciences, disordered materials, and solidification and growth
[PB85-132140] 11 p1737 N85-20927

Electron image simulation: A complementary processing technique
[DE85-000685] 12 p1941 N85-22190

TEM/FIM study of modulated microstructures in the Fe-Be system
[DE85-005379] 13 p2023 N85-22670

Grain boundaries in NiO
[DE85-006129] 13 p2025 N85-22687

Decomposition of VTAN alloy solid solution upon irradiation and thermal aging 13 p2029 N85-22712

Impurities in Kevlar 49 fibers
[DE85-004996] 13 p2038 N85-22767

A comprehensive review of black powder
[AD-A150455] 13 p2039 N85-22769

SEM (Scanning Electron Microscope) investigation of silicon diodes using the electron beam induced current method
[AD-A150356] 13 p2064 N85-22884

Structural characterization by intensity measurements of electron diffraction patterns
[DE85-004803] 13 p2184 N85-23427

New analysis aspects of the fatigue crack propagation behavior by SEM in situ microscopy
14 p2320 N85-24335

Secondary fluorescence effects on X-ray microanalysis
[DE85-005565] 15 p2506 N85-25457

Grain boundary composition and intergranular fracture of steels. Volume 1: Detection of grain boundary segregation in steels
[DE85-006850] 15 p2662 N85-26429

Low dose irradiation creep of pure nickel
[DE85-006320] 16 p2751 N85-26975

Tilt grain boundaries in NiO
[DE85-006839] 16 p2751 N85-26976

In situ HVEM studies of electron beam-driven composition changes in thin film alloys: Displacement-rate gradient effects
[DE85-007992] 17 p2931 N85-28082

Journal of Research of the National Bureau of Standards, volume 90, number 1, January - February 1985
[PB85-179083] 20 p3522 N85-31909

Modification of the grain size of sputtered copper with additions of oxygen, krypton, silver, or yttrium
[DE85-010975] 21 p3567 N85-32189

Z-contrast imaging and electron channeling analysis of dopants in semiconductors
[DE85-011410] 21 p3582 N85-32269

Aerosol formation by wave action over Ross Sea, Antartica 21 p3651 N85-32688
An electron microscopic study of urban aerosol
21 p3651 N85-32689
Three-dimensional reconstruction and data display of chromosome structure studied by electron microscope tomography
[DE85-011562] 22 p3825 N85-33697
Microstructures in rapidly solidified Ni-Mo alloys
[NASA-TM-87100] 23 p3915 N85-34266
High resolution electron microscopic characterization of interfaces in ceramics
[DE85-011207] 23 p3920 N85-34289
Intermolecular explosives
[DE85-009609] 23 p3921 N85-34296
The preparation of TEM specimens showing oxide scales in transverse cross-section
[AERE-R-11579] 24 p4078 N85-35276
Size and shape dependence of CO adsorption sites on sapphire supported Fe microcrystals
[NASA-CR-176171] 24 p4160 N85-35794
ELECTRON MOBILITY
Motion of electrons in non polar classical liquids
[DE84-013609] 05 p0727 N85-14672
High-efficiency solar-cell design modeling
06 p0829 N85-15262
Theory of silicon superlattices: Band structure and mobility enhancement 09 p1396 N85-18789
Microscopic structure of two-dimensional electron glass
[DE85-010265] 19 p3376 N85-30942
Air chemistry measurements 2
[AD-A156041] 24 p4117 N85-35520
ELECTRON MULTIPLIERS
U PHOTOMULTIPLIER TUBES
ELECTRON OPTICS
Method to render second order beam optics programs symplectic
[DE85-010631] 20 p3515 N85-31655
Practicality of electronic beam steering for MST/ST radars, part 6.2A 21 p3624 N85-32516
Electrostatic astigmatic tubular lens
21 p3695 N85-32955
ELECTRON ORBITALS
The 13C nuclear magnetic resonance in graphite intercalation compounds
[NASA-CR-174261] 07 p1040 N85-16601
Theoretical cross sections for inner-shell vacancy production by high-energy electrons
[DE84-007346] 11 p1721 N85-20827
ELECTRON OSCILLATIONS
Investigation of generation of oscillations using anomalous Doppler effect 13 p2078 N85-22980
ELECTRON PARAMAGNETIC RESONANCE
Studies of hydrogenated amorphous silicon
[DE84-013036] 01 p0067 N85-10443
Phase diagrams of organic superconductors
[DE84-016219] 05 p0731 N85-14699
EPR linewidth studies of unpaired electrons at the Si-SiO2
[DE84-016727] 05 p0733 N85-14712
Comparison of ionizing radiation and hot electron effects in MOS structures
[DE84-016766] 09 p1400 N85-18809
Characterization of acetylene-terminated resin cure states
[AD-A149463] 10 p1452 N85-19148
Charge-to-mass dispersion methods for abrasion-ablation fragmentation models
[NASA-TM-86340] 11 p1726 N85-20857
Control of electronic, magnetic and optical properties of doped polyacetylene conductors
[AD-A150117] 12 p1814 N85-21375
Ion and polymer chain motion in a superionic sodium-poly(ethylene oxide) complex
[AD-A152290] 16 p2755 N85-27001
Electron spin resonance study of interface states induced by electron injection in metal-oxide-semiconductor devices
[DE85-009502] 18 p3195 N85-29817
Defect formation in amorphous hydrated silicon subjected to laser radiation 21 p3682 N85-32873
An EPR (Electron-Paramagnetic-Resonance) and ENDOR (Electron-Nuclear-Double-Resonance) study of ferroelectric ammonium sulfate
[AD-A155580] 21 p3710 N85-33033
ELECTRON PATHS
U ELECTRON TRAJECTORIES
ELECTRON PHONON INTERACTIONS
Heterocontact effects in point contact electron-phonon spectroscopy of the alkali metals
[AD-A149760] 12 p1800 N85-21290
ELECTRON PHOTON CASCADES
Cascaded solar photovoltaic cells based on In-GaInPAs and InP-CdS heterostructures
02 p0268 N85-11749
Advanced high-efficiency concentrator cells
[DE84-013020] 09 p1344 N85-18459
Advanced high-efficiency concentrator cell
[DE85-000525] 14 p2351 N85-24533
SERI photovoltaic advanced research and development project: FY 1984 accomplishments
[DE85-002939] 18 p3128 N85-29368
Development of the Cascade inertial-confinement-fusion reactor
[DE85-010933] 19 p3357 N85-30812
Energy spectrum of extragalactic gamma-ray sources
[OG-2.7-13] 22 p3872 N85-33986
Fluctuations of development maximum depth and nuclear composition of primary cosmic radiation
[OG-5.1-13] 22 p3882 N85-34054
Coupled electron-photon transport calculations using the method of discrete ordinates
[DE85-009444] 23 p3967 N85-34597
High sensitive X-ray films to detect electron showers in 100 GeV region
[HE-3.1-13] 24 p4178 N85-35911
Comparison of big event with calculations of the air shower development
[HE-3.6-8] 24 p4185 N85-35956
Result of Monte-Carlo simulation of electron-photon cascades in lead and layers of lead-scintillator
[HE-3.6-11] 24 p4185 N85-35958
Theoretical study of EAS hadronic structure
24 p4189 N85-35991
Takhra-Tskaro complex intended for the investigations of EAS spatial characteristics near axis
24 p4190 N85-35995
Topological aspects of age parameter
[HE-4.3-13] 24 p4192 N85-36007
Lateral-angular and temporal characteristics of EAS optical radiation
[HE-4.4-19] 24 p4194 N85-36025
Energy spectrum of cascades generated by muons in Baksan underground scintillation telescope
[HE-5.1-15] 24 p4202 N85-36077
ELECTRON PLASMA
Charging of DMSP/F6 spacecraft in aurora on 10 January 1983 13 p1991 N85-22481
Average and worst-case specifications of precipitating auroral electron environment 13 p1991 N85-22482
The downshift of electron plasma oscillations in the electron foreshock region
[NASA-CR-175633] 14 p2423 N85-24945
Charge uncovering effects on flute instabilities in hot electron plasmas
[DE85-006957] 16 p2867 N85-27686
Plasma wake field accelerator
[DE85-010536] 18 p3191 N85-29791
Influence of ECR-heating on MHD activity of plasma in tokamak-10 installation 21 p3694 N85-32949
ELECTRON PRECIPITATION
Polar rain: Solar coronal electrons in the Earth's magnetosphere
[NASA-TM-86150] 07 p1060 N85-16726
Pitch angle scattering and particle precipitation in a pulsating aurora: An experimental study
[KGI-185] 09 p1355 N85-18523
The high latitude D region during electron precipitation events 11 p1664 N85-20484
High energy particle effects in the D region during and after geomagnetic storms 11 p1664 N85-20485
Electron and proton precipitation in magnetic substorms — auroral substorms
14 p2360 N85-24585
Coordinated balloon-satellite studies of energetic electron precipitation mechanisms
14 p2360 N85-24587
Observations during a magnetosphere substorm triggered by a Storm Sudden Commencement (SSC): A case study 14 p2361 N85-24588
Auroral X-rays and equatorial electrons in the morning sector — substorm 14 p2361 N85-24590
On the location of the source for X-ray microbursts
14 p2361 N85-24591
On-off characteristics of auroral pulsations
14 p2363 N85-24604
Multiple correlation between auroral and magnetic pulsations 14 p2363 N85-24605
X-ray intensification at balloon altitudes of the South Atlantic magnetic anomaly in association with geomagnetic activity
[INPE-3469-PRE/712] 16 p2827 N85-27437
ELECTRON PROBES
Materials characterization using ion, electron, and photon probes
[DE84-004518] 04 p0560 N85-13568
ELECTRON PUMPING
The 248 nm - new short wavelength for pumping lasers employing vapors of complex molecules
02 p0261 N85-11705
Pulsed excimer laser processing for cost-effective solar cells
[NASA-CR-175700] 14 p2351 N85-24530
ELECTRON RADIATION
NT BETA PARTICLES
NT ELECTRON BEAMS
NT RELATIVISTIC ELECTRON BEAMS
Periodic substorm activity in the geomagnetic tail
[NASA-CR-175629] 13 p2161 N85-23409
Radio-frequency radiation of storm clouds
21 p3692 N85-32939
ELECTRON RECOMBINATION
NT RADIATIVE RECOMBINATION
High lifetime solar cell processing and design
20 p3480 N85-31622
ELECTRON RING ACCELERATORS
U STORAGE RINGS (PARTICLE ACCELERATORS)
ELECTRON SCATTERING
Bremsstrahlung radiation from longitudinal plasma waves caused by subthermal electrons in plasma
02 p0264 N85-11730
Dirac single particle wave functions in inelastic electron scattering
[DE84-015129] 02 p0279 N85-11814
Electron collision processes in molecular gases
[AD-A148078] 03 p0418 N85-12671
Electromagnetic shower development and applications to sampling calorimeters
[DE84-016355] 04 p0493 N85-13142
Measurements of the A-dependence of deep-inelastic electron scattering from nuclei
[DE84-013865] 05 p0728 N85-14678
Comments on the image contrast from inelastically scattered electrons
[DE85-000899] 07 p1041 N85-16609
Pitch angle scattering and particle precipitation in a pulsating aurora: An experimental study
[KGI-185] 09 p1355 N85-18523
An extension of the multiconfiguration Hartree-Fock program for continuum functions
[DE85-002080] 09 p1379 N85-18672
Studies of P-shell nuclei by large momentum transfer electron scattering
[DE84-016803] 09 p1381 N85-18686
Microscopic determinations of lattice and electronic structures of solids
[DE84-017323] 09 p1399 N85-18806
Analytical electron microscopy: A potential new tool in the study of materials compatibility
[DE85-003271] 11 p1606 N85-20096
Effect of impurities on absorption in semiconductors and lasing of semiconductor lasers 11 p1716 N85-20797
Theoretical cross sections for inner-shell vacancy production by high-energy electrons
[DE84-007346] 11 p1721 N85-20827
Recent progress in electron scattering at SLAC
[DE85-002718] 11 p1723 N85-20840
Coincidence studies of secondary electron emission in light ion-atom collisions
[DE85-002373] 11 p1725 N85-20852
Recent advances in forward electron production studies in ion-atom and ion-solid collisions
[DE85-001255] 11 p1726 N85-20853
Activities in nuclear physics and high energy physics
11 p1728 N85-20866
Heterocontact effects in point contact electron-phonon spectroscopy of the alkali metals
[AD-A149760] 12 p1800 N85-21290
Theoretical study of near-threshold electron-molecule scattering
[DE85-004530] 12 p1930 N85-22126
Observation of pure resonance and threshold effects in electron impact experiments in high intensity laser fields
[AD-A150725] 14 p2309 N85-24293
Numerical solution of a first kind Fredholm integral equation arising in electron-atom scattering
[CWI-NM-R8414] 14 p2414 N85-24897
Slowing down of charged particles by the bound electrons in a plasma — ion beams, nuclear fusion
[LP-209] 14 p2419 N85-24929
Approximate closed-form expression for the electron-scattering-induced interaction between magnetic flux lines and grain boundaries
[DE85-004699] 15 p2660 N85-26417
Test of the electronic structure of Fe(100) by absorbed current spectroscopy
[DE85-004942] 15 p2661 N85-26422
Density of impurity states associated to inversion layers
[INPE-3406-PRE/675] 16 p2869 N85-27702
Wake fields and wake field acceleration
[DE85-006054] 17 p3031 N85-28750
Possible indication of an A-dependence of R in deep-inelastic electron scattering from nuclei
[DE85-006174] 17 p3033 N85-28763

Electron multiple, plural and single scattering
[DE85-010325] 18 p3181 N85-29721
Magnetic scattering and polarized neutrons
[DE85-009823] 19 p3355 N85-30794
Interaction of slow electrons with high-pressure gases (quasi-liquids): Synthesis of our knowledge on slow electron-molecule interactions
[DE85-010061] 19 p3355 N85-30800
Deep-inelastic lepton scattering by nuclei: The pion-exchange model
[DE85-010486] 19 p3359 N85-30828
Angle averaged Compton cross sections for degenerate electron gases
[AD-A154464] 19 p3371 N85-30906
Magnetoconductance in aluminum films, wires, and cylinders 19 p3374 N85-30928
Time-implicit Monte-Carlo collision algorithm for particle-in-cell electron transport models
[DE85-010759] 20 p3521 N85-31900
Inelastic Near-Surface Interactions. Proceedings of the Werner Brandt Workshop on Penetration Phenomena
[DE85-010579] 20 p3526 N85-31928
Metal-insulator-metal models of tunneling
20 p3536 N85-32006
Electron loss process and cross section of multiply charged ions by neutral atoms 23 p3981 N85-34685
X-ray spectra of bursting neutron stars
23 p3981 N85-34686
The propagation of solar flare particles in a turbulent coronal loop
[SH-1.1-3] 23 p3989 N85-34730
Analytical-numerical methods of calculations of energy and three-dimensional particle distributions in electromagnetic cascades
[HE-3.5-13] 24 p4164 N85-35950

ELECTRON SOURCES
Development of a continuous broad-energy-spectrum electron source 13 p1995 N85-22507

ELECTRON SPECTROSCOPY
Electron energy loss investigation of the electronic and structural properties of palladium
[NOTA-INTERNA-803] 02 p0289 N85-11888
A high transmission, 20 channel polychromator for the Thomson scattering diagnostic of TORTUR 3 — plasma diagnostics
[REPT-84-156] 03 p0422 N85-12694
The effect of thin-film growth mode on XPS/UPS/AES intensities
[AD-A146284] 03 p0434 N85-12763
Mossbauer spectroscopy and X-ray diffraction of samples from the Santa Catharina iron meteorite
06 p0885 N85-15624
Electron spectrometry experiments with the use of synchrotron radiation
[DE85-001286] 07 p1041 N85-16610
Nondestructive evaluation of titanium alloys. ESCA (Electron Spectroscopy for Chemical Analysis), ISS (Ion Scattering Spectroscopy), and SIMS (Secondary Ion Mass Spectrometry) examination of titanium alloy solid surfaces
[AD-P004135] 08 p1128 N85-17110
Simultaneous observations of electron spectra in the auroral zone and near the equatorial plane by the DMSP-5D-F2 and GEOS-1 Satellites
[KGI-184] 09 p1355 N85-18522
Surface physics instrumentation
[AD-A149304] 11 p1728 N85-20869
Some unique aspects of fouling on copper as compared to titanium or nickel
[AD-A150072] 12 p1806 N85-21332
Characterization of material surfaces exposed to atomic oxygen on space shuttle missions
12 p1946 N85-22220
Bonding information from Auger spectroscopy
[AD-A150864] 14 p2251 N85-23948
Chemical and localization effects in Auger lineshapes of transition metal compounds
[AD-A150865] 14 p2251 N85-23949
Threshold electron studies of gas-surface interactions
[AD-A151271] 15 p2647 N85-26326
Microscopic study of the influence of impurities on interface bonding
[AD-A151725] 16 p2743 N85-26929
Digital filters for application to data analysis in electron energy loss spectroscopy
[DE85-007932] 17 p2923 N85-28020
Self-sustaining coatings for fusion applications: Copper lithium alloys
[DE85-009740] 18 p3190 N85-29783
Method for predicting the performance of cathode materials
[AD-D011665] 19 p3257 N85-30198
Superconducting electronic film structures
[AD-A154196] 19 p3259 N85-30207
Study of solute segregation at interfaces using Auger electron spectroscopy
[DE85-005709] 20 p3423 N85-31247
Compositional analysis of silicon
20 p3480 N85-31626
Activities of the Physics Division
[DE85-000784] 21 p3702 N85-33002
Size and shape dependence of CO adsorption sites on sapphire supported Fe microcrystals
[NASA-CR-176171] 24 p4160 N85-35794

ELECTRON SPIN
Magnetic alignment theory and the interpretation of polarization 06 p0860 N85-15590
Collisional pumping for the production of intense spin-polarized, neutral beams: Target considerations
[DE85-003459] 11 p1723 N85-20841
Polarization of fast particle beams by collisional pumping
[DE85-011621] 22 p3838 N85-33764

ELECTRON SPIN RESONANCE
U ELECTRON PARAMAGNETIC RESONANCE

ELECTRON STATES
Singlet delta oxygen generator
[AD-D011206] 01 p0012 N85-10072
Actinides, the narrowest bands
[DE84-016463] 05 p0733 N85-14710
Modelling the local interstellar medium as a supernova remnant in a multiphase gas 06 p0879 N85-15585
Application of quantum chemistry of atmospheric chemistry
[AD-A147035] 07 p0922 N85-15843
Electronically excited atomic and molecular oxygen
[AD-A147732] 08 p1121 N85-17064
The Si/SiO2 intrinsic states and interface charges. Chapter 1: Origin, properties, models, impact
[HMI-B-413] 09 p1400 N85-18612
Temperature-dependent surface states and transitions of Si(111)-7x7
[AD-A149156] 10 p1562 N85-19850
Bonding information from Auger spectroscopy
[AD-A150864] 14 p2251 N85-23948
Experimental study of dissociative attachment in optically-pumped lithium molecules
[AD-A152800] 17 p3030 N85-28736
Monte Carlo simulation of thermalization of subexcitation electrons in He, Ne, Ar, Kr and Xe
[NAL-TR-843T] 18 p3178 N85-29702
Calculation of Franck-Condon factors for diatomic molecules
[AD-A154463] 19 p3353 N85-30784
A method to estimate the self-consistency effects on electronic structure calculations
[INPE-3536-PRE/752] 19 p3375 N85-30935
Calculation of molecular constants potential energy curves and Franck-Condon factors for lead oxide
[AD-A154521] 21 p3562 N85-32158
Nonradiative damping of molecular electronic excited states by metal surfaces
[AD-A154619] 21 p3701 N85-32994
Optical properties of heterostructures and superlattices
[AD-A156243] 24 p4162 N85-35802

ELECTRON SWEEPING
U SWEEP FREQUENCY

ELECTRON TELESCOPES
U PARTICLE TELESCOPES

ELECTRON TEMPERATURE
U ELECTRON ENERGY

ELECTRON TRAJECTORIES
Confinement of low-energy electrons near metallic surfaces for plasmon generation
[DE85-001119] 09 p1381 N85-18688
Electron acceleration by laser fields in a gas
[DE85-000575] 11 p1639 N85-20323
Laser measurements of distances from the ORELA neutron target to experiment stations along flight paths 1 and 6
[DE85-009457] 17 p2971 N85-28352
Hybrid two-dimensional Monte-Carlo electron transport in self-consistent electromagnetic fields
[DE85-010757] 19 p3346 N85-30756
Electron trajectories in a combined wiggler and alternating gradient quadrupole field
[DE85-010727] 22 p3842 N85-33794
Relativistic electron in curved magnetic fields
[OG-8.2-11] 22 p3890 N85-34110

ELECTRON TRANSFER
Solvent effects upon electrochemical kinetics: Influences of interfacial solvation and solvent relaxation dynamics
[AD-A145624] 02 p0173 N85-11156
The oxidation of transition-metal ions by molecular oxygen
[BLL-M-29593-(5828.4)] 02 p0175 N85-11172
Intramolecular electron transfer at metal surfaces. Dependence of tunneling probability upon donor-accep separation distance
[AD-A145611] 02 p0287 N85-118
Inclusion of electron transfer in the calculation of K multiple vacancy production by ion impact
[DE84-016596] 05 p0733 N85-1471
Electrochemistry in near-critical and supercritical flu I. Ammonia
[AD-A146429] 06 p0765 N85-14
Estimation of the rate of electron transfers between 2 contacting polymer surfaces
[AD-A148416] 08 p1122 N85-170
Homogeneous reaction involving components of different redox couples. 1: Theoretical considerations and digital simulation
[AD-A148686] 08 p1124 N85-170
The kinetics of electron transfer reactions in and at films of electroactive polymers
[AD-A148597] 08 p1134 N85-171
Electron production, electron attachment, and charge recombination process in high pressure gas discharge
[AD-A149535] 10 p1554 N85-197
Energy transfer and photochemistry in biomimetic sola conversion
[PB85-129112] 11 p1677 N85-20
Correlated 2 electron effects in collisions of multiply charged Au ions with He
[DE85-003064] 11 p1723 N85-208
Electronic transport in hydrogenated amorphous silica films
[DE85-002901] 13 p2164 N85-234
Noncontinuum solvent effects upon the intrins free-energy barrier for electron-transfer reactions
[AD-A150662] 14 p2250 N85-239
Intramolecular electron transfer at metal surfaces. Par 5: Pendant substituent effects upon thiocarboxylate-bridged Cobalt (3) reduction kinetics at mercury and gold electrodes
[AD-A150647] 14 p2254 N85-23
Sensitization and quenching in the conversion of ligh energy into chemical energy
[DE85-006301] 14 p2351 N85-24
Thermolysis of 4-methyl-4-(1-propenyl)malon peroxide: Mechanistic limits to chemiluminescence efficiency
[AD-A151567] 15 p2505 N85-254
Nitrolysis of the CN single bond and related chemistry of nitro and nitroso groups
[AD-A151753] 15 p2505 N85-254
Applications of photoinduced electron transfer and hydrogen abstraction reactions to chemical and electrochemical conversion processes
[DE85-006068] 15 p2506 N85-254
Optically triggered transferred-electron device microwave burst and single pulse generators
[AD-D011614] 16 p2778 N85-27141
Electrochemistry of polymer films not immersed in solution: Electron transfer on an ion budget
[AD-A152969] 17 p2920 N85-279
Photochemistry of coordination complexes: The phthalocyanines
[DE85-007693] 17 p2923 N85-280
Electrogenerated chemiluminescence
[AD-A153547] 18 p3070 N85-28
Germanium detectors with a built-in transverse dri field
[DE85-009944] 18 p3096 N85-291
One- and two-electron transfer processes in ion-surface scattering
[AD-A154208] 19 p3353 N85-307
Sulfate-reducing bacteria: Microbiology and physiology 21 p3659 N85-327
Electron photoejection in carbanions
[DE85-011747] 23 p3911 N85-342
Electron photoejection in carbanions
[DE85-011748] 23 p3912 N85-342
Study of photon emission by electron capture during solar nuclei acceleration, 1: Temperature-dependent cross section for charge changing processes
[SH-1.1-6] 23 p3990 N85-347
Vectorial electron transfer on designed surfaces
[PB85-204600] 24 p4076 N85-35

ELECTRON TRANSITIONS
Molecular beam scattering 03 p0417 N85-12
Oscillator strengths for OII ions
[NASA-CR-174153] 04 p0559 N85-13
Infrared emission and atomic transitions
[AD-A147840] 07 p1041 N85-16
Materials physics
[DE84-017103] 09 p1377 N85-18
Identification of spectra of highly ionized Mo, Nb, Z and Y atoms 09 p1390 N85-187
Indirect processes in electron-impact ionization of multiply-charged ions
[DE85-005237] 14 p2419 N85-24

Spectroscopic studies of lead oxide in a flow tube
[AD-A151849] 15 p2505 N85-25455
Spectroscopic studies of lasing transitions in the diatomic mercury halides
[AD-A151553] 15 p2563 N85-25809
Spectroscopy of quasimolecular X-rays with H-like decelerated ions
[DE85-006565] 15 p2649 N85-26337
The copper vapor laser 16 p2824 N85-27417
Field theory of the metal-insulator transitions in restricted symmetries
[NOTA-INTERNA-829] 18 p3196 N85-29826
Simplified analytical model for calculation of population inversion in channels of CW gasdynamic lasers operating at various transitions among levels pertaining to coupled upsilon 1 and upsilon 2 modes of CO2
[STN-2] 20 p3461 N85-31498
Multiple inner shell vacancies in laser-irradiated Au plasma 23 p3981 N85-34667

ELECTRON TUBES
NT CAMERA TUBES
NT CATHODE RAY TUBES
NT GAS DISCHARGE TUBES
NT HELITRONS
NT IMAGE DISSECTOR TUBES
NT KLYSTRONS
NT MAGNETRONS
NT MICROWAVE OSCILLATORS
NT MICROWAVE TUBES
NT PICTURE TUBES
NT RETURN BEAM VIDICONS
NT THERMICONS
NT THYRATRONS
NT TRAVELING WAVE TUBES
NT VACUUM TUBES
NT VIDICONS
Magnetically insulated diode for generating pulsed neutron and gamma ray emissions
[DE85-011658] 22 p3760 N85-33306
Los Alamos free-electron laser
[DE85-012666] 24 p4098 N85-35405

ELECTRON TUNNELING
Intramolecular electron transfer at metal surfaces. 4: Dependence of tunneling probability upon donor-acceptor separation distance
[AD-A145611] 02 p0287 N85-11876
Calculation of the scattering function of rotating molecules with emphasis on the tunnel spectra of absorbed molecules 03 p0427 N85-12725
GaAlAs Sb APD optimization
[AD-A149406] 10 p1480 N85-19344
Inelastic tunnel diodes
[NASA-CASE-LEW-13833-1] 12 p1832 N85-21492
Thin film technology of high-critical-temperature superconducting electronics
[AD-A150010] 12 p1940 N85-22185
Macroscopic quantum tunnelling in a current biased Josephson junction
[DE85-004603] 13 p2164 N85-23424
Tunneling in magnetic superconducting systems
[AD-A150677] 14 p2426 N85-24963
Research on superconductive signal-processing devices
[AD-A152703] 17 p2953 N85-28235
Variational transition state theory
[DE85-010665] 19 p3235 N85-30059
Metal-insulator-metal models of tunneling
20 p3536 N85-32006
A theory of exciton photoluminescence for two types of neutral acceptors in silicon. A study of the systems Si:(B, IN), Si:(Al), (Si), Si:(Ga, In), Si:(B, Al), Si:(B, Ga), and Si:(Al, GA)
[AD-A156452] 21 p3710 N85-33031
Design considerations for personnel access penetrations for the superconducting super collider
[DE85-013027] 24 p4162 N85-35807

ELECTRON-HOLE DROPS
Investigations of radiation-induced and carrier-enhanced conductivity 13 p1996 N85-22515

ELECTRON-ION RECOMBINATION
NT RADIATIVE RECOMBINATION
Ionic reactions of atmospheric importance
[AD-A147354] 07 p0997 N85-16333

ELECTRONIC AIRCRAFT
Electronic reconnaissance aircraft of the Soviet Union Navy
[AD-A154706] 21 p3551 N85-32091
DOD Value Engineering Conference report. Value Engineering (VE): A tool that benefits line management held at Leesburg, Virginia on 1-2 November 1984. Part 2. Plenary session
[AD-A156006] 24 p4163 N85-35811

ELECTRONIC AMPLIFIERS
U AMPLIFIERS

ELECTRONIC CONTROL
Motor/generator and electronic control considerations for energy storage flywheels 05 p0606 N85-13678
Commercialization of the power factor controller
[NASA-CR-171500] 17 p2951 N85-28221
Development of mass-producible line-focus tracking concentrating solar collectors. Category 2: Control systems
[DE85-007873] 17 p2967 N85-28459
Closed loop electrostatic levitation system
[NASA-CASE-NPO-15553-1] 18 p3092 N85-29142
Performance improvements of a highly integrated digital electronic control system for an F-15 airplane
[NASA-TM-86748] 21 p3556 N85-32120
A microprocessor-controlled, multichannel fluorimeter for analysis of sea water
[AD-A154986] 21 p3590 N85-32310
Qualification needs for advanced integrated aircraft
[NASA-TM-86731] 22 p3729 N85-33119

ELECTRONIC COUNTERMEASURES
NT CHAFF
Rivista Tecnica Selenia, volume 9, number 1
07 p0938 N85-15945
Equipment for preflight test of an Electronic Countermeasures (ECM) avionic system
07 p0939 N85-15949
Optimum jamming effects on frequency-hopping M-ary FSK (Frequency-Shift Keying) systems under certain ECCM (Electronic counter-countermeasures) receiver design strategies
[AD-A147766] 08 p1151 N85-17267
Integrated defense communications system antijamming antenna system
[AD-D011423] 08 p1154 N85-17285
Simulation of the performance of adaptively controlled Navstar antennas in battlefield scenarios
10 p1472 N85-19292
Research on adaptive antenna techniques 6
[AD-A149341] 11 p1624 N85-20228
Combat capable space systems for tactical support
11 p1713 N85-20775
A survey of radar ECM and ECCM
15 p2536 N85-25653
AN investigation into the control limitations of a bank to turn missile in the terminal homing phase
[AD-A152193] 16 p2704 N85-26696
Digital RF delay line for ECM (electronic countermeasure) look-through
[AD-A152120] 16 p2774 N85-27120
Adaptive nulling at HF using a compact array of active parasitic antennas
[AD-A152582] 17 p2948 N85-28203
An analysis of jamming effects on noncoherent digital receivers
[AD-A153791] 18 p3090 N85-29128

ELECTRONIC EQUIPMENT
NT AVALANCHE DIODES
NT BIPOLAR TRANSISTORS
NT CHARGE COUPLED DEVICES
NT CHARGE INJECTION DEVICES
NT CHARGE TRANSFER DEVICES
NT CMOS
NT DIODES
NT ELECTRONIC FILTERS
NT ELECTRONIC MODULES
NT ELECTRONIC PACKAGING
NT ELECTRONIC TRANSDUCERS
NT FIELD EFFECT TRANSISTORS
NT GALLIUM ARSENIDE LASERS
NT GERMANIUM DIODES
NT GUNN DIODES
NT HETEROJUNCTION DEVICES
NT JFET
NT JUNCTION DIODES
NT JUNCTION TRANSISTORS
NT LIGHT EMITTING DIODES
NT METAL OXIDE SEMICONDUCTORS
NT MIM (SEMICONDUCTORS)
NT MIM DIODES
NT MINIATURE ELECTRONIC EQUIPMENT
NT MIS (SEMICONDUCTORS)
NT MULTISPECTRAL LINEAR ARRAYS
NT PHOTODIODES
NT PHOTOTRANSISTORS
NT PHOTOVOLTAIC CELLS
NT PLASMA DIODES
NT RUBY LASERS
NT SCHOTTKY DIODES
NT SEMICONDUCTOR DEVICES
NT SEMICONDUCTOR DIODES
NT SEMICONDUCTOR LASERS
NT SILICON CONTROLLED RECTIFIERS
NT SILICON TRANSISTORS
NT SIS (SEMICONDUCTORS)
NT SOLID STATE DEVICES
NT SOLID STATE LASERS
NT SPACECRAFT ELECTRONIC EQUIPMENT
NT THERMISTORS
NT THYRISTORS
NT TRANSISTOR AMPLIFIERS
NT TRANSISTORS
NT TUNNEL DIODES
NT VARACTOR DIODES
NT VARISTORS
NT YAG LASERS
Polychlorinated biphenyls (PCBs) in transit system electrical equipment
[PB84-222207] 01 p0045 N85-10291
Center for Electronics and Electrical Engineering Technical Bulletin covering center programs with 1984 CEEE events calendar
[PB84-222785] 01 p0045 N85-10292
Center for Electronics and Electrical Engineering Technical Bulletin covering center programs with 1984 CEEE events calendar
[PB84-223684] 01 p0045 N85-10293
The psychology of technical devices and technical discourse
[AD-P003929] 02 p0246 N85-11609
Artificial intelligence approaches to monitoring system integrity
[AD-P003930] 02 p0246 N85-11610
Model-based probabilistic reasoning for electronics troubleshooting
[AD-P003937] 02 p0247 N85-11617
Knowledge based tools for electronic equipment maintenance
[AD-P003940] 02 p0248 N85-11620
LES: (Lockheed Expert System): A model-based expert system for electronic maintenance
[AD-P003944] 02 p0248 N85-11624
Characteristics of ion implanters for fabrication of electronic devices
[AD-P003949] 02 p0286 N85-11865
Electronics/avionics depots in the United States Air Force Warner Robins Air Logistics Center
[AD-P004000] 03 p0307 N85-11981
Training capabilities test of Electronics Equipment Maintenance Trainer (EEMT): Findings and conclusions
[AD-A146075] 03 p0359 N85-12302
Accelerated stress facility 1976-1983
[AD-A146101] 03 p0359 N85-12303
Ballpark reliability estimation techniques
[AD-A145971] 03 p0369 N85-12357
USSR report: Electronics and electrical engineering
[JPRS-UEE-84-010] 04 p0485 N85-13095
Electronic components for space applications
[CNES-NT-109] 04 p0496 N85-13169
Heavy duty precision pan and tilt head
[AD-A146669] 04 p0509 N85-13246
Space power management and distribution status and trends 05 p0610 N85-13696
USSR report: Electronics and electrical engineering
[JPRS-UEE-84-011] 06 p0789 N85-15042
High-power gate turn-off thyristors
06 p0793 N85-15071
Target detection using microwave irradiances from natural sources: A passive, local and global surveillance system
[NASA-CR-174260] 07 p0946 N85-15991
cost and benefits optimization model for fault-tolerant aircraft electronic systems
[NASA-CR-168043] 07 p0946 N85-15993
USSR report: Electronics and electrical engineering
[JPRS-UEE-84-017] 07 p0951 N85-16025
The electronic typesetting program programmer's manual
[AD-A147500] 07 p1025 N85-16506
Experience of one UK electronic equipment supplier with bite on engine/flight control systems over the past ten years 08 p1064 N85-16736
Outlook for expanding the Federal research in progress system
[AD-A148354] 08 p1229 N85-17737
Acceleration responses of typical LRU's subjected to bench handling and installation shock
09 p1334 N85-18365
Data acquisition, measurement devices at 1984 Leipzig Spring Fair 09 p1378 N85-18661
Vibration isolated cold plate assembly
[AD-D011444] 10 p1484 N85-19368
Design and calibration of a 35GHz dielectrometer
[AD-P004363] 12 p1826 N85-21457
Nose and inlet duct radomes for the firebolt aerial target
[AD-P004375] 12 p1827 N85-21469
Maintainability time standards for electronic equipment
[AD-A149684] 12 p1834 N85-21507
Algorithm for statistical simulation of electromagnetic compatibility characteristics of high-frequency transmission channels in radioelectronic facilities
12 p1842 N85-21560

The future of lightwave technology
[PB85-109759] 12 p1935 N85-22155
Control of cascaded induction generator systems
[AD-A150429] 13 p2065 N85-22897
USSR report: Electronics and electrical engineering
[JPRS-UEE-85-002] 13 p2066 N85-22907
Simple detonation meter 13 p2077 N85-22971
USSR report: Electronics and electrical engineering
[JPRS-UEE-85-001] 13 p2078 N85-22976
User's guide to calibration of analog electronic controllers in HVAC systems
[AD-A150803] 14 p2298 N85-24229
Laser spot welding in the electronics industry
14 p2306 N85-24287
Rain rate determinations from electronic weight measurements: Instrument description and data reduction techniques
[AD-A150765] 14 p2378 N85-24681
USSR report: Electronics and electrical engineering
[JPRS-UEE-85-005] 15 p2524 N85-25565
Evaluation of adequacy pf JP54 protection level for large electric machines 15 p2528 N85-25588
Electronic detection and concealment of film dirt
[BBC-RD-1985/4] 15 p2536 N85-25667
Structural analysis of electronic assembly housing
[DE85-005794] 15 p2580 N85-25913
Future directions in computers
15 p2626 N85-26183
Avionics integrity issues presented during NAECON (National Aerospace and Electronics Convention) 1984
[AD-A151923] 16 p2707 N85-26707
The replacement of precious metal thick film inks using conductive polymer technology
[AD-A152002] 16 p2749 N85-26965
Reliability report for communication networks
[AD-A153764] 18 p3090 N85-29127
Moisture content and gas sampling device
[NASA-CASE-MSC-18866-1] 18 p3103 N85-29213
Avionics and civil aircraft systems: The present and the future
[SNIAS-851-111-104] 20 p3392 N85-31038
Proceedings of the Electronic Test Equipment Division's Annual Program Review of Electronic Test Equipment Industry Response to Emerging Defense Requirements
[AD-A154455] 20 p3436 N85-31320
Air Force bid sample testing 20 p3437 N85-31323
France's LETI reports 1983 electronic components research 20 p3438 N85-31336
Electronics Division research and development
[DE85-011887] 20 p3540 N85-32032
Resistance of polyaniline films as a function of electrochemical potential and the fabrication of polyaniline-based microelectronic devices
[AD-A154999] 21 p3569 N85-32201
Prospects for a new kind of synthesis: Assembly of molecular components to achieve functions
[AD-A155023] 21 p3702 N85-32997
Adaptive modeling of electronic circuits
22 p3766 N85-33345
Conferences of quantum-radiooptics section
22 p3773 N85-33380
Electronic imaging system and technique
[DE85-005740] 23 p3935 N85-34393
Electronic information management and productivity
[DE85-013362] 24 p4164 N85-35818

ELECTRONIC EQUIPMENT TESTS
Investigation of the application of the marginal tension technique to test electronic devices, phase 3
[ESD-11-301] 02 p0206 N85-11360
Tests for susceptibility to electromagnetic attack
[SNIAS-842-422-101] 04 p0494 N85-13154
Practical application of electron beam testing in LSI and VLSI circuits
[BMFT-FB-T-84-185] 05 p0633 N85-14061
Equipment for preflight test of an Electronic Countermeasures (ECM) avionic system
07 p0939 N85-15949
Evaluation of test equipment for the detection of contamination on electronic circuits — spacecraft electronics
[ESA-STM-234] 08 p1159 N85-17316
Design of a bit-sliced processor array with built-in-self-test
[AD-A149785] 12 p1835 N85-21513
Built-in tests for VLSI (Very Large Scale Integration) finite-state machines
[AD-A149784] 12 p1911 N85-21997
Measurement of internal thermal resistance for quality control of semiconductor devices
13 p2074 N85-22963
The Avionics Flight Evaluation System (AFES) of DFVLR
[DFVLR-MITT-85-01] 17 p2897 N85-27864
Measurement methods for accurate microwave characterization and modeling of MESFET chips
[AD-A152360] 17 p2952 N85-28227
The GfW handbook for data compilation of irradiation tested electronic components, volume 3
[HMI-B-353-VOL-3] 17 p2956 N85-28256
Reliability derating procedures
[AD-A153744] 18 p3119 N85-29309
Ada compiler validation summary report, University of Karlsruhe-GMD/German MOD Siemens - BS 2000 version 7.30
[AD-A153747] 18 p3163 N85-29591
New measurement solutions for low frequency systems 20 p3437 N85-31325
East Europe report: Science and technology
[JPRS-ESA-85-021] 21 p3568 N85-32190
Transceiver test device
[AD-D011728] 22 p3786 N85-33458
Testbed for sensory control of intelligent machines
[DE85-012355] 24 p4099 N85-35412

ELECTRONIC FILTERS
Filtration of higher harmonic components in two-level digital computing synthesizers 22 p3778 N85-33410

ELECTRONIC LEVELS
U ELECTRON ENERGY
U ENERGY LEVELS

ELECTRONIC MAIL
Efficiency analysis of the electronic mail system (INFOMAIL) on the defense data network
[AD-A151894] 15 p2632 N85-26223
Interfacing the VAX 11/780 using berkeley UNIX 4.2BSD and Ethernet based Xerox Network Systems
[AD-A153174] 17 p3016 N85-28647

ELECTRONIC MODULES
The study of microstrip antenna arrays and related problems
[NASA-CR-174054] 02 p0189 N85-11265
Electronic bandwidth compression module
[AD-A145843] 03 p0366 N85-12343
Analyses to develop models to project failure rates and repair costs of electronic modules and subassemblies
[AD-A146509] 06 p0816 N85-15180
Electronic module insertion and retraction mechanism
[AD-D011309] 07 p0947 N85-16002
Diodes in photovoltaic modules and arrays
[NASA-CR-175454] 10 p1508 N85-19513
ESP (External-Stores Program): A pilot computer program for determining flutter-critical external-store configurations. Volume 3, part 1: Program compilation
[AD-A152270] 16 p2711 N85-26727
Maintenance of photovoltaic power systems
[AD-A152289] 16 p2819 N85-27390
Modular Optoelectronic Multispectral Scanner (MOMS) for Earth observation. First results of STS-7 mission
[MBB-UR-717/83-O] 16 p2874 N85-27732

ELECTRONIC PACKAGING
Component reliability and assembling technologies
[CNES-NT-106] 04 p0511 N85-13256
UCB cosmic ray experiment 09 p1417 N85-18941
The effects of water and hydrogen on materials used in integrated circuit packages
[AD-A151893] 15 p2518 N85-25529

ELECTRONIC PHOTOGRAPHY
U ELECTRO-OPTICAL PHOTOGRAPHY

ELECTRONIC SIGNAL MEASUREMENT
U SIGNAL MEASUREMENT

ELECTRONIC SPECTRA
Boundary condition effects in the energy loss spectrum of layered systems
[NOTA-INTERNA-802] 02 p0289 N85-11887
Scattering experiments on interactions of excited atoms: Differential cross sections of the system Na (3P)+K(4S)
[MPIS-6/1984] 05 p0728 N85-14677
Metal complexes of some heterocyclic ligands
15 p2504 N85-25446
Theory of electron-impact atomic ionization cross sections
[AD-A151763] 16 p2861 N85-27648
The electronic spectra of phthalocyanine radical anions and cations
[AD-A152328] 17 p2918 N85-27986
Local electron spectrum above 100 MeV derived from gamma-ray emissivity spectra
[OG-3.1-7] 22 p3874 N85-33995

ELECTRONIC STRUCTURE
U ATOMIC STRUCTURE

ELECTRONIC SWITCHES
U SWITCHING CIRCUITS

ELECTRONIC TRANSDUCERS
Electromagnetic Acoustic Transducers (EMATs) for erosion monitoring
[DE85-004834] 12 p1854 N85-21628
MFTF sensor verification computer program
[DE85-004452] 12 p1916 N85-22029
Robot use in FRG increases but sensor technology lags 15 p2531 N85-25605
Design of inductive shift transducers
22 p3771 N85-33368
Development of position sensors for microcomputer-oriented sensor systems
[BMFT-FB-T-85-021] 24 p4091 N85-35
Materials and process development for microcomputer-compatible pressure, temperature, and position sensors
[BMFT-FB-T-85-024] 24 p4097 N85-35

ELECTRONIC WARFARE
Simulation of the performance of adaptively controlled Navstar antennas in battlefield scenarios
10 p1472 N85-192
A survey of radar ECM and ECCM
15 p2536 N85-25
Fin line filters technology and electronic warfare
[AD-A154975] 21 p3576 N85-322

ELECTRONICS
Joint services electronics program
[AD-A145085] 01 p0042 N85-1027
Center for Electronics and Electrical Engineering Technical Bulletin covering center programs
[PB84-218056] 01 p0045 N85-102
NAVAIR's (Naval air systems command) AI (Artificial Intelligence) program for ATE (Automated Test Equipment)
[AD-P003935] 02 p0247 N85-11615
DRG theory on the basis of a discrete interaction model
[PR-215] 03 p0358 N85-122
Research activities of the Illinois University Coordinated Science Laboratory
[AD-A145589] 03 p0449 N85-125
Electrical/electronics working group summary
05 p0604 N85-13
USSR report: Electronics and electrical engineering
[JPRS-UEE-85-002] 13 p2066 N85-229
China report: Science and technology
[JPRS-CST-85-007] 15 p2533 N85-25
Tutorial discussion of electronic sampling systems for recording wide-bandwidth transient signals
[DE85-006577] 15 p2549 N85-257
Robotic arc welding 15 p2586 N85-259
On the relationship between electronics and chemistry
[DRIC-T-7480] 22 p3743 N85-33
Modeling of electronic circuits with high degree of component integration 22 p3766 N85-333
USSR report: Electronics and electrical engineering
[JPRS-UEE-84-003] 22 p3773 N85-3338

ELECTRONOGRAPHY
Photometric study of the Saturn E ring
15 p2671 N85-25

ELECTRONS
NT CONDUCTION ELECTRONS
NT FREE ELECTRONS
NT HIGH ENERGY ELECTRONS
NT HOT ELECTRONS
NT NEGATRONS
NT PHOTOELECTRONS
NT POLARONS
NT RELATIVISTIC ELECTRON BEAMS
NT SOLAR ELECTRONS
Monte Carlo simulation of thermalization of subexcitation electrons in molecular hydrogen
[NAL-TR-815T] 01 p0117 N85-107
Bremsstrahlung radiation from longitudinal plasma waves caused by subthermal electrons in plasma
02 p0264 N85-117
Exchange and correlation effects and pair potentials of inter-atomic interaction
[BLL-M-35745-(5828.4)] 02 p0277 N85-118
Electron traps in the GaAs permeable base transistor
[AD-A145399] 02 p0287 N85-1187
Relationships between electronic structure and stability of metallic glasses
[AD-A145506] 02 p0287 N85-1187
Forced oscillations theory for resonant extended interaction electron devices
[PR-206] 03 p0358 N85-1229
Mechanisms of electrical conductivity in olivine
[DE84-014333] 04 p0495 N85-131
Evidence for d-band conduction in metallic glasses containing transition metal elements
[DE84-014822] 04 p0570 N85-136
Motion of electrons in non polar classical liquids
[DE84-013609] 05 p0727 N85-14
The radiative hydrodynamics of flare loops heated by impulsive bursts of energetic electrons
05 p0745 N85-147
Generation of suprathermal electrons during plasma current startup by lower hybrid waves in a Tokamak
[IPPJ-697] 06 p0803 N85-154
Arc-evaporated carbon films: Optical properties and electron mean free paths
[DE85-001246] 06 p0867 N85-155
Application of the diffraction model to amorphous magnesium zinc alloys
[AD-A147369] 07 p0928 N85-158

Electron-irradiated effects in metals
[DE84-016989] 09 p1297 N85-18147
The role of fast electrons for the performance characteristics of hydrogen ion sources
09 p1303 N85-18189
Monte Carlo simulation of electron thermalization in rare gases
[NAL-TR-834T] 09 p1375 N85-18643
Electron bounce resonance heating in a bumpy cylinder
[DE85-001732] 10 p1561 N85-19845
Electron-plastic effect in metals
11 p1605 N85-20089
Correlated 2 electron effects in collisions of multiply charged Au ions with He
[DE85-003064] 11 p1723 N85-20837
ITS: The Integrated TIGER Series of coupled electron/photon Monte Carlo transport codes
[DE85-003719] 11 p1725 N85-20847
Velocity distributions of solar wind ions and electrons
12 p1954 N85-22273
Electron-positron pair equilibrium in strongly magnetized plasmas 12 p1957 N85-22296
Electron-positron pairs in a mildly relativistic plasma in active galactic nuclei 12 p1957 N85-22297
Galileo internal electrostatic discharge program
13 p1995 N85-22504
Discharge characteristics of dielectric materials examined in mono-, dual-, and spectral energy electron charging environments 13 p1995 N85-22510
On the choice of coordinates for semiconductor simulation
[AD-A152214] 16 p2870 N85-27708
Atom location by electron channeling analysis
[DE85-007549] 16 p2872 N85-27716
Effects of level broadening on the magnetothermal oscillations in two-dimensional electron systems
[AD-A152639] 17 p3029 N85-28732
Hall mobility in fluid argon
[DE85-007288] 17 p3045 N85-28840
A review of ionospheric effects on Earth-space propagation 18 p3106 N85-29233
Ionospheric limitations to time transfer by satellite
18 p3107 N85-29234
The prospects of the digital optical computer
18 p3188 N85-29771
Study of the equilibrium vacancy ensemble in aluminum using 1D- and 2D-angular correlation of annihilation radiation
[DE85-008957] 18 p3194 N85-29813
Experiments with stored heavy ions
[DE85-009976] 19 p3356 N85-30802
Monte Carlo electron/photon transport
[DE85-010799] 19 p3364 N85-30861
Localization of waves in a disordered medium
19 p3373 N85-30926
Microscopic structure of two-dimensional electron glass
[DE85-010265] 19 p3376 N85-30942
The influence of a turbulent region on the flux of auroral electrons
[KGI-PREPRINT-072] 20 p3494 N85-31723
Methods of Monte Carlo electron transport in particle-in-cell codes
[DE85-010702] 20 p3521 N85-31898
Runaway electrons and plasma turbulence in current ramping by lower hybrid waves in tokamak plasmas
[DE85-011390] 20 p3535 N85-31997
Detection of excited states by laser-induced fluorescence
[AD-A155558] 21 p3592 N85-32326
Solar modulation and interplanetary gradients of the galactic electron flux, 1977 - 1984
[PAPER-SH-4.7-4] 21 p3716 N85-33059
Electron-donor dopant, method of improving conductivity of polymers by doping therewith, and a polymer so treated
[DE85-011640] 22 p3752 N85-33257
Reestimation of the production spectra of cosmic ray secondary positrons and electrons in the ISM
[OG-6.2-8] 22 p3889 N85-34107
Electrons and positrons from expanding supernova envelopes in dense clouds
[OG-6.2-9] 22 p3889 N85-34108
The electron spectra in the synchrotron nebula of the supernova remnant G 29.7-0.3
[OG-6.2-10] 22 p3889 N85-34109
Atmospheric Emission Photometric Imaging (AEPI)
23 p3902 N85-34170
Measuring method and confirmation of H- (D-) ion current by sheet plasma 1
[IPPJ-730] 23 p3974 N85-34638
Electron dynamics and transport in a mirror field
23 p3977 N85-34856
Model of azimuthal non-uniformities induced by RF heating in RFC-XXM 23 p3977 N85-34858
The propagation of solar flare particles in a turbulent coronal loop
[SH-1.1-3] 23 p3989 N85-34730
Stochastic particle acceleration in solar flares
[SH-1.1-4] 23 p3989 N85-34731
Study of non-thermal photon production under different scenarios in solar flares. 2: The Compton inverse and Bremsstrahlung models and fittings
[SH-1.2-3] 23 p3991 N85-34739
Temporal evolution of an energetic electron population in an inhomogeneous medium: Application to solar hard X-ray bursts
[SH-1.2-6] 23 p3991 N85-34741
Quantitative analysis of flare accelerated electrons through their hard X-ray and microwave radiation
[SH-1.2-7] 23 p3991 N85-34742
Two types of electron events in solar flares
[SH-1.2-11] 23 p3992 N85-34746
The energy spectra of solar flare electrons
[SH-1.2-14] 23 p3992 N85-34749
The Jovian electron spectrum: 1978-1984
[SH-1.5-19] 23 p3996 N85-34782
Observations of solar energetic particles at a synchronous orbit
[SH-3.1-1] 23 p4001 N85-34806
Coronal propagation of flare associated electrons and protons
[SH-3.1-3] 23 p4001 N85-34808
Geometry of the diffusive propagation region in the August 14, 1982 solar electron event
[SH-3.1-5] 23 p4001 N85-34809
The dependence of solar modulation on the sign of the cosmic ray particle charge
[SH-4.2-23] 23 p4009 N85-34860
Onion-shell model for cosmic ray electrons and radio synchrotron emission in supernova remnants
[OG-8.1-10] 23 p4018 N85-34900
Pulsars as cosmic ray particle accelerators: Dynamics of electrons
[OG-8.2-23] 23 p4021 N85-34919
Solar modulation and interplanetary gradients of the galactic electrons flux, 1977 - 1984
[SH-4.7-4] 23 p4040 N85-35049
Additional flux of particles and albedo-electrons in upper atmosphere
[SH-6.1-6] 23 p4045 N85-35080
Pulsed-neutron-source models for the astrophysical s-process
[DE85-012927] 24 p4151 N85-35740
Studies of relativistic heavy ion collisions
[DE85-014686] 24 p4152 N85-35745
Mini-clusters
[HE-3.5-3] 24 p4183 N85-35942
Structure of super-families
[HE-3.5-7] 24 p4183 N85-35944
Extremely high energy hadron and gamma-ray families(3). Core structure of the halo of superfamily
[HE-3.5-8] 24 p4183 N85-35945
Numerical analysis of electromagnetic cascades in emulsion chambers
[HE-3.5-9] 24 p4184 N85-35946
An experimental study of correlations in the development of the electron-photon cascades
[HE-3.5-10] 24 p4184 N85-35947
Integral functions of electron lateral distribution and their fluctuations in electron-photon cascades
[HE-3.5-12] 24 p4184 N85-35949
Electrons, muons and hadrons in extensive air showers and how do they depend on nuclear interaction model, part 2 24 p4187 N85-35969
Electrons, muons and hadrons in extensive air showers and how do they depend on nuclear interaction model, part 1 24 p4187 N85-35972
Sensitivity of depth of maximum and absorption depth of EAS to hadron production mechanism
24 p4186 N85-35982
A critical analysis of air shower structure functions and size spectrum measurements with the NBU air shower array 24 p4188 N85-35983
Missing energies at pair creation
[HE-4.4-8] 24 p4193 N85-36016
The hump in the Cerenkov lateral distribution of gamma ray showers
[HE-4.5-9] 24 p4195 N85-36032
Simulation of gamma-initiated showers
[HE-4.5-10] 24 p4195 N85-36033
Phenomenological characteristic of the electron component in gamma-quanta initiated showers
[HE-4.5-11] 24 p4196 N85-36034
Nuclear cascades in electromagnetic showers produced by primary gamma-quanta in the atmosphere
[HE-4.5-16] 24 p4196 N85-36038
Longitudinal development of muons in large air showers studies from the arrival time distributions measured at 900m above sea level
[HE-4.7-4] 24 p4199 N85-36055
Arrival time distributions of electrons in air showers with primary energies above 10 (18)eV observed at 900m above sea level
[HE-4.7-5] 24 p4199 N85-36056
Analysis of the electron component of EAS at observational level 700 g x cm(-2) with a scale breaking interaction model and gammaisation hypothesis
[HE-5.4-8] 24 p4208 N85-36119
Study of photonuclear muon interactions at Baksan underground scintillation telescope
[HE-5.4-10] 24 p4208 N85-36122
Collimated groups of particles as possible manifestation of heavy meson production
[HE-5.4-14] 24 p4208 N85-36124

ELECTROPHORESIS
Opportunities for space bioprocessing
02 p0150 N85-11018
Advances in electrophoretic separations
02 p0156 N85-11054
Commentary on Salyut-7 electrophoresis, plugging mortar experiments 02 p0158 N85-11072
Commentary on derivation of biological materials, cosmonaut adaptation 02 p0158 N85-11074
Electronic autofluorography: Principles, problems and prospects
[DE84-016698] 05 p0639 N85-14097
Bioprocessing in space 05 p0690 N85-14436
Kidney cell electrophoresis
[NASA-CR-171889] 20 p3498 N85-31745
Task description for the 1983 catalog of tasks for the materials processing in space program
20 p3498 N85-31746
Kidney cell electrophoresis, continuing task
20 p3498 N85-31747
Effects of coating rectangular microscopic electrophoresis chamber with methylcellulose
20 p3498 N85-31748
Asymmetric electroosmotic flow and mobility measurements at nonstationary positions in the rectangular chamber 20 p3499 N85-31749
Theoretical prediction of stationary positions in the rectangular chamber during asymmetric electroosmotic flow 20 p3499 N85-31750
A computer program for determining the electrophoretic mobility of cells in a rectangular chamber during asymmetric electroosmotic flow
20 p3499 N85-31751
Operation of the Zeiss cytopherometer with Zn/ZnSO4 electrode system of Tenforde et al
20 p3499 N85-31752
Electrophoretic mobility of cells in a vertical Ficoll gradiant 20 p3499 N85-31753
Free-zone electrophoresis of animal cells. 1: Experiments on cell-cell interactions
20 p3499 N85-31754
Development anmd testing of electrophoresis solutions. Task I.1: Development of optimal buffer system
20 p3500 N85-31755
Electrophoretic mobilities of erythrocytes in various buffers 20 p3500 N85-31756
Effects of method of detachment on electrophoretic mobility of mammalian cells grown in monolayer culture
20 p3500 N85-31757
Preparative electrophoresis of cultured human cells: Effect of cell cycle phase 20 p3500 N85-31758
Size and DNA distributions of electrophoretically separated cultured human kidney cells
20 p3500 N85-31759
The role of cell size in density gradient electrophoretic separation of mouse leukemia cells according to position in the cell cycle 20 p3500 N85-31760
Electrophoretic mobilities of cultured human embryonic kidney cells in various buffers 20 p3501 N85-31761
Effect of passage number on electrophoretic mobility distributions of cultured human embryonic kidney cells
20 p3501 N85-31762
Density gradient electrophoresis of cultured human embryonic kidney cells 20 p3501 N85-31763
Identification and quantitation of morphological cell types in electrophoretically separated human embryonic kidney cell cultures 20 p3501 N85-31764
Urokinase production by electrophoretically separated cultured human embryonic kidney cells
20 p3501 N85-31765
Summary electrophoretic data base on human embryonic kidney cell strain 8514
20 p3501 N85-31766
Recommendations and calculations concerning physical characteristics of the EEVT apparatus
20 p3502 N85-31769
Evaluation of results of cell electrophoresis experiments on space shuttle STS-3 including pre-flight and post-flight laboratory experiments 20 p3502 N85-31772
Free zone electrophoresis simulation of static column electrophoresis in microgravity on shuttle flight STS-3
20 p3502 N85-31773

Microgravity electrophoresis: A study of the factors that affect free-fluid separation 20 p3502 N85-31774
Properties of electrophoretic fractions of human embryonic kidney cells separated on space shuttle flight STS-8 20 p3503 N85-31776
A computerized system for spot detection and analysis of two-dimensional electrophoresis images 23 p3958 N85-34531

ELECTROPHOTOMETERS
The Torun measuring system for astronomical spectra 07 p0966 N85-16130
The scanning heliometer 14 p2451 N85-25134
Program for observations of Halley's comet 22 p3732 N85-33138

ELECTROPHOTOMETRY
Offerings of the Astronomical Institute of Bonn 15 p2667 N85-26459
Photoelectric observations of contact binary stars [REPT-96] 15 p2667 N85-26460
Photoelectric observations of the dwarf nova VW Hydri during the November 1977 supermaximum [REPT-97] 15 p2667 N85-26461
Photoelectric observations of the eclipsing binary V 836 Cygni [REPT-98] 15 p2668 N85-26462

ELECTROPHYSICS
NT ELECTRO-OPTICS
NT MOLECULAR ELECTRONICS
Complex formation and temperature stability of electrophysical properties of GaAs seminsulating single crystals 02 p0258 N85-11689
Basic research in electronic (JSEP): Joint Services Electronics Program [AD-A147891] 07 p0948 N85-16007

ELECTROPHYSIOLOGY
Review on physiological and medical problems related to climates ranging from altitude to sub-tropics 05 p0687 N85-14417
Electrophysiologic changes in organophosphorus-induced delayed neurotoxicity [AD-P004025] 06 p0844 N85-15359
Natural electrical activity of human sympathetic nerve fibers, recorded from body surface 07 p1013 N85-16433
Electrosleep therapy advanced at medical institute 10 p1526 N85-19623
Functional system theory in practice 11 p1690 N85-20629
Psychological aspects of phenomenon of spatial synchronization of EEG potential 11 p1691 N85-20632
Topography of human brain electric potentials and dominance 11 p1691 N85-20633
Susceptibility of cat and squirrel monkey to motion sickness induced by visual stimulation: Correlation with susceptibility to vestibular stimulation 11 p1694 N85-20650
Brain mechanisms underlying individual differences in reaction to stress: An animal model [AD-A150195] 13 p2143 N85-23301
A model for generalization and specification by single neurons [AD-A150671] 14 p2391 N85-24724
The origin of brain potentials associated with selective visual attention [AD-A152291] 16 p2840 N85-27511
Interaction of opiate and phencyclidine derivatives with the acetylcholine receptor [AD-A155119] 21 p3664 N85-32761

ELECTROPLATING
Inhibition of hydrogen absorption during plating of high strength steels [AD-A144882] 01 p0028 N85-10174
Laser-assisted solar-cell metallization processing 06 p0831 N85-15282
Effect of rhodamine-B on the electrodeposition of lead on copper, revision [DE85-000674] 11 p1606 N85-20101
Laser-assisted solar cell metallization processing [NASA-CR-176124] 22 p3805 N85-33565
Electrolytic cell [DE85-011598] 22 p3807 N85-33578

ELECTROPOLISHING
An electrochemical study of hydrogen uptake and elimination by bare and gold-plated waspaloy [NASA-TM-86479] 02 p0182 N85-11222
Electrolytic lapping technique for vanadium [DE84-014710] 02 p0183 N85-11227

ELECTROSEISMIC EFFECT
U ELECTRIC CURRENT
U SEISMIC WAVES

ELECTROSLAG PROCESS
Steel castings by the electroslag casting technique [DE85-003812] 12 p1819 N85-21409

ELECTROSLAG REFINING
ESR (Electroslag Refining) technology in Australia: Laboratory research and industrial development [AD-A147776] 08 p1129 N85-17114

ELECTROSLAG WELDING
Institute's contribution to Soviet welding technology noted 16 p2767 N85-27072

ELECTROSTATIC CHARGE
Aerosol sampling bias from differential electrostatic charge and particle size 02 p0224 N85-11467
Charging of the DMSP F-2 spacecraft in the aurora on 10 January 1983 [AD-A146303] 03 p0324 N85-12086
Long-term light induced changes in dark conductivity of kapton [AD-A148791] 08 p1224 N85-17706
Measurement and control of electrostatic charges on solids in a gaseous suspension [DE85-001450] 09 p1291 N85-18105
Electrostatic potentials: A new method for interpreting and predicting molecular reactivities and for designing synthetic pathways. Applications to nitroaromatics, nitramines and nitrated [AD-A150120] 12 p1801 N85-21296
Direct measurements of severe spacecraft charging in auroral ionosphere 13 p1991 N85-22480
Average and worst-case specifications of precipitating auroral electron environment 13 p1991 N85-22482
Galileo internal electrostatic discharge program 13 p1995 N85-22504
Automatic charge control system for satellites 13 p1995 N85-22508
Discharge characteristics of dielectric materials examined in mono-, dual-, and spectral energy electron charging environments 13 p1995 N85-22510
Development and testing of a spacecraft surface potential monitor 13 p2007 N85-22582
Electrostatic discharge testing on a carbon fiber solar panel structure 13 p2007 N85-22584
EOS (electrical overstress) protection for VLSI (Very Large Scale Integration) devices [AD-A150333] 13 p2064 N85-22891
Electrostatic charging of the Giotto spacecraft due to neutral gas impact 14 p2244 N85-23913
Saturn electrostatic discharges 15 p2673 N85-26499
Statistical study of Saturnian electrostatic discharges observed by the Voyager Planetary Radio Astronomy experiment 15 p2673 N85-26500
Multivalued electrostatic potentials; chance or necessity for the charge of solid particles near Saturn? 15 p2677 N85-26529
On the electric charge carried by dust grain excitation of violent discharge — planetary rings 15 p2677 N85-26530
Oil tank electrostatic charging report [DRIC-T-6967] 20 p3436 N85-31319

ELECTROSTATIC ENGINES
Ion thruster performance model [NASA-CR-174810] 04 p0462 N85-12935
Ion thruster project [NASA-TM-77726] 07 p0917 N85-15805
Precision tunable resonant microwave cavity [NASA-CASE-LEW-13935-1] 11 p1628 N85-20248

ELECTROSTATIC EROSION
U SPARK MACHINING

ELECTROSTATIC FIELDS
U ELECTRIC FIELDS

ELECTROSTATIC GENERATORS
Closed loop electrostatic levitation system [NASA-CASE-NPO-15553-1] 18 p3092 N85-29142
A small-scale self-excited rotor electrostatic generator [AD-A155264] 21 p3581 N85-32265

ELECTROSTATIC GYROSCOPES
Suspension torques on a gimballed electrostatically supported gyroscope and requirements on the gyroscope and spacecraft for the relativity gyroscope experiment 12 p1851 N85-21608

ELECTROSTATIC PLASMA
U PLASMAS (PHYSICS)

ELECTROSTATIC PRECIPITATORS
Electrostatic augmentation of fabric filtration: Reverse-air pilot unit experience [PB84-230002] 03 p0343 N85-12207
A system for monitoring radon and its decay products in the atmosphere [INPE-3065-PRE/494] 03 p0391 N85-12502
Third US/USSR Symposium on Particulate Control [PB85-190890] 19 p3310 N85-30522
Evaluation of pilot ESP used with a spray dryer FGD system at Pittsburgh Energy Technology Center, Bruceton, Pennsylvania [DE85-011151] 22 p3746 N85-33217
A study of the control of particulate emissions from turbine engine test cells 24 p4067 N85-35205

ELECTROSTATIC PROBES
Ionic reactions of atmospheric importance [AD-A147354] 07 p0997 N85-163
A new fast response probe for diffusion studies in atmospheric air — pollution modeling [IC-AERO-84-01] 08 p1180 N85-17437
Cookbook for determining essential transmission characteristics of spherical section electrostatic analyzers [DE85-001404] 09 p1391 N85-18751
Ram-wake effects on plasma current collection of the PIX 2 Langmuir probe 13 p1993 N85-2249
Results of the Langmuir-probe experiment on board Intercosmos-18 — ionosphere-magnetosphere interaction 14 p2362 N85-245
Measuring elect.ical field fluctuations by Langmuir Double Probe Method 16 p2720 N85-287
Rocket measurements of mesospheric ionization irregularities [NASA-CR-176056] 20 p3494 N85-31721
Observations of mesospheric turbulence by rocket probe and VHF radar, part 2.4A 21 p3619 N85-32484
Recoverable Plasma Diagnostics Package (RPDP) 23 p3902 N85-34187
Langmuir probe on ISX-B [DE85-012066] 23 p3983 N85-348

ELECTROSTATIC PROPULSION
NT ION PROPULSION
Ion thruster performance model [NASA-CR-174810] 04 p0462 N85-12935

ELECTROSTATIC SHIELDING
High voltage isolation transformer [NASA-CASE-GSC-12817-1] 18 p3093 N85-2914

ELECTROSTATIC WAVES
Integral of wave kinetic equation of drift waves 02 p0283 N85-11848
Waves and instabilities in collisionless shocks [AD-A146689] 06 p0881 N85-15597
The flow of plasma in the solar terrestrial environment [NASA-CR-174301] 08 p1224 N85-17707
Simulation of the ion-beam-driven drift instability in a magnetic trap, 1 [AD-A149451] 10 p1452 N85-19147
Simulation of the ion-beam-driven drift instability in a magnetic trap, 2 [AD-A149452] 10 p1554 N85-1978
Pressure-gradient-driven Tokamak resistive MHD instability in the banana-plateau collisionality regime [DE85-004568] 12 p1937 N85-22171
Cosmic ray generation by plasma turbulence Development of a new paradigm in physics 12 p1955 N85-222
Generation and propagation of electron cyclotron harmonic waves 14 p2367 N85-2463
Theoretical studies of electric cyclotron harmonic (ECH) waves based on experimental data from GEOS 1 14 p2367 N85-2463
Anomalous heating of ionospheric components (thermal e- and He+) via intense Ion Cyclotron Waves (ICW's) 14 p2368 N85-2463
A method of solving the dispersion equation for electrostatic electron waves in magnetized plasma [KGI-PREPRINT-071] 16 p2869 N85-276
Quenching of the beam-plasma instability by 3-D spectra of large scale density fluctuations [NASA-CR-175969] 19 p3369 N85-309
Application of field similitude theory to calculation of stripline heating 22 p3780 N85-3341
Recoverable Plasma Diagnostics Package (RPDP) 23 p3902 N85-34187
Observation of mode-converted by ion Bernstein wave by an HCN laser scattering [IPPJ-724] 23 p3979 N85-34

ELECTROSTATICS
Research on large, highly accurate, inflatable reflectors [AD-A145080] 01 p0016 N85-100
Effects of core mixing on solar oscillation frequencies [DE84-015540] 03 p0449 N85-128
Solid state, surface and catalytic properties of oxides [DE85-002096] 06 p0867 N85-15512
Data appendix: F-number = 1.0 EMR with a flexible back electrode [NASA-CR-172477] 07 p0946 N85-159
Electrostatic wave observation during a space simulation Beam-Plasma-Discharge (BPD) [NASA-CR-174286] 07 p1045 N85-16
Large electrostatic accelerators [DE85-001120] 09 p1382 N85-18
High power pulsed accelerators with potential industrial applications [DE85-001710] 11 p1720 N85-20
Computerized study of several electrostatic surface-ionization ion-source configurations [DE85-001512] 11 p1721 N85-20

Electrostatic confinement in a bumpy torus
[DE85-003794] 12 p1936 N85-22164
Electrostatic forming and testing of polymer films on a 16-foot diameter test fixture
[NASA-TM-86328] 13 p2063 N85-22885
Evaluation of unimolecular rate constants for some outer-sphere electrochemical reactions
[AD-A150758] 14 p2250 N85-23946
VULTURE manual
[DE85-008873] 17 p3013 N85-28631
Global effects of double layers — plasma layers
[TRITA-EPP-84-12] 20 p3536 N85-32002
Electrostatic astigmatic tubular lens
21 p3695 N85-32955
Supermite vacuum interface design
[DE85-012881] 22 p3837 N85-33759
Design status of heavy ion injector program
[DE85-010751] 22 p3842 N85-33793
Friction, impact, and electrostatic discharge sensitivities of energetic materials
[DE85-013321] 24 p4083 N85-35309
The effect of power law body forces on a thermally-driven flow between concentric rotating spheres
[NASA-TM-87596] 24 p4093 N85-35374
Two-dimensional quasineutral description of particles and fields above discrete auroral arcs
[NASA-CR-176170] 24 p4116 N85-35517

ELECTROSTRICTION
Piezoelectric and electrostrictive materials for transducer applications
[AD-A145115] 01 p0043 N85-10277

ELECTROTHERMAL ENGINES
NT ARC JET ENGINES
NT PLASMA ENGINES
NT RESISTOJET ENGINES
Investigation of a pulsed electrothermal thruster system
[NASA-CR-174768] 02 p0169 N85-11132
Qualification of an electrothermal hydrazine thruster with a vacuum thrust of 0.5 to 2.0 N
[BMFT-FB-W-84-043] 07 p0917 N85-15806
Compatibility experiments of facilities, materials, and propellants for electrothermal thrusters
[NASA-TM-86956] 12 p1795 N85-21260

ELECTROWINNING
Using fuel cells or anode depolarization to reduce electrowinning energy consumption
[DE85-006187] 13 p2129 N85-23250

ELEMENT ABUNDANCE
U ABUNDANCE

ELEMENTARY EXCITATIONS
NT EXCITONS
NT MAGNONS
NT PHONONS
NT PLASMONS
NT POLARONS
Quasiparticle aggregation in the Fractional Quantum Hall Effect
[DE85-001574] 10 p1565 N85-19868
Elementary processes of electronically excited particles. Part 5: Deactivation of CHF (A1a' (O, V'2, O) after excitation by a pulsed dye laser
[MPIS-13/1984] 14 p2420 N85-24930
Quasiparticle excitations in valence-fluctuation materials: Effects of band structure and crystal fields
[DE85-010783] 19 p3359 N85-30824

ELEMENTARY PARTICLE INTERACTIONS
NT ELECTRON CAPTURE
NT NUCLEAR CAPTURE
NT NUCLEON-NUCLEON INTERACTIONS
Spline-Galerkin solution of integral equations for 3-body scattering above break-up
[TWISK-327] 01 p0109 N85-10738
Results on weak current from CHARM collaboration — neutrino interactions
[NOTA-INTERNA-810] 02 p0279 N85-11817
Computing the Kac determinant using dual mode techniques and more about the No-ghost theorem
[DE85-001329] 09 p1375 N85-18640
Activities in nuclear physics and high energy physics
11 p1728 N85-20866
Experimental studies of elementary particle interactions at high energies
[DE85-004795] 13 p2157 N85-23394
Glueball candidates
[DE85-003627] 14 p2418 N85-24921
Modern test of chiral anomalies
[DE85-005892] 17 p3020 N85-28680
Elementary particle theory
[DE85-006603] 17 p3034 N85-28771
Topics in intermediate vector boson physics
[NOTA-INTERNA-841] 18 p3184 N85-29743
Activities report of the Werner-Heisenberg Institute for Physics
[ISSN-0173-6256] 18 p3184 N85-29748
Introduction to the Standard Model — weak and electromagnetic interactions
[USIP-85-02] 20 p3532 N85-31970
Nucleon-nucleus interactions from JACEE
24 p4173 N85-35869

ELEMENTARY PARTICLES
NT ALPHA PARTICLES
NT ANTINEUTRINOS
NT ANTINUCLEONS
NT ANTIPARTICLES
NT ANTIPROTONS
NT BARYONS
NT BETA PARTICLES
NT BOSONS
NT COLD NEUTRONS
NT CONDUCTION ELECTRONS
NT DEUTERONS
NT ELECTRONS
NT FAST NEUTRONS
NT FERMIONS
NT FREE ELECTRONS
NT GLUONS
NT HADRONS
NT HIGH ENERGY ELECTRONS
NT HOT ELECTRONS
NT HYPERONS
NT KAONS
NT LEPTONS
NT LIGHT BEAMS
NT MAGNETIC MONOPOLES
NT MESONS
NT MUONS
NT NEGATRONS
NT NEUTRINOS
NT NEUTRON BEAMS
NT NEUTRONS
NT NUCLEONS
NT PHOTOELECTRONS
NT PHOTONS
NT PIONS
NT POLARONS
NT POSITRONS
NT PROTONS
NT QUARKS
NT SOLAR ELECTRONS
NT SOLAR NEUTRINOS
NT SOLAR PROTONS
NT TACHYONS
NT THERMAL NEUTRONS
NT VECTOR MESONS
Research program in theoretical high-energy physics
[DE84-013717] 01 p0119 N85-10817
Research in elementary particle physics
[DE84-013520] 02 p0279 N85-11815
Decaying particles do not heat up the Universe
[DE85-002191] 11 p1763 N85-21091
Cosmology, galactic astronomy and elementary particle physics 12 p1956 N85-22289
Los Alamos Science, Number 11, Summer-Fall, 1984
[DE85-004634] 14 p2419 N85-24926
Activities report of the Werner-Heisenberg Institute for Physics
[ISSN-0173-6256] 18 p3184 N85-29748
The SLC program
[DE85-011433] 19 p3357 N85-30813
Spin dependence of the lamda-nucleus interaction determined by observation of hypernuclear gamma rays
[DE85-011878] 19 p3364 N85-30863
Monte Carlo sampling strategies for lattice gauge calculations
[DE85-010756] 19 p3377 N85-30948
Research in the theory of condensed matter and elementary particles
[DE85-010447] 20 p3531 N85-31968
Phenomenology of the standard and nonstandard Higgs particles
[USIP-85-03] 20 p3532 N85-31971
Depth and size effects on cosmogenic nuclide production in meteorites
[SH-7.1-9] 23 p4048 N85-35101
The identification of gamma ray induced EAS
[HE-4.5-1] 24 p4195 N85-36026

ELEVATION
Prediction of deflections of the vertical by gravimetric methods
[PB84-213727] 01 p0072 N85-10478
Digital Terrain Elevation Data (DTED) anomaly removal through the use of an interactive Fourier frequency filtering process
[AD-A145433] 02 p0219 N85-11445
Special difficulties of retrieving surface elevation over continental ice — satellite radar altimetry
03 p0380 N85-12429
Digital elevation models improve processing of Alaskan gravity data 04 p0515 N85-13285
Automatic terrain elevation mapping and registration
08 p1148 N85-17242
A comparative test of photogrammetrically sampled digital elevation models 08 p1175 N85-17408
Digital elevation model computation using fast Poisson solutions 08 p1175 N85-17412
Sequential data processing for photogrammetric acquisition of digital elevation models
08 p1176 N85-17413
Hypsometric features on Venus
13 p1983 N85-22439
Mathematical modeling of results of geometric leveling in variable gravity field 13 p2114 N85-23170
Surface units on Venus derived from Pioneer-Venus altimetry, roughness, and reflectivity measurements
13 p2177 N85-23510
Derivation of model topography
18 p3141 N85-29449
Comparison of survey and photogrammetry methods to position gravity data, Yucca Mountain, Nevada
[DE85-011685] 21 p3590 N85-32316

ELEVATION ANGLE
Experimental test of the three subaperture method for estimating target elevation angle
[AD-A149687] 12 p1851 N85-21614
A star camera aspect system suitable for use in balloon experiments
[OG-9.3-10] 23 p4028 N85-34965

ELEVATIONS (DRAWINGS)
U DRAWINGS

ELEVATORS (CONTROL SURFACES)
Application of linear optimal control theory to the design of the elevator control system of the DHC-2 Beaver experimental aircraft
[VTH-LR-411] 16 p2711 N85-26729
Proposals for the determination of necessary elevator handling characteristics of sailplanes in high speed range
[DFVLR-FB-84-52] 17 p2900 N85-27882

ELEVATORS (LIFTS)
Hoist
[AD-D011458] 10 p1493 N85-19425
Automated, robotized forge-press systems viewed
14 p2284 N85-24153
Application of lightweight composite materials to naval weapons systems
[PB85-173607] 18 p3069 N85-28981

ELEVONS
Space shuttle elevon seal panel mechanism
08 p1101 N85-16961

ELIMINATION
NT DELETION
Comparison of two algebraic methods for curve/curve intersection 17 p3007 N85-28591

ELLIPSES
What is principal components analysis?
02 p0211 N85-11389
Symmetry breaking for a class of semi-linear elliptic problems
[AD-A149093] 10 p1546 N85-19748
A new method for calculating the flow field in a dump combustor
[AD-A149305] 11 p1631 N85-20271
On MGR (Upsilon) multigrid methods
[AD-A153687] 19 p3345 N85-30733
Use of a minimum-ellipse criterion in the study of ion-beam extraction systems
[DE85-012670] 24 p4148 N85-35721

ELLIPSOIDS
Two lunar global asymmetries
04 p0585 N85-13734
Automatic Monoellipsoidal Mirror Furnace Facility (AMMFF), volume 1 — spaceborne crystal growth
[AMF-RP.100-DS-015-VOL-1] 09 p1285 N85-18073
Computation of the inviscid velocity potential for general ellipsoids on a nearly quadratic surface grid
[REPT-25/84] 11 p1633 N85-20287
Dynamics of solid body with ellipsoidal cavity containing magnetic fluid 14 p2279 N85-24116
Singularity solutions for ellipsoids in Low-Reynolds-Number flows: With applications to the calculation of hydrodynamic interactions in suspensions of ellipsoids
[AD-A153503] 18 p3168 N85-29632
Speckle interferometry applied to asteroids and other solar system objects
[NASA-CR-175976] 19 p3384 N85-30995

ELLIPSOMETERS
Photon scattering and interaction analysis of interfacial corrosion and catalysis
[DE85-002534] 11 p1608 N85-20114
Time-resolved ellipsometry and reflectivity measurements of the optical properties of silicon during pulsed excimer laser irradiation
[DE85-005091] 13 p2096 N85-23079
Interfacial bonding stability 21 p3608 N85-32409

ELLIPTIC DIFFERENTIAL EQUATIONS
NT MONGE-AMPERE EQUATION
On the theory of coercitive linear partial differential operators
[ISSN-0355-0087] 03 p0414 N85-12646
Transformation of two and three-dimensional regions by elliptic systems
[NASA-CR-174176] 04 p0554 N85-13529
Swirling turbulent spray group combustion
09 p1289 N85-18095
Vectorization and implementation of an efficient multigrid algorithm for the solution of elliptic partial differential equations
[AD-A149049] 10 p1545 N85-19743
Domain decomposition techniques for solving elliptic partial differential equations on multiprocessors
[DE85-004446] 10 p1549 N85-19789
On the accuracy of least squares methods in the presence of corner singularities
[NASA-CR-172552] 12 p1919 N85-22050
Analysis of spectral operators in one-dimensional domains
[NASA-CR-172573] 15 p2633 N85-26228
A stability analysis of incomplete LU factorizations
[AD-A152056] 15 p2638 N85-26271
Generation of surface coordinates by elliptic partial differential equations 17 p3006 N85-28583
Numerical methods for stiff ordinary and elliptic partial differential equations
[AD-A153247] 17 p3020 N85-28675
Solving elliptic partial differential equations on the hypercube multiprocessor
[AD-A153464] 18 p3168 N85-29629
Optimization of a numerical method to calculate elliptic flows
[ESA-TT-889] 20 p3457 N85-31472
Some ideas for decomposing the domain of elliptic partial differential equations in the Schwarz process
[DE85-011844] 22 p3834 N85-33739
Absorbing boundary conditions for exterior problems
[NASA-CR-177944] 24 p4142 N85-35676

ELLIPTIC FUNCTIONS
Application of summability methods to Jackson theorems for splines
[AD-A146256] 03 p0412 N85-12635
Some scientific subroutines in LISP
[AD-A147889] 07 p1026 N85-16515
Feedback, adaptivity and A-posterior estimates in finite elements: Aims, theory and experience
[AD-A146869] 07 p1029 N85-16531
Computation of elliptical functions in problems of celestial mechanics 13 p1979 N85-22418
Incorporation of an elliptical boundary condition into the program POISSON
[DE85-006820] 16 p2849 N85-27584

ELLIPTIC INTEGRALS
U ELLIPTIC FUNCTIONS

ELLIPTICAL CYLINDERS
The unsteady boundary layer on an elliptic cylinder following the impulsive onset of translational and rotational motion — dynamic stall 14 p2209 N85-23699

ELLIPTICAL GALAXIES
The relationship between radio structures and stellar dynamics of nearby elliptical galaxies
08 p1236 N85-17794
A comparative study of dust and young stars in three small galaxies 09 p1415 N85-18926
X-ray emission from Centaurus A
[DE85-002030] 09 p1417 N85-18943
Dynamics of elliptical galaxies and the r sup 1/4 luminosity law 12 p1955 N85-22282

ELLIPTICAL ORBITS
NT INTERPLANETARY TRANSFER ORBITS
NT PERIGEES
NT PERIHELIONS
NT TRANSFER ORBITS
Periodic oscillation of gyrostat-satellite about its center of mass in an elliptical orbit 02 p0159 N85-11080
Nonlinear oscillations of 2 body system relative to center of mass in elliptical orbit 02 p0159 N85-11082
Some considerations on elliptic heliocentric orbits
[INPE-3217-PRE/570] 02 p0297 N85-11926
Averaging of equations of cometary orbital motion with allowance for nongravitational effects
13 p1978 N85-22411
Satellite oscillations in elliptical orbit
13 p1981 N85-22429
Periodic movements of axisymmetrical satellite about center of mass due to gravitational moment
13 p2042 N85-22783
Inclinations of the Uranian rings
15 p2672 N85-26487
Integrable cases of restricted doubly averaged 3-body problem 16 p2718 N85-26778
The 6 pi-periodic solutions of plane restricted elliptical 3-body problem in neighborhood of libration points
16 p2718 N85-26779
Dynamics and control of tethers in elliptical orbits
20 p3399 N85-31087

ELLIPTICAL PLASMAS
Elliptical X-ray analyzer spectrograph application to a laser-produced plasma
[DE85-013790] 24 p4097 N85-35398

ELLIPTICITY
Limits of possible operation of the R-Tokamak due to ideal MHD instabilities
[IPPJ-694] 06 p0863 N85-15486
Downwash in the plane of symmetry of an elliptically loaded wing
[NASA-TP-2414] 07 p0898 N85-15693
An experimental investigation of unexcited and exicted elliptic jets 15 p2554 N85-25755
Neoclassical diffusion including ellipticity in a heliotron-like configuration 23 p3978 N85-34667

ELONGATION
Equibiaxial extension of two polymer melts: Polystyrene and low density polyethylene
[AD-A144893] 01 p0032 N85-10200
Tensile properties and swelling of 20%-cold-worked Type 316 stainless steel irradiated in HFIR
[DE84-014080] 05 p0617 N85-13948
Development and characterization of ductile Long-Range-Ordered (LRO) alloys (Fe,Co, Ni)3V for high-temperature structural use
[DE84-016750] 06 p0769 N85-14921
Rheology of dissemination
[AD-A150006] 12 p1813 N85-21373
Magnetic method of inspecting mechanical properties of general purpose tubes
[BLL-M-36084-(5828.4)] 16 p2796 N85-27235
Effects of annealing treatments on superplasticity in a thermomechanically processed Aluminum-10.2%Mg-0.52%Mn
[AD-A154414] 19 p3239 N85-30080

EMANATION
U EMISSION

EMBEDDED COMPUTER SYSTEMS
NT AIRBORNE/SPACEBORNE COMPUTERS
Embedded-grid generation with complete continuity across interfaces for multi-element airfoils
02 p0133 N85-10911
Liquid payload moment equations
[AD-A145977] 03 p0362 N85-12319
The embedded test (BIT): Impact on the total cost of possession 08 p1063 N85-16734
Ada (trademark) primer
[AD-A148855] 10 p1539 N85-19703
HLLM software support
[AD-A154828] 21 p3671 N85-32805

EMBEDDING
Embedment system for ultrahigh-burning rate propellants of solid propulsion subsystems
[AD-D011257] 06 p0773 N85-14942
Immobilization of toxic waste by embedding it in bitumen
[OEFZS-4277] 07 p0995 N85-16322
Extracting embedded generalized networks from linear programming problems
[AD-A147565] 07 p1033 N85-16558
Monitoring the execution of plans in SIPE (System for Interactive Planning and Execution) monitoring
[AD-A149136] 10 p1544 N85-19731
Functional equation for the embedding of a homomorphism of the interval into a flow
[DE85-000655] 11 p1713 N85-20780
Embedding graphs in lines, trees and grids
19 p3334 N85-30652

EMBOLISMS
Pathogenesis and treatment of cerebral air embolism and associated disorders
[AD-A146723] 07 p1014 N85-16443

EMBRITTLEMENT
Effect of microstructure and trapping on the hydrogen embrittlement susceptibility of a titanium bearing HSLA steel 02 p0174 N85-11166
The influence of rare Earth elements on the temper embrittlement behaviour and mechanical properties of a low alloy steel 02 p0180 N85-11210
The effects of microstructure on the temper embrittlement susceptibility of a Cr-2-1/4 1Mo forging
[AERE-R-11110] 03 p0334 N85-12151
Susceptibility of 2 1/4 Cr-1Mo steel to liquid metal induced embrittlement by lithium-lead solutions
[DE85-000997] 09 p1294 N85-18130
Study of the mechanism for annealing embrittlement of an iron-based metallic glass
[DE84-016856] 09 p1300 N85-18164
Models for shock damage to marine structural materials 09 p1336 N85-18400
Patterns in the occurrence of the brittle topologically close-packed phases: Al
[DE85-000592] 11 p1607 N85-20109
Chemisorption theory: Adsorption on copper-nickel alloys and titanium surface embrittlement
[DE85-001815] 12 p1807 N85-21264
Influence of oxygen traces on the properties of tungsten heavy metals
[BLL-RARDE-TR-1177-(7291.7965)]
15 p2506 N85-25470
Radiation effects on structural materials
[DE85-007032] 15 p2649 N85-26230
Grain boundary composition and intergranular fracture of steels. Volume 1: Detection of grain boundary segregation in steels
[DE85-006850] 15 p2662 N85-25429
Effect of texture in steel on the susceptibility of hydrogen embrittlement
[BLL-BISI-TRANS-22026-(9022.06)]
17 p2926 N85-28046
Interfacial segregation and fracture
[DE85-009779] 18 p3075 N85-29019
Brittle fracture behaviour of cold formed, welded 10mm to 20 mm thick plate manufactured from plain carbon structural steels
[BLL-BISI-TRANS-21678-(9022.06)]
18 p3120 N85-29311

EMBRYOS
Effects on in vivo and in vitro exposure to excess gravity on growth and differentiation of mammalian embryos
15 p2612 N85-26086

EMERALD
U BERYL

EMERGENCIES
Materials for emergency repair of runways
[AD-A146139] 03 p0320 N85-12098
Design of a scientific information collation and dissemination system, volumes 1 thru 3
[AD-A146002] 03 p0436 N85-12791
Improved robotic equipment for radiological emergencies
[DE84-017637] 04 p0509 N85-13249
Energy supply problems for emergency telephones
05 p0663 N85-14255
Liposome-encapsulated hemoglobin for emergency resuscitation
[AD-A146794] 07 p1015 N85-16446
An approach to planning in the inflight emergency domain
[AD-A151869] 15 p2487 N85-25228
Survivable ground base sensor
[AD-D011647] 17 p2950 N85-28213
US Coast Guard High Frequency Emergency Network (HFEN) implementation plan
[PB85-174167] 18 p3092 N85-29141
Graphic display development program. Volume 2, revision 0: Appendices
[DE85-011078] 19 p3333 N85-30648
Hydrazine and the F-16 20 p3511 N85-31826
Emergency modeling of hazardous air pollutants
[AD-A155441] 21 p3614 N85-32481
Fire service emergency management handbook
[AD-A155760] 24 p4064 N85-35313

EMERGENCY LIFE SUSTAINING SYSTEMS
A life-saving device for ships
[NASA-TM-77670] 23 p3895 N85-34129

EMERGENCY LOCATOR TRANSMITTERS
Recommended improvements for second generation 121.5/243 MHz ELT's
[NASA-CR-175274] 08 p1080 N85-16841
Emergency Locator Transmitter (ELT) batteries guidance and recommendations
[NASA-TM-87436] 11 p1624 N85-20025
Improved legislated emergency locating transmitters and emergency position indicating radio beacons
[NASA-CASE-GSC-12892-1] 11 p1624 N85-20028
Emergency Locator Transmitter (ELT) batteries guidance and recommendations
[NASA-TM-87415] 11 p1672 N85-20533
The 121.5 MHz ELT: Past, present and future — Emergency Locator Transmitter (ELT)
20 p3401 N85-31105
Soviet Emergency Locator Transmitter/Emergency Position Indicating Radio Beacon (ELT/EPIRBs) at 121.5 and 406 MHz 20 p3402 N85-31107
A 406 MHz ELT processor for geostationary satellites — Emergency Locator Transmitter (ELT)
20 p3403 N85-31114
Navigation data for Emergency Position Indicating Radio Beacons (EPIRBs) 20 p3403 N85-31115
The 121.5/243 MHz ELT identification — Emergency Locator Transmitter (ELT) 20 p3404 N85-31118
SARSAT 406 MHz system technical evaluation
20 p3404 N85-31124

The COSPAS/SARSAT demonstration and evaluation. Results of the first year in the United States
20 p3405 N85-31128

EMISSION
NT ACOUSTIC EMISSION
NT BIOLUMINESCENCE
NT CATHODOLUMINESCENCE
NT CHEMILUMINESCENCE
NT CN EMISSION
NT ELECTROLUMINESCENCE
NT ELECTRON EMISSION
NT EXHAUST EMISSION
NT FIELD EMISSION
NT FLUORESCENCE
NT HYDROXYL EMISSION
NT INCANDESCENCE
NT ION EMISSION
NT LIGHT EMISSION
NT LUMINESCENCE
NT MICROWAVE EMISSION
NT NEUTRON EMISSION
NT OPTICAL RESONANCE
NT PARTICLE EMISSION
NT PHOSPHORESCENCE
NT PHOTOELECTRIC EFFECT
NT PHOTOELECTRIC EMISSION
NT PHOTOIONIZATION
NT PHOTOLUMINESCENCE
NT RADIO BURSTS
NT RADIO EMISSION
NT RESONANCE FLUORESCENCE
NT SECONDARY EMISSION
NT SHOCK WAVE LUMINESCENCE
NT SOLAR RADIO BURSTS
NT SOLAR RADIO EMISSION
NT SPECTRAL EMISSION
NT SPONTANEOUS EMISSION
NT STIMULATED EMISSION
NT THERMAL EMISSION
NT THERMIONIC EMISSION
NT THERMOLUMINESCENCE
NT TYPE 3 BURSTS
NT TYPE 4 BURSTS
NT WATER MASERS
NT X RAY FLUORESCENCE

Future scenarios and ozone change
[DE84-014781] 01 p0065 N85-10573

Harmonic emission from high power gyrotron oscillators
[AD-A145621] 02 p0200 N85-11335

Optical detection of alkali compounds
[DE84-015505] 03 p0328 N85-12117

Photoconductivity and emission from the impurity excited states in silicon
[DE84-015583] 04 p0479 N85-13052

VOC emissions from volatile organic liquid storage tanks: Background information for proposed standards
[PB84-237320] 04 p0532 N85-13403

Inclined dislocation emission at a shielded crack tip
[DE84-016703] 06 p0818 N85-15192

SWIR and visible atomic emission from laser-produced oxygen and nitrogen plasmas
[AD-A147526] 07 p1045 N85-16641

Bipolar flows and X-ray emission from young stellar object 08 p1234 N85-17779

Three dimensional ray tracing of the Jovian magnetosphere in the low frequency range
[NASA-CR-175462] 10 p1571 N85-19909

The spatial dependence of the Jovian auroral emissions 11 p1759 N85-21068

Increase in hydrogen emission of upper atmosphere following launches of space vehicles
13 p1961 N85-22431

Review of national emission standards for mercury
[PB85-153906] 16 p2622 N85-27406

Circular-beam ray tracing on a microcomputer
[DE85-010754] 19 p3338 N85-30685

Improved Nominal Operating Cell Temperature (NOCT) test procedure 21 p3612 N85-32449

Dynamics of emission from dye lasers employing synchronous pumping by limited picosecond pulse train
21 p3686 N85-32899

Spectral-luminescence characteristics and induced emission of Nd-3(+) ion in Gd(2-x)Nd(x)(WO4)3 crystals
21 p3688 N85-32912

SCRIBE data of October 23, 1983 flight
[AD-A154864] 21 p3705 N85-33012

The effect of anisotropic emission on the log N-log S curve of gamma-ray bursts
[OG-1.2-4] 22 p3862 N85-33914

Atmospheric Emission Photometric Imaging (AEPI)
23 p3902 N85-34170

Wide Angle Michelson Doppler Imaging Interferometer (WAMDII) 23 p3902 N85-34172

Results on nucleon life-time from the Kolar gold field experiment
[HE-6.2-3] 24 p4211 N85-36139

EMISSION SPECTRA

Local photometric standards for CaII emission stars
01 p0128 N85-10683

A spectroscopic survey of 113 nearby red dwarf stars
01 p0129 N85-10686

Photoluminescent properties of epitaxial p-GaSb
02 p0267 N85-11745

Variations of the H and K emission lines of singly ionized calcium in the eclipsing binary star system AR Lacertae
02 p0296 N85-11921

Lyman-Alpha aurora 02 p0302 N85-11953

Molecular hydrogen emission associated with high velocity flows. A tracer for low velocity shocks
03 p0443 N85-12819

The X-ray spectrum and time variability of narrow emission line galaxies
[NASA-TM-83859] 03 p0446 N85-12842

Local fields in strongly coupled plasmas
[DE84-013375] 04 p0567 N85-13611

Far-infrared line emission from the galaxy
[NASA-CR-174166] 04 p0580 N85-13702

Non-LTE considerations in spectral diagnostics of thermal transport and implosion experiments
[DE84-015187] 05 p0730 N85-14689

Physical conditions in low-luminosity active galactic nuclei 05 p0742 N85-14771

Lower atmospheric composition of Jupiter from Voyager infrared measurements
[NASA-CR-174196] 05 p0745 N85-14779

Supercell band structure calculations of the two peak photo-and inverse photoemission spectra in Ce and Pr compounds
[DE84-017485] 06 p0867 N85-15513

The IRAS galaxy 0421+040P06: An active spiral (?) galaxy with extended radio lobes
[NASA-CR-174206] 06 p0871 N85-15536

The nature of the soft X-ray emitting region in the direction of the North Polar spur
06 p0877 N85-15568

Polarization of radio molecular lines and mapping of magnetic field direction 06 p0878 N85-15581

The compact radio emission regions in active galactic nuclei — QUASAT VLBI mission
07 p1058 N85-16713

Air quality assessment model validation in complex terrain
[AD-A147690] 08 p1180 N85-17434

Photoemission, vibrational and stimulated desorption studies of metal-semiconductor interfaces and of chemisorbed atoms and molecules
[AD-A147709] 08 p1225 N85-17717

Observations of nonthermal radio emission from early-type stars 08 p1232 N85-17758

X-ray emission from PKS 2155-304 — BL Lac object
08 p1239 N85-17812

X-ray emission from Centaurus A — Vela 5B; radio galaxy 08 p1239 N85-17813

The X-ray spectra of NGC 4151 — Seyfert galaxy
08 p1239 N85-17815

The high energy X-ray spectrum of 3C 273 — quasar
08 p1240 N85-17818

A universal spectrum for AGNs and QSOs — Active Galactic Nuclei (AGN) 08 p1241 N85-17826

An inverse Compton model of the X-ray emission in Seyfert galaxies 08 p1241 N85-17827

Theoretical studies of emission line variability in type 1 Seyfert galaxies 08 p1242 N85-17839

On the stability of broad line clouds in active galactic nuclei 08 p1243 N85-17840

The 1.5 - 3.5 micron spectroscopy of the Orion H2 source 08 p1246 N85-17864

Far infrared spectroscopy of (O III) in M82
08 p1249 N85-17883

Interpretation of the far infrared emission from our external galaxies 08 p1249 N85-17884

Measurement procedures for the radar spectrum engineering criteria
[PB85-119022/GAR] 09 p1313 N85-18254

Effect of inner subshell ionization for emission lines of OIV ion 09 p1388 N85-18729

Applications of pulsed-laser techniques and thermographic phosphors to dynamic thermometry of rotating surfaces
[DE85-000403] 11 p1639 N85-20326

Ion quadrupole effects in spectral line broadening
[DE85-001504] 11 p1730 N85-20879

Subnanosecond time-resolved emission study of Cu2O and GaAs
[DE85-002070] 11 p1735 N85-20912

IUE spectroscopy of extragalactic H H regions
11 p1745 N85-20974

Coordinated multifrequency observations of the BL LAC objects MRK 180, MRK 421, and MRK 501
11 p1746 N85-20983

Fluorescent excitation of Fe 2, Mn 2, Ti 2, N 1 lines by V 4, N 5, O 6: Emission lines in the spectra of symbiotic stars and Seyfert galaxies 11 p1746 N85-20984

IUE observations of planetary nebulae in the Magellanic Clouds 11 p1747 N85-20986

1983 observations of the eclipsing nucleus of the bipolar planetary nebula NGC 2346 11 p1747 N85-20987

The changing ultraviolet spectrum of Herbig-Haro object No. 1 11 p1747 N85-20989

Short-wavelength observations of HH-2H and HH-24A
11 p1747 N85-20990

A search for young stellar chromospheres in NGC 2264 11 p1748 N85-20993

FP Cygni profiles in HL CMa
11 p1752 N85-21022

Variability of ultraviolet emission lines in the carbon star TX Psc 11 p1753 N85-21027

Temporal UV emission from the peculiar star RX Puppis 11 p1753 N85-21028

UV observations of epsilon aurigae during ingress and totality 11 p1755 N85-21038

Circumstellar material in Algols and Serpentids
11 p1757 N85-21051

Chromospheric emission lines in high-resolution LWR spectra (220 - 3000 alpha) of gamma CRU (M3 3) and alpha ORI (M2 lab) 11 p1758 N85-21058

Precise measurements of radial velocities of emission lines in the far-ultraviolet spectra of late-type stars
11 p1758 N85-21062

Long term variability of the IO torus
11 p1760 N85-21070

Calibrations of wavelengths in SWP echelle spectra
11 p1761 N85-21077

Formation of optical-line emitting regions in the jets of SS433 12 p1959 N85-22318

Impurities in Kevlar 49 fibers
[DE85-004996] 13 p2038 N85-22767

A standard aircraft diffusion flame: Spectral characteristics and a feasibility study for developing an alternate calibration source for aircraft optical fire detection systems
[AD-A150231] 13 p2039 N85-22768

Measurement of the large-scale anisotropy of the cosmic background radiation at 3 MM 13 p2206 N85-23680

The Fe XIII 10747 A and Fe XIV 5303 A coronal emission lines polarization 14 p2448 N85-25111

Sound emission by particle beam passing through hole in rigid shield 15 p2525 N85-25570

High pressure cosmochemistry applied to major planetary interiors: Experimental studies
[NASA-CR-175715] 15 p2679 N85-26544

A new luminosity component in 3C48
[NASA-CR-175840] 17 p3052 N85-28894

Method for predicting the performance of cathode materials
[AD-D011665] 19 p3257 N85-30198

Self-consistent models for the X-ray emission from supernova remnants 20 p3548 N85-32062

Aerosol analysis and emission spectrometry with free jets
[DE85-010576] 21 p3564 N85-32168

Ionospheric electron density profile and related studies
[AD-A155257] 21 p3632 N85-32567

Investigation of reproducibility of emission wavelength of helium-neon laser with external neon absorption cell (0.63 micrometers) 21 p3683 N85-32884

High-resolution spectrum of Cygnus X-1
[OG-2.4-12] 22 p3868 N85-33956

Inverse-Compton gamma rays in the galaxy
[OG-3.1-2] 22 p3873 N85-33990

Multicomponent analysis of total COS-B gamma-ray data at intermediate latitudes
[OG-3.1-3] 22 p3873 N85-33991

The galactic gamma-ray distribution and the radial cosmic ray gradient
[OG-3.1-4] 22 p3873 N85-33992

Local electron spectrum above 100 MeV derived from gamma-ray emissivity spectra
[OG-3.1-7] 22 p3874 N85-33995

The electron spectra in the synchrotron nebula of the supernova remnant G 29.7-0.3
[OG-6.2-10] 22 p3889 N85-34109

Time-resolved spectroscopic studies of detonating heterogeneous explosives
[DE85-009760] 23 p3921 N85-34297

Apparatus and method for the spectrochemical analysis of liquids using the laser spark
[DE85-005749] 23 p3935 N85-34387

The read-out system of spatial distribution of thermoluminescence in meteorites
[SH-9.1-16] 23 p4052 N85-35131

The structure of Herbig-Haro object 43 and Orion dark cloud extinction
[NASA-TM-87503] 24 p4166 N85-35831

The ionization structure of planetary nebulae. Part 4: NGC 7662
[NASA-CR-176151] 24 p4169 N85-35844

EMISSIVITY

Non equilibrium ionization in the local hot bubble
06 p0879 N85-15587

Experimental investigations of thermal radiation from potassium atoms in magnetohydrodynamic system: Preliminary report
[DE85-003715] 12 p1936 N85-22169

Emissivity enhancement of fused silica for space applications — solar cells 13 p2011 N85-22615

Periodic gamma-ray emissions from Geminga at or = 10(12) eV
[OG-2.4-2] 22 p3867 N85-33949

Search for periodicities near 59 s in the COS-B gamma-ray data of 2CG195+04 (Geminga)
[OG-2.4-3] 22 p3867 N85-33950

Search for gamma-rays above 400 GeV from Geminga
[OG-2.4-4] 22 p3867 N85-33951

Observations on TeV gamma rays from Geminga and PSR 0950+08
[OG-2.4-6] 22 p3868 N85-33953

HEAO 3 upper limits to the expected 1634 KeV line from SS 483
[OG-2.4-9] 22 p3868 N85-33954

EMISSOGRAPHS
U ACTINOMETERS
U RECORDING INSTRUMENTS

EMITTANCE

Energy dependence of the emittance of damping ring beams
[DE85-007080] 15 p2649 N85-26341

A calorimetric approach for measuring emittance and normal spectral absorptance at elevated temperatures
[AD-A151292] 15 p2651 N85-26351

Profile of a relativistic electron beam propagated through a linear wiggler and an axial guide field
[AD-A154403] 19 p3353 N85-30783

Emittance growth caused by current variation in a beam-transport channel
[DE85-010743] 19 p3363 N85-30849

Requirements for very high energy accelerators
[DE85-011173] 20 p3529 N85-31952

Observations of accelerated high current low emittance beams in the SLC Linac
[DE85-013073] 24 p4068 N85-35211

Beam potential measurement of an intense H(-) beam by use of the emissive probe technique
[DE85-012671] 24 p4155 N85-35762

High resolution beam profile monitors in the SLC
[DE85-013375] 24 p4157 N85-35774

Relation between field energy and RMS emittance in intense particle beams
[DE85-012655] 24 p4159 N85-35784

EMITTERS
NT THERMIONIC CATHODES
NT THERMIONIC EMITTERS

Strained-layer superlattice emitter and detector structures using modulation-doped active regions
[DE85-000064] 06 p0867 N85-15511

Power transfer from natural emitters to collection apertures at microwave wavelengths
[NASA-CR-174275] 07 p0945 N85-15989

Research on electroluminescence in thin film yttrium oxysulfide
[AD-A146909] 07 p1037 N85-16582

Study of surface damage in cathode composite materials in a high flux CO2 laser 10 p1444 N85-19098

Development of solid state infrared emitters for gas detection applications
[PB85-148450] 15 p2561 N85-25800

EMOTIONAL FACTORS

Influence of activation of ASFS-2 on human emotional status 08 p1194 N85-17522

Decision making in stressful conditions: A model based on the coping perspective
[FOA-C-55064-H3] 08 p1229 N85-17738

USSR report: Life sciences. Biomedical and behavioral sciences
[JPRS-UBB-85-011] 10 p1525 N85-19616

EMOTIONS

The Reports of Aeromedical Laboratory, volume 25, no. 1/2
[ISSN-0023-2856] 01 p0090 N85-10605

Psychological states (mood, affect or emotion) experienced by JASDF pilots through flying duties. 3: Flying conditions causing pilots psychological disturbances 01 p0090 N85-10606

The relationship between emotional tension scale and psychological uneasiness of JASDF pilots in flying situations 01 p0090 N85-10608

Functional role of type of person's temperament in individual and mutual activity 10 p1525 N85-19621

Electrosleep therapy advanced at medical institute
10 p1526 N85-19623

Methods of monitoring mental work efficiency, emotional activity 10 p1526 N85-19627

EMPENNAGE
U TAIL ASSEMBLIES

EMPLOYEE RELATIONS

Data processing professionals and DP application users' perceptions and expectations of operational roles of persons working in a DP/application user interface group 24 p4165 N85-35821

EMPLOYMENT

Exploratory assessment of second generation robotics and sensor-based systems
[PB85-132793] 11 p1648 N85-20368

A comparison of metropolitan and non-metropolitan employment characteristics: Indications of the size of non-metropolitan mobile communication services user classes
[NASA-CR-175648] 13 p2053 N85-22855

Application of the Hardman methodology to the Single Channel Ground-Airborne Radio System (SINCGARS)
[NASA-CR-175694] 14 p2218 N85-23756

Characteristics of recent science/engineering graduates, 1982: Detailed statistical tables
[PB85-149060] 15 p2683 N85-26437

EMULSIONS
NT NUCLEAR EMULSIONS
NT PHOTOGRAPHIC EMULSIONS

Mist flammability studies of candidate fire-resistant hydraulic fluids
[AD-A148572] 08 p1134 N85-17148

A study of organic chemical reactions in microemulsions
[AD-A150083] 12 p1796 N85-21265

A brief review of the technology of microemulsions and other micellar systems
[AD-A149759] 12 p1800 N85-21289

Research on microemulsions for storage and conversion of solar energy
[DE85-000181] 12 p1862 N85-21807

Combustion and micro-explosion of water/oil emulsions in high pressure environments
[AD-A152960] 17 p2919 N85-27997

Multidimensional analysis of data obtained in experiments with X-ray emulsion chambers and extensive air showers
[HE-3.6-2] 24 p4184 N85-35951

A new method of differential structural analysis of gamma-family basic parameters
[HE-3.6-3] 24 p4184 N85-35952

Hadrons registration in emulsion chamber with carbon block
[HE-3.7-3] 24 p4186 N85-35962

Structured events in Pamir carbon X-ray chambers
[HE-3.7-7] 24 p4186 N85-35965

Ultra high energy events in ECHOS series and primary energy spectrum
[HE-3.7-9] 24 p4186 N85-35966

Search for anomalons using plastic nuclear track detectors
[HE-6.2-12] 24 p4212 N85-36148

Observation of genetic relation among new phenomena Geminion, Chiron and mini-Centauro
[HE-6.2-16] 24 p4212 N85-36152

Detection threshold energy of high energy cascade showers using thermoluminescence PTFE-sheet and hot-gas reader
[HE-7.1-5] 24 p4213 N85-36159

Application of thermoluminescence for detection of cascade shower 2: Detection of cosmic ray cascade shower at Mount Fuji
[HE-7.1-12] 24 p4214 N85-36162

ENAMELS

Production process for steel with decarburized surface adapted for single coating enamelling
[BMFT-FB-T-85-022] 20 p3432 N85-31292

Features of behavior of gas bubbles in molten oxide films during enamelling: Communication 2
[BLL-M-35781-(5828.4)] 23 p3919 N85-34283

ENCAPSULATING

Investigation of liquid encapsulation Chochralski growth of InP
[AD-A146096] 03 p0433 N85-12760

Study program for encapsulation materials interface for Flat-plate Solar Array (FSA) project
[NASA-CR-174152] 04 p0530 N85-13385

Encapsulation design analysis
06 p0829 N85-15268

Encapsulation materials and processing
06 p0830 N85-15269

Photothermal degradation of encapsulants
06 p0830 N85-15270

Polymer-polymer interface bond stability
06 p0830 N85-15271

Polymer-metal interface bond stability
06 p0830 N85-15272

Module flammability research
06 p0830 N85-15274

Process research of non-Cz silicon material
06 p0830 N85-15275

Effect of sealants of the sound absorption coefficients of acoustical friable insulating materials
[AD-A148541] 08 p1218 N85-17674

WESF (173)Cs gamma ray sources
[DE85-000676] 11 p1727 N85-20[illegible]

Hot Isostatic Pressing (HIP): Techniques, applications and economical use
[JUEL-SPEZ-268] 17 p2939 N85-28141

Encapsulation and packaging of a semiconductor multielectrode array for cortical implantation
[AD-A153180] 17 p2998 N85-28605

Concretization of high level radioactive source in marine sediment
[AD-D011703] 19 p3249 N85-30146

Photothermal degradation studies of encapsulants
21 p3606 N85-32469

Encapsulation processing and manufacturing yield analysis 21 p3611 N85-32434

Investigation of test methods, material properties, and processes for solar cell encapsulants
[NASA-CR-176132] 23 p3945 N85-34446

ENCELADUS

The E-ring of Saturn 15 p2677 N85-26627

ENCKE COMET

Extended atmospheres of outer planet satellites and comets
[NASA-CR-174338] 08 p1258 N85-17916

Extended atmospheres of outer planet satellites and comets
[NASA-CR-174398] 09 p1416 N85-18933

ENCLOSURE

Heat-transfer enhancement in natural convection enclosure flow
[DE84-013048] 09 p1319 N85-18297

ENCLOSURES

Influence of Prandtl number on natural convection heat transfer correlations
[DE84-013006] 05 p0637 N85-14089

Moisture content and gas sampling device
[NASA-CASE-MSC-18866-1] 18 p3103 N85-29213

Plastic heliostat enclosure analysis
[DE85-009112] 18 p3130 N85-29387

Natural convection in square partitioned enclosures
[AD-A153707] 18 p3197 N85-29639

Sound-insulating enclosures — machine noise
[BMFT-FB-HA-85-005] 20 p3525 N85-31925

ENCODERS
U CODERS

ENCODING
U CODING

END MORAINES
U GLACIAL DRIFT

END-TO-END DATA SYSTEMS

The IRAS end-to-end data system
[NLR-MP-83056-U] 17 p3051 N85-28880

ENDANGERED SPECIES

Environmental management needs
[DE85-007859] 18 p3133 N85-29405

ENDOCRINE GLANDS
NT ADRENAL GLAND
NT PANCREAS
NT PARATHYROID GLAND
NT PITUITARY GLAND
NT THYMUS GLAND
NT THYROID GLAND

ENDOCRINE SECRETIONS
NT ADRENOCORTICOTROPIN (ACTH)
NT ALDOSTERONE
NT HORMONES
NT HYDROXYCORTICOSTEROID
NT INSULIN
NT PROSTAGLANDINS

ENDOCRINE SYSTEMS

Mathematical modeling of fluid-electrolyte alterations during weightlessness
[NASA-CR-171881] 15 p2617 N85-26125

ENDOCRINOLOGY

Endocrine responses to nonhypotensive gravitational stress: Vasopressin and aldosterone
05 p0693 N85-14459

Endocrine responses to hypotensive gravitational stress: Catecholamines, pancreatic polypeptide, and vasopressin 05 p0693 N85-14460

Changes in bone structure and metabolism during simulated weightlessness: Endocrine and dietary factors
[NASA-CR-175961] 18 p3153 N85-29521

ENDOLYMPH
Quantitation of Na+, K+-ATPase enzyme activity in tissues of the mammalian vestibular system
15 p2613 N85-26102

ENDURANCE
The effect of propranolol on the training response to endurance exercise in normal human adults
05 p0696 N85-14479

ENERGETIC PARTICLES
NT ARGON PLASMA
NT BETA PARTICLES
NT BOUNDARY LAYER PLASMAS
NT COLD PLASMAS
NT COLLISIONAL PLASMAS
NT COLLISIONLESS PLASMAS
NT CONDUCTION ELECTRONS
NT COSMIC PLASMA
NT CYLINDRICAL PLASMAS
NT DENSE PLASMAS
NT DEUTERIUM PLASMA
NT ELECTRON PLASMA
NT ELECTRONS
NT ELLIPTICAL PLASMAS
NT HELIUM PLASMA
NT HIGH ENERGY ELECTRONS
NT HIGH TEMPERATURE PLASMAS
NT HOT ELECTRONS
NT LASER PLASMAS
NT METALLIC PLASMAS
NT NEGATRONS
NT NITROGEN PLASMA
NT NONEQUILIBRIUM PLASMAS
NT NONUNIFORM PLASMAS
NT NUCLEI (NUCLEAR PHYSICS)
NT OXYGEN PLASMA
NT PLASMA FOCUS
NT PLASMAS (PHYSICS)
NT RELATIVISTIC PLASMAS
NT ROTATING PLASMAS
NT SEMICONDUCTOR PLASMAS
NT SOLAR WIND
NT SPACE PLASMAS
NT SPHERICAL PLASMAS
NT STELLAR WINDS
NT STRONGLY COUPLED PLASMAS
NT THERMAL PLASMAS
NT TOROIDAL PLASMAS
Atlas of polar cap energetic particle observations. Volume 1: TIROS-N, 1 January 1979 - 28 February 1981
[PB84-233402] 04 p0535 N85-13419
Hot plasma particles in the Earth's outer magnetosphere: New understandings during the IMS
[DE84-016826] 05 p0677 N85-14348
The radiative hydrodynamics of flare loops heated by impulsive bursts of energetic electrons
05 p0745 N85-14781
Fine structure of Alfven maser radiation
06 p0824 N85-15232
An atlas of polar cap energetic particle observations. Volume 2: NOAA-6, 8 July 1979 to 10 May 1983
[PB85-109072] 12 p1891 N85-21868
Suppression of tilting instability of a compact torus by energetic particle beams
[IPPJ-705] 12 p1935 N85-22157
Particle transport in planetary magnetospheres
12 p1954 N85-22275
Hot plasma and energetic particles in the Earth's outer magnetosphere: New understandings during the IMS
14 p2355 N85-24552
The access of energetic charged particles to satellite altitudes
[AD-A150799] 14 p2373 N85-24670
Boundary of modulation diffusion and stochastic instability of high energy protons in inner radiation belt
15 p2482 N85-25316
Substorms in energetic radiation belt particles according to data from Meteor artificial Earth satellite
16 p2719 N85-26788
Characteristics and sources of E-region ionization in the continuous aurora
[AD-A155018] 21 p3632 N85-32562
Contributions to the 19th International Cosmic Ray Conference
[NASA-CR-176060] 21 p3714 N85-33044
Solar coronal and photospheric abundances from solar energetic particle measurements
[PAPER-SH-2.1-5] 21 p3715 N85-33053
Search for gamma-rays from M31 and other extragalactic objects
[OG-2.7-3] 22 p3871 N85-33977
Cosmic rays in the 10(16) to 10(19) eV range from pulsars
[OG-5.4-3] 22 p3886 N85-34080
The primary cosmic ray mass composition at energies above 10(14) eV
[OG-5.4-6] 22 p3886 N85-34083
Two classes of solar energetic particle events associated with impulsive and long duration soft X-ray flares
[SH-1.2-12] 23 p3992 N85-34747
Energetic protons from a disappearing solar filament
[SH-1.3-7] 23 p3993 N85-34754
Injection of energetic particles following the gamma-ray flares on June 7, 1980, as observed on Helios 1
[SH-1.3-9] 23 p3993 N85-34756
Shock and statistical acceleration of energetic particles in the interplanetary medium
[SH-1.5-1] 23 p3996 N85-34771
Energetic ion acceleration at collisionless shocks
[SH-1.5-3] 23 p3996 N85-34772
Latitude dependence of co-rotating shock acceleration
[SH-1.5-14] 23 p3997 N85-34777
Elemental abundances in corotating events
[SH-1.5-15] 23 p3997 N85-34778
Solar and interplanetary particles at 2 to 4 MEV during solar cycles 21, solar cycle variations of event sizes, and compositions
[SH-1.5-16] 23 p3997 N85-34779
Energetic particle observations of the solar-gamma ray/neutron flare events of 3 Jun 1982 and 21 June 1980 isotopic and chemical composition
[SH-2.1-3] 23 p3998 N85-34784
Precision measurements of solar energetic particle elemental composition
[SH-2.1-4] 23 p3998 N85-34785
Solar Coronal and photospheric abundances from solar energetic particle measurements
[SH-2.1-5] 23 p3998 N85-34786
Variations in elemental composition of several MEV/nucleon ions observed in interplanetary space
[SH-2.1-7] 23 p3998 N85-34788
Diffusion in the chromosphere and the composition of the solar corona and energetic particles
[SH-2.1-9] 23 p3999 N85-34790
Anomalous abundances of solar energetic particles and coronal gas: Coulomb effects and First Ionization Potential (FIP) ordering
[SH-2.1-10] 23 p3999 N85-34791
The mean ionic charges of N, Ne, MG, SI and S in solar energetic particle events
[SH-2.1-11] 23 p3999 N85-34792
Calculations of heavy ion charge state distributions for nonequilibrium conditions
[SH-2.1-12] 23 p3999 N85-34793
Isotopic overabundances and the energetic particle model of solar flares
[SH-2.2-1] 23 p4000 N85-34796
Solar source regions of 3HE-rich particle events
[SH-2.2-4] 23 p4000 N85-34799
On the connection between the 3HE-enrichment and spectral index of solar energetic particles
[SH-2.2-9] 23 p4001 N85-34804
A cosmic ray driven instability
[OG-8.1-5] 23 p4018 N85-34895
Cosmogenic-nuclide production by primary cosmic-ray protons
[SH-7.1-6] 23 p4047 N85-35098
A silicon surface barrier telescope for solar particles identification
[SH-8.1-3] 23 p4050 N85-35118
Multiple vacancy production by high energy heavy ions
[DE85-004426] 24 p4162 N85-35805
A search for heavy long lived particles in high energy cosmic rays
[HE-6.2-7] 24 p4211 N85-36143

ENERGY
The energy cost of women walking and running in shoes and boots
[AD-A151022] 14 p2389 N85-24716
The 1000 GeV gamma rays from ms pulsars
[OG-2.3-12] 22 p3867 N85-33948

ENERGY ABSORPTION
NT ELECTROMAGNETIC ABSORPTION
NT GAMMA RAY ABSORPTION
NT INFRARED ABSORPTION
NT MOLECULAR ABSORPTION
NT MULTIPHOTON ABSORPTION
NT PHOTOABSORPTION
NT THERMAL ABSORPTION
NT THERMALIZATION (ENERGY ABSORPTION)
NT ULTRAVIOLET ABSORPTION
NT X RAY ABSORPTION
Mechanisms of laser annealing of semiconductors
02 p0267 N85-11744
Distribution of total solar radiation in Spain
04 p0523 N85-13344
Tests of the load-bearing and deformation behaviour of reinforced concrete spherical shells under point loading
[BLL-RISLEY-TR-4550-9091.9F)]
06 p0816 N85-15182
An orthogonal grid technique for studying internal deformation and energy absorption in target penetration
[AD-A149969] 12 p1860 N85-21665
Jet topologies in hadron-hadron collisions
[DE85-001328] 12 p1929 N85-22119
A plasma initiation-flow chamber to study CW laser beamed energy absorption in light gases
[AD-A151225] 15 p2562 N85-25806
Energy deposition from particle beams
[DE85-007382] 16 p2862 N85-27654
Energy deposition and its effects on the E+ capture section at Sector 20
[DE85-010964] 18 p3182 N85-29727
Impact dynamics research on composite transport structures
[NASA-TM-86391] 19 p3284 N85-30367
Cyclotron resonance in a nonneutral plasma
[AD-A155248] 21 p3707 N85-33017
Development of an energy-absorbing passenger seat for a transport aircraft 22 p3796 N85-33515
Design and testing of an energy-absorbing crewseat for the F/FB-111 aircraft, volume 1
[NASA-CR-3916] 23 p3896 N85-34133
Design and testing of an energy-absorbing crewseat for the F/FB-111 aircraft. Volume 2: Data from seat testing
[NASA-CR-3917] 24 p4064 N85-35184

ENERGY ABSORPTION FILMS
International Congress Centrum Berlin report on photovoltaics 12 p1877 N85-21773
Thin-film solar cells from sputtered and vapor-deposited amorphous silicon 12 p1879 N85-21792
Development of a CdSe thin film solar cell
12 p1880 N85-21796
Selective coatings for solar heat converters
17 p2939 N85-28144

ENERGY BANDS
NT BLOCH BAND
NT CONDUCTION BANDS
NT FORBIDDEN BANDS
Local contributions to the 0.6 keV diffuse X-ray background 06 p0877 N85-15569
Ultrasoft X-ray background observations of the local interstellar medium 06 p0877 N85-15571
Optically induced intervalence-band transitions in germanium by the absorption of 1.06 micrometers picosecond pulses
[DE85-000946] 09 p1399 N85-18803
Angle-resolved photoemission study of AuGa2 and AuIn2 intermetallic compounds
[AD-A150000] 12 p1940 N85-22183
Laser beam shaping system with reduced objective diameter 14 p2275 N85-24095
Electronic density of states for the double donor system Si:P, As
[INPE-3447-PRE/700] 16 p2869 N85-27700
Doping superlattices in organometallic VPE InP
[AD-A155151] 21 p3710 N85-33029

ENERGY BUDGETS
NT ATMOSPHERIC HEAT BUDGET
NT HEAT BUDGET
Energy-active zones in north Atlantic as manifestation of interannual variability of radiation balance
02 p0164 N85-11106
Cage regional energy budgets from the GLAS ATH order model 05 p0685 N85-14402
Eddy correlation measurements of energy partition for Amazonian forest
[INPE-3195-PRE/559] 06 p0827 N85-15252
The influence of deep cumulus convection on large-scale flow during AVE/SESAME 1, 10-11 April 1979
09 p1355 N85-18526
Testing an energy balance model for estimating actual evapotranspiration using remotely sensed data — Hannover, West Germany barley and wheat fields
13 p2125 N85-23236
Accurate albedos of the brightest regions on Io
13 p2195 N85-23618
Small component spectral model of annual course of zonal atmospheric circulation 14 p2337 N85-24453
The Martian climate: Energy balance models with CO2/H2O atmospheres
[NASA-CR-175722] 15 p2679 N85-26547

ENERGY CONSERVATION
ACEE program rationale and implementation
[NASA-TM-84549] 02 p0133 N85-10906
On-board near-optimal climb-dash energy management 02 p0137 N85-10931
Hybrid laminar flow control study
[NASA-CR-165930] 02 p0137 N85-10933

Energy efficient engine flight propulsion system preliminary analysis and design report
[NASA-CR-174701] 02 p0140 N85-10947
Energy-saving technological methods of obtaining controlled atmospheres
[BLL-M-35724-(5828.4)] 02 p0171 N85-11145
ECUT energy data reference series: Lightweight materials for ground transportation
[DE84-015269] 05 p0621 N85-13974
Hangar heating and energy conservation manual
[AD-A147893] 07 p0910 N85-15762
Development of design and economic parameters for passive solar systems
[AD-A147181] 07 p0993 N85-16303
Evaluation of the measured energy performance of four solar systems
[AD-A147912] 07 p0993 N85-16306
Oil-shale exploration expansion urged
07 p0994 N85-16317
MHD performance demonstration experiment, FY 1974 to FY 1984
[DE85-000854] 08 p1224 N85-17709
Collegium on aviation fuel conservation efforts
09 p1278 N85-18034
New lighting technologies, their status and impacts on power densities
[DE85-000712] 09 p1315 N85-18266
Effect of hitch positions on the performance of track-grouser systems
[AD-P004277] 09 p1406 N85-18853
Electrocatalysis research
[NASA-CR-174352] 10 p1437 N85-19054
DOE/ORNL electric systems program overview
[DE85-003334] 10 p1459 N85-19197
ElectriFleet Project
[DE85-001598] 10 p1570 N85-19898
Electric-Hybrid Vehicle (E-HV) demonstration-test project
[DE85-002370] 10 p1570 N85-19899
Power from the Sun: Light at night
[PB85-124097] 12 p1883 N85-21814
Using fuel cells or anode depolarization to reduce electrowinning energy consumption
[DE85-006187] 13 p2129 N85-23250
Deputy minister on civil aviation fuel conservation efforts 14 p2208 N85-23691
Aviation workers plenum reviews fuel conservation progress 15 p2461 N85-25197
USSR report: Transportation
[JPRS-UTR-84-014] 15 p2467 N85-25229
Ilyushin bureau designer on fuel conservation research
15 p2467 N85-25231
Aviation turbine fuels from tar sands bitumen and heavy oils. Part 1: Process analysis
[AD-A151319] 15 p2521 N85-25539
Planning fuel-conservative descents in an airline environmental using a small programmable calculator: Algorithm development and flight test results
[NASA-TP-2393] 16 p2707 N85-26705
General continuous formulations of atmospheric energy laws 16 p2830 N85-27448
A numerical solution technique for multitemperature plasma hydrodynamics
[AD-A152701] 17 p3039 N85-28801
On power effecient operation of the 2m x 2m transonic wind tunnel at the National Aerospace Laboratory
[NAL-TR-847] 18 p3064 N85-28953
Natural convection in square partitioned enclosures
[AD-A153707] 18 p3197 N85-29828
Improving the defense energy information system (DEIS)
[AD-A153524] 18 p3200 N85-29849
Energy accounting software
[DE85-010612] 19 p3340 N85-30694
Auto fuel efficiency standards, part 2
[GPO-41-169] 20 p3435 N85-31309
Energy efficient transport technology: Program summary and bibliography
[NASA-RP-1135] 22 p3729 N85-33116
Monitoring building energy performance: An informal review and characterization of research in progress
[BNL-51765] 23 p3923 N85-34308
Advanced heat pump research and development
[DE85-009540] 23 p3932 N85-34372
Energy Efficient Engine Program technology benefit/cost study, volume 2
[NASA-CR-174766-VOL-2] 24 p4066 N85-35198
Comparative analysis of operational forecasts versus actual weather conditions in airline flight planning, volume 1
[NASA-CR-167862] 24 p4119 N85-35534
Comparative analysis of operational forecasts versus actual weather conditions in airline flight planning, volume 2
[NASA-CR-167863] 24 p4119 N85-35535
Comparative analysis of operational forecasts versus actual weather conditions in airline flight planning, volume 3
[NASA-CR-167864] 24 p4120 N85-35536
Comparative analysis of operational forecasts versus actual weather conditions in airline flight planning, volume 4
[NASA-CR-167865] 24 p4120 N85-35537
Comparative analysis of operational forecasts versus actual weather conditions in airline flight planning: Summary report
[NASA-CR-167866] 24 p4120 N85-35538
Turbulent structure of stably stratified nocturnal slope flows
[AD-A155845] 24 p4123 N85-35559
Phase space factors in multiparticle processes
24 p4175 N85-35888

ENERGY CONSUMPTION
US energy for the rest of the century, 1984 edition
[PB84-207406] 04 p0531 N85-13393
Energy information exchange, 1983
[DE84-901446] 04 p0577 N85-13880
Hangar heating and energy conservation manual
[AD-A147893] 07 p0910 N85-15762
Biocatalyzed processes for production of commodity chemicals: Assessment of future research advances for N-butanol production
[NASA-CR-174264] 07 p0919 N85-15819
Development of design and economic parameters for passive solar systems
[AD-A147181] 07 p0993 N85-16303
Oil-shale exploration expansion urged
07 p0994 N85-16317
Study of low energy density photovoltaic applications under varying rate structures
[DE85-000165] 10 p1511 N85-19538
Synthetic fuels policy
[GPO-34-227] 11 p1613 N85-20143
Digital and color energy maps for graphic display of hourly data
[DE85-000526] 11 p1673 N85-20543
Feoktistov discusses need for space colonization
13 p1985 N85-22454
Using fuel cells or anode depolarization to reduce electrowinning energy consumption
[DE85-006187] 13 p2129 N85-23250
Field use of electric vehicles compared to prototype tests
[DE85-006887] 15 p2667 N85-26458
Improving the defense energy information system (DEIS)
[AD-A153524] 18 p3200 N85-29849
Wind tunnel results of advanced high speed propellers in the takeoff, climb and landing operating regimes
[NASA-TM-87054] 19 p3213 N85-29925
Energy accounting software
[DE85-010612] 19 p3340 N85-30694
Model documentation of the gas analysis modeling system. Volume 1: Model overview
[DE85-010952] 20 p3515 N85-31856
Development of a prototype energy meter
[PB85-196430] 22 p3789 N85-33476

ENERGY CONVERSION
NT BIOMASS ENERGY PRODUCTION
NT GEOTHERMAL ENERGY CONVERSION
NT OCEAN THERMAL ENERGY CONVERSION
NT PHOTOTHERMAL CONVERSION
NT SOLAR ENERGY CONVERSION
NT SOLAR TOTAL ENERGY SYSTEMS
NT WATERWAVE ENERGY CONVERSION
Shock electromechanical energy converter with permanent magnet
[AD-D011228] 01 p0115 N85-10781
Non-oxide ceramics: A new class of engineering materials 02 p0179 N85-11199
Material problems for high-temperature, high-power space energy-conversion systems
[AD-A145940] 03 p0385 N85-12466
FSA field test
[NASA-CR-174114] 04 p0526 N85-13373
Thermomagnetic generator
[DE84-017018] 04 p0530 N85-13388
Analysis of wind energy systems for selected electric utilities
[DE84-013025] 04 p0530 N85-13389
Electromechanical/electromagnetics working group summary 05 p0604 N85-13852
High-efficiency power conversion options for flywheel energy storage systems 05 p0607 N85-13876
Dynamic conversion working group summary
05 p0611 N85-13904
Thermoelectric and thermionic conversion technology
05 p0611 N85-13905
Advanced and nontraditional concepts working group report 05 p0612 N85-13909
Nitinol devices, phase 2, integration of slip ring system and tracking mechanism with memory drive
[BMFT-FB-W-84-032] 05 p0619 N85-13069
Optimization of energy conversion during locking of electron bunches by electromagnetic wave in longitudinal electrostatic field 06 p0786 N85-15025
Performance and cost of energy transport and storage systems for dish applications using reversible chemical reactions
[NASA-CR-174263] 07 p0992 N85-16298
Electrochemistry of polymer films. Applications to chemical analysis and energy conversion
[AD-A147737] 08 p1132 N85-17136
Air quality assessment model validation in complex terrain
[AD-A147690] 08 p1160 N85-17434
MHD performance demonstration experiment, FY 1974 to FY 1984
[DE85-000854] 08 p1224 N85-17709
Available energy method for evaluating thermodynamic performance of heat pump systems
[DE84-017223] 09 p1400 N85-18814
An electro-optic spatial light modulator for thermo-elastic generation of programmably focused ultrasound
[AD-A149078] 10 p1553 N85-19794
Advanced concepts in systems analysis and simulation
[DE85-002728] 11 p1702 N85-20701
JPL highlights
[NASA-CR-175517] 11 p1767 N85-21102
Oceanic role in terrestrial climate
[DE85-004422] 12 p1896 N85-21904
Modulation of light energy transduction in photosynthesis
[DE85-004711] 13 p2141 N85-23292
Spaceborne power systems preference analyses. Volume 1: Summary
[NASA-CR-175644] 14 p2349 N85-24517
Spaceborne power systems preference analyses. Volume 2: Decision analysis
[NASA-CR-175645] 14 p2349 N85-24518
Sensitivities of projected 1980 photovoltaic system costs to major system cost drivers
[NASA-CR-175669] 14 p2349 N85-24519
Test results of an organic Rankine-cycle power module for a small community solar thermal power experiment
[NASA-CR-175696] 14 p2350 N85-24524
Intermediate load modules for test and evaluation
[NASA-CR-175697] 14 p2350 N85-24526
Studies of photosynthetic Energy Conversion
[DE85-005973] 15 p2586 N85-25944
Exploratory wind-tunnel investigation of a wingtip-mounted vortex turbine for vortex energy recovery
[NASA-TP-2468] 16 p2699 N85-26667
Water brake convertor: A simple device to convert mechanical energy into heat energy
[DE85-006021] 16 p2716 N85-26786
General continuous formulations of atmospheric energy laws 16 p2830 N85-27448
Documents of the JPL Photovoltaics Program Analysis and Integration Center: An annotated bibliography
[NASA-CR-175873] 17 p2985 N85-28448
Energy data base: Subject categories and scope
[DE84-017376] 17 p3050 N85-28881
Technology for industrial waste heat recovery by organic Rankine cycle systems
[DE85-006719] 18 p3102 N85-29206
Exploratory study of coal conversion chemistry
[DE85-010393] 19 p3229 N85-30018
Metallophthalocyanine dimers incorporating five atom covalent bridges
[AD-A154365] 19 p3234 N85-30051
Uniform cost-estimation method for biomass production and conversion technologies
[DE85-011714] 19 p3380 N85-30970
Biocatalysis project
[NASA-CR-176044] 20 p3498 N85-31744
Energy from low temperature differences
[DE85-008817] 24 p4112 N85-35492

ENERGY CONVERSION EFFICIENCY
Energy efficient engine high pressure turbine test hardware detailed design report
[NASA-CR-167955] 02 p0147 N85-10985
Efficiency of photoelectric conversion of short radiation pulses 03 p0348 N85-12240
NASA Redox Storage System Development Project
[NASA-TM-83677] 03 p0385 N85-12465
Operating experience with potassium systems — thermal power stations
[OEFZS-4275] 03 p0387 N85-12473
Development and verification of MCD-2 and MOD-OA simulation models
[DE84-017389] 04 p0550 N85-13499

The spectrophotometric method of determining the transmission of solar energy in salt gradient solar ponds
05 p0666 N85-14283

The upwind power plant Manzanares
05 p0669 N85-14305

Gamma-ray to Cerenkov-light conversion efficiency for pure-silica-core optical fibers
[DE84-015041] 05 p0729 N85-14685

Proceedings of the 23rd Project Integration Meeting
[NASA-CR-174186] 06 p0829 N85-15260

High-efficiency silicon solar cell research
06 p0829 N85-15261

Efficiency estimation and sensitivity modeling
06 p0829 N85-15263

Barriers to achieving high efficiency
06 p0829 N85-15264

MBE growth for high-efficiency silicon solar cells
06 p0829 N85-15265

Development and analysis of silicon solar cells near 20% efficiency 06 p0829 N85-15267

Liquid-fueled Ramjet engines
07 p0918 N85-15814

Multijunction cells for concentrators: Technology prospects
[NASA-CR-174259] 07 p0991 N85-16295

Progress in developing tidal electric power plants reported 07 p0994 N85-16314

Actual versus design performance of solar systems in the National Solar Data Network
[DE85-001190] 09 p1344 N85-18456

Soft X-ray spectroscopy of laser produced plasmas
09 p1387 N85-18727

Development of high efficiency solar cells on silicon web
[NASA-CR-174435] 10 p1509 N85-19521

Research on the basic understanding of high efficiency in silicon solar cells
[DE85-000507] 11 p1672 N85-20537

Direct contact heat recovery from molten salt
[DE85-002830] 11 p1674 N85-20550

Performance of solar thermal systems with liquid metal MHD conversion
[DE85-002758] 11 p1675 N85-20555

Development of new process technologies for solar cells with high efficiency starting from purified silicon
12 p1878 N85-21785

Development of high-efficiency economic systems for photovoltaics 12 p1880 N85-21795

Nonlinearity and spectral mismatch problems of solar cells 13 p2010 N85-22605

High output photovoltaic conversion: The quadrispectral project — spacecraft power supplies
13 p2012 N85-22626

Reluctance and doubly-excited reluctance motors
[DE85-003585] 13 p2065 N85-22900

A theoretical analysis of solar-driven natural convection energy conversion systems
[DE84-004431] 13 p2128 N85-23245

Ways of optimization of light energy transformation in primary stages of photosynthesis. Necessity of optimization of photosynthetic unit structure and method for calculating efficiency 14 p2366 N85-24700

Modeling and optimization of a multiple-cell photovoltaic converter system 15 p2585 N85-25934

Development of high-efficiency solar cells on silicon web
[NASA-CR-175707] 15 p2585 N85-25939

Large-scale commercial combustion systems for producing energy from municipal solid waste
[DE85-007097] 15 p2587 N85-25946

Superconducting traveling wave accelerators
[DE85-006247] 15 p2661 N85-26424

Solar elements with distributed parameters
16 p2760 N85-27036

Documentation and solar cell modules
[NASA-CR-175769] 16 p2818 N85-27384

Design and development of a linear Fresnel lens air-cooled photovoltaic module and a stand-alone photovoltaic collector array
[DE85-006654] 16 p2819 N85-27391

Selection of promising sites for magma energy experiments
[DE85-006632] 16 p2820 N85-27393

Overview of the 1985 NASA Lewis Research Center SP-100 free-piston Stirling engine activities
[NASA-TM-87028] 16 p2860 N85-27769

A program for the calculation of paraboloidal-dish solar thermal power plant performance
[NASA-CR-175674] 17 p2985 N85-28449

Advanced evacuated tube collectors
[DE85-010271] 19 p3274 N85-30302

A mathematical model of reciprocating combustion engine dynamics for the diagnosis of deficient energy conversion 19 p3280 N85-30339

Develop and test fuel cell powered on-site integrated total energy systems. Phase 3: Full-scale power plant development
[NASA-CR-168338] 19 p3304 N85-30483

Research on the basic understanding of high efficiency in silicon solar cells
[DE85-006774] 19 p3305 N85-30487

Reciprocating Brayton cycle motor
[REPT-84-RR-336] 20 p3462 N85-31507

Silicon solar cell efficiency improvement: Status and outlook 20 p3479 N85-31619

Some practical considerations for economical back contact formation on high efficiency solar cells
20 p3479 N85-31620

High-efficiency cell concepts on low-cost silicon sheets 20 p3479 N85-31621

Processing technology for high efficiency silicon solar cells 20 p3483 N85-31642

Texture etching of (100) silicon for solar cells
20 p3483 N85-31643

User handbook for block 5 silicon solar cell modules
[NASA-CR-176043] 20 p3483 N85-31644

Nomographs for estimating the levelized cost of energy from flat-plate and concentrator photovoltaic systems
[NASA-CR-176048] 20 p3483 N85-31645

Photovoltaic concentrator research status
[DE85-010119] 20 p3483 N85-31647

Power generation efficiency of piezoelectric crystals
20 p3537 N85-32008

Status of boron combustion research
[AD-A154762] 21 p3563 N85-32160

High-efficiency crystalline silicon technology development 21 p3607 N85-32395

Summary of the high-efficiency crystalline solar cell research forum 21 p3607 N85-32396

High-efficiency module and array research
21 p3607 N85-32397

Flat-plate module efficiency versus cost tradeoffs
21 p3607 N85-32398

The future of crystalline silicon technology in the US Department of Energy program
21 p3607 N85-32399

Georgetown University Photovoltaic Higher Education National Exemplar Facility (PHENEF)
21 p3607 N85-32400

Block V module program 21 p3607 N85-32401

Photothermal degradation studies of encapsulants
21 p3608 N85-32403

Advanced module development overview
21 p3612 N85-32445

Stress and efficiency studies in EFG
[NASA-CR-176125] 22 p3751 N85-33251

Block 5 documentation and solar modules
[NASA-CR-176134] 22 p3805 N85-33564

Development of high-efficiency solar cells on silicon web
[NASA-CR-176101] 22 p3805 N85-33568

Advanced heat pump research and development
[DE85-009540] 23 p3932 N85-34372

Energy Efficient Engine Program technology benefit/cost study, volume 1
[NASA-CR-174766-VOL-1] 24 p4066 N85-35197

ENERGY CONVERTERS
U DIRECT POWER GENERATORS

ENERGY DENSITY
U FLUX DENSITY

ENERGY DISSIPATION

Electron energy loss rates in N-2, O-2 and air
[AD-A145158] 01 p0072 N85-10476

Electric conductivities, currents and energy dissipation in the polar ionosphere 02 p0227 N85-11483

Boundary condition effects in the energy loss spectrum of layered systems
[NOTA-INTERNA-802] 02 p0289 N85-11887

Electron energy loss investigation of the electronic and structural properties of palladium
[NOTA-INTERNA-803] 02 p0289 N85-11888

Reflection electron energy loss investigation of the H-GaAs(110) surface
[NOTA-INTERNA-811] 02 p0289 N85-11889

Theoretical studies of Field-Reversed Configurations (FRC) and experimental study of the FRC during translation
[DE84-016467] 04 p0568 N85-13603

Boundary conditions for artificial dissipation operators — convection
[FFA-TN-1984-53] 09 p1375 N85-18642

Confinement of low-energy electrons near metallic surfaces for plasmon generation
[DE85-001119] 09 p1381 N85-18688

Effect of hitch positions on the performance of track-grouser systems
[AD-P004277] 09 p1406 N85-18853

Carbon vaporization/condensation effects
[NASA-TM-87430] 10 p1436 N85-19048

Temperature-dependent surface states and transitions of Si(111)-7x7
[AD-A149156] 10 p1562 N85-19850

Vacuum ultraviolet electronic properties of liquids
[DE85-000305] 10 p1563 N85-19858

Winds and waves (4 min - 11 yrs) in the upper middle atmosphere (60-110 km) at Saskatoon, Canada (52 deg N, 107 deg W): MF radar (2.2 MHz) soundings 1973 - 1983 11 p1662 N85-20476

Excitation of impurities by heavy particles and radiative losses of thermonuclear plasma
11 p1719 N85-20816

Coincidence studies of secondary electron emission in light ion-atom collisions
[DE85-002373] 11 p1725 N85-20852

Reducing electric power losses in discharge chamber of induction plasmatron 12 p1841 N85-21553

Substorms in the Earth's atmosphere
[DE85-000654] 12 p1890 N85-21861

Dissipation of energy in composite material
13 p2027 N85-22703

Energy losses at leading edge of turbine blade during multirow jet cooling 13 p2049 N85-22826

Near Field/Far Field (NF/FF) energy loss in Electric Discharge Lasers (EDL's): A mode-medium interaction
[AD-A150299] 13 p2096 N85-23075

Special features of computations of vertical distribution of concentration of suspended sediments under marine conditions 13 p2106 N85-23125

Seismic waves and dispersion relations
13 p2116 N85-23181

Stability of the Galilean satellites in deep orbital resonance 13 p2172 N85-23477

Capture of planetesimals into a circumterrestrial swarm 13 p2179 N85-23522

Aspects of CSSR CMOS integrated circuits discussed
15 p2533 N85-25627

Elastic-workhardening SDF (Single-Degree-of-Freedom) system subjected to random blast excitations
[AD-A151866] 15 p2579 N85-25909

Energy deposition from particle beams
[DE85-007382] 16 p2862 N85-27654

Digital filters for application to data analysis in electron energy loss spectroscopy
[DE85-007932] 17 p2923 N85-28020

Energy considerations in second breakdown
[AD-A152389] 17 p2952 N85-28229

Tribological sinks: Money down the drain
[DE85-010019] 17 p2974 N85-28376

Magnetic steels with the lowest specific total losses
[BMFT-FB-T-84-263] 18 p3078 N85-29042

Interpretation of radar returns from the mesosphere, part 2.3A 21 p3619 N85-32485

All particle energy spectrum of cosmic rays in 10 to the 15th power - 10 to the 20th power eV region
[OG-5.1-15] 22 p3882 N85-34056

Monitoring building energy performance: An informal review and characterization of research in progress
[BNL-51765] 23 p3923 N85-34308

Twenty-two-year cycle of the upper limiting rigidity of Daly waves
[SH-4.5-5] 23 p4036 N85-35023

Spallogenic origin of nuclei in meteorites
[SH-7.1-10] 23 p4046 N85-35102

Prediction of turbulent internal recirculating flows with K-epsilon models 24 p4092 N85-35366

Turbulent structure of stably stratified nocturnal slope flows
[AD-A155845] 24 p4123 N85-35559

Proposed FRX-D experiment
[DE85-012766] 24 p4158 N85-35776

Experimental evidence of the decrease of kinetic energy of hadrons in passing through atomic nuclei
24 p4174 N85-35880

Analytical calculation of muon intensities under deep sea-water
[HE-5.2-16] 24 p4204 N85-36092

Photo nuclear energy loss term for muon-nucleus interactions based on xi scaling model of QCD
[HE-5.2-17] 24 p4204 N85-36093

Range fluctuations of high energy muons passing through matter
[HE-5.2-19] 24 p4204 N85-36095

Results from the UCSD magnetic monopole search
[HE-6.1-12] 24 p4210 N85-36137

ENERGY DISTRIBUTION
NT SPECTRAL ENERGY DISTRIBUTION

Measuring local ion energy distribution function in Tuman-3 Tokamak plasma 02 p0271 N85-11768

Emission mechanisms in the liquid metal ion source: A review
[AERE-R-11294] 03 p0418 N85-12675

Minimizing the energy spread within a single bunch by shaping its charge distribution
[DE84-016172] 05 p0727 N85-14676

The IRAS galaxy 0421+040P06: An active spiral (?) galaxy with extended radio lobes
[NASA-CR-174208] 06 p0871 N85-15536

Unidentified IRAS sources: Ultrahigh luminosity galaxies
[NASA-CR-174207] 06 p0872 N85-15537

Morphology of keV-electrons in the Earth's magnetosphere as observed by GEOS 1
[DRI-3-84] 09 p1350 N85-18496

Multifrequency observations of BL LAC objects and violently variable quasars 11 p1746 N85-20981

Ultraviolet observations of Population 2 Cepheids
11 p1754 N85-21034

Ultraviolet analysis of the peculiar F supergiant HD 112374 11 p1754 N85-21035

Acoustic energy balance method
13 p2000 N85-22537

Breakdown of thin plates by radiation
13 p2028 N85-22709

Theoretical thermodynamics of mixtures at high pressures 13 p2183 N85-23550

Measurement of charged secondary particle emission under ion and neutral impact --- Giotto mission
14 p2243 N85-23903

Energy dependence of the emittance of damping ring beams
[DE85-007080] 15 p2649 N85-26341

Time dependent and steady-state solutions of the electron energy distribution in a weakly ionized gas subject to an ac or dc electric field
[AD-A151829] 15 p2656 N85-26391

Ionization energies of liquids from energy distribution, quantum yield and second derivative curves
[AD-A152210] 16 p2746 N85-26946

Studies of hot B subdwarfs. Part 2: Energy distributions of three bright sdB/sdOB stars in the 950-5500 angstrom range
[NASA-CR-175854] 16 p2881 N85-27775

Influence of edge effects on performance of electrooptical lens 22 p3770 N85-33386

Observations on TeV gamma rays from Geminga and PSR 0950+08
[OG-2.4-6] 22 p3868 N85-33953

Composition of primary cosmic rays near the bend from a study of hadrons in air showers at sea level
[OG-5.2-2] 22 p3883 N85-34059

Composition of primary cosmic rays at energies 10(15) to approximately 10(16) eV
[OG-5.2-4] 22 p3883 N85-34061

Variations in elemental composition of several MEV/nucleon ions observed in interplanetary space
[SH-2.1-7] 23 p3998 N85-34788

On the retention of high-energy protons and nuclei with charges Z or equal to 2 in large solar flares after the process of their acceleration
[SH-2.1-8] 23 p3998 N85-34789

The response of ionization chambers to relativistic heavy nuclei
[OG-9.1-13] 23 p4024 N85-34938

Clusters and cycles in the cosmic ray age distributions of meteorites
[SH-7.1-11] 23 p4048 N85-35103

Status of the zeta(8.3)
[DE85-013070] 24 p4149 N85-35724

Lateral distribution of high energy hadrons and gamma ray in air shower cores observed with emulsion chambers
[HE-3.3-8] 24 p4180 N85-35926

Size distributions of air showers accompanied with high energy gamma ray bundles observed at Mt. Chacaltaya
[HE-3.3-9] 24 p4181 N85-35927

Comparison of absolute intensity between EAS with gamma-families and general EAS at Mount Norikura
[HE-3.3-11] 24 p4181 N85-35929

Analytical-numerical methods of calculations of energy and three-dimensional particle distributions in electromagnetic cascades
[HE-3.5-13] 24 p4184 N85-35950

Comparison of big event with calculations of the air shower development
[HE-3.6-8] 24 p4185 N85-35956

Character of energy flow in air shower core
24 p4189 N85-35985

The development of air shower in the iron absorber
24 p4189 N85-35987

Longitudinal trial functions and the cosmic ray energy scale 24 p4193 N85-36014

Primary chemical composition from simultaneous recording of muons induced cascades and accompanying muon group underground
[HE-5.1-13] 24 p4201 N85-36075

On method of muon spectrum measurements by the scintillation detectors of a large thickness T4t sub o
[HE-5.2-18] 24 p4204 N85-36094

Characteristics of slow particles emitted in the charged current interactions of neutrinos with emulsion nuclei
[HE-5.3-22] 24 p4207 N85-36113

Relationship of sea level muon charge ratio to primary composition including nuclear target effects
[HE-5.4-10] 24 p4208 N85-36121

ENERGY EFFICIENCY TRANSPORT PROGRAM
U ACEE PROGRAM

ENERGY EQUIPARTITION
U EQUIPARTITION THEOREM

ENERGY EXCHANGE
U ENERGY TRANSFER

ENERGY GAPS (SOLID STATE)

Refractive index of ternary and quaternary compound semiconductors below the fundamental absorption edge: Linear and nonlinear effects
[DE84-012325] 05 p0640 N85-14105

Material models and device structures for GaAs solar cells
[DE85-000501] 05 p0665 N85-14275

Repetitively pulsed metal ion beams for ion implantation
[DE84-014065] 05 p0732 N85-14704

Solar fuel synthesis based on colloidal and particulate semiconductors
[PB85-129104] 11 p1614 N85-20152

Method and apparatus for measuring minority carrier lifetime in a direct band-gap semiconductor
[NASA-CASE-NPO-163371-1] 11 p1628 N85-20251

Substituent effects on the electrical conductivities of the phenazine derivatives
[NASA-TM-77792] 14 p2249 N85-23938

Theory and calculations of the electronic structure of solids having directional bonding
[AD-A151062] 14 p2428 N85-24971

Novel materials properties of strained-layer superlattices
[DE85-003676] 14 p2430 N85-24989

Modeling and optimization of a multiple-cell photovoltaic converter system 15 p2585 N85-25934

Heavy doping effects in high efficiency silicon solar cells
[NASA-CR-175667] 15 p2585 N85-25937

Heavy doping effects in high efficiency silicon solar cells
[NASA-CR-175681] 15 p2586 N85-25940

The structural and electronic properties of amorphous silicon based alloy materials
[DE85-002909] 15 p2660 N85-26419

Shallow impurity cluster states in n-type semiconductors
[INPE-3495-PRE/732] 16 p2889 N85-27699

Optically nonlinear and bistable behaviour of direct gap semiconductors 18 p3186 N85-29759

Optical bistability in Cd(x)Hg(1-x)Te
18 p3186 N85-29760

Quantized Hall conductance as a topological invariant
[DE85-007798] 18 p3193 N85-29808

Lasertron simulation with a two-gap output cavity
[DE85-011213] 22 p3790 N85-33480

ENERGY LEVELS
NT ATOMIC ENERGY LEVELS
NT ELECTRON STATES
NT GROUND STATE
NT INTERMOLECULAR FORCES
NT MOLECULAR ENERGY LEVELS

Influence of translational and hyperfine relaxation on energy characteristics of oxygen-iodine laser
02 p0261 N85-11707

Determination of bound water in biological tissue and energy dissipated in bound water by low level microwaves
[AD-A143101] 03 p0399 N85-12547

Focussing and confinement
[DE84-016181] 05 p0640 N85-14106

Theoretical studies of atomic transition
[DE85-001325] 09 p1381 N85-18687

Spectroscopy of quasimolecular X-rays with H-like decelerated ions
[DE85-006565] 15 p2649 N85-26337

Fluorinated polyesters
[AD-D011611] 16 p2753 N85-26988

Boson degrees of freedom in Fermion many-body systems
[DE85-006997] 16 p2863 N85-27680

Multiple scattering effects in low energy alkali ion scattering: Application to the analysis of adsorbate ordering and bonding geometry
[DE85-007575] 17 p3032 N85-28757

Extension of the consistent Q formalism to odd-A nuclei in the W-Pt region
[DE85-006284] 17 p3034 N85-28770

Electronic structure calculations for low coverage adlayers
[DE85-007733] 18 p3179 N85-29709

Calculation of Franck-Condon factors for diatom molecules
[AD-A154463] 19 p3353 N85-3078

Strong-coupling approximations
[DE85-007829] 19 p3353 N85-3078

Atomic data for controlled fusion research. Volume 4: Spectroscopic data for iron
[DE85-009858] 19 p3354 N85-3078

Systematic view of transition intensities in the spectra of actinides and lanthanides in condensed phases
[DE85-010272] 19 p3354 N85-3078

Experimental level-structure determination in odd-odd actinide nuclei
[DE85-010476] 19 p3360 N85-3083

Microscopic structure of two-dimensional electron glass
[DE85-010265] 19 p3376 N85-3094

Antiproton-nucleus inelastic scattering and the spin-isospin dependence of the N anti N interaction
[DE85-010546] 20 p3526 N85-319

New O(6) region near A = 130 and the interplay of triaxiality and gamma-softness in the IBA
[DE85-010957] 20 p3530 N85-3196

Establishment of steady-state power level in pulse-periodic excimer laser 21 p3685 N85-32

Ionization detection of stimulated Raman spectra
[DE85-010672] 22 p3746 N85-3321

Vacuum ultraviolet laser
[DE85-011632] 22 p3790 N85-3347

Heavy quarks and CP: Moriond 1985
[DE85-010553] 22 p3841 N85-3379

Capture in the 1.15-keV iron resonance
[DE85-011913] 23 p3970 N85-3461

Duality of two-point functions for confined non-relativistic quark-antiquark systems
[DE85-012334] 23 p3971 N85-3461

Exact solutions for sporadic acceleration of cosmic rays
[OG-8.3-7] 23 p4022 N85-3492

Relativistic transport theory for cosmic-rays
[OG-8.3-8] 23 p4022 N85-349

The design of an experiment to detect low energy antiprotons
[OG-9.1-1] 23 p4022 N85-349

The response of ionization chambers to relativistic heavy nuclei
[OG-9.1-13] 23 p4024 N85-349

Gamma-ray production cross sections for alpha-particle induced reactions on F-19 and Na-23
[DE85-012603] 24 p4150 N85-3573

Standard value for the radiation length in air
[HE-4.4-4] 24 p4193 N85-360

ENERGY LOSSES
U ENERGY DISSIPATION

ENERGY METHODS
NT STRAIN ENERGY METHODS

A study of the recursion yn+1=yn+tau yn sup m
[CWI-NM-R8403] 05 p0723 N85-146

ENERGY OF FORMATION

Parameters of detonation waves excited in gas during concentrated release of energy
02 p0266 N85-1175

Energy of stacking fault and dislocation structure of titanium alloys 03 p0351 N85-122

Autenite transformation in powder-compacted chromium-nickel-molybdenum steels during continuous cooling
[BLL-M-35961-(5826.4)] 05 p0615 N85-139

ENERGY POLICY

The changing pattern of fossil fuel CO2 emissions
[DOE/OR-21400/2] 02 p0224 N85-114

Methane-fueled vehicle RD and D
[GPO-37-926] 04 p0481 N85-130

Information package on photovoltaics
05 p0661 N85-142

Stimulation of technologies towards photovoltaic energy conversion 05 p0661 N85-1425

Photovoltaic power supply units
05 p0662 N85-1425

Development and construction of a prototype photovoltaic energy supply unit
05 p0662 N85-1425

Siemens solar module: Status of the technique, development tendencies 05 p0662 N85-142

Development and utilization of CdS/Cu2S
05 p0662 N85-142

Solar generators made of amorphous silicon
05 p0662 N85-142

Fundamentals of solar energy conversion based on fluorescence collectors 05 p0662 N85-142

Biaxial tracking solar generator
05 p0663 N85-142

Energy storage with lead acid batteries in photovoltaic systems 05 p0663 N85-142

Energy storage for stationary and mobile operation as a buffer of power supply from additive energy sources
05 p0663 N85-14261

Utilization of solar energy for the production of hydrogen
05 p0663 N85-14262

The 16 photovoltaic pilot projects of the European Communities
05 p0663 N85-14263

Mains-connected photovoltaic system for a house
05 p0664 N85-14267

Project Pellworm: Solar electric energy supply for a health center
05 p0664 N85-14268

Photovoltaic pump systems 05 p0664 N85-14269

Realized field tests — solar generators
05 p0664 N85-14271

Utilization possibilities of photovoltaics in the private sector
05 p0664 N85-14272

Considerations on the dimensioning of photovoltaic supply systems in the low power range
05 p0665 N85-14273

Solar power supplies for ships
05 p0665 N85-14274

Measurement-Technical Investigations of Wind Energy Units
[JUEL-SPEZ-244] 05 p0667 N85-14293

Measurement-technical problems in the investigation of wind energy units 05 p0668 N85-14295

Design criteria for small wind turbines
[NLR-MP-83054-U] 07 p0994 N85-16310

Verification of the fatigue properties of (small) wind turbines
[NLR-MP-83055-U] 07 p0994 N85-16311

Energy and climate: Problems in Latin America
07 p1003 N85-16375

Blade technology program for large wind turbines, phase 1
[BMFT-FB-T-84-217] 08 p1179 N85-17426

The infrastructure for a surge in synfuels production: The potential role of the AE and C industry and of owner operators
[RAND/N-2172-SFC] 09 p1301 N85-18170

Assessment of wave power available at key United Kingdom sites
[IOS-186] 09 p1346 N85-18486

US Amorphous Silicon Research Project
[DE85-000536] 10 p1511 N85-19536

International Congress Centrum Berlin report on photovoltaics 12 p1877 N85-21773

Crystallization methods for solar cell silicon
12 p1877 N85-21774

Pin solar cells made of amorphous silicon
12 p1879 N85-21787

Physical-chemical investigations of copper sulfides for use in CdS/Cu2S solar cells 12 p1880 N85-21794

Development of a CdSe thin film solar cell
12 p1880 N85-21796

Solar process heat: Technology program
[BMFT-FB-T-84-234] 12 p1882 N85-21812

Hydrology and climatic conditions in Greenland
14 p2327 N85-24387

Ilyushin bureau designer on fuel conservation research
15 p2467 N85-25231

Solar house, Freiburg
[BMFT-FB-T-84-249] 15 p2588 N85-25953

Testing and further development of a solar absorption cooling plant
[BMFT-FB-T-84-264] 15 p2588 N85-25954

Transient behavior of a single-blade horizontal-axis wind turbine
[MBB-UD-421/84-O] 16 p2875 N85-27737

USSR report: Engineering and equipment
[JPRS-UEQ-85-004] 17 p2939 N85-28142

Navy geothermal plan
[AD-A152478] 17 p2985 N85-28450

Investigation of the transferability of measures of passive solar energy utilization in the USA to the Federal Republic of Germany
[BMFT-FB-T-84-284] 18 p3132 N85-29396

Environmental management needs
[DE85-007859] 18 p3133 N85-29405

Pacific Index, April 1983 - October 1984
[TI85-901335] 19 p3320 N85-30582

Wind energy in the north Netherlands region
20 p3485 N85-31661

Wind turbines and environment management
[CP-MEMO-1983-11] 20 p3485 N85-31662

Magnetohydrodynamics and the National Coal Science, Technology, and Engineering Development Acts
[S-HRG-98-1179] 20 p3535 N85-31994

Fusion facility siting considerations
[DE85-012894] 22 p3843 N85-33805

Magnetic Fusion Program plan
[DE85-009861] 22 p3846 N85-33823

Monitoring building energy performance: An informal review and characterization of research in progress
[BNL-51765] 23 p3923 N85-34308

Implementing agreement for cooperation in the development of large scale wind energy conversion systems
[JUEL-SPEZ-278] 24 p4110 N85-35473

General environmental aspects of large scale wind energy utilization 24 p4110 N85-35474

Environmental aspects of large-scale wind-power systems in the UK 24 p4110 N85-35478

Visit to test facility Stoetten (West Germany) May 9, 1984, including the Voith Wind Energy Converter (WEC) 520 turbine. The annual production of various wind energy plants in selected locations 24 p4112 N85-35487

ENERGY REQUIREMENTS

Energy and climate: Problems in Latin America
07 p1003 N85-16375

MHD performance demonstration experiment, FY 1974 to FY 1984
[DE85-000854] 08 p1224 N85-17709

Study of low energy density photovoltaic applications under varying rate structures
[DE85-000185] 10 p1511 N85-19538

The use of heat pumps in district heat supply
[BLL-OA-TRANS-2728-(6198.3)]
16 p2781 N85-27163

Studies related to the deep Earth gas: 1983
[PB85-171114] 16 p2816 N85-27373

Relative potentials of concentrating and two-axis tracking flat-plate photovoltaic arrays for central-station applications
[NASA-CR-175869] 17 p2985 N85-28446

ENERGY SOURCES

Simulation of automatic control of MFTF-B neutral beams
[DE85-010640] 20 p3530 N85-31960

Solar source regions of 3HE-rich particle events
[SH-2.2-4] 23 p4000 N85-34799

Atmospheric neutrinos observed in underground detectors
[HE-5.3-8] 24 p4205 N85-36102

Geophysical searches for three-neutrino oscillations
[HE-5.3-9] 24 p4205 N85-36103

ENERGY SPECTRA

NT ELECTRONIC SPECTRA
NT NEUTRON SPECTRA

Vowel phoneme identification in speech
[FUB-26-1983] 01 p0040 N85-10257

Equatorial energetic distributions of ions of terrestrial radiation belt as function of solar corona temperature response 02 p0160 N85-11087

Measuring local ion energy distribution function in Tuman-3 Tokamak plasma 02 p0271 N85-11768

Solar neutrinos: Prospects for detection and implications
[DE84-015522] 02 p0304 N85-11966

Chlorine and bromine solar neutrino experiments
[DE84-015720] 02 p0304 N85-11969

Comparison of forecast and observed energetics
05 p0683 N85-14389

Spectral energetics diagnoses and FGGE spectral observing periods and energetics analyses of forecast experiments with GLAS GCM 05 p0683 N85-14391

Aharonov-Bohm effect in absorption of electromagnetic wave 06 p0786 N85-15022

Annual energy spectrum for tracking arrays
06 p0832 N85-15297

On the broadband energy spectra of quasars and BL Lac objects 08 p1240 N85-17825

A compact time-of-flight energy analyzer of high resolution — for Tokamaks
[REPT-84-154] 09 p1324 N85-18318

An operational test of a time-of-flight analyzer at the ASDEX Tokamak
[REPT-84-155] 09 p1324 N85-18319

One-electron capture processes by highly charged ions from helium: Present status of HICE-IPP
09 p1369 N85-18736

The energy spectra of slowed-down neutrals from the heating beams in ASDEX — tokamak
[REPT-84-157] 09 p1394 N85-18772

Laser-Electron-Gamma-Source (LEGS)
[DE85-003204] 11 p1638 N85-20322

KMSF X-ray laser experiments, task no. 1
[DE85-001002] 11 p1639 N85-20325

Jet topologies in hadron-hadron collisions
[DE85-001328] 12 p1929 N85-22119

On the spectrum of longitudinal waves in the hot degenerate plasma 12 p1955 N85-22280

Measured electron contribution to Shuttle plasma environment: Abbreviated update
13 p1990 N85-22476

Development of a continuous broad-energy-spectrum electron source 13 p1995 N85-22507

Discharge characteristics of dielectric materials examined in mono-, dual-, and spectral energy electron charging environments 13 p1995 N85-22510

Nonlinearity and spectral mismatch problems of solar cells 13 p2010 N85-22605

Energy spectrum of processes of structural relaxation of amorphous alloy FeCo70Si15B10
13 p2035 N85-22750

Numerical investigation of evolution of energy spectrum of slightly nonlinear Rossby waves
13 p2106 N85-23124

Mean delta-ray energies in ion molecule collisions
[DE85-005524] 13 p2157 N85-23395

Kinetic energies of fragment ions produced by dissociative photoionization of NO
[NASA-CR-175721] 15 p2647 N85-26327

Restrike particle beam experiments on a dense plasma focus. Opening switch research on a dense plasma focus
[AD-A152991] 17 p3039 N85-28802

Comparison of forecast and observed energetics
18 p3143 N85-29459

On the group-theoretical approach to the energy spectra problem of charge carriers in cubic solids
[PREPRINT-435] 18 p3196 N85-29827

LINE: A code which simulates spectral line shapes for fusion reaction products generated by various speed distributions
[DE85-010833] 19 p3341 N85-30702

Comparison of simulation with experiment in an RFQ
[DE85-010770] 19 p3349 N85-30757

Time-resolved energy spectrum of the ion beam generated in the plasma focus 19 p3369 N85-30892

Paired ion chamber constants for fission gamma-neutron fields
[AD-A155069] 21 p3702 N85-32999

Changes in the energy spectrum of anomalous oxygen and helium during 1977 - 1985
[PAPER-SH-4.6-1] 21 p3715 N85-33056

Spectral measurements of magnetic energy and magnetic helicity between 0.29 and 0.97 AU
[IFSI-85-2] 22 p3850 N85-33844

Unthermalized plasma in bursts sources
[OG-1.1-5] 22 p3861 N85-33907

Gamma ray burst size-frequency distributions: Spectral selection effects
[OG-1.2-3] 22 p3862 N85-33913

Observation of an excess of cosmic ray muons of energies 2 TeV from the direction of Cygnus X-3
[OG-2.1-3] 22 p3863 N85-33920

Gamma rays of 0.3 to 30 MeV from PSR 0531+21
[OG-2.3-8] 22 p3866 N85-33945

Pulsed emission of TeV gamma rays from Vela pulsar
22 p3867 N85-33947

On the 1983 observations of the gamma-ray source 2CG195+4
[OG-2.4-5] 22 p3868 N85-33952

Low-energy gamma rays from Cygnus X-1
[OG-2.4-13] 22 p3868 N85-33957

Energy spectrum of extragalactic gamma-ray sources
[OG-2.7-13] 22 p3872 N85-33986

Ultrahigh energy gamma rays: Carriers of cosmological information
[OG-2.7-14] 22 p3872 N85-33987

On some problems of gamma-astronomy
[OG-2.7-15] 22 p3873 N85-33988

Spectrum of the gamma-ray diffuse component observed from HEAO-1
[OG-3.1-12] 22 p3874 N85-34000

Ninteenth International Cosmic Ray Conference. OG sessions, volume 2
[NASA-CP-2376-VOL-2] 22 p3875 N85-34006

Source spectral index of heavy cosmic ray nuclei
[OG-4.1-2] 22 p3875 N85-34008

Relative abundances of sub-iron to iron nuclei in low energy (50-250 MeV/N) cosmic rays as observed in the Skylab experiment
[OG-4.1-4] 22 p3876 N85-34010

Cosmic ray charge and energy spectrum measurements using a new large area Cerenkov x dE/dx telescope
[OG-4.1-5] 22 p3876 N85-34011

Energy spectra of elements with 18 or = Z or = 28 between 10 and 300 GeV/amu
[OG-4.1-8] 22 p3876 N85-34014

Primary cosmic ray spectra in the range 20-60 GeV/n
[OG-4.1-9] 22 p3877 N85-34015

Energy spectrum of cosmic-ray iron nucleus observed with emulsion chamber
[OG-4.1-10] 22 p3877 N85-34016

Measurement of the iron spectrum from 60 to 200 GeV per nucleon
[OG-4.1-11] 22 p3877 N85-34017

Composition and energy spectra of cosmic ray nuclei above 500 GeV/nucleon from the JACEE emulsion chambers
[OG-4.1-13] 22 p3877 N85-34019

Charge composition and energy spectral of cosmic ray primary particles for energies higher than 1 TeV
[OG-4.1-14] 22 p3877 N85-34020

ENERGY SPECTRA

Parametrized energy spectrum of cosmic-ray protons with kinetic energies down to 1 GeV
[OG-4.2-11] 22 p3878 N85-34025

Observations of ultraheavy cosmic ray particles at 10 GV cutoff rigidity
[OG-4.4-2] 22 p3879 N85-34035

Energy spectrum and arrival direction of primary cosmic rays of energy above 10 to the 18th power eV
[OG-5.1-1] 22 p3880 N85-34043

Ultra high energy cosmic ray spectrum
[OG-5.1-2] 22 p3881 N85-34044

The primary cosmic ray spectrum above 10 to the 18th power eV
[OG-5.1-3] 22 p3881 N85-34045

New calorimetric all-particle energy spectrum
[OG-5.1-4] 22 p3881 N85-34046

Primary cosmic ray spectrum in the 10 to the 12th power - 10 to the 16th power eV energy range from the NUSEX experiment
[OG-5.1-5] 22 p3881 N85-34047

A new measurement of the cosmic ray energy spectrum between 3 x 10 to the 15th power eV and 3 x 10 to the 16th power eV
[OG-5.1-6] 22 p3881 N85-34048

Study of composition of cosmic rays with energy .7 E 3 Ee
[OG-5.1-7] 22 p3881 N85-34049

The muon content of EAS as a function of primary energy
[OG-5.1-8] 22 p3881 N85-34050

A new method to determine the chemical composition of the cosmic rays beyond 10 to the 15th power eV
[OG-5.1-11] 22 p3882 N85-34052

Cosmic ray composition between 10 to the 15th power - 10 to the 17th power eV obtained by air shower experiments
[OG-5.1-12] 22 p3882 N85-34053

Fluctuations of development maximum depth and nuclear composition of primary cosmic radiation
[OG-5.1-13] 22 p3882 N85-34054

Estimation of composition of cosmic rays with E sub zero approximately equals 10(17) - 10(18) eV
[OG-5.1-14] 22 p3882 N85-34055

All particle energy spectrum of cosmic rays in 10 to the 15th power - 10 to the 20th power eV region
[OG-5.1-15] 22 p3882 N85-34056

EAS spectrum in the primary energy region above 10 to the 15th power eV by the Akeno and Yakutsk array data
[OG-5.1-16] 22 p3882 N85-34057

Cosmic ray spectra measurements at the Yakutsk EAS array
[OG-5.1-17] 22 p3882 N85-34058

The composition of cosmic rays near the Bend (10 to the 15th power eV) from a study of muons in air showers at sea level
[OG-5.2-3] 22 p3883 N85-34060

Composition of primary cosmic rays at energies 10(15) to approximately 10(16) eV
[OG-5.2-4] 22 p3883 N85-34061

The primary composition beyond 10 to the 5th power GeV as deduced from high energy hadrons and muons in air showers
[OG-5.2-6] 22 p3883 N85-34063

Implication of EAS data for the study of primary cosmic rays above 10 to the 5th power GeV
[OG-5.2-7] 22 p3883 N85-34064

High-energy multiple muons and heavy primary cosmic-rays
[OG-5.2-9] 22 p3883 N85-34065

Composition of primary cosmic rays near the knee
[OG-5.2-10] 22 p3884 N85-34066

EAS Cerenkov measurements of the composition of the cosmic ray flux around 10 to the 16th power eV
[OG-5.2-11] 22 p3884 N85-34067

Electron and muon parameters of EAS and the composition of primary cosmic rays in 10(15) to approximately 10(16) eV
[OG-5.2-12] 22 p3884 N85-34068

Arrival directions of large air showers, low-mu showers and old-age low-mu air showers observed at St. Chacaltaya
[OG-5.3-2] 22 p3884 N85-34069

Energy dependence of cosmic ray composition above 10(15) GeV/nucleus
[OG-5.4-4] 22 p3886 N85-34081

Implications of the experimental results on high energy cosmic rays with regard to their origin
[OG-5.4-5] 22 p3886 N85-34082

Virgo cluster as a high energy cosmic rays source
[OG-5.4-8] 22 p3886 N85-34085

Anisotropy and the knee of the energy spectrum
[OG-5.4-10] 22 p3887 N85-34087

Observed antiprotons and energy dependent confinement of cosmic rays: A conflict?
[OG-6.1-7] 22 p3888 N85-34098

Antiparticles in the extragalactic cosmic radiation
[OG-6.1-8] 22 p3888 N85-34099

Galactic cosmic ray antiprotons and supersymmetry
[OG-6.1-9] 22 p3888 N85-34100

Halo of NGC 4631 and models of cosmic-ray transport
[OG-6.2-3] 22 p3889 N85-34103

An observation of cosmic ray positrons from 10-20 GeV
[OG-6.2-6] 22 p3889 N85-34105

Reestimation of the production spectra of cosmic ray secondary positrons and electrons in the ISM
[OG-6.2-8] 22 p3889 N85-34107

The electron spectra in the synchrotron nebula of the supernova remnant G 29.7-0.3
[OG-6.2-10] 22 p3889 N85-34109

Study of non-thermal photon production under different scenarios in solar flares. 2: The Compton inverse and Bremsstrahlung models and fittings
[SH-1.2-3] 23 p3991 N85-34739

Observations of solar flare photon energy spectra from 20 keV to 7 MeV
[SH-1.2-9] 23 p3992 N85-34744

The energy spectra of solar flare electrons
[SH-1.2-14] 23 p3992 N85-34749

Source energy spectra from demodulation of solar particle data by interplanetary and coronal transport
[SH-1.3-13] 23 p3994 N85-34758

High energy neutron and gamma-radiation generated during the solar flares
[SH-1.4-8] 23 p3995 N85-34768

On the angular and energy distribution of solar neutrons generated in P-P reactions
[SH-1.4-9] 23 p3995 N85-34769

Acceleration of ions and electrons to near-cosmic ray energies in a perpendicular shock: The January 6, 1978 event
[SH-1.5-4] 23 p3996 N85-34773

The energy spectrum of Jovian electrons in interplanetary space
[SH-1.5-18] 23 p3997 N85-34781

Observation of the fluxes of nuclei with energies 10-20 MEV per nucleon during the solar flare of April 26, 1984
[SH-2.1-1] 23 p3998 N85-34783

Silicon to iron abundances in solar cosmic rays and in the sun
[SH-2.1-6] 23 p3998 N85-34787

The 1973-1984 solar modulation of cosmic ray nuclei
[SH-4.1-16] 23 p4006 N85-34838

A numerical study of diffusive shock acceleration of cosmic rays in supernova shocks
[OG-8.2-2] 23 p4019 N85-34903

The origins of cosmic rays and quantum effects on gravity
[OG-8.2-15] 23 p4020 N85-34911

Stochastic particle acceleration in flaring stars
[OG-8.3-9] 23 p4022 N85-34927

An experiment to measure the energy spectrum of cosmic ray antiprotons from 100 to 1000 MeV
[OG-9.1-3] 23 p4022 N85-34929

The development of a high energy cosmic ray detector for Spacelab-2
[OG-9.1-8] 23 p4023 N85-34934

An observatory to study 10 (10) to 10 (17) by EV gamma rays
[OG-9.4-6] 23 p4029 N85-34973

Mini and super mini arrays for the study of highest energy cosmic rays
[OG-9.4-9] 23 p4029 N85-34976

Detection of 10 (1) GeV cosmic neutrinos with a space station
[OG-9.4-10] 23 p4030 N85-34977

The difference in the energy spectra of galactic cosmic rays at the minima of the 19th and 20th solar activity cycles
[SH-4.4-18] 23 p4035 N85-35014

Solar tri-diurnal variation of cosmic rays in a wide range of rigidity
[SH-4.5-3] 23 p4036 N85-35021

Upper cut-off rigidity for corotation anisotropy during solar activity cycles 20 and 21
[SH-4.5-4] 23 p4036 N85-35022

Change of cosmic ray anisotropy with solar activity
[SH-4.5-20] 23 p4038 N85-35037

Changes in the energy spectrum of anomalous oxygen and helium during 1977-1985
[SH-4.6-1] 23 p4039 N85-35039

Radial and latitudinal gradients of anomalous oxygen during 1977 - 1985
[SH-4.6-4] 23 p4039 N85-35042

Observation of pick-up ions in the solar wind: Evidence for the source of the anomalous cosmic ray component?
[SH-4.6-5] 23 p4039 N85-35043

On the anomalous component
[SH-4.6-6] 23 p4039 N85-35044

Time and energy dependence of the cosmic ray gradient in the outer heliosphere
[SH-4.7-2] 23 p4040 N85-35047

Galactic cosmic ray radial gradients and the anomalous He component near maximum solar modulation and to radii beyond 34 AU from the Sun
[SH-4.7-5] 23 p4040 N85-35[illegible]

Rigidity spectrum of Forbush decrease
[SH-5.1-6] 23 p4042 N85-35[illegible]

Observations of cosmic-ray modulations in the fall, 1984
[SH-5.1-16] 23 p4043 N85-35[illegible]

Observation of energy spectrum of electron albedo in low latitude region at Hyderabad, India
[SH-6.1-7] 23 p4045 N85-35[illegible]

A bi-directional charged particle telescope to observe flux, energy spectrum and angular distribution of relativistic and non-relativistic particles
[SH-9.1-4] 23 p4050 N85-35119

A suggested standardized format for cosmic ray ground-level event data
[SH-9.1-15] 23 p4052 N85-35130

Measurement of low energy cosmic rays aboard Spacelab-1
[SH-10.1-6] 23 p4053 N85-35137

Scale separation closure and Alfven wave turbulence
[DE85-013124] 24 p4095 N85-35395

Los Alamos free-electron laser
[DE85-012668] 24 p4096 N85-35405

(NAT)Fe(n,n'x) spectra at 65.5 MeV
[AD-A155776] 24 p4150 N85-35730

Some rigorous results concerning spectral theory for ideal MHD
[DE85-013427] 24 p4156 N85-35770

Proton-air and proton-proton cross sections from air shower data
[HE-1.1-1] 24 p4170 N85-35849

Proton-air inelastic cross section at S(1/2) = 30 TeV
[HE-1.1-2] 24 p4170 N85-35850

Hadron cross sections at ultra high energies and unitarity bounds on diffraction dissociation
[HE-1.1-3] 24 p4170 N85-35851

On total cross sections and slopes at superhigh energies
[HE-1.1-4] 24 p4170 N85-35852

On a possibility of inelasticity partial coefficient K sub gamma determination in pi C and pi Pb interactions at 10 to the 14th power eV (experiment PAMIR 1)
[HE-1.1-12] 24 p4171 N85-35859

1Single particle momentum and angular distributions in hadron-hadron collisions at ultrahigh energies
[HE-1.2-1] 24 p4171 N85-35860

Empirical description of the hadron-hadron and hadron-nucleus interaction at the accelerator energy range
[HE-1.2-4] 24 p4171 N85-35862

Angular distribution and multiplicity of backward hadrons in hFe interactions at 0.5-5.0 TeV energies (PION Experiment)
[HE-1.2-8] 24 p4172 N85-35[illegible]

Scaling violation in the fragmentation region of inclusive nucleon spektrum 24 p4173 N85-35874

Intensities of high-energy cosmic rays at Mount Kanbala
[HE-3.1-2] 24 p4177 N85-35[illegible]

High energy gamma-rays and hadrons at Mount Fuji
[HE-3.1-3] 24 p4177 N85-35[illegible]

Hadron intensity and energy spectrum at 4380 m above level
[HE-3.1-7] 24 p4178 N85-35[illegible]

The nucleon intensity in the atmosphere and the Pt distribution
[HE-3.1-9] 24 p4178 N85-35[illegible]

Energy spectra of proton and nuclei of primary cosmic rays in energy region 10 TeV/particle
[HE-3.1-10] 24 p4178 N85-35[illegible]

Atmospheric interactions detected in both the upper and the lower chambers at Chacaltaya
[HE-3.3-7] 24 p4180 N85-35[illegible]

A cosmic ray super high multicore family event. 1: Experiment and general features
[HE-3.4-1] 24 p4181 N85-35[illegible]

Observation of super high energy big family with large scale Fe emulsion chambers
[HE-3.4-3] 24 p4182 N85-35[illegible]

Super-family P2 C-96-125 observed by Japan-USSR Joint Emulsion Chamber Experiment
[HE-3.4-8] 24 p4182 N85-35[illegible]

Integral functions of electron lateral distribution and their fluctuations in electron-photon cascades
[HE-3.5-12] 24 p4184 N85-35[illegible]

Comparison of big event with calculations of the air shower development
[HE-3.6-8] 24 p4185 N85-35[illegible]

Hadrons registration in emulsion chamber with carbon block
[HE-3.7-3] 24 p4186 N85-35962

Intensities of high-energy cosmic rays at Mount Kanbala
[HE-3.7-5] 24 p4186 N85-35964

Ultra high energy events in ECHOS series and primary energy spectrum
[HE-3.7-9] 24 p4186 N85-35966

The maximum depth of shower with E sub 0 larger than 10(17) eV on average characteristics of EAS different components 24 p4188 N85-35981

Monte Carlo simulation of EAS generated by 10(14) - 10(16) eV protons
[HE-4.3-14] 24 p4192 N85-36008

Lateral distribution of high energy muons in EAS of sizes Ne approximately equals 10(5) and Ne approximately equals 10(6)
[HE-4.3-16] 24 p4192 N85-36010

Energy calibration of the fly's eye detector
[HE-4.4-1] 24 p4192 N85-36011

The structure of EAS at E 0.1 EeV
[HE-4.4-2] 24 p4193 N85-36012

Longitudinal trial functions and the cosmic ray energy scale 24 p4193 N85-36014

EAS development curve at energy of 10(16) - 10(18) eV measured by optical Cerenkov light
[HE-4.4-7] 24 p4193 N85-36015

Missing energies at pair creation
[HE-4.4-8] 24 p4193 N85-36016

On the determination of the depth of EAS development maximum using the lateral distribution of Cerenkov light at distances 150 m from EAS axis
[HE-4.4-13] 24 p4194 N85-36019

Study of the energy spectrum of primary cosmic rays: EAS size fluctuations at a fixed primary energy
[HE-4.4-14] 24 p4194 N85-36020

Preliminary results of the Cerenkov EAS flashes the Crimean Astrophysical Observatory
[HE-4.4-17] 24 p4194 N85-36023

The experimental cascade curves of EAS at E sub 0 10(17) eV obtained by the method of detection of Cherenkov pulse shape
[HE-4.4-18] 24 p4194 N85-36024

Muons in gamma showers
[HE-4.5-3] 24 p4195 N85-36027

Muon spectrum in air showers initiated by gamma rays
[HE-4.5-4] 24 p4195 N85-36028

Expected rates with mini-arrays for air showers
[HE-4.7-8] 24 p4199 N85-36059

The spectrum of cosmic ray muons obtained with 100-ton scintillation detector underground and the analysis of recent experimental data
[HE-5.1-6] 24 p4201 N85-36071

A new world survey expression for cosmic ray vertical intensity vs. depth in standard rock
[HE-5.1-10] 24 p4201 N85-36073

Muon groups and primary composition at 10 to the 13th power to 10 to the 15th power eV
[HE-5.1-12] 24 p4201 N85-36074

On muon energy spectrum in muon groups underground
[HE-5.1-14] 24 p4201 N85-36076

Underwater measurements of muon intensity
[HE-5.1-16] 24 p4202 N85-36078

Hybrid TLC-pair meter for the Sphinx Project
[HE-5.2-10] 24 p4203 N85-36086

An upper limit of muon flux of energies above 100 TeV determined from horizontal air showers observed at Akeno
[HE-5.2-12] 24 p4203 N85-36088

Energy spectrum of cascade showers induced by cosmic ray muons in the range from 50 GeV to 5 TeV
[HE-5.2-14] 24 p4203 N85-36090

Analytical calculation of muon intensities under deep sea-water
[HE-5.2-16] 24 p4204 N85-36092

On method of muon spectrum measurements by the scintillation detectors of a large thickness T4t sub o
[HE-5.2-18] 24 p4204 N85-36094

Range fluctuations of high energy muons passing through matter
[HE-5.2-19] 24 p4204 N85-36095

The spectrum of neutrons at 60 hg m(-2)
[HE-5.2-20] 24 p4204 N85-36096

A transient digitiser for fast air shower events
[HE-5.2-21] 24 p4204 N85-36097

Results of low energy background measurements with the Liquid Scintillation Detector (LSD) of the Mont Blanc Laboratory
[HE-5.3-5] 24 p4205 N85-36099

Measurement of neutrino oscillations in MACRO experiment
[HE-5.3-10] 24 p4206 N85-36104

The capability of the existing network of installations for detecting the antineutrino burst from collapsing stars
[HE-5.3-13] 24 p4206 N85-36107

Energy spectra of high energy atmospheric neutrinos
[HE-5.3-14] 24 p4206 N85-36108

Relationship of sea level muon charge ratio to primary composition including nuclear target effects
[HE-5.4-10] 24 p4208 N85-36121

ENERGY STORAGE

NT ELECTRIC ENERGY STORAGE
NT HEAT STORAGE
NT MAGNETIC ENERGY STORAGE

NASA Redox Storage System Development Project
[NASA-TM-83677] 03 p0385 N85-12465

The limp flywheel
[AD-A146034] 03 p0386 N85-12467

Dynamic and other secondary benefits of compressed air energy storage
[DE84-015571] 03 p0386 N85-12468

Regenerative fuel cell energy storage system for a low Earth orbit space station
[NASA-CR-174802] 04 p0527 N85-13371

An Assessment of Integrated Flywheel System Technology
[NASA-CP-2346] 05 p0604 N85-13850

Rotating assembly working group summary
05 p0604 N85-13851

Electrical/electronics working group summary
05 p0604 N85-13853

Dynamics and controls working group summary
05 p0604 N85-13854

A summary of the 1983 Integrated Flywheel Technology Workshop 05 p0605 N85-13855

European development experience on energy storage wheels for space 05 p0605 N85-13856

Merits of flywheels for spacecraft energy storage
05 p0605 N85-13857

Comparative energy storage assessment item
05 p0605 N85-13858

Inertial storage for satellites 05 p0605 N85-13859

Perspectives on energy storage wheels for space station application 05 p0605 N85-13860

Flywheel-powered X-ray generator
05 p0605 N85-13861

Description of a laboratory model Annular Momentum Control Device (AMCD) 05 p0606 N85-13863

Generic composite flywheel designs
05 p0606 N85-13864

Flexible matrix composite laminated disk/ring flywheel
05 p0606 N85-13866

Flywheel containment and safety considerations
05 p0606 N85-13869

Magnetically suspended reaction wheel assembly
05 p0607 N85-13870

Magnetically suspended flywheel system study
05 p0607 N85-13873

Reaction wheels for kinetic energy storage
05 p0607 N85-13874

High-efficiency power conversion options for flywheel energy storage systems 05 p0607 N85-13876

Motor/generator and electronic control considerations for energy storage flywheels 05 p0608 N85-13878

Torque command steering law for double-gimbaled control moment gyros applied to rotor energy storage
05 p0608 N85-13879

Potential of flywheels for spacecraft energy storage
05 p0609 N85-13890

Space power management and distribution status and trends 05 p0610 N85-13896

Electrochemistry and storage panel report
05 p0611 N85-13903

Advanced and nontraditional concepts working group report 05 p0612 N85-13909

Engineering model system study for a regenerative fuel cell: Study report
[NASA-CR-174801] 07 p0991 N85-16292

Performance and cost of energy transport and storage systems for dish applications using reversible chemical reactions
[NASA-CR-174263] 07 p0992 N85-16296

Eigenvalues of rotating machinery
08 p1167 N85-17361

Hybrid system for producing and storing ice
[DE84-017474] 09 p1304 N85-18195

Comparison of energy storage systems in the United States chilled water versus two types of ice storage systems
[DE85-001102] 09 p1344 N85-18452

Ultrasonic characterization of advanced composite flywheels
[DE85-000158] 11 p1593 N85-20026

Underground pumped hydroelectric storage
[DE85-000288] 11 p1676 N85-20560

Power circuit utilizing self-excited Hall effect switch means
[AD-D011505] 12 p1832 N85-21496

Research on microemulsions for storage and conversion of solar energy
[DE85-000181] 12 p1882 N85-21807

Evaluation of ettringite and related compounds for use in solar energy storage
[DE85-003249] 12 p1882 N85-21809

Evaluation of ettringite and related compounds for use in solar energy storage
[PB85-146876] 12 p1883 N85-21816

Cyclic industrial robots with mechanical energy storing devices: Multipositional system with one or several degrees of freedom 13 p2045 N85-22803

Cyclic industrial robots with mechanical energy storing devices: Principles of drive design
13 p2046 N85-22807

Sensitization and quenching in the conversion of light energy into chemical energy
[DE85-006301] 14 p2351 N85-24535

The role of differential rotation in magnetic energy storage — coronal loops 14 p2449 N85-25119

Multikilowatt hydrogen-nickel oxide battery system
[DE85-003339] 15 p2550 N85-25737

Advanced energy storage systems
[AD-A152244] 16 p2741 N85-26915

Low pressure storage of methane on interlayered clays for potential vehicular applications
[DE85-006949] 16 p2758 N85-27017

Operating characteristics of a 0.87 kW-hr flywheel energy storage module
[NASA-TM-87036] 17 p2974 N85-28371

Relative potentials of concentrating and two-axis tracking flat-plate photovoltaic arrays for central-station applications
[NASA-CR-175889] 17 p2985 N85-28446

Documents of the JPL Photovoltaics Program Analysis and Integration Center: An annotated bibliography
[NASA-CR-175873] 17 p2985 N85-28448

SERI Solar Energy Storage Program: FY 1984
[DE85-002936] 18 p3130 N85-29385

Electrochemical Energy Storage Branch
[DE85-007592] 18 p3131 N85-29391

Control of energy-storage dc-to-dc converters: The large-signal time-domain approach
19 p3257 N85-30196

Thermal Energy Storage Program annual operating plan FY 1985
[DE85-008745] 19 p3307 N85-30499

Regenerative fuel cell systems for space station
20 p3443 N85-31372

System level electrochemical principles
20 p3443 N85-31375

Advances in rechargeable lithium molybdenum disulfide batteries 20 p3444 N85-31376

Capacitive energy storage at cryogenic temperatures
[AD-A154508] 21 p3579 N85-32253

A fast discharge excimer laser with symmetric geometry
[AD-A155294] 21 p3592 N85-32322

Transient two-dimensional simulation of SEU in a CMOS SRAM cell
[DE85-008419] 22 p3690 N85-34111

Series-counterpulse repetitive-pulse inductive storage circuit
[DE85-006438] 23 p3928 N85-34342

Reversing-counterpulse repetitive-pulse inductive storage circuit
[DE85-006409] 23 p3928 N85-34344

Evaluation of developmental membranes for the mixed reactant iron-chromium redox system
[NASA-TM-87074] 23 p3944 N85-34443

Wind energy battery storage, phase 2
[DE85-009753] 23 p3945 N85-34450

Solar heat pump
[DE85-011323] 23 p3946 N85-34453

Ion energy storage for post-flare loops
[SH-1.2-10] 23 p3992 N85-34745

Solar pond technology for Navy applications
[AD-A155877] 24 p4112 N85-35488

Strategic defense initiative
[DE85-012778] 24 p4150 N85-35735

Analysis of a pulsed power system containing rotating machine
[DE85-014128] 24 p4159 N85-35786

ENERGY STORAGE DEVICES

U ENERGY STORAGE

ENERGY TECHNOLOGY

NT GEOTHERMAL TECHNOLOGY

Solar heating and cooling R and D program coordination support
[DE84-013479] 01 p0068 N85-10449

Fusion and its future in Illinois
[DE84-014686] 01 p0122 N85-10833

Agribusiness and space: No limits to growth
02 p0152 N85-11029

Executive information system
[DE84-015355] 04 p0576 N85-13675

Activities report in technology [ISBN-951-38-1298-1] 04 p0577 N85-13681

Electrical/electronics working group summary 05 p0604 N85-13853

Merits of flywheels for spacecraft energy storage 05 p0605 N85-13857

Stimulation of technologies towards photovoltaic energy conversion 05 p0661 N85-14251

Photovoltaic power supply units 05 p0662 N85-14252

Development and construction of a prototype photovoltaic energy supply unit 05 p0662 N85-14254

Siemens solar module: Status of the technique, development tendencies 05 p0662 N85-14255

Solar energy supplied mobile water purification unit 05 p0664 N85-14270

Utilization possibilities of photovoltaics in the private sector ^5 p0664 N85-14272

Measurement-Technical Investigations of Wind Energy Units [JUEL-SPEZ-244] 05 p0667 N85-14293

Measurement-technical investigations of wind energy units in the short-time range — spectrum analysis 05 p0668 N85-14294

VOITH: Wind energy converter WEC 520 05 p0668 N85-14299

The upwind power plant Manzanares 05 p0669 N85-14305

USSR report: Engineering and equipment [JPRS-UEQ-84-007] 06 p0775 N85-14954

Viscosity measurements for thick-film pastes 06 p0831 N85-15280

Emerging role of the national laboratory in the development and transfer of materials technology [DE85-001252] 09 p1288 N85-18086

The influence of modern control techniques on the gas industry [ERS-E.395] 09 p1325 N85-18326

The 35 kilowatt peak power photovoltaic system [DE85-000189] 10 p1511 N85-19537

Advanced concepts in systems analysis and simulation [DE85-002728] 11 p1702 N85-20701

Materials refining for solar cell silicon 12 p1877 N85-21775

Flat-plate silicon for solar cells 12 p1877 N85-21776

Carbothermic production of silicon solar cells using high-purity starting materials 12 p1877 N85-21777

Development of silicon nitride materials for the casting of solar cell silicon 12 p1878 N85-21779

Photovoltaic roofing tile systems 12 p1878 N85-21783

Optimization of silicon-nitride-inversion layer solar cells 12 p1878 N85-21784

Development of new process technologies for solar cells with high efficiency starting from purified silicon 12 p1878 N85-21785

Development of new solar cells 12 p1880 N85-21797

Multi-year plan for Experimental Systems Research: Passive and hybrid solar energy program [DE85-004896] 12 p1882 N85-21810

Solar process heat: Technology program [BMFT-FB-T-84-234] 12 p1882 N85-21812

New high-efficiency silicon solar cells [NASA-CR-175643] 13 p2128 N85-23244

Production technology of an electrolyte for Na/S batteries [BMFT-FB-T-84-277] 15 p2550 N85-25742

Role of supercomputers in energy research programs [DE85-006865] 15 p2624 N85-26172

Energy Data Base: Subject thesaurus permutated listing. Revision 6, appendix [DE84-016963] 15 p2666 N85-26454

USSR report: Engineering and equipment [JPRS-UEQ-84-006] 16 p2760 N85-27035

Parametric study of potential early commercial power plants Task 3-A MHD cost analysis [NASA-CR-175639] 16 p2817 N85-27377

Wind energy technology program summary [DE85-007349] 16 p2820 N85-27392

Current alternative energy research and development in Illinois [PB85-163137] 16 p2820 N85-27397

Energy data base: Subject thesaurus [DE84-010566] 16 p2878 N85-27761

Documents of the JPL Photovoltaics Program Analysis and Integration Center: An annotated bibliography [NASA-CR-175873] 17 p2985 N85-28448

Shenandoah parabolic dish solar collector [DE85-008326] 17 p2987 N85-28460

Multicriteria decision analysis as an aid to strategic planning of energy research and development [REPT-84-02] 17 p3049 N85-28870

Energy data base: Subject categories and scope [DE84-017376] 17 p3050 N85-28881

Absorber coatings degradation [DE85-006628] 18 p3128 N85-29367

Improved acid electrolytes for fuel cells [PB85-176053] 18 p3132 N85-29397

Activities report in energy technology [OEFZS-4302] 18 p3199 N85-29846

Thermochemical energy transport using a hydrogen rich working fluid [AD-D011696] 19 p3233 N85-30042

Air Force Federal Photovoltaic Utilization Program [DE85-010612] 20 p3484 N85-31648

Renewable energy research and development outlook, volume 1 [DE85-011577] 20 p3540 N85-32033

Proceedings of the 24th Project Integration Meeting [NASA-CR-176058] 21 p3607 N85-32394

High-efficiency crystalline silicon technology development 21 p3607 N85-32395

Energy and Technology Review [DE85-011767] 21 p3716 N85-33061

Arctic and offshore research [DE85-001995] 22 p3818 N85-33653

Logical and physical modeling and design of scientific and statistical databases for energy research [DE85-006081] 22 p3833 N85-33737

Federal export assistance programs applicable to the US photovoltaic industry [NASA-CR-176114] 22 p3849 N85-33841

Monitoring building energy performance: An informal review and characterization of research in progress [BNL-51765] 23 p3923 N85-34308

New technologies at the forefront of industrial developments 24 p4061 N85-35168

Chemistry division report [DE85-010586] 24 p4071 N85-35228

Photovoltaics technology program summary [DE85-013098] 24 p4112 N85-35493

ENERGY TRANSFER

NT LINEAR ENERGY TRANSFER (LET)

Electronic-to-vibrational energy transfer studies of singlet molecular oxygen and hydrogen halides [AD-A145587] 02 p0277 N85-11802

Study of vibrational energy transfer at a liquid tin surface [AD-A145741] 02 p0277 N85-11804

High temperature gas energy transfer [AD-A146134] 03 p0328 N85-12113

Fluid layer between infinite elastic plates II. Distribution of power flow [AD-A146690] 03 p0361 N85-12312

Vector magnetic field analysis of Lorentz forces acting in the solar atmosphere [AD-A145941] 03 p0449 N85-12652

Study of combustion and flame processes initiated by laser-induced multiple-photon absorption [DE84-017095] 04 p0471 N85-12996

Laser-driven particle accelerators [DE84-015953] 04 p0506 N85-13227

Energy transfer in atom-molecule scattering experiments in the 1eV region with SF6-Ar, CF4-Ne and Xe-CO2 systems as examples [REPT-11/1983] 04 p0563 N85-13588

Energy information exchange, 1983 [DE84-901446] 04 p0577 N85-13680

The Interaction of Global Biochemical Cycles [NASA-CR-174184] 05 p0652 N85-14183

Biogeochemical cycles: Interactions in global metabolism 05 p0652 N85-14184

Power transfer from natural emitters to collection apertures at microwave wavelengths [NASA-CR-174275] 07 p0945 N85-15969

Collisional energy exchange in polyatomic molecules [AD-A147710] 08 p1219 N85-17679

Evaluation of the Fundamental Research on Explosives (FRE) program [DE85-001537] 09 p1301 N85-18172

Optical studies of dynamical processes in disordered materials [DE85-002400] 10 p1453 N85-19158

Thermal investigation of an electrical high-current arc with porous gas-cooled anode [NASA-TM-77769] 11 p1627 N85-20245

UK participation in the Middle Atmosphere Programme 11 p1655 N85-20426

Application of dimensional analysis to the problem of solar wind-magnetosphere energy coupling [DE85-002414] 11 p1674 N85-20551

Energy transfer and photochemistry in biomimetic solar conversion [PB85-129112] 11 p1677 N85-20566

Primary light harvesting system: The relationship of phycobilisomes to photosystem 1 and 2 [DE85-003075] 11 p1689 N85-20622

Saturation kinetics of active medium of oxygen- laser 11 p1718 N85-

Two-dimensional measurements of OH concentration and temperature in reactive flows [AD-A149849] 12 p1800 N85-21

Acoustic energy exchange in sheared mean flow - solid rocket motors 13 p1969 N85-22

Repetitive energy transfers from an inductive energy store 13 p2062 N85-22

Numerical investigation of evolution of energy spectra of slightly nonlinear Rossby waves 13 p2106 N85-231

The effects of internal waves on acoustic normal modes [AD-A150235] 13 p2155 N85-23

Molecular dynamics studies of energy transfer processes in crystal systems [AD-A150161] 13 p2163 N85-234

A fundamental study of liquid phase particle breakup. Revision [AD-A150791] 14 p2301 N85-24

The structure, stability, wave transmission and energy transfer at the Earth's magnetopause 14 p2372 N85-24

Ways of optimization of light energy transformation in primary stages of photosynthesis. Necessity of optimization of photosynthetic unit structure and method for calculating efficiency 14 p2386 N85-247

Ways of optimization of light energy transformation in primary stages of photosynthesis. Optimization of lattice structure of uniform photosynthetic unit 14 p2386 N85-247

Intermolecular energy transfer between the individual zero-field levels of triplet traps in an orientationally disordered solid [AD-A150751] 14 p2417 N85-24

Energy trapping, release, and transport in three-dimensional energetic solids and molecular crystals: Theory of defects and impurities [AD-A151071] 14 p2428 N85-24

Direct electron and ion fluid computation of high electrostatic fields in dense inhomogeneous plasmas with subsequent nonlinear optical and dynamical laser interaction 15 p2656 N85-2

Molecular dynamics studies of energy transfer processes in crystal systems [DE85-007247] 15 p2662 N85-2

Spectroscopic investigation of materials for frequency agile laser systems [AD-A151731] 16 p2790 N85-27

Electric field and energy transfer by magnetopause reconnection [INPE-3448-PRE/701] 16 p2826 N85-27

Rotational energy transfer in highly vibrationally excited hydrogen fluoride and deuterium fluoride [AD-A152003] 16 p2862 N85-27

Energy reflection coefficient for H+ ions at energies between 10 and 80 keV [DE85-007547] 16 p2863 N85-27

CALTECH-DOE program on numerical analysis, computing and fundamental studies of motion, energy and mass transfer in fluids [DE85-008106] 17 p2959 N85-2

Flow characteristics of a partially submerged liquid pickup [DE85-008744] 17 p2959 N85-2

Theory of laser-stimulated surface process. 2: A generalized-master-equation approach to energy transfer between an IR laser, an adspecies and phonons [AD-A153063] 17 p2970 N85-2

Average collisional vibrational energy transfer quantities and the inversion temperature [AD-A152674] 17 p3029 N85-2

Electronically excited alkaline earth oxides: Chemical production and collisional energy transfer processes [AD-A153172] 17 p3044 N85-2

Laser-stimulated vibrational excitation of an adspecies studied by a generalized master equation: Neutral atomic hydrogen on hydrated KCl(001) [AD-A153665] 18 p3112 N85-2

Thermochemical energy transport using a hydrogen rich working fluid [AD-D011696] 19 p3233 N85-30

Correction of calculated estimate of fatigue properties of materials under biharmonic loading 19 p3244 N85-301

A numerical solution of a nonisothermal wall using the two-dimensional Navier-Stokes equations [AD-A154467] 19 p3266 N85-30

Progress in inertial fusion at LLNL [DE85-010931] 19 p3277 N85-30

Production of gallium atoms by excimer laser photolysis of trimethyl gallium [DE85-010742] 19 p3278 N85-30

A study of the turbulent layer in the water at an air-water interface
[AD-A154117] 19 p3319 N85-30578

Vibrational energy transfer in benzene-argon collisions
[DE85-009803] 19 p3355 N85-30797

Energy transfer and excimer formation in rare gas solids 19 p3374 N85-30930

Solar-wind magnetosphere energy input functions
[NASA-CR-176021] 19 p3385 N85-31001

Meteorological weapons
[AD-A154735] 21 p3635 N85-32575

Resonant energy transfer during strong excitation
21 p3689 N85-32922

Implicit Monte Carlo methods and non-equilibrium Marshak wave radiative transport
[DE85-010711] 22 p3835 N85-33743

A dominant role for protons at the onset of solar flares
[SH-1.2-13] 23 p3992 N85-34748

Friction, impact, and electrostatic discharge sensitivities of energetic materials
[DE85-013321] 24 p4083 N85-35309

Scaling violation in hadron-nucleus interaction
[HE-3.2-8] 24 p4179 N85-35916

Few-particles generation channels in inelastic hadron-nuclear interactions at energy approximately equals 400 GeV
[HE-3.2-9] 24 p4179 N85-35917

Sub-luminal pulses from cosmic ray air showers
[HE-4.7-13] 24 p4200 N85-36063

ENGINE AIRFRAME INTEGRATION

Predicted performance benefits of an adaptive digital engine control system of an F-15 airplane
[NASA-TM-85916] 07 p0905 N85-15729

Energy efficient engine component development and integration program
[NASA-CR-172846] 19 p3219 N85-29958

ENGINE ANALYZERS

DEAN: A program for dynamic engine analysis
[NASA-TM-87033] 18 p3062 N85-28945

ENGINE CONTROL

NT ROCKET ENGINE CONTROL
NT TURBOJET ENGINE CONTROL

Study on control of ion engine system
[EL-847] 07 p0916 N85-15800

Energy Efficient Engine (E3) controls and accessories detail design report
[NASA-CR-168017] 19 p3218 N85-29957

Performance improvements of a highly integrated digital electronic control system for an F-15 airplane
[NASA-TM-86748] 21 p3556 N85-32120

ENGINE COOLANTS

Columbium chamber fabrication study
[AD-A145230] 01 p0017 N85-10102

Vortex-generating coolant-flow-passage design for increased film-cooling effectiveness and surface coverage
[NASA-TP-2388] 03 p0361 N85-12314

Improvement of gas turbine engine performance by water injection into turbine cooling air
09 p1307 N85-18209

Development of a high-temperature coolant for advanced diesel engines
[AD-A153680] 18 p3117 N85-29297

ENGINE DESIGN

NT ROCKET ENGINE DESIGN

Development trends and requirements of propulsion system technology for civil aircraft
01 p0011 N85-10066

Computational thermo-fluid dynamics contributions to advanced gas turbine engine design
[NASA-TM-86865] 01 p0011 N85-10069

Preliminary mechanical redesign of an existing gas-turbine engine to incorporate a high-efficiency, low-pressure-ratio, highly regenerative cycle for marine applications
[AD-A144808] 01 p0011 N85-10070

Free-piston Stirling engine development
[PB84-237787] 01 p0056 N85-10369

Energy efficient engine flight propulsion system preliminary analysis and design report
[NASA-CR-174701] 02 p0140 N85-10947

Energy efficient engine component development and integration program
[NASA-CR-170034] 02 p0146 N85-10990

Energy efficient engine ICLS Nacelle detail design report
[NASA-CR-167870] 02 p0146 N85-10993

Energy efficient engine. Low pressure turbine test hardware detailed design report
[NASA-CR-167956] 02 p0147 N85-10994

Energy efficient engine ICLS engine bearings, drives and configuration: Detail design report
[NASA-CR-167871] 02 p0147 N85-10997

External fuel vaporization study, phase 2
[NASA-CR-174079] 02 p0187 N85-11252

Liquid-piston Stirling machines
[DE84-014255] 02 p0205 N85-11351

Propulsion — jet aircraft engines
[PNR-90208] 03 p0320 N85-12062

Stirling material technology
[NASA-TM-86888] 04 p0472 N85-13007

Advanced automotive diesel assessment program
[NASA-CR-168285] 04 p0507 N85-13235

Advanced automotive diesel engine system study
04 p0508 N85-13240

A.A.D. engine noise evaluation
04 p0508 N85-13241

Boundary layer simulator improvement
[NASA-CR-174199] 05 p0597 N85-13802

Fabrication and quality assurance processes for superhybrid composite fan blades
[NASA-TM-83354] 06 p0763 N85-14882

USSR report: Engineering and equipment
[JPRS-UEQ-84-007] 06 p0775 N85-14954

Optimum thermogasdynamic design of gas turbine engines by characteristics of element prototypes
06 p0777 N85-14965

Cyclic endurance testing of the RB211-22B cast HP turbine blade 07 p0908 N85-15747

The aircraft engine of the future
[PNR-90226] 08 p1087 N85-16875

SSME lifetime prediction and verification, integrating environments, structures, materials: The challenge
08 p1095 N85-16918

Orbital Maneuvering system design evolution
08 p1098 N85-16943

Vehicle/engine integration — orbit transfer vehicles
08 p1109 N85-17008

Orbital transfer vehicle propulsion issues
08 p1109 N85-17009

USSR report: Engineering and equipment
[JPRS-UEQ-85-001] 09 p1305 N85-18200

On one design principle of surge protector for gas turbine engine compressor 09 p1306 N85-18206

Experimental study of influence of size of upper and lower laps on operational efficiency of centripetal full-inlet air driven microturbines 09 p1307 N85-18211

Advanced Gas Turbine (AGT) powertrain system development for automotive applications
[NASA-CR-174809] 09 p1403 N85-18831

SSME thrust chamber simulation using Navier-Stokes equations
[NASA-CR-171349] 10 p1430 N85-19017

Creep-rupture behavior of iron superalloys in high-pressure hydrogen
[NASA-CR-174411] 10 p1441 N85-19078

Analytical fuel property effects: Small combustors, phase 2
[NASA-CR-174848] 10 p1456 N85-19175

Initial testing of a variable-stroke Stirling engine
[NASA-TM-86875] 10 p1569 N85-19895

Lubrication and performance of high-speed rolling-element bearings
[NASA-TM-86958] 12 p1859 N85-21658

Some solar dish/heat engine design considerations
[DE85-003479] 12 p1881 N85-21802

Experimental determination of optimum ratio of runner blade height at exit to runner blade height at entrance of radial inward-flow microturbines
13 p2049 N85-22827

Hydrodynamic simulation of transient processes in injection system of aircraft engines during pump unswirling 13 p2050 N85-22829

Parameters of symmetric rhombic drive mechanism for single-cylinder Stirling engine 14 p2271 N85-24072

Special course on V/STOL aerodynamics: An assessment of European jet lift aircraft
[AGARD-R-710-ADDENDUM] 15 p2460 N85-25188

Ceramic technology for advanced heat engines project
[DE85-004798] 16 p2755 N85-27002

Ceramic applications in turbine engines
[NASA-CR-174715] 17 p2934 N85-28109

Analysis of physical-chemical processes governing SSME internal fluid flows
[NASA-CR-175893] 17 p2957 N85-28261

Use of ceramics in internal combustion engines
18 p3088 N85-29114

Reciprocating Brayton cycle motor
[REPT-84-RR-336] 20 p3462 N85-31507

Energy efficient engine. Fan and quarter-stage component performance report
[NASA-CR-168070] 23 p3897 N85-34141

Shroud segments for unshrouded blade turbines
[PNR-90260] 23 p3897 N85-34143

ENGINE FAILURE

Stall elimination and restart enhancement device
[AD-D011217] 01 p0010 N85-10062

A theory of post-stall transients in multistage axial compression systems
[NASA-CR-3878] 12 p1771 N85-21117

Effects of inlet distortion on a static pressure probe mounted on the engine hub in an F-15 airplane
[NASA-TP-2411] 13 p1974 N85-22394

Safety recommendation(s), A-84-128 through -133
[REPT-3996C/41] 15 p2466 N85-25221

Nonlinear global stability analysis of compressor stall phenomena
[NASA-CR-174908] 19 p3219 N85-29960

Fault detection and accommodation testing on an F100 engine in an F-15 airplane
[NASA-TM-86735] 19 p3219 N85-29962

Weibull distribution based on maximum likelihood with interval inspection data
[NASA-TM-86515] 21 p3678 N85-32647

ENGINE INLETS

A study of bird ingestions into large high bypass ratio turbine aircraft engines
[DOE/FAA/CT-84/13] 01 p0005 N85-10028

Effect of steady-state temperature distortion on inlet flow to a high-bypass-ration turbofan engine
[NASA-TM-86896] 07 p0904 N85-15725

Ramjet air induction system design for tactical missile application 07 p0918 N85-15811

Air intake efficiency at zero speed and lip suction — jet engines
[BAE-KRS-N-GEN-303] 09 p1272 N85-17996

Research and development for semi-spherical inflow control device
[NAL-TR-833] 09 p1281 N85-18056

Experimental study of aerodynamic shielding of turbojet engine air intake against exhaust gases
09 p1307 N85-18210

Description of a technique to measure spray distribution in an air stream
[AD-A149780] 12 p1771 N85-21122

Selection of air intake parameters for supersonic-flow operation 13 p2051 N85-22837

Shock waves in adjacent engine inlets
[ISL-R-104/84] 20 p3396 N85-31068

Calculation of compressible flow about three-dimensional inlets with auxiliary inlets, slats and vanes by means of a panel method
[NASA-CR-174975] 24 p4060 N85-35162

ENGINE MONITORING INSTRUMENTS

A comparative evaluation of EMADS (Engine Monitoring and Display System) and conventional engine instruments
[AD-A145901] 03 p0319 N85-12060

The applications of fibre optics in gas turbine engine instrumentation
[PNR-90209] 03 p0420 N85-12687

Advanced High Pressure O2/H2 Technology
[NASA-CP-2372] 16 p2733 N85-26862

A device to detect Top Dead Center (TDC) position in motored engines
[REPT-84-RR-347] 20 p3458 N85-31475

Design, development and operation of a high simultaneous capacity digital telemetry system — turbomachine blade flutter
[PNR-90261] 23 p3899 N85-34151

ENGINE NOISE

Energy efficient engine component development and integration program
[NASA-CR-169496] 02 p0146 N85-10989

Jet noise suppression by porous plug nozzles
[NASA-CR-3613] 02 p0275 N85-11790

Turbofan noise generation. Volume 2: Computer programs
[NASA-CR-167952] 02 p0275 N85-11791

A.A.D. engine noise evaluation
04 p0508 N85-13241

Experimental investigation of shock-cell noise reduction for dual-stream nozzles in simulated flight
[NASA-CR-3846] 04 p0557 N85-13549

Static jet noise test results of four 0.35 scale-model QCGAT mixer nozzles
[NASA-TM-86871] 04 p0558 N85-13551

Vibroacoustic control diagnostics of selected machines based on research on the slide bearing of an automobile engine and the alternator
[ISSN-0208-5658] 05 p0641 N85-14112

Research and development for semi-spherical inflow control device
[NAL-TR-833] 09 p1281 N85-18056

Fan noise suppression in turbofan engines
[B8560076] 17 p2398 N85-27872

Development of guidelines for setting physiological and hygienic standards for noise levels in aerospace medicine 19 p3323 N85-30584

Sound-insulating enclosures — machine noise
[BMFT-FB-HA-85-005] 20 p3525 N85-31925

Experimental study of engine knock
[DE85-009851] 22 p3754 N85-33268

ENGINE PARTS
Combustion modeling of a 2 cylinder cycle reciprocating engine
[AD-A144782] 01 p0055 N85-10364
Component-specific modeling
02 p0143 N85-10971
Constitutive model development for isotropic materials
02 p0144 N85-10975
Energy efficient engine ICLS engine bearings, drives and configuration: Detail design report
[NASA-CR-167871] 02 p0147 N85-10997
Jet engine blade repair at the Oklahoma Air Logistics Center, Propulsion Division
[AD-P004003] 03 p0307 N85-11983
Bulletin of the Faculty of Engineering, Hokkaido University, no. 123
[ISSN-0385-602-X] 04 p0482 N85-13075
Experimental study on the glow plug aided alcohol driven diesel engine 04 p0483 N85-13078
Roller crosshead analysis 04 p0507 N85-13238
Screw expander for light duty diesel engines
04 p0508 N85-13242
Thermal and mechanical analysis of major components for the advanced adiabatic diesel engine
04 p0508 N85-13243
Optimum thermogasdynamic design of gas turbine engines by characteristics of element prototypes
06 p0777 N85-14965
Longevity of thin-walled engine parts subjected to transient stresses under creep conditions
06 p0777 N85-14966
Constitutive modeling of engine materials
[AD-A146630] 06 p0817 N85-15189
Overview of the AGARD SMP activities on turbine engine materials technology in the 1972 - 1982 period
07 p0906 N85-15738
Cumulative damage modeling of fatigue crack growth
07 p0907 N85-15741
Problems and possibilities for life extension in gas turbine components 07 p0907 N85-15742
Disc fatigue life predictions for gas turbine engines
07 p0907 N85-15743
Life prediction at high temperature under multiaxial loading 07 p0907 N85-15745
Cyclic endurance testing of the RB211-22B cast HP turbine blade 07 p0908 N85-15747
An investigation of enhanced capability thermal barrier coating systems for diesel engine components
[NASA-CR-174820] 09 p1298 N85-18154
On selecting bypass mixers for turbofan engines
09 p1306 N85-18207
Influence of setting angle of jet cooling nozzles on temperature and stress state of a turbine wheel
09 p1306 N85-18208
Advanced Gas Turbine (AGT) powertrain system development for automotive applications
[NASA-CR-174809] 09 p1403 N85-18[illegible]31
Tribological systems as applied to aircraft engines
[NASA-TM-86965] 12 p1858 N85-2[illegible]357
Parameters of symmetric rhombic drive mechanism for single-cylinder Stirling engine 14 p2271 N85-24072
Estimate of fatigue stability of gas-turbine engine compressor vanes in probabilistic aspect
14 p2287 N85-24169
Laser drilling of aeroengine components
14 p2309 N85-24290
Fiat conducts R and D in ceramic parts for diesel engine 15 p2534 N85-25637
Advanced High Pressure O2/H2 Technology
[NASA-CP-2372] 16 p2733 N85-26862
Manufacturing and producibility technology
16 p2733 N85-26866
Ceramics for advanced O2/H2 application
16 p2734 N85-26868
Vacuum plasma coatings for turbine blades
16 p2734 N85-26869
Properties and microstructures for dual alloy combinations of three superalloys with alloy 901
[NASA-TM-86967] 16 p2749 N85-26963
Ceramic technology for advanced heat engines project
[DE85-004798] 16 p2756 N85-27002
Spacer structure
[AD-D011641] 17 p2897 N85-27866
Optical strain measurement system development
17 p2915 N85-27969
Ceramic applications in turbine engines
[NASA-CR-174715] 17 p2934 N85-28109
Determination of wear intensity and resource of crankshafts and cylinder liners of ZIL-130 and ZMZ-53 engines
[BLL-BISI-TRANS-21393-(9022.06)]
17 p2972 N85-28355
Ceramic turbochargers: A case study of a near-term application of high-strength ceramics
[DE85-006495] 17 p2975 N85-28379
Future of ceramic turbochargers: Promises and pitfalls
[DE85-006209] 17 p2975 N85-28380
Ceramic Technology for Advanced Heat Engines Project
[DE85-008755] 18 p3080 N85-29052
Energy efficient engine component development and integration program
[NASA-CR-172846] 19 p3219 N85-29958
Correction of calculated estimate of fatigue properties of materials under biharmonic loading
19 p3244 N85-30113
Creep fatigue life prediction for engine hot section materials (isotropic)
[NASA-CR-168228] 20 p3394 N85-31057
SSME seal test program: Test results for hole-pattern damper seals
[NASA-CR-171595] 20 p3395 N85-31059
Reliability of welds to repair defects in cast components made from CrMoV steel
[BLL-CE-TRANS-8054-(9022.09)]
20 p3461 N85-31501
Component-specific modeling
[NASA-CR-174925] 21 p3556 N85-32119

ENGINE STARTERS
Stall elimination and restart enhancement device
[AD-D011217] 01 p0010 N85-10062

ENGINE TESTS
NT COLD FLOW TESTS
NT STATIC FIRING
Cylinder power fault diagnosis in military diesel engines
[TT-8405] 01 p0053 N85-10354
Measurement and analysis of spark ignition engine pressure data to determine heat release profiles
[AD-A144770] 01 p0055 N85-10363
Dilution jet mixing 02 p0145 N85-10985
Combustion system for radiation investigations
02 p0145 N85-10986
HOST liner cyclic facilities: Facility description
02 p0146 N85-10988
Energy efficient engine component development and integration program
[NASA-CR-170034] 02 p0146 N85-10990
Advanced blade tip seal system, volume 2
[NASA-CR-167851] 02 p0147 N85-10999
The KZD-85 engine test. Engine type: 1 cylinder, 2 stroke motor 2100 Husquarna
[FWE-FO-1717] 02 p0205 N85-11354
Predicting changes in reliability characteristics of gas turbine engines during operation
06 p0776 N85-14964
Temperature distortion generator for turboshaft engine testing
[NASA-TM-83748] 07 p0893 N85-15658
Engine Cyclic Durability by Analysis and Testing
[AGARD-CP-368] 07 p0905 N85-15733
Accelerated Mission Endurance Testing (AMET)
07 p0906 N85-15736
Design and test requirements for development of today's engines 07 p0906 N85-15737
Cyclic endurance testing of the RB211-22B cast HP turbine blade 07 p0908 N85-15747
Qualification of an electrothermal hydrazine thruster with a vacuum thrust of 0.5 to 2.0 N
[BMFT-FB-W-84-043] 07 p0917 N85-15808
Integrated exhaust gas analysis system for aircraft turbine engine component testing
[NASA-TP-2424] 07 p0962 N85-16100
Laboratory simulation of smoke reduction from aircraft engine test cell exhaust using a fluidized bed filter
[AD-A148600] 08 p1089 N85-16886
Study of advanced fuel system concepts for commercial aircraft
[NASA-CR-174751] 11 p1584 N85-19978
China report: Science and technology
[JPRS-CST-84-032] 11 p1621 N85-20202
New air supply-prime mover facility for engine tests detailed 11 p1621 N85-20204
Diesel combustion: Advances in analysis and simulation 14 p2253 N85-23965
Ceramic applications in turbine engines
[NASA-CR-174715] 17 p2934 N85-28109
Determination of wear intensity and resource of crankshafts and cylinder liners of ZIL-130 and ZMZ-53 engines
[BLL-BISI-TRANS-21393-(9022.06)]
17 p2972 N85-28355
Energy efficient engine high-pressure turbine component rig performance test report
[NASA-CR-168189] 19 p3218 N85-29955
Free-piston Stirling engine/linear alternator 1000-hour endurance test
[NASA-CR-174771] 19 p3304 N85-30481
SSME seal test program: Test results for hole-pattern damper seals
[NASA-CR-171595] 20 p3395 N85-31059
Experimental study of engine knock
[DE85-009851] 22 p3754 N85-322
Energy efficient engine. Fan and quarter-stage component performance report
[NASA-CR-168070] 23 p3897 N85-34141
A study of the control of particulate emissions from turbine engine test cells 24 p4067 N85-3520

ENGINEERING
Experimenting with the Rolm Ada language workshop for specifying and designing 03 p0408 N85-1200
Emergency Mathematics and Science Education Act
[GPO-29-561] 03 p0435 N85-127
Write while you work: Painless technical writing for Sandia engineers
[DE84-010869] 04 p0577 N85-136
Computational mechanics: A perspective on problems and opportunities for increasing productivity and quality of engineering
[PB85-128106] 12 p1950 N85-2225
Characteristics of recent science/engineering graduates, 1982: Detailed statistical tables
[PB85-149060] 15 p2663 N85-2543
Academic science and engineering: Graduate enrollment and support, fall 1982 (detailed statistical tables)
[PB85-154730] 15 p2664 N85-2543
Academic science and engineering: R and D funds, fiscal year 1982 (detailed statistical tables)
[PB85-154763] 15 p2664 N85-2544
Engineering education based on computer simulation
[CFD/85/1] 20 p3512 N85-318

ENGINEERING DEVELOPMENT
U PRODUCT DEVELOPMENT

ENGINEERING DRAWINGS
High reliability mechanical-hydraulic converter
14 p2268 N85-240
Aircraft skin penetrator and agent applicator. Volume 2: Test and evaluation
[AD-A151609] 15 p2466 N85-252
An analysis of grid-based line drawing quantization methods
[AD-A151847] 15 p2522 N85-2554
An extension of a microcomputer based system for analysis of line drawing quantization schemes
[AD-A152008] 15 p2624 N85-26171
Water brake convertor: A simple device to convert mechanical energy into heat energy
[DE85-006021] 16 p2716 N85-267
X-ray satellite
[NASA-TM-77896] 20 p3407 N85-31144
Low-head hydroelectric power demonstration project City of Gonzales, Texas
[DE85-010403] 22 p3809 N85-335
A rational approach to cam design
23 p3923 N85-343

ENGINEERING MANAGEMENT
Computers and the consulting engineer
15 p2626 N85-261
Thin-film reliability and engineering overview
21 p3612 N85-324
DoD Value Engineering conference report. Value Engineering (VE): A tool that benefits line management. Part 4, Workshop B: VE on spare parts
[AD-A156070] 24 p4163 N85-358
DoD Value Engineering conference report. Value Engineering (VE): A tool that benefits line management. Part 7, Workshop E: VE in construction and archit engineer contracts
[AD-A156073] 24 p4164 N85-358

ENGINES
NT AIR BREATHING ENGINES
NT ARC JET ENGINES
NT BOOSTER ROCKET ENGINES
NT DIESEL ENGINES
NT DUCTED ROCKET ENGINES
NT ELECTROSTATIC ENGINES
NT ELECTROTHERMAL ENGINES
NT EXTERNAL COMBUSTION ENGINES
NT GAS TURBINE ENGINES
NT HYDRAZINE ENGINES
NT HYDROGEN OXYGEN ENGINES
NT INTERNAL COMBUSTION ENGINES
NT ION ENGINES
NT J-52 ENGINE
NT J-85 ENGINE
NT JET ENGINES
NT LIQUID PROPELLANT ROCKET ENGINES
NT MERCURY ION ENGINES
NT MICROROCKET ENGINES
NT ORBIT MANEUVERING ENGINE (SPACE SHUTTLE)
NT PISTON ENGINES
NT PLASMA ENGINES

NT PULSED JET ENGINES
NT RAMJET ENGINES
NT RESISTOJET ENGINES
NT REUSABLE ROCKET ENGINES
NT RIT ENGINES
NT RL-10 ENGINES
NT ROCKET ENGINES
NT ROTARY ENGINES
NT SOLID PROPELLANT ROCKET ENGINES
NT SPACE SHUTTLE MAIN ENGINE
NT SUPERSONIC COMBUSTION RAMJET ENGINES
NT TF-34 ENGINE
NT TURBINE ENGINES
NT TURBOFAN ENGINES
NT TURBOJET ENGINES
NT TURBOPROP ENGINES
NT TURBOROCKET ENGINES
NT UPPER STAGE ROCKET ENGINES
NT VARIABLE CYCLE ENGINES

Development of a Braun linear engine-driven, heat-actuated heat pump
[DE84-016647] 04 p0500 N85-13188

Effect of water on hydrogen permeability --- Stirling engines
[NASA-TM-86904] 06 p0761 N85-14864

A simulation model for Air Launched Cruise Missile engine management
[AD-A147018] 07 p1051 N85-16672

Technological and economic assessment of advanced ceramic materials. Volume 2: A case study of ceramics in heat engine applications
[PB85-113090] 12 p1815 N85-21384

Parameters of symmetric rhombic drive mechanism for single-cylinder Stirling engine 14 p2271 N85-24072

Nonlinear analysis of an axisymmetric structure subjected to non-axisymmetric loading
20 p3468 N85-31549

FAA/GAMA (Federal Aviation Administration/General Aviation Manufacturer's Association) propeller aircraft noise test program, Salina Municipal Airport, Salina, Kansas
[AD-A154818] 21 p3699 N85-32983

High temperature structural insulating material
[DE85-006361] 23 p3920 N85-34291

ENGLAND

Accidents and serious incidents to civil aircraft due to birdstrikes
[AD-P004180] 11 p1578 N85-19942

ENGLISH LANGUAGE

Research on knowledge delivery
[AD-A149585] 10 p1536 N85-19698

Character recognition using correlation techniques
[AD-A152006] 16 p2847 N85-27549

ENGRAVING

Fast and precise processing of material by means of an intensive electron beam
[BMFT-FB-T-84-123] 03 p0342 N85-12201

Applications of lasers in manufacturing
14 p2308 N85-24279

Automatic engraving of map frames in the revision of the TK 25, 1:25,000 topographical map
16 p2814 N85-27362

T sub EX font tables
[DE85-011394] 19 p3339 N85-30687

ENHANCEMENT
U AUGMENTATION

ENLARGING
U EXPANSION

ENRICHMENT
NT ISOTOPIC ENRICHMENT
NT JET MEMBRANE PROCESS

Development and demonstration of a spiral-wound thin-film composite membrane system for the economical production of oxygen-enriched air, phase 4
[DE85-012380] 23 p3920 N85-34288

Measurement of uranium enrichment for gaseous uranium at low pressure
[DE85-012697] 24 p4150 N85-35733

ENSKOG-CHAPMAN THEORY
U CHAPMAN-ENSKOG THEORY

ENSTATITE

High temperature deformation of hot-pressed polycrystalline orthoenstatite
[NASA-CR-174026] 02 p0285 N85-11861

The rheology of icy satellites
[NASA-CR-174024] 02 p0302 N85-11958

ENSTROPHY
U VORTICITY

ENTERPRISE (ORBITER)

Space shuttle flight readiness firing dress rehearsal for STS-1 08 p1097 N85-16929

ENTHALPY

Thermodynamic properties and environmental chemistry of chromium
[DE84-015123] 01 p0025 N85-10152

Thermodynamic properties of isobutane-isopentane mixtures from -40 to +600(0)F and up to 1000 psia
[DE84-015137] 01 p0124 N85-10850

Engineering method of calculating a turbulent diffusion flame
[BLL-M-35761-(5828.4)] 02 p0171 N85-11147

External fuel vaporization study, phase 2
[NASA-CR-174079] 02 p0187 N85-11252

Procedural aspects of testing aerodynamic models with combustion in high-enthalpy transient-mode installations
05 p0725 N85-14658

Hydrogen embrittlement of nickel
[AD-A148322] 08 p1129 N85-17119

Development of media for dynamic latent heat storage for the low-temperature range. Part 1: Thermal analyses of selected salt hydrate systems
[NASA-TM-77778] 10 p1507 N85-19510

The physical modelling of transition metal alloying: The roles that different levels of theory play
[DE85-000591] 11 p1607 N85-20105

Evaluation of ettringite and related compounds for use in solar energy storage
[DE85-003249] 12 p1882 N85-21809

Heat of mixing experiments for liquified gases
[PB85-183697] 18 p3084 N85-29081

The moist available energy of a conditionally unstable atmosphere 18 p3145 N85-29473

Determination of the vacancy formation enthalpy in chromium by positron annihilation
[DE85-010286] 19 p3239 N85-30084

PAS determination of the vacancy formation enthalpy in tungsten
[DE85-010283] 19 p3240 N85-30086

Liquid-phase compositions from vapor-phase analyses 2: Adaptation of the Prausnitz program to UF6 and some of its potential impurities
[DE85-011521] 21 p3673 N85-32619

Thermodynamic properties of alloys in the Fe-Ti system
[NPL-DMA(A)-96] 22 p3748 N85-33229

Drying of pulverized material with heated condensible vapor
[DE85-011656] 22 p3783 N85-33438

Enthalpy transients in fractured two-phase geothermal systems
[DE85-011988] 22 p3806 N85-33587

Enthalpies of formation of liquid Fe-Ce-Si and Fe-Ce-Al three-component alloys
[BLL-M-36296-(5828.4)] 23 p3913 N85-34247

Dynamics of the melting of chromium-manganese alloys in molten steel
[BLL-M-35850-(5828.4)] 23 p3914 N85-34252

Results of variable enthalpy tests of CPR-488 TIP panels in MSFC Hot Gas Facility
[NASA-CR-170889] 24 p4072 N85-35237

Thermodynamics of the corrosion of chromium in molten carbonates
[DE85-011407] 24 p4079 N85-35282

ENTIRE FUNCTIONS

Boundary behavior of analytic functions, analytic wave front sets and the intersection problem of Ehrenpreis
[PREPRINT-809] 01 p0114 N85-10778

On generating function of Weber parabolic cylinder functions with a negative integer index and radio pulse deformation by a medium
[PR-213] 03 p0354 N85-12276

Solutions of problems of miller and rubel
10 p1536 N85-19685

Pade tables of a class of entire functions
[CSIR-TWISK-337] 14 p2413 N85-24877

Annals of the Scientific Academy of Finland, series A. 1: Mathematics, volume 9
[ISSN-0066-1953] 15 p2633 N85-26229

Iteration of exponential functions
15 p2633 N85-26233

On the length of asymptotic paths of meromorphic functions of order zero 15 p2633 N85-26234

A note on integral operators
[REPT-83-26] 17 p3021 N85-28686

ENTRAINMENT

Experiments on turbulent mixing and chemical reactions in a liquid mixing layer 02 p0134 N85-10912

Characteristics of a turbulent plane offset jet
02 p0196 N85-11310

Particle entrainment in a compressible vortex
[ISL-CO-230/83] 04 p0500 N85-13192

The properties of a round turbulent buoyant jet
[NAL-TR-826] 06 p0808 N85-15136

A wind-tunnel study of the saltation of heterogeneous (size, density) sands 08 p1182 N85-17449

Simulation of entrainment at the top of the atmospheric boundary layer for use in General Circulation Models (GCM)
[DM-42] 09 p1355 N85-18525

The physics of the marine stratocumulus-capped mixed layer 15 p2593 N85-25979

Buoyant jet entrainment in stratified fluids
19 p3263 N85-30236

Density and confinement effects on mixing characteristics of an axisymmetrical CO(2) jet
[AD-A154486] 19 p3267 N85-30258

Performance characteristics of gravity-assisted potassium heat pipes
[DE85-010717] 19 p3287 N85-30387

ENTRAPMENT

Control of mammals at airports
[AD-P004192] 11 p1580 N85-19957

ENTROPY

Thermodynamic properties and environmental chemistry of chromium
[DE84-015123] 01 p0025 N85-10152

Research into topics in transonic flow theory
[AD-A148526] 08 p1078 N85-16837

Construction of solutions for two-dimensional Riemann problems
[DE85-003136] 10 p1549 N85-19770

Entrop production determination of the ambipolar solution nearest equilibrium
[DE85-003049] 10 p1560 N85-19836

Decaying particles do not heat up the Universe
[DE85-002191] 11 p1763 N85-21091

Entropy production during fatigue as a criterion for failure. A local theory of fracture in engineering materials
[AD-A151289] 15 p2576 N85-25902

Cluster production and entropy
[DE85-007626] 17 p3032 N85-28752

Heat of mixing experiments for liquified gases
[PB85-183697] 18 p3084 N85-29081

Entropy of He 2 and universality near the superfluid in He(4) 19 p3378 N85-30957

Biological modulation of planetary atmospheres: The early Earth scenario 22 p3854 N85-33867

ENTROPY (STATISTICS)
NT MAXIMUM ENTROPY METHOD
NT MINIMUM ENTROPY METHOD

Stochastic runaway of dynamical systems
[IPP-6/244] 11 p1708 N85-20745

The role of duality in optimization problems involving entropy functionals, with applications to information theory
[AD-A152336] 17 p3026 N85-28713

ENUMERATION

Isomer enumeration in polytertiary phosphines and related compounds
[AD-A148056] 09 p1290 N85-18099

ENVIRONMENT EFFECTS

Space Shuttle Environmental Effects: The First 5 Flights
[NASA-CR-171812] 01 p0069 N85-10457

State of knowledge of environmental concerns related to natural gas-fueled vehicles
[DE84-015894] 01 p0070 N85-10461

Land use/land cover 02 p0214 N85-11410

Analysis of potential combustion sorce impacts on acid deposition using an independently derived inventory, volume 1
[DE84-012005] 02 p0225 N85-11471

Design of alternate launch and recovery surfaces for environmental effects
[AD-A145800] 03 p0320 N85-12066

Dynamic and other secondary benefits of compressed air energy storage
[DE84-015571] 03 p0386 N85-12468

Modeling effects of toxicants on aquatic systems
[DE84-016594] 04 p0531 N85-13396

Health and environmental effects document for photovoltaic energy systems, 1983
[DE84-017179] 04 p0532 N85-13399

Ocean services user needs assessment. Volume 1: Survey results, conclusions and recommendations
[NASA-CR-174104] 04 p0541 N85-13445

Space nuclear safety program
[DE84-015983] 04 p0564 N85-13591

Global carbon - nitrogen - phosphorus cycle interactions: A key to solving the atmospheric CO2 balance problem?
05 p0652 N85-14188

Summary of salt gradient solar pond research
05 p0667 N85-14292

Activities report in Earth and planetary environments physics
[CRPE-NT-134] 05 p0734 N85-14720

Tides and tidal currents of the inland waters of Western Washington
[PB84-237379] 06 p0842 N85-15346

Ecological impacts of hydroelectric projects in Amazonia 07 p1003 N85-16374

The Amazon and climate 07 p1003 N85-16376

Simulating responses to expected climate change in eastern North America: Applications to decision-making in the forest industry
[DE85-001272] 07 p1008 N85-16406

Installation restoration program. Phase 2: Stage 1 problem confirmation study, Duluth International Airport Duluth, Minnesota
[AD-A148318] 08 p1089 N85-16885

Shuttle on-orbit contamination and environmental effects 08 p1104 N85-16980

Preliminary survey of wind generation in Washington: Site studies and selected wind speed data
[DE85-000058] 09 p1345 N85-18462

Monitoring environmental and related performance parameters for a Rankine-cycle turbine electric generator utilizing geothermal energy at the Gila Hot Springs, New Mexico
[DE84-901772] 09 p1345 N85-18465

Consideration of future climatic changes in three geologic settings
[DE85-001704] 09 p1357 N85-18537

A preliminary assessment of environmental noise from large Wind Energy Conversion Systems (WECS) based on experiences from Swedish prototypes
[FFA-TN-1984-48] 09 p1379 N85-18668

Airport site selection and design
[AD-P004193] 11 p1581 N85-19959

Effects of electromagnetic fields produced by high voltage transmission lines
[DE85-900034] 11 p1625 N85-20230

Effect of water vapor and water droplets on the RAM-1 (Real-Time Aerosol Monitor): Preliminary results
[PB85-109429] 11 p1637 N85-20313

Proceedings of a Workshop on Environment of West Antarctica: Potential CO2-induced changes
[PB85-110757] 11 p1671 N85-20527

Environmental effects of space activities
11 p1678 N85-20577

Combined effects of atmospheric deposition, internal acid production, and harvesting on nutrient gains and losses from forest ecosystems
[DE85-002325] 12 p1884 N85-21821

Ecological observations at the site of the 10 MWe solar thermal power system (1978-1984)
[DE85-004572] 12 p1885 N85-21827

Assessment of hazardous waste surface impoundment technology case studies and perspectives of experts
[PB85-117059] 12 p1886 N85-21834

Standard analytical procedures of the NOAA National Analytical Facility, 1984-85: Extractable toxic organic compounds
[PB85-126282] 12 p1887 N85-21840

Summary report of the Workshop on Structure Activity Concepts in Environmental Sciences
[PB85-137339] 12 p1887 N85-21841

Impact of aerosols on visibility and climate: A report prepared for Panel 3, Environmental Impact, of the NATO/CCMS Air Pollution Pilot Study on Air Pollution Control Strategies and Impact Modelling
[PB85-106744] 12 p1897 N85-21906

USC (University of Southern California) Sea Grant Program Directory, 1984-1985
[PB85-135051] 12 p1899 N85-21922

Effect of high ammonia content in closed environment on some parameters of human nitrogen and carbohydrate metabolism against background of a controlled diet
12 p1903 N85-21948

Areas with forest soils sensitive to acidic deposition under alternative damage hypotheses
[DE85-005257] 13 p2130 N85-23257

Effects of interactive transport and scavenging of smoke on the calculated temperature change resulting from large amounts of smoke
[DE85-006450] 14 p2378 N85-24684

A comparative evaluation of the effects of acid precipitation, natural acid production and harvesting of cation removal from forests
[DE85-005254] 15 p2589 N85-25961

The role of gravity on the reproduction of arabidopsis plants 15 p2607 N85-26069

Oil resistant silicone elastomers
[AD-131523] 16 p2753 N85-26987

Acid rain: Effects on fish and wildlife
[PB85-154672] 16 p2821 N85-27402

Impact of ozone on vegetation
[PB85-159937] 16 p2821 N85-27403

ELF (Extremely Low Frequency) communications system ecological monitoring program: Measurements of ELF electromagnetic fields for site selection and characterization, 1983
[AD-A153120] 17 p2949 N85-28209

Investigation of air pollution impact in Eastern Bavaria: Measurement results from August and September, 1984
[DFVLR-FB-85-03] 17 p2988 N85-28471

Ozone and temperature trends due to the injection of trace species in the atmosphere
[AERONOMICA-ACTA-A-288-1984]
18 p3132 N85-29399

Applied climatology — regional planning
18 p3147 N85-29486

Ambient air contamination: Characterization and detection techniques 18 p3157 N85-29546

Program planning using the GMAP procedure in SAS/GRAPH software
[DE85-006356] 18 p3199 N85-29842

Activities report in energy technology
[OEFZS-4302] 18 p3199 N85-29846

Environmental Sciences Division report
[DE85-010452] 19 p3308 N85-30506

Applied Science Division's Environmental Research Program
[DE85-010637] 19 p3308 N85-30510

Analysis of leachate production in closed hazardous waste landfills
[DE85-010978] 19 p3310 N85-30520

Aviation noise effects
[AD-A154319] 19 p3352 N85-30776

Annual environmental monitoring report, January-December 1984
[DE85-011689] 20 p3486 N85-31665

Ozone in the 21st century: Increase or decrease
[AERONOMICA-ACTA-A-291-1984]
20 p3489 N85-31687

Thin-film reliability and engineering overview
21 p3612 N85-32450

Effects of environment on spacecraft materials
22 p3733 N85-33144

Procedure for estimating orbital debris risks
[NASA-TP-2507] 22 p3738 N85-33169

Small-hydropower development: The process, pitfalls, and experience. Volume 1: Feasibility studies summary and analysis
[DE85-010639] 22 p3808 N85-33589

Acid rain in Europe
[COMMITTEE-PRINT-99-F] 22 p3810 N85-33601

Environmental monitoring at Lawrence Livermore National Laboratory: 1984 report
[DE85-011593] 22 p3811 N85-33606

A 1984 environmental summary: Sandia National Laboratories Tonopah Test Range, Tonopah, Nevada
[DE85-011145] 22 p3812 N85-33612

Nordic Association for Aerosol Research (NOSA) Aerosol Symposium: Program and abstracts
[FOA-E-40019] 22 p3812 N85-33616

Organic solvent alteration of hydraulic properties of sedimentary rocks of low permeability: A review
[DE85-012537] 22 p3815 N85-33635

Meteorology and Society: Statements presented at the 9th congress under agenda item 12 — World Meteorological Organization
[WMO-643] 22 p3817 N85-33644

Fusion facility siting considerations
[DE85-012894] 22 p3843 N85-33805

Near-threshold fatigue: An overview of the role of microstructure and environment
[DE85-009903] 23 p3941 N85-34431

Effects of acid rain on forest nutrient status
[DE85-012486] 23 p3947 N85-34463

Agents and effects of ozone trends in the atmosphere
[AERONOMICA-ACTA-A-287-1984]
23 p3948 N85-34466

Effect of hypokinesia and +Gz accelerations on transport function of human blood
23 p3952 N85-34497

Contribution to the properties of carbon fiber reinforced composites — structural mechanics
[ESA-TT-849] 24 p4074 N85-35246

Implementing agreement for cooperation in the development of large scale wind energy conversion systems
[JUEL-SPEZ-278] 24 p4110 N85-35473

General environmental aspects of large scale wind energy utilization 24 p4110 N85-35474

GROWIAN: First observations of the environmental impact at the GROWIAN site — wind energy converter
24 p4110 N85-35476

Environmental aspects of large-scale wind-power systems in the UK 24 p4110 N85-35478

Environmental Monitoring Burger Hill, Orkney wind turbine generator site and similar work at other UK WTG sites 24 p4111 N85-35482

Environmental aspects of the Netherlands wind farm project 24 p4111 N85-35485

ENVIRONMENT MANAGEMENT

EPA (Environmental Protection Agency) environmental data base and model directory, volume 1
[PB84-207562] 01 p0126 N85-10668

Proceedings of the Environmental Systems Symposium (13th) held at Bethesda, Md., 20-22 March 1984
[AD-A148194] 09 p1346 N85-18471

The application of emissions trading to DoD installations
[AD-P004136] 09 p1346 N85-18472

Compatible goals: Defense and environmental protection
[AD-P004137] 09 p1347 N85-18473

Environmental and energy audits of Air Force government owned-contractor operated installations
[AD-P004138] 09 p1347 N85-18474

Strategies for preparing and submitting a part B application for a DoD facility
[AD-P004139] 09 p1347 N85-18475

Assessment of environmental costs at ordnance activities
[AD-P004140] 09 p1347 N85-18476

Landscape management on airports for reduction of bird populations
[AD-P004194] 11 p1581 N85-19960

Inexpensive multipurpose landscaping
11 p1581 N85-19961

Reducing gull use of some attractions near airports
[AD-P004195] 11 p1581 N85-19962

Effectiveness of an overhead wire barrier in deterring gulls from feeding at a sanitary landfill
[AD-P004199] 11 p1582 N85-19966

Environmental management needs
[DE85-007859] 18 p3133 N85-29405

Wind turbines and environment management
[CP-MEMO-1983-11] 20 p3485 N85-31682

Marine environmental quality assessment program, five-year plan (FY 1984 - 1988)
[AD-A154715] 21 p3613 N85-32459

A guide for new environmental coordinators
[AD-A158327] 24 p4113 N85-35498

Land Disposal of Hazardous Waste
[PB85-196376] 24 p4113 N85-35500

ENVIRONMENT MODELS

EPA (Environmental Protection Agency) environmental data base and model directory, volume 1
[PB84-207562] 01 p0126 N85-10668

Measurements 12 p1787 N85-21222

The accuracy in calculations of intervisibility with digital terrain models — digital models
[FOA-C-20557-D6(E1)] 12 p1909 N85-21983

Empirical methods for predicting eutrophication in impoundments. Report 3. Phase 2. Model refinements
[AD-A155483] 21 p3614 N85-32462

Global environmental transport models for tritium
[DE85-011437] 22 p3816 N85-33639

Oxidation states of iron in the terrestrial planets: Evidence and implications for accretion models
22 p3852 N85-33864

ENVIRONMENT POLLUTION

NT AIR POLLUTION
NT GLOBAL AIR POLLUTION
NT INDOOR AIR POLLUTION
NT OIL POLLUTION
NT WATER POLLUTION

HS and E environmental sciences
[DE84-016183] 05 p0672 N85-14314

Something in the air at Windscale — radioactive contaminants from the Sellafield nuclear Complex for reprocessing and storing irradiated fuel
[BLL-RISLEY-TR-4998-(9091.9F)]
08 p1179 N85-17429

Penetration of the atmosphere by flammable mixtures as a result of spillage of LNG on the ground
08 p1179 N85-17432

Atmospheric acidification chemistry: A review
[PB84-215490] 09 p1350 N85-18486

Research in environmental biology reviewed
11 p1622 N85-20211

National Acid Precipitation Assessment Program. Report to the President and Congress (1983)
[PB85-116713] 11 p1679 N85-20581

China report: Science and technology
[JPRS-CST-84-036] 11 p1696 N85-20861

Report on the Second Annual Review Meeting of the National Acid Precipitation Assessment Program. Research to assist decisionmaking: Summary
[DE85-003003] 12 p1884 N85-21820

Feoktistov discusses need for space colonization
13 p1985 N85-22454

An ultrasensitive and element specific photoionization detection system for environmental analysis
[AD-A153365] 17 p2968 N85-28032

Technical support for geopressured-geothermal well activities in Louisiana
[DE85-010462] 18 p3102 N85-29200

North American acid deposition data base system (ADS) and its use in spatial analysis
[PB85-173235] 18 p3201 N85-29858

Environmental monitoring report for Pantex Plant covering, 1984
[DE85-010824] 19 p3308 N85-30509

Analysis of leachate production in closed hazardous waste landfills
[DE85-010978] 19 p3310 N85-30520

Radioactivity in gaseous waste discharged from the separations facilities during 1984
[DE85-011373] 19 p3360 N85-30831

Bulk and thermal properties of the functional Tuffaceous Beds in holes USW G-1, UE-25 no. 1, and USW G-2, Yucca Mountain, Nevada
[DE85-011181] 19 p3365 N85-30866
Soil extraction kit
[AD-D011736] 22 p3742 N85-33190

ENVIRONMENT PROTECTION
Estuaries of the Cape. Part 2: Synopses of available information on individual systems. Report no. 17: Lourens (CSW 7)
[CSIR-RR-416-PT-2] 01 p0087 N85-10586
National Photovoltaics Program Annual Review Meeting, abstracts
[DE84-013003] 04 p0530 N85-13390
Proceedings of the Environmental Systems Symposium (13th) held at Bethesda, Md., 20-22 March 1984
[AD-A148194] 09 p1346 N85-18471
Compatible goals: Defense and environmental protection
[AD-P004137] 09 p1347 N85-18473
Environmental and energy audits of Air Force government owned-contractor operated installations
[AD-P004138] 09 p1347 N85-18474
Strategies for preparing and submitting a part B application for a DoD facility
[AD-P004139] 09 p1347 N85-18475
Assessment of environmental costs at ordnance activities
[AD-P004140] 09 p1347 N85-18476
Remedial action of hazardous waste US Army Corps of Engineers, Anniston, Alabama
[AD-P004141] 09 p1347 N85-18477
Practical application of earth resistivity methods in phase 2 of the installation restoration program
[AD-P004148] 09 p1348 N85-18484
The Hazardous Materials Technical Center
[AD-P004149] 09 p1349 N85-18485
Community relations activities at Department of Defense sites
[AD-P004150] 09 p1349 N85-18486
Atmospheric diffusion in hilly region on middle reaches of the Chang Jiang 11 p1620 N85-20196
Urban climate and air hygiene before, during, and after the lifework of Hellmut Berg. Overview of a branch of applied meteorology 18 p3147 N85-29487
Radionuclide mobility in the shallow portion of an active high-temperature geothermal system
[DE85-010293] 18 p3182 N85-29729
Reference data source documentation for performance assessment studies, Basalt Waste Isolation Project, Hanford Site, Washington
[DE85-010543] 19 p3301 N85-30468
Magnetohydrodynamics and the National Coal Science, Technology, and Engineering Development Acts
[S-HRG-98-1179] 20 p3535 N85-31994
Corrosion resistant storage container for radioactive material
[DE85-011686] 22 p3838 N85-33765
A guide for new environmental coordinators
[AD-A156327] 24 p4113 N85-35498

ENVIRONMENT SIMULATION
NT ALTITUDE SIMULATION
NT SPACE ENVIRONMENT SIMULATION
NT THERMAL SIMULATION
NT WEIGHTLESSNESS SIMULATION
Evaluation of thermocouple junction temperature
[DE84-015159] 04 p0502 N85-13206
Growth of soil bacteria in presence of Martian soil analog, carbon dioxide and hydrogen peroxide
09 p1361 N85-18560
Ribbon burner simulation of T-700 turbine shroud for ceramic lined seals research
[NASA-TM-86940] 10 p1483 N85-19364
Potential bedforms on Venus: Wind tunnel simulations 13 p2189 N85-23583
Microdunes and other aeolian bedforms on Venus: Wind tunnel simulations 13 p2189 N85-23584
Simulated microgravity as a probe for understanding the mechanisms of early pattern specification
15 p2611 N85-26092
Testing of materials and coatings for jet engine components under simulated operational conditions
[B8560073] 17 p2899 N85-27873
An environmentally-controlled extended-use small animal hypobaric chamber
[AD-A153735] 19 p3221 N85-29974
The deep diving simulator TITAN: Physiological problems associated with staying in great depths of water 24 p4130 N85-35604

ENVIRONMENT SIMULATORS
NT SOLAR SIMULATORS
NT SPACE SIMULATORS
Impedance measurements on a VLF multi-turn loop antenna in a space plasma simulation chamber
[AD-A148104] 04 p0492 N85-13141
Natural exposure versus chamber simulation
[AD-A149538] 10 p1495 N85-19437

ENVIRONMENTAL CHAMBERS
U TEST CHAMBERS

ENVIRONMENTAL CHEMISTRY
NT AEROTHERMOCHEMISTRY
NT ATMOSPHERIC CHEMISTRY
NT BIOCHEMISTRY
NT BIOGEOCHEMISTRY
NT GEOCHEMISTRY
NT PHYSIOCHEMISTRY
Thermodynamic properties and environmental chemistry of chromium
[DE84-015123] 01 p0025 N85-10152
Estuaries of the Cape. Part 2: Synopses of available information on individual systems. Report no. 17: Lourens (CSW 7)
[CSIR-RR-416-PT-2] 01 p0087 N85-10586
Summary report of the Workshop on Structure Activity Concepts in Environmental Sciences
[PB85-137339] 12 p1887 N85-21841
Design of the National Trends Network for monitoring the chemistry of atmospheric precipitation
[GS-CIRC-964] 20 p3486 N85-31664
The 1984 effluent and environmental monitoring report for the Bettis Atomic Power Laboratory
[DE85-011533] 22 p3810 N85-33602

ENVIRONMENTAL CONTROL
Toxicological evaluation of Columbia spacecraft
01 p0094 N85-10631
Conceptual design and evaluation of selected Space Station concepts, volume 2
[NASA-TM-87384] 02 p0168 N85-11130
Challenges in the development of the orbiter atmosphere revitalization subsystem 08 p1095 N85-16920
Other challenges in the development of the orbiter environmental control hardware
08 p1096 N85-16924
Operating and maintenance guidelines for the kinergetics (trade name) environmental control system. Carbon dioxide scrubber model DH-10 and heat exchanger model CCU-01
[AD-A148107] 08 p1200 N85-17557
Control technology for fiber reinforced plastics industry at AMF Hatteras Yachts, New Bern Division, New Bern, North Carolina
[PB85-109015] 10 p1460 N85-19198
Extended mission life support systems
18 p3157 N85-29547
An environmentally-controlled extended-use small animal hypobaric chamber
[AD-A153735] 19 p3221 N85-29974
Space station ECLSS integration analysis: Simplified General Cluster Systems Model, ECLS System Assessment Program enhancements
[NASA-CR-176089] 21 p3670 N85-32796
Evaluation of source strength and dispersion model predications with data from large nitrogen tetroxide field experiments
[DE85-011855] 23 p3947 N85-34465

ENVIRONMENTAL ENGINEERING
Compilation of annual reports of the Navy ELF (Extremely Low Frequency) communications system ecological monitoring program. Volume 1: Tabs A-E
[AD-A148326] 08 p1152 N85-17272
Compilation of annual reports of the Navy ELF (Extremely Low Frequency) communications system ecological monitoring program (1983). Volume 2: Tabs F-J
[AD-A148327] 08 p1152 N85-17273
Research in environmental biology reviewed
11 p1622 N85-20211
Design of computer-related workstations in relation to job functions and productivity
[AD-A151938] 16 p2844 N85-27534
Recommendations for the design and equipping of engineering metrology laboratories
[NPL-MOM-22] 23 p3898 N85-34145

ENVIRONMENTAL LABORATORIES
Activities report in Earth and planetary environments physics
[CRPE-NT-134] 05 p0734 N85-14720
Environmental research laboratories (of the National Oceanic and Atmospheric Administration) programs and plans: FY 1983 programs and FY 1984 plans
[PB84-226729] 06 p0840 N85-15336
Making sure: A brief outline and history of ESA's test and checkout services
[ESA-BR-22] 09 p1286 N85-18077
Environmental Research Laboratories publication abstracts, FY 1984
[PB85-180594] 19 p3313 N85-30540
Environmental background measurement program
[AD-A153860] 19 p3319 N85-30577
Adaptive aiding for symbiotic human-computer control: Conceptual model and experimental approach
[AD-A153870] 19 p3332 N85-30644
European Space Tribology Laboratory: Facilities, services, capabilities
[ESA-BR-12] 20 p3398 N85-31080

ENVIRONMENTAL MONITORING
EPA (Environmental Protection Agency) environmental data base and model directory, volume 1
[PB84-207562] 01 p0126 N85-10868
Economic evaluation of space survey materials use in land improvement engineering field work
02 p0165 N85-11115
Analysis of radiocobalt in environmental samples
[DRIC-T-7334] 03 p0367 N85-12477
A system for monitoring radon and its decay products in the atmosphere
[INPE-3085-PRE/494] 03 p0391 N85-12502
A comparison of TIROS-N series satellite data and LANDSAT data over Scotland 05 p0656 N85-14210
Monitoring and mapping global vegetation cover using data from meteorological satellites
05 p0656 N85-14211
A geoinformation expert system for synergetic use of map and image data 05 p0659 N85-14233
Inventory and monitoring of national park landscapes — remote sensing 05 p0660 N85-14245
Environmental data inventory for the antarctic area
[PB85-107944] 06 p0819 N85-15195
Early detection of environmental exposure
[AD-P004039] 06 p0845 N85-15360
Compilation of annual reports of the Navy ELF (Extremely Low Frequency) communications system ecological monitoring program. Volume 1: Tabs A-E
[AD-A148326] 08 p1152 N85-17272
Compilation of annual reports of the Navy ELF (Extremely Low Frequency) communications system ecological monitoring program (1983). Volume 2: Tabs F-J
[AD-A148327] 08 p1152 N85-17273
Pilot climate data system
[NASA-CR-174321] 08 p1187 N85-17481
Remote sensing technology now playing practical roles 11 p1619 N85-20190
Environmental Monitoring Improvement Act
[GPO-39-742] 11 p1677 N85-20568
National Acid Precipitation Assessment Program. Report to the President and Congress (1983)
[PB85-116713] 11 p1679 N85-20581
On the P1 data from GMS-SEM
12 p1894 N85-21890
The development of image processing of NOAA AVHRR data and its application to sea surface temperature
12 p1895 N85-21891
Combined analysis of the dynamics of complex ecosystems based on repeated remote measurements
13 p1965 N85-22450
Data Collection and Platform Location by Satellite: ARGOS Users' Conference 14 p2237 N85-23869
The ARGOS system status report after 2 years operation 14 p2237 N85-23870
System performance, data distribution and technical files --- ARGOS project 14 p2237 N85-23871
Report on the panel discussion of the Workshop on Data Collection Platform Networks
14 p2239 N85-23880
The ARGOS system status report
14 p2239 N85-23884
Equipment for the ARGOS system from Eidsvoll Electronics A.S. 14 p2239 N85-23885
The ARGOS system main characteristics — satellite based localization 14 p2325 N85-24367
The ARGOS system after 3 years operation
14 p2325 N85-24368
Environmental satellites 14 p2328 N85-24392
Evaluation of carrying capacity and landscape damage in northern Kenya by multistage remote sensing
[DFVLR-FB-84-47] 14 p2347 N85-24514
The ARGOS program — satellite based localization
14 p2397 N85-24775
Thermally modulated electron affinity detector for priority pollutant analysis
[PB85-158145] 15 p2508 N85-25469
NOAA satellite operations: Programs briefing — Environmental satellites, LANDSAT, and space station polar platform 15 p2599 N85-26020
The impact of weather on aviation safety
[GPO-35-520] 16 p2703 N85-26685
Shuttle imaging radar-A (SIR-A) data analysis — geology of the Ozark Plateau of southern Missouri, land use in western Illinois, and vegetation types at Koonamore Station, Australia
[NASA-CR-175785] 16 p2809 N85-27324
Monitoring of marine environment
16 p2812 N85-27341

Contribution of the NOAA-7 and 8 and ARGOS partnership to white tuna fishing in the northeast Atlantic
16 p2813 N85-27355
Location and data collection satellite system ARGOS. User's guide — satellite based localization
16 p2816 N85-27371
Investigation of air pollution impact in Eastern Bavaria: Measurement results from August and September, 1984
[DFVLR-FB-85-03] 17 p2988 N85-28471
DFVLR measuring system for the determination of the spatial distribution of environmental parameters of the atmosphere by means of mobile instrumented platforms
[DFVLR-FB-85-09] 17 p2989 N85-28472
Technical support for geopressured-geothermal well activities in Louisiana
[DE85-010462] 18 p3102 N85-29203
Field measurements with the TAMS-2B and development of methods for measuring HCHO, HC3 and HONO in real air
[PB85-172955] 18 p3135 N85-29419
North American acid deposition data base system (ADS) and its use in spatial analysis
[PB85-173235] 18 p3201 N85-29856
Environmental Sciences Division report
[DE85-010452] 19 p3308 N85-30506
Environmental monitoring report for Pantex Plant covering, 1984
[DE85-010824] 19 p3308 N85-30508
Environmental monitoring at Argonne National Laboratory
[DE85-010613] 19 p3309 N85-30516
Radioactive liquid wastes discharged to ground in the 200 areas during 1984
[DE85-010619] 19 p3310 N85-30517
Environmental Research Laboratories publication abstracts, FY 1984
[PB85-180594] 19 p3313 N85-30540
Radioactivity in gaseous waste discharged from the separations facilities during 1984
[DE85-011373] 19 p3360 N85-30831
Design of the National Trends Network for monitoring the chemistry of atmospheric precipitation
[GS-CIRC-964] 20 p3486 N85-31664
Annual environmental monitoring report, January-December 1984
[DE85-011689] 20 p3486 N85-31665
Particulate contamination control in clean rooms by particle fallout (PFO) measurements
[ESA-PSS-01-204-ISSUE-1] 20 p3487 N85-31673
Offshore oceanographic and environmental monitoring services for the Strategic Petroleum Reserve, volume 3
[DE85-009907] 20 p3497 N85-31741
Environmental factors in corrosion and deterioration of materials 22 p3750 N85-33241
The 1984 effluent and environmental monitoring report for the Bettis Atomic Power Laboratory
[DE85-011533] 22 p3810 N85-33602
Environmental summary for calendar year 1984
[DE85-012020] 22 p3810 N85-33604
Environmental monitoring at Lawrence Livermore National Laboratory: 1984 report
[DE85-011593] 22 p3811 N85-33606
The 1984 environmental monitoring program report for Idaho National Engineering Laboratory site
[DE85-011209] 22 p3812 N85-33611
Dynamics of Mesoscale Weather Systems: 1984 Summer Colloquium
[PB85-168266] 22 p3817 N85-33648
Multi-solute subsurface transfer modeling for energy solid wastes: Highlights FY 1984
[DE85-012788] 23 p3966 N85-34591
Environmental Monitoring Burger Hill, Orkney wind turbine generator site and similar work at other UK WTG sites 24 p4111 N85-35482
Current inventory of anthropogenic carbon dioxide in the North Pacific Subarctic Gyre
[PB85-187938] 24 p4125 N85-35570

ENVIRONMENTAL QUALITY
NT AIR QUALITY
NT WATER QUALITY
Illinois Climate: Trends, Impacts and Issues
[PB84-211986] 01 p0086 N85-10577
Corporate use of information regarding natural resources and environmental quality
[PB84-222736] 03 p0439 N85-12794
Integrated global background monitoring network
[DE84-016996] 04 p0532 N85-13398
Air quality assessment model validation in complex terrain
[AD-A147690] 08 p1180 N85-17434
Quality assurance for environmental analytical chemistry, 1983
[DE84-016045] 09 p1349 N85-18489
China report: Science and technology
[JPRS-CST-84-040] 11 p1623 N85-20219
China report: Science and technology
[JPRS-CST-85-003] 13 p2166 N85-23433
China report: Science and technology
[JPRS-CST-85-009] 15 p2530 N85-25596
China report: Science and technology
[JPRS-CST-85-013] 15 p2536 N85-25652
China report: Science and technology
[JPRS-CST-85-011] 15 p2551 N85-25746
China report: Science and technology
[JPRS-CST-85-010] 15 p2564 N85-25819
An ultrasensitive and element specific photoionization detection system for environmental analysis
[AD-A153365] 17 p2968 N85-28332
Mathematical model of global processes in the biosphere 19 p3295 N85-30431
Assessment of the role of nitrogen oxides in nonurban ozone formation
[PB85-173680] 19 p3311 N85-30524
Marine environmental quality assessment program, five-year plan (FY 1984 - 1988)
[AD-A154715] 21 p3613 N85-32459
Air force technical objective document, Aerospace Medical Division, Fiscal Year 1986
[AD-A155195] 21 p3664 N85-32762
Practical consequences of the assessment of different energy health risks
[DE85-004538] 22 p3825 N85-33696

ENVIRONMENTAL SURVEYS
A geoinformation expert system for synergetic use of map and image data 05 p0659 N85-14233
Inventory and monitoring of national park landscapes — remote sensing 05 p0660 N85-14245
Helicopter noise survey performed at Las Vegas, Nevada, 19-21 January, 1984
[AD-A147392] 07 p1039 N85-16593
Extremely Low Frequency (ELF) Communications System Ecological Monitoring Program: Summary of 1983 progress
[AD-A147704] 08 p1151 N85-17265
Noise measurement flight test: Data-analyses Aerospatiale AS 350D AStar helicopter
[AD-A148496] 08 p1218 N85-17672
Marine environmental quality assessment program, five-year plan (FY 1984 - 1988)
[AD-A154715] 21 p3613 N85-32459
Environmental surveillance at Los Alamos during 1984
[DE85-011886] 22 p3811 N85-33605
Design analysis for a repository in crystalline rock
[DE85-011802] 22 p3839 N85-33771
Environmental-physical measurements and determination of atmospheric turbulence with the ASK-16 motor glider 24 p4122 N85-35549

ENVIRONMENTAL TEMPERATURE
U AMBIENT TEMPERATURE

ENVIRONMENTAL TESTS
NT CORROSION TESTS
NT HIGH TEMPERATURE TESTS
NT LOW TEMPERATURE TESTS
NT SALT SPRAY TESTS
NT UNDERWATER TESTS
Motion sensor evaluation using simulation
[DE84-014989] 01 p0050 N85-10331
Selection, procurement and description of Salem Limestone samples used to study the effects of acid rain
[PB84-231067] 04 p0484 N85-13068
Effects of restricted water intake on performance in a cold environment
[AD-A146904] 07 p1015 N85-16450
Initial investigation of cryogenic wind tunnel model filler materials
[NASA-TM-86363] 09 p1283 N85-18069
Acceleration responses of typical LRU's subjected to bench handling and installation shock
09 p1334 N85-18385
Impact of 810D on dynamic test laboratories
09 p1334 N85-18386
NBS (National Bureau of Standards) solar collector durability-reliability test program
[PB85-113603/GAR] 09 p1346 N85-18469
Natural exposure versus chamber simulation
[AD-A149538] 10 p1495 N85-19437
Evaluation of corrosion-erosion behavior of various ceramic materials
[AD-A149756] 12 p1812 N85-21367
Performance assessment of Class 1E pressure transmitters subjected to environmental stresses
[DE85-001623] 12 p1854 N85-21626
A study of fatigue crack growth in 2 1/4 Cr1Mo steel. Part 1: The influences of environment and material condition
[AERE-R-11472] 14 p2258 N85-23993
Ten year environmental test of glass fiber/epoxy pressure vessels
[NASA-TM-87058] 19 p3231 N85-30034
Module Hipot and ground continuity test results
21 p3612 N85-32447
Flight service evaluation of composite helicopter components
[NASA-CR-172562] 23 p3909 N85-34222

ENVIRONMENTS
NT AEROSPACE ENVIRONMENTS
NT CHROMOSPHERE
NT DEEP SPACE
NT EARTH ENVIRONMENT
NT EXTRATERRESTRIAL ENVIRONMENTS
NT GEOMAGNETIC TAIL
NT HELIUM HYDROGEN ATMOSPHERES
NT HIGH ALTITUDE ENVIRONMENTS
NT HIGH GRAVITY ENVIRONMENTS
NT HIGH TEMPERATURE ENVIRONMENTS
NT ICE ENVIRONMENTS
NT INNER RADIATION BELT
NT INTERPLANETARY SPACE
NT INTERSTELLAR SPACE
NT IONOSPHERE
NT JUPITER ATMOSPHERE
NT LOW TEMPERATURE ENVIRONMENTS
NT LOWER IONOSPHERE
NT LUNAR ATMOSPHERE
NT MAGNETOPAUSE
NT MAGNETOSPHERE
NT MARINE ENVIRONMENTS
NT MARS ATMOSPHERE
NT MARS ENVIRONMENT
NT MESOPAUSE
NT MESOSPHERE
NT MIDLATITUDE ATMOSPHERE
NT NEPTUNE ATMOSPHERE
NT PLANETARY ATMOSPHERES
NT PLANETARY ENVIRONMENTS
NT ROTATING ENVIRONMENTS
NT SATELLITE ATMOSPHERES
NT SATURN ATMOSPHERE
NT SOLAR ATMOSPHERE
NT SPACECRAFT ENVIRONMENTS
NT STELLAR ATMOSPHERES
NT THERMAL ENVIRONMENTS
NT URANUS ATMOSPHERE
NT VENUS ATMOSPHERE
Natural environment design criteria for the Advanced X-ray Astrophysics Facility (AXAF) definition and preliminary design
[NASA-TM-86481] 01 p0014 N85-10089
Software engineering environments for mission critical applications: STARS alternative programmatic approaches
[AD-A145285] 02 p0241 N85-11571
Human aspects in office automation
[PB84-240738] 06 p0847 N85-15376
Implementation of a Zilog Z-80 base realization library for the computer systems design environment
[AD-A146359] 06 p0853 N85-15420
USSR report: Life sciences. Biomedical and behavioral sciences
[JPRS-UBB-85-002] 09 p1360 N85-18559
Role of environments in managing data analysis
[DE85-000397] 09 p1369 N85-18602
Computing environments for data analysis. Part 1. Introduction
[AD-A148677] 09 p1373 N85-18632
Computing environments for data analysis. Part 2. Hardware
[AD-A148678] 09 p1374 N85-18633
Reliability of adhesive bonds under severe environments. Report of the Committee on Reliability of Adhesive Bonds in Severe Environments
[AD-A149010] 10 p1451 N85-19149
Construction and application of a questionnaire for the social scientific investigation of environmental noise effects
[NASA-TM-75492] 10 p1512 N85-19644
Development of satellite data presentation for environmental forecasting 11 p1712 N85-20770
Environmental cycling of cellulosic thermal insulation and its influence on fire performance
[DE85-004295] 13 p2041 N85-22776
Principles of software engineering environment design
[AD-A150352] 13 p2147 N85-23324
Recognition of objects in their natural environment — parallel processing 15 p2622 N85-26159
Computing environments for data analysis. Part 1: Introduction
[DE85-007919] 17 p3009 N85-28603
Computing environments for data analysis. Part 2: Hardware
[DE85-006320] 17 p3009 N85-28604
Use of environmental health-risk analysis for managing toxic substances
[DE85-008964] 18 p3160 N85-29574
Satellite measurements of atmospheric aerosols
[AD-A153807] 19 p3316 N85-30558

Anaerobic microbial transformations in subsurface environments: Project description
[DE85-012789] 23 p3951 N85-34486
Circuit approaches to increasing SRAM performance in total dose environments
[DE85-009441] 23 p3966 N85-34588
International flight planning handbook
[AD-A156330] 24 p4062 N85-35177
ENZYME ACTIVITY
NT FERMENTATION
Induced changes in the cholinergic system of sciatic nerve and slow and fast twitch muscle of rats
15 p2609 N85-26061
Neural mechanism by which gravitational stimulus and stress affect the secretion of renin and other hormones
15 p2610 N85-26083
Lipid hydrolysis in man during antiorthostatic hypokinesia 23 p3953 N85-34500
Lipogenesis in rat liver after flight aboard Cosmos-1129 biosatellite 23 p3954 N85-34508
ENZYMES
NT CATALASE
NT CHOLINESTERASE
NT OXIDASE
NT PROTEASE
NT TRYPSIN
Construction of a bacterium to convert cellulose to ethanol
[TI84-901639] 04 p0481 N85-13068
Acid phosphatase and protease activities in immobilized rat skeletal muscles
[NASA-CR-174340] 08 p1192 N85-17509
A comparison of rat myosin from fast and slow skeletal muscle and the effect of disuse
[NASA-CR-174339] 08 p1192 N85-17510
Ethanol production by enzymatic hydrolysis: Parametric analysis of a base-case process
[DE84-013105] 11 p1614 N85-20147
Development of a new class of chemical and biological ultrasensors: Ribonuclease contamination and control
[NASA-CR-175466] 11 p1635 N85-20296
USSR report: Space Biology and Aerospace Medicine, volume 18, no. 6, November - December 1984
[JPRS-USB-85-002] 12 p1900 N85-21931
Parameters of carbohydrate metabolism and blood serum enzyme activity after short-term spaceflights
12 p1903 N85-21951
Quantitative alterations in the function of bone forming cells due to reduced weight bearing
15 p2609 N85-26075
Quantitation of Na+, K+-ATPase enzyme activity in tissues of the mammalian vestibular system
15 p2613 N85-26102
Differential effect of denervation on free radical scavenging enzymes in slow and fast muscle of rat
[NASA-CR-175719] 15 p2614 N85-26110
Radiation damage and repair in cells and cell component, part 1
[DE85-008667] 18 p3152 N85-29519
Galactose oxidase in stereospecific oxidation of primary alcohols
[AD-A154059] 19 p3234 N85-30048
Blood serum enzyme activity following long term spaceflights 19 p3326 N85-30604
Biocatalysis project
[NASA-CR-176044] 20 p3498 N85-31744
Urokinase production by electrophoretically separated cultured human embryonic kidney cells
20 p3501 N85-31765
The Fibrin slide assay for detecting urokinase activity in human fetal kidney cells 20 p3502 N85-31768
Structural changes in thyroid due to high-altitude adaptation in Kirghizia 22 p3820 N85-33666
EOS
U LANDSAT SATELLITES
EOSS
In situ orbital debris experiment concepts
12 p1784 N85-21198
EPHEMERIDES
NT PLANET EPHEMERIDES
The solar system: Improving knowledge of the system
14 p2398 N85-24782
The astrometry network of the IHW and the P/Crommelin trial run results 14 p2435 N85-25016
The orbits of Comets Halley and Giocobini-Zinner
14 p2437 N85-25039
The work on Comet Halley's orbit at ESOC
14 p2438 N85-25041
Determination of the observation conditions of celestial bodies with the aid of the DISPO system
[NAS 1.15:77632] 14 p2438 N85-25044
Ephemeral regions versus pseudo ephemeral regions
18 p3208 N85-29901
EPHEMERIS TIME
Altimetry, orbits and tides
[E85-10066] 08 p1174 N85-17404

HEAO 3 upper limits to the expected 1634 KeV line from SS 483
[OG-2.4-9] 22 p3888 N85-33954
EPICYCLOIDS
High powered epicyclic gears: Some recent development 23 p3924 N85-34316
EPIDEMIOLOGY
USSR report: Life sciences. Biomedical and behavioral sciences
[JPRS-UBB-84-025] 04 p0543 N85-13453
Epidemiologic methods applied to the study of the relationship between climate and human health
05 p0687 N85-14418
The epidemiology and toxicology of Agent Orange
[AD-P004038] 06 p0845 N85-15368
USSR report: Life sciences. Biomedical and behavioral sciences
[JPRS-UBB-84-015] 07 p1010 N85-16416
Health examination findings among active civil airmen
[AD-A148325] 08 p1195 N85-17533
USSR report: Life sciences. Biomedical and behavioral sciences
[JPRS-UBB-85-002] 09 p1360 N85-18559
Review of epidemiological studies of human exposures to radiofrequency radiation 16 p2776 N85-27134
Geothermal hydrogen and health in Rotorua, New Zealand
[DE85-901283] 19 p3301 N85-30467
USSR report: Life sciences. Biomedical and behavioral sciences
[JPRS-UBB-85-017] 20 p3504 N85-31785
Using the information of cosmic rays to predict influence epidemic
[SH-10.1-2] 23 p4053 N85-35134
EPINEPHRINE
NT NOREPINEPHRINE
Distinctive morphological manifestations of acute stress reaction in adrenal cortex of hypokinetic rats
12 p1902 N85-21944
Studies of circulatory and metabolic changes during ketamine narcosis
[AD-A154512] 21 p3663 N85-32756
EPITAXY
NT ELECTROEPITAXY
NT LIQUID PHASE EPITAXY
NT MOLECULAR BEAM EPITAXY
NT VAPOR PHASE EPITAXY
Photoluminescent properties of epitaxial p-GaSb
02 p0287 N85-11745
Laser diodes for infrared spectroscopy
[BMFT-FB-T-84-131] 05 p0640 N85-14109
Efficiency estimation and sensitivity modeling
06 p0829 N85-15263
Formation of amorphous layers in Al2O3 by ion implantation
[DE85-001289] 09 p1397 N85-18794
Ion beam processes in Si
[DE85-001254] 09 p1399 N85-18808
Use of alternative solvents for low-temperature LPE growth of CdTe films
[AD-A149418] 10 p1562 N85-19853
Low stress semiconductor-insulator interface for cryogenic device applications
[NASA-CASE-NPO-16394-1] 11 p1734 N85-20906
Method for the fabrication of dielectric isolated junction field effect transistor and PNP transistor
[AD-D011500] 12 p1832 N85-21494
Method for the preparation of epitaxial films of mercury cadmium telluride
[AD-D011532] 12 p1938 N85-22175
Enhanced diffusion from interstitial trapping during solid-phase-epitaxial growth of silicon alloys
[DE85-001285] 12 p1941 N85-22193
Technology of thin silicon foils for the fabrication of monolithic integrated sensors
[BMFT-FB-T-84-209] 12 p1943 N85-22202
Clustering and ordering in 3-5 alloys
[AD-A150604] 13 p2022 N85-22670
Raman scattering of light in epitaxial films of solid phosphide-gallium arsenide solutions
15 p2643 N85-26301
Experimental method for measuring positronium reflection from surfaces
[DE85-010949] 20 p3531 N85-31967
Microwave semiconductor research: Materials, devices and circuits and gallium arsenide ballistic electron transistors
[AD-A154698] 21 p3709 N85-33024
Modulation doped GaAs/Al(x)Ga(1-x)As layered structures with applications to field effect transistors
[AD-A155360] 22 p3759 N85-33296
Process for improving the quality of epitaxial silicon films grown on insulating substrates
[AD-D011730] 22 p3847 N85-33828

EPITHELIUM
Preparative electrophoresis of cultured human cells: Effect of cell cycle phase 20 p3500 N85-31758
A critical synopsis: Continuous growth of proximal tubular kidney epithelial cells in hormone-supplemented serum-free medium 20 p3501 N85-31767
Mammalian tissue sensitivity to long-term exposure to high-intensity stationary magnetic fields
22 p3823 N85-33686
EPNL
U EFFECTIVE PERCEIVED NOISE LEVELS
EPOCHS
U TIME MEASUREMENT
EPOXIDES
U EPOXY COMPOUNDS
EPOXY COMPOUNDS
NT ETHYLENE OXIDE
Laboratory investigation on adhesives for Naval facilities construction
[AD-A147453] 07 p0932 N85-15909
Preliminary evaluation of an improved flammability test method for aircraft materials
[FAA-CT-84-22] 08 p1080 N85-16840
Rubber-modified epoxies. Part 2: Morphology, transitions, and mechanical properties
[AD-A147962] 08 p1132 N85-17137
Study of reaction kinetics and development of elastic properties in network polymerization systems by the impulse technique
[AD-A148187] 08 p1133 N85-17141
Crystallization behavior of poly(3,3-bis(Ethoxymethyl) oxentane) and poly(3,3-bis(Azidomethyl) oxetane)
[AD-A148271] 08 p1226 N85-17720
Evaluation of Epoxo 300-C nonskid coating for use on bridge decks
[PB85-108843] 12 p1819 N85-21412
Ten year environmental test of glass fiber/epoxy pressure vessels
[NASA-TM-87058] 19 p3231 N85-30034
Impact fracture mechanism of polymer plates containing a heavy inner material 23 p3908 N85-34215
Molecular biology of environmental aromatic hydrocarbons
[DE85-015036] 24 p4128 N85-35593
EPOXY MATRIX COMPOSITES
Investigating compression failure mechanisms in composite laminates with a transparent fiberglass-epoxy birefringent materials
[NASA-TM-86306] 02 p0170 N85-11137
Development of failure criterion for Kevlar-epoxy fabric laminates
[NASA-CR-172465] 02 p0170 N85-11138
The silane interphase of composites: Effects of process conditions on gamma-aminopropyltriethoxysilane
[AD-A145578] 02 p0171 N85-11143
Influence of test method and material stiffness on the damage produced by low velocity impacts on carbon-epoxy composites No. 45.387/1
[REPT-45.387/1] 03 p0326 N85-12100
Tough Composite Materials
[NASA-CP-2334] 04 p0463 N85-12941
Effects of constituent properties on compression failure mechanisms 04 p0464 N85-12946
Composite property dependence on the fiber, matrix, and the interphase 04 p0465 N85-12954
Variation of resin properties through the thickness of cured samples 04 p0468 N85-12974
Protective coverings for fiber reinforced epoxy composites
[PB84-231059] 04 p0480 N85-13063
Imide modified epoxy matrix resins
[NASA-CR-174695] 07 p0930 N85-15892
Ultrasonic analysis of spherical composite test specimens
[DE85-001591] 07 p0976 N85-16197
Fracture mechanics analysis and prediction of delamination growth in composite structures
[FFA-TN-1984-45] 09 p1289 N85-18092
Comparison of methods for predicting fiber stresses in a cracked Kevlar/epoxy monolayer
[DE84-016118] 11 p1593 N85-20022
Ultrasonic characterization of advanced composite flywheels
[DE85-000158] 11 p1593 N85-20026
Preliminary review of statistical treatment of S-glass/epoxy stress rupture data
[AD-A149610] 12 p1797 N85-21275
Directional dependent engineering properties of aluminum-aramid-epoxy laminates
[CCMS-85-02] 13 p2015 N85-22638
Development of a field repair technique for mini-sandwich Kevlar/epoxy aircraft skin
[AD-A151369] 15 p2503 N85-25439
Improved materials for composites and adhesive joints
[AD-A154918] 21 p3561 N85-32152

Improved materials for composite and adhesive joints
[AD-A155065] 21 p3562 N85-32153

EPOXY RESINS

Infrared spectroscopy study of the SP-250 epoxy resin system
[AD-A145860] 03 p0337 N85-12167

Investigation of toughened neat resins and their relations to advanced composite mechanical properties
04 p0464 N85-12949

The effect of cross-link density on the toughening mechanism of elastomer-modified epoxies
04 p0465 N85-12951

The chemical nature of the fiber/resin interface in composite materials 04 p0465 N85-12953

Modified epoxy composites 04 p0466 N85-12957

Variation of resin properties through the thickness of cured samples 04 p0468 N85-12974

Toughening mechanism in elastomer-modified epoxy resins, part 2
[NASA-CR-3852] 04 p0478 N85-13046

Investigation of the relations between neat resin and advanced composite mechanical properties. Volume 1: Results
[NASA-CR-172303] 05 p0612 N85-13911

Parametric study of the P9 HT glass fiber finish (Fatigue resistance). Lot no. 1: Report on the microfatigue tests
[CS-794] 05 p0620 N85-13968

Investigation of the relations between resin and advanced composite mechanical properties. Volume 2: Appendices
[NASA-CR-172303-VOL-2] 06 p0783 N85-14880

Imide modified epoxy matrix resins
[NASA-CR-174695] 07 p0930 N85-15892

Rubber-modified epoxies. 1: Cure, transitions, and morphology
[AD-A147377] 07 p0932 N85-15908

All-composite Airbus empennage
07 p0936 N85-15931

Monitoring cure of epoxy resins using a microdielectrometer
[AD-A148618] 08 p1119 N85-17054

Adhesive joint formation under field conditions
[AD-D011476] 10 p1453 N85-19153

Characterization of the network structure of a hardened epoxy resin (TGMDA/DDS system)
[ONERA-RT-3/3346-M] 11 p1613 N85-20140

Rubber modified epoxy adhesive
[AD-D011527] 12 p1810 N85-21354

SRM filament wound case resin characterization studies 12 p1944 N85-22212

Theoretical and experimental investigation of mechanically fastened composites
[AD-A150961] 14 p2248 N85-23935

Chemical interpretation of the relaxed permittivity during epoxy resin cure
[AD-A150955] 14 p2260 N85-24005

Compressive strength of epoxy resin chocks subjected to elevated temperatures
[AD-A152018] 15 p2519 N85-25532

Experimental study of the effect of moist environments on epoxy resin chocks
[AD-A152052] 15 p2568 N85-25849

Characterization-curing-property studies of HBRF 55A resin formulations
[NASA-CR-175836] 16 p2753 N85-26989

Evaluation of experimental epoxy monomers
[NASA-TM-87476] 16 p2754 N85-26996

New polymers for composites: A summary of research on polystyrylpyridines
[NASA-CR-175886] 17 p2933 N85-28106

Flight-service program for advanced composite rudders on transport aircraft
[NASA-CR-174537] 19 p3217 N85-29850

Development of fracture mechanics maps for composite materials, volume 1
[ESA-CR(P)-2017-VOL-1] 20 p3471 N85-31573

Development of fracture mechanics maps for composite materials, volume 2
[ESA-CR(P)-2017-VOL-2] 20 p3471 N85-31574

Development of fracture mechanics maps for composite materials. Volume 3: Appendices A-E
[ESA-CR(P)-2017-VOL-3] 20 p3472 N85-31575

Development of fracture mechanics maps for composite materials. Volume 4: Appendices F-K
[ESA-CR(P)-2017-VOL-4] 20 p3472 N85-31576

Improved materials for composite and adhesive joints
[AD-A155065] 21 p3562 N85-32153

The effect of mould size on the exothermic reaction and compressive strength of epoxy resin chocks
[AD-A155102] 21 p3570 N85-32203

Influence of cyclic thermal loading on internal stress in casted epoxy resin 23 p3908 N85-34211

Time and temperature dependence of fracture surface in soft epoxy resin 23 p3908 N85-34213

Study on fracture behavior of epoxy resin
23 p3909 N85-34216

Metal (2) 4,4',4',4'' phthalocyanine tetraamines as curing agents for epoxy resins
[NASA-CASE-ARC-11424-1] 23 p3918 N85-34281

Process for improving moisture resistance of epoxy resins by addition of chromium ions
[NASA-CASE-LAR-13226-1] 23 p3919 N85-34282

EQUALIZERS (CIRCUITS)

Adaptive signal processing for radio communications
10 p1473 N85-19295

Time and space domain filtering for improved HF communication 10 p1473 N85-19298

EQUATIONS

On the dependence of the convergence of Gummel's algorithm on the regularity of the solution
[AD-A154628] 21 p3675 N85-32832

EQUATIONS OF MOTION

NT EULER EQUATIONS OF MOTION
NT HELMHOLTZ VORTICITY EQUATION
NT HYDRODYNAMIC EQUATIONS
NT KINEMATIC EQUATIONS
NT KINETIC EQUATIONS
NT NAVIER-STOKES EQUATION
NT REYNOLDS EQUATION

Stable and chaotic dynamical systems and their singularities in the complex time plan
[DE84-011780] 01 p0035 N85-10222

K-shell yield scaling law for conventional PRS loads
[AD-A145155] 01 p0121 N85-10831

Control of lateral conjectory motion of spacecraft in atmosphere 02 p0160 N85-11085

Effect of the Basset term on particle relaxation behind normal shock waves
[AD-A145446] 02 p0198 N85-11320

Nonsteady motion of solid sphere in compressible viscous fluid 02 p0269 N85-11753

Propagation of longitudinal elastic waves in multilayered half-space 02 p0273 N85-11779

Numerical simulation of the subsonic wing-rock phenomenon 03 p0320 N85-12064

Damping synthesis for a spacecraft using substructure and component data
[CRC-1365] 03 p0323 N85-12082

A dynamical model for a towed linear sonar antenna
[REPT-6-84] 04 p0512 N85-13263

A numerical investigation of planetesimal collision trajectories with a Moon accumulating in Earth orbit
04 p0586 N85-13740

Laboratory electron beam simulation of cosmic radio jets
[DE84-016179] 04 p0590 N85-13764

Solving equations of movement with variable inertia moment
[BLL-M-35975-(5828.4)] 05 p0641 N85-14111

Saint Venant conditions in theory of piezoelastic shells
06 p0780 N85-14987

Motion of heavy symmetric body with flexible bars about stationary point 06 p0780 N85-14989

Analysis of the impact of a deformable missile model on a deformable obstruction
[BLL-RISLEY-TR-8534-(9091.9F)]
06 p0859 N85-15459

More than you want to know about maximum likelihood estimation
[NASA-TM-85905] 07 p0909 N85-15752

Bulk cavitation caused by a plane shock wave
[AD-A147031] 07 p0958 N85-16072

Optimum performance parameters for ski-jump operations of USAF fighter aircraft
[AD-A148532] 08 p1084 N85-16867

Acceleration of an electron ring in a modified betatron with transverse pressure
[AD-A148626] 08 p1221 N85-17688

On vortex transport in turbine channels
09 p1308 N85-18217

Parallel algorithms for robot dynamics
[DE84-016563] 09 p1369 N85-18605

A numerical approach for the vibration analysis of an axisymmetric shell structure with a nonuniform edge constraint
[AD-A149286] 11 p1651 N85-20402

Note of the dynamic behavior of a magnet system suspended by a thin fiber, with special reference to the Quartz Horizontal Magnetometer (QHM)
[DMI-GEOPHYS-PAPERS-R-70]
11 p1714 N85-20785

A Lagrange-D'Alembert formulation of the equations of motion of a helicopter carrying an externally suspended load
[NASA-TM-85864] 12 p1776 N85-21149

A 3-D treatment of convective flow in the Earth's mantle
[DE85-003734] 12 p1890 N85-21863

An analytic model for hydromagnetospheres --- stellar winds; pulsars; cosmic jets 12 p1959 N85-22313

Dynamics of solid body with ellipsoidal cavity containing magnetic fluid 14 p2279 N85-24116

Stability of permanent rotation modes of asymmetric heavy solid body 14 p2279 N85-24118

Stabilization of steady motion of mechanical systems
14 p2280 N85-24122

Quaternion algorithms of 3-dimensional inertial navigational systems 14 p2287 N85-24173

Motion of satellite with total dynamic symmetry around rotating aspherical Earth 14 p2287 N85-24174

Comets and nongravitational forces
14 p2437 N85-25038

The orbital motion of Comet Halley
14 p2437 N85-25040

A user's manual for AMEER flight path trajectory simulation code
[DE85-006580] 15 p2472 N85-25260

Vortex dynamics
[AD-A151278] 15 p2637 N85-26280

Optimum rotation of solid body with 1 axis of symmetry 16 p2718 N85-26781

Identification and control of structures in space
[NASA-CR-175790] 16 p2731 N85-26850

Effects of bearing deadbands on bearing loads and rotor stability 16 p2737 N85-26889

Use of quaternions in flight mechanics
[AD-A152616] 17 p2899 N85-27875

Incorporating control into the optimal structural design of large flexible space structures
[AD-A152858] 17 p2909 N85-27937

Stability in dynamical systems
[DE85-006698] 17 p3034 N85-28766

The role of thermal motions of air particles for fireballs
[PUBL-59] 17 p3053 N85-28900

Extraction of aerodynamic parameters for aircraft at extreme flight conditions
[NASA-TM-86730] 18 p3175 N85-29668

Application of Floquet theory to helicopter blade flapping stability
[AD-A154460] 19 p3218 N85-29852

Random vibration of nonlinear, parametrically excited systems 19 p3282 N85-30351

The initiation and growth of adiabatic shear bands
[AD-A154459] 19 p3287 N85-30382

Extended semiclassical calculations
[DE85-007824] 19 p3346 N85-30736

Robust adaptive control 20 p3417 N85-31207

Maximum likelihood estimation with emphasis on aircraft flight data 20 p3417 N85-31208

Transition in Turbines
[NASA-CP-2386] 20 p3452 N85-31430

Longitudinal tune control in synchrotrons
[DE85-010745] 20 p3527 N85-31937

Hadley circulation in planetary atmospheres
20 p3546 N85-32067

Optimal low thrust transfer using a first-order perturbation model
[AD-A154761] 21 p3676 N85-32835

Classical emission of relativistic charged particles during axial channeling 21 p3681 N85-32871

Theoretical foundations of turbulent flows
21 p3683 N85-32880

Equations of motion for electromagnetic waves in 4-dimensional Euclidian space 21 p3697 N85-32970

Space station rotational equations of motion
[NASA-TP-2511] 23 p3899 N85-34148

Optimisation in the computer aided design of mechanisms 23 p3924 N85-34321

Conjugated symmetrical coupler curves, produced by 4-bar linkages having the same transmission angles
23 p3924 N85-34322

Intermittent motion 23 p3925 N85-34323

The dynamics of articulated rigid bodies for purposes of animation 23 p3965 N85-34570

The model-independence of cosmic ray source determinations
[OG-7.2-1] 23 p4014 N85-34873

Identification and control of structures in space
[NASA-CR-176175] 24 p4069 N85-35214

The compliance of end effector force sensors for robot manipulator control 24 p4098 N85-35406

Time-dependent response of the climate to increasing atmospheric carbon dioxide 24 p4119 N85-35502

EQUATIONS OF STATE

NT HUGONIOT EQUATION OF STATE

Equation of state study for polar fluids
[PB84-222801] 01 p0025 N85-10157

Universal binding energy relations in metallic adhesion
[NASA-TM-86889] 03 p0331 N85-12132

On experimental equations of state for Boson gases
[PTB-ME-61] 04 p0574 N85-13659

Research in nuclear astrophysics: Stellar collapse and supernovae
[DE84-015559] 05 p0743 N85-14776

A virial equation of state option for the TIGER computer program
[AD-A147490] 07 p1025 N85-16507

A research proposal for the theoretical study of the thermodynamic and transport properties of dense plasmas
[AD-A148040] 08 p1224 N85-17708
Experimental high pressure equation of state of a very fast burning gun propellant
[DE85-001749] 10 p1456 N85-19184
A Galerkin method for the estimation of parameters in hybrid systems governing the vibration of flexible beams with tip bodies
[NASA-CR-172537] 10 p1544 N85-19734
User's manual for GRIZZLY
[DE85-001405] 11 p1702 N85-20702
Wavecode constitutive models: Nonhomogeneous mixtures
[DE85-000636] 12 p1798 N85-21278
Simple EOS for the silicone rubber Sylgard 184
[DE85-001394] 12 p1814 N85-21376
Potential at atomic boundaries in the TF (or TFD) model and equations of states 12 p1820 N85-21419
Control of nonlinear objects 12 p1842 N85-21561
Synthesis of digital control for object with lag
12 p1843 N85-21562
H-division materials physics progress
[DE85-004990] 13 p2165 N85-23430
Cooling of neutron stars with hyperons
[DE85-004641] 13 p2171 N85-23472
Impact cratering calculation 13 p2180 N85-23531
Reaction of piezoceramic shell to concentrated forces
14 p2279 N85-24115
Steady state solution of the Fokker-Planck equation combined with unidirectional quasilinear diffusion under detailed balance conditions
[DE85-004917] 14 p2425 N85-24959
Ionization equilibrium and equation of state in the solar interior 14 p2445 N85-25088
The sensitivity of solar eigenfrequencies to the treatment of the equation of state 14 p2445 N85-25089
Measurement of material properties to Mbar pressures using time-resolved shock wave techniques
[DE85-007319] 15 p2558 N85-25780
Equations of state of strongly coupled plasma mixtures
[DE85-006163] 15 p2657 N85-26393
Equation of state and two-body correlations for fluids of non-spherical molecules
[AD-A151969] 16 p2783 N85-27174
Cluster production and entropy
[DE85-007626] 17 p3032 N85-28752
Equation of state for detonation products
[DE85-009608] 18 p3084 N85-29079
A state variable approach to transient creep deformation in stress reduction experiments
[DE85-009492] 18 p3122 N85-29331
State variable theories based on Hart's formulation
[DE85-009474] 19 p3239 N85-30082
Shear deflection in a three-point bend beam of a solid circular cross-section
[AD-A154458] 19 p3287 N85-30381
Pion production and the nuclear equation of state
[DE85-009941] 19 p3365 N85-30670
Decentralized control synthesis method for large-scale interconnected systems
[DE85-000748] 20 p3518 N85-31878
BLAF: A blast field reconstruction program from pressure histories
[AD-A155300] 21 p3585 N85-32283
Liquid-phase compositions from vapor-phase analyses 2: Adaptation of the Prausnitz program to UF6 and some of its potential impurities
[DE85-011521] 21 p3673 N85-32819
A system of magnetohydrodynamic-type equations
21 p3693 N85-32946
A new problem in mathematical physics associated with the problem of coherent phase transformation
21 p3698 N85-32976
KRAK: A computer program for two-phase two-component porous flow and fracture
[LA-9703] 22 p3782 N85-33434
Planetary fluids He and NH3 at high shock pressures and temperatures
[DE85-011851] 22 p3859 N85-33896
Comparison of experimental data on detonation velocity and Chapman-Jouget pressure vs initial HE density with predictions from Ree's model equation of state
[DE85-007266] 23 p3922 N85-34304
Detonation of condensed explosives: Evolution of knowledge in the last 40 years
[ISL-CO-228/84] 23 p3923 N85-34307
Shock and release equation of state of calcite
[DE85-013151] 23 p3942 N85-34432
Calculations of heavy ion charge state distributions for nonequilibrium conditions
[SH-2.1-12] 23 p3999 N85-34793
Equation of state study for polar fluids
[PB85-204345] 24 p4076 N85-35262
Experimental technique for measuring the isentrope of hydrogen to several megabars
[DE85-014332] 24 p4095 N85-35386

EQUATORIAL ATMOSPHERE
Equatorial energetic distributions of ions of terrestrial radiation belt as function of solar corona temperature response 02 p0160 N85-11087
Inference of equatorial field-line integrated electron density values using whistlers
[AD-A145822] 03 p0392 N85-12507
Ionospheric scintillation: A brief review
04 p0522 N85-13337
Behavior of the ionospheric F region in low latitudes and in the equatorial region of Brazil during strong magnetic storms in the 1978 to 1983 period
[INPE-3231-PRE/581] 05 p0675 N85-14333
Medium- and large-scale wave disturbances and heterogeneities of electron concentration in outer ionosphere in middle and low latitudes
06 p0825 N85-15241
Equatorial transionospheric propagation conditions affecting digital communications
10 p1470 N85-19275
Ionospheric research at INPE
[INPE-3279-PRE/602] 10 p1514 N85-19556
Middle Atmosphere Program. Handbook for MAP, volume 7
[NASA-CR-175479] 11 p1656 N85-20437
PMP-2 report: Equatorial wave dynamics
11 p1657 N85-20442
Meteor wind results from Atlanta, USA, and Ramey, Puerto Rico 11 p1662 N85-20474
Kinetic Rayleigh-Taylor instability theory in the ionosphere near equator 13 p2067 N85-22911
Ionspheric effects of seasonal and diurnal variations of electric fields in equatorial F-region
14 p2338 N85-24459
Investigating statistical characteristics of atmospheric background brightness and star background density in equatorial region of celestial sphere
15 p2478 N85-25298
Determining effective rate of plasma heating in outer equatorial ionosphere using data from ISIS-1 and ISIS-2 satellites 16 p2721 N85-26797
Dependence of equatorial F-region plasma bubble rise velocity and dynamo electric field on solar cycle
[INPE-3439-PRE/696] 16 p2626 N85-27434

EQUATORIAL ELECTROJET
Role of equatorial Electron Cyclotron Harmonic (ECH) waves in the generation of diffuse auroras. Contribution of the GEOS IMS spacecraft 14 p2367 N85-24632

EQUATORIAL ORBITS
NT STATIONARY ORBITS

EQUATORIAL REGIONS
The marine geochemistry of the rare earth elements
[AD-A145132] 01 p0088 N85-10598
Near infrared modeling of the equatorial regions of Jupiter and Saturn 09 p1415 N85-18930
Investigations of the Mars cratered terrain: Smooth plains boundary in the eastern equatorial region
13 p2191 N85-23596
The French Ocean Climate in Equatorial Atlantic (FOCAL) Drifter Program, 1983-1984
14 p2329 N85-24399
Applications of ARGOS measurements in equatorial Pacific Ocean-atmosphere interaction studies
14 p2331 N85-24414
A study of the generation mechanisms of high latitude and equatorial F-region irregularities using DE-2 data
[NASA-CR-175745] 16 p2625 N85-27423
Equatorial F-region irregulerity latitudinal extension and dynamo electric field
[INPE-3494-PRE/731] 16 p2626 N85-27433
Thermal ion heating in the vicinity of the plasmapause
[NASA-CR-176030] 20 p3535 N85-31993
Equitorial scintillations: Advances since ISEA-6
[AD-A154962] 21 p3631 N85-32559

EQUATORS
NT MAGNETIC EQUATOR

EQUILIBRIUM
Thermodynamics of reactions of deoxidation of nickel melts
[BLL-M-35729-(5828.4)] 02 p0175 N85-11168
Exergetical analysis of turbojet engine cycle
13 p2049 N85-22825

EQUILIBRIUM DIAGRAMS
U PHASE DIAGRAMS

EQUILIBRIUM EQUATIONS
Radiation transport in the Earth atmosphere
04 p0522 N85-13341
Structural relaxation and isoconfigurational flow of a metallic glass near equilibrium
[AD-A147888] 07 p0933 N85-15915
Solar inverse theory 14 p2441 N85-25083
Computer-controlled carburizing
[BLL-OA-TRANS-3204-(6196.300)]
20 p3429 N85-31268
A new problem in mathematical physics associated with the problem of coherent phase transformation
21 p3698 N85-32976
Recombination and ionization in a nitrogen plasma
[AD-A155426] 22 p3845 N85-33813
Analysis of the nonlinear equations describing the elastic, thermal, and electromagnetic behavior of solids: Existence of solutions of semi-inverse problems
24 p4100 N85-35415

EQUILIBRIUM FLOW
NT FROZEN EQUILIBRIUM FLOW
Reducing numerical diffusion for incompressible flow calculations
[NASA-TM-83621] 06 p0756 N85-14840
Structural relaxation and isoconfigurational flow of a metallic glass near equilibrium
[AD-A147888] 07 p0933 N85-15915
Computer-Aided Structural Engineering (CASE) project. Seepage analysis of confined flow problems by the method of fragments (CFRAG)
[AD-A150015] 12 p1875 N85-21762
Time-dependent flow of stream swirled in vortex chamber 13 p2043 N85-22788
Interaction of cylindrical shell with concentrated mass moving along its inner surface 13 p2047 N85-22810
Elastohydrodynamic lubrication calculations used as a tool to study scuffing
[NASA-TM-87097] 23 p3938 N85-34408

EQUILIBRIUM METHODS
Modelling equilibrium and fractional crystallization in the system MgO-FeO-CaO-Al2O3-SiO2
13 p2184 N85-23552

EQUIPARTITION THEOREM
Equipartition threshold in nonlinear large Hamiltonian systems: The Fermi-Pasta-Ulam model
[NOTA-INTERNA-819] 02 p0255 N85-11670

EQUIPMENT
USSR report: Engineering and equipment
[JPRS-UEQ-85-001] 09 p1305 N85-18200
Plasma arc welding, equipment, installation and process control
[DE85-008481] 19 p3373 N85-30921
The CCIR satellite EPIRB coordinated trials programme --- Emergency Position Indicating Radio Beacon (EPIRB); International Radio Consultative Committee (CCIR) 20 p3402 N85-31111
The International Radio Consultative Committee (CCIR) recommended satellite Emergency Position Indicating Radio Beacon (EPIRB) system operating through geostationary satellites at 1.6 GHz
20 p3402 N85-31112

EQUIPMENT SPECIFICATIONS
UCB cosmic ray experiment 09 p1417 N85-18941
The helicopter transmission design process
14 p2221 N85-23772
Manufacturing considerations related to aircraft gearboxes 14 p2222 N85-23778
Practical considerations when using water quality and structure monitoring sensors as applied to portable ARGOS satellite transmitter equipment
14 p2330 N85-24405
Ariane launcher system. Pyrotechnics subsystem: Definition of chains and pyrotechnic components
[CNES-84/CT/DRT/SST/SE/242(1)]
20 p3398 N85-31081
Poseidon altimeter: Study of the hyperfrequency section and specifications of the prototype components
[CNES-84/DRT/TIT/HY/T/145]
20 p3419 N85-31219

EQUIPOTENTIALS
Plasma drift towards a plane equipotential surface
[TRITA-EPP-84-01] 02 p0285 N85-11860

EQUIVALENCE
Shear deformation plate continua of large double-layored space structures
01 p0059 N85-10391
A preliminary study of a cryogenic equivalence principle experiment on Shuttle
[NASA-CR-171300] 10 p1426 N85-18994
Fundamental equivalence of generalised state space systems
[MATHEMATICS-RESEARCH-182]
15 p2642 N85-26293
A trivariate version of Levy's equivalence
[AD-A153157] 17 p3025 N85-28705

EQUIVALENT CIRCUITS
Magnetic field calculation for ideal conductors by method of equivalent currents 06 p0788 N85-15035
An indirect measure of below-ground electric field, conductivity, and dielectric constant
[AD-A146518] 06 p0804 N85-15115

Battery response to pulse loads: A mathematical model
[DE85-001149] 09 p1316 N85-18277
Parameterization of a transient electromagnetic facility and test antennas from transient data
[DE85-006231] 15 p2545 N85-25710
Measurement methods for accurate microwave characterization and modeling of MESFET chips
[AD-A152360] 17 p2952 N85-28227
Magnetic field and equivalent circuit of induction motors with shielded poles 22 p3772 N85-33378

ERBE
U EARTH RADIATION BUDGET EXPERIMENT

ERBIUM
Spin dynamics of rare Earth ions in crystal fields probed by muon spin rotation
[DE84-013805] 02 p0278 N85-11610
Electron-oscillatory spectra of yttrium-erbium-aluminum garnet of crystals and their role in laser pumping
11 p1715 N85-20791
Contact properties of rare-earth silicides and germanides on Si and Ge 19 p3374 N85-30931

ERBIUM COMPOUNDS
Magnitude and range of the RKKy interaction in SmRh4B4
[DE85-012284] 23 p3985 N85-34712

ERECTION
U CONSTRUCTION

ERGODIC PROCESS
Omni transforms: Applications to renewal theory
[AD-A146939] 07 p1029 N85-16534
Conditionally heteroscedastic autoregressions
[AD-A147168] 07 p1035 N85-16567
A non-commutative quasi subadditive ergodic theorem
[AD-A146810] 07 p1037 N85-16581
On the ergodicity of bilinear time series models and some applications
[AD-A148032] 08 p1215 N85-17651
On ergodic actions whose self-joinings are graphs
[CWI-PM-R8408] 12 p1925 N85-22093
Ergodicity and Steady-State-Equilibrium conditions for Markov chains
[AD-A151038] 14 p2409 N85-24654
Sensitivity of the stationary distribution vector for an ergodic Markov chain
[DE85-006979] 16 p2857 N85-27621
Spectral transform approach to Backlund transformations
[PREPRINT-420] 18 p3172 N85-29663
Further results on the equipartition threshold in large nonlinear Hamiltonian systems
[PREPRINT-428] 18 p3173 N85-29668

ERGOMETERS
Comparison between cycle ergometers with different mechanical braking systems
[FOA-C-54058-H1] 07 p0975 N85-16193

ERGONOMICS
U HUMAN FACTORS ENGINEERING

EROSION
NT RAIN EROSION
NT SOIL EROSION
NT WATER EROSION
NT WIND EROSION
Simulation of contact surface erosion for impact problems 01 p0060 N85-10398
Erosion of sintered WC-Co alloys
02 p0179 N85-11201
Optical properties of laser erosion flares in plasma
02 p0270 N85-11764
Erosion of multiphase materials
[DE84-015816] 04 p0474 N85-13018
High-temperature erosion of plasma-sprayed, yttria-stabilized zirconia in a simulated turbine environment
[NASA-TP-2406] 04 p0478 N85-13045
Bridge erosion in electrical contacts
04 p0486 N85-13102
Back end valves: History and modifications
[DE84-009272] 05 p0646 N85-14145
Copper-nickel sheathing study, phase 2. Two-year service performance of test panels on the ARCO TEXAS
[PB84-242411] 06 p0775 N85-14952
Turbine blade test cascade modifications and orations, August 1982 - April 1983
[DE84-009268] 06 p0833 N85-15303
Proceedings of Workshop on Synergistic Effects in Surface Phenomena Related to Plasma-Wall Interactions
[IPPJ-AM-35] 06 p0864 N85-15488
Synergistic effects in fusion machines, session summary 06 p0864 N85-15489
Plasma surface interaction processes and possible synergisms 06 p0864 N85-15490
Synergisms in surface erosion, session summary
06 p0864 N85-15493
Synergism in materials erosion due to multispecies impact 06 p0864 N85-15494
Solar wind and cosmic ray irradiation of grains and ices - application to erosion and synthesis of organic compounds in the solar system
06 p0888 N85-15637
Arc erosion of metal in current interval of 1-10 amperes 07 p0953 N85-16042
Cavitation erosion resistant coatings for pumps
[PB85-120210/GAR] 09 p1300 N85-18167
Influence of turbulence on erosion by a particle-laden fluid jet
[DE84-014365] 09 p1320 N85-18301
Characterization of erosion of metallic materials under cavitation attack in a mineral oil
[NASA-TM-86934] 10 p1440 N85-19075
Study of surface damage in cathode composite materials in a high flux CO2 laser 10 p1444 N85-19098
Nautical charting with remotely sensed imagery, volume 1
[AD-A149361] 10 p1506 N85-19503
Nautical charting with remotely sensed imagery. Volume 2: Case studies
[AD-A149362] 10 p1506 N85-19504
California coastal erosion and storm damage during the winter 1982 - 1983, a reconnaissance report
[PB85-121705] 10 p1521 N85-19591
Effect of microstructure on solid particle erosion in multiphase materials
[DE85-000426] 11 p1608 N85-20109
Causes and means of prevention of erosion of exit edges of drive vanes in final stages of K-300-240 turbine
14 p2272 N85-24076
Brittle fracture resistance of electron beam-welded joints in titanium Alpha alloys 15 p2500 N85-25419
The influence of abrasive blast cleaning and corrosion inhibitors on protective paint coatings
15 p2517 N85-25522
Erosion of electrodes due to switching of capacitor-bank discharge circuits
[AD-A151207] 15 p2547 N85-25718
Self-sustaining low-Z coatings for fusion applications 2 - copper-lithium
[DE85-002553] 15 p2658 N85-26403
Erosion of multiphase materials
[DE85-006805] 18 p3068 N85-28978
Elevated temperature erosion corrosion of 9Cr1Mo steel
[DE85-008445] 18 p3074 N85-29016
Surface degradation of ductile metal in elevated temperature gas-particle streams
[DE85-008428] 18 p3074 N85-29017
Elevated temperature erosion of steels
[DE85-008503] 18 p3075 N85-29018
Corrosion-erosion rates/mechanisms of 9Cr1Mo steel
[DE85-008506] 18 p3076 N85-29029
The effect of temperature on the corrosion-erosion of 9Cr1Mo steel
[DE85-008507] 18 p3076 N85-29030
Long-Term Materials Test Program
[DE85-003248] 18 p3077 N85-29034
Cavitation erosion of plasma sprayed alloys
[DE85-009542] 18 p3077 N85-29036
A new theory aiming to define the mechanisms of material removal in electroerosion
[NASA-TM-77875] 18 p3176 N85-29689
Mechanical protection of DLC films on fused silica slides
[NASA-TM-87056] 19 p3248 N85-30138
Coastal erosion along Monterey Bay
[AD-A155610] 21 p3655 N85-32707
Operational window for a plasma erosion opening switch used for voltage multiplication on pulsed power generators
[AD-A155482] 21 p3707 N85-33020
Electrode erosion in arc discharges at atmospheric pressure
[NASA-TM-87087] 23 p3903 N85-34178
Influence of particle erosion on the microstructural changes in metals and alloys
[TI85-901384] 23 p3917 N85-34276

EROSIVE BURNING
Solid rocket motor certification to meet space shuttle requirements from challenge to achievement
08 p1098 N85-16941
Model of normal and erosive burning of composite propellants
[ONERA-NT-1984-3] 14 p2263 N85-24024

ERROR ANALYSIS
Diagnosis and therapy of geodetic satellite networks of Doppler type — error analysis
[SER-C-293] 01 p0015 N85-10090
An error analysis for the use of presently available lunar radio flux data in broadbeam antenna-system measurements
[PB84-218361] 01 p0016 N85-10097
Measurement assurance programs. Part 1: General introduction
[PB84-217868] 01 p0051 N85-10039
Performance of the h, p and h-p versions
01 p0058 N85-10050
The initialization of mesoscale models
01 p0079 N85-10525
A microcomputer aided measurement equipment for monitoring performance in digital radio relay systems
[FUB-4-1984] 01 p0101 N85-10686
Trajectory estimation using combined time-of-arrival and velocity measurements
[DE84-015872] 02 p0242 N85-11582
Boundary conditions in Chebyshev and Legendre methods
[NASA-CR-172469] 02 p0250 N85-11635
An asymptotic theory for logistic regression when some predictors are measured with error
[AD-A145673] 02 p0254 N85-11666
Unified approach to sensitivity and uncertainty analysis
[DE84-014049] 02 p0255 N85-11669
Minimization of anomalous errors in measuring systems employing search and testing devices
03 p0344 N85-12219
Diffusion of gases in porous solids: Simulation and measurements
[DE84-016292] 04 p0500 N85-13191
Time discretization of parabolic problems by the discontinuous Galerkin method
[CTH-MATH-1984-16] 04 p0556 N85-13543
TCAS 2 logic performance during phase one operational evaluation
[DOT/FAA/PM-84/20] 05 p0595 N85-13793
Submilliarcsecond VLBI using compact close pairs of radio sources: Error analysis 05 p0622 N85-13881
VLBI solutions for the time variation of DSN baselines: 1978 - 1983 05 p0623 N85-13883
Contributions to the error analysis in the relativity gyroscope experiment 05 p0638 N85-14095
The role of knowledge structures in fault diagnosis
05 p0703 N85-14509
Some error estimates for the p-version of the finite element method
[CTH-MATH-1984-21] 05 p0719 N85-14614
Use of least-squares method for estimating errors of turbine blade type parts during fabrication
06 p0776 N85-14863
NBS (National Bureau of Standards) and WR62 and WR90 reference noise standards
[PB84-235704] 07 p0942 N85-15977
Errors of analog of inertial coordinate systems modeled in astronavigation system 07 p0951 N85-16028
NBS (National Bureau of Standards) switching radiometers
[PB84-235894] 07 p0968 N85-16147
Modeling of human motion by computer considering measurement errors in initial data
07 p1012 N85-16429
A complete characterization of triply balanced matrices with applications to survey sampling
[AD-A147083] 07 p1031 N85-16542
Bayesian estimation of undetected errors
[AD-A147198] 07 p1031 N85-16545
Data stimulated on-line-checking (IROLD)
08 p1066 N85-16754
Altimetry, orbits and tides
[E85-10066] 08 p1174 N85-17404
Multimodels increase accuracy: Summary of an experiment — photogrammetry
08 p1175 N85-17409
A feedback finite element method with a posteriori error estimation. Part 1. The finite element method and some basic properties of the A posteriori error estimator
[AD-A148345] 08 p1212 N85-17631
Filter and passband problems
08 p1252 N85-17910
Cockpit resources management and the theory of the situation 09 p1276 N85-18022
Extrpolation in finite element analysis
09 p1331 N85-18385
An objective error measure for the comparison of calculated and measured transient response histories
09 p1335 N85-18395
A new method of approximating normal and t-tail areas
[AD-A149457] 10 p1548 N85-19761
Blunder detection using a sequential least squares adjustment
[AD-A149514] 10 p1548 N85-19765
On the application of compatibility checking techniques to dynamic flight test data
[ARL/AERO-R-161] 12 p1776 N85-21151
Estimating algorithmic error of digital recursive filters
12 p1839 N85-21543

Preliminary investigation into using the sun as a source for G/T (Gain to System Noise Temperature) measurements
[PB85-128148] 12 p1952 N85-22265

Expansion of functions describing planetary surface and gravity field 13 p1978 N85-22410

Analysis of systematic errors in systems of selenodetic coordinates 13 p1982 N85-22435

Noise tolerance of digital demodulator for complex signal system employing binary quantization
13 p2070 N85-22929

Influence of axial shaft load on operation of magnetoelastic torque transducer
14 p2270 N85-24065

Error analysis of heliostat alignment methods
14 p2281 N85-24128

Investigation of errors of acoustic goniometer information-measurement systems on rocking base
14 p2283 N85-24139

Geometric error analysis for shuttle imaging spectrometer experiment
[NASA-CR-175665] 14 p2305 N85-24269

Propagation of numerical errors in computers and numerical quality 14 p2396 N85-24760

Reliable computation with cellular automata
[AD-A150656] 14 p2399 N85-24790

Laser gyroscope random walk determination using a fast filtering technique 16 p2696 N85-26647

Simulation of a low orbit restitution. Covariance analysis of the position-velocity by Doppler and accelerometer measurements
[CNES-CT/DTI/MS/AE/166] 16 p2728 N85-26836

An evaluation of the performance of a new storm tracking methodology
[AD-A152234] 16 p2835 N85-27484

Evaluation of a fault tolerant system for an integrated avionics sensor configuration with TSRV flight data
[NASA-CR-172589] 18 p3062 N85-28941

Accepting error to make less error
[AD-A153949] 18 p3171 N85-29651

Satellite measurements of atmospheric aerosols
[AD-A153807] 19 p3316 N85-30556

Evaluation of curve-smoothing techniques
[HSE-TRANS-11108] 19 p3349 N85-30759

Simulations of strapdown-system errors and error compensation methods — transport aircraft navigation
[DFVLR-MITT-84-22] 20 p3392 N85-31040

Using regression analysis for determining air data sensor errors by means of an inertial navigation system
[ESA-TT-886] 20 p3392 N85-31041

Search and rescue satellite (SARSAT) error analysis of the 406 MHz system 20 p3403 N85-31118

Numerical experimentation with maximum likelihood identification in static distributed systems
20 p3418 N85-31214

Comparative analysis of laboratory and fullscale experimental data for metal flow displacements and speeds
[BLL-M-36266-(5828.4)] 20 p3430 N85-31276

Influence of error of determination of moire isotach orders on the stability of their approximation
[BLL-M-36277-(5828.4)] 20 p3450 N85-31423

Error spectrum of Goddard satellite models for the gravity field 20 p3491 N85-31704

Spaceborne gradiometer error analysis
20 p3492 N85-31707

TOPEX error budget 20 p3493 N85-31717

Performance and evaluation of real-time multicomputer control systems
[NASA-CR-176098] 21 p3673 N85-32821

Introduction to adaptive techniques for voice signal processing
[PUB-52-1983] 22 p3756 N85-33287

Design of inductive shift transducers
22 p3771 N85-33368

Error evaluation in measurements with thermoluminescent dosimeters
[ISS-T-84/6] 22 p3788 N85-33471

Implications of cross section errors for cosmic ray propagation
[OG-7.2-3] 23 p4014 N85-34875

Gravity gradiometer survey data processing
[AD-A156165] 24 p4117 N85-35522

A comparison between Falcon data and motor glider data 24 p4121 N85-35547

Accuracy and error analysis — airborne instruments
24 p4123 N85-35557

Study of fault tolerant software technology for dynamic systems
[NASA-CR-172618] 24 p4137 N85-35642

Specifying and verifying concurrent programs
[AD-A156190] 24 p4138 N85-35652

ERROR BAND
U ACCURACY

ERROR CORRECTING CODES

Throughput increase in frequency hopped multiple access channels by means of discrimination against partially overlapping interference
[AD-A145540] 02 p0191 N85-11275

Linear intersecting codes — error correction
[ENST-C-84002] 03 p0356 N85-12291

Simplified continued fraction calculation of spherical Bessel functions
[AD-A146644] 06 p0856 N85-15455

The algebraic structure of convolutional codes with application to code construction and decoding
[AD-A148770] 08 p1206 N85-17591

On the binary weight distribution of some Reed-Solomon codes
[NASA-CR-174375] 09 p1373 N85-18628

Error correction coding fur a self-adaptive modem: Theoretical and experimental results
10 p1474 N85-19303

Processing circuit with asymmetry corrector and convolutional encoder for digital data
[NASA-CASE-MSC-20187-1] 11 p1628 N85-20249

Reed-Solomon decoder — applicable to Galileo Project requirements
[NASA-CASE-NPO-15982-1] 11 p1699 N85-20680

Redundancy of codes for detection and correction of unidirectional errors 12 p1842 N85-21557

A concatenated coding scheme for error control
[NASA-CR-175504] 12 p1912 N85-22001

A concatenated coding scheme for error control
[NASA-CR-176006] 19 p3334 N85-30655

Error-correcting codes for computer memories
24 p4136 N85-35636

Pruned error-trellis decoding of certain non-systematic convolutional codes
[AD-A156122] 24 p4138 N85-35650

ERROR CORRECTING DEVICES

DISCUS multiprocessor enhancements — Distributed Control Microprocessor System (DISCUS)
[RSRE-MEMO-3591] 02 p0239 N85-11554

Methods of digital correction for channels of multichannel radar receivers 13 p2082 N85-23005

Decomposition in problem of correcting inertial navigation systems 14 p2287 N85-24172

SC filters and design centering of integrated circuits. Part 2: Design centering of integrated circuits
[BMFT-FB-T-84-265-PT-2] 17 p2956 N85-28257

Development and evaluation of a Fault-Tolerant Multiprocessor (FTMP) computer. Volume 3: FTMP test and evaluation
[NASA-CR-166073] 19 p3341 N85-30707

Satellite links in the ISO architecture: Models and performance evaluation
[ENST-84E017] 22 p3756 N85-33284

High-speed adaptation algorithm for harmonic corrector 22 p3765 N85-33336

ERROR DETECTION CODES

Analysis of the impact of error detection on computer performance
[NASA-CR-174167] 04 p0547 N85-13477

The undetected error probability for shortened hamming codes
[NASA-CR-174175] 04 p0555 N85-13535

Automatic error detection and recovery techniques in onboard intelligent units for space and avionic application 08 p1066 N85-16756

Meta-level control through fault detection and diagnosis
[AD-A149064] 10 p1540 N85-19709

Ada compiler validation summary report, Dansk Datamatik Center, VAX 11 compiler version 1.1
[AD-A149340] 11 p1699 N85-20681

The 20:16 block code for digital recording and transmission channels
[BBC-RD-1985/1] 12 p1824 N85-21443

Redundancy of codes for detection and correction of unidirectional errors 12 p1842 N85-21557

A concatenated coding scheme for error control
[NASA-CR-175504] 12 p1912 N85-22001

Error probability during optimal noncoherent reception of binary signals in multibeam channel
13 p2069 N85-22922

Experimental development of a failure detection scheme for large space structures 14 p2234 N85-23846

Care 3 model overview and user's guide, first revision
[NASA-TM-86404] 15 p2627 N85-26192

Development and evaluation of a Fault-Tolerant Multiprocessor (FTMP) computer. Volume 3: FTMP test and evaluation
[NASA-CR-166073] 19 p3341 N85-30707

Synthesis of tests for programmable logic arrays
22 p3777 N85-33408

Detection of and search for faults in programmable logic arrays 22 p3778 N85-33409

Study of fault tolerant software technology for dynamic systems
[NASA-CR-172618] 24 p4137 N85-35642

AUTOSIM: An automated repetitive software testing tool
[NASA-CR-177930] 24 p4137 N85-35643

Pruned error-trellis decoding of certain non-systematic convolutional codes
[AD-A156122] 24 p4138 N85-35650

Design of a microprogram control unit with concurrent error detection
[AD-A156447] 24 p4139 N85-35655

ERROR FUNCTIONS

The undetected error probability for shortened hamming codes
[NASA-CR-174175] 04 p0555 N85-13535

The method of residual minimization in compressible steady flows
[AD-A153924] 18 p3100 N85-29193

ERROR SIGNALS

Comparator with noise suppression
[NASA-CASE-LAR-13151-1] 11 p1627 N85-20247

Reception of signal with unknown amplitude and duration submerged in white noise 13 p2084 N85-23016

An error generator to support the trials of the ZODIAC prototype system — raster links
[PHL-1984-71] 14 p2293 N85-24216

Ziv-Zakai bound applied to an amplitude-comparison monopulse radar
[AD-A151937] 16 p2773 N85-27118

LANDSAT-4/5 image data quality analysis
[E85-10105] 24 p4107 N85-35463

ERRORS
NT BORESIGHT ERROR
NT INSTRUMENT ERRORS
NT PHASE ERROR
NT PILOT ERROR
NT POSITION ERRORS
NT RANDOM ERRORS
NT ROOT-MEAN-SQUARE ERRORS
NT TRUNCATION ERRORS

Metrological consequences of the hard optical boundary assumption
[PB84-223577] 01 p0121 N85-10827

EDS round-robin evaluation of type 308 austenitic stainless steel
[DE84-014574] 02 p0183 N85-11226

Eyelid motion sequences predictive of decision errors
[AD-A145702] 02 p0235 N85-11531

An asymptotic theory for logistic regression when some predictors are measured with error
[AD-A145673] 02 p0254 N85-11666

Accounting for error stochasticity in terminal homing of aircraft 04 p0489 N85-13115

Comparability and accuracy of industry codes in different data systems
[PB84-215607] 04 p0548 N85-13482

Treatment and expression of measurement uncertainties 05 p0630 N85-14042

Mean and random errors of visual roll rate perception from central and peripheral visual displays
05 p0704 N85-14519

Types of tracking errors induced by concurrent secondary manual task 05 p0711 N85-14561

Approximating true radioluminance distribution from observations on aperture synthesis systems
06 p0783 N85-15003

Indirect estimation of convective boundary layer structure for use in routine dispersion models
[PB84-236260] 06 p0834 N85-15308

Error analysis of wind determined using a VLF Omega sonde
[WSRL-0361-TM] 06 p0838 N85-15321

Computer science and technology: Overview of computer security certification and accreditation
[PB84-217819] 06 p0848 N85-15384

Array sidelobes, error tolerance, gain, and beamwidth
[AD-A147004] 07 p0940 N85-15956

High accuracy Doppler navigation employing optimum integrated position fix information
08 p1073 N85-16803

Error and uncertainty — metrology
[NPL-DPMA-2] 08 p1137 N85-17161

A moving finite element method for time dependent partial differential equations with error estimation and refinement
[AD-A147719] 08 p1210 N85-17617

A note on the prediction error for small time lags into the future
[AD-A148221] 08 p1215 N85-17654

The atmospheric extinction problem
08 p1251 N85-17901

Gain instabilities in photomultipliers: How accurate are photon counting measurements?
08 p1251 N85-17903

CCDs: Their cause and cure
08 p1252 N85-17905
Automatic land vehicle navigation using road map data
[DE84-017178] 09 p1278 N85-18043
Sampling errors. They may deprive the analytical results of any meaning
[BU-MINTEK-TR-1169-(5810.5758)]
09 p1373 N85-18625
Fixed vs. variable order Runge-Kutta
[DE85-001320] 09 p1374 N85-18639
Analysis of a visual performance experiment
[DE85-000710] 10 p1530 N85-19645
Rejection of anomalous observations when determining spacecraft trajectories 13 p1979 N85-22421
Analysis of systematic errors in systems of selenodetic coordinates 13 p1982 N85-22435
A Monte Carlo sampling plan for estimating network reliability
[AD-A150511] 13 p2065 N85-22898
Noise tolerance of diversity reception in frequency-adaptive digital transmission systems
13 p2086 N85-23024
Investigation of influence of communications link and synchronization error on noise tolerence of group transmission of binary information based on orthogonal Walsh function 13 p2086 N85-23026
Runge-Kutta formula with cheap error estimate
[DE85-005674] 13 p2152 N85-23363
Scheme for measuring specular reflection coefficient at 10.6 microns wavelength with zigzag-path cell and integrating sphere 14 p2275 N85-24097
Propagation of numerical errors in computers and numerical quality 14 p2396 N85-24760
Reliable computation with cellular automata
[AD-A150656] 14 p2399 N85-24790
Spline techniques for magnetic fields
[DE85-004919] 14 p2415 N85-24902
Astrometric plates obtained at the primary focus of large aperture reflectors 14 p2436 N85-25022
Problems and procedures of cometary astometry
14 p2436 N85-25024
Implications of observed frequencies of solar P modes
14 p2443 N85-25073
Evaluating identifiability in remote sensing problems
15 p2486 N85-25347
The effect of inaccuracies in structural models on the control of large space structures
[AD-A151794] 16 p2732 N85-26858
Estimates of errors of a gyroscope stabilized platform
16 p2763 N85-27050
Radial orbit error spectrum for Topex
16 p2805 N85-27292
Synthetic aperture side-looking radar image adjustment 16 p2806 N85-27304
Error reduction program — combustor performance evaluation codes
[NASA-CR-174776] 16 p2852 N85-27584
Inherent magnetic field error measurements in ELMO Bumpy Torus
[DE85-005855] 16 p2867 N85-27685
Spectral decomposition and verification of NOGAPS 500MB medium-range forecasts
[AD-A152550] 17 p2996 N85-28520
A high-accuracy optical linear algebra processor for finite element applications
[NASA-CR-175894] 17 p3017 N85-28658
Effects of inspection errors on curtailed Dorfman-type procedures
[AD-A152376] 17 p3024 N85-28699
Statistical effects of imperfect inspection sampling. Part 2: Double sampling, link sampling and grading
[AD-A152377] 17 p3024 N85-28700
A factored implicit scheme for numerical weather prediction with small factorization error
18 p3141 N85-29447
Error growth in operational 10-day forecasts
18 p3143 N85-29460
A constant altitude flight survey method for mapping atmospheric ambient pressures and systematic radar errors
[NASA-TM-86733] 19 p3217 N85-29951
The effect of sensor and actuator errors on static shape control for large space structures
[NASA-TM-86446] 19 p3225 N85-29998
Inherent angular tracking error in an amplitude comparison monopulse radar
[AD-A154212] 19 p3255 N85-30185
Filter induced errors in laser anemometer measurements using counter processors
[NASA-TM-87047] 19 p3272 N85-30288
Development and evaluation of a fault-tolerant multiprocessor (FTMP) computer. Volume 1: FTMP principles of operation
[NASA-CR-166071] 19 p3341 N85-30705
Wideband disturbance accomodation in precision flexible space structures 20 p3415 N85-31194
A comparison of millimeter wave, direct detect and heterodyne laser intersatellite links
[AD-A151964] 20 p3461 N85-31496
Errors and parameterizations of sub-grid scale processes in regional-scale atmospheric models
20 p3488 N85-31682
Hubble space telescope: Pointing error effects on nonlinear ball joints
[NASA-TM-86511] 20 p3545 N85-32058
In-situ measurement of wall thermal performance: Data interpretation and apparatus design recommendations
[DE85-011979] 21 p3586 N85-32289
Comparison of survey and photogrammetry methods to position gravity data, Yucca Mountain, Nevada
[DE85-011685] 21 p3590 N85-32316
Art of programming programmable microcalculators, part 4: errors of calculations 22 p3778 N85-33411
Search of the VAXintosh customizing VMS V4.0 for DCL windows
[DE85-011306] 22 p3831 N85-33729
Assessment of magnetic field asymmetries in ELMO Bumpy square
[DE85-011905] 22 p3846 N85-33819
Nonsimultaneous coupled laser velocimeter measurement technique: Error prediction for spatially noncoincident measurements
[NASA-TM-86718] 23 p3934 N85-34379
Comparative analysis of operational forecasts versus actual weather conditions in airline flight planning, volume 4
[NASA-CR-167665] 24 p4120 N85-35537
Comparative analysis of operational forecasts versus actual weather conditions in airline flight planning: Summary report
[NASA-CR-167666] 24 p4120 N85-35538
Error message recording and reporting in the SLC control system
[DE85-013057] 24 p4140 N85-35664
Multidimensional analysis of data obtained in experiments with X-ray emulsion chambers and extensive air showers
[HE-3.6-2] 24 p4184 N85-35951

ERS-1 (ESA SATELLITE)
ERS-1 radar altimeter data products — conferences
[ESA-SP-221] 03 p0379 N85-12419
The ESA remote sensing satellite system (ERS-1)
03 p0379 N85-12420
The ERS-1 radar altimeter: An overview
03 p0379 N85-12421
The ERS-1 radar altimeter instrument
03 p0379 N85-12422
The current formal status of the ERS-1 ground segment 03 p0380 N85-12423
Tracking requirements for precise ERS-1 orbit determination 03 p0380 N85-12431
Determination of geoid undulations and ocean heights from ERS-1 radar altimetry data
03 p0381 N85-12432
Factors affecting the archiving, processing and dissemination of ERS-1 altimeter data
03 p0381 N85-12435
ERS-1 altimeter ground segment relations to other sensors and programs 03 p0381 N85-12436
Impact of ERS-1 observations on wave forecasting in the North Sea 03 p0381 N85-12437
SEASAT altimeter data over the Mediterranean: Implications for ERS-1 03 p0382 N85-12443
The Precise Range and Range Rate Equipment (PRARE) and its possible support to the radar altimeter measurement for ERS-1 03 p0382 N85-12445
Determination of the altimetric geoid and gravity anomalies in the North Sea: Implications for a solution of the general circulation problem using ERS-1 data
03 p0382 N85-12446
Ice sheets as invariant surfaces for radar altimeter calibration and orbit determination
03 p0383 N85-12449
ERS-1 radar altimeter system performance evaluation and calibration 03 p0383 N85-12451
Simulation of information extraction from radar altimeter return echoes — ERS-1 (ESA satellite)
03 p0383 N85-12452
Lessons from the SEASAT and GEOS-3 altimeters data projects 03 p0384 N85-12457
Technology for the ERS-1 SAR antenna
05 p0626 N85-14008
ERS-1 and its potential for industrial utilization
05 p0659 N85-14235
Dissemination of ERS-1 low bit rate data and the use of L-band receiving stations
[NLR-TR-83049-U] 09 p1358 N85-18542
Quantization study for ERS-1 wave mode
[DFVLR-FB-84-39] 11 p1625 N85-20234
The ESA remote sensing satellite system (ERS-1)
11 p1713 N85-20777
Bonded stripline power splitter for ERS-1
[RML-009-84-124] 15 p2550 N85-25740
Comparison of ERS-1 scatterometer Monte Carlo performance simulations using a weighted nonlinear least squares and a maximum likelihood estimation method
20 p3420 N85-31226
AMI calibration study. Volume 1: SAR calibration. Volume 2: Ground Targets. Volume 3: Scatterometer calibration — Active Microwave Instrument (AMI) ERS-1
[C2248/4/4-VOL-1] 23 p3936 N85-34384

ERTS
U LANDSAT SATELLITES

ERTS-A
U LANDSAT 1

ERTS-D
U LANDSAT 4

ERYTHROCYTES
Hemopoiesis in rats submitted to weightlessness
01 p0091 N85-10813
Functional and structural changes in human erythrocyte surface after irradiation by UV waves of various wavelengths. Report 1: Expression of ABO and Rhesus system antigen 09 p1361 N85-18664
Functional and structural changes in human erythrocyte surface after irradiation by UV waves of various wavelenghts. Report 2: Adsorption of alcyan blue by external premembranous components
09 p1361 N85-18665
The effect of inert gases on ion transport across the erythrocyte membrane
[AD-A148889] 10 p1527 N85-19635
A detailed analysis of the erythropoietic control system in the human, squirrel, monkey, rat and mouse
[NASA-CR-171879] 15 p2614 N85-26107
Research opportunities in loss of red blood cell mass in space flight
[NASA-CR-175808] 16 p2841 N85-27517
Threshold effects and cellular recognition
[DE85-010816] 19 p3327 N85-30814
Electrophoretic mobilities of erythrocytes in various buffers 20 p3500 N85-31758
Evaluation of results of cell electrophoresis experiments on space shuttle STS-3 including pre-flight and post-flight laboratory experiments 20 p3502 N85-31772
Free zone electrophoresis simulation of static column electrophoresis in microgravity on shuttle flight STS-3
20 p3502 N85-31773
Microgravity electrophoresis: A study of the factors that affect free-fluid separation 20 p3502 N85-31774
Pre-flight report on cultured human embryonic kidney cell handling and cell electrophoresis. Prepared prior to continuous-flow electrophoretic separation experiments aboard space shuttle flight STS-8
20 p3503 N85-31775
A systems analysis of the erythropoietic responses to weightlessness. Volume 1: Mathematical model simulations of the erythropoietic responses to weightlessness
[NASA-CR-171890] 20 p3506 N85-31794
A systems analysis of the erythropoietic responses to weightlessness. Volume 2: Description of the model of erythropoiesis regulation. Part A: Model for regulation of erythropoiesis. Part B: Detailed description of the model for regulation of erythropoiesis
[NASA-CR-171891] 20 p3506 N85-31795
Spacelab 1 hematology experiment (INS103): Influence of space flight on erythrokinetics in man
[NASA-TM-58268] 22 p3824 N85-33693

ESA
U EUROPEAN SPACE AGENCY

ESA SATELLITES
NT COS-B SATELLITE
NT ERS-1 (ESA SATELLITE)
NT EUROPEAN COMMUNICATIONS SATELLITE
NT EXOSAT SATELLITE
NT GEOS SATELLITES (ESA)
NT HEOS B SATELLITE
NT L-SAT
NT METEOSAT SATELLITE
NT OTS (ESA)

ESA SPACECRAFT
NT COS-B SATELLITE
NT GIOTTO MISSION
NT L-SAT
NT METEOSAT SATELLITE
NT OTS (ESA)

ESAKI DIODES
U TUNNEL DIODES

ESCAPE (ABANDONMENT)
Study of several factors affecting crew escape trajectories from the Space Shuttle Orbiter at low-subsonic speeds
[NASA-TM-86303] 10 p1428 N85-19008

ESCAPE SYSTEMS
Aeronautical systems technology needs: Escape, rescue and survival, test facilities and test equipment and training-simulation equipment
[AD-A145059] 01 p0001 N85-10002
MC2989 escapement study
[DE84-014542] 05 p0645 N85-14143
A Generalized Escape System Simulation (GESS) computer program. Volume 2: GESS programmer's manual, version 2
[AD-A148363] 08 p1061 N85-16845
Personnel protection concepts for advance escape system design 10 p1532 N85-19658
Chemical and photographic evaluation of rigid explosive transfer lines
[AD-A149303] 11 p1613 N85-20145
Approach for service life extension of explosive devices for aircraft escape systems
[NASA-TM-86323] 13 p1971 N85-22361
Preliminary design of a limb restraint evaluator
[AD-A151749] 15 p2466 N85-25226
Generalized escape system simulation: Its purpose, recent modifications and potential
[DE85-005571] 16 p2703 N85-26689
Design and testing of an energy-absorbing crewseat for the F/FB-111 aircraft, volume 1
[NASA-CR-3916] 23 p3896 N85-34133
Design and testing of an energy-absorbing crewseat for the F/FB-111 aircraft. Volume 2: Data from seat testing
[NASA-CR-3917] 24 p4064 N85-35184

ESCARPMENTS
Lithologic and structural control on slope morphology in the Valles Marineris 13 p2201 N85-23651

ESCHERICHIA
Toxicity, mutagenesis and aging due to endogenous oxygen radicals
[AD-A150121] 12 p1900 N85-21928
Structural-functional changes in bacterial cells under spaceflight conditions 16 p2724 N85-26812

ESG (GYROSCOPES)
U ELECTROSTATIC GYROSCOPES

ESKERS
U GLACIAL DRIFT

ESRO
U EUROPEAN SPACE AGENCY

ESTERS
NT ACRYLATES
NT ASPARTATES
NT CELLULOSE NITRATE
NT DIISOCYANATES
NT GLUTAMATES
NT ISOCYANATES
NT MALEATES
NT NITRATE ESTERS
NT PETN
NT PHTHALATES
NT POLYCARBONATES
NT POLYESTERS
NT POLYETHYLENE TEREPHTHALATE
NT SULFONATES
NT URETHANES
Chemistry and metabolism of delayed neurotoxic organophosphorus esters
[AD-P004023] 06 p0844 N85-15357
Fluorinated diacrylic esters
[AD-D011328] 07 p0929 N85-15889
Acute oral toxicity (LD50) of 4-nitrophenyl monochloromethyl (Phenyl) phosphinate (TA009) in male rats
[AD-A148337] 08 p1192 N85-17513
Plasticizer system for propellant compositions
[AD-D011514] 12 p1817 N85-21393
Plasticizer system for propellant compositions
[AD-D011516] 12 p1817 N85-21394
Plasticizer system for propellant compositions
[AD-D011517] 12 p1817 N85-21395
Condensation of anhydrides or dicarboxylic acids with compounds containing active methylene groups. Part 19: Condensation of phthalic and substituted phthalic anhydrides with benzoylacetic ester
[NASA-TM-77885] 19 p3227 N85-30009
Condensation of anhydrides or dicarboxylic acids with compounds containing active methylene groups. Part 1: Condensation of phthalic anhydride with acetoacetic and malonic ester
[NASA-TM-77886] 19 p3227 N85-30010

ESTIMATES
NT COST ESTIMATES
Estimation of the potential and probable source regions for acid precipitation
[DE84-015119] 02 p0225 N85-11472
Nonparametric maximum penalized likelihood estimation of a density from arbitrarily right-censored observations
[AD-A145569] 02 p0251 N85-11644
Signal processing algorithms
[AD-A145748] 03 p0406 N85-12590
The ML (Maximum Likelihood) method for frequency estimation of real sinusoids in noise
[AD-A146053] 03 p0411 N85-12628
Measurement of range-resolved water vapor concentration by coherent CO2 differential absorption lidar
[PB84-236892] 04 p0535 N85-13420
Some error estimates for the p-version of the finite element method
[CTH-MATH-1984-21] 05 p0719 N85-14614
Numerical estimation of charge transfer time in charge-coupled device employing latent gallium arsenide channel 06 p0793 N85-15069
Repulsive force of magnetic clouds during solar flares and magnetospheric substorms
06 p0824 N85-15233
Characteristic scale of inner mixing layers in stably stratified atmosphere 06 p0824 N85-15235
Geostatistics for resource and reserve estimation
[PB85-105781/GAR] 07 p0989 N85-16286
Forest area estimates from LANDSAT MSS and forest inventory plot data
[PB85-105617/GAR] 07 p0990 N85-16290
Estimation for a semimartingale regression model using the method of sieves
[AD-A146809] 07 p1028 N85-16527
Determination of crustal and upper mantle structure from analysis of broadband teleseismic P-waveforms
08 p1181 N85-17440
A moving finite element method for time dependent partial differential equations with error estimation and refinement
[AD-A147719] 08 p1210 N85-17617
Research in stochastic processes
[AD-A148622] 08 p1216 N85-17660
On the local behaviour of solutions of degenerate parabolic equations with measurable coefficients
[AD-A147412] 09 p1373 N85-18631
Simple approximate variances for b-letter values. A sampling enquiry: Supplement
[DE85-001410] 09 p1376 N85-18647
Data-driven choice of a spectrum estimate: Extending the applicability of cross-validation methods
[DE85-001411] 10 p1437 N85-19058
On the modified likelihood for density estimation
[AD-A149437] 10 p1547 N85-19756
The inefficiency of least squares: Extensions of Kantorovich inequality
[AD-A149568] 10 p1549 N85-19768
Estimation of variance of the regression estimator
[AD-A149407] 10 p1551 N85-19780
Statistical analysis of autoregressive spectral estimates for noise corrupted autoregressive series
[AD-A149543] 11 p1708 N85-20747
AFOS (Automation of Field Operations and Services)-ERA forecast verification, September 1984
[PB85-137578] 12 p1897 N85-21912
An asymptotically efficient solution to the bandwidth problem of kernel density estimation, revision
[AD-A149600] 12 p1920 N85-22056
Estimation of gas turbine engine boost provided by injecting water behind compressor
13 p2051 N85-22838
Accuracy of approximation of Bayes estimates in presence of noninformative parameters
13 p2084 N85-23015
A note about the strong convergence of the nonparametric estimation of a regression function
[AD-A150325] 13 p2151 N85-23353
Runge-Kutta formula with cheap error estimate
[DE85-005674] 13 p2152 N85-23363
Monthly and Seasonal Weather Outlook for mid-December 1984 mid-January 1985, volume 38, number 24, 14 December 1984
14 p2379 N85-24687
Nonparametric estimation of density and hazard rate functions when samples are censored
[AD-A150946] 14 p2411 N85-24868
Residual oxygen pressure in contact gap upon diffusion welding of titanium 15 p2499 N85-25418
High frequency estimation of 2-dimensional cavity scattering
[AD-A151697] 15 p2542 N85-25696
The measurement of human time estimating ability using a modified jerison device
[AD-A151870] 15 p2620 N85-26141
Some estimates of harmonic majorants
15 p2634 N85-26237
A non-parametric probability density estimator and some applications
[AD-A151853] 15 p2641 N85-26287
Sensitivity of conditions for lumping finite Markov chains
[AD-A152122] 16 p2855 N85-27604
Formulas for updating the generalized inverse of a symmetric matrix perturbed by a symmetric rank 2 matrix composed of 2 nonsymmetric DYADS
[AD-A151736] 16 p2858 N85-27629
Conformational and mechanical properties at high strain rates
[AD-A153401] 17 p2959 N85-28272
Computer-aided thermohydraulic design of TEMA type E shell and tube heat exchangers for use in low pressure, liquid-to-liquid, single phase applications
[AD-A153779] 18 p3100 N85-29191
Extent to which least-squares cross-validation minimizes integrated square error in nonparametric density estimation
[AD-A153789] 18 p3174 N85-29679
Precipitation estimation using collocated GOES satellite and surface data
[AD-A154248] 19 p3317 N85-30559
Estimating ability with the wrong model
[AD-A154071] 19 p3335 N85-30663
The optimality of lower confidence limits for the reliability of series systems obtained by the method of key test results or other related techniques
[AD-A154880] 21 p3597 N85-32338
Parameter estimation in communication system tracking satellite observations
[AD-A155137] 21 p3636 N85-32582
Identification of unsteady aerodynamics and aeroelastic integro-differential systems
[NASA-TM-86749] 21 p3678 N85-32851
A simulation study of Sylvester's problem in three dimensions
[AD-A155266] 21 p3679 N85-32854
Procedure for estimating orbital debris risks
[NASA-TP-2507] 22 p3738 N85-33169
Estimating angular position of optical radiation source when received by array of photodetectors
22 p3778 N85-33413
Estimating the change in asymptotic direction due to secular changes in the geomagnetic field
[SH-6.1-13] 23 p4045 N85-35086
Optimal estimation of a high degree gravity field from a global set of 1 deg x 1 deg anomalies to degree and order 250
[AD-A156008] 24 p4117 N85-35519
Gravity gradiometer survey data processing
[AD-A156165] 24 p4117 N85-35522
Atlantic coast hindcast. Phase 2: Wave information, additional extremal estimates
[AD-A156137] 24 p4125 N85-35575
Error-correcting codes for computer memories
24 p4136 N85-35636

ESTIMATING
NT ORBITAL POSITION ESTIMATION
NT PARAMETER IDENTIFICATION
NT SYSTEM IDENTIFICATION
Recursive algorithms for adaptive arrays based on estimates
[REPT-5-84] 01 p0107 N85-10718
Construction of approximate confidence intervals for probability-of-kill via the bootstrap
[AD-A144761] 01 p0113 N85-10764
Decision tree rating scales for workload estimation: Theme and variations
[NASA-CR-174062] 02 p0237 N85-11544
Auto-regressive moving average spectral estimation using modified and least squares modified Yule-Walker estimates
[AD-A145516] 02 p0254 N85-11663
Programming effort estimation
[AD-A145839] 03 p0406 N85-12595
Maximum likelihood and Bayesian parameter estimation in item response theory
[AD-A145775] 03 p0413 N85-12644
Noise analysis of the Coarse Optical Power Spectrum Estimator (COPSE) data acquisition system
[AD-A145918] 03 p0419 N85-12677
Improved carrier tracking by smoothing estimators
05 p0623 N85-13989
Performance of Bayes-optimal angle-of-arrival estimators
[AD-A146594] 06 p0858 N85-15454
Efficient scores, variance decompositions and Monte Carlo swindles
[AD-A146673] 06 p0858 N85-15458
Electronics research at the University of Texas at Austin
[AD-A146900] 07 p0947 N85-15998
Bayesian estimation of undetected errors
[AD-A147198] 07 p1031 N85-16545
Hybrid state estimation approach to multiobject tracking for airborne surveillance radars
[AD-A148459] 08 p1153 N85-17279
Research on optimal control, stabilization and computational algorithms for aerospace applications
[NASA-CR-174318] 08 p1209 N85-17603

A feedback finite element method with a posteriori error estimation. Part 1. The finite element method and some basic properties of the A posteriori error estimator
[AD-A148345] 08 p1212 N85-17631

Antisampling for estimation: An overview
[AD-A148545] 08 p1216 N85-17659

Three position estimation procedures
[AD-A148748] 09 p1278 N85-18042

Comparing computing formulas for estimating concentration ratios
[DE84-008844] 09 p1349 N85-18490

Estimating the scale parameter of an exponential distribution from a sample of time-censored r-th order statistics
[AD-A149060] 09 p1375 N85-18644

Rain volume estimation over areas using satellite and radar data
[NASA-CR-174434] 10 p1518 N85-19588

Simulation of estimating periodicity of seasonally stationary time series
[DE85-003517] 11 p1708 N85-20748

Care 3 model overview and user's guide, first revision
[NASA-TM-86404] 15 p2627 N85-26192

Estimation theory applied to improving dynamic structural models
[DE85-004148] 15 p2630 N85-26210

Theory and Applications of State Estimation. NRIMS Summer Seminar Series
[CSIR-SWISK-37] 15 p2635 N85-26244

Nonlinear estimation 15 p2635 N85-26245

Some aspects of decentralized Kalman filtering
15 p2635 N85-26250

State estimation with interrupted observations
15 p2635 N85-26251

Estimation of maneuvering targets
15 p2636 N85-26253

Bayesian estimation of one dimensional discrete markov random fields
[AD-A151503] 15 p2640 N85-26284

Construction of efficient algorithms for the estimation of multivariate probability densities
[AD-A151509] 15 p2640 N85-26285

Estimation of launch vehicle performance parameters
[AD-A151927] 16 p2728 N85-26839

A data based algorithm for choosing the window width when estimating the integral of f2(x)
[AD-A152093] 16 p2847 N85-27553

Some new estimation methods for weighted regression when there are possible outliers
[AD-A152104] 16 p2854 N85-27602

Multivariable statistical modelling and its application
16 p2857 N85-27617

Methods for optimal recursive estimation of non-stationary time series, applications to atomic time and frequency metrology 17 p2965 N85-28312

Numerical estimation of the curvature of biological surfaces 17 p3006 N85-28588

Nonsmooth analysis and Frechet differentiability of M-functionals
[AD-A152932] 17 p3019 N85-28668

Nonparametric estimation of the probability of ruin
[AD-A153523] 18 p3174 N85-29674

A robust estimator of location using an adaptive spline model
[AD-A153662] 18 p3174 N85-29676

On the characterization of nonnegatively estimable linear combinations of variance components
[AD-A153786] 18 p3174 N85-29678

Estimating ability with the wrong model
[AD-A154071] 19 p3335 N85-30663

A comparison of four Monte Carlo methods for estimating the probability OF S=T connectedness
[AD-A154264] 19 p3348 N85-30749

Nomographs for estimating the levelized cost of energy from flat-plate and concentrator photovoltaic systems
[NASA-CR-176048] 20 p3483 N85-31645

A model parameter extraction procedure applicable to linear time-invariant dynamic systems
[NASA-CR-176120] 22 p3835 N85-33747

Monte Carlo techniques for analyzing deep penetration problems
[DE85-011426] 23 p3968 N85-34598

Estimation of flight mechanical variables by means of Kalman filters 24 p4062 N85-35171

LANDSAT-4/5 image data quality analysis
[E85-10105] 24 p4107 N85-35463

ESTIMATORS

Asymptotics for configural estimators
[AD-A150106] 12 p1924 N85-22087

ESTUARIES

The SANCOR estuaries programme, 1982-1986
[ISBN-0-7988-2662-2] 01 p0068 N85-10454

Ecology of estuarine channels of the pacific northwest coast: A community profile
[PB84-209709] 01 p0070 N85-10464

Estuaries of the Cape. Part 2: Synopses of available information on individual systems. Report 12: Buffels (WES) (CSW 1), Elsies (CSW 2), Sir Lowry's Pass (CSW8), Steenbras (CSW 9), and Buffels (OOS) (CSW 11)
[CSIR-RR-411-PT-2] 01 p0086 N85-10581

Estuaries of the Cape. Part 2: Synopses of available information on individual systems. Report 13: Silvermine (CSW 3)
[CSIR-RR-412-PT-2] 01 p0086 N85-10582

Estuaries of the Cape. Part 2: Synopses of available information on individual systems. Report no. 14: Sand (CSW 4)
[CSIR-RR-413-PT-2] 01 p0086 N85-10583

Estuaries of the Cape. Part 2: Synopses of available information on individual systems. Report no. 15: Zeekoe (CSW 5)
[CSIR-RR-414-PT-2] 01 p0087 N85-10584

Estuaries of the Cape. Part 2: Synopses of available information on individual systems. Report no. 16: Eerste (CSW 6)
[CSIR-RR-415-PT-2] 01 p0087 N85-10585

Estuaries of the Cape. Part 2: Synopses of available information on individual systems. Report no. 17: Lourens (CSW 7)
[CSIR-RR-416-PT-2] 01 p0087 N85-10586

Estuaries of the Cape. Part 2: Synopses of available information on individual systems. Report no. 18: Bot/Kleinmond system (CSW 13)
[CSIR-RR-417-PT-2] 01 p0087 N85-10587

Estuaries of the Cape. Part 2: Synposes of available information on individual systems. Report no. 19: Groot (WES) (CMS 23) and Sout (CMS 22)
[CSIR-RR-418] 01 p0087 N85-10588

Radiotracer studies of the dispersion of solid pollutants in marine and estuarial environment: Measurement of diffusion coefficients and the phenomenon of dispersion by currents
[BLL-DRIC-TRANS-7104-(3623.66)]
02 p0224 N85-11468

Verification of a model of the Eastern Scheldt
[RAND/R-3108-NETH] 09 p1354 N85-18518

Field-work report: Medway Estuary, 28 June - 18 July 1983
[RNC/NS/TR8] 13 p2041 N85-22773

Ecology of Pamlico River, North Carolina: An estuarine profile
[PB85-155703] 16 p2822 N85-27404

Review and annotated bibliography of benthic studies in coastal and estuarine areas of Florida with a selected compilation of worldwide benthic methodological references and southeastern United States benthic taxonomic references
[PB85-151041] 16 p2822 N85-27405

Water quantity and quality research for the Rhine Meuse estuary
[PUBL-325] 17 p2988 N85-28470

ETCHING

Fabrication of monocrystalline GaAs solar cells utilizing NaCl sacrificial substrates
[DE84-013016] 11 p1673 N85-20544

Laser-plasma interactions for the deposition and etching of semiconductor materials
[DE85-000458] 11 p1731 N85-20885

The characterisation of oxide films on treated aluminium alloys
[MQAD-R-849] 13 p2022 N85-22667

Apparatus for etching vertical junction solar cell wafers
[AD-D011653] 17 p2964 N85-28443

Morphology of GaAs/sub 1-x/P/sub x/ superlattices grown by MOCVD and chloride VPE
[DE85-002944] 17 p3045 N85-28842

Micro-reactions of metal contacts on various types of GaAs surfaces
[AD-A153650] 18 p3193 N85-29806

ETHANE

Laser schlieren, shock tube studies of high temperature hydrocarbon pyrolysis rates
[DE85-003314] 11 p1636 N85-20303

Mechanisms of heat and mass transfer across a double-diffusive interface
[PB85-148468] 12 p1848 N85-21594

Optical waveguide sensor for methane gas
[AD-D011691] 19 p3273 N85-30294

Shock tube measurements of growth constants in the branched-chain ethane-carbon monoxide-oxygen system
[NASA-TM-87068] 21 p3562 N85-32156

ETHERS

NT POLYPHENYL ETHER

Morphology and dynamic mechanical properties of diglycidyl ether of bisphenol-A toughened with carboxyl-terminated butadiene-acrylonitrile
04 p0466 N85-12958

Thermally stable thermoset resin compositions
[AD-D011274] 05 p0620 N85-13963

Fluorinated aliphatic polyalkylether lubricant additive composed of an aromatic phosphine with perfluoroalkylether groups
[AD-D011286] 06 p0770 N85-14

Plasticizer system for propellant compositions
[AD-D011508] 12 p1816 N85-21

Azido nitramino ether containing solid propellants
[AD-D011511] 12 p1816 N85-21

Plasticizer system for propellant compositions
[AD-D011516] 12 p1817 N85-21

Chemical interpretation of the relaxed permittivity during epoxy resin cure
[AD-A150955] 14 p2260 N85-2

Polyaromatic ether-sulfone-keytones fluoro-substituted-p-cyclophane units as cross-linking sites
[AD-D011649] 17 p2933 N85-2

Processable and stable conductive polymers
[AD-D011684] 19 p3249 N85-301

Synthesis and properties of aryletherśulfone thermoset systems
[AD-A154811] 21 p3569 N85-32

The use of perfluoroether lubricants in unprotected space environments 22 p3797 N85-33

ETHYL ALCOHOL

Construction of a bacterium to convert cellulose to ethanol
[TI84-901639] 04 p0481 N85-130

Bulletin of the Faculty of Engineering, Hokkaido University, no. 123
[ISSN-0385-602-X] 04 p0482 N85-130

Experimental study on the glow plug aided alcohol diesel engine 04 p0483 N85-1307

Alcohol fuel from Ohio farms: An introduction
[TI-84-901290] 05 p0621 N85-13

Renewable energy: Energy from agricultural products
[TI84-901769] 05 p0669 N85-14

Biocatalyzed processes for production of commodity chemicals: Assessment of future research advances N-butanol production
[NASA-CR-174264] 07 p0919 N85-15

Ethanol production by enzymatic hydrolysis: Parametric analysis of a base-case process
[DE84-013105] 11 p1614 N85-2014

Developments in the production and use of ethanol fuels
[GPO-40-678] 12 p1817 N85-21

Alcohol Fuels Program technical review, spring 19
[DE85-002919] 17 p2938 N85-281

Ignition characterization of LOX/hydrocarbon propellants
[NASA-CR-171884] 18 p3083 N85-2907

Ignition characterization of LOX/hydrocarbon propellants
[NASA-CR-171882] 18 p3083 N85-2907

ETHYL COMPOUNDS

Interactions of ketones and hexacarbons
[AD-P004019] 06 p0843 N85-153

Dynamics of vapor explosions
[DE85-008845] 18 p3101 N85-291

ETHYLENE

NT VINYLIDENE

A thermodynamic surface for the critical region of ethylene
[PB84-217850] 01 p0025 N85-101

Transport and relaxation processes in supercritical fluids
[DE84-006591] 05 p0731 N85-14

Field test results of experimental EPDM (Ethylene Propylene Diene Monomer) and PUF (Polyurethane Foam) roofing
[AD-A147697] 08 p1132 N85-1713

Cars temperature measurements in sooting, laminar diffusion flames
[AD-A148801] 09 p1319 N85-182

Laser schlieren, shock tube studies of high temperature hydrocarbon pyrolysis rates
[DE85-003314] 11 p1636 N85-2030

An indirect role for ethylene in shoot-inversion release of apical dominance in Pharbitis nil
15 p2611 N85-2

Participation of ethylene in two modes of gravistimulation of shoots 15 p2613 N85-261

Flash pyrolysis of biomass with reactive and non-reactive gases
[DE85-010962] 19 p3306 N85-30

Preparation of ethylenediamine dinitrate
[DE85-006423] 23 p3922 N85-34

ETHYLENE COMPOUNDS

NT CHLOROETHYLENE

NT ETHYLENEDIAMINE

Investigation of bromine complexed hydrogen/bromine regenerative fuel cells for portable electric power
[AD-A146401] 06 p0833 N85-153

Ionization energies of liquids from energy distribution, quantum yield and second derivative curves
[AD-A152210] 16 p2746 N85-26946

ETHYLENE OXIDE
Water absorption and conductivity in poly(ethylene oxide)-lithium tetrafluoroborate films
[AD-A147969] 10 p1450 N85-19136
Hazardous air pollutants: Wet removal rates and mechanisms
[PB85-139626] 12 p1887 N85-21842
Influence of hydrogen bonding in block copolymers and their blends 13 p2036 N85-22752
Characterization of poly(ethylene oxide) drawn by solid state extrusion
[AD-A150967] 14 p2260 N85-24006
Ion and polymer chain motion in a superionic sodium-poly(ethylene oxide) complex
[AD-A152290] 16 p2755 N85-27001

ETHYLENEDIAMINE
The IMX double direct process
[AD-A146250] 03 p0340 N85-12188
Ethylenediamine salt of 5-nitrotetrazole and preparation
[DE85-005738] 23 p3923 N85-34306

EUCLIDEAN GEOMETRY
NT ANALYTIC GEOMETRY
NT ANGLE OF ATTACK
NT ANGLES (GEOMETRY)
NT BRAGG ANGLE
NT CARTESIAN COORDINATES
NT CATENARIES
NT CIRCLES (GEOMETRY)
NT CIRCUMFERENCES
NT CONICS
NT DESCRIPTIVE GEOMETRY
NT ELEVATION ANGLE
NT ELLIPSES
NT EPICYCLOIDS
NT FIXED POINTS (MATHEMATICS)
NT GEODESIC LINES
NT HYPERBOLAS
NT INFLECTION POINTS
NT LINES (GEOMETRY)
NT LOCI
NT MERCATOR PROJECTION
NT OBLATE SPHEROIDS
NT PARABOLAS
NT PARALLELEPIPEDS
NT POINTS (MATHEMATICS)
NT POLYGONS
NT PROJECTIVE GEOMETRY
NT PYRAMIDS
NT RADII
NT RECTANGLES
NT SPHEROIDS
NT TANGENTS
NT TORUSES
Model diagnosis in two-way tables by means of row and column Euclidean maps
[CSIR-TWISK-307] 01 p0108 N85-10730
Schur-Ostrowski theorems for functionals on l1(0,1)
[AD-A150193] 13 p2150 N85-23346
A factorization approach to the linear regulator quadratic cost problem 20 p3413 N85-31178
A new description of combined trellis coding with asymmetric modulation
[NASA-CR-176197] 24 p4086 N85-35323

EUCLIDEAN SPACE
U EUCLIDEAN GEOMETRY

EULER BUCKLING
Interactive buckling of thin-walled structural components under static and dynamic loads
01 p0059 N85-10392
Nonlinear deformation and static linear buckling of structures under pressure
[CETIM-11-E-350] 04 p0514 N85-13261

EULER EQUATIONS OF MOTION
Shock capturing finite difference algorithms for supersonic flow past fighter and missile type configurations
[NASA-CR-174051] 02 p0134 N85-10913
Model equations describing unsteady fluid motion
[ESA-TT-850] 04 p0501 N85-13194
A comparative study of the nonuniqueness problem of the potential equation
[NASA-TP-2385] 07 p0898 N85-15694
A Van Leer shock capturing algorithm for the Euler equations
[AD-A148761] 08 p1163 N85-17335
Flow instabilities in transonic small disturbance theory
[NASA-TM-86251] 09 p1273 N85-18000
An implicit, conservative, zonal-boundary scheme for Euler equation calculations
[NASA-CR-3865] 09 p1318 N85-18290
Researched applied to transonic compressors in numerical fluid mechanics of inviscid flow and viscous flow
[NASA-CR-174353] 09 p1319 N85-18291
Algorithms for the Euler and Navier-Stokes equations for supercomputers
[NASA-CR-172543] 10 p1539 N85-19701
Collision detection for moving polyhedra
[AD-A148961] 10 p1544 N85-19735
Contribution to the study of a numerical implicit method for solving the Euler equations
[ESA-TT-872] 10 p1549 N85-19771
A convergent series expansion for hyperbolic systems of conservation laws
[NASA-CR-172557] 12 p1910 N85-21990
Calculation of harmonic aerodynamic forces of aerofoils and wings from the Euler equations
15 p2458 N85-25177
A new implicit plus minus splitting method for the solution of the Euler equations in the transonic flow regime
15 p2461 N85-25200
A 3-dimensional Navier-Stokes-Euler code for blunt-body flow computations
[NASA-TM-58266] 15 p2463 N85-25211
Vortex dynamics
[AD-A151278] 15 p2637 N85-26260
Redistribution of the inlet temperature profile through the SSME fuel turbine 16 p2739 N85-26901
Evaluation of an algorithm for the solution of the time-dependent Euler equations
[AD-A151993] 16 p2854 N85-27600
Upwind-difference methods for aerodynamic problems governed by the Euler equations
[REPT-84-23] 17 p2893 N85-27834
Unsteady flow in multistage turbines
17 p2911 N85-27946
Relaxation methods for hyperbolic equations
[REPT-84-20] 17 p3021 N85-28687
Chemical transformation modules for Eulerian acid deposition models. Volume 1: The gas-phase chemistry
[PB85-173714] 18 p3072 N85-29001
The dynamics and control of large flexible space structures, 8
[NASA-CR-175986] 19 p3225 N85-29996
An elliptic calculation procedure for 3-D viscous flow
21 p3587 N85-32297
Calculation of 3-D flow without numerical mixing
21 p3588 N85-32301
Three-dimensional hydrodynamic hot-spot model
[DE85-009587] 23 p3922 N85-34301
Compressible two-phase flow instabilities simulated with a hybrid Lagrange-Euler pseudospectral method
[DE85-009904] 23 p3931 N85-34361
A stream function approach to solving the conservative Euler equations for transonic flows
24 p4059 N85-35156
Numerical studies of 2-dimensional flows
[NASA-CR-3930] 24 p4060 N85-35160

EULER-CAUCHY EQUATIONS
A study of the recursion yn+1=yn+tau yn sup m
[CWI-NM-R8403] 05 p0723 N85-14648
Propagation of non-axisymmetric elastic waves through shell with filler under radial load at one end
17 p2943 N85-28169

EULER-LAGRANGE EQUATION
Hamiltonian and Lagrangian theory of gyrokinetic equations 02 p0283 N85-11845
The perfecting of the method of experimental-analytic solution of the problem of stationary plastic flow
[BLL-M-35938-(5828.4)] 05 p0634 N85-14065
Influence of turbulence on erosion by a particle-laden fluid jet
[DE84-014365] 09 p1320 N85-18301
Adaptive meshes in the 2DL code
[LA-9938-MS] 12 p1914 N85-22011
Elements of celestial mechanics
14 p2396 N85-24762
Development of a dynamic finite element model for unrestrained flexible structures
[AD-A151176] 15 p2636 N85-26259
FEMALE: Finite Element Method for Arbitrary Lagrangian and Eulerian elements
23 p3979 N85-34671
Two-dimensional simulation of LIB target implosion
23 p3980 N85-34678

EURECA (ESA)
European retrievable carrier (Eureca) and evolutionary space carrier for microgravity, Earth observation and technology demonstration 02 p0152 N85-11032
Botany facility, phase A study. Part 1: Executive summary — EURECA
[BF-DOC-10-VOL-1] 08 p1110 N85-17015
The EURECA Automatic Gradient Heating Facility (AGHF), phase A study
[ESA-CR(P)-1939] 11 p1591 N85-20005
Solution growth facility, phase A design study, executive summary — EURECA
[RPT/SGF/00014/TER] 11 p1591 N85-20006
Botany facility phase A study. Core payload number 6 EURECA carrier, volume 1
[ESA-CR(P)-1978-VOL-1] 17 p2906 N85-27918
Botany facility phase A study. Core payload number 6 for EURECA carrier, volume 2
[BF-TD-DRD-03-VOL-2] 17 p2906 N85-27919
German payloads for EURECA 1
[BMFT-FB-W-85-003] 20 p3419 N85-31223
The EURECA solution growth facility conceptual design study. Executive summary
[ESA-CR(P)-2007] 20 p3538 N85-32016

EUROPA
Multispectral and geomorphic studies of processed Voyager 2 images of Europa
[NASA-CR-174075] 03 p0448 N85-12848
Patterns of fracture and tidal stresses due to nonsynchronous rotation: Implications for fracturing on Europa 13 p2173 N85-23483
Planetary analogs in Antarctica: Icy satellites
13 p2193 N85-23605
Spectral units on Europa and Ganymede
13 p2196 N85-23621
Fault offsets and lateral crustal movement on Europa
13 p2201 N85-23656

EUROPE
Project COST 72 (The European weather radar project) today 01 p0084 N85-10561
Heat flow map of Europe: Brief summary of the geophysical implications
[REPT-562] 03 p0377 N85-12405
Terrestrial heat flow in Europe and general features of its regional distribution
[REPT-563] 03 p0377 N85-12406
Determination of the longitude differences Munich-Lissabon-San Fernando, Munich-Wettzell, and Munich-Karlsruhe-Niederreifenberg
[ASTRON-GEODAET-ARB-44]
04 p0524 N85-13353
Determination of astronomical longitude differences for the European longitude reference system for 1980. Relative right ascension corrections for 125 FK4 and FK4 Sup stars 04 p0524 N85-13354
European scientific notes. Volume 38, number 11
[AD-A148228] 08 p1230 N85-17745
West Europe report: Science and technology
[JPRS-WST-85-003] 09 p1309 N85-18224
Analysis of bird strikes reported by European airlines, 1976 - 1980
[AD-P004181] 11 p1578 N85-19943
West Europe report: Science and technology
[JPRS-WST-85-005] 11 p1592 N85-20013
West Europe report: Science and technology
[JPRS-WST-85-006] 11 p1618 N85-20183
The Middle Atmosphere Program: Winter in Northern Europe (MAP/WINE) 11 p1655 N85-20429
Winter in Northern Europe (WINE) project
11 p1657 N85-20439
Large scale winter time disturbances in meteor winds over central and eastern Europe
11 p1661 N85-20467
Changes in the ozone content over central Europe during reversals of stratospheric circulation in late winter
11 p1661 N85-20469
An air-breathing ballistic space transporter for Europe
[NASA-TM-77645] 12 p1792 N85-21244
Lateral inhomogeneity of mantle surface in western Eurasia 14 p2344 N85-24497
West Europe report: Science and technology
[JPRS-WST-85-014] 15 p2469 N85-25362
West Europe report: Science and technology
[JPRS-WST-84-012] 15 p2523 N85-25552
East European report: Science and technology
[JPRS-ESA-85-010] 15 p2524 N85-25560
West Europe report: Science and technology
[JPRS-WST-84-008] 15 p2531 N85-25606
East Europe report: Science and technology
[JPRS-ESA-84-016] 15 p2533 N85-25624
West Europe report: Science and technology
[JPRS-WST-84-020] 15 p2534 N85-25633
West Europe report: Science and technology
[JPRS-WST-84-003] 15 p2534 N85-25635
West Europe report: Science and technology
[JPRS-WST-84-010] 15 p2535 N85-25644
East Europe report: Science and technology
[JPRS-ESA-85-018] 15 p2537 N85-25658
Frequency dependence of Q in the mantle underlying the shield areas of eurasia
[AD-A151367] 15 p2592 N85-25978
East Europe report: Science and technology
[JPRS-ESA-84-032] 16 p2727 N85-26833
Rotterdam Airport and the Common Market
17 p2894 N85-27840

West Europe report: Science and technology
[JPRS-WST-84-024] 17 p2945 N85-26183
Air Weather Service (AWS) climatic briefs: Europe
[AD-A152528] 17 p2996 N85-26519
Forecast impact simulation studies
18 p3139 N85-29435
Reduced to pole long-wavelength magnetic anomalies of Africa and Europe 20 p3475 N85-31595
Euro-African MAGSAT anomaly-tectonic observations
20 p3475 N85-31596
Long-wavelength magnetic and gravity anomaly correlations on Africa and Europe
20 p3476 N85-31597
A transportable, machine oriented library of european sky and terrain radiance distributions with contemporary radiometric and meteorological profiles
[AD-A155254] 21 p3637 N85-32590
Supersaturation spect A of Ice Nuclei at different locations in Europe and over the North-Atlantic
21 p3640 N85-32615
Space-age Europe, 1957-1980
23 p4057 N85-35148
Introduction to European air traffic control
[AD-A156328] 24 p4062 N85-35176

EUROPEAN AIRBUS
NT A-310 AIRCRAFT
NT A-320 AIRCRAFT
Insight. Background information for multipurpose pilots: Flight phenomena 02 p0138 N85-10940
All-composite Airbus empennage
07 p0936 N85-15931
West Europe report: Science and technology
[JPRS-WST-85-006] 11 p1618 N85-20183
Airbus fatigue tests 11 p1618 N85-20186
A 320 to have combined automatic pilot, flight control system 14 p2289 N85-24186
West Europe report: Science and technology
[JPRS-WST-84-027] 15 p2532 N85-25612
MBB cost-reduction plan for Airbus construction described 15 p2532 N85-25616
FRG journal analyzes state, prospects of airbus programs: General analysis 15 p2535 N85-25638
Financial, economic commentary on Airbus, European aviation 15 p2536 N85-25649
Lightning-safe carbon fiber composite for Airbus tail unit 18 p3087 N85-29100
Avionics and civil aircraft systems: The present and the future
[SNIAS-851-111-104] 20 p3392 N85-31038

EUROPEAN COMMUNICATIONS SATELLITE
Station for in-orbit testing of satellites
[MBB-UR-708/84-O] 16 p2874 N85-27733

EUROPEAN LARGE TELECOMM SATELLITE
U L-SAT

EUROPEAN RETRIEVABLE CARRIER
U EURECA (ESA)

EUROPEAN SPACE AGENCY
Non-US approaches to space commercialization
02 p0150 N85-11012
Space research in Norway
[SAD-110-T] 03 p0321 N85-12072
Space research in Sweden 03 p0321 N85-12073
The ESA product assurance specification system: Explanatory note 04 p0511 N85-13259
International involvement in a civilian space station program 07 p0915 N85-15789
FRG study looks at participation in ESA, US space station 08 p1141 N85-17191
Making sure: A brief outline and history of ESA's test and checkout services
[ESA-BR-22] 09 p1286 N85-18077
Commercial space: Europe should have independent strategy 10 p1480 N85-19205
European views differ on space station concept
15 p2531 N85-25606
West Europe report: Science and technology
[JPRS-WST-84-010] 15 p2535 N85-25644
European space science horizon 2000
[ESA-SP-1070] 16 p2717 N85-26771
Timing of spacecraft date: Time accuracy requirements and timing facilities of the European Space Agency (ESA) 17 p2964 N85-28307
Documentation for the West German Federal Cabinet's space policy decision 17 p3051 N85-28886
Some Europeans voice opposition to space station participation 18 p3066 N85-28961
West Europe report: Science and technology
[JPRS-WST-84-022] 18 p3085 N85-29086
ESA presents plans for European manned space station 18 p3085 N85-29087
West Europe report: Science and technology
[JPRS-WST-84-032] 18 p3086 N85-29095
New ESA director on Ariane, space station, future trends 18 p3086 N85-29096
FRG weighs ESA participation, budget issues
18 p3088 N85-29110
The ESA field emission electric propulsion program
[ESA-STR-213] 20 p3420 N85-31229
Space-age Europe, 1957-1980
23 p4057 N85-35148

EUROPEAN SPACE PROGRAMS
Non-US approaches to space commercialization
02 p0150 N85-11012
European retrievable carrier (Eureca) and evolutionary space carrier for microgravity, Earth observation and technology demonstration 02 p0152 N85-11032
Space research in Norway
[SAD-110-T] 03 p0321 N85-12072
Space research in Sweden 03 p0321 N85-12073
Colloquium about Joint Projects within DFVLR/ISRO Cooperation
[DFVLR-MITT-84-12] 04 p0458 N85-12907
Presentation of Indian Space Research Organization (ISRO)/DFVLR cooperation 04 p0459 N85-12912
The Telecom 1 satellite telecommunication system
04 p0493 N85-13147
Antenna mechanical technologies within ESA
05 p0625 N85-14000
The METEOSAT exploitation project, operational use of a remote sensing system 05 p0658 N85-14223
Overview of German microgravity activities in the field of life science 05 p0696 N85-14476
Space research in Spain 08 p1231 N85-17751
United Kingdom report on space research
08 p1231 N85-17752
Space research in Denmark 08 p1231 N85-17753
Space activities in Finland 08 p1231 N85-17754
Space research in the Federal Republic of Germany
09 p1285 N85-18074
Gravity and biological systems: Emphasis on human physiology
[ESA-BR-21] 09 p1360 N85-18558
Activities report in space research in Austria
11 p1587 N85-19994
Preliminary concepts of candidate elements for a potential European participation in a manned space station
[MBB-UR-E-749-84-O] 11 p1587 N85-19996
Future launching systems, 3rd prospective phase
[SNIAS-S/DT/Y-25-063] 11 p1589 N85-19999
West Europe report: Science and technology
[JPRS-WST-85-013] 14 p2289 N85-24183
Science with the Solar and Heliospheric Observatory (SOHO) 14 p2449 N85-25121
Studies on rocket engines for future European launchers
[SEP-TPRL/K-19572/84] 15 p2495 N85-25393
European space science horizon 2000
[ESA-SP-1070] 16 p2717 N85-26771
European utilization aspects of a US manned space station, volume 1
[ESA-CR(P)-1987-VOL-1] 17 p2907 N85-27926
European utilization aspects of a US manned space station, volume 2
[ESA-CR(P)-1987-VOL-2] 17 p2907 N85-27927
In orbit infrastructura. Volume 1: Executive summary — European space programs
[RX011-002/84-VOL-1] 17 p2908 N85-27928
Documentation for the West German Federal Cabinet's space policy decision 17 p3051 N85-28886
In orbit infrastructure — european space programs
[SNIAS-S/DT-24-996] 18 p3064 N85-28956
Space station study
[BL-6167] 18 p3066 N85-28959
Maintenance of long life space systems, volume 1
[MATRA-0316/DX60-VOL-1] 18 p3066 N85-28964
Maintenance of long life space systems, volume 2
[MATRA-0350/DX60-VOL-2] 18 p3066 N85-28965
DFVLR official on areas of US-FRG Space Station cooperation 18 p3086 N85-29091
Ariane space general director on satellite launcher market 18 p3087 N85-29103
Study of a medium term flexible fixed satellite service mission
[DM51/CC-IM-0165.83] 18 p3091 N85-29136
Looking down looking forward: Earth observation, sciences and applications, a perspective
[ESA-SP-1073] 18 p3149 N85-29497
ERS economic impace study
[ESA-CR(P)-1979] 18 p3199 N85-29847
A study of the ESA-NAVSAT control segment
[ESA-CR(P)-2000] 20 p3398 N85-31079
Studies toward a manned space station: Participation of European industry in NASA space station (MSS)
[SNIAS-S/DT-Y-25-212] 20 p3418 N85-31217
Study of terrestrial mobile systems for personal communications
[MCS-8436] 20 p3441 N85-31357
Thermal protection systems for reentry vehicles
[CNES-NT-113] 23 p3900 N85-34157

EUROPEAN SPACE RESEARCH ORGANIZATION
U EUROPEAN SPACE AGENCY

EUROPIUM COMPOUNDS
Fluorescence quenching by metal semiconductor and insulator surfaces 19 p3374 N85-[illegible]

EUTECTIC ALLOYS
The influence of the carbide distribution on the [illegible] wear of ledeburitic chromium steels
01 p0054 N85-10[illegible]
Microstructure and creep behaviour at elevated temperature of unidirectionally solidified eutectic nickel base superalloys 02 p0181 N85-11216
Reciprocal solubility of phases in multi-component systems
[BLL-M-36003-(5828.4)] 07 p0926 N85-15670
Alloys and method of making
[AD-D011337] 07 p0927 N85-15674
Research on rapidly solidified alloys
[AD-A149360] 10 p1441 N85-1[illegible]
Dependence of superplastic flow on state of grain boundaries 13 p2025 N85-22[illegible]
Study of processes of modification of Al-Si alloys
13 p2026 N85-22[illegible]
Aluminum alloy ATs5K5 (5% Zn + 5% Cu) for superplastic forming 13 p2026 N85-22[illegible]
Influence of solidification parameters on the formation of the gamma-M7C3 eutectic structure of 2% C-12%Cr steel 15 p2512 N85-25[illegible]
Dissolution of solid solutions in absence of internal mass transfer
[BLL-M-36092-(5828.4)] 16 p2748 N85-2[illegible]
Ca-Ga, Sr-Ga and Ba-Ga binary systems
[DE85-006454] 16 p2751 N85-2[illegible]
Multi-phase crystallization of ferrous alloys
[BLL-BISI-TRANS-22441-(9022.06)]
17 p2925 N85-28007
Properties of heat resistant Ni-Al-Nb alloys with unidirectional eutectic structure
19 p3247 N85-3013[illegible]
Directional solidification of an eutectic Bi-MnBi alloy
[BLL-M-36270-(5828.4)] 20 p3430 N85-31275

EUTECTIC DIAGRAMS
U PHASE DIAGRAMS

EUTECTICS
NT EUTECTIC ALLOYS
Eutectic explosives containing ammonium nitrate
[DE84-015705] 01 p0034 N85-10213
The effect of heat treatment on wear resistance of gas-plasma eutectic coatings
[BLL-M-35756-(5828.4)] 03 p0329 N85-12132
The IMX double direct process
[AD-A146250] 03 p0340 N85-1218[illegible]
Effect of a thermal gradient applied to a sinusoidal surface profile
[DE84-015649] 03 p0434 N85-127[illegible]
Investigation of the dissolution of CaCrO4 in molten LiCl-KCl eutectic
[DE84-016394] 04 p0469 N85-12[illegible]
The growth of metastable peritectic compounds
[NASA-CR-171289] 07 p0920 N85-158[illegible]
Studies on copper alloys containing chromium on the copper side phase diagram
[NASA-TM-77752] 07 p0927 N85-158[illegible]
SPAR X technical report for experiment 76-22 directional solidification of magnetic composites
[NASA-CR-171271] 07 p0927 N85-158[illegible]
Advanced latent heat storage media for high-temperature industrial applications
[DE85-000907] 09 p1345 N85-184[illegible]
Development of media for dynamic latent heat storage for the low-temperature range. Part 1: Thermal analyses of selected salt hydrate systems
[NASA-TM-77776] 10 p1507 N85-19510
Influence of eutectic silicate inclusions on micro-processes during deformation and fracture of [illegible] steel
[BLL-BISI-TRANS-22296-(9022.06)]
17 p2929 N85-28073
Binary phase diagram determinations
[DE85-010856] 19 p3235 N85-300[illegible]
A study of freezing and melting with eutectic interactions 19 p3378 N85-30[illegible]
Influence of yttrium on eutectoid transformation in irons
[BLL-M-35787-(5828.4)] 24 p4078 N85-35[illegible]

EUTROPHICATION
Geographic variation in the relationships of temperature, salinity or sigma sub t versus plant nutrient concentrations in the world ocean — silicic acid, nitrate, and phosphate concentration
[NASA-CR-175621] 13 p2140 N85-23[illegible]
Empirical methods for predicting eutrophication in impoundments. Report 3. Phase 2. Model refinements
[AD-A155483] 21 p3614 N85-32[illegible]
Sulfur cycling in freshwater sediments
21 p3658 N85-32[illegible]

EUVE
U EXTREME ULTRAVIOLET EXPLORER SATELLITE

EVACUATING (TRANSPORTATION)
The helicopter, instrument of choice for health evacuation
[SNIAS-851-220-101] 20 p3393 N85-31051
EVACUATING (VACUUM)
Evacuate and backfill apparatus and method
[DE85-006016] 23 p3938 N85-34411
EVALUATION
NT TRAINING EVALUATION
Performance evaluation of A-10 aircraft mainteance units and aircraft using constrained facet analysis
[AD-A146955] 07 p0893 N85-15660
An evaluation and comparison of vertical profile data from the VISSR Atmospheric Sounder (VAS)
[NASA-TP-2425] 07 p1000 N85-16351
A survey and evaluation of software quality assurance
[AD-A147552] 07 p1026 N85-16510
Flight service evaluation of advanced composite ailerons on the L-1011 transport aircraft
[NASA-CR-172483] 08 p1118 N85-17049
Development and evaluation of techniques for using combined microwave and optical image data for vegetation studies 08 p1148 N85-17240
A study of Air Force Quality Circle program effectiveness as viewed through facilitator's perceptions
[AD-A147633] 08 p1170 N85-17377
Design of an evaluation system to measure performance degradation due to continuous operations
[AD-A148186] 08 p1200 N85-17558
Performance management system enhancement and maintenance
[NASA-CR-175271] 08 p1202 N85-17584
Evaluation of the Fundamental Research on Explosives (FRE) program
[DE85-001537] 09 p1301 N85-18172
Evaluation of the particulate levels occurring under 1.0/1.2 g/mi nitrogen oxide standards for light duty diesel vehicles and light duty diesel trucks
[PB85-115939/GAR] 09 p1350 N85-18494
Partial evaluation as a means of language extensibility
[AD-A148730] 09 p1368 N85-18596
Applicability of laboratory kinetics studies to the evaluation of aqueous phase atmospheric oxidation of sulfur-4
[DE85-000586] 12 p1883 N85-21819
Electrical characterization of analog microprocessors
[AD-A149629] 12 p1911 N85-21995
Operational performance of the photovoltaic-powered grain mill and water pump at Tangaye, Burkina Faso (formerly Upper Volta)
[NASA-TM-86970] 13 p2128 N85-23243
MSFC data analysis of the SAFE/DAE experiment
14 p2233 N85-23843
Robotic deburring. Part 2: Evaluation of cutters and noncompliant tooling
[DE85-006182] 14 p2311 N85-24306
US Army Aviation Engineering Flight Activity (USAAEFA) report bibliography update 1983 - 1984
[AD-A131381] 15 p2457 N85-25168
An evaluation of the performance of a new storm tracking methodology
[AD-A152234] 16 p2835 N85-27484
Evaluation of the PROFS (Program for Regional Observing and Forecasting Services) 1982, real-time forecast experiment
[PB85-159747] 16 p2837 N85-27495
Evaluation of used crankcase oils using computerized infrared spectrometry. Appendices
[AD-A152994] 17 p2920 N85-28000
On-orbit frequency stability analysis of the GPS NAVSTAR's 3 and 4 rubidium clocks and NAVSTAR's 5 and 6 cesium clocks 17 p2963 N85-28298
Test and evaluation plan for the Centralized Storm Information System 17 p2994 N85-28508
CSIS test and evaluation 17 p2994 N85-28509
DC-10 winglet flight evaluation
[NASA-CR-3704] 19 p3217 N85-29949
Fundamental studies related to failure of adhesively bonded structures
[AD-A154072] 19 p3285 N85-30374
Nickel cadmium cell design variable program data analysis 20 p3445 N85-31387
High discharge rate characteristics of nickel-cadmium batteries for pulse load filtering
20 p3446 N85-31391
Improved materials for composite and adhesive joints
[AD-A155065] 21 p3562 N85-32153
Fabrication and test of modified quadrupole mass spectrometer
[AD-A155186] 21 p3590 N85-32312
Photovoltaics technical information guide
[DE85-002924] 22 p3808 N85-33585
Fuel cell applications literature review
[DE85-011691] 22 p3809 N85-33592
Effect of interference on the performance of a minimum TCAS 2
[FAA-PM-84-33] 23 p3895 N85-34131
Evaluation of low-temperature geothermal potential in Utah and Goshen Valleys and adjacent areas, Utah. Part 2: Water temperature and chemistry
[DE85-009344] 23 p3943 N85-34438
Expert systems research in regional resource evaluation: Experiences in the application of microcomputer technologies 24 p4105 N85-35450
EVAPORATION
NT EVAPOTRANSPIRATION
NT PROPELLANT EVAPORATION
NT TRANSPIRATION
A comparison of evaporation duct models for IREPS (Integrated Refractive Effects Prediction System)
[AD-A146471] 06 p0799 N85-15103
Eddy correlation measurements of energy partition for Amazonian forest
[INPE-3195-PRE/559] 06 p0827 N85-15252
Practical application of IREPS (Integrated Refractive Effects Prediction System)
[AD-A146528] 06 p0838 N85-15323
Thermal evaporation in blast waves: A model for aneurism formation in the NRL (Naval Research Laboratory) LASER-HANE simulation experiment
[AD-A147006] 07 p0978 N85-16210
Climate at CRREL (Cold Regions Research and Engineering Laboratory) Hanover, New Hampshire
[AD-A148400] 08 p1189 N85-17495
Exciplex systems for vapor-liquid visualization of fuel sprays
[AD-A149360] 10 p1457 N85-19181
Modeling interception of rainfall by forests and the role of interception in the water balance
[DE85-002822] 12 p1884 N85-21825
Effects of temperature variation among droplets in an evaporating fuel spray 13 p2004 N85-22562
Fabrication and I-V characterization of AlGaAs/GaAs MODFETs with P-type surface layers grown by molecular beam epitaxy
[AD-A151695] 15 p2660 N85-26415
Research test facility for evaporation and combustion of alternative jet fuels at high air temperatures
[AD-A153830] 18 p3083 N85-29073
Analysis and model/data comparisons of large-scale releases of nitrogen tetroxide
[DE85-009989] 18 p3133 N85-29406
Laser-induced fluorescence measurement of vapor concentration surrounding evaporating droplets
[DE85-009409] 19 p3277 N85-30320
Influence of spatial variability of hydraulic characteristics of soils on surface parameters obtained from remote sensing data in infrared and microwaves
[NASA-TM-77902] 20 p3477 N85-31604
Vaporization from a heated surface into a saturated stream
[DE85-010484] 20 p3530 N85-31958
Emergency modeling of hazardous air pollutants
[AD-A155441] 21 p3614 N85-32461
Superheated fuel injection for combustion of liquid-solid slurries
[DE85-011624] 22 p3753 N85-33266
Volatile loss following very large impacts
22 p3853 N85-33862
Evaluation of source strength and dispersion model predications with data from large nitrogen tetroxide field experiments
[DE85-011855] 23 p3947 N85-34465
How are particle production, nucleon emission and target fragment evaporation processes interrelated in hadron-nucleus collisions? 24 p4174 N85-35878
EVAPORATION RATE
Vapor pressure and evaporation rate of certain heat-resistant compounds in a vacuum at high temperatures
[NASA-TM-77807] 10 p1434 N85-19036
EVAPORATIVE COOLING
NT FILM COOLING
NT SWEAT COOLING
Performance evaluation of an active solar cooling system utilizing low cost plastic collectors and an evaporatively-cooled absorption chiller
[DE84-010813] 12 p1880 N85-21798
Evaporatively cooled chiller for solar air conditioning systems design and field test
[DE84-014154] 20 p3484 N85-31652
EVAPORATORS
Development of a preprototype times wastewater recovery subsystem
[NASA-CR-171815] 03 p0388 N85-12480
Addendum: Development of a preprototype times wastewater recovery subsystem
[NASA-CR-171816] 03 p0388 N85-12481
Development of a preprototype times wastewater recovery subsystem: Appendices
[NASA-CR-171817] 03 p0388 N85-12482
Open cycle OTEC thermal-hydraulic systems analysis and parametric studies
[DE84-013011] 04 p0530 N85-13391
Open-cycle centrifugal vapor-compression heat pump
[PB85-113405/GAR] 09 p1328 N85-18348
Operation of a low temperature absorption chiller at rating point and at reduced evaporator temperature
[DE85-006306] 16 p2760 N85-27030
Spacecraft, straight-tube evaporator design
[AD-A154462] 19 p3226 N85-30003
An experimental apparatus to study nucleate pool boiling of R-114 and oil mixtures
[AD-A154077] 19 p3265 N85-30249
EVAPOTRANSPIRATION
Multispectral Imaging Science Working Group for Hydrologic Science: Executive summary
02 p0214 N85-11414
Remote Sensing of Snow and Evapotranspiration
[NASA-CP-2363] 13 p2123 N85-23223
General report of the researches of snowpack properties, snowmelt runoff and evapotranspiration in Japan 13 p2124 N85-23225
Estimation of regional evapotranspiration using remotely sensed land surface temperature. Part 1: Measurement of evapotranspiration at the Environmental Research Center and determination of Priestley-Taylor parameter
13 p2125 N85-23233
Estimation of regional evapotranspiration using remotely sensed land surface temperature. Part 2: Application of equilibrium evaporation model to estimate evapotranspiration by remote sensing technique — Japan 13 p2125 N85-23234
Testing an energy balance model for estimating actual evapotranspiration using remotely sensed data — Hannover, West Germany barley and wheat fields
13 p2125 N85-23236
Soil moisture and evapotranspiration estimates based on satellite data 15 p2596 N85-25998
EVASIVE ACTIONS
Simple-motion pursuit-evasion differential games in the plane
[CSIR-TWISK-336] 14 p2412 N85-24874
Stochastic pursuit-evasion differential games in the plane
[CSIR-TWISK-343] 14 p2412 N85-24875
EVECTION
U LUNAR ORBITS
U ORBIT PERTURBATION
U SOLAR GRAVITATION
EVEN-EVEN NUCLEI
Boson-fermion symmetries in the W-Pt region
[DE85-009755] 19 p3362 N85-30845
EVENTS
An investigation of the relationship between stressful life events and psychological, behavioral and physiological outcomes
[AD-A147754] 08 p1197 N85-17541
Software for event oriented processing on multiprocessor systems
[DE84-016720] 09 p1370 N85-18607
A replication and extension of the inducement of the availability heuristic
[AD-A149755] 12 p1923 N85-22083
A comparison of alternative analytic models for event related potential records
[AD-A151977] 15 p2618 N85-26134
EVOKED RESPONSE (PSYCHOPHYSIOLOGY)
An optically isolated amplifier
[CSIR-SR-ELEK-257] 01 p0049 N85-10321
Pattern reversal visual evoked potentials and reaction time
[CSIR-SR-PERS-354] 01 p0097 N85-10644
An investigation of the use of steady-state evoked potentials for human performance and workload assessment and control
[AD-A145727] 02 p0237 N85-11541
Visually evoked responses from non-occipital areas of the human cortex
[AD-A146079] 03 p0400 N85-12553
Evidence for multiple areas in the human auditory cortex
[AD-A146086] 03 p0401 N85-12555
Reflection of laterization of sound stimuli in evoked potentials of human brain 04 p0544 N85-13463
ERPS to monitor non-conscious mentation
05 p0707 N85-14536
Performance enhancements under dual-task conditions 05 p0707 N85-14537
In search of a visual-cortical describing function: A summary of work in progress 05 p0707 N85-14538
Measurement of workload: Physics, psychophysics, and metaphysics 05 p0708 N85-14539

Central regulation of sensory flow in human visual system 07 p1013 N85-16435
Visual evoked potentials with disrupted functioning of nonspecific cerebral systems 07 p1013 N85-16437
Nicholet MED-80 (trademark) programs in the Naval Biodynamics Laboratory evoked potential series
[AD-A147105] 07 p1016 N85-16451
Laboratory note: Effect on sleep latency of pre-sleep AEP (Auditory Evoked Potential) procedures
[AD-A147620] 08 p1194 N85-17527
Brain mechanisms underlying individual differences in reaction to stress: An animal model
[AD-A150195] 13 p2143 N85-23301
Effect of triphthasine and elenium on changes in evoked bioelectrical activity of the brain exposed to stationary magnetic field 19 p3325 N85-30601
Matched filtering of visual evoked potentials to detect acceleration (+Gz) induced blackout
[AD-A155912] 24 p4131 N85-35609

EVOLUTION
Sedimentary and tectonic evolution of the western Taiwan foredeep 03 p0389 N85-12491
Global aspects of stream evolution in the solar wind
[DE85-002207] 11 p1766 N85-21101

EVOLUTION (DEVELOPMENT)
NT ABIOGENESIS
NT BIOLOGICAL EVOLUTION
NT CHEMICAL EVOLUTION
NT GALACTIC EVOLUTION
NT LUNAR EVOLUTION
NT PLANETARY EVOLUTION
NT STELLAR EVOLUTION
NT STELLAR MASS ACCRETION
Phylogenic distribution of the large 55 rRNA from Halococcus morrhuae
[NASA-CR-174019] 02 p0234 N85-11523
Origin and evolution of the Uranian and Neptunian satellites: Some dynamical considerations
02 p0300 N85-11943
Composition, structure and evolution of Uranian and Neptunian satellites 02 p0300 N85-11944
Structure and evolution of the large scale solar and heliospheric magnetic fields 05 p0746 N85-14782
Evolutionary history of CI and CM chondrites
06 p0884 N85-15615
The development of the vestibular apparatus under conditions of weightlessness
[NASA-TM-77517] 07 p1011 N85-16422
The origin and evolution of terrestrial and Martian rock labyrinths
[NASA-CR-175511] 12 p1961 N85-22326
Asteroid collisional evolution studies
13 p2176 N85-23501
The legacy of science 14 p2432 N85-24995
Monitoring tropical cyclone growth using GOES VISSR/VAS and Nimbus-7 TOMS data
15 p2595 N85-25989
The evolution of meteor streams
15 p2678 N85-26539
Origin and evolution of ordinary chondrite meteorites
15 p2683 N85-26571
Origin of mesosiderites as a natural consequence of planet formation 15 p2683 N85-26574
Theoretical approach to evolution of solar magnetic field 18 p3204 N85-29674
The origin and evolution of the Earth's atmosphere and hydrosphere 19 p3312 N85-30533
The evolution of complex and higher organisms
[NASA-SP-478] 21 p3656 N85-32708
Heat transfer and brine evolution in magma-hydrothermal systems 24 p4104 N85-35441
Origin of sedimentary humic acids, potential carriers of ore-forming elements 24 p4104 N85-35443

EVOLUTION (LIBERATION)
NT GAS EVOLUTION
Evolution of strong inhomogeneities in ionospheric plasma, part 1 14 p2339 N85-24463

EXACTNESS
U PRECISION

EXAMINATION
Method of examining microcircuit patterns
[NASA-CASE-NPO-16299-1] 11 p1628 N85-20250

EXCAVATION
Impacts in ice: Commissions of solar system crater population 13 p2181 N85-23538

EXCHANGING
NT CHARGE EXCHANGE
NT GAS EXCHANGE
NT ION EXCHANGING
NT SPIN EXCHANGE
Deep-inelastic lepton scattering by nuclei: The pion-exchange model
[DE85-010498] 19 p3359 N85-30828
Tropospheric-stratospheric exchange, part 1.1A
21 p3615 N85-32488

EXCIMER LASERS
Manual for Raman cells
[NASA-TM-77756] 01 p0052 N85-10342
The 248 nm - new short wavelength for pumping lasers employing vapors of complex molecules
02 p0261 N85-11705
RF laser plasma measurements
[AD-A145936] 03 p0366 N85-12344
A high-repetition rate, inductively stabilized, long-pulse excimer laser
[DE84-016827] 04 p0506 N85-13229
Development of prototypes for versatile fast discharge systems for pulsed gas lasers, especially excimer lasers
[BMFT-FB-T-84-174] 06 p0813 N85-15165
Visible and ultraviolet lasers based on excimer transitions in the homonuclear halogens
[AD-D011311] 07 p0971 N85-16163
Excimer laser photofragmentation of organophosphonates. 1: Detection of the PO radical from dimethyl methyl phosphonate (DMMP)
[AD-A149471] 10 p1490 N85-19407
Pulsed excimer laser processing for cost-effective solar cells
[NASA-CR-174429] 10 p1509 N85-19517
Investigation of dye lasers pumped by high-power KrF laser radiation 11 p1718 N85-20806
Non-linear optical techniques for visible and UV lasers and thin film deposition
[AD-A150489] 13 p2096 N85-23077
Time-resolved ellipsometry and reflectivity measurements of the optical properties of silicon during pulsed excimer laser irradiation
[DE85-005091] 13 p2096 N85-23079
Low jitter trigger for an excimer laser
[DE85-005732] 13 p2097 N85-23080
Excimer laser annealing to fabricate low cost solar cells
[NASA-CR-175702] 14 p2351 N85-24529
Pulsed excimer laser processing for cost-effective solar cells
[NASA-CR-175700] 14 p2351 N85-24530
Kinetic studies following state selective laser excitations
[DE85-007173] 15 p2564 N85-25816
Discharge characteristics of high-pressure, fast-discharge XeCl excimer laser
15 p2564 N85-25820
Flat-plate solar array project process development area: Process research of non-CZ silicon material
[NASA-CR-175777] 16 p2818 N85-27382
Production of gallium atoms by excimer laser photolysis of trimethyl gallium
[DE85-010742] 19 p3278 N85-30331
Theoretical modeling of the discharge-pumped XeCl excimer laser 20 p3460 N85-31495
A fast discharge excimer laser with symmetric geometry
[AD-A155294] 21 p3592 N85-32322
Investigation of plasma processes in electronic transition lasers
[AD-A155598] 21 p3593 N85-32327
Pulsed excimer laser processing for cost-effective solar cells 21 p3611 N85-32432
Excimer laser annealing for fabrication of low-cost solar cells 21 p3611 N85-32433
Establishment of steady-state power level in pulse-periodic excimer laser 21 p3685 N85-32896
Saturation effect in multilevel lasing media
21 p3686 N85-32901
Excimer-laser generator of powerful UV picosecond pulses synchronized with picosecond pulses in visible and IR bands 21 p3686 N85-32903
Powerful XeCl excimer electric discharge laser with good temporal stability and fast response time
21 p3688 N85-32911
Sliding discharge in CO2 and excimer lasers
22 p3773 N85-33379
Flat-plate solar array project process development area process research of non-CZ silicon material
[NASA-CR-176117] 23 p3945 N85-34445
Generation of stimulated emission in the soft X-ray range by nonlinear processes with excimer lasers
[DE85-012465] 24 p4098 N85-35403

EXCIMERS
E-beam-induced fluorescence of excimers in cryogenic solutions
[DE85-010703] 19 p3278 N85-30328
Energy transfer and excimer formation in rare gas solids 19 p3374 N85-30930
A fast discharge excimer laser with symmetric geometry
[AD-A155294] 21 p3592 N85-32322

EXCITATION
NT ACOUSTIC EXCITATION
NT ATOMIC EXCITATIONS
NT MOLECULAR EXCITATION
NT SELF EXCITATION
NT WAVE EXCITATION
Experimental studies of atomic inner shell ionization phenomena
[DE84-013448] 01 p0118 N85-10
Excitation of quasi-static magnetic fields with axial structure 02 p0259 N85-11
Search for white dwarf companions of cool stars with peculiar element abundances
[NASA-CR-174030] 02 p0297 N85-1192
RF laser plasma measurements
[AD-A145936] 03 p0366 N85-1234
An inverse source problem for elastic waves
03 p0371 N85-12
Laser excitation of coupled surface electromagnetic and acoustic waves and of static structures in solids
05 p0723 N85-14
Raman study of neutron irradiated GaAs
[DE84-016056] 05 p0731 N85-1472
The correlation between excitation parameter and nebular luminosity for galactic HII regions with application to regions of star formation in M83
05 p0743 N85-1477
Flight test technique for evaluation of gust load alleviation analysis methodology
[NASA-TM-86344] 06 p0754 N85-148
Experimental determination of propagation rate of ELF signals employed by Omega radio navigation system for phase measurements 06 p0793 N85-150
Intense excitation source of blue-green laser
[AD-A147450] 07 p0971 N85-161
Theoretical study of laser-induced surface excitations on a grating
[AD-A147855] 07 p0972 N85-16172
Microwave resonator using lateral excitation
[AD-D011374] 07 p1039 N85-165
Pion inelastic scattering to the first three excited states of Lithium-6
[AD-A147560] 07 p1041 N85-166
Phase-dissipative mechanisms for laser-induced surface desorption-dissociation processes
[AD-A147961] 08 p1121 N85-170
Instrumentation for particle-beams research using laser excited merging beams
[AD-A147968] 08 p1220 N85-178
Degenerate four-wave mixing lineshapes in sodium vapor under pulsed excitation
[AD-A148211] 08 p1222 N85-178
Atomic and molecular collision processes
[DE85-001604] 09 p1362 N85-186
The coordinated research program at IAEA on atomic collision data for plasma diagnostics
09 p1390 N85-1874
A picosecond population modulation study of near interband resonances in semiconductors
09 p1396 N85-1875
Excitation modes and parameters of stress waves in metal exposed to single laser pulses
10 p1448 N85-191
Infrared excitation of clusters and ions of atmospheric interest
[DE85-002098] 10 p1516 N85-195
Plane-wave born collision strengths for electron-ion excitation: Comparison with other theoretical methods
[DE85-002348] 10 p1555 N85-196
Hydrodynamic response of a radiating Al plasma excited by a proton beam
[AD-A148904] 10 p1558 N85-196
KMSF X-ray laser experiments, task no. 2
[DE85-000291] 11 p1640 N85-202
Mini-modal testing of wind turbines using novel excitation
[DE85-000666] 11 p1654 N85-20417
Excitation of impurities by heavy particles and radiative losses of thermonuclear plasma
11 p1719 N85-208
Hydrogen vibrational population distributions and negative ion generation in tandem high density hydrogen discharges
[DE85-001207] 11 p1722 N85-208
Large amplitude forcing of a high speed 2-dimensional jet
[NASA-CR-175646] 13 p1974 N85-22
Use of markets to elucidate reacting sputtering processes
[DE85-005723] 13 p2018 N85-22
Extation of low-frequency resonance waves by moving conductor in space plasma 13 p2067 N85-22
Induction excitation of deep conducting zones
13 p2111 N85-23
Study of resolution of deep MT soundings by means of physical model 13 p2112 N85-23

Observation of a novel low-lying excited state in zinc complexes
[AD-A150188] 13 p2156 N85-23385

Sequential excitation preparation of molecular energy levels with special structural and chemical properties
[AD-A150301] 13 p2156 N85-23386

Electron stimulated desorption and the role of secondary electrons
[AD-A150974] 14 p2252 N85-23955

Computer simulations of rare earth sites in glass: Experimental tests and applications to laser materials
[DE85-006156] 14 p2261 N85-24013

Sensitization and quenching in the conversion of light energy into chemical energy
[DE85-006301] 14 p2351 N85-24535

Ion kinetics, small neutral and excited components in D-region with elevated ionization level. Part 2: Variations in small neutral and excited components
15 p2480 N85-25307

Electric discharge excitation and energy source integration
[AD-A151502] 15 p2562 N85-25806

Calculations of collision-induced optical gain in high-density mixtures of D2 or HD with a buffer gas
[AD-A151372] 15 p2648 N85-26330

Neutralization and excitation in low-energy ion-surface collisions
[AD-A151568] 15 p2660 N85-26414

A study of excitations during collisionally-induced electron detachment of negative ions
[AD-A152879] 17 p3030 N85-28739

Extension of the consistent Q formalism to odd-A nuclei in the W-Pt region
[DE85-008284] 17 p3034 N85-28770

Magnetically switched power supply systems for lasers
[NASA-CASE-NPO-16402-1] 18 p3112 N85-29265

Laser-stimulated vibrational excitation of an adspecies studied by a generalized master equation: Neutral atomic hydrogen on hydrated KCl(001)
[AD-A153665] 18 p3112 N85-29268

Review of short wavelength lasers
[DE85-009858] 18 p3114 N85-29277

Monte Carlo simulation of thermalization of subexcitation electrons in He, Ne, Ar, Kr and Xe
[NAL-TR-843T] 18 p3178 N85-29702

Excited state populations and charge-exchange of fast ions in solids
[DE85-009362] 18 p3180 N85-29714

Excited leptons contribution to muon g-2
[PREPRINT-432] 18 p3184 N85-29745

Alkali atom - SbCl(5) reactions: Blue-green chemiluminescence from an inverted population in SbCl
[AD-A154371] 19 p3276 N85-30315

Excitation of turbulence by density waves
[NASA-CR-3905] 19 p3314 N85-30546

Instrumentation for particle-beams research using excited merging beams
[AD-A154155] 19 p3356 N85-30807

Energy transfer and excimer formation in rare gas solids 19 p3374 N85-30930

Predamage threshold electron emission from insulator and semiconductor surfaces
[DE85-008968] 19 p3377 N85-30954

Antiproton-nucleus inelastic scattering and the spin-isospin dependence of the N anti N interaction
[DE85-010546] 20 p3526 N85-31935

Ab initio calculations of materials properties
[DE85-011167] 20 p3531 N85-31964

Detection of excited states by laser-induced fluorescence
[AD-A155558] 21 p3592 N85-32326

Toward a theory of excitation of atoms during nuclear and magnetic neutron scattering
21 p3689 N85-32918

Radiative-collision generation of sound in gases subjected to single-pulse optical excitation
21 p3689 N85-32920

Resonant energy transfer during strong excitation
21 p3689 N85-32922

Exotic events of p bar p-collider: Excited quark or excited color boson? 21 p3691 N85-32930

Vibrationally enhanced dissociation of diatomic molecules
[AD-A154827] 21 p3701 N85-32996

Electron photoejection in carbanions
[DE85-011748] 23 p3912 N85-34237

Pressure cross spectra in turbulent boundary layers in water
[AD-A156153] 24 p4094 N85-35378

Investigations of the molecular beam epitaxial growth and characteristics of external excitation induced non-equilibrium phases of immiscible 3-5 compound semiconductors
[AD-A156225] 24 p4162 N85-35804

Observations of far-infrared transitions between excited states of OH
[NASA-TM-86722] 24 p4167 N85-35833

EXCITED STATES
U EXCITATION

EXCITONS

Photophysical studies of triplet exciton processes in pure polymer films
[DE84-016258] 05 p0620 N85-13965

Spectroscopic investigation of materials for frequency agile laser systems
[AD-A151731] 16 p2790 N85-27206

Photophysical studies of triplet exciton processes in pure polymer films
[DE85-008571] 18 p3080 N85-29056

Stationary properties and switching characteristics of dispersive optical bistability in CuCl
18 p3186 N85-29763

A theory of exciton photoluminescence for two types of neutral acceptors in silicon. A study of the systems Si:(B, IN), Si:(Al), (Si), Si:(Ga, In), Si:(B, Al), Si:(B, Ga), and Si:(Al, GA)
[AD-A155452] 21 p3710 N85-33031

Time-resolved and infrared spectroscopy of excitons
[DE85-011879] 23 p3912 N85-34235

Pairing correction of particle-hole state densities for two kinds of fermions
[DE85-011549] 23 p3971 N85-34620

Optical properties of heterostructures and superlattices
[AD-A156243] 24 p4162 N85-35802

EXCLUSION

Some recent developments in systems reliability
[AD-A150661] 14 p2317 N85-24318

EXCRETION

Circadian dynamics of potassium excretion in urine as related to working on one and two shifts
19 p3325 N85-30568

EXECUTIVE AIRCRAFT
U GENERAL AVIATION AIRCRAFT
U PASSENGER AIRCRAFT

EXERCISE
U PHYSICAL EXERCISE

EXERCISE PHYSIOLOGY

Voluntary dehydration and electrolyte losses during prolonged exercise in the heat
[AD-A145157] 01 p0095 N85-10639

A machine for weight-lift testing
[AD-A146816] 07 p0973 N85-16182

Effects of restricted water intake on performance in a cold environment
[AD-A146904] 07 p1015 N85-16450

Thermoregulatory responses during exercise at graded hypohydration levels
[AD-A147733] 08 p1195 N85-17528

The effect of beta adrenergic blockade on ratings of perceived exertion
[AD-A148053] 08 p1195 N85-17530

Cognitive performance during successive sustained physical work episodes
[AD-A148061] 08 p1200 N85-17556

Blood viscosity responses to acute exercise and aerobic conditioning in women 09 p1363 N85-18573

Sleep deprivation and exercise tolerance
[AD-A150566] 13 p2142 N85-23296

Aerobic and anaerobic exercise tolerance in the heat: Effect and acclimatization 14 p2388 N85-24707

SPARTEN (Scientific Program of Aerobic and Resistance Training Exercise in the Navy): A total body fitness program for health and physical readiness
[AD-A150869] 14 p2388 N85-24711

Preparing Alberto Salazar for the heat of the 1984 Olympic Marathon
[AD-A150942] 14 p2389 N85-24714

Exercise-heat strain during hypohydration: Interaction with heat acclimation and aerobic fitness
[AD-A151023] 14 p2389 N85-24717

Physiological differences between men and women in exercise-heat tolerance and heat acclimation
[AD-A152048] 15 p2618 N85-26135

Comparative anaerobic power of males and females
[AD-A151960] 16 p2842 N85-27523

Relationship between the Army two mile run test and maximal oxygen uptake
[AD-A153914] 18 p3154 N85-29526

Regional circulation during testing on isokinetic dynamometer following 14-day bedrest
19 p3323 N85-30590

Heat injury: Prevention is the key
[AD-A153734] 19 p3328 N85-30622

Effect of short-term antiorthostatic hypokinesia on dynamics of cardiorespiratory parameters during graded physical exercise 22 p3822 N85-33677

Weight loss, rectal temperature and heart rates following the 1984 Boston Marathon
[AD-A155984] 24 p4132 N85-35612

Thirst and fluid intake following graded hypohydration levels in humans
[AD-A156201] 24 p4132 N85-35615

EXERTION
U PHYSICAL WORK

EXHAUST DIFFUSERS

Energy efficient engine combustor test hardware detailed design report
[NASA-CR-167945] 02 p0140 N85-10950

Strutless diffuser for gas turbine engine
[AD-D011662] 18 p3062 N85-28943

EXHAUST EMISSION

Size specific total particulate emission factors for mobile sources
[PB84-226653] 01 p0071 N85-10471

Mobile source exposure estimation
[PB84-224518] 01 p0095 N85-10643

Energy efficient engine component development and integration program
[NASA-CR-169496] 02 p0146 N85-10989

The changing pattern of fossil fuel CO2 emissions
[DOE/OR-21400/2] 02 p0224 N85-11469

Analysis of potential combustion sorce impacts on acid deposition using an independently derived inventory, volume 1
[DE84-012005] 02 p0225 N85-11471

Dissociated methanol vehicle test results
[DE84-004507] 04 p0509 N85-13248

Outline of a new emissions model for military and civilian aircraft facilities
[DE84-016455] 04 p0531 N85-13394

Facility safety study
[NASA-CR-174280] 07 p0910 N85-15759

Impact of aircraft emissions on air quality in the vicinity of airports. Volume 3: Air quality and emission modeling needs
[AD-A147951] 08 p1180 N85-17435

The application of emissions trading to DoD installations
[AD-P004136] 09 p1346 N85-18472

The influence on IR emission of engine parameters for an afterburn case. A sensitivity study on NATO infrared air target model (NIRATAM) version: 0.0
[AD-B089311L] 12 p1779 N85-21171

Stability of organic audit materials and results of source test analysis audits
[PB85-116184] 12 p1865 N85-21832

Composition and photochemical reactivity of turbine engine exhaust
[AD-A150559] 13 p2130 N85-23256

Emission inventory applications to regional acid deposition modeling
[PB85-157386] 16 p2760 N85-27033

Air quality benefit analysis for Los Angeles and San Francisco based on housing values and visibility
[PB85-166049] 16 p2822 N85-27409

Effect of traffic and meteorology on air pollution
16 p2830 N85-27452

Clean-burning diesel engines
[AD-A152606] 17 p2974 N85-28374

Mechanisms of exhaust pollutants and plume formation in continuous combustion
[AD-A154169] 20 p3435 N85-31310

Toxic hazards tests for vehicles and other equipment
[AD-A149164] 20 p3506 N85-31797

A study of the control of particulate emissions from turbine engine test cells 24 p4067 N85-35205

EXHAUST FLOW SIMULATION
NT ATMOSPHERIC ENTRY SIMULATION

Calculation of flow about posts and powerhead model — space shuttle main engine
[NASA-CR-171344] 10 p1483 N85-19362

The influence on IR emission of engine parameters for an afterburn case. A sensitivity study on NATO infrared air target model (NIRATAM) version: 0.0
[AD-B089311L] 12 p1779 N85-21171

Calculation of viscous compressible flows in small gas turbines 17 p2912 N85-27950

Numerical simulations of the effect of floor and ceiling venting on fire and smoke spread in aircraft cabins
[PB85-178333] 19 p3216 N85-29939

The highly underexpanded exhaust plume from nozzles with boundary layers
[DFVLR-FB-85-10] 20 p3421 N85-31230

EXHAUST GASES
NT FLUE GASES

Space Shuttle Environmental Effects: The First 5 Flights
[NASA-CR-171812] 01 p0069 N85-10457

Clean-burning diesel engines
[AD-A145515] 02 p0205 N85-11349

Impact of alcohol fuels on urban air pollution: Methanol photochemistry study
[DE84-012950] 04 p0531 N85-13397

Overview of waste heat utilization systems
[NASA-TM-86901] 04 p0578 N85-13692

Direct measurements of nitrous acid, nitrogen dioxide and formaldehyde in auto exhaust by differential optical absorption spectroscopy
[PB84-229269] 06 p0767 N85-14905
The toxicity of complex mixtures
[AD-P004033] 06 p0844 N85-15363
Integrated exhaust gas analysis system for aircraft turbine engine component testing
[NASA-TP-2424] 07 p0962 N85-16100
NOx emissions near a heat pump with gas motor
[BLL-WH-782-(9091.9F)] 07 p0995 N85-16319
Laboratory simulation of smoke reduction from aircraft engine test cell exhaust using a fluidized bed filter
[AD-A148600] 08 p1069 N85-16886
Impact of aircraft emissions on air quality in the vicinity of airports. Volume 3: Air quality and emission modeling needs
[AD-A147951] 08 p1180 N85-17435
An analytic model of gas turbine engine installations
[AD-A148708] 09 p1281 N85-18059
Natural gas the new locomotive fuel
[DE84-901824] 09 p1302 N85-18179
Experimental study of aerodynamic shielding of turbojet engine air intake against exhaust gases
09 p1307 N85-18210
Shock propagation in the exhaust gas handling system of the proposed large altitude rocket cell: Methods and preliminary analysis
[DE85-003055] 11 p1591 N85-20010
Diesel engine emissions of particulates and associated organic matter
[PB85-154425] 15 p2590 N85-25964
Papers from the Symposium on Emissions: The Value of Incentives and Guidelines for Control
[S-336] 15 p2590 N85-25967
Transformation of nitrogen oxides while sampling combustion products
[AD-A152184] 16 p2746 N85-26945
Measurements of two-phase exhaust flow parameters of a small caliber gun associated with muzzle flash phenomena
[ISL-CO-212/83] 16 p2784 N85-27182
High resolution spectroscopy of C13O16 in gas mixtures
[AD-A152625] 17 p2919 N85-27991
Clean-burning diesel engines
[AD-A152606] 17 p2974 N85-28374
Opacity control technique for jet engine test cells
[AD-D011668] 19 p3220 N85-29968
Analysis of aldehydes and ketones in the gas phase
[PB85-181865] 20 p3426 N85-31261
Comparative evaluation of three alternative power cycles for waste heat recovery from the exhaust of adiabatic diesel engines
[NASA-TM-86953] 20 p3542 N85-32043
Influence on an industrial site on the characteristics of CCN supersaturation with air masses of different origin
21 p3650 N85-32683
Ames Laboratory measurements of alkali levels in the Curtiss-Wright PFBC gas stream
[DE85-011357] 22 p3745 N85-33214
Modeling of auto exhaust smog chamber data for EKMA development
[PB85-186492] 22 p3813 N85-33619

EXHAUST JETS
U EXHAUST GASES

EXHAUST NOZZLES
NT CONVERGENT-DIVERGENT NOZZLES
NT PLUG NOZZLES
Density distribution in supersonic jet discharged into vacuum from nozzle with bevel tip
02 p0269 N85-11757
The preliminary checkout, evaluation and calibration of a 3-component force measurement system for calibrating propulsion simulators for wind tunnel models
[NASA-CR-174113] 04 p0458 N85-12903
Static jet noise test results of four 0.35 scale-model QCGAT mixer nozzles
[NASA-TM-86871] 04 p0558 N85-13551
Carbon/carbon rocket motor exit cone reinforcement
[AD-D011360] 07 p0916 N85-15799

EXHAUST SYSTEMS
Noise reduction of the exhaust from pneumatic tools
[BMFT-FB-HA-83-021] 02 p0276 N85-11799
Calculation of flow about posts and powerhead model — space shuttle main engine
[NASA-CR-171344] 10 p1483 N85-19362
Pneumatic clamping device
[AD-D011544] 12 p1858 N85-21656
Exhaust systems for passenger vehicles: Test procedure for resistance to internal corrosion of silencers
[BLL-BISI-TRANS-22360-(9022.06)]
17 p2973 N85-28361
Numerical simulations of the effect of floor and ceiling venting on fire and smoke spread in aircraft cabins
[PB85-178333] 19 p3216 N85-29939
Measurement of turbofan-turbojet thrust from tailpipe static pressure
[AD-A154036] 19 p3220 N85-29967

EXHAUST VELOCITY
Particle size, number, composition and velocity from solid rocket motors 12 p1785 N85-21201
Estimation of launch vehicle performance parameters
[AD-A151927] 16 p2728 N85-26839

EXISTENCE THEOREMS
The Boltzmann equation: Global existence for a rare gas in an infinite vacuum
[PREPRINT-78] 01 p0124 N85-10851
The Chinese remainder theorem and multi-PRF radars
[AD-A141375] 13 p2054 N85-22858

EXITS (DOORS)
U DOORS

EXOBIOLOGY
Space medicine and biology, continuing bibliography (supplement 263)
[NASA-SP-7011(263)] 01 p0094 N85-10636
Publications of the exobiology program for 1981: A special bibliography
[NASA-TM-86653] 01 p0099 N85-10657
Aerospace Medicine and Biology, a continuing bibliography with indexes
[NASA-SP-7011(264)] 02 p0234 N85-11525
A survey of space biology and space medicine
[ESA-BR-17] 04 p0545 N85-13466
Aerospace Medicine and Biology, a continuing bibliography with indexes
[NASA-SP-7011(265)] 04 p0545 N85-13467
Plant growth in space 05 p0691 N85-14444
Aerospace medicine and biology: A continuing bibliography with indexes
[NASA-SP-7011(266)] 08 p1194 N85-17525
Aerospace medicine and biology: A continuing bibliography with indexes, supplement 268
[NASA-SP-7011(268)] 08 p1194 N85-17526
Aerospace medicine and biology: A continuing bibliography with indexes
[NASA-SP-7011(269)] 10 p1526 N85-19628
Modular plant culture systems for life support functions
[NASA-CR-171853] 12 p1899 N85-21924
Second Soviet-French Symposium on Space Technology 15 p2483 N85-25326
Aerospace Medicine and Biology: A continuing bibliography with indexes
[NASA-SP-7011(270)] 15 p2615 N85-26114
Aerospace medicine and biology: A continuing bibliography with indexes, supplement 271, May 1985
[NASA-SP-7011(271)] 16 p2840 N85-27514
The cosmic history of the biogenic elements and compounds
[NASA-SP-476] 17 p3003 N85-28562
USSR report: Space Biology and Aerospace Medicine, volume 18, no. 5, September - October 1984
[JPRS-USB-84-007] 19 p3322 N85-30583
Changes in nephron and juxtaglomerular system of primate kidneys under the effect of antiorthostatic hypokinesia 19 p3326 N85-30605
Influence of limboreticular complex on some reactions of rabbits 19 p3326 N85-30607
Aerospace Medicine and Biology: A continuing bibliography with indexes (supplement 272)
[NASA-SP-7011(272)] 19 p3328 N85-30620
Sensitivity of human lymphocytes to microgravity in-vitro 20 p3510 N85-31820
Biostack experiments on STS-flights and the impact for man in space 20 p3510 N85-31821
The global sulfur cycle
[NASA-TM-87570] 21 p3656 N85-32710
Aerospace medicine and biology: A continuing bibliography with indexes, supplement 273
[NASA-SP-7011(273)] 21 p3663 N85-32755
Search for the universal ancestors
[NASA-SP-477] 21 p3667 N85-32777
USSR report: Space Biology and Aerospace Medicine, volume 19, no. 2, March - April 1985
[JPRS-USB-85-004] 22 p3820 N85-33667
Aerospace Medicine and Biology: A continuing bibliography with indexes (supplement 274)
[NASA-SP-7011(274)] 23 p3952 N85-34491
NASA Developmental Biology Workshop: A summary
[NASA-TM-86756] 24 p4126 N85-35578
Vertebrate development in space: Gravity is a drag (and has been for eons and eons) 24 p4126 N85-35580
Report of the NASA Mammalian Developmental Biology Working Group 24 p4126 N85-35581
Report of Amphibian Development Group
24 p4127 N85-35583
Report of the Insect Development Group
24 p4127 N85-35584
Aquatic Invertebrate Development Working Group
24 p4127 N85-35585
Report of the Microbial Development Working Group
24 p4127 N85-35586

EXOSAT SATELLITE
EXOSAT observations of active galactic nuclei
08 p1238 N85-17809
Soft X-ray emission from BL Lac objects
08 p1239 N85-17810

EXOSPHERE
Experimental investigation of neutral plasma beam propagation across a magnetic field
[AD-A150944] 14 p2423 N85-24047
Advances in technology development for exoatmospheric research
[AD-A152581] 17 p2992 N85-28485

EXOTHERMIC REACTIONS
Exothermic processes in solids under low temperatures, their physics and their cryogenic implications
[JUEL-1919] 03 p0414 N85-12651
Theoretical studies on N-bonded pyrazole derivatives of boron
[AD-A150036] 12 p1813 N85-21374
Physical chemistry of exothermic gas-aerosol calorimetry
[AD-A150872] 14 p2251 N85-22859
The effect of mould size on the exothermic reaction and compressive strength of epoxy resin chocks
[AD-A155102] 21 p3570 N85-32203
Optical waveguide along front of exothermic reaction
21 p3694 N85-32554
Pulsed hydrojet propulsion
[DE85-010771] 22 p3784 N85-33448

EXPANDABLE STRUCTURES
NT BALLOONS
NT HIGH ALTITUDE BALLOONS
NT INFLATABLE STRUCTURES
NT JIMSPHERE BALLOONS
NT METEOROLOGICAL BALLOONS
NT MICROBALLOONS
NT SUPERPRESSURE BALLOONS
NT TETHERED BALLOONS
LDR system concepts and technology
14 p2231 N85-23823

EXPANSION
NT GAS EXPANSION
NT KARHUNEN-LOEVE EXPANSION
NT PRANDTL-MEYER EXPANSION
NT SERIES EXPANSION
NT THERMAL EXPANSION
In-situ stress relief of expanded alloy 600 steam generator tubing
[DE84-014560] 04 p0513 N85-13273
Device for measuring relative axial expansion of turbine rotor employing space-vector tracking method
06 p0776 N85-14992
Basic studies of multiple free and confined jets
[AD-A149556] 10 p1485 N85-19374
Tenth-order expansion formulae for the orbital eccentricity function K (sub lpq)(e) obtained using a symbolic algebraic manipulation system
[AD-A153754] 18 p3170 N85-29647
Expedient runway surfacing with post tensioning system for expeditionary airfields
[AD-D011677] 19 p3222 N85-29976
An algorithm for the influence numbers in the expansion of the lumped gravitational potential coefficients in the presence of resonant inclination variation
[AD-A154229] 19 p3336 N85-30669
Acoustic radiation from concentric shells containing an inner fluid
[AD-A155476] 21 p3700 N85-32991

EXPANSION WAVES
U ELASTIC WAVES

EXPECTANCY HYPOTHESIS
Testing of inequality hypotheses in linear models using the Bayes method
[SER-C-292] 01 p0112 N85-10781

EXPENDABLE STAGES (SPACECRAFT)
The Expendable Launch Vehicle Commercialization Act
[GPO-30-838] 04 p0460 N85-12919
Commercial space launches
[S-REPT-98-656] 12 p1788 N85-21225

EXPERIMENT DESIGN
NT FACTORIAL DESIGN
Results of the technical exchange agreement between NASA and DuPont on the containerless drop tube solidification of NiAl3
[NASA-TM-86473] 01 p0014 N85-10087
Determination of vowel zones in speech — speech recognition
[FUB-16-1983] 01 p0040 N85-10253
Fast waves near the lower hybrid frequency
[DE84-015217] 01 p0123 N85-10841

Fluids Experiment Apparatus (FEA)
02 p0155 N85-11048

Design and implementation of a low-gravity solidification experiment package for the F-104
02 p0156 N85-11053

Advances in electrophoretic separations
02 p0156 N85-11054

Laser on copper and gold vapors with space diversity media 02 p0270 N85-11762

The Beatrice experiment and the luminance concept in Dante
[NOTA-INTERNA-823] 02 p0281 N85-11831

An underground search for massive slow particles (hunting Grand Unified Theory (GUT) monopoles)
[NOTA-INTERNA-821] 02 p0292 N85-11894

Definition of ground test for verification of large space structure control
[NASA-CR-171206] 05 p0602 N85-13838

Ground test experiment for large space structures, appendix I 05 p0603 N85-13847

Plant cell cultures in biological space experiments
05 p0690 N85-14434

Comparison of simulation of weightlessness by Head Down Tilt (HDT) and Water Immersion (WI)
05 p0692 N85-14454

Medication interference with space research: An example from a mass-discrimination experiment on Spacelab 1 05 p0695 N85-14472

Response surface designs
[AD-A147202] 07 p1035 N85-16569

Experiment description 08 p1143 N85-17210

UCB cosmic ray experiment 09 p1417 N85-18941

A preliminary study of a cryogenic equivalence principle experiment on Shuttle
[NASA-CR-171300] 10 p1426 N85-18994

Fluid slosh dynamics of surface tension tanks in three axis stabilized spacecraft
[MBB-UR-E-739-84-O] 11 p1634 N85-20291

Human assembly time versus levels of visual and tactile sensory input: Experimental results for five devices
[AD-A149962] 12 p1909 N85-21980

Investigation of dynamics of radiation spectrum of injection lasers by infrared impulse Fourier spectroscopy
13 p2090 N85-23047

Control Of Flexible Structures (COFS) flight experiment background and description 14 p2236 N85-23864

Electro-science requirements for shuttle-attached antenna flight experiments 14 p2237 N85-23866

Determining optimum service conditions for concentrator mirrors by methods of mathematically planned experiment 14 p2274 N85-24090

An interactive computer package for use with simulation models which performs multidimensional sensitivity analysis by employing the techniques of response surface methodology
[AD-A151956] 16 p2846 N85-27548

Botany facility phase A study. Core payload number 6 EURECA carrier, volume 1
[ESA-CR(P)-1978-VOL-1] 17 p2906 N85-27918

Botany facility phase A study. Core payload number 6 for EURECA carrier, volume 2
[BF-TD-DRD-03-VOL-2] 17 p2906 N85-27919

Laboratory research: A question of when, not if
[AD-A153296] 17 p3048 N85-28867

Optimization of single and multi-component analytical techniques
[HSE-TRANS-10967] 19 p3347 N85-30744

Experiments with stored heavy ions
[DE85-009976] 19 p3356 N85-30802

Efficiency tests of samplers for microbiological aerosols, a review
[FOA-C-40199-B1] 20 p3504 N85-31783

Design of simulation experiments
[FEW-123] 20 p3519 N85-31885

Apparatus for unilateral generation of a homogeneous magnetic field
[DE85-006001] 23 p3928 N85-34345

Experimental lithium system
[DE85-013252] 24 p4094 N85-35382

Model robust response surface designs: Scaling two-level factorials
[AD-A156218] 24 p4143 N85-35686

EXPERIMENTAL BREEDER REACTOR 2

SASSYS-1 computer code verification with EBR-2 test data
[DE85-012119] 24 p4139 N85-35657

EXPERIMENTATION

On thermomechanical testing in support of constitutive equation development for high temperature alloys
[NASA-CR-174879] 15 p2577 N85-25894

High pressure cosmochemistry applied to major planetary interiors: Experimental studies
[NASA-CR-175715] 15 p2679 N85-26544

Sensitivity and performance characterization of DINGU
[DE85-010750] 22 p3754 N85-33269

Experimental studies of chemical reactivity during shock initiation of hexanitrostilbene
[DE85-011726] 22 p3754 N85-33270

Separation of gas mixtures by supported complexes
[DE85-011996] 23 p3912 N85-34236

Evaluation of low-temperature geothermal potential in Utah and Goshen Valleys and adjacent areas, Utah. Part 2: Water temperature and chemistry
[DE85-009344] 23 p3943 N85-34438

Throughfall rate and chemistry studies: Whiteface Mountain
[DE85-012407] 23 p3947 N85-34464

The 1984 biotic studies of Yucca Mountain, Nevada test site, Nye County, Nevada
[DE85-011715] 23 p3951 N85-34487

The impact of supercomputers on experimentation: A view from a national laboratory
[NASA-TM-86822] 23 p3955 N85-34510

Analysis of transient radiation upset in a 16K SRAM
[DE85-008442] 23 p3965 N85-34586

Experimental technique for measuring the isentrope of hydrogen to several megabars
[DE85-014332] 24 p4095 N85-35386

EXPERT SYSTEMS

A relational approach to the development of expert diagnostic systems
[NASA-TM-86288] 01 p0099 N85-10658

Diagnosis via causal reasoning: Paths of interaction and the locality principle
[AD-P003920] 02 p0245 N85-11600

A representation for the functioning of devices that supports compilation of expert problem solving structures: An extended summary
[AD-P003921] 02 p0245 N85-11601

Application of the CSRL language to the design of expert diagnosis systems: The Auto-Mech experience
[AD-P003922] 02 p0245 N85-11602

An expert system for representing procedural knowledge
[AD-P003923] 02 p0245 N85-11603

Failure detection processes by pattern recognition and expert systems
[AD-P003924] 02 p0246 N85-11604

Designing an expert system for training automotive electrical troubleshooting
[AD-P003926] 02 p0246 N85-11606

Artificial intelligence approaches to monitoring system integrity
[AD-P003930] 02 p0246 N85-11610

Expert systems in maintenance diagnostics for self-repair of digital flight control systems
[AD-P003933] 02 p0247 N85-11613

DELTA: An expert system for diesel electric locomotive repair
[AD-P003941] 02 p0248 N85-11621

The ACE (Automated Cable Expert) experiment: Initial evaluation of an expert system for preventive maintenance
[AD-P003943] 02 p0248 N85-11623

LES: (Lockheed Expert System): A model-based expert system for electronic maintenance
[AD-P003944] 02 p0248 N85-11624

On the requirements of expert systems for fault isolation
[AD-P003947] 02 p0249 N85-11627

Memory-based expert systems
[AD-A145612] 02 p0249 N85-11628

Expert systems: The application of new computer methods to corrosion problems
[AERE-M-3395] 03 p0334 N85-12153

Power subsystem automation study
[NASA-CR-171213] 03 p0358 N85-12299

Psychological issues in the design of expert systems
[AD-A146081] 03 p0438 N85-12792

Expert systems in design and manufacture
[DE84-005522] 04 p0550 N85-13496

Minimal cut-set methodology for artificial intelligence applications
[DE84-016674] 04 p0553 N85-13518

A distributed expert system for Space Shuttle flight control 05 p0602 N85-13836

The role of expert systems in remote sensing
05 p0661 N85-14246

The application of artificial intelligence to contract management
[AD-A146681] 06 p0857 N85-15448

Mental models and cooperative problem solving with expert systems
[AD-A147843] 07 p1021 N85-16479

Automatic map name placement system
09 p1341 N85-18438

Expert systems in contract management: A pilot study
[AD-A149363] 10 p1566 N85-19873

ESOP expert system model described
11 p1619 N85-20187

The application of expert systems to corrosion problems
[AERE-M-3445] 12 p1804 N85-21316

An interactive environment for the development of an expert system in ZOG
[AD-A149954] 12 p1915 N85-22025

Characterizing the parallelism in rule-based expert systems
[DE85-002432] 12 p1919 N85-22047

Research Reports: 1984 NASA/ASEE Summer Faculty Fellowship Program
[NASA-CR-171317] 12 p1944 N85-22210

Evaluation of expert systems
12 p1947 N85-22229

An expert system for choosing the best combination of options in a general-purpose program for automated design synthesis
[NASA-TM-86329] 14 p2402 N85-24807

Gordon Conference on Fundamentals of Cybernetics
[AD-A151074] 14 p2408 N85-24842

Diagnosis: Using automatic test equipment and an artificial intelligence expert system
[AD-A151918] 16 p2851 N85-27576

Artificial intelligence in space platforms
[AD-A152078] 16 p2851 N85-27578

Composite loads spectra for select space propulsion structural components: Probabilistic load model development 17 p2912 N85-27954

Evidential reasoning in expert systems for image analysis
[AD-A153379] 17 p3013 N85-28627

Alternative theories of inference in expert systems for image analysis
[AD-A153649] 18 p3170 N85-29646

Expanding expertise by use of an expert system
[DE85-010759] 19 p3344 N85-30723

Data communications-Oriented Production System Language (CPSL)
[DE85-011457] 20 p3440 N85-31352

RESO: Expert system applied to company computer networks
[ENST-84E016] 20 p3518 N85-31874

Myoelectric control of a computer based expert system for flight control
[AD-A154981] 21 p3557 N85-32126

NASA space station automation: AI-based technology review
[NASA-CR-176094] 21 p3558 N85-32134

NASA space station automation: AI-based technology review. Executive summary
[NASA-CR-176096] 21 p3558 N85-32135

Research on an expert system for database operation of simulation-emulation math models. Volume 1, Phase 1: Results
[NASA-CR-176087] 21 p3669 N85-32792

Research on an expert system for database operation of simulation-emulation math models. Volume 2, Phase 1: Results
[NASA-CR-176088] 21 p3669 N85-32793

Design of an expert-system flight status monitor
[NASA-TM-86739] 21 p3669 N85-32794

A strategy planner for NASA robotics applications
[NASA-CR-175319] 22 p3834 N85-33736

Research issues in generating graphical explanations
23 p3959 N85-34539

Generative design in architecture using an expert system 23 p3965 N85-34582

Knowledge engineering application in image processing 23 p3965 N85-34583

Robot environment expert system
[NASA-CR-3915] 23 p3967 N85-34593

Implications of artificial intelligence on the design of future onboard systems
[SFENA-DPS/C/S3/84252A] 23 p3967 N85-34596

Expert systems research in regional resource evaluation: Experiences in the application of microcomputer technologies 24 p4105 N85-35450

AUTOSIM: An automated repetitive software testing tool
[NASA-CR-177930] 24 p4137 N85-35643

EXPIRED AIR

Gas analysis techniques for human physiological measurements in space — Spacelab
[A/6537] 20 p3507 N85-31803

EXPLODING CONDUCTOR CIRCUITS

U CIRCUITS
U EXPLODING WIRES

EXPLODING CONDUCTORS

U EXPLODING WIRES

EXPLODING WIRES

Modular detonator device
[AD-D011232] 03 p0340 N85-12184

Analysis of a potential hot-wire ignition problem
[DE84-017254] 09 p1301 N85-18174

Nonprimary-explosive, hot-wire detonator
[DE85-005195] 12 p1818 N85-21403

Lightning strikes on aircraft. The TRIP 82 experiment and 3-dimensional electromagnetic interferometry
[ONERA-RF-86/7154-PY] 16 p2703 N85-26690
Detonation velocity measurements of the explosives Detasheet C and Amatol
[AD-A152298] 16 p2757 N85-27015

EXPLOITATION
Orphans of the Valley: Abandoned surface mines in the Tennessee Valley. Volume 2: Maps
[DE85-901249] 19 p3301 N85-30485
Marine Sample Exploitation Project: Estimates regarding the sensitivity and technology for the detection of nuclear explosion debris in the marine environment
[DE85-013176] 23 p3947 N85-34462

EXPLORATION
NT LUNAR EXPLORATION
NT MINERAL EXPLORATION
NT OIL EXPLORATION
NT SPACE EXPLORATION
Geothermal exploration in Trans-Pecos, Texas/New Mexico
[DE84-015553] 01 p0064 N85-10424
Polar research in Earth sciences described
08 p1142 N85-17204
The discovery circumstances of Earth-approaching asteroids
[NASA-CR-174327] 08 p1256 N85-17920
Workshop on Remote Sensing/Lineament Applications for Energy Extraction
[DE84-009291] 12 p1875 N85-21763
Some recent deposit modeling efforts
24 p4106 N85-35453

EXPLORER SATELLITES
NT DYNAMICS EXPLORER 1 SATELLITE
NT EXPLORER 10 SATELLITE
NT EXPLORER 43 SATELLITE
NT EXPLORER 46 SATELLITE
NT EXPLORER 50 SATELLITE
NT EXPLORER 51 SATELLITE
NT EXTREME ULTRAVIOLET EXPLORER SATELLITE
NT FAR UV SPECTROSCOPIC EXPLORER
NT IMP
NT INTERNATIONAL SUN EARTH EXPLORER 1
NT INTERNATIONAL SUN EARTH EXPLORER 2
NT INTERNATIONAL SUN EARTH EXPLORER 3
NT INTERNATIONAL SUN EARTH EXPLORERS
NT SOLAR MESOSPHERE EXPLORER
Solar Corona Explorer: A mission for the physical diagnosis of the solar corona
[NASA-TM-87416] 10 p1572 N85-19912

EXPLORER 10 SATELLITE
Discovery of the solar wind 12 p1954 N85-22272

EXPLORER 43 SATELLITE
Reduction and analysis of data from the plasma wave instruments on the IMP-6 and IMP-8 spacecraft
[NASA-CR-175127] 04 p0460 N85-12918

EXPLORER 46 SATELLITE
Impacts on Explorer 46 from an Earth orbiting population 12 p1785 N85-21204

EXPLORER 50 SATELLITE
Reduction and analysis of data from the plasma wave instruments on the IMP-6 and IMP-8 spacecraft
[NASA-CR-175127] 04 p0460 N85-12918

EXPLORER 51 SATELLITE
Wakes and differential charging of large bodies in low Earth orbit 13 p1992 N85-22488

EXPLOSION SUPPRESSION
Explosion-proof properties and hydraulic resistance of fire-barrier elements based on knitted metallic screens
11 p1601 N85-20067

EXPLOSIONS
NT AERIAL EXPLOSIONS
NT CHEMICAL EXPLOSIONS
NT GAS EXPLOSIONS
NT NUCLEAR EXPLOSIONS
NT THERMONUCLEAR EXPLOSIONS
NT UNDERGROUND EXPLOSIONS
NT UNDERWATER EXPLOSIONS
Bulletin of the Faculty of Engineering, Hokkaido University, no. 123
[ISSN-0385-602-X] 04 p0482 N85-13075
Estimation of dynamic stresses around the shot point by scale model experiment 04 p0482 N85-13076
China report: Science and technology
[JPRS-CST-84-001] 04 p0557 N85-13545
Measurement of infrasonic waves from remotely detonated artificial explosion 04 p0557 N85-13546
Numerical reconstruction of part of an actual blast-wave flow field to agree with available experimental data
[UTIAS-TN-251] 07 p0956 N85-16061
Nonlinear wave propagation study
[AD-A147011] 07 p0996 N85-16329
Penguin warhead safety tests
08 p1115 N85-17031
The vulnerability of cast double base rocket motors to thermomechanical attack 08 p1115 N85-17033
Ballistic/detonic transition of propellants
08 p1117 N85-17041
Hazard assessment of a hypothetical large rocket motor 08 p1117 N85-17042
Penetration of short duration airblast into protective structures 09 p1336 N85-18404
Preventing explosive propagation in racks or containers of tactical missiles
[AD-P004342] 10 p1455 N85-19166
Analysis of the natural initiation of vapor explosions
[DE85-000186] 11 p1632 N85-20279
Piezoelectric stress transducer used for measurements of explosions in hard rock 11 p1638 N85-20316
Explosive instability of strong electromagnetic wave in plasma 11 p1719 N85-20817
An analysis of short-to-medium-range seismic attenuation tests using a multilayered viscoelastic seismic propagation model
[AD-A149771] 12 p1889 N85-21856
Biological effects of blast and impact waves
[FOA-C-52006-H4-D7] 12 p1906 N85-21968
Adaptive meshes in the 2DL code
[LA-9938-MS] 12 p1914 N85-22011
Electric and hybrid vehicle demonstration project
[DE85-003939] 13 p2169 N85-23455
Centrifuge impact cratering experiments
13 p2181 N85-23533
Hydrovolcanism 13 p2188 N85-23574
Empirical development of ground acceleration, velocity and displacement for accidental explosions at J5 or the proposed large altitude rocket cell at Arnold Engineering Development Center
[DE85-008324] 16 p2758 N85-27020
Pyrotechnic shock simulation using the controlled response of a resonating bar fixture
[DE85-006537] 16 p2784 N85-27181
Combustion and micro-explosion of water/oil emulsions in high pressure environments
[AD-A152960] 17 p2919 N85-27997
Constitutive modeling for blast-induced wave propagation
[AD-A153576] 18 p3099 N85-29187
Dynamics of vapor explosions
[DE85-006845] 18 p3101 N85-29194
Action of plasma and explosion products on silumins
19 p3242 N85-30100
Study of the explosive combustion of drops of sulphur at high temperatures
[HSE-TRANS-11182] 19 p3252 N85-30163
Strain-path modeling for geo-materials
[AD-A154378] 19 p3286 N85-30380
Supernova explosion in dense clouds in the galaxy and the COS-B gamma-ray sources
[OG-2.5-3] 22 p3869 N85-33960

EXPLOSIVE DEVICES
NT BOMBS (ORDNANCE)
NT DETONATORS
NT EXPLODING WIRES
NT INITIATORS (EXPLOSIVES)
NT SHAPED CHARGES
Approach for service life extension of explosive devices for aircraft escape systems
[NASA-TM-86323] 13 p1971 N85-22381

EXPLOSIVE FORMING
Dynamic compaction of powders
[DE85-001062] 11 p1612 N85-20137
Influence of behavior laws in the explosive deformation of metal plates
[ISL-R-122/83] 16 p2760 N85-27032
Computational methods for the explosive and impact compaction of powders
[AD-A156219] 24 p4139 N85-35653

EXPLOSIVE GASES
U FLAMMABLE GASES

EXPLOSIVE WELDING
Some features of the fabrication of multilayer fiber composites by explosive welding
[NASA-TM-77844] 14 p2248 N85-23932
Examination of the regions of the joint of sheets bonded by the explosive welding technique
[BLL-BISI-TRANS-22352-(9022.06)]
17 p2973 N85-28370
Determination of local deformation during explosive welding
[BLL-M-36279-(5828.4)] 20 p3462 N85-31503

EXPLOSIVES
NT CELLULOSE NITRATE
NT RDX
NT TATB
NT TRINITROTOLUENE
Computer simulation of the shock initiation of detonation in solid explosives
[PML-1984-23] 01 p0033 N85-10207
Eutectic explosives containing ammonium nitrate
[DE84-015705] 01 p0034 N85-10213
The 7-Amino-4,6-Dinitrobenzofuroxan, an insensitive high explosive
[AD-A145665] 02 p0188 N85-11257
Official journey to USA, November 1983. Symposium on the Compatibility of Explosives; Mound Laboratory, Naval Surface Weapons Center
[FOA-C-20548-D1] 04 p0482 N85-13072
Laser for determining the ignition conditions of a pyrotechnic mixture
[FOA-C-20542-D1] 04 p0506 N85-13220
Aircraft accident report, Western Helicopters, Inc., Bell UH-1B, N87701, Valencia, California, July 23, 1982
[PB84-910414] 05 p0594 N85-13780
Effects of surface interactions and mechanical properties of PBXs (plastic bonded explosives) on explosive sensitivity
[AD-A146366] 06 p0773 N85-14944
Deformation, fracture and explosive properties of reactive materials
[AD-A146396] 06 p0774 N85-14945
Making high explosive bodies for shaped charges by casting or pressing. Shaped charge research at Research Institute of National Defence (FOA) in 1972 - 1983, part 1
[FOA-C-20554-D4-PT-1] 07 p0935 N85-15923
Sensitiveness and explosiveness assessment at Perme Waltham Abbey 08 p1115 N85-17029
Numerical simulation of the shock detonation transition 08 p1116 N85-17030
Mass spectrometry/mass spectrometry as a screening method for detecting explosive vapors
[DE85-001276] 09 p1292 N85-18110
Evaluation of the Fundamental Research on Explosives (FRE) program
[DE85-001537] 09 p1301 N85-18172
LX-10 and LX-17 moisture content and release
[DE84-016579] 09 p1301 N85-18173
Incineration of explosives contaminated soils
[AD-P004142] 09 p1347 N85-18478
Polymeric liner selection for military waste impoundments
[AD-P004143] 09 p1348 N85-18479
NATO AC/310 activities report on NATO STANAG 4170 and Allied Ordnance Publication 7 (Manual of Tests for Qualification of Explosive Materials for Military Use)
[AD-P004341] 10 p1454 N85-19165
A thermal-mechanical model of deflagration-to-detonation in granular energetic materials
[AD-P004346] 10 p1455 N85-19170
A summary of the mechanism of delayed detonation
[AD-P004347] 10 p1455 N85-19171
Some aspects of the micromechanics of hot spot formation in energetic materials
[AD-P004348] 10 p1456 N85-19172
Thermodynamics of the reactive flow model
[DE85-004405] 10 p1565 N85-19870
Polymer blends as high explosive binders
[DE85-001210] 11 p1611 N85-20131
Design of explosive logic elements
[DE84-009611] 11 p1614 N85-20146
The response of explosive systems to thermal stimuli. A state-of-the-art assessment
[DE85-000919] 11 p1614 N85-20148
DOE hazard classification for Insensitive High Explosives (IHE)
[DE84-017002] 11 p1614 N85-20149
Waveform control and application of detonation wave in explosives 12 p1820 N85-21420
A comprehensive review of black powder
[AD-A150455] 13 p2039 N85-22769
IHE material qualification tests description and criteria
[DE85-004649] 13 p2040 N85-22770
Detonations of solid explosives
[AD-A152012] 15 p2521 N85-25540
Detonation velocity measurements of the explosives Detasheet C and Amatol
[AD-A152298] 16 p2757 N85-27015
Surveillance program for the dissection and analysis of explosive and pyrotechnic components
[DE85-006105] 16 p2757 N85-27016
A review of safety practices and safety training for the explosives field
[AD-A152295] 16 p2759 N85-27028
Inversion of Rayleigh wave group velocities from high-explosive tests
[AD-A152172] 16 p2783 N85-27175
Detonation behavior of LX-14 and PBX-9404: Theoretical aspect
[DE85-010038] 18 p3084 N85-29076
The shock desensitization of PBX-9404 and composition B-3
[DE85-009604] 18 p3084 N85-29077
Equation of state for detonation products
[DE85-009606] 18 p3084 N85-29079

Diagnostic verification of the GLAS (Goddard Laboratory for Atmospheric Sciences) general circulation model as applied to a case of extratropical maritime explosive cyclogenesis
[AD-A153686] 18 p3148 N85-29494
Deformation, fracture and explosive properties of reactive materials
[AD-A154073] 19 p3251 N85-30157
Burn rates of explosives at high pressures
[DE85-010606] 19 p3251 N85-30159
X-ray photoelectron spectroscopy study of the compatibility of the explosive PETN with candidate plastic bonding materials
[DE85-010604] 19 p3251 N85-30161
SAFEORD: Safety of explosive ordnance databank
[AD-A154058] 19 p3380 N85-30972
Electrochemistry of Hexanitroazobenzene (HNAB)
[DE85-010607] 21 p3565 N85-32171
The determination of dinitrotoluene in single base propellants
[AD-A154672] 21 p3571 N85-32209
TNT equivalency of EAK explosive
[AD-A155737] 21 p3571 N85-32211
Explosive containment study
[DE85-011719] 22 p3753 N85-33267
Sensitivity and performance characterization of DINGU
[DE85-010750] 22 p3754 N85-33269
Experimental studies of chemical reactivity during shock initiation of hexanitrostilbene
[DE85-011726] 22 p3754 N85-33270
Modeling granular explosive detonations with shear band concepts
[DE85-011823] 22 p3754 N85-33271
Hydrazine nitrate based explosives
[ISL-CO-229/84] 22 p3754 N85-33272
Intermolecular explosives
[DE85-009609] 23 p3921 N85-34296
Pressure-shear loading of PBX-9404
[DE85-009862] 23 p3921 N85-34298
Modeling heterogeneous high explosive burn with an explicit hot-spot process
[DE85-009593] 23 p3922 N85-34300
Detonation of condensed explosives: Evolution of knowledge in the last 40 years
[ISL-CO-226/84] 23 p3923 N85-34307
Computational methods for the explosive and impact compaction of powders
[AD-A156219] 24 p4139 N85-35653

EXPONENTIAL FUNCTIONS
NT LOGARITHMS
Simulation uses of the exponential distribution
[AD-A144940] 01 p0112 N85-10756
Likelihood estimation for generalized mixed exponential distributions
[AD-A145675] 02 p0252 N85-11651
A power transformation exponential regression model for censored failure time data
[AD-A148377] 08 p1212 N85-17632
Estimating the scale parameter of an exponential distribution from a sample of time-censored r-th order statistics
[AD-A148060] 09 p1375 N85-18644
Modelling and residual analysis of nonlinear auto-regressive time series in exponential variables
[AD-A149047] 10 p1550 N85-19776
Attainable rates of convergence of maxima
[AD-A150838] 14 p2408 N85-24847
Iteration of exponential functions
15 p2633 N85-26233
Asymptotic expansions of the distribution of test statistics associated with several two parameter exponential distributions
[AD-A151906] 15 p2641 N85-26289
Exponential order statistic models of software reliability growth
[NASA-CR-3909] 20 p3515 N85-31852
Survival function of hypo-exponential distributions
[AD-A155518] 21 p3672 N85-32814

EXPORTS
U INTERNATIONAL TRADE

EXPOSURE
The oxidation behaviour of a 20 percent Cr/25 percent Ni/Nb stabilized stainless steel in carbon dioxide at high temperatures and its improvement by cerium and yttrium
[AERE-R-11228] 01 p0029 N85-10162
Instability in semiconductors exposed to ionizing radiation 02 p0267 N85-11747
NAAQS (National Ambient Air Quality Standards) Exposure Model (NEM) applied to carbon monoxide
[PB84-242551] 06 p0834 N85-15310
Early detection of environmental exposure
[AD-P004039] 06 p0845 N85-15369
Using a Gossen light meter to produce enlarged interpositive film copies from glass plates — astronomical photography 07 p0964 N85-16118
Carotid baroreceptor influences on peripheral circulatory and thermal responses during cold exposure
[AD-A146806] 07 p1015 N85-16447
A crew exposure study. Volume 1: Offshore
[AD-A146884] 07 p1015 N85-16449
Exposure modelling of particle beam lithography
[AD-A147849] 08 p1219 N85-17678
Long-term light induced changes in dark conductivity of kapton
[AD-A148791] 08 p1224 N85-17706
Natural exposure versus chamber simulation
[AD-A149536] 10 p1495 N85-19437
Effects of overall vibration and noise on operational personnel 10 p1523 N85-19606
Mercury health effects update: Health issue assessment
[PB85-123925] 10 p1528 N85-19639
Effect of long-term repeated exposure to high-intensity stationary magnetic field on adrenomedullary activity
12 p1904 N85-21955
Characterization of material surfaces exposed to atomic oxygen on space shuttle missions
12 p1946 N85-22220
The effect of occupational exposure and the body weight to height ratio on exhaled methylene chloride breath concentration in females at one, eighteen and sixty-six hours post exposure 14 p2388 N85-24708
Spectroscopic analysis of radiation-generated changes in tensile properties of a polyetherimide film
[NASA-TP-2429] 15 p2502 N85-25435
A study of the methods for evaluating the noise impact of a proposed airport on a community
15 p2588 N85-25957
Damage caused to polyurethane foams by aging, simulated sunlight exposure, heat and fire
[AD-A152040] 16 p2754 N85-26998
Experiments in microwave exposure in the rat: Body temperature, serum chemistry and the use of chemical restraint
[PB85-156834] 16 p2840 N85-27512
Low-profile fastener
[AD-D011667] 19 p3280 N85-30343
Los Alamos optical materials reliability, maintainability, and exposure testing program
[DE85-011894] 21 p3613 N85-32456
A crew exposure study. Phase II. Volume 2. At sea. Part A
[AD-A155233] 21 p3666 N85-32774
Estimating risks of lead-induced hemoglobin decrements under conditions of uncertainty: Methodology, pilot judgments and illustrative calculations
[DE85-012293] 23 p3952 N85-34493

EXPRESSIONS (MATHEMATICS)
U FORMULAS (MATHEMATICS)

EXPULSION
Electro-expulsive separation system
[NASA-CASE-ARC-11613-1] 18 p3094 N85-29150

EXTENDED DURATION SPACE FLIGHT
U LONG DURATION SPACE FLIGHT

EXTENSIONS
On shrinkage and molecular extension
[AD-A149100] 10 p1451 N85-19144
ODIN: An extensible software environment. Report and user's reference manual
[DE85-008459] 18 p3164 N85-29600

EXTENSOMETERS
Recommendations for the use of Ni-Cr-base alloy extensometers for measurement of creep strain
[NPL-DMA(A)-81] 08 p1164 N85-17342
Some advances in experimentation supporting development of viscoplastic constitutive models
[NASA-CR-174855] 16 p2799 N85-27260
A simple optical extensometer achieving high accuracy
[NPL-DMA(A)-95] 20 p3458 N85-31474
Some advances in experimentation supporting development of viscoplastic constitutive models
20 p3468 N85-31545
Results of an interlaboratory fatigue test program conducted on alloy 800H at room and elevated temperatures
[NASA-CR-174940] 21 p3597 N85-32340
Tensile testing apparatus
[NASA-CASE-LAR-13243-1] 23 p3933 N85-34375

EXTERNAL COMBUSTION ENGINES
Stirling material technology
[NASA-TM-86886] 04 p0472 N85-13007

EXTERNAL STORE SEPARATION
Implementation of the supersonic triplet singularity into the USTORE computer code
[CSIR-NIAST-83/47] 01 p0001 N85-10006
Remote pivot decoupler pylon: Wing/store suppression
[NASA-CASE-LAR-13173-1] 11 p1584 N85-19981
Slide release mechanism — for space shuttle orbiter/external tank connection device
[NASA-CASE-MSC-20080-1] 19 p3279 N85-30334

EXTERNAL STORES
NT PODS (EXTERNAL STORES)
External tank aft cargo carrier
02 p0155 N85-11050
UH-60A external stores support system fixed provision fairings drag determination
[AD-A147188] 07 p0902 N85-15719
ESP (External-Stores Program): A pilot computer program for determining flutter-critical external-store configurations. Volume 3, part 2. Program compilation
[AD-A152271] 16 p2706 N85-26703
ESP (External-Stores Program): A pilot computer program for determining flutter-critical external-store configurations. Volume 1: User's manual
[AD-A152268] 16 p2710 N85-26725
ESP (External-Stores Program): A pilot computer program for determining flutter-critical external-store configurations. Volume 2: Final report on program enhancement and delivery
[AD-A152269] 16 p2711 N85-26726
ESP (External-Stores Program): A pilot computer program for determining flutter-critical external-store configurations. Volume 3, part 1: Program compilation
[AD-A152270] 16 p2711 N85-26727
Flight trials of a modified gulfstream commander carrying external stores
[AD-A153376] 17 p2896 N85-27859
Results of variable enthalpy tests of CPR-488 TIP panels in MSFC Hot Gas Facility
[NASA-CR-170669] 24 p4072 N85-35237

EXTERNAL SURFACE CURRENTS
SEPAC (space experiments with particle accelerators)
01 p0014 N85-10085
Rocket body charge neutralization processes in ARAKS experiment (data from two launches)
13 p1980 N85-22426
Electric field effects on ion currents in satellite wakes
13 p1991 N85-22485
Calculation of secondary-electron escape currents from inclined-spacecraft surfaces in a magnetic field
13 p1992 N85-22491
Surface interactions and high-voltage current collection 13 p1993 N85-22493
Development of a continuous broad-energy-spectrum electron source 13 p1995 N85-22507
Development and testing of a spacecraft surface potential monitor 13 p2007 N85-22562

EXTERNAL TANKS
Vibration, acoustic, and shock design and test criteria for components on the Solid Rocket Boosters (SRB), Lightweight External Tank (LWT), and Space Shuttle Main Engines (SSME)
[NASA-RP-1127] 01 p0081 N85-10405
External tank aft cargo carrier
02 p0155 N85-11050
The variable polarity plasma arc welding process: Its application to the Space Shuttle external tank
[NASA-TM-86482] 05 p0641 N85-14115
Preliminary airworthiness evaluation AH-1S (MC) helicopter with external fuel tanks installed
[AD-A148091] 08 p1084 N85-16865
Space shuttle external tank performance improvements: The challenge 08 p1094 N85-16916
External tank processing from barge to pad
08 p1096 N85-16927
Cryogenic propellant management: Integration of design, performance and operational requirements
08 p1098 N85-16939
External tank GH2 vent arm 08 p1102 N85-16969
Thermal design of the space shuttle external tank
08 p1103 N85-16977
BI-PAC F-15 external fuel tank container modification
[AD-A148836] 09 p1280 N85-18053
STS-1 Pogo analysis
[NASA-TM-87433] 11 p1591 N85-20007
Artificial gravity: Tethers and containers
11 p1645 N85-20367
Results of aeroheating DFI and ET design-data test on a 0.0175-scale model 60-OTS conducted in the Von Karman Gas Dynamics Facility (VKF) 40' supersonic and the 50' hypersonic wind tunnels A and C
[NASA-CR-167693] 13 p1988 N85-22466
Results of a M = 5.3 heat transfer test of the integrated vehicle using phase-change paint techniques on the 0.0175-scale model 56-OTS in the NASA/Ames Research Center 3.5-foot hypersonic wind tunnel
[NASA-CR-167695] 13 p1988 N85-22468
Development of acceptance criteria for batches of silane primer for external tank thermal protection system bonding applications
[NASA-CR-171428] 14 p2259 N85-23998

Development of acceptance criteria for batches of silane primer for external tank thermal protection system bonding applications
[NASA-CR-171436] 15 p2518 N85-25523
Development of acceptance criteria for batches of silane primer for external tank thermal protection system bonding applications
[NASA-CR-175650] 16 p2754 N85-26995
Analysis of heat-transfer measurements from 2 AEDC wind tunnels on the Shuttle external tank
[NASA-CR-171470] 17 p2957 N85-28263
Slide release mechanism — for space shuttle orbiter/external tank connection device
[NASA-CASE-MSC-20060-1] 19 p3279 N85-30334
Results of a study to build a gamma-ray telescope in an external tank
[OG-9.3-3] 23 p4027 N85-34958

EXTINCTION
NT INTERSTELLAR EXTINCTION
Atmospheric extinction in critical environments
[AD-A146102] 03 p0396 N85-12527
Extinction by dielectric particles at optical and infrared wavelengths
[AD-A146305] 03 p0413 N85-12640
Dust in the region of Herbig-Haro objects: The case of NGC 1999 11 p1747 N85-20991
The UV extinction laws in two very young clusters, NGC 6530 in the galaxy and NGC 2100 in the LMC
11 p1748 N85-20994
On the inversion of the lidar equation
[AD-A149653] 12 p1856 N85-21641
Phase function, backscatter, extinction, and absorption for standard radiation atmosphere and El Chichon aerosol models at visible and near-infrared wavelengths
[NASA-TM-86379] 12 p1892 N85-21874
Characteristics and behavior of atmospheric aerosols; application to prediction of infrared extinction
[AD-A150691] 14 p2372 N85-24665
SAM II measurements of the polar stratospheric aerosol. Volume 6: April to October 1981
[NASA-RP-1141] 16 p2825 N85-27422
Visibility and vertical structure measurements in southern Germany
[AD-A154714] 21 p3635 N85-32574
Ice fog as an electro-optical obscurant
[AD-A155059] 21 p3705 N85-33015

EXTINGUISHERS
U FIRE EXTINGUISHERS

EXTINGUISHING
Vortex dynamics simulation of conserved scalar dissipation 22 p3745 N85-33210

EXTRACTION
NT GEOTHERMAL ENERGY EXTRACTION
NT ION EXTRACTION
NT SOLVENT EXTRACTION
Extractor for spring-lock pin connectors
[AD-D011235] 01 p0043 N85-10280
Positron flux concentrator: An update
[DE84-016260] 04 p0561 N85-13576
Solar cell coverslide extraction method and apparatus
[AD-D011275] 05 p0669 N85-14306
Application of extraction replicas and analytical electron microscopy to precipitate phase studies
[DE85-001253] 06 p0769 N85-14919
Analyses of energy extraction efficiency of unstable resonators
[AD-A146391] 06 p0813 N85-15161
Extracting embedded generalized networks from linear programming problems
[AD-A147565] 07 p1033 N85-16556
Parachute extraction device for ultralight gliders
[CH-643499-A5] 16 p2699 N85-26663
Slow extraction of LAMPF 2
[DE85-010744] 19 p3356 N85-30805
Soil extraction kit
[AD-D011736] 22 p3742 N85-33190
Geologic, technical, and economic sensitivity analysis in support of the GRI (Gase Research Institute) tight gas reservoirs project area
[PB85-192276] 22 p3802 N85-33559
Use of a minimum-ellipse criterion in the study of ion-beam extraction systems
[DE85-012670] 24 p4148 N85-35721
Measurement of uranium enrichment for gaseous uranium at low pressure
[DE85-012697] 24 p4150 N85-35733
Synchronous timing of multi-energy fast beam extraction during a single AGS cycle
[DE85-011829] 24 p4158 N85-35781

EXTRAGALACTIC LIGHT
U EXTRATERRESTRIAL RADIATION
U LIGHT (VISIBLE RADIATION)

EXTRAGALACTIC MEDIA
U INTERGALACTIC MEDIA

EXTRAGALACTIC RADIO SOURCES
NT RADIO GALAXIES
Documentation for the machine-readable version of A Catalogue of Extragalactic Radio Source Identifications (Veron-Cetty and Veron 1983)
[NASA-TM-87373] 03 p0405 N85-12587
Dynamical models for radio jets
03 p0449 N85-12854
VLBI solutions for the time variation of DSN baselines: 1978 - 1983 05 p0623 N85-13983
Metric-wave and decimetric-wave aperture synthesis systems (review) 06 p0762 N85-14996
Research in geodesy based upon radio interferometric observations of extragalactic radio sources
[AD-A147581] 07 p0988 N85-16280
The extragalactic nature of H0323+022
08 p1237 N85-17802
Morphology and optical polarization of the 3C 273 jet — radio jet 08 p1238 N85-17803
Spatially resolved optical spectroscopy of the radio jet of the X-ray galaxy NGC 2110 08 p1238 N85-17804
Characteristics of X-ray spectra from galactic and extragalactic X-ray sources 08 p1239 N85-17811
Comments on the physics of active galactic nuclei
08 p1240 N85-17823
The origin of the X-ray background
08 p1243 N85-17841
VLBI observations of compact double radio sources
09 p1417 N85-18940
Arcsecond positions for milliarcsecond VLBI nuclei of extragalactic radio sources. Part 3: 74 sources
10 p1463 N85-19225
Jets in galaxies 12 p1958 N85-22309
All-Union conference of radio astronomers
13 p1977 N85-22406
Extragalactic origin or gamma-ray bursts, revision 1
[DE85-005822] 15 p2686 N85-26588
Evolution of the luminosity function of extragalactic objects
[NASA-CR-175977] 18 p3201 N85-29860
Frequent observations of extragalactic compact sources at 24 GHz 19 p3386 N85-31003
New VLBI technology developments
20 p3491 N85-31702
Variations in the small-scale galactic magnetic field and short time-scale intensity variations of extragalactic radio sources 20 p3549 N85-32084
Observation of gamma-rays from LMC X-4 above 10(16) eV
[OG-2.6-10] 22 p3870 N85-33972
Search for TeV gamma rays from extragalactic sources and the Galactic Center
[OG-2.7-1] 22 p3871 N85-33976
Search for gamma-rays from M31 and other extragalactic objects
[OG-2.7-3] 22 p3871 N85-33977
Energy spectrum of extragalactic gamma-ray sources
[OG-2.7-13] 22 p3872 N85-33986
Ultrahigh energy gamma rays: Carriers of cosmological information
[OG-2.7-14] 22 p3872 N85-33987
Propagation of cosmic rays and new evidence for distributed acceleration
[OG-8.3-5] 23 p4022 N85-34924

EXTRAPOLATION
Signal processing algorithms
[AD-A145748] 03 p0406 N85-12590
Searching for impact craters using space shuttle photography 06 p0889 N85-15645
Combustion kinetics of metal oxide and halide radicals
[AD-A148521] 08 p1122 N85-17076
A note on the prediction error for small time lags into the future
[AD-A148221] 08 p1215 N85-17654
Extrpolation in finite element analysis
09 p1331 N85-18365
Fixed vs. variable order Runge-Kutta
[DE85-001320] 09 p1374 N85-18639
Proposed preliminary design criteria model environment for the 1990's 12 p1784 N85-21194
Real-time enhancement of a climatology or forecast of ocean thermal structure using observed ocean temperatures
[AD-A151118] 15 p2604 N85-26049
Extrapolation methods for multi-dimensional quadrature of singular and regular integrand functions
[DE85-009665] 18 p3172 N85-29655
Extrapolation methods in the finite element method
[BONNER-MATHE-SCHR-156]
19 p3345 N85-30729
An objective analysis technique for extrapolating tidal fields 20 p3493 N85-31715
Changes in lattice cell parameter of film intermetallic compounds RT2
[BLL-M-35874-(5828.4)] 23 p3915 N85-34261

EXTRATERRESTRIAL ENVIRONMENTS
NT CHROMOSPHERE
NT DEEP SPACE
NT HELIUM HYDROGEN ATMOSPHERES
NT INTERPLANETARY SPACE
NT INTERSTELLAR SPACE
NT JUPITER ATMOSPHERE
NT LUNAR ATMOSPHERE
NT MARS ATMOSPHERE
NT MARS ENVIRONMENT
NT NEPTUNE ATMOSPHERE
NT PLANETARY ATMOSPHERES
NT PLANETARY ENVIRONMENTS
NT SATELLITE ATMOSPHERES
NT SATURN ATMOSPHERE
NT SOLAR ATMOSPHERE
NT STELLAR ATMOSPHERES
NT URANUS ATMOSPHERE
NT VENUS ATMOSPHERE
The velocity-age relation for B and A stars
05 p0740 N85-14782
Natural environment design criteria for the Space Station definition and preliminary design
[NASA-TM-86498] 12 p1789 N85-21222

EXTRATERRESTRIAL INTELLIGENCE
The search for extraterrestrial intelligence
15 p2689 N85-2[illegible]
Where is everybody? An account of Fermi's question
[DE85-011898] 19 p3383 N85-3[illegible]

EXTRATERRESTRIAL LIFE
The impact ejection of living organisms into space
15 p2682 N85-2[illegible]
Microbial ecology of extreme environments: Antarctic yeasts and growth in substrate-limited habitats
[NASA-CR-176005] 19 p3326 N85-30[illegible]
Where is everybody? An account of Fermi's question
[DE85-011898] 19 p3383 N85-3[illegible]

EXTRATERRESTRIAL MATTER
NT COSMIC GASES
NT COSMIC PLASMA
NT INTERSTELLAR GAS
NT NEUTRAL GASES
Minor elements in relict olivine grains of deep-sea spheres: Match with Mg-rich olivines from C2 meteorites 06 p0683 N85-15610
Activities report of the Institute for Extraterrestrial Physics
[MPI-PAE/EXTRATERR-187] 17 p3053 N85-28[illegible]
Lead and uranium group abundances in cosmic rays
[OG-7.1-3] 23 p4013 N85-34[illegible]

EXTRATERRESTRIAL RADIATION
NT CIRCUMSOLAR RADIATION
NT EXTRATERRESTRIAL RADIO WAVES
NT GALACTIC COSMIC RAYS
NT GALACTIC RADIATION
NT GALACTIC RADIO WAVES
NT GAMMA RAY BURSTS
NT INTERSTELLAR RADIATION
NT LUNAR RADIATION
NT NORTH POLAR SPUR (ASTRONOMY)
NT PLANETARY RADIATION
NT PRIMARY COSMIC RAYS
NT RADIO BURSTS
NT SOLAR CORPUSCULAR RADIATION
NT SOLAR COSMIC RAYS
NT SOLAR ELECTRONS
NT SOLAR NEUTRINOS
NT SOLAR PROTONS
NT SOLAR RADIATION
NT SOLAR RADIO BURSTS
NT SOLAR RADIO EMISSION
NT SOLAR WIND
NT SOLAR X-RAYS
NT STELLAR RADIATION
NT STELLAR WINDS
NT SUNLIGHT
NT TYPE 3 BURSTS
NT TYPE 4 BURSTS
NT ZODIACAL LIGHT
Fluctuations during observations of extraterrestrial sources from outer space through Earth's atmosphere
07 p0953 N85-16040
Cosmology 07 p1056 N85-16701
IUE spectroscopy of extragalactic H H regions
11 p1745 N85-20974
Research in particles and fields
[NASA-CR-175472] 12 p1963 N85-22337
Space radiation monitor observations from Salyut-4 orbital station 15 p2482 N85-25317
Spectroscopic analysis of radiation-generated changes in tensile properties of a polyetherimide film
[NASA-TP-2429] 15 p2502 N85-25435
Space radiation studies — Spacelab 2 Payload
[NASA-CR-171410] 15 p2665 N85-26884

Activities report of the Institute for Extraterrestrial Physics
[MPI-PAE/EXTRATERR-187] 17 p3053 N85-28898
Radio counterparts of galactic gamma-ray sources
20 p3549 N85-32085
Results from radiation monitoring equipment experiments on STS-41C, 41D, 41G and 51A
[AD-A154676] 21 p3560 N85-32142
Nineteenth International Cosmic Ray Conference. Conference program and author index
[NASA-CP-2376] 22 p3860 N85-33901
Standard value for the radiation length in air
[HE-4.4-4] 24 p4193 N85-36013
Samarkand complex setup for investigation of cosmic ray variation in the energy range of 7 10 (9) - 10 (15) eV
[HE-4.6-14] 24 p4198 N85-36050
High energy neutrino astronomy with MACRO
[HE-5.3-12] 24 p4203 N85-36106

EXTRATERRESTRIAL RADIO WAVES
NT GALACTIC RADIO WAVES
NT NORTH POLAR SPUR (ASTRONOMY)
NT RADIO BURSTS
NT SOLAR RADIO BURSTS
NT SOLAR RADIO EMISSION
NT TYPE 3 BURSTS
NT TYPE 4 BURSTS
Solar radio bursts, proton events and geomagnetic activity
[AD-A149018] 10 p1571 N85-19906
Forecast verification of the 10.7 centimeter solar flux and the Ap daily geomagnetic activity indices
[AD-A152959] 17 p2993 N85-28499
High energy radiation from neutron stars
[DE85-014353] 24 p4169 N85-35843

EXTRATERRESTRIAL RESOURCES
Studies on the processing methods for extraterrestrial materials
[NASA-CR-175776] 16 p2716 N85-26768
Hydrogen recovery from extraterrestrial materials using microwave energy
[DE85-006717] 16 p2883 N85-27789

EXTRATERRESTRIAL ROVING VEHICLES
U ROVING VEHICLES

EXTRAVEHICULAR ACTIVITY
EVA of cosmonauts Savitskaya and Dzhanibekov
02 p0158 N85-11076
Commentary on hand tool used in cosmonaut EVA
02 p0159 N85-11077
Further details in welding, spray-coating tool
02 p0159 N85-11078
The human role in space. Volume 1: Executive summary
[NASA-CR-171223] 04 p0546 N85-13473
Aerospace Safety Advisory Panel
[NASA-TM-87426] 13 p1970 N85-22373
Astronaut hazard during free-flight polar EVA
13 p1997 N85-22522
A concept for a mobile remote manipulator system
14 p2236 N85-23859
Assembly Concept for Construction of Erectible Space Structure (ACCESS) neutral buoyancy testing results
14 p2236 N85-23862
National Space Transportation Systems Program mission report
[NASA-TM-87454] 14 p2242 N85-23899
The human role in space (THURIS)
18 p3158 N85-29557
Experiences with neutral buoyance testing mockups
18 p3159 N85-29571
Space station automation and robotics study. Operator-systems interface
[NASA-CR-176095] 22 p3736 N85-33172

EXTRAVEHICULAR MOBILITY UNITS
Challenges in the development of the shuttle extravehicular mobility unit 08 p1095 N85-16922
Swing-arm beam erector (SABER) concept for single astronaut assembly of space structure
[NASA-TP-2379] 10 p1429 N85-19015

EXTREMA
U RANGE (EXTREMES)

EXTREME ULTRAVIOLET EXPLORER SATELLITE
The 1986 National Aeronautics and Space Administration authorization
[GPO-47-635] 24 p4166 N85-35829

EXTREME ULTRAVIOLET RADIATION
A normal-incidence monochromator branch line on the FEL-undulator for experimental studies in the 5 to 30 eV region
[DE84-014379] 04 p0505 N85-13225
Voyager EUV and FUV observations
06 p0875 N85-15554
Absorption and emission of EUV radiation by the local ISM 06 p0876 N85-15563
Measuring EUV line emission from the hot interstellar medium 06 p0880 N85-15595
Spectroscopic instrumentation for Tokamak diagnostics 09 p1368 N85-18732
Research in extreme ultraviolet and far ultraviolet astronomy
[NASA-CR-174432] 10 p1570 N85-19902
Solar flare and IMF sector structure effects in the lower ionosphere 11 p1664 N85-20486
Edge diagnostics for tandem mirror machines
[DE85-001209] 11 p1733 N85-20902
Tasks for observations of close binary systems in the extreme ultraviolet 11 p1757 N85-21054
Studies on radiative collisional and ultraviolet lasers
[AD-A151004] 14 p2310 N85-24296
Free electron lasers for the EUV spectral region
[DE85-006804] 15 p2563 N85-25815
Review of short wavelength lasers
[DE85-009858] 18 p3114 N85-29277
Four-photon resonant third harmonic generation
[DE85-010070] 19 p3367 N85-30883

EXTREMELY HIGH FREQUENCIES
The Finnish approach to microwave remote sensing of snow 05 p0656 N85-14212
The development of a 90 GHz solid state noise source
[CD.6500695] 05 p0733 N85-14715
Potential affiliate stations to work with the EVN — European VLBI Network; QUASAT
07 p1057 N85-16708
Design of mode converters from TE circular om modes in circular waveguides to TE rectangular mo modes in rectangular waveguides for high power applications in the frequency range 1 to 30 GHz
[IPF-84-7] 09 p1395 N85-18781
The effects of mode impurity of Ka-band system performance 10 p1463 N85-19227
EHF air-to-air communications
10 p1469 N85-19273
EHF MILSATCOM systems for tactical users
11 p1709 N85-20755
Tactical military communications by satellite relay at high latitudes 11 p1709 N85-20756
Design and calibration of a 35GHz dielectrometer
[AD-P004363] 12 p1826 N85-21457
Digital processing of passive Ka-band microwave images for sea-ice classification
[AD-A150686] 14 p2347 N85-24511
Analysis of space diversity techniques for EHF (Extremely High Frequency) satellite downlinks
[AD-A151900] 15 p2544 N85-25705
Radiometry: A useful prediction tool — atmospheric attenuation
[ESA-SP-1071] 20 p3399 N85-31084
Preliminary investigations concerning a 90 GHz radiometer satellite experiment
[ESA-TT-860] 20 p3420 N85-31225
Thirty GHz low noise GaAs FET amplifiers — satellite-ground communication
[CD.6500686] 20 p3449 N85-31413
An experimental study of dielectric rod antennas for millimeter-wave imaging applications
[AD-A155832] 24 p4086 N85-35328

EXTREMELY LOW FREQUENCIES
Experimental determination of propagation rate of ELF signals employed by Omega radio navigation system for phase measurements 06 p0793 N85-15066
Electrostatic wave observation during a space simulation Beam-Plasma-Discharge (BPD)
[NASA-CR-174286] 07 p1045 N85-16639
Extremely Low Frequency (ELF) Communications System Ecological Monitoring Program: Summary of 1983 progress
[AD-A147704] 08 p1151 N85-17265
Compilation of annual reports of the Navy ELF (Extremely Low Frequency) communications system ecological monitoring program. Volume 1: Tabs A-E
[AD-A148326] 08 p1152 N85-17272
Compilation of annual reports of the Navy ELF (Extremely Low Frequency) communications system ecological monitoring program (1983). Volume 2: Tabs F-J
[AD-A148327] 08 p1152 N85-17273
Energetic electron anisotropy and ELF waves onboard GEOS. How does quasi-linear diffusion work
14 p2366 N85-24623
ELF chorus in the Earth's outer magnetosphere
14 p2366 N85-24624
Conjugacy of ELF-VHF emissions near L=6 — chorus phenomenon, hiss 14 p2367 N85-24629
Biological and human health effects of extremely low frequency electromagnetic fields. Post-1977 literature review
[AD-A152731] 17 p2999 N85-28539
Numerical modeling of subsurface communication
[DE85-012818] 21 p3577 N85-32249

EXTREMELY LOW RADIO FREQUENCIES
The propagation and growth of whistler mode waves generated by electron beams in Earth's bow shock
[AD-A145572] 02 p0228 N85-11492
Energy correlation between natural extra-low-frequency noises at various frequencies 06 p0784 N85-15010
Propagation of electromagnetic fields along the sea/sea-bed interface
[AD-A149523] 10 p1467 N85-19257
The ULF/ELF/VLF electromagnetic fields generated in a sea of finite depth by elevated dipole sources
[AD-A149638] 12 p1828 N85-21470
Dielectric measurements in infralow-frequency band
13 p2087 N85-23034
Spatial characteristics of ULF pulsations and their modification by the ionosphere: IMS results
14 p2364 N85-24612
An evaluation of the contributions of the IMS to experimental and theoretical studies of ULF plasma
14 p2365 N85-24614
Results of ULF-wave investigations in the USSR
14 p2369 N85-24644
Satellite, auroral radar and ground magnometer observations of transient ULF pulsations
14 p2369 N85-24645

EXTREMUM VALUES
NT LIMITS (MATHEMATICS)
NT MAXIMA
Distributions of extreme values of sequences of autocorrelated random variables
[PB84-240746] 06 p0858 N85-15456
Master Fit users' guide, version 1.0
[DE85-014199] 24 p4140 N85-35667

EXTRUDING
NT PULTRUSION
Optimizing conductive polymer compounds
[BMFT-FB-T-84-145] 03 p0338 N85-12177
Optimization of the die entrance shape for polymeric extrusion
[DE85-001586] 06 p0772 N85-14937
Computer-aided design of extrusion dies by metal-flow simulation 06 p0797 N85-15094
Modelling temperature changes during hot working operations 06 p0798 N85-15095
Materials of the fourth scientific-technical Conference on Questions of the Extrusion of Metals (Selected articles)
[AD-A148578] 08 p1130 N85-17121
High temperature properties of equiatomic FeAl with ternary additions
[NASA-TM-86936] 10 p1439 N85-19072
Evaluation of 7010 aluminium alloy extruded tube in the T76 condition
[BR92019] 11 p1596 N85-20039
Characterization of poly(ethylene oxide) drawn by solid state extrusion
[AD-A150967] 14 p2260 N85-24006
Effect of initial structure on texture of pressed titanium alloy bars 15 p2515 N85-25518
Strain fields for aluminum at different tooling temperatures and extrusion ratios
[DE85-008257] 18 p3075 N85-29020
Downdraw extrusion of ULE(TM) glass
[AD-A153783] 18 p3079 N85-29048
Characterization of modified 9 Cr Mo steel extruded pipe
[DE85-012056] 23 p3941 N85-34430
Solid-state co-extrusion of nylon 6 gel
[AD-A156187] 24 p4082 N85-35298
Establishment of a Computer-Aided Design (CAD)-Computer-Aided Manufacturing (CAM) process for the production of cold forged gears
[AD-A155756] 24 p4137 N85-35644

EYE (ANATOMY)
NT NYSTAGMUS
NT OCULOMOTOR NERVES
NT RETINA
A limbus-sensing eye movement recorder
[AD-A144772] 01 p0049 N85-10323
Eyes for computers 07 p1012 N85-16428
The effect of modified spectacles on the field of view of the helmet display unit of the integrated helmet and display sighting system
[AD-A148693] 09 p1281 N85-18055
Photorefractor ocular screening system
[NASA-CASE-MFS-26011-1SB]
11 p1692 N85-20639
Retinal information mapping system
[AD-D011531] 12 p1849 N85-21601
Application of the system identification technique to goal-directed saccades
[AD-A150132] 12 p1906 N85-21967
Technical support for microwave experiments on the eye lens
[AD-A149702] 12 p1933 N85-22144

Applications of compound eye configurations to smart sensor design
[AD-A150731] 14 p2420 N85-24935
Test and evaluation of the 2.4-micron photorefractor ocular screening system
[NASA-TM-86492] 15 p2615 N85-26115
The 10 MWe solar thermal central receiver pilot plant: Beam safety tests and analyses
[SAND-83-8035] 16 p2818 N85-27379
Pursuit tracking performance and flash disruption: The effects of training the non-dominant eye on target reacquisition
[AD-A153404] 17 p2999 N85-28541
Predictive model of electron beam induced flashblindness
[AD-A155260] 21 p3664 N85-32763

EYE DISEASES
NT CATARACTS
Photorefractor ocular screening system
[NASA-CASE-MFS-26011-1SB]
11 p1692 N85-20639

EYE MOVEMENTS
NT NYSTAGMUS
NT SACCADIC EYE MOVEMENTS
A limbus-sensing eye movement recorder
[AD-A144772] 01 p0049 N85-10323
Eyelid motion sequences predictive of decision errors
[AD-A145702] 02 p0235 N85-11531
Development and evaluation of a performance-based test of saccadic and vestibulo-ocular control
[AD-A145367] 02 p0237 N85-11545
Computerized sleep staging by detecting eye and hand movement, delta EEG activity and EMG, using portable solid state technique — spaceborne experiments
05 p0695 N85-14475
Visual attention to radar displays
05 p0704 N85-14514
No fatigue effect on blink rate
05 p0712 N85-14564
Neuro-linguistic programming: Eye movements as indicators of representational systems
[AD-A147541] 07 p1016 N85-16454
Vestibular and oculomotor function during Gz variations 11 p1693 N85-20645
Prediction of seasickness susceptibility
11 p1693 N85-20647
Sensory and motor properties of the cerebellar uvula and modulus 15 p2613 N85-26104
Eye movement in response to single and multiple targets
[AD-A151115] 15 p2617 N85-26126
Electrooculographic measurement, fatigue and variability of performance in simulated aircraft flight
19 p3217 N85-29948
An error-dependent model of instrument-scanning behavior in commercial airline pilots
[NASA-CR-3908] 21 p3665 N85-32765
The human engineering eye movement measurement research facility
[AD-A156099] 24 p4132 N85-35613

F

F CENTERS
U COLOR CENTERS
F DISPLAYS
U F REGION
F LAYER
U F REGION
F REGION
NT F 2 REGION
Global maps of foF2 derived from observations and theoretical values
[AD-A145866] 03 p0392 N85-12509
Behavior of the ionospheric F region in low latitudes and in the equatorial region of Brazil during strong magnetic storms in the 1978 to 1983 period
[INPE-3231-PRE/581] 05 p0675 N85-14333
Nocturnal increases of ionization in the ionospheric F region in the low latitude of Brazil during magnetic storms
[INPE-3271-PRE/596] 05 p0675 N85-14334
Experience with proposed improvements of the International Reference Ionosphere (IRI)
[PB84-235670] 05 p0678 N85-14353
Observations of plasma bubbles and their zonal drift using polarimeters
[INPE-3219-PRE/572] 06 p0729 N85-14688
Dynamics of the low-latitude thermosphere and ionosphere 09 p1351 N85-18501
Ionspheric effects of seasonal and diurnal variations of electric fields in equatorial F-region
14 p2338 N85-24459
Influence of internal gravity waves on F layer
14 p2338 N85-24460
Anisoptropy of Alfven wave absorption in ionosphere
14 p2339 N85-24464
Fabry-Perot interferometer and skymapping photometer determinations of midlatitude f-region neutral winds and temperatures and airglow enhancement/depletions
[AD-A150730] 14 p2373 N85-24866
Fast ion polarization jet in subauroral F-layer and its manifestation in structure of high latitude ionosphere
15 p2480 N85-25306
Influence of tropical F region in ionosphere on propagation of short radio waves
16 p2721 N85-26798
A study of the generation mechanisms of high latitude and equatorial F-region irregularities using DE-2 data
[NASA-CR-175745] 16 p2825 N85-27423
Equatorial F-region irregularity latitudinal extension and dynamo electric field
[INPE-3494-PRE/731] 16 p2826 N85-27433
Dependence of equatorial F-region plasma bubble rise velocity and dynamo electric field on solar cycle
[INPE-3439-PRE/696] 16 p2826 N85-27434
EISCAT electron density studies
[AD-A152820] 17 p2993 N85-28498
Small-scale structure of ionospherie F-region
19 p3297 N85-30440
Equitorial scintillations: Advances since ISEA-6
[AD-A154962] 21 p3631 N85-32559

F 2 REGION
Response of the F2 layer to the polarity of the interplanetary magnetic field
[REPT-561] 03 p0377 N85-12404
Foreshortened short-wave scattering on artificial ionospheric inhomogeneities 14 p2340 N85-24468

F-80 AIRCRAFT
U T-33 AIRCRAFT

F-8 AIRCRAFT
Analytical redundancy management mechanization and flight data analysis for the F-8 digital fly-by-wire aircraft flight control sensors
[NASA-CR-170396] 06 p0757 N85-14844
F-8 refueling boom ground vibration test
[NASA-TM-84914] 07 p0902 N85-15713

F-14 AIRCRAFT
A safety evaluation of the relocation of the ACM (Air Combat Maneuver) panel in the F-14 ( )/AIP (Avionics Integration Program)
[AD-A149596] 12 p1777 N85-21158
F-14A aircraft high-speed flow simulations
[NASA-CR-172559] 14 p2209 N85-23702

F-15 AIRCRAFT
The F-15 flight loads tracking program
07 p0894 N85-15666
Predicted performance benefits of an adaptive digital engine control system of an F-15 airplane
[NASA-TM-85016] 07 p0905 N85-15729
BI-PAC F-15 external fuel tank container modification
[AD-A148836] 09 p1280 N85-18053
Impacts of Space Shuttle thermal protection system tile on F-15 aircraft vertical tile
[NASA-TM-85904] 12 p1792 N85-21245
Effects of inlet distortion on a static pressure probe mounted on the engine hub in an F-15 airplane
[NASA-TP-2411] 13 p1974 N85-22394
Diagnosis: Using automatic test equipment and an artificial intelligence expert system
[AD-A151918] 16 p2851 N85-27576
Fault detection and accommodation testing on an F100 engine in an F-15 airplane
[NASA-TM-86735] 19 p3219 N85-29962
Recent developments in rotary-balance testing of fighter aircraft configurations at NASA Ames Research Center
[NASA-TM-86714] 21 p3551 N85-32090
Performance improvements of a highly integrated digital electronic control system for an F-15 airplane
[NASA-TM-86746] 21 p3556 N85-32120
Development of control laws for a flight test maneuver autopilot for an F-15 aircraft
[NASA-TM-86736] 22 p3730 N85-33122

F-16 AIRCRAFT
F-16 force management, yesterday, today and tomorrow 07 p0895 N85-15674
Implications of guidance and control technology on human factors considerations 10 p1532 N85-19656
Automated radome testing
[AD-P004362] 12 p1826 N85-21456
Dynamic wind-tunnel testing of active controls by the NASA Langley Research Center
13 p1966 N85-22353
Multivariable control law design for the AFTI/F-16 with a failed control surface
[AD-A151908] 15 p2474 N85-25271
Flight control system reconfiguration design using quantitative feedback theory
[AD-A151771] 16 p2710 N85-26722
Application of AFTI/F-16 task-tailored control modes in advanced multirole fighters 17 p2901 N85-27888
Selection procedures for F-16 pilots in the Belgian Air Force 20 p3510 N85-31822

F-17 AIRCRAFT
Dynamic wind-tunnel testing of active controls by the NASA Langley Research Center
13 p1966 N85-22353

F-18 AIRCRAFT
The F-18: A new era for human factors
10 p1534 N85-19671

F-20 AIRCRAFT
Development of the F-20 nose radome
[AD-P004374] 12 p1827 N85-21469

F-27 AIRCRAFT
Safety recommendation(s), A-84-126 through -133
[REPT-3996C/41] 15 p2468 N85-25221
Static longitudinal stability and control characteristics of the Fokker F27 Friendship calculated by simple handbook methods
[VTH-LR-394] 16 p2711 N85-26728

F-104 AIRCRAFT
Testing of the digital flight control system of the German CCV fighter experimental aircraft
13 p1968 N85-22361

F-106 AIRCRAFT
Electromagnetic resonances of cylinders and aircraft model with resistive wires
[NASA-CR-174203] 06 p0838 N85-15319
Comparison of wind velocity in thunderstorms determined from measurements by a ground-based Doppler radar and an F-106B airplane
[NASA-TM-86348] 16 p2703 N85-26687

F-111 AIRCRAFT
Interactions between F-111 fuselage fuel tank sealants. Part 2: Variation in performance properties of polysulfides after contact with polyester degradation products
[AD-A149777] 12 p1812 N85-21368
Automatic flight control modes for the AFTI/F-111 mission adaptive wing aircraft 16 p2714 N85-26756
Automatic flight control modes for the AFTI/F-111 mission adaptive wing aircraft 17 p2905 N85-27909
F-111 automatic test equipment replacement program
20 p3437 N85-31322
Design and testing of an energy-absorbing crewseat for the F/FB-111 aircraft. Volume 3: Data from crew module testing
[NASA-CR-3918] 23 p3896 N85-34134

FAB (PROGRAMMING LANGUAGE)
U FORTRAN

FABRICATION
NT SPACE MANUFACTURING
Development of copper sulfide/cadmium sulfide thin-film solar cells
[DE84-004513] 01 p0044 N85-10287
Automated apparatus for producing gradient gels
[DE84-014507] 01 p0107 N85-10716
Acoustic resonator and method of making same
[DE84-014655] 01 p0116 N85-10792
Characteristics of ion implanters for fabrication of electronic devices
[AD-P003949] 02 p0286 N85-11865
Weld metal solidification cracking in a carbon-manganese steel 03 p0330 N85-12126
Novel techniques for the fabricating and characterization of GaAs MIS (Metal Insulator Semiconductor) structures
[AD-A145766] 03 p0358 N85-12301
Chemical derivatization of an array of three gold microelectrodes with polypyrrole: Fabrication of a molecule-based transistor
[AD-A146221] 03 p0359 N85-12304
The design, fabrication and delivery of a spacelab neutral buoyancy Instrument Pointing System (IPS) mockup – underwater training simulator
[NASA-CR-171233] 04 p0462 N85-12934
Ceramic/ceramic seals by microwave heating
[DE84-007486] 04 p0479 N85-13050
Materials for high-temperature fuel cells
[DE84-016316] 04 p0479 N85-13054
NMOS test chip for a course in semiconductor parameter measurements
[PB84-216506] 04 p0497 N85-13174
Development and demonstration of a vertical axis wind turbine POWERHOUSE
[DE84-901449] 04 p0527 N85-13369
Advanced amorphous materials for photovoltaic conversion
[DE84-017198] 04 p0529 N85-13384
Health and environmental effects document for photovoltaic energy systems, 1983
[DE84-017179] 04 p0532 N85-13399
Design, ancillary testing, analysis and fabrication data for the advanced composite stabilizer for Boeing 737 aircraft, volume 2
[NASA-CR-166011] 05 p0612 N85-13914
The variable polarity plasma arc welding process: Its application to the Space Shuttle external tank
[NASA-TM-86482] 05 p0641 N85-14115

Forming fluorine-containing threads from vinylidene fluoride-tetrafluoroethylene copolymer by dry method
06 p0762 N85-14873

Preparation of fire-resistant infusible polycaproamide fiber
06 p0763 N85-14877

Fabrication and quality assurance processes for superhybrid composite fan blades
[NASA-TM-83354] 06 p0763 N85-14882

Effect of substituted phenylnadimides on processing and properties of PMR polyimide composites
[NASA-TM-86902] 06 p0770 N85-14929

Use of least-squares method for estimating errors of turbine blade type parts during fabrication
06 p0776 N85-14963

Oxide charge characteristics of low temperature MOS (Metal-Oxide-Silicon) oxide films
[AD-A146447] 06 p0803 N85-15113

Design and development of a sealed 100-Ah nickel-hydrogen battery
[DE84-016935] 06 p0805 N85-15128

Research on submicrometer structures
[AD-A146578] 06 p0867 N85-15508

Development of short gate FET's
[AD-A147033] 07 p0947 N85-15999

Control technology for integrated circuit fabrication at Micro-Circuit Engineering, Incorporated, West Palm Beach, Florida
[PB85-100717/GAR] 07 p0949 N85-16013

Infrared technology for satellite power conversion --- antenna arrays and bolometers
[NASA-CR-174266] 07 p0991 N85-16293

Switchable zero order diffraction gratings as light valves
[AD-A147575] 07 p1044 N85-16633

Advances in composites technology
[NASA-TM-86353] 08 p1118 N85-17048

Materials of the fourth scientific-technical Conference on Questions of the Extrusion of Metals (Selected articles)
[AD-A148578] 08 p1130 N85-17121

Ceramic fabrication process before firing-surface treatment of ceramic powder
[NASA-TM-77437] 08 p1131 N85-17129

Investigation on experimental techniques to detect, locate and quantify gear noise in helicopter transmissions
[NASA-CR-3847] 08 p1217 N85-17667

The fabrication, processing and characterization of multidimensionally braided graphite/epoxy composite materials
[AD-A148729] 09 p1288 N85-18090

An inexpensive vector thin film magnetometer
[AD-A148725] 09 p1323 N85-18310

Mask aligner for solar cell fabrication
[AD-D011450] 10 p1510 N85-19529

Conceptual design of a 10 MW shore-based OTEC plant
[DE84-015808] 10 p1511 N85-19532

Develop and demonstrate manufacturing processes for fabricating graphite filament reinforced polymide (Gr/PI) composite structural elements
[NASA-CR-172497] 11 p1592 N85-20019

Fabrication and properties of tungsten heavy metal alloys containing 30% - 90% tungsten
[DE85-000152] 11 p1607 N85-20103

Fabrication of fiber-reinforced ceramic composites by chemical vapor infiltration
[DE85-003809] 11 p1611 N85-20132

Control technology for integrated circuit fabrication at Honeywell Optoelectronics Division, Richardson, Texas
[PB85-109023] 11 p1616 N85-20162

Pultrusion process for fabrication of tethers (preliminary concepts) 11 p1646 N85-20371

Excimer laser annealing to fabricate low cost solar cells
[NASA-CR-174394] 11 p1673 N85-20536

Research on separators for alkaline zinc batteries
[DE85-003082] 12 p1836 N85-21523

New high resolution scanning ion microprobe and focused ion beam applications
[AD-A149992] 12 p1852 N85-21616

Low capacitance e-beam fabricated beam-lead Schottky barrier diodes
[AD-A150236] 13 p2063 N85-22888

New high-efficiency silicon solar cells
[NASA-CR-175643] 13 p2128 N85-23244

Structural design of the Sandia 34-M Vertical Axis Wind Turbine
[DE85-002831] 13 p2129 N85-23247

A normal incidence, high resolution X-ray telescope for solar coronal observations
[NASA-CR-175622] 13 p2169 N85-23461

Technology for pressure-instrumented thin airfoil models, phase 1
[NASA-CR-3891] 14 p2227 N85-23804

Extreme precision antenna reflector study results
14 p2232 N85-23830

Some features of the fabrication of multilayer fiber composites by explosive welding
[NASA-TM-77844] 14 p2248 N85-23932

Milling of spherical zones in parts
14 p2266 N85-24041

Fabrication of turbine parts with transportable tools
14 p2267 N85-24046

Design, fabrication and testing of a multibeam forming network
[NASA-CR-175695] 14 p2298 N85-24228

High resistance and raised modulus carbon fibers
[NASA-TM-76884] 15 p2502 N85-25436

Glass, carbon fibers made at Fibre et Mica in France
15 p2534 N85-25634

Welding technology: Japan — Conference
[ISBN-0-85300177-4] 15 p2565 N85-25823

Welding technology and organisation in steel construction 15 p2566 N85-25828

Design and fabrication of a unique electromechanical machine for long-term fatigue testing
[DE85-006524] 15 p2580 N85-25912

Development of a new faster process for the fabrication of ceramic fiber-reinforced ceramic composites by chemical vapor infiltration
[DE85-007550] 16 p2756 N85-27007

Method of fabricating acceleration resistant crystal resonators and acceleration resistant crystal resonators so formed
[AD-D011630] 16 p2778 N85-27145

Method of fabricating material for the electrodes of gas discharge devices
[DE85-007452] 16 p2780 N85-27157

Production and compaction of amorphous metal powders
[BLL-BISI-TRANS-22387-(9022.06)]
17 p2929 N85-28080

Process for making electrodes for discharge tubes
[DE85-008898] 17 p2955 N85-28247

Electrode for flash discharge lamps
[DE85-008896] 17 p2955 N85-28252

Effects of processing chemistry on electrical properties of high field ZnO varistors
[DE85-007688] 17 p2956 N85-28254

Laser welder for fabricating neutron tubes
[DE85-009965] 17 p2974 N85-28377

Inspection of welds and the factors improving its effectiveness in welded structure fabrication
[BLL-BISI-TRANS-22194-(9022.06)]
17 p2976 N85-28387

Low density inorganic foams fabricated using microwaves
[DE85-007708] 18 p3080 N85-29051

Molten carbonate fuel cell cathode material development
[DE85-010268] 18 p3081 N85-29057

LFMR definition study
[AD-A153691] 18 p3090 N85-29126

Coal-Fired MHD Combustor Development Project, Phase 3D
[DE85-008822] 18 p3192 N85-29795

Solar rocket component study
[AD-A154186] 19 p3227 N85-30007

Method for production of ceramic oxide and carbide bodies by polymer inclusion and decomposition
[DE85-011668] 19 p3250 N85-30152

Heterojunction Schottky gate MESFET with lower channel ridge barrier
[AD-D011673] 19 p3258 N85-30199

Glow discharge deposition at high rates using disilane
[DE85-010236] 19 p3263 N85-30235

Design and operation of epitaxial reactor
[DE85-011089] 19 p3306 N85-30491

Materials and techniques for model construction
[NASA-CR-172620] 20 p3396 N85-31066

Design and fabrication of durable owner-built wind turbine blades
[DE85-009200] 20 p3484 N85-31650

Resistance of polyaniline films as a function of electrochemical potential and the fabrication of polyaniline-based microelectronic devices
[AD-A154999] 21 p3569 N85-32201

Parallel simulation of digital LSI circuits
[AD-A154745] 21 p3580 N85-32258

Fabrication and test of modified quadrupole mass spectrometer
[AD-A155166] 21 p3590 N85-32312

Three-dimensional photochemical machining with lasers
[AD-A154711] 21 p3591 N85-32320

Tape casting as an approach to an all-ceramic turbine shroud seal
[NASA-TM-87078] 21 p3596 N85-32333

Status of high-efficiency module design and fabrication 21 p3612 N85-32446

Method of bonding silver to glass and mirrors produced according to this method
[DE85-011642] 22 p3792 N85-33495

Automatic rotary valve actuator
[DE85-012797] 22 p3794 N85-33505

Block 5 documentation and solar modules
[NASA-CR-176134] 22 p3805 N85-33564

Poly-functional building material from fiberglass (its fabrication and properties) 23 p3906 N85-34209

Evacuate and backfill apparatus and method
[DE85-006018] 23 p3938 N85-34411

Electrolyte resevoir for carbonate fuel cells
[DE85-005736] 23 p3947 N85-34460

Method of preparing thin porous sheets of ceramic material
[DE85-006399] 24 p4082 N85-35300

Single-point diamond crushing of Zerodur with in-situ polishing and metrology on a diamond turning machine
[DE85-012918] 24 p4083 N85-35305

SLC arc transport system: Magnet design and construction
[DE85-014289] 24 p4159 N85-35789

FABRICS

NT PARACHUTE FABRICS
NT WOOL

Zero adhesion system
[AD-D011237] 01 p0015 N85-10093

The theory of elastic modulus of fabric composites and its examination by experiments
[NAL-TR-808] 01 p0022 N85-10133

Development of failure criterion for Kevlar-epoxy fabric laminates
[NASA-CR-172465] 02 p0170 N85-11136

Testing of three different flight suits in fire environment — fuel fire
[FOA-C-59012-H1] 02 p0238 N85-11552

Thermoplastic-carbon fiber hybrid yarn
[NASA-CR-3849] 03 p0325 N85-12093

Fabric filter system study
[PB84-229749] 03 p0342 N85-12206

Electrostatic augmentation of fabric filtration: Reverse-air pilot unit experience
[PB84-230002] 03 p0343 N85-12207

Flame-resistant materials for use in pyrotechnic safety clothing
[AD-A146857] 07 p0931 N85-15901

Measurement of stress in clothing: A literature review and methods selected
[AD-A147674] 08 p1132 N85-17132

Ceramic fabric material testing
[DE84-012014] 09 p1300 N85-18165

Improved electron emission by use of a cloth fiber cathode
[AD-A149250] 10 p1480 N85-19340

Hot melt adhesive attachment pad
[NASA-CASE-LAR-12894-1] 11 p1610 N85-20125

Finger materials for air cushion vehicles. Volume 2: Base fabrics for finger materials
[AD-A149701] 12 p1819 N85-21408

Removable cleanable antireflection shield
[AD-D011735] 22 p3844 N85-33810

FABRY-PEROT INTERFEROMETERS

Fabry-Perot interferometer and skymapping photometer determinations of midlatitude f-region neutral winds and temperatures and airglow enhancement/depletions
[AD-A150730] 14 p2373 N85-24666

Evaluation of a magneto-optical filter and a Fabry-Perot interferometer for the measurement of solar velocity fields from space 14 p2442 N85-25067

Linewidth and bandwidth measurements of the q-branch of h2 using CW coherent anti-Stokes Raman spectroscopy
[AD-A151868] 15 p2506 N85-25456

Thermospheric winds observed by OI6300A Doppler shifts at 23 deg S in the Brazilian sector
[INPE-3384-RPE/470] 16 p2834 N85-27479

Optically bistable devices using InSb
18 p3186 N85-29758

Optical bistability in Cd(x)Hg(1-x)Te
18 p3186 N85-29760

Optical modulators and bistable devices using molecular gases 18 p3186 N85-29761

A simple optical extensometer achieving high accuracy
[NPL-DMA(A)-95] 20 p3458 N85-31474

FABRY-PEROT LASERS

U LASERS

FABRY-PEROT SPECTROMETERS

High precision measurement of stellar radial velocity variations 08 p1250 N85-17896

FACE CENTERED CUBIC LATTICES

Kohn anomaly in metastable fcc lanthanum at low temperatures
[DE84-015459] 04 p0569 N85-13626

Irradiation creep induced anisotropy in a/2110 dislocation populations
[DE84-016623] 06 p0868 N85-15520
Computer simulation of grain-boundary properties in ionic crystals and metals
[DE85-000577] 11 p1734 N85-20906
Observation of surface vibrational resonances on (110) surfaces of FCC metals
[AD-A150469] 13 p2163 N85-23419
Defect production and recovery in FCC metals irradiated at 4.2 K
[DE85-010477] 20 p3538 N85-32014

FACETS
U FLAT SURFACES

FACILITIES
Corrosion and coatings review of specifications and drawings of facilities for the Oman Military Construction Program at Masirah Island, Oman
[AD-A149739] 12 p1812 N85-21366

FACSIMILE COMMUNICATION
Facsimile transmission of microforms
[AD-A144855] 01 p0038 N85-10236
APOLLO system requirements specification — electronic document delivery
[ESA-SP-1068] 04 p0494 N85-13150

FACSIMILE TRANSMISSION
U FACSIMILE COMMUNICATION

FACTOR ANALYSIS
Factor analysis applied to a silane coupling agent on E-glass fiber system
[AD-A145687] 02 p0187 N85-11249
What is principal components analysis?
02 p0211 N85-11389
Principal components: A review
02 p0211 N85-11390
A factor analysis for time series
[AD-A147495] 07 p1036 N85-16574
Studies in quality improvement. Part 1: Dispersion effects from fractional designs, revised
[AD-A153516] 18 p3119 N85-29308
Chemometric analysis of multisensor arrays
[AD-A153805] 18 p3174 N85-29680
Factor analysis of atmospheric pollution by polycyclic aromatic hydrocarbons
[HSE-TRANS-10988] 19 p3311 N85-30528
Bayesian factor analysis
[AD-A154184] 19 p3347 N85-30747
Development of improved capabilities for computation of gas supercompressibility factors and other properties
[PB85-188316] 20 p3436 N85-31315
Telecommunication market research processing
[ENST-83E018] 23 p3926 N85-34331

FACTORIAL DESIGN
Model robust response surface designs: Scaling 2-level factorials
[AD-A147494] 07 p1033 N85-16556
Analyzing two-level fractional factorial experiments for possible dispersion effects
[AD-A149455] 10 p1548 N85-19760
Studies in quality improvement. Part 1: Dispersion effects from fractional designs, revised
[AD-A153516] 18 p3119 N85-29308
Model robust response surface designs: Scaling two-level factorials
[AD-A156218] 24 p4143 N85-35686

FACTORIALS
Analysis of unreplicated factorials allowing for possibly faulty observations
[AD-A154813] 21 p3678 N85-32848

FACTORIES
U INDUSTRIAL PLANTS

FACTORIZATION
Augmented weak forms and element-by-element preconditioners: Efficient iterative strategies for structural finite elements. A preliminary study
01 p0058 N85-10384
Most wanted factorizations using the quadratic sieve
[DE84-016208] 05 p0718 N85-14609
Supersonic nonlinear potential analysis
[NASA-CR-172456] 07 p0897 N85-15685
Analysis of inviscid transonic flow around an airfoil by diagonal form of IAF scheme
[NAL-TR-831] 10 p1420 N85-18955
Factorized algorithms for combined spatial and temporal processing of radar signals 13 p2081 N85-22997
A stability analysis of incomplete LU factorizations
[AD-A152058] 15 p2638 N85-26271
Symbolic Givens reduction in large sparse least squares problems
[DE85-008685] 17 p3021 N85-28681
A factored implicit scheme for numerical weather prediction with small factorization error
18 p3141 N85-29447
Intermediate boundary conditions for LOD, ADI and approximate factorization methods
[NASA-CR-172591] 18 p3167 N85-29626
Pipelined Givens method for computing the QR factorization of a sparse matrix
[DE85-009772] 18 p3171 N85-29653
Approximate factorization method for computation of nonhydrostatic mesoscale flows
[DE85-007259] 19 p3313 N85-30537
Bayesian factor analysis
[AD-A154184] 19 p3347 N85-30747
A factorization approach to the linear regulator quadratic cost problem 20 p3413 N85-31178

FACULAE
Variability of the quiet photospheric network
14 p2452 N85-25144
Contribution functions for Zeeman-split lines, and line formation in photospheric faculae
18 p3207 N85-29893

FADDEEV EQUATIONS
Spline-Galerkin solution of integral equations for 3-body scattering above break-up
[TWISK-327] 01 p0109 N85-10738
Configuration space Faddeev calculations
[DE85-005813] 16 p2872 N85-27721

FADING
NT SELECTIVE FADING
NT SIGNAL FADING
Propagation influences on the performance of a reduced bandwidth quadrature phase shift keyed digital radio system 10 p1470 N85-19274
Equatorial transionospheric propagation conditions affecting digital communications
10 p1470 N85-19275
The fading of R coronae borealis
11 p1753 N85-21029
DMSK: A practical 2400-bps receiver for the mobile satellite service: An MSAT-X Report
[NASA-CR-176194] 24 p4066 N85-35324

FAHRENHEIT TEMPERATURE SCALE
U TEMPERATURE SCALES

FAIL-SAFE SYSTEMS
Automatic flight control modes for the AFTI/F-111 mission adaptive wing aircraft 17 p2905 N85-27909
Graphic display development program. Volume 2, revision 0: Appendices
[DE85-011078] 19 p3333 N85-30648

FAILURE
NT ENGINE FAILURE
NT STRUCTURAL FAILURE
NT SYSTEM FAILURES
Fracture, failure, and fragmentation
01 p0059 N85-10390
Life distribution properties of devices subject to deterioration
[AD-A145554] 02 p0206 N85-11358
On discrete failure models
[AD-A145579] 02 p0206 N85-11359
Vertical crustal movements in southern California, 1974 to 1978
[GS-CIRC-905] 02 p0228 N85-11491
Failure detection processes by pattern recognition and expert systems
[AD-P003924] 02 p0246 N85-11604
Luminous points and breakdown in structure of GaAs transistors 02 p0257 N85-11684
Contributions to the 7th International Acoustic Emission Symposium
[AD-A145368] 02 p0275 N85-11792
On-line fatigue life prediction under stochastic loading by the time series modeling 03 p0370 N85-12362
Dynamic shear failure of shallow-buried flat-roofed reinforced concrete structures subjected to blast loading
[AD-A145974] 03 p0373 N85-12376
A comparison of methods for predicting ductile crack growth instability
[AERE-R-11199] 03 p0374 N85-12387
Effects of constituent properties on compression failure mechanisms 04 p0464 N85-12946
Allowable surge currents and failure mechanisms in semiconductor power devices in various modes of operation 06 p0795 N85-15080
Analyses to develop models to project failure rates and repair costs of electronic modules and subassemblies
[AD-A146509] 06 p0816 N85-15180
Predicting electrochemical breakdown in terrestrial photovoltaic modules 06 p0830 N85-15273
Challenges in the development of the orbiter active thermal control subsystem 08 p1096 N85-16923
Completely monotone regression estimates of software failure rates
[NASA-CR-174319] 08 p1204 N85-17575
A power transformation exponential regression model for censored failure time data
[AD-A148377] 08 p1212 N85-17632
Evaluation of failure criterion for graphite/epoxy fabric laminates
[NASA-CR-172547] 10 p1431 N85-19025
Flashover failures from wet-wire arcing and tracking
[AD-A149055] 10 p1478 N85-[illegible]
Fractographic features of titanium alloy fatigue failure under repeated static stress and high frequency vibration 11 p1601 N85-[illegible]
Systems vulnerability and lethality in the development phase
[AD-A149737] 12 p1924 N85-[illegible]
Reliability bounds for fault-tolerant systems with competing responses to component failures
[NASA-TP-2409] 13 p2100 N85-[illegible]
Effects of assuming independent component failure times, if they are actually dependent, in a series system
[AD-A150562] 13 p2101 N85-[illegible]
Sizing capability of automated ultrasonic time-of-flight diffraction in thick section steel and aspects of reliable inspection in practice
[AERE-R-11548] 15 p2571 N85-[illegible]
VLSI (Very large scale integrated circuits) device reliability models
[AD-A153268] 17 p2954 N85-[illegible]
Inequalities for distributions with increasing failure rate
[AD-A152812] 17 p2976 N85-[illegible]
Optimally robust redundancy relations for failure in uncertain systems
[NASA-CR-175953] 17 p2976 N85-[illegible]
Critical conditions for failure in materials subjected to high rates of loading
[AD-A153135] 17 p2980 N85-[illegible]
Nonparametric estimation of the probability of ruin
[AD-A153523] 18 p3174 N85-[illegible]
Deformation, fracture and explosive properties of reactive materials
[AD-A154073] 19 p3251 N85-30157
Effect of confinement on failure in 95 TATB/5 KEL-F
[DE85-010790] 19 p3251 N85-30158
The value of DMT in the selection of pilots
[RAE-TRANS-2127] 19 p3330 N85-[illegible]
Fundamental investigations of failure during superplastic forming process
[AD-A154647] 21 p3566 N85-32184
Accelerated stress factors and failure/degradation mechanisms in terrestrial solar cells
21 p3613 N85-32451
Analysis of long bone and vertebral failure patterns
[AD-A154796] 21 p3663 N85-[illegible]
Method of characterizing critical timing paths and analyzing timing related failure modes in very large scale integrated circuits
[AD-D011731] 22 p3759 N85-[illegible]

FAILURE ANALYSIS
Review of aircraft accident data: US General Aviation
[PB84-230960] 01 p0005 N85-10027
Stochastic properties of a sequence of interfailure times under minimal repair and under revival
[AD-A145003] 01 p0113 N85-[illegible]
Airfoil deposition model 02 p0144 N85-[illegible]
Development of failure criterion for Kevlar-epoxy fabric laminates
[NASA-CR-172465] 02 p0170 N85-[illegible]
Effect of stress concentrations in composite structures
[NASA-CR-173976] 02 p0170 N85-[illegible]
Efficient methods for mechanical and structural reliability analysis and design 02 p0205 N85-11355
LES: (Lockheed Expert System): A model-based expert system for electronic maintenance
[AD-P003944] 02 p0248 N85-[illegible]
On the requirements of expert systems for fault isolation
[AD-P003947] 02 p0249 N85-11627
Composite fracture toughness and impact characterization 04 p0466 N85-[illegible]
Evaluation of fuzzy rulemaking for expert systems for failure detection 05 p0703 N85-[illegible]
Analytical redundancy management mechanization and flight data analysis for the F-8 digital fly-by-wire aircraft flight control sensors
[NASA-CR-170396] 06 p0757 N85-[illegible]
On the effects of delamination damage in fibre composite laminates
[ARL/STRUC-R-403] 06 p0763 N85-[illegible]
Investigation of accelerated stress factors and failure/degradation mechanisms
06 p0832 N85-[illegible]
Investigation of the HPFTP first stage impeller crack
[NASA-CR-171281] 07 p0977 N85-[illegible]
Built-in-test for first line testing
08 p1064 N85-[illegible]
Automatic error detection and recovery techniques in onboard intelligent units for space and avionic application 08 p1066 N85-[illegible]
Ballistic/detonic transition of propellants
08 p1117 N85-[illegible]
Advances in composites technology
[NASA-TM-86353] 08 p1118 N85-[illegible]

Prematurely terminated sequential tests for MIL-STD 781C
[AD-A148417] 08 p1216 N85-17657
finite element analysis of bi-material systems with applications in hydraulic fracturing
09 p1332 N85-18369
Comparison of property regeneration techniques and life prediction procedures applied to laboratory tested and service exposed Ni-Cr alloys
[NPL-DMA(A)-91] 09 p1333 N85-18374
Material flow in the manufacturing system: Fault-diagnosis systems as support for the maintenance of highly automated manufacturing systems
[PNR-90236] 09 p1371 N85-18618
Reliability studies of ceramic capacitors
[AD-A149126] 10 p1479 N85-19338
Theoretical and experimental study of crack resistance and macrocrack growth rate in organic fiber reinforced plastic under pure shear condition
11 p1598 N85-20053
Method of constructing diagram of bimetal fatigue failure 11 p1599 N85-20058
Electric vehicle demonstration project
[DE85-002167] 11 p1741 N85-20943
Environment definition, large particles
12 p1787 N85-21220
A summary and assessment of historical reliability and maintainability data for solar hot water and space conditioning systems
[DE84-004521] 12 p1876 N85-21770
Results of the AFRSI rewaterproofing systems screening test in the NASA/Ames Research Center (ARC) 2 x 2-foot transonic wind tunnel
[NASA-CR-167094] 13 p1988 N85-22467
Reliability of robotized welding apparatus
13 p2034 N85-22741
Characteristics of surface crack development in ATtsS aluminum alloy during slow-cycle loading
13 p2034 N85-22745
Advanced life analysis methods. Volume 1: Cracking data survey and NDI (nondestructive inspection) assessment for attachment lugs
[AD-A150419] 13 p2103 N85-23108
A theoretical basis for the analysis of redundant software subject to coincident errors
[NASA-TM-86369] 13 p2145 N85-23317
Contribution of instrumentation and control software to system reliability
[DE85-004693] 13 p2149 N85-23340
Load capacity of cages of roller bearings for planet wheels 14 p2221 N85-23775
Condition monitoring of helicopter gearboxes using automatic vibration analysis techniques
14 p2223 N85-23790
The observation and interpretation of gear tooth failures 14 p2224 N85-23792
Experimental development of a failure detection scheme for large space structures 14 p2234 N85-23846
Convolution of the IFRA (Increasing Failure Rate Average) scaled-mins class
[AD-A151070] 14 p2411 N85-24870
On failure modeling, revised
[AD-A151411] 15 p2637 N85-26263
How to handle failures in advanced flight control systems of future transport aircraft 16 p2714 N85-26752
Recent failures of weather satellites
[S-HRG-99-1070] 16 p2731 N85-26855
Reusable rocket engine turbopump condition monitoring 16 p2740 N85-26907
ACT applied to helicopter flight control
17 p2902 N85-27891
Experimental measurements and analysis of heat transfer and gas dynamics in a rotating turbine stage
17 p2911 N85-27949
Strength and failure analysis of composite laminates with holes at room and elevated temperatures
[AD-A153263] 17 p2917 N85-27981
Influence of thermochemical treatment on properties of low-carbon steel
[BLL-BISI-TRANS-22410-(9022.06)]
17 p2927 N85-28055
Inequalities for distributions with increasing failure rate
[AD-A152812] 17 p2976 N85-28390
Optimally robust redundancy relations for failure in uncertain systems
[NASA-CR-175953] 17 p2976 N85-28391
Method of assessment of start of slow crack growth by acoustic emission technique
[BLL-BISI-TRANS-21762-(9022.06)]
17 p3027 N85-28722
Properties of polyethylene gas piping materials
[PB85-187045] 18 p3082 N85-29068
Fault detection and accommodation testing on an F100 engine in an F-15 airplane
[NASA-TM-86735] 19 p3219 N85-29962
Study of failure mechanism of fibrous composition materials taking into account physicochemical reactions of components 19 p3243 N85-30106
Effect of matrix plasticity on durability of fibrous composition materials 19 p3243 N85-30107
Resistance to corrosion fatigue in aluminum alloy 1561 in sea water 19 p3243 N85-30108
Correction of calculated estimate of fatigue properties of materials under biharmonic loading
19 p3244 N85-30113
Deformation, fracture and explosive properties of reactive materials
[AD-A154073] 19 p3251 N85-30157
Effects of high mean stress on the high-cycle fatigue behavior of PWA 1480
[NASA-CR-176020] 19 p3287 N85-30388
Impurity and particle control systems for tokamak reactor experiments
[DE85-006124] 19 p3386 N85-30873
Failure modes experienced on spacecraft NiCd batteries 20 p3445 N85-31386
The failure mechanism of a nickel electrode in a nickel-hydrogen cell 20 p3448 N85-31406
Automated FMEA (Failure Modes and Effects Analysis) techniques
[AD-A154161] 20 p3464 N85-31518
A comparison of two contemporary creep-fatigue life prediction methods 20 p3467 N85-31538
Geothermal COMPAX drill hit development
[DE85-011353] 20 p3469 N85-31556
Failure mechanisms in metal-sheathed thermocouples
[DE85-011929] 21 p3590 N85-32317
Dynamic fracture of concrete and other heterogeneous materials
[AD-A154513] 21 p3598 N85-32343
Development of improved dynamic failure models
[AD-A155586] 21 p3600 N85-32354
Failure analysis of thin-film amorphous-silicon solar-cell modules 21 p3613 N85-32452
Methods of reliability design of semiconductor power devices 22 p3770 N85-33365
Nonlinear response and failure characteristics of internally pressurized composite cylindrical panels
[NASA-CR-176148] 22 p3800 N85-33546
Data Base Workshop: Availability-Reliability Modeling
[DE85-011570] 22 p3829 N85-33713
Detonation in tungsten-loaded HMX
[DE85-009606] 23 p3922 N85-34299
The use of ultrasound to monitor incipient failure of rolling element bearings 23 p3924 N85-34317
Method and apparatus for transfer function simulator for testing complex systems
[NASA-CASE-NPO-15696-1] 23 p3926 N85-34333
Short-time creep of ice
[NRC/CNR-TT-2111] 23 p3941 N85-34428
A preliminary evaluation of a failure detection filter for detecting and identifying control element failures in a transport aircraft
[NASA-TM-87576] 24 p4067 N85-35204
Reliability prediction of the series system with spares subject to Weibull failure 24 p4100 N85-35413
State-of-the-art of solid-state motor controllers
[TI85-006674] 24 p4162 N85-35806
FAILURE MODES
Determination sample sizes for diversified reliability test programs
[DE84-015003] 04 p0511 N85-13255
General Electric composite ring-disk flywheel: Recent and potential developments 05 p0606 N85-13867
Centrifuge tests to provide closure bounds for switches subjected to random vibration
[DE85-002003] 10 p1482 N85-19357
Characterization of mode 1 and mixed-mode failure of adhesive bonds between composite adherends
[NASA-TM-86355] 12 p1797 N85-21270
Supported liquid membrane battery separators
[DE85-001031] 12 p1836 N85-21519
Use of acoustical emission method to study specifics of fracture of boron reinforced plastic structural elements 13 p2026 N85-22696
Layered composite analysis capability
15 p2573 N85-25868
Signal analysis techniques for incipient failure detection in turbomachinery 16 p2736 N85-26884
The effects of pin elasticity, clearance, and friction on the stresses in a pin-loaded orthotropic plate
[NASA-CR-175816] 16 p2743 N85-26927
Creep-fatigue interaction of notched 304 stainless steel bars 16 p2796 N85-27249
Determination of failure characteristics of materials and structures
[AD-A152073] 16 p2800 N85-27266
Photovoltaic cell reliability research: Investigation of accelerated stress factors and failure-degradation mechanisms in terrestrial solar cells
[NASA-CR-175815] 16 p2819 N85-27388
Recent progress in the dynamic plastic behaviour of structures, part 4 17 p2978 N85-28402
On validity of threshold values of fatigue strength of steel structures
[BLL-BISI-TRANS-22192-(9022.06)]
17 p2978 N85-28408
Properties of polyethylene gas piping materials
[PB85-187045] 18 p3082 N85-29068
Automated FMEA (Failure Modes and Effects Analysis) techniques
[AD-A154161] 20 p3464 N85-31518
A continuous damage model based on stepwise-stress creep rupture tests
[NASA-CR-174941] 21 p3597 N85-32341
Thin-film reliability and engineering overview
21 p3612 N85-32450
Circuit approaches to increasing SRAM performance in total dose environments
[DE85-009441] 23 p3966 N85-34588
Mechanical characterization and failure modes of fiber reinforced angle-ply composites
24 p4072 N85-35234
Structure and properties of polyethylene films used in heavy lift balloons
[NASA-CR-176227] 24 p4083 N85-35306
FAIRCHILD MILITARY AIRCRAFT
U MILITARY AIRCRAFT
FAIRINGS
UH-60A external stores support system fixed provision fairings drag determination
[AD-A147188] 07 p0902 N85-15719
Space shuttle elevon seal panel mechanism
08 p1101 N85-16961
Automating the study of error in discrete aerodynamic fairing design 14 p2288 N85-24176
The development of staging mechanisms for the Japanese satellite launcher Mu-3SII
22 p3798 N85-33528
An automated technique for encasing specific payloads with low-drag fairings 24 p4063 N85-35183
FALKNER-SKAN EQUATION
Numerical solutions of turbulent models for flow over a flat plate with angle of attack
[DE85-010360] 21 p3585 N85-32286
FALLING SPHERES
Computing parameters characterizing possibility of planets falling in star camera field of view during space survey 15 p2487 N85-25351
Applied research and development for falling-sphere air density measuring systems
[AD-A155227] 21 p3552 N85-32099
FALLOUT
Particle size distribution on surfaces in clean rooms
[AD-A146057] 03 p0326 N85-12109
Assessment of radiation dosages obtained by intake of radioactive fallout contaminated food
[VTT-292] 07 p1017 N85-16480
Development and validation of a new fallout transport method using variable spectral winds
[AD-A151871] 15 p2599 N85-26022
On the design of a global detection system for airborne radioactivity
[CM-68] 20 p3487 N85-31670
FAN BLADES
Energy efficient engine. Volume 2. Appendix A: Component development and integration program
[NASA-CR-173085] 02 p0146 N85-10991
Basic study of bladed disk structural response
[AD-A146226] 03 p0319 N85-12061
Fabrication and quality assurance processes for superhybrid composite fan blades
[NASA-TM-83354] 06 p0763 N85-14882
Strength analysis of fan-shaped wing considering temperature deformation and creep deformations
06 p0779 N85-14983
A comparison of measured and predicted unsteady pressure on a fan blade in unstalled supersonic flutter
[PNR-90223] 08 p1079 N85-16839
Fluctuating pressures on fan blades of a turbofan engine, flight test investigation
[NASA-TP-2381] 10 p1553 N85-19790
Effects of vane/blade ratio and spacing on fan noise, volume 1
[NASA-CR-174664] 10 p1553 N85-19791
Effects of vane/blade ratio and spacing on fan noise. Volume 2: Data supplement
[NASA-CR-174665] 10 p1553 N85-19792
Numerical analyses in aerodynamic design of aero-engine fan 16 p2692 N85-26618
Energy Efficient Engine Program technology benefit/cost study, volume 1
[NASA-CR-174766-VOL-1] 24 p4066 N85-35197
FAN IN WING AIRCRAFT
Strength analysis of fan-shaped wing considering temperature deformation and creep deformations
06 p0779 N85-14983

FANS

Sources, paths, and concepts for reduction of noise in the test section of the NASA Langley 4x7m wind tunnel
[NASA-CR-172446-VOL-1] 05 p0726 N85-14866

Comparison of options for reduction of noise in the test section of the NASA Langley 4x7m wind tunnel, including reduction of nozzle area
[NASA-CR-172446-VOL-2] 05 p0726 N85-14867

FAR FIELDS

Transonic wing and far field test data on a high aspect ratio transport wing for three dimensional computational method evaluation 01 p0004 N85-10021

Case study of sample spacing in planar near-field measurement of high gain antennas
[NASA-TM-86872] 01 p0037 N85-10234

Characteristic boundary conditions for three-dimensional transonic unsteady aerodynamics
[NASA-TM-86292] 02 p0134 N85-10915

Time variability of directionality properties of pulsed EB-EDL (Electron Beam-Electric Discharge Laser) N2-CO2 lasers
[AD-A145546] 02 p0202 N85-11344

Efficient computation of reflector antenna aperture distributions and far field patterns
[AD-A147367] 07 p0940 N85-15962

Radiation patterns of a pyramidal horn antenna 09 p1311 N85-18236

A conformal mapping suitable for problems involving interaction between given geometries and known far fields
[AD-A149050] 10 p1545 N85-19744

Near Field/Far Field (NF/FF) energy loss in Electric Discharge Lasers (EDL's): A mode-medium interaction
[AD-A150299] 13 p2096 N85-23075

Space processing of acoustic signals in plane-parallel waveguide — antenna arrays 15 p2525 N85-25572

The method of residual minimization in compressible steady flows
[AD-A153924] 18 p3100 N85-29193

Notes on unsteady transonic cascade flows
[AD-A154829] 21 p3552 N85-32096

Reducing grating lobes due to subarray amplitude tapering
[AD-D011723] 23 p3927 N85-34339

FAR INFRARED RADIATION

Effects of atmospheric water vapor and clouds on NOAA (National Oceanic and Atmospheric Administration) AVHRR (Advanced Very High Resolution Radiometer) satellite data
[AD-A145425] 02 p0280 N85-11824

Developments in far-infrared detection techniques
[AD-A146290] 03 p0420 N85-12683

Far-infrared observations of some regions of star formation 03 p0442 N85-12814

Far-infrared photometry of compact extragalactic sources: OJ 187 and BL Lac
[NASA-TM-86022] 04 p0580 N85-13701

Far-infrared line emission from the galaxy
[NASA-CR-174166] 04 p0580 N85-13702

Far-infrared laser diagnostic on EBT and extreme far-forward laser scattering on ISX
[DE85-001788] 07 p1046 N85-16643

The Lear Jet Observatory: Fifteen years of discovery and rebirth 08 p1244 N85-17850

Far infrared and submillimeter observations of the giant planets 08 p1245 N85-17856

Far-infrared spectroscopy of interstellar gas 08 p1245 N85-17858

Multi-spectral observations of the star formation: The role of far infrared photometry 08 p1245 N85-17859

The Orion molecular cloud at far-infrared wavelengths 08 p1245 N85-17860

First results of submillimeter polarimetry 08 p1246 N85-17861

NGC 2024: Multi-wavelength infrared and radio observations 08 p1246 N85-17865

Far-infrared photometry of low-mass pre-main-sequence stars with broad CO wings 08 p1246 N85-17866

High sensitivity, high angular resolution far-infrared photometry from the KAO 08 p1246 N85-17867

Star formation in globules 08 p1247 N85-17868

Far infrared observations of molecular clouds in the outer galaxy 08 p1247 N85-17869

Far infrared emission from galaxies 08 p1248 N85-17875

Far infrared continuum emission from the galactic center 08 p1248 N85-17876

The 157 micron (C II) luminosity of the galaxy 08 p1248 N85-17877

Variation of oxygen and nitrogen abundances in the galaxy 08 p1248 N85-17878

Far IR observations of the Magellanic clouds 08 p1248 N85-17879

Dust reradiation from NGC 6946 08 p1248 N85-17880

Starbursts in galaxies: Implications of molecular and far-infrared observations 08 p1248 N85-17881

Far-infrared spectroscopy of galaxies: The 158 micron C(+) line 08 p1249 N85-17882

Interpretation of the far infrared emission from our external galaxies 08 p1249 N85-17884

A far infrared Echelle spectrometer for the Kuiper Airborne Observatory 08 p1249 N85-17886

Far-infrared interferometry/polarimetry on the ISX-B Tokamak
[DE84-015401] 10 p1558 N85-19827

Far-infrared line observations of planetary nebulae. 1: The O 3 spectrum
[NASA-TM-86670] 10 p1570 N85-19900

FIR interferometer/polarimeter system on ISX-B Tokamak
[DE85-001129] 11 p1731 N85-20887

Balloon-borne, He-cooled Fourier transform spectrometer for far infrared astronomy
[MPE-IR-41] 17 p3053 N85-28899

Far-infrared emission lines of CO and OH in the Orion-KL molecular shock
[NASA-TM-86721] 24 p4167 N85-35832

Observations of far-infrared transitions between excited states of OH
[NASA-TM-86722] 24 p4167 N85-35833

FAR ULTRAVIOLET RADIATION

NT LYMAN ALPHA RADIATION

Voyager EUV and FUV observations 06 p0875 N85-15554

Radiation/catalytic augmented combustion
[AD-A148758] 09 p1290 N85-18101

Evaluation of miniature vacuum ultraviolet lamps for stability and operating characteristics, Lyman-Alpha task
[NASA-CR-171345] 10 p1477 N85-19323

Vacuum ultraviolet electronic properties of liquids
[DE85-000305] 10 p1563 N85-19858

Research in extreme ultraviolet and far ultraviolet astronomy
[NASA-CR-174432] 10 p1570 N85-19902

Ultraviolet observations of circumstellar matter in Algol type binary systems 11 p1756 N85-21043

Strange F + Be binary star systems 11 p1756 N85-21045

The solar stellar connection in the far ultraviolet 11 p1757 N85-21055

Precise measurements of radial velocities of emission lines in the far-ultraviolet spectra of late-type stars 11 p1758 N85-21062

Documentation for the machine-readable version of the Revised S210 Catalog of Far-Ultraviolet Objects (Page, Carruthers and Heckathorn 1982)
[NASA-TM-87439] 14 p2438 N85-25047

Stimulated Brillouin scattering reflectivity in the presence of various aberrators
[AD-A151750] 15 p2563 N85-25812

Studies of collisional and nonlinear radiative process for development of coherent UV and XUV sources
[AD-A152001] 16 p2865 N85-27670

Photoionization mass spectrometry with VUV hydrogen laser source
[AD-A153362] 17 p2921 N85-28009

Lifetime and quenching measurements of C2H emission produced by vacuum ultraviolet photolysis of C2H2
[DE85-010769] 19 p3278 N85-30330

Energy transfer and excimer formation in rare gas solids 19 p3374 N85-30930

Tuning system for capacitively loaded 1/4 accelerating cavity
[DE85-012516] 24 p4091 N85-35358

FAR UV SPECTROSCOPIC EXPLORER

Future ultraviolet experiments, including FUSE/COLUMBUS 11 p1744 N85-20969

FARADAY EFFECT

Shock electromechanical energy converter with permanent magnet
[AD-D011228] 01 p0115 N85-10781

Beam pulse length determination by spectral analysis
[CSIR-NAC-83-05] 01 p0116 N85-10793

Magnetosphere, rings, and moons of Uranus 02 p0301 N85-11951

The response of mid-latitude total electron content to solar activity 04 p0522 N85-13336

A warm magnetoactive plasma in a large volume of space 06 p0878 N85-15579

Influence of Faraday effect in ionosphere on nonmutuality of meteor radio channel 07 p0952 N85-16037

Current measurements by Faraday rotation in single mode optical fibers
[DE85-002025] 09 p1384 N85-18707

The Faraday rotation experiment — solar corona 16 p2866 N85-27805

Sensitive detection of tunable diode laser absorption by polarization rotation
[DE85-009621] 19 p3277 N85-30322

Variations in the small-scale galactic magnetic field and short time-scale intensity variations of extragalactic radio sources 20 p3549 N85-32084

The Faraday effect in ruby and corundum in strong magnetic fields 21 p3697 N85-32967

Injector losses on Mite
[DE85-012356] 24 p4090 N85-35355

FARADAY ROTATION

U FARADAY EFFECT

FARM CROPS

NT ALFALFA
NT BARLEY
NT CORN
NT FRUITS
NT GRAINS (FOOD)
NT LEGUMINOUS PLANTS
NT OATS
NT POTATOES
NT RICE
NT SUGAR BEETS
NT SUGAR CANE
NT WHEAT

Spatial estimation from remotely sensed data via empirical Bayes models 07 p0985 N85-16256

The climate in food production in Latin America 07 p1001 N85-16359

The challenge of food production: The importance of climate 07 p1001 N85-16361

The management of atmospheric resources in food production 07 p1002 N85-16362

Some stability and control problems with trailed farm tankers on slopes
[AD-P004291] 09 p1408 N85-18898

Characterization of LANDSAT-4 TM and MSS image quality for the interpretation of California's agricultural resources — Central Valley 13 p2118 N85-23190

Evaluation of the area and severity of last night's frosts
[REPT-109] 16 p2833 N85-27473

Irradiation of northwest agricultural products
[DE85-012455] 22 p3843 N85-33803

FARMLANDS

Evaluation of SIR-B imagery for geologic and geomorphic mapping, hydrology, and oceanography in Australia 08 p1146 N85-17229

Remote sensing research for agricultural applications — San Joaquin County, California and Snake River Plain and Twin Falls area, Idaho
[E85-10090] 12 p1873 N85-21752

Characterization of LANDSAT-4 TM and MSS image quality for the interpretation of California's agricultural resources — Central Valley 13 p2118 N85-23190

An initial analysis of LANDSAT-4 Thematic Mapper data for the discrimination of agricultural, forested wetlands, and urban land cover — Poinsett County, Arkansas; and Reelfoot Lake and Union City, Tennessee 13 p2118 N85-23193

Preliminary evaluation of TM for soils information 13 p2121 N85-23259

The use of Thematic Mapper data for land cover discrimination: Preliminary results from the UK SATMaP programme 13 p2121 N85-23207

Mathematical model of the nitrogen cycle in a nonsaturated area of cultivated soil 20 p3478 N85-31610

FAST FOURIER TRANSFORMATIONS

On maximum entropy signal analysis
[AD-A144374] 03 p0410 N85-12616

Fast method for calculating radiation patterns of nonequidistant radiator systems 06 p0791 N85-15052

An adaptive Fast Fourier Transform weighting technique to increase small target sensitivity
[AD-D011424] 08 p1154 N85-17286

Computing convolution of multifrequency signal employing truncated fast Fourier transform algorithms 13 p2065 N85-23019

Spectral information from gapped data. A comparison of technique 14 p2444 N85-25080

Hardware schemes for fast Fourier transform, part 7.4A 21 p3626 N85-32528

Interpolation problems in meteor radar analysis, part 7.6A 21 p3626 N85-32529

Generalization of discrete Fourier transform for interpolation in time domain 22 p3775 N85-33396

Generalization of discrete Fourier transformation for interpolation in time domain 22 p3776 N85-33400

Matched filtering of visual evoked potentials to detect acceleration (+Gz) induced blackout
[AD-A155912] 24 p4131 N85-35809

FAST NEUTRONS

Raman study of neutron irradiated GaAs
[DE84-016056] 05 p0731 N85-14702

Measurement of oxygen contamination in titanium alloy ingots by fast neutron activation analysis
[AD-P004133] 08 p1126 N85-17108

Sulfur activation at the Little Boy-Comet Critical Assembly: A replica of the Hiroshima bomb
[DE85-010261] 20 p3527 N85-31938
Fast-neutron interaction with niobium
[DE85-011471] 24 p4150 N85-35731

FAST NUCLEAR REACTORS
NT EXPERIMENTAL BREEDER REACTOR 2
NT FAST TEST REACTORS
NT LIQUID METAL FAST BREEDER REACTORS
Expected behavior of plutonium in the IFR fuel cycle
[DE85-006225] 18 p3181 N85-29725
A review of the SIMMER-2 analyses of liquid-metal-cooled fast breeder reactor core-disruptive accident fuel escape
[DE85-010603] 19 p3366 N85-30676

FAST TEST REACTORS
Application of robotics in remote fuel fabrication operations
[DE84-011481] 05 p0646 N85-14144
Liquid metal reactor programs: Safeguards and program assurance
[DE85-010621] 19 p3331 N85-30635

FASTENERS
NT ANCHORS (FASTENERS)
NT BOLTS
NT LOCKS (FASTENERS)
NT NUTS (FASTENERS)
NT PINS
NT RIVETS
NT SCREWS
The influence of fastener flexibility on load transfer and fatigue life predictions for multirow bolted and riveted joints — aircraft structures
[LBF-FB-172/84] 07 p0979 N85-16219
Eddy current test probe with circumferential segments and method of testing material surrounding fastener holes
[AD-D011554] 12 p1850 N85-21603
Finite element analysis of problems associated with life enhancement techniques
[ARL/STRUC-R-404] 12 p1862 N85-21676
On the stress analysis of bonded inserts
[ARL/STRUC-R-407] 12 p1865 N85-21698
Stresses in a half-plane containing either a pressurized hole or an interference-fit disc
[ARL/STRUC-R-409] 12 p1865 N85-21700
Elastic response of a half-plane to a bonded interference-fit disc of the same material
[ARL/STRUC-R-408] 12 p1865 N85-21701
Theoretical and experimental investigation of mechanically fastened composites
[AD-A150961] 14 p2248 N85-23935
Daze fasteners
[NASA-CASE-LAR-13009-1] 18 p3116 N85-29285
Mechanical fastener
[NASA-CASE-LAR-12738-2] 19 p3279 N85-30335
Low-profile fastener
[AD-D011667] 19 p3280 N85-30343
Load transfer by analytical methods
[SNIAS-851-111-109] 20 p3470 N85-31561
Mechanical connection for a tubular assembly
[DE85-011590] 22 p3792 N85-33497
Automatic capability to store and retrieve component data and to calculate structural integrity of these components
[DE85-012429] 22 p3831 N85-33726

FASTING
Effect of prolonged hunger during experimental hikes
11 p1692 N85-20637

FATIGUE (BIOLOGY)
NT AUDITORY FATIGUE
NT FLIGHT FATIGUE
NT MUSCULAR FATIGUE
The Reports of Aeromedical Laboratory, volume 25, no. 1/2
[ISSN-0023-2858] 01 p0090 N85-10605
A study of fatigue of shiftworkers in air traffic control and weather service groups in JASDF
01 p0090 N85-10610
The effect of sleep loss on the human visual event-related potential
[AD-A145364] 02 p0234 N85-11528
Man's physical tolerance to heat. Heat storage, burn injury
[FOA-C-54055-H1] 02 p0235 N85-11533
No fatigue effect on blink rate
05 p0712 N85-14564
Human factors survey: C-5 pilots
[AD-A147108] 07 p1020 N85-16477
Methods of monitoring mental work efficiency, emotional activity 10 p1526 N85-19627
Electrooculographic measurement, fatigue and variability of performance in simulated aircraft flight
19 p3217 N85-29946
Human performance in continuous/sustained operations and the demands of extended work/rest schedules. An annotated bibliography
[AD-A155619] 21 p3666 N85-32771
Physiological responses to unvarying (steady) and 2-2-1 shifts: Miami International Flight Service Station
[AD-A155751] 24 p4133 N85-35619

FATIGUE (MATERIALS)
NT BENDING FATIGUE
NT METAL FATIGUE
NT STRUCTURAL STRAIN
NT THERMAL FATIGUE
Influence of aluminum metalization coatings on corrosion fatigue properties of steel
01 p0018 N85-10112
Retardation analytical model to extend service life
[NASA-CR-171177] 01 p0057 N85-10376
Estimation of the threshold in fatigue crack initiation models: A Bayesian approach
[AD-A144847] 01 p0062 N85-10410
Turbine Engine Hot Section Technology (HOST)
[NASA-TM-83022] 02 p0140 N85-10951
Benchmark notch test for life prediction
02 p0140 N85-10953
Life prediction and constitutive models for anisotropic materials 02 p0144 N85-10976
The effect of overload on three different kinds of steel
02 p0174 N85-11165
The adhesion of hard and wear resistant coatings
02 p0179 N85-11203
Fatigue-impact studies in laminated composites
[AD-A142841] 03 p0326 N85-12097
High temperature low-cycle fatigue mechanisms in single crystals of nickel-based superalloy Mar-M 200
[NASA-CR-174739] 03 p0331 N85-12130
Kinetics of fatigue factor of AT3 titanium alloys in air, distilled water and 3.5% aqueous NaCl solution
03 p0350 N85-12255
Fatigue limit analysis involving biaxial stress components 03 p0370 N85-12363
The TA6Zr5D (IMI 685) characterization in strain controlled tests. (Specimens obtained from a forged spinning wheel) no. M4-45870
[M4-45870] 03 p0373 N85-12384
Composite structural materials
[NASA-CR-174077] 04 p0467 N85-12966
Fatigue in composite materials
04 p0467 N85-12968
Ultrasound interaction with partially closed fatigue cracks
[DE84-016360] 04 p0514 N85-13276
Development of damage in fatigue loaded carbon fiber reinforced plastics 05 p0650 N85-14172
Fatigue behavior of bolted joints made of carbon fiber reinforced epoxy resins 05 p0650 N85-14173
Fatigue behavior of sintered steels and measurement criteria for sintered prefabricated parts
05 p0650 N85-14174
Fatigue behavior of continuous fiber silicon-carbide-aluminum composites
[NASA-TM-86332] 06 p0763 N85-14879
On the effects of delamination damage in fibre composite laminates
[ARL/STRUC-R-403] 06 p0763 N85-14881
Study of fatigue fracture in hardened and tempered carbon steel. Report 1: Microscopic observation of the fatigue crack formation process
[BLL-PNR-90242-(8019.3153)]
06 p0767 N85-14909
Investigations into the fatigue crack growth behaviour of X6CrNi 18 11 (1.4948) austenitic stainless steel
[BLL-RISLEY-TR-4544-(9091.9F)]
06 p0768 N85-14911
Influence of the shape and distribution of inclusions of the fatigue strength of bearing steels in rotary bending
[BLL-PNR-90243-(8019.3153)]
06 p0768 N85-14912
The effect of potential on the corrosion fatigue behavior of a precipitation hardened aluminum alloy
[AD-A146537] 06 p0768 N85-14916
Three-dimensional crack location by acoustic emission
[AERE-R-11277] 06 p0818 N85-15193
Operational Loads Data
[AGARD-CP-375] 07 p0894 N85-15664
Operational loads measurement: A philosophy and its implementation 07 p0894 N85-15665
The F-15 flight loads tracking program
07 p0894 N85-15666
Structural load measurements on a Northrop NF-5A
07 p0894 N85-15667
Operational loads data evaluation for individual aircraft fatigue monitoring 07 p0895 N85-15669
In-flight evalution of LCF life consumption of critical rotor components subjected to high transient thermal stress
07 p0906 N85-15734
Monitoring engine thermal stresses
07 p0906 N85-15735
Mechanical aspects of high temperature coatings
07 p0908 N85-15749
Study of residual stresses introduced into TA6ZrD (685) cylinders by quenching
[BLL-PNR-90240-(8019.3153)]
07 p0925 N85-15859
Experimental compliance calibration of the NASA Lewis Research Center Mode 2 fatigue specimen
[NASA-TM-86908] 07 p0977 N85-16205
Verification of the fatigue properties of (small) wind turbines
[NLR-MP-83055-U] 07 p0994 N85-16311
Applicability of linear elastic fracture mechanics to fatigue in polymers and short-fiber composites
09 p1298 N85-18152
Determination of blade service life under irregular loading conditions 09 p1309 N85-18222
Assessing expired fatigue life in large turbine shafts
[DE84-016676] 09 p1340 N85-18427
Fracture resistance of surface layer with technological defects under cyclical loading 10 p1448 N85-19126
Mechanism and pattern of fatigue crack growth in aluminum alloys 11 p1597 N85-20047
Method of constructing diagram of bimetal fatigue failure 11 p1599 N85-20058
Finger materials for air cushion vehicles. Volume 2: Base fabrics for finger materials
[AD-A149701] 12 p1819 N85-21408
The residual strength of cracked specimens representing a section of the mirage into wing main spar
[ARL/STRUC-R-406] 12 p1865 N85-21699
Proceedings of the 9th Biennial Army Symposium on Solid Mechanics. Advances in Solid Mechanics for Design and Analysis
[AD-A150042] 12 p1867 N85-21710
Characterisation of fatigue crack extension by quantitative acoustic emission
[AERE-R-11289] 12 p1868 N85-21721
Experimental and numerical analysis of electric currents and electromagnetic blunting of cracks in thin plates
[AD-A150418] 13 p2022 N85-22669
Long-term strength and fracture criteria for EI698VD alloy under complex stress conditions
13 p2030 N85-22723
Some specifics of development of fatigue and creep in heat-resistant alloys with asymmetrical multicycle loading
13 p2031 N85-22724
Load capacity of cages of roller bearings for planet wheels 14 p2221 N85-23775
A study of frequency effects and damage accumulation during the fatigue of graphite/epoxy and glass/epoxy composite materials 14 p2247 N85-23930
An investigation of elevated temperature fatigue crack initiation in 2 and 1/4 cR-1 MO low alloy steel
[AD-A150670] 14 p2255 N85-23973
Variability in constant-load-amplitude fatigue crack growth rates in marine environments
[AD-A150786] 14 p2255 N85-23975
Role of passive surface films on corrosion fatigue crack initiation
[DE85-000436] 14 p2257 N85-23985
Fatigue Crack Topography
[AGARD-CP-376] 14 p2318 N85-24321
Essential features in fatigue fractures and remarkable phenomena in fatigue crack growth
14 p2318 N85-24322
Fatigue fracture topography 14 p2318 N85-24323
Generation of marker lines by means of marker loads
14 p2318 N85-24327
Generation of marker lines on fatigue fracture surfaces 14 p2319 N85-24328
Periodic loading sequences for the systematic marking of fatigue crack fracture surfaces
14 p2319 N85-24329
Modifications of flight by flight load sequences to provide for good fracture surface readability
14 p2319 N85-24330
Effect of fatigue and thermal loads on silicon carbide fiber reinforced glass matrix composites
[DE85-006069] 15 p2503 N85-25441
Mechanisms of corrosion fatigue in high strength I/M (Ingot Metallurgy) and P/M (Powder Metallurgy) aluminum alloys
[AD-A151177] 15 p2509 N85-25478
Damage development during low cycle fatigue of carbon-black loaded SBR
[DE85-006234] 15 p2519 N85-25533
Entropy production during fatigue as a criterion for failure. A local theory of fracture in engineering materials
[AD-A151289] 15 p2578 N85-25902
Crack closure characteristics considering center cracked and compact tension specimens
[AD-A151702] 15 p2579 N85-25907

FATIGUE DIAGRAMS

Creep ratcheting simplified methods experience from structural design of elevated temperature components [DE85-007433] 15 p2580 N85-25915

Fatigue criterion to system design, life and reliability [NASA-TM-87017] 16 p2793 N85-27226

Fatigue damage and small crack growth during biaxial loading 16 p2797 N85-27247

Creep-fatigue interaction of notched 304 stainless steel bars 16 p2798 N85-27249

Elevated temperature biaxial fatigue [NASA-CR-175795] 16 p2800 N85-27263

Initiation, growth and coalescence of small fatigue cracks [AD-A151799] 16 p2800 N85-27265

The practical and theoretical significance of small cracks: An evaluation [VTH-LR-432] 16 p2803 N85-27283

Structural Integrity and Durability of Reusable Space Propulsion Systems [NASA-CP-2381] 17 p2910 N85-27941

Interaction of high-cycle and low-cycle fatigue of Haynes 188 alloy at 1400 F deg 17 p2913 N85-27961

Reexamination of cumulative fatigue damage laws 17 p2914 N85-27962

The synergistic actions of stress corrosion cracking and corrosion fatigue [BLL-BISI-TRANS-22334-(9022.06)] 17 p2926 N85-28045

Characterization of the fatigue and slow crack growth behavior of partially stabilized zirconia ceramics [DE85-005240] 17 p2934 N85-28113

Relaxation properties and fatigue fracture resistance of austenitic spring steel [BLL-BISI-TRANS-22300-(9022.06)] 17 p2978 N85-28406

Fatigue crack propagation characteristics and fatigue fracture toughness in 780 MPa grade high strength steel weldments at low temperature [BLL-BISI-TRANS-22369-(9022.06)] 17 p2979 N85-28411

Fatigue of synthetic fibers for marine rope applications [MIT-R84-2] 17 p2979 N85-28414

Fatigue behavior of synthetic fibers, yarns and ropes 17 p2979 N85-28415

The effects of sea water and concentrated salt solutions on the fatigue of nylon 6,6 fibers 17 p2979 N85-28416

Interaction among inhomogeneities and inclusions [AD-A153114] 17 p2979 N85-28419

Evaluation of interpolative modeling concepts for fatigue crack growth at elevated temperature [AD-A153222] 17 p2980 N85-28422

Fatigue strength of Inconel 625 plate and weldments used in the DIII-D configuration vacuum vessel [DE85-008276] 17 p2981 N85-28427

Fatigue and chromium-ferritic steels at elevated temperatures [DE85-007735] 18 p3074 N85-29015

Fatigue behavior of HY-130 steel weldments containing fabrication discontinuities [AD-A153630] 18 p3122 N85-29326

Study of the influence of metallurgical factors on fatigue and fracture of aerospace structural materials [AD-A153913] 18 p3122 N85-29329

Study of failure mechanism of fibrous composition materials taking into account physicochemical reactions of components 19 p3243 N85-30106

Correction of calculated estimate of fatigue properties of materials under biharmonic loading 19 p3244 N85-30113

Fatigue resistance of VT3-1 titanium alloy related to surface cold working 19 p3245 N85-30120

Fatigue resistance of homogeneous and heterogeneous welded joints of TS5 titanium alloy 19 p3246 N85-30126

Acoustic emission study of fatigue crack extension position in a stress cycle 19 p3263 N85-30355

Residual stress distributions in (plastically) surface deformed two-phase materials 19 p3263 N85-30356

Experimental and theoretical study of fatigue crack initiation in metals 19 p3263 N85-30357

Multiaxial fatigue and fracture: A literature review [ARL/STRUC-R-410] 19 p3265 N85-30370

Hold-time effects in elevated temperature fatigue crack propagation [AD-A154146] 19 p3266 N85-30376

Fatigue-crack propagation behavior of alloy A-286 [DE85-007460] 19 p3268 N85-30391

Fatigue-crack growth and ductile fracture toughness behavior of ASTM A387 Grade 91 steel [DE85-008495] 20 p3431 N85-31286

Two simplified procedures for predicting cyclic material response from a strain history 20 p3467 N85-31543

The effect of abrasive blasting on the fatigue and corrosion of an aluminium-copper alloy [AD-A154954] 21 p3586 N85-32182

Measurement and analysis of critical crack tip processes during fatigue crack growth [NASA-CR-172597] 21 p3598 N85-32342

Tensile fatigue of glass fibers and composites with conventional and surface compressed fibers [RR-84-4] 22 p3742 N85-33196

Fatigue behavior of chromium-containing ferritic steels at elevated temperature [DE85-012309] 22 p3748 N85-33231

Application of traction drives as servo mechanisms 22 p3797 N85-33520

Near-threshold fatigue: An overview of the role of microstructure and environment [DE85-009903] 23 p3941 N85-34431

Fatigue damage detection in steels by optical correlation [AD-A155830] 24 p4079 N85-35277

Effect of microstructure on the fatigue behavior of Fe-C-X alloys [DE85-011749] 24 p4080 N85-35285

FATIGUE DIAGRAMS
U S-N DIAGRAMS

FATIGUE LIFE

Distributions of fatigue life and fatigue strength in notched specimens of a carbon 8-harness-satin laminate [NAL-TR-809T] 01 p0061 N85-10407

Life prediction and constitutive behavior: Overview 02 p0143 N85-10973

Investigation of chemical durability mechanisms in fluoride glasses [AD-A145420] 02 p0186 N85-11241

The influence of sublaminate cracks on the tension fatigue behavior of a graphite epoxy laminate [FFA-TN-1984-32] 02 p0210 N85-11386

The in-flight estimation and indication of cumulative fatigue damage to helicopter gears [ARL/AERO-R-164] 03 p0317 N85-12050

On-line fatigue life prediction under stochastic loading by the time series modeling 03 p0370 N85-12362

Turbine blade damping study, introduction 04 p0456 N85-12891

Effect of lubricant extreme-pressure additives on surface fatigue life of AISI 9310 spur gears [NASA-TP-2408] 04 p0507 N85-13234

Mechanical properties of aligned short carbon fiber reinforced PES and PI laminates [DFVLR-FB-84-24] 05 p0613 N85-13918

The fourth LBF colloquium [ISSN-0721-5320] 05 p0648 N85-14163

Welcome and introduction — materials strength 05 p0649 N85-14164

Critical evaluation of methods to calculate fatigue life 05 p0649 N85-14165

Possibilities of fatigue life estimation in the higher cycle range 05 p0649 N85-14166

Low cycle fatigue strength for multiaxial loading of ductile materials 05 p0649 N85-14167

Fatigue life improvement due to mechanically induced compressive residual stresses 05 p0650 N85-14175

Processes to increase the fatigue life of constructions with already initiated cracks 05 p0650 N85-14176

Evaluation of the crack initiation life behavior of fatigue loaded automotive components made from high strength aluminium alloys [ESA-TT-733] 05 p0651 N85-14181

Operational loads measurement: A philosophy and its implementation 07 p0894 N85-15665

The F-15 flight loads tracking program 07 p0894 N85-15666

Navy operational loads data sources and systems 07 p0895 N85-15668

Structural flight load measurement demonstration of structural integrity 07 p0895 N85-15670

Advanced fatigue monitoring on service aircraft 07 p0895 N85-15671

Flight parameters recording for structure fatigue life monitoring 07 p0896 N85-15682

Disc fatigue life predictions for gas turbine engines 07 p0907 N85-15743

Experiences with the material bevaviour and high temperature low cycle fatigue life prediction of the IN 738 blading alloy 07 p0908 N85-15746

Thermal-mechanical fatigue crack growth in Inconel X-750 [NASA-CR-174740] 07 p0927 N85-15877

Fatigue strength of different sintered steels and design criteria for porous material (PM) parts [LBF-FB-170/84] 07 p0928 N85-15886

Fundamentals of microcrack nucleation mechanics [NASA-CR-3851] 07 p0975 N85-16195

Possibilities for a more accurate life prediction of components — gas turbine disks 07 p0976 N85-16196

The influence of fastener flexibility on load transfer and fatigue life predictions for multirow bolted and riveted joints — aircraft structures [LBF-FB-172/84] 07 p0979 N85-1821

A comparison of fatigue lives under a complex and a much simplified flight-by-flight testing sequence — Mirage 3 aircraft [ARL/STRUC-TM-388] 09 p1280 N85-190

Fatigue-creep interaction in + or - 45 deg carbon-resin composites — aircraft construction materials [ONERA-RT/40/7086/M] 11 p1594 N85-200

Effect of stress concentration fatigue resistance of refractory nickel alloys under asymmetrical multicycle loading, communication 1 11 p1604 N85-200

Fatigue crack growth in Aramid Reinforced Aluminum Laminates (ARALL): Mechanisms and predictions [DFVLR-FB-84-37] 11 p1609 N85-2011

Fatigue crack propagation in mirage 1110 wing main spar specimens and the effects of spectrum truncation on life [ARL/STRUC-R-405] 12 p1776 N85-2115

Finite element analysis of problems associated with life enhancement techniques [ARL/STRUC-R-404] 12 p1862 N85-2167

On the stress analysis of bonded inserts [ARL/STRUC-R-407] 12 p1865 N85-216

Fatigue and corrosion fatigue resistance of aluminum casting alloy VAL10 and forging alloy AK6 13 p2025 N85-22

Fatigue life, crack initiation, and propagation of 304 stainless steel with non-proportional axial/torsional strain-paths 13 p2101 N85-230

Resistance of hydrogenated alpha-titanium alloys to corrosion-fatigue fracture 15 p2499 N85-2541

Fatigue life, fatigue crack propagation and fracture toughness study of 7075 aluminum alloy subjected to thermomechanical processing 15 p2573 N85-258

A review of fracture mechanics life technology 16 p2733 N85-268

Fatigue life extension 16 p2733 N85-268

Thrust chamber life prediction 16 p2733 N85-268

Rolling contact fatigue life of chromium ion plated 440C bearing steel 16 p2736 N85-268

Fatigue life analysis of a turboprop reduction gearbox [NASA-TM-87014] 16 p2793 N85-272

Experimental measurements and analysis of heat transfer and gas dynamics in a rotating turbine stage 17 p2911 N85-279

Flow-induced vibration of SSME main injector liquid-oxygen posts 17 p2912 N85-2795

Further investigations to improve the fatigue life of the Mirage 1110 wing main span [ARL/STRUC-TM-397] 18 p3061 N85-28

Low-rate discharge of various electrochemical batteries for use with oceanographic instruments [AD-A153965] 18 p3095 N85-291

Corrosion fatigue cooperative testing program statistical analysis [AD-A153686] 19 p3238 N85-300

Load-carrying capabilities of refractory alloys for space reactor power applications [DE85-010566] 19 p3240 N85-300

Effect of prolonged high temperature on durability of coated high-temperature nickel alloys 19 p3243 N85-301

Experimental and theoretical study of fatigue crack initiation in metals 19 p3283 N85-303

Fatigue characterization of fabricated ship details for design [SSC-318] 19 p3285 N85-303

Effects of high mean stress on the high-cycle fatigue behavior of PWA 1480 [NASA-CR-176020] 19 p3287 N85-30

Creep fatigue life prediction for engine hot section materials (isotropic) [NASA-CR-168228] 20 p3394 N85-310

Mechanical properties of aligned short carbon fiber reinforced PES and PI laminates [ESA-TT-898] 20 p3422 N85-312

Influence of recrystallization and solution on the tenacity of the 7010 and 7475 alloys. Olygocyclic fatigue of the 7010 alloy [ONERA-RT-19/5069-M] 20 p3432 N85-312

Effect of speed and press fit on fatigue life of roller-bearing inner-race contact [NASA-TP-2496] 20 p3463 N85-315

A comparison of two contemporary creep-fatigue life prediction methods 20 p3467 N85-315

Influence of moisture and elevated temperature on the fatigue properties of WTS-3 glass fiber blade material — wind turbine blade (WTS-3) [FFA-TN-1984-58] 20 p3470 N85-315

Controlled indentation flaws for the construction of toughness and fatigue master maps [PB85-179067] 20 p3473 N85-315

Voyager 0.2-lbf thruster valve assembly short pulse test report
[NASA-CR-176121] 22 p3741 N85-33185
Joint design for improved fatigue life of diffusion-bonded box-stiffened panels
[NASA-TP-2480] 22 p3799 N85-33537
Corrosion fatigue strength and crack growth in prestrained 0.16% C carbon steel
23 p3905 N85-34192
Statistical pooling method of fatigue data for reliability design 23 p3906 N85-34198
The character of observed porosity and its possible effects on rolling contact fatigue life of M-50 steel
[AD-A155930] 24 p4079 N85-35279
Effect of prior warm rolling on the retained austenite content and hardening response of VIM-VAR (vacuum-induction melted-vacuum-arc remelted) AISI M-50 steel
[AD-A156145] 24 p4079 N85-35281
Development of a mathematical model for predicting the percentage fatigue life increase resulting from shot peened components
[AD-A155774] 24 p4101 N85-35425

FATIGUE TESTING MACHINES
Design and fabrication of a unique electromechanical machine for long-term fatigue testing
[DE85-006524] 15 p2580 N85-25912

FATIGUE TESTS
Strength of welded joints in VT23 alloy upon repeated static loading 01 p0020 N85-10120
Effect of penetrant on fatigue of aluminum alloy lap joints
[NLR-TR-82104-U] 01 p0056 N85-10373
Flight simulation fatigue crack propagation in metal/carbon-epoxy laminates
[NLR-TR-83006-U] 01 p0063 N85-10416
The effect of overload on three different kinds of steel
02 p0174 N85-11165
The influence of sublaminate cracks on the tension fatigue behavior of a graphite epoxy laminate
[FFA-TN-1984-32] 02 p0210 N85-11386
Cyclic endurance testing of the RB211-22B cast HP turbine blade — high pressure (HP)
[PNR-90210] 03 p0320 N85-12063
The TA6Zr5D (IMI 685) characterization in strain controlled tests. (Specimens obtained from a forged spinning wheel) no. M4-45870
[M4-45870] 03 p0373 N85-12384
Parametric study of the P9 HT glass fiber finish (Fatigue resistance). Lot no. 1: Report on the microfatigue tests
[CS-794] 05 p0620 N85-13968
Critical evaluation of methods to calculate fatigue life
05 p0649 N85-14165
Possibilities of fatigue life estimation in the higher cycle range 05 p0649 N85-14166
Advanced fatigue monitoring on service aircraft
07 p0895 N85-15671
Design and test requirements for development of today's engines 07 p0906 N85-15737
Inconel 718 alloy resistance to crack propagation
07 p0907 N85-15740
Engine cyclic durability by analysis and material testing 07 p0907 N85-15744
Effect of five lubricants on life of AISI 9310 spur gears
[NASA-TP-2419] 07 p0962 N85-16099
Low cycle fatigue of MAR-M 200 single crystals at 760 and 870 deg C
[NASA-TM-86933] 10 p1440 N85-19074
Airbus fatigue tests 11 p1618 N85-20186
Deflection model of a CT4-A undercarriage
[AD-A149778] 12 p1777 N85-21156
Characterization of mode 1 and mixed-mode failure of adhesive bonds between composite adherends
[NASA-TM-86355] 12 p1797 N85-21270
Comparison of the fatigue resistance (initiation, propagation) of cast TA6V with hot rolled TA6V — titanium alloy
[DGT-25369-PT-1] 12 p1808 N85-21341
Fatigue and corrosion fatigue resistance of aluminum casting alloy VAL10 and forging alloy AK6
13 p2025 N85-22690
Use of acoustical emission method to study specifics of fracture of boron reinforced plastic structural elements 13 p2026 N85-22696
Advanced life analysis methods. Volume 1: Cracking data survey and NDI (nondestructive inspection) assessment for attachment lugs
[AD-A150419] 13 p2103 N85-23108
Analysis and design of hydraulic servo systems within the scope of the improvement of a fatigue testing installation of the Royal Dutch Army
[LEOK-TR-1984-09] 14 p2265 N85-24033
Study of fatigue strength of shafts with segmented channels 14 p2282 N85-24138
Durability calculation of wing panel element
14 p2285 N85-24159
Two recent cases of marker load applications on cargo/fighter aircraft fatigue tests
14 p2318 N85-24325
Generation of marker lines by means of marker loads
14 p2318 N85-24327
Fatigue of clad aluminum materials D16T and 2024-T3 with stepped loading 15 p2496 N85-25397
Fatigue strength of alpha-titanium alloys under cophasal action of variable normal and tangential stresses
15 p2498 N85-25407
The effect of frictional forces on fatigue crack growth in lugs
[AD-A151994] 15 p2578 N85-25898
Initial quality of advanced joining concepts
[AD-A152241] 16 p2759 N85-27027
Lubricant and additive effects on spur gear fatigue life
[NASA-TM-87044] 17 p2974 N85-28373
Tests of low-cycle fatigue of elected steels of class 11
[BLL-BISI-TRANS-22039-(9022.06)]
17 p2978 N85-28404
Fatigue and chromium-ferritic steels at elevated temperatures
[DE85-007735] 18 p3074 N85-29015
Fatigue behavior of HY-130 steel weldments containing fabrication discontinuities
[AD-A153630] 18 p3122 N85-29326
Rolling contact fatigue testing of thermomechanically processed M-50 steel
[AD-A153640] 18 p3122 N85-29327
Corrosion fatigue cooperative testing program statistical analysis
[AD-A153886] 19 p3238 N85-30077
Influence of interface ply orientation on fatigue damage of adhesively bonded composite joints
[NASA-TM-86443] 19 p3284 N85-30365
Investigation of fatigue strength of spring steel after high-temperature thermomechanical working (HTMW) by helical drawing
[BLL-M-36274-(5828.4)] 20 p3465 N85-31525
Multiaxial fatigue low cycle fatigue testing
20 p3468 N85-31544
Influence of the molding joint plane on the fatigue resistance of the alloys 7010 and 7050. Test Report No. M1-631600
[PV-M1-631600] 20 p3470 N85-31562
Design and fabrication of durable owner-built wind turbine blades
[DE85-009200] 20 p3484 N85-31650
The effect of abrasive blasting on the fatigue and corrosion of an aluminium-copper alloy
[AD-A154954] 21 p3566 N85-32182
Results of an interlaboratory fatigue test program conducted on alloy 800H at room and elevated temperatures
[NASA-CR-174940] 21 p3597 N85-32340
Rotating bending fatigue strength of silicon carbide and alumina-fiber reinforced aluminum
23 p3907 N85-34206
Fatigue lives of specimens representing critical locations in Mirage 3 spars under Australian and Swiss test spectra
[ARL-STRUC-R-415] 24 p4064 N85-35187

FATS
NT CHOLINE
Prediction of percent body fat for U.S. Navy women from body circumferences and height
[AD-A146456] 06 p0845 N85-15370

FATTY ACIDS
NT BENZOIC ACID
NT CARBOXYLIC ACIDS
NT DICARBOXYLIC ACIDS
The lipid composition and its alteration during the growth stage in pathogenic fungus, epidermophyton floccosum
[NASA-TM-77440] 07 p1011 N85-16421
Fatty and aromatic acid catabolizing bacteria from methanogenic ecosystems
[DE85-008133] 17 p2998 N85-28537

FAULT MECHANICS
U FRACTURE MECHANICS

FAULT TOLERANCE
Assessing the reliability of computer software and computing networks: An opportunity for partnership with computer scientists
[AD-A145131] 01 p0104 N85-10697
Communications protocols for a fault tolerant, integrated local area network for Space Station applications
[NASA-TM-86304] 01 p0106 N85-10711
Fault tolerant computing research
[AD-A145640] 02 p0244 N85-11590
An expert system for representing procedural knowledge
[AD-P003923] 02 p0245 N85-11603
A generalized model of fault-isolation performance
[AD-P003928] 02 p0246 N85-11608
Artificial intelligence approaches to monitoring system integrity
[AD-P003930] 02 p0246 N85-11610
Depot level problems in the testing of printed circuit boards
[AD-P003932] 02 p0247 N85-11612
Technologies for space station autonomy
[NASA-CR-174112] 04 p0458 N85-12906
Analysis of the impact of error detection on computer performance
[NASA-CR-174167] 04 p0547 N85-13477
Test experience on an ultrareliable computer communication network
[NASA-TM-85915] 04 p0552 N85-13514
cost and benefits optimization model for fault-tolerant aircraft electronic systems
[NASA-CR-166043] 07 p0946 N85-15993
Local area network evaluation by MICROSS extensions
[AD-A146773] 07 p1027 N85-16521
Investigating version dependence in fault-tolerant software 08 p1065 N85-16749
Evolution of shuttle avionics redundancy management/fault tolerance 08 p1090 N85-16890
SSME digital control design characteristics
08 p1091 N85-16893
A unified model for performance and reliability of Fault-Tolerant/Multi-Mode systems
[AD-A148789] 08 p1208 N85-17601
Research on optimal control, stabilization and computational algorithms for aerospace applications
[NASA-CR-174318] 08 p1209 N85-17603
Extended Stochastic Petri Nets: Applications and analysis
[AD-A148439] 08 p1213 N85-17633
SPADE: Series-parallel directed acyclic graph evaluator
[AD-A148458] 09 p1368 N85-18592
Beyond fault trees to fault graphs
[DE84-017022] 09 p1370 N85-18608
An ultra reliable computer communication network: The dispersed sensor processing mesh
09 p1372 N85-18620
AIRLAB: A laboratory for flight-crucial-electronics system research 13 p1968 N85-22362
Reliability bounds for fault-tolerant systems with competing responses to component failures
[NASA-TP-2409] 13 p2100 N85-23090
A theoretical basis for the analysis of redundant software subject to coincident errors
[NASA-TM-86369] 13 p2145 N85-23317
Measurement of SIFT operating system overhead
[NASA-TM-86322] 13 p2149 N85-23337
An experiment in software reliability
[NASA-CR-172553] 14 p2403 N85-24813
Care 3 model overview and user's guide, first revision
[NASA-TM-86404] 15 p2627 N85-26192
An abstract specification language for Markov reliability models
[NASA-TM-86423] 16 p2857 N85-27616
Efficient VLSI (Very Large Scale Integration) fault simulation
[AD-A152661] 17 p2953 N85-28233
Optimal design and use of retry in fault tolerant real-time computer systems
[NASA-CR-175920] 17 p3015 N85-28643
Evaluation of a fault tolerant system for an integrated avionics sensor configuration with TSRV flight data
[NASA-CR-172589] 18 p3062 N85-28941
Guidance on planning and implementing computer system reliability
[PB85-177996] 18 p3161 N85-29581
Research on optimal control, stabilization and computational algorithms for aerospace applications
[NASA-CR-172528] 19 p3221 N85-29970
Ultrareliable, fault-tolerant control systems: A conceptual description
[NASA-TM-86017] 19 p3221 N85-29972
Graceful fault tolerance in large networks of microcomputers 19 p3332 N85-30643
Development and evaluation of a Fault-Tolerant Multiprocessor (FTMP) computer. Volume 2: FTMP software
[NASA-CR-166072] 19 p3341 N85-30706
Development and evaluation of a Fault-Tolerant Multiprocessor (FTMP) computer. Volume 3: FTMP test and evaluation
[NASA-CR-166073] 19 p3341 N85-30707
Fault-tolerant computing research
[AD-A154082] 19 p3342 N85-30710
Implementation of a serial communication process for a fault tolerant, real time, multitransputer operating system
[AD-A154237] 19 p3343 N85-30714

Performance and evaluation of real-time multicomputer control systems
[NASA-CR-176096] 21 p3673 N85-32821
A new fault-tolerant algorithm for clock synchronization
[AD-A154771] 21 p3676 N85-32836
A dual, fault-tolerant aerospace actuator
22 p3798 N85-33530
Design of a dual fault tolerant space shuttle payload deployment actuator 22 p3798 N85-33531
Modeling and measurement of fault-tolerant multiprocessors
[NASA-CR-3920] 22 p3833 N85-33732
Study of fault tolerant software technology for dynamic systems
[NASA-CR-172618] 24 p4137 N85-35642

FAULT TREES
Minimal cut-set methodology for artificial intelligence applications
[DE84-016674] 04 p0553 N85-13518
Avionics fault tree analysis and artifical intelligence for future aircraft maintenance 08 p1066 N85-16755
Beyond fault trees to fault graphs
[DE84-017022] 09 p1370 N85-18608
Calculation through Fault Tree Analysis of the probability of a warhead being armed prior to launch
[AD-P004339] 10 p1454 N85-19163
Contribution of instrumentation and control software to system reliability
[DE85-004693] 13 p2149 N85-23340

FAULTS
Models of natural intelligence in fault diagnosis tasks: Implications for training and aiding of maintenance personnel
[AD-P003927] 02 p0246 N85-11607
Battery control and fault detection method
[AD-D011384] 07 p0993 N85-16307

FAUNA
U ANIMALS

FCC LATTICES
U FACE CENTERED CUBIC LATTICES

FDMA
U FREQUENCY DIVISION MULTIPLE ACCESS

FEAR
NT FEAR OF FLYING

FEAR OF FLYING
The Reports of Aeromedical Laboratory, volume 25, no. 1/2
[ISSN-0023-2858] 01 p0090 N85-10605
The relationship between emotional tension scale and psychological uneasiness of JASDF pilots in flying situations 01 p0090 N85-10606

FEASIBILITY
A preliminary study of the feasibility of detecting the floating macrophytes by means of digital processing of MSS/LANDSAT data
[E85-10005] 02 p0215 N85-11418
Initial feasibility ground test of a proposed photogrammetric system for measuring the shapes of ice accretions on helicopter rotor blades during forward flight
[NASA-TM-87381] 04 p0455 N85-12887

FEASIBILITY ANALYSIS
Exploratory investigation of the need for and feasibility of a Lower Atmosphere Research Satellite (LARS) program
[NASA-CR-1[illegible]181] 01 p0015 N85-10091
Prospectus of the utilization of leafy spurge (Euphorbia Esula L.) as a source of liquid fuel and biomass
[DE84-015203] 01 p0034 N85-10208
Theory of near-field phased arrays for electromagnetic susceptibility testing
[PB84-217836] 01 p0042 N85-10273
The development of a diode laser Doppler velocimeter for boundary layer measurements under ice: A feasibility investigation
[AD-A145076] 01 p0053 N85-10348
Robotics investment decision model user's manual
[AD-A145467] 02 p0204 N85-11347
Research on gallium arsenide diffused junction solar cells
[NASA-CR-174057] 02 p0222 N85-11457
SLIM TDMA ANIK B pilot project
[CRC-REPT-1366] 03 p0354 N85-12278
Feasibility study of a satellite-borne 90 GHz radiometer 04 p0459 N85-12914
Methodology for the implementation of a domestic satellite communications network
04 p0493 N85-13148
Measurement of range-resolved water vapor concentration by coherent CO2 differential absorption lidar
[PB84-236892] 04 p0535 N85-13420
Feasibility of long duration ballooning in Antarctica
[PB84-240571] 04 p0541 N85-13443
Report of the reference designs study group on the superconducting super collider
[DE84-015567] 04 p0569 N85-13630
Results of principal NASA studies on space station uses and functional requirements 07 p0914 N85-15787
Feasibility of producing a range of food products from a limited range of undifferenitiated major food components
[NASA-CR-177329] 07 p1020 N85-16473
NSW (National Software Works) lessons learned
[AD-A146737] 07 p1023 N85-16494
Feasibility of measuring technical productivity improvements in Air Force Logistics Command depot-level maintenance using the Data Envelopment Analysis (DEA) and Constrained Facet Analysis (CFA) models
[AD-A147329] 07 p1052 N85-16676
Proposal for a small scheme implementation
[AD-A148707] 09 p1388 N85-18595
Magnetic heat pump feasibility assessment
[DE85-002806] 11 p1632 N85-20276
Advanced glazings research
[DE85-000539] 11 p1674 N85-20549
Feasibility of producing commodities and electricity for space shuttle operations at Vandenberg Air Force Base
[DCN-84-203-001-80-21] 12 p1789 N85-21230
Technological and economic assessment of advanced ceramic materials. Volume 6: A case study of ceramic cutting tools
[PB85-113132] 12 p1815 N85-21387
Shallow magma targets in the western US
[DE85-003274] 12 p1881 N85-21803
Using a data base management system for modelling SSME test history data 12 p1944 N85-22211
A standard aircraft diffusion flame: Spectral characteristics and a feasibility study for developing an alternate calibration source for aircraft optical fire detection systems
[AD-A150231] 13 p2039 N85-22768
Multifunctional elements for integrated optics
13 p2068 N85-22918
Technical and cost analyses of manganese nodule processing techniques and their significant variations
[PB85-148815] 14 p2258 N85-23992
Feasibility study of an installation to simulate the flow of propellant gases in a gun barrel, part 2
[ISL-R-128/83-PT-2] 14 p2303 N85-24263
Feasibility of optical instruments based on multiaperture optics
[AD-A150868] 14 p2421 N85-24936
FRG opinion on Spacelab benefits, space station participation 15 p2532 N85-25618
Application of infrared radiometers for airborne detection of clear air turbulence and low level wind shear, airborne infrared low level wind shear detection test
[NASA-CR-175725] 15 p2594 N85-25985
A practical system for collecting reliable data on the space-time behavior of people
[AD-A151174] 15 p2619 N85-26140
A feasibility study for using low boiling point fluids to change aircraft tire deflection
[AD-A152096] 16 p2706 N85-26701
Feasibility study on Laser Doppler Anemometer (LDA) wind velocity measurements using pulsed visible laser light
[ISL-CO-224/83] 16 p2836 N85-27489
Preliminary technology utilization assessment of the robotic fruit harvester
[NASA-CR-175834] 16 p2844 N85-27532
On various Fourier series utilized for solution of structural mechanics problems
[VTH-LR-429] 16 p2856 N85-27615
Transverse electron resonance accelerator
[DE85-008289] 17 p3032 N85-28758
Some Europeans voice opposition to space station participation 18 p3066 N85-28961
Personal mobile communications by satellite
[REPT-15-4572] 18 p3091 N85-29135
Stability and feasibility of model ecosystems
[PREPRINT-431] 18 p3134 N85-29408
Feasibility study of a fission-suppressed Tokamak fusion breeder
[DE85-009099] 18 p3190 N85-29786
Note for a research feasibility project: High reliability design in the aeronautical field
[REPT-84-RR-350] 20 p3387 N85-31005
Future prospects for a combined INMARSAT polar communication and search and rescue satellite system
20 p3406 N85-31137
Large space structure flight experiment
20 p3410 N85-31163
Preliminary investigations concerning a 90 GHz radiometer satellite experiment
[ESA-TT-860] 20 p3420 N85-31225
Improved turbopump dynamics
[NASA-TM-86514] 20 p3462 N85-31509
Rain volume estimation over areas using satellite and radar data
[NASA-CR-176050] 21 p3634 N85-32570
Feasibility of applications of Competition Decision Assist Package (CDAP) to spare parts
[AD-A154716] 21 p3712 N85-33038
Deficit irrigation feasibility study and demonstration project
[DE85-011531] 22 p3802 N85-33565
Diffusion welding of Cassegrainian concentrator cell stack assemblies
[NASA-CR-176104] 22 p3805 N85-33598
Small-hydropower development: The process, pitfalls, and experience. Volume 1: Feasibility studies summary and analysis
[DE85-010639] 22 p3806 N85-33599
Technology transfer report: Feasibility study for the use of geothermal brine in the Ashdod area, Israel
[DE85-013316] 22 p3810 N85-33606
Thermal protection systems for reentry vehicles
[CNES-NT-113] 23 p3900 N85-34157
Calculations on the feasibility of ultrasonic inspection of steam generator tubing in pressurized water reactors
[AERE-R-10960] 23 p3940 N85-34419
SP-100 Thermionic Technology Program
[DE85-012311] 23 p3972 N85-34625
Miniature infra-red data acquisition and telemetry system
[NASA-CR-177953] 24 p4096 N85-35200

FEATHERING
Study to eliminate ground resonance using active controls
[NASA-CR-166609] 07 p0902 N85-15716
Optimally designed propellers constrained by noise
24 p4065 N85-35196

FEATURE EXTRACTION
U PATTERN RECOGNITION

FECES
Improved orbiter waste collection system study
[NASA-CR-171830] 08 p1199 N85-17548
Space Shuttle Orbiter waste collection system conceptual study
[NASA-CR-171844] 08 p1199 N85-17553
Preliminary assessment of climatic change during late Wisconsin time, southwest Great Basin and vicinity, Arizona, California and Nevada
[DE85-006343] 16 p2836 N85-27488

FEDERAL BUDGETS
Department of Housing and Urban Development, and certain independent agencies appropriations for fiscal year 1985, part 2
[S-REPT-98-889-PT-2] 01 p0127 N85-10870
National Aeronautics and Space Administration
01 p0127 N85-10871
The status of synthetic fuels and cost-shared energy R and D facilities
[GPO-36-903] 03 p0339 N85-12182
Financing considerations and Federal budget impacts
07 p0915 N85-15792
Outlook for expanding the Federal research in progress system
[AD-A148354] 08 p1229 N85-17737
1984 science and technology posture hearing with the director of the Office of Science and Technology Policy
[GPO-41-060] 12 p1949 N85-22244
An agenda for a study of government science policy
[GPO-40-860] 12 p1949 N85-22245
President's private sector survey on cost control, report on research and development
[PB84-173269] 12 p1951 N85-22253
Summary of activities of the Committee on Science and Technology
[H-REPT-98-1189] 12 p1964 N85-22341
Department of Housing and Urban Development-independent agencies appropriations for 1986. Part 6: National Aeronautics and Space Administration
[GPO-47-235] 16 p2879 N85-27768
Selected university laboratory needs in support of national security
[AD-A153511] 18 p3197 N85-29833
Department of Housing and Urban Development-Independent Agencies Appropriation Bill, 1986
[H-REPT-99-212] 19 p3382 N85-30979
National Aeronautics and Space Administration
19 p3382 N85-30980
NASA authorization, 1986, volume 1
[GPO-46-385] 20 p3541 N85-32039
Department of Housing and Urban Development-Independent Agencies Appropriation Act, 1986 20 p3542 N85-32041
National Aeronautics and Space Administration research and development 20 p3542 N85-32042

Testimony of Robert A. Frosch before the Subcommittee on HUD and Independent Agencies of the Senate Committee on Appropriations
[NASA-TM-87496] 22 p3738 N85-33173
Department of Housing and Urban Development Independent Agencies Appropriation Bill, 1986
[S-REPT-99-129] 23 p3987 N85-34720
National Aeronautics and Space Administration research and development: Program description
23 p3987 N85-34721
Progress report on implementing the recommendations of the White House Science Council's Federal Laboratory Review Panel, volume 1
[PB85-185072] 24 p4164 N85-35819

FEDERAL REPUBLIC OF GERMANY
U WEST GERMANY

FEED SYSTEMS
Feed system design considerations for large space antenna systems. Part 1: Multiple apertures with non-overlapping feeds 14 p2234 N85-23852
Feed system design considerations for large space antenna systems. Part 2: Single aperture with overlapping feeds 14 p2235 N85-23853
Auxiliary units for Robots 14 p2285 N85-24161
Inspection evaluation and repair of the flawed feedwater nozzle of the 50 MWe Dodewaard GKN boiling water reactor
[ISBN-90-353-0017-3] 17 p2977 N85-26394

FEEDBACK
NT BIOFEEDBACK
NT NEGATIVE FEEDBACK
NT NONLINEAR FEEDBACK
NT SENSORY FEEDBACK
Optimizing search with positive information feedback
[CSIR-TWISK-313] 01 p0125 N85-10855
Qualitative results for distributed systems with discrete damping and stiffness with application to control
[AD-A145525] 02 p0209 N85-11362
Self-modulation of injection laser emission intensity due to external optical feedback 02 p0261 N85-11706
An appraisal of an out-of-phase feed-back system for the variation of damping of dynamic wind-tunnel models
[NMI-169] 03 p0320 N85-12065
Investigation of cloud feedback in the GLAS model
05 p0685 N85-14404
Feedback, adaptivity and A-posterior estimates in finite elements: Aims, theory and experience
[AD-A146669] 07 p1029 N85-16531
Unstable optical resonator with cancelling edge waves
[AD-D011379] 07 p1042 N85-16618
A feedback finite element method with a posteriori error estimation. Part 1. The finite element method and some basic properties of the A posteriori error estimator
[AD-A148345] 08 p1212 N85-17631
A note on the disturbance decoupling problem for retarded systems
[AD-A149045] 10 p1543 N85-19730
The eigenstructure assignment of deadbeat control systems
[AD-A149761] 12 p1834 N85-21510
Total energy-rate feedback for automatic glide-slope tracking during wind-shear penetration
[NASA-TP-2412] 14 p2226 N85-23801
Practical methods for the compensation and control of multivariable systems
[AD-A151047] 14 p2407 N85-24841
Stochastic pursuit-evasion differential games in the plane
[CSIR-TWISK-343] 14 p2412 N85-24875
Positioning of a robotic manipulator through the use of visual feedback
[AD-A151933] 16 p2851 N85-27577
Principles of designing digital compensating accelerometers 17 p2944 N85-28172
Short and long-term robot feedback
[PB85-180735] 19 p3281 N85-30347
Interactive computer program for the analysis and design of linear time invariant systems
[AD-A154076] 19 p3335 N85-30664
Self Q-modulation and generation of short pulses in distributed-feedback lasers 21 p3687 N85-32907

FEEDBACK AMPLIFIERS
Efficiency in integral active antennas
06 p0792 N85-15060
Method of improving dynamic characteristics of DC voltage stabilizers with compound regulation
15 p2528 N85-25589
Eye movement in response to single and multiple targets
[AD-A151115] 15 p2617 N85-26126
Synthesis of high-speed devices using integrated operational amplifiers 22 p3781 N85-33426

FEEDBACK CIRCUITS
Experimental performance of a frequency measurement circuit
[AD-A152951] 17 p2953 N85-28239
A study of reflex optoelectronic switching matrices and their derivatives
[CRC-TN-720] 19 p3253 N85-30169

FEEDBACK CONTROL
NT CASCADE CONTROL
Interactive aircraft flight control and aeroelastic stabilization
[NASA-CR-174025] 02 p0148 N85-11003
Optimal nonlinear feedback control of spacecraft attitude maneuvers 02 p0167 N85-11126
Smith predictor and self-tuning control of muscle relaxant drug administration
[RR-257] 02 p0235 N85-11534
On a class of suboptimal controls for infinite-dimensional bilinear systems
[RR-258] 02 p0249 N85-11630
Control and identification of time varying systems
[AD-A145638] 02 p0252 N85-11649
The numerical range: A tool for robust stability studies — multivariable feedback systems
[RR-255] 02 p0253 N85-11660
CONTROL: A suite of interactive transfer-function analysis programs
[OUEL-1527/84] 03 p0408 N85-12609
On the relationship between Lehtomaki's robustness test and an inverse Nyquist based test
[OUEL-1526/84] 03 p0409 N85-12616
Non-linear systems in infinite dimensional state spaces
[AD-A145828] 03 p0410 N85-12623
Return difference feedback design for robust uncertainty tolerance in stochastic multivariable control systems
[AD-A145861] 03 p0411 N85-12624
Control of linear stationary objects subject to external actions by means of various types of feedback
04 p0488 N85-13114
Frequency response design methods for large scale systems
[DE84-014161] 04 p0553 N85-13517
Experiments in control of flexible structures with uncertain parameters 05 p0602 N85-13837
The acquisition, processing, and use of tactile sensor data in robot control 05 p0641 N85-14114
A nonlinear filter for compensating for time delays in manual control systems 05 p0700 N85-14493
Does McKuer's law hold for heart rate control via biofeedback display? 05 p0706 N85-14528
Active sticks: A new dimension in controller design
05 p0706 N85-14531
An H-infinity-minimax approach to the design of robust control systems
[OUEL-1537/84] 05 p0717 N85-14600
Improvement of the transient response in the finite settling time control
[NAL-TR-823] 06 p0757 N85-14843
Flutter control with unsteady aerodynamic models
[AD-A147858] 07 p0909 N85-15753
Precise control of flexible manipulators
[NASA-CR-174210] 07 p0973 N85-16178
Multivariable flight control with time-scale separation
[NASA-CR-174320] 08 p1067 N85-16873
Time series analysis of closed-loop pilot vehicle dynamics 08 p1067 N85-16876
Research on optimal control, stabilization and computational algorithms for aerospace applications
[NASA-CR-174318] 08 p1209 N85-17603
Improved stability and performance bounds using approximate models — control system design
[RR-260] 08 p1209 N85-17606
Utilization of numerical optimization techniques in the design of robust multi-input, multi-output control systems
[AD-A148289] 08 p1212 N85-17630
Servo operated anti-G suit pressurization system
[AD-D011468] 10 p1531 N85-19651
A note on the disturbance decoupling problem for retarded systems
[AD-A149045] 10 p1543 N85-19730
Tethered satellite system project overview
11 p1642 N85-20341
Analytically redundant output feedback scheme for reduction of structural loads of a flexible transport aircraft
[TT-8303] 12 p1777 N85-21154
Modal control of structural systems
[AD-A149734] 12 p1790 N85-21235
Stability analysis of flexible spacecraft with PID controller
[CRC-1372] 12 p1792 N85-21247
NASA/MSFC ground experiment for large space structure control verification
[NASA-TM-86496] 12 p1792 N85-21248
The eigenstructure assignment of deadbeat control systems
[AD-A149761] 12 p1834 N85-21510
Control of nonlinear objects 12 p1842 N85-21561
Dynamic visual servo control of robots: An adaptive image-based approach
[AD-A150057] 12 p1860 N85-21667
Practical considerations for noninteracting control synthesis
[AD-A150130] 12 p1918 N85-22046
Testing of the digital flight control system of the German CCV fighter experimental aircraft
13 p1968 N85-22361
Periodic binary sequence generators: VLSI circuits considerations
[NASA-CR-175649] 13 p2063 N85-22886
Control of cascaded induction generator systems
[AD-A150429] 13 p2065 N85-22897
Design of multivariable feedback control systems via spectral assignment using reduced-order models and reduced-order observers
[NASA-CR-3889] 14 p2226 N85-23800
Dynamic verification of large space structures
14 p2234 N85-23847
A mathematical formulation of the Scole control problem, part 1
[NASA-CR-172581] 14 p2243 N85-23903
Two-stage gyrocompass 14 p2273 N85-24060
Computer program TRAMP: Inclusion of state space facilities and the analysis of non-linear elements
[BAE-BT-12643] 15 p2626 N85-26181
The modeling and simulation of feedback control systems
[NASA-CR-171875] 15 p2632 N85-26225
Flight control system reconfiguration design using quantitative feedback theory
[AD-A151771] 16 p2710 N85-26722
Application of linear optimal control theory to the design of the elevator control system of the DHC-2 Beaver experimental aircraft
[VTH-LR-411] 16 p2711 N85-26729
Flight testing and development of the F/A-18A digital flight control system 16 p2713 N85-26743
OLGA: An open loop gust alleviation
16 p2713 N85-26744
Optimal open loop and nonlinear feedback control for remote orbital capture
[AD-A151967] 16 p2732 N85-26859
Nonintrusive shaft speed sensor
16 p2740 N85-26908
Digital RF delay line for ECM (electronic countermeasure) look-through
[AD-A152120] 16 p2774 N85-27120
Development of graphical time response using the OPTSYSX program
[AD-A152221] 16 p2848 N85-27557
Stabilizing force feedback in bio-actuated control systems
[AD-D011634] 17 p3002 N85-28560
Closed loop electrostatic levitation system
[NASA-CASE-NPO-15553-1] 18 p3092 N85-29142
An interactive computer aid for the design and analysis of linear, single input/single output digital and continuous control systems
[AD-A153704] 18 p3162 N85-29589
Research on optimal control, stabilization and computational algorithms for aerospace applications
[NASA-CR-172528] 19 p3221 N85-29970
Evaluation of methods used for the determination of acidity in acid rain samples
[PB85-178309] 19 p3237 N85-30070
Phase and amplitude feedback control system for the Los Alamos free-electron laser
[DE85-010787] 19 p3277 N85-30325
High gain adaptive control of decentralized systems
[DE85-001566] 19 p3343 N85-30717
Multivariable control of a soft coupled space station
20 p3408 N85-31151
Automatic assembly of space stations
20 p3409 N85-31153
Antenna pointing of large flexible telecommunications spacecraft 20 p3409 N85-31156
Proceedings of the Workshop on Identification and Control of Flexible Space Structures, volume 2
[NASA-CR-176052] 20 p3411 N85-31170
Approximation techniques for parameter estimation and feedback control for distributed models of large flexible structures 20 p3413 N85-31179
Parametric stiffness control of flexible structures
20 p3414 N85-31187
Wideband disturbance accomodation in precision flexible space structures 20 p3415 N85-31194
Proceedings of the Workshop on Identification and Control of Flexible Space Structures, volume 3
[NASA-CR-176053] 20 p3415 N85-31195
Eigenvalue placement and stabilization by constrained optimization 20 p3416 N85-31198
Self-tuning adaptive-controller using online frequency identification 20 p3417 N85-31205

Feedforward-feedback control logic for robust target-tracking 20 p3436 N85-31317

Decentralized control synthesis method for large-scale interconnected systems
[DE85-000748] 20 p3518 N85-31878

Ultrasonic position reference systems for an autonomous sentry robot and a robot manipulator arm
[AD-A155481] 21 p3596 N85-32336

Flight test experience and controlled impact of a large, four-engine, remotely piloted airplane
[NASA-TM-86738] 22 p3730 N85-33123

Decentralized control of dynamically interconnected systems
[BU-111] 22 p3835 N85-33744

Method and apparatus for transfer function simulator for testing complex systems
[NASA-CASE-NPO-15696-1] 23 p3926 N85-34333

Feedback regulated induction heater for a flowing fluid
[DE85-006508] 23 p3939 N85-34414

A graph theoretic procedure for the design of feedback patterns
[REPT-110] 24 p4142 N85-35673

Design of dynamic compensators of prescribed pattern
[BU-109] 24 p4142 N85-35674

Spreading the control complexity in decentralized control of interconnected systems
[BU-117] 24 p4144 N85-35688

Decentralized stabilization by high gain feedback
[BU-115] 24 p4144 N85-35689

FEEDERS

Stability indicators for front end loaders
[AD-P004293] 09 p1408 N85-18870

Leak monitoring in high pressure preheaters by a noninvasive ultrasonic method
[CISE-2373] 11 p1650 N85-20394

Leak detection by acoustic emission monitoring in power plant high pressure preheaters
[CISE-2392] 11 p1650 N85-20395

New technique for fluid feed in simultaneous multisurface grinding 13 p2045 N85-2280

FEEDFORWARD CONTROL

Decentralized control synthesis method for large-scale interconnected systems
[DE85-000748] 20 p3518 N85-3187

FEELINGS

U SENSORY FEEDBACK

FEET (ANATOMY)

Translating rudder pedal system
[AD-D011510] 12 p1780 N85-2117

FELDSPARS

Concordant bands of augen gneiss within metasedimentary rocks in the Big Delta C-2 quadrangle east-central Alaska 04 p0516 N85-1329

Solar cosmic ray produced neon in lunar soils and their implication for gas-rich meteorite studies
06 p0887 N85-15636

Interim rock mass properties and conditions for analyses of a repository in crystalline rock
[DE85-010700] 18 p3125 N85-29352

Conditions for formation of parageneses containing kyanite-orthoclase in region of Mount Provender and Pratt Peak (Shackleton Range, Antarctica)
19 p3298 N85-30447

Primordial magmaspheres and their lasting consequences 22 p3857 N85-33882

FEMALES

Challenges in the development of the shuttle extravehicular mobility unit 08 p1095 N85-16922

Aviation-related cardiorespiratory effects of blood donation in female pilots
[AD-A148045] 08 p1195 N85-17529

An investigation of spinal injury potential from the use of the ACES 2 ejection seat by lower weight female pilots
[AD-A148449] 08 p1196 N85-17537

Blood viscosity responses to acute exercise and aerobic conditioning in women 09 p1363 N85-18573

Assessment of muscle strength and prediction of lifting capacity in US Army personnel
[AD-A148846] 10 p1527 N85-19633

The effect of occupational exposure and the body weight to height ratio on exhaled methylene chloride breath concentration in females at one, eighteen and sixty-six hours post exposure 14 p2388 N85-24708

The energy cost of women walking and running in shoes and boots
[AD-A151022] 14 p2389 N85-24716

Perceived heterogeneity and its effect on various typas of tasks
[AD-A151003] 14 p2392 N85-24729

Physiological differences between men and women in exercise-heat tolerance and heat acclimation
[AD-A152048] 15 p2618 N85-26135

Cosmonaut Savitskaya says many women in cosmonaut training 16 p2717 N85-26774

Comparative anaerobic power of males and females
[AD-A151960] 16 p2842 N85-27523

FEMUR

Locomotion research for the analysis of the human gait and for the determination of the maximum loads of the pelvis-leg skeleton. Volume 1: Two-dimensional analysis
[BMFT-FB-T-83-187-VOL-1] 02 p0236 N85-11535

FENCES (BARRIERS)

Deer control using 7 strand vertical fence
11 p1581 N85-19958

Reducing gull use of some attractions near airports
[AD-P004195] 11 p1581 N85-19962

Effectiveness of an overhead wire barrier in deterring gulls from feeding at a sanitary landfill
[AD-P004199] 11 p1582 N85-19966

FERMENTATION

DOE supported research in alcohol fuel technology development
[DE84-007686] 06 p0774 N85-14948

ECUT, Energy Conversion and Utilization Technologies program: Technical and economic assessment of processes for the production of butanol and acetone. Phase 2: Analysis of research advances
[NASA-CR-175471] 10 p1434 N85-19034

Ethanol production by enzymatic hydrolysis: Parametric analysis of a base-case process
[DE84-013105] 11 p1614 N85-20147

Anaerobic microbial transformations in subsurface environments
[DE85-012790] 22 p3819 N85-33659

Production of butanol by fermentation in the presence of cocultures of clostridium
[NASA-CASE-NPO-16203-1] 24 p4071 N85-35227

FERMI LIQUIDS

Quasiparticle excitations in valence-fluctuation materials: Effects of band structure and crystal fields
[DE85-010783] 19 p3359 N85-30824

FERMI SURFACES

Kohn anomaly in metastable fcc lanthanum at low temperatures
[DE84-015459] 04 p0569 N85-13628

Electronic properties of intercalated graphite and amorphous metals
[AD-A147664] 08 p1225 N85-17716

Fermi surface study of CeSb
[DE85-002532] 10 p1564 N85-19862

First principles theory of Fermi-surface driven concentration waves in Cu/sub c/Pd/sub 1-c/ alloys
[DE85-005367] 13 p2024 N85-22681

Further results on the equipartition threshold in large nonlinear Hamiltonian systems
[PREPRINT-428] 18 p3173 N85-29668

Quantized Hall conductance as a topological invariant
[DE85-007796] 18 p3193 N85-29808

Aspects of silicon bulk lifetimes
20 p3479 N85-31617

FERMI-DIRAC STATISTICS

Potential at atomic boundaries in the TF (or TFD) model and equations of states 12 p1820 N85-21419

First-order shock acceleration in solar flares
[SH-1.1-5] 23 p3989 N85-34732

FERMIONS

NT ANTINEUTRINOS
NT BARYONS
NT COLD NEUTRONS
NT CONDUCTION ELECTRONS
NT FAST NEUTRONS
NT HYPERONS
NT LEPTONS
NT MUONS
NT NEUTRINOS
NT NEUTRONS
NT PROTONS
NT SOLAR NEUTRINOS
NT SOLAR PROTONS
NT THERMAL NEUTRONS

Constraints to the radiative lifetime of a light neutral fermion in the galactic halo from IUE
[NOTA-INTERNA-817] 02 p0279 N85-11820

Measurement of the induced moment magnetic form factor of a heavy fermion superconductor
[DE85-004165] 12 p1942 N85-22194

Canonical analysis of the fermion sector in higher-derivative supergravity
[DE85-007828] 16 p2859 N85-27635

Boson degrees of freedom in Fermion many-body systems
[DE85-006997] 16 p2863 N85-27660

Microscopic analysis of angular momentum projected HFB-states in terms of interacting bosons
[DE85-007629] 16 p2863 N85-27661

Comment on quantum effects on 4-dimensional space-time symmetries
[DE85-007780] 16 p2872 N85-27722

On the definition of topological susceptibility via lattice anomalous Ward identities and its perturbative tail
[PREPRINT-416] 18 p3184 N85-29744

Neutron scattering study of the heavy fermion system UBe-13
[DE85-010955] 19 p3356 N85-30804

Boson-fermion symmetries in the W-Pt region
[DE85-009755] 19 p3362 N85-30845

Monte Carlo simulations of fermion systems: The determinant method
[DE85-010706] 19 p3376 N85-30947

Pairing correction of particle-hole state densities for two kinds of fermions
[DE85-011549] 23 p3971 N85-34820

FERRATES

Analysis of ferrates and ferrites of three transition metals using Moessbauer effects
[BLL-CE-TRANS-8019-(9022.09)]
20 p3430 N85-31273

FERRIC IONS

Dynamics of graphite fiber intercalation: In situ resistivity measurements with a four point probe
[NASA-TM-86858] 01 p0017 N85-10106

FERRIMAGNETS

Static and dynamic disordering in amorphous magnets and crystals 03 p0422 N85-12099

FERRITES

Study to optimize Cr-Mo steels to resist hydrogen and temper embrittlement. A study of carbides formed in low alloy Cr-Mo steels
[DE84-015208] 01 p0029 N85-10179

Symmetry of exchange interaction in crystalline magnetic films 02 p0259 N85-11694

Stability of several substituted ferrites in a reducing atmosphere
[AD-A146108] 03 p0328 N85-12112

Effects of prior austenite and ferrite grain size on fracture properties of a plain carbon steel
[AD-A146276] 03 p0332 N85-12138

Anisotropy and relaxation effects of Co2+ ions in LiTi ferrite
[AD-A146550] 06 p0861 N85-15480

Fundamental tribological properties of ceramics
[NASA-TM-86915] 07 p0930 N85-15893

Defective nature of the crystalline lattice of nickel ferrite-based solid solutions
[BLL-WH-595-(9091.9F)] 07 p1046 N85-16645

Replacement of Fe-3+ ions in nickel ferrites by nonmagnetic Al-3+ and Sc-3+ ions
[BLL-WH-594-(9091.9F)] 08 p1125 N85-17090

Defective nature of the crystalline lattice of nickel ferrite-based solid solutions
[BLL-TRANS-WH-595-(9091.9F)]
10 p1439 N85-19068

Permanent magnet motors
[DE85-000660] 10 p1482 N85-19355

Magnetic and structural properties of shock-synthesized zinc ferrite
[DE85-000469] 11 p1736 N85-20915

Humidity effects on adhesion of nickel-zinc ferrite in elastic contact with magnetic tape and itself
[NASA-TP-2449] 12 p1811 N85-21359

Quenching effects on iron site partitioning in the Apollo 17 orange glass composition 13 p2184 N85-22553

Studies of ferritic filler metals for welding 9 percent nickel steel 15 p2565 N85-25825

Effects of wear on structure-sensitive magnetic properties of ceramic ferrite in contact with magnetic tape
[NASA-TM-87007] 16 p2753 N85-26891

Mechanical stabilization of austenite against epsilon martensite and its effect on deformation behavior in high manganese steels
[DE85-007654] 17 p2932 N85-28097

Analysis of ferrates and ferrites of three transition metals using Moessbauer effects
[BLL-CE-TRANS-8019-(9022.09)]
20 p3430 N85-31273

FERRITIC STAINLESS STEELS

Alloying effects of reactive elements in ferritic stainless steels 02 p0178 N85-11186

Sour-gas cracking in ferritic steels
[AERE-R-10908] 03 p0333 N85-12148

The role of void nucleation in the swelling resistance of ferritic steel
[AERE-R-11525] 11 p1610 N85-20122

Thickness effects of fracture toughness
[DE85-002974] 11 p1653 N85-20409

Investigation of the development possibilities of a ferritic creep and oxidation-resistant steel for application under creep conditions above 650 deg C
[BMFT-FB-T-84-244] 12 p1808 N85-21344

The ferrite permanent magnet AC motor: A technical and economical assessment
[DE85-002480] 13 p2066 N85-22903

Rapid solidification of candidate ferritic steels
[DE85-008596] 16 p2750 N85-26971
Properties of corrosion resistant stabilized ferritic steels
[BLL-BISI-TRANS-22519-(9022.06)]
17 p2925 N85-28039
Stainless steels: Application and welding
[BLL-BISI-TRANS-22357-(9022.06)]
17 p2927 N85-28059
Fatigue behavior of chromium-containing ferritic steels at elevated temperature
[DE85-012309] 22 p3748 N85-33231

FERROALLOYS
U IRON ALLOYS

FERROELECTRICITY
Center for dielectric studies
[AD-A146183] 03 p0434 N85-12761
Ferroelectric tungsten bronze bulk crystals and epitaxial thin films for electro-optic device applications
[AD-A151044] 14 p2427 N85-24970
Capacitive energy storage at cryogenic temperatures
[AD-A154508] 21 p3579 N85-32253
Materials used by industry for the production of piezoelectric transducers. The state of the art of research work performed in the field of PZT ceramics and ferroelectric polymers
[ISL-CO-211/84] 24 p4089 N85-35344
Ferroelectric homopolymer PVF2 and P (VDF-TrFe) copolymers 24 p4089 N85-35347

FERROFLUIDS
Use of ferrofluids in machining of metals
13 p2045 N85-22802
Linear motion valve
[NASA-CASE-MSC-20148-1] 18 p3115 N85-29284

FERROMAGNETIC FILMS
Magnetization of very thin Ni films in epitaxial metal film sandwiches of Cu
[DE85-001640] 10 p1563 N85-19860
Study of amorphous strips and microconductors by ferromagnetic resonance method
15 p2497 N85-25402
Dielectric mirror with ferromagnetic substrate
21 p3696 N85-32966

FERROMAGNETIC MATERIALS
NT FERROFLUIDS
NT FERROMAGNETIC FILMS
NT MAGNETITE
Contributions to the 7th International Acoustic Emission Symposium
[AD-A145366] 02 p0275 N85-11792
Use of magnetic compression based on amorphous alloys as a drive for induction linacs
[DE84-014524] 02 p0277 N85-11805
Nonlinear electromagnetic waves in ferromagnetic conducting media 03 p0346 N85-12232
Effect of external magnetic field on characteristics of current-carrying steel tape 06 p0788 N85-15034
Advanced artificial dielectric materials for millimeter wavelength applications
[AD-A148960] 10 p1431 N85-19027
Application of hysteresis modelling to the non-destructive inspection of stress
[DE85-003081] 11 p1650 N85-20393
The UFe4P12 and CeFe4P12: Non-metallic isotopes of superconducting LaFe4P12
[DE85-003724] 12 p1942 N85-22195
Annealing effects in ferromagnetic amorphous alloys
[AD-A150648] 14 p2255 N85-23972
NMR manometer for measuring high pressures at liquid-helium temperatures 17 p2944 N85-28171
An evaluation and preparation of ferromagnetic liquid composites for use at millimeter wavelengths
[AD-A153939] 18 p3069 N85-28980
Magnetically-localizable, polymerized lipid vesicles and method of disrupting same
[AD-D011686] 19 p3249 N85-30144
An experimental study of the magnetoelastic bending of thin plates made of soft ferromagnetic material
19 p3282 N85-30352
Very low temperature studies of hyperfine effects in metals
[DE85-013367] 22 p3749 N85-33236
Magnetic search system
[PB85-165108] 23 p3949 N85-34477

FERROMAGNETIC RESONANCE
Ferromagnetic resonance in a Ni-Mo superlattice
[DE85-003039] 11 p1735 N85-20911
Study of amorphous strips and microconductors by ferromagnetic resonance method
15 p2497 N85-25402

FERROMAGNETISM
Ferromagnetism in metals at finite temperatures
[DE85-000698] 09 p1377 N85-18656
The Fermi surface and momentum space densities of ferromagnetic Gd using the Positron technique
09 p1396 N85-18788
Fermi surface study of CeSb
[DE85-002532] 10 p1564 N85-19862
Investigation of electric and magnetic properties of intercalated graphite
[AD-A149801] 12 p1797 N85-21274
Magnetic X-ray scattering studies of the rare Earth metal holmium
[DE85-003608] 12 p1807 N85-21335
Behavior of small ferromagnetic particles in traveling magnetic field 12 p1843 N85-21564
Paramagnetic scattering from Ni
[DE85-004207] 12 p1942 N85-22198
Magnetovolume effects in some Y-Ni intermetallic compounds
[ISSN-0066-2003] 13 p2021 N85-22663
Anomalous magnetism of CeRh3B2 under pressure
[DE85-003069] 13 p2164 N85-23425
Material research in microgravity
[NASA-TM-77628] 14 p2228 N85-23811
Peltier heat of a small polaron in a magnetic semiconductor
[DE85-000470] 14 p2430 N85-24983
Lattice overview
[DE85-007282] 15 p2662 N85-26427
Central limit theorems in the area of large deviations for some dependent random variables
[AD-A153125] 17 p3043 N85-28831
A theoretical model for the study of nonlinear dynamics of magnetic bearings 20 p3462 N85-31505
Electronics Division research and development
[DE85-011887] 20 p3540 N85-32032

FERROUS METALS
Strain hardening and strain aging in Fe-Al-Mn alloys
02 p0178 N85-11196
The origin of the Moon 04 p0588 N85-13754
Unsinkability of ferromanganese nodules
06 p0819 N85-15202
Mineralogical-geochemical characteristics of ferromanganese formations in Arabian-Indian Ocean Ridge 19 p3293 N85-30416
Pitting corrosion of ferrous alloys
[AERE-R-11490] 24 p4078 N85-35273
Assessment of metal heating technologies for ferrous forging: A pilot study of the form value of natural gas
[PB85-204394] 24 p4084 N85-35314
Cobalt-rich ferromanganese crusts in the oceans
24 p4104 N85-35444

FERTILITY
Microbial ecology of extreme environments: Antarctic yeasts and growth in substrate-limited habitats
[NASA-CR-175810] 16 p2839 N85-27509

FERTILIZATION
An automatic device for amphibian egg fertilization in space: Technical aspects and biological requirements
05 p0689 N85-14427
Combined effects of atmospheric deposition, internal acid production, and harvesting on nutrient gains and losses from forest ecosystems
[DE85-002325] 12 p1884 N85-21821
Effects of simulated weightlessness on mammalian development. Part 2: Meiotic maturation of mouse oocytes during clinostat rotation 15 p2612 N85-26094

FERTILIZERS
Growth and reflectance characteristics of winter wheat canopies
[E85-10080] 10 p1505 N85-19494
Salinity driven oceanographic upwelling
[DE85-011664] 22 p3818 N85-33652

FET (TRANSISTORS)
U FIELD EFFECT TRANSISTORS

FEVER
China report: Science and technology
[JPRS-CST-84-008] 13 p1972 N85-22384

FEYNMAN DIAGRAMS
Introduction to LINE: A Feynman diagram graphic operator
[DE85-009299] 17 p3013 N85-28632
A test of the Feynman scaling in the fragmentation region
[HE-1.2-9] 24 p4172 N85-35867
General consequences of the violated Feynman scaling 24 p4173 N85-35872

FFT
U FAST FOURIER TRANSFORMATIONS

FIBER COMPOSITES
NT CARBON FIBER REINFORCED PLASTICS
NT GLASS FIBER REINFORCED PLASTICS
Fracture toughness of fibrous composite materials
[NASA-TP-2370] 02 p0170 N85-11136
Microstructural basis of strength and toughness in hardmetals 02 p0177 N85-11185
Effective moduli of elasticity of unidirectional fibrous composite 02 p0265 N85-11733
Tough Composite Materials
[NASA-CP-2334] 04 p0463 N85-12941
Characterization of interlaminar crack growth in composites with the double cantilever beam specimen
04 p0463 N85-12942
Characterizing delamination resistance of toughened resin composites 04 p0464 N85-12943
Composite materials characterization and development at AFWAL 04 p0464 N85-12944
Effect of impact damage and open holes on the compression strength of tough resin/high strain fiber laminates 04 p0464 N85-12945
Effects of constituent properties on compression failure mechanisms 04 p0464 N85-12946
The effect of matrix and fiber properties on impact resistance 04 p0464 N85-12947
Fundamental studies of composite toughness
04 p0464 N85-12948
European development experience on energy storage wheels for space 05 p0605 N85-13856
Generic composite flywheel designs
05 p0606 N85-13864
The creep and creep rupture of SMC-R50 under different thermomechanical conditions 05 p0648 N85-14160
Design procedures for fiber composite structural components: Panels subjected to combined in-plane loads
[NASA-TM-86909] 07 p0919 N85-15823
Titanium Matrix/Continuous Fiber/Continuous fiber composite interface interactions and their influence on mechanical properties
[AD-A147504] 07 p0920 N85-15829
Composite batteries 07 p0936 N85-15932
Applicability of linear elastic fracture mechanics to fatigue in polymers and short-fiber composites
09 p1298 N85-18152
Tribological properties of graphite-fiber-reinforced, partially fluorinated polyimide composites
[NASA-TM-86926] 09 p1298 N85-18153
Calculating residual stresses in composite materials
10 p1443 N85-19095
Spreading upon compacting of fiber composite materials with porous metal matrix 10 p1443 N85-19096
Quantitative estimate of compatibility of fiber composite material components 10 p1444 N85-19099
SEP of France manufactures its first silicon carbide fibers 11 p1618 N85-20184
Estimating degree of development of physical-chemical interaction among components in Al-B fiber composite material 13 p2027 N85-22705
Segregation of silicon in silumin-carbon fiber composites 13 p2028 N85-22706
Some features of the fabrication of multilayer fiber composites by explosive welding
[NASA-TM-77844] 14 p2246 N85-23932
Outlook for polymer composite materials
15 p2497 N85-25403
Research, development of composite materials described 15 p2497 N85-25404
The accuracy of approximate solutions in the analysis of fracture of composites
[NASA-CR-175738] 15 p2503 N85-25437
Homogeneity of pristine and bromine intercalated graphite fibers
[NASA-TM-87016] 15 p2517 N85-25521
Mechanical jointing in Aramid fiber composites: An experimental study
[VTH-LR-371] 16 p2802 N85-27280
Designing for fiber composite structural durability in hygrothermomechanical environment
[NASA-TM-87045] 17 p2917 N85-27976
Titanium metal-matrix composites
[AD-D011643] 17 p2930 N85-28086
Light weight fire resistant graphite composites
[NASA-CASE-ARC-11615-1-SB]
18 p3068 N85-28976
Development of carbon based brake lining materials without asbestos content in the form of carbon-carbon composites and carbon-metal or carbon-carbide composites
[BMFT-FB-T-85-014] 18 p3082 N85-29067
Lightning-safe carbon fiber composite for Airbus tail unit 18 p3087 N85-29100
Arc spray fabrication of metal matrix composite monotape
[NASA-CASE-LEW-13828-1] 19 p3230 N85-30027
Polymer matrix and graphite fiber interface study
[NASA-CR-177357] 19 p3232 N85-30036
Structural characteristics of high temperature composites
[NASA-CR-175998] 19 p3232 N85-30037
Basic cryogenics and materials. Phase 1
[NASA-CR-177932] 21 p3572 N85-32215
Measurement of damping of graphite epoxy materials
[NASA-CR-176073] 21 p3596 N85-32334
Substitution of asbestos by aramid fibers and fiber blends in industrial textiles and composites with organic binders
[BMFT-FB-T-85-006] 23 p3920 N85-34294

FIBER OPTICS
Peripheral vision displays: The future
01 p0009 N85-10058
New type of unique frequency laser communications
[AD-A145126] 01 p0038 N85-10239
Center for Electronics and Electrical Engineering Technical Bulletin covering center programs
[PB84-216056] 01 p0045 N85-10296
Environmentally independent fiber optic rotation sensor
[AD-D011219] 01 p0119 N85-10818
The development of an optoelectronic assembly applied to computer systems
[AD-A145028] 01 p0120 N85-10821
Optical pin apparatus for measuring the arrival time and velocity of shock waves and particles
[DE84-014501] 01 p0120 N85-10824
Fine grained hodoscopes based on scintillating optical fibers
[DE84-014849] 01 p0120 N85-10825
Two novel plasma diagnostic tools: Fiber sensors and phase conjugation
[DE84-014033] 01 p0123 N85-10840
Dual (GaAl) As-heterostructure based injection laser traveling wave amplifier 02 p0261 N85-11708
Fiber cable in optical system with brightness amplifier
02 p0263 N85-11724
Nonlinear symmetrization of picosecond pulses in optical fibers 02 p0264 N85-11725
Using fiber-optics light guides in diagnosing intense shock waves 02 p0272 N85-11773
The effect of temperature on the radiation induced losses of large diameter GPS (Germanium phosphosilicate) and GBS core optical fibers
[AD-A145409] 02 p0280 N85-11823
Fore-optics systems designed for electronic streak cameras using fiber optics
[DE84-014525] 02 p0281 N85-11830
Multiple object spectroscopy: The MX spectrometer design 02 p0296 N85-11920
ONR (Office of Naval Research) Far east Scientific Bulletin, Volume 9, Number 2, April - June 1984
[AD-A145681] 02 p0305 N85-11974
East Europe report: Science and technology
[JPRS-ESA-84-036] 03 p0343 N85-12210
Fiber optics development, prospects assessed
03 p0343 N85-12214
Frequency shifting in multimode fiber optic phase modulation devices 03 p0347 N85-12239
Influence of mode noise suppression in multimode fiber optic light guides 03 p0348 N85-12242
Microshell (trademark)-tipped optical fibers as sensors of high-pressure pulses in adverse environments
[DE84-015520] 03 p0365 N85-12338
Holographic displacement analysis with fiber optics
[AD-A146185] 03 p0420 N85-12680
The applications of fibre optics in gas turbine engine instrumentation
[PNR-90209] 03 p0420 N85-12687
High-temperature optically activated GaAs power switching for aircraft digital electronic control
[NASA-CR-174711] 04 p0457 N85-12901
China report: Science and technology
[JPRS-CST-84-003] 04 p0491 N85-13132
New telecommunications optical fiber developed
04 p0492 N85-13135
Fiber optic data bus using Frequency Division Multiplexing (FDM) and an asymmetric coupler
[NASA-TM-86015] 04 p0492 N85-13139
Scintillator-fiber charged particle track-imaging detector
[NASA-CR-174160] 04 p0559 N85-13560
Fiber optic, Fabry-Perot high temperature sensor
[NASA-CR-174712] 04 p0564 N85-13594
High-bandwidth multichannel fiber optic system for measuring gamma rays
[DE84-014526] 04 p0564 N85-13596
Measuring transient radiation effects in optical fibers
[DE84-015044] 04 p0565 N85-13598
Application of commercial star couplers to increase signal dynamic range
[DE84-014769] 04 p0565 N85-13600
Optical characterization of radiation-resistant fibers
[DE84-015248] 05 p0620 N85-13964
Characterization of fiber optic cables under large tensile loads
[DE84-016816] 05 p0651 N85-14180
Clinical measurements using fiber optics and optrodes
[DE84-015043] 05 p0696 N85-14481
Psychophysical research in development of a fiber-optic helmet mounted display 05 p0701 N85-14501
Contribution to the study and realization of the CARTHAGE multiservice local network
[ENST-84E006] 05 p0716 N85-14595
Gamma-ray to Cerenkov-light conversion efficiency for pure-silica-core optical fibers
[DE84-015041] 05 p0729 N85-14685
100 MHz fiber optic single transient gamma ray detection system
[DE84-016818] 05 p0729 N85-14686
Transient attenuation in optical fibers
[DE84-016487] 05 p0729 N85-14687
A single optical fiber telephone system
[AD-D011293] 06 p0799 N85-15107
Lithium battery safety: A fiber-optic application for safe observation of lithium cells under severe tests
[AD-A146646] 06 p0804 N85-15119
Qualitative and quantitative compositional analysis of shale derived by gas chromatography and combined gas Chromatography/Mass spectrometry. Executive summary
[AD-A146369] 07 p0924 N85-15851
The relationship between radiation sensitivity and redox equilibria — glass processing variables
[AD-A147216] 07 p0932 N85-15906
Holographic directional coupler for fiber optic systems
[AD-D011365] 07 p0937 N85-15939
Micro-waveguide transformers of coherent optical signals 07 p0950 N85-16022
Helmet mounted telescope
[AD-D011355] 07 p1019 N85-16467
Multiwavelength bidirectional coupler-decouplers
[AD-A147009] 07 p1043 N85-16625
Optical fibers with reduced pressure sensitivity to high frequency acoustic field
[AD-D011306] 07 p1043 N85-16627
Bragg cell spectrum analyzer specification
[AD-D011320] 07 p1044 N85-16629
Analytic models for radiation induced loss in optical fibers 2: A physical model
[AD-A147442] 07 p1044 N85-16632
Research and technology, 1984 report
[NASA-TM-83096] 07 p1061 N85-16730
Helicopter Guidance and Control Systems for Battlefield Support
[AGARD-CP-359] 08 p1072 N85-16797
Telecommunications equipment at 1984 Leipzig Spring Fair 08 p1140 N85-17179
East Europe report: Science and technology
[JPRS-ESA-84-047] 08 p1140 N85-17183
UK, FRG, France: R and D in sensors, related fields
08 p1142 N85-17197
RF fiber optic link
[AD-A148679] 08 p1155 N85-17290
Optical frequency domain reflectometry
08 p1222 N85-17695
Application of fiber optics and compound collectors
08 p1253 N85-17912
The fiber-optic helmet-mounted display
[AD-P004330] 09 p1270 N85-17984
Binocular overlap in a fiber optic helmet mounted display
[AD-P004331] 09 p1270 N85-17985
Current measurements by Faraday rotation in single mode optical fibers
[DE85-002025] 09 p1384 N85-18707
Radiation response of optical fibers in a nuclear reactor
[DE84-017221] 09 p1385 N85-18710
Self-induced nonlinear effects in optical fibers: A unified approach
[FUB-67-1982] 09 p1385 N85-18713
Low voltage two wire to four wire telephone circuit converter apparatus
[AD-D011449] 10 p1468 N85-19261
Worldwide report: Telecommunications policy, research and development
[JPRS-TTP-85-002] 10 p1475 N85-19309
NTT (Nippon Telegraph and Telephone Public Corporation) develops new optical fiber
10 p1476 N85-19311
West Europe report: Science and technology
[JPRS-WST-85-008] 11 p1617 N85-20174
Siemens-Corning plant to manufacture optical fibers
11 p1617 N85-20175
Photonic methods of high speed analog data recording
[DE84-016723] 11 p1637 N85-20308
Report of the Technology and Test Panel
11 p1646 N85-20370
Polarization transformation by single-mode fibers --- optical fibers
[FI-452-TBR-59] 11 p1729 N85-20876
Wide-field-of-view, helmet-mounted infinity display system development
[AD-A149641] 12 p1777 N85-21159
Optical fiber communications link design in compliance with systems performance standards
[PB85-111037] 12 p1830 N85-21489
1.5 to 1.7 micrometers LEDs (Light-Emitting Diode)
[AD-A149685] 12 p1834 N85-21508
Temperature-insensitive optical fibers
[AD-D011551] 12 p1933 N85-22142
Design of an optical proximity sensor using multiple cones of light for measuring surface shape — application to a robot manipulator
[AD-A150050] 12 p1934 N85-22152
The future of lightwave technology
[PB85-109759] 12 p1935 N85-22155
Analysis of fiber-gyroscopes discussed
13 p2052 N85-22846
Interference immunity of fiber-optic communication line with spectral multiplexing of channels
13 p2069 N85-22924
AL-124 light-emitting diode in 30 Mbit/s fiber-optic communication line 13 p2069 N85-22925
Optical reflectometer for multimode fiber lightpipes
13 p2075 N85-22961
Dispersion characteristics of small-mode gradient optical fibers 13 p2082 N85-23004
Technical Digest: Symposium on Optical Fiber measurements, 1984
[PB85-114700] 13 p2160 N85-23407
Feasibility study for an AFGL fiber optic data link at WSMR sounding rocket launch area
[AD-A150652] 14 p2240 N85-23884
Use of focons in combination with brightness amplifiers 14 p2274 N85-24086
Research study of fiber-optic interferometry at very low frequencies
[AD-A150906] 14 p2421 N85-24807
Experimental report on a fiber optic light guide made by Galileo Electro-Optics Corporation
[DE85-006161] 14 p2421 N85-24841
Fiber optics applications for MIL-STD-1760
[AD-A151113] 15 p2470 N85-25251
Instrument for measuring dispersional distortions in optical fibers and cables 15 p2530 N85-25586
Wideband fiber optic communications link
[AD-A151704] 15 p2542 N85-25687
Wavelength dependent, tunable, optical time delay system for electrical signals
[AD-D011584] 15 p2548 N85-25725
Length dependent, optical time delay/filter device for electrical signals
[AD-D011594] 15 p2549 N85-25732
Mode dependent, optical time delay system for electrical signals
[AD-D011596] 15 p2653 N85-26580
Three new fiber-optic components
[DE85-006269] 15 p2653 N85-26584
Fiber optic Raman thermometer for Space Shuttle main engine preburner profiling 16 p2739 N85-26904
Reusable rocket engine turbopump condition monitoring 16 p2740 N85-26907
Wavelength multiplexer-demultiplexer
[AD-D011606] 16 p2777 N85-27140
Phase-lock fiber optic interferometer
[AD-D011603] 16 p2786 N85-27191
The utilization of optical fibers in holography
[ISL-R-102/83] 16 p2787 N85-27196
Ultrafast holography using optical fibers
[ISL-CO-238/83] 16 p2788 N85-27204
In-situ stratospheric ozone measurements: Recent results and their implications 16 p2824 N85-27419
A study of topologies and protocols for fiber optic local area network
[NASA-CR-175771] 16 p2864 N85-27690
Performance evaluation of fiber-optic converters
17 p2941 N85-28154
Derated application of parts for (Electronic Systems Division) systems development. Revision
[AD-A153299] 17 p2955 N85-28246
Studies of optical-beam phase-conjugation by nonlinear refraction
[AD-A152865] 17 p3037 N85-28786
Preparation of heavy metal fluoride glasses in the bulk form
[AD-A153784] 18 p3079 N85-29049
West Europe report: Science and technology
[JPRS-WST-84-031] 18 p3086 N85-29099
Philips researches gallium arsenide use for lasers
18 p3087 N85-29106
Rifa of Sweden conducts research in 3-5 materials
18 p3088 N85-29107
Optical fiber magnetic field sensor with nanosecond response time
[DE85-008409] 18 p3110 N85-29259
Optical fiber coupling method and apparatus
[NASA-CASE-NPO-15464-1] 18 p3184 N85-29749
Fiber optics in high dose radiation fields
[DE85-008649] 18 p3185 N85-29750
Fiber optic sensors operating at dc
[AD-D011674] 19 p3271 N85-30392

Fiber optic gyroscope with alternating output signal
[AD-D011689] 19 p3271 N85-30284

Optical 3-D signature device for detecting chemical agents
[AD-D011669] 19 p3272 N85-30293

One-frequency laser interferometer using the optic fiber as a polarization-independent interference phase detector
[DE85-010544] 19 p3277 N85-30326

Fiber optic expanded beam connector
[AD-A154057] 19 p3367 N85-30880

Fiber optics in transient radiation fields
[DE85-010721] 19 p3368 N85-30886

Swedish program for sensor research, development
20 p3438 N85-31338

Data communications-Oriented Production System Language (CPSL)
[DE85-011457] 20 p3440 N85-31352

Optical multiplexing on monomode fibers
[ENST-83E016] 20 p3533 N85-31982

R and D activities of the Systems Engineering Division
20 p3540 N85-32027

Methods for measuring and analyzing dispersion properties of multimode fiber optic lightpipes (a review)
21 p3695 N85-32960

USSR report: Electronics and electrical engineering
[JPRS-UEE-84-015] 22 p3762 N85-33314

Comparative characteristics of optical multiposition pulse signals with intersymbol distortion
22 p3764 N85-33329

Refraction of narrow probing light beam in multilayer optical fiber 22 p3764 N85-33330

Temperature sensitivity of fiber-optic transmission line
22 p3764 N85-33331

Fiber optic moisture sensor
[DE85-011651] 22 p3787 N85-33462

Optical-fiber/microprocessor-based remote velocity sensor
[DE85-010071] 22 p3788 N85-33470

The use of optical fibers in pulsed laser holography
[ISL-CO-226/84] 23 p3936 N85-34395

Fiber optics interface for a dye laser oscillator and method
[DE85-005765] 23 p3973 N85-34633

Bevalac calibration of the SOFIE range and hodoscope detectors
[OG-9.1-7] 23 p4023 N85-34933

Akeno 20 km (2) air shower array (Akeno Branch)
[OG-9.4-8] 23 p4029 N85-34975

Center for Electronics and Electrical Engineering technical progress bulletin covering center programs, July-September with 1985 CEEE events calendar
[PB85-191393] 24 p4091 N85-35363

Optical synthetic aperture techniques
[AD-A156151] 24 p4154 N85-35752

On the possibilities of large-scale radio and fiber optics detectors in cosmic rays
[HE-4.6-2] 24 p4196 N85-36039

FIBER ORIENTATION

Fracture toughness of fibrous composite materials
[NASA-TP-2370] 02 p0170 N85-11136

Experimental study on transonic flutter characteristics of sweptback wing with core composite plates having different fiber orientations
[NAL-TR-827] 06 p0756 N85-14842

Studies of structure and mechanical properties of carbon-reinforced plastic based on spirally reinforced filler 10 p1444 N85-19100

Initial fracture stages of orthogonally reinforced composite material 11 p1599 N85-20055

Strength properties of unidirectionally reinforced hybrid composites 11 p1599 N85-20056

The orientation distribution of nonspherical aerosol particles within a cloud
[AD-A150600] 13 p2092 N85-23061

Technical Digest: Symposium on Optical Fiber measurements, 1984
[PB85-114700] 13 p2160 N85-23407

Literature survey of discontinuous-fiber-reinforced composites with emphasis on pressure vessels
[DE85-010386] 19 p3232 N85-30038

Strength properties of glassfiber reinforced thermoplastics 23 p3908 N85-34212

FIBER REINFORCED COMPOSITES

Inorganic composites for space applications
02 p0155 N85-11047

Contributions to the 7th International Acoustic Emission Symposium
[AD-A145368] 02 p0275 N85-11792

Thermoplastic-carbon fiber hybrid yarn
[NASA-CR-3849] 03 p0325 N85-12093

Matrix resin characterization in cured graphite composites using diffuse reflectance-FTIR
04 p0486 N85-12959

Composite structural materials
[NASA-CR-174077] 04 p0487 N85-12966

Protective coverings for fiber reinforced epoxy composites
[PB84-231059] 04 p0480 N85-13063

Prefabricated panels for rapidly runway repair and expedient airfield surfacing
[AD-D011277] 05 p0597 N85-13804

On the effects of delamination damage in fibre composite laminates
[ARL/STRUC-R-403] 06 p0763 N85-14881

Carbon fibre reinforced aluminum matrix composites: A critical review
[AD-A146367] 06 p0764 N85-14883

Characterization of newly developed conductive composites
[AD-A146652] 06 p0764 N85-14884

System for rapid repair of damaged airfield runways
[AD-D011325] 07 p0909 N85-15754

Unidirectional fibers and polyurethane elastomer matrix based composites synthesis and properties
[NASA-TM-77501] 07 p0920 N85-15826

Titanium Matrix/Continuous Fiber/Continuous fiber composite interface interactions and their influence on mechanical properties
[AD-A147504] 07 p0920 N85-15829

Verification of the fatigue properties of (small) wind turbines
[NLR-MP-83055-U] 07 p0994 N85-16311

Effects of high energy radiation on the mechanical properties of epoxy-graphite fiber reinforced composites
[NASA-CR-174314] 08 p1118 N85-17047

Disclinations in carbon-carbon composites
[AD-A148290] 08 p1119 N85-17052

The response of metallic structures to dynamic loading 08 p1172 N85-17389

The fabrication, processing and characterization of multidimensionally braided graphite/epoxy composite materials
[AD-A148729] 09 p1288 N85-18090

A comprehensive study on sublaminate crack growth stability and its effects on the load-carrying capacity
[AD-A149037] 10 p1432 N85-19028

Proceedings of Colloquium/Workshop on Composite Materials and Structures, Standardization, Qualification, Certification held at washington, D.C. on 8-10 May 1984
[AD-A149039] 10 p1432 N85-19029

The problem of protecting the structure of a packet composite of optimal thinwall elements
10 p1444 N85-19101

Fiber composite materials with titanium matrix
10 p1445 N85-19105

Fracture toughness of fiber reinforced concrete
[AD-A149403] 10 p1496 N85-19441

Thermoviscoelastic analysis of dimensionally stable fiber composite space structures
[AD-A149275] 11 p1593 N85-20021

Fatigue crack growth in Aramid Reinforced Aluminum Laminates (ARALL): Mechanisms and predictions
[DFVLR-FB-84-37] 11 p1609 N85-20118

Fabrication of fiber-reinforced ceramic composites by chemical vapor infiltration
[DE85-003809] 11 p1611 N85-20132

Aerostructure nondestructive evaluation by thermal field detection. Phase 2: Technique refinement and quantitative determination of flaw detection capabilities
[AD-A149622] 12 p1777 N85-21155

Nonlinear analysis for high-temperature multilayered fiber composite structures — turbine blades
[NASA-TM-83754] 12 p1797 N85-21273

Behavior of fiber-reinforced composites under dynamic tension
[AD-A150619] 13 p2015 N85-22641

Fibre composite laminated plate analysis using a card programmable calculator (HP41C/CV)
[NIAST-83/88] 13 p2103 N85-23106

Monitoring of laminate cure with microdielectrometry
[AD-A150863] 14 p2248 N85-23934

Synthesis of hydrophobic, crosslinkable resins
[AD-A150658] 14 p2260 N85-24002

Research on composite materials for structural design
[AD-A150802] 14 p2260 N85-24004

A model for the compressive buckling of extended chain polymers
[AD-A151025] 14 p2260 N85-24008

Local elastoplastic fracture of fibrous composite materials 15 p2497 N85-25405

A preliminary investigation into transverse fracture of unidirectional fiber composites
[AERE-R-11494] 15 p2503 N85-25438

Effect of fatigue and thermal loads on silicon carbide fiber reinforced glass matrix composites
[DE85-006069] 15 p2503 N85-25441

Mechanics of polymers and composites: Research opportunities
[DE85-007052] 15 p2503 N85-25442

Fabrication of fiber reinforced ceramic composites by chemical vapor infiltration
[DE85-007565] 15 p2520 N85-25536

Design overview of fiber-reinforced superalloy composites for the Space Shuttle main engine
16 p2734 N85-26871

Nonlinear structural analysis for fiber-reinforced superalloy turbine blades 16 p2737 N85-26887

NASA/aircraft industry standard specification for graphite fiber toughened thermoset resin composite material
[NASA-RP-1142] 16 p2742 N85-26923

Effect of low-velocity or ballistic impact damage on the strength of thin composite and aluminum shear panels
[NASA-TP-2441] 16 p2742 N85-26924

Durability of Aramid reinforced aluminum laminate (ARALL)
[VTH-LR-423] 16 p2744 N85-26933

The effect of low sheet thicknesses on the fracture toughness of an Al alloy (7075-T6) — Aramid Reinforced Aluminum Laminate (ARALL)
[VTH-LR-425] 16 p2752 N85-26984

Development of a new faster process for the fabrication of ceramic fiber-reinforced ceramic composites by chemical vapor infiltration
[DE85-007550] 16 p2756 N85-27007

The application of BRILES rivets for mechanical jointing of Aramid Reinforced Aluminum Laminate (ARALL)
[VTH-LR-387] 16 p2802 N85-27279

Reaction-bonded and fiber-reinforced SIC static and dynamic gas turbine components
[BMFT-FB-T-84-302] 17 p2899 N85-27874

Aluminum-lithium alloys: The answer of the aluminum industry to the threat of advanced fiber-reinforced materials
[VTH-LR-406] 17 p2932 N85-28102

DFVLR research in aluminum-lithium alloys
18 p3067 N85-29105

Fatigue behavior of unidirectional FP-Al composites with circular holes
[AD-A153466] 18 p3121 N85-29322

Ten year environmental test of glass fiber/epoxy pressure vessels
[NASA-TM-87058] 19 p3231 N85-30034

Literature survey of discontinuous-fiber-reinforced composites with emphasis on pressure vessels
[DE85-010386] 19 p3232 N85-30038

Study of failure mechanism of fibrous composition materials taking into account physicochemical reactions of components 19 p3243 N85-30106

Effect of matrix plasticity on durability of fibrous composition materials 19 p3243 N85-30107

BN coating of ceramic fibers for ceramic fiber composites
[AD-D011700] 19 p3249 N85-30145

Tensile fatigue of glass fibers and composites with conventional and surface compressed fibers
[RR-84-4] 22 p3742 N85-33196

Improved process for the preparation of fiber-reinforced ceramic composites by chemical vapor deposition
[DE85-011584] 22 p3752 N85-33255

Stresses and deformations in cross-ply composite tubes subjected to a uniform temperature change: Elasticity and Approximate Solutions
[NASA-CR-176147] 22 p3800 N85-33545

X-ray measurement of thermal stresses in tungsten fiber-copper composites 23 p3907 N85-34205

Evaluation methods of ceramic fiber reinforced metal matrix composite 23 p3907 N85-34206

Fracture behavior of aluminum composites reinforced with fiber 23 p3907 N85-34207

Rotating bending fatigue strength of silicon carbide and alumina-fiber reinforced aluminum
23 p3907 N85-34208

Mechanical properties of SiC fiber-reinforced reaction-bonded Si3N4 composites
[NASA-TM-87085] 23 p3908 N85-34223

Viscoelastic behavior of short-fiber composite materials
[DE85-011233] 23 p3910 N85-34225

Three-dimensional finite element failure model for predicting failure in fibre reinforced bolted joints
[BR94778] 23 p3940 N85-34423

Mechanical characterization and failure modes of fiber reinforced angle-ply composites
24 p4072 N85-35234

Quantitative non-destructive evaluation of composite materials based on ultrasonic wave propagation
[NASA-CR-176176] 24 p4074 N85-35244

Determination of characteristic values for fiber reinforced materials 24 p4074 N85-35247

Computational techniques for fiber reinforced components 24 p4075 N85-35250

A research program to reduce the interior noise in general aviation aircraft, index and summary
[NASA-CR-176178] 24 p4145 N85-35695

FIBER STRENGTH

High performance fibers for structurally reliable metal and ceramic composites — advanced gas turbine engine materials
[NASA-TM-86878] 03 p0325 N85-12095

Qualitative and quantitative compositional analysis of shale derived by gas chromatography and combined gas Chromatography/Mass spectrometry. Executive summary
[AD-A148369] 07 p0924 N85-15851

Damage to boron fibers during thermal cycling and annealing 10 p1445 N85-19107

High resistance and raised modulus carbon fibers
[NASA-TM-76884] 15 p2502 N85-25436

Effect of surface state on durability of aluminized boron fibers 19 p3244 N85-30115

FIBERGLASS
U GLASS FIBERS

FIBERS
NT BORON FIBERS
NT CARBON FIBERS
NT CERAMIC FIBERS
NT GLASS FIBERS
NT METAL FIBERS
NT NYLON (TRADEMARK)
NT REINFORCING FIBERS
NT SYNTHETIC FIBERS
NT WOOL

Dynamics of graphite fiber intercalation: In situ resistivity measurements with a four point probe
[NASA-TM-86858] 01 p0017 N85-10105

Preparation of silicon carbide fibers
[DE84-014661] 01 p0022 N85-10137

Evaluation of hollow fiber ultrafiltration as a pretreatment for reverse osmosis desalinaton of seawater
[PB84-212406] 01 p0026 N85-10160

Stability of bromine intercalated graphite fibers
[NASA-TM-86859] 01 p0031 N85-10187

Research in quantitative NDE techniques
[AD-A145990] 03 p0369 N85-12358

Gamma-ray to Cerenkov-light conversion efficiency for pure-silica-core optical fibers
[DE84-015041] 05 p0729 N85-14685

Transient attenuation in optical fibers
[DE84-016487] 05 p0729 N85-14687

Fire retardant cellulosehydrate fibers
06 p0761 N85-14870

Improved uniformity of viscous textile fibers obtained by altering drying procedures 06 p0762 N85-14871

Synthesis of antimicrobial chemical fibers and fibrous materials containing quaternary ammonium compounds and their utilization 06 p0762 N85-14872

Forming fluorine-containing threads from vinylidene fluoride-tetrafluoroethylene copolymer by dry method
06 p0762 N85-14873

Study of effectiveness of fire-resistant activity of antipyrenes for fibers of aromatic polyamides
06 p0762 N85-14874

Polymer-carbon black interaction in electrically conducting fiber-forming composites
06 p0762 N85-14875

Effect of polymer matrix on properties of fibers obtained by caking polymer dispersions 06 p0762 N85-14876

Preparation of fire-resistant infusible polycaproamide fiber 06 p0763 N85-14877

Creep of chemically vapor deposited SiC fibers
[NASA-TM-86897] 06 p0763 N85-14878

Flame resistant fibrous materials development
[NASA-CR-167817] 07 p0920 N85-15827

Improved solid-state laser sources, volume 2
[DE85-000759] 09 p1325 N85-18330

Gel drawn fibers of poly(vinyl alcohol)
[AD-A149062] 10 p1435 N85-19040

Behavior and specifics of fracture of porous fiber materials in extension 10 p1447 N85-19118

Thermophysical properties of porous fiber materials
11 p1601 N85-20068

West Europe report: Science and technology
[JPRS-WST-85-006] 11 p1618 N85-20183

Impurities in Kevlar 49 fibers
[DE85-004996] 13 p2038 N85-22767

A model for the compressive buckling of extended chain polymers
[AD-A151025] 14 p2260 N85-24008

Changes in the cholinergic system of rat sciatic nerve and skeletal muscle following suspension induced disuse
[NASA-CR-175718] 15 p2615 N85-26111

A micrographic and gravimetric study of intercalation and deintercalation of graphite fibers
[NASA-TM-87026] 17 p2934 N85-28110

Experiments and micromechanical models for creep-rupture in polymer matrix composites
[DE85-009633] 17 p2935 N85-28118

Thermal expansion coefficients of a 30% glass fiber filled PEEK pyrotechnic charge holder
[DE85-010805] 19 p3251 N85-30155

Woven heat exchanger
[DE85-011633] 22 p3763 N85-33439

Development and characterization of carbon-bonded carbon fiber insulation for radioisotope space power systems
[DE85-013365] 24 p4082 N85-35299

FIBERS (MATHEMATICS)

Annals of the Fourier Institute, volume 34, no. 4
11 p1698 N85-20668

Contribution of the cup-product of Milnor's fiber with /I/ sup 2 lambda poles 11 p1698 N85-20672

Riemann foliations on simply connected varieties
11 p1699 N85-20677

FIBRILLATION

Mapping of mammalian arrhythmias with the cardiac laser scanner 03 p0399 N85-12545

FIBRIN

The Fibrin slide assay for detecting urokinase activity in human fetal kidney cells 20 p3502 N85-31768

FIBROBLASTS

Repair of DNA treated with lambda-irradiation and chemical carcinogens
[DE85-010298] 19 p3327 N85-30616

FIBROUS MATERIALS
U FIBERS

FIDELITY
U ACCURACY

FIELD COILS

Superconducting toroidal field coil current densities for the TFCX
[DE85-010265] 20 p3530 N85-31959

FIELD EFFECT TRANSISTORS
NT JFET

Luminous points and breakdown in structure of GaAs transistors 02 p0257 N85-11684

Novel techniques for the fabricating and characterization of GaAs MIS (Metal Insulator Semiconductor) structures
[AD-A145766] 03 p0356 N85-12301

High-temperature optically activated GaAs power switching for aircraft digital electronic control
[NASA-CR-174711] 04 p0457 N85-12901

Glow spots and breakdown in GaAs transistor structure 04 p0487 N85-13107

Gamma-induced leakage in junction field-effect transistors
[DE84-014990] 04 p0570 N85-13634

Radiation hardened ion-implanted GaAs field effect transistor and method for making the same specification
[AD-D011264] 05 p0731 N85-14697

Dual-gate MESFET variable gain constant output power amplifier
[AD-D011334] 07 p0945 N85-15982

Development of short gate FET's
[AD-A147033] 07 p0947 N85-15999

Linear wideband microwave amplifiers for monolithic integrated microcircuits 07 p0955 N85-16051

Fluctuation phenomena studies in chemically sensitive field effect transistor. Part 1: Corrosion of aluminum
[AD-A148240] 08 p1129 N85-17116

Fluctuation phenomena studies in chemically sensitive field effect transistors. Part 2: Corrosion of silicon oxynitride
[AD-A148227] 08 p1157 N85-17302

A transistor oscillator-doubler
[AD-D011406] 08 p1158 N85-17307

Thin film transistors for addressing flat panel displays
[BMFT-FB-T-84-210] 08 p1227 N85-17726

Transient response of a small-signal microwave GaAs FET to X-rays
[DE85-000066] 09 p1315 N85-18265

Tally cell circuit
[AD-D011492] 11 p1629 N85-20254

Determination of the mobility profile in GaAs-MESFETs
[NASA-TM-77818] 11 p1734 N85-20905

High-voltage, high-power, solid-state remote power controllers for aerospace applications
[NASA-TP-2437] 12 p1795 N85-21263

Factors affecting SOS (Silicon-On-Sapphire) yield and reliability
[AD-A150004] 12 p1835 N85-21515

Pulse transformer package for impedance matching a laser diode to a transmission line
[AD-D011499] 12 p1855 N85-21632

Process for making a heterojunction source-drain insulated gate field-effect transistors utilizing diffusion to form the lattice
[AD-D011536] 12 p1939 N85-22176

Electrical performance of semiconductor devices at cryogenic temperatures 12 p1948 N85-22239

Advanced detectors and signal processing for bubble memories
[NASA-CR-172534] 14 p2297 N85-24219

Proceedings of the Cold Electronics Workshop
[NASA-CR-175662] 14 p2297 N85-24220

Physical electronics of cooled operation of very short compound semiconductor transistors
14 p2297 N85-24223

Si MOS devices at low temperatures
14 p2297 N85-24225

Cryogenically-cooled, low-noise microwave receivers: Present status and future needs
14 p2298 N85-24229

InGaAs/GaAs, Strained-Layer Superlattice (SLS), junction photodetectors, LED's, injection LASER's and FET's for optoelectronic IC applications
[DE85-001940] 14 p2430 N85-24886

Cascode and differential amplifier using field-effect transistors 15 p2520 N85-25881

Assessment of present and future large-scale semiconductor detector systems
[DE85-006606] 15 p2662 N85-26430

Impurity bands associated with MOS inversion layers
[INPE-3483-PRE/726] 16 p2870 N85-27704

A study of Ga(.47)In(.53)As and Al(.48)In(.52)As for very high frequency device applications
[AD-A151995] 16 p2870 N85-27706

Effect of dislocations on gallium arsenide FETs
[AD-A152249] 16 p2870 N85-27709

Measurement methods for accurate microwave characterization and modeling of MESFET chips
[AD-A152360] 17 p2952 N85-28227

Communications and logic systems at millimeter wave frequencies
[NASA-CR-175859] 17 p3042 N85-28824

Communications and logic systems at millimeter wave frequencies, summary 17 p3042 N85-28825

Leakage effects in n-GaAs MESFET with n-GaAs buffer layer 17 p3043 N85-28826

GaAs MESFET with lateral non-uniform doping
17 p3043 N85-28827

Further development of high voltage SIPMOS FET's to fulfill market needs
[BMFT-FB-T-84-255] 17 p3045 N85-28843

Rifa of Sweden conducts research in 3-5 materials
18 p3088 N85-29107

The ESFET: Evaporated Sensing Field Effect Transistor 19 p3256 N85-30180

High speed GaAs device and integrated circuit modeling and simulation 19 p3256 N85-30181

High voltage lateral power transisters: Theory and design 19 p3257 N85-30184

Heterojunction Schottky gate MESFET with lower channel ridge barrier
[AD-D011673] 19 p3258 N85-30189

Self-aligned GaAs FET with low 1/F noise
[AD-D011687] 19 p3260 N85-30215

Optical injection locking of solid-state oscillators by frequency-multiplexed injection-locked, laser diodes
[AD-D011695] 19 p3275 N85-30307

Design and fabrication of monolithic broadband microwave GaAs low noise FET amplifiers
20 p3443 N85-31370

Thirty GHz low noise GaAs FET amplifiers — satellite-ground communication
[CD.6500686] 20 p3449 N85-31410

Evaluation of semiconductor devices for Electric and Hybrid Vehicle (EHV) ac-drive applications, volume 2
[NASA-CR-176103] 22 p3750 N85-33294

Modulation doped GaAs/Al(x)Ga(1-x)As layered structures with applications to field effect transistors
[AD-A155360] 22 p3759 N85-33298

Study of nonlinear distortion in microwave amplifiers using Schottky gate field effect transistors
22 p3780 N85-33423

Two-dimensional numerical modeling of ion implanted GaAs MESFET devices 24 p4086 N85-35341

FIELD EMISSION

Virtual cathode oscillator study
[AD-A149268] 10 p1480 N85-19342

On the electric charge carried by dust grain excitation of violent discharge — planetary rings
15 p2677 N85-26530

Apparatus for mounting a field emission cathode
[NASA-CASE-LEW-14108-1] 18 p3094 N85-29140

Resolution at its current limit: Applications of the Berkeley ARM
[DE85-009959] 19 p3274 N85-30301

The ESA field emission electric propulsion program
[ESA-STR-213] 20 p3420 N85-31229

FIELD INTENSITY METERS

Methodical approaches to determination of sanitation protective zone dimensions around TV centers and TV retransmitters 09 p1361 N85-18660

Automated TEM (Transverse electromagnetic) cell calibration system
[PB85-134377] 11 p1638 N85-20010

FIELD OF VIEW
Investigation of several aspects of LANDSAT 4/5 data quality
[E85-10038] 04 p0525 N85-13357
Direction judgement errors in perspective displays
05 p0705 N85-14520
Helmet mounted telescope
[AD-D011355] 07 p1019 N85-16467
Binocular overlap in a fiber optic helmet mounted display
[AD-P004331] 09 p1270 N85-17965
The effect of modified spectacles on the field of view of the helmet display unit of the integrated helmet and display sighting system
[AD-A148693] 09 p1261 N85-18055
On the error of typhoon intensity estimation by means of IR Dvorak technique occurring when the eye is very small 12 p1894 N85-21886
Focal plane array optical proximity sensor
[NASA-CASE-NPO-15155-1] 12 p1932 N85-22139
Computing parameters characterizing possibility of planets falling in star camera field of view during space survey 15 p2487 N85-25351
FIELD STRENGTH
NT ELECTRIC FIELD STRENGTH
NT MAGNETIC FLUX
Automated TEM (Transverse electromagnetic) cell calibration system
[PB85-134377] 11 p1638 N85-20319
User's manual for the University of Houston individual heliostat layout and performance code
[DE85-004643] 12 p1882 N85-21808
Exact design formulas for field intensity of dipole deployed above flat homogeneous Earth with finite conductivity 13 p2081 N85-22998
MHD channel development
[DE85-008305] 18 p3192 N85-29796
Solar monochromatic images in magneto-sensitive spectral lines and maps of vector magnetic fields
18 p3207 N85-29897
Magnetic field-vector measurements in quiescent prominences via the Hanle effect: Analysis of prominences observed at Pic-du-Midi and at Sacramento Peak
18 p3208 N85-29898
Fractal structure of the interplanetary magnetic field
[NASA-TM-86212] 19 p3383 N85-30987
Short perturbations of cosmic ray intensity and electric field in atmosphere
[SH-6.1-18] 23 p4046 N85-35090
FIELD THEORY (ALGEBRA)
NT QUADRATIC EQUATIONS
Annals of the Fourier Institute, volume 34, no. 4
11 p1698 N85-20668
On the distribution of integral and prime divisors with equal norms 11 p1698 N85-20669
The Milnor link of a local field to a perfect residue field 11 p1698 N85-20670
Nonlinear sigma-models and integration methods
[DE85-004447] 12 p1922 N85-22071
Field theory analysis using the finite element method to determine the deliberation curves of three dimensional fracture mechanics specimens with a semicircular surface crack applying the electrical direct current potential method for crack depth measurement
[GKSS-84-E-53] 17 p2982 N85-28434
Special relativity of Kaluza-Klein
[DE85-007838] 17 p3046 N85-28847
FIELD THEORY (PHYSICS)
NT INSTANTONS
NT QUANTUM CHROMODYNAMICS
NT STRONG INTERACTIONS (FIELD THEORY)
NT UNIFIED FIELD THEORY
NT WEAK INTERACTIONS (FIELD THEORY)
Scattering theory by Enss' method for operator valued matrices: Dirac operator in an electric field
[REPT-84] 01 p0045 N85-10290
Research program in theoretical high-energy physics
[DE84-013717] 01 p0119 N85-10617
Linear conformal gravitation 02 p0265 N85-11735
Renormalization theory in four dimensional scalar fields
[NOTA-INTERNA-824] 02 p0292 N85-11895
Toward unification of elementary particle physics and cosmology in 10-dimensions
[DE84-013650] 05 p0727 N85-14674
Analyses of energy extraction efficiency of unstable resonators
[AD-A146391] 06 p0813 N85-15161
Supermanifolds and Berezin's new integral
[DE85-001833] 11 p1706 N85-20732
Ultraviolet divergences and supersymmetric theories
[DE85-001649] 11 p1729 N85-20875
Research in theoretical physics
[DE85-004286] 12 p1944 N85-22207
Standard model and beyond
[DE85-004269] 14 p2418 N85-24919
Research in theoretical nuclear physics
[DE85-006172] 14 p2418 N85-24920
Los Alamos Science, Number 11, Summer-Fall, 1984
[DE85-004634] 14 p2419 N85-24926
Lattice Monte Carlo calculations of finite temperature QCD
[DE85-004035] 14 p2431 N85-24992
Gravitational effects in theories with interacting fields: Two studies 15 p2663 N85-26435
Solutions of field equations in General Relativity with spinor connection 15 p2663 N85-26436
Neutrino measurements on the Moon
[DE85-007700] 16 p2884 N85-27791
Coherent state description of non-topological solitons and momentum projection
[DE85-007814] 17 p3033 N85-28761
Cavityless optical bistability in systems of two-level atoms 18 p3186 N85-29764
Operation of HFTF to test the MIT 12 T coil
[DE85-010409] 18 p3195 N85-29821
Field theory of the metal-insulator transitions in restricted symmetries
[NOTA-INTERNA-829] 18 p3196 N85-29826
Constructing a bit string universe
[DE85-006317] 18 p3197 N85-29829
Theory of high energy collision processes
[DE85-010183] 19 p3362 N85-30846
The standard model and beyond
[DE85-010239] 19 p3362 N85-30847
Wave propagation and methods of solution of the wave equation for moving disturbances sources
[ESA-TT-824] 20 p3522 N85-31906
Research in the theory of condensed matter and elementary particles
[DE85-010447] 20 p3531 N85-31968
Introduction to the Standard Model — weak and electromagnetic interactions
[USIP-85-02] 20 p3532 N85-31970
Some dynamic electronic properties of semiconductor surfaces and interfaces 20 p3537 N85-32007
Bergson and the unification of the sciences
[DE85-009961] 20 p3538 N85-32018
Lattice theory for nonspecialists, lecture notes
[NIKHEF-H/84-11] 20 p3539 N85-32019
Monopole search below the Parker limit with the MACRO detector at Gran Sasso
[HE-6.1-5] 24 p4209 N85-36131
Limits on monopole fluxes from KFG experiment
[HE-6.1-6] 24 p4209 N85-36132
An experiment to detect gut monopoles
[HE-6.1-7] 24 p4210 N85-36133
FIGHTER AIRCRAFT
NT F-8 AIRCRAFT
NT F-14 AIRCRAFT
NT F-15 AIRCRAFT
NT F-16 AIRCRAFT
NT F-17 AIRCRAFT
NT F-18 AIRCRAFT
NT F-27 AIRCRAFT
NT F-104 AIRCRAFT
NT F-106 AIRCRAFT
NT F-111 AIRCRAFT
NT HARRIER AIRCRAFT
NT JAGUAR AIRCRAFT
NT JET PROVOST AIRCRAFT
NT MIG AIRCRAFT
NT MIRAGE AIRCRAFT
NT MIRAGE 3 AIRCRAFT
Prediction of aerodynamic characteristics of fighter wings at high angles of attack
[AD-A145107] 01 p0003 N85-10017
Shock capturing finite difference algorithms for supersonic flow past fighter and missile type configurations
[NASA-CR-174051] 02 p0134 N85-10913
Avionics Integrity Program (Avip). Volume 2: Hardware case studies
[AD-A145689] 02 p0139 N85-10944
Status and prospects of computational fluid dynamics for unsteady transonic viscous flows
[NASA-TM-86018] 03 p0315 N85-12037
Quantification of cross-coupling and motion feedthrough for multiaxis controllers used in an air combat flying task
05 p0700 N85-14491
China report: Science and technology
[JPRS-CST-84-042] 06 p0747 N85-14789
New fighter aircraft reported — Jian-8 aircraft
06 p0747 N85-14790
F-7 supersonic day fighter viewed — Jian-7 aircraft
06 p0747 N85-14791
Operational Loads Data
[AGARD-CP-375] 07 p0894 N85-15664
Structural load measurements on a Northrop NF-5A
07 p0894 N85-15667
Navy operational loads data sources and systems
07 p0895 N85-15668
Structural flight load measurement demonstration of structural integrity 07 p0895 N85-15670
Display Techniques for Advanced Crew Stations (DTACS). Phase 1: Display techniques study
[AD-A146022] 07 p0904 N85-15722
Can the Aggressors continue to be effective in the F-5E?
[AD-A146861] 07 p1019 N85-16465
Computer sizing of fighter aircraft
[NASA-TM-86351] 08 p1067 N85-16759
International aviation (selected articles)
[AD-A148704] 08 p1067 N85-16762
Full scale experiments into the use of large eddy breakup devices for drag reduction on aircraft
08 p1071 N85-16790
Optimum performance parameters for ski-jump operations of USAF fighter aircraft
[AD-A148532] 08 p1084 N85-16867
Advances in composites technology
[NASA-TM-86353] 08 p1118 N85-17048
Development of an electro-pneumatic anti-G valve for high performance fighter aircraft
[AD-A148468] 08 p1201 N85-17561
Some fighter aircraft trends
[NASA-TM-86352] 10 p1420 N85-18954
Pictorial format display evaluation
[AD-A149252] 10 p1425 N85-18986
A technical solution to fadings in tactical satellite digital transmissions 10 p1473 N85-19297
Human Factors Considerations in High Performance Aircraft
[AGARD-CP-371] 10 p1532 N85-19653
Aircrew and avionics: Friends or Foes?
10 p1532 N85-19654
Military pilot ergonomics 10 p1532 N85-19655
Impact of future aircombat characteristics on pilot performance and cockpit design
10 p1533 N85-19661
Grasp of information by the pilot in future combat aircraft 10 p1533 N85-19662
The cockpit of the year 2000: How big a step?
10 p1534 N85-19667
Flight mechanics analysis of dynamic derivatives of the Dornier variable wind tunnel model
[ESA-TT-854] 11 p1577 N85-19937
Don't fowl out
[AD-P004179] 11 p1578 N85-19941
Robustness of discrete-time dynamical systems: Application to the multivariable digital control of combat aircraft
[ONERA-NT-1984-2] 11 p1585 N85-19986
Potential impact of Navstar GPS on NATO tactical operations 11 p1711 N85-20763
Development of the F-20 nose radome
[AD-P004374] 12 p1827 N85-21468
Laser clock
[AD-D011513] 12 p1855 N85-21634
Low-speed stability and control wind-tunnel investigations of effects of spanwise blowing on fighter flight characteristics at high angles of attack — Langely 12-ft low-speed tunnel and 30- by 60-ft tunnel
[NASA-TP-2431] 14 p2210 N85-23706
Status and prospects of computational fluid dynamics for unsteady transonic flow 15 p2459 N85-25180
West Europe report: Science and technology
[JPRS-WST-84-012] 15 p2523 N85-25552
Low-resolution target classification from a staring infrared sensor
[AD-A151690] 15 p2652 N85-26358
Some aspects of how to design cost-effective flight control systems 16 p2695 N85-26639
Application of AFTI/F-16 task-tailored control modes in advanced multirole fighters 16 p2712 N85-26735
The STOL and maneuver technology program integrated control system 16 p2715 N85-26757
Some aspects of how to design cost-effective flight control systems
[MBB-LKE-32/S/PUB/143] 16 p2873 N85-27729
Operational and developmental experience with the F/A-18A digital flight control system
17 p2902 N85-27895
Flight testing and development of the F/A-18A digital flight control system 17 p2902 N85-27896
The flight control system for the Experimental Aircraft Programme (EAP) demonstration aircraft
17 p2904 N85-27906
Design and implementation of input signals for identification of pilot/aircraft models
[ESA-TT-880] 20 p3394 N85-31055
Modifications of flight-by-flight load sequences to provide for good fracture surface readability
[NLR-MP-84012-U] 20 p3472 N85-31577
Maintenance and the military environment
22 p3750 N85-33243

Fatigue lives of specimens representing critical locations in Mirage 3 spars under Australian and Swiss test spectra
[ARL-STRUC-R-415] 24 p4064 N85-35187
RAFTS: A T-38 replacement for the 21st century
[AD-A156103] 24 p4065 N85-35191

FIGURE OF MERIT
Transversely reinforced piezoelectric composites
[AD-D011676] 19 p3260 N85-30214

FILAMENT WINDING
The fabrication, processing and characterization of multidimensionally braided graphite/epoxy composite materials
[AD-A148729] 09 p1288 N85-18090
Studies of structure and mechanical properties of carbon-reinforced plastic based on spirally reinforced filler 10 p1444 N85-19100
SRM filament wound case resin characterization studies 12 p1944 N85-22212
Testing of wound materials for strength with loading in the reinforcement plane 13 p2027 N85-22701
Glass, carbon fibers made at Fibre et Mica in France 15 p2534 N85-25634
SRB filament wound case material property study
[NASA-CR-171469] 17 p2910 N85-27940
Filament wound structures in PSP carbon composite
[RV10/84424] 22 p3743 N85-33198

FILAMENT WOUND CONSTRUCTION
U FILAMENT WINDING

FILAMENTS
Dynamics of liquid filament breakup
[DE84-016008] 04 p0500 N85-13187
Ultrasonic girth weld evaluation for aluminum substrate of spherical Kevlar-epoxy test specimens
[DE85-001592] 06 p0816 N85-15161
Magnetization measurements on multifilamentary Nb3Sn and NbTi conductors
[DE85-001237] 11 p1737 N85-20923
Current enhancement in a conducting channel
[AD-A155418] 22 p3645 N85-33812

FILAMENTS (SOLAR PHYSICS)
U SOLAR PROMINENCES

FILE MAINTENANCE (COMPUTERS)
Storage in the LLNL Octopus network: An overview and reflections
[DE84-014711] 01 p0106 N85-10712
Proceedings of the 5th LAN-Transport Workshop
[PB84-232667] 01 p0107 N85-10715
WXR (hydrologic weather wire and PLT product software package)
[PB84-237221] 04 p0541 N85-13442
OBLOG: Designed to create and maintain a 40 hour observation log file
[PB85-109528] 10 p1519 N85-19579
The identification of semantics for the file/database problem domain and their use in a template-based software environment 14 p2401 N85-24803
An adaptive technique and its application in database design 16 p2677 N85-27748
VIDTEX
[PB85-175669] 19 p3318 N85-30567
Recovery of lost files from VAX/WMS disk structures: A case study
[DE85-010652] 19 p3333 N85-30650
CMP: Code Maintenance Package reference manual, version 2.0
[DE85-011396] 19 p3340 N85-30697
Analysis of spacecraft data
[NASA-CR-171597] 21 p3669 N85-32790
CARE 3 user friendly interface user's guide
[NASA-CR-172608] 21 p3669 N85-32791
CARE 3 MENU maintenance manual
[NASA-CR-172609] 22 p3828 N85-33706
User's operating procedures. Volume 1: Scout project information programs
[NASA-CR-177948] 23 p3956 N85-34518
Using LINE as an interactive graphics package. Interfacing line and Topdraw in 43 and 24 VM
[DE85-012007] 23 p3965 N85-34585

FILLERS
Numerical modeling of complex interaction of shell of revolution and its filler with allowance for friction 06 p0779 N85-14980
Initial investigation of cryogenic wind tunnel model filler materials
[NASA-TM-86363] 09 p1283 N85-18069
Studies of structure and mechanical properties of carbon-reinforced plastic based on spirally reinforced filler 10 p1444 N85-19100
The effect of filler wire and flux compositions on the microstructure and properties of microalloyed steel weld metal
[AD-A149529] 10 p1492 N85-19423
Studies of ferritic filler metals for welding 9 percent nickel steel 15 p2565 N85-25625
Propagation of non-axisymmetric elastic waves through shell with filler under radial load at one end 17 p2943 N85-28169
Comparison of TT-F-1098 solvent-thinned block fillers with water-thinnable block fillers
[AD-A154207] 19 p3249 N85-30142
Results of tests of weathered K5NA closeout material in the MSFC Hot Gas Facility
[NASA-CR-170893] 24 p4073 N85-35239

FILLETS
Fillet weld stress using finite element methods 15 p2576 N85-25884

FILLING
NT REFILLING
Modifications to SOLA-VOF for flow dynamics in spinning cylinders
[AD-A154093] 19 p3265 N85-30250
Robotic order picking
[AD-D011737] 22 p3792 N85-33493
AUTSKED: An addendum
[DE85-010410] 22 p3829 N85-33712
An analysis and algorithm for filling propagation 23 p3961 N85-34551

FILM BOILING
Theoretical description of film boiling in a two phase flow calculation
[IKE-2-66] 05 p0638 N85-14092
Instability of film boiling of moving liquids
[BLL-WH-603-(9091.9F)] 07 p0956 N85-16056

FILM CONDENSATION
Heat transfer due to film condensation on vertical fluted tubes
[AD-A147258] 07 p0959 N85-16079
Filmwise condensation of steam on low integral-finned tubes
[AD-A152220] 16 p2783 N85-27176
Film condensation of steam on externally finned horizontal tubes
[AD-A155642] 21 p3585 N85-32285

FILM COOLING
Vortex-generating coolant-flow-passage design for increased film-cooling effectiveness and surface coverage
[NASA-TP-2388] 03 p0361 N85-12314
Heat transfer results and operational characteristics of the NASA Lewis Research Center Hot Section Cascade Test Facility
[NASA-TM-86890] 06 p0808 N85-15133
Flow visualization study of the effect of injection hole geometry on an inclined jet in crossflow
[NASA-TM-86936] 11 p1631 N85-20269
Advanced liner-cooling techniques for gas turbine combustors
[NASA-TM-86952] 12 p1770 N85-21115
Optimization of combined convective and film cooling of perforated baffle blades in gas turbines 14 p2270 N85-24067
The effect of injection-stream turbulence on film cooling effectiveness and heat transfer coefficients 20 p3451 N85-31424
Vortex generating flow passage design for increased film cooling effectiveness
[NASA-CASE-LEW-14039-1] 22 p3762 N85-33433

FILM THICKNESS
Effect of interconnection of the ends of a sliding bearing on film thickness
[AD-A147736] 08 p1132 N85-17135
Mechanical interactions of rough surfaces
[DE85-000814] 10 p1494 N85-19434
Nonuniform interference coatings with thickness-dependent refractive index 14 p2281 N85-24131
Fast approach for calculating film thicknesses and pressures in elastohydrodynamically lubricated contacts at high loads
[NASA-TM-87032] 19 p3264 N85-30242
Influence of surface films of petroleum products on conditions for absorption of solar radiation by upper water layer 19 p3289 N85-30396

FILMS
Rep rated long life capacitor development: Phase 1 and 2
[DE85-000719] 11 p1629 N85-20256
Modification of the grain size of sputtered copper with additions of oxygen, krypton, silver, or yttrium
[DE85-010975] 21 p3567 N85-32189
A new large-scale, high-resolution multicolor software display concept
[AD-A155404] 22 p3627 N85-33703

FILTERING
U FILTRATION

FILTERS
Calibration and use of filter test facility orifice plates
[DE84-016851] 04 p0500 N85-13190
Intermediate results of a 1-year study of a laser spectrometer in the DOE filter test facilities
[DE84-016478] 04 p0506 N85-132[illegible]
Theory of optimum M-filtration of signals against background of correlated interference 13 p2069 N85-22[illegible]
Sigma filter 18 p3142 N85-29[illegible]

FILTRATION
NT SPATIAL FILTERING
Noise isolation system for high-speed circuits
[DE84-014229] 01 p0043 N85-10[illegible]
Ultrafiltration as pretreatment for the preparation of drinking water by reverse osmosis onboard ships
[PML-1984-32] 01 p0098 N85-10[illegible]
Fabric filter system study
[PB84-229740] 03 p0342 N85-122[illegible]
Electrostatic augmentation of fabric filtration: Reverse-air pilot unit experience
[PB84-230002] 03 p0343 N85-122[illegible]
Characteristics of absorption and frequency filtration of ULF electromagnetic waves in the ionosphere 03 p0376 N85-124[illegible]
A method of making the gas-electric removal of highly dispersed particles more effective
[BLL-M-36030-(5828.4)] 06 p0765 N85-14[illegible]
Laboratory simulation of smoke reduction from aircraft engine test cell exhaust using a fluidized bed filter
[AD-A148600] 08 p1069 N85-16[illegible]
Carbon filter plates for aluminum filtration at casting
[BMFT-FB-T-84-242] 12 p1806 N85-2134[illegible]
Local behavior of solutions of an elliptic-parabolic equation
[AD-A149624] 12 p1920 N85-22057
Acoustic agglomeration methods and apparatus
[NASA-CASE-NPO-15466-1] 12 p1927 N85-22104
Fine filtration: An attractive route towards lower helicopter operating costs 14 p2221 N85-23774
High-latitude filtering in a global grid-point model using model normal modes 18 p3140 N85-29[illegible]
The investigation of natural and artificial ice nuclei by the improved membrane filter method 21 p3642 N85-32[illegible]
Determination of sensitivity functions for discrete dynamic systems from results of function modeling on digital computer 22 p3760 N85-33[illegible]
Nonlinear filtration of clutter 22 p3777 N85-33404

FINANCE
Financial issues for commercial space ventures: Paying for the dreams 02 p0150 N85-11[illegible]
Siemens, Philips megaproject to yield superchip in 5 years 11 p1592 N85-20[illegible]
A microcomputer tutorial on spreadsheets and databases with a simulated budget preparation
[AD-A155516] 21 p3672 N85-32[illegible]

FINANCIAL MANAGEMENT
Space commercialization: Analysis of R and D investments with long time horizons 02 p0155 N85-11[illegible]
Satellite servicing: A business opportunity? 02 p0156 N85-110[illegible]
Development and testing of a rural credit supervision system at the level of counties and rural properties utilizing remote sensing techniques
[E85-10018] 02 p0217 N85-114[illegible]
Evaluation of the effectiveness of the weighted guidelines to induce contractor's investment in cost reducing facilities equipment
[AD-A147586] 07 p1053 N85-16[illegible]
Activities report of the aerospace industry in West Germany
[ISSN-0722-3838] 07 p1053 N85-16[illegible]
Activities report of the aerospace industry in West Germany
[ISSN-0722-3838] 07 p1054 N85-16[illegible]
Digest of the Deutsche Lufthansa report, 1982
[ISSN-0415-603X] 09 p1418 N85-18[illegible]
An analysis of a dynamic project cost problem
[CSIR-TWISK-338] 13 p2149 N85-23[illegible]
FRG journal analyzes state, prospects of [illegible] programs: General analysis 15 p2535 N85-25[illegible]
Management communication and financial modeling 15 p2627 N85-2[illegible]
Information technology applications in voluntary sector transport operations. SP1: Objectives and programme of work
[TT-8501] 15 p2667 N85-2[illegible]
A microcomputer tutorial on spreadsheets and databases with a simulated budget preparation
[AD-A155516] 21 p3672 N85-32[illegible]
User's operating procedures. Volume 1: Scout project financial analysis program
[NASA-CR-177949] 23 p3956 N85-34[illegible]

FINE STRUCTURE
Study of deformation and fracture of AMg6N [illegible] aluminum alloy by method of acoustic emission 03 p0352 N85-12[illegible]

EXAFS studies of sodium silicate glasses containing dissolved actinides
[DE84-015805] 04 p0479 N85-13051
Extended X-ray absorption fine structure (Exafs) studies of the actinides
[DE84-015839] 04 p0559 N85-13561
Surface structure determination with ARPEFS
[DE84-016904] 04 p0571 N85-13644
Asymmetrical harmonic oscillator and fine-structure constant
[FUB-8-1984] 09 p1401 N85-18818
Synchrotron X-ray fluorescence and extended X-ray absorption fine structure analysis
[DE85-003606] 10 p1436 N85-19063
Structural studies of sputtered Ni-As-O films
[DE85-003229] 11 p1605 N85-20095
Documentation for the machine-readable version of A Finding List for the Multiplet Tables of NSRDS-NBS 3, Sections 1-10 (Adelman, Adelman, Fischel and Warren 1984)
[NASA-TM-87440] 14 p2436 N85-25048
Fine structure of solar acoustic oscillations due to rotation 14 p2445 N85-25087
The intern. rotation of the Sun inferred from the rotational splitting of acoustic and gravity mode multiplets
14 p2449 N85-25122
Effect of zirconium on forming ultrafine-grained structure in Al-Mg-Zr alloy 15 p2513 N85-25504
Test of the electronic structure of Fe(100) by absorbed current spectroscopy
[DE85-004942] 15 p2661 N85-26422
Characterization of thin films and layered structures using X-ray absorption and reflection at grazing incidence
[DE85-006560] 15 p2662 N85-26429

FINES
Drying of pulverized material with heated condensible vapor
[DE85-011656] 22 p3783 N85-33438

FINGERS
Finger materials for air cushion vehicles. Volume 1: Flexible coatings for finger materials
[AD-A151438] 15 p2522 N85-25545

FINISHES
NT ENAMELS
NT GLAZES
NT LACQUERS

FINITE DIFFERENCE THEORY
Development and applications of algorithms for calculating the transonic flow about harmonically oscillating wings
[NASA-CR-172376] 01 p0002 N85-10007
ICARUS: A general one-dimensional heat conduction code
[DE84-018125] 01 p0047 N85-10310
Upwind compact finite difference schemes
[CSIR-TWISK-334] 01 p0110 N85-10742
Shock capturing finite difference algorithms for supersonic flow past fighter and missile type configurations
[NASA-CR-174051] 02 p0134 N85-10913
Finite-difference synthetic seismograms for SH waves
[AD-A145834] 03 p0392 N85-12506
Difference schemes for equations of Schrodinger type
[AD-A145812] 03 p0410 N85-12622
Return difference feedback design for robust uncertainty tolerance in stochastic multivariable control systems
[AD-A145861] 03 p0411 N85-12624
Simulation of separated transonic airfoil flow by finite-difference viscous-inviscid interaction
05 p0591 N85-13768
Numerical methods for bluff body aerodynamics
05 p0593 N85-13782
Numerical integrations of the Navier-Stokes equations for flow over surface-mounted obstacles
05 p0593 N85-13784
Numerical investigations into the parabolized Navier-Stokes equations 05 p0635 N85-14075
Implicit numerical methods in meteorology
05 p0686 N85-14408
A compact finite element method for elastic bodies
[NASA-CR-172487] 06 p0817 N85-15185
An exploratory study of finite difference grids for transonic unsteady aerodynamics
[NASA-TM-84583] 07 p0899 N85-15696
High Marangoni number convection in a square cavity
[NASA-CR-174283] 07 p0959 N85-16078
Laminar flow over a backward-facing step
[AD-A147469] 07 p0960 N85-16084
Finite difference calculations of buoyant convection in an enclosure. Part 2: Verification of the nonlinear algorithm
[PB85-104065/GAR] 07 p0961 N85-16089
A finite difference method for inverse mode calculations of a three-dimensional boundary layer
[ESA-TT-863] 09 p1274 N85-18007
Researched applied to transonic compressors in numerical fluid mechanics of inviscid flow and viscous flow
[NASA-CR-174353] 09 p1319 N85-18291
Accuracy of the finite analytic method for scalar transport calculations
[DE85-001474] 09 p1320 N85-18300
The implementation of irregular grid systems for the finite difference solution of partial differential equations
[LU-MATH-RES-181] 09 p1373 N85-18630
Boundary conditions for artificial dissipation operators — convection
[FFA-TN-1984-53] 09 p1375 N85-18642
Vectorization and implementation of an efficient multigrid algorithm for the solution of elliptic partial differential equations
[AD-A149049] 10 p1545 N85-19743
Numerical solution of semilinear elliptic problems on unbounded domains
[AD-A149559] 10 p1549 N85-19767
Developments in the simulation of compressible inviscid and viscous flow on supercomputers
[NASA-TM-86674] 11 p1575 N85-19924
A fast algorithm of the finite difference method for computation of the transonic flow past an arbitrary airfoil with the conservative full-potential equation
11 p1619 N85-20191
A mixed finite difference analysis of the internal and external transonic flow fields of inlets with centerbody
11 p1619 N85-20192
Finite difference method for solving turbulent boundary layer equations 11 p1619 N85-20193
Finite difference computation of the flow around airfoils in two-dimensional transonic slotted wall wind tunnel
11 p1623 N85-20216
Calculation of oscillating turbulent flows in open channels
[KU-SFB-80/T/226] 11 p1633 N85-20289
Spectral methods in time for parabolic problems
[NASA-CR-172539] 11 p1706 N85-20730
The split-coefficient matrix method for supersonic three dimensional flow 12 p1821 N85-21425
Numerical studies of fluid spin-up from rest in a partially-filled cylinder
[AD-A150079] 12 p1847 N85-21586
Robust calculation of three-dimensional transonic potential flow based on the nonlinear gas multigrid method and a mixed incomplete lower upper decomposition/strongly implicit procedure (ILU/SIP) algorithm
[NLR-MP-84003-U] 12 p1848 N85-21593
Structural sensitivity analysis: Methods, applications and needs
[NASA-TM-85827] 12 p1865 N85-21695
Intensification of tropical instabilities
[AD-A149985] 12 p1896 N85-21899
Asymptotics for configural estimators
[AD-A150106] 12 p1924 N85-22087
Workshop on Nuclear Dynamics 3
[INC-40007-24] 12 p1931 N85-22130
Machine analysis of resonance characteristics of plate-type radio electronic equipment constructions
13 p2085 N85-23018
Calculation of level surface in problems of large-scale ocean circulation 13 p2108 N85-23136
Parallel processing for computational continuum dynamics
[AD-A150513] 13 p2147 N85-23327
Application of adaptive grids in solving the partial differential equations governing fluid flow
[AD-A151175] 15 p2555 N85-25766
Vibration and buckling of rotating, pretwisted, preconed beams including Cooriolis effects
[NASA-TM-87004] 15 p2577 N85-25893
Inviscid upwind finite difference model for two dimensional vertical axis wind turbines
15 p2585 N85-25933
Recent progress in the development and application of the parabolic equation
[AD-A151475] 15 p2637 N85-26265
Some numerical analyses of flows with separation
16 p2632 N85-26616
Finite-difference computations of rotor loads
[NASA-TM-86682] 16 p2700 N85-26669
A computer analysis program for interfacing thermal and structural codes
[NASA-TM-87021] 16 p2800 N85-27264
Error reduction program — combustor performance evaluation codes
[NASA-CR-174776] 16 p2852 N85-27584
Evaluation of an algorithm for the solution of the time-dependent Euler equations
[AD-A151993] 16 p2854 N85-27600
Analysis and modeling for thermal focal plane arrays
[AD-A153156] 17 p2968 N85-28329
A discussion of adaptive grids and their applicability in numerical hydrodynamic modeling
[AD-A151843] 17 p3017 N85-28659
Spatial differencing for finite difference codes
[DE85-008902] 17 p3021 N85-28684
A numerical solution technique for multitemperature plasma hydrodynamics
[AD-A152701] 17 p3039 N85-28801
A study of aerodynamic control in stalled flight long laminar separation bubble analysis
[AD-A153850] 18 p3059 N85-28930
Numerical simulation of unsteady motion in a turbulent mixing layer
[NAL-TR-849T] 18 p3099 N85-29183
Limiting processes laser CVD
[DE85-008846] 18 p3114 N85-29279
A model for the combustion of polymethyl methacrylate in air in a laminar diffusion flame
[VTH-LR-439] 18 p3165 N85-29606
Intermediate boundary conditions for LOD, ADI and approximate factorization methods
[NASA-CR-172591] 18 p3167 N85-29626
Shock capturing
[NASA-CR-172592] 18 p3168 N85-29627
Study of second order upwind differencing in a recirculating flow
[NASA-CR-174939] 19 p3264 N85-30243
On the convergence of difference approximations to scalar conservation laws
[NASA-CR-172614] 19 p3344 N85-30726
Floating shock-fitting in transonic potential flow calculations 20 p3387 N85-31007
An implicit finite-difference code for a two-equation turbulence model for three-dimensional flows
[NASA-TM-86752] 20 p3454 N85-31448
Nonnewtonian, unsteady flow in a convergent divergent duct 20 p3456 N85-31463
Generation of three-dimensional body-fitted coordinates using hyperbolic partial differential equations
[NASA-TM-86753] 20 p3519 N85-31867
Calculation of transonic steady and oscillatory pressures on a low aspect ratio model and comparison with experiment
[NASA-TM-86449] 21 p3551 N85-32092
A numerical study of Taylor-Vortex flow
[AD-A154787] 21 p3584 N85-32277
Performance evaluation of flow in turbomachinery blade rows 21 p3587 N85-32299
Numerical solution of the Navier-Stokes equations for 3-D internal flows: An emerging capability
21 p3588 N85-32300
An investigation into the comparisons of the underwater shock effects on a stiffened flat plate to the predictive nature of a computer model
[AD-A155612] 21 p3600 N85-32355
Generalized formulation of a class of explicit and implicit TVD schemes
[NASA-TM-86775] 21 p3675 N85-32830
Oscillatory solutions of the Peaceman-Rachford alternating direction implicit method and a comparison of methods for the solution of the two dimensional heat diffusion equation
[AD-A154670] 21 p3675 N85-32833
Gradient scaling for nonuniform meshes
[DE85-009625] 22 p3784 N85-33443
Selecting step sizes in sensitivity analysis by finite differences
[NASA-TM-86382] 22 p3799 N85-33538
KIVA computer program for multidimensional chemically reactive fluid flows with fuel sprays
[DE85-012730] 22 p3830 N85-33722
Use of a hyperbolic grid generation scheme in simulating supersonic viscous flow about three-dimensional winged configuration
[NASA-TM-85344] 23 p3893 N85-34116
A versatile computer package for mechanism analysis
23 p3924 N85-34314
Block-implicit calculations of three-dimensional laminar flow in strongly curved ducts
[DE85-003047] 23 p3931 N85-34363
Numerical and analytic descriptions of cosmic-ray transport
[SH-4.1-4] 23 p4005 N85-34830
Finite analytic solutions of supersonic flows in two-dimensional non-symmetrical channels
24 p4059 N85-35154
Numerical studies of 2-dimensional flows
[NASA-CR-3930] 24 p4060 N85-35160
Two-dimensional numerical modeling of ion implanted GaAs MESFET devices 24 p4088 N85-35341
Stress analysis of axisymmetric sandwich shells of variable thickness 24 p4101 N85-35419
Thermal evolution of coastal California with implications for hydrocarbon maturation 24 p4115 N85-35509

Three-dimensional finite deformation viscoelastic model accounting for damage effects
[DE85-012951] 24 p4139 N85-35660

The finite element-difference method
24 p4141 N85-35672

FINITE ELEMENT METHOD

Finite element computation on nearest neighbor connected machines 01 p0057 N85-10379

Initial experience with distributing structural calculations among computers operating in parallel
01 p0058 N85-10381

Performance of the h, p and h-p versions
01 p0058 N85-10383

Augmented weak forms and element-by-element preconditioners: Efficient iterative strategies for structural finite elements. A preliminary study
01 p0058 N85-10384

Stress-derivative control of keystoning deformation in finite element codes 01 p0058 N85-10385

A triangular finite element for thin plates and shells
01 p0058 N85-10386

Crashworthiness of light aircraft fuselage structures: A numerical and experimental investigation
01 p0060 N85-10399

Finite element modelling of buried structures
01 p0061 N85-10403

On the computer analysis of structures and mechanical systems 01 p0061 N85-10404

Solution of contaminant transport equations using an orthogonal-upstream finite element scheme
[DE84-014266] 01 p0070 N85-10463

Applications of a finite-element regional model to very-short-range forecasting 01 p0080 N85-10531

Recursive calculation of curved finite element stiffness matrices
[CSIR-TWISK-303] 01 p0108 N85-10726

Constitutive model development for isotropic materials
02 p0144 N85-10975

The CMC/3DPNS computer program for prediction of three-dimensional, subsonic, turbulent aerodynamic juncture region flow. Volume 3: Programmers' manual
[NASA-CR-165998] 02 p0197 N85-11318

Finite element analysis of thermoelasticity problems
02 p0208 N85-11369

STARS: A general-purpose finite element computer program for analysis of engineering structures
[NASA-RP-1129] 02 p0209 N85-11378

Parallel triangularization of substructured finite element problems
[NASA-CR-172466] 02 p0241 N85-11569

A finite element projection method for the solution of particle transport problems with anisotropic scattering
[AD-A145382] 02 p0250 N85-11637

Numerical methods for singularly perturbed differential equations with applications
[AD-A145639] 02 p0252 N85-11650

Pointwise iterations of finite element modeling of advection-diffusion equations
[DE84-015284] 02 p0253 N85-11656

A finite element method for the solution of two-dimensional transonic flows in cascades
[PNR-90216] 03 p0316 N85-12045

A comparative study of the finite element and boundary element methods as applied to a boundary value problem of a harmonic function
[AD-A146018] 03 p0411 N85-12627

Moving finite elements in 2-D
[AD-A146266] 03 p0412 N85-12637

Analysis of piezoelectric disks and cylinders using finite element method
[AD-A146323] 03 p0414 N85-12650

Numerical calculations of stratified Ekman layer flow over ridges with a finite element model
[DE84-014482] 04 p0499 N85-13179

Finite element method for a class of viscoelastic flows in deforming domains applied to jet breakup
[DE84-014571] 04 p0500 N85-13186

NIKE3D: An implicit, finite-deformation, finite element code for analyzing the static and dynamic response of three-dimensional solids, revision 1
[DE84-017161] 04 p0514 N85-13277

Comparison of free component mode synthesis techniques using MSC/NASTRAN
[DE84-014451] 04 p0514 N85-13278

The determination of eddy current losses in electrical equipment
[DE84-016340] 05 p0632 N85-14050

A finite element method for three dimensional cavity circulation 05 p0635 N85-14071

Dynamic testing of NOVA laser switchyard tower
[DE84-014450] 05 p0640 N85-14103

Finite element method calculation of a necking tension specimen including heat transfer influence
[RUB-IFM-MITT-40] 05 p0648 N85-14162

Some error estimates for the p-version of the finite element method
[CTH-MATH-1984-21] 05 p0719 N85-14814

A lumped mass finite element method with quadrature for a nonlinear parabolic problem
[CTH-MATH-1984-22] 05 p0719 N85-14815

Applications of finite and wave envelope element approximations to acoustic radiation from turbofan engine inlets in flight 05 p0726 N85-14664

Element methods for calculation of sound fields
[RUB-IFM-MITT-41] 05 p0726 N85-14665

A study of crashworthiness of light aircraft fuselage structures: A numerical and experimental investigation
[UTIAS-286] 06 p0750 N85-14803

Iterative method of calculating strength of airframe members using finite element method
06 p0775 N85-14955

Process Modeling Applied to Metal Forming and Thermomechanical Processing
[AGARD-LS-137] 06 p0796 N85-15086

Finite element simulation of forging processes
06 p0797 N85-15093

Computer-aided design of extrusion dies by metal-flow simulation 06 p0797 N85-15094

A simple extension to multidimensional problems of the artificial viscosity due to Lapidus
06 p0808 N85-15134

A compact finite element method for elastic bodies
[NASA-CR-172487] 06 p0817 N85-15185

Verification of a computer program for vibration analysis of composite wing cores
[NAL-TR-825] 06 p0817 N85-15187

CFM 56-2. Oligocyclic fatigue of the turbofan disk: Dimensionning and tests for verification and improvements 07 p0908 N85-15750

A study of interply layer effects on the free-edge stress field of angleplied laminates
[NASA-TM-86924] 07 p0919 N85-15822

Finite element procedures applicable to nonlinear analysis of reinforced concrete shell structures
[AD-A146796] 07 p0978 N85-16209

Buckling analysis of cracked, floating ice sheets
[AD-A147330] 07 p0988 N85-16277

Feedback, adaptivity and A-posterior estimates in finite elements: Aims, theory and experience
[AD-A146869] 07 p1029 N85-16531

Solution of finite element problems by preconditioned conjugate gradient and Lanczos methods
[AD-A146921] 07 p1029 N85-16532

Performance of the h, p and h-p versions of the finite element method
[AD-A146940] 07 p1029 N85-16535

A counterexample to a result of Strang and Fix concerning controlled approximation
[AD-A147360] 07 p1032 N85-16550

Splitting methods for the numerical solution of the incompressible Navier-Stokes equations
[AD-A147463] 07 p1032 N85-16554

Analysis of a penalty finite element approximation of the Navier Stokes equations 08 p1161 N85-17321

Finite element calculation for a Y-joint and comparison of results with strain measurements
[BLL-RISLEY-TR-4526-(9091.9F)]
08 p1171 N85-17381

Computational methods for nonlinear dynamics problems in solid and structural mechanics
[AD-A148352] 08 p1172 N85-17392

Response of saturated porous nonlinear materials to dynamic loadings
[AD-A146526] 08 p1173 N85-17394

A moving finite element method for time dependent partial differential equations with error estimation and refinement
[AD-A147719] 08 p1210 N85-17617

A local refinement finite element method for time dependent partial differential equations
[AD-A147943] 08 p1211 N85-17620

A feedback finite element method with a posteriori error estimation. Part 1. The finite element method and some basic properties of the A posteriori error estimator
[AD-A148345] 08 p1212 N85-17631

Analytical and experimental investigation of rubbing interaction in labyrinth seals for a liquid hydrogen fuel pump — space shuttle main engine
[NASA-CR-174857] 09 p1287 N85-18064

Nonlinear analysis of composite laminates
09 p1288 N85-18087

Defect tolerance in pipeline girth welds
[ERS-E.353] 09 p1328 N85-18347

Finite element computation of structural design sensitivity analysis 09 p1330 N85-18353

A finite element analysis of viscoelastic materials with varying time scales 09 p1330 N85-18355

Extrpolation in finite element analysis
09 p1331 N85-18365

finite element analysis of bi-material systems with applications in hydraulic fracturing
09 p1332 N85-1

Existence, uniqueness and stability conditions for general finite element methods in linear elasticity
09 p1332 N85-18372

Nonlinear finite element analysis of elastic and elastic-plastic buckling of cylinders under complex combined loads 09 p1332 N85-18373

Alternative shock characterizations for consistent shock test specifications 09 p1335 N85-1

Determination of shear coefficient of a general beam cross section by finite element method
09 p1339 N85-18413

System software for the finite element machine
[NASA-CR-3870] 09 p1372 N85-1

A 3-dimensional mass conserving element for compressible flows
[NASA-CR-172513] 09 p1373 N85-1

Grouser effect studies
[AD-P004278] 09 p1406 N85-1

Condensed antenna structural models for dynamics analysis 10 p1463 N85-1

Finite element analysis of nonlinear oscillations and flutter of shells of revolution
[AD-A149071] 10 p1496 N85-19440

A program design for an adaptive, non-linear finite element solver
[AD-A148880] 10 p1539 N85-19705

SOLIDGEN: A solid finite element data generator. User's manual
[AD-A149490] 10 p1541 N85-19715

Controlled approximation and a characterization of the local approximation order
[AD-A149095] 10 p1546 N85-19750

Calculation of transmission line impedances using the ANSYS finite element program
[DE84-016715] 11 p1629 N85-20261

Local strain redistribution corrections for a simplified inelastic analysis procedure based on an elastic finite-element analysis
[NASA-TP-2421] 11 p1651 N85-20386

Dynamic investigations of a spherical tank structure filled with liquid using ANSYS three-dimensional fluid elements
[MBB-UR-E-737-83-O] 11 p1654 N85-20418

Resolution of 2-dimensional seismologic problems by a finite element approximation. Application to the Love wave propagation through the Atlantic border of the Iberic Peninsula 11 p1681 N85-20594

Resolution of 2-dimensional seismologic problems by a finite element approximation. Application to the Love wave propagation through the Atlantic border of the Iberic Peninsula. Appendix: Graphs of results — Lagrange coordinates 11 p1681 N85-20595

PASLIB programmer's guide for the finite element machine, revision 2.1-A
[NASA-CR-172281] 11 p1705 N85-20727

Finite element method for solving neutron transport problems
[DE85-001075] 11 p1722 N85-20829

Si-on-insulator formation using a line-source electron beam
[DE85-003449] 11 p1737 N85-20925

Advanced stress analysis methods applicable to turbine engine structures
[NASA-CR-175573] 12 p1778 N85-21165

Nonlinear analysis for high-temperature multilayered fiber composite structures — turbine blades
[NASA-TM-83754] 12 p1797 N85-21273

Algorithm for the simulation of transient viscoelastic flows with free surfaces
[DE85-002713] 12 p1848 N85-21590

Finite element analysis of problems associated with life enhancement techniques
[ARL/STRUC-R-404] 12 p1862 N85-21676

3-D inelastic analysis methods for hot section components (base program) — turbine blades, turbine vanes, and combustor liners
[NASA-CR-174700] 12 p1863 N85-21686

Recent advances in hybrid/mixed finite elements
[NASA-CR-175574] 12 p1863 N85-21687

A study of coupling the boundary and finite element methods in two-dimensional elastostatics
[AD-A149619] 12 p1865 N85-21702

A solution method for large deformation contact problems
[AD-A149642] 12 p1866 N85-21707

Nonlinear analysis of layered composite plates and shells
[PB85-127181] 12 p1868 N85-21718

Geometrically nonlinear analysis of laminated elastic structures
[NASA-CR-175609] 12 p1868 N85-21720

A 3-D treatment of convective flow in the Earth's mantle
[DE85-003734] 12 p1880 N85-21883

On the accuracy of least squares methods in the presence of corner singularities
[NASA-CR-172552] 12 p1919 N85-22050

Experimental and numerical analysis of electric currents and electromagnetic blunting of cracks in thin plates
[AD-A150416] 13 p2022 N85-22669

Micromechanical modeling of microstructural damage in creeping alloys
[DE85-003625] 13 p2022 N85-22671

Analysis of interaction of dynamically adjustable gyroscopes on elastic platform by finite-element method
13 p2046 N85-22822

Pre- and post-processing for stream-function eddy current calculations
[AD-A150417] 13 p2065 N85-22896

HPFTP flow diverter analysis
[NASA-CR-171424] 13 p2091 N85-23057

On Hybrid and mixed finite element methods
[NASA-CR-175551] 13 p2101 N85-23096

Advanced life analysis methods. Volume 2: Crack growth analysis methods for attachment lugs
[AD-A150420] 13 p2103 N85-23109

Exploiting parallel computing with limited program changes using a network of microcomputers
[NASA-TM-86367] 13 p2146 N85-23318

User's and programmer's guide to the mechanics of moving finite element code
[DE85-008165] 13 p2152 N85-23365

Magnetic field interactions with material discontinuities
[AD-A150197] 13 p2154 N85-23373

Unified constitutive material models for nonlinear finite-element structural analysis — gas turbine engine blades and vanes
[NASA-TM-86985] 14 p2320 N85-24338

Stress in axially symmetrical heavy metal projectiles during discharge — numerical simulation
[ISL-CO-219/83] 14 p2321 N85-24345

Finite element model for creep in composite masonry
[PB85-150324] 14 p2322 N85-24347

Space Mathematics for the Preparation and Development of satellite Exploitation
[ISBN-2-85428-115-2] 14 p2395 N85-24753

Finite element methods in space mathematics
14 p2396 N85-24757

Runstreams for using ASKA
[MAST-84/27] 14 p2403 N85-24812

Implementation of a C1 triangular element based on the p-version of the finite element method
[AD-A150904] 14 p2404 N85-24825

Constrained parabolic approximation of curves in the finite element method
[CSIR-TWISK-340] 14 p2408 N85-24843

Finite Element Methods in South Africa 1983 — conference
[S-332] 14 p2410 N85-24863

Design, fabrication and test of composite curved frames for helicopter fuselage structure
[NASA-CR-172438] 15 p2470 N85-25247

Summary of recent investigations of the mechanical properties of polycrystalline solids
[DE85-006776] 15 p2511 N85-25492

A finite element, Navier-Stokes study of the confined, laminar flow over a downstream facing step
15 p2553 N85-25754

Thirteenth NASTRAN Users' Colloquium
[NASA-CP-2373] 15 p2573 N85-25863

New enhancements in April 85 NASTRAN release
15 p2573 N85-25864

Crack elements for COSMIC/NASTRAN
15 p2573 N85-25866

Layered composite analysis capability
15 p2573 N85-25868

NPLOT: An interactive plotting program for NASTRAN finite element models 15 p2573 N85-25869

COSMIC/NASTRAN-PATRAN interface
15 p2574 N85-25870

Isoparametric 3-D finite element mesh generation using interactive computer graphics 15 p2574 N85-25873

A new NASTRAN capability for data reduction
15 p2574 N85-25874

Symmetric composite laminate stress analysis
15 p2575 N85-25878

On the interconnection of incompatible solid finite element meshes using multipoint constraints
15 p2575 N85-25879

NASTRAN's application in agricultural engineering
15 p2575 N85-25880

Use of COSMIC NASTRAN in a design department
15 p2575 N85-25881

An elastic analysis of a plated bone to determine fracture gap motion 15 p2575 N85-25882

Learjet Model 55 wing analysis with landing loads
15 p2575 N85-25883

Fillet weld stress using finite element methods
15 p2576 N85-25884

The structural finite element model of the C-5A
15 p2576 N85-25885

Using NASTRAN to model missile inertia loads
15 p2576 N85-25886

Experience with free bodies 15 p2576 N85-25887

NASTRAN analysis comparison to shock tube tests used to simulate nuclear overpressures
15 p2576 N85-25888

Finite element prediction of loss factors for structures with frequency-dependent damping treatments
15 p2576 N85-25889

Direct transient analysis of a fuze assembly by axisymmetric solid elements 15 p2576 N85-25890

Transient analysis of a magnetic heat pump
15 p2576 N85-25891

Effect of internal pressure on flexibility and stress intensification factors for pipe elbows analyzed by the finite element method
[AD-A151161] 15 p2578 N85-25901

An experimental investigation into the dynamic response of a stiffened flat plate loaded impulsively by an underwater shockwave
[AD-A151321] 15 p2578 N85-25903

Crack closure characteristics considering center cracked and compact tension specimens
[AD-A151702] 15 p2579 N85-25907

GRID: A FORTRAN program for using a digitizing table to enter a finite element GRID
[AD-A151317] 15 p2628 N85-26196

Enhanced thermal-structural analysis by integrated finite elements
[AD-A151103] 15 p2636 N85-26258

Development of a dynamic finite element model for unrestrained flexible structures
[AD-A151176] 15 p2636 N85-26259

SPLOT: A plot program for finite element data, function versus distance
[DE85-007129] 15 p2638 N85-26273

Sliding interfaces with contact-impact in large scale Lagrangian computations
[DE85-006451] 15 p2639 N85-26277

Two computational methods for cascade flows
16 p2692 N85-26617

The effect of inaccuracies in structural models on the control of large space structures
[AD-A151794] 16 p2732 N85-26858

Theoretical and experimental comparisons of nearfield electrogalvanic fields due to nonlinear polarization layers
[AD-A152085] 16 p2779 N85-27149

Solution of Onsager's equation for a rotating compressible fluid in a multiply-connected domain
[DE85-007048] 16 p2784 N85-27178

Computer modeling of vibrational energy levels of potential laser candidates (diatomic molecules)
[AD-A151765] 16 p2790 N85-27209

Automatic tracking of crack growth via finite elements
16 p2797 N85-27246

Finite axisymmetric deformation of a thin shell of revolution 16 p2798 N85-27251

A computer analysis program for interfacing thermal and structural codes
[NASA-TM-87021] 16 p2800 N85-27264

The nonlinear analysis of thick composite plates using a cubic spline function
[AD-A152115] 16 p2801 N85-27268

Numerical resolution calculation for elastic-plastic impact problems
[AD-A152292] 16 p2801 N85-27270

Hopkinson bar simulation using DYNA2D
[DE85-006766] 16 p2802 N85-27275

Stress analysis of the space telescope focal plane structure joint
[NASA-CR-175797] 16 p2803 N85-27284

A general purpose scatter storage subsystem and a comparison of hashing methods
[NASA-CR-175814] 16 p2845 N85-27542

Finite elements and the method of conjugate gradients on a concurrent processor
[NASA-CR-175812] 16 p2853 N85-27588

Analysis of the convergence of mixed finite element methods
[HTKK-MAT-A227] 16 p2856 N85-27613

Probabilistic finite element development
17 p2913 N85-27956

Probabilistic finite element: Variational theory
17 p2913 N85-27957

Designing for fiber composite structural durability in hygrothermomechanical environment
[NASA-TM-87045] 17 p2917 N85-27978

Analytical shear buckling investigation of curved composite panels
[AD-A153136] 17 p2960 N85-28421

Field theory analysis using the finite element method to determine the deliberation curves of three dimensional fracture mechanics specimens with a semicircular surface crack applying the electrical direct current potential method for crack depth measurement
[GKSS-84-E-53] 17 p2962 N85-28434

Implementation of a general finite element code on an IBM PC compatible microcomputer
[AD-A152681] 17 p3011 N85-28615

TRINITY: A pre- and post-processing program for 2-dimensional finite element data
[DE85-008029] 17 p3013 N85-28628

Numerical benchmark study for the finite element computer code NEPTUNE
[DE85-008400] 17 p3013 N85-28630

A high-accuracy optical linear algebra processor for finite element applications
[NASA-CR-175894] 17 p3017 N85-28658

A discussion of adaptive grids and their applicability in numerical hydrodynamic modeling
[AD-A151843] 17 p3017 N85-28659

A fast implementation of explicit time stepping algorithms with the finite element method for a class of nonlinear evolution problems
[REPT-84-03] 17 p3021 N85-28686

Finite element thermal-structural analysis of cable-stiffened space structures
[AD-A153822] 18 p3066 N85-28963

Localized ionic currents from a corroding iron-copper galvanic couple
[AD-A153627] 18 p3074 N85-29011

Structural Analysis
[DFVLR-MITT-84-21] 18 p3120 N85-29313

Field consistency and the finite element analysis of multifield structural problems 18 p3120 N85-29316

Scattering by distributions of small thin particles
19 p3253 N85-30172

Use of a two-dimensional flow model to quantify aquatic habitat
[AD-A154287] 19 p3266 N85-30253

Comparison and evaluation of field and numerical results from the Site A heater test at Avery Island
[DE85-010625] 19 p3268 N85-30269

Forced structural response using component mode synthesis
[DE85-006479] 19 p3287 N85-30363

Three-dimensional finite element impact analysis of a nuclear waste truck cask
[DE85-010653] 19 p3288 N85-30389

Combined finite element meshing techniques using SUPERTAB
[DE85-011393] 19 p3340 N85-30696

Nested dissection on a mesh-connected processor array
[AD-A154068] 19 p3342 N85-30711

Extrapolation methods in the finite element method
[BONNER-MATHE-SCHR-158]
19 p3345 N85-30729

Asymptotic expansions for finite element eigenvalues and finite element solution 19 p3345 N85-30730

Asymptotic expansions for the finite element approximation of parabolic functions
19 p3345 N85-30731

Superconvergence of finite element approximation for Navier-Stokes equations 19 p3345 N85-30732

Space station parametric models
20 p3413 N85-31180

A control concept for large flexible spacecraft using order reduction techniques 20 p3415 N85-31193

Delamination micromechanics analysis
[NASA-CR-172598] 20 p3422 N85-31237

SPAR improved structural-fluid dynamic analysis capability
[NASA-CR-171549] 20 p3454 N85-31449

A new finite element approach: Progress in inviscid flow computations
[NASA-TM-86434] 20 p3454 N85-31450

Application of finite element method to the sizing of mechanical parts — helicopter design
[SNIAS-851-210-105] 20 p3463 N85-31515

Constitutive modeling of superalloy single crystals and directionally solidified materials
20 p3466 N85-31535

A numerical algorithm for endochronic plasticity and comparison with experiment 20 p3467 N85-31539

Finite element modeling of cracked bodies using the Bodner-Partom flow law 20 p3468 N85-31547

Nonlinear analysis of an axisymmetric structure subjected to non-axisymmetric loading
20 p3468 N85-31549

Efficient solution methods for nonlinear finite element analysis 20 p3519 N85-31886

A variable node finite element method applied to the gas dynamics equations
[AD-A155211] 21 p3584 N85-32281

Ductile fracture of dynamically loaded naval structures-compact tension specimen tests and analyses
[AD-A155472] 21 p3600 N85-32353
An investigation into the comparisons of the underwater shock effects on a stiffened flat plate to the predictive nature of a computer model
[AD-A155812] 21 p3600 N85-32355
Analysis of inclined growth of silicon sheet
21 p3612 N85-32442
Edge-defined film-fed growth of thin silicon sheets
21 p3612 N85-32443
Concurrent implementation of the Crank-Nicolson method for heat transfer analysis
[NASA-TM-86446] 21 p3674 N85-32822
DYNA3D, INGRID, and TAURUS: An integrated, interactive software system for crashworthiness engineering
[DE85-010626] 21 p3677 N85-32846
Photo-acoustic effect in finite-dimensional semiconductors 21 p3682 N85-32876
Finite element methods for viscoelastic flow
[AD-A154877] 22 p3783 N85-33437
Selecting step sizes in sensitivity analysis by finite differences
[NASA-TM-86382] 22 p3796 N85-33536
Elevated temperature crack growth
[NASA-CR-174957] 22 p3798 N85-33540
A review of path-independent integrals in elastic-plastic fracture mechanics, task 4
[NASA-CR-174956] 22 p3799 N85-33541
Slideline verification for multilayer pressure vessels and piping analysis including strain hardening
[DE85-005816] 22 p3801 N85-33549
SANCHO: A finite element computer program for the quasistatic, large deformation, inelastic response of two-dimensional solids
[DE85-011456] 22 p3829 N85-33714
Numerical simulation of interior and terminal ballistics phenomena. Investigation of the effects of the parameters and application examples
[ISL-R-112/84] 22 p3831 N85-33731
Behaviors of stress waves in a conical bar
23 p3904 N85-34182
Experimental study of collapse of thick-walled tube under external pressure and axial force
23 p3904 N85-34186
Proceedings of the Mechanisms Conference, volume 1 23 p3923 N85-34309
Proceedings of the Mechanisms Conference, volume 2 23 p3924 N85-34316
An introduction to finite elements
23 p3924 N85-34319
Inertial stresses and deformations in mechanisms
23 p3924 N85-34320
Thermal stress analysis of a new turbine shroud seal concept
[NASA-TM-87062] 23 p3938 N85-34406
Three-dimensional finite element failure model for predicting failure in fibre reinforced bolted joints
[BR94778] 23 p3940 N85-34423
Stresses and strains in a plate resulting from two closely-spaced interference-fit fasteners
[ARL/STRUC-TM-409] 23 p3941 N85-34429
FEMALE: Finite Element Method for Arbitrary Lagrangian and Eulerian elements
23 p3979 N85-34671
Analysis of incompressible cascade flows using state-of-the-art computer programs
[AD-A155850] 24 p4062 N85-35173
Design and behavior of coped beams
24 p4100 N85-35417
Stress-intensity factors for circumferential surface cracks in pipes and rods under tension and bending loads
[NASA-TM-87594] 24 p4101 N85-35424
Prediction of plasticity characteristics for three-dimensional fracture specimens comparison with experiment
[AD-A156425] 24 p4102 N85-35430
The finite element-difference method
24 p4141 N85-35672
A new method for boundary value problems
[AD-A156934] 24 p4143 N85-35683

FINITE IMPULSE RESPONSE FILTERS
U FIR FILTERS

FINITE VOLUME METHOD
Theoretical contributions to transonic flow analysis for transport aircraft
[BMFT-FB-W-84-036] 08 p1078 N85-16838
Thermodynamic evaluation of transonic compressor rotors using the finite volume approach
[NASA-CR-175811] 16 p2706 N85-26712
Unsteady flow in multistage turbines
17 p2911 N85-27946
Calculation of flow around the SF 310 airplane using a full potential equation method
[FFA-TN-1984-63] 20 p3369 N85-31022

FINITE-STATE MACHINES
U TURING MACHINES

FINLAND
Space activities in Finland 08 p1231 N85-17754
Finnair, LOT, SAS reps in USSR on present operations, plans 09 p1278 N85-18035
Precipitation and snow cover data, 1977
[ISBN-951-697-215-2] 17 p2995 N85-28514

FINS
NT COOLING FINS
NT NOSE FINS
The effect of channel convergence on heat transfer in a passage with short pin fins
[NASA-TM-83801] 01 p0046 N85-10303
An experimental study on the induced normal force on tail-fins due to wing-tail interference
[NAL-TR-814] 03 p0318 N85-12051
Oil-flow study of a Space Shuttle orbiter tip-fin controller
[NASA-TM-86276] 04 p0460 N85-12920
Finlet injector
[AD-D011245] 06 p0765 N85-14891
Repair of composites 08 p1120 N85-17056
Modeling and simulation of a fin actuation system
[AD-A149443] 10 p1428 N85-19005
Optimization of a ground coupled heat pump
[DE85-000273] 10 p1486 N85-19380
An exploratory investigation of sharp fin-induced shock wave/turbulent boundary layer interactions at high shock strengths
[AD-A151571] 15 p2556 N85-25772
Subsonic and transonic aerodynamics of a wraparound fin configuration
[AD-A153646] 18 p3059 N85-28927
A computation of fin-line impedance
[AD-A154080] 19 p3256 N85-30204
Fin line filters technology and electronic warfare
[AD-A154975] 21 p3576 N85-32237
Film condensation of steam on externally finned horizontal tubes
[AD-A155642] 21 p3585 N85-32285
Computer simulation of a cruise missile using brushless dc motor fin control
[AD-A155835] 24 p4089 N85-35349

FIR FILTERS
Use of Walsh functions for calculating characteristics of digital filters with impulse response of finite duration
13 p2083 N85-23011

FIRE CONTROL
Voice command weapons launching system
[AD-D011378] 07 p0937 N85-15940
Methodology improvement program for the second generation miss distance radar (MIDI 2)
[AD-A148467] 08 p1153 N85-17281
Acta Electronica Sinica (selected articles)
[AD-A148829] 11 p1626 N85-20252
Ground evaluation of helicopter air-to-air warfare
13 p1967 N85-22360
Research Flight Simulator for Helicopters (RFSH): Description and application to fire control system design
[SNIAS-851-210-106] 20 p3393 N85-31050

FIRE DAMAGE
Testing of three different flight suits in fire environment — fuel fire
[FOA-C-59012-H1] 02 p0238 N85-11552
Post fire interview: Development and field validation of the behavioral sequence interview technique
[NBS-GCR-84-477] 04 p0454 N85-12881
Thermal radiation hazards from Liquified Petroleum Gas (LPG) fireballs
[VTT-304] 09 p1293 N85-18122
Pathophysiological study of poisoning due to thermal degradation of materials — aircraft cabins
[CERMA-84-15] 11 p1692 N85-20640
The role of aircraft panel materials in cabin fires and their properties
[FAA-CT-84-30] 21 p3553 N85-32104
Photovoltaic module spread-of-flame testing
21 p3612 N85-32448

FIRE EXTINGUISHERS
Flow of nitrogen-pressurized Halon 1301 in fire extinguishing systems
[NASA-CR-174271] 07 p0900 N85-15701
Aircraft skin penetrator and agent applicator. Volume 1: Working model development and construction
[AD-A150498] 13 p1970 N85-22374

FIRE FIGHTING
The experimental mod 3 firefighters' aluminized crash-rescue, fire-proximity hood
[AD-A144993] 01 p0098 N85-10655
Fire research publications, 1983
[PB84-217066] 03 p0343 N85-12208
Suppression and control of Class C cargo compartment fires
[FAA-CT-84-21] 12 p1773 N85-21133
Firefighters' communication transceiver test plan
[NASA-CR-171419] 13 p2053 N85-22284
Aircraft skin penetrator and agent applicator. Volume 2: Test and evaluation
[AD-A151609] 15 p2486 N85-25225
Fire protection review revisit no. 2, Argonne National Laboratory, Argonne, Illinois
[DE85-013245] 22 p3755 N85-33276
Fire research publications, 1984
[PB85-208502] 24 p4166 N85-35827

FIRE PREVENTION
Fire research publications, 1983
[PB84-217066] 03 p0343 N85-12208
Fire prevention and control
[GPO-30-743] 04 p0482 N85-13074
The development of fire evaluation system for detention and correctional occupancies
[NBSIR-84-2976] 10 p1459 N85-19182
Legislation to improve airline safety
[GPO-38-222] 12 p1773 N85-21132
Fire resistant polymers based on 1-(diorgano oxyphosphonyl)methyl-2,4- and 2,6-diamino benzenes
[NASA-CASE-ARC-11512-2] 12 p1811 N85-21382
Test results from a comparative evaluation of a condensation nuclei fire detector
[NASA-CR-3874] 12 p1862 N85-21675
Fiscal year 1986 technical objective document
[AD-A151039] 14 p2432 N85-25000
Hazards in welding due to oxygen changes in the workplace atmosphere
[BLL-WI-TRANS-684-(9312.57)]
16 p2792 N85-27224
Evaluation of pyrotechnic fire suppression system for six pyrotechnic compositions
[AD-A152995] 17 p2937 N85-28130
Practical real-time quality control of antimisting kerosene
[DE/FAA/CT-85/1] 18 p3083 N85-29072
Fire protection review revisit no. 2, Argonne National Laboratory, Argonne, Illinois
[DE85-013245] 22 p3755 N85-33276
Scaling parameters of flashover
[NBS-GCR-85-497] 23 p3911 N85-34229
Review of zirconium-zircaloy pyrophoricity
[DE85-011169] 23 p3916 N85-34270
Investigation of experimental lightweight firewall materials for A/C engine bay applications
[AD-A155765] 24 p4062 N85-35175
Proceedings of the 7th Joint Panel Meeting of the UJNR Panel on Fire Research and Safety
[PB85-199545] 24 p4065 N85-35317
Fire research publications, 1984
[PB85-208502] 24 p4166 N85-35827

FIRE RESISTANCE
U FLAMMABILITY

FIRE RETARDANTS
U FLAME RETARDANTS

FIREBREAKS
Explosion-proof properties and hydraulic resistance of fire-barrier elements based on knitted metallic screens
11 p1601 N85-20087
Scaling parameters of flashover
[NBS-GCR-85-497] 23 p3911 N85-34229

FIREPROOFING
Module flammability research
06 p0830 N85-15274
Flame-resistant materials for use in pyrotechnic safety clothing
[AD-A146857] 07 p0931 N85-15801
Environmental cycling of cellulosic thermal insulation and its influence on fire performance
[DE85-004295] 13 p2041 N85-22776
Fire performance of interstitial space construction system
[NBSIR-85-3158] 20 p3436 N85-31316
Aviation safety (aircraft passenger survivability and cabin safety)
[GPO-39-847] 23 p3895 N85-34130
Investigation of experimental lightweight firewall materials for A/C engine bay applications
[AD-A155765] 24 p4062 N85-35175
Fire research publications, 1984
[PB85-208502] 24 p4166 N85-35827

FIRES
The pyrolysis toxic gas analysis of aircraft interior materials
[AD-A146265] 03 p0328 N85-12115
Fire research publications, 1983
[PB84-217066] 03 p0343 N85-12208
Post fire interview: Development and field validation of the behavioral sequence interview technique
[NBS-GCR-84-477] 04 p0454 N85-12881

Fire prevention and control
[GPO-30-743] 04 p0482 N85-13074
Modeling of aircraft cabin fires
[PB85-137685/GAR] 09 p1277 N85-18031
Suppression and control of Class C cargo compartment fires
[FAA-CT-84-21] 12 p1773 N85-21133
A study of intumescent reaction mechanisms
[AD-A149605] 12 p1812 N85-21365
Collection and use of lightning strike data in the western US during summer 1983
[PB85-110534] 12 p1897 N85-21907
Determination of toxicity of combustion products of habitability foams concurrently with flammability studies of these materials
[AD-A149647] 12 p1905 N85-21961
Aircraft skin penetrator and agent applicator. Volume 1: Working model development and construction
[AD-A150496] 13 p1970 N85-22374
Environmental cycling of cellulosic thermal insulation and its influence on fire performance
[DE85-004295] 13 p2041 N85-22776
Thermal response of aircraft cabin ceiling materials during a post-crash, external fuel-spill, fire scenario
[PB85-145647] 14 p2220 N85-23764
Safety recommendation(s), A-84-76 through -78
[REPT-3751E] 15 p2486 N85-25224
Hydrocarbon pool and vapor fire data analysis
[DE85-005857] 15 p2523 N85-25550
Fire pit tests of blue flight coverall program
[AD-A151884] 15 p2620 N85-26149
Evaluation of pyrotechnic fire suppression system for six pyrotechnic compositions
[AD-A152995] 17 p2937 N85-26130
Laboratory modeling of aspects of large fires
[AD-A153152] 17 p2938 N85-26136
Numerical simulations of the effect of floor and ceiling venting on fire and smoke spread in aircraft cabins
[PB85-176333] 19 p3216 N85-29939
Fire performance of interstitial space construction system
[NBSIR-85-3156] 20 p3436 N85-31318
Aviation safety (aircraft passenger survivability and cabin safety)
[GPO-39-847] 23 p3895 N85-34130
The application of models to the assessment of fire hazard from consumer products
[NBSIR-85-3219] 23 p3925 N85-34325

FIREWORKS
U PYROTECHNICS

FIRING (IGNITING)
NT STATIC FIRING
NT TEST FIRING
CP DDT detonators. Part 1: Design sensitivity study
[DE84-017255] 09 p1302 N85-18180
A computer code IB-KB for interior ballistics of recoiling and recoilless guns
[FOA-C-20566-D2] 18 p3164 N85-29602

FISCHER-TROPSCH PROCESS
Michelle-derived catalysts for extended Schulz-Flory
[DE85-005658] 17 p2922 N85-28012
Catalyst and reactor development for a liquid phase Fischer-Tropsch process
[DE85-005694] 17 p2922 N85-28014
CO + H2 reaction over nitrogn-modified iron catalysts
[DE85-013791] 24 p4072 N85-35231

FISH
U FISHES

FISHERIES
The Marine Resources Experiment Program (MAREX)
[NASA-TM-87368] 01 p0086 N85-10580
Climate and fisheries: A Peruvian case study
07 p1003 N85-16373
The use of hydrometeorological data in explaining shrimp cycles in Guyana 07 p1004 N85-16381
Automatic buoys to assist the tuna fishery off the Azores 14 p2238 N85-23879
Contribution of the NOAA-7 and 8 and ARGOS partnership to white tuna fishing in the northeast Atlantic
16 p2813 N85-27355
Ecology of Pamlico River, North Carolina: An estuarine profile
[PB85-155703] 16 p2822 N85-27404

FISHES
NT SHARKS
Modeling effects of toxicants on aquatic systems
[DE84-016694] 04 p0531 N85-13396
The development of the vestibular apparatus under conditions of weightlessness
[NASA-TM-77517] 07 p1011 N85-16422
Mercury health effects update: Health issue assessment
[PB85-123925] 10 p1526 N85-19639
Acid rain: Effects on fish and wildlife
[PB85-154672] 16 p2821 N85-27402
Pollutant body burdens and reproduction in Platichthys stellatus from San Francisco Bay
[DE85-010407] 19 p3306 N85-30509
Chemoreception and detection of micropollutants by means of a telemetric bionic detector
[DRIC-T-7460] 22 p3810 N85-33600

FISHTAILING
U YAW

FISSION
Tests of the lunar hypothesis
04 p0584 N85-13730
A reappraisal of Darwin's fission hypothesis and a possible limit to the primordial angular momentum of the Earth 04 p0585 N85-13736
Numerical simulations of fission
04 p0585 N85-13737
The dynamic fission instability and the origin of the Moon 04 p0586 N85-13738
On the origin of the Moon by rotational fission
04 p0587 N85-13746
Geochemical evidence for the formation of the Moon by impact induced fission of the proto-Earth
04 p0587 N85-13747
Workshop on Nuclear Dynamics 3
[INC-40007-24] 12 p1931 N85-22130
Methodology for evaluating P sub nu distributions: Results to date
[DE85-007286] 20 p3530 N85-31956
Paired ion chamber constants for fission gamma-neutron fields
[AD-A155069] 21 p3702 N85-32999
Nuclear data for MCNP
[DE85-010794] 22 p3840 N85-33782

FISSION PRODUCTS
Hydrolysis, formation and ionization constants at 25(0)C, and at high temperature-high ionic strength
[DE85-010645] 19 p3236 N85-30061
MELCOR Accident Consequence Code System (MACCS)
[DE85-009712] 19 p3339 N85-30689
Source Term Experiments Project (STEP): Aerosol characterization system
[DE85-010248] 19 p3361 N85-30839
Consolidated fuel reprocessing program
[DE85-008750] 19 p3366 N85-30871
Paired ion chamber constants for fission gamma-neutron fields
[AD-A155069] 21 p3702 N85-32999
Neutron detector counting capabilities for (10) B-lined and (235) U fission chambers in high gamma-ray fluxes
[DE85-011893] 22 p3840 N85-33780
Marine Sample Exploitation Project: Estimates regarding the sensitivity and technology for the detection of nuclear explosion debris in the marine environment
[DE85-013176] 23 p3947 N85-34462
Downstream behavior of volatile fission product species
[DE85-012124] 23 p3971 N85-34617
Application of evaluated fission-product delayed-neutron precursor data in reactor kinetics calculations
[DE85-012728] 23 p3972 N85-34624

FISSURES (GEOLOGY)
Radar observations of fissure-fed basaltic lava flows, Craters of the Moon, Idaho 13 p2199 N85-23640
Interpretation of space photolineaments
15 p2487 N85-25353
Transport properties of Topopah Spring tuff
[DE85-010448] 19 p3270 N85-30278

FITNESS
NT PHYSICAL FITNESS

FITTING
Use of ranks to fit a linear model to cross-sectional data with an application to biological rhythms
[MATHEMATICS-RESEARCH-169]
12 p1923 N85-22081
Macro for fitting nonlinear models to Poisson distributed data
[DE84-008569] 14 p2412 N85-24871
A prototype test chamber for fit testing of protective masks in the field
[FOA-C-40208-C1(C2)] 20 p3512 N85-31834

FITTINGS
Tube coupling device
[NASA-CASE-MFS-25964-1] 11 p1647 N85-20378
Development and test of advanced composite components. Center Directors discretionary fund program
[NASA-TM-86512] 21 p3561 N85-32147

FIXED POINT ARITHMETIC
Interval interation methods for nonlinear equation systems: Theory and comparison on computer
[INTERVALL-BER-84/6] 05 p0719 N85-14612

FIXED POINTS (MATHEMATICS)
Towards a uniform topological treatment of streams and functions on streams
[CWI-CS-R8422] 17 p3014 N85-28639

FIXED WINGS
Flight testing the fixed-wing configuration of the Rotor Systems Research Aircraft (RSRA)
[NASA-TM-86782] 23 p3896 N85-34135

FIXED-WING AIRCRAFT
U AIRCRAFT CONFIGURATIONS
U FIXED WINGS

FIXTURES
An alignment fixture for a 2-Degree-of-Freedom (TDF) gyroscope
[AD-A148885] 10 p1422 N85-18969
Electrostatic forming and testing of polymer films on a 16-foot diameter test fixture
[NASA-TM-86328] 13 p2063 N85-22885

FLAME FRONTS
U FLAME PROPAGATION

FLAME HOLDERS
Computational analysis of scramjet dual mode operation
[NASA-CR-174250] 07 p0956 N85-16060
Flameholder with integrated air mixer
[AD-D011549] 12 p1778 N85-21161
The mechanisms of flame holding in the wake of a bluff body
[NASA-CR-3866] 12 p1779 N85-21166
On the coupling of an anchored flame with an acoustic field
[COLL-AERON-8434] 12 p1799 N85-21282

FLAME INTERACTION
U CHEMICAL REACTIONS
U FLAME PROPAGATION

FLAME IONIZATION
Ionization and time structure of flames
[LE-484/1-2] 05 p0614 N85-13925
Large eddy structures in transitional and turbulent flames
[AD-A154520] 21 p3562 N85-32157

FLAME PROBES
Ionization and time structure of flames
[LE-484/1-2] 05 p0614 N85-13925

FLAME PROPAGATION
Gravitational effects on premixed particle cloud flames
02 p0171 N85-11144
Diffusive combustion of fluids with free surface
02 p0274 N85-11785
Laminar flame propagation/quench for a parallel-wall duct
[DE84-009773] 04 p0470 N85-12993
Combustion waves in dispersed-2-phase mixtures
[CFD/84/13] 04 p0472 N85-13003
Ionization and time structure of flames
[LE-484/1-2] 05 p0614 N85-13925
Numerical calculation of the cold-flow characteristics of a bluff-body flame stabilizer
[CFD/84/14] 08 p1124 N85-17068
Radiation/catalytic augmented combustion
[AD-A148758] 09 p1290 N85-18101
Flame propagation and stabilization studies using Rayleigh scattering and laser Doppler velocimetry
[AD-A148802] 09 p1290 N85-18102
Burner stabilized flames in fluids
[DE84-017429] 09 p1291 N85-18109
Turbulent premixed flame study
[DE85-003220] 09 p1292 N85-18112
Long range effect of turbulent pressure pulsations in plane-parallel flows at different velocities with various flame fronts 09 p1308 N85-18220
A thermal-mechanical model of deflagration-to-detonation in granular energetic materials
[AD-P004346] 10 p1455 N85-19170
Research in nonlinear problems of energy: Informal technical report
[DE85-001529] 11 p1595 N85-20031
Flame spread on combustible solar collector glazing materials
[DE85-002598] 11 p1595 N85-20032
Behavior of the lean methane-air flame at zero-gravity
[NASA-CR-175586] 12 p1799 N85-21283
Hydrogen flame acceleration and transition to detonation
[DE85-000611] 12 p1802 N85-21299
Limiting factor of flame propagation in mono-sized sprays of low-volatility fuels
[NAL-TR-839T] 15 p2521 N85-25538
Affect of angle of incidence on plasmas generated during laser welding
[DE85-005724] 15 p2569 N85-25852
Modeling the role of radicals in the ignition of and flame propagation in hydrogen-air and methane-air mixtures
16 p2744 N85-26935
LDA study of non-steady flame propagation in a constant volume duct
[DE85-007233] 16 p2746 N85-26948
On the analytic calculation of premixed flames
[VTH-LR-417] 16 p2747 N85-26954

Significant parameters for predicting flame spread
[PB85-178002] 16 p2760 N85-27034
Polynomial approaches for the characteristic velocity and flame temperature as a function of mixing compounding and pressure for the systems PMMA/O2, PMMA/air, PE/O2, PE/air, PS/O2 and PS/air
[VTH-LR-421] 17 p2924 N85-28024
Laboratory modeling of aspects of large fires
[AD-A153152] 17 p2938 N85-28138
Flame acceleration mechanisms under conditions of partial confinement
[PB85-184083] 18 p3073 N85-29004
LDA study of the unburned gas motion induced by nonsteady flame propagation in a constant volume duct
[DE85-009938] 19 p3270 N85-30277
Wall flames and implications for upward flame spread
[FAA-CT-85-2] 21 p3553 N85-32103
Optical waveguide along front of exothermic reaction
21 p3694 N85-32954
Multiparameter conditionally sampled laser velocimetry measurements during flame propagation in a spark ignition engine
[DE85-009850] 22 p3793 N85-33502
Investigation of the flame speeds of propane/methanol gas mixtures
[DE85-012817] 23 p3912 N85-34239
The use of austenitic stainless steel versus monel (Ni-cu) alloy in pressurized Gaseous Oxygen (GOX) life support systems
[AD-A156305] 24 p4134 N85-35825

FLAME QUENCHING
U EXTINGUISHING
U QUENCHING (COOLING)

FLAME RETARDANTS
Fire retardent cellulosehydrate fibers
06 p0761 N85-14870
Study of effectiveness of fire-resistant activity of antipyrenes for fibers of aromatic polyamides
06 p0762 N85-14874
Preparation of fire-resistant infusible polycaproamide fiber 06 p0763 N85-14877
Flame resistant fibrous materials development
[NASA-CR-167817] 07 p0920 N85-15827
A study of intumescent reaction mechanisms
[AD-A149605] 12 p1812 N85-21365
Polyesters: A review of the literature on products of combustion and toxicity
[NBSIR-85-3139] 20 p3433 N85-31298
Photovoltaic module spread-of-flame testing
21 p3612 N85-32448
Investigation of experimental lightweight firewall materials for A/C engine bay applications
[AD-A155765] 24 p4062 N85-35175
Fire research publications, 1984
[PB85-208502] 24 p4166 N85-35827

FLAME SPECTROSCOPY
Laser Raman techniques for studying flows and flames 11 p1576 N85-19929
Advanced diagnostics for reacting flows
[AD-A150675] 14 p2301 N85-24246
Spectroscopic studies of lead oxide in a flow tube
[AD-A151849] 15 p2505 N85-25455
Shock tube measurements of growth constants in the branched-chain ethane-carbon monoxide-oxygen system
[NASA-TM-87068] 21 p3562 N85-32156

FLAME SPRAYING
Detonation flame spraying extends life of automotive parts 15 p2513 N85-25507
Thermal barrier coating system
[NASA-CASE-LEW-14057-1] 24 p4072 N85-35233

FLAME STABILITY
Linear long-wave stability of cylindrical steady laminar flame in rotating medium 02 p0268 N85-11752
Numerical calculation of the cold-flow characteristics of a bluff-body flame stabilizer
[CFD/84/14] 08 p1124 N85-17088
The mechanisms of flame holding in the wake of a bluff body
[NASA-CR-3888] 12 p1779 N85-21166
Radiative augmented combustion
[AD-A154137] 20 p3423 N85-31246
Wall flames and implications for upward flame spread
[FAA-CT-85-2] 21 p3553 N85-32103

FLAME TEMPERATURE
New concepts for measuring flame spread properties
[NBSIR-84-2943] 03 p0327 N85-12104
Cars temperature measurements in sooting, laminar diffusion flames
[AD-A148801] 09 p1319 N85-18294
Ionic mechanisms of soot formation in flames
[AD-A150119] 12 p1801 N85-21297
The influence of fuel quality upon flame-tube temperature and flame radiation in a model gas-turbine primary zone
[K233] 13 p1974 N85-22396
The influence of fuel molecular composition upon flame-tube temperature and flame radiation in a model gas-turbine primary zone
[K234] 13 p2017 N85-22646
Laser diagnostic analyses of sooting flames
[AD-A150478] 13 p2017 N85-22649
On the analytic calculation of premixed flames
[VTH-LR-417] 16 p2747 N85-26954
Elementary reactions of importance in oxidation, combustion ignition and flame inhibitions
[AD-A153139] 17 p2921 N85-28004
Polynomial approaches for the characteristic velocity and flame temperature as a function of mixing compounding and pressure for the systems PMMA/O2, PMMA/air, PE/O2, PE/air, PS/O2 and PS/air
[VTH-LR-421] 17 p2924 N85-28024

FLAMEOUT
The mechanisms of flame holding in the wake of a bluff body
[NASA-CR-174058] 02 p0172 N85-11149

FLAMES
NT DIFFUSION FLAMES
NT PREMIXED FLAMES
Limiting effects during turbulent combustion
02 p0274 N85-11784
Raman and fluorescence spectroscopy in a methane-nitrous oxide laminar flame
[AD-A146092] 03 p0328 N85-12111
Study of combustion and flame processes initiated by laser-induced multiple-photon absorption
[DE84-017095] 04 p0471 N85-12996
The structure of dilute combusting sprays
[NASA-CR-174838] 07 p0905 N85-15728
Burner stabilized flames in fluids
[DE84-017429] 09 p1291 N85-18109
Mechanisms and reaction dynamics related to methane combustion
[PB85-129690] 10 p1438 N85-19065
Theory of flammability limits. Flow gradient effects and flame stretch
[PB85-135077] 10 p1439 N85-19067
Behavior of the lean methane-air flame at zero-gravity
[NASA-CR-175586] 12 p1799 N85-21283
Two-dimensional measurements of OH concentration and temperature in reactive flows
[AD-A149849] 12 p1800 N85-21292
Ionic mechanisms of soot formation in flames
[AD-A150119] 12 p1801 N85-21297
Picosecond lidar techniques in laboratory and field diagnostics
[AD-A150755] 14 p2309 N85-24294
An experimental investigation of two-dimensional flame-vortex interactions 16 p2744 N85-26934
Modeling the role of radicals in the ignition of and flame propagation in hydrogen-air and methane-air mixtures
16 p2744 N85-26935
Elementary reactions of importance in oxidation, combustion ignition and flame inhibitions
[AD-A153139] 17 p2921 N85-28004
Investigation of several low-lying levels of X doublet pi state of NCO using argon laser excited fluorescence
[AD-A153693] 18 p3071 N85-28994
Theoretical studies of combustion chemistry
[DE85-010284] 19 p3237 N85-30069
Intermittency, conditional sampling and turbulent combustion 20 p3424 N85-31249
Rayleigh scattering for density measurements in premixed flames: One point, time series data
20 p3424 N85-31253
Recent measurements in turbulent jet flames at Sandia Combustion Research Facility 20 p3424 N85-31254
Large eddy structures in transitional and turbulent flames
[AD-A154520] 21 p3562 N85-32157
Status of boron combustion research
[AD-A154762] 21 p3563 N85-32160
In-cavity laser IR spectrum analyzer for investigating non-steady-state processes 21 p3685 N85-32894
Experimental study of engine knock
[DE85-009851] 22 p3754 N85-33268
Effects of ambient pressure on the instability of a liquid boiling explosively at the superheat limit
[DE85-009476] 23 p3932 N85-34370
Electronic imaging system and technique
[DE85-005740] 23 p3935 N85-34393
Radiation measurements on magnesium flames
[BLL-CE-TRANS-8110-(9022.09)]
24 p4075 N85-35254

FLAMMABILITY
Development of new and improved polymer matrix resin systems, phase 1
[NASA-CR-166595] 01 p0017 N85-10104
Quasi-steady analysis of aircraft panel flammability
[AD-A145461] 02 p0138 N85-10936
New concepts for measuring flame spread properties
[NBSIR-84-2943] 03 p0327 N85-12104
Modeling of aircraft cabin fires
[NBS-GCR-84-473] 04 p0454 N85-12880
Standardization of flammability tests for hydraulic fluids
[AD-A146468] 06 p0771 N85-14892
Module flammability research
06 p0830 N85-15274
Preliminary evaluation of an improved flammability test method for aircraft materials
[FAA-CT-84-22] 08 p1060 N85-16840
Mist flammability studies of candidate fire-resistant hydraulic fluids
[AD-A148572] 08 p1134 N85-17148
Penetration of the atmosphere by flammable mixture as a result of spillage of LNG on the ground
08 p1179 N85-17432
Theory of flammability limits. Flow gradient effects and flame stretch
[PB85-135077] 10 p1439 N85-19067
Determination of toxicity of combustion products of habitability foams concurrently with flammability studies of these materials
[AD-A149647] 12 p1905 N85-21981
Light weight fire resistant graphite composites
[NASA-CASE-ARC-11615-1-SB]
18 p3066 N85-28978
Practical real-time quality control of antimisting kerosene
[DE/FAA/CT-85/1] 18 p3083 N85-29072
Working with flammable solvents, thinners, paints and adhesives
[HSE-TRANS-11066] 19 p3250 N85-30154
The role of aircraft panel materials in cabin fires and their properties
[FAA-CT-84-30] 21 p3553 N85-32104
Photovoltaic module spread-of-flame testing
21 p3612 N85-32448
Review of zirconium-zircaloy pyrophoricity
[DE85-011169] 23 p3916 N85-34270
The use of a laser Doppler velocimeter in a standard flammability tube
[NASA-CR-174960] 24 p4096 N85-35389

FLAMMABLE GASES
NT GASEOUS FUELS
NT LIQUEFIED NATURAL GAS
Investigation of the flame speeds of propane/methanol gas mixtures
[DE85-012817] 23 p3912 N85-34239

FLANGE WRINKLING
Design, fabrication and test of composite curved frames for helicopter fuselage structure
[NASA-CR-172436] 15 p2470 N85-25247

FLANGES
High temperature ultra-high vacuum infrared window seal
[AD-D011333] 07 p0929 N85-15880
Fuel cell separator plate with bellows-type sealing flanges
[DE85-005991] 23 p3947 N85-34458

FLAP CONTROL
U AIRCRAFT CONTROL
U FLAPS (CONTROL SURFACES)

FLAPERONS
Wing buffeting active control testing on a transport aircraft configuration in a large sonic windtunnel
17 p2904 N85-27903

FLAPPING
Stochastic motor blade dynamics
[AD-A146312] 03 p0316 N85-12054
Computer analysis of wind turbine blade dynamic loads
[DE85-000530] 12 p1867 N85-21714

FLAPS (CONTROL SURFACES)
NT FLAPERONS
NT JET FLAPS
NT LEADING EDGE FLAPS
NT LEADING EDGE SLATS
NT TRAILING EDGE FLAPS
NT VORTEX FLAPS
NT WING FLAPS
Development of the space shuttle body flap actuation subsystem 08 p1102 N85-16988
An experimental investigation of flap turbulent heat transfer and pressure characteristics in hypersonic flow
12 p1821 N85-21426
Flow over a biconic configuration with an afterbody compression flap
[AD-A151882] 15 p2557 N85-25778
Additional flow field studies of the GA(W)-1 airfoil with 30-percent chord Fowler flap including slot-gap variations and cove shape modifications
[NASA-CR-3887] 19 p3212 N85-29818

FLARE STARS
On the most probable number of flare stars in the Pleiades field 05 p0739 N85-14755

Activity and magnetic fields on stars from radio observations
[NASA-CR-175966] 18 p3202 N85-29861
Stochastic particle acceleration in flaring stars
[OG-8.3-9] 23 p4022 N85-34927

FLASH
Production of thin-walled electricity welded tubes with reduced internal flash
[BLL-BISI-TRANS-22381-(9022.06)] 17 p2973 N85-28364

FLASH BLINDNESS
Pursuit tracking performance and flash disruption: The effects of training the non-dominant eye on target reacquisition
[AD-A153404] 17 p2999 N85-28541
Predictive model of electron beam induced flashblindness
[AD-A155260] 21 p3664 N85-32763

FLASH LAMPS
Electronics Engineering Department: EE technical review
[DE84-016124] 01 p0044 N85-10286
Flares and photoflash items
[AD-A145442] 02 p0187 N85-11253
Performance of a large area flash chamber prototype
[NOTA-INTERNA-807] 02 p0201 N85-11338
An evaluation of flashtube signal characteristics
[AD-A149569] 10 p1423 N85-18974
Characteristics of unstable resonators in flashlamp-pumped organic-compound lasers
11 p1717 N85-20800
Electrodes for flash discharge lamps
[DE85-008897] 17 p2955 N85-28250
Electrode for flash discharge lamps
[DE85-008896] 17 p2955 N85-28252
Dye laser traveling wave amplifier
[NASA-CR-175989] 19 p3275 N85-30308
Switching power supply
[DE85-005993] 22 p3761 N85-33312

FLASH POINT
Removal of longitudinal internal flash from electrically welded tubes
[BLL-BISI-TRANS-22380-(9022.06)] 17 p2938 N85-28136

FLASH TUBES
U FLASH LAMPS

FLASHING (VAPORIZING)
Critical flashing flow of subcooled fluids in nozzles with contour discontinuities
[DE84-017229] 09 p1319 N85-18296

FLASHOVER
Development of power system management
[PB84-216530] 04 p0497 N85-13173
Flashover failures from wet-wire arcing and tracking
[AD-A149055] 10 p1478 N85-19332
Flash radiography 14 p2317 N85-24316
Vacuum interface flashover with bipolar electric fields
[DE85-012027] 22 p3755 N85-33275
Scaling parameters of flashover
[NBS-GCR-85-497] 23 p3911 N85-34229

FLASKS
Dynamic pressure test unit-ratio method
[AD-D011486] 10 p1488 N85-19392
Transmissive Dewar cooling chamber for optically pumped semiconductor ring lasers
[AD-D011550] 12 p1855 N85-21636

FLAT COAXIAL TRANSMISSION LINES
U MICROSTRIP TRANSMISSION LINES

FLAT PLATES
Approximate solution of a laminar flow over a flat plate with suction and pressure gradient
[AD-A145482] 02 p0198 N85-11321
Modular photovoltaic array field
[SAND-83-7028] 02 p0222 N85-11454
Total area of diffusion elements in a reverberation chamber and measured degree of sound absorption
[NRC/CNR-TT-2110] 03 p0415 N85-12653
FSA field test
[NASA-CR-174114] 04 p0526 N85-13373
Thin polymer film collectors as a contribution to the solar industry
[DE84-015299] 04 p0529 N85-13383
Proceedings of the 22nd Project Integration Meeting
[DE85-000334] 06 p0833 N85-15302
A second-order accurate parabolized Navier-Stokes algorithm for internal flows
[NASA-CR-174258] 07 p0956 N85-16059
Free surface effects on the wake of a flat plate
[AD-A146988] 07 p0958 N85-16071
A free shear layer prediction of the turbulent wake of a flat plate towed below a free surface
[AD-A146690] 09 p1319 N85-18293
An experimental investigation into the effects of plate eccentricity and elastic deformation on orifice meter accuracy
[ERS-E.391] 09 p1325 N85-18325
The dependence of soil bearing capacity and drawbar pull on the spacing between track
[AD-P004273] 00 p1406 N85-18849
A multistage time-stepping scheme for the Navier-Stokes equations
[NASA-CR-172527] 10 p1483 N85-19365
MOD silver metallization for photovoltaics
[NASA-CR-175460] 10 p1510 N85-19526
LOVEL-84: A LOw-VELocity aerodynamic heating code for flat plates, wedges, and cones
[DE85-002604] 11 p1576 N85-19933
Pre-turbulence: Transitional Laminar-turbulent flows
11 p1716 N85-20793
Numerical study of large-eddy breakup and its effect on the drag characteristics of boundary layers
[NASA-CR-3884] 12 p1797 N85-21272
Interaction of part-through cracks in a flat plate
[NASA-CR-175588] 12 p1864 N85-21692
A new model for thin plates with rapidly varying thickness. Part 3: Comparison of different scalings
[AD-A149748] 12 p1866 N85-21704
Scattered data interpolation using thin plate splines with tension
[AD-A149803] 12 p1866 N85-21705
Nonlinear analysis of layered composite plates and shells
[PB85-127181] 12 p1868 N85-21719
Calculating isothermal flow in wake beyond injection zone 14 p2287 N85-24175
Heat transfer to vertical flat plates in a rectangular gas-fluidized bed
[AD-A150785] 14 p2301 N85-24248
Silicon-sheet and thin-film cell and module technology potential: Issue study
[NASA-CR-175654] 14 p2349 N85-24520
Intermediate load modules for test and evaluation
[NASA-CR-175697] 14 p2350 N85-24526
Periodic vortex shedding in the supersonic wake of a planar plate
[NASA-TM-77854] 15 p2463 N85-25207
Flow past a flat plat with a vortex/sink combination
[JIAA-TR-58] 15 p2464 N85-25215
An experimental investigation into the dynamic response of a stiffened flat plate loaded impulsively by an underwater shockwave
[AD-A151321] 15 p2578 N85-25903
Electrical research on solar cells and photovoltaic materials
[NASA-CR-175699] 15 p2585 N85-25935
Turbulent flow of fluid near trailing edge of plate in stream at zero angle of attack 16 p2764 N85-27057
Acceleration sensitivity reduction method
[AD-D011631] 16 p2778 N85-27146
MOD silver metallization for photovoltaics
[NASA-CR-175773] 16 p2818 N85-27381
Turbulent wake of a submerged flat plate
[AD-A153776] 18 p3100 N85-29190
Underwater shock-induced responses of stiffened flat plates: An investigation into the predictive capabilities of the USA-STAGS code
[AD-A154245] 19 p3286 N85-30377
Using PVFORM, a systems performance model, to determine optimum mounting configurations for flat-plate photovoltaic modules
[DE85-011181] 19 p3306 N85-30495
Sub-optimal control of nonlinear flexible space structures 20 p3414 N85-31190
A mathematical analysis of the effect of free stream turbulence on the Blasius boundary layer
20 p3451 N85-31430
Experimental observation of transition behavior on a flat plate 20 p3452 N85-31437
Dynamical study of flat plates by nonlinear elasticity theory
[STN-8] 20 p3471 N85-31572
An analysis of the feasibility of producing silicon for solar cells by a dichlorosilane/fluidized-bed reactor process
[NASA-CR-176036] 20 p3478 N85-31614
Proceedings of the Flat-Plate Solar Array Project Research Forum on High-Efficiency Crystalline Silicon Solar Cells
[NASA-CR-176047] 20 p3478 N85-31615
Nomographs for estimating the levelized cost of energy from flat-plate and concentrator photovoltaic systems
[NASA-CR-176048] 20 p3483 N85-31645
Instability and chaotic behavior in a free-surface flow
[AD-A154879] 21 p3584 N85-32279
Numerical solutions of turbulent models for flow over a flat plate with angle of attack
[DE85-010380] 21 p3585 N85-32286
An investigation into the comparisons of the underwater shock effects on a stiffened flat plate to the predictive nature of a computer model
[AD-A155612] 21 p3600 N85-32355
Proceedings of the 24th Project Integration Meeting
[NASA-CR-176058] 21 p3607 N85-32394
Flat-plate module efficiency versus cost tradeoffs
21 p3607 N85-32398
Block V module program 21 p3607 N85-32401
Reliability physics 21 p3608 N85-32402
MOD silver metallization for photovoltaics
21 p3610 N85-32426
Development of artificially produced perturbations in supersonic boundary layer 21 p3683 N85-32879
Fuel cell separator plate with bellows-type sealing flanges
[DE85-005991] 23 p3947 N85-34459
Vortex boundary-layer interactions
[NASA-CR-176192] 24 p4093 N85-35373

FLAT SURFACES
Local stability analysis for a planar shock wave
[NASA-TP-2387] 04 p0452 N85-12864
An experimental investigation of a turbulent junction vortex
[NASA-CR-175915] 17 p2957 N85-28259
Boundary to constructive solid geometry mappings: A focus on 2-D issues 17 p3004 N85-28570
Numerical estimation of the curvature of biological surfaces 17 p3006 N85-28588

FLATNESS
Development of a measuring procedure for the automatic evaluation of the flatness of reflective surfaces
[BMFT-FB-T-84-168] 03 p0421 N85-12688

FLATS (LANDFORMS)
Surface soil moisture measurements of the White Sands, New Mexico
[NOAA-TM-NESDIS-7] 02 p0219 N85-11441

FLATTENING
Computation of thermal shock-free straightening conditions for aluminum-magnesium alloy welded structures 10 p1449 N85-19131

FLAVOR (PARTICLE PHYSICS)
Heavy quarks and CP: Moriond 1985
[DE85-010553] 22 p3841 N85-33790

FLAW DETECTION
U NONDESTRUCTIVE TESTS

FLAWS
U DEFECTS

FLEXIBILITY
Two- and three-dimensional model and wall data from a flexible-walled transonic test section
03 p0312 N85-12015
Synthesis study of nondestructive testing devices for use in overlay thickness design of flexible pavements
[PB84-218080] 06 p0774 N85-14950
Random vibrations of aircraft engine blades
06 p0777 N85-14967
The influence of fastener flexibility on load transfer and fatigue life predictions for multirow bolted and riveted joints --- aircraft structures
[LBF-FB-172/84] 07 p0979 N85-16219
A Galerkin method for the estimation of parameters in hybrid systems governing the vibration of flexible beams with tip bodies
[NASA-CR-172537] 10 p1544 N85-19734
Simplified theory for the behaviour of buried flexible cylinders under the influence of uniform hoop compression
[PB85-116531] 11 p1654 N85-20419
Finger materials for air cushion vehicles. Volume 2: Base fabrics for finger materials
[AD-A149701] 12 p1819 N85-21408
Effects of triazine components on physicochemical properties of polybutadiene: urethane block copolymers
13 p2014 N85-22635
Optimum design and automated dynamic analysis of flexible mechanisms
[AD-A150152] 13 p2099 N85-23088
A research program in active control/aeroelasticity
[NASA-CR-175674] 14 p2212 N85-23752
Systems design and application of computers with flexible architecture 14 p2401 N85-24800
Effect of internal pressure on flexibility and stress intensification factors for pipe elbows analyzed by the finite element method
[AD-A151161] 15 p2578 N85-25901
Control of a flexible beam
[DE85-007243] 15 p2580 N85-25914
Development of a new faster process for the fabrication of ceramic fiber-reinforced ceramic composites by chemical vapor infiltration
[DE85-007550] 16 p2756 N85-27007
On the accuracy of modelling the dynamics of large space structures 19 p3225 N85-29995
Modeling and analysis of pinhole occulter experiment: Initial study phase
[NASA-CR-175978] 19 p3272 N85-30287
Dynamic response of a flexible space beam
[NASA-TM-86441] 19 p3285 N85-30368
Sub-optimal control of nonlinear flexible space structures 20 p3414 N85-31190

An overview of latest model reduction and control methods of large flexible space structures 20 p3414 N85-31191
A control concept for large flexible spacecraft using order reduction techniques 20 p3415 N85-31193
Wideband disturbance accomodation in precision flexible space structures 20 p3415 N85-31194
STPI/LARC: A 200 deg C polyimide adhesive [NASA-TM-86447] 20 p3433 N85-31297
An analysis of multi-fingered hands 20 p3462 N85-31504
User's guide for computer program CGFAG, Concrete General Flexure Analysis with Graphics [AD-A155555] 21 p3570 N85-32204
Thin-film reliability and engineering overview 21 p3612 N85-32450
Removable cleanable antireflection shield [AD-D011735] 22 p3844 N85-33810
Strength properties of glassfiber reinforced thermoplastics 23 p3908 N85-34212

FLEXIBLE BODIES
NT FLEXIBLE SPACECRAFT
Measurement of the inertial constants of a rigid or flexible structure of arbitrary share through a vibration test [NASA-TM-77557] 02 p0209 N85-11381
Experiments in control of flexible structures with uncertain parameters 05 p0602 N85-13837
Low-loss flexible dielectric waveguide for millimeter-wave transmission and its appication to devices [AD-A147848] 07 p0948 N85-16006
Flexible line support assembly [AD-D011391] 07 p0972 N85-16177
Precise control of flexible manipulators [NASA-CR-174210] 07 p0973 N85-16178
Identification of vibration parameters of flexible structures 09 p1331 N85-18360
A deformation analysis of flat flexible gear and its equation of original curved surfaces [NASA-TM-77493] 12 p1859 N85-21660
Planar dynamics of a uniform beam with rigid bodies affixed to the ends [NASA-CR-175566] 12 p1864 N85-21693
Developments in deployable masts to support flexible solar arrays 13 p2012 N85-22620
Spline-based Rayleigh-Ritz methods for the approximation of the natural modes of vibration for flexible beams with tip bodies [NASA-CR-172566] 13 p2102 N85-23100
AFWAL space control technology program 14 p2233 N85-23839
Control Of Flexible Structures (COFS) flight experiment background and description 14 p2236 N85-23864
Modeling and control of large flexible structures, phase 1 [AD-A150736] 14 p2403 N85-24817
Model reduction techniques applied to the control of large space structures [AD-A151784] 16 p2731 N85-26857
Addition of flexible body option to the TOLA computer program, part 1 [NASA-CR-132732-1] 17 p2896 N85-27855
Addition of flexible body option to the TOLA computer program. Part 2: User and programmer documentation [NASA-CR-132732-2] 17 p2896 N85-27856
LFMR definition study [AD-A153691] 18 p3090 N85-29126
Spillover minimization: An approach for actuators and sensors placement in distributed parameter study [INPE-3525-PRE/746] 19 p3272 N85-30289
Application of deformable body mean-axis to dynamics of flexible mechanical systems 19 p3283 N85-30359
AFWAL control technology programs 20 p3406 N85-31150
Attitude control tradeoff study between the use of a flexible beam and a tether configuration for the connection of two bodies in orbit 20 p3412 N85-31174
Approximation techniques for parameter estimation and feedback control for distributed models of large flexible structures 20 p3413 N85-31179
Approximation of optimal infinite dimensional compensators for flexible structures 20 p3413 N85-31181
Control of a flexible space antenna: A finite dimensional perspective based on distributed parameter theory 20 p3413 N85-31182
Optimization of controlled structures 20 p3414 N85-31186
A nonlinear dual-adaptive control strategy for identification and control of flexible structures 20 p3416 N85-31203
Combined state and parameter estimation for a static model of the Maypole (Hoop-Column) antenna suface 20 p3417 N85-31210
Experimental verification of identification algorithms for control of flexible structures 20 p3418 N85-31211
Non-rigid body motion 23 p3964 N85-34576
Analysis of flexible aircraft longitudinal dynamics and handling qualities. Volume 1: Analysis methods [NASA-CR-177943-VOL-1] 24 p4066 N85-35202
Analysis of flexible aircraft longitudinal dynamics and handling qualities. Volume 2: Data [NASA-CR-177943-VOL-2] 24 p4067 N85-35203

FLEXIBLE SPACECRAFT
Modular design attitude control system [NASA-CR-171182] 01 p0016 N85-10098
Qualitative results for distributed systems with discrete damping and stiffness with application to control [AD-A145525] 02 p0209 N85-11382
A user's guide to the Flexible Spacecraft Dynamics and Control Program [NASA-TM-87389] 03 p0405 N85-12586
Damping models for flexible communications satellites by substructural damping synthesis [UTIAS-287] 14 p2237 N85-23868
A mathematical formulation of the Scole control problem, part 1 [NASA-CR-172581] 14 p2243 N85-23903
Numerical experiments on flexible spacecraft with the aid of the Dynamic Control and Analysis Package (DCAP) [ESA-STM-229] 15 p2493 N85-25382
The effect of sensor and actuator errors on static shape control for large space structures [NASA-TM-86446] 19 p3225 N85-29996
Dynamic response of a flexible space beam [NASA-TM-86441] 19 p3265 N85-30368
Proceedings of the Workshop on Identification and Control of Flexible Space Structures, volume 1 [NASA-CR-176051] 20 p3408 N85-31148
Dynamic performance of several large antenna concepts 20 p3409 N85-31155
Antenna pointing of large flexible telecommunications spacecraft 20 p3409 N85-31156
Control of flexible structures 20 p3410 N85-31161
Experiments in structural dynamics and control using a grid 20 p3410 N85-31165
Rationale for an experimental test for flexible space structure attitude control 20 p3411 N85-31167
Numerical and experimental evaluation for single-axis control of an LSS laboratory model 20 p3411 N85-31168
Proceedings of the Workshop on Identification and Control of Flexible Space Structures, volume 2 [NASA-CR-176052] 20 p3411 N85-31170
Vibration/libration interaction dynamics during the orbiter based deployment of flexible members 20 p3411 N85-31171
Design of multivariable controllers using the Integrated Analysis Capability (IAC) 20 p3412 N85-31172
An integrated control and minimum mass structural optimization algorithm for large space structures 20 p3413 N85-31183
ISAAC (Integrated Structural Analysis and Control) via continuum modeling and distributed frequency domain design techniques 20 p3414 N85-31185
Parametric stiffness control of flexible structures 20 p3414 N85-31187
Vibrational stabilization of flexible structures 20 p3414 N85-31188
Stiffness control of large space structures 20 p3414 N85-31189
Proceedings of the Workshop on Identification and Control of Flexible Space Structures, volume 3 [NASA-CR-176053] 20 p3415 N85-31195
Matrix transfer function design for flexible structures: An application 20 p3416 N85-31199
On the stability of collocated controllers in the presence or uncertain nonlinearities and other perils 20 p3416 N85-31201
Maximum likelihood estimation with emphasis on aircraft flight data 20 p3417 N85-31208
Enhancement of the flexible spacecraft dynamics program for open spacecraft [NASA-CR-175309] 24 p4137 N85-35641

FLEXIBLE WINGS
Transonic pressure distribution computations of a flexible wing 11 p1622 N85-20213
Analytically redundant output feedback scheme for reduction of structural loads of a flexible transport aircraft [TT-8303] 12 p1777 N85-21154
Transonic calculations for a flexible supercritical wing and comparison with experiment [NASA-TM-86439] 20 p3388 N85-31012

FLEXING
Long-term thermal aging of 2 graphite-polyimide composite materials [NASA-TP-2369] 03 p0325 N85-12094
Effect of coupled torsional-flexural vibration of a geared shaft system on the dynamic tooth load 09 p1336 N85-18415
Variable flexing device for targets in internal beams of charged particle accelerators 13 p2044 N85-22797
Machine analysis of resonance characteristics of plate-type radio electronic equipment constructions 13 p2065 N85-23018
Load carrying capacity of double circular arc gears 14 p2221 N85-23776
Reflection and transmission of flexural waves at discontinuities 15 p2572 N85-25861
On geoid heights and flexure of the lithosphere at seamounts [AD-A151220] 15 p2604 N85-26050
Buckling and bracing of cantilevers [CE-42] 17 p2979 N85-28413
Study on a flexure hinged pendulum accelerometer [NAL-TR-844] 18 p3104 N85-29220
Buckling and post-buckling behavior of sparsely connected built-up columns 19 p3283 N85-30358
Graphite/PMR polyimide composites with improved toughness [NASA-TM-87061] 21 p3561 N85-32146
Reliability of two sintered silicon nitride materials [NASA-TM-87092] 23 p3919 N85-34284

FLEXURE
U FLEXING

FLICKER
An evaluation of flashtube signal characteristics [AD-A149569] 10 p1423 N85-18874
Variations in the small-scale galactic magnetic field and short time-scale intensity variations of extragalactic radio sources 20 p3549 N85-32084

FLIGHT ALTITUDE
Global matrix of thermospheric density values for selected solar/geomagnetic conditions and spacecraft orbital attitudes [NASA-TM-86478] 04 p0533 N85-13400
Safety recommendation(s), A-84-82 through -84 [REPT-3957] 14 p2217 N85-23746

FLIGHT CHARACTERISTICS
Airworthiness and flight characteristics test of the JOH-6A light combat helicopter configured with a wire strike protection system [AD-A144880] 01 p0006 N85-10038
Airworthiness and Flight Characteristics (A and FC) test of the EH - 1X/EH - 1H helicopter configurations [AD-A144881] 01 p0007 N85-10039
Active control technology experience with the Space Shuttle in the landing regime [NASA-TM-85910] 01 p0012 N85-10071
YO-3A acoustics research aircraft systems manual [NASA-TM-85968] 01 p0012 N85-10074
Simulator study of flight characteristics of several large, dissimilar, cargo transport airplanes during approach and landing [NASA-TP-2357] 02 p0148 N85-11002
Aircrew-aircraft integration: A summary of US Army research programs and plans [NASA-TM-85991] 02 p0148 N85-11004
Flying qualities and control system characteristics for superaugmented aircraft [NASA-CR-170419] 05 p0596 N85-13800
An in-flight investigation of a twin fuselage configuration in approach and landing [NASA-CR-172366] 05 p0596 N85-13801
STOL simulation requirements for development of integrated flight/propulsion control systems 05 p0701 N85-14499
Maximum normalized rate as a flying qualities parameter 05 p0702 N85-14503
The Sternberg task as a workload metric in flight handling qualities research 05 p0712 N85-14508
Effects of aircraft and flight parameters on energy-efficient profile descents in time-based metered traffic [NASA-CR-172338-ADD] 07 p0901 N85-15706
Airworthiness and flight characteristics test of the RC-12D Guardrail V [AD-A148046] 08 p1064 N85-16864
Realization and testing of an experimental color display system for general aviation helicopters and aircraft [BMFT-FB-W-84-042] 08 p1066 N85-16872
Time series analysis of closed-loop pilot vehicle dynamics 08 p1067 N85-16876
Low-speed longitudinal orbiter qualities 08 p1092 N85-16905
Aerodynamic challenges of ALT 08 p1094 N85-16911
The design of sport and touring aircraft [NASA-TM-77783] 10 p1423 N85-18875
In-flight investigation of the effects of time delay in control system on flying qualities in landing approach [DFVLR-FB-84-35] 11 p1586 N85-19969
Technical evaluation report on the FDP Symposium on Flight Test Techniques [AGARD-AR-208] 12 p1777 N85-21157

Low-speed stability and control wind-tunnel investigations of effects of spanwise blowing on fighter flight characteristics at high angles of attack --- Langely 12-ft low-speed tunnel and 30- by 60-ft tunnel
[NASA-TP-2431] 14 p2210 N85-23708

The design of high-performance gliders
[NASA-TM-77772] 14 p2217 N85-23750

Simulation of aircraft behaviour on and close to the ground
[NASA-TM-87480] 14 p2218 N85-23754

Preliminary helicopter design decision making based on flight performance factors
[AD-A151488] 15 p2471 N85-25254

Study of longitudinal landing flying qualities evaluation using pilot model theory
[AD-A152194] 16 p2706 N85-26702

Technical evaluation report on the Flight Mechanics Symposium on Active Control Systems: Review, Evaluation and Projections
[AGARD-AR-220] 16 p2711 N85-26730

The state-of-the-art and future of flight control systems 16 p2712 N85-26732

In-flight investigation of the influence of pitch damping and pitch control effectiveness on landing approach flying qualities of statically unstable transport aircraft
[DFVLR-FB-84-12] 17 p2900 N85-27880

Helicopter Aeromechanics
[AGARD-LS-139] 18 p3057 N85-28913

Helicopter aeromechanics: Introduction and historical review 18 p3057 N85-28914

In-flight evaluation of pure time delays in pitch and roll
[NASA-TM-86744] 21 p3556 N85-32123

Ground-based and in-flight simulator studies of flight characteristics of a twin-fuselage passenger transport airplane during approach and landing
[NASA-TP-2451] 23 p3898 N85-34144

Estimation of flight mechanical variables by means of Kalman filters 24 p4062 N85-35171

FLIGHT CLOTHING

The water vapor resistances of some clothing assemblies used by flying personnel of the Swedish Armed Forces: A series of model studies
[FOA-C-59011-H1] 02 p0238 N85-11551

Testing of three different flight suits in fire environment --- fuel fire
[FOA-C-59012-H1] 02 p0238 N85-11552

Acceptance-testing procedures for air-line supplied-air suits
[DE84-016980] 05 p0712 N85-14569

The new Navy flier's fire-resistant blue coverall
[AD-A146611] 06 p0846 N85-15375

SPH-4 US Army flight helmet performance, 1972 - 1983
[AD-A148674] 08 p1201 N85-17562

The application of anthropometric survey data to aircrew clothing sizing
[AD-A150545] 13 p2143 N85-23304

Fire pit tests of blue flight coverall program
[AD-A151884] 15 p2620 N85-26149

FLIGHT COMPUTERS

U AIRBORNE/SPACEBORNE COMPUTERS

FLIGHT CONDITIONS

TAF verification (airport weather forecasts)
[GEOPHYSBDBW-FM-205] 05 p0687 N85-14420

Weather satellite products in the Flight Service Automation System (FSAS)
[AD-A146520] 06 p0759 N85-14855

The Altitude Wind Tunnel (AWT): A unique facility for propulsion system and adverse weather testing
[NASA-TM-86921] 09 p1283 N85-18067

Direct-strike lightning photographs, swept-flash attachment patterns, and flight conditions for storm hazards 1982
[NASA-TM-86347] 12 p1892 N85-21877

Safety recommendation(s), A84-111 through -115
[HEPT-4011C/27] 14 p2216 N85-23744

Extraction of aerodynamic parameters for aircraft at extreme flight conditions
[NASA-TM-86730] 18 p3175 N85-29686

FLIGHT CONTROL

NT AUTOMATIC FLIGHT CONTROL
NT AUTOMATIC LANDING CONTROL
NT FLY BY WIRE CONTROL
NT POINTING CONTROL SYSTEMS
NT THRUST VECTOR CONTROL

LED multifunction keyboard engineering study
[AD-A145199] 01 p0010 N85-10061

Modal simplification of flight control systems
02 p0147 N85-11000

Interactive aircraft flight control and aeroelastic stabilization
[NASA-CR-174025] 02 p0148 N85-11003

Aircrew-aircraft integration: A summary of US Army research programs and plans
[NASA-TM-85991] 02 p0148 N85-11004

Definition of acceptable levels of mismatch for equivalent systems of augmented CTOL (Conventional Take-Off and Landing) aircraft
[AD-A145619] 02 p0149 N85-11007

Expert systems in maintenance diagnostics for self-repair of digital flight control systems
[AD-P003933] 02 p0247 N85-11613

Computer equipment for research in statistics
[AD-A145755] 03 p0406 N85-12591

A unified method for evaluating real-time computer controllers: A case study --- aircraft control
[NASA-CR-174168] 04 p0547 N85-13478

Flying qualities and control system characteristics for superaugmented aircraft
[NASA-CR-170419] 05 p0596 N85-13800

A distributed expert system for Space Shuttle flight control 05 p0602 N85-13836

Statistical time series models of pilot control with applications to instrument discrimination
05 p0700 N85-14489

Quantification of cross-coupling and motion feedthrough for multiaxis controllers used in an air combat flying task
05 p0700 N85-14491

A nonlinear filter for compensating for time delays in manual control systems 05 p0700 N85-14493

Predictions of cockpit simulator experimental outcome using system models 05 p0702 N85-14504

Twentieth Annual Conference on Manual Control, volume 2
[NASA-CP-2341-VOL-2] 05 p0707 N85-14535

Performance measures for aircraft landings as a function of aircraft dynamics 05 p0712 N85-14565

Terminal control of gliding in atmosphere
06 p0777 N85-14968

Aircraft thrust control scheme for terrain following system
[AD-D011387] 07 p0901 N85-15711

Effect of aerodynamic and angle-of-attack uncertainties on the May 1979 entry flight control system of the Space Shuttle from Mach 8 to 1.5
[NASA-TP-2365] 07 p0913 N85-15778

Literature review of voice recognition and generation technology for Army helicopter applications
[AD-A146878] 07 p0939 N85-15954

cost and benefits optimization model for fault-tolerant aircraft electronic systems
[NASA-CR-166043] 07 p0946 N85-15993

Experience of one UK electronic equipment supplier with bite on engine/flight control systems over the past ten years 08 p1064 N85-16738

Helicopter Guidance and Control Systems for Battlefield Support
[AGARD-CP-359] 08 p1072 N85-16797

Integrated digital/electric aircraft concepts study
[NASA-CR-3841] 08 p1083 N85-16861

Reference energy-altitude descent guidance: Simulator evaluation --- aircraft descent and fuel conservation
[NASA-TP-2383] 08 p1085 N85-16868

Multivariable flight control with time-scale separation
[NASA-CR-174320] 08 p1087 N85-16873

Shuttle avionics software development trials: Tribulations and successes, the backup flight system
08 p1091 N85-16892

SSME digital control design characteristics
08 p1091 N85-16893

Development and implementation of the verification process for the shuttle avionics system
08 p1091 N85-16896

Some effects of digital sampling on orbiter flight control system operation 08 p1092 N85-16903

The development and application of aerodynamic uncertainties: And flight test verification for the space shuttle orbiter 08 p1093 N85-16910

Space Shuttle Technical Conference, part 2
[NASA-CP-2342-PT-2] 08 p1098 N85-16937

Space shuttle rudder/speedbrake actuation subsystem
08 p1102 N85-16965

Design and test of a four channel motor for electromechanical flight control actuation
[NASA-CR-171838] 08 p1156 N85-17294

Implications of guidance and control technology on human factors considerations 10 p1532 N85-19656

Interactive Graphics Simulator: Design, development and effectiveness/cost evaluation
[AD-A149417] 10 p1540 N85-19712

Robustness of discrete-time dynamical systems: Application to the multivariable digital control of combat aircraft
[ONERA-NT-1984-2] 11 p1585 N85-19986

Robustness of continuous multivariable flight controls
[ONERA-RT-12/7224-SY] 11 p1586 N85-19987

Robustness of continuous multivariable flight controls
[ONERA-RT-11/7224-SY] 11 p1586 N85-19988

Translating rudder pedal system
[AD-D011510] 12 p1780 N85-21172

Analytical and flight investigation of the influence of rotor and other high-order dynamics on helicopter flight-control system bandwidth
[NASA-TM-86696] 12 p1780 N85-21174

Optimal symmetric flight studies
[NASA-CR-172508] 12 p1780 N85-21176

Integrated control system engineering support
[AD-A149742] 12 p1780 N85-21177

Activities in flight mechanics and flight control
[ISSN-0720-7808] 14 p2227 N85-23803

On-orbit systems identification of flexible spacecraft Technol., 1984, Pt. 2 p 465-481
14 p2233 N85-23841

High specific power aircraft turn maneuvers: Tradeoff of time-to-turn versus change in specific energy
[AD-A151701] 15 p2471 N85-25257

Effects of side-stick controllers on rotorcraft handling qualities for terrain flight
[NASA-TM-86688] 15 p2473 N85-25267

Multistep orbital correction algorithms for an Earth satellite using low thrust engine
15 p2479 N85-25303

Harrier 15 p2687 N85-26595

Cost Effective and Affordable Guidance and Control Systems
[AGARD-CP-360] 16 p2695 N85-26638

Some aspects of how to design cost-effective flight control systems 16 p2695 N85-26639

Navigation: Accounting for copy
16 p2695 N85-26641

A cost-efficient control procedure for the benefit of all airspace users 16 p2697 N85-26651

Study of longitudinal landing flying qualities evaluation using pilot model theory
[AD-A152194] 16 p2706 N85-26702

Flight control system reconfiguration design using quantitative feedback theory
[AD-A151771] 16 p2710 N85-26722

A modern control design methodology with application to the CH-47 helicopter
[AD-A151946] 16 p2710 N85-26723

The state-of-the-art and future of flight control systems 16 p2712 N85-26732

A perspective on superaugmented flight control advantages and problems 16 p2712 N85-26733

Aspects of application of ACT systems for pilot workload alleviation 16 p2712 N85-26734

Application of AFTI/F-16 task-tailored control modes in advanced multirole fighters 16 p2712 N85-26735

X-29A digital flight control system design
16 p2712 N85-26736

ACT applied to helicopter flight control
16 p2712 N85-26738

Some flight test results with redundant digital flight control systems 16 p2712 N85-26739

An update on experience on the fly by wire Jaguar equipped with a full-time digital flight control system
16 p2712 N85-26740

ACT flight research experience
16 p2713 N85-26741

Operational and developmental experience with the F/A-18A digital flight control system
16 p2713 N85-26742

Flight testing and development of the F/A-18A digital flight control system 16 p2713 N85-26743

Active control technology experience with the Space Shuttle in the landing regime 16 p2713 N85-26747

How to handle failures in advanced flight control systems of future transport aircraft 16 p2714 N85-26752

Interactive design of specifications for airborne software set (GISELE) 16 p2714 N85-26753

The flight control system for the Experimental Aircraft Programme (EAP) demonstrator aircraft
16 p2714 N85-26755

Automatic flight control modes for the AFTI/F-111 mission adaptive wing aircraft 16 p2714 N85-26756

The STOL and maneuver technology program integrated control system 16 p2715 N85-26757

The evolution of active control technology systems for the 1990's helicopter 16 p2715 N85-26758

Some aspects of how to design cost-effective flight control systems
[MBB-LKE-32/S/PUB/143] 16 p2873 N85-27729

Analysis of control system from a viewpoint of desired pole placement and desired degree of robustness
[AD-A152627] 17 p2899 N85-27876

Design of robust controllers for a multiple input-multiple output control system with uncertain parameters application to the lateral and longitudinal modes of the KC-135 transport aircraft
[AD-A153100] 17 p2900 N85-27877

Controller requirements for uncoupled aircraft motion, volume 1
[AD-A153173] 17 p2900 N85-27878

Active Control Systems: Review, Evaluation and Projections
[AGARD-CP-384] 17 p2901 N85-27883
The state-of-the-art and future of flight control systems 17 p2901 N85-27885
A perspective on superaugmented flight control advantages and problems 17 p2901 N85-27886
ACT applied to helicopter flight control
17 p2902 N85-27891
Some flight test results with redundant digital flight control systems 17 p2902 N85-27892
Active control technology experience with the Space Shuttle in the landing regime 17 p2903 N85-27900
The aerodynamics of control
17 p2903 N85-27901
The STOL and maneuver technology program integrated control system development 17 p2905 N85-27910
The evolution of active control technology systems for the 1990's helicopter 17 p2905 N85-27911
Advanced secondary power system for transport aircraft
[NASA-TP-2463] 18 p3062 N85-28944
Piloted simulation of an algorithm for onboard control of time-optimal intercept
[NASA-TP-2445] 18 p3063 N85-28949
Extraction of aerodynamic parameters for aircraft at extreme flight conditions
[NASA-TM-86730] 18 p3175 N85-29686
Development and evaluation of a Fault-Tolerant Multiprocessor (FTMP) computer. Volume 2: FTMP software
[NASA-CR-166072] 19 p3341 N85-30706
Interactive aircraft flight control and aeroelastic stabilization
[NASA-CR-176035] 20 p3396 N85-31064
Ergonomic problems regarding the interactive touch input via screens in onboard and ground-based flight control
[NASA-TM-77814] 20 p3512 N85-31832
Flight control system for a computer controlled aircraft with limited sensors
[AD-A155107] 21 p3555 N85-32115
Myoelectric control of a computer based expert system for flight control
[AD-A154981] 21 p3557 N85-32126
Flutter clearance of the Schweizer 1-36 deep-stall sailplane
[NASA-TM-85917] 22 p3729 N85-33118
Flight test experience and controlled impact of a large, four-engine, remotely piloted airplane
[NASA-TM-86738] 22 p3730 N85-33123
The interpretation of flying qualities requirements for flight control system design
[NASA-CR-177942] 22 p3730 N85-33125
Intelligent redundant actuation system requirements and preliminary system design
[NASA-CR-177368] 23 p3896 N85-34136

FLIGHT CREWS
NT SPACECREWS
Analysis of on-board CIG (Computer Image Generator) applications for aircrew training
[AD-A145214] 01 p0013 N85-10079
Dark focus: Intersubject variation, intrasubject stability, and relationship to near retinoscopy
[AD-A145489] 02 p0235 N85-11530
System status display information
[NASA-CR-172347] 04 p0455 N85-12889
Decision tree rating scales for workload estimation: Theme and variations 05 p0708 N85-14541
Intelligent interfaces for tactical airborne platforms
06 p0752 N85-14820
Establishment of posture and working movements of pilot in air crash enquiries 07 p1010 N85-16417
Human factors survey: C-5 pilots
[AD-A147106] 07 p1020 N85-16477
An analysis of constraints to coordinated tactical crew interaction in the P-3C aircraft
[AD-A147220] 07 p1021 N85-16478
Video concepts in CRM training
09 p1276 N85-18015
A systems analysis of alternative concepts for aircrew cold weather clothing
[AD-A148805] 09 p1365 N85-18580
Human Factors Considerations in High Performance Aircraft
[AGARD-CP-371] 10 p1532 N85-19653
Aircrew and avionics: Friends or Foes?
10 p1532 N85-19654
Observations of physiological and psychological effects of terrain following flight based on in-flight test experience 10 p1532 N85-19657
Personnel protection concepts for advence escape system design 10 p1532 N85-19658
Results of a longitudinal study of airsickness incidence during Naval flight officer training
11 p1694 N85-20649
Preflight and postflight motion sickness testing of the Spacelab 1 crew 11 p1694 N85-20652
Psychological components in the development and prevention of air sickness 11 p1695 N85-20659
Assessing the behavior and performance of teams in organizations: The case of air transport crews
[AD-A150359] 13 p2143 N85-23302
The application of anthropometric survey data to aircrew clothing sizing
[AD-A150545] 13 p2143 N85-23304
Torso restraint system
[AD-D011609] 16 p2702 N85-26684
Statistical study of the dynamic analysis of the workload in the A310 certification campaign
16 p2844 N85-27531
Guidelines of the Federal Minister of Transportation for the formation and examination of airline personnel, part 4 17 p3002 N85-28556
Human factors in cockpit automation: A field study of flight crew transition
[NASA-CR-177333] 19 p3215 N85-29937
U.S. Civil airmen statistics for calendar year 1984
[AD-A156326] 24 p4059 N85-35153
Introduction to European air traffic control
[AD-A156328] 24 p4062 N85-35176
Models for assessing workload of aircrews on long distance flights 24 p4129 N85-35599

FLIGHT FATIGUE
Tolerance, fatigue, physiological and performance effects of sustained and oscillating lateral accelerations
10 p1533 N85-19659
Mental workload measurement: Event-related potentials and ratings of workload and fatigue
[NASA-CR-177354] 15 p2619 N85-26139

FLIGHT HAZARDS
NT METEOROID HAZARDS
Study of effects of lightning on aircraft systems stressed 03 p0310 N85-12005
Don't fowl out
[AD-P004179] 11 p1578 N85-19941
Analysis of bird strikes reported by European airlines, 1976 - 1980
[AD-P004181] 11 p1578 N85-19943
Birds and aircraft engine strike rates
[AD-P004184] 11 p1579 N85-19946
The use of falconry as mean to persuade the birds to stay out of the airport vicinity 11 p1580 N85-19956
Airport bird hazards associated with solid waste disposal facilities
[AD-P004197] 11 p1581 N85-19964
Evaluation of effectiveness of bird scaring operations at a sanitary landfill site near CFB Trenton, Ontario, Canada
[AD-P004201] 11 p1582 N85-19968
Development of bird hazard reduction for airport operational safety
[AD-P004202] 11 p1582 N85-19969
The bird strike situation and its ecological background in the Copenhagen Airport, Kastrup
[AD-P004203] 11 p1582 N85-19970
Bird control program Orlando International Airport
[AD-P004204] 11 p1583 N85-19971
Staff assistance to bases for bird hazards
[AD-P004205] 11 p1583 N85-19972
Bird strike avoidance system for Dover AFB, Delaware
[AD-P004206] 11 p1583 N85-19973
The potential of the NEXRAD radar system for warning of bird hazards
[AD-P004210] 11 p1583 N85-19977
First stage of equipping a Do 28 as a research aircraft for icing, and first research results
[ESA-TT-855] 11 p1584 N85-19982
An analysis of the impacts of the Airport Radar Service Area (ARSA)
[AD-A150954] 14 p2217 N85-23749
Helicopter user survey: Traffic alert and collision avoidance system (TCAS)
[FAA-PM-85-6] 15 p2468 N85-25236
The impact of weather on aviation safety
[GPO-35-520] 16 p2703 N85-26685
Aircraft accident report: United Airlines Flight 663, Boeing 727-222, N7647U, Denver, Colorado, May 31, 1984
[PB85-910405] 16 p2703 N85-26686
Flying in spite of the weather
[NLR-MP-84021-U] 17 p2895 N85-27847
Contributions on the subject of longitudinal movements of aircraft in wind shears
[NASA-TM-77837] 18 p3139 N85-29432
Space Station crew safety alternatives study. Volume 2: Threat development
[NASA-CR-3855] 21 p3558 N85-32133
System safety study of minimum TCAS 2 for instrument weather conditions
[FAA-PM-85-12] 22 p3728 N85-33113

FLIGHT INSTRUMENTS
NT APPROACH INDICATORS
NT ATTITUDE INDICATORS
NT AUTOMATIC PILOTS
NT FLIGHT TEST INSTRUMENTS
NT GYRO HORIZONS
NT HORIZON SCANNERS
NT RADIO ALTIMETERS
The Malcolm horizon: History and future
01 p0008 N85-1
A comparative evaluation of EMADS (Engine Monitoring and Display System) and conventional engine instruments
[AD-A145901] 03 p0319 N85-1
Commerce Laboratory: Mission analysis payload integration study
[NASA-CR-171298] 07 p0911 N85-157
LPI-radar for helicopter obstacle warning
08 p1074 N85-16
Crewstation assessment of reach as applied to the OH-58A helicopter
[AD-A149413] 10 p1531 N85-19
Air Force Academy Aeronautics Digest
[AD-A149614] 12 p1760 N85-211
A preliminary investigation of handling qualities requirements for helicopter instrument flight during decelerating approach maneuvers and overshoot
[NRC-24173] 17 p2896 N85-27
A guide to USAF helicopter instrument flight procedures
[AD-A156102] 24 p4063 N85-35
Accuracy and error analysis --- airborne instruments
24 p4123 N85-35

FLIGHT LOAD RECORDERS
Operational Loads Data
[AGARD-CP-375] 07 p0894 N85-15
Operational loads measurement: A philosophy and its implementation 07 p0894 N85-15
The F-15 flight loads tracking program
07 p0894 N85-15
Operational loads data evaluation for individual aircraft fatigue monitoring 07 p0895 N85-15
US Army helicopter operational flight loads
07 p0895 N85-15
Flight parameters recording for structure fatigue life monitoring 07 p0896 N85-15
USAF approach to airborne structural data recording Airborne Data Acquisition Multifunction System (ADAMS)
07 p0897 N85-15

FLIGHT MANAGEMENT SYSTEMS
Ground and flight testing for aircraft guidance and control
[AGARD-AG-262] 13 p1966 N85-22
Civil avionics flight testing with the RAE(B) BAC1-11
13 p1967 N85-22
A flight management algorithm and guidance for fuel-conservative descents in a time-based metered air traffic environment: Development and flight test results
13 p1967 N85-22
Users guide: The LaRC human-operator-simulator-based pilot model
[NASA-TM-86367] 14 p2390 N85-24721
Planning fuel-conservative descents in an airline environmental using a small programmable calculator: Algorithm development and flight test results
[NASA-TP-2393] 16 p2707 N85-26705

FLIGHT MECHANICS
AGARD bulletin technical programme, 1985
[AGARD-BUL-84-2] 02 p0305 N85-11871
Flight test of the Open Loop Gust Alleviation (OLGA) system
[BMFT-FB-W-84-038] 08 p1066 N85-16
Flight mechanics analysis of dynamic derivatives of the Dornier variable wind tunnel model
[ESA-TT-854] 11 p1577 N85-19
Technical evaluation report on the FDP Symposium on Flight Test Techniques
[AGARD-AR-206] 12 p1777 N85-21157
Optimal symmetric flight studies
[NASA-CR-172506] 12 p1780 N85-21176
Dynamic wind tunnel testing for active control research 13 p1966 N85-22
Activities in flight mechanics and flight control
[ISSN-0720-7806] 14 p2227 N85-23
Use of quaternions in flight mechanics
[AD-A152616] 17 p2890 N85-27875
Active Control Systems: Review, Evaluation and Projections
[AGARD-CP-384] 17 p2901 N85-278
Flight-mechanics test with a restricted flying aircraft model in a wind tunnel
[ESA-TT-885] 20 p3394 N85-310
The Naval Postgraduate School Flight Mechanics Laboratory: A feasibility study
[AD-A154578] 21 p3557 N85-321

Lectures of a Flight Mechanics Conference --- conferences
[ESA-TT-891] 24 p4061 N85-35165
Development of flight mechanics research in Brunswick 24 p4061 N85-35166
The contribution made by flight mechanics to civil aviation 24 p4061 N85-35169
The effect of instrumentation system parameters on the results of a flight mechanical system identification
24 p4061 N85-35170
Estimation of flight mechanical variables by means of Kalman filters 24 p4062 N85-35171
Gust simulation for flight mechanical wind tunnel tests
24 p4062 N85-35172
Control variables in vertical wind determination using simple flight-mechanical equations
24 p4121 N85-35546

FLIGHT OPERATIONS
NT CREW PROCEDURES (INFLIGHT)
New runway enables IL-76 flights to Tenkeli in far north 12 p1769 N85-21108
Ministry officials on improving aircraft technical servicing 14 p2208 N85-23687
Disturbance to the population due to flight operations at landing fields. Questionnaire on community reaction to non-commercial and sporting aviation
[NASA-TM-76531] 14 p2353 N85-24537
Space station systems technology study (add-on task). Volume 2: Trade study and technology selection
[NASA-CR-171416] 15 p2475 N85-25279

FLIGHT OPTIMIZATION
On-board near-optimal climb-dash energy management 02 p0137 N85-10931
Computer assisted flight schedule optimization
[AD-A151689] 16 p2858 N85-27623

FLIGHT PATHS
NT GLIDE PATHS
On-board near-optimal climb-dash energy management 02 p0137 N85-10931
Command flight path display. Phase I and II: Appendix F
[AD-A145858] 03 p0318 N85-12058
Effects of aircraft and flight parameters on energy-efficient profile descents in time-based metered traffic
[NASA-CR-172338-ADD] 07 p0901 N85-15706
Predicted performance benefits of an adaptive digital engine control system of an F-15 airplane
[NASA-TM-85916] 07 p0905 N85-15729
Investigation of semiautomatic aircraft control processes employing time redundancy in on-board digital trajectory control computers 07 p0954 N85-16048
Hot radome boresight error measurements
[AD-P004364] 12 p1826 N85-21458
Minimum time turns using vectored thrust
[AD-A151693] 15 p2471 N85-25256
High specific power aircraft turn maneuvers: Tradeoff of time-to-turn versus change in specific energy
[AD-A151701] 15 p2471 N85-25257
A user's manual for AMEER flight path trajectory simulation code
[DE85-006580] 15 p2472 N85-25260
A method of estimating aircraft attitude from fly by wire flight control system data 16 p2697 N85-26653
Terrain following without use of forward looking sensors 16 p2698 N85-26659
Generation of flight paths using heuristic search
[AD-A151949] 16 p2704 N85-26694
Planning fuel-conservative descents in an airline environmental using a small programmable calculator: Algorithm development and flight test results
[NASA-TP-2393] 16 p2707 N85-26705
Aspects of application of ACT systems for pilot workload alleviation 16 p2712 N85-26734
Probabilistic computer model of optimal runway turnoffs
[NASA-CR-172549] 16 p2715 N85-26760
Status of air traffic control system
[S-HRG-98-1197] 20 p3391 N85-31036
User's manual of the BNDSCO computer program for solving constrained optimal control problems
[DFVLR-MITT-85-05] 20 p3516 N85-31865
Guidelines for the evaluation of visual approach slope indicators
[ARL/SYS-R-32] 23 p3896 N85-34132
Determination of instrument errors by compatibility checking: Results from dynamic flight test data
[ARL/AERO-R-162] 23 p3896 N85-34137
International flight planning handbook
[AD-A156330] 24 p4062 N85-35177
Comparative analysis of operational forecasts versus actual weather conditions in airline flight planning, volume 2
[NASA-CR-167863] 24 p4119 N85-35535
Comparative analysis of operational forecasts versus actual weather conditions in airline flight planning, volume 3
[NASA-CR-167864] 24 p4120 N85-35536
Comparative analysis of operational forecasts versus actual weather conditions in airline flight planning, volume 4
[NASA-CR-167865] 24 p4120 N85-35537
Comparative analysis of operational forecasts versus actual weather conditions in airline flight planning: Summary report
[NASA-CR-167866] 24 p4120 N85-35538

FLIGHT PERFORMANCE
U FLIGHT CHARACTERISTICS

FLIGHT PLANS
Kovtunenko comments on Vega flight plan, instrumentation 15 p2482 N85-25318
International flight planning handbook
[AD-A156330] 24 p4062 N85-35177
Comparative analysis of operational forecasts versus actual weather conditions in airline flight planning, volume 1
[NASA-CR-167862] 24 p4119 N85-35534
Comparative analysis of operational forecasts versus actual weather conditions in airline flight planning, volume 2
[NASA-CR-167863] 24 p4119 N85-35535
Comparative analysis of operational forecasts versus actual weather conditions in airline flight planning: Summary report
[NASA-CR-167866] 24 p4120 N85-35538

FLIGHT RULES
NT INSTRUMENT FLIGHT RULES
NT VISUAL FLIGHT RULES

FLIGHT SAFETY
Flight [illegible]ease status monitor study. Phase 1: Systems concepts
[DOT/FAA/PM-84/18] 03 p0317 N85-12046
Aircraft navigation and landing technology: Status of implementation
[GPO-38-615] 04 p0454 N85-12683
Flight Training Technology for Regional/Commuter Airline Operations: Regional Airline Association/NASA Workshop Proceedings
[NASA-CP-2348] 09 p1275 N85-18009
Dynamic training devices in CRM training
09 p1276 N85-18018
Safety awareness, pilot education, and incident reporting programs 09 p1276 N85-18020
The aviation safety reporting system
09 p1276 N85-18021
Pilot education and safety awareness programs
09 p1277 N85-18026
Legislation to improve airline safety
[GPO-38-222] 12 p1773 N85-21132
Aerospace Safety Advisory Panel
[NASA-TM-87428] 12 p1774 N85-21135
Improvements in personnel needed for better flight safety 14 p2208 N85-23693
Safety recommendation(s), A84-111 through -115
[REPT-4011C/27] 14 p2216 N85-23744
An analysis of the impacts of the Airport Radar Service Area (ARSA)
[AD-A150954] 14 p2217 N85-23749
Official on Soviet research in deicing techniques
15 p2460 N85-25191
Safety recommendation(s), A-84-96
[REPT-3983A/217] 15 p2466 N85-25223
Safety recommendation(s), A-84-76 through -78
[REPT-3751E] 15 p2466 N85-25224
The impact of weather on aviation safety
[GPO-35-520] 16 p2703 N85-26685
Aircraft accident report: United Airlines Flight 663, Boeing 727-222, N7647U, Denver, Colorado, May 31, 1984
[PB85-910405] 16 p2703 N85-26686
Lightning-safe carbon fiber composite for Airbus tail unit 18 p3087 N85-29100
Hydrazine and the F-16 20 p3511 N85-31826

FLIGHT SIMULATION
Pressure distribution on a swept wing aircraft in flight
01 p0004 N85-10025
A mathematical simulation model of the CH-47B helicopter, volume 1
[NASA-TM-84351-VOL-1] 01 p0006 N85-10033
The Malcolm horizon: History and future
01 p0008 N85-10046
Active control technology experience with the Space Shuttle in the landing regime
[NASA-TM-85910] 01 p0012 N85-10071
Effect of penetrant on fatigue of aluminum alloy lap joints
[NLR-TR-82104-U] 01 p0056 N85-10373
Flight simulation fatigue crack propagation in metal/carbon-epoxy laminates
[NLR-TR-83006-U] 01 p0063 N85-10416
Airborne performance measurement system design: C-5 aircraft
[AD-A145436] 02 p0236 N85-11539
Cyclic endurance testing of the RB211-22B cast HP turbine blade --- high pressure (HP)
[PNR-90210] 03 p0320 N85-12063
A spatial model of wind shear and turbulence for flight simulation 03 p0395 N85-12518
An in-flight investigation of a twin fuselage configuration in approach and landing
[NASA-CR-172366] 05 p0596 N85-13801
Investigation of pilot behavior in flight tests with a rate command/attitude hold control system
[DFVLR-FB-84-25] 05 p0699 N85-14486
Quantification of cross-coupling and motion feedthrough for multiaxis controllers used in an air combat flying task
05 p0700 N85-14491
A method for measuring the effective throughput time delay in simulated displays involving manual control
05 p0701 N85-14497
Maximum normalized rate as a flying qualities parameter 05 p0702 N85-14503
Measuring workload differences between short-term memory and long-term memory scenarios in a simulated flight environment 05 p0703 N85-14513
Use of linear perspective scene cues in a simulated height regulation task 05 p0704 N85-14517
Accuracy of system step response roll magnitude estimation from central and peripheral visual displays and simulator cockpit motion 05 p0705 N85-14522
Fractographic observation and estimation of crack growth curve of aluminum alloy under ramdom flight simulation loading
[NAL-TR-824] 06 p0768 N85-14913
NyKINM, a further development of KINM 22 --- simulation of a robot attack on an aircraft
[FOA-C-20559-D8(E3)] 07 p0903 N85-15720
Practice makes perfect
[AD-A147124] 07 p1019 N85-16486
Advanced flight simulation for helicopter development
08 p1075 N85-16815
Assessment of simulation fidelity using measurements of piloting technique in flight 08 p1075 N85-16817
The IMAGE 3 Conference Proceedings
[AD-A148636] 09 p1267 N85-17962
Visual perceptual aspects of low level high speed flight and flight simulation
[AD-P004310] 09 p1267 N85-17964
Low altitude high speed flight simulation using video disc technology
[AD-P004312] 09 p1268 N85-17966
SODERN Visualization System (SVS) for flight simulation
[AD-P004320] 09 p1269 N85-17974
CIG (Computer Image Generator) goes to war: The tactical illusion
[AD-P004336] 09 p1271 N85-17990
AVTS (Advanced Visual Technology System): A high fidelity visual simulator
[AD-P004338] 09 p1271 N85-17992
Flight crew training technology: A review
09 p1275 N85-18010
Low-cost training technology
09 p1275 N85-18011
Initiative uses of aircraft for flight training
09 p1277 N85-18027
Innovative approaches to recurrent training
09 p1277 N85-18028
In-flight investigation of the effects of time delay in control system on flying qualities in landing approach
[DFVLR-FB-84-35] 11 p1586 N85-19969
Crack growth geometry in aluminum alloy sheet material under flight simulation loading. 1: A comparison between TWIST and miniTWIST FALSTAFF and short FALSTAFF. 2: Effect of truncating high loads
[VTH-LR-441] 11 p1609 N85-20119
Simulation of aircraft behaviour on and close to the ground
[NASA-TM-67460] 14 p2218 N85-23754
Flight simulation for inertial navigation system
14 p2273 N85-24081
Users guide: The LaRC human-operator-simulator-based pilot model
[NASA-TM-86367] 14 p2390 N85-24721
YAV-8B Harrier 15 p2686 N85-26605
Piloted simulation of one-on-one helicopter air combat at NOE flight levels
[NASA-TM-86686] 16 p2710 N85-26720
The effect of load factor on aircraft handling qualities
[AD-A152118] 16 p2710 N85-26724
Design and specification of a local area network architecture for use in real-time flight simulation
[AD-A152242] 16 p2716 N85-26762
Flight Experiment Demonstration System (FEDS) functional description and interface document
[NASA-CR-175290] 16 p2717 N85-26769

Research and development. Technical and scientific reports 1984 16 p2873 N85-27724
Advanced flight simulation for helicopter development
[MBB-UD-416/84-O] 16 p2874 N85-27731
Technical evaluation of the Naval Automated Pilot Aptitude Measurement System (NAPAMS)
[AD-A152361] 17 p3000 N85-28547
Adding computationally efficient realism to Monte Carlo turbulence simulation
[NASA-TP-2469] 17 p3025 N85-28708
Helicopter Aeromechanics
[AGARD-LS-139] 18 p3057 N85-28913
Visual and part-task manipulations for teaching simulated carrier landings
[AD-A153622] 18 p3154 N85-29529
Electrooculographic measurement, fatigue and variability of performance in simulated aircraft flight
19 p3217 N85-29948
Crew systems and flight station concepts for a 1995 transport aircraft
[NASA-CR-166068] 19 p3221 N85-29973
X-ray satellite
[NASA-TM-77696] 20 p3407 N85-31144
Modifications of flight-by-flight load sequences to provide for good fracture surface readability
[NLR-MP-84012-U] 20 p3472 N85-31577
Learning and self adaptation applied to the simulation of a human pilot
[ONERA-RT-24/5122-SY] 20 p3511 N85-31828
A preliminary investigation of handling qualities requirements for helicopter instrument flight during decelerating approach maneuvers and overshoot
[AD-A154650] 21 p3557 N85-32125
The interpretation of flying qualities requirements for flight control system design
[NASA-CR-177942] 22 p3730 N85-33125
Energy management of three-dimensional minimum-time intercept
[NASA-CR-176174] 24 p4064 N85-35186
Comparative analysis of operational forecasts versus actual weather conditions in airline flight planning, volume 2
[NASA-CR-167963] 24 p4119 N85-35535

FLIGHT SIMULATORS
NT COCKPIT SIMULATORS
Evaluation of the Malcolm horizon in a moving-base flight simulator 01 p0008 N85-10051
Content, variety, and augmentation of simulated visual scenes for teaching air-to-ground attack
[AD-A145218] 01 p0013 N85-10080
Simulator study of flight characteristics of several large, dissimilar, cargo transport airplanes during approach and landing
[NASA-TP-2357] 02 p0148 N85-11002
Air Force Human Resources Laboratory report: Fiscal year, 1983
[AD-A145647] 02 p0236 N85-11548
Models for the effects of G-seat cuing on roll-axis tracking performance 05 p0707 N85-14532
Determining training device requirements in Army aviation systems 05 p0711 N85-14558
Measuring pilot workload in a moving-base simulator. Part 2: Building levels of workload
05 p0712 N85-14566
Simulation evaluation of two VTOL control/display systems in IMC approach and shipboard landing
[NASA-TM-85996] 06 p0756 N85-14841
Situational interactive micro/graphic simulator system for improving maintenance performance
[AD-A146677] 06 p0757 N85-14846
Reference energy-altitude descent guidance: Simulator evaluation — aircraft descent and fuel conservation
[NASA-TP-2393] 06 p1086 N85-16868
Proceedings of a Workshop on Research Issues in Simulator Sickness
[AD-A148543] 08 p1196 N85-17536
Using a limited field of view simulator to instruct high speed, low altitude flying skills
[AD-P004309] 09 p1267 N85-17963
Altitude control using action-demanding interactive displays: Toward an active psychophysics
[AD-P004311] 09 p1267 N85-17965
Simulating speed and height cues in the C-130 weapon system trainer
[AD-P004313] 09 p1268 N85-17967
Automated and interactive data base generation
[AD-P004316] 09 p1268 N85-17970
An overview of the research program at the visual technology research simulator
[AD-P004321] 09 p1269 N85-17975
Considerations in an optical variable acuity display system
[AD-P004323] 09 p1269 N85-17977
Design considerations for an eye tracked AOI (Area of Interest) display system
[AD-P004324] 09 p1269 N85-17978
The effects of time delay in man-machine control systems: Implications for design of flight simulator Visual-Display-Delay compensation
[AD-P004329] 09 p1270 N85-17983
Binocular overlap in a fiber optic helmet mounted display
[AD-P004331] 09 p1270 N85-17985
Global optical metrics for self-motion perception
[AD-P004333] 09 p1271 N85-17987
Simulator sickness: Sensorimotor disturbances induced in flight simulators
[AD-P004334] 09 p1271 N85-17988
Simulation 09 p1277 N85-18024
Low cost training aids and devices
09 p1277 N85-18025
Pictorial format display evaluation
[AD-A149252] 10 p1425 N85-18986
Interactive Graphics Simulator: Design, development and effectiveness/cost evaluation
[AD-A149417] 10 p1540 N85-19712
Inflight IFR procedures simulator
[NASA-CASE-KSC-11218-1] 11 p1586 N85-19990
Simulator sickness: Reaction to a transformed perceptual world. 6: Preliminary site surveys
11 p1694 N85-20853
Transportation
[JPRS-UTR-85-004] 12 p1769 N85-21105
New flight simulators at Vnukovo permit less in-flight training 12 p1769 N85-21107
Visual simulation requirements for aircraft aspect recognition at real world distances
[AD-A151040] 14 p2228 N85-23810
Roundtable on effective use of flight simulators
15 p2460 N85-25190
The evaluation of ACS for helicopters: Conceptual simulation studies to preliminary design
16 p2712 N85-26737
Advanced flight simulation for helicopter development
[MBB-UD-416/84-O] 16 p2874 N85-27731
The role of simulation 18 p3058 N85-28919
The use of flight simulators in measuring and improving training effectiveness
[AD-A153817] 18 p3084 N85-28954
A systematic determination of skill and simulator requirements for airline transport pilot certification
[AD-A154135] 19 p3330 N85-30630
Advanced simulator for pilot training and helmet-mounted visual display configuration comparisons
[AD-A155326] 21 p3667 N85-32776
Man-vehicle systems research facility advanced aircraft flight simulator throttle mechanism
22 p3796 N85-33527
Langley aeronautics and space test highlights, 1984
[NASA-TM-87585] 23 p4057 N85-35151

FLIGHT STABILITY TESTS
Flight test of the Open Loop Gust Alleviation (OLGA) system
[BMFT-FB-W-84-036] 08 p1088 N85-16881
Identification of gust input and gust response characteristics from Do 28 TNT flight test data
[DFVLR-FB-84-48] 17 p2900 N85-27881
Proposals for the determination of necessary elevator handling characteristics of sailplanes in high speed range
[DFVLR-FB-84-52] 17 p2900 N85-27882
Real scale test of the Petit Canard aircraft in the number 3 section, 47 sqm, of the SIMA wind tunnel, May 1984
[ONERA-PV-1/0772-GY] 20 p3389 N85-31018

FLIGHT STRESS (BIOLOGY)
NT SPACE FLIGHT STRESS
The Reports of Aeromedical Laboratory, volume 25, no. 1/2
[ISSN-0023-2858] 01 p0090 N85-10605
Psychological states (mood, affect or emotion) experienced by JASDF pilots through flying duties. 3: Flying conditions causing pilots psychological disturbances 01 p0090 N85-10606
The relationship between emotional tension scale and psychological uneasiness of JASDF pilots in flying situations 01 p0090 N85-10608
Results of a longitudinal study of airsickness during naval flight officer training: Executive summary
[AD-A150687] 14 p2388 N85-24712
Blood serum enzyme activity following long term spaceflights 19 p3326 N85-30604
Microorganisms in space flight
23 p3951 N85-34490

FLIGHT TECHNICAL ERROR
U PILOT ERROR

FLIGHT TEST INSTRUMENTS
Flight test support aircraft Advanced Technologies Testing Aircraft System (ATTAS) for the DFVLR
[MBB-FE-732/S/PUB/154] 16 p2674 N85-27730

FLIGHT TEST VEHICLES
Flight test support aircraft Advanced Technologies Testing Aircraft System (ATTAS) for the DFVLR
[MBB-FE-732/S/PUB/154] 16 p2674 N85-27730
B-52B/DTV (Drop Test Vehicle) flight test results: Drop test missions
[NASA-CR-171530] 19 p3215 N85-29984

FLIGHT TESTS
NT FLIGHT STABILITY TESTS
NT SPACE TRANSPORTATION SYSTEM FLIGHTS
NT SPACE TRANSPORTATION SYSTEM 1 FLIGHT
NT SPACE TRANSPORTATION SYSTEM 3 FLIGHT
NT SPACE TRANSPORTATION SYSTEM 4 FLIGHT
Pressure distribution on a swept wing aircraft in flight
01 p0004 N85-10025
Airworthiness and flight characteristics test of the JOH-6A light combat helicopter configured with a wire strike protection system
[AD-A144860] 01 p0006 N85-10038
Airworthiness and Flight Characteristics (A and FC) test of the EH - 1X/EH - 1H helicopter configurations
[AD-A144861] 01 p0007 N85-10039
A preliminary flight evaluation of the peripheral vision display using the NT-33A aircraft
[AD-A145123] 01 p0010 N85-10060
YO-3A acoustics research aircraft systems manual
[NASA-TM-85968] 01 p0012 N85-10074
Nonlinear system identification methodology development based on F-4S flight test data analysis
[AD-A146289] 03 p0318 N85-12063
Flight and wind-tunnel comparisons of the inlet-airframe interaction of the F-15 airplane
[NASA-TP-2374] 04 p0455 N85-12884
Flight tests of the Digital Integrated Automatic Landing System (DIALS)
[NASA-CR-3859] 04 p0457 N85-12900
The DG400 propulsed glider
[CEV/IS/SE/AV/84] 05 p0596 N85-13786
Maximum normalized rate as a flying qualities parameter 05 p0702 N85-14508
Maximum likelihood estimation of parameters in linear systems from flight test data: A FORTRAN program
[AD-B087198L] 05 p0715 N85-14598
Flight test technique for evaluation of gust load alleviation analysis methodology
[NASA-TM-86344] 06 p0754 N85-14833
Flight test results on stall characteristics of a large jet transport
[NAL-TR-617] 06 p0754 N85-14835
Structural flight load measurement demonstration of structural integrity 07 p0895 N85-15570
CF-5 vertical stabilizer flight load survey
07 p0895 N85-15573
Ground-effect analysis of a jet transport airplane
[NASA-TM-85920] 07 p0897 N85-15587
The UH-1H helicopter icing flight test program: An overview
[NASA-TM-86825] 07 p0900 N85-15702
Flight testing of Litton laser gyro strapdown system LTN-90 for general aviation
[DFVLR-MITT-84-16] 07 p0901 N85-15709
Noise measurement flight test: Data-analyses aerospatiale AS-355F TwinStar helicopter
[AD-A147497] 07 p1039 N85-16595
Built-in-test for first line testing
08 p1064 N85-16739
Flight tests with a new helicopter Force Feel System (FFS) 08 p1075 N85-16818
Development and flight test of a helicopter compact, portable, precision landing system concept
08 p1076 N85-16821
Airworthiness and flight characteristics test of the RC-12D Guardrail V
[AD-A148046] 08 p1084 N85-16884
Preliminary airworthiness evaluation AH-1S (MC) helicopter with external fuel tanks installed
[AD-A148091] 08 p1084 N85-16885
Noise measurement flight test for Boeing Vertol 234/CH 47-d helicopter: Data/analyses
[AD-A148172] 08 p1218 N85-17670
Noise measurement flight test: Data-analyses Aerospatiale AS 350D AStar helicopter
[AD-A148496] 08 p1218 N85-17672
Noise measurement flight test: Data-analyses, Sikorsky S-76A helicopter
[AD-A148525] 08 p1218 N85-17673
Activities at Mil Experimental Design Bureau
09 p1278 N85-18036
Modeling of aircraft performance from flight test results using quasi steady-state test techniques
09 p1279 N85-18047
A comparison of fatigue lives under a complex and a much simplified flight-by-flight testing sequence — Mirage 3 aircraft
[ARL/STRUC-TM-388] 09 p1280 N85-18052

NASA-VCOSS dynamic test facility
[NASA-TM-86491] 10 p1427 N85-18998
Observations of physiological and psychological effects of terrain following flight based on in-flight test experience 10 p1532 N85-19657
Collision avoidance for Naval training aircraft
[FAA-PM-84-4] 12 p1774 N85-21136
On the application of compatibility checking techniques to dynamic flight test data
[ARL/AERO-R-161] 12 p1776 N85-21151
Technical evaluation report on the FDP Symposium on Flight Test Techniques
[AGARD-AR-208] 12 p1777 N85-21157
Civil avionics flight testing with the RAE(B) BAC1-11
13 p1967 N85-22354
Guidance and control research flight testing with HFB 320 test aircraft 13 p1967 N85-22355
A flight management algorithm and guidance for fuel-conservative descents in a time-based metered air traffic environment: Development and flight test results
13 p1967 N85-22356
Avionics Flight Evaluation System (AFES)
13 p1967 N85-22357
Improved Y-11 general-purpose transport designated Y-12 13 p1972 N85-22385
Operational loads measurement: A philosophy and its implementation — aircraft structures
[AD-A149445] 13 p2144 N85-23306
Glider Nimbus 3-24.5. Partial certification test results for importation in the U category
[REPT-CEV/IS/SE/AV/84] 14 p2220 N85-23763
Solar Array Experiment (SAE) flight experience
14 p2236 N85-23861
Location and data collection for long stratospheric balloon flights 14 p2326 N85-24377
US Army Aviation Engineering Flight Activity (USAAEFA) report bibliography update 1983 - 1984
[AD-A151381] 15 p2457 N85-25168
Trajectory measurements for take-off and landing tests and other short-range applications, volume 16
[AGARD-AG-160-VOL-16] 15 p2561 N85-25801
Navigation and flight director guidance for the NASA/FAA helicopter MLS curved approach flight test program
[NASA-CR-177350] 16 p2704 N85-26691
Planning fuel-conservative descents in an airline environmental using a small programmable calculator: Algorithm development and flight test results
[NASA-TP-2393] 16 p2707 N85-26705
Development and flight test of a helicopter, X-band, portable precision landing system concept
[NASA-TM-86710] 16 p2710 N85-26721
A modern control design methodology with application to the CH-47 helicopter
[AD-A151946] 16 p2710 N85-26723
The effect of load factor on aircraft handling qualities
[AD-A152118] 16 p2710 N85-26724
Some flight test results with redundant digital flight control systems 16 p2712 N85-26739
Flight testing and development of the F/A-18A digital flight control system 16 p2713 N85-26743
OLGA: An open loop gust alleviation
16 p2713 N85-26744
Space Shuttle program communication and tracking systems interface analysis
[NASA-CR-171882] 16 p2729 N85-26841
In-situ stratospheric ozone measurements: Recent results and their implications 16 p2824 N85-27419
Station for in-orbit testing of satellites
[MBB-UR-708/84-O] 16 p2874 N85-27733
USSR report: Transportation
[JPRS-UTR-84-025] 17 p2894 N85-27841
Test flight of IL-76TD long-range transport variant
17 p2894 N85-27842
A preliminary investigation of handling qualities requirements for helicopter instrument flight during decelerating approach maneuvers and overshoot
[NRC-24173] 17 p2896 N85-27857
Flight trials of a modified gulfstream commander carrying external stores
[AD-A153376] 17 p2896 N85-27859
Parameter identification results of tests in nonsteady symmetric flight with the Hawker Hunter Mk 7
[NLR-TR-83042-U] 17 p2897 N85-27860
The Avionics Flight Evaluation System (AFES) of DFVLR
[DFVLR-MITT-85-01] 17 p2897 N85-27864
In-flight investigation of the influence of pitch damping and pitch control effectiveness on landing approach flying qualities of statically unstable transport aircraft
[DFVLR-FB-84-12] 17 p2900 N85-27880
Some flight test results with redundant digital flight control systems 17 p2902 N85-27892
ACT flight research experience
17 p2902 N85-27894
Flight testing and development of the F/A-18A digital flight control system 17 p2902 N85-27896
OLGA: An open loop gust alleviation system
17 p2903 N85-27897
Flight testing for performance and flying qualities
18 p3058 N85-28920
DC-10 winglet flight evaluation
[NASA-CR-3704] 19 p3217 N85-29949
Flight testing the Litton LTN 90 laser gyro strapdown system for civil aviation
[ESA-TT-904] 20 p3392 N85-31042
Design and implementation of input signals for identification of pilot/aircraft models
[ESA-TT-880] 20 p3394 N85-31055
Large space structure flight experiment
20 p3410 N85-31163
Design, manufacture and testing of a medium accuracy star tracker
[REPT-TR/84-048] 20 p3459 N85-31488
Artificial and natural icing tests YEH-60A quick fix helicopter
[AD-A155147] 21 p3555 N85-32116
Design of an expert-system flight status monitor
[NASA-TM-86739] 21 p3669 N85-32794
Qualification needs for advanced integrated aircraft
[NASA-TM-86731] 22 p3729 N85-33119
Development of a temperature-compensated hot-film anemometer system for boundary-layer transition detection on high-performance aircraft
[NASA-TM-86732] 22 p3730 N85-33121
Development of control laws for a flight test maneuver autopilot for an F-15 aircraft
[NASA-TM-86736] 22 p3730 N85-33122
Flight test experience and controlled impact of a large, four-engine, remotely piloted airplane
[NASA-TM-86738] 22 p3730 N85-33123
The interpretation of flying qualities requirements for flight control system design
[NASA-CR-177942] 22 p3730 N85-33125
Flight testing the fixed-wing configuration of the Rotor Systems Research Aircraft (RSRA)
[NASA-TM-86762] 23 p3896 N85-34135
Determination of instrument errors by compatibility checking: Results from dynamic flight test data
[ARL/AERO-R-162] 23 p3896 N85-34137
A comparison between Falcon data and motor glider data 24 p4121 N85-35547
FLIGHT TIME
General aviation activity and avionics survey
[AD-A149572] 12 p1769 N85-21103
FLIGHT TRAINING
NT SPACE FLIGHT TRAINING
Analysis of on-board CIG (Computer Image Generator) applications for aircrew training
[AD-A145214] 01 p0013 N85-10079
Workload demand and CNS depressant stressor effects on spatial orientation information processing
[AD-A145211] 01 p0098 N85-10651
Airborne performance measurement system design: C-5 aircraft
[AD-A145436] 02 p0236 N85-11539
Air Force Human Resources Laboratory report: Fiscal year, 1983
[AD-A145647] 02 p0238 N85-11548
Can the Aggressors continue to be effective in the F-5E?
[AD-A146861] 07 p1019 N85-16465
Practice makes perfect
[AD-A147124] 07 p1019 N85-16466
Directions of the West German Ministry of Transport for education and control of airline personnel (section 3, chapters 2 and 12) 08 p1081 N85-16848
Directions of the West German Ministry of Transport for education and control or airline personnel, Report 6; chapters 3/A and 3/B 08 p1081 N85-16849
The value and utility of inflight onboard simulation
[AD-A148033] 08 p1198 N85-17543
Flight Training Technology for Regional/Commuter Airline Operations: Regional Airline Association/NASA Workshop Proceedings
[NASA-CP-2348] 09 p1275 N85-18009
Flight crew training technology: A review
09 p1275 N85-18010
Low-cost training technology
09 p1275 N85-18011
Captain development training at US Air
09 p1275 N85-18012
Management training for cockpit crews at Piedmont flight 09 p1276 N85-18013
Integrated approach to flight crew training
09 p1276 N85-18014
Video concepts in CRM training
09 p1276 N85-18015
Use of simplifier scenarios for CRM training
09 p1276 N85-18016
Use of airplanes for loft training
09 p1276 N85-18019
Low cost training aids and devices
09 p1277 N85-18025
Initiative uses of aircraft for flight training
09 p1277 N85-18027
Innovative approaches to recurrent training
09 p1277 N85-18028
Interactive Graphics Simulator: Design, development and effectiveness/cost evaluation
[AD-A149417] 10 p1540 N85-19712
Inflight IFR procedures simulator
[NASA-CASE-KSC-11218-1] 11 p1586 N85-19990
Results of a longitudinal study of airsickness incidence during Naval flight officer training
11 p1694 N85-20649
New flight simulators at Vnukovo permit less in-flight training 12 p1769 N85-21107
Results of a longitudinal study of airsickness during naval flight officer training: Executive summary
[AD-A150887] 14 p2388 N85-24712
Roundtable on effective use of flight simulators
15 p2460 N85-25190
Trends shaping advanced aircrew training capabilities through the 1990s
[AD-A152277] 16 p2843 N85-27530
Guidelines of the Federal Minister of Transportation for the formation and examination of airline personnel, part 4 17 p3002 N85-28556
The use of flight simulators in measuring and improving training effectiveness
[AD-A153817] 18 p3064 N85-28954
Visual and part-task manipulations for teaching simulated carrier landings
[AD-A153622] 18 p3154 N85-29529
FLIGHT VEHICLES
Approximate analytic method of calculating trajectories of movement of a flight vehicle in the atmosphere
14 p2279 N85-24121
FLIP-FLOPS
Experimental test of the three subaperture method for estimating target elevation angle
[AD-A149887] 12 p1851 N85-21614
A two-cycle shift register with error detection
[AD-A150768] 14 p2400 N85-24791
FLIR DETECTORS
Some thoughts on the implementation of pilot night vision devices for helicopters 06 p0751 N85-14814
Application of infrared radiometers for airborne detection of clear air turbulence and low level wind shear, airborne infrared low level wind shear detection test
[NASA-CR-175725] 15 p2594 N85-25985
An analysis of the economic impact of the AN/APS-134 FLAR (Forward Looking Airborne Radar) retrofit on Coast Guard HC-130 aircraft
[AD-A152619] 17 p2949 N85-28204
Thin film phase transition materials development program
[AD-A154260] 19 p3259 N85-30209
FLOAT ZONES
Research on the basic understanding of high efficiency in silicon solar cells
[DE85-000507] 11 p1672 N85-20537
Microgravity silicon zoning investigation
[NASA-CR-171531] 20 p3397 N85-31073
Advanced module development overview
21 p3612 N85-32445
FLOATING
Development of a floating element wall shear transducer
[AD-A144794] 01 p0049 N85-10324
Buckling analysis of cracked, floating ice sheets
[AD-A147330] 07 p0988 N85-16277
FLOATING POINT ARITHMETIC
Function algorithms for MPP scientific subroutines, volume 1
[NASA-CR-175246] 01 p0102 N85-10678
Floating-point function generation routines for 16-bit microcomputers
[NASA-TM-83783] 01 p0102 N85-10683
ES devices at fair 08 p1141 N85-17187
Programmable realtime interface between a block floating point processor and memory
[AD-D011431] 08 p1203 N85-17571
Hardware math for the 6502 microprocessor
[NASA-TM-86517] 23 p3955 N85-34511
FLOATS
Air carrier overwater emergency equipment and procedures
[PB85-917006] 21 p3553 N85-32105
FLOCCULATING
Mechanism and process of flocculation by polymeric flocculant 09 p1303 N85-18185

FLOOD PLAINS
Deforestation, floodplain dynamics, and carbon biogeochemistry in the Amazon Basin
08 p1144 N85-17216
Application of hierarchical data structures to geographical information systems
[AD-A152169] 16 p2877 N85-27753
FLOOD PREDICTIONS
NESDIS operational precipitation estimation techniques 01 p0076 N85-10505
Short period forecasts in West Africa using Meteosat data 01 p0079 N85-10526
Parameterizing extreme still water levels and waves in design level studies
[IOS-183] 03 p0398 N85-12542
FLOODS
Paleohydrology and geomorphology of selected reaches of the upper Wabash Valley, Indiana
02 p0226 N85-11481
Heat sources in the tropics and large scale flow anomalies associated with precipitation anomalies in northeast Brazil
[INPE-3211-TDL/175] 04 p0538 N85-13421
Probable maximum flood estimation - Eastern United States
[AD-A146536] 06 p0839 N85-15324
Droughts and floods in South America due to the 1982-83 El Nino-southern oscillation episode
[INPE-3408-PRE/677] 09 p1357 N85-18535
Catastrophic-flood features in Swedish Lapland as a terrestrial analog for Martian channel flows
13 p2190 N85-23587
Flood-runoff forecasting with HEC1F
[AD-A154286] 19 p3300 N85-30456
Military hydrology. Report 9: State-of-the-art review and annotated bibliography of dam-breach flood forecasting
[AD-A155383] 22 p3801 N85-33553
FLOORS
Full-scale crash-test evaluation of two load-limiting subfloors for general aviation airframes
[NASA-TP-2380] 04 p0512 N85-13267
The development of a method for the shock-resistant securing of large batteries in submarines
09 p1335 N85-18391
Fire performance of interstitial space construction system
[NBSIR-85-3158] 20 p3436 N85-31318
Airborne sound transmission loss characteristics of wood-frame construction
[AD-A154174] 20 p3524 N85-31919
FLOQUET THEOREM
Application of Floquet theory to helicopter blade flapping stability
[AD-A154460] 19 p3218 N85-29952
FLORA
U PLANTS (BOTANY)
FLORIDA
Water resources data, Florida, water year 1982. Volume 4: Northwest Florida
[PB84-223445] 01 p0066 N85-10437
Revised Uniform Summary of Surface Weather Observations (RUSSWO). Parts A-F: Homestead AFB, Florida
[AD-A147203] 07 p1007 N85-16396
Surface pressure produced by Space Transportation System flight 41B
[AD-A150793] 14 p2242 N85-23901
Review and annotated bibliography of benthic studies in coastal and estuarine areas of Florida with a selected compilation of worldwide benthic methodological references and southeastern United States benthic taxonomic references
[PB85-151041] 16 p2822 N85-27405
FLOTATION
Investigations into the improvement of processing of Bolivian tin ores
[BMFT-FB-T-84-184] 07 p0917 N85-15807
Flotation tires and subsurface compaction
[AD-P004299] 09 p1409 N85-18876
Investigation of foam flotation and phase partitioning techniques 12 p1945 N85-22216
FLOTATION SYSTEMS
U FLOATS
FLOUR (FOOD)
Compilation of elemental concentration data for NBS (National Bureau of Standards) biological, geological and environmental standard reference materials, 1982
[PB84-218338] 01 p0025 N85-10156
FLOW CHAMBERS
Jet pump-drive system for heat removal
[NASA-CASE-NPO-16494-1-CU]
18 p3099 N85-29182
Fluidic angular velocity sensor
[NASA-CASE-NPO-16479-1-CU]
18 p3104 N85-29219
FLOW CHARACTERISTICS
NT BOUNDARY LAYER STABILITY
NT FLAME STABILITY
NT FLOW DISTRIBUTION
NT FLOW STABILITY
NT FLOW VELOCITY
NT MAGNETOHYDRODYNAMIC STABILITY
NT WEIBEL INSTABILITY
Coolant passage heat transfer with rotation
02 p0143 N85-10968
Vortex-generating coolant-flow-passage design for increased film-cooling effectiveness and surface coverage
[NASA-TP-2388] 03 p0361 N85-12314
Modelling the aerodynamics in a system of continuous channels and experimentation procedure
[BLL-M-35923-(5828.4)] 05 p0634 N85-14067
Analytical modeling of circuit aerodynamics in the new NASA Lewis wind tunnel
[NASA-TM-88912] 07 p0897 N85-15688
Flow of nitrogen-pressurized Halon 1301 in fire extinguishing systems
[NASA-CR-174271] 07 p0900 N85-15701
Turbulent bouyent flow and pressure variations around a circular cylinder in a cross uniform flow near the ground 09 p1316 N85-18287
Flow through very porous screens
[NASA-TP-2436] 11 p1631 N85-20270
A probe for direct measurement of flow direction
[ESA-TT-853] 11 p1637 N85-20310
TRACR3D: A model of flow and transport in porous/fractured media
[LA-9667-MS] 12 p1845 N85-21576
Calibration of wind tunnel flow quality
13 p1976 N85-22399
Hydraulic brakes for industrial robots
13 p2046 N85-22806
Design of piping for oil drain from turbine bearings
14 p2271 N85-24073
Analysis of selected problems involving vortical flows
[NASA-CR-177347] 15 p2463 N85-25212
Flow past a flat plat with a vortex/sink combination
[JIAA-TR-58] 15 p2464 N85-25215
The effect of air holes on combustor liner wall temperature profile: Experiments
[NAL-TR-840] 15 p2504 N85-25443
Flow through very porous inclined screens
[NASA-TM-86979] 15 p2565 N85-25761
Inviscid upwind finite difference model for two dimensional vertical axis wind turbines
15 p2585 N85-25933
Fuel and oxidizer turbine loss analysis
16 p2739 N85-26900
Analysis of the NASA/MSFC airborne Doppler lidar results from San Gorgonio Pass, California
[NASA-CR-3901] 16 p2832 N85-27463
New flow physical aspects in aerodynamics
[MBB-FE-122/S/PUB/138] 16 p2873 N85-27725
Dependence of characteristics of centrifugal magnetohydrodynamic conduction pump on electrical conductance of end walls. Part 1: Experiment
17 p2939 N85-28146
Transport characteristics of slurries in pipelines: Flow regimes and pressure drop
[DE85-009453] 18 p3101 N85-29198
Inferred flows of electric currents in solar active regions 18 p3208 N85-29899
Microgravity silicon zoning investigation
[NASA-CR-171531] 20 p3397 N85-31073
Flow characteristics of the Cascade granular blanket
[DE85-010932] 20 p3420 N85-31227
Flow modeling at the base region of missiles
[SNIAS-851-320-101] 20 p3420 N85-31228
Detailed studies of aviation fuel flowability
[NASA-CR-174936] 20 p3435 N85-31308
A comparison of two bench scale tests of fuel low temperature flow properties
[AD-A154477] 20 p3435 N85-31311
Transition in Turbines
[NASA-CP-2386] 20 p3452 N85-31433
Investigation of influence of gas exit modes on characteristics of N2O - N2 - He discharge laser
21 p3684 N85-32888
Compressible two-phase flow instabilities simulated with a hybrid Lagrange-Euler pseudospectral method
[DE85-009904] 23 p3931 N85-34361
FLOW CHARTS
Flowcharting with D-charts
[NASA-CR-175641] 14 p2402 N85-24806
A test methodology for an automated and interactive software development environment
[AD-A152857] 17 p3011 N85-28618
Resource management for the tagged token dataflow architecture
[AD-A154773] 21 p3667 N85-32779
A rational approach to cam design
23 p3923 N85-34311
FLOW COEFFICIENTS
Measurement of the development of the boundary layer in the annulus walls of a fourstage compressor
[CUED/A-TURBO-TR-121] 01 p0046 N85-10029
Analysis of experimental shaft seal data for high-performance turbomachines, as for Space Shuttle main engines
[NASA-TM-86928] 12 p1544 N85-21589
FLOW DEFLECTION
Turbulent flow around circular cylinder uniformly rotating in infinite incompressible fluid 14 p2277 N85-24109
FLOW DIRECTION INDICATORS
NT WIND VANES
Determination of corrections to flow direction measurements obtained with a wing-tip mounted sensor
[NASA-CR-174412] 10 p1421 N85-18982
Miniature electrooptical air flow sensor
[NASA-CASE-LAR-13065-1] 11 p1635 N85-20295
Determination of boundary line between reverse jet and surrounding stream 13 p2043 N85-22779
FLOW DISTORTION
On vortex bursting
[NASA-TM-77587] 01 p0002 N85-10008
Natural environment analysis
[NASA-CR-171333] 10 p1428 N85-19010
Experimental and analytical investigation of fan flow interaction with downstream struts
[NASA-CR-175756] 15 p2462 N85-25201
Development of artificially produced perturbations in supersonic boundary layer 21 p3683 N85-32879
FLOW DISTRIBUTION
Numerical analysis of the 3-dimensional inviscid hypersonic flow around capsule-type bodies by the alternate directional implicit method
[NAL-TR-799] 01 p0002 N85-10012
Computational methods for complex flowfields
[AD-A145219] 01 p0004 N85-10019
Measurement of the development of the boundary layer in the annulus walls of a fourstage compressor
[CUED/A-TURBO-TR-121] 01 p0046 N85-10029
Oil flow patterns of separated flow on a hemispherical cylinder at incidence
[DFVLR-FB-84-20] 01 p0048 N85-10033
Estuaries of the Cape. Part 2: Synposes of available information on individual systems. Report no. 19: Groot (WES) (CMS 23) and Sout (CMS 22)
[CSIR-RR-418] 01 p0087 N85-10598
Experimental trim drag values and flow-field measurements for a wide-body transport model with conventional and supercritical wings
[NASA-TP-2071] 02 p0135 N85-10880
Hot section laser anemometry
02 p0142 N85-10962
Jet array impingement flow distributions and heat transfer characteristics: Effects of initial crossflow and nonuniform array geometry 02 p0142 N85-10967
Energy efficient engine high pressure turbine test hardware detailed design report
[NASA-CR-167955] 02 p0147 N85-10985
An experimental study of jet impingement on a circular cylinder
[AD-A145583] 02 p0198 N85-11328
Problem of reduction to ideal wind tunnel in experimental aerodynamics 02 p0260 N85-11702
Navier-Stokes solution of 3-dimensional hypersonic afterbody flowfields over capsule-type vehicles
[NAL-TR-819] 03 p0311 N85-12010
Wind Tunnel Wall Interference Assessment and Correction, 1983
[NASA-CP-2319] 03 p0311 N85-12011
Wall interference measurements for three-dimensional models in transonic wind tunnels: Experimental difficulties 03 p0311 N85-12012
Survey of ONERA activities on adaptive-wall applications and computation of residual corrections
03 p0312 N85-12013
Investigations of flow field perturbations induced on slotted transonic-tunnel walls 03 p0312 N85-12016
NLR activities in the field of wind tunnel wall interference 03 p0313 N85-12024
Interaction between an airfoil and a streamwise vortex
[AD-A145823] 03 p0316 N85-12041
An inviscid computational method for supersonic inlets
[AD-A145997] 03 p0316 N85-12042
Structure and properties of titanium alloys after isothermal deformation at low speeds
03 p0351 N85-12280
Fluid layer between infinite elastic plates II. Distribution of power flow
[AD-A148690] 03 p0361 N85-12312
Fluid motion in a rotating and nutating container
[AD-A146175] 03 p0362 N85-12322

Laser velocimeter measurements and analysis in turbulent flows with combustion. Part 3: A correction lens for laser Doppler measurements in a cylindrical tube
[AD-A146208] 03 p0366 N85-12348

Terrestrial heat flow in Europe and general features of its regional distribution
[REPT-583] 03 p0377 N85-12406

Dynamic occlusion analysis in optical flow fields
[AD-A145805] 03 p0406 N85-12594

A study of flow past an airfoil with a jet issuing from its lower surface
[NASA-CR-168610] 04 p0451 N85-12860

Viscous-inviscid aerodynamic analysis of two-dimensional thrust augmentors
[NASA-CR-177321] 04 p0451 N85-12861

Development of computational fluid dynamics at NASA Ames Research Center
[NASA-TM-86021] 04 p0452 N85-12866

An experimental investigation of two-dimensional thrust augmenting ejectors, part 2
[NASA-CR-174110] 04 p0456 N85-12895

The preliminary checkout, evaluation and calibration of a 3-component force measurement system for calibrating propulsion simulators for wind tunnel models
[NASA-CR-174113] 04 p0458 N85-12903

Calibration and use of filter test facility orifice plates
[DE84-016851] 04 p0500 N85-13190

Model equations describing unsteady fluid motion
[ESA-TT-860] 04 p0501 N85-13194

Effect of two inner-ring oil-flow distribution schemes on the operating characteristics of a 35 millimeter bore ball bearing to 2.5 million DN
[NASA-TP-2404] 04 p0507 N85-13233

Magnetohydrodynamic and gasdynamic theories for planetary bow waves
[NASA-CR-174135] 04 p0589 N85-13760

Experimental studies of transonic airfoil trailing edge and wake flowfield properties 05 p0592 N85-13773

Flow Around Bluff Bodies: Numerical and Experimental Approaches — conferences
[VKI-LS-1984-06] 05 p0593 N85-13778

Flow around bluff bodies 05 p0593 N85-13779

Acceleration of bluff bodies through fluids
05 p0593 N85-13786

Direct numerical simulation of curved turbulent channel flow 05 p0635 N85-14072

Experiments on the structure of turbulent reattaching flow 05 p0635 N85-14074

Vaneless diffusers — flow in centrifugal compressors
05 p0637 N85-14084

Theoretical approach to labyrinth seal forces - cross-coupled stiffness of a straight-through labyrinth seal 05 p0643 N85-14127

Experimental investigation of lateral forces induced by flow through model labyrinth glands
05 p0643 N85-14128

Analysis of dynamic characteristics of fluid force induced by labyrinth seal 05 p0643 N85-14129

Friction and heat exchange in laminar and turbulent boundary layers with axisymmetrical bodies exposed to heterogeneous supersonic flow
05 p0724 N85-14655

A three-dimensional axisymmetric calculation procedure for turbulent flows in a radial vaneless diffuser
[NASA-TM-86903] 06 p0749 N85-14798

Analysis of physical-chemical processes governing SSME internal fluid flows
[NASA-CR-174245] 06 p0760 N85-14862

Special topics reports for the reference tandem mirror fusion breeder: Liquid metal MHD pressure drop effects in the pocket bed blanket, volume 1
[DE85-002142] 06 p0865 N85-15500

Supersonic nonlinear potential analysis
[NASA-CR-172456] 07 p0697 N85-15685

An exploratory study of finite difference grids for transonic unsteady aerodynamics
[NASA-TM-84583] 07 p0699 N85-15696

Analysis of the flow field about a T-45 using PANAIR
[AD-A146811] 07 p0699 N85-15699

Columbia: The first 5 flights entry heating data series. Volume 1: An overview
[NASA-CR-171820] 07 p0913 N85-15777

High altitude chemically reacting gas particle mixtures. Volume 1: A theoretical analysis and development of the numerical solution — rocket nozzle and orbital plume flow fields
[NASA-CR-171826] 07 p0916 N85-15801

High altitude chemically reacting gas particle mixtures. Volume 2: Program manual for RAMP2 — rocket nozzle and orbital plume flow fields
[NASA-CR-171827] 07 p0916 N85-15802

High altitude chemically reacting gas particle mixtures. Volume 3: Computer code user's and applications manual — rocket nozzle and orbital plume flow fields
[NASA-CR-171828] 07 p0917 N85-15803

Computational analysis of scramjet dual mode operation
[NASA-CR-174250] 07 p0956 N85-16060

Numerical reconstruction of part of an actual blast-wave flow field to agree with available experimental data
[UTIAS-TN-251] 07 p0956 N85-16061

Numerical studies of interacting vortices
[NASA-TM-86325] 07 p0957 N85-16062

Aero-optics experimental techniques
[AD-A146755] 07 p0957 N85-16067

Bulk cavitation caused by a plane shock wave
[AD-A147031] 07 p0958 N85-16072

Contamination and distortion of steady flow field induced by discrete frequency in aircraft gas turbines
[AD-A147092] 07 p0958 N85-16073

High Marangoni number convection in a square cavity
[NASA-CR-174283] 07 p0959 N85-16078

Calculation of the velocity field generated by a helicopter main and tail rotors in hover
[AD-A147731] 08 p1078 N85-16833

The orbiter air data system 08 p1094 N85-16912

Shuttle system ascent aerodynamic and plume heating 08 p1103 N85-16975

Aerothermal tests of a 12.5 percent cone at Mach 6.7 for various Reynolds numbers, angles of attack and nose shapes — conducted in Langley 8-foot high temperature tunnel
[NASA-TP-2345] 08 p1161 N85-17322

Computation of flow and heat transfer in flow around a 180 deg bend
[AD-A146065] 08 p1162 N85-17330

Steady flow model user's guide
[DE85-002001] 08 p1163 N85-17337

Genesis of unsteady separation
[AD-P004173] 09 p1266 N85-17958

Corrections for attached sidewall boundary-layer effects in 2-dimensional airfoil testing
[NASA-CR-3873] 09 p1272 N85-17997

Effect of jet exit vanes on flow pulsations in an open-jet wind tunnel
[NASA-TM-86299] 09 p1273 N85-17999

Theory of wing rock 09 p1282 N85-18064

Flow quality of NAL 2-dimensional transonic wind tunnel. Part 2: Extensive and systematic pressure fluctuations study in the settling chamber, test section and second throat of the NAL 2-D transonic wind tunnel
[NAL-TR-836-PT2] 09 p1283 N85-18066

On vortex transport in turbine channels
09 p1308 N85-18217

Analysis of sudden expansion flow in a two-dimensional duct with and without side-wall injection using the k-epsilon turbulence model 09 p1317 N85-18262

The boundary layer on compressor cascade blades
[NASA-CR-174369] 09 p1319 N85-18292

Force balance limiting current for charged particle beams
[DE84-016976] 09 p1381 N85-18685

Hydrodynamic flow structures in quantum field theory
[DE84-015513] 09 p1401 N85-18817

Aerodynamic improvements by discrete wing tip jets
[AD-A148981] 10 p1421 N85-18964

Capabilities of laser diagnostics for combustion and flow fields
[DE85-002861] 10 p1436 N85-19064

Theory of flammability limits. Flow gradient effects and flame stretch
[PB85-135077] 10 p1439 N85-19067

A shock wave capability for the improved Two-Dimensional Kinetics (TDK) computer program
[NASA-CR-171302] 10 p1483 N85-19360

A frozen vorticity approach to the axisymmetric strong interaction problem
[AD-A149101] 10 p1484 N85-19369

Averaging effects in models of three-dimensional two-phase flows
[AD-A149313] 10 p1484 N85-19371

Optimization of a ground coupled heat pump
[DE85-000273] 10 p1486 N85-19380

Mixing chemical reaction and flow field development in ducted rockets
[DE85-002710] 11 p1591 N85-20009

A mixed finite difference analysis of the internal and external transonic flow fields of inlets with centerbody
11 p1619 N85-20192

Flow through very porous screens
[NASA-TP-2436] 11 p1631 N85-20270

A new method for calculating the flow field in a dump combustor
[AD-A149305] 11 p1631 N85-20271

A study of degenerate and nondegenerate critical points in three-dimensional flow fields
[DFVLR-FB-84-36] 11 p1633 N85-20288

A study of eddy-mean flow interactions using Eliassen-Palm diagnostics: FGGE SOP-1 data and the NASA GLAS general circulation model compared
[NASA-CR-175508] 11 p1686 N85-20604

Reconstruction of a 3-dimensional transonic rotor flow field from holographic interferogram data
[NASA-TM-86680] 12 p1770 N85-21112

An investigation of turbulence mechanisms in V/STOL upwash flow fields
[AD-A149786] 12 p1772 N85-21123

Unsteady flows around 3-dimensional wings
[AD-A149993] 12 p1772 N85-21124

Investigation of flowfields found in typical combustor geometries
[NASA-CR-3869] 12 p1779 N85-21167

Aerodynamic behavior of ventilated wind tunnel walls
13 p1968 N85-22363

On the solution of the three-dimensional flowfield about a flow-through nacelle
[NASA-TM-87448] 13 p1969 N85-22371

Results of the AFRSI rewaterproofing systems screening test in the NASA/Ames Research Center (ARC) 2 x 2-foot transonic wind tunnel
[NASA-CR-167694] 13 p1988 N85-22467

HPFTP flow diverter analysis
[NASA-CR-171424] 13 p2091 N85-23057

Centrifuge impact cratering experiments
13 p2181 N85-23533

The nature of Martian flow ejecta craters
13 p2183 N85-23545

Interaction of Martian flow ejecta blankets with pre-existing impact craters: Morphological observations
13 p2183 N85-23546

Comparison of measured and computed boundary layers at the tail-end of an axisymmetric body in an air-jet
[AMTE(N)-TM-83053] 14 p2209 N85-23700

Estimating unsteady aerodynamic forces on a cascade in a three-dimensional turbulence field
[NASA-TM-86701] 14 p2209 N85-23704

Transonic merging separated flows
[AD-A150667] 14 p2213 N85-23724

Mixing, chemical reaction and flow field development in ducted rockets
[DE85-004083] 14 p2247 N85-23928

Experimental simulation of the flow inside a gun barrel
[ISL-CO-208/83] 14 p2302 N85-24252

Measurements in the flow field of a cylinder with a laser transit anemometer and a drag rake in the Langley 0.3 m transonic cryogenic tunnel
[NASA-TM-86389] 14 p2305 N85-24270

A study of the turbulent layer in the water at an air-water interface 14 p2378 N85-24679

A new implicit plus minus splitting method for the solution of the Euler equations in the transonic flow regime
15 p2461 N85-25200

A 3-dimensional Navier-Stokes-Euler code for blunt-body flow computations
[NASA-TM-58266] 15 p2463 N85-25211

An experimental study of hairpin-type vortices as a potential flow structure of turbulent boundary layers
15 p2553 N85-25751

The influence of jet-grid turbulence on heat transfer from the stagnation region of a cylinder in crossflow
[NASA-TM-87011] 15 p2554 N85-25760

Flow over a biconic configuration with an afterbody compression flap
[AD-A151862] 15 p2557 N85-25778

Viscous effects on blast wave flowfields
[AD-A152013] 15 p2558 N85-25779

Numerical analysis of supersonic reactive flow in wake of reverse step 15 p2643 N85-26303

An evaluation of proposed acoustic treatments for the NASA LaRC 4 x 7 meter wind tunnel
[NASA-CR-172577] 15 p2646 N85-26319

Navier-Stokes solution of hypersonic blunt-nosed body flowfields 16 p2693 N85-26624

The role of computational fluid dynamics in aeronautical engineering 16 p2694 N85-26629

A method for simulating 3-D aircraft flow fields with jet plume effects
[NASA-CR-175802] 16 p2699 N85-26664

Application of CFD techniques toward the validation of nonlinear aerodynamic models
[NASA-TM-86715] 16 p2700 N85-26671

Measurements in low pressure flow using an electronic beam detector — wind tunnel tests
16 p2701 N85-26676

Turbulence characteristics of swirling flowfields
[NASA-CR-174918] 16 p2709 N85-26717

Numerical analysis of flow non-uniformity in the hot gas manifold of the Space Shuttle main engine
16 p2738 N85-26899

Analysis of combustion oscillations in heterogeneous systems
[AD-A151999] 16 p2745 N85-26942

Simulation of interior ballistics flows in a shock tube
[ISL-CO-222/83] 16 p2784 N85-27183

Structural stability and bifurcation in conical flow fields
[VTH-LR-424] 16 p2803 N85-27282

Static and dynamic pressure measurements on a NACA 0012 airfoil in the Ames High Reynolds Number Facility
[NASA-TP-2485] 17 p2891 N85-27823
User's manual for airfoil flow field computer code SRAIR
[NASA-CR-172585] 17 p2891 N85-27825
Predictions and measurements of isothermal flowfields in axisymmetric combustor geometries
[NASA-CR-174916] 17 p2898 N85-27867
The gust simulation apparatus of the 3m x 3m low speed wind tunnel of the DFVLR in Goettingen, West Germany
[DFVLR-FB-85-04] 17 p2906 N85-27920
Simulation of multistage turbine flows
17 p2911 N85-27945
Unsteady flow in multistage turbines
17 p2911 N85-27946
Feasibility of mapping velocity flow fields in SSME powerhead by laser anemometry techniques
17 p2915 N85-27971
Proceedings of the 9th US Air Force and the Federal Republic of Germany Data Exchange Agreement Meeting. Viscous and Interacting Flow Field Effects
[AD-A153020] 17 p2958 N85-28266
Vortices in non-Newtonian fluids
[AD-A153169] 17 p2958 N85-28269
Numerical computation of space shuttle orbiter flow field
[NASA-CR-175912] 18 p3058 N85-28921
Transverse vorticity measurements using an array of four hot-wire probes
[FSFL-R-85-006] 18 p3099 N85-29184
On the origin of streamwise vortices in a turbulent boundary layer
[AD-A153651] 18 p3100 N85-29188
The method of residual minimization in compressible steady flows
[AD-A153924] 18 p3100 N85-29193
A model for the combustion of polymethyl methacrylate in air in a laminar diffusion flame
[VTH-LR-439] 18 p3165 N85-29606
Wake effects of the aerodynamic performance of horizontal axis wind turbines 19 p3211 N85-29915
Additional flow field studies of the GA(W)-1 airfoil with 30-percent chord Fowler flap including slot-gap variations and cove shape modifications
[NASA-CR-3887] 19 p3212 N85-29919
Vapor-screen technique for flow visualization in the Langley Unitary Plan Wind Tunnel
[NASA-TM-86384] 19 p3214 N85-29929
Turbine blade-tip clearance excitation forces
[NASA-CR-171534] 19 p3220 N85-29963
Flow field effects on nucleation in a reacting mixing layer
[ARL/AERO-R-165] 19 p3263 N85-30237
Highly accurate shock flow calculations with moving grids and mesh refinements, revision 1
[DE85-010929] 19 p3267 N85-30260
SANDRAG: A computer code for predicting drag of bodies of revolution at zero angle of attack in incompressible flow
[DE85-011170] 19 p3336 N85-30684
A theory of quasi-conical solutions of noninteger degree — flow fields on supersonic wings
[UTH-LR-420] 20 p3390 N85-31024
Mechanisms of exhaust pollutants and plume formation in continuous combustion
[AD-A154169] 20 p3435 N85-31310
An experimental investigation of confined, multiple, turbulent jet mixing with recirculation
20 p3451 N85-31426
Numerical and experimental investigation of turbomachinery rotor flow fields
20 p3451 N85-31429
Direct simulation techniques for the Boltzmann equation
[DFVLR-FB-85-13] 20 p3457 N85-31470
Geologic and hydrologic characterization and evaluation of the basin and range province relative to the disposal of high-level radioactive waste. Part 1: Introduction and guidelines
[GS-CIRC-904-A] 20 p3526 N85-31932
Geologic and hydrologic characterization and evaluation of the basin and range province relative to the disposal of high-level radioactive waste. Part 2: Geologic and hydrologic characterization
[GS-CIRC-904-B] 20 p3526 N85-31933
BLAF: A blast field reconstruction program from pressure histories
[AD-A155300] 21 p3585 N85-32283
Techniques for the study of gravity waves and turbulence (keynote paper), part 4 21 p3621 N85-32499
Calculation of steady and unsteady airfoil flow fields via the Navier-Stokes equations
[NASA-CR-3899] 22 p3727 N85-33105
Sandia Cooperative Group on the Aerothermochemistry of Turbulent Combustion. Discussion record of the second meeting
[DE85-007493] 22 p3743 N85-33203
Pressure correlations in turbulent reacting flows
22 p3744 N85-33205
Second order modelling in non-constant density flows
22 p3744 N85-33206
KRAK: A computer program for two-phase two-component porous flow and fracture
[LA-9703] 22 p3762 N85-33434
A three-dimensional viscous flow analysis for the helicopter tip vortex generation problem
[NASA-CR-3906] 23 p3893 N85-34114
A comparison of laser Doppler anemometry and probe measurements within the boundary layer of an airfoil at subsonic flow
[ISL-CO-219/84] 23 p3895 N85-34127
Prediction of the flow-field interference induced by the long-range laser velocimeter in the Ames 40- by 80-foot and the 80- by 120-foot wind tunnels
[NASA-TM-86763] 23 p3896 N85-34146
A three-dimensional turbulent boundary layer undergoing transverse strain and streamwise pressure gradient
[NASA-TM-86768] 23 p3930 N85-34358
Block-implicit calculations of three-dimensional laminar flow in strongly curved ducts
[DE85-003047] 23 p3931 N85-34363
Mathematical modeling of ultimate heat sink cooling ponds
[TI85-009747] 23 p3932 N85-34369
General design method for 3-dimensional, potential flow fields. Part 2: Computer program DIN3D1 for simple, unbranched ducts
[NASA-CR-3926] 24 p4060 N85-35159
Calculation of compressible flow about three-dimensional inlets with auxiliary inlets, slats and vanes by means of a panel method
[NASA-CR-174975] 24 p4060 N85-35162
The effect of power law body forces on a thermally-driven flow between concentric rotating spheres
[NASA-TM-87596] 24 p4093 N85-35374
The kinematic structure of cold frontal rainbands
24 p4119 N85-35531

FLOW EQUATIONS
NT HELMHOLTZ VORTICITY EQUATION
NT VORTICITY EQUATIONS
Second order modeling of scalar turbulent flows
03 p0360 N85-12311
Multigrid iteration solution procedure for solving two-dimensional sets of coupled equations
[DE84-016554] 04 p0555 N85-13533
Vectorizable multigrid algorithms for transonic flow calculations
[NASA-CR-174326] 06 p1077 N85-16827
Front tracking for gas dynamics
[DE85-000571] 08 p1163 N85-17336
Closure problem and numerical studies of turbulence
08 p1209 N85-17808
Numerical approach for the aerodynamic analysis if airfoils with laminar separation
[NASA-CR-172496] 09 p1273 N85-18001
Notes on compressible flow equations for thermodynamics of hot jets
[BAE-KRS-N-GEN-273] 09 p1318 N85-18289
An implicit, conservative, zonal-boundary scheme for Euler equation calculations
[NASA-CR-3865] 09 p1318 N85-18290
Accuracy of the finite analytic method for scalar transport calculations
[DE85-001474] 09 p1320 N85-18300
Nicolai maps and stochastic observables from a coupling constant flow
[BONN-HE-84-26] 09 p1376 N85-18653
Triple layer system for numerical integration of equations of gas dynamics and nonlinear heat conduction equation
[DE85-000297] 11 p1632 N85-20277
Evaluation of time integrators for the shallow water equations
[CWI-NM-R8406] 11 p1634 N85-20292
High order difference schemes with reduced dispersion for hyperbolic differential equations
[CWI-NM-R8408] 11 p1634 N85-20293
Space nuclear-power reactor design based on combined neutronic and thermal-fluid analyses
[DE85-002433] 11 p1727 N85-20864
Calculation of harmonic aerodynamic forces of aerofoils and wings from the Euler equations
15 p2458 N85-25177
Mathematical modeling of the AEDC (Arnold Engineering Development Center) propulsion wind tunnel (16T)
[AD-A151293] 15 p2475 N85-25275
Solution of Onsager's equation for a rotating compressible fluid in a multiply-connected domain
[DE85-007048] 16 p2784 N85-27178
Steady, incompressible, inviscid flow through a finite collapsible tube under longitudinal tension
[REPT-84-01] 17 p2959 N85-[illegible]
A second-order pressure-correction method for viscous incompressible flow
[REPT-84-15] 17 p2960 N85-[illegible]
Flow through finite collapsible tubes: A branching problem
[REPT-84-29] 17 p2960 N85-[illegible]
On Long's solution to hydrostatic flow over mountains
[DFVLR-MITT-84-02] 17 p2994 N85-[illegible]
Relaxation methods for hyperbolic equations
[REPT-84-20] 17 p3021 N85-[illegible]
Fluid modeling of magnetized plasmas
[DE85-007679] 17 p3039 N85-[illegible]
An investigation of hydraulic transients in combination free surface and pressurized flows
19 p3264 N85-[illegible]
Use of a two-dimensional flow model to quantify aquatic habitat
[AD-A154287] 19 p3266 N85-30[illegible]
An implicit finite-difference code for a two-equation turbulence model for three-dimensional flows
[NASA-TM-86752] 20 p3454 N85-314[illegible]
Some remarks on the constitutive equations of stratified gas-liquid flow
[EME-137] 20 p3456 N85-314[illegible]
Optimization of a numerical method to calculate elliptic flows
[ESA-TT-889] 20 p3457 N85-31472
The calculation of fully three dimensional flow through any type of turbomachine blade row
21 p3587 N85-32[illegible]
Tabular and graphical solutions of regular and Mach reflections in pseudo-stationary frozen and vibrational-equilibrium flows, part 1
[UTIAS-283-PT-1] 23 p3893 N85-34117
Tabular and graphical solutions of regular and Mach reflections in pseudo-stationary frozen and vibrational-equilibrium flows, part 2
[UTIAS-283-PT-2] 23 p3894 N85-34118

FLOW FIELDS
U FLOW DISTRIBUTION

FLOW GEOMETRY
Geometric characteristics of turbulent boundary layer separation upon action with direct shock wave in conical flows 02 p0269 N85-11785
An improved computer model for prediction of axial gas turbine performance losses
[NASA-CR-174246] 07 p0904 N85-15724
TRACR3D: A model of flow and transport in porous/fractured media
[LA-9667-MS] 12 p1645 N85-21576
Grid generation for a pump collector
[AD-A150217] 13 p2092 N85-23[illegible]
Numerical calculation of subsonic jets in crossflow with reduced numerical diffusion
[NASA-TM-87003] 15 p2472 N85-25[illegible]
Computational aerodynamics in designing aircraft
16 p2693 N85-26[illegible]
Boundary layer and parabolic flows
[DFVLR-FB-84-46] 17 p2960 N85-28[illegible]

FLOW MEASUREMENT
Pressure distribution on a swept wing aircraft in flight
01 p0004 N85-10[illegible]
Measurement of the development of the boundary layer in the annulus walls of a fourstage compressor
[CUED/A-TURBO-TR-121] 01 p0046 N85-10[illegible]
Development in UK of a method for calculating tunnel wall corrections from flow measurements
03 p0314 N85-120[illegible]
Comparative review of laser Doppler and laser two-focus anemometry in turbomachinery applications
[VKI-TM-34] 03 p0367 N85-12[illegible]
Study of the structure of turbulent shear flows at supersonic speeds and high Reynolds number
[NASA-CR-174144] 04 p0452 N85-12[illegible]
Magnetic inductive flowmeter for low conducting liquids
[BMFT-FB-T-84-136] 04 p0504 N85-13216
Flow Around Bluff Bodies: Numerical and Experimental Approaches — conferences
[VKI-LS-1984-06] 05 p0593 N85-13778
Experimental techniques and instrumentation for bluff body aerodynamics 05 p0593 N85-13781
Experimental observation of the flow in impellers and diffusers — centrifugal compressors
05 p0636 N85-140[illegible]
Turbulence measurement interferometer apparatus
[AD-D011377] 07 p0970 N85-161[illegible]
Investigation of the ice dynamics in the marginal ice zone
[AD-A146729] 07 p1009 N85-16411
Advanced diagnostics for reacting flows
[AD-A148479] 08 p1162 N85-17[illegible]

Halogen mass flow rate detection system
[AD-D011398] 08 p1166 N85-17352
Experimental study of aerodynamic shielding of turbojet engine air intake against exhaust gases
09 p1307 N85-18210
Modeling turbulent flow in compressible fluids: Metrological aspects — conferences
11 p1575 N85-19926
Comparison of two-dimensional laser and hot-wire velocimetry for a supersonic turbulent boundary layer
11 p1576 N85-19927
Characterization of jet turbulence using infrared radiometry
11 p1576 N85-19928
Laser Raman techniques for studying flows and flames
11 p1576 N85-19929
Velocity and volumetric measurement in free jets
11 p1576 N85-19931
Laser Doppler Anemometry (LDA) signal triggering and effective particle size range
[KU-SFB-210/E/5] 11 p1634 N85-20290
Miniature electrooptical air flow sensor
[NASA-CASE-LAR-13065-1] 11 p1635 N85-20295
Examples of environment services: Hydrological and pollution measurements in the Po River (Italy)
[CISE-2299] 11 p1679 N85-20578
Liquid mass flow rate computer
13 p2075 N85-22962
Turbulent flows of surfacant solutions
[AD-B089137L] 13 p2092 N85-23058
Mean flow and turbulence in complex terrain NPS (Naval Postgraduate School)/Vandenberg measurement system
[AD-A150184] 13 p2138 N85-23274
Field measurements of the 1983 Royal Gardens lava flows, Kilauea Volcano, and 1984 Mauna Loa lava flows, Hawaii 13 p2186 N85-23565
Calibration of sonic valves for the laminar flow control, leading-edge flight test
[NASA-TP-2423] 14 p2210 N85-23707
Advanced diagnostics for reacting flows
[AD-A150675] 14 p2301 N85-24246
Experimental and analytical investigation of fan flow interaction with downstream struts
[NASA-CR-175756] 15 p2462 N85-25201
Measurements in low pressure flow using an electronic beam detector — wind tunnel tests
16 p2701 N85-26676
Measurements of two-phase exhaust flow parameters of a small caliber gun associated with muzzle flash phenomena
[ISL-CO-212/83] 16 p2784 N85-27182
Vibration-free Raman Doppler velocimeter
[NASA-CASE-LAR-13268-1] 18 p3104 N85-29216
Use of a two-dimensional flow model to quantify aquatic habitat
[AD-A154287] 19 p3286 N85-30253
Accuracy in determining velocity of fluid movement by Doppler method 19 p3293 N85-30419
Measurement and analysis of two-phase flow through low permeability media, task 3
[PB85-168373] 20 p3435 N85-31313
Velocity visualization in gaseous flows
[NASA-CR-174854] 20 p3453 N85-31445
Study of requirements for and method of multidimensional acoustic imaging — spaceborne experiments
[ESA-CR(P)-2020] 20 p3525 N85-31924
Injection of drag reducing additives into turbulent water flows: Two-component velocity measurements and mixing length model predictions
[AD-A154604] 21 p3563 N85-32274
Laser Doppler Anemometer (LDA) measurements in the turbulent near-wake of blunt bodies
[ISL-CO-212/84] 22 p3785 N85-33450
Measurement of velocity and concentration in free jets
[ISL-CO-215/84] 22 p3786 N85-33451
Improved flow cytometer measurement of binding assays
[DE85-006407] 23 p3935 N85-34390
FLOW PATTERNS
U FLOW DISTRIBUTION
FLOW RATE
U FLOW VELOCITY
FLOW REGULATORS
Research and development for semi-spherical inflow control device
[NAL-TR-833] 09 p1281 N85-18056
Flow through very porous inclined screens
[NASA-TM-86970] 15 p2555 N85-25761
Combined riblet and LEBU drag reduction system
[NASA-CASE-LAR-13286-1] 18 p3058 N85-28922
Fluidized bed desulfurization
[NASA-CASE-NPO-15824-1] 24 p4075 N85-35253
FLOW RESISTANCE
NT AERODYNAMIC DRAG
NT FRICTION DRAG
NT VISCOUS DRAG
Turbulent flows of surfacant solutions
[AD-B089137L] 13 p2092 N85-23058
FLOW SEPARATION
U BOUNDARY LAYER SEPARATION
U SEPARATED FLOW
FLOW STABILITY
NT BOUNDARY LAYER STABILITY
NT FLAME STABILITY
NT MAGNETOHYDRODYNAMIC STABILITY
NT WEIBEL INSTABILITY
On vortex bursting
[NASA-TM-77587] 01 p0002 N85-10008
Stability of fluid flow in a cylindrical annulus
[NASA-TM-77720] 01 p0046 N85-10300
Computation of the nonequilibrium flow in a gasdynamic laser
[AD-A141022] 04 p0505 N85-13224
Experiences with nonsynchronous forced vibration in centrifugal compressors 05 p0642 N85-14119
Preliminary investigation of labyrinth packing pressure drops at onset of swirl-induced rotor instability
05 p0644 N85-14132
Stability of lubricant film in gas dynamic bearing
06 p0778 N85-14977
Stability of rigid motions and rollers in bicomponent flows of immiscible liquids
[AD-A147302] 07 p0960 N85-16081
An experimental study on the instability of a mixing-layer with laminar wake as the initial condition
08 p1076 N85-16824
Flow instabilities in transonic small disturbance theory
[NASA-TM-86251] 09 p1273 N85-18000
Acoustic energy balance method
13 p2000 N85-22537
Lyapunov stability of very simple steady solutions of prognostic systems 14 p2333 N85-24429
Stability calculations of the two-dimensional boundary layer along a concave wall: Part 1: A numerical method of solution for the simultaneous ordinary differential equations governing disturbances
[NAL-TR-841] 15 p2554 N85-25758
Instability of solar wind near streamlined bodies
16 p2720 N85-26794
Vortex shedding flowmeters for liquids at high flow velocities 16 p2740 N85-26906
A numerical study of nonspherical black hole accretion 16 p2881 N85-27780
Generation of capillary instabilities by external disturbances in a liquid jet
[NASA-TM-87041] 19 p3265 N85-30246
Development of thermoconvective instabilities in porous media. Influence of boundary conditions
20 p3456 N85-31461
Moist barotropic instability in the tropics
20 p3489 N85-31683
Experiments on the influence of active walls on the initial amplitudes and growths of instability waves
[AD-A154630] 21 p3583 N85-32275
Instability and chaotic behavior in a free-surface flow
[AD-A154879] 21 p3584 N85-32279
Stability of implosion dynamics
23 p3980 N85-34680
Couette flow of two fluids between concentric cylinders
[AD-A155827] 24 p4093 N85-35376
FLOW THEORY
NT MIXING LENGTH FLOW THEORY
Magnetohydrodynamic and gasdynamic theories for planetary bow waves
[NASA-CR-174135] 04 p0589 N85-13760
Acceleration of bluff bodies through fluids
05 p0593 N85-13786
Wave propagation in compliant tubes containing a heat-conducting viscous fluid
[WTHD-163] 05 p0638 N85-14094
Flow-based analyses of metal deformation processes: An overview 06 p0796 N85-15087
Investigation of the local mass transfer of a laminar and turbulent falling liquid film
[BLL-T6368/BG/WH792/84] 06 p0807 N85-15130
The stability of an infinite elastic pipe with uniform mean flow
[AD-A146686] 08 p1161 N85-17326
Large deformations of a nonlinear elastic solid and the diffusion of an ideal fluid treated as interacting continua
09 p1330 N85-18356
Study proposal for the possible use of ISS as an aerodynamic facility for aerospace applications
11 p1646 N85-20374
Computational aerodynamics in designing aircraft
16 p2693 N85-26622
La Recherche Aerospatiale Bimonthly Bulletin Number 1984-2, 219/March-April
[ESA-TT-878] 16 p2694 N85-26635
Conical stagnation points in the flow around an external corner — delta wings
[VTH-LR-396] 16 p2701 N85-26680
New flow physical aspects in aerodynamics
[MBB-FE-122/S/PUB/133] 16 p2873 N85-27725
Calculation of viscous compressible flows in small gas turbines 17 p2912 N85-27950
Boundary layer and parabolic flows
[DFVLR-FB-84-46] 17 p2960 N85-28285
Progress in the development of a two-fluid model of turbulence: A set of 42 lecture panels
[CFD/84/20] 20 p3457 N85-31469
Explosion in flight 21 p3683 N85-32883
A curvilinear coordinate method for the solutions of initial value problems using the third-order upwind differencing scheme
[IPPJ-734] 23 p3975 N85-34642
Bibliography on tidal hydraulics. Report 2. Supplement 9: Supplementary material compiled from June 1980 - June 1983. Tidal flows in rivers and harbors
[AD-A155990] 24 p4125 N85-35574
FLOW VELOCITY
NT SOLAR WIND VELOCITY
Water resources data for Michigan, water year 1983
[PB84-225176] 01 p0066 N85-10442
Chemical vapor deposition of amorphous silicon films produced by using higher order silanes
[DE84-004519] 01 p0123 N85-10647
Laser anemometer optimization
02 p0142 N85-10963
Characteristics of a turbulent plane offset jet
02 p0196 N85-11310
Some of the features of movement of gas through a layer of free-flowing substances
[BLL-M-35732-(5828.4)] 02 p0196 N85-11312
NLR activities in the field of wind tunnel wall interference 03 p0313 N85-12024
Flow around bluff bodies 05 p0593 N85-13779
A finite element method for three dimensional cavity circulation 05 p0635 N85-14071
Flow rates and pressure profiles for one to four axially aligned Borda inlets
[NASA-TP-2390] 05 p0636 N85-14078
Plasma and magnetospheric research
[NASA-CR-171293] 08 p1183 N85-17451
Studies on reactive mufflers. Part 2: Mufflers with air flow 09 p1303 N85-18184
Determination of total pressure losses in stepped annular diffusors with curvilinear outer walls and uniform velocity field at inlet 09 p1306 N85-18203
Influence of secondary flow rate on dynamic stresses in turbine rotor blades 09 p1306 N85-18205
Long range effect of turbulent pressure pulsations in plane-parallel flows at different velocities with various flame fronts 09 p1308 N85-18220
Developing a flowmeter for streams with high solids content
[DE84-016643] 09 p1323 N85-18316
Optical flow and texture variables useful in detecting decelerating and accelerating self-motion
[AD-A148718] 09 p1384 N85-18703
Critical velocities in He II for independently varied superfluid and normal fluid velocities
09 p1396 N85-18784
Velocity measurements in a 3D shock wave laminar boundary layer interaction. Part 1: Low speed 2D LDV measurements
[AD-A149533] 10 p1485 N85-19373
Computation of the inviscid velocity potential for general ellipsoids on a nearly quadratic surface grid
[REPT-25/84] 11 p1633 N85-20287
Preliminary analysis of tone-excited two-stream jet velocity decay
[NASA-TM-86951] 12 p1770 N85-21114
Liquid mass flow rate computer
13 p2075 N85-22962
Turbulence measurements in shock induced flows
13 p2091 N85-23055
Hydraulic characteristics of reduction installation valves 14 p2289 N85-24080
Heat transfer to vertical flat plates in a rectangular gas fluidized bed
[AD-A150785] 14 p2301 N85-24248
Modeling longitudinal motions of thermal O+ and H+ ions in magnetic field tube convective through daytime polar cusp 15 p2481 N85-25314
An experimental technique for the study of velocity profiles in a laminar jet using a pulsed nitrogen laser
[AD-A151496] 15 p2556 N85-25771
Fuel and oxidizer turbine loss analysis
16 p2739 N85-26900
Vortex shedding flowmeters for liquids at high flow velocities 16 p2740 N85-26906
Aerodynamic forces developing in channels between vanes in turbine drive wheels 16 p2765 N85-27062

Flow rate and pressure profiles for 1 to 4 axially alined orifice inlets
[NASA-TP-2460] 16 p2782 N85-27165
Supersonic flow around blunt wedge
17 p2942 N85-28158
Flow quality of National Aerospace Laboratory two-dimensional transonic wind tunnel. Part 3: Flow turbulence level and measuring method
[NAL-TR-842-PT-3] 18 p3064 N85-28952
Burner rig corrosion of SiC at 1000 deg C
[NASA-TM-87061] 19 p3227 N85-30011
Transient combustion dynamics
[AD-A154430] 19 p3235 N85-30052
Improved fluid flow meter for measuring the rate of fluid flow in a conduit
[NASA-CASE-MFS-28030-1] 19 p3271 N85-30296
Accuracy in determining velocity of fluid movement by Doppler method 19 p3293 N85-30419
Combustor turbulence 20 p3452 N85-31434
Preliminary results of a study of the relationship between free-stream turbulence and stagnation region heat transfer 20 p3452 N85-31435
Transition in a disturbed environment
20 p3452 N85-31436
Velocity visualization in gaseous flows
[NASA-CR-174954] 20 p3453 N85-31445
A panel method study of vortex sheets with special emphasis on sheets of axisymmetric geometry
[NASA-CR-177365] 21 p3552 N85-32095
A comparison of laser Doppler anemometry and probe measurements within the boundary layer of an airfoil at subsonic flow
[ISL-CO-219/84] 23 p3895 N85-34127
Flow modifying device
[NASA-CASE-LEW-13562-2] 24 p4065 N85-35195
The use of a laser Doppler velocimeter in a standard flammability tube
[NASA-CR-174960] 24 p4096 N85-35369

FLOW VISUALIZATION
NT NUMERICAL FLOW VISUALIZATION
On vortex bursting
[NASA-TM-77587] 01 p0002 N85-10008
Pressure distributions measured on research wing M86 mounted on an axisymmetric body
01 p0004 N85-10024
Oil flow patterns of separated flow on a hemispherical cylinder at incidence
[DFVLR-FB-84-20] 01 p0048 N85-10313
Three dimensional separation and vortex formation
02 p0196 N85-11308
New approaches to hydrodynamic flow visualization on surfaces
[AD-A145528] 02 p0198 N85-11324
Preliminary results using a rapid photographic wake traverse system — in a wind tunnel
[RAE-TM-AERO-1987] 02 p0200 N85-11332
Experiences with a high-blockage model tested in the NASA Ames 12-foot pressure wind tunnel
03 p0315 N85-12032
Flow visualization study of a vortex-wing interaction
[NASA-TM-86656] 03 p0316 N85-12040
The role of freestream turbulence scale in subsonic flow separation
[NASA-CR-174172] 04 p0452 N85-12870
An experimental investigation of the parallel blade-vortex interaction
[NASA-TM-86005] 05 p0592 N85-13777
A collection of flow visualization techniques used in the Aerodynamic Research Branch
[NASA-TM-85998] 06 p0808 N85-15135
Channel constructed to provide well defined boundary layers for vorticity optical probe measurements
[AD-A146679] 06 p0809 N85-15140
Investigation of light source and scattering medium related to vapor-screen flow visualization in a supersonic wind tunnel
[NASA-TM-86290] 06 p0810 N85-15144
Unsteady flow characteristics in the near-wake of a two-dimensional obstacle
[NASA-TM-77762] 07 p0897 N85-15684
Unsteady pressure measurements on a biconvex airfoil in a transonic oscillating cascade
[NASA-TM-86914] 07 p0898 N85-15689
A 3-dimensional turbulent boundary layer upstream and around a junction vortex flow 08 p1160 N85-17319
Advanced diagnostics for reacting flows
[AD-A148479] 08 p1162 N85-17334
Simultaneous flow visualization and unsteady lift measurement on an oscillating lifting surface
[AD-P004157] 09 p1264 N85-17942
A visual study of a delta wing in steady and unsteady motion
[AD-P004158] 09 p1264 N85-17943
Comparative visualization of accelerating flow around various bodies, starting from rest
[AD-P004159] 09 p1264 N85-17944
Unsteady separated flows: Generation and use by insects
[AD-P004168] 09 p1266 N85-17953
Aerodynamic improvements by discrete wing tip jets
[AD-A148961] 10 p1421 N85-18964
Capabilities of laser diagnostics for combustion and flow fields
[DE85-002861] 10 p1438 N85-19064
Mixing characteristics of an underexpanded multiple jet ejector
[AD-A149557] 10 p1485 N85-19375
Momentum and heat transfers in a complex, but well-defined turbulent fluid flow
[DE85-002857] 10 p1486 N85-19381
Flow visualization study of the effect of injection hole geometry on an inclined jet in crossflow
[NASA-TM-86936] 11 p1631 N85-20269
Experimental investigation of a pulse combustor: Flow visualization by Schlieren photography
[DE85-002862] 11 p1636 N85-20304
Use of laser flow visualization techniques in reactor component thermal-hydraulic studies
[DE84-014766] 11 p1639 N85-20330
Unsteady flows around 3-dimensional wings
[AD-A149993] 12 p1772 N85-21124
Continuous laminar smoke generator
[NASA-CASE-LAR-13014-1] 12 p1781 N85-21176
Experimental studies of Quasi-Two-Dimensional and three-dimensional viscous interaction regions induced by skewed-shock and swept-shock boundary layer interactions
[AD-A150080] 12 p1847 N85-21587
Deflected jet experiments in a turbulent combustor flowfield
[NASA-CR-174863] 13 p1973 N85-22390
An experimental investigation of the chopping of helicopter main rotor tip vortices by the tail rotor
[NASA-CR-177338] 13 p2154 N85-23376
Stability of vortex structures during separation flow past array of wings 14 p2278 N85-24110
Advanced diagnostics for reacting flows
[AD-A150675] 14 p2301 N85-24246
Fluid mechanics and heat transfer spirally fluted tubing
[AD-A150774] 14 p2301 N85-24247
Experimental simulation of the flow inside a gun barrel
[ISL-CO-206/83] 14 p2302 N85-24252
Visualization of velocity fields with Doppler images
[ISL-CO-218/83] 14 p2302 N85-24256
Experimental and theoretical investigation of the motion of particles in a compressible vortex
[ISL-R-129/83] 14 p2303 N85-24264
Modifications to the nozzle test chamber to extend nozzle static-test capability
[NASA-TM-86368] 15 p2464 N85-25216
An experimental study of hairpin-type vortices as a potential flow structure of turbulent boundary layers
15 p2553 N85-25751
An experimental investigation of unexcited and excited elliptic jets 15 p2554 N85-25755
An experimental technique for the study of velocity profiles in a laminar jet using a pulsed nitrogen laser
[AD-A151496] 15 p2556 N85-25771
Simulation of interior ballistics flows in a shock tube
[ISL-CO-222/83] 16 p2784 N85-27183
Convective storm downdraft outflows detected by NASA/MSFC's Airborne 10.6 micron pulsed Doppler Lidar System
[NASA-CR-3898] 17 p2995 N85-28511
Multi-ducted inlet combustor research and development
[AD-A153753] 18 p3063 N85-28946
Lee-side flow over delta wings at supersonic speeds
[NASA-TP-2430] 19 p3212 N85-29921
Vapor-screen technique for flow visualization in the Langley Unitary Plan Wind Tunnel
[NASA-TM-86384] 19 p3214 N85-29929
Density and confinement effects on mixing characteristics of an axisymmetrical CO(2) jet
[AD-A154468] 19 p3267 N85-30258
Flow visualization study of inverted annular flow of post dryout heat transfer region
[DE85-010482] 19 p3269 N85-30275
An experimental investigation of confined, multiple, turbulent jet mixing with recirculation
20 p3451 N85-31426
Preliminary results of a study of the relationship between free-stream turbulence and stagnation region heat transfer 20 p3452 N85-31435
Velocity visualization in gaseous flows
[NASA-CR-174954] 20 p3453 N85-31445
Two-phase flow visualization in a transparent, atmospheric pressure, boiling water loop
[DE84-016857] 21 p3586 N85-32208
Computer and water-model simulation of flow through poppet valves
[CFD/85/2] 22 p3785 N85-33449
Experimental simulation of in-bore flows using a high pressure shock tube
[ISL-CO-217/84] 22 p3785 N85-33
Circulation control lift generation experiment: Hardware development 22 p3799 N85-33
The influence of helicopter tail shape on drag: An aerodynamic study using a low speed wind tunnel
[AD-A156304] 24 p4062 N85-35

FLOWMETERS
NT GAS METERS
NT HOT-WIRE FLOWMETERS
NT RHEOMETERS
Magnetic inductive flowmeter for low conducting liquids
[BMFT-FB-T-84-136] 04 p0504 N85-13216
Dynamic response of electromagnetic current meters
[PB84-229731] 06 p0842 N85-1534
Flow measurement device
[AD-D011432] 08 p1168 N85-17
Developing a flowmeter for streams with high solids content
[DE84-016643] 09 p1323 N85-18
Miniature electrooptical air flow sensor
[NASA-CASE-LAR-13065-1] 11 p1635 N85-20
State-of-charge coulometer
[NASA-CASE-NPO-15759-1] 12 p1849 N85-21
Field-work report: Medway Estuary, 28 June - 18 July 1983
[RNC/NS/TR8] 13 p2041 N85-227
Vortex shedding flowmeters for liquids at high flow velocities 16 p2740 N85-2
Improved fluid flow meter for measuring the rate of fluid flow in a conduit
[NASA-CASE-MFS-28030-1] 19 p3271 N85-30
MHD generator CDIF
[DE85-011389] 20 p3536 N85-32
IEA-SSPS CRS calibration report: Calibration of relevant measuring sensors
[DE85-010174] 22 p3788 N85-33
Acoustic cross-correlation flowmeter for solid-gas flow
[DE85-005688] 23 p3935 N85-34

FLUCTUATION
U VARIATIONS

FLUCTUATION THEORY
Range fluctuations of high energy muons passing through matter
[HE-5.2-19] 24 p4204 N85-36

FLUE GASES
Comparative usefulness of flue gas oxygen and carbon dioxide analysis
[BLL-TRANS-T6356/BG/WH783/84]
08 p1179 N85-174
Components of the combustion gases of propellant charge powders after reaction in the high pressure bomb in the pressure range up to 1000 MPa. Part 1: Nitroglycerine powder GB Pa 125
[ISL-CO-217/83-PT-1] 14 p2264 N85-2
Development of corrosion resistant heat exchangers for flue gas desulfurization
[BMFT-FB-T-84-281] 18 p3103 N85-2
Evaluation of the Santee limestone for use in flue-gas desulfurization systems
[DE85-901277] 19 p3249 N85-3014
Evaluation of pilot ESP used with a spray dryer FGD system at Pittsburgh Energy Technology Center, Bruceton, Pennsylvania
[DE85-011151] 22 p3748 N85-33217

FLUENCE
Critical assessment of low fluence irradiation creep mechanisms
[DE84-015578] 02 p0184 N85-112
Beam profiling in gigawatt 1064-nm lasers used in research on optical materials at Livermore
[DE84-087226] 04 p0505 N85-13
Structure and properties of ion-implanted Al sub 2 O sub 3
[DE85-005374] 14 p2430 N85-24
Incorporation of Monte Carlo electron interface studies into photon general cavity theory
[DE85-007674] 17 p3034 N85-2877
Solar flare gamma-ray line spectroscopy
[SH-2.1-14] 23 p3999 N85-347

FLUID AMPLIFICATION
U FLUID AMPLIFIERS

FLUID AMPLIFIERS
Design guide for fluidic laminar proportional amplifiers and laminar jet angular rate sensors
[AD-A147730] 08 p1161 N85-17

FLUID BOUNDARIES
NT GAS-SOLID INTERFACES
NT JET BOUNDARIES
NT LIQUID-LIQUID INTERFACES
NT LIQUID-SOLID INTERFACES
NT LIQUID-VAPOR INTERFACES
Instability of film boiling of moving liquids
[BLL-WH-603-(9091.9F)] 07 p0858 N85-16

Perturbation of a multiple eigenvalue in the Benard problem for two fluid layers
[AD-A148068] 10 p1546 N85-19745

Application of the MHD energy principle to magnetostatic atmospheres
[NASA-CR-176987] 18 p3136 N85-29420

An investigation of hydraulic transients in combination free surface and pressurized flows
19 p3264 N85-30239

The Konstantinov effect and absorption of sound in inhomogeneous media 21 p3680 N85-32661

FLUID DYNAMICS
NT AERODYNAMICS
NT AEROTHERMODYNAMICS
NT COMPUTATIONAL FLUID DYNAMICS
NT CYLINDRICAL PLASMAS
NT ELASTOHYDRODYNAMICS
NT ELECTROHYDRODYNAMICS
NT GAS DYNAMICS
NT HYDRODYNAMICS
NT INTERACTIONAL AERODYNAMICS
NT MAGNETOHYDRODYNAMICS
NT RAREFIED GAS DYNAMICS
NT ROTONS
NT ROTOR AERODYNAMICS
NT SUPERSONICS
NT VORTEX SHEDDING

The properties of plane turbulent buoyant jet
[NAL-TR-796] 01 p0046 N85-10304

Highlights of the Institute of Sound and Vibration Research 01 p0131 N85-10905

Further development of a transonic cascade analysis
[AD-A145410] 02 p0198 N85-11319

USSR report: Physics and mathematics
[JPRS-UPM-84-004] 02 p0266 N85-11737

AGARD bulletin technical programme, 1985
[AGARD-BUL-84-2] 02 p0305 N85-11971

Report of the Department of Aerospace Engineering
03 p0307 N85-11977

Fluid motion in a rotating and nutating container
[AD-A146175] 03 p0362 N85-12322

Report of the Division of Atmospheric Physics, 1980-1983 03 p0391 N85-12501

Flow in Centrifugal Compressors — conferences
[VKI-LS-1984-07] 05 p0636 N85-14079

Salt-gradient solar ponds: Summary of US Department of Energy sponsored research
[NASA-CR-174183] 06 p0667 N85-14286

Solar pond fluid dynamics and heat transfer
05 p0667 N85-14288

Intraocular fluid dynamics in microgravity
05 p0693 N85-14455

USSR report: Physics and mathematics
[JPRS-UPM-84-007] 05 p0729 N85-14651

A method for solving the inverse problem of transonic cascade flow
[AD-A146739] 07 p0899 N85-15688

Dynamical characteristics of weak turbulence
[AD-A147166] 07 p0959 N85-16075

Solution of partial differential equations on vector and parallel computers
[NASA-CR-172500] 07 p1028 N85-16525

Advanced diagnostics for reacting flows
[AD-A148479] 08 p1162 N85-17334

Researched applied to transonic compressors in numerical fluid mechanics of inviscid flow and viscous flow
[NASA-CR-174363] 09 p1319 N85-18291

Solution of the h-equation for a single point source emission of magnitude K
[DE84-017574] 09 p1374 N85-18636

Materials physics
[DE84-017103] 09 p1377 N85-18658

Effect of alpha particles on the stability of Elmo Bumpy Torus (EBT) reactor
[DE84-017206] 09 p1392 N85-18758

Summer study program in geophysical fluid dynamics, the Woods Hole Oceanographic Institution, dynamic differentiation
[AD-A148386] 10 p1521 N85-19595

Fluid temperature and concentration gradient measurement study — for spaceborne experiments
[CISE-R/FL/1/04] 11 p1637 N85-20309

MAP in India 11 p1655 N85-20424

The Middle Atmosphere Program: A special project for the Antarctic Middle Atmosphere (AMA)
11 p1656 N85-20430

Three-dimensional baroclinic instability of a Hadley cell for small Richardson number
[NASA-TP-2450] 11 p1687 N85-20605

Advanced research and technology programs for advanced high-pressure oxygen-hydrogen rocket propulsion
[NASA-TM-86966] 12 p1769 N85-21231

Numerical studies of fluid spin-up from rest in a partially-filled cylinder
[AD-A150079] 12 p1847 N85-21586

Analysis of the NASA/MSFC Airborne Doppler Lidar results from San Gorgonio Pass, California
[NASA-CR-171355] 12 p1892 N85-21873

Research Reports: 1984 NASA/ASEE Summer Faculty Fellowship Program
[NASA-CR-171317] 12 p1944 N85-22210

A study of the compatibility of an existing CFD package with a broader class of material constitutions
12 p1945 N85-22219

Evaluation of PHOENICS as a design analysis tool for SSME 12 p1949 N85-22240

Oversight review of the five-year outlook report on science and technology
[GPO-41-058] 12 p1949 N85-22243

Current problems in turbomachinery fluid dynamics
[AD-A150639] 13 p1974 N85-22397

The low frequency behaviour of an immersed structure at a standstill in a high density fluid with free surface
[TP-1983-31] 13 p2103 N85-23105

Effect of apparent fluid masses on natural vibration frequencies of impellers of multistage centrifugal pumps
14 p2277 N85-24109

Determination of gravity wave envelope solitons on surface of stratified fluid interacting with wind
14 p2334 N85-24433

One physical mechanism of formation of fine structure of ocean waters 14 p2334 N85-24436

Circulation statistics based on FGGE (First GARP Global Experiment) level 3-B analyses produced by GFDL (Geophysics Fluid Dynamics Laboratory)
[PB85-149318] 14 p2379 N85-24668

Magneto-fluid-dynamic issues for fusion first wall and blanket systems
[DE85-004022] 14 p2424 N85-24954

Heat transfer and fluid mechanics measurements in the turbulent reattaching flow behind a backward-facing step
15 p2553 N85-25753

Gasdynamic evaluation of choking cascade turns
[AD-A151854] 15 p2557 N85-25776

Geophysical Fluid Dynamics Laboratory activities, FY84, plans, FY85
[PB85-147601] 15 p2558 N85-25783

USSR report: Physics and mathematics
[JPRS-UPM-85-003] 15 p2642 N85-26300

Mean free paths, viscosity, and the limitations of perfect fluid hydrodynamics in the description of the quark-gluon plasma
[DE85-005501] 15 p2649 N85-26339

Progress of computational fluid dynamics in the world
16 p2691 N85-26612

Flow dynamic environment data base development for the SSME 16 p2736 N85-26885

Experimental evaluation of an advanced Space Shuttle main engine hot-gas manifold design concept
16 p2738 N85-26898

Analytical study of flow phenomena in SSME turnaround duct geometries 16 p2739 N85-26902

Liquid rocket combustor computer code development
16 p2740 N85-26910

Laser Schlieren and ultraviolet diagnostics of rocket combustion 16 p2740 N85-26911

USSR report: Engineering and equipment
[JPRS-UEQ-84-006] 16 p2760 N85-27035

An incremental multigrid strategy for the fluid dynamics equations
[AD-A151953] 16 p2783 N85-27172

A study of the effect of gently varying terrain on atmospheric flow near the surface
16 p2823 N85-27411

Fluid-dynamic model of a downburst
[UTIAS-271] 16 p2829 N85-27441

Air flow of the western coastal boundary of South Africa and its influence on the ocean 16 p2831 N85-27459

Apparatus for measuring velocity of sound in fluids
17 p2944 N85-28175

Vortices in non-Newtonian fluids
[AD-A153169] 17 p2958 N85-28269

FLOWPLOT 2: A fluid dynamics and heat transfer plotting package
[DE85-009802] 17 p2969 N85-28277

Morphological stability and fluid dynamics of vapor crystal growth
[NASA-CR-175879] 17 p3042 N85-28822

Morphological stability and fluid dynamics of vapor crystal growth
[NASA-CR-175880] 17 p3042 N85-28823

Activities of the Department of Aerospace Engineering
18 p3199 N85-29844

Buoyant jet entrainment in stratified fluids
19 p3263 N85-30238

Modifications to SOLA-VOF for flow dynamics in spinning cylinders
[AD-A154093] 19 p3265 N85-30250

Destruction of density jumps in ocean by turbulence
19 p3291 N85-30407

A device for generating motive force through the expansion of a non-elastic dense fluid
[NASA-TM-77664] 20 p3454 N85-31446

Notes on unsteady transonic cascade flows
[AD-A154829] 21 p3552 N85-32096

Experiments on the influence of active walls on the initial amplitudes and growths of instability waves
[AD-A154630] 21 p3583 N85-32275

Characteristics of a numerical fluid dynamics simulator
[DE85-009602] 21 p3586 N85-32290

Simulation of instability of cylindrically converging shock waves 23 p3960 N85-34679

FLUID FILLED SHELLS
NT LIQUID FILLED SHELLS

Acoustic radiation from concentric shells containing an inner fluid
[AD-A155476] 21 p3700 N85-32991

FLUID FILMS
NT SQUEEZE FILMS

Investigation of the local mass transfer of a laminar and turbulent falling liquid film
[BLL-T6366/BG/WH792/84] 06 p0807 N85-15130

Effect of interconnection of the ends of a sliding bearing on film thickness
[AD-A147736] 08 p1132 N85-17135

Tunable microwave transversal filters
[AD-A148370] 08 p1158 N85-17304

Mechanical interactions of rough surfaces
[DE85-000814] 10 p1494 N85-19434

FLUID FILTERS
NT AIR FILTERS

Laboratory simulation of smoke reduction from aircraft engine test cell exhaust using a fluidized bed filter
[AD-A145600] 08 p1089 N85-16866

Carbon filter plates for aluminum filtration at casting
[BMFT-FB-T-84-242] 12 p1808 N85-21343

Molecular and macromolecular sieving by asymmetric ultrafiltration membranes
[PB85-157766] 24 p4077 N85-35266

FLUID FLOW
NT AIR CURRENTS
NT AIR FLOW
NT AIR JETS
NT ANNULAR FLOW
NT AXIAL FLOW
NT AXISYMMETRIC FLOW
NT BAROTROPIC FLOW
NT BASE FLOW
NT BLASIUS FLOW
NT BLOOD FLOW
NT BOUNDARY LAYER FLOW
NT BOUNDARY LAYER SEPARATION
NT CAPILLARY FLOW
NT CASCADE FLOW
NT CAVITATION FLOW
NT CHANNEL FLOW
NT COAXIAL FLOW
NT COMBUSTIBLE FLOW
NT COMPRESSIBLE FLOW
NT CONICAL FLOW
NT CONTINUUM FLOW
NT CONVECTIVE FLOW
NT CORE FLOW
NT CORNER FLOW
NT COUETTE FLOW
NT COUNTERFLOW
NT CRITICAL FLOW
NT CROSS FLOW
NT DUCTED FLOW
NT EQUILIBRIUM FLOW
NT EQUIPOTENTIALS
NT FREE FLOW
NT FREE MOLECULAR FLOW
NT FROZEN EQUILIBRIUM FLOW
NT FUEL FLOW
NT GAS FLOW
NT HELICAL FLOW
NT HYPERSONIC FLOW
NT HYPERVELOCITY FLOW
NT INCOMPRESSIBLE FLOW
NT INLET FLOW
NT INVISCID FLOW
NT ISOTHERMAL FLOW
NT JET FLOW
NT JET MIXING FLOW
NT JET STREAMS (METEOROLOGY)
NT KNUDSEN FLOW
NT LAMINAR FLOW
NT LIQUID FLOW
NT MAGNETOHYDRODYNAMIC FLOW
NT MASS FLOW
NT MERIDIONAL FLOW
NT MOLECULAR FLOW
NT MULTIPHASE FLOW

NT NONEQUILIBRIUM FLOW
NT NONNEWTONIAN FLOW
NT NONUNIFORM FLOW
NT NOZZLE FLOW
NT ONE DIMENSIONAL FLOW
NT OPEN CHANNEL FLOW
NT ORIFICE FLOW
NT OSCILLATING FLOW
NT OUTLET FLOW
NT PARALLEL FLOW
NT PIPE FLOW
NT PLASTIC FLOW
NT POTENTIAL FLOW
NT PRESSURE HEADS
NT PROPELLANT TRANSFER
NT RADIAL FLOW
NT REATTACHED FLOW
NT RECIRCULATIVE FLUID FLOW
NT REVERSED FLOW
NT SECONDARY FLOW
NT SEPARATED FLOW
NT SHEAR FLOW
NT SMALL PERTURBATION FLOW
NT SOLIDS FLOW
NT STAGNATION FLOW
NT STEADY FLOW
NT STOKES FLOW
NT STRATIFIED FLOW
NT SUBCRITICAL FLOW
NT SUBSONIC FLOW
NT SUPERCRITICAL FLOW
NT SUPERSONIC FLOW
NT SUPERSONIC JET FLOW
NT THREE DIMENSIONAL FLOW
NT TRANSITION FLOW
NT TRANSONIC FLOW
NT TRESCA FLOW
NT TURBULENT FLOW
NT TWO DIMENSIONAL FLOW
NT TWO PHASE FLOW
NT UNIFORM FLOW
NT UNSTEADY FLOW
NT VERTICAL AIR CURRENTS
NT VISCOUS FLOW
NT WALL FLOW
NT WATER FLOW
NT WEDGE FLOW

Implementation of the supersonic triplet singularity into the USTORE computer code
[CSIR-NIAST-83/47] 01 p0001 N85-10006

Collapsable seal member
[DE84-014300] 01 p0056 N85-10367

Observations of the vertical structure of the eddy field in the Kuroshio extension
[AD-A145178] 01 p0089 N85-10599

Upwind compact finite difference schemes
[CSIR-TWISK-334] 01 p0110 N85-10742

Experiments on turbulent mixing and chemical reactions in a liquid mixing layer 02 p0134 N85-10912

Spatial relationships in stream flow residuals
02 p0212 N85-11397

A study on dynamic characteristics of liquid oxygen pumps for rocket engines
[NAL-TR-806] 03 p0324 N85-12086

NBS (National Bureau of Standards): Materials measurements
[NASA-CR-174036] 03 p0332 N85-12143

Analysis of physical-chemical processes governing SSME internal fluid flows
[NASA-CR-171247] 04 p0451 N85-12859

A preliminary study of numerical simulation of thermosolutal convection of interest to crystal growth
[NASA-TP-2394] 04 p0498 N85-13175

Analysis of dynamic characteristics of fluid force induced by labyrinth seal 05 p0643 N85-14129

Atmospheric studies in complex terrain
[DE84-008553] 05 p0676 N85-14345

Analysis of physical-chemical processes governing SSME internal fluid flows
[NASA-CR-174245] 06 p0760 N85-14862

Towing tank studies of stratified flow over ridges and valleys
[DE84-011418] 06 p0839 N85-15329

Stability of rigid motions and rollers in bicomponent flows of immiscible liquids
[AD-A147302] 07 p0960 N85-16081

Numerical solutions for steady natural convection in a square cavity
[PB84-245752] 07 p0961 N85-16090

Steady flow model user's guide
[DE85-002001] 08 p1163 N85-17337

New discovery in supersonic flight research
09 p1278 N85-18041

Supercritical fluid chromatography/supersonic jet spectroscopy
[DE85-003310] 09 p1292 N85-18115

Microscopic study of fluid flow
09 p1317 N85-18280

Convective heat transfer coefficients for pipe flow with curvature induced secondary motion
09 p1318 N85-18285

Accuracy of the finite analytic method for scalar transport calculations
[DE85-001474] 09 p1320 N85-18300

Thermal striping downstream of a horizontal elbow under thermally stratified transient flow conditions
[DE84-014687] 09 p1320 N85-18302

Survey of remote data monitoring systems
[DE85-001385] 09 p1323 N85-18313

Analysis of compact heat exchanger performance
[DE84-012624] 10 p1485 N85-19377

Perturbation of a multiple eigenvalue in the Benard problem for two fluid layers
[AD-A149068] 10 p1546 N85-19745

Thermodynamics of the reactive flow model
[DE85-004405] 10 p1565 N85-19870

Leakage-flow-induced vibration of a tube-in-tube slip joint
[DE84-007301] 11 p1652 N85-20406

Flow-induced tube vibration thresholds in heat exchangers from shellside water tests
[DE84-008803] 11 p1652 N85-20407

Algorithm for the simulation of transient viscoelastic flows with free surfaces
[DE85-002713] 12 p1848 N85-21590

Response time correlations for platinum resistance thermometers in flowing fluids
[NASA-CR-172523] 12 p1850 N85-21606

A two-axis, self-nulling skin friction balance
[NASA-CASE-LAR-13294-1] 12 p1851 N85-21610

Computer-Aided Structural Engineering (CASE) project. Seepage analysis of confined flow problems by the method of fragments (CFRAG)
[AD-A150015] 12 p1875 N85-21762

Results of the AFRSI rewaterproofing systems screening test in the NASA/Ames Research Center (ARC) 2 x 2-foot transonic wind tunnel
[NASA-CR-167694] 13 p1968 N85-22467

Workshop report: Swirl Enhanced Combustion
13 p2005 N85-22564

HPFTP flow diverter analysis
[NASA-CR-171424] 13 p2091 N85-23057

Effects of fracture roughness on fluid flow through a single deformable fracture
[DE85-004593] 13 p2092 N85-23062

Emplacement of long lava flows on Mauna Loa (Hawaii) and Alba (Mars) 13 p2186 N85-23563

Thermal infrared observations of lava flows during the 1984 Mauna Loa eruption 13 p2186 N85-23564

Surface structures of Hawaiian lavas
13 p2186 N85-23566

Basaltic pressure ridges: Formation and relationship to flow emplacement 13 p2186 N85-23567

Model of friction bearing hydrodynamics
14 p2288 N85-24178

Application of adaptive grids in solving the partial differential equations governing fluid flow
[AD-A151175] 15 p2555 N85-25766

Thermal traction contact performance evaluation under fully flooded and starved conditions
[NASA-CR-168173] 15 p2568 N85-25848

Variational bounds on Darcy's constant
[DE85-008638] 15 p2580 N85-25916

The effect of the Benthic Boundary Layer on the physics of intense mesoscale eddies
[AD-A153193] 17 p2958 N85-28270

Experimental and theoretical studies on transport processes in laser welding
[DE84-008672] 17 p2975 N85-28378

Numerical benchmark study for the finite element computer code NEPTUNE
[DE85-008400] 17 p3013 N85-28630

Fluid modeling of magnetized plasmas
[DE85-007679] 17 p3039 N85-28804

Multi-ducted inlet combustor research and development
[AD-A153753] 18 p3063 N85-28946

Theoretical and experimental studies of the mechanics of viscoelastic liquids
[AD-A153505] 18 p3070 N85-28987

Variational bounds on Darcy's constant
[DE85-008958] 18 p3101 N85-29195

Transport characteristics of slurries in pipelines: Flow regimes and pressure drop
[DE85-009453] 18 p3101 N85-29198

Laboratory investigation of formation damage of an artificial fracture at simulated geothermal conditions
[DE85-010301] 18 p3102 N85-29201

Applications of Caruto's method to Rayleigh-Taylor-initiated turbulence
[DE85-010835] 18 p3102 N85-29202

Pressure measurement: Short course
[DE85-008644] 18 p3102 N85-29[illegible]

Conceptual hydrologic model of flow in the unsaturated zone, Yucca Mountain, Nevada
[DE85-008346] 18 p3125 N85-29[illegible]

Interim rock mass properties and conditions for analyses of a repository in crystalline rock
[DE85-010700] 18 p3125 N85-29[illegible]

Collodial particle transport with simultaneous birth, growth and capture
[DE85-010388] 19 p3235 N85-300[illegible]

The stability and dynamics of elastic structures and fluid flows
[AD-A154186] 19 p3266 N85-302[illegible]

A method for predicting additive drag reduction from small-diameter pipe flows
[AD-A154411] 19 p3266 N85-30254

Mathematics of oil production
[DE85-011235] 19 p3267 N85-302[illegible]

Pressure recovery in a cylindrical heat pipe at high radial Reynolds numbers and at high Mach numbers
[DE85-010718] 19 p3269 N85-30274

LDA study of the unburned gas motion induced by nonsteady flame propagation in a constant volume duct
[DE85-009938] 19 p3270 N85-30277

Improved fluid flow meter for measuring the rate of fluid flow in a conduit
[NASA-CASE-MFS-28030-1] 19 p3271 N85-302[illegible]

Accuracy in determining velocity of fluid movement by Doppler method 19 p3293 N85-30419

Preliminary evaluation of alterant geophysical tomography in welded tuff
[DE85-010826] 19 p3302 N85-304[illegible]

KIVA: A computer program for two- and three-dimensional fluid flows with chemical reactions and fuel sprays
[DE85-010334] 19 p3339 N85-30[illegible]

Observations of the use of the setapoint detector
[AD-A154533] 21 p3571 N85-322[illegible]

Weak shock waves propagating in fluid-gas mixtures
[AD-A154759] 21 p3584 N85-32276

Finite element methods for viscoelastic flow
[AD-A154877] 22 p3783 N85-334[illegible]

Gradient scaling for nonuniform meshes
[DE85-009625] 22 p3784 N85-334[illegible]

Linear boundary detection using pressure buildup tests
[DE85-009926] 22 p3784 N85-33444

KIVA computer program for multidimensional chemically reactive fluid flows with fuel sprays
[DE85-012730] 22 p3830 N85-337[illegible]

The application of models to the assessment of fire hazard from consumer products
[NBSIR-85-3219] 23 p3925 N85-34[illegible]

Refrigerated dynamic seal to 6.9 MPa (1000 psi)
[NASA-TM-87108] 23 p3930 N85-34[illegible]

Feedback regulated induction heater for a flowing fluid
[DE85-008508] 23 p3939 N85-34414

Studies in thermo-hydro-chemical transport in porous and fractured media
[DE85-012555] 23 p3949 N85-34473

Flow modifying device
[NASA-CASE-LEW-13562-2] 24 p4065 N85-35[illegible]

The effect of power law body forces on a thermally-driven flow between concentric rotating spheres
[NASA-TM-87596] 24 p4093 N85-353[illegible]

Noise-sustained structure, intermittency and the Ginzburg-Landau equation
[DE85-009626] 24 p4094 N85-353[illegible]

Transient three-phase three-component systems. Part 1: Formulation of the system of differential equations
[DE85-013267] 24 p4095 N85-353[illegible]

FLUID INJECTION
NT DEEP WELL INJECTION (WASTES)
NT GAS INJECTION
NT LIQUID INJECTION
NT WATER INJECTION

Geothermal injection treatment: Process chemistry, field experiences, and design options
[DE85-002873] 11 p1675 N85-20[illegible]

Calculating isothermal flow in wake beyond injection zone 14 p2287 N85-24175

Micro-scale methods for characterization of supercritical fluid extraction and fractionation processes
[DE85-010968] 20 p3455 N85-314[illegible]

FLUID JET AMPLIFIERS
U FLUID AMPLIFIERS

FLUID JETS
NT AIR JETS
NT FREE JETS
NT GAS JETS
NT HYDRAULIC JETS
NT VAPOR JETS

Supercritical fluid chromatography/supersonic jet spectroscopy
[DE84-016199] 04 p0471 N85-12[illegible]

Transition and mixing in axisymmetric jets and vortex rings
05 p0591 N85-13769

Influence of turbulence on erosion by a particle-laden fluid jet
[DE84-014365] 09 p1320 N85-18301

Algorithm for the simulation of transient viscoelastic flows with free surfaces
[DE85-002713] 12 p1848 N85-21590

Fluid-dynamic model of a downburst
[UTIAS-271] 16 p2829 N85-27441

Buoyant jet entrainment in stratified fluids
19 p3263 N85-30238

Generation of capillary instabilities by external disturbances in a liquid jet
[NASA-TM-87041] 19 p3265 N85-30246

Supercritical fluid chromatography/supersonic jet spectroscopy
[DE85-007005] 22 p3746 N85-33221

FLUID MANAGEMENT

Space station task force perspective
08 p1106 N85-16992

Technology requirements to be addressed by the NASA Lewis Research Center Cryogenic Fluid Management Facility program
[NASA-TM-87048] 19 p3224 N85-29987

FLUID MECHANICS

NT AERODYNAMICS
NT AEROTHERMODYNAMICS
NT COMPUTATIONAL FLUID DYNAMICS
NT CYLINDRICAL PLASMAS
NT ELASTOHYDRODYNAMICS
NT ELECTROHYDRODYNAMICS
NT FLUID DYNAMICS
NT GAS DYNAMICS
NT HYDRODYNAMICS
NT HYDROMECHANICS
NT HYDROSTATICS
NT INTERACTIONAL AERODYNAMICS
NT MAGNETOHYDRODYNAMICS
NT PNEUMATICS
NT RAREFIED GAS DYNAMICS
NT ROTONS
NT ROTOR AERODYNAMICS
NT SUPERSONICS
NT VORTEX SHEDDING

Equation of state study for polar fluids
[PB84-222801] 01 p0025 N85-10157

Space research and the new approach to the mechanics of fluid media in cosmos
[TRITA-EPP-84-04] 03 p0447 N85-12844

Experimental and theoretical study of a solar thermochemical receiver module
[NASA-CR-174107] 04 p0528 N85-13374

USSR report: Engineering and equipment
[JPRS-UEQ-84-007] 06 p0775 N85-14954

Large-eddy simulation. Guidelines for its application to planetary boundary layer research
[AD-A146381] 06 p0890 N85-15651

An update of the Canada/USA augmentor-wing project
08 p1070 N85-16781

USSR report: Engineering and equipment
[JPRS-UEQ-85-001] 09 p1305 N85-18200

An experimental study of single and multiple turbulent buoyant jets in crossflow
09 p1317 N85-18281

Evaluation of inviscid/boundary layer and parabolized Navier-Stokes solutions for design of reentry vehicles
[DE84-014329] 10 p1428 N85-19006

Overview of leading-edge research at French CNRS lab
11 p1618 N85-20179

Acoustic resonance in heat exchanger tube banks
[DE85-004385] 11 p1632 N85-20281

Advanced research and technology programs for advanced high-pressure oxygen-hydrogen rocket propulsion
[NASA-TM-86969] 12 p1789 N85-21231

Heated subcritical flows within supercritical systems
[NASA-TM-86980] 12 p1845 N85-21574

Arc-driven rail gun research
[NASA-CR-174816] 12 p1859 N85-21662

Space research and the new approach to the mechanics of fluid media in cosmos
12 p1953 N85-22271

USSR report: Engineering and equipment
[JPRS-UEQ-85-003] 13 p2042 N85-22782

Coupling between velocity oscillations and solid propellant combustion
[AD-A151081] 14 p2247 N85-23927

Abatement of noise and vibration in pipelines of hydro systems
14 p2276 N85-24102

USSR report: Engineering and equipment
[JPRS-UEQ-84-005] 14 p2285 N85-24157

Fluid mechanics and heat transfer spirally fluted tubing
[AD-A150774] 14 p2301 N85-24247

Adaptive grid generation for numerical solution of Burger's equation
[AD-A152217] 16 p2855 N85-27606

USSR report: Engineering and equipment
[JPRS-UEQ-85-004] 17 p2939 N85-28142

Buildup of oscillation of bodies in stratified fluid
17 p2941 N85-28157

Fluid surface behavior in low gravity. Center discretionary fund no. 83-21
[NASA-TP-2486] 17 p2957 N85-28260

TRINITY: A pre- and post-processing program for 2-dimensional finite element data
[DE85-008029] 17 p3013 N85-28628

Turbulent wake of a submerged flat plate
[AD-A153776] 18 p3100 N85-29190

Pattern selection and instability in nonlinear wave equation: An aspect of soliton and chaos
[DE85-009578] 18 p3101 N85-29197

Dynamic stability of a spinning tube conveying a flowing fluid
[DE85-007583] 18 p3102 N85-29207

Highly accurate shock flow calculations with moving grids and mesh refinements, revision 1
[DE85-010929] 19 p3267 N85-30260

Analysis of seismic sloshing of reactor tanks considering submerged components and seismic isolation
[DE85-010499] 19 p3269 N85-30273

Transition in Turbines
[NASA-CP-2386] 20 p3452 N85-31433

Heat transfer and fluid mechanics measurements in transitional boundary layer flows
20 p3453 N85-31439

R and D activities of the Aerodynamics Division
20 p3539 N85-32023

Bubble dynamics in polymer solutions undergoing shear
[AD-A154575] 21 p3568 N85-32193

Experiments on the influence of active walls on the initial amplitudes and growths of instability waves
[AD-A154630] 21 p3583 N85-32275

USSR report: Physics and mathematics
[JPRS-UPM-85-004] 21 p3680 N85-32860

Basic research on pulse-combustion phenomena
[PB85-200228] 24 p4077 N85-35265

FLUID POWER

Fluid layer between infinite elastic plates II. Distribution of power flow
[AD-A146690] 03 p0361 N85-12312

Rotordynamic Instability Problems in High-Performance Turbomachinery
[NASA-CP-2338] 05 p0642 N85-14116

Lateral fluid forces acting on a whirling centrifugal impeller in vaneless and vaned diffuser
05 p0643 N85-14123

Two-dimensional unsteady analysis of fluid forces on a whirling centrifugal impeller in a volute
05 p0643 N85-14126

FLUID PRESSURE

NT WATER PRESSURE

Evaluation of subsurface fracture geometry using fluid pressure response to solid earth tidal strain
[DE85-003294] 12 p1890 N85-21864

Investigation, development, and certification of a burst disk for cryogenic fuel tanks
[GCP-3/MT-CM-21-2546] 18 p3067 N85-28972

Damping seal for turbomachinery
[NASA-CASE-MFS-25842-2] 19 p3280 N85-30341

Polymer solution-supercritical fluid behavior
[AD-A154514] 21 p3568 N85-32192

FLUID SWITCHING ELEMENTS

An investigation into the advantages of fluidics in fluid processing. Part 1: An overview of fluidics
[FFA-TN-1984-15-PT-1] 02 p0199 N85-11328

FLUID TRANSMISSION LINES

Dynamic response of fluid transmission lines
[AD-A151926] 16 p2782 N85-27171

FLUID TRANSPIRATION

U TRANSPIRATION

FLUID-SOLID INTERACTIONS

NT GAS-METAL INTERACTIONS
NT GAS-SOLID INTERACTIONS

Normal mode method of solving problem forced oscillations of rib-reinforced shell of revolution in liquid
02 p0273 N85-11781

Leakage-flow induced vibrations of a chimney structure suspended in a liquid flow — nuclear reactors
09 p1339 N85-18420

Effect of air cavity on the vibration analysis of loaded drums 09 p1339 N85-18422

FLUIDIC CIRCUITS

NT FLIP-FLOPS

An investigation into the advantages of fluidics in fluid processing. Part 1: An overview of fluidics
[FFA-TN-1984-15-PT-1] 02 p0199 N85-11328

FLUIDICS

An investigation into the advantages of fluidics in fluid processing. Part 1: An overview of fluidics
[FFA-TN-1984-15-PT-1] 02 p0199 N85-11328

Design guide for fluidic laminar proportional amplifiers and laminar jet angular rate sensors
[AD-A147730] 08 p1161 N85-17328

Dynamic response of fluid transmission lines
[AD-A151926] 16 p2782 N85-27171

FLUIDIZED BED PROCESSORS

Overall heat transfer coefficients for a horizontal cylinder in a fluidized bed
[AD-A144878] 01 p0124 N85-10849

Dynamics of burnout of solid fuel in fluidized bed of finely divided inert particles 02 p0273 N85-11782

Electrochemical production of silicon
06 p0832 N85-15290

JPL in-house fluidized-bed reactor research
06 p0832 N85-15291

Advanced technology cogeneration system conceptual design study: Closed cycle gas turbines
[NASA-CR-168222] 07 p0992 N85-16300

Laboratory simulation of smoke reduction from aircraft engine test cell exhaust using a fluidized bed filter
[AD-A148600] 08 p1089 N85-16886

Liquid phase methanol process development unit: Installation, operation, and support studies
[DE85-001311] 09 p1301 N85-18171

Heat transfer to vertical flat plates in a rectangular gas-fluidized bed
[AD-A150785] 14 p2301 N85-24248

Conversion of methanol to gasoline: Engineering and construction of the demonstration plant
[DE85-003237] 17 p2937 N85-28133

Current status of TVA's atmospheric fluidized bed combustion development efforts
[DE85-901209] 19 p3306 N85-30507

An analysis of the feasibility of producing silicon for solar cells by a dichlorosilane/fluidized-bed reactor process
[NASA-CR-176036] 20 p3478 N85-31614

An investigation into the fluidization and heat transfer of low density particles in a fluidized bed with applications
[AD-A155259] 21 p3584 N85-32282

A fluidized-bed reactor for silane pyrolysis
21 p3609 N85-32413

JPL in-house fluidized-bed reactor research
21 p3609 N85-32414

Modeling of the silane FBR system
21 p3609 N85-32415

Solids mixing in a three phase fluidized bed containing spherically shaped-porous solid particles
[PB85-187961] 22 p3785 N85-33453

Fluidized bed desulfurization
[NASA-CASE-NPO-15924-1] 24 p4075 N85-35253

FLUIDS

On the co-variant formulation of the law of motion of passive particles in a field of turbulence
[REPT-564] 03 p0377 N85-12407

Convection heat transfer in the critical region of fluid mixtures
[DE85-001282] 11 p1633 N85-20285

Self-charging metering and dispensing device for fluids
[NASA-CASE-MSC-20275-1] 12 p1848 N85-21595

Dynamics of solid body with ellipsoidal cavity containing magnetic fluid 14 p2279 N85-24116

Mathematical modeling of fluid-electrolyte alterations during weightlessness
[NASA-CR-171881] 15 p2617 N85-26125

An experimental study of the pressure in a fast bottom beneath the apex of an overlying fluid wedge
[AD-A153618] 18 p3177 N85-29696

FLUORESCENCE

NT PHOSPHORESCENCE
NT RESONANCE FLUORESCENCE
NT X RAY FLUORESCENCE

Raman and fluorescence spectroscopy in a methane-nitrous oxide laminar flame
[AD-A146092] 03 p0326 N85-12111

Microfluorescence studies of zirconium oxide
[DE84-016116] 03 p0329 N85-12118

Time-resolved spectroscopy of evanescent-wave excited fluorescence
[DE84-015213] 04 p0473 N85-13013

Fluorescent dyes for luminescent solar concentrators
[BMFT-FB-T-84-164] 04 p0480 N85-13061

Secondary fluorescence effects on X-ray microanalysis
[DE84-016600] 05 p0618 N85-13951

Determining lamp/ballast system performance with a temperature-controlled integrating chamber
[DE84-014806] 05 p0631 N85-14049

Fundamentals of solar energy conversion based on fluorescence collectors 05 p0662 N85-14258

Fundamental equations of the LIF hydroxyl measurements, appendix A 05 p0676 N85-14338

Saturation phenomena in LIF measurements, appendix B 05 p0676 N85-14339

Detailed performance calculations: Wayne State University and Ford Motor Company, appendix C
05 p0676 N85-14340

Detailed performance calculations: Portland State Group, appendix F 05 p0676 N85-14343

Detailed performance calculations: Harvard Group, appendix G 05 p0676 N85-14344

Clinical measurements using fiber optics and optrodes
[DE84-015043] 05 p0696 N85-14481

Measurements of X-ray spectra from laser produced plasma 06 p0746 N85-14794

Solar energy conversion based on the principle of fluorescent collectors. Installation of a test collector to deliver several Watts power
[BMFT-FB-T-84-192] 07 p0993 N85-16308

Solar energy conversion based on the principle of fluorescent collectors
[BMFT-FB-T-84-193] 07 p0994 N85-16309

Combustion kinetics of metal oxide and halide radicals
[AD-A148521] 08 p1122 N85-17076

New lighting technologies, their status and impacts on power densities
[DE85-000712] 09 p1315 N85-18266

Alignment of high Ryberg states in hydrogen
[DE85-000582] 09 p1380 N85-18677

Developments and applications of laser fluorescence spectroscopy for studies of particle bahaviours in fusion plasmas 09 p1389 N85-18735

Measurements of electric fields in plasmas by using beam probe and laser fluorescence techniques
09 p1389 N85-18737

Laser-induced-fluorescence-spectroscopy of atomic processes under a high magnetic field
09 p1389 N85-18740

The fluorescence of cometary OH and CN
09 p1411 N85-18896

Exciplex systems for vapor-liquid visualization of fuel sprays
[AD-A149360] 10 p1457 N85-19181

Excimer laser photofragmentation of organophosphonates. 1: Detection of the PO radical from dimethyl methyl phosphonate (DMMP)
[AD-A149471] 10 p1490 N85-19407

Applications of pulsed-laser techniques and thermographic phosphors to dynamic thermometry of rotating surfaces
[DE85-000403] 11 p1639 N85-20328

Fluorescent excitation of Fe 2, Mn 2, Ti 2, N 1 lines by V 4, N 5, O 6: Emission lines in the spectra of symbiotic stars and Seyfert galaxies 11 p1746 N85-20984

Two-dimensional measurements of OH concentration and temperature in reactive flows
[AD-A149849] 12 p1800 N85-21292

Application of fluorescence to measurement of surface temperature in solid propellants
13 p2002 N85-22548

Luminescence in the ocean
[AD-B089136L] 13 p2140 N85-23288

Ion transport in beam-plasma interactions
[AD-A150145] 13 p2161 N85-23410

Computer simulations of rare earth sites in glass: Experimental tests and applications to laser materials
[DE85-006156] 14 p2261 N85-24013

Application of atomic fluorescence to measurement of combustion temperature in solid propellants
[AD-A150733] 14 p2263 N85-24021

Secondary fluorescence effects on X-ray microanalysis
[DE85-005565] 15 p2506 N85-25457

Water vapor 16 p2824 N85-27420

Measurement of Franck-Condon factors for the $v'=0$ progression in the B-X system of PO
[AD-A152734] 17 p2919 N85-27993

Investigation of several low-lying levels of X doublet pi state of NCO using argon laser excited fluorescence
[AD-A153693] 18 p3071 N85-28994

Measurement of radical species concentrations and polycyclic aromatic hydrocarbons in flames by fluorescence and absorption using a tunable dye laser
[DE85-008624] 18 p3113 N85-29274

Quantitative studies for photoabsorption and fluorescence of HCl
[NASA-CR-175965] 19 p3233 N85-30043

Measurement of combustion species by electron impact fluorescence
[DE85-011163] 19 p3236 N85-30065

Improvements in the energy resolution and high-count-rate performance of bismuth germanate
[DE85-010763] 19 p3240 N85-30092

Laser-induced fluorescence measurement of vapor concentration surrounding evaporating droplets
[DE85-009409] 19 p3277 N85-30320

E-beam-induced fluorescence of excimers in cryogenic solutions
[DE85-010703] 19 p3278 N85-30328

Development of a technique for in situ detection of stratospheric nitrogen dioxide 19 p3312 N85-30534

Fluorescence quenching by metal semiconductor and insulator surfaces 19 p3374 N85-30929

Chromophores with auxochrome-like function
[NASA-TM-77849] 20 p3421 N85-31233

Recent measurements in turbulent jet flames at Sandia Combustion Research Facility 20 p3424 N85-31254

Velocity visualization in gaseous flows
[NASA-CR-174954] 20 p3453 N85-31445

Multidimensional luminescence measurements
[AD-A154950] 21 p3563 N85-32162

A microprocessor-controlled, multichannel fluorimeter for analysis of sea water
[AD-A154986] 21 p3590 N85-32310

Detection of excited states by laser-induced fluorescence
[AD-A155558] 21 p3592 N85-32326

Photofragment fluorescence as a sensitive probe for gas-phase alkali compounds and their photochemistry
[DE85-010707] 22 p3746 N85-33219

Laser probes of natural gas ignition chemistry
[PB85-200210] 24 p4077 N85-35264

Atmospheric nitrogen oxides: Their detection and chemistry
[PB85-193910] 24 p4114 N85-35502

Lateral-angular and temporal characteristics of EAS optical radiation
[HE-4.4-19] 24 p4194 N85-36025

Air fluorescence detection of large air showers below the horizon
[HE-4.6-6] 24 p4197 N85-36043

FLUORESCENT EMISSION
U FLUORESCENCE

FLUORIDES
NT BERYLLIUM FLUORIDES
NT BORON FLUORIDES
NT CADMIUM FLUORIDES
NT CALCIUM FLUORIDES
NT DEUTERIUM FLUORIDES
NT DIFLUORIDES
NT HYDROFLUORIC ACID
NT LITHIUM FLUORIDES
NT MAGNESIUM FLUORIDES
NT METAL FLUORIDES
NT OXYFLUORIDES
NT POLYVINYL FLUORIDE
NT STRONTIUM FLUORIDES
NT SULFUR FLUORIDES
NT URANIUM FLUORIDES

Method for the preparation of poly(carbonyl fluoride) oligomers
[AD-D011207] 01 p0030 N85-10184

Comparison study of analytical methods for the determination of fluoride, chloride, and bromide in plastics
[DE84-015008] 04 p0470 N85-12989

Effects of silver and group 2 fluorides addition to plasma sprayed chromium carbide high temperature solid lubricant for foil gas bearing to 650 deg C
[NASA-TM-86895] 06 p0770 N85-14928

Compositional, structural, and physical studies of some graphite hexafluoroarsenates and their relatives
[DE85-000855] 10 p1432 N85-19030

Optically pumped iodine monofluoride laser
[AD-D011555] 12 p1855 N85-21637

Synthesis and characterization of poly(vinylidene fluoride)
[AD-A150291] 13 p2037 N85-22759

Mixed valence materials
[AD-A151009] 14 p2252 N85-23959

Preparation of heavy metal fluoride glasses in the bulk form
[AD-A153784] 18 p3079 N85-29049

RAY-O-VAC BR2325 lithium carbon monofluoride cell performance 20 p3444 N85-31382

Method for fluorination of actinide fluorides and oxyfluorides using O2F2
[DE85-011646] 22 p3743 N85-33202

Environmental surveillance at Los Alamos during 1984
[DE85-011886] 22 p3811 N85-33605

A new large-scale, high-resolution multicolor software display concept
[AD-A155404] 22 p3827 N85-33703

FLUORINATION

Fluorinated diamond particles bonded in a filled fluorocarbon resin matrix
[DE84-014444] 01 p0022 N85-10136

Method for introducing fluorine into an aromatic ring
[AD-D011397] 08 p1120 N85-17061

Effective antireflection coatings of transparent polymeric materials by gas-phase surface fluorination
[DE84-013027] 09 p1385 N85-18711

Fluorinated polyesters
[AD-D011611] 16 p2753 N85-26988

Method for fluorination of actinide fluorides and oxyfluorides using O2F2
[DE85-011646] 22 p3743 N85-33202

FLUORINE

Nuclear moments and nuclear structure
[DE84-015847] 04 p0561 N85-13573

Forming fluorine-containing threads from vinylidene fluoride-tetrafluoroethylene copolymer by dry method
06 p0762 N85-14873

Alabama Tin Belt: Metallogenesis and mineral resource evaluation. Year-end report
[DE84-901335] 07 p0989 N85-16[illegible]

Method for introducing fluorine into an aromatic ring
[AD-D011397] 08 p1120 N85-17061

Time dependent Hartree-Fock theory of ion-atom collisions: Application to F(9+) + Ne
[DE85-003083] 11 p1723 N85-20838

Preparation of nitrocompounds
[AD-A153687] 18 p3071 N85-28[illegible]

Slow chemistry effects in a turbulent mixing layer
20 p3424 N85-31252

Synthesis of energetic materials
[AD-A154887] 21 p3571 N85-32210

Vacuum ultraviolet laser
[DE85-011632] 22 p3790 N85-33475

FLUORINE COMPOUNDS
NT BERYLLIUM FLUORIDES
NT BORON FLUORIDES
NT CADMIUM FLUORIDES
NT CALCIUM FLUORIDES
NT CARBON TETRAFLUORIDE
NT DEUTERIUM FLUORIDES
NT DIFLUORIDES
NT DIFLUORO COMPOUNDS
NT FLUORIDES
NT FLUORINE ORGANIC COMPOUNDS
NT FLUORITE
NT FLUORO COMPOUNDS
NT FLUOROCARBONS
NT FLUOROHYDROCARBONS
NT FLUOROPOLYMERS
NT HYDROFLUORIC ACID
NT LITHIUM FLUORIDES
NT MAGNESIUM FLUORIDES
NT METAL FLUORIDES
NT OXYFLUORIDES
NT PERFLUOROALKANE
NT POLYTETRAFLUOROETHYLENE
NT POLYVINYL FLUORIDE
NT STRONTIUM FLUORIDES
NT SULFUR FLUORIDES
NT URANIUM FLUORIDES

Synthesis of pentafluorotellurium hypofluorite
[AD-D011212] 01 p0023 N85-10139

Electron oxidation of graphite by fluorospecies
[DE85-001196] 11 p1595 N85-20034

New catalysts and new electrolytes for acid fuel cells
[DE85-009940] 19 p3307 N85-30498

FLUORINE ORGANIC COMPOUNDS
NT CARBON TETRAFLUORIDE
NT FLUOROCARBONS
NT FLUOROHYDROCARBONS
NT FLUOROPOLYMERS
NT PERFLUOROALKANE
NT POLYVINYL FLUORIDE

Development and application of fluorine-containing reagents in the gas chromatography of carbonyl compounds
[BLL-DRIC-TRANS-7205-(3623.66)]
01 p0023 N85-10140

FLUORITE

A mixed-basis band structure interpolation schem applied to the fluorite structure compounds NiSi2, AuAl2, AuGa2 and AuIn2
[AD-A150131] 12 p1940 N85-22187

FLUORO COMPOUNDS
NT CARBON TETRAFLUORIDE
NT DIFLUORO COMPOUNDS
NT FLUORINE ORGANIC COMPOUNDS
NT FLUOROCARBONS
NT FLUOROHYDROCARBONS
NT FLUOROPOLYMERS
NT PERFLUOROALKANE
NT POLYTETRAFLUOROETHYLENE

Measurement of state and dynamic solid state propertie in nonmetals using excited probe nuclei on the Erlange 12 MeV tandem accelerator 03 p0428 N85-1273

Pseudo-p-1,2,2,9,9,10,10-octofluoro (2,2)-p-cyclophan bis-acid chloride
[AD-D011393] 07 p0919 N85-1581

Water-resistance and some other properties of polyal fluorophosphate glasses 14 p2281 N85-2413

Improved acid electrolytes for fuel cells
[PB85-176053] 18 p3132 N85-2

FLUOROCARBONS
Fluorinated diamond particles bonded in a filled fluorocarbon resin matrix
[DE84-014444] 01 p0022 N85-10136
Apparatus for measuring dielectric characteristics of polymer materials in millimetric range of wavelengths at 4.2-300 K temperatures 06 p0788 N85-15032
Cross-Appalachian Tracer Experiment (CAPTEX '83)
[PB84-236641] 06 p0834 N85-15307
New approaches to functionalized fluorocarbons
[AD-A154205] 19 p3248 N85-30141
Basic research in novel inorganic reagents and fluorocarbon chemistry
[AD-A155340] 21 p3564 N85-32165
Reaction of uranium and the fluorocarbon FC-75
[DE85-012322] 22 p3843 N85-33802

FLUOROHYDROCARBONS
NT CARBON TETRAFLUORIDE
Working medium for sorption heat pumps
[BLL-T6360/BG/WH785/84] 06 p0807 N85-15131
Fluorinated diacrylic esters
[AD-D011326] 07 p0929 N85-15889
Elementary processes of electronically excited particles. Part 5: Deactivation of CHF (A1a' (O, V'2, O) after excitation by a pulsed dye laser
[MPIS-13/1984] 14 p2420 N85-24930
New approaches to functionalized fluorocarbons
[AD-A154205] 19 p3248 N85-30141
Atmospheric chlorofluromethanes as tracers of ocean circulation and mixing: Measurement and calibration techniques and studies in the Greenland and Norwegian Seas 19 p3319 N85-30573

FLUOROMICA
U MICA

FLUOROPLASTICS
U FLUOROPOLYMERS

FLUOROPOLYMERS
NT POLYTETRAFLUOROETHYLENE
NT POLYVINYL FLUORIDE
NT TEFLON (TRADEMARK)
Fluorinated aliphatic polyalkylether lubricant with an additive composed of an aromatic phosphine substituted with perfluoroalkylether groups
[AD-D011286] 06 p0770 N85-14927
Fluorinated diacrylic esters
[AD-D011326] 07 p0929 N85-15889
Dynamic polymer pressure transducer with temperature compensation
[AD-D011373] 07 p0967 N85-16142
Polymer blends as high explosive binders
[DE85-001210] 11 p1611 N85-20131
Fluorinated polyurethanes
[AD-D011526] 12 p1810 N85-21353
Ion transporting composite membranes. 1: Nafion impregnated gore-tex
[AD-A151020] 14 p2252 N85-23960

FLUSHING
Nitrogen flushing during exposure of large Schmidt telescope plates 07 p0963 N85-16109

FLUTING
U GROOVING

FLUTTER
NT AEROELASTIC RESEARCH WINGS
NT SUBSONIC FLUTTER
NT SUPERSONIC FLUTTER
NT TRANSONIC FLUTTER
Results of winglet development studies for DC-10 derivatives
[NASA-CR-3677] 02 p0138 N85-10936
Interactive aircraft flight control and aeroelastic stabilization
[NASA-CR-174025] 02 p0148 N85-11003
Status and prospects of computational fluid dynamics for unsteady transonic viscous flows
[NASA-TM-86018] 03 p0315 N85-12037
Flutter parametric studies of cantilevered twin-engine-transport type wing with and without winglet. Volume 1: Low-speed investigations
[NASA-CR-172410-VOL-1] 04 p0513 N85-13269
Flutter parametric studies of cantilevered twin-engine transport type wing with and without winglet. Volume 2: Transonic and density effect investigations
[NASA-CR-172410-VOL-2] 04 p0513 N85-13270
Flutter control with unsteady aerodynamic models
[AD-A147858] 07 p0909 N85-15753
Finite element analysis of nonlinear oscillations and flutter of shells of revolution
[AD-A149071] 10 p1496 N85-19440
Remote pivot decoupler pylon: Wing/store suppression
[NASA-CASE-LAR-13173-1] *1 p1584 N85-19981
Flutter taming: A new tool for the aeroelastic designer
[AD-A150834] 14 p2226 N85-23802
Transonic Unsteady Aerodynamics and its Aeroelastic Applications
[AGARD-CP-374] 15 p2457 N85-25171
Status and prospects of computational fluid dynamics for unsteady transonic flow 15 p2459 N85-25180
Application of time-linearized methods to oscillating wings in transonic flow and flutter
15 p2459 N85-25182
The application of transonic unsteady methods for calculation of flutter airloads 15 p2460 N85-25186
The design and operation of a simple low-speed flutter-suppression model
[AD-A151610] 15 p2474 N85-25269
Active control of forward swept wings with divergence and flutter aeroelastic instabilities
[AD-A151837] 15 p2474 N85-25270
Aerodynamic detuning analysis of an unstalled supersonic turbofan cascade
[NASA-TM-87001] 16 p2700 N85-26670
ESP (External-Stores Program): A pilot computer program for determining flutter-critical external-store configurations. Volume 3, part 2. Program compilation
[AD-A152271] 16 p2706 N85-26703
ESP (External-Stores Program): A pilot computer program for determining flutter-critical external-store configurations. Volume 1: User's manual
[AD-A152268] 16 p2710 N85-26725
ESP (External-Stores Program): A pilot computer program for determining flutter-critical external-store configurations. Volume 2: Final report on program enhencement and delivery
[AD-A152269] 16 p2711 N85-26726
ESP (External-Stores Program): A pilot computer program for determining flutter-critical external-store configurations. Volume 3, part 1: Program compilation
[AD-A152270] 16 p2711 N85-26727
Flight trials of a modified gulfstream commander carrying external stores
[AD-A153376] 17 p2896 N85-27859
The application of bispectral analyses to aeroelastic phenomena 24 p4060 N85-35157
Unsteady flow in a supersonic cascade with two in-passage shocks
[NASA-CR-3925] 24 p4060 N85-35158

FLUTTER ANALYSIS
NT AEROELASTIC RESEARCH WINGS
Flutter parametric studies of cantilevered twin-engine-transport type wing with and without winglet. Volume 1: Low-speed investigations
[NASA-CR-172410-VOL-1] 04 p0513 N85-13269
Viscous effects on transonic airfoil stability and response
[NASA-TM-86374] 10 p1421 N85-18961
Exploratory flutter test in a cryogenic wind tunnel
[NASA-TM-86380] 12 p1863 N85-21689
Dynamic wind-tunnel testing of active controls by the NASA Langley Research Center
13 p1966 N85-22353
Two degree-of-freedom flutter solution for a personal computer
[NASA-TM-86361] 13 p1971 N85-22379
Experience with transonic unsteady aerodynamic calculations 15 p2456 N85-25176
A semi-empirical unsteady transonic method with supersonic free stream 15 p2458 N85-25179
A study of transonic flutter of a two-dimensional airfoil using the U-g and p-k methods
[AD-A151463] 15 p2473 N85-25266
Verification of calculation methods for unsteady airloads in the precipitation of transonic flutter
[NLR-MP-84016-U] 20 p3390 N85-31027
Flutter clearance of the Schweizer 1-36 deep-stall sailplane
[NASA-TM-85917] 22 p3729 N85-33116
Design, development and operation of a high simultaneous capacity digital telemetry system — turbomachine blade flutter
[PNR-90261] 23 p3899 N85-34151

FLUX
Stellar ultraviolet flux distributions in the 912-1200 A wavelength range 11 p1762 N85-21081
Limits on deeply penetrating particles in the 10(17) eV cosmic ray flux
[HE-5.3-1] 24 p4205 N85-36098
Atmospheric neutrinos observed in underground detectors
[HE-5.3-8] 24 p4205 N85-36102

FLUX (RATE PER UNIT AREA)
U FLUX DENSITY

FLUX (RATE)
NT HEAT FLUX
NT MAGNETIC FLUX
NT SOLAR FLUX
Method and apparatus for determining the content and distribution of a thermal neutron absorbing material in an object
[DE84-014319] 01 p0117 N85-10801
Mid-infrared spectroscopy of planetary nebulae
08 p1247 N85-17872
The high latitude D region during electron precipitation events 11 p1664 N85-20484
Absolute measurements of radiation intensity from Cassiopeia-A, Cygnus-A and crab nebula in 60-100 cm band 13 p2076 N85-22976
Study of integral and spectral direct solar radiation over Atlantic 14 p2341 N85-24475
The behavior of the atmosphere in the desert planetary boundary layer
[AD-A151266] 15 p2592 N85-25977
Proposed solar neutrino experiment using (81)Br(nu,e(-e)) (81)Kr
[DE85-004802] 15 p2684 N85-26579
Periodicity of variations in galactic cosmic ray fluxes and solar activity parameters near 20th cycle minimum
16 p2720 N85-26791
Variations in intensity of secondary cosmic radiation observed on 10-11 August 1981
16 p2721 N85-26796
Measurements of fluxes of high-energy protons and electrons by 2 oppositely oriented spectrometers aboard Cosmos-368 artificial Earth satellite
16 p2722 N85-26800
On the choice of coordinates for semiconductor simulation
[AD-A152214] 16 p2870 N85-27708
Parameterization of surface fluxes in the VVR Fourth Order GCM 18 p3142 N85-29454
On the global distribution of three-dimensional Eliassen-Palm fluxes by stationary waves
18 p3145 N85-29469
Dynamic models of flux tubes in the interpretation of polarization measurements 18 p3206 N85-29891
The influence of a turbulent region on the flux of auroral electrons
[KGI-PREPRINT-072] 20 p3494 N85-31723
Use of the VAD technique and measurements of momentum flux in the stratosphere at Aercibo, part 4.3A
21 p3622 N85-32505
Momentum flux measurements: Techniques and needs, part 4.5A 21 p3623 N85-32506
Characteristics and sources of E-region ionization in the continuous aurora
[AD-A155018] 21 p3632 N85-32562
Horizontal and vertical structure of velocity, potential vorticity and energy in the gulf stream
[AD-A154753] 21 p3655 N85-32702
Sulfur Cycle 21 p3662 N85-32748
Solar cycle variation of ephemeral regions
[AD-A154967] 21 p3723 N85-33097
Scientific Opportunities with Advanced Facilities for Neutron Scattering
[DE85-012113] 22 p3839 N85-33770
Neutron flux, spectrum and dose equivalent measurements for a 4500-W(th) 238 PuO2 general purpose heat source
[DE85-011361] 22 p3841 N85-33786
Observations of the Crab Nebula at energies 4.10(11)
[OG-2.3-1] 22 p3865 N85-33938
Search for gamma-rays above 400 GeV from Geminga
[OG-2.4-4] 22 p3867 N85-33951
Balloon observations of hard X-rays from some galactic X-ray sources
[OG-2.5-11] 22 p3870 N85-33966
All sky Northern Hemisphere 10(15) EV gamma-ray survey
[OG-2.6-3] 22 p3870 N85-33968
Search for the gamma-ray fluxes with energies above 10915) eV from various objects
[OG-2.6-14] 22 p3871 N85-33975
Cosmic rays in the 10(16) to 10(19) eV range from pulsars
[OG-5.4-3] 22 p3886 N85-34080
The primary cosmic ray mass composition at energies above 10(14) eV
[OG-5.4-6] 22 p3886 N85-34083
UHE particle production in close binary systems
[OG-5.4-7] 22 p3886 N85-34084
Modeling cosmic ray anisotropies near 10(18) eV
[OG-5.4-9] 22 p3886 N85-34086
A search for solar neutrons on a long duration balloon flight
[SH-1.4-6] 23 p3995 N85-34766
Observation of the fluxes of nuclei with energies 10-20 MEV per nucleon during the solar flare of April 26, 1984
[SH-2.1-1] 23 p3998 N85-34783
The 3HE in solar non-relativistic electron events
[SH-2.2-5] 23 p4000 N85-34800
The dependence of solar modulation on the sign of the cosmic ray particle charge
[SH-4.2-23] 23 p4009 N85-34860
Scaling from Jupiter to pulsars and the acceleration of cosmic ray particles by pulsars, 3
[OG-8.2-3] 23 p4019 N85-34904

The design of an experiment to detect low energy antiprotons
[OG-9.1-1] 23 p4022 N85-34928

Cosmic ray modulation by high-speed solar wind fluxes
[SH-5.1-22] 23 p4044 N85-35074

Additional flux of particles and albedo-electrons in upper atmosphere
[SH-6.1-6] 23 p4045 N85-35080

Empirical model for the Earth's cosmic ray shadow at 400 KM: Prohibited cosmic ray access
[SH-6.1-14] 23 p4046 N85-35087

Limiter
[DE85-011620] 24 p4150 N85-35736

Hadron intensity and energy spectrum at 4360 m above level
[HE-3.1-7] 24 p4178 N85-35905

Scaling violation in fragmentation region at energies above 10-15 eV based on the data on cosmic ray hadron component
[HE-3.1-11] 24 p4178 N85-35909

Monte Carlo simulations of electron lateral distributions in the core region of 10(13) - 10(16) eV air showers
24 p4190 N85-35992

The Nagoya cosmic-ray muon spectrometer 3, part 1: Preliminary observations
[HE-5.2-2] 24 p4202 N85-36080

Angular distribution of muons produced by cosmic ray neutrinos in rock
[HE-5.3-24] 24 p4207 N85-36115

Muon and neutrino fluxes
[HE-6.2-18] 24 p4213 N85-36154

FLUX DENSITY
NT CURRENT DENSITY
NT ELECTRON FLUX DENSITY
NT ILLUMINANCE
NT IRRADIANCE
NT LUMINANCE
NT LUMINOUS INTENSITY
NT NEUTRON FLUX DENSITY
NT PARTICLE FLUX DENSITY
NT PHOTON DENSITY
NT PROTON FLUX DENSITY
NT RADIANCE
NT RADIANT FLUX DENSITY
NT SOLAR CONSTANT
NT SOLAR FLUX DENSITY
NT SOUND INTENSITY

An error analysis for the use of presently available lunar radio flux data in broadbeam antenna-system measurements
[PB84-218361] 01 p0016 N85-10097

Bremsstrahlung radiation from longitudinal plasma waves caused by subthermal electrons in plasma
02 p0264 N85-11730

X-ray observations of the Seyfert 1 galaxies AKN120 and MCG8-11-11
[NASA-TM-80663] 03 p0446 N85-12839

Positron flux concentrator: An update
[DE84-016260] 04 p0561 N85-13576

Potential of flywheels for spacecraft energy storage
05 p0609 N85-13890

Diurnal variation harmonics and spatial change in cosmic ray flux 06 p0824 N85-15230

Grain boundary structure in NiO
[DE84-016242] 06 p0866 N85-15519

The nature of the soft X-ray emitting region in the direction of the North Polar spur
06 p0877 N85-15568

Inverse relations between 0.25 keV counts and local interstellar dust 06 p0877 N85-15572

The Orion molecular cloud at far-infrared wavelengths
08 p1245 N85-17860

Techniques for measuring intercepted and absorbed PAR in corn canopies
[E85-10081] 10 p1505 N85-19495

Study of low energy density photovoltaic applications under varying rate structures
[DE85-000185] 10 p1511 N85-19536

Quasi-thermodynamic prediction of hydrogen reemission behavior from titanium films
[DE85-003867] 10 p1564 N85-19864

Assessment of satellite power flux-density limits in the 2025-2300 MHz frequency range, part 2
[PB85-101244] 11 p1625 N85-20236

Absorption of ozone molecules in strong field of tea CO2 injection laser 11 p1718 N85-20808

Coordinated multifrequency observations of the BL LAC objects MRK 180, MRK 421, and MRK 501
11 p1746 N85-20983

The physical implications of an isothermal model for the hot intracluster medium
[NASA-TM-86174] 11 p1763 N85-21089

Mass analysis of neutral particles and ions released during electrical breakdowns on spacecraft surfaces
[NASA-CR-175585] 12 p1793 N85-21250

Magnetic field in main gap of separator
12 p1843 N85-21563

Dual electrochemical system
[AD-D011616] 16 p2817 N85-27376

Investigation of pseudo bi-polar nickel cadmium batteries as filter elements for pulsed power loads
[AD-A152112] 16 p2819 N85-27389

High efficiency ionizer using a hollow cathode discharge plasma
[DE85-006690] 16 p2866 N85-27693

Nickel-cadmium cell design variable program data analysis
[NASA-TM-86198] 19 p3258 N85-30203

Frequent observations of extragalactic compact sources at 24 GHz 19 p3366 N85-31003

Results of analysis on the design variable cells
20 p3445 N85-31388

Improved specific energy Ni-H2 cell
20 p3447 N85-31399

Density gradient electrophoresis of cultured human embryonic kidney cells 20 p3501 N85-31763

Spectral methods for the estimation of acoustic intensity, energy density, and surface velocity using a multimicrophone probe 20 p3524 N85-31916

Hit-size effectiveness theory applied to high doses of low LET radiation for pink mutations in Tradescantia
[DE85-011835] 22 p3619 N85-33657

Very high energy gamma rays from the Crab Nebula
[OG-2.3-3] 22 p3866 N85-33940

Periodic gamma-ray emissions from Geminga at or = 10(12) eV
[OG-2.4-2] 22 p3867 N85-33949

On the 1983 observations of the gamma-ray source 2CG195+4
[OG-2.4-5] 22 p3868 N85-33952

SMM detection of interstellar Al-26 gamma radiation
[OG-3.2-1] 22 p3874 N85-34001

The muon content of EAS as a function of primary energy
[OG-5.1-6] 22 p3881 N85-34050

EAS spectrum in the primary energy region above 10 to the 15th power eV by the Akeno and Yakutsk array data
[OG-5.1-16] 22 p3882 N85-34057

Composition of primary cosmic rays at energies 10(15) to approximately 10(16) eV
[OG-5.2-4] 22 p3883 N85-34061

Implication of EAS data for the study of primary cosmic rays above 10 to the 5th power GeV
[OG-5.2-7] 22 p3883 N85-34064

EAS Cerenkov measurements of the composition of the cosmic ray flux around 10 to the 16th power eV
[OG-5.2-11] 22 p3884 N85-34067

Analytic and numerical calculations of the ambipolar electric field in a stellarator 23 p3978 N85-34665

Spectral analyses of the Forbush decrease of 13 July 1982
[SH-5.1-7] 23 p4042 N85-35061

Transient cosmic ray increase associated with a geomagnetic storm
[SH-5.1-8] 23 p4042 N85-35062

Short perturbations of cosmic ray intensity and electric field in atmosphere
[SH-6.1-16] 23 p4046 N85-35090

Diurnal variations of cosmic ray geomagnetic cut-off threshold rigidities
[SH-6.1-21] 23 p4046 N85-35092

The influence of the Earth's magnetosphere on the high-energy solar protons
[SH-6.1-22] 23 p4046 N85-35093

Observation of nuclei with energies 8-30 MeV per nucleon in the Earth's magnetosphere at the altitudes 350 KM
[SH-10.1-5] 23 p4053 N85-35136

Proton-air and proton-proton cross sections from air shower data
[HE-1.1-1] 24 p4170 N85-35849

Multiplicity distributions in interaction models used for cascade simulations
[HE-1.2-5] 24 p4172 N85-35863

Connection between variations of the atmosphere temperature profile and variations of the meson component intensity
[HE-3.1-12] 24 p4178 N85-35910

The model of independent particles emission in the multiparticle production theory
[HE-3.2-10] 24 p4179 N85-35918

A critical analysis of air shower structure functions and size spectrum measurements with the NBU air shower array 24 p4188 N85-35983

Measurement of the local density spectrum
24 p4189 N85-35984

Transition effect of air shower particles in plastic scintillators
[HE-4.4-9] 24 p4193 N85-36017

On the determination of the depth of EAS development maximum using the lateral distribution of Cerenkov light at distances 150 m from EAS axis
[HE-4.4-13] 24 p4194 N85-36019

An upper limit of muon flux of energies above 100 TeV determined from horizontal air showers observed at Akeno
[HE-5.2-12] 24 p4203 N85-36088

Energy spectrum of cascade showers induced by cosmic ray muons in the range from 50 GeV to 5 TeV
[HE-5.2-14] 24 p4203 N85-36089

Measurement of muon intensity by Cerenkov method
[HE-5.2-15] 24 p4204 N85-36091

Analytical calculation of muon intensities under deep sea-water
[HE-5.2-16] 24 p4204 N85-36092

The spectrum of neutrons at 60 hg m(-2)
[HE-5.2-20] 24 p4204 N85-36096

Geophysical searches for three-neutrino oscillations
[HE-5.3-9] 24 p4205 N85-36103

Angular distribution of muons produced by cosmic ray neutrinos in rock
[HE-5.3-24] 24 p4207 N85-36115

Atmospheric muons and neutrinos, and the neutrino-induced muon flux underground
[HE-5.4-7] 24 p4207 N85-36118

Results of investigation of muon fluxes of superhigh energy cosmic rays with X-ray emulsion chambers
[HE-5.4-16] 24 p4208 N85-36125

FLUX MAPPING
U FLUX DENSITY
U MAPPING

FLUX PINNING

Flux-line pinning by the grain boundary in niobium bicrystals
[DE84-016668] 04 p0570 N85-13888

Ballooning instabilities on a magnetic separatrix
[DE85-010855] 19 p3372 N85-30815

Flux pinning and flux flow studies in superconductors using flux flow noise techniques
[DE85-010814] 19 p3376 N85-30845

FLUXES

Suppressing porosity in weld joints of 1420 aluminum alloy 01 p0020 N85-10123

Densification of submicron YSZ (Yttria-Stabilized Zirconia) powders with alumina and borate additives
[AD-A149520] 10 p1452 N85-19150

The effect of filler wire and flux compositions on the microstructure and properties of microalloyed steel weld metal
[AD-A149529] 10 p1402 N85-19423

Automatic multi-layer welding of thick cylindrical structures under flux 13 p2036 N85-22746

Microcomputer-controlled system for measuring atmospheric particle fluxes
[DE85-007910] 17 p2986 N85-28480

FLUXMETERS
U MAGNETIC MEASUREMENT
U MEASURING INSTRUMENTS

FLY ASH

Compressive strength-maturity relationships of mortar containing fly ash
[AD-A148705] 09 p1339 N85-19420

Adherence of ash particles from the combustion of micronized coal
[DE85-008600] 19 p3229 N85-30023

Third US/USSR Symposium on Particulate Control
[PB85-190890] 19 p3310 N85-30522

Evaluation of pilot ESP used with a spray dryer FGD system at Pittsburgh Energy Technology Center, Bruceton, Pennsylvania
[DE85-011151] 22 p3746 N85-33217

FLY BY WIRE CONTROL

Role of research aircraft in technology development
[NASA-TM-85913] 02 p0137 N85-10802

Integrated digital/electric aircraft concepts study
[NASA-CR-3841] 08 p1083 N85-16961

Some aspects of the design of a fly-by-wire flying control system for a supersonic V/STOL fighter aircraft
[COLL-AERON-8413] 12 p1780 N85-21175

Guidance and control research flight testing with HFB 320 test aircraft 13 p1967 N85-22355

Multivariable control law design for the X-29 aircraft
[AD-A151826] 15 p2472 N85-25259

A method of estimating aircraft attitude from fly by wire flight control system data 16 p2687 N85-26863

An update on experience on the fly by wire Jaguar equipped with a full-time digital flight control system
16 p2712 N85-26740

Application of AFTI/F-16 task-tailored control modes in advanced multirole fighters 17 p2901 N85-27888

X-29 digital flight control system design
17 p2901 N85-27889

An update of experience on the fly by wire Jaguar equipped with a full-time digital flight control system
17 p2902 N85-27893

Operational and developmental experience with the F/A-18A digital flight control system
17 p2902 N85-27895
How to handle failures in advanced flight control systems of future transport aircraft 17 p2904 N85-27905
The flight control system for the Experimental Aircraft Programme (EAP) demonstration aircraft
17 p2904 N85-27906
Crew systems and flight station concepts for a 1995 transport aircraft
[NASA-CR-166068] 19 p3221 N85-29973

FLYBY MISSIONS
NT ASTEROID MISSIONS
NT GIOTTO MISSION
Sample return from a comet flyby
06 p0889 N85-15646
The violet absorber on Io: Disulfur monoxide derivatives 13 p2173 N85-23482
Dark halo craters and the thickness of grooved terrain on Ganymede 13 p2173 N85-23484
Formation of bright terrain bands on Ganymede by unstable lithosphere extension 13 p2173 N85-23485
Dynamical studies of Saturn's rings
13 p2174 N85-23489
The astrometry network of the IHW and the P/Crommelin trial run results 14 p2435 N85-25016
Comments on Vega mission 15 p2482 N85-25319
Press conference on flight of Vega spacecraft
15 p2482 N85-25320
Interpretation of Venus gravitational anomalies
15 p2483 N85-25322
TASS update on flights of Vega-1 and Vega-2
16 p2722 N85-26803
Kovtunenko discuses Vega Project
16 p2722 N85-26804

FLYING BEDSTEAD AIRCRAFT
U FLYING PLATFORMS

FLYING PERSONNEL
NT AIRCRAFT PILOTS
NT ASTRONAUTS
NT COSMONAUTS
NT FLIGHT CREWS
NT PILOTS (PERSONNEL)
NT SPACECREWS
Review of US manual of clinical aviation medicine
12 p1904 N85-21957
Review of US guide on medication and flying
12 p1904 N85-21958

FLYING PLATFORM STABILITY
U AERODYNAMIC STABILITY
U FLYING PLATFORMS

FLYING PLATFORMS
Intelligent interfaces for tactical airborne platforms
06 p0752 N85-14820

FLYING QUALITIES
U FLIGHT CHARACTERISTICS

FLYWHEELS
The limp flywheel
[AD-A146034] 03 p0386 N85-12467
An Assessment of Integrated Flywheel System Technology
[NASA-CP-2346] 05 p0604 N85-13850
Rotating assembly working group summary
05 p0604 N85-13851
Electromechanical/electromagnetics working group summary 05 p0604 N85-13852
Electrical/electronics working group summary
05 p0604 N85-13853
Dynamics and controls working group summary
05 p0604 N85-13854
A summary of the 1983 Integrated Flywheel Technology Workshop 05 p0605 N85-13855
European development experience on energy storage wheels for space 05 p0605 N85-13856
Merits of flywheels for spacecraft energy storage
05 p0605 N85-13857
Comparative energy storage assessment item
05 p0605 N85-13858
Inertial storage for satellites 05 p0605 N85-13859
Flywheel-powered X-ray generator
05 p0605 N85-13861
Generic composite flywheel designs
05 p0606 N85-13864
Summary results of the DOE flywheel development effort 05 p0606 N85-13865
Flexible matrix composite laminated disk/ring flywheel
05 p0606 N85-13866
General Electric composite ring-disk flywheel: Recent and potential developments 05 p0606 N85-13867
The multipurpose composite flywheel
05 p0606 N85-13868
Flywheel containment and safety considerations
05 p0606 N85-13869
Magnetically suspended flywheel system study
05 p0607 N85-13873
Reaction wheels for kinetic energy storage
05 p0607 N85-13874
High-efficiency power conversion options for flywheel energy storage systems 05 p0607 N85-13876
Motor/generator and electronic control considerations for energy storage flywheels 05 p0608 N85-13878
Torque command steering law for double-gimbaled control moment gyros applied to rotor energy storage
05 p0608 N85-13879
Potential of flywheels for spacecraft energy storage
05 p0609 N85-13890
Ultrasonic characterization of advanced composite flywheels
[DE85-000158] 11 p1593 N85-20026
Operating characteristics of a 0.87 kW-hr flywheel energy storage module
[NASA-TM-87036] 17 p2974 N85-28371
Strategic defense initiative
[DE85-012778] 24 p4150 N85-35735

FOAMS
Design, manufacture, and testing of compliant coatings for reduction of turbulent drag
[AD-A145510] 02 p0198 N85-11323
Insulation bonding test system
[NASA-CASE-MFS-25862-1] 11 p1610 N85-20126
X-ray gauge measures areal density variations as small as 0.1%
[DE85-003774] 12 p1854 N85-21629
Hydrolysis of plastic wastes with the aim of recovering and reprocessing the starting components (recycling)
[BMFT-FB-T-84-250] 12 p1885 N85-21828
Determination of toxicity of combustion products of habitability foams concurrently with flammability studies of these materials
[AD-A149647] 12 p1905 N85-21961
Exploratory development of foams from liquid crystal polymers
[NASA-CR-172510] 13 p2036 N85-22754
Development of nitrile rubbers and foams having a high static modulus and low creep
[BR91465] 14 p2259 N85-24001
Atmospheric frontal zone studies
[NASA-CR-175293] 16 p2833 N85-27469
Low density inorganic foams fabricated using microwaves
[DE85-007708] 18 p3080 N85-29051
Dynamics of thin-film breakup in a constricted pore
[DE85-008442] 18 p3101 N85-29199
Foamglass solar window collector
[DE85-009197] 18 p3129 N85-29374
Results of variable enthalpy tests of CPR-488 TIP panels in MSFC Hot Gas Facility
[NASA-CR-170889] 24 p4072 N85-35237
Results of tests of Insta-Foam Thermal Protection System (TPS) material for protection of equipment inside the SRB aft skirt
[NASA-CR-170892] 24 p4081 N85-35295

FOCI
NT PLASMA FOCUS
New focal plane detector system for the broad range spectrometer
[DE85-005370] 16 p2788 N85-27201

FOCUSING
NT DEFOCUSING
NT SELF FOCUSING
Ultrasonic synthetic aperture focusing using unfocused pulse-echo transducers
[AERE-R-11230] 01 p0057 N85-10374
Dark focus: Intersubject variation, intrasubject stability, and relationship to near retinoscopy
[AD-A145489] 02 p0235 N85-11530
Focusing beam of 1-GeV protons with volumetric capture to the mode of channeling by bent single crystal
02 p0268 N85-11750
Focusing effects of a laser beam in the nonresonant multiphoton ionization (MPI) of gases
[LP-207] 04 p0506 N85-13231
Focussing and confinement
[DE84-016181] 05 p0640 N85-14106
Calculated parameters for the initial part of an accelerator with high-frequency quadrupole focusing
[RAE-TRANS-2122] 07 p1040 N85-16600
Emerging technology of synthetic aperture focusing for ultrasonic testing
[DE85-000373] 09 p1378 N85-18664
Subreflector focusing techniques applied to new DSS-15 and DSS-45 34-meter antennas
10 p1464 N85-19233
Axial focusing of signal from distant point radiator reflected twice in deep paraboloid
13 p2078 N85-22979
Effects of focusing on HRS focal-plane polarimeter measurements
[DE85-004627] 13 p2160 N85-23406
Design of a variable-focal-length optical system
[NASA-CR-175710] 15 p2651 N85-26349
Streak tube characterization
[DE85-009674] 17 p2956 N85-28255
DOE/Sandia point-focus concentrator program, draft
[DE85-008209] 17 p3038 N85-28793
Mass spectrometry technology at the Jet Propulsion Laboratory (JPL) 18 p3157 N85-29552
Applications and investigations of second harmonic generation 19 p3367 N85-30878
Advanced ultrasonic imaging of piping in Dresden and Vermont Yankee reactors
[TI85-010049] 20 p3464 N85-31520
Particle sizing from forward scattered light at two angles using a Variable-Focal-Length optical system
[AD-A154164] 20 p3533 N85-31980
Background equatorial astronomical measurements focal plane assembly (refurbished HI STAR SOUTH)
[AD-A155215] 21 p3590 N85-32313
Existence of smooth solutions in problems of electromagnetic radiation focusing
21 p3697 N85-32972
Theoretical and computational research on the focused transport of intense charged particle beams
[DE85-012980] 23 p3972 N85-34621
Parametric stability of analytical close-range photogrammetry 24 p4107 N85-35461

FOG
An operational numerical model for prediction of fog and stratus 01 p0080 N85-10537
A 1-dimensional model with a sub-grid scale condensation scheme for stratiform clouds and fog
01 p0080 N85-10538
An operational forecasting system for stratus and fog with sodar 01 p0081 N85-10539
Preparation steps for the use of one-dimensional interpretation models for nowcasting purposes in the German weather net 01 p0081 N85-10540
Studies of the ocean surface and the coupling between the sea and the atmosphere
[AD-A146546] 06 p0841 N85-15339
An evaluation of an advection fog prediction model
[AD-A147436] 07 p1008 N85-16403
Fog advection in the Namib 16 p2831 N85-27454
Fog activation and supersaturation
21 p3650 N85-32678
The interaction of polynuclear aromatic hydrocarbons PAH's with water vapor and their role as condensation nuclei in the formation of haze and fog
21 p3652 N85-32695
Ice fog as an electro-optical obscurant
[AD-A155059] 21 p3705 N85-33015

FOIL BEARINGS
Effects of silver and group 2 fluorides addition to plasma sprayed chromium carbide high temperature solid lubricant for foil gas bearing to 650 deg C
[NASA-TM-86895] 06 p0770 N85-14928

FOILS (MATERIALS)
NT METAL FOILS
Progress on solar absorber selective paint research
[DE84-015536] 04 p0480 N85-13059
Strong-coupling superconductivity of Mg in proximity to Ta
[DE84-015462] 04 p0569 N85-13627
Pulsed electric discharge laser technology. Electron beam window foil material
[AD-A146420] 06 p0813 N85-15162
Electron beam propagation along charged foils
[DE85-002137] 06 p0861 N85-15472
High efficiency electron beam gun foil support
[AD-D011434] 08 p1159 N85-17312
Beam-foil spectroscopy of highly ionized aluminum atoms 09 p1390 N85-18746
AEM with a convergent beam
[DE85-000667] 11 p1714 N85-20784
Time-integrated yield for the Joint European Torus (JET), April - September 1984
[AERE-M-3449] 17 p3038 N85-28797
Flux pinning and flux flow studies in superconductors using flux flow noise techniques
[DE85-010814] 19 p3376 N85-30945
Plasma mass and effective inductance in a small railgun
[AD-A154644] 21 p3589 N85-32304
Plating density standards
[DE85-010014] 21 p3591 N85-32318
Rhodium-103 and Indium-115 inelastic scattering reactions for fission neutron dosimetry
21 p3703 N85-33004
Buildup of electric charge in foil dielectrics during gamma irradiation 22 p3770 N85-33363
Fast shutter apparatus
[DE85-006501] 23 p3928 N85-34343
System expectations for Pioneer 1 foil implosion experiments
[DE85-014129] 24 p4091 N85-35359

Diagnostics for Pioneer 1 imploding plasma experiments
[DE85-014120] 24 p4159 N85-35787

FOKKER AIRCRAFT
NT F-27 AIRCRAFT

FOKKER BOND TESTERS
U ADHESION TESTS

FOKKER F 27 AIRCRAFT
U F-27 AIRCRAFT

FOKKER FRIENDSHIP AIRCRAFT
U F-27 AIRCRAFT

FOKKER-PLANCK EQUATION
Stochastic methods for the description of multiparticle production
[DE84-009981] 10 p1556 N85-19810
Beam loss due to the aperture limitation resulting from intrabeam scattering
[DE85-005138] 12 p1930 N85-22124
On filter binary processes
[AD-A150328] 13 p2063 N85-22890
Steady state solution of the Fokker-Planck equation combined with unidirectional quasilinear diffusion under detailed balance conditions
[DE85-004917] 14 p2425 N85-24959
Kinetic theory and simulation of multi-species plasmas in Tokamaks excited with ICRF microwaves
[DE85-008119] 16 p2868 N85-27691
Random vibration of nonlinear, parametrically excited systems 19 p3282 N85-30351
Fokker-Planck calculation of hot electron formation in the thermal barrier region of tandem mirror Gamma-10
[IPPJ-726] 23 p3979 N85-34669
Pitch angle distributions of solar energetic particles and the local scattering properties of the interplanetary magnetic field
[SH-3.1-13] 23 p4002 N85-34816
Numerical descriptions of cosmic-ray transport
[SH-4.1-3] 23 p4004 N85-34829

FOLDING STRUCTURES
Large-diameter astromast development
[NASA-CR-171201] 03 p0342 N85-12200
High performance deployable antenna structures 05 p0625 N85-14001
Development of a foldline concept for automatic refolding of a flexible blanket (folding analysis) --- spaceborne solar generators
[ESA-CR(P)-1933] 08 p1179 N85-17426
Deployable folded antenna apparatus
[AD-D011503] 12 p1832 N85-21495
Variable geometry truss concept
[REPT-614] 12 p1865 N85-21697
SPOT solar array 13 p2009 N85-22595
Retractable Rigid Solar Generator (GSR) 13 p2009 N85-22597
Blanket integrated cushioning of foldable and retractable solar arrays 13 p2011 N85-22612
Synchronously deployable tetrahedral truss reflector 14 p2231 N85-23827
Retractable Rigid Solar Generator (GSR)
[SNIAS-851-440-101] 20 p3484 N85-31654
The SPOT solar array
[SNIAS-851-440-103] 20 p3485 N85-31656

FOLDS (GEOLOGY)
Structural observations in the Circle quadrangle, Yukon-Tanana Upland, Alaska 04 p0517 N85-13298
Structural investigation of the Grenville Province by radar and other imaging and nonimaging sensors 08 p1147 N85-17237
Structural morphology and associated strain within parts of the US section of the Kootenay Arc, NE, Washington 09 p1352 N85-18505
Normal-fault and fold development in sedimentary rocks above a pre-existing basement normal fault 13 p2131 N85-23259
Mechanisms of basalt-plains ridge formation 13 p2198 N85-23643
Terrestrial analogs for planetary wrinkle ridges 13 p2199 N85-23644
Using remote photographs in prospecting for hydrocarbons on the Kerch Peninsula 22 p3735 N85-33154

FOLIAGE
Scattering from foliage covered terrain
[AD-A154724] 21 p3574 N85-32226
Throughfall rate and chemistry studies: Whiteface Mountain
[DE85-012407] 23 p3947 N85-34464

FOOD
Assessment of radiation dosages obtained by intake of radioactive fallout contaminated food
[VTT-292] 07 p1017 N85-16460
Characterization of heat transfer in nutrient materials --- space flight feeding
[NASA-CR-171841] 08 p1199 N85-17551
Controlled Ecological Life Support Systems (CELSS) 15 p2688 N85-26604

FOOD CHAIN
Hollings hungry mantid model for the invertebrate functional response considered as a Markov process. Part 3: Mathematical elaborations
[CWI-AM-R8407-PT-3] 05 p0722 N85-14639
Models and parameters for environmental radiological assessments
[DE81-027154] 11 p1678 N85-20573
From microbial communities to cells 21 p3659 N85-32728
The 1984 environmental monitoring report, Sandia National Laboratories, Albuquerque, New Mexico
[DE85-011175] 22 p3811 N85-33607
The 1984 environmental monitoring program report for Idaho National Engineering Laboratory site
[DE85-011209] 22 p3812 N85-33611
Chemical composition of Musca domestica L. larval and pupal biomass when developing in organic waste of biological life-support system for man 22 p3824 N85-33691

FOOD PROCESSING
NT CANNING
NT PRESERVING
USSR report: Life sciences. Biomedical and behavioral sciences
[JPRS-UBB-84-015] 07 p1010 N85-16416
Feasibility of producing a range of food products from a limited range of undifferenitiated major food components
[NASA-CR-177329] 07 p1020 N85-16473
Food Service and Nutrition for the Space Station
[NASA-CP-2370] 14 p2393 N85-24733
The context for food service and nutrition in the space station 14 p2393 N85-24734
Food service management 14 p2393 N85-24736
Preparation methods: Past and potential methods of food preparation for space 14 p2393 N85-24738
Use of irradiated foods 14 p2393 N85-24740
Equipment for hot-to-serve foods 14 p2393 N85-24741
Packaging's contribution for the effectiveness of the space station's food service operation 14 p2394 N85-24746
Packaging for food service 14 p2394 N85-24747

FORBIDDEN BANDS
Forbidden lines of oxygen in comet spectra 02 p0163 N85-11105
Formation of lattice defects by nitrogen laser exposure in A2B6 semiconductors with wide forbidden band 02 p0258 N85-11692
Nonlinear absorption of laser radiation in InP and in GaAs 02 p0266 N85-11740
Magnetoabsorption of weak light wave in presence of intense light wave in semiconductor with narrow forbidden band 02 p0267 N85-11743
Cascaded solar photovoltaic cells based on InP-GaInPAs and InP-CdS heterostructures 02 p0268 N85-11749

FORBIDDEN TRANSITIONS
Collision-induced dipole moments
[AD-A147682] 08 p1121 N85-17063
Theoretical studies of atomic transition
[DE85-001325] 09 p1381 N85-18687
Excitation of some alkaline Earth-like ions
[DE85-010737] 20 p3529 N85-31951
Ionization detection of stimulated Raman spectra
[DE85-010672] 22 p3746 N85-33216

FORBUSH DECREASES
Some features of the interplanetary medium during Forbush decreases
[NOTA-INTERNA-836] 18 p3202 N85-29866
The longitudinal asymmetry of the interplanetary perturbation producing Forbush decreases
[IFSI-84-18] 20 p3546 N85-32065
Interplanetary disturbances during Forbush decreases
[IFSI-84-10] 20 p3547 N85-32075
Some properties of flare-not-associated Forbush decreases
[IFSI-84-13] 20 p3548 N85-32077
the role of shock waves in modulation of galactic cosmic rays
[SH-4.1-7] 23 p4005 N85-34831
The intensity recovery of Forbush-type decreases as a function of heliocentric distance and its relationship to the 11-year variation
[SH-4.1-9] 23 p4005 N85-34832
Cumulative effect of Forbush decreases in the heliospheric modulation during the present solar cycle
[SH-4.1-10] 23 p4005 N85-34833
Drift and Forbush decreases
[SH-5.1-2] 23 p4041 N85-35056
Anomalous short-term increases in the galactic cosmic ray intensity: Are they related to the interplanetary magnetic cloud-like structures?
[SH-5.1-3] 23 p4041 N85-35057
The flare origin of Forbush decreases not associated with solar flares on the visible hemisphere of the Sun
[SH-5.1-4] 23 p4041 N85-35058
Longitudinal dependence of the interplanetary perturbation produced by energetic type 4 solar flares and of the associated cosmic ray modulation
[SH-5.1-5] 23 p4042 N85-35059
Rigidity spectrum of Forbush decrease
[SH-5.1-6] 23 p4042 N85-35060
Spectral analysis of the Forbush decrease of 13 July 1982
[SH-5.1-7] 23 p4042 N85-35061
The theoretical and experimental investigation of cosmic ray Forbush-effects
[SH-5.1-20] 23 p4044 N85-35072
Peculiarities of Galactic Cosmic Ray (GCR) anisotropy variation in connection with the recurrent and sporadic Forbush effects
[SH-5.1-21] 23 p4044 N85-35073
Cosmic ray modulation by high-speed solar wind fluxes
[SH-5.1-22] 23 p4044 N85-35074
The neutron moderated detector and groundbased cosmic ray modulation studies
[SH-9.1-13] 23 p4052 N85-35128
The influences of the galactic cosmic ray on the atmospheric ozone
[SH-10.1-1] 23 p4053 N85-35138

FORBUSH EFFECT
U FORBUSH DECREASES

FORCE
Primer for mass metrology
[PB85-121424/GAR] 09 p1305 N85-18199

FORCE DISTRIBUTION
Control of the dynamic response of a damped membrane by distributed forces
[CSIR-TWISK-312] 01 p0061 N85-10406
Flight and wind-tunnel comparisons of the inlet-airframe interaction of the F-15 airplane
[NASA-TP-2374] 04 p0455 N85-12894
Mathematical modeling of assembly processes involving use of sensitized robots 04 p0488 N85-13111
On the use of marker loads and replicas for measuring growth rates for small cracks 14 p2319 N85-24331
Experimental and theoretical determination of the wing-induced lateral wind on the tail surfaces in oscillating rolling motion. Part 1: Application of the Mobile Oscillating Derivatives (MOD) on an experimental part
[IFD-1/84-PT-1] 18 p3061 N85-28939
Application of two-dimensional unsteady aerodynamic to a free-tip rotor response analysis
[NASA-CR-177348] 19 p3215 N85-28953
Turbine blade-tip clearance excitation forces
[NASA-CR-171534] 19 p3220 N85-28980
On high strain rate fragmentation of a closed vessel 23 p3904 N85-34187

FORCE FIELDS
U FIELD THEORY (PHYSICS)

FORCE-FREE MAGNETIC FIELDS
Measurements of Solar Vector Magnetic Fields
[NASA-CP-2374] 18 p3203 N85-28869
On the numerical computation of nonlinear force-free magnetic fields 18 p3203 N85-28871
Modeling solar magnetic structures 18 p3203 N85-28872

FORCED CONVECTION
Internal forced convection to low Prandtl number gas mixtures
[AD-A148932] 10 p1484 N85-19398
Heat transfer in aeropropulsion systems
[NASA-TM-87066] 20 p3453 N85-31444
Forced convection on solar collector arrays
[DE85-010381] 21 p3585 N85-32287

FORCED OSCILLATION
U FORCED VIBRATION

FORCED VIBRATION
Normal mode method of solving problem forced oscillations of rib-reinforced shell of revolution in liquid 02 p0273 N85-11781
The Shock and Vibration Digest, volume 16, no. 9
[AD-A146779] 07 p0976 N85-16200
A review of approximate methods for determining the vibrational modes of membranes 09 p1331 N85-18363
Journal of Research of the National Bureau of Standards, volume 89, number 2, March - April 1984
[PB85-115426] 12 p1926 N85-22103
A preliminary investigation of the dynamic force-calibration of a magnetic suspension and balance system
[NASA-CR-172580] 14 p2226 N85-23806
Study of dynamic characteristics of prefabricated gas turbine compressor rotor 14 p2272 N85-24079
A study of internal and distributed damping for vibrating turbomachiner blades
[NASA-CR-175901] 17 p2898 N85-27868

FORCED VIBRATORY MOTION EQUATIONS
U EQUATIONS
U FORCED VIBRATION
FOREBODIES
NT NOSE CONES
NT NOSES (FOREBODIES)
Effects of body shape on the aerodynamics of a body of revolution at Mach numbers from 1.6 to 4.6
[NASA-TM-86345] 07 p0893 N85-15657
Free-surface boundary layer and the origin of bow vortices
[AD-A147427] 07 p0960 N85-16083
FORECASTING
NT DELPHI METHOD (FORECASTING)
NT LONG RANGE WEATHER FORECASTING
NT NOWCASTING
NT NUMERICAL WEATHER FORECASTING
NT PATTERN METHOD (FORECASTING)
NT PERFORMANCE PREDICTION
NT PREDICTION ANALYSIS TECHNIQUES
NT PROFILE METHOD (FORECASTING)
NT STATISTICAL WEATHER FORECASTING
NT TECHNOLOGICAL FORECASTING
NT WEATHER FORECASTING
Future scenarios and ozone change
[DE84-014781] 01 p0085 N85-10573
Outline of a new emissions model for military and civilian aircraft facilities
[DE84-016455] 04 p0531 N85-13294
Subhourly wind forecasting techniques for wind turbine operations
[DE84-016205] 04 p0539 N85-13427
General model of earthquakes and the place of warnings in it 07 p0981 N85-16232
Earthquake forecasting research in the Ukraine
07 p0981 N85-16233
Crop yield forecasting 07 p1001 N85-16360
A note on using the integrated form of ARIMA forecasts
[AD-A146965] 07 p1030 N85-16536
Life cycle cost management master plan for the Defense Communications Agency
[AD-A146876] 07 p1050 N85-16668
The Air Force can improve its forecasts of aircraft spare parts requirements
[AD-A147911] 07 p1053 N85-16682
On seismic waves 08 p1171 N85-17383
An HF communications frequency-management procedure for forecasting the frequency of optimum transmission
[AD-A149191] 10 p1467 N85-19254
A model for forecasting runway surface temperature and verification with subjective forecasts
[TR-28] 10 p1518 N85-19569
Bootstrapping the Kalman filter
[AD-A150509] 13 p2153 N85-23370
Real-time enhancement of a climatology or forecast of ocean thermal structure using observed ocean temperatures
[AD-A151118] 15 p2604 N85-26049
Role of supercomputers in energy research programs
[DE85-008865] 15 p2624 N85-26172
Kalman filtering and exponential smoothing in economics 15 p2635 N85-26246
Intermediate term forecasting techniques for management
[AD-A151370] 15 p2637 N85-26262
Satellite provided customer promises services, a forecast of potential domestic demand through the year 2000. Volume 4: Sensitivity analysis
[NASA-CR-174662] 16 p2769 N85-27092
Use of forest modeling to project acid rain effects
[DE85-005251] 16 p2821 N85-27400
An evaluation of discretized conditional probability and linear regression threshold techniques in model output statistics forecasting of visibility over the north Atlantic Ocean
[AD-A151955] 16 p2857 N85-27619
Historical perspective on the Moon base: The British perspective
[DE85-005905] 17 p2907 N85-27925
Forecast verification of the 10.7 centimeter solar flux and the Ap daily geomagnetic activity indices
[AD-A152959] 17 p2993 N85-28499
Discovery in earthquake forecasting and seismic zoning recorded 19 p3295 N85-30426
Flood-runoff forecasting with HEC1F
[AD-A154286] 19 p3300 N85-30456
Optimization of single and multi-component analytical techniques
[HSE-TRANS-10987] 19 p3347 N85-30744
New estimating procedures for surface runoff, sediment yield, and contaminant transport in Los Alamos County, New Mexico
[DE85-011690] 21 p3606 N85-32393
Forecasting atmospheric visibility over the summer north Atlantic using the principal discriminant method
[AD-A155637] 21 p3637 N85-32593
Study to encourage and facilitate industrial investment and involvement in space
[NASA-CR-176152] 23 p3898 N85-34147
The NORDA/FNOC (Naval Ocean Research and Development Activity's/Fleet Numerical Oceanography Center) Polar Ice Prediction System (PIPS)-Arctic: A technical description
[AD-A156332] 24 p4126 N85-35577
FORECASTS
U FORECASTING
FOREIGN POLICY
NT INTERNATIONAL COOPERATION
NT INTERNATIONAL RELATIONS
NT OUTER SPACE TREATY
FORENSIC SCIENCES
U LAW (JURISPRUDENCE)
FOREST FIRE DETECTION
Aerospace technology determines forest-fire danger
19 p3295 N85-30427
FOREST MANAGEMENT
The 1984 NASA/ASEE summer faculty fellowship program
[NASA-CR-174138] 04 p0574 N85-13663
Modeling long-term changes in forested landscapes and their relation to the Earth's energy balance
05 p0653 N85-14194
Forest cover monitoring by remote sensing in Great Britain 05 p0656 N85-14214
Integrative investigation on forest damage detection based on airborne Multispectral Scanner data
05 p0656 N85-14215
Response of unmanaged forests to CO2-induced climate change: Available information, initial tests and data requirements
[DOE/NSB-0053] 12 p1683 N85-21817
Remote sensing used for study of forest resources
13 p1983 N85-22440
Technologies to sustain tropical forest resources
[TI85-901085] 13 p2126 N85-23241
FORESTS
NT RAIN FORESTS
Fungi of Mt. Babia Gora. 2: Indicative value of macromycetes in forest associations. A: Initial considerations
[NASA-TM-77485] 01 p0094 N85-10632
Fungi of Mount Babia Gora. 3: The indicating value of macromycetes in the forest associations
[NASA-TM-77486] 01 p0094 N85-10633
Remote sensing applied to forest resources
[E85-10012] 02 p0216 N85-11425
Shuttle Experimental Radar for Geological Exploration (SERGE) project: Field work relating to the Shuttle Experimental Radar A (SIR-A) in Brazil (phase 2)
[NASA-CR-174033] 02 p0219 N85-11444
Some principles of plant resources evaluation using remotely sensed data 04 p0543 N85-13459
Integrative investigation on forest damage detection based on airborne Multispectral Scanner data
05 p0656 N85-14215
Acid rain and tree physiology: Some hypotheses for observed changes in forest productivity
[DE84-016568] 05 p0672 N85-14318
Image variance and spatial structure in remotely sensed scenes — South Dakota, California, Missouri, Kentucky, Louisiana, Tennessee, District of Columbia, and Oregon
07 p0986 N85-16265
Forest area estimates from LANDSAT MSS and forest inventory plot data
[PB85-105617/GAR] 07 p0990 N85-16290
Deciduous forest radiation regimes: Effects of forest structure, phenology and Earth-Sun geometry upon their spatial, temporal and spectral variability
[AD-A146804] 07 p0996 N85-16327
Simulating responses to expected climate change in eastern North America: Applications to decision-making in the forest industry
[DE85-001272] 07 p1008 N85-16406
New Zealand SIR-B science investigations
08 p1144 N85-17218
Microwave and optical remote sensing of forest vegetation 08 p1146 N85-17228
The extension of an invertible coniferous forest canopy reflectance model using SIR-B and LANDSAT data
08 p1149 N85-17246
Test plan for the forest-echo experiment
[DE84-017175] 09 p1343 N85-18447
Smoother terrain-machine
[AD-P004296] 09 p1409 N85-18873
UHF radiowave propagation through forests
[AD-A149518] 10 p1467 N85-19256
UHF communications through forested propagation channels 10 p1470 N85-19260
Analysis of data acquired by synthetic aperture radar and LANDSAT Multispectral Scanner over Kershaw County, South Carolina, during the summer season
[E85-10071] 10 p1503 N85-19485
Anaysis of the quality of image data required by the LANDSAT-4 Thematic Mapper and Multispectral Scanner — agricultural and forest cover types in California
[E85-10074] 10 p1504 N85-19488
Effects of air pollution and acid rain on forest decline
[GPO-37-458] 12 p1683 N85-21818
Modeling interception of rainfall by forests and the role of interception in the water balance
[DE85-002822] 12 p1684 N85-21825
The use of Thematic Mapper data for land cover discrimination: Preliminary results from the UK SATMaP programme 13 p2121 N85-23207
Areas with forest soils sensitive to acidic deposition under alternative damage hypotheses
[DE85-005257] 13 p2130 N85-23257
A comparative evaluation of the effects of acid precipitation, natural acid production and harvesting of cation removal from forests
[DE85-005254] 15 p2589 N85-25961
Use of forest modeling to project acid rain effects
[DE85-005251] 16 p2821 N85-27400
A transport theory of millimeter wave propagation in woods and forests
[AD-A151883] 17 . p2947 N85-28196
A comparative evaluation of the effects of acid precipitation, natural acid production and harvesting on cation removal from forests
[DE85-010821] 19 p3309 N85-30511
Study of the formation of particles from natural hydrocarbons released by vegetation
21 p3644 N85-32640
Snow cover in the Siberian forest-steppe
[NASA-TM-77914] 23 p3943 N85-34435
Effects of acid rain on forest nutrient status
[DE85-012486] 23 p3947 N85-34463
FORGING
Calculation of the optimum conditions for the forging of plates
[BLL-M-35757-(5828.4)] 02 p0189 N85-11260
Tensile and crack propagation tests on aluminum alloys of the 2000 and 7000 series in laminated plate and forged products
[M2-678300] 03 p0373 N85-12383
The role of microstructure in the modelling of plastic flow in P/M superalloys at forging temperatures and strain rate 06 p0796 N85-15090
Control of microstructure during hot working of Ti-6242 06 p0797 N85-15091
Static and dynamic fracture toughness characterization of SA508 forging and SA533B welded plate — pressure vessel steels
[CISE-2258] 08 p1131 N85-17127
Application of electricity to the reheating of metals prior to forming. Forging, lamination, induction
[BLL-TR-T6399/BG/MRS14903/84]
08 p1137 N85-17160
Engineering property comparisons of PM and IM aluminum alloy forgings
[AD-B088146L] 08 p1173 N85-17398
Correction of engraving stamp for forming blanks of gas turbine engine blades 09 p1307 N85-18213
Robotized blanks loader for new forge press
10 p1461 N85-19216
Dependence of mechanical properties of large VT3-1 alloy forgings on microstructure parameters
11 p1602 N85-20072
Weldability and mechanical property characterization of weld clad alloy 800H tubesheet forging
[DE85-001737] 11 p1609 N85-20116
USSR report: Machine tools and metalworking equipment
[JPRS-UMM-85-005] 13 p2051 N85-22839
Experience in use of optical theodolite for machine construction 14 p2267 N85-24049
Clutchless mechanism for engagement of forging press 14 p2268 N85-24051
USSR report: Machine tools and metalworking equipment
[JPRS-UMM-85-004] 14 p2284 N85-24152
Automated, robotized forge-press systems viewed
14 p2264 N85-24153
Robots for application in forge-press operation
14 p2284 N85-24154
Titanium alloys, products, standards listed
15 p2533 N85-25626
Automatic manipulators for forging rollers
16 p2762 N85-27042
Industrial robots and automatic manipulators for forging and pressing operations at Second International Exhibition 16 p2762 N85-27044

Precision die forging of blades or gas turbines
17 p2940 N85-28148

Mechanizing of handling operations in drop forging with hammers and presses (conducted ergonomical examinations)
[BMFT-FB-HA-84-051] 17 p3002 N85-28561

Powder metallurgy forged gear development
[NASA-TM-87483] 18 p3117 N85-29295

Distribution of density in closed-impression die forging of axisymmetrical products from metal powders
19 p3245 N85-30118

Influence of the molding joint plane on the fatigue resistance of the alloys 7010 and 7050. Test Report No. M1-631600
[PV-M1-631600] 20 p3470 N85-31562

Assessment of metal heating technologies for ferrous forging: A pilot study of the form value of natural gas
[PB85-204394] 24 p4084 N85-35314

Establishment of a Computer-Aided Design (CAD)-Computer-Aided Manufacturing (CAM) process for the production of cold forged gears
[AD-A155796] 24 p4137 N85-35644

FORM
U SHAPES

FORM FACTORS

Dirac single particle wave functions in inelastic electron scattering
[DE84-015129] 02 p0279 N85-11814

Measurement of the induced moment magnetic form factor of a heavy fermion superconductor
[DE85-004165] 12 p1942 N85-22194

Paramagnetic form factors from itinerant electron theory
[DE85-005272] 16 p2750 N85-26973

FORM PERCEPTION
U SPACE PERCEPTION

FORMALDEHYDE

Direct measurements of nitrous acid, nitrogen dioxide and formaldehyde in auto exhaust by differential optical absorption spectroscopy
[PB84-229269] 06 p0767 N85-14905

Long term durability of urea formaldehyde glued joints removed from Vampire aircraft
[AD-A149053] 10 p1424 N85-18985

The decomposition of gas phase formaldehyde by plasma discharge
[AD-A153202] 17 p2921 N85-28007

Synthesis of 2,4,8,10-tetroxaspiro5,5undecane
[NASA-CASE-ARC-11243-2] 22 p3741 N85-33187

Oxidation of formaldehyde solutions used for the preservation of reverse osmosis membranes
[PB85-185585] 22 p3742 N85-33194

Modeling of auto exhaust smog chamber data for EKMA development
[PB85-186482] 22 p3813 N85-33619

FORMALISM

Model theory for infinitely deep languages
[ISSN-0355-0087] 01 p0101 N85-10674

On the formal description and derivation of temporal proof rules for program properties
[TUM-I8405] 01 p0101 N85-10675

Experimental techniques of formal specifications for the design of tested and reliable computer programs
[ENST-84E007] 05 p0716 N85-14591

The period of orbit as a test of the general theory of relativity
05 p0742 N85-14772

Analysis of the impact of a deformable missile model on a deformable obstruction
[BLL-RISLEY-TR-8534-(9091.9F)]
06 p0859 N85-15459

Self-induced nonlinear effects in optical fibers: A unified approach
[FUB-67-1982] 09 p1385 N85-18713

An algorithm to test for confluence in a system of left to right rewrite rules
[AD-A154066] 19 p3335 N85-30662

FORMAT

Standardization of data formats for radar altimeter data
03 p0384 N85-12455

WXR (hydrologic weather wire and PLT product software package)
[PB84-237221] 04 p0541 N85-13442

Formats for numerical and textual data in data processing
[DFVLR-MITT-84-07] 04 p0551 N85-13504

Distribution of the K-corona over the polar regions of the solar disk: 1965-1983
[PB84-230077] 06 p0835 N85-15317

Standard SHEF (Standard Hydrometeorologic Exchange Format) decoder Version 1.1
[PB85-106508/GAR] 06 p0840 N85-15332

RATFOR user's guide version 2.0
[NASA-CR-166601] 07 p1023 N85-16490

Document interchange format
[PB84-217033] 07 p1027 N85-16517

Technical order managers handbook: Utilization assessment
[AD-A147579] 07 p1055 N85-16604

Introduction to LBL graphics
[DE85-000389] 09 p1369 N85-18600

Pictorial format display evaluation
[AD-A148252] 10 p1425 N85-18986

Standardized format for computer series
[PB85-109668] 11 p1705 N85-20734

Atmospheric handbook: Atmospheric data tables available on computer tape
[PB85-108512] 12 p1891 N85-21867

The four forms of omega
[AD-A149694] 12 p1915 N85-22020

M68000 RNF text formatter user's manual
[NASA-TM-86327] 13 p2146 N85-23320

Multiple resources and display formatting: The implications of task integration in a simulated air traffic control task
[AD-A150713] 14 p2292 N85-24205

Factors affecting dwell times on digital displaying
[NASA-TM-86406] 14 p2390 N85-24722

Use of COSMIC NASTRAN in a design department
15 p2575 N85-25881

User manual for IMAGER: The DREO (Defence Research Establishment Ottawa) image processing system
[AD-A151754] 15 p2653 N85-26362

Design of an interface to an information retrieval network
16 p2877 N85-27750

A method to calculate the parameters of wings of arbitrary planform
[AD-A152669] 17 p2892 N85-27831

Airport and airway system cost allocation model. Volume 7: User's manual
[AD-A152677] 17 p2906 N85-27917

VIDTEX
[PB85-175669] 19 p3318 N85-30567

Cultural data base implementation study and computer-aided scene modeling system users manual
[AD-A154232] 19 p3333 N85-30646

T sub EX font tables
[DE85-011394] 19 p3339 N85-30687

A model for a document maintenance system
23 p3960 N85-34542

FORMATION

Ionic mechanisms of soot formation in flames
[AD-A150119] 12 p1801 N85-21297

FORMATION HEAT
U HEAT OF FORMATION

FORMATIONS

A paleomagnetic study of the Prince William terrane and Nixon Fork terrane, Alaska 02 p0226 N85-11478

Paleozoic limestones of the Crazy Mountains and vicinity, Circle quadrangle, east-central Alaska
04 p0517 N85-13296

Late Paleozoic and early Mesozoic radiolarians in the Circle quadrangle, east-central Alaska
04 p0517 N85-13297

Morphology and mechanics of terraces in lunar craters
13 p2182 N85-23543

Application of far-field models to the disposal of nuclear waste in geologic formations
[DE85-005489] 14 p2420 N85-24932

Thermal-cycle testing of the G-tunnel heated block
[DE85-006408] 18 p3126 N85-29359

Implications for the Earth of the early dynamical environment 21 p3719 N85-33079

FORMING TECHNIQUES
NT CASTING
NT CENTRIFUGAL CASTING
NT COLD ROLLING
NT COLD WORKING
NT ELECTROFORMING
NT ELECTROHYDRAULIC FORMING
NT EXPLOSIVE FORMING
NT EXTRUDING
NT FORGING
NT HOT WORKING
NT INJECTION MOLDING
NT MAGNETIC FORMING
NT METAL DRAWING
NT METAL SPINNING
NT PRESSING (FORMING)
NT PULTRUSION
NT ROLL FORMING
NT SLIP CASTING
NT STAMPING

International Conference on Recent Developments in Specialty Steels and Hard Materials. Conference abstracts
[CSIR-S-256] 02 p0176 N85-11177

Process Modeling Applied to Metal Forming and Thermomechanical Processing
[AGARD-LS-137] 06 p0796 N85-15086

Microstructure, texture and formability of thin aluminum sheets 06 p0796 N85-1[illegible]

Numerical methods in metalforming
06 p0797 N85-1[illegible]

Finite element simulation of forging processes
06 p0797 N85-1[illegible]

Heliostat tested 07 p0994 N85-1[illegible]

USSR report: Machine tools and metalworking equipment
[JPRS-UMM-85-001] 08 p1139 N85-1717[illegible]

Electromagnetic processing of materials
[AD-A148804] 09 p1311 N85-18[illegible]

Factors influencing the ball milling of Si3N4 in water
[NASA-TM-86032] 10 p1450 N85-19[illegible]

Developments in GDR metal forming technology assessed 11 p1617 N85-20[illegible]

Aluminum alloy ATs5K5 (5% Zn + 5% Cu) for superplastic forming 13 p2026 N85-22[illegible]

Electrostatic forming and testing of polymer films on a 16-foot diameter test fixture
[NASA-TM-86328] 13 p2063 N85-22[illegible]

Equipment for performing surfaces of optical parts
14 p2286 N85-24[illegible]

Powder metallurgy production problems
15 p2497 N85-25[illegible]

New material, process spins off from Volvo LCP 2000 program 15 p2536 N85-25[illegible]

Preparation of metal for cold upsetting
[BLL-BISI-TRANS-22383-(9022.06)]
17 p2926 N85-28[illegible]

Application of 4-wire submerged arc method to welding UOE pipe
[BLL-BISI-TRANS-22417-(9022.06)]
17 p2972 N85-28[illegible]

State of stress and penetration of plastic deformation in forming
[BLL-BISI-22199-(9022.06)] 17 p2977 N85-28[illegible]

French, UK, Swedish research in powder metallurgy, HIP 18 p3088 N85-29[illegible]

FORMULAS (MATHEMATICS)

Model theory for infinitely deep languages
[ISSN-0355-0087] 01 p0101 N85-10[illegible]

What formulas are good for representing dipole and generalized oscillator-strength spectra
[DE84-014641] 02 p0278 N85-11[illegible]

Spatial mechanics formulas and exercises
05 p0601 N85-13[illegible]

Consolidation theory with consideration of finite plasticity
[REPT-9/1984] 16 p2796 N85-27[illegible]

Formulas for updating the generalized inverse of a symmetric matrix perturbed by a symmetric rank 2 matrix composed of 2 nonsymmetric DYADS
[AD-A151736] 16 p2858 N85-27[illegible]

The method of residual minimization in compressible steady flows
[AD-A153924] 18 p3100 N85-29[illegible]

About product formulas with variable step-size
[AD-A153527] 18 p3160 N85-29[illegible]

Tenth-order expansion formulae for the orbital eccentricity function K (sub lpq)(e) obtained using a symbolic algebraic manipulation system
[AD-A153754] 18 p3170 N85-29[illegible]

Aspects of SAR image segmentation
[AD-A154965] 21 p3575 N85-32[illegible]

FORMULATIONS

Finding the largest l(p)-ball in a polyhedral set
[AD-A153542] 18 p3170 N85-29[illegible]

FORTRAN

Three degree of freedom steady state point performance program: Updated version 1
[CSIR-NIAST-83/48] 01 p0001 N85-10005

Application guide for Hydrological Simulation Program FORTRAN (HSPF)
[PB84-215763] 01 p0064 N85-10427

Manual of phosphoric acid fuel cell stack three-dimensional model and computer program
[NASA-CR-174722] 01 p0067 N85-10447

ADS: A FORTRAN program for automated design synthesis, version 1.00
[NASA-CR-172460] 01 p0102 N85-10[illegible]

The CMC/3DPNS computer program for prediction of three-dimensional, subsonic, turbulent aerodynamic juncture region flow. Volume 3: Programmers' manual
[NASA-CR-165998] 02 p0197 N85-11316

Phosphoric acid fuel cell power plant system performance model and computer program
[NASA-CR-174638] 02 p0222 N85-11456

Proposal for a semiautomatic program testing system
[INPE-3262-TDL/178] 02 p0240 N85-11561

SMILE user's guide: A macro preprocessor for extending FORTRAN
[DE84-015984] 02 p0243 N85-11584

Programmer's guide for ASKF 77: A tool for programming of dialogs in FORTRAN and PASCAL
[FOA-C-30366-E1] 02 p0243 N85-11585

Convergent Technologies, mega frame, CTIX FORTRAN 77 version 2.1
[PB84-227768] 03 p0404 N85-12580
Digital Equipment Corp., VAX-11/782, VAX FORTRAN version 4.0
[PB84-227701] 03 p0405 N85-12582
Conversion of FEB (Fast and Easy Binary) utilities to ASCII FORTRAN
[AD-A145840] 03 p0406 N85-12596
Vertical coherence along a macroray path in an inhomogeneous anisotropic ocean
[AD-A145902] 03 p0416 N85-12660
Prime Computer, Inc., PRIME 750, FORTRAN-77 revision 19.4
[PB84-227628] 04 p0548 N85-13467
Control Data Corporation CYBER 205 model 442, FORTRAN 200 (G201-25)
[PB84-216290] 04 p0551 N85-13510
United Information Services, Inc., CRAY 1-S/2000, FORTRAN CFT 1.10
[PB84-227685] 04 p0552 N85-13512
Multigrid iteration solution procedure for solving three-dimensional sets of coupled equations
[DE84-018515] 04 p0555 N85-13532
Use of monitors in FORTRAN: A tutorial on the barrier, self-scheduling DO-loop and Askfor monitors
[DE84-018506] 05 p0715 N85-14567
Efficient sorting routines in FORTRAN 77
[OUEL-1529/84] 05 p0716 N85-14590
Some implementations of multigrid linear system solvers
[CWI-NM-R8401] 05 p0720 N85-14626
Digital Research incorporated, IBM PC XT, FORTRAN-77 V4.0
[PB84-243633] 06 p0849 N85-15388
Perkin-Elmer, Perkin-Elmer 3230, FORTRAN 7 D R00-00
[PB84-243682] 06 p0849 N85-15389
Gould Incorporated, Gould PS-3000, Gould PS-3000 FORTRAN 77 V2.1
[PB84-229178] 06 p0849 N85-15390
Digital Equipment Corporation, PDP-11/23-PLUS PDP-11 FORTRAN-77 V5.0
[PB84-227610] 06 p0851 N85-15405
Plexus Computers, Inc., Plexus P/60, Plexus FORTRAN 77 Version 1.1
[PB84-227659] 06 p0851 N85-15407
Modular Computer Systems, incorporated, MODCOMP CLASSIC 7860, MODCOMP FORTRAN 77/16 Version A.0
[PB84-230556] 06 p0852 N85-15411
Modular Computer Systems, Incorporated, MODCOMP CLASSIC 7860, MODCOMP NASA EXTENDED FORTRAN 76 Version A.40
[PB84-230549] 06 p0852 N85-15412
Sperry Corporation, 1100/80 ASC2 FORTRAN Level 11R1
[PB84-229194] 06 p0852 N85-15416
Wang Laboratories, Incorporated, Wang VS100, FORTRAN 77 Version 01.00.02
[PB84-228014] 06 p0852 N85-15419
Digital Equipment Corporation, DECSYSTEM-20 2060 Model B, FORTRAN-20 Version 10
[PB84-227974] 06 p0853 N85-15422
Convergent Technologies, NGEN CP001, CT FORTRAN Version 9.0
[PB84-229210] 06 p0856 N85-15442
Simplified continued fraction calculation of spherical Bessel functions
[AD-A146844] 06 p0858 N85-15455
RATFOR user's guide version 2.0
[NASA-CR-166601] 07 p1023 N85-16490
NOISEMAP 4.4 computer program update, operator's manual, addendum 1
[AD-A147091] 07 p1025 N85-16503
FORTRAN version of the quantitative energy-dispersive electron beam X-ray analysis program FRAME C
[PB84-240836] 07 p1027 N85-16519
Using the control system design environment in the design of a data link receiver unit for the Coast Guard HH-65A helicopter
[AD-A148624] 08 p1088 N85-16860
Validation of the communications link analysis and simulation system (CLASS) 08 p1100 N85-16954
Developing double sampling plans for attributes to meet sample size criteria
[AD-A148144] 08 p1205 N85-17587
COPES/ADS (Control Program for Engineering Synthesis) (Automated Design Synthesis) using the ADS optimization program
[AD-A148576] 08 p1206 N85-17588
Multitasking kernel for the C and FORTRAN programming languages
[DE85-001799] 09 p1370 N85-18609
Documentation for an instrument database system
[DE84-017302] 09 p1402 N85-18826
FORTRAN 66 analyser: User's manual
[PB85-111748] 10 p1542 N85-19724
DOS 21: PCDOS 2.0 support subroutine package for the IBM personal computer
[LA-10142-MS] 12 p1914 N85-22012
HGRAPH: A subroutine package for the IBM personal computer to support the Hercules Graphic Card
[LA-10144-MS] 12 p1914 N85-22013
ZTLCK: A subroutine package for the IBM personal computer to support the Zietech ZT1488 real time clock
[LA-10146-MS] 12 p1914 N85-22014
Ryan-McFarland Corporation, IBM PC model XT, RM/FORTRAN, version 2.0.0
[PB85-107993] 12 p1917 N85-22037
Ryan-McFarland Corporation, sun microsystem with sky fast floating point processor, RM/FORTRAN version 1.5.0
[PB85-108009] 12 p1917 N85-22038
Selection and use of general-purpose programming-language: Program examples, volume 2
[PB85-122000] 12 p1917 N85-22039
Selection and use of general-purpose programming language: Overview, volume 1
[PB85-122018] 12 p1917 N85-22040
Validation summary report, Burroughs Corporation, 820 FORTRAN release 4.0
[PB84-227792] 13 p2145 N85-23316
FORTRAN in the 90's
[DE85-006154] 13 p2148 N85-23332
Guidelines for development structured FORTRAN programs
[NASA-TM-86407] 14 p2402 N85-24806
Easyplot: An interactive, user-friendly graphics program
[AD-A150779] 14 p2404 N85-24824
A fast ray tracing routine for laterally inhomogeneous media
[AD-A150984] 14 p2421 N85-24936
A FORTRAN program for deep space sensor analysis
[AD-A151700] 15 p2489 N85-25366
The interactive plotting program: GRAPH
[AD-A151371] 15 p2623 N85-26185
GRID: A FORTRAN program for using a digitizing table to enter a finite element GRID
[AD-A151317] 15 p2628 N85-26196
Recent trends in software technology for vector processors 16 p2691 N85-26615
Pulsewidth modulated speed control of brushless dc motors
[AD-A151968] 16 p2778 N85-27148
An interactive computer package for use with simulation models which performs multidimensional sensitivity analysis by employing the techniques of response surface methodology
[AD-A151956] 16 p2846 N85-27548
Development of graphical time response using the OPTSYSX program
[AD-A152221] 16 p2848 N85-27557
Graphics package, version 4: User reference manual
[DE85-007694] 18 p3163 N85-29596
Introduction to programming multiple-processor computers
[DE85-010274] 18 p3164 N85-29599
Using MATHLIB on the IBM computer and sundry plotting examples with a taste of IMSL
[DE85-011395] 19 p3340 N85-30695
HANDTC: A FORTRAN program to calculate inner-zone terrain corrections
[DE85-011196] 19 p3340 N85-30699
Reliability of void detection in structural ceramics using scanning laser acoustic microscopy
[NASA-TM-87035] 21 p3597 N85-32337
SIGMA - A stochastic-integration global minimization algorithm
[AD-A154878] 21 p3671 N85-32806
A device-independent 2D plotting package written in FORTRAN
[RSRE-MEMO-3776] 23 p3956 N85-34514
CRAYCDC
[NASA-CR-177374] 24 p4137 N85-35639
CDCCRAY
[NASA-CR-177375] 24 p4137 N85-35640

FORWARD LOOKING INFRARED DETECTORS
U FLIR DETECTORS

FORWARD SCATTERING
Characterization of atmospheric conditions along transmission paths from a remotely piloted vehicle
[AD-A145527] 02 p0232 N85-11511
Description of amplitude scintillations on a 11 GHz slant path in terms of forward scattering from turbulent layers
[FI-455-TBR-76] 11 p1625 N85-20232
Surface forward scattering and reflection
[AD-A150115] 12 p1926 N85-22112
Application of forward scattering renormalization to scattering in turbid media
[AD-A153232] 17 p2959 N85-28271
Particle sizing from forward scattered light at two angles using a Variable-Focal-Length optical system
[AD-A154164] 20 p3533 N85-31980

FOSSIL FUELS
NT COAL
NT CRUDE OIL
NT LIGNITE
NT NATURAL GAS
NT PEAT
Analysis of potential combustion sorce impacts on acid deposition using an independently derived inventory, volume 1
[DE84-012005] 02 p0225 N85-11471
Humidity/cloud-radiation feedback on possible climate perturbation due to fossil fuel utilization
[DE85-008886] 18 p3133 N85-29402
Coal-Fired MHD Combustor Development Project, Phase 3D
[DE85-008822] 18 p3192 N85-29795
Control of acid deposition precursors through dry scrubbing
[DE85-010281] 19 p3235 N85-30056
Fracture detection and mapping for geothermal reservoir definition: An assessment of current technology, research, and research needs
[DE85-010627] 19 p3301 N85-30464
Current status of TVA's atmospheric fluidized bed combustion development efforts
[DE85-901209] 19 p3308 N85-30507
Technical guide for estimating fugitive dust impacts from coal handling operations. Volume 1: Project summary
[DE85-010948] 19 p3309 N85-30515

FOSSIL METEORITE CRATERS
U FOSSILS
U METEORITE CRATERS

FOSSILS
Post-Sonoman conodont biofacies of the Triassic of northwestern Nevada 03 p0390 N85-12497
Geographic and stratigraphic distribution of Miocene palynomorphs in north Idaho 03 p0390 N85-12498
Constraints on lunar origin: Evidence preserved in Precambrian stromatolites 04 p0584 N85-13731
Preliminary assessment of climatic change during late Wisconsin time, southwest Great Basin and vicinity, Arizona, California and Nevada
[DE85-006343] 16 p2836 N85-27488
Cyanobacterial mats: Microanalysis of community metabolism 21 p3661 N85-32743
Indications of mineral zoning in a fossil hydrothermal system at the Meager Creek geothermal prospect, British Columbia, Canada from induced polarization studies
[DE85-011962] 22 p3815 N85-33636

FOULING
NT ANTIFOULING
Operating experiences of reverse osmosis plants treating Rand Water Board (RWB) water: Pitfalls and problems 01 p0023 N85-10142
An electrochemical approach to the prevention of biofouling phenomena
[PB84-202613] 01 p0025 N85-10155
Bifouling and corrosion studies at the Seacoast Test Facility in Hawaii
[DE84-014643] 01 p0029 N85-10180
Hot-gas cleanup for molten carbonate fuel cells-dechlorination and soot formation
[DE84-003072] 01 p0066 N85-10450
Copper-nickel sheathing study, phase 2. Two-year service performance of test panels on the ARCO TEXAS
[PB84-242411] 06 p0775 N85-14952
Study of deposition control using transpiration
[DE85-002339] 10 p1485 N85-19378
Ocean energy systems
[PB85-110656] 11 p1676 N85-20564
Investigation of the initial events in biofouling
[AD-A149995] 12 p1900 N85-21927
Heat transfer monitor for measurements of fouling of industrial heat exchangers
[DE85-010257] 20 p3455 N85-31455
Ocean thermal energy conversion
[DE85-012291] 23 p3946 N85-34456

FOUNDATIONS
NT PILE FOUNDATIONS
Response and characteristics of structures subjected to S-H waves 01 p0060 N85-10398
The effect of an elastic foundation and of dissipative forces on the stability of fluid conveying pipes
[TAE-563] 12 p1863 N85-21688
Analysis of slabs-on-grade for a variety of loading and support conditions
[AD-A150965] 14 p2264 N85-24030
Repair of the DSS-14 pedestal concrete
16 p2772 N85-27108

FOUNDRIES
Theoretical and experimental investigations of dust loaded flow fields in industrial halls
[BMFT-FB-HA-84-044] 12 p1819 N85-21411

FOUR BODY PROBLEM
Investigations of the structure and electromagnetic interactions of few-body systems
[DE85-002854] 11 p1721 N85-20624
FOURIER ANALYSIS
NT FOURIER SERIES
Analysis of the Frascati and Geneva gravitational wave antenna background exhibiting the one half sideral day period
[NOTA-INTERNA-801] 02 p0192 N85-11283
Hardware and software selection for experimental model analysis 02 p0208 N85-11373
Digital Terrain Elevation Data (DTED) anomaly removal through the use of an interactive Fourier frequency filtering process
[AD-A145430] 02 p0219 N85-11445
Local geomagnetic characteristics of solar activity (Dourbes 1960-1978) 04 p0521 N85-13328
Development of holographic particle field data reduction by Fourier analysis
[AD-A148664] 08 p1165 N85-17348
Precision measurement of torsional oscillations induced by gear errors 09 p1338 N85-18416
The eigenvalues of the pseudospectral Fourier approximation to the operator sin (2x) d/dx
[NASA-CR-172538] 11 p1706 N85-20729
Research in image understanding as applied to 3-D tomographic imaging with near optical resolution
[AD-A150098] 12 p1829 N85-21483
Mathematical simulation of thermal prrocesses involved in electron-beam treatment 12 p1843 N85-21565
A two-dimensional smoothing spline and a regression problem
[AD-A149624] 12 p1921 N85-22067
Nonlinear behavior and stability of thin spherical shells subjected to non-axisymmetrical loading
13 p2048 N85-22821
Analysis of short-period changes in intensity of hard X-radiation of solar flares registered aboard Venera-13 and Venera-14 spacecraft 16 p2723 N85-26806
The development and implementation of an optical communications laboratory
[AD-A151682] 16 p2772 N85-27111
Head-on scattering of a tubular cylinder of finite length for radar target identification purposes
[AD-A155608] 21 p3577 N85-32246
Analysis of spacecraft data
[NASA-CR-171587] 21 p3669 N85-32789
SCRIBE data of October 23, 1983 flight
[AD-A154864] 21 p3705 N85-33012
Clusters and cycles in the cosmic ray age distributions of meteorites
[SH-7.1-11] 23 p4046 N85-35103
FOURIER SERIES
Controlled approximation and a characterization of the local approximation order
[AD-A149095] 10 p1546 N85-19750
A numerical approach for the vibration analysis of an axisymmetric shell structure with a nonuniform edge constraint
[AD-A149286] 11 p1651 N85-20402
Nonparametric estimation of density and hazard rate functions when samples are censored
[AD-A150946] 14 p2411 N85-24988
Natural convection in cylindrical containers
15 p2555 N85-25763
On various Fourier series utilized for solution of structural mechanics problems
[VTH-LR-429] 16 p2856 N85-27615
Extension of three theorems of Fourier series on the disc to the torus
[AD-A153017] 17 p3019 N85-28669
Fourier coding and reconstruction of complicated contours
[REPT-84-39] 17 p3022 N85-28691
Sigma filter 18 p3142 N85-29450
An extension to complex-valued functions of an algorithm for numerically inverting the Laplace transform
[DE85-010701] 19 p3347 N85-30743
Stress analysis of axisymmetric sandwich shells of variable thickness 24 p4101 N85-35419
FOURIER TRANSFORMATION
NT FAST FOURIER TRANSFORMATIONS
Shift-variant multidimensional systems
[AD-A144756] 01 p0111 N85-10752
Beam pulse length determination by spectral analysis
[CSIR-NAC-83-05] 01 p0116 N85-10793
Fast Fourier transform for unequally spaced data
01 p0128 N85-10876
Holographic subtraction of images by Fourier plane recording and spatial filtration with a narrow beam
02 p0263 N85-11721
Optical constant determination of thin polymer films in the infrared
[AD-A145669] 02 p0287 N85-11877
Thermomechanical cracking in layered media from moving friction load
[AD-A146022] 03 p0373 N85-12379
Meteorological analysis for clusters of wind turbines
[DE84-013164] 04 p0539 N85-13425
Surface structure determination with ARPEFS
[DE84-016904] 04 p0571 N85-13644
Phase problem in aperture synthesis systems
06 p0782 N85-15002
Micro-waveguide transformers of coherent optical signals 07 p0950 N85-16022
GC-FTIR (Fourier Transform Infrared Spectrometry) of jet fuels
[AD-A148272] 08 p1135 N85-17155
Signal reconstruction from Fourier transform sign information
[AD-A148039] 08 p1211 N85-17624
Molecular dynamics in nitramines and modified nitramines
[AD-A148515] 08 p1220 N85-17686
Effect of ultraviolet radiation on transparent polymer films as determined using in situ FTIR-RA spectroscopy. Volume 2: Photophysics of poly(vinylidene fluoride) films
[DE84-013040] 09 p1299 N85-18159
Shock response analysis by personal computer using the extended IFT algorithm 09 p1335 N85-18397
PCB analysis by capillary gas chromatography coupled with matrix isolation-Fourier transform infrared spectroscopy
[DE84-009201] 10 p1437 N85-19059
An object-oriented signal processing environment: The knowledge-based signal processing package
[AD-A148963] 10 p1466 N85-19251
Some qualitative properties of bivariate Euler-Frobenius polynomials
[AD-A149408] 10 p1547 N85-19755
Characteristic functional of a probability measure absolutely continuous with respect to a Gaussien radon measure
[AD-A149482] 10 p1548 N85-19763
Fourier densitometry: A new optical method for measuring density fluctuations by Rayleigh scattering -- turbulent jets 11 p1576 N85-19932
Interim protocol for the automated analysis of semivolatile organic compounds by Gas Chromatography/Fourier Transfer Infrared (GC/FT-IR) spectrometry
[PB85-115186] 11 p1595 N85-20035
Signal processing and range spreading in the FM-CW radar
[PB85-108256] 11 p1626 N85-20239
Classic Fourier microdistributions in the real analytic case 11 p1698 N85-20673
Carbon monoxide adsorption on a platinum electrode studied by polarization modulated FT-IRRAS (Fourier Transform-IR Reflections Adsorption Spectroscopy). Part 1: CO adsorbed in the double layer potential region and its oxidation in acids
[AD-A149751] 12 p1800 N85-21288
Effect of ultraviolet radiation on transparent polymer films as determined using in situ FTIR-RA spectroscopy. Volume 1: Photodegradation of transparent polymer films
[DE84-013039] 12 p1814 N85-21377
Application of the system identification technique to goal-directed saccades
[AD-A150132] 12 p1906 N85-21967
Acousto-optically addressed Fourier transform matched filters
[AD-A150298] 13 p2063 N85-22889
Processing of signals in experiments with scattering of short radio pulses by conducting sphere
13 p2068 N85-22917
Synthesis of quasi-optimum algorithms for signal recognition against background of correlated noise employing discrete spectral transformations
13 p2085 N85-23020
New convolution and discrete Fourier transformation algorithms based on rectangular transformations over field of roots of unity 13 p2085 N85-23022
Algorithms for reconstruction of partially known, band limited Fourier transform pairs from noisy data
[AD-A150194] 13 p2150 N85-23347
Optical processing in radon space
[AD-A150289] 13 p2159 N85-23402
Wave propagation in heterogeneous media
[AD-A150800] 14 p2321 N85-24341
Fourier transform of wave data on ARGOS buoys
14 p2323 N85-24351
Detection of solar gravity mode oscillations
14 p2442 N85-25070
Processing speech for analysis using optical Fourier techniques
[AD-A151896] 15 p2544 N85-25704
Rayleigh criteria resolution of optical correlations
[AD-A151711] 15 p2652 N85-26359
An experimental investigation of two-dimensional flame-vortex interactions 16 p2744 [illegible]
Fourier transform infrared spectrophotometric analysis of resin mix stoichiometry, revision 1
[DE85-007272] 16 p2747 N85-26851
Techniques for computing the DFT using the residue Fermat number systems and VLSI
16 p2770 N85-27087
Balloon-borne, He-cooled Fourier transform spectrometer for far infrared astronomy
[MPE-IR-41] 17 p3053 [illegible]
Transform domain adaptive filtering using a recursive DFT
[DE85-006965] 18 p3172 [illegible]
Novel analytical approaches to coal beneficiation
[DE85-010437] 19 p3229 N85-30021
An extension to complex-valued functions of an algorithm for numerically inverting the Laplace transform
[DE85-010701] 19 p3347 N85-30743
Highly dispersed metal atoms in zeolites
[DE85-010515] 19 p3354 N85-30792
Speciation of hazardous inorganic compounds by Fourier transform infrared (FTIR) spectroscopy
[PB85-188969] 20 p3426 N85-31282
On the solution for the sound field in a semi-infinite uniform duct with sheared mean flow
20 p3523 N85-31912
In-situ measurement of wall thermal performance: Data interpretation and apperatus design recommendations
[DE85-011979] 21 p3586 N85-32289
Qualitative analysis of sign-bit processing
[AD-A154776] 21 p3671 N85-32804
Adaptive corrector operating in frequency domain
22 p3765 N85-33337
Substructure coupling in the frequency domain
[NASA-CR-176140] 22 p3800 N85-33543
Pulse effect in a light ion beam propagation through a Z-discharge plasma channel 23 p3961 N85-34894
The conjecture concerning time variations in the solar neutrino flux
[SH-8.1-6] 23 p4049 N85-35111
Methods and software for cosmic ray scintillation studies
[SH-9.1-17] 23 p4052 N85-35132
FRACTALS
Stable distribution and Levy process in fractal turbulence 02 p0283 N85-11848
A case of a not-so-strange strange attractor
[CWI-AM-R8406] 08 p1214 N85-17643
Fractal structure of the interplanetary magnetic field
[NASA-TM-86212] 19 p3383 N85-30987
On the multifractal nature of fully developed turbulence and chaotic systems
[PREPRINT-413] 20 p3455 N85-31458
Attractors for the Kuramoto-Sivashinsky equations
[DE85-009631] 20 p3520 N85-31882
FRACTIONATION
NT CHEMICAL FRACTIONATION
Geophysical and geochemical constraints favoring the capture hypothesis 04 p0581 N85-13710
Synthesis and characterization of a 1,4 Polybutadiene/Isotactic polypropylene block copolymer
[AD-A148199] 08 p1133 N85-17142
Molecular toxicology of chromatin: The role of Poly(ADP-Ribose) in gene control
[AD-A154415] 19 p3327 N85-30811
Micro-scale methods for characterization of supercritical fluid extraction and fractionation processes
[DE85-010968] 20 p3455 N85-31456
Supercritical fluid chromatography/supersonic jet spectroscopy
[DE85-007005] 22 p3746 N85-33221
Nebular volatile fractionations associated with chondrule formation 22 p3852 N85-33855
FRACTOGRAPHY
Applications of synchrotron X-ray diffraction topography to fractography
[DE84-016257] 04 p0513 N85-13274
Fractographic study of stress corrosion cracking of SUS 304 stainless steel in various environments
[BLL-RISLEY-TR-4598-(9091.9F)]
05 p0815 N85-13828
Fractographic observation and estimation of crack growth curve of aluminum alloy under ramdom flight simulation loading
[NAL-TR-824] 06 p0768 N85-14913
Damage to boron fibers during thermal cycling and annealing 10 p1445 N85-19107
Fractographic features of titanium alloy fatigue failure under repeated static stress and high frequency vibration 11 p1601 N85-20070
Micrographic and fractographic examination of alloys 2214 and 2024 for conditions which would cause burning of the metal on being put into solution, trial 17/175
[DGT-23.419] 11 p1609 N85-20117

Fatigue Crack Topography
[AGARD-CP-376] 14 p2318 N85-24321
Fatigue fracture topography 14 p2318 N85-24323
Fatigue crack propagation and fracture in 7050 and 7091 aluminum alloy forgings 14 p2318 N85-24324
Two recent cases of marker load applications on cargo/fighter aircraft fatigue tests
14 p2318 N85-24325
Effect of flight sequences in complex load histories on crack front marking 14 p2318 N85-24326
Generation of marker lines by means of marker loads
14 p2318 N85-24327
Generation of marker lines on fatigue fracture surfaces 14 p2319 N85-24328
Fatigue crack topography and crack growth analysis --- wrought and cast aluminum 14 p2319 N85-24333
Application of optical and electron microscopic techniques in the fractographic determination of fatigue crack growth rates 14 p2320 N85-24334
New analysis aspects of the fatigue crack propagation behavior by SEM in situ microscopy
14 p2320 N85-24335
Crack propagation under constant and variable stress amplitudes: A comparison of calculations based on the Striation spacing and tests 14 p2320 N85-24336
Journal of Research of the National Bureau of Standards, volume 89, no. 6, November - December 1984
[PB85-179042] 20 p3472 N85-31580
Indentation fractography: A measure of brittleness
[PB85-179059] 20 p3473 N85-31581
A fractographic study on mode 2 and mode 3 SCC crack growth in an Al-Zn-Mg alloy 23 p3905 N85-34191
Fractographic analysis for nonpropagating conditions of fatigue crack at high stress ratios in mild steel
23 p3905 N85-34194

FRACTURE MECHANICS
USSR report: Materials science and metallurgy, no. 93
[JPRS-84810] 01 p0018 N85-10110
Influence of annealing on properties of AT3 alloy welded joints 01 p0019 N85-10118
The effects of radial yarns, 3-dimensionally reinforced carbon-carbon composite
[AD-A144751] 01 p0022 N85-10134
On the treatment of material laws for approximate J-estimation methods
[GKSS-84-E-15] 01 p0062 N85-10414
HOST high temperature crack propagation
02 p0144 N85-10977
Tensile strength of composite sheets with unidirectional stringers and crack-like damage: A brief report
[NASA-TM-86310] 02 p0170 N85-11139
Toughness in high speed steels and hard metals
02 p0176 N85-11181
The role of molybdenum as an alloy element in adhesive wear resistance 02 p0181 N85-11212
A study of environmental characterization of conventional and advanced aluminum alloys for selection and design. Phase 2: The breaking load test method
[NASA-CR-172387-PHASE-2] 02 p0182 N85-11219
Short cracks and crack closure in AL 2024-T3
[FFA-TN-1984-40] 02 p0210 N85-11387
Effective moduli of elasticity of unidirectional fibrous composite 02 p0265 N85-11733
European Scientific Notes, Number 38-9
[AD-A145683] 02 p0306 N85-11975
Study of delamination cracking under static and cyclic loads of carbon-epoxy composite materials
[REPT-42-727/F] 03 p0327 N85-12102
The influence of aluminum on the qualities of low and medium carbon steel
[BLL-M-35754-(5828.4)] 03 p0330 N85-12123
Sour-gas cracking in ferritic steels
[AERE-R-10906] 03 p0333 N85-12148
Thermal ageing studies of 9%Cr 1%Mo steel
[AERE-R-11109] 03 p0333 N85-12149
Stress-driven solute enrichment of crack-tips during low ductility intergranular fracture of low-alloy steel
[AERE-R-11120] 03 p0333 N85-12150
Microstructure of ceramics fabricated by unidirectional solidification
[NASA-TM-77423] 03 p0336 N85-12157
HIP glassmaking for high nitrogen compositions in the Y-Si-Al-O-N system
[DE84-015546] 03 p0338 N85-12175
Features of plastic deformation and fracture of EP 741 nickel alloy under thermal strain
03 p0349 N85-12250
Kinetics of fatigue factor of AT3 titanium alloys in air, distilled water and 3.5% aqueous NaCl solution
03 p0350 N85-12255
Structure of two-phase titanium alloys with different microstructures 03 p0351 N85-12257
Penetrator/armour interactions: Background to Australian work
[MRL-R-936] 03 p0367 N85-12353
Viscoplastic finite element analysis of rapid fracture
03 p0370 N85-12365
Applications of integral equations with strong singularities in fracture mechanics
03 p0371 N85-12367
Bending strength studies on hot-pressed silicon carbide
[NASA-TM-77512] 03 p0371 N85-12369
Stress intensity factors for a circular ring with uniform array of radial cracks of unequal depth
[AD-A145893] 03 p0372 N85-12377
Thermomechanical cracking due to moving frictional loads
[AD-A146271] 03 p0373 N85-12381
Eta values for compact geometry specimens to calculate the J integral
[AERE-R-11126] 03 p0374 N85-12385
Removal of singularities in Tresca and Mohr-Coulomb yield functions
[OUEL-1528/84] 03 p0413 N85-12642
Morphology and dynamic mechanical properties of diglycidyl ether of bisphenol-A toughened with carboxyl-terminated butadiene-acrylonitrile
04 p0466 N85-12958
Composite fracture toughness and impact characterization 04 p0466 N85-12963
Constituent properties and interrelationships
04 p0467 N85-12964
Impact of NDE unreliability on pressure vessel fracture predictions
[DE84-015586] 05 p0647 N85-14151
Welcome and introduction --- materials strength
05 p0649 N85-14164
Fatigue behavior of continuous fiber silicon-carbide-aluminum composites
[NASA-TM-86332] 06 p0763 N85-14879
Study of fatigue fracture in hardened and tempered carbon steel. Report 1: Microscopic observation of the fatigue crack formation process
[BLL-PNR-90242-(8019.3153)]
06 p0767 N85-14909
Deformation, fracture and explosive properties of reactive materials
[AD-A146396] 06 p0774 N85-14945
Constitutive modeling of engine materials
[AD-A146630] 06 p0817 N85-15189
Three-dimensional crack location by acoustic emission
[AERE-R-11277] 06 p0818 N85-15193
Engine Cyclic Durability by Analysis and Testing
[AGARD-CP-368] 07 p0905 N85-15733
Investigation of the creep behaviour of soft soldered joints with solder L-SnAg5 at ambient temperature
[BLL-T6383/BG/WH798/84] 07 p0926 N85-15865
Influence of pressure on compaction during compression of powders of iron and 40Kh and 10R6MS steels
[BLL-M-35995-(5828.4)] 07 p0926 N85-15866
Nondestructive tests and fracture mechanics investigations in the Component Integrity Research Programme
[BLL-RISLEY-TR-4541-(9091.9F)]
07 p0976 N85-16199
A general theory of circuit analogy in fracture diagnosis
[AD-A147177] 07 p0978 N85-16212
A hydrogen partitioning model for hydrogen assisted crack growth
[AD-A147385] 07 p0978 N85-16214
New aspects of thermoelastic contact
[AD-A147554] 07 p0979 N85-16217
Buckling analysis of cracked, floating ice sheets
[AD-A147330] 07 p0988 N85-16277
Crack growth in propellants 08 p1116 N85-17034
Shock and impact response of solid rocket propellants: Experimental and theoretical 08 p1116 N85-17040
The influence of strain rate and porosity on the deformation and fracture of titanium and nickel
[AD-A148670] 08 p1130 N85-17123
The influence of porosity on the deformation and fracture of alloys
[AD-A148766] 08 p1130 N85-17124
High pressure physics research focusing on composite materials 08 p1140 N85-17185
Electrodes for repairing power engineering equipment made from creep resisting steel
[BLL-CE-TRANS-8064-(9022.09)]
08 p1167 N85-17360
Numerical solution of elastodynamic problems in fracture mechanics 08 p1171 N85-17385
Tensile test of pressureless-sintered silicon nitride at elevated temperature
[NASA-TM-77777] 08 p1172 N85-17390
A simple engineering treatment of center cracked tension panels in the regime of nonlinear fracture mechanics under plane stress conditions
[GKSS-84-E-38] 08 p1173 N85-17396
Modeling of large-scale accretionary wedge and thin-skinned trust-and-fold belt mechanics
08 p1181 N85-17442
Fracture mechanics analysis and prediction of delamination growth in composite structures
[FFA-TN-1984-45] 09 p1269 N85-18092
Deformation and fracture of P/M (Powder/Metallurgy) titanium alloys
[AD-A148672] 09 p1294 N85-18128
Applicability of linear elastic fracture mechanics to fatigue in polymers and short-fiber composites
09 p1298 N85-18152
Analysis of a potential hot-wire ignition problem
[DE84-017254] 09 p1301 N85-18174
Method of testing carbide inserts for premature fracture by face milling of cylindrical workpieces
09 p1303 N85-18183
Determination of blade service life under irregular loading conditions 09 p1309 N85-18222
finite element analysis of bi-material systems with applications in hydraulic fracturing
09 p1332 N85-18369
The influence of mechanical damage on transmission pipeline integrity
[ERS-E.351] 09 p1340 N85-18431
Recent studies of the significance of mechanical damage in pipelines
[ERS-E.367] 09 p1341 N85-18433
Fracture resistance of surface layer with technological defects under cyclical loading 10 p1448 N85-19126
Crack problems for bonded nonhomogeneous materials under antiplane shear loading
[NASA-CR-172532] 10 p1495 N85-19438
Interaction between a crack and a soft inclusion
[NASA-CR-172533] 10 p1495 N85-19439
Fracture toughness of fiber reinforced concrete
[AD-A149403] 10 p1496 N85-19441
Mechanisms of damage accumulation in time-dependent cyclic deformation
[DE85-001004] 10 p1496 N85-19443
European Scientific Notes. Volume 39, number 2
[AD-A148994] 10 p1573 N85-19919
Fracture analysis of notched composites
[NASA-CR-172563] 11 p1593 N85-20020
Rapidly solidified NiAl and FeAl
[NASA-TM-86941] 11 p1597 N85-20042
Initial fracture stages of orthogonally reinforced composite material 11 p1599 N85-20055
Direct comparison of unloading compliance and potential drop techniques in J-integral testing
[DE85-001550] 11 p1650 N85-20392
Effect of input distributions on the probabilistic fracture mechanics analysis of reactor pressure vessels
[DE85-000832] 11 p1652 N85-20403
Thickness effects of fracture toughness
[DE85-002974] 11 p1653 N85-20409
Simulation of brittle fracture via molecular dynamics
[DE85-001061] 11 p1653 N85-20410
Requirements of quantitative NDE in developing fracture control plans
[DE85-003147] 11 p1654 N85-20415
Translational and extensional energy release rates (the J- and M-integrals) for a crack layer in thermoelasticity
[NASA-CR-174872] 12 p1863 N85-21685
Fracture analysis of cracks in complete cylindrical shells
[AD-A150091] 12 p1867 N85-21711
Evaluation of subsurface fracture geometry using fluid pressure response to solid earth tidal strain
[DE85-003294] 12 p1890 N85-21864
Reliability of structural brittle materials
12 p1946 N85-22222
Longitudinal splitting in unidirectional composites, analysis and experiments
[NASA-CR-3881] 13 p2015 N85-22639
Behavior of fiber-reinforced composites under dynamic tension
[AD-A150619] 13 p2015 N85-22641
Creep crack growth in ductile alloys
[DE85-003937] 13 p2023 N85-22676
Long-term strength and fracture criteria for EI698VD alloy under complex stress conditions
13 p2030 N85-22723
Advanced life analysis methods. Volume 2: Crack growth analysis methods for attachment lugs
[AD-A150420] 13 p2103 N85-23109
Scattering of elastic waves on fractures randomly distributed in a three-dimensional medium
13 p2111 N85-23151
Patterns of fracture and tidal stresses due to nonsynchronous rotation: Implications for fracturing on Europa 13 p2173 N85-23483
Research on composite materials for structural design
[AD-A150802] 14 p2260 N85-24004
On the corner singularity of a 3-D Griffith crack
[AD-A150989] 14 p2321 N85-24342

A preliminary investigation into transverse fracture of unidirectional fiber composites
[AERE-R-11494] 15 p2503 N85-25438

Influence of oxygen traces on the properties of tungsten heavy metals
[BLL-RARDE-TR-1177-(7291.7965)] 15 p2508 N85-25470

Transformation toughened ceramics: A potential material for light diesel engine application
[AD-A151421] 15 p2518 N85-25526

The effect of overload cycles on fatigue crack propagation in structural steels
15 p2577 N85-25897

Fracture problems in power law viscoelastic materials
[AD-A149221] 15 p2578 N85-25900

Crack closure characteristics considering center cracked and compact tension specimens
[AD-A151702] 15 p2579 N85-25907

A study of the time dependence in fracture processes relating to service prediction of adhesive joints and advanced composites
[AD-A152064] 15 p2579 N85-25910

A review of fracture mechanics life technology
16 p2733 N85-26863

Microscopic study of the influence of impurities on interface bonding
[AD-A151725] 16 p2743 N85-26928

Multiaxial and thermomechanical fatigue considerations in damage tolerant design
[NASA-TM-87022] 16 p2749 N85-26964

Automatic tracking of crack growth via finite elements
16 p2797 N85-27246

Full statistical characteristics of microdeformation
[BLL-M-36076-(5828.4)] 16 p2798 N85-27254

Predicting fully plastic mode 2 crack growth from an asymmetric defect
[AD-A152227] 16 p2801 N85-27269

Interaction of high-cycle and low-cycle fatigue of Haynes 188 alloy at 1400 F deg 17 p2913 N85-27961

Experiments and micromechanical models for creep-rupture in polymer matrix composites
[DE85-009533] 17 p2935 N85-28118

Conformational and mechanical properties at high strain rates
[AD-A153401] 17 p2959 N85-28272

Inspection evaluation and repair of the flawed feedwater nozzle of the 50 MWe Dodewaard GKN boiling water reactor
[ISBN-90-353-0017-3] 17 p2977 N85-28394

Measurement of fracture macro-geometry in evaluating fracture toughness
[BLL-BISI-TRANS-22241-(9022.06)] 17 p2978 N85-28403

Fracture mechanics analysis of cold drawn Si-Cr valve steel
[BLL-BISI-TRANS-22216-(9022.06)] 17 p2978 N85-28405

Relaxation properties and fatigue fracture resistance of austenitic spring steel
[BLL-BISI-TRANS-22300-(9022.06)] 17 p2978 N85-28406

Critical conditions for failure in materials subjected to high rates of loading
[AD-A153135] 17 p2980 N85-28420

High temperature fracture mechanics of silicon nitride
[BMFT-FB-T-84-285] 17 p2981 N85-28433

Field theory analysis using the finite element method to determine the deliberation curves of three dimensional fracture mechanics specimens with a semicircular surface crack applying the electrical direct current potential method for crack depth measurement
[GKSS-84-E-53] 17 p2982 N85-28434

Laboratory investigation of formation damage of an artificial fracture at simulated geothermal conditions
[DE85-010301] 18 p3102 N85-29201

Brittle fracture behaviour of cold formed, welded 10mm to 20 mm thick plate manufactured from plain carbon structural steels
[BLL-BISI-TRANS-21678-(9022.06)] 18 p3120 N85-29311

An effective substructure technique applied to crack problems 18 p3121 N85-29319

Study of the influence of metallurgical factors on fatigue and fracture of aerospace structural materials
[AD-A153913] 18 p3122 N85-29328

Fracture of laminated composite materials
19 p3230 N85-30030

The mechanics of internal stress and microcrack toughening mechanisms in ceramics
[AD-A154049] 19 p3248 N85-30139

Fracture mechanics formulas on microcomputers
[NASA-TM-77850] 19 p3284 N85-30362

Computational methods in advanced stress and durability analyses
[AD-A154119] 19 p3286 N85-30375

Micromechanism of fracture for stage 1 hydrogen-induced crack growth
[DE85-010027] 19 p3288 N85-30390

Delamination micromechanics analysis
[NASA-CR-172598] 20 p3422 N85-31237

Prediction of lifetime for ceramic materials in the elastic and viscoelastic region by fracture mechanical methods
[ESA-TT-825] 20 p3434 N85-31305

On elastic-plastic fracture criterion
20 p3466 N85-31528

Numerical study of ductile rupture in plane deformations
[ONERA-RT-23/7169-RY-072-R] 20 p3469 N85-31557

Numerical study of tensile fracture in plane stress
[ONERA-RT-22/7169-RY-070-R] 20 p3470 N85-31563

On the variation of the stress intensity factor along the front of a surface flaw
[OUEL-1565/85] 20 p3471 N85-31566

Development of fracture mechanics maps for composite materials, volume 1
[ESA-CR(P)-2017-VOL-1] 20 p3471 N85-31573

Development of fracture mechanics maps for composite materials, volume 2
[ESA-CR(P)-2017-VOL-2] 20 p3471 N85-31574

Development of fracture mechanics maps for composite materials. Volume 3: Appendices A-E
[ESA-CR(P)-2017-VOL-3] 20 p3472 N85-31575

Development of fracture mechanics maps for composite materials. Volume 4: Appendices F-K
[ESA-CR(P)-2017-VOL-4] 20 p3472 N85-31576

The three-dimensional J-integral. An investigation into its use for post-yield fracture safety assessment
[WTHD-167] 20 p3472 N85-31578

Indentation fractography: A measure of brittleness
[PB85-179059] 20 p3473 N85-31581

Simulation model of acoustic emission due to microscopic fracture in metals
[BLL-BISI-TRANS-22367-(9022.06)] 20 p3523 N85-31909

Influence of the resin on interlaminar mixed-mode fracture
[NASA-TM-87571] 21 p3561 N85-32150

Comparisons of various configurations of the edge delamination test for interlaminar fracture toughness
[NASA-TM-86433] 21 p3561 N85-32151

Effects of weak interfaces on thermostructural behavior of carbon-carbon composites
[AD-A155330] 21 p3562 N85-32154

The shearing contribution in transformation toughening of brittle materials
[AD-A154656] 21 p3568 N85-32195

Stress corrosion of ceramic materials
[AD-A155020] 21 p3570 N85-32202

Dynamic fracture behavior of structural materials
[AD-A154568] 21 p3598 N85-32345

Ductile fracture of dynamically loaded naval structures-compact tension specimen tests and analyses
[AD-A155472] 21 p3600 N85-32353

Development of improved dynamic failure models
[AD-A155586] 21 p3600 N85-32354

Relating corrosion maintenance to environmental factors 22 p3750 N85-33247

Elevated temperature crack growth
[NASA-CR-174957] 22 p3799 N85-33540

A review of path-independent integrals in elastic-plastic fracture mechanics, task 4
[NASA-CR-174956] 22 p3799 N85-33541

Proceedings of the Twentyseventh Japan Congress on Materials Research
[ISSN-0368-3141] 23 p3903 N85-34180

On the methods to determine the stress intensity factors in boundary element method 23 p3905 N85-34189

Experimental study on time and temperature dependent behavior of crack growth in viscoelastic strip
23 p3905 N85-34193

Fatigue crack retardation phenomenon caused by single-multiple overloads in 2017-T3 aluminum allow
23 p3906 N85-34196

Fracture behavior of aluminum composites reinforced with fiber 23 p3907 N85-34207

Time and temperature dependence of fracture surface in soft epoxy resin 23 p3908 N85-34213

Impact fracture mechanism of polymer plates containing a heavy inner material 23 p3908 N85-34215

Study on fracture behavior of epoxy resin
23 p3909 N85-34216

1983 review of experimental stress and strain analysis
[DRIC-T-7469] 24 p4101 N85-35422

Subcritical fracture propagation in rocks: An examination using the methods of fracture mechanics and non-destructive testing 24 p4116 N85-35516

FRACTURE RESISTANCE
U FRACTURE STRENGTH

FRACTURE STRENGTH

Fracture toughness characteristics of welded joints in VT65 and AT6 titanium alloys 01 p0020 N85-10121

Delayed fracture of high-strength steels in spherical tanks for LP gas
[BLL-RISLEY-TR-4926-(9091.9F)] 01 p0026 N85-10162

Fracture toughness of fibrous composite materials
[NASA-TP-2370] 02 p0170 N85-11136

Development of powder metallurgy 2XXX series Al alloys for high temperature aircraft structural applications
[NASA-CR-172408] 02 p0182 N85-11220

Effects of prior austenite and ferrite grain size on fracture properties of a plain carbon steel
[AD-A146276] 03 p0332 N85-12138

Structure and ductility of fracture of joints produced by electron-beam welding of VT6ch titanium alloy parts
03 p0351 N85-12201

An experimental evaluation of the J integral in 50% sidegrooved compact geometry specimens
[AERE-R-11202] 03 p0374 N85-12286

Tough Composite Materials
[NASA-CP-2334] 04 p0463 N85-12941

Characterization of interlaminar crack growth in composites with the double cantilever beam specimen
04 p0463 N85-12942

Characterizing delamination resistance of toughened resin composites 04 p0464 N85-12943

Composite materials characterization and development at AFWAL 04 p0464 N85-12944

Fundamental studies of composite toughness
04 p0464 N85-12948

The effect of cross-link density on the toughening mechanism of elastomer-modified epoxies
04 p0465 N85-12951

Toughening mechanism in elastomer-modified epoxy resins, part 2
[NASA-CR-3852] 04 p0478 N85-13046

Effects of irradiation fluence and creep on fracture toughness of 347/348 stainless steel
[DE84-016091] 05 p0618 N85-13953

Welcome and introduction --- materials strength
05 p0649 N85-14164

Influence of residual stresses resulting from manufacturing on the fatigue strength of welded joints
05 p0650 N85-14177

Applicability of fatigue strength data obtained from small separately cast specimens on large cast components
05 p0651 N85-14178

Effect of crack-tip region constraint on fracture in the ductile-to-brittle transition
[PB84-237395] 06 p0770 N85-14926

Strength analysis of fan-shaped wing considering temperature deformation and creep deformations
06 p0779 N85-14983

Inconel 718 alloy resistance to crack propagation
07 p0907 N85-15740

Dispersed metal-toughened ceramics and ceramic brazing
[NASA-CR-174284] 07 p0933 N85-15916

Static and dynamic fracture toughness characterization of SA508 forging and SA533B welded plate --- pressure vessel steels
[CISE-2258] 08 p1131 N85-17127

A discussion of problems encountered in the dynamic fracture toughness testing of materials
[OUEL-1524/84] 08 p1173 N85-17387

Engineering property comparisons of PM and IM aluminum alloy forgings
[AD-B088146L] 08 p1173 N85-17398

Surface mechanical properties and wear behavior of ion implanted TiB2
[DE85-001130] 09 p1295 N85-18133

Fabrication of ceramic-ceramic composites by chemical vapor deposition
[DE85-000981] 09 p1298 N85-18155

Fracture toughness of austenitic stainless steel weld metal at 4 K
[DE84-016636] 09 p1340 N85-18425

Preliminary report on tests of tensile specimens with a part-through surface notch for a filament wound graphite/epoxy material
[NASA-CR-172545] 10 p1431 N85-19026

K sub 1* -n diagram of cyclical crack resistance of aluminum alloys 10 p1442 N85-19080

Influence of excess phases on fracture toughness of cast alumiun-magnesium-zinc alloy
10 p1442 N85-19081

Strength and failure of ceramic-metallic material
10 p1446 N85-19112

Behavior and specifics of fracture of porous fiber materials in extension 10 p1447 N85-19118

Influence of gaseous hydrogen on strength and ductility of nickel heat-resistant alloys 10 p1447 N85-19119

Fracture toughness of fiber reinforced concrete
[AD-A149403] 10 p1496 N85-19441

Effect of ingot structure of failure ductility of pressed semifinished products of high-durability aluminum alloys
11 p1597 N85-20045

Thickness effects of fracture toughness
[DE85-002974] 11 p1653 N85-20409

Slit-ring test for evaluating fracture in tubular cross sections
[DE85-003550] 11 p1654 N85-20416

Fatigue crack propagation in mirage 1110 wing main spar specimens and the effects of spectrum truncation on life
[ARL/STRUC-R-405] 12 p1776 N85-21152

Stress corrosion cracking and oxidation characteristics of boride-strenghened microcrystalline iron and nickel based alloys
[AD-A149805] 12 p1806 N85-21328

Effects of neutron irradiation on the fracture properties of HT-9 weld
[DE85-001069] 12 p1807 N85-21339

Fracture toughness of materials
[DE85-004306] 12 p1867 N85-21713

Interlaminar fracture toughness in resin matrix composites
[AD-A150585] 13 p2015 N85-22640

Particulate toughened silicon carbide
[DE85-004797] 13 p2016 N85-22643

Prediction of the resistance of structural materials to cavitation erosion
[BLL-DRIC-TRANS-7435-(3623.66)]
13 p2020 N85-22659

Fatigue and corrosion fatigue resistance of aluminum casting alloy VAL10 and forging alloy AK6
13 p2025 N85-22690

Structural strenght of strip D16T aluminum alloy with low copper and magnesium content
13 p2025 N85-22691

Use of acoustical emission method to study specifics of fracture of boron reinforced plastic structural elements 13 p2026 N85-22696

Mechanical properties and brittle fracture resistance of welded multilayer elements for high pressure vessels
13 p2033 N85-22736

Analysis of strength and ductility of welded joints in AMtsS and AMg5 aluminum alloys
13 p2033 N85-22737

Effect of protective medium on durability and fracture structure on seam zones of thin-walled titanium articles produced by diffusion welding 13 p2033 N85-22738

Dispersed-metal-toughened alumina
[NASA-CR-174687] 13 p2037 N85-22758

Fracture mechanics evaluation of GaAs
[NASA-CR-175657] 13 p2102 N85-23101

The effect of notch acuity on the fracture toughness of silicon carbide/aluminum metal matrix composites
[AD-A150970] 14 p2248 N85-23936

Fracture toughness of HY-130 steel weld metals
[AD-A150841] 14 p2255 N85-23976

Cast-iron technology: Metallographic and mechanical testing results
[DE85-002684] 14 p2257 N85-23984

Effect of elevated-temperature neutron irradiation on fracture toughness of ceramics
[DE85-000652] 14 p2261 N85-24010

Correlation of uniaxial and biaxial fracture strengths of ceramics
[DE85-003779] 14 p2261 N85-24011

Effect of deep cooling on crack resistance and low-temperature hardening of aluminum alloys
15 p2496 N85-25396

Fatigue strength of alpha-titanium alloys under cophasal action of variable normal and tangential stresses
15 p2498 N85-25407

The accuracy of approximate solutions in the analysis of fracture of composites
[NASA-CR-175738] 15 p2503 N85-25437

Fatigue life, fatigue crack propagation and fracture toughness study of 7075 aluminum alloy subjected to thermomechanical processing 15 p2573 N85-25862

Tensile and fracture toughness properties of Mirage III spars
[AR-003-019] 15 p2578 N85-25899

Particulate and whisker toughened alumina composites
[DE85-005239] 16 p2743 N85-26930

Simultaneous chemical vapor deposition of SiC-dispersed phase composites
[DE85-007751] 16 p2744 N85-26931

The effect of low sheet thicknesses on the fracture toughness of an Al alloy (7075-T6) — Aramid Reinforced Aluminum Laminate (ARALL)
[VTH-LR-425] 16 p2752 N85-26984

An improved torsional method for determining the fracture toughness of stiff materials and of adhesive joints
[AD-A152091] 16 p2800 N85-27267

Reaction-bonded and fiber-reinforced SiC static and dynamic gas turbine components
[BMFT-FB-T-84-302] 17 p2899 N85-27874

Fracture toughness of MgCr(sub)2O(sub)4-ZrO(sub)2
[DE85-007945] 17 p2917 N85-27982

Preparation of metal for cold upsetting
[BLL-BISI-TRANS-22363-(9022.06)]
17 p2926 N85-28043

Measurement of fracture macro-geometry in evaluating fracture toughness
[BLL-BISI-TRANS-22241-(9022.06)]
17 p2976 N85-28403

On validity of threshold values of fatigue strength of steel structures
[BLL-BISI-TRANS-22192-(9022.06)]
17 p2976 N85-28406

Specimen thickness effects for elastic-plastic CTOD toughness of A36 steel
[DE85-006992] 18 p3077 N85-29036

Load-carrying capabilities of refractory alloys for space reactor power applications
[DE85-010586] 19 p3240 N85-30087

Mechanism of strength degradation for hot corrosion of alpha-SiC
[NASA-TM-87052] 19 p3248 N85-30135

The mechanics of internal stress and microcrack toughening mechanisms in ceramics
[AD-A154049] 19 p3248 N85-30139

Fatigue-crack growth and ductile fracture toughness behavior of ASTM A387 Grade 91 steel
[DE85-008495] 20 p3431 N85-31286

Application of the unloading compliance methods in fracture toughness measurements of a quenched and tempered steel
[BLL-CE-TRANS-7953-(9022.09)]
20 p3465 N85-31523

Assessment of dynamic test methods for the measurement of fracture toughness — steels
[OUEL-1561/85] 20 p3470 N85-31565

The Hopkinson pressure bar: An alternative to the instrumented pendulum for Charpy tests
[OUEL-1566/85] 20 p3471 N85-31569

Journal of Research of the National Bureau of Standards, volume 89, no. 6, November - December 1984
[PB85-179042] 20 p3472 N85-31580

Indentation fractography: A measure of brittleness
[PB85-179059] 20 p3473 N85-31581

Controlled indentation flaws for the construction of toughness and fatigue master maps
[PB85-179067] 20 p3473 N85-31582

Influence of the resin on interlaminar mixed-mode fracture
[NASA-TM-87571] 21 p3561 N85-32150

Comparisons of various configurations of the edge delamination test for interlaminar fracture toughness
[NASA-TM-86433] 21 p3561 N85-32151

Metallurgical origins of fracture toughness and microstructure and fracture toughness of an HSLA (High-Strength/Low-Alloy) steel
[AD-A155530] 21 p3567 N85-32187

Thin-film reliability and engineering overview
21 p3612 N85-32450

Dispersion toughened ceramic composites and method for making same
[DE85-011601] 22 p3751 N85-33252

KRAK: A computer program for two-phase two-component porous flow and fracture
[LA-9703] 22 p3782 N85-33434

On high strain rate fragmentation of a closed vessel
23 p3904 N85-34187

Study on fracture behavior of epoxy resin
23 p3909 N85-34216

FRACTURE TOUGHNESS
U FRACTURE STRENGTH

FRACTURES (MATERIALS)

Delayed fracture of high-strength steels in spherical tanks for LP gas
[BLL-RISLEY-TR-4926-(9091.9F)]
01 p0026 N85-10162

Turbine Engine Hot Section Technology (HOST)
[NASA-TM-83022] 02 p0140 N85-10951

Contributions to the 7th International Acoustic Emission Symposium
[AD-A145368] 02 p0275 N85-11792

Study of deformation and fracture of AMg6N weldable aluminum alloy by method of acoustic emission
03 p0352 N85-12266

Influence of cyclic tangential loading on indentation fracture
[DE84-015969] 03 p0373 N85-12382

Investigation of toughened neat resins and their relations to advanced composite mechanical properties
04 p0464 N85-12949

Numerical investigation of the micromechanics of composite fracture 04 p0467 N85-12970

Fundamental tribological properties of ceramics
[NASA-TM-86915] 07 p0930 N85-15893

Effects of fracture roughness on fluid flow through a single deformable fracture
[DE85-004593] 13 p2092 N85-23062

Scattering of elastic waves on fractures randomly distributed in a three-dimensional medium
13 p2111 N85-23151

Study of resolution of deep MT soundings by means of physical model 13 p2112 N85-23156

Durability calculation of wing panel element
14 p2285 N85-24159

Essential features in fatigue fractures and remarkable phenomena in fatigue crack growth
14 p2318 N85-24322

Generation of marker lines on fatigue fracture surfaces 14 p2319 N85-24328

Periodic loading sequences for the systematic marking of fatigue crack fracture surfaces
14 p2319 N85-24329

Modifications of flight by flight load sequences to provide for good fracture surface readability
14 p2319 N85-24330

The effect of overload cycles on fatigue crack propagation in structural steels
15 p2577 N85-25897

Creep-fatigue interaction of notched 304 stainless steel bars 16 p2798 N85-27249

Laboratory investigation of formation damage of an artificial fracture at simulated geothermal conditions
[DE85-010301] 18 p3102 N85-29201

Multiaxial fatigue and fracture: A literature review
[ARL/STRUC-R-410] 19 p3285 N85-30370

Dynamic fracture behavior of structural materials
[AD-A154568] 21 p3598 N85-32345

Automatic capability to store and retrieve component data and to calculate structural integrity of these components
[DE85-012429] 22 p3831 N85-33728

Special features of the fracture of ball-bearing steel close to non-metallic inclusion eutectics
[BLL-M-35809-(5828.4)] 23 p3914 N85-34258

On size effects in plane stress crack-growth resistance
[AD-A155926] 24 p4102 N85-35426

FRACTURING
NT CRUSTAL FRACTURES

Fracture, failure, and fragmentation
01 p0059 N85-10390

Quantum characteristics of kinetic fracturing of solids
02 p0265 N85-11732

Composite materials characterization and development at AFWAL 04 p0464 N85-12944

Effects of irradiation fluence and creep on fracture toughness of 347/348 stainless steel
[DE84-016091] 05 p0618 N85-13953

Tests of the load-bearing and deformation behaviour of reinforced concrete spherical shells under point loading
[BLL-RISLEY-TR-4550-9091.9F)]
06 p0816 N85-15182

Modelling of deformation and fracture in high-temperature structural materials
[DE84-016906] 06 p0818 N85-15191

Role of hydrogen in processes of deformation and fracture of metals 10 p1449 N85-19132

Rock mechanics: Issues and research needs in the disposal of wastes in hydraulic fractures
[DE85-001399] 10 p1556 N85-19809

Micro-deformation of quartz under dynamic action and its applications 11 p1620 N85-20201

Simulation of brittle fracture via molecular dynamics
[DE85-001061] 11 p1653 N85-20410

Requirements of quantitative NDE in developing fracture control plans
[DE85-003147] 11 p1654 N85-20415

Reliability of structural brittle materials
12 p1946 N85-22222

Physiography of the Martian west equatorial uplift
12 p1961 N85-22325

Hydrogen effects in austenitic stainless steels based on the Fe-Cr-Mn-N system
[DE85-003617] 13 p2023 N85-22672

Hydrovolcanism 13 p2188 N85-23574

Structural Integrity and Durability of Reusable Space Propulsion Systems
[NASA-CP-2381] 17 p2910 N85-27941

Designing for fiber composite structural durability in hygrothermomechanical environment
[NASA-TM-87045] 17 p2917 N85-27978

Part played by non-metallic inclusions during deformation and fracture of steel with different grain sizes
[BLL-BISI-TRANS-22321-(9022.06)]
17 p2928 N85-28072

Laboratory investigation of formation damage of an artificial fracture at simulated geothermal conditions
[DE85-010301] 18 p3102 N85-29201
Hot Dry Rock Geothermal Energy Developement Program
[DE85-010570] 19 p3288 N85-30264
Failure analysis of fractured capscrews in centrifugal coolant compressor
[DE85-010029] 19 p3287 N85-30384
Comprehensive fracture diagnostics experiement. Part 2: Comparison of seven fracture azimuth measurements
[DE85-011707] 23 p3948 N85-34470

FRAGMENTATION
Fracture, failure, and fragmentation
01 p0059 N85-10390
Theoretical studies in molecular fragmentation: Processes, energetics and diagnostics
[AD-A146310] 03 p0418 N85-12673
The fragmentation of molecular clouds and the IMF
05 p0740 N85-14759
Study of the transition from deflagration to detonation of previously fragmented propellants
08 p1115 N85-17032
Experiment on triggered fragmentation on a molten copper droplet in water
[BLL-WH-602-(9091.9F)] 08 p1125 N85-17091
A T-matrix theory of galactic heavy-ion fragmentation
[NASA-TP-2363] 08 p1221 N85-17690
Fragmentation and turbulence in collapsing gas clouds
[DE85-003745] 11 p1633 N85-20282
Statistical theory of fragmentation processes
[DE85-002206] 11 p1653 N85-20414
Charge-to-mass dispersion methods for abrasion-ablation fragmentation models
[NASA-TM-86340] 11 p1726 N85-20857
Workshop on Nuclear Dynamics 3
[INC-40007-24] 12 p1931 N85-22130
Hydrovolcanism 13 p2188 N85-23574
Collisional outcomes in the asteroid belt
15 p2678 N85-26538
Frangibility of obstacles at airports
[NLR-MP-84002-U] 17 p2981 N85-28431
On high strain rate fragmentation of a closed vessel
23 p3904 N85-34187
On the importance of interstellar helium for the propagation of heavy cosmic rays
[OG-7.2-11] 23 p4015 N85-34879
Measurements of the fragmentation of (40)Ar, (28)Si and (12)C in CH2C and H targets between 300 and 1500 MeV/nuc at the Bevalac
[OG-7.2-19] 23 p4016 N85-34886
Measurements of Fe and Ar fragmentation cross sections
[OG-7.2-20] 23 p4016 N85-34887
Cross sections for the production of fragments with Z greater than or equal to 8 by fragmentation of Z greater than or equal to 9 and less than or equal to 26 nuclei
[OG-7.2-22] 23 p4016 N85-34889
Experimental data for characterizing perforating impacts: Fragmentation processes
[AD-A156370] 24 p4102 N85-35427
A test of the Feynman scaling in the fragmentation region
[HE-1.2-9] 24 p4172 N85-35867
Scaling violation in fragmentation region at energies above 10-15 eV based on the data on cosmic ray hadron component
[HE-3.1-11] 24 p4178 N85-35909
Peculiarities of gamma-quanta distribution at 20 TeV energy
[HE-3.7-10] 24 p4186 N85-35967

FRAGMENTS
Holographic assembly for measuring velocity fields of supersonic ballistic splinters at a large distance
[ISL-CO-203/84] 20 p3459 N85-31487
How are particle production, nucleon emission and target fragment evaporation processes interrelated in hadron-nucleus collisions? 24 p4174 N85-35878

FRAMES
NT AIRFRAMES
NT CHASSIS
NT UNDERCARRIAGES
Studies on reliability of structural systems
02 p0206 N85-11362
Iterative method for determining the distortion of elastic-plastic frames
[ISSN-0208-5658] 05 p0647 N85-14156
A general theory of circuit analogy in fracture diagnosis
[AD-A147177] 07 p0978 N85-16212
A study on a medium-sized rocket with Burnout frame
[NAL-TR-821] 09 p1287 N85-18082
Alternative approximation concepts for space frame synthesis
[NASA-CR-172526] 12 p1776 N85-21150
Spline curves, wire frames and B-value
17 p3006 N85-28587
Airborne sound transmission loss characteristics of wood-frame construction
[AD-A154174] 20 p3524 N85-31919

FRAMES (DATA PROCESSING)
Low-resolution target classification from a staring infrared sensor
[AD-A151690] 15 p2652 N85-26358
ZOG-Vinson technology demonstration project. Volume 2: System description
[AD-A153871] 19 p3333 N85-30645
ZOG/VINSON technology demonstration project system description. Volume 1
[AD-A154211] 19 p3342 N85-30713

FRAMING CAMERAS
Design and fabrication of a CCD camera for use with relay optics in solar X-ray astronomy
[NASA-CR-174334] 08 p1164 N85-17344

FRANCE
The French weather radar network: A status report
01 p0082 N85-10550
Deformation mechanisms associated with mesoscopic kinkbands, Jura Mountains (Switzerland) and Chaines Subalpines (France) 03 p0369 N85-12492
French commentary on Soviet industrial espionage
10 p1461 N85-19210
French panel makes specific proposals for robotics research. Current state of French robotics
11 p1618 N85-20180
French research minister on policy, technology transfer 11 p1618 N85-20182
SEP of France manufactures its first silicon carbide fibers 11 p1618 N85-20184
French activities relevant to middle atmosphere research 11 p1655 N85-20423
Statistics of french Armee de l'air ejections 1970 - 1980 12 p1906 N85-21971
Evaluation of wave energy resources on the French Atlantic seaboard 14 p2325 N85-24369
The ARGOS system and hydrology: The use of Platform Terminal Transmitter (PTT) with built-in memory and direct reception by the Seine basin hydrology service
14 p2328 N85-24389
Second Soviet-French Symposium on Space Cytology
14 p2386 N85-24699
West Europe report: Science and technology
[JPRS-WST-84-007] 15 p2530 N85-25600
Search and rescue of aircraft in distress in France. Organization, means 20 p3401 N85-31096
Specific aspects of maritime search and rescue in French metropolitan and overseas territories: Expected benefits from a detection and location of distress system by satellites 20 p3401 N85-31097
The SARSAT-COSPAS demonstration in France
20 p3405 N85-31131

FRANCK-CONDON PRINCIPLE
Measurement of Franck-Condon factors for the v'=0 progression in the B-X system of PO
[AD-A152734] 17 p2919 N85-27993
Calculation of Franck-Condon factors for diatomic molecules
[AD-A154463] 19 p3353 N85-30784

FRAUNHOFER LINES
Ten years observations of long-period oscillations of the Sun 14 p2450 N85-25123

FRAUNHOFER REGION
U FAR FIELDS

FREDHOLM EQUATIONS
Numerical solution of a first kind Fredholm integral equation arising in electron-atom scattering
[CWI-NM-R8414] 14 p2414 N85-24897
A program for solving first kind Fredholm integral equations by means of regularization
[CWI-NM-R8416] 17 p3022 N85-28697

FREDHOLM OPERATORS
U FREDHOLM EQUATIONS
U OPERATORS (MATHEMATICS)

FREE ATMOSPHERE
C2 sub n (optical) studies in the free atmosphere based on rawinsonde data
[AD-A147307] 07 p0997 N85-16332
A turbulent closure model for the free atmosphere
09 p1351 N85-18502

FREE BOUNDARIES
Diffusive combustion of fluids with free surface
02 p0274 N85-11785
Regularity of the free boundary for the porous medium equation
[AD-A147299] 08 p1210 N85-17611
Initial velocity of the emerging free boundary in a two-phase Stefan problem with imposed flux
[DE85-003813] 11 p1631 N85-20272
A new approach to queer differential equations
[AD-A149321] 15 p2638 N85-26272
A Navier-Stokes capillary free boundary in open boat crystal growth
[REPT-84-34] 17 p2980 N85-28[illegible]

FREE CONVECTION
Vertical channel free convection for a power law fluid with a constant heat flux
[DE84-014551] 01 p0047 N85-10311
Influence of Prandtl number on natural convection heat transfer correlations
[DE84-013006] 05 p0637 N85-14089
Theoretical description of film boiling in a two phase flow calculation
[IKE-2-66] 05 p0636 N85-14082
Unsteady free-convection heat transfer inside an annular cavity
[CFD/84/16] 08 p1163 N85-17339
Natural convection during heat accumulation by substances with change of aggregate state
13 p2043 N85-22707
Numerical benchmark study for the finite element computer code NEPTUNE
[DE85-008400] 17 p3013 N85-28630
Surface temperature distribution along a thin liquid layer due to thermocapillary convection
[NASA-TM-87115] 23 p3930 N85-34357

FREE ELECTRON LASERS
NRL (Naval Research Laboratory) FEL (Free Electron Laser) program
[AD-A145057] 01 p0052 N85-10347
Free electron lasers
[AD-A145109] 01 p0053 N85-10349
A covariant derivation of the ponderomotive force
[AD-A145054] 01 p0121 N85-10630
Summary discussion: Theoretical aspects of XUV free electron lasers
[AD-A145475] 02 p0202 N85-11343
Theory of free-electron lasers with focusing pumping field 02 p0262 N85-11714
Linear theory of free-electron lasers with cylindrical interaction space 02 p0262 N85-11718
A normal-incidence monochromator branch line on the FEL-undulator for experimental studies in the 5 to 30 eV region
[DE84-014379] 04 p0505 N85-13225
Laser-driven particle accelerators
[DE84-015953] 04 p0506 N85-13227
Accelerator Technology Program
[DE84-017083] 04 p0563 N85-13586
A proton laser accelerator by means of the inverse free electron laser mechanism
[DE85-000231] 06 p0813 N85-15183
Rippled-field magnetron apparatus
[AD-D011354] 07 p0969 N85-16154
A new free electron laser using a relativistic beam with spiralling electron
[AD-D011318] 07 p0971 N85-16165
Technology for satellite power conversion
[NASA-CR-174335] 09 p1343 N85-18451
Two-stage free electron laser research
[AD-A148951] 10 p1489 N85-19402
The axial velocity spread acceptance of free electron lasers
[AD-A149024] 10 p1489 N85-19403
A free electron laser with a rotating quadrupole wiggler
[AD-A149052] 10 p1489 N85-19404
Construction tolerances for low loss, dielectric coated, metallic waveguide for transmission optical radiation
[DE85-004056] 10 p1558 N85-19822
A free electron laser with two-component wiggler
11 p1623 N85-20217
Progress toward free-electron lasers for applications
[DE85-002208] 11 p1639 N85-20326
Optical guiding in a free electron laser
[DE85-003141] 11 p1639 N85-20327
Novel probe for determining the size and position of a relativistic electron beam
[DE85-001044] 11 p1723 N85-20836
Betatron-synchrotron detrapping in a tapered wiggler free electron laser
[AD-A149686] 12 p1856 N85-21642
Resonance between betatron and synchrotron oscillations in a free electron laser: A 3-D numerical study
[AD-A150059] 12 p1857 N85-21645
Enhancing the performance of a high-gain free electron laser operating at millimeter wavelengths
[DE85-000862] 12 p1857 N85-21646
Los Alamos free electron laser: Accelerator performance
[DE85-005722] 13 p2097 N85-23084
Principle and design of a medium-enhanced free-electron laser 15 p2561 N85-25802
Stimulated Brillouin scattering reflectivity in the presence of various aberrators
[AD-A151750] 15 p2563 N85-25812

Free electron lasers for the EUV spectral region
[DE85-008804] 15 p2563 N85-25815
Microwave emission from relativistic electron beams
[AD-A151472] 15 p2648 N85-26333
Two-beam accelerator
[DE85-004662] 15 p2649 N85-26335
Low voltage free electron laser development
[AD-A152917] 17 p2970 N85-28342
Resonator optical designs for free electron lasers
[DE85-007678] 17 p2971 N85-28347
Report of the Working Group on Other Acceleration Schemes
[DE85-008447] 17 p3033 N85-28764
Review of short wavelength lasers
[DE85-009858] 18 p3114 N85-29277
The free electron laser variable bridge coupler
[DE85-009630] 18 p3114 N85-29278
Hamiltonian picture of the free electron laser and unitary symmetries
[PREPRINT-436] 18 p3114 N85-29281
Phase and amplitude considerations for the 2-beam accelerator
[DE85-008455] 18 p3180 N85-29715
Coherent X-rays and vacuum-ultraviolet radiation from storage-ring-based undulators and free electron lasers
[DE85-009988] 18 p3183 N85-29736
Conversion efficiencies of charged particle beam driven free electron lasers
[AD-A154404] 19 p3276 N85-30316
Recent results of the Los Alamos free-electron laser oscillator experiment
[DE85-010736] 19 p3277 N85-30324
Phase and amplitude feedback control system for the Los Alamos free-electron laser
[DE85-010787] 19 p3277 N85-30325
Los Alamos Free-Electron Laser (FEL) RF system
[DE85-010718] 19 p3278 N85-30329
High-brightness photoemitter development for electron accelerator injectors
[DE85-009548] 19 p3355 N85-30796
Grazing incidence beam expander
[DE85-010784] 19 p3368 N85-30889
New concepts in free electron lasers
20 p3460 N85-31493
Cerenkov maser and Cerenkov laser devices
[AD-A155443] 21 p3592 N85-32324
ATA upgrade to 150 MeV
[DE85-013174] 24 p4096 N85-35404
Los Alamos free-electron laser
[DE85-012666] 24 p4096 N85-35405

FREE ELECTRONS
A free electron laser with two-component wiggler
11 p1623 N85-20217
RF-Primed high power halogen vial apparatus
[AD-D011545] 12 p1935 N85-22156

FREE ENERGY
Thermodynamic properties and environmental chemistry of chromium
[DE84-015123] 01 p0025 N85-10152
Equation of state study for polar fluids
[PB84-222801] 01 p0025 N85-10157
Free energy and effective mass of the polaron at finite temperatures
[TUM-M8401] 03 p0417 N85-12687
Correlation of electronic charge transfer transitions and electrochemical potentials. The Bipyrazine(Tetracarbonyl)Molybdenum(O) system in various solvents
[AD-A147660] 08 p1120 N85-17062
Simple EOS for the silicone rubber Sylgard 184
[DE85-001394] 12 p1814 N85-21376
Low-dimensional behavior of the pattern formation Cahn-Hilliard equation
[DE85-003727] 12 p1922 N85-22072
Green's function solution of the Kondo problems and universality of the thermodynamic properties
[DE85-002739] 12 p1943 N85-22206
Noncontinuum solvent effects upon the intrinsic free-energy barrier for electron-transfer reactions
[AD-A150662] 14 p2250 N85-23943
Detonation behavior of LX-14 and PBX-9404: Theoretical aspect
[DE85-010038] 18 p3084 N85-29076
Influence of particle arrangement on sintering
[AD-A155337] 21 p3599 N85-32352

FREE FALL
Research relative to the development of a cryogenic microwave cavity gradiometer for orbital use
[NASA-CR-174249] 07 p0962 N85-16095
Reinterpretation of otolith input as a primary factor in space motion sickness 20 p3509 N85-31812

FREE FLIGHT
Thermal and cryogenic design study for space infrared telescope facility (SIRTF)
[NASA-CR-166613] 07 p0915 N85-15793

FREE FLIGHT TEST APPARATUS
The effect of instrumentation system parameters on the results of a flight mechanical system identification
24 p4061 N85-35170

FREE FLOW
Numerical analysis of the 3-dimensional inviscid hypersonic flow around capsule-type bodies by the alternate directional implicit method
[NAL-TR-799] 01 p0002 N85-10012
Preliminary results of a study of the relationship between free stream turbulence and stagnation region heat transfer
[NASA-TM-86864] 02 p0197 N85-11317
Solid sorbent air sampler
[NASA-CASE-MSC-20653-1] 11 p1636 N85-20301
Investigation of internal friction of free-flowing material during discharge
[BLL-M-36141-(5828.4)] 15 p2553 N85-25752
Study of the coupling between average, coherent and turbulent fields in a circular excited free jet
[ISL-R-115/83] 16 p2785 N85-27184
Computation model of turbulent free flow: Application to axisymmetric jets
[ISL-R-126/83] 16 p2785 N85-27185
Analyses of orderly structures in jets and the relationship with emitted noise
[ISL-R-117/83] 16 p2861 N85-27646
Transverse vorticity measurements using an array of four hot-wire probes
[FSFL-R-85-006] 18 p3069 N85-29184
On Fofonoff's mode 18 p3145 N85-29471
Transient combustion dynamics
[AD-A154430] 19 p3235 N85-30052
An investigation of hydraulic transients in combination free surface and pressurized flows
19 p3264 N85-30239
An experimental investigation of curvature and freestream turbulence effects on heat transfer and fluid mechanics in transitional boundary layer flows
19 p3264 N85-30240
Vortex simulation of v-shaped flame
20 p3425 N85-31259
A mathematical analysis of the effect of free stream turbulence on the Blasius boundary layer
20 p3451 N85-31430
Preliminary results of a study of the relationship between free-stream turbulence and stagnation region heat transfer 20 p3452 N85-31435
Vaporization from a heated surface into a saturated stream
[DE85-010484] 20 p3530 N85-31958
Experiments on the influence of active walls on the initial amplitudes and growths of instability waves
[AD-A154630] 21 p3583 N85-32275
Numerical solutions of turbulent models for flow over a flat plate with angle of attack
[DE85-010380] 21 p3585 N85-32286
Nozzle wall roughness effects on free-stream noise and transition in the pilot low-disturbance tunnel
[NASA-TM-86389] 23 p3930 N85-34355
Experimental study of free and mixed convective flow of air in a heated cavity
[DE85-012538] 24 p4094 N85-35380

FREE JETS
Computation of noise radiation from a free jet perpendicular to its axis via laser anemometry measurements
[ESA-TT-870] 09 p1379 N85-18669
Basic studies of multiple free and confined jets
[AD-A149556] 10 p1485 N85-19374
Velocity and volumetric measurement in free jets
11 p1576 N85-19931
Fourier densitometry: A new optical method for measuring density fluctuations by Rayleigh scattering -- turbulent jets 11 p1576 N85-19932
Time-dependent flow of stream swirled in vortex chamber 13 p2043 N85-22786
Application of laser anemometry to jets in combustion chambers
[ISL-CO-210/83] 14 p2302 N85-24253
Laser anemometry two dimensional measurement of velocity fluctuations in an excited jet
[ISL-CO-213/83] 14 p2302 N85-24254
An automatic traversing system for Laser Doppler Anemometer (LDA) applications to wind tunnels and to free jets
[ISL-CO-225/83] 16 p2636 N85-27490
Aerosol analysis and emission spectrometry with free jets
[DE85-010576] 21 p3564 N85-32168
Measurement of velocity and concentration in free jets
[ISL-CO-215/84] 22 p3786 N85-33451

FREE MOLECULAR FLOW
Relation of core structure to high velocity outflow in G35.2-0.74 and other molecular clouds
03 p0443 N85-12818

FREE OSCILLATIONS
U FREE VIBRATION

FREE RADICALS
NT HYDROXYL RADICALS
Analysis of glow discharges for understanding the process of film formation
[NASA-TM-83750] 01 p0022 N85-10138
USSR report: Chemistry
[JPRS-UCH-84-012] 06 p0761 N85-14865
Time-resolved studies of free radicals and laser-initiated chain reactions
[DE85-002100] 09 p1326 N85-18332
Characterization of acetylene-terminated resin cure states
[AD-A149463] 10 p1452 N85-19148
Synthesis of hydrophobic, crosslinkable resins
[AD-A150658] 14 p2260 N85-24002
Free radicals in the stratosphere: A new observational technique 16 p2624 N85-27415
Role and fate of ozone in the atmosphere
16 p2624 N85-27421
Chemical transformation modules for Eulerian acid deposition models. Volume 1: The gas-phase chemistry
[PB85-173714] 18 p3072 N85-29001
Shock tube measurements of growth constants in the branched-chain ethane-carbon monoxide-oxygen system
[NASA-TM-87068] 21 p3562 N85-32156

FREE STREAM EFFECTS
U FREE FLOW

FREE STREAMS
U FREE FLOW

FREE VIBRATION
A rigid body mechanism in structural dynamics
02 p0206 N85-11361
The Shock and Vibration Digest, volume 16, no. 9
[AD-A146779] 07 p0976 N85-16200
A review of approximate methods for determining the vibrational modes of membranes
09 p1331 N85-18363
Effect of coupled torsional-flexural vibration of a geared shaft system on the dynamic tooth load
09 p1338 N85-18415
Effect of air cavity on the vibration analysis of loaded drums 09 p1339 N85-18422
A study of internal and distributed damping for vibrating turbomachiner blades
[NASA-CR-175901] 17 p2898 N85-27868
Applications of the Galerkin formalism in the coupling of the earth's free oscillations 24 p4116 N85-35514

FREEZE DRYING
Polyactic-polyglycolic acid copolymer combined with decalcified freeze-dried bone for use as a bone repair material
[AD-D011438] 10 p1451 N85-19142

FREEZING
NT ZONE MELTING
Forecasting water temperature decline and freeze-up in rivers
[AD-A147068] 07 p0967 N85-16274
Diurnal freeze-thaw frequencies in selected regions of the high latitudes
[AD-A147276] 07 p1007 N85-16400
Lake ice occurrence as a possible detector of atmospheric CO2 effects on climate
[DE85-002951] 11 p1687 N85-20606
Jet fuel property changes and their effect on producibility and cost in the U.S., Canada, and Europe
[NASA-CR-174840] 16 p2757 N85-27012
Fuel freeze point investigations
[AD-A152801] 17 p2937 N85-28129
The distribution of higher n-alkanes in partially frozen middle distillate fuels
[AD-A153840] 18 p3083 N85-29074
Onset of freezing in residential air-to-air heat exchangers
[DE85-009960] 19 p3267 N85-30259
A study of freezing and melting with eutectic interactions 19 p3378 N85-30956
On the problem of possible mechanism of ice nuclei formation in convective clouds 21 p3640 N85-32610
Supersaturation spect A of Ice Nuclei at different locations in Europe and over the North-Atlantic
21 p3640 N85-32615
Concentrations of ice nuclei of different modes of activities 21 p3641 N85-32616
Ice nucleating characteristics of Capparis Aphylla, an Indian herb 21 p3641 N85-32619
Ice-forming efficiency of the soluble and insoluble portions of dust contained in snow
21 p3643 N85-32631
Critical supersaturations with respect to water for fast condensation-freezing ice nucleation
21 p3643 N85-32632

Aircraft accident report: World Airways Inc., Flight 30H, McDonnell Douglas DC-10-30CF, N113WA, Boston-Logan International Airport, Boston, Massachusetts, January 23, 1982
[PB85-910406] 22 p3726 N85-33114
Land vehicle corrosion management
22 p3750 N85-33246
Refrigerated dynamic seal to 6.9 MPa (1000 psi)
[NASA-TM-87106] 23 p3930 N85-34356
Lake ice occurence as a possible detector of atmospheric CO2 effects on climate
[DE85-012987] 23 p3950 N85-34480

FREEZING POINTS
U MELTING POINTS

FREIGHT
U CARGO

FRENCH SATELLITES
NT SPOT (FRENCH SATELLITE)

FRENCH SPACE PROGRAMS
Non-US approaches to space commercialization
02 p0150 N85-11012
The 2 GHz network and the network operations center — satellite tracking 05 p0589 N85-13817
MATRA has Europe's largest white room for satellites
10 p1477 N85-19320
CNES, INRA do joint remote-sensing research
10 p1477 N85-19321
Activities in French aerospace
11 p1587 N85-19995
France officially proposes development of Ariane 5 to ESA 15 p2532 N85-25613
SEP of France to make Ariane HM-60 cryogenic engine 15 p2532 N85-25614
The French space program 22 p3731 N85-33127

FREON
Characteristics of controlled-oscillating annular cascade test facility with Freon gas
[NAL-TR-812] 01 p0003 N85-10014
Challenges in the development of the orbiter active thermal control subsystem 06 p1096 N85-16923
A feasibility study for using low boiling point fluids to change aircraft tire deflection
[AD-A152096] 16 p2706 N85-26701
Special features of the temperature dependence of the capillary constant in the vicinity of the critical point
[BLL-T6438/BG/LRS/LRST750/85]
16 p2859 N85-27632
Thermodynamic study of CO2-organic compound interaction at high pressures and temperatures
[DE85-010999] 19 p3268 N85-30266

FREQUENCIES
NT AUDIO FREQUENCIES
NT BEAT FREQUENCIES
NT BROADBAND
NT C BAND
NT CARRIER FREQUENCIES
NT CRITICAL FREQUENCIES
NT CYCLOTRON FREQUENCY
NT EXTREMELY HIGH FREQUENCIES
NT EXTREMELY LOW FREQUENCIES
NT EXTREMELY LOW RADIO FREQUENCIES
NT HIGH FREQUENCIES
NT INFRASONIC FREQUENCIES
NT INTERMEDIATE FREQUENCIES
NT LOW FREQUENCIES
NT MICROWAVE FREQUENCIES
NT PLASMA FREQUENCIES
NT RADIO FREQUENCIES
NT RESONANT FREQUENCIES
NT SUPERHIGH FREQUENCIES
NT SWEEP FREQUENCY
NT ULTRAHIGH FREQUENCIES
NT VERY HIGH FREQUENCIES
NT VERY LOW FREQUENCIES
Anomalies in frequency characteristics of solid-state ring laser 02 p0271 N85-11765
Characteristics of light diffraction by two acoustic waves, one with complex frequency composition
03 p0348 N85-12243
The investigation of short wave signal structure in the vicinity of the caustic by means of a high-directed antenna
[PR-194] 03 p0354 N85-12277
The ML (Maximum Likelihood) method for frequency estimation of real sinusoids in noise
[AD-A146053] 03 p0411 N85-12628
Analysis of frequency-selective integrated circuits in system of normal coordinates 04 p0489 N85-13119
Two programs for the HP9836C computer to acquire frequency or voltage data from a source
[AD-A146632] 06 p0854 N85-15430
An evaluation of flashtube signal characteristics
[AD-A149569] 10 p1423 N85-18974
Condensed antenna structural models for dynamics analysis 10 p1463 N85-19230
Spectrum resource assessment of the Aeronautical Mobile Service between 400 MHz and 17.7 GHz
[PB85-125995] 11 p1626 N85-20241
Frequency spectra of turbulent pulsations in stability of laminar boundary layer 11 p1716 N85-20795
Study of light shifts in laser pumped quantum discriminator frequency 11 p1716 N85-20798
Externally compensated crystal oscillator (ECXO) study
[AD-A150335] 13 p2064 N85-22893
Programmable filter with fanned interdigital surface acoustic wave transducer 13 p2083 N85-23006
Adsorption site, adsorption energy and normal vibration frequency of H/Ni(100) via total energy calculations
[AD-A150555] 13 p2156 N85-23388
A study of frequency effects and damage accumulation during the fatigue of graphite/epoxy and glass/epoxy composite materials 14 p2247 N85-23930
Design and measured performance of a broadband Archimedes spiral antenna
[R-NIAS-22] 14 p2290 N85-24194
The sensitivity of solar eigenfrequencies to the treatment of the equation of state 14 p2445 N85-25089
Frequency selective signals-to-noise enhancer/limiter apparatus
[AD-D011583] 15 p2548 N85-25724
Adjustment of the frequency-temperature characteristics of crystal oscillators
[AD-D011588] 15 p2548 N85-25726
An atlas of pure water vapor spectra from 500 to 5000/cm, Volume 2
[AD-A151757] 16 p2745 N85-26940
Relationship between Allan variances and Kalman Filter parameters 18 p3107 N85-29238
Temperature sensitive oscillator
[NASA-CASE-GSC-12958-1] 19 p3258 N85-30201
Experimental determination of the mixing frequency parameter for coalescence/dispersion modeling of turbulent combustion
[DE85-011468] 19 p3270 N85-30280
Some studies in filtering of atmospheric turbulence
[AD-A154042] 19 p3316 N85-30557
The problem of brightness enhancement during laser frequency doubling 21 p3686 N85-32897
International prototype network in Dubna experimental satellite communications system
22 p3773 N85-33383
Gradiental adaptive corrector with optimum tuning step 22 p3776 N85-33403
Calculating dominant (quasi-t) mode group velocity in shielded microstrip line 22 p3780 N85-33422

FREQUENCY ANALYZERS
Magnetostatic wave frequency analyzer apparatus
[AD-D011249] 05 p0631 N85-14044
Use of electronic coding-frequency meters to measure parameters of pulsed radio signals
13 p2076 N85-22964
Rotor blade test apparatus
[AD-D011725] 23 p3934 N85-34381

FREQUENCY ASSIGNMENT
Planning guide for the review of telecommunications systems for frequency availability and electromagnetic compatibility
[PB84-210238] 01 p0041 N85-10268
Radar frequency selection strategies
[AD-A147493] 07 p0941 N85-15967
A commentray on the utilization of real-time channel evaluation systems in HF spectrum management
[AD-A148616] 08 p1154 N85-17289
A description of the NRL oblique-incidence-ionogram data base
[AD-A148625] 08 p1230 N85-17748
Spectrum resource assessment of the 1530-1660.5 MHz band
[NTIA/REPT-84/160] 10 p1469 N85-19268
Spectrum resource assessment of the 7125-8500 MHz band
[PB85-127413] 11 p1626 N85-20242
Spectrum resource assessment of the fixed and mobile services in the 947-17,700 MHz band, phase 1
[PB85-128288] 11 p1626 N85-20243
Engineering calculations for communications satellite systems planning
[NASA-CR-175552] 12 p1789 N85-21233
Frequency selection for dispersion signal in satellite communication lines 15 p2528 N85-25584
Propagation considerations in land mobile satellite transmission
[NASA-CR-175733] 15 p2540 N85-25684
Optimal frequencies for broadcast transmitters in the UHF domain: Report
[TUM-M8404] 16 p2769 N85-27088
Generalized graph coloring: A frequency assignment method for VHF broadcasting
[TUM-M8405] 16 p2844 N85-27535
Criteria for site selection and frequency allocation (keynote paper), part 5 21 p3623 N85-32511
Frequency and site selection criteria for MST radars, part 5.1A 21 p3624 N85-32512

FREQUENCY BANDS
U FREQUENCIES

FREQUENCY CONTROL
NT AUTOMATIC FREQUENCY CONTROL
Diagnostic apparatus for radar pulse repetition frequency control circuit card
[AD-D011364] 07 p0937 N85-15938
Low noise multiple crystal-controlled oscillator
[AD-D011401] 07 p0948 N85-16010
Improved magnetic bias and delay linearity in a magnetostatic wave delay line
[AD-D011441] 10 p1479 N85-19337
Stereo decoder without subcarrier restoration
13 p2068 N85-22921
Gyrator frequency selectors with bandwidth independent of input signal level 13 p2083 N85-23009
System of phase-lock automatic frequency control with acoustoelectronic convolver 15 p2526 N85-25573
Simultaneous phase and frequency control of a three-phase inductor-convertor bridge
[DE85-006197] 18 p3096 N85-29184
Rubidium and cesium frequency standards status and performance on the GPS program
18 p3106 N85-29228
A miniature tactical Rb frequency standard
18 p3106 N85-29229
The Rubidium-Crystal Oscillator Hybrid Development Program 18 p3106 N85-29230
New features of different frequency generating systems due to the use of electrodeless rigidly mounted VBA quartz crystal resonator 18 p3106 N85-29231
The system design of a rubidium maser frequency standard 18 p3106 N85-29232
Maintenance of time and frequency in the Jet Propulsion Laboratory's Deep Space Network using the Global Positioning System 18 p3109 N85-29249
A variable frequency control for three-phase induction motors 19 p3256 N85-30190

FREQUENCY CONVERSION
U FREQUENCY CONVERTERS

FREQUENCY CONVERTERS
NT DOWN-CONVERTERS
NT FREQUENCY DIVIDERS
NT FREQUENCY MULTIPLIERS
NT FREQUENCY SYNTHESIZERS
NT PARAMETRIC FREQUENCY CONVERTERS
NT UP-CONVERTERS
15 kW general purpose frequency changer performance improvement
[AD-A145503] 02 p0194 N85-11287
A means of extending streak camera recording into the important 1300-1600 nm wavelength regime: Parametric frequency upconversion
[DE84-015666] 04 p0503 N85-13208
VLBI system (BLK I) IF-video down conversion design
05 p0625 N85-13996
Charge depletion meter
[AD-D011484] 10 p1488 N85-19383
Development of a 20 GHz modulator for the payload of a satellite for propagation and transmission experiments, including the required converters of the test equipment
[BMFT-FB-W-84-044] 11 p1590 N85-20004
Wideband phase keyers 12 p1839 N85-21544
Magnetic noise in single-machine rotating frequency converters 13 p2077 N85-22969
Converters of sum/differnce of codes to frequency
15 p2526 N85-25578
Lidar ER2 (ozone). Crystal characterization for harmonic conversion — laser systems
[CERT-2/6129-00] 16 p2672 N85-27717

FREQUENCY DISCRIMINATORS
Multiple passband transducers for tone selection from a frequency comb generator
[RSRE-MEMO-3647] 02 p0184 N85-11295
Analysis of characteristics of digital discriminators for phase-shift keyed signals 13 p2070 N85-22930

FREQUENCY DISTRIBUTION
Three algorithms for parametric frequency domain system identification
[DE85-002801] 11 p1706 N85-20735
Problem of frequency space variation of sonic field in stratified media 11 p1715 N85-20787
Noise immunity of information transmission system with pseudorandom frequency switching under worst-case interference conditions 13 p2086 N85-23025
A statistical treatment of the regional slope characteristics of Venus and Earth
13 p2178 N85-23517
Transient combustion dynamics
[AD-A154430] 19 p3235 N85-30052

The determination of daily usage or occupancy in the land-mobile band 138-174 MHz at Montreal
[CRC-1383] 19 p3253 N85-30167
Scattering by distributions of small thin particles
19 p3253 N85-30172
Coding schemes for improving MST radar performance, part 7.1A 21 p3625 N85-32520
Gamma ray burst size-frequency distributions: Spectral selection effects
[OG-1.2-3] 22 p3862 N85-33913
Burst size distributions in the digitized data of the ion chambers t Mt. Norikura and sea level stations
[SH-9.1-9] 23 p4051 N85-35124
Performance of a local electron density trigger to select extensive air showers at sea level
[HE-4.6-11] 24 p4198 N85-36048

FREQUENCY DIVIDERS
Investigation of characteristics of phased antenna array considering interaction between radiators and properties of power divider 06 p0790 N85-15051
A noise-suppressing digital frequency meter
06 p0796 N85-15084

FREQUENCY DIVISION MULTIPLE ACCESS
Throughput increase in frequency hopped multiple access channels by means of discrimination against partially overlapping interference
[AD-A145540] 02 p0191 N85-11275

FREQUENCY DIVISION MULTIPLEXING
Fiber optic data bus using Frequency Division Multiplexing (FDM) and an asymmetric coupler
[NASA-TM-86015] 04 p0492 N85-13139
Preliminary estimation of mutual interference between fixed satellite service systems 15 p2528 N85-25586

FREQUENCY HOPPING
Throughput increase in frequency hopped multiple access channels by means of discrimination against partially overlapping interference
[AD-A145540] 02 p0191 N85-11275
Spread-spectrum communications
[AD-A146135] 03 p0355 N85-12285
Optimum jamming effects on frequency-hopping M-ary FSK (Frequency-Shift Keying) systems under certain ECCM (Electronic counter-countermeasures) receiver design strategies
[AD-A147766] 08 p1151 N85-17267
Research on adaptive antenna techniques 6
[AD-A149341] 11 p1624 N85-20228
Tactical satellite terminals for land and airborne C3 applications 11 p1710 N85-20760
Spread spectrum mobile radio communications
[AD-A149936] 12 p1829 N85-21477
FH/MFSK performance in multitone jamming
[NASA-CR-175667] 14 p2290 N85-24197
Spectroscopic investigation of materials for frequency agile laser systems
[AD-A151731] 16 p2790 N85-27208
Measured noise performance of a new method of frequency hopping
[AD-A152679] 17 p2953 N85-28234

FREQUENCY MEASUREMENT
Spectral noise density and random errors of pulse frequency characteristic meters
03 p0346 N85-12231
A group delay standard for the MHz frequency range
05 p0630 N85-14040
Infralow-frequency digital phase meter
06 p0787 N85-15031
A noise-suppressing digital frequency meter
06 p0796 N85-15084
NBS frequency measurement system from a user's viewpoint
[DE84-016782] 09 p1315 N85-18268
Historical cost curves for hydrogen masers and cesium beam frequency and timing standards
10 p1465 N85-19245
Use of electronic coding-frequency meters to measure parameters of pulsed radio signals
13 p2076 N85-22964
Space-based antenna measurement system concepts for space station operation 14 p2236 N85-23860
Experimental performance of a frequency measurement circuit
[AD-A152951] 17 p2953 N85-28239
New time and frequency services at the National Bureau of Standards 17 p2961 N85-28289
Methods for optimal recursive estimation of non-stationary time series, applications to atomic time and frequency metrology 17 p2965 N85-28312
Ionospheric limitations to time transfer by satellite
18 p3107 N85-29234
Maintenance of time and frequency in the Jet Propulsion Laboratory's Deep Space Network using the Global Positioning System 18 p3109 N85-29249
Using GPS and VLBI technology to maintain 14 digit synchronization 18 p3109 N85-29250
Performance test results of a low cost GPS time and frequency monitor 18 p3109 N85-29252
Fiber optic sensors operating at dc
[AD-D011674] 19 p3271 N85-30283
New measurement solutions for low frequency systems 20 p3437 N85-31325
Characterization of microstrip discontinuities in the time and frequency domains
[NASA-CR-176190] 24 p4088 N85-35342

FREQUENCY MODULATION
NT FREQUENCY SHIFT KEYING
NT PULSE FREQUENCY MODULATION
Self-modulation of injection laser emission intensity due to external optical feedback 02 p0261 N85-11706
Analog voice processing for FM transmission in a telephone channel
[INPE-2798-PRE/359] 03 p0354 N85-12279
Radio telemetry formula applications. A practical users guide
[AD-A146247] 03 p0356 N85-12286
Television transmission in frequency modulation
04 p0493 N85-13146
Structure of frequency modulated and phase-shift keyed signals reflected from ionosphere at near-critical frequencies 07 p0952 N85-16035
BBC receiving terminal for the European orbital test satellite
[BBC-RD-1984/15] 08 p1142 N85-17205
EMC enhanced constant Z modulator
[AD-A147715] 08 p1157 N85-17297
Subjective evaluation of the effect of noise and interference on frequency modulated NTSC television signals
[CRC-1367] 09 p1310 N85-18230
Generation of Alfven waves due to thermal modulation of the electrical conductivity
[AD-A149389] 10 p1558 N85-19826
Signal processing and range spreading in the FM-CW radar
[PB85-108256] 11 p1626 N85-20239
Space-time response characteristics of acoustooptic filter for compression of linearly frequency-modulated signal 13 p2071 N85-22937
Simple detonation meter 13 p2077 N85-22971
Synthesis of optimum single-channel discrete signals and filters 13 p2080 N85-22990
Analysis of interference caused by interfering radio signals in communications systems with frequency separation of telephone channels and frequency modulation 13 p2086 N85-23025
Preliminary estimation of mutual interference between fixed satellite service systems 15 p2528 N85-25586
An analysis of jamming effects on noncoherent digital receivers
[AD-A153791] 18 p3090 N85-29128
Analog frequency modulated laser using magnetostriction
[AD-D011701] 19 p3276 N85-30318
Use of radar with frequency modulation for studying atmospheric boundary layer 19 p3296 N85-30437
Controllable companding in low-frequency FM radio communication systems 22 p3776 N85-33402
Device for frequency modulation of a laser output spectrum
[DE85-011634] 22 p3790 N85-33479

FREQUENCY MULTIPLIERS
Infralow-frequency digital phase meter
06 p0787 N85-15031
A phase-locked frequency multiplier for the signal averaging of the vibration of the Wessex helicopter input spiral bevel pinion
[AD-A154914] 21 p3555 N85-32113

FREQUENCY RANGES
Statistical properties of geomagnetic pulsations at the Observatory of Fuerstenfeldbruck determined with the aid of pulsation indices. Part 2: Periodicity in the occurrence of pulsations
[REPT-556] 03 p0376 N85-12399
Propagation and scattering considerations for the 0.2-3.0 GHz frequency range for a space-based radar
[AD-A148504] 08 p1153 N85-17282
Solid Rocket Motor Case (SRMC) dynamic sensitivity to changes in composite properties
12 p1948 N85-22238
Observations of intermediate-degree solar oscillations
14 p2442 N85-25069
The medical results of human exposures to radio frequency radiation 16 p2776 N85-27133
Frequent observations of extragalactic compact sources at 24 GHz 19 p3386 N85-31003
VLF (Very low frequency) workshop held at San Diego California, 24-25 January 1985
[AD-A154652] 21 p3573 N85-32224

FREQUENCY REGULATION
U FREQUENCY CONTROL

FREQUENCY RESPONSE
Complex frequency analysis of damped thin-walled beams with open cross sections
03 p0371 N85-12366
Frequency response design methods for large scale systems
[DE84-014161] 04 p0553 N85-13517
Application of the hydraulic system frequency response program to propellant feed systems
[AD-A151824] 16 p2741 N85-26914
An interactive computer aid for the design and analysis of linear, single input/single output digital and continuous control systems
[AD-A153704] 18 p3162 N85-29589

FREQUENCY REUSE
Mechanical/thermal design of a polarization sensitive reflector — communication satellites
05 p0626 N85-14009

FREQUENCY SCANNING
Optical 3-D signature device for detecting chemical agents
[AD-D011669] 19 p3272 N85-30293

FREQUENCY SHIFT
Frequency shifting in multimode fiber optic phase modulation devices 03 p0347 N85-12239
Tropospheric and ionospheric phase perturbations and Doppler frequency shift effects
[AD-A148579] 08 p1154 N85-17283
Atmospheric limitations in stellar seismology: Should one measure radial velocity or brightness fluctuations?
08 p1251 N85-17899
Propagation effects on the Doppler frequency shift of satellite transmissions 10 p1470 N85-19276
Nonlinear saturation of stimulated Raman scattering in homogeneous plasma
[DE85-003120] 10 p1560 N85-19837
Study of light shifts in laser pumped quantum discriminator frequency 11 p1716 N85-20798
Experimental studies of low temperature surface interactions of atomic hydrogen using maser technique
[AD-A150216] 13 p2017 N85-22647
Acceleration-resistant crystal resonator
[AD-D011627] 16 p2778 N85-27144
On the accuracy of Cs beam primary frequency standards 18 p3105 N85-29224
Performance data of US Naval Observatory VLG-11 hydrogen masers since September, 1983
18 p3108 N85-29244
Accuracy in determining velocity of fluid movement by Doppler method 19 p3293 N85-30419
Design of a jamming simulator for a binary communication system
[AD-A154617] 21 p3573 N85-32221
Mesospheric measurements of irregularity patches using a 3-antenna interferometer, part 3.6B
21 p3621 N85-32498
Doppler spectrometer for measuring narrow photochemical gaps in inhomogeneously broadened spectra 21 p3669 N85-32921
HEAO 3 upper limits to the expected 1634 KeV line from SS 483
[OG-2.4-9] 22 p3868 N85-33954
Search for gamma ray lines from SS433
[OG-2.4-11] 22 p3868 N85-33955
DMSK: A practical 2400-bps receiver for the mobile satellite service: An MSAT-X Report
[NASA-CR-176194] 24 p4086 N85-35324
Scale separation closure and Alfven wave turbulence
[DE85-013124] 24 p4095 N85-35385

FREQUENCY SHIFT KEYING
Optimum jamming effects on frequency-hopping M-ary FSK (Frequency-Shift Keying) systems under certain ECCM (Electronic counter-countermeasures) receiver design strategies
[AD-A147766] 08 p1151 N85-17267
Ionospheric distortions of digital signals with wideband modulation 13 p2072 N85-22945
FH/MFSK performance in multitone jamming
[NASA-CR-175667] 14 p2290 N85-24197
Rational pulse-shaping filters for almost MSK-like modulation
[AD-A153065] 17 p2949 N85-28208

FREQUENCY STABILITY
Frequency stabilized laser
[AD-D011223] 01 p0053 N85-10351
Device for frequency stabilization of microwave oscillators 06 p0788 N85-15033
Reference oscillator stability effect on clutter cancellation in a radar system 07 p0938 N85-15946
Low noise multiple crystal-controlled oscillator
[AD-D011401] 07 p0948 N85-16010
The Statistical Loop Analyzer (SLA)
08 p1100 N85-16955
Measurement procedures for the radar spectrum engineering criteria
[PB85-119022/GAR] 09 p1313 N85-18254

best copy available

Synthesis of digital nonrecursive band-elimination filters for moving-target selectors 12 p1840 N85-21545
Coupled acoustic and hydrodynamic wave instabilities 13 p2000 N85-22538
Spectral frequency of eigenvalues in optimal problems of stability of cylindrical shells of variable thickness 13 p2047 N85-22815
Effect of variance of photoreceiver frequency characteristics on characteristics of measuring instruments 13 p2076 N85-22965
Experimental study of high-stability oscillator with surface-acoustic-wave resonator in feedback loop 13 p2090 N85-23053
Separating the variances of noise components in the Global Positioning System
[AD-P004578] 17 p2963 N85-28295
A new precision time and frequency source for stationary PTTI applications 17 p2963 N85-28297
On-orbit frequency stability analysis of the GPS NAVSTAR's 3 and 4 rubidium clocks and NAVSTAR's 5 and 6 cesium clocks 17 p2963 N85-28298
Improved master clock reference system at USNO 17 p2963 N85-28300
Test results for prototype GPS rubidium clocks 17 p2964 N85-28302
Clock characterization tutorial 17 p2965 N85-28311
The measurement of linear frequency drift in oscillators 17 p2966 N85-28316
High performances from a new design of crystal oscillator 17 p2966 N85-28318
Recent results on the peformance of EFOS, NP and NX hydrogen masers 17 p2966 N85-28320
Physics element design aspects for a tactical rubidium frequency standard 17 p2967 N85-28321
Proceedings of the Sixteenth Annual Precise Time and Time Interval (PTTI) Applications and Planning Meeting
[NASA-TM-87561] 18 p3105 N85-29221
On-orbit frequency stability analysis of the GPS NAVSTAR-1 quartz clock and the NAVSTARs-6 and -8 rubidium clocks 18 p3105 N85-29227
Investigation of fast reaction SAW (Surface Acoustic Wave) accelerometer
[AD-A153676] 19 p3216 N85-29943
Self-tuning adaptive-controller using online frequency identification 20 p3417 N85-31205
RF stabilization of interchange-ballooning modes
[DE85-012080] 24 p4090 N85-35353

FREQUENCY STANDARDS
Portable real-time clock
[AD-A146218] 03 p0364 N85-12336
NBS frequency measurement system from a user's viewpoint
[DE84-016782] 09 p1315 N85-18268
Experimental studies of low temperature surface interactions of atomic hydrogen using maser technique
[AD-A150216] 13 p2017 N85-22647
Lifetime and reliability of rubidium discharge lamps for use in atomic frequency standards
[AD-A150787] 14 p2417 N85-24915
Maintenance of time and frequency in the DSN using the global positioning system 16 p2771 N85-27105
New time and frequency services at the National Bureau of Standards 17 p2961 N85-28289
Recent improvements in the atomic time scales of the National Bureau of Standards 17 p2962 N85-28290
Enhacements to the TTS-502 time transfer system 17 p2963 N85-28296
A new precision time and frequency source for stationary PTTI applications 17 p2963 N85-28297
Improved master clock reference system at USNO 17 p2963 N85-28300
Test results for prototype GPS rubidium clocks 17 p2964 N85-28302
Timing-system design considerations for a mobile astrolabe 17 p2965 N85-28309
A plan for the development of inertial reconstruction of initial state clock (IRIS) 17 p2966 N85-28317
Physics element design aspects for a tactical rubidium frequency standard 17 p2967 N85-28321
The superconducting cavity stability ruby maser oscillator 17 p2967 N85-28324
Proceedings of the Sixteenth Annual Precise Time and Time Interval (PTTI) Applications and Planning Meeting
[NASA-TM-87561] 18 p3105 N85-29221
Prospects for atomic frequency standards 18 p3105 N85-29222
Frequency and time standards based on stored ions 18 p3105 N85-29223
On the accuracy of Cs beam primary frequency standards 18 p3105 N85-29224
Methods to recover the narrow Dicke sub-Doppler feature in evacuated wall-coated cells without restrictions on cell size 18 p3105 N85-29225
Diode laser 87Rb optical pumping in an evacuated wall-coated cell 18 p3105 N85-29226
Rubidium and cesium frequency standards status and performance on the GPS program 18 p3106 N85-29228
A miniature tactical Rb frequency standard 18 p3106 N85-29229
The Rubidium-Crystal Oscillator Hybrid Development Program 18 p3106 N85-29230
New features of different frequency generating systems due to the use of electrodeless rigidly mounted VBA quartz crystal resonator 18 p3106 N85-29231
The system design of a rubidium maser frequency standard 18 p3106 N85-29232
Maser and secondary clock in telecommunications networks 18 p3108 N85-29246
The time and frequency comparisons via Loran-C and National TV Network in Yugoslavia 18 p3109 N85-29248
The role of long term lamp fluctuations in the random walk of frequency behavior of the rubidium frequency standard: A case study
[AD-A155338] 21 p3590 N85-32314

FREQUENCY SYNCHRONIZATION
Fundamental limits to synchronization and tracking
[AD-A149623] 12 p1833 N85-21504
Foreshortened short-wave scattering on artificial ionospheric inhomogeneities 14 p2340 N85-24466
Clock synchronization by the Symphonie and Laser Synchronization from Stationary Orbit (LASSO) geostationary satellites 14 p2398 N85-24776
Timing accuracy of LF and TV synchronization techniques 17 p2961 N85-28288
The role of a low Earth orbiter in intercontinental time synchronization via GPS satellites 17 p2964 N85-28306
Using GPS and VLBI technology to maintain 14 digit synchronization 18 p3109 N85-29250
Global positioning system carrier phase: Description and use
[PB85-174126] 19 p3216 N85-29946
General design principles of high speed frequency synthesizers based on phase synchronization systems 22 p3779 N85-33417

FREQUENCY SYNTHESIZERS
EMC enhanced constant Z modulator
[AD-A147715] 08 p1157 N85-17297
Transdigitizer for relaying signals from Global Positioning System (GPS) satellites
[AD-D011442] 10 p1422 N85-18970
Regular synthesis of pairs of phase-keyed binary minimax signals 13 p2069 N85-22923
Theory of optimum M-filtration of signals against background of correlated interference 13 p2069 N85-22927
Optimal synthesis of surface acoustic wave filters 13 p2070 N85-22933
Simple sweep frequency generator 13 p2075 N85-22960
Reactanceless synthesized impedance bandpass amplifier
[NASA-CASE-GSC-12788-1] 18 p3093 N85-29145
A low noise synthesizer for autotuning and performance testing of hydrogen masers 18 p3108 N85-29242
Design of high-order analog and digital filters with identical sections 22 p3786 N85-33341
General design principles of high speed frequency synthesizers based on phase synchronization systems 22 p3779 N85-33417

FREQUENCY TRANSLATION
U FREQUENCY CONVERTERS

FRESH WATER
Identification and parameter estimation of phosphate balance models in drinking water reservoirs
[PUBL-313] 08 p1181 N85-17439
Operational performance of the photovoltaic-powered grain mill and water pump at Tangaye, Burkina Faso (formerly Upper Volta)
[NASA-TM-86970] 13 p2128 N85-23243
Sulfur cycling in freshwater sediments 21 p3658 N85-32726

FRESNEL DIFFRACTION
Optimization piezoelectric transducer width of acousto-optical devices 07 p0950 N85-16024
The evaluation of a deformable diffraction grating for a stigmatic EUV spectroheliometer
[NASA-CR-174248] 07 p1042 N85-16621
Morphology of the scattering targets: Fresnel and turbulent mechanisms, part 2.1A 21 p3618 N85-32481

FRESNEL LENSES
Research on materials and components for opto-electronic signal processing
[AD-A145806] 03 p0433 N85-12754
A second generation WAVIDS (Wide Angle Virtual Image Display System)
[AD-P004328] 09 p1270 N85-17982
Phase 2 fabrication and construction of the Sky Harbor Airport, solar photovoltaic concentrator project
[DE85-000019] 11 p1678 N85-20581
Design and development of a linear Fresnel lens air-cooled photovoltaic module and a stand-alone photovoltaic collector array
[DE85-008854] 16 p2819 N85-27301
Development of a second-generation linear Fresnel Photovoltaic and Thermal (PVT) concentrator array, including fabrication and installation of a 200 square meter collector field
[DE85-008473] 17 p2988 N85-28485
DOE/Sandia point-focus concentrator program, draft
[DE85-008209] 17 p3038 N85-28790
Visual and part-task manipulations for teaching simulated carrier landings
[AD-A153622] 18 p3154 N85-29629

FRESNEL REFLECTORS
Magnetism at interfaces and surfaces, as probed by neutron scattering
[DE85-007987] 18 p3176 N85-29890

FRESNEL REGION
A modified Fresnel scattering model for the parameterization of Fresnel returns, part 2.3A 21 p3618 N85-32483

FRETTING
Fretting corrosion and fretting fatigue of medium carbon steels 01 p0054 N85-10358
Effect of humidity on fretting wear of several pure metals
[NASA-TP-2403] 04 p0472 N85-13006
Comparison of the fatigue resistance (initiation, propagation) of cast TA6V with hot rolled TA6V — titanium alloy
[DGT-25369-PT-1] 12 p1806 N85-21341

FRETTING CORROSION
Fretting corrosion and fretting fatigue of medium carbon steels 01 p0054 N85-10358

FRICTION
NT AERODYNAMIC DRAG
NT DRY FRICTION
NT FLOW RESISTANCE
NT FRICTION DRAG
NT INTERNAL FRICTION
NT KINETIC FRICTION
NT SKIN FRICTION
NT SLIDING FRICTION
NT VISCOUS DRAG
Pavement friction measurements on nontangent sections of roadways, vol. 1
[PB84-219732] 01 p0036 N85-10227
Laminar flow heat exchangers. Viscosity induced non-uniform flow
[AD-A144777] 01 p0047 N85-10307
Structure and wear workshop colloquium 01 p0054 N85-10356
The influence of surface layers on the friction and wear behavior of materials 01 p0054 N85-10357
Friction and wear of polymers and polymer composite materials 01 p0054 N85-10361
Friction, wear and structure of heterogeneous materials 01 p0055 N85-10362
Surface segregation of sulfur during oscillatory pin-on-plate wear studies of precious metal electrical contact alloys. 1: Friction and electrical contact resistance
[DE84-006962] 02 p0195 N85-11369
Comparison of predicted and measured friction for a tilt-pad thrust bearing with crown and roughness under hydrodynamic and mixed lubrication
[AD-A145752] 03 p0371 N85-12371
Thermomechanical cracking in layered media from moving friction load
[AD-A146022] 03 p0373 N85-12379
Roller crosshead analysis 04 p0507 N85-13228
Alternatives for runway rubber removal from porous friction surfaces
[DOT/FAA/PM-84/28] 05 p0597 N85-13603
An Iwatsubo-based solution for labyrinth seals - comparison with experimental results 05 p0644 N85-14131
Analysis for leakage and rotordynamic coefficients of surface roughened tapered annular gas seals 05 p0644 N85-14135
Conditions for assembling dies for drawing under hydrodynamic friction conditions
[BLL-M-35054-(5828.4)] 05 p0647 N85-14159
Friction and heat exchange in laminar and turbulent boundary layers with axisymmetrical bodies exposed to heterogeneous supersonic flow 05 p0724 N85-14665
The fate of globular clusters 05 p0739 N85-14751
Effects of silver and group 2 fluorides addition to plasma sprayed chromium carbide high temperature solid lubricant for foil gas bearing to 650 deg C
[NASA-TM-86895] 06 p0770 N85-14999

Fundamental tribological properties of ceramics
[NASA-TM-86915] 07 p0930 N85-15893
Experimental test program for evaluation of solid lubricant coating as applied to compliant foil gas bearings to 315 deg C
[NASA-CR-174637] 07 p0930 N85-15895
Surface effects of corrosive media on hardness, friction, and wear of materials
[NASA-TM-83711] 07 p0930 N85-15896
Antifriction nickel-phosphorous coatings on aluminum alloy products 09 p1309 N85-18221
Temperature prediction in mechanical components, an analytical approach 09 p1327 N85-18339
Stochastic dynamic analysis of a structure with frictional joints 09 p1337 N85-18408
Antifriction properties of gas thermal coatings of clad carbine powders 10 p1447 N85-19115
Effect of implantation species on the tribological response of stainless steel surfaces
[DE85-003530] 10 p1493 N85-19432
Techniques to analyze vehicle coastdown data
[DE85-005159] 12 p1772 N85-21127
Tribological properties of boron nitride synthesized by ion beam deposition
[NASA-TM-86962] 12 p1810 N85-21355
Tribological systems as applied to aircraft engines
[NASA-TM-86965] 12 p1858 N85-21657
Skid steering of wheeled and tracked vehicles: Analysis with Coulomb friction assumptions
[AD-A149826] 12 p1860 N85-21664
Dissipation of energy in composite material
13 p2027 N85-22703
High temperature antifriction properties of Ti sub 1-sub xNb sub x C sub 0.5N sub 0.5 alloys
13 p2029 N85-22715
Effect of zero-wear in friction pairs operating in abrasive media 13 p2045 N85-22801
Model of friction bearing hydrodynamics
14 p2288 N85-24178
Hermetic sealing of nonlubricated gas seal and friction characteristics, chapter 7
[DE85-006375] 15 p2569 N85-25851
Metal armatures for railguns
[AD-A152129] 16 p2728 N85-26838
Breakway friction and dynamic friction/wear measurements of various ceramic matenals from 25 C (75 F) to 650 C (1200 F)
[NASA-CR-174803] 16 p2754 N85-26994
Friction and wear behavior of aluminum and composite I-beam stiffened airplane skins
[NASA-TM-86418] 17 p2895 N85-27852
Studies on surface processes during friction and wear
[AD-A153509] 18 p3117 N85-29296
Study of the chemical mechanism in lubrication
[DE85-010766] 19 p3228 N85-30013
Mechanical modification of friction surfaces of aluminum alloys by friction transfer 19 p3241 N85-30097
Numerical solutions of turbulent models for flow over a flat plate with angle of attack
[DE85-010380] 21 p3585 N85-32286
Surface roughness effects in elastohydrodynamic contacts
[NASA-TP-2488] 21 p3595 N85-32329
The stress distribution in pin-loaded orthotropic plates
[NASA-CR-176146] 22 p3800 N85-33547
Three body abrasive wear in various metal combinations 23 p3906 N85-34200
Lubrication and cooling for high speed gears
[NASA-TM-87096] 23 p3938 N85-34407
Friction, impact, and electrostatic discharge sensitivities of energetic materials
[DE85-013321] 24 p4083 N85-35309
The use of austenitic stainless steel versus monel (Ni-cu) alloy in pressurized Gaseous Oxygen (GOX) life support systems
[AD-A156305] 24 p4134 N85-35625

FRICTION COEFFICIENT
U COEFFICIENT OF FRICTION

FRICTION DRAG
NT AERODYNAMIC DRAG
NT VISCOUS DRAG
Distributed energy store railguns experiment and analysis 09 p1313 N85-18256
A survey of the turbulent drag reduction using passive devices
[NMI-R-193] 11 p1630 N85-20268
Design of apparatus for the determination of aerodynamic drag coefficients of automobiles
[AD-A151842] 15 p2484 N85-25219
Calculation of friction at spherical bearing journals in turbomachines 17 p2940 N85-28150
Combined riblet and LEBU drag reduction system
[NASA-CASE-LAR-13286-1] 18 p3058 N85-28922
Drag-compensated, precision-powered hinge system
22 p3796 N85-33517

FRICTION FACTOR
Numerical modeling of complex interaction of shell of revolution and its filler with allowance for friction
06 p0779 N85-14960
Experimental study of heat transfer from shaft in cooled radial bearing of GNT-25 gas turbine
14 p2270 N85-24068
Study of axial bearings without oil bath with radial cooling of blocks 14 p2286 N85-24164
Turbine blade friction damping study
16 p2736 N85-26886

FRICTION LOSS COEFFICIENT
U FRICTION FACTOR

FRICTION MEASUREMENT
Skin friction measurements for 2 relatively thick airfoil sections at high Reynolds number
[AD-A150021] 12 p1772 N85-21125
A two-axis, self-nulling skin friction balance
[NASA-CASE-LAR-13294-1] 12 p1851 N85-21610

FRICTION PRESSURE DROP
U SKIN FRICTION

FRICTION REDUCTION
Microscopic aspects of the effect of friction reducers at the lubrication limit
[NASA-TM-77413] 03 p0367 N85-12354
Implantation of Ti + C for reduced friction and wear of steels
[DE85-001606] 09 p1295 N85-18135
The analysis by the lumped parameter method of blade platform friction dampers used in the high pressure fuel turbopump on the space shuttle main engine
09 p1338 N85-18417
Selection of bearing type for large steam turbines
14 p2271 N85-24069
Study of axial bearings without oil bath with radial cooling of blocks 14 p2286 N85-24164
Lubricant and additive effects on spur gear fatigue life
[NASA-TM-87044] 17 p2974 N85-28373
Tribological sinks: Money down the drain
[DE85-010019] 17 p2974 N85-28376
Mechanical modification of friction surfaces of aluminum alloys by friction transfer 19 p3241 N85-30097

FRICTION WELDING
Welding of PM-superalloys
[MTU-TB-910/84] 07 p0975 N85-16191

FRINGE MULTIPLICATION
Measurement of ultrasonic fields in transparent media using a scanning differential interferometer
[NASA-CR-175921] 17 p3028 N85-28726

FRINGE PATTERNS
U DIFFRACTION PATTERNS

FROGS
Spacelab mission D1 Frog statolith experiment STATEX: Hardware family and experiment operational sequence
05 p0689 N85-14426

FRONTAL AREAS (METEOROLOGY)
U FRONTS (METEOROLOGY)

FRONTAL WAVES
Frontal nature of Cromwell Current
14 p2336 N85-24445

FRONTS (METEOROLOGY)
NT COLD FRONTS
Layered sloping mesoscale structures and rainbands in atmospheric frontal regions and their relation to symmetric instability 01 p0075 N85-10497
About the influence of nonadiabatic processes on frontogenesis near the ground 01 p0075 N85-10498
Black Sea coastal frontogenesis
01 p0075 N85-10500
Doppler radar analysis of a frontal zone prior to convective development 01 p0077 N85-10515
Plans for the NRL/NORDA (Naval Research Laboratory-Naval Ocean Research and Development Activity) fine-scale variability experiment - 1984 (FVX-84)
[AD-A146041] 03 p0398 N85-12540
A study of the adequacy of quasi-geostrophic dynamics for modeling the effect of frontal cyclones on the larger scale flow 05 p0684 N85-14398
Meridional penetration of frontal systems in South America and its relation to organized convection in the Amazon
[INPE-3407-PRE/676] 10 p1518 N85-19572
Numerical studies of frontal dynamics
15 p2598 N85-26014
The sensitivity of mesoscale cyclogenesis forecasts to detailed three-dimensional isentropic initial analyses and varied vertical model resolution
15 p2598 N85-26015
A survey of major east coast snowstorms, 1960-1983. Part 2. Summary of surface and upperlevel characteristics
[NASA-TM-86195] 16 p2833 N85-27471
A survey of major east coast snowstorms, 1960-1983. Part 2: Case studies of eighteen storms
[NASA-TM-86196] 16 p2833 N85-27472
Statistical interpretation of the ECMWF model using MOS to predict surface wind and temperature
[WSR-2] 17 p2995 N85-28515
Automatic detection of gust fronts
[FAA-PM-85-11] 17 p2995 N85-28516
A study of the adequacy of quasi-geostrophic dynamics for modeling the effect of frontal cyclones on the larger scale flow
[NASA-CR-176065] 20 p3495 N85-31731
Observations of frontal zone structures with a VHF Doppler radar and radiosondes, part 1.2A
21 p3616 N85-32469
Thunderstorm phenomena and weather radar scanning strategies
[DOT/FAA/PM-85/14] 21 p3634 N85-32573

FROST
Frost nowcasting in the agricultural area of Valencia (Spain) — meteorological satellites
05 p0656 N85-14225
Salt action on concrete
[AD-A147812] 07 p0933 N85-15912
Ice segregation and frost heaving
[PB85-122430] 10 p1460 N85-19199
The violet absorber on Io: Disulfur monoxide derivatives 13 p2173 N85-23482

FROST DAMAGE
Evaluation of the area and severity of last night's frosts
[REPT-109] 16 p2833 N85-27473

FROZEN EQUILIBRIUM FLOW
Tabular and graphical solutions of regular and Mach reflections in pseudo-stationary frozen and vibrational-equilibrium flows, part 1
[UTIAS-283-PT-1] 23 p3893 N85-34117
Tabular and graphical solutions of regular and Mach reflections in pseudo-stationary frozen and vibrational-equilibrium flows, part 2
[UTIAS-283-PT-2] 23 p3894 N85-34118

FROZEN SOILS
U PERMAFROST

FRUITS
Packaging for food service 14 p2394 N85-24747
Preliminary technology utilization assessment of the robotic fruit harvester
[NASA-CR-175834] 16 p2844 N85-27532

FUEL CAPSULES
General-purpose heat source development: Safety test program. Postimpact evaluation, design iteration test 4
[LA-10217-SR] 12 p1930 N85-22128
General-purpose heat source development: Safety test program. Postimpact evaluation, design iteration test 5
[LA-10232-SR] 12 p1931 N85-22129
Evacuate and backfill apparatus and method
[DE85-006018] 23 p3938 N85-34411

FUEL CELL CATALYSTS
U ELECTROCATALYSTS

FUEL CELL POWER PLANTS
Phosphoric and electric utility fuel cell technology development
[NASA-CR-174215] 06 p0805 N85-15124
Electric utility acid fuel cell stack technology advancement
[NASA-CR-174804] 08 p1178 N85-17422
Development of molten carbonate fuel cell power plant technology
[DE84-016839] 14 p2352 N85-24536
Effects of H2S on molten carbonate fuel cells
[DE85-008310] 18 p3130 N85-29386
Development of molten carbonate fuel cell power plant, volume 1
[DE85-008743] 18 p3131 N85-29394
F-CAP documentation
[DE85-003369] 19 p3307 N85-30503
Reactant pressure differential control for fuel cell gases
[NASA-CASE-MSC-20127-2] 23 p3937 N85-34403

FUEL CELLS
NT PHOSPHORIC ACID FUEL CELLS
NT REGENERATIVE FUEL CELLS
Advanced fuel cell development
[DE84-014847] 01 p0044 N85-10289
Hot-gas cleanup for molten carbonate fuel cells-dechlorination and soot formation
[DE84-003072] 01 p0068 N85-10450
P-doping of (CH)x to the metallic regime with gaseous oxygen. Application to oxygen fuel cell type electrodes
[AD-A145477] 02 p0186 N85-11242
Effects of H2S on molten carbonate fuel cells
[DE84-015166] 02 p0195 N85-11307
Electrochemical and surface science research on fuel cells
[DE84-015062] 03 p0359 N85-12307
Materials for high-temperature fuel cells
[DE84-016316] 04 p0479 N85-13054

Phosphoric and electric utility fuel cell technology development
[NASA-CR-174215] 06 p0805 N85-15124
Space shuttle electrical power generation and reactant supply system 08 p1099 N85-16947
5 kW sleeps inverter. Revision
[AD-A149526] 10 p1510 N85-19528
High-temperature, solid oxide electrolyte fuel cell power generation system
[DE85-002976] 11 p1675 N85-20552
Using fuel cells or anode depolarization to reduce electrowinning energy consumption
[DE85-006187] 13 p2129 N85-23250
Molten carbonate fuel cell performance model update, draft
[DE85-005423] 13 p2129 N85-23252
Cathode materials for molten carbonate fuel cells
[DE85-004078] 13 p2130 N85-23254
Electricity production from coal through molten-carbonate fuel cells
[TI85-005072] 14 p2351 N85-24534
Long-life high performance fuel cell program
[NASA-CR-174874] 15 p2494 N85-25384
Molten carbonate fuel cell performance model update
[DE85-003356] 17 p2986 N85-28454
Fuel cells: A bibliography
[DE85-004565] 18 p3128 N85-29371
Effects of H2S on molten carbonate fuel cells
[DE85-006310] 18 p3130 N85-29386
Improved acid electrolytes for fuel cells
[PB85-176053] 18 p3132 N85-29397
Plasma spray screen repair method
[AD-D011713] 19 p3281 N85-30346
Advanced fuel cell development
[DE85-009662] 19 p3306 N85-30497
F-CAP documentation
[DE85-003369] 19 p3307 N85-30503
Integrated current collector and catalyst support
[DE85-011616] 22 p3761 N85-33311
Molten carbonate fuel cell separator
[DE85-011615] 22 p3806 N85-33577
Effects of H2S on molten carbonate fuel cells. Literature review on the impact of SO2 in the oxidant supplied to molten carbonate fuel cells
[DE85-011698] 22 p3808 N85-33586
Transfer of battery technology developed by the US Department of Energy
[DE85-009668] 22 p3808 N85-33588
Fuel cell applications literature review
[DE85-011691] 22 p3809 N85-33592
Reactant pressure differential control for fuel cell gases
[NASA-CASE-MSC-20127-2] 23 p3937 N85-34403
Evaluation of developmental membranes for the mixed reactant iron-chromium redox system
[NASA-TM-87074] 23 p3944 N85-34443
Fuel cell separator plate with bellows-type sealing flanges
[DE85-005991] 23 p3947 N85-34459
Electrolyte reservoir for carbonate fuel cells
[DE85-005736] 23 p3947 N85-34460
Thermodynamics of the corrosion of chromium in molten carbonates
[DE85-011407] 24 p4079 N85-35282

FUEL COMBUSTION
Combustion gas properties I-ASTM jet A fuel and dry air
[NASA-TP-2359] 01 p0010 N85-10064
The mechanisms of flame holding in the wake of a bluff body
[NASA-CR-174058] 02 p0172 N85-11149
Alternate fuels combustion research
[AD-A145691] 02 p0188 N85-11256
Analysis of potential combustion sorce impacts on acid deposition using an independently derived inventory, volume 1
[DE84-012005] 02 p0225 N85-11471
Dynamics of burnout of solid fuel in fluidized bed of finely divided inert particles 02 p0273 N85-11782
Combustion waves in dispersed-2-phase mixtures
[CFD/84/13] 04 p0472 N85-13003
Liquid-fueled Ramjet engines
07 p0918 N85-15814
Ramjets with supersonic combustion
07 p0918 N85-15817
Catalytic ignition and combustion of lean mixtures
[AD-A148101] 08 p1121 N85-17067
Radiation/catalytic augmented combustion
[AD-A148756] 09 p1290 N85-18101
Mechanisms and reaction dynamics related to methane combustion
[PB85-129680] 10 p1436 N85-19065
Fuels combustion research
[AD-A149106] 10 p1457 N85-19178
The mechanisms of flame holding in the wake of a bluff body
[NASA-CR-3866] 12 p1779 N85-21166
Ignition of mixtures of SiH sub 4, CH sub 4, O sub 2, and Ar or N sub 2 behind reflected shock waves
[NASA-TP-2415] 13 p1974 N85-22395
The influence of fuel quality upon flame-tube temperature and flame radiation in a model gas-turbine primary zone
[K233] 13 p1974 N85-22396
Workshop report: Swirl Enhanced Combustion
13 p2005 N85-22564
The influence of fuel molecular composition upon flame-tube temperature and flame radiation in a model gas-turbine primary zone
[K234] 13 p2017 N85-22646
Laser diagnostic analyses of sooting flames
[AD-A150478] 13 p2017 N85-22649
Dependence of combustion of homogeneous kerosene-air mixtures on humidity of air
13 p2051 N85-22835
Diesel combustion: Advances in analysis and simulation 14 p2253 N85-23965
Shock tube study of the fuel structure effects on the chemical kinetic mechanisms responsible for soot formation, part 2
[NASA-CR-174880] 15 p2504 N85-25444
Influence of fuel properties on gas turbine combustion performance
[AD-A151464] 15 p2504 N85-25448
Studies of the combustion of model fuels with low hydrogen content (pyrolysis of polycyclic aromatics-detection of soot precursors)
[DE85-005422] 15 p2521 N85-25541
Numerical analysis of supersonic reactive flow in wake of reverse step 15 p2643 N85-26303
Analytical fuel property effects--small combustors
[NASA-CR-174738] 16 p2708 N85-26709
Research test facility for evaporation and combustion of alternative jet fuels at high air temperatures
[AD-A153830] 18 p3063 N85-29073
An experimental investigation of fuel regression rate control in solid fuel ramjets
[AD-A154251] 19 p3227 N85-30008
The effect of surface reactions in catalytic combustion
[AD-A154217] 19 p3234 N85-30049
Injection, atomization, ignition and combustion of liquid fuels in high-speed air streams
[AD-A154056] 19 p3251 N85-30156
Investigation of the behavior of fuel in the intake manifold and its relation to SI engines, 1980 - 1983
19 p3279 N85-30337
Fuel-rich catalytic combustion: A soot-free technique for in situ hydrogen-like enrichment
[NASA-TP-2496] 20 p3423 N85-31244
Toxic hazards tests for vehicles and other equipment
[AD-A149164] 20 p3506 N85-31797
Jet flows: Modelling and experiments
22 p3744 N85-33208
Ames Laboratory measurements of alkali levels in the Curtiss-Wright PFBC gas stream
[DE85-011257] 22 p3745 N85-33214
Current inventory of anthropogenic carbon dioxide in the North Pacific Subarctic Gyre
[PB85-187938] 24 p4125 N85-35570

FUEL CONSUMPTION
ACEE program rationale and implementation
[NASA-TM-84549] 02 p0133 N85-10908
Fuel efficiency through new airframe technology
[NASA-TM-84548] 02 p0133 N85-10909
Hybrid laminar flow control study
[NASA-CR-165930] 02 p0137 N85-10933
Energy efficient engine flight propulsion system preliminary analysis and design report
[NASA-CR-174701] 02 p0140 N85-10947
Energy efficient engine. Volume 1: Component development and integration program
[NASA-CR-173084] 02 p0146 N85-10992
Analysis and simulation of the I C engine Otto cycle using the second law of thermodynamics
02 p0291 N85-11891
Advanced Automotive Diesel Assessment Program, executive summary 04 p0507 N85-13236
Dissociated methanol vehicle test results
[DE84-004507] 04 p0509 N85-13248
Combined cycle ramjet engine
[AD-D011247] 06 p0760 N85-14859
Copper-nickel sheathing study, phase 2. Two-year service performance of test panels on the ARCO TEXAS
[PB84-242411] 06 p0775 N85-14952
Reference energy-altitude descent guidance: Simulator evaluation — aircraft descent and fuel conservation
[NASA-TP-2393] 08 p1085 N85-16866
Collegium on aviation fuel conservation efforts
09 p1278 N85-18034
Dissociated methanol citation
[DE85-000505] 10 p1458 N85-19188
Fiat introduces 1000-CC engine
11 p1618 N85-20186
Effect of water injection into air for turbine cooling on economy of operation of gas turbine engine with afterburning 13 p2050 N85-22930
Deputy minister on civil aviation fuel conservation efforts 14 p2208 N85-23691
Safety recommendation(s), A-84-103
[REPT-3909B/101B] 14 p2216 N85-23745
Aviation workers plenum reviews fuel conservation progress 15 p2461 N85-25197
Ilyushin bureau designer on fuel conservation research
15 p2467 N85-25231
Planning fuel-conservative descents in an airline environmental using a small programmable calculator: Algorithm development and flight test results
[NASA-TP-2393] 16 p2707 N85-26776
Energy efficient engine high-pressure turbine component rig performance test report
[NASA-CR-168189] 19 p3218 N85-29955
Energy efficient engine integrated core/low spool test hardware design report
[NASA-CR-168137] 19 p3218 N85-29958
Energy Efficient Engine (E3) controls and accessories detail design report
[NASA-CR-168017] 19 p3218 N85-29957
Auto fuel efficiency standards, part 2
[GPO-41-189] 20 p3435 N85-31309
FAA requirements for model to support capacity, delay, noise and energy programs
[AD-A155815] 24 p4063 N85-35179
Comparative analysis of operational forecasts versus actual weather conditions in airline flight planning, volume 1
[NASA-CR-167862] 24 p4119 N85-35534
Comparative analysis of operational forecasts versus actual weather conditions in airline flight planning, volume 2
[NASA-CR-167863] 24 p4119 N85-35535
Comparative analysis of operational forecasts versus actual weather conditions in airline flight planning, volume 3
[NASA CR-167864] 24 p4120 N85-35536
Comparative analysis of operational forecasts versus actual weather conditions in airline flight planning, volume 4
[NASA-CR-167865] 24 p4120 N85-35537

FUEL CONTAMINATION
Sound speed measurements in liquid oxygen-liquid nitrogen mixtures
[NASA-TP-2464] 24 p4083 N85-35307

FUEL CONTROL
Engine wear and cold startability of methanol fueled engines.
[DE85-001208] 11 p1647 N85-20081
Energy Efficient Engine (E3) controls and accessories detail design report
[NASA-CR-168017] 19 p3218 N85-29957
An experimental investigation of fuel regression rate control in solid fuel ramjets
[AD-A154251] 19 p3227 N85-30008

FUEL ELEMENTS (NUCLEAR REACTORS)
U NUCLEAR FUEL ELEMENTS

FUEL FLOW
NT PROPELLANT TRANSFER
Energy efficient engine high-pressure turbine component rig performance test report
[NASA-CR-168189] 19 p3218 N85-29955
Detailed studies of aviation fuel flowability
[NASA-CR-174938] 20 p3435 N85-31306
A comparison of two bench scale tests of fuel low temperature flow properties
[AD-A154477] 20 p3435 N85-31311

FUEL GAGES
Assessment study of liquid content measurement methods applicable to space missions — Infrared Space Observatory
[TU-HH-TRI-ESA-84-2] 17 p2938 N85-28135

FUEL INJECTION
Combustion modeling of a 2 cylinder cycle reciprocating engine
[AD-A144782] 01 p0055 N85-10084
Finlet injector
[AD-D011245] 06 p0765 N85-14891
Experimental study of the spray characteristics of a research airblast atomizer
[NASA-TM-86911] 07 p0904 N85-15727
Catalytic ignition and combustion of lean mixtures
[AD-A148101] 08 p1121 N85-17067
A study of air breathing rockets. Part 4: Direct fuel injection into a secondary combustor
[NAL-TR-832] 09 p1287 N85-18093

Hypergolic combustion demonstration in a reciprocating internal combustion engine
[AD-A150846] 14 p2311 N85-24303

Small gas turbine combustor study: Fuel injector performance in a transpiration-cooled liner
[NASA-TM-86969] 15 p2473 N85-25264

Installation, maintenance and operating manual for the Lucas-type fuel injection system of the 3 B rotary engine
[NASA-TM-77872] 15 p2566 N85-25846

Numerical analysis of supersonic reactive flow in wake of reverse step 15 p2643 N85-26303

Segmented zoned fuel injection system for use with a combustor
[AD-D011640] 17 p2897 N85-27865

Research test facility for evaporation and combustion of alternative jet fuels at high air temperatures
[AD-A153830] 18 p3083 N85-29073

Injection, atomization, ignition and combustion of liquid fuels in high-speed air streams
[AD-A154056] 19 p3251 N85-30156

The design of Direct Injection (DI) diesel engines. Injection system by a numerical optimization technique
[REPT-84-RR-346] 20 p3462 N85-31506

Superheated fuel injection for combustion of liquid-solid slurries
[DE85-011624] 22 p3753 N85-33266

FUEL OILS

US energy for the rest of the century, 1984 edition
[PB84-207406] 04 p0531 N85-13393

USSR report: Energy
[JPRS-UEN-84-038] 07 p0994 N85-16312

Oil tank electrostatic charging report
[DRIC-T-6967] 20 p3436 N85-31319

FUEL PRODUCTION

Alcohol fuel from Ohio farms: An introduction
[TI-84-901290] 05 p0621 N85-13970

Application of robotics in remote fuel fabrication operations
[DE84-011481] 05 p0646 N85-14144

Advancement of remote technology: Past perspectives and future plans
[DE85-000934] 09 p1327 N85-18342

Catalytic conversion of C3-C4 paraffins to gasoline
[DE85-004181] 10 p1458 N85-19187

Test report for Getty Synthetic Fuels, Inc., Calumet City, Illinois
[PB85-119493] 10 p1459 N85-19191

Research and development of shallow algal mass culture systems for the production of oils
[DE85-000518] 11 p1690 N85-20624

Microalgae culture collection, 1984-1985
[DE84-013035] 11 p1690 N85-20626

Developments in the production and use of ethanol fuels
[GPO-40-678] 12 p1817 N85-21386

Trifunctional catalysts for conversion of syngas to alcohols
[DE85-004577] 13 p2040 N85-22771

Anaerobic digestion of biomass: status summary and research development needs, 1983
[PB85-161925] 13 p2040 N85-22772

PSA, Renault work on all fuel automobile engine
15 p2531 N85-25604

Jet fuel property changes and their effect on producibility and cost in the U.S., Canada, and Europe
[NASA-CR-174840] 16 p2757 N85-27012

Technical and economic analysis of liquid fuel production from microalgae
[DE85-002926] 16 p2758 N85-27018

Conversion of methanol to gasoline: Engineering and construction of the demonstration plant
[DE85-003237] 17 p2937 N85-28133

Alcohol: An alternate energy resource for community use
[DE85-007731] 18 p3084 N85-29075

Feasibility study of a fission-suppressed Tokamak fusion breeder
[DE85-009099] 18 p3190 N85-29786

Consolidated fuel reprocessing program
[DE85-010591] 19 p3358 N85-30818

Linking R and D to problems experienced in solids processing
[AD-A154238] 19 p3380 N85-30968

FUEL PUMPS

Analytical and experimental investigation of rubbing interaction in labyrinth seals for a liquid hydrogen fuel pump — space shuttle main engine
[NASA-CR-174657] 09 p1287 N85-18084

Hydrodynamic simulation of transient processes in injection system of aircraft engines during pump unswirling 13 p2050 N85-22829

HPFTP flow diverter analysis
[NASA-CR-171424] 13 p2091 N85-23057

Ceramics for advanced O2/H2 application
16 p2734 N85-26868

FUEL SPRAYS

Exciplex systems for vapor-liquid visualization of fuel sprays
[AD-A149360] 10 p1457 N85-19181

Liquid fuel spray processes in high-pressure gas flow
[NASA-TM-86944] 12 p1844 N85-21570

Research test facility for evaporation and combustion of alternative jet fuels at high air temperatures
[AD-A153830] 18 p3083 N85-29073

KIVA: A computer program for two- and three-dimensional fluid flows with chemical reactions and fuel sprays
[DE85-010334] 19 p3339 N85-30693

Particle sizing from forward scattered light at two angles using a Variable-Focal-Length optical system
[AD-A154164] 20 p3533 N85-31980

KIVA computer program for multidimensional chemically reactive fluid flows with fuel sprays
[DE85-012730] 22 p3830 N85-33722

FUEL SYSTEMS

NT AIRCRAFT FUEL SYSTEMS

Application of the CSRL language to the design of expert diagnosis systems: The Auto-Mech experience
[AD-P003922] 02 p0245 N85-11602

Heat management system for aircraft
[AD-D011658] 18 p3061 N85-28936

Energy Efficient Engine (E3) controls and accessories detail design report
[NASA-CR-168017] 19 p3216 N85-29957

Special tools used by cosmonauts in EVA
22 p3731 N85-33129

FUEL TANKS

NT WING TANKS

Aircraft wing fuel tank environmental simulator tests for evaluation of antimisting fuels
[FAA-CT-84-15] 07 p0934 N85-15920

Distribution and storage of aviation turbine fuel for military operations in northern Australia
[AD-A147180] 07 p0935 N85-15921

Preliminary airworthiness evaluation AH-1S (MC) helicopter with external fuel tanks installed
[AD-A148091] 08 p1084 N85-16865

BI-PAC F-15 external fuel tank container modification
[AD-A148836] 09 p1280 N85-18053

Interactions between F-111 fuselage fuel tank sealants. Part 2: Variation in performance properties of polysulfides after contact with polyester degradation products
[AD-A149777] 12 p1812 N85-21368

Fuel freeze point investigations
[AD-A152801] 17 p2937 N85-28129

Investigation, development, and certification of a burst disk for cryogenic fuel tanks
[GCP-3/MT-CM-21-2546] 18 p3067 N85-28972

Fuel containment and damage tolerance in large composite primary aircraft structures
[NASA-CR-166083] 19 p3231 N85-30032

Fuel containment and damage tolerance for large composite primary aircraft structures. Phase 1: Testing
[NASA-CR-166091] 24 p4073 N85-35241

FUEL TESTS

NT REACTOR STARTUP TESTS

Rapid estimation of concentration of aromatic classes in middistillate fuels by high-performance liquid chromatography
[NASA-TP-2495] 20 p3434 N85-31307

Observations of the use of the setapoint detector
[AD-A154533] 21 p3571 N85-32206

FUEL VALVES

Man-vehicle systems research facility advanced aircraft flight simulator throttle mechanism
22 p3798 N85-33527

FUEL-AIR RATIO

Gas dynamics of combustion of gas-air mixture in semi-closed space with relief of pressure into gasless adjacent space 02 p0260 N85-11699

Finlet injector
[AD-D011245] 06 p0765 N85-14891

Catalytic ignition and combustion of lean mixtures
[AD-A148101] 08 p1121 N85-17067

Combustion gas properties. 2: Natural gas fuel and dry air
[NASA-TP-2435] 12 p1779 N85-21168

Behavior of the lean methane-air flame at zero-gravity
[NASA-CR-175586] 12 p1799 N85-21283

The behaviour of detonation waves in single phase heterogeneous systems
[AD-A149825] 12 p1846 N85-21581

Dependence of combustion of homogeneous kerosene-air mixtures on humidity of air
13 p2051 N85-22835

Limiting factor of flame propagation in mono-sized sprays of low-volatility fuels
[NAL-TR-839T] 15 p2521 N85-25536

Detailed chemical kinetic study of the effect of molecular structure on autoignition of fuel-air mixtures
[DE85-004424] 17 p2921 N85-28010

The effect of surface reactions in catalytic combustion
[AD-A154217] 19 p3234 N85-30049

Experimental determination of the mixing frequency parameter for coalescence/dispersion modeling of turbulent combustion
[DE85-011468] 19 p3270 N85-30280

Flow modifying device
[NASA-CASE-LEW-13562-2] 24 p4065 N85-35195

FUELING

U REFUELING

FUELS

NT ACTIVATED CARBON
NT AIRCRAFT FUELS
NT AUTOMOBILE FUELS
NT CERAMIC NUCLEAR FUELS
NT CHARCOAL
NT CHEMICAL FUELS
NT COAL
NT CRYOGENIC ROCKET PROPELLANTS
NT DIESEL FUELS
NT DOUBLE BASE ROCKET PROPELLANTS
NT FOSSIL FUELS
NT FUEL OILS
NT GASEOUS FUELS
NT GASOHOL (FUEL)
NT GASOLINE
NT HYDROCARBON FUELS
NT HYDROGEN FUELS
NT HYPERGOLIC ROCKET PROPELLANTS
NT JET ENGINE FUELS
NT JP-4 JET FUEL
NT JP-5 JET FUEL
NT JP-8 JET FUEL
NT KEROSENE
NT LIQUEFIED NATURAL GAS
NT LIQUID FUELS
NT LIQUID ROCKET PROPELLANTS
NT MONOPROPELLANTS
NT NUCLEAR FUELS
NT PEAT
NT SLURRY PROPELLANTS
NT SOLID ROCKET PROPELLANTS
NT SPENT FUELS
NT SYNTHETIC FUELS

External fuel vaporization study, phase 2
[NASA-CR-174079] 02 p0187 N85-11252

DOE supported research in alcohol fuel technology development
[DE84-007686] 06 p0774 N85-14948

Phase 1-A development kinematic Stirling/Rankine commercial gas-fired heat pump research program
[PB85-100931/GAR] 07 p0936 N85-15928

Research and development of alcohol fuel usage in spark ignited engines 09 p1301 N85-18175

Morbidity and mortality associated with exposure to Otto Fuel II in the U.S. Navy 1966-1979
[AD-A148726] 09 p1363 N85-18574

Investigation of fuel additive effects on sooting flames
[AD-A149154] 10 p1457 N85-19179

Alternative fuels for buses: Current assessment and future perspectives
[PB85-116325] 10 p1459 N85-19190

Peat resources of Maine. Volume 2: Penobscot County
[DE85-004195] 11 p1670 N85-20522

Peat resources of Maine. Volume 5: Washington County
[DE85-004197] 11 p1670 N85-20523

Limiting factor of flame propagation in mono-sized sprays of low-volatility fuels
[NAL-TR-839T] 15 p2521 N85-25536

Evaluation of used crankcase oils using computerized infrared spectrometry
[AD-A152993] 17 p2920 N85-27999

Alcohol Fuels Program technical review, spring 1984
[DE85-002919] 17 p2938 N85-28134

Urban vehicle research project
[DE85-005444] 17 p3052 N85-28669

Effects of H2S on molten carbonate fuel cells
[DE85-006310] 18 p3130 N85-29386

Impact of alcohol fuels on urban air pollution: Methanol photochemistry study
[DE85-009539] 18 p3133 N85-29403

Investigation of the behavior of fuel in the intake manifold and its relation to SI engines, 1980 - 1983
19 p3279 N85-30337

Coal slurry ignition in a diesel engine simulator
[DE85-010987] 20 p3463 N85-31513

FULL SCALE TESTS

Full-scale testing, production and cost analysis data for the advanced composite stabilizer for Boeing 737 aircraft. Volume 1: Technical summary
[NASA-CR-3649] 05 p0612 N85-13912

Full-scale testing, production and cost analysis data for the advanced composite stabilizer for Boeing 737 aircraft, volume 2
[NASA-CR-166012] 05 p0613 N85-13915

FUMES
Pathophysiological study of poisoning due to thermal degradation of materials — aircraft cabins
[CERMA-84-15] 11 p1692 N85-20640
Material thermolysis product toxicity: Definition of a hazard evaluation methodology
[CERMA-84-06] 11 p1692 N85-20641

FUMIGATION
Methanol vaporization: Effects on volumetric efficiency and on determination of optimum fuel delivery system
[PB84-243914] 09 p1302 N85-18181

FUNCTION GENERATORS
Technical data on new engineering products
10 p1460 N85-19201
Precision linear ramp function generator
[DE85-011647] 22 p3760 N85-33304

FUNCTION SPACE
NT BANACH SPACE
NT HILBERT SPACE
NT SOBOLEV SPACE
Partitions of unity and approximation
[AD-A144717] 01 p0110 N85-10746
A simple transport model 02 p0284 N85-11853
Condenser capacities and removable sets in W1p1
10 p1536 N85-19682
Asymptotic behavior of matrix coefficients related to reductive symmetric spaces
[CWI-PM-R8410] 12 p1925 N85-22095
A problem of Burkholder and the existence of harmonic majorants of the absolute value of x sup p in certain domains in R sup d 15 p2634 N85-26236
Quadratic spaces over discrete Hodge algebras
16 p2853 N85-27593
A study of the effect of a mismatch in gamma and gamma prime phase lattice spacings on the high temperature strength characteristics of dispersion-hardened nickel alloys
[BLL-CE-TRANS-8048-(9022.09)]
20 p3430 N85-31279

FUNCTIONAL ANALYSIS
NT BANACH SPACE
NT CONVOLUTION INTEGRALS
NT FOURIER TRANSFORMATION
NT FREDHOLM EQUATIONS
NT HARMONIC ANALYSIS
NT HILBERT SPACE
NT HILBERT TRANSFORMATION
NT INTEGRAL EQUATIONS
NT INTEGRAL TRANSFORMATIONS
NT J INTEGRAL
NT LAPLACE TRANSFORMATION
NT SINGULAR INTEGRAL EQUATIONS
NT SOBOLEV SPACE
NT TESSERAL HARMONICS
NT VOLTERRA EQUATIONS
NT WIENER HOPF EQUATIONS
NT ZONAL HARMONICS
Markovian control problems: Functional equations and algorithms
[MCTH-97] 01 p0107 N85-10717
Applications of functional analytic and Martingale methods
[AD-A145555] 02 p0255 N85-11672
Nonlinear regression with emphasis on spline methods
[AD-A146192] 03 p0412 N85-12633
Interpolating sequences for H to infinity in the ball
[CTH-MATH-1984-15] 04 p0556 N85-13542
Simplified proofs of some basic theorems for quasiregular mappings 10 p1535 N85-19677
Functional equation for the embedding of a homomorphism of the interval into a flow
[DE85-000655] 11 p1713 N85-20780
Schur-Ostrowski theorems for functionals on l1(0,1)
[AD-A150193] 13 p2150 N85-23346
A database design for the Brazilian Air Force Flying Unit Operational Control System
[AD-A151848] 15 p2666 N85-26452
Infinite dimensional linear systems with unbounded control and observation: A functional analytic approach
[AD-A153535] 18 p3169 N85-29639
Conceptualizing in assembly tasks
[AD-A155564] 21 p3665 N85-32770

FUNCTIONAL DESIGN SPECIFICATIONS
Vibration, acoustic, and shock design and test criteria for components on the Solid Rocket Boosters (SRB), Lightweight External Tank (LWT), and Space Shuttle Main Engines (SSME)
[NASA-RP-1127] 01 p0061 N85-10405
The multipurpose composite flywheel
05 p0606 N85-13868
Operational problems with radiation survey meters: The university and accelerator
[DE84-015703] 06 p0811 N85-15151
Design study of technology requirements for high performance single-propeller-driven business airplanes
[NASA-CR-3863] 07 p0898 N85-15692
A digital piloting system for the combat helicopter
08 p1074 N85-16806
The orbiter mate/demate device
08 p1103 N85-16972
High level languages in protocol specification and verification
[FUB-51-1983] 09 p1370 N85-18611
Parallel input and feedback in dialogue cells
[CWI-CS-R8413] 11 p1703 N85-20708
Possible technological answers to new design requirements for power transmission systems
14 p2222 N85-23779
SC filters and design centering of integrated circuits. Part 2: Design centering of integrated circuits
[BMFT-FB-T-84-265-PT-2] 17 p2956 N85-28257
Search of the VAXintosh customizing VMS V4.0 for DCL windows
[DE85-011306] 22 p3831 N85-33729
Product definition: Technical specification of needs
[SNIAS-851-430-104] 23 p3910 N85-34226

FUNCTIONALS
Analytical construction of flight vehicle surfaces
06 p0775 N85-14957
On the probability generating functional for point processes
[AD-A147692] 08 p1210 N85-17615
A data based algorithm for choosing the window width when estimating the integral of f2(x)
[AD-A152093] 16 p2847 N85-27553
Stability of functionals determined by moment conditions
[TRITA-NA-8310] 16 p2852 N85-27585
The role of duality in optimization problems involving entropy functionals, with applications to information theory
[AD-A152336] 17 p3026 N85-28713
Comments on estimating quantiles for Gaussian functionals by simulation
[AD-A154302] 19 p3348 N85-30750

FUNCTIONS
Statistical comparison of pooled nitrogen washout data of various altitude decompression response groups
[NASA-TM-58265] 15 p2639 N85-26278
DLA: Data/data base administration analysis
[AD-A153031] 17 p3050 N85-28879

FUNCTIONS (MATHEMATICS)
NT ABEL FUNCTION
NT AIRY FUNCTION
NT ANALYTIC FUNCTIONS
NT ASYMPTOTES
NT BOOLEAN FUNCTIONS
NT COMPOSITE FUNCTIONS
NT CONFORMAL MAPPING
NT COORDINATE TRANSFORMATIONS
NT DELTA FUNCTION
NT DISCRETE FUNCTIONS
NT DISCRIMINANT ANALYSIS (STATISTICS)
NT DISTRIBUTION FUNCTIONS
NT ELLIPTIC FUNCTIONS
NT ENTIRE FUNCTIONS
NT ERROR FUNCTIONS
NT EXPONENTIAL FUNCTIONS
NT FOURIER TRANSFORMATION
NT GAMMA FUNCTION
NT GREEN'S FUNCTIONS
NT HAMILTONIAN FUNCTIONS
NT HARMONIC FUNCTIONS
NT HYPERBOLIC FUNCTIONS
NT HYPERGEOMETRIC FUNCTIONS
NT KERNEL FUNCTIONS
NT LAGUERRE FUNCTIONS
NT LAPLACE TRANSFORMATION
NT LEGENDRE FUNCTIONS
NT LIAPUNOV FUNCTIONS
NT LINEAR TRANSFORMATIONS
NT LOGARITHMS
NT LORENTZ TRANSFORMATIONS
NT MAXWELL-BOLTZMANN DENSITY FUNCTION
NT MEROMORPHIC FUNCTIONS
NT MODULATION TRANSFER FUNCTION
NT MONOTONE FUNCTIONS
NT NORMAL DENSITY FUNCTIONS
NT OPTICAL TRANSFER FUNCTION
NT ORTHOGONAL FUNCTIONS
NT ORTHONORMAL FUNCTIONS
NT PEARSON DISTRIBUTIONS
NT PENALTY FUNCTION
NT PERIODIC FUNCTIONS
NT POINT SPREAD FUNCTIONS
NT POISSON DENSITY FUNCTIONS
NT PROBABILITY DENSITY FUNCTIONS
NT PROBABILITY DISTRIBUTION FUNCTIONS
NT RAMP FUNCTIONS
NT RAYLEIGH DISTRIBUTION
NT RECURSIVE FUNCTIONS
NT SPACE-TIME FUNCTIONS
NT SPHERICAL HARMONICS
NT SPLINE FUNCTIONS
NT STRESS FUNCTIONS
NT TANGENTS
NT TIME FUNCTIONS
NT TRANSCENDENTAL FUNCTIONS
NT TRANSFER FUNCTIONS
NT WALSH FUNCTION
NT WEIBULL DENSITY FUNCTIONS
NT WEIGHTING FUNCTIONS
Implementation of the supersonic triplet singularity in the USTORE computer code
[CSIR-NIAST-83/47] 01 p0001 N85-10008
Simultaneous rational approximation of a function and its derivatives in the complex plane
[CSIR-TWISK-311] 01 p0109 N85-10739
On two concepts of fundamental matching
[CSIR-TWISK-335] 01 p0110 N85-10743
Computing the reliability of k out of n systems
[AD-A145505] 02 p0206 N85-11357
About ambiguity and Q-functions
[AD-A145293] 02 p0250 N85-11638
Algebraic functions of H-functions with specific dependency structure
[AD-A145598] 02 p0252 N85-11647
Maximum likelihood estimation of the survival functions of N stochastically ordered random variables
[AD-A145429] 02 p0254 N85-11662
A proposal for standard basic functions in Ada
[NPL-DITC-45/84] 05 p0715 N85-14584
The resistance and mobility functions of two equal spheres in low Reynolds number flow
[AD-A147301] 07 p0959 N85-16080
Estimation for a semimartingale regression model using the method of sieves
[AD-A146809] 07 p1028 N85-16527
Conjunctive and disjunctive item response functions
[AD-A147815] 07 p1033 N85-16561
Modules of continuum structures, revised
[AD-A148620] 08 p1213 N85-17639
Bounding the stochastic performance of continuum structure functions 1
[AD-A148621] 08 p1213 N85-17640
Generating positively correlated random variables from a sequence of independent random variables with symmetric logarithmically concave densities
[AD-A148438] 08 p1216 N85-17658
Generalized convex functions: Properties, optimality and duality
[DE85-001553] 09 p1376 N85-18852
On rotation automorphic functions with descrete rotation groups 10 p1536 N85-19686
Computable real analysis
[AD-A149079] 10 p1546 N85-19747
Bounding the stochastic performance of continuum structure functions 2
[AD-A149458] 10 p1546 N85-19762
Sequential minimization for sum of squares of unknown functions
[DE85-004162] 11 p1707 N85-20738
Axiomatic characterizations of continuum structure functions
[AD-A149617] 12 p1866 N85-21706
Software for special functions
[DE85-004684] 12 p1917 N85-22033
A note about the strong convergence of the nonparametric estimation of a regression function
[AD-A150325] 13 p2151 N85-23353
The complexity of reliability computations in planar and acyclic graphs
[AD-A150759] 14 p2408 N85-24845
Disproof of the Mertens conjecture
[CWI-NM-R8412] 14 p2414 N85-24886
A remark on the conformal capacity of Groetzsch's condenser in space 15 p2634 N85-26240
Schubert varieties are arithmetically Cohen-Macaulay
16 p2853 N85-27592
Convergence of Newton's method for a single real equation
[NASA-TP-2489] 17 p3017 N85-28658
The origin of the binary-search paradigm
[AD-A154367] 19 p3337 N85-30677
On the solution for the sound field in a semi-infinite uniform duct with sheared mean flow
20 p3523 N85-31912
On the dependence of the convergence of Gummel's algorithm on the regularity of the solution
[AD-A154628] 21 p3675 N85-32832

New developments on the core function for efficient implementation of the difficult residue number system operations
[AD-A154678] 21 p3676 N85-32834
USSR report: Physics and mathematics
[JPRS-UPM-85-004] 21 p3680 N85-32860
Two methods of global data assimilation
[AD-A155961] 24 p4143 N85-35684

FUNGI
NT YEAST
Aquatic plant control research program. Evaluation of Fusarium roseum Culmorum as a biological control agent for Hydrilla verticillata
[AD-A145228] 01 p0069 N85-10459
Fungi of Mt. Babia Gora. 2: Indicative value of macromycetes in forest associations. A: Initial considerations
[NASA-TM-77485] 01 p0094 N85-10632
Fungi of Mount Babia Gora. 3: The indicating value of macromycetes in the forest associations
[NASA-TM-77486] 01 p0094 N85-10633
Fungi of Mt. Babia Gora. 1: Mycoflora of forests
[NASA-TM-77484] 02 p0234 N85-11522
Architecture of dermatophyte cell Walls: Electron microscopic and biochemical analysis
[NASA-TM-77441] 03 p0399 N85-12546
Structure and functions of fungal cell surfaces
[NASA-TM-77439] 06 p0842 N85-15347
The structure and function of fungal cells
[NASA-TM-77443] 06 p0842 N85-15348
The lipid composition and its alteration during the growth stage in pathogenic fungus, epidermophyton floccosum
[NASA-TM-77440] 07 p1011 N85-16421
Nitrogen control of photosynthetic protein synthesis
[DE85-003513] 11 p1690 N85-20623

FUNNELS
Proposed use of the radio-frequency quadrupole structure to funnel high-current ion beams
[DE85-010746] 19 p3364 N85-30857

FURAN RESINS
NT KEVLAR (TRADEMARK)
NT POLYAMIDE RESINS

FURANS
NT TETRAHYDROFURAN

FURLABLE ANTENNAS
Offset unfurlable antenna concepts
05 p0625 N85-14002
Antenna Technology for QUASAT application --- radio antenna for very long base interferometry missions
14 p2231 N85-23828

FURNACES
NT ELECTRIC FURNACES
NT IMAGE FURNACES
NT SOLAR FURNACES
NT VACUUM FURNACES
Results of the technical exchange agreement between NASA and DuPont on the containerless drop tube solidification of NiAl3
[NASA-TM-86473] 01 p0014 N85-10087
Some of the features of movement of gas through a layer of free-flowing substances
[BLL-M-35732-(5828.4)] 02 p0196 N85-11312
Development of a capacitive sensor system for high temperature application
[BMFT-FB-HA-84-027] 05 p0646 N85-14147
Procedure for investigating high-temperature properties of iron-ore materials
[BLL-M-36020-(5828.4)] 07 p0926 N85-15868
Heliostat tested 07 p0994 N85-16318
Application of electricity to the reheating of metals prior to forming. Forging, lamination, induction
[BLL-TR-T6399/BG/MRS14903/84]
08 p1137 N85-17160
Comparative usefulness of flue gas oxygen and carbon dioxide analysis
[BLL-TRANS-T6358/BG/WH783/84]
08 p1179 N85-17430
The EURECA Automatic Gradient Heating Facility (AGHF), phase A study
[ESA-CR(P)-1939] 11 p1591 N85-20005
Development of AK18 alloy production technology based on electrothermic silumin
11 p1598 N85-20048
Three-dimensional analysis of heat transfer and gas flow in a radiant furnace
[DE84-011732] 11 p1633 N85-20284
Study of a constricted electric arc cooled by transpiration
[NASA-TM-77846] 17 p3038 N85-28798
Concept development evaluation for John Deere/UA STS middeck experiment location
[NASA-CR-171541] 20 p3397 N85-31071
High-frequency furnace
[DE85-011210] 21 p3586 N85-32291
The design, construction and operation of a large-area, high-temperature, thermal conductance apparatus --- furnace insulation
[NPL-DMA(A)-84] 22 p3786 N85-33455

FUSELAGE MOUNTING
U AIRCRAFT PRODUCTION

FUSELAGES
Crashworthiness of light aircraft fuselage structures: A numerical and experimental investigation
01 p0060 N85-10399
Analysis of a transport fuselage section drop test
01 p0060 N85-10400
Modeling of aircraft cabin fires
[NBS-GCR-84-473] 04 p0454 N85-12880
Second sailplane project: The RP-2
04 p0468 N85-12977
An in-flight investigation of a twin fuselage configuration in approach and landing
[NASA-CR-172366] 05 p0596 N85-13801
A study of crashworthiness of light aircraft fuselage structures: A numerical and experimental investigation
[UTIAS-286] 06 p0750 N85-14803
Turbulent drag reduction research
06 p1071 N85-16788
Forced corrosion tests of construction components of passenger aircraft fuselages 11 p1600 N85-20062
Study for prediction of rotor/wake/fuselage interference, part 1
[NASA-CR-177340-VOL-1] 13 p1965 N85-22346
Study for prediction of rotor/wake/fuselage interference. Part 2: Program users guide
[NASA-CR-177340-VOL-2] 13 p1966 N85-22347
Redesign of fuselage compartments by method of special contours 13 p2042 N85-22784
Normal mode calculations for fuselage type intricate structures by regarding them as systems with superposed constraints 13 p2048 N85-22817
Development of a fuselage forward section in Carbon Fiber Reinforced Plastic (CFRP) type of construction
[MBB/LFA34/CFK/PUB/008] 17 p2895 N85-27851
A survey of recent development in helicopter aerodynamics 18 p3057 N85-28915
Impact dynamics research on composite transport structures
[NASA-TM-86391] 19 p3284 N85-30367
Fuselage upwash effects on RSRA rotor systems
[NASA-CR-177349] 20 p3388 N85-31015
Estimation of dynamic rotor loads for the rotor systems research aircraft: Methodology development and validation
[NASA-CR-177362] 20 p3393 N85-31045
Simulation and analysis of airborne antenna radiation patterns 20 p3439 N85-31342
Wind tunnel drag evaluations of helicopter nose sections
[AD-A155489] 21 p3553 N85-32100
Aerodynamic characteristics of a distinct wing-body configuration at Mach 6: Experiment, theory, and the hypersonic isolation principle
[NASA-TP-2467] 22 p3727 N85-33107
Ground-based and in-flight simulator studies of flight characteristics of a twin-fuselage passenger transport airplane during approach and landing
[NASA-TP-2451] 23 p3898 N85-34144

FUSES (ORDNANCE)
Safing and arming mechanism
[AD-D011261] 05 p0621 N85-13969
Calculation through Fault Tree Analysis of the probability of a warhead being armed prior to launch
[AD-P004339] 10 p1454 N85-19163
Direct transient analysis of a fuze assembly by axisymmetric solid elements 15 p2576 N85-25890
Properties of Ti-6Al-4V spun formed fuze supports
[DE85-011968] 22 p3792 N85-33498

FUSIFORM SHAPES
U CONES

FUSION
The 1984 review of the Applied Plasma Physics Program
[DE85-002136] 10 p1560 N85-19840

FUSION (MELTING)
Biform resolidification and amorphous phases in a laser and electron beam processed tantalum-iridium alloy
[DE84-013334] 02 p0184 N85-11234
Induction heating gun
[NASA-CASE-LAR-13181-1] 18 p3085 N85-29083
Development of low-melting fused salts 8: Formation of molybdenum film from molten ammonium formate bath
[BLL-OA-TRANS-3195-(6196.300)]
20 p3429 N85-31264
Preparation and use of very pure o-D2
[DE85-009415] 22 p3843 N85-33800
Summary of activities, 1983
[LBL-18500] 23 p3969 N85-34805

FUSION REACTORS
NT SPHEROMAKS
Engineering Physics Division
[DE84-007778] 02 p0274 N85-11767
Review: Role of refractory metal alloys in fusion reactor applications
[AERE-R-11317] 03 p0422 N85-12695
Volatility of vanadium from a candidate fusion tractor alloy
[DE84-015277] 05 p0618 N85-13965
Passive stabilization of vertical instability in Tokamak reactor 06 p0775 N85-14958
Proceedings of Workshop on Synergistic Effects in Surface Phenomena Related to Plasma-Wall Interactions
[IPPJ-AM-35] 06 p0864 N85-15488
Synergistic effects in fusion machines, session summary 06 p0864 N85-15489
Plasma surface interaction processes and possible synergisms 06 p0864 N85-15490
Steady state hydrogen transport in solids
06 p0864 N85-15492
Special topics reports for the reference tandem mirror fusion breeder: Liquid metal MHD pressure drop effects in the packet bed blanket, volume 1
[DE85-002142] 06 p0865 N85-15500
Identification of spectra of highly ionized Mo, Nb, Zr and Y atoms 09 p1390 N85-18745
CTR plasma engineering studies
[DE84-017447] 09 p1392 N85-18762
Magnetic fusion energy plasma interactive and high heat flux components. Volume 2: Technical assessment of the critical issues and problem areas in high heat flux materials and component development
[DE85-001155] 09 p1393 N85-18764
Magnetic fusion energy plasma interactive and high heat flux components. Volume 3: Strategy for international collaborations in the areas of plasma materials interactions and high heat flux materials and components development
[DE85-001145] 10 p1559 N85-19829
Small, octopole-stabilized tandem mirror reactor
[DE85-002144] 10 p1559 N85-19832
Fusion Energy Division
[DE85-001701] 11 p1731 N85-20884
Magneto-fluid-dynamic issues for fusion first wall and blanket systems
[DE85-004022] 14 p2424 N85-24954
Nagoya bumpy torus 15 p2655 N85-26377
Basic research on inertial confinement fusion by LIMAY-I 15 p2655 N85-26383
Plasma theory and computations
15 p2655 N85-26384
Ballooning beta limits of dee and bean shaped Tokamaks
[IPPJ-713] 16 p2866 N85-27676
TOKASTAR: A Tokamak stellarator hybrid with possible bean-shaped operation
[IPPJ-718] 16 p2866 N85-27680
Prospects for developing attractive magnetic fusion concepts
[DE85-006925] 16 p2867 N85-27684
Fusion-power-core design of a Compact Reversed-Field Pinch Reactor (CRFPR)
[DE85-007710] 16 p2868 N85-27692
Heavy ion fusion accelerator research in the US
[DE85-008465] 17 p3034 N85-28767
An Impurity Control Test Facility (ICTF) for the study of fusion reactor/plasma edge materials
[DE85-007946] 17 p3040 N85-28810
Radiation damage experiments and lifetime estimates for beryllium components in fusion systems
[DE85-008038] 17 p3040 N85-28811
Two-dimensional TBR calculations for conceptual compact reversed-field pinch reactor blanket
[DE85-007636] 17 p3040 N85-28812
Pulse star inertial confinement fusion reactor
[DE85-010940] 18 p3181 N85-29726
Inertial fusion reactors and magnetic fields
[DE85-009571] 18 p3191 N85-29789
SHAPS-2: A three-dimensional computer program for linear/non-linear, static/dynamic analyses of piping systems
[DE85-010500] 19 p3335 N85-30658
Test cell modeling and optimization for FPD-2
[DE85-010836] 19 p3358 N85-30821
TFCK shielding optimization
[DE85-010503] 19 p3359 N85-30826
Qualitative comparison of fusion reactor materials for waste handling and disposal
[DE85-010473] 19 p3360 N85-30830
Poloidal variations in toroidal fusion reactor wall power loadings
[DE85-009505] 19 p3362 N85-30848
Tritium system design for the mirror reactors FPD-1, FPD-2 and FPD-3
[DE85-010490] 19 p3363 N85-30852

Molten salt cooling/17Li-83Pb breeding blanket concept
[DE85-010522] 19 p3363 N85-30854
Magnetic fusion 1985: What next?
[DE85-009953] 19 p3365 N85-30868
Steady-state spheromak reactor studies
[DE85-009585] 19 p3372 N85-30916
Current state of development and expected performance of copper-lithium alloys as an impurity control system in fusion applications
[DE85-009673] 19 p3372 N85-30917
Fusion reactions at low energy
[DE85-010561] 20 p3528 N85-31944
MFTF-(alpha) + T shield design
[DE85-010496] 20 p3529 N85-31948
Superconducting toroidal field coil current densities for the TFCX
[DE85-010285] 20 p3530 N85-31959
Fusion facility siting considerations
[DE85-012894] 22 p3843 N85-33805
Key issues of fusion nuclear technology development (FINESSE)
[DE85-012599] 22 p3845 N85-33817
Fusion Power Demonstration (FPD) maintenance and disassembly considerations
[DE85-011413] 22 p3846 N85-33820
Magnetic Fusion Program plan
[DE85-009861] 22 p3846 N85-33823
Blanket optimization studies for Cascade
[DE85-010002] 22 p3846 N85-33824
Data on the backscattering coefficients on light ions from solids: A revision
[IPPJ-AM-41-REV] 23 p3982 N85-34689
Advanced Toroidal Facility (ATF)
[DE85-011567] 23 p3983 N85-34699
Perspective on the next ten years in plasma physics
[DE85-011849] 23 p3984 N85-34706
ECH tokamak
[DE85-012074] 23 p3984 N85-34707

FUSION WELDING
NT ARC WELDING
NT BRAZING
NT ELECTRON BEAM WELDING
NT ELECTROSLAG WELDING
NT GAS TUNGSTEN ARC WELDING
NT LOW TEMPERATURE BRAZING
NT PLASMA ARC WELDING
New application possibilities for clad steel by reducing surface treatment expenditure and by using improved welding technology
[BMFT-FB-T-84-236] 12 p1861 N85-21672

FUZZY SETS
An investigation into fuzzy clustering and classification
[AD-A145571] 02 p0251 N85-11645
Induction of fuzzy decision rules
[INPE-3053-PRE/474] 04 p0554 N85-13525
R and D project selection with nonnumerical returns
[INPE-2760-PRE/335] 04 p0575 N85-13665
Evaluation of fuzzy rulemaking for expert systems for failure detection 05 p0703 N85-14508
Looking at multivariate data through fuzzy sets
[DE85-000684] 11 p1702 N85-20706
Some applications of fuzzy sets and the analytical hierarchy process to decision making
[AD-A150720] 14 p2412 N85-24676
Fuzzy hierarchical analysis
[DE85-008149] 17 p3021 N85-28685
Applications of fuzzy set theory to satellite soundings
18 p3141 N85-29445
Applications of some artificial intelligence methods to satellite soundings 18 p3141 N85-29446

FUZZY SYSTEMS
The R and D project selection problem with fuzzy coefficients
[INPE-3329-PRE/626] 10 p1565 N85-19871
Looking at multivariate data through fuzzy sets
[DE85-000684] 11 p1702 N85-20706
Applications of fuzzy clustering techniques to stratified by tropopause MSU temperature retrievals
18 p3141 N85-29444

F8U AIRCRAFT
U F-8 AIRCRAFT

G

G FORCE
U ACCELERATION (PHYSICS)

GADOLINIUM
Thermomagnetic generator
[DE84-017018] 04 p0530 N85-13388
The Fermi surface and momentum space densities of ferromagnetic Gd using the Positron technique
09 p1396 N85-16788
Structural, morphological and optical characteristics of KGd(WO4)2 crystals 14 p2280 N85-24126
Spectral-luminescence characteristics and induced emission of Nd-3(+) ion in Gd(2-x)Nd(x)(WO4)3 crystals
21 p3688 N85-32912

GAGES
U MEASURING INSTRUMENTS

GAIN (AMPLIFICATION)
U AMPLIFICATION

GALACTIC CLUSTERS
NT ANDROMEDA GALAXIES
NT VIRGO GALACTIC CLUSTER
Fractals: From snow flakes to galactic clusters
[NOTA-INTERNA-796] 02 p0296 N85-11918
Multiple object spectroscopy: The MX spectrometer design 02 p0296 N85-11920
On syntheses of the X-ray background with power-law sources
[NASA-TM-82173] 03 p0446 N85-12840
Galaxy and cluster formation in a universe dominated by cold dark matter
[DE84-015879] 04 p0580 N85-13706
On the scale of distances of the galaxy
05 p0737 N85-14735
Cosmology 07 p1056 N85-16701
A search for young stellar chromospheres in NGC 2264 11 p1748 N85-20993
The UV extinction laws in two very young clusters, NGC 6530 in the galaxy and NGC 2100 in the LMC
11 p1748 N85-20994
The physical implications of an isothermal model for the hot intracluster medium
[NASA-TM-86174] 11 p1763 N85-21089
Recent heavy particle decay in a matter dominated universe
[NASA-CR-175501] 11 p1764 N85-21095
Plasma in the clusters of galaxies
12 p1957 N85-22299
Morphology and energetics of narrow angle tail radio sources 14 p2455 N85-25164
A program of ground-based astronomy to complement einstein observations
[AD-A151111] 15 p2668 N85-26466
Spectral constraints on models of gas in clusters of galaxies
[NASA-TM-86186] 15 p2669 N85-26468
Formation of galaxies
[DE85-009537] 18 p3202 N85-29863
Further studies of X-ray structure of the Perseus cluster
[OG-2.5-12] 22 p3870 N85-33967
Cosmic gamma rays from quasars
[OG-2.7-10] 22 p3872 N85-33983

GALACTIC COSMIC RAYS
Characteristics of latitude effect on cosmic ray charged component in atmosphere at altitudes 3-5 KM
13 p1978 N85-22413
Periodicity of variations in galactic cosmic ray fluxes and solar activity parameters near 20th cycle minimum
16 p2720 N85-26791
Tables of nuclear cross sections for galactic cosmic rays: Absorption cross sections
[NASA-RP-1134] 16 p2864 N85-27665
Diffuse galactic annihilation radiation from supernova nucleosynthesis
[OG-3.2-8] 22 p3875 N85-34004
Cosmic ray intensity and the tilt of the neutral sheet
[SH-4.2-8] 23 p4007 N85-34846
Differential measurement of cosmic-ray gradient with respect to interplanetary current sheet
[SH-4.2-9] 23 p4007 N85-34847
Spatial variation of cosmic rays near the heliospheric current sheet
[SH-4.2-10] 23 p4007 N85-34848
Effects of a wavy neutral sheet on cosmic ray anisotropies
[SH-4.2-11] 23 p4008 N85-34849
Effects of solar magnetic field on cosmic rays
[SH-4.2-12] 23 p4008 N85-34850
Determination of galactic cosmic ray latitudinal gradient using Earth based detectors
[SH-4.2-13] 23 p4008 N85-34851
The expected cosmic ray density and stream distributions at the heliolatitudinal asymmetry of solar wind
[SH-4.2-14] 23 p4008 N85-34852
Latitudinal gradients of cosmic rays and the polarity reversal of the heliospheric magnetic field: A preliminary evaluation
[SH-4.2-16] 23 p4008 N85-34853
The influence of nonstationarity of the solar activity and general solar field on modulation of cosmic rays
[SH-4.2-17] 23 p4008 N85-34854
The effect of the neutral sheet structure of the interplanetary magnetic field on cosmic ray distribution in space
[SH-4.2-18] 23 p4008 N85-34855
On the influence of the heliomagnetospheric periphery on the galactic cosmic rays
[SH-4.2-19] 23 p4009 N85-34856
Spatial distribution of cosmic rays in magnetic cycles of the Sun
[SH-4.2-20] 23 p4009 N85-34857
11- and 22-year variations of the cosmic ray density and of the solar wind speed
[SH-4.2-21] 23 p4009 N85-34858
Difference between even and odd 11-year cycles in cosmic ray intensity
[SH-4.2-22] 23 p4009 N85-34859
The dependence of solar modulation on the sign of the cosmic ray particle charge
[SH-4.2-23] 23 p4009 N85-34860
An update on the correlation between the cosmic radiation intensity and the geomagnetic AA index
[SH-4.2-24] 23 p4009 N85-34861
Cosmic ray secondary nuclei and the structure of the galaxy
[OG-7.2-4] 23 p4014 N85-34876
Why do leaky-box models work so fine?
[OG-7.2-8] 23 p4014 N85-34877
On the importance of interstellar helium for the propagation of heavy cosmic rays
[OG-7.2-11] 23 p4015 N85-34879
A model for the origin of high-energy cosmic rays
[OG-8.1-8] 23 p4018 N85-34888
Astrophysical applications of high angular resolution array-telescopes
[OG-9.5-7] 23 p4031 N85-34964
Recording system for the solar neutron monitoring at Mt. Norikura
[SH-9.1-8] 23 p4051 N85-35123
Burst size distributions in the digitized data of the ion chambers t Mt. Norikura and sea level stations
[SH-9.1-9] 23 p4051 N85-35124
Sensitivity of single and multiple cosmic ray neutrons to the surrounding medium in a lead-free monitor
[SH-9.1-10] 23 p4051 N85-35125
Plastic scintillators in coincidence for the study of multi-particle production of sea level cosmic rays in dense medium
[SH-9.1-11] 23 p4052 N85-35126
The neutron moderated detector and groundbased cosmic ray modulation studies
[SH-9.1-13] 23 p4052 N85-35128
New Matsushiro underground cosmic ray station (220 M.W.E. in depth)
[SH-9.1-14] 23 p4052 N85-35129
Methods and software for cosmic ray scintillation studies
[SH-9.1-17] 23 p4052 N85-35132
The influences of the galactic cosmic ray on the atmospheric ozone
[SH-10.1-1] 23 p4053 N85-35133
Observation of nuclei with energies 8-30 MeV per nucleon in the Earth's magnetosphere at the altitudes 350 KM
[SH-10.1-5] 23 p4053 N85-35136
Measurement of low energy cosmic rays aboard Spacelab-1
[SH-10.1-6] 23 p4053 N85-35137
Heavy cosmic ray measurement aboard Spacelab-1
[SH-10.1-7] 23 p4053 N85-35138

GALACTIC EVOLUTION
The Belikt experiment 02 p0159 N85-11079
Galaxy and cluster formation in a universe dominated by cold dark matter
[DE84-015879] 04 p0580 N85-13706
Fifth Conference on Star Clusters and Associations and Their Relation to the Evolution of the Galaxy
[PUBL-56] 05 p0736 N85-14732
Structural properties of open star clusters and their relation to the galaxy 05 p0736 N85-14733
Open star clusters and the evolution of the galactic disk 05 p0736 N85-14734
Local galactic kinematics 05 p0741 N85-14765
The structure and dynamics of ringed galaxies
09 p1415 N85-18625
Comments on the origins and variations of carbon and nitrogen in the ISM of galaxies as evident from IUE spectroscopy of H 2 regions 11 p1745 N85-20973
Axions in astrophysics and cosmology
[DE85-002720] 11 p1763 N85-21094
Recent heavy particle decay in a matter dominated universe
[NASA-CR-175501] 11 p1764 N85-21095
Cosmology, galactic astronomy and elementary particle physics 12 p1956 N85-22298
Jets in galaxies 12 p1958 N85-22309
Galaxy formation 12 p1960 N85-22321
Research on the early history of the solar system
13 p2180 N85-23527

Dark matter, galaxies, and large scale structure in the universe
[DE85-006053] 16 p2882 N85-27786
Formation of galaxies
[DE85-009537] 18 p3202 N85-29863
Integral constraints on stress energy perturbations in general relativity and applications to cosmology
19 p3383 N85-30985
Activities report of the Institute of Astronomy
20 p3545 N85-32059
Primary gamma-rays with E gamma or = to 10(15) eV: Evidence for ultrahigh energy particle acceleration in galactic sources
[OG-2.6-13] 22 p3871 N85-33974
Implications of the experimental results on high energy cosmic rays with regard to their origin
[OG-5.4-5] 22 p3886 N85-34082
Anisotropy of cosmic rays above 10(14) eV
[OG-5.4-11] 22 p3887 N85-34088
A model for the proton spectrum and cosmic ray anisotropy
[OG-5.4-12] 22 p3887 N85-34089
Why do leaky-box models work so fine?
[OG-7.2-8] 23 p4014 N85-34877
Cosmic-ray exposure records and origins of meteorites
[SH-7.1-7] 23 p4047 N85-35099

GALACTIC MAGNETIC FIELDS
U INTERSTELLAR MAGNETIC FIELDS

GALACTIC NUCLEI
Star formation in interacting galaxies
03 p0444 N85-12826
Infrared mapping of galaxian centers: Star forming regions with kiloparsec scale sizes
03 p0444 N85-12827
Spectral components at visual and infrared wavelengths in active galactic nuclei
[NASA-CR-174133] 03 p0445 N85-12832
Continuum distributions of active galactic nuclei
05 p0742 N85-14770
Physical conditions in low-luminosity active galactic nuclei 05 p0742 N85-14771
The IRAS galaxy 0421+040P06: An active spiral (?) galaxy with extended radio lobes
[NASA-CR-174208] 06 p0871 N85-15536
Some aspects of active galactic nuclei
07 p1056 N85-16702
The environment of active galactic nuclei
07 p1057 N85-16712
The compact radio emission regions in active galactic nuclei — QUASAT VLBI mission
07 p1058 N85-16713
Very Long Base Interferometry (VLBI) in space and X-ray observations of compact sources in active galactic nuclei 07 p1058 N85-16716
X-ray and UV Emission from Active Galactic Nuclei — conference
[MPE-184] 08 p1236 N85-17790
Optical and UV emission of active galactic nuclei
08 p1236 N85-17791
BL Lacertae objects: Multifrequency observations and model applications 08 p1236 N85-17792
Radio Seyferts and the forbidden line region
08 p1236 N85-17793
Active inner regions of isolated galaxies
08 p1237 N85-17795
A new estimate of the local luminosity function of Seyfert 1 nuclei 08 p1237 N85-17796
Optical studies of X-ray selected Active Galactic Nuclei (AGN) in the direction of the Large Magellanic Cloud (LMC) 08 p1237 N85-17797
Continuous transition from star burst galaxies to Seyfert galaxies 08 p1237 N85-17798
Preliminary results on the ultraviolet observations of a complete X-ray selected sample of Active Galactic Nuclei (AGN) — HEAO 2 08 p1237 N85-17800
Spatially resolved optical spectroscopy of the radio jet of the X-ray galaxy NGC 2110 08 p1238 N85-17804
Extragalactic cosmic rays from active galaxies
08 p1238 N85-17805
A comparison of some photometric parameters of active and normal spiral galaxies 08 p1238 N85-17806
X-ray emission from active galactic nuclei
08 p1238 N85-17808
EXOSAT observations of active galactic nuclei
08 p1238 N85-17809
Characteristics of X-ray spectra from galactic and extragalactic X-ray sources 08 p1239 N85-17811
X-ray emission from PKS 2155-304 — BL Lac object
08 p1239 N85-17812
X-ray spectra of accretion disks — active galactic nuclei 08 p1239 N85-17814
EXO 1102.8+2539, an X-ray variable Active Galactic Nucleus (AGN) 08 p1239 N85-17816
UV and X-ray observations of AGN: Two comparisons with other wave lengths — Active Galactic Nuclei (AGN)
08 p1240 N85-17819
Comments on the physics of active galactic nuclei
08 p1240 N85-17823
Physical processes in relativistic plasmas — active galactic nuclei 08 p1240 N85-17824
A universal spectrum for AGNs and QSOs — Active Galactic Nuclei (AGN) 08 p1241 N85-17826
Shock acceleration in active galactic nuclei and quasars 08 p1241 N85-17828
Power law X- and gamma-ray emission from relativistic thermal plasmas 08 p1241 N85-17829
Pair production at moderate optical depths — galactic nuclei X ray spectra 08 p1241 N85-17830
On the hydrodynamical equations of astrophysical jets — active galactic nuclei 08 p1241 N85-17831
Collimated winds from active galactic nuclei
08 p1241 N85-17832
An alternative to relativistic beaming in AGN — Active Galactic Nuclei (AGN) 08 p1242 N85-17833
Centrifugally driven magnetohydrodynamic (MHD) winds and the nonthermal emission regions in Active Galactic Nuclei (AGN) 08 p1242 N85-17835
Macroscopic currents and wind perturbations in the frame of the wind and shock model — galactic nuclei
08 p1242 N85-17836
Duelling winds: A model for broad-line regions — galactic nuclei 08 p1242 N85-17837
X-ray spectra of accretion disks — active galactic nuclei 08 p1242 N85-17838
On the stability of broad line clouds in active galactic nuclei 08 p1243 N85-17840
Active galactic nuclei and their cosmological evolution
08 p1243 N85-17842
Very long base interferometry (VLBI) and X-ray observations of complete samples of radio selected active galactic nuclei 08 p1243 N85-17847
Ultraviolet and X-ray observations of active galactic nuclei: Constraints on models of the broad emission line region 11 p1744 N85-20966
Structure of the Seyfert broad line region and absorption region of NGC 4151 11 p1746 N85-20978
Broad emission features in active galactic nuclei
11 p1746 N85-20979
Coordinated multifrequency observations of the BL LAC objects MRK 180, MRK 421, and MRK 501
11 p1746 N85-20983
Interstellar extinction in the nucleus of H PER
11 p1749 N85-21001
X-ray emission from active galactic nuclei
[NASA-TM-86175] 11 p1763 N85-21088
Consequences of hot gas in the broad line region of active galactic nuclei
[NASA-TM-86176] 11 p1763 N85-21090
Electron-positron pairs in a mildly relativistic plasma in active galactic nuclei 12 p1957 N85-22297
Hydrodynamics of astrophysical jets — active galactic nuclei 12 p1958 N85-22307
Viscous jets — extragalactic jets
12 p1958 N85-22308
Small scale structure and the Spinar model for active galactic nuclei 12 p1959 N85-22316
All-Union conference of radio astronomers
13 p1977 N85-22406
IRAS observations of active galaxies
[NASA-CR-175720] 15 p2668 N85-26483
Interactions of galaxies and their nuclear activity
20 p3545 N85-32060
The hydrodynamic effects of nuclear active galaxy winds on host galaxies 20 p3545 N85-32062
Spectra and positions of galactic gamma-ray sources
[OG-2.5-7] 22 p3869 N85-33963
Search for TeV gamma rays from extragalactic sources and the Galactic Center
[OG-2.7-1] 22 p3871 N85-33976
Gamma-radiation with E gamma 5 MeV detected from Seyfert galaxy 3C120 and region with 1' = 190 deg and b' = 20 deg
[OG-2.8-8] 22 p3871 N85-33981
Galactic distribution of interstellar Al-26
[OG-3.2-3] 22 p3874 N85-34002
Cosmic rays in the 10(16) to 10(19) eV range from pulsars
[OG-5.4-3] 22 p3886 N85-34080
Energy dependence of cosmic ray composition above 10(15) GeV/nucleus
[OG-5.4-4] 22 p3886 N85-34081
The 1973-1984 solar modulation of cosmic ray nuclei
[SH-4.1-16] 23 p4006 N85-34838
The effects of newly measured cross sections in hydrogen on the production of secondary nuclei during the propagation of cosmic rays through interstellar H
[OG-7.2-2] 23 p4014 N85-34874
The central engine of quasars and AGNs: A relativistic proton radiative shock
[OG-8.1-7] 23 p4018 N85-34897
Cerenkov light images of EAS produced by primary gamma
[OG-9.5-3] 23 p4030 N85-34979

GALACTIC RADIATION
NT GALACTIC COSMIC RAYS
NT GALACTIC RADIO WAVES
NT NORTH POLAR SPUR (ASTRONOMY)
Constraints to the radiative lifetime of a light neutral fermion in the galactic halo from IUE
[NOTA-INTERNA-817] 02 p0279 N85-11820
Star formation in interacting galaxies
03 p0444 N85-12826
Infrared mapping of galaxian centers: Star forming regions with kiloparsec scale sizes
03 p0444 N85-12827
Spectral components at visual and infrared wavelengths in active galactic nuclei
[NASA-CR-174133] 03 p0445 N85-12832
Far-infrared line emission from the galaxy
[NASA-CR-174166] 04 p0580 N85-13702
The IRAS galaxy 0421+040P06: An active spiral (?) galaxy with extended radio lobes
[NASA-CR-174208] 06 p0871 N85-15536
Optical emission line studies and the warm, ionized component of the local interstellar medium
06 p0875 N85-15555
On the record of galactic cosmic ray flux and traffic break-ups in iron meteorites 06 p0887 N85-15634
The ultraviolet spectra of the narrow line active galaxies NGC 3081 and NGC 4507 08 p1237 N85-17799
Low excitation absorptions in the spectrum of the quasar PKS 1327-206 due to the galaxy MCG 03-34-085
08 p1237 N85-17801
The origin of the X-ray background
08 p1243 N85-17841
Far infrared emission from galaxies
08 p1248 N85-17875
Far infrared continuum emission from the galactic center 08 p1248 N85-17876
Dust reradiation from NGC 6946
08 p1248 N85-17880
Far-infrared spectroscopy of galaxies: The 158 micron C(+) line 08 p1249 N85-17882
Interpretation of the far infrared emission from our external galaxies 08 p1249 N85-17884
X-ray emission from Centaurus A
[DE85-002030] 09 p1417 N85-18943
Coordinated multifrequency observations of the BL LAC objects MRK 180, MRK 421, and MRK 501
11 p1746 N85-20983
IRAS observations of Seyfert galaxies
[NASA-CR-175557] 12 p1953 N85-22267
Morphology and energetics of narrow angle tail radio sources 14 p2455 N85-25164
Results from the Helios galactic and solar cosmic ray experiment (E7) 16 p2886 N85-27807
Differential measurement of cosmic-ray gradient with respect to interplanetary current sheet
[PAPER-SH-4.2-9] 21 p3715 N85-33055
Galactic gamma-ray sources, SNOBs, and giant H2 regions
[OG-2.5-4] 22 p3869 N85-33961
Inverse-Compton gamma rays in the galaxy
[OG-3.1-2] 22 p3873 N85-33990
Radial distribution of cosmic ray intensity in the galaxy from gamma-ray data
[OG-3.1-5] 22 p3873 N85-33993
Local electron spectrum above 100 MeV derived from gamma-ray emissivity spectra
[OG-3.1-7] 22 p3874 N85-33995
Relevance of cosmic gamma rays to the mass of gas in the galaxy
[OG-3.1-8] 22 p3874 N85-33996
A measurement of the cosmic ray elements C to Fe in the two energy intervals 0.5-2.0 GeV/n and 20-60 GeV/n
[OG-4.1-6] 22 p3876 N85-34012
Cosmic ray nuclei of energy 50 GeV/NUC
[OG-4.1-12] 22 p3877 N85-34018
Interstellar propagation and the isotopic composition of hydrogen in the galactic cosmic rays
[OG-4.2-1] 22 p3877 N85-34021
Measurements of galactic hydrogen and helium isotopes from 1978 through 1983
[OG-4.2-2] 22 p3877 N85-34022
Galactic propagation models consistent with the cosmic ray lifetime derived from Be-10 measurements
[OG-4.3-1] 22 p3878 N85-34026
Implications of new measurements of O-16 + p + C-12,13, N-14,15 for the abundances of C, N isotopes at the cosmic ray source
[OG-4.3-2] 22 p3878 N85-34027

The isotopic composition of cosmic ray chlorine
[OG-4.3-3] 22 p3878 N85-34028
Cosmic ray isotope measurements with a new Cerenkov X total energy telescope
[OG-4.3-4] 22 p3878 N85-34029
The isotopic composition of cosmic ray calcium
[OG-4.3-5] 22 p3879 N85-34030
A new analysis of cosmic ray isotopes at 3 GeV/n from HEA03-C2 data
[OG-4.3-6] 22 p3879 N85-34031
The energy dependence of the neon-22 excess in the cosmic radiation
[OG-4.3-7] 22 p3879 N85-34032
Ariel 6 measurements of ultra-heavy cosmic ray fluxes in the region 34 or = Z or = 48
[OG-4.4-3] 22 p3879 N85-34036
Ariel 6 measurements of ultra-heavy cosmic ray fluxes in the region Z or = 48
[OG-4.4-4] 22 p3880 N85-34037
Elemental abundances of cosmic rays with Z 33 as measured on HEAO-3
[OG-4.4-5] 22 p3880 N85-34036
Capabilities of the LDEF-2 heavy nuclei collection
[OG-4.4-8] 22 p3880 N85-34040
Energy spectrum and arrival direction of primary cosmic rays of energy above 10 to the 18th power eV
[OG-5.1-1] 22 p3880 N85-34043
Ultra high energy cosmic ray spectrum
[OG-5.1-2] 22 p3881 N85-34044
The primary cosmic ray spectrum above 10 to the 19th power eV
[OG-5.1-3] 22 p3881 N85-34045
Estimation of composition of cosmic rays with E sub zero approximately equals 10(17) - 10(18) eV
[OG-5.1-14] 22 p3882 N85-34055
On galactic origin of cosmic rays with energy up to 10(19) eV
[OG-5.4-15] 22 p3887 N85-34091
Galactic cosmic ray antiprotons and supersymmetry
[OG-6.1-9] 22 p3888 N85-34100
Effect of seeds of heavy charged particles of galactic cosmic radiation 23 p3954 N85-34505
Abundances from solar-flare gamma-ray line spectroscopy
[SH-2.1-13] 23 p3999 N85-34794
Type 3 solar radio bursts and 3HE-rich events
[SH-2.2-3] 23 p4000 N85-34798
the role of shock waves in modulation of galactic cosmic rays
[SH-4.1-7] 23 p4005 N85-34831
Propagation of the phase of solar modulation
[SH-4.1-12] 23 p4005 N85-34835
Germanium and lead: Significant differences between meteoritic and photospheric abundances?
[OG-7.1-2] 23 p4012 N85-34864
Implications of source abundances of ultraheavy cosmic rays
[OG-7.1-4] 23 p4013 N85-34866
Propagation and nucleosynthesis of ultraheavy cosmic rays
[OG-7.1-5] 23 p4013 N85-34867
On the importance of interstellar helium for the propagation of heavy cosmic rays
[OG-7.2-11] 23 p4015 N85-34879
Cosmic-ray transport in the galactic magnetosphere
[OG-7.2-17] 23 p4016 N85-34884
The role of cosmic rays and Alfven waves in the structure of the galactic halo
[OG-7.2-18] 23 p4016 N85-34885
Do supernovae of type 1 paly a role in cosmic-ray production?
[OG-8.2-5] 23 p4019 N85-34905
Neutron-rich nuclei in cosmic rays and Wolf-Rayet stars
[OG-8.2-6] 23 p4019 N85-34906
Bursting star formation and the overabundance of Wolf-Rayet stars
[OG-8.2-8] 23 p4019 N85-34907
Interstellar (Na-22) as a possible source of the excess (Ne-22) in the galactic cosmic ray
[OG-8.2-12] 23 p4020 N85-34908
The electromagnetic ram action of the plasma focus as a paradigm for the generation of cosmic rays and the gigantic jets in active galaxies
[OG-8.2-14] 23 p4020 N85-34910
The origins of cosmic rays and quantum effects on gravity
[OG-8.2-15] 23 p4020 N85-34911
Influence of the source distribution on the age distribution of galactic cosmic rays
[OG-8.3-1] 23 p4021 N85-34920
Explanation of the secondary to primary ratio within the continuous Fermi accelerator model
[OG-8.3-2] 23 p4021 N85-34921
Propagation of cosmic rays and new evidence for distributed acceleration
[OG-8.3-5] 23 p4022 N85-34924
High resolution Cherenkov detectors for cosmic ray isotope experiment
[OG-9.1-4] 23 p4023 N85-34930
A high resolution gas Cerenkov detector for the superconducting magnet facility
[OG-9.1-6] 23 p4023 N85-34932
Mass resolution optimization in a large isotopic composition experiment
[OG-9.1-9] 23 p4023 N85-34935
The difference in the energy spectra of galactic cosmic rays at the minima of the 19th and 20th solar activity cycles
[SH-4.4-18] 23 p4035 N85-35014
Azimuthal and meridional asymmetries of the solar wind and quasiperiodic variations of intensity of Galactic Cosmic Rays (GCR)
[SH-4.4-20] 23 p4035 N85-35016
Long-term modulation of galactic cosmic rays in high-energy region
[SH-4.4-22] 23 p4035 N85-35018
The first three harmonics of solar daily variation caused by the diffusive propagation of galactic cosmic rays through the heliosphere
[SH-4.5-1] 23 p4035 N85-35019
Diurnal variation of galactic cosmic ray intensity on quiet days
[SH-4.5-11] 23 p4037 N85-35029
Solar modulation and interplanetary gradients of the galactic electrons flux, 1977 - 1984
[SH-4.7-4] 23 p4040 N85-35049
Galactic cosmic ray radial gradients and the anomalous He component near maximum solar modulation and to radii beyond 34 AU from the Sun
[SH-4.7-5] 23 p4040 N85-35050
Voyager 1 and 2 measurements of radial and latitudinal cosmic ray gradients during 1981 - 1984
[SH-4.7-6] 23 p4041 N85-35051
The large-scale modulation of cosmic rays in mid-1982: Its dependence on heliospheric longitude and radius
[SH-4.7-9] 23 p4041 N85-35053
Nonstationary modulation of galactic cosmic rays in a nonlinear model
[SH-4.7-10] 23 p4041 N85-35054
Dimensions of the solar wind cavity and of the region of interplanetary cosmic ray modulation
[SH-4.7-11] 23 p4041 N85-35055
Drift and Forbush decreases
[SH-5.1-2] 23 p4041 N85-35056
Anomalous short-term increases in the galactic cosmic ray intensity: Are they related to the interplanetary magnetic cloud-like structures?
[SH-5.1-3] 23 p4041 N85-35057
Longitudinal dependence of the interplanetary perturbation produced by energetic type 4 solar flares and of the associated cosmic ray modulation
[SH-5.1-5] 23 p4042 N85-35059
Galactic cosmic ray currents and magnetic field irregularity degree in high-speed solar wind streams
[SH-5.1-9] 23 p4042 N85-35063
Influence of magnetic clouds on cosmic ray intensity variations
[SH-5.1-12] 23 p4042 N85-35065
Cosmic rays 10Be biennal data and their relationship to aurorae and sunspots
[SH-7.1-1] 23 p4047 N85-35094
Cosmogenic-nuclide production by primary cosmic-ray protons
[SH-7.1-6] 23 p4047 N85-35098
Accelerator experiments on the contribution of secondary particles to the production of cosmogenic nuclides in meteorites
[SH-7.1-8] 23 p4048 N85-35100
Depth and size effects on cosmogenic nuclide production in meteorites
[SH-7.1-9] 23 p4048 N85-35101
A search for cosmic sources of high energy neutrinos with small underground detectors
[HE-5.3-16] 24 p4206 N85-36110

GALACTIC RADIO WAVES
NT NORTH POLAR SPUR (ASTRONOMY)
Radio Seyferts and the forbidden line region
08 p1236 N85-17793
The relationship between radio structures and stellar dynamics of nearby elliptical galaxies
08 p1236 N85-17794
All-Union conference of radio astronomers
13 p1977 N85-22408
Radio counterparts of galactic gamma-ray sources
20 p3549 N85-32085

GALACTIC ROTATION
On a spectral theory of the excitation mechanism of galactic spirals 12 p1955 N85-22284

The study of the physics of cometary nuclei
[NASA-CR-175917] 17 p3054 N85-28605
A simulation of high energy cosmic ray propagation 2
[OG-5.4-2] 22 p3885 N85-34079

GALACTIC STRUCTURE
The galactic distribution of open clusters of different ages and the angular velocity of the spiral structure
05 p0737 N85-14737
On collective effects in the rotation of stars in clusters and associations 05 p0737 N85-14739
Excitation of spiral patterns in responsible density wave theory 05 p0740 N85-14764
Local galactic kinematics 05 p0741 N85-14765
Some aspects of active galactic nuclei
07 p1056 N85-16702
The galactic gamma-ray distribution: Implications for galactic structure and the radial cosmic ray gradient
[NASA-TM-86173] 07 p1061 N85-16729
The relationship between radio structures and stellar dynamics of nearby elliptical galaxies
08 p1236 N85-17794
Continuous transition from star burst galaxies to Seyfert galaxies 08 p1237 N85-17798
The structure and dynamics of ringed galaxies
09 p1415 N85-18928
On the morphology of spiral modes — disk galaxies
12 p1955 N85-22283
Drift-accretion theory of the spiral structure of galaxies
12 p1957 N85-22298
Some constraints on magnetic fields in galactic spiral arms 12 p1957 N85-22300
Small scale structure and the Spiner model for active galactic nuclei 12 p1959 N85-22316
The color excesses of classical cepheids and the structure of our galaxy 13 p2169 N85-23459
Gas dynamics of the barred spiral galaxy NGC 3359
13 p2170 N85-23465
Dynamics of gas disks in triaxial galaxies
13 p2171 N85-23466
A rocket-borne X-ray observation of SN1006 with the imaging gas scintillation proportional counter
14 p2435 N85-25014
Formation of galaxies
[DE85-009537] 18 p3202 N85-29960
Cosmic ray secondary nuclei and the structure of the galaxy
[OG-7.2-4] 23 p4014 N85-34876
High energy cosmic ray signature of quark nuggets
[HE-6.2-11] 24 p4212 N85-36147

GALACTOSE
Galactose oxidase in stereospecific oxidation of primary alcohols
[AD-A154059] 19 p3234 N85-30048

GALAXIES
NT ANDROMEDA GALAXIES
NT BARRED GALAXIES
NT DISK GALAXIES
NT ELLIPTICAL GALAXIES
NT GALACTIC CLUSTERS
NT MAGELLANIC CLOUDS
NT MILKY WAY GALAXY
NT RADIO GALAXIES
NT SEYFERT GALAXIES
NT SPIRAL GALAXIES
NT VIRGO GALACTIC CLUSTER
IRAS observations of external galaxies
03 p0443 N85-12825
Galaxy and cluster formation in a universe dominated by cold dark matter
[DE84-015879] 04 p0580 N85-13706
Unidentified IRAS sources: Ultrahigh luminosity galaxies
[NASA-CR-174207] 06 p0872 N85-15537
Supersymmetric inflationary cosmology
[DE85-001331] 06 p0881 N85-15598
Far infrared emission from galaxies
08 p1248 N85-17875
Starbursts in galaxies: Implications of molecular and far-infrared observations 08 p1248 N85-17881
Far-infrared spectroscopy of galaxies: The 158 micron C(+) line 08 p1249 N85-17882
Far infrared spectroscopy of (O III) in M82
08 p1249 N85-17883
Data reduction 09 p1412 N85-18903
Combined ultraviolet studies of astronomical sources
[NASA-CR-174361] 09 p1413 N85-18910
Research in extreme ultraviolet and far ultraviolet astronomy
[NASA-CR-174432] 10 p1570 N85-19902
International Ultraviolet Explorer observations of amorphous hot galaxies
[NASA-CR-174354] 10 p1571 N85-19904
Future of Ultraviolet Astronomy Based on Six Years of IUE Research
[NASA-CP-2349] 11 p1743 N85-20981

Galactic absorption lines measured from the IUE low dispersion spectra of active galaxies
11 p1745 N85-20977
University of Cambridge Institute of Astronomy report of activities 13 p2170 N85-23464
Studies of galactic HI in 21-centimeter absorption
13 p2170 N85-23466
Color evolution in high redshift galaxies
20 p3544 N85-32055
Activities report of the Institute of Astronomy
20 p3545 N85-32059
The kinematic and radial properties of normal luminous SC galaxies 20 p3545 N85-32061
Activities report of the Department of Astrophysics
20 p3546 N85-32064
Search for positron annihilation line and continuum radiation from the Galactic Center
[OG-2.5-5] 22 p3869 N85-33962
Charge 4/3 leptons in cosmic rays
[HE-6.2-14] 24 p4212 N85-36150

GALAXY AIRCRAFT
U C-5 AIRCRAFT

GALERKIN METHOD
The convergence of Garlerkin approximation schemes for second-order hyperbolic equations with dissipation
[CSIR-TWISK-325] 01 p0109 N85-10736
Spline-Galerkin solution of integral equations for 3-body scattering above break-up
[TWISK-327] 01 p0109 N85-10738
Approximation of discontinuous solutions of hyperbolic partial differential equations
[NRIMS-TWISK-302] 02 p0250 N85-11631
Time discretization of parabolic problems by the discontinuous Galerkin method
[CTH-MATH-1984-16] 04 p0556 N85-13543
A lumped mass finite element method with quadrature for a nonlinear parabolic problem
[CTH-MATH-1984-22] 05 p0719 N85-14615
Algorithm for the simulation of transient viscoelastic flows with free surfaces
[DE85-002713] 12 p1848 N85-21590
Low-dimensional behavior of the pattern formation Cahn-Hilliard equation
[DE85-003727] 12 p1922 N85-22072
Spline-based Rayleigh-Ritz methods for the approximation of the natural modes of vibration for flexible beams with tip bodies
[NASA-CR-172566] 13 p2102 N85-23100
Solution of Onsager's equation for a rotating compressible fluid in a multiply-connected domain
[DE85-007048] 16 p2784 N85-27178
A study of internal and distributed damping for vibrating turbomachiner blades
[NASA-CR-175901] 17 p2898 N85-27868
A fast implementation of explicit time stepping algorithms with the finite element method for a class of nonlinear evolution problems
[REPT-84-03] 17 p3021 N85-28686
Applications of the Galerkin formalism in the coupling of the earth's free oscillations 24 p4116 N85-35514

GALILEAN SATELLITES
NT CALLISTO
NT EUROPA
NT GANYMEDE
NT IO
Stability of the Galilean satellites in deep orbital resonance 13 p2172 N85-23477
Creep of ice: Further studies
13 p2201 N85-23655
The Galilean Satellite Geological Mapping Program, 1984 13 p2203 N85-23664
Voyager cartography 13 p2203 N85-23668
The control networks of the satellites of Jupiter and Saturn 13 p2204 N85-23671
Interpretation of photometric measurements of airless bodies 22 p3855 N85-33871

GALILEO MISSION
U GALILEO PROJECT

GALILEO PROBE
Galileo 15 p2688 N85-26601

GALILEO PROJECT
Mission science value-cost savings from the Advanced Imaging Communication System (AICS)
[NASA-CR-174170] 04 p0458 N85-12905
Reed-Solomon decoder — applicable to Galileo Project requirements
[NASA-CASE-NPO-15982-1] 11 p1699 N85-20680
The 1986 National Aeronautics and Space Administration authorization
[GPO-47-635] 24 p4166 N85-35829

GALILEO SPACECRAFT
Transient vibration test criteria for spacecraft hardware — galileo spacecraft 09 p1338 N85-18418
Solid particle environment and protection for the Galileo Orbiter 12 p1786 N85-21207
Galileo internal electrostatic discharge program
13 p1995 N85-22504
Galileo battery testing and the impact of test automation 20 p3444 N85-31381
The Galeleo spacecraft magnetometer boom
22 p3796 N85-33513

GALL
Biligenic function of white rat liver
01 p0093 N85-10624

GALLIUM
Development of high responsitivity Ga:Ga photoconductors
[DE84-016902] 04 p0571 N85-13643
IUE observations of the gaseous component of the local interstellar medium 06 p0874 N85-15553
Research on the basic understanding of high efficiency in silicon solar cells
[DE85-000507] 11 p1672 N85-20537
Angle-resolved photoemission study of AuGa2 and AuIn2 intermetallic compounds
[AD-A150000] 12 p1940 N85-22183
Annealing of radiation damage in boron and gallium doped silicon solar cells 13 p2012 N85-22624
Improvement in magnetic field properties of vanadium-gallium superconductors by enhancement of spin-orbit scattering
[DE85-002693] 13 p2164 N85-23422
Specificity of (71)Ga(p,n) (71)Ge at 35 MeV for Gamow-Teller strength
[DE85-011837] 23 p3971 N85-34615

GALLIUM ANTIMONIDES
Photoluminescent properties of epitaxial p-GaSb
02 p0267 N85-11745
Cascaded solar photovoltaic cells based on InP-GaInPAs and InP-CdS heterostructures
02 p0268 N85-11749
Raman scattering from metastable GaSb(1-x) Ge(2x) alloys
[AD-A145897] 03 p0327 N85-12108
Inter-zone auger recombination in GaSb laser structures 21 p3682 N85-32875

GALLIUM ARSENIDE LASERS
Space-time characteristics of radiation of single-mode injection lasers 02 p0269 N85-11758
Heatsink requirements for coherent operation of high-power semiconductor laser arrays
[AD-A146184] 03 p0366 N85-12346
Design and chemical synthesis of iodine-containing molecules for application to solar-pumped I* lasers
[NASA-CR-176010] 19 p3275 N85-30310
Phase locked loops for optical homodyne detection, volume 2 — spaceborne receivers
[ESA-CR(P)-2029-VOL-2] 20 p3442 N85-31368
Low-threshold injection InGaAsP/GaAs double heterostructure lasers with separate limiting obtained by liquid-phase epitaxy (lambda = 0.78 divided by 0.87 microns, I sub thr = 460 A/cm 2, T = 300 K)
21 p3687 N85-32908
Influence of technological factors on luminescence characteristics of InGaAsP/InP heterolasers (lambda = 1.55 microns) 21 p3688 N85-32910

GALLIUM ARSENIDES
NT ALUMINUM GALLIUM ARSENIDES
NT SUPERLATTICES
An investigation of the solubility and diffusivity of chromium in gallium arsenide
[AD-A144949] 01 p0024 N85-10148
Solution of the Boltzmann transport equations for a permeable base transistor
[AD-A144969] 01 p0112 N85-10757
Acoustic resonator and method of making same
[DE84-014655] 01 p0116 N85-10792
Plasma deposited diamondlike carbon on GaAs and InP
[NASA-TM-86870] 01 p0123 N85-10844
Producing gallium arsenide crystals in space
02 p0151 N85-11023
Research directions and progress in the SERI advanced high efficiency concept program
[DE84-004592] 02 p0223 N85-11462
Luminous points and breakdown in structure of GaAs transistors 02 p0257 N85-11684
Composition of metal films on gallium arsenide surface 02 p0257 N85-11685
Impurity trapping during gas phase epitaxy of gallium arsenide 02 p0257 N85-11686
Spectral distribution of radiation in n junctions of GaAs during avalanche breakdown 02 p0258 N85-11688
Complex formation and temperature stability of electrophysical properties of GaAs seminsulating single crystals 02 p0258 N85-11689
Reversible change in parameters of GaAs-based surface-barrier metal-semiconductor diodes induced by hydrogen absorption-desorption
02 p0258 N85-11690
Nonlinear absorption of laser radiation in InP and in GaAs 02 p0266 N85-11740
Injection lasers based on AlGaAsSb/GaSb and InGaAsSb/GaSb heterostructures
02 p0270 N85-11761
Splitting of surface polariton spectrum by holographic grating 02 p0272 N85-11771
Electron traps in the GaAs permeable base transistor
[AD-A145399] 02 p0287 N85-11871
Reflection electron energy loss investigation of the H-GaAs(110) surface
[NOTA-INTERNA-811] 02 p0289 N85-11889
Raman scattering from metastable GaSb(1-x) Ge(2x) alloys
[AD-A145897] 03 p0327 N85-12108
Studies of grown-in defects versus growth parameters in 3-4 compound semiconductors
[AD-A145864] 03 p0433 N85-12755
Folded acoustic and quantized optic phonons in semiconductor superlattices
[AD-A145935] 03 p0433 N85-12756
High-temperature optically activated GaAs power switching for aircraft digital electronic control
[NASA-CR-174711] 04 p0457 N85-12901
Effect of barrier height on friction behavior of the semiconductors silicon and gallium arsenide in contact with pure metals
[NASA-TP-2405] 04 p0478 N85-13044
Glow spots and breakdown in GaAs transistor structure 04 p0487 N85-13107
Lifetime of excess charge carriers in weakly doped epitaxial GaAs layers 04 p0487 N85-13108
Trends in space photovoltaic technology
05 p0609 N85-13888
Material models and device structures for GaAs solar cells
[DE85-000501] 05 p0665 N85-14275
Material models and device structures for GaAs solar cells, introduction 05 p0665 N85-14276
GaAs material properties and models
05 p0665 N85-14277
Comparison of SCAPID/GaAs to experiment
05 p0665 N85-14279
Radiation hardened ion-implanted GaAs field effect transistor and method for making the same specification
[AD-D011264] 05 p0731 N85-14697
Photoluminescence studies of Ga(As,P) strained-layer superlattices
[DE84-015709] 05 p0731 N85-14701
Raman study of neutron irradiated GaAs
[DE84-016056] 05 p0731 N85-14702
Numerical estimation of charge transfer time in charge-coupled device employing latent gallium arsenide channel 06 p0793 N85-15069
Galium-arsenide power devices
06 p0794 N85-15076
Gallium arsenide compounds tested nondestructively with X-rays 07 p0936 N85-15934
Development of short gate FET's
[AD-A147033] 07 p0947 N85-15999
X-ray and backscattering analysis of ion implantation phenomena in GaAs and related compounds
[AD-A147449] 07 p1048 N85-16659
Aluminum nitride insulator for 3-5 MIS (Metal-Insulator-Semiconductor) applications
[AD-A147842] 07 p1049 N85-16662
French research on gallium arsenide devices
08 p1141 N85-17196
Automated assembly of Gallium Arsenide and 50-micron thick silicon solar cell modules
[NASA-CR-174331] 08 p1168 N85-17364
Characterization of thermally treated gallium arsenide by laser-Raman and Auger spectroscopy
[AD-A148414] 08 p1226 N85-17721
Ion implantation in 3-5 compound semiconductors
[AD-A148462] 08 p1226 N85-17723
ONR (Office of Naval Research) Far East Scientific Bulletin, volume 9, number 3, July to September 1984
[AD-A147282] 08 p1262 N85-17930
Transient response of a small-signal microwave GaAs FET to X-rays
[DE85-000066] 09 p1315 N85-18265
A picosecond population modulation study of near interband resonances in semiconductors
09 p1396 N85-18787
Effect of hydrostatic pressure on trapping centers in strained-layer superlattice structures
[DE85-001362] 09 p1399 N85-18807
Material growth and characterization for solid state devices
[NASA-CR-174410] 10 p1561 N85-19847
Surface and interfacial properties of Ga(0.47) In(0.53)As alloys
[AD-A148891] 10 p1562 N85-19849

Fabrication of monocrystalline GaAs solar cells utilizing NaCl sacrificial substrates
[DE84-013016] 11 p1673 N85-20544
Determination of the mobility profile in GaAs-MESFETs
[NASA-TM-77818] 11 p1734 N85-20905
Low stress semiconductor-insulator interface for cryogenic device applications
[NASA-CASE-NPO-16394-1] 11 p1734 N85-20906
AlAs/GaAs superlattice barrier unipolar diode structure
[DE85-001904] 11 p1736 N85-20921
GaAs and 3-5 compound solar cells status and prospects for use in space
[NASA-TM-86960] 12 p1795 N85-21261
Distributed Gunn effect devices; a numerical analysis of microstrip circuits on thin active GaAs substrates
[FOA-C-30363-E] 12 p1837 N85-21527
New high resolution scanning ion microprobe and focused ion beam applications
[AD-A149992] 12 p1852 N85-21616
Characterization of high purity Si-doped molecular beam epitaxial GaAs
[AD-A149651] 12 p1939 N85-22181
Semiconductor materials for high frequency solid state sources
[AD-A150020] 12 p1940 N85-22186
Evaluation of implantation-disordering of (InGa)As/GaAs strained-layer superlattices
[DE85-003533] 12 p1942 N85-22200
Gallium arsenide arrays versus silicon arrays for space application 13 p2006 N85-22574
Space qualified AlGaAs/GaAs solar cells
13 p2006 N85-22575
Availability of AlGaAs/GaAs solar cells in space
13 p2006 N85-22576
Comparative study of GaAs solar cell potentialities for space applications 13 p2006 N85-22577
Investigation of high output gallium arsenide solar cells 13 p2006 N85-22578
Development of very thin large area GaAs solar cells for space application 13 p2006 N85-22579
GaAs and 3-5 compound solar cells status and prospects for use in space 13 p2007 N85-22580
GaAlAs-GaAs solar cell development: Prospective for space applications under concentration
13 p2007 N85-22581
Investigation of the degradation of GaAs photovoltaic cells by proton and electron irradiation
13 p2008 N85-22587
Isotropic proton irradiation of GaAs solar cells
13 p2012 N85-22622
High output photovoltaic conversion: The quadrispectral project — spacecraft power supplies
13 p2012 N85-22626
Thermally stimulated conductivity in semi-insulating gallium arsenide 13 p2088 N85-23036
Fracture mechanics evaluation of GaAs
[NASA-CR-175657] 13 p2102 N85-23101
Some observations of heated gallium arsenide heteroface solar cells
[NASA-TM-86388] 14 p2246 N85-23925
Physical electronics of cooled operation of very short compound semiconductor trasnsistors
14 p2297 N85-24223
Cryogenically-cooled, low-noise microwave receivers: Present status and future needs
14 p2298 N85-24226
Advanced high-efficiency concentrator cell
[DE85-000525] 14 p2351 N85-24533
Infrared nonlinear processes in semiconductors
[AD-A150966] 14 p2427 N85-24968
Ion implantation disorder in strained-layer superlattices
[DE85-004466] 14 p2430 N85-24984
Dual species ion implantation of ternary compounds based on In-Ga-As
[AD-D011617] 16 p2869 N85-27698
A study of Ga(.47)In(.53)As and Al(.48)In(.52)As for very high frequency device applications
[AD-A151995] 16 p2870 N85-27706
Effect of dislocations on gallium arsenide FETs
[AD-A152249] 16 p2870 N85-27709
TEM investigation of polar-on-nonpolar epitaxy: GaAs-AlGaAs on (100) Ge
[DE85-007613] 16 p2871 N85-27714
Random access memory technologies
[AD-A153069] 17 p3008 N85-28597
Optical waveguide characterization using grating couplers
[AD-A153063] 17 p3037 N85-28789
Activities of the Solid State Physics Research Institute
[NASA-CR-175899] 17 p3042 N85-28818
Leakage effects in n-GaAs MESFET with n-GaAs buffer layer 17 p3043 N85-28826
GaAs MESFET with lateral non-uniform doping
17 p3043 N85-28827
Materials-process interactions in ternary alloy semiconductors
[AD-A153133] 17 p3043 N85-28832
Development of photodetectors
[AD-A153773] 18 p3095 N85-29158
Evaluation of VLSI technology — space applications
[CD.6501702] 18 p3098 N85-29177
Mechanically-stacked multijunction solar cells
[DE85-010389] 18 p3129 N85-29377
Prospects for parallel nonlinear optical signal processing using GaAs etalons and ZnS interference filters
18 p3187 N85-29765
Micro-reactions of metal contacts on various types of GaAs surfaces
[AD-A153650] 18 p3193 N85-29806
TEM combined with Al/sub x/Ga/sub 1-x/ as marker layers as a technique for the study of GaAs MBE growth
[DE85-008451] 18 p3194 N85-29809
Summary of recent studies on AlGaAs/GaAs radiation hardened photodiodes
[DE85-009501] 18 p3194 N85-29812
The photochemical oxidation of GaAs
[AD-A153689] 19 p3233 N85-30045
High speed GaAs device and integrated circuit modelling and simulation 19 p3256 N85-30191
Heterojunction Schottky gate MESFET with lower channel ridge barrier
[AD-D011673] 19 p3258 N85-30199
Self-aligned GaAs FET with low 1/F noise
[AD-D011687] 19 p3260 N85-30215
High-efficiency, low-cost, passively-cooled PV concentrator module
[DE85-010013] 19 p3305 N85-30490
Design and operation of epitaxial reactor
[DE85-011089] 19 p3306 N85-30491
Crystal growth of device quality GaAs in space
[NASA-CR-176024] 19 p3375 N85-30935
A method to estimate the self-consistency effects on electronic structure calculations
[INPE-3536-PRE/752] 19 p3375 N85-30936
Leading-edge microelectronics research at Sweden's Chalmers 20 p3438 N85-31337
Design and fabrication of monolithic broadband microwave GaAs low noise FET amplifiers
20 p3443 N85-31370
Thirty GHz low noise GaAs FET amplifiers — satellite-ground communication
[CD.6500686] 20 p3449 N85-31413
Millimetre wave pulse technology — satellite mapping
[ESA-CR(P)-2004] 20 p3478 N85-31611
Recent improvements in materials for thin GaAs and multibandgap solar cells
[DE85-008800] 20 p3484 N85-31651
Gallium arsenide arrays versus silicon arrays for space application
[SNIAS-851-440-104] 20 p3485 N85-31657
Some dynamic electronic properties of semiconductor surfaces and interfaces 20 p3537 N85-32007
NASA space station automation: AI-based technology review
[NASA-CR-176094] 21 p3558 N85-32134
LSI/VLSI ion implanted planar GaAs IC processing
[AD-A155110] 21 p3581 N85-32262
Effect of powerful pulsed low-energy ion streams on GaAs 21 p3682 N85-32877
Microwave semiconductor research: Materials, devices and circuits and gallium arsenide ballistic electron transistors
[AD-A154698] 21 p3709 N85-33024
Microscopic control of semiconductor surface oxidation
[AD-A154799] 21 p3709 N85-33026
Determination of kinetic parameters of molecular beam epitaxy
[AD-A155222] 21 p3710 N85-33030
Raman scattering studies in solids
[AD-A155528] 21 p3710 N85-33032
Sixty GHz IMPATT diode development
[NASA-CR-174969] 22 p3758 N85-33293
In-situ observations of the development of heavy-ion damage in semiconductors
[DE85-010289] 22 p3761 N85-33307
Numerical simulation of nonisothermal transient processes in GaAs diode structures
22 p3767 N85-33350
Diffusion welding of Cassegrainian concentrator cell stack assemblies
[NASA-CR-176104] 22 p3805 N85-33566
Two-dimensional numerical modeling of ion implanted GaAs MESFET devices 24 p4088 N85-35341
Center for Electronics and Electrical Engineering technical progress bulletin covering center programs, July-September with 1985 CEEE events calendar
[PB85-191393] 24 p4091 N85-35363

GALLIUM COMPOUNDS
NT ALUMINUM GALLIUM ARSENIDES
NT GALLIUM ANTIMONIDES
NT GALLIUM ARSENIDES
NT GALLIUM PHOSPHIDES
Ca-Ga, Sr-Ga and Ba-Ga binary systems
[DE85-008454] 16 p2751 N85-2[illegible]
Production of gallium atoms by excimer laser photolysis of trimethyl gallium
[DE85-010742] 19 p3278 N85-30301

GALLIUM PHOSPHIDES
Photoluminescence studies of Ga(As,P) strained-layer superlattices
[DE84-015709] 05 p0731 N85-14701
A picosecond population modulation study of new interband resonances in semiconductors
09 p1396 N85-18787
Effect of hydrostatic pressure on trapping centers in strained-layer superlattice structures
[DE85-001362] 09 p1399 N85-18807
In-situ observations of the development of heavy-ion damage in semiconductors
[DE85-010289] 22 p3761 N85-33307
Time-resolved and infrared spectroscopy of excitons
[DE85-011879] 23 p3912 N85-34236

GALVANIC CELLS
U ELECTROLYTIC CELLS

GALVANIC SKIN RESPONSE
Effects of tasks on responses of human skin mechanoreceptors 11 p1691 N85-20636

GALVANIZING
U ZINC COATINGS

GALVANOMAGNETIC EFFECTS
NT NERNST-ETTINGSHAUSEN EFFECT
Standardization of amplitude characteristics of galvanometric seismographs in the KAPG network
[REPT-552] 03 p0375 N85-12395
Study of resolution of deep MT soundings by means of physical model 13 p2112 N85-23155

GALVANOMAGNETISM
U GALVANOMAGNETIC EFFECTS

GALVANOMETERS
Standardization of amplitude characteristics of galvanometric seismographs in the KAPG network
[REPT-552] 03 p0375 N85-12395
SVKD and SVKM-3 seismographs with a low-sensitivity channel
[REPT-553] 03 p0376 N85-12396
Short-period seismograph SVSN-6
[REPT-554] 03 p0376 N85-12397

GAME THEORY
NT SADDLE POINTS (GAME THEORY)
Model theory for infinitely deep languages
[ISSN-0355-0087] 01 p0101 N85-10674
Effects of alternative chromatic mixed graphics displays in decision support systems
[AD-A145561] 02 p0242 N85-11578
Homomonotone games and monocore solutions, revised
[AD-A146216] 03 p0413 N85-12545
The design and use of subtasks in part training and their relationship to the whole task
05 p0711 N85-14559
A computer-based gaming system for assessing recognition performance (RECOG)
[AD-A149752] 12 p1915 N85-22022
Simple-motion pursuit-evasion differential games in the plane
[CSIR-TWISK-336] 14 p2412 N85-24874
Stochastic pursuit-evasion differential games in the plane
[CSIR-TWISK-343] 14 p2412 N85-24875
A formal analysis of the evolution of cooperation
[AD-A152539] 17 p3018 N85-28602
An extended two-target differential game model for medium-range air combat game analysis
[NASA-CR-175968] 18 p3175 N85-29697
A formulation and analysis of combat games
[NASA-TP-2487] 22 p3835 N85-33745

GAMETOCYTES
Effects of simulated weightlessness on mammalian development. Part 2: Meiotic maturation of mouse oocytes during clinostat rotation 15 p2612 N85-26094

GAMMA FUNCTION
On a random difference equation for matrices and a characterization of the gamma distribution
[AD-A146958] 07 p1029 N85-16529

GAMMA RADIATION
U GAMMA RAYS

GAMMA RAY ABSORPTIOMETRY
Local interstellar medium and gamma-ray astronomy
[OG-3.1-1] 22 p3873 N85-33989

GAMMA RAY ABSORPTION

Electronic structure and lattice dynamics of solid state substances from gamma nuclear resonance absorption and angular correlation measurements
03 p0427 N85-12728

Facilities for studing radiation damage in nonmetals during irradiation
[DE85-000590] 10 p1554 N85-19601

Observations of ultraheavy cosmic ray particles at 10 GV cutoff rigidity
[OG-4.4-2] 22 p3879 N85-34035

GAMMA RAY ASTRONOMY

Choice of orbit for scientific satellites: SIGMA, the submillimeter telescope — Ariane-borne gamma imagery satellite (SIGMA) 05 p0600 N85-13828

Instrumental background in balloon-borne gamma-ray spectrometers and techniques for its reduction
[NASA-TM-86162] 09 p1413 N85-18911

Shuttle flight test of an advanced gamma-ray detection system
[AD-A150316] 13 p1986 N85-22489

Nineteenth International Cosmic Ray Conference. OG sessions, volume 1
[NASA-CP-2376-VOL-1] 22 p3860 N85-33902

Observations of Cygnus X-3 above 10(15) eV from 1979 - 1984
[OG-2.1-6] 22 p3863 N85-33923

Experimental results on gamma-ray sources at E sub 0 = 10(13) - 10(14) eV
[OG-2.2-12] 22 p3865 N85-33937

A coded aperture imaging system optimized for hard X-ray and gamma ray astronomy
[OG-9.2-3] 23 p4024 N85-34942

The Gamma-Ray Imaging Spectrometer (GRIS): A new balloon-borne experiment for gamma-ray line astronomy
[OG-9.2-4] 23 p4025 N85-34943

Operating characteristics of a prototype high energy gamma-ray telescope
[OG-9.2-7] 23 p4025 N85-34946

The gamma-ray telescope Gamma-1
[OG-9.2-10] 23 p4026 N85-34949

The Figaro experiment for the observation of time marked sources in the low energy gamma-ray range
[OG-9.2-11] 23 p4026 N85-34950

GeV gamma-ray astronomy telescopes with high angular resolution
[OG-9.3-4] 23 p4027 N85-34959

The final COS-B database now publicly available
[OG-9.3-6] 23 p4028 N85-34963

The University of Durham Mark 3 very high energy gamma ray telescope
[OG-9.4-2] 23 p4028 N85-34969

Application of imaging to the atmospheric Cherenkov technique
[OG-9.5-4] 23 p4030 N85-34981

A new statistic for the analysis of circular data in gamma-ray astronomy
[OG-9.5-13] 23 p4031 N85-34989

GAMMA RAY BEAMS

Observations of Cygnus X-3 above 10(15) eV from 1979 - 1984
[OG-2.1-6] 22 p3863 N85-33923

1000 GeV gamma rays from Cygnus X-3: An update
[OG-2.1-8] 22 p3863 N85-33925

Evidence for long-term variability in the ultra high energy photon flux from Cygnus X-3
[OG-2.1-10] 22 p3863 N85-33926

A search for gamma-ray point sources with the Carpet shower array
[OG-2.1-12] 22 p3864 N85-33928

GAMMA RAY BURSTS

Pair production at moderate optical depths — galactic nuclei X ray spectra 08 p1241 N85-17830

Gamma-ray burster recurrence timescales
[NASA-TM-86157] 09 p1417 N85-18942

Old and new neutron stars
[DE85-002716] 11 p1762 N85-21065

Extragalactic origin or gamma-ray bursts, revision 1
[DE85-005622] 15 p2686 N85-26588

HEAO-1 observations of gamma ray bursts
[OG-1.1-1] 22 p3860 N85-33903

Soft-spectrum gamma-ray bursts
[OG-1.1-2] 22 p3860 N85-33904

Annihilation radiation in cosmic gamma-ray bursts
[OG-1.1-3] 22 p3861 N85-33905

On the emission region of gamma ray bursts
[OG-1.1-4] 22 p3861 N85-33906

Unthermalized plasma in bursts sources
[OG-1.1-5] 22 p3861 N85-33907

Optical monitoring of gamma-ray source fields
[OG-1.1-7] 22 p3861 N85-33908

Search for optical bursts from the gamma ray burst source GBS 0526-66
[OG-1.1-8] 22 p3861 N85-33909

Search for infrared counterparts of gamma-ray bursters
[OG-1.1-9] 22 p3861 N85-33910

A second catalog of gamma ray bursts: 1978 - 1980 localizations from the interplanetary network
[OG-1.2-1] 22 p3861 N85-33912

Gamma ray burst size-frequency distributions: Spectral selection effects
[OG-1.2-3] 22 p3862 N85-33913

The effect of anisotropic emission on the log N-log S curve of gamma-ray bursts
[OG-1.2-4] 22 p3862 N85-33914

Limits to the burster repetition rate as deduced from the 2nd catalog of the interplanetary network
[OG-1.2-5] 22 p3862 N85-33915

An internally consistent gamma ray burst time history phenomenology
[OG-1.2-6] 22 p3862 N85-33916

Gamma-ray burst variability above 4 MeV
[OG-1.2-7] 22 p3862 N85-33917

Relationships between log N-log S and celestial distribution of gamma-ray bursts
[OG-1.2-10] 22 p3862 N85-33918

Observations of Cygnus X-3 above 10(15) eV from 1979 - 1984
[OG-2.1-6] 22 p3863 N85-33923

On gamma and neutrino radiation from Cyg X-3
[OG-2.1-7] 22 p3863 N85-33924

Variability in the high energy gamma ray emission from Cyg X-3 over a two-year period (1983 - 1984) at E 4 x 10(11) eV
[OG-2.1-11] 22 p3864 N85-33927

Cyg X-3: Not seen in high-energy gamma rays by COS-B
[OG-2.2-2] 22 p3864 N85-33929

Relevance of the observation of UHE gammas to hard X-ray astronomy
[OG-2.2-6] 22 p3865 N85-33932

500 TeV gamma rays from Hercules X-1
[OG-2.2-7] 22 p3865 N85-33933

A model for the UHE gamma-rays from Hercules X-1
[OG-2.2-8] 22 p3865 N85-33934

Hercules X-1: Pulsed gamma-rays detected above 150 GeV
[OG-2.2-9] 22 p3865 N85-33935

Microburst of TeV gamma rays from the Crab pulsar
[OG-2.3-4] 22 p3866 N85-33941

Secondary periodicities of microbursts of TeV gamma rays from the Crab pulsar
[OG-2.3-5] 22 p3866 N85-33942

Search for bursts in air shower data
[OG-5.3-10] 22 p3885 N85-34076

The 1983 international intercomparison of nuclear accident dosimetry systems at Oak Ridge National Laboratory
[DE85-011303] 23 p3934 N85-34382

Helios 1 energetic particle observations of the solar gamma ray flare events of 7, 21 June 1980 and 3 June 1982
[SH-1.3-8] 23 p3993 N85-34755

Injection of energetic particles following the gamma-ray flares on June 7, 1980, as observed on Helios 1
[SH-1.3-9] 23 p3993 N85-34756

Ultrarelativistic electrons and solar flare gamma-radiation
[SH-1.3-11] 23 p3993 N85-34757

North-south asymmetry in activity on the Sun and cosmic ray density gradients
[SH-4.2-7] 23 p4007 N85-34845

Burst and Transient Source Experiment (BATSE) for the Gamma Ray Observatory (GRO)
[OG-9.2-14] 23 p4026 N85-34953

Gamma-ray burst spectroscopy capabilities of the BATSE/GRO experiment
[OG-9.2-15] 23 p4026 N85-34954

Capabilities of the GRO/BATSE for monitoring of discrete sources
[OG-9.2-16] 23 p4026 N85-34955

Astrophysical applications of high angular resolution array-telescopes
[OG-9.5-7] 23 p4031 N85-34984

Angular resolution of an EAS array for gamma ray astronomy energies 5 x 10 (13) eV
[OG-9.5-8] 23 p4031 N85-34985

Note on the detection of high energy primary cosmic gamma rays by air shower observation
[OG-9.5-9] 23 p4031 N85-34986

A new approach to evaluate gamma-ray measurements
[OG-9.5-11] 23 p4031 N85-34988

A new statistic for the analysis of circular data in gamma-ray astronomy
[OG-9.5-13] 23 p4031 N85-34989

Multidimensional analysis of data obtained in experiments with X-ray emulsion chambers and extensive air showers
[HE-3.6-2] 24 p4184 N85-35951

A new method of differential structural analysis of gamma-family basic parameters
[HE-3.6-3] 24 p4184 N85-35952

Relation between gamma-ray family and EAS core: Monte-Carlo simulation of EAS core
[HE-3.6-7] 24 p4185 N85-35955

Comparison of big event with calculations of the air shower development
[HE-3.6-8] 24 p4185 N85-35956

Result of Monte-Carlo simulation of electron-photon cascades in lead and layers of lead-scintillator
[HE-3.6-11] 24 p4185 N85-35958

A study of gamma-families generated in nucleon-nucleus (NA) and pion-nucleus (pi A) interactions
[HE-3.7-2] 24 p4186 N85-35961

New analysis of nuclear interaction observed by Mt. Kanbara emulsion chamber experiment
[HE-3.7-4] 24 p4186 N85-35963

Intensities of high-energy cosmic rays at Mount Kanbala
[HE-3.7-5] 24 p4186 N85-35964

Ultra high energy events in ECHOS series and primary energy spectrum
[HE-3.7-9] 24 p4186 N85-35966

Peculiarities of gamma-quanta distribution at 20 TeV energy
[HE-3.7-10] 24 p4186 N85-35967

Results of low energy background measurements with the Liquid Scintillation Detector (LSD) of the Mont Blanc Laboratory
[HE-5.3-5] 24 p4205 N85-36099

The research program of the Liquid Scintillation Detector (LSD) in the Mont Blanc Laboratory
[HE-5.3-6] 24 p4205 N85-36100

Muon and neutrino fluxes
[HE-6.2-18] 24 p4213 N85-36154

Search for acoustic signals from high energy cascades
[HE-7.1-1] 24 p4213 N85-36155

Exploring results of the possibility on detecting cosmic ray particles by acoustic way
[HE-7.1-3] 24 p4213 N85-36157

GAMMA RAY OBSERVATORY

The Figaro experiment for the observation of time marked sources in the low energy gamma-ray range
[OG-9.2-11] 23 p4026 N85-34950

High energy gamma ray balloon instrument
[OG-9.2-12] 23 p4026 N85-34951

Burst and Transient Source Experiment (BATSE) for the Gamma Ray Observatory (GRO)
[OG-9.2-14] 23 p4026 N85-34953

Gamma-ray burst spectroscopy capabilities of the BATSE/GRO experiment
[OG-9.2-15] 23 p4026 N85-34954

An observatory to study 10 (10) to 10 (17) by EV gamma rays
[OG-9.4-6] 23 p4029 N85-34973

GAMMA RAY SPECTRA

Advances in room-temperature solid-state gamma-ray spectrometry
[DE84-015944] 04 p0469 N85-12967

Fast neutron capture with a white neutron source
[DE84-016799] 04 p0562 N85-13580

Power law X- and gamma-ray emission from relativistic thermal plasmas 08 p1241 N85-17829

A 200-MeV pi(+) induced nucleon removal from 24Mg
17 p3042 N85-28821

Paired ion chamber constants for fission gamma-neutron fields
[AD-A155069] 21 p3702 N85-32999

Kalman filter time series analysis of gamma-ray data from NaI(T1) detectors for the ND6620 computer
[AD-A154995] 21 p3705 N85-33014

Measurement of radionuclides in waste packages
[DE85-011674] 22 p3838 N85-33766

Gamma-ray line intensities for depleted uranium
[DE85-012674] 22 p3843 N85-33804

Soft-spectrum gamma-ray bursts
[OG-1.1-2] 22 p3860 N85-33904

The effect of anisotropic emission on the log N-log S curve of gamma-ray bursts
[OG-1.2-4] 22 p3862 N85-33914

Search for gamma ray lines from SS433
[OG-2.4-11] 22 p3868 N85-33955

Low-energy gamma rays from Cygnus X-1
[OG-2.4-13] 22 p3868 N85-33957

Spectral evolution of gamma-rays from adiabatically expanding sources in dense clouds
[OG-2.5-2] 22 p3869 N85-33959

Capture in the 1.15-keV iron resonance
[DE85-011913] 23 p3870 N85-34612

Abundances from solar-flare gamma-ray line spectroscopy
[SH-2.1-13] 23 p3999 N85-34794
Solar flare gamma-ray line spectroscopy
[SH-2.1-14] 23 p3999 N85-34795
The Gamma-Ray Imaging Spectrometer (GRIS): A new balloon-borne experiment for gamma-ray line astronomy
[OG-9.2-4] 23 p4025 N85-34943
Modeling a high energy gamma-ray telescope
[OG-9.2-5] 23 p4025 N85-34944
Secondary gamma-ray production in a coded aperture mask
[OG-9.2-6] 23 p4025 N85-34945
An experimental assessment of the imaging quality of the low energy gamma-ray telescope ZEBRA
[OG-9.2-8] 23 p4025 N85-34947
Advanced techniques for high resolution spectroscopic observations of cosmic gamma-ray sources
[OG-9.2-9] 23 p4025 N85-34948
The gamma-ray telescope Gamma-1
[OG-9.2-10] 23 p4026 N85-34949
The Figaro experiment for the observation of time marked sources in the low energy gamma-ray range
[OG-9.2-11] 23 p4026 N85-34950
Measured performance of the new University of California gamma ray telescope
[OG-9.2-13] 23 p4026 N85-34952
Burst and Transient Source Experiment (BATSE) for the Gamma Ray Observatory (GRO)
[OG-9.2-14] 23 p4026 N85-34953
Gamma-ray burst spectroscopy capabilities of the BATSE/GRO experiment
[OG-9.2-15] 23 p4026 N85-34954
An improved time of flight gamma-ray telescope to monitor diffuse gamma-ray in the energy range 5 MeV - 50 MeV
[OG-9.3-2] 23 p4027 N85-34957
Neutron-induced 2.2 MeV background in gamma ray telescopes
[OG-9.3-6] 23 p4027 N85-34961
Measurement control for plutonium isotopic measurements using gamma-ray spectrometry
[DE85-013394] 24 p4097 N85-35397
Gamma-ray production cross sections for alpha-particle induced reactions on F-19 and Na-23
[DE85-012603] 24 p4150 N85-35732

GAMMA RAY SPECTROMETERS
Description of the SSB/A (Special Sensor B/Aerospace X-ray spectrometer
[AD-A150040] 12 p1790 N85-21236
Method and apparatus for mapping the distribution of chemical elements in an extended medium
[NASA-CASE-GSC-12808-1] 12 p1796 N85-21279
Proceedings of the Fifth International Conference on Nuclear Methods in Environmental and Energy Research
[DE84-017348] 19 p3310 N85-30521
A miroprocessor based multiscaling data acquisition system for Mossbauer spectroscopy
[USIP-85-01] 20 p3518 N85-31875
Neutral pion production in solar flares
[SH-1.4-7] 23 p3995 N85-34767
A coded aperture imaging system optimized for hard X-ray and gamma ray astronomy
[OG-9.2-3] 23 p4024 N85-34942
The Gamma-Ray Imaging Spectrometer (GRIS): A new balloon-borne experiment for gamma-ray line astronomy
[OG-9.2-4] 23 p4025 N85-34943
Advanced techniques for high resolution spectroscopic observations of cosmic gamma-ray sources
[OG-9.2-9] 23 p4025 N85-34948
Gamma-ray burst spectroscopy capabilities of the BATSE/GRO experiment
[OG-9.2-15] 23 p4026 N85-34954
Monte Carlo calibration of the SMM gamma ray spectrometer for high energy gamma rays and neutrons
[SH-9.1-6] 23 p4051 N85-35121
Noiseless coding for the Gamma Ray spectrometer
[NASA-CR-176201] 24 p4069 N85-35219
Measurement control for plutonium isotopic measurements using gamma-ray spectrometry
[DE85-013394] 24 p4097 N85-35397

GAMMA RAY TELESCOPES
Measurement of nuclear lines with a dual Ge(Li) telescope aboard a stratospheric balloon
[INPE-3360-TDL/185] 11 p1762 N85-21083
Determination of angular resolution of coded aperture gamma-ray telescope 13 p1981 N85-22432
Search for positron annihilation line and continuum radiation from the Galactic Center
[OG-2.5-5] 22 p3869 N85-33962
North-south asymmetry in activity on the Sun and cosmic ray density gradients
[SH-4.2-7] 23 p4007 N85-34845
A balloon-borne imaging gamma-ray telescope
[OG-9.2-2] 23 p4024 N85-34941
Modeling a high energy gamma-ray telescope
[OG-9.2-5] 23 p4025 N85-34944
Operating characteristics of a prototype high energy gamma-ray telescope
[OG-9.2-7] 23 p4025 N85-34946
An experimental assessment of the imaging quality of the low energy gamma-ray telescope ZEBRA
[OG-9.2-8] 23 p4025 N85-34947
The gamma-ray telescope Gamma-1
[OG-9.2-10] 23 p4026 N85-34949
High energy gamma ray balloon instrument
[OG-9.2-12] 23 p4026 N85-34951
Measured performance of the new University of California gamma ray telescope
[OG-9.2-13] 23 p4026 N85-34952
An improved time of flight gamma-ray telescope to monitor diffuse gamma-ray in the energy range 5 MeV - 50 MeV
[OG-9.3-2] 23 p4027 N85-34957
Results of a study to build a gamma-ray telescope in an external tank
[OG-9.3-3] 23 p4027 N85-34958
GeV gamma-ray astronomy telescopes with high angular resolution
[OG-9.3-4] 23 p4027 N85-34959
An approach of reducing the background induced by neutrons
[OG-9.3-5] 23 p4027 N85-34960
A Cerenkov imaging telescope for high energy gamma rays
[OG-9.3-13] 23 p4028 N85-34968
The University of Durham Mark 3 very high energy gamma ray telescope
[OG-9.4-2] 23 p4028 N85-34969
A new ultra high energy gamma ray telescope at Ohya mine
[OG-9.4-3] 23 p4029 N85-34970
An observatory to study 10 (10) to 10 (17) by EV gamma rays
[OG-9.4-6] 23 p4029 N85-34973
A method to improve observations of gamma-ray sources near 10 (15) eV
[OG-9.5-5] 23 p4030 N85-34982
Angular resolution of an EAS array for gamma ray astronomy energies 5 x 10 (13) eV
[OG-9.5-8] 23 p4031 N85-34985
The angular resolution of air shower gamma ray telescopes
[OG-9.5-14] 23 p4031 N85-34990
Construction of a cosmic ray air shower telescope
[HE-4.5-14] 24 p4196 N85-36036
Thickness of the particle swarm in cosmic ray air showers
[HE-4.7-14] 24 p4200 N85-36064
Charge 4/3 leptons in cosmic rays
[HE-6.2-14] 24 p4212 N85-36150

GAMMA RAYS
NT GAMMA RAY BURSTS
Observation of gamma radiation from crab nebula in 5-100 MeV range 02 p0162 N85-11096
Investigation of internal fields and motions, radiation damages and recovery processes using beta and gamma active probe nuclei 03 p0427 N85-12726
High-bandwidth multichannel fiber optic system for measuring gamma rays
[DE84-014526] 04 p0564 N85-13596
Gamma-ray to Cerenkov-light conversion efficiency for pure-silica-core optical fibers
[DE84-015041] 05 p0729 N85-14685
100 MHz fiber optic single transient gamma ray detection system
[DE84-016818] 05 p0729 N85-14686
A microchannel plate streak camera
[DE84-016536] 06 p0811 N85-15153
The galactic gamma-ray distribution: Implications for galactic structure and the radial cosmic ray gradient
[NASA-TM-86173] 07 p1061 N85-16729
The HEAO-1 diffuse component spectrum from 15 to above 500 keV — X and gamma rays
08 p1240 N85-17820
P-I-N CdTe gamma-ray detectors by Liquid Phase Epitaxy (LPE)
[DE84-012276] 09 p1323 N85-18315
Comparison of ionizing radiation and hot electron effects in MOS structures
[DE84-016766] 09 p1400 N85-18809
Directivity of Bremsstrahlung radiation from relativistic beams and the Gamma-Rays from solar flares
[NASA-CR-174433] 10 p1572 N85-19913
Physical aspects of the prediction of solar flares
[NASA-CR-175487] 10 p1572 N85-19915
Laser-Electron-Gamma-Source (LEGS)
[DE85-003204] 11 p1638 N85-20322
Behavior degradation due to 1100-RAD pulsed radiation exposure (5.8:1 neutron/gamma ratio)
[AD-A149284] 11 p1689 N85-20621
MCNP code
[DE85-002565] 11 p1702 N85-20705
WESF (173)Cs gamma ray sources
[DE85-000676] 11 p1727 [illegible]
A remote source system for measuring relative positron annihilation line widths in individual slab cylindrical samples
[AERE-R-10549] 12 p1938 N85-22173
Neutron and gamma-ray signatures for particle acceleration in solar flares 12 p1954 N85-22276
Research in particles and fields
[NASA-CR-175472] 12 p1963 N85-22337
Basic principles of industrial radiography
14 p2316 N85-24310
Radiological safety aspects of industrial radiography
14 p2316 N85-24312
The gamma thermometer: A new type of fixed internal instrumentation developed by EDF
[BLL-CE-TRANS-8080-(9022.09)]
15 p2560 N85-25791
Interstellar Al-26 and excess Mg-26
15 p2680 N85-26551
Results from radiation monitoring equipment experiment on STS-11
[AD-A152531] 17 p2908 N85-27932
Measurement and interpretation of electron angle at MABE beam stop
[DE85-008583] 17 p3032 N85-28755
Incorporation of Monte Carlo electron interface studies into photon general cavity theory
[DE85-007674] 17 p3034 N85-28772
High energy gamma rays from complex particle collisions
[DE85-007871] 17 p3036 N85-28783
Results from radiation monitoring equipment experiment on STS-8
[AD-A153241] 17 p3055 N85-28911
Radiation-induced degradation of trichloroethylene and tetrachloroethylene in drinking water
[OEFZS-4298] 18 p3134 N85-29409
Comparison of calculations and measurements of the off-axis radiation dose (SI) in liquid nitrogen as a function of radiation length
[AD-A153676] 18 p3178 N85-29704
Three-dimensional and tomographic imaging device for X-ray and gamma-ray emitting objects
[NASA-CASE-GSC-12851-1] 19 p3271 N85-30281
Chromosome aberrations in Crepis capillaris exposed to gamma radiation and clinostat
19 p3325 N85-30600
Study of a novel shielding principle for protection against intense gamma-ray beams
[AD-A154374] 19 p3357 N85-30808
Correlation analysis of 1 to 30 MeV celestial gamma rays 20 p3549 N85-32083
Radio counterparts of galactic gamma-ray sources
20 p3549 N85-32085
Study of proton and neutron activation of metal samples in low Earth orbit
[NASA-CR-171596] 21 p3558 N85-32120
Results from radiation monitoring equipment experiments on STS-41C, 41D, 41G and 51A
[AD-A154676] 21 p3560 N85-32142
A practical guide to ionization chamber dosimetry at the AFRRI reactor
[AD-A155185] 21 p3703 N85-33003
Empirical correlation of residual gamma radiation resulting from operation of the Health Physics Research Reactor
[DE85-012075] 21 p3704 N85-33008
Kalman filter time series analysis of gamma-ray data from NaI(T1) detectors for the ND6620 computer
[AD-A154995] 21 p3705 N85-33014
A balloon-borne imaging gamma-ray telescope
[OG-9.2-2] 21 p3714 N85-33049
Balloon-borne video cassette recorders for digital data storage
[OG-9.3-11] 21 p3715 N85-33050
Research in particles and fields
[NASA-CR-176069] 21 p3724 N85-33103
Magnetically insulated diode for generating pulsed neutron and gamma ray emissions
[DE85-011658] 22 p3760 N85-33306
Apparatus and method for identification of matrix materials in which transuranic elements are embedded using thermal neutron capture gamma-ray emission
[DE85-011659] 22 p3786 N85-33454
Control technology for radioactive emissions to the atmosphere at US Department of Energy facilities: The Los Alamos Meson Physics Facility
[DE85-011402] 22 p3811 N85-33609
The degradation of pollutants in water and waste water by means of electron or gamma irradiation
[OEFZS-4317] 22 p3812 N85-33615

Neutron detector counting capabilities for (10) B-lined and (235) U fission chambers in high gamma-ray fluxes
[DE85-011893] 22 p3840 N85-33780

Use of gamma radiation as a form of preservation of sweet potatoes
[DE85-011898] 22 p3841 N85-33787

Gamma-ray line intensities for depleted uranium
[DE85-012674] 22 p3843 N85-33804

Nineteenth International Cosmic Ray Conference. OG sessions, volume 1
[NASA-CP-2376-VOL-1] 22 p3860 N85-33902

Search for gamma rays of energy 10(15) eV from Cygnus X-3
[OG-2.1-1] 22 p3862 N85-33919

Gamma rays of energy or = 10(15) eV from Cyg X-3
[OG-2.1-5] 22 p3863 N85-33922

Experimental results on gamma-ray sources at E sub 0 = 10(13) - 10(14) eV
[OG-2.2-12] 22 p3865 N85-33937

Observations of the Crab Nebula at energies 4.10(11)
[OG-2.3-1] 22 p3865 N85-33938

Search for excess showers from Crab Nebula
[OG-2.3-2] 22 p3866 N85-33939

Very high energy gamma rays from the Crab Nebula
[OG-2.3-3] 22 p3866 N85-33940

Detection of gamma-ray lines from the direction of the Crab Nebula
22 p3866 N85-33943

Gamma rays of 0.3 to 30 MeV from PSR 0531+21
[OG-2.3-6] 22 p3866 N85-33945

The 1000 GeV gamma ray emission from radio pulsars
22 p3867 N85-33946

Pulsed emission of TeV gamma rays from Vela pulsar
22 p3867 N85-33947

The 1000 GeV gamma rays from ms pulsars
[OG-2.3-12] 22 p3867 N85-33948

Periodic gamma-ray emissions from Geminga at or = 10(12) eV
[OG-2.4-2] 22 p3867 N85-33949

Search for periodicities near 59 s in the COS-B gamma-ray data of 2CG195+04 (Geminga)
[OG-2.4-3] 22 p3867 N85-33950

Search for gamma-rays above 400 GeV from Geminga
[OG-2.4-4] 22 p3867 N85-33951

On the 1983 observations of the gamma-ray source 2CG195+4
[OG-2.4-5] 22 p3868 N85-33952

Observations on TeV gamma rays from Geminga and PSR 0950+08
[OG-2.4-6] 22 p3868 N85-33953

HEAO 3 upper limits to the expected 1634 KeV line from SS 433
[OG-2.4-9] 22 p3868 N85-33954

Search for gamma ray lines from SS433
[OG-2.4-11] 22 p3868 N85-33955

High-resolution spectrum of Cygnus X-1
[OG-2.4-12] 22 p3868 N85-33956

Excess gamma-rays in the direction of the rho Ophiuchi cloud: An exotic object?
[OG-2.5-1] 22 p3868 N85-33958

Supernova explosion in dense clouds in the galaxy and the COS-B gamma-ray sources
[OG-2.5-3] 22 p3869 N85-33960

Spectra and positions of galactic gamma-ray sources
[OG-2.5-7] 22 p3869 N85-33963

A search in the COS-B data base for correlated time variability in regions containing objects of interest
[OG-2.5-9] 22 p3869 N85-33964

Radio observations of four anticenter 2CG gamma-ray sources
[OG-2.5-10] 22 p3869 N85-33965

Further studies of X-ray structure of the Perseus cluster
[OG-2.5-12] 22 p3870 N85-33967

All sky Northern Hemisphere 10(15) EV gamma-ray survey
[OG-2.6-3] 22 p3870 N85-33968

A search for sources of ultra high energy gamma rays at air shower energies with Ooty EAS array
[OG-2.6-8] 22 p3870 N85-33970

Observations of potential ultra high energy gamma-ray sources above 10(15) eV
[OG-2.6-9] 22 p3870 N85-33971

Observation of gamma-rays from LMC X-4 above 10(16) eV
[OG-2.6-10] 22 p3870 N85-33972

Primary gamma-rays with E gamma or = to 10(15) eV: Evidence for ultrahigh energy particle acceleration in galactic sources
[OG-2.6-13] 22 p3871 N85-33974

Search for TeV gamma rays from extragalactic sources and the Galactic Center
[OG-2.7-1] 22 p3871 N85-33976

Search for gamma-rays from M31 and other extragalactic objects
[OG-2.7-3] 22 p3871 N85-33977

Some evidence for high energy gamma-ray sources at large galactic latitudes
[OG-2.7-5] 22 p3871 N85-33978

CEN A observation at MeV-energies
[OG-2.7-7] 22 p3871 N85-33980

Gamma-radiation with E gamma 5 MeV detected from Seyfert galaxy 3C120 and region with 1' = 190 deg and b' = 20 deg
[OG-2.8-6] 22 p3871 N85-33981

The universal spectrum of AGNs and QSOs
[OG-2.7-9] 22 p3872 N85-33982

Cosmic gamma rays from quasars
[OG-2.7-10] 22 p3872 N85-33983

Some evidence for large gravitational redshift in Seyfert galaxy NGC 4151
[OG-2.7-11] 22 p3872 N85-33984

Limits on the Doppler factor in relativistic jets by means of gamma-ray observations
[OG-2.7-12] 22 p3872 N85-33985

Energy spectrum of extragalactic gamma-ray sources
[OG-2.7-13] 22 p3872 N85-33986

Ultrahigh energy gamma rays: Carriers of cosmological information
[OG-2.7-14] 22 p3872 N85-33987

On some problems of gamma-astronomy
[OG-2.7-15] 22 p3873 N85-33988

Local interstellar medium and gamma-ray astronomy
[OG-3.1-1] 22 p3873 N85-33989

Inverse-Compton gamma rays in the galaxy
[OG-3.1-2] 22 p3873 N85-33990

Multicomponent analysis of total COS-B gamma-ray data at intermediate latitudes
[OG-3.1-3] 22 p3873 N85-33991

The galactic gamma-ray distribution and the radial cosmic ray gradient
[OG-3.1-4] 22 p3873 N85-33992

Radial distribution of cosmic ray intensity in the galaxy from gamma-ray data
[OG-3.1-5] 22 p3873 N85-33993

Constraints on the galactic distribution of cosmic rays from the COS-B gamma-ray data
[OG-3.1-6] 22 p3873 N85-33994

Local electron spectrum above 100 MeV derived from gamma-ray emissivity spectra
[OG-3.1-7] 22 p3874 N85-33995

Relevance of cosmic gamma rays to the mass of gas in the galaxy
[OG-3.1-8] 22 p3874 N85-33996

COS-B gamma-ray sources and interstellar gas
[OG-3.1-9] 22 p3874 N85-33997

Excess gamma rays from the Loop I supernova remnant
[OG-3.1-10] 22 p3874 N85-33998

Spectrum of the gamma-ray diffuse component observed from HEAO-1
[OG-3.1-12] 22 p3874 N85-34000

SMM detection of interstellar Al-26 gamma radiation
[OG-3.2-1] 22 p3874 N85-34001

Galactic distribution of interstellar Al-26
[OG-3.2-3] 22 p3874 N85-34002

Gamma-ray line emission from Al-26 produced by Wolf-Rayet stars
[OG-3.2-5] 22 p3875 N85-34003

Gamma ray line production from cosmic ray spallation reactions
22 p3875 N85-34005

On the possibility of the determining the average mass composition near 10 to the 14th power eV through the solar magnetic field
[OG-5.1-9] 22 p3882 N85-34051

Arrival directions of large air showers, low-mu showers and old-age low-mu air showers observed at St. Chacaltaya
[OG-5.3-2] 22 p3884 N85-34069

Arrival directions of cosmic rays of E .4 EeV
[OG-5.3-4] 22 p3884 N85-34071

Air shower arrival directions measured at Buckland Park
[OG-5.3-11] 22 p3885 N85-34077

UHE particle production in close binary systems
[OG-5.4-7] 22 p3886 N85-34084

Anisotropy of cosmic rays above 10(14) eV
[OG-5.4-11] 22 p3887 N85-34088

Improved method for the stabilization of NaI-photomultiplier gamma detectors against thermal and other drift
[DE85-011830] 23 p3970 N85-34613

Study of non-thermal photon production under different scenarios in solar flares. 1: Scenarios and formulations
[SH-1.2-2] 23 p3991 N85-34738

Study of non-thermal photon production under different scenarios in solar flares. 2: The Compton inverse and Bremsstrahlung models and fittings
[SH-1.2-3] 23 p3991 N85-34739

The starting conditions for an optically small solar gamma ray flare
[SH-1.3-2] 23 p3993 N85-34751

Observations of solar flare gamma-rays and protons
[SH-1.3-6] 23 p3993 N85-34753

Time extended production of neutrons during a solar flare
[SH-1.4-1] 23 p3994 N85-34762

Further observations of protons resulting from the decay of neutrons ejected by solar flares
[SH-1.4-2] 23 p3994 N85-34763

Suggestions for improving the efficiency of ground-based neutron monitors for detecting solar neutrons
[SH-1.4-3] 23 p3995 N85-34764

Search for solar neutrons using NM-64 equipment
[SH-1.4-5] 23 p3995 N85-34765

Neutral pion production in solar flares
[SH-1.4-7] 23 p3995 N85-34767

High energy neutron and gamma-radiation generated during the solar flares
[SH-1.4-8] 23 p3995 N85-34768

Possible detection of flare-generated positrons by Helios 1 on 3 Jun 1982
[SH-1.4-10] 23 p3996 N85-34770

Energetic particle observations of the solar-gamma ray/neutron flare events of 3 Jun 1982 and 21 June 1980 isotopic and chemical composition
[SH-2.1-3] 23 p3998 N85-34784

Geometry of the diffusive propagation region in the August 14, 1982 solar electron event
[SH-3.1-5] 23 p4001 N85-34809

A very important process of nucleosynthesis in stars
[OG-7.1-11] 23 p4014 N85-34872

Bursting star formation and the overabundance of Wolf-Rayet stars
[OG-8.2-8] 23 p4019 N85-34907

Giant molecular clouds as regions of particle acceleration
23 p4020 N85-34913

A balloon-borne imaging gamma-ray telescope
[OG-9.2-2] 23 p4024 N85-34941

Secondary gamma-ray production in a coded aperture mask
[OG-9.2-6] 23 p4025 N85-34945

The final COS-B database now publicly available
[OG-9.3-8] 23 p4026 N85-34963

The Buckland Park air shower array
[OG-9.4-4] 23 p4029 N85-34971

An EAS experiment at mountain altitude for the detection of gamma-ray sources
[OG-9.4-5] 23 p4029 N85-34972

A new array for the study of ultra high energy gamma-ray sources
[OG-9.4-7] 23 p4029 N85-34974

Cerenkov light images of EAS produced by primary gamma
[OG-9.5-3] 23 p4030 N85-34979

Shower disc sampling and the angular resolution of gamma-ray shower detectors
[OG-9.5-2] 23 p4030 N85-34980

Photometric and spectroscopic gamma-ray observations of solar transient phenomena using long duration balloons
[SH-9.1-5] 23 p4051 N85-35120

Total integrated dose testing of solid-state scientific CD4011, CD4013, and CD4060 devices by irradiation with CO-60 gamma rays
[NASA-CR-176196] 24 p4161 N85-35795

Experiment Pamir-3. Coplanar emission of high energy gamma-quanta at interaction of hadrons with nuclei of air atoms at energies above 10 to the 7th power GeV
[HE-1.4-12] 24 p4177 N85-35899

High energy gamma-rays and hadrons at Mount Fuji
[HE-3.1-3] 24 p4177 N85-35903

The multiplicity and the spectra of secondaries correlated with the leading particle energy
[HE-3.2-11] 24 p4179 N85-35919

Study of hadron bundles observed in Chacaltaya two-story emulsion chamber
[HE-3.3-4] 24 p4180 N85-35922

Lateral distribution of high energy hadrons and gamma ray in air shower cores observed with emulsion chambers
[HE-3.3-8] 24 p4180 N85-35926

Size distributions of air showers accompanied with high energy gamma ray bundles observed at Mt. Chacaltaya
[HE-3.3-9] 24 p4181 N85-35927

EAS accompanied by gamma-families at Mt. Norikura and comparison with Monte Carlo simulation
[HE-3.3-10] 24 p4181 N85-35928

Comparison of absolute intensity between EAS with gamma-families and general EAS at Mount Norikura
[HE-3.3-11] 24 p4181 N85-35929

A cosmic ray super high multicore family event. 1: Experiment and general features
[HE-3.4-1] 24 p4181 N85-35930

A halo event created at 200 m above the Chacaltaya emulsion chamber
[HE-3.4-5] 24 p4182 N85-35933

A binocular-type atmospheric interaction generating sequential exotic features
[HE-3.4-6] 24 p4182 N85-35934
Gamma-hadron families and scaling violation
[HE-3.4-7] 24 p4182 N85-35935
Super-family P2 C-96-125 observed by Japan-URSS Joint Emulsion Chamber Experiment
[HE-3.4-8] 24 p4182 N85-35936
On the halo events observed by Mount Fuji and Mount Kanbala Emulsion Chamber Experiments
[HE-3.4-9] 24 p4182 N85-35937
Experiment Pamir-2. Flanit: A giant super-family with halo (Epsilon sub 0 at approximately 10(17) eV)
[HE-3.4-10] 24 p4182 N85-35938
Experiment Pamir-4: Analysis of superfamily with halo of electromagnetic nature detected in deep XEC
[HE-3.4-11] 24 p4183 N85-35939
Particle interactions at energies over 1000 TeV inferred from gamma-families observed at Mount Fuji
[HE-3.5-1] 24 p4183 N85-35940
A search for mini-clusters in Japan-USSR Joint Experiment at Pamir
[HE-3.5-2] 24 p4183 N85-35941
Mini-clusters
[HE-3.5-3] 24 p4183 N85-35942
Giant mini-clusters as possible origin of halo phenomena observed in super-families
[HE-3.5-4] 24 p4183 N85-35943
The electromagnetic component of albedo from superhigh energy cascades in dense media
[HE-3.5-11] 24 p4184 N85-35948
Integral functions of electron lateral distribution and their fluctuations in electron-photon cascades
[HE-3.5-12] 24 p4184 N85-35949
A comparative analysis of gamma and hadron families at the superhigh energies recorded in experiment Pamir
[HE-3.7-1] 24 p4185 N85-35960
Nineteenth International Cosmic Ray Conference. HE Sessions, volume 7
[NASA-CP-2376-VOL-7] 24 p4186 N85-35968
New aspects in nucleon-nucleus collisions and EAS properties around 10(6) GeV 24 p4187 N85-35974
Application of photodiodes to the detection of electromagnetic bursts 24 p4189 N85-35988
Lateral distribution on charged particles in EAS
[HE-4.3-15] 24 p4192 N85-36009
Longitudinal trial functions and the cosmic ray energy scale 24 p4193 N85-36014
Missing energies at pair creation
[HE-4.4-8] 24 p4193 N85-36016
The identification of gamma ray induced EAS
[HE-4.5-1] 24 p4195 N85-36026
Muons in gamma showers
[HE-4.5-3] 24 p4195 N85-36027
Muon spectrum in air showers initiated by gamma rays
[HE-4.5-4] 24 p4195 N85-36028
Development of electromagnetic cascades in the atmosphere including the Landau-Pomeranchuk-Migdal effect
[HE-4.5-5] 24 p4195 N85-36029
Electromagnetic and muonic structure of showers initiated by gamma-rays and by hadrons
[HE-4.5-6] 24 p4195 N85-36030
The muon content of gamma-ray showers
[HE-4.5-7] 24 p4195 N85-36031
The hump in the Cerenkov lateral distribution of gamma ray showers
[HE-4.5-9] 24 p4195 N85-36032
Simulation of gamma-initiated showers
[HE-4.5-10] 24 p4195 N85-36033
Phenomenological characteristic of the electron component in gamma-quanta initiated showers
[HE-4.5-11] 24 p4196 N85-36034
Construction of a cosmic ray air shower telescope
[HE-4.5-14] 24 p4196 N85-36036
Nuclear cascades in electromagnetic showers produced by primary gamma-quanta in the atmosphere
[HE-4.5-16] 24 p4196 N85-36038
Comments on the measurements of multiple muon phenomena
[HE-5.2-13] 24 p4203 N85-36089
High energy neutrino astronomy with MACRO
[HE-5.3-12] 24 p4206 N85-36106
Analysis of the electron component of EAS at observational level 700 g x cm(-2) with a scale breaking interaction model and gammaisation hypothesis
[HE-5.4-8] 24 p4208 N85-36119
Collimated groups of particles as possible manifestation of heavy meson production
[HE-5.4-14] 24 p4208 N85-36124

GANGLIA
NT NERVES
NT NEURONS

GANTRIES
U GANTRY CRANES

GANTRY CRANES
Specifications, applications of gantry robots viewed
10 p1461 N85-19215

GANYMEDE
Dark halo craters and the thickness of grooved terrain on Ganymede 13 p2173 N85-23484
Formation of bright terrain bands on Ganymede by unstable lithosphere extension 13 p2173 N85-23485
Polar cap formation on Ganymede
13 p2174 N85-23486
Giant planets and their satellites: Cosmochemistry, evolution and structure 13 p2175 N85-23494
Ripple ring basins on Ganymede and Callisto
13 p2183 N85-23547
Planetary analogs in Antarctica: Icy satellites
13 p2193 N85-23605
Spectral units on Europa and Ganymede
13 p2196 N85-23621
Three-layer generic Ganymedes: Structure and evolution 13 p2202 N85-23657
Lineaments on Ganymede: New evidence for late tectonic activity 13 p2202 N85-23658
Global tectonics on Ganymede
13 p2202 N85-23659
Tectonics of the Galileo Regio on Ganymede
13 p2202 N85-23660
Importance of the tectonic motions on Ganymede
13 p2202 N85-23661
Geology of the Ganymede quadrangle Jg7
13 p2203 N85-23665
Ganymede and Callisto: Beauty is only skin deep
15 p2680 N85-26552

GAPS
NT ENERGY GAPS (SOLID STATE)
NT SPARK GAPS
Investigation of current setting procedures for sector magnets
[CSIR-NAC-83-03] 01 p0117 N85-10795
Benthic boundary layer, IOS observational programme: Discovery Gap measurements, March 1984 — Institute of Oceanographic Sciences (IOS)
[ISO-180] 09 p1359 N85-18552
Magnetic field in main gap of separator
12 p1843 N85-21563
Correlation of ring current and ionospheric gap in morning and evening hours 14 p2339 N85-24466
Residual oxygen pressure in contact gap upon diffusion welding of titanium 15 p2499 N85-25418
The radiation of the Vela pulsar
20 p3548 N85-32080
SRB attach ring phenolic TPS fishtail seal evaluation tests
[NASA-CR-170887] 24 p4098 N85-35407

GAPS (GEOLOGY)
Ridged plains of Lunae Planum: Thickness distribution revised 13 p2185 N85-23559
Mechanisms of basalt-plains ridge formation
13 p2199 N85-23643
Terrestrial analogs for planetary wrinkle ridges
13 p2199 N85-23644

GARBAGE
Effectiveness of an overhead wire barrier in deterring gulls from feeding at a sanitary landfill
[AD-P004199] 11 p1582 N85-19966

GARNETS
NT YTTRIUM-ALUMINUM GARNET
NT YTTRIUM-IRON GARNET
Metamorphic petrology of the Table Mountain area, Circle quadrangle, Alaska 04 p0516 N85-13295
Spectroscopic investigation of materials for frequency agile laser systems
[AD-A151731] 16 p2790 N85-27208
Anorthositic oceanic crust in the Archean Earth
21 p3719 N85-33077
Advanced detectors and signal processing
[NASA-CR-176193] 24 p4088 N85-35343

GARP
U GLOBAL ATMOSPHERIC RESEARCH PROGRAM

GAS ANALYSIS
NT OZONOMETRY
The pyrolysis toxic gas analysis of aircraft interior materials
[AD-A146285] 03 p0328 N85-12115
Portable microprocessor-controlled instrument for sensing, identifying and monitoring gaseous chemicals
[DE84-013431] 04 p0504 N85-13214
Portable instrument for the detection and identification of air pollutants
[DE84-014767] 05 p0672 N85-14316
Formation of reference signals in laser-type gas analyzers with mechanical switching of optical channels
06 p0787 N85-15027
Integrated exhaust gas analysis system for aircraft turbine engine component testing
[NASA-TP-2424] 07 p0962 N85-16100
Analysis of gases in the Earth's crust
[PB85-113397/GAR] 07 p0990 N85-16287
Evaluation of interstitial gas contamination in titanium alloys using induced magnetic field analysis
[AD-P004130] 08 p1127 N85-17106
Evaluation of the thermoelectric method for determination of interstitial gases in titanium
[AD-P004132] 08 p1127 N85-17107
Comparative evaluation of GC/MS (Gas Chromatography/Mass Spectrometry) data analysis processing
[PB85-125664] 11 p1596 N85-20037
Edge diagnostics for tandem mirror machines
[DE85-001209] 11 p1733 N85-20902
Diagnostic verification of the GLAS (Goddard Laboratory for Atmospheric Sciences) general circulation model as applied to a case of extratropical maritime explosive cyclogenesis
[AD-A153686] 18 p3148 N85-29484
Analysis of aldehydes and ketones in the gas phase
[PB85-181865] 20 p3426 N85-31281
Gas analysis techniques for human physiological measurements in space — Spacelab
[A/6537] 20 p3507 N85-31603
Model documentation of the gas analysis modeling system. Volume 1: Model overview
[DE85-010952] 20 p3515 N85-31659
Gas sensing with surface acoustic wave devices
[DE85-009125] 20 p3524 N85-31921
Participation of singlet oxygen in photodestruction of air-saturated solutions of coumarin dyes
21 p3685 N85-32891
The possibilities of remote analysis of atmospheric gases based on Raman scattering spectroscopy
21 p3685 N85-32892
Experimental studies of glass refining
[NASA-CR-176130] 22 p3751 N85-33246
Method for controlling the viscosity of siloxane oils
[DE85-011586] 23 p3909 N85-34221
Oxygen analyzer
[DE85-006002] 23 p3935 N85-34392
Gas analysis of ore-forming fluids
24 p4105 N85-35447

GAS ATOMIZATION
Rapid solidification of candidate ferritic steels
[DE85-006596] 16 p2750 N85-28971
Atomized magnetism-aluminum protective coatings
19 p3244 N85-30116

GAS BEARINGS
Development of gas-lubricated pistons for heavy duty diesel engine technology program
[NASA-CR-174746] 03 p0441 N85-12808
Stability of lubricant film in gas dynamic bearing
06 p0778 N85-14977
Experimental test program for evaluation of solid lubricant coating as applied to compliant foil gas bearings to 315 deg C
[NASA-CR-174837] 07 p0930 N85-15985
The series 2000: A miniature gas bearing DTG for low cost strapdown guidance and control
16 p2696 N85-28648

GAS CHROMATOGRAPHY
Development and application of fluorine-containing reagents in the gas chromatography of carbonyl compounds
[BLL-DRIC-TRANS-7205-(3623.66)]
01 p0023 N85-10140
The pyrolysis toxic gas analysis of aircraft interior materials
[AD-A146285] 03 p0328 N85-12115
Helium ionization detection apparatus
[NASA-TM-77505] 03 p0364 N85-12332
Measurements of atmospheric carbon disulfide using aircraft platforms and a GC/MS isotopic dilution analysis technique 03 p0391 N85-12500
Gas chromatographic separation of hydrogen isotopes using metal hydrides
[DE84-014455] 04 p0469 N85-12980
Photoelectrochemistry with chemically modified electrodes
[DE84-016796] 04 p0471 N85-12997
Development of acceptance criteria for batches of silane primer for external tank thermal protection system bonding applications
[NASA-CR-171266] 04 p0478 N85-13043
Volatile organic emissions from adhesives with indoor applications
[DE84-015965] 05 p0620 N85-13988
USSR report: Chemistry
[JPRS-UCH-84-012] 06 p0761 N85-14885
Gas chromatographic determination of content of harmful substances in air of industrial locations
06 p0761 N85-14888
Description and operation of a thermal decomposition unit-gas chromatographic system
[PB84-248362] 07 p0968 N85-16146

GC-FTIR (Fourier Transform Infrared Spectrometry) of jet fuels
[AD-A148272] 08 p1135 N85-17155

Multiplex gas chromatography for use in space craft
[NASA-TM-86666] 09 p1290 N85-18097

Prediction of retention indices of polynuclear aromatic hydrocarbons. Part 2: Capillary gas chromatography
[DE85-001301] 10 p1437 N85-19053

PCB analysis by capillary gas chromatography coupled with matrix isolation-Fourier transform infrared spectroscopy
[DE84-009201] 10 p1437 N85-19059

Interim protocol for the automated analysis of semivolatile organic compounds by Gas Chromatography/Fourier Transfer Infrared (GC/FT-IR) spectrometry
[PB85-115186] 11 p1595 N85-20035

Comparative evaluation of GC/MS (Gas Chromatography/Mass Spectrometry) data analysis processing
[PB85-125864] 11 p1596 N85-20037

User's guide for the computer program response factor (REFAC)
[PB85-138600] 11 p1705 N85-20726

Study of the kinetics of hydrogenation using aged catalysts
[DE85-004373] 12 p1802 N85-21302

Isolation, concentration and subsequent analysis by capillary gas chromatography of trace amounts of organophosphorus compounds from aqueous samples
[AD-B089301L] 12 p1803 N85-21306

A GC/MS (Gas Chromatograph/Mass Spectrometer) data management process. Part 1: User's guide, version 1.0
[PB85-116051] 12 p1803 N85-21309

A GC/MS (Gas Chromatograph/Mass Spectrometer) data management process. Part 2: Program documentation, version 1.0
[PB85-116069] 12 p1803 N85-21310

Thermally modulated electron affinity detector for priority pollutant analysis
[PB85-158145] 15 p2506 N85-25469

An ultrasensitive and element specific photoionization detection system for environmental analysis
[AD-A153365] 17 p2966 N85-28332

Gas chromatography: Possible application of advanced instrumentation developed for solar system exploration to space station cabin atmospheres
18 p3157 N85-29551

Technical and administrative activities of the Analytical Chemistry Laboratory (ACL)
[DE85-010150] 19 p3236 N85-30063

Identification and quantification of nitropolynuclear aromatic hydrocarbons in ambient and indoor air particulate samples
[PB85-176790] 19 p3311 N85-30525

Atmospheric chlorofluromethanes as tracers of ocean circulation and mixing: Measurement and calibration techniques and studies in the Greenland and Norwegian Seas 19 p3319 N85-30573

Micro-scale methods for characterization of supercritical fluid extraction and fractionation processes
[DE85-010966] 20 p3455 N85-31456

The determination of dinitrotoluene in single base propellants
[AD-A154672] 21 p3571 N85-32209

Determination of organobromide compounds in water by gas chromatography-negative ion chemical ionisation mass spectrometry
[DRIC-T-7411] 22 p3743 N85-33199

Method for measuring surface activity of silicon nitride powder
[NASA-TM-77906] 24 p4073 N85-35242

Aspects of high-resolution gas chromatography as applied to the analysis of hydrocarbon fuels and other complex organic mixtures. Volume 1
[AD-A156154] 24 p4076 N85-35257

GAS COMPOSITION

NT CARBON DIOXIDE CONCENTRATION

Combustion gas properties I-ASTM jet A fuel and dry air
[NASA-TP-2359] 01 p0010 N85-10064

Analysis of gases in the Earth's crust
[PB85-113397/GAR] 07 p0990 N85-16287

Instrumentation for Application Number 1: Mass spectrometric analysis of the boundary layer associated with the tethered satellite 11 p1646 N85-20372

Possible uses of tunable diode lasers in infrared spectroscopy
[ESA-TT-888] 15 p2564 N85-25818

Equipment for monitoring low concentrations of volatile substances in gases or liquid metals
[BLL-DOUNREAY-TR-949-(9091.9F)]
16 p2786 N85-27190

Comparison of observed and predicted short-term tracer-gas concentrations in the atmosphere
[DE85-007566] 16 p2821 N85-27399

Moisture content and gas sampling device
[NASA-CASE-MSC-18886-1] 18 p3103 N85-29213

Combustion gas properties. Part 3: Hydrogen gas fuel and dry air
[NASA-TP-2477] 20 p3395 N85-31058

Gas composition and molecule velocity in the detonation products of pentaerythritol tetranitrate (PETN) in expansion in a high vacuum container. Analysis by mass spectroscopy and time of flight spectrometry
[ISL-R-109/84] 22 p3747 N85-33226

GAS COOLED REACTORS

NT HIGH TEMPERATURE GAS COOLED REACTORS

NT HIGH TEMPERATURE NUCLEAR REACTORS

Technical assessment of thermal-hydraulics for high heat flux fusion components
[DE85-013178] 23 p3930 N85-34359

Liquid uranium alloy-helium fission reactor
[DE85-006511] 23 p3970 N85-34607

GAS COOLING

Gas cooled fuel cell systems technology development
[NASA-CR-174732] 07 p0991 N85-16291

Exploration of new methods to produce efficient sources of coherent near millimeter wave radiation
[AD-A150094] 12 p1829 N85-21481

Method of calculating cooldown process in cryostat of cryogenic electric machine 12 p1843 N85-21567

GAS DENSITY

Emergency modeling of hazardous air pollutants
[AD-A155441] 21 p3614 N85-32461

Local interstellar medium and gamma-ray astronomy
[OG-3.1-1] 22 p3873 N85-33989

Inverse-Compton gamma rays in the galaxy
[OG-3.1-2] 22 p3873 N85-33990

Radial distribution of cosmic ray intensity in the galaxy from gamma-ray data
[OG-3.1-5] 22 p3873 N85-33993

Excess gamma rays from the Loop I supernova remnant
[OG-3.1-10] 22 p3874 N85-33998

GAS DETECTORS

Investigation of the gas-content of gas-liquid systems
[BLL-M-35748-(5828.4)] 02 p0171 N85-11146

Portable instrument for the detection and identification of air pollutants
[DE84-014767] 05 p0672 N85-14316

Gas contamination detection device
[AD-D011386] 07 p0921 N85-15833

History, design and performance of the space shuttle hazardous gas detection system
08 p1098 N85-16936

General theory and design considerations for optical waveguide chemical vapor sensors
[AD-A148505] 08 p1223 N85-17702

Monte Carlo simulation of gas Cerenkov detectors
[DE85-002422] 10 p1488 N85-19394

Technological and economic assessment of advanced ceramic materials. Volume 5: A case study of ceramic toxic and combustible gas sensors
[PB85-113124] 12 p1815 N85-21386

Portable remote laser sensor for methane leak detection
[NASA-CASE-NPO-15790-1] 12 p1855 N85-21631

Development of solid state infrared emitters for gas detection applications
[PB85-148450] 15 p2561 N85-25800

Development of a stationary carbon monoxide detector
[BMFT-FB-T-84-253] 18 p3134 N85-29413

Field measurements with the TAMS-2B and development of methods for measuring HCHO, HC3 and HONO in real air
[PB85-172955] 18 p3135 N85-29419

Surface acoustic wave devices as chemical vapor microsensors
[AD-A153752] 18 p3177 N85-29698

Gas sensing with surface acoustic wave devices
[DE85-009125] 20 p3524 N85-31921

GAS DIFFUSION

U GASEOUS DIFFUSION

GAS DISCHARGE COUNTERS

U COUNTERS

U GAS DISCHARGE TUBES

GAS DISCHARGE TUBES

NT THYRATRONS

Theoretical elements of photometry
[BLL-RISLEY-TR-5022-(9091.9F)]
02 p0279 N85-11821

Development of novel lamps for study of enhanced production of resonance by low-density mercury discharges
[DE84-016889] 05 p0632 N85-14053

Lifetime and reliability of rubidium discharge lamps for use in atomic frequency standards
[AD-A150787] 14 p2417 N85-24915

Method of fabricating material for the electrodes of gas discharge devices
[DE85-007452] 16 p2780 N85-27157

Process for making electrodes for discharge tubes
[DE85-008896] 17 p2955 N85-28247

Schottky theory of three component plasmas
[AD-A154461] 19 p3371 N85-30907

Space-time characteristics of field in longitudinal pulse-period discharge typical in pumping of self-terminating lasers 21 p3687 N85-32909

GAS DISCHARGES

Bibliography of data on electrical breakdown in gases
[PB84-218049] 01 p0045 N85-10294

Development of prototypes for versatile fast discharge systems for pulsed gas lasers, especially excimer lasers
[BMFT-FB-T-84-174] 06 p0813 N85-15165

An experimental and theoretical investigation of optogalvanic effects
[AD-A148089] 08 p1157 N85-17299

An experimental and theoretical investigation of optogalvanic effects
[AD-A148456] 08 p1223 N85-17700

Evaluation of miniature vacuum ultraviolet lamps for stability and operating characteristics, Lyman-Alpha task
[NASA-CR-171345] 10 p1477 N85-19323

Electron production, electron attachment, and charge recombination process in high pressure gas discharges
[AD-A149535] 10 p1554 N85-19799

RF-Primed high power halogen vial apparatus
[AD-D011545] 12 p1935 N85-22156

Turbulence effects on a glow discharge as derived from continuity and energy considerations
[AD-A151838] 15 p2557 N85-25775

Electric discharge excitation and energy source integration
[AD-A151502] 15 p2562 N85-25808

Predischarge parameters of SF6-CO2 determined by laser 15 p2564 N85-25821

Investigation of electron attachment and dissociation rates in C2F6/CH4 electric gas discharges
[AD-A151796] 16 p2862 N85-27649

The decomposition of gas phase formaldehyde by plasma discharge
[AD-A153202] 17 p2921 N85-28007

GAS DISSOCIATION

Electron collision processes in molecular gases
[AD-A146078] 03 p0418 N85-12671

Dissociated methanol citation
[DE85-000505] 10 p1458 N85-19186

GAS DYNAMICS

NT AERODYNAMICS

NT AEROTHERMODYNAMICS

NT INTERACTIONAL AERODYNAMICS

NT RAREFIED GAS DYNAMICS

NT ROTOR AERODYNAMICS

NT SUPERSONICS

Compressibility and fugacity of gaseous hydrogen
[NLR-TR-83079-U] 01 p0025 N85-10154

DYNKIN: A computer program for the description of detailed gas reactions in interaction with gas dynamics
[AD-B085364] 01 p0046 N85-10298

Gas dynamics of combustion of gas-air mixture in semi-closed space with relief of pressure into gasless adjacent space 02 p0260 N85-11699

Ultraviolet observations of Uranus and Neptune below 3000 Angstrom 02 p0298 N85-11932

Magnetohydrodynamic and gasdynamic theories for planetary bow waves
[NASA-CR-174132] 03 p0448 N85-12850

On experimental equations of state for Boson gases
[PTB-ME-61] 04 p0574 N85-13659

Magnetohydrodynamic and gasdynamic theories for planetary bow waves
[NASA-CR-174135] 04 p0589 N85-13760

Multiple steady states for characteristic initial value problems
[NASA-CR-172466] 06 p0749 N85-14800

Optimum thermogasdynamic design of gas turbine engines by characteristics of element prototypes
06 p0777 N85-14965

Kinematics of nearby gas and stars
06 p0880 N85-15591

A Van Leer shock capturing algorithm for the Euler equations
[AD-A148761] 08 p1163 N85-17335

Front tracking for gas dynamics
[DE85-000571] 08 p1163 N85-17336

On limits of applicability of linear models to dynamics of gas channels in aircraft engines
09 p1308 N85-18219

Microscopic study of fluid flow
09 p1317 N85-18280

GAS EVACUATING

Preliminary analysis of selected gas dynamic problems — space shuttle main engine main combustion transients and IUS nozzle flow
[NASA-CR-171343] 10 p1483 N85-19361
TVENT1P user's manual, a computer code for analyzing tornado induced gas dynamic transients in flow networks
[DE85-002346] 10 p1486 N85-19379
Triple layer system for numerical integration of equations of gas dynamics and nonlinear heat conduction equation
[DE85-000297] 11 p1632 N85-20277
Model calculations for a CO2 mixing laser with screen nozzle
[ESA-TT-859] 11 p1640 N85-20336
Study proposal for the possible use of ISS as an aerodynamic facility for aerospace applications
11 p1646 N85-20374
Characteristics of flow of oscillatory-relaxing gas in nozzles with constant cross-sections in throat region
11 p1716 N85-20794
Advanced research and technology programs for advanced high-pressure oxygen-hydrogen rocket propulsion
[NASA-TM-86969] 12 p1789 N85-21231
Front tracking and two dimensional Riemann problems: A conference report
[DE85-002209] 12 p1847 N85-21589
Ideal gas thermodynamic properties for the phenyl, phenoxy, and o-biphenyl radicals
[NASA-TM-83800] 12 p1943 N85-22204
Viscous jets — extragalactic jets
12 p1958 N85-22308
Development of a Global 3-D magnetohydrodynamic computational model for solar wind-cometary and planetary studies
[NASA-CR-175490] 12 p1962 N85-22331
Internal fluid mechanism of solid propellant rocket motors 13 p2001 N85-22544
Hypersonic flow about triangular airfoil at large angles of attack 13 p2044 N85-22792
Gas dynamics of the barred spiral galaxy NGC 3359
13 p2170 N85-23465
Dynamics of gas disks in triaxial galaxies
13 p2171 N85-23469
Automating the study of error in discrete aerodynamic fairing design 14 p2288 N85-24176
Discrete models for the numerical analysis of time-dependent multidimensional gas dynamics
[NASA-CR-172574] 14 p2300 N85-24239
Thirty-three years of research with shock tubes in the Franco-German Research Institute, Saint Louis (France)
[ISL-CO-226/83] 14 p2302 N85-24257
Gasdynamic evaluation of choking cascade turns
[AD-A151654] 15 p2557 N85-25776
Results of recent large-scale NH3 and N2O4 dispersion experiments
[DE85-004988] 15 p2589 N85-25960
Numerical analysis of supersonic reactive flow in wake of reverse step 15 p2643 N85-26303
Numerical modeling of gas dynamic phenomena during supersonic flow of viscous gas in channel with electrical flow discharge 15 p2643 N85-26304
Fluid and gas dynamics 16 p2738 N85-26897
Coadsorption studies on transition metals
[PB85-183713] 18 p3072 N85-29003
Velocity visualization in gaseous flows
[NASA-CR-174954] 20 p3453 N85-31445
R and D activities of the Propulsion Division
20 p3539 N85-32025
A variable node finite element method applied to the gas dynamics equations
[AD-A155211] 21 p3584 N85-32261
The 2-D simulations of the NRL (Naval Research Laboratory) laser experiment
[AD-A154915] 21 p3592 N85-32321
Mechanics of a gaseous film barrier to lubricant wetting of elastohydrodynamically lubricated conjunctions
[NASA-TP-2500] 21 p3595 N85-32330
A comparison of experimental and theoretical results for rotordynamic coefficients of four annular gas seals
[NASA-CR-176086] 21 p3596 N85-32332
Preliminary considerations for the gasdynamic precompression of solid molecular hydrogen
[DE85-013256] 22 p3784 N85-33445
Separation of gas mixtures by supported complexes
[DE85-011996] 23 p3912 N85-34236
Numerical model of a pulse combustor
[DE85-011717] 23 p3912 N85-34240

GAS EVACUATING
U EVACUATING (VACUUM)

GAS EVOLUTION
Change in the nitrogen content when nitrided alloys are heated
[BLL-M-35946-(5828.4)] 05 p0615 N85-13929
Chemical composition and kinetics of libration of gases upon welding of aluminum alloys 19 p3247 N85-30131
Means for reducing hydrogen concentration upon surfacing of antifriction aluminum alloys with powder electrode 19 p3247 N85-30132

GAS EXCHANGE
Interaction between lung mechanics and gas exchange by low volume high frequency pulmonary ventilation in patients with respiratory failure
[AD-A146604] 06 p0846 N85-15372
External respiration, gas exchange and energy expenditures of man in weightlessness
12 p1900 N85-21932
Contribution to theory of ocean-atmosphere gas exchange 13 p2108 N85-23134
Influence of bubbles formed upon breaking of waves on gas exchange between ocean and atmosphere
14 p2335 N85-24439
Controlled Ecological Life Support Systems (CELSS)
15 p2688 N85-26604
Photosynthetic acclimation of Acer saccharum
[DE85-008247] 17 p2998 N85-28536
Atmosphere behavior in gas-closed mouse-algal systems: An experimental and modelling study
18 p3155 N85-29536
Effect of 120-day antiorthostatic bedrest on gas exchange and pulmonary circulation in man
19 p3323 N85-30589

GAS EXPANSION
Regularity of the free boundary for the porous medium equation
[AD-A147289] 08 p1210 N85-17611
Partial bleed expander cycle for low thrust LOX/LH2 rocket engine
[NAL-TR-837T] 10 p1430 N85-19018
Study of stresses on surface of flat barrier immersed in under expanded jet of rarefied gas
16 p2765 N85-27061
The highly underexpanded exhaust plume from nozzles with boundary layers
[DFVLR-FB-85-10] 20 p3421 N85-31230
Expansion ratio influence on population inversion in CO2/Ar CW gasdynamic lasers operating at various transitions within coupled upsilon 1 and upsilon 2 modes of CO2
[STN-4] 22 p3790 N85-33485
Spectral evolution of gamma-rays from adiabatically expanding sources in dense clouds
[OG-2.5-2] 22 p3869 N85-33959
Real time analysis of PETN detonation products
[DE85-009581] 23 p3922 N85-34303

GAS EXPLOSIONS
Experiment on triggered fragmentation on a molten copper droplet in water
[BLL-WH-602-(9091.9F)] 08 p1125 N85-17091
Thermal radiation hazards from Liquified Petroleum Gas (LPG) fireballs
[VTT-304] 09 p1293 N85-18122
Explosion in flight 21 p3683 N85-32883

GAS FLOW
NT AIR CURRENTS
NT AIR FLOW
NT CONTINUUM FLOW
NT EQUILIBRIUM FLOW
NT FREE MOLECULAR FLOW
NT FROZEN EQUILIBRIUM FLOW
NT JET STREAMS (METEOROLOGY)
NT KNUDSEN FLOW
NT MERIDIONAL FLOW
NT MOLECULAR FLOW
NT NONEQUILIBRIUM FLOW
NT PIPE FLOW
NT TRANSITION FLOW
NT VERTICAL AIR CURRENTS
Preliminary mechanical redesign of an existing gas-turbine engine to incorporate a high-efficiency, low-pressure-ratio, highly regenerative cycle for marine applications
[AD-A144808] 01 p0011 N85-10070
Chemical vapor deposition of amorphous silicon films produced by using higher order silanes
[DE84-004519] 01 p0123 N85-10847
Some of the features of movement of gas through a layer of free-flowing substances
[BLL-M-35732-(5828.4)] 02 p0196 N85-11312
Multigrid iteration solution procedure for solving two-dimensional sets of coupled equations
[DE84-016554] 04 p0555 N85-13533
Influence of inter-layer effect on charge gas-permeability
[BLL-M-35919-(5828.4)] 05 p0616 N85-13940
Front tracking for gas dynamics
[DE85-000571] 08 p1163 N85-17336
Replaceable blade turbine and stationary specimen corrosion testing facility
[NASA-TM-86931] 09 p1294 N85-18126
Designing the profile of turbine blades using an iteration technique 09 p1305 N85-18201
Calculating secondary nonviscous gas flows in spatial cascades of turbines 09 p1305 N85-18202
Developments in gas metering technology
[ERS-E.346] 09 p1321 N85-18307
Internal forced convection to low Prandtl number gas mixtures
[AD-A148932] 10 p1484 N85-19366
Averaging effects in models of three-dimensional two-phase flows
[AD-A149313] 10 p1484 N85-19371
Characteristics of flow of oscillatory-relaxing gas in nozzles with constant cross-sections in throat region
11 p1716 N85-20794
Explorations into thermodynamics analogies and critical points in reference to gas-solid transport
[DE85-000616] 11 p1738 N85-20939
Front tracking and two dimensional Riemann problems: A conference report
[DE85-002209] 12 p1847 N85-21589
An investigation of aerowindows for solar receivers
[DE84-010931] 12 p1877 N85-21772
Some unique features of isentrophic flow of gas under high pressures 13 p2043 N85-22790
Efficiency of algorithms for gas-air channel diagnostics in gas turbine engines based on gas thermodynamic parameters 13 p2048 N85-22823
Mathematical modeling of transient performance of gas turbine engine 13 p2050 N85-22834
Model for high rate gas flows in deformable and reactive porous beds
[DE85-006140] 14 p2253 N85-23994
Effect of diaphragm leakage on turbine stage characteristics 14 p2286 N85-24169
Heat transfer to vertical flat plates in a rectangular gas-fluidized bed
[AD-A150765] 14 p2301 N85-24248
The significance for laser anemometry of particles carried along in a gas flow
[ISL-CO-205/83] 14 p2301 N85-24251
Experimental simulation of the flow inside a gun barrel
[ISL-CO-206/83] 14 p2302 N85-24252
Solid state compressor
[AD-A150790] 14 p2311 N85-24302
Turbulence effects on a glow discharge as derived from continuity and energy considerations
[AD-A151838] 15 p2557 N85-25775
Numerical modeling of gas dynamic phenomena during supersonic flow of viscous gas in channel with electrical flow discharge 15 p2643 N85-26304
Waveguide phenomena in dense relaxing gases and their use in chemical and gas-dynamic lasers
15 p2644 N85-26308
Aerodynamic forces developing in channels between vanes in turbine drive wheels 16 p2765 N85-27062
Hypersonic nonequilibrium gas flow past zero-aspect wing 16 p2765 N85-27063
Calculation of viscous compressible flows in small gas turbines 17 p2912 N85-27800
Flow characteristics of a partially submerged liquid pickup
[DE85-006744] 17 p2959 N85-28276
Numerical computation of space shuttle orbiter flow field
[NASA-CR-175912] 18 p3058 N85-28821
Unsymmetrical flow in a centrifuge
[DE85-009021] 18 p3103 N85-29209
Computer program for the control/operating system of the gas flow installation for the solid fuel combustion chamber
[VTH-LR-430] 18 p3165 N85-29585
Adherence of ash particles from the combustion of micronized coal
[DE85-006600] 19 p3229 N85-30023
Mathematics of oil production
[DE85-011235] 19 p3267 N85-30201
Development and application of a high power ND-glass laser instrument
[AD-A154366] 19 p3276 N85-3021
Development of improved capabilities for computation of gas supercompressibility factors and other properties
[PB85-188316] 20 p3436 N85-3131
Vaporization from a heated surface into a saturated stream
[DE85-010484] 20 p3530 N85-319
BLAF: A blast field reconstruction program fr pressure histories
[AD-A155300] 21 p3585 N85-32
Investigation of influence of gas exit mode characteristics of N2O - N2 - He discharge laser
21 p3684 N85-3
Integrated current collector and catalyst support
[DE85-011616] 22 p3761 N85-3
Vortex generating flow passage design for incre film cooling effectiveness
[NASA-CASE-LEW-14039-1] 22 p3782 N85-3

Unsteady transonic heat transfer in a transient facility
[NASA-CR-176145] 23 p3930 N85-34354

GAS GENERATOR ENGINES
U ENGINES
U GAS GENERATORS

GAS GENERATORS
Singlet delta oxygen generator
[AD-D011208] 01 p0012 N85-10072
Qualification of a hydrazine gas generator system with electrothermal/catalytic gas generator
[BMFT-FB-W-84-040] 08 p1110 N85-17016
Curvilinear solid propellant grain
[AD-D011457] 10 p1458 N85-19183

GAS GIANT PLANETS
NT JUPITER (PLANET)
NT NEPTUNE (PLANET)
NT SATURN (PLANET)
NT URANUS (PLANET)
NT URANUS RINGS
Far infrared and submillimeter observations of the giant planets 08 p1245 N85-17856
Shock compression of liquid helium to 56 GPa (560) kbar 13 p2184 N85-23551

GAS GUNS
NT LIGHT GAS GUNS
Performance of the 10 KSI Wilson valve breech
[DE85-000258] 10 p1493 N85-19430
Behavior of fiber-reinforced composites under dynamic tension
[AD-A150619] 13 p2015 N85-22641
Design and fabrication of projectiles for round bore railguns
[DE85-011871] 20 p3398 N85-31078
Low temperature experimental capability for use with gas guns
[DE85-010418] 22 p3801 N85-33548
Shock and release equation of state of calcite
[DE85-013151] 23 p3942 N85-34432

GAS HEATING
Experimentally determined characteristics of vortex heaters 13 p2050 N85-22833
High Temperature Heating System (HTHS)
[PB85-188340] 24 p4084 N85-35316

GAS INJECTION
Alloying specially low carbon silicon-bearing steel with nitrogen
[BLL-M-35707-(5828.4)] 02 p0175 N85-11170
A 50-kW electric-discharge CO2 laser
[AD-A149779] 12 p1857 N85-21644
Characteristics of heat exchange in the region of injection into a supersonic high-temperature flow
[NASA-TM-77833] 15 p2555 N85-25762
An experimental investigation of fuel regression rate control in solid fuel ramjets
[AD-A154251] 19 p3227 N85-30008

GAS IONIZATION
NT ATMOSPHERIC IONIZATION
NT AURORAL IONIZATION
NT FLAME IONIZATION
Helium ionization detection apparatus
[NASA-TM-77505] 03 p0364 N85-12332
Focusing effects of a laser beam in the nonresonant multiphoton ionization (MPI) of gases
[LP-207] 04 p0506 N85-13231
Highly ionized gas associated with the small Magellanic cloud 11 p1745 N85-20976
Frictional and structural characterization of ion-nitrided low and high chromium steels
[NASA-TM-86991] 13 p2098 N85-23085
Giotto residual ionization 14 p2244 N85-23909
Relative abundances of elements (20 or = Z or = 28) at energies up to 70 GeV/amu using relativistic rise in ion chambers
[OG-4.1-7] 22 p3876 N85-34013
Breakdown of intrinsic ambipolarity for the radial diffusion due to a rotating RF field 23 p3977 N85-34660

GAS JETS
Mechanism of brittle heat fracture of inhomogeneous solids by high temperature gas jets
02 p0265 N85-11731
Study of the velocity-acoustic pressure correlation in a cold jet, centered on the sign and the amplitude of the velocity fluctuations
[ISL-R-124/83] 04 p0501 N85-13193
A neutral gas jet in a low velocity shock front at the boundary of the Draco Nebula 06 p0878 N85-15576
Development of the sonic pump levitator
[NASA-CR-171382] 12 p1782 N85-21186
Apparatus and method to keep the walls of a free-space reactor free from deposits of solid materials
[NASA-CASE-NPO-15851-1] 12 p1858 N85-21652
Ion sensor signal fluctuations during operation of spacecraft reaction engines 16 p2724 N85-26815
Uniaxial angular accelerometers
17 p2944 N85-28173

GAS LASERS
NT CARBON DIOXIDE LASERS
NT CARBON MONOXIDE LASERS
NT DF LASERS
NT EXCIMER LASERS
NT HCN LASERS
NT HELIUM-NEON LASERS
NT HF LASERS
NT KRYPTON FLUORIDE LASERS
NT NITROGEN LASERS
NT TEA LASERS
NT ULTRAVIOLET LASERS
NT XENON CHLORIDE LASERS
NT XENON FLUORIDE LASERS
Peripheral vision displays: The future
01 p0009 N85-10058
Development of prototypes for versatile fast discharge systems for pulsed gas lasers, especially excimer lasers
[BMFT-FB-T-84-174] 06 p0813 N85-15165
High efficiency electron beam gun foil support
[AD-D011434] 08 p1159 N85-17312
Axial flow laser cavity
[AD-D011506] 12 p1855 N85-21633
Optically pumped iodine monofluoride laser
[AD-D011555] 12 p1855 N85-21637
Laser with a hollow copper cathode
[ISL-R-119/83] 14 p2310 N85-24300
DARPA/TTO program IR binary optics
[AD-A152196] 16 p2865 N85-27672
Photochemical ignition studies. 1: Laser ignition of flowing premixed gases
[AD-A153048] 17 p2920 N85-28002
Magnetically switched power supply systems for lasers
[NASA-CASE-NPO-16402-1] 18 p3112 N85-29265
Development of a resistive load for PBFA 2 rimfire gas switch simultaneity and laser triggering tests
[DE85-011060] 19 p3365 N85-30869
Theoretical modeling of the discharge-pumped XeCl excimer laser 20 p3460 N85-31495
Vacuum ultraviolet laser
[DE85-011632] 22 p3790 N85-33478

GAS LIQUEFACTION
U CONDENSING

GAS LUBRICANTS
Dual clearance squeeze film damper
[NASA-CASE-LEW-13506-1] 22 p3791 N85-33490

GAS LUBRICATED BEARINGS
U GAS BEARINGS

GAS MASERS
NT HYDROGEN MASERS

GAS METERS
A simple electronic apparatus for determining the oxidation stability of lubricants and other organic compounds
[AD-A146080] 03 p0338 N85-12172
Developments in gas metering technology
[ERS-E.348] 09 p1321 N85-18307
Buckling and eccentricity effects on orifice metering accuracy --- gas meters
[ERS-E.350] 09 p1324 N85-18321
An experimental investigation into the effects of plate eccentricity and elastic deformation on orifice meter accuracy
[ERS-E.391] 09 p1325 N85-18325

GAS MIXTURES
NT AIR
NT COMPRESSED AIR
NT EXPIRED AIR
NT LIQUID AIR
Experimental properties of an inhomogeneously broadened He-Xe unstable ring laser
[AD-A144824] 01 p0052 N85-10344
Experimental and theoretical study of condensation in multicomponent vapors
[DE84-015610] 02 p0174 N85-11164
Recent advances in gaseous dielectrics
[DE84-014279] 02 p0195 N85-11304
Gas dynamics of combustion of gas-air mixture in semi-closed space with relief of pressure into gasless adjacent space 02 p0260 N85-11699
Combustion and detonation of hydrogen-air mixture in free spaces 02 p0274 N85-11783
NaK chemiluminescence
[AD-A146077] 03 p0328 N85-12110
PRIAMUS, a computer program for the calculation of thermophysical properties of gas mixtures containing O2, N2, CO, CO2, He, H2O, H2, CH4
[JUEL-1916] 04 p0472 N85-13002
Experiments with hydrox at 1.3 MPa (13 atm) --- for divers
[FOA-C-58014-H1] 04 p0545 N85-13471
Cardiac output measured by mass spectroscopy
05 p0692 N85-14449
Cardiac output measurement with soluble gases
05 p0692 N85-14450
Hypersonic flow of mixture around blunt body
06 p0778 N85-14979
Hydrogen-oxygen (hydrox) breathing at 1.3MPa
[FOA-C-58015-H1] 09 p1364 N85-18577
Separation of gas mixtures with coordination complexes
[DE85-000363] 10 p1438 N85-19062
Influence of temperature on wear resistance of detonation coatings of alloy powders
10 p1447 N85-19116
Internal forced convection to low Prandtl number gas mixtures
[AD-A148932] 10 p1484 N85-19366
Diffusion separation of reacting gas mixtures
11 p1718 N85-20810
Basic studies of gases for fast switches
[AD-A149828] 12 p1835 N85-21514
Resonant coherent anti-Stokes Raman scattering
[ESA-TT-876] 15 p2507 N85-25466
Predischarge parameters of SF6-CO2 determined by laser 15 p2564 N85-25821
Calculations of collision-induced optical gain in high-density mixtures of D2 or HD with a buffer gas
[AD-A151372] 15 p2648 N85-26330
Optical waveguide sensor for methane gas
[AD-D011691] 19 p3273 N85-30294
Combustion gas properties. Part 3: Hydrogen gas fuel and dry air
[NASA-TP-2477] 20 p3395 N85-31058
Weak shock waves propagating in fluid-gas mixtures
[AD-A154759] 21 p3584 N85-32276
Asymptotically stable solutions of some nonlinear equations 21 p3698 N85-32974
Separation of gas mixtures by supported complexes
[DE85-011996] 23 p3912 N85-34236
Investigation of the flame speeds of propane/methanol gas mixtures
[DE85-012817] 23 p3912 N85-34239

GAS PHASES
U VAPOR PHASES

GAS PIPES
The influence of mechanical damage on transmission pipeline integrity
[ERS-E.351] 09 p1340 N85-18431
Results of an EPRG round robin test programme with DWTT specimens --- drop weight test (DWTT);pipe steels
[ERS-E.365] 09 p1341 N85-18432

GAS POCKETS
Western gas sands
[DE85-001985] 18 p3126 N85-29360

GAS PRESSURE
Gas pressure and electron density at the level of the active zone of hollow cathode arc discharges
[NASA-TM-77477] 03 p0414 N85-12648
Gas pressure and electron density in the active zone level of hollow cathode arc discharges
[NASA-TM-77468] 07 p0945 N85-15988
Improvement of gas-tightness of OTTG and TBO-5 threaded pipe couplings
[BLL-M-35993-(5828.4)] 07 p0972 N85-16175
Simulation in the design of gas pressure control equipment
[ERS-E.352] 09 p1324 N85-18322
Ignition phenomena of bulk aluminum alloy as a function of oxygen pressure 13 p1999 N85-22531
Molecular dynamics of propellant gases, part 2
13 p2002 N85-22552
Residual oxygen pressure in contact gap upon diffusion welding of titanium 15 p2490 N85-25418
A feasibility study for using low boiling point fluids to change aircraft tire deflection
[AD-A152096] 16 p2700 N85-26701
The loss of material from the cathode of metal arcs
[NASA-TM-77845] 17 p2918 N85-27985
Determination of individual tolerance in hyperbaric oxygen 23 p3954 N85-34507

GAS RECOVERY
Separation of gas mixtures with coordination complexes
[DE85-000363] 10 p1438 N85-19062
Diffusion separation of reacting gas mixtures
11 p1718 N85-20810
Improved model for fluid-driven cracks in jointed rock
[DE85-008963] 18 p3125 N85-29349

GAS SPECTROSCOPY
NT FLAME SPECTROSCOPY

GAS STREAMS
Stability of lubricant film in gas dynamic bearing
06 p0776 N85-14977
Linear problem of harmonic vibrator acting at supercritical frequencies in subsonic boundary layer
06 p0779 N85-14978
Discharge pulse phenomenology
13 p1995 N85-22509

Method of calculating separation flow of subsonic gas stream around wings 17 p2942 N85-28161
Surface degradation of ductile metal in elevated temperature gas-particle streams
[DE85-008428] 18 p3074 N85-29017

GAS TEMPERATURE
HOST instrumentation R and D program overview
02 p0141 N85-10957
Dynamic gas temperature measurement system
02 p0141 N85-10958

GAS TRANSPORT
Aircraft measurements of tracer gas during the 1983 cross Appalachian tracer experiment (CAPTEX)
[DE84-015292] 04 p0531 N85-13395
Mechanisms of gas permeation through polymer membranes
[DE84-017423] 09 p1293 N85-18117
Formaldehyde and tracer gas transfer between airstreams in enthalpy-type air-to-air heat exchangers
[DE84-016951] 11 p1631 N85-20274
Principal patterns of functional changes of human respiratory system in adaptation to high pressure
14 p2387 N85-24704

GAS TUNGSTEN ARC WELDING
Minor element effects on gas tungsten arc weld penetration
[PB84-222579] 01 p0056 N85-10370
Recommended aluminum pipe welding procedures for corps of engineers construction
[AD-A146712] 06 p0815 N85-15172
Characterization of the heat source distribution of a typical GTAW welding arc
[DE85-004322] 12 p1861 N85-21670
Sensor control of robot arc welding
12 p1948 N85-22233
Fracture toughness of HY-130 steel weld metals
[AD-A150841] 14 p2255 N85-23976
Laser welding of 6Al-4V titanium alloy
[DE85-012019] 23 p3936 N85-34413
Interaction of trace elements and welding parameters on GTA weld shape
[DE85-004046] 24 p4060 N85-35284

GAS TURBINE ENGINES
NT J-52 ENGINE
NT J-85 ENGINE
NT JET ENGINES
NT RAMJET ENGINES
NT SUPERSONIC COMBUSTION RAMJET ENGINES
NT TURBOFAN ENGINES
NT TURBOJET ENGINES
NT TURBOPROP ENGINES
Computational thermo-fluid dynamics contributions to advanced gas turbine engine design
[NASA-TM-86865] 01 p0011 N85-10069
Thermal fatigue of gas turbine engine blades made of material based on silicon nitride and silicon carbide
01 p0019 N85-10115
A review and analysis of boundary layer transition data for turbine application
[NASA-TM-86880] 01 p0047 N85-10306
Energy efficient engine flight propulsion system: preliminary analysis and design report
[NASA-CR-174701] 02 p0140 N85-10947
Turbine Engine Hot Section Technology (HOST)
[NASA-TM-83022] 02 p0140 N85-10951
Equivalent damage: A critical assessment
02 p0140 N85-10952
Benchmark notch test for life prediction
02 p0140 N85-10953
Nonlinear structural and life analyses of a turbine blade 02 p0141 N85-10954
Nonlinear structural and life analyses of a combustor liner 02 p0141 N85-10955
Pre-HOST high temperature crack propagation
02 p0141 N85-10956
High temperature static strain sensor development program 02 p0141 N85-10959
Burner liner thermal/structural load modelling
02 p0143 N85-10970
Component-specific modeling
02 p0143 N85-10971
The 3-D inelastic analysis methods for hot section components: Brief description 02 p0143 N85-10972
Creep-fatigue life prediction for engine hot section materials (isotropic) 02 p0144 N85-10974
Constitutive model development for isotropic materials
02 p0144 N85-10975
Life prediction and constitutive models for anisotropic materials 02 p0144 N85-10976
Surface protection overview 02 p0144 N85-10978
Airfoil deposition model 02 p0144 N85-10979
Effects of surface chemistry on hot corrosion life: Overview 02 p0145 N85-10980
Combustion hot section technology
02 p0145 N85-10981
Aerothermal modeling 02 p0145 N85-10982
Aerothermal modeling program
02 p0145 N85-10983
Dilution zone mixing studies 02 p0145 N85-10984
Studies on the hot corrosion of a nickel-base superalloy, Udimet 700
[NASA-TM-86882] 02 p0183 N85-11224
Hot isostatically pressed manufacture of high strength MERL 76 disk and seal shapes
[NASA-CR-165550] 02 p0183 N85-11225
External fuel vaporization study, phase 2
[NASA-CR-174079] 02 p0187 N85-11252
Biaxial constitutive equation development for single crystals
[NASA-CR-174056] 02 p0286 N85-11862
High performance fibers for structurally reliable metal and ceramic composites — advanced gas turbine engine materials
[NASA-TM-86878] 03 p0325 N85-12095
Development and fabrication of refractory bodies for gas turbine engines
[BMFT-FB-T-84-160] 04 p0457 N85-12899
High-temperature erosion of plasma-sprayed, yttria-stabilized zirconia in a simulated turbine environment
[NASA-TP-2406] 04 p0478 N85-13045
Ceramic technology for advanced heat engines program plan
[DE84-013567] 04 p0479 N85-13055
Fabrication and quality assurance processes for superhybrid composite fan blades
[NASA-TM-83354] 06 p0763 N85-14882
Predicting changes in reliability characteristics of gas turbine engines during operation
06 p0776 N85-14964
Optimum thermogasdynamic design of gas turbine engines by characteristics of element prototypes
06 p0777 N85-14965
Mounting construction for turbine vane assembly
[AD-D011395] 07 p0904 N85-15723
Control system design language implementation of a gas turbine starting controller
[AD-A147896] 07 p0905 N85-15732
Overview of the AGARD SMP activities on turbine engine materials technology in the 1972 - 1982 period
07 p0906 N85-15738
Comparison between the properties of conventional wrought and powder metallurgical alloys for turbine disc applications 07 p0906 N85-15739
Cumulative damage modeling of fatigue crack growth
07 p0907 N85-15741
Disc fatigue life predictions for gas turbine engines
07 p0907 N85-15743
Engine cyclic durability by analysis and material testing 07 p0907 N85-15744
Life prediction at high temperature under multiaxial loading 07 p0907 N85-15745
Experiences with the material bevaviour and high temperature low cycle fatigue life prediction of the IN 738 blading alloy 07 p0908 N85-15746
Verification of life prediction through component testing 07 p0908 N85-15748
View of future requirements for engine cyclic durability by analysis and testing 07 p0908 N85-15751
Current problems in turbomachinery fluid dynamics
[AD-A147127] 07 p0958 N85-16074
Integrated exhaust gas analysis system for aircraft turbine engine component testing
[NASA-TP-2424] 07 p0962 N85-16100
The solid rocket booster auxiliary power unit: Meeting the challenge 08 p1099 N85-16946
The effects of manufacturing automation on the surge and mobilization capabilities of the gas turbine engine industry
[AD-A147285] 08 p1137 N85-17162
Development of high temperature ceramic parts for vehicular gas turbines
[PNR-90245] 09 p1282 N85-18062
On one design principle of surge protector for gas turbine engine compressor 09 p1306 N85-18206
Influence of setting angle of jet cooling nozzles on temperature and stress state of a turbine wheel
09 p1306 N85-18208
Improvement of gas turbine engine performance by water injection into turbine cooling air
09 p1307 N85-18209
Correction of engraving stamp for forming blanks of gas turbine engine blades 09 p1307 N85-18213
Advanced Gas Turbine (AGT) powertrain system development for automotive applications
[NASA-CR-174809] 09 p1403 N85-18831
Structural ceramics in transportation: Fuel implications and economic impacts
[DE85-003024] 11 p1611 N85-20130
Introducing engine innovations: An examination of future markets for Brayton and Stirling automotive engines
[DE84-016319] 11 p1647 N85-20362
Assuring structural integrity in Army systems
[NASA-CR-175492] 11 p1651 N85-203
Advanced liner-cooling techniques for gas turbine combustors
[NASA-TM-86952] 12 p1770 N85-2111
Combustion research for gas turbine engines
[NASA-TM-86963] 12 p1778 N85-211
Evaluation results of the 700 deg C Chinese strain gauges — for gas turbine engine
[NASA-TM-86973] 12 p1850 N85-21
Advanced thin film thermocouples
[NASA-CR-175541] 12 p1850 N85-21
Current problems in turbomachinery fluid dynamics
[AD-A150533] 13 p1974 N85-22
Development of a multiplane multispeed balancing system for turbine systems
[NASA-CR-174750] 13 p1976 N85-22
The influence of fuel molecular composition upon flame-tube temperature and flame radiation in a model gas-turbine primary zone
[K234] 13 p2017 N85-22
Efficiency of algorithms for gas-air channel diagnostics in gas turbine engines based on gas thermodynamic parameters 13 p2048 N85-22
Effect of water injection into air for turbine cooling on economy of operation of gas turbine engine with afterburning 13 p2050 N85-22
effect of gas stream sweeping past the effluent of a perforated plate on heat transfer inside the perforations
13 p2051 N85-22
Estimation of gas turbine engine boost provided by injecting water behind compressor
13 p2051 N85-22
Thermal state of cooled thin-walled nozzle blade
14 p2270 N85-240
Optimization of combined convective and film cooling of perforated baffle blades in gas turbines
14 p2270 N85-240
Experimental study of heat transfer from shaft in cooled radial bearing of GNT-25 gas turbine
14 p2270 N85-240
Estimate of fatigue stability of gas-turbine engine compressor vanes in probabilistic aspect
14 p2287 N85-241
Investigation of gas-turbine engine blower impeller vibrations with change in engine intake conditions
14 p2287 N85-2417
Laser drilling of aeroengine components
14 p2309 N85-242
Experiments in dilution jet mixing effects of multiple rows and non-circular orifices
[NASA-TM-86996] 15 p2473 N85-25
Crack closure characteristics considering center cracked and compact tension specimens
[AD-A151702] 15 p2579 N85-25
Analytical fuel property effects--small combustors
[NASA-CR-174738] 16 p2708 N85-26
Multiaxial and thermomechanical fatigue considerations in damage tolerant design
[NASA-TM-87022] 16 p2740 N85-26
Structural tailoring of SSME blades (vanes)
17 p2913 N85-27
An investigation into the soot production processes in a gas turbine engine
[AD-A152710] 17 p2919 N85-27
Ceramic applications in turbine engines
[NASA-CR-174715] 17 p2934 N85-28
Report to Congress on the Automotive Technology Development Program
[DE85-005640] 17 p3052 N85-28
Strutless diffuser for gas turbine engine
[AD-D011662] 18 p3062 N85-28
Energy efficient engine high-pressure turbine component rig performance test report
[NASA-CR-168189] 19 p3218 N85-29
Energy efficient engine integrated core/low spool test hardware design report
[NASA-CR-168137] 19 p3218 N85-29
Advanced Gas Turbine (AGT) technology project
[NASA-CR-174798] 19 p3219 N85-29
Hold-time effects in elevated temperature fatigue crack propagation
[AD-A154146] 19 p3266 N85-30
Creep fatigue life prediction for engine hot section materials (isotropic)
[NASA-CR-168228] 20 p3394 N85-31
Gas turbines: Operating conditions, material selection and development
[NLR-MP-83046-U] 20 p3395 N85-31
Flat-plate transition 20 p3452 N85-31
A review and analysis of boundary layer transition data for turbine application 20 p3453 N85-31
R and D activities of the Propulsion Division
20 p3539 N85-32

Tape casting as an approach to an all-ceramic turbine shroud seal
[NASA-TM-87078] 21 p3596 N85-32333
Dual clearance squeeze film damper
[NASA-CASE-LEW-13506-1] 22 p3791 N85-33490
Elevated temperature crack growth
[NASA-CR-174957] 22 p3799 N85-33540
Shroud segments for unshrouded blade turbines
[PNR-90260] 23 p3897 N85-34143
The development and evaluation of the creep and corrosion resistant alloy IN6201
[PNR-90253] 23 p3917 N85-34278
Directionally solidified gas turbine alloys
[PNR-90264] 23 p3917 N85-34279
Oxidizing seal for a turbine tip gas path
[NASA-CASE-LEW-14053-1] 23 p3937 N85-34402
Cost effective single crystals: The Rolls Royce approach — gas turbine components
[PNR-90262] 23 p3985 N85-34717
Energy Efficient Engine Program technology benefit/cost study, volume 2
[NASA-CR-174766-VOL-2] 24 p4066 N85-35198
Energy efficient engine, high pressure turbine thermal barrier coating. Support technology report
[NASA-CR-168037] 24 p4066 N85-35199
Development of advanced high-temperature heat flux sensors. Phase 2: Verification testing
[NASA-CR-174973] 24 p4096 N85-35391

GAS TURBINES
Variable inlet vane assembly for a gas turbine combustion
[AD-D011220] 01 p0010 N85-10063
Preliminary mechanical redesign of an existing gas-turbine engine to incorporate a high-efficiency, low-pressure-ratio, highly regenerative cycle for marine applications
[AD-A144806] 01 p0011 N85-10070
Selecting the proper ceramic material for a regenerator experiencing large temperature gradients
[AD-A144796] 01 p0032 N85-10199
The effect of channel convergence on heat transfer in a passage with short pin fins
[NASA-TM-83601] 01 p0046 N85-10303
Gas side heat transfer: 2-D flow
02 p0142 N85-10965
Jet array impingement flow distributions and heat transfer characteristics: Effects of initial crossflow and nonuniform array geometry 02 p0142 N85-10967
Coolant passage heat transfer with rotation
02 p0143 N85-10968
Structural analysis 02 p0143 N85-10969
Alternate fuels combustion research
[AD-A145691] 02 p0188 N85-11258
Air force plasma spray at SA-ALC (San Antonio Air Logistics Center)
[AD-P004004] 03 p0308 N85-11984
Features of plastic deformation and fracture of EP 741 nickel alloy under thermal strain
03 p0349 N85-12250
Additives for heat engine coal slurry fuels
[DE84-016434] 05 p0621 N85-13971
Control of rotordynamic instability in a typical gas turbine's power system 05 p0642 N85-14120
High pressure combustion test facility for gas turbine research
[NAL-TR-801] 06 p0757 N85-14845
Heat transfer results and operational characteristics of the NASA Lewis Research Center Hot Section Cascade Test Facility
[NASA-TM-86890] 06 p0808 N85-15133
An improved computer model for prediction of axial gas turbine performance losses
[NASA-CR-174246] 07 p0904 N85-15724
In-flight evalution of LCF life consumption of critical rotor components subjected to high transient thermal stress
07 p0906 N85-15734
Accelerated Mission Endurance Testing (AMET)
07 p0906 N85-15736
Mechanical aspects of high temperature coatings
07 p0908 N85-15749
Contamination and distortion of steady flow field induced by discrete frequency in aircraft gas turbines
[AD-A147092] 07 p0958 N85-16073
Possibilities for a more accurate life prediction of components — gas turbine disks
07 p0976 N85-16198
Advanced technology cogeneration system conceptual design study: Closed cycle gas turbines
[NASA-CR-168222] 07 p0992 N85-16300
Combustion chamber floatwall panel attachment arrangement
[AD-D011358] 07 p1047 N85-16647
Experience of one UK electronic equipment supplier with life on engine/flight control systems over the past ten years
08 p1064 N85-16738
An analytic model of gas turbine engine installations
[AD-A148708] 09 p1281 N85-18059
High pressure combustion test facility for gas turbine research
[NAL-TR-801] 09 p1283 N85-18065
Comparison of property regeneration techniques and life prediction procedures applied to laboratory tested and service exposed Ni-Cr alloys
[NPL-DMA(A)-91] 09 p1333 N85-18374
NASA Lewis Research Center/University Graduate Research Program on Engine Structures
[NASA-TM-86916] 09 p1333 N85-18375
Exciplex systems for vapor-liquid visualization of fuel sprays
[AD-A149360] 10 p1457 N85-19181
Internal forced convection to low Prandtl number gas mixtures
[AD-A148932] 10 p1484 N85-19366
Evaluation of corrosion-erosion behavior of various ceramic materials
[AD-A149756] 12 p1812 N85-21367
Cost comparison of small gas turbines versus electric motors in a variable load industrial application
[PB85-149783] 12 p1837 N85-21530
High pressure turbine rotor two-piece blade retainer
[AD-D011498] 12 p1858 N85-21653
Closed cycle versus open cycle gas turbines. A review of A.D. Little's ICOP report, vol. 3
[DE85-000564] 12 p1861 N85-21671
Optimal design efforts in Shanghai described
13 p1972 N85-22386
Oxidation resistant materials for hot gas turbines and jet engines
[AD-B087399L] 13 p1973 N85-22389
Composition and photochemical reactivity of turbine engine exhaust
[AD-A150559] 13 p2130 N85-23256
Construction of profiles of intermediate blade sections from master profiles given on conical surfaces
14 p2272 N85-24075
Causes and means of prevention of erosion of exit edges of drive vanes in final stages of K-300-240 turbine
14 p2272 N85-24076
Oscillations of gas turbine installation rotors under operating conditions 14 p2272 N85-24077
Study of dynamic characteristics of prefabricated gas turbine compressor rotor 14 p2272 N85-24078
Effect of diaphragm leakage on turbine stage characteristics 14 p2286 N85-24168
Fiscal year 1986 technical objective document
[AD-A151039] 14 p2432 N85-25000
Small gas turbine combustor study: Fuel injector performance in a transpiration-cooled liner
[NASA-TM-86989] 15 p2473 N85-25264
Study of the primary zone of gas turbine hearths
[ONERA-RTS-22/3256-EY] 16 p2709 N85-26719
Transformation of nitrogen oxides while sampling combustion products
[AD-A152184] 16 p2746 N85-26945
Future fundamental combustion research for aeropropulsion systems
[NASA-TM-87049] 17 p2898 N85-27870
Reaction-bonded and fiber-reinforced SiC static and dynamic gas turbine components
[BMFT-FB-T-84-302] 17 p2899 N85-27874
Detailed chemical kinetic study of the effect of molecular structure on autoignition of fuel-air mixtures
[DE85-004424] 17 p2921 N85-28010
Development of high temperature resistant, noncorrosible, non-metallic ceramic materials, especially silicon nitride in gas turbine application
[BMFT-FB-T-85-015] 17 p2936 N85-28125
Development of high temperature resistant noncorrodible silicon carbide components for gas turbine applications, follow-up report
[BMFT-FB-T-85-016] 17 p2936 N85-28126
Precision die forging of blades or gas turbines
17 p2940 N85-28148
Stressed-strained state of tightening buckles in sectional runners of gas turbines 17 p2940 N85-28149
Long-Term Materials Test Program
[DE85-003248] 18 p3077 N85-29034
Research test facility for evaporation and combustion of alternative jet fuels at high air temperatures
[AD-A153830] 18 p3083 N85-29073
Adherence of ash particles from the combustion of micronized coal
[DE85-008600] 19 p3229 N85-30023
Optimisation of MCr Al coating compositions for marine gas turbines
[BR91159] 20 p3394 N85-31056
Mechanisms of exhaust pollutants and plume formation in continuous combustion
[AD-A154169] 20 p3435 N85-31310
A comparison of two bench scale tests of fuel low temperature flow properties
[AD-A154477] 20 p3435 N85-31311
Nonlinear analysis of an axisymmetric structure subjected to non-axisymmetric loading
20 p3468 N85-31549
The effect of stress and hot corrosion on nickel-base superalloys
[AD-A154722] 21 p3566 N85-32181
High powered epicyclic gears: Some recent development 23 p3924 N85-34316
Heat transfer characteristics for two-dimensional arrays of impinging jets with initial crossflow
24 p4092 N85-35365

GAS VALVES
Slow opening valve — valve design for shuttle portable oxygen system
[NASA-CASE-MSC-20112-1] 11 p1642 N85-20338

GAS VISCOSITY
Viscous jets — extragalactic jets
12 p1958 N85-22308

GAS WELDING
NT BRAZING
NT LOW TEMPERATURE BRAZING

GAS-GAS INTERACTIONS
KRAK: A computer program for two-phase two-component porous flow and fracture
[LA-9703] 22 p3782 N85-33434

GAS-LIQUID INTERACTIONS
NT AIR SEA ICE INTERACTIONS
NT AIR WATER INTERACTIONS
Investigation of the gas-content of gas-liquid systems
[BLL-M-35748-(5828.4)] 02 p0171 N85-11146
Development of a mass transfer machine for gas/liquid operations in the absence of gravity
[BMFT-FB-W-84-027] 05 p0637 N85-14091
Intermittent gas-liquid flow modeling in horizontal or weakly inclined pipes
[EME-132] 20 p3456 N85-31465
Mechanics of a gaseous film barrier to lubricant wetting of elastohydrodynamically lubricated conjunctions
[NASA-TP-2500] 21 p3595 N85-32330

GAS-METAL INTERACTIONS
Compressibility and fugacity of gaseous hydrogen
[NLR-TR-83079-U] 01 p0025 N85-10154
Determining the optimum heating parameters for precision alloys — iron-nickel alloys
[BLL-M-35718-(5824.4)] 02 p0174 N85-11167
Hydrogen trapping, diffusion, and recombination in austenitic stainless steels
[DE85-001871] 09 p1294 N85-18129
Hydrogen induced cracking in pipeline steels
[ERS-E.327] 09 p1340 N85-18429
Mechanism of hydrogen induced cracking in pipeline steels
[ERS-E.349] 09 p1340 N85-18430
Effects of MAR-M247 substrate (modified) composition on coating oxidation coating/substrate interdiffusion — protective coatings for hot section components of gas turbine engines
[NASA-CR-174851] 10 p1440 N85-19073
Influence of gaseous hydrogen on strength and ductility of nickel heat-resistant alloys 10 p1447 N85-19119
Role of hydrogen in processes of deformation and fracture of metals 10 p1449 N85-19132
Quasi-thermodynamic prediction of hydrogen reemission behavior from titanium films
[DE85-003667] 10 p1564 N85-19864
Oxidation of PT-7M and OT4-1 titanium alloys in air
11 p1600 N85-20063
Hydrogen attack of steel
[DE85-002645] 11 p1606 N85-20113
Electrochemical cell to measure corrosion rates in noncondensing environments
[DE85-003148] 12 p1807 N85-21338
Oxidation and hot corrosion of hot-pressed Si3N4 at 1000 deg C
[NASA-TM-86977] 12 p1811 N85-21358
Change in microstructure of heat-resistant nickel alloys upon thermal cycling in a current of gas
13 p2031 N85-22725
Hartree-Fock interaction between a helium atom and lithium-metal: A test for the effective medium theory
[AD-A150468] 13 p2156 N85-23367
Effect of protective atmosphere composition on durability of welded joints of niobium alloys
15 p2502 N85-25432
Hot Isostatic Pressing (HIP): Techniques, applications and economical use
[JUEL-SPEZ-288] 17 p2939 N85-28141
Changes of structure of EP648-VI alloy as a result of high-temperature gas corrosion
19 p3243 N85-30110
Means for reducing hydrogen concentration upon surfacing of antifriction aluminum alloys with powder electrode 19 p3247 N85-30132

Hydrogen embrittlement testing
[DE85-007352] 23 p3916 N85-34273
GAS-SOLID INTERACTIONS
NT GAS-METAL INTERACTIONS
An investigation of the role of sintering in gas-solid interactions
[DE84-015461] 02 p0288 N85-11884
High temperature gas energy transfer
[AD-A146134] 03 p0326 N85-12113
High altitude chemically reacting gas particle mixtures. Volume 1: A theoretical analysis and development of the numerical solution — rocket nozzle and orbital plume flow fields
[NASA-CR-171826] 07 p0916 N85-15801
Influence of size grading of sintering ore on the sintering process
[BLL-M-36004-(5828.4)] 07 p0924 N85-15854
Separation of gas mixtures with coordination complexes
[DE85-000363] 10 p1438 N85-19062
High pressure cosmochemistry of major planetary interiors: Laboratory studies of the water-rich region of the system ammonia-water 13 p2183 N85-23549
Threshold electron studies of gas-surface interactions
[AD-A151271] 15 p2647 N85-26328
GAS-SOLID INTERFACES
Space charge, interfacial kinetics, and electrical response of condensed matter
[AD-A146364] 06 p0765 N85-14893
Laser studies of chemical dynamics at the gas-solid interface
[DE84-017590] 11 p1736 N85-20920
GASDYNAMIC LASERS
Microwave discharge in a supersonic flow for the excitation of a gas dynamic CO laser
[ESA-TT-833] 09 p1326 N85-18337
Model calculations for a CO2 mixing laser with screen nozzle
[ESA-TT-859] 11 p1640 N85-20336
Waveguide phenomena in dense relaxing gases and their use in chemical and gas-dynamic lasers
15 p2644 N85-26306
Simplified analytical model for calculation of population inversion in channels of CW gasdynamic lasers operating at various transitions among levels pertaining to coupled upsilon 1 and upsilon 2 modes of CO2
[STN-2] 20 p3461 N85-31498
Requirements for attaining Treanor's distribution of vibrational energy among CO2 levels in CW gasdynamic laser flows
[STN-3] 20 p3461 N85-31499
Expansion ratio influence on population inversion in CO2/Ar CW gasdynamic lasers operating at various transitions within coupled upsilon 1 and upsilon 2 modes of CO2
[STN-4] 22 p3790 N85-33485
GASEOUS CAVITATION
U CAVITATION FLOW
U GAS FLOW
GASEOUS DIFFUSION
NT GASEOUS SELF-DIFFUSION
Mechanisms of gas permeation through polymer membranes
[DE84-017423] 09 p1293 N85-18117
Diffusion separation of reacting gas mixtures
11 p1718 N85-20810
Diffusion of water vapor in Carbon Fiber Reinforced Plastics (CFRP). Measurement of the diffusion coefficient under influence of concentration
[DFVLR-FB-84-41] 14 p2262 N85-24018
Diffusion of gases in porous solids: Simulation and measurements
[DE85-006870] 18 p3101 N85-29196
Diffusion of trace gases in the ground level boundary layer 18 p3148 N85-29489
Technology for increasing the uranium-235 isotopic abundance in natural uranium feed on a productive scale
[DE85-011252] 19 p3357 N85-30810
Preliminary wind tunnel experiments to investigate the effect of heat transfer on the dispersion of cold dense gases
[OUEL-1546/84] 20 p3456 N85-31467
Study of molecular diffusivity influence on mass transfer rate at a water-atmosphere interface
22 p3747 N85-33222
WIPP horizon in situ permeability measurements
[DE85-012667] 22 p3802 N85-33557
GASEOUS FUELS
Status of gaseous fuels for use in highway transportation: A 1983 perspective
[DE84-015205] 01 p0034 N85-10211
GASEOUS ROCKET PROPELLANTS
Ignition characterization of LOX/hydrocarbon propellants
[NASA-CR-171884] 18 p3083 N85-29070
Ignition characterization of LOX/hydrocarbon propellants
[NASA-CR-171882] 18 p3083 N85-29071
GASEOUS SELF-DIFFUSION
Two phase discharge of liquefied gases through pipes. Field experiments with ammonia and theoretical model
[FOA-B-40139-C1] 18 p3103 N85-28209
GASES
NT AIR
NT ARGON
NT ARGON ISOTOPES
NT ARGON PLASMA
NT BOUNDARY LAYER PLASMAS
NT CARBON DIOXIDE
NT CARBON MONOXIDE
NT CHARGED PARTICLES
NT COLD GAS
NT COLD PLASMAS
NT COLLISIONAL PLASMAS
NT COLLISIONLESS PLASMAS
NT COMPRESSED AIR
NT COMPRESSED GAS
NT CONDUCTION ELECTRONS
NT COSMIC GASES
NT DENSE PLASMAS
NT DEUTERIUM
NT DEUTERIUM PLASMA
NT DIATOMIC GASES
NT DISSOLVED GASES
NT ELECTRON PLASMA
NT ELLIPTICAL PLASMAS
NT EVEN-EVEN NUCLEI
NT EXHAUST GASES
NT EXPIRED AIR
NT FLAMMABLE GASES
NT FLUE GASES
NT GAS MIXTURES
NT GAS STREAMS
NT HEAVY NUCLEI
NT HELIUM
NT HELIUM ATOMS
NT HELIUM ISOTOPES
NT HELIUM PLASMA
NT HIGH TEMPERATURE GASES
NT HIGH TEMPERATURE PLASMAS
NT HYDROGEN
NT HYDROGEN ATOMS
NT HYDROGEN IONS
NT HYDROGEN ISOTOPES
NT HYDROGEN PLASMA
NT HYPERNUCLEI
NT IDEAL GAS
NT INTERSTELLAR GAS
NT IONIZED GASES
NT KRYPTON
NT LASER PLASMAS
NT LIQUEFIED GASES
NT LIQUEFIED NATURAL GAS
NT LIQUID AIR
NT LIQUID AMMONIA
NT LIQUID HELIUM
NT LIQUID HELIUM 2
NT LIQUID HYDROGEN
NT LIQUID NITROGEN
NT LIQUID OXYGEN
NT LORENTZ GAS
NT METALLIC PLASMAS
NT MOLECULAR GASES
NT NATURAL GAS
NT NEON
NT NEON ISOTOPES
NT NEUTRAL GASES
NT NITROGEN
NT NITROGEN IONS
NT NITROGEN PLASMA
NT NONCONDENSABLE GASES
NT NUCLEI (NUCLEAR PHYSICS)
NT ODD-EVEN NUCLEI
NT ODD-ODD NUCLEI
NT OXYGEN
NT OXYGEN ATOMS
NT OXYGEN IONS
NT OXYGEN ISOTOPES
NT OXYGEN PLASMA
NT OZONE
NT POLAR GASES
NT RADON
NT RADON ISOTOPES
NT RARE GASES
NT RAREFIED GASES
NT RELATIVISTIC PLASMAS
NT ROTATING PLASMAS
NT SOLAR WIND
NT SOLIDIFIED GASES
NT STELLAR WINDS
NT STRONGLY COUPLED PLASMAS
NT THERMAL PLASMAS
NT TRITIUM
NT XENON
NT XENON ISOTOPES
NT XENON 129
Combustion gas properties I-ASTM jet A fuel and
air
[NASA-TP-2359] 01 p0010 N85-10
Bibliography of data on electrical breakdown in
[PB84-218049] 01 p0045 N85-10
Recent advances in gaseous dielectrics
[DE84-014279] 02 p0195 N85-11304
Effects of H2S on molten carbonate fuel cells
[DE84-015166] 02 p0195 N85-11
Laboratory investigation of coefficients of absorption of air at Lambda = 10.6 microns 02 p0263 N85-117
Characterization of ion implanted deuterium traps in nickel by equilibration with deuterium gas
[DE84-014958] 02 p0288 N85-11
The pyrolysis toxic gas analysis of aircraft interior materials
[AD-A146285] 03 p0326 N85-121
The effect of heat treatment on wear resistance of gas-plasma eutectic coatings
[BLL-M-35756-(5828.4)] 03 p0329 N85-12132
Pulsed neodymium glass laser system for investigating nonlinear optical phenomena in gases
03 p0348 N85-12241
China report: Science and technology
[JPRS-CST-84-003] 04 p0491 N85-13132
Magnetohydrodynamic flow of two-component gas analyzed 04 p0491 N85-13133
Velocity-changing collisional effects in nonlinear atomic spectroscopy and photon echo decay in gases
[NASA-CR-174159] 04 p0559 N85-13
A method of making the gas-electric removal of highly dispersed particles more effective
[BLL-M-36030-(5828.4)] 06 p0765 N85-14
Homogeneous condensation of gaseous mixtures of S, Fe, O, N, and C in relative cosmic abundance and implications for astronomical condensation
06 p0667 N85-15
Apparatus for determining the liquid water content of a gas
[AD-D011297] 07 p0922 N85-15
A study of the chemical interaction of gases with activated carbon
[AD-A147342] 07 p0923 N85-15
Identification of leaks: Internal acoustic method, phase 2
[PB85-101947/GAR] 07 p0936 N85-15
Phase 1-A development kinematic Sterling/Rankine commercial gas-fired heat pump research program
[PB85-100931/GAR] 07 p0936 N85-15
Convection heat transfer in the critical region of fluid mixtures
[DE85-002118] 07 p0961 N85-16
A virial equation of state option for the TIGER computer program
[AD-A147490] 07 p1025 N85-16
Measurement and control of electrostatic charges on solids in a gaseous suspension
[DE85-001450] 09 p1291 N85-18
Measurement of gas compressibility factor data for natural gas and synthetic gas components and their mixtures
[PB85-129047] 11 p1614 N85-20151
Electron acceleration by laser fields in a gas
[DE85-000575] 11 p1639 N85-20
Interaction of large meteoroids with the atmosphere
11 p1656 N85-20
Photoacoustic effect and its applications
12 p1820 N85-21
Stability of organic audit materials and results of source test analysis audits
[PB85-116184] 12 p1885 N85-21
A computer controlled mass spectrometer system for investigating the decomposition of non-metallic materials under atmospheric conditions 12 p1948 N85-22
Physical chemistry of exothermic gas-aerosol calorimetry
[AD-A150872] 14 p2251 N85-23
Recording of acoustic wave in gaseous medium with thin-film pyroelectric transducers
15 p2525 N85-25
Mixing across a gas-gas interface
[AD-A151471] 15 p2556 N85-25
Action of plasma and explosion products on alumina
19 p3242 N85-30
Crosswell acoustic surveying in gas sands: Travel-time pattern recognition, seismic Q and channel waves
[DE85-010777] 19 p3352 N85-30
Interaction of slow electrons with high-pressure gases (quasi-liquids): Synthesis of our knowledge on slow electron-molecule interactions
[DE85-010061] 19 p3355 N85-30

Radioactivity in gaseous waste discharged from the separations facilities during 1984
[DE85-011373] 19 p3360 N85-30831
Gas hydrates
[DE85-001966] 20 p3477 N85-31607
Toxic hazards tests for vehicles and other equipment
[AD-A149164] 20 p3506 N85-31707
Emergency modeling of hazardous air pollutants
[AD-A155441] 21 p3614 N85-32461
Model that predicts pulse charged gas switching breakdown phenomena
[DE85-013119] 22 p3761 N85-33313
Control technology for radioactive emissions to the atmosphere at US Department of Energy facilities: The Los Alamos Meson Physics Facility
[DE85-011402] 22 p3811 N85-33609
Excess gamma-rays in the direction of the rho Ophiuchi cloud: An exotic object?
[OG-2.5-1] 22 p3868 N85-33958
Description of a test site for large-scale heavy gas dispersion and combustion experiments
[DE85-004987] 23 p3911 N85-34231
Features of behavior of gas bubbles in molten oxide films during enamelling: Communication 2
[BLL-M-35781-(5828.4)] 23 p3919 N85-34283
The cosmic-ray shock structure problem for relativistic shocks
[OG-8.1-1] 23 p4017 N85-34891
Measurement of uranium enrichment for gaseous uranium at low pressure
[DE85-012697] 24 p4150 N85-35733

GASIFICATION
NT COAL GASIFICATION
Biomass thermochemical conversion program
[DE84-017177] 05 p0621 N85-13972
Gasification of boron oxide drops and boron slurry agglomerates in combustion gases
13 p1999 N85-22529
Alcohol Fuels Program technical review, spring 1984
[DE85-002919] 17 p2938 N85-28134
Mechanism of the catalytic gasification and reactivity of graphite
[DE85-009932] 19 p3229 N85-30020
Laminar diffusion flames, carbon gasification, and laser diagnostics applied to combustion systems. 1: Laminar diffusion flames with cylindrical symmetry. 2: Diffusion-controlled gasification of carbon particles. 3: Laser diagnostics applied to combustion systems
20 p3423 N85-31243
Biomass thermochemical conversion program
[DE85-011867] 21 p3572 N85-32213

GASKETS
Response of a BWR Mark 2 containment vessel head to loads beyond the design basis
[DE85-010524] 24 p4103 N85-35432

GASOHOL (FUEL)
Dissociated methanol citation
[DE85-000505] 10 p1458 N85-19188
Developments in the production and use of ethanol fuels
[GPO-40-678] 12 p1817 N85-21398

GASOLINE
Converting gasoline farm tractors to run efficiently on farm-produced alcohol
[DE84-015796] 02 p0205 N85-11350
Some characteristics of automotive gasolines and their performance in a light aircraft engine
[FAA-CT-84-12] 07 p0934 N85-15919
Cooling system investigation of the 3-kW MEP models 016A, 021A, and 026A (60Hz, 400-Hz and 28-V dc) gasoline-engine-driven generator sets
[AD-A147571] 07 p0974 N85-16185
Catalytic conversion of C3-C4 paraffins to gasoline
[DE85-004181] 10 p1458 N85-19187
Volatility of in-use gasoline and gasoline-methanol blends
[PB85-117976] 10 p1459 N85-19189
Trends of petroleum fuels
[DE85-000116] 14 p2263 N85-24023
Conversion of methanol to gasoline: Engineering and construction of the demonstration plant
[DE85-003237] 17 p2937 N85-28133
Durability of oxygen sensors
[PB85-183093] 22 p3789 N85-33477

GASP
U GLOBAL AIR SAMPLING PROGRAM

GASTROINTESTINAL SYSTEM
NT INTESTINES
NT RECTUM
Influence of chemical form, feeding regimen, and animal species on the gastrointestinal absorption of plutonium
[DE85-010291] 21 p3662 N85-32751
Investigation of spectrum of human bile acids during 120-day antiorthostatic hypokinesia
22 p3821 N85-33674
Lipid hydrolysis in man during antiorthostatic hypokinesia 23 p3953 N85-34500

GATES (CIRCUITS)
NT THRESHOLD GATES
Glow spots and breakdown in GaAs transistor structure 04 p0487 N85-13107
High-power gate turn-off thyristors
06 p0793 N85-15071
High-speed power devices with field control
06 p0794 N85-15073
Development of short gate FET's
[AD-A147033] 07 p0947 N85-15999
Development of a 2 micrometer silicon-gate-CMOS-technology for microcomputer oriented VLSI circuits with a supply voltage range between 1.5 and 5 V
[BMFT-FB-T-84-203] 07 p0949 N85-16012
Two carrier dual injector apparatus
[AD-D011357] 07 p1047 N85-16646
A new very high voltage semiconductor switch
[NASA-TM-86957] 11 p1627 N85-20246
Automatic pickup of trajectory by method of sequential analysis taking into account deviation of radar markers from center of strobe 12 p1838 N85-21535
Basic EMC (electromagnetic interference) technology advancement for c3 systems. Volume 3A: Probabilistic analysis of combinational circuits with random delays
[AD-A150349] 13 p2055 N85-22666
All-optical logic gates with external switching by laser and incoherent radiation 18 p3187 N85-29766
Electro-optic techniques for VLSI interconnect
18 p3188 N85-29774
Energizing arrangement for charge coupled device control electrodes
[AD-D011712] 19 p3261 N85-30220
Digital integrated circuits 21 p3669 N85-32787

GAUGE INVARIANCE
Magnetic helicity in the solar corona
05 p0745 N85-14780
Cocycles and magnetic monopole
[DE85-007797] 16 p2856 N85-27612
Canonical analysis of the fermion sector in higher-derivative supergravity
[DE85-007828] 16 p2859 N85-27635
Summary of the discussion of the theory of radiative processes
[DE85-007812] 19 p3371 N85-30914
The dimensional reduction transition
[DE85-003948] 19 p3383 N85-30990
Gauge invariance and fractional quantized Hall effect
[DE85-007832] 23 p3985 N85-34716

GAUGE THEORY
Linear conformal gravitation 02 p0265 N85-11735
Gauge Theory on a Lattice, 1984: Proceedings
[DE84-014856] 02 p0291 N85-11892
Particle physics
[DE84-013834] 05 p0727 N85-14673
SU(2) x U(1) vacuum and the Centauro events
[NASA-TM-86082] 08 p1260 N85-17926
Nicolai maps and stochastic observables from a coupling constant flow
[BONN-HE-84-26] 09 p1376 N85-18653
Standard model and beyond
[DE85-004269] 14 p2418 N85-24919
Lattice overview
[DE85-007282] 15 p2662 N85-26427
Overview of the physics issues at the SSC
[DE85-007074] 16 p2859 N85-27634
Topics in intermediate vector boson physics
[NOTA-INTERNA-841] 18 p3184 N85-29743
Search for neutrino oscillations at the Brookhaven AGS
[DE85-009766] 20 p3530 N85-31957
Effects of CP violation in SU(2) sub L x SU(2) sub R x U(1) electroweak models
[DE85-010801] 20 p3531 N85-31965
Introduction to the Standard Model — weak and electromagnetic interactions
[USIP-85-02] 20 p3532 N85-31970
Does low-energy physics depend on the potential of a heavy Higgs-particle
[NIKHEF-H/85-1] 22 p3836 N85-33763

GAUSS EQUATION
A research program in active control/aeroelasticity in the JIAFS at NASA Langley Research Center
[NASA-CR-174052] 02 p0148 N85-11001
Equivocation limits in Gaussian additive channels
[INPE-2828-PRE/380] 04 p0492 N85-13137
Stochastic dynamic analysis of a structure with frictional joints 09 p1337 N85-18408
Checking the shape of discrete distributions
[DE85-000177] 11 p1706 N85-20733
Mathematical simulation of thermal prrocesses involved in electron-beam treatment 12 p1843 N85-21565
MATRIX: A program that shows how row and column orderings affect matrix fill-in
[DE85-007522] 15 p2630 N85-26213
Special relativity of Kaluza-Klein
[DE85-007638] 17 p3046 N85-28847
Analysis and model/data comparisons of large-scale releases of nitrogen tetroxide
[DE85-009969] 18 p3133 N85-29406
Nested dissection on a mesh-connected processor array
[AD-A154068] 19 p3342 N85-30711
Extended semiclassical calculations
[DE85-007824] 19 p3346 N85-30736
Comments on estimating quantiles for Gaussian functionals by simulation
[AD-A154302] 19 p3348 N85-30750
MANHIST user's guide
[DE85-010684] 19 p3348 N85-30754
Modulation transfer function for two-point and periodic objects using Gaussian and Lorentzian resolution functions
[PB85-187557] 19 p3368 N85-30891
An overview of latest model reduction and control methods of large flexible space structures
20 p3414 N85-31191
Frequency domain control design of large space structures: A practical approach
20 p3415 N85-31192
Diakoptic calculation of characteristics for optimization of linear circuits with respect to parameters of individual branches 22 p3767 N85-33346
Observations of Cygnus X-3 above 10(15) eV from 1979 - 1984
[OG-2.1-6] 22 p3863 N85-33923
Evaluation of source strength and dispersion model predications with data from large nitrogen tetroxide field experiments
[DE85-011655] 23 p3947 N85-34465
Master Fit users' guide, version 1.0
[DE85-014199] 24 p4140 N85-35667

GAUSS FUNCTION
U GAUSS EQUATION

GAUSS-MARKOV THEOREM
Nonlinear digital phase-locked loops with application to Loran-C receivers 24 p4063 N85-35178

GAUSSIAN DISTRIBUTIONS
U NORMAL DENSITY FUNCTIONS

GAUSSIAN NOISE
U RANDOM NOISE

GAUSSMETERS
U MAGNETOMETERS

GCR (REACTORS)
U GAS COOLED REACTORS

GEAR TEETH
Effect of coupled torsional-flexural vibration of a geared shaft system on the dynamic tooth load
09 p1338 N85-18415
Precision measurement of torsional oscillations induced by gear errors 09 p1338 N85-18416
Advanced gearbox technology in small turbo propeller engines 14 p2221 N85-23771
Software for designing teeth for reduction gears and transmissions 14 p2221 N85-23773
Load carrying capacity of double circular arc gears
14 p2221 N85-23776
Manufacturing perspective in the design of bevel gearing 14 p2221 N85-23777
Root stresses in conformal gears-strain gauge and photoelastic investigations 14 p2223 N85-23787
Gear noise origins 14 p2224 N85-23791
The observation and interpretation of gear tooth failures 14 p2224 N85-23792
New technology of finish cutting teeth in large gear blanks 14 p2267 N85-24047
Milling machine with numerical programmed control for cutting teeth 14 p2268 N85-24052
Tooth wear in worm gears in vacuum
16 p2766 N85-27070
Study of meshing of beveled gears with normally decreasing arc teeth
[NASA-TM-77866] 18 p3117 N85-29293
Improvement of conditions for meshing spiral bevel gears
[NASA-TM-77867] 18 p3117 N85-29294
Planetary-gear-support bearing test rig design
[NASA-CR-174927] 24 p4064 N85-35185

GEARS
Energy efficient engine ICLS engine bearings, drives and configuration: Detail design report
[NASA-CR-167871] 02 p0147 N85-10997
Vibrational power transmission of an idealised gearbox
[ISVR-TR-124] 02 p0204 N85-11346
The in-flight estimation and indication of cumulative fatigue damage to helicopter gears
[ARL/AERO-R-164] 03 p0317 N85-12050

Effect of lubricant extreme-pressure additives on surface fatigue life of AISI 9310 spur gears
[NASA-TP-2408] 04 p0507 N85-13234
MC2969 escapement study
[DE84-014542] 05 p0645 N85-14143
Effect of five lubricants on life of AISI 9310 spur gears
[NASA-TP-2419] 07 p0962 N85-16099
Gear case vibration isolation in a geared turbine generator 09 p1336 N85-18414
Precision measurement of torsional oscillations induced by gear errors 09 p1336 N85-18416
The guidelines to design the lever turning gears in articulated vehicles
[AD-P004301] 09 p1409 N85-18678
Characteristics of the elevation drive suspension of the 64-meter antennas 10 p1464 N85-19240
Missile launcher integral shock isolation and running gear system
[AD-D011490] 11 p1589 N85-19996
A deformation analysis of flat flexible gear and its equation of original curved surfaces
[NASA-TM-77493] 12 p1859 N85-21660
Gears and Power Transmission Systems for Helicopters and Turboprops
[AGARD-CP-369] 14 p2220 N85-23765
Summary of drive-train component technology in helicopters 14 p2220 N85-23766
Current transmission systems
14 p2220 N85-23767
Helicopter transmission lubricants
14 p2220 N85-23768
Advanced gearbox technology in small turbo propeller engines 14 p2221 N85-23771
Software for designing teeth for reduction gears and transmissions 14 p2221 N85-23773
Load capacity of cages of roller bearings for planet wheels 14 p2221 N85-23775
Load carrying capacity of double circular arc gears
14 p2221 N85-23776
Manufacturing perspective in the design of bevel gearing 14 p2221 N85-23777
Case depth on flanks of gears for helicopter gearboxes 14 p2222 N85-23780
The characteristics of surface roughness important to gear and rolling bearing problems
14 p2222 N85-23782
Significant parameters of the behavior and of the surface damage of the lubricated Hertzian contact: An application to gears 14 p2222 N85-23783
Problems of elastic hydrodynamic lubrication of helicopter transmission gears 14 p2222 N85-23784
Chemical-mechanical interaction in gears
14 p2223 N85-23785
Root stresses in conformal gears-strain gauge and photoelastic investigations 14 p2223 N85-23787
Transmission of gear noise to aircraft interiors prediction methods 14 p2223 N85-23788
Evolution of the design techniques for helicopter main transmission gearboxes 14 p2223 N85-23789
Condition monitoring of helicopter gearboxes using automatic vibration analysis techniques
14 p2223 N85-23790
Gear noise origins 14 p2224 N85-23791
Problems regarding the practical evaluation of efficiency of worm gears 14 p2224 N85-23793
Transmission error measurements in gearbox development 14 p2224 N85-23794
Modernization of running gear of crane
14 p2286 N85-24163
Tooth wear in worm gears in vacuum
16 p2766 N85-27070
A description of the 64-meter antenna elevation drive gears and their strange wear 16 p2771 N85-27107
An analytical investigation of dynamic coupling in nonlinear, geared rotor systems
16 p2792 N85-27218
Life and reliability modeling of bevel gear reductions
[NASA-TM-87006] 16 p2793 N85-27227
Fatigue life analysis of a turboprop reduction gearbox
[NASA-TM-87014] 16 p2793 N85-27228
Study of a test method for assessing machinability in gear cutting operations
[BLL-BISI-TRANS-22345-(9022.06)]
17 p2972 N85-28359
Assessing the machinability of gearwheel steels during manufacture
[BLL-BISI-TRANS-22343-(9902.06)]
17 p2973 N85-28365
Multi-mesh gear dynamics program evaluation and enhancements
[NASA-CR-174747] 17 p2974 N85-28372
Lubricant and additive effects on spur gear fatigue life
[NASA-TM-87044] 17 p2974 N85-28373
Study of meshing of beveled gears with normally decreasing arc teeth
[NASA-TM-77866] 18 p3117 N85-29293
Improvement of conditions for meshing spiral bevel gears
[NASA-TM-77867] 18 p3117 N85-29294
Powder metallurgy forged gear development
[NASA-TM-87483] 18 p3117 N85-29295
Spiral bevel and circular arc helical gears: Tooth contact analysis and the effect of misalignment on circular arc helical gears
[NASA-TM-87013] 20 p3395 N85-31060
A device for generating motive force through the expansion of a non-elastic dense fluid
[NASA-TM-77664] 20 p3454 N85-31446
A computer-controlled traverse gear for the Oxford wind engineering research group's 4 metre x 2 metre wind tunnel
[OUEL-1525/84] 20 p3483 N85-31514
A phase-locked frequency multiplier for the signal averaging of the vibration of the Wessex helicopter input spiral bevel pinion
[AD-A154914] 21 p3555 N85-32113
Proposal for modifications to the Wessex helicopter main rotor gearbox vibration monitoring program
[AD-A155196] 21 p3555 N85-32117
Department of Energy gear drive unit final prototype testing and design evaluation
[DE85-003296] 22 p3793 N85-33499
The design and development of a spacecraft appendage tie down mechanism 22 p3797 N85-33522
Some problems in high speed gears and gearing
23 p3923 N85-34312
High powered epicyclic gears: Some recent development 23 p3924 N85-34316
The design and analysis of single flank transmission error testor for loaded gears
[NASA-CR-176163] 23 p3937 N85-34404
Generated spiral bevel gears: Optimal machine-tool settings and tooth contact analysis
[NASA-TM-87075] 23 p3937 N85-34405
Lubrication and cooling for high speed gears
[NASA-TM-87096] 23 p3938 N85-34407
Elastohydrodynamic lubrication calculations used as a tool to study scuffing
[NASA-TM-87097] 23 p3938 N85-34408
Planetary-gear-support bearing test rig design
[NASA-CR-174927] 24 p4064 N85-35185
Establishment of a Computer-Aided Design (CAD)-Computer-Aided Manufacturing (CAM) process for the production of cold forged gears
[AD-A155756] 24 p4137 N85-35644

GEL PERMEATION CHROMATOGRAPHY
U LIQUID CHROMATOGRAPHY

GELATION
Study of reaction kinetics and development of elastic properties in network polymerization systems by the impulse technique
[AD-A148187] 08 p1133 N85-17141
Polymers and macromolecules
[DE85-003176] 10 p1454 N85-19160

GELS
NT DOUBLE BASE ROCKET PROPELLANTS
NT SILICA GEL
Automated apparatus for producing gradient gels
[DE84-014507] 01 p0107 N85-10716
Structural evolution during the gel to glass conversion
[DE84-014954] 06 p0772 N85-14939
Turbulent shear fields for dispersion of aqueous drops in organic liquids and application to gel-sphere processes
[DE84-016562] 06 p0809 N85-15141
Gel drawn fibers of poly(vinyl alcohol)
[AD-A149062] 10 p1435 N85-19040
Electrical and thermal performance during charging and discharging a Phase 1 gel cell battery
[PB85-114312] 11 p1677 N85-20565
Sol-gel processing of lead zirconate titanate films
[ATR-85(8343)-2] 18 p3073 N85-29010
A gel-halo sample pellet: The best of both worlds? Stubby zones without a constricted sample gate
20 p3502 N85-31770
Solid-state co-extrusion of nylon 6 gel
[AD-A156187] 24 p4082 N85-35298

GENERAL AVIATION AIRCRAFT
NT AGRICULTURAL AIRCRAFT
NT CESSNA 402B AIRCRAFT
NT DHC 2 AIRCRAFT
NT DO-28 AIRCRAFT
Review of aircraft accident data: US General Aviation
[PB84-230960] 01 p0005 N85-10027
Full-scale crash-test evaluation of two load-limiting subfloors for general aviation airframes
[NASA-TP-2380] 04 p0512 N85-13267
Annual review of aircraft accident data: US general aviation, calendar year, 1981
[PB84-230960] 06 p0750 N85-14805
Design study of technology requirements for high performance single-propeller-driven business airplanes
[NASA-CR-3863] 07 p0866 N85-1
Some characteristics of automotive gasolines and their performance in a light aircraft engine
[FAA-CT-84-12] 07 p0934 N85-1
Aerodynamic-structural study of canard wing, dual wing, and conventional wing systems for general aviation applications
[NASA-CR-172529] 08 p1077 N85-1
The design of sport and touring aircraft
[NASA-TM-77783] 10 p1423 N85-1
Wind-tunnel investigation of a full-scale canard-configured general aviation airplane
[NASA-TP-2382] 11 p1575 N85-1
Circulation control propellers for general aviation, including a BASIC computer program
[NASA-CR-165968] 19 p3219 N85-2
FAA regulation of 9-seat and under passenger aircraft
[GPO-42-703] 20 p3391 N85-3102
Quest for performance: The evolution of modern aircraft
[NASA-SP-468] 21 p3551 N85-32

GENERAL DYNAMICS AIRCRAFT
NT CL-41 AIRCRAFT
NT CV-990 AIRCRAFT
NT F-106 AIRCRAFT
NT F-111 AIRCRAFT

GENERAL DYNAMICS MILITARY AIRCRAFT
U MILITARY AIRCRAFT

GENERATION
Fuel cell applications literature review
[DE85-011891] 22 p3809 N85-33

GENERATORS
Continuous laminar smoke generator
[NASA-CASE-LAR-13014-1] 12 p1781 N85-2117
Coal-Fired MHD Combustor Development Project, Phase 3D
[DE85-008822] 18 p3192 N85-2
Design of a generator for near-tangential transonic swirling outflow
[AD-A155163] 21 p3584 N85-32
Control system for fluid heated steam generator
[DE85-005734] 23 p3939 N85-34417
Development of the osmium-191 yields iridium-191m radionuclide generator
[DE85-011185] 23 p3970 N85-34611
Current status of the Os-191 yields Ir-191m generator
[DE85-008306] 23 p3971 N85-34614

GENETIC CODE
Genetics in methylotrophic bacteria
[DE85-011460] 19 p3327 N85-30815

GENETIC ENGINEERING
Genetic engineering of plants: Agricultural research opportunities and policy concerns
[DE85-006771] 16 p2840 N85-27513
East Europe report: Science and technology
[JPRS-ESA-85-023] 21 p3572 N85-32217

GENETICS
NT GENETIC CODE
NT MUTATIONS
USSR report: Life sciences. Biomedical and behavioral sciences
[JPRS-UBB-84-025] 04 p0543 N85-134
Study of mathematical models of mutation and selection in multi-locus systems
[DE85-000873] 09 p1376 N85-1
Genetic effects of microwave exposure on mammalian cells in vitro. Volume 2, Appendix A: Cytogenetics and growth kinetics data, 850 MHz
[AD-A148866] 10 p1522 N85-1
Oversight review of the five-year outlook report on science and technology
[GPO-41-058] 12 p1949 N85-22
USSR report: Life sciences. Biomedical and behavioral sciences
[JPRS-UBB-85-012] 14 p2386 N85-24
Towards a statistical analysis of genetic sequences data with particular reference to protein sequences
[AD-A153605] 18 p3152 N85-29515
Chromosome aberrations in Crepis capillaris exposed to gamma radiation and clinostat
19 p3325 N85-30
Genetics in methylotrophic bacteria
[DE85-011460] 19 p3327 N85-30815
Biocatalysis project
[NASA-CR-176044] 20 p3498 N85-31744
Organization of the R region in maize
[DE85-011273] 20 p3504 N85-317
Search for the universal ancestors
[NASA-SP-477] 21 p3667 N85-32777
USSR report: Life sciences. Biomedical and behavioral sciences
[JPRS-UBB-85-018] 22 p3819 N85-33

Three-dimensional reconstruction and data display of chromosome structure studied by electron microscope tomography
[DE85-011582] 22 p3825 N85-33697

Genetic and physiological control of protective antigen synthesis by bacillus anthracis
[AD-A158324] 24 p4133 N85-35617

GENITOURINARY SYSTEM
NT BLADDER

GEOASTROPHYSICS
U ASTROPHYSICS
U GEOPHYSICS

GEOBOTANY

Remote sensing as a mineral prospecting technique
[E85-10010] 02 p0216 N85-11423

NASA's land remote sensing plans for the 1980's
13 p2124 N85-23224

Carbon isotope geochemistry and geobiology
21 p3657 N85-32716

GEOCENTRIC COORDINATES

Increasing the accuracy of processing radar pictures by excluding systematic point coordinate error component
15 p2488 N85-25356

Global coordinate system
[AD-A153878] 19 p3299 N85-30454

GEOCHEMISTRY
NT BIOGEOCHEMISTRY

Thermodynamic properties and environmental chemistry of chromium
[DE84-015123] 01 p0025 N85-10152

Hydrogeochemical investigation of thermal springs in the Black Canyon-Hoover Dam area, Nevada and Arizona
[PB84-202472] 01 p0064 N85-10428

The marine geochemistry of the rare earth elements
[AD-A145132] 01 p0068 N85-10596

The Alaskan mineral resources assessment program: Guide to information contained in the folio of geologic and mineral-resource maps of the Medfra Quadrangle, Alaska
[GS-CIRC-928] 02 p0219 N85-11443

The petrology and geochemistry of high cascade volcanics in southern Washington: Mount Saint Helens volcano and the Indian Heaven basalt field
02 p0227 N85-11487

Geology and geochemistry of early Tertiary submarine volcanic rocks of the Aleutian Islands, and their bearing on the development of the Aleutian Island Arc
03 p0389 N85-12493

The United States Geological Survey in Alaska: Accomplishments during 1981
[USGS-CIRC-868] 04 p0515 N85-13283

Geology and geochemical evolution of the Lost River, Alaska, tin deposit 04 p0533 N85-13405

Geophysical and geochemical constraints favoring the capture hypothesis 04 p0581 N85-13710

Tests of the lunar hypothesis
04 p0584 N85-13730

Geochemical evidence for the formation of the Moon by impact induced fission of the proto-Earth
04 p0587 N85-13747

An integrated dynamical and geochemical approach to lunar origin modelling 04 p0587 N85-13748

A circumterrestrial compositional filter
04 p0588 N85-13753

Summaries of physical research in the geosciences
[DE85-001862] 06 p0818 N85-15194

Manganese in recent sediments of Ukrainian SSR Black Sea shelf 06 p0819 N85-15200

Geochemical data for rock samples from the Petersburg and parts of the Port Alexander and Sumdum quadrangles, southeastern Alaska (documentation)
[PB84-234434] 06 p0836 N85-15318

Alabama Tin Belt: Metallogenesis and mineral resource evaluation. Year-end report
[DE84-001335] 07 p0989 N85-16283

Analysis of gases in the Earth's crust
[PB85-113397/GAR] 07 p0990 N85-16287

Earth Sciences Division report, 1983
[DE85-001036] 09 p1341 N85-18436

Correlation and petrological interpretation of abyssal and terrestrial tephra layers 09 p1353 N85-18512

Relationship of gold content to gravity fields in Far East 10 p1501 N85-19475

Radioactive waste isolation in salt: Peer review of the Office of Nuclear Waste Isolation's report on the organic geochemistry of deep groundwaters from the Palo Duro Basin, Texas
[DE85-001439] 10 p1556 N85-19811

Research and development related to the Nevada nuclear waste storage investigations
[DE85-002303] 12 p1932 N85-22138

Reports of the Planetary Geology and Geophysics Program, 1984
[NASA-TM-87563] 13 p2172 N85-23474

Hibonite: Crystal chemistry and origin of blue coloration in meteoritic assemblages 13 p2184 N85-23555

Basalts of Mars: Constraints on volatile evolution
13 p2194 N85-23610

USSR report: Earth sciences
[JPRS-UES-85-004] 14 p2332 N85-24424

Most important geochemical barrier zones in ocean (with example of Atlantic Ocean basin)
14 p2343 N85-24491

Geological information content of reflected wave record form 14 p2345 N85-24502

Deep source gas
[DE85-001964] 18 p3126 N85-29358

Radionuclide mobility in the shallow portion of an active high-temperature geothermal system
[DE85-010293] 18 p3182 N85-29729

Geochemistry of manganese in ocean
19 p3291 N85-30406

Mineralogical-geochemical characteristics of ferromanganese formations in Arabian-Indian Ocean Ridge 19 p3293 N85-30416

Petrologic and geochemical characterization of the Topopah Spring Member of the Paintbrush Tuff: Outcrop samples used in waste package experiments
[DE85-010449] 19 p3302 N85-30470

Proceedings of the Fifth International Conference on Nuclear Methods in Environmental and Energy Research
[DE84-017346] 19 p3310 N85-30521

Subsurface petroleum geology of Santa Rosa sandstone (Triassic), northeast New Mexico
[TI85-901364] 19 p3313 N85-30536

Clay identification and amount measured by laboratory techniques compared to well log responses: Application to tight gas sands and shales
[DE85-010411] 19 p3362 N85-30843

The U.S. Geological Survey in Alaska: Accomplishments during 1982
[US-GEOL-SURV-CIRC-939] 20 p3493 N85-31719

Global Mega-Geomorphology
[NASA-CP-2312] 21 p3600 N85-32357

Carbon isotope geochemistry and geobiology
21 p3657 N85-32716

Geology and geochemistry of sulfide and sulfate deposition 21 p3658 N85-32723

Microbiology of solar salt ponds
21 p3658 N85-32724

Workshop on the Early Earth: The Interval from Accretion to the Older Archean
[NASA-CR-176037] 21 p3717 N85-33062

The relation between the age of the subconducting slab and the recycling of sediments into the mantle
21 p3717 N85-33063

The 3.5 b.y. old Onverwacht Group: A remnant of ancient oceanic crust 21 p3718 N85-33073

A review of noble gas geochemistry in relation to early Earth history 21 p3720 N85-33081

The Aravalli sequence of Rajasthan, India: A Precambrian continental margin?
21 p3720 N85-33084

Carbon and nitrogen in the deep Earth
21 p3721 N85-33085

Chemical evolution of the Earth: Equilibrium or disequilibrium process? 21 p3721 N85-33088

Thermal, dynamic and compositional aspects of the core-forming Earth 21 p3722 N85-33091

Geologic processes on Venus: An update
22 p3857 N85-33883

Geochemical confirmation of the lunar magmasphere hypothesis 22 p3859 N85-33895

Thermally induced chemical migration: A natural analog approach
[DE85-012308] 23 p3949 N85-34474

Chemistry division report
[DE85-010586] 24 p4071 N85-35228

The role of regional subsurface geochemistry in resource assessment in the central United States
24 p4104 N85-35440

The development of assessment techniques program
24 p4106 N85-35457

The Alaska Mineral Resources Assessment Program
24 p4107 N85-35460

GEOCHRONOLOGY

Erosion and sedimentation chronology of three watersheds in Maryland
[PB84-207356] 01 p0071 N85-10467

On gravity from SST, geoid from Seasat, and plate age and fracture zones in the Pacific
[E85-10020] 02 p0217 N85-11433

The United States Geological Survey in Alaska: Accomplishments during 1981
[USGS-CIRC-868] 04 p0515 N85-13283

Reconnaissance geology of the northern part of the Unalakleet quadrangle 04 p0516 N85-13291

Newly recognized sedimentary environments in the Shelikof Formation, Alaska 04 p0516 N85-13292

New ages of radiolarian chert from the Rampart district, east-central Alaska 04 p0516 N85-13293

Paleozoic limestones of the Crazy Mountains and vicinity, Circle quadrangle, east-central Alaska
04 p0517 N85-13296

Late Paleozoic and early Mesozoic radiolarians in the Circle quadrangle, east-central Alaska
04 p0517 N85-13297

Structural observations in the Circle quadrangle, Yukon-Tanana Upland, Alaska 04 p0517 N85-13298

Lacustrine and eolian deposits of Wisconsin age at Riverside Bluff in the upper Tanana River valley, Alaska
04 p0517 N85-13299

Glacial-lake deposits in the Mount Harper area, Yukon-Tanana Upland 04 p0517 N85-13300

Paleogene volcanic rocks of the Matanuska Valley area and the displacement history of the Castle Mountain fault 04 p0518 N85-13303

Progress in lead/uranium zircon studies of lower paleozoic rocks of the southern Alexander terrane
04 p0518 N85-13304

Geology and geochemical evolution of the Lost River, Alaska, tin deposit 04 p0533 N85-13405

The I-Pu-Xe age of the Moon
04 p0584 N85-13729

Constraints on lunar origin: Evidence preserved in Precambrian stromatolites 04 p0584 N85-13731

A tectonic and metamorphic history of the north-central Klamath Mountains, California 05 p0673 N85-14323

Tectonic history of a continent: Island arc boundary, west-central Idaho 05 p0673 N85-14324

Geophysical investigation of precambrian crustal structure and Laramide effects across a precambrian suture in southeastern Wyoming
05 p0674 N85-14328

Quaternary stratigraphy, geochronology and carbon isotope geology of alluvial deposits in the Texas panhandle 09 p1353 N85-18514

Major glaciation events of the past and their geological significance 10 p1497 N85-19450

Post-carboniferous tectonics in the Anadarko Basin, Oklahoma: Evidence from side-looking radar imagery
[NASA-CR-175458] 10 p1505 N85-19496

Crustal dynamics studies in China
[NASA-CR-175617] 13 p2132 N85-23265

Why not a constant early lunar impact rate?
13 p2181 N85-23536

Martian terrain ages 13 p2181 N85-23537

The geology of Mt. Hope, a silicic volcanic center in West Central Arizona 13 p2187 N85-23571

Geomorphology and geology of the Southwestern Margaritifer Sinus and Argyre regions of Mars. Part 2: Crater size-frequency distribution curves and geomorphic unit ages 13 p2192 N85-23601

Chondrule-like particles provide evidence of early Archean meteorite impacts, South Africa and western Australia 15 p2682 N85-26562

Structural and tectonic history of the Golconda allochton, southern Toiyabe Range, Nevada
19 p3312 N85-30529

Global Mega-Geomorphology
[NASA-CP-2312] 21 p3600 N85-32357

Some observations on paleogeomorphology
21 p3601 N85-32363

Landscape inheritance: Report of Working Group Number 2 21 p3604 N85-32383

Precambrian evolution and the rock record
21 p3656 N85-32711

Origin of life 21 p3657 N85-32713

The 3.5 b.y. old Onverwacht Group: A remnant of ancient oceanic crust 21 p3718 N85-33073

Archean sedimentary systems and crustal evolution
21 p3720 N85-33082

The Aravalli sequence of Rajasthan, India: A Precambrian continental margin?
21 p3720 N85-33084

Chemical constraints on the evolution of Archean continental crust 21 p3722 N85-33093

Dating Archean zircon by ion microprobe: New light on an old problem 21 p3722 N85-33094

Geology and petroleum resources of basins in western China
[DE85-013038] 23 p3948 N85-34469

Early and middle Cenozoic volcanic synthesis
24 p4105 N85-35449

Hydrogeology of the lower Glen Rose Aquifer, south-central Texas 24 p4108 N85-35466

GEOCORONAL EMISSIONS

High resolution geocoronal Balmer alpha observations
20 p3489 N85-31686

GEODESIC LINES

Harmonic analysis and Radon transforms on pencils of geodesics
[CWI-PM-R8413] 12 p1922 N85-22074

Reflected wave travel-time curves in stratified media with vertically heterogeneous layers and slightly sloping curved boundaries 13 p2114 N85-23167

Informative geometry of probability spaces
[AD-A150510] 13 p2153 N85-23371

GEODESY

NT CELESTIAL GEODESY

Global positioning system: Geodetic applications
[AD-A144904] 01 p0005 N85-10030

Prediction of deflections of the vertical by gravimetric methods
[PB84-213727] 01 p0072 N85-10478

Use and value of a geodetic reference system
[PB84-216167] 03 p0379 N85-12418

Investigation of several aspects of LANDSAT 4/5 data quality
[E85-10038] 04 p0525 N85-13357

An interactive FORTRAN program for determining reliability of pseudo-range geodetic point positioning using the global positioning system
[AD-A147133] 07 p0988 N85-16275

Altimetry, orbits and tides
[E85-10066] 08 p1174 N85-17404

Mathematical aspects of digital terrain information; Report from International Society for Photogrammetry and Remote Sensing (ISPRS) working group 3:3, 1980 - 1984 — photogrammetry 08 p1175 N85-17407

Using the global positioning system (GPS) phase observable for relative geodesy: Modeling, processing, and results 09 p1341 N85-18437

Activities report of the Department of Applied Research 78 for satellite geodesy of the Technical University, Munich
[ASTRON-GEODAET-ARB-45]
09 p1342 N85-18440

Continental networks: Report on the activities of the International Association of Geodesy (IAG) Commission 10, 1979 - 1983 — geodesy
[SER-B-266] 09 p1342 N85-18441

World Geodetic System, 1984
[AD-A147409] 09 p1342 N85-18445

Computer programs for the adjustment of indirect observation with condition equations between the unknowns
[SER-B-268-MITT-170] 09 p1370 N85-18612

Utilization of mobile VLBI for geodetic measurements
10 p1466 N85-19248

Study of tectonic earthquake precursors by geodetic methods 10 p1502 N85-19479

Geodetic accuracy of LANDSAT 4 Multispectral Scanner and Thematic Mapper data — Washington, DC, California, Alabama, South Dakota, and Illinois
11 p1667 N85-20504

Geometric accuarcy assessment of LANDSAT-4 Multispectral Scanner (MSS) data
11 p1667 N85-20505

Program INNAVSAT: Global Positioning System (GPS): Test and demonstration program
[BMFT-FB-W-84-047] 12 p1775 N85-21145

Hybrid method of mapping and photogeodetic control network densification
[PB85-133775] 12 p1876 N85-21766

Use of three omega radionavigation system position lines for solving problems in marine geodesy
13 p2107 N85-23131

Determining vector of radiointerferometer base from observations of natural radio emission with narrow spectrum 13 p2112 N85-23158

Development, achievements in China's cartography work 13 p2166 N85-23434

A unified lunar control network
13 p2203 N85-23669

The control network of Mars: October 1984
13 p2203 N85-23670

The control networks of the satellites of Jupiter and Saturn 13 p2204 N85-23671

Shape of Io 13 p2204 N85-23672

Application of space methods in geodesy
16 p2724 N85-26817

Radial orbit error spectrum for Topex
16 p2805 N85-27292

Astrometric method advances Astronomy, geodesy
16 p2806 N85-27306

Reports on cartography and geodesy. Series 1: Original reports, no. 94
[ISSN-0469-4236] 16 p2814 N85-27357

Use of vector processors in cartographic raster data processing, with special regard to the AP-120B vector processor 16 p2814 N85-27358

Standards and specifications for geodetic control networks
[PB85-166478] 16 p2816 N85-27374

Water vapor radiometry research and development phase
[NASA-CR-175887] 17 p2995 N85-28512

Information relative to cartography and geodesy. Series 2: Translations, number 42, volume 1
[ISSN-0469-4244] 18 p3123 N85-29338

Reports on cartography and geodesy. Series 1: Original reports, number 93
[ISSN-0469-4236] 18 p3124 N85-29343

Use of stereographic projection in marine geodesy
19 p3294 N85-30421

HANDTC: A FORTRAN program to calculate inner-zone terrain corrections
[DE85-011196] 19 p3340 N85-30699

Geodyn systems development
20 p3492 N85-31708

Crustal dynamics project data analysis fixed station VLBI geodetic results
[NASA-TM-86229] 21 p3615 N85-32465

SPLINES. Their equivalence to collocation
[AD-A155250] 21 p3632 N85-32566

Crustal Dynamics Project: Catalogue of site information
[NASA-TM-86216] 22 p3801 N85-33552

GEODETIC ACCURACY

Global positioning system: Geodetic applications
[AD-A144904] 01 p0005 N85-10030

An investigation of several aspects of LANDSAT-5 data quality — Palmer County, Shelby, mt; White sands, NM; Great Salt Lake, UT; San Matted Bridge and Sacramento, California
[E85-10096] 13 p2122 N85-23214

Minimizing influence of Earth's curvature in projective rectification of space photographs into photoplans and photomaps 16 p2727 N85-26829

New VLBI technology developments
20 p3491 N85-31702

Error spectrum of Goddard satellite models for the gravity field 20 p3491 N85-31704

GEODETIC COORDINATES

Diagnosis and therapy of geodetic satellite networks of Doppler type — error analysis
[SER-C-293] 01 p0015 N85-10090

A strategy for the adjustment and analysis of densification networks — geodetic networks
[SER-C-295] 01 p0063 N85-10420

Testing of a field portable GPS (Global Positioning System) geodetic receiver
[AD-A148336] 08 p1082 N85-16859

Continental networks: Report on the activities of the International Association of Geodesy (IAG) Commission 10, 1979 - 1983 — geodesy
[SER-B-266] 09 p1342 N85-18441

A three-dimensional geometric-physical model for conventional geodetic observations-observables, parameter estimation, and deformation analysis
[SER-C-298] 11 p1665 N85-20493

The 1980 diagnostic adjustment of the German main triangulation network. 4: Network adjustment (part 3)
[SER-B-267-PT-3-MITT-168] 11 p1665 N85-20494

The 1980 diagnostic adjustment of the German main triangulation network. 4: Network adjustment (part 1)
[SER-B-267-PT-1-MITT-168] 11 p1670 N85-20525

The 1980 diagnostic adjustment of the German main triangulation network. 4: Network adjustment (part 2)
[SER-B-267-PT-2-MITT-168] 11 p1670 N85-20526

Evaluating accuracy in determining position of Earth's center of mass and elements of orientation of geodetic coordinate system 13 p1983 N85-22441

Determining vector of radiointerferometer base from observations of natural radio emission with narrow spectrum 13 p2112 N85-23158

Study of phase radiogeodetic systems with phase-locked loops 13 p2115 N85-23172

Location and synchronization — space-time coordinates 14 p2397 N85-24768

UTM (Universal Transverse Mercator) determinations from geographical data
[AD-A152293] 16 p2856 N85-27610

Allowance for differences in ellipsoids and geodetic control coordinate systems in determining ship's position using radio navigation systems
19 p3292 N85-30413

Global coordinate system
[AD-A153878] 19 p3299 N85-30454

Comparing SLR and VLBI geodetic parameters
20 p3491 N85-31703

Basic formulae for the computation of the deflection of the vertical from astronomical star observations
[AD-A154912] 21 p3605 N85-32390

GEODETIC SATELLITES

NT GEOS 1 SATELLITE
NT GEOS 2 SATELLITE
NT GEOS 3 SATELLITE

The motion of the Earth by Doppler observing campaign (MEDOC) 05 p0801 N85-13831

Establishment of hydrographic shore control by Doppler satellite techniques
[AD-A150709] 14 p2347 N85-24512

GEODETIC SURVEYS

NASA Geodynamics Program
[NASA-TM-87359] 01 p0063 N85-10418

Basic research for the geodynamics program
[NASA-CR-174055] 02 p0228 N85-11480

Tides and tidal currents of the inland waters of Western Washington
[PB84-237379] 06 p0842 N85-15346

Continental networks: Report on the activities of the International Association of Geodesy (IAG) Commission 10, 1979 - 1983 — geodesy
[SER-B-266] 09 p1342 N85-18441

Utilization of mobile VLBI for geodetic measurements
10 p1466 N85-19248

A three-dimensional geometric-physical model for conventional geodetic observations-observables, parameter estimation, and deformation analysis
[SER-C-298] 11 p1665 N85-20493

The 1980 diagnostic adjustment of the German main triangulation network. 4: Network adjustment (part 1)
[SER-B-267-PT-1-MITT-168] 11 p1670 N85-20525

The 1980 diagnostic adjustment of the German main triangulation network. 4: Network adjustment (part 2)
[SER-B-267-PT-2-MITT-168] 11 p1670 N85-20526

Hybrid method of mapping and photogeodetic control network densification
[PB85-133775] 12 p1876 N85-21766

Planetary cartography in the next decade (1984 - 1994)
[NASA-SP-475] 12 p1980 N85-22323

Consideration of heterogeneity of gravity fields in local high precision geodetic constructions
13 p2114 N85-23169

Mathematical modeling of results of geometric leveling in variable gravity field 13 p2114 N85-23170

Crustal dynamics project: Catalogue of site information
[NASA-TM-87452] 13 p2131 N85-23258

Establishment of hydrographic shore control by Doppler satellite techniques
[AD-A150709] 14 p2347 N85-24512

Preliminary processing of laser ranging data from LAGEOS artificial Earth satellite during short merit program observation period 15 p2488 N85-25365

Increasing the accuracy of processing radar pictures by excluding systematic point coordinate error component
15 p2488 N85-25366

Application of the Siemens Computer Aided Computer (Sicad) system to the surveying management in Baden-Wuerttemberg 16 p2814 N85-27361

Derivation of model topography
18 p3141 N85-29449

A comparison of methods of least squares adjustment of traverses
[AD-A153612] 18 p3170 N85-29645

Application of GPS in a high precision engineering survey network
[DE85-010556] 19 p3313 N85-30538

Carbon fiber strainmeter studies in southern California
[PB85-196889] 24 p4118 N85-35528

GEODYNAMICS

NASA Geodynamics Program
[NASA-TM-87359] 01 p0063 N85-10418

The SANCOR programme on coastal processes, April 1982 - March 1988
[REPT-68] 01 p0069 N85-10455

Basic research for the geodynamics program
[NASA-CR-174055] 02 p0228 N85-11480

General model of earthquakes and the place of warnings in it 07 p0981 N85-16232

Earthquake forecasting research in the Ukraine
07 p0981 N85-16233

Activities report of the Department of Applied Research 78 for satellite geodesy of the Technical University, Munich
[ASTRON-GEODAET-ARB-45]
09 p1342 N85-18440

Structural morphology and associated strain within parts of the US section of the Kootenay Arc, NE, Washington
09 p1352 N85-18506

Mesozoic magmatism of Mongolian-Okhotsk Belt and its possible geodynamic interpretation
10 p1502 N85-19481

Science Applications, part 2 11 p1643 N85-20047

Summary presentation of the Science Applications Panel 11 p1644 N85-20055

Absolute movement of Pacific Ocean plate during last 120 million years 13 p2107 N85-23128

Crustal dynamics project: Catalogue of site information
[NASA-TM-87452] 13 p2131 N85-23258

Crustal dynamics studies in China
[NASA-CR-175617] 13 p2132 N85-23265

Reference systems — in space mechanics
14 p2399 N85-24784

Example of joint use of data from surface studies and space photographs in investigating dynamics of zone of North Zeravshan seismogenic faults
15 p2485 N85-25342

Basic research for the geodynamics program
[NASA-CR-175751] 16 p2825 N85-27424
Kuril-Aleutian subduction 19 p3290 N85-30402
Investigation of dynamic noise affecting geodynamics information in a tethered subsatellite
[NASA-CR-176031] 20 p3476 N85-31602
Geodynamics Branch research program
[NASA-TM-86223] 20 p3489 N85-31688
The Earth's wobble and associated ocean motions
20 p3490 N85-31696
NASA/GSFC TOPEX gravity model operations group
20 p3492 N85-31709
Precambrian evolution and the rock record
21 p3656 N85-32711
Thermal, dynamic and compositional aspects of the core-forming Earth 21 p3722 N85-33091
Mapping of dynamics of deltas by space photography
22 p3737 N85-33163

GEOELECTRICITY
NT TELLURIC CURRENTS
Possible effects of interaction of electric seismic fields with the ionosphere 06 p0823 N85-15228
Brazil future plans in upper atmosphere research in Antarctica
[INPE-3400-PRE/669] 10 p1515 N85-19559
Discrimination of normal and anomalous magnetic and electric fields in geoelectromagnetic variations
13 p2114 N85-23166
Electromagnetic fields migration method
14 p2343 N85-24487
Report of the geomagnetic and geoelectric observations, 1983 (rapid variations)
[REPT-24] 15 p2591 N85-25975

GEOFRACTURES
U GEOLOGICAL FAULTS

GEOGRAPHIC INFORMATION SYSTEMS
Use and value of a geodetic reference system
[PB84-216167] 03 p0379 N85-12418
Building a functional, integrated GIS/remote sensing resource analysis and planning system — Utah
[E85-10092] 12 p1874 N85-21754

GEOGRAPHY
NT HYPSOGRAPHY
NT OROGRAPHY
Environmental geologic atlas of the North Carolina coastal zone: Dare, Hyde, Tyrrell and Washington Counties
[PB84-222975] 01 p0068 N85-10439
The Multispectral Imaging Science Working Group. Volume 1: Executive summary
[E85-10001] 02 p0213 N85-11404
The Multispectral Imaging Science Working Group. Volume 2: Working group reports
[E85-10002] 02 p0213 N85-11405
Geographic and stratigraphic distribution of Miocene palynomorphs in north Idaho 03 p0390 N85-12498
Calculation of the area covered by mobile radio systems using geographic data stored in a computer
[FUB-43-1983] 09 p1312 N85-18247
The sharing of remote sensing techniques in Brazilian geographic research
[INPE-3307-PRE/617] 10 p1506 N85-19502
Review of computer mapping and display techniques applicable to regional analysis
[DE85-003545] 12 p1875 N85-21764
Hexagonal data base study
[AD-A150176] 13 p2167 N85-23448
MAP3S precipitation chemistry network
[DE85-006324] 14 p2353 N85-24539
Activities report of the Laboratory for Computer Science (FOA 32)
[FOA-C-30384-E1] 20 p3516 N85-31861
Applied computer graphics in a geographic information system: Problems and successes
23 p3962 N85-34563

GEOIDS
On gravity from SST, geoid from Seasat, and plate age and fracture zones in the Pacific
[E85-10020] 02 p0217 N85-11433
Determination of geoid undulations and ocean heights from ERS-1 radar altimetry data
03 p0381 N85-12432
Satellite altimetry for sea-surfacing topography determination and geoid improvement
03 p0382 N85-12444
Determination of the altimetric geoid and gravity anomalies in the North Sea: Implications for a solution of the general circulation problem using ERS-1 data
03 p0382 N85-12446
Local geoid determination in mountain regions
[AD-A145799] 03 p0384 N85-12458
Lithospheric structure in the Pacific geoid
[NASA-CR-174155] 04 p0526 N85-13365
Altimetry, orbits and tides
[E85-10066] 08 p1174 N85-17404
Simultaneous determination of the xi and eta components of vertical deflection with a prism astrolabe
[SER-B-270-MITT-171] 09 p1343 N85-18450
The Gauss-Krueger projection of the Earth ellipsoid with direct calculation of elliptic integrals through Landen transformations
[SER-C-296] 11 p1666 N85-20495
Physiography of the Martian west equatorial uplift
12 p1961 N85-22325
On geoid heights and flexure of the lithosphere at seamounts
[AD-A151220] 15 p2604 N85-26050
Altimetry data and the elastic stress tensor of subduction zones
[NASA-CR-175796] 16 p2825 N85-27425
Application of GPS in a high precision engineering survey network
[DE85-010556] 19 p3313 N85-30539
Evolution of the oceanic upper mantle and effects on sea floor subsidence geoid height and heat flow
19 p3319 N85-30575
Spaceborne gradiometer error analysis
20 p3492 N85-31707
Global mean sea surface based upon a combination of the GEOS-3 and SEASAT altimeter data
20 p3492 N85-31710
The time averaged circulation of the oceans from satellite altimetry 20 p3493 N85-31713
Dynamic compensation of Venus's geoid: A comparison with Earth 22 p3858 N85-33888
A dynamic model of Venus's gravity field
[NASA-CR-176173] 24 p4169 N85-35845

GEOLOGICAL FAULTS
NT SAN ANDREAS FAULT
Seismic studies in southern Alaska
04 p0515 N85-13286
Paleogene volcanic rocks of the Matanuska Valley area and the displacement history of the Castle Mountain fault 04 p0518 N85-13303
Petrologic model of the northern Mississippi embayment based on satellite magnetic and ground based geophysical data
[NASA-TM-85075] 04 p0533 N85-13406
Blind zones and aspect ratio bias in acquisition of discontinuity orientation data
[DE84-002718] 04 p0533 N85-13410
Rio Grande rift: Problems and perspectives
[DE84-015492] 04 p0534 N85-13417
Synthesis of proterozoic data as a prerequisite for tectonic and thermal modeling
[NASA-CR-174252] 07 p0995 N85-16323
New Zealand SIR-B science investigations
08 p1144 N85-17218
Analysis of SIR-B radar illumination of geometry for depth of penetration and surface feature and vegetation detection, Nevada and California
08 p1149 N85-17248
Modeling of large-scale accretionary wedge and thin-skinned trust-and-fold belt mechanics
08 p1181 N85-17442
Mesozoic ophiolitic olistostromes and Cenozoic imbricate thrust faulting in the northern California coast ranges: Geology of the Mysterious Valley area, Napa County 08 p1182 N85-17445
Thermal conditions and thinning of lithosphere in late cenozoic in southwestern US 10 p1501 N85-19473
Tectonic position and formation of young alkaline provinces of continents and oceans
10 p1502 N85-19480
Nonlinear seismology 10 p1503 N85-19482
Statistical study of anthropogenic seismic noise with IVK-7 computer system 10 p1503 N85-19483
SIR-A imagery in geologic studies of the Sierra Madre Oriental, northeastern Mexico. Part 1 (Regional stratigraphy): The use of morphostratigraphic units in remote sensing mapping
[NASA-CR-175457] 10 p1505 N85-19497
Post-carboniferous tectonics in the Anadarko Basin, Oklahoma: Evidence from side-looking radar imagery
[NASA-CR-175458] 10 p1505 N85-19498
Tectonic lineaments in the cenozoic volcanics of southern Guatemala: Evidence for a broad continental plate boundary zone
[NASA-CR-175456] 10 p1505 N85-19499
Arctic-North Atlantic rift megasystem
13 p2105 N85-23117
Crustal and upper mantle density model of Owen fault zone 13 p2110 N85-23144
Numerical modeling of plane stick-slip fault
13 p2111 N85-23150
Study of geological media based on scattered earthquake waves 13 p2114 N85-23168
Crustal dynamics project: Catalogue of site information
[NASA-TM-87452] 13 p2131 N85-23258
Normal-fault and fold development in sedimentary rocks above a pre-existing basement normal fault
13 p2131 N85-23259
Crustal dynamics studies in China
[NASA-CR-175617] 13 p2132 N85-23265
Volcanism and rift formation in Beta Regio, Venus: New radar results 13 p2176 N85-23507
Volcanic debris flows in the Elysium region of Mars
13 p2185 N85-23560
Geomorphology and geology of the Southwestern Margaritifer Sinus and Argyre regions of Mars. Part 1: Geological and geomorphological overview
13 p2192 N85-23600
On the absence of strike-slip faults from the planets and satellites 13 p2200 N85-23645
Lunar mascon loading: An example of the importance of fault initiation depth on fault type predictions from stresses on planetary surfaces
13 p2200 N85-23646
Elysium region, Mars: Tests of lithospheric loading models for the formation of tectonic features
13 p2200 N85-23650
Creep of ice: Further studies
13 p2201 N85-23655
Fault offsets and lateral crustal movement on Europa
13 p2201 N85-23656
Laboratory investigation of formation damage of an artificial fracture at simulated geothermal conditions
[DE85-010301] 18 p3102 N85-29201
Structure of Reykjanes Ridge rift zone and Icelandic thermal anomaly 19 p3289 N85-30395
Discovery in earthquake forecasting and seismic zoning recorded 19 p3295 N85-30426
Tectonic structure features of some deep faults in Atlantic and Pacific Oceans (according to deep seismic sounding-reflected waves method data)
19 p3295 N85-30428
Fracture detection and mapping for geothermal reservoir definition: An assessment of current technology, research, and research needs
[DE85-010627] 19 p3301 N85-30464
Comparative study of fracture planes computed from topography and lineaments from imagery with structures and mineralization in the magnetic belt of Washington State
[DE85-010972] 20 p3477 N85-31608
Design of a freestanding noise measurement and recording system to predict the intensity and location of electromagnetic radiation from earthquakes
[AD-A155070] 21 p3632 N85-32563
Spacecraft-aided research discussed at geology Congress 22 p3734 N85-33147
Landscape interpretation capabilities using space photographs of regions of a multistage platform mantle structure 22 p3734 N85-33151
Fracture detection and characterization for geothermal reservoir definition
[DE85-008677] 22 p3815 N85-33630
Indications of mineral zoning in a fossil hydrothermal system at the Meager Creek geothermal prospect, British Columbia, Canada from induced polarization studies
[DE85-011962] 22 p3815 N85-33636
Compressional environment in the location and orientation of planetary dorsa and terrestrial earthquake fault structures 22 p3857 N85-33885
Comprehensive fracture diagnostics experiement. Part 2: Comparison of seven fracture azimuth measurements
[DE85-011707] 23 p3948 N85-34470
Studies in thermo-hydro-chemical transport in porous and fractured media
[DE85-012555] 23 p3949 N85-34473
Geophysical-geological studies of possible extensions of the New Madrid fault zone
[TI85-901341] 23 p3949 N85-34475
Geology: Structural history and fluvial geomorphology of the southern Death Valley Fault Zone, Inyo and San Bernardino Counties, California
24 p4114 N85-35506
Structural development of the west-central Grant Range, Nye County, Nevada 24 p4115 N85-35508

GEOLOGICAL SURVEYS
Evaluating effectiveness of using space information in specialized hydrogeological research
02 p0164 N85-11114
The United States Geological Survey in Alaska: Accomplishments during 1981
[USGS-CIRC-868] 04 p0515 N85-13283
Summary of LANDSAT quadrangle studies in Alaska
04 p0515 N85-13284
Digital elevation models improve processing of Alaskan gravity data 04 p0515 N85-13285
The Kanayut Conglomerate in the westernmost Brooks Range, Alaska 04 p0516 N85-13289
Progress in lead/uranium zircon studies of lower paleozoic rocks of the southern Alexander terrane
04 p0518 N85-13304

Report of the field work performed in the Basins of the Quebra Osso and Tanque Petro Rivers in the Catas Altas quadrangle, Minas Gerais
[INPE-3268-NTE/225] 04 p0525 N85-13359

Methods for correlating geological, geochemical and geophysical data with satellite imagery in central Ireland
05 p0655 N85-14208

Maritime prospecting, mining discussed
07 p0960 N85-16226

Integrated analysis of remote sensing products from basic geological surveys -- Brazil
[E85-10052] 07 p0984 N85-16248

Organogenic structures (submerged reefs) in Silhetian limestone of west Bengal basin
10 p1500 N85-19464

LANDSAT 4 investigations of Thematic Mapper and Multispectral Scanner applications -- Drum Mountains, Utah and Tonopath, Nevada
[E85-10095] 12 p1874 N85-21757

GADB: A database facility for modelling naturally occuring geophysical fields 13 p2122 N85-23217

NASA's land remote sensing plans for the 1980's
13 p2124 N85-23224

Remote sensing: New tool for China's geologists
14 p2283 N85-24141

Investigative report on using geological research to promote prospecting 14 p2283 N85-24142

Temperature anomalies above ore bodies
14 p2345 N85-24500

Results of studies of wave field internal structure in prediction of geological cross section
14 p2346 N85-24504

Experience in automation of data processing in interpretation and defining of linear elements from space photographs 15 p2486 N85-25349

Interpretation of the data of USGS seismic refraction profile across the Arabian Shield in western Saudi Arabia 17 p2991 N85-28488

Technical support for geopressured-geothermal well activities in Louisiana
[DE85-010462] 18 p3102 N85-29203

Revised draft: Southeastern regional geologic characterization report
[DE85-008285] 18 p3125 N85-29351

Space methods for geological research
19 p3295 N85-30429

Highly important features of regional tectonics of Earth's Arctic sector 19 p3298 N85-30449

Engineering geology of selected areas, US army engineer division, lower Mississippi valley. The American bottom area, MO-IL. Volume 1
[AD-A154258] 19 p3299 N85-30455

Fracture detection and mapping for geothermal reservoir definition: An assessment of current technology, research, and research needs
[DE85-010627] 19 p3301 N85-30464

Evaluation of geothermal potential of Rio Grande rift and Basin and Range province, New Mexico
[DE85-901380] 19 p3301 N85-30466

Melt zones beneath five volcanic complexes in California: An assessment of shallow magma occurrences
[DE85-010644] 19 p3305 N85-30489

Crosswell acoustic surveying in gas sands: Travel-time pattern recognition, seismic Q and channel waves
[DE85-010777] 19 p3352 N85-30778

Petroleum and mineral resources of Antarctica
[US-GEOL-SURV-CIRC-909] 20 p3477 N85-31605

The U.S. Geological Survey in Alaska: Accomplishments during 1982
[US-GEOL-SURV-CIRC-939] 20 p3493 N85-31719

Worldwide directory of national Earth-science agencies and related international organizations
[GS-CIRC-934] 21 p3605 N85-32386

Fracture detection and characterization for geothermal reservoir definition
[DE85-008677] 22 p3815 N85-33630

Indications of mineral zoning in a fossil hydrothermal system at the Meager Creek geothermal prospect, British Columbia, Canada from induced polarization studies
[DE85-011962] 22 p3815 N85-33636

The United States Geological Survey in Alaska: Accomplishments during 1983
[USGS-CIRC-945] 23 p3946 N85-34468

The transient electromagnetic depth sounding technique applied to hydrocarbons and geothermal exploration
[MITT-42] 23 p3949 N85-34476

The development of assessment techniques program
24 p4106 N85-35457

The Conterminous United States Mineral Assessment Program 24 p4106 N85-35458

Federal Mineral Land Information System
24 p4106 N85-35459

The Alaska Mineral Resources Assessment Program
24 p4107 N85-35460

USGS coastal research, studies and maps: A source of information for coastal decision making
[USGS-CIRC-883] 24 p4106 N85-35465

Evaluation: Close-range photogrammetry for slope inventory and monitoring
[PB85-192755] 24 p4106 N85-35470

GEOLOGY
NT CONES (VOLCANOES)
NT CROSSBEDDING (GEOLOGY)
NT GEOCHRONOLOGY
NT GEOMORPHOLOGY
NT GLACIOLOGY
NT HYDROGEOLOGY
NT LITHOLOGY
NT LUNAR GEOLOGY
NT MARS VOLCANOES
NT OROGRAPHY
NT PETROGRAPHY
NT PETROLOGY
NT PHOTOGEOLOGY
NT RADAR GEOLOGY
NT STRUCTURAL PROPERTIES (GEOLOGY)
NT SUBDUCTION (GEOLOGY)
NT TECTONICS
NT VOLCANOES
NT VOLCANOLOGY

A summary of geothermal studies in Montana, through 1983
[DE84-014325] 01 p0064 N85-10422

Geology and geomorphology of the southern central Blue Ridge: An indexed bibliography
[PB84-225119] 01 p0072 N85-10480

Commentary on cosmonauts geological mapping, photography 02 p0158 N85-11069

The Multispectral Imaging Science Working Group. Volume 1: Executive summary
[E85-10001] 02 p0213 N85-11404

The Multispectral Imaging Science Working Group. Volume 2: Working group reports
[E85-10002] 02 p0213 N85-11405

Workshop on the Use of Future Multispectral Imaging Capabilities for Lithologic Mapping: Workshop summary
02 p0214 N85-11413

Remote sensing as a mineral prospecting technique
[E85-10010] 02 p0216 N85-11423

The Alaskan mineral resources assessment program: Guide to information contained in the folio of geologic and mineral-resource maps of the Medfra Quadrangle, Alaska
[GS-CIRC-928] 02 p0219 N85-11443

Sedimentary and tectonic evolution of the western Taiwan foredeep 03 p0389 N85-12491

Abstracts of papers submitted in 1983 for publication
[PB84-217579] 03 p0398 N85-12543

Reconnaissance geology of the northern part of the Unalakleet quadrangle 04 p0516 N85-13291

Archean sedimentation and tectonics in southern Africa
[NASA-CR-174156] 04 p0533 N85-13406

Mars polar volatiles: Topographic and geologic setting
[NASA-CR-174089] 04 p0581 N85-13708

Crystalline rocks of the northeastern United States
[DE84-013674] 05 p0677 N85-14347

Report on United States Antarctic research activities, February 1983 - October 1984 and United States Antarctic research activities planned for October 1984 - September 1985
[PB84-231265] 05 p0677 N85-14352

Potential geological natural landmarks of the East Gulf Coastal Plain
[PB84-230317] 06 p0835 N85-15316

Exploring ocean's mineral wealth
07 p0960 N85-16227

Evaluation of SIR-B imagery for geologic and geomorphic mapping, hydrology, and oceanography in Australia 08 p1146 N85-17229

Boring information and subsurface data base package user's guide
[AD-A148823] 08 p1230 N85-17747

Earth Sciences Division report, 1983
[DE85-001036] 09 p1341 N85-18436

Glacial geology of Barron County, Wisconsin
09 p1351 N85-18500

Late precambrian to ordovician metamorphism and orogenesis in the Blue Ridge and western Piedmont, Virginia Appalachians 09 p1352 N85-18503

Quaternary stratigraphy, geochronology and carbon isotope geology of alluvial deposits in the Texas panhandle 09 p1353 N85-18514

Consideration of future climatic changes in three geologic settings
[DE85-001704] 09 p1357 N85-18537

Spatial distribution of auroras and its relationship to geological structure of Norilsk region
10 p1497 N85-19447

China report: Science and technology
[JPRS-CST-84-040] 11 p1623 N85-20219

Low-temperature geothermal assessment of the Jordan Valley Salt Lake County, Utah
[DE85-000616] 11 p1670 N85-20524

Proceedings of the 1st Glacier Bay Science Symposium
[PB85-115913] 11 p1682 N85-20590

Geological remote sensing develops rapidly, finds broad applications 13 p2052 N85-22946

Application of field X-ray: Radiometric analysis in exploratory geology and means for its improvement
13 p2115 N85-23176

Possibilities of aerial electric prospecting by long cable method for detecting poorly conducting strata
13 p2115 N85-23177

Proceedings of the Geoscience Instrumentation Workshop
[DE85-004359] 13 p2132 N85-23268

China report: Science and technology
[JPRS-CST-85-003] 13 p2166 N85-23433

Rapid advancus in geological work
13 p2166 N85-23437

Dark halo craters and the thickness of grooved terrain on Ganymede 13 p2173 N85-23484

Polar cap formation on Ganymede
13 p2174 N85-23486

Studies of planetary rings 13 p2174 N85-23488

Mapping and geological analysis of Mercury and Venus radar ranging data 13 p2198 N85-23633

Bouguer images of the North American craton
13 p2200 N85-23648

China report: Science and technology
[JPRS-CST-84-012] 14 p2283 N85-24140

Evaluating structure-forming role of late Paleozoic and Mesozoic-Cenozoic tectonic movements in Baltic Sea region 14 p2337 N85-24469

Geological information content of reflected wave record form 14 p2345 N85-24502

Use of space information in petroleum- and gas-prospecting work (example of Southern Mangyshlak)
15 p2485 N85-25341

Spectral reflectance of carbonate minerals and rocks in the visible and near infrared (0.35 - 2.55 microns) and its applications in carbonate petrology
[NASA-CR-175763] 15 p2591 N85-25973

Organizing geological work tasks for 1985 outlined
16 p2806 N85-27303

Shales and other argillaceous strata in the United States
[DE85-010453] 18 p3125 N85-29353

Implications about in situ stress at Yucca Mountain
[DE85-008068] 18 p3126 N85-29356

Western gas sands
[DE85-001985] 18 p3126 N85-29360

Sixth All-Union Marine Geology School
19 p3294 N85-30420

Stratigraphic analysis of Pennsylvania rocks using hierarchy of transgressive-regressive units
19 p3312 N85-30531

Inhomogeneous deformation: The theory and geological application of finite strain compatibility
19 p3312 N85-30532

Subsurface petroleum geology of Santa Rosa sandstone (Triassic), northeast New Mexico
[TI85-901364] 19 p3313 N85-30538

Improving the geological interpretation of magnetic and gravity satellite anomalies
[E85-10103] 20 p3473 N85-31585

Geologic analysis of averaged magnetic satellite anomalies 20 p3474 N85-31586

Statistical magnetic anomalies from satellite measurements for geologic analysis
20 p3474 N85-31589

Binning of satellite magnetic anomalies
20 p3474 N85-31590

The south-central United States magnetic anomaly
20 p3474 N85-31591

The south-central United States magnetic anomaly
20 p3475 N85-31592

Gas hydrates
[DE85-001986] 20 p3477 N85-31607

Global Mega-Geomorphology
[NASA-CP-2312] 21 p3600 N85-32367

Space imagery and some geomorphological problems of the Guiana Shield, South America
21 p3602 N85-32368

One application of mega-geomorphology in education
21 p3602 N85-32370

Worldwide directory of national Earth-science agencies and related international organizations
[GS-CIRC-934] 21 p3605 N85-32386

Carbon and sulfur cycling through geologic time
21 p3658 N85-32720

Geology and geochemistry of sulfide and sulfate deposition 21 p3658 N85-32723

Spacecraft-aided research discussed at geology Congress 22 p3734 N85-33147
Tectonic stability and expected ground motion at Yucca Mountain
[DE85-012004] 22 p3814 N85-33829
Bedrock geology of the Brattleboro Quadrangle, Vermont-New Hampshire
[DE85-011027] 22 p3815 N85-33834
Geology and petroleum resources of basins in western China
[DE85-013036] 23 p3948 N85-34469
GEOMAGNETIC ANOMALIES
U MAGNETIC ANOMALIES
GEOMAGNETIC CROTCHETS
U SUDDEN IONOSPHERIC DISTURBANCES
GEOMAGNETIC EFFECTS
U MAGNETIC EFFECTS
GEOMAGNETIC EQUATOR
U MAGNETIC EQUATOR
GEOMAGNETIC FIELD
U GEOMAGNETISM
GEOMAGNETIC HOLLOW
The IMS advances in understanding terrestrial myriametric radiation 14 p2365 N85-24618
Altimetry data and the elastic stress tensor of subduction zones
[NASA-CR-175796] 16 p2825 N85-27425
GEOMAGNETIC LATITUDE
Paleomagnetic latitude of paleocene volcanic rocks of the Cantwell Formation, central Alaska
04 p0517 N85-13302
An atlas of polar cap energetic particle observations. Volume 2: NOAA-6, 8 July 1979 to 10 May 1983
[PB85-109072] 12 p1891 N85-21868
Characteristics of latitude effect on cosmic ray charged component in atmosphere at altitudes 3-5 KM
13 p1978 N85-22413
Deuteron whistlers at low latitudes in the low altitude topside ionosphere 14 p2366 N85-24625
Low-latitude ducted whistlers observed at Sanya, Hainan, China 14 p2367 N85-24626
Whistler observation at Okinawa, Japan during the IMS 14 p2367 N85-24627
The latitudinal variation of geomagnetic pulsation amplitude and phase 14 p2370 N85-24646
GEOMAGNETIC PULSATIONS
Statistical properties of geomagnetic pulsations at the Observatory of Fuerstenfeldbruck determined with the aid of pulsation indices. Part 2: Periodicity in the occurrence of pulsations
[REPT-556] 03 p0376 N85-12399
Seasonal variations of reflexibility and transmissibility of ULF waves propagating through the ionosphere of geomagnetic mid-latitudes
[REPT-560] 03 p0376 N85-12403
Fine structure of Alfven maser radiation
06 p0824 N85-15232
Interpretation of directional magnetotelluric soundings by analytical continuation method
14 p2343 N85-24488
Excitation of geomagnetic Pci-2 and pulsations with decreasing period during microsubstorms
14 p2344 N85-24494
Directional analysis of wave packets of magnetotelluric field 14 p2344 N85-24495
On-off characteristics of auroral pulsations
14 p2363 N85-24604
Multiple correlation between auroral and magnetic pulsations 14 p2363 N85-24605
Multiple correlation between auroral and magnetic pulsations. Part 2: Determination of electric currents and electric fields around a pulsating auroral patch
14 p2363 N85-24606
Pc 1-2 pulsations and related phenomena: A review — geomagnetic pulsations 14 p2364 N85-24611
Spatial characteristics of ULF pulsations and their modification by the ionosphere: IMS results
14 p2364 N85-24612
Contribution of the Scandinavian Twin Auroral Radar Experiment (STARE) radar to the understanding of the physical mechanisms associated with Pc5 pulsations
14 p2364 N85-24613
Short-period magnetic pulsations during substorms
14 p2366 N85-24636
Substorm associated Pc 1 emission in the morning sub-cleft latitudes 14 p2368 N85-24637
Pc 1 pulsation source regions and their relationship to the plasma pause 14 p2368 N85-24638
Long-period magnetospheric pulsations observed with an electric field experiment in the magnetosphere
14 p2369 N85-24639
Magnetospheric pulsations observed by ISEE 1 and 2 satellites 14 p2369 N85-24640
The SAMBO-GEOS experiment: A Ps-6 event from ground-satellite observations 14 p2369 N85-24641
Sudden Storm Commencement (SSC) associated hydromagnetic variations at geosynchronous altitude and on the ground 14 p2369 N85-24642
Observations of a pulsation event from the ground with balloons and with a geostationary satellite
14 p2369 N85-24643
Results of ULF-wave investigations in the USSR
14 p2369 N85-24644
Satellite, auroral radar and ground magnometer observations of transient ULF pulsations
14 p2369 N85-24645
The latitudinal variation of geomagnetic pulsation amplitude and phase 14 p2370 N85-24646
Magnetic pulsations recorded in northern Scandinavia during the IMS; a study of Pc 4-5 events
14 p2370 N85-24647
Characteristics of Pc 4,5 pulsations and their source mechanisms 14 p2370 N85-24648
Ground magnetic observations of high-latitude Pi2 pulsations: Scandinavian magnetometer array results
14 p2370 N85-24649
Pi2 pulsations and the substorm current wedge - ground observations 14 p2370 N85-24650
Ground-satellite observations of substorm related Pi 2 pulsations and current systems
14 p2370 N85-24651
Implications of the global appearance of Pi2 and Pc 3 bursts 14 p2371 N85-24652
A structural classification of geomagnetic pulsations
14 p2371 N85-24657
Correlated fluctuations of charged particle fluxes and magnetic field according to data from Intercosmos-10 satellite 16 p2722 N85-26802
GEOMAGNETIC STORMS
U MAGNETIC STORMS
GEOMAGNETIC TAIL
Plasma flow in the near and distant geomagnetic tail
[DE84-014029] 04 p0534 N85-13415
Polar rain: Solar coronal electrons in the Earth's magnetosphere
[NASA-TM-86150] 07 p1060 N85-16726
Periodic substorm activity in the geomagnetic tail
[NASA-CR-175629] 13 p2161 N85-23409
Response of magnetospheric substorm activity to changes in the interplanetary magnetized plasma
14 p2357 N85-24563
Magnetotail current sheet and energetic particles observed on ISEE-1 14 p2357 N85-24566
Estimate of the amplitude of transient electric fields in the magnetotail 14 p2358 N85-24568
Timing between particle injections at the geostationary orbit and particle flux decreases in the distant geomagnetic tail during substorms 14 p2358 N85-24569
Streaming reversal of energetic particles in the magnetotail during a substorm 14 p2358 N85-24571
The near Earth current sheet: ISEE-1 and -2 case studies 14 p2358 N85-24573
The dawn-dusk asymmetry of particles near the neutral sheet of geomagnetotail 14 p2358 N85-24574
The ionospheric O+ streams in the magnetotail between 22 RE and 6 RE 14 p2360 N85-24582
Pi2 pulsations and the substorm current wedge - ground observations 14 p2370 N85-24650
Hydromagnetic vortices: An interpretation for dawnside events as on December 11, 1977 — magnetotail
14 p2371 N85-24653
Structure of the distant geotail: ISEE-3 observations
20 p3488 N85-31678
Magnetotails of the terrestrial planets: A comparative study 22 p3856 N85-33875
GEOMAGNETICALLY TRAPPED PARTICLES
U RADIATION BELTS
GEOMAGNETISM
Precipitation of protons with E sub p approximately 1 MeV near plasmopause 02 p0161 N85-11093
The south-central United States magnetic anomaly
[E85-10025] 02 p0218 N85-11438
Basic research for the geodynamics program
[NASA-CR-174055] 02 p0228 N85-11490
Geophysical Works during 1981, volume 29, no. 547-566 03 p0375 N85-12389
Characteristics of absorption and frequency filtration of ULF electromagnetic waves in the ionosphere
03 p0376 N85-12402
Continental and oceanic crustal magnetization modelling
[E85-10034] 03 p0378 N85-12413
Asymptotic orbit theory for trapped electrons in inhomogeneous Whistler field
[AD-A146178] 03 p0392 N85-12510
Scientific contributions in commemoration of Ebro Observatory's 75th anniversary — conference
[ISBN-84-00-05380-X] 04 p0518 N85-13308
Present practice for the recording of the Earth magnetic field — geophysical observatories
04 p0519 N85-13317
Advantages and limitations of spherical harmonic analyses of geomagnetic data 04 p0519 N85-13318
Analysis of the daily geomagnetic variation with the use of MAGSAT data — MAGSAT satellites
04 p0520 N85-13319
Research directions in recent studies of the lunar geomagnetic effects 04 p0520 N85-13320
On derivation and significance of geomagnetic equivalent amplitude indices 04 p0520 N85-13321
A directly obtained geomagnetic activity measure, J3
04 p0520 N85-13322
Resonance model of Pc3 in subtropical regions — geomagnetism 04 p0520 N85-13323
Daily magnetic variations at Ebro, Spain
04 p0520 N85-13325
On the annual and semiannual variation of S sub R at l'Aquila — geomagnetism 04 p0520 N85-13326
On some new features of semiannual variation of the geomagnetic field 04 p0520 N85-13327
Local geomagnetic characteristics of solar activity (Dourbes 1960-1978) 04 p0521 N85-13328
Geomagnetic secular variation: A jerk in 1970
04 p0521 N85-13329
Comparisons of secular variation in two-dipole and spherical harmonic models with observatory data in Eurasia, 1965-1975 04 p0521 N85-13330
Geomagnetic secular variation at Ebro Observatory during the past 70 years 04 p0521 N85-13331
Reversals of the Earth's magnetic field
04 p0521 N85-13332
Petrologic model of the northern Mississippi embayment based on satellite magnetic and ground based geophysical data
[NASA-TM-85075] 04 p0533 N85-13406
Global matrix of thermospheric density values for selected solar/geomagnetic conditions and spacecraft orbital attitudes
[NASA-TM-86478] 04 p0533 N85-13409
Statistical relationship of strong earthquakes with planetary geomagnetic field activity
06 p0820 N85-15209
Anomalous magnetic field in northwestern Pacific Ocean and Pacific Ocean plate kinematics
06 p0820 N85-15210
Correlation radius of gravitational and magnetic anomalies and methods of its determination
06 p0821 N85-15213
Spectrum of geomagnetic field variations in the range of periods between 1 and 10 years
06 p0821 N85-15215
Processes of smooth increase and dropoff in intensity of glow line lambda' = 5577 A with exposure of ionosphere to electron beam 06 p0822 N85-15219
Earth's radiation belts
[AD-A147927] 07 p0996 N85-16339
Artificial ionospheric disturbances caused by powerful radio waves
[AD-A148077] 08 p1186 N85-17473
Algorithm for space-time analysis of data on geomagnetic field
[NASA-TM-77804] 08 p1209 N85-17609
Recent investigations at INPE in magnetospheric physics and geomagnetism
[INPE-3280-PRE/603] 10 p1514 N85-19555
Brazil future plans in upper atmosphere research in Antarctica
[INPE-3400-PRE/669] 10 p1515 N85-19559
Solar radio bursts, proton events and geomagnetic activity
[AD-A149018] 10 p1571 N85-19906
Precursors for Brazilian magnetic anomalies from 1922 to 1969
[INPE-3283-PRE/605] 11 p1681 N85-20590
Solar-Geophysical Data. Part 1: (Prompt reports)
[PB85-112068] 11 p1766 N85-21100
Calculation of ionospheric profiles by inverting VLF/LF reflection data. 2. Anisotropic propagation
[AD-A150105] 12 p1890 N85-21859
Circulation and internal waves in a cold Gulf Stream waves
[AD-A149704] 12 p1898 N85-21918
Research on ocean floor electrical surveys
[AD-A149831] 12 p1899 N85-21920
Models of the upper atmosphere
12 p1945 N85-22217
Particle transport in planetary magnetospheres
12 p1954 N85-22275
One-dimensional model of auroral magnetic force with longitudinal current and cyclotron heating of ions
13 p1980 N85-22424
Auroral-polar cap environment and its impact on spacecraft plasma interactions 13 p1991 N85-22484
Calculation of secondary-electron escape currents from inclined-spacecraft surfaces in a magnetic field
13 p1992 N85-22491

Geomagnetic precursors of intensive earthquakes in the 1-0.-2 Hz frequency range of geomagnetic pulsations
13 p2116 N85-23178

Solution of direct magnetometric problem on spherical Earth 13 p2116 N85-23179

Geomagnetic field dynamics 13 p2116 N85-23182

MAGSAT anomaly field data of the crustal properties of Australia
[E85-10100] 13 p2122 N85-23215

GADB: A database facility for modelling naturally occuring geophysical fields 13 p2122 N85-23217

Data selection techniques in the interpretation of MAGSAT data over Australia 13 p2123 N85-23218

USSR report: Earth sciences
[JPRS-UES-85-004] 14 p2332 N85-24424

Diurnal variations in terrestrial magnetic field and structure of magnetosphere 14 p2344 N85-24493

Dynamic spectra of mean monthly values of geomagnetic field elements based on spectral-time analysis data 14 p2344 N85-24496

Achievements of the International Magnetospheric Study (IMS) — conference
[ESA-SP-217] 14 p2354 N85-24544

The measurements of Prognoz-4, -5, -6, -7 during IMS
14 p2355 N85-24548

The structure and dynamics of the magnetosphere: Progress in the IMS 14 p2355 N85-24550

Magnetic field observations at the dayside magnetopause: ISEE-1 and -2 contributions during the IMS 14 p2356 N85-24555

Magnetic field in the Earth's outer magnetosphere: Prognoz-6, -7 data 14 p2356 N85-24556

Sudden Storm Commencement (SSC) associated hydromagnetic variations at geosynchronous altitude and on the ground 14 p2369 N85-24642

Advances in magnetospheric plasma-wave research during the IMS 14 p2372 N85-24662

The access of energetic charged particles to satellite altitudes
[AD-A150799] 14 p2373 N85-24670

The first effect of the amplitude of a solar cycle
14 p2452 N85-25143

Report of the geomagnetic and geoelectric observations, 1983 (rapid variations)
[REPT-24] 15 p2591 N85-25975

Geophysical responses of dynamics of solar wind transition region 16 p2721 N85-26795

Solar-Geophysical Data Number 484, December 1984. Part 1 (prompt reports): Data for November 1984, October 1984 and late data
[NASA-CR-175829] 16 p2888 N85-27819

The influence of the heliospheric current sheet and angular separation on flare accelerated solar wind
[NASA-CR-175962] 18 p3209 N85-29907

MAGSAT scalar anomaly map of South America
20 p3473 N85-31586

MAGSAT satellite magnetic anomaly map over South America 20 p3474 N85-31587

Geologic analysis of averaged magnetic satellite anomalies 20 p3474 N85-31588

Statistical magnetic anomalies from satellite measurements for geologic analysis
20 p3474 N85-31589

Binning of satellite magnetic anomalies
20 p3474 N85-31590

The south-central United States magnetic anomaly
20 p3474 N85-31591

The south-central United States magnetic anomaly
20 p3475 N85-31592

Reduced to pole long-wavelength magnetic anomalies of Africa and Europe 20 p3475 N85-31595

Euro-African MAGSAT anomaly-tectonic observations
20 p3475 N85-31596

Continental and oceanic magnetic anomalies: Enhancement through GRM 20 p3476 N85-31598

Continental magnetic anomaly constraints on continental reconstruction 20 p3476 N85-31599

Regional magnetic anomaly constraints on continental rifting 20 p3476 N85-31600

Thermal ion heating in the vicinity of the plasmapause
[NASA-CR-176030] 20 p3535 N85-31993

Fluxgate magnetometer (SSM) for the defense meteorological satellite program (DMSP) block 5D-2, flight 7
[AD-A155229] 21 p3560 N85-32143

Planetary Dynamos
[NASA-CR-176001] 21 p3679 N85-32857

A real time index of geomagnetic background noise for the MAD (Magnetic Anomaly Detection) frequency band
[AD-A155717] 22 p3814 N85-33627

Absolute measurement of Declination (D) by means of a proton magnetometer
[DMI-GEOPHYS-PAPERS-R-68]
22 p3836 N85-33751

Current enhancement in a conducting channel
[AD-A155418] 22 p3845 N85-33812

Planetary surface processes: A review
22 p3855 N85-33869

The magnetic field of planets
22 p3858 N85-33891

Magnetic field generation in the cores of terrestrial bodies 22 p3859 N85-33894

Linear filters as a method of real-time prediction of geomagnetic activity
[DE85-010760] 22 p3860 N85-33899

An update on the correlation between the cosmic radiation intensity and the geomagnetic AA index
[SH-4.2-24] 23 p4009 N85-34881

Dynamics of two-year cosmic ray variations inferred from the data of spacecraft and stratospheric measurements and from the neutron monitor data in 1959-1981
[SH-4.4-21] 23 p4035 N85-35017

Formulation of cosmic-ray solar daily variation and its seasonal variation, produced from generalized stationary anisotropy of solar origin
[SH-4.5-2] 23 p4036 N85-35020

Diurnal variation of galactic cosmic ray intensity on quiet days
[SH-4.5-11] 23 p4037 N85-35029

A relation between the short time variations of cosmic rays and geomagnetic field change
[SH-5.1-14] 23 p4043 N85-35067

Anomalous low level of cosmic ray intensity decreases observed during 1980
[SH-5.1-15] 23 p4043 N85-35068

Frequency spectra of short-period variations of cosmic ray
[SH-5.1-17] 23 p4043 N85-35070

Re-evaluation of cosmic ray cutoff terminology
[SH-6.1-11] 23 p4045 N85-35084

The use of the McIlwain L-parameter to estimate cosmic ray vertical cutoff rigidities for different epochs of the geomagnetic field
[SH-6.1-12] 23 p4045 N85-35085

Estimating the change in asymptotic direction due to secular changes in the geomagnetic field
[SH-6.1-13] 23 p4045 N85-35086

Empirical model for the Earth's cosmic ray shadow at 400 KM: Prohibited cosmic ray access
[SH-6.1-14] 23 p4046 N85-35087

Diurnal variations of cosmic ray geomagnetic cut-off threshold rigidities
[SH-6.1-21] 23 p4046 N85-35092

The influence of the Earth's magnetosphere on the high-energy solar protons
[SH-6.1-22] 23 p4046 N85-35093

Correlation between solar neutrino flux and other solar phenomena 23 p4049 N85-35109

Heavy cosmic ray measurement aboard Spacelab-1
[SH-10.1-7] 23 p4053 N85-35138

Radio wave emitted by an extensive air showers in 10KHz to 1MHz region
[HE-4.6-15] 24 p4198 N85-36051

Measurement of neutrino oscillations in MACRO experiment
[HE-5.3-10] 24 p4206 N85-36104

GEOMETRIC ACCURACY

Canadian plans for Thematic Mapper data
11 p1668 N85-20513

LANDSAT-4 Science Characterization Early Results. Volume 3, part 2: Thematic Mapper (TM)
[E85-10068] 12 p1869 N85-21724

A preliminary assessment of LANDSAT-4 Thematic Mapper data — Windsor, Ontario and Medicine Hat areas, Canada 12 p1869 N85-21728

TM geometric performance: Line to Line Displacement Analysis (LLDA) — New Mexico
12 p1870 N85-21732

A preliminary evaluation of LANDSAT-4 Thematic Mapper data for their geometric and radiometric accuracies 12 p1871 N85-21739

GEOMETRIC RECTIFICATION (IMAGERY)

Specification and preliminary design of the CARTA system for satellite cartography
[E85-10035] 03 p0378 N85-12414

Rectification of single and multiple frames of satellite scanner imagery using points and edges as control
07 p0986 N85-16263

The influence of the number of ground control points on the scene-to-map registration accuracy — Kansas, Louisiana, Mississipp, and Missouri
07 p0986 N85-16264

Anaysis of the quality of image data required by the LANDSAT-4 Thematic Mapper and Multispectral Scanner — agricultural and forest cover types in California
[E85-10074] 10 p1504 N85-19488

Summary of MSS characterization investigations
11 p1666 N85-20497

Radiometric calibration and geocoded precision processing of LANDSAT-4 Multispectral Scanner products by the Canada Centre for Remote Sensing
11 p1667 N85-20501

Geometric accuracy of LANDSAT-4 MSS image data
11 p1667 N85-20503

Geometric accuarcy assessment of LANDSAT-4 Multispectral Scanner (MSS) data
11 p1667 N85-20505

LS-4 MSS geometric correction: Methods and results
11 p1668 N85-20507

An overview of the Thematic Mapper geometric correction system 11 p1668 N85-20511

Analysis and evaluation of the LANDSAT-4 MSS and TM sensors and ground data processing systems: Early results 13 p2117 N85-23169

Correction and geological analysis of lunar 3.8 cm radar data 13 p2196 N85-23604

Minimizing influence of Earth's curvature in projective rectification of space photographs into photoplans and photomaps 16 p2727 N85-26829

Looking at more than three dimensions
[DE85-007764] 17 p3009 N85-28603

Reports on cartography and geodesy. Series 1: Original reports, number 93
[ISSN-0469-4236] 18 p3124 N85-29343

Dynamic rectification of airborne scanner digital image recordings 18 p3124 N85-29344

LANDSAT-4/5 image data quality analysis
[E85-10105] 24 p4107 N85-35463

GEOMETRICAL ACOUSTICS

High-frequency asymptotic behavior of reflected and transmitted waves during scattering of sound by hollow elastic sphere filled with fluid 02 p0268 N85-11739

Wave description of sound propagation through stratified moving atmosphere 15 p2525 N85-25587

GEOMETRICAL HYDROMAGNETICS

U MAGNETOHYDRODYNAMICS

GEOMETRICAL OPTICS

Theoretical elements of photometry
[BLL-RISLEY-TR-5022-(9091.9F)]
02 p0279 N85-11821

Influence of geometric conditions on the indicatrix of reflection of the perfect reflecting diffuser
[PTB-OPT-16] 03 p0420 N85-12866

An iteration method for complex scattering problems
[AD-A150038] 12 p1934 N85-22151

Dependence of properties of optical cavity on misalignment 14 p2276 N85-24099

Analytical techniques used to calculate the fields due to refraction and diffraction of electromagnetic waves
[AD-A151705] 15 p2543 N85-25688

Performance evaluation of fiber-optic converters
17 p2941 N85-28154

Optical phenomena in computer vision
[AD-A152970] 17 p3008 N85-28595

Solvability of some inverse problems in laser radiation focusing 21 p3696 N85-32963

Existence of smooth solutions in problems of electromagnetic radiation focusing
21 p3697 N85-32972

Edge detection and geometric methods in computer vision
[AD-A155873] 24 p4135 N85-35630

GEOMETRICAL THEORY OF DIFFRACTION

On aircraft antennas and basic scattering studies
[AD-A146017] 03 p0355 N85-12282

Interpolation methods for GTD analysis of shaped reflectors 10 p1483 N85-19231

Scattering of waves by axisymmetrical edge
13 p2060 N85-22967

Analytical techniques used to calculate the fields due to refraction and diffraction of electromagnetic waves
[AD-A151705] 15 p2543 N85-25688

Guided-mode launching in a slab waveguide by way of diffraction at the edge of a conducting screen residing on one surface of the slab
[AD-A154886] 21 p3575 N85-32202

GEOMETRODYNAMICS

U RELATIVITY

GEOMETRY

NT ANALYTIC GEOMETRY
NT ANGLE OF ATTACK
NT ANGLES (GEOMETRY)
NT BRAGG ANGLE
NT CARTESIAN COORDINATES
NT CATENARIES
NT CIRCLES (GEOMETRY)
NT CIRCUMFERENCES
NT COLLINEARITY
NT CONICS
NT COPLANARITY
NT CRACK GEOMETRY
NT CURVATURE
NT CURVES (GEOMETRY)
NT DESCRIPTIVE GEOMETRY

NT DIFFERENTIAL GEOMETRY
NT DUCT GEOMETRY
NT ELEVATION ANGLE
NT ELLIPSES
NT EPICYCLOIDS
NT EUCLIDEAN GEOMETRY
NT FIXED POINTS (MATHEMATICS)
NT FLOW GEOMETRY
NT FRACTALS
NT GEODESIC LINES
NT HOMOTOPY THEORY
NT HYPERBOLAS
NT INFLECTION POINTS
NT LIE GROUPS
NT LINES (GEOMETRY)
NT LINKS (MATHEMATICS)
NT LOCI
NT MERCATOR PROJECTION
NT METRIC SPACE
NT NOZZLE GEOMETRY
NT OBLATE SPHEROIDS
NT PARABOLAS
NT PARALLELEPIPEDS
NT POINTS (MATHEMATICS)
NT POLYGONS
NT PROJECTIVE GEOMETRY
NT PYRAMIDS
NT RADII
NT RECTANGLES
NT RIEMANN MANIFOLD
NT SPECIMEN GEOMETRY
NT SPHEROIDS
NT SPINOR GROUPS
NT TANGENTS
NT TENSOR ANALYSIS
NT TOPOLOGY
NT TORUSES
NT VECTOR ANALYSIS
NT VORTICITY

Halfspace representations of extrusions, solids of revolution and pyramids
[DE84-015005] 01 p0104 N85-10700

Response of propellants to high dynamic stresses: The uses of gun launch techniques
[DE84-013223] 02 p0188 N85-11259

SMP: A solid modeling program
[NASA-CR-172473] 02 p0241 N85-11570

Formation of radio images by scanning around circle
02 p0264 N85-11727

Analysis of in-plane and out-of-plane ground motions using the boundary element method
[AD-A146229] 03 p0355 N85-12287

An experimental evaluation of the J integral in 50% sidegrooved compact geometry specimens
[AERE-R-11202] 03 p0374 N85-12386

Investigation of an ejector heat pump by analytical methods
[DE84-016675] 04 p0500 N85-13189

Computer-aided design of extrusion dies by metal-flow simulation 06 p0797 N85-15094

Investigation of the creep behaviour of soft soldered joints with solder L-SnAg5 at ambient temperature
[BLL-T8383/BG/WH796/84] 07 p0926 N85-15865

A simple prediction model for soil compaction under various wheel loads and geometries as an aid to vehicle design
[AD-P004298] 09 p1409 N85-18675

A conformal mapping suitable for problems involving interaction between given geometries and known far fields
[AD-A149050] 10 p1545 N85-19744

Geometric Hamiltonian structures and perturbation theory
[DE85-002005] 11 p1707 N85-20737

Experimental study of main rotor tip geometry and tail rotor interactions in hover. Volume 1. Text and figures
[NASA-CR-177336-VOL-1] 13 p1965 N85-22344

Experimental study of main rotor tip geometry and tail rotor interactions in hover. Volume 2: Run log and tabulated data
[NASA-CR-177336-VOL-2] 13 p1965 N85-22345

Magnetostatic-wave propagation in a finite YIG-Loaded rectangular waveguide
[AD-A150332] 13 p2055 N85-22865

Mathematical modeling of results of geometric leveling in variable gravity field 13 p2114 N85-23170

Introduction to combinatorial geometry
[DE85-003266] 13 p2152 N85-23364

Informative geometry of probability spaces
[AD-A150510] 13 p2153 N85-23371

Quantitative analyses of planetary reflectance spectra
13 p2197 N85-23625

Problems regarding the practical evaluation of efficiency of worm gears 14 p2224 N85-23793

Global positioning system: A modification to the baseline satellite constellation for improved geometric performance
[AD-A151692] 15 p2469 N85-25239

Optimum geometry of interblade passages in impellers of thermomolecular vacuum pump
16 p2764 N85-27058

Scattering center analysis for radar cross section modification 16 p2769 N85-27085

Probabilistic structural analysis of SSME turbopump blades: Probabilistic geometry effects
17 p2913 N85-27958

Computational Geometry and Computer-Aided Design
[NASA-CP-2379] 17 p3003 N85-28563

Multivariate spline algorithms for CAGD
17 p3003 N85-28566

Improving the effectiveness of integral property calculation in a CSG solid modeling system by exploiting predictability 17 p3006 N85-28586

A study of aerodynamic control in stalled flight leading-edge vortex formation analysis
[AD-A153758] 18 p3059 N85-28928

Study of meshing of beveled gears with normally decreasing arc teeth
[NASA-TM-77868] 18 p3117 N85-29293

Geometry, velocity structure and penetration depths of descending slabs in the western Pacific
19 p3319 N85-30574

Fast and optimal solution to the Rankine-Hugoniot problem
[NASA-TM-86214] 19 p3344 N85-30724

Mathematics of surfaces
[DE85-010439] 19 p3346 N85-30742

A fast discharge excimer laser with symmetric geometry
[AD-A155294] 21 p3592 N85-32322

Photo-acoustic effect in finite-dimensional semiconductors 21 p3682 N85-32876

MORSE-CGA: A Monte Carlo radiation transport code with array geometry capability
[DE85-012063] 22 p3830 N85-33718

Report of Workshop on Computational Geometry and summary of related research
[AD-A155399] 22 p3833 N85-33734

Thermal transport measurements of UV laser irradiated spherical targets
[DE85-011038] 23 p3931 N85-34365

System maintenance manual for master modeling of aerodynamic surfaces by three-dimensional explicit representation
[NASA-CR-178224] 23 p3956 N85-34517

A simple but systematic CSG system
23 p3963 N85-34569

Low cost geometric modelling system for CAM
23 p3964 N85-34578

GEOMORPHOLOGY

Geology and geomorphology of the southern central Blue Ridge: An indexed bibliography
[PB84-225119] 01 p0072 N85-10460

Estuaries of the Cape. Part 2: Synopses of available information on individual systems. Report no. 18: Bot/Kleinmond system (CSW 13)
[CSIR-RR-417-PT-2] 01 p0087 N85-10587

Geographic science: Executive summary
02 p0214 N85-11408

Geographic science 02 p0214 N85-11409

Geomorphology 02 p0214 N85-11411

Paleohydrology and geomorphology of selected reaches of the upper Wabash Valley, Indiana
02 p0226 N85-11481

Mars-Earth geographical comparisons: A pictorial view
[NASA-TM-86166] 02 p0302 N85-11957

Geology and geochemistry of early Tertiary submarine volcanic rocks of the Aleutian Islands, and their bearing on the development of the Aleutian Island Arc
03 p0389 N85-12493

Metamorphic petrology of the Table Mountain area, Circle quadrangle, Alaska 04 p0516 N85-13295

Paleozoic limestones of the Crazy Mountains and vicinity, Circle quadrangle, east-central Alaska
04 p0517 N85-13296

Late Paleozoic and early Mesozoic radiolarians in the Circle quadrangle, east-central Alaska
04 p0517 N85-13297

Lacustrine and eolian deposits of Wisconsin age at Riverside Bluff in the upper Tanana River valley, Alaska
04 p0517 N85-13299

Landform evaluation through integrated remote sensing methods. A case study in parts of Haryana, India
05 p0657 N85-14221

Some methodological aspects of study of layer associations in continents and oceans
06 p0820 N85-15205

Tectonic, volcanic, and climatic geomorphology study of the Sierras Pampeanas Andes, northwestern Argentina 08 p1144 N85-17215

Geological, structural, and geomorphological analyses from SIR-B 08 p1145 N85-17226

Interlobate comparison of glacial-depositional style as evidenced by small-relief glacial landscape features in Illinois, Indiana, and Ohio, utilizing SIR-B
08 p1146 N85-17231

Evaluation of the L-band scattering characteristics of volcanic terrain in aid of lithologic identification, assessment of SIR-B calibration, and development of planetary geomorphic analogs 08 p1146 N85-17232

Soil formation on tertiary landsurfaces of the New Jersey coastal plain 08 p1181 N85-17441

Post-Laramide history of North Central Wyoming
08 p1181 N85-17444

Structural morphology and associated strain within parts of the US section of the Kootenay Arc, NE, Washington
09 p1352 N85-18505

Basic structural features and probable mechanism of formation of the Kuril Island system
10 p1501 N85-19472

Assessment of LANDSAT for rangeland mapping, Rush Valley, Utah
[E85-10072] 10 p1503 N85-19486

An integrated GIS/remote sensing data base in North Cache soil conservation district, Utah: A pilot project for the Utah Department of Agriculture's RIMS (Resource Inventory and Monitoring System)
[E85-10073] 10 p1504 N85-19487

Nautical charting with remotely sensed imagery, volume 1
[AD-A149361] 10 p1506 N85-19503

Nautical charting with remotely sensed imagery. Volume 2: Case studies
[AD-A149362] 10 p1506 N85-19504

Study of the physical properties of crystalline rocks in the southeast Voronezh anteclise
[NASA-TM-77823] 10 p1514 N85-19551

Physiography of the Martian west equatorial uplift
12 p1961 N85-22325

Planetary geology in the 1980s
[NASA-SP-467] 13 p2169 N85-23457

Geomorphic classification of lava flows on Io
13 p2173 N85-23480

Martian terrain ages 13 p2181 N85-23537

Average spacing for rings of individual multi-ring basins is 2.0(0.5)D 13 p2182 N85-23541

Ring-diameter ratios for multi-ring basins average 2.0(0.5)D 13 p2182 N85-23542

Morphology and mechanics of terraces in lunar craters
13 p2182 N85-23543

Interaction of Martian flow ejecta blankets with pre-existing impact craters: Morphological observations
13 p2183 N85-23546

Ripple ring basins on Ganymede and Callisto
13 p2183 N85-23547

Morphologic evolution of the Mount St. Helens crater area, Washington 13 p2187 N85-23568

The geology of Mt. Hope, a silicic volcanic center in West Central Arizona 13 p2187 N85-23571

A silicic shield volcano in Bolivia
13 p2187 N85-23572

Martian fretted terrain morphometry interpreted using principal components analysis 13 p2192 N85-23597

Distribution and properties of large symmetric knobs on Mars 13 p2192 N85-23598

Enigmatic hills of the mottled plains, Mare Acidalium quadrangle (MC-4), Mars 13 p2192 N85-23599

Geomorphology and geology of the Southwestern Margaritifer Sinus and Argyre regions of Mars. Part 1: Geological and geomorphological overview
13 p2192 N85-23600

Geomorphology and geology of the Southwestern Margaritifer Sinus and Argyre regions of Mars. Part 2: Crater size-frequency distribution curves and geomorphic unit ages 13 p2192 N85-23601

Geomorphology and geology of the Southwestern Margaritifer Sinus and Argyre regions of Mars. Part 3: Valley types and distribution 13 p2193 N85-23602

Geomorphology and geology of the Southwestern Margaritifer Sinus and Argyre regions of Mars. Part 4: Flow ejecta crater distribution 13 p2193 N85-23603

The geomorphology of Rhea
13 p2193 N85-23606

Kasei Vallis of Mars: Dating the interplay of tectonics and geomorphology 13 p2201 N85-23654

Chondrule-like particles provide evidence of early Archean meteorite impacts, South Africa and western Australia 15 p2682 N85-26562

The Mars ancient cratered terrain, smooth plains boundary: Implications of Viking color data for evolution of the Amenthes Region 15 p2682 N85-26564

Closer look at lunar volcanism
[DE85-006663] 15 p2683 N85-26576

Space methods for geological research
19 p3295 N85-30429

Engineering geology of selected areas, US army engineer division, lower Mississippi valley. The American bottom area, MO-IL. Volume 1
[AD-A154256] 19 p3299 N85-30455

Geologic and hydrologic characterization and evaluation of the basin and range province relative to the disposal of high-level radioactive waste. Part 1: Introduction and guidelines
[GS-CIRC-904-A] 20 p3526 N85-31932

Global Mega-Geomorphology
[NASA-CP-2312] 21 p3600 N85-32357

A new global geomorphology?
21 p3601 N85-32358

Global geomorphology 21 p3601 N85-32359

Mega-geomorphology: Mars vis a vis Earth
21 p3601 N85-32360

Geomorphological similarity and uniqueness
21 p3601 N85-32361

Regional landform thresholds
21 p3601 N85-32362

Some observations on paleogeomorphology
21 p3601 N85-32363

Ancient landscapes: Their nature and significance for the question of inheritance 21 p3601 N85-32364

Geomorphology, tectonics, and exploration
21 p3601 N85-32365

Mega-geomorphology and neotectonics
21 p3602 N85-32366

Andrean examples of mega-geomorphology themes
21 p3602 N85-32367

Space imagery and some geomorphological problems of the Guiana Shield, South America
21 p3602 N85-32368

Deep sea mega-geomorphology: Progress and problems 21 p3602 N85-32369

One application of mega-geomorphology in education
21 p3602 N85-32370

Use of the synoptic view: Examples from Earth and other planets 21 p3602 N85-32371

Geomorphic classification of Icelandic and Martian volcanoes: Limitations of comparative planetology research from LANDSAT and Viking orbiter images
21 p3603 N85-32372

Aeolian geomorphology from the global perspective
21 p3603 N85-32373

Geomorphic analyses from space imagery
21 p3603 N85-32374

The problem of scale in planetary geomorphology
21 p3603 N85-32375

Quantitative analysis in megageomorphology
21 p3603 N85-32376

Use of spaceborne imaging radar in regional geomorphic studies 21 p3603 N85-32377

Techniques, problems and uses of mega-geomorphological mapping
21 p3604 N85-32378

Quantitative analysis of geomorphic processes using satellite image data at different scales
21 p3604 N85-32380

Quantitative geomorphologic studies from spaceborne platforms 21 p3604 N85-32381

Global geomorphology: Report of Working Group Number 1 21 p3604 N85-32382

Process thresholds: Report of Working Group Number 3 21 p3604 N85-32384

Planetary perspective. Report of Working Group Number 4 21 p3605 N85-32385

Precambrian evolution and the rock record
21 p3656 N85-32711

Considerations of large scale impact and the early Earth 21 p3718 N85-33070

Geologic processes on Venus: An update
22 p3857 N85-33683

The United States Geological Survey in Alaska: Accomplishments during 1983
[USGS-CIRC-945] 23 p3948 N85-34468

Geology and geomorphology of the Roraima group, southeastern Venezuela 24 p4115 N85-35511

GEON (TRADEMARK)
U POLYVINYL CHLORIDE

GEOPHYSICAL FLUIDS

Magnetic location of Earth's core-mantle boundary and estimates of the adjacent fluid motion
13 p2131 N85-23260

GEOPHYSICAL OBSERVATORIES
NT OGO

Scientific contributions in commemoration of Ebro Observatory's 75th anniversary — conference
[ISBN-84-00-05380-X] 04 p0518 N85-13308

The Ebro Observatory and international scientific organizations 04 p0518 N85-13309

Use of Ebro Observatory data at Word Data Center A for Solar-Terrestrial Physics 04 p0518 N85-13310

Present practice for the recording of the Earth magnetic field — geophysical observatories
04 p0519 N85-13317

Daily magnetic variations at Ebro, Spain
04 p0520 N85-13325

On the annual and semiannual variation of S sub R at l'Aquila — geomagnetism 04 p0520 N85-13326

GEOPHYSICAL SATELLITES
NT COSMOS SATELLITES
NT EXPLORER 10 SATELLITE
NT INTERCOSMOS SATELLITES
NT OGO

Application of satellite accelerometer data to improve density models
[AD-A154904] 21 p3631 N85-32558

GEOPHYSICS

Seafloor geosciences division: Missions, technical specialties, accomplishments, and activities, calendar year 1983
[AD-A144849] 01 p0087 N85-10592

A bibliography of planetary geology and geophysics principal investigators and their associates, 1983 - 1984
[NASA-TM-87361] 01 p0127 N85-10874

Cosmonauts complete 4th month aboard Salyut-7
02 p0157 N85-11065

Geophysical experiments, photography aboard Salyut-7 02 p0157 N85-11066

Orbit of Salyut-7 station boosted
02 p0157 N85-11067

Salyut-7 crew in orbit 150 days
02 p0157 N85-11068

Use of gravitational stabilization in performance of experiments 02 p0160 N85-11084

Development of a method for exploring low-reflectance areas through the combined use of different geophysical methods taking the north-west German basin as an example
[BMFT-FB-T-83-180] 02 p0220 N85-11450

Project review on geophysical and ocean sound speed profile inversion
[AD-A145717] 02 p0276 N85-11797

Geophysical Works during 1981, volume 29, no. 547-566 03 p0375 N85-12389

SVKD and SVKM-3 seismographs with a low-sensitivity channel
[REPT-553] 03 p0376 N85-12396

Abstracts of papers submitted in 1983 for publication
[PB84-217579] 03 p0398 N85-12543

International Geosphere/Biosphere Program: 1984
[GPO-39-222] 04 p0578 N85-13691

Activities at the Lunar and Planetary Institute
[NASA-CR-174069] 04 p0579 N85-13694

Activities at the Lunar and Planetary Institute, introduction 04 p0579 N85-13695

NASA's SESAC report on research and analysis in space and Earth sciences 04 p0579 N85-13697

Geophysical and geochemical constraints favoring the capture hypothesis 04 p0581 N85-13710

Geophysical investigation of precambrian crustal structure and Laramide effects across a precambrian suture in southeastern Wyoming
05 p0674 N85-14328

Geology and resources of the Tar Sand Triangle, southeastern Utah
[DE84-012017] 05 p0677 N85-14346

USSR report: Earth sciences
[JPRS-UES-84-007] 06 p0819 N85-15196

Selection of spacing of modular and gradient measurement surveys based on statistical characteristics of measured geomagnetic field
06 p0821 N85-15214

Solar-geophysical data number 478, June 1984. Part 1 (prompt reports): Data for May 1984, Apr. 1984, and late data
[PB84-243153] 06 p0890 N85-15653

Solar-geophysical data number 478, June 1984. Part 2 (comprehensive reports): Data for December 1983 and miscellanea
[PB84-243161] 06 p0890 N85-15654

Deployment of a regional array in Norway
[AD-A147032] 07 p0997 N85-16330

Microprocessors in geophysical instruments discussed
08 p1142 N85-17199

Ground-based measurements of mesosphere temperatures by optical means
08 p1183 N85-17453

A research in support of NASA's space science
[NASA-CR-174267] 08 p1227 N85-17728

European scientific notes. Volume 38, number 11
[AD-A148228] 08 p1230 N85-17745

Air Force space technology center space technology: Emphasis 84 09 p1333 N85-18381

Earth Sciences Division report, 1983
[DE85-001036] 09 p1341 N85-18436

Solar-geophysical data number 476, April 1984. Part 1: (Prompt reports). Data for March 1984, February 1984 and late data
[PB84-215060] 09 p1416 N85-[illegible]

Solar-geophysical data number 476, April 1984. Part 2: (Comprehensive reports). Data for October 1982, June 1981 and miscellanea
[PB84-215078] 09 p1417 N85-[illegible]

USSR report: Earth sciences
[JPRS-UES-85-003] 10 p1497 N85-[illegible]

Organogenic structures (submerged reefs) in Sylhet limestone of west Bengal basin
10 p1500 N85-[illegible]

MIZEX (Marginal Ice Zone Program): A program for mesoscale air-ice-ocean interaction experiments in Arctic marginal ice zones. 5. MIZEX 84. Summer experiment PI (Principal Investigator) preliminary reports
[AD-A148986] 10 p1521 N85-[illegible]

Summer study program in geophysical fluid dynamics, the Woods Hole Oceanographic Institution, dynamic differentiation
[AD-A149366] 10 p1521 N85-[illegible]

Structure and application of extremely large geophysical data bases
[DE85-003527] 10 p1568 N85-[illegible]

The global meteor observation system (GLOBMET)
11 p1656 N85-[illegible]

Global meteor observation system (GLOBMET)
11 p1656 N85-[illegible]

Large natural geophysical events: Planetary planning
[DE85-000859] 11 p1763 N85-[illegible]

Solar-geophysical data number 479, July 1984. Part 1: (Prompt reports). Data for June 1984, May 1984 and later data
[NASA-CR-175542] 12 p1962 N85-[illegible]

Aeronautical Engineering: A continuing bibliography with indexes, supplement 185
[NASA-SP-7037(185)] 13 p1965 N85-22342

USSR report: Earth sciences
[JPRS-UES-85-002] 13 p2105 N85-23116

Application of field X-ray: Radiometric analysis in exploratory geology and means for its improvement
13 p2115 N85-[illegible]

Reports of the Planetary Geology and Geophysics Program, 1984
[NASA-TM-87563] 13 p2172 N85-23474

Planetary interior modeling and tectonic implications
13 p2200 N85-[illegible]

USSR report: Earth sciences
[JPRS-UES-85-004] 14 p2332 N85-[illegible]

Electromagnetic field of currents and its use to estimate total conductivity of sedimentary deposits in Western Black Sea 14 p2334 N85-[illegible]

New methods for interpreting seismic time fields in media with variable velocities 14 p2343 N85-[illegible]

Possibility of retrieving dynamics of reflected wave method records beneath low-velocity zone
14 p2346 N85-[illegible]

Observation model and parameter partials for the JPL VLBI parameter estimation software MASTERFIT-F 2.0
[NASA-CR-175640] 14 p2347 N85-[illegible]

Spectral analysis of diurnal nonuniformity of Earth's rotation 15 p2477 N85-[illegible]

High-capacity real-time computer system for processing hydrophysical data 15 p2625 N85-[illegible]

Telescope in lunar orbit 15 p2682 N85-[illegible]

Tenth Conference of Working Group of Socialist Countries on Remote Sensing of Earth under Intercosmos Program 16 p2725 N85-[illegible]

USSR report: Earth sciences
[JPRS-UES-85-005] 16 p2807 N85-[illegible]

Surface exploration geophysics applied to the Moon
[DE85-006714] 16 p2884 N85-[illegible]

Solar-Geophysical Data Number 484, December 1984. Part 1 (prompt reports): Data for November 1984, October 1984 and late data
[NASA-CR-175829] 16 p2888 N85-[illegible]

Solar-Geophysical Data Number 484, December 1984. Part 2 (comprehensive reports): Data for June 1984, January 1982 and Miscellanea
[NASA-CR-175826] 16 p2888 N85-[illegible]

Yearbook of the Bureau of Mineral Resources, Geology and Physics: Geoscientific research, resource assessment, and database development, 1 Jul. 1983 to 30 Jun. 1984
[BMR-84] 17 p2989 N85-[illegible]

Geophysical plasmas and atmospheric modeling
[AD-A152805] 17 p2993 N85-[illegible]

Earth Resources: A continuing bibliography with indexes, issue 45
[NASA-SP-7041(45)] 18 p3123 N85-[illegible]

Deep source gas
[DE85-001984] 18 p3126 N85-[illegible]

Geological-geophysical and gas-biochemical studies in Bering Sea 19 p3291 N85-[illegible]

Projects of the Computer Center of the academy's Siberian branch 19 p3295 N85-30425
Preliminary evaluation of alterant geophysical tomography in welded tuff
[DE85-010826] 19 p3302 N85-30469
Melt zones beneath five volcanic complexes in California: An assessment of shallow magma occurrences
[DE85-010644] 19 p3305 N85-30489
Environmental background measurement program
[AD-A153860] 19 p3319 N85-30577
Contemporary plate motions from LAGEOS
20 p3489 N85-31689
The Earth's wobble and associated ocean motions
20 p3490 N85-31696
Geodyn systems development
20 p3492 N85-31706
Global Mega-Geomorphology
[NASA-CP-2312] 21 p3600 N85-32357
Deep sea mega-geomorphology: Progress and problems 21 p3602 N85-32369
The origin of continental crust: Outlines of a general theory 21 p3720 N85-33083
Landscape interpretation capabilities using space photographs of regions of a multistage platform mantle structure 22 p3734 N85-33151
Questions about Mercury's role in comparative planetary geophysics 22 p3853 N85-33861
Geophysical-geological studies of possible extensions of the New Madrid fault zone
[TI85-901341] 23 p3949 N85-34475
Some geophysical guides to ore in southern and southwestern Alaska 24 p4103 N85-35436
The development of assessment techniques program
24 p4106 N85-35457
The Alaska Mineral Resources Assessment Program
24 p4107 N85-35460
Procedure for editing the fluxgate magnetometer data of the AFGL (Air Force Geophysics Laboratory) magnetometer network
[AD-A156331] 24 p4117 N85-35523

GEOPOTENTIAL
NT GEOPOTENTIAL HEIGHT
Geopotential harmonics of order 15 and 30, from analysis of the orbit of satellite 1971-10B
[RAE-TR-84008] 02 p0165 N85-11121
Individual geopotential coefficients of order 15 and 30, from resonant satellite orbits
[AD-A146887] 06 p0826 N85-15256
Individual geopotential coefficients of order 15 and 30, from resonant satellite orbits
[RAE-TR-84021] 08 p1105 N85-16985
Science Applications, part 2 11 p1643 N85-20347
Approximate perturbing part of geopotential by polynomials of stipulated form 13 p1984 N85-22448
Potential models — Earth gravity
14 p2396 N85-24764
Optimization of system for observing Northern Hemisphere atmospheric pressure field
15 p2485 N85-25338
Satellite physical and orbital characteristics
16 p2804 N85-27287
Radial orbit error spectrum for Topex
16 p2805 N85-27292
The selection of the starting field: General versus tailored model 16 p2805 N85-27294
Improving the geological interpretation of magnetic and gravity satellite anomalies
[E85-10103] 20 p3473 N85-31585
A comparative study of spherical and flat-Earth geopotential modeling at satellite elevations
20 p3475 N85-31593
A comparative study of spherical and flat-Earth geopotential modeling at satellite elevations
20 p3475 N85-31594
Continental and oceanic magnetic anomalies: Enhancement through GRM 20 p3476 N85-31598
Spaceborne gradiometer error analysis
20 p3492 N85-31707
Troposphere-stratosphere (surface-55 km) monthly general circulation statistics for the Northern Hemisphere-four year averages
[NASA-TM-86182] 20 p3495 N85-31730

GEOPOTENTIAL HEIGHT
Middle Atmosphere Program. Handbook for MAP, volume 7
[NASA-CR-175479] 11 p1656 N85-20437
Workshop on Comparison of Data and Derived Dynamical Quantities During Northern Hemisphere (PMP-1) Winters 11 p1657 N85-20444
Changes in the ozone content over central Europe during reversals of stratospheric circulation in late winter
11 p1661 N85-20469
On geoid heights and flexure of the lithosphere at seamounts
[AD-A151220] 15 p2604 N85-26050
The seasonal cycle of storminess as measured by band-pass fluctuations 18 p3144 N85-29467

GEORGIA
Revised Uniform Summary of Surface Weather Observations (RUSSWO). Dobbins AFB, Georgia, parts A-F
[AD-A148916] 07 p1005 N85-16387
Meteor wind results from Atlanta, USA, and Ramey, Puerto Rico 11 p1662 N85-20474
Geometric accuracy of LANDSAT-4 MSS image data
11 p1667 N85-20503

GEOS SATELLITES (ESA)
The structure and dynamics of the magnetosphere: Progress in the IMS 14 p2355 N85-24550
Terrestrial continuum radiation study during the IMS
14 p2365 N85-24619
Contribution of relaxation sounding experiments to the understanding of magnetospheric processes
14 p2371 N85-24655
Contribution of mutual impedance experiments to the understanding of magnetospheric processes — GEOS satellites 14 p2371 N85-24656

GEOS SATELLITES (ESRO)
U GEOS SATELLITES (ESA)

GEOS 1 SATELLITE
Simultaneous observations of electron spectra in the auroral zone and near the equatorial plane by the DMSP-5D-F2 and GEOS-1 Satellites
[KGI-184] 09 p1355 N85-18522
Results from the GEOS-1 and GEOS-2 spacecraft and their contributions to the IMS 14 p2354 N85-24545
Morphology of 2keV-electrons observed by GEOS 1
14 p2360 N85-24581
Energetic electron anisotropy and ELF waves onboard GEOS. How does quasi-linear diffusion work
14 p2366 N85-24623
Theoretical studies of electric cyclotron harmonic (ECH) waves based on experimental data from GEOS 1
14 p2367 N85-24631
Advances in magnetospheric plasma diagnosis by active experiments — IMS satellites 14 p2371 N85-24654
Contribution of relaxation sounding experiments to the understanding of magnetospheric processes
14 p2371 N85-24655

GEOS 2 SATELLITE
Results from the GEOS-1 and GEOS-2 spacecraft and their contributions to the IMS 14 p2354 N85-24545
The GEOS-2 electric field observations at times of solar wind discontinuities 14 p2360 N85-24584
Coordinated balloon-satellite studies of energetic electron precipitation mechanisms
14 p2360 N85-24587
The GEOS-2 E-field behavior during dynamic auroral development near the satellite footpoint
14 p2362 N85-24598
Role of equatorial Electron Cyclotron Harmonic (ECH) waves in the generation of diffuse auroras. Contribution of the GEOS IMS spacecraft 14 p2367 N85-24632
Long-period magnetospheric pulsations observed with an electric field experiment in the magnetosphere
14 p2369 N85-24639
The SAMBO-GEOS experiment: A Ps-6 event from ground-satellite observations 14 p2369 N85-24641
Observations of a pulsation event from the ground with balloons and with a geostationary satellite
14 p2369 N85-24643
Satellite, auroral radar and ground magnometer observations of transient ULF pulsations
14 p2369 N85-24645
Advances in magnetospheric plasma diagnosis by active experiments — IMS satellites 14 p2371 N85-24654

GEOS 3 SATELLITE
Intercomparison of GEOS 3/SEASAT wave data and wave model data 03 p0381 N85-12438
Lessons from the SEASAT and GEOS-3 altimeters data projects 03 p0384 N85-12457
Global mean sea surface based upon a combination of the GEOS-3 and SEASAT altimeter data
20 p3492 N85-31710

GEOS-B SATELLITE
U GEOS 2 SATELLITE

GEOS-C SATELLITE
U GEOS 3 SATELLITE

GEOSTATIONARY OPERATIONAL ENVIRON SATS
U GOES SATELLITES

GEOSTATIONARY PLATFORMS
U SYNCHRONOUS PLATFORMS

GEOSTATIONARY SATELLITES
U SYNCHRONOUS SATELLITES

GEOSTROPHIC WIND
The inducement of planetary boundary layer mass convergence associated with varying vorticity beneath tropospheric wind maximum 01 p0074 N85-10494
An alternative to reduction of surface pressure to sea level
[NASA-CR-174174] 04 p0538 N85-13422
A study of the adequacy of quasi-geostrophic dynamics for modeling the effect of frontal cyclones on the larger scale flow 05 p0684 N85-14398
Spectral modeling of a potential vorticity equation for a barotropic flow on a beta-plane
[CWI-AM-R8408] 08 p1186 N85-17478
Sea-ice motion in response to geostrophic winds
14 p2323 N85-24357
Numerical experiments of jet streak ageostrophic circulations using pseudo-geostrophic initialization and perspectives 15 p2590 N85-25969
Numerical studies of frontal dynamics
15 p2596 N85-26014
A study of the adequacy of quasi-geostrophic dynamics for modeling the effect of frontal cyclones on the larger scale flow
[NASA-CR-176065] 20 p3495 N85-31731

GEOSYNCHRONOUS ORBITS
Relationships between Ariane trajectories and satellite orbits 05 p0599 N85-13815
Satellite positioning — in geosynchronous orbit
05 p0600 N85-13823
Perturbations in geostationary orbit
05 p0600 N85-13824
Stationkeeping strategies for geostationary satellites
05 p0600 N85-13825
Moderate lift-to-drag aeroassist
08 p1107 N85-16995
OTV propulsion tecnology programmatic overview
08 p1107 N85-16997
The rationale and suggested approaches for research geosynchronous satellite measurements for severe storm and mesoscale investigations
[NASA-TM-86185] 09 p1356 N85-18532
Efficient structures for geosynchronous spacecraft solar arrays
[NASA-CR-174448] 10 p1428 N85-19004
Assessment of satellite collision hazards by simulated sampling in space 12 p1784 N85-21195
Geosynchronous satellite collision avoidance
12 p1784 N85-21197
The long term behaviour of Earth orbits and the implications for debris control 12 p1786 N85-21213
Debris in the geostationary orbit ring, the endless shooting gallery: The necessity for a disposal policy
12 p1786 N85-21214
The international environment UNISPACE '82 and the ITU: A relationship between orbit-spectrum resource allocation and orbital debris 12 p1787 N85-21215
Radiation exposure and performance of multiple burn LEO-GEO orbit transfer trajectories
[NASA-TM-86946] 12 p1788 N85-21228
SCATHA (spacecraft charging at high altitudes) plasma interaction experiment: SC-3 high energy particle spectrometer; SC-8 energetic ion composition experiment
[AD-A149728] 12 p1793 N85-21252
Design guidelines for assessing and controlling spacecraft charging effects 13 p1994 N85-22500
Development of a continuous broad-energy-spectrum electron source 13 p1995 N85-22507
Automatic charge control system for satellites
13 p1995 N85-22508
Observations of energetic electron and ion distributions near the magnetopause at geosynchronous orbit and related ground effects 14 p2356 N85-24560
Timing between particle injections at the geostationary orbit and particle flux decreases in the distant geomagnetic tail during substorms 14 p2358 N85-24569
Results of the SCATHA ion composition experiment during the IMS 14 p2359 N85-24580
Sudden Storm Commencement (SSC) associated hydromagnetic variations at geosynchronous altitude and on the ground 14 p2369 N85-24642
Costs, payload of Ariane, US Space Shuttle compared
15 p2530 N85-25601
Station for in-orbit testing of satellites
[MBB-UR-708/84-O] 16 p2874 N85-27733
Geostationary orbit capacity study
[REPT-44-3558] 18 p3091 N85-29134
A 406 MHz geostationary satellite SARSAT experiment 20 p3403 N85-31113
Civilian Space Stations and the US future in Space
[OTA-STI-242] 20 p3418 N85-31215
Geosynchronous performance of a lithium-titanium disulfide battery 20 p3444 N85-31377

GEOSYNCLINES
Deformation mechanisms associated with mesoscopic kinkbands, Jura Mountains (Switzerland) and Chaines Subalpines (France) 03 p0369 N85-12492
Conditions for formation of parageneses containing kyanite-orthoclase in region of Mount Provender and Pratt Peak (Shackleton Range, Antarctica)
19 p3296 N85-30447

Stratigraphic analysis of Pennsylvania rocks using hierarchy of transgressive-regressive units
19 p3312 N85-30531

GEOTECHNICAL ENGINEERING
Engineering geology of selected areas, US army engineer division, lower Mississippi valley. The American bottom area, MO-IL. Volume 1
[AD-A154258] 19 p3299 N85-30455

GEOTEMPERATURE
Geophysical Works during 1981, volume 29, no. 547-566 03 p0375 N85-12389
Heat flow map of Europe: Brief summary of the geophysical implications
[REPT-562] 03 p0377 N85-12405
Terrestrial heat flow in Europe and general features of its regional distribution
[REPT-563] 03 p0377 N85-12406
Diagenesis of niagaran (middle silurian) pinnacle reefs, northwest Michigan 09 p1352 N85-18506
Thermal conditions and thinning of lithosphere in late cenozoic in southwestern US 10 p1501 N85-19473
Low-temperature geothermal assessment of the Jordan Valley Salt Lake County, Utah
[DE85-000616] 11 p1670 N85-20524
Determining deep heat flow and rate of horizontal percolation from temperature measurements in aquifer
13 p2116 N85-23180
Temperature anomalies above ore bodies
14 p2345 N85-24500
Crustal radiogenic heat production and the selective survival of ancient continental crust
21 p3721 N85-33066

GEOTHERMAL ANOMALIES
Seismic discrimination of a geothermal field: Cerro Prieto
[DE84-014581] 01 p0064 N85-10425
Interpreting geothermal anomalies by special points method 07 p0982 N85-16238

GEOTHERMAL ENERGY CONVERSION
International test and demonstration of a 1-MW wellhead generator: Helical screw expander power plant
[NASA-CR-174161] 04 p0527 N85-13372
USSR report: Energy
[JPRS-UEN-84-038] 07 p0994 N85-16312
Deputy Minister discusses plans for geothermal power
07 p0994 N85-16313
Geothermal injection treatment: Process chemistry, field experiences, and design options
[DE85-002873] 11 p1675 N85-20554
Silica problem in the design of geothermal power plants
[DE85-008245] 17 p2986 N85-28453
Solar energy education. Renewable energy: A background text
[DE85-010365] 23 p3946 N85-34452

GEOTHERMAL ENERGY EXTRACTION
Geothermal wells drilled in Transcarpathians
07 p0994 N85-16315
Thermohydrodynamic model: Hydrothermal system, shallowly seated magma chamber
13 p2115 N85-23173
Western gas sands
[DE85-001985] 18 p3126 N85-29360
Technology transfer report: Feasibility study for the use of geothermal brine in the Ashdod area, Israel
[DE85-013316] 22 p3810 N85-33598

GEOTHERMAL ENERGY UTILIZATION
Deputy Minister discusses plans for geothermal power
07 p0994 N85-16313
Optimization of design and control strategies for geothermal space heating systems
[DE85-000496] 09 p1344 N85-18458
Monitoring environmental and related performance parameters for a Rankine-cycle turbine electric generator utilizing geothermal energy at the Gila Hot Springs, New Mexico
[DE84-901772] 09 p1345 N85-18465
Two-phase flow in geothermal systems
[DE85-004692] 12 p1848 N85-21591
Leak detectors for organic Rankine cycle power plants: On-line and manual methods
[DE85-002792] 12 p1852 N85-21617
Selection of promising sites for magma energy experiments
[DE85-006832] 16 p2820 N85-27393
Pagosa Springs geothermal project
[DE85-011308] 22 p3807 N85-33583
Enthalpy transients in fractured two-phase geothermal systems
[DE85-011968] 22 p3808 N85-33587

GEOTHERMAL RESOURCES
NT GEYSERS
NT VOLCANOES
A summary of geothermal studies in Montana, through 1983
[DE84-014325] 01 p0064 N85-10422
Geothermal resources of the Laramie, Hanna, and Shirley Basins, Wyoming
[DE84-016104] 01 p0064 N85-10423
Geothermal exploration in Trans-Pecos, Texas/New Mexico
[DE84-015553] 01 p0064 N85-10424
Seismic discrimination of a geothermal field: Cerro Prieto
[DE84-014581] 01 p0064 N85-10425
Hydrogeochemical investigation of thermal springs in the Black Canyon-Hoover Dam area, Nevada and Arizona
[PB84-202472] 01 p0064 N85-10428
Investigation of mineral and thermomineral springs in the Eifel Mountains regarding thermal indications
[BMFT-FB-T-84-019] 02 p0220 N85-11451
Similarity considerations in 1-component 2-phase flow
[DE84-016370] 04 p0499 N85-13184
Geothermal studies in Alaska: Conditions at Prudhoe Bay 04 p0516 N85-13290
Geothermal resource assessment for North Dakota
[DE84-016128] 04 p0526 N85-13367
Geothermal assessment of the lower Bear River drainage and northern East Shore ground-water areas, Box Elder County, Utah
[DE84-017358] 04 p0526 N85-13368
International test and demonstration of a 1-MW wellhead generator: Helical screw expander power plant
[NASA-CR-174161] 04 p0527 N85-13372
CO-2-silica geothermometer for low temperature geothermal resource assessment, with application to resources in the Safford Basin, Arizona
[DE84-013958] 04 p0534 N85-13411
Subsurface temperatures in northeastern Wyoming measured by bottom hole temperature records
[TI84-901610] 04 p0534 N85-13413
Thermal energy resources of thermal waters in Kazakhstan 06 p0820 N85-15208
Geothermal assessment of a portion of the Escalante Valley, Utah
[DE84-015964] 06 p0828 N85-15257
Analysis of gases in the Earth's crust
[PB85-113397/GAR] 07 p0990 N85-16287
Coso Monitoring Program, January 1981 through December 1983
[AD-A147694] 07 p0998 N85-16338
Earth Sciences Division report, 1983
[DE85-001036] 09 p1341 N85-18436
Geothermal assessment of part of the east shore area, Davis and Weber Counties, Utah
[DE84-016817] 09 p1342 N85-18446
Heat cycle research program
[DE84-017015] 09 p1344 N85-18455
Field testing of aquifer thermal energy storage
[DE85-000399] 09 p1344 N85-18457
Results from geopressured-geothermal subsidence studies
[DE84-016279] 09 p1354 N85-18520
Low-temperature geothermal assessment of the Jordan Valley Salt Lake County, Utah
[DE85-000616] 11 p1670 N85-20524
Geothermal injection treatment: Process chemistry, field experiences, and design options
[DE85-002873] 11 p1675 N85-20554
Heat Cycle Research Experimental Program report, FY-84
[DE85-003558] 12 p1882 N85-21811
Evaluation of subsurface fracture geometry using fluid pressure response to solid earth tidal strain
[DE85-003294] 12 p1890 N85-21864
Normal and anomalous geothermal fields and their relationship to hierarchy of geological bodies
13 p2113 N85-23163
Thermohydrodynamic model: Hydrothermal system, shallowly seated magma chamber
13 p2115 N85-23173
Navy geothermal plan
[AD-A152478] 17 p2985 N85-28450
Laboratory investigation of formation damage of an artificial fracture at simulated geothermal conditions
[DE85-010301] 18 p3102 N85-29201
Hot Dry Rock Geothermal Energy Developement Program
[DE85-010570] 19 p3268 N85-30264
Lost circulation in geothermal wells: Research and development status
[DE85-009636] 19 p3268 N85-30267
Evaluation of geothermal potential of Rio Grande rift and Basin and Range province, New Mexico
[DE85-901380] 19 p3301 N85-30466
Geothermal hydrogen and health in Rotorua, New Zealand
[DE85-901283] 19 p3301 N85-30467
Linear boundary detection using pressure buildup tests
[DE85-009926] 22 p3784 N85-33444
Pagosa Springs geothermal project
[DE85-011308] 22 p3807 N85-33583
Enthalpy transients in fractured two-phase geotherma
systems
[DE85-011968] 22 p3606 N85-
Technology transfer report: Feasibility study for the u
of geothermal brine in the Ashdod area, Israel
[DE85-013316] 22 p3810 N85-
Fracture detection and characterization for geotherma
reservuir definition
[DE85-008677] 22 p3815 N85-
Proposed resource evaluation plan. Salton Sea scienti
drilling program
[DE85-011294] 22 p3815 N85-
Geothermal resources of the Laramie, Hanna and Shirle
Basins, Wyoming
[DE85-005005] 23 p3943 N85-34
Depletion modeling of liquid dominated geotherma
reservoirs
[DE85-009923] 23 p3943 N85-3442
Evaluation of low-temperature geothermal potential i
Utah and Goshen Valleys and adjacent areas, Utah. Pa
2: Water temperature and chemistry
[DE85-009344] 23 p3943 N85-34
Modeling of geothermal systems
[DE85-012553] 23 p3943 N85-34
Workshop on Recent Research in the Valles Calde
[DE85-010569] 23 p3949 N85-3447
Early and middle Cenozoic volcanic synthesis
24 p4105 N85-354
Evaluation of low-temperature geothermal potential i
north-central Box Elder County, Utah
[DE85-009541] 24 p4112 N85-354
Geothermal resources of the Washakie and Great Divid
basins, Wyoming
[DE85-013004] 24 p4112 N85-3549

GEOTHERMAL TECHNOLOGY
NT GEOTHERMAL ENERGY CONVERSION
NT GEOTHERMAL ENERGY EXTRACTION
NT GEOTHERMAL ENERGY UTILIZATION
Optimization of design and control strategies fo
geothermal space heating systems
[DE85-000496] 09 p1344 N85-1845
Geothermal injection treatment: Process chemistry, fie
experiences, and design options
[DE85-002873] 11 p1675 N85-2055
Two-phase flow in geothermal systems
[DE85-004692] 12 p1848 N85-2159
Thermophysical properties of working fluids for bina
geothermal cycles
[DE85-000365] 12 p1881 N85-2180
Alternative heat sources for heat pumps
[DE85-007610] 17 p2959 N85-2827
Hot Dry Rock Geothermal Energy Developmen
Program
[DE85-010570] 19 p3268 N85-3026
The transient electromagnetic depth sounding techniqu
applied to hydrocarbons and geothermal exploration
[MITT-42] 23 p3949 N85-3447

GEOTHERMOMETRY
U GEOTEMPERATURE

GEOTROPISM
Gravity and cell differentiation in lentil roots
06 p0690 N85-143

GEP TELESCOPES
U PARTICLE TELESCOPES

GERDIEN ARC HEATERS
U HEATING EQUIPMENT

GERMAN DEMOCRATIC REPUBLIC
U EAST GERMANY

GERMANATES
Recent progress in BGO development for high resolutio
calorimetry
[MPI-PAE/EXP-E1-129] 01 p0124 N85-1084
Improvements in the energy resolution an
high-count-rate performance of bismuth germanate
[DE85-010763] 19 p3240 N85-300

GERMANIDES
Contact properties of rare-earth silicides and germanide
on Si and Ge 19 p3374 N85-309

GERMANIUM
NT GERMANIUM ISOTOPES
Relationships between electronic structure and stabili
of metallic glasses
[AD-A145141] 01 p0028 N85-1017
Development of high responsivity Ge:G
photoconductors
[DE84-016902] 04 p0571 N85-13
On the origins of structural defects in BF2(+)-implante
and rapid thermally annealed silicon: Conditions for defe
free regrowth
[DE84-016060] 04 p0572 N85-13
Ge abundances in the lunar mantle and implications
for the origin of the Moon 04 p0582 N85-137
IUE observations of the gaseous component of the loca
interstellar medium 06 p0874 N85-15

Electronic structure, chemical bonding, and superconductivity of silver films on germanium
[AD-A147720] 08 p1128 N85-17112
Optically induced intervalence-band transitions in germanium by the absorption of 1.06 micrometers picosecond pulses
[DE85-000946] 09 p1399 N85-18803
Metal-nonmetal transitions in N-doped many-valley Si and Ge
[INPE-3358-PRE/636] 10 p1562 N85-19648
Impurity complexes in pure elemental semiconductors
11 p1736 N85-20919
Germanium resistance thermometer calibration at superfluid helium temperatures
12 p1947 N85-22226
Shuttle flight test of an advanced gamma-ray detection system
[AD-A150316] 13 p1988 N85-22469
Time resolved X-ray studies during pulsed laser irradiation of Ge
[DE85-005263] 13 p2097 N85-23083
Infrared nonlinear processes in semiconductors
[AD-A150966] 14 p2427 N85-24968
TEM investigation of polar-on-nonpolar epitaxy: GaAs-AlGaAs on (100) Ge
[DE85-007613] 16 p2871 N85-27714
Germanium detectors with a built-in transverse drift field
[DE85-009944] 18 p3096 N85-29165
Method for producing high quality germanium-germanium nitride interfaces for germanium semiconductors and device produced thereby
[AD-D011702] 19 p3260 N85-30218
Bismuth germanate scintillators: Applications in nuclear safeguards and health physics
[DE85-010730] 19 p3365 N85-30665
New adatom model for Si(11) 7X7 and Si(111)Ge 5X5 reconstructed surfaces 20 p3480 N85-31625
Thermoelectric properties of beta-boron and some boron compounds
[DE85-011976] 21 p3582 N85-32270
Absorption of 10.6 micrometer laser radiation in electron-hole condensate in germanium
21 p3681 N85-32870
Raman scattering studies in solids
[AD-A155528] 21 p3710 N85-33032
Specificity of (71)Ga(p,n) (71)Ge at 35 MeV for Gamow-Teller strength
[DE85-011837] 23 p3971 N85-34615
Germanium and lead: Significant differences between meteoritic and photospheric abundances?
[OG-7.1-2] 23 p4012 N85-34864

GERMANIUM ALLOYS
Raman scattering from metastable GaSb(1-x) Ge(2x) alloys
[AD-A145897] 03 p0327 N85-12106
Optical properties of composite materials
[AD-A146768] 07 p0920 N85-15828
Alloy supercooling on Salyut-7
11 p1604 N85-20083
Structure and aging of amorphous chromium-germanium alloys 15 p2497 N85-25401
Compensation of dangling bonds in A-Si, Ge:H alloys
[DE85-002905] 15 p2662 N85-26433
LPCVD tungsten deposition on Si-Ge alloy
[DE85-005588] 16 p2750 N85-26970
Theoretical studies on the structures of insulating and metallic glasses
[DE85-010022] 18 p3194 N85-29814
Development of improved thermoelectric materials for space nuclear power systems
[DE85-013079] 22 p3844 N85-33807

GERMANIUM COMPOUNDS
NT GERMANATES
NT GERMANIDES
NT GERMANIUM OXIDES
The effect of temperature on the radiation induced losses of large diameter GPS (Germanium phosphosilicate) and GBS core optical fibers
[AD-A145409] 02 p0280 N85-11823
1985 Amorphous Silicon Review Meeting
[DE85-008794] 22 p3807 N85-33582

GERMANIUM DIODES
Measurement of nuclear lines with a dual Ge(Li) telescope aboard a stratospheric balloon
[INPE-3380-TDL/185] 11 p1762 N85-21083
Intercomparison of the calculated absolute efficiency values between true coaxial and true closed-end coaxial Ge (Li) and NaI detectors
[REPT-5-1984] 20 p3532 N85-31976

GERMANIUM ISOTOPES
Results of ultra-low level 71ge counting for application in the Gallex-solar neutrino experiment at the Gran Sasso Underground Physics Laboratory
[SH-8.1-2] 23 p4049 N85-35106

GERMANIUM OXIDES
The relationship between radiation sensitivity and redox equilibria — glass processing variables
[AD-A147216] 07 p0932 N85-15906

GERMANIUM RECTIFIERS
U GERMANIUM DIODES

GERMANY
Determination of the longitude differences Munich-Lissabon-San Fernando, Munich-Wettzell, and Munich-Karlsruhe-Niederreifenberg
[ASTRON-GEODAET-ARB-44]
04 p0524 N85-13353
Determination of astronomical longitude differences for the European longitude reference system for 1980. Relative right ascension corrections for 125 FK4 and FK4 Sup stars 04 p0524 N85-13354
Determination of astronomical longitude differences: Munich, Karlsruhe, Niederreifenberg in 1974
04 p0524 N85-13355
Limited surface observatins climatic summary (LISOCS). Ansback AHP, Germany
[AD-A147205] 07 p1007 N85-16398

GERMINATORS
U PHYTOTRONS

GERT
A Q-GERT network simulation model for examining pipeline time in the Navy's J-52 intermediate level jet engine repair cycle
[AD-A147269] 07 p0894 N85-15663
Simulation of estimating periodicity of seasonally stationary time series
[DE85-003517] 11 p1708 N85-20748
SINOGRAFO: A system for influencing and forecasting weather
[INPE-3349-PRE/628] 16 p2834 N85-27475

GETTERS
Studies on impurity control and hydrogen pumping with chromium gettering in ISX-B
[DE85-001896] 09 p1394 N85-18771
Neutral beam injector oxygen impurity measurements and concentration reduction via gettering processes
[DE85-000861] 12 p1836 N85-21521
Development of new process technologies for solar cells with high efficiency starting from purified silicon
12 p1878 N85-21785
Vacuum system for the Argonne 6 GeV synchrotron light source
[DE85-012286] 24 p4157 N85-35773

GEYSERS
Categorization of nocturnal drainage flows within the Brush Creek valley in western Colorado and the variability of sigma theta in complex terrain
[DE85-011291] 19 p3300 N85-30461

GIACOBINI-ZINNER COMET
The astrometry network of the IHW and the P/Crommelin trial run results 14 p2435 N85-25016
The IHW reference star catalogs for Comets Halley and Giocobini-Zinner 14 p2436 N85-25031
The orbits of Comets Halley and Giocobini-Zinner
14 p2437 N85-25039
Astrometric needs for the ISEE-3/ICE mission to Comet Giocobini-Zinner 14 p2438 N85-25043
The International Cometary Explorer (ICE)wallsheet teacher's guide
[NASA-TM-87498] 23 p3988 N85-34727

GIANT STARS
NT CARBON STARS
NT RED GIANT STARS
Photoelectric photometry of globular cluster giants
01 p0128 N85-10884
Outer atmospheres of giant and supergiant stars
[NASA-CR-174165] 04 p0580 N85-13703
The behaviour of brighter binaries and yellow giants in open clusters 05 p0737 N85-14738
On the content of nitrogen in atmospheres of late giants derived from molecular bands on NH in the UV spectral range 05 p0740 N85-14761
Theoretical studies of chromospheres and winds in cool stars
[NASA-CR-174204] 06 p0880 N85-15596
The essence of binary star coalescence: A coordinated ground-based photometric and IUE ultraviolet study of FK Comae 11 p1756 N85-21044
Chromospheric activity in M giants
11 p1757 N85-21056
Rotational modulation of chromospheric emission in cool giants and hybrid stars 11 p1759 N85-21064
Stellar granulation 14 p2451 N85-25132

GIMBALS
Orbital transfer vehicle propulsion issues
08 p1109 N85-17009
Determination of directional gyro parameters
14 p2287 N85-24171
Impact of magnetic isolation on pointing system performance in the presence of structural flexibility
[NASA-CR-172481] 16 p2732 N85-26861
A Gimbal sizing analysis for an IPACS rotating assembly
[NASA-CR-172524] 16 p2741 N85-26913

GIOTTO MISSION
A cometary ion mass spectrometer
[NASA-CR-174328] 08 p1164 N85-17343
Giotto solar array: Design, manufacture and test
13 p2008 N85-22589
The Giotto spacecraft impact-induced plasma environment
[ESA-SP-224] 14 p2243 N85-23905
Measurement of charged secondary particle emission under ion and neutral impact — Giotto mission
14 p2243 N85-23906
Contactless determination of the conductivity of the white paint PCB-Z — Giotto spacecraft thermal control coating 14 p2243 N85-23907
Measurements of integral yields of charged secondary particles using neutral beams simulating a cometary fly-by — Giotto mission 14 p2244 N85-23908
Giotto residual ionization 14 p2244 N85-23909
Impact ionization from gold, aluminum and PCB-Z — Giotto spacecraft paint PCB-Z 14 p2244 N85-23910
Experimental investigations on ion emission with dust impact on solid surfaces — Giotto spacecraft
14 p2244 N85-23911
Ion emission from solid surfaces: Comparison of dust impact with other excitations — Giotto mission
14 p2244 N85-23912
Electrostatic charging of the Giotto spacecraft due to neutral gas impact 14 p2244 N85-23913
A model of plasma cloud expansion generated by a dust particle impact — Giotto mission
14 p2245 N85-23914
Giotto plasmasheath and wake charging near Halley's Comet: Revised parameters 14 p2245 N85-23915
Simulations of satellite-plasma interaction, including electron space charges — Giotto mission
14 p2245 N85-23916
Anticipated impact plasma problems for the COPERNIC-RPA experiment in the cometary environment — Giotto mission 14 p2245 N85-23917
An impact plasma monitor for cometary missions — Giotto , VEGA 14 p2245 N85-23918
Plasma environment effects on the Giotto Ion Mass Spectrometer 14 p2245 N85-23919
Thermal design of the Giotto spacecraft
14 p2245 N85-23920
Spacecraft environment during the Giotto-Halley encounter: A summary 14 p2246 N85-23921
Towards the Halley Comet 14 p2399 N85-24783

GLACIAL DRIFT
Glacier dynamics and the development of glacial landforms in the eastern Puget lowland, Washington
03 p0389 N85-12490
The pleistocene geology of Vilas County, Wisconsin
09 p1353 N85-18509

GLACIERS
Late quarterly glaciolacustrine and vegetational history of the Copper River Basin, south-central Alaska
03 p0391 N85-12499
Glacial-lake deposits in the Mount Harper area, Yukon-Tanana Upland 04 p0517 N85-13300
Paleoclimatologists use past to predict weather patterns 06 p0819 N85-15197
Surging as a potential response of ice sheets to CO2-induced changes in the polar environment (SPICAE)
[DE84-016472] 06 p0841 N85-15341
Consideration of future climatic changes in three geologic settings
[DE85-001704] 09 p1357 N85-18537
Decade of the Varilov Kupola
10 p1497 N85-19448
Major glaciation events of the past and their geological significance 10 p1497 N85-19450
Proceedings of the 1st Glacier Bay Science Symposium
[PB85-115913] 11 p1682 N85-20599
Catastrophic-flood features in Swedish Lapland as a terrestrial analog for Martian channel flows
13 p2190 N85-23587
Greenland ice sheet mass balance
15 p2603 N85-26043
Potential climatic effects on the Greenland ice sheet
15 p2603 N85-26044
Modern sedimentation in the northern Barents Sea: Input, dispersal and deposition of suspended sediments from glacial meltwater
[AD-A152520] 17 p2997 N85-28530

GLACIOFLUVIAL DEPOSITS
U GLACIAL DRIFT

GLACIOLOGY
Late quaternary glacial cycles in the Bahamian deep basins and in the adjacent Atlantic Ocean
02 p0226 N85-11476

Interlobate comparison of glacial-depositional style as evidenced by small-relief glacial landscape features in Illinois, Indiana, and Ohio, utilizing SIR-B
08 p1146 N85-17231

Glacial geology of Barron County, Wisconsin
09 p1351 N85-18500

The pleistocene geology of Vilas County, Wisconsin
09 p1353 N85-18509

Decade of the Varilov Kupola
10 p1497 N85-19448

Major glaciation events of the past and their geological significance 10 p1497 N85-19450

Antarctic glaciation, or what are catastrophes in Earth's history 13 p2105 N85-23118

Numerical experiments with simple model of ocean climate 13 p2106 N85-23123

Reports of the Planetary Geology and Geophysics Program, 1984
[NASA-TM-87563] 13 p2172 N85-23474

GLANDS (ANATOMY)
NT ADRENAL GLAND
NT PANCREAS
NT PARATHYROID GLAND
NT PITUITARY GLAND
NT THYMUS GLAND
NT THYROID GLAND

GLANDS (SEALS)

Life testing of rubber seals — aircraft hydraulic systems
[AD-A143193] 13 p2098 N85-23086

GLARE

Removable cleanable antireflection shield
[AD-D011735] 22 p3844 N85-33610

GLASS
NT BOROSILICATE GLASS
NT GLASS FIBERS
NT METALLIC GLASSES
NT S GLASS
NT SILICA GLASS
NT SPIN GLASS

Potential utilization of glass experiments in space
02 p0151 N85-11020

Inorganic composites for space applications
02 p0155 N85-11047

Investigation of chemical durability mechanisms in fluoride glasses
[AD-A145420] 02 p0186 N85-11241

Silicon nitride joining
[AD-A145668] 02 p0187 N85-11248

Structure of vibrational spectrum and selection rules in Raman and hyper-Raman light scattering spectra of inorganic glasses 02 p0271 N85-11769

Thermal deformation measurements of heat-resistant structural materials for aircraft by electro optical displacement transducer
[NAL-TR-810] 03 p0325 N85-12092

HIP glassmaking for high nitrogen compositions in the Y-Si-Al-O-N system
[DE84-015546] 03 p0338 N85-12175

Evaluation of laterally loaded laminated glass units by theory and experiment
[PB84-216423] 03 p0339 N85-12179

EXAFS studies of sodium silicate glasses containing dissolved actinides
[DE84-015835] 04 p0479 N85-13051

Abundancies of Ni, Cr, CO and major elements in the silicate portion of the Moon: Constraints from primary lunar magmas 04 p0582 N85-13720

Volatile elements in and on lunar volcanic glasses: What do they tell us about lunar genesis?
04 p0584 N85-13728

High temperature corrosion of ceramics
[DE84-017084] 05 p0620 N85-13967

Polyimide-glass multilayer printed wiring boards
[DE84-015092] 05 p0631 N85-14048

Polarization in chemically doped hydrogen-rich glasses
[DE84-017486] 06 p0771 N85-14936

The influence of gravitational body force in meteoritic chondrule and lunar glass formation
06 p0884 N85-15614

Method for bonding insulator to insulator
[AD-D011340] 07 p0929 N85-15891

The relationship between radiation sensitivity and redox equilibria — glass processing variables
[AD-A147218] 07 p0932 N85-15906

Cryogenic glass-to-metal seal
[AD-D011370] 07 p0933 N85-15911

Glass corrosion in liquid lithium
[DE85-002086] 09 p1299 N85-18162

Study of charge transport in the thermoelectret state of some ceramics and glasses
[DE85-001763] 09 p1300 N85-18163

Evaluation of laterally loaded laminated glass units by theory and experiment
[PB85-111532/GAR] 09 p1300 N85-18166

Stabilization of contaminated soils by in situ vitrification
[AD-P004144] 09 p1348 N85-18480

Optical studies of dynamical processes in disordered materials
[DE85-002400] 10 p1453 N85-19158

Ultrasonic characterization of advanced composite flywheels
[DE85-000158] 11 p1593 N85-20026

Kinetics of reaction of metals and non-metals during diffusion welding 11 p1602 N85-20076

Ab initio calculations of the optical properties of ions in glass
[DE85-001008] 11 p1612 N85-20133

Magnetically-induced luminescence of (Ir(2-phos)(2)C10(4)
[AD-A149659] 12 p1799 N85-21286

Ring-on-ring tests and load capacity of cladding glass
[PB85-106391] 12 p1868 N85-21717

Densification and deformation in the presence of a liquid phase
[DE85-005101] 13 p2038 N85-22763

Experimental methods for quenching structures in lunar-analog silicate melts: Variations as a function of quench media and composition
13 p2184 N85-23554

A study of frequency effects and damage accumulation during the fatigue of graphite/epoxy and glass/epoxy composite materials 14 p2247 N85-23930

Computer simulations of rare earth sites in glass: Experimental tests and applications to laser materials
[DE85-006156] 14 p2261 N85-24013

Density and thermal expansion measurements of several mixed oxide glasses in the solid and liquid regions
[DE85-006134] 14 p2261 N85-24014

Power control of induction equipment for founding optical glass in array of platinum crucibles
14 p2267 N85-24044

Water-resistance and some other properties of polyalkali fluorophosphate glasses 14 p2281 N85-24133

USSR report: Materials science and metallurgy
[JPRS-UMS-85-001] 15 p2496 N85-25395

A statistical approach to relaxation in glassy materials
[AD-A151265] 15 p2516 N85-25524

Low-temperature thermal expansion of glass
15 p2645 N85-26315

Impurity studies
[DE85-006235] 15 p2661 N85-26423

Impact of optical inhomogeneity in sintered interface between glasses on laser emission characteristics
16 p2763 N85-27053

Spectroscopic investigation of materials for frequency agile laser systems
[AD-A151731] 16 p2790 N85-27208

Mechanical properties of lunar materials under anhydrous, hard vacuum conditions: Applications of lunar glass structural components
[DE85-006682] 16 p2801 N85-27271

Accuracy of the calculated stress field around a craze
[DE85-005520] 16 p2801 N85-27272

Dendritic growth from amorphous matrix
[DE85-007630] 16 p2871 N85-27712

Investigation of charge transport in the thermoelectret state of some ceramics and glasses
[DE85-009318] 17 p2936 N85-28122

Investigation of semiconductor clad optical waveguides
[NASA-CR-175870] 17 p3036 N85-28785

Preparation of heavy metal fluoride glasses in the bulk form
[AD-A153784] 18 p3079 N85-29049

Foamglass solar window collector
[DE85-009197] 18 p3129 N85-29374

Structural characteristics of high temperature composites
[NASA-CR-175998] 19 p3232 N85-30037

Weldability/microstructure relationships of high nickel alloys for header applications
[DE85-009337] 19 p3241 N85-30094

Thermal expansion coefficients of a 30% glass fiber filled PEEK pyrotechnic charge holder
[DE85-010805] 19 p3251 N85-30155

Microscopic structure of two-dimensional electron glass
[DE85-010265] 19 p3376 N85-30942

Silicon nitride protective coatings for silvered glass mirrors
[DE85-011637] 20 p3433 N85-31300

Development of processes for the inclusion of radioactive waste in glass-metal compounds and ceramic materials
[BLL-CE-TRANS-8014-(9022.09)]
20 p3526 N85-31931

EVA-glass interface bond stability
21 p3608 N85-32408

Thin-film reliability and engineering overview
21 p3612 N85-[illegible]

Luminescence and absorption of indium-activated potassium-borate glasses subjected to high-power excitation 21 p3661 N85-[illegible]

Tensile fatigue of glass fibers and composites with conventional and surface compressed fibers
[RR-84-4] 22 p3742 N85-33196

Experimental studies of glass refining
[NASA-CR-176130] 22 p3751 N85-[illegible]

Research study for gel precursors as glass and ceramic starting materials for space processing applications research
[NASA-CR-176113] 22 p3751 N85-[illegible]

Sodium nitrate containing mixture for producing ceramic-glass-ceramic seal by microwave heating
[DE85-011610] 22 p3751 N85-33254

Method of bonding silver to glass and mirrors produced according to this method
[DE85-011642] 22 p3792 N85-[illegible]

Technology of off-gas treatment for liquid-fed ceramic melters
[DE85-012467] 22 p3812 N85-[illegible]

Iron and manganese in oxide minerals and in glasses: Preliminary consideration of Eh buffering potential at Yucca Mountain, Nevada
[DE85-011892] 23 p3916 N85-34271

The effect of liquid-liquid phase separation of glass on the properties and crystallization behavior
[NASA-TM-77890] 23 p3919 N85-34285

Single-point diamond crushing of Zerodur with in-situ polishing and metrology on a diamond turning machine
[DE85-012918] 24 p4063 N85-35335

GLASS COATINGS

Advanced glazings research
[DE85-000539] 11 p1674 N85-20540

Development of corrosion resistant heat exchangers for flue gas desulfurization
[BMFT-FB-T-84-281] 18 p3103 N85-29211

Tensile fatigue of glass fibers and composites with conventional and surface compressed fibers
[RR-84-4] 22 p3742 N85-33196

Laser sealed evacuated window glazings
[DE85-000512] 22 p3754 N85-33273

GLASS FIBER REINFORCED PLASTICS

Prediction of long term strength of glass reinforced plastics in wet environments
[NPL-DMA(A)-80] 04 p0477 N85-13041

Non-linear data fitting for the analysis of creep rupture data on GRP materials in aggressive environments — glass reinforced plastics (GRP)
[NPL-DMA(A)-79] 04 p0512 N85-13261

Prefabricated panels for rapidly runway repair and expedient airfield surfacing
[AD-D011277] 05 p0597 N85-13894

System for rapid repair of damaged airfield runways
[AD-D011325] 07 p0909 N85-15754

Stresses in pin-loaded orthotropic plates using photoelasticity
[NASA-CR-172496] 07 p0977 N85-16204

Review of the mechanical properties of SMC and GRP materials
[NPL-DMA(A)-88] 08 p1131 N85-17128

Initial fracture stages of orthogonally reinforced composite material 11 p1599 N85-20055

Strength properties of unidirectionally reinforced hybrid composites 11 p1599 N85-20056

Preliminary review of statistical treatment of S-glass/epoxy stress rupture data
[AD-A148810] 12 p1797 N85-21275

Scale-up of vanadium trineodecanoate
[AD-A149935] 12 p1813 N85-21370

Stability of three-layer glass-reinforced plastic shells of rotation 13 p2047 N85-22813

Finland, Sweden cooperate in composites research
17 p2946 N85-28184

Expedient runway surfacing with post tensioning system for expeditionary airfields
[AD-D011677] 19 p3222 N85-29978

Influence of moisture and elevated temperature on the fatigue properties of WTS-3 glass fiber blade material — wind turbine blade (WTS-3)
[FFA-TN-1984-58] 20 p3470 N85-31558

Long-term strength of glass fibre/phenolic resin composites
[NPL-DMA(A)-98] 22 p3742 N85-33195

Poly-functional building material from fiberglass (its fabrication and properties) 23 p3908 N85-34209

Stress distribution of fiberglass reinforced plastic beam with a delamination under three-point bending
23 p3908 N85-34210

Strength properties of glassfiber reinforced thermoplastics 23 p3908 N85-34212

Effect of strain rate on the initial failure of notched GRP laminates 23 p3908 N85-34214

Design of transversely stiffenend FRP panels under compressive load — fiber reinforced plastic (FRP) ships
[AMTE(S)-R-84104] 23 p3940 N85-34424

GLASS FIBERS

Lightweight composite launcher pod
[AD-D011236] 01 p0015 N85-10092

Investigating compression failure mechanisms in composite laminates with a transparent fiberglass-epoxy birefringent materials
[NASA-TM-86306] 02 p0170 N85-11137

Parametric study of the P9 HT glass fiber finish (Fatigue resistance). Lot no. 1: Report on the microfatigue tests
[CS-794] 05 p0620 N85-13968

Telephoning with light and sun — glass fibers, solar cells 05 p0663 N85-14264

Qualitative and quantitative compositional analysis of shale derived by gas chromatography and combined gas Chromatography/Mass spectrometry. Executive summary
[AD-A148369] 07 p0924 N85-15851

Composite batteries 07 p0936 N85-15932

Preliminary evaluation of an improved flammability test method for aircraft materials
[FAA-CT-84-22] 08 p1080 N85-16840

Studies of structure and mechanical properties of carbon-reinforced plastic based on spirally reinforced filler 10 p1444 N85-19100

Stress-relieving interlayers for bituminous resurfacings
[PB85-136885] 12 p1820 N85-21415

Development and study of two-matrix glass fiber composite with increased transverse deformation
13 p2027 N85-22700

Theoretical and experimental investigation of mechanically fastened composites
[AD-A150961] 14 p2248 N85-23935

Glass, carbon fibers made at Fibre et Mica in France
15 p2534 N85-25634

Ten year environmental test of glass fiber/epoxy pressure vessels
[NASA-TM-87058] 19 p3231 N85-30034

Transversely reinforced piezoelectric composites
[AD-D011676] 19 p3260 N85-30214

Tensile fatigue of glass fibers and composites with conventional and surface compressed fibers
[RR-84-4] 22 p3742 N85-33196

GLASS LASERS

Pulsed neocymium glass laser system for investigating nonlinear optical phenomena in gases
03 p0348 N85-12241

The development of a high average power glass laser source
[AD-A147471] 07 p0971 N85-16169

Improved solid-state laser sources, volume 2
[DE85-000759] 09 p1325 N85-18330

Research, development of laser glasses in China
13 p2166 N85-23439

Operation of solid state lasers exposed to electron beam 21 p3685 N85-32895

GLASSY CARBON

Experimental study of enthalpy of quasimonocrystal of graphite and carbon glass in temperature range of 2890-3618 deg K 13 p2036 N85-22751

Glassy metals: New highly resistant material
[BLL-BISI-TRANS-21764-(9022.06)]
17 p2926 N85-28049

GLAUERT COEFFICIENT

U AERODYNAMIC FORCES
U MACH NUMBER

GLAZES

Evaluation of laterally loaded laminated glass units by theory and experiment
[PB85-111532/GAR] 09 p1300 N85-18166

Flame spread on combustible solar collector glazing materials
[DE85-002598] 11 p1595 N85-20032

Advanced glazings research
[DE85-000539] 11 p1674 N85-20549

Vertical solar louver project
[DE84-017335] 11 p1676 N85-20558

Improvements in glazings: SERI materials research in progress
[DE84-013049] 12 p1814 N85-21378

Laser sealed evacuated window glazings
[DE85-000512] 22 p3754 N85-33273

GLIDE ANGLES

U GLIDE PATHS

GLIDE LANDINGS

NT HORIZONTAL SPACECRAFT LANDING

Terminal control of gliding in atmosphere
06 p0777 N85-14968

GLIDE PATHS

Realistic localizer courses for aircraft instrument landing simulators
[NASA-CR-172333] 04 p0455 N85-12885

A cockpit-display concept for executing a multiple glide-slope approach for wake-vortex avoidance
[NASA-TP-2386] 08 p1085 N85-16869

Total energy-rate feedback for automatic glide-slope tracking during wind-shear penetration
[NASA-TP-2412] 14 p2226 N85-23801

Theoretical investigation of single-frequency 8-element localizer signal scattering for critical area determination
[FAA-PM-85-4] 20 p3391 N85-31037

GLIDE SLOPES

U GLIDE PATHS

GLIDERS

NT HANG GLIDERS
NT HYPERSONIC GLIDERS

Minimax optimal control in the reentry of a space glider 02 p0167 N85-11124

A comparison of Wortmann airfoil computer-generated lift and drag polars with flight and wind tunnel results
[NASA-TM-86035] 04 p0452 N85-12868

Initial sailplane project: The RP-1
04 p0468 N85-12976

Second sailplane project: The RP-2
04 p0468 N85-12977

The DG400 propulsed glider
[CEV/IS/SE/AV/84] 05 p0595 N85-13795

The design of high-performance gliders
[NASA-TM-77772] 14 p2217 N85-23750

Glider Nimbus 3-24.5. Partial certification test results for importation in the U category
[REPT-CEV/IS/SE/AV/84] 14 p2220 N85-23763

Parachute extraction device for ultralight gliders
[CH-643499-A5] 16 p2699 N85-26663

Three powered sailplanes as meteorological instrumentation for atmospheric boundary layer studies at DFVLR
[DFVLR-FB-84-50] 17 p2897 N85-27862

Proposals for the determination of necessary elevator handling characteristics of sailplanes in high speed range
[DFVLR-FB-84-52] 17 p2900 N85-27882

Flutter clearance of the Schweizer 1-36 deep-stall sailplane
[NASA-TM-85917] 22 p3729 N85-33118

Proceedings of Meteorological Motor Glider (MEMO) Workshop '84
[DFVLR-MITT-85-04] 24 p4121 N85-35542

Motor glider meteorology 24 p4121 N85-35543

Typical and historical aspects of motor gliders as meteorological measuring aircraft
24 p4121 N85-35544

A comparison between Falcon data and motor glider data 24 p4121 N85-35547

Environmental-physical measurements and determination of atmospheric turbulence with the ASK-16 motor glider 24 p4122 N85-35549

Partitioning of the vertical turbulent energy transport into positive and negative contributions — meteorology
24 p4122 N85-35551

Aircraft measurements during the Bonn Experiment (BONEX 1) — meteorology 24 p4122 N85-35552

Motor glider measurements during the Urban Atmosphere Energy Budget Experiment (EESA 1)
24 p4122 N85-35553

Meteorological measurements with motor gliders in Poland 24 p4122 N85-35555

GLIDING

Terminal control of gliding in atmosphere
06 p0777 N85-14968

The study of thermal forecasting for gliding
16 p2830 N85-27453

GLOBAL AIR POLLUTION

Integrated global background monitoring network
[DE84-016996] 04 p0532 N85-13398

Global model of transport of pollutants in atmosphere
19 p3297 N85-30439

The global sulfur cycle
[NASA-TM-87570] 21 p3656 N85-32710

GLOBAL AIR SAMPLING PROGRAM

GASP cloud- and particle-encounter statistics and their application to LFC aircraft studies. Volume 2: Appendixes
[NASA-TM-85835-VOL-2] 03 p0395 N85-12522

GLOBAL ATMOSPHERIC RESEARCH PROGRAM

Global Scale Atmospheric Processes Research Program Review
[NASA-CP-2344] 05 p0679 N85-14360

Observational-numerical study of maritime extratropical cyclones using FGGE data 05 p0685 N85-14400

Polar regions and climatic change
[PB84-237023] 05 p0688 N85-14421

Global scale diagnoses of FGGE data
[NASA-CR-174356] 09 p1356 N85-18533

A study of eddy-mean flow interactions using Eliassen-Palm diagnostics: FGGE SOP-1 data and the NASA GLAS general circulation model compared
[NASA-CR-175508] 11 p1686 N85-20604

The ARGOS contribution to the First GARP Global Experiment (FGGE) study of drifting buoys
14 p2325 N85-24371

Circulation statistics based on FGGE (First GARP Global Experiment) level 3-B analyses produced by GFDL (Geophysics Fluid Dynamics Laboratory)
[PB85-149318] 14 p2379 N85-24688

Characteristics of precipitation regimes during first global atmospheric research project global experiments
[AD-A151572] 15 p2599 N85-26021

Comparison of circulation statistics based on FGGE (First GARP Global Experiment) level 3-B analyses produced by GFDL (Geophysics Fluid Dynamics Laboratory) and ECMWF (European Centre for Medium Range Weather Forecasts) for special observing periods
[PB85-153948] 16 p2836 N85-27492

Experiments using atmospheric forcing from a FGGE analysis to drive an upper ocean model
[INPE-3503-PRE/738] 19 p3319 N85-30576

Generation of available potential energy and the energy cycle during the global weather experiment
[NASA-CR-175301] 21 p3634 N85-32572

GLOBAL POSITIONING SYSTEM

Global positioning system: Geodetic applications
[AD-A144904] 01 p0005 N85-10030

Autonomous navigation of USAF spacecraft
03 p0321 N85-12074

Time comparison with GPS technique and first results with the DFVLR C/A code receiver
[DFVLR-MITT-84-05] 05 p0595 N85-13794

NAVSTAR GPS (Global Positioning System) marine receiver performance analysis
[AD-A146414] 06 p0753 N85-14831

An interactive FORTRAN program for determining reliability of pseudo-range geodetic point positioning using the global positioning system
[AD-A147133] 07 p0988 N85-16275

Satellite navigation
[S-HRG-98-856] 08 p1082 N85-16851

Installation options for the NAVSTAR global positioning system in surface ships
[AD-A148190] 08 p1082 N85-16856

Testing of a field portable GPS (Global Positioning System) geodetic receiver
[AD-A148336] 08 p1082 N85-16859

Using the global positioning system (GPS) phase observable for relative geodesy: Modeling, processing, and results 09 p1341 N85-18437

Transdigitizer for relaying signals from Global Positioning System (GPS) satellites
[AD-D011442] 10 p1422 N85-18970

Technical evaluation report on the 46th Symposium of the Avionics Panel on Space System Applications to Tactical Operations
[AGARD-AR-203] 10 p1425 N85-18986

Simulation of the performance of adaptively controlled Navstar antennas in battlefield scenarios
10 p1472 N85-19292

The Global Positioning System (GPS): Program status update 11 p1710 N85-20761

GPS system field testing 11 p1711 N85-20762

Potential impact of Navstar GPS on NATO tactical operations 11 p1711 N85-20763

Coverage and buildup of the Navstar constellation
11 p1711 N85-20764

Tactical applications of GPS user equipment
11 p1711 N85-20765

Program INNAVSAT: Global Positioning System (GPS): Test and demonstration program
[BMFT-FB-W-84-047] 12 p1775 N85-21145

Hybrid method of mapping and photogeodetic control network densification
[PB85-133775] 12 p1876 N85-21766

Accurate baseline determination by radio interferometry on NAVSTAR GPS satellite transmissions
[AD-A150681] 14 p2291 N85-24202

The TRANSIT and Global Positioning System (GPS) systems. Precision navigation and localization
14 p2398 N85-24777

Global positioning system: A modification to the baseline satellite constellation for improved geometric performance
[AD-A151692] 15 p2469 N85-25239

A replenishment phase study for the NAVSTAR global positioning system
[AD-A152030] 16 p2704 N85-26695

Analysis of orbit transfer vehicles for GPS Block 3 satellites
[AD-A152021] 16 p2732 N85-26860

Maintenance of time and frequency in the DSN using the global positioning system 16 p2771 N85-27105

Real-time position determinations using the GPS TI4100/GEOSTAR receiver
[AD-A152551] 17 p2894 N85-27845

Proceedings of the Fifteenth Annual Precise Time and Time Interval (PTTI) Applications and Planning Meeting [AD-A149163] 17 p2961 N85-28287
International time comparison by a GPS timing receiver 17 p2962 N85-28293
First results of GPS time transfer to Australia 17 p2962 N85-28294
Separating the variances of noise components in the Global Positioning System [AD-P004576] 17 p2963 N85-28295
Enhacements to the TTS-502 time transfer system 17 p2963 N85-28296
On-orbit frequency stability analysis of the GPS NAVSTAR's 3 and 4 rubidium clocks and NAVSTAR's 5 and 6 cesium clocks 17 p2963 N85-28298
CPS navigation experiment using high precision GPS timing receivers 17 p2963 N85-28299
The steering of GPS time 17 p2964 N85-28301
Test results for prototype GPS rubidium clocks 17 p2964 N85-28302
International time transfer and portable clock evaluation using GPS timing receivers: Preliminary results 17 p2964 N85-28303
Unattended TV time transfer results 17 p2964 N85-28305
The role of a low Earth orbiter in intercontinental time synchronization via GPS satellites 17 p2964 N85-28306
Review and evaluation of plans to incorporate NAVSTAR global positioning system user equipment on military sealift command ships [AD-A153799] 18 p3060 N85-28934
On-orbit frequency stability analysis of the GPS NAVSTAR-1 quartz clock and the NAVSTARs-6 and -8 rubidium clocks 18 p3105 N85-29227
Rubidium and cesium frequency standards status and performance on the GPS program 18 p3106 N85-29228
Maintenance of time and frequency in the Jet Propulsion Laboratory's Deep Space Network using the Global Positioning System 18 p3109 N85-29249
Using GPS and VLBI technology to maintain 14 digit synchronization 18 p3109 N85-29250
A simplified GPS C/A reciever front end with low noise performance 18 p3109 N85-29251
Performance test results of a low cost GPS time and frequency monitor 18 p3109 N85-29252
Global positioning system carrier phase: Description and use [PB85-174126] 19 p3216 N85-29946
Application of GPS in a high precision engineering survey network [DE85-010556] 19 p3313 N85-30539
A study of the application of differential techniques to the global positioning system for a helicopter precision approach [NASA-CR-177326] 20 p3391 N85-31035
The NAVSTAR Global Positioning System (GPS) receiver development program, phase 1 [BMFT-FB-W-85-002] 20 p3399 N85-31085
Time comparisons using the Global Positioning System (GPS). Method and first results obtained using the DFVLR C/A receiver [ESA-TT-894] 20 p3460 N85-31490
The potential of the NAVSTAR global positioning system for the Corps of Engineers, civil works [AD-A154913] 21 p3554 N85-32109
A derivation of relativistic effects in satellite tracking [AD-A154620] 21 p3558 N85-32132

GLOBAL TRACKING NETWORK
The MEDOC 2: Experimental Doppler measurement of Earth kinematics 14 p2399 N85-24786
CPS navigation experiment using high precision GPS timing receivers 17 p2963 N85-28299

GLOBULAR CLUSTERS
Photoelectric photometry of globular cluster giants 01 p0128 N85-10884
Spectroscopic data for globular cluster giants. 1: Stars of the red giant tip 01 p0128 N85-10885
Fifth Conference on Star Clusters and Associations and Their Relation to the Evolution of the Galaxy [PUBL-56] 05 p0736 N85-14732
The galactic distribution of open clusters of different ages and the angular velocity of the spiral structure 05 p0737 N85-14737
Binaries and evolution of globular clusters 05 p0738 N85-14744
Evolution of globular clusters 05 p0738 N85-14745
Evolution of globular clusters 05 p0738 N85-14746
Investigation of central parts of globular clusters, performed in PUlkovo 05 p0738 N85-14747
Brightness distribution in globular clusters derived by the narrow-slit scanning method 05 p0738 N85-14748
Lessons from the globular cluster NGC 5466 05 p0739 N85-14749
Galactic orbits of globular clusters 05 p0739 N85-14750
The fate of globular clusters 05 p0739 N85-14751

GLOBULES
Dark cloud and globule distribution for galactic longitudes 230 to 360 degrees 06 p0878 N85-15575
Star formation in globules 08 p1247 N85-17868

GLOBULINS
The influence of angiotensin on the maintenance of venous tone. The effect of Lower Body Negative Pressure (LBNP) and angiotensin blockade 05 p0693 N85-14457

GLOSSARIES
U DICTIONARIES

GLOTRAC (TRACKING NETWORK)
U GLOBAL TRACKING NETWORK

GLOW
U LUMINESCENCE

GLOW DISCHARGES
Analysis of glow discharges for understanding the process of film formation [NASA-TM-83750] 01 p0022 N85-10138
Numerical investigation of characteristics of current flow for different methods of obtaining discharge in high speed lasers. Mechanism underlying current flow in positive glow discharge column 02 p0264 N85-11728
Glow discharge amorphous silicon tin alloys [DE84-013001] 05 p0618 N85-13952
Nitriding of titanium and its alloys by N2, NH3 or mixtures of N2 + H2 in a dc arc plasma at low pressures (or = to torr) [NASA-TM-83803] 06 p0814 N85-15168
Silent discharge carbon dioxide gas laser machining facility [BLL-CTO-2267-(9091.9F)] 07 p0969 N85-16150
Evaluation of miniature vacuum ultraviolet lamps for stability and operating characteristics, Lyman-Alpha task [NASA-CR-171345] 10 p1477 N85-19323
Program for controlling electrical measuring contact instrument on glow-discharge indicator panel 12 p1842 N85-21558
Frictional and structural characterization of ion-nitrided low and high chromium steels [NASA-TM-86991] 13 p2098 N85-23085
Explosive emission cathode plasmas in intense relativistic electron beam diodes [AD-A150669] 14 p2417 N85-24912
Spatial resolution of small particles in silane discharge [AD-A150953] 14 p2423 N85-24948
Diagnostics of a glow discharge used to produce hydrogenated amorphous silicon films [DE85-002914] 15 p2661 N85-26420
The structure of ion plated films in relation to coating properties [NASA-TM-87055] 18 p3085 N85-29085
Influence of type of processing of AK4 alloy on its surface state and strength of bonding of plasma coatings 19 p3242 N85-30103
Characteristics of optogalvanic effect in media with inverse populations 21 p3693 N85-32944
Investigation of space-time structure of glow of laser plasma colliding with flat screen 21 p3693 N85-32947

GLUCOSE
Glucose tolerance in trained and untrained subjects during head-down tilt (6 deg) 05 p0693 N85-14461
Investigation of adaptive distinctions of mechanism of controlled glycemia in Macaca rhesus monkeys 12 p1902 N85-21946

GLUES
Long term durability of urea formaldehyde glued joints removed from Vampire aircraft [AD-A149053] 10 p1424 N85-18965

GLUONS
Quark models of hadronic interactions [DE84-013787] 04 p0561 N85-13570
Very high energy probes of the quark-gluon plasma [DE84-016992] 09 p1392 N85-18763
Glueball candidates [DE85-003627] 14 p2418 N85-24921
Resonances in photon-photon scattering [DE85-004607] 14 p2419 N85-24928
Eleven lectures on the physics of the quark-gluon plasma [DE85-004321] 15 p2662 N85-26431
Some comments on SSC physics [DE85-008444] 18 p3179 N85-29712
A comprehensive study of psi meson production [DE85-006094] 18 p3180 N85-29718
Quark structure of nuclei [DE85-010781] 22 p3842 N85-33795
Detectors for relativistic nuclear collisions (report from the Fixed-Target Hadron Group) 24 p4146 N85-35701
Very high energy probes of the quark-gluon plasma 24 p4147 N85-3[illegible]
Propagation of cosmic rays through the atmosphere in the quark-gluon strings model 24 p4173 N85-3[illegible]
The phi-meson and Chiral-mass-meson production in heavy-ion collisions as potential probes of quark-gluon-plasma and Chiral symmetry transitions 24 p4175 N85-3[illegible]
Heavy flavours production in quark-gluon plasma formed in high energy nuclear reactions 24 p4175 N85-3[illegible]
A cosmic ray super high energy multicore family event. 2: Structure and fragmentation characteristics of the jets [HE-3.4-2] 24 p4181 N85-3[illegible]
Peculiarities of gamma-quanta distribution at 20 TeV energy [HE-3.7-10] 24 p4186 N85-3[illegible]
The maximum depth of shower with E sub 0 larger than 10(17) eV on average characteristics of EAS different components 24 p4188 N85-3[illegible]
Calculation of intensity of high energy muon groups observed deep underground [HE-5.4-13] 24 p4208 N85-3612[illegible]

GLUTAMATES
Response of amino acids in hindlimb muscles to recovery from hypogravity and unloading by tail-cast suspension [NASA-CR-176183] 24 p4128 N85-35589
Response of rat hindlimb muscles to 12 hours recovery from tail-cast suspension [NASA-CR-176182] 24 p4128 N85-35590

GLUTAMINE
Response of amino acids in hindlimb muscles to recovery from hypogravity and unloading by tail-cast suspension [NASA-CR-176183] 24 p4128 N85-35589
Response of rat hindlimb muscles to 12 hours recovery from tail-cast suspension [NASA-CR-176182] 24 p4128 N85-35590

GLUTATHIONE
Distribution and abundance of organic thiols 21 p3657 N85-32717
Glutathione in cyanobacteria 21 p3661 N85-32745

GLYCINE
Investigation of spectrum of human bile acids during 120-day antiorthostatic hypokinesia 22 p3821 N85-33674

GLYCOGENS
Possible mechanism for changes in glycogen metabolism in unloaded soleus muscle [NASA-CR-176184] 24 p4127 N85-35588
Muscle protein and glycogen responses to recovery from hypogravity and unloading by tail-cast suspension [NASA-CR-176181] 24 p4128 N85-35591

GLYCOLS
Investigation of bromine complexed hydrogen/bromine regenerative fuel cells for portable electric power [AD-A146401] 06 p0833 N85-15300
Ionization energies of liquids from energy distribution, quantum yield and second derivative curves [AD-A152210] 16 p2746 N85-28946
Stabilized unsaturated polyesters [NASA-CASE-NPO-16103-1] 18 p3078 N85-29043
Threshold effects and cellular recognition [DE85-010816] 19 p3327 N85-30814
Electron-donor dopant, method of improving conductivity of polymers by doping therewith, and a polymer so treated [DE85-011640] 22 p3752 N85-33257

GNEISS
Concordant bands of augen gneiss within metasedimentary rocks in the Big Delta C-2 quadrangle, east-central Alaska 04 p0516 N85-13[illegible]
Conditions for formation of parageneses containing kyanite-orthoclase in region of Mount Provender and Pratt Peak (Shackleton Range, Antarctica) 19 p3296 N85-30447
Dating Archean zircon by ion microprobe: New light on an old problem 21 p3722 N85-33[illegible]

GNOMONIC PROJECTION
Use of stereographic projection in marine geodesy 19 p3294 N85-30421

GOALS
Review of Space Shuttle requirements, operations, and future plans [GPO-39-101] 04 p0461 N85-12[illegible]
Constituent properties and interrelationships 04 p0467 N85-12[illegible]
Broadening the debate 07 p0914 N85-15785
Toward a goal-oriented civilian space program 07 p0914 N85-157[illegible]
Summary of activities of Aeronautics and Space Engineering Board [NASA-CR-174294] 08 p1228 N85-177[illegible]

High-technology ceramics in Japan
[PB85-125029] 12 p1815 N85-21389

National aeronautical R and D goals: Technology for America's future 19 p3379 N85-30964

Long-term goals for solar thermal technology
[DE85-013032] 22 p3809 N85-33597

GOBI DESERT

Measurements of the surface energy budget in the southern Gobi Desert of China, and in the Rocky Mountains of Colorado
[NASA-CR-175506] 12 p1888 N85-21847

GODDARD EXPERIMENT PACKAGE TELESCOPE

U PARTICLE TELESCOPES

GOERTLER INSTABILITY

Stability calculations of the two-dimensional boundary layer along a concave wall: Part 1: A numerical method of solution for the simultaneous ordinary differential equations governing disturbances
[NAL-TR-841] 15 p2554 N85-25758

GOES SATELLITES

NT GOES 5

Report of the First Session of the International Working Group on Data Management for the International Satellite Cloud Climatology Project (ISCCP)
[WCP-42] 01 p0073 N85-10483

Cloud cover sampling capability of various satellite combinations for ISCCP 01 p0073 N85-10484

ISCCP Cloud Algorithm Intercomparison Workshop
01 p0073 N85-10485

ISSCP Cloud Algorithm Intercomparison Workshop
01 p0073 N85-10486

Use of satellite soundings and imagery for nowcasting and very-short-range forecasting
01 p0076 N85-10504

NESDIS operational precipitation estimation techniques 01 p0076 N85-10505

Geostationary satellite cloud and precipitation analysis using an interactive computer system
01 p0076 N85-10506

A scheme for the delineation and extrapolation of thunderstorms from GOES satellite data
01 p0076 N85-10507

Convective scale weather analysis and forecasting
[NASA-CR-174185] 06 p0838 N85-15320

Solar-geophysical data number 478, June 1984. Part 2 (comprehensive reports): Data for December 1983 and miscellanea
[PB84-243161] 06 p0890 N85-15654

Geostationary Operational Environmental Satellite Data Collection System 14 p2328 N85-24393

Soil moisture and evapotranspiration estimates based on satellite data 15 p2596 N85-25998

New GOES satellite synchronized time code generation 18 p3109 N85-29247

A 406 MHz geostationary satellite SARSAT experiment 20 p3403 N85-31113

Rain volume estimation over areas using satellite and radar data
[NASA-CR-176050] 21 p3634 N85-32570

GOES 5

Test results from RAINSAT 01 p0076 N85-10508

GOGGLES

Some thoughts on the implementation of pilot night vision devices for helicopters 06 p0751 N85-14814

The effect of modified spectacles on the field of view of the helmet display unit of the integrated helmet and display sighting system
[AD-A148693] 09 p1281 N85-18055

GOLD

Ion chromatographic determination of gold in plating baths
[DE84-016187] 02 p0184 N85-11230

Influence of aluminum oxide film on thermocompression bonding of gold wire to evaporated aluminum film
[NASA-TM-77503] 03 p0330 N85-12127

Chemical derivatization of an array of three gold microelectrodes with polypyrrole: Fabrication of a molecule-based transistor
[AD-A146221] 03 p0359 N85-12304

Sputtering of gold irradiated with thermal neutrons
03 p0429 N85-12738

The adsorption of acrylonitrile at a gold electrode: An EMIRS measurement of the electrochemical stark effect
[AD-A148664] 08 p1123 N85-17082

Stability of amorphous metals on semiconductor substrates
[DE84-017256] 09 p1295 N85-18134

Lithography radiation effects study
[AD-A149552] 10 p1468 N85-19260

Relationship of gold content to gravity fields in Far East 10 p1501 N85-19475

Angle-resolved photoemission study of AuGa2 and AuIn2 intermetallic compounds
[AD-A150000] 12 p1940 N85-22183

A mixed-basis band structure interpolation scheme applied to the fluorite structure compounds NiSi2, AuAl2, AuGa2 and AuIn2
[AD-A150131] 12 p1940 N85-22187

High energy facilities advanced projects: Intrabeam scattering for a beam of gold ions
[DE85-000687] 12 p1941 N85-22192

Study of energy versus misorientation for grain boundaries in gold by crystallite rotation method. 1: 001 twist boundaries
[DE85-004596] 12 p1943 N85-22201

WRAP-RIB antenna technology development
14 p2231 N85-23824

Ligand structural influences upon electrochemical reactivity: Organic substituent effects upon Carboxylatopentaamminecobalt(3) reductions at mercury and gold electrodes
[AD-A150885] 14 p2250 N85-23944

Characterization of supported metal catalysts by imaging, microdiffraction and microanalysis techniques
[DE85-005567] 14 p2253 N85-23961

The effects of water and hydrogen on materials used in integrated circuit packages
[AD-A151893] 15 p2518 N85-25529

Current understanding of point defects and diffusion processes in silicon 20 p3481 N85-31632

Resistance of polyaniline films as a function of electrochemical potential and the fabrication of polyaniline-based microelectronic devices
[AD-A154999] 21 p3569 N85-32201

Multiple inner shell vacancies in laser-irradiated Au plasma 23 p3961 N85-34687

Elliptical X-ray analyzer spectrograph application to a laser-produced plasma
[DE85-013790] 24 p4097 N85-35398

Mineral deposit models: Theory and practice
24 p4105 N85-35448

Some recent deposit modeling efforts
24 p4106 N85-35453

The Conterminous United States Mineral Assessment Program 24 p4106 N85-35458

Stopping relativistic Xe, Ho, Au and U nuclei in nuclear emulsions 24 p4173 N85-35876

GOLD ALLOYS

Surface segregation of sulfur during oscillatory pin-on-plate wear studies of precious metal electrical contact alloys. 1: Friction and electrical contact resistance
[DE84-006962] 02 p0195 N85-11303

Critical evaluation of binary rare earth phase diagrams
[DE84-015057] 05 p0614 N85-13922

Surface physics and crystallography
[DE85-003128] 11 p1735 N85-20910

Atomistic studies of grain boundaries with segregated impurities
[DE85-000063] 11 p1737 N85-20924

Sputter-induced compositional modifications in a Ni-Au alloy
[DE85-002771] 12 p1807 N85-21333

Pulsed electrodeposition
[DE85-007057] 16 p2747 N85-26950

Studies of the crystallization process of aluminum-silicon alloys using a high temperature microscope
[NASA-TM-77869] 24 p4078 N85-35272

GOLD COATINGS

Impact ionization from gold, aluminum and PCB-Z — Giotto spacecraft paint PCB-Z 14 p2244 N85-23910

GOLD PLATE

U GOLD COATINGS

GONIOMETERS

NT PHOTOGONIOMETERS

Structural, morphological and optical characteristics of KGd(WO4)2 crystals 14 p2280 N85-24126

Investigation of errors of acoustic goniometer information-measurement systems on rocking base
14 p2283 N85-24139

GOODNESS OF FIT

Kolmogorov-Smirnov goodness-of-fit test: Corrected for use with EEG-like data
[AD-A144711] 01 p0110 N85-10745

Sequential minimization for sum of squares of unknown functions
[DE85-004162] 11 p1707 N85-20738

Tests of fit based on normalized spacings
[AD-A149749] 12 p1921 N85-22062

Identification of a mathematical model 1: Goodness of fit criterion
[HSE-TRANS-11109] 19 p3341 N85-30703

A guide to the statistical analysis of the results of linear and nonlinear least-squares data fitting
[NPL-DITC-53/84] 20 p3521 N85-31895

GORGES

U CANYONS

GOVERNMENT PROCUREMENT

Benefit value to the Air Force of the GIDEP (Government Industry Data Exchange Program) alert
[AD-A145470] 02 p0292 N85-11897

System engineering and integration contract for implementation of the National Airspace System plan, volume 1, sections 1.0-4.0, 6.0
[AD-A145783] 03 p0317 N85-12046

Introduction to software packages
[PB84-217843] 06 p0856 N85-15441

Survey relating to the implementation of cost/schedule control systems criteria within the Department of Defense and industry
[AD-A146664] 06 p0870 N85-15526

A buyer's guide to space infrastructure
07 p0914 N85-15784

Synopsis of the OTA Workshop on Cost Containment of Civilian Infrastructure (Civilian Space Station) Elements 07 p0915 N85-15790

An evaluation of the effect of establishing a minimum Economic Order Quantity (EOQ) on the Air Force EOQ item management system
[AD-A147121] 07 p1051 N85-16673

Evaluation of the effectiveness of the weighted guidelines to induce contractor's investment in cost reducing facilities equipment
[AD-A147586] 07 p1053 N85-16681

An analysis of production competition and award methodology
[AD-A147775] 08 p1228 N85-17733

Excessive Air Force inventories result from duplicative spare parts requirements
[AD-A147777] 08 p1228 N85-17734

Cost-plus-percentage-of-costs in government contracts
[AD-A147779] 08 p1228 N85-17735

Prototype concept design for US Army type 3A Air Traffic Control Tower (ATCT)
[AD-A148840] 09 p1284 N85-18070

Program manager: The Journal of the Defense Systems Management College. Volume 13, Number 6, November-December 1984
[AD-A149546] 11 p1739 N85-20933

Copyright law, computer software, and government acquisition
[AD-A150347] 13 p2168 N85-23453

Life cycle costing in government procurement
[AD-A151878] 15 p2688 N85-26456

Navy program manager's guide, 1985 edition
[AD-A151925] 16 p2876 N85-27744

Automation of the reporting and tracking requirements of architect-engineering type contracts
[AD-A152218] 16 p2876 N85-27745

Cost savings from multiyear contracting
[AD-A153564] 18 p3197 N85-29634

Overhead management guide for aerospace procurements
[AD-A153626] 18 p3198 N85-29635

Capital investment motivational techniques used by prime contractors on subcontractors
[AD-A153660] 18 p3198 N85-29637

Using incentives to improve maintainability
[AD-A153792] 18 p3199 N85-29641

The evolution of the U.S. helicopter industry
[AD-A154290] 19 p3211 N85-29913

Civilian Space Stations and the US future in Space
[OTA-STI-242] 20 p3418 N85-31215

Feasibility of applications of Competition Decision Assist Package (CDAP) to spare parts
[AD-A154716] 21 p3712 N85-33036

GOVERNMENT/INDUSTRY RELATIONS

Second Symposium on Space Industrialization — space commercialization
[NASA-CP-2313] 02 p0149 N85-11011

Non-US approaches to space commercialization
02 p0150 N85-11012

Legal considerations and cooperative opportunities for space commercial activities 02 p0150 N85-11013

Land remote sensing commercialization: A status report 02 p0151 N85-11024

Comments on the commercialization of expendable launch vehicles 02 p0153 N85-11034

Concept for a commercial space station laboratory
02 p0153 N85-11035

Commercial space services 02 p0153 N85-11039

Space commercialization: Analysis of R and D investments with long time horizons
02 p0155 N85-11052

Doing business in space: How to get there from here
02 p0156 N85-11057

Contracting for computer software development: Serious problems require management attention to avoid wasting additional millions
[FGMSD-80-4] 02 p0241 N85-11567

Land Remote-Sensing Commercialization Act
[S-REPT-98-458] 05 p0654 N85-14201

GOVERNMENTS

Financing considerations and Federal budget impacts
07 p0915 N85-15792
A weapon system design approach to diagnostics
08 p1066 N85-16752
GIDEP representative interaction
[DE84-016792] 09 p1401 N85-18820
Activities report in aerospace in West Germany
[ISSN-0070-3966] 09 p1418 N85-18947
Electric-Hybrid Vehicle (E-HV) demonstration-test project
[DE85-002370] 10 p1570 N85-19699
1984 science and technology posture hearing with the director of the Office of Science and Technology Policy
[GPO-41-060] 12 p1949 N85-22244
Transfer of technology
[S-REPT-98-664] 12 p1949 N85-22246
Status of the U.K. N.D.T. industry today
14 p2316 N85-24309
Financial, economic commentary on Airbus, European aviation 15 p2536 N85-25649
Criteria for qualifying for FRG federal CAD/CAM subsidies 15 p2536 N85-25651
Biotechnology in Japan
[PB85-169464] 15 p2615 N85-26113
The evolution of the U.S. helicopter industry
[AD-A154290] 19 p3211 N85-29913

GOVERNMENTS
Major institutional arrangements affecting ground water in New York state
[PB84-202506] 01 p0065 N85-10429
Lagging development of biotechnology described
01 p0115 N85-10787
International cooperation and competition in space
[GPO-38-001] 02 p0295 N85-11911
Statement of Otho E. Eskin, Director, Office of Advanced Technology, Department of State
02 p0295 N85-11914
Statement of John H. McElroy, Assistant Administrator for Environmental Satellite, Data and Information Services, National Oceanic and Atmospheric Administration
02 p0295 N85-11915
NESDIS international activities, appendix 2
02 p0295 N85-11917
Ways to improve management of Federal funded computerized models
[LCD-75-111] 03 p0435 N85-12771
Federal Telecommunications Privacy Act of 1984
[H-REPT-98-815] 03 p0441 N85-12807
International comparative study of systems for the government advancement of research and development
[NASA-TM-77589] 04 p0578 N85-13689
Area handbook series. Honduras: A country study
[AD-A146510] 06 p0827 N85-15253
Toward an improved FIPS cost-benefit methodology. Phase 2: Descriptive models, general purpose application software development and maintenance
[PB84-226943] 06 p0870 N85-15527
Publications of the Executive Office of the President: January 20, 1981 - June 30, 1984
[PB84-230671] 06 p0871 N85-15533
Government contract contingent liabilities. The anti-deficiency act, and the hobgoblin of little minds
[AD-A147919] 07 p1053 N85-16684
Provision of Federal government publication in electronic format to depository libraries
[S-PRT-98-260] 10 p1567 N85-19880
Organizations as information processing systems. Toward a strategic contingencies model of budget related influence in municipal government organizations
[AD-A149364] 10 p1567 N85-19883
Airport bird hazards associated with solid waste disposal facilities
[AD-P004197] 11 p1581 N85-19964
The FAA grant-in-aid assurances: FAR part 139, and airport hazards
[AD-P004209] 11 p1583 N85-19976
Oversight review of the five-year outlook report on science and technology
[GPO-41-058] 12 p1949 N85-22243
1984 science and technology posture hearing with the director of the Office of Science and Technology Policy
[GPO-41-060] 12 p1949 N85-22244
A 5-year research plan, 1985-1990. Wind energy technology: Generating power from the wind
[DE85-008427] 17 p2987 N85-28463
U.S.-China conference on science policy
[PB85-176345] 19 p3360 N85-30971
Methodology for assessing benefits and costs of government information collection
[DE85-010594] 19 p3361 N85-30975

GOVERNORS
U SPEED REGULATORS

GRABENS
U GEOLOGICAL FAULTS

GRADIENT INDEX OPTICS
Supersonic missile seeker lens system using gradient index material for first element lens
[AD-A151478] 15 p2490 N85-25367

GRADIENTS
NT ELECTRON DENSITY PROFILES
NT POTENTIAL GRADIENTS
NT PRESSURE GRADIENTS
NT TEMPERATURE GRADIENTS
NT THERMOCLINES
A trivariate Clough-Tocher scheme for tetrahedral data
[AD-A144740] 01 p0111 N85-10751
Solar pond overview 05 p0667 N85-14287
Summary of salt gradient solar pond research
05 p0667 N85-14292
Doubly diffusive linear stability with nonconstant gradients
[DE84-013008] 05 p0670 N85-14310
Modeling localized stress fields in composite laminates
[AD-A148630] 08 p1120 N85-17056
Measurement of the vertical gradient of the semidiurnal tidal wind phase in winter at the 95 km level
11 p1662 N85-20478
Rotating squid magnetometers and gradiometers
[AD-D011529] 12 p1849 N85-21600
Determining object orientation from a single image using multiple information sources
[AD-A149980] 12 p1933 N85-22146
Edge detection in SAR imagery using gradient operators — synthetic aperture radar (SAR)
[AD-A149411] 13 p2054 N85-22882
Method for processing broad-profile data
13 p2117 N85-23185
Alternating gradient synchrotron
[DE85-005950] 17 p3033 N85-28759
3d calculations of a fixed field alternating gradient synchrotron magnet
[DE85-002742] 18 p3183 N85-29739
Electron trajectories in a combined wiggler and alternating gradient quadrupole field
[DE85-010727] 22 p3842 N85-33794
Differential measurement of cosmic-ray gradient with respect to interplanetary current sheet
[SH-4.2-9] 23 p4007 N85-34847
Determination of galactic cosmic ray latitudinal gradient using Earth based detectors
[SH-4.2-13] 23 p4008 N85-34851
The expected cosmic ray density and stream distributions at the heliolatitudinal asymmetry of solar wind
[SH-4.2-14] 23 p4008 N85-34852
Latitudinal gradients of cosmic rays and the polarity reversal of the heliospheric magnetic field: A preliminary evaluation
[SH-4.2-16] 23 p4008 N85-34853
The dependence of solar modulation on the sign of the cosmic ray particle charge
[SH-4.2-23] 23 p4009 N85-34860
Voyager 1 and 2 measurements of radial and latitudinal cosmic ray gradients during 1981 - 1984
[SH-4.7-6] 23 p4041 N85-35051

GRADIOMETERS
U MAGNETOMETERS

GRADUATION
U CALIBRATING

GRAFTING
Low temperature synthesis of polycaproamide copolymers grafted with polydimethylaminothylmethacrylate
06 p0761 N85-14868

GRAIN BOUNDARIES
Granular boundary segregation in low-alloyed titanium-vanadium alloys 01 p0019 N85-10117
Process Research of Polycrystalline Silicon Material (PROPSM)
[NASA-CR-173838] 01 p0067 N85-10446
Swaged Mo-5 percent W alloy and recrystallized commercially pure molybdenum
02 p0180 N85-11208
Diffusion of Cr-51 tracer in Cr-2O-3 and the growth of Cr-2O-3 films
[AERE-R-11314] 03 p0333 N85-12146
Thermal ageing studies of 9%Cr 1%Mo steel
[AERE-R-11109] 03 p0333 N85-12149
Analysis techniques for tracer studies of oxidation
[NASA-CR-174796] 03 p0336 N85-12162
Structure of two-phase titanium alloys with different microstructures 03 p0351 N85-12257
Transport processes during the growth of oxide films at elevated temperature
[AERE-R-11293] 03 p0434 N85-12766
Ion contrasting chamber for discrimination of grains and textures
[BMFT-FB-T-84-151] 04 p0477 N85-13036
Structure and properties of grain boundaries
[DE84-014366] 04 p0570 N85-13688
Flux-line pinning by the grain boundary in niobium bicrystals
[DE84-016668] 04 p0570 N85-13689
The influence of manganese on intercrystalline internal adsorption of arsenic in low carbon steel
[BLL-M-35965-(5828.4)] 05 p0615 N85-13901
Process Research On Polycrystalline Silicon Material (PROPSM) 06 p0830 N85-15276
Grain boundary structure in NiO
[DE84-016242] 06 p0868 N85-15519
Characterization of bicrystal grain boundary properties using device structures
[DE84-004509] 06 p0869 N85-15523
Design of ordered intermetallic alloys for high-temperature structural use
[DE85-000697] 07 p0926 N85-15665
Grain refining and microstructural modification during solidification
[AD-A147705] 08 p1128 N85-17111
Hydrogen embrittlement of nickel
[AD-A148322] 08 p1129 N85-17119
In-situ formation of a grain boundary in field ion microscopy using a laser
[AD-A148225] 08 p1166 N85-17365
Sub-eutectic densification and second phase formation in Al2O3 - CaO
[DE85-002065] 09 p1398 N85-18796
High temperature properties of equiatomic FeAl with ternary additions
[NASA-TM-86938] 10 p1439 N85-19072
Comparisons between computed and observed grain boundary structures and properties in metals
[DE85-002596] 10 p1442 N85-19085
Investigation of vanadium solid solution and zeta phase regions of vanadium-carbon system
[DE85-002676] 11 p1605 N85-20092
Contributions of segregated phosphorus to the intergranular stress corrosion cracking of nickel
[DE85-003112] 11 p1606 N85-20099
Computer simulation of grain-boundary properties in ionic crystals and metals
[DE85-000577] 11 p1734 N85-20903
Atomistic studies of grain boundaries with segregated impurities
[DE85-000063] 11 p1737 N85-20924
Effects of scatterer spacing statistics on ultrasonic backscatter signal spectra
[DE85-003259] 12 p1926 N85-22114
Study of energy versus misorientation for grain boundaries in gold by crystallite rotation method. 1: 001 twist boundaries
[DE85-004598] 12 p1943 N85-22201
Micromechanical modeling of microstructural damage in creeping alloys
[DE85-003925] 13 p2022 N85-22671
Grain boundaries in NiO
[DE85-006129] 13 p2025 N85-22687
Dependence of superplastic flow on state of grain boundaries 13 p2025 N85-22689
Drift fields and boundary conditions at grain boundaries in bipolar P/N junction silicon devices
13 p2062 N85-22879
Investigation of the effect of annealing on the dislocation and sub-grain boundary content of solvent-evaporation-grown CdTe
[AD-A144087] 13 p2162 N85-23415
Relationship between symmetrical tilt, twist, special, and favored grain boundaries
[DE85-004024] 14 p2429 N85-24982
Structural unit/grain boundary dislocation model for twist boundaries in cubic crystals
[DE85-000425] 14 p2430 N85-24985
Superplasticity in a thermo-mechanically processed Aluminum-10.2%Mg-0.52%Mn alloy
[AD-A152016] 15 p2510 N85-25485
Variation in the spacing of dislocations in subgrain boundaries with creep strain in Type 304 stainless steel
[DE85-006184] 15 p2511 N85-25493
Structure of condensed aluminum thin film metallizations 15 p2512 N85-25501
Approximate closed-form expression for the electron-scattering-induced interaction between magnetic flux lines and grain boundaries
[DE85-004699] 15 p2660 N85-26417
Grain boundary composition and intergranular fracture of steels. Volume 1: Detection of grain boundary segregation in steels
[DE85-006850] 15 p2662 N85-26428
Tilt grain boundaries in NiO
[DE85-006839] 16 p2751 N85-26878
Electrons and grain boundary energies in metals
[DE85-009530] 17 p2932 N85-28089
Interfacial segregation and fracture
[DE85-009779] 18 p3076 N85-28919

Quantitative analysis of defects in silicon-characterization of UCP, HAMCO, and microcrystalline material
[NASA-CR-175988] 18 p3079 N85-29046
Effects of annealing treatments on superplasticity in a thermomechanically processed Aluminum-10.2%Mg-0.52%Mn
[AD-A154414] 19 p3239 N85-30080
State variable theories based on Hart's formulation
[DE85-006474] 19 p3239 N85-30082
Structural defects in crystalline silicon
20 p3461 N85-31630
The effect of stress and hot corrosion on nickel-base superalloys
[AD-A154722] 21 p3566 N85-32181
The effect of diffusive hydrogen segregation on fracture of polycrystalline nickel
[AD-A155238] 21 p3567 N85-32186
Influence of particle arrangement on sintering
[AD-A155337] 21 p3599 N85-32352
Electrotransport in thin films
[AD-A155584] 21 p3710 N85-33034
Electronic phenomena near semiconductor grain boundaries
[DE85-011543] 21 p3711 N85-33035
An enhanced photoresponse at dislocation subgrain boundaries revealed by X-ray topography of polysilicon solar cells 22 p3806 N85-33572
Investigation of the microstructure and photovoltaic properties of semicrystalline silicon
22 p3806 N85-33573
High resolution electron microscopic characterization of interfaces in ceramics
[DE85-011207] 23 p3920 N85-34269
Grain boundary and surface diffusion in oxide systems
[DE85-007291] 23 p3985 N85-34715
GRAIN SIZE
Structural recrystallization in titanium
03 p0351 N85-12258
Dependence of microplasticity of beryllium on grain size and heat treatment 03 p0353 N85-12273
Center for dielectric studies
[AD-A146183] 03 p0434 N85-12761
Microstructure, texture and formability of thin aluminium sheets 06 p0796 N85-15088
The role of microstructure in the modelling of plastic flow in P/M superalloys at forging temperatures and strain rate 06 p0796 N85-15090
Grainsize evolution and differential comminution in an experimental regolith 06 p0888 N85-15638
Influence of grain size distribution on the undrained dynamic properties of saturated sand
[PB85-102382/GAR] 09 p1305 N85-18197
Mechanical stabilization of austenite against epsilon martensite and its effect on deformation behavior in high manganese steels
[DE85-007654] 17 p2932 N85-28097
Electrohydrodynamic process for the production of large area polycrystalline silicon sheet
[DE85-008781] 19 p3261 N85-30225
Modification of the grain size of sputtered copper with additions of oxygen, krypton, silver, or yttrium
[DE85-010975] 21 p3567 N85-32189
Nonequilibrium kinetics of growth of oxide layer grains during laser heating of metals in air
21 p3689 N85-32919
Influence of technology of atomization of naturally alloyed iron on grain-size characteristics of powder material
[BLL-M-35810-(5828.4)] 23 p3914 N85-34257
GRAINS
Electron channeling and EBIC studies of polycrystalline silicon sheets
[DE84-004515] 05 p0670 N85-14309
Solar wind and cosmic ray irradiation of grains and ices - application to erosion and synthesis of organic compounds in the solar system
06 p0888 N85-15637
GRAINS (FOOD)
NT BARLEY
NT CORN
NT OATS
NT RICE
NT WHEAT
Determination of the conservation state of long conservation agricultural products by means of capacitive sensors
[NOTA-INTERNA-799] 02 p0220 N85-11447
Alcohol fuel from Ohio farms: An introduction
[TI-84-001290] 05 p0621 N85-13970
Crop yield forecasting 07 p1001 N85-16360
Operational performance of the photovoltaic-powered grain mill and water pump at Tangaye, Burkina Faso (formerly Upper Volta)
[NASA-TM-86970] 13 p2128 N85-23243
Gravity perception and response in shoot of cereal grasses 15 p2611 N85-26091
GRAMMARS
Information-theoretic properties of languages and their grammars
[AD-A146688] 06 p0799 N85-15106
Speech analysis by parametric methods: A survey
[ENST-84C004] 09 p1313 N85-18251
Research on knowledge delivery
[AD-A149565] 10 p1538 N85-19696
An algorithm for generating abstract syntax trees
[NASA-CR-172541] 12 p1912 N85-22003
Construction of a menu-based system
[NASA-CR-172560] 13 p2146 N85-23321
Language design, computers and brains
[AD-A152819] 17 p3006 N85-28594
Polylith: The early goals
[DE85-012534] 24 p4139 N85-35658
GRANITE
Contribution to the radiogeology of Sao Roque, SP, granites
[INPE-3079-PRE/492] 03 p0391 N85-12503
Geology and geochemical evolution of the Lost River, Alaska, tin deposit 04 p0533 N85-13405
Geology, petrology, and tectonic setting of the Mafic rocks of the 1480 Ma old granite-rhyolite terrane of Missouri, USA 05 p0674 N85-14327
Alabama Tin Belt: Metallogenesis and mineral resource evaluation. Year-end report
[DE84-901335] 07 p0989 N85-16283
Creep deformation of compacted decomposed granite soils 09 p1303 N85-18187
GRANTS
National Science Foundation grants and awards for fiscal year 1983, volume 2
[PB84-212323] 01 p0125 N85-10854
A research in support of NASA's space science
[NASA-CR-174267] 08 p1227 N85-17728
Small business innovation research: Abstracts of 1984. Phase 1 awards
[NASA-TM-87427] 13 p2165 N85-23431
GRANULAR MATERIALS
Weak shocks and steady waves in a nonlinear elastic rod or granular material
[AD-A145715] 02 p0209 N85-11383
Influence of inter-layer effect on charge gas-permeability
[BLL-M-35919-(5828.4)] 05 p0616 N85-13940
Atmospheric heating of meteorites: Results from nuclear track studies 06 p0882 N85-15607
Carbon granule probe microphone for leak detection -- recovery boilers
[NASA-CASE-NPO-16027-1] 12 p1849 N85-21597
Large-size fine-granular graphite for solar techniques
12 p1878 N85-21780
Effect of annealing procedures on structure and properties of VT6 alloy with initial large-grained structure
15 p2496 N85-25410
The Jovian ring 15 p2672 N85-26492
Voyager planetary radio astronomy: Grain and particle impacts shot noise in Saturn's ring plane
15 p2673 N85-26496
Single-pulse Raman and photoacoustic spectroscopy studies of Triaminotrinitrobenzene (TATB) and related compounds
[DE85-010072] 18 p3084 N85-29078
Granular Flow Project
[DE85-010015] 19 p3270 N85-30279
Effect of nonuniform size on internal stresses in a rapid, simple shear flow of granular materials. Part 1: Two grain sizes
[AD-A154045] 19 p3285 N85-30372
Effect of nonuniform size on internal stresses in a rapid, simple shear flow of granular materials. Part 2: Multiple grain sizes
[AD-A154046] 19 p3285 N85-30373
Flow characteristics of the Cascade granular blanket
[DE85-010932] 20 p3420 N85-31227
Modeling granular explosive detonations with shear band concepts
[DE85-011823] 22 p3754 N85-33271
GRAPH THEORY
A comparative evaluation of algorithms for generalized network problems
[TWISK-289] 01 p0107 N85-10721
New labeling procedures for the basis graph in generalized networks
[AD-A146217] 03 p0407 N85-12601
On the formal development of graph theoretical algorithms by transformation
[TUM-I8403] 04 p0553 N85-13522
The traveling salesman problem on a graph and some related integer polyhedra
[AD-A147953] 08 p1211 N85-17621
Some facets of the tri-index assignment polytope
[AD-A149195] 10 p1547 N85-19753
On large matchings and cycles in sparse random graphs
[AD-A149194] 10 p1550 N85-19778
On matchings and Hamiltonian cycles in random graphs
[AD-A151015] 14 p2409 N85-24851
Generalized graph coloring: A frequency assignment method for VHF broadcasting
[TUM-M8405] 16 p2844 N85-27535
Embedding graphs in lines, trees and grids
19 p3334 N85-30652
Graph-theoretical exorcism
[DE85-011916] 23 p3955 N85-34512
A graph theoretic procedure for the design of feedback patterns
[REPT-110] 24 p4142 N85-35673
Design of dynamic compensators of prescribed pattern
[BU-109] 24 p4142 N85-35674
GRAPHIC ARTS
Description of a data matrix structure and model diagnosis by means of row and column Euclidean maps
02 p0211 N85-11392
Application of correspondence analysis to meteorological data 02 p0211 N85-11393
Representing multidimensional systems using visual displays 05 p0711 N85-14560
Television animation store: Recording pictures on a parallel transfer magnetic disc
[BBC-RD-1984/17] 10 p1462 N85-19220
Draftsman displays: A graphical technique for exploratory data analysis
[AD-A150515] 13 p2041 N85-22775
Digital laser platemaker modifications
[AD-A150190] 13 p2096 N85-23074
Image synthesis: Optical identity or pictorial communication? 23 p3963 N85-34565
GRAPHIC EVALUATION AND REVIEW TECHNIQUES
U GERT
GRAPHITE
NT PYROLYTIC GRAPHITE
Dynamics of graphite fiber intercalation: In situ resistivity measurements with a four point probe
[NASA-TM-86858] 01 p0017 N85-10105
Stability of bromine intercalated graphite fibers
[NASA-TM-86859] 01 p0031 N85-10187
Preparation and properties of evaporated CdTe films compared with single crystal CdTe
[DE85-000502] 02 p0222 N85-11452
Fundamental electronic properties of donor-type graphite intercalated compounds
[AD-A146148] 03 p0326 N85-12099
Influence of test method and material stiffness on the damage produced by low velocity impacts on carbon-epoxy composites No. 45.387/1
[REPT-45.387/1] 03 p0326 N85-12100
Matrix resin characterization in cured graphite composites using diffuse reflectance-FTIR
04 p0466 N85-12959
Thermal contact conductance measurements on Doublet 3 armor title traphite
[DE84-013554] 05 p0613 N85-13916
Metallographic evaluation of the reactions between boronated graphite and Fe-Ni-Cr alloys
[DE84-015374] 06 p0769 N85-14922
Development of intercalated wire and cable
[AD-A146502] 06 p0774 N85-14949
An investigation of the electrical conductivity in highly oriented graphite intercalation compounds
[AD-A146539] 06 p0804 N85-15116
Experimental test program for evaluation of solid lubricant coating as applied to compliant foil gas bearings to 315 deg C
[NASA-CR-174837] 07 p0930 N85-15895
The 13C nuclear magnetic resonance in graphite intercalation compounds
[NASA-CR-174261] 07 p1040 N85-16601
Structure-property relationships in intercalated graphite
[AD-A147949] 08 p1219 N85-17680
Electronic properties of intercalated graphite and amorphous metals
[AD-A147664] 08 p1225 N85-17716
The fabrication, processing and characterization of multidimensionally braided graphite/epoxy composite materials
[AD-A148729] 09 p1288 N85-18090
Tribological properties of graphite-fiber-reinforced, partially fluorinated polyimide composites
[NASA-TM-86926] 09 p1296 N85-18153
Compositional, structural, and physical studies of some graphite hexafluoroarsenates and their relatives
[DE85-000855] 10 p1432 N85-19030
Method of determining thermal stability of heat-resistant coatings on graphite 10 p1447 N85-19117

Electron oxidation of graphite by fluorospecies
[DE85-001196] 11 p1595 N85-20034

Effect of macrostructure on durability of polycrystalline graphite 11 p1605 N85-20091

Investigation of electric and magnetic properties of intercalated graphite
[AD-A149801] 12 p1797 N85-21274

Electric and magnetic properties of intercalated graphite
[AD-A149848] 12 p1798 N85-21276

Fine-grained, isotropic graphite for use as NBS (National Bureau of Standards) thermophysical property RM's from 5 to 2500 K
[PB85-112886] 12 p1814 N85-21381

Large-size fine-granular graphite for solar techniques
12 p1878 N85-21780

Sound velocity of carbon at high pressures
[DE85-002016] 12 p1928 N85-22113

Neutron scattering studies of graphite intercalation compounds
[DE85-003079] 12 p1942 N85-22196

Silicon carbide-silicon nitride fibers: Preparation and characterization of polycarbosilazane precursors
12 p1945 N85-22214

Experimental study of enthalpy of quasimonocrystal of graphite and carbon glass in temperature range of 2890-3818 deg K 13 p2036 N85-22751

High-temperature X-ray diffraction study of coating-substrate compatibility in yttria-coated graphite
[DE85-005916] 14 p2262 N85-24016

Homogeneity of pristine and bromine intercalated graphite fibers
[NASA-TM-87016] 15 p2517 N85-25521

Carbon isotopes in bulk carbonaceous chondrites
15 p2681 N85-26557

Graphite fiber intercalation: Dynamics of the bromine intercalation process
[NASA-TM-87015] 16 p2742 N85-26921

NASA/aircraft industry standard specification for graphite fiber toughened thermoset resin composite material
[NASA-RP-1142] 16 p2742 N85-26923

Microscopic study of the influence of impurities on interface bonding
[AD-A151725] 16 p2743 N85-26928

Environmental stability of intercalated graphite fibers
[NASA-TM-87025] 16 p2753 N85-26992

Effects of the cooling rate on the structure of the graphite in inoculated irons
[BLL-BISI-TRANS-22305-(9022.06)]
17 p2930 N85-28083

A micrographic and gravimetric study of intercalation and deintercalation of graphite fibers
[NASA-TM-87026] 17 p2934 N85-28110

Bifunctional oxygen electrodes
[DE85-006871] 17 p2955 N85-28248

Light weight fire resistant graphite composites
[NASA-CASE-ARC-11615-1-SB]
18 p3068 N85-28976

Mechanism of the catalytic gasification and reactivity of graphite
[DE85-009932] 19 p3229 N85-30020

Polymer matrix and graphite fiber interface study
[NASA-CR-177357] 19 p3232 N85-30036

USSR report: Materials Science and Metallurgy
[JPRS-UMS-85-005] 19 p3241 N85-30095

New form of graphite 19 p3243 N85-30111

Thermodynamics of high temperature materials
[AD-A154269] 19 p3378 N85-30958

Long-term thermal aging of Celion/V378A composite materials
[NASA-TM-86362] 20 p3421 N85-31236

Electrical and mechanical properties of intercalated graphite fibers
[AD-A155560] 21 p3570 N85-32205

Paired ion chamber constants for fission gamma-neutron fields
[AD-A155069] 21 p3702 N85-32999

Multistage spent particle collector and a method for making same
[NASA-CASE-LEW-13914-1] 22 p3791 N85-33489

Oxidation resistant slurry coating for carbon-based materials
[NASA-CASE-LEW-13923-1] 24 p4077 N85-35267

Applications of the mineral resources data system and the international strategic minerals inventory in mineral-resource assessments by region and commodity
24 p4105 N85-35451

GRAPHITE-EPOXY COMPOSITES

Distributions of fatigue life and fatigue strength in notched specimens of a carbon 8-harness-satin laminate
[NAL-TR-809T] 01 p0061 N85-10407

Advanced composite stabilizer for Boeing 737 aircraft
[NASA-CR-168451] 02 p0137 N85-10934

Deformation measurements of composite multi-span beam shear specimens by Moire interferometry
[NASA-CR-3844] 02 p0169 N85-11135

Fracture toughness of fibrous composite materials
[NASA-TP-2370] 02 p0170 N85-11136

The influence of sublaminate cracks on the tension fatigue behavior of a graphite epoxy laminate
[FFA-TN-1984-32] 02 p0210 N85-11366

Accelerated viscoelastic characterization of T300/5208 graphite-epoxy laminates 03 p0325 N85-12091

Study of delamination cracking under static and cyclic loads of carbon-epoxy composite materials
[REPT-42-727/F] 03 p0327 N85-12102

Effect of impact damage and open holes on the compression strength of tough resin/high strain fiber laminates 04 p0464 N85-12945

Investigation of toughened neat resins and their relations to advanced composite mechanical properties
04 p0464 N85-12949

Composite structural materials
[NASA-CR-174077] 04 p0467 N85-12966

Fatigue in composite materials
04 p0467 N85-12968

Experimental and theoretical studies of moisture and temperature effects on the mechanical properties of graphite/epoxy laminates and neat resins
04 p0467 N85-12969

Free-edge failures of composite laminates
04 p0467 N85-12971

Quantification of Saint-Venant's principle for a general prismatic member 04 p0467 N85-12972

Test report no. 17.208: Statistics of the basic characteristics of carbon-epoxy composites
[DGT-23.426/A] 04 p0468 N85-12979

Influence of relaxation on the mechanical characteristics of a carbon-epoxy composite. Report no. 45.427/1
04 p0468 N85-12980

Polyimide resin characteristics, test
[DGT-24.322] 04 p0479 N85-13049

The dimensional stability of advanced composite antenna reflectors: Analytical and test evaluation — satellite antennas 05 p0626 N85-14014

Passive Orbital Disconnect Strut (PODS 3) structural test program
[NASA-CR-177325] 08 p1113 N85-17020

Effects of high energy radiation on the mechanical properties of epoxy-graphite fiber reinforced composites
[NASA-CR-174314] 08 p1118 N85-17047

Flight service evaluation of advanced composite ailerons on the L-1011 transport aircraft
[NASA-CR-172483] 08 p1118 N85-17049

Contact behavior, impact response and damage in graphite-epoxy laminates subjected to initial stresses
08 p1171 N85-17386

Delamination growth in graphite epoxy laminates under compressive loads 09 p1288 N85-18088

The fabrication, processing and characterization of multidimensionally braided graphite/epoxy composite materials
[AD-A146729] 09 p1288 N85-18090

Simulation of repetitively-pulsed laser irradiation of graphite-epoxy composite
[AD-A148698] 09 p1325 N85-18329

Verification and application of the Iosipescu shear test method
[NASA-CR-174346] 09 p1333 N85-18376

Evaluation of failure criterion for graphite/epoxy fabric laminates
[NASA-CR-172547] 10 p1431 N85-19025

Preliminary report on tests of tensile specimens with a part-through surface notch for a filament wound graphite/epoxy material
[NASA-CR-172545] 10 p1431 N85-19026

Evaluation and prediction of long-term environmental effects of nonmetallic materials
[NASA-CR-171353] 10 p1450 N85-19137

Interleaved array antenna technology development
[NASA-CR-171845] 10 p1477 N85-19326

Characterization of mode 1 and mixed-mode failure of adhesive bonds between composite adherends
[NASA-TM-86355] 12 p1797 N85-21270

Accelerated viscoelastic characterization of T300-5208 graphite-epoxy laminates
[NASA-CR-3871] 12 p1797 N85-21271

Rubber modified epoxy adhesive
[AD-D011527] 12 p1810 N85-21354

SRM filament wound case resin characterization studies 12 p1944 N85-22212

Longitudinal splitting in unidirectional composites, analysis and experiments
[NASA-CR-3881] 13 p2015 N85-22639

Development of epoxy matrices for filament-wound graphite structures
[DE85-003674] 13 p2015 N85-22642

WRAP-RIB antenna technology development
14 p2231 N85-23824

A study of frequency effects and damage accumulation during the fatigue of graphite/epoxy and glass/epoxy composite materials 14 p2247 N85-[illegible]

Measurement of damping of graphite epoxy materials
[NASA-CR-175663] 14 p2248 N85-[illegible]

Design, fabrication and test of composite curved frames for helicopter fuselage structure
[NASA-CR-172436] 15 p2470 N85-[illegible]

Crack growth direction in unidirectional off-axis graphite epoxy
[NASA-CR-175752] 15 p2502 N85-[illegible]

In-plane shear properties of graphite Fibre/Epoxy composites for aerospace applications: Evaluation of test methods by the decision analysis technique
[AD-A151593] 15 p2503 N85-[illegible]

The physical effects of different stress situations on graphite/epoxy compounds 15 p2687 N85-[illegible]

Effect of low-velocity or ballistic impact damage on the strength of thin composite and aluminum shear panels
[NASA-TP-2441] 16 p2742 N85-[illegible]

Measurement of damping of graphite expoxy materials
[NASA-CR-175793] 16 p2743 N85-[illegible]

Temperature: Curvature relationships for unsymmetric graphite-epoxy laminates
[VPI-E-85-08] 16 p2743 N85-[illegible]

Directional thermal conductivities of graphite-epoxy composites: 0/90 and 0/ + or - 45/90
[AD-A152209] 16 p2743 N85-[illegible]

The effect of center delamination on the instability of composite cylindrical panels
[AD-A153494] 18 p3069 N85-28979

DFVLR research in aluminum-lithium alloys
18 p3087 N85-29105

Flight-service program for advanced composite rudders on transport aircraft
[NASA-CR-174537] 19 p3217 N85-[illegible]

Fuel containment and damage tolerance in large composite primary aircraft structures
[NASA-CR-166083] 19 p3231 N85-30032

Influence of interface ply orientation on fatigue damage of adhesively bonded composite joints
[NASA-TM-86443] 19 p3284 N85-[illegible]

Residual thermal and moisture influences on the strain energy release rate analysis of edge delamination
[NASA-TM-86437] 20 p3422 N85-[illegible]

Development and test of advanced composite components. Center Directors discretionary fund program
[NASA-TM-86512] 21 p3561 N85-32147

Comparisons of various configurations of the edge delamination test for interlaminar fracture toughness
[NASA-TM-86433] 21 p3561 N85-32151

Measurement of damping of graphite epoxy materials
[NASA-CR-176073] 21 p3596 N85-[illegible]

Nonlinear response and failure characteristics of internally pressurized composite cylindrical panels
[NASA-CR-176148] 22 p3600 N85-[illegible]

Flight service evaluation of composite helicopter components
[NASA-CR-172562] 23 p3809 N85-34222

Damage induced stress redistribution in composite laminates 24 p4072 N85-[illegible]

Fuel containment and damage tolerance for large composite primary aircraft structures. Phase 1: Testing
[NASA-CR-166091] 24 p4073 N85-35241

Quantitative non-destructive evaluation of composite materials based on ultrasonic wave propagation
[NASA-CR-176176] 24 p4074 N85-35244

Effects of temperature on the tensile strength and elastic modulus of composite material
[AD-A156112] 24 p4075 N85-35251

A normal incidence X-ray telescope sounding rocket payload
[NASA-CR-176169] 24 p4153 N85-[illegible]

GRAPHITE-POLYIMIDE COMPOSITES

Long-term thermal aging of 2 graphite-polyimide composite materials
[NASA-TP-2369] 03 p0325 N85-12094

Develop and demonstrate manufacturing processes for fabricating graphite filament reinforced polyimide (Gr/PI) composite structural elements
[NASA-CR-172497] 11 p1592 N85-20019

Effect of counterface material type and its topography on the tribological properties of polyimide composites
[NASA-TM-87036] 16 p2754 N85-[illegible]

DFVLR research in aluminum-lithium alloys
18 p3087 N85-29105

Graphite/PMR polyimide composites with improved toughness
[NASA-TM-87081] 21 p3561 N85-32148

Thermal expansion of selected graphite reinforced polyimide-, epoxy-, and glass-matrix composite
[NASA-TM-87572] 21 p3561 N85-32149

GRAPHITIZATION
Influence of hydrogen saturation and prior heat treatment on graphitization of white cast iron
[BLL-M-35964-(5828.4)] 05 p0615 N85-13932
Rubber modified epoxy adhesive
[AD-D011527] 12 p1810 N85-21354
Directional thermal conductivities of graphite-epoxy composites: 0/90 and 0/ + or - 45/90
[AD-A152209] 16 p2743 N85-26929
GRAPHOEPITAXY
Research on submicrometer structures
[AD-A146578] 06 p0867 N85-15508
GRAPHS (CHARTS)
Planarity criteria in electromagnetic topology
[AD-A145279] 01 p0036 N85-10241
A method for evaluating the contamination of steel in relation to the solidification curve
[BLL-M-35735-(5828.4)] 02 p0175 N85-11171
On the formal development of graph theoretical algorithms by transformation
[TUM-I8403] 04 p0553 N85-13522
Drifting buoy data from equatorial Pacific Ocean, 31 Aug. 1980 - 30 Apr. 1982
[PB85-120046] 10 p1522 N85-19598
Atlas of the Beaufort Sea
[AD-A149545] 11 p1689 N85-20619
Maximum matchings in a class of random graphs
[AD-A149663] 12 p1920 N85-22060
Introduction to CHART: A graphic analysis and display system, revision
[DE85-004812] 13 p2148 N85-23335
The complexity of reliability computations in planar and acyclic graphs
[AD-A150756] 14 p2406 N85-24845
On matchings and Hamiltonian cycles in random graphs
[AD-A151015] 14 p2409 N85-24851
Graphic simulation of a machine-repairman model
[AD-A151761] 16 p2694 N85-26633
Reliability models for dataflow computer systems
[NASA-CR-175813] 16 p2646 N85-27543
Algorithm for determination of isomorphic graphs
22 p3769 N85-33357
GRASHOF NUMBER
Experimental study of free and mixed convective flow of air in a heated cavity
[DE85-012536] 24 p4094 N85-35380
GRASSES
Relationships between grass canopy characteristics and LANDSAT Thematic Mapper bands
02 p0213 N85-11402
Study of the motion of agricultural vehicles on steep grass-covered slopes
[AD-P004290] 09 p1408 N85-18867
Gravity perception and response in shoot of cereal grasses 15 p2611 N85-26091
GRASSLANDS
Direct regression analysis of remote sensing data (using example of grass cover) 22 p3736 N85-33157
GRASSMANN ALGEBRA
U VECTOR SPACES
GRATINGS (SPECTRA)
NT ECHELETTE GRATINGS
Splitting of surface polariton spectrum by holographic grating 02 p0272 N85-11771
Research on materials and components for opto-electronic signal processing
[AD-A145606] 03 p0433 N85-12754
Method of producing a buried long period grating
[AD-D011351] 07 p0969 N85-16153
Theoretical study of laser-induced surface excitations on a grating
[AD-A147655] 07 p0972 N85-16172
Switchable zero order diffraction gratings as light valves
[AD-A147575] 07 p1044 N85-16633
The evaluation of a deformable diffraction grating for a stigmatic EUV spectroheliometer
[NASA-CR-174350] 09 p1322 N85-18309
STS atmospheric luminosities
[NASA-CR-175514] 12 p1791 N85-21240
Solar energy converter using surface plasma waves
[NASA-CASE-LEW-13827-1] 12 p1876 N85-21768
High resolution diffraction grating
[AD-D011541] 12 p1933 N85-22141
Properties of chirped grating lenses in optical waveguides
[AD-A150023] 12 p1934 N85-22149
Switchable zero order diffraction gratings as light valves
[AD-A150129] 12 p1934 N85-22153
Study of the potential usefulness of superfine holographic x-ray gratings in AXAF and astrophysics in general 12 p1945 N85-22215
Reflex attachment for line alignment in spectral diffraction devices 13 p2044 N85-22794
Millimeter-wave diffraction devices and materials
[AD-A150876] 14 p2418 N85-24917
Mirror accessory for line straightening in diffraction spectrometers 16 p2764 N85-27054
New image deblurring method described
16 p2806 N85-27305
Optical waveguide characterization using grating couplers
[AD-A153063] 17 p3037 N85-28769
Bandpass filter formed by serial gratings operating in a wood's anomaly region
[AD-D011660] 18 p3093 N85-29148
Switchable zero order diffraction gratings as light valves
[AD-A154471] 20 p3533 N85-31961
Picosecond-pulse damage studies of diffraction gratings
[DE85-010785] 22 p3790 N85-33481
On the convergence of an iterative formulation of the electromagnetic scattering from an infinite grating of thin wires 24 p4085 N85-35319
Redefining the scratch standards
[PB85-194736] 24 p4154 N85-35755
GRAVIMETRY
Analysis of highly precise gravity measurements
[SER-C-294] 01 p0071 N85-10472
Prediction of deflections of the vertical by gravimetric methods
[PB84-213727] 01 p0072 N85-10478
Development of a method for exploring low-reflectance areas through the combined use of different geophysical methods taking the north-west German basin as an example
[BMFT-FB-T-83-180] 02 p0220 N85-11450
Morphological study of monkeys submitted to antiorthostatic hypokinesia 12 p1902 N85-21942
Determination of density of the crust and upper mantle from deep seismic sounding and gravimetry, 2
13 p2111 N85-23153
Polynomial parameterization in inverse gravimetric problem 13 p2115 N85-23174
Determination of crust and upper mantle density based on deep seismic sounding and gravimetry data, part 1
14 p2345 N85-24498
Attempts to localize and identify the gravity sensing device of plant seedlings 15 p2607 N85-26064
Standards and specifications for geodetic control networks
[PB85-166478] 16 p2816 N85-27374
A micrographic and gravimetric study of intercalation and deintercalation of graphite fibers
[NASA-TM-87026] 17 p2934 N85-28110
GRAVIRECEPTORS
NT OTOLITH ORGANS
Mammalian gravity receptors: Structure and metabolism 15 p2605 N85-26055
Effects of weightlessness of Aurelia Ephyra differentiation and statolith synthesis
15 p2605 N85-26056
Gravity perception and cardiac function in the spider
15 p2606 N85-26058
Amyloplast sedimentation kinetics in corn roots
15 p2606 N85-26059
Polyamines as possible modulators of gravity induced calcium transport in plants 15 p2606 N85-26060
Calcium and calmodulin localization in gravitropically-responding plant organs
15 p2606 N85-26061
Role of Ca++ in shoot gravitropism — avena
15 p2607 N85-26065
A possible explanation of why gravitropic growth is detected earlier than straight growth
15 p2607 N85-26067
Gravitropism in leafy dicot stems
15 p2610 N85-26086
Mutant peas as probes in the understanding of growth and gravitropism 15 p2611 N85-26088
Gravity perception and response in shoot of cereal grasses 15 p2611 N85-26091
Are living cells generally sensitive to gravity?
24 p4130 N85-35602
GRAVITATION
NT ARTIFICIAL GRAVITY
NT GRAVITY ANOMALIES
NT PLANETARY GRAVITATION
NT REDUCED GRAVITY
NT SOLAR GRAVITATION
Use of gravitational stabilization in performance of experiments 02 p0160 N85-11084
Gravitational vacuum 02 p0265 N85-11734
Linear conformal gravitation 02 p0265 N85-11735
A geometrical theory of spin motion
[DE84-016537] 04 p0574 N85-13658
Observation of the contractile vacuolar system of Paramecium caudatum on the fast running clinostat
05 p0689 N85-14431
Gravity and cell differentiation in lentil roots
05 p0690 N85-14433
The use of horizontal clinostats in studies of plant statocyte development 05 p0690 N85-14435
Stability of stellar disk and ratio of halo to disk masses in the galaxy 05 p0740 N85-14763
World Geodetic System, 1984
[AD-A147409] 09 p1342 N85-18445
A preliminary study of a cryogenic equivalence principle experiment on Shuttle
[NASA-CR-171300] 10 p1426 N85-18994
Venus gravity: Global field results
13 p2177 N85-23512
The interaction of calcium and auxin in the gravitropic response of roots 15 p2606 N85-26062
Attempts to localize and identify the gravity sensing device of plant seedlings 15 p2607 N85-26064
The role of gravity on the reproduction of arabidopsis plants 15 p2607 N85-26069
Importance of gravity for plant growth and behavior
15 p2608 N85-26070
Structural development and gravity
15 p2608 N85-26071
SU(N,1) inflation
[DE85-003952] 15 p2669 N85-26469
Fluid surface behavior in low gravity. Center discretionary fund no. 83-21
[NASA-TP-2486] 17 p2957 N85-28260
Gravitational properties of antimatter
[DE85-009601] 18 p3197 N85-29832
Research relative to the development of a cryogenic microwave cavity gradiometer for orbital use
[NASA-CR-176002] 19 p3222 N85-29980
Primordial inflation and supergravity
[DE85-009538] 19 p3383 N85-30989
The effect of power law body forces on a thermally-driven flow between concentric rotating spheres
[NASA-TM-87596] 24 p4093 N85-35374
Aeromagnetic and gravity models of the pluton below the Lake City caldera, Colorado
24 p4104 N85-35442
Three-dimensional gravity ideal body studies in rough terrain
[DE85-014097] 24 p4118 N85-35525
GRAVITATION THEORY
Stability questions for gravity in 4 and higher dimensions 05 p0734 N85-14716
The determination of the post-Newtonian parameters in gravitational theory using laser ranging to the Lageos satellite 09 p1414 N85-18924
Supermanifolds and Berezin's new integral
[DE85-001833] 11 p1706 N85-20732
Cosmology in theories with extra dimensions
18 p3202 N85-29864
GRAVITATIONAL COLLAPSE
NT BLACK HOLES (ASTRONOMY)
Iron core collapse models of Type 2 supernovae
[DE84-013909] 05 p0743 N85-14775
Research in nuclear astrophysics: Stellar collapse and supernovae
[DE84-015559] 05 p0743 N85-14776
Fragmentation and turbulence in collapsing gas clouds
[DE85-003745] 11 p1633 N85-20262
Inflation from extra dimensions
[DE85-007834] 16 p2883 N85-27787
GRAVITATIONAL EFFECTS
NT GRAVITATIONAL LENSES
NT LAGRANGIAN EQUILIBRIUM POINTS
NT STELLAR GRAVITATION
Some notes on a tangent plane oriented heading reference — stabilized platforms
[RAE-TM-IEE-144] 02 p0136 N85-10928
Rapid nonresonant rotation of a spacecraft in nominally periodic orbits in limited 3 body problem
02 p0160 N85-11083
Gravitational effects on premixed particle cloud flames
02 p0171 N85-11144
Transport phenomena in the boundary layer during solution solidification under microgravity. Ice growth from a water-salt solution
[BMFT-FB-W-84-031] 03 p0329 N85-12121
Tidal disruption and the origin of the Moon
04 p0586 N85-13739
A testable gravitational capture model for the origin of the Earth's Moon 04 p0586 N85-13742
Orbit perturbation — satellites
05 p0598 N85-13810
Investigation of the Ostwald ripening of separated particles in liquid-liquid systems under microgravity conditions
[BMFT-FB-W-84-037] 05 p0615 N85-13927
Biogeochemical cycles: Interactions in global metabolism 05 p0652 N85-14184
Life Sciences Research in Space — conference
[ESA-SP-212] 05 p0689 N85-14425

Influence of simulated weightlessness on the motility of the acellular slime mold Physarum polycephalum
05 p0689 N85-14430

Observation of the contractile vacuolar system of Paramecium caudatum on the fast running clinostat
05 p0689 N85-14431

Gravity and cell differentiation in lentil roots
05 p0690 N85-14433

The influence of gravitational body force in meteoritic chondrule and lunar glass formation
06 p0884 N85-15614

The growth of metastable peritectic compounds
[NASA-CR-171290] 07 p0920 N85-15825

SPAR X technical report for experiment 76-22 directional solidification of magnetic composites
[NASA-CR-171271] 07 p0927 N85-15880

Comparative effects of auxin and abscisic acid on growth, hydrogen ion efflux and gravitropism in primary roots of maize
[NASA-CR-174355] 09 p1342 N85-18444

Gravity and biological systems: Emphasis on human physiology
[ESA-BR-21] 09 p1360 N85-18558

The restricted problem of 2 + N bodies
09 p1414 N85-18925

Approximation of difference in water table positions by horizontal stratum in studies of their influence on gravity
10 p1502 N85-19478

Influence of gravitoinertial force level on apparent magnitude of coriolis cross-coupled angular accelerations and motion sickness 11 p1693 N85-20644

Vestibular and oculomotor function during Gz variations 11 p1693 N85-20645

Averaging of equations of cometary orbital motion with allowance for nongravitational effects
13 p1978 N85-22411

Lagrangian solutions in photogravitational restricted circular three-body problem 13 p1979 N85-22416

Periodic movements of axisymmetrical satellite about center of mass due to gravitational moment
13 p2042 N85-22783

Problems of space biology. Volume 50: Nystagmometry for evaulation of the status of the vestibular function
[NASA-TM-77616] 14 p2385 N85-24694

Systematic and random deformations of orbits of long-period comets 15 p2479 N85-25299

Resonant rotations of satellite in polar orbit in magnetic and gravitational fields 15 p2479 N85-25302

Investigation of internal friction of free-flowing material during discharge
[BLL-M-36141-(5828.4)] 15 p2553 N85-25752

NASA Space Biology Program: 9th Annual Symposium
[NASA-CP-2336] 15 p2605 N85-26054

Mammalian gravity receptors: Structure and metabolism 15 p2605 N85-26055

Effects of weightlessness of Aurelia Ephyra differentiation and statolith synthesis
15 p2605 N85-26056

Gravity perception in a Cladoceran-Zooplankter: Anatomy of antennal socket setae of Daphnia magna
15 p2605 N85-26057

Gravity perception and cardiac function in the spider
15 p2606 N85-26058

Gravistimulus production in roots of corn
15 p2607 N85-26066

Neural mechanism by which gravitational stimulus and stress affect the secretion of renin and other hormones
15 p2610 N85-26083

Gravity, body mass and composition, and metabolic rate 15 p2610 N85-26084

Homeostasis in primates in the hyperdynamic environment — circadian timekeeping and effects of lower body positive pressure on sleep
15 p2610 N85-26085

Plant growth biophysics: The basis for growth asymmetry induced by gravity 15 p2611 N85-26089

An indirect role for ethylene in shoot-inversion release of apical dominance in Pharbitis nil
15 p2611 N85-26090

Gravity perception and response in shoot of cereal grasses 15 p2611 N85-26091

Simulated microgravity as a probe for understanding the mechanisms of early pattern specification
15 p2611 N85-26092

Development and maturation of the neuromuscular juncition in cell culture under conditions of simulated zero-gravity 15 p2611 N85-26093

Effects of simulated weightlessness on mammalian development. Part 2: Meiotic maturation of mouse oocytes during clinostat rotation 15 p2612 N85-26094

Effects on in vivo and in vitro exposure to excess gravity on growth and differentiation of mammalian embryos
15 p2612 N85-26095

Gravitational effects on reproduction, growth and development of mammals 15 p2612 N85-26097

Participation of ethylene in two modes of gravistimulation of shoots 15 p2613 N85-26101

Isolation of hybridomas for golgi-associated proteins and a plant calmodulin 15 p2613 N85-26103

Differential wall growth in gravistimulated corn roots: Its timing and regulation 15 p2614 N85-26105

Gravitational effects in theories with interacting fields: Two studies 15 p2663 N85-26435

The gravitational interaction between inclined, elliptical rings — Uranus rings 15 p2675 N85-26514

Dense but collisionless orbiting rings — Saturn rings
15 p2675 N85-26517

The gravito-electrodynamics of charged dust in planetary ring systems 15 p2677 N85-26531

Effects of posture and water immersion on diaphragmatic function 16 p2840 N85-27515

Optical best arc RMS test results
20 p3492 N85-31706

Sensitivity of human lymphocytes to microgravity in-vitro 20 p3510 N85-31820

G-induced Loss of Consciousness (GLC)
20 p3510 N85-31823

Study of requirements for and method of multidimensional acoustic imaging — spaceborne experiments
[ESA-CR(P)-2020] 20 p3525 N85-31924

Tolerance to +Gz and +Gx accelerations of individuals in older age groups in good health and with early signs of arteriosclerosis 23 p3952 N85-34496

NASA Developmental Biology Workshop: A summary
[NASA-TM-86756] 24 p4126 N85-35578

Effects of microgravity and hypergravity on invertebrate development 24 p4126 N85-35579

Vertebrate development in space: Gravity is a drag (and has been for eons and eons) 24 p4126 N85-35580

Report of the NASA Mammalian Developmental Biology Working Group 24 p4126 N85-35581

Report of the Avian Development Working Group
24 p4127 N85-35582

Report of Amphibian Development Group
24 p4127 N85-35583

Report of the Insect Development Group
24 p4127 N85-35584

Aquatic Invertebrate Development Working Group
24 p4127 N85-35585

Report of the Microbial Development Working Group
24 p4127 N85-35586

Cardiovascular responses to orthostatism and weightlessness 24 p4130 N85-35601

Are living cells generally sensitive to gravity?
24 p4130 N85-35602

Simulation of high +Gz onset in the dynamic environment simulator
[AD-A155963] 24 p4131 N85-35610

GRAVITATIONAL FIELDS

NT STELLAR GRAVITATION

Solution generating technique for the Einstein equations 03 p0435 N85-12768

Digital elevation models improve processing of Alaskan gravity data 04 p0515 N85-13285

Relationship of gold content to gravity fields in Far East 10 p1501 N85-19475

Consideration of heterogeneity of gravity fields in local high precision geodetic constructions
13 p2114 N85-23169

Mathematical modeling of results of geometric leveling in variable gravity field 13 p2114 N85-23170

Polynomial parameterization in inverse gravimetric problem 13 p2115 N85-23174

Gravity field of Venus and comparison with Earth
13 p2178 N85-23514

The support of long wavelength loads on Venus
13 p2178 N85-23515

Gravity field of the Jovian system from Pioneer and Voyager tracking data 13 p2180 N85-23529

A study of terrain reductions, density anomalies and geophysical inversion methods in gravity field modelling
[AD-A150788] 14 p2373 N85-24668

Local covariance functions and density distributions
[AD-A150792] 14 p2373 N85-24669

Potential models — Earth gravity
14 p2396 N85-24764

Elementary sunspot energy model
15 p2476 N85-25287

One method for constructing model of point masses of planetary gravity field 15 p2479 N85-25300

Resonant rotations of satellite in polar orbit in magnetic and gravitational fields 15 p2479 N85-25302

Interpretation of Venus gravitational anomalies
15 p2483 N85-25322

Distribution of gravity and plumb line deflection at Martian surface 15 p2483 N85-25324

Optimization of system for observing Northern Hemisphere atmospheric pressure field
15 p2485 N85-25338

The gravitational interaction between inclined, elliptical rings — Uranus rings 15 p2675 N85-26514

Heliocentric sail problem with variable gravity field reduction 16 p2724 N85-26816

On gravitational waves 16 p2759 N85-27028

Topex Gravity Model Development Team activities during fiscal year 1984
[NASA-TM-86208] 16 p2804 N85-27286

Status of the observational data sets — TOPEX
16 p2804 N85-27288

Satellite selection criteria 16 p2804 N85-27289

Optical best arc RMS test results
16 p2804 N85-27290

The size of a gravitational field model for Topex
16 p2805 N85-27293

The selection of the starting field: General versus tailored model 16 p2805 N85-27294

Comparison of gravity field solution techniques
16 p2805 N85-27295

Gravitational properties of antimatter
[DE85-009601] 18 p3197 N85-29832

An algorithm for the influence numbers in the expansion of the lumped gravitational potential coefficients in the presence of resonant inclination variation
[AD-A154229] 19 p3336 N85-30689

Geodynamics Branch research program
[NASA-TM-86223] 20 p3489 N85-31686

New optical satellite data 20 p3492 N85-31705

Spaceborne gradiometer error analysis
20 p3492 N85-31707

NASA/GSFC TOPEX gravity model operations group
20 p3492 N85-31709

The time averaged circulation of the oceans from satellite altimetry 20 p3493 N85-31713

Global geoid and gravity anomaly predictions using the collocation and point mass techniques
[AD-A154517] 21 p3605 N85-32387

The evolution of complex and higher organisms
[NASA-SP-478] 21 p3656 N85-32708

The effect of power law body forces on a thermally-driven flow between concentric rotating spheres
[NASA-TM-87596] 24 p4093 N85-35374

A dynamic model of Venus's gravity field
[NASA-CR-176173] 24 p4169 N85-35845

GRAVITATIONAL LENSES

QUASAT, gravitational lenses, and studies of the interstellar, intracluster and intergalactic medium
07 p1056 N85-16715

University of Cambridge Institute of Astronomy report of activities 13 p2170 N85-23464

Milliarcsecond morphology of the twin quasar 0957 + 56A,B: The view through a gravitational lens
20 p3544 N85-32054

GRAVITATIONAL PHYSIOLOGY

A survey of space biology and space medicine
[ESA-BR-17] 04 p0545 N85-13468

Spacelab mission D1 Frog statolith experiment STATEX: Hardware family and experiment operational sequence
05 p0689 N85-14426

Experiment 1ES031 on Spacelab 1: Are cells sensitive to gravity? — lymphocyte proliferation
05 p0689 N85-14428

Ultrasonic study of early cardiovascular adaptation to zero gravity 05 p0691 N85-14445

Three-dimensional ballistocardiography in weightlessness (experiment 1ES 028) — Spacelab
05 p0691 N85-14447

Miniature personal physiological tape recorder (experiment 1ES 30) — Spacelab
05 p0692 N85-14448

Physical performance capacity after a 7 day head-down tilt (-6 deg) 05 p0692 N85-14451

Intraocular fluid dynamics in microgravity
05 p0693 N85-14455

Endocrine responses to nonhypotensive gravitational stress: Vasopressin and aldosterone
05 p0693 N85-14459

Endocrine responses to hypotensive gravitational stress: Catecholamines, pancreatic polypeptide, and vasopressin 05 p0693 N85-14460

Sleep physiology in weightlessness (experiment 1ES 030) — Spacelab 05 p0695 N85-14474

Gravity and biological systems: Emphasis on human physiology
[ESA-BR-21] 09 p1360 N85-16558

Modular plant culture systems for life support functions
[NASA-CR-171853] 12 p1899 N85-21924

Evaluation of Results of Space Experiments in Physiology and Medicine and Informal Briefings by the F-16 Medical Working Group 20 p3508 N85-31805

GRAVITATIONAL POTENTIAL

U GRAVITATIONAL FIELDS

GRAVITATIONAL RADIATION

U GRAVITATIONAL WAVES

GRAVITATIONAL WAVE ANTENNAS

Analysis of the Frascati and Geneva gravitational wave antenna background exhibiting the one half sideral day period
[NOTA-INTERNA-601] 02 p0192 N85-11283

Some considerations on the capacitive calibration used for the 2.3 ton cryogenic antenna at CERN — gravitational antennas
[NOTA-INTERNA-609] 02 p0192 N85-11284

Sensitivity improvement of a two-mode gravitational radiation detector through the use of a transducer not perfectly tuned to the antenna
[NOTA-INTERNA-612] 02 p0192 N85-11285

GRAVITATIONAL WAVES

Analysis of the Frascati and Geneva gravitational wave antenna background exhibiting the one half sideral day period
[NOTA-INTERNA-601] 02 p0192 N85-11283

Sensitivity improvement of a two-mode gravitational radiation detector through the use of a transducer not perfectly tuned to the antenna
[NOTA-INTERNA-612] 02 p0192 N85-11285

Improved sensitivities in laser interferometers for the detection of gravitational waves
[MPQ-88] 04 p0506 N85-13232

Internal gravity waves in real atmosphere
06 p0825 N85-15236

Determination of gravity wave envelope solitons on surface of stratified fluid interacting with wind
14 p2334 N85-24433

Two-cycle mechanism of dissipation of tidal energy in ocean 14 p2335 N85-24438

The Record of Electrical and Communication Engineering Conversazione, volume 53, no. 2, November 1984
[ISSN-0385-7719] 16 p2758 N85-27022

On gravitational waves 16 p2759 N85-27026

Interplanetary plasma turbulence and the Doppler detection of a gravitational background radiation
[IFSI-85-1] 20 p3546 N85-32066

Some aspects of internal gravity waves in a multi-layered moving stratified flow 24 p4092 N85-35369

GRAVITROPISM

Comparative effects of auxin and abscisic acid on growth, hydrogen ion efflux and gravitropism in primary roots of maize
[NASA-CR-174355] 09 p1342 N85-18444

Role of Ca++ in shoot gravitropism — avena
15 p2607 N35-26065

Gravitropism in leafy dicot stems
15 p2610 N85-26086

Mutant peas as probes in the understanding of growth and gravitropism 15 p2611 N85-26088

GRAVITY

U GRAVITATION

GRAVITY ANOMALIES

On gravity from SST, geoid from Seasat, and plate age and fracture zones in the Pacific
[E85-10020] 02 p0217 N85-11433

Generalized linear inversion of 2.5 - dimensional gravity and magnetic anomalies 02 p0226 N85-11480

Determination of the altimetric geoid and gravity anomalies in the North Sea: Implications for a solution of the general circulation problem using ERS-1 data
03 p0382 N85-12446

Local geoid determination in mountain regions
[AD-A145799] 03 p0384 N85-12458

Lithospheric structure in the Pacific geoid
[NASA-CR-174155] 04 p0526 N85-13365

Models for volcanic processes in Long Valley, California: Testing by continental drilling
[DE84-014943] 04 p0534 N85-13414

Correlation radius of gravitational and magnetic anomalies and methods of its determination
06 p0821 N85-15213

Selection of spacing of modular and gradient measurement surveys based on statistical characteristics of measured geomagnetic field
06 p0821 N85-15214

Gravity anomaly map of Mars and Moon and analysis of Venus gravity field: New analysis procedures
[NASA-CR-174295] 08 p1258 N85-17919

Prospects and means for development of theory and practice of interpretation of gravitational and magnetic anomalies 10 p1501 N85-19474

Polynomial parameterization in inverse gravimetric problem 13 p2115 N85-23174

Gravity field of Venus and comparison with Earth
13 p2178 N85-23514

The support of long wavelength loads on Venus
13 p2178 N85-23515

Impacts in ice: Commissions of solar system crater population 13 p2181 N85-23536

Interpretation of Venus gravitational anomalies
15 p2483 N85-25322

Improving the geological interpretation of magnetic and gravity satellite anomalies
[E85-10103] 20 p3473 N85-31585

A comparative study of spherical and flat-Earth geopotential modeling at satellite elevations
20 p3475 N85-31593

A comparative study of spherical and flat-Earth geopotential modeling at satellite elevations
20 p3475 N85-31594

Long-wavelength magnetic and gravity anomaly correlations on Africa and Europe
20 p3476 N85-31597

Comparison of survey and photogrammetry methods to position gravity data, Yucca Mountain, Nevada
[DE85-011685] 21 p3590 N85-32316

Global geoid and gravity anomaly predictions using the collocation and point mass techniques
[AD-A154517] 21 p3605 N85-32387

Upward continuation of surface gravity anomalies
[AD-A154973] 21 p3631 N85-32560

Geologic processes on Venus: An update
22 p3857 N85-33883

The non-hydrostatic figures of the terrestrial planets
22 p3858 N85-33887

Optimal estimation of a high degree gravity field from a global set of 1 deg x 1 deg anomalies to degree and order 250
[AD-A156008] 24 p4117 N85-35519

Gravity gradiometer survey data processing
[AD-A156165] 24 p4117 N85-35522

A dynamic model of Venus's gravity field
[NASA-CR-176173] 24 p4169 N85-35845

GRAVITY GRADIENT SATELLITES

NT ATS

Application Number 3: Using tethers for attitude control 11 p1646 N85-20373

GRAVITY GRADIOMETERS

Research relative to the development of a cryogenic microwave cavity gradiometer for orbital use
[NASA-CR-174249] 07 p0962 N85-16095

A preliminary study of a cryogenic equivalence principle experiment on Shuttle
[NASA-CR-171300] 10 p1426 N85-18994

Gravity gradiometer survey data processing
[AD-A156165] 24 p4117 N85-35522

GRAVITY PROBE B

Optical contacting for gravity probe star tracker
[NASA-TM-86475] 01 p0120 N85-10819

Optical analysis of the star-tracker telescope for Gravity Probe
[NASA-TM-86474] 01 p0129 N85-10888

GRAVITY WAVES

NT BAROCLINIC WAVES

Wave phase velocity in a wind gradient — gravity waves 04 p0523 N85-13343

Effect of mountain wave dynamics on orographic storms
[DE84-014713] 04 p0540 N85-13433

Theoretical and observed dispersion of acoustic-gravity waves in atmosphere 04 p0557 N85-13547

Dispersion properties of moving ionospheric perturbations 07 p0952 N85-16036

The interpretation of SIR-B imagery of surface waves and other oceanographic features using in-situ, meteorological satellite, and infrared satellite data
08 p1143 N85-17212

On the classification and nonlinear solution of one type of stratified shear flow
[AD-A148832] 09 p1319 N85-18295

Internal Gravity Waves and Small-Scale Turbulence: Proceedings of the 2nd 'Aha Huliko'a Hawaiian Winter Workshop
[AD-A149510] 10 p1522 N85-19597

PMP-2 report: Equatorial wave dynamics
11 p1657 N85-20442

Winds and waves (4 min - 11 yrs) in the upper middle atmosphere (60-110 km) at Saskatoon, Canada (52 deg N, 107 deg W): MF radar (2.2 MHz) soundings 1973 - 1983 11 p1662 N85-20476

Mesh effects on the computation of non-linear gravity waves of arbitrary discharge
[COLL-AERON-8501] 12 p1888 N85-21848

Radio scintillations observed during atmospheric occultations of Voyager: Internal gravity waves at Titan and magnetic field orientations at Jupiter and Saturn
[NASA-CR-175554] 12 p1961 N85-22327

Analysis and interpretation of observations of airglow at 297 nm in the Venus thermosphere
13 p2172 N85-23473

Influence of internal gravity waves on F layer
14 p2338 N85-24460

Long nonlinear waves in layers of sudden changes in wind velocity 14 p2340 N85-24470

Numerical simulations of convectively excited gravity waves 14 p2444 N85-25082

Resonance generation of inertial waves (in the atmosphere) by Doppler-shift of inertio-gravity modes
15 p2590 N85-25968

Role of frontal circulations and gravity waves in initiating convective storm systems 15 p2598 N85-26010

Wave propagation in density stratified fluids
16 p2781 N85-27162

Turbopause as source of internal gravity waves
16 p2808 N85-27314

Wave dynamics and transport in the stratosphere
[NASA-CR-175789] 16 p2823 N85-27413

Symposium on Atmospheric Sciences in South Africa
[CSIR-S-331] 16 p2829 N85-27442

Atmospherically forced, coastally trapped, long period gravity waves off the south coast of southern Africa
16 p2832 N85-27461

Propagation of gravity waves in the atmosphere and around critical levels
[KNMI-WR-85-1] 18 p3137 N85-29428

High-latitude filtering in a global grid-point model using model normal modes 18 p3140 N85-29442

A laser slope gauge and a spar buoy wave gauge: Tools for the validation of microwave remote sensors
[AD-A154038] 19 p3272 N85-30290

Middle Atmosphere Program. Handbook for MAP. Volume 14: URSI/SCOSTEP Workshop on Technical Aspects of MST Radar
[NASA-CR-176085] 21 p3615 N85-32466

Excerpts from the paper: Research Status and Recommendation from the Alaska Workshop on Gravity Waves and Turbulence in the Middle Atmosphere, part 1.3A 21 p3616 N85-32470

Gravity waves from the stratosphere to the mesosphere, part 1.3B 21 p3616 N85-32471

The suppression of convective wavebreaking by radiative transfer processes, part 1.3C
21 p3616 N85-32472

A simple model for testing the effects of gravity-wave-produced vertical oscillations of scattering irregularities on spaced-antenna, horizontal drift measurements 21 p3619 N85-32489

Interferometer applications of VHF radars, part 3.6A
21 p3621 N85-32497

Techniques for the study of gravity waves and turbulence (keynote paper), part 4 21 p3621 N85-32499

Spectral measurements of turbulence and gravity waves, part 4.2A 21 p3622 N85-32501

Gravity-wave spectra in the atmosphere observed by MST radar, part 4.2B 21 p3622 N85-32502

High resolution evidence for the Garrett-Munk spectrum of stratospheric gravity waves 21 p3622 N85-32503

On the spectrum of atmospheric velocity fluctuations seen by MST/ST radar and their interpretation
21 p3622 N85-32504

Use of the VAD technique and measurements of momentum flux in the stratosphere at Aercibo, part 4.3A
21 p3622 N85-32505

Momentum flux measurements: Techniques and needs, part 4.5A 21 p3623 N85-32508

Tropospheric gravity waves observed by three closely spaced ST radars 21 p3623 N85-32509

Determination of horizontal and vertical wavelengths of gravity waves in the mesosphere by spaced wind measurements 21 p3623 N85-32510

On the limiting configuration of interfacial gravity waves
[AD-A154821] 21 p3631 N85-32557

A new hypothesis for the observed vertical distribution of atmospheric aerosols 21 p3645 N85-32646

GRAZING FLOW

The effect of grazing flow on the impedance of the Helmholtz resonator 05 p0635 N85-14076

GRAZING INCIDENCE

Study of magnetism at surfaces by scattering of neutrons at grazing incidence
[DE84-015850] 10 p1564 N85-19865

A new generation of spectrometer designs for ultraviolet astronomy 11 p1761 N85-21079

Grazing incidence beam expander
[DE85-010784] 19 p3368 N85-30889

GRAZING LANDS

U GRASSLANDS

GREASES

An evaluation of grease type ball bearing lubricants operating in various environments
[NASA-TM-86480] 02 p0185 N85-11239

Performance evaluation of automotive wheel bearing greases
[AD-A145948] 03 p0337 N85-12168

Grease versus oil lubrication of wheel bearings in Army equipment
[AD-A147546] 07 p0973 N85-16184

Corrosion properties of second-generation conductive materials 07 p1000 N85-16348

Protection products for the conductors of high voltage overhead lines
[BLL-OA-TRANS-3219-(6196.300)]
20 p3429 N85-31269

GREAT BRITAIN
U UNITED KINGDOM

GREAT LAKES (NORTH AMERICA)
Homogeneous macroclimatic zones of the lake states
[PB84-215821] 04 p0540 N85-13436
Two-dimensional lake wave prediction system
[PB84-231034] 06 p0841 N85-15342
PATHFINDER: A trajectory prediction system for the Great Lakes
[PB85-115335] 10 p1506 N85-19506
Great Lakes winter weather and ice conditions for 1982-83
[PB85-165009] 16 p2637 N85-27498
EPA (Environmental Protection Agency) research program guide, FY-1985, October 1, 1984 - September 30, 1985
[PB85-181881] 20 p3467 N85-31676
Great Lakes hydrometeorologic and hydraulic data needs 20 p3496 N85-31739

GREAT PLAINS CORRIDOR (NORTH AMERICA)
The influence of soil moisture distribution on the severe-storm environment of the southern Great Plains: A numerical study of the SESAME 4 case
09 p1357 N85-18534

GREEN THEOREM
U GREEN'S FUNCTIONS

GREEN'S FUNCTIONS
An inverse source problem for elastic waves
03 p0371 N85-12368
Applications of Green's boundary formula
05 p0718 N85-14607
Green function in theory of microstrip antennas
06 p0790 N85-15050
A first-order Green's function approach to supersonic oscillatory flow: A mixed analytic and numeric treatment
[NASA-CR-172207] 09 p1273 N85-18002
Noise transmission loss of a rectangular plate in an infinite baffle
[NASA-TP-2398] 12 p1927 N85-22109
Green's function solution of the Kondo problems and universality of the thermodynamic properties
[DE85-002739] 12 p1943 N85-22206
Elastic wave scattering from an interface crack in a layered half space 13 p2101 N85-23095
Surface scattering
[AD-A150252] 13 p2153 N85-23386
Reaction of piezoceramic shell to concentrated forces
14 p2279 N85-24115
First- and second-order charged particle optics
[DE85-006310] 14 p2421 N85-24940
Investigation of the numerical method of moments for digital computer determination of differential equations
[AD-A151896] 15 p2638 N85-26266
Local density theory of heats of formation and short-range order parameters in substitutionally disordered alloys
[DE85-009811] 18 p3075 N85-29021
A first-order time-domain Green's function approach to supersonic unsteady flow
[NASA-CR-172208] 19 p3214 N85-29930
Mutual coupling analysis for conformal microstrip antennas
[AD-A154292] 19 p3259 N85-30210
Integral constraints on stress energy perturbations in general relativity and applications to cosmology
19 p3363 N85-30965
Wave propagation and methods of solution of the wave equation for moving disturbances sources
[ESA-TT-824] 20 p3522 N85-31906
A cracked orthotropic sheet stiffened by a semi-infinite orthotropic sheet
[NASA-TP-2455] 21 p3597 N85-32339
Exact solutions of singular equations for viscous transonic flows 21 p3683 N85-32882

GREENHOUSE EFFECT
A study of greenhouse effects using zero, 1 and 2 dimensional climate models 02 p0230 N85-11498
Carbon dioxide, the greenhouse effect and climate: A primer
[GPO-33-444] 03 p0395 N85-12519
Paleoclimatologists use past to predict weather patterns 06 p0819 N85-15197
Surging as a potential response of ice sheets to CO2-induced changes in the polar environment (SPICAE)
[DE84-016472] 06 p0841 N85-15341
Carbon dioxide and the greenhouse effect
[GPO-39-043] 11 p1677 N85-20569
Modeling of mechanism of positive feedback between mean Earth surface temperature and atmospheric carbon dioxide in geologic time scale 13 p2106 N85-23122
Greenhouse effect in Earth's primordial atmosphere
16 p2807 N85-27310
Humidity/cloud-radiation feedback on possible climate perturbation due to fossil fuel utilization
[DE85-008888] 18 p3133 N85-29402
Climatic consequences of very high CO2 levels in Earth's early atmosphere 22 p3854 N85-33865
Volatiles on satellites of the outer solar system
22 p3854 N85-33868
Carbon dioxide and climate: A working glossary
[DE85-013535] 24 p4124 N85-35562

GREENLAND
Investigation of ice dynamics in the marginal ice zone
[AD-A145110] 01 p0088 N85-10597
Revised Uniform Summary of Surface Weather Observations (RUSSWO). Sondestrom AB, Greenland, parts A-F
[AD-A148919] 07 p1005 N85-16390
Structure and stratigraphy of Midterhuken Peninsula, Bellsund, West Spitsbergen 09 p1353 N85-18513
Hydrology and climatic conditions in Greenland
14 p2327 N85-24387
North Atlantic Deep Water Formation
[NASA-CP-2367] 15 p2601 N85-26028
Oceanographic variations in recent decades and their impact on the fertility of the Iceland Sea
15 p2602 N85-26034
North Atlantic Deep Water formation: Information from ice cores 15 p2602 N85-26035
Greenland ice sheet mass balance
15 p2603 N85-26043
Potential climatic effects on the Greenland ice sheet
15 p2603 N85-26044
Origin of the Greenland ice sheet
15 p2604 N85-26046
Mining cosmic dust from the blue ice lakes of Greenland 15 p2682 N85-26563
Operational experiences with the ARGOS system in Greenland 16 p2813 N85-27353
AWS (Air Weather Service) climatic briefs: North America
[AD-A152161] 16 p2835 N85-27483

GRIDS
Comparison of the multigrid and ICCG methods in solving the diffusion equation
[DE84-014409] 02 p0253 N85-11657
Transformation of two and three-dimensional regions by elliptic systems
[NASA-CR-174176] 04 p0554 N85-13529
Multigrid iteration solution procedure for solving three-dimensional sets of coupled equations
[DE84-016515] 04 p0555 N85-13532
Characteristics of polarization grids made of parallel metal strips during hemispherical scanning
06 p0792 N85-15062
An exploratory study of finite difference grids for transonic unsteady aerodynamics
[NASA-TM-84583] 07 p0899 N85-15696
Semianalytic modeling of aerodynamic shapes
[NASA-TP-2413] 12 p1771 N85-21120
An orthogonal grid technique for studying internal deformation and energy absorption in target penetration
[AD-A149989] 12 p1880 N85-21665
Grid generation for a pump collector
[AD-A150217] 13 p2092 N85-23059
GRID: A FORTRAN program for using a digitizing table to enter a finite element GRID
[AD-A151317] 15 p2628 N85-26196
An incremental multigrid strategy for the fluid dynamics equations
[AD-A151953] 16 p2783 N85-27172

GRIDS (MATHEMATICS)
U COMPUTATIONAL GRIDS

GRIFFITH CRACK
On the corner singularity of a 3-D Griffith crack
[AD-A150989] 14 p2321 N85-24342

GRINDING (COMMINUTION)
Milling of Si3N4 with Si3N4 hardware
[NASA-TM-86864] 01 p0031 N85-10191
Metallographic grinding efficiency
[DE85-001520] 09 p1304 N85-18194
Ammonia formation caused by the presence of water in the wet grinding of silicon nitride powder
[NASA-TM-77748] 14 p2249 N85-23937
Drying of pulverized material with heated condensible vapor
[DE85-011656] 22 p3783 N85-33438
Spectral characteristics of grinding sparks used for identification of scrap metals
[PB85-196570] 24 p4080 N85-35290

GRINDING (MATERIAL REMOVAL)
NT METAL GRINDING
In-situ annular face grinder
[AD-D011422] 08 p1168 N85-17367
Factors influencing the ball milling of Si3N4 in water
[NASA-TM-86932] 10 p1450 N85-19136
Parametric evaluation of ball milling of SiC in water
[NASA-TM-86974] 12 p1811 N85-21368
New technique for fluid feed in simultaneous multisurface grinding 13 p2046 N85-22880
Robotic deburring. Part 2: Evaluation of cutters and noncompliant tooling
[DE85-006182] 14 p2311 N85-24308
Study of a test method for assessing machinability in gear cutting operations
[BLL-BISI-TRANS-22345-(9022.06)]
17 p2972 N85-28358

GRINDING MACHINES
In-situ annular face grinder
[AD-D011422] 08 p1168 N85-17367
Diamond cutters' grinders 13 p2051 N85-22841
Role of fluid lubricant-coolant in fine grinding of optical glass by diamond tool 14 p2280 N85-24125
Non-contact hydrostatic bearings
16 p2762 N85-27046
Very high speed lap with positive lift effect
[AD-D011710] 19 p3280 N85-30344
Very high speed lap with negative lift effect
[AD-D011711] 19 p3281 N85-30345

GRINDING MILLS
Milling of Si3N4 with Si3N4 hardware
[NASA-TM-86864] 01 p0031 N85-10191
Improved silicon grinding method and apparatus
[NASA-CASE-NPO-16336-1-CU]
12 p1819 N85-21407
Operational performance of the photovoltaic-powered grain mill and water pump at Tangaye, Burkina Faso (formerly Upper Volta)
[NASA-TM-86970] 13 p2126 N85-23243

GRIT
Process development for the production of technically high quality monocrystalline diamond grits
[BMFT-FB-T-84-204] 08 p1138 N85-17168

GROOVES
Annular groove in compressor casing as device for control of air stream 13 p2050 N85-22832
An X-ray study of residual stresses in narrow groove TIG weldments
[DE85-006485] 16 p2802 N85-27274
Monogroove heat pipe design: Insulated liquid channel with bridging wick
[NASA-CASE-MSC-20497-1] 18 p3098 N85-29180

GROOVING
Stress concentration due to axial tension of loaded nonsymmetric-shaped grooves
[AD-A149425] 10 p1496 N85-19442

GROUND BASED CONTROL
NT AIR TRAFFIC CONTROL
NT AUTOMATED EN ROUTE ATC
NT RADAR APPROACH CONTROL
Planned office and facility consolidations: To improve system effectiveness and efficiency, FY 1985-87
[AD-A150441] 13 p1970 N85-22976
Helios ground operations 16 p2887 N85-27811
Simulation studies of time-control procedures for the advanced air traffic control system
[NASA-TP-2493] 21 p3553 N85-32101
The development of assessment techniques program
24 p4106 N85-35457

GROUND EFFECT (AERODYNAMICS)
Ground-effect analysis of a jet transport airplane
[NASA-TM-85920] 07 p0897 N85-15687
Hover test results of a small-scale twin-tilt nacelle model
[NASA-TM-86685] 14 p2210 N85-23706
Structures and Dynamics Division research and technology plans for FY 1985 and accomplishments for FY 1984
[NASA-TM-86417] 15 p2577 N85-25865
Effect of ground and/or ceiling planes on thrust of rotors in hover
[NASA-TM-86754] 20 p3388 N85-31014
Aerodynamic measurement of the wind flow in the number two section of the SIMA wind tunnel
[ONERA-PV-1/8138-GY] 20 p3389 N85-31019
Ground effect on helicopter aerodynamics and stability
20 p3395 N85-31060

GROUND EFFECT (COMMUNICATIONS)
Development of the microwave antenna range of the national antenna test facility at Paardefontein
[R-NIAS-21] 15 p2539 N85-25988
A short range, high accuracy radar ranging system
[AD-A152195] 16 p2774 N85-27122
Most desirable terrain, e.g., flat vs valley location, part 5.1B 21 p3624 N85-32513

GROUND EFFECT MACHINES
NT CUSHIONCRAFT GROUND EFFECT MACHINE
Finger materials for air cushion vehicles. Volume 2: Base fabrics for finger materials
[AD-A149701] 12 p1819 N85-21406

Impact studies of a 1/3-scale model of an air cushion vehicle
[NASA-TM-86380] 14 p2218 N85-23757
Finger materials for air cushion vehicles. Volume 1: Flexible coatings for finger materials
[AD-A151436] 15 p2522 N85-25545
Operational noise data for the LACV-30 air cushion vehicle
[AD-A154063] 19 p3351 N85-30773
GROUND HANDLING
Mechanical features of the shuttle rotating service structure 08 p1102 N85-16967
Payload transportation at KSC
08 p1103 N85-16970
STS payload ground handling mechanism at John F. Kennedy Space Center 08 p1103 N85-16971
Computer aided processing using laser measurements
08 p1103 N85-16973
GROUND RESONANCE
Study to eliminate ground resonance using active controls
[NASA-CR-166609] 07 p0902 N85-15715
Aerodynamic performance of a wing in ground effect using the PANAIR program
[AD-A153303] 17 p2892 N85-27832
GROUND SPEED
Geomagnetic velocimeter
[AD-D011672] 19 p3218 N85-29953
GROUND STATE
Spurious center of mass effects in a dynamically determined basis
[CSIR-TWISK-310] 01 p0109 N85-10732
Stark broadening of H(-) resonances in large electric fields
[DE84-016974] 04 p0496 N85-13164
Variational calculation of the 2D H2 molecule
[INPE-3304-PRE/615] 10 p1554 N85-19796
Quasiparticle aggregation in the Fractional Quantum Hall Effect
[DE85-001574] 10 p1565 N85-19868
Control of electronic, magnetic and optical properties of doped polyacetylene conductors
[AD-A150117] 12 p1814 N85-21375
Ab initio calculations of materials properties
[DE85-011167] 20 p3531 N85-31964
GROUND STATIONS
NT EARTH TERMINALS
NT POLYSTATION DOPPLER TRACKING SYSTEM
The application of microprocessors in the command and control of satellites by the MECB stations
[INPE-3202-RPE/466] 02 p0239 N85-11553
Determination of astronomical longitude differences: Munich, Karlsruhe, Niederreifenberg in 1974
04 p0524 N85-13355
Mark IVA DSN 26-meter subnet
05 p0624 N85-13995
Antenna microwave subsystem
05 p0625 N85-13997
Potential affiliate stations to work with the EVN — European VLBI Network; QUASAT
07 p1057 N85-16708
Dissemination of ERS-1 low bit rate data and the use of L-band receiving stations
[NLR-TR-83049-U] 09 p1356 N85-18542
The Telecommunications and Data Acquisition Report
[NASA-CR-174366] 10 p1462 N85-19224
Brazilian remote sensing receiving, recording and processing ground systems in the 1980's
[E85-10079] 10 p1504 N85-19493
Computer-assisted data processing and analysis system for ground-based meteorological data collection, report on the Sierra Cooperative Pilot Project
[PB85-115350] 10 p1520 N85-19537
The spot operational remote sensing satellite system: Current status and perspectives
11 p1713 N85-20776
The ARGOS VHF direct readout mini-station and CML-80-MP data collection Platform Transmitter Terminals (PTTs) 14 p2238 N85-23873
ARGOS VHF direct readout mini-station
14 p2239 N85-23886
Consultative Committee for Space Data Systems. Panel 1: Support
[NASA-CR-175786] 16 p2769 N85-27090
The Telecommunications and Data Acquisition Report
[NASA-CR-175842] 16 p2770 N85-27094
A description of the 64-meter antenna elevation drive gears and their strange wear 16 p2771 N85-27107
Repair of the DSS-14 pedestal concrete
16 p2772 N85-27108
Canadian Astronautics Limited's SARSAT ground stations 20 p3401 N85-31104
Ground segment of COSPAS system
20 p3402 N85-31108
The COSPAS/SARSAT local user terminal in Tromso, Norway. Special considerations and experience with high latitude location (69 deg, 43 min N)
20 p3402 N85-31109
Fault tolerant multiprocessor SARSAT-COSPAS 406 MHz local user terminal 20 p3404 N85-31123
The COSPAS-SARSAT system evaluation in Norway
20 p3406 N85-31133
GROUND SUPPORT EQUIPMENT
New airport ground traffic control system planned
03 p0310 N85-12006
National airspace system configuration management interface control document. Maintenance processor subsystem to remote monitoring subsystems and remote monitoring subsystem concentrators
[NAS-MD-790] 07 p0900 N85-15705
Equipment for preflight test of an Electronic Countermeasures (ECM) avionic system
07 p0939 N85-15949
External tank processing from barge to pad
08 p1096 N85-16927
Mechanical features of the shuttle rotating service structure 08 p1102 N85-16967
Payload transportation at KSC
08 p1103 N85-16970
STS payload ground handling mechanism at John F. Kennedy Space Center 08 p1103 N85-16971
Airport ground equipment under development at Riga
09 p1278 N85-18038
Improvements in Kazan airport equipment, facilities
09 p1278 N85-18039
Ministry officials on improving aircraft technical servicing 14 p2208 N85-23697
GROUND SUPPORT SYSTEMS
Integration of ground and on-board system for terminal count 08 p1092 N85-16898
Space shuttle flight readiness firing dress rehearsal for STS-1 08 p1097 N85-16929
Mathematical models for space shuttle ground systems 08 p1097 N85-16933
Support systems design and analysis
08 p1097 N85-16935
Impact of activation optimization on the Vandenberg Ground Support System using Q-GERT analysis
[AD-A148446] 08 p1105 N85-16986
Study of application of space telescope science operations software for SIRTF use
[NASA-CR-177337] 09 p1287 N85-18080
NASA-VCOSS dynamic test facility
[NASA-TM-86491] 10 p1427 N85-18996
MAP-related activities in the United States
11 p1655 N85-20427
A mathematical formulation of the problem of optimal use of ground resources for future space missions
12 p1947 N85-22232
GROUND TESTS
NT COLD FLOW TESTS
NT STATIC FIRING
Definition of ground test for verification of large space structure control
[NASA-CR-171206] 05 p0602 N85-13838
Level of effort 05 p0602 N85-13839
Oral presentation of first year final report, appendix A
05 p0602 N85-13840
Simplified planar model of ground test verification structure, appendix B 05 p0603 N85-13841
Definition of ground test for Large Space Structure (LSS) control verification, appendix G
05 p0603 N85-13845
Ground test experiment for large space structures, appendix I 05 p0603 N85-13847
Test signal generator for coherent air-to-ground radars
[AD-D011278] 05 p0626 N85-14025
A rig for testing the soft soil performance of track systems
[AD-P004272] 09 p1405 N85-18848
NASA-VCOSS dynamic test facility
[NASA-TM-86491] 10 p1427 N85-18996
Ground test experiment for large space structures
[NASA-TM-86489] 10 p1429 N85-19013
NASA/MSFC ground experiment for large space structure control verification
[NASA-TM-86496] 12 p1792 N85-21248
Definition of ground test for Large Space Structure (LSS) control verification
[NASA-TM-86495] 12 p1792 N85-21249
Spacecraft environmental interactions: A joint Air Force and NASA research and technology program
13 p1997 N85-22517
Scientific requirements for ozone measurements
13 p2105 N85-23113
Damping models for flexible communications satellites by substructural damping synthesis
[UTIAS-287] 14 p2237 N85-23868
A suggested standardized format for cosmic ray ground-level event data
[SH-9.1-15] 23 p4052 N85-35130
GROUND TRACKS
NT SATELLITE GROUND TRACKS
Mobility of the small combine (track type) on soft ground-relationship between the position of the center of gravity and the mobility
[AD-P004265] 09 p1407 N85-18862
Distributed control of circuits in multiuser communication networks with circuit precedence and path suitability criteria using failsafe routing concepts
[AD-A151825] 16 p2772 N85-27113
GROUND TRUTH
Evaluating effectiveness of using space information in specialized hydrogeological research
02 p0164 N85-11114
Active microwave measurements of sea ice under fall conditions: The RADARSAT/FIREX fall experiment — in the Canadian Arctic
[E85-10019] 02 p0217 N85-11432
Study of the improvement in analyzing passive microwave remote sensing data by integrated use of ground data 05 p0656 N85-14226
Classification of vegetation communities in the Battle Mountain SE quadrangle, Nevada with MSS digital data
[E85-10043] 06 p0826 N85-15246
Effective use of remote sensing products in litigation
[E85-10048] 06 p0827 N85-15250
Exploring the use of structural models to improve remote sensing agricultural estimates 07 p0985 N85-16259
The influence of the number of ground control points on the scene-to-map registration accuracy — Kansas, Louisiana, Mississipp, and Missouri
07 p0986 N85-16264
Amplitude calibration experiment for SIR-B
08 p1146 N85-17227
Ground truth for SIR-B images obtained by SIR system 8 impulse radar 08 p1149 N85-17251
Spectroradiometric calibration of the Thematic Mapper and Multispectral Scanner system
[E85-10077] 10 p1504 N85-19491
Preliminary evaluation of the airborne imaging spectrometer for vegetation analysis
[NASA-CR-174440] 10 p1505 N85-19496
Intra-eruption geologic map from an x-band radar image during the May 18, 1980 eruption of Mount St. Helens, Washington 13 p2199 N85-23639
Recent VAS imaging/sounding research
15 p2597 N85-26004
Simultaneous Earth observations from 2 satellites
[NASA-TM-86204] 16 p2810 N85-27325
Handbook for obtaining and using aerial photography to map aquatic plant distribution
[AD-A154584] 21 p3605 N85-32388
Interpretation of multiband photographs made during Telefoto-80 experiment for the purpose of discriminating agricultural crops 22 p3735 N85-33152
Direct regression analysis of remote sensing data (using example of grass cover) 22 p3736 N85-33157
LANDSAT-4/5 image data quality analysis
[E85-10105] 24 p4107 N85-35463
GROUND WATER
An evaluation of the electrodialysis reversal process (Edr) for the desalination of brackish water from the Omaruru delta (SWA/Namibia)
01 p0023 N85-10141
Major institutional arrangements affecting ground water in New York state
[PB84-202506] 01 p0065 N85-10429
Water resources data, Mississippi, water year 1982
[PB84-224559] 01 p0065 N85-10434
Water resources data, Florida, water year 1982. Volume 4: Northwest Florida
[PB84-223445] 01 p0066 N85-10437
The use of fixed-bed adsorber models to predict the fluxes of toxic substances in groundwaters and soil environments
[PB84-202563] 01 p0071 N85-10468
The application of remote sensing to resource management and environmental quality programs in Kansas
[E85-10023] 02 p0218 N85-11436
Water resources data for Florida, water year 1983. Volume 3B: Southwest Florida ground water
[PB84-220662] 03 p0384 N85-12459
Water resources data for California, water year 1982. Volume 1: Southern Great Basin from Mexican border to Mono Lake Basin and Pacific Slope Basins from Tijuana River to Santa Maria River
[PB84-220670] 03 p0384 N85-12461
Water resources data for Florida, water year 1982. Volume 3A: Southwest Florida surface water
[PB84-223080] 03 p0384 N85-12462
Water resources data for Nebraska, water year 1982
[PB84-223688] 03 p0385 N85-12463

Water resources data for California, water year 1982. Volume 3: Southern Central Valley Basins and Great Basins from Walker River to Truckee River
[PB84-223726] 03 p0385 N85-12464

Geothermal assessment of the lower Bear River drainage and northern East Shore ground-water areas, Box Elder County, Utah
[DE84-017358] 04 p0526 N85-13368

Subsurface temperatures in northeastern Wyoming measured by bottom hole temperature records
[TI84-901610] 04 p0534 N85-13413

Fate and disposition of trichloroethylene in surface soils
[AD-A147918] 07 p0995 N85-16321

Installation restoration program. Phase 2: Stage 1 problem confirmation study, Duluth International Airport Duluth, Minnesota
[AD-A148318] 08 p1089 N85-16885

Application of SIR-B data for groundwater exploration in the Arabian shield and sand-drift monitoring in the AN Nafud and Al Jafurah fringe areas, Kingdom of Saudi Arabia 08 p1144 N85-17214

German Radar Observation Shuttle Experiment (ROSE) 08 p1148 N85-17245

Electrical resistivity technique to assess the integrity of geomembrane liners
[PB85-122414/GAR] 09 p1325 N85-18327

Geothermal assessment of part of the east shore area, Davis and Weber Counties, Utah
[DE84-016817] 09 p1342 N85-18446

Ground-water level data and preliminary potentiometric-surface maps, Yucca Mountain and vicinity, Nye County, Nevada
[DE85-001771] 09 p1343 N85-18448

Applying an innovative approach to field investigations at a remedial action site
[AD-P004145] 09 p1348 N85-18481

Analysis of geohydrologic data by kriging
[AD-P004152] 09 p1349 N85-18488

Approximation of difference in water table positions by horizontal stratum in studies of their influence on gravity
10 p1502 N85-19478

Nationwide urban runoff program. Relationship of urban runoff to land use and groundwater resources
[PB85-114692] 10 p1506 N85-19505

Water resources data for Illinois, water year 1983. Volume 1: Illinois except Illinois River Basin
[PB85-125755] 10 p1507 N85-19508

Radioactive waste isolation in salt: Peer review of the Office of Nuclear Waste Isolation's report on the organic geochemistry of deep groundwaters from the Palo Duro Basin, Texas
[DE85-001439] 10 p1556 N85-19811

ELECT groundwater transport research code
[DE85-003284] 12 p1884 N85-21824

Shallow land burial technology: Humid
[DE85-004432] 12 p1932 N85-22136

Research and development related to the Nevada nuclear waste storage investigations
[DE85-002303] 12 p1932 N85-22138

Protecting the nation's groundwater from contamination, volume 1
[PB85-154201] 15 p2590 N85-25965

Protecting the nation's groundwater from contamination, volume 2
[PB85-154219] 15 p2590 N85-25966

Report on regional groundwater flow modeling for the Palo Duro Basin, Texas
[DE85-007490] 16 p2815 N85-27370

Groundwater model for an island aquifer: Bribie Island groundwater study
[CE-44] 16 p2821 N85-27396

In situ Tuff water migration/heater experiment
[DE85-010415] 18 p3101 N85-29200

Interim rock mass properties and conditions for analyses of a repository in crystalline rock
[DE85-010700] 18 p3125 N85-29352

Chlorine isotopes as environmental tracers in Columbia River basalt groundwaters
[DE85-011392] 19 p3302 N85-30473

Microwave hydrology: A trilogy
[NASA-CR-176042] 20 p3477 N85-31603

State-of-the-art of aquifer restoration. Volume 1: Sections 1 through 8
[PB85-181071] 20 p3478 N85-31612

State-of-the-art of aquifer restoration. Volume 2: Appendices A through G
[PB85-181089] 20 p3478 N85-31613

EPA (Environmental Protection Agency) research program guide, FY-1985, October 1, 1984 - September 30, 1985
[PB85-181881] 20 p3487 N85-31676

Geologic and hydrologic characterization and evaluation of the basin and range province relative to the disposal of high-level radioactive waste. Part 1: Introduction and guidelines
[GS-CIRC-904-A] 20 p3526 N85-31932

Geologic and hydrologic characterization and evaluation of the basin and range province relative to the disposal of high-level radioactive waste. Part 2: Geologic and hydrologic characterization
[GS-CIRC-904-B] 20 p3526 N85-31933

Geologic and hydrologic characterization and evaluation of the basin and range province relative to the disposal of high-level radioactive waste. Part 3: Geologic and hydrologic evaluation
[GS-CIRC-904-A] 20 p3526 N85-31934

Source-term considerations for a potential radioactive-waste repository located in unsaturated tuff
[DE85-010090] 20 p3529 N85-31953

Stochastic groundwater flow modeling using the second-order method
[DE85-011250] 22 p3802 N85-33556

Environmental surveillance at Los Alamos during 1984
[DE85-011886] 22 p3811 N85-33605

The 1984 environmental monitoring program report for Idaho National Engineering Laboratory site
[DE85-011209] 22 p3812 N85-33611

Anaerobic microbial transformations in subsurface environments: Project description
[DE85-012789] 23 p3951 N85-34486

State-of-the-art construction technology for deep tunnels and shafts in rock
[AD-A156362] 24 p4099 N85-35411

The geostatistical approach to the inverse problem in two-dimensional steady state groundwater modeling
24 p4107 N85-35462

Simulated effects of increased recharge on the ground-water flow system of Yucca Mountain and vicinity, Nevada-California
[DE85-012985] 24 p4108 N85-35469

Evaluation of low-temperature geothermal potential in north-central Box Elder County, Utah
[DE85-009541] 24 p4112 N85-35490

Geothermal resources of the Washakie and Great Divide basins, Wyoming
[DE85-013004] 24 p4112 N85-35491

Groundwater radon studies for earthquake precursors in southern California
[PB85-196871] 24 p4118 N85-35529

GROUND WAVE PROPAGATION

Synoptic observations of the radio noise background in the frequency range 150-180 kHz to provide design data for the low frequency communications designer
[AD-A147438] 07 p0941 N85-15965

Measurements and predictions of HF ground wave radio propagation over irregular, inhomogeneous terrain
[PB85-110666] 12 p1830 N85-21487

GROUND WIND

Atmospheric environment for Space Shuttle (STS-41G) launch
[NASA-TM-86486] 07 p0995 N85-16320

Revised Uniform Summary of Surface Weather Observations (RUSSWO). Alconbury RAF United Kingdom, parts A-F
[AD-A146913] 07 p1004 N85-16384

Revised Uniform Summary of Surface Weather Observations (RUSSWO). McChord AFB, Washington, parts A-F
[AD-A146914] 07 p1005 N85-16385

Revised Uniform Summary of Surface Weather Observations (RUSSWO). Mildenhall RAF, United Kingdom, parts A-F
[AD-A146915] 07 p1005 N85-16386

Revised Uniform Summary of Surface Weather Observations (RUSSWO). Dobbins AFB, Georgia, parts A-F
[AD-A146916] 07 p1005 N85-16387

Revised Uniform Summary of Surface Weather Observations (RUSSWO). Shemya AFB, Alaska, parts A-F
[AD-A146917] 07 p1005 N85-16388

Revised Uniform Summary of Surface Weather Observations (RUSSWO). Pope AFB, Fayetteville, North Carolina, parts A-F
[AD-A146918] 07 p1005 N85-16389

Revised Uniform Summary of Surface Weather Observations (RUSSWO). Sondestrom AB, Greenland, parts A-F
[AD-A146919] 07 p1005 N85-16390

Revised Uniform Summary of Surface Weather Observations (RUSSWO). England AFB, Alexandria, Lousiana, parts A-F
[AD-A146920] 07 p1006 N85-16391

Revised Uniform Summary of Surface Weather Observations (RUSSWO). Parts A-F: Homestead AFB, Florida
[AD-A147203] 07 p1007 N85-16396

On the formation of the nocturnal coastal surface wind speed maximum 09 p1356 N85-18[illegible]

Data catalog for the 1982 DFVLR observational Foehn experiment — alpine wind
[DFVLR-FB-84-33] 09 p1358 N85-18543

Natural environment analysis
[NASA-CR-171333] 10 p1428 N85-19010

Wind shear detection technology
[GPO-38-920] 12 p1893 N85-21979

Preliminary study of inphase gusts and moment force wind loads over the first 150 meters at KSC, Florida
[NASA-TM-86501] 13 p2137 N85-22373

Summary of Meteorological Observations, Surface (SMOS), Bermuda
[AD-A150537] 13 p2138 N85-22378

Summary of Meteorological Observations, Surface (SMOS), Beaufort, South Carolina
[AD-A150538] 13 p2138 N85-22379

Mountain barrier baroclinity effects on surface winds along the Alaskan Arctic coast 14 p2238 N85-23877

Application of infrared radiometers for airborne detection of clear air turbulence and low level wind shear, airborne infrared low level wind shear detection test
[NASA-CR-175725] 15 p2594 N85-25985

Air flow of the western coastal boundary of South Africa and its influence on the ocean 16 p2831 N85-27489

The determination of lee circulation during the foehn wind 24 p4122 N85-35504

Turbulent structure of stably stratified nocturnal slope flows
[AD-A155845] 24 p4123 N85-35509

GROUND-AIR-GROUND COMMUNICATION

Combat capable space systems for tactical support
11 p1713 N85-20775

GROUP BEHAVIOR

U GROUP DYNAMICS

GROUP DYNAMICS

Command control group behaviors. Objective 1: A methodology for and identification of command control group behaviors
[AD-A145690] 02 p0191 N85-11278

An analysis of constraints to coordinated tactical crew interaction in the P-3C aircraft
[AD-A147220] 07 p1021 N85-16478

Integrated approach to flight crew training
09 p1276 N85-18014

Video concepts in CRM training
09 p1276 N85-18015

Research opportunities in human behavior and performance
[NASA-CR-175473] 10 p1529 N85-19640

Effect of prolonged hunger during experimental hikes
11 p1692 N85-20937

Team dimensions: Their identity, their measurement and their relationships
[AD-A149662] 12 p1906 N85-21978

Perceived heterogeneity and its effect on various types of tasks
[AD-A151003] 14 p2392 N85-24729

Individual characteristics and unit performance: A review of research and methods
[AD-A153145] 17 p3001 N85-28550

The impact of group processing on achievement in cooperative learning groups
[AD-A153168] 17 p3001 N85-28551

Oral discussion, group-to-individual transfer and achievement in cooperative learning groups
[AD-A153209] 17 p3001 N85-28552

The effects of controversy and concurrence seeking on effective decision making
[AD-A153370] 17 p3002 N85-28555

Symbolic and interactional perspectives on leadership: An integrative framework
[AD-A155247] 21 p3665 N85-32789

USSR report: Space Biology and Aerospace Medicine, vol. 19, no. 3, May - June 1985
[JPRS-USB-85-005] 23 p3952 N85-34484

GROUP THEORY

NT AUTOMORPHISMS

NT HOMOMORPHISMS

Trilinear alternating forms on a vector space of dimension 7
[CWI-PM-R8402] 05 p0722 N85-14644

Nonlinear semigroups and evolution governed by accretive operators
[AD-A147556] 07 p1033 N85-16557

A note on the G-space version of Glicksberg's theorem
[CWI-PM-R8405] 08 p1217 N85-17885

Chemical applications of topology and group theory. 18: Polyhedral isomerizations of seven-coordinate complexes
[AD-A149461] 10 p1436 N85-19647

Annals of the Fourier Institute, volume 34, no. 4
11 p1686 N85-20888

The Milnor link of a local field to a perfect residue field 11 p1698 N85-20670

A continuous Helson surface in R3 11 p1698 N85-20674

Finite products of commutators in C* algebras 11 p1698 N85-20676

Multi-sample cluster analysis as an alternative to multiple comparison procedures [AD-A148960] 12 p1923 N85-22084

On ergodic actions whose self-joinings are graphs [CWI-PM-R8406] 12 p1925 N85-22093

On localization of injective modules [CSIR-TWISK-342] 14 p2413 N85-24878

On positive vectors, positive matrices and the specialization ordering [CWI-PM-R8407] 14 p2414 N85-24899

Old and new in Moebius groups 15 p2634 N85-26235

Cocycles and magnetic monopole [DE85-007797] 16 p2856 N85-27612

Probabilistic algorithms in group theory [AD-A152253] 16 p2859 N85-27630

On the transformation of derivatives of distributions on surfaces [PREPRINT-434] 18 p3173 N85-29670

On the group-theoretical approach to the energy spectra problem of charge carriers in cubic solids [PREPRINT-435] 18 p3196 N85-29827

GROUP VELOCITY

Dispersion characteristics of small-mode gradient optical fibers 13 p2062 N85-23004

Calculating dominant (quasi-t) mode group velocity in shielded microstrip line 22 p3780 N85-33422

GROUP 7A COMPOUNDS

U HALOGEN COMPOUNDS

GROUT

Mixtures experiment where the amount of the mixture is a factor under study [DE85-010974] 19 p3250 N85-30153

Experimental characterization and stability of salt- and nonsalt-containing grouts and mortars (BCT-1F- and BCT-1FF-related) [DE85-012339] 22 p3753 N85-33263

GROWTH

NT CROP GROWTH
NT CRYSTAL GROWTH
NT CZOCHRALSKI METHOD
NT DIRECTIONAL SOLIDIFICATION (CRYSTALS)
NT ELECTROEPITAXY
NT EPITAXY
NT HYDROTHERMAL CRYSTAL GROWTH
NT LIQUID PHASE EPITAXY
NT MOLECULAR BEAM EPITAXY
NT TRAVELING SOLVENT METHOD
NT VAPOR PHASE EPITAXY
NT VEGETATION GROWTH

Effect of 1,25-dihydroxycholecalciferol and 24,25 dihydroxycholecalciferol on growth and alteration of rat bones during hypokinesa (histomorphometric study) 01 p0092 N85-10622

Acid rain and tree physiology: Some hypotheses for observed changes in forest productivity [DE84-016568] 05 p0672 N85-14318

Comparative effects of auxin and abscisic acid on growth, hydrogen ion efflux and gravitropism in primary roots of maize [NASA-CR-174355] 09 p1342 N85-18444

The use of image registration technique in Brasilia's urban growth monitoring [INPE-3302-PRE/614] 10 p1569 N85-19896

Mechanism and pattern of fatigue crack growth in aluminum alloys 11 p1597 N85-20047

User's guide to the TAMW wheat model as implemented on the IBM 360/195 computer [E85-10084] 12 p1873 N85-21749

Purification and cultivation of human pituitary growth hormone secreting cells [NASA-CR-171848] 12 p1899 N85-21923

Investigation of the MBE growth of InSb and novel quantum well structures [AD-A151014] 14 p2427 N85-24969

Role of Ca++ in shoot gravitropism — avena 15 p2607 N85-26065

A possible explanation of why gravitropic growth is detected earlier than straight growth 15 p2607 N85-26067

Constant fiber number during skeletal muscle atrophy and modified arachidonate metabolism during hypertrophy 15 p2609 N85-26078

Development and maturation of the neuromuscular junction in cell culture under conditions of simulated zero-gravity 15 p2611 N85-26093

Effects on in vivo and in vitro exposure to excess gravity on growth and differentiation of mammalian embryos 15 p2612 N85-26095

Gravitational effects on reproduction, growth and development of mammals 15 p2612 N85-26097

Numerical estimation of the curvature of biological surfaces 17 p3006 N85-28588

Cloud droplet nucleation and initial growth derived from lidar depolarization studies 21 p3644 N85-32635

Chemolithotrophy and physiology of bacterial nutrient limitation 21 p3659 N85-32730

Sulfate-reducing bacteria: Microbiology and physiology 21 p3659 N85-32732

Microbial colonization and growth on metal sulfides and other mineral surfaces 21 p3662 N85-32747

Screening and characterizing oleaginous microalgal species from the southeastern United States [DE85-008787] 23 p3951 N85-34488

GROWTH CHAMBERS

U PHYTOTRONS

GRUMMAN AIRCRAFT

NT F-14 AIRCRAFT
NT F-111 AIRCRAFT
NT OV-1 AIRCRAFT

GRUMMAN OV-1C AIRCRAFT

U OV-1 AIRCRAFT

GRUNEISEN CONSTANT

Low-temperature thermal expansion of glass 15 p2645 N85-26315

GUANIDINES

NT TRIAMINOGUANIDINIUM AZIDE

GUATEMALA

Tectonic lineaments in the cenozoic volcanics of southern Guatemala: Evidence for a broad continental plate boundary zone [NASA-CR-175456] 10 p1505 N85-19499

GUAYULE

Guayule research [GPO-29-562] 04 p0477 N85-13042

Process development for commercial production of natural rubber from Guayule [PB85-124956] 12 p1815 N85-21388

GUIDANCE (MOTION)

NT AIRCRAFT GUIDANCE
NT COMMAND GUIDANCE
NT INERTIAL GUIDANCE
NT LASER GUIDANCE
NT MAP MATCHING GUIDANCE
NT REENTRY GUIDANCE
NT RENDEZVOUS GUIDANCE
NT SATELLITE GUIDANCE
NT SPACECRAFT GUIDANCE
NT STRAPDOWN INERTIAL GUIDANCE
NT TERMINAL GUIDANCE

On-board near-optimal climb-dash energy management 02 p0137 N85-10931

Certification of advanced systems 06 p0753 N85-14829

USSR report: Engineering and equipment [JPRS-UEQ-85-001] 09 p1305 N85-18200

Optimization of guidance and control using function minimization and NAVSTAR/GPS [AD-A149956] 12 p1775 N85-21141

Determination of directional gyro parameters 14 p2287 N85-24171

Multi-rate digital autopilot modeling methodology [AD-A152044] 15 p2474 N85-25272

A cost-efficient control procedure for the benefit of all airspace users 16 p2697 N85-26651

GUIDANCE SENSORS

Study of alternate optical and fine guidance sensor designs for the space infrared telescope facility (SIRTF) [NASA-CR-166614] 07 p0915 N85-15794

Evaluation of nose, roof, and mast mounted sensor platforms for piloting and sighting, integrated in future combat helicopters 08 p1074 N85-16808

Fourth International Conference on Robot Vision and Sensory Controls [AD-A149524] 10 p1492 N85-19422

Gyrolaser guidance system for medium range missiles 16 p2696 N85-26649

The impact of VLSI on guidance and control system design 16 p2697 N85-26654

GUIDE VANES

NT JET VANES

Variable inlet vane assembly for a gas turbine combustion [AD-D011220] 01 p0010 N85-10063

Development and certification of a new stall warning and avoidance system 05 p0702 N85-14507

Mounting construction for turbine vane assembly [AD-D011395] 07 p0904 N85-15723

Influence of normalized frequency on time-dependent aerodynamic characteristics of vane blading profiles 09 p1306 N85-18204

Gasdynamic evaluation of choking cascade turns [AD-A151854] 15 p2557 N85-25776

Spacer structure [AD-D011641] 17 p2897 N85-27866

GUINEA PIGS

Measurement of cochlear acoustic pressure in guinea pigs [ISL-CO-234/83] 16 p2861 N85-27644

Spontaneous transitional cell carcinoma in the urinary bladder of a strain 13 guinea pig [AD-A155645] 21 p3665 N85-32764

GULF OF MEXICO

Hurricane experience levels of coastal county populations: Texas to Maine [PB85-111383] 10 p1520 N85-19561

GULF STREAM

The gulf stream deflection and meander energetics experiment. Current meter and bottom pressure gauge data report for the September, 1981 to April, 1982 mooring period [AD-A144977] 01 p0088 N85-10595

Circulation and internal waves in a cold Gulf Stream waves [AD-A149704] 12 p1898 N85-21918

Biological processes in the water column of the South Atlantic Bight. Volume 1: Published manuscripts [DE85-004610] 12 p1900 N85-21929

Circulation pattern of the North Atlantic, part of the warmwater sphere research effort at Kiel University 14 p2239 N85-23888

Horizontal and vertical structure of velocity, potential vorticity and energy in the gulf stream [AD-A154753] 21 p3655 N85-32702

Numerical simulations of the response of intense ocean currents to atmospheric forcing [AD-A155161] 21 p3655 N85-32704

GULFS

NT GULF OF MEXICO

GUM VULCANIZATES

U VULCANIZED ELASTOMERS

GUMBEL THEORY

U RANGE (EXTREMES)

GUN LAUNCHERS

Response of propellants to high dynamic stresses: The uses of gun launch techniques [DE84-013223] 02 p0188 N85-11259

Response of propellants to high dynamic stresses: The uses of gun launch techniques 08 p1116 N85-17035

Experimental simulation of the flow inside a gun barrel [ISL-CO-208/83] 14 p2302 N85-24252

A method of calculating the aim point for an unguided projectile fired at a moving target [BAE-BT-12717] 15 p2489 N85-25365

Telemetry system for the transmission of data from projectiles during the acceleration phase in the gun barrel [ISL-CO-207/84] 22 p3739 N85-33178

Experimental simulation of in-bore flows using a high pressure shock tube [ISL-CO-217/84] 22 p3785 N85-33452

GUN PROPELLANTS

Response of propellants to high dynamic stresses: The uses of gun launch techniques [DE84-013223] 02 p0188 N85-11259

Thrust characterization of very high burning rate propellants [AD-A145891] 03 p0340 N85-12186

Response of propellants to high dynamic stresses: The uses of gun launch techniques 08 p1116 N85-17035

Effects of perforation L/D ratio and slotting on stick propellant combustion [AD-A148854] 10 p1456 N85-19177

A review of hazard assessment procedures for liquid gun propellants [AD-A149470] 10 p1457 N85-19182

Experimental high pressure equation of state of a very fast burning gun propellant [DE85-001749] 10 p1458 N85-19184

Twenty-first JANNAF Combustion Meeting, volume 1 [AD-A150981] 13 p1998 N85-22526

Study on the combustion of nitramine propulsion powder up to 1500 MPa and comparison of the performance with that of classical propulsion powders [ISL-CO-203/83] 14 p2264 N85-24025

Fiber reinforcement of gun propellant [AD-A152296] 16 p2757 N85-27014

Liquid propellants for use in guns: A review [AD-A153051] 17 p2937 N85-28131

The determination of dinitrotoluene in single base propellants [AD-A154672] 21 p3571 N85-32209

GUNFIRE

Measurements of two-phase exhaust flow parameters of a small caliber gun associated with muzzle flash phenomena [ISL-CO-212/83] 16 p2784 N85-27182

GUNN DIODES
Low frequency noise in oscillator with limited space-charge accumulation 06 p0786 N85-15024
Development of a 20/30 GHz receiving station for propagation experiments with L-SAT
[AD-A148261] 08 p1152 N85-17271
A coaxial cavity gunn oscillator using probe coupled microstrip
[AD-D011437] 10 p1479 N85-19334
An integrated varactor tuned coaxial gunn oscillator for 60 GHz operation
[AD-D011439] 10 p1479 N85-19335
Filter reflection image guide oscillator and solid state line scanning device
[AD-D011440] 10 p1479 N85-19336
Millimetre wave pulse technology — satellite mapping
[ESA-CR(P)-2004] 20 p3478 N85-31611

GUNN EFFECT
Distributed Gunn effect devices; a numerical analysis of microstrip circuits on thin active GaAs substrates
[FOA-C-30383-E] 12 p1837 N85-21527

GUNPOWDER
U GUN PROPELLANTS

GUNS (ORDNANCE)
NT ARTILLERY
Response of propellants to high dynamic stresses: The uses of gun launch techniques
06 p1116 N85-17035
Sealing assembly
[AD-D011463] 10 p1452 N85-19151
An orthogonal grid technique for studying internal deformation and energy absorption in target penetration
[AD-A149869] 12 p1860 N85-21665
Modified Landolt C-ring test to measure the effects of laser filters on visual acuity
[AD-A151164] 15 p2617 N85-26127
Liquid propellants for use in guns: A review
[AD-A153051] 17 p2937 N85-28131
A computer code IB-KB for interior ballistics of recoiling and recoilless guns
[FOA-C-20566-D2] 18 p3164 N85-29602
Inertial navigation system - LAS II for SGT YORK testing
[AD-A154204] 19 p3216 N85-29944
Using synchro-ballistic cameras to determine the velocity and spin rate of high-velocity projectiles
[DE85-010829] 19 p3367 N85-30884
Next generation gunship
[AD-A156361] 24 p4065 N85-35193

GUST ALLEVIATORS
Flight test technique for evaluation of gust load alleviation analysis methodology
[NASA-TM-86344] 06 p0754 N85-14833
Helicopter active control with rotor blades relaxation
06 p1075 N85-16819
Flight test of the Open Loop Gust Alleviation (OLGA) system
[BMFT-FB-W-84-038] 06 p1088 N85-16881
OLGA: An open loop gust alleviation
16 p2713 N85-26744
OLGA: An open loop gust alleviation system
17 p2903 N85-27897
Gust load alleviation of a cantilevered rectangular elastic wing. Wind tunnel experiment and analysis
[NAK-TR-86] 18 p3063 N85-28950

GUST LOADS
Flight test technique for evaluation of gust load alleviation analysis methodology
[NASA-TM-86344] 06 p0754 N85-14833
Evaluating wind flow around buildings on heliport placement
[FAA-PM-84-25] 12 p1893 N85-21881
Dynamic wind tunnel testing for active control research 13 p1986 N85-22352
Qualification of the T2 wind tunnel in cryogenic operation. A: Thermal field, preliminary study of a schematic model
[NASA-TM-77781] 14 p2227 N85-23805
Identification of gust input and gust response characteristics from Do 28 TNT flight test data
[DFVLR-FB-84-48] 17 p2900 N85-27881
OLGA: An open loop gust alleviation system
17 p2903 N85-27897
Gust load alleviation of a cantilevered rectangular elastic wing. Wind tunnel experiment and analysis
[NAK-TR-86] 18 p3063 N85-28950

GUSTS
Aerodynamics of airfoils subject to 3-dimensional periodic gusts
[AD-A145149] 01 p0003 N85-10018
Altitude control using action-demanding interactive displays: Toward an active psychophysics
[AD-P004311] 09 p1267 N85-17965
Unsteady aerodynamic characterization of a military aircraft in vertical gusts
[NASA-TM-77810] 12 p1770 N85-21110
Transonic interactions of unsteady vortical flows
[NASA-TM-86658] 12 p1770 N85-21113
Qualification of the T2 wind tunnel in cryogenic operation. B: Flow fluctuations, particle detection and qualification
[NASA-TM-77782] 14 p2227 N85-23806
Synthesis study: Validation of a gust generator in the presence of a model in a wind tunnel
[ONERA-RT-16/5108-RY-051]
16 p2701 N85-26678
The gust simulation apparatus of the 3m x 3m low speed wind tunnel of the DFVLR in Goettingen, West Germany
[DFVLR-FB-85-04] 17 p2906 N85-27920
Automatic detection of gust fronts
[FAA-PM-85-11] 17 p2995 N85-28516
Lectures of a Flight Mechanics Conference — conferences
[ESA-TT-831] 24 p4061 N85-35165
Gust simulation for flight mechanical wind tunnel tests
24 p4062 N85-35172

GUY WIRES
A novel type of stayed tower for wind turbines
[ISD-295] 15 p2587 N85-25952
Dynamic and aeroelastic action of guy cables
[VTT-18] 16 p2802 N85-27276

GUYANA
The use of hydrometeorological data in explaining shrimp cycles in Guyana 07 p1004 N85-16381

GYMNASTICS
U PHYSICAL EXERCISE

GYRATION
NT EARTH ROTATION
NT MOLECULAR ROTATION
NT MUON SPIN ROTATION
NT PLANETARY ROTATION
NT PRECESSION
NT QUENCHING (ATOMIC PHYSICS)
NT REVOLVING
NT ROTATION
NT SATELLITE ROTATION
NT SOLAR ROTATION
NT STELLAR ROTATION

GYRATORS
NT MICROWAVE FILTERS
Gyrator frequency selectors with bandwidth independent of input signal level 13 p2083 N85-23009
Quasioptical gyroklystron
[AD-D011666] 19 p3356 N85-30801

GYRES
Current inventory of anthropogenic carbon dioxide in the North Pacific Subarctic Gyre
[PB85-187938] 24 p4125 N85-35570

GYRO HORIZONS
Attitude data consistence check of rocket payloads
[BMFT-FB-W-84-049] 12 p1790 N85-21239
Perception of roll rate from an artificial horizon and peripheral displays
[VTH-LR-403] 17 p3002 N85-28557

GYROCOMPASSES
Low cost gyrocompass
[AD-A146295] 08 p1082 N85-16857
Design of single-wheel gyrocompass with correction
14 p2272 N85-24079
Two-stage gyrocompass 14 p2273 N85-24080
Simulation of gyrocompassing alignment and calibration of strapdown inertial navigation system in a swaying vehicle
[DFVLR-MITT-84-20] 17 p2895 N85-27850
Elastic wave gyrometer
[REPT-26/4924/HF] 20 p3459 N85-31484

GYROINTERACTION
U MAGNETIC RIGIDITY

GYROMAGNETISM
Nonlocal and nonadiabatic expression for the ponderomotive force near cyclotron resonance
[IPPJ-736] 23 p3974 N85-34636

GYROPLANES
U HELICOPTERS

GYROS
U GYROSCOPES

GYROSCOPES
NT ATTITUDE GYROS
NT CONTROL MOMENT GYROSCOPES
NT ELECTROSTATIC GYROSCOPES
NT GYRO HORIZONS
NT GYROCOMPASSES
NT GYROSTABILIZERS
NT LASER GYROSCOPES
NT OPTICAL GYROSCOPES
NT ROTARY GYROSCOPES
Periodic oscillation of gyrostat-satellite about its center of mass in an elliptical orbit 02 p0159 N85-11060
Gyrotron beam generation with helical magnetic fields
[AD-A145987] 03 p0417 N85-12670
Development program: Nuclear magnetic resonance gyroscope (NMR-gyro). Phase 1: Development of an experimental model
[BMFT-FB-W-84-041] 05 p0639 N85-14191
Measurement of electromagnetic field components from arbitrarily oriented gyro platforms
06 p0787 N85-15008
A gyro sensor block suspension
[AD-D011411] 08 p1154 N85-17294
Loop radiating elements
[AD-D011409] 08 p1158 N85-17298
Data analysis techniques for vehicle attitudinal, positional and experimental measurements
[AD-A147752] 08 p1188 N85-17484
An alignment fixture for a 2-Degree-of-Freedom (TDF) gyroscope
[AD-A148885] 10 p1422 N85-[illegible]
Analysis of interaction of dynamically adjustable gyroscopes on elastic platform by finite-element method
13 p2048 N85-[illegible]
Determination of directional gyro parameters
14 p2287 N85-24171
Superconducting gyroscope research
[NASA-CR-171406] 15 p2560 N85-25786
Preguidance and piloting with the aid of composite inertial sensors 16 p2696 N85-26646
The series 2000: A miniature gas bearing DTG for low cost strapdown guidance and control
16 p2696 N85-26648
Low cost two gimbal inertial platform and its system integration 16 p2698 N85-26661
Positions of relative equilibrium of satellite-gyrostat
16 p2718 N85-26777
USSR report: Engineering and equipment
[JPRS-UEQ-84-006] 16 p2760 N85-27035
Estimates of errors of a gyroscope stabilized platform
16 p2763 N85-27050
Errors in compensating for image oscillation by means of a gyroscopic head 16 p2763 N85-27051
The DREO (Defence Research Establishment Ottawa) Inertial Navigation Laboratory: Development and test capabilities
[AD-A154425] 19 p3216 N85-29945
Test evaluation of the Honeywell GG1111 Single-Degree-of-Freedom (SDF) strapdown gyroscope
[AD-A154768] 21 p3589 N85-32307
Determining an azimuth with a north seeking gyro
[AD-A155860] 24 p4063 N85-35180

GYROSCOPIC DRIFT
U GYROSCOPES
U GYROSCOPIC STABILITY

GYROSCOPIC STABILITY
Contributions to the error analysis in the relativity gyroscope experiment 05 p0638 N85-14095
Flight dynamics of axisymmetrical rotating bodies in air medium 13 p2043 N85-22791
Test evaluation of the Honeywell GG1111 Single-Degree-of-Freedom (SDF) strapdown gyroscope
[AD-A154768] 21 p3589 N85-32307

GYROSTABILIZERS
Optimum parameters of aerogyroscopic satellite orientation system 16 p2716 N85-26782

GYROSTATS
U GYROSCOPES

GYROTRONS
U CYCLOTRON RESONANCE DEVICES

H

H ALPHA LINE
A warm magnetoactive plasma in a large volume of space 06 p0878 N85-15579
Theoretical studies of chromospheres and winds in cool stars
[NASA-CR-174204] 06 p0880 N85-15596
Increase in hydrogen emission of upper atmosphere following launches of space vehicles
13 p1961 N85-22431

H LINES
NT H ALPHA LINE
Variations of the H and K emission lines of singly ionized calcium in the eclipsing binary star system AR Lacertae
02 p0296 N85-11921
Photoionization structure of the Orion Nebula
08 p1246 N85-17863
The kinematic and radial properties of normal luminous SC galaxies 20 p3545 N85-32081

HABITABILITY
Human response to vibroacoustic environments of space vehicles
[NASA-TM-86316] 01 p0116 N85-10759
NASA's land remote sensing plans for the 1980's
13 p2124 N85-23224

Proceedings of the Seminar on Space Station Human Productivity [NASA-TM-86673] 18 p3156 N85-29539
Space station crew safety: Human factors interaction model 18 p3156 N85-29540
Space station crew safety alternatives study, third quarter briefing 18 p3156 N85-29541
Habitability sleep accommodations 18 p3159 N85-29566
Rockwell experience applications to Ames space station mockup habitability/productivity studies 18 p3159 N85-29572

HABITATS
Ecology of estuarine channels of the pacific northwest coast: A community profile [PB84-209709] 01 p0070 N85-10464
The use of digital spaceborne SAR data for the delineation of surface features indicative of malaria vector breeding habitats 08 p1146 N85-17230
Birds on airports: The reason for their presence 11 p1580 N85-19955
Use of a two-dimensional flow model to quantify aquatic habitat [AD-A154287] 19 p3266 N85-30253
Microbial ecology of extreme environments: Antarctic yeasts and growth in substrate-limited habitats [NASA-CR-176005] 19 p3326 N85-30609

HADRONS
NT BARYONS
NT KAONS
NT MESONS
NT MUONS
NT VECTOR MESONS
A concept for a hadron calorimeter with photodiode readout [MPI-PAE/EXP-E1-130] 01 p0050 N85-10332
High intensity hadron accelerators [DE84-014063] 01 p0119 N85-10812
Stochastic cell model for hadronic multiparticle distributions [DE84-018480] 04 p0562 N85-13578
Stochastic methods for the description of multiparticle production [DE84-009981] 10 p1556 N85-19810
Jet topologies in hadron-hadron collisions [DE85-001328] 12 p1929 N85-22119
Glueball candidates [DE85-003627] 14 p2418 N85-24921
Parton dynamics in hadronic processes [DE85-006072] 14 p2418 N85-24922
Space station as quark matter factory [DE85-004806] 15 p2685 N85-26585
Measurements of heavy quark and lepton lifetimes [DE85-008321] 18 p3181 N85-29724
Electron-proton collider option for the superconducting super collider [DE85-010146] 18 p3196 N85-29822
Detector problems at the SSC [DE85-010217] 21 p3703 N85-33007
Generalized string amplitude and wave equation for hadrons [DE85-011492] 22 p3842 N85-33798
Composition of primary cosmic rays near the bend from a study of hadrons in air showers at sea level [OG-5.2-2] 22 p3883 N85-34059
The composition of cosmic rays near the Bend (10 to the 15th power eV) from a study of muons in air showers at sea level [OG-5.2-3] 22 p3883 N85-34060
The primary composition beyond 10 to the 5th power GeV as deduced from high energy hadrons and muons in air showers [OG-5.2-6] 22 p3883 N85-34063
Observations of cosmic-ray modulations in the fall, 1984 [SH-5.1-16] 23 p4043 N85-35069
Detector requirements for intensity interferometry measurements 24 p4147 N85-35709
Status of the zeta(8.3) [DE85-013070] 24 p4149 N85-35724
Hadron cross sections at ultra high energies and unitarity bounds on diffraction dissociation [HE-1.1-3] 24 p4170 N85-35851
On total cross sections and slopes at superhigh energies [HE-1.1-4] 24 p4170 N85-35852
Hadron thermodynamics in relativistic nuclear collisions [HE-1.1-8] 24 p4171 N85-35856
Estimation of the total inelasticity coefficient in interaction of greater than or equal to 20 TeV hadrons with lead [HE-1.1-9] 24 p4171 N85-35857
1Single particle momentum and angular distributions in hadron-hadron collisions at ultrahigh energies [HE-1.2-1] 24 p4171 N85-35860
Empirical description of the hadron-hadron and hadron-nucleus interaction at the accelerator energy range [HE-1.2-4] 24 p4171 N85-35862
Low P sub T hadron-nucleus interactions [HE-1.2-7] 24 p4172 N85-35865
Angular distribution and multiplicity of backward hadrons in hFe interactions at 0.5-5.0 TeV energies (PION Experiment) [HE-1.2-8] 24 p4172 N85-35866
Nucleon-nucleus interactions from JACEE 24 p4173 N85-35869
A unification of the interactions and the diffractive processes 24 p4173 N85-35870
Is the inelastic charge-exchange contribution constant at the large X and superhigh energies? Qaut 01Kuchin, I. A. 24 p4173 N85-35871
General consequences of the violated Feynman scaling 24 p4173 N85-35872
Propagation of cosmic rays through the atmosphere in the quark-gluon strings model 24 p4173 N85-35873
Scaling violation in the fragmentation region of inclusive nucleon spektrum 24 p4173 N85-35874
Physical meaning of the multiplicities of emitted nucleons in hadron-nucleus collisions 24 p4174 N85-35877
How are particle production, nucleon emission and target fragment evaporation processes interrelated in hadron-nucleus collisions? 24 p4174 N85-35878
Experimental study of the space-time development of the particle production process in hadron-nucleon collisions, using massive target nucleus as a detector 24 p4174 N85-35879
Experimental evidence of the decrease of kinetic energy of hadrons in passing through atomic nuclei 24 p4174 N85-35880
Energy-range relations for hadrons in nuclear matter 24 p4174 N85-35881
Scattering and stopping of hadrons in nuclear matter 24 p4174 N85-35882
Measurements of hadron mean free path for the particle-producing collisions in nuclear matter 24 p4174 N85-35883
The phi-meson and Chiral-mass-meson production in heavy-ion collisions as potential probes of quark-gluon-plasma and Chiral symmetry transitions 24 p4175 N85-35884
Heavy flavours production in quark-gluon plasma formed in high energy nuclear reactions 24 p4175 N85-35886
Observation of direct hadronic pairs in nucleus-nucleus collisions in JACEE emulsion chambers [HE-1.4-5] 24 p4176 N85-35893
Inclusive angular distribution of alpha and Li fragments produced in the Fe-C and Fe-Pb collisions at 1.88 GeV/u [HE-1.4-11] 24 p4177 N85-35898
Experiment Pamir-3. Coplanar emission of high energy gamma-quanta at interaction of hadrons with nuclei of air atoms at energies above 10 to the 7th power GeV [HE-1.4-12] 24 p4177 N85-35899
Japan - USSR joint emulsion chamber experiment at Pamir [HE-3.1-1] 24 p4177 N85-35901
Intensities of high-energy cosmic rays at Mount Kanbala [HE-3.1-2] 24 p4177 N85-35902
High energy gamma-rays and hadrons at Mount Fuji [HE-3.1-3] 24 p4177 N85-35903
Hadron intensity and energy spectrum at 4380 m above level [HE-3.1-7] 24 p4178 N85-35905
Some characteristic cosmic ray events and an attempt at their explanation [HE-3.1-8] 24 p4178 N85-35906
Scaling violation in fragmentation region at energies above 10-15 eV based on the data on cosmic ray hadron component [HE-3.1-11] 24 p4178 N85-35909
Jets in air-jet family [HE-3.2-1] 24 p4179 N85-35912
Scaling violation in hadron-nucleus interaction [HE-3.2-8] 24 p4179 N85-35916
Few-particles generation channels in inelastic hadron-nuclear interactions at energy approximately equals 400 GeV [HE-3.2-9] 24 p4179 N85-35917
Study of hadron bundles observed in Chacaltaya two-story emulsion chamber [HE-3.3-4] 24 p4180 N85-35922
Penetrative nature of high energy showers observed in Chacaltaya emulsion chamber [HE-3.3-5] 24 p4180 N85-35923
Anomalous correlation between hadron and electromagnetic particles in hadron and gamma-ray families [HE-3.3-6] 24 p4180 N85-35924
Atmospheric interactions detected in both the upper and the lower chambers at Chacaltaya [HE-3.3-7] 24 p4180 N85-35925
Lateral distribution of high energy hadrons and gamma ray in air shower cores observed with emulsion chambers [HE-3.3-8] 24 p4180 N85-35926
A cosmic ray super high energy multicore family event. 2: Structure and fragmentation characteristics of the jets [HE-3.4-2] 24 p4181 N85-35931
Observation of super high energy big family with large scale Fe emulsion chambers [HE-3.4-3] 24 p4182 N85-35932
A halo event created at 200 m above the Chacaltaya emulsion chamber [HE-3.4-5] 24 p4182 N85-35933
A binocular-type atmospheric interaction generating sequential exotic features [HE-3.4-6] 24 p4182 N85-35934
Gamma-hadron families and scaling violation [HE-3.4-7] 24 p4182 N85-35935
Super-family P2 C-96-125 observed by Japan-URSS Joint Emulsion Chamber Experiment [HE-3.4-8] 24 p4182 N85-35936
Experiment Pamir-2. Fianit: A giant super-family with halo (Epsilon sub 0 at approximately 10(17) eV) [HE-3.4-10] 24 p4182 N85-35938
Experiment Pamir-4: Analysis of superfamily with halo of electromagnetic nature detected in deep XEC [HE-3.4-11] 24 p4183 N85-35939
A search for mini-clusters in Japan-USSR Joint Experiment at Pamir [HE-3.5-2] 24 p4183 N85-35941
Mini-clusters [HE-3.5-3] 24 p4183 N85-35942
Giant mini-clusters as possible origin of halo phenomena observed in super-families [HE-3.5-4] 24 p4183 N85-35943
LPM effect and primary energy estimations [HE-3.6-4] 24 p4185 N85-35953
Experimental basis for the models of cascade propagation in atmosphere [HE-3.6-6] 24 p4185 N85-35954
Relation between gamma-ray family and EAS core: Monte-Carlo simulation of EAS core [HE-3.6-7] 24 p4185 N85-35955
Comparison of big event with calculations of the air shower development [HE-3.6-8] 24 p4185 N85-35956
On mini-cluster observed by Chacaltaya emulsion chamber experiment [HE-3.6-12] 24 p4185 N85-35959
A comparative analysis of gamma and hadron families at the superhigh energies recorded in experiment Pamir [HE-3.7-1] 24 p4185 N85-35960
Hadrons registration in emulsion chamber with carbon block [HE-3.7-3] 24 p4186 N85-35962
Intensities of high-energy cosmic rays at Mount Kanbala [HE-3.7-5] 24 p4186 N85-35964
Structured events in Pamir carbon X-ray chambers [HE-3.7-7] 24 p4186 N85-35965
Analysis of the hadron component in E.A.S. 24 p4187 N85-35971
Electrons, muons and hadrons in extensive air showers and how do they depend on nuclear interaction model, part 1 24 p4187 N85-35972
High energy hadrons in extensive air showers 24 p4187 N85-35976
Dependence of the average spatial and energy characteristics of the hadron-lepton cascade on the strong interaction parameters at superhigh energies 24 p4188 N85-35977
Hadronic components of EAS by rigorous saddle point method in the energy range between 10(5) and 10(8) GeV 24 p4188 N85-35978
About increase of the large transvere momentum processes fraction in hA interactions at energies 5.10(14) - 10(16) eV according to the data on E.A.S. hadrons 24 p4188 N85-35979
Phenomenology of soft hadron interactions and the relevant EAS data 24 p4188 N85-35980
The maximum depth of shower with E sub 0 larger than 10(17) eV on average characteristics of EAS different components 24 p4188 N85-35981
Sensivity of depth of maximum and absorption depth of EAS to hadron production mechanism 24 p4188 N85-35982
Theoretical study of EAS hadronic structure 24 p4189 N85-35991
Muon spectrum in air showers initiated by gamma rays [HE-4.5-4] 24 p4195 N85-36028

Electromagnetic and muonic structure of showers initiated by gamma-rays and by hadrons
[HE-4.5-6] 24 p4195 N85-36030
The muon content of gamma-ray showers
[HE-4.5-7] 24 p4195 N85-36031
Simulation of gamma-initiated showers
[HE-4.5-10] 24 p4195 N85-36033
Nuclear cascades in electromagnetic showers produced by primary gamma-quanta in the atmosphere
[HE-4.5-16] 24 p4196 N85-36038
Investigation of cosmic rays in very short time scales
[HE-4.6-7] 24 p4197 N85-36044
A facility for investigation of multiple hadrons at cosmic-ray energies
[HE-4.6-8] 24 p4197 N85-36045
Sub-luminal pulses from cosmic ray air showers
[HE-4.7-13] 24 p4200 N85-36063
Anomalies in cosmic rays: New particles versus charm?
[HE-5.4-9] 24 p4208 N85-36120
Collimated groups of particles as possible manifestation of heavy meson production
[HE-5.4-14] 24 p4208 N85-36124
Energetic delayed hadrons in large air showers observed at 5200m above sea level
[HE-6.2-9] 24 p4211 N85-36145
Observation of genetic relation among new phenomena Geminion, Chiron and mini-Centauro
[HE-6.2-16] 24 p4212 N85-36152
Tien-Shan effect and charmed particles
[HE-6.2-17] 24 p4212 N85-36153

HAFNIUM
Long range ordered alloys modified by addition of niobium and cerium
[DE85-011661] 20 p3431 N85-31285

HAFNIUM ALLOYS
Temperature variation of resistivity of certain alloys based on transition and simple metals in amorphous and crystalline states 15 p2496 N85-25399

HALF LIFE
The I-Pu-Xe age of the Moon
04 p0584 N85-13729
Study of proton and neutron activation of metal samples in low Earth orbit
[NASA-CR-171596] 21 p3558 N85-32130

HALF PLANES
Stresses in a half-plane containing either a pressurized hole or an interference-fit disc
[ARL/STRUC-R-409] 12 p1865 N85-21700
Elastic response of a half-plane to a bonded interference-fit disc of the same material
[ARL/STRUC-R-406] 12 p1865 N85-21701

HALF SPACES
Halfspace representations of extrusions, solids of revolution and pyramids
[DE84-015005] 01 p0104 N85-10700
Propagation of longitudinal elastic waves in multilayered half-space 02 p0273 N85-11779
Acoustic emission waveforms in a half space
[AD-A146322] 03 p0417 N85-12664
Elastic wave scattering from an interface crack in a layered half space 13 p2101 N85-23095
Interaction among inhomogeneities and inclusions
[AD-A153114] 17 p2979 N85-28419
Transient dynamic solutions of some half space problems by the boundary element method
19 p3283 N85-30360
Numerical experiment of elastic wave propagation by framework model
[DRIC-T-7462] 22 p3795 N85-33511

HALIDES
NT ALKALI HALIDES
NT ALUMINUM CHLORIDES
NT BERYLLIUM FLUORIDES
NT BORON FLUORIDES
NT BROMIDES
NT CADMIUM FLUORIDES
NT CALCIUM CHLORIDES
NT CALCIUM FLUORIDES
NT CARBON TETRACHLORIDE
NT CESIUM IODIDES
NT CHLORIDES
NT COPPER CHLORIDES
NT DICHLORIDES
NT DIFLUORIDES
NT FLUORIDES
NT HYDROBROMIC ACID
NT HYDROCHLORIC ACID
NT HYDROFLUORIC ACID
NT HYDROGEN CHLORIDES
NT IRON CHLORIDES
NT LITHIUM CHLORIDES
NT LITHIUM FLUORIDES
NT MAGNESIUM CHLORIDES
NT MAGNESIUM FLUORIDES
NT METAL HALIDES
NT OXYFLUORIDES
NT OXYHALIDES
NT POTASSIUM CHLORIDES
NT SILVER CHLORIDES
NT SILVER HALIDES
NT SILVER IODIDES
NT SODIUM CHLORIDES
NT SODIUM IODIDES
NT STRONTIUM FLUORIDES
NT SULFUR FLUORIDES
NT TITANIUM CHLORIDES
NT URANIUM FLUORIDES
NT ZINC CHLORIDES
Electronic-to-vibrational energy transfer studies of singlet molecular oxygen and hydrogen halides
[AD-A145587] 02 p0277 N85-11802
Combustion kinetics of metal oxide and halide radicals
[AD-A148521] 08 p1122 N85-17076
Spectroscopic studies of lasing transitions in the diatomic mercury halides
[AD-A151553] 15 p2563 N85-25809
Metal vapor lasers and their applications
[ISL-CO-218/84] 22 p3791 N85-33488
Thermodynamic data for mineral technology
[PB85-184331] 22 p3803 N85-33560

HALL COEFFICIENT
U HALL EFFECT

HALL CURRENTS
U ELECTRIC CURRENT
U HALL EFFECT

HALL EFFECT
Calibration of hall probes
[CSIR-NAC-83-04] 01 p0116 N85-10794
A study of defects in neutron transmutation doped silicon: Gallium by hall effect analysis
[AD-A146047] 03 p0433 N85-12758
Implications of the chiral anomaly for quantum Hall effect devices
[NUB-2662] 05 p0629 N85-14029
Motion of electrons in non polar classical liquids
[DE84-013609] 05 p0727 N85-14672
Anomalous electronic transport in boron carbides
[DE84-015620] 06 p0868 N85-15518
Quasiparticle aggregation in the Fractional Quantum Hall Effect
[DE85-001574] 10 p1565 N85-19868
Power circuit utilizing self-excited Hall effect switch means
[AD-D011505] 12 p1832 N85-21496
High temperature position sensors based on monolithic GaAs Hall IC
[BMFT-FB-T-84-266] 17 p2969 N85-28337
Activities of the Solid State Physics Research Institute
[NASA-CR-175899] 17 p3042 N85-28818
Hall mobility in fluid argon
[DE85-007288] 17 p3045 N85-28840
Quantized Hall conductance as a topological invariant
[DE85-007796] 18 p3193 N85-29808
Quantized Hall effect in two-dimensional electron systems
[AD-A154347] 19 p3259 N85-30211
Fractional statistics and fractional quantized Hall effect
[DE85-007833] 19 p3375 N85-30940
Electrical properties of bulk grown nitrogen doped silicon
[AD-A155471] 21 p3581 N85-32266
Gauge invariance and fractional quantized Hall effect
[DE85-007832] 23 p3985 N85-34716

HALLEY'S COMET
A cometary ion mass spectrometer
[NASA-CR-174328] 08 p1164 N85-17343
Airborne observations of comets
08 p1244 N85-17853
Extended atmospheres of outer planet satellites and comets
[NASA-CR-174398] 09 p1416 N85-18933
The international VEGA 'Venus-Halley' (1984-1986 experiment: Description and scientific objectives
[NASA-TM-77536] 12 p1960 N85-22324
Averaging of equations of cometary orbital motion with allowance for nongravitational effects
13 p1978 N85-22411
History and future views on solar cells of Japanese scientific satellites 13 p2005 N85-22566
Giotto solar array: Design, manufacture and test
13 p2008 N85-22589
Development of Halley's Comet explorer PLANET-A solar array 13 p2010 N85-22608
Research in planetary studies and operation of Mauna Kea Observatory
[NASA-CR-175618] 13 p2169 N85-23460
Halley's Comet, a bibliography
[LC-84-600109] 13 p2204 N85-23674
Giotto plasmasheath and wake charging near Halley's Comet: Revised parameters 14 p2245 N85-23915
Anticipated impact plasma problems for the COPERNIC-RPA experiment in the cometary environment — Giotto mission 14 p2245 N85-2391
An impact plasma monitor for cometary missions — Giotto, VEGA 14 p2245 N85-2391
Spacecraft environment during the Giotto-Halley encounter: A summary 14 p2246 N85-2392
Towards the Halley Comet 14 p2399 N85-2470
The astrometry network of the IHW and the P/Crommelin trial run results 14 p2435 N85-2501
Near-nucleus studies of Comet Halley
14 p2435 N85-2501
Kitt Peak measurements of P/Halley positions
14 p2436 N85-2502
The astrometry network of observers in China
14 p2436 N85-2502
The astrometry network of observers in Japan
14 p2436 N85-2502
The astrometry network of observers in USSR
14 p2436 N85-2502
The IHW reference star catalogs for Comets Halley and Giocobini-Zinner 14 p2436 N85-2503
The orbits of Comets Halley and Giocobini-Zinner
14 p2437 N85-2503
The orbital motion of Comet Halley
14 p2437 N85-2504
The work on Comet Halley's orbit at ESOC
14 p2438 N85-2504
Astrometric needs for the ISEE-3/ICE mission to Comet Giocobini-Zinner 14 p2438 N85-2504
Determination of the observation conditions of celestial bodies with the aid of the DISPO system
[NAS 1.15:77632] 14 p2438 N85-2504
Kovtunenko comments on Vega flight plan, instrumentation 15 p2482 N85-2531
Comments on Vega mission 15 p2482 N85-2531
Press conference on flight of Vega spacecraft
15 p2482 N85-2532
Sixteenth Lunar and Planetary Science Conference. Press abstracts
[NASA-CR-175692] 15 p2680 N85-2654
Dust emission of Comet Halley at large heliocentric distances 15 p2681 N85-265
TASS update on flights of Vega-1 and Vega-2
16 p2722 N85-2680
Kovtunenko discusses Vega Project
16 p2722 N85-2680
French and West German equipment for Vega Project
16 p2722 N85-2680
Swedish space program includes research satellite
18 p3088 N85-29113
Program for observations of Halley's comet
22 p3732 N85-3313
The 1986 National Aeronautics and Space Administration authorization
[GPO-47-635] 24 p4166 N85-3552
Comet Halley returns: A teachers' guide 1985-19
[NASA-EP-197] 24 p4168 N85-3553

HALOCARBONS
NT FLUOROCARBONS
Flow of nitrogen-pressurized Halon 1301 in fire extinguishing systems
[NASA-CR-174271] 07 p0900 N85-1570
New liquid cathodes for lithium batteries. Part A: Halocarbons
[AD-A148433] 08 p1178 N85-1743

HALOGEN COMPOUNDS
NT ALKALI HALIDES
NT ALUMINUM CHLORIDES
NT AMMONIUM PERCHLORATES
NT BERYLLIUM FLUORIDES
NT BORON FLUORIDES
NT BROMIDES
NT BROMINE COMPOUNDS
NT CADMIUM FLUORIDES
NT CALCIUM CHLORIDES
NT CALCIUM FLUORIDES
NT CARBON TETRACHLORIDE
NT CARBON TETRAFLUORIDE
NT CESIUM IODIDES
NT CHLORIDES
NT CHLORINE COMPOUNDS
NT CHLORINE OXIDES
NT CHLOROSILANES
NT COPPER CHLORIDES
NT DDT
NT DICHLORIDES
NT DIFLUORIDES
NT DIFLUORO COMPOUNDS
NT FLUORIDES
NT FLUORINE COMPOUNDS
NT FLUORINE ORGANIC COMPOUNDS
NT FLUORITE
NT FLUORO COMPOUNDS
NT FLUOROCARBONS
NT FLUOROHYDROCARBONS

NT FLUOROPOLYMERS
NT HALIDES
NT HALOCARBONS
NT HYDROBROMIC ACID
NT HYDROCHLORIC ACID
NT HYDROFLUORIC ACID
NT HYDROGEN CHLORIDES
NT IODIDES
NT IODINE COMPOUNDS
NT IRON CHLORIDES
NT LITHIUM CHLORIDES
NT LITHIUM FLUORIDES
NT LITHIUM IODATES
NT MAGNESIUM CHLORIDES
NT MAGNESIUM FLUORIDES
NT METAL FLUORIDES
NT METAL HALIDES
NT OXYFLUORIDES
NT OXYHALIDES
NT PERCHLORATES
NT PERFLUOROALKANE
NT POLYTETRAFLUOROETHYLENE
NT POTASSIUM CHLORIDES
NT POTASSIUM PERCHLORATES
NT SILVER CHLORIDES
NT SILVER HALIDES
NT SILVER IODIDES
NT SODIUM CHLORIDES
NT SODIUM IODIDES
NT STRONTIUM FLUORIDES
NT SULFUR FLUORIDES
NT TITANIUM CHLORIDES
NT URANIUM FLUORIDES
NT ZINC CHLORIDES

Catalyzed low burning rate propellants for upper-stage solid rocket motor
[NAL-TR-805] 03 p0339 N85-12181

Structural phase transitions in doped hexahalogen metallates 03 p0426 N85-12721

HALOGENATION
NT CHLORINATION
NT FLUORINATION

Process for functionalizing alkanes
[DE85-006420] 23 p3909 N85-34219

HALOGENS
NT BROMINE
NT BROMINE ISOTOPES
NT CHLORINE
NT FLUORINE
NT IODINE
NT IODINE ISOTOPES

Determination of halogens and sulfur in organic compounds and polymers by combustion-ion chromatography
[DE84-016186] 05 p0614 N85-13921

Polymerization and halogen scrambling behavior of phenyl-substituted cyclotriphosphazenes
[AD-A146366] 06 p0771 N85-14930

Halogen mass flow rate detection system
[AD-D011398] 08 p1166 N85-17352

Adsorption thermodynamics and surface transport of metal catalyst poisons
[DE85-003750] 12 p1802 N85-21301

RF-Primed high power halogen vial apparatus
[AD-D011545] 12 p1935 N85-22156

HALOS

Highly ionized gas associated with the small Magellanic cloud 11 p1745 N85-20976

Galactic absorption lines measured from the IUE low dispersion spectra of active galaxies
11 p1745 N85-20977

Dark halo craters and the thickness of grooved terrain on Ganymede 13 p2173 N85-23484

Jupiter's ring system resolved: Physical properties inferred from the Voyager images
20 p3546 N85-32069

Evidence for a dynamical halo around the edge-on galaxy NGC 4631
[OG-6.2-1] 22 p3869 N85-34102

Halo of NGC 4631 and models of cosmic-ray transport
[OG-6.2-3] 22 p3869 N85-34103

The extent of the local hi halo
[NASA-CR-176115] 23 p3987 N85-34724

A cosmic ray super high multicore family event. 1: Experiment and general features
[HE-3.4-1] 24 p4181 N85-35930

A halo event created at 200 m above the Chacaltaya emulsion chamber
[HE-3.4-5] 24 p4182 N85-35933

On the halo events observed by Mount Fuji and Mount Kanbala Emulsion Chamber Experiments
[HE-3.4-8] 24 p4182 N85-35937

Experiment Pamir-2. Fianit: A giant super-family with halo (Epsilon sub 0 at approximately 10(17) eV)
[HE-3.4-10] 24 p4182 N85-35938

Experiment Pamir-4: Analysis of superfamily with halo of electromagnetic nature detected in deep XEC
[HE-3.4-11] 24 p4183 N85-35939

Giant mini-clusters as possible origin of halo phenomena observed in super-families
[HE-3.5-4] 24 p4183 N85-35943

Structure of super-families
[HE-3.5-7] 24 p4183 N85-35944

Extremely high energy hadron and gamma-ray families(3). Core structure of the halo of superfamily
[HE-3.5-8] 24 p4183 N85-35945

Numerical analysis of electromagnetic cascades in emulsion chambers
[HE-3.5-9] 24 p4184 N85-35946

HAMILTON-JACOBI EQUATION

The period of orbit as a test of the general theory of relativity 05 p0742 N85-14772

Viscosity solutions of Hamilton-Jacobi equations at the boundary
[AD-A147444] 07 p1032 N85-16553

Neumann type boundary conditions for Hamilton-Jacobi equations
[AD-A149069] 10 p1546 N85-19746

Hamilton-Jacobi equations in infinite dimensions. Part 1. Uniqueness of viscosity solutions
[AD-A149094] 10 p1546 N85-19749

A remark on regularization in Hilbert spaces
[AD-A149046] 10 p1552 N85-19787

HAMILTONIAN FUNCTIONS

Stable and chaotic dynamical systems and their singularities in the complex time plan
[DE84-011780] 01 p0035 N85-10222

Spurious center of mass effects in a dynamically determined basis
[CSIR-TWISK-310] 01 p0109 N85-10732

Equipartition threshold in nonlinear large Hamiltonian systems: The Fermi-Pasta-Ulam model
[NOTA-INTERNA-819] 02 p0255 N85-11670

Stochasticity and transport in Hamiltonian systems
02 p0282 N85-11836

Long-time tail in the two-wave model
02 p0282 N85-11837

On existence and uniqueness of solutions of Hamilton-Jacobi equations
[AD-A147597] 07 p1033 N85-16560

An invariant measure for the equation u sub tt - u sub xx + u3 = O
[AD-A147300] 08 p1210 N85-17612

Periodic solutions of prescribed energy for a class of Hamiltonian systems
[AD-A149487] 10 p1548 N85-19764

Geometric Hamiltonian structures and perturbation theory
[DE85-002005] 11 p1707 N85-20737

Covariant lie-transformed plasma action principle
[DE85-000285] 11 p1732 N85-20691

Accidental degeneracies, hidden supersymmetries, and spectrum-generating superalgebras
[DE85-003547] 11 p1738 N85-20930

A method of calculating periodic solutions of second order dynamical systems
[AD-A149634] 12 p1920 N85-22058

Stability of permanent rotation modes of asymmetric heavy solid body 14 p2279 N85-24118

Elements of celestial mechanics
14 p2396 N85-24762

On matchings and Hamiltonian cycles in random graphs
[AD-A151015] 14 p2409 N85-24851

Application of quaternions to problems of solid body dynamics in the atmosphere 15 p2481 N85-25313

Eigenvalue approximation methods for quantum lattice Hamiltonians 16 p2858 N85-27627

Hamiltonian picture of the free electron laser and unitary symmetries
[PREPRINT-436] 18 p3114 N85-29281

A numerical investigation of the overlap distribution among pure states in the spin glass phase
[PREPRINT-414] 18 p3172 N85-29659

The Hamiltonian structure of a complex version of the Burgers hierarchy
[PREPRINT-423] 18 p3173 N85-29665

Reduction techniques for infinite-dimensional Hamiltonian systems: Some ideas and applications
[PREPRINT-424] 18 p3173 N85-29666

Further results on the equipartition threshold in large nonlinear Hamiltonian systems
[PREPRINT-426] 18 p3173 N85-29668

Exact invariants in resonance form for time-dependent potentials
[DE85-010733] 19 p3346 N85-30739

One- and two-electron transfer processes in ion-surface scattering
[AD-A154206] 19 p3353 N85-30782

Interacting Boson approximation
[DE85-003016] 22 p3837 N85-33756

Width of nonlinear difference resonances
[DE85-013026] 24 p4148 N85-35719

HAND (ANATOMY)
NT FINGERS

Computerized sleep staging by detecting eye and hand movement, delta EEG activity and EMG, using portable solid state technique — spaceborne experiments
05 p0695 N85-14475

A control model: Interpretation of Fitts' law
05 p0706 N85-14526

Mechanical properties for the grasp of a robotic hand
[AD-A150062] 12 p1860 N85-21669

Instrument for determining spatial coordination of hand movements 14 p2387 N85-24702

Investigation of the requirement for auxiliary heating of Canadian forces personnel
[AD-A151950] 16 p2841 N85-27522

Hand controllers for teleoperation. A state-of-the-art technology survey and evaluation
[NASA-CR-175890] 17 p3002 N85-28559

An analysis of multi-fingered hands
20 p3462 N85-31504

HANDBOOKS
NT USER MANUALS (COMPUTER PROGRAMS)

Information Center handbook
[PB84-211341] 03 p0439 N85-12795

Economic analysis handbook
[AD-A146263] 03 p0441 N85-12805

Vibration data analysis system for SNLA area 3 reference manual
[DE84-016207] 04 p0514 N85-13275

National Bureau of Standards passive solar test facility: Instrumentation and site handbook
[PB85-100451/GAR] 07 p0968 N85-16148

Project manager's handbook for special projects
[AD-A147913] 07 p1053 N85-16683

Technical order managers handbook: Utilization assessment
[AD-A147579] 07 p1055 N85-16694

User's guide for the Photochemical Box Model (PBM)
[PB85-137164] 11 p1682 N85-20602

Instructor's handbook on meteorological instrumentation
[PB85-105930] 11 p1688 N85-20615

Atmospheric handbook: Atmospheric data tables available on computer tape
[PB85-108512] 12 p1891 N85-21867

Review of US guide on medication and flying
12 p1904 N85-21958

An overview of the MIL-HDBK-5 program
[AD-A147788] 14 p2254 N85-23970

Installation, maintenance and operating manual for the Lucas-type fuel injection system of the 3 B rotary engine
[NASA-TM-77872] 15 p2568 N85-25846

AWS (Air Weather Service) climatic briefs: Asia
[AD-A151944] 16 p2835 N85-27481

The GfW handbook for data compilation of irradiation tested electronic components, volume 3
[HMI-B-353-VOL-3] 17 p2956 N85-28258

Handbook on superconductivity: The large-scale applications. Chapter 4
[DE85-008170] 17 p3044 N85-28838

State Weights and Measures Laboratories: Program handbook
[PB85-183358] 18 p3111 N85-29263

Technical guide for estimating fugitive dust impacts from coal handling operations. Volume 1: Project summary
[DE85-010948] 19 p3309 N85-30515

Human Engineering Guide to Equipment Design (HEGED)
[AD-A154087] 19 p3331 N85-30631

User handbook for block 5 silicon solar cell modules
[NASA-CR-176043] 20 p3483 N85-31644

Middle Atmosphere Program. Handbook for MAP, volume 11
[NASA-CR-176107] 22 p3814 N85-33625

International flight planning handbook
[AD-A156330] 24 p4062 N85-35177

Fire service emergency management handbook
[AD-A155780] 24 p4084 N85-35313

A guide for new environmental coordinators
[AD-A156327] 24 p4113 N85-35496

Air university commander's and supervisor's guide on substance abuse
[AD-A156336] 24 p4133 N85-35622

Recommendations for content revision and alternate delivery modes for the Human Engineering Guide to Equipment Design (HEGED)
[AD-A155781] 24 p4134 N85-35624

Time domain reflectometry for SLC BPM system
[DE85-012389] 24 p4155 N85-35758

HANDLING EQUIPMENT
NT CRANES
NT GANTRY CRANES

Depot modernization at the Defense Logistics Agency
[AD-P004008] 03 p0308 N85-11966

Dental multi-purpose slowspeed handpieces test and evaluation
[AD-A155764] 24 p4130 N85-35606

HANDLING QUALITIES
U CONTROLLABILITY

HANG GLIDERS
An assessment of the suitability of the BHGA structural test rig for aerodynamic testing of hang gliders
[CA-8505] 17 p2896 N85-27853

HANGARS
Hangar destratification investigation
[AD-A145049] 01 p0012 N85-10076
Hangar heating and energy conservation manual
[AD-A147893] 07 p0910 N85-15762

HARBORS
USSR report: Transportation
[JPRS-UTR-84-008] 14 p2208 N85-23694
LORAN-C harbor and harbor entrance survey: Charleston, South Carolina
[AD-A154875] 21 p3554 N85-32108
Bibliography on tidal hydraulics. Report 2. Supplement 9: Supplementary material compiled from June 1980 - June 1983. Tidal flows in rivers and harbors
[AD-A155990] 24 p4125 N85-35574

HARDENERS
Structure and abrasive resistance of iron based alloys rich in hardening components 01 p0054 N85-10360

HARDENING
Influence of heat treatment parameters on the properties of induction hardened Ni-Cr-Mo steels
[BLL-BISI-TRANS-2499-(9022.06)] 17 p2926 N85-28053

HARDENING (MATERIALS)
NT CARBURIZING
NT HOT PRESSING
NT NITRIDING
NT PRECIPITATION HARDENING
NT PULSE HEATING
NT SHOT PEENING
NT SILICONIZING
NT STRAIN HARDENING
NT WORK HARDENING
USSR report: Machine tools and metalworking equipment
[JPRS-UMM-84-019] 01 p0035 N85-10214
Electro-spark case-hardening of contoured surfaces 01 p0035 N85-10216
Directional nature of strengthening during thermomechanical treatment
[BLL-M-35746-(5828.4)] 02 p0175 N85-11174
An investigation into the superhardening effect in molybdenum-free steel with specific reference to alloy substitution 02 p0180 N85-11209
The determination of soluble and insoluble boron in steel by emission spectrometry using an inductively coupled plasma and a scanning monochromator 02 p0180 N85-11211
Defining effect of hardening on mean yield strength in deformation zone
[BLL-M-35934-(5828.4)] 05 p0647 N85-14154
Study of superplastic alloys based on Al-Zn-Ca 10 p1442 N85-19092
Influence of laser hardening on mechanical properties of type 45 steel with various preliminary heat treatments 10 p1446 N85-19111
Diffusion welding with forced deformation of heat-resistant nickel-based dispersion hardened alloy 10 p1449 N85-19130
Thermal hardening of welded joints in titanium alloys with various structures 13 p2032 N85-22734
Influence of short-range order on deformation mechanisms in solid solutions
[DE85-006374] 14 p2258 N85-23989
Trapping model analysis of annihilation line narrowing in some plastically deformed metals and alloys
[AERE-R-10593] 14 p2258 N85-23995
Laser surface treatments 14 p2306 N85-24284
Effect of deep cooling on crack resistance and low-temperature hardening of aluminum alloys 15 p2496 N85-25396
Hardening of titanium alloy electric-arc welded joints 15 p2514 N85-25513
Determination of failure characteristics of materials and structures
[AD-A152073] 16 p2800 N85-27266
On the accurate representation of large strain non-proportional plastic flow in ductile materials
[DE85-007106] 16 p2801 N85-27273
Heat resistant Carbon Fiber Reinforced Plastics (CFRP) hardening equipment
[MBB/LFA33/CFK/PUB/007] 17 p2916 N85-27976
X-ray crystallography of steel U8 after pulsed laser hardening
[BLL-BISI-22444-(9022.06)] 17 p2925 N85-28038
Internal structure of GP zones in dilute Al-Cu alloys 19 p3238 N85-30073
Effect of ScAl3 phase dispersion on hardening of alloy Al-6.3 percent Mg-0.21 percent Sc 19 p3241 N85-30096
Durability of reinforced hard-alloy draw plates
[BLL-M-36278-(5828.4)] 20 p3465 N85-31526
Effect of prior warm rolling on the retained austenite content and hardening response of VIM-VAR (vacuum-induction melted-vacuum-arc remelted) AISI M-50 steel
[AD-A156145] 24 p4079 N85-35281

HARDENING (SYSTEMS)
Invited papers: DNA ICBM technical R and D program 09 p1333 N85-18379
Ground shock effect on soil field inclusions 09 p1336 N85-18403

HARDNESS
NT KNOOP HARDNESS
NT MICROHARDNESS
Sintered silicon nitride workpiece
[NASA-TM-77600] 01 p0021 N85-10129
Some reflections on the competition among different hard materials in industrial applications 02 p0177 N85-11192
The chemical nature of the fiber/resin interface in composite materials 04 p0485 N85-12953
Creep-rupture behavior of iron superalloys in high-pressure hydrogen
[NASA-CR-174411] 10 p1441 N85-19078
Effect of temperature and deformation rate on hardness of copper 11 p1605 N85-20090
Investigation of vanadium solid solution and zeta phase regions of vanadium-carbon system
[DE85-002678] 11 p1605 N85-20092
Deposition of diamondlike carbon films
[NASA-CASE-LEW-14080-1] 11 p1615 N85-20153
Case depth on flanks of gears for helicopter gearboxes 14 p2222 N85-23780
Sintering reactions, structure and properties of a cobalt free nonconventional hard material
[DE85-007704] 18 p3076 N85-29025
Age hardening and atomic structure of an aluminum-6 at. % silver alloy
[DE85-009977] 18 p3077 N85-29031
Tests on zirconium nitride coatings applied to SW 18 steel using the chemical vapor deposition method 24 p4078 N85-35271
Effect of thermal ageing on the mechanical properties of PWR pressure vessel steels and weldments
[AERE-R-11460] 24 p4078 N85-35275

HARDNESS TESTS
Laboratory evaluation of Electromagnetic Pulse (EMP) hardness testing concepts for electrical conduit systems
[AD-A145466] 02 p0190 N85-11273

HARDWARE
Microcomputers in Hungary 01 p0115 N85-10786
ATE user's view on design for maintainability 08 p1064 N85-16737
Hardware/software codesign for maintainable systems 08 p1066 N85-16753
Fast arithmetic for microcomputers 08 p1140 N85-17180
VICOM technical description
[REPT-611-0012-REV-A] 08 p1202 N85-17563
Development and operation of a real-time data acquisition system for the NASA-LaRC differential absorption lidar
[NASA-CR-174384] 09 p1366 N85-18583
DDL system: Design systhesis of digital systems
[NASA-CR-170759] 09 p1366 N85-18584
National Machine Tools Conference slated for 1985: Conference agenda, papers 10 p1460 N85-19202
A low-cost, general purpose image processing system
[INPE-3292-PRE/607] 10 p1537 N85-19690
ZTLCK: A subroutine package for the IBM personal computer to support the Ziatech ZT1488 real time clock
[LA-10146-MS] 12 p1914 N85-22014
USSR report: Cybernetics, computers and automation technology
[JPRS-UCC-85-003] 15 p2625 N85-26174
Active control technology: Past, present, future 16 p2711 N85-26731
Flight Experiment Demonstration System (FEDS) functional description and interface document
[NASA-CR-175290] 16 p2717 N85-26769
Multiple array processors for ocean acoustic problems
[AD-A152174] 16 p2860 N85-27641
Shuttle-tethered satellite system definition study extension
[NASA-CR-171473] 17 p2907 N85-27923
Hardware test program for evaluation of baseline range/range rate sensor concept
[NASA-CR-175910] 17 p2947 N85-28194
Synchronization and fault-masking in redundant real-time systems
[NASA-TM-87476] 17 p3015 N85-28644
Energy efficient engine integrated core/low spool fan hardware design report
[NASA-CR-168137] 19 p3218 N85-29864
Methods for design and evaluation of integrated hardware-software systems for concurrent computation
[NASA-CR-176066] 20 p3515 N85-31801

HARMONIC ANALYSIS
NT TESSERAL HARMONICS
NT ZONAL HARMONICS
Harmonizable, Cramer, and Karhunen classes of processes
[AD-A144964] 01 p0113 N85-10767
Stochastic motor blade dynamics
[AD-A146312] 03 p0318 N85-12254
NATFREQ users manual: A FORTRAN 4 program for computing natural frequencies, mode shapes and drag coefficients for taut strumming cables with attached masses and spring-mass combinations
[AD-A146058] 03 p0407 N85-12800
Linear harmonic analysis for Stirling machines and second law analysis of four important losses
[DE84-016595] 04 p0573 N85-13866
Linear harmonic analysis of Stirling engine thermodynamics
[DE84-016646] 04 p0574 N85-13867
Effects of vane/blade ratio and spacing on fan noise, volume 1
[NASA-CR-174664] 10 p1553 N85-19791
A study for calculating rotor loads using free vortex concept 11 p1620 N85-20184
Three algorithms for parametric frequency domain system identification
[DE85-002801] 11 p1706 N85-20735
A deformation analysis of flat flexible gear and its equation of original curved surfaces
[NASA-TM-77493] 12 p1859 N85-21680
Harmonic analysis and Radon transforms on pencils of geodesics
[CWI-PM-R8413] 12 p1922 N85-22074
Harmonic analysis of the solar magnetic field 14 p2454 N85-25154
Acoustic radiation from concentric shells containing an inner fluid
[AD-A155476] 21 p3700 N85-32981
Hardy spaces and the L sup P-Neumann problem for Laplace's equation in a Lipschitz domain
[CTH-MATH-1985-02] 22 p3836 N85-33749
Arrival directions of large air showers, low-mu showers and old-age low-mu air showers observed at Mt. Chacaltaya
[OG-5.3-2] 22 p3884 N85-34069
Anisotropy of cosmic rays of energy 10 (15) eV to 10 (17) eV observed at Akeno
[OG-5.3-3] 22 p3884 N85-34070
Anisotropy and the knee of the energy spectrum
[OG-5.4-10] 22 p3887 N85-34087
Characteristics of cosmic ray pole-equator anisotropy derived from spherical harmonic analysis of neutron monitor data
[SH-4.3-12] 23 p4032 N85-34986
Magnetic fluctuation and cosmic ray diurnal variations
[SH-4.5-21] 23 p4038 N85-35038
On the solar cycle variation in the barometer coefficients of high latitude neutron monitors
[SH-6.1-2] 23 p4044 N85-35077
The conjecture concerning time variations in the solar neutrino flux
[SH-8.1-6] 23 p4049 N85-35111
Optimal estimation of a high degree gravity field from a global set of 1 deg x 1 deg anomalies to degree and order 250
[AD-A156008] 24 p4117 N85-35510

HARMONIC CONTROL
Data processing on the rotor test stand at DFVLR in Brunswick: Microprogrammable interfaces and array processor as key components in a PDP 11 real time data acquisition and processing system
[DFVLR-MITT-85-03] 17 p2906 N85-27821
Fixed gain and adaptive techniques for rotorcraft vibration control
[NASA-CR-177344] 22 p3726 N85-33111
High-speed adaptation algorithm for harmonic corrector 22 p3765 N85-33336

HARMONIC FUNCTIONS
Some families of near-orthonormal analytic and harmonic functions
[AD-A144722] 01 p0110 N85-10748
On some exact solutions in elastostatics in terms of harmonic functions 09 p1332 N85-18387
Annuals of the Finnish Academy of Sciences, series A. 1: Mathematics, volume 8, part 2
[ISSN-0066-1953] 10 p1535 N85-19873
On harmonic functions with integrable maximum modulus 10 p1536 N85-19881
On the integral representation of bisubharmonic functions in Rn 10 p1536 N85-19884

Intertwining functions on compact Lie groups
[CWI-TRACT-5] 14 p2414 N85-24895
Annals of the Scientific Academy of Finland, series A. 1: Mathematics, volume 9
[ISSN-0066-1953] 15 p2633 N85-26229
Harmonic univalent functions
15 p2633 N85-26230
A problem of Burkholder and the existence of harmonic majorants of the absolute value of x sup p in certain domains in R sup d 15 p2634 N85-26236
Some estimates of harmonic majorants
15 p2634 N85-26237
The first three harmonics of solar daily variation caused by the diffusive propagation of galactic cosmic rays through the heliosphere
[SH-4.5-1] 23 p4035 N85-35019

HARMONIC GENERATIONS
Multimode harmonic power measurement of 40 MW pulsed S-band klystrons
[DE85-001560] 09 p1316 N85-18272
Optical second harmonic generation for surface studies
[DE85-000670] 11 p1640 N85-20333
Digital detector of harmonic signals
12 p1840 N85-21549
Four-photon resonant third harmonic generation
[DE85-010070] 19 p3367 N85-30683

HARMONIC GENERATORS
Theory of harmonic generation of finite amplitude ultrasonic waves in solids of hexagonal symmetry
[AD-A146636] 06 p0860 N85-15465
Quasi-optical harmonic gyrotron and gyroklystron
[AD-D011306] 07 p0947 N85-16001

HARMONIC OSCILLATION
Flow instabilities in transonic small disturbance theory
[NASA-TM-86251] 09 p1273 N85-18000
Precision measurement of torsional oscillations induced by gear errors 09 p1338 N85-18416
Finite element analysis of nonlinear oscillations and flutter of shells of revolution
[AD-A149071] 10 p1496 N85-19440
Errors in compensating for image oscillation by means of a gyroscopic head 16 p2763 N85-27051
Approximate solution of the problem of fluid oscillations in cavities of revolution 16 p2764 N85-27056
Study of oscillations of composite cylindrical shells using a dynamic stiffness technique 16 p2766 N85-27066
Analysis of unsteady pressure measurements on a supercritical airfoil with a harmonically oscillating trailing edge flap at subsonic and transonic speeds
[DFVLR-FB-84-49] 17 p2893 N85-27837
Filtration of higher harmonic components in two-level digital computing synthesizers 22 p3778 N85-33410
Role of ECRH in potential formation for tandem mirrors
[DE85-011859] 22 p3848 N85-33834

HARMONIC OSCILLATORS
Harmonic emission from high power gyrotron oscillators
[AD-A145621] 02 p0200 N85-11335
Reference oscillator stability effect on clutter cancellation in a radar system 07 p0938 N85-15946
Applications of molecular dynamics to the study of shock-induced chemistry
[AD-A148017] 08 p1121 N85-17066
A transistor oscillator-doubler
[AD-D011406] 08 p1158 N85-17307
Asymmetrical harmonic oscillator and fine-structure constant
[FUB-9-1984] 09 p1401 N85-18618
Coupled-cavity gyrotrons with mode conversion
13 p2076 N85-22967
Optical injection locking of solid-state oscillators by frequency-multiplexed injection-locked, laser diodes
[AD-D011695] 19 p3275 N85-30307
A multiplying slot array
[AD-A155570] 21 p3576 N85-32245

HARMONIC RADIATION
Generation and propagation of electron cyclotron harmonic waves 14 p2367 N85-24630
Theoretical studies of electric cyclotron harmonic (ECH) waves based on experimental data from GEOS 1
14 p2367 N85-24631
Role of equatorial Electron Cyclotron Harmonic (ECH) waves in the generation of diffuse auroras. Contribution of the GEOS IMS spacecraft 14 p2367 N85-24632
Measurement of RF fields associated with ISM equipment as it relates to aeronautical services
[FAA-ES-84-2] 19 p3254 N85-30180
The problem of brightness enhancement during laser frequency doubling 21 p3686 N85-32897
Cerenkov radiation from periodic electron bunches for finite emission length in air
[AD-A156156] 24 p4090 N85-35352

HARMONICS
NT HARMONIC GENERATIONS
NT HARMONIC OSCILLATION
NT SPHERICAL HARMONICS
NT TESSERAL HARMONICS
NT ZONAL HARMONICS
Use of a first-harmonic RF system in the NSLS booster
[DE84-016432] 02 p0277 N85-11806
Recent observations of tides and tidal currents from the northeastern Bering Sea shelf
[PB84-241785] 04 p0543 N85-13452
Linear problem of harmonic vibrator acting at supercritical frequencies in subsonic boundary layer
06 p0779 N85-14978
Perceptibility of nonlinear distortions in power amplifier
06 p0789 N85-15041
Individual geopotential coefficients of order 15 and 30, from resonant satellite orbits
[AD-A146687] 06 p0828 N85-15256
Nonlinear ultrasonic characterization of oxygen impurities in titanium
[AD-P004123] 08 p1126 N85-17098
Analysis of inverter models and harmonic propagation. Part 1: A physical simulator for large solar cell arrays
[DE85-002312] 09 p1315 N85-18271
Analysis of inverter models and harmonic propagation. Part 2: Harmonic propagation
[DE85-000198] 10 p1482 N85-19356
Some individual differences in human response to infrasound
[UTIAS-282] 12 p1905 N85-21960
The effects of internal waves on acoustic normal modes
[AD-A150235] 13 p2155 N85-23379
Propagation of sound in matter
[AD-A151052] 14 p2416 N85-24908
Internal resonance in nonlinear vibrating systems
[REPT-15/1984] 16 p2797 N85-27245
Guided and radiation wave interactions in periodic dielectric waveguides 19 p3253 N85-30173
An algorithm for the influence numbers in the expansion of the lumped gravitational potential coefficients in the presence of resonant inclination variation
[AD-A154229] 19 p3336 N85-30669
Four-photon resonant third harmonic generation
[DE85-010070] 19 p3367 N85-30683
Upward continuation of surface gravity anomalies
[AD-A154973] 21 p3631 N85-32560
Electro-optic harmonic conversion to switch a laser beam out of a cavity
[DE85-011619] 22 p3790 N85-33483
Sidereal variations deep underground in Tasmania
[SH-4.4-4] 23 p4033 N85-35002
The effect of the interplanetary magnetic field on sidereal variations observed at medium depth underground detectors
[SH-4.4-5] 23 p4033 N85-35003
Cosmic ray intensity variations observed at Matsushiro (220 M.W.E. in depth)
[SH-4.4-9] 23 p4034 N85-35007

HARNESSES
Impact tests of adjusters for the HBU-12 lap belt
[AD-A148021] 08 p1060 N85-16843
Impact tests of automatic lap belt configurations
[AD-A148034] 08 p1061 N85-16844
Double pinch-push contact insertion end-effector
[AD-D011485] 10 p1459 N85-19196
Tight Ribbon Arm Protection (TRAP) for aircrewman ejection
[AD-A150464] 13 p2143 N85-23303
Torso restraint system
[AD-D011609] 16 p2702 N85-26684
Improving inflight negative Gz restraint for aircrewmen
[AD-A151909] 16 p2703 N85-26688
Features of the solar array drive mechanism for the space telescope 22 p3798 N85-33532

HARRIER AIRCRAFT
Multivariable flight control with time-scale separation
[NASA-CR-174320] 08 p1087 N85-16873
Harrier 15 p2687 N85-26595
YAV-8B Harrier 15 p2688 N85-26605

HARTREE APPROXIMATION
Spurious center of mass effects in a dynamically determined basis
[CSIR-TWISK-310] 01 p0109 N85-10732
An extension of the multiconfiguration Hartree-Fock program for continuum functions
[DE85-002080] 09 p1379 N85-18672
Time dependent Hartree-Fock theory of ion-atom collisions: Application to F(9+) + Ne
[DE85-003083] 11 p1723 N85-20836
Hartree-Fock interaction between a helium atom and lithium-metal: A test for the effective medium theory
[AD-A150468] 13 p2156 N85-23387
Microscopic analysis of angular momentum projected HFB-states in terms of interacting bosons
[DE85-007629] 16 p2863 N85-27661
Multiple inner shell vacancies in laser-irradiated Au plasma 23 p3981 N85-34687

HARTREE-APPLETON APPROXIMATION
U HARTREE APPROXIMATION

HARTREE-FOCK APPROXIMATION
U HARTREE APPROXIMATION

HASTELLOY (TRADEMARK)
Elevated temperature biaxial fatigue
[NASA-CR-175795] 16 p2800 N85-27263
A comparison of smooth specimen and analytical simulation techniques for notched members at elevated temperatures 20 p3468 N85-31546

HAULING
A Lagrange-D'Alembert formulation of the equations of motion of a helicopter carrying an externally suspended load
[NASA-TM-85864] 12 p1776 N85-21149

HAWAII
An improved analytical theory of Rossby wave driven Eulerian and Lagrangian mean flows along non-zonal barriers with application to the Hawaiian Ridge
[AD-A144951] 01 p0088 N85-10593
Thermosonde C2N measurements in Hawaii--August 1982
[AD-A148016] 08 p1189 N85-17489
Lidar observations of stratospheric aerosol over Mauna Loa Observatory, 1974 - 1981
[PB85-115061] 11 p1682 N85-20597
Emplacement of long lava flows on Mauna Loa (Hawaii) and Alba (Mars) 13 p2186 N85-23563
Thermal infrared observations of lava flows during the 1984 Mauna Loa eruption 13 p2186 N85-23564
Field measurements of the 1983 Royal Gardens lava flows, Kilauea Volcano, and 1984 Mauna Loa lava flows, Hawaii 13 p2186 N85-23565
Surface structures of Hawaiian lavas
13 p2186 N85-23566

HAWKER SIDDELEY AIRCRAFT
NT DH 115 AIRCRAFT
NT HARRIER AIRCRAFT

HAYNES STELLITE
U STELLITE (TRADEMARK)

HAZARDOUS MATERIAL DISPOSAL (IN SPACE)
A model for the evolution of on-orbit manmade debris environment 12 p1784 N85-21196

HAZARDS
NT AIRCRAFT HAZARDS
NT FLIGHT HAZARDS
NT METEOROID HAZARDS
NT OPERATIONAL HAZARDS
NT RADIATION HAZARDS
NT TOXIC HAZARDS
Review of USAF treatment of solid propellant rocket motor hazards 08 p1114 N85-17027
Sensitiveness and explosiveness assessment at Perme Waltham Abbey 08 p1115 N85-17029
Analysis of Deflagration to Shock to Detonation Transition (DSDT) in porous energetic solid propellants
08 p1115 N85-17030
The vulnerability of cast double base rocket motors to thermomechanical attack 08 p1115 N85-17033
Hazard assessment of a hypothetical large rocket motor 08 p1117 N85-17042
The use of synthetic aperture radar imagery to detect hazards to navigation
[AD-A149324] 10 p1422 N85-18971
The 1984 JANNAF Propulsion Systems Hazards Subcommittee Meeting, volume 1
[AD-A148865] 10 p1454 N85-19162
Report on AGARD Meeting: Hazards Studies for Solid Propellant Rocket Motors
[AD-P004340] 10 p1454 N85-19164
Antiplane cracks in solid propellants
[AD-P004344] 10 p1455 N85-19166
Laser Hazards Bibliography, October 1984
[AD-A149534] 10 p1490 N85-19406
Successful control of gulls and other birds at a sanitary landfill
[AD-P004198] 11 p1582 N85-19965
DOE hazard classification for Insensitive High Explosives (IHE)
[DE84-017002] 11 p1614 N85-20149
A model for the evolution of on-orbit manmade debris environment 12 p1784 N85-21196
Preliminary design of an Earth-based debris detection system using current technology and existing installations 12 p1784 N85-21199
Orbital debris policy issues: Battelle involvement and some personal observations 12 p1787 N85-21218
Spacecraft hazard and shielding requirements
12 p1788 N85-21224
Hazardous air pollutants: Dry-deposition phenomena
[PB85-138279] 12 p1887 N85-21843

Astronaut hazard during free-flight polar EVA
13 p1997 N85-22522
Electric and hybrid vehicle demonstration project
[DE85-003939] 13 p2169 N85-23455
Innovation in earthquake and natural hazards research: Determining soil liquefaction potential
[PB85-149573] 14 p2374 N85-24676
Criteria for the classification of hydrographic positioning data
[AD-A152283] 16 p2705 N85-26697
A review of safety practices and safety training for the explosives field
[AD-A152295] 16 p2759 N85-27028
Hazards in welding due to oxygen changes in the workplace atmosphere
[BLL-WI-TRANS-684-(9312.57)]
16 p2792 N85-27224
Space station crew safety alternatives study, third quarter briefing 18 p3156 N85-29541
Facility for large-scale hazardous gas testing
[DE85-011852] 21 p3564 N85-32169
Fire protection review revisit no. 2, Argonne National Laboratory, Argonne, Illinois
[DE85-013245] 22 p3755 N85-33276
Description of a test site for large-scale heavy gas dispersion and combustion experiments
[DE85-004967] 23 p3911 N85-34231
The application of models to the assessment of fire hazard from consumer products
[NBSIR-85-3219] 23 p3925 N85-34325
Estimating risks of lead-induced hemoglobin decrements under conditions of uncertainty: Methodology, pilot judgments and illustrative calculations
[DE85-012293] 23 p3952 N85-34493
The investigation of tethered satellite system dynamics
[NASA-CR-176180] 24 p4069 N85-35215
Fire service emergency management handbook
[AD-A155780] 24 p4084 N85-35313
Investigation of the lightning vulnerability of nuclear explosive test systems at the Nevada Test Site
[DE85-011761] 24 p4124 N85-35563
National program for inspection of non-federal dams. Woodward reservoir dam (VT 00209), Connecticut River Basin, Plymouth, Vermont. Phase 1 inspection report
[AD-A156256] 24 p4144 N85-35693

HAZE
Method for measuring haze in transparencies
[AD-D011233] 01 p0120 N85-10823
Arctic haze: Meteorological aspects of long-range transport 02 p0230 N85-11499
Water-ice clouds on Mars: Location and seasonal variation 13 p2194 N85-23611
Chemical composition of coastal haze aerosol
14 p2338 N85-24456
Haze over eastern North America. Part 1: Haze properties
[PB85-181857] 19 p3311 N85-30526
Atmospheric cross sections for the Arctic gas and aerosol sampling program, March - April 1983
[NASA-CR-176027] 19 p3314 N85-30541
The measurement of aircraft windscreen haze and its effect on visual performance
[AD-A154949] 21 p3555 N85-32114
Airborne measurements of the vertical distribution of Arctic haze 21 p3647 N85-32657
Condensation nuclei and aerosol size distribution measurements in Arctic haze 21 p3647 N85-32658
The interaction of polynuclear aromatic hydrocarbons PAH's with water vapor and their role as condensation nuclei in the formation of haze and fog
21 p3652 N85-32695

HAZE DETECTION
Haze over eastern North America. Part 1: Haze properties
[PB85-181857] 19 p3311 N85-30526

HBNQ
U NITROGUANIDINE

HC-1 HELICOPTER
U CH-47 HELICOPTER

HCMM
U HEAT CAPACITY MAPPING MISSION

HCN LASERS
Observation of mode-converted by ion Bernstein wave by an HCN laser scattering
[IPPJ-724] 23 p3979 N85-34668

HEAD (ANATOMY)
NT SKULL
Powered articulated headrest system
[AD-D011353] 07 p0901 N85-15710
SPH-4 US Army flight helmet performance, 1972 - 1983
[AD-A148674] 08 p1201 N85-17562
Psychometric evaluation of head injury among fliers referred to the AF School of Aerospace Medicine
[AD-A151479] 15 p2617 N85-26129

Investigation of spectrum of human bile acids during 120-day antiorthostatic hypokinesia
22 p3821 N85-33674
Vascular mechanisms of adaptation to antiorthostatic position 22 p3822 N85-33675
Cerebral hemodynamics and ventricular function in -15 deg antiorthostatic position 22 p3822 N85-33676
Effect of short-term antiorthostatic hypokinesia on dynamics of cardiorespiratory parameters during graded physical exercise 22 p3822 N85-33677
Investigation of some aspects of amino acid metabolism in man during brief exposure to antiorthostatic hypokinesia combined with ultraviolet radiation
22 p3822 N85-33678

HEAD (FLUID MECHANICS)
NT PRESSURE HEADS

HEAD (PRESSURE)
U PRESSURE HEADS

HEAD MOVEMENT
Development and evaluation of a performance-based test of saccadic and vestibulo-ocular control
[AD-A145367] 02 p0237 N85-11545
Inverse modelling to obtain head movement controller signal 05 p0705 N85-14525
Effects of external loads on human head movement control systems 05 p0707 N85-14534
Vestibular and oculomotor function during Gz variations 11 p1693 N85-20645
Analysis of head motion during simulated, rough water operation of a 2200 ton surface effect ship
11 p1695 N85-20656
Sensory and motor properties of the cerebellar uvula and modulus 15 p2613 N85-26104

HEAD-UP DISPLAYS
The value and utility of inflight onboard simulation
[AD-A148033] 08 p1188 N85-17543
Some effects of display format variables on the perception of aircraft spatial orientation
10 p1534 N85-19666
A safety evaluation of the relocation of the ACM (Air Combat Maneuver) panel in the F-14 ( )/AIP (Avionics Integration Program)
[AD-A149596] 12 p1777 N85-21158
Crew systems and flight station concepts for a 1995 transport aircraft
[NASA-CR-166068] 19 p3221 N85-29973

HEADSETS
U EARPHONES

HEALING
Polyactic-polyglycolic acid copolymer combined with decalcified freeze-dried bone for use as a bone repair material
[AD-D011438] 10 p1451 N85-19142

HEALTH
NT HEALTH PHYSICS
NT MENTAL HEALTH
NT PUBLIC HEALTH
Differences in health risks by aircraft model among US Navy pilots
[AD-A146147] 03 p0401 N85-12556
Report of the Meeting of Experts on Climate and Human Health
[WCP-78] 05 p0687 N85-14413
Organization of the session 05 p0687 N85-14414
Difficulties encountered in determining the potential involvement of consultants on health problems in various climatic zones 05 p0687 N85-14416
Epidemiologic methods applied to the study of the relationship between climate and human health
05 p0687 N85-14418
An update on the capabilities of the Air Force Computerized Occupational Health Program (COHP)
[AD-P004037] 06 p0845 N85-15367
Health examination findings among active civil airmen
[AD-A148325] 08 p1195 N85-17533
Robotic safety
[DE85-002314] 10 p1493 N85-19431
Health standards for general vibration
10 p1523 N85-19607
Assessing the short- and long-term health effects of decompression sickness among US Navy divers
[AD-A151887] 15 p2618 N85-26132
Development of guidelines for setting physiological and hygienic standards for noise levels in aerospace medicine 19 p3323 N85-30584
Flow cytometry for health monitoring in space
[DE85-009572] 19 p3329 N85-30625

HEALTH PHYSICS
NT PUBLIC HEALTH
Symposium on Military Aviation Medicine summarized
11 p1696 N85-20663
The biological effects of radiofrequency radiation
16 p2775 N85-27131
Review of epidemiological studies of human exposures to radiofrequency radiation 16 p2776 N85-27134

Practical consequences of the assessment of differen energy health risks
[DE85-004538] 22 p3825 N85-33
Wholebody radiation counting system
[AD-A155842] 24 p4131 N85-35

HEALTH PHYSICS RESEARCH REACTOR
Empirical correlation of residual gamma radiatio resulting from operation of the Health Physics Research Reactor
[DE85-012075] 21 p3704 N85-33

HEAO
NT HEAO 1
NT HEAO 2
NT HEAO 3
Optical observations of HEAO-B objects
17 p3052 N85-28

HEAO A
U HEAO 1

HEAO B
U HEAO 2

HEAO C
U HEAO 3

HEAO 1
Local contributions to the 0.6 keV diffuse X-ray background 06 p0877 N85-15569
HEAO-1 diffuse soft X-ray sky maps
06 p0877 N85-15570
Inverse relations between 0.25 keV counts and local interstellar dust 06 p0877 N85-15572
The HEAO-1 diffuse component spectrum from 15 to above 500 keV — X and gamma rays
06 p1240 N85-17820
HEAO-1 observations of gamma ray bursts
[OG-1.1-1] 22 p3860 N85-33903
Spectra and positions of galactic gamma-ray sources
[OG-2.5-7] 22 p3869 N85-339

HEAO 2
Is the ratio of observed X-ray luminosity to bolometric luminosity in early-type stars really a constant?
08 p1234 N85-17777
Preliminary results on the ultraviolet observations of a complete X-ray selected sample of Active Galactic Nuclei (AGN) — HEAO 2 08 p1237 N85-17800
X-ray surveys of quasars with the Einstein observatory
08 p1238 N85-17807
Interacting binary systems 11 p1744 N85-20967
A soft X-ray survey of galactic supernova remnants with the Einstein Observatory 14 p2434 N85-25013
Optical pulsar in the Large Magellanic Cloud remnant 0540-69.3
[DE85-006707] 16 p2883 N85-27758

HEAO 3
HEAO 3 upper limits to the expected 1634 KeV line from SS 483
[OG-2.4-9] 22 p3868 N85-33954
High-resolution spectrum of Cygnus X-1
[OG-2.4-12] 22 p3868 N85-3395
Energy spectra of elements with 18 or = Z or = 28 between 10 and 300 GeV/amu
[OG-4.1-8] 22 p3876 N85-34014

HEARING
NT BINAURAL HEARING
Auditory impairment and the onset of disability and handicap in noise-induced hearing loss
[ISVR-TR-126] 20 p3507 N85-31801

HEARING LOSS
U AUDITORY DEFECTS

HEART
NT CARDIAC VENTRICLES
NT MYOCARDIUM
Effect of hyperoxia and increased gas atmosphere density on contractile function of the right ventricle
01 p0093 N85-106
Influence of geomagnetic disturbances o cardiovascular function of athletes
08 p1193 N85-175
The EM algorithm for censored data
[AD-A148136] 08 p1212 N85-176
Development of the osmium-191 yields iridium-191 radionuclide generator
[DE85-011185] 23 p3970 N85-346
Current status of the Os-191 yields Ir-191m general
[DE85-008306] 23 p3971 N85-346

HEART DISEASES
NT CORONARY ARTERY DISEASE
Cardiovascular disease among U.S. Navy pilots
[AD-A145871] 03 p0400 N85-125
An investigation of the relationship between stres life events and psychological, behavioral and physiolog outcomes
[AD-A147754] 08 p1197 N85-175
Medically disqualified airline pilots
[AD-A149454] 10 p1528 N85-19
Longitudinal study of cardiovascular disease in US N pilots
[AD-A154331] 19 p3328 N85-30

HEART FUNCTION
Frequency and nature of electrocardiographic disturbances in dogs during single and repeated exposure to +G sub z accelerations 01 p0092 N85-10619
Mapping of mammalian arrhythmias with the cardiac laser scanner 03 p0399 N85-12545
Left heart ventricular function during a 7 day zero-g simulation (6 deg head down tilt) 05 p0691 N85-14446
Cardiac output measured by mass spectroscopy 05 p0692 N85-14449
Cardiac output measurement with soluble gases 05 p0692 N85-14450
Hemodynamics responses to upright tilt at sea level and high altitude
[AD-A148848] 10 p1527 N85-19634
Morphological study of monkeys submitted to antiorthostatic hypokinesia 12 p1902 N85-21942
Changes in cardiovascular function: Weightlessness and ground-based studies 20 p3509 N85-31815
Oxygenation and regional circulation in gingival mucosa during exposure to lower body negative pressure 23 p3953 N85-34496
HEART RATE
NT ARRHYTHMIA
Heart rate variability during 7 day head-down tilt (6 deg) 05 p0692 N85-14453
Does McKuer's law hold for heart rate control via biofeedback display? 05 p0706 N85-14528
Scattering of electromagnetic waves by human body and its applications 09 p1363 N85-18572
Variability of cardiac rhythm during information loading 10 p1525 N85-19619
Exercise-heat strain during hypohydration: Interaction with heat acclimation and aerobic fitness
[AD-A151023] 14 p2389 N85-24717
Development of an EM-Based lifeform detector
[AD-A153504] 18 p3151 N85-29512
Studies of circulatory and metabolic changes during ketamine narcosis
[AD-A154512] 21 p3663 N85-32756
Mathematical analysis of heart rhythm assessment of distinctive features in adaptation to spaceflight conditions 22 p3733 N85-33142
Effect of water immersion of parameters of central hemodynamics in individuals over 45 years old 23 p3953 N85-34499
Effect of acute hypoxia on coronary and systemic hemodynamics 23 p3953 N85-34503
Weight loss, rectal temperature and heart rates following the 1984 Boston Marathon
[AD-A155984] 24 p4132 N85-35612
HEAT
NT PROCESS HEAT
Change in energetics of muscular contraction as a result of hyperoxia 01 p0093 N85-10629
Thermite and Fe/KClO4: Some thermodynamic calculations
[DE84-016945] 04 p0573 N85-13653
An atropinized heat-stressed rat model: Dose response effects and pharmacokinetics
[AD-A146851] 07 p1011 N85-16423
Thermal radiation hazards from Liquified Petroleum Gas (LPG) fireballs
[VTT-304] 09 p1293 N85-18122
Heat cycle research program
[DE84-017015] 09 p1344 N85-18455
A one dimensional dynamical model of ocean/atmosphere interactions 09 p1358 N85-18545
Correlation of zeolite ZSM-5 acid strength with catalytic activity and selectivity
[DE85-005415] 17 p2922 N85-28013
Heat injury: Prevention is the key
[AD-A153734] 19 p3328 N85-30622
Advanced regenerative heat recovery system
[PB85-199602] 24 p4064 N85-35315
HEAT ACCLIMATIZATION
Skeletal muscle metabolism during exercise is influenced by heat acclimation
[AD-A148845] 10 p1527 N85-19632
Preventive effect of acute heat factors during hypokinesia 12 p1902 N85-21945
Preparing Alberto Salazar for the heat of the 1984 Olympic Marathon
[AD-A150942] 14 p2389 N85-24714
Physiological differences between men and women in exercise-heat tolerance and heat acclimation
[AD-A152048] 15 p2616 N85-26135
HEAT BALANCE
Breakdown of thin plates by radiation 13 p2026 N85-22709
Accurate albedos of the brightest regions on Io 13 p2195 N85-23618
Mathematical models relating to human thermoregulation: Basic assumptions, validation, and application. Parts A and B
[AD-A151556] 15 p2616 N85-26130
Heating parameter estimation using coaxial thermocouple gages in wind tunnel test articles
[AD-A153039] 17 p2968 N85-28328
Maintenance of blocking anticyclones in a general circulation model
[PB85-190866] 24 p4124 N85-35567
HEAT BUDGET
NT ATMOSPHERIC HEAT BUDGET
Razrezy program research in the tropical Atlantic 07 p0961 N85-16229
Tropical Ocean and Global Atmosphere (TOGA) heat exchange project: A summary report
[NASA-CR-176038] 20 p3496 N85-31738
HEAT CAPACITY
U SPECIFIC HEAT
HEAT CAPACITY MAPPING MISSION
Combining Heat Capacity Mapping Mission (HCMM) LANDSAT and thematic map information into a unique high precision merged multichannel system — climatology 05 p0660 N85-14239
A multiple approach in remote sensing for structural and lithological mapping by use Modular Optoelectronic Multispectral Scanner (MOMS)/LANDSAT/Heat Capacity Mapping Mission (HCMM) data 05 p0660 N85-14244
Comparison of measurement and simulation results of radiation temperatures applied to the thermal mapping of Munich
[DFVLR-FB-85-06] 17 p2984 N85-28442
HEAT CONDUCTION
U CONDUCTIVE HEAT TRANSFER
HEAT CONTENT
U ENTHALPY
HEAT DISSIPATION
U COOLING
HEAT DISSIPATION CHILLING
U COOLING
HEAT EFFECTS
U TEMPERATURE EFFECTS
HEAT EQUATIONS
U THERMODYNAMICS
HEAT EXCHANGERS
NT TUBE HEAT EXCHANGERS
Bifouling and corrosion studies at the Seacoast Test Facility in Hawaii
[DE84-014643] 01 p0029 N85-10180
Laminar flow heat exchangers. Viscosity induced non-uniform flow
[AD-A144777] 01 p0047 N85-10307
Heat exchanger
[DE84-014299] 01 p0047 N85-10309
Research approaches to qualify aluminum for Ocean Thermal Energy Conversion (OTEC) systems
[DE84-013007] 04 p0476 N85-13034
Evaluation of selected advanced heat exchangers for waste heat recuperation of high temperature streams
[DE84-016299] 04 p0499 N85-13180
Review of SERI solar pond work 05 p0667 N85-14269
Allowing for the temperature field in the wall thickness of checkerwork in thermal calculation
[BLL-M-36015-(5828.4)] 07 p0956 N85-16058
Challenges in the development of the orbiter active thermal control subsystem 08 p1096 N85-16923
Operating and maintenance guidelines for the kinergetics (trade name) environmental control system. Carbon dioxide scrubber model DH-10 and heat exchanger model CCU-01
[AD-A148107] 08 p1200 N85-17557
Corrosion of ceramics in heat exchanger applications
[DE84-017459] 09 p1299 N85-18161
Hybrid system for producing and storing ice
[DE84-017474] 09 p1304 N85-18195
Monitoring environmental and related performance parameters for a Rankine-cycle turbine electric generator utilizing geothermal energy at the Gila Hot Springs, New Mexico
[DE84-901772] 09 p1345 N85-18465
Acoustic imaging in a water filled metallic pipe — monitoring heat exchangers in nuclear power reactors
[DE84-016051] 09 p1378 N85-18665
Effect of inclination, transverse intertip spacing, and logitudinal pitch on crossflow heat transfer from an array of finned tubes 10 p1482 N85-19359
Analysis of compact heat exchanger performance
[DE84-012624] 10 p1485 N85-19377
Heat and mass exchange in a partially stratified fluid
[DE85-000528] 10 p1486 N85-19384
Conceptual design of a 10 MW shore-based OTEC plant
[DE84-015808] 10 p1511 N85-19532
Research on heat-exchanger corrosion
[PB85-126316] 11 p1616 N85-20164
Formaldehyde and tracer gas transfer between airstreams in enthalpy-type air-to-air heat exchangers
[DE84-016951] 11 p1631 N85-20274
Acoustic resonance in heat exchanger tube banks
[DE85-004395] 11 p1632 N85-20281
Theoretical and experimental analysis of vertical, concentric-tube ground-coupled heat exchangers
[DE85-000474] 11 p1633 N85-20286
Slit-ring test for evaluating fracture in tubular cross sections
[DE85-003550] 11 p1654 N85-20416
Direct contact heat recovery from molten salt
[DE85-002830] 11 p1674 N85-20550
Theoretical analysis of condensation in the presence of noncondensable gases as applied to open cycle OTEC condensers
[DE84-015809] 11 p1675 N85-20556
Steam generator tube vibration tests
[DE85-003599] 12 p1867 N85-21712
Direct-contact condensers for solar pond power production
[DE84-004510] 12 p1876 N85-21771
Development of a single-family absorption chiller for use in a solar heating and cooling system, phase 3, volume 2
[DE85-003218] 13 p2130 N85-23253
Advanced radiator concepts
[NASA-TM-87008] 14 p2300 N85-24245
Equipment for monitoring low concentrations of volatile substances in gases or liquid metals
[BLL-DOUNREAY-TR-949-(9091.9F)] 16 p2786 N85-27190
DOE/ANL/HTRI heat exchanger tube vibration data bank: Addendum 5
[DE85-007730] 17 p2980 N85-28425
Heat management system for aircraft
[AD-D011658] 18 p3061 N85-28936
Research test facility for evaporation and combustion of alternative jet fuels at high air temperatures
[AD-A153830] 18 p3083 N85-29073
Reciprocating magnetic refrigerator employing tandem porous matrices within a reciprocating displacer
[NASA-CASE-NPO-16257-1] 18 p3085 N85-29082
Development of corrosion resistant heat exchangers for flue gas desulfurization
[BMFT-FB-T-84-281] 18 p3103 N85-29211
Experimental investigation of turbulent heat transfer in straight and curved rectanguler ducts
[AD-A154413] 19 p3266 N85-30255
Onset of freezing in residential air-to-air heat exchangers
[DE85-009960] 19 p3267 N85-30259
Intrinsically irreversible acoustic heat engines
[DE85-007672] 19 p3270 N85-30276
Stability analysis of direct contact heat exchangers subject to system perturbations
[DE85-011780] 20 p3455 N85-31452
An investigation into the fluidization and heat transfer of low density particles in a fluidized bed with applications
[AD-A155259] 21 p3584 N85-32282
One method of solving the problem of unsteady heat exchange of a body and its ablation 22 p3733 N85-33146
Woven heat exchanger
[DE85-011633] 22 p3783 N85-33439
Heat-mass flow enhancement system for a metal hydride assembly
[DE85-010698] 22 p3783 N85-33441
Ocean thermal energy conversion
[DE85-012291] 23 p3946 N85-34456
High Temperature Heating System (HTHS)
[PB85-188340] 24 p4064 N85-35316
Experimental lithium system
[DE85-013252] 24 p4094 N85-35382
HEAT FLOW
U HEAT TRANSMISSION
HEAT FLUX
Evaluation of surface sensible heat flux effects on the generation and modification of mesoscale circulations 01 p0079 N85-10527
Heat flux sensors for burner liners and turbine blades and vanes 02 p0142 N85-10961
Numerical analysis of flow and heat transfer in the VAFB LOX storage Dewar tank
[NASA-CR-171203] 02 p0197 N85-11315
Resistance of Navy shipboard outerwear garments and fire-resistant fabrics to extreme heat
[AD-A145414] 02 p0236 N85-11546
The areal pattern of latent and sensible heat fluxes: The combination of soil physics and remotely sensed data 05 p0656 N85-14213
Modeling influence of three layer cloud cover on outgoing thermal radiation 06 p0825 N85-15242

High temperature thermocouple and heat flux gauge using a unique thin film-hardware hot juncture
[NASA-TM-86896] 07 p0962 N85-16096

Self-generated magnetic fields and thermal flux inhibition
[AD-A147405] 07 p0971 N85-16166

New aspects of thermoelastic contact
[AD-A147554] 07 p0979 N85-16217

Subcooled flow boiling at high heat flux
[OUEL-1540/84] 08 p1163 N85-17338

Magnetic fusion energy plasma interactive and high heat flux components. Volume 2: Technical assessment of the critical issues and problem areas in high heat flux materials and component development
[DE85-001155] 09 p1393 N85-18764

Analysis of the dissipation mechanism within an instationary cathode spot of metal vapor arcs
[AD-A149258] 10 p1558 N85-19625

Thermal investigation of an electrical high-current arc with porous gas-cooled anode
[NASA-TM-77759] 11 p1627 N85-20245

Aspects of planetary wave transports in the middle atmosphere 11 p1661 N85-20471

Envelope thermal test unit: Technical description
[DE84-012254] 11 p1674 N85-20548

Heat flux in Lorentzian plasma
[IPPJ-704] 12 p1935 N85-22158

Experimental investigations of thermal radiation from potassium atoms in magnetohydrodynamic system: Preliminary report
[DE85-003715] 12 p1936 N85-22169

Coupling between velocity oscillations and solid propellant combustion
[AD-A151061] 14 p2247 N85-23927

Parameterization of apparent and latent heat fluxes above water surface in calm weather under natural conditions 14 p2337 N85-24454

Thermal and magnetic properties of neutron stars
16 p2660 N85-27774

Experimental measurements and analysis of heat transfer and gas dynamics in a rotating turbine stage
17 p2911 N85-27949

Heat flux sensor calibrator 17 p2915 N85-27970

Conformational and mechanical properties at high strain rates
[AD-A153401] 17 p2959 N85-28272

Analysis of ocean surface wind fields using SEASAT-A scatterometer data 18 p3139 N85-29434

Objective determination of heat wave patterns
18 p3140 N85-29437

Preliminary results from numerical experiments on the summer 1980 heat wave and drought
18 p3140 N85-29438

Enhanced thermal coupling by a repetitively pulsed laser
[AD-A154435] 19 p3276 N85-30317

Experiments using atmospheric forcing from a FGGE analysis to drive an upper ocean model
[INPE-3503-PRE/738] 19 p3319 N85-30576

One-dimensional model hindcasts of warm anomalies in the North Pacific Ocean
[AD-A154128] 19 p3320 N85-30579

Experimental observation of transition behavior on a flat plate 20 p3452 N85-31437

Stability analysis of direct contact heat exchangers subject to system perturbations
[DE85-011780] 20 p3455 N85-31452

Wall flames and implications for upward flame spread
[FAA-CT-85-2] 21 p3553 N85-32103

Facility for large-scale hazardous gas testing
[DE85-011852] 21 p3564 N85-32169

Technical assessment of thermal-hydraulics for high heat flux fusion components
[DE85-013178] 23 p3930 N85-34359

Sequential regularization solution of the inverse heat conduction problem
[DE85-010857] 23 p3931 N85-34362

Forced convective, nonequilibrium, post-CHF heat transfer experiment data and correlation comparison report
[TI85-009331] 23 p3932 N85-34371

On the heat flux derived by the moment method in Lorentzian plasma between hot and cold walls
23 p3980 N85-34682

Integral representation for nonlinear heat transport
23 p3981 N85-34683

High Temperature Heating System (HTHS)
[PB85-188340] 24 p4084 N85-35316

Development of advanced high-temperature heat flux sensors. Phase 2: Verification testing
[NASA-CR-174973] 24 p4096 N85-35391

Case studies for flux measurements along a low-flying route to the south of Munich 24 p4121 N85-35548

Two-point closure study of covariance budgets for turbulent Rayleigh-Benard convection
[PB85-189108] 24 p4124 N85-35568

HEAT GAIN
U HEATING

HEAT GENERATION

Temperature prediction in mechanical components, an analytical approach 09 p1327 N85-18339

Thermal profiles of thermite reactions
[DE85-003308] 10 p1438 N85-19061

U, Th, K content, heat production and thermal conductivity of Sao Paulo, Brazil continental shelf sediments: A reconnaissance work
[INPE-3401-PRE/670] 10 p1515 N85-19556

Two-d heat transfer through porous media with heat generation
[AD-A151965] 16 p2783 N85-27173

Generated spiral bevel gears: Optimal machine-tool settings and tooth contact analysis
[NASA-TM-87075] 23 p3937 N85-34405

HEAT MEASUREMENT

A concept for a hadron calorimeter with photodiode readout
[MPI-PAE/EXP-E1-130] 01 p0050 N85-10332

Time resolved calorimetry of 30 nm Te-films during laser annealing
[AD-A145047] 01 p0052 N85-10346

Recent progress in BGO development for high resolution calorimetry
[MPI-PAE/EXP-E1-129] 01 p0124 N85-10848

Accurate measurement of heat capacity by differential scanning calorimetry 04 p0466 N85-12975

Thermal performance testing of passive solar components in NBS (National Bureau of Standards) calorimeter
[PB85-119345/GAR] 09 p1346 N85-18470

Calorimetric investigation into the possibility of a charge density wave ground state in alkali metals
[DE85-002006] 09 p1397 N85-18795

Synthesis and thermomechanical properties of new AT-Phenylene R systems
[AD-A149961] 12 p1813 N85-21372

Transient technique for measuring heat transfer coefficients on stator airfoils in a jet engine environment
[NASA-TM-87005] 15 p2560 N85-25794

Heat flux sensor calibrator 17 p2915 N85-27970

Objective determination of heat wave patterns
18 p3140 N85-29437

Guest molecules in coal
[DE85-010435] 19 p3228 N85-30016

The effect of prior parent phase cold work on martensite transformation in Cu-Zn-Al shape memory alloys
[AD-A155140] 21 p3566 N85-32183

Cryogenic laser calorimetry for impurity analysis
[NASA-CR-176179] 24 p4097 N85-35395

X-ray film chamber with carbon target of Tien-Shan complex array 24 p4179 N85-35915

HEAT OF FORMATION

Local density theory of heats of formation and short-range order parameters in substitutionally disordered alloys
[DE85-009811] 18 p3075 N85-29021

Heats of formation of gas phase organosulfur molecules, radicals and ions measured by PEPICO and application of (17)O and (33)S NMR spectroscopy to structure determination of organosulfur compounds
[DE85-010556] 24 p4071 N85-35229

HEAT OF FUSION

Natural convection during heat accumulation by substances with change of aggregate state
13 p2043 N85-22787

HEAT OF VAPORIZATION

Analysis of the natural initiation of vapor explosions
[DE85-000188] 11 p1632 N85-20279

HEAT PIPES

Corrosion in alkali metal/molybdenum heat pipes
[DE84-014039] 02 p0184 N85-11233

Titanium-potassium heat pipe corrosion studies
[DE84-015526] 05 p0637 N85-14090

Procedures for testing and evaluating spacecraft-type heat pipes
[AD-A146671] 06 p0809 N85-15139

Power flattening techniques for radioisotopic thermoelectric generators
[AD-A146365] 06 p0833 N85-15299

Thermally isolated structural support link
[AD-D011349] 07 p0972 N85-16176

Capillary Pump Loop (CPL) heat pipe development status report
[NASA-CR-175273] 08 p1161 N85-17323

An evaluation of liquid and two-phase cooling techniques for use in electrical machinery
[AD-A149528] 10 p1484 N85-19372

Space heat rejection radiators: Meteoroid/debris consideration 12 p1786 N85-21210

Heat pipe cooled probe
[NASA-CASE-LAR-12568-1] 12 p1844 N85-21568

Modeling of transient heat pipe operation
[NASA-CR-175496] 12 p1844 N85-21571

Use of heat pipes for heat collection and transmission in solar plants 14 p2265 N85-24037

Sodium and lithium corrosion in molybdenum heat pipes
[DE85-005561] 16 p2784 N85-27179

Heat pipe and method of making same
[AD-D011654] 17 p2959 N85-28273

High thermal power density heat transfer apparatus providing electrical isolation at high temperature using heat pipes
[NASA-CASE-LEW-12950-2] 18 p3098 N85-29179

Pressure recovery in a cylindrical heat pipe at high radial Reynolds numbers and at high Mach numbers
[DE85-010718] 19 p3269 N85-30274

Performance characteristics of gravity-assisted potassium heat pipes
[DE85-010717] 19 p3287 N85-30387

Infrared generation and wave-mixing studies in cesium
[DE85-012883] 24 p4063 N85-35304

Development of a high-efficiency, gas-fired, heat pipe, warm-air heating system
[PB85-199636] 24 p4085 N85-35318

HEAT PUMPS

Chemical heat pump state-of-the-art survey
[DE84-013552] 01 p0048 N85-10312

Determination of optimum Curie point as a function of source and sink temperatures for magnetic heat pumps
[DE84-016995] 04 p0499 N85-13182

Magnetic heat pump cycles for industrial waste heat recovery
[DE84-017016] 04 p0499 N85-13183

Development of a Braun linear engine-driven, heat-actuated heat pump
[DE84-016647] 04 p0500 N85-13188

Investigation of an ejector heat pump by analytical methods
[DE84-016675] 04 p0500 N85-13189

A refined computer program for the transient simulation of ground coupled heat pump systems
[DE84-014098] 05 p0637 N85-14088

Open-cycle vapor compression heat pump
[PB85-101475/GAR] 06 p0775 N85-14861

Working medium for sorption heat pumps
[BLL-T6360/BG/WH785/84] 06 p0807 N85-15131

Phase 1-A development kinematic Sterling/Rankine commercial gas-fired heat pump research program
[PB85-100931/GAR] 07 p0936 N85-15909

NOx emissions near a heat pump with gas motor
[BLL-WH-782-(9091.9F)] 07 p0995 N85-16319

Rotary magnetic heat pump
[DE84-017017] 09 p1320 N85-18303

Sulfuric acid chemical heat pump program, March - November 1982
[DE84-017436] 09 p1320 N85-18304

Open-cycle centrifugal vapor-compression heat pump
[PB85-113405/GAR] 09 p1328 N85-18348

Comparison of energy storage systems in the United States chilled water versus two types of ice storage systems
[DE85-001102] 09 p1344 N85-18452

Available energy method for evaluating thermodynamic performance of heat pump systems
[DE84-017223] 09 p1400 N85-18814

DOE/ORNL electric systems program overview
[DE85-003334] 10 p1459 N85-19197

Optimization of a ground coupled heat pump
[DE85-000273] 10 p1486 N85-19380

An assessment of ground-coil heat-pump technology
[DE85-002567] 10 p1486 N85-19382

Development and demonstration of a Stirling/Rankine heat activated heat pump. Phase 3B: Engine technology development testing
[DE85-004368] 10 p1486 N85-19383

Development and test of a high COP Rankine heat pump for generation of process steam. Phase 2: Fabrication and test
[DE85-002600] 11 p1632 N85-20275

Magnetic heat pump feasibility assessment
[DE85-002606] 11 p1632 N85-20276

Theoretical and experimental analysis of vertical, concentric-tube ground-coupled heat exchangers
[DE85-000474] 11 p1633 N85-20286

Performance evaluation of an active solar cooling system utilizing low cost plastic collectors and an evaporatively-cooled absorption chiller
[DE84-010813] 12 p1680 N85-21798

Magnetic refrigeration and heat pumping design options
[DE85-003405] 13 p2092 N85-23094

Cooling performance improvement of a horizontal ground coupled heat pump
[DE85-002470] 13 p2093 N85-23095

A review of development and application of heat pump technology
[CSIR-RR-585] 14 p2300 N85-24241

Mass and heat transfer in reflux condensers of absorption heat pumps
[DFVLR-FB-83-43] 14 p2304 N85-24266
Transient analysis of a magnetic heat pump
15 p2576 N85-25891
The use of heat pumps in district heat supply
[BLL-OA-TRANS-2720-(6196.3)]
16 p2781 N85-27163
Alternative heat sources for heat pumps
[DE85-007610] 17 p2959 N85-28275
Simplified analysis of Stirling engines and heat pumps
[DE85-008753] 17 p2986 N85-28457
Comparative evaluation of ground-coupled heat pumps that use solar energy
[DE85-010950] 20 p3484 N85-31649
Solid state radiative heat pump
[DE85-011605] 22 p3760 N85-33303
Heat-mass flow enhancement system for a metal hydride assembly
[DE85-010696] 22 p3783 N85-33441
Advanced heat pump research and development
[DE85-009540] 23 p3932 N85-34372
Solar heat pump
[DE85-011323] 23 p3946 N85-34453

HEAT RADIATORS
NT SPACECRAFT RADIATORS
Methods for heat transfer and temperature field analysis of the insulated diesel
[NASA-CR-174783] 07 p1056 N85-16699
Challenges in the development of the orbiter radiator system 08 p1096 N85-16925

HEAT REGULATION
U TEMPERATURE CONTROL

HEAT REJECTION DEVICES
U HEAT RADIATORS

HEAT RESISTANCE
U THERMAL RESISTANCE

HEAT RESISTANT ALLOYS
NT MOLYBDENUM ALLOYS
NT NIOBIUM ALLOYS
NT REFRACTORY METAL ALLOYS
NT RENE 95
NT RHENIUM ALLOYS
NT TANTALUM ALLOYS
NT TUNGSTEN ALLOYS
NT UDIMET ALLOYS
NT WASPALOY
Weldability of aged heat resistant nickel alloys
01 p0021 N85-10125
Morphological changes of gamma prime precipitates in nickel-base superalloy single crystals
[NASA-TM-83698] 01 p0026 N85-10165
The effects of seven alloying elements on the microstructure and stress-rupture behavior of nickle-base superalloys
[NASA-TM-83791] 01 p0027 N85-10168
High temperature static strain sensor development program 02 p0141 N85-10959
The structure of rapidly solidified nickel-base alloys
02 p0181 N85-11215
Microstructure and creep behaviour at elevated temperature of unidirectionally solidified eutectic nickel base superalloys 02 p0181 N85-11216
The transient oxidation of single crystal NiAl + Zr
[NASA-CR-174756] 02 p0182 N85-11221
The effect of tantalum and carbon on the structure/properties of a single crystal nickel-base superalloy
[NASA-CR-174779] 02 p0182 N85-11223
Studies on the hot corrosion of a nickel-base superalloy, Udimet 700
[NASA-TM-86862] 02 p0183 N85-11224
Plastic strain localization in superalloy single crystals
[AD-A145705] 02 p0288 N85-11878
Materials for advanced turbine engines. Project 2: Rene 150 directionally solidified superalloy turbine blades, volume 2
[NASA-CR-167993] 03 p0319 N85-12059
Verification tests of durable TPS concepts
[NASA-TM-86313] 03 p0323 N85-12085
Effects of tin on microstructure and mechanical behavior of Inconel 718
[NASA-TM-86866] 03 p0330 N85-12129
High temperature low-cycle fatigue mechanisms in single crystals of nickel-based superalloy Mar-M 200
[NASA-CR-174739] 03 p0331 N85-12130
The effects of Cr, Co, Al, Mo and Ta on the cyclic oxidation behavior of a prototype cast Ni-base superalloy based on a 2(5) composite statistically designed experiment
[NASA-TM-83764] 03 p0331 N85-12131
The effect of orientation on fatigue growth in a nickel-based single crystal superalloy
[PNR-90207] 03 p0332 N85-12141
Analysis techniques for tracer studies of oxidation
[NASA-CR-174796] 03 p0336 N85-12162
Time-temperature dependence of the strength of commercial zirconia ceramics
[AD-A146233] 03 p0338 N85-12173
Features of plastic deformation and fracture of EP 741 nickel alloy under thermal strain
03 p0349 N85-12250
Structural stability of nickel heat resistant alloys at high temperatures 03 p0350 N85-12251
Interactions between corrosion and creep of uncoated and coated superalloys in sulfate melts
04 p0477 N85-13036
COST 50 - materials for gas turbines, part 1 and 2 3UK9
[NPL-DMA(A)-74] 05 p0617 N85-13943
The microstructural characteristics of revert superalloys --- for turbine blades
05 p0617 N85-13945
Controlled directionally solidified precision casting for superalloys and steels
[BMFT-FB-T-84-198] 05 p0619 N85-13960
Method for predicting the creep rupture life of nickel-base precipitation-hardened superalloys from their chemical composition
[BLL-PNR-90241-(6019.3153)]
06 p0768 N85-14910
The role of microstructure in the modelling of plastic flow in P/M superalloys at forging temperatures and strain rate 06 p0796 N85-15090
Method for making alloy additions to base metals having higher melting points
[AD-D011403] 07 p0926 N85-15884
Welding of PM-superalloys
[MTU-TB-910/84] 07 p0975 N85-16191
The effect of the test atmosphere on the formation and propagation of creep cracks in commercial high temperature alloys
[JUEL-1939] 07 p0980 N85-16221
Grain refining and microstructural modification during solidification
[AD-A147705] 08 p1128 N85-17111
Materials of the fourth scientific-technical Conference on Questions of the Extrusion of Metals (Selected articles)
[AD-A148576] 08 p1130 N85-17121
The effect of tantalum on the structure/properties of two polycrystalline nickel-base superalloys: B-1900 + Hf MAR-M247
[NASA-CR-174847] 09 p1294 N85-18127
Resistivity of alloys
[DE85-000906] 09 p1296 N85-18138
Adaptation of remelting procedures for the use of recycled metal in nickel-base superalloy castings
[PNR-90232] 09 p1297 N85-18149
Effects of MAR-M247 substrate (modified) composition on coating oxidation coating/substrate interdiffusion --- protective coatings for hot section components of gas turbine engines
[NASA-CR-174851] 10 p1440 N85-19073
Low cycle fatigue of MAR-M 200 single crystals at 760 and 870 deg C
[NASA-TM-86933] 10 p1440 N85-19074
Creep-rupture behavior of iron superalloys in high-pressure hydrogen
[NASA-CR-174411] 10 p1441 N85-19078
Influence of gaseous hydrogen on strength and ductility of nickel heat-resistant alloys 10 p1447 N85-19119
Estimation of endurance characteristics of heat resistant materials. Report 2: Determination of endurance limit of heat resistant alloys over a broad temperature range
10 p1447 N85-19120
Metals and Ceramics Division Materials Science Program
[DE85-003795] 11 p1592 N85-20012
The physical modelling of transition metal alloying: The roles that different levels of theory play
[DE85-000591] 11 p1607 N85-20105
Patterns in the occurrence of the brittle topologically close-packed phases: AI
[DE85-000592] 11 p1607 N85-20106
Weldability and mechanical property characterization of weld clad alloy 800H tubesheet forging
[DE85-001737] 11 p1609 N85-20116
Effect of reduction of strategic Columbium addition in 718 Alloy on the structure and properties
[NASA-CR-174841] 12 p1805 N85-21320
Investigation of the development possibilities of a ferritic creep and oxidation-resistant steel for application under creep conditions above 650 deg C
[BMFT-FB-T-84-244] 12 p1808 N85-21344
Orientation and temperature dependence of some mechanical properties of the single-crystal nickel-base superalloy Rene N4. 3: Tension-compression anisotropy
[NASA-TM-86982] 13 p2021 N85-22660
USSR report: Materials science and metallurgy
[JPRS-UMS-85-002] 13 p2025 N85-22688
Comparison of dynamic-tension and constant-load strength characteristics of heat-resistant materials
13 p2030 N85-22722
Some specifics of development of fatigue and creep in heat-resistant alloys with asymmetrical multicycle loading
13 p2031 N85-22724
Change in microstructure of heat-resistant nickel alloys upon thermal cycling in a current of gas
13 p2031 N85-22725
Softening of metal near seam during welding of heat-resistant nickel alloys 13 p2035 N85-22747
Effect of zero-wear in friction pairs operating in abrasive media 13 p2045 N85-22801
The cyclic stress-strain behavior of nickel-base superalloy poly- and single crystals
14 p2254 N85-23969
Research directed advanced high temperature coating system beyond current state-of-the art systems
[AD-A150696] 14 p2255 N85-23974
Role of passive surface films on corrosion fatigue crack initiation
[DE85-000436] 14 p2257 N85-23985
Contact point and seam welding of heat-resistant alloys 15 p2501 N85-25429
An investigation of the structure and high temperature mechanical properties of oxide dispersion strengthened alloys
[AD-A151107] 15 p2509 N85-25477
Optimizing hot workability and controlling microstructures in difficult to process high strength and high temperature materials
[AD-D011586] 15 p2510 N85-25482
Design of ductile polycrystaline Ni3Al alloys
[DE85-005572] 15 p2511 N85-25491
Reduced-chromium stainless steel substitutes containing silicon and aluminum
[PB85-160786] 15 p2513 N85-25502
Mechanisms of buildup and properties of aluminum coatings on heat-resistant nickel alloys
15 p2513 N85-25508
Modified aluminosilicide coating for heat-resistant nickel alloys 15 p2514 N85-25509
On thermomechanical testing in support of constitutive equation development for high temperature alloys
[NASA-CR-174879] 15 p2577 N85-25894
Crack closure characteristics considering center cracked and compact tension specimens
[AD-A151702] 15 p2579 N85-25907
Fatigue life extension 16 p2733 N85-26864
Design overview of fiber-reinforced superalloy composites for the Space Shuttle main engine
16 p2734 N85-26871
Materials for advanced rocket engine turbopump turbine blades 16 p2734 N85-26872
Development of hydrogen resistant alloys
16 p2735 N85-26873
Relationships between microstructure and microfissuring in alloy 718 16 p2735 N85-26876
Nonlinear structural analysis for fiber-reinforced superalloy turbine blades 16 p2737 N85-26887
Iron rich low cost superalloys
[NASA-CR-174900] 16 p2748 N85-26962
Effects of high mean stress on high-cycle fatigue behavior of PWA 1480 17 p2914 N85-27964
Constitutive cyclic deformation behavior in single-crystal and directionally solidified SSME high-pressure fuel turbopump airfoil materials 17 p2914 N85-27965
High-thermal-gradient superalloy crystal growth
17 p2914 N85-27966
Role of hydrogen and structure on CMSX-2
17 p2915 N85-27967
The characteristic structure of weld metal of high temperature alloy X20CrMoV 121
[BLL-BISI-TRANS-21623-(9022.06)]
17 p2928 N85-28069
Precision die forging of blades or gas turbines
17 p2940 N85-28148
High-temperature oxidation of alloys in mixed oxidants
[DE85-009706] 18 p3077 N85-29035
Study of the influence of metallurgical factors on fatigue and fracture of aerospace structural materials
[AD-A153913] 18 p3122 N85-29328
Effect of prolonged high temperature on durability of coated high-temperature nickel alloys
19 p3243 N85-30105
Properties of heat resistant Ni-Al-Nb alloys with unidirectional eutectic structure
19 p3247 N85-30133
Effects of high mean stress on the high-cycle fatigue behavior of PWA 1480
[NASA-CR-176020] 19 p3287 N85-30388
Mechanical behavior of Ni-Cr-base superalloys in forms and conditions representative of service
[NPL-DMA(A)-94] 20 p3431 N85-31262

Long range ordered alloys modified by addition of niobium and cerium
[DE85-011061] 20 p3431 N85-31265
Micromechanics of high temperature deformation and failure 20 p3466 N85-31534
Constitutive modeling of superalloy single crystals and directionally solidified materials
20 p3466 N85-31535
On the use of internal state variables in thermoviscoplastic constitutive equations
20 p3466 N85-31536
Finite element modeling of cracked bodies using the Bodner-Partom flow law 20 p3466 N85-31547
The effect of stress and hot corrosion on nickel-base superalloys
[AD-A154722] 21 p3566 N85-32181
Strain rate sensitivity estimation from high velocity impact data
[AD-A154703] 21 p3599 N85-32347
Nitriding of super alloys for enhancing physical properties
[DE85-005762] 23 p3917 N85-34275
The development and evaluation of the creep and corrosion resistant alloy IN6201
[PNR-90253] 23 p3917 N85-34278
Directionally solidified gas turbine alloys
[PNR-90264] 23 p3917 N85-34279
Microshrink, tensile properties, and the detection of microshrink
[AD-A155875] 24 p4079 N85-35278

HEAT SHIELDING
NT REENTRY SHIELDING
NT REUSABLE HEAT SHIELDING
Passive storage technologies
06 p1108 N85-17003
Erosion of corrosion-resistant surface treatments on alloy steels
[DE85-008446] 17 p2932 N85-28100
Mechanical fastener
[NASA-CASE-LAR-12738-2] 19 p3279 N85-30335
Experimental aerodynamic heating to simulated space shuttle tiles in laminar and turbulent boundary layers with variable flow angles at a nominal Mach number of 7
[NASA-TP-2307] 23 p3929 N85-34351
Results of tests on a specimen of the SRB aft skirt heat shield curtain in the MSFC LRLF
[NASA-CR-170883] 24 p4070 N85-35221
Results of tests of the SRB aft skirt heat shield curtain in the MSFC Hot Gas Facility
[NASA-CR-170886] 24 p4070 N85-35223

HEAT SINKS
Hot hollow cathode gun assembly
[DE84-014312] 01 p0121 N85-10832
Heatsink requirements for coherent operation of high-power semiconductor laser arrays
[AD-A146184] 03 p0366 N85-12346
Determination of optimum Curie point as a function of source and sink temperatures for magnetic heat pumps
[DE84-016995] 04 p0499 N85-13182
Evaluation of some photovoltaic concentrator solar cell-heat sink coupling materials
[DE84-016027] 04 p0529 N85-13378
High-efficiency, low-cost, passively-cooled PV concentrator module
[DE85-010013] 19 p3305 N85-30490
Heat sinking for printed circuitry
[DE85-011585] 22 p3783 N85-33440
Mathematical modeling of ultimate heat sink cooling ponds
[TI85-009747] 23 p3932 N85-34369

HEAT SOURCES
NT GEOTHERMAL RESOURCES
NT GEYSERS
NT THERMAL RESOURCES
Metallography of Kovar/glass/thermite interfaces
[DE84-015247] 02 p0195 N85-11302
General-purpose heat source development: Safety test program. Postimpact evaluation, design iteration test 2
[DE84-015978] 04 p0564 N85-13592
Infrared thermography of burn front propagation in heat powders
[DE85-003307] 10 p1438 N85-19060
Thermal profiles of thermite reactions
[DE85-003308] 10 p1438 N85-19061
Consolidation around a point heat source
[PB85-116549] 11 p1662 N85-20601
General-purpose heat source development: Safety test program. Postimpact evaluation, design iteration test 4
[LA-10217-SR] 12 p1930 N85-22128
General-purpose heat source development: Safety test program. Postimpact evaluation, design iteration test 5
[LA-10232-SR] 12 p1931 N85-22129
General-purpose heat source development: Safety test program. Postimpact evaluation, design iteration test 1
[LA-9980-SR] 12 p1931 N85-22131
Long-term exposure of pressed plutonium oxide heat sources to aquatic environments
[DE85-007385] 15 p2495 N85-25392
Low gravity exothermic heating/cooling apparatus
[NASA-CASE-MSC-25707-1] 18 p3104 N85-29214
Burn front velocity as a function of pellet density in iron-potassium perchlorate heat powders
[DE85-011448] 21 p3572 N85-32214
Crustal radiogenic heat production and the selective survival of ancient continental crust
21 p3721 N85-33088
Neutron flux, spectrum and dose equivalent measurements for a 4500-W(th) 238 PuO2 general purpose heat source
[DE85-011361] 22 p3841 N85-33786
Contrasts in evolution of Venus and Earth
22 p3857 N85-33880
General-purpose heat source development: Safety test program. Postimpact evaluation, design iteration test
[LA-10034-SR] 23 p3960 N85-34606
Development and characterization of carbon-bonded carbon fiber insulation for radioisotope space power systems
[DE85-013365] 24 p4082 N85-35299

HEAT STORAGE
Man's physical tolerance to heat. Heat storage, burn injury
[FOA-C-54055-H1] 02 p0235 N85-11533
Thermal energy storage at 900 deg C
[DE84-004589] 04 p0530 N85-13387
Possibilities of conjugating binary solutions for thermal energy storage
[DE84-016704] 04 p0531 N85-13392
Trends in concentrator, receiver, and storage development for terrestrial applications
05 p0609 N85-13891
A refined computer program for the transient simulation of ground coupled heat pump systems
[DE84-014096] 05 p0637 N85-14088
Thermodynamical characteristics of heat storage reactors using metal hydrides
[NAL-TR-822] 06 p0869 N85-15524
Thermal energy storage
[DE85-001492] 09 p1344 N85-18454
Field testing of aquifer thermal energy storage
[DE85-000399] 09 p1344 N85-18457
Advanced latent heat storage media for high-temperature industrial applications
[DE85-000907] 09 p1345 N85-18461
Development of media for dynamic latent heat storage for the low-temperature range. Part 1: Thermal analyses of selected salt hydrate systems
[NASA-TM-77778] 10 p1507 N85-19510
Direct contact heat recovery from molten salt
[DE85-002830] 11 p1674 N85-20550
Latent heat storage technology and application workshop. Summary report: Session 6
[DE85-001097] 12 p1882 N85-21806
Phase change thermal energy storage and the model building codes
[PB85-111201] 12 p1883 N85-21813
Natural convection during heat accumulation by substances with change of aggregate state
13 p2043 N85-22787
Latent heat storage in cooling systems
[DE85-005355] 13 p2129 N85-23248
Overview of latent storage for passive solar applications
[DE85-005354] 13 p2129 N85-23249
Central solar heating plants with seasonal storage. Evaluation of systems concepts based on heat storage in aquifers
[DE85-006788] 16 p2820 N85-27396
High temperature composite thermal storage systems
[DE85-005073] 17 p2966 N85-28455
Performance of an active/passive hybrid solar system utilizing vapor transport
[DE85-008627] 17 p2968 N85-28466
Solar pond research at the Los Alamos National Laboratory
[DE85-008631] 18 p3128 N85-29366
High temperature sensible heat storage options
[DE85-000534] 18 p3129 N85-29375
Salt-gradient solar ponds
[DE85-008626] 18 p3129 N85-29380
SERI Solar Energy Storage Program: FY 1984
[DE85-002936] 18 p3130 N85-29385
Stable density stratification solar pond
[NASA-CASE-NPO-15419-2] 19 p3303 N85-30474
Calibration of relevant measuring sensors
[DE85-009620] 19 p3306 N85-30492
DHC: A diurnal heat capacity program for microcomputers
[DE85-009645] 20 p3518 N85-31869
Solar energy education: Renewable energy activities for chemistry and physics
[DE85-010371] 23 p3948 N85-344

HEAT STROKE
An atropinized heat-stressed rat model: Dose response effects and pharmacokinetics
[AD-A146851] 07 p1011 N85-1642

HEAT TESTS
U HIGH TEMPERATURE TESTS

HEAT TOLERANCE
Man's physical tolerance to heat. Heat storage, burn injury
[FOA-C-54055-H1] 02 p0235 N85-1153
Tolerance endpoint for evaluating the effects of heat stress in dogs
[AD-A148104] 08 p1192 N85-17511
Heat stress and personal protective equipment
[DE85-003552] 10 p1532 N85-1962
Preventive effect of acute heat factors during hypokinesia 12 p1902 N85-2184
Physiological differences between men and women in exercise-heat tolerance and heat acclimation
[AD-A152048] 15 p2618 N85-2613

HEAT TRANSFER
NT AERODYNAMIC HEAT TRANSFER
NT CONDUCTIVE HEAT TRANSFER
NT CONVECTIVE HEAT TRANSFER
NT HYPERSONIC HEAT TRANSFER
NT LAMINAR HEAT TRANSFER
NT RADIATIVE HEAT TRANSFER
NT TURBULENT HEAT TRANSFER
Turbulent boundary layers over rough surface hypersonic flow
[AD-A145040] 01 p0003 N85-10016
Real time sensing and control of out-of-plane distortion due to line heating by laser
[AD-A144773] 01 p0027 N85-10169
The effect of channel convergence on heat transfer in a passage with short pin fins
[NASA-TM-83801] 01 p0046 N85-10303
Second All-Union Seminar on Hydromechanics and Heat and Mass Exchange in Weightlessness, summaries of reports
[NASA-TM-77590] 01 p0047 N85-10305
A review and analysis of boundary layer transition data for turbine application
[NASA-TM-86880] 01 p0047 N85-10306
Measurement and analysis of spark ignition engine pressure data to determine heat release profiles
[AD-A144770] 01 p0055 N85-10360
Turbine Engine Hot Section Technology (HOST)
[NASA-TM-83022] 02 p0140 N85-10851
Turbine heat transfer 02 p0142 N85-10864
Gas side heat transfer: 2-D flow
02 p0142 N85-10865
Gas flow environment and heat transfer nonrotating 3D program 02 p0142 N85-10866
Jet array impingement flow distributions and heat transfer characteristics: Effects of initial crossflow and nonuniform array geometry 02 p0142 N85-10867
Coolant passage heat transfer with rotation
02 p0143 N85-10869
Burner liner thermal/structural load modelling
02 p0143 N85-10870
Some of the features of movement of gas through a layer of free-flowing substances
[BLL-M-35732-(5828.4)] 02 p0196 N85-11312
Numerical analysis of flow and heat transfer in the VAFB LOX storage Dewar tank
[NASA-CR-171203] 02 p0197 N85-11315
Preliminary results of a study of the relationship between free stream turbulence and stagnation region heat transfer
[NASA-TM-86884] 02 p0197 N85-11317
Experimental and predicted heating distributions for biconics at incidence in air at Mach 10
[NASA-TP-2334] 03 p0361 N85-12313
Heat transfer and pressure drop in blade cooling channels with turbulence promoters
[NASA-CR-3837] 03 p0361 N85-12315
Oil-flow study of a Space Shuttle orbiter tip-fin controller
[NASA-TM-86276] 04 p0460 N85-1258
Proposal for wall function for friction and heat transfer in the presence of roughness and mass transfer
[CFD/84/12] 04 p0501 N85-1319
Multigrid iteration solution procedure for solving three-dimensional sets of coupled equations
[DE84-016515] 04 p0555 N85-1350
Multigrid iteration solution procedure for solving two-dimensional sets of coupled equations
[DE84-016554] 04 p0555 N85-1350
The Interaction of Global Biochemical Cycles
[NASA-CR-174184] 05 p0682 N85-1418
Air-sea heat exchange, an element of the water cycle
05 p0682 N85-1418

Salt-gradient solar ponds: Summary of US Department of Energy sponsored research
[NASA-CR-174183] 05 p0667 N85-14266

Solar pond fluid dynamics and heat transfer
05 p0667 N85-14268

Cage regional energy budgets from the GLAS ATH order model 05 p0685 N85-14402

Analysis of physical-chemical processes governing SSME internal fluid flows
[NASA-CR-174245] 06 p0760 N85-14862

Heat transfer results and operational characteristics of the NASA Lewis Research Center Hot Section Cascade Test Facility
[NASA-TM-86890] 06 p0808 N85-15133

Energy active areas of ocean
06 p0820 N85-15204

Indirect estimation of convective boundary layer structure for use in routine dispersion models
[PB84-226260] 06 p0834 N85-15306

Thermodynamical characteristics of heat storage reactors using metal hydrides
[NAL-TR-822] 06 p0869 N85-15524

Engine Cyclic Durability by Analysis and Testing
[AGARD-CP-368] 07 p0905 N85-15733

Monitoring engine thermal stresses
07 p0906 N85-15735

Heat transfer due to film condensation on vertical fluted tubes
[AD-A147258] 07 p0959 N85-16079

High temperature thermocouple and heat flux gauge using a unique thin film-hardware hot juncture
[NASA-TM-86896] 07 p0962 N85-16096

Razrezy program research in the tropical Atlantic
07 p0981 N85-16229

Frazil ice formation
[AD-A147425] 07 p0988 N85-16279

Experiment on triggered fragmentation on a molten copper droplet in water
[BLL-WH-602-(9091.9F)] 08 p1125 N85-17091

Capillary Pump Loop (CPL) heat pipe development status report
[NASA-CR-175273] 08 p1161 N85-17323

Computation of flow and heat transfer in flow around a 180 deg bend
[AD-A148065] 08 p1162 N85-17330

Subcooled flow boiling at high heat flux
[OUEL-1540/84] 08 p1163 N85-17338

Characterization of heat transfer in nutrient materials -- space flight feeding
[NASA-CR-171841] 08 p1199 N85-17551

Numerical investigation of phase change heat transfer in a horizontal cylinder including effects of natural convection 09 p1318 N85-18286

Heat-transfer enhancement in natural convection enclosure flow
[DE84-013048] 09 p1319 N85-18297

Optimization of design and control strategies for geothermal space heating systems
[DE85-000496] 09 p1344 N85-18458

Heat transfer and mechanical interactions in fusion nuclear systems
[DE84-016233] 09 p1392 N85-18761

A diffuser heat transfer code
[AD-A148270] 10 p1430 N85-19022

Investigation on the burning of unpulverized coal in a self excited acoustic field
[INPE-3295-PRE/610] 10 p1434 N85-19035

Design of low loss helix circuits for interference fitted and brazed circuits
[NASA-CR-168313] 10 p1476 N85-19328

Effect of inclination, transverse intertip spacing, and logitudinal pitch on crossflow heat transfer from an array of finned tubes 10 p1482 N85-19359

Experimental study of ceramic coated tip seals for turbojet engines
[NASA-TM-86939] 10 p1483 N85-19363

Ribbon burner simulation of T-700 turbine shroud for ceramic lined seals research
[NASA-TM-86940] 10 p1483 N85-19364

Internal forced convection to low Prandtl number gas mixtures
[AD-A148832] 10 p1484 N85-19366

Analysis of compact heat exchanger performance
[DE84-012824] 10 p1485 N85-19377

Momentum and heat transfers in a complex, but well-defined turbulent fluid flow
[DE85-000857] 10 p1486 N85-19381

Heat and mass exchange in a partially stratified fluid
[DE85-000526] 10 p1486 N85-19384

SBPS-CRS advanced sodium receiver: Construction experience report
[DE85-000825] 10 p1511 N85-19533

LOVEL-84: A LOw-VELocity aerodynamic heating code for flat plates, wedges, and cones
[DE85-000804] 11 p1576 N85-19933

Thickness effect in low-density insulation
[DE85-003065] 11 p1631 N85-20273

Envelope thermal test unit: Technical description
[DE84-012254] 11 p1674 N85-20548

Magnetic fluctuations, field reversal maintenance, and anomalous thermal transport in the reversed field pinch
[DE85-003804] 11 p1732 N85-20892

Numerical model for swirl cooling in high-heat-flux particle beam targets and the design of a swirl-flow-based plasma limiter
[DE85-003824] 11 p1732 N85-20894

Advanced liner-cooling techniques for gas turbine combustors
[NASA-TM-86952] 12 p1770 N85-21115

Aerostructure nondestructive evaluation by thermal field detection. Phase 2: Technique refinement and quantitative determination of flaw detection capabilities
[AD-A149622] 12 p1777 N85-21155

Improvements in glazings: SERI materials research in progress
[DE84-013049] 12 p1814 N85-21378

Method of calculating cooldown process in cryostat of cryogenic electric machine 12 p1843 N85-21567

Nested subcritical flows within supercritical systems
[NASA-TM-86960] 12 p1845 N85-21574

Mechanisms of heat and mass transfer across a double-diffusive interface
[PB85-148468] 12 p1848 N85-21594

Response time correlations for platinum resistance thermometers in flowing fluids
[NASA-CR-172523] 12 p1850 N85-21606

Experimental study of steam condensation on water in countercurrent flow in presence of inert gases
[DE84-013028] 12 p1861 N85-21800

Multi-year plan for Experimental Systems Research: Passive and hybrid solar energy program
[DE85-004698] 12 p1862 N85-21810

Heat Cycle Research Experimental Program report, FY-84
[DE85-003558] 12 p1862 N85-21811

Multiyear plan for experimental systems research passive and hybrid solar energy program
[PB85-146868] 12 p1863 N85-21815

General-purpose heat source development: Safety test program. Postimpact evaluation, design iteration test 1
[LA-9680-SR] 12 p1931 N85-22131

Coupling between velocity oscillations and solid propellant combustion 13 p2000 N85-22536

Pressure drop and coefficients of internal heat transfer necessary for transpiration cooling
13 p2050 N85-22831

effect of gas stream sweeping past the effluent of a perforated plate on heat transfer inside the perforations
13 p2051 N85-22836

Two-dimensional numerical model of sensible and latent heat transport in an irrigated field under advective conditions 13 p2131 N85-23261

H-division materials physics progress
[DE85-004990] 13 p2165 N85-23430

Classification of circular features on Venus
13 p2177 N85-23511

Hydrovolcanism 13 p2188 N85-23574

Physics of the inner heliosphere: Mechanisms, models and observational signatures
[NASA-CR-175632] 13 p2205 N85-23677

Experimental study of heat transfer from shaft in cooled radial bearing of GNT-25 gas turbine
14 p2270 N85-24068

Fluid mechanics and heat transfer spirally fluted tubing
[AD-A150774] 14 p2301 N85-24247

Heat transfer to vertical flat plates in a rectangular gas-fluidized bed
[AD-A150785] 14 p2301 N85-24248

Effect of form and clearance of a piston launched in a tube on the boundary layer and the heat transfer
[ISL-CO-216/83] 14 p2302 N85-24255

Mass and heat transfer in reflux condensers of absorption heat pumps
[DFVLR-FB-83-43] 14 p2304 N85-24266

Parameterization of apparent and latent heat fluxes above water surface in calm weather under natural conditions 14 p2337 N85-24454

Equipment for hot-to-serve foods
14 p2393 N85-24741

Two-phase fluid thermal transport for spacecraft
[AD-A151316] 15 p2493 N85-25376

Manrating orbital transfer vehicle propulsion
[NASA-TM-87019] 15 p2494 N85-25385

Heat transfer and fluid mechanics measurements in the turbulent reattaching flow behind a backward-facing step
15 p2553 N85-25753

The influence of jet-grid turbulence on heat transfer from the stagnation region of a cylinder in crossflow
[NASA-TM-87011] 15 p2554 N85-25760

Flow over a biconic configuration with an afterbody compression flap
[AD-A151882] 15 p2557 N85-25776

Transient technique for measuring heat transfer coefficients on stator airfoils in a jet engine environment
[NASA-TM-87005] 15 p2560 N85-25794

NASTRAN's application in agricultural engineering
15 p2575 N85-25880

Summaries of FY 1984 engineering research
[DE85-006273] 15 p2664 N85-26442

Advanced rocket engine cryogenic turbopump bearing thermal model 16 p2735 N85-26879

Analysis of combustion oscillations in heterogeneous systems
[AD-A151999] 16 p2745 N85-26942

The use of heat pumps in district heat supply
[BLL-OA-TRANS-2728-(6196.3)]
16 p2761 N85-27103

Two-d heat transfer through porous media with heat generation
[AD-A151965] 16 p2783 N85-27173

Component-specific modeling
[NASA-CR-174765] 16 p2799 N85-27261

A computer analysis program for interfacing thermal and structural codes
[NASA-TM-87021] 16 p2800 N85-27264

Fog advection in the Namib 16 p2831 N85-27454

Adaptive grid generation for numerical solution of Burger's equation
[AD-A152217] 16 p2855 N85-27606

Future fundamental combustion research for aeropropulsion systems
[NASA-TM-87049] 17 p2898 N85-27870

Investigation of heat transfer to a turbine blade cascade using a shock tube
[AD-A153090] 17 p2898 N85-27871

Overview of aerothermodynamic loads definition study
17 p2910 N85-27942

Fuel freeze point investigations
[AD-A152801] 17 p2937 N85-28129

Stefan-Maxwell relations for plasma diffusion currents in magnetic field 17 p2942 N85-28160

FLOWPLOT 2: A fluid dynamics and heat transfer plotting package
[DE85-009802] 17 p2959 N85-28277

Heating parameter estimation using coaxial thermocouple gages in wind tunnel test articles
[AD-A153039] 17 p2968 N85-28328

Experimental and theoretical studies on transport processes in laser welding
[DE84-008572] 17 p2975 N85-28378

Simplified analysis of Stirling engines and heat pumps
[DE85-006753] 17 p2986 N85-28457

Performance of an active/passive hybrid solar system utilizing vapor transport
[DE85-006627] 17 p2988 N85-28466

TRINITY: A pre- and post-processing program for 2-dimensional finite element data
[DE85-008029] 17 p3013 N85-28628

Large, energetic cluster impacts on surfaces
[DE85-006559] 17 p3034 N85-28769

Handbook on superconductivity: The large-scale applications. Chapter 4
[DE85-008170] 17 p3044 N85-28838

Heat management system for aircraft
[AD-D011658] 18 p3061 N85-28936

High thermal power density heat transfer apparatus providing electrical isolation at high temperature using heat pipes
[NASA-CASE-LEW-12950-2] 18 p3098 N85-29179

Monogroove heat pipe design: Insulated liquid channel with bridging wick
[NASA-CASE-MSC-20497-1] 18 p3098 N85-29180

Circulation and transport in the middle atmosphere: Tropouphere and lower atmosphere
18 p3148 N85-29491

Circulation and transport in the middle atmosphere: Mesosphere and lower thermosphere
18 p3148 N85-29492

Energy deposition and its effects on the E+ capture section at Sector 20
[DE85-010964] 18 p3182 N85-29727

Thermochemical energy transport using a hydrogen rich working fluid
[AD-D011696] 19 p3233 N85-30042

An experimental investigation of curvature and freestream turbulence effects on heat transfer and fluid mechanics in transitional boundary layer flows
19 p3264 N85-30240

Turbulent transport and length scale measurement experiments with confined coaxial jets
[NASA-CR-174831] 19 p3266 N85-30245

Mathematics of oil production
[DE85-011236] 19 p3267 N85-30261

Design and operation of solar thermal heat transfer systems
[DE85-009837] 19 p3267 N85-30263

Comparison and evaluation of field and numerical results from the Site A heater test at Avery Island
[DE85-010625] 19 p3268 N85-30269

Loss-of-flow transient characterization in carbide-fueled LMFBRs
[DE85-009552] 19 p3269 N85-30270

Flow visualization study of inverted annular flow of post dryout heat transfer region
[DE85-010482] 19 p3269 N85-30275

Intrinsically irreversible acoustic heat engines
[DE85-007672] 19 p3270 N85-30276

Heat flow through ocean floor and its relationship to lithosphere structure and thickness
19 p3294 N85-30422

Transition in Turbines
[NASA-CP-2386] 20 p3452 N85-31433

Preliminary results of a study of the relationship between free-stream turbulence and stagnation region heat transfer 20 p3452 N85-31435

Transition in a disturbed environment
20 p3452 N85-31436

Flat-plate transition 20 p3452 N85-31438

Heat transfer and fluid mechanics measurements in transitional boundary layer flows
20 p3453 N85-31439

A review and analysis of boundary layer transition data for turbine application 20 p3453 N85-31440

Heat transfer in aeropropulsion systems
[NASA-TM-87066] 20 p3453 N85-31444

Stability analysis of direct contact heat exchangers subject to system perturbations
[DE85-011780] 20 p3455 N85-31452

Heat transfer monitor for measurements of fouling of industrial heat exchangers
[DE85-010257] 20 p3455 N85-31455

Preliminary wind tunnel experiments to investigate the effect of heat transfer on the dispersion of cold dense gases
[OUEL-1546/84] 20 p3456 N85-31467

PHOENICS 84: A multi-dimensional multi-phase general-purpose computer simulator for fluid flow, heat transfer and combustion: 36 lecture panels
[CFD/84/18] 20 p3457 N85-31468

Influence of spatial variability of hydraulic characteristics of soils on surface parameters obtained from remote sensing data in infrared and microwaves
[NASA-TM-77902] 20 p3477 N85-31604

R and D activities of the Propulsion Division
20 p3539 N85-32025

Wall flames and implications for upward flame spread
[FAA-CT-85-2] 21 p3553 N85-32103

Imbedded thermocouples as a solid propellant combustion probe
[AD-A155630] 21 p3564 N85-32167

An investigation into the fluidization and heat transfer of low density particles in a fluidized bed with applications
[AD-A155259] 21 p3584 N85-32282

Numerical solutions of turbulent models for flow over a flat plate with angle of attack
[DE85-010360] 21 p3585 N85-32286

Forced convection on solar collector arrays
[DE85-010361] 21 p3585 N85-32287

Resolution of thermal striping issue downstream of a horizontal pipe elbow in stratified pipe flow
[DE85-006195] 21 p3586 N85-32292

Concurrent implementation of the Crank-Nicolson method for heat transfer analysis
[NASA-TM-86446] 21 p3674 N85-32822

Oscillatory solutions of the Peaceman-Rachford alternating direction implicit method and a comparison of methods for the solution of the two dimensional heat diffusion equation
[AD-A154670] 21 p3675 N85-32833

SHELTER: Description of a program code — indoor climate
[FOA-C-58002-H1] 22 p3755 N85-33278

TEMO and TEB thermoelectronic devices
22 p3779 N85-33415

Local heat-transfer measurements on a large, scale-model turbine blade airfoil using a composite of a heater element and liquid crystals
[NASA-TM-86900] 22 p3782 N85-33435

Heat-mass flow enhancement system for a metal hydride assembly
[DE85-010698] 22 p3783 N85-33441

Advances in open-cycle solid desiccant cooling
[DE85-006797] 22 p3808 N85-33590

Microwave radiation and thermoregulation
[AD-A155718] 22 p3816 N85-33654

Component-specific modeling
[NASA-CR-174765] 23 p3897 N85-34140

Numerical model of a pulse combustor
[DE85-011717] 23 p3912 N85-34240

The application of models to the assessment of fire hazard from consumer products
[NBSIR-85-3219] 23 p3925 N85-34325

Technical assessment of thermal-hydraulics for high heat flux fusion components
[DE85-013178] 23 p3930 N85-34359

Preliminary SPR thermal model description and results for WH-11 and BM-4
[DE85-013171] 23 p3931 N85-34360

Thermal transport measurements of UV laser irradiated spherical targets
[DE85-011036] 23 p3931 N85-34365

Vapor phase heat transport concepts
[DE85-009550] 23 p3931 N85-34366

Forced convective, nonequilibrium, post-CHF heat transfer experiment data and correlation comparison report
[TI85-009331] 23 p3932 N85-34371

Determination of properties of zeolite/refrigerant combinations for solar refrigeration systems
[DE85-012009] 23 p3945 N85-34448

Ocean thermal energy conversion
[DE85-012291] 23 p3946 N85-34456

Studies in thermo-hydro-chemical transport in porous and fractured media
[DE85-012555] 23 p3949 N85-34473

Advanced regenerative heat recovery system
[PB85-199602] 24 p4084 N85-35315

High Temperature Heating System (HTHS)
[PB85-186340] 24 p4084 N85-35316

Heat transfer characteristics for two-dimensional arrays of impinging jets with initial crossflow
24 p4092 N85-35365

A two-phase flow and heat transfer model for zero gravity
[AD-A156097] 24 p4094 N85-35377

Experimental study of free and mixed convective flow of air in a heated cavity
[DE85-012538] 24 p4094 N85-35380

Enhanced heat transfer computations for internally cooled cable superconductor
[DE85-011697] 24 p4095 N85-35383

Transient three-phase three-component systems. Part 1: Formulation of the system of differential equations
[DE85-013267] 24 p4095 N85-35384

Heat transfer and brine evolution in magma-hydrothermal systems 24 p4104 N85-35441

Computer code calculations of the TMI-2 accident: Initial and boundary conditions
[DE85-012613] 24 p4140 N85-35666

Analysis of reactor material experiments investigating oxide fuel crust stability and heat transfer in jet impingement flow
[DE85-012097] 24 p4151 N85-35739

HEAT TRANSFER COEFFICIENTS

Laminar flow heat exchangers. Viscosity induced non-uniform flow
[AD-A144777] 01 p0047 N85-10307

Overall heat transfer coefficients for a horizontal cylinder in a fluidized bed
[AD-A144878] 01 p0124 N85-10849

Internal heat transfer and pressure drop measurements in a variously baffled shell and tube heat exchanger
03 p0360 N85-12310

Calculating heat transfer coefficients for turbine profiles taking surface curvature and elevated flow turbulence into account 09 p1307 N85-18212

Convection heat transfer in the critical region of fluid mixtures
[DE85-001282] 11 p1633 N85-20285

Transport processes in the upper atmosphere
11 p1646 N85-20375

Turbulent convecting flow in a square duct with a 180 deg bend: An experimental and numerical study
[AD-A149989] 12 p1846 N85-21563

Two-phase fluid thermal transport for spacecraft
[AD-A151316] 15 p2493 N85-25378

Characteristics of heat exchange in the region of injection into a supersonic high-temperature flow
[NASA-TM-77833] 15 p2555 N85-25762

Filmwise condensation of steam on low integral-finned tubes
[AD-A152220] 16 p2783 N85-27176

An experimental apparatus to study nucleate pool boiling of R-114 and oil mixtures
[AD-A154077] 19 p3265 N85-30249

The effect of injection-stream turbulence on film cooling effectiveness and heat transfer coefficients
20 p3451 N85-31424

The influence of oil contamination on the nucleate pool-boiling behavior of R-114 from a structured surface
[AD-A155809] 21 p3585 N85-32284

Local heat-transfer measurements on a large, scale-model turbine blade airfoil using a composite of a heater element and liquid crystals
[NASA-TM-86900] 22 p3782 N85-33435

Heat transfer coefficients for particles in liquid in axially rotating cans 24 p4093 N85-35378

A two-phase flow and heat transfer model for zero gravity
[AD-A156097] 24 p4094 N85-35377

HEAT TRANSMISSION
NT AERODYNAMIC HEAT TRANSFER
NT CONDUCTIVE HEAT TRANSFER
NT CONVECTIVE HEAT TRANSFER
NT HEAT TRANSFER
NT HYPERSONIC HEAT TRANSFER
NT LAMINAR HEAT TRANSFER
NT RADIATIVE HEAT TRANSFER
NT TURBULENT HEAT TRANSFER

Investigation of heat exchange on models in subsonic jets of induction plasmatron 02 p0260 N85-11756

Heat flow map of Europe: Brief summary of the geophysical implications
[REPT-562] 03 p0377 N85-12405

Terrestrial heat flow in Europe and general features of its regional distribution
[REPT-563] 03 p0377 N85-12406

Megaregolith thickness, heat flow, and the bulk composition of the Moon 04 p0583 N85-13723

Procedural aspects of testing aerodynamic models with combustion in high-enthalpy transient-mode installations
05 p0725 N85-14659

Interpreting geothermal anomalies by special points method 07 p0982 N85-16239

Thermal conditions and thinning of lithosphere in late cenozoic in southwestern US 10 p1501 N85-19473

Characterization of the heat source distribution of a typical GTAW welding arc
[DE85-004322] 12 p1861 N85-21670

Normal and anomalous geothermal fields and their relationship to hierarchy of geological bodies
13 p2113 N85-23163

Determining deep heat flow and rate of horizontal percolation from temperature measurements in aquifer
13 p2116 N85-23180

Use of heat pipes for heat collection and transmission in solar plants 14 p2265 N85-24037

Structure of cold film in water-air boundary layer
14 p2335 N85-24443

Determination of permissible heating rate of metal
[BLL-M-36107-(5828.4)] 16 p2748 N85-26987

Evolution of the oceanic upper mantle and effects on sea floor subsidence geoid height and heat flow
19 p3319 N85-30575

Stability analysis of direct contact heat exchangers subject to system perturbations
[DE85-011780] 20 p3455 N85-31452

MPS solidification model. Analysis and calculation of macrosegregation in a casting ingot
[NASA-CR-171589] 21 p3566 N85-32178

In-situ measurement of wall thermal performance: Data interpretation and apparatus design recommendations
[DE85-011979] 21 p3586 N85-32289

On the importance of viscous dissipation in Io
22 p3855 N85-33873

Adiabatic thermal models for planetary bodies
22 p3857 N85-33881

Spectral evolution of gamma-rays from adiabatically expanding sources in dense clouds
[OG-2.5-2] 22 p3869 N85-33959

Detailed validation of a liquid and heat flow code against field performance
[DE85-009901] 23 p3932 N85-34380

Advanced regenerative heat recovery system
[PB85-199602] 24 p4084 N85-35315

Geothermal resources of the Washakie and Great Divide basins, Wyoming
[DE85-013004] 24 p4112 N85-35491

HEAT TREATMENT
NT ANNEALING
NT LASER ANNEALING
NT NITRIDING
NT PULSE HEATING
NT STRESS RELIEVING
NT TEMPERING

Heat treatment of welded joints in OT4 and VT20 titanium alloys 01 p0020 N85-10119

Injection molding of silicon carbide capable of being sintered without pressure
[NASA-TM-77736] 01 p0035 N85-10221

Energy-saving technological methods of obtaining controlled atmospheres
[BLL-M-35724-(5828.4)] 02 p0171 N85-11145

Metallurgy of a 12 percent chromium stainless steel
02 p0178 N85-11196

Mechanism of brittle heat fracture of inhomogeneous solids by high temperature gas jets
02 p0265 N85-11731

The effect of heat treatment on wear resistance of gas-plasma eutectic coatings
[BLL-M-35758-(5828.4)] 03 p0329 N85-12122

A study of precipitation and boron distribution in 20 Cr 29Ni base stainless steels
[AERE-M-3353] 03 p0334 N85-12154

Effect of heat treatment on phase composition and crystal structure of thin WSi2 films on silicon substrates
03 p0350 N85-12253

Effect of oxidizing medium and heat treatment on stoichiometry of ZnSe crystal surface
03 p0353 N85-12272

Dependence of microplasticity of beryllium on grain size and heat treatment 03 p0353 N85-12273

The disordering process in an L1sub2 ordered alloy
[DE84-016599] 04 p0475 N85-13028

Change in the nitrogen content when nitrided alloys are heated
[BLL-M-35946-(5828.4)] 05 p0615 N85-13929

Impact toughness of wire after cold deformation and annealing
[BLL-M-35941-(5828.4)] 05 p0615 N85-13930

Influence of hydrogen saturation and prior heat treatment on graphitization of white cast iron
[BLL-M-35964-(5828.4)] 05 p0615 N85-13932

Creep of chemically vapor deposited SiC fibers
[NASA-TM-86897] 06 p0763 N85-14878

The effect of potential on the corrosion fatigue behavior of a precipitation hardened aluminum alloy
[AD-A146537] 06 p0768 N85-14916

Development of high-efficiency solar cells on silicon web
[NASA-CR-174212] 06 p0828 N85-15259

Problems and possibilities for life extension in gas turbine components 07 p0907 N85-15742

The formation of isolated phase precipitates during the decomposition of high-coercive force Fe-Cr-Co alloys
[BLL-M-36028-(5828.4)] 07 p0924 N85-15855

Procedure for investigating high-temperature properties of iron-ore materials
[BLL-M-36020-(5828.4)] 07 p0926 N85-15868

On heat-treatable copper-chromium alloy, 1
[NASA-TM-77753] 07 p0927 N85-15879

Method for bonding insulator to insulator
[AD-D011340] 07 p0929 N85-15891

Dependence of breakdown voltage for p-n junction on parameters of ion implantation and semiconductor heat treatment 07 p0954 N85-16046

Effects of oxygen on the microstructure and properties of titanium 6211 alloys
[AD-P004122] 08 p1126 N85-17097

Electromagnetic processing of materials
[AD-A148804] 09 p1311 N85-18241

New method for heat treatment of metals
10 p1446 N85-19110

Influence of laser hardening on mechanical properties of type 45 steel with various preliminary heat treatments
10 p1446 N85-19111

The response of cobalt-free Udimet 700 type alloy to modified heat treatments
[NASA-TM-86942] 11 p1597 N85-20043

USSR report: Materials science and metallurgy
[JPRS-UMS-84-006] 11 p1597 N85-20044

Micrographic and fractographic examination of alloys 2214 and 2024 for conditions which would cause burning of the metal on being put into solution, trial 17/175
[DGT-23.419] 11 p1609 N85-20117

Chemical and photographic evaluation of rigid explosive transfer lines
[AD-A149303] 11 p1613 N85-20145

Method for refining microstructures of cast titanium articles
[AD-D011518] 12 p1804 N85-21318

Microstructural and electronic characteristics of metallic spin glasses
[AD-A149950] 12 p1813 N85-21371

Influence of laser treatment of structure and mechanical properties if MA21 alloy 13 p2029 N85-22713

Specifics of laser heat treatment of high steel tools
13 p2029 N85-22714

Specifics of kinetics of polymorphous conversion upon heating of low carbon steels 13 p2030 N85-22721

Effect of zero-wear in friction pairs operating in abrasive media
13 p2045 N85-22801

Stability of three-layer glass-reinforced plastic shells of rotation
13 p2047 N85-22813

Microstructural study on the processing and properties of high-field A15 superconducting materials
[DE85-004652] 13 p2164 N85-23423

Case depth on flanks of gears for helicopter gearboxes
14 p2222 N85-23780

Synthesis and properties of elevated temperature P/M aluminum alloys
[AD-A151031] 14 p2256 N85-23961

Role of residual stresses in stress corrosion cracking in alloy 600 tubes. Part 1: Determination of throughwall residual stresses and their modification by transient heat treatment
[DE85-004648] 14 p2257 N85-23988

Robotized system for treating gear wheels
14 p2285 N85-24162

Influence of phosphorus content and heat treatment on the machinability of electroless nickel deposits
[DE85-007250] 15 p2522 N85-25546

Properties and microstructures for dual alloy combinations of three superalloys with alloy 901
[NASA-TM-86967] 16 p2749 N85-26963

Thermodynamic analysis of the plasma nitriding of ferrovanadium
[BLL-BISI-TRANS-22237-(9022.06)]
17 p2924 N85-28032

Thermomechanical softening treatment for bearing and tool steels
[BLL-BISI-TRANS-22432-(9022.06)]
17 p2925 N85-28035

Improving the properties of copper and copper alloys through heat treatment and alloying
[BLL-BISI-TRANS-21939-(9022.06)]
17 p2926 N85-28047

The state of martensite after quenching in a magnetic field
[BLL-BISI-TRANS-22297-(9022.06)]
17 p2926 N85-28051

Influence of heat treatment parameters on the properties of induction hardened Ni-Cr-Mo steels
[BLL-BISI-TRANS-2499-(9022.06)]
17 p2926 N85-28053

Textural transformations taking place during heat and mechanical treatment in triplex steels
[BLL-BISI-TRANS-22404-(9022.06)]
17 p2927 N85-28063

Effects of the phase compositions of cast low-pearlite steels micro-alloyed with vanadium and titanium of their structure and properties
[BLL-BISI-TRANS-22301-(9022.06)]
17 p2928 N85-28067

Technological apparatus for laser treatment of materials 17 p2944 N85-28174

Local heat treatment of welded joints of pipes and rotary vessels
[BLL-BISI-TRANS-22197-(9022.06)]
17 p2972 N85-28354

Technical information: Weldability of stainless steel. Part 1: Austenitic stainless steel
[BLL-BISI-TRANS-22456-(9022.06)]
17 p2973 N85-28362

Effects of the structural state in thermo-bimetals on their resistance to microscopic plastic deformation
[BLL-BISI-TRANS-22403-(9022.06)]
17 p2979 N85-28412

Plasma processing of materials
[AD-A152396] 17 p3039 N85-28800

Evaluation of 7XXX-series aluminum alloys for the W87 aft support ring
[DE85-009967] 18 p3076 N85-29027

Rolling contact fatigue testing of thermomechanically processed M-50 steel
[AD-A153640] 18 p3122 N85-29327

Internal structure of GP zones in dilute Al-Cu alloys
19 p3238 N85-30073

Effects of heat treatment and tracer element impurities on the impact properties of the 12Cr steels
[DE85-010676] 19 p3240 N85-30088

Possible causes of modification and strengthening of aluminum by scandium 19 p3241 N85-30099

Effect of thermochemical processing on fatigue resistance of titanium alloys 19 p3244 N85-30112

Structure and properties of VT23 alloy welded joints after thermocyclic processing 19 p3246 N85-30125

Method for the preparation of photochromic insulating crystals
[DE85-011606] 19 p3262 N85-30229

Plasma spray screen repair method
[AD-D011713] 19 p3281 N85-30346

Long-term thermal aging of Celion/V378A composite materials
[NASA-TM-86362] 20 p3421 N85-31236

Structural transformation of a 9% Cr - 2%Mo steel (type Z10CDNbV 09-02) for use in steam generators for fast neutron reactors
[BLL-CE-TRANS-7943-(9022.09)]
20 p3430 N85-31271

Influence of gamma-phase on magnetic properties and structure of KhK15YuB alloy during strain-aging
[BLL-M-36281-(5828.4)] 20 p3431 N85-31280

Influence of recrystallization and solution on the tenacity of the 7010 and 7475 alloys. Olygocyclic fatigue of the 7010 alloy
[ONERA-RT-19/5069-M] 20 p3432 N85-31289

Electrical and structural characterization of web dendrite crystals 20 p3481 N85-31633

Metallurgical origins of fracture toughness and microstructure and fracture toughness of an HSLA (High-Strength/Low-Alloy) steel
[AD-A155530] 21 p3567 N85-32187

Electrical and mechanical properties of intercalated graphite fibers
[AD-A155560] 21 p3570 N85-32205

Strain rate sensitivity estimation from high velocity impact data
[AD-A154703] 21 p3599 N85-32347

Maintenance and the military environment
22 p3750 N85-33243

The study of the effect of residual microimpurities on the fatigue strength of 55S2 steel
[BLL-M-36317-(5828.4)] 23 p3913 N85-34246

The effect of pre-heating on the structure and properties of chromiun-molybdenum steels
[BLL-M-35897-(5828.4)] 23 p3914 N85-34255

Properties of tungsten-free steel for cutting tools
[BLL-M-35808-(5828.4)] 23 p3915 N85-34259

Stress corrosion cracking susceptibility of types 316NG and 316 stainless steel in an impurity environment
[TI85-006864] 23 p3917 N85-34277

The read-out system of spatial distribution of thermoluminescence in meteorites
[SH-9.1-16] 23 p4052 N85-35131

Studies of the crystallization process of aluminum-silicon alloys using a high temperature microscope
[NASA-TM-77869] 24 p4078 N85-35272

The dynamic strain ageing of A533B class 1 nuclear pressure vessel steel
[AERE-R-11485] 24 p4078 N85-35274

Effect of thermal ageing on the mechanical properties of PWR pressure vessel steels and weldments
[AERE-R-11460] 24 p4078 N85-35275

The character of observed porosity and its possible effects on rolling contact fatigue life of M-50 steel
[AD-A155930] 24 p4079 N85-35279

Development of a high strength isothermally heat-treated nodular iron road wheel arm
[AD-A155755] 24 p4099 N85-35406

HEATERS

Experimental study on the glow plug aided alcohol driven diesel engine 04 p0483 N85-13078

Heater block assembly for use in thermal oxidation testing of jet fuel
[AD-D011430] 08 p1123 N85-17077

Experimentally determined characteristics of vortex heaters 13 p2050 N85-22833

Heat resistant sheathed insulated electrical conductors
[AD-D011644] 17 p2951 N85-28219

Physiochemically controlled scour jet array system
[AD-D011688] 19 p3306 N85-30505

Toxic hazards tests for vehicles and other equipment
[AD-A149164] 20 p3506 N85-31797

Feedback regulated induction heater for a flowing fluid
[DE85-006508] 23 p3939 N85-34414

HEATING

NT AERODYNAMIC HEATING
NT ATMOSPHERIC HEATING
NT ELECTRON CYCLOTRON HEATING
NT GAS HEATING
NT INDUCTION HEATING
NT IONOSPHERIC HEATING
NT KINETIC HEATING
NT LASER HEATING
NT PLASMA HEATING
NT PULSE HEATING
NT RADIANT HEATING
NT RADIO FREQUENCY HEATING
NT RESISTANCE HEATING
NT SHOCK HEATING
NT SOLAR HEATING
NT SPACE HEATING (BUILDINGS)
NT SUPERHEATING
NT TRANSIENT HEATING
NT WATER HEATING

Treating silicon carbide sinter by heating in nitrogen
[NASA-TM-77601] 01 p0021 N85-10130

Real time sensing and control of out-of-plane distortion due to line heating by laser
[AD-A144773] 01 p0027 N85-10169

Determining the optimum heating parameters for precision alloys — iron-nickel alloys
[BLL-M-35718-(5824.4)] 02 p0174 N85-11167

Robotization of technological processes in high-frequency heating and welding
03 p0345 N85-12226

Dynamic thermal episodes in the protosolar nebula: Development of models from observations on CAI's
06 p0667 N85-15633
Analysis of the heating process of a body in a melt
[BLL-M-36014-(5828.4)] 07 p0956 N85-16057
The Origin of Nonradiative Heating/Momentum in Hot Stars
[NASA-CP-2358] 08 p1231 N85-17755
Evidence for non-radiative activity in stars with T sub eff 10000 K
08 p1231 N85-17757
Non-radiative energy from differential rotation in hot stars
08 p1234 N85-17778
Nonradiative heating and enhanced mass-loss due to shear turbulence in massive hot stars
08 p1235 N85-17780
A leaky waveguide model for MHD wave driven winds from coronal holes
08 p1235 N85-17781
Radiatively driven winds and what they imply: A review of radiative driven instabilities and their importance in hot stars
08 p1235 N85-17782
Magnetic effects in the heating and modification of flows in the outer stellar atmospheres with application to early type star case
08 p1235 N85-17783
ORNL ECR multicharged ion source
[DE85-001283] 09 p1380 N85-18681
On shrinkage and molecular extension
[AD-A149100] 10 p1451 N85-19144
Method of heating quartz resonators
[AD-D011454] 10 p1481 N85-19347
Picosecond laser pulse interactions with metallic and semiconductor surfaces
[AD-A149112] 10 p1490 N85-19405
VHF radar observations in the stratosphere and mesosphere during a stratospheric warming
11 p1661 N85-20466
Improvements in glazings: SERI materials research in progress
[DE84-013049] 12 p1814 N85-21378
Re-design of ARL/HLF (Heated Laminar Flow) body nose region
[AD-A150063] 12 p1846 N85-21585
Influence of substrate heating and thermal annealing on the surface crystallinity in single Si crystals implanted with high doses of (16)O
[DE85-005264] 13 p2164 N85-23428
Thermal and thermoelastic effects in rolling/sliding contacts
[AD-A150435] 13 p2165 N85-23429
Railgun conductor heating from multiple current pulses
[DE85-005333] 14 p2265 N85-24031
Equipment for hot-to-serve foods
14 p2393 N85-24741
New control design principles based on measured performance and energy analysis of HVAC (Heating, Ventilating, and Air-Conditioning) systems
[AD-A151708] 15 p2522 N85-25546
Numerical simulation of boundary layer excitation by surface heating/cooling
[NASA-CR-172575] 15 p2554 N85-25756
A feasibility study for using low boiling point fluids to change aircraft tire deflection
[AD-A152096] 16 p2706 N85-26701
Metal armatures for railguns
[AD-A152129] 16 p2728 N85-26836
Microwave processing of lunar materials: Potential applications
[DE85-007223] 16 p2755 N85-27003
Investigation of the requirement for auxiliary heating of Canadian forces personnel
[AD-A151950] 16 p2841 N85-27522
Hydrogen recovery from extraterrestrial materials using microwave energy
[DE85-006717] 16 p2883 N85-27789
Thermal donor removal by rapid thermal annealing: Infrared absorption
[DE85-010092] 18 p3081 N85-29059
Low gravity exothermic heating/cooling apparatus
[NASA-CASE-MSC-25707-1] 18 p3104 N85-29214
Tokamak ignition/burn experimental research device
[DE85-009999] 18 p3190 N85-29785
The nature of the anomalies on the polytherms of the properties of molten metallic alloys
[BLL-M-36265-(5828.4)] 20 p3430 N85-31277
Self-heating to ignition measurements and computation of critical size for solar energy collector materials
[PB85-183374] 20 p3485 N85-31663
Development of a prototype energy meter
[PB85-196430] 22 p3769 N85-33476

HEATING EQUIPMENT
NT BOILERS
NT ELECTRIC FURNACES
NT EVAPORATORS
NT FURNACES
NT IMAGE FURNACES
NT SOLAR FURNACES
NT VACUUM FURNACES
NT VAPORIZERS
FORTRAN 77 computer program for test procedure calculations of vented heaters
[PB85-109627/GAR] 09 p1305 N85-18198
Leak monitoring in high pressure preheaters by a noninvasive ultrasonic method
[CISE-2373] 11 p1650 N85-20394
Leak detection by acoustic emission monitoring in power plant high pressure preheaters
[CISE-2392] 11 p1650 N85-20395
Investigation of the requirement for auxiliary heating of Canadian forces personnel
[AD-A151950] 16 p2841 N85-27522
Precision manipulator heating and cooling apparatus for use in UHV systems with sample transfer capability
[NASA-CASE-LAR-13040-1] 18 p3116 N85-29286
Measurement of radiated emissions from industrial heating device equipment as it relates to aeronautical services
[FAA-ES-85-2] 19 p3255 N85-30181
Development of a high-efficiency, gas-fired, heat pipe, warm-air heating system
[PB85-199636] 24 p4085 N85-35318

HEAVING
Ice segregation and frost heaving
[PB85-122430] 10 p1460 N85-19199

HEAVY COSMIC RAY PRIMARIES
U HEAVY NUCLEI
U PRIMARY COSMIC RAYS

HEAVY ELEMENTS
NT AMERICIUM
NT AMERICIUM ISOTOPES
NT AMERICIUM 241
NT CALIFORNIUM ISOTOPES
NT CURIUM
NT CURIUM 244
NT PLUTONIUM
NT PLUTONIUM ISOTOPES
NT PLUTONIUM 238
NT PLUTONIUM 239
NT TRANSURANIUM ELEMENTS
Pulsed-neutron-source models for the astrophysical s-process
[DE85-012927] 24 p4151 N85-35740
Some nuclear data needs in astrophysics
[DE85-012916] 24 p4168 N85-35842

HEAVY IONS
The Berkeley mini-collider
[DE84-014594] 01 p0118 N85-10808
Do the satellites of Uranus control its magnetosphere?
02 p0301 N85-11952
Utilization of a tandem accelerator for the investigation of solid state properties by means of heavy ions
03 p0429 N85-12733
The radiobiological advanced Biostack experiment on Spacelab 1
05 p0691 N85-14442
Research in nuclear astrophysics: Stellar collapse and supernovae
[DE84-015559] 05 p0743 N85-14776
The (20)Ne interaction in extended matter
[NASA-TM-86312] 07 p1061 N85-16728
A T-matrix theory of galactic heavy-ion fragmentation
[NASA-TP-2363] 08 p1221 N85-17690
Forward electron production in heavy ion-atom and ion-solid collisions
[DE85-001256] 09 p1381 N85-18683
Beam-foil spectroscopy of highly ionized aluminum atoms
09 p1390 N85-18746
Applications of the Heavy-Iron Rutherford Backscattering Spectrometry (HIRBS) to the analysis of contact structures on GaAs and Ge
[DE85-000671] 10 p1564 N85-19861
Heavy ion induced crystallization in amorphous phases
[DE85-003114] 11 p1606 N85-20098
Charge-to-mass dispersion methods for abrasion-ablation fragmentation models
[NASA-TM-86340] 11 p1726 N85-20857
Operating experience and construction status of ATLAS — Argonne tandem-linac accelerator
[DE85-002741] 11 p1735 N85-20914
Workshop on Nuclear Dynamics 3
[INC-40007-24] 12 p1931 N85-22130
High energy facilities advanced projects: Intrabeam scattering for a beam of gold ions
[DE85-000887] 12 p1941 N85-22192
Laser-induced fluorescence of metal-atom impurities in a neutral beam
[DE85-004980] 14 p2310 N85-24298
X-ray emission in heavy ion collisions
[DE85-006350] 14 p2419 N85-24927
Future accelerator studies of high energy heavy ion collisions
[DE85-005885] 15 p2650 N85-26346
Nuclear spectroscopic studies
[DE85-006894] 16 p2862 N85-27682
Tables of nuclear cross sections for galactic cosmic rays: Absorption cross sections
[NASA-RP-1134] 16 p2864 N85-27685
Nonrelativistic theory of heavy-ion collisions
[DE85-007536] 17 p3031 N85-28747
Experiments and detectors for high energy heavy ion colliders
[DE85-007927] 17 p3031 N85-28748
Spin distributions in heavy ion fusion at and below the Coulomb barrier
[DE85-007817] 17 p3031 N85-28751
Theoretical studies of heavy ion scattering processes
[DE85-008823] 17 p3032 N85-28753
Heavy ion physics at BNL, the AGS and RHIC
[DE85-005951] 17 p3033 N85-28760
Heavy ion fusion accelerator research in the US
[DE85-008465] 17 p3034 N85-28767
Inertial fusion reactors and magnetic fields
[DE85-009571] 18 p3191 N85-29789
Experiments with stored heavy ions
[DE85-009976] 19 p3356 N85-30802
Research activities of the Physics Division
[DE85-006958] 19 p3357 N85-30811
Ion beam-plasma interactions
[DE85-010202] 19 p3371 N85-30913
Biostack experiments on STS-flights and the impact for man in space
20 p3510 N85-31921
Fusion reactions at low energy
[DE85-010561] 20 p3528 N85-31944
In-situ observations of the development of heavy-ion damage in semiconductors
[DE85-010289] 22 p3761 N85-33307
Ultrahigh vacuum system of the heavy ion transport line at Brookhaven
[DE85-011836] 22 p3840 N85-33778
Heavy ion medical accelerator options
[DE85-011204] 22 p3841 N85-33784
Design status of heavy ion injector program
[DE85-010751] 22 p3842 N85-33793
Physics Division annual review, 1 April 1983 - 31 March 1984
[ANL-84-24] 23 p3969 N85-34602
Summary of activities, 1983
[LBL-18500] 23 p3969 N85-34605
Low-energy sputterings with the Monte Carlo Program ACAT
[IPPJ-AM-40] 23 p3962 N85-34690
Calculations of heavy ion charge state distributions for nonequilibrium conditions
[SH-2.1-12] 23 p3999 N85-34793
The heavy ion composition in 3HE-rich solar flares
[SH-2.2-7] 23 p4000 N85-34802
The plasma mechanism for preferential acceleration of heavy ions
[SH-2.2-10] 23 p4001 N85-34805
A high resolution gas Cerenkov detector for the superconducting magnet facility
[OG-9.1-6] 23 p4023 N85-34852
The heavy ions in space experiment
[OG-9.1-10] 23 p4023 N85-34856
The response of ionization chambers to relativistic heavy nuclei
[OG-9.1-13] 23 p4024 N85-34858
Detector calibration of the Indian cosmic ray experiment (IONS) in Space-Shuttle Spacelab-13
[SH-9.1-2] 23 p4050 N85-35117
Proceedings of the Workshop on Detectors for Relativistic Nuclear Collisions
[LBL-18225] 24 p4146 N85-35700
Summary of the working group on penetrating probes in collider experiments. 1: The collider environment
24 p4146 N85-35704
Fractional charge resolution in music
24 p4147 N85-35712
Calculation of heavy-ion tracks in liquid water
[DE85-012101] 24 p4149 N85-35725
Considerations on collective ion acceleration as an intense ion injector
[DE85-012706] 24 p4155 N85-35757
Ion source development for the Los Alamos heavy ion fusion injector
[DE85-012682] 24 p4156 N85-35766
Applications of decelerated ions
[DE85-011832] 24 p4156 N85-35767
Numerical studies of high current beam compression in heavy ion fusion
[DE85-011874] 24 p4158 N85-35780
Multiple vacancy production by high energy heavy ions
[DE85-004428] 24 p4162 N85-35805
The phi-meson and Chiral-mass-meson production in heavy-ion collisions as potential probes of quark-gluon-plasma and Chiral symmetry transitions
24 p4175 N85-3588

On the mechanism of anomalous nucleus-nucleus interactions at energies above 1 TeV/nucleon
[HE-1.4-8] 24 p4177 N85-35896
Meson multiplicity in nucleus-nucleus collisions above 4 GeV/amu
[HE-1.4-10] 24 p4177 N85-35897
Multidimensional analysis of data obtained in experiments with X-ray emulsion chambers and extensive air showers
[HE-3.6-2] 24 p4184 N85-35951

HEAVY NUCLEI
Anomalon search — heavy cosmic ray interactions
[NOTA-INTERNA-825] 02 p0305 N85-11970
Radiobiological studies on egg systems exposed to heavy nuclei of cosmic galactic radiation — insects
05 p0690 N85-14440
Preliminary results of advanced Biostack experiments with plant seeds and spores — cosmic ray effects
05 p0691 N85-14441
The radiobiological advanced Biostack experiment on Spacelab 1 05 p0691 N85-14442
The propagation of ultraheavy cosmic rays
15 p2665 N85-26582
Heavy ion physics at BNL, the AGS and RHIC
[DE85-005951] 17 p3033 N85-28760
Contributions to the 19th International Cosmic Ray Conference
[NASA-CR-176049] 20 p3543 N85-32044
Energy spectra of elements with 18 less than or equal to Z less than or equal to 28 between 10 and 300 GeV/amu 20 p3543 N85-32045
Elemental abundances of cosmic rays with Z33 as measured on HEAO-3 20 p3543 N85-32046
Abundances of secondary elements among the ultra heavy cosmic rays: Results from HEAO-3
20 p3543 N85-32047
Lead, platinum, and other heavy elements in the primary cosmic radiation: HEAO-3 results sac wg032961 cb553097 20 p3543 N85-32048
Implications of source abundances of ultraheavy cosmic rays 20 p3543 N85-32049
Interactions of heavy nuclei, Kr, Xe and Ho, in light targets 20 p3544 N85-32050
The response of ionization chambers to relativistic heavy nuclei 20 p3544 N85-32051
Source spectral index of heavy cosmic ray nuclei
[OG-4.1-2] 22 p3875 N85-34008
Energy spectra of elements with 18 or = Z or = 28 between 10 and 300 GeV/amu
[OG-4.1-6] 22 p3876 N85-34014
Elemental abundances of cosmic rays with Z 33 as measured on HEAO-3
[OG-4.4-5] 22 p3880 N85-34038
Abundances of secondary elements among the ultra heavy cosmic rays: Results from HEAO-3
[OG-4.4-6] 22 p3880 N85-34039
Capabilities of the LDEF-2 heavy nuclei collection
[OG-4.4-8] 22 p3880 N85-34040
Ultraheavy cosmic ray tracks in meteorites: A reappraisal, based on calibrations with relativistic ions
[OG-4.4-10] 22 p3880 N85-34041
High-energy multiple muons and heavy primary cosmic-rays
[OG-5.2-9] 22 p3883 N85-34065
Electron and muon parameters of EAS and the composition of primary cosmic rays in 10(15) to approximately 10(16) eV
[OG-5.2-12] 22 p3884 N85-34068
Implications of the experimental results on high energy cosmic rays with regard to their origin
[OG-5.4-5] 22 p3886 N85-34082
The heavy ion composition in 3HE-rich solar flares
[SH-2.2-7] 23 p4000 N85-34802
Variations in the propagation of UH-nuclei
[OG-7.1-1] 23 p4012 N85-34863
Propagation and nucleosynthesis of ultraheavy cosmic rays
[OG-7.1-5] 23 p4013 N85-34867
Sources of the ultraheavy cosmic rays
[OG-7.1-7] 23 p4013 N85-34868
Interactions of heavy nuclei, Kr, Xe and Ho, in light targets
[OG-7.2-21] 23 p4016 N85-34886
The response of ionization chambers to relativistic heavy nuclei
[OG-9.1-13] 23 p4024 N85-34938
The response of ionization chambers to relativistic heavy nuclei
[OG-9.1-13] 23 p4024 N85-34939
Measurement of low energy cosmic rays aboard Spacelab-1
[SH-10.1-6] 23 p4053 N85-35137
Heavy cosmic ray measurement aboard Spacelab-1
[SH-10.1-7] 23 p4053 N85-35138
The response of a scintillation counter below an emulsion chamber to heavy nucleus interactions in the chamber 24 p4175 N85-35889
Heavy nucleus collisions between 20 and 60 GeV/nucleon
[HE-1.4-2] 24 p4175 N85-35890
Characteristics of central collision events in Fe-nucleus interactions for 20 - 60 GeV/nucleon
[HE-1.4-3] 24 p4176 N85-35891
Nucleus-nucleus interaction above several hundred GeV/n
[HE-1.4-4] 24 p4176 N85-35892
Experiment Pamir-3. Coplanar emission of high energy gamma-quanta at interaction of hadrons with nuclei of air atoms at energies above 10 to the 7th power GeV
[HE-1.4-12] 24 p4177 N85-35899
Intensities of high-energy cosmic rays at Mount Kanbala
[HE-3.1-2] 24 p4177 N85-35902
Multidimensional analysis of data obtained in experiments with X-ray emulsion chambers and extensive air showers
[HE-3.6-2] 24 p4184 N85-35951
On mini-cluster observed by Chacaltaya emulsion chamber experiment
[HE-3.6-12] 24 p4185 N85-35959
Monte Carlo simulations of electron lateral distributions in the core region of 10(13) - 10(16) eV air showers
24 p4190 N85-35992
Comparison of simulation results with sea-level experimental data on 10(14) - 10(16) air shower cores
24 p4190 N85-35993
Relevance of multiple muons detected underground to the mass composition of primary cosmic rays
[HE-5.1-4] 24 p4201 N85-36069
Search for stellar collapse with the MACRO detector at Gran Sasso
[HE-5.3-11] 24 p4206 N85-36105
Spatial distribution read-out system for thermoluminescence sheets
[HE-7.1-7] 24 p4213 N85-36161

HEIGHT
The estimation of persistance statistics from cumulative probabilities of wave height
[NMI-R183] 03 p0397 N85-12534
Prediction of wave height of wind-generated seas in finite water depth
[AD-A145996] 03 p0398 N85-12539
Components of the time variation of sea surface height from SEASAT altimeter data 05 p0658 N85-14227
Applications of TOMS ozone data and clustering techniques in satellite soundings
05 p0661 N85-14379
Prediction of percent body fat for U.S. Navy women from body circumferences and height
[AD-A146456] 06 p0845 N85-15370
The 500 millibar sign frequency teleconnection charts: Winter
[PB85-106276/GAR] 07 p1009 N85-16410
Analysis of the inflow layer and air-sea interactions in Hurricane Frederic (1979)
[NASA-CR-175616] 13 p2137 N85-23271
A laser slope gauge and a spar buoy wave gauge: Tools for the validation of microwave remote sensors
[AD-A154038] 19 p3272 N85-30290
Troposphere-stratosphere (surface-55 km) monthly general circulation statistics for the Northern Hemisphere-four year averages
[NASA-TM-86182] 20 p3495 N85-31730
Practical use of a tropopause height determination algorithm on an MST radar data set, part 1.8B
21 p3618 N85-32479

HEISENBERG THEORY
Lattice actions improved by block-spin renormalisation group and maximally symmetric lattices
[DE85-007416] 17 p3045 N85-28841

HELICAL ANTENNAS
Measured performance of a broadband matching section for peripherally fed helical antennas
[R-NIAS-25] 15 p2539 N85-25670
Dual sense, circularly polarized helical antenna
[AD-D011680] 19 p3254 N85-30175

HELICAL FLOW
International test and demonstration of a 1-MW wellhead generator: Helical screw expander power plant
[NASA-CR-174161] 04 p0527 N85-13372
Spectral measurements of magnetic energy and magnetic helicity between 0.29 and 0.97 AU
[IFSI-85-2] 22 p3850 N85-33844
Behavior of helically-trapped fast ion orbits in heliotron E 23 p3978 N85-34666
Neoclassical diffusion including ellipticity in a heliotron-like configuration 23 p3978 N85-34667

HELICOPTER ATTITUDE INDICATORS
U ATTITUDE INDICATORS
U HELICOPTERS

HELICOPTER CONTROL
The design and development of an integrated core system for battlefield helicopters
08 p1074 N85-16811
A review of US Army aircrew-aircraft integration research programs 08 p1075 N85-16814
Flight tests with a new helicopter Force Feel System (FFS) 08 p1075 N85-16818
Helicopter active control with rotor blades relaxation
08 p1075 N85-16819
Flight research on visual aids and navigation equipment for helicopter low-level flight at night
08 p1076 N85-16820
A preliminary investigation of handling qualities requirements for helicopter instrument flight during decelerating approach maneuvers and overshoot
[NRC-24173] 17 p2896 N85-27857
The evolution of ACS for helicopters: Conceptual simulation studies to preliminary design
17 p2902 N85-27890
ACT applied to helicopter flight control
17 p2902 N85-27891
The evolution of active control technology systems for the 1990's helicopter 17 p2905 N85-27911
Data processing on the rotor test stand at DFVLR in Brunswick: Microprogrammable interfaces and array processor as key components in a PDP 11 real time data acquisition and processing system
[DFVLR-MITT-85-03] 17 p2906 N85-27921
Helicopter Aeromechanics
[AGARD-LS-139] 18 p3057 N85-28913
The role of simulation 18 p3058 N85-28919

HELICOPTER DESIGN
Helicopter rotor blade design for minimum vibration
[NASA-CR-3825] 01 p0006 N85-10032
DFVLR rotorcraft: Construction and engineering
[NASA-TM-77740] 01 p0006 N85-10035
Applications of numerical optimization methods to helicopter design problems: A survey
[NASA-TM-86010] 01 p0006 N85-10036
YO-3A acoustics research aircraft systems manual
[NASA-TM-85968] 01 p0012 N85-10074
Data input, processing and presentation — helicopter rotor balance measurement
[NASA-TM-77739] 01 p0125 N85-10856
Manufacturing Methods and Technology (MM/T) specifications for miniature cathode ray tube
[AD-A145597] 02 p0194 N85-11298
Avionics system design for requirements for the United States Coast Guard HH-65A Dolphin
06 p0753 N85-14827
Speed benefits of tilt-rotor designs for LHX
[NASA-CR-166437] 07 p0902 N85-15717
Operational requirements versus technological capabilities 08 p1072 N85-16798
Integration of sensor fusion in advanced helicopter cockpit design 08 p1074 N85-16813
Advanced flight simulation for helicopter development
08 p1075 N85-16815
Integrated technology rotor/flight research rotor concept definition study
[NASA-CR-166446] 10 p1424 N85-18980
Transmission efficiency measurements and correlations with physical characteristics of the lubricant
14 p2222 N85-23781
Problems of elastic hydrodynamic lubrication of helicopter transmission gears 14 p2222 N85-23784
Evolution of the design techniques for helicopter main transmission gearboxes 14 p2223 N85-23789
Preliminary helicopter design decision making based on flight performance factors
[AD-A151468] 15 p2471 N85-25254
Determination of quantitative relationships between selected critical helicopter design parameters
[AD-A152034] 16 p2706 N85-26700
The evaluation of ACS for helicopters: Conceptual simulation studies to preliminary design
16 p2712 N85-26737
Advanced flight simulation for helicopter development
[MBB-UD-416/84-O] 16 p2874 N85-27731
Design of helicopter rotor blades for optimum dynamic characteristics
[NASA-CR-176076] 20 p3393 N85-31044
Application of finite element method to the sizing of mechanical parts — helicopter design
[SNIAS-851-210-105] 20 p3463 N85-31515

HELICOPTER PERFORMANCE
DFVLR rotorcraft: Construction and engineering
[NASA-TM-77740] 01 p0006 N85-10035
Applications of numerical optimization methods to helicopter design problems: A survey
[NASA-TM-86010] 01 p0006 N85-10036
Airworthiness and flight characteristics test of the JOH-6A light combat helicopter configured with a wire strike protection system
[AD-A144880] 01 p0006 N85-10038

Airworthiness and Flight Characteristics (A and FC) test of the EH - 1X/EH - 1H helicopter configurations
[AD-A144881] 01 p0007 N85-10039
Estimation of helicopter performance using a program based on blade element analysis
[AD-A146341] 03 p0318 N85-12055
The need for a dedicated public service helicopter design 06 p0753 N85-14828
Preliminary airworthiness evaluation AH-1S (MC) helicopter with external fuel tanks installed
[AD-A148091] 08 p1084 N85-16865
Preliminary helicopter design decision making based on flight performance factors
[AD-A151488] 15 p2471 N85-25254
Wind-tunnel evaluation of a 21-percent-scale powered model of a prototype advanced scout helicopter
[NASA-TP-2420] 18 p3058 N85-28923
Effect of ground and/or ceiling planes on thrust of rotors in hover
[NASA-TM-86754] 20 p3388 N85-31014
Standardization of helicopter certification requirements in the western world
[SNIAS-851-210-103] 20 p3393 N85-31046
The effects of parameter variation on helicopter performance
[AD-A156027] 24 p4064 N85-35189
Development of NATOPS performance software for the SH-3D and SH-3H helicopters
[AD-A156140] 24 p4065 N85-35192

HELICOPTER PROPELLER DRIVE
The in-flight estimation and indication of cumulative fatigue damage to helicopter gears
[ARL/AERO-R-164] 03 p0317 N85-12050
The helicopter transmission design process
14 p2221 N85-23772
Fine filtration: An attractive route towards lower helicopter operating costs 14 p2221 N85-23774
Possible technological answers to new design requirements for power transmission systems
14 p2222 N85-23779

HELICOPTER ROTORS
U ROTARY WINGS

HELICOPTER TAIL ROTORS
Calculation of the velocity field generated by a helicopter main and tail rotors in hover
[AD-A147731] 08 p1078 N85-16833
Numerical analysis of the first static calibration of the RSRA helicopter active-isolator rotor balance system
[NASA-TM-85975] 08 p1083 N85-16863
Repair of composites 08 p1120 N85-17058
Reconstruction of a 3-dimensional transonic rotor flow field from holographic interferogram data
[NASA-TM-86690] 12 p1770 N85-21112
Experimental study of main rotor tip geometry and tail rotor interactions in hover. Volume 1. Text and figures
[NASA-CR-177336-VOL-1] 13 p1965 N85-22344
Experimental study of main rotor tip geometry and tail rotor interactions in hover. Volume 2: Run log and tabulated data
[NASA-CR-177336-VOL-2] 13 p1965 N85-22345
Rotorcraft research testing in the National Full-Scale Aerodynamics Complex at NASA Ames Research Center
[NASA-TM-86687] 17 p2896 N85-27854
Fuselage upwash effects on RSRA rotor systems
[NASA-CR-177349] 20 p3388 N85-31015

HELICOPTER WAKES
Study for prediction of rotor/wake/fuselage interference, part 1
[NASA-CR-177340-VOL-1] 13 p1965 N85-22346
Study for prediction of rotor/wake/fuselage interference. Part 2: Program users guide
[NASA-CR-177340-VOL-2] 13 p1966 N85-22347
Unsteady analysis of rotor blade tip flow
[NASA-CR-3868] 15 p2482 N85-25202
Ground effect on helicopter aerodynamics and stability
20 p3395 N85-31063

HELICOPTERS
NT BO-105 HELICOPTER
NT CH-47 HELICOPTER
NT MILITARY HELICOPTERS
NT P-531 HELICOPTER
NT RIGID ROTOR HELICOPTERS
NT UH-1 HELICOPTER
NT UH-60A HELICOPTER
Rotor systems research aircraft airplane configuration flight-test results
[NASA-TM-85911] 01 p0006 N85-10034
Transonic flow analysis for rotors. Part 1: Three-dimensional quasi-steady, full-potential calculation
[NASA-TP-2375-PT-1] 02 p0134 N85-10914
Aircrew-aircraft integration: A summary of US Army research programs and plans
[NASA-TM-85891] 02 p0146 N85-11004
Structural design guidelines for heliports
[FAA-PM-84-23] 02 p0149 N85-11010
The effects of helicopter vibration on the spinal system
[AD-A146274] 03 p0402 N85-12582
Prediction and modeling of helicopter noise
[AD-A145784] 03 p0415 N85-12656
Initial feasibility ground test of a proposed photogrammetric system for measuring the shapes of ice accretions on helicopter rotor blades during forward flight
[NASA-TM-87391] 04 p0455 N85-12887
Aircraft accident report, Western Helicopters, Inc., Bell UH-1B, N87701, Valencia, California, July 23, 1982
[PB84-910414] 05 p0594 N85-13789
Helicopter pilot performance for discrete-maneuver flight tasks 05 p0702 N85-14502
Technical Workshop: Advanced Helicopter Cockpit Design
[NASA-CP-2351] 06 p0750 N85-14806
Superaugmented rotorcraft program
06 p0750 N85-14807
Helicopter human factors programs and plans
06 p0751 N85-14808
Guidance and navigation programs and plans
06 p0751 N85-14809
Army aviation today and tomorrow
06 p0751 N85-14810
Marine helicopter missions 06 p0751 N85-14811
Civil law enforcement missions
06 p0751 N85-14812
SAR maritime missions 06 p0751 N85-14813
Some thoughts on the implementation of pilot night vision devices for helicopters 06 p0751 N85-14814
HH-65A Dolphin digital integrated avionics
06 p0751 N85-14815
Integrated cockpit design for the Army helicopter improvement program 06 p0751 N85-14816
HH-60D night hawk helicopter
06 p0752 N85-14817
Operational requirements - system concepts
06 p0752 N85-14823
Avionics technology - system concepts
06 p0753 N85-14824
Man-machine interface requirements - advanced technology 06 p0753 N85-14825
Attack helicopter (AH-1T) cockpit systems integration
06 p0753 N85-14826
Avionics system design for requirements for the United States Coast Guard HH-65A Dolphin
06 p0753 N85-14827
The need for a dedicated public service helicopter design 06 p0753 N85-14828
Certification of advanced systems
06 p0753 N85-14829
Operational Loads Data
[AGARD-CP-375] 07 p0894 N85-15664
Helicopter data acquisition in WHL
07 p0896 N85-15676
The UH-1H helicopter icing flight test program: An overview
[NASA-TM-86925] 07 p0900 N85-15702
Study to eliminate ground resonance using active controls
[NASA-CR-166609] 07 p0902 N85-15715
Literature review of voice recognition and generation technology for Army helicopter applications
[AD-A146878] 07 p0939 N85-15954
Helicopter noise survey performed at Las Vegas, Nevada, 19-21 January, 1984
[AD-A147382] 07 p1039 N85-16593
Noise measurement flight test: Data-analyses aerospatiale AS-355F TwinStar helicopter
[AD-A147497] 07 p1039 N85-16595
Helicopter Guidance and Control Systems for Battlefield Support
[AGARD-CP-359] 08 p1072 N85-16797
Automatic briefing and mission management systems for battlefield support 08 p1073 N85-16799
A Computer-generated topographic display system for navigation and mission planning in helicopters
08 p1073 N85-16800
Map display for helicopters 08 p1073 N85-16801
Development of a Helicopter integrated navigation system 08 p1073 N85-16802
Standard Attitude Heading Reference System (SAHRS) full scale development program
08 p1073 N85-16804
Integrated control and display systems for helicopter battlefield mission management
08 p1073 N85-16805
Recent methods for calibrating the anemometry of helicopters at low speeds 08 p1074 N85-16809
LPI-radar for helicopter obstacle warning
08 p1074 N85-16810
Advanced flight simulation for helicopter development
08 p1075 N85-16815
Development and flight test of a helicopter compact, portable, precision landing system concept
08 p1076 N85-16821
Helicopter model rotor-blade vortex interaction impulsive noise: Scalability and parametric variations
[NASA-TM-86007] 08 p1077 N85-16822
Development, production and testing of central control and display unit for helicopters
[BMFT-FB-W-84-039] 08 p1085 N85-16871
Investigation on experimental techniques to detect, locate and quantify gear noise in helicopter transmissions
[NASA-CR-3847] 08 p1217 N85-17867
Noise measurement flight test: Data-analyses Aerospatiale AS 350D AStar helicopter
[AD-A148496] 08 p1218 N85-17872
Noise measurement flight test: Data-analyses, Sikorsky S-76A helicopter
[AD-A148525] 08 p1218 N85-17873
A feasibility study of free-tip rotor application as a passive cyclic control device 09 p1279 N85-18046
Discrete modifications to continuous dynamic structural systems 09 p1337 N85-18410
Inviscid analysis of unsteady blade tip flow correlation studies
[NASA-CR-172506] 10 p1420 N85-18958
Integrated Technology Rotor/Flight Research Rotor (ITR/FRR) concept definition study
[NASA-CR-166444] 10 p1424 N85-18981
Crewstation assessment of reach as applied to the OH-58A helicopter
[AD-A149413] 10 p1531 N85-19650
A Lagrange-D'Alembert formulation of the equations of motion of a helicopter carrying an externally suspended load
[NASA-TM-85864] 12 p1776 N85-21140
Analytical and flight investigation of the influence of rotor and other high-order dynamics on helicopter flight-control system bandwidth
[NASA-TM-86696] 12 p1780 N85-21174
Evaluating wind flow around buildings on heliport placement
[FAA-PM-84-25] 12 p1893 N85-21881
Study for prediction of rotor/wake/fuselage interference, part 1
[NASA-CR-177340-VOL-1] 13 p1965 N85-22346
Study for prediction of rotor/wake/fuselage interference. Part 2: Program users guide
[NASA-CR-177340-VOL-2] 13 p1966 N85-22347
Ground evaluation of helicopter air-to-air warfare
13 p1967 N85-22380
A community survey of helicopter noise annoyance conducted under controlled noise exposure conditions
[NASA-TM-86400] 13 p2154 N85-23374
An experimental investigation of the chopping of helicopter main rotor tip vortices by the tail rotor
[NASA-CR-177338] 13 p2154 N85-23376
Basic consideration of the lifting capability of stoppable rotors
[AD-A150850] 14 p2219 N85-23759
Gears and Power Transmission Systems for Helicopters and Turboprops
[AGARD-CP-369] 14 p2220 N85-23765
Summary of drive-train component technology in helicopters 14 p2220 N85-23766
Current transmission systems
14 p2220 N85-23767
Helicopter transmission lubricants
14 p2220 N85-23768
A state of the art assessment of turboprop transmission technology and projected needs for the next generation
14 p2220 N85-23770
Case depth on flanks of gears for helicopter gearboxes 14 p2222 N85-23780
Condition monitoring of helicopter gearboxes using automatic vibration analysis techniques
14 p2223 N85-23783
Transmission error measurements in gearbox development 14 p2224 N85-23784
Do new aircraft need new technologies and certification rules? 14 p2224 N85-23785
Establishment and maintenance of certification standards for helicopter and turboprop power transmission systems 14 p2224 N85-23786
Recent developments in the dynamics of advanced rotor systems
[NASA-TM-86669] 14 p2317 N85-24320
MI-8 helicopter cargo loading experiment for Arctic shipping 14 p2332 N85-24455
Investigation of technology needs for avoiding helicopter pilot error related accidents
[NASA-CR-3895] 15 p2465 N85-25239
Helicopter user survey: Traffic alert and collision avoidance system (TCAS)
[FAA-PM-85-6] 15 p2468 N85-25276

Calibration loading of a strain-gauged diverless helicopter weapon recovery system
[AD-A151486] 15 p2471 N85-25253
Effects of side-stick controllers on rotorcraft handling qualities for terrain flight
[NASA-TM-86688] 15 p2473 N85-25267
Rotorcraft digital advanced avionics system (Rodass)
15 p2688 N85-26606
The use of a self-compensated magnetometer in an economical navigation system for the helicopter
16 p2697 N85-26650
Finite-difference computations of rotor loads
[NASA-TM-86682] 16 p2700 N85-26669
Rotor blade flap-lag stability and response in forward flight in turbulent flows 16 p2705 N85-26698
Determination of quantitative relationships between selected critical helicopter design parameters
[AD-A152034] 16 p2706 N85-26700
Development and flight test of a helicopter, X-band, portable precision landing system concept
[NASA-TM-86710] 16 p2710 N85-26721
The evaluation of ACS for helicopters: Conceptual simulation studies to preliminary design
16 p2712 N85-26737
ACT applied to helicopter flight control
16 p2712 N85-26738
The evolution of active control technology systems for the 1990's helicopter 16 p2715 N85-26758
The NAVTAG (Naval Tactical Game) system and its modification to include the SH-60B helicopter
[AD-A152004] 16 p2858 N85-27624
Investigation of imaging and flight guidance concepts for rotorcraft zero visibility approach and landing
[NASA-CR-166571] 17 p2894 N85-27843
Helicopter Aeromechanics
[AGARD-LS-139] 18 p3057 N85-28913
Helicopter aeromechanics: Introduction and historical review 18 p3057 N85-28914
A survey of recent development in helicopter aerodynamics 18 p3057 N85-28915
Rotorcraft noise 18 p3057 N85-28916
Recent developments in the dynamics of advanced rotor systems 18 p3057 N85-28917
Mission requirements and handling qualities
18 p3057 N85-28918
The role of simulation 18 p3058 N85-28919
Flight testing for performance and flying qualities
18 p3058 N85-28920
The evolution of the U.S. helicopter industry
[AD-A154290] 19 p3211 N85-29913
Application of two-dimensional unsteady aerodynamic to a free-tip rotor response analysis
[NASA-CR-177348] 19 p3215 N85-29933
Correlation of rheological characteristics of lubricants with transmission efficiency measurements
[NASA-TM-86986] 19 p3280 N85-30342
A study of the application of differential techniques to the global positioning system for a helicopter precision approach
[NASA-CR-177326] 20 p3391 N85-31035
Standardization of helicopter certification requirements in the western world
[SNIAS-851-210-103] 20 p3393 N85-31048
Automated fabrication of composite structures for helicopters
[SNIAS-851-210-104] 20 p3393 N85-31049
The helicopter, instrument of choice for health evacuation
[SNIAS-851-220-101] 20 p3393 N85-31051
Ground effect on helicopter aerodynamics and stability
20 p3395 N85-31063
Impulsive noise due to transonic blade-vortex interactions 20 p3523 N85-31913
R and D activities of the Structural Sciences Division
20 p3539 N85-32026
Wind tunnel drag evaluations of helicopter nose sections
[AD-A155469] 21 p3553 N85-32100
A phase-locked frequency multiplier for the signal averaging of the vibration of the Wessex helicopter input spiral bevel pinion
[AD-A154914] 21 p3555 N85-32113
Artificial and natural icing tests YEH-60A quick fix helicopter
[AD-A155147] 21 p3556 N85-32116
Proposal for modifications to the Wessex helicopter main rotor gearbox vibration monitoring program
[AD-A155196] 21 p3555 N85-32117
Helicopter noise survey for selected cities in the contiguous US
[AD-A154693] 21 p3699 N85-32965
A three-dimensional viscous flow analysis for the helicopter tip vortex generation problem
[NASA-CR-3906] 23 p3893 N85-34114
An evaluation of three helicopter rotor sections
[NASA-TM-86719] 23 p3893 N85-34115
Flight service evaluation of composite helicopter components
[NASA-CR-172562] 23 p3909 N85-34222
Some problems in high speed gears and gearing
23 p3923 N85-34312
U.S. Civil airmen statistics for calendar year 1984
[AD-A156326] 24 p4059 N85-35153
Laboratory vibration schedules
[AD-A155856] 24 p4084 N85-35188
Development of NATOPS (Naval Air Training and Operating Procedure Standardization) performance software for the H-46D helicopter
[AD-A156089] 24 p4084 N85-35190
Development of NATOPS performance software for the SH-3D and SH-3H helicopters
[AD-A156140] 24 p4085 N85-35192

HELIOCENTRIC ORBITS
U SOLAR ORBITS

HELIOGRAPHS
U SPECTROHELIOGRAPHS

HELIOGRAPHY
U SPECTROHELIOGRAPHS

HELIOMAGNETISM
U SOLAR MAGNETIC FIELD

HELIOMETERS
NT PYROHELIOMETERS
The evaluation of a deformable diffraction grating for a stigmatic EUV spectroheliometer
[NASA-CR-174350] 09 p1322 N85-18309
The scanning heliometer 14 p2451 N85-25134

HELIOMETRY
U HELIOMETERS
U PYROHELIOMETERS

HELIOS PROJECT
Ten years of Helios
[ISBN-3-88135-156-6] 16 p2884 N85-27794
The Helios missions 16 p2884 N85-27795
Zodiacal light: A replica of the interplanetary dust cloud — Helios space probe 16 p2885 N85-27796
The micrometeorite experiment on Helios — inner solar system 16 p2885 N85-27797
Results from the Helios galactic and solar cosmic ray experiment (E7) 16 p2886 N85-27807
The significance of Helios for Europe
16 p2886 N85-27808
Managerial benefits of Helios for the European industry 16 p2887 N85-27809
The technological gains of Helios for the European industry 16 p2887 N85-27810
Helios project support 16 p2887 N85-27812

HELIOS SATELLITES
NT HELIOS 1
NT HELIOS 2
Data analysis of electron measurements of the plasma experiment aboard the HELIOS probes
[MPE-185] 09 p1416 N85-18935

HELIOS 1
Ten years of Helios
[ISBN-3-88135-156-6] 16 p2884 N85-27794
Ten years solar wind experiments on Helios 1 and Helios 2 16 p2885 N85-27798
Results of the magnetic field experiments E2 and E4 onboard Helios 1 and Helios 2 — magnetometer development 16 p2885 N85-27799
Plasma waves in the solar wind: Ten years of Helios observations 16 p2885 N85-27801
The Helios radio astronomy experiment
16 p2886 N85-27803
Remote sensing of the plasma with time delay measurements (coronal sounding)
16 p2886 N85-27804
The Faraday rotation experiment — solar corona
16 p2886 N85-27805
The fast individualists in the solar system: Cosmic rays 16 p2886 N85-27806
Helios ground operations 16 p2887 N85-27811
Solar wind observations associated with a slow forward shock wave at 0.31 AU
[MPAE-W-79-84-46] 17 p3055 N85-28909
Parallel fast-forward shock within 1 AU: Helios-1 and 2 observations
[MPAE-W-79-84-27] 24 p4169 N85-35847

HELIOS 2
Ten years of Helios
[ISBN-3-88135-156-6] 16 p2884 N85-27794
Ten years solar wind experiments on Helios 1 and Helios 2 16 p2885 N85-27798
Results of the magnetic field experiments E2 and E4 onboard Helios 1 and Helios 2 — magnetometer development 16 p2885 N85-27799
Plasma waves in the solar wind: Ten years of Helios observations 16 p2885 N85-27801
Evidence concerning the generation mechanism of solar type 3 radio bursts 16 p2886 N85-27802
The Helios radio astronomy experiment
16 p2886 N85-27803
Remote sensing of the plasma with time delay measurements (coronal sounding)
16 p2886 N85-27804
The Faraday rotation experiment — solar corona
16 p2886 N85-27805
The fast individualists in the solar system: Cosmic rays 16 p2886 N85-27806
Helios ground operations 16 p2887 N85-27811
Parallel fast-forward shock within 1 AU: Helios-1 and 2 observations
[MPAE-W-79-84-27] 24 p4169 N85-35847

HELIOSEISMOLOGY
Solar Seismology From Space. A conference at Snowmass, Colorado
[NASA-CR-175661] 14 p2441 N85-25060
Overview of solar seismology: Oscillations as probes of internal structure and dynamics in the Sun
14 p2441 N85-25061
What would a dynamo theorist like to know about the dynamics of the solar convection zone?
14 p2441 N85-25062
Solar inverse theory 14 p2441 N85-25063
Rotational inversion from global solar oscillations
14 p2442 N85-25064
Sensitivity of inferred subphotospheric velocity field to mode selection, analysis technique and noise
14 p2442 N85-25065
Evaluation of a magneto-optical filter and a Fabry-Perot interferometer for the measurement of solar velocity fields from space 14 p2442 N85-25067
Optimized response functions for 2-dimensional observations of solar oscillations
14 p2443 N85-25075
The effects of image motion on the l-nu diagram
14 p2443 N85-25076
An excitation mechanism for solar 5-minute oscillation of intermediate and high degree
14 p2444 N85-25085
Solar oscillations 14 p2445 N85-25092
Global solar oscillations in irradiance and velocity: A comparison 14 p2446 N85-25094
The intern. rotation of the Sun inferred from the rotational splitting of acoustic and gravity mode multiplets
14 p2449 N85-25122
Magnetic probing of the solar interior
[NASA-CR-176025] 19 p3385 N85-30998

HELIOSPHERE
Physics of the inner heliosphere 1-10R sub O plasma diagnostics and models
[NASA-CR-174010] 02 p0304 N85-11964
Structure and evolution of the large scale solar and heliospheric magnetic fields 05 p0746 N85-14782
Changes of LISM characteristics in the heliospheric interface 06 p0873 N85-15542
Broadening of the interplanetary helium cone structure due to elastic collisions of LISM helium atoms with solar wind ions 06 p0873 N85-15543
A new radio emission at 3 kHz in the outer heliosphere 12 p1959 N85-22312
Science with the Solar and Heliospheric Observatory (SOHO) 14 p2449 N85-25121
The influence of the heliospheric current sheet and angular separation on flare accelerated solar wind
[NASA-CR-175962] 18 p3209 N85-29907
Ninteenth International Cosmic Ray Conference. SH sessions, volume 4
[NASA-CP-2376-VOL-4] 23 p3989 N85-34729
Latitude dependence of co-rotating shock acceleration
[SH-1.5-14] 23 p3997 N85-34777
The intensity recovery of Forbush-type decreases as a function of heliocentric distance and its relationship to the 11-year variation
[SH-4.1-9] 23 p4005 N85-34832
Cumulative effect of Forbush decreases in the heliospheric modulation during the present solar cycle
[SH-4.1-10] 23 p4005 N85-34833
Latitude variation of recurrent fluxes in the outer solar system
[SH-4.1-13] 23 p4006 N85-34836
Longitudinal distribution of cosmic rays in the heliosphere
[SH-4.1-14] 23 p4006 N85-34837
Evidence for regions of negligible cosmic-ray modulation in the inner heliosphere (10 AU)
[SH-4.1-21] 23 p4006 N85-34840
Drift and observations in cosmic-ray modulation, 1
[SH-4.2-4] 23 p4007 N85-34842
Cosmic ray intensity and the tilt of the neutral sheet
[SH-4.2-8] 23 p4007 N85-34846
Spatial variation of cosmic rays near the heliospheric current sheet
[SH-4.2-10] 23 p4007 N85-34848
Effects of a wavy neutral sheet on cosmic ray anisotropies
[SH-4.2-11] 23 p4008 N85-34849

Determination of galactic cosmic ray latitudinal gradient using Earth based detectors
[SH-4.2-13] 23 p4008 N85-34851
Latitudinal gradients of cosmic rays and the polarity reversal of the heliospheric magnetic field: A preliminary evaluation
[SH-4.2-16] 23 p4008 N85-34853
The effect of the neutral sheet structure of the interplanetary magnetic field on cosmic ray distribution in space
[SH-4.2-18] 23 p4008 N85-34855
On the influence of the heliomagnetospheric periphery on the galactic cosmic rays
[SH-4.2-19] 23 p4009 N85-34856
The dependence of solar modulation on the sign of the cosmic ray particle charge
[SH-4.2-23] 23 p4009 N85-34860
An update on the correlation between the cosmic radiation intensity and the geomagnetic AA index
[SH-4.2-24] 23 p4009 N85-34861
Ninteenth International Cosmic Ray Conference. SH sessions, volume 5
[NASA-CP-2376-VOL-5] 23 p4031 N85-34991
Gradients and anisotropies of high energy cosmic rays in the outer heliosphere
[SH-4.3-7] 23 p4032 N85-34992
IMF-sense-dependent cosmic ray anisotropy produced from diffusion-convection in heliosphere
[SH-4.3-9] 23 p4032 N85-34994
The effect of the interplanetary magnetic field on sidereal variations observed at medium depth underground detectors
[SH-4.4-5] 23 p4033 N85-35003
The first three harmonics of solar daily variation caused by the diffusive propagation of galactic cosmic rays through the heliosphere
[SH-4.5-1] 23 p4035 N85-35019
Time and energy dependence of the cosmic ray gradient in the outer heliosphere
[SH-4.7-2] 23 p4040 N85-35047
The large scale dynamics of the outer heliosphere and the long-term modulation of galactic cosmic rays
[SH-4.7-3] 23 p4040 N85-35048
Voyager 1 and 2 measurements of radial and latitudinal cosmic ray gradients during 1981 - 1984
[SH-4.7-6] 23 p4041 N85-35051
The recovery of the cosmic ray flux from maximum solar modulation at IMP-8 (1 AU) and at Pioneer (R 30 AU)
[SH-4.7-7] 23 p4041 N85-35052
The large-scale modulation of cosmic rays in mid-1982: Its dependence on heliospheric longitude and radius
[SH-4.7-9] 23 p4041 N85-35053
Cosmic rays 10Be biennal data and their relationship to aurorae and sunspots
[SH-7.1-1] 23 p4047 N85-35094

HELIOSTATS
Heliostat tested 07 p0994 N85-16318
User's manual for the University of Houston individual heliostat layout and performance code
[DE85-004643] 12 p1882 N85-21808
Ecological observations at the site of the 10 MWe solar thermal power system (1978-1984)
[DE85-004572] 12 p1885 N85-21827
Error analysis of heliostat alignment methods
14 p2281 N85-24128
The 10 MWe solar thermal central receiver pilot plant: Beam safety tests and analyses
[SAND-83-8035] 16 p2818 N85-27379
Plastic heliostat enclosure analysis
[DE85-009112] 18 p3130 N85-29387
Receiver loss study of optimized solar central receiver systems as a function of receiver thermal loss per unit area
[DE85-010831] 19 p3268 N85-30265
Calibration of relevant measuring sensors
[DE85-009820] 19 p3306 N85-30492
Theory of cellwise optimization for solar central receiver system
[DE85-012586] 22 p3807 N85-33579

HELIPORTS
Heliport snow and ice control methods and guidelines
[DOT/FAA/PM-84/22] 01 p0012 N85-10073
Structural design guidelines for heliports
[FAA-PM-84-23] 02 p0149 N85-11010
Evaluating wind flow around buildings on heliport placement
[FAA-PM-84-25] 12 p1893 N85-21881
Microwave landing systems for heliport operators, owners and users
[FAA-PM-85-7] 19 p3216 N85-29940

HELITRONS
Present status of Heliotron E experiment
09 p1387 N85-18721
Spectroscopic measurement on Heliotron E
09 p1387 N85-18722
Behavior of helically-trapped fast ion orbits in heliotron E 23 p3976 N85-34666
Neoclassical diffusion including ellipticity in a heliotron-like configuration 23 p3976 N85-34667

HELIUM
NT HELIUM ATOMS
NT HELIUM IONS
NT HELIUM ISOTOPES
NT LIQUID HELIUM
NT LIQUID HELIUM 2
Experimental studies of atomic inner shell ionization phenomena
[DE84-013448] 01 p0118 N85-10805
Momentum distributions in superfluid helium: Bose condensate fraction
[DE84-014676] 05 p0731 N85-14700
Pioneer 10 and Voyager observations of the interstellar medium in scattered emission of the He 584 A and H Lya 1216 A lines 06 p0873 N85-15541
Broadening of the interplanetary helium cone structure due to elastic collisions of LISM helium atoms with solar wind ions 06 p0873 N85-15543
Thermal and cryogenic design study for space infrared telescope facility (SIRTF)
[NASA-CR-166613] 07 p0915 N85-15793
Critical velocities in He II for independently varied superfluid and normal fluid velocities
09 p1396 N85-18784
Atomistic studies of grain boundaries with segregated impurities
[DE85-000063] 11 p1737 N85-20924
IUE spectrophotometry of the hot helium-rich PG1159 DO degenerates 11 p1751 N85-21015
A Jamin interferometer to determine the helium abundance in the atmosphere of Jupiter
[BONN-IR-83-17] 12 p1961 N85-22329
NMR imaging and spectroscopy of the mammalian central nervous system after heavy ion radiation
[DE85-004509] 14 p2386 N85-24896
Theoretical and experimental studies of stabilized metastable helium
[AD-A150706] 14 p2417 N85-24913
Infrared telescope
[NASA-CR-171392] 15 p2668 N85-26465
Reciprocating magnetic refrigerator employing tandem porous matrices within a reciprocating displacer
[NASA-CASE-NPO-16257-1] 18 p3085 N85-29082
Intrinsically irreversible acoustic heat engines
[DE85-007672] 19 p3270 N85-30276
Flash pyrolysis of biomass with reactive and non-reactive gases
[DE85-010962] 19 p3306 N85-30496
Possibilities for studying short-lived nuclei produced at LAMPF
[DE85-010740] 19 p3365 N85-30864
Reciprocating Brayton cycle motor
[REPT-84-RR-336] 20 p3462 N85-31507
Design of a helium-cooled molten salt fusion breeder
[DE85-010474] 20 p3528 N85-31943
Investigation of influence of gas exit modes on characteristics of N2O - N2 - He discharge laser
21 p3684 N85-32888
Selective population of N = 3 OVIII level during expansion of laser plasma in helium
21 p3688 N85-32914
Changes in the energy spectrum of anomalous oxygen and helium during 1977 - 1985
[PAPER-SH-4.6-1] 21 p3715 N85-33056
Solar cycle variations of the anomalous cosmic ray component
[PAPER-SH-4.6-2] 21 p3715 N85-33057
Tritium-helium effects in metals
[DE85-011507] 22 p3749 N85-33235
Planetary fluids He and NH3 at high shock pressures and temperatures
[DE85-011851] 22 p3859 N85-33896
Absolute rigidity spectrum of protons and helium nuclei above 10 GV/c
[OG-4.1-1] 22 p3875 N85-34007
The flux of secondary anti-deuterons and antihelium produced in the interstellar medium
[OG-6.1-5] 22 p3888 N85-34096
Combined cold compressor/ejector helium refrigerator
[DE85-006408] 23 p3925 N85-34326
Technical assessment of thermal-hydraulics for high heat flux fusion components
[DE85-013178] 23 p3930 N85-34359
Determination of individual tolerance in hyperbaric oxygen 23 p3954 N85-34507
Observations on (3)He neutron spectrometry
[DE85-010731] 23 p3970 N85-34608
On the importance of interstellar helium for the propagation of heavy cosmic rays
[OG-7.2-11] 23 p4015 N85-34879
Changes in the energy spectrum of anomalous oxygen and helium during 1977-1985
[SH-4.6-1] 23 p4039 N85-35039
Experimental technique for measuring the isentrope of hydrogen to several megabars
[DE85-014332] 24 p4095 N85-35286
Search for magnetic monopoles using proportional counters filled with helium gas
[HE-6.1-1] 24 p4209 N85-36127
Magnetic monopole search by 130 m(2)sr He gas proportional counter
[HE-6.1-2] 24 p4209 N85-36128
Results from the UCSD magnetic monopole search
[HE-6.1-12] 24 p4210 N85-36137

HELIUM ATOMS
Helium atoms in interstellar and interplanetary media, part 3: Temperature and velocity of interstellar wind
02 p0160 N85-11098
Helium atoms in interstellar and interplanetary space. II: Determination of direction of interstellar gas motion relative to Sun 13 p1980 N85-22425
Hartree-Fock interaction between a helium atom and lithium-metal: A test for the effective medium theory
[AD-A150468] 13 p2156 N85-23387

HELIUM HYDROGEN ATMOSPHERES
Shock compression of liquid helium to 56 GPa (560) kbar 13 p2184 N85-23651

HELIUM IONS
Helium ionization detection apparatus
[NASA-TM-77505] 03 p0364 N85-12332
One-electron capture processes by highly charged ions from helium: Present status of HICE-IPP
09 p1389 N85-18736
Anomalous heating of ionospheric components (thermal e- and He+) via intense Ion Cyclotron Waves (ICW's)
14 p2368 N85-24633
Data on the backscattering coefficients on light ions from solids: A revision
[IPPJ-AM-41-REV] 23 p3982 N85-34699
Injection of energetic particles following the gamma-ray flares on June 7, 1980, as observed on Helios 1
[SH-1.3-9] 23 p3993 N85-34758
Spectra of solar proton ground level events using neutron monitor and neutron moderated detector recordings
[SH-1.3-14] 23 p3994 N85-34759
Observation of pick-up ions in the solar wind: Evidence for the source of the anomalous cosmic ray component?
[SH-4.6-5] 23 p4039 N85-35043

HELIUM ISOTOPES
Structure and kinetics of physisorption, properties of helium during reduction of the dimension
03 p0432 N85-12749
Development program: Nuclear magnetic resonance gyroscope (NMR-gyro). Phase 1: Development of an experimental model
[BMFT-FB-W-84-041] 05 p0639 N85-14101
Solar He-3-rich events and non-relativistic electron events: A new association
[NASA-TM-86179] 06 p0890 N85-15652
Outlook for realization of proximity effect and Josephson direct current in helium-2 13 p2074 N85-22958
Entropy of He 2 and universality near the superfluid in He(4) 19 p3378 N85-30967
Cosmic ray He3 measurements
[OG-4.2-3] 21 p3714 N85-33045
Constraints on early atmosphere from planetary accretion processes 21 p3717 N85-33064
The degassing history of the Earth: Noble gas studies of Archaean cherts and zero age glassy submarine basalts 21 p3718 N85-33072
Interstellar propagation and the isotopic composition of hydrogen in the galactic cosmic rays
[OG-4.2-1] 22 p3877 N85-34021
Measurements of galactic hydrogen and helium isotopes from 1978 through 1983
[OG-4.2-2] 22 p3877 N85-34022
Cosmic ray He-3 measurements
[OG-4.2-3] 22 p3878 N85-34023
Analysis of experimental data on interstellar antiprotons in the light of measurements of high-energy electrons and He-3 nuclei
[OG-6.1-6] 22 p3886 N85-34087
Type 3 solar radio bursts and 3HE-rich events
[SH-2.2-3] 23 p4000 N85-34798
Solar source regions of 3HE-rich particle events
[SH-2.2-4] 23 p4000 N85-34799
The 3HE in solar non-relativistic electron events
[SH-2.2-5] 23 p4000 N85-34800
The heavy ion composition in 3HE-rich solar flares
[SH-2.2-7] 23 p4000 N85-34802
The mean ionic charge of silicon in 3HE-rich solar flares
[SH-2.2-8] 23 p4000 N85-34803

On the connection between the 3HE-enrichment and spectral index of solar energetic particles
[SH-2.2-9] 23 p4001 N85-34604
Breakdown of helium nuclei in matter processed near black holes
[OG-8.2-20] 23 p4021 N85-34916
The 4He1H ratios in the chemical compositions of solar flare particles and the primordial solar nebula
[SH-7.1-12] 23 p4046 N85-35104

HELIUM PLASMA
Low plasma edge temperatures for the self-pumped limiter
[DE85-010155] 18 p3189 N85-29782
The dependence of solar modulation on the sign of the cosmic ray particle charge
[SH-4.2-23] 23 p4009 N85-34860

HELIUM STARS
U B STARS

HELIUM 2
U HELIUM ISOTOPES
U LIQUID HELIUM

HELIUM 3
U HELIUM ISOTOPES

HELIUM 4
U HELIUM ISOTOPES

HELIUM-NEON LASERS
Scheme for measuring specular reflection coefficient at 10.6 microns wavelength with zigzag-path cell and integrating sphere 14 p2275 N85-24097
Applications of laser technology described
21 p3572 N85-32218
Investigation of reproducibility of emission wavelength of helium-neon laser with external neon absorption cell (0.63 micrometers) 21 p3683 N85-32884
Dielectric mirror with ferromagnetic substrate
21 p3696 N85-32966

HELIX TUBES
U TRAVELING WAVE TUBES

HELIXES
U CURVES (GEOMETRY)

HELMET MOUNTED DISPLAYS
Psychophysical research in development of a fiber-optic helmet mounted display 05 p0701 N85-14501
Helmet mounted telescope
[AD-D011355] 07 p1019 N85-16467
The use of lasers in wide-angle visual systems
[AD-P004322] 09 p1269 N85-17976
Design considerations for an eye tracked AOI (Area of Interest) display system
[AD-P004324] 09 p1269 N85-17978
Air combat visual simulation using a head slaved projector
[AD-P004327] 09 p1270 N85-17981
The fiber-optic helmet-mounted display
[AD-P004330] 09 p1270 N85-17984
Binocular overlap in a fiber optic helmet mounted display
[AD-P004331] 09 p1270 N85-17985
The effect of modified spectacles on the field of view of the helmet display unit of the integrated helmet and display sighting system
[AD-A148693] 09 p1281 N85-18055
Wide-field-of-view, helmet-mounted infinity display system development
[AD-A149641] 12 p1777 N85-21159
Trends shaping advanced aircrew training capabilities through the 1990s
[AD-A152277] 16 p2843 N85-27530
Advanced simulator for pilot training and helmet-mounted visual display configuration comparisons
[AD-A155326] 21 p3667 N85-32776

HELMETS
Direct view helmet mounted telescope
[AD-D011291] 06 p0755 N85-14839
Helmet mounted telescope
[AD-D011355] 07 p1019 N85-16467
SPH-4 US Army flight helmet performance, 1972 - 1983
[AD-A148674] 08 p1201 N85-17562

HELMHOLTZ EQUATIONS
The numerical solution of the Helmholtz equation for wave propagation problems in underwater acoustics
[NASA-CR-172454] 02 p0250 N85-11634
Spheroidal functions: Properties and tabulation. Application to antenna synthesis
14 p2396 N85-24758

HELMHOLTZ RESONATORS
The effect of grazing flow on the impedance of the Helmholtz resonator 05 p0635 N85-14076
A broadband matching network
[AD-D011406] 08 p1219 N85-17675
A research program to reduce the interior noise in general aviation aircraft, index and summary
[NASA-CR-176178] 24 p4145 N85-35695

HELMHOLTZ VORTICITY EQUATION
Diffraction of plane polarized waves by noncircular cylindrical cavity 02 p0269 N85-11754
Three-dimensional, direct and vectorized elliptic solvers for various boundary conditions
[AD-B088266L] 08 p1206 N85-17595
An introduction to vortex breakdown and vortex core bursting
[NAE-AN-28] 17 p2892 N85-27829
On the use of internal state variables in thermoviscoplastic constitutive equations
20 p3466 N85-31536

HELOS (SATELLITE)
U EXOSAT SATELLITE

HEMATOCRIT RATIO
A systems analysis of the erythropoietic responses to weightlessness. Volume 1: Mathematical model simulations of the erythropoietic responses to weightlessness
[NASA-CR-171890] 20 p3506 N85-31794

HEMATOLOGY
Multiple regression method used to assess animal adaptation to hypoxic hypoxia 12 p1902 N85-21947
Chemical characterization and toxicologic evaluation of airborne mixtures. Inhalation toxicology of diesel fuel obscurant aerosol in Sprague-Dawley rats. Phase 3. Subchronic exposures
[AD-A150100] 12 p1905 N85-21966
Research opportunities in loss of red blood cell mass in space flight
[NASA-CR-175808] 16 p2841 N85-27517

HEMATOPOIESIS
Hemopoiesis in rats submitted to weightlessness
01 p0091 N85-10613
Functional and structural changes in human erythrocyte surface after irradiation by UV waves of various wavelengths. Report 1: Expression of ABO and Rhesus system antigen 09 p1361 N85-18564
Functional and structural changes in human erythrocyte surface after irradiation by UV waves of various wavelentights. Report 2: Adsorption of alcyan blue by external premembranous components
09 p1361 N85-18565
A systems analysis of the erythropoietic responses to weightlessness. Volume 1: Mathematical model simulations of the erythropoietic responses to weightlessness
[NASA-CR-171890] 20 p3506 N85-31794
A systems analysis of the erythropoietic responses to weightlessness. Volume 2: Description of the model of erythropoiesis regulation. Part A: Model for regulation of erythropoiesis. Part B: Detailed description of the model for regulation of erythropoiesis
[NASA-CR-171891] 20 p3506 N85-31795

HEMATOPOIETIC SYSTEM
A detailed analysis of the erythropoietic control system in the human, squirrel, monkey, rat and mouse
[NASA-CR-171879] 15 p2614 N85-26107

HEMODYNAMIC RESPONSES
Distribution of blood flow to brain, kidneys, gut, spleen and posterior extremities in cats in acute hypoxia
07 p1013 N85-16434
Nature of postural changes in human hemodynamics with intake of sydnocarb alone and in combination with obsidan 19 p3325 N85-30597
Analysis of the transient response of temporal artery blood flow data relative to various anti-G suit pressure schedules
[AD-A155242] 21 p3666 N85-32775
Formation of new microvessels in skeletal muscles of rats exposed to hypobaric hypoxia for one week
22 p3820 N85-33662
Effect of hypokinesia and +Gz accelerations on transport function of human blood
23 p3952 N85-34497
Oxygenation and regional circulation in gingival mucosa during exposure to lower body negative pressure
23 p3953 N85-34498
Effect of water immersion of parameters of central hemodynamics in individuals over 45 years old
23 p3953 N85-34499
Effect of acute hypoxia on coronary and systemic hemodynamics 23 p3953 N85-34503

HEMODYNAMICS
NT LOWER BODY NEGATIVE PRESSURE
Compensatory and adaptive regional hemodynamic reactions to weightlessness during long-term spaceflights 01 p0091 N85-10616
Hemodynamics and plasma arginine vasopressin during water immersion in normal man
05 p0693 N85-14458
Hemodynamics responses to upright tilt at sea level and high altitude
[AD-A148848] 10 p1527 N85-19634
Regional circulation during testing on isokinetic dynamometer following 14-day bedrest
19 p3323 N85-30590
Primate adrenal reactions to antiorthostatic hypokinesia 19 p3324 N85-30591
Long term exposure of animals to antiorthostatis (-90 deg) as a model of critical homeostatic disturbances
19 p3324 N85-30592
Nature of postural changes in human hemodynamics with intake of sydnocarb alone and in combination with obsidan 19 p3325 N85-30597
Results and prospects of physiological research during spaceflights 22 p3732 N85-33139
Intracardiac hemodynamics and human heart function in simulated weightlessness 22 p3733 N85-33140
Cosmonauts' cardiovascular system function during long-term orbital flights aboard Salyut-6 station
22 p3733 N85-33141
Effects of blood volume overload on myocardial ultrastructure in relation to adaptation to high altitude hypoxia 22 p3820 N85-33664
USSR report: Space Biology and Aerospace Medicine, volume 19, no. 2, March - April 1985
[JPRS-USB-85-004] 22 p3820 N85-33667
Typological characteristics of hemodynamic states of healthy subjects in orthostatic position
22 p3821 N85-33673
Cerebral hemodynamics and ventricular function in -15 deg antiorthostatic position 22 p3822 N85-33676
Morphological manifestations of hemodynamic changes in lungs of monkeys submitted to antiorthostatic hypokinesia 22 p3824 N85-33688
USSR report: Space Biology and Aerospace Medicine, vol. 19, no. 3, May - June 1985
[JPRS-USB-85-005] 23 p3952 N85-34494
Effect of dibazol on parameters of nonspecific resistance of subjects in pressurized cabins
23 p3954 N85-34504

HEMOGLOBIN
NT OXYHEMOGLOBIN
Effect of maximum physical load on oxygen-transport properties of blood 01 p0093 N85-10627
A systems analysis of the erythropoietic responses to weightlessness. Volume 1: Mathematical model simulations of the erythropoietic responses to weightlessness
[NASA-CR-171890] 20 p3506 N85-31794
A systems analysis of the erythropoietic responses to weightlessness. Volume 2: Description of the model of erythropoiesis regulation. Part A: Model for regulation of erythropoiesis. Part B: Detailed description of the model for regulation of erythropoiesis
[NASA-CR-171891] 20 p3506 N85-31795
Estimating risks of lead-induced hemoglobin decrements under conditions of uncertainty: Methodology, pilot judgments and illustrative calculations
[DE85-012293] 23 p3952 N85-34493

HEMORRHAGES
Fatal hemorrhagic shock and acetate solutions
[AD-A146754] 07 p1014 N85-16444

HEOS B SATELLITE
The Earth magnetosphere: A charged particle accelerator 04 p0519 N85-13315

HEOS SATELLITES
NT HEOS B SATELLITE

HERBICIDES
Proceedings of the 14th Conference on Environmental Toxicology
[AD-A146400] 06 p0843 N85-15350
The epidemiology and toxicology of Agent Orange
[AD-P004038] 06 p0845 N85-15368
Toxicity, mutagenesis and aging due to endogenous oxygen radicals
[AD-A150121] 12 p1900 N85-21928

HERBIG-HARO OBJECTS
Bipolar molecular outflows: T Tauri stars and Herbig-Haro objects 03 p0446 N85-12837
Non-stable motions and instability in stellar associations 05 p0739 N85-14754
UV observations and results on pre-main sequence stars 11 p1744 N85-20970
The changing ultraviolet spectrum of Herbig-Haro object No. 1 11 p1747 N85-20989
Short-wavelength observations of HH-2H and HH-24A
11 p1747 N85-20990
Dust in the region of Herbig-Haro objects: The case of NGC 1999 11 p1747 N85-20991
Plasma processes in Herbig-Haro objects
12 p1957 N85-22301
Low-excitation Herbig-Haro objects and interstellar extinction
[NASA-CR-176142] 23 p3988 N85-34726
The structure of Herbig-Haro object 43 and Orion dark cloud extinction
[NASA-TM-87503] 24 p4166 N85-35831

HERCULES NOVA
EXOSAT observations of the 35d intensity variations of Her X-1 — X ray binary source
11 p1742 N85-20956
Pulse phase spectroscopy of Her X-1 with EXOSAT — X ray binary source
11 p1743 N85-20957
HERMES SATELLITE
U COMMUNICATIONS TECHNOLOGY SATELLITE
HERMETIC SEALS
Qualitative and quantitative compositional analysis of shale derived by gas chromatography and combined gas Chromatography/Mass spectrometry. Executive summary
[AD-A148369] 07 p0924 N85-15851
Method for bonding insulator to insulator
[AD-D011340] 07 p0929 N85-15891
Experimental stiffness of tapered bore seals
[NASA-TM-86978] 15 p2568 N85-25847
Hermetic sealing of nonlubricated gas seal and friction characteristics, chapter 7
[DE85-006375] 15 p2569 N85-25851
Inhibited anticorrosion protection of automotive steel strip in the NLMK
[BLL-M-36250-(5828.4)] 20 p3430 N85-31274
A device for generating motive force through the expansion of a non-elastic dense fluid
[NASA-TM-77664] 20 p3454 N85-31446
X-ray residual stress analysis on the coarse grain of copper and its application to the brazed copper
23 p3907 N85-34202
Hermetic chip carrier compliant soldering pads
[AD-D011722] 23 p3938 N85-34410
HERMITIAN POLYNOMIAL
Montonicity preserving bicubic interpolation, revision 1
[DE85-007976] 17 p3021 N85-28683
HERTZSPRUNG-RUSSELL DIAGRAM
X-ray spectra of bursting neutron stars
23 p3981 N85-34686
HESSIAN MATRICES
Quasi-Newton algorithms for large scale nonlinear systems
02 p0208 N85-11370
Software for estimating sparse Hessian matrices
[DE85-008121] 17 p3013 N85-28629
HETEROCYCLIC COMPOUNDS
NT ADENOSINE DIPHOSPHATE
NT ADENOSINE TRIPHOSPHATE
NT ADENOSINES
NT ATROPINE
NT AZINES
NT AZOLES
NT CARBAZOLES
NT METHYLENE BLUE
NT OXAZOLE
NT PHTHALOCYANIN
NT PHYLLOQUINONE
NT PYRROLES
NT RDX
NT TETRAHYDROFURAN
NT THIAZINE (TRADEMARK)
NT TRYPTOPHAN
Method of obtaining heterocyclic polymers
[AD-A145127] 01 p0033 N85-10202
Method for making heterocyclic block copolymers
[AD-D011446] 10 p1451 N85-19143
Spray pyrolysis as a synthetic tool
[AD-A153891] 19 p3234 N85-30047
HETERODYNING
NT OPTICAL HETERODYNING
Quantum noise and excess noise in optical homodyne and heterodyne receivers
[AD-A148298] 08 p1157 N85-17303
Pulse heterodyne equipment for measurements of range and velocity of moving targets-pulse radar
[ESA-TT-845] 09 p1312 N85-18246
Injection controlled laser transmitter with twin local oscillators
[AD-D011577] 15 p2563 N85-25810
A comparison of electronic heterodyne moire deflectometry and electronic heterodyne holographic interferometry for flow measurements
[NASA-TM-87071] 21 p3586 N85-32302
Recording small frequency drifts of microwave oscillators
22 p3771 N85-33372
Heterodyne holographic interferometry for visualization of surface acoustic waves
[AD-A155405] 22 p3836 N85-33753
HETEROGENEITY
Friction, wear and structure of heterogeneous materials
01 p0055 N85-10362
Transformation of heterogeneous surface waves by skewed streams
02 p0250 N85-11697
Numerical investigation of characteristics of current flow for different methods of obtaining discharge in high speed lasers. Mechanism underlying current flow in positive glow discharge column
02 p0264 N85-11728
The 6th International Summer Institute in Surface Science 1983)
[AD-A146253] 03 p0434 N85-12762
Heterogeneous data base access
05 p0735 N85-14724
Characteristic scale of inner mixing layers in stably stratified atmosphere
06 p0824 N85-15235
Transformation of electromagnetic waves in plasma with randomly-heterogeneous magnetic field
07 p0953 N85-16039
Fluctuations during observations of extraterrestrial sources from outer space through Earth's atmosphere
07 p0953 N85-16040
In situ monitoring of electrochemical reactions by surface enhanced Raman scattering
[PB85-149789] 12 p1803 N85-21312
The behaviour of detonation waves in single phase heterogeneous systems
[AD-A149825] 12 p1846 N85-21581
Temperature effects of heterogenizated annealing on structure and properties of V95 aluminum alloy
13 p2025 N85-22692
Consideration of heterogeneity of gravity fields in local high precision geodetic constructions
13 p2114 N85-23169
Wave propagation in heterogeneous media
[AD-A150800] 14 p2321 N85-24341
Perceived heterogeneity and its effect on various types of tasks
[AD-A151003] 14 p2392 N85-24729
Analysis of combustion oscillations in heterogeneous systems
[AD-A151999] 16 p2745 N85-26942
Quality testing to the specifications of the Stahl-Eisen-Pruefblatt 1570/71 using an automatic image analysis system
[BLL-BISI-TRANS-22253-(9022.06)]
17 p2976 N85-28385
Mechanism of heterogeneous deposition ice nucleation near water-saturation
21 p3638 N85-32597
HETEROJUNCTION DEVICES
Thin film (Al, Ga)As heterojunction solar cells
02 p0258 N85-11691
Preparation and evaluation of ZnSe and ZnS sub X Se sub 1-x epitaxial layers on Ge substrates for applications in surface passivation and heterojunction devices
[AD-A147432] 07 p1048 N85-16657
Heterocontact effects in point contact electron-phonon spectroscopy of the alkali metals
[AD-A149760] 12 p1800 N85-21290
Comparative study of GaAs solar cell potentialities for space applications
13 p2006 N85-22577
GaAs and 3-5 compound solar cells status and prospects for use in space
13 p2007 N85-22580
Photovoltaic cells of InP-CdS heterojunction type and their temperature characteristics under A-M illumination
14 p2275 N85-24092
Physical electronics of cooled operation of very short compound semiconductor trasnsistors
14 p2297 N85-24223
Self-detecting optical sensors
[AD-D011657] 18 p3185 N85-29751
Modulation doped GaAs/Al(x)Ga(1-x)As layered structures with applications to field effect transistors
[AD-A155360] 22 p3759 N85-33296
HETEROJUNCTIONS
Low-threshold injection lasers on grown GaInPAs/InP heterostructures (1.2-1.6 micrometers wavelengths)
02 p0258 N85-11693
Research activities of the Illinois University Coordinated Science Laboratory
[AD-A145589] 03 p0449 N85-12856
The growth and properties of semiconductor strained-layer superlattices
[DE84-012979] 06 p0868 N85-15515
Diffusion barrier for long wavelength laser diodes
[AD-D011390] 07 p0970 N85-16157
Effect of neutron irradiation on the high temperature operation of injection laser diodes
[DE85-000068] 09 p1326 N85-18333
Liquid-phase epitaxial growth of CdTe on HgCdTe
[AD-D011482] 10 p1561 N85-19846
Surface and allied studies in silicon solar cells
[NASA-CR-174447] 11 p1671 N85-20531
Preliminary studies on the low cost preparation of chalcogenide semiconductors from solution depositions
[DE85-000538] 11 p1736 N85-20918
Multiple double heterojunction buried laser device
[AD-D011519] 12 p1855 N85-21635
Process for making a heterojunction source-drain insulated gate field-effect transistors utilizing diffusion to form the lattice
[AD-D011536] 12 p1939 N85-22176
Development of a planar heterojunction bipolar transistor for very high speed logic
[AD-A150374] 13 p2064 N85-22895
Thin film cadmium telluride and zinc phosphide solar cells
[DE85-002904] 15 p2587 N85-25880
Polycrystalline semiconductor heterojunction modeling (CdS/CuInSe(sub)2)
[DE85-002913] 16 p2871 N85-27713
The construction and study of improved Al(x)Ga(1-x)As-GaAs heterostructure devices
[AD-A153264] 17 p2954 N85-28244
Zn3P2 as an improved semiconductor for photovoltaic solar cells
[DE85-008772] 18 p3007 N85-29171
Heterojunction Schottky gate MESFET with lower channel ridge barrier
[AD-D011673] 19 p3258 N85-30199
Cadmium sulfide/copper ternary heterojunction cell research
[DE85-008778] 19 p3305 N85-30486
Photoelectronic properties of zinc phosphide crystals and heterojunctions
[DE85-008777] 19 p3307 N85-30501
Optical properties of heterostructures and superlattices
[AD-A156243] 24 p4162 N85-35802
HETEROTROPHS
Chemical composition of Musca domestica L. larval and pupal biomass when developing in organic waste of biological life-support system for man
22 p3824 N85-33681
HEURISTIC METHODS
An expert system for representing procedural knowledge
[AD-P003923] 02 p0245 N85-11603
The search for regularity: Four aspects of scientific discovery
[AD-A145939] 03 p0368 N85-12355
New uses for sensitivity analysis: How different movement tasks effect limb model parameter sensitivity
05 p0706 N85-14529
Automatic map name placement system
09 p1341 N85-18438
Spacefilling curves and the planer travelling salesman problem
[AD-A149337] 10 p1551 N85-19786
Heuristics based on spacefilling curves for combinatorial problems in the plane
[AD-A149320] 10 p1552 N85-19788
Learning to search. From weak methods to domain-specific heuristics
[AD-A149949] 12 p1918 N85-22045
A replication and extension of the inducement of the availability heuristic
[AD-A149755] 12 p1923 N85-22063
State dependent priority rules for scheduling
[AD-A149972] 12 p1924 N85-22090
Solving set covering problems using heuristics with branch and bound
[AD-A151905] 15 p2638 N85-26289
Generation of flight paths using heuristic search
[AD-A151949] 16 p2704 N85-26884
A heuristic solution to the spacing problem: Maximizing the minimum Euclidean distance among N points in a convex region
[AD-A152116] 16 p2855 N85-27003
Identifying solution paths in cognitive diagnosis
[AD-A152463] 17 p3000 N85-28549
A practical approach to Karmarkar's algorithm
[AD-A155714] 21 p3673 N85-32818
Heuristic rules for visualization
23 p3965 N85-34584
HEWLETT-PACKARD COMPUTERS
System test: Hewlett-Packard draft
[A-9] 18 p3166 N85-29613
HEXANITROSTILBENE
Experimental studies of chemical reactivity during shock initiation of hexanitrostilbene
[DE85-011726] 22 p3754 N85-33270
HEXENES
Influence of structural parameters of zeolite catalysts on their activity and selectivity
[BMFT-FB-T-83-253] 03 p0329 N85-12119
HF LASERS
Short Wavelength Chemical Laser (SWCL) Workshop
[AD-A151959] 16 p2790 N85-27211
Operating characteristics, absorptivity/reflectivity measurements, and pulse system design of the NPS (Naval Postgraduate School) hydrogen fluoride/deuterium fluoride laser
[AD-A152712] 17 p2970 N85-28341
Chemical lasers
[ISL-R-107/84] 23 p3936 N85-34400
HICAT (RADAR TECHNIQUE)
U HIGH RESOLUTION COVERAGE ANTENNAS
HiCAT PROJECT
U HIGH RESOLUTION COVERAGE ANTENNAS

HIERARCHIES
Approximating hierarchical normal priors using a vague component
[CSIR-TWISK-284] 01 p0107 N85-10720
Evidence accumulation for spatial reasoning
07 p0985 N85-16261
Research into self-timed VLSI circuits
[AD-A149140] 10 p1479 N85-19339
A circuit grammer for operational amplifier design
[AD-A149566] 10 p1481 N85-19346
Normal and anomalous geothermal fields and their relationship to hierarchy of geological bodies
13 p2113 N85-23163
The hierarchical database decomposition approach to database concurrency control
[AD-A150612] 13 p2168 N85-23450
Some applications of fuzzy sets and the analytical hierarchy process to decision making
[AD-A150720] 14 p2412 N85-24876
Multigrid algorithms on the hypercube multiprocessor
[AD-A152200] 16 p2847 N85-27556
Application of hierarchical data structures to geographical information systems
[AD-A152169] 16 p2877 N85-27753
Fuzzy hierarchical analysis
[DE85-008149] 17 p3021 N85-28685
The Hamiltonian structure of a complex version of the Burgers hierarchy
[PREPRINT-423] 18 p3173 N85-29665
Inference in hierarchic classification — data bases
[ENST-84E014] 20 p3518 N85-31873
Models for multidimensional tests and hierarchically structured training materials
[AD-A155231] 21 p3665 N85-32768
Hierarchical chamfer matching
[FOA-C-30387-E1] 22 p3802 N85-33558
A hierarchy of knowledge levels implemented in a rule-based production system to calculate bounds on the size of intersections and unions of simple sets
[AD-A155291] 22 p3848 N85-33836
Selection of segment similarity measures for hierarchical picture segmentation 23 p3960 N85-34548
Source hierarchy list. Volume 1: A through H
[AD-A156300] 24 p4165 N85-35825
Source hierarchy list. Volume 2: I through Z
[AD-A156301] 24 p4165 N85-35826

HIGH ACCELERATION
Further cell biology experiments with Physarum polycephalum for a reflight of Biorack
05 p0689 N85-14429

HIGH ALTITUDE
Magnetospheric plasma studies using data from the dynamics high and low altitude plasma instruments
[AD-A145751] 03 p0392 N85-12505
Structure of temperature field based on observations of refraction from high meteorological mast
06 p0819 N85-15199
Hemodynamics responses to upright tilt at sea level and high altitude
[AD-A148848] 10 p1527 N85-19634
Design considerations for high-altitude, long-endurance, microwave-powered aircraft
[NASA-TM-86403] 14 p2218 N85-23751
High altitude sampling program: Radioactivity in the stratosphere
[DE85-005824] 14 p2374 N85-24676
Spectral characteristics of protons at low and high altitudes during geomagnetic storm of 29 July 1977
16 p2719 N85-26786
Technological experiments on high-altitude rockets
16 p2725 N85-26818
Applied research and development for falling-sphere air density measuring systems
[AD-A155227] 21 p3552 N85-32099
Effects of blood volume overload on myocardial ultrastructure in relation to adaptation to high altitude hypoxia 22 p3820 N85-33664
Cardiorespiratory function and work performance during adaptation to industrial labor in midalpine conditions
22 p3820 N85-33665
Structural changes in thyroid due to high-altitude adaptation in Kirghizia 22 p3820 N85-33666
An EAS experiment at mountain altitude for the detection of gamma-ray sources
[OG-9.4-5] 23 p4029 N85-34972
Short perturbations of cosmic ray intensity and electric field in atmosphere
[SH-6.1-18] 23 p4046 N85-35090

HIGH ALTITUDE BALLOONS
NT JIMSPHERE BALLOONS
NT SUPERPRESSURE BALLOONS
Thin film strain transducer --- suitable for in-flight measurement of scientific balloon strain
[NASA-CASE-WLP-10055-2] 12 p1849 N85-21598
Observation of cosmic ray flux variations in stratosphere 13 p1981 N85-22430

HIGH ALTITUDE BREATHING
Hemodynamics and neurodynamics of the human brain during exposure to moderate hypoxic hypoxia
01 p0094 N85-10630
Results of study of hypoxia problems
04 p0544 N85-13462

HIGH ALTITUDE ENVIRONMENTS
Fungi of Mt. Babia Gora. 1: Mycoflora of forests
[NASA-TM-77484] 02 p0234 N85-11522
Armed forces special Symposium on Medicine of Altitudes 13 p2166 N85-23441
High-altitude testing of selective optical coatings for solar radiators and collectors 17 p2939 N85-28143

HIGH ALTITUDE FLIGHT
U HIGH ALTITUDE

HIGH ALTITUDE PRESSURE
Cut-off lows and their influence on the weather in Switzerland
[REPT-45] 10 p1519 N85-19574
Formation of new microvessels in skeletal muscles of rats exposed to hypobaric hypoxia for one week
22 p3820 N85-33662
Effects of immobilization and high-altitude adaptation on energy metabolism in rats 22 p3820 N85-33663

HIGH ALTITUDE TESTS
High-altitude testing of selective optical coatings for solar radiators and collectors 17 p2939 N85-28143
The design of an experiment to detect low energy antiprotons
[OG-9.1-1] 23 p4022 N85-34928

HIGH ASPECT RATIO
Flutter parametric studies of cantilevered twin-engine transport type wing with and without winglet. Volume 2: Transonic and density effect investigations
[NASA-CR-172410-VOL-2] 04 p0513 N85-13270
Aileron effectiveness for a subsonic transport model with a high-aspect-ratio supercritical wing
[NASA-TM-85674] 07 p0898 N85-15695
Comparison of analytical and experimental steadyand unsteady-pressure distributions at Mach number 0.78 for a high-aspect-ratio supercritical wing model with oscillating control surfaces
[NASA-TM-84589] 07 p0899 N85-15697
Numerical simulation of transonic flutter of a high-aspect ratio transport wing 16 p2694 N85-26630
Low-speed tests of a high-aspect-ratio, supercritical-wing transport model equipped with a high-lift flap system in the Langley 4- by 7-meter and Ames 12-foot pressure tunnels
[NASA-TP-2097] 20 p3388 N85-31010

HIGH ASPECT RATIO WINGS
U SLENDER WINGS

HIGH CURRENT
A 10/sup 11/W high current pulse electron beam accelerator described 11 p1620 N85-20200
High-current measurement techniques
[PB85-100444] 11 p1637 N85-20311
Surface interactions and high-voltage current collection 13 p1993 N85-22493
Collective acceleration of ions using high current relativistic electron beams
[DE85-004889] 13 p2157 N85-23393
Development of theory of high-current high-pressure pulsed arc 15 p2645 N85-26314
High current beam hollowing instability study
[AD-A151301] 15 p2648 N85-26329
Plasma erosion opening switch
[DE85-011384] 20 p3535 N85-31998
Observations of accelerated high current low emittance beams in the SLC Linac
[DE85-013073] 24 p4066 N85-35211
Numerical studies of high current beam compression in heavy ion fusion
[DE85-011874] 24 p4158 N85-35783

HIGH ECCENTRIC LUNAR OCCULTATION SATELLITE
U EXOSAT SATELLITE

HIGH ENERGY ASTRONOMY OBSERVATORIES
U HEAO

HIGH ENERGY ASTRONOMY OBSERVATORY A
U HEAO 1

HIGH ENERGY ASTRONOMY OBSERVATORY B
U HEAO 2

HIGH ENERGY ASTRONOMY OBSERVATORY C
U HEAO 3

HIGH ENERGY ASTRONOMY OBSERVATORY 1
U HEAO 1

HIGH ENERGY ASTRONOMY OBSERVATORY 2
U HEAO 2

HIGH ENERGY ASTRONOMY OBSERVATORY 3
U HEAO 3

HIGH ENERGY ELECTRONS
NT RELATIVISTIC ELECTRON BEAMS
Energetic electrons in impulsive solar flares
02 p0303 N85-11962
Asymptotic orbit theory for trapped electrons in inhomogeneous Whistler field
[AD-A146178] 03 p0392 N85-12510
Morphology of keV-electrons in the Earth's magnetosphere as observed by GEOS 1
[DRI-3-84] 09 p1350 N85-18496
High energy pulsed particle accelerator
[AD-A149247] 10 p1554 N85-19797
The high latitude D region during electron precipitation events 11 p1664 N85-20484
High energy particle effects in the D region during and after geomagnetic storms 11 p1664 N85-20485
Latitudinal dependence of the energy input into the mesosphere by high energy electrons
11 p1664 N85-20489
Longitude and pitch-angle distributions of streams of high-energy electrons under Earth's radiation belts
13 p1978 N85-22415
The keV electrons and 80 keV protons in the vicinity of the high latitude magnetosphere and at the bow shock 14 p2355 N85-24554
Morphology of 2keV-electrons observed by GEOS 1
14 p2360 N85-24581
Electron flux with electron energies above 40 MeV at altitudes of about 500 km in region where capture is possible and outside it when L is 3 or greater
15 p2481 N85-25315
Measurements of fluxes of high-energy protons and electrons by 2 oppositely oriented spectrometers aboard Cosmos-368 artificial Earth satellite
16 p2722 N85-26800
Fast electromagnetic (EM) shower simulation
[NOTA-INTERNA-831] 18 p3175 N85-29683
Low-energy gamma rays from Cygnus X-1
[OG-2.4-13] 22 p3868 N85-33957
Analysis of experimental data on interstellar antiprotons in the light of measurements of high-energy electrons and He-3 nuclei
[OG-6.1-6] 22 p3888 N85-34097
Spectral shape variation of interstellar electrons at high energies
[OG-6.2-7] 22 p3889 N85-34106
Collisional relaxation of electron tail distribution
[IPPJ-729] 23 p3974 N85-34635
On the retention of high-energy protons and nuclei with charges Z or equal to 2 in large solar flares after the process of their acceleration
[SH-2.1-6] 23 p3998 N85-34789
The influence of the Earth's magnetosphere on the high-energy solar protons
[SH-6.1-22] 23 p4046 N85-35093

HIGH ENERGY INTERACTIONS
NT STRONG INTERACTIONS (FIELD THEORY)
High energy-resolution inelastic X-ray scattering
[DE84-014565] 01 p0118 N85-10804
Research program in theoretical high-energy physics
[DE84-013717] 01 p0119 N85-10817
Response of propellants to high dynamic stresses: The uses of gun launch techniques
08 p1116 N85-17035
Dynamics and mechanisms of catalytic processes and hot chemistry
[DE85-002899] 09 p1292 N85-18114
High energy physics study
[DE84-015803] 09 p1363 N85-18700
Very high energy probes of the quark-gluon plasma
[DE84-016992] 09 p1392 N85-18763
Supersymmetric inflationary cosmology
[DE85-001332] 09 p1415 N85-18929
Experimental and theoretical high energy physics
[DE85-000844] 11 p1726 N85-20856
Activities in nuclear physics and high energy physics
11 p1728 N85-20868
Research and technology: Fiscal year 1984 report
[NASA-TM-85231] 12 p1964 N85-22340
Experimental studies of elementary particle interactions at high energies
[DE85-004795] 13 p2157 N85-23394
Los Alamos Science, Number 11, Summer-Fall, 1984
[DE85-004634] 14 p2419 N85-24926
Summaries of FY 1984 research in high energy physics
[DE85-005641] 14 p2420 N85-24934
Physics, Computer Science and Mathematics Div.
[DE85-006868] 15 p2642 N85-26296
Two-beam accelerator
[DE85-004662] 15 p2649 N85-26335
Mean free paths, viscosity, and the limitations of perfect fluid hydrodynamics in the description of the quark-gluon plasma
[DE85-005501] 15 p2649 N85-26339
Future accelerator studies of high energy heavy ion collisions
[DE85-005885] 15 p2650 N85-26346
Overview of the physics issues at the SSC
[DE85-007074] 16 p2859 N85-27834

USSR report: Engineering and equipment
[JPRS-UEQ-85-004] 17 p2939 N85-28142

Neutron scattering and reactions on 59Co from 1 to 20 MeV
[AERE-R-11439] 17 p3028 N85-28729

Heavy ion physics at BNL, the AGS and RHIC
[DE85-005951] 17 p3033 N85-28760

Particle physics: Recent successes and future prospects
[DE85-008175] 17 p3033 N85-28765

Activities report in nuclear physics and high energy physics
[JF40026] 17 p3035 N85-28777

Physics of (very) high energy e(+)-e(-) colliders
[DE85-008177] 17 p3036 N85-28780

Theoretical studies of high energy phenomenon: Analysis of models of CP and T violation
[DE85-007455] 17 p3036 N85-28782

Physics of High Energy Particle Accelerators. AIP Conference Proceedings no. 127
[DE85-008891] 18 p3182 N85-29733

Slow extraction of LAMPF 2
[DE85-010744] 19 p3356 N85-30805

Theory of high energy collision processes
[DE85-010183] 19 p3362 N85-30846

High-energy particle Monte Carlo at Los Alamos
[DE85-010716] 19 p3363 N85-30856

Work in Amsterdam on local intelligence — artificial intelligence
[NIKHEF-H/84-9] 20 p3518 N85-31877

Requirements for very high energy accelerators
[DE85-011173] 20 p3529 N85-31952

Research in the theory of condensed matter and elementary particles
[DE85-010447] 20 p3531 N85-31968

High-energy Physics Institute building 3-trillion-ev accelerator 21 p3691 N85-32934

Gamma rays of 0.3 to 30 MeV from PSR 0531+21
[OG-2.3-6] 22 p3866 N85-33945

Search for gamma-rays above 400 GeV from Geminga
[OG-2.4-4] 22 p3867 N85-33951

Primary gamma-rays with E gamma or = to 10(15) eV: Evidence for ultrahigh energy particle acceleration in galactic sources
[OG-2.6-13] 22 p3871 N85-33974

Some evidence for high energy gamma-ray sources at large galactic latitudes
[OG-2.7-5] 22 p3871 N85-33978

High-energy multiple muons and heavy primary cosmic-rays
[OG-5.2-9] 22 p3883 N85-34065

Composition of primary cosmic rays near the knee
[OG-5.2-10] 22 p3884 N85-34066

Electron and muon parameters of EAS and the composition of primary cosmic rays in 10(15) to approximately 10(16) eV
[OG-5.2-12] 22 p3884 N85-34068

The primary cosmic ray mass composition at energies above 10(14) eV
[OG-5.4-6] 22 p3886 N85-34083

Summary of activities, 1983
[LBL-18500] 23 p3969 N85-34505

Calculation of improved spallation cross sections
[OG-7.2-23] 23 p4017 N85-34890

Cerenkov counters for high energy nuclei: Some new developments
[OG-9.1-5] 23 p4023 N85-34931

SONTRAC: A solar neutron track chamber detector
[SH-9.1-12] 23 p4052 N85-35127

A survey of multiplicities and rapidity densities from existing emission data on hadron-nucleus nucleus-nucleus collisions 24 p4146 N85-35706

A simulation of ultra-relativistic nucleus-nucleus collisions 24 p4146 N85-35707

Very high energy probes of the quark-gluon plasma
24 p4147 N85-35708

Detector requirements for intensity interferometry measurements 24 p4147 N85-35709

Forty-five years of e(+)e(-) annihilation physics: 1956 to 2001
[DE85-013052] 24 p4149 N85-35723

Neutrino production of like sign dimuons
[DE85-013594] 24 p4151 N85-35741

SLC Energy Upgrade Program at SLAC
[DE85-014290] 24 p4160 N85-35790

Development of observational and instrumental techniques in hard X-ray and medium energy gamma-ray astronomy
[NASA-CR-176172] 24 p4168 N85-35841

Nineteenth International Cosmic Ray Conference. HE Sessions, volume 6
[NASA-CP-2376-VOL-6] 24 p4170 N85-35848

Estimation of the total inelasticity coefficient in interaction of greater than or equal to 20 TeV hadrons with lead
[HE-1.1-9] 24 p4171 N85-35857

The method for the study of the inelastic cross-section for high energy protons by means of shower arrays with the large calorimetric area
[HE-1.1-11] 24 p4171 N85-35858

On a possibility of inelasticity partial coefficient K sub gamma determination in pi C and pi Pb interactions at 10 to the 14th power eV (experiment PAMIR 1)
[HE-1.1-12] 24 p4171 N85-35859

QCD-motivated description of very high energy particle interactions
[HE-1.2-2] 24 p4171 N85-35861

Empirical description of the hadron-hadron and hadron-nucleus interaction at the accelerator energy range
[HE-1.2-4] 24 p4171 N85-35862

Multiplicity distributions in interaction models used for cascade simulations
[HE-1.2-5] 24 p4172 N85-35863

Transverse momentum distribution of pion deg in the fragmentation region of super high energy interactions
24 p4180 N85-35921

Penetrative nature of high energy showers observed in Chacaltaya emulsion chamber
[HE-3.3-5] 24 p4180 N85-35923

Lateral distribution of high energy hadrons and gamma ray in air shower cores observed with emulsion chambers
[HE-3.3-8] 24 p4180 N85-35926

Size distributions of air showers accompanied with high energy gamma ray bundles observed at Mt. Chacaltaya
[HE-3.3-9] 24 p4181 N85-35927

An experimental study of correlations in the development of the electron-photon cascades
[HE-3.5-10] 24 p4184 N85-35947

A comparative analysis of gamma and hadron families at the superhigh energies recorded in experiment Pamir
[HE-3.7-1] 24 p4185 N85-35960

Nineteenth International Cosmic Ray Conference. HE Sessions, volume 7
[NASA-CP-2376-VOL-7] 24 p4186 N85-35968

Analysis of the hadron component in E.A.S.
24 p4187 N85-35971

Electrons, muons and hadrons in extensive air showers and how do they depend on nuclear interaction model, part 1 24 p4187 N85-35972

Simulation of EAS properties on the basis of high energy interaction model deduced from the accelerator data
24 p4187 N85-35973

High energy hadrons in extensive air showers
24 p4187 N85-35976

Dependence of the average spatial and energy characteristics of the hadron-lepton cascade on the strong interaction parameters at superhigh energies
24 p4188 N85-35977

Hadronic components of EAS by rigorous saddle point method in the energy range between 10(5) and 10(8) GeV 24 p4188 N85-35978

Phenomenology of soft hadron interactions and the relevant EAS data 24 p4188 N85-35980

Development of electromagnetic cascades in the atmosphere including the Landau-Pomeranchuk-Migdal effect
[HE-4.5-5] 24 p4195 N85-36029

Nuclear cascades in electromagnetic showers produced by primary gamma-quanta in the atmosphere
[HE-4.5-16] 24 p4196 N85-36038

Energy spectrum of cascade showers induced by cosmic ray muons in the range from 50 GeV to 5 TeV
[HE-5.2-14] 24 p4203 N85-36090

Range fluctuations of high energy muons passing through matter
[HE-5.2-19] 24 p4204 N85-36095

High energy neutrino astronomy with MACRO
[HE-5.3-12] 24 p4206 N85-36106

The capability of the existing network of installations for detecting the antineutrino burst from collapsing stars
[HE-5.3-13] 24 p4206 N85-36107

Energy spectra of high energy atmospheric neutrinos
[HE-5.3-14] 24 p4206 N85-36108

A standard source for high energy neutrino astronomy
[HE-5.3-15] 24 p4206 N85-36109

A search for cosmic sources of high energy neutrinos with small underground detectors
[HE-5.3-16] 24 p4206 N85-36110

Characteristics of slow particles emitted in the charged current interactions of neutrinos with emulsion nuclei
[HE-5.3-22] 24 p4207 N85-36113

Multiple muons of conventional and exotic origin in DUMAND
[HE-5.4-4] 24 p4207 N85-36117

Study of photonuclear muon interactions at Baksan underground scintillation telescope
[HE-5.4-10] 24 p4208 N85-36122

Calculation of intensity of high energy muon groups observed deep underground
[HE-5.4-13] 24 p4208 N85-36123

Results of investigation of muon fluxes of superhigh energy cosmic rays with X-ray emulsion chambers
[HE-5.4-16] 24 p4208 N85-36126

High energy cosmic ray signature of quark nuggets
[HE-6.2-11] 24 p4212 N85-36147

HIGH ENERGY PROPELLANTS

The DDT process for high energy propellants
08 p1116 N85-17033

Analysis of deflagration to detonation transition in high-energy solid propellants
[AD-A148302] 08 p1135 N85-17158

Analysis of Shock to Detonation Transition (SDT) of porous high energy propellant from ramp-wave compression loading
[AD-A149333] 10 p1457 N85-19180

Analysis of deflagration to detonation transition in high-energy solid propellants 16 p2757 N85-27010

HIGH FREQUENCIES

Resistance to HF jamming interference in mobile radio networks by an adaptive, distributed reconfiguration technique
[AD-A145117] 01 p0038 N85-10250

High frequency radar software reference manual for Product Two
[PB84-210079] 01 p0041 N85-10270

Nonlinear propagation in a depth-dependent ocean
[AD-A145079] 01 p0116 N85-10791

Robotization of technological processes in high-frequency heating and welding
03 p0345 N85-12226

Observations and prognosis of HF wave propagation via the sporadic E layer
[UIO-SR-84-04] 03 p0356 N85-12294

Special Developments and Methods in High Frequency Measuring Techniques — conferences
[PTB-E-24] 05 p0629 N85-14030

Present status and development tendencies in the field of high frequency measuring techniques
05 p0629 N85-14031

Admittance measurement with twin-T devices in the frequency range between 1 and 300 MHz
05 p0629 N85-14032

A computer controlled measuring system for the calibration of HF components 05 p0630 N85-14037

Voltage dependence of the relative AC-DC transfer difference for HF voltage-transfer standards
05 p0630 N85-14039

A group delay standard for the MHz frequency range
05 p0630 N85-14040

Optical fibers with reduced pressure sensitivity to high frequency acoustic field
[AD-D011306] 07 p1043 N85-16627

Tactical HF communication for military helicopters using the NVIS mode 08 p1074 N85-16807

A commentray on the utilization of real-time channel evaluation systems in HF spectrum management
[AD-A148616] 08 p1154 N85-17280

Standing wave pattern of HF radio waves in the ionospheric reflection region. Part 1: General formulas
[UIO-SR-84-05-PT-1] 09 p1313 N85-18253

An HF communications frequency-management procedure for forecasting the frequency of optimum transmission
[AD-A149191] 10 p1467 N85-19254

Multipath and Doppler observations during transatlantic digital HF propagation experiments
10 p1471 N85-19281

An ionospheric mode detection system for HF communications application 10 p1471 N85-19282

An H.F. simulator for use with real time channel evaluation systems 10 p1473 N85-19283

Time and space domain filtering for improved HF communication 10 p1473 N85-19286

Overview of RADC adaptive antenna developments for communications 10 p1474 N85-19289

Serial data transmission with large output on the HF channel 10 p1475 N85-19305

Effect of interfacial characteristics of metal clad polymeric substrates on electrical high frequency interconnection performance
[NASA-TM-86948] 11 p1624 N85-20023

The Ferranti Tactical SHF SATCOM station (MANSAT) 11 p1710 N85-20759

An electronically-steerable active receiving array for h.f.
[BBC-RD-1985/2] 12 p1822 N85-21430

Surface forward scattering and reflection
[AD-A150115] 12 p1926 N85-22112

Stress compensation crystal device
[AD-D011497] 12 p1941 N85-22189

Computer aided antenna design and frequency selection for HF communications
[AD-A150485] 13 p2055 N85-[illegible]

Coupled-cavity gyrotrons with mode conversion
13 p2076 N85-22967

Alternatives for satellite sound broadcast systems at HF and VHF
14 p2229 N85-23815
Physical electronics of cooled operation of very short compound semiconductor trasnsistors
14 p2297 N85-24223
Observations of the MF-HF plasma wave emissions in active auroras by the sounding rocket experiments at Syowa station
14 p2386 N85-24620
High frequency estimation of 2-dimensional cavity scattering
[AD-A151697] 15 p2542 N85-25696
Scattering center analysis for radar cross section modification
16 p2769 N85-27065
Predicting the effects of non-Gaussian interference in HF (High-Frequency) broadcasting. Part 1: A methodology for an analytic approach
[PB85-171544] 18 p3092 N85-29140
US Coast Guard High Frequency Emergency Network (HFEN) implementation plan
[PB85-174167] 18 p3092 N85-29141
Recovery of pyroshock data from distorted acceleration records
[NASA-TP-2494] 20 p3407 N85-31141
Seismic discrimination
[AD-A154167] 20 p3494 N85 31722
Field antenna handbook
[AD-A155204] 21 p3576 N85-32242
High-frequency furnace
[DE85-011210] 21 p3586 N85-32291
Multitrunk high-frequency multiplexing of antenna-waveguide channels 22 p3774 N85-33385
Transmitter spectrum analyzer
22 p3774 N85-33389
Optimality criterion for high-frequency channel in receivers of discrete radio signals
22 p3776 N85-33401
KT3127A, KT3128A transistors
22 p3779 N85-33414

HIGH GAIN
Case study of sample spacing in planar near-field measurement of high gain antennas
[NASA-TM-86872] 01 p0037 N85-10234
The axial velocity spread acceptance of free electron lasers
[AD-A149024] 10 p1489 N85-19403
Instabilities and chaotic behavior of active and passive laser systems
[AD-A153366] 17 p2971 N85-28346
High gain adaptive control of decentralized systems
[DE85-010040] 19 p3339 N85-30688

HIGH GRAVITY (ACCELERATION)
U HIGH GRAVITY ENVIRONMENTS

HIGH GRAVITY ENVIRONMENTS
Effects on in vivo and in vitro exposure to excess gravity on growth and differentiation of mammalian embryos
15 p2612 N85-26095
Physical training and G tolerance
20 p3511 N85-31824
Centrifuge operations and training in the Royal Netherlands Air Force 20 p3511 N85-31825
Effects of microgravity and hypergravity on invertebrate development 24 p4126 N85-35579

HIGH INTENSITY LASERS
U HIGH POWER LASERS

HIGH LATITUDES
U POLAR REGIONS

HIGH LEVEL LANGUAGES
NT ADA (PROGRAMMING LANGUAGE)
Floating-point function generation routines for 16-bit microcomputers
[NASA-TM-83783] 01 p0102 N85-10683
THLL (TRIDENT Higher Level Language) reference manual
[AD-A145116] 01 p0104 N85-10696
DATAPLOT: Introduction and overview
[PB84-214055] 01 p0105 N85-10706
Tree Query Language Flat (TQLF) specifications
[PB84-217116] 06 p0855 N85-15438
Relational Query Language Flat (RQLF) specifications
[PB84-217405] 06 p0855 N85-15439
Network Query Language Flat (NQLF) specifications
[PB84-217538] 06 p0855 N85-15440
Software test handbook
[AD-A146844] 07 p1024 N85-16498
Representation and refinement of visual specifications in PegaSys
[AD-A146733] 09 p1368 N85-18598
High level languages in protocol specification and verification
[FUB-51-1983] 09 p1370 N85-18611
A Gypsy-to-Ada program compiler
[TR-39] 12 p1913 N85-22005
Very-high level concurrent programming
[AD-A150009] 12 p1916 N85-22026
Flowcharting with D-charts
[NASA-CR-175641] 14 p2402 N85-24606
Design and analysis of a complete relational interface for a multi-backend database system
[AD-A151501] 15 p2628 N85-26198
Harnessing computional power: Distributed combinator reduction
[DE85-005967] 15 p2631 N85-26216
An abstract specification language for Markov reliability models
[NASA-TM-86423] 16 p2857 N85-27616
Multicomputer operating systems and applications
[AD-A153205] 17 p3016 N85-28648
MC TRICOMP user's guide
[AD-A154339] 19 p3337 N85-30673
VAX TRICOMP user's guide
[AD-A154341] 19 p3337 N85-30675
Implementation assessment of the OSI network service. The test definition language
[NPL-DITC-52/84] 20 p3514 N85-31849
Study of the applicability of higher order languages for on-board satellite software production
[ESA-CR(P)-2024] 20 p3516 N85-31864
HLLM software support
[AD-A154828] 21 p3671 N85-32805
The formal specification of an abstract machine: Design and implementation
[AD-A155167] 21 p3672 N85-32808
Evaluation of a software design approach: Develop a threat resolution module in Ada (trademark)
[AD-A155599] 21 p3672 N85-32815

HIGH MELTING COMPOUNDS
U REFRACTORY MATERIALS

HIGH PASS FILTERS
Frequency-spreading coupler
[AD-D011683] 19 p3258 N85-30200

HIGH POWER LASERS
NT NOVA LASER SYSTEM
Summary discussion: Theoretical aspects of XUV free electron lasers
[AD-A145475] 02 p0202 N85-11343
High energy laser mirror
[AD-D011255] 06 p0812 N85-15158
High power metal vapor laser
[AD-D011271] 06 p0813 N85-15159
The development of a high average power glass laser source
[AD-A147471] 07 p0971 N85-16169
High-power radiating plasma
[NASA-TM-77784] 07 p1045 N85-16637
Status of specific FRG high tech research funded by BMFT 11 p1618 N85-20181
Potential of high-average-power solid state lasers
[DE85-003884] 11 p1639 N85-20329
Research, development of laser glasses in China
13 p2166 N85-23439
Observation of pure resonance and threshold effects in electron impact experiments in high intensity laser fields
[AD-A150725] 14 p2309 N85-24293
Ground-up-to-Space (GUTS) laser propagation code description and manual
[AD-A150783] 14 p2309 N85-24295
High energy lasers: A primer on directed energy weapons for space use
[AD-A151279] 15 p2562 N85-25807
Discharge characteristics of high-pressure, fast-discharge XeCl excimer laser
15 p2564 N85-25820
Predischarge parameters of SF6-CO2 determined by laser 15 p2564 N85-25821
West Europe report: Science and technology
[JPRS-WST-84-032] 18 p3086 N85-29095
Results of Italian research in high power lasers
18 p3086 N85-29097
Magnetically switched power supply systems for lasers
[NASA-CASE-NPO-16402-1] 18 p3112 N85-29265
Intense excitation source for high power laser
[AD-A153424] 18 p3112 N85-29267
A simple power meter for high energy pulsed lasers
[AD-D011661] 18 p3113 N85-29271
1.5 micrometer GaInAsP high pulsed power diode lasers
[AD-A153568] 18 p3193 N85-29805
Development and application of a high power ND-glass laser instrument
[AD-A154366] 19 p3276 N85-30314
Research with high-power short-wavelength lasers
[DE85-010329] 19 p3278 N85-30332
High-power two-frequency CW dye laser
21 p3686 N85-32900

HIGH PRESSURE
Energy efficient engine high pressure turbine ceramic shroud support technology report
[NASA-CR-168036] 02 p0147 N85-10996
Energy efficient engine. High pressure compressor detail design report
[NASA-CR-165558] 02 p0147 N85-10998
High pressure cosmochemistry applied to major planetary interiors: Experimental studies
[NASA-CR-174032] 02 p0302 N85-11956
Mechanochemical reactions of polymethyl methacrylate and polystyrene at high pressure
[DRIC-T-7307] 03 p0337 N85-12165
Qualification of noninvasive systems for on-line leak detection in high pressure feed water preheaters
[CISE-2341] 04 p0558 N85-13555
Design and off-design performance prediction of high pressure ratio centrifugal compressors
05 p0636 N85-14082
High pressure combustion test facility for gas turbine research
[NAL-TR-801] 06 p0757 N85-14845
Understanding the high pressure properties of molecular solids and molecular surfaces deposited on hetrogeneous substrates
[NASA-CR-174262] 07 p1047 N85-16649
High pressure physics research focusing on composite materials 08 p1140 N85-17185
Thermodynamic properties of aqueous NaCl from 273 to 823 K with estimates for higher temperatures
[DE85-000392] 09 p1292 N85-18116
Experimental high pressure equation of state of a very fast burning gun propellant
[DE85-001749] 10 p1458 N85-19184
Electron production, electron attachment, and charge recombination process in high pressure gas discharges
[AD-A149535] 10 p1554 N85-19799
Leak monitoring in high pressure preheaters by a noninvasive ultrasonic method
[CISE-2373] 11 p1650 N85-20394
Leak detection by acoustic emission monitoring in power plant high pressure preheaters
[CISE-2392] 11 p1650 N85-20395
Liquid fuel spray processes in high-pressure gas flow
[NASA-TM-86944] 12 p1844 N85-21570
A 50-kW electric-discharge CO2 laser
[AD-A149779] 12 p1857 N85-21644
High pressure turbine rotor two-piece blade retainer
[AD-D011498] 12 p1858 N85-21653
Sound velocity of carbon at high pressures
[DE85-002016] 12 p1928 N85-22113
High-pressure rocket engine turnaround duct computational fluid dynamics analysis
13 p2003 N85-22556
Possibility of producing monolithic composite materials based on niobium carbide 13 p2028 N85-22707
Some unique features of isentrophic flow of gas under high pressures 13 p2043 N85-22788
High pressure cosmochemistry of major planetary interiors: Laboratory studies of the water-rich region of the system ammonia-water 13 p2183 N85-23549
Theoretical thermodynamics of mixtures at high pressures 13 p2183 N85-23550
Applications of high pressure differential scanning calorimetry to aviation fuel thermal stability research
[NASA-TM-87002] 14 p2249 N85-23941
Stability of turbine runners in sliding bearings under external circulation forces 14 p2272 N85-24074
Hypergolic combustion demonstration in a reciprocating internal combustion engine
[AD-A150846] 14 p2311 N85-24303
Principal patterns of functional changes of human respiratory system in adaptation to high pressure
14 p2387 N85-24704
Hydrogen resistance of VT1-0 titanium under 150 MPa pressure at room temperature 15 p2499 N85-25414
Calorimeter for measuring high-energy optical pulses
[PB85-160695] 15 p2561 N85-25799
Discharge characteristics of high-pressure, fast-discharge XeCl excimer laser
15 p2564 N85-25820
Development of theory of high-current high-pressure pulsed arc 15 p2645 N85-26314
High pressure cosmochemistry applied to major planetary interiors: Experimental studies
[NASA-CR-175715] 15 p2679 N85-26544
Material technology 16 p2734 N85-26870
Ignition of metals in high pressure oxygen
16 p2735 N85-26874
High-pressure hydrogen testing of single crystal superalloys for advanced rocket engine turbopump turbine blades 16 p2735 N85-26875
Graphite fiber intercalation: Dynamics of the bromine intercalation process
[NASA-TM-87015] 16 p2742 N85-26921
Fog advection in the Namib 16 p2831 N85-27454
Combustion and micro-explosion of water/oil emulsions in high pressure environments
[AD-A152960] 17 p2919 N85-27997
Steel Tubes
[BLL-BISI-TRANS-22064-(9022.06)]
17 p2973 N85-28369

Principal quality assurance measures in the manufacture of HF-welded high-pressure linepipe
[BLL-BISI-TRANS-21690-(9022.06)] 17 p2976 N85-26389
Energy efficient engine high-pressure turbine component rig performance test report
[NASA-CR-168189] 19 p3218 N85-29955
Burn rates of explosives at high pressures
[DE85-010806] 19 p3251 N85-30159
Thermodynamic study of CO2-organic compound interaction at high pressures and temperatures
[DE85-010999] 19 p3266 N85-30266
Evaluation of a high pressure proportional counter for the detection of radioactive noble gases
[AD-A154436] 19 p3272 N85-30292
Damping seal for turbomachinery
[NASA-CASE-MFS-25842-2] 19 p3280 N85-30341
The use of superoxide mixtures as air-revitalization chemicals in hyperbaric, self-contained, closed-circuit breathing apparatus
[NASA-TM-86709] 20 p3512 N85-31831
High pressure working mode of hollow cathode arc discharges
[NASA-TM-77680] 20 p3535 N85-31992
Identification of vibrational-rotational transitions of Os-192O4 within frequency tuning limits of high pressure CO2 waveguide laser 21 p3689 N85-32917
Static high pressure study of nitric oxide chemistry: Proposed mechanism for nitric oxide detonation
[DE85-010795] 22 p3746 N85-33220
High pressure compressor component performance report
[NASA-CR-168245] 23 p3897 N85-34138
Hollow cathodes in high pressure arc discharges
[NASA-TM-87096] 23 p3903 N85-34179
Determination of individual tolerance in hyperbaric oxygen 23 p3954 N85-34507
Experimental technique for measuring the isentrope of hydrogen to several megabars
[DE85-014332] 24 p4095 N85-35386

HIGH Q
U Q FACTORS

HIGH RESISTANCE
Properties of nitrogen containing stainless alloy designed for high resistance to pitting
[DE85-006282] 17 p2931 N85-28095

HIGH RESOLUTION
The development of a diode laser Doppler velocimeter for boundary layer measurements under ice: A feasibility investigation
[AD-A145076] 01 p0053 N85-10348
Vibration data analysis system for SNLA area 3 reference manual
[DE84-016207] 04 p0514 N85-13275
GLAS fourth order model 05 p0679 N85-14361
Psychophysical research in development of a fiber-optic helmet mounted display 05 p0701 N85-14501
High resolution photoacoustic and photothermal imaging 05 p0723 N85-14649
A geometric approach to high resolution TVD schemes
[NASA-CR-172484] 06 p0857 N85-15449
Topics in high resolution spectroscopy of stored ions
[DE85-002093] 06 p0861 N85-15470
Future studies of the local interstellar medium with Space Telescope and Columbus 06 p0880 N85-15593
A nonlinear technique for high-resolution data processing
[AD-D011415] 08 p1203 N85-17570
Improved real-time ultra-high resolution image projection display using laser-addressed liquid crystal light valve
[AD-D011414] 08 p1223 N85-17705
Acoustic microscopy at cryogenic temperatures
[AD-A146755] 09 p1384 N85-18704
Improved performance for large area triple layer microchannel plate detector for a neutral spectrometer in Doublet III
[DE85-001719] 10 p1488 N85-19395
A progress report on the analysis of long exposure SWP high resolution spectra of cool stars
11 p1758 N85-21057
Statistical classification of IUE low-dispersion stellar spectra: Progress report 11 p1760 N85-21075
Research in image understanding as applied to 3-D tomographic imaging with near optical resolution
[AD-A150098] 12 p1829 N85-21483
New high resolution scanning ion microprobe and focused ion beam applications
[AD-A149992] 12 p1852 N85-21616
High time resolution thermospheric temperature and wind studies in the Arctic
[AD-A150114] 12 p1890 N85-21860
HREELS and Auger studies of conducting polymers
[DE85-004541] 13 p2038 N85-22764
Hot spots on Io: Correlation of infrared emission and visible reflectance 13 p2172 N85-23475
Surfaces of asteroids and cometary nuclei
13 p2176 N85-23503
Venus surface composition from radio/radar measurements 13 p2177 N85-23509
Automated extraction of absorption bands from reflectance spectra 13 p2197 N85-23624
Viking Lander mosaics of Mars
13 p2203 N85-23667
High time-resolution studies of the auroral ionosphere
[AD-A150945] 14 p2409 N85-24850
Investigations of high resolution imaging through the Earth's atmosphere using speckle interferometry
[AD-A150680] 14 p2439 N85-25053
High resolution hard X-ray spectra of solar and cosmic sources 14 p2455 N85-25163
Asteroid amphitrite: Surface composition and prospects for the possible Galileo flyby 15 p2680 N85-26549
Scheme for atmospheric thermal sensing from satellites with enhanced vertical resolution
16 p2726 N85-26823
High resolution powder diffraction
[DE85-006287] 17 p2922 N85-28015
The HURRA high resolution experimental radar system sampling unit
[FOA-C-30376-E1] 18 p3091 N85-29133
The determination of dinitrotoluene in single base propellants
[AD-A154672] 21 p3571 N85-32209
Antenna induced range smearing in MST radars
21 p3620 N85-32495
High resolution evidence for the Garrett-Munk spectrum of stratospheric gravity waves 21 p3622 N85-32503
The design, development, testing, fabrication, calibration and integration of a High Resolution Imager (HRI) for the Roentgen Satellite (ROSAT)
[NASA-CR-175302] 22 p3741 N85-33184
Ionization detection of stimulated Raman spectra
[DE85-010672] 22 p3746 N85-33218
Electron beam enhanced surface modification for making highly resolved structures
[DE85-011609] 22 p3760 N85-33305
Determination of band oscillator strengths of atmospheric molecules from high resolution vacuum ultraviolet cross section measurements
[NASA-CR-176150] 22 p3814 N85-33624
Heterodyne holographic interferometry for visualization of surface acoustic waves
[AD-A155405] 22 p3836 N85-33753
High-resolution spectrum of Cygnus X-1
[OG-2.4-12] 22 p3868 N85-33956
High resolution electron microscopic characterization of interfaces in ceramics
[DE85-011207] 23 p3920 N85-34289
Acceleration of ions and electrons to near-cosmic ray energies in a perpendicular shock: The January 6, 1978 event
[SH-1.5-4] 23 p3996 N85-34773
Advanced techniques for high resolution spectroscopic observations of cosmic gamma-ray sources
[OG-9.2-9] 23 p4025 N85-34948
High-resolution spectroscopy and dynamics of multiphoton processes in atoms and molecules
[AD-A155862] 24 p4147 N85-35714
High resolution beam profile monitors in the SLC
[DE85-013375] 24 p4157 N85-35774

HIGH RESOLUTION COVERAGE ANTENNAS
Information for space radar designers: Required dynamic range vs resolution and antenna calibration using the Amazon rain forest 06 p1147 N85-17239

HIGH REYNOLDS NUMBER
Study of the structure of turbulent shear flows at supersonic speeds and high Reynolds number
[NASA-CR-174144] 04 p0452 N85-12865
Aeroacoustic data for high Reynolds number supersonic axisymmetric jets
[NASA-TM-86296] 07 p1038 N85-16587
A survey of the turbulent drag reduction using passive devices
[NMI-R-193] 11 p1630 N85-20268
Transition fixing and simulation of high Reynolds number flow at transonic velocities 14 p2212 N85-23721
Investigation of the aerodynamic forces on bluff bodies at high Reynolds numbers
[DFVLR-MITT-84-19] 14 p2213 N85-23727
Mach-10 high Reynolds number development in the NSWC (Naval Surface Weapons Center) hypervelocity facility
[AD-A151241] 15 p2474 N85-25274
Simultaneous measurement of velocity and density in a turbulent nonpremixed flame 22 p3744 N85-33209

HIGH SPEED
Noise isolation system for high-speed circuits
[DE84-014229] 01 p0043 N85-10283
Results of winglet development studies for DC-10 derivatives
[NASA-CR-3677] 02 p0138 N85-10936
Gyrotron beam generation with helical magnetic fields
[AD-A145967] 03 p0417 N85-1287
Effect of two inner-ring oil-flow distribution schemes on the operating characteristics of a 35 millimeter bore ball bearing to 2.5 million DN
[NASA-TP-2404] 04 p0507 N85-1322
High-speed power thyristors with excellent switching and load characteristics 06 p0793 N85-1507
Visual perceptual aspects of low level high speed flight and flight simulation
[AD-P004310] 09 p1267 N85-1786
Low altitude high speed flight simulation using video disc technology
[AD-P004312] 09 p1268 N85-178
Study on controllability and stability of high speed tracked vehicles
[AD-P004302] 09 p1409 N85-1887
High-speed intercity rail passenger service
[GPO-35-896] 10 p1570 N85-1988
Diesel fuel alternatives for engines in civil works prime movers
[AD-A149736] 12 p1817 N85-2140
Lubrication and performance of high-speed rolling-element bearings
[NASA-TM-86958] 12 p1859 N85-2165
Development of a multiplane multispeed balancing system for turbine systems
[NASA-CR-174750] 13 p1976 N85-2240
Specifics of laser heat treatment of high steel tools
13 p2029 N85-2271
Transition fixing in the high speed range for the development of civil aircraft wings
14 p2211 N85-2371
Advanced gearbox technology in small turbo propeller engines 14 p2221 N85-2377
Gear-cutting tools made of ultra high speed steel coated with TiN
[BLL-RISLEY-TR-5109-(9091.9F)]
15 p2567 N85-2
Wind tunnel results of advanced high speed propellers in the takeoff, climb and landing operating regimes
[NASA-TM-87054] 19 p3213 N85-2

HIGH SPEED CAMERAS
NT FRAMING CAMERAS
High-speed, eight-frame electro-optic camera with multipulsed ruby laser illuminator
[DE85-001748] 09 p1323 N85-1831
Positioning errors of commutating lenses and their influence on characteristics of high speed movie cameras 14 p2273 N85-240

HIGH SPEED FLIGHT
U HIGH SPEED

HIGH SPEED PHOTOGRAPHY
Measurement of shock and induced reaction in rocket propellants by nanosecond infrared radiometry and photography
[DE84-013209] 04 p0482 N85-1307
Development of a dynamic radiographic capability using high-speed video
[DE84-016477] 04 p0511 N85-1325
Method and apparatus for high speed, sustained recording of infrared laser beam patterns
[AD-D011585] 15 p2563 N85-2581
Solids mixing in a three phase fluidized bed containing spherically shaped-porous solid particles
[PB85-187961] 22 p3785 N85-3340

HIGH STRENGTH
Microstructural basis of strength and toughness in hardmetals 02 p0177 N85-1118
Description of a laboratory model Annular Momentum Control Device (AMCD) 05 p0606 N85-1388
Improvement of gas-tightness of OTTG and TBO-4 threaded pipe couplings
[BLL-M-35993-(5828.4)] 07 p0972 N85-1817
Research, development of composite materials described 15 p2497 N85-2540
High resistance and raised modulus carbon fibers
[NASA-TM-76884] 15 p2502 N85-254
Chain dynamics and structure property relation in high impact strength polycarbonate plastic
[AD-A152011] 15 p2519 N85-255
Development of a high strength isothermally heat-treated nodular iron road wheel arm
[AD-A155755] 24 p4099 N85-354

HIGH STRENGTH ALLOYS
NT HIGH STRENGTH STEELS
NT MARAGING STEELS
Methods for producing platinum-group metal coatings from molten alkali cyanides
[PB84-225994] 01 p0029 N85-1018
Design of strong, ductile, duplex low alloy steels
02 p0177 N85-111
A study of environmental characterization of conventional and advanced aluminum alloys for selection and design. Phase 1: Literature review
[NASA-CR-172387-PHASE-1] 02 p0181 N85-1121

Hot isostatically pressed manufacture of high strength MERL 76 disk and seal shapes
[NASA-CR-165550] 02 p0183 N85-11225

Improved reinforcement metal
03 p0353 N85-12271

Study of high performance alloy electroforming
[NASA-CR-174276] 07 p0927 N85-15875

Distribution of hydrogen in multi-layer welded joints of alloyed steels 11 p1603 N85-20079

The role of hydrogen in the stress corrosion failure of high strength Al-Zn-Mg alloys
[AD-A150691] 14 p2256 N85-23978

Sweden develops new rapid solidification process
15 p2531 N85-25610

High-pressure hydrogen testing of single crystal superalloys for advanced rocket engine turbopump turbine blades 16 p2735 N85-26875

Corrosion test on high-alloy steels
[BLL-BISI-TRANS-21627-(9022.06)]
17 p2926 N85-28046

The influence of temperature on static and dynamic SCC crack growth behavior in aluminum alloy
23 p3905 N85-34190

HIGH STRENGTH STEELS

NT MARAGING STEELS

Delayed fracture of high-strength steels in spherical tanks for LP gas
[BLL-RISLEY-TR-4926-(9091.9F)]
01 p0026 N85-10162

Research on high-strength steels with an improved resistance against weld cracking
[AD-A144830] 01 p0027 N85-10170

Inhibition of hydrogen absorption during plating of high strength steels
[AD-A144882] 01 p0028 N85-10174

Effect of microstructure and trapping on the hydrogen embrittlement susceptibility of a titanium bearing HSLA steel 02 p0174 N85-11166

International Conference on Recent Developments in Specialty Steels and Hard Materials. Conference abstracts
[CSIR-S-256] 02 p0176 N85-11177

Microstructural design and control of sintered hard materials 02 p0176 N85-11180

Toughness in high speed steels and hard metals
02 p0176 N85-11181

Copper-boron low alloy high strength steels
02 p0176 N85-11183

Stress-driven solute enrichment of crack-tips during low ductility intergranular fracture of low-alloy steel
[AERE-R-11120] 03 p0333 N85-12150

Optimization of toughness properties of HSCA shielded metal arc welding electrodes
[BMFT-FB-T-84-166] 05 p0646 N85-14148

Hydrogen induced cracking in pipeline steels
[ERS-E.327] 09 p1340 N85-18429

Mechanism of hydrogen induced cracking in pipeline steels
[ERS-E.349] 09 p1340 N85-18430

Fatigue resistance of welded joints of high strength steels produced by electron beam welding
10 p1449 N85-19127

Assessment of the need for an advanced high-strength chromium-molybdenum steel for construction of third-generation gasifier pressure vessels
[DE85-002865] 11 p1606 N85-20097

High strength steel sheet with dual phase structure
[BMFT-FB-T-84-219] 12 p1808 N85-21342

An investigation of elevated temperature fatigue crack initiation in 2 and 1/4 cR-1 MO low alloy steel
[AD-A150670] 14 p2255 N85-23973

A study of fatigue crack growth in 2 1/4 Cr1Mo steel. Part 1: The influences of environment and material condition
[AERE-R-11472] 14 p2258 N85-23993

Development of high strength ship hull steel for high heat input welding --- controlled rolling and accelerated cooling 15 p2565 N85-25827

High-strength weldable steel 03G4N2MAF Sh with improved ductility
[BLL-BISI-TRANS-22233-(9022.06)]
17 p2924 N85-28031

Corrosion test on high-alloy steels
[BLL-BISI-TRANS-21627-(9022.06)]
17 p2926 N85-28046

Effect of texture in steel on the susceptibility of hydrogen embrittlement
[BLL-BISI-TRANS-22026-(9022.06)]
17 p2926 N85-28048

Influence of preliminary cold deformation on fineness of pearlite
[BLL-BISI-TRANS-22409-(9022.06)]
17 p2927 N85-28054

Hydrogen embrittlement of high-strength steel
[illegible] 17 p2933 N85-28103

Fatigue crack propagation characteristics and fatigue fracture toughness in 780 MPa grade high strength steel weldments at low temperature
[BLL-BISI-TRANS-22369-(9022.06)]
17 p2979 N85-28411

Tendency of selected low-carbon steels to corrosion cracking in nitrates
[BLL-BISI-TRANS-22262-(9022.06)]
18 p3073 N85-29006

Fatigue behavior of HY-130 steel weldments containing fabrication discontinuities
[AD-A153630] 18 p3122 N85-29326

Metallurgical origins of fracture toughness and microstructure and fracture toughness of an HSLA (High-Strength/Low-Alloy) steel
[AD-A155530] 21 p3567 N85-32187

Mechanical properties of Shielded Metal Arc (SMA) and Submerged Arc (SA) welded joints in a steel Raex 386 P Arctic
[VTT-339] 22 p3601 N85-33551

HIGH TEMPERATURE

Stability of bromine intercalated graphite fibers
[NASA-TM-86859] 01 p0031 N85-10187

Equivalent damage: A critical assessment
02 p0140 N85-10952

Benchmark notch test for life prediction
02 p0140 N85-10953

Pre-HOST high temperature crack propagation
02 p0141 N85-10956

Development of powder metallurgy 2XXX series Al alloys for high temperature aircraft structural applications
[NASA-CR-172408] 02 p0182 N85-11220

Mechanism of brittle heat fracture of inhomogeneous solids by high temperature gas jets
02 p0265 N85-11731

High temperature deformation of hot-pressed polycrystalline orthoenstatite
[NASA-CR-174026] 02 p0285 N85-11861

The rheology of icy satellites
[NASA-CR-174024] 02 p0302 N85-11959

Effects of tin on microstructure and mechanical behavior of Inconel 718
[NASA-TM-86866] 03 p0330 N85-12129

NBS (National Bureau of Standards): Materials measurements
[NASA-CR-174038] 03 p0332 N85-12143

Structural stability of nickel heat resistant alloys at high temperatures 03 p0350 N85-12251

High-temperature optically activated GaAs power switching for aircraft digital electronic control
[NASA-CR-174711] 04 p0457 N85-12901

Solid electrolytes for medium temperature steam electrolysis
[DE84-014384] 04 p0463 N85-12938

Surface diffusion of high temperature vapors in porous alumina
[DE84-015968] 04 p0479 N85-13053

Materials for high-temperature fuel cells
[DE84-016316] 04 p0479 N85-13054

High temperature mechanical properties of ceramics
[DE84-016492] 04 p0480 N85-13058

Diffusion of gases in porous solids: Simulation and measurements
[DE84-016292] 04 p0500 N85-13191

Study of the reactive-element effect in oxidation of Fe-Cr alloys using transverse section analytical electron microscopy
[DE84-016237] 04 p0571 N85-13641

High temperature thermoelectric energy conversion
05 p0610 N85-13694

Tensile properties and swelling of 20%-cold-worked Type 316 stainless steel irradiated in HFIR
[DE84-014060] 05 p0617 N85-13948

Effects of irradiation fluence and creep on fracture toughness of 347/348 stainless steel
[DE84-016091] 05 p0618 N85-13953

High temperature corrosion of ceramics
[DE84-017084] 05 p0620 N85-13967

Hydrogen production employing high-temperature solid oxide cells
[DE84-014559] 06 p0766 N85-14901

Development and characterization of ductile Long-Range-Ordered (LRO) alloys (Fe,Co, Ni)3V for high-temperature structural use
[DE84-016750] 06 p0769 N85-14921

Metallographic evaluation of the reactions between boronated graphite and Fe-Ni-Cr alloys
[DE84-015374] 06 p0769 N85-14922

Effects of silver and group 2 fluorides addition to plasma sprayed chromium carbide high temperature solid lubricant for foil gas bearing to 650 deg C
[NASA-TM-86895] 06 p0770 N85-14928

Evaluation of the ion implantation process for production of solar cells from silicon sheet materials
06 p0831 N85-15281

The soft X-ray diffuse background: Implications for the nature of the local interstellar medium
06 p0876 N85-15566

Life prediction at high temperature under multiaxial loading 07 p0907 N85-15745

Experiences with the material bevaviour and high temperature low cycle fatigue life prediction of the IN 738 blading alloy 07 p0908 N85-15746

Mechanical aspects of high temperature coatings
07 p0908 N85-15749

Design of ordered intermetallic alloys for high-temperature structural use
[DE85-000697] 07 p0928 N85-15885

Dispersed metal-toughened ceramics and ceramic brazing
[NASA-CR-174284] 07 p0933 N85-15916

Transformation toughened ceramics for the heavy duty diesel engine technology program
[NASA-CR-174689] 07 p1055 N85-16696

Thermodynamic properties of aqueous NaCl from 273 to 823 K with estimates for higher temperatures
[DE85-000392] 09 p1292 N85-18116

Hydrolysis of iodine: Equilibria at high temperatures
[DE84-016713] 09 p1293 N85-18119

Notes on compressible flow equations for thermodynamics of hot jets
[BAE-KRS-N-GEN-273] 09 p1318 N85-18289

High temperature properties of equiatomic FeAl with ternary additions
[NASA-TM-86938] 10 p1439 N85-19072

Problems in high temperature thermocouple thermometry
[DE85-000808] 10 p1488 N85-19397

Sputter-induced compositional modifications in a Ni-Au alloy
[DE85-002771] 12 p1807 N85-21333

Chemical approach for controlling nadimide cure temperature and rate
[NASA-CASE-LEW-13770-5] 12 p1810 N85-21352

High-temperature-stable detonators
[DE85-005188] 12 p1818 N85-21402

A millimeter wave apparatus for free-space measurement of dielectric constants at high temperature
[AD-P004361] 12 p1826 N85-21455

3-D inelastic analysis methods for hot section components (base program) --- turbine blades, turbine vanes, and combustor liners
[NASA-CR-174700] 12 p1863 N85-21686

Fast times at high temperatures
[DE85-003306] 12 p1943 N85-22205

High temperature antifriction properties of Ti sub 1-sub xNb sub x C sub 0.5N sub 0.5 alloys
13 p2029 N85-22715

Degassification of silicon nitride powders of various origins 13 p2030 N85-22718

Research directed advanced high temperature coating system beyond current state-of-the art systems
[AD-A150696] 14 p2255 N85-23974

Stability of turbine runners in sliding bearings under external circulation forces 14 p2272 N85-24074

Biophysical evaluation of the wet globe temperature index (Botsball) at high air movements and constant dew point temperature
[AD-A151065] 14 p2378 N85-24683

Structural changes with one- and two-stage aging of alloys Ti-Al-Mo-Fe and Ti-Zr-V-Al-Sn
15 p2499 N85-25415

Swelling behavior of manganese-bearing AISI 216 steel
[DE85-005712] 15 p2512 N85-25495

A calorimetric approach for measuring emittance and normal spectral absorptance at elevated temperatures
[AD-A151292] 15 p2651 N85-26351

Studies on the processing methods for extraterrestrial materials
[NASA-CR-175778] 16 p2716 N85-26768

Multiaxial and thermomechanical fatigue considerations in damage tolerant design
[NASA-TM-87022] 16 p2749 N85-26964

Low dose irradiation creep of pure nickel
[DE85-006320] 16 p2751 N85-26975

Method of investigating accumulations of damage to weld joints in the case of low-cycle creep
[BLL-CE-TRANS-8088-(9022.09)]
16 p2792 N85-27219

Strength and failure analysis of composite laminates with holes at room and elevated temperatures
[AD-A153263] 17 p2917 N85-27981

Improving the properties of copper and copper alloys through heat treatment and alloying
[BLL-BISI-TRANS-21939-(9022.06)]
17 p2926 N85-28047

Powder-metallurgy alloys and steels
[BLL-BISI-TRANS-22239-(9022.06)]
17 p2926 N85-28050

The characteristic structure of weld metal of high temperature alloy X20CrMoV 121
[BLL-BISI-TRANS-21623-(9022.06)] 17 p2926 N85-28069
Influence of eutectic silicate inclusions on micro-processes during deformation and fracture of 12GS steel
[BLL-BISI-TRANS-22296-(9022.06)] 17 p2929 N85-28073
Overload effects on sustained load crack growth at elevated temperature
[AD-A153223] 17 p2931 N85-28091
Electrodes for flash discharge lamps
[DE85-008697] 17 p2955 N85-28250
Evaluation of interpolative modeling concepts for fatigue crack growth at elevated temperature
[AD-A153222] 17 p2980 N85-28422
Average collisional vibrational energy transfer quantities and the inversion temperature
[AD-A152674] 17 p3029 N85-28733
Elevated temperature erosion corrosion of 9Cr1Mo steel
[DE85-008445] 18 p3074 N85-29016
Surface degradation of ductile metal in elevated temperature gas-particle streams
[DE85-008426] 18 p3074 N85-29017
Elevated temperature erosion of steels
[DE85-008503] 18 p3075 N85-29018
Synthesis chemistry of ceramics by solid-state combustion processes in micro-gravity
[DE85-009595] 18 p3081 N85-29061
Research test facility for evaporation and combustion of alternative jet fuels at high air temperatures
[AD-A153830] 18 p3083 N85-29073
Development of a high-temperature coolant for advanced diesel engines
[AD-A153680] 18 p3117 N85-29297
Behavior of reinforced concrete at elevated temperatures
[DE85-009032] 18 p3123 N85-29332
Structural characteristics of high temperature composites
[NASA-CR-175998] 19 p3232 N85-30037
Catalytic hydrotreatment studies with model compounds
[DE85-010187] 19 p3236 N85-30064
An investigation of the irradiation swelling mechanisms in refractory metals at high temperatures
[AD-A154149] 19 p3238 N85-30079
CP DDT detonators. 4: Thermal aging
[DE85-011172] 19 p3251 N85-30160
Thermodynamic study of CO2-organic compound interaction at high pressures and temperatures
[DE85-010999] 19 p3266 N85-30266
Creep fatigue life prediction for engine hot section materials (isotropic)
[NASA-CR-168228] 20 p3394 N85-31057
STPI/LARC: A 200 deg C polyimide adhesive
[NASA-TM-86447] 20 p3433 N85-31297
Investigation of fatigue strength of spring steel after high-temperature thermomechanical working (HTMW) by helical drawing
[BLL-M-36274-(5828.4)] 20 p3465 N85-31525
Constitutive modeling of superalloy single crystals and directionally solidified materials
20 p3466 N85-31535
On numerical integration and computer implementation of viscoplastic models 20 p3467 N85-31542
A comparison of smooth specimen and analytical simulation techniques for notched members at elevated temperatures 20 p3468 N85-31546
Analytical simulation of weld effects in creep range
20 p3468 N85-31550
Current understanding of point defects and diffusion processes in silicon 20 p3481 N85-31632
Recession of graphitic nozzles in rocket motors
21 p3560 N85-32144
Shock tube measurements of growth constants in the branched-chain ethane-carbon monoxide-oxygen system
[NASA-TM-87068] 21 p3562 N85-32156
The effect of stress and hot corrosion on nickel-base superalloys
[AD-A154722] 21 p3566 N85-32181
High temperature electronics technology: Life test report
[AD-A154681] 21 p3580 N85-32257
Results of an interlaboratory fatigue test program conducted on alloy 800H at room and elevated temperatures
[NASA-CR-174940] 21 p3597 N85-32340
Fatigue behavior of chromium-containing ferritic steels at elevated temperature
[DE85-012309] 22 p3748 N85-33231
Multistage spent particle collector and a method for making same
[NASA-CASE-LEW-13914-1] 22 p3791 N85-33489
Reaction of uranium and the fluorocarbon FC-75
[DE85-012322] 22 p3843 N85-33802
X-ray measurement of thermal stresses in tungsten fiber-copper composites 23 p3907 N85-34205
Dynamics of the melting of chromium-manganese alloys in molten steel
[BLL-M-35850-(5828.4)] 23 p3914 N85-34252
High temperature structural insulating material
[DE85-006361] 23 p3920 N85-34291
Depletion modeling of liquid dominated geothermal reservoirs
[DE85-009923] 23 p3943 N85-34437
Effects of temperature on the tensile strength and elastic modulus of composite material
[AD-A156112] 24 p4075 N85-35251

HIGH TEMPERATURE ALLOYS
U HEAT RESISTANT ALLOYS

HIGH TEMPERATURE ENVIRONMENTS
Component-specific modeling
02 p0143 N85-10971
The 3-D inelastic analysis methods for hot section components: Brief description 02 p0143 N85-10972
Life prediction and constitutive behavior: Overview
02 p0143 N85-10973
HOST high temperature crack propagation
02 p0144 N85-10977
Surface protection overview 02 p0144 N85-10978
Airfoil deposition model 02 p0144 N85-10979
A coaxial probe for measuring the current density profile of intense electron beams
[AD-D011407] 08 p1164 N85-17347
Development of a pressure transducer for usage in high-temperature and vibration environments. Phase 1: Feasibility investigation
[AD-A148695] 08 p1165 N85-17349
High-temperature, solid oxide electrolyte fuel cell power generation system
[DE85-002978] 11 p1675 N85-20552
Heat pipe cooled probe
[NASA-CASE-LAR-12588-1] 12 p1844 N85-21568
Evaluation results of the 700 deg C Chinese strain gauges — for gas turbine engine
[NASA-TM-86973] 12 p1850 N85-21605
Design and fabrication of a unique electromechanical machine for long-term fatigue testing
[DE85-006524] 15 p2580 N85-25912
Gas turbines: Operating conditions, material selection and development
[NLR-MP-83046-U] 20 p3395 N85-31062
Thermal barrier coating system
[NASA-CASE-LEW-14057-1] 24 p4072 N85-35233

HIGH TEMPERATURE FLUIDS
NT HIGH TEMPERATURE GASES
Standardization of flammability tests for hydraulic fluids
[AD-A146468] 06 p0771 N85-14932

HIGH TEMPERATURE GAS COOLED REACTORS
Inquiry into disintegration control of irradiated low enrichment uranium for high temperature gas cooled reactors
[OEFZS-7281] 07 p1042 N85-16615
Consolidated fuel reprocessing program
[DE85-006750] 19 p3366 N85-30871

HIGH TEMPERATURE GASES
Hot-gas cleanup for molten carbonate fuel cells-dechlorination and soot formation
[DE84-003072] 01 p0068 N85-10450
High temperature gas energy transfer
[AD-A146134] 03 p0328 N85-12113
Local Interstellar Medium. International Astronomical Union Colloquium No. 81
[NASA-CP-2345] 06 p0872 N85-15539
Modelling the local interstellar medium as a supernova remnant in a multiphase gas 06 p0879 N85-15585
Noncontact photo-thermal probe-beam deflection measurement of thermal diffusivity in an confined hot gas
[AD-A147461] 07 p0971 N85-16170
The environment of active galactic nuclei
07 p1057 N85-16712
Some aspects of the micromechanics of hot spot formation in energetic materials
[AD-P004348] 10 p1456 N85-19172
Consequences of hot gas in the broad line region of active galactic nuclei
[NASA-TM-86176] 11 p1763 N85-21090
Molecular dynamics of propellant gases, part 2
13 p2002 N85-22552
Characteristics of heat exchange in the region of injection into a supersonic high-temperature flow
[NASA-TM-77833] 15 p2555 N85-25762
Fluid and gas dynamics 16 p2738 N85-26897
Experimental evaluation of an advanced Space Shuttle main engine hot-gas manifold design concept
16 p2738 N85-26898
Influence of thermochemical treatment on properties of low-carbon steel
[BLL-BISI-TRANS-22410-(9022.06)]
17 p2927 N85-28
Changes of structure of EP648-VI alloy as a result of high-temperature gas corrosion
19 p3243 N85-3011
Results of tests of weathered KSNA closeout material in the MSFC Hot Gas Facility
[NASA-CR-170893] 24 p4073 N85-35
Study of NSI and related cable performance during tests performed in the NASA Hot Gas Facility
[NASA-CR-170886] 24 p4101 N85-354

HIGH TEMPERATURE MATERIALS
U REFRACTORY MATERIALS

HIGH TEMPERATURE NUCLEAR REACTORS
NT HIGH TEMPERATURE GAS COOLED REACTORS
Reaction of uranium and the fluorocarbon FC-75
[DE85-012322] 22 p3843 N85-338

HIGH TEMPERATURE PLASMAS
Ion-density correlations and enhancement of thermonuclear reaction rate in dense, inertially confined fusion plasmas 02 p0284 N85-118
Hot plasma particles in the Earth's outer magnetosphere: New understandings during the IMS
[DE84-016626] 05 p0677 N85-143
Atomic and molecular collision processes
[DE85-001604] 09 p1382 N85-18
X-ray spectroscopy of high-Z and high-density plasmas 09 p1387 N85-187
Identification of spectra of highly ionized Mo, Nb, Zr and Y atoms 09 p1390 N85-187
Plasma surface interaction processes and possible synergisms
[DE85-001861] 09 p1391 N85-187
Application of layered synthetic microstructures to high temperature plasma diagnostics
[DE85-002035] 10 p1559 N85-18
Effects of the solar-terrestrial environment on satellite operations
[DE85-002413] 11 p1590 N85-20
Excitation of impurities by heavy particles and radiative losses of thermonuclear plasma
11 p1719 N85-20
Design, construction and initial evaluation of an absolute, time-integrating/time-resolving spectrometer for the diagnostics of pulsed, high temperature plasma X-ray sources in the 100-10,000 eV region
[DE85-003526] 11 p1732 N85-20
Light diffraction with collective, thermal electron density fluctuation in plasmas with several ionic components
[IPF-84-5] 11 p1733 N85-20
On the spectrum of longitudinal waves in the hot degenerate plasma 12 p1955 N85-222
Electron-positron pair equilibrium in strongly magnetized plasmas 12 p1957 N85-2229
Electron-positron pairs in a mildly relativistic plasma in active galactic nuclei 12 p1957 N85-2229
Spacecraft-environment interaction: The environmental plasma aspect 13 p1990 N85-224
Ruby wavefront-conjugation laser for obtaining high temperature plasma 13 p2044 N85-227
Hot plasma and energetic particles in the Earth's outer magnetosphere: New understandings during the IMS
14 p2355 N85-24
Equations of state of strongly coupled plasma mixtures
[DE85-006163] 15 p2657 N85-26
Charge uncovering effects on flute instabilities in hot electron plasmas
[DE85-006957] 16 p2867 N85-27
LINE: A code which simulates spectral line shapes for fusion reaction products generated by various speed distributions
[DE85-010833] 19 p3341 N85-307
Double layer formation due to contact of different temperature plasmas
[IPPJ-722] 19 p3370 N85-30
Unthermalized plasma in bursts sources
[OG-1.1-5] 22 p3861 N85-33
Calculations of heavy ion charge state distributions for nonequilibrium conditions
[SH-2.1-12] 23 p3999 N85-347
A cosmic ray driven instability
[OG-8.1-5] 23 p4018 N85-34

HIGH TEMPERATURE TESTS
Silicon nitride joining
[AD-A145868] 02 p0187 N85-112
Special features of the deformation of molybdenum at high temperatures
[BLL-M-36027-(5828.4)] 07 p0924 N85-15
Tensile test of pressureless-sintered silicon nitride at elevated temperature
[NASA-TM-77777] 08 p1172 N85-17
Kinetics of oxidation of titanium alloy upon heating to 1000 deg C 10 p1448 N85-191

Compatibility experiments of facilities, materials, and propellants for electrothermal thrusters
[NASA-TM-86958] 12 p1795 N85-21260

Development of a high temperature single impact rain erosion test capability
[AD-P004371] 12 p1827 N85-21465

Analysis of experimental shaft seal data for high-performance turbomachines, as for Space Shuttle main engines
[NASA-TM-86928] 12 p1844 N85-21539

Performance of Chromel versus Alumel and Nicrosil versus Nisil thermocouple assemblies in vacuum and argon between 1000 deg C and 1200 deg C
[DE85-000810] 12 p1853 N85-21624

Experimental study of enthalpy of quasimonocrystal of graphite and carbon glass in temperature range of 2980-3818 deg K 13 p2036 N85-22751

Exploratory corrosion tests on materials and fluids for advanced high-temperature molten-salt storage
[DE85-002911] 14 p2258 N85-23991

Influence of thermochemical treatment on properties of low-carbon steel
[BLL-BISI-TRANS-22410-(9022.06)]
17 p2927 N85-28055

Evaluation of 7XXX-series aluminum alloys for the W87 aft support ring
[DE85-008887] 18 p3076 N85-29027

Burner rig corrosion of SiC at 1000 deg C
[NASA-TM-87061] 19 p3227 N85-30011

Effect of prolonged high temperature on durability of coated high-temperature nickel alloys
19 p3243 N85-30105

Nonlinear Constitutive Relations for High Temperature Application, 1984
[NASA-CP-2369] 20 p3465 N85-31530

Influence of moisture and elevated temperature on the fatigue properties of WTS-3 glass fiber blade material -- wind turbine blade (WTS-3)
[FFA-TN-1984-58] 20 p3470 N85-31558

Friction and wear of solid-lubricated contact in gas turbine engine bearings
[AD-A155042] 21 p3596 N85-32335

The design, construction and operation of a large-area, high-temperature, thermal conductance apparatus -- furnace insulation
[NPL-DMA(A)-84] 22 p3786 N85-33455

Space shuttle SRB TPS protective paint test and evaluation in NASA Hot Gas Facility and AEDC Tunnel C
[NASA-CR-170884] 24 p4061 N85-35294

HIGH VACUUM

Interaction of a stream of dielectric spheres in an electric field in a high vacuum
[DE84-014714] 01 p0115 N85-10782

Field installed brazed thermocouple feedthroughs for high vacuum experiments
[DE84-013556] 04 p0503 N85-13207

Vacuum chamber pressure effects on thrust measurements of low Reynolds number nozzles
[NASA-TM-86955] 12 p1794 N85-21259

Cutting structural materials in vacuum
14 p2296 N85-24165

Diffusion vacuum welding 15 p2489 N85-25416

Prospective uses for diffusion welding in vacuum
22 p3733 N85-33145

HIGH VOLTAGES

Resistance and inductance calculations for helical flux compression generators
[DE84-015086] 02 p0195 N85-11306

Circuit transients due to negative bias arcs on a high-voltage solar array in low Earth orbit
[NASA-TP-2407] 06 p0760 N85-14858

Choice of criteria for rejection of insulating components in high-voltage surge equipment
06 p0785 N85-15021

Semiconductor high-voltage power devices: State of art and outlook 06 p0794 N85-15074

Repetitive pulse generation with inductive energy storage: A new technology for defense
[DE84-017080] 06 p0805 N85-15122

Diagnosis of insulation defects in 1000+ V distribution networks with insulated neutral
07 p0954 N85-16044

High voltage effects measured on dummy mannequin
07 p1012 N85-16432

High voltage disconnect protection
[AD-D011480] 10 p1481 N85-19353

Effects of electromagnetic fields produced by high voltage transmission lines
[DE85-000034] 11 p1625 N85-20230

A new very high voltage semiconductor switch
[NASA-TM-86957] 11 p1627 N85-20246

High voltage RF coaxial cable
[AD-D011463] 11 p1629 N85-20255

Adaptation of an air-dielectric RF cable for use as an oil-filled high voltage pulse transmission line
[DE84-017414] 11 p1630 N85-20265

Study of electric field and ion effects on HVDC lines
[DE85-002975] 12 p1833 N85-21503

Spacecraft Environmental Interactions Technology, 1983
[NASA-CP-2359] 13 p1989 N85-22470

Non-self-maintained high-voltage low-pressure discharge 13 p2086 N85-23037

Further development of high voltage SIPMOS FET's to fulfill market needs
[BMFT-FB-T-84-255] 17 p3045 N85-28843

High voltage isolation transformer
[NASA-CASE-GSC-12817-1] 18 p3093 N85-29146

High voltage power supply
[NASA-CASE-GSC-12818-1] 18 p3093 N85-29147

High voltage lateral power transistors: Theory and design 19 p3257 N85-30194

Protection products for the conductors of high voltage overhead lines
[BLL-OA-TRANS-3219-(6196.300)]
20 p3429 N85-31269

Improvements in safety testing of lithium cells
20 p3444 N85-31379

Outline of CCVT (Coupling Capacitor Voltage Transformer) calibration procedure, EPRI-NBS (Electric Power Research Institute/National Bureau of Standards) prototype system. Supplement to EPRI report EL-890 (Field Calibration System for CCVTs, April 1978)
[PB85-182566] 20 p3450 N85-31418

Plasma erosion opening switch
[DE85-011384] 20 p3535 N85-31998

Module Hipot and ground continuity test results
21 p3612 N85-32447

Partial discharges in and electric strength of high-voltage polymer insulation at cryogenic temperatures
22 p3770 N85-33364

Photoconductive pulse power switches: A review
[DE85-014125] 24 p4091 N85-35360

HIGHLANDS

Mapping structures characteristic of the highland boundary scarp on Mars 13 p2191 N85-23595

Mars: Stratigraphy of western highlands and polar regions 13 p2201 N85-23653

HIGHLY MANEUVERABLE AIRCRAFT

Closing the design loop on HiMAT (highly maneuverable aircraft technology)
[NASA-TM-85923] 06 p0754 N85-14836

Autofocus motion compensation for synthetic aperture radar and its compatibility with strapdown inertial navigation sensors on highly maneuverable aircraft
[AD-A151940] 16 p2704 N85-26693

HIGHWAYS

Predictor model for seasonal variations in skid resistance, volume 1
[PB84-226612] 01 p0036 N85-10229

Skid resistance of bituminous surfaces in Ohio
[PB84-234491] 04 p0484 N85-13086

Optimal design efforts in Shanghai described
13 p1972 N85-22366

USSR report: Transportation
[JPRS-UTR-84-008] 14 p2206 N85-23694

HIJACKING
U AIR PIRACY

HILBERT SPACE
NT BANACH SPACE
NT SOBOLEV SPACE

On the commutant of an irreducible set of operators in real Hilbert space
[TUM-M8316] 01 p0114 N85-10774

Orthogonal polynomials and rigged Hilbert space
[TUM-M8313] 03 p0414 N85-12647

Analytic and sequential feynman integrals on abstract Wiener and Hilbert spaces, and A Cameron-Martin formula. Revision
[AD-A146969] 07 p1030 N85-16537

Chandrasekhar equations for infinite dimensional systems
[NASA-CR-172515] 09 p1376 N85-18851

A non-hypoelliptic Dirichlet problem from stochastics
10 p1537 N85-19687

A remark on regularization in Hilbert spaces
[AD-A149046] 10 p1552 N85-19787

Fake topological Hilbert spaces and characterizations of dimension in terms of negligibility
[CWI-TRACT-2] 14 p2414 N85-24693

Characteristic functionals of stochastic wave processes
[REPT-14/1984] 16 p2768 N85-27084

Finite control in underdamped distributed parameter systems 20 p3412 N85-31176

A factorization approach to the linear regulator quadratic cost problem 20 p3413 N85-31178

HILBERT TRANSFORMATION

Orthogonal polynomials and a Dirichlet problem related to the Hilbert transform
[CWI-PM-R8406] 05 p0723 N85-14647

HILL CURVES
U HILL METHOD

HILL METHOD

Magnetohydrodynamic equilibrium and stability of spheromak with spheroidal plasma-vacuum interface
[IPPJ-732] 23 p3974 N85-34640

HILLER MILITARY AIRCRAFT
U MILITARY AIRCRAFT

HILSCH TUBES

Experimentally determined characteristics of vortex heaters 13 p2050 N85-22833

HIMALAYAS

Diet of first Soviet expedition on Mount Everest
19 p3323 N85-30586

HIMAT
U HIGHLY MANEUVERABLE AIRCRAFT

HINDRANCE
U CONSTRAINTS

HINGE MOMENTS
U TORQUE

HINGED ROTOR BLADES
U HINGES
U ROTARY WINGS

HINGELESS ROTORS
U RIGID ROTORS

HINGES

In-orbit performance of INTELSAT V communications antennas deployment systems 05 p0627 N85-14018

Drag-compensated, precision-powered hinge system
22 p3796 N85-33517

HISS

VLF emissions observed by ISIS Satellites during the IMS 14 p2366 N85-24621

Conjugacy of ELF-VHF emissions near L=6 -- chorus phenomenon, hiss 14 p2367 N85-24629

HISTOCHEMICAL ANALYSIS

New techniques for studying calcium gradients
15 p2609 N85-26076

The Fibrin slide assay for detecting urokinase activity in human fetal kidney cells 20 p3502 N85-31766

HISTOGRAMS

Determining object orientation from a single image using multiple information sources
[AD-A149980] 12 p1933 N85-22146

Normal and anomalous geothermal fields and their relationship to hierarchy of geological bodies
13 p2113 N85-23163

CHIL: A comprehensive histogramming language
[DE85-005356] 14 p2405 N85-24630

Nonparametric estimation of density and hazard rate functions when samples are censored
[AD-A150946] 14 p2411 N85-24668

A cluster analysis method for identification of subpopulations of cells in flow cytometric list-mode arrays 20 p3503 N85-31779

How map designers can represent their ideas in thematic maps: Effective user interfaces for thematic map design
23 p3962 N85-34562

Study of spectral/radiometric characteristics of the Thematic Mapper for land use applications
[E85-10106] 24 p4107 N85-35464

Edge information in color images based on histograms of differences
[AD-A156002] 24 p4154 N85-35751

HISTOLOGY

Effect of 1,25-dihydroxycholecalciferol and 24,25 dihydroxycholecalciferol on growth and alteration of rat bones during hypokinesia (histomorphometric study)
01 p0092 N85-10622

Morphological study of monkeys submitted to antiorthostatic hypokinesia 12 p1902 N85-21942

Actual and simulated weightlessness inhibit osteogenesis in long bone metaphysis by different mechanisms 15 p2608 N85-26074

Histological and compositional responses of bone to immobilization and other experimental conditions
[NASA-CR-175837] 16 p2641 N85-27518

Spontaneous transitional cell carcinoma in the urinary bladder of a strain 13 guinea pig
[AD-A155645] 21 p3665 N85-32764

HISTORIES

The Malcolm horizon: History and future
01 p0008 N85-10046

Estuaries of the Cape. Part 2: Synopses of available information on individual systems. Report no. 18: Bot/Kleinmond system (CSW 13)
[CSIR-RR-417-PT-2] 01 p0067 N85-10587

Synthesis of current measurements in Puget Sound, Washington. Volume 1: Index to current measurements made in Puget Sound from 1908-1980 with daily and record averages for selected measurements
[PB84-214105] 01 p0080 N85-10603

Space research benefits national economy
02 p0163 N85-11107
The identification of the scientific community's choice criteria in the history of scientific research: The case of quantum mechanics
[NOTA-INTERNA-797] 02 p0291 N85-11683
Propulsion — jet aircraft engines
[PNR-90206] 03 p0320 N85-12062
Lunar magnetic history 04 p0582 N85-13715
A historical overview of the electrical power systems in the US manned and some US unmanned spacecraft
[NASA-CR-174806] 05 p0612 N85-13810
Men in Space: National Historic Landmark Theme Study
[PB85-107233/GAR] 07 p0911 N85-15766
Polar research in Earth sciences described
08 p1142 N85-17204
Post-Laramide history of North Central Wyoming
08 p1181 N85-17444
The beginnings of airborne astronomy, 1920 - 1930: An historical narrative 08 p1244 N85-17846
History of photometric precision
08 p1250 N85-17893
Chronology of KSC and KSC related events for 1983
[NASA-TM-87400] 08 p1261 N85-17927
On the frontier: Flight research at Dryden 1946-1981
[NASA-SP-4303] 08 p1263 N85-17934
The Prandtl Hargesell project of a national research establishment for aeronautics
[ESA-TT-835] 09 p1272 N85-17993
Flight crew training technology: A review
09 p1275 N85-18010
Making sure: A brief outline and history of ESA's test and checkout services
[ESA-BR-22] 09 p1286 N85-18077
An objective error measure for the comparison of calculated and measured transient response histories
09 p1335 N85-18395
Some fighter aircraft trends
[NASA-TM-86352] 10 p1420 N85-18954
Major glaciation events of the past and their geological significance 10 p1497 N85-19450
A history of full-scale testing of aircraft structures at the National Aeronautical Establishment
[NAE-AN-24] 12 p1777 N85-21153
Discovery of the solar wind 12 p1954 N85-22272
Chronology of KSC and KSC related events for 1983
[NASA-TM-87435] 12 p1963 N85-22339
Feoktistov recalls period leading to Gagarin spaceflight 13 p1985 N85-22451
Model research: The National Advisory Committee for Aeronautics, 1915-1958, volume 1
[NASA-SP-4103-VOL-1] 14 p2207 N85-23683
Model research, the National Advisory Committee for Aeronautics, 1915-1958, volume 2
[NASA-SP-4103-VOL-2] 14 p2207 N85-23684
Basic principles of industrial radiography
14 p2316 N85-24310
Some historical and other notes about the Mertens conjecture and its recent disproof
[CWI-NM-R8415] 14 p2414 N85-24898
O. F. Mossotti and the physics of molecules
[NOTA-INTERNA-822] 14 p2420 N85-24931
Special course on V/STOL aerodynamics: An assessment of European jet lift aircraft
[AGARD-R-710-ADDENDUM] 15 p2460 N85-25188
A climatic data bank for Northern Hemisphere land areas, 1851-1980
[DE85-007663] 16 p2835 N85-27486
The revolution in military affairs and the Soviet system
[AD-P004566] 17 p3048 N85-28863
Air traffic: Instruments, airports, companies, post, cargo and passengers 18 p3060 N85-28932
Environmental management needs
[DE85-007859] 18 p3133 N85-29405
Numerical meteorology 18 p3147 N85-29484
Early study of muons and muon decay
[NOTA-INTERNA-835] 18 p3184 N85-29742
The evolution of the U.S. helicopter industry
[AD-A154290] 19 p3211 N85-29913
The international scope of data evaluation
[DE85-005953] 19 p3349 N85-30760
Historical perspective of barriers to achieving high-efficiency silicon solar cells
20 p3479 N85-31616
Monte Carlo: In the beginning and some great expectations
[DE85-010789] 20 p3518 N85-31872
Quest for performance: The evolution of modern aircraft
[NASA-SP-468] 21 p3551 N85-32089
Ancient landscapes: Their nature and significance for the question of inheritance 21 p3601 N85-32364
One application of mega-geomorphology in education
21 p3602 N85-32370
Space research in the United Kingdom: An assessment
[AD-A155334] 21 p3712 N85-33036
Noble gases and the early history of the Earth: Inappropriate paradigms and assumptions inhibit research and communication 21 p3719 N85-33075
150 years of meteorology in Belgium
22 p3817 N85-33642
An internally consistent gamma ray burst time history phenomenology
[OG-1.2-6] 22 p3882 N85-33916
A spacefaring people: Perspectives on early spaceflight
[NASA-SP-4405] 23 p4056 N85-35142
The next assignment: The state of the literature on space 23 p4057 N85-35146
Opportunities for policy historians: The evolution of the US civilian space program 23 p4057 N85-35147
Space-age Europe, 1957-1980
23 p4057 N85-35148
Space activities in the Soviet Union, Japan, and the People's Republic of China 23 p4057 N85-35149
The idea of space exploration
23 p4057 N85-35150
Development of flight mechanics research in Brunswick 24 p4061 N85-35166
Typical and historical aspects of motor gliders as meteorological measuring aircraft
24 p4121 N85-35544

HMX
HMX combustion modification
[AD-A145071] 01 p0024 N85-10149
Critical analysis of nitramine decomposition data. Preliminary comments on autoacceleration and autoinhibition in HMX and RDX decomposition
[AD-A146570] 06 p0774 N85-14946
Molecular dynamics in nitramines and modified nitramines
[AD-A148515] 08 p1220 N85-17686
Effects of HMX addition on the combustion of energetic binders 13 p2004 N85-22560
The chemistry of RDX and HMX cluster ions
13 p2004 N85-22561
Detonation in tungsten-loaded HMX
[DE85-009606] 23 p3922 N85-34299

HNST
U HEXANITROSTILBENE

HODOGRAPHS
Classical free-streamline flow over a polygonal obstacle
[NASA-CR-172448] 01 p0046 N85-10301
Transonic jets: A numerical approach in the hodograph plane 05 p0592 N85-13774

HODOSCOPES
Fine grained hodoscopes based on scintillating optical fibers
[DE84-014849] 01 p0120 N85-10825
Bevalac calibration of the SOFIE range and hodoscope detectors
[OG-9.1-7] 23 p4023 N85-34933
The response of a scintillation counter below an emulsion chamber to heavy nucleus interactions in the chamber 24 p4175 N85-35869
Results of a search for monopoles and tachyons in horizontal cosmic ray flux
[HE-6.1-3] 24 p4209 N85-36129
Search for acoustic signals from high energy cascades
[HE-7.1-1] 24 p4213 N85-36155

HOGBACKS
U RIDGES

HOHMANN TRAJECTORIES
U ELLIPTICAL ORBITS
U TRANSFER ORBITS

HOHMANN TRANSFER ORBITS
U ELLIPTICAL ORBITS
U TRANSFER ORBITS

HOLDERS
NT FLAME HOLDERS
Contact insertion and wire lay robotic end effector apparatus
[AD-D011451] 10 p1492 N85-19424
Classification of holding jigs for objects of robotized assembly 14 p2266 N85-24039
Apparatus for mounting a field emission cathode
[NASA-CASE-LEW-14108-1] 18 p3094 N85-29149
Thermal expansion coefficients of a 30% glass fiber filled PEEK pyrotechnic charge holder
[DE85-010805] 19 p3251 N85-30155
Results of tests of MTA-2 TPS on the SRB hold-down bolt blast container
[NASA-CR-170891] 24 p4070 N85-35224

HOLE DISTRIBUTION (ELECTRONICS)
Absorption of 10.6 micrometer laser radiation in electron-hole condensate in germanium
21 p3681 N85-32870

HOLE DISTRIBUTION (MECHANICS)
Final magnetic shimming of vacuum chamber suspension holes on the sector magnets
[CSIR-NAC-83-02] 01 p0117 N85-[illegible]

HOLE GEOMETRY (MECHANICS)
Stress analysis of pin-loaded orthotropic plates using orthotropic photoelasticity 02 p0207 N85-113[illegible]
Stress intensity factors for corner cracks at holes located near an edge
[FFA-TN-1984-20] 04 p0514 N85-132[illegible]
Flow visualization study of the effect of injection hole geometry on an inclined jet in crossflow
[NASA-TM-86936] 11 p1631 N85-20[illegible]
Finite element analysis of problems associated with life enhancement techniques
[ARL/STRUC-R-404] 12 p1862 N85-2167[illegible]
An approximation to the problem of a pin-loaded hole in an orthothropic plate
[VTH-LR-386] 16 p2802 N85-2727[illegible]
Effect of edge distance on yield initiation in a remotely loaded half-plane containing interference-fit disc of the same material
[ARL/STRUC-R-413] 19 p3285 N85-30[illegible]

HOLE MOBILITY
High-efficiency solar-cell design modeling
06 p0829 N85-152[illegible]
Collective modes, effective interaction and superconductivity in the electron-hole liquid
20 p3537 N85-32[illegible]

HOLES
Stresses in a half-plane containing either a pressurized hole or an interference-fit disc
[ARL/STRUC-R-409] 12 p1865 N85-21700
Elastic response of a half-plane to a bonded interference-fit disc of the same material
[ARL/STRUC-R-406] 12 p1865 N85-21701

HOLES (ELECTRON DEFICIENCIES)
Theoretical analysis of physical processes of lasing medium degradation in semiconductor lasers
02 p0269 N85-[illegible]
Electron and hole effective masses for two-dimensional transport in strained-layer superlattices
[DE84-016222] 04 p0570 N85-13607
Inclusion of electron transfer in the calculation of K(alpha)L(n) multiple vacancy production by ion impact
[DE84-016596] 05 p0733 N85-14711
Photoluminescent and electroluminescent properties of Cd sub 0.95 Mn sub 0.05 Se electrodes
[AD-A146775] 07 p0946 N85-15[illegible]
Two carrier dual injector apparatus
[AD-D011357] 07 p1047 N85-16[illegible]
Chaotic dynamics of instabilities in solids
[DE85-004909] 14 p2429 N85-24[illegible]
On the group-theoretical approach to the energy spectra problem of charge carriers in cubic solids
[PREPRINT-435] 18 p3196 N85-29[illegible]
Collective modes, effective interaction and superconductivity in the electron-hole liquid
20 p3537 N85-32[illegible]
Dangling bonds and sub-gap optical absorption in silicon
[DE85-011752] 24 p4082 N85-35[illegible]
Optical properties of heterostructures and superlattices
[AD-A156243] 24 p4162 N85-35802
Multiple vacancy production by high energy heavy ions
[DE85-004426] 24 p4162 N85-35[illegible]

HOLLAND
U NETHERLANDS

HOLLOW CATHODES
Hot hollow cathode gun assembly
[DE84-014312] 01 p0121 N85-108[illegible]
Gas pressure and electron density at the level of the active zone of hollow cathode arc discharges
[NASA-TM-77477] 03 p0414 N85-12[illegible]
Extended performance technology study 30-cm thruster
[NASA-CR-168259] 07 p0917 N85-15[illegible]
Gas pressure and electron density in the active zone level of hollow cathode arc discharges
[NASA-TM-77468] 07 p0945 N85-15[illegible]
Measurements of electric fields in plasmas by using beam probe and laser fluorescence techniques
09 p1389 N85-1[illegible]
Advanced ion thruster research
[NASA-CR-174862] 10 p1430 N85-1[illegible]
Proposal for hollow cathode electron gun for electron cooling
[DE85-002721] 11 p1630 N85-20[illegible]
Hollow cathode apparatus
[NASA-CASE-NPO-15560-1] 12 p1632 N85-21[illegible]
Journal of Research of the National Bureau of Standards, volume 89, number 2, March - April 1984
[PB85-115426] 12 p1926 N85-22[illegible]
Laser with a hollow copper cathode
[ISL-R-119/83] 14 p2310 N85-24[illegible]

High efficiency ionizer using a hollow cathode discharge plasma
[DE85-006890] 18 p2868 N85-27693
A liquid nitrogen cooled composite wall hollow cathode — molecular spectroscopy
[UBP-85-07] 20 p3526 N85-31930
High pressure working mode of hollow cathode arc discharges
[NASA-TM-77880] 20 p3535 N85-31992
Heaterless ignition of inert gas ion thruster hollow cathodes
[NASA-TM-87086] 23 p3903 N85-34177
Hollow cathodes in high pressure arc discharges
[NASA-TM-87090] 23 p3903 N85-34179

HOLMIUM
Spin dynamics of rare Earth ions in crystal fields probed by muon spin rotation
[DE84-013605] 02 p0278 N85-11810
Magnetic X-ray scattering studies of the rare Earth metal holmium
[DE85-003608] 12 p1807 N85-21335
Interactions of heavy nuclei, Kr, Xe and Ho, in light targets
[OG-7.2-21] 23 p4016 N85-34888
Stopping relativistic Xe, Ho, Au and U nuclei in nuclear emulsions 24 p4173 N85-35876

HOLOGRAMMETRY
Development of holographic particle field data reduction by Fourier analysis
[AD-A148684] 08 p1165 N85-17348
Optical processor for synthetic aperture radar
11 p1621 N85-20203
Hologram-like transmission of pictures
23 p3961 N85-34552

HOLOGRAPHIC INTERFEROMETRY
Distortional measurement of antennas under space simulation conditions by means of holography
06 p0825 N85-14005
Reconstruction of a 3-dimensional transonic rotor flow field from holographic interferogram data
[NASA-TM-86690] 12 p1770 N85-21112
Interferometric velocity measurements in ballistics
[ISL-CO-239/83] 14 p2306 N85-24276
Description of an holographic interferometry nondestructive test installation: Application to bond tests
[SNIAS-851-430-101] 20 p3464 N85-31521
A comparison of electronic heterodyne moire deflectometry and electronic heterodyne holographic interferometry for flow measurements
[NASA-TM-87071] 21 p3568 N85-32302
New method for compensating and measuring any motion of three-dimensional objects in holographic interferometry
[ISL-CO-216/84] 22 p3769 N85-33474
Heterodyne holographic interferometry for visualization of surface acoustic waves
[AD-A155405] 22 p3836 N85-33753
Practical aspects of laser holographic interferometry in wind tunnels
[NASA-TM-86788] 23 p3933 N85-34378

HOLOGRAPHIC SPECTROSCOPY
Simultaneous measuring absorption spectrometer
[BMFT-FB-T-84-132] 03 p0365 N85-12339
Bibliography of Soviet laser developments, number 65, May - June 1983
[AD-A146189] 03 p0366 N85-12347
Investigations of photochemistry using holography and photoacoustic spectroscopy
[AD-A146837] 06 p0810 N85-15149
Fourier transform infrared spectrophotometric analysis of resin mix stoichiometry, revision 1
[DE85-007272] 16 p2747 N85-26951
Holographic corrector in objective with compound main mirror 17 p2941 N85-28153

HOLOGRAPHIC SUBTRACTION
Effect of hydrogen on formation of energy spectrum of multiply charged and copper ions
02 p0203 N85-11720
Holographic subtraction of images by Fourier plane recording and spatial filtration with a narrow beam
02 p0203 N85-11721

HOLOGRAPHY
NT ACOUSTICAL HOLOGRAPHY
NT MICROWAVE HOLOGRAPHY
NT WHITE LIGHT HOLOGRAPHY
Peripheral vision displays: The future
01 p0009 N85-10056
A determination of the photochemical quantum yields from 2 excited triplet states of biacetyl using holography
[AD-A146091] 01 p0050 N85-10326
Acoustic emission linear pulse holography
[DE84-014519] 01 p0050 N85-10330
Formation of radio images by scanning around circle
02 p0264 N85-11727
Modeling holographic recognition system by using number-theory convolution transformation
02 p0272 N85-11774
Holographic displacement analysis with fiber optics
[AD-A146185] 03 p0420 N85-12880
Hologram bleaching 06 p0789 N85-15038
Recording holograms on thin films of titanium dioxide
06 p0789 N85-15039
A collection of flow visualization techniques used in the Aerodynamic Research Branch
[NASA-TM-85998] 06 p0808 N85-15135
Wavelength coded image transmission and holographic optical elements
[AD-A146490] 06 p0810 N85-15147
Investigations of photochemistry using holography and photoacoustic spectroscopy
[AD-A146837] 06 p0810 N85-15149
Holographic directional coupler for fiber optic systems
[AD-D011365] 07 p0937 N85-15939
Solid state research
[NASA-CR-174285] 07 p1048 N85-16656
Advanced diagnostics for reacting flows
[AD-A148479] 08 p1162 N85-17334
Holographic FLI for detection of defects
[AD-A148339] 08 p1164 N85-17345
Development of holographic particle field data reduction by Fourier analysis
[AD-A148684] 08 p1165 N85-17348
Critical flashing flow of subcooled fluids in nozzles with contour discontinuities
[DE84-017229] 09 p1319 N85-18296
Diffraction diffusion screen with holographically-suppressed zero-order beam
[AD-D011445] 10 p1487 N85-19387
X-ray holography of biological specimens
[DE85-002437] 10 p1489 N85-19398
Optical implementation of the synthetic discriminant function
[AD-A149582] 10 p1557 N85-19817
Electronics Engineering Department: EE technical review
[DE85-004380] 11 p1629 N85-20259
KMSF X-ray laser experiments, task no. 2
[DE85-000291] 11 p1640 N85-20335
Study of the potential usefulness of superfine holographic x-ray gratings in AXAF and astrophysics in general 12 p1945 N85-22215
Solid propellant combustion diagnostics and automated data retrieval from holograms 13 p1998 N85-22527
Laser applications in last 10 years reviewed
13 p2052 N85-22844
Space-variant optical systems
[AD-A151032] 14 p2421 N85-24939
Holography in space 15 p2476 N85-25285
Holographic lens for optical correlator
16 p2763 N85-27052
Holoswitch, phase 1
[AD-A152212] 16 p2787 N85-27196
Digital image analysis of four-frame holographic plasma and neutral gas interferograms
[DE85-008397] 16 p2788 N85-27200
Ultrafast holography using optical fibers
[ISL-CO-236/83] 16 p2788 N85-27204
Holographic intensity correlator with PRIS-type photoelectro-optical controlled transparency
17 p2940 N85-28152
Holographic corrector in objective with compound main mirror 17 p2941 N85-28153
Morphological stability and fluid dynamics of vapor crystal growth
[NASA-CR-175879] 17 p3042 N85-28822
Holographic investigation of solid propellant combustion in a two-dimensional motor
[AD-A153546] 18 p3070 N85-28989
Holographic assembly for measuring velocity fields of supersonic ballistic splinters at a large distance
[ISL-CO-203/84] 20 p3459 N85-31487
Infrared laser holography used in fusion plasma studies 21 p3687 N85-32905
Signal processing in quasi-holographic system as an inverse problem 22 p3762 N85-33315
Digital holographic synthesis of pattern-forming transparencies for ring antenna arrays
22 p3763 N85-33326
Depth dimension compression of 3-D images
22 p3764 N85-33332
Pulsed lasers for filming color holographic film images
22 p3781 N85-33426
Holographic cinematography with the help of a pulse YAG laser
[ISL-CO-213/84] 22 p3788 N85-33472
Cineholography
[ISL-CO-214/84] 22 p3788 N85-33473
Methods for the optical processing of signals
[DRIC-T-7439] 22 p3844 N85-33809
Modular digital holographic fringe data processing system
[NASA-CR-177952] 23 p3933 N85-34376
Applications of holography to X-ray imaging
[DE85-010984] 23 p3934 N85-34384
The use of optical fibers in pulsed laser holography
[ISL-CO-226/84] 23 p3936 N85-34395
Fatigue damage detection in steels by optical correlation
[AD-A155830] 24 p4079 N85-35277
Holoswitch
[AD-A155841] 24 p4096 N85-35392

HOLOMORPHISM
U ANALYTIC FUNCTIONS

HOMEOSTASIS
Effects of hypothermia on brain metabolism
11 p1682 N85-20636
Fluid metabolism of monkeys during two-week antiorthostatic hypokinesia 12 p1902 N85-21943
Alterations in gut transport of minerals and in binding proteins during simulated weightlessness
[NASA-CR-175637] 14 p2388 N85-24709
Homeostasis in primates in the hyperdynamic environment — circadian timekeeping and effects of lower body positive pressure on sleep
15 p2610 N85-26095
Primate experiments on SLS-1
15 p2687 N85-26592
Long term exposure of animals to antiorthostatis (-90 deg) as a model of critical homeostatic disturbances
19 p3324 N85-30682
Effect of dibazol on parameters of nonspecific resistance of subjects in pressurized cabins
23 p3954 N85-34504

HOMING
Accounting for error stochasticity in terminal homing of aircraft 04 p0489 N85-13115
Determining an azimuth with a north seeking gyro
[AD-A155880] 24 p4063 N85-35180

HOMING DEVICES
Dual mode radio frequency-infrared frequency system
[AD-D011402] 08 p1061 N85-16850
Applications of compound eye configurations to smart sensor design
[AD-A150731] 14 p2420 N85-24935
Supersonic missile seeker lens system using gradient index material for first element lens
[AD-A151476] 15 p2480 N85-25367
Preguidance and piloting with the aid of composite inertial sensors 16 p2696 N85-26646

HOMODYNE RECEPTION
Quantum noise and excess noise in optical homodyne and heterodyne receivers
[AD-A148298] 08 p1157 N85-17303
Phase-locked loops for optical homodyne detection, volume 1 — spaceborne receivers
[ESA-CR(P)-2029-VOL-1] 20 p3442 N85-31367
Phase locked loops for optical homodyne detection, volume 2 — spaceborne receivers
[ESA-CR(P)-2029-VOL-2] 20 p3442 N85-31368

HOMOGENEITY
Scanning photoacoustic microscopy of aluminum with aluminum oxide, roughness standards and rubber
[AD-A149480] 10 p1441 N85-19081
Surface scattering
[AD-A150252] 13 p2153 N85-23366
Homogeneity of pristine and bromine intercalated graphite fibers
[NASA-TM-87016] 15 p2517 N85-25521
Numerical modeling of subsurface communication
[DE85-012818] 21 p3577 N85-32249
A cracked orthotropic sheet stiffened by a semi-infinite orthotropic sheet
[NASA-TP-2455] 21 p3597 N85-32339
On the principle of uniformity of satellite communications systems 22 p3773 N85-33382
Apparatus for unilateral generation of a homogeneous magnetic field
[DE85-008001] 23 p3926 N85-34345
Why do leaky-box models work so fine?
[OG-7.2-8] 23 p4014 N85-34877

HOMOGENEOUS TURBULENCE
Vortex dynamics simulation of conserved scalar dissipation 22 p3745 N85-33210

HOMOGENIZATION
U HOMOGENIZING

HOMOGENIZING
Optimum convection conditions for Czochralski growth of semiconductors
[INPE-3395-PRE/695] 16 p2670 N85-27703
Effect of polymer additives on characteristics of direct-current motor with liquid dielectric filler
22 p3772 N85-33376

HOMOJUNCTIONS
Comparison of SCAPID/GaAs to experiment
05 p0665 N85-14279

Comparative study of GaAs solar cell potentialities for space applications 13 p2006 N85-22577
Investigation of high output gallium arsenide solar cells 13 p2006 N85-22578
GaAs and 3-5 compound solar cells status and prospects for use in space 13 p2007 N85-22580

HOMOLOGY
Contribution of the cup-product of Milnor's fiber with /1/ sup 2 lambda poles 11 p1698 N85-20672

HOMOMORPHISMS
NT AUTOMORPHISMS
On Bezout domains, elementary divisor rings, and pole assignability
[CSIR-TWISK-330] 01 p0110 N85-10740

HOMOPOLAR GENERATORS
Westinghouse programs in pulsed homopolar power supplies 05 p0606 N85-13862

HOMOSPHERE
NT MIDDLE ATMOSPHERE
NT STRATOSPHERE

HOMOTOPY THEORY
A fast ray tracing routine for laterally inhomogeneous media
[AD-A150984] 14 p2421 N85-24938

HONDURAS
Area handbook series. Honduras: A country study
[AD-A146510] 06 p0827 N85-15253
Interrelationship of atmospheric parameters in Honduras
[AD-A147371] 07 p1007 N85-16401

HONEYCOMB CORES
Nonlinear dynamic analysis of sandwich panels 01 p0060 N85-10394
Integrated insulation wall assembly — for a solid rocket motor case
[AD-D011553] 12 p1794 N85-21257
Aircraft safety improvement 15 p2686 N85-26602
Stress analysis of axisymmetric sandwich shells of variable thickness 24 p4101 N85-35419

HONEYCOMB STRUCTURES
NT HONEYCOMB CORES
Quasi-steady analysis of aircraft panel flammability
[AD-A145461] 02 p0138 N85-10938
Air Force honeycomb shaping at SM-ALC (Sacramento Air Logistics Center)
[AD-P004005] 03 p0308 N85-11985
Verification tests of durable TPS concepts
[NASA-TM-86313] 03 p0323 N85-12085
Composite repair of aircraft structures 08 p1120 N85-17059
Technological parameters of diffusion welding processes in honeycomb titanium alloy structures 13 p2033 N85-22739
Computational methods for the explosive and impact compaction of powders
[AD-A156219] 24 p4139 N85-35653

HOOP COLUMN ANTENNAS
Vibration control experiment design for the 15-m hoop/column antenna 20 p3409 N85-31159

HOOPS
Direct transient analysis of a fuze assembly by axisymmetric solid elements 15 p2576 N85-25890

HORIZON
Stimulus factors in motion perception and spatial orientation 01 p0006 N85-10049
Early Air Force Flight Test Center (AFFTC) experience with Peripheral Vision Horizon Displays (PVHD) 01 p0009 N85-10057
Cockpit window edge proximity effects on judgements of horizon vertical displacement 05 p0704 N85-14518
Mean and random errors of visual roll rate perception from central and peripheral visual displays 05 p0704 N85-14519

HORIZON SCANNERS
Personal experience with the PVHD and opinion of situations in which a wide Field Of View (FOV) PVHD might be helpful 01 p0008 N85-10045
Evaluation of the Malcolm horizon in a moving-base flight simulator 01 p0008 N85-10051
Peripheral vision horizon display on the single seat night attack A-10 01 p0009 N85-10053
Infrared horizon sensor modeling for attitude determination and control: Analysis and mission experience
[NASA-TM-86181] 10 p1429 N85-19016
Autonomous state determination for an Earth orbiting satellite using horizon and star sensors
[AD-A151827] 15 p2493 N85-25379
Studies of the solar mesosphere explorer: Dynamics and horizon sensor performance. Part A: Spin axis precession and atmospheric drag. Part B: Clouds
[NASA-CR-175308] 24 p4069 N85-35213

HORIZON SENSING
U HORIZON SCANNERS

HORIZONTAL ORIENTATION
The Malcolm horizon: History and future 01 p0008 N85-10046
Comparison of wind derived from the LIMS (Limb Infrared Monitor of the Stratosphere) satellite instrument with rocket observations
[NASA-CR-174083] 04 p0541 N85-13444
Experiments in forecasting atmospheric marine horizontal visibility using model output statistics with conditional probabilities of discretized parameters
[AD-A147574] 07 p1008 N85-16404
Intensification of tropical instabilities
[AD-A149865] 12 p1896 N85-21899
Horizontal deflection TS-257 13 p2069 N85-22926
Experimentally determined distribution of stress around a horizontally loaded model pile in dense sand
[CE-43] 16 p2796 N85-27239
Wake effects on the aerodynamic performance of horizontal axis wind turbines
[NASA-CR-174920] 18 p3127 N85-29364
Resolution of thermal striping issue downstream of a horizontal pipe elbow in stratified pipe flow
[DE85-006195] 21 p3586 N85-32292
On the spectrum of atmospheric velocity fluctuations seen by MST/ST radar and their interpretation 21 p3622 N85-32504
Tropospheric gravity waves observed by three closely spaced ST radars 21 p3623 N85-32509
Determination of horizontal and vertical wavelengths of gravity waves in the mesosphere by spaced wind measurements 21 p3623 N85-32510
Horizontal and vertical structure of velocity, potential vorticity and energy in the gulf stream
[AD-A154753] 21 p3655 N85-32702

HORIZONTAL SPACECRAFT LANDING
Active control technology experience with the Space Shuttle in the landing regime 17 p2903 N85-27900

HORIZONTAL STABILIZERS
U STABILIZERS (FLUID DYNAMICS)

HORIZONTAL TAIL SURFACES
Experimental trim drag values and flow-field measurements for a wide-body transport model with conventional and supercritical wings
[NASA-TP-2071] 02 p0135 N85-10920

HORMONE METABOLISMS
Effect of modulated ultrahigh frequency field on behavior and hormone level in female rats under emotional stress 09 p1361 N85-18562
The behavior of renal-regulating hormones during hypogravic stress
[NASA-CR-171877] 15 p2616 N85-26123
Rat plasma hormone levels following flight aboard Cosmos-1129 biosatellite 22 p3823 N85-33681

HORMONES
NT ADRENOCORTICOTROPIN (ACTH)
NT ALDOSTERONE
NT CORTICOSTEROIDS
NT CORTISONE
NT HYDROXYCORTICOSTEROID
NT PROSTAGLANDINS
Modulation of the cytosolic androgen receptor in striated muscle by sex steroids
[NASA-CR-174173] 04 p0545 N85-13468
Comparative effects of auxin and abscisic acid on growth, hydrogen ion efflux and gravitropism in primary roots of maize
[NASA-CR-174355] 09 p1342 N85-18444
Purification and cultivation of human pituitary growth hormone secreting cells
[NASA-CR-171846] 12 p1899 N85-21923
Transduction of the root gravitropic stimulus: Can apical calcium regulate auxin distribution? 15 p2606 N85-26063
Attempts to localize and identify the gravity sensing device of plant seedlings 15 p2607 N85-26064
The salutary effect of dietary calcium on bone mass in a rat model of simulated weightlessness 15 p2608 N85-26073
Neural mechanism by which gravitational stimulus and stress affect the secretion of renin and other hormones 15 p2610 N85-26083
Morphological study of primate hypothalamus and hypophysis after experiment with antiorthostatic hypokinesia 19 p3325 N85-30603
A critical synopsis: Continuous growth of proximal tubular kidney epithelial cells in hormone-supplemented serum-free medium 20 p3501 N85-31767

HORN ANTENNAS
Radiation patterns of a pyramidal horn antenna 09 p1311 N85-18236
Beamwidth control in pyramidal horns
[R-NIAS-27] 13 p2053 N85-22853
Prime-focus parabolic reflector antenna: Theory and measurement
[R-NIAS-20] 14 p2291 N85-24199
Dual sense, circularly polarized helical antenna
[AD-D011680] 19 p3254 N85-3017
Fin-line horn antennas
[AD-A154597] 21 p3580 N85-322

HORSEPOWER
Tractor power selection with compaction constraints
[AD-P004300] 09 p1409 N85-1897

HOT ATOMS
Observations of absorption lines from highly ionized atoms 06 p0876 N85-155

HOT CATHODES
Hot hollow cathode gun assembly
[DE84-014312] 01 p0121 N85-108
Analysis of the dissipation mechanism within a nstationary cathode spot of metal vapor arcs
[AD-A149258] 10 p1558 N85-19

HOT CORROSION
NT TEMPERATURE DEPENDENCE
Effects of surface chemistry on hot corrosion life: Overview 02 p0145 N85-10
Studies on the hot corrosion of a nickel-base superalloy, Udimet 700
[NASA-TM-86882] 02 p0183 N85-1124
Kinetics of oxidation of titanium alloy upon heating to 1000 deg C 10 p1448 N85-1912
High temperature corrosion of ceramics
[DE85-002179] 11 p1612 N85-2013
Digital temperature and velocity control of mach 0.3 atmospheric pressure durability testing burner rigs in long time, unattended cyclic testing
[NASA-TM-86959] 12 p1805 N85-2132
Oxidation and hot corrosion of hot-pressed Si3N4 at 1000 deg C
[NASA-TM-86977] 12 p1811 N85-2138
Effects of surface chemistry on hot corrosion life
[NASA-CR-174915] 16 p2708 N85-26711
Burner rig corrosion of SiC at 1000 deg C
[NASA-TM-87061] 19 p3227 N85-30011
Changes of structure of EP648-VI alloy as a result of high-temperature gas corrosion 19 p3243 N85-30110
High-temperature oxidation of reaction-roasted silicon nitride with various additives 19 p3244 N85-30114
Mechanism of strength degradation for hot corrosion of alpha-SiC
[NASA-TM-87052] 19 p3248 N85-30135
A multiple linear regression analysis of hot corrosion attack on a series of nickel base turbine alloys
[NASA-TM-87020] 20 p3431 N85-31284
The effect of stress and hot corrosion on nickel-base superalloys
[AD-A154722] 21 p3566 N85-32181
Thin-film reliability and engineering overview 21 p3612 N85-3245
High temperature corrosion of ceramics
[DE85-013481] 24 p4060 N85-3530

HOT CYCLE PROPULSION SYSTEM
U TIP DRIVEN ROTORS

HOT ELECTRONS
Non-LTE considerations in spectral diagnostics of thermal transport and implosion experiments
[DE84-015187] 05 p0730 N85-148
Stabilization of the hot electron precessional mode in a symmetric tandem mirror by the axial variation of radial electric field
[DE84-016389] 05 p0730 N85-1482
The flow of plasma in the solar terrestrial environment
[NASA-CR-174301] 08 p1224 N85-1770
Comparison of ionizing radiation and hot electron effects in MOS structures
[DE84-016766] 09 p1400 N85-180
A microchannel plate pinhole camera for 20 to 100 ke
X-ray imaging
[DE85-001572] 10 p1486 N85-190
Measurement of hot-electron production and microwave emission by laser-irradiated CH targets
[DE85-003139] 11 p1640 N85-20
Anomalous heating of ionospheric components (therm e- and He+) via intense Ion Cyclotron Waves (ICW's) 14 p2368 N85-24
Hard X-ray measurements of the hot electron rings Nagoya BUMPY TORUS (NBT-1M)
[IPPJ-720] 19 p3370 N85-30
Stability of a hot symmetric tandem mirror with therm barrier
[DE85-010539] 19 p3377 N85-30
Plug and thermal barrier potential formation in Gam 10 23 p3976 N85-34
Effect of ECH and ICH on ambipolar potential NBT-1M 23 p3978 N85-34
Simulation studies on stability of hot electron plas 23 p3978 N85-34
Fokker-Planck calculation of hot electron formatio the thermal barrier region of tandem mirror Gamm
[IPPJ-726] 23 p3979 N85-3

HOT EXTRUDING
U EXTRUDING
HOT FORMING
U HOT WORKING
HOT GAS SYSTEMS
U HIGH TEMPERATURE GASES
HOT GASES
U HIGH TEMPERATURE GASES
HOT JET EXHAUST
U HIGH TEMPERATURE GASES
U JET EXHAUST
HOT JETS
U JET FLOW
HOT PLASMAS
U HIGH TEMPERATURE PLASMAS
HOT PRESSING
Processing ceramics
[NASA-TM-77603] 01 p0031 N85-10188
Fabrication and characterization of Si3N4 ceramics without additives by high pressure hot pressing
[NASA-TM-77724] 01 p0031 N85-10189
Hot isostatically pressed manufacture of high strength MERL 76 disk and seal shapes
[NASA-CR-165550] 02 p0183 N85-11225
High temperature deformation of hot-pressed polycrystalline orthoenstatite
[NASA-CR-174026] 02 p0285 N85-11861
HIP glassmaking for high nitrogen compositions in the Y-Si-Al-O-N system
[DE84-015546] 03 p0338 N85-12175
Development and fabrication of refractory bodies for gas turbine engines
[BMFT-FB-T-84-180] 04 p0457 N85-12899
Development and production of improved alpha-phase silicon nitride powders for hot pressing and sintering
[BMFT-FB-T-84-208] 07 p0921 N85-15830
Development and production of improved silicon carbide powder for pressureless sintering and hot pressing
[BMFT-FB-T-84-211] 07 p0934 N85-15917
Ti-6Al-4V alloy castings prepared in zircon sand molds and the effect of hot isostatic pressing
[PB85-109932/GAR] 09 p1298 N85-18150
Oxidation and hot corrosion of hot-pressed Si3N4 at 1000 deg C
[NASA-TM-86977] 12 p1611 N85-21358
Pressureless sintered silicon nitride as a promising candidate for radome materials
[AD-P004367] 12 p1626 N85-21461
Particulate toughened silicon carbide
[DE85-004797] 13 p2016 N85-22643
Dispersed-metal-toughened alumina
[NASA-CR-174687] 13 p2037 N85-22758
Sweden invents new ceramic for more durable cutting tools 15 p2536 N85-25645
Development of high temperature resistant, noncorrosible, non-metallic ceramic materials, especially silicon nitride in gas turbine application
[BMFT-FB-T-85-015] 17 p2936 N85-28125
Development of high temperature resistant noncorrodible silicon carbide components for gas turbine applications, follow-up report
[BMFT-FB-T-85-016] 17 p2936 N85-28126
Hot Isostatic Pressing (HIP): Techniques, applications and economical use
[JUEL-SPEZ-288] 17 p2939 N85-28141
Sintering reactions, structure and properties of a cobalt free nonconventional hard material
[DE85-007704] 18 p3076 N85-29025
Hot isostatically pressed Sm(2)(TM)17 magnets
[AD-A155479] 21 p3582 N85-32267
System for electro-optical ceramic recrystallization
21 p3682 N85-32872
HOT STARS
NT A STARS
NT B STARS
NT BLUE STARS
NT O STARS
NT SYMBIOTIC STARS
NT WHITE DWARF STARS
NT WOLF-RAYET STARS
Observations of absorption lines from highly ionized atoms 06 p0876 N85-15562
Stromgren trails of hot white dwarfs
06 p0879 N85-15589
The Origin of Nonradiative Heating/Momentum in Hot Stars
[NASA-CP-2358] 08 p1231 N85-17755
Evidence for non-radiative activity in hot stars
08 p1231 N85-17756
Evidence for non-radiative activity in stars with T sub eff 10000 K 08 p1231 N85-17757
Bipolar ejection of matter from hot stars
08 p1233 N85-17767
Stellar winds: Observational evidence for a hot-cool star connection 08 p1233 N85-17768
Corotating interaction regions in stellar winds: Particle acceleration and non-thermal radio emission in hot stars
08 p1234 N85-17773
Synchrotron emission from chaotic stellar winds
08 p1234 N85-17774
Winds from rotating, magnetic, hot stars
08 p1234 N85-17775
Non-radiative energy from differential rotation in hot stars 08 p1234 N85-17776
Bipolar flows and X-ray emission from young stellar object 08 p1234 N85-17779
Nonradiative heating and enhanced mass-loss due to shear turbulence in massive hot stars
08 p1235 N85-17780
A leaky waveguide model for MHD wave driven winds from coronal holes 08 p1235 N85-17781
Magnetic effects in the heating and modification of flows in the outer stellar atmospheres with application to early type star case 08 p1235 N85-17783
Radiative amplification of acoustic waves in hot stars
08 p1235 N85-17786
On the role played by lines in radiatively driven stellar winds depending on the position of the stars in the HR diagram 08 p1236 N85-17787
Summary of the origin of nonradiative heating/momentum in hot stars
08 p1236 N85-17789
International Ultraviolet Explorer observations of amorphous hot galaxies
[NASA-CR-174354] 10 p1571 N85-19904
Radiative ion beams: Hot stellar reactions in the laboratory
[DE85-001570] 11 p1722 N85-20833
IUE absorption line studies of highly ionized interstellar gas 11 p1743 N85-20962
Hot stars: Six years of progress
11 p1743 N85-20963
The usual hot stars in unusual galaxies
11 p1745 N85-20975
The variation of galactic interstellar extenction in the ultraviolet 11 p1749 N85-21000
Coronal effects of the winds of early-type stars
11 p1749 N85-21002
Coordinated ultraviolet and visual observations of Omega Orionis 1982-1983 11 p1750 N85-21007
An episodic red-wing structure of SiIV, lambda 1394A, in gamma Cas 11 p1750 N85-21009
IUE spectrophotometry of the hot helium-rich PG1159 DO degenerates 11 p1751 N85-21015
Eclipse observations of Epsilon Aurigae
11 p1755 N85-21037
Egress spectra of the new eclipsing supergiant 22 Vulfeculae 11 p1755 N85-21039
HOT SURFACES
Problems with electrical interference between solar generators and shunt type regulators
13 p2010 N85-22607
Component-specific modeling
[NASA-CR-174765] 23 p3897 N85-34140
HOT WEATHER
Heat injury: Prevention is the key
[AD-A153734] 19 p3328 N85-30622
HOT WORKING
Mechanical properties of a leaded, resulfurized, rephosphorized steel in various thermo/mechanical conditions
[PB84-216464] 03 p0333 N85-12144
Process Modeling Applied to Metal Forming and Thermomechanical Processing
[AGARD-LS-137] 06 p0796 N85-15086
Control of microstructure during hot working of Ti-6242 06 p0797 N85-15091
Modelling temperature changes during hot working operations 06 p0798 N85-15095
ESR (Electroslag Refining) technology in Australia: Laboratory research and industrial development
[AD-A147776] 08 p1129 N85-17114
Summaries of press automation conference presented
08 p1139 N85-17173
Hot rolling of ceramics by the use of self propagating synthesis
[AD-D011486] 10 p1453 N85-19154
Comparison of the fatigue resistance (initiation, propagation) of cast TA6V with hot rolled TA6V --- titanium alloy
[DGT-25369-PT-1] 12 p1808 N85-21341
Optimizing hot workability and controlling microstructures in difficult to process high strength and high temperature materials
[AD-D011586] 15 p2510 N85-25482
New material, process spins off from Volvo LCP 2000 program 15 p2536 N85-25648
Effect of prior warm rolling on the retained austenite content and hardening response of VIM-VAR (vacuum-induction melted-vacuum-arc remelted) AISI M-50 steel
[AD-A156145] 24 p4079 N85-35281
HOT-FILM ANEMOMETERS
Analysis of the Viking Lander 1 surface wind vector for sols 45 to 375
[NASA-CR-174349] 09 p1416 N85-18932
Development of a temperature-compensated hot-film anemometer system for boundary-layer transition detection on high-performance aircraft
[NASA-TM-86732] 22 p3730 N85-33121
HOT-WIRE ANEMOMETERS
Aero-optics experimental techniques
[AD-A146755] 07 p0957 N85-16067
An experimental investigation of unexcited and exicted elliptic jets 15 p2554 N85-25755
Velocity and transient measurements in a shock tube using a hot-wire anemometer
[AD-A154894] 21 p3569 N85-32305
HOT-WIRE FLOWMETERS
Comparison of two-dimensional laser and hot-wire velocimetry for a supersonic turbulent boundary layer
11 p1576 N85-19927
Surface shear stress characteristics in turbulent flows
19 p3211 N85-29914
HOT-WIRE TURBULENCE METERS
U HOT-WIRE FLOWMETERS
U TURBULENCE METERS
HOUSEHOLDER TRANSFORMATIONS
Implementation of some concurrent algorithms
[DE85-004687] 13 p2148 N85-23334
HOUSINGS
NT COWLINGS
NT RADOMES
Flywheel containment and safety considerations
05 p0606 N85-13869
Thermally isolated structural support link
[AD-D011349] 07 p0972 N85-16176
Housing flexibility effects on rotor stability
16 p2738 N85-26896
Refrigerated dynamic seal to 6.9 MPa (1000 psi)
[NASA-TM-87108] 23 p3930 N85-34356
HOVERCRAFT
U GROUND EFFECT MACHINES
HOVERING
Reconstruction of a 3-dimensional transonic rotor flow field from holographic interferogram data
[NASA-TM-86690] 12 p1770 N85-21112
Experimental study of main rotor tip geometry and tail rotor interactions in hover. Volume 1. Text and figures
[NASA-CR-177336-VOL-1] 13 p1965 N85-22344
Experimental study of main rotor tip geometry and tail rotor interactions in hover. Volume 2: Run log and tabulated data
[NASA-CR-177336-VOL-2] 13 p1965 N85-22345
Hover test results of a small-scale twin-tilt nacelle model
[NASA-TM-86665] 14 p2210 N85-23706
Harrier 15 p2687 N85-26595
Effect of ground and/or ceiling planes on thrust of rotors in hover
[NASA-TM-86754] 20 p3388 N85-31014
HPRR
U HEALTH PHYSICS RESEARCH REACTOR
HR DIAGRAM
U HERTZSPRUNG-RUSSELL DIAGRAM
HTGR
U HIGH TEMPERATURE GAS COOLED REACTORS
HTPB PROPELLANTS
Study of HTPB-based SOFRAM fuels
[FOA-C-20563-D3] 11 p1614 N85-20150
Effect of variable solid phase thermal properties on propellant combustion 13 p2002 N85-22547
HU-1 HELICOPTER
U UH-1 HELICOPTER
HUBBLE CONSTANT
Ultrahigh energy gamma rays: Carriers of cosmological information
[OG-2.7-14] 22 p3872 N85-33967
HUBBLE DIAGRAM
Cosmology 07 p1056 N85-16701
On the role played by lines in radiatively driven stellar winds depending on the position of the stars in the HR diagram 08 p1236 N85-17787
HUBBLE SPACE TELESCOPE
Algorithm for astronomical, extended source, signal-to-noise radio calculations
[NASA-TP-2396] 03 p0445 N85-12833
Algorithm for astronomical, point source, signal to noise ratio calculations
[NASA-TP-2397] 03 p0445 N85-12834
Local Interstellar Medium. International Astronomical Union Colloquium No. 81
[NASA-CP-2345] 06 p0872 N85-15539

Future studies of the local interstellar medium with Space Telescope and Columbus 06 p0880 N85-15593
Study of application of space telescope science operations software for SIRTF use
[NASA-CR-177337] 09 p1287 N85-18080
Future ultraviolet experiments, including FUSE/COLUMBUS 11 p1744 N85-20906
IUE observations of faint standard stars for calibration of the space telescope 11 p1781 N85-21076
Innovative research in the design and operation of large telescopes for space: Aspects of giant telescopes in space
[NASA-CR-175826] 13 p2170 N85-23462
Telescope in lunar orbit 15 p2582 N85-25566
Hubble space telescope: Pointing error affects on nonlinear ball joints
[NASA-TM-86511] 20 p3546 N85-32058
Astron telescope stabilization system
22 p3732 N85-33133
Features of the solar array drive mechanism for the space telescope 22 p3798 N85-33532
Appendange deployment mechanism for the Hubble Space Telescope program 22 p3798 N85-33533

HUBS
Extended aeroelastic analysis for helicopter rotors with prescribed hub motion and blade appended pendulum vibration absorbers
[NASA-CR-172455] 03 p0315 N85-12036
Integrated technology rotor/flight research rotor hub concept definition
[NASA-CR-166447] 09 p1290 N85-18051
Integrated Technology Rotor/Flight Research Rotor (ITR/FRR) concept definition
[NASA-CR-166443] 10 p1423 N85-18978
Integrated Technology Rotor/Flight Research Rotor (ITR/FRR) concept definition
[NASA-CR-166445] 10 p1423 N85-18979
Integrated technology rotor/flight research rotor concept definition study
[NASA-CR-166446] 10 p1424 N85-18980
Integrated Technology Rotor/Flight Research Rotor (ITR/FRR) concept definition study
[NASA-CR-166444] 10 p1424 N85-18981
Self-locking mechanical center joint
[NASA-CASE-LAR-12864-1] 19 p3279 N85-30336
A new main rotor hub for the AS 332 Super Puma
[SNIAS-861-210-102] 20 p3393 N85-31047

HUGHES MILITARY AIRCRAFT
U MILITARY AIRCRAFT

HUGONIOT ADIABAT
U HUGONIOT EQUATION OF STATE

HUGONIOT EQUATION OF STATE
Dynamic compaction of a monosized spherical tungsten powder
[DE85-014808] 24 p4080 N85-35299

HULLS (STRUCTURES)
NT SHIP HULLS

HUMAN BEHAVIOR
Mathematical Models of the Circadian Sleep-Wake Cycle
[AD-A146712] 02 p0236 N85-11532
Patterns of behavior in lodgings exposed to traffic noise
[NASA-TM-77750] 03 p0387 N85-12479
Evaluation of the National Library of Medicine's programs in the medical behavior sciences. Coverage of the Medical Behavioral Sciences (MBS) literature in monographic databases, study 5
[PB84-230531] 03 p0439 N85-12797
Evaluation of the National Library of Medicine's programs in the medical behavior sciences. Online searchers' reactions to database and vendor capabilities in the Medical Behavioral Sciences (MBS), study 4
[PB84-230523] 03 p0439 N85-12798
Evaluation of the National Library of Medicine's programs in the medical behavior sciences. Quality of indexing: The development and testing of a methodology comparing databases covering the Medical Behavioral Sciences (MBS) literature, study 3
[PB84-230515] 03 p0439 N85-12799
Evaluation of the National Library of Medicine's programs in the medical behavior sciences. Test retrievals in five major databases covering the Medical Behavioral Sciences (MBS) literature, study 2
[PB84-230507] 03 p0440 N85-12800
Evaluation of the National Library of Medicine's programs in the medical behavior sciences. Coverage, overlaps and gaps in bibliographic databases dealing with the Medical Behavioral Sciences (MBS) literature, study 1
[PB84-230499] 03 p0440 N85-12801
Evaluation of the National Library of Medicine's program in the medical behavior sciences. An analysis of the National Library of Medicine's (NLM) handling of Medical Behavioral Sciences (MBS) literatures: Some research tests of methods for evaluating bibliographic databases, executive summary
[PB84-230481] 03 p0440 N85-12802
USSR report: Life Sciences: Biomedical and behavioral sciences
[JPRS-UBB-84-026] 04 p0543 N85-13457
Reflection of lateralization of sound stimuli in evoked potentials of human brain 04 p0544 N85-13463
The human role in space. Volume 2: Research analysis and technology report
[NASA-CR-171224] 04 p0546 N85-13474
The human role in space. Volume 3: Generalizations on human roles in space
[NASA-CR-171225] 04 p0546 N85-13475
Evaluation of fuzzy rulemaking for expert systems for failure detection 05 p0703 N85-14506
An investigation of the relationship between stressful life events and psychological, behavioral and physiological outcomes
[AD-A147754] 08 p1197 N85-17541
Compatibility effects and preference reversals
[AD-A148399] 08 p1198 N85-17544
European scientific notes. Volume 38, number 11
[AD-A148228] 08 p1230 N85-17745
Communications skills for CRM training
09 p1276 N85-18017
European Scientific Notes, volume 38, number 12
[AD-A148713] 09 p1418 N85-18946
USSR report: Life sciences. Biomedical and behavioral sciences
[JPRS-UBB-85-011] 10 p1525 N85-19616
Functional role of type of person's temperament in individual and mutual activity 10 p1525 N85-19621
Research opportunities in human behavior and performance
[NASA-CR-175473] 10 p1529 N85-19640
Aircrew-aircraft integration issues in future US Army helicopters 10 p1535 N85-19672
USSR report: Life sciences. Biomedical and behavioral sciences
[JPRS-UBB-85-010] 11 p1690 N85-20628
Psychological aspects of phenomenon of spatial synchronization of EEG potential
11 p1691 N85-20632
Effect of prolonged hunger during experimental hikes
11 p1692 N85-20637
Psychological components in the development and prevention of air sickness 11 p1695 N85-20659
Assessing the behavior and performance of teams in organizations: The case of air transport crews
[AD-A150359] 13 p2143 N85-23302
Predictors of cold weather health behaviors
[AD-A151910] 16 p2843 N85-27529
Shape with and without redundant colour as coding mechanism for simulated radar displays in a time-extended simple vigilance task
[AD-A151683] 16 p2844 N85-27533
Identifying solution paths in cognitive diagnosis
[AD-A152483] 17 p3000 N85-28549
Individual characteristics and unit performance: A review of research and methods
[AD-A153145] 17 p3001 N85-28550
A formal analysis of the evolution of cooperation
[AD-A152539] 17 p3018 N85-28662
European Science Notes, Volume 39, Number 3
[AD-A152448] 17 p3027 N85-28717
Verbal information processing paradigms: A review of theory and methods
[AD-A153229] 17 p3050 N85-28880
Psychological issues relevant to astronaut selection for long-duration space flight: A review of the literature
[AD-A154051] 19 p3330 N85-30627
Resource allocation in cerebral specialization of function: Behavioral and electrophysiological studies
[AD-A155092] 21 p3664 N85-32759
Rapid determination of cadet discipline by projective tests 22 p3821 N85-33671
Effects of low level carbon monoxide (CO) on tracking and monitoring. An attempt to replicate the findings of Putz et al. (1976) protocol 2
[AD-A155722] 22 p3825 N85-33694
USSR report: Life sciences. Biomedical and behavioral sciences
[JPRS-UBB-85-021] 23 p3951 N85-34489

HUMAN BEINGS
USSR report: Space Biology and Aerospace Medicine, volume 18, no. 4, July - August 1984
[JPRS-USB-84-006] 01 p0091 N85-10611
Functional capacities of elderly subjects exposed to simulated spaceflight factors 01 p0091 N85-10617
Models of natural intelligence in fault diagnosis tasks: Implications for training and aiding of maintenance personnel
[AD-P003927] 02 p0246 N85-11097
Report of the Meeting of Experts on Climate and Human Health
[WCP-78] 05 p0687 N85-14413
Organization of the session 05 p0687 N85-14414
Difficulties encountered in determining the potential involvement of consultants on health problems in various climatic zones 05 p0687 N85-14416
Modeling of human motion by computer considering measurement errors in initial data
07 p1012 N85-16439
Management of vibration sickness in coal mines by hyperbaric oxygenation 10 p1523 N85-19608
Comparative assessment of different treatment modalities in miners with vibration- and noise-induced disease 10 p1524 N85-19610
Aircraft noise effects: An interdisciplinary study of the effects of aircraft noise on man. Part 1: Basic report
[NASA-TM-75819] 10 p1526 N85-19629
Health assessment document for carbon tetrachloride
[PB85-124196] 10 p1528 N85-19639
The effect of jamming/deception on decision making
[AD-A149740] 12 p1828 N85-21472
Human cognition and intelligence: Towards an integrated theoretical perspective
[CSIR-SR-PERS-350] 13 p2143 N85-23300
Photoreactivation and other ultraviolet/visible light effects on DNA in human skin
[DE85-005135] 14 p2390 N85-24719
Functional impairment and structureal cervical injuries in human surrogates
[PB85-167436] 15 p2619 N85-26137
The origin of brain potentials associated with selective visual attention
[AD-A152291] 16 p2840 N85-27511
Evaluation of a field expedient technique for sweat sample collection
[AD-A151918] 16 p2841 N85-27521
Collected epidemiological studies of the late effects of internal radium in man, and mechanistic investigations of those effects, part 2
[DE85-011174] 19 p3331 N85-30626
Task description for the 1983 catalog of tasks for the materials processing in space program
20 p3498 N85-31746
Review of the psychological issues relating to the effectiveness of structured programming
[AD-A154593] 21 p3665 N85-32769
Spacelab 1 hematology experiment (INS103): Influence of space flight on erythrokinetics in man
[NASA-TM-58268] 22 p3824 N85-33683
Tritium hazard via the ingestion pathway
[DE85-012897] 24 p4133 N85-35618

HUMAN BODY
Non-invasive techniques for determining musculoskeleton body composition
[DE84-015718] 04 p0545 N85-13470
Introduction to human biometeorology
05 p0687 N85-14415
In vivo neutron activation analysis: Body composition studies in health and disease
[DE84-014092] 05 p0696 N85-14480
Comparison of thermal responses between rest and leg exercise in water
[AD-A146818] 07 p1015 N85-16449
Effects of body mass and morphology on thermal responses in water
[AD-A147558] 07 p1016 N85-16455
Technique for measuring body circumferences and skinfold thicknesses
[AD-A148166] 08 p1195 N85-17532
Gravity and biological systems: Emphasis on human physiology
[ESA-BR-21] 09 p1360 N85-18558
Scattering of electromagnetic waves by human body and its applications 09 p1363 N85-18572
Health standards for general vibration
10 p1523 N85-19607
The medical results of human exposure to radio frequency radiation
[AD-A149718] 12 p1905 N85-21982
Study of effective physiological temperature
13 p2042 N85-22780
Distribution of radium and plutonium in human bone
[DE85-005025] 13 p2142 N85-23298
Mathematical models relating to human thermoregulation: Basic assumptions, validation, and application. Parts A and B
[AD-A151556] 15 p2618 N85-26130
Human body dimensions: Body outlines and envelope curves at different normal positions and movements
[HSE-TRANS-10866] 19 p3332 N85-30640

Kidney cell electrophoresis, continuing task 20 p3498 N85-31747
A mechanical model of the human body and its application 24 p4129 N85-35598
HUMAN CENTRIFUGES
Susceptability to kinetoses and the amplitude perceived from sensory illusions 11 p1694 N85-20651
Centrifuge operations and training in the Royal Netherlands Air Force 20 p3511 N85-31825
HUMAN ENGINEERING
U HUMAN FACTORS ENGINEERING
HUMAN FACTORS ENGINEERING
NT MOTION SIMULATION
LED multifunction keyboard engineering study [AD-A145199] 01 p0010 N85-10061
USSR report: Machine tools and metalworking equipment [JPRS-UMM-84-019] 01 p0035 N85-10214
A review of selected studies of computerized speech recognition conducted at the Naval Postgraduate School [AD-A144841] 01 p0037 N85-10235
The Reports of Aeromedical Laboratory, volume 25, no. 1/2 [ISSN-0023-2858] 01 p0090 N85-10605
Assessment of the inflating characteristics of the modified anti-G suit 01 p0090 N85-10609
Human response to vibroacoustic environments of space vehicles [NASA-TM-86316] 01 p0116 N85-10789
Highlights of the Institute of Sound and Vibration Research 01 p0131 N85-10905
Aircrew-aircraft integration: A summary of US Army research programs and plans [NASA-TM-85991] 02 p0148 N85-11004
Human engineering laboratory grounding analysis: Project Helga [AD-A145728] 02 p0195 N85-11300
Decision tree rating scales for workload estimation: Theme and variations [NASA-CR-174062] 02 p0237 N85-11544
Respiratory protection for children 3 - 6 years of age [FOA-C-40197-C2] 02 p0236 N85-11550
Auditory information systems in military aircraft: Current configurations versus the state of the art [AD-A145469] 02 p0275 N85-11794
A management workstation concept [AD-A145617] 02 p0294 N85-11906
Study of annoyance due to urban automobile traffic. Annex 4: A catalog of the characteristics of noise at different measuring points [NASA-TM-77516] 03 p0387 N85-12478
Patterns of behavior in lodgings exposed to traffic noise [NASA-TM-77750] 03 p0387 N85-12479
The human operator and system effectiveness [AD-A146326] 03 p0402 N85-12563
Climate-chamber experiments to improve pilots' work conditions 04 p0543 N85-13454
Impact of space medicine on Earth-based medicine: Academician Ye. I. Chazov comments on the work in orbit of physician O. Atkov 04 p0543 N85-13458
The human role in space. Volume 2: Research analysis and technology report [NASA-CR-171224] 04 p0546 N85-13474
The human role in space. Volume 3: Generalizations on human roles in space [NASA-CR-171225] 04 p0546 N85-13475
Investigation and development of multicolored liquid crystal display systems for automotive dashboard application and large format information boards [BMFT-FB-T-84-187] 04 p0572 N85-13652
Twentieth Annual Conference on Manual Control, volume 1 [NASA-CP-2341-VOL-1] 05 p0699 N85-14487
Time series modeling of human operator dynamics in manual control tasks 05 p0699 N85-14488
Quantification of cross-coupling and motion feedthrough for multiaxis controllers used in an air combat flying task 05 p0700 N85-14491
Evaluation of fuzzy rulemaking for expert systems for failure detection 05 p0703 N85-14508
The role of knowledge structures in fault diagnosis 05 p0703 N85-14509
Twentieth Annual Conference on Manual Control, volume 2 [NASA-CP-2341-VOL-2] 05 p0707 N85-14535
Measurement of workload: Physics, psychophysics, and metaphysics 05 p0708 N85-14539
A comparative study of alternative controls and displays for by the severely physically handicapped 05 p0709 N85-14549
Performance measures for aircraft landings as a function of aircraft dynamics 05 p0712 N85-14565
Measuring pilot workload in a moving-base simulator. Part 2: Building levels of workload 05 p0712 N85-14566
Technical Workshop: Advanced Helicopter Cockpit Design [NASA-CP-2351] 06 p0750 N85-14806
Helicopter human factors programs and plans 06 p0751 N85-14808
Human factors in cockpit automation 06 p0752 N85-14819
Intelligent interfaces for tactical airborne platforms 06 p0752 N85-14820
Human factors of visual displays 06 p0752 N85-14821
Crewstation design and validation 06 p0752 N85-14822
Avionics technology - system concepts 06 p0753 N85-14824
Man-machine interface requirements - advanced technology 06 p0753 N85-14825
Attack helicopter (AH-1T) cockpit systems integration 06 p0753 N85-14826
Avionics system design for requirements for the United States Coast Guard HH-65A Dolphin 06 p0753 N85-14827
Human aspects in office automation [PB84-240738] 06 p0847 N85-15376
Human engineer's guide to auditory displays. Volume 2: Elements of signal reception and resolution affecting auditory displays [AD-A146513] 06 p0859 N85-15462
Human engineer's guide to auditory displays. Volume 1. Elements of perception and memory affecting auditory displays [AD-A146601] 06 p0860 N85-15464
Biodynamic resistant control stick [AD-D011380] 07 p0904 N85-15721
USSR report: Life sciences. Biomedical and behavioral sciences [JPRS-UBB-84-015] 07 p1010 N85-16416
Human factors and training research in military organizations and systems [AD-A146832] 07 p1020 N85-16475
Human factors characteristics of the Joint Tactical Fusion Test Bed: Field test 467 results [AD-A146856] 07 p1020 N85-16476
Mental models and cooperative problem solving with expert systems [AD-A147843] 07 p1021 N85-16479
Operational requirements versus technological capabilities 08 p1072 N85-16798
A Computer-generated topographic display system for navigation and mission planning in helicopters 08 p1073 N85-16800
A review of US Army aircrew-aircraft integration research programs 08 p1075 N85-16814
Impact tests of adjusters for the HBU-12 lap belt [AD-A148021] 08 p1080 N85-16843
Automatic speech recognition in severe environments [AD-A148461] 08 p1153 N85-17260
Waste collection subsystem study [NASA-CR-171836] 08 p1199 N85-17552
Space Shuttle Orbiter waste collection system conceptual study [NASA-CR-171844] 08 p1199 N85-17553
A computer aided Multi-Man-Machine Work Area Design and Evaluation System (MAWADES) [AD-A147950] 08 p1199 N85-17554
Development of an electro-pneumatic anti-G valve for high performance fighter aircraft [AD-A148468] 08 p1201 N85-17561
Simulating speed and height cues in the C-130 weapon system trainer [AD-P004313] 09 p1268 N85-17967
The fiber-optic helmet-mounted display [AD-P004330] 09 p1270 N85-17984
Dual arm master controller concept [DE85-001901] 09 p1327 N85-18344
USSR report: Life sciences. Biomedical and behavioral sciences [JPRS-UBB-85-002] 09 p1360 N85-18559
Role of engineering psychology 09 p1361 N85-18561
Further development in ride quality assessment [AD-P004280] 09 p1406 N85-18856
European Scientific Notes, volume 38, number 12 [AD-A148713] 09 p1418 N85-18946
Pictorial format display evaluation [AD-A149252] 10 p1425 N85-18986
Production turret lathe retrofitted with robot 10 p1461 N85-19214
Be healthy, pilot 10 p1526 N85-19626
Guide to human factors information sources [AD-A149102] 10 p1531 N85-19649
Human Factors Considerations in High Performance Aircraft [AGARD-CP-371] 10 p1532 N85-19653
Aircrew and avionics: Friends or Foes? 10 p1532 N85-19654
Military pilot ergonomics 10 p1532 N85-19655
Implications of guidance and control technology on human factors considerations 10 p1532 N85-19656
Observations of physiological and psychological effects of terrain following flight based on in-flight test experience 10 p1532 N85-19657
Impact of future aircombat characteristics on pilot performance and cockpit design 10 p1533 N85-19661
Electronic displays: Their strengths and weaknesses for advanced high performance aircraft 10 p1533 N85-19664
Changing system and display concepts and their impact on aircrew performance 10 p1533 N85-19665
Some effects of display format variables on the perception of aircraft spatial orientation 10 p1534 N85-19666
Pilot workload, performance and aircraft control automation 10 p1534 N85-19670
The F-18: A new era for human factors 10 p1534 N85-19671
Aircrew-aircraft integration issues in future US Army helicopters 10 p1535 N85-19672
European Scientific Notes. Volume 39, number 2 [AD-A148994] 10 p1573 N85-19919
Proceedings of the 14th Army Science Conference. Volume 1: Principal Authors A through H [AD-A149200] 10 p1573 N85-19920
Biomechanics finds practical applications in aerospace research 11 p1621 N85-20205
Functional system theory in practice 11 p1690 N85-20629
Aviation medicine's role in modern airforce discussed 11 p1696 N85-20662
Symposium on Military Aviation Medicine summarized 11 p1696 N85-20663
Man/machine interface for a nuclear cask remote handling control station: System design requirements [DE85-000256] 11 p1697 N85-20667
Computer-generated display system guidelines. Volume 1: Display design [DE85-000679] 11 p1701 N85-20699
Proceedings of the 6th Advanced Aircrew Display Symposium [AD-A150044] 12 p1778 N85-21160
Human assembly time versus levels of visual and tactile sensory input: Experimental results for five devices [AD-A149962] 12 p1909 N85-21980
Proceedings of the 6th Human Factors Workshop on Aviation [AD-A150043] 12 p1909 N85-21982
NASA: Model development for human factors interfacing [NASA-CR-175584] 12 p1910 N85-21985
Shoulder and hip joint for hard space suits and the like [NASA-CASE-ARC-11543-1] 12 p1910 N85-21986
Torso sizing ring construction for hard space suit [NASA-CASE-ARC-11616-1] 12 p1910 N85-21987
Very-high level concurrent programming [AD-A150009] 12 p1916 N85-22026
TASS update on unmanned flight of Salyut-7 13 p1977 N85-22404
Construction of a menu-based system [NASA-CR-172560] 13 p2146 N85-23321
Principles of software engineering environment design [AD-A150352] 13 p2147 N85-23324
Complex program of ergonomic studies Pilot described 14 p2386 N85-24698
Users guide: The LaRC human-operator-simulator-based pilot model [NASA-TM-86367] 14 p2390 N85-24721
Programmer/analyst workstation evaluation report [NASA-CR-175289] 14 p2394 N85-24749
Streamlined Test Reporting And Planning (STRAP): Computerized human factors questionnaire [AD-A150811] 14 p2395 N85-24751
Current approaches for the biophysical and physiological evaluation of combat clothing for environmental extremes [AD-A151012] 14 p2395 N85-24752
Investigation of technology needs for avoiding helicopter pilot error related accidents [NASA-CR-3895] 15 p2465 N85-25220
Preliminary design of a limb restraint evaluator [AD-A151749] 15 p2466 N85-25226
Rotorcraft digital advanced avionics system (RODAAS) functional description [NASA-CR-166611] 15 p2468 N85-25237
US Army human Engineering Laboratory Communications Survey: A Pilot Study (HELCOMS-PS) [AD-A151434] 15 p2521 N85-25544
An introductory study of automatic speech recognition systems [BAE-BT-12266] 15 p2539 N85-25677

A portable battery for objective, non-obstrusive measures of human performances
[NASA-CR-171868] 15 p2586 N85-25942
Computerized biophysical data acquisition system for motion sickness studies
[AD-A151691] 15 p2618 N85-26131
A practical system for collecting reliable data on the space-time behavior of people
[AD-A151174] 15 p2619 N85-26140
Proceedings of the BAe human factors seminar
[BAE-BT-11873] 15 p2620 N85-26145
Human factors department 1981 publications
[BAE-BT-12685] 15 p2620 N85-26147
The human engineering of laboratory data acquisition and control systems
[AD-A151576] 15 p2620 N85-26148
Activities report for FOA 53: Laboratory for man and information systems
[FOA-C-53019-H] 15 p2621 N85-26150
Development of a user support package for CPESIM 2 (a computer simulation for CPE (Computer Performance Evaluation) use
[AD-A151899] 15 p2624 N85-26170
A comparison of pictorial and speech warning messages in the modern cockpit
[AD-A151917] 16 p2707 N85-26706
The introduction of new cockpit technology: A human factors study
[NASA-TM-86659] 16 p2843 N85-27528
Shape with and without redundant colour as coding mechanism for simulated radar displays in a time-extended simple vigilance task
[AD-A151683] 16 p2844 N85-27533
Design of computer-related workstations in relation to job functions and productivity
[AD-A151938] 16 p2844 N85-27534
Corrective-predictive systems
[BLL-M-36063-(5828.4)] 16 p2851 N85-27573
Information presentation in power plant control rooms
[VTT-320] 16 p2864 N85-27668
Optimizing computational efficiency and user convenience in plasma simulation codes
[DE85-007661] 16 p2866 N85-27682
Utilization of an automated riveting system in aircraft construction
[MBB-UT-11/84-O] 16 p2875 N85-27736
Space Station crew safety alternatives study. Volume 5: Space Station safety plan
[NASA-CR-3858] 17 p2908 N85-27930
Robotic safety systems and methods: Savannah River site
[DE85-008261] 17 p2974 N85-28375
Hand controllers for teleoperation. A state-of-the-art technology survey and evaluation
[NASA-CR-175890] 17 p3002 N85-28559
Mechanizing of handling operations in drop forging with hammers and presses (conducted ergonomical examinations)
[BMFT-FB-HA-84-051] 17 p3002 N85-28561
Space Station crew safety alternatives study. Volume 4: Appendices
[NASA-CR-3857] 18 p3065 N85-28958
The POK project; studies of information handling problems with a new kind of communication device — precoded signals
[FOA-A-53001-H2] 18 p3091 N85-29131
CELSS transportation analysis
18 p3156 N85-29538
Proceedings of the Seminar on Space Station Human Productivity
[NASA-TM-86673] 18 p3156 N85-29539
Space station crew safety: Human factors interaction model 18 p3156 N85-29540
Internal contamination in the space station
18 p3157 N85-29549
The human role in space (THURIS) .
18 p3158 N85-29557
Overview: Human factors issues in space station architecture 18 p3158 N85-29558
Human factors issues in space station architecture
18 p3158 N85-29560
Man-machine tradeoff study 18 p3158 N85-29561
Some ideas and questions regarding space station design for human use 18 p3158 N85-29562
Human productivity experience and undersea habitat design 18 p3159 N85-29563
Considerations for space station interior architecture
18 p3159 N85-29564
Human factors in space station architecture: The ECLSS module concept 18 p3159 N85-29565
Habitability sleep accommodations
18 p3159 N85-29566
Customer and mission influence on space station architecture 18 p3159 N85-29567
Simulation for human factors research. A central question: Fidelity 18 p3159 N85-29568
Mockups and human productivity studies
18 p3159 N85-29570
Rockwell experience applications to Ames space station mockup habitability/productivity studies
18 p3159 N85-29572
Human factors in cockpit automation: A field study of flight crew transition
[NASA-CR-177333] 19 p3215 N85-29937
Space station crew safety alternatives study. Volume 3: Safety impact of human factors
[NASA-CR-3856] 19 p3223 N85-29984
Space station crew safety alternatives study, volume 1
[NASA-CR-3854] 19 p3223 N85-29985
Human Engineering Guide to Equipment Design (HEGED)
[AD-A154087] 19 p3331 N85-30631
Physical dimensions of humans; values; the effect of clothing, working clothes and protective equipment on the design of work places
[HSE-TRANS-10868] 19 p3331 N85-30638
The design of working systems on ergonomic principles. The importance of clothes and protective equipment in the design of the workplace
[HSE-TRANS-10865] 19 p3332 N85-30639
Human body dimensions: Body outlines and envelope curves at different normal positions and movements
[HSE-TRANS-10866] 19 p3332 N85-30640
Space Station man-machine automation trade-off analysis
[NASA-CR-176046] 20 p3408 N85-31147
Study to determine potential flight applications and human factors design guidelines for voice recognition and synthesis systems
[NASA-CR-172590] 20 p3440 N85-31349
Ergonomic problems regarding the interactive touch input via screens in onboard and ground-based flight control
[NASA-TM-77814] 20 p3512 N85-31832
The blind and the paralyzed. The notion of the tool revealed and integrated in a different organization environment
[SNIAS-851-422-104] 20 p3513 N85-31835
Human factors engineering contracts in Sweden: An overview
[FOA-C-56043-H2] 20 p3513 N85-31836
Human factors engineering data sources; an overview
[FOA-C-56044-H2] 20 p3513 N85-31837
Physical dimensions of humans, values, envelope curves in different postures
[HSE-TRANS-10869] 20 p3513 N85-31838
Noise reduction in the automotive test cell of the Motor Institute of Naples
[REPT-85-RR-361] 20 p3524 N85-31917
Sound-insulating enclosures — machine noise
[BMFT-FB-HA-85-005] 20 p3525 N85-31925
Space Station crew safety alternatives study. Volume 2: Threat development
[NASA-CR-3855] 21 p3558 N85-32133
USSR report: Life sciences. Biomedical and behavioral sciences
[JPRS-UBB-85-020] 21 p3663 N85-32752
Living aloft: Human requirements for extended spaceflight
[NASA-SP-483] 21 p3666 N85-32772
Design guidelines for user-system interface software
[AD-A154907] 21 p3671 N85-32807
USSR report: Life sciences. Biomedical and behavioral sciences
[JPRS-UBB-85-018] 22 p3819 N85-33660
Speech analysis system for assessing pilots' working fitness 22 p3819 N85-33661
Using percent-done program indicators to enhance user interfaces 23 p3960 N85-34546
Calculation of trajectories of detached wind turbine blades and prediction of site risk levels associated with failures of HAWT's 24 p4110 N85-35475
The human engineering eye movement measurement research facility
[AD-A156099] 24 p4132 N85-35613
Recommendations for content revision and alternate delivery modes for the Human Engineering Guide to Equipment Design (HEGED)
[AD-A155781] 24 p4134 N85-35624
Attacking software crisis: A macro approach
[AD-A155846] 24 p4138 N85-35645

HUMAN PATHOLOGY
Material thermolysis product toxicity: Definition of a hazard evaluation methodology
[CERMA-84-08] 11 p1692 N85-20641
Selection procedures for F-16 pilots in the Belgian Air Force 20 p3510 N85-31822
Analogies of control mechanisms in flight guidance and medicine 24 p4129 N85-35597

HUMAN PERFORMANCE
NT ASTRONAUT PERFORMANCE
NT OPERATOR PERFORMANCE
NT PILOT PERFORMANCE
The perceptual quality of smoke screens: An analysis of the Oldebroek 2 trials, May 1981
[IZF-1984-20] 01 p0095 N85-10841
The prediction of observer responses from photometric data on smoke screens; an analysis of the Oldebroek 2 trials, May 1981
[IZF-1984-21] 01 p0096 N85-10842
Self-paced instruction. Factors critical to implementation in Air Force technical training: A preliminary inquiry
[AD-A145098] 01 p0097 N85-10847
Ada (trademark) training curriculum. Software engineering for managers m101 teacher's exercise guide
[AD-A145094] 01 p0104 N85-[illegible]
Airborne performance measurement system design: C-5 aircraft
[AD-A145436] 02 p0236 N85-11539
An investigation of the use of steady-state evoked potentials for human performance and workload assessment and control
[AD-A145727] 02 p0237 N85-11541
The effects of feedback and predictability of human judgment
[AD-A145744] 02 p0237 N85-11542
Using gross outline features in long range target identification
[FOA-C-53018-H2] 02 p0237 N85-11543
Overview of training and aiding
[AD-P003917] 02 p0245 N85-11597
The role of physical and physiological capacities and their modification on the tolerance to various stress experienced by Air Force personnel
[AD-A145779] 03 p0400 N85-12560
Experiments with hydrox at 1.3 MPa (13 atm) – for divers
[FOA-C-58014-H1] 04 p0545 N85-13471
Human reliability data bank: Feasibility study
[DE84-015215] 04 p0546 N85-13476
Physical performance capacity after a 7 day head-down tilt (-6 deg) 05 p0692 N85-14451
Medication interference with space research: An example from a mass-discrimination experiment on Spacelab 1 05 p0695 N85-14472
Estimating number, time and length; a baseline study
05 p0695 N85-14473
The effect of propranolol on the training response to endurance exercise in normal human adults
05 p0696 N85-14479
Catecholamine excretion and subjective ratings of tension during autogenic training and mental stress
[REPT-172] 05 p0697 N85-[illegible]
Time series modeling of human operator dynamics in manual control tasks 05 p0699 N85-[illegible]
Multiloop manual control of dynamic systems
05 p0702 N85-[illegible]
The role of knowledge structures in fault diagnosis
05 p0703 N85-[illegible]
Fitts' law? A test of the relationship between information load and movement precision 05 p0705 N85-[illegible]
A production system model of capturing reactive moving targets 05 p0706 N85-[illegible]
Models for the effects of G-seat cuing on roll-axis tracking performance 05 p0707 N85-[illegible]
Subjective workload assessment and voluntary control of effort in a tracking task 05 p0708 N85-[illegible]
Classification systems for individual differences in multiple-task performance and subjective estimates of workload 05 p0708 N85-[illegible]
The representation of action plans in long term memory 05 p0709 N85-[illegible]
On choosing between two probabilistic choice sub-models in a dynamic multitask environment
05 p0711 N85-[illegible]
No fatigue effect on blink rate
05 p0712 N85-[illegible]
Situational interactive micro/graphic simulator system for improving maintenance performance
[AD-A146677] 06 p0757 N85-[illegible]
Performance evaluation of A-10 aircraft maintenance units and aircraft using constrained facet analysis
[AD-A146955] 07 p0883 N85-[illegible]
Nondestructive inspection: Improved capabilities of technicians
[AD-A147388] 07 p0975 N85-[illegible]
Effects of restricted water intake on performance in a cold environment
[AD-A146904] 07 p1015 N85-[illegible]
On the structure of information in software
[AD-A147580] 07 p1026 N85-[illegible]
Efforts to improve aviation medical examiner performance through continuing medical education and annual performance reports
[AD-A148078] 08 p1195 N85-[illegible]

Training high performance skills: Fallacies and guidelines
[AD-A148574] 08 p1198 N85-17545

Design of an evaluation system to measure performance degradation due to continuous operations
[AD-A148186] 08 p1200 N85-17556

Decision making in stressful conditions: A model based on the coping perspective
[FOA-C-55064-H3] 08 p1229 N85-17738

Work capacity of heat and electric power plant operations working 12 hour day and night shifts
09 p1362 N85-18567

Success in learning occupation of chemical production technician as function of certain personality traits and development of psychophysiological functions
09 p1362 N85-18568

Hydrogen-oxygen (hydrox) breathing at 1.3MPa
[FOA-C-58015-H1] 09 p1364 N85-18577

Neurocognitive pattern analysis of an auditory and visual numeric motor control task. Part 1: Development of methods
[AD-A145809] 09 p1364 N85-18578

Bibliography of unclassified reports, FY 1984
[AD-A148836] 09 p1401 N85-18819

Research opportunities in human behavior and performance
[NASA-CR-175473] 10 p1529 N85-19640

The multiple resources model of human performance: Implications for display design 10 p1534 N85-19669

Laboratory tests of motion sickness susceptibility
11 p1694 N85-20646

Space motion sickness monitoring experiment: Spacelab 1 11 p1695 N85-20654

Psychological components in the development and prevention of air sickness 11 p1695 N85-20659

Team dimensions: Their identity, their measurement and their relationships
[AD-A149662] 12 p1906 N85-21978

Human assembly time versus levels of visual and tactile sensory input: Experimental results for five devices
[AD-A149982] 12 p1909 N85-21980

NASA: Model development for human factors interfacing
[NASA-CR-175584] 12 p1910 N85-21985

The man-machine interface
[AD-A149971] 12 p1910 N85-21989

Task influences in the analytic-intuitive approach to decision making
[AD-A149870] 12 p1950 N85-22250

Assessing the behavior and performance of teams in organizations: The case of air transport crews
[AD-A150359] 13 p2143 N85-23302

Personal decision making: The influence of perceived locus of control and degree of rationality on information seeking strategies 13 p2167 N85-23446

Multiple resources and display formatting: The implications of task integration in a simulated air traffic control task
[AD-A150713] 14 p2292 N85-24205

Plans for adaptation research during Antarctic expedition 14 p2333 N85-24426

Instrument for determining spatial coordination of hand movements 14 p2387 N85-24702

The effect of set size on color matching
[AD-A150889] 14 p2388 N85-24713

The effect of set size on color recognition
[AD-A150868] 14 p2391 N85-24726

The effect of strategy in second order manual control on resource competition with a sternberg memory search task
[AD-A150886] 14 p2391 N85-24727

Analysis of team performance in a programmed environment
[NASA-CR-175634] 14 p2392 N85-24728

Perceived heterogeneity and its effect on various types of tasks
[AD-A151003] 14 p2392 N85-24729

Psychophysiological studies. 1: Performance and physiological response in learning, short-term memory and discrimination tasks
[AD-A151018] 14 p2392 N85-24731

US Army human Engineering Laboratory Communications Survey: A Pilot Study (HELCOMS-PS)
[AD-A151434] 15 p2521 N85-25544

A portable battery for objective, non-obstrusive measures of human performances
[NASA-CR-171868] 15 p2586 N85-25942

Measurement and modification of sensory system EEG (electroencephalographic) characteristics during visual-motor performance
[AD-A151601] 15 p2618 N85-26133

Visual search strategy predictions: The use of aspect ratio as a cue
[BAE-BT-12665] 15 p2619 N85-26138

A practical system for collecting reliable data on the space-time behavior of people
[AD-A151174] 15 p2619 N85-26140

Skilled memory
[AD-A152063] 15 p2620 N85-26143

Sleep deprivation and performance: Older age performance and limited sleep period use
[AD-A153102] 17 p2999 N85-28540

Performance Evaluation Tests for Environmental Research (PETER) evaluation of 112 measures
[AD-A152317] 17 p2999 N85-28543

The levels of processing conceptualization of human memory: Some empirical and theoretical issues
[AD-A152321] 17 p3000 N85-28544

The relationship between performance and satisfaction: A utility analysis
[AD-A152342] 17 p3000 N85-28546

Individual characteristics and unit performance: A review of research and methods
[AD-A153145] 17 p3001 N85-28550

Biofeedback and performance: An update
[AD-A153228] 17 p3001 N85-28553

Relationship between the Army two mile run test and maximal oxygen uptake
[AD-A153914] 18 p3154 N85-29526

A task battery for applied human performance assessment research
[AD-A153677] 18 p3154 N85-29530

Proceedings of the Seminar on Space Station Human Productivity
[NASA-TM-86673] 18 p3156 N85-29539

Space station crew safety: Human factors interaction model 18 p3156 N85-29540

Human factors issues in space station architecture
18 p3158 N85-29560

Human factors in cockpit automation: A field study of flight crew transition
[NASA-CR-177333] 19 p3215 N85-29937

Performance envelopes and optimal appropriateness measurement
[AD-A154129] 19 p3330 N85-30629

The design of working systems on ergonomic principles. The importance of clothes and protective equipment in the design of the workplace
[HSE-TRANS-10665] 19 p3332 N85-30639

Individual observer data for the 1955 Stiles-Burch 2 deg pilot investigation — color vision
[NPL-QU-68] 20 p3512 N85-31830

Resource allocation in cerebral specialization of function: Behavioral and electrophysiological studies
[AD-A155092] 21 p3664 N85-32759

Conceptualizing in assembly tasks
[AD-A155564] 21 p3665 N85-32770

Performance of rolling ball and isometric joystick on a 2-D target alignment task
[RSRE-MEMO-3695] 22 p3826 N85-33699

The relationship between personality and performance
24 p4129 N85-35600

The effect of an unphysiological oxygen supply on the organism 24 p4130 N85-35605

An exploratory study of the effect of screen size and resolution on the legibility of graphics in automated job performance aids
[AD-A155989] 24 p4136 N85-35632

HUMAN REACTIONS

A limbus-sensing eye movement recorder
[AD-A144772] 01 p0049 N85-10323

Psychological states (mood, affect or emotion) experienced by JASDF pilots through flying duties. 3: Flying conditions causing pilots psychological disturbances 01 p0090 N85-10606

Post fire interview: Development and field validation of the behavioral sequence interview technique
[NBS-GCR-84-477] 04 p0454 N85-12881

Human reactions to ELF (Extremely Low Frequency) electric and magnetic fields. An annotated bibliography of current literature, fourth edition
[PB84-230358] 04 p0545 N85-13472

Endocrine responses to nonhypotensive gravitational stress: Vasopressin and aldosterone
05 p0693 N85-14459

Fitts' law? A test of the relationship between information load and movement precision 05 p0705 N85-14523

A production system model of capturing reactive moving targets 05 p0705 N85-14524

Inverse modelling to obtain head movement controller signal 05 p0705 N85-14525

A control model: Interpretation of Fitts' law
05 p0706 N85-14526

Human reactions to transient electric currents, volume 12
[PB84-231483] 06 p0846 N85-15374

Construction and application of a questionnaire for the social scientific investigation of environmental noise effects
[NASA-TM-75492] 10 p1512 N85-19544

Functional role of type of person's temperament in individual and mutual activity 10 p1525 N85-19621

Restructuring of the process of visual recognition as perception conditions alter 10 p1526 N85-19624

Effects of tasks on responses of human skin mechanoreceptors 11 p1691 N85-20635

Role of mental work in human tolerance in total-body vibration 12 p1901 N85-21940

Parameters of carbohydrate metabolism and blood serum enzyme activity after short-term spaceflights
12 p1903 N85-21951

Some individual differences in human response to infrasound
[UTIAS-282] 12 p1905 N85-21960

Predictors of transfer adjustment: A longitudinal study
[AD-A152462] 17 p3000 N85-28548

Aviation noise effects
[AD-A154319] 19 p3352 N85-30776

Zinc: Biological effects. Facts and fiction
[USIP-84-12] 20 p3507 N85-31798

The 1984 environmental monitoring report, Sandia National Laboratories, Albuquerque, New Mexico
[DE85-011175] 22 p3811 N85-33607

HUMAN RELATIONS

An investigation of the relationship between stressful life events and psychological, behavioral and physiological outcomes
[AD-A147754] 08 p1197 N85-17541

HUMAN RESOURCES

Strategic management for organizational effectiveness. The effect of human resource planning on retention and related issues, volume 1
[AD-A149398] 10 p1566 N85-19874

Strategic management for organizational effectiveness. The effect of human resource planning on retention and related issues, volume 2
[AD-A149399] 10 p1566 N85-19875

Strategic management for organizational effectiveness. The effect of human resource planning on retention and related issues, volume 3
[AD-A149400] 10 p1566 N85-19876

Strategic management for organizational effectiveness. The effect of human resource planning on retention and related issues: Methodological appendix
[AD-A149401] 10 p1566 N85-19877

Air Force Human Resources Laboratory research and development summary
[AD-A154310] 19 p3331 N85-30632

The Human Resource Management Information Network (HRMIN): A cost comparison in accordance with Office of Management and Budget (OMB) Circular no. A-76, 5 April 1979
[AD-A154583] 21 p3713 N85-33039

HUMAN TOLERANCES

The Reports of Aeromedical Laboratory, volume 25, no. 1/2
[ISSN-0023-2858] 01 p0090 N85-10605

The effects of isotonic training on +Gz tolerance
01 p0090 N85-10607

Assessment of the inflating characteristics of the modified anti-G suit 01 p0090 N85-10609

Effect of fluid and salt supplements to food allowance on endurance of head-to-pelvis accelerations following 7-day dry immersion and under ordinary motor activity conditions 01 p0092 N85-10618

Hemodynamics and neurodynamics of the human brain during exposure to moderate hypoxic hypoxia
01 p0094 N85-10630

Impact of space medicine on Earth-based medicine: Academician Ye. I. Chazov comments on the work in orbit of physician O. Atkov 04 p0543 N85-13458

Endocrine responses to hypotensive gravitational stress: Catecholamines, pancreatic polypeptide, and vasopressin 05 p0693 N85-14460

Glucose tolerance in trained and untrained subjects during head-down tilt (6 deg) 05 p0693 N85-14461

Vityaz specialists study human adaptability to ocean depths 07 p0980 N85-16225

Aircraft noise effects: An inter-disciplinary study of the effect of aircraft noise on man. Part 3: Supplementary analyses of the social-scientific portion of the study on aircraft noise conducted by the DFG
[NASA-TM-75802] 10 p1527 N85-19631

Tolerance, fatigue, physiological and performance effects of sustained and oscillating lateral accelerations
10 p1533 N85-19659

Air quality criteria for ozone and other photochemical oxidants. External review draft, volume 5
[PB85-126076-VOL-5] 11 p1679 N85-20583

Some individual differences in human response to infrasound
[UTIAS-282] 12 p1905 N85-21960

Research on the effect of noise at different times of day: Models, methods and findings
[NASA-CR-3886] 13 p2154 N85-23375

Nutritional criteria for military rations and effects of prolonged feeding on acceptability
14 p2394 N85-24742
Physiological differences between men and women in exercise-heat tolerance and heat acclimation
[AD-A152048] 15 p2618 N85-26135
Positive Gz accelerations tolerance of individuals 41 to 56 years of age 19 p3323 N85-30588
Effect of 120-day antiorthostatic bedrest on gas exchange and pulmonary circulation in man
19 p3323 N85-30589
Pressure chamber simulation of 450-meter dive
20 p3505 N85-31786
Physical training and G tolerance
20 p3511 N85-31824
Centrifuge operations and training in the Royal Netherlands Air Force 20 p3511 N85-31825
Cosmonauts' cardiovascular system function during long-term orbital flights aboard Salyut-6 station
22 p3733 N85-33141
Environmental surveillance at Los Alamos during 1984
[DE85-011886] 22 p3811 N85-33605
Determination of individual tolerance in hyperbaric oxygen 23 p3954 N85-34507

HUMAN WASTES
NT FECES
NT SWEAT
NT URINE
Design concept definition study for an improved shuttle waste collection subsystem
[NASA-CR-171834] 08 p1198 N85-17546
Improved orbiter waste collection system study
[NASA-CR-171830] 08 p1199 N85-17548
Improved orbiter waste collection system study, appendix D
[NASA-CR-171833] 08 p1199 N85-17549
Gas analysis techniques for human physiological measurements in space --- Spacelab
[A/6537] 20 p3507 N85-31803

HUMIDITY
RADC/NBS (Rome Air Development Center/National Bureau of Standards) Workshop. Moisture Measurement and Control for Semiconductor Devices, 3
[PB84-219559] 01 p0051 N85-10337
Spectroradiometric calibration of the Thematic Mapper and Multispectral Scanner system
[E85-10026] 02 p0218 N85-11439
Low-frequency sound absorption measurements in air
[NASA-RP-1128] 02 p0275 N85-11789
Effect of humidity on fretting wear of several pure metals
[NASA-TP-2403] 04 p0472 N85-13006
Climate at CRREL (Cold Regions Research and Engineering Laboratory) Hanover, New Hampshire
[AD-A148400] 08 p1180 N85-17495
Survey of remote data monitoring systems
[DE85-001385] 09 p1323 N85-18313
Effect of water vapor and water droplets on the RAM-1 (Real-Time Aerosol Monitor): Preliminary results
[PB85-109429] 11 p1637 N85-20313
Humidity effects on adhesion of nickel-zinc ferrite in elastic contact with magnetic tape and itself
[NASA-TP-2449] 12 p1811 N85-21359
Study of effective physiological temperature
13 p2042 N85-22760
Two-dimensional numerical model of sensible and latent heat transport in an irrigated field under advective conditions 13 p2131 N85-23261
Portable Automated Mesonet (PAM) data from the 1980 experiment in Anderson Creek Valley
[DE85-004361] 13 p2139 N85-23282
Experimental study of the effect of moist environments on epoxy resin chocks
[AD-A152062] 16 p2566 N85-25849
Proper quality of anticorrosion work no matter how bad the atmospheric conditions
[BLL-BISI-TRANS-22080-(9022.06)]
17 p2975 N85-28383
Humidity/cloud-radiation feedback on possible climate perturbation due to fossil fuel utilization
[DE85-008886] 18 p3133 N85-29402
Urban climate and air hygiene before, during, and after the lifework of Hellmut Berg. Overview of a branch of applied meteorology 18 p3147 N85-29487
Variability of air humidity profiles over ocean determined by lidar sounding 19 p3296 N85-30436
Ice active bacteria as condensation nuclei
21 p3639 N85-32603
Ice crystal nucleation on hygroscopic aerosols
21 p3639 N85-32605
Variation of the submicron aerosol structure
21 p3647 N85-32661
Condensation properties of atmospheric aerosol
21 p3649 N85-32672
Measurements of the critical supersaturation of 0.029 to 0.035 micron radius particles at Washington, District of Columbia 21 p3649 N85-32676
Protective systems and maintenance policies for marine environments 22 p3750 N85-33245
Air-sea interaction with SSM/I and altimeter
[NASA-CR-176105] 22 p3818 N85-33650
Millimeter-wave propagation in moist air: Model versus path data
[AD-A156040] 24 p4087 N85-35331

HUMIDITY MEASUREMENT
Climate-chamber experiments to improve pilots' work conditions 04 p0543 N85-13454
Technology development for thin-film-trace humidity sensors
[BMFT-FB-T-84-288] 17 p2969 N85-28338
Effects of relative humidity gradients on the evaluation of submicron aerosol flux measurements in the atmospheric surface layer
[DE85-010510] 19 p3316 N85-30555
Tropical Ocean and Global Atmosphere (TOGA) heat exchange project: A summary report
[NASA-CR-176036] 20 p3496 N85-31738

HUNGARY
Microcomputers in Hungary 01 p0115 N85-10786

HUNTING P-84 AIRCRAFT
U JET PROVOST AIRCRAFT

HURRICANES
Nowcasting: Advances with McIDAS 3 --- Man-computer Interactive Data System System (McIDAS)
01 p0082 N85-10553
Setting hurricane conditions of readiness with high confidence
[AD-A144785] 01 p0085 N85-10570
Mesoscale and convective-scale characteristics of mature hurricanes 03 p0394 N85-12516
Fastest-mile wind speeds in Hurricane Alicia
[PB84-220771] 03 p0397 N85-12532
Hurricane Alicia, Galveston and Houston, Texas, 17-18 August 1983
[PB84-237056] 04 p0541 N85-13441
Annual data and verification tabulation for Eastern North Pacific tropical storms and hurricanes, 1983
[PB85-109635] 10 p1520 N85-19580
Hurricane experience levels of coastal county populations: Texas to Maine
[PB85-111383] 10 p1520 N85-19581
Hurricane plotting program
[PB85-121432] 10 p1521 N85-19592
Hurricane storm surge research
[GPO-40-048] 12 p1893 N85-21880
Hurricane alicia storm surge and wave data
[AD-A149668] 12 p1895 N85-21896
Analysis of the inflow layer and air-sea interactions in Hurricane Frederic (1979)
[NASA-CR-175616] 13 p2137 N85-23271
Hurricane structure and dynamics from stereoscopic and infrared satellite observations and radar data
15 p2594 N85-25988
Analysis of the inflow and air-sea interactions in hurricane Frederic 15 p2595 N85-25990
Forecast of Atlantic seasonal hurricane activity for 1985 16 p2833 N85-27470
Hurricane Research Division, fiscal year 1984 programs, fiscal year 1985 projections 16 p2836 N85-27491
Airborne research meteorological data collected by the National Hurricane Research Laboratory (Hurricane Research Division/AOML) during the 1982-1983 hurricane seasons: Inventory and availability
[PB85-163881] 17 p2997 N85-28528
Forecast of Atlantic seasonal hurricane activity for 1985 20 p3495 N85-31732
Parameter estimation in communication system tracking satellite observations
[AD-A155137] 21 p3636 N85-32582
Kinematic analysis of Hurricane Frederick (1979) using satellite, aircraft and rawinsonde data
[NASA-CR-176167] 24 p4119 N85-35533

HYBRID CIRCUITS
Planning of hybrid integrated circuits for microwave band oscillators 04 p0490 N85-13124
Qualification of a thick film hybrid
[BMFT-FB-W-84-024] 04 p0497 N85-13170
New designs from electronics R and D center
15 p2538 N85-25666
Hybrid two-dimensional Monte-Carlo electron transport in self-consistent electromagnetic fields
[DE85-010757] 19 p3348 N85-30756
Modeling of electronic circuits with high degree of component integration 22 p3766 N85-33343

HYBRID COMPUTERS
Experiments on the influence of active walls on the initial amplitudes and growths of instability waves
[AD-A154630] 21 p3583 N85-32275

HYBRID NAVIGATION SYSTEMS
Terrain following without use of forward looking sensors 16 p2598 N85-26659

HYBRID PROPULSION
Oxygen-hydrogen thrusters for Space Station auxiliary propulsion systems
[NASA-CR-175691] 15 p2484 N85-25083
Hybrid propulsion technologies for urban bus transit
[PB85-157469] 16 p2880 N85-27773

HYBRID STRUCTURES
Joint services electronics program
[AD-A145065] 01 p0042 N85-10276
Hybrid vehicle program
[DE85-000326] 09 p1410 N85-18998
INEL electric vehicle laboratory qualification: Transition test results and comparisons with JPL ETV1-2 data
[DE85-008006] 16 p2880 N85-27772
Elastic equilibrium of composite shells with finite shear rigidity 17 p2942 N85-28160

HYBRIDS (BIOLOGY)
U GENETIC ENGINEERING

HYDRATES
Development of media for dynamic latent heat storage for the low-temperature range. Part 1: Thermal analyses of selected salt hydrate systems
[NASA-TM-77778] 10 p1507 N85-19610
Chemical weathering of soils from the dry valleys of Antarctica: A terrestrial analog of Martian weathering processes 13 p2197 N85-23623
Volatiles in the outer solar system. 1: Thermodynamics of clathrate hydrates. 2: Ethane ocean on Titan. 3: Evolution of primordial Titan atmosphere
19 p3382 N85-30884
Gas hydrates
[DE85-001986] 20 p3477 N85-31607
Theoretical studies of structure and stability of hydrates of atmospheric sulfur species 21 p3650 N85-32884
Defect formation in amorphous hydrated silicon subjected to laser radiation 21 p3682 N85-32873

HYDRATION
Effect of fluid and salt supplements to food allowance on endurance of head-to-pelvis accelerations following 7-day dry immersion and under ordinary motor activity conditions 01 p0092 N85-10818
Neutron diffraction studies of the hydrogen bonding and water molecules in zeolites
[DE84-016431] 06 p0766 N85-14000
Mechanical properties of adhesively bonded aluminum structures protected with hydration inhibitors
[AD-A148123] 08 p1133 N85-17130
Mechanical properties of adhesively bonded aluminum structures protected with hydration inhibitors
[AD-A153755] 18 p3079 N85-20047
Hydrothermal alteration in the 3.5 b.y. old Onverwacht Group of South Africa 21 p3718 N85-30071

HYDRAULIC ACTUATORS
U ACTUATORS
U HYDRAULIC EQUIPMENT

HYDRAULIC ANALOGIES
Verification of a model of the Eastern Scheldt
[RAND/R-3108-NETH] 09 p1354 N85-18518
Catastrophic-flood features in Swedish Lapland as a terrestrial analog for Martian channel flows
13 p2190 N85-22887

HYDRAULIC CONTROL
Automation of coastal engineering modelling facilities
[CSIR-T/SEA-8304] 01 p0035 N85-10219
Powered articulated headrest system
[AD-D011353] 07 p0901 N85-15710
Hydraulic brakes for industrial robots
13 p2046 N85-22806

HYDRAULIC EQUIPMENT
NT AIRCRAFT HYDRAULIC SYSTEMS
Vehicle-to-vehicle connection mechanism
[AD-D011267] 05 p0645 N85-14142
A study of wear characteristics due to pressure for hydraulic fixed displacement vane pumps
[AD-A146023] 06 p0814 N85-15180
Vehicle anchoring system
[AD-D011292] 06 p0815 N85-15173
Space shuttle orbiter auxiliary power unit development challenges 08 p1099 N85-16845
Materials of the fourth scientific-technical Conference on Questions of the Extrusion of Metals (Selected articles)
[AD-A148578] 08 p1130 N85-17181
Multiple rate shock isolator damping valve
[AD-D011429] 08 p1168 N85-17399
Turning behaviour of articulated frame steering tractor
[AD-P004304] 09 p1409 N85-18881
Integrated paratroop door
[AD-D011507] 12 p1776 N85-21146
Analysis and design of hydraulic servo systems within the scope of the improvement of a fatigue testing installation of the Royal Dutch Army
[LEOK-TR-1984-09] 14 p2265 N85-24033

Pneumohydraulic drive 14 p2268 N85-24050
High reliability mechanical-hydraulic converter
14 p2268 N85-24055
Manufacture of drive wheel vanes for hydraulic turbines on program controlled machine tools
14 p2269 N85-24058
Hydraulic characteristics of reduction installation valves 14 p2269 N85-24060
Hydraulic drag of rod with artificial microroughness in longitudinal flow 14 p2276 N85-24111
Locking of Automotive Products hydraulic selector valves
[BAE-EXPER/NOTE-459] 15 p2567 N85-25839
User's guide for concrete strength investigation and design (CSTR)
[AD-A151617] 15 p2579 N85-25906
Application of the hydraulic system frequency response program to propellant feed systems
[AD-A151824] 16 p2741 N85-26914
Active control landing gear for ground load alleviation
17 p2903 N85-27902
Use of a two-dimensional flow model to quantify aquatic habitat
[AD-A154287] 19 p3266 N85-30253

HYDRAULIC FLUIDS
Standardization of flammability tests for hydraulic fluids
[AD-A146466] 06 p0771 N85-14902
Toxic hazards research
[AD-A147857] 07 p1011 N85-16425
Mist flammability studies of candidate fire-resistant hydraulic fluids
[AD-A148572] 08 p1134 N85-17148
Hydraulic drag of rod with artificial microroughness in longitudinal flow 14 p2276 N85-24111
Organic solvent alteration of hydraulic properties of sedimentary rocks of low permeability: A review
[DE85-012537] 22 p3615 N85-33635

HYDRAULIC HEATING SOURCES
U HEAT SOURCES
U HYDRAULIC EQUIPMENT

HYDRAULIC JETS
Potential application of robotics and state-of-the art end effectors at Letterkenny Army Depot
[AD-P004015] 03 p0309 N85-11994
Characterization of jet-contaminant interaction flow in chemical decontamination
[AD-A147298] 08 p1161 N85-17327
The hydrosynclastic infundibulum
[AD-A153649] 18 p3100 N85-29192
Pulsed hydrojet propulsion
[DE85-010771] 22 p3764 N85-33446

HYDRAULIC PUMPS
U HYDRAULIC EQUIPMENT
U PUMPS

HYDRAULIC SHOCK
Rock mechanics: Issues and research needs in the disposal of wastes in hydraulic fractures
[DE85-001399] 10 p1556 N85-19609
Comprehensive fracture diagnostics experiement. Part 2: Comparison of seven fracture azimuth measurements
[DE85-011707] 23 p3948 N85-34470

HYDRAULIC SYSTEMS
U HYDRAULIC EQUIPMENT

HYDRAULIC TEST TUNNELS
The effects of microbubbles on turbulent boundary layer skin friction 20 p3451 N85-31425

HYDRAULIC VALVES
U HYDRAULIC EQUIPMENT
U VALVES

HYDRAULICS
Multigrid iteration solution procedure for solving three-dimensional sets of coupled equations
[DE84-016515] 04 p0555 N85-13532
Hydraulic locking boltwork system
[AD-D011299] 06 p0815 N85-15174
Great Lakes hydrometeorologic and hydraulic data needs 20 p3496 N85-31739
Computer code calculations of the TMI-2 accident: Initial and boundary conditions
[DE85-012613] 24 p4140 N85-35666

HYDRAZINE ENGINES
Heat resistant sheathed insulated electrical conductors
[AD-D011644] 17 p2951 N85-28219

HYDRAZINE NITRATE
Hydrazine nitrate based explosives
[ISL-CO-229/84] 22 p3754 N85-33272

HYDRAZINES
Qualification of a hydrazine gas generator system with electrothermal/catalytic gas generator
[BMFT-FB-W-84-040] 08 p1110 N85-17016
The use of hydrazine as an alternate source of energy
[NASA-CR-175635] 12 p1817 N85-21397
Atmospheric dispersion of hypergolic liquid rocket fuels, volume 1
[AD-A149597] 12 p1817 N85-21399
Hydrazine and the F-16 20 p3511 N85-31826

HYDRIDES
NT BORANES
NT BORON HYDRIDES
NT CARBORANE
NT CHLOROSILANES
NT METAL HYDRIDES
NT PHOSPHINES
NT SILANES
NT ZIRCONIUM HYDRIDES
Influence of 5f electrons on structures and bonding in the actinide-hydrogen intermetallics
[DE84-013893] 01 p0118 N85-10807
Mossbauer effect and contactless conductivity studies of superconducting actinides intermetallics and hydrides. Mossbauer high pressure studies
03 p0430 N85-12743
Neutron scattering for the investigation of solid state materials, utilization in chemical structures
03 p0432 N85-12752
Formation of a limiting composition in the preparation of ternary 3-5 semiconductors by the VPE (Vapor Phase Epitaxy) Hydride technique
[AD-A147639] 08 p1225 N85-17713
An infrared study of the hydrogenation of carbon dioxide on supported rhodium catalysts
[AD-A149477] 10 p1436 N85-19049
Ten degree Kelvin hydride refrigerator
[NASA-CASE-NPO-16393-1-CU]
18 p3085 N85-29084
Method for preparing hydride configurations and reactive metal surface
[DE85-006443] 23 p3917 N85-34274

HYDROACOUSTICS
U UNDERWATER ACOUSTICS

HYDROAEROMECHANICS
U AERODYNAMICS

HYDROBAROPHONES
U HYDROPHONES

HYDROBROMIC ACID
Study of the liquid vapor equilibrium in the bromine-hydrobromic acid-water system
[NASA-TM-77787] 07 p0921 N85-15836
A study of liquid-vapor equilibria of the bromine-hydrobromic acid-water system
[NASA-TM-77748] 14 p2249 N85-23940

HYDROCARBON COMBUSTION
Combustion in high speed air flows
[AD-A148371] 08 p1122 N85-17070
Comprehensive mechanisms for combustion chemistry: An experimental and numerical study with emphasis on applied sensitivity analysis
[DE85-000173] 13 p2019 N85-22656

HYDROCARBON FUEL PRODUCTION
NT ATMOSPHERIC ENERGY SOURCES
Bioenergy, solar biotech research in France, Europe
15 p2536 N85-25646

HYDROCARBON FUELS
NT DIESEL FUELS
NT FOSSIL FUELS
NT GASOLINE
NT JET ENGINE FUELS
NT JP-4 JET FUEL
NT JP-5 JET FUEL
NT JP-8 JET FUEL
Chemistry of fuel deposits and sediments and their predursors
[NASA-CR-174778] 01 p0034 N85-10209
Liquid hydrocarbon fuels from syngas
[DE84-015942] 04 p0482 N85-13069
Analysis of middle distillate fuels by high resolution field ionization mass spectrometry
[AD-A147724] 08 p1135 N85-17153
Combustion gas properties. 2: Natural gas fuel and dry air
[NASA-TP-2435] 12 p1779 N85-21168
PSA, Renault work on all fuel automobile engine
15 p2531 N85-25604
Improved catalysts for liquid hydrocarbon fuels from syngas
[DE85-006569] 16 p2746 N85-26947
Ignition characterization of LOX/hydrocarbon propellants
[NASA-CR-171884] 18 p3083 N85-29070
Ignition characterization of LOX/hydrocarbon propellants
[NASA-CR-171882] 18 p3083 N85-29071
Liquid hydrocarbon fuels from syngas
[DE85-009613] 19 p3226 N85-30017
Fuel-rich catalytic combustion: A soot-free technique for in situ hydrogen-like enrichment
[NASA-TP-2498] 20 p3423 N85-31244
Rapid estimation of concentration of aromatic classes in middistillate fuels by high-performance liquid chromatography
[NASA-TP-2495] 20 p3434 N85-31307
Aspects of high-resolution gas chromatography as applied to the analysis of hydrocarbon fuels and other complex organic mixtures. Volume 1
[AD-A156154] 24 p4076 N85-35257

HYDROCARBONS
NT ACETYLENE
NT ALKANES
NT ALKENES
NT ALKYNES
NT ANTHRACENE
NT BENZENE
NT BUTADIENE
NT BUTANES
NT BUTENES
NT CAROTENE
NT CYCLIC HYDROCARBONS
NT CYCLOHEXANE
NT CYCLOPROPANE
NT DIENES
NT DURENE
NT ETHANE
NT ETHYLENE
NT HEXENES
NT KEROGEN
NT LIQUEFIED NATURAL GAS
NT METHANE
NT METHYLENE
NT NAPHTHALENE
NT NATURAL GAS
NT NITROPROPANE
NT PARAFFINS
NT PENTANES
NT PROPANE
NT PROPYLENE
NT PYRENES
NT TOLUENE
NT TRIPHENYLS
NT VINYLIDENE
Plasma deposited diamondlike carbon on GaAs and InP
[NASA-TM-86870] 01 p0123 N85-10844
Systematic data interpretation of remote sensing in the reception of hydrocarbons, volume 1
[E85-10008] 02 p0215 N85-11421
Development of a method for exploring low-reflectance areas through the combined use of different geophysical methods taking the north-west German basin as an example
[BMFT-FB-T-83-180] 02 p0220 N85-11450
Magnetic resonance studies of transient radicals and radical ions
[DE84-011699] 03 p0328 N85-12116
Polycyclic aromatic hydrocarbons on the inner surfaces of copper tubing
[AD-A145979] 03 p0337 N85-12169
Organic aerosol formation: OH(hydroxyl radical) versus ozone oxidation pathways
[PB84-219880] 03 p0386 N85-12484
Structure determination of molecular adsorbates with dynamical LEED and HREELS
[DE85-002007] 06 p0861 N85-15473
Analysis of gases in the Earth's crust
[PB85-113397/GAR] 07 p0990 N85-16287
Homogeneous reaction involving components of different redox couples. 1: Theoretical considerations and digital simulation
[AD-A148666] 08 p1124 N85-17084
Impact of aircraft emissions on air quality in the vicinity of airports. Volume 4. Nitrogen dioxide and hydrocarbons
[AD-A148253] 08 p1180 N85-17436
On the importance of light hydrocarbons in multiphase atmospheric systems
[JUEL-1942] 08 p1190 N85-17496
Aromatics determination in middle distillate petroleum fractions by spectrophotometric titration
[PNR-90239] 09 p1293 N85-18123
Initial results for supercritical cycle experiments using pure and mixed-hydrocarbon working fluids
[DE84-017008] 09 p1345 N85-18460
Prediction of retention indices of polynuclear aromatic hydrocarbons. Part 1: HPLC on nitrogen containing normal phase packing materials
[DE85-001302] 10 p1436 N85-19051
Prediction of retention indices of polynuclear aromatic hydrocarbons. Part 2: Capillary gas chromatography
[DE85-001301] 10 p1437 N85-19053
Vapor pressure studies of the solubilization of hydrocarbons by surfactant micelles
[DE85-004319] 12 p1803 N85-21306
Oxidation and gum formation in jet fuels
[AD-A149934] 12 p1818 N85-21401

The body burden of organic vapors in artificial air trial measurements aboard a moored submarine
[AD-A149696] 12 p1910 N85-21988
Applications of high pressure differential scanning calorimetry to aviation fuel thermal stability research
[NASA-TM-87002] 14 p2249 N85-23941
Modelling of photodegradation in solar cell modules of substrate and superstrate design made with ethylene-vinyl acetate as pottant material
[NASA-CR-175690] 14 p2350 N85-24527
C2H(n) fragments on metal surfaces
[AD-A151474] 15 p2505 N85-25449
Studies of the combustion of model fuels with low hydrogen content (pyrolysis of polycyclic aromatics-detection of soot precursors)
[DE85-005422] 15 p2521 N85-25541
The remote detection of polynuclear aromatic hydrocarbons using laser-induced fluorescence
[AD-A152294] 16 p2757 N85-27013
Systematic nomenclature of the nitrogen, oxygen and sulfur functional polycyclic aromatic hydrocarbons
[DE85-007426] 17 p2916 N85-27974
Fuel rich catalytic comustion: The first stage of a two-stage combustor
[NASA-TM-87042] 18 p3069 N85-28983
Study of synthesis gas conversion over metal oxides
[DE85-010136] 18 p3072 N85-28999
Measurement of radical species concentrations and polycyclic aromatic hydrocarbons in flames by fluorescence and absorption using a tunable dye laser
[DE85-008624] 18 p3113 N85-29274
Mechanism of the catalytic gasification and reactivity of graphite
[DE85-009932] 19 p3229 N85-30020
Thermodynamic study of CO2-organic compound interaction at high pressures and temperatures
[DE85-010999] 19 p3268 N85-30266
Identification and quantification of nitropolynuclear aromatic hydrocarbons in ambient and indoor air particulate samples
[PB85-176790] 19 p3311 N85-30525
Factor analysis of atmospheric pollution by polycyclic aromatic hydrocarbons
[HSE-TRANS-10988] 19 p3311 N85-30528
Study of the formation of particles from natural hydrocarbons released by vegetation
21 p3644 N85-32640
The interaction of polynuclear aromatic hydrocarbons PAH's with water vapor and their role as condensation nuclei in the formation of haze and fog
21 p3652 N85-32695
Using remote photographs in prospecting for hydrocarbons on the Kerch Peninsula
22 p3735 N85-33154
Method for removing chlorine compounds from hydrocarbon mixtures
[DE85-011608] 22 p3742 N85-33191
Effect of polymer additives on characteristics of direct-current motor with liquid dielectric filler
22 p3772 N85-33376
Environmental summary for calendar year 1984
[DE85-012020] 22 p3810 N85-33604
Development of a chemical kinetic mechanism for the US EPA (Environmental Protection Agency) regional oxidant model
[PB85-185858] 22 p3813 N85-33618
Modeling of auto exhaust smog chamber data for EKMA development
[PB85-186492] 22 p3813 N85-33619
Process for functionalizing alkanes
[DE85-006420] 23 p3909 N85-34219
FTIR studies of hydrocarbon synthesis on Pd/ZSM5 catalysts
[DE85-012430] 24 p4071 N85-35230
The Conterminous United States Mineral Assessment Program 24 p4106 N85-35458
Thermal evolution of coastal California with implications for hydrocarbon maturation 24 p4115 N85-35509
Molecular biology of environmental aromatic hydrocarbons
[DE85-015036] 24 p4128 N85-35593
Few-particles generation channels in inelastic hadron-nuclear interactions at energy approximately equals 400 GeV
[HE-3.2-9] 24 p4179 N85-35917

HYDROCHLORIC ACID
Photoelectron studies of autoionizing Rydberg states in HCl
[DE85-011813] 21 p3702 N85-33001
A study of the chemistry of alkali metals in the upper atmosphere
[AD-A156349] 24 p4117 N85-35524

HYDROCLIMATOLOGY
Hydrometric telemetry in Canada
14 p2239 N85-23882

HYDRODYNAMIC COEFFICIENTS
Hydraulic brakes for industrial robots
13 p2046 N85-22806
Influence of spatial variability of hydraulic characteristics of soils on surface parameters obtained from remote sensing data in infrared and microwaves
[NASA-TM-77902] 20 p3477 N85-31604

HYDRODYNAMIC EQUATIONS
NT HELMHOLTZ VORTICITY EQUATION
Self-similar expansion of dense matter due to heat transfer by nonlinear conduction
[MPQ-81] 01 p0046 N85-10297
Reduction of nonlinear problems to Schroedinger or heat equations: Formation of Kepler orbits, singular solutions for hydrodynamical equations
[REPT-72] 01 p0129 N85-10892
Equations of plasma transport in a curved magnetic field
[DE84-015625] 05 p0730 N85-14690
On the hydrodynamical equations of astrophysical jets — active galactic nuclei 08 p1241 N85-17831
Nonlinear waves in the magnetosphere of pulsars
12 p1955 N85-22281
An analytic model for hydromagnetospheres — stellar winds; pulsars: cosmic jets 12 p1959 N85-22313
Contribution to the theory of stationary separation areas
[NASA-TM-77825] 14 p2300 N85-24244
Lyapunov stability of very simple steady solutions of prognostic systems 14 p2333 N85-24429
General continuous formulations of atmospheric energy laws 16 p2830 N85-27448
Singularity solutions for ellipsoids in Low-Reynolds-Number flows: With applications to the calculation of hydrodynamic interactions in suspensions of ellipsoids
[AD-A153503] 18 p3168 N85-29632
Method for computing evolution of random hydropdynamic fields on basis of adjoint equations
19 p3292 N85-30412
The cosmic-ray shock structure problem for relativistic shocks
[OG-8.1-1] 23 p4017 N85-34891

HYDRODYNAMIC STABILITY
U FLOW STABILITY

HYDRODYNAMICS
NT CYLINDRICAL PLASMAS
NT ELASTOHYDRODYNAMICS
NT ELECTROHYDRODYNAMICS
NT MAGNETOHYDRODYNAMICS
HULL users' manual
[AD-A145000] 01 p0103 N85-10691
A perturbation solution for rigid dumbbell suspensions in steady shear flow
[AD-A144876] 01 p0111 N85-10755
New approaches to hydrodynamic flow visualization on surfaces
[AD-A145528] 02 p0198 N85-11324
Experiences with a high-blockage model tested in the NASA Ames 12-foot pressure wind tunnel
03 p0315 N85-12032
Comparison of predicted and measured friction for a tilt-pad thrust bearing with crown and roughness under hydrodynamic and mixed lubrication
[AD-A145752] 03 p0371 N85-12371
Algebra of hydrodynamic flows of an ideal fluid and the prediction of the behaviour of a system of particles of a passive admixture on Riemann surfaces with a variable curvature
[REPT-565] 03 p0377 N85-12408
Dynamical models for radio jets
03 p0449 N85-12854
Flash radiography as a quantitative tool
[DE84-016465] 04 p0503 N85-13211
Supernova envelope shock origin of cosmic rays: A review
[DE84-016479] 04 p0590 N85-13763
Rotordynamic Instability Problems in High-Performance Turbomachinery
[NASA-CP-2338] 05 p0642 N85-14116
Hydraulic forces on a centrifugal impeller undergoing synchronous whirl 05 p0643 N85-14124
Hydrodynamic impeller stiffness, damping, and inertia in the rotordynamics of centrifugal flow pumps
05 p0643 N85-14125
Damping capacity of a sealed squeeze film bearing
05 p0645 N85-14139
Conditions for assembling dies for drawing under hydrodynamic friction conditions
[BLL-M-35954-(5828.4)] 05 p0647 N85-14153
The radiative hydrodynamics of flare loops heated by impulsive bursts of energetic electrons
05 p0745 N85-14781
Characterization of jet-contaminant interaction flow in chemical decontamination
[AD-A147298] 08 p1161 N85-17327
Hydrodynamic flow structures in quantum field theory
[DE84-015513] 09 p1401 N85-1
New methods for numerical solution of one class of strongly nonlinear partial differential equations with applications in hydrodynamics
[AD-A149026] 10 p1545 N85-1
Hydrodynamic response of a radiating Al plasma excited by a proton beam
[AD-A148904] 10 p1558 N85-1
Ion velocity distributions from spherical 1054 nm and 351 nm laser plasmas
[DE85-002816] 10 p1559 N85-1
Parallel processing experiences on the Denelcor HEP computer
[DE85-000653] 11 p1702 N85-20
Hydrodynamic simulations of recurrent novae
11 p1753 N85-21
Investigation of the initial events in biofouling
[AD-A149995] 12 p1900 N85-21
Processes and problems in secondary star formation
[DE85-003623] 12 p1960 N85-22
Coupled acoustic and hydrodynamic wave instabilities
13 p2000 N85-22
Application of modulated hydrodynamic voltammetry to the study of anodic electrocatalysis
[DE85-004182] 13 p2018 N85-22
Turbulent flows of surfactant solutions
[AD-B089137L] 13 p2092 N85-23
Calculation of level surface in problems of large-scale ocean circulation 13 p2106 N85-23
Double and inverse Taylor-Hogg vortices in a stratified ocean 13 p2108 N85-23137
Model for high rate gas flows in deformable and reactive porous beds
[DE85-006140] 14 p2253 N85-23
Model of friction bearing hydrodynamics
14 p2288 N85-24
USSR report: Earth sciences
[JPRS-UES-85-004] 14 p2332 N85-24
Numerical study of a two-fluid hydrodynamical model of interstellar medium and population 1 stars
14 p2440 N85-25
The design and construction of a flow channel and rig for corrosion studies
[AERE-M-3455] 15 p2508 N85-25474
Laboratory for laser energetics report
[DE85-007235] 15 p2563 N85-25814
Gravity perception in a Cladoceran-Zooplankter: Anatomy of antennal socket setae of Daphnia magna
15 p2605 N85-26057
Mean free paths, viscosity, and the limitations of perfect fluid hydrodynamics in the description of the quark-gluon plasma
[DE85-005501] 15 p2649 N85-26
Instability of solar wind near streamlined bodies
16 p2720 N85-26
Characteristic functionals of stochastic
processes
[REPT-14/1984] 16 p2768 N85-27
Optimum convection conditions for Czochralski growth of semiconductors
[INPE-3395-PRE/665] 16 p2870 N85-27703
Catalyst and reactor development for a liquid phase Fischer-Tropsch process
[DE85-005894] 17 p2922 N85-28014
A discussion of adaptive grids and their applicability in numerical hydrodynamic modeling
[AD-A151843] 17 p3017 N85-28
A numerical solution technique for multitemperature plasma hydrodynamics
[AD-A152701] 17 p3039 N85-28
Multi-ducted inlet combustor research and development
[AD-A153753] 18 p3063 N85-28
Dynamics of thin-film breakup in a constricted pore
[DE85-008442] 18 p3101 N85-29
Numerical techniques for steady two-dimensional transcritical stratified flow problems, with an application to the intermediate field dynamics of ocean thermal energy conversion plants
[DE85-008347] 18 p3151 N85-29
Study of the chemical mechanism in lubrication
[DE85-010768] 19 p3228 N85-30013
Flow visualization study of inverted annular flow of post dryout heat transfer region
[DE85-010482] 19 p3269 N85-30
Space photographs confirm 40-year-old hydrodynamics discovery 19 p3289 N85-30
Use of adjoint equations in problems of evaluating
of random hydrodynamic fields
19 p3289 N85-30
SHAPS-2: A three-dimensional computer program for linear/non-linear, static/dynamic analyses of piping systems
[DE85-010500] 19 p3335 N85-30

Hybrid two-dimensional Monte-Carlo electron transport in self-consistent electromagnetic fields
[DE85-010757] 19 p3348 N85-30756

Venus thermospheric circulation
[PB85-180420] 19 p3364 N85-30997

Activities report of the Laboratory of Mechanics and Energetics 20 p3437 N85-31328

Hydrodynamic solutions for the diffusion of components in confined media 20 p3456 N85-31464

Hydrodynamics and sanitation
[CT-579] 20 p3487 N85-31672

Compressible Lagrangian hydrodynamics without Lagrangian cells
[DE85-008597] 20 p3520 N85-31891

Self-consistent models for the X-ray emission from supernova remnants 20 p3548 N85-32082

Discovery of a nonpropagating hydrodynamic soliton
[AD-A155569] 21 p3582 N85-32268

Mechanics of a gaseous film barrier to lubricant wetting of elastohydrodynamically lubricated conjunctions
[NASA-TP-2509] 21 p3595 N85-32330

Effect of polymer additives on characteristics of direct-current motor with liquid dielectric filler
22 p3772 N85-33376

Dual clearance squeeze film damper
[NASA-CASE-LEW-13506-1] 22 p3791 N85-33490

Volatile loss following very large impacts
22 p3853 N85-33862

Three-dimensional hydrodynamic hot-spot model
[DE85-009587] 23 p3922 N85-34301

Numerical simulation in astrophysics: Smoothed particle methods 23 p3979 N85-34674

Numerical calculations on shock loaded materials
23 p3980 N85-34676

Dissipation terms in one-dimensional hydrodynamic code for ICF target 23 p3980 N85-34677

Two-dimensional simulation of LIB target implosion
23 p3980 N85-34678

Stability of implosion dynamics
23 p3980 N85-34680

Pulse effect in a light ion beam propagation through a Z-discharge plasma channel 23 p3981 N85-34684

Adaptive rezoner in a two-dimensional Lagrangian hydrodynamic code
[DE85-010108] 24 p4094 N85-35381

HYDROELASTICITY

Time dependent interaction of internal pressure wave with system of two spherical shells
13 p2046 N85-22809

Thermal and thermoelastic effects in rolling/sliding contacts
[AD-A150435] 13 p2165 N85-23429

HYDROELECTRIC POWER STATIONS

International test and demonstration of a 1-MW wellhead generator: Helical screw expander power plant
[NASA-CR-174161] 04 p0527 N85-13372

Ecological impacts of hydroelectric projects in Amazonia 07 p1003 N85-16374

Underground pumped hydroelectric storage
[DE85-000288] 11 p1676 N85-20560

Small-hydropower development: The process, pitfalls, and experience. Volume 1: Feasibility studies summary and analysis
[DE85-010639] 22 p3806 N85-33589

Low-head hydroelectric power demonstration project: City of Gonzales, Texas
[DE85-010403] 22 p3809 N85-33595

Small Hydroelectric Power Plan Demonstration Project
[DE85-011343] 23 p3946 N85-34454

HYDROELECTRICITY

Monitoring environmental and related performance parameters for a Rankine-cycle turbine electric generator utilizing geothermal energy at the Gila Hot Springs, New Mexico
[DE84-901772] 09 p1345 N85-18465

Small-hydropower development: The process, pitfalls, and experience. Volume 1: Feasibility studies summary and analysis
[DE85-010639] 22 p3808 N85-33589

Solar energy education. Renewable energy: A background text
[DE85-010365] 23 p3946 N85-34452

Small Hydroelectric Power Plan Demonstration Project
[DE85-011343] 23 p3946 N85-34454

HYDROFLUORIC ACID

Rotational energy transfer in highly vibrationally excited hydrogen fluoride and deuterium fluoride
[AD-A152003] 16 p2862 N85-27650

Rotational relaxation studies of hydrogen fluoride
[AD-A152711] 17 p3029 N85-28734

HYDROFOIL BOATS

U HYDROFOIL CRAFT

HYDROFOIL CRAFT

A broadband kevlar radome for shipboard
[AD-P004365] 12 p1826 N85-21459

HYDROGEN

NT DEUTERIUM
NT DEUTERIUM PLASMA
NT HYDROGEN ATOMS
NT HYDROGEN IONS
NT HYDROGEN ISOTOPES
NT HYDROGEN PLASMA
NT LIQUID HYDROGEN
NT METALLIC HYDROGEN
NT TRITIUM

Compressibility and fugacity of gaseous hydrogen
[NLR-TR-83079-U] 01 p0025 N85-10154

Inhibition of hydrogen absorption during plating of high strength steels
[AD-A144882] 01 p0026 N85-10174

Monte Carlo simulation of thermalization of subexcitation electrons in molecular hydrogen
[NAL-TR-815T] 01 p0117 N85-10788

Observations of the pulsating hydrogen: Deficient star BD+13 deg 3224, during 1980 - 1981
01 p0128 N85-10882

An electrochemical study of hydrogen uptake and elimination by bare and gold-plated waspaloy
[NASA-TM-86479] 02 p0182 N85-11222

Effects of H2S on molten carbonate fuel cells
[DE84-015166] 02 p0195 N85-11307

Reversible change in parameters of GaAs-based surface-barrier metal-semiconductor diodes induced by hydrogen absorption-desorption
02 p0258 N85-11690

Combustion and detonation of hydrogen-air mixture in free spaces 02 p0274 N85-11783

Surface production of negative hydrogen ions
[AD-A145437] 02 p0277 N85-11801

Molecular hydrogen emission associated with high velocity flows. A tracer for low velocity shocks
03 p0443 N85-12819

Interaction of hydrogen with defects in metals
[DE84-016781] 04 p0476 N85-13032

Theoretical studies of highly ionized species
[DE84-016797] 04 p0561 N85-13574

Influence of hydrogen saturation and prior heat treatment on graphitization of white cast iron
[BLL-M-35964-(5828.4)] 05 p0615 N85-13932

Effect of water on hydrogen permeability --- Stirling engines
[NASA-TM-86904] 06 p0761 N85-14664

Investigation of bromine complexed hydrogen/bromine regenerative fuel cells for portable electric power
[AD-A146401] 06 p0833 N85-15300

Synergisms in hydrogen recycling, session summary
06 p0864 N85-15491

Steady state hydrogen transport in solids
06 p0864 N85-15492

Pioneer 10 and Voyager observations of the interstellar medium in scattered emission of the He 584 A and H Lya 1216 A lines 06 p0873 N85-15541

Absorption line studies and the distribution of neutral gas in the local interstellar medium
06 p0873 N85-15544

Synthesis of data on the local interstellar medium
06 p0874 N85-15545

Non-local origin of a substantial portion of the soft X-ray background 06 p0877 N85-15567

The Draco Nebula, a molecular cloud associated with a high velocity cloud? 06 p0878 N85-15577

Nearby molecular hydrogen 06 p0879 N85-15582

Radio and UV observations of high latitude HI
06 p0879 N85-15583

The results of hydrogen hypersensitization of photoemulsions --- astronomical photography
07 p0963 N85-16108

The fundamentals of dislocation transport of hydrogen in bcc iron
[AD-A148143] 08 p1129 N85-17117

Photoionization structure of the Orion Nebula
08 p1246 N85-17863

The 1.5 - 3.5 micron spectroscopy of the Orion H2 source 08 p1246 N85-17864

Interpretation of the far infrared emission from our external galaxies 08 p1249 N85-17884

Simultaneous flow visualization and unsteady lift measurement on an oscillating lifting surface
[AD-P004157] 09 p1264 N85-17942

NMR study on rotational fluctuation in solid hydrogen and deuterium 09 p1289 N85-18093

Hydrogen trapping, diffusion, and recombination in austenitic stainless steels
[DE85-001871] 09 p1294 N85-18129

Hydrogen-oxygen (hydrox) breathing at 1.3MPa
[FOA-C-58015-H1] 09 p1364 N85-18577

Alignment of high Ryberg states in hydrogen
[DE85-000582] 09 p1380 N85-18677

Developments and applications of laser fluorescence spectroscopy for studies of particle bahaviours in fusion plasmas 09 p1389 N85-18735

Molecular hydrogen and thermal phases in astrophysics 09 p1414 N85-18922

Theoretical studies of the ignition and combustion of silane-hydrogen-air mixtures
[NASA-CR-3876] 10 p1433 N85-19032

Separation of gas mixtures with coordination complexes
[DE85-000363] 10 p1438 N85-19062

Improved operation of transversely exited N2O lasers
[AD-D011488] 10 p1490 N85-19409

Variational calculation of the 2D H2 molecule
[INPE-3304-PRE/615] 10 p1554 N85-19796

Quasi-thermodynamic prediction of hydrogen reemission behavior from titanium films
[DE85-003687] 10 p1564 N85-19864

Effect of hydrogen on fatigue of VT6 alloy
11 p1601 N85-20071

Distribution of hydrogen in multi-layer welded joints of alloyed steels 11 p1603 N85-20079

Low energy antiproton interaction studies at Brookhaven
[DE85-001228] 11 p1720 N85-20820

Vibrational relaxation in H-2 molecules by wall collisions: Applications to negative ion source processes
[DE85-000852] 11 p1721 N85-20828

Direct measurement of the temperature dependence of the velocity of the reaction of deuterium atoms with vibration-excited hydrogen molecules
[MPIS-12/1984] 11 p1726 N85-20856

Atomistic studies of grain boundaries with segregated impurities
[DE85-000063] 11 p1737 N85-20924

Feasibility of producing commodities and electricity for space shuttle operations at Vandenberg Air Force Base
[DCN-84-203-001-80-21] 12 p1789 N85-21230

Hydrogen flame acceleration and transition to detonation
[DE85-000611] 12 p1802 N85-21299

Increase in hydrogen emission of upper atmosphere following launches of space vehicles
13 p1981 N85-22431

Adsorption site, adsorption energy and normal vibration frequency of H/Ni(100) via total energy calculations
[AD-A150555] 13 p2156 N85-23388

Gas dynamics of the barred spiral galaxy NGC 3359
13 p2170 N85-23465

Hydrogen on impurity-covered iron surfaces
14 p2254 N85-23968

Hydrogen resistance of VT1-0 titanium under 150 MPa pressure at room temperature 15 p2499 N85-25414

Linewidth and bandwidth measurements of the q-branch of h2 using CW coherent anti-Stokes Raman spectroscopy
[AD-A151868] 15 p2506 N85-25456

Applications of photoinduced electron transfer and hydrogen abstraction reactions to chemical and electrochemical conversion processes
[DE85-006068] 15 p2506 N85-25459

The effects of water and hydrogen on materials used in integrated circuit packages
[AD-A151893] 15 p2518 N85-25529

Numerical analysis of supersonic reactive flow in wake of reverse step 15 p2643 N85-26303

Compensation of dangling bonds in A-Si, Ge:H alloys
[DE85-002905] 15 p2662 N85-26433

Development of hydrogen resistant alloys
16 p2735 N85-26873

Modeling the role of radicals in the ignition of and flame propagation in hydrogen-air and methane-air mixtures
16 p2744 N85-26935

Transitional metal activation and functionalization of C-H bonds
[DE85-006816] 16 p2746 N85-26949

Study of the kinetics and thermodynamics of hydrogen in Pd-based alloys
[DE85-007341] 16 p2750 N85-26969

Spin-polarized quantum systems
[DE85-006914] 16 p2864 N85-27667

The structure of galactic HI in directions of low total column density
[NASA-CR-175709] 16 p2882 N85-27785

An analysis of alternate hydrogen sources for lunar manufacture
[DE85-007234] 16 p2884 N85-27792

Role of hydrogen and structure on CMSX-2
17 p2915 N85-27967

Photoionization mass spectrometry with VUV hydrogen laser source
[AD-A153362] 17 p2921 N85-28009

Effect of texture in steel on the susceptibility of hydrogen embrittlement
[BLL-BISI-TRANS-22026-(9022.06)]
17 p2926 N85-28048

Construction techniques of a molecular hydrogen laser
[AD-A152928] 17 p2970 N85-28343

Thermodynamic calculations of equilibrium states in metal-carbon-hydrogen-oxygen system
[BLL-BISI-TRANS-22092-(9022.06)] 17 p3045 N85-28844

Hydrogen absorption in metals: A field ion microscopy study
[DE85-010299] 18 p3076 N85-29026

Feasibility of electrolytic hydrogen production in the Pacific Northwest
[DE85-009856] 18 p3084 N85-29080

Electron capture to the continuum from atomic hydrogen
[DE85-005269] 18 p3181 N85-29722

Effect of polarized radiative transfer on the Hanle magnetic field determination in prominences: Analysis of hydrogen H alpha line observations at Pic-du-Midi
18 p3207 N85-29894

Determining partial molar volume of hydrogen in titanium alloys 19 p3245 N85-30119

Means for reducing hydrogen concentration upon surfacing of antifriction aluminum alloys with powder electrode 19 p3247 N85-30132

Flash pyrolysis of biomass with reactive and non-reactive gases
[DE85-010962] 19 p3306 N85-30496

Tables of generalized hydrogen diffusion profiles and permeating fluxes for fusion applications
[DE85-006876] 19 p3372 N85-30919

Slow chemistry effects in a turbulent mixing layer
20 p3424 N85-31252

Assessment of superlayer contribution to the conserved scalar PDF in a hydrogen turbulent jet diffusion flame
20 p3425 N85-31255

Surface passivation and junction formation using low energy hydrogen implants 20 p3480 N85-31628

EBIC characterization and hydrogen passivation in silicon sheet 20 p3481 N85-31634

Detection of excited states by laser-induced fluorescence
[AD-A155556] 21 p3592 N85-32326

Sulfate-reducing bacteria: Microbiology and physiology 21 p3659 N85-32732

Thermophysical properties of fluids for the gas industry
[PB85-196471] 22 p3747 N85-33227

Use of low energy hydrogen ion implants in high efficiency crystalline silicon solar cells
[NASA-CR-176109] 22 p3806 N85-33571

Separation of gas mixtures by supported complexes
[DE85-011996] 23 p3912 N85-34236

Method for preparing hydride configurations and reactive metal surface
[DE85-006443] 23 p3917 N85-34274

Low noise polycrystalline semiconductor resistors by hydrogen passivation
[AD-D011721] 23 p3927 N85-34336

Dual-chamber plasma deposition of A-Si:H solar cells at high rates using disilane
[DE85-011828] 23 p3946 N85-34451

The extent of the local hi halo
[NASA-CR-176115] 23 p3967 N85-34724

Low-excitation Herbig-Haro objects and interstellar extinction
[NASA-CR-176142] 23 p3968 N85-34726

On the detectability of key-MeV solar protons through their nonthermal Lyman-alpha emission
[SH-1.3-5] 23 p3993 N85-34752

The effects of newly measured cross sections in hydrogen on the production of secondary nuclei during the propagation of cosmic rays through interstellar H
[OG-7.2-2] 23 p4014 N85-34874

On the importance of interstellar helium for the propagation of heavy cosmic rays
[OG-7.2-11] 23 p4015 N85-34879

Interactions of heavy nuclei, Kr, Xe and Ho, in light targets
[OG-7.2-21] 23 p4016 N85-34886

CO + H2 reaction over nitrogn-modified iron catalysts
[DE85-013791] 24 p4072 N85-35231

Fluidized bed desulfurization
[NASA-CASE-NPO-15924-1] 24 p4075 N85-35253

Pressure measurements in a hydrogen combustion environment: Hydrogen-air combustion test series 1 and 2 in the FITS tank, volume 1
[TI85-009899] 24 p4076 N85-35259

Vectorial electron transfer on designed surfaces
[PB85-204600] 24 p4076 N85-35263

Effect of temperature and ionic impurities at very low concentrations on stress corrosion cracking of Type 304 stainless steel
[TI85-003048] 24 p4079 N85-35283

Experimental technique for measuring the isentrope of hydrogen to several megabars
[DE85-014332] 24 p4085 N85-35366

Characterization of catalysts with metal-support effects and of the species adsorbed on their surfaces
[DE85-012254] 24 p4096 N85-35394

Cooling high intensity atomic hydrogen beams to liquid helium temperatures
[DE85-012515] 24 p4148 N85-35718

Limiter
[DE85-011620] 24 p4150 N85-35736

Circumstellar shells of late-type stars: A study at millimeter and infrared wavelengths
24 p4167 N85-35836

Some nuclear data needs in astrophysics
[DE85-012916] 24 p4168 N85-35842

HYDROGEN ATOMS

Electron capture by multiply charged ions from hydrogen atoms at low energies
[DE84-016560] 06 p0861 N85-15475

Reactions of butadiyne. 1: The reaction with hydrogen atoms
[NASA-TM-77805] 07 p0921 N85-15834

Dipole active surface vibrational resonances on clean and hydrogen covered Ni(110)
[AD-A150546] 13 p2163 N85-23420

Super hydrides
[AD-A153499] 18 p3070 N85-28986

HYDROGEN BONDS

Influence of hydrogen bonding in block copolymers and their blends 13 p2036 N85-22752

HYDROGEN CHLORIDES

NT HYDROCHLORIC ACID

Space Shuttle Environmental Effects: The First 5 Flights
[NASA-CR-171812] 01 p0069 N85-10457

Measurements on the diffusion of hydrogen chloride in the waste gas plume of incineration ships in the North Sea. Part 1: Methodology, instrumentation and presentation of data
[GKSS-84-E-23-PT-1] 05 p0672 N85-14319

Process for the epitaxial deposition of III-V compounds utilizing a continuous in-situ hydrogen chloride etch
[AD-D011557] 12 p1939 N85-22177

Quantitative studies for photoabsorption and fluorescence of HCl
[NASA-CR-175965] 19 p3233 N85-30043

HYDROGEN CLOUDS

NT ORION NEBULA

The z-dependence of the spin temperature of HI
06 p0878 N85-15580

Cosmic ray secondary nuclei and the structure of the galaxy
[OG-7.2-4] 23 p4014 N85-34876

HYDROGEN COMPOUNDS

NT BORANES
NT BORON HYDRIDES
NT CARBORANE
NT CHLOROSILANES
NT DEUTERIUM COMPOUNDS
NT DEUTERIUM FLUORIDES
NT HYDRIDES
NT HYDROGEN PEROXIDE
NT HYDROGEN SULFIDE
NT METAL HYDRIDES
NT PHOSPHINES
NT SILANES
NT ZIRCONIUM HYDRIDES

Preparation and properties of single crystals of hydrogen bis(phthalocyaninato) neodymium(3)
[AD-A144933] 01 p0123 N85-10846

Electronic-to-vibrational energy transfer studies of singlet molecular oxygen and hydrogen halides
[AD-A145587] 02 p0277 N85-11802

Reflection electron energy loss investigation of the H-GaAs(110) surface
[NOTA-INTERNA-811] 02 p0289 N85-11889

Calculations of collision-induced optical gain in high-density mixtures of D2 or HD with a buffer gas
[AD-A151372] 15 p2648 N85-26330

Intermolecular explosives
[DE85-009609] 23 p3921 N85-34296

HYDROGEN EMBRITTLEMENT

Compressibility and fugacity of gaseous hydrogen
[NLR-TR-83079-U] 01 p0025 N85-10154

Delayed fracture of high-strength steels in spherical tanks for LP gas
[BLL-RISLEY-TR-4926-(9091.9F)]
01 p0026 N85-10162

Study to optimize Cr-Mo steels to resist hydrogen and temper embrittlement. A study of carbides formed in low alloy Cr-Mo steels
[DE84-015208] 01 p0029 N85-10179

Lattice dilation in metal-hydrogen systems
[BLL-M-35758-(5825.4)] 02 p0176 N85-11176

Detection of hydrogen assisted crack growth
[DE84-015920] 02 p0183 N85-11228

Environment-induced embrittlement: Effect of impurity segregation and state of stress
[DE84-015436] 02 p0184 N85-1123

Detection of hydrogen assisted crack growth by measurement of modulus changes and acoustic emission
[DE84-015752] 02 p0184 N85-1123

A hydrogen partitioning model for hydrogen assisted crack growth
[AD-A147385] 07 p0978 N85-16214

Hydrogen embrittlement of nickel
[AD-A148322] 08 p1129 N85-17119

Effect of microstructure and trapping on the hydrogen embrittlement susceptibility of a ti-bearing HSLA steel
[AD-A148610] 08 p1130 N85-17122

Hydrogen induced cracking in pipeline steels
[ERS-E.327] 09 p1340 N85-18489

Mechanism of hydrogen induced cracking in pipeline steels
[ERS-E.349] 09 p1340 N85-18490

Statistical aspects of shear fracture propagation
[ERS-E.368] 09 p1341 N85-18494

Influence of gaseous hydrogen on strength and ductility of nickel heat-resistant alloys 10 p1447 N85-19119

Role of hydrogen in processes of deformation and fracture of metals 10 p1449 N85-19132

Mechanism of titanium impact on brittle tendency in delayed deformation of martensite-aging steels
11 p1604 N85-20087

Hydrogen attack of steel
[DE85-002645] 11 p1906 N85-20113

Hydrogen embrittlement of cadmium-plated ultra-high strength steels in paint strippers
[ARL/MAT-R-117] 12 p1806 N85-21120

Delayed cracking strength of experimental grades of 42 CD 4 steel in aqueous H2S surroundings
[BLL-T6419/BG/LRS/LRST738/84]
13 p2020 N85-22868

Hydrogen effects in austenitic stainless steels based on the Fe-Cr-Mn-N system
[DE85-003617] 13 p2023 N85-22872

The role of hydrogen in the stress corrosion failure of high strength Al-Zn-Mg alloys
[AD-A150891] 14 p2256 N85-23878

A study of fatigue crack growth in 2 1/4 Cr1Mo steel. Part 1: The influences of environment and material condition
[AERE-R-11472] 14 p2258 N85-23880

Hydrogen induced crack growth in Grade-12 Titanium
[BNL-NUREG-35598] 16 p2751 N85-26876

Study to optimize Cr-Mo steels to resist hydrogen and temper embrittlement
[DE85-005492] 17 p2932 N85-28096

Hydrogen degradation of pipeline steels
[DE85-008930] 17 p2932 N85-28101

Hydrogen embrittlement of high-strength steel
[B8580075] 17 p2933 N85-28100

Feasibility of electrolytic hydrogen production in the Pacific Northwest
[DE85-009856] 18 p3084 N85-29080

Kinetics of H-induced stress corrosion cracking. Part 1: Important features of cracking in respect of high strength steels
[BLL-BISI-TRANS-(9022.06)] 19 p3282 N85-30080

Failure analysis of fractured capscrews in centrifugal coolant compressor
[DE85-010029] 19 p3287 N85-30084

Micromechanism of fracture for stage 1 hydrogen-induced crack growth
[DE85-010027] 19 p3288 N85-30090

The effect of diffusive hydrogen segregation on fracture of polycrystalline nickel
[AD-A155238] 21 p3567 N85-32186

Hydrogen embrittlement testing
[DE85-007352] 23 p3916 N85-34273

HYDROGEN FLUORIDES

U HYDROFLUORIC ACID

HYDROGEN FUELS

Combustion gas properties. Part 3: Hydrogen gas fuel and dry air
[NASA-TP-2477] 20 p3395 N85-31058

Jet flows: Modelling and experiments
22 p3744 N85-33209

HYDROGEN IONS

Hydrogen passivation of electrically active defects in crystalline silicon solar cells
[DE84-004590] 02 p0223 N85-11461

Stark broadening of H(-) resonances in large electric fields
[DE84-016974] 04 p0496 N85-13164

Focusing effects of a laser beam in the nonresonant multiphoton ionization (MPI) of gases
[LP-207] 04 p0506 N85-13201

The role of fast electrons for the performance characteristics of hydrogen ion sources
09 p1303 N85-18169

Comparative effects of auxin and abscisic acid on growth, hydrogen ion efflux and gravitropism in primary roots of maize
[NASA-CR-174355] 09 p1342 N85-18444

Hydrogen vibrational population distributions and negative ion generation in tandem high density hydrogen discharges
[DE85-001207] 11 p1722 N85-20834

Collisional pumping for the production of intense spin-polarized, neutral beams: Target considerations
[DE85-003459] 11 p1723 N85-20841

Three-dimensional calculation of shuttle charging in polar orbit 13 p1992 N85-22486

Hydrogen vibrational population distributions and negative ion generation in tandem high-density hydrogen discharges
[DE85-006764] 16 p2863 N85-27657

Energy reflection coefficient for H+ ions at energies between 10 and 80 keV
[DE85-007547] 16 p2863 N85-27662

Shifts and widths of hydrogenic ion lines
[DE85-011375] 19 p3277 N85-30323

Heating of the deep chromosphere during solar flares
[AD-A155256] 21 p3723 N85-33100

Some physical differences between sheet plasma and multicusp plasma as volume produced H- or D- ion sources
[IPPJ-726] 23 p3974 N85-34637

Data on the backscattering coefficients on light ions from solids: A revision
[IPPJ-AM-41-REV] 23 p3982 N85-34689

HYDROGEN ISOTOPES
NT DEUTERIUM
NT METALLIC HYDROGEN
NT TRITIUM

Gas chromatographic separation of hydrogen isotopes using metal hydrides
[DE84-014455] 04 p0469 N85-12983

Stable isotope studies
[DE84-016752] 04 p0562 N85-13583

Advanced mass spectrometers for hydrogen isotope analyses
[DE85-000716] 06 p0811 N85-15150

Ion beam studies of hydrogen in metals
[DE84-017422] 09 p1297 N85-18145

Plasma-edge studies using carbon resistance probes
[DE85-005589] 14 p2424 N85-24955

Hydrogen recovery from extraterrestrial materials using microwave energy
[DE85-006717] 16 p2883 N85-27789

Cosmic ray He3 measurements
[OG-4.2-3] 21 p3714 N85-33045

Interstellar propagation and the isotopic composition of hydrogen in the galactic cosmic rays
[OG-4.2-1] 22 p3877 N85-34021

Measurements of galactic hydrogen and helium isotopes from 1978 through 1983
[OG-4.2-2] 22 p3877 N85-34022

The 4He1H ratios in the chemical compositions of solar flare particles and the primordial solar nebula
[SH-7.1-12] 23 p4048 N85-35104

HYDROGEN MASERS

Historical cost curves for hydrogen masers and cesium beam frequency and timing standards
10 p1465 N85-19245

Experimental studies of low temperature surface interactions of atomic hydrogen using maser technique
[AD-A150216] 13 p2017 N85-22647

Proceedings of the Fifteenth Annual Precise Time and Time Interval (PTTI) Applications and Planning Meeting
[AD-A149163] 17 p2961 N85-28287

First results of GPS time transfer to Australia
17 p2962 N85-28294

Improved master clock reference system at USNO
17 p2963 N85-28300

Recent results on the peformance of EFOS, NP and NX hydrogen masers 17 p2966 N85-28320

Methods to recover the narrow Dicke sub-Doppler feature in evacuated wall-coated cells without restrictions on cell size 18 p3105 N85-29225

Development of hydrogen masers for K-3 VLBI system
18 p3106 N85-29239

Atomic hydrogen maser active oscillator cavity and bulb design optimization 18 p3106 N85-29240

Hydrogen maser oscillation at 10 K
18 p3106 N85-29241

A low noise synthesizer for autotuning and performance testing of hydrogen masers 18 p3106 N85-29242

Atomic hydrogen maser measurements with wall surfaces of carbon tetrafluoride
18 p3106 N85-29243

Performance data of US Naval Observatory VLG-11 hydrogen masers since September, 1983
18 p3106 N85-29244

HYDROGEN OXYGEN ENGINES

LOX/LH2 propulsion system for launch vehicle upper stage, test results
[NASA-TM-77727] 03 p0324 N85-12089

Nonlinear control model of an H2O steam reactor
[DFVLR-FB-84-30] 07 p0975 N85-16192

Cryogenic propellant management: Integration of design, performance and operational requirements
08 p1098 N85-16939

Advanced research and technology programs for advanced high-pressure oxygen-hydrogen rocket propulsion
[NASA-TM-86969] 12 p1789 N85-21231

Advanced High Pressure O2/H2 Technology
[NASA-CP-2372] 16 p2733 N85-26862

Ceramics for advanced O2/H2 application
16 p2734 N85-26868

An evaluation of oxygen-hydrogen propulsion systems for the Space Station
[NASA-TM-87050] 18 p3067 N85-28971

Status of advanced orbital transfer propulsion
[NASA-TM-87069] 24 p4071 N85-35225

HYDROGEN PEROXIDE

Attempted measurement of gaseous H-2O-2 in the ambient atmosphere
[DE85-001937] 06 p0834 N85-15306

Oxygen isotopic study of the oxidation of SO2 by H2O2 in the atmosphere
[DE85-004017] 17 p2988 N85-28468

Chemical transformation in acid rain. Volume 1: New methodologies for sampling and analysis of gas-phase peroxide
[PB85-173425] 19 p3311 N85-30527

HYDROGEN PLASMA
NT DEUTERIUM PLASMA

Density measurements of atomic hydrogen in NBT-IM by laser-induced fluorescence spectroscopy
09 p1369 N85-18739

Control of surface composition and hydrogen recycling by plasma conditioning
[DE85-001859] 11 p1731 N85-20889

Frictional and structural characterization of ion-nitrided low and high chromium steels
[NASA-TM-86991] 13 p2098 N85-23085

Injection of hydrogen macroparticles into T-10 tokamak 21 p3692 N85-32937

HYDROGEN PRODUCTION

Surface production of negative hydrogen ions
[AD-A145437] 02 p0277 N85-11801

Solid electrolytes for medium temperature steam electrolysis
[DE84-014384] 04 p0463 N85-12938

High-temperature steam electrolysis: Technical and economic evaluation of alternative process designs
[DE84-015702] 04 p0469 N85-12986

Hydrogen technology evaluation center at Brookhaven National Laboratory
[DE84-014099] 04 p0470 N85-12988

Development and testing of thin film cells for high temperature water vapor electrolysis
[BMFT-FB-T-84-146] 04 p0471 N85-13001

Utilization of solar energy for the production of hydrogen 05 p0663 N85-14262

Hydrogen production employing high-temperature solid oxide cells
[DE84-014559] 06 p0766 N85-14901

Production of hydrogen by cyanobacteria
[PB85-113421/GAR] 07 p0935 N85-15925

Hydrogen from solar energy
[DE85-001914] 10 p1437 N85-19055

Artificial photosynthesis with algal and reconstituted systems
[DE85-002557] 10 p1523 N85-19604

Alternative anodic reactions in water splitting
[DE85-004159] 12 p1802 N85-21300

Solar-assisted hydrogen generation by photoelectrocatalysis
[PB85-149706] 12 p1804 N85-21314

The effect of water chemistry on the rates of hydrogen generation for galvanized steel corrosion at post-loca conditions
[NUREG/CR-3361] 14 p2253 N85-23963

Solid state hydrogen pumping and storage material
[AD-D011610] 16 p2757 N85-27011

Hydrogen recovery from extraterrestrial materials using microwave energy
[DE85-006717] 16 p2683 N85-27789

HYDROGEN RECOMBINATIONS

Hydrogen trapping, diffusion, and recombination in austenitic stainless steels
[DE85-001871] 09 p1294 N85-18129

Spin-polarized quantum systems
[DE85-006914] 16 p2864 N85-27667

HYDROGEN SULFIDE

The Jovian atmospheric window at 2.7 microns: A search for H2S
[NASA-TM-86861] 03 p0445 N85-12836

Thio and seleno compounds of the transition metals with the d (o) configuration
[BLL-MINTEK-TR-1177-(5810.5759)]
07 p0925 N85-15863

Effects of H2S on molten carbonate fuel cells
[DE85-008310] 18 p3130 N85-29386

Geothermal hydrogen and health in Rotorua, New Zealand
[DE85-901283] 19 p3301 N85-30467

Sulfur transformations at the hydrogen sulfide/oxygen interface in stratified waters and in cyanobacterial mats
21 p3657 N85-32715

The identification of compounds in mustard hydrolysate
[AD-A156381] 24 p4076 N85-35258

HYDROGEN 2
U DEUTERIUM

HYDROGEN 3
U TRITIUM

HYDROGEN-BASED ENERGY

Solid state hydrogen pumping and storage material
[AD-D011610] 16 p2757 N85-27011

Design principles for nickel hydrogen cells and batteries 20 p3447 N85-31396

HYDROGENATION

Studies of hydrogenated amorphous silicon
[DE84-013038] 01 p0067 N85-10443

Process research of polycrystalline silicon material (PROPSM)
[NASA-CR-174130] 05 p0619 N85-13962

Process Research On Polycrystalline Silicon Material (PROPSM) 06 p0830 N85-15276

Cation promotion effects in zeolite-supported F-T catalysts
[DE85-001708] 09 p1291 N85-18106

Process Research on Polycrystalline Silicon Material (PROPSM)
[NASA-CR-175461] 10 p1509 N85-19523

Study of the kinetics of hydrogenation using aged catalysts
[DE85-004373] 12 p1802 N85-21302

Synthesis, static and reactive characterization of supported organometallics
[DE85-004265] 12 p1808 N85-21340

Fire resistant polymers based on 1-(diorgano oxyphosphonyl)methyl-2,4- and 2,6-diamino benzenes
[NASA-CASE-ARC-11512-2] 12 p1811 N85-21362

Resistance of hydrogenated alpha-titanium alloys to corrosion-fatigue fracture 15 p2499 N85-25413

Process Research on Polycrystalline Silicon Material (PROPSM)
[NASA-CR-175761] 15 p2587 N85-25951

Optical properties of hydrogenated amorphous carbon films grown from methane plasma
[NASA-TM-86995] 15 p2658 N85-26406

Chemical vapor deposition of amorphous semiconductor films
[DE85-002917] 15 p2661 N85-26421

Study of synthesis gas conversion over metal oxides
[DE85-010136] 18 p3072 N85-28999

Study of the kinetics of hydrogenation using aged catalysts
[DE85-010427] 19 p3230 N85-30025

Catalytic hydrotreatment studies with model compounds
[DE85-010187] 19 p3236 N85-30064

Effect of thermochemical processing on fatigue resistance of titanium alloys 19 p3244 N85-30112

Reduction of the trapping of positrons in dislocated single crystals of iron when charged with hydrogen
[DE85-010235] 19 p3377 N85-30950

Mechanistic and kinetic studies of the elementary processes in catalytic combustion of methane
[PB85-188308] 20 p3435 N85-31314

HYDROGENOLYSIS

Properties of supported metal catalysts
[DE85-003927] 12 p1802 N85-21303

Exploratory study of coal conversion chemistry
[DE85-010393] 19 p3229 N85-30018

HYDROGEOLOGY

Hydrogeochemical investigation of thermal springs in the Black Canyon-Hoover Dam area, Nevada and Arizona
[PB84-202472] 01 p0064 N85-10428

Seafloor geosciences division: Missions, technical specialties, accomplishments, and activities, calendar year 1983
[AD-A144849] 01 p0087 N85-10592

Evaluating effectiveness of using space information in specialized hydrogeological research
02 p0164 N85-11114

Paleohydrology and geomorphology of selected reaches of the upper Wabash Valley, Indiana 02 p0226 N85-11481
Submarine sand ridges: Geology and development, New Jersey, USA 02 p0227 N85-11482
Glacier dynamics and the development of glacial landforms in the eastern Puget lowland, Washington 03 p0369 N85-12490
Activities of the Coastal Research Center [PB84-231323] 05 p0672 N85-14320
Application of SIR-B data for groundwater exploration in the Arabian shield and sand-drift monitoring in the AN Nafud and Al Jafurah fringe areas, Kingdom of Saudi Arabia 08 p1144 N85-17214
Deforestation, floodplain dynamics, and carbon biogeochemistry in the Amazon Basin 08 p1144 N85-17216
Radioactive waste isolation in salt: Peer review of the Office of Nuclear Waste Isolation's report on the organic geochemistry of deep groundwaters from the Palo Duro Basin, Texas [DE85-001439] 10 p1556 N85-19811
Structure and application of extremely large geophysical data bases [DE85-003527] 10 p1568 N85-19868
Mars: Long term changes in the state and distribution of H2O 13 p2191 N85-23593
Equipment for the ARGOS system from Eidsvoll Electronics A.S. 14 p2239 N85-23885
Remote sensing: New tool for China's geologists 14 p2283 N85-24141
Investigative report on using geological research to promote prospecting 14 p2283 N85-24142
Protecting the nation's groundwater from contamination, volume 1 [PB85-154201] 15 p2590 N85-25965
Protecting the nation's groundwater from contamination, volume 2 [PB85-154219] 15 p2590 N85-25966
Geologic and hydrologic characterization and evaluation of the basin and range province relative to the disposal of high-level radioactive waste. Part 2: Geologic and hydrologic characterization [GS-CIRC-904-B] 20 p3526 N85-31933
Geologic and hydrologic characterization and evaluation of the basin and range province relative to the disposal of high-level radioactive waste. Part 3: Geologic and hydrologic evaluation [GS-CIRC-904-A] 20 p3526 N85-31934
Deep sea mega-geomorphology: Progress and problems 21 p3602 N85-32369
Understanding coherence losses incurred by bottom-retained signals [AD-A155559] 21 p3701 N85-32992
Indications of mineral zoning in a fossil hydrothermal system at the Meager Creek geothermal prospect, British Columbia, Canada from induced polarization studies [DE85-011962] 22 p3815 N85-33636
Hydrogeology of the lower Glen Rose Aquifer, south-central Texas 24 p4108 N85-35466

HYDROGRAPHY
The Long Term Upper Ocean Study (LOTUS). Cruise summary [AD-A145767] 03 p0397 N85-12536
The long term upper ocean study (LOTUS). Cruise summary and hydrographic data report, OCEANUS 154, May 1984 [AD-A147906] 07 p1009 N85-16414
Advanced technology for hydrographic mapping [FOA-C-30371-E1] 08 p1176 N85-17418
Deep water mass circulation in the Western Alboran Basin: Measurements in July and September 1980 (Alboran I experiment) [AD-A148586] 08 p1191 N85-17504
Analysis of flow within the coastal boundary layer off Long Island, New York [DE85-001364] 09 p1359 N85-18550
Nautical charting with remotely sensed imagery, volume 1 [AD-A149361] 10 p1506 N85-19503
Nautical charting with remotely sensed imagery. Volume 2: Case studies [AD-A149362] 10 p1506 N85-19504
Establishment of hydrographic shore control by Doppler satellite techniques [AD-A150709] 14 p2347 N85-24512
Study of Volga river delta using space photosurvey materials 15 p2485 N85-25340
Report of the Hydrographic Service Royal Australian Navy for the year ended 30th june 1984, issue number 20 [AD-A151480] 15 p2583 N85-25932
Criteria for the classification of hydrographic positioning data [AD-A152283] 16 p2705 N85-26597
Status of computer aided mapping in hydrographic services 16 p2815 N85-27366
A comparison of methods of least squares adjustment of traverses [AD-A153612] 18 p3170 N85-29645
Hydrographic data from the OPTOMA (Ocean Prediction Through Observations, Modeling and Analysis) program: OPTOMA15, 24 January to 23 February 1985 [AD-A155012] 21 p3655 N85-32703
Federal Mineral Land Information System 24 p4106 N85-35459

HYDROKINETICS
U HYDROMECHANICS

HYDROLOGY
NT HYDROGEOLOGY
A summary of geothermal studies in Montana, through 1983 [DE84-014325] 01 p0064 N85-10422
Application guide for Hydrological Simulation Program FORTRAN (HSPF) [PB84-215763] 01 p0064 N85-10427
Water resources data, Mississippi, water year 1982 [PB84-224559] 01 p0065 N85-10434
Water resources data, Florida, water year 1982. Volume 4: Northwest Florida [PB84-223445] 01 p0066 N85-10437
Water resources data for Michigan, water year 1983 [PB84-225176] 01 p0066 N85-10442
Ecology of estuarine channels of the pacific northwest coast: A community profile [PB84-208709] 01 p0070 N85-10464
Estuaries of the Cape. Part 2: Synopses of available information on individual systems. Report no. 16: Bot/Kleinmond system (CSW 13) [CSIR-RR-417-PT-2] 01 p0087 N85-10587
The Multispectral Imaging Science Working Group. Volume 1: Executive summary [E85-10001] 02 p0213 N85-11404
The Multispectral Imaging Science Working Group. Volume 2: Working group reports [E85-10002] 02 p0213 N85-11405
Multispectral Imaging Science Working Group for Hydrologic Science: Executive summary 02 p0214 N85-11414
WXR (hydrologic weather wire and PLT product software package) [PB84-237221] 04 p0541 N85-13442
Contributions to remote sensing : Applications of thermal infrared [COMMUN-34/1984] 06 p0654 N85-14196
USSR report: Earth sciences [JPRS-UES-84-008] 07 p0980 N85-16223
Hydrologic characteristics of the Mediterranean and Black Sea 07 p0981 N85-16228
Razrezy program research in the tropical Atlantic 07 p0981 N85-16229
Evaluation of SIR-B imagery for geologic and geomorphic mapping, hydrology, and oceanography in Australia 08 p1146 N85-17229
Earth Sciences Division report, 1983 [DE85-001036] 09 p1341 N85-18436
Analysis of geohydrologic data by kriging [AD-P004152] 09 p1349 N85-18488
Retrieval procedures for hydrologic data from ARS (Agricultural Research Service) experimental watersheds in the US (REPHLEX) [PB85-111326/GAR] 09 p1402 N85-18826
Ice segregation and frost heaving [PB85-122430] 10 p1480 N85-19199
Water resources data for Alabama, water year 1983 [PB85-123842] 10 p1507 N85-19507
Water resources data for Colorado, water year 1983. Volume 1: Missouri River Basin, Arkansas River Basin and Rio Grande Basin [PB85-123859] 11 p1671 N85-20528
Water resources data for Colorado, water year 1983. Volume 2: River Basin above Dolores River [PB85-123867] 11 p1671 N85-20529
Review of computer mapping and display techniques applicable to regional analysis [DE85-003545] 12 p1875 N85-21764
Hydrographic data collected in 1982 and 1983 for EPOCS (Equatorial Pacific Ocean Climate Studies) [PB85-110799] 12 p1876 N85-21765
Catalog of submarine volcanoes and hydrological phenomena associated with volcanic events: 1500 BC to 31 Dec. 1899 [PB85-117984] 12 p1891 N85-21869
Effects of fracture roughness on fluid flow through a single deformable fracture [DE85-004593] 13 p2092 N85-23062
Snow reflectance from Thematic Mapper 13 p2120 N85-23205
Hydrovolcanism 13 p2186 N85-23574
Paleohydrologic implications of valley networks of Mars 13 p2190 N85-23585
Catastrophic-flood features in Swedish Lapland as a terrestrial analog for Martian channel flows 13 p2190 N85-2
The ARGOS system and hydrology. Results obtained by ORSTROM and benefits of a degree of standardization 14 p2239 N85-23
Automatic hydrological data collection facility using ARGOS 14 p2324 N85-24
Hydrology and climatic conditions in Greenland 14 p2327 N85-24
Hydrological data collection from Swedish mountain areas 14 p2327 N85-24
The ARGOS system and hydrology: The use of Platform Terminal Transmitter (PTT) with built-in memory and direct reception by the Seine basin hydrology service 14 p2328 N85-24
Preliminary report on the results of hydrological measurements in the southern Tyrrhenian Sea, in the Messina strait and in the western Ionian sea [PREPRINT-433] 14 p2382 N85-24
Organizing geological work tasks for 1985 outlined 16 p2806 N85-27
Present stage of utilization of the ARGOS system by the ORSTOM hydrological service for hydrometric data collection 16 p2813 N85-27
The ARGOS system in Brazil — hydrology 16 p2813 N85-27
Report on regional groundwater flow modeling for the Palo Duro Basin, Texas [DE85-007490] 16 p2815 N85-27370
Ecology of Pamlico River, North Carolina: An estuarine profile [PB85-155703] 16 p2822 N85-27404
Potential climatic impacts of increasing atmospheric CO2 with emphasis on water availability and hydrology in the United States [NASA-TM-87479] 17 p2995 N85-28617
Earth Resources: A continuing bibliography with indexes, issue 45 [NASA-SP-7041(45)] 18 p3123 N85-29
Conceptual hydrologic model of flow in the unsaturated zone, Yucca Mountain, Nevada [DE85-008346] 18 p3125 N85-29
Shales and other argillaceous strata in the United States [DE85-010453] 18 p3125 N85-29
Surface hydrologic characteristics of proposed repository locations in the Palo Duro Basin of the Texas Panhandle [DE85-010530] 18 p3126 N85-29
CSIN (Chemical Substances Information Network) workbook: US Geological Survey training course for Chemical Substances Information Network [PB85-170058] 18 p3200 N85-29
Use of a two-dimensional flow model to quantify aquatic habitat [AD-A154287] 19 p3266 N85-30253
Chlorine isotopes as environmental tracers in Columbia River basalt groundwaters [DE85-011392] 19 p3302 N85-30473
Synthetic rainfall and its use in hydrologic modeling 19 p3314 N85-30542
Microwave hydrology: A trilogy [NASA-CR-176042] 20 p3477 N85-31
SEASAT altimetry for surface height of inland seas 20 p3493 N85-31714
Geologic and hydrologic characterization and evaluation of the basin and range province relative to the disposal of high-level radioactive waste. Part 3: Geologic and hydrologic evaluation [GS-CIRC-904-A] 20 p3526 N85-31
Mega-geomorphology and neotectonics 21 p3602 N85-32
Space imagery and some geomorphological problems of the Guiana Shield, South America 21 p3602 N85-32
Changes in the organic material in lakes in the blast zone of Mount St. Helens, Washington: Hydrologic effects of the eruptions [GS-CIRC-850-1] 21 p3630 N85-32551
Military hydrology. Report 9: State-of-the-art review and annotated bibliography of dam-breach flood forecasting [AD-A155383] 22 p3801 N85-33553
Meteorology and Society: Statements presented at the 9th congress under agenda item 12 — World Meteorological Organization [WMO-643] 22 p3817 N85-33
Hydrology [PB85-182954] 23 p3944 N85-34
USGS coastal research, studies and maps: A source of information for coastal decision making [USGS-CIRC-883] 24 p4108 N85-35
Two-dimensional inversion of resistivity monitoring data from the Cerro Prieto geothermal field [DE85-012554] 24 p4113 N85-35

HYDROLOGY MODELS
Hydrologic and economic models for watershed evaluation and research
[PB84-222371] 01 p0086 N85-10438
The use of fixed-bed adsorber models to predict the fates of toxic substances in groundwaters and soil environments
[PB84-202583] 01 p0071 N85-10466
Identification and parameter estimation of phosphate balance models in drinking water reservoirs
[PUBL-313] 06 p1181 N85-17439
Verification of a model of the Eastern Scheldt
[RAND/R-3108-NETH] 09 p1354 N85-18518
World ocean level oscillations and their relationship to change in inflow of continental waters
13 p2108 N85-23133
Remote Sensing of Snow and Evapotranspiration
[NASA-CP-2363] 13 p2123 N85-23223
Snowmelt-runoff model utilizing remotely-sensed data
13 p2124 N85-23226
Snowmelt runoff model in Japan
13 p2124 N85-23227
Application of Martinec-Rango model to river basin in Japan 13 p2124 N85-23228
Applications of Kalman filtering and recursive least-squares in river flow modelling
15 p2636 N85-26254
Identification and characterization of watershed models for evaluation of impacts of climate change on hydrology
[DE85-008576] 18 p3125 N85-29348
Hydrology
[PB85-182954] 23 p3944 N85-34440
The development of assessment techniques program
24 p4106 N85-35457
HYDROLYSIS
Ceramic microstructure development
[AD-A145753] 03 p0337 N85-12166
Research in phase transfer catalysis
[AD-A148286] 08 p1121 N85-17068
Hydrolysis of iodine: Equilibria at high temperatures
[DE84-016713] 09 p1293 N85-18119
ECUT, Energy Conversion and Utilization Technologies program: Technical and economic assessment of processes for the production of butanol and acetone. Phase 2: Analysis of research advances
[NASA-CR-175471] 10 p1434 N85-19034
Ethanol production by enzymatic hydrolysis: Parametric analysis of a base-case process
[DE84-013105] 11 p1614 N85-20147
Hydrolysis of plastic wastes with the aim of recovering and reprocessing the starting components (recycling)
[BMFT-FB-T-84-250] 12 p1885 N85-21828
Kinetics of hydrolysis and products of hydrolysis and photolysis of tetryl
[AD-A153144] 17 p2921 N85-28005
Model for the growth of fractal silica polymers
[DE85-007884] 17 p2935 N85-28115
Lipid hydrolysis in man during antiorthostatic hypokinesia 23 p3953 N85-34500
The identification of compounds in mustard hydrolysate
[AD-A156381] 24 p4076 N85-35258
Aqueous volatile weak electrolyte equilibria to 300 C
[DE85-013840] 24 p4076 N85-35261
HYDROMAGNETIC FLOW
U MAGNETOHYDRODYNAMIC FLOW
HYDROMAGNETIC STABILITY
U MAGNETOHYDRODYNAMIC STABILITY
HYDROMAGNETIC WAVES
U MAGNETOHYDRODYNAMIC WAVES
HYDROMAGNETICS
U MAGNETOHYDRODYNAMICS
HYDROMAGNETISM
U MAGNETOHYDRODYNAMICS
HYDROMECHANICS
NT ELASTOHYDRODYNAMICS
NT ELECTROHYDRODYNAMICS
NT HYDRODYNAMICS
NT HYDROSTATICS
NT MAGNETOHYDRODYNAMICS
Second All-Union Seminar on Hydromechanics and Heat and Mass Exchange in Weightlessness, summaries of reports
[NASA-TM-77590] 01 p0047 N85-10305
Free surface effects on the wake of a flat plate
[AD-A148986] 07 p0958 N85-16071
Experiments on the influence of active walls on the initial amplitudes and growths of instability waves
[AD-A154630] 21 p3583 N85-32275
HYDROMETEOROLOGY
NT MARINE METEOROLOGY
Bibliography of climate textbooks and studies
[WCP-84] 02 p0231 N85-11505
Standard SHEF (Standard Hydrometeorologic Exchange Format) decoder Version 1.1
[PB85-108508/GAR] 06 p0840 N85-15332
Use of minicomputers for the formation of hydrological data banks 07 p1001 N85-16358
Water and climate, study of one case
07 p1002 N85-16369
The use of hydrometeorological data in explaining shrimp cycles in Guyana 07 p1004 N85-16381
A scheme for short-term prediction of hydrometeors using advection and physical forcing
[AD-A148011] 08 p1158 N85-17487
Atmospheric research aircraft — conductivity/charge measurements
[ONERA-RS-87/7154/PY] 11 p1682 N85-20596
Analysis of hydrometeorological conditions in Antarctic coastal waters according to data from hydrological and satellite observations 15 p2487 N85-25354
Great Lakes hydrometeorologic and hydraulic data needs 20 p3406 N85-31739
Effects of hydrometeors on electromagnetic wave propagation
[AD-A155379] 22 p3759 N85-33297
HYDROPHONES
Effect of axisymmetric vibration modes on sensitivity and directivity characteristics of piezoceramic sphere — hydrophones 15 p2525 N85-25569
Transversely reinforced piezoelectric composites
[AD-D011676] 19 p3260 N85-30214
HYDROPLANING
Runway rubber removal specification development field evaluation procedures development
[FAA-PM-84-27] 12 p1781 N85-21179
Very high speed lap with positive lift effect
[AD-D011710] 19 p3280 N85-30344
HYDROPONICS
Hydroponics developments for spaceship garden
21 p3663 N85-32754
HYDROPOWER STATIONS
U HYDROELECTRIC POWER STATIONS
HYDROSPHERE (EARTH)
U EARTH HYDROSPHERE
HYDROSTATIC PRESSURE
Processing ceramics
[NASA-TM-77603] 01 p0031 N85-10188
Special topics reports for the reference tandem mirror fusion breeder: Liquid metal MHD pressure drop effects in the packet bed blanket, volume 1
[DE85-002142] 06 p0865 N85-15500
Effect of hydrostatic pressure on trapping centers in strained-layer superlattice structures
[DE85-001362] 09 p1399 N85-18807
Hydrostatic bearing pad maximum load and overturning conditions for the 70-meter antenna
10 p1465 N85-19241
Simplified theory for the behaviour of buried flexible cylinders under the influence of uniform hoop compression
[PB85-116531] 11 p1654 N85-20419
Human lung fluid content during 7-day head-down tilt
12 p1902 N85-21941
High pressure environmental conditioning systems and chamber rehabilitation
[AD-A150039] 12 p1905 N85-21964
Effects of posture and water immersion on diaphragmatic function 16 p2840 N85-27515
Distribution of density in closed-impression die forging of axisymmetrical products from metal powders
19 p3245 N85-30118
HYDROSTATICS
Development of gas-lubricated pistons for heavy duty diesel engine technology program
[NASA-CR-174746] 03 p0441 N85-12808
Behavior and characteristics of storm cold outflows
09 p1356 N85-18529
Hydrostatic compression of Fe1-chi 0 wustite.
15 p2508 N85-25472
Non-contact hydrostatic bearings
16 p2762 N85-27046
On Long's solution to hydrostatic flow over mountains
[DFVLR-MITT-84-02] 17 p2994 N85-28503
Planetary reorientation by surface loads
22 p3858 N85-33886
HYDROTHERMAL CRYSTAL GROWTH
Hydrothermal alteration of CM carbonaceous chondrites: Implications of the identification of tochilinite as one type of meteoritic PCP 06 p0884 N85-15616
HYDROTHERMAL STRESS ANALYSIS
Designing for fiber composite structural durability in hygrothermomechanical environment
[NASA-TM-87045] 17 p2917 N85-27978
EVA-glass interface bond stability
21 p3608 N85-32408
Hydrothermal alteration in the 3.5 b.y. old Onverwacht Group of South Africa 21 p3718 N85-33071
HYDROTHERMAL SYSTEMS
Field testing of aquifer thermal energy storage
[DE85-000399] 09 p1344 N85-18457
Thermohydrodynamic model: Hydrothermal system, shallowly seated magma chamber
13 p2115 N85-23173
Determining deep heat flow and rate of horizontal percolation from temperature measurements in aquifer
13 p2116 N85-23180
Structure of Reykjanes Ridge rift zone and Icelandic thermal anomaly 19 p3289 N85-30395
Melt zones beneath five volcanic complexes in California: An assessment of shallow magma occurrences
[DE85-010644] 19 p3305 N85-30489
Submarine hydrothermal environments as sites for the origin and evolution of life 21 p3719 N85-33074
Indications of mineral zoning in a fossil hydrothermal system at the Meager Creek geothermal prospect, British Columbia, Canada from induced polarization studies
[DE85-011962] 22 p3815 N85-33636
Workshop on Recent Research in the Valles Caldera
[DE85-010569] 23 p3949 N85-34472
Heat transfer and brine evolution in magma-hydrothermal systems 24 p4104 N85-35441
Massive sulfide deposits from the southern Juan de Fuca Ridge 24 p4105 N85-35446
A comparison of LANDSAT thematic mapper, multispectral scanner and airborne sensors for mapping the distribution of alteration minerals: Examples from the southwestern United States 24 p4106 N85-35452
Preliminary results of an ALVIN dive program on active hydrothermal vents at the southern Juan de Fuca Ridge
24 p4106 N85-35454
Ore genesis at the Monterrosas deposit in the Coastal Batholith, Ica, Peru 24 p4115 N85-35510
HYDROX ENGINES
U HYDROGEN OXYGEN ENGINES
HYDROXIDES
NT POTASSIUM HYDROXIDES
The alpha-form of the hydroxides of bivalent metals
[NASA-TM-77506] 04 p0473 N85-13009
Evaluation of ettringite and related compounds for use in solar energy storage
[DE85-003249] 12 p1682 N85-21609
Exploratory corrosion tests on alloys in molten salts at 900(0)C
[DE85-000511] 14 p2257 N85-23963
High performance size exclusion chromatography (IX) bulk and component analysis of silanol groups in polydimethylsiloxanes: Process development endeavor
[DE85-006853] 15 p2506 N85-25456
Sintering phenomena of non-oxide silicon compounds
[DE85-006676] 15 p2520 N85-25535
Investigation of the reaction system NOX/ClOX/HOX under tropospheric and stratospheric conditions
[BPT-11/84] 18 p3137 N85-29427
HYDROXYCORTICOSTEROID
NT CORTISONE
Biochemical status of adrenocortical dysfunction following spaceflight 12 p1901 N85-21935
HYDROXYL COMPOUNDS
NT ALCOHOLS
NT ETHYL ALCOHOL
NT GLYCOLS
NT METHYL ALCOHOLS
NT PHENOLS
NT POLYVINYL ALCOHOL
HYDROXYL EMISSION
Fundamental equations of the LIF hydroxyl measurements, appendix A 05 p0676 N85-14338
Orographic disturbances of upper atmosphere emissions 11 p1663 N85-20480
Twilight intensity variation of the infrared hydroxyl airglow 11 p1663 N85-20481
Far-infrared emission lines of CO and OH in the Orion-KL molecular shock
[NASA-TM-86721] 24 p4167 N85-35832
Observations of far-infrared transitions between excited states of OH
[NASA-TM-86722] 24 p4167 N85-35833
HYDROXYL RADICALS
Organic aerosol formation: OH(hydroxyl radical) versus ozone oxidation pathways
[PB84-219680] 03 p0388 N85-12484
Detailed performance calculations: Wayne State University and Ford Motor Company, appendix C
05 p0676 N85-14340
Detailed performance calculations: Portland State Group, appendix F 05 p0676 N85-14343
Detailed performance calculations: Harvard Group, appendix G 05 p0676 N85-14344
The fluorescence of cometary OH and CN
09 p1411 N85-18896
Application of Monte Carlo and molecular dynamics methods to the calculation of thermodynamic properties of molten salts
[AD-A148697] 10 p1565 N85-19869

Electron stimulated desorption and the role of secondary electrons
[AD-A150974] 14 p2252 N85-23955
The copper vapor laser 16 p2624 N85-27417
Water vapor 16 p2624 N85-27420
Resonant CARS detection of OH radicals
[AD-A153842] 18 p3071 N85-28995
Measurement of radical species concentrations and polycyclic aromatic hydrocarbons in flames by fluorescence and absorption using a tunable dye laser
[DE85-006624] 18 p3113 N85-29274
Passive Q-modulation of optical cavities by KCl crystals containing OH(-) -ions 21 p3666 N85-32915
HYGRAL PROPERTIES
Remote sensing as a mineral prospecting technique
[E85-10010] 02 p0216 N85-11423
Designing for fiber composite structural durability in hygrothermomechanical environment
[NASA-TM-87045] 17 p2917 N85-27978
HYGROMETERS
Trace water sensor
[NASA-CASE-NPO-15722-1] 18 p3103 N85-29212
Fog activation and supersaturation
21 p3650 N85-32678
HYGROSCOPICITY
Structure and property formation mechanism in magnetite alloy-binder composite
10 p1444 N85-19103
Water-resistance and some other properties of polyalkali fluorophosphate glasses 14 p2261 N85-24133
HYPERBARIC CHAMBERS
Hyperbaric physiology (status and prospects)
08 p1194 N85-17521
Management of vibration sickness in coal mines by hyperbaric oxygenation 10 p1523 N85-19609
Peripheral changes in regional sweating responses to exercise in hypobaric environments
[AD-A150757] 14 p2388 N85-24710
Medical planning criteria for implementation of clinical hyperbaric facilities
[AD-A151001] 14 p2389 N85-24715
Light-weight oxygen delivery hood assembly for hyperbaric chamber
[AD-D011709] 19 p3331 N85-30634
Determination of individual tolerance in hyperbaric oxygen 23 p3954 N85-34507
HYPERBOLAS
Efficient parallel solution of linear systems with hyperbolic rotations
[AD-A152355] 17 p3018 N85-28661
Hyperbolic phenomena in the flow of viscoelastic fluids
[AD-A153533] 18 p3099 N85-29186
HYPERBOLIC COORDINATES
Generation of three-dimensional body-fitted coordinates using hyperbolic partial differential equations
[NASA-TM-86753] 20 p3519 N85-31887
HYPERBOLIC DIFFERENTIAL EQUATIONS
The convergence of Garlerkin approximation schemes for second-order hyperbolic equations with dissipation
[CSIR-TWISK-325] 01 p0109 N85-10736
Approximation of discontinuous solutions of hyperbolic partial differential equations
[NRIMS-TWISK-302] 02 p0250 N85-11631
A pseudospectral Legendre method for hyperbolic equations with an improved stability condition
[NASA-CR-172475] 03 p0410 N85-12617
On explicit difference schemes for hyperbolic systems with variable coefficient 2
[PREPRINT-808] 03 p0413 N85-12641
Loeb Sobolev spaces with applications to variational integrals and differential equations
[CTH-MATH-1984-19] 04 p0556 N85-13544
Generation of 3-dimensional body fitted coordinates using hyperbolic partial differential equations
[AD-A148059] 09 p1274 N85-18006
Contribution to the study of a numerical implicit method for solving the Euler equations
[ESA-TT-872] 10 p1549 N85-19771
High order difference schemes with reduced dispersion for hyperbolic differential equations
[CWI-NM-R8408] 11 p1634 N85-20293
A convergent series expansion for hyperbolic systems of conservation laws
[NASA-CR-172557] 12 p1910 N85-21990
Results for second order hyperbolic systems with viscous dumping
[AD-A151100] 15 p2555 N85-25765
On functions with a finite or locally bounded Dirichlet integral 15 p2635 N85-26243
Relaxation methods for hyperbolic equations
[REPT-84-20] 17 p3021 N85-28687
Use of a hyperbolic grid generation scheme in simulating supersonic viscous flow about three-dimensional winged configuration
[NASA-TM-85344] 23 p3893 N85-34116
Workshop report on Simulation Techniques for Shock Wave Phenomena and Characteristics of Plasmas in Inertial Confinement Fusion
[IPPJ-725] 23 p3979 N85-34670
Cubic interpolated pseudo-particle method (CIP) for solving hyperbolic-type equation
23 p3979 N85-34673
Absorbing boundary conditions for exterior problems
[NASA-CR-177944] 24 p4142 N85-35676
HYPERBOLIC FUNCTIONS
Some scientific subroutines in LISP
[AD-A147889] 07 p1026 N85-16515
Generalized formulation of a class of explicit and implicit TVD schemes
[NASA-TM-86775] 21 p3675 N85-32830
HYPERBOLIC NAVIGATION
NT LORAN
NT LORAN C
HYPERBOLIC SPACE
U HYPERBOLIC COORDINATES
HYPERBOLIC SYSTEMS
The experimental computer control of a two-dimensional hyperbolic system 20 p3411 N85-31166
HYPERCAPNIA
Dynamics of external respiration and gas metabolism under combined effect of hypoxia and hypercapnia
08 p1193 N85-17519
Factors determining effectiveness of voluntary decrease in ventilation during muscular work using instrumented feedback 08 p1193 N85-17520
HYPERFINE STRUCTURE
Investigation of solid state problems using the hyperfine interaction between static and dynamic internal fields with short live excited probe nuclei 03 p0428 N85-12729
EXAFS and Moessbauer study of small metal clusters isolated in rare-gas solids
[DE84-015976] 04 p0470 N85-12994
Investigation on K (4 2P3/2) Hg interaction at collision energies from 0.5 to 5.7 eV
[MPIS-15/1983] 04 p0563 N85-13589
The evaluation of a deformable diffraction grating for a stigmatic EUV spectroheliometer
[NASA-CR-174248] 07 p1042 N85-16621
Hyperfine structure and lifetime measurements on electronically excited long-life molecules in a beam experiment
[MPIS-11/1984] 11 p1726 N85-20855
Very low temperature studies of hyperfine effects in metals
[DE85-013367] 22 p3749 N85-33236
HYPERGEOMETRIC FUNCTIONS
Asymptotic expansion of Jacobi polynomials
[REPT-84-35] 17 p3021 N85-28689
HYPERGOLIC ROCKET PROPELLANTS
Atmospheric dispersion of hypergolic liquid rocket fuels, volume 1
[AD-A149597] 12 p1817 N85-21399
Atmospheric dispersion of hypergolic liquid rocket fuels, volume 2
[AD-A150699] 14 p2263 N85-24020
HYPERKINESIA
Alterations in skeletal muscle with disuse atrophy
[NASA-CR-174195] 06 p0843 N85-15349
HYPERNEA
Factors determining effectiveness of voluntary decrease in ventilation during muscular work using instrumented feedback 08 p1193 N85-17520
HYPERNUCLEI
A 1-2 GeV/c beam line for hypernuclear and kaon research
[DE85-007623] 16 p2863 N85-27659
Spin dependence of the lamda-nucleus interaction determined by observation of hypernuclear gamma rays
[DE85-011878] 19 p3364 N85-30863
HYPERONS
Cooling of neutron stars with hyperons
[DE85-004641] 13 p2171 N85-23472
HYPEROXIA
Effect of hyperoxia and increased gas atmosphere density on contractile function of the right ventricle
01 p0093 N85-10628
Change in energetics of muscular contraction as a result of hyperoxia 01 p0093 N85-10629
Mechanisms of oxygen toxicity and methods of protection
[AD-A145830] 03 p0400 N85-12551
Distribution and abundance of organic thiols
21 p3657 N85-32717
HYPERSONIC AIRCRAFT
NT HYPERSONIC GLIDERS
Aerodynamic heating rate distributions induced by trailing edge controls on hypersonic aircraft configurations at Mach 8
[NASA-TM-87453] 13 p1969 N85-22370
Aerodynamic characteristics of a distinct wing-body configuration at Mach 6: Experiment, theory, and the hypersonic isolation principle
[NASA-TP-2467] 22 p3727 N85-[illegible]
HYPERSONIC BOUNDARY LAYER
Experimental studies of Quasi-Two-Dimensional and three-dimensional viscous interaction regions induced by skewed-shock and swept-shock boundary layer interactions
[AD-A150080] 12 p1847 N85-[illegible]
Proceedings of the 9th US Air Force and the Federal Republic of Germany Data Exchange Agreement Meeting. Viscous and Interacting Flow Field Effects
[AD-A153020] 17 p2958 N85-[illegible]
A numerical solution of a nonisothermal wall using the two-dimensional Navier-Stokes equations
[AD-A154467] 19 p3286 N85-[illegible]
HYPERSONIC FLOW
Numerical analysis of the 3-dimensional inviscid hypersonic flow around capsule-type bodies by the alternate directional implicit method
[NAL-TR-799] 01 p0002 N85-10012
Turbulent boundary layers over rough surfaces hypersonic flow
[AD-A145040] 01 p0003 N85-10018
Experimental and predicted heating distributions for biconics at incidence in air at Mach 10
[NASA-TP-2334] 03 p0361 N85-12313
Aerodynamic and thermal characteristics of slender bodies in hypersonic flow of rarefied gas at angle of attack 06 p0778 N85-14874
Hypersonic flow of mixture around blunt body
06 p0779 N85-14879
Laminar heat-transfer distributions on biconics at incidence in hypersonic-hypervelocity flows
[NASA-TP-2213] 07 p0957 N85-10086
Instrumentation for Application Number 1: Mass spectrometric analysis of the boundary layer associated with the tethered satellite 11 p1646 N85-20372
Hypersonic flow about triangular airfoil at large angles of attack 13 p2044 N85-22782
A 3-dimensional Navier-Stokes-Euler code for blunt-body flow computations
[NASA-TM-58266] 15 p2463 N85-25211
Flow over a biconic configuration with an afterbody compression flap
[AD-A151882] 15 p2557 N85-25778
Hypersonic nonequilibrium gas flow past zero-aspect wing 16 p2765 N85-27083
Cone drag in the transition from continuum to free molecular flow
[OUEL-1538/84] 20 p3390 N85-31023
One method of solving the problem of unsteady heat exchange of a body and its ablation
22 p3733 N85-33146
Experimental aerodynamic heating to simulated space shuttle tiles in laminar and turbulent boundary layers with variable flow angles at a nominal Mach number of 7
[NASA-TP-2307] 23 p3929 N85-34351
Mach 14 flow restrictor thermal stress analysis
[AD-A156215] 24 p4067 N85-35208
HYPERSONIC GLIDERS
Flight tests of experimental shuttle craft described
15 p2533 N85-25825
HYPERSONIC HEAT TRANSFER
Experimental investigation of heat transfer to bluff cylinders and cones in hypersonic rarefied gas flow
11 p1620 N85-20196
An experimental investigation of flap turbulent heat transfer and pressure characteristics in hypersonic flow
12 p1821 N85-21426
HYPERSONIC REENTRY
NT UNCONTROLLED REENTRY (SPACECRAFT)
Columbia: The first 5 flights entry heating data series. Volume 1: An overview
[NASA-CR-171820] 07 p0913 N85-15777
HYPERSONIC SPEED
Fiber reinforced fused silica for hypersonic radome applications
[AD-P004366] 12 p1826 N85-21480
HYPERSONIC VEHICLES
NT HYPERSONIC AIRCRAFT
NT HYPERSONIC GLIDERS
NT LIFTING REENTRY VEHICLES
A model of hypersonic two-dimensional oblique detonation wave ramjet
[UTIAS-TN-257] 23 p3897 N85-34139
HYPERSONIC WIND TUNNELS
NT CASCADE WIND TUNNELS
Aeronautical facilities catalogue. Volume 1: Wind tunnels
[NASA-RP-1132] 10 p1426 N85-18801
Mach-10 high Reynolds number development in the NSWC (Naval Surface Weapons Center) hypervelocity facility
[AD-A151241] 15 p2474 N85-25274

Mach 14 flow restrictor thermal stress analysis
[AD-A156215] 24 p4067 N85-35206
HYPERTENSION
NT POLYPEPTIDES
HYPERTHERMIA
Effects of hyperthermia on free amino acids in rat brain and in subcellular fractions 11 p1691 N85-20631
HYPERTONIA
U OSMOSIS
HYPERTROPHY
U GROWTH
HYPERVELOCITY
Electromagnetic acceleration of macroparticles to hypervelocities in axisymmetric geometry
[IPPJ-696] 06 p0863 N85-15484
Mach-10 high Reynolds number development in the NSWC (Naval Surface Weapons Center) hypervelocity facility
[AD-A151241] 15 p2474 N85-25274
HYPERVELOCITY ACCELERATORS
U HYPERVELOCITY GUNS
HYPERVELOCITY CRATERING
U HYPERVELOCITY PROJECTILES
U PROJECTILE CRATERING
HYPERVELOCITY FLOW
Laminar heat-transfer distributions on biconics at incidence in hypersonic-hypervelocity flows
[NASA-TP-2213] 07 p0957 N85-16065
HYPERVELOCITY GUNS
NASA-Ames vertical gun 04 p0579 N85-13696
Electromagnetic rail launcher as a circuit element
[AD-A150067] 12 p1835 N85-21516
An orthogonal grid technique for studying internal deformation and energy absorption in target penetration
[AD-A149989] 12 p1860 N85-21665
Design and fabrication of projectiles for round bore railguns
[DE85-011871] 20 p3398 N85-31078
HYPERVELOCITY IMPACT
Particle velocity experiments in anorthosite and gabbro
[NASA-CR-174158] 04 p0533 N85-13407
Orbital Debris
[NASA-CP-2360] 12 p1783 N85-21188
Manmade orbital debris studies at NASA Langley
12 p1783 N85-21192
Hypervelocity impacts on Skylab 4/Apollo windows
12 p1785 N85-21202
Hypervelocity impact investigations and meteoroid shielding experience related to Apollo and Skylab
12 p1785 N85-21206
Debris impact on Earth-orbiting spacecraft
12 p1948 N85-22234
Plasma production by meteoroid impact
13 p2174 N85-23492
Progress on studies of early intense cratering
13 p2181 N85-23535
Martian terrain ages 13 p2181 N85-23537
Morphology and mechanics of terraces in lunar craters
13 p2182 N85-23543
Newly discovered Martian impact basins
13 p2182 N85-23544
Impact ionization from gold, aluminum and PCB-Z --- Giotto spacecraft paint PCB-Z 14 p2244 N85-23910
Experimental investigations on ion emission with dust impact on solid surfaces --- Giotto spacecraft
14 p2244 N85-23911
Voyager planetary radio astronomy: Grain and particle impacts shot noise in Saturn's ring plane
15 p2673 N85-26498
Experimental data for characterizing perforating impacts: Fragmentation processes
[AD-A156370] 24 p4102 N85-35427
HYPERVELOCITY LAUNCHERS
Preliminary analysis of space mission applications for electromagnetic launchers
[NASA-CR-174067] 03 p0321 N85-12071
Use of the computer programa PARA 80 to study results from firing the railgun ERGS-1M
[MRL-R-900] 22 p3738 N85-33167
HYPERVELOCITY PROJECTILES
Rail accelerator technology and applications
[NASA-TM-86947] 12 p1794 N85-21258
Arc-driven rail gun research
[NASA-CR-174816] 12 p1859 N85-21662
Ion emission from solid surfaces: Comparison of dust impact with other excitations --- Giotto mission
14 p2244 N85-23912
A method of accurizing rail guns
[LA-10028-MS] 22 p3737 N85-33166
Experimental data for characterizing perforating impacts: Fragmentation processes
[AD-A156370] 24 p4102 N85-35427
HYPERVELOCITY WIND TUNNELS
NT CASCADE WIND TUNNELS
HYPOBARIC ATMOSPHERES
Small animal hypobaric chamber
[AD-A148196] 03 p0364 N85-12335
An environmentally-controlled extended-use small animal hypobaric chamber
[AD-A153735] 19 p3221 N85-29974
HYPOKINESIA
Dynamics of morphological changes in articulation nervous system under hypokinetic conditions as a model of a spaceflight factor 01 p0092 N85-10621
Effect of 1,25-dihydroxycholecalciferol and 24,25 dihydroxycholecalciferol on growth and alteration of rat bones during hypokinesa (histomorphometric study)
01 p0092 N85-10622
Dynamics of some parameters of carbohydrate and lipid metabolism in recovery period following long-term hypokinesa 01 p0093 N85-10623
Biligenic function of white rat liver
01 p0093 N85-10624
Effect of short-term hypokinesia on rat opioid system reaction 01 p0093 N85-10625
Skeletal muscle metabolism in hypokinetic rats
[NASA-CR-174059] 02 p0233 N85-11520
General resistance of organism of rats under hypokinesia 05 p0694 N85-14462
Effects of prolonged hypokinesia on nervous system
08 p1194 N85-17524
Study of bodily functional status and quality of controlling action of power unit operators with various intensities of labor 09 p1362 N85-18569
Characteristics of human masseter under conditions of hypokinesia 11 p1691 N85-20630
Morphological study of monkeys submitted to antiorthostatic hypokinesia 12 p1902 N85-21942
Fluid metabolism of monkeys during two-week antiorthostatic hypokinesia 12 p1902 N85-21943
Distinctive morphological manifestations of acute stress reaction in adrenal cortex of hypokinetic rats
12 p1902 N85-21944
Preventive effect of acute heat factors during hypokinesia 12 p1902 N85-21945
Rat tissue opioid peptide content during long-term hypokinesia 12 p1904 N85-21954
Effects of muscle atrophy on motor control: Cage size effects 15 p2609 N85-26080
Induced changes in the cholinergic system of sciatic nerve and slow and fast twitch muscle of rats
15 p2609 N85-26081
Use and disuse and the control of acetylcholinesterase activity in fast and slow twitch muscle of rat
[NASA-CR-175717] 15 p2614 N85-26109
Changes in the cholinergic system of rat sciatic nerve and skeletal muscle following suspension induced disuse
[NASA-CR-175718] 15 p2615 N85-26111
Analysis of head-down tilt as an analog of weightlessness using a mathematical simulation model
[NASA-CR-171870] 15 p2616 N85-26118
Regional circulation during testing on isokinetic dynamometer following 14-day bedrest
19 p3323 N85-30590
Primate adrenal reactions to antiorthostatic hypokinesia 19 p3324 N85-30591
Distinctions of rat lymphatic organ reactions to acute stress factor during hypokinesia
19 p3324 N85-30596
Morphological study of primate hypothalamus and hypophysis after experiment with antiorthostatic hypokinesia 19 p3325 N85-30603
Changes in nephron and juxtaglomerular system of primate kidneys under the effect of antiorthostatic hypokinesia 19 p3326 N85-30605
Rat blood serum and liver carbohydrates and lipids in recovery period after 15-day hypokinesia
19 p3326 N85-30606
Analysis of long bone and vertebral failure patterns
[AD-A154796] 21 p3663 N85-32758
Results and prospects of physiological research during spaceflights 22 p3732 N85-33139
Effects of immobilization and high-altitude adaptation on energy metabolism in rats 22 p3820 N85-33663
Investigation of spectrum of human bile acids during 120-day antiorthostatic hypokinesia
22 p3821 N85-33674
Effect of short-term antiorthostatic hypokinesia on dynamics of cardiorespiratory parameters during graded physical exercise 22 p3822 N85-33677
Investigation of some aspects of amino acid metabolism in man during brief exposure to antiorthostatic hypokinesia combined with ultraviolet radiation
22 p3822 N85-33678
Morphological study of antiorthostatic hypokinesia in monkeys 22 p3822 N85-33680
Morphological manifestations of hemodynamic changes in lungs of monkeys submitted to antiorthostatic hypokinesia 22 p3824 N85-33688
Effect of hypokinesia and +Gz accelerations on transport function of human blood
23 p3952 N85-34497
Lipid hydrolysis in man during antiorthostatic hypokinesia 23 p3953 N85-34500
Rat skeletal muscles with simulation of physiological effects of weightlessness (morphological study)
23 p3953 N85-34502
Possible mechanism for changes in glycogen metabolism in unloaded soleus muscle
[NASA-CR-176184] 24 p4127 N85-35586
HYPOTHALAMUS
Influence of hyperthermia on body temperature and content of catecholamines in white rat hypothalamus
10 p1524 N85-19615
Neural mechanism by which gravitational stimulus and stress affect the secretion of renin and other hormones
15 p2610 N85-26083
Morphological study of primate hypothalamus and hypophysis after experiment with antiorthostatic hypokinesia 19 p3325 N85-30603
HYPOTHERMIA
Influence of hyperthermia on body temperature and content of catecholamines in white rat hypothalamus
10 p1524 N85-19615
Effects of hypothermia on brain metabolism
11 p1692 N85-20636
Changes in pentose and glucuronate pathway dehydrogenases in rat brains following single or multiple hypothermic episodes 20 p3505 N85-31790
Electroanesthesia as a means of controlling cold stress of local hypothermia 22 p3823 N85-33687
HYPOTHESES
NT EXPECTANCY HYPOTHESIS
NT NULL HYPOTHESIS
NT VORTICITY TRANSPORT HYPOTHESIS
Distributed hypothesis testing in distributed sensor networks
[AD-A145434] 02 p0294 N85-11905
The search for regularity: Four aspects of scientific discovery
[AD-A145939] 03 p0368 N85-12355
Development of structured regression hypotheses/interactive descriptive geometry through five dimensions
[INT-324] 04 p0554 N85-13524
Invariant tests and likelihood ratio tests for multivariate elliptically contoured distributions
[AD-A155844] 24 p4142 N85-35679
HYPOXEMIA
Pulmonary blood flow and oxygenation of arterial blood in a healthy subject upon 7 days hypokinesia
07 p1014 N85-16439
The effect of an unphysiological oxygen supply on the organism 24 p4130 N85-35605
HYPOXIA
Hemodynamics and neurodynamics of the human brain during exposure to moderate hypoxic hypoxia
01 p0094 N85-10630
The effect of naproxen on acute mountain sickness and vascular responses to hypoxia
[AD-A145144] 01 p0095 N85-10638
USSR report: Life Sciences: Biomedical and behavioral sciences
[JPRS-UBB-84-026] 04 p0543 N85-13457
Results of study of hypoxia problems
04 p0544 N85-13462
Distribution of blood flow to brain, kidneys, gut, spleen and posterior extremities in cats in acute hypoxia
07 p1013 N85-16434
Biochemical evaluation of bodily influence of high and low temperatures 07 p1014 N85-16441
Dynamics of external respiration and gas metabolism under combined effect of hypoxia and hypercapnia
08 p1193 N85-17519
Aviation-related cardiorespiratory effects of blood donation in female pilots
[AD-A148045] 08 p1195 N85-17529
Multiple regression method used to assess animal adaptation to hypoxic hypoxia 12 p1902 N85-21947
Peripheral changes in regional sweating responses to exercise in hypobaric environments
[AD-A150757] 14 p2386 N85-24710
Oxygen uptake as an indicator of animal adaptation to altitude hypoxia 19 p3324 N85-30595
Formation of new microvessels in skeletal muscles of rats exposed to hypobaric hypoxia for one week
22 p3820 N85-33662
Effects of blood volume overload on myocardial ultrastructure in relation to adaptation to high altitude hypoxia 22 p3820 N85-33664
Structural changes in thyroid due to high-altitude adaptation in Kirghizia 22 p3820 N85-33666
Effect of acute hypoxia on coronary and systemic hemodynamics 23 p3953 N85-34503

Monitoring dosage of volatile compounds in tests at low barometric pressure 23 p3954 N85-34506
HYPSOGRAPHY
Hypsometric features on Venus
13 p1983 N85-22439
HYSTERESIS
Input-output stability analysis with magnetic hysteresis non-linearity: A class of multipliers
[AD-A145729] 02 p0253 N85-11654
Theory of the double critical state in type-2 superconductors
[DE84-015461] 02 p0289 N85-11886
Variation of resin properties through the thickness of cured samples 04 p0468 N85-12974
Internal hysteresis experienced on a high pressure syn gas compressor 05 p0642 N85-14122
Anisotropy and relaxation effects of Co2+ ions in LiTi ferrite
[AD-A146550] 06 p0861 N85-15469
Magnetostatic problems in nonlinear media with hysteresis
[DE85-003701] 10 p1482 N85-19358
Application of hysteresis modelling to the non-destructive inspection of stress
[DE85-003081] 11 p1650 N85-20393
Studies in electron phenomena in MOS structures: The pulsed C-V method 15 p2659 N85-26407
An experimental nonlinear optical waveguide device
18 p3186 N85-29762
Application of traction drives as servo mechanisms
22 p3797 N85-33520
Electrical resistivity and hysteresis of the equiatomic nickel-titanium alloy near the martensitic transformation temperature 23 p3904 N85-34181
Monotonous stress-strain properties of structural steel subjected to nonstationary repetitive pre-loading
23 p3904 N85-34185

I

I BEAMS
Yield joint condition for three-dimensional I-beams
[ILR-MITT-137] 12 p1867 N85-21716
Buckling and bracing of cantilevers
[CE-42] 17 p2979 N85-28413
Impact dynamics research on composite transport structures
[NASA-TM-86391] 19 p3284 N85-30367
IBM COMPUTERS
IBM Corporation, IBM 5381 model 5, system/38 COBOL release 6
[PB84-227677] 03 p0405 N85-12584
Digital Research Incorporated, IBM PC XT, FORTRAN-77 V4.0
[PB84-243633] 06 p0849 N85-15388
Northern Telecom, Incorporated, IBM 3033 (compilation), NTI-585/565 (execution), XCOBOL Release 4.1 Version H(01)
[PB84-227875] 06 p0850 N85-15400
ZTL: A subroutine package for the IBM personal computer to support the Ziatech ZT1488 IEEE-488 controller
[LA-10141-MS] 12 p1913 N85-22010
DOS 21: PCDOS 2.0 support subroutine package for the IBM personal computer
[LA-10142-MS] 12 p1914 N85-22012
TRANIO: A subroutine package for the IBM personal computer to support the transfer 6002 CAMAC crate controller
[LA-10145-MS] 12 p1914 N85-22015
ICBM (MISSILES)
U INTERCONTINENTAL BALLISTIC MISSILES
ICE
NT GLACIERS
NT ICE FLOES
NT ICEBERGS
NT LAKE ICE
NT LAND ICE
NT PRESSURE ICE
NT SEA ICE
The development of a diode laser Doppler velocimeter for boundary layer measurements under ice: A feasibility investigation
[AD-A145076] 01 p0053 N85-10348
Executive report: Results of the IRGA-CNPq/INPE experimental project
[E85-10011] 02 p0216 N85-11424
Transport phenomena in the boundary layer during solution solidification under microgravity. Ice growth from a water-salt solution
[BMFT-FB-W-84-031] 03 p0329 N85-12121
Measurement of snow cover thickness by radar sounding 03 p0344 N85-12216
Ice sheets as invariant surfaces for radar altimeter calibration and orbit determination
03 p0383 N85-12449
Initial feasibility ground test of a proposed photogrammetric system for measuring the shapes of ice accretions on helicopter rotor blades during forward flight
[NASA-TM-87391] 04 p0455 N85-12887
Evaluation of thermocouple junction temperature
[DE84-015159] 04 p0502 N85-13206
Solar wind and cosmic ray irradiation of grains and ices - application to erosion and synthesis of organic compounds in the solar system
06 p0888 N85-15637
Salt action on concrete
[AD-A147812] 07 p0933 N85-15912
Pulse transmission through frozen silt
[AD-A147108] 07 p0940 N85-15958
Buckling analysis of cracked, floating ice sheets
[AD-A147330] 07 p0988 N85-16277
Deuterium diffusion in a soil-water-ice mixture
[AD-A148457] 08 p1176 N85-17415
Hybrid system for producing and storing ice
[DE84-017474] 09 p1304 N85-18195
The pleistocene geology of Vilas County, Wisconsin
09 p1353 N85-18509
A model for the climatic behavior of water on Mars
09 p1415 N85-18931
Atlas of snow and ice resources
10 p1497 N85-19449
Freeze-up, breakup and date of maximum ice thickness for the Saint Lawrence River, 1971 - 1978
[PB85-119451] 10 p1507 N85-19509
Ground-based snow and ice crystal observation system used in Sierra Nevada winter orographic storms
[PB85-115343] 10 p1520 N85-19584
MIZEX (Marginal Ice Zone Program): A program for mesoscale air-ice-ocean interaction experimemts in Arctic marginal ice zones. 5. MIZEX 84. Summer experiment PI (Principal Investigator) preliminary reports
[AD-A148986] 10 p1521 N85-19594
Lake ice occurrence as a possible detector of atmospheric CO2 effects on climate
[DE85-002951] 11 p1687 N85-20606
Implications of the presence of S2 in cometary ice
11 p1760 N85-21072
Latent heat storage in cooling systems
[DE85-005355] 13 p2129 N85-23248
Variation of Arctic cloud cover in summer
[DE85-004507] 13 p2139 N85-23285
Patterns of fracture and tidal stresses due to nonsynchronous rotation: Implications for fracturing on Europa 13 p2173 N85-23483
Comet thermal modeling 13 p2176 N85-23505
High pressure cosmochemistry of major planetary interiors: Laboratory studies of the water-rich region of the system ammonia-water 13 p2183 N85-23549
Transformation of polar ice sublimate residue into Martian circumpolar sand 13 p2189 N85-23580
Mars: Long term changes in the state and distribution of H2O 13 p2191 N85-23593
Creep of ice: Further studies
13 p2201 N85-23655
North Atlantic Deep Water Formation
[NASA-CP-2367] 15 p2601 N85-26028
Macrostructure and microphysics of Saturn's E-ring
15 p2677 N85-26528
Permafrost, seasonally frozen ground, snow cover and vegetation in the USSR
[AD-A153628] 18 p3124 N85-29346
Active and passive remote sensing of ice
[AD-A154406] 19 p3300 N85-30459
A study of freezing and melting with eutectic interactions 19 p3378 N85-30956
Mesoscale features and atmospheric refraction conditions of the Arctic marginal ice zone
[AD-A155139] 21 p3636 N85-32584
The nucleation of ice at very low temperatures and pressures 21 p3641 N85-32617
The capture of ice nucleating and non ice-nucleating aerosols by ice phase precipitation
21 p3641 N85-32620
Short-time creep of ice
[NRC/CNR-TT-2111] 23 p3941 N85-34428
Lake ice occurence as a possible detector of atmospheric CO2 effects on climate
[DE85-012967] 23 p3950 N85-34480
Elemental tracers of source regions of contaminants in precipitation
[DE85-012858] 24 p4113 N85-35499
ICE ENVIRONMENTS
Sea ice data buoys in the Weddell Sea
[AD-A144953] 01 p0086 N85-10594
Investigation of ice dynamics in the marginal ice zone
[AD-A145110] 01 p0088 N85-10597
Cryospheric data products available through satellite altimetry 03 p0380 N85-12439
Surging as a potential response of ice sheets to CO2-induced changes in the polar environment (SPICAE)
[DE84-016472] 06 p0841 N85-15341
Proceedings of a Workshop on Environment of West Antarctica: Potential CO2-induced changes
[PB85-110757] 11 p1671 N85-20527
Planetary analogs in Antarctica: Icy satellites
13 p2193 N85-23565
Ganymede and Callisto: Beauty is only skin deep
15 p2680 N85-26502
The NORDA/FNOC (Naval Ocean Research and Development Activity's/Fleet Numerical Oceanography Center) Polar Ice Prediction System (PIPS)-Arctic: A technical description
[AD-A156332] 24 p4126 N85-35577
ICE FLOES
Meteorite concentrations in Antarctica: How complete is the picture? 06 p0889 N85-15944
Parachute expedition to Arctic
07 p0962 N85-16040
Mining cosmic dust from the blue ice lakes of Greenland 15 p2682 N85-26868
ICE FORMATION
Automated aircraft icing forecast technique
[AD-A144853] 01 p0065 N85-10571
The rheology of icy satellites
[NASA-CR-174024] 02 p0302 N85-11899
Icing rate on stationary structures under marine conditions
[AD-A145795] 03 p0395 N85-12524
The UH-1H helicopter icing flight test program: An overview
[NASA-TM-86925] 07 p0900 N85-15702
The NASA Altitude Wind Tunnel (AWT): Its role in advanced icing research and development
[NASA-TM-86920] 07 p0910 N85-15759
Frazil ice formation
[AD-A147425] 07 p0988 N85-16276
Snow characterization measurements from SNOW-TWO/Smoke Week 6
[AD-A147423] 07 p1006 N85-16402
Icing flight research: Aerodynamic effects of ice and ice shape documentation with stereo photography
[NASA-TM-86906] 09 p1279 N85-18049
Ice segregation and frost heaving
[PB85-122430] 10 p1460 N85-19199
Frozen precipitation and concurrent weather: A case study for Munchen-Riem, West Germany
[AD-A149227] 10 p1519 N85-19577
First stage of equipping a Do 28 as a research aircraft for icing, and first research results
[ESA-TT-855] 11 p1584 N85-19992
Analysis of hydrometeorological conditions in Antarctic coastal waters according to data from hydrological and satellite observations 15 p2487 N85-25354
Characteristics of snow cover on sea ice and formation of snow ice II 15 p2582 N85-25924
Ice multiplication in summertime cumulus clouds in the BEWMEX area 16 p2829 N85-27445
Ice shapes and the resulting drag increase for a NACA 0012 airfoil
[NASA-TM-83556] 17 p2894 N85-27839
On the state of knowledge on meteorologically caused icing of aircraft in clouds
[ESA-TT-861] 20 p3496 N85-31736
Artificial and natural icing tests YEH-60A quick fix helicopter
[AD-A155147] 21 p3555 N85-32116
Ice nucleation of single water droplet by silver iodide: A laboratory observation 21 p3643 N85-32630
Ice-forming efficiency of the soluble and insoluble portions of dust contained in snow
21 p3643 N85-32631
Monte Carlo studies of H2O layers adsorbed on a model basal face of AgI 21 p3643 N85-32633
Aircraft accident report: World Airways Inc., Flight 30H, McDonnell Douglas DC-10-30CF, N113WA, Boston-Logan International Airport, Boston, Massachusetts, January 23, 1982
[PB85-910406] 22 p3728 N85-33114
Permafrost features on Earth and Mars: Similarities, differences 22 p3655 N85-33670
ICE MAPPING
Ice-soil mixtures: Visual and near-infrared remote sensing techniques
[NASA-CR-174087] 04 p0525 N85-13358
Technology development for unmanned untethered submersible vehicle systems
[AD-A148794] 09 p1304 N85-18190
Analysis of hydrometeorological conditions in Antarctic coastal waters according to data from hydrological and satellite observations 15 p2487 N85-25354

ICE NUCLEI
Ice multiplication in summertime cumulus clouds in the BEWMEX area
16 p2629 N85-27445
SCPP (Sierra Cooperative Pilot Project) data collection and analysis. Volume 1: Executive summary
[PB85-156065] 16 p2637 N85-27494
Eleventh International Conference on Atmospheric Aerosols, Condensation and Ice Nuclei, volume 2
[PB85-182416] 21 p3638 N85-32596
Mechanism of heterogeneous deposition ice nucleation near water-saturation 21 p3638 N85-32597
Experimental studies of the kinetics of deposition nucleation on an ice nucleant used in weather modification 21 p3638 N85-32598
Inactivation of silver iodide by atmospheric nucleation inhibitors 21 p3638 N85-32599
Ice nucleation by silver iodine particles with nearly critical sizes 21 p3638 N85-32600
Photoinduced active sites on ice nucleating aerosol of silver iodide 21 p3639 N85-32601
Experimental investigation of properties of ice-forming reagents 21 p3639 N85-32602
Ice active bacteria as condensation nuclei
21 p3639 N85-32603
The effect of supersaturation, temperature and particle size on ice-nucleating ability of atmospheric aerosol
21 p3639 N85-32604
Ice crystal nucleation on hygroscopic aerosols
21 p3639 N85-32605
On the efficiency of the mechanism of ice particles formation in the vapor supersaturation field around a freezing droplet 21 p3639 N85-32606
Generation of lead, lead iodide and iodide aerosols and their ice nucleation 21 p3639 N85-32607
The nucleation of ice crystals during the freezing of large supercooled drops 21 p3640 N85-32608
Ice nucleus measurements 21 p3640 N85-32609
On the problem of possible mechanism of ice nuclei formation in convective clouds 21 p3640 N85-32610
Bacterial ice nuclei of marine origin: Some recent observations 21 p3640 N85-32611
Airborne measurements of atmospheric ice nuclei
21 p3640 N85-32612
Aircraft observations of condensation and ice nuclei at a tropical station 21 p3640 N85-32613
A statistical analysis of ice nuclei concentrations at urban and rural sites in Valladolid, Spain
21 p3640 N85-32614
Supersaturation spect A of Ice Nuclei at different locations in Europe and over the North-Atlantic
21 p3640 N85-32615
Concentrations of ice nuclei of different modes of activities 21 p3641 N85-32616
Observations of the atmospheric ice nucleus at northwest China 21 p3641 N85-32618
Ice nucleating characteristics of Capparis Aphylla, an Indian herb 21 p3641 N85-32619
The capture of ice nucleating and non ice-nucleating aerosols by ice phase precipitation
21 p3641 N85-32620
The investigation of natural and artificial ice nuclei by the improved membrane filter method
21 p3642 N85-32626
Basic ice nucleation mechanisms on mono and microcrystals and ice forming nuclei. Theoretical analysis and experimental results achieved in the laboratory over the past ten years: Review paper
21 p3642 N85-32629
Ice-forming efficiency of the soluble and insoluble portions of dust contained in snow
21 p3643 N85-32631
Critical supersaturations with respect to water for fast condensation-freezing ice nucleation
21 p3643 N85-32632
Concentration and source areas of ice nuclei in the Alaskan atmosphere 21 p3643 N85-32634
Eleventh International Conference on Atmospheric Aerosols, Condensation and Ice Nuclei, volume 1
[PB85-182400] 21 p3644 N85-32636
Effect of ions on cloud formation and its role in solar terrestrial relationship 21 p3653 N85-32697

ICE OBSERVATION
U ICE REPORTING

ICE PACKS
U SEA ICE

ICE PREVENTION
Heliport snow and ice control methods and guidelines
[DOT/FAA/PM-84/22] 01 p0012 N85-10073
To take off and to land safely, Hoechst 1678 for ice and snow free runways 05 p0595 N85-13791
Analytical and physical modeling program for the NASA Lewis Research Center's Altitude Wind Tunnel (AWT)
[NASA-TM-86919] 07 p0909 N85-15757

ICE REPORTING
Cryospheric data products available through satellite altimetry 03 p0380 N85-12428
Special difficulties of retrieving surface elevation over continental ice — satellite radar altimetry
03 p0380 N85-12429
Sea ice characteristics derived from airborne altimetry
03 p0382 N85-12440
Radar altimetry over sea ice 03 p0382 N85-12441
Use of SIR-B multiincidence-angle imagery to study iceberg detectability and offshore ocean feature extraction 08 p1145 N85-17225
Data report on variations in the composition of sea ice during MIZEX/East'83 with the Nimbus-7 SMMR
[NASA-TM-86170] 09 p1342 N85-18443
Data collection and winter ice dynamics in the Beaufort Sea 14 p2236 N85-23878
Results of the MIZEX preliminary campaign: 29 June to 19 July 1983 — Marginal Ice Zone Experiment (MIZEX), satellite observation
[CNES-84/142/T/CT/DRT/TIT/RL]
20 p3478 N85-31609

ICE SHELVES
U LAND ICE

ICEBERGS
Arctic ice island and sea ice movements and mechanical properties
[DE84-016323] 04 p0542 N85-13450
Use of SIR-B multiincidence-angle imagery to study iceberg detectability and offshore ocean feature extraction 08 p1145 N85-17225
The use of the ARGOS system for the study of the drift of Antarctic icebergs 14 p2240 N85-23890
Main features of Antarctic Ocean circulation as revealed by satellite tracking of icebergs
14 p2325 N85-24372
Radar measurement of thickness of drifting ocean ice employing cepstral signal processing
15 p2644 N85-26313

ICELAND
The structure of the Iceland-Faeroe ridge, derived from geophysical measurements
[DRIC-T-7255] 03 p0397 N85-12535
Structure of Iceland and ocean floor spreading
13 p2112 N85-23159
Oceanographic variations in recent decades and their impact on the fertility of the Iceland Sea
15 p2602 N85-26034
Geomorphic classification of Icelandic and Martian volcanoes: Limitations of comparative planetology research from LANDSAT and Viking orbiter images
21 p3603 N85-32372

ICING
U ICE FORMATION

IDAHO
Geology of selected migmatite zones within the bitterroot lobe of the Idaho batholith, Idaho and Montana
03 p0389 N85-12489
Geographic and stratigraphic distribution of Miocene palynomorphs in north Idaho 03 p0390 N85-12498
Multi crop area estimation in Idaho using EDITOR
[E85-10054] 06 p0827 N85-15251
Depositional modeling of tetrahedrite in the Coeur d'Alene district, Idaho 08 p1182 N85-17448
The geology of East Butte, a rhyolitic volcanic dome on the Eastern Snake River Plain, Idaho
13 p2187 N85-23570

IDEAL FLUIDS
Algebra of hydrodynamic flows of an ideal fluid and the prediction of the behaviour of a system of particles of a passive admixture on Riemann surfaces with a variable curvature
[REPT-565] 03 p0377 N85-12406
Large deformations of a nonlinear elastic solid and the diffusion of an ideal fluid treated as interacting continua
09 p1330 N85-18356

IDEAL GAS
Calculating secondary nonviscous gas flows in spatial cascades of turbines 09 p1305 N85-18202
Ideal gas thermodynamic properties for the phenyl, phenoxy, and o-biphenyl radicals
[NASA-TM-83800] 12 p1943 N85-22204

IDENTIFY FRIEND OR FOE
U IFF SYSTEMS (IDENTIFICATION)

IDENTIFYING
NT CROP IDENTIFICATION
NT IFF SYSTEMS (IDENTIFICATION)
NT PARAMETER IDENTIFICATION
NT RAPID BALLISTICS IDENTIFICATION
NT SYSTEM IDENTIFICATION
NT TIMBER IDENTIFICATION
Identification as a function of familiarity for known voices talking over an unprocessed channel and an LPC (Linear Predictive Coding) voice processor
[AD-A145545] 02 p0191 N85-11276
Microscopic identification of feathers in order to improve birdstrike statistics
[AD-P004187] 11 p1579 N85-19950
Approximation in optimal control and identification of large space structures
[AD-A150323] 13 p2151 N85-23351
Stereotype traits can be processed automatically
[AD-A150947] 14 p2391 N85-24725
The 121.5/243 MHz ELT identification — Emergency Locator Transmitter (ELT) 20 p3404 N85-31119
A cluster analysis method for identification of subpopulations of cells in flow cytometric list-mode arrays 20 p3503 N85-31779
Distributed name management
[AD-A154785] 21 p3712 N85-33037
Results of a search for deuterium at 25-50 GC/c using a magnetic spectrometer
[OG-4.2-4] 22 p3878 N85-34024

IFF SYSTEMS (IDENTIFICATION)
A computer analysis of the RF performance of a ground-mounted, air-supported radome
[AD-P004352] 12 p1824 N85-21446

IFR (RULES)
U INSTRUMENT FLIGHT RULES

IGFET
U FIELD EFFECT TRANSISTORS

IGNEOUS ROCKS
NT ANORTHOSITE
NT BASALT
NT ECLOGITE
NT GRANITE
NT PERIDOTITE
Petrology of deep crustal xenoliths from the eastern Snake River Plain, Idaho 02 p0226 N85-11477
Particle velocity experiments in anorthosite and gabbro
[NASA-CR-174158] 04 p0533 N85-13407
Two lunar global asymmetries
04 p0585 N85-13734
Crystalline rocks of the northeastern United States
[DE84-013674] 05 p0677 N85-14347
The search for igneous materials at the Viking landing sites 13 p2194 N85-23609
Bouguer images of the North American craton
13 p2200 N85-23648
Region-to-area screening methodology for the Crystalline Repository Project
[DE85-009892] 18 p3125 N85-29354
Design analysis for a repository in crystalline rock
[DE85-011802] 22 p3839 N85-33771
Aeromagnetic and gravity models of the pluton below the Lake City caldera, Colorado
24 p4104 N85-35442

IGNIMBRITE
U IGNEOUS ROCKS

IGNITERS
NT DETONATORS
NT INITIATORS (EXPLOSIVES)
Metallography of Kovar/glass/thermite interfaces
[DE84-015247] 02 p0195 N85-11302
Hollow cathode apparatus
[NASA-CASE-NPO-15560-1] 12 p1832 N85-21491
Oxygen-hydrogen thrusters for Space Station auxiliary propulsion systems
[NASA-CR-175691] 15 p2494 N85-25383
Low gravity exothermic heating/cooling apparatus
[NASA-CASE-MSC-25707-1] 18 p3104 N85-29214

IGNITION
NT SOLID PROPELLANT IGNITION
NT SPARK IGNITION
Effect of oxide coated thickness on thermal ignition of titanium-based pyrotechnics
[DE84-013081] 04 p0481 N85-13065
Bulletin of the Faculty of Engineering, Hokkaido University, no. 123
[ISSN-0385-602-X] 04 p0482 N85-13075
Experimental study on the glow plug aided alcohol driven diesel engine 04 p0483 N85-13078
Laser for determining the ignition conditions of a pyrotechnic mixture
[FOA-C-20542-D1] 04 p0506 N85-13230
Catalytic ignition and combustion of lean mixtures
[AD-A148101] 08 p1121 N85-17067
Fuel-rich solid propellant boron combustion
[AD-A148522] 08 p1136 N85-17157
Spontaneous ignition of organic solids by radiant heating 09 p1289 N85-18096
Evaluation of minimum ignition energy measurement techniques used at P.E.R.M.E.
[SG83/A256] 09 p1301 N85-18169
Analysis of a potential hot-wire ignition problem
[DE84-017254] 09 p1301 N85-18174
Parameters affecting hot wire ignition of thermite mixtures
[DE84-016941] 09 p1301 N85-18176
Theoretical studies of the ignition and combustion of silane-hydrogen-air mixtures
[NASA-CR-3876] 10 p1433 N85-19032

Mechanisms and reaction dynamics related to methane combustion
[PB85-129690] 10 p1436 N85-19065

Laser-initiated combustion studies on metallic alloys in pressurized oxygen
[PB85-128114] 10 p1436 N85-19066

Theory of flammability limits. Flow gradient effects and flame stretch
[PB85-135077] 10 p1439 N85-19067

Fuels combustion research
[AD-A149106] 10 p1457 N85-19178

Hydrogen flame acceleration and transition to detonation
[DE85-000611] 12 p1802 N85-21299

Ignition of mixtures of SiH sub 4, CH sub 4, O sub 2, and Ar or N sub 2 behind reflected shock waves
[NASA-TP-2415] 13 p1974 N85-22385

Ignition phenomena of bulk aluminum alloy as a function of oxygen pressure 13 p1999 N85-22531

Combustion of zirconium carbide
13 p1999 N85-22532

Limiting factor of flame propagation in mono-sized sprays of low-volatility fuels
[NAL-TR-839T] 15 p2521 N85-25538

Ignition of metals in high pressure oxygen
16 p2735 N85-26874

Modeling the role of radicals in the ignition of and flame propagation in hydrogen-air and methane-air mixtures
16 p2744 N85-26935

Design of a Mobile Combustion Diagnostic Fixture (MCDF)
[AD-A151814] 16 p2745 N85-26941

Elementary reactions of importance in oxidation, combustion ignition and flame inhibitions
[AD-A153139] 17 p2921 N85-28004

Whist code calculations of ignition margin in an ignition Tokamak
[DE85-009507] 18 p3190 N85-29784

Measurement of combustion species by electron impact fluorescence
[DE85-011163] 19 p3236 N85-30065

Injection, atomization, ignition and combustion of liquid fuels in high-speed air streams
[AD-A154056] 19 p3251 N85-30156

Deformation, fracture and explosive properties of reactive materials
[AD-A154073] 19 p3251 N85-30157

Burn rates of explosives at high pressures
[DE85-010806] 19 p3251 N85-30159

Coal slurry ignition in a diesel engine simulator
[DE85-010967] 20 p3463 N85-31513

Self-heating to ignition measurements and computation of critical size for solar energy collector materials
[PB85-183374] 20 p3485 N85-31663

Burn front velocity as a function of pellet density in iron-potassium perchlorate heat powders
[DE85-011448] 21 p3572 N85-32214

Scaling parameters of flashover
[NBS-GCR-85-497] 23 p3911 N85-34229

Laser probes of natural gas ignition chemistry
[PB85-200210] 24 p4077 N85-35264

Neutral pumping rates for a next step tokamak ignition device
[DE85-012780] 24 p4157 N85-35776

IGNITION LIMITS

New concepts for measuring flame spread properties
[NBSIR-84-2943] 03 p0327 N85-12104

Evaluation of minimum ignition energy measurement techniques used at P.E.R.M.E.
[SG83/A258] 09 p1301 N85-18169

Theory of flammability limits. Flow gradient effects and flame stretch
[PB85-135077] 10 p1439 N85-19067

Behavior of the lean methane-air flame at zero-gravity
[NASA-CR-175586] 12 p1799 N85-21283

The use of a laser Doppler velocimeter in a standard flammability tube
[NASA-CR-174960] 24 p4096 N85-35389

IGNITION SYSTEMS

Analysis and simulation of the I C engine Otto cycle using the second law of thermodynamics
02 p0291 N85-11891

Studies of ignition and combustion wave propagation in exothermic systems using high-speed photography
[DE84-016482] 04 p0471 N85-12995

Laser ignition of explosives
[FOA-C-20550-D1] 07 p0972 N85-16173

Study of bridgewire size and pyrotechnic density relationships on all-fire levels
[DE84-016946] 09 p1302 N85-18177

Development of a PETN DDT detonator
[DE84-016944] 09 p1302 N85-18178

Tokamak ignition/burn experimental research device
[DE85-009999] 18 p3190 N85-29785

Experimental study of engine knock
[DE85-009651] 22 p3754 N85-33268

IGNITION TEMPERATURE

NT FLASH POINT

Catalytic ignition and combustion of lean mixtures
[AD-A148101] 08 p1121 N85-17067

A program to develop thermite reactions to produce refractory borides and carbides
[AD-A148972] 10 p1434 N85-19037

The reaction of oxygen-nitrogen mixtures with granular activated carbons below the spontaneous ignition temperature
[AD-A149041] 10 p1434 N85-19039

Review of zirconium-zircaloy pyrophoricity
[DE85-011169] 23 p3916 N85-34270

ILLINOIS

Illinois Climate: Trends, Impacts and Issues
[PB84-211986] 01 p0096 N85-10577

Revised Uniform Summary of Surface Weather Observations (RUSSWO). O'Hare International Airport, Chicago, parts A-F
[AD-A147206] 07 p1007 N85-16399

Interlobate comparison of glacial-depositional style as evidenced by small-relief glacial landscape features in Illinois, Indiana, and Ohio, utilizing SIR-B
08 p1146 N85-17231

Water resources data for Illinois, water year 1983. Volume 1: Illinois except Illinois River Basin
[PB85-125755] 10 p1507 N85-19508

Geodetic accuracy of LANDSAT 4 Multispectral Scanner and Thematic Mapper data — Washington, DC, California, Alabama, South Dakota, and Illinois
11 p1667 N85-20504

Evaluation of the radiometric quality of the TM data using clustering, linear transformations and multispectral distance measures — Illinois 12 p1870 N85-21731

Current alternative energy research and development in Illinois
[PB85-163137] 16 p2820 N85-27397

ILLUMINANCE

Effect of aberration in optical system on illuminance distribution over image of strip in semicoherent light
06 p0777 N85-14970

Correlations of solar irradiance and daylight illuminance for building energy analysis
[DE85-001736] 06 p0839 N85-15326

Quantitative analyses of planetary reflectance spectra
13 p2197 N85-23625

Photovoltaic cells of InP-CdS heterojunction type and their temperature characteristics under A-M illumination
14 p2275 N85-24092

Solar cells with distributed parameters: Current-voltage characteristics under uniform and nonuniform illumination 14 p2275 N85-24093

Issue of sky conditions
[DE85-010590] 19 p3317 N85-30562

Immediate visibility after red and white adaptation
[AD-A156271] 24 p4132 N85-35615

ILLUMINATING

Theoretical elements of photometry
[BLL-RISLEY-TR-5022-(9091.9F)]
02 p0279 N85-11821

Evaluation of arctic test of improved tritium radioluminescent lighting
[DE84-014887] 05 p0597 N85-13805

Human factors of visual displays
06 p0752 N85-14821

Analysis of a visual performance experiment
[DE85-000710] 10 p1530 N85-19645

Lighting for remote viewing systems
[DE85-001898] 11 p1729 N85-20673

Power from the Sun: Light at night
[PB85-124097] 12 p1883 N85-21814

Development of robots and application to industrial processes
[NASA-CR-175754] 15 p2567 N85-25840

Use of Goudrian model in studying laws of reflection in vegetation-soil system in optical range. 2: Influence of illumination conditions on spectral brightness coefficients 16 p2726 N85-26827

Electrodeless HID lamp study
[DE85-010626] 18 p3096 N85-29167

Terrain illumination conditions when taking scanning photographs from space 22 p3736 N85-33159

Electrochromic display device
[AD-D011733] 22 p3759 N85-33299

ILLUMINATION

Laser illuminated nano-second microscope
[DE84-016200] 06 p0811 N85-15152

NBS (National Bureau of Standards) daylight availability database
[PB84-245745] 07 p1054 N85-16688

ILLUMINATORS

High-speed, eight-frame electro-optic camera with multipulsed ruby laser illuminator
[DE85-001748] 09 p1323 N85-18314

Analysis of a visual performance experiment
[DE85-000710] 10 p1530 N85-19645

ILLUSIONS

Bulletin of the Faculty of Engineering, Hokkaido University, no. 123
[ISSN-0385-602-X] 04 p0482 N85-13075

A mathematical model of visual perception regarding peripheral vision and its application to the Hermann's illusion 04 p0483 N85-13080

Susceptability to kinetoses and the amplitude perceived from sensory illusions 11 p1694 N85-20651

Effect of body position and immobilization on intensity of spatial illusions in weightlessness
22 p3821 N85-33672

ILS (LANDING SYSTEMS)

U INSTRUMENT LANDING SYSTEMS

ILYUSHIN AIRCRAFT

Testing solution for IL-76 braking system problem
08 p1067 N85-16766

IMAGE ANALYSIS

The Multispectral Imaging Science Working Group. Volume 1: Executive summary
[E85-10001] 02 p0213 N85-11404

The Multispectral Imaging Science Working Group. Volume 2: Working group reports
[E85-10002] 02 p0213 N85-11406

Information Science Panel joint meeting with Imaging Science Panel 02 p0214 N85-11415

Integrated analysis of remote sensing products from basic geological surveys — Brazil
[E85-10052] 07 p0984 N85-16248

LANDSAT-4 Thematic Mapper Modulation Transfer Function (MFT) evaluation — California and New Mexico
[E85-10055] 07 p0984 N85-16250

Proceedings of the Second Annual Symposium on Mathematical Pattern Recognition and Image Analysis Program
[E85-10056] 07 p0984 N85-16251

Estimating location parameters in a mixture
07 p0984 N85-16252

Nonparametric analysis of Minnesota spruce and aspen tree data and LANDSAT data 07 p0984 N85-16253

Texture classification using autoregressive filtering
07 p0984 N85-16254

Bayesian estimation of normal mixture parameters
07 p0985 N85-16255

Spatial estimation from remotely sensed data via empirical Bayes models 07 p0985 N85-16256

Evidence accumulation for spatial reasoning
07 p0985 N85-16261

Power spectral onsity of markov texture fields
07 p0986 N85-16262

Rectification of single and multiple frames of satellite scanner imagery using points and edges as control
07 p0986 N85-16263

The influence of the number of ground control points on the scene-to-map registration accuracy — Kansas, Louisiana, Mississipp, and Missouri
07 p0986 N85-16264

Image variance and spatial structure in remotely sensed scenes — South Dakota, California, Missouri, Kentucky, Louisiana, Tennessee, District of Columbia, and Oregon
07 p0986 N85-16265

Image-to-image correspondence: Linear structure matching 07 p0988 N85-16266

Metric aspects of digital images and digital image processing
[AD-A147211] 07 p0988 N85-16276

The interpretation of SIR-B imagery of surface waves and other oceanographic features using in-situ, meteorological satellite, and infrared satellite data
08 p1143 N85-17212

Southern ocean sea-ice morphology and kinematics
08 p1144 N85-17217

Automatic analysis of speckle photographs by microcomputer
[NPL-DITC-47/84] 09 p1322 N85-18306

Anaysis of the quality of image data required by the LANDSAT-4 Thematic Mapper and Multispectral Scanner — agricultural and forest cover types in California
[E85-10074] 10 p1504 N85-19488

Study of spectral/radiometric characteristics of the Thematic Mapper for land use applications
[E85-10075] 10 p1504 N85-19489

Geodetic accuracy of LANDSAT 4 Multispectral Scanner and Thematic Mapper data — Washington, DC, California, Alabama, South Dakota, and Illinois
11 p1667 N85-20504

Geometric accuarcy assessment of LANDSAT-4 Multispectral Scanner (MSS) data
11 p1667 N85-20505

Canadian plans for Thematic Mapper data
11 p1668 N85-20513

Image lobe analysis for large radomes
[AD-P004359] 12 p1825 N85-21453

The use of linear feature detection to investigate Thematic Mapper data performance and processing
12 p1872 N85-21740

Method for approximating autocorrelation functions for describing areal photoimage features
13 p1983 N85-22443

Experience in automated interpretation of aerospace photographs 13 p1983 N85-22444

Geoindication method for interpreting aerial and space photographs: Status and prospects
13 p1984 N85-22445

Edge detection in SAR imagery using gradient operators — synthetic aperture radar (SAR)
[AD-A149411] 13 p2054 N85-22862

An investigation of several aspects of LANDSAT-5 data quality — Palmer County, Shelby, mt; White sands, NM; Great Salt Lake, UT; San Matted Bridge and Sacramento, California
[E85-10096] 13 p2122 N85-23214

Photometric analysis of Jupiter-illuminated images of Io 13 p2196 N85-23620

Using color to separate reflection components
[AD-A150999] 14 p2405 N85-24828

Optical flow-patterns of image velocity and their potential use in guidance and image interpretation
[BAE-BT-12091] 15 p2651 N85-26347

The impact of VLSI on guidance and control system design 16 p2697 N85-26654

Digital image analysis of four-frame holographic plasma and neutral gas interferograms
[DE85-008397] 16 p2788 N85-27200

Air photo analysis, photo interpretation logic, and feature extraction
[AD-A153826] 18 p3124 N85-29347

Alternative theories of inference in expert systems for image analysis
[AD-A153649] 18 p3170 N85-29646

Resource allocation in cerebral specialization of function: Behavioral and electrophysiological studies
[AD-A155092] 21 p3664 N85-32759

Experiments and discussions on the analysis of interferograms with closed-loop fringes
[NPL-MOM-68] 23 p3956 N85-34515

Non-rigid body motion 23 p3964 N85-34576

IMAGE CONTRAST

Ion contrasting chamber for discrimination of grains and textures
[BMFT-FB-T-84-151] 04 p0477 N85-13036

Human factors of visual displays
06 p0752 N85-14821

Comments on the image contrast from inelastically scattered electrons
[DE85-000899] 07 p1041 N85-16609

Alphabet-constrained data compression
[AD-A152887] 17 p3019 N85-28667

Colour spaces and colour contrast
23 p3963 N85-34567

IMAGE CONVERTERS

NT THERMICONS

Use of focons in combination with brightness amplifiers 14 p2274 N85-24088

Beam tests of phosphorescent screens
[DE85-009843] 18 p3097 N85-29170

IMAGE CORRELATORS

Holographic lens for optical correlator
16 p2763 N85-27052

IMAGE DISSECTOR TUBES

Dynamic visual servo control of robots: An adaptive image-based approach
[AD-A150057] 12 p1880 N85-21667

IMAGE ENHANCEMENT

Effect of hydrogen on formation of energy spectrum of multiply charged and copper ions
02 p0263 N85-11720

Holographic subtraction of images by Fourier plane recording and spatial filtration with a narrow beam
02 p0263 N85-11721

Noise removal in multichannel images
[NASA-CR-174116] 04 p0554 N85-13526

Investigative findings of image enhancement techniques
[AD-A146392] 06 p0853 N85-15424

Information extraction and transmission techniques for spaceborne synthetic aperture radar images
[NASA-CR-174341] 08 p1150 N85-17256

Resolution enhancement of multichannel microwave imagery from the Nimbus-7 SMMR for maritime rainfall analysis
[NASA-CR-174367] 10 p1462 N85-19221

A concept for the processing and display of Thematic Mapper data 13 p2119 N85-23196

A quantitative image evaluation study of a concurrent photon amplification treated emulsion
[AD-A151831] 15 p2560 N85-25796

Looking at more than three dimensions
[DE85-007764] 17 p3009 N85-28600

First results of oceanography utilization of infrared high resolution picture transmission images
[KNMI-TR-59] 18 p3151 N85-29511

Quantizer of images of heat fields obtained by Rubin-type infra-red imagers 22 p3771 N85-33369

IMAGE FILTERS

Investigative findings of image enhancement techniques
[AD-A146392] 06 p0853 N85-15424

On edge detection
[AD-A148573] 08 p1223 N85-17703

Improved continuum definition in high-background IUE images 11 p1761 N85-21078

Hexagonal uniformly redundant arrays for coded-aperture imaging
[OG-9.2-1] 21 p3714 N85-33048

IMAGE FURNACES

Automatic Monoellipsoidal Mirror Furnace Facility (AMMFF), volume 1 — spaceborne crystal growth
[AMF-RP.100-DS-015-VOL-1] 09 p1285 N85-18073

IMAGE INTENSIFIERS

Programmable optical sensor
[AD-D011244] 02 p0281 N85-11829

Development of a dynamic radiographic capability using high-speed video
[DE84-016477] 04 p0511 N85-13256

Electronic autofluorography: Principles, problems and prospects
[DE84-016698] 05 p0639 N85-14097

STS atmospheric luminosities
[NASA-CR-175514] 12 p1791 N85-21240

Research in the optical sciences
[AD-A150196] 13 p2159 N85-23401

Holographic intensity correlator with PRIS-type photoelectro-optical controlled transparency
17 p2940 N85-28152

Quantizer of images of heat fields obtained by Rubin-type infra-red imagers 22 p3771 N85-33369

Application of thermoluminescence for detection of cascade shower 1: Hardware and software of reader system
[HE-7.1-6] 24 p4213 N85-36160

Spatial distribution read-out system for thermoluminescence sheets
[HE-7.1-7] 24 p4213 N85-36161

Application of thermoluminescence for detection of cascade shower 2: Detection of cosmic ray cascade shower at Mount Fuji
[HE-7.1-12] 24 p4214 N85-36162

IMAGE MOTION COMPENSATION

Predicting optical image displacement velocity in survey of Earth's surface 02 p0165 N85-11116

Study of alternate optical and fine guidance sensor designs for the space infrared telescope facility (SIRTF)
[NASA-CR-166614] 07 p0915 N85-15794

Processing dynamic image sequences from a moving sensor
[AD-A149984] 12 p1934 N85-22148

Autofocus motion compensation for synthetic aperture radar and its compatibility with strapdown inertial navigation sensors on highly maneuverable aircraft
[AD-A151940] 16 p2704 N85-26693

Errors in compensating for image oscillation by means of a gyroscopic head 16 p2763 N85-27051

New method for compensating and measuring any motion of three-dimensional objects in holographic interferometry
[ISL-CO-216/84] 22 p3789 N85-33474

IMAGE PROCESSING

NT GEOMETRIC RECTIFICATION (IMAGERY)

Analysis of on-board CIG (Computer Image Generator) applications for aircrew training
[AD-A145214] 01 p0013 N85-10079

Detection and coding techniques of contours in image signals
[FUB-8-1983] 01 p0039 N85-10251

Image signals encoding techniques oriented towards the reduction of perceptive redundance
[FUB-23-1983] 01 p0040 N85-10256

Methods for the design of quantizers for image signals
[FUB-38-1983] 01 p0041 N85-10263

A system for meteorological satellite, radar, conventional data and model analysis 01 p0082 N85-10551

A human visual system investigation applicable to image contour coding
[FUB-36-1983] 01 p0095 N85-10640

Detection and estimation of image contours
[FUB-35-1983] 01 p0112 N85-10760

East Europe report: Science and technology
[JPRS-ESA-84-029] 01 p0115 N85-10783

Methods, applications of image processing
01 p0115 N85-10785

LANDSAT data and interactive computer mapping
02 p0152 N85-11028

Technological approach to automation of specialized processing of survey data 02 p0165 N85-11118

The application of principal components analysis to LANDSAT MSS data 02 p0212 N85-11398

Information Science Panel joint meeting with Imaging Science Panel 02 p0214 N85-11415

Mapping land use changes in the carboniferous region of Santa Catarina, report 2
[E85-10017] 02 p0217 N85-11430

Application of digital analysis of MSS to agro-environmental studies
[E85-10024] 02 p0218 N85-11437

Description of the logical support for an image processing system
[INPE-2783-PRE/349] 02 p0240 N85-11563

SITIM system: Object manager module
[INPE-3284-NTE/226] 02 p0240 N85-11564

SITIM system: Supervisor utilization
[INPE-3287-NTE/224] 02 p0240 N85-11565

Utilization of interpolation and transformation for the compression of digital image data
[INPE-3061-PRE/479] 02 p0240 N85-11566

Design of edge detectors for reduced images
[AD-A145700] 02 p0252 N85-11653

Tomographic reconstruction of neutron radiograph images
[AD-A145682] 02 p0280 N85-11826

Production of optically correlated SEASAT-A (SEA satellite) SAR (Synthetic Aperture Radar) imagery at DREO (Defence Research Establishment Ottawa)
[AD-A145970] 03 p0355 N85-12281

LANDAT-4/5 image data quality analysis
[E85-10039] 03 p0379 N85-12417

Automatic recognition and turbuling objects
[AD-A145908] 03 p0419 N85-12676

Multispectral and geomorphic studies of processed Voyager 2 images of Europa
[NASA-CR-174075] 03 p0446 N85-12848

Research activities of the Illinois University Coordinated Science Laboratory
[AD-A145589] 03 p0449 N85-12856

Mission science value-cost savings from the Advanced Imaging Communication System (AICS)
[NASA-CR-174170] 04 p0458 N85-12905

Digital image processing; report from a conference and study trip to the USA and Canada, summer 1984
[FOA-C-30369-E1] 04 p0494 N85-13153

LANDSAT instruments characterization
[E85-10032] 04 p0524 N85-13356

Coastal Zone Color Scanner (CZCS): Imagery of near-surface phytoplankton pigment concentrations from the first coastal ocean dynamics experiment (CODE-1), March - July 1981
[NASA-CR-174169] 04 p0542 N85-13447

Restoration of multichannel microwave radiometric images
[NASA-CR-174115] 04 p0554 N85-13527

Time-resolved tomographic images of a relativistic electron beam
[DE84-015021] 04 p0565 N85-13597

Tomographic reconstruction of axially symmetric objects from a single radiograph
[DE84-016783] 04 p0565 N85-13599

Imaging of surfaces and defects of crystals
[DE84-016449] 04 p0570 N85-13632

Characterizing the scientific potential of satellite sensors
[E85-10031] 05 p0654 N85-14200

The Interactive Planetary Image Processing System (IPIPS): A major facility for research and teaching in remote sensing 05 p0655 N85-14203

Digital comparison and correlation techniques of remote sensing images with differing spatial resolutions
05 p0655 N85-14204

The integrated use of digital cartographic data and remotely sensed imagery 05 p0655 N85-14206

Methodological research in connection with the handling of LANDSAT satellite data for archaeology
05 p0655 N85-14207

The areal pattern of latent and sensible heat fluxes: The combination of soil physics and remotely sensed data 05 p0656 N85-14213

Integration of multispectral data obtained at different view angles for vegetation analysis
05 p0657 N85-14218

Landform evaluation through integrated remote sensing methods. A case study in parts of Haryana, India
05 p0657 N85-14221

Modular Optoelektronischer Multispektraler Scanner (MOMS), interpretation and evaluation of the MOMS image Arica, West Coast of South America — STS-7 flight
05 p0657 N85-14222

A methodology for an integrated spatial data model and its application to image classification
05 p0659 N85-14234

Application of high frequency 2-D digital filtering to remote sensing image processing
05 p0660 N85-14242

best copy available

A multiple approach in remote sensing for structural and lithological mapping by use Modular Optoelectronic Multispectral Scanner (MOMS)/LANDSAT/Heat Capacity Mapping Mission (HCMM) data
05 p0660 N85-14244

Image texture study for the operational meteorological satellites NOAA 6 and NOAA 7 and its variation with time. Application to the Beauce region
[ENST-84E009] 05 p0661 N85-14249

Vector quantization of digital images
05 p0714 N85-14580

Automatic determination of motion in an image sequence. The interest for interpretation
[ENST-84E012] 05 p0716 N85-14592

Linear associative mapping
[ESA-TT-868] 05 p0719 N85-14611

Some techniques in image processing
05 p0721 N85-14629

Multi-disciplinary techniques for understanding time-varying space-based imagery
[AD-A144357] 05 p0726 N85-14681

Fly's eye sensor nonlinear signal processing
[AD-D011290] 05 p0729 N85-14684

Selection of parameters for image decomposition by television system for recognition of group of point sources 06 p0785 N85-15018

Hologram bleaching 06 p0789 N85-15038

Wavelength coded image transmission and holographic optical elements
[AD-A146490] 06 p0810 N85-15147

Geological effectiveness of automated processing of highly precise aeromagnetic surveys in Caspian region
06 p0821 N85-15216

Experiences with digital processing of images at INPE
[E85-10045] 06 p0826 N85-15247

An integrated LANDSAT/ancillary data classification of desert rangeland
[E85-10046] 06 p0826 N85-15248

A geographic information system for resource managers based on multi-level remote sensing data
[E85-10047] 06 p0827 N85-15249

Effective use of remote sensing products in litigation
[E85-10048] 06 p0827 N85-15250

Support for the Naval Research Laboratory Passive Microwave Clutter Analysis Program
[AD-A146771] 07 p0939 N85-15951

White-light optical information processing and holography
[AD-A146938] 07 p0967 N85-16138

Characterizing the scientific potential of satellite sensors — San Francisco, California
[E85-10044] 07 p0983 N85-16244

Integrated analysis of remote sensing products from basic geological surveys — Brazil
[E85-10052] 07 p0984 N85-16248

Metric aspects of digital images and digital image processing
[AD-A147211] 07 p0988 N85-16276

Enhancement of multispectral scanner images by digital filtering
[ESA-TT-824] 07 p0989 N85-16284

JPL Robotics Laboratory computer vision software library
[NASA-CR-174272] 07 p1023 N85-16491

Surface reconstruction preserving discontinuities
[AD-A146741] 07 p1028 N85-16526

Ultrasonic measurements, X-ray photographs and image processing
[BLL-RISLEY-TR-4586-(9091.9F)]
07 p1037 N85-16583

Rule-based evidence accrual system for image understanding
[AD-A147835] 07 p1044 N85-16634

Manual and automated line generalization and feature displacement: Appendixes
[AD-A143251] 07 p1054 N85-16689

Functional built-in-test in a pipelined image processor
08 p1064 N85-16740

UK, FRG, France: R and D in sensors, related fields
08 p1142 N85-17197

Development and evaluation of techniques for using combined microwave and optical image data for vegetation studies 08 p1148 N85-17240

Automatic terrain elevation mapping and registration
08 p1148 N85-17242

An investigation of ionospheric irregularity effects on SIR-B image processing and information extraction
08 p1149 N85-17247

Analysis of SIR-B radar illumination of geometry for depth of penetration and surface feature and vegetation detection, Nevada and California
08 p1149 N85-17248

Information extraction and transmission techniques for spaceborne synthetic aperture radar images
[NASA-CR-174341] 08 p1150 N85-17256

Hierarchical data structures and algorithms for digital stereoscopical mensuration 08 p1175 N85-17410

Digital elevation model computation using fast Poisson solutions 08 p1175 N85-17412

Interactive digital image processing for terrain data extraction
[AD-A148580] 08 p1176 N85-17417

An auroral X-ray imaging spectrometer
[AD-A147756] 08 p1185 N85-17469

Atmospheric wind and diffusion from analysis of an SF6 release at 350 km altitude
[AD-A147965] 08 p1185 N85-17471

VICOM technical description
[REPT-611-0012-REV-A] 08 p1202 N85-17563

Hybrid data processing research facility
[AD-A148092] 08 p1202 N85-17567

Image quality on the KAO 08 p1249 N85-17885

A CCD system for photometry of direct and spectroscopic images 08 p1252 N85-17904

The IMAGE 3 Conference Proceedings
[AD-A148636] 09 p1267 N85-17962

The use of lasers in wide-angle visual systems
[AD-P004322] 09 p1269 N85-17976

A second generation WAVIDS (Wide Angle Virtual Image Display System)
[AD-P004328] 09 p1270 N85-17982

Military applications of the Singer Link-Miles IMAGE visual system
[AD-P004337] 09 p1271 N85-17991

AVTS (Advanced Visual Technology System): A high fidelity visual simulator
[AD-P004338] 09 p1271 N85-17992

The evaluation of a deformable diffraction grating for a stigmatic EUV spectroheliometer
[NASA-CR-174350] 09 p1322 N85-18309

Field implementation of geophysical diffraction tomography
[DE84-017594] 09 p1343 N85-18449

Data reduction 09 p1412 N85-18903

Diffraction diffusion screen with holographically-suppressed zero-order beam
[AD-D011445] 10 p1487 N85-19387

LANDSAT 4 investigation of Thematic Mapper and Multispectral Scanner applications
[E85-10076] 10 p1504 N85-19490

Thematic Mapper: Design through flight evaluation
[E85-10078] 10 p1504 N85-19492

Processing of Global Area Coverage (GAC) data of the TIROS-N/NOAA series polar orbiters
[AD-A148992] 10 p1519 N85-19576

A low-cost, general purpose image processing system
[INPE-3292-PRE/607] 10 p1537 N85-19690

One-dimensional processing for adaptive image restoration
[AD-A149314] 10 p1557 N85-19815

Image Understanding: Proceedings of the 15th Workshop
[AD-A149496] 10 p1557 N85-19816

The use of image registration technique in Brasilia's urban growth monitoring
[INPE-3302-PRE/614] 10 p1569 N85-19896

LS-4 MSS geometric correction: Methods and results
11 p1668 N85-20507

An overview of LANDSAT-4 and the Thematic Mapper
11 p1668 N85-20509

TM digital image products for applications
11 p1668 N85-20512

Characterization of radiometric calibration of LANDSAT-4 reflective bands 11 p1669 N85-20516

Contour line generalization using digital image processing methods
[SER-C-291] 11 p1700 N85-20688

Digital imaging processing
[INPE-3325-PRE/624] 11 p1701 N85-20696

A modern approach of a synthetic aperture radar processor and its technological aspects
11 p1713 N85-20778

Improved continuum definition in high-background IUE images 11 p1761 N85-21076

Image processing instrumentation for speckle interferometry and imaging
[AD-A149306] 11 p1762 N85-21084

Conclusion of Viking Lander Imaging Investigation: Picture catalog of experiment data record
[NASA-RP-1137] 11 p1765 N85-21099

Wide-field-of-view, helmet-mounted infinity display system development
[AD-A149641] 12 p1777 N85-21150

Imaging apparatus for transverse electrode electro-optic tunable filter
[AD-D011524] 12 p1832 N85-21497

Integrating non-semantic knowledge into image segmentation processes
[AD-A149571] 12 p1851 N85-21612

Relative radiometric calibration of LANDSAT TM reflective bands 12 p1869 N85-21725

Preliminary evaluation of the radiometric calibration of LANDSAT-4 Thematic Mapper data by the Canada Centre for Remote Sensing 12 p1870 N85-2172

The use of linear feature detection to investigate Thematic Mapper data performance and processing
12 p1872 N85-2174

The development of image processing of NOAA AVHRR data and its application to sea surface temperature
12 p1895 N85-219

Instrumentation award
[AD-A150061] 12 p1912 N85-219

Processing dynamic image sequences from a moving sensor
[AD-A149984] 12 p1934 N85-2214

Electron image simulation: A complementary processing technique
[DE85-000685] 12 p1941 N85-2218

Method for approximating autocorrelation functions for describing areal photoimage features
13 p1983 N85-2243

Electronic generation of text for television
[BBC-RD-1984/14] 13 p2053 N85-22

Nature of seismic images with amplitude and time fluctuations of recorded oscillations
13 p2112 N85-2315

LANDSAT-4 Science Characterization Early Results. Volume 4: Applications — agriculture, soils land use, geology, hydrology, wetlands, water quality, biomass identification, and snow mapping
[E85-10070] 13 p2117 N85-2318

A concept for the processing and display of Thematic Mapper data 13 p2119 N85-2319

Early results of investigations of LANDSAT 4 Thematic Mapper and Multispectral Scanner applications — Washington, D.C. 13 p2119 N85-2320

Comparative techniques used to evaluate Thematic Mapper data for land cover classification in Logan County, West Virginia 13 p2121 N85-2320

Comparison of MSS and TM data for landcover classification in the Chesapeake Bay area: A preliminary report — Taylor's Island, Maryland
13 p2121 N85-2321

Distribution of snow and maximum snow water equivalent obtained by LANDSAT data and degree day method 13 p2124 N85-2322

Feature extraction assessment study
[AD-A150189] 13 p2126 N85-2322

On a mathematical structure for an image algebra
[AD-A150228] 13 p2150 N85-2334

Image data compression using uneven knots selection
[AD-A150602] 13 p2152 N85-2335

Hexagonal data base study
[AD-A150176] 13 p2167 N85-2344

Hot spots on Io: Correlation of infrared emission and visible reflectance 13 p2172 N85-2347

Bouguer images of the North American craton
13 p2200 N85-2364

Participation in the Mars Data Analysis Program: Analysis of cloud forms in Viking and Mariner 9 images
[NASA-CR-175604] 13 p2204 N85-2367

New developments in industrial radiography
14 p2317 N85-2431

Evaluation of carrying capacity and landscape damage in northern Kenya by multistage remote sensing
[DFVLR-FB-84-47] 14 p2347 N85-2451

Visual recognition of simple objects by a connection network
[AD-A151043] 14 p2389 N85-2471

Perceptual organization and visual recognition
[AD-A150826] 14 p2391 N85-2472

Synthetic aperture radar data processing
14 p2396 N85-2478

Studies in parallel image processing
14 p2399 N85-2478

Execution of cellular logic operations in spatially continuous, bit slice processor 14 p2401 N85-2479

The Multimission Image Processing Laboratory's virtual frame buffer interface
[NASA-CR-175655] 14 p2402 N85-2480

Video animation system
[DE85-005494] 14 p2405 N85-2483

Photoacoustic imaging
[AD-A150823] 14 p2416 N85-2490

Feasibility of optical instruments based on multiaperture optics
[AD-A150868] 14 p2421 N85-2492

Space-variant optical systems
[AD-A151032] 14 p2421 N85-2492

High resolution Z-contrast imaging and lattice location analysis of dopants in ion-implanted silicon
[DE85-005261] 14 p2429 N85-249

Efficient contextual measures for classification of multispectral image data 14 p2433 N85-250

Near-nucleus studies of Comet Halley
14 p2435 N85-250

Kitt Peak measurements of P/Halley positions
14 p2436 N85-25023

Problems and procedures of cometary astometry
14 p2436 N85-25024

Desired characteristics of catalogs for cometary astrometry 14 p2436 N85-25030

Investigations of high resolution imaging through the Earth's atmosphere using speckle interferometry
[AD-A150980] 14 p2439 N85-25053

Research on atmospheric dust formations using satellite observation data 15 p2485 N85-25339

Evaluating radiation distortions of optical image of Earth's surface in horizontally inhomogeneous atmosphere 15 p2486 N85-25345

Evaluating identifiability in remote sensing problems
15 p2486 N85-25347

Identifying land use structures of multizonal aerospace photographs using digital data processing
15 p2486 N85-25348

Using SM-4 Omega system in checking and editing digital terrain information 15 p2487 N85-25350

Increasing the accuracy of processing radar pictures by excluding systematic point coordinate error component
15 p2488 N85-25356

French firm develops new kind of CTD camera for robots 15 p2523 N85-25556

Microcomputer controlled image acquisition system
15 p2537 N85-25654

Statistical techniques for signal processing
[AD-A151231] 15 p2541 N85-25690

Experimental investigation of the electric breakdown in SF6
[BLL-CE-TRANS-7987-(9022.09)]
15 p2546 N85-25714

Superfine laser position control using statistically enhanced resolution in real time
[DE85-005643] 15 p2564 N85-25817

Three-dimensional/perspective display techniques for meteorological data sets 15 p2599 N85-26018

Test and evaluation of the 2.4-micron photorefractor ocular screening system
[NASA-TM-86492] 15 p2615 N85-26115

Workshop on Parallel Computer Architectures in Pattern Recognition and Image Processing
[BMFT-FB-DV-84-006] 15 p2622 N85-26154

Posing of the problem, status, and future of parallel computer architecture for image processing
15 p2622 N85-26155

Industrial applications of pattern recognition and image processing 15 p2622 N85-26157

Recognition of objects in their natural environment — parallel processing 15 p2622 N85-26158

Innovative image processing architectures
15 p2622 N85-26159

Influence and possibilities of Very Large Scale Integration (VLSI) in pattern recognition and image processing 15 p2622 N85-26160

Computer architecture for image processing and pattern recognition in the Federal Republic of Germany. Status 1983, a review 15 p2623 N85-26161

Design specifications for IMAGER: The DREO (Defence Research Establishment Ottawa) image processing system
[AD-A151752] 15 p2624 N85-26168

Feasibility studies of optical processing of image bandwidth compression schemes
[AD-A151254] 15 p2651 N85-26350

User manual for IMAGER: The DREO (Defence Research Establishment Ottawa) image processing system
[AD-A151754] 15 p2653 N85-26362

Image formation in terms of the transport equation
[DE85-004993] 15 p2653 N85-26365

SVIT complex for analysis of space photography
16 p2725 N85-26819

Contribution to space program reviewed
16 p2727 N85-26834

Polarimetric image recorder
[AD-D011605] 16 p2787 N85-27192

New image deblurring method described
16 p2806 N85-27305

CNPq/INPE LANDSAT system: Report of activities from October 1, 1983 to September 30, 1984 — Brazil
[E85-10097] 16 p2808 N85-27318

Noise correction on LANDSAT images using a spline-like algorithm
[E85-10098] 16 p2808 N85-27319

Study of the urban evolution of Brasilia with the use of LANDSAT data
[E85-10101] 16 p2809 N85-27321

System of interpretation of remote sensing data when hydrocarbons are present, volume 2
[INPE-3087-TDL/162-VOL-2] 16 p2810 N85-27326

Symbiosis between postgraduate training and research projects: A successful experience
[INPE-3216-PRE/589] 16 p2810 N85-27330

Reports on cartography and geodesy. Series 1: Original reports, no. 94
[ISSN-0469-4236] 16 p2814 N85-27357

Realization of cartographic tasks on the multiprocessor system EGPA — image processing
16 p2814 N85-27360

A concept for map updating using digital image processing methods 16 p2815 N85-27364

Contour line generalization using digital image processing methods 16 p2815 N85-27367

What does digital image processing perform in the production of orthophotomaps 16 p2815 N85-27368

Free-surface phenomena under low- and zero-gravity conditions
[NASA-CR-175885] 17 p2907 N85-27922

Techniques for operating Charge Coupled Devices (CCD's) in very high speed framing mode
[AD-A152678] 17 p2953 N85-28238

Sub-nanosecond cinematography in laser fusion research: Current techniques and applications at the Lawrence Livermore Laboratory
[DE85-007252] 17 p2968 N85-28334

Evidential reasoning in expert systems for image analysis
[AD-A153379] 17 p3013 N85-28627

Application of artificial intelligence (AI) to radar image understanding
[AD-A152519] 17 p3017 N85-28654

Deconvolution methods for multi-sensors
[AD-A152351] 17 p3018 N85-28660

Further study of digital matching of dissimilar images
[AD-A153112] 17 p3019 N85-28672

Spatial light modulator having a capacitively coupled photoconductor
[AD-D011646] 17 p3037 N85-28790

Axial topography from digitized real time radiography
[DE85-006767] 18 p3091 N85-29130

Reports on cartography and geodesy. Series 1: Original reports, number 93
[ISSN-0469-4236] 18 p3124 N85-29343

An information theoretical method for automatic noise elimination in digital image processing
18 p3124 N85-29345

Air photo analysis, photo interpretation logic, and feature extraction
[AD-A153926] 18 p3124 N85-29347

Image processing: Mathematics, engineering or art
[DE85-007666] 18 p3154 N85-29527

The multiple processor machine for image processing, volume 5
[ESA-CR(P)-1976-VOL-5] 18 p3164 N85-29603

Research on signal detection and block truncation cooling for image compression
[AD-A153444] 18 p3168 N85-29628

Alternative theories of inference in expert systems for image analysis
[AD-A153649] 18 p3170 N85-29646

Solar physics applications of computer graphics and image processing 18 p3208 N85-29903

Graphic displays of vector magnetograph data
18 p3209 N85-29904

Approaches to digital image registration and recognition 19 p3257 N85-30197

Projects of the Computer Center of the academy's Siberian branch 19 p3295 N85-30425

Texture perception and shape from texture
[AD-A154276] 19 p3336 N85-30672

Target discrimination using infrared techniques: Theoretical considerations
[AD-A154070] 19 p3350 N85-30762

Methods for design and evaluation of integrated hardware-software systems for concurrent computation
[NASA-CR-176066] 20 p3515 N85-31851

Activities report of the Laboratory for Computer Science (FOA 32)
[FOA-C-30384-E1] 20 p3516 N85-31861

Electronics Division research and development
[DE85-011887] 20 p3540 N85-32032

Aspects of SAR image segmentation
[AD-A154965] 21 p3575 N85-32236

Microcomputer processing of LANDSAT Thematic Mapper data for the acquisition of military tactical terrain data
[AD-A154781] 21 p3605 N85-32389

Object identification and manipulation using silhouette moments
[AD-A154755] 21 p3705 N85-33011

Depth dimension compression of 3-D images
22 p3764 N85-33332

Pulsed lasers for filming color holographic film images
22 p3781 N85-33426

Hierarchical chamfer matching
[FOA-C-30387-E1] 22 p3802 N85-33558

Optimal Bayesian estimators for image segmentation and surface reconstruction
[AD-A155732] 22 p3827 N85-33704

Microcomputer controlled image processor
[AD-D011734] 22 p3833 N85-33735

Electronic imaging system and technique
[DE85-005740] 23 p3936 N85-34393

Production of initial estimates of photogrammetric variables
[NPL-MOM-66] 23 p3943 N85-34434

A model for graphics interface tool development
23 p3960 N85-34545

A general purpose image processing package
23 p3961 N85-34549

A new approach to linear quadtrees
23 p3961 N85-34550

Image synthesis: Optical identity or pictorial communication? 23 p3963 N85-34565

Knowledge engineering application in image processing 23 p3965 N85-34583

The read-out system of spatial distribution of thermoluminescence in meteorites
[SH-9.1-16] 23 p4052 N85-35131

Raster functionality for a VDI
[DE85-006734] 24 p4097 N85-35396

Strain measurement using point recognition picture processing
[DRIC-T-7407] 24 p4101 N85-35421

Selected publications in image understanding and computer vision from 1974 to 1983
[AD-A156196] 24 p4136 N85-35634

Edge information in color images based on histograms of differences
[AD-A156002] 24 p4154 N85-35751

Application of thermoluminescence for detection of cascade shower 1: Hardware and software of reader system
[HE-7.1-6] 24 p4213 N85-36160

Spatial distribution read-out system for thermoluminescence sheets
[HE-7.1-7] 24 p4213 N85-36161

Application of thermoluminescence for detection of cascade shower 2: Detection of cosmic ray cascade shower at Mount Fuji
[HE-7.1-12] 24 p4214 N85-36162

IMAGE RECONSTRUCTION

Shift-variant multidimensional systems
[AD-A144756] 01 p0111 N85-10752

Effect of hydrogen on formation of energy spectrum of multiply charged and copper ions
02 p0263 N85-11720

Wavelength coded image transmission and holographic optical elements
[AD-A146490] 06 p0810 N85-15147

One-dimensional processing for adaptive image restoration
[AD-A149314] 10 p1557 N85-19815

Diffraction-limited imaging of space objects 2
[AD-A149344] 11 p1728 N85-20870

Image data compression using uneven knots selection
[AD-A150602] 13 p2152 N85-23359

Holographic intensity correlator with PRIS-type photoelectro-optical controlled transparency
17 p2940 N85-28152

Deconvolution methods for multi-sensors
[AD-A152351] 17 p3018 N85-28660

Optimal Bayesian estimators for image segmentation and surface reconstruction
[AD-A155732] 22 p3827 N85-33704

Advanced instrumentation for Positron Emission Tomography
[DE85-011147] 22 p3840 N85-33779

Hologram-like transmission of pictures
23 p3961 N85-34552

IMAGE RESOLUTION

Test measurements of the 100 m telescope at lambda = 7 mm
[TR-18] 01 p0129 N85-10890

The Multispectral Imaging Science Working Group. Volume 1: Executive summary
[E85-10001] 02 p0213 N85-11404

The Multispectral Imaging Science Working Group. Volume 2: Working group reports
[E85-10002] 02 p0213 N85-11405

Formation of radio images by scanning around circle
02 p0264 N85-11727

Characterizing the scientific potential of satellite sensors
[E85-10031] 05 p0654 N85-14200

A study on the imaging potential of QUASAT — spaceborne VLBI 07 p1057 N85-16707

Potential affiliate stations to work with the EVN — European VLBI Network; QUASAT
07 p1057 N85-16708

Image quality on the KAO 08 p1249 N85-17885

Resolution enhancement of multichannel microwave imagery from the Nimbus-7 SMMR for maritime rainfall analysis
[NASA-CR-174367] 10 p1462 N85-19221

Research in image understanding as applied to 3-D tomographic imaging with near optical resolution
[AD-A150098] 12 p1829 N85-21483

LANDSAT-4 Science Characterization Early Results. Volume 3, part 2: Thematic Mapper (TM)
[E85-10069] 12 p1869 N85-21724

TM geometric performance: Line to Line Displacement Analysis (LLDA) — New Mexico
12 p1870 N85-21732

A preliminary evaluation of LANDSAT-4 Thematic Mapper data for their geometric and radiometric accuracies 12 p1871 N85-21739

Processing dynamic image sequences from a moving sensor
[AD-A149984] 12 p1934 N85-22148

Overview of TM applications research reports
13 p2117 N85-23187

Analysis and evaluation of the LANDSAT-4 MSS and TM sensors and ground data processing systems: Early results 13 p2117 N85-23189

Characterization of LANDSAT-4 TM and MSS image quality for the interpretation of California's agricultural resources — Central Valley 13 p2118 N85-23190

Preliminary evaluation of Thematic Mapper image data quality 13 p2118 N85-23194

Use of focons in combination with brightness amplifiers 14 p2274 N85-24088

A quantitative image evaluation study of a concurrent photon amplification treated emulsion
[AD-A151831] 15 p2560 N85-25796

Holographic intensity correlator with PRIS-type photoelectro-optical controlled transparency
17 p2940 N85-28152

The design, development, testing, fabrication, calibration and integration of a High Resolution Imager (HRI) for the Roentgen Satellite (ROSAT)
[NASA-CR-175302] 22 p3741 N85-33184

An analysis and algorithm for filling propagation
23 p3961 N85-34551

Hologram-like transmission of pictures
23 p3961 N85-34552

An exploratory study of the effect of screen size and resolution on the legibility of graphics in automated job performance aids
[AD-A155869] 24 p4136 N85-35632

IMAGE ROTATION

Three-dimensional data display on the two-dimensional screen
[AD-A153699] 18 p3160 N85-29577

IMAGE TRANSDUCERS

Fly's eye sensor nonlinear signal processing
[AD-D011290] 05 p0729 N85-14884

Construction and analysis of a PRIZ spatial light modulator exhibiting dynamic image selection
[AD-A152318] 17 p3037 N85-28787

Acoustic imaging systems (for robotic object acquisition)
[AD-A154043] 19 p3351 N85-30772

IMAGE TUBES

NT THERMICONS

IMAGE VELOCITY SENSORS

Predicting optical image displacement velocity in survey of Earth's surface 02 p0165 N85-11116

IMAGERY

NT ACOUSTICAL HOLOGRAPHY
NT AERIAL PHOTOGRAPHY
NT ALL SKY PHOTOGRAPHY
NT ASTRONOMICAL PHOTOGRAPHY
NT AUTORADIOGRAPHY
NT BLACK AND WHITE PHOTOGRAPHY
NT CINEMATOGRAPHY
NT CLOUD PHOTOGRAPHY
NT COLOR INFRARED PHOTOGRAPHY
NT COLOR PHOTOGRAPHY
NT COMPUTER AIDED TOMOGRAPHY
NT ELECTRO-OPTICAL PHOTOGRAPHY
NT HOLOGRAPHY
NT INFRARED IMAGERY
NT INFRARED PHOTOGRAPHY
NT LUNAR PHOTOGRAPHY
NT MICROWAVE HOLOGRAPHY
NT MICROWAVE IMAGERY
NT NEUTRON RADIOGRAPHY
NT PHOTOMICROGRAPHY
NT PHOTORECONNAISSANCE
NT RADAR IMAGERY
NT RADAR PHOTOGRAPHY
NT RADIOGRAPHY
NT REPRODUCTION (COPYING)
NT SATELLITE IMAGERY
NT SATELLITE-BORNE PHOTOGRAPHY
NT SCHLIEREN PHOTOGRAPHY
NT SHADOWGRAPH PHOTOGRAPHY
NT SPACEBORNE PHOTOGRAPHY
NT SPECTROHELIOGRAPHS
NT STEREOPHOTOGRAPHY
NT STEREOSCOPY
NT TOMOGRAPHY
NT ULTRAVIOLET PHOTOMETRY
NT WHITE LIGHT HOLOGRAPHY
NT X RAY IMAGERY

Formation of radio images by scanning around circle
02 p0264 N85-11727

Multi-disciplinary techniques for understanding time-varying space-based imagery
[AD-A144357] 05 p0726 N85-14881

Image variance and spatial structure in remotely sensed scenes — South Dakota, California, Missouri, Kentucky, Louisiana, Tennessee, District of Columbia, and Oregon
07 p0986 N85-16265

Analysis of subpixel registration
07 p0986 N85-16267

Radar calibration using direct measurement equipment and oblique photometry
[AD-D011530] 12 p1822 N85-21433

Relationship between brightness spectrum of photographic image and spectrum of rises on a water surface with waves 13 p2115 N85-23171

An assessment of the potential role of multispectral imagery in bathymetric charting
[AD-A152460] 17 p2984 N85-28438

Improved cloud and surface fields derived from HIRS2/MSU 18 p3140 N85-29439

Jupiter's ring system resolved: Physical properties inferred from the Voyager images
20 p3546 N85-32069

Geomorphic classification of Icelandic and Martian volcanoes: Limitations of comparative planetology research from LANDSAT and Viking orbiter images
21 p3603 N85-32372

Geomorphic analyses from space imagery
21 p3603 N85-32374

Process thresholds: Report of Working Group Number 3 21 p3604 N85-32384

Recognition and clear representation of handwritten electronic diagrams 23 p3960 N85-34541

Selected publications in image understanding and computer vision from 1974 to 1983
[AD-A156196] 24 p4136 N85-35634

IMAGES

NT RETINAL IMAGES

Range-residuated mappings
[AD-A145148] 01 p0112 N85-10759

Aircraft flow effects on cloud droplet images and concentrations
[AD-A146176] 03 p0396 N85-12529

Analysis of accretion and deletion at boundaries in dynamic scenes
[AD-A145944] 03 p0419 N85-12678

Weather satellite products in the Flight Service Automation System (FSAS)
[AD-A146520] 06 p0759 N85-14855

Effect of aberration in optical system on illuminance distribution over image of strip in semicoherent light
06 p0777 N85-14970

Matrix display simulation
[AD-D011371] 07 p1055 N85-16695

Development and evaluation of techniques for using combined microwave and optical image data for vegetation studies 08 p1148 N85-17240

Filter reflection image guide oscillator and solid state line scanning device
[AD-D011440] 10 p1479 N85-19336

Wide-angle flat field telescope
[NASA-CASE-GSC-12825-1] 11 p1728 N85-20668

Diffraction-limited imaging of space objects 2
[AD-A148344] 11 p1728 N85-20870

Integrating non-semantic knowledge into image segmentation processes
[AD-A149571] 12 p1851 N85-21612

Determining object orientation from a single image using multiple information sources
[AD-A149960] 12 p1933 N85-22146

A posteriori increase of resolving power of optical system forming averaged monochromatic images
13 p2082 N85-23003

Vision algorithms and psychophysics
[AD-A151868] 15 p2620 N85-26142

Asteroid amphitrite: Surface composition and prospects for the possible Galileo flyby 15 p2680 N85-26549

The development and implementation of an optical communications laboratory
[AD-A151682] 16 p2772 N85-27111

Further study of digital matching of dissimilar images
[AD-A153112] 17 p3019 N85-28672

System of white-light density pseudocolor encoding with three primary colors
[AD-D011651] 17 p3037 N85-28791

Images of the Earth's aurora and geocorona from the Dynamics Explorer Mission
[NASA-CR-175983] 18 p3136 N85-29423

Solar monochromatic images in magneto-sensitive spectral lines and maps of vector magnetic fields
18 p3207 N85-[illegible]

Infrared laser holography used in fusion plasma studies 21 p3687 N85-[illegible]

Optical image of bounded objects
21 p3697 N85-[illegible]

Depth dimension compression of 3-D images
22 p3764 N85-[illegible]

LI481 and LI482 vidicons for two-tube color TV camera with improved image quality 22 p3764 N85-[illegible]

Optimal Bayesian estimators for image segmentation and surface reconstruction
[AD-A155732] 22 p3827 N85-33704

Image synthesis: Optical identity or pictorial communication? 23 p3963 N85-[illegible]

Shadow volumes for non-planar polygons
23 p3965 N85-[illegible]

Remote sensing of hydrologic transport processes using spot simulation data
[DE85-012412] 24 p4108 N85-35487

Edge information in color images based on histograms of differences
[AD-A156002] 24 p4154 N85-35701

IMAGING RADAR

3D (Three-Dimensional) sensor for adaptive suspension vehicle
[AD-A150921] 14 p2311 N85-24305

The Boot Lake MF imaging radar
21 p3628 N85-32507

IMAGING TECHNIQUES

East Europe report: Science and technology
[JPRS-ESA-84-029] 01 p0115 N85-10763

Methods, applications of image processing
01 p0115 N85-10766

Imaging Science Panel. Multispectral Imaging Science Working Group joint meeting with Information Science Panel: Introduction 02 p0213 N85-11406

Workshop on the Use of Future Multispectral Imaging Capabilities for Lithologic Mapping: Workshop summary
02 p0214 N85-11413

Multispectral Imaging Science Working Group for Hydrologic Science: Executive summary
02 p0214 N85-11414

Information Science Panel joint meeting with Imaging Science Panel 02 p0214 N85-11415

Executive report: Results of the IRGA-CNPq/INPE experimental project
[E85-10011] 02 p0216 N85-11424

Application of digital analysis of MSS to agro-environmental studies
[E85-10024] 02 p0218 N85-11437

Holographic subtraction of images by Fourier plane recording and spatial filtration with a narrow beam
02 p0263 N85-11721

Near infrared imaging of Uranus and Neptune
02 p0299 N85-11934

Lyman-Alpha aurora 02 p0302 N85-11963

Infrared images of the Uranian rings
02 p0302 N85-11965

Restoration of multichannel microwave radiometric images
[NASA-CR-174115] 04 p0554 N85-12627

Scintillator-fiber charged particle track-imaging detector
[NASA-CR-174160] 04 p0559 N85-12650

High-speed videography for optical and X-ray imaging
[DE84-012661] 04 p0564 N85-12695

A method for measuring the effective throughput time delay in simulated displays involving manual control
05 p0701 N85-14407

Representing multidimensional systems using visual displays 05 p0711 N85-14500

Some techniques in image processing
05 p0721 N85-14629

High resolution photoacoustic and photothermal imaging 05 p0723 N85-14640

Synthesis of radio image on RATAN-600 radiotelescope 06 p0783 N85-15004

Investigative findings of image enhancement techniques
[AD-A146392] 06 p0853 N85-15424

Image-to-image correspondence: Linear structure matching 07 p0986 N85-16298

The electronic typesetting program programmer's manual
[AD-A147500] 07 p1025 N85-16508

Use of the analytic signal in ultrasonic imaging
[DE84-016843] 07 p1039 N85-16538

Application and calibration of the subsurface mapping capability of SIR-B in desert regions
08 p1148 N85-17244

A cometary ion mass spectrometer
[NASA-CR-174328] 08 p1164 N85-17343

A CCD system for photometry of direct and spectroscopic images 08 p1252 N85-17904

CCDs: Their cause and cure
08 p1252 N85-17905

Automated and interactive data base generation
[AD-P004316] 09 p1268 N85-17970

Geographic subdivision and top level data structures, Columbus, Magellan, and expanding CIG (Computer Image Generation) horizons
[AD-P004317] 09 p1268 N85-17971

CIG (Computer Image generation) data bases in an instance: Bits and pieces
[AD-P004318] 09 p1269 N85-17972

The generation of three-dimensional data bases using a building block approach
[AD-P004319] 09 p1269 N85-17973

SODERN Visualization System (SVS) for flight simulation
[AD-P004320] 09 p1269 N85-17974

An overview of the research program at the visual technology research simulator
[AD-P004321] 09 p1269 N85-17975

Design considerations for an eye tracked AOI (Area of interest) display system
[AD-P004324] 09 p1269 N85-17978

Control systems analysis program: A tool for analysis of the GE-VSCDP (General Electric-Visual System Component Display Program) image display system
[AD-P004325] 09 p1270 N85-17979

Progress report on an eye-slaved area-of-interest visual display
[AD-P004326] 09 p1270 N85-17980

Baffled eye and confounded brain or using visual illusions to train blind pilots
[AD-P004332] 09 p1271 N85-17986

On-board Computer Image Generator (CIG) applications
[AD-P004335] 09 p1271 N85-17989

CIG (Computer Image Generator) goes to war: The tactical illusion
[AD-P004336] 09 p1271 N85-17990

Military applications of the Singer Link-Miles IMAGE visual system
[AD-P004337] 09 p1271 N85-17991

Acoustic imaging in a water filled metallic pipe --- monitoring heat exchangers in nuclear power reactors
[DE84-016051] 09 p1378 N85-18665

A microchannel plate pinhole camera for 20 to 100 keV X-ray imaging
[DE85-001572] 10 p1486 N85-19396

X-ray holography of biological specimens
[DE85-002437] 10 p1489 N85-19398

Fourth International Conference on Robot Vision and Sensory Controls
[AD-A149524] 10 p1492 N85-19422

Imaging through a multiple scattering medium
[DE85-002051] 10 p1557 N85-19821

Airborne remote sensing CCD imaging system
11 p1623 N85-20220

A modern approach of a synthetic aperture radar processor and its technological aspects
11 p1713 N85-20778

Multiparticle 3D imaging technique to study the structure of molecular ions
[DE85-001843] 12 p1929 N85-22122

Grain boundaries in NiO
[DE85-008129] 13 p2025 N85-22687

A posteriori increase of resolving power of optical system forming averaged monochromatic images
13 p2082 N85-23003

Electroacoustical imaging technique for encoding incoherent radiance fields as Gabor elementary signals
[NASA-TM-88372] 13 p2094 N85-23067

Image data compression using uneven knots selection
[AD-A150602] 13 p2152 N85-23359

Optical system
[NASA-CASE-NPO-15801-1] 13 p2158 N85-23396

Photoacoustic imaging
[AD-A150823] 14 p2416 N85-24905

Connection between time- and frequency-domain three-dimensional inverse problems for the Schroedinger equation
[DE85-005914] 15 p2639 N85-26274

Occultation detection of a Neptune ring segment
15 p2681 N85-26558

Validation of the ERBE scanner scene identification methodology: Analysis with Nimbus-7 ERB data
[NASA-CR-172596] 16 p2832 N85-27466

Holographic intensity correlator with PRIS-type photoelectro-optical controlled transparency
17 p2940 N85-28152

Techniques for operating Charge Coupled Devices (CCD's) in very high speed framing mode
[AD-A152876] 17 p2953 N85-28238

Generation and display apparatus
[AD-D011630] 17 p3006 N85-28599

System of white-light density pseudocolor encoding with three primary colors
[AD-D011651] 17 p3037 N85-28791

Digital image mapping of Antarctica using NOAA-7 AVHRR imagery 18 p3124 N85-29340

Graphic displays of vector magnetograph data
18 p3209 N85-29904

Three-dimensional and tomographic imaging device for X-ray and gamma-ray emitting objects
[NASA-CASE-GSC-12851-1] 19 p3271 N85-30261

Texture perception and shape from texture
[AD-A154276] 19 p3336 N85-30672

Acoustic imaging systems (for robotic object acquisition)
[AD-A154043] 19 p3351 N85-30772

Short-time spectroscopic measurement of the temperature of solids
[ISL-CO-202/84] 20 p3459 N85-31486

EBIC characterization and hydrogen passivation in silicon sheet 20 p3481 N85-31634

The temporal evolution of a small auroral substorm as viewed from high altitudes with Dynamics Explorer 1
[NASA-CR-176064] 20 p3493 N85-31718

Study of requirements for and method of multidimensional acoustic imaging — spaceborne experiments
[ESA-CR(P)-2020] 20 p3525 N85-31924

Z-contrast imaging and electron channeling analysis of dopants in semiconductors
[DE85-011410] 21 p3582 N85-32269

One application of mega-geomorphology in education
21 p3602 N85-32370

Hexagonal uniformly redundant arrays for coded-aperture imaging
[OG-9.2-1] 21 p3714 N85-33048

An image compression survey and algorithm switching based on scene activity
[NASA-TP-2458] 22 p3727 N85-33106

Physico-geographical regionalization of Caspian lowland based on space survey materials
22 p3736 N85-33162

Conceptual design and analysis of high-speed electronic imaging
[LA-10072-MS] 22 p3756 N85-33292

Quantizer of images of heat fields obtained by Rubin-type infra-red imagers 22 p3771 N85-33369

Advanced instrumentation for Positron Emission Tomography
[DE85-011147] 22 p3840 N85-33779

Method and apparatus for Delta Kappa synthetic aperture radar measurement of ocean current
[NASA-CASE-NPO-15704-1] 23 p3925 N85-34327

Applications of holography to X-ray imaging
[DE85-010984] 23 p3934 N85-34384

A theoretical and empirical analysis of coherent ray-tracing 23 p3957 N85-34524

Frame buffer algorithms for stochastic models
23 p3957 N85-34525

Specifying stochastic objects in a hierarchical graphics system 23 p3957 N85-34526

Computer analysis techniques for the temporal evaluation of cardiac wall motion
23 p3958 N85-34530

A computerized system for spot detection and analysis of two-dimensional electrophoresis images
23 p3958 N85-34531

An image management kernel for the design of relational and pictorial data bases 23 p3958 N85-34532

Animengine: An engineering animation system
23 p3959 N85-34535

3D computer animation: More an evolution problem than a motion problem 23 p3959 N85-34536

Towards an integrated view of 3-D computer character animation 23 p3959 N85-34538

Research issues in generating graphical explanations
23 p3959 N85-34539

The scientific and technical issues in integrating remotely sensed imagery with geocoded data bases
23 p3960 N85-34547

Selection of segment similarity measures for hierarchical picture segmentation 23 p3960 N85-34548

Hexagonal uniformly redundant arrays for coded-aperture imaging
[OG-9.2-1] 23 p4024 N85-34940

A coded aperture imaging system optimized for hard X-ray and gamma ray astronomy
[OG-9.2-3] 23 p4024 N85-34942

An experimental assessment of the imaging quality of the low energy gamma-ray telescope ZEBRA
[OG-9.2-8] 23 p4025 N85-34947

Advanced techniques for high resolution spectroscopic observations of cosmic gamma-ray sources
[OG-9.2-9] 23 p4025 N85-34948

A Cerenkov imaging telescope for high energy gamma rays
[OG-9.3-13] 23 p4028 N85-34958

The University of Durham Mark 3 very high energy gamma ray telescope
[OG-9.4-2] 23 p4028 N85-34959

Application of imaging to the atmospheric Cherenkov technique
[OG-9.5-4] 23 p4030 N85-34961

An experimental study of dielectric rod antennas for millimeter-wave imaging applications
[AD-A155832] 24 p4086 N85-35328

Strain measurement using point recognition picture processing
[DRIC-T-7407] 24 p4101 N85-35421

Processing of LANDSAT imagery to map surface mineral alteration on the Alaska Peninsula, Alaska
24 p4106 N85-35455

Selected publications in image understanding and computer vision from 1974 to 1983
[AD-A156196] 24 p4136 N85-35634

Optical synthetic aperture techniques
[AD-A156151] 24 p4154 N85-35752

IMIDES

Development of new and improved polymer matrix resin systems, phase 1
[NASA-CR-168595] 01 p0017 N85-10104

A method for obtaining new cyclical imides of derivative benzimidazoles
[AD-A145042] 01 p0017 N85-10106

A new heat-resistant polymer from dimer diamine bismaleimide. Part 1: Preparation and free radical cure of dimer diamine bismaleimide
[AD-A145864] 02 p0186 N85-11247

Polyimide-glass multilayer printed wiring boards
[DE84-015092] 05 p0631 N85-14048

Imide modified epoxy matrix resins
[NASA-CR-174695] 07 p0930 N85-15892

Phosphorus-containing imide resins
[NASA-CASE-ARC-11368-2] 12 p1809 N85-21347

High performance mixed bisimide resins and composites based thereon
[NASA-CASE-ARC-11536-1-SB]
19 p3231 N85-30033

IMINES

A soluble linear Schiff-base coordination polymer containing eight-coordinate zirconium(4)
[AD-A151446] 15 p2518 N85-25527

Polyethylene imine-metal salt solid electrolyte
[AD-D011678] 19 p3305 N85-30485

IMMERSION

U SUBMERGING

IMMISCIBILITY

U SOLUBILITY

IMMITTANCE

U ELECTRICAL IMPEDANCE

IMMOBILIZATION

Effect of disuse on sarcoplasmic reticulum in fast and slow skeletal muscle
[NASA-CR-174337] 08 p1191 N85-17508

Acid phosphatase and protease activities in immobilized rat skeletal muscles
[NASA-CR-174340] 08 p1192 N85-17509

A comparison of rat myosin from fast and slow skeletal muscle and the effect of disuse
[NASA-CR-174339] 08 p1192 N85-17510

Histological and compositional responses of bone to immobilization and other experimental conditions
[NASA-CR-175837] 16 p2841 N85-27518

IMMUNITY

Induction of immunity to toxins with anti-idiotypic antibody
[AD-A146793] 07 p1014 N85-16445

Phenomenon of universal rosette-forming cell stimulation by extreme stress 20 p3505 N85-31789

IMMUNOASSAY

Proceedings of the 14th Army Science Conference. Volume 1: Principal Authors A through H
[AD-A149200] 10 p1573 N85-19920

IMMUNOLOGY

USSR report: Life sciences. Biomedical and behavioral sciences
[JPRS-UBB-84-015] 07 p1010 N85-16416

The effects of simulated weightlessness on susceptibility to viral and bacterial infections using a murine model
15 p2613 N85-26100

Rapid rate-kinetic turbidometric assay for quantitation of antiviral complement-fixing antibodies
[AD-A153644] 18 p3152 N85-29516

USSR report: Life sciences. Biomedical and behavioral sciences
[JPRS-UBB-85-017] 20 p3504 N85-31785

East Europe report: Science and technology
[JPRS-ESA-85-021] 21 p3568 N85-32190

East Europe report: Science and technology
[JPRS-ESA-85-023] 21 p3572 N85-32217

IMP
Pluribus satellite IMP development mobile access terminal network
[AD-A147675] 08 p1151 N85-17264
IMP-I
U EXPLORER 43 SATELLITE
IMP-J
U EXPLORER 50 SATELLITE
IMP-6
U EXPLORER 43 SATELLITE
IMP-8
U EXPLORER 50 SATELLITE
IMPACT
NT ECONOMIC IMPACT
NT ELECTRON IMPACT
NT HYPERVELOCITY IMPACT
NT ION IMPACT
Impact phenomena as factors in the evolution of the Earth
[NASA-CR-174015] 01 p0072 N85-10474
Impact of alcohol fuels on urban air pollution: Methanol photochemistry study
[DE84-012960] 04 p0531 N85-13397
Lunar magma ocean and its implication for origin of the Moon 04 p0581 N85-13711
Lunar origin: role of giant impacts
04 p0587 N85-13749
Lunar origin from impact on the Earth
04 p0588 N85-13757
Evaluation of the birdstrike threat to the F-15 present fleet, rapid deployment force, and dual role fighter transparencies
[AD-A148954] 10 p1421 N85-18966
Impacts on Explorer 46 from an Earth orbiting population 12 p1785 N85-21204
Stagnation zone impaction on a simple terrain feature in stable flow 13 p2130 N85-23255
Lunar origin: Role of giant impacts
13 p2179 N85-23519
Impact cratering calculation 13 p2180 N85-23531
Impact crater scaling laws 13 p2181 N85-23532
Sliding interfaces with contact-impact in large scale Lagrangian computations
[DE85-006451] 15 p2639 N85-26277
Volatile loss following very large impacts
22 p3853 N85-33862
Friction, impact, and electrostatic discharge sensitivities of energetic materials
[DE85-013321] 24 p4083 N85-35309
IMPACT ACCELERATION
Biomechanical studies of impact acceleration research
[AD-A149077] 10 p1522 N85-19601
Telemetry system for the transmission of data from projectiles during the acceleration phase in the gun barrel
[ISL-CO-207/84] 22 p3739 N85-33178
IMPACT DAMAGE
NT METEORITIC DAMAGE
Simulation of contact surface erosion for impact problems 01 p0060 N85-10396
Single-drop impact damage prediction for low density, coated ceramic materials — rain erosion
01 p0061 N85-10402
Influence of test method and material stiffness on the damage produced by low velocity impacts on carbon-epoxy composites No. 45.387/1
[REPT-45.387/1] 03 p0326 N85-12100
Effect of impact damage and open holes on the compression strength of tough resin/high strain fiber laminates 04 p0464 N85-12945
The effect of matrix and fiber properties on impact resistance 04 p0464 N85-12947
Development of a heterogeneous laminating resin
04 p0465 N85-12956
On the effects of delamination damage in fibre composite laminates
[ARL/STRUC-R-403] 06 p0763 N85-14881
Contact behavior, impact response and damage in graphite-epoxy laminates subjected to initial stresses
06 p1171 N85-17386
A study of constitutive relations for polycrystalline aluminum during finite dynamic plastic deformation
06 p1172 N85-17388
Water impact laboratory and flight test results for the space shuttle solid rocket booster aft skirt
09 p1335 N85-18394
The influence of mechanical damage on transmission pipeline integrity
[ERS-E.351] 09 p1340 N85-18431
Recent studies of the significance of mechanical damage in pipelines
[ERS-E.367] 09 p1341 N85-18433
Smoother terrain-machine
[AD-P004296] 09 p1409 N85-18873
Birds and aviation
[AD-P004177] 11 p1578 N85-19939
Avoiding serious bird strike incidents
[AD-P004178] 11 p1578 N85-19940
Accidents and serious incidents to civil aircraft due to birdstrikes
[AD-P004180] 11 p1578 N85-19942
Worldwide birdstrike statistics of Lufthansa German Airlines
[AD-P004183] 11 p1579 N85-19945
Birds and aircraft engine strike rates
[AD-P004184] 11 p1579 N85-19946
Orbital Debris
[NASA-CP-2360] 12 p1783 N85-21188
A model for the evolution of on-orbit manmade debris environment 12 p1784 N85-21196
Geosynchronous satellite collision avoidance
12 p1784 N85-21197
In situ orbital debris experiment concepts
12 p1784 N85-21198
General-purpose heat source development: Safety test program. Postimpact evaluation, design iteration test 5
[LA-10232-SR] 12 p1931 N85-22129
Anticipated impact plasma problems for the COPERNIC-RPA experiment in the cometary environment — Giotto mission 14 p2245 N85-23917
Considerations of large scale impact and the early Earth 21 p3718 N85-33070
Design and testing of an energy-absorbing crewseat for the F/FB-111 aircraft, volume 1
[NASA-CR-3916] 23 p3896 N85-34133
Quantitative non-destructive evaluation of composite materials based on ultrasonic wave propagation
[NASA-CR-176176] 24 p4074 N85-35244
IMPACT DECELERATION
U DECELERATION
U IMPACT ACCELERATION
IMPACT FUSION
Investigation of electromagnetic launcher behavior for impact fusion
[DE84-017401] 04 p0563 N85-13585
IMPACT LOADS
Fatigue-impact studies in laminated composites
[AD-A142641] 03 p0326 N85-12097
Constitutive features of solids at shock-wave loading rates
[DE84-015715] 03 p0362 N85-12325
Tests of the load-bearing and deformation behaviour of reinforced concrete spherical shells under point loading
[BLL-RISLEY-TR-4550-9091.9F)]
06 p0816 N85-15182
Analysis of the impact of a deformable missile model on a deformable obstruction
[BLL-RISLEY-TR-8534-(9091.9F)]
06 p0859 N85-15459
Crack growth in propellants 06 p1116 N85-17034
Alternative shock characterizations for consistent shock test specifications 09 p1335 N85-18396
Subreflector focusing techniques applied to new DSS-15 and DSS-45 34-meter antennas
10 p1464 N85-19233
Biological effects of blast and impact waves
[FOA-C-52006-H4-D7] 12 p1906 N85-21968
A search for evidence of large body Earth impacts associated with biological crisis zones in the fossil record 15 p2682 N85-26567
General Aviation Crashworthiness Project. Phase 2: Impact severity and potential injury prevention in general aviation accidents
[PB85-917002] 19 p3215 N85-29938
Analysis of rotorcraft crash dynamics for development of improved crashworthiness design criteria
[FAA-CT-85-11] 20 p3391 N85-31031
Space station dynamic modeling, disturbance accommodation, and adaptive control
20 p3409 N85-31154
Preliminary considerations for the gasdynamic precompression of solid molecular hydrogen
[DE85-013256] 22 p3784 N85-33445
Safety and reliability of steel structural materials under random service impact loads 23 p3906 N85-34197
IMPACT MELTS
Centrifuge impact cratering experiments
13 p2181 N85-23533
Progress on studies of early intense cratering
13 p2181 N85-23535
Why not a constant early lunar impact rate?
13 p2181 N85-23536
IMPACT PREDICTION
Structural modifications by viscoelastic elements
09 p1337 N85-18407
General-purpose heat source development: Safety test program. Postimpact evaluation, design iteration test 1
[LA-9980-SR] 12 p1931 N85-22131
IMPACT PRESSURES
U IMPACT LOADS
IMPACT RESISTANCE
Sensitivity analysis of limit state functions for probability-based plastic design
01 p0059 N85-10[illegible]
The influence of inert particulate material on the properties of RDX/polyethylene wax compositions
[MRL-R-929] 03 p0336 N85-121[illegible]
The effect of matrix and fiber properties on impact resistance 04 p0464 N85-12947
Fundamental studies of composite toughness
04 p0464 N85-1294[illegible]
Development of a heterogeneous laminating resin
04 p0465 N85-1295[illegible]
Modified epoxy composites 04 p0466 N85-1295[illegible]
Nonlinear analysis of composite laminates
09 p1288 N85-180[illegible]
Development of a heterogeneous laminating resin system
[NASA-CR-172459] 09 p1288 N85-180[illegible]
General-purpose heat source development: Safety test program. Postimpact evaluation, design iteration test 4
[LA-10217-SR] 12 p1930 N85-2212[illegible]
Remote control of an impact demonstration vehicle
[NASA-TM-85925] 14 p2225 N85-2[illegible]
Development of an impact- and solvent-resistant thermoplastic composite matrix, phase 3
[NASA-CR-172568] 20 p3422 N85-312[illegible]
Strain rate sensitivity estimation from high velocity impact data
[AD-A154703] 21 p3599 N85-323[illegible]
IMPACT SENSITIVITY
U IMPACT RESISTANCE
IMPACT STRENGTH
Tough Composite Materials
[NASA-CP-2334] 04 p0463 N85-12941
Impact toughness of wire after cold deformation and annealing
[BLL-M-35941-(5828.4)] 05 p0615 N85-13[illegible]
Proceedings of the International Conference and Exposition on Structural Impact and Crashworthiness
[AD-A147845] 07 p0900 N85-157[illegible]
Contact behavior, impact response and damage in graphite-epoxy laminates subjected to initial stresses
06 p1171 N85-17386
Impact toughness of composites with layered microstructure of OT4 titanium alloy
10 p1445 N85-19104
Fiber composite materials with titanium matrix
10 p1445 N85-19105
Prediction of the resistance of structural materials to cavitation erosion
[BLL-DRIC-TRANS-7435-(3623.66)]
13 p2020 N85-22[illegible]
Chain dynamics and structure property relation in high impact strength polycarbonate plastic
[AD-A152011] 15 p2519 N85-2553[illegible]
Effect of low-velocity or ballistic impact damage on the strength of thin composite and aluminum shear panels
[NASA-TP-2441] 16 p2742 N85-2[illegible]
High-strength weldable steel 03G4N2MAF Sh with improved ductility
[BLL-BISI-TRANS-22233-(9022.06)]
17 p2924 N85-2[illegible]
Effects of heat treatment and tracer element impurities on the impact properties of the 12Cr steels
[DE85-010676] 19 p3240 N85-30[illegible]
Impact fracture mechanism of polymer plates containing a heavy inner material 23 p3906 N85-34215
IMPACT TESTING MACHINES
Instrumented impact testing machine with reduced specimen oscillation effects
[VTT-290] 04 p0504 N85-1321[illegible]
IMPACT TESTS
NT CHARPY IMPACT TEST
Eutectic explosives containing ammonium nitrate
[DE84-015705] 01 p0034 N85-10213
Crashworthiness of light aircraft fuselage structures: A numerical and experimental investigation
01 p0060 N85-10[illegible]
Analysis of a transport fuselage section drop test
01 p0060 N85-10400
Deformation measurements of composite multi-span beam shear specimens by Moire interferometry
[NASA-CR-3844] 02 p0169 N85-1110[illegible]
Influence of test method and material stiffness on the damage produced by low velocity impacts on carbon-epoxy composites No. 45.387/1
[REPT-45.387/1] 03 p0326 N85-12100
Full-scale crash-test evaluation of two load-limiting subfloors for general aviation airframes
[NASA-TP-2380] 04 p0512 N85-13[illegible]
NASA-Ames vertical gun 04 p0579 N85-13[illegible]
Deformation, fracture and explosive properties of reactive materials
[AD-A146396] 06 p0774 N85-14[illegible]

Impact tests of adjusters for the HBU-12 lap belt
[AD-A148021] 08 p1060 N85-16843

Impact tests of automatic lap belt configurations
[AD-A148034] 08 p1061 N85-16844

Sensitivity tests for solid propellants in Germany
08 p1115 N85-17028

Development of a high temperature single impact rain erosion test capability
[AD-P004371] 12 p1827 N85-21465

General-purpose heat source development: Safety test program. Postimpact evaluation, design iteration test 4
[LA-10217-SR] 12 p1930 N85-22128

Behavior of fiber-reinforced composites under dynamic tension
[AD-A150619] 13 p2015 N85-22641

IHE material qualification tests description and criteria
[DE85-004649] 13 p2040 N85-22770

Progress on Experimental impact studies
13 p2181 N85-23534

Impact studies of a 1/3-scale model of an air cushion vehicle
[NASA-TM-86360] 14 p2218 N85-23757

Six-inch HYGE vertical impact facility
[AD-A150665] 14 p2226 N85-23809

Impact ionization from gold, aluminum and PCB-Z — Giotto spacecraft paint PCB-Z 14 p2244 N85-23910

Experimental investigations on ion emission with dust impact on solid surfaces — Giotto spacecraft
14 p2244 N85-23911

Ion emission from solid surfaces: Comparison of dust impact with other excitations — Giotto mission
14 p2244 N85-23912

Dynamic shock studies of PZT 95/5 ferroelectric ceramic
[DE85-006137] 14 p2261 N85-24015

Hopkinson bar simulation using DYNA2D
[DE85-006766] 16 p2802 N85-27275

Constitutive modeling for blast-induced wave propagation
[AD-A153576] 18 p3099 N85-29187

Effect of thermochemical processing on fatigue resistance of titanium alloys 19 p3244 N85-30112

Study of intermediate velocity penetration of steel spheres into deep aluminum targets
[DE85-010419] 19 p3287 N85-30385

Flight test experience and controlled impact of a large, four-engine, remotely piloted airplane
[NASA-TM-86738] 22 p3730 N85-33123

Design and testing of an energy-absorbing crewseat for the F/FB-111 aircraft, volume 1
[NASA-CR-3916] 23 p3896 N85-34133

Design and testing of an energy-absorbing crewseat for the F/FB-111 aircraft. Volume 3: Data from crew module testing
[NASA-CR-3918] 23 p3896 N85-34134

Design and testing of an energy-absorbing crewseat for the F/FB-111 aircraft. Volume 2: Data from seat testing
[NASA-CR-3917] 24 p4064 N85-35184

IMPACT TOLERANCES

Impacts of Space Shuttle thermal protection system tile on F-15 aircraft vertical tile
[NASA-TM-85904] 12 p1792 N85-21245

Design and testing of an energy-absorbing crewseat for the F/FB-111 aircraft. Volume 2: Data from seat testing
[NASA-CR-3917] 24 p4064 N85-35184

IMPACTORS

Progress on studies of early intense cratering
13 p2181 N85-23535

Why not a constant early lunar impact rate?
13 p2181 N85-23536

Martian terrain ages 13 p2181 N85-23537

Interaction of Martian flow ejecta blankets with pre-existing impact craters: Morphological observations
13 p2183 N85-23546

Development of a microorifice uniform deposit cascade impactor
[DE85-006765] 22 p3812 N85-33614

IMPATT DIODES

U AVALANCHE DIODES

IMPEDANCE

NT ACOUSTIC IMPEDANCE
NT CONTACT RESISTANCE
NT ELECTRICAL IMPEDANCE
NT ELECTRICAL RESISTANCE

Admittance measurement with twin-T devices in the frequency range between 1 and 300 MHz
05 p0629 N85-14032

Space charge, interfacial kinetics, and electrical response of condensed matter
[AD-A146364] 06 p0765 N85-14893

Scattering of H10-mode wave by narrow conducting plate inside rectangular waveguide
06 p0788 N85-15036

The dc SQUID as a tuned radiofrequency amplifier
[DE85-000701] 06 p0805 N85-15123

Investigation of the pressure-and velocity-coupled responses of solid propellants using impedance tube method 09 p1300 N85-18168

Calculation of transmission line impedances using the ANSYS finite element program
[DE84-016715] 11 p1629 N85-20261

Driven global Alfven eigenmodes
[DE85-001056] 11 p1732 N85-20890

Thermocouple modeling
[DE85-005172] 14 p2306 N85-24273

Discharge characteristics of high-pressure, fast-discharge XeCl excimer laser
15 p2564 N85-25820

Measurement of damping of graphite expoxy materials
[NASA-CR-175793] 16 p2743 N85-26925

Ionospheric effects on antenna impedance
[BMFT-FB-W-84-052] 17 p2950 N85-28217

Nonlinear plasma reactions on the antenna impedance of high transmission power satellites
[BMFT-FB-W-84-053] 18 p3192 N85-29799

Mutual coupling analysis for conformal microstrip antennas
[AD-A154292] 19 p3259 N85-30210

Characterization of microstrip discontinuities in the time and frequency domains
[NASA-CR-176190] 24 p4088 N85-35342

IMPEDANCE MATCHING

A broadband matching network
[AD-D011406] 08 p1219 N85-17675

Pulse transformer package for impedance matching a laser diode to a transmission line
[AD-D011499] 12 p1855 N85-21632

Measured performance of a broadband matching section for peripherally fed helical antennas
[R-NIAS-25] 15 p2539 N85-25670

Switching mixer
[AD-D011602] 16 p2777 N85-27139

IMPEDANCE MEASUREMENT

An automated immittance measuring system for electroacoustic transducers
[AD-A145701] 02 p0200 N85-11336

Impedance measurements on a VLF multi-turn loop antenna in a space plasma simulation chamber
[AD-A145104] 04 p0492 N85-13141

Admittance measurement with twin-T devices in the frequency range between 1 and 300 MHz
05 p0629 N85-14032

Experimental verification of eddy-current flaw theory
[DE85-001288] 09 p1329 N85-18350

Generalized method for the calibration of 4-terminal-pair type digital impedance meters
[PB85-128122] 11 p1638 N85-20318

Thermocouple modeling
[DE85-005172] 14 p2306 N85-24273

IMPEDANCE PROBES

Contribution of mutual impedance experiments to the understanding of magnetospheric processes — GEOS satellites 14 p2371 N85-24656

IMPELLER BLADES

U ROTOR BLADES (TURBOMACHINERY)

IMPELLERS

NT PUMP IMPELLERS

Experimental observation of the flow in impellers and diffusers — centrifugal compressors
05 p0636 N85-14080

Answering thermodynamic questions with three-dimensional viscous flow calculations
05 p0636 N85-14081

Lateral fluid forces acting on a whirling centrifugal impeller in vaneless and vaned diffuser
05 p0643 N85-14123

Hydraulic forces on a centrifugal impeller undergoing synchronous whirl 05 p0643 N85-14124

Hydrodynamic impeller stiffness, damping, and inertia in the rotordynamics of centrifugal flow pumps
05 p0643 N85-14125

Two-dimensional unsteady analysis of fluid forces on a whirling centrifugal impeller in a volute
05 p0643 N85-14126

Group technology for working turbine drive wheel disks 14 p2269 N85-24061

Effect of apparent fluid masses on natural vibration frequencies of impellers of multistage centrifugal pumps
14 p2277 N85-24108

Investigation of gas-turbine engine blower impeller vibrations with change in engine intake conditions
14 p2287 N85-24170

Fluidic angular velocity sensor
[NASA-CASE-NPO-16479-1-CU]
18 p3104 N85-29219

A 3-D Euler method for internal transonic flows computation with a multi-domain approach
21 p3587 N85-32298

IMPERFECTIONS

U DEFECTS

IMPERIAL VALLEY (CA)

Investigation of radiometric properties of LANDSAT-4 MSS — California, North Carolina, South Carolina, and New England 11 p1666 N85-20500

IMPINGEMENT

NT JET IMPINGEMENT

Materials characterization with intense positron beams
[DE85-011850] 22 p3839 N85-33769

Experimental aerodynamic heating to simulated space shuttle tiles in laminar and turbulent boundary layers with variable flow angles at a nominal Mach number of 7
[NASA-TP-2307] 23 p3929 N85-34351

Computation of three-dimensional shock wave and boundary-layer interactions
[NASA-TM-86780] 24 p4093 N85-35372

IMPLANTATION

NT ION IMPLANTATION

Ion-implantation doping of strained-layer superlattices
[DE85-001903] 09 p1400 N85-18811

Percutaneous connectors
[NASA-CR-175627] 16 p2839 N85-27508

A communications link for an implantable electrode array
[AD-A152238] 16 p2840 N85-27510

Design evaluation of high reliability lithium batteries
20 p3444 N85-31380

IMPLANTED ELECTRODES (BIOLOGY)

Encapsulation and packaging of a semiconductor multielectrode array for cortical implantation
[AD-A153180] 17 p2998 N85-28535

IMPLOSIONS

K-shell yield scaling law for conventional PRS loads
[AD-A145155] 01 p0121 N85-10831

Imploding plasma radiation sources: Basic concepts
[AD-A145542] 02 p0284 N85-11856

Non-LTE considerations in spectral diagnostics of thermal transport and implosion experiments
[DE84-015187] 05 p0730 N85-14689

Imploding plasma X-ray laser research
[DE85-000057] 09 p1326 N85-18331

Study of opacity effects on line radiation from pellet implosions
[DE85-000380] 10 p1491 N85-19413

Prediction of the resistance of structural materials to cavitation erosion
[BLL-DRIC-TRANS-7435-(3623.66)]
13 p2020 N85-22659

Research with high-power short-wavelength lasers
[DE85-010329] 19 p3278 N85-30332

Workshop report on Simulation Techniques for Shock Wave Phenomena and Characteristics of Plasmas in Inertial Confinement Fusion
[IPPJ-725] 23 p3979 N85-34670

Moving finite element method for ICF target implosion
23 p3980 N85-34675

Two-dimensional simulation of LIB target implosion
23 p3980 N85-34678

Stability of implosion dynamics
23 p3980 N85-34680

System expectations for Pioneer 1 foil implosion experiments
[DE85-014129] 24 p4091 N85-35359

Diagnostics for Pioneer 1 imploding plasma experiments
[DE85-014120] 24 p4159 N85-35787

IMPREGNATING

Theory of kinetics of impregnation of porous bodies
[BLL-M-35917-(5828.4)] 06 p0616 N85-13942

The fabrication, processing and characterization of multidimensionally braided graphite/epoxy composite materials
[AD-A148729] 09 p1288 N85-18090

Utilization of microwave measuring systems for the automation of composite materials manufacturing
[SNIAS-851-430-102] 22 p3742 N85-33197

Implementation of polymer impregnation as a bridge deck sealant
[PB85-185718] 22 p3753 N85-33265

IMPROVEMENT

Improved coordinate measuring machine calibration and control
[DE85-012053] 21 p3590 N85-32315

Land vehicle corrosion management
22 p3750 N85-33246

The properties of VSt3sp inoculated steel
[BLL-M-35894-(5828.4)] 23 p3915 N85-34263

IMPULSE GENERATORS

Fast response impulse generator
[AD-D011283] 06 p0759 N85-14853

Application of pulsed power in the simulation of severe natural lightning
[DE85-012666] 24 p4124 N85-35564

IMPULSES
Axisymmetrical oscillations of shell systems subjected to impulse loads 13 p2047 N85-22814
The Record of Electrical and Communication Engineering Conversazione, volume 53, no. 2, November 1984
[ISSN-0385-7719] 16 p2758 N85-27022
Proposal of a method for evaluating accuracy of estimated impulse response of a system
16 p2759 N85-27024
Development of the relativistic impulse approximation
[DE85-008506] 18 p3179 N85-29711

IMPURITIES
NT PSEUDOPOTENTIALS
Nonlinear ultrasonic characterization of oxygen impurities in titanium, 2
[AD-A144857] 01 p0027 N85-10171
Milling of Si3N4 with Si3N4 hardware
[NASA-TM-86864] 01 p0031 N85-10191
Environment-induced embrittlement: Effect of impurity segregation and state of stress
[DE84-015436] 02 p0184 N85-11235
Impurity trapping during gas phase epitaxy of gallium arsenide 02 p0257 N85-11686
RF laser plasma measurements
[AD-A145836] 03 p0368 N85-12344
Investigation of the interaction of atoms with lattice defects using probe methods 03 p0429 N85-12737
Spectroscopic investigations on neutron induced impurity atoms and radiation defects
03 p0430 N85-12742
Paramagnetic impurity effects in NMR determinations of hydrogen diffusion and electronic structure in metal hydrides. Cerium in YH-2 and LaH-2.25
[DE84-014127] 04 p0472 N85-13005
Preparation of low-silicon vanadium metal
[DE84-014818] 04 p0476 N85-13031
Effects of monolayer converages on substrate sputtering yields
[DE84-016312] 04 p0476 N85-13033
Silicon for solar cells
[DE84-004503] 04 p0529 N85-13381
Contamination analysis of Ti-O2 thin films deposited using ion assisted deposition
[DE84-014944] 05 p0732 N85-14705
Mechanisms of impurity diffusion in rutile
[DE84-014741] 06 p0766 N85-14902
JPL in-house fluidized-bed reactor research
06 p0832 N85-15291
Determination of moments of initial estimate during linear approximation of distribution of ejected impurity
07 p0954 N85-16045
Dependence of breakdown voltage for p-n junction on parameters of ion implantation and semiconductor heat treatment 07 p0954 N85-16046
Prototype wash water renovation system integration with government-furnished wash fixture
[NASA-CR-171829] 08 p1196 N85-17547
Spectroscopic measurement on Heliotron E
09 p1387 N85-18722
Radial profiles of high resolution X-ray spectra from the Alcator C Tokamak 09 p1387 N85-18723
Impurity control by additional current rise and gas puffing during ICRF heating in JIPP T-IIU Tokamak
09 p1387 N85-18725
Sources, densities, and transport of impurities in neutral-beam injected Tokamaks
09 p1388 N85-18731
Transport experiments in the Texas experimental Tokamak 09 p1389 N85-18741
Impact of atomic data on Tokamak modeling
09 p1390 N85-18743
Extended abstract: Ergodic magnetic limiter experiments on TEXT with a 7/3 resonance
[DE85-001390] 09 p1391 N85-18754
Studies on impurity control and hydrogen pumping with chromium gettering in ISX-B
[DE85-001896] 09 p1394 N85-18771
An infrared study of the hydrogenation of carbon dioxide on supported rhodium catalysts
[AD-A149477] 10 p1436 N85-19049
Variational calculation of the 2D H2 molecule
[INPE-3304-PRE/615] 10 p1554 N85-19796
Investigation of vanadium solid solution and zeta phase regions of vanadium-carbon system
[DE85-002678] 11 p1605 N85-20092
Phonon-impurity relaxation and acoustic wave absorption in yttrium-aluminum garnet crystals with impurities 11 p1715 N85-20790
Excitation of impurities by heavy particles and radiative losses of thermonuclear plasma
11 p1719 N85-20816
Atomic processes involving impurities in the plasma edge
[DE85-001277] 11 p1730 N85-20882
Impurity complexes in pure elemental semiconductors
11 p1736 N85-20919
Atomistic studies of grain boundaries with segregated impurities
[DE85-000063] 11 p1737 N85-20924
Electrochemical processes at the sodium (BETA)" alumina interface
[DE85-004653] 12 p1802 N85-21305
Neutral beam injector oxygen impurity measurements and concentration reduction via gettering processes
[DE85-000861] 12 p1836 N85-21521
Spectroscopic study of sources and control of impurities in TMX-U: Revision 1
[DE85-004423] 12 p1937 N85-22170
Americium metal preparation on the multigram scale
[DE85-003735] 13 p2024 N85-22683
Impurities in Kevlar 49 fibers
[DE85-004996] 13 p2038 N85-22767
Hydrogen on impurity-covered iron surfaces
14 p2254 N85-23966
Recent developments in semiconductor research
14 p2297 N85-24222
Laser-induced fluorescence of metal-atom impurities in a neutral beam
[DE85-004980] 14 p2310 N85-24298
Self-substaining low-Z coatings for impurity control. Part 1: General considerations
[DE85-000427] 14 p2425 N85-24956
Energy trapping, release, and transport in three-dimensional energetic solids and molecular crystals: Theory of defects and impurities
[AD-A151071] 14 p2428 N85-24973
Effect of protective atmosphere composition on durability of welded joints of niobium alloys
15 p2502 N85-25432
Structure and properties of VT20L titanium alloy with 0.1-0.3 percent content 15 p2515 N85-25517
Dynamics of recrystallization and redistribution of impurities in semiconductors subjected to millisecond laser pulses 15 p2643 N85-26302
Performance of a copper-lithium alloy as an impurity control system surface material for a fusion reactor
[DE85-006494] 15 p2657 N85-26396
Impurity studies
[DE85-006235] 15 p2661 N85-26423
Microscopic study of the influence of impurities on interface bonding
[AD-A151725] 16 p2743 N85-26928
Sodium and lithium corrosion in molybedenum heat pipes
[DE85-005561] 16 p2784 N85-27179
Periodic cluster simulation of a disordered impurity system
[INPE-3453-PRE/705] 16 p2858 N85-27628
Shallow impurity cluster states in n-type semiconductors
[INPE-3495-PRE/732] 16 p2869 N85-27699
Electronic density of states for the double donor system Si:P, As
[INPE-3447-PRE/700] 16 p2869 N85-27700
On some physical impurity properties of doped-indirect gap semiconductors at low and intermediate concentrations
[INPE-3452-PRE/704] 16 p2869 N85-27701
Density of impurity states associated to inversion layers
[INPE-3406-PRE/675] 16 p2869 N85-27702
Atom location by electron channeling analysis
[DE85-007549] 16 p2872 N85-27716
An Impurity Control Test Facility (ICTF) for the study of fusion reactor/plasma edge materials
[DE85-007948] 17 p3040 N85-28810
Impurity control and vacuum pumping system design and analysis for next-generation Tokamaks
[DE85-009291] 17 p3041 N85-28815
The transport of neutral H, D, T and He and O in the boundary layers of a Tokamak plasma
[REPT-84-153] 17 p3041 N85-28817
Magnetic impurities in superconductors
[DE85-008372] 18 p3196 N85-29825
Anisotropic electron-impurity scattering in dilute AlLi: (Small) corrections to the local density approximation
[DE85-002946] 19 p3238 N85-30076
Effects of heat treatment and tracer element impurities on the impact properties of the 12Cr steels
[DE85-010676] 19 p3240 N85-30086
Method of reducing impurity and antisite defects in semiconductor crystal materials, and device and apparatus respectively produced from and utilizing same
[AD-D011698] 19 p3260 N85-30216
Impurity and particle control systems for tokamak reactor experiments
[DE85-006124] 19 p3366 N85-30873
Current state of development and expected performance of copper-lithium alloys as an impurity control system in fusion applications
[DE85-009673] 19 p3372 N85-[illegible]
Compositional analysis of silicon
20 p3460 N85-[illegible]
Oxygen and carbon impurities and related defects in silicon 20 p3481 N85-[illegible]
Z-contrast imaging and electron channeling analysis of dopants in semiconductors
[DE85-011410] 21 p3582 N85-[illegible]
Raman scattering studies in solids
[AD-A155526] 21 p3710 N85-[illegible]
Cryogenic laser calorimetry for impurity analysis
[NASA-CR-176102] 22 p3743 N85-[illegible]
The study of the effect of residual microimpurities on the fatigue strength of 55S2 steel
[BLL-M-36317-(5828.4)] 23 p3913 N85-[illegible]
Stress corrosion cracking susceptibility of types 316NG and 316 stainless steel in an impurity environment
[TI85-006664] 23 p3917 N85-34277
Effect of temperature and ionic impurities at very low concentrations on stress corrosion cracking of Type 304 stainless steel
[TI85-003048] 24 p4079 N85-[illegible]
Cryogenic laser calorimetry for impurity analysis
[NASA-CR-176179] 24 p4097 N85-[illegible]
X-ray fluorescence analysis of uranium concentrates
[DE85-013189] 24 p4148 N85-35717

IMS
U INTERNATIONAL MAGNETOSPHERIC STUDY

IN-FLIGHT MONITORING
Wind shear measuring on board an airliner
[NASA-TM-77463] 03 p0395 N85-12521
Tornado: Structural Usage Monitoring System (SUMS) 07 p0896 N85-[illegible]
Flight parameters recording for structure fatigue life monitoring 07 p0896 N85-[illegible]
USAF approach to airborne structural data recording: Airborne Data Acquisition Multifunction System (ADAMS)
07 p0897 N85-[illegible]

INACTIVATION
U DEACTIVATION

INCANDESCENCE
Personal experience with the PVHD and opinion of situations in which a wide Field Of View (FOV) PVHD might be helpful 01 p0008 N85-10046
Brightness comparison of electroluminescent versus incandescent lighting: A photometric validation
[AD-A145395] 02 p0280 N85-11822

INCENTIVES
NT CONTRACT INCENTIVES
Papers from the Symposium on Emissions: The Value of Incentives and Guidelines for Control
[S-336] 15 p2590 N85-[illegible]

INCIDENCE
NT GRAZING INCIDENCE
Oil flow patterns of separated flow on a hemispherical cylinder at incidence
[DFVLR-FB-84-20] 01 p0048 N85-10313
A Monte Carlo comparison of the recovery of winds near upwind and downwind from the SASS-1 model function by means of the sum of squares algorithm and a maximum likelihood estimator
[NASA-CR-3839] 01 p0064 N85-10421
Performance of Bayes-optimal angle-of-arrival estimators
[AD-A146594] 06 p0858 N85-15454
The effect of changes in the angle of incidence in the event of a richochet at a float step
[RAE-TRANS-2120] 07 p0902 N85-15712
Quantitative use of multiincidence-angle SAR for geologic mapping 08 p1145 N85-17220
Investigation of SIR-B images for lithologic mapping
08 p1148 N85-17241
Australian Multiexperimental Assessment of SIR-B (AMAS) 08 p1148 N85-[illegible]
German Radar Observation Shuttle Experiment (ROSE) 08 p1148 N85-[illegible]
A probe for direct measurement of flow direction
[ESA-TT-853] 11 p1637 N85-[illegible]
Influence of turbulence of incident stream on three dimensional boundary layer 14 p2278 N85-24113
Diffuse reflection of light from turbid conservative medium of finite thickness with incidence of beam on surface of scattering glancing 14 p2342 N85-[illegible]
Characterization of terrestrial solar cells for space applications: Electrical characteristics of the Westinghouse dendritic web cells as a function of solar intensity, temperature, and incidence angle
[NASA-CR-175642] 14 p2349 N85-[illegible]
Measurement and interpretation of electron angle at MABE beam stop
[DE85-008583] 17 p3032 N85-[illegible]

OMEGA: Optoelectronic measurement of the incidence angle of a projectile
[ISL-CO-223/84] 23 p3974 N85-34634

A normal incidence X-ray telescope sounding rocket payload
[NASA-CR-176169] 24 p4153 N85-35749

INCIDENT RADIATION

Spontaneous ignition of organic solids by radiant heating 09 p1289 N85-18096

Texture etching of (100) silicon for solar cells
20 p3483 N85-31643

Propagation and reflection of a finite amplitude ultrasonic beam including harmonic content: A numeric model
20 p3523 N85-31914

Formulation of cosmic-ray solar daily variation and its seasonal variation, produced from generalized stationary anisotropy of solar origin
[SH-4.5-2] 23 p4036 N85-35020

INCINERATION

U INCINERATORS

INCINERATORS

Measurements on the diffusion of hydrogen chloride in the waste gas plume of incineration ships in the North Sea. Part 1: Methodology, instrumentation and presentation of data
[GKSS-84-E-23-PT-1] 05 p0672 N85-14319

Description and operation of a thermal decomposition unit-gas chromatographic system
[PB84-246362] 07 p0968 N85-16146

Incineration of explosives contaminated soils
[AD-P004142] 09 p1347 N85-18478

Large-scale commercial combustion systems for producing energy from municipal solid waste
[DE85-007097] 15 p2587 N85-25946

Reduction of pollutant formation in combustion processes
[DE85-010181] 19 p3309 N85-30512

INCLUSIONS

Effect of impact damage and open holes on the compression strength of tough resin/high strain fiber laminates 04 p0464 N85-12945

Inclusion formation during solidification of steels with improved machinability
[BMFT-FB-T-84-160] 05 p0619 N85-13957

Influence of the shape and distribution of inclusions of the fatigue strength of bearing steels in rotary bending
[BLL-PNR-90243-(8019.3153)]
06 p0768 N85-14912

Unexplained Fe, Ni and S anomalies in CV chondrite components 06 p0884 N85-15618

Investigation of granules of molybdenum-base alloys obtained with pulsed discharges
[BLL-M-36012-(5828.4)] 07 p0926 N85-15871

Ground shock effect on soil field inclusions
09 p1336 N85-18403

Interaction between a crack and a soft inclusion
[NASA-CR-172533] 10 p1495 N85-19439

Some recent developments in systems reliability
[AD-A150661] 14 p2317 N85-24318

Fracture toughness of MgCr(sub)2O(sub)4-ZrO(sub)2
[DE85-007945] 17 p2917 N85-27982

Weldability of micro-alloy steels as reaction of structure and inclusions
[BLL-BISI-TRANS-22196-(9022.06)]
17 p2924 N85-28027

Physio-chemical mechanisms of the processes of the formation of globular inclusions in ball-bearing metal
[BLL-BISI-TRANS-22235-(9022.06)]
17 p2924 N85-28030

The behaviour of nitride inclusions in nickel-base alloys
[BLL-BISI-TRANS-22396-(9022.06)]
17 p2927 N85-28058

Quality testing to the specifications of the Stahl-Eisen-Pruefblatt 1570/71 using an automatic image analysis system
[BLL-BISI-TRANS-22253-(9022.06)]
17 p2976 N85-28365

Method for production of ceramic oxide and carbide bodies by polymer inclusion and decomposition
[DE85-011668] 19 p3250 N85-30152

Deep-burial diagenesis in carbonates
[DE85-011224] 22 p3802 N85-33554

Viscoelastic behavior of short-fiber composite materials
[DE85-011233] 23 p3910 N85-34225

Special features of the fracture of ball-bearing steel close to non-metallic inclusion eutectics
[BLL-M-35809-(5828.4)] 23 p3914 N85-34258

INCOHERENCE

Fundamental limits to synchronization and tracking
[AD-A149623] 12 p1833 N85-21504

New image deblurring method described
16 p2806 N85-27305

All-optical logic gates with external switching by laser and incoherent radiation 18 p3187 N85-29766

INCOHERENT SCATTER RADAR

Sources of information concerning the ionosphere
04 p0521 N85-13334

Incoherent scatter radar studies of the mesosphere
08 p1184 N85-17463

The magnetospheric convection electric field at ionospheric altitudes: A case study based on STARE and Saint-Santin data 14 p2362 N85-24594

EISCAT electron density studies
[AD-A152820] 17 p2993 N85-28496

Active and passive remote sensing of ice
[AD-A154406] 19 p3300 N85-30459

The Proust radar 21 p3629 N85-32547

INCOHERENT SCATTERING

Incoherent scatter radar studies of the mesosphere
08 p1184 N85-17463

Error probability during optimal noncoherent reception of binary signals in multibeam channel
13 p2069 N85-22922

A spatially incoherent and temporally coherent source
[AD-A151281] 13 p2157 N85-23390

The Sondrestrom radar: Progress and proposed upgrades for ST work 21 p3628 N85-32541

INCOMPRESSIBILITY

Numerical methods in metalforming
06 p0797 N85-15092

Nonlinear waves in a rod. Results for incompressible elastic materials
[AD-A147485] 07 p0979 N85-16216

Vortices in non-Newtonian fluids
[AD-A153169] 17 p2958 N85-28269

INCOMPRESSIBLE BOUNDARY LAYER

Experimental investigation of a turbulent incompressible boundary layer on a curved wall
11 p1577 N85-19936

Stability of an oscillating boundary layer
[NASA-TM-77827] 14 p2299 N85-24238

A method of determining the suction velocity for laminar flow control of two-dimensional airfoil in incompressible flow
[NAL-TR-845] 18 p3059 N85-28925

INCOMPRESSIBLE FLOW

NT STOKES FLOW

Classical free-streamline flow over a polygonal obstacle
[NASA-CR-172448] 01 p0046 N85-10301

Review of some vortex relations
[NASA-CR-172452] 01 p0046 N85-10302

Accelerated convergence for incompressible flow calculations
[NASA-TM-86863] 02 p0140 N85-10949

Linear long-wave stability of cylindrical steady laminar flame in rotating medium 02 p0268 N85-11752

Incompressible lifting-surface aerodynamics for a rotor-stator combination
[NASA-TM-83767] 03 p0316 N85-12039

Wall effects on the slow steady motion of a particle in a viscous incompressible fluid
[PREPRINT-828] 03 p0363 N85-12327

Algebra of hydrodynamic flows of an ideal fluid and the prediction of the behaviour of a system of particles of a passive admixture on Riemann surfaces with a variable curvature
[REPT-565] 03 p0377 N85-12408

Reducing numerical diffusion for incompressible flow calculations
[NASA-TM-83621] 06 p0756 N85-14840

Laminar flow over a backward-facing step
[AD-A147489] 07 p0960 N85-16084

Numerical solutions for steady natural convection in a square cavity
[PB84-245752] 07 p0961 N85-16090

Calculation of the velocity field generated by a helicopter main and tail rotors in hover
[AD-A147731] 08 p1078 N85-16833

Analysis of sudden expansion flow in a two-dimensional duct with and without side-wall injection using the k-epsilon turbulence model 09 p1317 N85-18282

Algorithms for the Euler and Navier-Stokes equations for supercomputers
[NASA-CR-172543] 10 p1539 N85-19701

Experimental investigation of a breakdown criterion for a vortex in an incompressible flow — delta wing
[ONERA-RT-27/1147-AY] 11 p1577 N85-19935

A three-dimensional spectral algorithm for simulations of transition and turbulence
[NASA-CR-172561] 12 p1845 N85-21575

Local behavior of solutions of an elliptic-parabolic equation
[AD-A149624] 12 p1920 N85-22057

Turbulent flow around circular cylinder uniformly rotating in infinite incompressible fluid 14 p2277 N85-24109

Turbulent flow of fluid near trailing edge of plate in stream at zero angle of attack 16 p2764 N85-27057

Steady, incompressible, inviscid flow through a finite collapsible tube under longitudinal tension
[REPT-84-01] 17 p2959 N85-28278

A second-order pressure-correction method for viscous incompressible flow
[REPT-84-15] 17 p2960 N85-28280

A method of determining the suction velocity for laminar flow control of two-dimensional airfoil in incompressible flow
[NAL-TR-845] 18 p3059 N85-28925

A computational method for wings of arbitrary planform
[AD-A153788] 18 p3059 N85-28929

The hydrosynclastic infundibulum
[AD-A153849] 18 p3100 N85-29192

Dynamic stability of a spinning tube conveying a flowing fluid
[DE85-007583] 18 p3102 N85-29207

A method for computing the core flow in three-dimensional leading-edge vortices
[NASA-TM-87489] 19 p3214 N85-29932

SANDRAG: A computer code for predicting drag of bodies of revolution at zero angle of attack in incompressible flow
[DE85-011170] 19 p3338 N85-30684

Turbulent reacting flows 20 p3451 N85-31427

Numerical and experimental investigation of turbomachinery rotor flow fields
20 p3451 N85-31429

Turbulence modeling in a two-dimensional wake
20 p3452 N85-31431

Turbulent solutions of equations of fluid motion
20 p3453 N85-31441

An implicit finite-difference code for a two-equation turbulence model for three-dimensional flows
[NASA-TM-86752] 20 p3454 N85-31448

Experiments on the influence of active walls on the initial amplitudes and growths of instability waves
[AD-A154630] 21 p3583 N85-32275

Generation by conformal mappings of aerofoil sections and of certain other simple shapes suitable for both aerodynamic and stress-concentration problems
[AD-A154901] 22 p3728 N85-33112

Modelling of unsteady, incompressible separation on an aerofoil using an inviscid flow algorithm
[GU-AERO-8412] 23 p3894 N85-34122

Calculation of flow kinetics of composite media
[BLL-M-35819-(5828.4)] 23 p3929 N85-34348

Stability of two-dimensional immiscible flow to viscous fingering
[DE85-011403] 23 p3931 N85-34364

New semi-implicit method for solving the time-dependent conservation equations for incompressible flow
[DE85-010926] 23 p3931 N85-34367

A curvilinear coordinate method for the solutions of initial value problems using the third-order upwind differencing scheme
[IPPJ-734] 23 p3975 N85-34642

General design method for 3-dimensional, potential flow fields. Part 2: Computer program DIN3D1 for simple, unbranched ducts
[NASA-CR-3926] 24 p4060 N85-35159

INCOMPRESSIBLE FLUIDS

Splitting methods for the numerical solution of the incompressible Navier-Stokes equations
[AD-A147463] 07 p1032 N85-16554

Local behavior of solutions of an elliptic-parabolic equation
[AD-A149624] 12 p1920 N85-22057

Stability of steady rotation of a cylinder filled with a stratified viscous incompressible fluid
14 p2278 N85-24112

Finite element methods for viscoelastic flow
[AD-A154877] 22 p3783 N85-33437

INCONEL (TRADEMARK)

Benchmark notch test for life prediction
02 p0140 N85-10953

Effects of tin on microstructure and mechanical behavior of Inconel 718
[NASA-TM-86866] 03 p0330 N85-12129

Investigation of the isothermal precipitation behavior of nickel-base alloys using electrochemical phase extraction
[JUEL-1903] 05 p0619 N85-13958

Inconel 718 alloy resistance to crack propagation
07 p0907 N85-15740

Experiences with the material bevaviour and high temperature low cycle fatigue life prediction of the IN 738 blading alloy 07 p0908 N85-15746

Thermal-mechanical fatigue crack growth in Inconel X-750
[NASA-CR-174740] 07 p0927 N85-15877

Possibilities for a more accurate life prediction of components — gas turbine disks
07 p0976 N85-16198

Elevated temperature creep behavior of Inconel alloy 625
[DE84-015836] 09 p1297 N85-18144
Non-isothermal irradiation creep of nickel alloys Inconel 706 and PE-16
[DE85-000842] 11 p1607 N85-20102
Stress relief of transition zones
[DE85-000234] 11 p1653 N85-20411
Effect of reduction of strategic Columbium addition in 718 Alloy on the structure and properties
[NASA-CR-174841] 12 p1805 N85-21320
Fatigue life extension 16 p2733 N85-26864
Fatigue strength of Inconel 625 plate and weldments used in the DIII-D configuration vacuum vessel
[DE85-008276] 17 p2981 N85-28427
Preliminary results of the Inconel 617 optimization program. Advanced gas cooled reactor materials program
[DE85-008235] 18 p3075 N85-29024
Hold-time effects in elevated temperature fatigue crack propagation
[AD-A154146] 19 p3286 N85-30376
Finite element analysis of notch behavior using a state variable constitutive equation 20 p3468 N85-31548
Decomposition of sulfuric acid using solar thermal energy
[DE85-012288] 21 p3564 N85-32170
The effect of stress and hot corrosion on nickel-base superalloys
[AD-A154722] 21 p3566 N85-32181

INDENTATION
Influence of cyclic tangential loading on indentation fracture
[DE84-015869] 03 p0373 N85-12382
Elastic fields under a spherical indenter
[AD-A146519] 06 p0817 N85-15188
Journal of Research of the National Bureau of Standards, volume 89, no. 6, November - December 1984
[PB85-179042] 20 p3472 N85-31580
Indentation fractography: A measure of brittleness
[PB85-179059] 20 p3473 N85-31581
Controlled indentation flaws for the construction of toughness and fatigue master maps
[PB85-179067] 20 p3473 N85-31582

INDEPENDENT VARIABLES
NT LATTICE PARAMETERS
A preliminary study of using a strain-gauged balance and parameter estimation techniques for the determination of aerodynamic forces on a model in a very short duration wind tunnel
[AD-A146473] 06 p0810 N85-15145
Some applications of penalty functions in mathematical programming
[AD-A147443] 07 p1032 N85-16552
Optimum performance parameters for ski-jump operations of USAF fighter aircraft
[AD-A148532] 08 p1064 N85-16867
Estimation of launch vehicle performance parameters
[AD-A151927] 16 p2728 N85-26839
An interactive computer package for use with simulation models which performs multidimensional sensitivity analysis by employing the techniques of response surface methodology
[AD-A151956] 16 p2846 N85-27548
Development factors and field dependence-independence
[AD-A152337] 17 p3000 N85-28545
Turbulent wake of a submerged flat plate
[AD-A153776] 18 p3100 N85-29190
Computer program for plotting and fairing wind-tunnel data
[NASA-TM-85648] 20 p3387 N85-31009
On the interpretation of variables — simulation and regression models
[FEW-136] 20 p3522 N85-31903
Diakoptic calculation of characteristics for optimization of linear circuits with respect to parameters of individual branches 22 p3767 N85-33346
The effects of parameter variation on helicopter performance
[AD-A156027] 24 p4064 N85-35189
The NORDA/FNOC (Naval Ocean Research and Development Activity's/Fleet Numerical Oceanography Center) Polar Ice Prediction System (PIPS)-Arctic: A technical description
[AD-A156332] 24 p4126 N85-35577

INDEXES (DOCUMENTATION)
Synthesis of current measurements in Puget Sound, Washington. Volume 1: Index to current measurements made in Puget Sound from 1908-1980 with daily and record averages for selected measurements
[PB84-214105] 01 p0089 N85-10803
Catalogue of earthquakes for the territory of Czechoslovakia for the period 1957 - 1980
[REPT-555] 03 p0376 N85-12398
NASA Thesaurus supplement: A 3-part cumulative supplement to the 1982 edition of the NASA Thesaurus
[NASA-SP-7051(SUPPL-2)] 03 p0437 N85-12785
Criss-cross directory of NASA N numbers and DOD AD numbers, 1962-1978 04 p0575 N85-13869
Index of Air Weather Service technical publications, 1 July 1983-30 June 1984
[AD-A148051] 08 p1189 N85-17491
A research in support of NASA's space science
[NASA-CR-174267] 08 p1227 N85-17728
Abstract and index collection
[PB85-119501] 10 p1569 N85-19892
Index to published geologic maps in the region around the potential Yucca Mountain nuclear waste repository site, southern Nye County, Nevada
[DE85-000260] 11 p1669 N85-20518
Aerospace Medicine and Biology: A continuing bibliography with indexes, supplement 267, January 1985
[NASA-SP-7011(267)] 12 p1904 N85-21959
The intelligent database machine
12 p1949 N85-22242
Medical subject headings, tree structures, 1985
[PB84-216092] 12 p1952 N85-22261
Permuted medical subject headings, 1985
[PB84-216100] 12 p1952 N85-22262
NASA Thesaurus supplement, a three part cumulative supplement to the 1982 edition of the NASA Thesaurus
[NASA-SP-7051(SUPPL-3)] 14 p2432 N85-25002
Schema theory in the representation and analysis of text 14 p2433 N85-25004
Air Force Office of Scientific Research (AFOSR): Technical report summaries. Fourth quarter (CY)
[AD-A150860] 14 p2456 N85-25167
DOD manual for standard data elements, part 1
[AD-A152201] 16 p2878 N85-27754
DoD manual for standard data elements, part 2
[AD-A152202] 16 p2878 N85-27755
DoD manual for standard data elements, part 3
[AD-A152203] 16 p2878 N85-27756
DoD manual for standard data elements, part 4
[AD-A152204] 16 p2878 N85-27757
DoD manual for standard data elements, part 5
[AD-A152205] 16 p2878 N85-27758
Bibliography of Lewis Research Center technical publications announced in 1984
[NASA-TM-87012] 17 p3049 N85-28876
Inference in hierarchic classification — data bases
[ENST-84E014] 20 p3518 N85-31873
Air Force Office of Scientific Research (AFOSR). Technical report summaries: First quarter (CY)
[AD-A154757] 21 p3713 N85-33041
Ninteenth International Cosmic Ray Conference. Conference program and author index
[NASA-CP-2376] 22 p3860 N85-33901
Index of laser program publications and related reports, calendar year 1984
[DE85-011863] 23 p3936 N85-34398
Role of solar flare index in long term modulation of cosmic ray intensity
[SH-4.4-12] 23 p4034 N85-35009
A research program to reduce the interior noise in general aviation aircraft, index and summary
[NASA-CR-176178] 24 p4145 N85-35695
Source hierarchy list. Volume 1: A through H
[AD-A156300] 24 p4165 N85-35825
Source hierarchy list. Volume 2: I through Z
[AD-A156301] 24 p4165 N85-35826

INDEXES (RATIOS)
On derivation and significance of geomagnetic equivalent amplitude indices 04 p0520 N85-13321
A directly obtained geomagnetic activity measure, J3
04 p0520 N85-13322
Index cycles simulated by a low order forced barotropic model 07 p1002 N85-16364
The application of a technology index to aircraft turbine engine cost estimating relationships
[AD-A147701] 08 p1087 N85-16874
Biophysical evaluation of the wet globe temperature index (Botsball) at high air movements and constant dew point temperature
[AD-A151065] 14 p2378 N85-24683
Forecast verification of the 10.7 centimeter solar flux and the Ap daily geomagnetic activity indices
[AD-A152959] 17 p2993 N85-28499
Objective determination of heat wave patterns
18 p3140 N85-29437
Performance envelopes and optimal appropriateness measurement
[AD-A154129] 19 p3330 N85-30629
A real time index of geomagnetic background noise for the MAD (Magnetic Anomaly Detection) frequency band
[AD-A155717] 22 p3814 N85-33627

INDIA
Review on physiological and medical problems related to climates ranging from altitude to sub-tropics
05 p0667 N85-14417
MAP in India 11 p1655 N85-2040
Relationship of Indian monsoon intensity to time of onset 13 p2106 N85-2212
Influence of land surface processes on the Indian monsoon: A numerical study 18 p3146 N85-2947
Observation of energy spectrum of electron albedo in low latitude region at Hyderabad, India
[SH-6.1-7] 23 p4045 N85-3509
Proton albedo spectrum observation in low latitude region at Hyderabad, India
[SH-6.1-8] 23 p4045 N85-3509

INDIAN OCEAN
Sea-level in the world ocean. Part 7: The Indian Ocean, a catalogue of measurements
[CSIR-T/SEA-8303-7] 01 p0067 N85-1059
Tide tables 1985, high and low water predictions, central and western Pacific Ocean and Indian Ocean
[PB84-238393] 04 p0542 N85-13481
Late Quaternary deep-water paleoceanography of the eastern equatorial Indian Ocean: Evidence from Benthic foraminifers, carbonate dissolution, and stable isotopes
08 p1182 N85-17446
Surface currents of the Indian Ocean (to 25 deg S, 100 deg E.)
[IOS-187] 10 p1521 N85-1958
Remenent magnetization model for the broken ridge satellite magnetic anomaly 13 p2123 N85-2221
The BALSAMINE experiment
14 p2238 N85-2367
The Indian Ocean surface dynamics experiment (SINODE) 14 p2325 N85-24370
Parameters of magnetically active layers of Indian Ocean determined from deep drilling data and magnetic surveys
14 p2337 N85-24401
Characteristics of North Indian Ocean tropical cyclone activity
[AD-A153085] 17 p2997 N85-2852
Mineralogical-geochemical characteristics of ferromanganese formations in Arabian-Indian Ocean Ridge 19 p3293 N85-30418
Variability of air humidity profiles over ocean determined by lidar sounding 19 p3296 N85-30436
Mariners weather log, volume 28, number 4, fall 1984
[PB85-178406] 19 p3318 N85-30571
On the interannual variability of the Indian monsoon and the Southern Oscillation 20 p3495 N85-31728

INDIAN SPACE PROGRAM
Colloquium about Joint Projects within DFVLR/ISRO Cooperation
[DFVLR-MITT-84-12] 04 p0458 N85-12907
The Monocular Electro-Optical Stereo Scanner Experiment (MEOSS) 04 p0459 N85-12910
Overview of Autonomous Payload Control Experiment
04 p0459 N85-12911
The space flight of the Soviet-Indian crew
[NASA-TM-77615] 12 p1786 N85-21226

INDIAN SPACE RESEARCH ORGANIZATION
U ISRO

INDIAN SPACECRAFT
An overview of Multispectral Electro-Optical Stereo Scanner (MEOSS) mission 04 p0458 N85-12908
Status of Stretched Rohini Satellite System (SROSS) and Augmented Satellite Launch Vehicle Project (ASLV)
04 p0459 N85-12909
Time synchronization experiments with APPLE
17 p2967 N85-2832

INDIANA
Interlobate comparison of glacial-depositional style as evidenced by small-relief glacial landscape features in Illinois, Indiana, and Ohio, utilizing SIR-B
08 p1146 N85-1723

INDICATING INSTRUMENTS
NT ANEMOMETERS
NT APPROACH INDICATORS
NT ASTROLABES
NT ATTITUDE INDICATORS
NT CLOUD HEIGHT INDICATORS
NT FLOW DIRECTION INDICATORS
NT GYRO HORIZONS
NT GYROCOMPASSES
NT HOT-FILM ANEMOMETERS
NT HOT-WIRE ANEMOMETERS
NT LASER ANEMOMETERS
NT MICROBALANCES
NT MICROWAVE SENSORS
NT PLAN POSITION INDICATORS
NT POSITION INDICATORS
NT RADIO DIRECTION FINDERS
NT SMOKE DETECTORS
NT SPACECRAFT POSITION INDICATORS
NT SPEED INDICATORS

NT TACHOMETERS
NT WEIGHT INDICATORS
NT WIND VANES
Decision tree rating scales for workload estimation: Theme and variations
[NASA-CR-174062] 02 p0237 N85-11544
Fuse status indicator system
[AD-D011294] 06 p0804 N85-15121
Stability indicators for front end loaders
[AD-P004293] 09 p1406 N85-18870
The multiple resources model of human performance: Implications for display design 10 p1534 N85-19669
Adjustable indicating device for load position
[NASA-CASE-MFS-28008-1] 11 p1635 N85-20300

INDIUM
Use of alternative solvents for low-temperature LPE growth of CdTe films
[AD-A149418] 10 p1562 N85-19853
Low cost, sprayed CuInSe2 solar cell research
[DE85-003467] 12 p1881 N85-21799
Angle-resolved photoemission study of AuGa2 and AuIn2 intermetallic compounds
[AD-A150000] 12 p1940 N85-22183
A mixed-basis band structure interpolation scheme applied to the fluorite structure compounds NiSi2, AuAl2, AuGa2 and AuIn2
[AD-A150131] 12 p1940 N85-22187
Effect of dislocations on gallium arsenide FETs
[AD-A152249] 16 p2870 N85-27709
Post-deposition heat treatments of CdS/CuInSe2 solar cells
[DE85-002943] 18 p3128 N85-29373
Optically bistable devices using InSb
18 p3186 N85-29758
Luminescence and absorption of indium-activated potassium-borate glasses subjected to high-power excitation 21 p3661 N85-32868

INDIUM ANTIMONIDES
InAsSb strained-layer superlattices (SLSs) for long wavelength detector applications
[DE84-016111] 05 p0732 N85-14706
Quaternary narrow-band semiconductors (HgTe)x (InSb)1-x for far-infrared detectors
[AD-A149350] 10 p1562 N85-19852

INDIUM ARSENIDES
InAsSb strained-layer superlattices (SLSs) for long wavelength detector applications
[DE84-016111] 05 p0732 N85-14706
Evaluation of implantation-disordering of (InGa)As/GaAs strained-layer superlattices
[DE85-003533] 12 p1942 N85-22200
Ion implantation disorder in strained-layer superlattices
[DE85-004466] 14 p2430 N85-24984
A study of Ga(.47)In(.53)As and Al(.48)In(.52)As for very high frequency device applications
[AD-A151995] 16 p2870 N85-27706
Mechanically-stacked multijunction solar cells
[DE85-010369] 18 p3129 N85-29377
Low-threshold injection InGaAsP/GaAs double heterostructure lasers with separate limiting obtained by liquid-phase epitaxy (lambda = 0.78 divided by 0.87 microns, I sub thr = 460 A/cm 2, T = 300 K)
21 p3687 N85-32908
Adjustment of radiation wavelength of multimode InP-GaInAsP injection heterolasers
21 p3688 N85-32913

INDIUM COMPOUNDS
NT INDIUM ANTIMONIDES
NT INDIUM ARSENIDES
NT INDIUM PHOSPHATES
NT INDIUM PHOSPHIDES
NT INDIUM TELLURIDES
CuInSe2-based photoelectrochemical cells: Their use in characterization of thin CuInSe2 films, and as photovoltaic cells per se
[DE84-004514] 04 p0529 N85-13379
Surface and interfacial properties of Ga(0.47) In(0.53)As alloys
[AD-A148891] 10 p1562 N85-19849
Transport studies of several novel organic conductors
[DE85-003950] 14 p2429 N85-24979
A study of the stability of cadmium sulfide/copper sulfide and cadmium sulfide copper-indium-diselenide solar cells
[DE85-002902] 15 p2587 N85-25947
Dual species ion implantation of ternary compounds based on In-Ga-As
[AD-D011617] 16 p2869 N85-27698
Materials-process interactions in ternary alloy semiconductors
[AD-A153133] 17 p3043 N85-28832
Development of photodetectors
[AD-A153773] 18 p3095 N85-29158
Liquid crystal light valve structures
[NASA-CASE-MSC-20036-1] 22 p3847 N85-33826

INDIUM PHOSPHATES
Cascaded solar photovoltaic cells based on InP-GaInPAs and InP-CdS heterostructures
02 p0298 N85-11749

INDIUM PHOSPHIDES
Plasma deposited diamondlike carbon on GaAs and InP
[NASA-TM-86870] 01 p0123 N85-10844
Studies of grown-in defects versus growth parameters in 3-4 compound semiconductors
[AD-A145864] 03 p0433 N85-12755
Investigation of liquid encapsulation Chochralski growth of InP
[AD-A146096] 03 p0433 N85-12760
Characterization of surface electronic properties of semi-insulating InP
[AD-A146553] 06 p0866 N85-15507
A picosecond population modulation study of near interband resonances in semiconductors
09 p1396 N85-18787
Material growth and characterization for solid state devices
[NASA-CR-174410] 10 p1561 N85-19847
Method for synthesizing indium phosphide
[AD-D011475] 10 p1563 N85-19855
InP materials
[AD-A152341] 17 p3043 N85-28828
Development of photodetectors
[AD-A153773] 18 p3095 N85-29158
Influence of technological factors on luminescence characteristics of InGaAsP/InP heterolasers (lambda = 1.55 microns) 21 p3686 N85-32910
Adjustment of radiation wavelength of multimode InP-GaInAsP injection heterolasers
21 p3688 N85-32913

INDIUM TELLURIDES
Preliminary studies on the low-cost preparation of chalcogenide semiconductors from solution depositions
[DE85-000538] 11 p1736 N85-20918

INDOLES
NT TRYPTOPHAN

INDONESIA
Geologic mapping of Indonesian rain forest with analysis of multiple SIR-B incidence angles
08 p1145 N85-17221
Microwave propagation studies, measurements and education in Surabaya, Indonesia
[B8464633] 24 p4088 N85-35339

INDOOR AIR POLLUTION
A dispersion model for airborne particulates inside a building
[DE84-014961] 02 p0225 N85-11473
Volatile organic emissions from adhesives with indoor applications
[DE84-015965] 05 p0620 N85-13966
Effect of sealants of the sound absorption coefficients of acoustical friable insulating materials
[AD-A148541] 08 p1218 N85-17674
Formaldehyde and tracer gas transfer between airstreams in enthalpy-type air-to-air heat exchangers
[DE84-016951] 11 p1631 N85-20274
Identification and quantification of nitropolynuclear aromatic hydrocarbons in ambient and indoor air particulate samples
[PB85-176790] 19 p3311 N85-30525

INDUCED FLUID FLOW
U FLUID FLOW

INDUCTANCE
NT PROXIMITY EFFECT (ELECTRICITY)
Magnetic and photoconductive repetitive rail-gun opening switches
[DE84-017080] 04 p0496 N85-13163
Plasma mass and effective inductance in a small rainbow
[MRL-R-947] 12 p1936 N85-22162
Piezoelectric filter with low-Q inductances
13 p2070 N85-22932
Plasma mass and effective inductance in a small railgun
[AD-A154644] 21 p3589 N85-32304
Use of the computer programa PARA 80 to study results from firing the railgun ERGS-1M
[MRL-R-900] 22 p3738 N85-33167
Predicting electrical performance parameters of underwater cables 22 p3775 N85-33391
New formulation for linear accelerator design
[DE85-011171] 22 p3842 N85-33792

INDUCTION
DC switching regulated power supply for driving an inductive load
[DE84-014238] 01 p0044 N85-10285
Induction voidmeter
[DE84-014321] 01 p0050 N85-10329
RADLAC technolgy review
[DE85-011995] 23 p3982 N85-34691

INDUCTION (MATHEMATICS)
Induction of fuzzy decision rules
[INPE-3053-PRE/474] 04 p0554 N85-13525

INDUCTION HEATING
High frequency plasma generator for ion thrusters
[NASA-CR-174772] 08 p1114 N85-17023
The heat sensitivity of solid propellants
08 p1117 N85-17043
Application of electricity to the reheating of metals prior to forming. Forging, lamination, induction
[BLL-TR-T6399/BG/MRS14903/84]
08 p1137 N85-17160
Underwater pipeline: Welding by high frequency induction
[BLL-WI-TRANS-682-(9312.57)]
16 p2792 N85-27221
Influence of heat treatment parameters on the properties of induction hardened Ni-Cr-Mo steels
[BLL-BISI-TRANS-2499-(9022.06)]
17 p2926 N85-28053
Induction heating gun
[NASA-CASE-LAR-13161-1] 18 p3085 N85-29083
Feedback regulated induction heater for a flowing fluid
[DE85-006508] 23 p3939 N85-34414
Effect of ECH and ICH on ambipolar potential in NBT-1M 23 p3978 N85-34661
Transports studies of ECH and ICRH-heated bumpy torus plasma in NBT-1M 23 p3978 N85-34662

INDUCTION MOTORS
Variable speed generator technology options for wind turbine generators
[RR-84-4] 10 p1478 N85-19331
Solar powered actuator with continuously variable auxiliary power control
[NASA-CASE-MFS-25637-1] 12 p1876 N85-21769
Power control for ac motor
[NASA-CASE-MFS-25861-1] 13 p2062 N85-22877
Magnetic noise in single-machine rotating frequency converters 13 p2077 N85-22969
The performance of an alternating-current thyristor-controlled motor 15 p2546 N85-25716
Commercialization of the power factor controller
[NASA-CR-171500] 17 p2951 N85-28221
A variable frequency control for three-phase induction motors 19 p3256 N85-30190
Induction motors with minimum waste of magnetic iron
22 p3772 N85-33377
Magnetic field and equivalent circuit of induction motors with shielded poles 22 p3772 N85-33378
Evaluation of half wave induction motor drive for use in passenger vehicles
[NASA-CR-176119] 23 p3926 N85-34334
State-of-the-art of solid-state motor controllers
[TI85-008674] 24 p4162 N85-35806

INDUCTION SYSTEMS
U INTAKE SYSTEMS

INDUCTORS
Characteristics of the boat inductor for keeping liquid metal in the suspended state
[NASA-TM-77816] 12 p1851 N85-21611
Plasma erosion opening switch
[DE85-011384] 20 p3535 N85-31996

INDUSTRIAL AREAS
Influence on an industrial site on the characteristics of CCN supersaturation with air masses of different origin
21 p3650 N85-32683

INDUSTRIAL ENERGY
Advanced technology cogeneration system conceptual design study: Closed cycle gas turbines
[NASA-CR-168222] 07 p0992 N85-16300
Linking R and D to problems experienced in solids processing
[AD-A154238] 19 p3380 N85-30968

INDUSTRIAL MANAGEMENT
NT ENGINEERING MANAGEMENT
NT INVENTORY CONTROLS
NT INVENTORY MANAGEMENT
NT PERSONNEL MANAGEMENT
Business planning for information services under special consideration of German management information systems
[BMFT-FB-ID-83-007] 02 p0294 N85-11910
Primer on the registration of technical information in industry 03 p0438 N85-12786
Value analysis — industrial competition
[CNES-NT-110] 04 p0577 N85-13684
Evaluation of the effectiveness of the weighted guidelines to induce contractor's investment in cost reducing facilities equipment
[AD-A147586] 07 p1053 N85-16681
USSR report: Machine tools and metalworking equipment
[JPRS-UMM-85-001] 08 p1139 N85-17172
Summaries of press automation conference presented
08 p1139 N85-17173

Plans, developments in robotics
14 p2260 N85-24191

Mini-Seminar on Non-Destructive Testing
[CSIR-TSD-0009/83] 14 p2316 N85-24306

Status of the U.K. N.D.T. industry today
14 p2316 N85-24309

Robot use in FRG increases but sensor technology lags
15 p2531 N85-25605

The development and implementation of advanced welding technology
15 p2565 N85-25824

Robotic arc welding
15 p2566 N85-25830

Welding techniques in pressure part technology
15 p2566 N85-25835

Industrial applications of pattern recognition and image processing
15 p2622 N85-26157

Quality analysis
21 p3666 N85-32785

DOD Value Engineering Conference report. Value Engineering (VE): A tool that benefits line management held at Leesburg, Virginia on 1-2 November 1984. Part 1. Executive summary
[AD-A156067] 24 p4163 N85-35810

DOD Value Engineering Conference report. Value Engineering (VE): A tool that benefits line management held at Leesburg, Virginia on 1-2 November 1984. Part 2. Plenary session
[AD-A156068] 24 p4163 N85-35811

INDUSTRIAL PLANTS

NT FOUNDRIES

User experience of existing corrosion monitoring techniques and the development of Thin Layer Activation (TLA) for corrosion monitoring
[AERE-R-11248] 01 p0029 N85-10183

Growth, future of Soviet robotics sector analyzed
01 p0035 N85-10217

Advanced technology cogeneration system conceptual design study: Closed cycle gas turbines
[NASA-CR-168222] 07 p0992 N85-16300

Manufacturing methods and technology project summary reports
[AD-A146209] 08 p1138 N85-17163

The infrastructure for a surge in synfuels production: The potential role of the AE and C industry and of owner operators
[RAND/N-2172-SFC] 09 p1301 N85-18170

Scania, ASEA of Sweden use robots for all production phases
09 p1310 N85-18229

Thermal energy storage
[DE85-001492] 09 p1344 N85-18454

Flexible applications robot used in Moscow training course
10 p1462 N85-19217

Institute director surveys industrial automation drive
11 p1617 N85-20167

Increased use of CNC in machine tool construction
11 p1617 N85-20170

Siemens-Corning plant to manufacture optical fibers
11 p1617 N85-20175

French panel makes specific proposals for robotics research. Current state of French robotics
11 p1618 N85-20180

Aviation repair plant directors on quality control measures
12 p1769 N85-21106

Optoelectronic safety system for robotized technological complex
13 p2046 N85-22805

Robotized system for treating gear wheels
14 p2285 N85-24162

Mini-Seminar on Non-Destructive Testing
[CSIR-TSD-0009/83] 14 p2316 N85-24306

West Europe report: Science and technology
[JPRS-WST-84-012] 15 p2523 N85-25552

MBB uses new CFC form tool for titanium alloy air intake
15 p2523 N85-25553

French robotics research at Grenoble labs
15 p2523 N85-25555

West Europe report: Science and technology
[JPRS-WST-84-007] 15 p2530 N85-25600

Robot use in FRG increases but sensor technology lags
15 p2531 N85-25605

Pechiney strategy includes development of new materials
15 p2531 N85-25607

MBB/Erno's views, future plans in aerospace activities
15 p2531 N85-25609

West Europe report: Science and technology
[JPRS-WST-84-027] 15 p2532 N85-25612

West Europe report: Science and technology
[JPRS-WST-84-014] 15 p2536 N85-25647

Updating model RPD-1.25 industrial robot
16 p2762 N85-27043

New stage in robotics development
16 p2762 N85-27045

Review of national emission standards for mercury
[PB85-153906] 16 p2822 N85-27406

Conversion of methanol to gasoline: Engineering and construction of the demonstration plant
[DE85-003237] 17 p2937 N85-28133

Robots, automatic devices inside VW's Wolfsburg plant
17 p2946 N85-28186

USSR report: Machine tools and metalworking equipment
[JPRS-UMM-84-014] 17 p2946 N85-28188

Component problems plague French robotics industry
18 p3065 N85-29088

West Europe report: Science and technology
[JPRS-WST-84-031] 18 p3066 N85-29089

Multinational program to develop intelligent robots
18 p3066 N85-29094

West Europe report: Science and technology
[JPRS-WST-84-037] 18 p3088 N85-29108

Some examples of the application of automatically guided vehicle systems
[HSE-TRANS-11134] 19 p3281 N85-30348

Environmental monitoring report for Pantex Plant covering, 1984
[DE85-010624] 19 p3306 N85-30508

West Europe report: Science and technology
[JPRS-WST-85-020] 20 p3438 N85-31333

Centralized surveillance of flexible workshops for the manufacturing of composite materials
[SNIAS-851-430-103] 23 p3910 N85-34227

Solar thermal technologies program summary
[DE85-012253] 23 p3945 N85-34449

INDUSTRIAL SAFETY

Early detection of environmental exposure
[AD-P004039] 06 p0845 N85-15369

Facility safety study
[NASA-CR-174280] 07 p0910 N85-15759

High voltage effects measured on dummy mannequin
07 p1012 N85-16432

A crew exposure study. Volume 1: Offshore
[AD-A146884] 07 p1015 N85-16449

Study of bodily functional status and quality of controlling action of power unit operators with various intensities of labor
09 p1362 N85-18569

Robotic safety
[DE85-002314] 10 p1493 N85-19431

USSR report: Life sciences. Biomedical and behavioral sciences
[JPRS-UBB-85-008] 10 p1523 N85-19605

Health standards for general vibration
10 p1523 N85-19607

Effects of overall vibration and noise on operational personnel
10 p1523 N85-19608

Comparative assessment of different treatment modalities in miners with vibration- and noise-induced disease
10 p1524 N85-19610

Control technology for integrated circuit fabrication at Honeywell Optoelectronics Division, Richardson, Texas
[PB85-109023] 11 p1616 N85-20162

The audiomat: An automatic audiometer for use in occupational audiometry
[DRIC-T-7138] 13 p2142 N85-23294

Safety with industrial manufacturing lasers
14 p2308 N85-24281

Robotic safety systems and methods: Savannah River site
[DE85-008261] 17 p2974 N85-28375

Sound-insulating enclosures — machine noise
[BMFT-FB-HA-85-005] 20 p3525 N85-31925

A crew exposure study. Phase II. Volume 2. At sea. Part A
[AD-A155233] 21 p3666 N85-32774

INDUSTRIAL WASTES

High-level waste processing and disposal
[DE85-003564] 11 p1726 N85-20865

Technology for industrial waste heat recovery by organic Rankine cycle systems
[DE85-006719] 18 p3102 N85-29206

Pollutant body burdens and reproduction in Platichthys stellatus from San Francisco Bay
[DE85-010407] 19 p3308 N85-30509

INDUSTRIES

NT AEROSPACE INDUSTRY
NT AIRCRAFT INDUSTRY
NT CONSTRUCTION INDUSTRY
NT DEFENSE INDUSTRY

Lagging development of biotechnology described
01 p0115 N85-10787

Space commercialization: Analysis of R and D investments with long time horizons
02 p0155 N85-11052

Development, production, application of robots assessed
03 p0343 N85-12211

Modular electromechanical industrial robots
03 p0345 N85-12223

International exhibition: Industrial Robots, 1982
03 p0345 N85-12224

Robotization of electric welding processes
03 p0345 N85-12225

Robotization of technological processes in high-frequency heating and welding
03 p0345 N85-12226

Improving operational reliability and productivity of robotized technological complexes
03 p0346 N85-12227

USSR report: Chemistry
[JPRS-UCH-84-012] 06 p0781 N85-14[illegible]

New concepts for industrial robots outlined
06 p0815 N85-15170

West Europe report: Science and technology
[JPRS-WST-84-039] 07 p0936 N85-15[illegible]

Airport ground equipment under development at Riga
09 p1278 N85-18[illegible]

The infrastructure for a surge in synfuels production: The potential role of the AE and C industry and of owner operators
[RAND/N-2172-SFC] 09 p1301 N85-18170

Scania, ASEA of Sweden use robots for all production phases
09 p1310 N85-18229

East Europe report: Science and technology
[JPRS-ESA-85-005] 09 p1377 N85-18[illegible]

Advanced industrial robot control systems
[PB85-110773] 11 p1648 N85-20[illegible]

Advanced industrial robot control systems
[PB85-110781] 11 p1648 N85-20[illegible]

Technological and economic assessment of advanced ceramic materials. Volume 5: A case study of ceramic toxic and combustible gas sensors
[PB85-113124] 12 p1815 N85-21[illegible]

Cost comparison of small gas turbines versus electric motors in a variable load industrial application
[PB85-149763] 12 p1837 N85-21530

The future of lightwave technology
[PB85-109759] 12 p1935 N85-22155

Current plans for development of chemical industry
13 p2014 N85-22[illegible]

USSR report: Machine tools and metalworking equipment
[JPRS-UMM-85-006] 14 p2263 N85-24146

Basic principles of industrial radiography
14 p2316 N85-24310

Standing of industrial radiography in South Africa
14 p2316 N85-24311

Radiological safety aspects of industrial radiography
14 p2316 N85-24312

Ultrasonic non-destructive testing technique
14 p2316 N85-24313

Mercedes-Benz auto 2000 achieves low drag coefficient
15 p2530 N85-25602

West Europe report: Science and technology
[JPRS-WST-84-020] 15 p2534 N85-25633

West Europe report: Science and technology
[JPRS-WST-84-003] 15 p2534 N85-25635

West Europe report: Science and technology
[JPRS-WST-84-009] 15 p2535 N85-25639

USSR report: Engineering and equipment
[JPRS-UEQ-85-004] 17 p2939 N85-28142

West Europe report: Science and technology
[JPRS-WST-84-024] 17 p2945 N85-28183

Space station study
[BL-6167] 18 p3066 N85-2[illegible]

CEMA cooperation in development of robotics, FMS viewed
20 p3436 N85-31331

Spin-offs from technical commercial infrastructures, no. 2
20 p3540 N85-32055

Quality analysis
21 p3666 N85-32785

New innovative businesses from industry. Experience in the Netherlands in the successful transfer of technology from university to industry
22 p3849 N85-33843

Forecasting future industrial SO2 and NO/sub x/ emissions, revised
23 p3947 N85-34461

INELASTIC BODIES

U RIGID STRUCTURES

INELASTIC COLLISIONS

Monte Carlo simulation of thermalization of subexcitation electrons in molecular hydrogen
[NAL-TR-815T] 01 p0117 N85-10798

Energy transfer in atom-molecule scattering experiments in the 1eV region with SF6-Ar, CF4-Ne and Xe-CO2 systems as examples
[REPT-11/1983] 04 p0563 N85-13588

Capture of planetesimals into a circumterrestrial swarm
13 p2179 N85-23522

Accumulation of the terrestrial planets
13 p2179 N85-23524

Kinetic studies following state selective laser excitations
[DE85-007173] 15 p2564 N85-25818

Size distribution in collisional systems — planetary rings
15 p2674 N85-26608

Inelastic Near-Surface Interactions. Proceedings of the Werner Brandt Workshop on Penetration Phenomena
[DE85-010579] 20 p3526 N85-31926

Propagation and secondary production of low energy antiprotons in the atmosphere
[OG-6.1-3] 22 p3887 N85-34094

On a possibility of inelasticity partial coefficient K sub gamma determination in pi C and pi Pb interactions at 10 to the 14th power eV (experiment PAMIR 1)
[HE-1.1-12] 24 p4171 N85-35859

Determination of primary energy in nucleus-nucleus collisions and the high P(sub)T tail of alpha-particles
24 p4173 N85-35875

INELASTIC SCATTERING

Study of structure of nuclei with neutrons and nuclear data measurements for MFE
[DE84-015126] 01 p0117 N85-10802

High energy-resolution inelastic X-ray scattering
[DE84-014565] 01 p0118 N85-10804

Dirac single particle wave functions in inelastic electron scattering
[DE84-015129] 02 p0279 N85-11814

Diffuse elastic and inelastic neutron scattering of disorder transitions and boundaries. Phase determination of structure factors 03 p0424 N85-12708

Inelastic neutron scattering on crystals for the clarification of structure and semiconductor properties
03 p0425 N85-12714

Measurements on the triple axis spectrometer UNIDAS for the investigation of dynamic processes in crystals using inelastic neutron scattering 03 p0426 N85-12716

Structural properties of amorphous metals by Raman scattering
[DE84-016047] 04 p0475 N85-13027

Local fields in strongly coupled plasmas
[DE84-013375] 04 p0567 N85-13611

Particle physics
[DE84-013634] 05 p0727 N85-14673

Measurements of the A-dependence of deep-inelastic electron scattering from nuclei
[DE84-013665] 05 p0728 N85-14678

Pion inelastic scattering to the first three excited states of Lithium-6
[AD-A147560] 07 p1041 N85-16606

Comments on the image contrast from inelastically scattered electrons
[DE85-000699] 07 p1041 N85-16609

Notes for lectures in China: The Bethe theory of inelastic collisions of fast charged particles with atoms and molecules
[DE84-017487] 09 p1380 N85-18676

Neutral-current x-distributions
[DE84-016522] 09 p1382 N85-18691

Microscopic determinations of lattice and electronic structures of solids
[DE84-017323] 09 p1399 N85-18806

Theoretical cross sections for inner-shell vacancy production by high-energy electrons
[DE84-007346] 11 p1721 N85-20827

Recent progress in electron scattering at SLAC
[DE85-002718] 11 p1723 N85-20840

Theoretical nuclear physics
[DE85-003466] 12 p1932 N85-22135

Theoretical aspects of the nucleon-nucleon workshop
[DE85-003740] 14 p2420 N85-24933

Neutron scattering and reactions on 59Co from 1 to 20 MeV
[AERE-R-11439] 17 p3028 N85-28729

Experimental studies of diffractive phenomena
[DE85-006812] 17 p3031 N85-28749

Possible indication of an A-dependence of R in deep-inelastic electron scattering from nuclei
[DE85-008174] 17 p3033 N85-28763

New experimental results in two photon physics
[NIKHEF-H/84-16] 17 p3035 N85-28776

SPECTER: Neutron damage calculations for materials irradiations
[DE85-005791] 18 p3180 N85-29716

Intermediate energy nuclear theory
[DE85-010440] 18 p3182 N85-29731

Deep-inelastic lepton scattering by nuclei: The pion-exchange model
[DE85-010496] 19 p3359 N85-30828

Discussion session: Nucleon- and antinucleon-nucleus inelastic scattering and charge exchange
[DE85-010723] 19 p3364 N85-30860

Energy-advanced nuclear data: Measurements and physical interpretations
[DE85-006196] 19 p3366 N85-30872

Magnetoconductance in aluminum films, wires, and cylinders 19 p3374 N85-30928

Inelastic Near-Surface Interactions. Proceedings of the Werner Brandt Workshop on Penetration Phenomena
[DE85-010579] 20 p3526 N85-31928

Antiproton-nucleus inelastic scattering and the spin-isospin dependence of the N anti N interaction
[DE85-010546] 20 p3526 N85-31935

Toward the question of multi-quark configurations in nuclei 21 p3691 N85-32929

Evaluated nuclear-data file for niobium
[DE85-012095] 21 p3704 N85-33009

Calculation of heavy-ion tracks in liquid water
[DE85-012101] 24 p4149 N85-35725

Fast-neutron interaction with niobium
[DE85-011471] 24 p4150 N85-35731

Proton-air and proton-proton cross sections from air shower data
[HE-1.1-1] 24 p4170 N85-35849

Proton-air inelastic cross section at S(1/2) = 30 TeV
[HE-1.1-2] 24 p4170 N85-35850

Hadron cross sections at ultra high energies and unitarity bounds on diffraction dissociation
[HE-1.1-3] 24 p4170 N85-35851

Determination of the cross section of the proton, pion and neutron inelastic interaction with lead and carbon nuclei at 0.5 - 5.0 TeV energies (PION experiment)
[HE-1.1-5] 24 p4170 N85-35853

Estimation of the total inelasticity coefficient in interaction of greater than or equal to 20 TeV hadrons with lead
[HE-1.1-9] 24 p4171 N85-35857

The method for the study of the inelastic cross-section for high energy protons by means of shower arrays with the large calorimetric area
[HE-1.1-11] 24 p4171 N85-35858

Forward particle production in inelastic Ne-22 inteVractions in emulsion at 4.1 A Ge/c
[HE-1.4-7] 24 p4176 N85-35895

Meson multiplicity in nucleus-nucleus collisions above 4 GeV/amu
[HE-1.4-10] 24 p4177 N85-35897

On the characteristics of emulsion chamber family events produced in low heights
[HE-3.1-6] 24 p4178 N85-35904

A study of gamma-families generated in nucleon-nucleus (NA) and pion-nucleus (pi A) interactions
[HE-3.7-2] 24 p4186 N85-35961

QCD analysis of neutrino charged current structure function F2 in deep inelastic scattering
[HE-5.3-23] 24 p4207 N85-36114

INELASTIC STRESS

The 3-D inelastic analysis methods for hot section components: Brief description 02 p0143 N85-10972

Local strain redistribution corrections for a simplified inelastic analysis procedure based on an elastic finite-element analysis
[NASA-TP-2421] 11 p1651 N85-20396

3-D inelastic analysis methods for hot section components (base program) — turbine blades, turbine vanes, and combustor liners
[NASA-CR-174700] 12 p1863 N85-21686

Unified constitutive material models for nonlinear finite-element structural analysis — gas turbine engine blades and vanes
[NASA-TM-86985] 14 p2320 N85-24338

Elastic-plastic analysis for cyclic loading using a linearized yield condition
[PB85-149607] 14 p2322 N85-24346

A survey of unified constitutive theories
20 p3466 N85-31531

Monotonous stress-strain properties of structural steel subjected to nonstationary repetitive pre-loading
23 p3904 N85-34165

Subcritical fracture propagation in rocks: An examination using the methods of fracture mechanics and non-destructive testing 24 p4116 N85-35516

INEQUALITIES

NT SCHWARTZ INEQUALITY

A weighted polynomial inequality
[CSIR-TWISK-332] 01 p0110 N85-10741

On two concepts of fundamental matching
[CSIR-TWISK-335] 01 p0110 N85-10743

Testing of inequality hypotheses in linear models using the Bayes method
[SER-C-292] 01 p0112 N85-10761

An integral inequality with applications to order statistics
[AD-A145081] 01 p0113 N85-10770

Constrained optimization using iterated partial Kuhn-Tucker vectors
[AD-A145476] 02 p0251 N85-11641

Stable monotone variational inequalities
[AD-A147123] 07 p1031 N85-16544

Generating positively correlated random variables from a sequence of independent random variables with symmetric logarithmically concave densities
[AD-A148438] 08 p1216 N85-17658

On the local behaviour of solutions of degenerate parabolic equations with measurable coefficients
[AD-A147412] 09 p1373 N85-18631

Solutions of problems of miller and rubel
10 p1536 N85-19685

Bounding the stochastic performance of continuum structure functions 2
[AD-A149458] 10 p1548 N85-19762

The inefficiency of least squares: Extensions of Kantorovich inequality
[AD-A149568] 10 p1549 N85-19766

Schur-Ostrowski theorems for functionals on l1(0,1)
[AD-A150193] 13 p2150 N85-23346

Nonlinear 0-1 programming. 1: Linearization techniques, revision
[AD-A150960] 14 p2405 N85-24826

Maintaining solution invariants in the numerical solution of ODEs
[DE85-005918] 14 p2410 N85-24857

Squares of Gegenbauer polynomials and Milin type inequalities
[CWI-PM-R8412] 14 p2410 N85-24862

Entire functions with spiral limits
15 p2634 N85-26241

An inequality and its application to the truncated distributions 17 p3020 N85-28673

On the convergence of difference approximations to scalar conservation laws
[NASA-CR-172614] 19 p3344 N85-30726

On the dependence of the convergence of Gummel's algorithm on the regularity of the solution
[AD-A154628] 21 p3675 N85-32832

Sobolev-Poincare's inequality and the Neumann problem for u sub t = divergence of the absolute value of the gradient u to the p-2 power x the gradient u
[AD-A154786] 21 p3676 N85-32839

INERT ATMOSPHERE

Apparatus and method for the horizontal, crucible-free growth of silicon sheet crystals
[DE85-011586] 22 p3847 N85-33829

INERT GASES

U RARE GASES

INERTIA

Vibrational power transmission of an idealised gearbox
[ISVR-TR-124] 02 p0204 N85-11346

Measurement of the inertial constants of a rigid or flexible structure of arbitrary share through a vibration test
[NASA-TM-77557] 02 p0209 N85-11381

A geometrical theory of spin motion
[DE84-016537] 04 p0574 N85-13656

Hydrodynamic impeller stiffness, damping, and inertia in the rotordynamics of centrifugal flow pumps
05 p0643 N85-14125

Effects of fluid inertia and turbulence on force coefficients for squeeze film dampers
05 p0645 N85-14137

Effects of external loads on human head movement control systems 05 p0707 N85-14534

A tracked vehicle test plant for the simulation of dynamic operation
[AD-P004305] 09 p1410 N85-18862

Resonance generation of inertial waves (in the atmosphere) by Doppler-shift of inertio-gravity modes
15 p2590 N85-25966

The Shock and Vibration Digest, volume 17, no. 2
[AD-A153129] 17 p2977 N85-28400

Recent progress in the dynamic plastic behaviour of structures, part 4 17 p2978 N85-28402

INERTIA MOMENTS

U MOMENTS OF INERTIA

INERTIA WHEELS

U COUNTER-ROTATING WHEELS

U REACTION WHEELS

INERTIAL CONFINEMENT FUSION

NT IMPACT FUSION

Ion-density correlations and enhancement of thermonuclear reaction rate in dense, inertially confined fusion plasmas 02 p0284 N85-11849

Vacuum inductive pulsed power compression for inertial confinement fusion
[DE84-010935] 03 p0421 N85-12693

Inertial confinement fusion: Present status and future potential
[DE84-016177] 04 p0567 N85-13616

Progress in inertial confinement fusion at Lawrence Livermore National Laboratory
[DE84-016227] 04 p0568 N85-13621

Quality assurance in the Antares Laser Fusion Construction Project
[DE84-015493] 05 p0640 N85-14104

Recent ICF research by GEKKO 12 glass layer at ILE Osaka 09 p1387 N85-18726

Basic research on inertial confinement fusion by LIMAY-I 15 p2655 N85-26383

Pulse star inertial confinement fusion reactor
[DE85-010940] 18 p3181 N85-29726

Inertial fusion reactors and magnetic fields
[DE85-009571] 18 p3191 N85-29789

Progress in inertial fusion at LLNL
[DE85-010931] 19 p3277 N85-30321

Summary of research for the Inertial Confinement Fusion Program at Los Alamos National Laboratory
[DE85-010330] 19 p3361 N85-30836

Advances in ICF power reactor design
[DE85-010930] 19 p3361 N85-30841
Ion beam-plasma interactions
[DE85-010202] 19 p3371 N85-30913
Flow characteristics of the Cascade granular blanket
[DE85-010932] 20 p3420 N85-31227
Thomson scattering on Elmo Bumpy Torus
[DE85-010584] 20 p3527 N85-31941
Transparent electrode for optical switch
[DE85-011618] 22 p3761 N85-33310
Workshop report on Simulation Techniques for Shock Wave Phenomena and Characteristics of Plasmas in Inertial Confinement Fusion
[IPPJ-725] 23 p3979 N85-34670
Stellarator approach to fusion plasma confinement
[DE85-011420] 23 p3984 N85-34704

INERTIAL FORCES
U INERTIA

INERTIAL FUSION (REACTOR)
Accelerator Technology Program
[DE84-017083] 04 p0563 N85-13586
Opacity determinations for Inertial Confinement Fusion (ICF) materials using an average atom model
12 p1957 N85-22295
Heavy ion fusion accelerator research in the US
[DE85-008465] 17 p3034 N85-28767
Megajoule-class single-pulse KrF laser test facility as a logical step toward inertial fusion commercialization
[DE85-009590] 18 p3191 N85-29794
Progress in inertial fusion at LLNL
[DE85-010931] 19 p3277 N85-30321
Ion source development for the Los Alamos heavy ion fusion injector
[DE85-012682] 24 p4156 N85-35766

INERTIAL GUIDANCE
NT STRAPDOWN INERTIAL GUIDANCE
Polaris guidance system
[AD-D011324] 07 p0900 N85-15704
Distance-inertial guidance of launch vehicle described
12 p1820 N85-21417
Gyrolaser guidance system for medium range missiles
16 p2696 N85-26649

INERTIAL MEASURING UNITS
U INERTIAL PLATFORMS

INERTIAL NAVIGATION
Errors of analog of inertial coordinate systems modeled in astronavigation system 07 p0951 N85-16026
A discussion of coning errors exhibited by inertial navigation systems
[RAE-TM-RAD-NAV-243] 08 p1062 N85-16854
Potential impact of Navstar GPS on NATO tactical operations 11 p1711 N85-20763
Avionics Flight Evaluation System (AFES)
13 p1967 N85-22357
Flight simulation for inertial navigation system
14 p2273 N85-24081
Decomposition in problem of correcting inertial navigation systems 14 p2287 N85-24172
Quaternion algorithms of 3-dimensional inertial navigational systems 14 p2287 N85-24173
Non-linear methods for inertial navigation system alignment
[BAE-BT-12683] 15 p2468 N85-25232
Assessment of a nonlinear method of INS alignment — inertial navigation systems (INS)
[BAE-BT-12684] 15 p2468 N85-25233
Implementation of an inertial navigation algorithm using a limited wordlength microprocessor for a strapdown navigation computer
[BAE-BT-12792] 15 p2468 N85-25234
Application of quaternions to problems of solid body dynamics in the atmosphere 15 p2481 N85-25313
Combinatorial performance/cost analysis of an autonomous navigation system for aircraft
16 p2695 N85-26640
Navigation: Accounting for copy
16 p2695 N85-26641
Low cost two gimbal inertial platform and its system integration 16 p2698 N85-26661
Observability in problem of correction of inertial navigation systems using additional information from artificial Earth satellite 16 p2719 N85-26785
A system for take-off and landing measurements (STALINS)
[B8580072] 17 p2895 N85-27849
Simulation of gyrocompassing alignment and calibration of strapdown inertial navigation system in a swaying vehicle
[DFVLR-MITT-84-20] 17 p2895 N85-27850
The AFTI/F16 terrain-aided navigation system
[DE85-008411] 18 p3060 N85-28935
Investigation of fast reaction SAW (Surface Acoustic Wave) accelerometer
[AD-A153876] 19 p3216 N85-29943
Inertial navigation system - LAS II for SGT YORK testing
[AD-A154204] 19 p3216 N85-29944
The DREO (Defence Research Establishment Ottawa) Inertial Navigation Laboratory: Development and test capabilities
[AD-A154425] 19 p3216 N85-29945
Simulations of strapdown-system errors and error compensation methods — transport aircraft navigation
[DFVLR-MITT-84-22] 20 p3392 N85-31040
Using regression analysis for determining air data sensor errors by means of an inertial navigation system
[ESA-TT-886] 20 p3392 N85-31041
Development of an active laser gyro for inertial rotation sensing in attitude/heading reference and inertial navigation systems, phase 1
[BMFT-FB-W-85-001] 20 p3460 N85-31489

INERTIAL PLATFORMS
Low cost two gimbal inertial platform and its system integration 16 p2698 N85-26661
The DREO (Defence Research Establishment Ottawa) Inertial Navigation Laboratory: Development and test capabilities
[AD-A154425] 19 p3216 N85-29945

INERTIAL REFERENCE SYSTEMS
Attitude measurements and determination
14 p2397 N85-24767
Reference systems — in space mechanics
14 p2399 N85-24784
Materialization of a reference system via a star catalog 14 p2399 N85-24787
Non-linear methods for inertial navigation system alignment
[BAE-BT-12683] 15 p2468 N85-25232
Assessment of a nonlinear method of INS alignment — inertial navigation systems (INS)
[BAE-BT-12684] 15 p2468 N85-25233
Relating the planetary ephemerides and the radio reference frame 16 p2770 N85-27095

INERTIAL UPPER STAGE
Preliminary analysis of selected gas dynamic problems — space shuttle main engine main combustion transients and IUS nozzle flow
[NASA-CR-171343] 10 p1483 N85-19361

INFARCTION
NT MYOCARDIAL INFARCTION

INFECTIONS
U INFECTIOUS DISEASES

INFECTIOUS DISEASES
NT INFLUENZA
The use of digital spaceborne SAR data for the delineation of surface features indicative of malaria vector breeding habitats 08 p1146 N85-17230
The effects of simulated weightlessness on susceptibility to viral and bacterial infections using a murine model
15 p2613 N85-26100
Differences in susceptibility of inbred mice to bacillus anthracis
[AD-A155646] 21 p3662 N85-32750
Legionnaires' disease bacteria in power plant cooling systems: Phase 2
[DE85-011546] 22 p3825 N85-33695
Molecular biology of environmental aromatic hydrocarbons
[DE85-015036] 24 p4128 N85-35593

INFERENCE
Lower level inference control in statistical database systems
[DE84-016005] 05 p0735 N85-14729
Ambiguity and uncertainty in probabilistic inference
[AD-A147378] 07 p1035 N85-16572
Research in stochastic processes
[AD-A148622] 08 p1216 N85-17660
Multivariate analysis and its applications
[AD-A150324] 13 p2151 N85-23352
The HORNE reasoning system, revision
[AD-A150983] 14 p2405 N85-24827
Inference and state estimation for stochastic point processes
[AD-A151216] 15 p2640 N85-26281
A complete inference system for regular processes with silent moves
[CWI-CS-R8420] 17 p3014 N85-28638
Alternative theories of inference in expert systems for image analysis
[AD-A153649] 18 p3170 N85-29646
Bayesian inference and diagnostics for the 3 parameter logistic model
[AD-A153840] 18 p3175 N85-29681
Manual and computer-aided sequential diagnostic inference
[AD-A156229] 24 p4133 N85-35620

INFESTATION
Irradiation of northwest agricultural products
[DE85-012455] 22 p3843 N85-33803

INFILTRATION
Fabrication of fiber-reinforced ceramic composites by chemical vapor infiltration
[DE85-003809] 11 p1611 N85-20132
Development of a new faster process for the fabrication of ceramic fiber-reinforced ceramic composites by chemical vapor infiltration
[DE85-007550] 16 p2758 N85-27007
Development of high temperature resistant noncorrodible silicon carbide components for gas turbine applications, follow-up report
[BMFT-FB-T-85-016] 17 p2906 N85-28129
Laboratory investigation of formation damage of an artificial fracture at simulated geothermal conditions
[DE85-010301] 18 p3102 N85-29331

INFINITY
Model theory for infinitely deep languages
[ISSN-0355-0087] 01 p0101 N85-10674
A note on the G-space version of Glicksberg's theorem
[CWI-PM-R8405] 08 p1217 N85-17666
Infinite dimensional linear systems with unbounded control and observation: A functional analytic approach
[AD-A153535] 18 p3169 N85-29639
On the convergence of an iterative formulation of the electromagnetic scattering from an infinite grating of thin wires 24 p4065 N85-35319

INFLATABLE DEVICES
U INFLATABLE STRUCTURES

INFLATABLE STRUCTURES
NT BALLOONS
NT HIGH ALTITUDE BALLOONS
NT JIMSPHERE BALLOONS
NT METEOROLOGICAL BALLOONS
NT MICROBALLOONS
NT SUPERPRESSURE BALLOONS
NT TETHERED BALLOONS
Research on large, highly accurate, inflatable reflectors
[AD-A145080] 01 p0016 N85-10009
Collapseable seal member
[DE84-014300] 01 p0055 N85-10067
Large spaceborne antenna reflectors using inflatable space rigidized structures 05 p0625 N85-14004
Tire inflation/deflation system
[AD-D011459] 10 p1493 N85-19426
Tire deflation mechanism
[AD-D011460] 10 p1493 N85-19427
Air bag restraint system
[AD-D011671] 19 p3215 N85-29936

INFLATING
The Reports of Aeromedical Laboratory, volume 25, no. 1/2
[ISSN-0023-2858] 01 p0090 N85-10605
Assessment of the inflating characteristics of the modified anti-G suit 01 p0090 N85-10609
A theoretical view on the stress analysis of fully inflated parachute canopies
[AD-A148387] 08 p1078 N85-16835
SU(N,1) inflation
[DE85-003952] 15 p2869 N85-26489

INFLECTION POINTS
Construction of solutions for two-dimensional Riemann problems
[DE85-003136] 10 p1549 N85-19770

INFLUENCE COEFFICIENT
Development and application of a unified balancing approach with multiple constraints
16 p2737 N85-26891

INFLUENZA
Advances in study of cold injury in Army
14 p2283 N85-24145
Using the information of cosmic rays to predict influenza epidemic
[SH-10.1-2] 23 p4053 N85-35134

INFORMATION
A proposed integration among organizational information requirements, media richness and structural design
[AD-A149317] 10 p1567 N85-19881
Report on the Second Annual Review Meeting of the National Acid Precipitation Assessment Program. Research to assist decisionmaking: Summary
[DE85-003003] 12 p1884 N85-21620
Accomplishments of Institute of Cartography summarized 13 p2166 N85-23435
National Telecommunications and Information Administration authorization
[GPO-38-660] 16 p2679 N85-27766
Verbal information processing paradigms: A review of theory and methods
[AD-A153229] 17 p3050 N85-28860
Summary of archived Atlantic coast wave information study pressure, wind, wave, and water level data
[AD-A153782] 18 p3151 N85-29668

Hybrid uncertainty theory
[DE85-008367] 18 p3167 N85-29822
Fracture detection and characterization for geothermal reservoir definition
[DE85-008677] 22 p3815 N85-33630
Colour coding scales and computer graphics
23 p3963 N85-34568

INFORMATION ADAPTIVE SYSTEM
Alphabet-constrained data compression
[AD-A152887] 17 p3019 N85-28667

INFORMATION DISSEMINATION
NT MESSAGES
NT SELECTIVE DISSEMINATION OF INFORMATION
Nowcasting using lightning location techniques
01 p0084 N85-10568
Estuaries of the Cape. Part 2: Synopses of available information on individual systems. Report no. 16: Eerste (CSW 6)
[CSIR-RR-415-PT-2] 01 p0087 N85-10585
Sea-level in the world ocean. Part 6: The South Atlantic and South Pacific Oceans, a catalogue of measurements
[CSIR-T/SEA-8303-6] 01 p0087 N85-10590
Sea-level in the world ocean. Part 7: The Indian Ocean, a catalogue of measurements
[CSIR-T/SEA-8303-7] 01 p0087 N85-10591
Improving technical documents
[AD-B084855] 01 p0126 N85-10866
Depository librarians' views on GPO's administration of the depository library program. Report to the Chairman, Joint Committee on Printing
[PB84-212265] 01 p0126 N85-10867
Opportunities for commercial organizations
02 p0156 N85-11055
A system for the management of requests at an image data bank
[E85-10014] 02 p0216 N85-11427
Remote sensing applications program
[E85-10022] 02 p0218 N85-11435
Artificial Intelligence in Maintenance: Proceedings of the Joint Services Workshop
[AD-A145349] 02 p0244 N85-11592
Benefit value to the Air Force of the GIDEP (Government Industry Data Exchange Program) alert
[AD-A145470] 02 p0292 N85-11897
Collection overlap and coordinated collection development 02 p0293 N85-11902
AGARD Highlights
[AGARD-HIGHLIGHTS-84/2] 02 p0305 N85-11972
Catalogue of earthquakes for the territory of Czechoslovakia for the period 1957 - 1980
[REPT-555] 03 p0376 N85-12398
Factors affecting the archiving, processing and dissemination of ERS-1 altimeter data
03 p0381 N85-12435
NSSDC and WDC-A-R and S document availability and distribution services
[NASA-TM-87374] 03 p0438 N85-12787
Design of a scientific information collation and dissemination system, volumes 1 thru 3
[AD-A146002] 03 p0438 N85-12791
Scientific communications and national security
[GPO-36-093] 04 p0492 N85-13138
The 1984 ASEE-NASA summer faculty fellowship program (aeronautics and research)
[NASA-TM-87393] 04 p0575 N85-13664
FY 1984 scientific and technical reports, articles, papers and presentations
[NASA-TM-86470] 04 p0575 N85-13670
Economic value of consumer information: A selected, annotated bibliography
[PB84-235795] 04 p0576 N85-13673
Energy information exchange, 1983
[DE84-901446] 04 p0577 N85-13680
An electronic documentation system
[SNIAS-842-111-101] 04 p0577 N85-13683
The availability of Japanese scientific and technical information in the United States
[GPO-35-241] 05 p0735 N85-14726
Oceanographic data for development of the US exclusive economic zone
[PB85-108458/GAR] 07 p1010 N85-16415
Outlook for expanding the Federal research in progress system
[AD-A148354] 08 p1229 N85-17737
Safety awareness, pilot education, and incident reporting programs 09 p1276 N85-18020
The aviation safety reporting system
09 p1276 N85-18021
Community relations activities at Department of Defense sites
[AD-P004150] 09 p1349 N85-18488
GIDEP representative interaction
[DE84-016792] 09 p1401 N85-18820
The establishment and experience of the Carbon Dioxide Information Center (CDIC)
[DE85-001934] 09 p1402 N85-18825
Automation of information services furnished by documentation centers and specialized libraries
[FUB-6-1984] 09 p1402 N85-18827
French commentary on Soviet industrial espionage
10 p1461 N85-19210
Proceedings of the 17th Symposium on Electromagnetic Windows, part 1
[AD-A149185] 10 p1466 N85-19253
Commentary on start of scientific data transmissions with USSR 10 p1476 N85-19319
Computer center CDC libraries
[AD-A149005] 10 p1540 N85-19707
Provision of Federal government publication in electronic format to depository libraries
[S-PRT-98-280] 10 p1567 N85-19880
Keyword thesaurus: A list of terms and codes to identify areas of interest for research and other types of sponsored programs (revised October 1984)
[PB85-136893] 10 p1568 N85-19890
Air Force Office of Scientific Research (AFOSR) technical report summaries. Third quarter (CY)
[AD-A148965] 10 p1573 N85-19918
French research minister on policy, technology transfer 11 p1616 N85-20182
Information systems issues 11 p1701 N85-20693
Computer and communications security and privacy
[GPO-39-741] 12 p1911 N85-21994
Electronics Engineering Department EE Technical Review
[UCRL-50025-84-1] 13 p2083 N85-22887
Evaluating the appropriateness of microcomputers for litigation document management using the analytic hierarchy process 14 p2399 N85-24788
The Effect of Computers on the Generation and Use of Technical Data
[NBSIR-84-2907] 14 p2400 N85-24792
Progress through cooperation and exchange of ideas and experiences 15 p2626 N85-26186
Management communication and financial modeling
15 p2627 N85-26190
Energy Data Base: Subject thesaurus permutated listing. Revision 6, appendix
[DE84-016963] 15 p2666 N85-26454
Span graphics display utilities handbook, first edition
[NASA-TM-86500] 16 p2849 N85-27567
Scientific data bases on a VAX-11/780 running VMS
[DE85-007925] 16 p2878 N85-27760
Australian seismological report, 1980
[REPT-252] 17 p2989 N85-28473
Defense data network support concept analysis
[AD-A153214] 17 p3016 N85-28649
Origin, processing, and dissemination of scientific news, with examples from 20 research institutes
[JUEL-1940] 17 p3050 N85-28882
The POK project; studies of information handling problems with a new kind of communication device — precoded signals
[FOA-A-53001-H2] 18 p3091 N85-29131
Combined catalog of ionosphere vertical soundings data
[PB85-168494] 18 p3138 N85-29430
INEL User Network Exchange, volume 1-85, Jan./Feb. 1985
[DE85-006108] 18 p3166 N85-29615
Notes for medical catalogers, 1984
[PB85-180206] 18 p3200 N85-29853
System enhancements of Mesoscale Analysis and Space Sensor (MASS) computer system
[NASA-CR-171483] 19 p3342 N85-30708
The application of artificial intelligence techniques to large distributed networks
[NASA-CR-177346] 19 p3344 N85-30721
TMI-2 technical information and examination program
[DE85-010614] 19 p3359 N85-30827
Human factors engineering contracts in Sweden: An overview
[FOA-C-56043-H2] 20 p3513 N85-31836
Data base management: MSTRAC (keynote paper), part 8 21 p3626 N85-32530
USSR Space Life Sciences Digest
[NASA-CR-3922] 21 p3656 N85-32709
Remote medical diagnosis 21 p3663 N85-32753
The Human Resource Management Information Network (HRMIN): A cost comparison in accordance with Office of Management and Budget (OMB) Circular no. A-76, 5 April 1979
[AD-A154583] 21 p3713 N85-33039
The flow of scientific and technical information in the US Army Research Laboratories
[AD-A155050] 21 p3713 N85-33043
USGS coastal research, studies and maps: A source of information for coastal decision making
[USGS-CIRC-863] 24 p4108 N85-35465

INFORMATION FLOW
Standards for commercially emerging technologies: A preliminary cost-benefit assessment for the Optical Digital data disk (OD3) technology for mass data storage applications
[PB84-223593] 01 p0101 N85-10089
Information requirements analysis: An application
[AD-A144896] 01 p0125 N85-10858
Information flow in event-driven large-scale systems
[DE84-014167] 05 p0736 N85-14728
Methodology investigation. Streamlined Test Reporting and Planning (STRAP): Data flow procedures
[AD-A146463] 06 p0871 N85-15531
Model of information-reference dialogue system for working with document abstracts
12 p1903 N85-21949
The availability of Japanese scientific and technical information in the United States
[GPO-39-478] 12 p1951 N85-22254
The application of artificial intelligence techniques to large distributed networks
[NASA-CR-177346] 19 p3344 N85-30721
The flow of scientific and technical information in the US Army Research Laboratories
[AD-A155050] 21 p3713 N85-33043
Assured information flow capping architecture
[AD-A155392] 22 p3756 N85-33283

INFORMATION MANAGEMENT
User requirements for very-short-range weather forecasts: Some key issues 01 p0084 N85-10562
Sea-level in the world ocean. Part 6: The South Atlantic and South Pacific Oceans, a catalogue of measurements
[CSIR-T/SEA-8303-6] 01 p0087 N85-10590
Sea-level in the world ocean. Part 7: The Indian Ocean, a catalogue of measurements
[CSIR-T/SEA-8303-7] 01 p0087 N85-10591
Information requirements analysis: An application
[AD-A144896] 01 p0125 N85-10858
Data dictionary systems and their role in information resource management
[AD-A144905] 01 p0125 N85-10859
Collection overlap and coordinated collection development 02 p0293 N85-11902
A management workstation concept
[AD-A145617] 02 p0294 N85-11906
Inclusion of audiovisual media in information services for the special subjects journalism and communication science (pilot study)
[BMFT-FB-ID-83-004] 02 p0294 N85-11909
Business planning for information services under special consideration of German management information systems
[BMFT-FB-ID-83-007] 02 p0294 N85-11910
A research program in computer technology
[AD-A145776] 03 p0402 N85-12565
Five-year plan for meeting the automatic data processing and telecommunications needs of the Federal Government. Volume 1: Planning strategies
[PB84-214501] 03 p0436 N85-12777
Five-year plan for meeting the automatic data processing and telecommunications needs of the Federal Government. Volume 2: Major information technology systems acquisition plans of Federal executive agencies, 1984-1989
[PB84-214519] 03 p0436 N85-12778
Interdisciplinary structure of information science
03 p0436 N85-12779
Information processing for better utilization: Assessing the CLER model as organizer for innovation diffusion and planned change information reported in selected studies in the ERIC system 03 p0437 N85-12780
An approach to interfacing data bases in WWMCCS ADP
[AD-A146350] 03 p0439 N85-12793
Corporate use of information regarding natural resources and environmental quality
[PB84-222736] 03 p0439 N85-12794
IRM (Information Resources Management) long-range plan: Fiscal year 1984-1988 (update). Volume 2: ADP and telecommunications acquisition plan
[PB84-229244] 03 p0439 N85-12796
The 1984 ASEE-NASA summer faculty fellowship program (aeronautics and research)
[NASA-TM-87393] 04 p0575 N85-13664
Economic value of consumer information: A selected, annotated bibliography
[PB84-235795] 04 p0576 N85-13673
Executive information system
[DE84-015355] 04 p0576 N85-13675
Energy information exchange, 1983
[DE84-901446] 04 p0577 N85-13680
Use of minicomputers for the formation of hydrological data banks 07 p1001 N85-16358
Document interchange format
[PB84-217033] 07 p1027 N85-16517

A study of the relationship between user attitudes and the success of the MAJCOM and AFRCE work information management system
[AD-A146956] 07 p1051 N85-16671
Organizations and information processing: A field study of research and development units within the United States Air Force Systems Command
[AD-A147361] 07 p1054 N85-16691
Data user's manual 08 p1150 N85-17254
The establishment and experience of the Carbon Dioxide Information Center (CDIC)
[DE85-001934] 09 p1402 N85-18825
The evolution from data processing to information resource management
[AD-A149429] 10 p1567 N85-19878
The conservation and utilization of scientific research documents: Practical aspects and organization
[NOTA-INTERNA-834] 14 p2433 N85-25008
White paper on new intern..tional satellite systems
[PB85-162501] 16 p2775 N85-27127
Information presentation in power plant control rooms
[VTT-320] 16 p2864 N85-27688
Distributed systems management in wide area networks
[CWI-CS-R8419] 17 p3016 N85-28651
A hierarchy of knowledge levels implemented in a rule-based production system to calculate bounds on the size of intersections and unions of simple sets
[AD-A155291] 22 p3848 N85-33636
Research report program of the US Army in Europe
24 p4061 N85-35167
Electronic information management and productivity
[DE85-013362] 24 p4164 N85-35818
Records Disposal: A guidebook for laboratory offices
[AD-A156064] 24 p4165 N85-35823

INFORMATION RETRIEVAL
Compilation of data sources for existing chemicals
[GSF-A-2/84] 01 p0017 N85-10103
Intelligent information retrieval from on-line technical documentation
[AD-P003946] 02 p0249 N85-11626
Distributed hypothesis testing in distributed sensor networks
[AD-A145434] 02 p0294 N85-11905
Information processing for better utilization: Assessing the CLER model as organizer for innovation diffusion and planned change information reported in selected studies in the ERIC system 03 p0437 N85-12780
NASA Thesaurus supplement: A 3-part cumulative supplement to the 1982 edition of the NASA Thesaurus
[NASA-SP-7051(SUPPL-2)] 03 p0437 N85-12785
Research activities of the Illinois University Coordinated Science Laboratory
[AD-A145569] 03 p0449 N85-12856
FY 1984 scientific and technical reports, articles, papers and presentations
[NASA-TM-86470] 04 p0575 N85-13670
Automated Library Search System (ALSS) user's manual
[DE84-015952] 04 p0576 N85-13672
Some attributes of online search intermediaries that relate to search outcome 05 p0734 N85-14721
Role of DESIGNMANAGER in information engineering
[DE84-016807] 05 p0736 N85-14730
Setting time standards at NISTARS (Naval Integrated Storage and Retrieval System)
[AD-A146371] 06 p0870 N85-15529
Distributed knowledge base systems for diagnosis and information retrieval
[AD-A146690] 07 p1054 N85-16690
Commerce Lab: Mission analysis. Payload integration study
[NASA-CR-171285] 08 p1104 N85-16982
Benchmarking database systems in multiple backend configurations
[AD-A148191] 08 p1202 N85-17568
Performance evaluation of a database system in multiple backend configurations
[AD-A148192] 08 p1229 N85-17743
Boring information and subsurface data base package user's guide
[AD-A148623] 08 p1230 N85-17747
Analytical modeling of a polling protocol — airline information network
[ENST-84H001] 09 p1277 N85-18029
GIDEP representative interaction
[DE84-016782] 09 p1401 N85-18820
Methodology for evaluating related databases and a computerized algorithm for merging their output
09 p1401 N85-18821
Online database search strategies and thesaural relationship models 09 p1402 N85-18822
The establishment and experience of the Carbon Dioxide Information Center (CDIC)
[DE85-001934] 09 p1402 N85-18825
Automation of information services furnished by documentation centers and specialized libraries
[FUB-6-1984] 09 p1402 N85-18827
Retrieval procedures for hydrologic data from ARS (Agricultural Research Service) experimental watersheds in the US (REPHLEX)
[PB85-111326/GAR] 09 p1402 N85-18828
Guide to human factors information sources
[AD-A149102] 10 p1531 N85-19649
The integrated library system design concepts for a complete serials control subsystem
[AD-A149379] 10 p1568 N85-19884
Post-processing of bibliographic citations from DOE/Recon, NASA/Recon, and DOD/DROLS
[DE85-000617] 11 p1739 N85-20938
AID: Access to Informal Documentation
[DE85-000418] 11 p1740 N85-20939
Requirements formulation subtask 1.A of the Major Item System Mapping (MISM) project
[DE85-000978] 11 p1740 N85-20940
Model of information-reference dialogue system for working with document abstracts
12 p1903 N85-21949
The EEC's information technology program: An update
[AD-A150022] 12 p1951 N85-22258
Evaluation of the vocabulary switching systems
[PB85-127157] 12 p1951 N85-22260
Precedency control and other semantic integrity issues in a workbench database 13 p2123 N85-23220
General design considerations of an Air Force information system
[AD-A150611] 13 p2168 N85-23449
MMCIAC (Metal Matrix Composites Information Analysis Center)
[AD-A150654] 14 p2248 N85-23933
Invariant system of technological preparation of production 14 p2268 N85-24056
Research needs for artificial intelligence applications in support of C3 (Command, Control, and Communication)
[AD-A150867] 14 p2292 N85-24210
Evaluating the appropriateness of microcomputers for litigation document management using the analytic hierarchy process 14 p2399 N85-24786
NASA Thesaurus supplement, a three part cumulative supplement to the 1982 edition of the NASA Thesaurus
[NASA-SP-7051(SUPPL-3)] 14 p2432 N85-25002
The retrieval expert model of information retrieval
14 p2433 N85-25003
Schema theory in the representation and analysis of text 14 p2433 N85-25004
The conservation and utilization of scientific research documents: Practical aspects and organization
[NOTA-INTERNA-834] 14 p2433 N85-25008
Document retrieval from a relational database management system: An investigation of multiple-line query formulation using SEQUEL
15 p2665 N85-26447
A database design for the Brazilian Air Force Flying Unit Operational Control System
[AD-A151848] 15 p2666 N85-26452
Forward library searching of previously-quantitated peaks, using a scan list created from a quantitation list by a novel FORTRAN program for the INCOS data system
[PB85-165835] 16 p2845 N85-27541
Retrieval performance in a full text journal article database 16 p2877 N85-27747
Access path optimization for network database retrieval 16 p2877 N85-27749
Design of an interface to an information retrieval network 16 p2877 N85-27750
Organization of scientific, technical information services 17 p3049 N85-28873
Energy data base: Subject categories and scope
[DE84-017376] 17 p3050 N85-28881
Avionics Data Base users manual
[AD-A153610] 18 p3062 N85-28942
Information science in toxicology
[DE85-007746] 18 p3200 N85-29851
National Archives and Records Service (NARS) twenty year preservation plan
[PB85-177640] 18 p3200 N85-29854
CSIN (Chemical Substances Information Network) workbook: US Geological Survey training course for Chemical Substances Information Network
[PB85-170058] 18 p3200 N85-29855
Using MATHLIB on the IBM computer and sundry plotting examples with a taste of IMSL
[DE85-011395] 19 p3340 N85-30695
SAFEORD: Safety of explosive ordnance databank
[AD-A154056] 19 p3380 N85-30972
Modified dynamic hashing
[DE85-011166] 19 p3381 N85-30974
Individual differences in online search behavior: The effect of learning styles and cognitive abilities on process and outcome 20 p3541 N85-3
Technology transfer system automation implementation
[PB85-177335] 22 p3649 N85-3
User's operating procedures. Volume 3: Projects directorate information programs
[NASA-CR-177950] 23 p3956 N85-34
NAPGEN: Automatic NAPLPS page generator
23 p3964 N85-34
LOCAT: A data retrieval program
[AD-A156004] 24 p4165 N85-35
Source header list, supplement 3
[AD-A156100] 24 p4165 N85-35
Source hierarchy list. Volume 1: A through H
[AD-A156300] 24 p4165 N85-35
Source hierarchy list. Volume 2: I through Z
[AD-A156301] 24 p4165 N85-35

INFORMATION SYSTEMS
NT ATMOSPHERIC & OCEANOGRAPHIC INFORM SYS
NT GEOGRAPHIC INFORMATION SYSTEMS
NT INFORMATION ADAPTIVE SYSTEM
NT MANAGEMENT INFORMATION SYSTEMS
Analysis of computer and communication information processing and system development
[AD-A144966] 01 p0100 N85-10
A technique to model and design physical database systems
[DE84-015337] 01 p0128 N85-10
A system for the management of requests at an image data bank
[E85-10014] 02 p0216 N85-1142
Yearly report for programming productivity enhancement by the use of application generators
[AD-A145623] 02 p0242 N85-1157
Implications of artificial intelligence for a user defined technical information system
[AD-P003938] 02 p0248 N85-1161
The application of artificial intelligence to a maintenance and diagnostic information system
[AD-P003945] 02 p0249 N85-116
Memory-based expert systems
[AD-A145612] 02 p0249 N85-116
Auditory information systems in military aircraft: Current configurations versus the state of the art
[AD-A145469] 02 p0275 N85-1179
An operational system for subject switching between controlled vocabularies: A computational linguistics approach
[NASA-CR-3838] 02 p0293 N85-1190
Distributed hypothesis testing in distributed sensor networks
[AD-A145434] 02 p0294 N85-119
Use of prototyping for man-machine interface requirements definition on the AWDS (Automated Weather Distribution System) program
[AD-A146033] 03 p0396 N85-125
Five-year plan for meeting the automatic data processing and telecommunications needs of the Federal Government. Volume 1: Planning strategies
[PB84-214501] 03 p0436 N85-1277
Five-year plan for meeting the automatic data processing and telecommunications needs of the Federal Government. Volume 2: Major information technology systems acquisition plans of Federal executive agencies, 1984-1989
[PB84-214519] 03 p0436 N85-1277
Information processing for better utilization: Assessing the CLER model as organizer for innovation diffusion and planned change information reported in selected studies in the ERIC system 03 p0437 N85-1278
Preserving the time dimension in information systems
03 p0437 N85-1278
Design of a scientific information collection and dissemination system, volumes 1 thru 3
[AD-A146002] 03 p0438 N85-127
IRM (Information Resources Management) long-range plan: Fiscal year 1984-1988 (update). Volume 2: ADP and telecommunications acquisition plan
[PB84-229244] 03 p0439 N85-127
Evaluation of the National Library of Medicine's programs in the medical behavior sciences. Coverage of the Medical Behavioral Sciences (MBS) literature in monographic databases, study 5
[PB84-230531] 03 p0439 N85-127
Evaluation of the National Library of Medicine's programs in the medical behavior sciences. Online searchers' reactions to database and vendor capabilities in the Medical Behavioral Sciences (MBS), study 4
[PB84-230523] 03 p0439 N85-127

Evaluation of the National Library of Medicine's programs in the medical behavior sciences. Quality of indexing: The development and testing of a methodology comparing databases covering the Medical Behavioral Sciences (MBS) literature, study 3
[PB84-230515] 03 p0439 N85-12799

Evaluation of the National Library of Medicine's programs in the medical behavior sciences. Test retrievals in five major databases covering the Medical Behavioral Sciences (MBS) literature, study 2
[PB84-230507] 03 p0440 N85-12800

Evaluation of the National Library of Medicine's programs in the medical behavior sciences. Coverage, overlaps and gaps in bibliographic databases dealing with the Medical Behavioral Sciences (MBS) literature, study 1
[PB84-230499] 03 p0440 N85-12801

Evaluation of the National Library of Medicine's program in the medical behavior sciences. An analysis of the National Library of Medicine's (NLM) handling of Medical Behavioral Sciences (MBS) literatures: Some research tests of methods for evaluating bibliographic databases, executive summary
[PB84-230481] 03 p0440 N85-12802

Competitive assessment of the US information services industry
[PB84-174804] 03 p0440 N85-12803

Research activities of the Illinois University Coordinated Science Laboratory
[AD-A145589] 03 p0449 N85-12856

Human reliability data bank: Feasibility study
[DE84-015215] 04 p0546 N85-13476

INFORM system 2-year plan, FY 1984-1985
[DE84-016044] 04 p0576 N85-13674

International information networks for material properties
[DE84-013836] 04 p0576 N85-13676

Archiving and exchange of a computerized marine seismic database: The ROSE data archive system
[DE84-901453] 04 p0576 N85-13677

Nuclear criticality information system: Database examples
[DE84-014462] 04 p0576 N85-13678

Activities report in technology
[ISBN-951-38-1996-1] 04 p0577 N85-13681

Information flow in event-driven large-scale systems
[DE84-014167] 05 p0735 N85-14728

Recommended documentation for computer users at ANL
[DE84-016286] 06 p0855 N85-15434

Toward an improved FIPS cost-benefit methodology. Phase 2: Descriptive models, general purpose application software development and maintenance
[PB84-226943] 06 p0870 N85-15527

UK, FRG, France: R and D in sensors, related fields
08 p1142 N85-17197

EDP computer tapes described
08 p1142 N85-17203

DDN directory
[AD-A148213] 08 p1230 N85-17744

Analytical modeling of a polling protocol — airline information network
[ENST-84H001] 09 p1277 N85-18029

Integrating heterogeneous non-geometric information systems using RIM
[DE84-017600] 09 p1402 N85-18823

Online directory of databases for material properties
[DE84-016511] 09 p1402 N85-18824

Retrieval procedures for hydrologic data from ARS (Agricultural Research Service) experimental watersheds in the US (REPHLEX)
[PB85-111326/GAR] 09 p1402 N85-18828

Concepts and tools for the software life cycle
10 p1464 N85-19236

Guide to human factors information sources
[AD-A149102] 10 p1531 N85-19649

The multiple resources model of human performance: Implications for display design 10 p1534 N85-19669

Management challenges encountered in CAD implementation
[DE85-002072] 10 p1541 N85-19716

Predicting the performance of distributed knowledge-based systems: A modeling approach
[AD-A149021] 10 p1545 N85-19736

Structure and application of extremely large geophysical data bases
[DE85-003527] 10 p1566 N85-19888

Research needs on the interaction between information systems and their users: Report of a workshop
[PB85-121523] 10 p1566 N85-19891

Air Force Office of Scientific Research (AFOSR) technical report summaries. Third quarter (CY)
[AD-A148965] 10 p1573 N85-19916

Information systems issues 11 p1701 N85-20693

Requirements formulation subtask 1.A of the Major Item System Mapping (MISM) project
[DE85-000976] 11 p1740 N85-20940

Sourcebook: Gaining access to US government information on the environment and natural resources
[DE84-017419] 11 p1740 N85-20941

Model of information-reference dialogue system for working with document abstracts
12 p1903 N85-21949

The EEC's information technology program: An update
[AD-A150022] 12 p1951 N85-22258

Performance evaluation of distributed systems with unbalanced flows: An analysis of the INFOPLEX data storage hierarchy
[AD-A150528] 13 p2147 N85-23328

Intel IDIS evaluation
[DE85-003748] 13 p2168 N85-23451

MMCIAC (Metal Matrix Composites Information Analysis Center)
[AD-A150654] 14 p2246 N85-23933

An introduction to USAFETAC (USAF Environmental Technical Applications Center)
[AD-A150971] 14 p2378 N85-24682

Selection criteria and computer aided design (CAD) systems
[NLR-MP-84037-U] 14 p2406 N85-24834

Air Force Office of Scientific Research (AFOSR): Technical report summaries. Fourth quarter (CY)
[AD-A150860] 14 p2456 N85-25167

Computerized biophysical data acquisition system for motion sickness studies
[AD-A151691] 15 p2618 N85-26131

Procedures for use in compiling requirements specifications for computerized library systems
[CSTI-76] 15 p2665 N85-26446

Energy Data Base: Subject thesaurus permutated listing. Revision 6, appendix
[DE84-016983] 15 p2666 N85-26454

Information technology applications in voluntary sector transport operations. SP1: Objectives and programme of work
[TT-8501] 15 p2667 N85-26457

Historical perspectives on information transmission engineering 16 p2759 N85-27023

Diagnostic system
[INPE-3350-PRE/659] 16 p2841 N85-27519

Internation information networks for material properties: Revision 1
[DE85-007412] 16 p2850 N85-27572

Compilation of abstracts of theses submitted by candidates for degrees
[AD-A151722] 16 p2875 N85-27739

DoD manual for standard data elements, part 2
[AD-A152202] 16 p2878 N85-27755

DoD manual for standard data elements, part 3
[AD-A152203] 16 p2878 N85-27756

DoD manual for standard data elements, part 4
[AD-A152204] 16 p2878 N85-27757

DoD manual for standard data elements, part 5
[AD-A152205] 16 p2878 N85-27758

Energy data base: Subject thesaurus
[DE84-010568] 16 p2878 N85-27761

The interactive generation of specifications for an onboard software series (GISELE)
17 p2904 N85-27906

US Naval Observatory collection and utilization of time comparison data 17 p2962 N85-28292

Centralized Storm Information System (CSIS)
[NASA-CR-175898] 17 p2994 N85-28506

A report from the Space Science and Engineering Center, the University of Wisconsin-Madison, Madison, Wisconsin 17 p2994 N85-28507

Test and evaluation plan for the Centralized Storm Information System 17 p2994 N85-28508

Efforts at office automation and information systems utilization at Martin Marietta Energy Systems, Incorporated
[DE85-006154] 17 p3013 N85-28633

USSR report: Science and technology policy
[JPRS-UST-85-008] 17 p3049 N85-28872

Organization of scientific, technical information services 17 p3049 N85-28873

The development of information systems at NLR
[B8580079] 17 p3051 N85-28884

Avionics Data Base users manual
[AD-A153810] 18 p3062 N85-28942

Data base of all known, published data on trace elements in oil shale and its products
[DE85-003399] 18 p3126 N85-29357

Ada (trademark) compiler validation summary report. Honeywell information systems GCOS6 Ada version 1.1
[AD-A153746] 18 p3162 N85-29590

Information science in toxicology
[DE85-007746] 18 p3200 N85-29851

Local automation model software benchmarking: Test plan
[AD-A154349] 19 p3337 N85-30676

The international scope of data evaluation
[DE85-005953] 19 p3349 N85-30760

SAFEORD: Safety of explosive ordnance databank
[AD-A154058] 19 p3380 N85-30972

Evaluative report on the Institute for Computer Sciences and Technology, National Bureau of Standards, fiscal year 1984
[PB85-176097] 20 p3514 N85-31848

Activities report of the Laboratory for Computer Science (FOA 32)
[FOA-C-30384-E1] 20 p3518 N85-31861

Individual differences in online search behavior: The effect of learning styles and cognitive abilities on process and outcome 20 p3541 N85-32037

Navy information systems: Planning, policy, organization, and management
[PB85-176113] 20 p3541 N85-32038

Design guidelines for user-system interface software
[AD-A154907] 21 p3671 N85-32907

The flow of scientific and technical information in the US Army Research Laboratories
[AD-A155050] 21 p3713 N85-33043

Fuel cell applications literature review
[DE85-011891] 22 p3809 N85-33592

User's operating procedures. Volume 1: Scout project information programs
[NASA-CR-177948] 23 p3956 N85-34518

User's operating procedures. Volume 1: Scout project financial analysis program
[NASA-CR-177949] 23 p3956 N85-34519

Applied computer graphics in a geographic information system: Problems and successes
23 p3962 N85-34563

Procedure for editing the fluxgate magnetometer data of the AFGL (Air Force Geophysics Laboratory) magnetometer network
[AD-A156331] 24 p4117 N85-35523

Electronic information management and productivity
[DE85-013362] 24 p4164 N85-35818

INFORMATION THEORY

Approximating hierarchical normal priors using a vague component
[CSIR-TWISK-284] 01 p0107 N85-10720

The inferring of preferences from indifferences in multicriteria decision analysis
[CSIR-TWISK-306] 01 p0108 N85-10729

Optimizing search with positive information feedback
[CSIR-TWISK-313] 01 p0125 N85-10855

A mathematical theory of command and control structures
[AD-A145608] 02 p0256 N85-11675

Distributed hypothesis testing in distributed sensor networks
[AD-A145434] 02 p0294 N85-11905

On update semantics and relational views
[AD-A145622] 02 p0294 N85-11907

Spread-spectrum communications
[AD-A146135] 03 p0355 N85-12285

East Europe report: Science and technology
[JPRS-ESA-84-041] 04 p0484 N85-13090

Theory of information, automation in Czechoslovakia
04 p0485 N85-13091

Equivocation limits in Gaussian additive channels
[INPE-2828-PRE/380] 04 p0492 N85-13137

Process algebra for communication and mutual excitation
[CWI-CS-R8409] 05 p0720 N85-14622

Lower level inference control in statistical database systems
[DE84-016005] 05 p0735 N85-14729

Information-theoretic properties of languages and their grammars
[AD-A146688] 06 p0799 N85-15106

Study of spectral/radiometric characteristics of the Thematic Mapper for land use applications
[E85-10057] 07 p0987 N85-16268

Rule-based evidence accrual system for image understanding
[AD-A147835] 07 p1044 N85-16634

On the complexity of distributed decision problems
[AD-A147174] 07 p1052 N85-16674

Hardware/software codesign for maintainable systems
08 p1066 N85-16753

Data stimulated on-line-checking (IROLD)
08 p1066 N85-16754

Symbol structure, information content and visual form: A carto-semiotic theory of map signs
09 p1342 N85-18439

Smoothing with split linear fits
[AD-A149032] 10 p1545 N85-19740

Relative-entropy minimization with uncertain constraints—theory and application to spectrum analysis
[AD-A149192] 10 p1546 N85-19752

The use of analytical models to interpret data properly [ERS-E.341] 11 p1651 N85-20399
Investigation of influence of communications link and synchronization error on noise tolerance of group transmission of binary information based on orthogonal Walsh function 13 p2086 N85-23026
A preliminary comparison of the information content of data from the LANDSAT 4 Thematic Mapper and Multispectral Scanner -- Arkansas 13 p2119 N85-23199
A perspective on multiaccess channels [AD-A150183] 13 p2146 N85-23322
Internation information networks for material properties: Revision 1 [DE85-007412] 16 p2850 N85-27572
Future information technology, 1984: Telecommunications [NBS/SP-500/119] 16 p2878 N85-27762
Chemical applications of topology and group theory. 17: An information theoretical approach to polyhedral symmetry [AD-A152821] 17 p2919 N85-27995
A software simulation study of a (255,223) Reed-Solomon encoder-decoder [NASA-CR-175872] 17 p2947 N85-28192
Distributed memory [AD-A153364] 17 p3001 N85-28554
Language design, computers and brains [AD-A152819] 17 p3008 N85-28594
Counting is easy -- Turing machines [CWI-CS-R8423] 17 p3009 N85-28606
The role of duality in optimization problems involving entropy functionals, with applications to information theory [AD-A152336] 17 p3026 N85-28713
An information theoretical method for automatic noise elimination in digital image processing 18 p3124 N85-29345
Evaluation of curve-smoothing techniques [HSE-TRANS-11108] 19 p3349 N85-30759

INFORMATION TRANSFER
Architecture for a demonstration radar-communication link [AD-A147635] 06 p1150 N85-17260
The Hazardous Materials Technical Center [AD-P004149] 09 p1349 N85-18485
Graphics translators for computer-aided drafting and design: Interface alternatives for the A/E community [AD-A148892] 10 p1540 N85-19706
Oral discussion, group-to-individual transfer and achievement in cooperative learning groups [AD-A153209] 17 p3001 N85-28552
Study of raster metafile formats [AD-A153322] 17 p3012 N85-28624
Interfacing the VAX 11/780 using berkeley UNIX 4.2BSD and Ethernet based Xerox Network Systems [AD-A153174] 17 p3016 N85-28647
Myoelectric control of a computer based expert system for flight control [AD-A154981] 21 p3557 N85-32126
Tight bounds on the complexity of parallel sorting [AD-A154726] 21 p3667 N85-32778
The flow of scientific and technical information in the US Army Research Laboratories [AD-A155050] 21 p3713 N85-33043

INFORMATION TRANSMISSION
U DATA TRANSMISSION

INFRARED ABSORPTION
Study of combustion and flame processes initiated by laser-induced multiple-photon absorption [DE84-017095] 04 p0471 N85-12996
Development of acceptance criteria for batches of silane primer for external tank thermal protection system bonding applications [NASA-CR-171266] 04 p0478 N85-13043
An analysis of the data obtained by a simultaneous observation of GMS and GMS-2: A study of the difference between the brightness temperatures by GMS and those by GMS-2 12 p1894 N85-21888
VISSR infrared calibration by means of calculated radiances 12 p1894 N85-21889
Infrared aerosol absorption index 13 p2110 N85-23147
A brief comparison of Egyptian with West German atmospheric transmission data in the 8 to 11.5 micron waveband [BAE-BT-12829] 15 p2594 N85-25983
Infrared absorption of oxygen complexes in electron-irradiated silicon [FOA-C-30379-E1,E2,E3,E4] 20 p3538 N85-32015

INFRARED ASTRONOMY
Infrared thermal radiation of Venus 02 p0163 N85-11101
Near infrared imaging of Uranus and Neptune 02 p0299 N85-11934
Documentation for the machine-readable version of The Revised AFGL Infrared Sky Survey Catalog (Price and Murdock 1983) [NASA-TM-87377] 03 p0405 N85-12586
IRAS observations of galactic star formation 03 p0442 N85-12813
IRAS observations of external galaxies 03 p0443 N85-12825
Far-infrared line emission from the galaxy [NASA-CR-174186] 04 p0580 N85-13702
SIRTF: The next step [NASA-TM-86663] 07 p1059 N85-16724
Airborne Astronomy Symposium. A symposium commemorating the tenth anniversary of operations of the Kuiper Airborne Observatory [NASA-CP-2353] 08 p1244 N85-17848
The Lear Jet Observatory: Fifteen years of discovery and rebirth 08 p1244 N85-17850
Exploration of the solar system by airborne astronomy 08 p1244 N85-17851
Extreme limb profiles of the Sun at far infrared and submillimeter wavelengths 08 p1244 N85-17852
Airborne observations of comets 08 p1244 N85-17853
Measurements of H2O in Jupiter's atmosphere from 5 microns airborne observations 08 p1244 N85-17854
The 1.5 - 3.5 micron spectroscopy of the Orion H2 source 08 p1246 N85-17864
Far-infrared photometry of low-mass pre-main-sequence stars with broad CO wings 08 p1246 N85-17866
Star formation in globules 08 p1247 N85-17868
Far infrared continuum emission from the galactic center 08 p1248 N85-17876
The 157 micron (C II) luminosity of the galaxy 08 p1248 N85-17877
Variation of oxygen and nitrogen abundances in the galaxy 08 p1248 N85-17878
Far IR observations of the Magellanic clouds 08 p1248 N85-17879
Dust reradiation from NGC 6946 08 p1248 N85-17880
Far infrared spectroscopy of (O III) in M82 08 p1249 N85-17883
Infrared astronomical satellite (IRAS) catalogs and atlases. Explanatory supplement [NASA-CR-174311] 09 p1411 N85-18898
Infrared astronomical satellite (IRAS) catalogs and atlases: Introduction 09 p1412 N85-18899
The IRAS mission 09 p1412 N85-18901
Sky coverage, confusion, completeness and reliability 09 p1412 N85-18906
BIG MAC: A bolometer array for mid-infrared astronomy, Center Director's Discretionary Fund [NASA-TM-86502] 13 p2170 N85-23463
Current ideas on the nature of comets 14 p2435 N85-25017
IRAS observations of active galaxies [NASA-CR-175720] 15 p2668 N85-26463
The infrared astronomical satellite 15 p2668 N85-26464
A new luminosity component in 3C48 [NASA-CR-175840] 17 p3052 N85-28894
Balloon-borne, He-cooled Fourier transform spectrometer for far infrared astronomy [MPE-IR-41] 17 p3053 N85-28899
The 8.3 and 12.4 micron imaging of the Galactic Center source complex with the Goddard infrared array camera [NASA-TM-86225] 19 p3382 N85-30982
Activities report of the Aeronomy Department [G-774-1984] 21 p3633 N85-32569
Evaluation study of mechanical refrigeration systems for application to space missions -- infrared astronomy [SNIAS-1029ACA/LL/V] 22 p3755 N85-33277
Mosaic Infrared Sensor for Space Astronomy (MIRSSA) [NASA-CR-176154] 22 p3786 N85-33456

INFRARED ASTRONOMY SATELLITE
In-orbit experiments on IRAS for application to the ISO satellite [FOK-TR-R-84-057] 03 p0322 N85-12078
IRAS observations of galactic star formation 03 p0442 N85-12813
IRAS observations of external galaxies 03 p0443 N85-12825
High sensitivity, high angular resolution far-infrared photometry from the KAO 08 p1246 N85-17867
Infrared astronomical satellite (IRAS) catalogs and atlases: Explanatory supplement [NASA-CR-174311] 09 p1411 N85-18898
Infrared astronomical satellite (IRAS) catalogs and atlases: Introduction 09 p1412 N85-18899
Satellite description 09 p1412 N85-18900
The IRAS mission 09 p1412 N85-18901
In-flight tests 09 p1412 N85-18902
Data reduction 09 p1412 N85-18903
Flux reconstruction and calibration 09 p1412 N85-
Analysis of processing 09 p1412 N85-
The low-resolution spectra 09 p1413 N85-
The formats of the IRAS catalogs and atlases 09 p1413 N85-
Dynamics of long-period comets 13 p2176 N85-
The infrared astronomical satellite 15 p2668 N85-
IRAS: Space technology from the Netherlands [B8561841] 17 p2908 N85-27
The IRAS end-to-end data system [NLR-MP-83056-U] 17 p3051 N85-
The attitude control model tests for the Infrared Astronomical Satellite (IRAS) [B8580071] 18 p3067 N85-
The 1986 National Aeronautics and Space Administration authorization [GPO-47-635] 24 p4186 N85-

INFRARED DETECTORS
NT FLIR DETECTORS
Moving object detection system using infrared scanning [AD-D011222] 01 p0120 N85-1022
Developments in far-infrared detection techniques [AD-A146290] 03 p0420 N85-128
Preliminary study for an IR-vidicon for the 8 to 14 micron range, phase 1 [BMFT-FB-W-84-025] 05 p0633 N85-140
InAsSb strained-layer superlattices (SLSs) for long wavelength detector applications [DE84-016111] 05 p0732 N85-147
Data handling for the Spectral Radiometer (SPERAD) [FOA-C-30368-E1,E4] 07 p0988 N85-1616
Electro-optical target detection [AD-D011366] 07 p1042 N85-1681
Buried junction enhanced Schottky barrier device [AD-D011399] 07 p1044 N85-168
Study in spurious sensitivity of electronics in space [AD-A148386] 08 p1158 N85-1730
In-flight tests 09 p1412 N85-1890
Elimination of sensor artifacts from infrared data [AD-A149048] 10 p1556 N85-1961
Liquid-phase epitaxial growth of CdTe on HgCdTe [AD-D011482] 10 p1561 N85-196
Quaternary narrow-band semiconductors (HgTe)x (InSb)1-x for far-infrared detectors [AD-A149350] 10 p1562 N85-1965
Aerostructure nondestructive evaluation by thermal field detection. Phase 2: Technique refinement and quantitative determination of flaw detection capabilities [AD-A149622] 12 p1777 N85-2115
Monolithic short wave infrared (SWIR) detector array [NASA-CR-175264] 12 p1874 N85-217
Performance estimate of a reflecting light pipe for infrared detectors [AD-A141269] 13 p2158 N85-23
BIG MAC: A bolometer array for mid-infrared astronomy, Center Director's Discretionary Fund [NASA-TM-86502] 13 p2170 N85-234
Performance of charge-injection-device infrared detector arrays at low and moderate backgrounds [NASA-TM-86667] 15 p2560 N85-257
Low-resolution target classification from a staring infrared sensor [AD-A151690] 15 p2652 N85-26
Simulation of solidification in a Bridgman cell [NASA-CR-175638] 16 p2870 N85-277
Analysis and modeling for thermal focal plane arrays [AD-A153156] 17 p2968 N85-28
The 8.3 and 12.4 micron imaging of the Galactic Center source complex with the Goddard infrared array camera [NASA-TM-86225] 19 p3382 N85-309
Background equatorial astronomical measurements focal plane assembly (refurbished HI STAR SOUTH) [AD-A155215] 21 p3590 N85-321
Absorption and scattering properties of aerosols of aggregated particles in the infrared spectral region [AD-A155475] 21 p3637 N85-32
Bayesian vs MAP multiple model adaptive estimation for field of view expansion in tracking airborne targets [AD-A155466] 21 p3679 N85-32
Enhancing precision of remote temperature sensing data from satellites under cloudy atmospheric conditions 22 p3734 N85-331
Determination of altitude of cloud cover top from Meteor satellite data 22 p3734 N85-331
Mosaic Infrared Sensor for Space Astronomy (MIRSSA) [NASA-CR-176154] 22 p3788 N85-334

INFRARED HORIZON SCANNERS
U HORIZON SCANNERS
U INFRARED SCANNERS

INFRARED IMAGERY
Near infrared imaging of Uranus and Neptune
02 p0299 N85-11934
Image texture study for the operational meteorological satellites NOAA 6 and NOAA 7 and its variation with time. Application to the Beauce region
[ENST-84E009] 05 p0661 N85-14249
An integrated remote sensing approach for identifying ecological range sites — parker mountain
[E85-10050] 07 p0983 N85-16246
Rule-based evidence accrual system for image understanding
[AD-A147836] 07 p1044 N85-16634
The interpretation of SIR-B imagery of surface waves and other oceanographic features using in-situ, meteorological satellite, and infrared satellite data
08 p1143 N85-17212
Evaluation of the radar response to land surfaces and volumes: Examination of theoretical models, target statistics, and applications 08 p1149 N85-17250
Scanning photoacoustic microscopy of aluminum with aluminum oxide, roughness standards and rubber
[AD-A149480] 10 p1441 N85-19081
Civil weather satellite systems
11 p1711 N85-20768
Meteorological and oceanographic support during the Falklands conflict 11 p1712 N85-20769
LANDSAT 4 band 6 data evaluation
[E85-10093] 12 p1874 N85-21755
On the error of typhoon intensity estimation by means of IR Dvorak technique occurring when the eye is very small 12 p1894 N85-21886
A supplement study on the subsynoptic cloud system off the south coast of Japan 12 p1895 N85-21892
Proposed use of system ARGOS with data buoys for calibration of thermal infrared imagery of North British waters for sea surface temperature maps
14 p2240 N85-23889
Hurricane structure and dynamics from stereoscopic and infrared satellite observations and radar data
15 p2594 N85-25988
INPE's line imaging camera: Preliminary results
[INPE-3476-PRE/719] 16 p2787 N85-27194
Technique that uses satellite, radar, and conventional data for analyzing and short-range forecasting of precipitation from extratropical cyclones
[PB85-164994] 16 p2837 N85-27499
Target discrimination using infrared techniques: Theoretical considerations
[AD-A154070] 19 p3350 N85-30762
The 8.3 and 12.4 micron imaging of the Galactic Center source complex with the Goddard infrared array camera
[NASA-TM-86225] 19 p3382 N85-30962
Influence of spatial variability of hydraulic characteristics of soils on surface parameters obtained from remote sensing data in infrared and microwaves
[NASA-TM-77902] 20 p3477 N85-31604
Object identification and manipulation using silhouette moments
[AD-A154755] 21 p3705 N85-33011
Quantizer of images of heat fields obtained by Rubin-type infra-red imagers 22 p3771 N85-33369
Surface cyclogenesis as indicated by satellite imagery
[PB85-191815] 24 p4124 N85-35566
Far-infrared observations of young clusters embedded in the R Coronae Austrinae and RHO Ophiuchi dark clouds
[NASA-TM-86681] 24 p4167 N85-35834
INFRARED INSPECTION
Pulsed photothermal radiometry for remote sensing of spectroscopic and physical properties of thin film
[AD-A149060] 10 p1435 N85-19041
Characterization of the heat source distribution of a typical GTAW welding arc
[DE85-004322] 12 p1861 N85-21670
INFRARED INSTRUMENTS
NT FLIR DETECTORS
NT INFRARED DETECTORS
NT INFRARED INTERFEROMETERS
NT INFRARED SCANNERS
NT INFRARED SPECTROMETERS
NT INFRARED SPECTROPHOTOMETERS
Infrared thermography of burn front propagation in heat powders
[DE85-003307] 10 p1436 N85-19060
An airborne infrared thermal scanning system for easy use on Navy P-3 aircraft
[AD-A149690] 12 p1933 N85-22143
Instrumentation for sensing moisture content of material using a transient thermal pulse
[NASA-CASE-NPO-15493-2] 23 p3933 N85-34373
INFRARED INTERFEROMETERS
A Jamin interferometer to determine the helium abundance in the atmosphere of Jupiter
[BONN-IR-83-17] 12 p1961 N85-22329
Analysis of atmospheric interferometer data
[AD-A150682] 14 p2372 N85-24663
Special topics in infrared interferometry — Michelson interferometer development
[NASA-TM-87472] 17 p3038 N85-28794
SCRIBE data of October 23, 1983 flight
[AD-A154864] 21 p3706 N85-33012
INFRARED LASERS
Thick film radiation detector
[AD-D011211] 01 p0048 N85-10318
Laser diodes for infrared spectroscopy
[BMFT-FB-T-84-131] 05 p0640 N85-14109
Advanced infrared laser modulator development
[NASA-CR-172479] 06 p0862 N85-15479
Upgrading flexible infrared waveguides
[AD-A146763] 07 p0970 N85-16160
Design and testing of a refractive laser beam homogenizer
[AD-A146997] 07 p0970 N85-16162
Far-infrared laser diagnostic on EBT and extreme far-forward laser scattering on ISX
[DE85-001788] 07 p1046 N85-16643
RF fiber optic link
[AD-A148679] 08 p1155 N85-17290
Multilayer reflecting systems based on glassy chalcogenides for infrared lasers
14 p2274 N85-24089
Laser with a hollow copper cathode
[ISL-R-119/83] 14 p2310 N85-24300
Laser induced damage of zinc sulphide
[BAE-BT-13363] 15 p2562 N85-25803
Method and apparatus for high speed, sustained recording of infrared laser beam patterns
[AD-D011585] 15 p2563 N85-25811
Theory of laser-stimulated surface process. 2: A generalized-master-equation approach to energy transfer between an IR laser, an adspecies and phonons
[AD-A153083] 17 p2970 N85-28344
Laser-stimulated vibrational excitation of an adspecies studied by a generalized master equation: Neutral atomic hydrogen on hydrated KCl(001)
[AD-A153665] 18 p3112 N85-29268
Spectroscopic investigation of materials for tunable infrared lasers
[AD-A154124] 19 p3272 N85-30291
Cerenkov maser and Cerenkov laser devices
[AD-A155443] 21 p3592 N85-32324
Infrared laser holography used in fusion plasma studies 21 p3687 N85-32905
INFRARED MASERS
U INFRARED LASERS
INFRARED PHOTOGRAPHY
NT COLOR INFRARED PHOTOGRAPHY
Measurement of shock and induced reaction in rocket propellants by nanosecond infrared radiometry and photography
[DE84-013209] 04 p0482 N85-13070
The need for integrating ground thermal measurements with thermal aircraft imagery 05 p0660 N85-14243
Astronomical applications of new infrared films
07 p0964 N85-16111
Infrared presensitization photography
[AD-A146866] 07 p0967 N85-16139
Measurement of shock induced reaction in rocket propellants by nanosecond infrared radiometry and photography
[AD-P004349] 10 p1456 N85-19173
Infrared presensitization photography
16 p2786 N85-27189
The 8.3 and 12.4 micron imaging of the Galactic Center source complex with the Goddard infrared array camera
[NASA-TM-86225] 19 p3382 N85-30962
Interpretation of multiband photographs made during Telefoto-80 experiment for the purpose of discriminating agricultural crops 22 p3735 N85-33152
INFRARED PHOTOMETRY
Far-infrared photometry of compact extragalactic sources: OJ 187 and BL Lac
[NASA-TM-86022] 04 p0580 N85-13701
Multi-spectral observations of the star formation: The role of far infrared photometry 08 p1245 N85-17859
Far-infrared photometry of low-mass pre-main-sequence stars with broad CO wings 08 p1246 N85-17866
High sensitivity, high angular resolution far-infrared photometry from the KAO 08 p1246 N85-17867
INFRARED RADIATION
NT FAR INFRARED RADIATION
NT NEAR INFRARED RADIATION
A limbus-sensing eye movement recorder
[AD-A144772] 01 p0049 N85-10323
Diagnostics of ionization in air produced by infrared radiation from A pulse CO2 laser
[AD-A145376] 02 p0201 N85-11342
Infrared images of the Uranian rings
02 p0302 N85-11965
Infrared mapping of galaxian centers: Star forming regions with kiloparsec scale sizes
03 p0444 N85-12927
A means of extending streak camera recording into the important 1300-1600 nm wavelength regime: Parametric frequency upconversion
[DE84-015666] 04 p0503 N85-13206
Unidentified IRAS sources: Ultrahigh luminosity galaxies
[NASA-CR-174207] 06 p0872 N85-15537
Upgrading flexible infrared waveguides
[AD-A146763] 07 p0970 N85-16160
Variation in spectral response of soybeans with respect to illumination, view, and canopy geometry
[E85-10040] 07 p0982 N85-16241
SWIR and visible atomic emission from laser-produced oxygen and nitrogen plasmas
[AD-A147526] 07 p1045 N85-16641
Radiation parameterization programs for use in general circulation models
[AD-A148015] 08 p1186 N85-17488
Evidence for non-radiative activity in hot stars
08 p1231 N85-17756
Infrared horizon sensor modeling for attitude determination and control: Analysis and mission experience
[NASA-TM-86181] 10 p1429 N85-19016
Infrared excitation of clusters and ions of atmospheric interest
[DE85-002096] 10 p1516 N85-19564
Elimination of sensor artifacts from infrared data
[AD-A149046] 10 p1556 N85-19814
Liquid-phase epitaxial growth of CdTe on HgCdTe
[AD-D011482] 10 p1561 N85-19846
PMP-1: A coordinated study of the behavior of the middle atmosphere in winter 11 p1654 N85-20421
Distortion of temporal characteristics during parametric up-conversion of ultrashort laser pulses
11 p1717 N85-20803
Absorption of ozone molecules in strong field of tea CO2 injection laser 11 p1718 N85-20808
Evaluation of infrared reflectance as a technique for measuring absorber materials degradation
[DE85-002171] 11 p1729 N85-20874
Infrared modulation of photoluminescence in glow discharge amorphous silicon
[DE85-016993] 11 p1737 N85-20922
New results on PU VUL 11 p1753 N85-21023
The influence on IR emission of engine parameters for an afterburn case. A sensitivity study on NATO infrared air target model (NIRATAM) version: 0.0
[AD-B089311L] 12 p1779 N85-21171
Carbon monoxide adsorption on a platinum electrode studied by polarization modulated FT-IRRAS (Fourier Transform-IR Reflections Adsorption Spectroscopy). Part 1: CO adsorbed in the double layer potential region and its oxidation in acids
[AD-A149751] 12 p1800 N85-21288
Progress on transparent yttria
[AD-P004370] 12 p1827 N85-21484
Infrared material optical damage by rain
[AD-P004372] 12 p1827 N85-21486
Intense, broadband, pulsed I-R source at the National Synchrotron Light Source
[DE84-010542] 12 p1935 N85-22154
Below-room-temperature water-vapor continuum absorption within the 8- to 10 micron atmospheric transmission window
[TR-0084(4945-09)-1] 13 p2132 N85-23268
Measurement of the nighttime infrared luminosity of Spacelab 1 in the H- and K-bands
[NASA-TM-85972] 14 p2434 N85-25011
Low-resolution target classification from a staring infrared sensor
[AD-A151690] 15 p2652 N85-26358
Mechanism of formation of low temperatures in nighttime Venusian thermosphere 16 p2723 N85-26807
Scheme for atmospheric thermal sensing from satellites with enhanced vertical resolution
16 p2726 N85-26823
Analysis and modeling for thermal focal plane arrays
[AD-A153156] 17 p2968 N85-28329
On the definition of topological susceptibility via lattice anomalous Ward identities and its perturbative tail
[PREPRINT-416] 18 p3184 N85-29744
Laser forward and backscattering in particulate media
[AD-A154136] 19 p3275 N85-30312
Comparison of 8 to 12 micrometer and 3 to 5 micrometer CVF transmissometer data with LOWTRAN calculations
[AD-A154218] 19 p3350 N85-30763
Double photon excitation of high-Rydberg atoms as a long-lived submillimeter detector
[NASA-CASE-NPO-16372-1] 19 p3352 N85-30779
Calibration and use of clutter data for simulation
[AD-A154793] 21 p3574 N85-32229

Absorption and scattering properties of aerosols of aggregated particles in the infrared spectral region
[AD-A155475] 21 p3637 N85-32591
Ice fog as an electro-optical obscurant
[AD-A155059] 21 p3705 N85-33015
Solid state radiative heat pump
[DE85-011605] 22 p3760 N85-33303
Search for infrared counterparts of gamma-ray bursters
[OG-1.1-9] 22 p3861 N85-33910
Hercules X-1: Pulsed gamma-rays detected above 150 GeV
[OG-2.2-9] 22 p3865 N85-33935
Further studies of X-ray structure of the Perseus cluster
[OG-2.5-12] 22 p3870 N85-33967
Infrared generation and wave-mixing studies in cesium
[DE85-012663] 24 p4063 N85-35304
Miniature infra-red data acquisition and telemetry system
[NASA-CR-177953] 24 p4096 N85-35390
Electronic structure and lattice dynamics of dimensionally constrained and disordered solids
[AD-A155927] 24 p4161 N85-35797

INFRARED RADIOMETERS
Measurement of shock and induced reaction in rocket propellants by nanosecond infrared radiometry and photography
[DE84-013209] 04 p0482 N85-13070
Comparison of wind derived from the LIMS (Limb Infrared Monitor of the Stratosphere) satellite instrument with rocket observations
[NASA-CR-174083] 04 p0541 N85-13444
Remote sensing of plant stress and diseases
05 p0657 N85-14216
Characterization of jet turbulence using infrared radiometry 11 p1576 N85-19928
Analysis of SMIRR data for volcanic and sedimentary terrains of the trans-Pecos region, Texas
13 p2197 N85-23626

INFRARED REFLECTION
Evaluation of infrared reflectance as a technique for measuring absorber materials degradation
[PB85-108488] 11 p1677 N85-20567
The nature and geometry of infrared reflection nebulae 24 p4167 N85-35835

INFRARED SCANNERS
ISSCP Cloud Algorithm Intercomparison Workshop
01 p0073 N85-10486
Description of the Dutch-Danish (DUDA) scanner — thermal signatures
[AD-B084893] 01 p0121 N85-10826
Infrared-thermal wave scanner for NDE of naval thermal spray coatings
[DE85-002237] 11 p1650 N85-20391
An airborne infrared thermal scanning system for easy use on Navy P-3 aircraft
[AD-A149690] 12 p1933 N85-22143
Thermal infrared observations of lava flows during the 1984 Mauna Loa eruption 13 p2186 N85-23564
Design specifications for IMAGER: The DREO (Defence Research Establishment Ottawa) image processing system
[AD-A151752] 15 p2624 N85-26168
User manual for IMAGER: The DREO (Defence Research Establishment Ottawa) image processing system
[AD-A151754] 15 p2653 N85-26362
Thermal Infrared Multispectral Scanner (TIMS): An investigator's guide to TIMS data
[NASA-CR-175875] 17 p2961 N85-28286
Developments in remote sensing
[B8560069] 17 p2984 N85-28441
Comparison of measurement and simulation results of radiation temperatures applied to the thermal mapping of Munich
[DFVLR-FB-85-06] 17 p2984 N85-28442

INFRARED SPECTRA
Middle infrared spectral studies of geologic materials in their natural state using photothermal beam deflection spectroscopy
[AD-A144894] 01 p0120 N85-10820
Infrared spectroscopy study of the SP-250 epoxy resin system
[AD-A145860] 03 p0337 N85-12167
Spectral components at visual and infrared wavelengths in active galactic nuclei
[NASA-CR-174133] 03 p0445 N85-12832
The Jovian atmospheric window at 2.7 microns: A search for H2S
[NASA-TM-86861] 03 p0445 N85-12836
Development of acceptance criteria for batches of silane primer for external tank thermal protection system bonding applications
[NASA-CR-171266] 04 p0478 N85-13043
Advanced amorphous materials for photovoltaic conversion
[DE84-017198] 04 p0529 N85-13384
Lower atmospheric composition of Jupiter from Voyager infrared measurements
[NASA-CR-174196] 05 p0745 N85-14779
In situ analysis of corrosive and passive surfaces by laser-excited Raman spectroscopy — lead, galvanized iron, and asbestos-cement pipes
[PB84-229756] 06 p0767 N85-14904
Nitriding of titanium and its alloys by N2, NH3 or mixtures of N2 + H2 in a dc arc plasma at low pressures (or = to torr)
[NASA-TM-83803] 06 p0814 N85-15168
Spectral reflectance studies on the orientale region of the Moon 06 p0886 N85-15639
Demonstration of transparent solar array module design
[NASA-CR-174257] 07 p0992 N85-16302
Infrared emission and atomic transitions
[AD-A147840] 07 p1041 N85-16607
Far infrared and submillimeter observations of the giant planets 08 p1245 N85-17856
Mid-infrared spectroscopy of planetary nebulae
08 p1247 N85-17872
Aromatics determination in middle distillate petroleum fractions by spectrophotometric titration
[PNR-90239] 09 p1293 N85-18123
The formats of the IRAS catalogs and atlases
09 p1413 N85-18906
Near infrared modeling of the equatorial regions of Jupiter and Saturn 09 p1415 N85-18930
PCB analysis by capillary gas chromatography coupled with matrix isolation-Fourier transform infrared spectroscopy
[DE84-009201] 10 p1437 N85-19059
Satellite support to the Sierra Cooperative Pilot Project: 1979/80 and 1980/81
[PB85-115079] 10 p1520 N85-19583
Far-infrared line observations of planetary nebulae. 1: The O 3 spectrum
[NASA-TM-86670] 10 p1570 N85-19900
Thermal band characterization of the LANDSAT-4 Thematic Mapper 12 p1869 N85-21727
The effects of atmospheric water vapor on infrared propagation
[AD-A150030] 12 p1934 N85-22150
IRAS observations of Seyfert galaxies
[NASA-CR-175557] 12 p1953 N85-22267
A method for estimating soil moisture availability
[NASA-CR-175806] 13 p2126 N85-23238
Water-ice clouds on Mars: Location and seasonal variation 13 p2194 N85-23611
Reassignment of the iron (3) absorption bands in the spectra of Mars 13 p2195 N85-23614
Participation in the Mars Data Analysis Program: Analysis of cloud forms in Viking and Mariner 9 images
[NASA-CR-175604] 13 p2204 N85-23673
Radiation effects induced in pin photodiodes by 40- and 85-MeV protons
[NASA-CR-175678] 14 p2426 N85-24960
Selection of a model of Earth's albedo radiation, practical calculation of its effect on the trajectory of a satellite
[NASA-TM-77870] 15 p2591 N85-25972
Estimation of convective rainfall from visible and infrared satellite data 15 p2596 N85-25999
Infrared observations of the Uranian rings
15 p2672 N85-26488
A measurement of the vibrational band strength for the upsilon sub 3 band of the HO2 radical
[NASA-CR-175858] 16 p2744 N85-26936
Fourier transform infrared spectrophotometric analysis of resin mix stoichiometry, revision 1
[DE85-007272] 16 p2747 N85-26951
Evaluation of used crankcase oils using computerized infrared spectrometry
[AD-A152993] 17 p2920 N85-27999
Evaluation of used crankcase oils using computerized infrared spectrometry. Appendices
[AD-A152994] 17 p2920 N85-28000
The spectroscopy and reaction kinetics of coordinated unsaturated metal carbonyls
[AD-A153079] 17 p2920 N85-28003
Thermal donor removal by rapid thermal annealing: Infrared absorption
[DE85-010092] 18 p3081 N85-29059
Screening phase transitions in two-dimensional Coulomb gas
[NOTA-INTERNA-830] 18 p3192 N85-29796
Technical and administrative activities of the Analytical Chemistry Laboratory (ACL)
[DE85-010150] 19 p3236 N85-30063
Compatibility, contamination and IR microspectrophotometry
[DE85-010809] 19 p3273 N85-30297
Comparison of 8 to 12 micrometer and 3 to 5
CVF transmissometer data with LOWTRAN
[AD-A154218] 19 p3350
Speciation of hazardous inorganic compounds by
transform infrared (FTIR) spectroscopy
[PB85-186969] 20 p3426
Stress corrosion of ceramic materials
[AD-A155020] 21 p3570
Absorption and scattering properties of
aggregated particles in the infrared spectral
[AD-A155475] 21 p3637
In-cavity laser IR spectrum analyzer for
non-steady-state processes 21 p3685
Voigt line profile computation of infrared lines in
stratosphere and mesosphere
[AERONOMICA-ACTA-A-294-1985]
22 p3813
Acetonitrile in the Earth's atmosphere: An upper
deduced from infrared solar spectra
[AERONOMICA-ACTA-A-295-1985]
22 p3813
FTIR studies of hydrocarbon synthesis on Pd/
catalysts
[DE85-012430] 24 p4071
Infrared generation and wave-mixing studies in
[DE85-012663] 24 p4063

INFRARED SPECTROMETERS
A high transmission, 20 channel polychromator for
Thomson scattering diagnostic of TORTUR 3 —
diagnostics
[REPT-84-156] 03 p0422
Instruments for characterization of carbon black
polymers
[AD-A146475] 06 p0810
Construction of a superheterodyne receiver for
micron waves to be put on a Cassegrain optics
for spectroscopic research on the Mars and
atmospheres
[MPE-183] 06 p0872
GC-FTIR (Fourier Transform Infrared Spectrometry)
jet fuels
[AD-A148272] 08 p1135
The low-resolution spectra 09 p1413
Preliminary evaluation of the airborne
spectrometer for vegetation analysis
[NASA-CR-174440] 10 p1505
Hot spots on Io: Correlation of infrared emission
visible reflectance 13 p2172
Evaluation of used crankcase oils using
infrared spectrometry. Appendices
[AD-A152994] 17 p2920
Balloon-borne, He-cooled Fourier
spectrometer for far infrared astronomy
[MPE-IR-41] 17 p3053

INFRARED SPECTROPHOTOMETERS
Evaluation of used crankcase oils using
infrared spectrometry
[AD-A152993] 17 p2920

INFRARED SPECTROSCOPY
Middle infrared spectral studies of geologic
in their natural state using photothermal beam
spectroscopy
[AD-A144894] 01 p0120
Optical constant determination of thin polymer
the infrared
[AD-A145669] 02 p0287
Properties of the upper tropospheres of Uranus
Neptune derived from observations at
near-infrared wavelengths 02 p0298
The 6th International Summer Institute in
Science 1983)
[AD-A146253] 03 p0434
Development of acceptance criteria for batches of
primer for external tank thermal protection system
applications
[NASA-CR-171266] 04 p0478
Investigations regarding process analysis of
the 1 to 2 micrometer spectral range
[BMFT-FB-T-84-169] 05 p0614
Carbon monoxide study, Anchorage, Alaska,
22, 1982 to February 11, 1983
[PB84-236595] 06 p0673
Polymer-polymer interface bond stability
06 p0830
A study of the chemical interaction of gases
activated carbon
[AD-A147342] 07 p0923
Analysis of Nonvolatile Residue (NVR) from
systems
[NASA-TM-86184] 08 p1113
Modulated surface vibrational
electrode/electrolyte interfaces
[AD-A148665] 08 p1123
Molecular dynamics in nitramines and
nitramines
[AD-A148515] 08 p1220

The Lear Jet Observatory: Fifteen years of discovery and rebirth 08 p1244 N85-17850
Far-infrared spectroscopy of interstellar gas
08 p1245 N85-17858
Mid-infrared spectroscopy of planetary nebulae
08 p1247 N85-17872
Interstellar grain mantles 08 p1247 N85-17874
Far infrared spectroscopy of (O III) in M82
08 p1249 N85-17883
A far infrared Echelle spectrometer for the Kuiper Airborne Observatory 08 p1249 N85-17886
An infrared study of isotopic exchange during methanation over supported rhodium catalysts; an inverse spillover effect
[AD-A148090] 10 p1435 N85-19046
An infrared study of the oxidation of carbon monoxide over supported rhodium catalysts
[AD-A149478] 10 p1436 N85-19050
Water absorption and conductivity in poly(ethylene oxide)-lithium tetrafluoroborate films
[AD-A147989] 10 p1450 N85-19138
Characterization of acetylene-terminated resin cure states
[AD-A149463] 10 p1452 N85-19148
Fundamental study of catalysts using laser Raman, infrared, auger electron spectroscopy and low energy electron diffraction
[DE85-001813] 11 p1595 N85-20033
Middle atmosphere NO and NO2 observed by means of the Spacelab one grille spectrometer
[AERONOMICA-ACTA-A-293-1984]
11 p1680 N85-20588
An infrared study of the dissociation of carbon dioxide over supported rhodium catalysts
[AD-A149613] 12 p1800 N85-21291
Investigation of dynamics of radiation spectrum of injection lasers by infrared impulse Fourier spectroscopy
13 p2090 N85-23047
Spectral reflectance of carbonate minerals and rocks in the visible and near infrared (0.35 - 2.55 microns) and its applications in carbonate petrology
[NASA-CR-175763] 15 p2591 N85-25973
Molecular spectroscopy from the Kuiper Airborne Observatory
[NASA-CR-175748] 16 p2882 N85-27783
Evaluation of used crankcase oils using computerized infrared spectrometry
[AD-A152993] 17 p2920 N85-27999
Evaluation of used crankcase oils using computerized infrared spectrometry. Appendices
[AD-A152994] 17 p2920 N85-28000
Formation and fate of toxic chemicals in California's atmosphere
[PB85-172609] 18 p3134 N85-29414
Lithium cell reactions
[AD-A154429] 19 p3305 N85-30484
Speciation of hazardous inorganic compounds by Fourier transform infrared (FTIR) spectroscopy
[PB85-169969] 20 p3426 N85-31262
Infrared studies of the influence of alkali metals on the C-O bond in chemisorbed carbon monoxide
[DE85-005306] 23 p3911 N85-34232
Time-resolved and infrared spectroscopy of excitons
[DE85-011879] 23 p3912 N85-34235

INFRARED STARS
Documentation for the machine-readable version of The Revised AFGL Infrared Sky Survey Catalog (Price and Murdock 1983)
[NASA-TM-87377] 03 p0405 N85-12588
Compact infrared sources: Protostars before IRAS
03 p0442 N85-12612

INFRARED SUPPRESSION
Airworthiness and flight characteristics test of the RC-12D Guardrail V
[AD-A148046] 08 p1084 N85-16864

INFRARED TELESCOPES
NT SPACE INFRARED TELESCOPE FACILITY
Thermal and cryogenic design study for space infrared telescope facility (SIRTF)
[NASA-CR-166613] 07 p0915 N85-15793
Study of alternate optical and fine guidance sensor designs for the space infrared telescope facility (SIRTF)
[NASA-CR-166614] 07 p0915 N85-15794
Pointing and control system design study for the space infrared telescope facility (SIRTF)
[NASA-CR-166612] 07 p0915 N85-15795
SIRTF: The next step
[NASA-TM-86863] 07 p1059 N85-16724
SIRTF: The next step 08 p1250 N85-17891
The removal, mechanical handling and installation procedures for declination tachometer and Itek encoder — United Kingdom Infrared Telescope
[UKIRT-17] 09 p1414 N85-18915
The mechanical procedures for the 8 channel bolometer — United Kingdom Infrared Telescope
[UKIRT-18] 09 p1414 N85-18916
Procedures for the bonding of the E.M.C. mirror onto its INVAR mirror flange — United Kingdom Infrared Telescope
[UKIRT-19] 09 p1414 N85-18917
In situ washing procedures for the UKIRT 3.8 meter primary mirror — United Kingdom Infrared Telescope (UKIRT)
[UKIRT-20] 09 p1414 N85-18918
The removal, mechanical handling and installation procedures for the RA Itek encoder
[UKIRT-21] 09 p1414 N85-18919
The UKIRT centre section structural investigation — United Kingdom Infrared Telescope (UKIRT)
[UKIRT-22] 09 p1414 N85-18920
UKIRT spectro-photometry system — United Kingdom Infrared Telescope (UKIRT)
[UKIRT-23] 09 p1414 N85-18921
LDR system concepts and technology
14 p2231 N85-23823
Precision antenna reflector structures
14 p2232 N85-23834
Infrared telescope
[NASA-CR-171392] 15 p2668 N85-26465
IRAS: Space technology from the Netherlands
[B8561841] 17 p2908 N85-27929
Long life feasibility study for the shuttle infrared telescope facility
[NASA-CR-3722] 17 p3052 N85-28893
The nature and geometry of infrared reflection nebulae 24 p4167 N85-35835

INFRARED TRACKING
Dual mode radio frequency-infrared frequency system
[AD-D011402] 08 p1081 N85-16850
Elimination of sensor artifacts from infrared data
[AD-A149048] 10 p1556 N85-19614
Presentations at the Tri-Service Cloud Modeling Workshop (2nd), held at the Naval Surface Weapons Center, White Oak, Maryland, 26-27 June 1984, volume 1
[AD-A152735] 17 p2996 N85-28522

INFRARED WINDOWS
High temperature ultra-high vacuum infrared window seal
[AD-D011333] 07 p0929 N85-15890
Continuum absorption by H2O in the 700-1200 cm(-1) and 2400-280 cm(-1) windows
[AD-A147391] 07 p0997 N85-16334

INFRASONIC FREQUENCIES
China report: Science and technology
[JPRS-CST-84-001] 04 p0557 N85-13545
Measurement of infrasonic waves from remotely detonated artificial explosion 04 p0557 N85-13546
Theoretical and observed dispersion of acoustic-gravity waves in atmosphere 04 p0557 N85-13547
Long-distance propagation of infrasound in atmosphere near Earth's surface 06 p0825 N85-15238
Seismic observation of infrasonic signals
[AD-A149574] 12 p1889 N85-21853
Some individual differences in human response to infrasound
[UTIAS-282] 12 p1905 N85-21960
Field of point source of low-frequency sound in atmosphere with altitudinally nonuniform wind
15 p2524 N85-25566

INGESTION (BIOLOGY)
NT EATING

INGESTION (ENGINES)
Temperature distortion generator for turboshaft engine testing
[NASA-TM-83748] 07 p0893 N85-15658
Avoiding serious bird strike incidents
[AD-P004178] 11 p1578 N85-19940
Accidents and serious incidents to civil aircraft due to birstrikes
[AD-P004180] 11 p1578 N85-19942
Birds and aircraft engine strike rates
[AD-P004184] 11 p1579 N85-19946
Review of engine ingestions to wide body transport aircraft
[AD-P004185] 11 p1579 N85-19947

INGOTS
Engineering property comparisons of PM and IM aluminum alloy forgings
[AD-B088146L] 08 p1173 N85-17398
USSR report: Materials science and metallurgy
[JPRS-UMS-84-005] 11 p1597 N85-20044
Effect of ingot structure of failure ductility of pressed semifinished products of high-durability aluminum alloys
11 p1597 N85-20045
Nondestructive testing of stainless steel to improve quality and output efficiency of the processing of ingot and continuous casting
[BMFT-FB-T-84-240] 12 p1808 N85-21345
Mechanisms of corrosion fatigue in high strength I/M (Ingot Metallurgy) and P/M (Powder Metallurgy) aluminum alloys
[AD-A151177] 15 p2509 N85-25478
MPS solidification model. Analysis and calculation of macrosegregation in a casting ingot
[NASA-CR-171589] 21 p3586 N85-32178

INHALATION
U RESPIRATION

INHIBITION (PSYCHOLOGY)
Inhibition of return: Neural basis and function
[AD-A145242] 01 p0098 N85-10652

INHIBITORS
NT WEAR INHIBITORS
Mechanical properties of adhesively bonded aluminum structures protected with hydration inhibitors
[AD-A148123] 08 p1133 N85-17139
Effects of pyridostigmine on psychomotor and visual performance
[AD-A148553] 08 p1196 N85-17539
Adsorption thermodynamics and surface transport of metal catalyst poisons
[DE85-002868] 10 p1441 N85-19084
Corrosion inhibitor formulation for molybdenum, tungsten and other metals
[AD-D011593] 15 p2510 N85-25486
Mechanical properties of adhesively bonded aluminum structures protected with hydration inhibitors
[AD-A153755] 18 p3079 N85-29047
Effect of multi-functional inhibitors on the electrochemistry within corrosion crack
19 p3238 N85-30075
Molecular biology of environmental aromatic hydrocarbons
[DE85-015036] 24 p4128 N85-35593

INHOMOGENEITY
Mechanism of brittle heat fracture of inhomogeneous solids by high temperature gas jets
02 p0265 N85-11731
Crack problems for bonded nonhomogeneous materials under antiplane shear loading
[NASA-CR-172532] 10 p1495 N85-19438
Boundary velocities of longitudinal seismic waves and lateral inhomogeneities of upper ocean mantle
13 p2113 N85-23165
Spreading of greatly extended inhomogeneities in upper ionosphere 14 p2339 N85-24462
Evolution of strong inhomogeneities in ionospheric plasma, part 1 14 p2339 N85-24463
Waves in inhomogeneous media — magnetohydrodynamic waves; solar atmosphere
14 p2449 N85-25116
Structural inhomogeneities in amorphous nickel-phosphorus alloy
[BLL-M-36103-(5828.4)] 16 p2748 N85-26960
Impact of optical inhomogeneity in sintered interface between glasses on laser emission characteristics
16 p2763 N85-27053
Optimum convection conditions for Czochralski growth of semiconductors
[INPE-3395-PRE/665] 16 p2870 N85-27703
Reflection of acoustic beam from inhomogeneous boundary 21 p3680 N85-32864
Relaxation lens in inhomogeneous binary mixture
21 p3695 N85-32957
Vortex dynamics simulation of conserved scalar dissipation 22 p3745 N85-33210
Cosmic ray secondary nuclei and the structure of the galaxy
[OG-7.2-4] 23 p4014 N85-34876

INITIAL VALUE PROBLEMS
U BOUNDARY VALUE PROBLEMS

INITIATION
Computer simulation of the shock initiation of detonation in solid explosives
[PML-1984-23] 01 p0033 N85-10207
Analysis of the natural initiation of vapor explosions
[DE85-000188] 11 p1632 N85-20279
Evidence concerning the generation mechanism of solar type 3 radio bursts 16 p2886 N85-27802
Experimental studies of chemical reactivity during shock initiation of hexanitrostilbene
[DE85-011726] 22 p3754 N85-33270

INITIATORS (EXPLOSIVES)
NT DETONATORS
NT EXPLODING WIRES
Fast response impulse generator
[AD-D011283] 06 p0759 N85-14853
Laser ignition of explosives
[FOA-C-20550-D1] 07 p0972 N85-16173
Study of bridgewire size and pyrotechnic density relationships on all-fire levels
[DE84-016946] 09 p1302 N85-18177
Generation of detonation waves of given spatial and temporal characteristics
[ISL-R-103/83] 16 p2758 N85-27021

Deformation, fracture and explosive properties of reactive materials
[AD-A154073] 19 p3251 N85-30157

INJECTION
NT CARRIER INJECTION
NT DEEP WELL INJECTION (WASTES)
NT FLUID INJECTION
NT FUEL INJECTION
NT GAS INJECTION
NT ION INJECTION
NT LIQUID INJECTION
NT WATER INJECTION
Transonic shock interaction with a tangentially-injected turbulent boundary layer 06 p1072 N85-16796
Simulation of the ion-beam-driven drift instability in a magnetic trap, 2
[AD-A149452] 10 p1554 N85-19796
A new very high voltage semiconductor switch
[NASA-TM-86957] 11 p1627 N85-20246
Mechanisms of exhaust pollutants and plume formation in continuous combustion
[AD-A154169] 20 p3435 N85-31310
The effect of injection-stream turbulence on film cooling effectiveness and heat transfer coefficients
20 p3451 N85-31424
Method of characterizing critical timing paths and analyzing timing related failure modes in very large scale integrated circuits
[AD-D011731] 22 p3759 N85-33298
Computer simulation of integrated injection logic
22 p3767 N85-33349
Method for determining depth and shape of a sub-surface conductive object
[DE85-006502] 23 p3935 N85-34389

INJECTION CARBURETORS
U FUEL INJECTION

INJECTION LASERS
Low-threshold injection lasers on grown GaInPAs/InP heterostructures (1.2-1.6 micrometers wavelengths)
02 p0258 N85-11693
Self-modulation of injection laser emission intensity due to external optical feedback 02 p0261 N85-11706
Spectrally matched modulation of radiation of injection laser in traveling-wave amplifier below 2 GHz
02 p0262 N85-11712
Space-time characteristics of radiation of single-mode injection lasers 02 p0269 N85-11758
Quantum noise effects in single-mode injection lasers
[FUB-11-1984] 09 p1327 N85-18336
The noise of laser diodes with modulated injection current
[FI-465-TBR-23] 11 p1625 N85-20233
Investigation of dynamics of radiation spectrum of injection lasers by infrared impulse Fourier spectroscopy
13 p2090 N85-23047
Injection controlled laser transmitter with twin local oscillators
[AD-D011577] 15 p2563 N85-25810
Injection laser structure design
[AD-A153210] 17 p2971 N85-28345
Definition of requirements for injection locking of pulsed UV lasers
[DE85-010126] 18 p3113 N85-29275
Arrangement for damping the resonance in a laser diode
[NASA-CASE-NPO-15960-1] 19 p3274 N85-30305
Dye laser traveling wave amplifier
[NASA-CR-175969] 19 p3275 N85-30308
Low-threshold injection InGaAsP/GaAs double heterostructure lasers with separate limiting obtained by liquid-phase epitaxy (lambda = 0.76 divided by 0.87 microns, I sub thr = 480 A/cm 2, T = 300 K)
21 p3687 N85-32908
Adjustment of radiation wavelength of multimode InP-GaInAsP injection heterolasers
21 p3688 N85-32913

INJECTION LOCKING
Definition of requirements for injection locking of pulsed UV lasers
[DE85-010126] 18 p3113 N85-29275
Optical injection locking of solid-state oscillators by frequency-multiplexed injection-locked, laser diodes
[AD-D011695] 19 p3275 N85-30307
Dye laser traveling wave amplifier
[NASA-CR-175969] 19 p3275 N85-30308

INJECTION MOLDING
Injection molding of silicon carbide capable of being sintered without pressure
[NASA-TM-77736] 01 p0035 N85-10221
Optimization of the injection process for thermostatic polyether-ether-ketone (Peek) thermoplastics reinforced with short carbon fibers
[SNIAS-842-422-102] 04 p0480 N85-13062

INJECTORS
Finlet injector
[AD-D011245] 06 p0765 N85-14891
Low loss injector for liquid propellant rocket engines
[NASA-CASE-MFG-25980-1] 11 p1591 N85-20006
Oxygen-hydrogen thrusters for Space Station auxiliary propulsion systems
[NASA-CR-175691] 15 p2494 N85-25383
Segmented zoned fuel injection system for use with a combustor
[AD-D011640] 17 p2897 N85-27885
Physiochemically controlled scour jet array system
[AD-D011688] 19 p3308 N85-30505
High-brightness photoemitter development for electron accelerator injectors
[DE85-009548] 19 p3355 N85-30796
Design status of heavy ion injector program
[DE85-010751] 22 p3842 N85-33793
Solid state high power amplifier for driving the SLC injector klystron
[DE85-013063] 24 p4090 N85-35356

INJURIES
NT BAROTRAUMA
NT BURNS (INJURIES)
NT CRASH INJURIES
NT EJECTION INJURIES
NT LESIONS
NT NOISE INJURIES
NT PULMONARY LESIONS
NT RADIATION INJURIES
Establishment of posture and working movements of pilot in air crash enquiries 07 p1010 N85-16417
Fatal hemorrhagic shock and acetate solutions
[AD-A146754] 07 p1014 N85-16444
An investigation of spinal injury potential from the use of the ACES 2 ejection seat by lower weight female pilots
[AD-A148449] 08 p1196 N85-17537
SPH-4 US Army flight helmet performance, 1972 - 1983
[AD-A148674] 08 p1201 N85-17562
Interaction of metals and metalloids with biomembranes
[DE85-004902] 13 p2141 N85-23293
Psychometric evaluation of head injury among fliers referred to the AF School of Aerospace Medicine
[AD-A151479] 15 p2617 N85-26129
Heat injury: Prevention is the key
[AD-A153734] 19 p3328 N85-30622
The helicopter, instrument of choice for health evacuation
[SNIAS-851-220-101] 20 p3393 N85-31051
Design and testing of an energy-absorbing crewseat for the F/FB-111 aircraft, volume 1
[NASA-CR-3916] 23 p3896 N85-34133

INKS
Mod silver metallization for photovoltaics
[NASA-CR-174444] 10 p1509 N85-19518
Use of optical techniques in studies of wear rates of anodized aluminum and polymer coatings on aluminum
14 p2259 N85-23997
Procedure for certifying quantity of volatile organic compounds emitted by paint, ink and other coatings
[PB85-159044] 15 p2520 N85-25537
Ink jet printing of silver metallization for photovoltaics
[NASA-CR-175793] 15 p2586 N85-25943
The replacement of precious metal thick film inks using conductive polymer technology
[AD-A152002] 16 p2749 N85-26965
Ink jet printing of silver metallization for photovoltaics
[NASA-CR-176019] 19 p3343 N85-30720
Ink jet printing of silver metallization for photovoltaics
[NASA-CR-176054] 22 p3805 N85-33569

INLAND WATERS
NT GROUND WATER
Investigation of mineral and thermomineral springs in the Eifel Mountains regarding thermal indications
[BMFT-FB-T-84-019] 02 p0220 N85-11451

INLET AIRFRAME CONFIGURATIONS
Flight and wind-tunnel comparisons of the inlet-airframe interaction of the F-15 airplane
[NASA-TP-2374] 04 p0455 N85-12884
Some aspects of engine and airframe integration for Ramjet and Ramrocket powered missiles
07 p0918 N85-15812
Performance and surge limits of a TF30-P-3 turbofan engine/axisymmetric mixed-compression inlet propulsion system at Mach 2.5
[NASA-TP-2461] 15 p2472 N85-25261

INLET FLOW
Flow rates and pressure profiles for one to four axially alined Borda inlets
[NASA-TP-2390] 05 p0636 N85-14078
Experimental observation of the flow in impellers and diffusers — centrifugal compressors
05 p0636 N85-14080
Effect of steady-state temperature distortion on inlet flow to a high-bypass-ration turbofan engine
[NASA-TM-86896] 07 p0904 N85-15725
Some aspects of engine and airframe integration for Ramjet and Ramrocket powered missiles
07 p0918 N85-15812
Current problems in turbomachinery fluid dynamics
[AD-A147127] 07 p0958 N85-16074
Interest of internal bleed for a two-dimensional air intake operating in a wide Mach number range (1.8-3 plus)
08 p1071 N85-16790
Research and development for semi-spherical inflow control device
[NAL-TR-833] 09 p1281 N85-18080
Determination of total pressure losses in stepped annular diffusers with curvilinear outer walls and uniform velocity field at inlet 09 p1306 N85-18283
A mixed finite difference analysis of the internal and external transonic flow fields of inlets with centerbody
11 p1619 N85-20192
Effects of inlet distortion on a static pressure probe mounted on the engine hub in an F-15 airplane
[NASA-TP-2411] 13 p1974 N85-22384
Experimentally determined characteristics of vortex heaters 13 p2050 N85-22803
Dependents of velocity distribution in exit section of converging channel on shape of inlet channel in regulating valve 14 p2277 N85-24108
Aerodynamic detuning analysis of an unstalled supersonic turbofan cascade
[NASA-TM-87001] 16 p2700 N85-26870
A numerical simulation of the NFAC (National Full-scale Aerodynamics Complex) open-return wind tunnel inlet flow
[NASA-TM-86724] 16 p2700 N85-26872
Flow rate and pressure profiles for 1 to 4 axially alined orifice inlets
[NASA-TP-2460] 16 p2762 N85-27185
SSME turbopump turbine computations
17 p2911 N85-27944
Analysis of physical-chemical processes governing SSME internal fluid flows
[NASA-CR-175893] 17 p2957 N85-28261
Application of computational fluid dynamics to complex inlet ducts
[NASA-TM-87060] 19 p3265 N85-30247

INLET NOZZLES
Heat exchanger
[DE84-014299] 01 p0047 N85-10309
Experimental observation of the flow in impellers and diffusers — centrifugal compressors
05 p0636 N85-14080
Vaned diffusers — in centrifugal compressors
05 p0637 N85-14085
Low solidity cascade diffusers for wide flow range centrifugal blowers 05 p0637 N85-14086
Interest of internal bleed for a two-dimensional air intake operating in a wide Mach number range (1.8-3 plus)
08 p1071 N85-16790
Investigation of heat transfer to a turbine blade cascade using a shock tube
[AD-A153090] 17 p2898 N85-27871
Inspection evaluation and repair of the flawed feedwater nozzle of the 50 MWe Dodewaard GKN boiling water reactor
[ISBN-90-353-0017-3] 17 p2977 N85-28094
Quasi non-intrusive sampling and analysis of gases associated with the boundary layer on the tethered satellite and similar supersonic and hypersonic research vehicle
[NASA-CR-176075] 20 p3407 N85-31140

INLET PRESSURE
Inlet and airframe compatibility for a V/STOL fighter/attack aircraft with top-mounted inlets
[NASA-TM-84252] 01 p0003 N85-10015
Flow rates and pressure profiles for one to four axially alined Borda inlets
[NASA-TP-2390] 05 p0636 N85-14078
Investigation of heat transfer to a turbine blade cascade using a shock tube
[AD-A153090] 17 p2898 N85-27871

INLET TEMPERATURE
Methanol vaporization: Effects on volumetric efficiency and on determination of optimum fuel delivery system
[PB84-243914] 09 p1302 N85-18181
Redistribution of the inlet temperature profile through the SSME fuel turbine 16 p2739 N85-26901
SSME fuel preburner two-dimensional analysis
17 p2911 N85-27943
Onset of freezing in residential air-to-air heat exchangers
[DE85-009960] 19 p3267 N85-30259

INLETS (DEVICES)
U INTAKE SYSTEMS

INLETS (TOPOGRAPHY)
NT BAYOUS

INNER RADIATION BELT
Boundary of modulation diffusion and stochastic instability of high energy protons in inner radiation belt
15 p2482 N85-25316

INOCULATION
Induction of immunity to toxins with anti-idiotypic antibody
[AD-A146793] 07 p1014 N85-16445
Inoculation of non-metallic inclusions in steel 17GS
[BLL-BISI-TRANS-22431-(9022.06)]
17 p2925 N85-28042
Effects of the cooling rate on the structure of the graphite in inoculated irons
[BLL-BISI-TRANS-22305-(9022.06)]
17 p2930 N85-28083
INORGANIC CHEMISTRY
The synthesis, structural characterization and reactions of closo-Rhodacarborane Anions containing a formal d8 metal vertex 1,2
[AD-A149640] 12 p1799 N85-21285
Abstracts of the 36th Southeastern Regional Meeting of the American Chemical Society
[AD-A151506] 15 p2496 N85-25394
Basic research in novel inorganic reagents and fluorocarbon chemistry
[AD-A155340] 21 p3564 N85-32165
INORGANIC COATINGS
NT ANODIC COATINGS
NT CERAMIC COATINGS
INORGANIC COMPOUNDS
NT AMMONIA
NT LIQUID AMMONIA
Structure of vibrational spectrum and selection rules in Raman and hyper-Raman light scattering spectra of inorganic glasses 02 p0271 N85-11769
USSR report: Chemistry
[JPRS-UCH-84-012] 06 p0761 N85-14865
High capacity inorganic oxyhalide electrochemical cell
[AD-D011321] 07 p0923 N85-15845
Preliminary report on the results of hydrological measurements in the southern Tyrrhenian Sea, in the Messina strait and in the western Ionian sea
[PREPRINT-433] 14 p2382 N85-24693
Chemicals identified in human biological media, a data base, volume 6, part 1
[DE85-008768] 17 p2999 N85-28542
Aerobic sulfur-oxidizing bacteria: Environmental selection and diversification 21 p3656 N85-32712
Anaerobic microbial transformations in subsurface environments: Project description
[DE85-012789] 23 p3951 N85-34486
INORGANIC NITRATES
NT AMMONIUM NITRATES
NT HYDRAZINE NITRATE
NT SODIUM NITRATES
INORGANIC PEROXIDES
NT HYDROGEN PEROXIDE
The use of superoxide mixtures as air-revitalization chemicals in hyperbaric, self-contained, closed-circuit breathing apparatus
[NASA-TM-86709] 20 p3512 N85-31831
Improved oxygen sources for breathing apparatus
[NASA-TM-86671] 24 p4134 N85-35623
INORGANIC SULFIDES
NT BARIUM SULFIDES
NT CADMIUM SULFIDES
NT CALCIUM SULFIDES
NT COPPER SULFIDES
NT HYDROGEN SULFIDE
NT MOLYBDENUM DISULFIDES
NT POLYSULFIDES
NT ZINC SULFIDES
INPUT
Determination of the input-output characteristics of time-invariant memoryless nonlinear devices
[FUB-41-1983] 01 p0100 N85-10667
Theory of diaphragm light modulators with electrical input signal 13 p2082 N85-23002
Gyrator frequency selectors with bandwidth independent of input signal level 13 p2083 N85-23009
Multivariable statistical modelling and its application
16 p2857 N85-27617
A study of error rates in voice recognition
[AD-A153282] 17 p2949 N85-28211
The touch panel system: Design and development
[AD-A153014] 17 p3008 N85-28596
A comparison of numeric data entry with touch-sensitive and conventional numeric keypads
[AD-A153276] 17 p3008 N85-28598
Frequency-spreading coupler
[AD-D011683] 19 p3259 N85-30200
Bayesian factor analysis
[AD-A154184] 19 p3347 N85-30747
Microwave SAW (Surface Acoustic Wave) monochromator
[AD-D011718] 21 p3590 N85-32311
Visibility and vertical structure measurements in southern Germany
[AD-A154714] 21 p3635 N85-32574
Issues and techniques in touch-sensitive tablet input (executive summary) 23 p3960 N85-34543
Aspects of input signal design for order and parameter estimation in linear dynamical systems
[ER-83/05] 24 p4091 N85-35382
Software maintenance relating to the input translator and z-80 realization volume of the computer systems design environment
[AD-A155849] 24 p4138 N85-35646
INPUT/OUTPUT ROUTINES
THLL (TRIDENT Higher Level Language) reference manual
[AD-A145118] 01 p0104 N85-10696
Input-output stability analysis with magnetic hysteresis non-linearity: A class of multipliers
[AD-A145729] 02 p0253 N85-11654
NATFREQ users manual: A FORTRAN 4 program for computing natural frequencies, mode shapes and drag coefficients for taut strumming cables with attached masses and spring-mass combinations
[AD-A146058] 03 p0407 N85-12600
Investigative findings of image enhancement techniques
[AD-A148392] 06 p0853 N85-15424
High altitude chemically reacting gas particle mixtures. Volume 3: Computer code user's and applications manual — rocket nozzle and orbital plume flow fields
[NASA-CR-171828] 07 p0917 N85-15803
Console I/O routines
[DE85-002644] 11 p1702 N85-20700
New enhancements in April 85 NASTRAN release
15 p2573 N85-25864
Sample problems for STAGSC-1
[AD-A153142] 17 p3012 N85-28621
Complete development and implement AFIT/ENG database management system, volume 1
[AD-A153043] 17 p3048 N85-28866
An interactive computer aid for the design and analysis of linear, single input/single output digital and continuous control systems
[AD-A153704] 18 p3162 N85-29580
MC TRICOMP user's guide
[AD-A154339] 19 p3337 N85-30673
BP (Basic Processor) TRICOMP user's guide
[AD-A154340] 19 p3337 N85-30674
VAX TRICOMP user's guide
[AD-A154341] 19 p3337 N85-30675
Flight control system for a computer controlled aircraft with limited sensors
[AD-A155107] 21 p3555 N85-32115
Flexible satellite communications systems simulator, phase 3
[AD-A155647] 21 p3577 N85-32247
INSAT SATELLITES
U INDIAN SPACECRAFT
INSECT DAMAGE
U INFESTATION
INSECTICIDES
NT DDT
NT URETHANES
INSECTS
NT LARVAE
Radiobiological studies on egg systems exposed to heavy nuclei of cosmic galactic radiation — insects
05 p0690 N85-14440
Unsteady separated flows: Generation and use by insects
[AD-P004168] 09 p1266 N85-17953
Irradiation of northwest agricultural products
[DE85-012455] 22 p3843 N85-33603
Effects of microgravity and hypergravity on invertebrate development 24 p4126 N85-35579
Report of the Insect Development Group
24 p4127 N85-35584
INSENSITIVITY
U SENSITIVITY
INSERTION
Electronic module insertion and retraction mechanism
[AD-D011309] 07 p0947 N85-16002
Developments in gas metering technology
[ERS-E.348] 09 p1321 N85-18307
INSERTION LOSS
Fiber optic expanded beam connector
[AD-A154057] 19 p3367 N85-30880
INSERTS
NT NOZZLE INSERTS
Method of testing carbide inserts for premature fracture by face milling of cylindrical workpieces
09 p1303 N85-18183
Ultrasonic test evaluation of the insert bond on hermetic connectors
[DE85-008394] 18 p3120 N85-29310
INSHORE ZONES
U BEACHES
INSOLATION
Solar energy resource assessment in Eastern New Mexico and solar and wind energy resource assessment in Eastern New Mexico
[DE84-901511] 04 p0527 N85-13370
Global radiation in West Germany — solar generators
05 p0662 N85-14253
Weather data for simplified energy calculation methods. Volume 3. Western United States: TRY data
[DE85-000495] 09 p1358 N85-18540
Weather data for simplified energy calculation methods. Volume 1. Eastern United States: TRY data
[DE85-000493] 09 p1358 N85-18541
Weather data for simplified energy calculation methods. Volume 2: Middle United States. TRY data
[DE85-00[illegible]94] 11 p1687 N85-20606
Some solar dish/heat engine design considerations
[DE85-003479] 12 p1881 N85-21802
Evaluation of satellite derived estimates of solar radiation
[E85-10067] 14 p2346 N85-24507
Screening ceramic materials for intense radiant heat applications
[DE85-006989] 16 p2756 N85-27006
The influence of global dust storms on the mean seasonal daily insolations at the Martian surface
[AERONOMICA-ACTA-A-289-1984]
18 p3203 N85-29868
View-limiting shrouds for insolation radiometers
[NASA-CR-176041] 20 p3458 N85-31476
Insolation changes on Pluto caused by orbital element variations
[AERONOMICA-ACTA-A-290-1984]
20 p3546 N85-32070
Improved Nominal Operating Cell Temperature (NOCT) test procedure 21 p3612 N85-32449
Resource evaluation and site selection for microalgae production systems
[DE85-008807] 23 p3951 N85-34485
INSPECTION
NT INFRARED INSPECTION
NT X RAY INSPECTION
Advanced blade tip seal system, volume 2
[NASA-CR-167851] 02 p0147 N85-10999
Modernization of IDTs-6 ultrasonic installation
[BLL-M-35716-(5828.4)] 02 p0206 N85-11356
Procedures for precap visual inspection
[NASA-RP-1122] 04 p0495 N85-13156
Nondestructive inspection: Improved capabilities of technicians
[AD-A147388] 07 p0975 N85-16196
Mobile accelerator neutron radiography system
[AD-A148608] 09 p1323 N85-18311
Ultrasonic inspection of alloyed tungsten bars
[AD-A148900] 10 p1495 N85-19435
Electromagnetic inspection of wire ropes using sensor arrays
[AD-A149016] 10 p1495 N85-19436
Application of hysteresis modelling to the non-destructive inspection of stress
[DE85-003081] 11 p1650 N85-20393
Aerostructure nondestructive evaluation by thermal field detection. Phase 2: Technique refinement and quantitative determination of flaw detection capabilities
[AD-A149622] 12 p1777 N85-21155
The state of the art in printed wiring board inspection
[AD-A149671] 12 p1862 N85-21679
Sizing capability of automated ultrasonic time-of-flight diffraction in thick section steel and aspects of reliable inspection in practice
[AERE-R-11548] 15 p2571 N85-25855
Magnetic flux leakage inspection: Principles and applications
[BLL-BISI-TRANS-22248-(9022.06)]
17 p2975 N85-28382
Inspection of welds and the factors improving its effectiveness in welded structure fabrication
[BLL-BISI-TRANS-22194-(9022.06)]
17 p2976 N85-28387
Effects of inspection errors on curtailed Dorfman-type procedures
[AD-A152376] 17 p3024 N85-28699
Statistical effects of imperfect inspection sampling. Part 2: Double sampling, link sampling and grading
[AD-A152377] 17 p3024 N85-28700
Production verification of the acoustic emission weld monitor
[AD-A154168] 20 p3464 N85-31519
In-service supervision of a pressurized concrete pressure vessel
[OEFZS-4308] 20 p3470 N85-31564
Infrared laser holography used in fusion plasma studies 21 p3687 N85-32905
Corrosion management strategies for aircraft and related systems 22 p3749 N85-33239

Relating corrosion maintenance to environmental factors 22 p3750 N85-33247
Towards the year 2000: Developments in inspection and product assurance to be anticipated during the next 15 years — aircraft engines
[PNR-90258] 23 p3940 N85-34421
National program for inspection of non-federal dams. Woodward reservoir dam (VT 00209), Connecticut River Basin, Plymouth, Vermont. Phase 1 inspection report
[AD-A156256] 24 p4144 N85-35693

INSTABILITY
U STABILITY

INSTALLATION
U INSTALLING

INSTALLATION MANUALS
Installation, maintenance and operating manual for the Lucas-type fuel injection system of the 3 B rotary engine
[NASA-TM-77872] 15 p2568 N85-25846

INSTALLING
Automated installation methods for photovoltaic arrays 2
[SAND-84-7035] 02 p0222 N85-11453
Installation options for the NAVSTAR global positioning system in surface ships
[AD-A148190] 08 p1082 N85-16856
The removal, mechanical handling and installation procedures for the RA Ilek encoder
[UKIRT-21] 09 p1414 N85-18919
Plasma arc welding, equipment, installation and process control
[DE85-008481] 19 p3373 N85-30921

INSTANTONS
Stability questions for gravity in 4 and higher dimensions 05 p0734 N85-14716
Strong-coupling approximations
[DE85-007829] 19 p3353 N85-30785

INSTITUTIONS
Model research: The National Advisory Committee for Aeronautics, 1915-1958, volume 1
[NASA-SP-4103-VOL-1] 14 p2207 N85-23683
Model research, the National Advisory Committee for Aeronautics, 1915-1958, volume 2
[NASA-SP-4103-VOL-2] 14 p2207 N85-23684

INSTRUCTION SETS (COMPUTERS)
System of microprocessor instructions 22 p3770 N85-33362

INSTRUCTIONS
U EDUCATION

INSTRUCTORS
Ada (trademark) training curriculum. Advanced Ada topics L305 teacher's guide exercises
[AD-A154621] 21 p3670 N85-32798

INSTRUMENT APPROACH
Realistic localizer courses for aircraft instrument landing simulators
[NASA-CR-172333] 04 p0455 N85-12885
Safety recommendation(s), A-84-123 and -124
[REPT-3694B/93] 15 p2486 N85-25222

INSTRUMENT COMPENSATION
NT TEMPERATURE COMPENSATION
Compensation of skew passband of a SAW filter using predistortion 12 p1821 N85-21422
Sphericity gauge for wavefront of laser radiation 14 p2275 N85-24096
The use of a self-compensated magnetometer in an economical navigation system for the helicopter 16 p2697 N85-26650
Development of a prototype energy meter
[PB85-196430] 22 p3789 N85-33476
The final COS-B database: In-flight calibration of instrumental parameters
[OG-9.3-9] 23 p4028 N85-34964

INSTRUMENT DRIFT
U DRIFT (INSTRUMENTATION)

INSTRUMENT ERRORS
Problem of reduction to ideal wind tunnel in experimental aerodynamics 02 p0260 N85-11702
Minimization of anomalous errors in measuring systems employing search and testing devices 03 p0344 N85-12219
Buckling and eccentricity effects on orifice metering accuracy — gas meters
[ERS-E.350] 09 p1324 N85-18321
An experimental investigation into the effects of plate eccentricity and elastic deformation on orifice meter accuracy
[ERS-E.391] 09 p1325 N85-18325
On the application of compatibility checking techniques to dynamic flight test data
[ARL/AERO-R-161] 12 p1776 N85-21151
On the wind error of the Finnish raingauge
[REPT-37] 12 p1893 N85-21883

INSTRUMENT FLIGHT RULES
National airspace review: Airport radar service area operational confirmation report
[DOT/FAA/AT-84/2] 07 p0901 N85-15707
A guide to USAF helicopter instrument flight procedures
[AD-A156102] 24 p4063 N85-35182

INSTRUMENT LANDING SYSTEMS
NT ALL-WEATHER LANDING SYSTEMS
NT AUTOMATIC LANDING CONTROL
Use of microprocessor techniques and new antenna systems to improve the navigation aids very high frequency omnidirectional radar (VOR), Doppler VOR and Instrument Landing System (ILS)
[BMFT-FB-W-84-026] 02 p0137 N85-10930
Realistic localizer courses for aircraft instrument landing simulators
[NASA-CR-172333] 04 p0455 N85-12885
Investigation of pilot behavior in flight tests with a rate command/attitude hold control system
[DFVLR-FB-84-25] 05 p0699 N85-14486
Measurement of signal separation between radio service and air navigation service
[IRT-TB-B-40/82] 08 p1083 N85-16860
A preliminary investigation of handling qualities requirements for helicopter instrument flight during decelerating approach maneuvers and overshoot
[AD-A154650] 21 p3557 N85-32125

INSTRUMENT ORIENTATION
The design, fabrication and delivery of a spacelab neutral buoyancy Instrument Pointing System (IPS) mockup — underwater training simulator
[NASA-CR-171233] 04 p0462 N85-12934
Operational experience with ion concentration sensors in orientation systems 13 p1980 N85-22422
Evaluating accuracy in orientation of topographic photograph and satellite-centered direction from star photograph 13 p1983 N85-22442
Mobile antenna and beam pointing studies for satellite mobile communications
[NASA-CR-175736] 15 p2540 N85-25679
Modeling and analysis of pinhole occulter experiment: Initial study phase
[NASA-CR-175976] 19 p3272 N85-30287

INSTRUMENT PACKAGES
Recommended improvements for second generation 121.5/243 MHz ELT's
[NASA-CR-175274] 08 p1080 N85-16841

INSTRUMENT RECEIVERS
Development of a 20/30 GHz receiving station for propagation experiments with L-SAT
[AD-A148261] 08 p1152 N85-17271

INSTRUMENTAL ANALYSIS
U ANALYZING
U AUTOMATION

INSTRUMENTATION
U INSTRUMENTS

INSTRUMENTS
HOST instrumentation R and D program overview 02 p0141 N85-10957
Magnetospheric plasma studies using data from the dynamics high and low altitude plasma instruments
[AD-A145751] 03 p0392 N85-12505
Instrumentation technology overview 16 p2739 N85-26903

INSULATING MATERIALS
U INSULATION

INSULATION
NT ELECTRICAL INSULATION
NT MULTILAYER INSULATION
NT THERMAL INSULATION
Manifold insulated with knitted impregnated sleeve
[AD-D011270] 06 p0814 N85-15167
Passive storage technologies 08 p1108 N85-17003
Effect of sealants of the sound absorption coefficients of acoustical friable insulating materials
[AD-A148541] 08 p1218 N85-17674
High voltage RF coaxial cable
[AD-D011493] 11 p1629 N85-20255
Advanced glazings research
[DE85-000539] 11 p1674 N85-20549
International Conference on Defects in Insulating Crystals
[AD-A149611] 12 p1939 N85-22180
Optimization of overall dimensions of enclosures for low-voltage devices and equipment 13 p2087 N85-23033
AlN insulator for 3-5 MIS applications
[AD-A150674] 14 p2426 N85-24962
Theory and calculations of the electronic structure of solids having directional bonding
[AD-A151062] 14 p2428 N85-24971
Electrical research on solar cells and photovoltaic materials
[NASA-CR-175699] 15 p2585 N85-25935
Theoretical studies on the structures of insulating and metallic glasses
[DE85-010022] 18 p3194 N85-29814
Processable and stable conductive polymers
[AD-D011684] 19 p3249 N85-30148
Method for the preparation of photochromic insulating crystals
[DE85-011606] 19 p3262 N85-30223
A numerical solution of a nonisothermal wall using the two-dimensional Navier-Stokes equations
[AD-A154467] 19 p3266 N85-30257
Basic cryogenics and materials. Phase 1
[NASA-CR-177932] 21 p3572 N85-32216
Induction motors with minimum waste of magnetic iron 22 p3772 N85-33377
Results of variable enthalpy tests of CPR-488 TIP panels in MSFC Hot Gas Facility
[NASA-CR-170889] 24 p4072 N85-35227
Development and characterization of carbon-bonded carbon fiber insulation for radioisotope space power systems
[DE85-013365] 24 p4082 N85-35289
Injector losses on Mite
[DE85-012356] 24 p4090 N85-35355
Laser and electron beam processing of semiconductors
[AD-A155914] 24 p4161 N85-35796

INSULATORS
Optimized conditions for the formation of buried insulating layers in Si by high dose implantation of oxygen
[DE84-015369] 02 p0288 N85-11862
Effect of doping on the voltage holdoff performance of alumina insulators in vacuum
[DE84-017163] 04 p0480 N85-13080
Development of power system management
[PB84-216530] 04 p0497 N85-13173
Technology status of thermionic fuel elements for space nuclear power 05 p0610 N85-13860
Method for bonding insulator to insulator
[AD-D011340] 07 p0929 N85-15881
Moisture absorbing anti-arcing coating and method for applying same
[AD-D011310] 07 p0932 N85-15904
Dispersed metal-toughened ceramics and ceramic brazing
[NASA-CR-174284] 07 p0933 N85-15916
Two carrier dual injector apparatus
[AD-D011357] 07 p1047 N85-16646
Determination of threshold and maximum operating electric stresses for selected high voltage insulation. Task 3: Investigation of high voltage capacitor insulation
[DE84-017051] 09 p1316 N85-18274
Optical studies of dynamical processes in disordered materials
[DE85-002400] 10 p1453 N85-19158
Self-consistent simulation of plasma interactions with secondary-emitting insulators 13 p1993 N85-22482
Investigation of charge transport in the thermoelectric state of some ceramics and glasses
[DE85-009318] 17 p2936 N85-28122
Field theory of the metal-insulator transitions in restricted symmetries
[NOTA-INTERNA-829] 18 p3196 N85-29828
Fluorescence quenching by metal semiconductor and insulator surfaces 19 p3374 N85-30929
Predamage threshold electron emission from insulator and semiconductor surfaces
[DE85-008968] 19 p3377 N85-30954
Nuclear responses in INTOR plasma stabilization elements
[DE85-010489] 20 p3535 N85-31895
Metal-insulator-metal models of tunneling 20 p3536 N85-32008
Electronic structure and lattice dynamics of dimensionally constrained and disordered solids
[AD-A155927] 24 p4161 N85-35797

INSULIN
Investigation of adaptive distinctions of mechanism of controlled glycemia in Macaca rhesus monkeys 12 p1902 N85-21946

INTAKE SYSTEMS
NT AIR INTAKES
NT ENGINE INLETS
NT INLET AIRFRAME CONFIGURATIONS
NT SUPERSONIC INLETS
Inlet and airframe compatibility for a V/STOL fighter/attack aircraft with top-mounted inlets
[NASA-TM-84252] 01 p0003 N85-10015
A study of bird ingestions into large high bypass ratio turbine aircraft engines
[DOE/FAA/CT-84/13] 01 p0005 N85-10028
Developed turbulent flow under conditions of internal and external problems 02 p0260 N85-11700
Flow rates and pressure profiles for one to four axially alined Borda inlets
[NASA-TP-2390] 05 p0636 N85-14079

Applications of finite and wave envelope element approximations to acoustic radiation from turbofan engine inlets in flight
05 p0726 N85-14664

Continuous laminar smoke generator
[NASA-CASE-LAR-13014-1] 12 p1781 N85-21176

The role of convective perturbations in supercritical inlet oscillations
13 p2004 N85-22563

Performance and surge limits of a TF30-P-3 turbofan engine/axisymmetric mixed-compression inlet propulsion system at Mach 2.5
[NASA-TP-2461] 15 p2472 N85-25261

Multi-ducted inlet combustor research and development
[AD-A153753] 18 p3063 N85-28946

An experimental investigation of fuel regression rate control in solid fuel ramjets
[AD-A154251] 19 p3227 N85-30008

Investigation of the behavior of fuel in the intake manifold and its relation to SI engines, 1980 - 1983
19 p3279 N85-30337

Calculation of compressible flow about three-dimensional inlets with auxiliary inlets, slats and vanes by means of a panel method
[NASA-CR-174975] 24 p4060 N85-35162

INTEGERS

Formats for numerical and textual data in data processing
[DFVLR-MITT-84-07] 04 p0551 N85-13504

VLSI architectures for the multiplication of integers modulo a Fermat number 05 p0624 N85-13993

Techniques for computing the DFT using the residue Fermat number systems and VLSI
16 p2770 N85-27097

INTEGRAL CALCULUS

On the integral representation of bisubharmonic functions in Rn 10 p1536 N85-19684

INTEGRAL EQUATIONS
NT FREDHOLM EQUATIONS
NT J INTEGRAL
NT SINGULAR INTEGRAL EQUATIONS
NT VOLTERRA EQUATIONS
NT WIENER HOPF EQUATIONS

Integral equation of lifting surfaces in Laplace domain and analytic continuation of its pressure kernel
[NAL-TR-795T] 01 p0002 N85-10009

Spline-Galerkin solution of integral equations for 3-body scattering above break-up
[TWISK-327] 01 p0109 N85-10738

An integral method for analyzing incompressible two dimensional turbulent boundary layers with separation
02 p0196 N85-11309

Applications of integral equations with strong singularities in fracture mechanics
03 p0371 N85-12367

Loeb Sobolev spaces with applications to variational integrals and differential equations
[CTH-MATH-1984-19] 04 p0556 N85-13544

A theoretical design method for 3-dimensional transonic wings
[NAL-TR-830] 06 p0754 N85-14834

Analytic and sequential feynman integrals on abstract Wiener and Hilbert spaces, and A Cameron-Martin formula. Revision
[AD-A146969] 07 p1030 N85-16537

Single integral constitutive equations for viscoelastic fluids
[AD-A149410] 10 p1547 N85-19756

Algebraic decay in self-similar Markov chains
[DE85-003162] 11 p1707 N85-20740

Evaluation of resonant modes in isolated dielectric resonators using a surface integral equation formulation
[PB85-110831] 12 p1837 N85-21528

Noise transmission loss of a rectangular plate in an infinite baffle
[NASA-TP-2396] 12 p1927 N85-22109

Magnetostatic-wave propagation in a finite YIG-Loaded rectangular waveguide
[AD-A150332] 13 p2055 N85-22865

Axisymmetric magnetofluidistatic (MFS) equilibria of solar coronal loops: An integral equation approach
14 p2449 N85-25118

On the relation between upwind-differencing schemes of Godunov, Engquist-Osher and Roe
[NASA-CR-175805] 16 p2652 N85-27583

On Long's solution to hydrostatic flow over mountains
[DFVLR-MITT-84-02] 17 p2994 N85-28503

Quantized Hall effect in two-dimensional electron systems
[AD-A154347] 19 p3259 N85-30211

Solving Volterra integral equations with ODE codes
[DE85-011216] 19 p3346 N85-30740

A cracked orthotropic sheet stiffened by a semi-infinite orthotropic sheet
[NASA-TP-2455] 21 p3597 N85-32339

Some properties of Loeb-Sobolev spaces
[CTH-MATH-1985-01] 22 p3835 N85-33748

Integral equation formulation for three-dimensional unsteady transonic flow
[ARL/STRUC-R-416] 23 p3894 N85-34119

Nonlinear adhesive behavior effects in a cracked orthotropic sheet stiffened by a semi-infinite orthotropic sheet
[NASA-TM-87584] 23 p3941 N85-34426

A new method of differential structural analysis of gamma-family basic parameters
[HE-3.6-3] 24 p4184 N85-35952

INTEGRAL FUNCTIONS
U ENTIRE FUNCTIONS

INTEGRAL TRANSFORMATIONS
NT CONVOLUTION INTEGRALS
NT FAST FOURIER TRANSFORMATIONS
NT FOURIER TRANSFORMATION
NT HILBERT TRANSFORMATION
NT LAPLACE TRANSFORMATION

Simplified proofs of some basic theorems for quasiregular mappings 10 p1535 N85-19677

The Gauss-Krueger projection of the Earth ellipsoid with direct calculation of elliptic integrals through Landen transformations
[SER-C-296] 11 p1666 N85-20495

A note on the use of polynomial transformations in evaluating singular integrals
[MATHEMATICS-RESEARCH-165]
12 p1920 N85-22053

The implementation of the Tanh transformations in the evaluation of singular integrals
[MATHEMATICS-RESEARCH-171]
12 p1920 N85-22054

Uniform asymptotic expansions of integrals
[CWI-AM-R8412] 17 p3022 N85-28694

Dynamical systems and numerical integration
[CWI-AM-R8413] 17 p3022 N85-28695

Spectral transform approach to Backlund transformations
[PREPRINT-420] 18 p3172 N85-29663

On the solution for the sound field in a semi-infinite uniform duct with sheared mean flow
20 p3523 N85-31912

INTEGRALS

Recursive calculation of curved finite element stiffness matrices
[CSIR-TWISK-303] 01 p0108 N85-10726

An integral inequality with applications to order statistics
[AD-A145081] 01 p0113 N85-10770

Integral of wave kinetic equation of drift waves
02 p0283 N85-11848

Analytic and sequential feynman integrals on abstract Wiener and Hilbert spaces, and A Cameron-Martin formula. Revision
[AD-A146969] 07 p1030 N85-16537

On the distribution of integral and prime divisors with equal norms 11 p1696 N85-20669

Supermanifolds and Berezin's new integral
[DE85-001833] 11 p1706 N85-20732

Translational and extensional energy release rates (the J- and M-integrals) for a crack layer in thermoelasticity
[NASA-CR-174872] 12 p1863 N85-21685

An integral representation of the generalized Euler-Mascheroni constants
[NASA-TP-2456] 13 p2144 N85-23305

Study of integral and spectral direct solar radiation over Atlantic 14 p2341 N85-24475

On the boundary behaviour of a rotation automorphic function with finite spherical Dirichlet integral
15 p2634 N85-26238

A remark on the conformal capacity of Groetzsch's condenser in space 15 p2634 N85-26240

Extrapolation methods for multi-dimensional quadrature of singular and regular integrand functions
[DE85-009665] 18 p3172 N85-29655

Admissible convergence of Poisson integrals in symmetric spaces
[CTH-MATH-1985-04] 22 p3836 N85-33750

Applications of the Kirchoff-Helmholtz integral to problems in body wave seismology
24 p4116 N85-35515

INTEGRATED CIRCUITS
NT LARGE SCALE INTEGRATION
NT TTL INTEGRATED CIRCUITS
NT VERY LARGE SCALE INTEGRATION
NT VHSIC (CIRCUITS)

RADC/NBS (Rome Air Development Center/National Bureau of Standards) Workshop. Moisture Measurement and Control for Semiconductor Devices, 3
[PB84-219569] 01 p0051 N85-10337

Hardware implementation of a support system for the 2501 Western digital LSI, complete controller of the second level, first version of the CCITT 25 (CAP) recommendations
[FUB-60-1982] 01 p0100 N85-10666

Cosmic ray effects on microelectronics. Part 3: Propagation of cosmic rays in the atmosphere
[AD-A145026] 01 p0131 N85-10902

Microwave susceptibility experiments
[DE84-016188] 02 p0192 N85-11281

Investigation of the application of the marginal tension technique to test electronic devices, phase 3
[ESD-11-301] 02 p0206 N85-11380

Guided-wave optic devices for integrated optic information processing
[AD-A145695] 02 p0280 N85-11827

Influence of aluminum oxide film on thermocompression bonding of gold wire to evaporated aluminum film
[NASA-TM-77503] 03 p0330 N85-12127

West Europe report: Science and technology, no. 166
[JPRS-84845] 03 p0341 N85-12190

Integrated circuits, MBM's, form focus of work at French LETI 03 p0341 N85-12194

Problems in CEMA microelectronic cooperation noted
03 p0341 N85-12196

Numerical investigation of diffraction models of microwave integrated circuits 03 p0347 N85-12233

Functional checking of microprocessors and microprocessor systems 03 p0347 N85-12236

Basic EMC (Electromagnetic Compatibility) technology advancement for C3 systems, macromodeling of digital circuits, volume 2B
[AD-A146333] 03 p0359 N85-12306

VLSI (Very Large Scale Integration) design tools reference manual, release 1.0
[AD-A146273] 03 p0408 N85-12604

Research activities of the Illinois University Coordinated Science Laboratory
[AD-A145589] 03 p0449 N85-12856

Analysis of frequency-selective integrated circuits in system of normal coordinates 04 p0489 N85-13119

Machine computation of delay and capacitance of transistor structures of subnanosecond large integrated circuits 04 p0490 N85-13120

Comparison analysis of algorithm for construction of functional tests for combined large-scale integrated circuits 04 p0490 N85-13121

Quasi-three dimensional modeling of functionally-integrated elements of large-scale integrated circuits 04 p0490 N85-13122

Analysis of dynamic characteristics and ways of development of bipolar main memory with miniaturization of integrated circuit elements 04 p0490 N85-13123

Planning of hybrid integrated circuits for microwave-band oscillators 04 p0490 N85-13124

Propagation of acoustic shear waves through active periodic structure 04 p0490 N85-13125

Standard cell initial placement strategy
[DE84-016921] 05 p0632 N85-14051

User-oriented development and production of integrated circuits in small and medium quantities
[BMFT-FB-T-84-171] 05 p0633 N85-14059

Practical application of electron beam testing in LSI and VLSI circuits
[BMFT-FB-T-84-185] 05 p0633 N85-14061

Fly's eye sensor nonlinear signal processing
[AD-D011290] 05 p0729 N85-14684

Efficiency in integral active antennas
06 p0792 N85-15060

Computer investigation of effects of high injection in transistor large integrated circuit structures
06 p0793 N85-15068

Trends in development of bipolar power transistors
06 p0793 N85-15072

Quality control of integrated circuits by parametric identification methods 06 p0796 N85-15085

Characterization of MMIC devices for active array antennas
[NASA-TM-86907] 07 p0913 N85-15779

Investigation of planar waveguides and components for millimeter-wave integrated circuits
[AD-A147380] 07 p0946 N85-16005

Control technology for integrated circuit fabrication at Micro-Circuit Engineering, Incorporated, West Palm Beach, Florida
[PB85-100717/GAR] 07 p0949 N85-16013

Linear wideband microwave amplifiers for monolithic integrated microcircuits 07 p0955 N85-16051

Trends in development of software for computer-aided analysis of large-scale integrated circuits
07 p0955 N85-16055

Built-in test and self repair mechanisms in a digital correlator integrated circuit 08 p1064 N85-16741

Chemical, material electronics studies established
08 p1142 N85-17200

General assessment of GDR microelectronics industry, applications 08 p1142 N85-17202

Data acquisition channel apparatus
[AD-D011426] 08 p1159 N85-17311

Configuration study for a 30 GHz monolithic receive array: Technical assessment [NASA-CR-174697] 09 p1311 N85-18236
Device modeling for advanced integrated circuits 09 p1314 N85-18258
The planned expansion of microelectronics capability at Sandia National Laboratory [TI85-004326] 09 p1314 N85-18260
An inexpensive vector thin film magnetometer [AD-A148725] 09 p1323 N85-18310
DDL system: Design sythesis of digital systems [NASA-CR-170759] 09 p1366 N85-18584
Semiconductors at Leipzig Spring Fair 09 p1377 N85-18660
Bondability of Al-Si thin film in thermosonic gold wire bonding — integrated circuits [NASA-TM-77795] 10 p1439 N85-19071
Researchers, projects at French intelligent machine center 10 p1460 N85-19207
Siemens' CAD system designs VLSI circuits 10 p1461 N85-19209
Research into self-timed VLSI circuits [AD-A149140] 10 p1479 N85-19339
Qualitative of analysis of MOS circuits [AD-A149267] 10 p1480 N85-19341
Advanced inverter technology [AD-A149335] 10 p1480 N85-19343
Integrated circuit tunable cavity oscillator [AD-D011474] 10 p1481 N85-19351
Linear, position-sensitive X-ray detector used for real-time calculations of small-angle scattering parameters with submillisecond resolution [DE85-002530] 10 p1489 N85-19401
Liquid-phase epitaxial growth of CdTe on HgCdTe [AD-D011482] 10 p1561 N85-19846
Control technology for integrated circuit fabrication at Honeywell Optoelectronics Division, Richardson, Texas [PB85-109023] 11 p1616 N85-20162
China report: Science and technology [JPRS-CST-84-039] 11 p1621 N85-20206
High quality super-large circuits developed 11 p1622 N85-20209
Method of examining microcircuit patterns [NASA-CASE-NPO-16299-1] 11 p1628 N85-20250
Design of a semi-custom integrated circuit for the SLAC SLC timing control system [DE85-003091] 11 p1629 N85-20258
Description of 8048 microcomputer operation published 11 p1700 N85-20665
Method for the fabrication of dielectric isolated junction field effect transistor and PNP transistor [AD-D011500] 12 p1832 N85-21494
Monolithic thin film SAW (Surface Acoustic Wave) structures [AD-A149782] 12 p1835 N85-21511
Concurrent simulation techniques exploiting hierarchy [AD-A149783] 12 p1835 N85-21512
Design of a bit-sliced processor array with built-in-self-test [AD-A149785] 12 p1835 N85-21513
Factors affecting SOS (Silicon-On-Sapphire) yield and reliability [AD-A150004] 12 p1835 N85-21515
Universal file processing program for field programmable integrated circuits [DE85-004384] 12 p1837 N85-21526
Built-in tests for VLSI (Very Large Scale Integration) finite-state machines [AD-A149784] 12 p1911 N85-21997
X-ray lithography and VLSI circuits 13 p2052 N85-22846
Basic EMC (electromagnetic interference) technology advancement for c3 systems. Volume 3A: Probabilistic analysis of combinational circuits with random delays [AD-A150349] 13 p2055 N85-22866
Advanced mixed-mode simulation techniques 13 p2062 N85-22883
Low capacitance e-beam fabricated beam-lead Schottky barrier diodes [AD-A150238] 13 p2063 N85-22888
EOS (electrical overstress) protection for VLSI (Very Large Scale Integration) devices [AD-A150333] 13 p2064 N85-22891
High sheet resistance, arsenic implanted polycrystalline silicon for integrated circuit resistors [DE85-004355] 13 p2065 N85-22902
Algorithm in Walsh function basis for analysis of integrated microcircuits on MOS-structures 13 p2083 N85-23006
Synthesis of optimum smooth transition in microstrip through line on microwave integrated circuit 13 p2089 N85-23041
Parallel test method for LSI (Large Scale Integration) microprocessors [AD-A150237] 13 p2144 N85-23310
Design for tactical avionics maintainability, technical evaluation report [AGARD-AR-204] 14 p2225 N85-23798
Onboard demand scheduling of a multibeam SS/TDMA satellite with integrated circuit and packet switching 14 p2229 N85-23812
Plans, developments in robotics 14 p2289 N85-24191
Proceedings of the Cold Electronics Workshop [NASA-CR-175662] 14 p2297 N85-24220
Cold electronics: An overview 14 p2297 N85-24221
The effects of cooling on delay-time limits in IC's 14 p2297 N85-24224
Bipolar nonswitching logic arrays: Universal components of function expanders for computation of elementary functions 14 p2400 N85-24797
UW/NW (University of Washington/Northwest) VLSI Consortium [AD-A150740] 14 p2404 N85-24818
The effects of water and hydrogen on materials used in integrated circuit packages [AD-A151893] 15 p2518 N85-25520
Computer-aided identification of complete constitution model of transistor structure for design of subnanosecond large-scale-integrated circuits 15 p2529 N85-25594
Developments in microelectronics: Past and future 15 p2530 N85-25597
East Europe report: Science and technology [JPRS-ESA-84-016] 15 p2533 N85-25624
Aspects of CSSR CMOS integrated circuits discussed 15 p2533 N85-25627
Recent developments 15 p2533 N85-25628
MHB4046 phase-lock circuit 15 p2533 N85-25629
Improved, cheaper SIPMOS circuits no. 10, 1983 p 370 15 p2534 N85-25630
Phase-locked loop design with MHB4046 15 p2534 N85-25631
Additional PLL designs 15 p2534 N85-25632
New designs from electronics R and D center 15 p2538 N85-25666
Conversion of algorithms to custom integrated circuit devices [AD-A151288] 15 p2547 N85-25720
Analysis of the capability to effectively design complementary metal oxide semiconductor integrated circuits [AD-A151832] 15 p2548 N85-25728
Designing VLSI (Very Large Scale Integrated) circuits for testability [AD-A151834] 15 p2549 N85-25729
A microcomputer-based program for printing check plots of integrated circuits specified in Caltech intermediate form [AD-A151715] 15 p2629 N85-26205
Technical evaluation report on Avionics Panel Specialists' Meeting on Digital Optical Circuit Technology [AGARD-AR-202] 15 p2653 N85-26367
The impact of VLSI on guidance and control system design 16 p2697 N85-26654
An integrated UNIX-based CAD system for the design and testing of custom VLSI chips 16 p2771 N85-27102
System design of automated VLSI (Very Large Scale Integrated) test station and implementation of selected system aspects [AD-A151961] 16 p2778 N85-27147
Radiation hardening for VLSI applications [DE85-005493] 16 p2780 N85-27155
Bond test data acquisition and analysis system [DE85-007021] 16 p2780 N85-27158
The systematic integration of very large scale integrated circuit computer-aided design tools into a toolkit optimized for academic applications [AD-A151813] 16 p2845 N85-27538
East Europe report: Science and technology [JPRS-ESA-85-017] 17 p2945 N85-28177
Goals, achievements of microelectronics program 17 p2945 N85-28179
Uses of, experiences in production of custom designed IC's 17 p2945 N85-28180
Modern equipment for manufacture of IC's in Hungary 17 p2945 N85-28181
SC filters and design centering of integrated circuits. Part 2: Design centering of integrated circuits [BMFT-FB-T-84-265-PT-2] 17 p2956 N85-28257
Investigation of semiconductor clad optical waveguides [NASA-CR-175870] 17 p3036 N85-28785
Development of thin film hybrid IC active filter for video band use [NHK-LABS-NOTE-312] 18 p3094 N85-29153
System design of multi-layer (3-dimensional) integrated circuits [AD-A153468] 18 p3094 N85-29154
The use of VLSI technology for the real-time generation of graphics displays: A proposal [AD-A153766] 18 p3160 N85-29673
The potential of semiconductors for optical integrated circuits 18 p3187 N85-29795
Split-cross-bridge resistor for testing for proper fabrication of integrated circuits [NASA-CASE-NPO-16021-1] 19 p3256 N85-30157
High speed GaAs device and integrated circuit modeling and simulation 19 p3256 N85-30161
A comparison of the radiation hardness of various VLSI technologies for defense applications [DE85-006973] 19 p3263 N85-30209
Leading-edge microelectronics research at Sweden's Chalmers 20 p3438 N85-31397
Globally-asynchronous locally-synchronous systems [AD-A154624] 21 p3573 N85-32222
Parallel simulation of digital LSI circuits [AD-A154745] 21 p3580 N85-32258
GAO (General Accounting Office) assessment of DOD's Very High Speed Integrated Circuits (VHSIC) technology program [AD-A155109] 21 p3581 N85-32261
LSI/VLSI ion implanted planar GaAs IC processing [AD-A155110] 21 p3581 N85-32262
Tight bounds on the complexity of parallel sorting [AD-A154726] 21 p3667 N85-32776
Digital integrated circuits 21 p3669 N85-32787
Development of a dedicated speech work station [AD-A155465] 21 p3674 N85-32824
Adaptive modeling of electronic circuits 22 p3766 N85-33346
Software for frequency analysis of microwave circuits 22 p3768 N85-33362
USSR report: Electronics and electrical engineering [JPRS-UEE-84-003] 22 p3773 N85-33381
Multidiode integrated-circuit protective device 22 p3781 N85-33425
Synthesis of metrico-topological model for layout of topology of large-scale-integration arrays 22 p3781 N85-33427
Synthesis of high-speed devices using integrated operational amplifiers 22 p3781 N85-33429
Joint services electronics program [AD-A154748] 23 p3927 N85-34336
Multi-robot assembly of IC's 23 p3964 N85-34577
Analog, still without fear [AD-A155920] 24 p4069 N85-35346
A methodology for the design of testable custom large-scale integrated circuits [AD-A156098] 24 p4090 N85-35351
Monolithic photovoltaic series array for an energy coupler [BMFT-FB-T-85-023] 24 p4113 N85-35496
Computer Aided Design (CAD) methods for very large scale integration systems [BMFT-FB-T-85-029] 24 p4141 N85-35696
Laser and electron beam processing of semiconductors [AD-A155914] 24 p4161 N85-35796

INTEGRATED ENERGY SYSTEMS
An Assessment of Integrated Flywheel System Technology [NASA-CP-2346] 05 p0604 N85-13859
Comparative energy storage assessment item 05 p0605 N85-13868
Develop and test fuel cell powered on-site integrated total energy systems. Phase 3: Full-scale power plant development [NASA-CR-174887] 15 p2586 N85-25941

INTEGRATED OPTICS
Guided-wave optic devices for integrated optic information processing [AD-A145695] 02 p0280 N85-11627
Advanced infrared laser modulator development [NASA-CR-172479] 06 p0862 N85-15479
Technological and economic assessment of advanced ceramic materials. Volume 1: Summary and conclusions [PB85-113082] 12 p1815 N85-21380
Technological and economic assessment of advanced ceramic materials: Volume 4: A case study of integrated optic devices [PB85-113116] 12 p1815 N85-21386
Technological and economic assessment of advanced ceramic materials. Volume 6: A case study of ceramic cutting tools [PB85-113132] 12 p1815 N85-21387
Multifunctional elements for integrated optics 13 p2068 N85-22916
Integrated optical components utilizing acoustooptic and electrooptic diffraction in micro-waveguides 13 p2069 N85-22944
Investigation of semiconductor clad optical waveguides [NASA-CR-175870] 17 p3036 N85-28785

Digital Optical Circuit Technology
[AGARD-CP-362] 18 p3185 N85-29757
Integrated electrooptical components using dielectric substrates 18 p3187 N85-29767
Solar adaptive optics
[AD-A155494] 21 p3724 N85-33101
INTEGRATION (REAL VARIABLES)
U MEASURE AND INTEGRATION
INTEGRATORS
NT DIGITAL INTEGRATORS
Integrated control and display systems for helicopter battlefield mission management
08 p1073 N85-16805
Evaluation of time integrators for the shallow water equations
[CWI-NM-R8406] 11 p1634 N85-20292
Numerical optical computing at the Ohio State University 18 p3188 N85-29775
INTEGRITY
NT COMPUTER PROGRAM INTEGRITY
Avionics integrity program (Avip). Volume 4: Force management. Economic life considerations
[AD-A145592] 02 p0138 N85-10941
Artificial intelligence approaches to monitoring system integrity
[AD-P003930] 02 p0246 N85-11610
INTEGRODIFFERENTIAL EQUATIONS
U DIFFERENTIAL EQUATIONS
U INTEGRAL EQUATIONS
INTELLECT
Manual and computer-aided sequential diagnostic inference
[AD-A156229] 24 p4133 N85-35620
INTELLIGENCE
NT ARTIFICIAL INTELLIGENCE
NT EXPERT SYSTEMS
NT EXTRATERRESTRIAL INTELLIGENCE
NT INTELLECT
Conjunctive and disjunctive item response functions
[AD-A147815] 07 p1033 N85-16561
Transfer of technology
[S-REPT-98-664] 12 p1949 N85-22248
Human cognition and intelligence: Towards an integrated theoretical perspective
[CSIR-SR-PERS-350] 13 p2143 N85-23300
Military journal on US intelligence satellites
16 p2727 N85-26832
Design and implementation of an intelligence database
[AD-A154095] 19 p3381 N85-30973
INTELLIGIBILITY
NT SPEECH RECOGNITION
Hearing protection and speech intelligibility of two nonstandard inflight communication headsets
[AD-A148110] 03 p0355 N85-12284
INTELSAT SATELLITES
Television transmission in frequency modulation
04 p0493 N85-13146
Electrical design of the Intelsat 6 solar generator
13 p2008 N85-22592
INTENSIFICATION
U AMPLIFICATION
INTENSIFIER TUBES
U IMAGE INTENSIFIERS
INTENSIFIERS
NT IMAGE INTENSIFIERS
INTENSITY
Interplanetary cosmic ray intensity: 1972-1984 and out to 32 AU
[AD-A145130] 01 p0131 N85-10903
Beam profiling in gigawatt 1064-nm lasers used in research on optical materials at Livermore
[DE84-087226] 04 p0505 N85-13223
Hurricane Alicia, Galveston and Houston, Texas, 17-18 August 1983
[PB84-237056] 04 p0541 N85-13441
Magnetic constraints on early lunar evolution revisited: Limits on accuracy imposed by methods of paleointensity measurements 04 p0582 N85-13716
Effect of stationary magnetic field on bleeding time
12 p1904 N85-21956
INTERACTIONAL AERODYNAMICS
Calculation of unsteady transonic separated flows by viscous-inviscid interaction 15 p2458 N85-25178
An experimental and analytical study of the aerodynamic interference effects between two Sears-Haack bodies at Mach 2.7
[NASA-TM-85729] 16 p2700 N85-26673
Flow around rotating and nonmoving circular cylinder near flat screen. Report 1: Aerodynamic forces in cylinder 16 p2765 N85-27059
Study of stresses on surface of flat barrier immersed in under expanded jet of rarefied gas
16 p2765 N85-27061
Propulsion efficiency of vibrating bodies in subsonic gas stream 17 p2942 N85-28159
INTERACTIONS
Metal-support interactions: Their effects upon adsorption, electronics, and activity/selectivity properties of cobalt in hydrogenation
[DE85-003316] 09 p1282 N85-18113
Electromagnetic pulse (EMP) interaction with electric power systems. Power Systems Technology Program
[DE85-000166] 09 p1312 N85-18244
A frozen vorticity approach to the axisymmetric strong interaction problem
[AD-A149101] 10 p1484 N85-19369
INTERACTIVE CONTROL
Interactive graphics nonlinear constrained optimization
01 p0058 N85-10367
Interactive color-graphics interface for energy monitoring and control systems
[AD-A147538] 07 p1025 N85-16509
MINDS: A microcomputer interactive data system for 8086-based controllers
[NASA-TP-2378] 08 p1204 N85-17576
Further development of an Interactive Control Engineering Computer Analysis Package (ICECAP) for discrete and continuous systems
[AD-A151783] 16 p2846 N85-27546
A modern control theory enhancement to an interactive Control Engineering Computer Analysis Package (ICECAP)
[AD-A153249] 17 p3012 N85-28622
Interactive computer program for the analysis and design of linear time invariant systems
[AD-A154076] 19 p3335 N85-30664
Interactive aircraft flight control and aeroelastic stabilization
[NASA-CR-176035] 20 p3396 N85-31064
INTERACTIVE GRAPHICS
U COMPUTER GRAPHICS
INTERATOMIC FORCES
Quantum characteristics of kinetic fracturing of solids
02 p0265 N85-11732
Atomistic studies of grain boundaries with segregated impurities
[DE85-000063] 11 p1737 N85-20924
Planetary fluids He and NH3 at high shock pressures and temperatures
[DE85-011851] 22 p3859 N85-33896
INTERCALATION
Dynamics of graphite fiber intercalation: In situ resistivity measurements with a four point probe
[NASA-TM-86858] 01 p0017 N85-10105
Stability of bromine intercalated graphite fibers
[NASA-TM-86859] 01 p0031 N85-10187
Reaction mechanisms in the formation of intercalation complexes, and properties of intercalated molecules
03 p0431 N85-12745
An investigation of the electrical conductivity in highly oriented graphite intercalation compounds
[AD-A146539] 06 p0804 N85-15116
The 13C nuclear magnetic resonance in graphite intercalation compounds
[NASA-CR-174261] 07 p1040 N85-16601
Structure-property relationships in intercalated graphite
[AD-A147949] 08 p1219 N85-17680
Electronic properties of intercalated graphite and amorphous metals
[AD-A147664] 08 p1225 N85-17716
Compositional, structural, and physical studies of some graphite hexafluoroarsenates and their relatives
[DE85-000655] 10 p1432 N85-19030
Investigation of electric and magnetic properties of intercalated graphite
[AD-A149601] 12 p1797 N85-21274
Electric and magnetic properties of intercalated graphite
[AD-A149848] 12 p1798 N85-21276
Neutron scattering studies of graphite intercalation compounds
[DE85-003079] 12 p1942 N85-22196
Homogeneity of pristine and bromine intercalated graphite fibers
[NASA-TM-87016] 15 p2517 N85-25521
Graphite fiber intercalation: Dynamics of the bromine intercalation process
[NASA-TM-87015] 16 p2742 N85-26921
Environmental stability of intercalated graphite fibers
[NASA-TM-87025] 16 p2753 N85-26992
A micrographic and gravimetric study of intercalation and deintercalation of graphite fibers
[NASA-TM-87026] 17 p2934 N85-28110
Structural and physical studies on a new class of low-dimensional conducting material: FeOCl intercalated with TTF and related molecules
[DE85-009701] 18 p3196 N85-29824
INTERCEPTION
LPI-radar for helicopter obstacle warning
08 p1074 N85-16810
Modeling interception of rainfall by forests and the role of interception in the water balance
[DE85-002822] 12 p1884 N85-21825
Space interception guidance with uncertain factors
13 p2042 N85-22781
INTERCEPTOR AIRCRAFT
U FIGHTER AIRCRAFT
INTERCONNECTION
U JOINING
INTERCONTINENTAL BALLISTIC MISSILES
NT MINUTEMAN ICBM
Invited papers: DNA ICBM technical R and D program 09 p1333 N85-18379
INTERCOSMOS SATELLITES
Space-time features of solar cosmic ray penetration into high latitude regions of Earth's magnetosphere based on Intercosmos-19 satellite data 15 p2481 N85-25310
Interkosmos program of space communication development 15 p2528 N85-25585
INTERDIGITAL TRANSDUCERS
Experimental study of high-stability oscillator with surface-acoustic-wave resonator in feedback loop
13 p2090 N85-23053
Compensation of acoustic wave devices
[AD-D011582] 15 p2646 N85-26322
Microwave SAW (Surface Acoustic Wave) monochromator
[AD-D011718] 21 p3590 N85-32311
INTERFACE STABILITY
Thermal conductivity and interface resistance of particle-filled silicone resin
[DE84-011681] 04 p0479 N85-13056
Polymer-polymer interface bond stability
06 p0830 N85-15271
Polymer-metal interface bond stability
06 p0630 N85-15272
Instability of film boiling of moving liquids
[BLL-WH-603-(9091.9F)] 07 p0956 N85-16056
Instability at the interface between two shearing fluids in a channel
[AD-A153532] 18 p3099 N85-29185
Application of the MHD energy principle to magnetostatic atmospheres
[NASA-CR-175967] 18 p3136 N85-29420
Compressible two-phase flow instabilities simulated with a hybrid Lagrange-Euler pseudospectral method
[DE85-009904] 23 p3931 N85-34381
INTERFACES
NT FLUID BOUNDARIES
NT GAS-SOLID INTERFACES
NT JET BOUNDARIES
NT LIQUID-LIQUID INTERFACES
NT LIQUID-SOLID INTERFACES
NT LIQUID-VAPOR INTERFACES
NT SOLID-SOLID INTERFACES
Automation of coastal engineering modelling facilities
[CSIR-T/SEA-8304] 01 p0035 N85-10219
Electronics Engineering Department: EE technical review
[DE84-016124] 01 p0044 N85-10286
PDSS/IMC CIS user's guide
[NASA-CR-171179] 01 p0102 N85-10682
Surface environmental effects in electrochemical kinetics: Outer-sphere chromium (3) reductions at mercury, gallium, lead, and thallium surfaces
[AD-A145607] 02 p0172 N85-11155
Pluribus satellite IMP (Interface Message Provision) development mobile access terminal network
[AD-A145346] 02 p0190 N85-11269
Multiplexing the ethernet interface among VAX/VMS users
[AD-A145539] 02 p0243 N85-11588
Checking optical-polarization measurements at interfaces 02 p0271 N85-11770
An approach to interfacing data bases in WWMCCS ADP
[AD-A146350] 03 p0439 N85-12793
The chemical nature of the fiber/resin interface in composite materials 04 p0465 N85-12953
Composite property dependence on the fiber, matrix, and the interphase 04 p0465 N85-12954
Study program for encapsulation materials interface for Flat-plate Solar Array (FSA) project
[NASA-CR-174152] 04 p0530 N85-13385
Physical database processor preliminary interface specifications
[PB84-217561] 04 p0548 N85-13483
Elastodynamic stress intensity factors of an interface finite-width crack
[DE84-016906] 06 p0817 N85-15190
High speed magnetic tape interface for a microcomputer
[CSIRO-TP-7] 06 p0847 N85-15377
A standard operating system interface for microcomputer software development
[AD-A146884] 06 p0854 N85-15426

Design and analysis of an SQL (Structured Query Language) interface for a multi-backend database system
[AD-A146534] 08 p0856 N85-15447
Titanium Matrix/Continuous Fiber/Continuous fiber composite interface interactions and their influence on mechanical properties
[AD-A147504] 07 p0920 N85-15829
Interactive color-graphics interface for energy monitoring and control systems
[AD-A147538] 07 p1025 N85-16509
Hardware/software codesign for maintainable systems 08 p1066 N85-16753
Integrated design checkout of shuttle payload avionics interfaces 08 p1092 N85-16899
Kernel Ada Programming Support Environment (KAPSE) interface team public report, volume 4
[AD-A147648] 08 p1205 N85-17581
Electrochemical interfaces and electrode processes
[AD-A147414] 09 p1290 N85-18096
Photoacoustic spectroscopy at electrode-solution interface
[DE85-001872] 09 p1292 N85-18111
Nondestructive characterization of semiconductor surfaces and interfaces 09 p1329 N85-18349
Influence of the amorphous-crystalline interface morphology on dislocation nucleation in pre-amorphized silicon
[DE85-002068] 09 p1398 N85-18800
A comprehensive study on sublaminate crack growth stability and its effects on the load-carrying capacity
[AD-A149037] 10 p1432 N85-19028
Numerical simulations of liquid propellant combustion instability: Onset and growth
[DE85-000743] 10 p1458 N85-19186
Man-machine interaction: Operator
[AD-A149075] 10 p1531 N85-19648
Management challenges encountered in CAD implementation
[DE85-002072] 10 p1541 N85-19716
Effect of interfacial characteristics of metal clad polymeric substrates on electrical high frequency interconnection performance
[NASA-TM-86948] 11 p1624 N85-20223
Elastic compliance of imperfect interfaces: Review and relationship to ultrasonic scattering
[DE85-003088] 11 p1652 N85-20404
Electrochemical processes at the sodium (BETA)" alumina interface
[DE85-004653] 12 p1802 N85-21305
DOS 21: PCDOS 2.0 support subroutine package for the IBM personal computer
[LA-10142-MS] 12 p1914 N85-22012
ZTLCK: A subroutine package for the IBM personal computer to support the Ziatech ZT1488 real time clock
[LA-10146-MS] 12 p1914 N85-22014
Interface specifications for SCR (Software Cost Reduction) (A-7E) extended computer module, revised
[AD-A149948] 12 p1915 N85-22024
A formal method for specifying computer resources in an implementation independent manner
[AD-A149955] 12 p1918 N85-22043
Numerical methods for tracking interfaces
[LA-9917-MS] 12 p1919 N85-22052
Nucleation of phase transitions in the vicinity of phase boundary. Part 1: Comparison of various idolated mechanisms. Part 2: Coupled cluster growth processes
[N-0206-5658] 12 p1936 N85-22174
Problems with electrical interference between solar generators and shunt type regulators
13 p2010 N85-22607
Presentation based user interfaces
[AD-A150311] 13 p2144 N85-23311
A design analysis and implementation of a user-friendly interface for the UNIX operating system
[AD-A150558] 13 p2145 N85-23312
The Multimission Image Processing Laboratory's virtual frame buffer interface
[NASA-CR-175655] 14 p2402 N85-24805
A fast ray tracing routine for laterally inhomogeneous media
[AD-A150964] 14 p2421 N85-24938
Electroreflectance spectroscopy as a probe of the electronic structure at the metal-electronic interface
[DE85-003541] 14 p2428 N85-24976
Mixing across a gas-gas interface
[AD-A151471] 15 p2556 N85-25770
COSMIC/NASTRAN-PATRAN interface
15 p2574 N85-25870
Orbiter middeck/payload standard interfaces control document
[NASA-TM-87473] 16 p2729 N85-26840
Microscopic study of the influence of impurities on interface bonding
[AD-A151725] 16 p2743 N85-26928
Continued development and implementation of the Universal Network Interface Device (UNID) 2 in the Digital Engineering Laboratory Network (DELNET), volume 2
[AD-A151947] 16 p2850 N85-27570
A new technique for system-to-system transfer of surface data 17 p3007 N85-28589
CAMAC 488 module: 68000 based GPIB interface module
[DE85-009367] 17 p3014 N85-28635
Incorporation of Monte Carlo electron interface studies into photon general cavity theory
[DE85-007674] 17 p3034 N85-28772
The effect of ion-bombardment-induced atomic mixing on depth-profiling of interfaces
[AD-A153199] 17 p3044 N85-28834
LDV multiplexer interface
[NASA-CASE-ARC-11536-1] 19 p3258 N85-30202
Method for producing high quality germanium-germanium nitride interfaces for germanium semiconductors and device produced thereby
[AD-D011702] 19 p3260 N85-30218
VUV synchrotron light as a technique for studying the interface quality and properties of thin overlayers
[DE85-009822] 19 p3262 N85-30227
BREED: A CDC-7600 computer program for the automation of breeder reactor design analysis (LWBR Development Program)
[DE85-010327] 19 p3338 N85-30686
Photoeffects of semiconductor electrolyte interfaces
[AD-A154163] 20 p3449 N85-31411
Chemical structure of interfaces
20 p3480 N85-31629
Effects of contact area of an interface on acoustic wave transmission characteristics
[DE85-009935] 20 p3524 N85-31920
Some dynamic electronic properties of semiconductor surfaces and interfaces 20 p3537 N85-32007
Improved materials for composite and adhesive joints
[AD-A155065] 21 p3562 N85-32153
Interface chemistry of Hg(1-x)Cd(x)Te
[AD-A154876] 21 p3563 N85-32161
EVA-glass interface bond stability
21 p3608 N85-32408
Interfacial bonding stability 21 p3608 N85-32409
On the limiting configuration of interfacial gravity waves
[AD-A154821] 21 p3631 N85-32557
Experimental studies of chemical reactivity during shock initiation of hexanitrostilbene
[DE85-011726] 22 p3754 N85-33270
Module for interfacing microprocessors and microcomputer 22 p3774 N85-33390
Supermite vacuum interface design
[DE85-012861] 22 p3837 N85-33759
High resolution electron microscopic characterization of interfaces in ceramics
[DE85-011207] 23 p3920 N85-34289
The interactive planning work station: A graphics-based UNIX (trademark) tool for application users and developers 23 p3957 N85-34527
An image management kernel for the design of relational and pictorial data bases 23 p3958 N85-34532
Graphics Interaction in databases
23 p3958 N85-34534
Issues and techniques in touch-sensitive tablet input (executive summary) 23 p3960 N85-34543
Efficient recovery and reversal in graphical user interfaces generated by the Higgens system
23 p3960 N85-34544
A model for graphics interface tool development
23 p3960 N85-34545
Using percent-done program indicators to enhance user interfaces 23 p3960 N85-34546
The CADME approach to the interface of solid modellers 23 p3961 N85-34554
An innovative user interface for microcomputer-based computer-aided design 23 p3961 N85-34555
How map designers can represent their ideas in thematic maps: Effective user interfaces for thematic map design
23 p3962 N85-34562
Pluribus satellite IMP (Interface Message Processors) development mobile access terminal network
[AD-A155754] 24 p4068 N85-35216
Raster functionality for a VDI
[DE85-006734] 24 p4097 N85-35396
DSS/MIS (Decision Support Systems/Management Information Systems) design and implementation for LAMPS Mk 3 utilizing a microcomputer and a maintenance personnel assignment program
[AD-A155852] 24 p4135 N85-35629
Research on GaSb/AlSb multi-quantum well superlattices
[AD-A156060] 24 p4161 N85-35800

INTERFACIAL ENERGY
HgCdTe surface and defect study program
[AD-A156079] 24 p4161 N85-35799

INTERFACIAL STRAIN
U INTERFACIAL TENSION

INTERFACIAL TENSION
Minor element effects on gas tungsten arc weld penetration
[PB84-222579] 01 p0056 N85-10970
Evaluation of interfacial stresses from the amplitude of reflected ultrasonic signal
[DE84-015472] 02 p0276 N85-11798
NBS (National Bureau of Standards): Materials measurements
[NASA-CR-174038] 03 p0332 N85-12143
Dynamics of liquid filament breakup
[DE84-016008] 04 p0500 N85-13187
Contact angle and surface tension measurements of a five-ring polyphenyl ether
[NASA-TM-86927] 07 p0930 N85-15887
Investigation of surface tension phenomena using the KC-135 aircraft
[NASA-TM-82506] 10 p1426 N85-18996
Characterization and adhesive bonding of poly(etheretherketone) resins and composites
[DE85-002526] 11 p1593 N85-20020
Fluid slosh dynamics of surface tension tanks in three axis stabilized spacecraft
[MBB-UR-E-739-84-O] 11 p1634 N85-20281
Dynamic investigations of a spherical tank structure filled with liquid using ANSYS three-dimensional fluid elements
[MBB-UR-E-737-83-O] 11 p1654 N85-20418
Vapor pressure studies of the solubilization of hydrocarbons by surfactant micelles
[DE85-004319] 12 p1803 N85-21306
Tribological properties of boron nitride synthesized by ion beam deposition
[NASA-TM-86962] 12 p1810 N85-21355
Properties of materials using acoustic waves
[AD-A150465] 13 p2155 N85-23382
Mixing across a gas-gas interface
[AD-A151471] 15 p2556 N85-25770
Effects of thermal fluctuations on systems with small surface tension
[PREPRINT-437] 18 p3152 N85-29520
Effects of weak interfaces on thermostructural behavior of carbon-carbon composites
[AD-A155330] 21 p3562 N85-32154
Hertzian contact in two and three dimensions
[NASA-TP-2473] 21 p3596 N85-32331
The Konstantinov effect and absorption of sound in inhomogeneous media 21 p3680 N85-32861
Hydrogen embrittlement testing
[DE85-007352] 23 p3916 N85-34273

INTERFERENCE
Using two-beam interference method for measuring wavelength of tunable pulse lasers
02 p0272 N85-11772
Experiments suitable for wind tunnel wall interference assessment/correction 03 p0313 N85-12021
Asymptotic methods for wind tunnel wall corrections at transonic speed 03 p0313 N85-12022
NLR activities in the field of wind tunnel wall interference 03 p0313 N85-12024
Progress in wind tunnel wall interference assessment/correction procedures at the NAE
03 p0314 N85-12025
The susceptibility of aeronautical navigational aids to interference from adjacent-band broadcast transmissions
[BBC-RD-1984/12] 09 p1311 N85-18234
Pseudospectral calculations of two-dimensional transonic flow (Task 1). Numerical investigation of VTOL aerodynamics (Task 2)
[AD-A150123] 12 p1772 N85-21126

INTERFERENCE DRAG
Installed nacelle drag-improvement tests of an M = 0.8 turboprop transport configuration
[NASA-TM-84302] 07 p0902 N85-15718

INTERFERENCE GRATING
Extraction of signals from background interference with unknown parameters in quantized sample
13 p2084 N85-23013
Probability of detection of pulsed signals employing zero-gating interference suppression
13 p2085 N85-23021
Laser plasma LINAC
[DE85-008294] 17 p2971 N85-28348
Measurement of ultrasonic fields in transparent media using a scanning differential interferometer
[NASA-CR-175921] 17 p3028 N85-28728
Prospects for parallel nonlinear optical signal processing using GaAs etalons and ZnS interference filters
18 p3187 N85-29756
Modular digital holographic fringe data processing system
[NASA-CR-177952] 23 p3933 N85-34376

INTERFERENCE IMMUNITY
Interference immunity of digital equipment for coherent processing of wideband signals
04 p0486 N85-13100
Interference immunity of fiber-optic communication lines with spectral multiplexing of channels
13 p2069 N85-22924
Interference immunity of binary systems with second-order phase-difference modulation in various reception modes 13 p2072 N85-22944
Playback amplifier with high interference immunity
13 p2077 N85-22970
Interference immunity of optical radar system with phased antenna array 15 p2526 N85-25575
INTERFERENCE LIFT
Assessment of lift- and blockage-induced wall interference in a three-dimensional adaptive-wall tunnel
03 p0312 N85-12016
Wind tunnel wall interference correction for aircraft models 03 p0314 N85-12029
INTERFERENCE MONOCHROMATIZATION
U DIFFRACTION
U MONOCHROMATIZATION
INTERFEROGRAMS
U INTERFEROMETRY
INTERFEROMETERS
NT FABRY-PEROT INTERFEROMETERS
NT INFRARED INTERFEROMETERS
NT MICHELSON INTERFEROMETERS
NT MICROWAVE INTERFEROMETERS
NT RADIO INTERFEROMETERS
Neutron interferometry and double diffractometer for condensed matter 03 p0424 N85-12705
Imaging polarimeter-interferometer arrays for Tokamak measurements
[DE84-015916] 05 p0730 N85-14693
Decimetric-wave aperture synthesis system at Scientific Research Institute of Radiophysics
06 p0782 N85-15000
Software for Crimea-Pushchino radiointerferometer
06 p0783 N85-15007
Turbulence measurement interferometer apparatus
[AD-D011377] 07 p0970 N85-16156
Far-infrared interferometry/polarimetry on the ISX-B Tokamak
[DE84-015401] 10 p1558 N85-19627
KMSF X-ray laser experiments, task no. 2
[DE85-000291] 11 p1640 N85-20335
FIR interferometer/polarimeter system on ISX-B Tokamak
[DE85-001129] 11 p1731 N85-20887
Comparison reference etalon of unit laser radiation power 13 p2074 N85-22957
Phase-lock fiber optic interferometer
[AD-D011603] 16 p2786 N85-27191
Fiber optic gyroscope with alternating output signal
[AD-D011689] 19 p3271 N85-30284
Mesospheric measurements of irregularity patches using a 3-antenna interferometer, part 3.6B
21 p3621 N85-32498
Automatic sphericity interferometer for testing lens radii
[AD-A155736] 22 p3786 N85-33457
Optical synthetic aperture techniques
[AD-A156151] 24 p4154 N85-35752
INTERFEROMETRY
NT DIFFERENTIAL INTERFEROMETRY
NT HOLOGRAPHIC INTERFEROMETRY
NT LASER INTERFEROMETRY
NT MOIRE INTERFEROMETRY
NT VERY LONG BASE INTERFEROMETRY
Two novel plasma diagnostic tools: Fiber sensors and phase conjugation
[DE84-014033] 01 p0123 N85-10840
Modern radioastronomical aperture synthesis systems (review) 06 p0782 N85-14997
SIR-B interferometric topography
08 p1145 N85-17224
Two-photon coherent state light - its generation and potential applications
[AD-A148245] 08 p1166 N85-17356
Diffraction-limited imaging of space objects 2
[AD-A149344] 11 p1728 N85-20870
Research study of fiber-optic interferometry at very low frequencies
[AD-A150906] 14 p2421 N85-24937
Investigations of high resolution imaging through the Earth's atmosphere using speckle interferometry
[AD-A150880] 14 p2439 N85-25053
Optical monitoring of photo-acoustic pulse propagation in silicon wafers
[AD-A151333] 15 p2651 N85-26352
Digital image analysis of four-frame holographic plasma and neutral gas interferograms
[DE85-008397] 16 p2788 N85-27200
Acoustooptic pulse-echo transducer system
[NASA-CR-175919] 17 p2951 N85-28224
Transport in aqueous battery systems
[DE85-007246] 17 p2955 N85-28251
Water vapor radiometry research and development phase
[NASA-CR-175887] 17 p2995 N85-28512
Prospects for parallel nonlinear optical signal processing using GaAs etalons and ZnS interference filters
18 p3187 N85-29765
Dual differential interferometer
[NASA-CASE-LAR-12986-1] 19 p3271 N85-30282
Interferometric creep testing
[AD-A154249] 19 p3286 N85-30378
Speckle interferometry applied to asteroids and other solar system objects
[NASA-CR-175976] 19 p3384 N85-30995
Status of the Jicamarca radar
21 p3627 N85-32535
SCRIBE data of October 23, 1983 flight
[AD-A154864] 21 p3705 N85-33012
Ranging system which compares an object reflected component of a light beam to a reference component of the light beam
[NASA-CASE-NPO-15865-1] 23 p3973 N85-34629
INTERGALACTIC MEDIA
Star formation in interacting galaxies
03 p0444 N85-12826
QUASAT, gravitational lenses, and studies of the interstellar, intracluster and intergalactic medium
07 p1058 N85-16715
Extragalactic cosmic rays from active galaxies
08 p1236 N85-17805
Extragalactic origin or gamma-ray bursts, revision 1
[DE85-005622] 15 p2686 N85-26588
Interactions of heavy nuclei, Kr, Xe and Ho, in light targets 20 p3544 N85-32050
Activities report of the Department of Astrophysics
20 p3546 N85-32064
Galactic antiprotons of 0.2-2 GeV energy
[OG-6.1-11] 22 p3888 N85-34101
Evidence for a dynamical halo around the edge-on galaxy NGC 4631
[OG-6.2-1] 22 p3889 N85-34102
Interstellar turbulence, random density variations, and scintillation measurements
[OG-7.2-13] 23 p4015 N85-34880
INTERGRANULAR CORROSION
Bending strength studies on hot-pressed silicon carbide
[NASA-TM-77512] 03 p0371 N85-12369
In-situ stress relief of expanded alloy 600 steam generator tubing
[DE84-014560] 04 p0513 N85-13273
Testing of non-alloyed and low-alloyed steels for their behaviour with respect to intercrystalline stress corrosion cracking
[BLL-RISLEY-TR-4546-(9091.9F)]
07 p0925 N85-15861
Contributions of segregated phosphorus to the intergranular stress corrosion cracking of nickel
[DE85-003112] 11 p1606 N85-20099
Stress relief of transition zones
[DE85-000234] 11 p1653 N85-20411
Role of segregated P and S in intergranular stress corrosion cracking of nickel
[DE85-004547] 13 p2024 N85-22679
Crack tip chemistry modeling of intergranular stress corrosion cracks of nickel containing segregated phosphorus and sulphur
[DE85-010059] 18 p3076 N85-29028
Electrochemical method for investigation of the susceptibility of corrosion-resistant steels to intercrystalline corrosion
[BLL-CE-TRANS-8082-(9022.09)]
24 p4077 N85-35269
INTERIM STAGES (SPACECRAFT)
NT INERTIAL UPPER STAGE
INTERIM UPPER STAGE (STS)
U INERTIAL UPPER STAGE
INTERIOR BALLISTICS
Intercomparison between West Germany and US thermodynamic codes
[AD-A146822] 06 p0889 N85-15525
Experimental high pressure equation of state of a very fast burning gun propellant
[DE85-001749] 10 p1458 N85-19184
Averaging effects in models of three-dimensional two-phase flows
[AD-A149313] 10 p1484 N85-19371
Molecular dynamics of propellant gases, part 2
13 p2002 N85-22552
Experimental simulation of the flows in front of and behind a projectile with and without gas slippage
[ISL-CO-232/83] 14 p2302 N85-24258
The utilization of a light-gas gun to simulate interior ballistic flow
[ISL-CO-233/83] 14 p2303 N85-24259
Unsteady flows in a tube with combustion reaction
[ISL-R-116/83] 14 p2303 N85-24261
Feasibility study of an installation to simulate the flow of propellent gases in a gun barrel, part 2
[ISL-R-128/83-PT-2] 14 p2303 N85-24263
Simulation of interior ballistics flows in a shock tube
[ISL-CO-222/83] 16 p2784 N85-27183
A computer code IB-KB for interior ballistics of recoiling and recoilless guns
[FOA-C-20566-D2] 18 p3164 N85-29602
Experimental simulation of internal ballistic flows
[ISL-CO-208/84] 20 p3435 N85-31312
Telemetry system for the transmission of data from projectiles during the acceleration phase in the gun barrel
[ISL-CO-207/84] 22 p3739 N85-33178
Experimental simulation of in-bore flows using a high pressure shock tube
[ISL-CO-217/84] 22 p3785 N85-33452
Numerical simulation of interior and terminal ballistics phenomena. Investigation of the effects of the parameters and application examples
[ISL-R-112/84] 22 p3831 N85-33731
INTERLACING DRAINAGE
U DRAINAGE PATTERNS
INTERLAYERS
NT MULTILAYER INSULATION
Influence of inter-layer effect on charge gas-permeability
[BLL-M-35919-(5828.4)] 05 p0616 N85-13940
Stress-relieving interlayers for bituminous resurfacings
[PB85-136865] 12 p1820 N85-21415
Graphite fiber intercalation: Dynamics of the bromine intercalation process
[NASA-TM-87015] 16 p2742 N85-26921
X-ray diffractometric measurements and calculations of limiting values of discrepancy between lattices and layer thicknesses, preventing generation of dislocations during growth of multilayer heterostructures
21 p3681 N85-32866
INTERLOCKING
U LOCKING
INTERMEDIATE FREQUENCIES
VLBI system (BLK I) IF-video down conversion design
05 p0625 N85-13998
Digital coherent detector
[AD-D011560] 12 p1833 N85-21501
Observations of the MF-HF plasma wave emissions in active auroras by the sounding rocket experiments at Syowa station 14 p2366 N85-24620
Coherently pumped two-frequency laser-type devices
[AD-A154065] 19 p3275 N85-30311
INTERMEDIATE RANGE BALLISTIC MISSILES
NT POLARIS MISSILES
INTERMETALLICS
Influence of 5f electrons on structures and bonding in the actinide-hydrogen intermetallics
[DE84-013893] 01 p0118 N85-10607
Photoelectric effect in liquid crystals
02 p0259 N85-11695
Magnetic properties of intermetallic phases and simple systems — neutron diffraction 03 p0422 N85-12697
Magnetism of the rare earth compounds — intermetallic compounds 03 p0424 N85-12707
Mossbauer effect and contactless conductivity studies of superconducting actinides intermetallics and hydrides. Mossbauer high pressure studies
03 p0430 N85-12743
Cerium compounds in the fashion of the light actinides
[DE84-014642] 04 p0475 N85-13024
Storage life of thermal detents
[DE84-016934] 04 p0476 N85-13030
Thermomagnetic generator
[DE84-017016] 04 p0530 N85-13386
Electronic bandstructure of an incommensurate crystal
[DE84-016891] 05 p0733 N85-14714
High temperature properties of equiatomic FeAl with ternary additions
[NASA-TM-86938] 10 p1439 N85-19072
The B2 aluminides as alternative materials
[NASA-TM-86937] 10 p1440 N85-19076
Alloys based on NiAl for high temperature applications
[NASA-TM-86976] 12 p1805 N85-21322
Angle-resolved photoemission study of AuGa2 and AuIn2 intermetallic compounds
[AD-A150000] 12 p1940 N85-22183
A mixed-basis band structure interpolation scheme applied to the fluorite structure compounds NiSi2, AuAl2, AuGa2 and AuIn2
[AD-A150131] 12 p1940 N85-22187
Magnetic studies of Ni3Al(Fe) compounds
[DE85-005262] 13 p2025 N85-22686

Structure and aging of amorphous chromium-germanium alloys 15 p2497 N85-25401

Experimental studies of the electronic structure of 1-2 and 1-3 intermetallic compounds [DE85-006978] 15 p2662 N85-26432

Changes in lattice cell parameter of film intermetallic compounds RT2 [BLL-M-35874-(5828.4)] 23 p3915 N85-34261

Oxidizing seal for a turbine tip gas path [NASA-CASE-LEW-14053-1] 23 p3937 N85-34402

Oxidation resistant slurry coating for carbon-based materials [NASA-CASE-LEW-13923-1] 24 p4077 N85-35267

INTERMITTENCY

Diffusion and intermittency in an extended one-dimensional maps 02 p0282 N85-11834

Characterization of intermittancy in chaotic systems [PREPRINT-429] 18 p3173 N85-29669

Intermittent gas-liquid flow modeling in horizontal or weakly inclined pipes [EME-132] 20 p3456 N85-31465

Intermittent motion 23 p3925 N85-34323

Noise-sustained structure, intermittency and the Ginzburg-Landau equation [DE85-009626] 24 p4094 N85-35379

INTERMODULATION

Simulation of a transmission circuit composed of slightly nonlinear elements. Computation of the intermodulation on signals composed of N carriers [CNES-NT-105] 04 p0496 N85-13167

The susceptibility of aeronautical navigational aids to interference from adjacent-band broadcast transmissions [BBC-RD-1984/12] 09 p1311 N85-18234

INTERMOLECULAR FORCES

Some unique features of isentrophic flow of gas under high pressures 13 p2043 N85-22788

Molecular dynamics studies of energy transfer processes in crystal systems [DE85-007247] 15 p2662 N85-26426

Simulation studies for surfaces and materials strength [NASA-CR-175786] 16 p2800 N85-27262

INTERMONTANE FLOORS

U VALLEYS

INTERNAL COMBUSTION ENGINES

NT DIESEL ENGINES

NT GAS TURBINE ENGINES

NT J-52 ENGINE

NT J-85 ENGINE

NT JET ENGINES

NT RAMJET ENGINES

NT ROTARY ENGINES

NT SUPERSONIC COMBUSTION RAMJET ENGINES

NT TURBOFAN ENGINES

NT TURBOJET ENGINES

NT TURBOPROP ENGINES

Measurement and analysis of spark ignition engine pressure data to determine heat release profiles [AD-A144770] 01 p0055 N85-10363

The KZD-85 engine test. Engine type: 1 cylinder, 2 stroke motor 2100 Husquarna [FWE-FO-1717] 02 p0205 N85-11354

Advanced concepts for methanol fuel vehicles [DE84-013612] 04 p0482 N85-13071

Detailed performance analysis of the A.A.D. - concept B 04 p0507 N85-13237

A.A.D. engine noise evaluation 04 p0508 N85-13241

Phase 1-A development kinematic Starling/Rankine commercial gas-fired heat pump research program [PB85-100931/GAR] 07 p0936 N85-15928

Cooling system investigation of the 3-kW MEP models 016A, 021A, and 026A (60Hz, 400-Hz and 28-V dc) gasoline-engine-driven generator sets [AD-A147571] 07 p0974 N85-16185

Research and development of alcohol fuel usage in spark ignited engines 09 p1301 N85-18175

Knock syndrome: Its cures and its victims [NASA-CR-174395] 10 p1458 N85-19185

Modeling the internal combustion engine [NASA-RP-1094] 10 p1544 N85-19733

Structural ceramics in transportation: Fuel implications and economic impacts [DE85-003024] 11 p1611 N85-20130

NDE for heat engine ceramics [NASA-TM-86949] 11 p1649 N85-20389

Stratified charge rotary aircraft engine technology enablement program [NASA-CR-174812] 12 p1778 N85-21163

Laboratory tests of reciprocating internal combustion engines [AD-A150143] 13 p2098 N85-23087

Hypergolic combustion demonstration in a reciprocating internal combustion engine [AD-A150846] 14 p2311 N85-24303

Exhaust systems for passenger vehicles: Test procedure for resistance to internal corrosion of silencers [BLL-BISI-TRANS-22360-(9022.06)] 17 p2973 N85-28361

Urban vehicle research project [DE85-005444] 17 p3052 N85-28889

Use of ceramics in internal combustion engines 18 p3088 N85-29114

KIVA: A comprehensive model for 2D and 3D engine simulations [DE85-005562] 18 p3118 N85-29298

Investigation of the behavior of fuel in the intake manifold and its relation to SI engines, 1960 - 1983 19 p3279 N85-30337

KIVA: A computer program for two- and three-dimensional fluid flows with chemical reactions and fuel sprays [DE85-010334] 19 p3339 N85-30693

Friction and wear of solid-lubricated contact in gas turbine engine bearings [AD-A155042] 21 p3596 N85-32335

INTERNAL CONVERSION

Inelastic scattering in condensed matter with high intensity Moessbauer radiation [DE85-003531] 12 p1854 N85-21627

INTERNAL ENERGY

Investigation of internal fields and motions, radiation damages and recovery processes using beta and gamma active probe nuclei 03 p0427 N85-12726

Investigation of solid state problems using the hyperfine interaction between static and dynamic internal fields with short live excited probe nuclei 03 p0428 N85-12729

On the use of internal state variables in thermoviscoplastic constitutive equations 20 p3466 N85-31536

INTERNAL FRICTION

Internal friction, microstructure and radiation effects [DE84-013905] 02 p0288 N85-11880

Control of rotordynamic instability in a typical gas turbine's power system 05 p0642 N85-14120

Interaction of cylindrical shell with concentrated mass moving along its inner surface 13 p2047 N85-22810

Steady-state reaction of three-layered cylindrical shell to effect of moving load 13 p2047 N85-22811

Investigation of internal friction of free-flowing material during discharge [BLL-M-36141-(5828.4)] 15 p2553 N85-25752

Acoustic oscillations of rods and plates 17 p2944 N85-28170

Experimental investigations of the unsteady turbulent friction behavior with pressure impulses in a circular pipe [IWAWI-MITT-102] 18 p3103 N85-29210

INTERNAL PRESSURE

Optimization of pressure vessels with standard intercepting spheres [INPE-3276-PRE/600] 11 p1651 N85-20397

Effect of internal pressure on flexibility and stress intensification factors for pipe elbows analyzed by the finite element method [AD-A151161] 15 p2578 N85-25901

Mechanical ratcheting behaviors of a steel pipe under combined cyclic axial load and internal pressure 23 p3904 N85-34184

INTERNAL STRESS

U RESIDUAL STRESS

INTERNAL WAVES

NT PLANETARY WAVES

An improved analytical theory of Rossby wave driven Eulerian and Lagrangian mean flows along non-zonal barriers with application to the Hawaiian Ridge [AD-A144951] 01 p0088 N85-10593

Internal waves in ocean 06 p0819 N85-15201

Internal gravity waves in real atmosphere 06 p0825 N85-15236

The investigation of selected oceanographic applications of spaceborne synthetic-aperture radar 08 p1146 N85-17233

SAR internal wave signature experiment 08 p1149 N85-17253

Solitons and SEASAT [AD-A148396] 08 p1176 N85-17414

On the classification and nonlinear solution of one type of stratified shear flow [AD-A148832] 09 p1319 N85-18295

Internal Gravity Waves and Small-Scale Turbulence: Proceedings of the 2nd 'Aha Huliko'a Hawaiian Winter Workshop [AD-A149510] 10 p1522 N85-19597

The imaging of internal waves by the SEASAT-A synthetic aperture radar [AD-A149806] 12 p1875 N85-21761

Circulation and internal waves in a cold Gulf Stream waves [AD-A149704] 12 p1898 N85-21918

The imaging of internal waves by the SEASAT-A synthetic aperture radar [ARE(PORTLAND)TN-720/84] 13 p2054 N85-

The effects of internal waves on acoustic normal modes [AD-A150235] 13 p2155 N85-23

Influence of internal gravity waves on F layer 14 p2338 N85-244

SEASAT report [AD-A151283] 15 p2583 N85-259

Sound propagation through directional internal wave fields [AD-A151166] 15 p2646 N85-262

Wave propagation in density stratified fluids 16 p2781 N85-2714

Internal waves in layers of Earth's upper mantle 16 p2807 N85-2731

Turbopause as source of internal gravity waves 16 p2808 N85-2731

Internal waves in marine straits [PREPRINT-415] 18 p3151 N85-2951

Excerpts from the paper: Research Status and Recommendation from the Alaska Workshop on Gravity Waves and Turbulence in the Middle Atmosphere, part 1.3A 21 p3616 N85-3247

On the limiting configuration of interfacial gravity waves [AD-A154821] 21 p3631 N85-325

Theory of soliton waves [AD-A154784] 21 p3676 N85-328

Some aspects of internal gravity waves in a multi-layered moving stratified flow 24 p4092 N85-353

INTERNATIONAL COMETARY EXPLORER

U INTERNATIONAL SUN EARTH EXPLORER 3

INTERNATIONAL COOPERATION

NT OUTER SPACE TREATY

Space Research in Japan. National report 01 p0013 N85-1008

SEPAC (space experiments with particle accelerators) 01 p0014 N85-1009

Balloon observations 01 p0014 N85-1009

Availability of transmission systems in continental and intercontinental connections — telecommunication [FUB-33-1983] 01 p0040 N85-102

Solar heating and cooling R and D program coordination support [DE84-013479] 01 p0068 N85-104

Report of the First Session of the International Working Group on Data Management for the International Satellite Cloud Climatology Project (ISCCP) [WCP-42] 01 p0073 N85-104

Cloud cover sampling capability of various satellite combinations for ISCCP 01 p0073 N85-104

ISCCP Cloud Algorithm Intercomparison Workshop 01 p0073 N85-104

ISSCP Cloud Algorithm Intercomparison Workshop 01 p0073 N85-104

Project COST 72 (The European weather radar project) today 01 p0084 N85-105

Development of space instrumentation of Intercosmos member countries 02 p0163 N85-111

International cooperation and competition in space [GPO-38-001] 02 p0295 N85-1191

International cooperation and competition in space. Introduction 02 p0295 N85-1191

Statement of Kenneth S. Pedersen, Director, International Affairs Division, National Aeronautics and Space Administration 02 p0295 N85-1191

Statement of Otho E. Eskin, Director, Office of Advanced Technology, Department of State 02 p0295 N85-1191

Statement of John H. McElroy, Assistant Administrator for Environmental Satellite, Data and Information Services, National Oceanic and Atmospheric Administration 02 p0295 N85-1191

International cooperation and competition in civilian space activities, summary, appendix 1 02 p0295 N85-1191

NESDIS international activities, appendix 2 02 p0295 N85-1191

AGARD Highlights [AGARD-HIGHLIGHTS-84/2] 02 p0306 N85-119

West Europe report: Science and technology [JPRS-WST-84-004] 03 p0309 N85-11

French, Soviets decide to launch Sigma space telescope 03 p0341 N85-121

International banking of satellite and in-situ wave data by the Marine Information and Advisory Services (MIAS) 03 p0381 N85-124

Competitive assessment of the US information services industry [PB84-174804] 03 p0440 N85-12

The structures and the role of an international agency for the control of satellites [NASA-TM-76765] 03 p0441 N85-12

Colloquium about Joint Projects within DFVLR/ISRO Cooperation
[DFVLR-MITT-84-12] 04 p0458 N85-12907
Presentation of Indian Space Research Organization (ISRO)/DFVLR cooperation 04 p0459 N85-12912
Launching systems
[CNES-NT-111] 04 p0460 N85-12917
The Ebro Observatory and international scientific organizations 04 p0518 N85-13309
Use of Ebro Observatory data at Word Data Center A for Solar-Terrestrial Physics 04 p0518 N85-13310
International coordination in scientific research
04 p0519 N85-13311
International cooperation in remote sensing applications 05 p0656 N85-14209
International Conference on Physics of Clouds
06 p0819 N85-15198
Broadening the debate 07 p0914 N85-15785
International involvement in a civilian space station program 07 p0915 N85-15789
West Europe report: Science and technology
[JPRS-WST-84-039] 07 p0936 N85-15929
Maritime prospecting, mining discussed
07 p0960 N85-16226
The challenge of food production: The importance of climate 07 p1001 N85-16361
The potential contributions of the World Climate Program (WCP) to the economies of developing countries
07 p1003 N85-16371
International projects, other work of Aeroproyekt Institute 08 p1066 N85-16767
FRG study looks at participation in ESA, US space station 08 p1141 N85-17191
UK, FRG, France: R and D in sensors, related fields
08 p1142 N85-17197
International cooperation and competition in civilian space activities
[OTA-ISC-240] 08 p1231 N85-17750
High-technology ceramics in Japan
[TI85-900369] 09 p1299 N85-18157
The Venus Balloon Project 10 p1465 N85-19243
Commentary on start of scientific data transmissions with USSR 10 p1476 N85-19319
Magnetic fusion energy plasma interactive and high heat flux components. Volume 3: Strategy for international collaborations in the areas of plasma materials interactions and high heat flux materials and components development
[DE85-001145] 10 p1559 N85-19829
Window on science visit to the USA, 21 March - 22 April, 1984 — ramjets and solid propellant rocketry
[VTH-LR-426] 11 p1592 N85-20011
FRG's DFVLR ready for participation in space station
11 p1618 N85-20176
TCS Satellite overview 11 p1642 N85-20343
The Middle Atmosphere Program: A special project for the Antarctic Middle Atmosphere (AMA)
11 p1656 N85-20430
Large natural geophysical events: Planetary planning
[DE85-000859] 11 p1763 N85-21092
INMARSAT marine satellite organization
13 p1985 N85-22456
The astrometry network of the IHW and the P/Crommelin trial run results 14 p2435 N85-25016
International conference on COSPAS-SARSAT system
15 p2484 N85-25336
Financial, economic commentary on Airbus, European aviation 15 p2536 N85-25649
NOAA satellite operations: Programs briefing — Environmental satellites, LANDSAT, and space station polar platform 15 p2599 N85-26020
Progress through cooperation and exchange of ideas and experiences 15 p2626 N85-26186
AGARD bulletin: Meetings, publications, membership
[AGARD-BUL-85-1] 15 p2686 N85-26589
Tass reports program for Salyut-7 fully completed
16 p2717 N85-26773
East Europe report: Science and technology
[JPRS-ESA-85-019] 16 p2767 N85-27077
International cooperation in space exploration
16 p2766 N85-27079
The relevance of remote sensing to Brazil
[INPE-3421-PRE/666] 16 p2811 N85-27332
International information networks for material properties: Revision 1
[DE85-007412] 16 p2850 N85-27572
East-West cooperation in outer space
[S-HRG-98-1064] 16 p2879 N85-27767
Construction 1976-1980: Design, manufacturing, calibration of the German-Dutch wind tunnel (DNW)
17 p2905 N85-27913
European utilization aspects of a US manned space station, volume 1
[ESA-CR(P)-1987-VOL-1] 17 p2907 N85-27926
European utilization aspects of a US manned space station, volume 2
[ESA-CR(P)-1987-VOL-2] 17 p2907 N85-27927
Finland, Sweden cooperate in composites research
17 p2946 N85-28184
New ESA director on space station, military space
18 p3066 N85-28982
West Europe report: Science and technology
[JPRS-WST-84-031] 18 p3086 N85-29089
DFVLR official on areas of US-FRG Space Station cooperation 18 p3086 N85-29091
New ESA director on Ariane, space station, future trends 18 p3086 N85-29096
FRG weighs ESA participation, budget issues
18 p3088 N85-29110
DFVLR study recommends European independence in space systems 18 p3088 N85-29111
United States participation in International Energy Agency Task IX, Subtask (C): Pyranometry. 1984 participation
[DE85-009615] 18 p3110 N85-29256
Forecast impact simulation studies
18 p3139 N85-29435
Standards Committee activities of the National Bureau of Standards: 1984 highlights
[PB85-183362] 19 p3350 N85-30784
Report to the Working Group on Technology, Growth and Employment
[DE85-010320] 19 p3372 N85-30920
Cost and schedule implications of multinational coproduction
[AD-A154358] 19 p3380 N85-30969
The international organization of maritime search and rescue 20 p3400 N85-31089
Search and rescue services for international civil aviation 20 p3400 N85-31090
Maritime search and rescue cooperation and planning
20 p3400 N85-31093
The development of an institutional structure for the Future Global Satellite System for Search and Rescue
20 p3406 N85-31138
Studies toward a manned space station: Participation of European industry in NASA space station (MSS)
[SNIAS-S/DT-Y-25-212] 20 p3418 N85-31217
CEMA cooperation in development of robotics, FMS viewed 20 p3438 N85-31331
Antarctica
[S-HRG-98-1161] 20 p3473 N85-31584
United States-Soviet satellite accord: SARSAT/Cospas search-and-rescue program
[GPO-41-113] 20 p3541 N85-32040
International prototype network in Dubna experimental satellite communications system
22 p3773 N85-33383
Research report program of the US Army in Europe
24 p4061 N85-35167
Microwave propagation studies, measurements and education in Surabaya, Indonesia
[B8464633] 24 p4066 N85-35339

INTERNATIONAL GEOSPHERE-BIOSPHERE PROGRAM
International Geosphere/Biosphere Program: 1984
[GPO-39-222] 04 p0578 N85-13691

INTERNATIONAL LAW
NT AIR LAW
NT SPACE LAW

INTERNATIONAL MAGNETOSPHERIC STUDY
Achievements of the International Magnetospheric Study (IMS) — conference
[ESA-SP-217] 14 p2354 N85-24544
Results from the GEOS-1 and GEOS-2 spacecraft and their contributions to the IMS 14 p2354 N85-24545
Observations of auroras and related plasma phenomena by the Kyokko and Jikiken satellite in IMS — EXOS-A and B satellite 14 p2354 N85-24547
The measurements of Prognoz-4, -5, -6, -7 during IMS
14 p2355 N85-24548
The Earth's magnetopause — International Magnetospheric Study 14 p2355 N85-24549
The structure and dynamics of the magnetosphere: Progress in the IMS 14 p2355 N85-24550
Observations of the magnetospheric boundary layers — International Magnetospheric Study
14 p2355 N85-24551
Hot plasma and energetic particles in the Earth's outer magnetosphere: New understandings during the IMS
14 p2355 N85-24552
Magnetic field observations at the dayside magnetopause: ISEE-1 and -2 contributions during the IMS 14 p2356 N85-24555
Ground-based and near-Earth observations during the IMS 14 p2359 N85-24575
IMS advances in studies of field-aligned currents and their related electrodynamics 14 p2359 N85-24578
Results of the SCATHA ion composition experiment during the IMS 14 p2359 N85-24580
Achievements of the plasma composition experiment on ISEE-1 during the IMS 14 p2360 N85-24583
A brief summary of results derived from Scandinavian Twin Auroral Radar Experiment (STARE) observations during IMS — ionospheric electric fields
14 p2362 N85-24595
Characteristics of the electrodynamics of auroral arcs as inferred from rocket and ground-base observations during IMS 14 p2363 N85-24601
An evaluation of the contributions of the IMS to experimental and theoretical studies of ULF plasma
14 p2365 N85-24614
The IMS advances in understanding terrestrial myriametric radiation 14 p2365 N85-24618
Terrestrial continuum radiation study during the IMS
14 p2365 N85-24619
VLF emissions observed by ISIS Satellites during the IMS 14 p2366 N85-24621
Whistler mode waves near the plasmapause: Results from the IMS VLF experiment at Halley, Antarctica
14 p2367 N85-24628
Role of equatorial Electron Cyclotron Harmonic (ECH) waves in the generation of diffuse auroras. Contribution of the GEOS IMS spacecraft 14 p2367 N85-24632
Results of ULF-wave investigations in the USSR
14 p2369 N85-24644
Magnetic pulsations recorded in northern Scandinavia during the IMS; a study of Pc 4-5 events
14 p2370 N85-24647
Advances in magnetospheric plasma diagnosis by active experiments — IMS satellites 14 p2371 N85-24654
The IMS contributions to the understanding of auroral precipitation, transport and particle sources
14 p2372 N85-24660
Advances in magnetospheric plasma-wave research during the IMS 14 p2372 N85-24662
IMS (International Magnetospheric Study) contributions to the understanding of auroral precipitation, transport, and particle sources
[AD-A152320] 17 p2992 N85-28492

INTERNATIONAL PRACTICAL TEMPERATURE
U TEMPERATURE SCALES

INTERNATIONAL RELATIONS
NT INTERNATIONAL COOPERATION
NT OUTER SPACE TREATY
Technology transfer to the Middle East
[PB85-127744] 12 p1952 N85-22264
East-West cooperation in outer space
[S-HRG-98-1064] 16 p2879 N85-27767
Technology and Soviet political choices
[AD-P004566] 17 p3048 N85-28861
Close encounters with S/T (science and technology) in the Soviet Union
[AD-P004570] 17 p3048 N85-28864
Sub-committee on advanced technology and technology transfer
[AD-A153645] 18 p3196 N85-29836
U.S.-China conference on science policy
[PB85-176345] 19 p3380 N85-30971

INTERNATIONAL SATS FOR IONOSPHERIC STUDY
U ISIS SATELLITES

INTERNATIONAL SUN EARTH EXPLORER 1
Observation of a westward travelling surge from satellites at low, medium and high altitudes
[NASA-TM-87434] 09 p1342 N85-18442
Anomalously high potentials observed on ISEE
13 p1994 N85-22503
Some contributions to knowledge of the magnetospheric plasma by ISEE-1 investigators
14 p2354 N85-24546
Magnetic field observations at the dayside magnetopause: ISEE-1 and -2 contributions during the IMS 14 p2356 N85-24555
Magnetotail current sheet and energetic particles observed on ISEE-1 14 p2357 N85-24566
Plasma sheet dynamics deduced from ISEE-1 and -2 energetic particle flux data 14 p2358 N85-24570
The near Earth current sheet: ISEE-1 and -2 case studies 14 p2358 N85-24573
Achievements of the plasma composition experiment on ISEE-1 during the IMS 14 p2360 N85-24583
Magnetospheric pulsations observed by ISEE 1 and 2 satellites 14 p2369 N85-24640
Advances in magnetospheric plasma diagnosis by active experiments — IMS satellites 14 p2371 N85-24654
The downshift of electron plasma oscillations in the electron foreshock region
[NASA-CR-175833] 14 p2423 N85-24945
On the use of a sunward-libration-point orbiting spacecraft as an IMF monitor for magnetospheric studies
[NASA-CR-175809] 16 p2825 N85-27426
Interaction between an interplanetary shock and the Earth's magnetosphere on 27 August 1978: ISEE-1 electric field and ISEE-2 plasma observations
[IFSI-84-15] 20 p3548 N85-32078

ISEE-1 data reduction and analysis plasma composition experiment
[NASA-CR-175306] 21 p3630 N85-32552

INTERNATIONAL SUN EARTH EXPLORER 2

Magnetic field observations at the dayside magnetopause: ISEE-1 and -2 contributions during the IMS 14 p2356 N85-24555

Plasma sheet dynamics deduced from ISEE-1 and -2 energetic particle flux data 14 p2358 N85-24570

The near Earth current sheet: ISEE-1 and -2 case studies 14 p2358 N85-24573

Magnetospheric pulsations observed by ISEE 1 and 2 satellites 14 p2369 N85-24640

Interaction between an interplanetary shock and the Earth's magnetosphere on 27 August 1978: ISEE-1 electric field and ISEE-2 plasma observations
[IFSI-84-15] 20 p3548 N85-32078

INTERNATIONAL SUN EARTH EXPLORER 3

Isotopic composition of primary cosmic rays H-Fe for ISEE-C
[NASA-CR-175266] 06 p0746 N85-14783

Astrometric needs for the ISEE-3/ICE mission to Comet Giacobini-Zinner 14 p2438 N85-25043

On the use of a sunward-libration-point orbiting spacecraft as an IMF monitor for magnetospheric studies
[NASA-CR-175809] 16 p2825 N85-27426

Measurements of galactic hydrogen and helium isotopes from 1978 through 1983
[OG-4.2-2] 22 p3877 N85-34022

The International Cometary Explorer (ICE)wallsheet teacher's guide
[NASA-TM-87496] 23 p3988 N85-34727

INTERNATIONAL SUN EARTH EXPLORERS
NT INTERNATIONAL SUN EARTH EXPLORER 1
NT INTERNATIONAL SUN EARTH EXPLORER 2
NT INTERNATIONAL SUN EARTH EXPLORER 3

The structure and dynamics of the magnetosphere: Progress in the IMS 14 p2355 N85-24550

Terrestrial continuum radiation study during the IMS 14 p2365 N85-24619

Contribution of relaxation sounding experiments to the understanding of magnetospheric processes 14 p2371 N85-24655

The boundary layers as the primary transport regions of the Earth's magnetotail
[AD-A152714] 17 p2992 N85-28496

INTERNATIONAL TRADE

East Europe report: Science and technology
[JPRS-ESA-84-036] 03 p0343 N85-12210

International airport study: How to improve the effect of airports on trade and on export-related industries
[PB85-124923] 11 p1586 N85-19992

Transfer of technology
[S-REPT-98-664] 12 p1949 N85-22246

Transfer of technology
[S-HRG-98-986] 12 p1949 N85-22247

Sub-committee on advanced technology and technology transfer
[AD-A153645] 18 p3198 N85-29836

Irradiation of northwest agricultural products
[DE85-012455] 22 p3843 N85-33803

Federal export assistance programs applicable to the US photovoltaic industry
[NASA-CR-176114] 22 p3849 N85-33841

INTERNATIONAL ULTRAVIOLET EXPLORER
U IUE

INTERORBITAL TRAJECTORIES

Radiation exposure and performance of multiple burn LEO-GEO orbit transfer trajectories
[NASA-TM-86946] 12 p1788 N85-21228

INTERPERSONAL RELATIONS
U HUMAN RELATIONS

INTERPLANETARY COMMUNICATION

Performance analysis of the DSN baseband assembly (Bba) Real-Time Combiner (RTC)
[NASA-CR-175878] 17 p2946 N85-28190

INTERPLANETARY DUST
NT ZODIACAL DUST

Discovery of nuclear tracks in interplanetary dust 06 p0869 N85-15847

Evolution of grains in a turbulent solar nebula 13 p2179 N85-23525

A model of plasma cloud expansion generated by a dust particle impact — Giotto mission 14 p2245 N85-23914

Dynamics of neutral small particles — in the solar system 15 p2676 N85-26521

Dynamics of charged small particles — Jupiter, Saturn magnetospheres 15 p2676 N85-26522

Diffusion of dust around a central body — Keplerian orbits 15 p2676 N85-26523

On the electric charge carried by dust grain excitation of violent discharge — planetary rings 15 p2677 N85-26530

French and West German equipment for Vega Project 16 p2722 N85-26805

The influence of global dust storms on the mean seasonal daily insolations at the Martian surface
[AERONOMICA-ACTA-A-289-1984] 18 p3203 N85-29868

Elemental abundance differences between nuclei accelerated in CIR shocks and solar flares
[SH-2.2-6] 23 p4000 N85-34801

INTERPLANETARY FLIGHT
NT ASTEROID MISSIONS
NT LONG DURATION SPACE FLIGHT

Towards the Halley Comet 14 p2399 N85-24783

TASS update on flights of Vega-1 and Vega-2 16 p2722 N85-26803

Kovtunenko discusses Vega Project 16 p2722 N85-26804

Far travelers: The exploring machines
[NASA-SP-480] 22 p3731 N85-33126

INTERPLANETARY MAGNETIC FIELDS

Response of the F2 layer to the polarity of the interplanetary magnetic field
[REPT-561] 03 p0377 N85-12404

Relations between the particle precipitation events in mid-latitudes, the ring current intensity and the polarity of the interplanetary magnetic field 04 p0519 N85-13316

Sun-aligned polar cap auroral arcs
[AD-A148052] 08 p1185 N85-17472

Solar-geophysical data number 476, April 1984. Part 1: (Prompt reports). Data for March 1984, February 1984 and late data
[PB84-215060] 09 p1416 N85-18936

Partial penetration of IMF B(sub y) into the magnetosphere
[DRI-5-84] 10 p1514 N85-19554

Plans for Interbol satellite experiment 13 p1977 N85-22407

The measurements of Prognoz-4, -5, -6, -7 during IMS 14 p2355 N85-24548

Response of magnetospheric substorm activity to changes in the interplanetary magnetized plasma 14 p2357 N85-24563

On the use of a sunward-libration-point orbiting spacecraft as an IMF monitor for magnetospheric studies
[NASA-CR-175809] 16 p2825 N85-27426

An interplanetary magnetic field ensemble at 1 AU
[NASA-TM-86209] 16 p2882 N85-27784

Results of the magnetic field experiments E2 and E4 onboard Helios 1 and Helios 2 — magnetometer development 16 p2885 N85-27799

Rome/Goddard Space Flight Center (GSFC) magnetic field experiment: A summary of results — flux gate magnetometer 16 p2885 N85-27800

Images of the Earth's aurora and geocorona from the Dynamics Explorer Mission
[NASA-CR-175983] 18 p3136 N85-29423

Fractal structure of the interplanetary magnetic field
[NASA-TM-86212] 19 p3383 N85-30987

Solar-wind magnetosphere energy input functions
[NASA-CR-176021] 19 p3385 N85-31001

The longitudinal asymmetry of the interplanetary perturbation producing Forbush decreases
[IFSI-84-16] 20 p3546 N85-32065

Interplanetary disturbances during Forbush decreases
[IFSI-84-10] 20 p3547 N85-32075

Spectral measurements of magnetic energy and magnetic helicity between 0.29 and 0.97 AU
[IFSI-85-2] 22 p3850 N85-33844

Interplanetary magnetic field control of high-latitude electric fields and currents determined from Greenland magnetometer data
[DMI-GEOPHYS-PAPERS-R-69] 22 p3850 N85-33845

Linear filters as a method of real-time prediction of geomagnetic activity
[DE85-010760] 22 p3860 N85-33899

Determination of the pitch-angle distribution and transverse anisotropy of interplanetary particles
[SH-3.1-11] 23 p4002 N85-34815

Pitch angle distributions of solar energetic particles and the local scattering properties of the interplanetary magnetic field
[SH-3.1-13] 23 p4002 N85-34816

Channeled propagation of solar particles
[SH-3.2-3] 23 p4003 N85-34819

The propagation of solar energetic particles in magnetic channels
[SH-3.2-4] 23 p4003 N85-34820

The local characteristic function of interplanetary particle propagation
[SH-3.2-8] 23 p4003 N85-34823

On reflecting boundary behind the Earth's orbit at propagation of fast particles from solar flares
[SH-3.2-13] 23 p4004 N85-34827

The intensity recovery of Forbush-type decreases as a function of heliocentric distance and its relationship to the 11-year variation
[SH-4.1-9] 23 p4005 N85-34

Cosmic ray modulatin and merged interaction regions
[SH-4.1-11] 23 p4005 N85-34

Cosmic ray modulation in a random anisotropic magnetic field
[SH-4.1-20] 23 p4006 N85-34

Drift and observations in cosmic-ray modulation, 1
[SH-4.2-4] 23 p4007 N85-34

Drift and observations in cosmic-ray modulation, 2
[SH-4.2-5] 23 p4007 N85-34

Cosmic ray north-south anisotropy 1981 - 1983
[SH-4.2-6] 23 p4007 N85-34

Cosmic ray intensity and the tilt of the neutral sheet
[SH-4.2-8] 23 p4007 N85-34

Differential measurement of cosmic-ray gradient with respect to interplanetary current sheet
[SH-4.2-9] 23 p4007 N85-34

Spatial variation of cosmic rays near the heliospheric current sheet
[SH-4.2-10] 23 p4007 N85-34

The effect of the neutral sheet structure of the interplanetary magnetic field on cosmic ray distribution in space
[SH-4.2-18] 23 p4008 N85-34

The dependence of solar modulation on the sign of the cosmic ray particle charge
[SH-4.2-23] 23 p4009 N85-34

An update on the correlation between the cosmic radiation intensity and the geomagnetic AA index
[SH-4.2-24] 23 p4009 N85-34

Isotropic intensity waves and features of their occurrence
[SH-4.3-6] 23 p4032 N85-34

IMF-sense-dependent cosmic ray anisotropy produced from diffusion-convection in heliosphere
[SH-4.3-9] 23 p4032 N85-34

Characteristics of cosmic ray pole-equator anisotropy derived from spherical harmonic analysis of neutron monitor data
[SH-4.3-12] 23 p4032 N85-34

The corotating variation of the north-south anisotropy of cosmic rays
[SH-4.3-15] 23 p4033 N85-34

Sidereal variations deep underground in Tasmania
[SH-4.4-4] 23 p4033 N85-350

The effect of the interplanetary magnetic field on sidereal variations observed at medium depth underground detectors
[SH-4.4-5] 23 p4033 N85-350

Corrected sidereal anisotropy for underground muons
[SH-4.4-7] 23 p4033 N85-350

A study of periodicities and recurrences in solar activity and cosmic ray modulation
[SH-4.4-14] 23 p4034 N85-35010

Solar wind velocity and daily variation of cosmic rays
[SH-4.5-6] 23 p4036 N85-350

Magnetic fluctuation and cosmic ray diurnal variations
[SH-4.5-21] 23 p4038 N85-350

Observation of pick-up ions in the solar wind: Evidence for the source of the anomalous cosmic ray component?
[SH-4.6-5] 23 p4039 N85-350

Possible origin of the anomalous component of cosmic rays
[SH-4.6-7] 23 p4039 N85-350

Anomalous short-term increases in the galactic cosmic ray intensity: Are they related to the interplanetary magnetic cloud-like structures?
[SH-5.1-3] 23 p4041 N85-350

Galactic cosmic ray currents and magnetic field irregularity degree in high-speed solar wind streams
[SH-5.1-9] 23 p4042 N85-35

Influence of magnetic clouds on cosmic ray intensity variations
[SH-5.1-12] 23 p4042 N85-35

Solar activity beyond the disk and variations of the cosmic ray gradient
[SH-5.1-23] 23 p4044 N85-350

Parallel fast-forward shock within 1 AU: Helios-1 and 2 observations
[MPAE-W-79-84-27] 24 p4169 N85-35

INTERPLANETARY MEDIUM
NT INTERPLANETARY DUST
NT ZODIACAL DUST

Helium atoms in interstellar and interplanetary media, part 3: Temperature and velocity of interstellar wind 02 p0160 N85-11

Dust properties determined from backscattering in the interplanetary and interstellar medium 03 p0446 N85-12

Broadening of the interplanetary helium cone structure due to elastic collisions of LISM helium atoms with solar wind ions 06 p0873 N85-15

Solar-geophysical data number 476, April 1984. Part 2: (Comprehensive reports). Data for October 1983, June 1981 and miscellanea
[PB84-218078] 09 p1417 N85-18937
Hydromagnetic precursors of interplanetary plasma burst 13 p1978 N85-22414
Interplanetary shock waves during April and May of 1981 13 p1982 N85-22434
Some features of the interplanetary medium during Forbush decreases
[NOTA-INTERNA-838] 18 p3202 N85-29866
Shocks in the solar wind between 1 and 8.5 AU: Voyager 1 observations
[NASA-CR-175911] 18 p3209 N85-29905
Interplanetary plasma turbulence and the Doppler detection of a gravitational background radiation
[IFSI-85-1] 20 p3546 N85-32066
Interplanetary disturbances during Forbush decreases
[IFSI-84-10] 20 p3547 N85-32075
Some properties of flare-not-associated Forbush decreases
[IFSI-84-13] 20 p3548 N85-32077
Interaction between an interplanetary shock and the Earth's magnetosphere on 27 August 1978: ISEE-1 electric field and ISEE-2 plasma observations
[IFSI-84-15] 20 p3548 N85-32078
Nineteenth International Cosmic Ray Conference. SH sessions, volume 4
[NASA-CP-2376-VOL-4] 23 p3989 N85-34729
Source energy spectra from demodulation of solar particle data by interplanetary and coronal transport
[SH-1.3-13] 23 p3994 N85-34756
Shock and statistical acceleration of energetic particles in the interplanetary medium
[SH-1.5-1] 23 p3996 N85-34771
Energetic ion acceleration at collisionless shocks
[SH-1.5-3] 23 p3996 N85-34772
Particle acceleration due to shocks in the interplanetary field: High time resolution data and simulation results
[SH-1.5-5] 23 p3996 N85-34774
Pitch angle distributions of 35-1000 keV protons at quasi-perpendicular interplanetary shocks
[SH-1.5-6] 23 p3996 N85-34775
Spatial dependence of the local diffusion coefficient measured upstream of the November 12, 1978 interplanetary traveling shock
[SH-1.5-12] 23 p3996 N85-34776
Solar and interplanetary particles at 2 to 4 MEV during solar cycles 21, solar cycle variations of event sizes, and compositions
[SH-1.5-16] 23 p3997 N85-34779
Cosmic ray acceleration by stellar wind. Simulation for heliosphere
[SH-1.5-17] 23 p3997 N85-34780
Low energy proton bidirectional anisotropies and their relation to transient interplanetary magnetic structures: ISEE-3 observations
[SH-3.1-9] 23 p4002 N85-34813
Latitudinal gradients of cosmic rays and the polarity reversal of the heliospheric magnetic field: A preliminary evaluation
[SH-4.2-16] 23 p4006 N85-34853
Solar modulation and interplanetary gradients of the galactic electrons flux, 1977 - 1984
[SH-4.7-4] 23 p4040 N85-35049
Anomalous short-term increases in the galactic cosmic ray intensity: Are they related to the interplanetary magnetic cloud-like structures?
[SH-5.1-3] 23 p4041 N85-35057
A suggested standardized format for cosmic ray ground-level event data
[SH-9.1-15] 23 p4052 N85-35130
INTERPLANETARY MONITORING PLATFORM
U IMP
INTERPLANETARY NAVIGATION
Interplanetary navigation 14 p2398 N85-24781
INTERPLANETARY PROPULSION
U INTERPLANETARY SPACECRAFT
U ROCKET ENGINES
INTERPLANETARY SPACE
Interplanetary cosmic ray intensity: 1972-1984 and out to 32 AU
[AD-A145130] 01 p0131 N85-10903
Interplanetary radio storms. 2: Emission levels and solar wind speed in the range 0.05-0.8 AU
[NASA-TM-84946] 04 p0589 N85-13761
Electric fields in Earth orbital space
[AD-A146448] 06 p0835 N85-15313
Dependence of the high latitude middle atmosphere ionization on structures in interplanetary space
11 p1664 N85-20487
The Helios radio astronomy experiment
16 p2886 N85-27803
The energy spectrum of Jovian electrons in interplanetary space
[SH-1.5-10] 21 p3715 N85-33051
Possible detection of flare-generated positrons by Helios 1 on 3 Jun 1982
[SH-1.4-10] 23 p3996 N85-34770
Variations in elemental composition of several MEV/nucleon ions observed in interplanetary space
[SH-2.1-7] 23 p3998 N85-34788
On the retention of high-energy protons and nuclei with charges Z or equal to 2 in large solar flares after the process of their acceleration
[SH-2.1-8] 23 p3998 N85-34789
Isotopic overabundances and the energetic particle model of solar flares
[SH-2.2-1] 23 p4000 N85-34798
Radial transport of approximately 1 MeV/nucleon ions during the 22 November 1977 solar particle event
[SH-3.2-5] 23 p4003 N85-34821
Investigation of cosmic ray propagation in interplanetary space
[SH-3.2-9] 23 p4004 N85-34824
Monte Carlo calculations of relativistic solar proton propagation in interplanetary space
[SH-3.2-11] 23 p4004 N85-34826
The influence of nonstationarity of the solar activity and general solar field on modulation of cosmic rays
[SH-4.2-17] 23 p4006 N85-34854
The cosmic ray interplanetary radial gradient from 1972 - 1985
[SH-4.7-1] 23 p4040 N85-35046
The large scale dynamics of the outer heliosphere and the long-term modulation of galactic cosmic rays
[SH-4.7-3] 23 p4040 N85-35048
Study of cosmic ray scintillations from 5-minute data of the scintillations telescope Izmran and world-wide network stations
[SH-5.1-18] 23 p4043 N85-35071
The theoretical and experimental investigation of cosmic ray Forbush-effects
[SH-5.1-20] 23 p4044 N85-35072
Observation of nuclei with energies 8-30 MeV per nucleon in the Earth's magnetosphere at the altitudes 350 KM
[SH-10.1-5] 23 p4053 N85-35136
INTERPLANETARY SPACECRAFT
NT GALILEO PROBE
NT GALILEO SPACECRAFT
NT JUPITER PROBES
NT MARINER 5 SPACE PROBE
NT MARINER 9 SPACE PROBE
NT MARS PROBES
NT PIONEER SPACE PROBES
NT PIONEER VENUS SPACECRAFT
NT PIONEER 10 SPACE PROBE
NT VENERA SATELLITES
NT VENERA 11 SATELLITE
NT VENUS PROBES
NT VIKING LANDER SPACECRAFT
NT VIKING LANDER 1
NT VIKING ORBITER SPACECRAFT
NT VIKING SPACECRAFT
NT VOYAGER 1 SPACECRAFT
NT VOYAGER 2 SPACECRAFT
Interplanetary plasma turbulence and the Doppler detection of a gravitational background radiation
[IFSI-85-1] 20 p3546 N85-32066
Far travelers: The exploring machines
[NASA-SP-480] 22 p3731 N85-33126
INTERPLANETARY TRAJECTORIES
Interplanetary trajectories 05 p0600 N85-13827
Towards the Halley Comet 14 p2399 N85-24783
INTERPLANETARY TRANSFER ORBITS
Interplanetary trajectories 05 p0600 N85-13827
INTERPOLATION
Interpolation formulas for viscosity of six gases: Air, nitrogen, carbon dioxide, helium, argon and oxygen
[PB84-217801] 01 p0026 N85-10161
Floating-point function generation routines for 16-bit microcomputers
[NASA-TM-83783] 01 p0102 N85-10683
Oscillatory integrals by Hermite interpolatory rules
[CSIR-TWISK-301] 01 p0108 N85-10725
A trivariate Clough-Tocher scheme for tetrahedral data
[AD-A144740] 01 p0111 N85-10751
Utilization of interpolation and transformation for the compression of digital image data
[INPE-3061-PRE/479] 02 p0240 N85-11566
Application of summability methods to Jackson theorems for splines
[AD-A146256] 03 p0412 N85-12635
Spatial and temporal interpolation of NEROS radiosonde winds
[PB84-232545] 04 p0540 N85-13436
Interpolating sequences for H to infinity in the ball
[CTH-MATH-1984-15] 04 p0556 N85-13542
Comparison of optimum interpolation and Cressman analyses 05 p0680 N85-14371
Analytical construction of flight vehicle surfaces
06 p0775 N85-14957
Robust prediction and interpolation for vector stationary processes, part 3
[AD-A147860] 07 p1036 N85-16579
Analysis of geohydrologic data by kriging
[AD-P004152] 09 p1349 N85-18486
Interpolation methods for GTD analysis of shaped reflectors 10 p1463 N85-19231
Some qualitative properties of bivariate Euler-Frobenius polynomials
[AD-A149408] 10 p1547 N85-19755
Scattered data interpolation using thin plate splines with tension
[AD-A149803] 12 p1866 N85-21705
A mixed-basis band structure interpolation scheme applied to the fluorite structure compounds NiSi2, AuAl2, AuGa2 and AuIn2
[AD-A150131] 12 p1940 N85-22187
Digital standards conversion: Interpolation theory and aperture synthesis
[BBC-RD-1984/20] 13 p2053 N85-22857
Analysis of spectral operators in one-dimensional domains
[NASA-CR-172573] 15 p2633 N85-26228
Scattered data interpolation and approximation
[DE85-007495] 15 p2641 N85-26290
An incremental multigrid strategy for the fluid dynamics equations
[AD-A151953] 16 p2783 N85-27172
An interpolation method with the possibility of first derivative correction
[INPE-3352-PRE/631] 16 p2853 N85-27590
Surface interpolation using weighted splines
[INPE-3387-PRE/658] 16 p2853 N85-27591
Evaluation of interpolative modeling concepts for fatigue crack growth at elevated temperature
[AD-A153222] 17 p2980 N85-28422
Shape preserving spline interpolation
17 p3003 N85-28564
A survey of patch methods 17 p3003 N85-28567
Convex interpolating splines of arbitrary degree
17 p3004 N85-28574
A natural bias approach to cardinal spline curves
17 p3004 N85-28575
Montonicity preserving bicubic interpolation, revision 1
[DE85-007976] 17 p3021 N85-28683
Confidence intervals based on interpolated order statistics
[AD-A152607] 17 p3025 N85-28701
A study of aerodynamic control in stalled flight leading-edge vortex formation analysis
[AD-A153758] 18 p3059 N85-28928
Comparison of optimum interpolation and Cressman analyses 18 p3141 N85-29448
Development and testing of the variable vertical resolution Fourth Order GCM 18 p3142 N85-29453
Developement of an optimum interpolation analysis method for the CYBER 205 18 p3143 N85-29456
Scattered data interpolation codes
[DE85-007337] 18 p3164 N85-29601
Monotonicity preserving bicubic interpolation
[DE85-004206] 18 p3172 N85-29657
Interpolation and differentiation for periodic functions
[PREPRINT-419] 18 p3172 N85-29662
Mathematics of surfaces
[DE85-010439] 19 p3346 N85-30742
An objective analysis technique for extrapolating tidal fields 20 p3493 N85-31715
Interpolation problems in meteor radar analysis, part 7.6A 21 p3626 N85-32528
Heterodyne holographic interferometry for visualization of surface acoustic waves
[AD-A155405] 22 p3836 N85-33753
The improved display of 625-line television pictures: Adaptive interpolation
[BBC-RD-1985/5] 23 p3925 N85-34328
Reports from the German Meteorological Service. No. 166: The optimal spectral density of climatological station networks
[ISBN-3-88148-214-8] 23 p3950 N85-34478
Geometric continuity with interpolating Bezier curves
23 p3963 N85-34570
Users guide for optimum interpolation method of global data assimilation
[AD-A155929] 24 p4138 N85-35648
Two methods of global data assimilation
[AD-A155961] 24 p4143 N85-35684
INTERPOLATORS
U REPEATERS
INTERPROCESSOR COMMUNICATION
Activities of the MIT Laboratory for Computer Science
[AD-A145134] 01 p0100 N85-10661
REMOTE: Modem Communicator Program for the IBM personal computer
[DE84-015047] 01 p0100 N85-10665

Numerical algorithms and parallel tasking
[AD-A145090] 01 p0104 N85-10693

The development of an optoelectronic assembly applied to computer systems
[AD-A145028] 01 p0120 N85-10621

Multiplexing the ethernet interface among VAX/VMS users
[AD-A145539] 02 p0243 N85-11588

The design and performance analysis of an arbiter for a multi-processor shared-memory system
[AD-A146074] 03 p0403 N85-12566

Requirements and overview of the LINCS distributed operating system architecture
[DE84-013721] 05 p0714 N85-14577

Design and analysis of an SQL (Structured Query Language) interface for a multi-backend database system
[AD-A146534] 06 p0856 N85-15447

Decentralized control of scheduling in distributed systems
[AD-A147446] 07 p1022 N85-16487

Local area network evaluation by MICROSS extensions
[AD-A146773] 07 p1027 N85-16521

Decentralized control of scheduling in distributed systems
[AD-A147445] 07 p1028 N85-16523

Architecture for a demonstration radar-communication link
[AD-A147635] 08 p1150 N85-17260

NSWC-NADC interactive communication links for AN/UYS-1 loadtape creation and retrieval
[AD-A148418] 08 p1153 N85-17277

Adapting logistics models to a microcomputer for interface with computer-aided design systems
[AD-A147066] 08 p1202 N85-17566

Benchmarking database systems in multiple backend configurations
[AD-A148191] 08 p1202 N85-17568

Some experiences of testing protocol implementations — open systems interconnection
[NPL-DITC-46/84] 08 p1204 N85-17574

EGP (Exterior Gateway Protocol) gateway under Berkeley UNIX 4.2
[AD-A148056] 08 p1208 N85-17597

Performance evaluation and control of distributed computer communication networks
[AD-A148103] 08 p1208 N85-17598

Asynchronous distributed flow control algorithms
[AD-A148452] 08 p1208 N85-17600

Performance evaluation of a database system in multiple backend configurations
[AD-A148192] 08 p1229 N85-17743

Gateway testing techniques — computer system interconnection
[NPL-DITC-49/84] 09 p1372 N85-18621

Distributed data processing design methodology
[AD-A148668] 10 p1537 N85-19692

Pluribus Satellite IMP (Interface Message Provision) development mobile access terminal network
[AD-A151201] 15 p2541 N85-25688

Evaluating computer-communication networks with simulation techniques
[AD-A151652] 15 p2632 N85-26222

Interfacing the VAX 11/780 using Berkeley Unix 4.2.BSD and Ethernet based Xerox network systems, volume 1
[AD-A152953] 17 p3015 N85-28645

A real-time executive for multiple-computer clusters
[AD-A152961] 17 p3015 N85-28646

Interfacing the VAX 11/780 using berkeley UNIX 4.2BSD and Ethernet based Xerox Network Systems
[AD-A153174] 17 p3016 N85-28647

Multicomputer operating systems and applications
[AD-A153205] 17 p3016 N85-28648

Distributed elections in a ring of processors using Archimedean time
[CWI-CS-R8416] 17 p3016 N85-28653

Reliability report for communication networks
[AD-A153764] 18 p3090 N85-29127

Performance evaluation of stochastic timed decision-free Petri Nets
[AD-A153987] 18 p3171 N85-29652

Computer center policy
[AD-A154416] 19 p3336 N85-30681

VLSI structures for numerical and digital signal processing computations 20 p3439 N85-31340

Implementation assessment of the OSI network service. The test definition language
[NPL-DITC-52/84] 20 p3514 N85-31849

Broadcasting topology and routing information in computer networks
[AD-A155668] 21 p3674 N85-32827

Parallel Cholesky factorization in message-passing multiprocessor environments
[DE85-012070] 22 p3830 N85-33717

Interprocess communication
[AD-A156337] 24 p4088 N85-35337

INTERRELATIONSHIPS
U RELATIONSHIPS

INTERROGATION

Design and analysis of an SQL (Structured Query Language) interface for a multi-backend database system
[AD-A146534] 06 p0856 N85-15447

Steps towards parsing of query sequences to a database
[AD-A146769] 08 p1206 N85-17590

Design of a pictorial program reference language
[AD-A149323] 10 p1540 N85-19711

INTERRUPTION

A single server queue with mixed types of interruptions
[AD-A148536] 08 p1213 N85-17637

Current interruption by density depression
[DE85-013120] 24 p4169 N85-35846

INTERSECTIONS

An iterative procedure for obtaining I-projections onto the intersection of convex sets
[AD-A145402] 02 p0251 N85-11639

Comparison of two algebraic methods for curve/curve intersection 17 p3007 N85-28591

A comparison of three curve intersection algorithms 17 p3007 N85-28592

Intersection of three-dimensional geometric surfaces
[NASA-TP-2454] 20 p3513 N85-31839

INTERSTELLAR CHEMISTRY

Distribution and properties of molecular clouds in the galaxy 03 p0442 N85-12810

Relation of core structure to high velocity outflow in G35.2-0.74 and other molecular clouds 03 p0443 N85-12818

Time-dependent chemistry of molecular clouds 03 p0443 N85-12822

IUE observations of interstellar lines 11 p1748 N85-20996

Observations of Mg 1 and Mg 2 in the local ISM 11 p1748 N85-20997

The dependence of interstellar element depletions on mean space density 11 p1749 N85-20998

INTERSTELLAR COMMUNICATION

Interstellar mission 04 p0459 N85-12916

The search for extraterrestrial intelligence 15 p2669 N85-26609

Where is everybody? An account of Fermi's question
[DE85-011898] 19 p3383 N85-30988

INTERSTELLAR EXTINCTION

Local interstellar extinction with an emphasis on uvby beta results 06 p0875 N85-15559

Do the arching HI filaments show in local reddening data? 06 p0876 N85-15561

Inverse relations between 0.25 keV counts and local interstellar dust 06 p0877 N85-15572

Nearby molecular hydrogen 06 p0879 N85-15582

The atmospheric extinction problem 08 p1251 N85-17901

Magellanic cloud objects 11 p1744 N85-20965

The variation of galactic interstellar extenction in the ultraviolet 11 p1749 N85-21000

Interstellar extinction in the nucleus of H PER 11 p1749 N85-21001

The UV extinction of HR 5999 11 p1753 N85-21026

Physical models for the UV continua of symbiotic stars 11 p1756 N85-21048

IUE and optical observations of LMC X-ray binaries 11 p1757 N85-21050

Tasks for observations of close binary systems in the extreme ultraviolet 11 p1757 N85-21054

Dynamics of long-period comets 13 p2176 N85-23506

The structure of Herbig-Haro object 43 and Orion dark cloud extinction
[NASA-TM-87503] 24 p4166 N85-35831

INTERSTELLAR GAS
NT NEUTRAL GASES

Relation of core structure to high velocity outflow in G35.2-0.74 and other molecular clouds 03 p0443 N85-12818

Changes of LISM characteristics in the heliospheric interface 06 p0873 N85-15542

Probe of the nearby interstellar medium by the vacant line of sight to Beta CMa 06 p0874 N85-15551

IUE observations of the gaseous component of the local interstellar medium 06 p0874 N85-15553

Optical emission line studies and the warm, ionized component of the local interstellar medium 06 p0875 N85-15555

A high-resolution study of local interstellar sodium 06 p0875 N85-15556

Optical observations of nearby interstellar gas 06 p0875 N85-15557

Local interstellar extinction with an emphasis in uvby beta results 06 p0875 N85-1555[illegible]

Do the arching HI filaments show in local reddening data? 06 p0876 N85-155[illegible]

Absorption and emission of EUV radiation by the local ISM 06 p0876 N85-15[illegible]

Observations of highly-ionized interstellar iron 06 p0876 N85-15[illegible]

Local contributions to the 0.6 keV diffuse X-ray background 06 p0877 N85-15[illegible]

Inverse relations between 0.25 keV counts and local interstellar dust 06 p0877 N85-1557[illegible]

Dark cloud and globule distribution for galactic longitudes 230 to 360 degrees 06 p0878 N85-1557[illegible]

The smallest sizes of diffuse interstellar clouds 06 p0878 N85-1557[illegible]

Polarization of radio molecular lines and mapping of magnetic field direction 06 p0878 N85-158[illegible]

Nearby molecular hydrogen 06 p0879 N85-1558[illegible]

Modelling the local interstellar medium as a supernova remnant in a multiphase gas 06 p0879 N85-158[illegible]

Kinematics of nearby gas and stars 06 p0880 N85-1559[illegible]

The environment of active galactic nuclei 07 p1057 N85-1671[illegible]

Radio Seyferts and the forbidden line region 08 p1236 N85-177[illegible]

On the stability of broad line clouds in active galactic nuclei 08 p1243 N85-178[illegible]

Far-infrared spectroscopy of interstellar gas 08 p1245 N85-178[illegible]

Multi-spectral observations of the star formation: The role of far infrared photometry 08 p1245 N85-178[illegible]

First results of submillimeter polarimetry 08 p1246 N85-178[illegible]

Far-infrared spectroscopy of galaxies: The 158 micron C(+) line 08 p1249 N85-178[illegible]

Molecular hydrogen and thermal phases in astrophysics 09 p1414 N85-18[illegible]

IUE absorption line studies of highly ionized interstellar gas 11 p1743 N85-209[illegible]

Supernova remnants and the carbon abundance in M33 11 p1745 N85-2097[illegible]

The UV extinction laws in two very young clusters, NGC 6530 in the galaxy and NGC 2100 in the LMC 11 p1748 N85-209[illegible]

Observations of Mg 1 and Mg 2 in the local ISM 11 p1748 N85-209[illegible]

The dependence of interstellar element depletions on mean space density 11 p1749 N85-209[illegible]

High-velocity interstellar gas in the line-of-sight to HD 50896 11 p1749 N85-209[illegible]

Helium atoms in interstellar and interplanetary space. II: Determination of direction of interstellar gas motion relative to Sun 13 p1980 N85-224[illegible]

Numerical study of a two-fluid hydrodynamical model of interstellar medium and population 1 stars 14 p2440 N85-25[illegible]

Spectral constraints on models of gas in clusters of galaxies
[NASA-TM-86186] 15 p2669 N85-26[illegible]

The structure of galactic HI in directions of low total column density
[NASA-CR-175709] 16 p2882 N85-27[illegible]

The extent of the local hi halo
[NASA-CR-176115] 23 p3967 N85-347[illegible]

On the influence of the heliomagnetospheric periphery on the galactic cosmic rays
[SH-4.2-19] 23 p4009 N85-34[illegible]

On the importance of interstellar helium for the propagation of heavy cosmic rays
[OG-7.2-11] 23 p4015 N85-34[illegible]

The role of cosmic rays in magnetic hydrodynamics of interstellar medium
[OG-7.2-15] 23 p4015 N85-34[illegible]

The HEAO-2 Guest Investigator Program: Non-linear growth of instabilities in line-driven stellar winds
[NASA-CR-176168] 24 p4168 N85-35[illegible]

INTERSTELLAR MAGNETIC FIELDS

Models of nonkeplerian accretion disks based on dynamo magnetic field: Application to Active Galactic Nuclei (AGN) 08 p1242 N85-178[illegible]

Some constraints on magnetic fields in galactic spiral arms 12 p1957 N85-2[illegible]

Variations in the small-scale galactic magnetic field and short time-scale intensity variations of extragalactic radio sources 20 p3549 N85-3[illegible]

A simulation of high energy cosmic ray propagation 1
[OG-5.4-1] 22 p3885 N85-3[illegible]

Modeling cosmic ray anisotropies near 10(18) eV
[OG-5.4-9] 22 p3886 N85-34[illegible]

On galactic origin of cosmic rays with energy up to 10(18) eV
[OG-5.4-15] 22 p3887 N85-34[illegible]

Relativistic electron in curved magnetic fields
[OG-6.2-11] 22 p3890 N85-341[illegible]

Angular resolution of an EAS array for gamma ray astronomy energies 5 x 10 (13) eV
[OG-9.5-5] 23 p4031 N85-34965
Change of cosmic ray anisotropy with solar activity
[SH-4.5-30] 23 p4038 N85-35037

INTERSTELLAR MASERS
An infrared study of the bi-polar outflow region GGD 12-15
[NASA-TM-86655] 03 p0445 N85-12835
The relevance of QUASAT to the star formation problem 07 p1058 N85-16718
Galactic OH and H2O masers — QUASAT project
07 p1058 N85-16719
Water maser outburst 07 p1058 N85-16720
Water masers and distance measurements: The impact of QUASAT 07 p1059 N85-16721

INTERSTELLAR MATTER
Helium atoms in interstellar and interplanetary media, part 2: Temperature and velocity of interstellar wind
02 p0160 N85-11066
Molecules in external galaxies
03 p0444 N85-12828
Detection of submillimeter polarization in the Orion Nebula
[NASA-TM-86013] 04 p0579 N85-13700
Structural properties of open star clusters and their relation to the galaxy 05 p0736 N85-14733
The dynamical evolution of the environment of an OB association 05 p0739 N85-14752
Local Interstellar Medium. International Astronomical Union Colloquium No. 81
[NASA-CP-2345] 06 p0872 N85-15539
Absorption line studies and the distribution of neutral gas in the local interstellar medium
06 p0873 N85-15544
Synthesis of data on the local interstellar medium
06 p0874 N85-15545
Observations of interstellar HI toward nearby late-type stars 06 p0874 N85-15546
Observations of local interstellar Mg I and Mg II
06 p0874 N85-15547
Mg II spectra of late type stars used to probe the LISM 06 p0874 N85-15548
FeII and MgII in the nearby interstellar medium
06 p0874 N85-15549
A type stars as probes of the local interstellar medium
06 p0874 N85-15550
Deuterium abundance in the local interstellar medium
06 p0874 N85-15552
Voyager EUV and FUV observations
06 p0875 N85-15554
Distances of local clouds from optical line observations 06 p0875 N85-15558
Optical polarization as a probe of the local interstellar medium 06 p0875 N85-15560
Do the arching HI filaments show in local reddening data? 06 p0876 N85-15561
Observations of absorption lines from highly ionized atoms 06 p0876 N85-15562
Absorption and emission of EUV radiation by the local ISM 06 p0876 N85-15563
Detection of narrow C 4 and Si 4 absorption features in spectra of stars within 200 pc f the Sun
06 p0876 N85-15564
Observations of highly-ionized interstellar iron
06 p0876 N85-15565
The soft X-ray diffuse background: Implications for the nature of the local interstellar medium
06 p0876 N85-15566
Non-local origin of a substantial portion of the soft X-ray background 06 p0877 N85-15567
Local contributions to the 0.6 keV diffuse X-ray background 06 p0877 N85-15569
HEAO-1 diffuse soft X-ray sky maps
06 p0877 N85-15570
Ultrasoft X-ray background observations of the local interstellar medium 06 p0877 N85-15571
Inverse relations between 0.25 keV counts and local interstellar dust 06 p0877 N85-15572
Molecular clouds within 100 pc
06 p0877 N85-15573
A wide latitude CO survey of molecular clouds in the northern Milky Way 06 p0877 N85-15574
Non equilibrium ionization in the local hot bubble
06 p0879 N85-15587
Large-scale bubble structure of the interstellar medium (ISM) and properties of the Local Spiral Arm (LSA)
06 p0879 N85-15588
Stromgren trails of hot white dwarfs
06 p0879 N85-15589
Magnetic alignment theory and the interpretation of polarization 06 p0880 N85-15590
Dark matter near the sun: Simulated star counts and the Oort limit 06 p0880 N85-15592
Future studies of the local interstellar medium with Space Telescope and Columbus 06 p0880 N85-15593
Observations of local ISM emission with the Berkeley EUV/FUV shuttle telescope 06 p0880 N85-15594
Measuring EUV line emission from the hot interstellar medium 06 p0880 N85-15595
Far-infrared spectroscopy of interstellar gas
08 p1245 N85-17858
Multi-spectral observations of the star formation: The role of far infrared photometry 08 p1245 N85-17859
The 1.5 - 3.5 micron spectroscopy of the Orion H2 source 08 p1246 N85-17864
High sensitivity, high angular resolution far-infrared photometry from the KAO 08 p1246 N85-17867
Interstellar grain mantles 08 p1247 N85-17874
Boundary conditions for the paleoenvironment: Chemical and physical processes in the pre-solar nebula — molecular clouds, interstellar matter, and abundance
[NASA-CR-174370] 10 p1570 N85-19901
Future of Ultraviolet Astronomy Based on Six Years of IUE Research
[NASA-CP-2349] 11 p1743 N85-20961
Magellanic cloud objects 11 p1744 N85-20965
Comments on the origins and variations of carbon and nitrogen in the ISM of galaxies as evident from IUE spectroscopy of H 2 regions 11 p1745 N85-20973
IUE observations of interstellar lines
11 p1748 N85-20996
Dynamics of long-period comets
13 p2176 N85-23506
A soft X-ray survey of galactic supernova remnants with the Einstein Observatory 14 p2434 N85-25013
The propagation of ultraheavy cosmic rays
15 p2665 N85-26582
The soft X-ray background as a supernova blast wave viewed from inside: Solar abundance models
[NASA-CR-175767] 16 p2867 N85-27813
Photoabsorption and photodissociation of molecules important in the interstellar medium
[NASA-CR-175916] 19 p3383 N85-30986
The hydrodynamic effects of nuclear active galaxy winds on host galaxies 20 p3545 N85-32062
Local interstellar medium and gamma-ray astronomy
[OG-3.1-1] 22 p3873 N85-33989
Multicomponent analysis of total COS-B gamma-ray data at intermediate latitudes
[OG-3.1-3] 22 p3873 N85-33991
Constraints on the galactic distribution of cosmic rays from the COS-B gamma-ray data
[OG-3.1-6] 22 p3873 N85-33994
Relevance of cosmic gamma rays to the mass of gas in the galaxy
[OG-3.1-8] 22 p3874 N85-33996
COS-B gamma-ray sources and interstellar gas
[OG-3.1-9] 22 p3874 N85-33997
SMM detection of interstellar Al-26 gamma radiation
[OG-3.2-1] 22 p3874 N85-34001
Galactic distribution of interstellar Al-26
[OG-3.2-3] 22 p3874 N85-34002
Interpretation of cosmic-ray anisotropy below 10(14) eV
[OG-5.4-13] 22 p3887 N85-34090
The flux of secondary anti-deuterons and antihelium produced in the interstellar medium
[OG-6.1-5] 22 p3888 N85-34096
Analysis of experimental data on interstellar antiprotons in the light of measurements of high-energy electrons and He-3 nuclei
[OG-6.1-6] 22 p3888 N85-34097
Spectral shape variation of interstellar electrons at high energies
[OG-6.2-7] 22 p3889 N85-34106
Reestimation of the production spectra of cosmic ray secondary positrons and electrons in the ISM
[OG-6.2-8] 22 p3889 N85-34107
Variations in the propagation of UH-nuclei
[OG-7.1-1] 23 p4012 N85-34863
Electron capture decay of cosmic rays: A model of the inhomogeneous interstellar medium
[OG-7.1-10] 23 p4014 N85-34871
The effects of newly measured cross sections in hydrogen on the production of secondary nuclei during the propagation of cosmic rays through interstellar H
[OG-7.2-2] 23 p4014 N85-34874
Interstellar turbulence, random density variations, and scintillation measurements
[OG-7.2-13] 23 p4015 N85-34880
Interstellar (Na-22) as a possible source of the excess (Ne-22) in the galactic cosmic ray
[OG-8.2-12] 23 p4020 N85-34908
Giant molecular clouds as regions of particle acceleration 23 p4020 N85-34913
Secondary to primary ratio and the continuous acceleration
[OG-8.3-4] 23 p4022 N85-34923
Exact solutions for sporadic acceleration of cosmic rays
[OG-8.3-7] 23 p4022 N85-34925

INTERSTELLAR MICROWAVE SPECTRA
U INTERSTELLAR RADIATION
U MICROWAVE SPECTRA

INTERSTELLAR RADIATION
Polarization of radio molecular lines and mapping of magnetic field direction 06 p0878 N85-15581
Radiation exposure and performance of multiple burn LEO-GEO orbit transfer trajectories
[NASA-TM-86946] 12 p1788 N85-21228
Pulsars and interstellar medium
12 p1960 N85-22320
Contributions to the 19th International Cosmic Ray Conference
[NASA-CR-176060] 21 p3714 N85-33044
Observations of Cygnus X-3 above 10(15) eV from 1979 - 1984
[OG-2.1-6] 22 p3863 N85-33923
Interstellar propagation and the isotopic composition of hydrogen in the galactic cosmic rays
[OG-4.2-1] 22 p3877 N85-34021
Influence of the source distribution on the age distribution of galactic cosmic rays
[OG-8.3-1] 23 p4021 N85-34920

INTERSTELLAR REDDENING
U INTERSTELLAR EXTINCTION

INTERSTELLAR SPACE
Dust properties determined from backscattering in the interplanetary and interstellar medium
03 p0446 N85-12836
Helium and hydrogen of the local interstellar mdium observed in the vicinity of the Sun
06 p0873 N85-15540
Pioneer 10 and Voyager observations of the interstellar medium in scattered emission of the He 584 A and H Lya 1216 A lines 06 p0873 N85-15541
Changes of LISM characteristics in the heliospheric interface 06 p0873 N85-15542
Broadening of the interplanetary helium cone structure due to elastic collisions of LISM helium atoms with solar wind ions 06 p0873 N85-15543
Synthesis of data on the local interstellar medium
06 p0874 N85-15545
Magnetic alignment theory and the interpretation of polarization 06 p0880 N85-15590
QUASAT, gravitational lenses, and studies of the interstellar, intracluster and intergalactic medium
07 p1058 N85-16715
Pulsars and interstellar medium
12 p1960 N85-22320
Activities report of the Institute for Astronomy and Astrophysics
[MITT-5] 14 p2434 N85-25012
On the influence of the heliomagnetospheric periphery on the galactic cosmic rays
[SH-4.2-19] 23 p4009 N85-34856
Cosmic ray secondary nuclei and the structure of the galaxy
[OG-7.2-4] 23 p4014 N85-34876
On the cosmic ray diffusion in a violent interstellar medium
[OG-7.2-14] 23 p4015 N85-34881
The role of cosmic rays in magnetic hydrodynamics of interstellar medium
[OG-7.2-15] 23 p4015 N85-34882

INTERSTELLAR SPACECRAFT
Interstellar mission 04 p0459 N85-12916

INTERSTELLAR TRAVEL
Where is everybody? An account of Fermi's question
[DE85-011898] 19 p3383 N85-30988

INTERSTITIALS
Investigation of the interaction of atoms with lattice defects using probe methods 03 p0429 N85-12737
Interaction of hydrogen with defects in metals
[DE84-016781] 04 p0476 N85-13032
Evaluation of interstitial gas contamination in titanium alloys using induced magnetic field analysis
[AD-P004130] 08 p1127 N85-17105
Electromagnetic NDE of interstitial contamination in titanium alloy weldments
[AD-P004131] 08 p1127 N85-17106
Evaluation of the thermoelectric method for determination of interstitial gases in titanium
[AD-P004132] 08 p1127 N85-17107
Enhanced diffusion from interstitial trapping during solid-phase-epitaxial growth of silicon alloys
[DE85-001285] 12 p1941 N85-22193
Current understanding of point defects and diffusion processes in silicon 20 p3481 N85-31632

INTERTROPICAL CONVERGENT ZONES
Plans for the NRL/NORDA (Naval Research Laboratory-Naval Ocean Research and Development Activity) fine-scale variability experiment - 1984 (FVX-84)
[AD-A148041] 03 p0398 N85-12540
Simple prediction of convergence zone propagation in waters around australia
[AD-A145986] 03 p0416 N85-12659

INTERVALS
Construction of approximate confidence intervals for probability-of-kill via the bootstrap
[AD-A144761] 01 p0113 N85-10764
Interval mathematics reports
[REPT-84/1] 04 p0556 N85-13536
Interval-mathematical treatment of initial value problems of ordinary differential equations
04 p0556 N85-13538
Interval interation methods for nonlinear equation systems: Theory and comparison on computer
[INTERVALL-BER-84/6] 05 p0719 N85-14612
Bootstrap confidence intervals
[AD-A147572] 07 p1033 N85-16559
Exact simultaneous confidence intervals for pairwise comparisons of three normal means
[AD-A148751] 09 p1375 N85-18645
Confidence intervals using the regenerative method for simulation output analysis
[AD-A150147] 13 p2149 N85-23343
Better bootstrap confidence intervals
[AD-A150798] 14 p2408 N85-24846
The measurement of human time estimating ability using a modified jerison device
[AD-A151870] 15 p2620 N85-26141
Proceedings of the Sixteenth Annual Precise Time and Time Interval (PTTI) Applications and Planning Meeting
[NASA-TM-87561] 18 p3105 N85-29221
Fixed width interval estimation in linear regression
[AD-A153633] 18 p3174 N85-29675
Weibull distribution based on maximum likelihood with interval inspection data
[NASA-TM-86515] 21 p3676 N85-32847
Precision microwave attenuation measurement by time interval ratio
[RSRE-85005] 22 p3755 N85-33280
Limits to the burster repetition rate as deduced from the 2nd catalog of the interplanetary network
[OG-1.2-5] 22 p3862 N85-33915
INTESTINES
NT RECTUM
Distinctions of SPF rats used in experiments aboard biosatellites 07 p1012 N85-16427
Dynamics of quantitative and qualitative changes in conditionally pathogenic microflora of the human intestine during long-term hypokinesia 12 p1903 N85-21953
INTOXICATION
A manual control test for the detection and deterrence of impaired drivers 05 p0709 N85-14550
INTRAMOLECULAR STRUCTURES
Intramolecular electron transfer at metal surfaces. Part 5: Pendant substituent effects upon thiocarboxylate-bridged Cobalt (3) reduction kinetics at mercury and gold electrodes
[AD-A150647] 14 p2254 N85-23971
Determination of the intramolecular potential flow from a neutron diffraction experiment
[B8563199] 20 p3532 N85-31978
INTRAOCULAR PRESSURE
Intraocular fluid dynamics in microgravity
05 p0693 N85-14455
INTRAVEHICULAR ACTIVITY
The human role in space. Volume 1: Executive summary
[NASA-CR-171223] 04 p0546 N85-13473
INTRUSION
Slope water intrusions within the nearshore waters off Long Island, New York
[DE85-001386] 09 p1359 N85-18549
One physical mechanism of formation of fine structure of ocean waters 14 p2334 N85-24436
Device for preventing intrusion of a blade during vibration cutting of intermittent cutting with a lathe
16 p2794 N85-27232
Explanation of Russian models: Saudi Arabian seismic refraction profile 17 p2991 N85-28487
INVALIDITY
U ERRORS
INVARIANCE
NT GAUGE INVARIANCE
Time invariant memoryless nonlinear systems identification method
[FUB-9-1983] 01 p0114 N85-10773
Trilinear alternating forms on a vector space of dimension 7
[CWI-PM-R8402] 05 p0722 N85-14644
An invariant measure for the equation u sub tt - u sub xx + u3 = O
[AD-A147300] 08 p1210 N85-17612
Recognition of complex 3-dimensional objects using 3-dimensional moment invariants
[AD-A148119] 08 p1212 N85-17625
Connected simple systems and the Conley index of isolated invariant sets
[AD-A149383] 10 p1552 N85-19789
Invariant differential operators on a semisimple symmetric space and finite multiplicities in a Plancherel formula
[CWI-PM-R8409] 12 p1325 N85-22094
Practical methods for the compensation and control of multivariable systems
[AD-A151047] 14 p2407 N85-24841
Generalised translation invariance and systems theory
[CRM-8501] 17 p3017 N85-28657
Exact invariants in resonance form for time-dependent potentials
[DE85-010733] 19 p3346 N85-30739
Application of adaptive noise cancellation to Coast Guard voice communications
[AD-A154798] 21 p3574 N85-32230
A graph theoretic procedure for the design of feedback patterns
[REPT-110] 24 p4142 N85-35673
INVENTIONS
Parabolic tapers for overmoded waveguides
[DE84-014237] 01 p0039 N85-10247
A high-voltage discharger
[AD-A145659] 02 p0194 N85-11299
Novel drives for machine tools
14 p2268 N85-24053
Equipment for monitoring low concentrations of volatile substances in gases or liquid metals
[BLL-DOUNREAY-TR-949-(9091.9F)]
16 p2786 N85-27190
East Europe report: Science and technology
[JPRS-ESA-85-021] 21 p3568 N85-32190
INVENTORIES
NT CROP INVENTORIES
NT TIMBER INVENTORY
International strategic minerals inventory. Summary report: Manganese
[GS-CIRC-930-A] 02 p0219 N85-11442
On some common interests among reliability, inventory and queuing
[AD-A145595] 02 p0251 N85-11646
Environmental data inventory for the antarctic area
[PB85-107944] 06 p0819 N85-15195
Setting time standards at NISTARS (Naval Integrated Storage and Retrieval System)
[AD-A146371] 06 p0870 N85-15529
Excessive Air Force inventories result from duplicative spare parts requirements
[AD-A147777] 08 p1228 N85-17734
Inventory policy for high backorder items
[AD-A153696] 18 p3198 N85-29840
INVENTORY CONTROLS
Probability distribution of leadtime demand
[AD-A144952] 01 p0113 N85-10766
Setting time standards at NISTARS (Naval Integrated Storage and Retrieval System)
[AD-A146371] 06 p0870 N85-15529
An application of Markov chains to the problem of migration in inventory systems
[AD-A151954] 16 p2857 N85-27618
EOQ (Economic Order Quantity) range model
[AD-A153709] 19 p3379 N85-30965
Discrete simulation models - their role in the design, development and management of inventory control systems
[PNR-90249] 23 p3986 N85-34719
INVENTORY MANAGEMENT
NT INVENTORY CONTROLS
Ministry wants better commo facilities for agroaviation
03 p0310 N85-12003
A methodology for comparing the variable costs of the continuous and periodic review models
[AD-A146351] 03 p0436 N85-12776
An evaluation of the effect of establishing a minimum Economic Order Quantity (EOQ) on the Air Force EOQ item management system
[AD-A147121] 07 p1051 N85-16673
The Air Force stock fund and aircraft availability
[AD-A148653] 08 p1067 N85-16761
Inventory policy for high backorder items
[AD-A153696] 18 p3198 N85-29840
EOQ (Economic Order Quantity) range model
[AD-A153709] 19 p3379 N85-30965
INVERSE SCATTERING
The development of new methods for solving the target identification or inverse scattering problem for time-harmonic acoustic and electromagnetic waves
[AD-A145821] 03 p0415 N85-12657
Multidimensional inverse scattering for first order systems
[AD-A148711] 08 p1214 N85-17642
Lax-pair operators for squared-sum and squared-difference eigenfunctions
[AD-B089063L] 09 p1386 N85-18718
Nonlinear sigma-models and integration methods
[DE85-004447] 12 p1922 N85-22071
Connection between time- and frequency-domain three-dimensional inverse problems for the Schrodinger equation
[DE85-005914] 15 p2639 N85-[illegible]
Solvability of some inverse problems in laser radiation focusing 21 p3696 N85-[illegible]
Inverse-Compton gamma rays in the galaxy
[OG-3.1-2] 22 p3873 N85-[illegible]
Multicomponent analysis of total COS-B gamma-ray data at intermediate latitudes
[OG-3.1-3] 22 p3873 N85-[illegible]
Calculation of heavy-ion tracks in liquid water
[DE85-012101] 24 p4149 N85-3573
INVERSIONS
NT CENTRIFUGING STRESS
NT MAGNETIC FIELD INVERSIONS
NT POPULATION INVERSION
NT TEMPERATURE INVERSIONS
Project review on geophysical and ocean sound speed profile inversion
[AD-A145717] 02 p0276 N85-1178
An extension of the Born inversion method to a depth dependent reference profile
[AD-A146469] 06 p0659 N85-1548
A method for solving the inverse problem of transonic cascade flow
[AD-A146739] 07 p0899 N85-15[illegible]
Ill-posed problems and regularization analysis in early vision
[AD-A147753] 08 p1222 N85-17[illegible]
Characteristic functional of a probability measure absolutely continuous with respect to a Gaussian radon measure
[AD-A149482] 10 p1548 N85-19[illegible]
On the inversion of the lidar equation
[AD-A149653] 12 p1856 N85-2184
Determining conductivity by boundary measurements. Part 2: Interior results
[AD-A149750] 12 p1921 N85-22[illegible]
Inverse behavior of silicon photovoltaic cells
13 p2010 N85-22[illegible]
Algorithms for reconstruction of partially known, band limited Fourier transform pairs from noisy data
[AD-A150194] 13 p2150 N85-2347
Born inversion with a stratified reference velocity
[AD-A149222] 16 p2853 N85-2759
Efficient parallel solution of linear systems
[AD-A152663] 17 p3018 N85-28[illegible]
INVERTEBRATES
NT INSECTS
NT LARVAE
NT PROTOZOA
NT SPIDERS
Hollings hungry mantid model for the invertebrate functional response considered as a Markov process. Part 3: Mathematical elaborations
[CWI-AM-R8407-PT-3] 05 p0722 N85-14[illegible]
Effects of acid rain on forest nutrient status
[DE85-012486] 23 p3947 N85-34[illegible]
Aquatic Invertebrate Development Working Group
24 p4127 N85-355[illegible]
INVERTED CONVERTERS (DC TO AC)
Analysis of inverter models and harmonic propagation. Part 1: A physical simulator for large solar cell arrays
[DE85-002312] 09 p1315 N85-1827
Analysis of inverter models and harmonic propagation. Part 2: Harmonic propagation
[DE85-000198] 10 p1482 N85-19[illegible]
5 kW sleeps inverter. Revision
[AD-A149526] 10 p1510 N85-19[illegible]
Analysis of inverter models and harmonic propagation. Part 3. Transient processes in inverter models
[DE85-000191] 10 p1510 N85-19[illegible]
Airport solar photovoltaic concentrator phase 3
[DE85-006773] 18 p3128 N85-29[illegible]
INVERTERS
Advanced inverter technology
[AD-A149335] 10 p1480 N85-19[illegible]
IREB (Intense Relativistic Electron Beam) converter to ac pulses
[AD-D011479] 10 p1554 N85-19[illegible]
Numerical simulation of inverters with I2L elements including effects of high doping level
13 p2068 N85-23[illegible]
Evaluation of half wave induction motor drive for use in passenger vehicles
[NASA-CR-176119] 23 p3926 N85-34[illegible]
INVESTIGATION
NT ACCIDENT INVESTIGATION
NT AIRCRAFT ACCIDENT INVESTIGATION
NT INTERNATIONAL MAGNETOSPHERIC STUDY
Holographic investigation of solid propellant combustion in a two-dimensional motor
[AD-A153546] 18 p3070 N85-[illegible]

Studies in quality improvement 2. An analysis for unreplicated fractional factorials
[AD-A153539] 18 p3169 N85-29640

INVESTMENTS
Capital investment motivational techniques used by prime contractors on subcontractors
[AD-A153680] 18 p3196 N85-29837

INVISCID FLOW
NT STAGNATION FLOW
Numerical analysis of the 3-dimensional inviscid hypersonic flow around capsule-type bodies by the alternate directional implicit method
[NAL-TR-799] 01 p0002 N85-10012
Review of some vortex relations
[NASA-CR-172452] 01 p0046 N85-10302
Gas side heat transfer: 2-D flow
02 p0142 N85-10965
Linear long-wave stability of cylindrical steady laminar flame in rotating medium 02 p0268 N85-11752
An inviscid computational method for supersonic inlets
[AD-A145997] 03 p0316 N85-12042
Incorporation of viscous-inviscid interactions in turbomachinery design
[PNR-90219] 04 p0457 N85-12897
The numerical simulation of steady transonic rotational flow using a dual potential formulation
05 p0591 N85-13770
A comparative study of the nonuniqueness problem of the potential equation
[NASA-TP-2385] 07 p0898 N85-15694
Analysis of the flow field about a T-45 using PANAIR
[AD-A146811] 07 p0899 N85-15699
A second-order accurate parabolized Navier-Stokes algorithm for internal flows
[NASA-CR-174258] 07 p0956 N85-16059
Recent advances in computational methods to solve the high-lift multi-component airfoil problem
08 p1068 N85-16774
Inviscid compressible flow past a multi-element aerofoil 08 p1069 N85-16776
Theoretical study of boundary-layer control
08 p1070 N85-16784
Leading edge separation criterion for an oscillating airfoil
[AD-P004175] 09 p1267 N85-17960
Development of multigrid algorithms for problems from fluid dynamics
[GMD-111] 09 p1321 N85-18305
Analysis of inviscid transonic flow around an airfoil by diagonal form of IAF scheme
[NAL-TR-831] 10 p1420 N85-18955
Inviscid analysis of unsteady blade tip flow correlation studies
[NASA-CR-172506] 10 p1420 N85-18958
Efficient self-consistent viscous-inviscid solutions for unsteady transonic flow
[NASA-TM-86335] 10 p1420 N85-18959
Computation of the inviscid velocity potential for general ellipsoids on a nearly quadratic surface grid
[REPT-25/84] 11 p1633 N85-20287
Wind tunnel wall interference
[AD-A151212] 15 p2474 N85-25273
Flow through very porous inclined screens
[NASA-TM-86979] 15 p2555 N85-25761
Investigation of potential and viscous flow effects contributing to dynamic stall
[AD-A151696] 15 p2557 N85-25773
Inviscid upwind finite difference model for two dimensional vertical axis wind turbines
15 p2585 N85-25933
Numerical simulation of inviscid compressible flow through three-dimensional cascade
16 p2682 N85-26619
The role of computational fluid dynamics in aeronautical engineering 16 p2694 N85-26629
Theoretical investigation of three-dimensional shock wave turbulent boundary layer interactions. Part 3
[AD-A152251] 16 p2783 N85-27177
On the relation between upwind-differencing schemes of Godunov, Engquist-Osher and Roe
[NASA-CR-175805] 16 p2852 N85-27583
Steady, incompressible, inviscid flow through a finite collapsible tube under longitudinal tension
[REPT-84-01] 17 p2959 N85-28278
Numerical computation of space shuttle orbiter flow field
[NASA-CR-175912] 18 p3058 N85-28921
Inviscid analysis of two supercritical laminar-flow-control airfoils at design and off-design conditions
[NASA-TM-84657] 19 p3212 N85-29920
Numerical and experimental investigation of turbomachinery rotor flow fields
20 p3451 N85-31429
A new finite element approach: Progress in inviscid flow computations
[NASA-TM-86434] 20 p3454 N85-31450
An evaluation of four methods of numerical analysis for two-dimensional airfoil flows
[AD-A155202] 21 p3552 N85-32098
An analysis of flow models: From Navier-Stokes to potential flow equations 21 p3587 N85-32295
Numerical solution of the Navier-Stokes equations for 3-D internal flows: An emerging capability
21 p3588 N85-32300
Calculation of 3-D flow without numerical mixing
21 p3588 N85-32301
Generation by conformal mappings of aerofoil sections and of certain other simple shapes suitable for both aerodynamic and stress-concentration problems
[AD-A154901] 22 p3726 N85-33112
Modelling of unsteady, incompressible separation on an aerofoil using an inviscid flow algorithm
[GU-AERO-8412] 23 p3894 N85-34122

INVISIBILITY
U VISIBILITY

IO
Do the satellites of Uranus control its magnetosphere?
02 p0301 N85-11952
Temporal and spatial variations in the intensity of ultraviolet emissions from Jupiter and the Io torus
03 p0448 N85-12846
Outer satellite atmospheres: Their nature and planetary interactions
[NASA-CR-174146] 04 p0589 N85-13759
Analysis of Jovian low frequency radio emissions
[NASA-CR-174449] 10 p1571 N85-19906
A modeling analysis program for the JPL Table Mountain Io sodium cloud data
[NASA-CR-175493] 11 p1681 N85-20589
Coincidence techniques to study electron emission in ion-atom collisions
[DE85-003635] 11 p1724 N85-20846
Long term variability of the IO torus
11 p1760 N85-21070
Research in planetary studies and operation of Mauna Kea Observatory
[NASA-CR-175618] 13 p2169 N85-23460
Hot spots on Io: Correlation of infrared emission and visible reflectance 13 p2172 N85-23475
Io: Generation of silicate magma by shear melting at the base of a basaltic lithosphere
13 p2172 N85-23476
Topographic evidence for shield volcanism on Io
13 p2172 N85-23478
Sulfur volcanoes on Io? 13 p2173 N85-23479
Sulfur oxygen processes on Io
13 p2173 N85-23481
The violet absorber on Io: Disulfur monoxide derivatives 13 p2173 N85-23482
Emplacement of long lava flows on Mauna Loa (Hawaii) and Alba (Mars) 13 p2186 N85-23563
Accurate albedos of the brightest regions on Io
13 p2195 N85-23618
Io: Precise comparison of Voyager spectral curves with laboratory measurements 13 p2196 N85-23619
Photometric analysis of Jupiter-illuminated images of Io 13 p2196 N85-23620
Shape of Io 13 p2204 N85-23672
A modeling analysis program for the JPL table mountain Io sodium cloud
[NASA-CR-175851] 16 p2833 N85-27468
On the importance of viscous dissipation in Io
22 p3855 N85-33873
Models of planetary structure and evolution: The case of Io 22 p3855 N85-33874

IODATES
NT LITHIUM IODATES

IODIDES
NT CESIUM IODIDES
NT SILVER IODIDES
NT SODIUM IODIDES
Structural and synthetic organosilicon chemistry
[AD-A147101] 07 p0919 N85-15820
Mercuric iodide photodetectors for scintillation spectroscopy
[DE85-001437] 10 p1437 N85-19056
Generation of lead, lead iodide and iodide aerosols and their ice nucleation 21 p3639 N85-32607
New and revised methods of purifying mercuric iodide
[DE85-011684] 22 p3749 N85-33237
Stable n-CuInSe/sub 2/iodide-iodine photoelectrochemical cell
[DE85-011597] 22 p3806 N85-33576

IODINE
NT IODINE ISOTOPES
Spectrophotometric studies of iodine complexes in an aluminum chloride - butylpyridinium chloride ionic liquid
[AD-A145074] 01 p0024 N85-10150
Hydrolysis of iodine: Equilibria at high temperatures
[DE84-016713] 09 p1293 N85-18119
Ice nucleating characteristics of Capparis Aphylla, an Indian herb 21 p3641 N85-32619
Ice nucleation of single water droplet by silver iodide: A laboratory observation 21 p3643 N85-32630
Monte Carlo studies of H2O layers adsorbed on a model basal face of AgI 21 p3643 N85-32633
Technology of off-gas treatment for liquid-fed ceramic melters
[DE85-012467] 22 p3812 N85-33610
Aqueous volatile weak electrolyte equilibria to 300 C
[DE85-013640] 24 p4076 N85-35261
A new drawing technique for nylon 6 by reversible plasticization with iodine
[AD-A156272] 24 p4162 N85-35803

IODINE COMPOUNDS
NT CESIUM IODIDES
NT IODIDES
NT LITHIUM IODATES
NT SILVER IODIDES
NT SODIUM IODIDES
Spectrophotometric studies of iodine complexes in an aluminum chloride - butylpyridinium chloride ionic liquid
[AD-A145074] 01 p0024 N85-10150
Environmental stability of intercalated graphite fibers
[NASA-TM-87025] 16 p2753 N85-26992

IODINE ISOTOPES
The I-Pu-Xe age of the Moon
04 p0584 N85-13729
Design and chemical synthesis of iodine-containing molecules for application to solar-pumped I* lasers
[NASA-CR-176010] 19 p3275 N85-30310

IODINE LASERS
Saturation kinetics of active medium of oxygen-iodine laser 11 p1718 N85-20807
Optically pumped iodine monofluoride laser
[AD-D011555] 12 p1855 N85-21637
Laser-induced fluorescence measurement of vapor concentration surrounding evaporating droplets
[DE85-009409] 19 p3277 N85-30320
Optical inhomogeneities in a nanosecond-pulse iodine photodissociation laser with slow UV radiation pumping
21 p3686 N85-32902

ION ACCELERATORS
The Berkeley mini-collider
[DE84-014594] 01 p0118 N85-10808
High intensity hadron accelerators
[DE84-014063] 01 p0119 N85-10812
Laser source of neutral atoms for collective-field particle accelerator 02 p0263 N85-11719
Preliminary grouping in A strong-current linear ion accelerator with a low injection energy
[DE84-017192] 04 p0563 N85-13587
Explosive emission cathode plasmas in intensive relativistic electron beam diodes
[AD-A147917] 07 p1046 N85-16642
Status of RF superconductivity at Argonne National Laboratory
[DE85-002145] 09 p1312 N85-18245
Mobile accelerator neutron radiography system
[AD-A148808] 09 p1323 N85-18311
Large electrostatic accelerators
[DE85-001120] 09 p1382 N85-18689
Operating experience and construction status of ATLAS — Argonne tandem-linac accelerator
[DE85-002741] 11 p1735 N85-20914
Theoretical study of collective ion acceleration in the Luce diode
[AD-A150107] 12 p1929 N85-22116
Workshop on Nuclear Dynamics 3
[INC-40007-24] 12 p1931 N85-22130
Effects of magnetic shear on lower hybrid waves in the suprauroral region
[AD-A151960] 15 p2656 N85-26392
Heavy ion physics at BNL, the AGS and RHIC
[DE85-005951] 17 p3033 N85-28760
Heavy ion fusion accelerator research in the US
[DE85-008465] 17 p3034 N85-28767
Ultrahigh vacuum system of the heavy ion transport line at Brookhaven
[DE85-011838] 22 p3840 N85-33778
Heavy ion medical accelerator options
[DE85-011204] 22 p3841 N85-33784
Energetic ion acceleration at collisionless shocks
[SH-1.5-3] 23 p3996 N85-34772
Considerations on collective ion aceleration as an intense ion injector
[DE85-012706] 24 p4155 N85-35757
Applications of decelerated ions
[DE85-011832] 24 p4156 N85-35767
Heavy nucleus collisions between 20 and 60 GeV/nucleon
[HE-1.4-2] 24 p4175 N85-35890
Meson multiplicity in nucleus-nucleus collisions above 4 GeV/amu
[HE-1.4-10] 24 p4177 N85-35897

ION ACOUSTIC WAVES
Arguments for fundamental emission by the parametric process L yields T + S in interplanetary type III bursts — langmuir, electromagnetic, ion acoustic waves (L, T, S) 12 p1958 N85-22311
Research with high-power short-wavelength lasers [DE85-010329] 19 p3278 N85-30332
Ion-acoustic double layer in a magnetic picket fence configuration [INPE-3552-PRE/764] 19 p3369 N85-30896
Investigation of ion-acoustic plasma turbulence in field of powerful electromagnetic wave by CO2-laser radiation scattering 21 p3691 N85-32935
Current interruption by density depression [DE85-013120] 24 p4169 N85-35846

ION ATOM INTERACTIONS
Experimental studies of atomic inner shell ionization phenomena [DE84-013448] 01 p0118 N85-10805
Progress in numerical calculations of ion-atom collisions [DE84-016596] 06 p0861 N85-15474
Electron capture by multiply charged ions from hydrogen atoms at low energies [DE84-016560] 06 p0861 N85-15475
Forward electron production in heavy ion-atom and ion-solid collisions [DE85-001256] 09 p1381 N85-18683
Time dependent Hartree-Fock theory of ion-atom collisions: Application to F(9+) + Ne [DE85-003063] 11 p1723 N85-20838
Inner shell contribution to multiple ionization in ion-atom collisions [DE85-003107] 11 p1723 N85-20839
Classical rainbow scattering of alkali ions on metal surfaces. Application to the investigation of unknown surface structures [MPIS-10/1984] 11 p1726 N85-20854
Vacancy-rearrangement theory in the first Magnus approximation [DE85-004435] 12 p1930 N85-22123
Convoy electron production by heavy ions in solids [DE85-005256] 15 p2660 N85-26418
Spin distributions in heavy ion fusion at and below the Coulomb barrier [DE85-007817] 17 p3031 N85-28751
Theoretical studies of heavy ion scattering processes [DE85-008823] 17 p3032 N85-28753
The production and destruction of metastable negative ions [DE85-011056] 19 p3364 N85-30858

ION BEAMS
Manufacturing methods for microwave circuits [AD-A145237] 01 p0043 N85-10278
Beam pulse length determination by spectral analysis [CSIR-NAC-83-05] 01 p0116 N85-10793
Metastable phase formation in ion implanted metals [DE84-014945] 02 p0183 N85-11229
Neutral beam interactions with materials [AD-A145636] 02 p0285 N85-11857
Materials modification by ion beam mixing [AD-P003948] 02 p0286 N85-11864
The use of ion implantation for materials processing [AD-A145438] 02 p0287 N85-11873
Emission mechanisms in the liquid metal ion source: A review [AERE-R-11294] 03 p0418 N85-12675
Vacuum inductive pulsed power compression for inertial confinement fusion [DE84-010935] 03 p0421 N85-12693
Fast ions as probes in solid state research 03 p0430 N85-12740
Ion beam lithography [BMFT-FB-T-84-182] 04 p0504 N85-13219
Low energy ion-molecule reaction dynamics and chemiionization kinetics [DE84-015881] 04 p0559 N85-13562
Intense non-relativistic cesium ion beam [DE84-012575] 04 p0560 N85-13566
Performing (p vector, |c|n), (d vector, n) and (n vector, n) measurements with a rotating magnet beam swinger [DE84-017003] 04 p0562 N85-13582
Ion beam and laser induced surface modifications [DE84-016569] 04 p0571 N85-13642
Repetitively pulsed metal ion beams for ion implantation [DE84-014065] 05 p0732 N85-14704
Ion cluster beam deposition research 06 p0831 N85-15283
Extended performance technology study 30-cm thruster [NASA-CR-168259] 07 p0917 N85-15806
The (20)Ne interaction in extended matter [NASA-TM-86312] 07 p1061 N85-16728
Exposure modelling of particle beam lithography [AD-A147849] 08 p1219 N85-17678
Effect of resonant microwave power on a PIG ion source [DE85-001396] 09 p1379 N85-18673
The energy spectra of slowed-down neutrals from the heating beams in ASDEX — tokamak [REPT-84-157] 09 p1394 N85-18772
Fundamental aspects on ion-beam surface modification: Defect production and migration processes [DE85-000093] 09 p1399 N85-18804
Ion beam processes in Si [DE85-001254] 09 p1399 N85-18808
Advanced ion thruster research [NASA-CR-174862] 10 p1430 N85-19021
Simulation of the ion-beam-driven drift instability in a magnetic trap, 1 [AD-A149451] 10 p1452 N85-19147
Amorphization of ceramics by ion beams [DE85-000936] 10 p1453 N85-19156
Hydrodynamic response of a radiating Al plasma excited by a proton beam [AD-A148904] 10 p1558 N85-19824
Oxidation protection coatings for polymers [NASA-CASE-LEW-14072-1] 11 p1611 N85-20129
Deposition of diamondlike carbon films [NASA-CASE-LEW-14080-1] 11 p1615 N85-20153
Radiative ion beams: Hot stellar reactions in the laboratory [DE85-001570] 11 p1722 N85-20833
Diamondlike flakes [NASA-CASE-LEW-13837-2] 12 p1796 N85-21267
Ion-beam nitriding of steels [NASA-CASE-LEW-14104-1] 12 p1805 N85-21324
Sputter-induced compositional modifications in a Ni-Au alloy [DE85-002771] 12 p1807 N85-21333
New high resolution scanning ion microprobe and focused ion beam applications [AD-A149992] 12 p1852 N85-21616
Beam loss due to the aperture limitation resulting from intrabeam scattering [DE85-005136] 12 p1930 N85-22124
Sheath ionization model of beam emissions from large spacecraft 13 p1992 N85-22489
System for forming and focusing high current beam of deuterium ions 13 p2045 N85-22798
Collective acceleration of ions using high current relativistic electron beams [DE85-004889] 13 p2157 N85-23393
Ion transport in beam-plasma interactions [AD-A150145] 13 p2161 N85-23410
Influences of thermal spikes in ion beam mixing [DE85-006130] 14 p2419 N85-24924
Slowing down of charged particles by the bound electrons in a plasma — ion beams, nuclear fusion [LP-209] 14 p2419 N85-24929
Ion beam mixing of marker layers in Al and Si [DE85-006227] 15 p2511 N85-25490
Effects of ion bombardment on the morphology of lead films [DE85-007232] 15 p2511 N85-25494
Annual Review, April 1983 - March 1984 [ISSN-0547-1567] 15 p2654 N85-26369
Heavy ion beam study of potential formation in bumpy torus plasma [IPPJ-711] 15 p2656 N85-26386
Survey of experimental and theoretical electron-impact ionization cross sections for transition metal ions in low stages of ionization [DE85-007605] 16 p2863 N85-27658
Surface modification of solids [DE85-007543] 16 p2871 N85-27715
Uniaxial angular accelerometers 17 p2944 N85-28173
Heavy ion fusion accelerator research in the US [DE85-008465] 17 p3034 N85-28767
Restrike particle beam experiments on a dense plasma focus. Opening switch research on a dense plasma focus [AD-A152991] 17 p3039 N85-28802
Intense ion beam diode diagnostics using a tunable dye laser [DE85-008079] 18 p3113 N85-29272
Generation of intense negative ion beams [NASA-CASE-NPO-16061-1-CU] 18 p3178 N85-29701
Wide-angle optics with strong magnetic fields for efficient generation of secondary-particle beams [DE85-007727] 18 p3179 N85-29713
Ion beam sputter-deposited thin film coatings for protection of spacecraft polymers in low Earth orbit [NASA-TM-87051] 19 p3248 N85-30137
Experiments with stored heavy ions [DE85-009976] 19 p3356 N85-30802
Emittance growth caused by current variation in a beam-transport channel [DE85-010743] 19 p3363 N85-30849
Proposed use of the radio-frequency quadrupole structure to funnel high-current ion beams [DE85-010746] 19 p3364 N85-30857
Time-resolved energy spectrum of the ion beam generated in the plasma focus 19 p3369 N85-30892
Ion beam-plasma interactions [DE85-010202] 19 p3371 N85-30913
Analysis of beam interaction of the electrical thruster RIT 10 (particle emission) with surfaces [ESA-TT-826] 20 p3421 N85-31231
The response of ionization chambers to relativistic heavy nuclei 20 p3544 N85-32081
In-situ observations of the development of heavy-ion damage in semiconductors [DE85-010289] 22 p3761 N85-33327
Ultrahigh vacuum system of the heavy ion transport line at Brookhaven [DE85-011838] 22 p3840 N85-33778
Heavy ion medical accelerator options [DE85-011204] 22 p3841 N85-33784
Design status of heavy ion injector program [DE85-010751] 22 p3842 N85-33790
Calculation of mixed depth for some metal-Si systems [DE85-011907] 23 p3871 N85-34616
Diamondlike carbon protective coatings for IR materials [NASA-TM-87083] 23 p3873 N85-34631
Numerical calculations on shock loaded materials 23 p3880 N85-34676
Dissipation terms in one-dimensional hydrodynamic code for ICF target 23 p3880 N85-34677
Pulse effect in a light ion beam propagation through a Z-discharge plasma channel 23 p3881 N85-34684
Repetitive pulse accelerator technology for light ion inertial confinement fusion [DE85-012030] 23 p3882 N85-34690
Light ion sources for ICF [DE85-011544] 23 p3883 N85-34702
Method of precisely modifying predetermined surface layers of a workpiece by cluster ion impact therewith [DE85-006519] 23 p3884 N85-34710
Survey of mixing in metal/insulator systems [DE85-011938] 23 p3885 N85-34714
Injection of energetic particles following the gamma-ray flares on June 7, 1980, as observed on Helios 1 [SH-1.3-9] 23 p3893 N85-34756
Use of a minimum-ellipse criterion in the study of ion-beam extraction systems [DE85-012670] 24 p4148 N85-35721
Neutron production by Ne and Si ions on a thick Cu target at 670 MeV/A with application to radiation protection [DE85-014526] 24 p4152 N85-35746
Ion source development for the Los Alamos heavy ion fusion injector [DE85-012682] 24 p4156 N85-35766
Applications of decelerated ions [DE85-011832] 24 p4156 N85-35767

ION CHAMBERS
U IONIZATION CHAMBERS

ION CHARGE
Relative abundances of sub-iron to iron nuclei in low energy (50-250 MeV/N) cosmic rays as observed in the Skylab experiment [OG-4.1-4] 22 p3876 N85-34010
The mean ionic charges of N, Ne, MG, Si and S in solar energetic particle events [SH-2.1-11] 23 p3999 N85-34792
The mean ionic charge of silicon in 3HE-rich solar flares [SH-2.2-8] 23 p4000 N85-34803

ION CONCENTRATION
Measuring system with ion selective electrodes [BMFT-FB-T-84-170] 05 p0639 N85-14100
Maximum current densities from tandem high density systems [DE85-008966] 18 p3180 N85-29730

ION CURRENTS
NT ION BEAMS
Rocket and satellite observations of electric fields and ion convection in the dayside auroral ionosphere [TRITA-EPP-84-05] 02 p0229 N85-11497
Quasielastic neutron scattering on single crystals of solid ionic conductor 03 p0426 N85-12719
Solid electrolytes: Mechanisms for achieving optimal conductivity [AD-A150116] 12 p1801 N85-21285
Achievements of the plasma composition experiment on ISEE-1 during the IMS 14 p2380 N85-24586
Ionic conduction and water diffusion in Li (BETA)-alumina [DE85-007548] 16 p2755 N85-27706
Electrochemistry of polymer films not immersed in solution: Electron transfer on an ion budget [AD-A152989] 17 p2920 N85-27980

Localized ionic currents from a corroding iron-copper galvanic couple
[AD-A153827] 16 p3074 N85-29011
Maximum current densities from tandem high density systems
[DE85-008966] 18 p3180 N85-29720
Ion waves generated by ion loss-cone distributions or drifting particles
[KGI-PREPRINT-070] 20 p3549 N85-32087
Some physical differences between sheet plasma and multicusp plasma as volume produced H- or D- ion sources
[IPPJ-728] 23 p3974 N85-34637
Measuring method and confirmation of H- (D-) ion current by sheet plasma 1
[IPPJ-730] 23 p3974 N85-34638
Feasibility study of radar-transmitting materials
[AD-A155839] 24 p4087 N85-35329
Ion composition measurements of the disturbed and quiet D-region in 1980 - 1981
[AD-A156055] 24 p4117 N85-35521
ION CYCLOTRON RADIATION
Slow wave antenna coupling to ion Bernstein waves for plasma heating in ICRF
[AD-B089084L] 09 p1386 N85-18717
Impurity control by additional current rise and gas puffing during ICRF heating in JIPP T-IIU Tokamak
09 p1387 N85-18725
Electron bounce resonance heating in a bumpy cylinder
[DE85-001732] 10 p1561 N85-19845
Analysis of Jovian low frequency radio emissions
[NASA-CR-174449] 10 p1571 N85-19908
Monte Carlo studies of tandem mirror plasmas interacting with waves in the Ion Cyclotron Range of Frequencies (ICRF)
[DE85-002988] 11 p1731 N85-20883
Lower hybrid heating and current drive, and ion cyclotron heating experiments on the Alcator C and the Versator II Tokamaks
[DE85-004918] 13 p2161 N85-23412
Theory and computer simulation of auroral kilometric radiation 14 p2365 N85-24617
Anomalous heating of ionospheric components (thermal e- and He+) via intense Ion Cyclotron Waves (ICW's)
14 p2368 N85-24633
Propagation and amplification of Ion Cyclotron Waves (ICW's) in a multicomponent plasma. The Earth magnetosphere as a giant maser for Alfven waves
14 p2368 N85-24634
Pc 1 pulsation source regions and their relationship to the plasma pause 14 p2368 N85-24638
Preparatory experiments. 1: JIPP T-IIU
15 p2654 N85-26374
Radio frequency containment
15 p2654 N85-26375
Computational study on excitation, propagation and 3 omega -heating due to the ion Bernstein wave
[IPPJ-733] 23 p3975 N85-34641
Transport issues in Phaedrus-type plasmas
23 p3976 N85-34653
Bounce resonance heating and radial transport of electrons 23 p3977 N85-34655
Effect of ECH and ICH on ambipolar potential in NBT-1M 23 p3978 N85-34661
Simulation studies on stability of hot electron plasma
23 p3978 N85-34664
Observation of mode-converted by ion Bernstein wave by an HCN laser scattering
[IPPJ-724] 23 p3979 N85-34668
ION DENSITY (CONCENTRATION)
NT IONOSPHERIC ION DENSITY
NT MAGNETOSPHERIC ION DENSITY
NT MAGNETOSPHERIC PROTON DENSITY
NT PROTON DENSITY (CONCENTRATION)
Ion-density correlations and enhancement of thermonuclear reaction rate in dense, inertially confined fusion plasmas 02 p0284 N85-11849
Many-body correlations in strongly-coupled plasmas
02 p0284 N85-11850
Analysis of Jovian low frequency radio emissions
[NASA-CR-174449] 10 p1571 N85-19908
Hydrogen vibrational population distributions and negative ion generation in tandem high density hydrogen discharges
[DE85-001207] 11 p1722 N85-20834
Development of Faraday cup onboard MS-T5 for solar wind measurements
[REPT-616] 12 p1794 N85-21255
Ionic mechanisms of soot formation in flames
[AD-A150119] 12 p1801 N85-21297
Study of electric field and ion effects on HVDC lines
[DE85-002975] 12 p1833 N85-21503
Theoretical study of collective ion acceleration in the Luce diode
[AD-A150107] 12 p1929 N85-22116
Evolution of strong inhomogeneities in ionospheric plasma, part 1 14 p2339 N85-24463
Correlation of ring current and ionospheric gap in morning and evening hours 14 p2339 N85-24466
Hydrogen vibrational population distributions and negative ion generation in tandem high-density hydrogen discharges
[DE85-006764] 16 p2863 N85-27857
Electron and ion distributions at high latitudes as measured by the Air Force polar orbiting satellites
[AD-A153242] 17 p2983 N85-28500
Ion thruster performance model
20 p3420 N85-31226
Yakutsk Institute's cosmic ray research facility
22 p3732 N85-33135
ION DISTRIBUTION
Measuring local ion energy distribution function in Tuman-3 Tokamak plasma 02 p0271 N85-11768
Ion velocity distributions from spherical 1054 nm and 351 nm laser plasmas
[DE85-002616] 10 p1559 N85-19833
Observations of energetic electron and ion distributions near the magnetopause at geosynchronous orbit and related ground effects 14 p2356 N85-24560
Results of the SCATHA ion composition experiment during the IMS 14 p2359 N85-24580
Ion sensor signal fluctuations during operation of spacecraft reaction engines 16 p2724 N85-26815
Ion waves generated by ion loss-cone distributions or drifting particles
[KGI-PREPRINT-070] 20 p3549 N85-32087
Stability of ion distribution in strong ion shock structure 23 p3960 N85-34681
Solar Coronal and photospheric abundances from solar energetic particle measurements
[SH-2.1-5] 23 p3998 N85-34786
ION EMISSION
Emission mechanisms in the liquid metal ion source: A review
[AERE-R-11294] 03 p0418 N85-12675
Measurements of integral yields of charged seconcary particles using neutral beams simulating a cometary fly-by — Giotto mission 14 p2244 N85-23908
Impact ionization from gold, aluminum and PCB-Z — Giotto spacecraft paint PCB-Z 14 p2244 N85-23910
Experimental investigations on ion emission with dust impact on solid surfaces — Giotto spacecraft
14 p2244 N85-23911
Ion emission from solid surfaces: Comparison of dust impact with other excitations — Giotto mission
14 p2244 N85-23912
The ESA field emission electric propulsion program
[ESA-STR-213] 20 p3420 N85-31229
Workshop report on Simulation Techniques for Shock Wave Phenomena and Characteristics of Plasmas in Inertial Confinement Fusion
[IPPJ-725] 23 p3979 N85-34670
ION ENGINES
NT MERCURY ION ENGINES
NT RIT ENGINES
Investigation of a pulsed electrothermal thruster system
[NASA-CR-174768] 02 p0169 N85-11132
Study on control of ion engine system
[EL-847] 07 p0916 N85-15800
Advanced ion thruster research
[NASA-CR-174862] 10 p1430 N85-19021
Precision tunable resonant microwave cavity
[NASA-CASE-LEW-13935-1] 11 p1628 N85-20248
Multistep orbital correction algorithms for an Earth satellite using low thrust engine
15 p2479 N85-25303
Ion thruster performance model
20 p3420 N85-31226
The ESA field emission electric propulsion program
[ESA-STR-213] 20 p3420 N85-31229
Heaterless ignition of inert gas ion thruster hollow cathodes
[NASA-TM-87086] 23 p3903 N85-34177
ION EXCHANGE MEMBRANE ELECTROLYTES
Research and development work on a single cation specific membrane for the recovery of raw materials with electrodialysis
[BMFT-FB-T-84-163] 03 p0329 N85-12120
Measuring system with ion selective electrodes
[BMFT-FB-T-84-170] 05 p0639 N85-14100
Research and development work concerning liquid membranes
[BMFT-FB-T-84-227] 08 p1124 N85-17087
Development of a lithium secondary battery separator
20 p3444 N85-31378
Evaluation of developmental membranes for the mixed reactant iron-chromium redox system
[NASA-TM-87074] 23 p3944 N85-34443
ION EXCHANGE RESINS
Ion transporting composite membranes. 1: Nafion impregnated gore-tex
[AD-A151020] 14 p2252 N85-23960
Luminescence probe studies of ionomers. I: Steady-state measurements from nafion membrane
[AD-A152475] 17 p3029 N85-28730
Determination of the association constant for pertechnetic acid
[DE85-010224] 19 p3235 N85-30057
Polyethylene solidification of low-level wastes
[DE85-012566] 22 p3843 N85-33799
ION EXCHANGING
Trivalent ion exchange in beta alumina
[AD-A145373] 02 p0172 N85-11151
Ion chromatographic determination of gold in plating baths
[DE84-016187] 02 p0184 N85-11230
Workshop on membrane biophysics
[AD-A148238] 08 p1192 N85-17512
Solid electrolytes: Mechanisms for achieving optimal conductivity
[AD-A150116] 12 p1801 N85-21296
Ion transport in beam-plasma interactions
[AD-A150145] 13 p2161 N85-23410
Feasibility study for small group water desalination equipment
[AD-A155106] 21 p3563 N85-32164
Oxidation of formaldehyde solutions used for the preservation of reverse osmosis membranes
[PB85-185585] 22 p3742 N85-33194
Multi-solute subsurface transfer modeling for energy solid wastes: Highlights FY 1984
[DE85-012788] 23 p3966 N85-34591
ION EXTRACTION
Extended performance technology study 30-cm thruster
[NASA-CR-168259] 07 p0917 N85-15806
Reconsideration of sheath related to negative ion extraction
[IPPJ-706] 12 p1935 N85-22159
Some physical differences between sheet plasma and multicusp plasma as volume produced H- or D- ion sources
[IPPJ-728] 23 p3974 N85-34637
ION GAGES
U IONIZATION GAGES
ION IMPACT
Inclusion of electron transfer in the calculation of K(n)L(v) multiple vacancy production by ion impact
[DE84-016596] 05 p0733 N85-14711
Synergism in materials erosion due to multispecies impact 06 p0864 N85-15494
Measurement of charged secondary particle emission under ion and neutral impact — Giotto mission
14 p2243 N85-23906
Inelastic Near-Surface Interactions. Proceedings of the Werner Brandt Workshop on Penetration Phenomena
[DE85-010579] 20 p3526 N85-31928
Method of precisely modifying predetermined surface layers of a workpiece by cluster ion impact therewith
[DE85-006519] 23 p3984 N85-34710
Air chemistry measurements 2
[AD-A156041] 24 p4117 N85-35520
ION IMPLANTATION
Implantation of ionized monomer into aluminum alloy 6061 for marine corrosion protection
[AD-A144874] 01 p0028 N85-10172
The oxidation behaviour of a 20 percent Cr/25 percent Ni/Nb stabilized stainless steel in carbon dioxide at high temperatures and its improvement by cerium and yttrium
[AERE-R-11228] 01 p0029 N85-10182
Metastable phase formation in ion implanted metals
[DE84-014945] 02 p0183 N85-11229
Studies of laser melting and rapid solidification using amorphous silicon
[DE84-014737] 02 p0202 N85-11345
Proceedings of the Ion Implantation for Army Needs Workshop
[AD-A145474] 02 p0286 N85-11863
Materials modification by ion beam mixing
[AD-P003948] 02 p0286 N85-11864
Characteristics of ion implanters for fabrication of electronic devices
[AD-P003949] 02 p0286 N85-11865
Review of the University of Manchester Ion Implantation Conference
[AD-P003950] 02 p0286 N85-11866
Research and development requirements for ion implantation
[AD-P003951] 02 p0286 N85-11867
Navy programs on ion implantation for materials modification
[AD-P003952] 02 p0286 N85-11868

Use of ion implantation to modify the corrosion behavior of metals
[AD-P003953] 02 p0266 N85-11869

The modification of metallic corrosion by ion implantation: Engineering applications and fundamentals studies
[AD-P003954] 02 p0266 N85-11870

The use of ion implantation for materials processing
[AD-A145438] 02 p0267 N85-11873

Characterization of ion implanted deuterium traps in nickel by equilibration with deuterium gas
[DE84-014958] 02 p0268 N85-11879

Optimized conditions for the formation of buried insulating layers in Si by high dose implantation of oxygen
[DE84-015369] 02 p0268 N85-11882

Characterization of amorphous surface layers in Fe implanted with Ti and C
[DE84-014960] 02 p0269 N85-11885

Annealing of implanted Al-2O-3 in a reducing environment
[DE84-015370] 03 p0332 N85-12140

Formation of subsurface Al2O3 layers in aluminum by oxygen ion implantation
[DE84-015599] 04 p0474 N85-13020

Ion beam and laser induced surface modifications
[DE84-016569] 04 p0571 N85-13642

On the origins of structural defects in BF2(+)-implanted and rapid thermally annealed silicon: Conditions for defect free regrowth
[DE84-016060] 04 p0572 N85-13650

Radiation hardened ion-implanted GaAs field effect transistor and method for making the same specification
[AD-D011264] 05 p0731 N85-14697

Repetitively pulsed metal ion beams for ion implantation
[DE84-014065] 05 p0732 N85-14704

Process for producing carbide coatings
[AD-D011295] 06 p0764 N85-14885

Evaluation of the ion implantation process for production of solar cells from silicon sheet materials
06 p0831 N85-15261

Evidence for pairing of implanted nitrogen in silicon
[DE84-015622] 06 p0868 N85-15517

Dependence of breakdown voltage for p-n junction on parameters of ion implantation and semiconductor heat treatment 07 p0954 N85-16046

Ion implantation and laser processing of III-V compound semiconductors with applications to the fabrication of microwave devices
[AD-A146848] 07 p1047 N85-16651

Laser annealing of ion implanted semiconductors
[AD-A146979] 07 p1047 N85-16652

X-ray and backscattering analysis of ion implantation phenomena in GaAs and related compounds
[AD-A147449] 07 p1048 N85-16659

Ion implantation in 3-5 compound semiconductors
[AD-A148462] 08 p1226 N85-17723

Surface mechanical properties and wear behavior of ion implanted TiB2
[DE85-001130] 09 p1295 N85-18133

Implantation of Ti + C for reduced friction and wear of steels
[DE85-001606] 09 p1295 N85-18135

Ion implantation of surgical Ti-6Al-4V alloy
[DE85-000943] 09 p1296 N85-18142

Ion beam studies of hydrogen in metals
[DE84-017422] 09 p1297 N85-18145

Formation of amorphous layers in Al2O3 by ion implantation
[DE85-001289] 09 p1397 N85-18794

Reactivity of ion implanted silicon carbide
[DE85-001543] 09 p1399 N85-18802

Fundamental aspects on ion-beam surface modification: Defect production and migration processes
[DE85-000093] 09 p1399 N85-18804

Amorphization of ceramics by ion beams
[DE85-000936] 10 p1453 N85-19156

Effect of implantation species on the tribological response of stainless steel surfaces
[DE85-003530] 10 p1493 N85-19432

Pulsed excimer laser processing for cost-effective solar cells
[NASA-CR-175465] 10 p1509 N85-19520

Fundamental studies of growth, doping and transformation in beta silicon carbide
[AD-A148339] 10 p1562 N85-19651

Ion implanted lateral in 2Ga 8As/GaAs strained-layer superlattice photodector
[DE85-001365] 10 p1563 N85-19659

Analysis of diffusion in an ion-implanted alloy using a phenomenological model
[AERE-R-11527] 11 p1609 N85-20120

Excimer laser annealing to fabricate low cost solar cells
[NASA-CR-174394] 11 p1673 N85-20538

Effects of B, Ti and Ta implantation on the wear resistance of Fe and Ni-plated Fe
[AD-A149947] 12 p1806 N85-21330

Enhanced diffusion from interstitial trapping during solid-phase-epitaxial growth of silicon alloys
[DE85-001285] 12 p1941 N85-22193

Evaluation of implantation-disordering of (InGa)As/GaAs strained-layer superlattices
[DE85-003533] 12 p1942 N85-22200

Experiences with implanted Back Surface Field (BSF) solar cells 13 p2005 N85-22571

Use of markets to elucidate reacting sputtering processes
[DE85-005723] 13 p2018 N85-22655

Study of the effects of implantation on the high Fe-Ni-Cr and Ni-Cr-Al alloys
[NASA-CR-175625] 13 p2021 N85-22661

High sheet resistance, arsenic implanted polycrystalline silicon for integrated circuit resistors
[DE85-004355] 13 p2065 N85-22902

Activation of Si-N modes in silicon by pulsed laser annealing
[DE85-003966] 13 p2097 N85-23082

Influence of substrate heating and thermal annealing on the surface crystallinity in single Si crystals implanted with high doses of (16)O
[DE85-005264] 13 p2164 N85-23428

Measurements of radiation-induced segregation and diffusion in ion irradiated alloy using implanted manganese
[AERE-R-11526] 14 p2258 N85-23994

Improvement by cerium and yttrium ion implantation of oxidation behaviour of stabilised stainless steel in carbon dioxide
[AERE-R-11523] 14 p2259 N85-23996

Excimer laser annealing to fabricate low cost solar cells
[NASA-CR-175702] 14 p2351 N85-24529

Laser annealing of ion implanted HgCdTe
[AD-A150675] 14 p2427 N85-24966

High resolution Z-contrast imaging and lattice location analysis of dopants in ion-implanted silicon
[DE85-005261] 14 p2429 N85-24980

Ion implantation disorder in strained-layer superlattices
[DE85-004466] 14 p2430 N85-24984

Structure and properties of ion-implanted Al sub 2 O sub 3
[DE85-005374] 14 p2430 N85-24987

Fundamental studies of growth, doping and transformation in beta silicon carbide
[AD-A152047] 15 p2660 N85-26416

Thin-film polycrystalline silicon research
[DE85-002908] 15 p2683 N85-26434

Dual species ion implantation of ternary compounds based on In-Ga-As
[AD-D011617] 16 p2869 N85-27698

Surface modification of solids
[DE85-007543] 16 p2871 N85-27715

High temperature position sensors based on monolithic GaAs Hall IC
[BMFT-FB-T-84-266] 17 p2969 N85-28337

Electrical research on solar cells and photovoltaic materials
[NASA-CR-175897] 17 p2986 N85-28452

Communications and logic systems at millimeter wave frequencies, summary 17 p3042 N85-28825

Crack tip chemistry modeling of intergranular stress corrosion cracks of nickel containing segregated phosphorus and sulphur
[DE85-010059] 18 p3076 N85-29028

Oxygen-nitrogen interactions in ion-implanted silicon
[DE85-010091] 18 p3195 N85-29819

Wear improvement in titanium alloys by ion implantation
[AD-D011694] 19 p3239 N85-30081

Spectroscopic investigation of materials for tunable infrared lasers
[AD-A154124] 19 p3272 N85-30291

Amorphous alloys of ion-implanted Fe-Ti-C
[DE85-010656] 19 p3360 N85-30834

Leading-edge microelectronics research at Sweden's Chalmers 20 p3436 N85-31337

Surface passivation and junction formation using low energy hydrogen implants 20 p3480 N85-31628

Processing technology for high efficiency silicon solar cells 20 p3483 N85-31642

Use of low energy hydrogen ion implants in high efficiency crystalline silicon solar cells
[NASA-CR-176109] 22 p3806 N85-33571

Calculation of mixed depth for some metal-Si systems
[DE85-011907] 23 p3971 N85-34616

Formation of amorphous silicon by light ion damage
[DE85-012606] 23 p3972 N85-34623

Two-dimensional numerical modeling of ion implanted GaAs MESFET devices 24 p4088 N85-35341

ION INJECTION

Argon ion pollution of the magnetosphere
13 p1998 N85-[illegible]

Timing between particle injections at the geostationary orbit and particle flux decreases in the distant geomagnetic tail during substorms 14 p2358 N85-[illegible]

Experimental study of laser produced ions for collective ion acceleration 20 p3460 N85-[illegible]

ISEE-1 data reduction and analysis plasma composition experiment
[NASA-CR-175306] 21 p3630 N85-[illegible]

Effect of powerful pulsed low-energy ion streams on GaAs 21 p3662 N85-[illegible]

Ultrahigh vacuum system of the heavy ion transport line at Brookhaven
[DE85-011836] 22 p3840 N85-[illegible]

Design status of heavy ion injector program
[DE85-010751] 22 p3842 N85-[illegible]

ION IRRADIATION

NT DEUTERON IRRADIATION

NT PROTON IRRADIATION

Metastable phase formation in ion implanted metals
[DE84-014945] 02 p0183 N85-11129

Hydrogen passivation of electrically active defects in crystalline silicon solar cells
[DE84-004590] 02 p0223 N85-11461

Review: Role of refractory metal alloys in fusion reactor applications
[AERE-R-11317] 03 p0422 N85-12695

Radiation induced defects in superconductors of type 2 03 p0429 N85-12734

Experimental determination of the critical cavity radius in Fe-10% Cr for ion irradiation
[DE84-016570] 04 p0571 N85-13646

Ion beam studies of hydrogen in metals
[DE84-017422] 09 p1297 N85-18145

Plasma surface interaction processes and possible synergisms
[DE85-001861] 09 p1391 N85-18752

Amorphization of ceramics by ion beams
[DE85-000936] 10 p1453 N85-19156

Heavy ion induced crystallization in amorphous phases
[DE85-003114] 11 p1606 N85-20088

Effects of ion bombardment on the morphology of lead films
[DE85-007232] 15 p2511 N85-25494

Neutralization and excitation in low-energy ion-surface collisions
[AD-A151568] 15 p2660 N85-26414

Secondary ion mass spectrometry studies of solids and surfaces
[AD-A151744] 16 p2745 N85-26939

Energy reflection coefficient for H+ ions at energies between 10 and 80 keV
[DE85-007547] 16 p2863 N85-27692

Surface modification of solids
[DE85-007543] 16 p2871 N85-27715

The effect of ion-bombardment-induced atomic mixing on depth-profiling of interfaces
[AD-A153199] 17 p3044 N85-28634

An investigation of the irradiation swelling mechanisms in refractory metals at high temperatures
[AD-A154149] 19 p3238 N85-30079

An investigation of cementation and carbonitriding by means of ionic bombardment
[BLL-OA-TRANS-3203-(6196.300)]
20 p3429 N85-31285

Breakdown of intrinsic ambipolarity for the radial diffusion due to a rotating RF field 23 p3977 N85-34690

Size and shape dependence of CO adsorption sites on sapphire supported Fe microcrystals
[NASA-CR-176171] 24 p4160 N85-35794

ION MICROSCOPES

Ion microscopy of metals and semiconductors
[AD-A147118] 07 p1043 N85-16636

In-situ formation of a grain boundary in field ion microscopy using a laser
[AD-A148225] 08 p1166 N85-17355

New high resolution scanning ion microprobe and focused ion beam applications
[AD-A149992] 12 p1852 N85-21618

Hydrogen absorption in metals: A field ion microscopy study
[DE85-010299] 18 p3076 N85-29029

Chemical constraints on the evolution of Archean continental crust 21 p3722 N85-33083

ION MOTION

Trivalent ion exchange in beta alumina
[AD-A145373] 02 p0172 N85-11151

Simulation of the ion-beam-driven drift instability in a magnetic trap, 1
[AD-A149451] 10 p1452 N85-19147

Fast ion polarization jet in subauroral F-layer and its manifestation in structure of high latitude ionosphere
15 p2480 N85-25308

Ion and polymer chain motion in a superionic sodium-poly(ethylene oxide) complex
[AD-A152290] 16 p2755 N85-27001
Velocity space diffusion of high energy ions induced by a lower hybrid wave in a nonuniform magnetic field
[IPPJ-714] 16 p2866 N85-27681
Behavior of helically-trapped fast ion orbits in heliotron E
23 p3978 N85-34666

ION OSCILLATION
U PLASMA OSCILLATIONS

ION PLATING
Ion chromatographic determination of gold in plating baths
[DE84-010187] 02 p0184 N85-11230
Tribological properties of boron nitride synthesized by ion beam deposition
[NASA-TM-86962] 12 p1810 N85-21355
Corrosion of aircraft Al and Al-Zn ion plated steel fasteners 13 p2021 N85-22066
The structure of ion plated films in relation to coating properties
[NASA-TM-87055] 18 p3085 N85-29065
New metal coating method developed
21 p3568 N85-32191
Advances in sputtered and ion plated solid film lubrication 22 p3797 N85-33524

ION PROBES
Materials characterization using ion, electron, and photon probes
[DE84-004518] 04 p0560 N85-13568
Heavy ion beam study of potential formation in bumpy torus plasma
[IPPJ-711] 15 p2656 N85-26386
Studies in mixed species charged particle beam dynamics
[OUEL-1545/84] 20 p3531 N85-31969

ION PRODUCTION RATES
Modeling longitudinal motions of thermal O+ and H+ ions in magnetic field tube convective through daytime polar cusp 15 p2481 N85-25314

ION PROPULSION
Characterization of 8-cm engineering model thruster
[NASA-CR-174673] 02 p0169 N85-11131
Study on control of ion engine system
[EL-847] 07 p0916 N85-15800
Ion thruster project
[NASA-TM-77726] 07 p0917 N85-15805
Advanced ion thruster research
[NASA-CR-174862] 10 p1430 N85-19021
Ring-cusp ion thruster with shell anode
[NASA-CASE-LEW-13881-1] 12 p1794 N85-21256
The ESA field emission electric propulsion program
[ESA-STR-213] 20 p3420 N85-31229

ION PUMPS
Design study of the vacuum pump of the ESRP --- synchrotron radiation
[NIKHEF-MTG-21] 08 p1138 N85-17167
Measurement of NSLS distributed diode sputter ion pump characteristics
[DE85-006550] 16 p2760 N85-27031

ION RECOMBINATION
Surface and allied studies in silicon solar cells
[NASA-CR-175468] 10 p1508 N85-19516
Trends in the electric field enhancement of dielectronic recombination cross sections
[DE85-006920] 16 p2871 N85-27711

ION SCATTERING
Structure of adsorbed monolayers. The surface chemical bond
[DE84-016679] 06 p0861 N85-15471
Chemical information from ion scattering spectrometry
[AD-A148287] 08 p1121 N85-17069
Analysis of Jovian low frequency radio emissions
[NASA-CR-174449] 10 p1571 N85-19906
Classical rainbow scattering of alkali ions on metal surfaces. Application to the investigation of unknown surface structures
[MPIS-10/1984] 11 p1726 N85-20654
Theoretical studies of heavy ion scattering processes
[DE85-008623] 17 p3032 N85-28753
Multiple scattering effects in low energy alkali ion scattering: Application to the analysis of adsorbate ordering and bonding geometry
[DE85-007575] 17 p3032 N85-28757
Solar flare gamma-ray line spectroscopy
[SH-2.1-14] 23 p3999 N85-34795

ION SELECTIVE ELECTRODES
Measuring system with ion selective electrodes
[BMFT-FB-T-84-170] 05 p0639 N85-14100

ION SHEATHS
Advanced ion thruster research
[NASA-CR-174862] 10 p1430 N85-19021
Some physical differences between sheet plasma and multicusp plasma as volume produced H- or D- ion sources
[IPPJ-728] 23 p3974 N85-34637

ION SOURCES
NT PLASMATRONS
Plasma deposited diamondlike carbon on GaAs and InP
[NASA-TM-86870] 01 p0123 N85-10844
Surface production of negative hydrogen ions
[AD-A145437] 02 p0277 N85-11801
Effect of resonant microwave power on a PIG ion source
[DE85-001396] 09 p1379 N85-18673
ORNL ECR multicharged ion source
[DE85-001283] 09 p1380 N85-18681
Vibrational relaxation in H-2 molecules by wall collisions: Applications to negative ion source processes
[DE85-000852] 11 p1721 N85-20828
Hydrogen vibrational population distributions and negative ion generation in tandem high density hydrogen discharges
[DE85-001207] 11 p1722 N85-20834
Collisional pumping for the production of intense spin-polarized, neutral beams: Target considerations
[DE85-003459] 11 p1723 N85-20841
Theoretical study of collective ion acceleration in the Luce diode
[AD-A150107] 12 p1929 N85-22116
Development of an apparatus for obtaining molecular beams in the energy range from 2 to 200 eV
[NASA-TM-77835] 15 p2647 N85-26326
Plasma heating 15 p2654 N85-26372
Maximum current densities from tandem high density systems
[DE85-006966] 18 p3180 N85-29720
An alpha particle diagnostic beam line system to generate an intense Li(O) beam with an ORNL SITEX source
[DE85-010564] 18 p3182 N85-29730
Experimental study of laser produced ions for collective ion acceleration 20 p3460 N85-31494
Aerosol analysis and emission spectrometry with free jets
[DE85-010576] 21 p3564 N85-32168
Acceleration of polarized H(-) in the BNL 200 MeV linac
[DE85-011836] 22 p3840 N85-33777
Improved negative ion source
[DE85-006445] 23 p3912 N85-34241
Negative ion sources equipped with continuous annular and spherical geometry surface ionizers
[DE85-011939] 23 p3971 N85-34619
Light ion sources for ICF
[DE85-011544] 23 p3983 N85-34702
Beam intensity increases at the intense pulsed neutron source accelerator
[DE85-012377] 24 p4155 N85-35764

ION SPECTROMETERS
U MASS SPECTROMETERS

ION STORAGE
Frequency and time standards based on stored ions
18 p3105 N85-29223

ION STRIPPING
Large electrostatic accelerators
[DE85-001120] 09 p1382 N85-18669

ION TEMPERATURE
Equatorial energetic distributions of ions of terrestrial radiation belt as function of solar corona temperature response 02 p0160 N85-11087
Measuring local ion energy distribution function in Tuman-3 Tokamak plasma 02 p0271 N85-11768
A research in support of NASA's space science
[NASA-CR-174267] 08 p1227 N85-17728
Determination of ion temperature and rotation velocity profiles by visible, UV and X-ray spectroscopy on Doublet 3 09 p1388 N85-18734
Beam probe spectroscopic technique for ion temperature and magnetic field measurements
09 p1389 N85-18738
Background calculations for the measurement of the ion temperature in a deuterium plasma
[DE84-016546] 09 p1393 N85-18768
Development of Faraday cup onboard MS-T5 for solar wind measurements
[REPT-616] 12 p1794 N85-21255
Ionic mechanisms of soot formation in flames
[AD-A150119] 12 p1801 N85-21297
Low plasma edge temperatures for the self-pumped limiter
[DE85-010155] 18 p3189 N85-29782
Two-point theory of current-driven ion-cyclotron turbulence
[DE85-010114] 19 p3372 N85-30918
Thermal ion heating in the vicinity of the plasmapause
[NASA-CR-176030] 20 p3535 N85-31993
Low frequency instabilities driven by an ion temperature anisotropy
[AD-A154902] 21 p3707 N85-33016
Soft X-ray polychromator for the Solar Maximum Mission
[NASA-CR-175297] 21 p3723 N85-33096
Transports studies of ECH and ICRH-heated bumpy torus plasma in NBT-1M 23 p3978 N85-34662
Langmuir probe on ISX-B
[DE85-012066] 23 p3983 N85-34697

IONIC COLLISIONS
Theoretical studies of highly ionized species
[DE84-016797] 04 p0561 N85-13574
Monte Carlo studies of transport in stellarators
[DE84-017633] 04 p0568 N85-13625
Particle physics
[DE84-013834] 05 p0727 N85-14673
Inclusion of electron transfer in the calculation of K(n)L(v) multiple vacancy production by ion impact
[DE84-016598] 05 p0733 N85-14711
Progress in numerical calculations of ion-atom collisions
[DE84-016596] 06 p0861 N85-15474
Electron capture by multiply charged ions from hydrogen atoms at low energies
[DE84-016560] 06 p0861 N85-15475
Collision-induced dipole moments
[AD-A147682] 08 p1121 N85-17063
Forward electron production in heavy ion-atom and ion-solid collisions
[DE85-001256] 09 p1381 N85-18663
Plane-wave born collision strengths for electron-ion excitation: Comparison with other theoretical methods
[DE85-002348] 10 p1555 N85-19802
Recent advances in forward electron production studies in ion-atom and ion-solid collisions
[DE85-001255] 11 p1726 N85-20853
Bibliography of atomic and molecular processes, 1983
[DE85-000662] 12 p1929 N85-22121
Multiparticle 3D imaging technique to study the structure of molecular ions
[DE85-001843] 12 p1929 N85-22122
Vacancy-rearrangement theory in the first Magnus approximation
[DE85-004435] 12 p1930 N85-22123
Mean delta-ray energies in ion molecule collisions
[DE85-005524] 13 p2157 N85-23395
Influences of thermal spikes in ion beam mixing
[DE85-006130] 14 p2419 N85-24924
X-ray emission in heavy ion collisions
[DE85-006350] 14 p2419 N85-24927
Many-electron effects in electron impact ionization of multiply charged ions
[DE85-005570] 15 p2649 N85-26340
Convoy electron production by heavy ions in solids
[DE85-005256] 15 p2660 N85-26418
Nuclear spectroscopic studies
[DE85-006894] 16 p2862 N85-27652
Homogeneous processes of atmospheric interest
[NASA-CR-175770] 17 p2969 N85-28475
Experimental approaches to the measurement of dielectronic recombination
[DE85-006927] 17 p3030 N85-28743
Nonrelativistic theory of heavy-ion collisions
[DE85-007538] 17 p3031 N85-28747
Excited state populations and charge-exchange of fast ions in solids
[DE85-009362] 18 p3180 N85-29714
Resonant-transfer-and-excitation for highly charged ions (16 or = Z or = 23) in collisions with helium
[DE85-010550] 19 p3359 N85-30823
A theoretical study of electron capture in ion-ion and ion-atom collisions
[DE85-011154] 19 p3362 N85-30842
Inelastic Near-Surface Interactions. Proceedings of the Werner Brandt Workshop on Penetration Phenomena
[DE85-010579] 20 p3526 N85-31928
Study of photon emission by electron capture during solar nuclei acceleration, 1: Temperature-dependent cross section for charge changing processes
[SH-1.1-8] 23 p3990 N85-34735
Multiple vacancy production by high energy heavy ions
[DE85-004426] 24 p4162 N85-35805
Heavy nucleus collisions between 20 and 60 GeV/nucleon
[HE-1.4-2] 24 p4175 N85-35890
Nucleus-nucleus interaction above several hundred GeV/n
[HE-1.4-4] 24 p4176 N85-35892
Observation of direct hadronic pairs in nucleus-nucleus collisions in JACEE emulsion chambers
[HE-1.4-5] 24 p4176 N85-35893
Excessive production of electron pairs by soft photons in low multiplicity ion interactions
[HE-1.4-6] 24 p4176 N85-35894
On the mechanism of anomalous nucleus-nucleus interactions at energies above 1 TeV/nucleon
[HE-1.4-8] 24 p4177 N85-35896

Inclusive angular distribution of alpha and Li fragments produced in the Fe-C and Fe-Pb collisions at 1.88 GeV/u
[HE-1.4-11] 24 p4177 N85-35896

IONIC CONDUCTIVITY
U ION CURRENTS

IONIC CRYSTALS
Computer simulation of grain-boundary properties in ionic crystals and metals
[DE85-000577] 11 p1734 N85-20906
Ionic crystals
[DE85-009462] 24 p4163 N85-35809

IONIC DIFFUSION
Spreading of greatly extended inhomogeneities in upper ionsphere 14 p2339 N85-24462
Electrogenerated chemiluminescence
[AD-A153547] 18 p3070 N85-28990
Diffusion welding of aluminum with vacuum-tight corundum ceramic 19 p3247 N85-30130
Changes in the impedance and bioelectrical activity of the cerebral cortex of rats under the action of anaesthetic drugs
[HSE-TRANS-10371] 19 p3327 N85-30617
The plasma mechanism for preferential acceleration of heavy ions
[SH-2.2-10] 23 p4001 N85-34805

IONIC MOBILITY
The effect of inert gases on ion transport across the erythrocyte membrane
[AD-A148889] 10 p1527 N85-19635
An investigation of tropospheric ions
16 p2823 N85-27412

IONIC PROPELLANTS
U ION ENGINES

IONIC REACTIONS
Ionic reactions of atmospheric importance
[AD-A147354] 07 p0997 N85-16333
Alternative anodic reactions in water splitting
[DE85-004159] 12 p1802 N85-21300
Use of markets to elucidate reacting sputtering processes
[DE85-005723] 13 p2018 N85-22655
International Conference on Coordination Chemistry (23rd) held at Boulder, Colorado on 29 July - 3 August, 1984
[AD-A150960] 14 p2252 N85-23956
Polymer-water interaction studies
21 p3609 N85-32411
Resonant energy transfer during strong excitation
21 p3689 N85-32922

IONIC WAVES
A new maser effect in plasma turbulence
02 p0284 N85-11852
Caviton collapse of SRS by SBS
[DE85-009605] 20 p3535 N85-31999
Resonant ion acceleration by oblique magnetosonic shock wave in a collisionless plasma
[IPPJ-735] 23 p3975 N85-34643

IONIZATION
NT ATMOSPHERIC IONIZATION
NT AURORAL IONIZATION
NT AUTOIONIZATION
NT FLAME IONIZATION
NT GAS IONIZATION
NT ION PRODUCTION RATES
NT NONEQUILIBRIUM IONIZATION
NT PHOTOIONIZATION
NT SURFACE IONIZATION
Diagnostics of ionization in air produced by infrared radiation from A pulse CO2 laser
[AD-A145376] 02 p0201 N85-11342
Comparison of wide aperture and short residence time ion lenses
[DE84-015274] 03 p0420 N85-12685
Oscillator strengths for OII ions
[NASA-CR-174153] 04 p0559 N85-13556
Non-LTE considerations in spectral diagnostics of thermal transport and implosion experiments
[DE84-015187] 05 p0730 N85-14689
Analysis of middle distillate fuels by high resolution field ionization mass spectrometry
[AD-A147724] 08 p1135 N85-17153
An experimental and theoretical investigation of optogalvanic effects
[AD-A148456] 08 p1223 N85-17700
Effect of scattering on instabilities in line-driven stellar winds 08 p1235 N85-17784
Laser ablation studies using RIS
[DE85-001118] 09 p1326 N85-18336
Effect of inner subshell ionization for emission lines of OIV ion 09 p1368 N85-18729
Identification of spectra of highly ionized Mo, Nb, Zr and Y atoms 09 p1390 N85-18745
The coordinated research program at IAEA on atomic collision data for plasma diagnostics
09 p1390 N85-18747
Ozone measurements in the mesosphere during a solar proton event 11 p1665 N85-20490
Time dependent Hartree-Fock theory of ion-atom collisions: Application to F(9+) + Ne
[DE85-003083] 11 p1723 N85-20838
Inner shell contribution to multiple ionization in ion-atom collisions
[DE85-003107] 11 p1723 N85-20839
Stellar winds in the young galactic cluster NGC 6530
11 p1750 N85-21004
Sheath ionization model of beam emissions from large spacecraft 13 p1992 N85-22489
A simple model of electron beam initiated dielectric breakdown 13 p1996 N85-22516
Mean delta-ray energies in ion molecule collisions
[DE85-005524] 13 p2157 N85-23395
Impact ionization from gold, aluminum and PCB-Z — Giotto spacecraft paint PCB-Z 14 p2244 N85-23910
Correlation of ring current and ionospheric gap in morning and evening hours 14 p2339 N85-24466
Indirect processes in electron-impact ionization of multiply-charged ions
[DE85-005237] 14 p2419 N85-24925
Ionization equilibrium and equation of state in the solar interior 14 p2445 N85-25088
The sensitivity of solar eigenfrequencies to the treatment of the equation of state 14 p2445 N85-25089
Ion kinetics, small neutral and excited components in D-region with elevated ionization level. Part 2: Variations in small neutral and excited components
15 p2480 N85-25307
Survey of experimental and theoretical electron-impact ionization cross sections for transition metal ions in low stages of ionization
[DE85-007605] 16 p2863 N85-27658
Resonance ionization mass spectrometry of carbon
[DE85-009040] 17 p2923 N85-28018
Recent advances in optical measurement methods in physics and chemistry
[DE85-008695] 17 p3037 N85-28792
Numerical studies of ablation and ionization of railgun materials
[DE85-010741] 19 p3223 N85-29963
A study of Co and Mn in ZnO varistors
[DE85-011193] 19 p3263 N85-30233
Atomic data for controlled fusion research. Volume 4: Spectroscopic data for iron
[DE85-009658] 19 p3354 N85-30787
Electron-atom collision studies using optically state selected beams
[DE85-010848] 19 p3368 N85-30888
Predamage threshold electron emission from insulator and semiconductor surfaces
[DE85-008968] 19 p3377 N85-30954
Effects of coronal disturbances on the ionization state of the solar wind
[NASA-CR-175997] 19 p3385 N85-31000
Contributions to the 19th International Cosmic Ray Conference
[NASA-CR-176049] 20 p3543 N85-32044
Energy spectra of elements with 16 less than or equal to Z less than or equal to 26 between 10 and 300 GeV/amu 20 p3543 N85-32045
Elemental abundances of cosmic rays with Z33 as measured on HEAO-3 20 p3543 N85-32046
Abundances of secondary elements among the ultra heavy cosmic rays: Results from HEAO-3
20 p3543 N85-32047
Self-consistent models for the X-ray emission from supernova remnants 20 p3548 N85-32082
Ionization detection of stimulated Raman spectra
[DE85-010872] 22 p3746 N85-33216
Electron impact ionization of multicharged ions at ORNL: 1980-1984
[DE85-013104] 23 p3972 N85-34622
Stability of ion distribution in strong ion shock structure 23 p3980 N85-34681
Solar Coronal and photospheric abundances from solar energetic particle measurements
[SH-2.1-5] 23 p3996 N85-34786
The detection and study of molecular species using time resolved laser spectroscopy
[AD-A155910] 24 p4075 N85-35256
Aqueous volatile weak electrolyte equilibria to 300 C
[DE85-013840] 24 p4076 N85-35261
Infrared generation and wave-mixing studies in cesium
[DE85-012883] 24 p4083 N85-35304
The ionization structure of planetary nebulae. Part 4: NGC 7662
[NASA-CR-176151] 24 p4169 N85-35844
Sub-luminal pulses from cosmic ray air showers
[HE-4.7-13] 24 p4200 N85-36083
Search for acoustic signals from high energy cascades
[HE-7.1-1] 24 p4213 N85-36155

IONIZATION CHAMBERS
NT BUBBLE CHAMBERS
NT CLOUD CHAMBERS
NT PROPORTIONAL COUNTERS
NT SPARK CHAMBERS
Photon and electron dosimetry at the Physikalische-Technische Bundesanstalt in [illegible]
[PTB-DOS-9] 01 p0119 N85-10[illegible]
Measurement of soft X-ray absorption spectra with a fluorescent ion chamber detector
[AD-A142213] 07 p0922 N85-1[illegible]
Results from a Bragg curve spectrometer
[DE85-007870] 18 p3176 N85-[illegible]
The response of ionization chambers to relativistic heavy nuclei 20 p3544 N85-3205[illegible]
Paired ion chamber constants for fission gamma-neutron fields
[AD-A155069] 21 p3702 N85-3[illegible]
A practical guide to ionization chamber dosimetry at the AFRRI reactor
[AD-A155185] 21 p3703 N85-3[illegible]
Digital characterization of particle tracks for microdosimetry
[DE85-012896] 22 p3846 N85-3[illegible]
Relative abundances of elements (20 or = Z or = 28) at energies up to 70 GeV/amu using relativistic rise in ion chambers
[OG-4.1-7] 22 p3876 N85-34013
Energy spectra of elements with 16 or = Z or = 26 between 10 and 300 GeV/amu
[OG-4.1-8] 22 p3876 N85-34014
Observations on (3)He neutron spectrometry
[DE85-010731] 23 p3970 N85-34[illegible]
The response of ionization chambers to relativistic heavy nuclei
[OG-9.1-13] 23 p4024 N85-34[illegible]
Sidereal anisotropy of cosmic rays
[SH-4.4-8] 23 p4034 N85-3[illegible]
Long term changes in cosmic ray diurnal variations observed by ion chambers in Hong Kong and Japan
[SH-4.5-14] 23 p4037 N85-35031
Burst size distributions in the digitized data of the ion chambers t Mt. Norikura and sea level stations
[SH-9.1-9] 23 p4051 N85-35124
The influences of the galactic cosmic ray on the atmospheric ozone
[SH-10.1-1] 23 p4053 N85-35133
Fractional charge resolution in music
24 p4147 N85-35712
X-ray film chamber with carbon target of Tien-Shan complex array 24 p4179 N85-35915
Peculiarities of gamma-quanta distribution at 20 TeV energy
[HE-3.7-10] 24 p4186 N85-35967
Observation of genetic relation among new phenomena Geminion, Chiron and mini-Centauro
[HE-6.2-16] 24 p4212 N85-36152

IONIZATION COEFFICIENTS
Ionization coefficient for atomic collisions in meteor trail 16 p2720 N85-26792
Air chemistry measurements 2
[AD-A156041] 24 p4117 N85-35520

IONIZATION COUNTERS
U IONIZATION CHAMBERS
U RADIATION COUNTERS

IONIZATION CROSS SECTIONS
Progress in numerical calculations of ion-atom collisions
[DE84-016596] 06 p0861 N85-15474
Theoretical studies of Rydberg atom collisions
[AD-A148558] 08 p1220 N85-17697
Laser-induced-fluorescence-spectroscopy of atomic processes under a high magnetic field
09 p1389 N85-18740
K and L-shell cross-sections for X-ray microanalysis in an AEM
[DE85-002733] 11 p1721 N85-208[illegible]
Correlated 2 electron effects in collisions of multiply charged Au ions with He
[DE85-003064] 11 p1723 N85-20837
Inner shell contribution to multiple ionization in ion-atom collisions
[DE85-003107] 11 p1723 N85-20839
Many-electron effects in electron impact ionization of multiply charged ions
[DE85-005570] 15 p2649 N85-26340
Theory of electron-impact atomic ionization cross sections
[AD-A151763] 16 p2861 N85-27648
Investigation of electron attachment and dissociation rates in C2F6/CH4 electric gas discharges
[AD-A151796] 16 p2862 N85-27649
Survey of experimental and theoretical electron-impact ionization cross sections for transition metal ions in low stages of ionization
[DE85-007605] 16 p2863 N85-27658

Nuclear data needs for fusion energy development
[DE85-010445] 20 p3536 N85-32000
Toward a theory of excitation of atoms during nuclear and magnetic neutron scattering
21 p3689 N85-32918
Contributions to the 19th International Cosmic Ray Conference
[NASA-CR-176080] 21 p3714 N85-33044
Charge and energy dependence of the residence time of cosmic ray nuclei below 15 GeV/nucleon
[OG-4.1-3] 22 p3876 N85-34009
Electron impact ionization of multicharged ions at ORNL: 1980-1984
[DE85-013104] 23 p3972 N85-34622
Electron loss process and cross section of multiply charged ions by neutral atoms 23 p3981 N85-34665
On the importance of interstellar helium for the propagation of heavy cosmic rays
[OG-7.2-11] 23 p4015 N85-34879
EAS accompanied by gamma-families at Mt. Norikura and comparison with Monte Carlo simulation
[HE-3.3-10] 24 p4181 N85-35928

IONIZATION GAGES
Helium ionization detection apparatus
[NASA-TM-77505] 03 p0364 N85-12332
Test results from a comparative evaluation of a condensation nuclei fire detector
[NASA-CR-3874] 12 p1862 N85-21675

IONIZATION POTENTIALS
Photoionization structure of the Orion Nebula
06 p1246 N85-17863
Radiation data and standards for Tokamak diagnostics
09 p1390 N85-18742
Relationship between topological and magnetic order in small metal clusters
[AD-A150547] 13 p2018 N85-22651
GloGo residual ionization 14 p2244 N85-23909
Ionization energies of liquids from energy distribution, quantum yield and second derivative curves
[AD-A152210] 16 p2746 N85-26946
On the role of the magnetic field strength in critical ionization velocity interaction
[TRITA-EPP-85-01] 20 p3536 N85-32003
Contributions to the 19th International Cosmic Ray Conference
[NASA-CR-176080] 21 p3714 N85-33044
Modulated voltage metastable ionization detector
[NASA-CASE-ARC-11503-1] 23 p3933 N85-34374
Anomalous abundances of solar energetic particles and coronal gas: Coulomb effects and First Ionization Potential (FIP) ordering
[SH-2.1-10] 23 p3999 N85-34791
Variations in the propagation of UH-nuclei
[OG-7.1-1] 23 p4012 N85-34863
Germanium and lead: Significant differences between meteoritic and photospheric abundances?
[OG-7.1-2] 23 p4012 N85-34864
Implications of source abundances of ultraheavy cosmic rays
[OG-7.1-4] 23 p4013 N85-34866

IONIZED GASES
NT ARGON PLASMA
NT BOUNDARY LAYER PLASMAS
NT CATIONS
NT CHARGED PARTICLES
NT COLD PLASMAS
NT COLLISIONAL PLASMAS
NT COLLISIONLESS PLASMAS
NT CONDUCTION ELECTRONS
NT COSMIC PLASMA
NT DENSE PLASMAS
NT ELECTRON PLASMA
NT ELLIPTICAL PLASMAS
NT EVEN-EVEN NUCLEI
NT HEAVY NUCLEI
NT HELIUM PLASMA
NT HIGH TEMPERATURE PLASMAS
NT HYPERNUCLEI
NT LASER PLASMAS
NT METALLIC PLASMAS
NT NITROGEN PLASMA
NT NUCLEI (NUCLEAR PHYSICS)
NT ODD-EVEN NUCLEI
NT ODD-ODD NUCLEI
NT PLASMA CLOUDS
NT PLASMA JETS
NT PLASMA LAYERS
NT PLASMA SHEATHS
NT PLASMAS (PHYSICS)
NT RELATIVISTIC PLASMAS
NT ROTATING PLASMAS
NT SEMICONDUCTOR PLASMAS
NT SOLAR WIND
NT SPACE PLASMAS
NT STELLAR WINDS
NT STRONGLY COUPLED PLASMAS
NT THERMAL PLASMAS
NT TOROIDAL PLASMAS
Optical emission line studies and the warm, ionized component of the local interstellar medium
06 p0875 N85-15555
Photoionization structure of the Orion Nebula
06 p1246 N85-17863
Hollow cathode apparatus
[NASA-CASE-NPO-15560-1] 12 p1832 N85-21491
Time dependent and steady-state solutions of the electron energy distribution in a weakly ionized gas subject to an ac or dc electric field
[AD-A151829] 15 p2656 N85-26391
Anomalous abundances of solar energetic particles and coronal gas: Coulomb effects and First Ionization Potential (FIP) ordering
[SH-2.1-10] 23 p3999 N85-34791
The mean ionic charges of N, Ne, MG, SI and S in solar energetic particle events
[SH-2.1-11] 23 p3999 N85-34792

IONIZED PLASMAS
U PLASMAS (PHYSICS)

IONIZERS
High efficiency ionizer using a hollow cathode discharge plasma
[DE85-006690] 16 p2868 N85-27693

IONIZING RADIATION
NT ALPHA PARTICLES
NT BETA PARTICLES
NT COSMIC RAY SHOWERS
NT COSMIC RAYS
NT COSMIC X RAYS
NT EXTREME ULTRAVIOLET RADIATION
NT FAR ULTRAVIOLET RADIATION
NT GALACTIC COSMIC RAYS
NT GAMMA RAY BEAMS
NT GAMMA RAY BURSTS
NT GAMMA RAYS
NT LYMAN ALPHA RADIATION
NT PRIMARY COSMIC RAYS
NT SECONDARY COSMIC RAYS
NT SOLAR COSMIC RAYS
NT SOLAR X-RAYS
NT ULTRAVIOLET RADIATION
NT X RAYS
Radiation measuring system using transistor flux sensors
[AD-D011239] 01 p0050 N85-10328
Energy deposition in microvolumes of silicon from high energy proton reactions
[AD-A144713] 01 p0123 N85-10845
Critical assessment of low fluence irradiation creep mechanisms
[DE84-015576] 02 p0184 N85-11232
Instability in semiconductors exposed to ionizing radiation 02 p0267 N85-11747
A total dose characterization of five commercial analog multiplexers
[AD-A146886] 07 p0946 N85-15997
Chemical protection against ionizing radiation
[AD-A147822] 07 p1016 N85-16457
Beam-foil spectroscopy of highly ionized aluminum atoms 09 p1390 N85-18746
Comparison of ionizing radiation and hot electron effects in MOS structures
[DE84-016766] 09 p1400 N85-18609
Strange F + Be binary star systems
11 p1756 N85-21045
Periodic substorm activity in the geomagnetic tail
[NASA-CR-175629] 13 p2161 N85-23409
Investigation of basic characteristics of laser heating in thermoluminescence and of laser-stimulated luminescence
[AD-A152143] 16 p2790 N85-27212
Study of the degradation of short-circuit current and the open-circuit tension of spatial solar cells as a function of the fluency of 1MeV electrons
[INPE-3356-PRE/634] 16 p2887 N85-27814
Radiation damage and repair in cells and cell component, part 1
[DE85-008667] 18 p3152 N85-29519
Working safely with ionizing radiation sources at the Interuniversity Reactor Institute (IRI) (meant for the introduction of new collaborators)
[IRI-190-84-01] 18 p3160 N85-29576
Fiber optics in transient radiation fields
[DE85-010721] 19 p3368 N85-30686
Development of a recombinant DNA assay system for the detection of genetic change in astronauts cells
[DE85-010103] 20 p3504 N85-31781
The DNA metabolism and poly-(ADP-ribose) synthesis in lymphocytes of persons exposed to low doses of ionizing radiation
[OEFZS-4307] 20 p3507 N85-31800
USAFSAM review and analysis of radiofrequency radiation bioeffects literature
[AD-A155113] 21 p3684 N85-32760
Lower bounds of propagation velocity of steady ionizing waves in field of strong electromagnetic wave
21 p3692 N85-32940
Buildup of electric charge in foil dielectrics during gamma irradiation 22 p3770 N85-33363
The 1984 environmental monitoring program report for Idaho National Engineering Laboratory site
[DE85-011209] 22 p3812 N85-33611
Study of composition of cosmic rays with energy .7 E 3 Ee
[OG-5.1-7] 22 p3881 N85-34049
Composition of primary cosmic rays near the bend from a study of hadrons in air showers at sea level
[OG-5.2-2] 22 p3883 N85-34059

IONOGRAMS
A description of the NRL oblique-incidence-ionogram data base
[AD-A148625] 08 p1230 N85-17748

IONOSONDES
On the study of ionospheric disturbances
04 p0522 N85-13335

IONOSPHERE
NT D REGION
NT E REGION
NT F REGION
NT F 2 REGION
NT LOWER IONOSPHERE
NT SPORADIC E LAYER
NT UPPER IONOSPHERE
USSR report: Space
[JPRS-USP-84-005] 02 p0156 N85-11060
Magnetospheric structures: Uranus and Neptune
02 p0301 N85-11949
Characteristics of absorption and frequency filtration of ULF electromagnetic waves in the ionosphere
03 p0376 N85-12402
Seasonal variations of reflectibility and transmissibility of ULF waves propagating through the ionosphere of geomagnetic mid-latitudes
[REPT-560] 03 p0376 N85-12403
Scientific contributions in commemoration of Ebro Observatory's 75th anniversary -- conference
[ISBN-84-00-05360-X] 04 p0518 N85-13308
Experience with proposed improvements of the International Reference Ionosphere (IRI)
[PB84-235870] 05 p0678 N85-14353
Artificial defocusing lens in ionosphere
05 p0724 N85-14654
Activities report in Earth and planetary environments physics
[CRPE-NT-134] 05 p0734 N85-14720
Processes of smooth increase and dropoff in intensity of glow line lambda' = 5577 A with exposure of ionosphere to electron beam 06 p0822 N85-15219
Mechanism of damping of plasma oscillations in initial stage of injection of electron beams from spacecraft into ionosphere in active experiments
06 p0823 N85-15225
Influence of Faraday effect in ionosphere on nonmutuality of meteor radio channel
07 p0952 N85-16037
Region 1 birkeland currents from a global MHD simulation of the magnetosphere
[AD-A147435] 07 p0997 N85-16335
An investigation of ionospheric irregularity effects on SIR-B image processing and information extraction
08 p1149 N85-17247
X rays from the aurora
[AD-A149828] 08 p1186 N85-17477
A research in support of NASA's space science
[NASA-CR-174267] 08 p1227 N85-17726
Current carriers for the field-aligned current system
[NASA-TM-86161] 08 p1260 N85-17925
Ionospheric research at INPE
[INPE-3279-PRE/602] 10 p1514 N85-19556
Winter anomaly of the lower ionosphere and its possible causes 11 p1680 N85-20459
S3-3 ONR-118 data analysis
[AD-A149725] 12 p1889 N85-21855
Calculation of ionospheric profiles by inverting VLF/LF reflection data. 2. Anisotropic propagation
[AD-A150105] 12 p1890 N85-21859
Direct measurements of severe spacecraft charging in auroral ionosphere 13 p1991 N85-22480
Polar plasmas as observed by Dynamics Explorers 1 and 2 13 p1991 N85-22483
Ionospheric distortions of digital signals with wideband modulation 13 p2072 N85-22945
Evolution of strong inhomogeneities in ionospheric plasma, part 1 14 p2339 N85-24463
Correlation of ring current and ionospheric gap in morning and evening hours 14 p2339 N85-24466

Numberical simulation of the effects of radially injected barium plasma in the ionosphere
[NASA-CR-175636] 14 p2354 N85-24542

Ground-based and near-Earth observations during the IMS 14 p2359 N85-24575

IMS advances in studies of field-aligned currents and their related electrodynamics 14 p2359 N85-24578

Electrodynamics of magnetosphere-ionosphere coupling 14 p2359 N85-24579

Results of the Langmuir-probe experiment on board Intercosmos-18 — ionosphere-magnetosphere interaction 14 p2362 N85-24596

Comparison of magnetospheric and ionospheric electric fields using different empirical mapping factors
14 p2362 N85-24597

Magnetosphere-ionosphere interaction through hydromagnetic waves 14 p2364 N85-24610

Spatial characteristics of ULF pulsations and their modification by the ionosphere: IMS results
14 p2364 N85-24612

High time-resolution studies of the auroral ionosphere
[AD-A150945] 14 p2409 N85-24850

Magnetic field penetration into cometary ionosphere
15 p2477 N85-25290

Turbopause as source of internal gravity waves
16 p2806 N85-27314

Ionospheric effects on antenna impedance
[BMFT-FB-W-84-052] 17 p2950 N85-28217

The boundary layers as the primary transport regions of the Earth's magnetotail
[AD-A152714] 17 p2992 N85-28496

EISCAT electron density studies
[AD-A152820] 17 p2993 N85-28498

Combined catalog of ionosphere vertical soundings data
[PB85-166494] 18 p3136 N85-29430

Shuttle Molecular Gun: Smog. Potential experiment for the electrodynamic Tethered Satellite System (TSS) mission
[IFSI-84-17] 20 p3419 N85-31221

Fluxgate magnetometer (SSM) for the defense meteorological satellite program (DMSP) block 5D-2, flight 7
[AD-A155229] 21 p3560 N85-32143

Doppler satellite data characteristics
[AD-A154868] 21 p3575 N85-32231

Further developments of EISCAT as an MST radar
21 p3627 N85-32534

Urbana radar systems: Possibilities and limitations
21 p3628 N85-32540

The Sondrestrom radar: Progress and proposed upgrades for ST work 21 p3628 N85-32541

The Adelaide VHF radar: Capabilities and future plans
21 p3629 N85-32546

Ionospheric electron density profile and related studies
[AD-A155257] 21 p3632 N85-32567

Beam diffusion in linear ionospheric layer
21 p3695 N85-32958

Yakutsk Institute's cosmic ray research facility
22 p3732 N85-33135

Magnetotails of the terrestrial planets: A comparative study 22 p3856 N85-33675

Waves in Space Plasmas (WISP)
23 p3901 N85-34164

Electrodynamic tether 23 p3902 N85-34168

Atmospheric Emission Photometric Imaging (AEPI)
23 p3902 N85-34170

IONOSPHERIC ABSORPTION
U ELECTROMAGNETIC ABSORPTION
U IONOSPHERIC PROPAGATION

IONOSPHERIC COMPOSITION

Middle atmospheric ionization. Observations and chemistry 04 p0522 N85-13340

IONOSPHERIC CONDUCTIVITY

Electric conductivities, currents and energy dissipation in the polar ionosphere 02 p0227 N85-11483

Field-aligned currents observed in the vicinity of a moving auroral arc 14 p2363 N85-24603

Multiple correlation between auroral and magnetic pulsations 14 p2363 N85-24605

Multiple correlation between auroral and magnetic pulsations. Part 2: Determination of electric currents and electric fields around a pulsating auroral patch
14 p2363 N85-24606

Effects of Birkeland current limitation on high latitude convection patterns
[TRITA-EPP-84-10] 20 p3494 N85-31725

IONOSPHERIC CURRENTS
NT AURORAL ELECTROJETS
NT ELECTROJETS
NT EQUATORIAL ELECTROJET

Electric conductivities, currents and energy dissipation in the polar ionosphere 02 p0227 N85-11483

Research directions in recent studies of the lunar geomagnetic effects 04 p0520 N85-13320

Dayside cusp aurora 04 p0521 N85-13333

Longitudinal current before westward propagating auroral bend 06 p0823 N85-15223

One-dimensional model of auroral magnetic force with longitudinal current and cyclotron heating of ions
13 p1980 N85-22424

Direct measurements of severe spacecraft charging in auroral ionosphere 13 p1991 N85-22480

Three-dimensional calculation of shuttle charging in polar orbit 13 p1992 N85-22486

Ionspheric effects of seasonal and diurnal variations of electric fields in equatorial F-region
14 p2338 N85-24459

Solar wind control of electric fields and currents in the magnetosphere and ionosphere
14 p2364 N85-24608

Ionosphere-magnetosphere coupling and convection
14 p2364 N85-24609

Effects of Birkeland current limitation on high latitude convection patterns
[TRITA-EPP-84-10] 20 p3494 N85-31725

IONOSPHERIC DISTURBANCES
NT IONOSPHERIC STORMS
NT SUDDEN IONOSPHERIC DISTURBANCES
NT TRAVELING IONOSPHERIC DISTURBANCES

Solar-geophysical data number 477, May 1984. Part 1: (Prompt reports). Data for April 1984, March 1984 and late data. Explanation of data reports issued as number 474 (supplement) February 1984
[PB84-225026] 01 p0131 N85-10901

Global maps of foF2 derived from observations and theoretical values
[AD-A145866] 03 p0392 N85-12509

Occurrences of the polar slant E condition (SEC) at Narssarssuaq, Godhavn, Thule 1982
03 p0393 N85-12514

On the study of ionospheric disturbances
04 p0522 N85-13335

Experimental results of study of artificial perturbation region in upper and lower ionosphere disturbance by the method of vertical probing 06 p0784 N85-15011

Relation between polarization of artificial low frequency radiation and parameters of auroral ionosphere
06 p0785 N85-15016

Possible effects of interaction of electric seismic fields with the ionosphere 06 p0823 N85-15226

Ionospheric turbulence: Interchange instabilities and chaotic fluid behavior
[AD-A147810] 07 p0998 N85-16337

Remote sensing of the high latitude ionosphere
[AD-A147881] 07 p1006 N85-16405

Tropospheric and ionospheric phase perturbations and Doppler frequency shift effects
[AD-A148579] 08 p1154 N85-17283

Artificial ionospheric disturbances caused by powerful radio waves
[AD-A148077] 08 p1186 N85-17473

Ionospheric and magnetospheric modifications caused by VLF waves
[AD-A148210] 08 p1186 N85-17475

X rays from the aurora
[AD-A148628] 08 p1186 N85-17477

Method and apparatus for calibrating the ionosphere and application to surveillance of geophysical events
[NASA-CASE-NPO-15430-1] 12 p1887 N85-21846

Kinetic Rayleigh-Taylor instability theory in the ionosphere near equator 13 p2067 N85-22911

Disturbances in structure of lower ionosphere at terminators based on results of winde-band LW sounding 14 p2339 N85-24467

Foreshortened short-wave scattering on artificial ionospheric inhomogeneities 14 p2340 N85-24468

Disturbance of midlatitude electrodynamic parameters due to the magnetospheric convection
14 p2362 N85-24593

Experimental research on ionospheric disturbance caused by cumulative barium vapor injection
16 p2719 N85-26787

Full shadow phenomenon in Earth's upper atmosphere 16 p2806 N85-27316

Remote sensing of irregularities in the equatorial ionosphere using the radio scintillation technique
16 p2806 N85-27317

Scintillation using NNSS satellites
[AD-A152604] 17 p2949 N85-28207

The Shock and Vibration Digest, volume 17, no. 2
[AD-A153129] 17 p2977 N85-28400

The effects of seismic waves
17 p2978 N85-28401

Ionospheric limitations to time transfer by satellite
18 p3107 N85-29234

Equitorial scintillations: Advances since ISEA-6
[AD-A154962] 21 p3631 N85-32559

Vehicle Charging And Potential (VCAP)
23 p3902 N85-34173

Sporadic radio emission connected with a definite manifestation of solar activity in the near Earth space
[SH-10.1-8] 23 p4053 N85-[illegible]

Near Earth space sporadic radio emission bursts occuring during sunrise
[SH-10.1-9] 23 p4054 N85-[illegible]

Ion composition measurements of the disturbed and quiet D-region in 1980 - 1981
[AD-A156055] 24 p4117 N85-[illegible]

IONOSPHERIC DRIFT

Rocket and satellite observations of electric fields and ion convection in the dayside auroral ionosphere
[TRITA-EPP-84-05] 02 p0229 N85-[illegible]

Fast ion polarization jet in subauroral F-layer and its manifestation in structure of high latitude ionosphere
15 p2480 N85-[illegible]

A study of the generation mechanisms of high latitude and equatorial F-region irregularities using DE-2 data
[NASA-CR-175745] 16 p2825 N85-[illegible]

Geophysical plasmas and atmospheric modeling
[AD-A152605] 17 p2993 N85-[illegible]

A simple model for testing the effects of gravity-wave-produced vertical oscillations of scattering irregularities on spaced-antenna, horizontal drift measurements 21 p3619 N85-[illegible]

Effects of line-of-sight velocity on spaced-antenna measurements, part 3.5A 21 p3621 N85-[illegible]

IONOSPHERIC ELECTRON DENSITY

Two-level model for formation of night ionosphere of Venus from radio occulation experiments
02 p0162 N85-[illegible]

Theoretical study of electron concentration in Venusian atmosphere as function of zenith angle of sun and solar activity in areas of photochemical equilibrium
02 p0163 N85-11104

Inference of equatorial field-line integrated electron density values using whistlers
[AD-A145822] 03 p0392 N85-12507

On the study of ionospheric disturbances
04 p0522 N85-13335

The response of mid-latitude total electron content to solar activity 04 p0522 N85-13336

Middle atmospheric ionization. Observations and chemistry 04 p0522 N85-13340

Observations of plasma bubbles and their zonal drift using polarimeters
[INPE-3219-PRE/572] 05 p0729 N85-14[illegible]

Medium- and large-scale wave disturbances and heterogeneities of electron concentration in outer ionosphere in middle and low latitudes
06 p0825 N85-15241

Partial reflection D-region electron densities
08 p1184 N85-17461

Dynamics of the low-latitude thermosphere and ionosphere 09 p1351 N85-[illegible]

Neutral atmosphere properties determining D-region electron densities 11 p1658 N85-20481

Variation of derived mesospheric nitric oxide in relation to wind and temperature in winter
11 p1658 N85-20482

Indirect phase height measurements in central and eastern Europe for monitoring D region plasma
11 p1659 N85-20486

Measurements of partial reflections at 3.18 MHz using the CW radar technique 11 p1659 N85-20487

Method and apparatus for calibrating the ionosphere and application to surveillance of geophysical events
[NASA-CASE-NPO-15430-1] 12 p1887 N85-21846

Rocket observations of the ionosphere during the eclipse of 26 February 1979
[NASA-CR-175513] 12 p1886 N85-[illegible]

Ionspheric effects of seasonal and diurnal variations of electric fields in equatorial F-region
14 p2338 N85-24459

Universal time effects in polar ionosphere
14 p2338 N85-24461

Determination of ionospheric electron density profiles from satellite UV (ultraviolet) emission measurements
[AD-A150734] 14 p2373 N85-[illegible]

Influence of tropical F region in ionosphere on propagation of short radio waves
16 p2721 N85-[illegible]

Full shadow phenomenon in Earth's upper atmosphere 16 p2806 N85-27316

Ionospheric electron density profile and related studies
[AD-A155257] 21 p3632 N85-32567

IONOSPHERIC HEATING

Magnetospheric plasma studies using data from the dynamics high and low altitude plasma instruments
[AD-A145751] 03 p0392 N85-12505

IONOSPHERIC ION DENSITY

Middle atmospheric ionization. Observations and chemistry 04 p0522 N85-13340

Analysis of ionization sources in D region based on theoretical models 06 p0825 N85-15240

One-dimensional model of auroral magnetic force with longitudinal current and cyclotron heating of ions
13 p1960 N85-22424

Results of the SCATHA ion composition experiment during the IMS
14 p2359 N85-24580

The ionospheric O+ streams in the magnetotail between 22 RE and 6 RE
14 p2360 N85-24582

Radar echoes at 2.66 and 40.92 MHz from the mesosphere, part 2.6A
21 p3619 N85-32486

IONOSPHERIC NOISE
NT WHISTLERS

A system for measuring the characteristics of the ionospheric channel by digital transmissions
10 p1472 N85-19267

Sporadic radio emission connected with a definite manifestation of solar activity in the near Earth space
[SH-10.1-6] 23 p4053 N85-35139

IONOSPHERIC PROPAGATION

Convection of plasma in polar ionosphere, comparison of measurements from Cosmos-184 with model dependent on interplanetary magnetic field vector
02 p0160 N85-11066

Observations and prognosis of HF wave propagation via the sporadic E layer
[UIO-SR-84-04] 03 p0356 N85-12294

Geophysical Works during 1981, volume 29, no. 547-566
03 p0375 N85-12369

Impedance measurements on a VLF multi-turn loop antenna in a space plasma simulation chamber
[AD-A145104] 04 p0492 N85-13141

Sources of information concerning the ionosphere
04 p0521 N85-13334

On the study of ionospheric disturbances
04 p0522 N85-13335

Ionospheric scintillation: A brief review
04 p0522 N85-13337

The winter anomaly in ionospheric absorption (with special reference to the results obtained in Spain)
04 p0522 N85-13338

Possible anomaly prediction system for the middle atmosphere — ionospheric absorption
04 p0522 N85-13339

Distortions of radio pulses during reflection from maximum region of ionospheric layer
06 p0792 N85-15061

Medium- and large-scale wave disturbances and heterogeneities of electron concentration in outer ionosphere in middle and low latitudes
06 p0825 N85-15241

Development of a 20/30 GHz receiving station for propagation experiments with L-SAT
[AD-A148261] 08 p1152 N85-17271

Propagation and scattering considerations for the 0.2-3.0 GHz frequency range for a space-based radar
[AD-A148504] 08 p1153 N85-17282

Standing wave pattern of HF radio waves in the ionospheric reflection region. Part 1: General formulas
[UIO-SR-84-05-PT-1] 09 p1313 N85-18253

Equatorial transionospheric propagation conditions affecting digital communications
10 p1470 N85-19275

A system for measuring the characteristics of the ionospheric channel by digital transmissions
10 p1472 N85-19267

A modem with pseudo-orthogonal codes: Experimental results
10 p1474 N85-19302

Error correction coding for a self-adaptive modem: Theoretical and experimental results
10 p1474 N85-19303

Serial data transmission with large output on the HF channel
10 p1475 N85-19305

Ionospheric absorption on 1539 kHz in relation to solar ionizing radiation
11 p1659 N85-20455

Indirect phase height measurements in central and eastern Europe for monitoring D region plasma
11 p1659 N85-20456

Measurements of partial reflections at 3.18 MHz using the CW radar technique
11 p1659 N85-20457

Autumn and winter anomalies in ionospheric absorption as measured by riometers
11 p1660 N85-20460

A model of the influence of neutral air dynamics on the seasonal variation in the low ionosphere
11 p1660 N85-20462

Calculation of ionospheric profiles by inverting VLF/LF reflection data. 2. Anisotropic propagation
[AD-A150105] 12 p1890 N85-21859

Anisoptropy of Alfven wave absorption in ionosphere
14 p2339 N85-24464

Deuteron whistlers at low latitudes in the low altitude topside ionosphere
14 p2366 N85-24625

Ionosphere effects may replace some communications satellites
15 p2484 N85-25337

Influence of tropical F region in ionosphere on propagation of short radio waves
16 p2721 N85-26796

Results of simultaneous measurements of absorption and polarization of radio waves reflected from ionosphere
16 p2807 N85-27313

Proceedings of the Sixteenth Annual Precise Time and Time Interval (PTTI) Applications and Planning Meeting
[NASA-TM-87561] 18 p3105 N85-29221

A review of ionospheric effects on Earth-space propagation
18 p3106 N85-29233

Ionospheric limitations to time transfer by satellite
18 p3107 N85-29234

Waves in Space Plasmas (WISP)
23 p3901 N85-34164

IONOSPHERIC REFLECTION
U IONOSPHERIC PROPAGATION

IONOSPHERIC SOUNDING

Sources of information concerning the ionosphere
04 p0521 N85-13334

Partial reflection D-region electron densities
08 p1184 N85-17461

D1 LF wind measurements in the 90 to 100 km height range
08 p1185 N85-17468

Indirect phase height measurements in central and eastern Europe for monitoring D region plasma
11 p1659 N85-20456

Measurements of partial reflections at 3.18 MHz using the CW radar technique
11 p1659 N85-20457

Method and apparatus for calibrating the ionosphere and application to surveillance of geophysical events
[NASA-CASE-NPO-15430-1] 12 p1887 N85-21846

Remote sensing of irregularities in the equatorial ionosphere using the radio scintillation technique
16 p2806 N85-27317

Small-scale structure of ionospheric F-region
19 p3297 N85-30440

IONOSPHERIC STORMS
NT SUDDEN IONOSPHERIC DISTURBANCES

Cold streams of ionospheric oxygen in the plasma sheet during the CDAW-6 event of March 22, 1979
[NASA-CR-174064] 03 p0393 N85-12513

IONOSPHERIC TEMPERATURE

Determining effective rate of plasma heating in outer equatorial ionosphere using data from ISIS-1 and ISIS-2 satellites
16 p2721 N85-26797

IONOSPHERICS
NT DAWN CHORUS
NT HISS

IONS
NT ANIONS
NT ANTIPROTONS
NT CATIONS
NT CESIUM IONS
NT DEUTERONS
NT FERRIC IONS
NT HEAVY IONS
NT HELIUM IONS
NT HYDROGEN IONS
NT LIGHT IONS
NT METAL IONS
NT MOLECULAR IONS
NT NEGATIVE IONS
NT NITROGEN IONS
NT OXYGEN IONS
NT POSITIVE IONS
NT PROTONS
NT RECOIL IONS
NT SOLAR PROTONS
NT TRIVALENT IONS

Spectrophotometric studies of iodine complexes in an aluminum chloride - butylpyridinium chloride ionic liquid
[AD-A145074] 01 p0024 N85-10150

Trivalent ion exchange in beta alumina
[AD-A145373] 02 p0172 N85-11151

Surface production of negative hydrogen ions
[AD-A145437] 02 p0277 N85-11801

Spin dynamics of rare Earth ions in crystal fields probed by muon spin rotation
[DE84-013805] 02 p0278 N85-11810

Absolute transition probabilities of lines in the spectra of astrophysical atoms, molecules, and ions
[NASA-CR-174141] 04 p0580 N85-13705

Determination of halogens and sulfur in organic compounds and polymers by combustion-ion chromatography
[DE84-016166] 05 p0614 N85-13921

Non-LTE considerations in spectral diagnostics of thermal transport and implosion experiments
[DE84-015187] 05 p0730 N85-14689

Measurement of oxide ion concentration in NaCl-ZnCl2 molten salt and several applications
[BLL-AWRE-TRANS-74-(9091.9F)]
06 p0764 N85-14886

Topics in high resolution spectroscopy of stored ions
[DE85-002093] 06 p0861 N85-15470

Observations of local interstellar Mg I and Mg II
06 p0874 N85-15547

FeII and MgII in the nearby interstellar medium
06 p0874 N85-15549

Research relative to plasma transport across the magnetopause
[NASA-CR-174300] 07 p1045 N85-16636

A cometary ion mass spectrometer
[NASA-CR-174326] 08 p1164 N85-17343

Effect of disuse on sarcoplasmic reticulum in fast and slow skeletal muscle
[NASA-CR-174337] 08 p1191 N85-17508

Instrumentation for particle-beams research using laser excited merging beams
[AD-A147968] 08 p1220 N85-17681

Time-of-flight spectroscopy of ionic and metastable fragments from dissociating molecules
[AD-A148068] 08 p1220 N85-17683

Microstructural analysis of ion containing polymers
[DE85-001594] 10 p1453 N85-19157

Ab initio calculations of the optical properties of ions in glass
[DE85-001008] 11 p1612 N85-20133

Superionized species and winds in low luminosity B and Be stars
11 p1749 N85-21003

Efficient heating and confinement of ions in an axisymmetric magnetic mirror supplemented with dc electric field
[IPPJ-707] 12 p1935 N85-22160

Strong iron accelerating by collisionless magnnetosonic shock wave propagating perpendicular to a magnetic field
[IPPJ-709] 12 p1935 N85-22161

Velocity distributions of solar wind ions and electrons
12 p1954 N85-22273

Operational experience with ion concentration sensors in orientation systems
13 p1960 N85-22422

The chemistry of RDX and HMX cluster ions
13 p2004 N85-22561

Interaction of the magnetospheric ions with the surfaces of the icy satellites of Saturn
13 p2174 N85-23491

Plasma environment effects on the Giotto Ion Mass Spectrometer
14 p2245 N85-23919

Kinetic energies of fragment ions produced by dissociative photoionization of NO
[NASA-CR-175721] 15 p2647 N85-26327

Spectroscopy of quasimolecular X-rays with H-like decelerated ions
[DE85-006565] 15 p2649 N85-26337

Comparison of computational results of a few representative three-dimensional transonic potential flow analysis programs
16 p2693 N85-26628

Velocity space diffusion of high energy ions induced by a lower hybrid wave in a nonuniform magnetic field
[IPPJ-714] 16 p2866 N85-27681

Selective detection of species in complex matrices by SIMS (Secondary Ion Mass Spectrometry)
[AD-D011685] 19 p3235 N85-30053

Systematic view of transition intensities in the spectra of actinides and lanthanides in condensed phases
[DE85-010272] 19 p3354 N85-30789

Resonant-transfer-and-excitation for highly charged ions (16 or = Z or = 23) in collisions with helium
[DE85-010550] 19 p3359 N85-30823

Effect of inner subshell ionization on emission lines OIV ions
[IPPJ-719] 19 p3370 N85-30903

Excitation of some alkaline Earth-like ions
[DE85-010737] 20 p3529 N85-31951

Thermal ion heating in the vicinity of the plasmapause
[NASA-CR-176030] 20 p3535 N85-31993

Production of stable embryo particles in dense ion tracks of alpha particle emissions in the atmosphere
21 p3644 N85-32638

Formation of particles in the air of the humid tropical forests
21 p3644 N85-32639

Effect of ions on cloud formation and its role in solar terrestrial relationship
21 p3653 N85-32697

Electrostatic ion cyclotron instability due to a nonuniform electric field perpendicular to the external magnetic field
[AD-A155474] 21 p3707 N85-33019

Relative abundances of sub-iron to iron nuclei in low energy (50-250 MeV/N) cosmic rays as observed in the Skylab experiment
[OG-4.1-4] 22 p3876 N85-34010

Measuring method and confirmation of H- (D-) ion current by sheet plasma 1
[IPPJ-730] 23 p3974 N85-34636

Low frequency instability in a mirror field
23 p3977 N85-34657

Model of azimuthal non-uniformities induced by RF heating in RFC-XXM
23 p3977 N85-34658

Experimental measurements of the ion cyclotron antennas' coupling and RF characteristics
[DE85-011569] 23 p3962 N85-34694

Study of photon emission by electron capture during solar nuclei acceleration, 1: Temperature-dependent cross section for charge changing processes
[SH-1.1-6] 23 p3990 N85-34735
Quantitative analysis of flare accelerated electrons through their hard X-ray and microwave radiation
[SH-1.2-7] 23 p3991 N85-34742
Ion energy storage for post-flare loops
[SH-1.2-10] 23 p3992 N85-34745
Energetic protons from a disappearing solar filament
[SH-1.3-7] 23 p3993 N85-34754
Ion composition measurements of the disturbed and quiet D-region in 1980 - 1981
[AD-A156055] 24 p4117 N85-35521
Generalized reduced fluid model with finite ion-gyroradius effects
[DE85-013123] 24 p4157 N85-35777
Noise in sodium beta alumina crystals
[AD-A156025] 24 p4161 N85-35796

IOWA
Shortwave infrared detection of vegetation
[E85-10064] 08 p1174 N85-17402
Quaternary stratigraphy of the lower Iowa and Cedar River Valleys, southeast Iowa 09 p1352 N85-18504
Scan angle and detector effects in Thematic Mapper radiometry — Iowa and Arkansas
12 p1871 N85-21735
Investigation of TM band-to-band registration using the JSC registration processor 12 p1872 N85-21745

IP (IMPACT PREDICTION)
U COMPUTERIZED SIMULATION

IRAN
Microwave hydrology: A trilogy
[NASA-CR-176042] 20 p3477 N85-31603

IRAS
U INFRARED ASTRONOMY SATELLITE

IRAS-ARAKI-ALCOCK COMET
Implications of the presence of S2 in cometary ice
11 p1760 N85-21072
Research in planetary studies and operation of Mauna Kea Observatory
[NASA-CR-175618] 13 p2169 N85-23460

IRASERS
U INFRARED LASERS

IRIDIUM
Magnetically-induced luminescence of (Ir(2=phos)(2)C10(4)
[AD-A149659] 12 p1799 N85-21286
Development of the osmium-191 yields iridium-191m radionuclide generator
[DE85-011165] 23 p3970 N85-34611
Current status of the Os-191 yields Ir-191m generator
[DE85-006306] 23 p3971 N85-34614

IRON
NT FERRIC IONS
NT IRON ISOTOPES
NT IRON 59
Low-gravity solidification of cast iron and space technology applications 02 p0151 N85-11022
Directional solidification of flake and nodular cast iron during KC-135 low-g maneuvers
02 p0154 N85-11040
The reactions of cobalt, iron and nickel in SO-2 atmospheres: Similarities and differences
[NASA-TM-86866] 02 p0181 N85-11217
Detection of hydrogen assisted crack growth
[DE84-015920] 02 p0183 N85-11226
Characterization of amorphous surface layers in Fe implanted with Ti and C
[DE84-014960] 02 p0289 N85-11885
EXAFS and Moessbauer study of small metal clusters isolated in rare-gas solids
[DE84-015676] 04 p0470 N85-12994
The problem of iron partition between Earth and Moon during simultaneous formation as a double planet system 04 p0587 N85-13744
Origin of the Moon 04 p0587 N85-13745
Influence of hydrogen saturation and prior heat treatment on graphitization of white cast iron
[BLL-M-35964-(5828.4)] 05 p0615 N85-13932
Iron core collapse models of Type 2 supernovae
[DE84-013909] 05 p0743 N85-14775
Thermal conductivity of aluminum, copper, iron and tungsten for temperature from 1 K to the melting point
[PB84-235678] 06 p0770 N85-14924
FeII and MgII in the nearby interstellar medium
06 p0874 N85-15549
IUE observations of the gaseous component of the local interstellar medium 06 p0874 N85-15553
Observations of highly-ionized interstellar iron
06 p0876 N85-15565
Procedure for investigating high-temperature properties of iron-ore materials
[BLL-M-36020-(5828.4)] 07 p0926 N85-15866
Surface effects of corrosive media on hardness, friction, and wear of materials
[NASA-TM-83711] 07 p0930 N85-15896
The mineralogy of global magnetic anomalies
[E85-10061] 07 p0987 N85-16272
The fundamentals of dislocation transport of hydrogen in bcc iron
[AD-A148143] 08 p1129 N85-17117
Effect of iron on the performance of IN 625 weld deposits
[BR91456] 08 p1169 N85-17376
Metal-support interactions: Their effects upon adsorption, electronics, and activity/selectivity properties of cobalt in hydrogenation
[DE85-003316] 09 p1292 N85-18113
Alloying effects and microstructure of iron aluminides
[DE85-000903] 09 p1295 N85-18137
Study of the mechanism for annealing embrittlement of an iron-based metallic glass
[DE84-016856] 09 p1300 N85-18164
Liquid phase methanol process development unit: Installation, operation, and support studies
[DE85-001311] 09 p1301 N85-18171
The feasibility of low-G grey solidification of nodular iron in the F-104 experimental furnace package
[NASA-TM-82527] 10 p1426 N85-18996
High temperature properties of equiatomic FeAl with ternary additions
[NASA-TM-86936] 10 p1439 N85-19072
Residual stress after laser processing
11 p1600 N85-20065
Electrical resistance measurements of metals to 40 GPa in the diamond cell
[DE85-001009] 11 p1629 N85-20262
A circum-terrestrial compositional filter
13 p2179 N85-23520
Reassignment of the iron (3) absorption bands in the spectra of Mars 13 p2195 N85-23614
Hydrogen on impurity-covered iron surfaces
14 p2254 N85-23968
The Fe XIII 10747 A and Fe XIV 5303 A coronal emission lines polarization 14 p2448 N85-25111
Weldability of Ni3Al-type aluminide alloys
[DE85-006932] 15 p2512 N85-25496
Test of the electronic structure of Fe(100) by absorbed current spectroscopy
[DE85-004942] 15 p2661 N85-26422
Effect of nickel addition on the thermal, magnetic and magnetomechanical properties of Fe(80)B(15)Si(5)
[AD-A152281] 16 p2749 N85-26967
Effect of superconducting solenoid model cores on spanwise iron magnet roll control
[NASA-TM-86378] 17 p2905 N85-27915
The loss of material from the cathode of metal arcs
[NASA-TM-77845] 17 p2918 N85-27985
Multi-phase crystallization of ferrous alloys
[BLL-BISI-TRANS-22441-(9022.06)]
17 p2925 N85-28037
Effect of the agressive action of soil on metallic pipelines. New possibilities for the passive and active corrosion protection
[BLL-BISI-TRANS-21630-(9022.06)]
17 p2928 N85-28070
Kinetics of the formation of a complex alloyed boride coating on iron and its properties
[BLL-BISI-TRANS-22303-(9022.06)]
17 p2930 N85-28084
Temperature and manganese content dependences of tensile deformation in iron-high manganese binary alloys
[DE85-007656] 17 p2932 N85-28098
Uniaxial stress induced symmetry breaking for muon sites in Fe 17 p3042 N85-28820
Localized ionic currents from a corroding iron-copper galvanic couple
[AD-A153627] 18 p3074 N85-29011
Mineralogical-geochemical characteristics of ferromanganese formations in Arabian-Indian Ocean Ridge 19 p3293 N85-30416
Atomic data for controlled fusion research. Volume 4: Spectroscopic data for iron
[DE85-009658] 19 p3354 N85-30787
Reduction of the trapping of positrons in dislocated single crystals of iron when charged with hydrogen
[DE85-010235] 19 p3377 N85-30950
Concept development evaluation for John Deere/UA STS middeck experiment location
[NASA-CR-171541] 20 p3397 N85-31071
Determination of edge and screw dislocation density in single crystals of high-purity iron
[DE85-010237] 20 p3537 N85-32012
Burn front velocity as a function of pellet density in iron-potassium perchlorate heat powders
[DE85-011448] 21 p3572 N85-32214
Microanalysis of dissolved iron and phosphate in pore waters of hypersaline sediment
21 p3661 N85-32744
Multiphoton production and detection of atoms
[AD-A155561] 21 p3702 [illegible]
Initial results from the Caltech/DSRI balloon-borne isotope experiment
[OG-4.3-8] 21 p3714 [illegible]
Measurements of Fe and Ar fragmentation cross sections
[PAPER-OG-7.2-20] 21 p3714 [illegible]
Was core formation violent enough to homogenize the early mantle? 21 p3718 [illegible]
The problem of the Earth's CO2 content and the iron core 21 p3718 [illegible]
Tritium-helium effects in metals
[DE85-011507] 22 p3749 [illegible]
Induction motors with minimum waste of magnetic iron
22 p3772 [illegible]
Oxidation states of iron in the terrestrial planets: Evidence and implications for accretion models
22 p3852 [illegible]
Relative abundances of sub-iron to iron nuclei in low energy (50-250 MeV/N) cosmic rays as observed in the Skylab experiment
[OG-4.1-4] 22 p3876 N85-34010
A measurement of the cosmic ray elements C to Fe in the two energy intervals 0.5-2.0 GeV/n and 20-60 GeV/n
[OG-4.1-6] 22 p3876 N85-34012
Energy spectrum of cosmic-ray iron nucleus observed with emulsion chamber
[OG-4.1-10] 22 p3877 N85-34016
Measurement of the iron spectrum from 60 to 200 GeV per nucleon
[OG-4.1-11] 22 p3877 N85-34017
A new analysis of cosmic ray isotopes at 3 GeV/n from HEA03-C2 data
[OG-4.3-6] 22 p3879 N85-34031
Calculation of activities of components in liquid alloys of iron with yttrium
[BLL-M-35868-(5828.4)] 23 p3914 N85-34253
Capture in the 1.15-keV iron resonance
[DE85-011913] 23 p3970 N85-34612
Silicon to iron abundances in solar cosmic rays and in the sun
[SH-2.1-6] 23 p3998 N85-34787
Influence of yttrium on eutectoid transformation in irons
[BLL-M-35787-(5828.4)] 24 p4078 N85-35270
Development of a high strength isothermally heat-treated nodular iron road wheel arm
[AD-A155755] 24 p4099 [illegible]
Development of electrodes for the NASA iron/chromium
[NASA-CR-174724] 24 p4109 N85-35471
Ore genesis at the Monterrosas deposit in the Coastal Batholith, Ica, Peru 24 p4115 N85-35510
Size and shape dependence of CO adsorption sites on sapphire supported Fe microcrystals
[NASA-CR-176171] 24 p4160 N85-35794
Characteristics of central collision events in Fe-nucleus interactions for 20 - 60 GeV/nucleon
[HE-1.4-3] 24 p4176 [illegible]
The electromagnetic component of albedo from superhigh energy cascades in dense media
[HE-3.5-11] 24 p4184 [illegible]
The development of air shower in the iron absorber
24 p4189 [illegible]
Monte Carlo simulations of electron lateral distributions in the core region of 10(13) - 10(16) eV air showers
24 p4190 [illegible]
The longitudinal development of muons in cosmic ray air showers at energies 10(15) - 10(17) eV
[HE-4.3-12] 24 p4192 [illegible]
Multiple muons in MACRO
[HE-5.2-1] 24 p4202 [illegible]
The Nagoya cosmic-ray muon spectrometer 3, part 2: Track detector
[HE-5.2-3] 24 p4202 N85-36081

IRON ALLOYS
NT AUSTENITIC STAINLESS STEELS
NT CARBON STEELS
NT CHROMIUM STEELS
NT FERRITIC STAINLESS STEELS
NT HIGH STRENGTH STEELS
NT LOW CARBON STEELS
NT MARAGING STEELS
NT MARTENSITIC STAINLESS STEELS
NT NICKEL STEELS
NT STAINLESS STEELS
NT STEELS
Structure and abrasive resistance of iron based alloys rich in hardening components 01 p0054 [illegible]
Determining the optimum heating parameters for precision alloys — iron-nickel alloys
[BLL-M-35718-(5824.4)] 02 p0174 [illegible]
Rapid solidification of steels: Model and commercial alloys 02 p0176 [illegible]

Effect of annealing in transverse magnetic field on magnetic permeability of amorphous Fe5Co70Si15B10 alloy 03 p0349 N85-12247
Magnetic properties of and superfine interactions in amorphous Fe-Cr-Co-Si-B alloys 03 p0349 N85-12248
Metallurgy Institute's developments for alloy and aircraft producers 03 p0353 N85-12268
Stirling material technology [NASA-TM-86888] 04 p0472 N85-13007
Radiation effects in amorphous metallic alloys [DE84-014302] 04 p0475 N85-13025
Thermal conductivity of iron/potassium perchlorate heat powder [DE84-017071] 04 p0476 N85-13035
Thermomagnetic generator [DE84-017018] 04 p0530 N85-13388
Study of the reactive-element effect in oxidation of Fe-Cr alloys using transverse section analytical electron microscopy [DE84-016237] 04 p0571 N85-13641
Experimental determination of the critical cavity radius in Fe-10% Cr for ion irradiation [DE84-016570] 04 p0571 N85-13646
Metallographic evaluation of the reactions between boronated graphite and Fe-Ni-Cr alloys [DE84-015374] 06 p0769 N85-14922
A study of tetrataenite 06 p0885 N85-15623
Low temperature diffusion coefficients in the Fe-Ni and FeNiP systems: Application to meteorite cooling rates 06 p0886 N85-15626
Speculations on the formation of metallic meteorite phases 06 p0889 N85-15648
The formation of isolated phase precipitates during the decomposition of high-coercive force Fe-Cr-Co alloys [BLL-M-36028-(5828.4)] 07 p0924 N85-15855
Laser-initiated combustion studies on metallic alloys in pressurized oxygen [PB85-128114] 10 p1438 N85-19066
Creep-rupture behavior of iron superalloys in high-pressure hydrogen [NASA-CR-174411] 10 p1441 N85-19078
Development of AK18 alloy production technology based on electrothermic silumin 11 p1598 N85-20048
Electron-diffraction structural examination of amorphous iron-tin alloys 11 p1604 N85-20084
Heavy ion induced crystallization in amorphous phases [DE85-003114] 11 p1606 N85-20098
Initial development of nickel and nickel-iron aluminides for structural uses [DE84-016641] 11 p1608 N85-20108
Development of an automated miniature Charpy test method [DE85-003011] 11 p1652 N85-20405
Atomistic studies of grain boundaries with segregated impurities [DE85-000063] 11 p1737 N85-20924
Effects of chromium and aluminum on mechanical and oxidation properties of iron-nickel-base superalloys based on CG-27 [NASA-TP-2443] 12 p1805 N85-21323
Stress corrosion cracking and oxidation characteristics of boride-strengthened microcrystalline iron and nickel based alloys [AD-A149605] 12 p1806 N85-21328
Formation of alumina layers on iron-base alloys [BLL-T6418/BG/LRS/LRST737/84] 13 p2020 N85-22657
Study of the effects of implantation on the high Fe-Ni-Cr and Ni-Cr-Al alloys [NASA-CR-175625] 13 p2021 N85-22661
TEM/FIM study of modulated microstructures in the Fe-Be system [DE85-005379] 13 p2023 N85-22678
Corrosion-resistant amorphous alloys 13 p2035 N85-22748
Structure of amorphous films of alloys based on Fe, condensed from laser erosion products 13 p2035 N85-22749
Energy spectrum of processes of structural relaxation of amorphous alloy FeCo70Si15B10 13 p2035 N85-22750
Cast-iron technology: Metallographic and mechanical testing results [DE85-002864] 14 p2257 N85-23984
Contact point and seam welding of heat-resistant alloys 15 p2501 N85-25429
Mossbauer spectrometry: Testing of a new computer based system and its application to a study of an aluminum-iron-cerium alloy [AD-A151826] 15 p2510 N85-25483
Reduced-chromium stainless steel substitutes containing silicon and aluminum [PB85-160786] 15 p2513 N85-25502
Iron rich low cost superalloys [NASA-CR-174900] 16 p2748 N85-26962
The disordering process in an L12 ordered alloy [DE85-008152] 17 p2931 N85-28093
Hydrogen absorption in metals: A field ion microscopy study [DE85-010299] 18 p3076 N85-29026
Investigation for low-cost permanent magnets [AD-A154367] 19 p3260 N85-30212
Experimental and theoretical study of fatigue crack initiation in metals 19 p3283 N85-30357
Long range ordered alloys modified by addition of niobium and cerium [DE85-011661] 20 p3431 N85-31285
Cells for measuring thermoelectromotive force and electrical resistance of metals in temperature range of 20-950 degrees Celsius [BLL-M-36240-(5828.4)] 20 p3457 N85-31473
Metallic glass composition [DE85-011594] 22 p3751 N85-33253
Enthalpics of formation of liquid Fe-Ce-Si and Fe-Ce-Al three-component alloys [BLL-M-36296-(5828.4)] 23 p3913 N85-34247
Influence of technology of atomization of naturally alloyed iron on grain-size characteristics of powder material [BLL-M-35810-(5826.4)] 23 p3914 N85-34257
Thermal barrier coating system [NASA-CASE-LEW-14057-1] 24 p4072 N85-35233

IRON CHLORIDES
Coexistence of antiferromagnetism and spin-glass ordering in the Ising system FeO 55MgO 45Cl2 [DE85-004164] 12 p1942 N85-22197
Environmental stability of intercalated graphite fibers [NASA-TM-87025] 16 p2753 N85-26992

IRON COMPOUNDS
NT CHROMITES
NT FERRATES
NT FERRITES
NT IRON CHLORIDES
NT IRON CYANIDES
NT IRON OXIDES
NT LIMONITE
NT MAGNETITE
NT PYRITES
NT SIDERITES
NT TROILITE
A circumterrestrial compositional filter 04 p0588 N85-13753
Chemically modified electrodes and related solution chemistry [DE84-017110] 05 p0614 N85-13924
Electrochemical features of the ferric sulfate leaching of CuFeS2/C aggregates [AD-A148661] 08 p1123 N85-17081
The UFe4P12 and CeFe4P12: Non-metallic isotopes of superconducting LaFe4P12 [DE85-003724] 12 p1942 N85-22195
Mixed valence materials [AD-A151009] 14 p2252 N85-23959
Effects of the cooling rate on the structure of the graphite in inoculated irons [BLL-BISI-TRANS-22305-(9022.06)] 17 p2930 N85-28083
Lithium-alloy/iron sulfide battery design studies [DE85-007991] 18 p3131 N85-29389

IRON CYANIDES
Development and evaluation of sulfonated polysulfone membranes for the zinc-ferricyanide battery [DE85-009104] 24 p4090 N85-35357
Cationic exchange membrane for the zinc-ferricyanide battery [DE85-013152] 24 p4112 N85-35489

IRON ISOTOPES
NT IRON 59
Diffusion of Fe-55 in Fe-2O-3 single crystals [AERE-R-11286] 03 p0333 N85-12147
Measurements of Fe and Ar fragmentation cross sections [OG-7.2-20] 23 p4016 N85-34887
The response of ionization chambers to relativistic heavy nuclei [OG-9.1-13] 23 p4024 N85-34939

IRON METEORITES
Fractionation of siderophiles in cosmic spherules and its implications 06 p0884 N85-15613
Mossbauer spectroscopy and X-ray diffraction of samples from the Santa Catharina iron meteorite 06 p0885 N85-15624
Structural development in the Santa Catharina meteorite 06 p0886 N85-15625
Extreme incompatibility of Pb during the crystallization of magmatic iron meteorites 06 p0886 N85-15627
Experimental and theoretical study of the formation of the 2AB, 3AB, and 9A meteorite chemical groups from the parent liquid 06 p0886 N85-15628
Investigations concerning the magmatic iron meteorites: Static vs. dynamic experiments 06 p0886 N85-15629
On the record of galactic cosmic ray flux and traffic break-ups in iron meteorites 06 p0887 N85-15634
The low-energy secondary cosmic ray flux: Detectors in iron meteorites 06 p0887 N85-15635
Differentiated meteorites and the components of chondrites [NASA-CR-174201] 06 p0890 N85-15649
Origin of mesosiderites as a natural consequence of planet formation 15 p2683 N85-26574

IRON ORES
Distribution of oxygen between metal and basic slags [BLL-M-35932-(5828.4)] 05 p0616 N85-13935
World iron ore reserves [BLL-BISI-TRANS-22280-(9022.06)] 17 p2983 N85-28435

IRON OXIDES
NT CHROMITES
NT MAGNETITE
Effects of additives and KOH electrolyte concentration on dissolution of iron electrodes [DE84-014840] 02 p0173 N85-11162
An investigation of the role of sintering in gas-solid interactions [DE84-015481] 02 p0288 N85-11884
Diffusion of Fe-55 in Fe-2O-3 single crystals [AERE-R-11286] 03 p0333 N85-12147
Thermite and Fe/KClO4: Some thermodynamic calculations [DE84-016945] 04 p0573 N85-13653
The bulk-Moon MgO/FeO ratio: A highlands perspective 04 p0583 N85-13724
Solid state, surface and catalytic properties of oxides [DE85-002096] 06 p0867 N85-15512
Kinetics of interaction between carbon and iron oxides of metallized materials in solid phase [BLL-M-36023-(5828.4)] 07 p0926 N85-15873
Mechanism of burning rate enhancement by ferric oxide 13 p2002 N85-22546
Iron oxides of Mars: Evidence for contemporary weathering 13 p2195 N85-23613
Hydrostatic compression of Fe1-chi 0 wustite. 15 p2508 N85-25472
Influence of eutectic silicate inclusions on micro-processes during deformation and fracture of 12GS steel [BLL-BISI-TRANS-22296-(9022.06)] 17 p2929 N85-28073
Carbon reduction of mixtures of MnO(2) and Fe(2)O(3) [BLL-M-36260-(5828.4)] 20 p3422 N85-31241
Iron and manganese in oxide minerals and in glasses: Preliminary consideration of Eh buffering potential at Yucca Mountain, Nevada [DE85-011892] 23 p3916 N85-34271
Features of behavior of gas bubbles in molten oxide films during enamelling: Communication 2 [BLL-M-35781-(5828.4)] 23 p3919 N85-34283

IRON 59
Mechanisms of impurity diffusion in rutile [DE84-014741] 06 p0766 N85-14902

IROQUOIS HELICOPTER
U UH-1 HELICOPTER

IRRADIANCE
NT ILLUMINANCE
NT SOLAR CONSTANT
New concepts for measuring flame spread properties [NBSIR-84-2943] 03 p0327 N85-12104
Annual energy spectrum for tracking arrays 06 p0832 N85-15297
Correlations of solar irradiance and daylight illuminance for building energy analysis [DE85-001736] 06 p0839 N85-15326
User's guide for the Nimbus 7 ERB Solar Analysis Tape (ESAT) [NASA-TM-86143] 10 p1572 N85-19914
MSG-7: Atmospheric penetration of solar radiation in the range of Schumann-Runge bands 11 p1657 N85-20443
Report on the Workshop on Intercomparison of Solar UV Irradiance Measurements and Related Instrument Calibration 11 p1658 N85-20448
Optical radiation emissions from selected sources. Part 2: High intensity discharge lamps [PB85-149136] 15 p2523 N85-25551
Simple solar spectral model for direct and diffuse irradiance on horizontal and tilted planes at the Earth's surface for cloudless atmospheres [DE85-002933] 18 p3137 N85-29424
Solar Ultraviolet Spectral Irradiance Monitor (SUSIM) 23 p3901 N85-34160
Active Cavity Radiometer (ACR) 23 p3901 N85-34163

IRRADIATION
NT AURORAL IRRADIATION
NT DEUTERON IRRADIATION
NT ELECTRON IRRADIATION
NT ION IRRADIATION
NT NEUTRON IRRADIATION
NT PROTON IRRADIATION
NT X RAY IRRADIATION
Formation of lattice defects by nitrogen laser exposure in A2B6 semiconductors with wide forbidden band
02 p0258 N85-11692
Isotopes in day to day life
[IAEA/PI/A.6E-84-00924] 03 p0417 N85-12668
A study of defects in neutron transmutation doped silicon: Gallium by hall effect analysis
[AD-A146047] 03 p0433 N85-12758
Radiation effects in amorphous metallic alloys
[DE84-014302] 04 p0475 N85-13025
Tensile properties and swelling of 20%-cold-worked Type 316 stainless steel irradiated in HFIR
[DE84-014080] 05 p0617 N85-13948
Raman study of neutron irradiated GaAs
[DE84-016056] 05 p0731 N85-14702
Solar wind and cosmic ray irradiation of grains and ices - application to erosion and synthesis of organic compounds in the solar system
06 p0888 N85-15637
Synergistic sputtering properties of binary alloys
[DE84-017493] 09 p1297 N85-18148
Simulation of repetitively-pulsed laser irradiation of graphite-epoxy composite
[AD-A146696] 09 p1325 N85-18329
Fundamental aspects on ion-beam surface modification: Defect production and migration processes
[DE85-000093] 09 p1399 N85-18804
Radiation-induced compositional redistribution and local phase transformation in irradiated alloys
[DE85-000080] 10 p1441 N85-19062
Facilities for studing radiation damage in nonmetals during irradiation
[DE85-000590] 10 p1554 N85-19801
Study of microstructure of aluminum and copper alloys after processing with continuous CO2 laser beam
11 p1601 N85-20066
Non-isothermal irradiation creep of nickel alloys Inconel 706 and PE-16
[DE85-000642] 11 p1607 N85-20102
Measurement of hot-electron production and microwave emission by laser-irradiated CH targets
[DE85-003139] 11 p1640 N85-20331
Development of an automated miniature Charpy test method
[DE85-003011] 11 p1652 N85-20405
Design and use of nonstandard tensile specimens for irradiated materials testing
[DE85-001071] 11 p1652 N85-20408
Plasma states near surface of metal irradiated by CO2 laser 11 p1719 N85-20815
Irradiation effects on fuels for space reactors
[DE84-016460] 12 p1931 N85-22134
Decomposition of VTAN alloy solid solution upon irradiation and thermal aging 13 p2020 N85-22712
Specifics of laser heat treatment of high steel tools
13 p2029 N85-22714
Time-resolved ellipsometry and reflectivity measurements of the optical properties of silicon during pulsed excimer laser irradiation
[DE85-005091] 13 p2096 N85-23079
Time resolved X-ray studies during pulsed laser irradiation of Ge
[DE85-005263] 13 p2097 N85-23083
Time-resolved reflectivity measurement of extrinsic silicon during pulsed laser irradiation
[AD-A150350] 13 p2159 N85-23403
Local phase transformation in alloys during charged-particle irradiation
[DE85-005012] 14 p2258 N85-23990
Sphericity gauge for wavefront of laser radiation
14 p2275 N85-24096
Use of irradiated foods 14 p2393 N85-24740
Experimental report on a fiber optic light guide made by Galileo Electro-Optics Corporation
[DE85-006161] 14 p2421 N85-24941
Solar gravity modes from ACRIM-SWM irradiance data
14 p2443 N85-25071
Observations of low-degree modes from the solar maximum mission (extended abstract)
14 p2443 N85-25072
Image formation in terms of the transport equation
[DE85-004903] 15 p2653 N85-26365
Low dose irradiation creep of pure nickel
[DE85-006320] 16 p2751 N85-26975
Influence of composition on the microstructural evolution and mechanical properties of irradiated Fe-Ni-Cr ternaries
[DE85-007462] 17 p2931 N85-28094
Effects of gamma-ray irradiation on dislocations in sodium nitrate single crystals
[DE85-008291] 18 p3195 N85-29816
Historical review of californium-252 discovery and development
[DE85-010223] 19 p3362 N85-30644
Defect production and recovery in FCC metals irradiated at 4.2 K
[DE85-010477] 20 p3538 N85-32014
Theoretical modeling of laser induced optical degradation
[AD-A155302] 21 p3592 N85-32323
Effect of powerful pulsed low-energy ion streams on GaAs 21 p3682 N85-32877
Current internal-dosimetry practices at US Department of Energy facilities
[DE85-011718] 22 p3787 N85-33466
Irradiation of northwest agricultural products
[DE85-012455] 22 p3843 N85-33803
Calibration of a high-level photon irradiation
[DE85-013044] 24 p4151 N85-35738
Total integrated dose testing of solid-state scientific CD4011, CD4013, and CD4060 devices by irradiation with CO-60 gamma rays
[NASA-CR-176196] 24 p4161 N85-35795
IRREGULARITIES
Irregularity decay in an isolated plasma bubble
[AD-A145782] 03 p0392 N85-12506
Spectral evaluation of irregularity of superconducting coaxial cables 13 p2062 N85-23000
A study of the generation mechanisms of high latitude and equatorial F-region irregularities using DE-2 data
[NASA-CR-175745] 16 p2825 N85-27423
Mesospheric measurements of irregularity patches using a 3-antenna interferometer, part 3.6B
21 p3621 N85-32496
IRRIGATION
Deficit irrigation feasibility study and demonstration project
[DE85-011531] 22 p3802 N85-33555
IRRITATION
NT TOXICITY AND SAFETY HAZARD
IRROTATIONAL FLOW
U POTENTIAL FLOW
IRS (INDIAN SPACECRAFT)
U INDIAN SPACECRAFT
ISEE
U INTERNATIONAL SUN EARTH EXPLORERS
ISENTROPE
Experimental technique for measuring the isentrope of hydrogen to several megabars
[DE85-014332] 24 p4095 N85-35386
ISENTROPIC PROCESSES
Isentropic objective analysis
[PB85-112167] 11 p1686 N85-20617
Use and interpretation of isentropic analyses
[PB85-132694] 11 p1688 N85-20618
Isotropic plotter
[PB85-175651] 18 p3150 N85-29504
Preliminary considerations for the gasdynamic precompression of solid molecular hydrogen
[DE85-013256] 22 p3784 N85-33445
ISING MODEL
U FERROMAGNETISM
U MATHEMATICAL MODELS
ISIS SATELLITES
NT ALOUETTE 2 SATELLITE
VLF emissions observed by ISIS Satellites during the IMS 14 p2366 N85-24621
ISLAND ARCS
Earthquakes and tectonics of Pacific Ocean margins
06 p0820 N85-15206
Magmatism in continent-ocean transition zone (development of ideas of A. N. Zavaritskiy)
13 p2113 N85-23161
Kuril-Aleutian subduction 19 p3290 N85-30402
ISLANDS
NT ALEUTIAN ISLANDS (US)
NT BERMUDA
NT CUBA
NT GREENLAND
NT HAWAII
NT ICELAND
NT INDONESIA
NT JAPAN
NT KURILE ISLANDS
NT NEW ZEALAND
NT PACIFIC ISLANDS
NT PUERTO RICO
NT TASMANIA
Satellite photographs suggest arctic volcano
07 p0962 N85-16239
Catalog of submarine volcanoes and hydrological phenomena associated with volcanic events: 1500 BC to 31 Dec. 1899
[PB85-117984] 12 p1891 N85-21869
Groundwater model for an island aquifer: Bri
groundwater study
[CE-44] 16 p2821 N85-27
ISOBUTANE
U BUTANES
ISOBUTYLENE
U BUTENES
ISOCHORIC PROCESSES
The isochoric heat capacity of fluid substances in the critical region. Pre-examinations for a Spac
experiment
[BMFT-FB-W-84-034] 05 p0723 N85-14
ISOCYANATES
NT DIISOCYANATES
Moisture absorbing anti-arcing coating and method
applying same
[AD-D011310] 07 p0932 N85-15
Fluorinated polyurethanes
[AD-D011526] 12 p1810 N85-21
ISOENERGETIC PROCESSES
Application of the isoenergy principle and the A weightin
to evaluate lesion risks due to noise in a milita
environment
[ISL-CO-231/83] 14 p2390 N85-24
ISOLATION
A generalized model of fault-isolation performanc
[AD-P003926] 02 p0246 N85-11
Battery control and fault detection method
[AD-D011384] 07 p0993 N85-16
High voltage disconnect protection
[AD-D011490] 10 p1481 N85-19
High voltage isolation transformer
[NASA-CASE-GSC-12817-1] 18 p3093 N85-29
Molten carbonate fuel cell separator
[DE85-011615] 22 p3806 N85-33
ISOLATORS
NT VIBRATION ISOLATORS
An optically isolated amplifier
[CSIR-SR-ELEK-257] 01 p0049 N85-10
Numerical analysis of the first static calibration of the
RSRA helicopter active-isolator rotor balance system
[NASA-TM-85975] 07 p1063 N85-16
Multiple rate shock isolator damping valve
[AD-D011429] 08 p1166 N85-17
Transients during the switching of SF6-insulat
isolating switches
[BLL-CE-TRANS-7986-(9022.09)]
15 p2546 N85-25
ISOMERIZATION
Chemical applications of topology and group theory. 18
Polyhedral isomerizations of seven-coordina
complexes
[AD-A149461] 10 p1436 N85-19
Chemical applications of topology and group theory. 17
An information theoretical approach to polyhed
symmetry
[AD-A152821] 17 p2919 N85-27
ISOMERS
EXAFS and Moessbauer study of small metal cluste
isolated in rare-gas solids
[DE84-015976] 04 p0470 N85-12
Isomer enumeration in polytertiary phosphines and
related compounds
[AD-A148058] 09 p1290 N85-18
PCB analysis by capillary gas chromatography coupl
with matrix isolation-Fourier transform infrar
spectroscopy
[DE84-009201] 10 p1437 N85-19
Interpretation of 119 Sn isomer shifts and 3
5/2-core-level shifts based on Dirac-Slater calculations o
a number of ionic states
[USIP-85-06] 20 p3532 N85-31
Noble metals as incipient transition metals
[DE85-013283] 24 p4080 N85-35
ISOMORPHISM
Moessbauer study of amorph
Fe(67)Co(18)B(14)S(1)
[AERE-R-11526] 11 p1737 N85-20
Algorithm for determination of isomorphic graphs
22 p3769 N85-33
ISOPARAMETRIC FINITE ELEMENTS
Recursive calculation of curved finite element stiffne
matrices
[CSIR-TWISK-303] 01 p0108 N85-10
Nonlinear analysis of composite laminates
09 p1288 N85-18
Improved accuracy in solid isoparametric elements
selectively reduced integration 15 p2573 N85-
A 4-node bilinear isoparametric element in
NASTRAN 15 p2573 N85-
ISOPLETHS
U NOMOGRAPHS
ISOPYCNIC PROCESSES
Local mechanism of equatorial countercurrents
14 p2336 N85-24

ISOSTATIC PRESSURE

HIP glassmaking for high nitrogen compositions in the Y-Si-Al-O-N system
[DE84-015646] 03 p0338 N85-12175

Mechanical properties and microstructure of centrifugally cast alloy 718
[AD-A147800] 06 p1129 N85-17116

Hot Isostatic Pressing (HIP): Techniques, applications and economical use
[JUEL-SPEZ-286] 17 p2939 N85-28141

Hot isostatically pressed Sm(2)(TM)17 magnets
[AD-A156479] 21 p3562 N85-32267

ISOSTERIC PROCESSES
U ISOPYCNIC PROCESSES

ISOTENSOID STRUCTURES

Mechanics of composite materials, theory and application
[VTH-LR-431] 18 p3123 N85-29334

ISOTHERMAL FLOW

Theoretical and experimental investigations of dust loaded flow fields in industrial halls
[BMFT-FB-HA-84-044] 12 p1819 N85-21411

Calculating isothermal flow in wake beyond injection zone 14 p2287 N85-24175

Predictions and measurements of isothermal flowfields in axisymmetric combustor geometries
[NASA-CR-174916] 17 p2698 N85-27867

Turbulent reacting flows 20 p3451 N85-31427

Nonequilibrium chemistry in an isothermal turbulent flow 22 p3745 N85-33211

ISOTHERMAL LAYERS

The physical implications of an isothermal model for the hot intracluster medium
[NASA-TM-86174] 11 p1763 N85-21089

ISOTHERMAL PROCESSES

Structure and properties of titanium alloys after isothermal deformation at low speeds
03 p0351 N85-12260

ECUT, Energy Conversion and Utilization Technologies program: isothermal separation processes update
[NASA-CR-175463] 10 p1433 N85-19033

Joining of sintered composite TiC-steel materials by welding
[BLL-M-36253-(5828.4)] 20 p3461 N85-31502

Numerical simulation of nonisothermal transient processes in GaAs diode structures
22 p3767 N85-33350

ISOTHERMS

Accurate measurement of heat capacity by differential scanning calorimetry 04 p0468 N85-12975

Application of computer methods for calculation of multicomponent phase diagrams of high temperature structural ceramics
[AD-A148138] 08 p1133 N85-17140

A survey of major east coast snowstorms, 1960-1983. Part 2. Summary of surface and upperlevel characteristics
[NASA-TM-86195] 16 p2833 N85-27471

ISOTOPE EFFECT

Deuterium isotope effect on the compatibility between polystyrene and polybutadiene
[AD-A148551] 08 p1134 N85-17145

Variational transition state theory
[DE85-010686] 19 p3235 N85-30059

Constraints on the development of the early continental crust from isotopic data 21 p3719 N85-33076

Electron photoejection in carbanions
[DE85-011748] 23 p3912 N85-34237

ISOTOPE SEPARATION

Gas chromatographic separation of hydrogen isotopes using metal hydrides
[DE84-014455] 04 p0469 N85-12963

Methodology for economic evaluation of process technologies in the early research and development stages
[DE84-015863] 05 p0736 N85-14731

An infrared study of isotopic exchange during methanation over supported rhodium catalysts; an inverse spillover effect
[AD-A148390] 10 p1435 N85-19046

Definition of requirements for injection locking of pulsed UV lasers
[DE85-010126] 18 p3113 N85-29275

EDS operator and control software
[DE85-010470] 19 p3340 N85-30698

Possibilities for studying short-lived nuclei produced at LAMPF
[DE85-010740] 19 p3365 N85-30864

ISOTOPE SHIFT
U ISOTOPE EFFECT

ISOTOPES
NT ALUMINUM ISOTOPES
NT ALUMINUM 26
NT AMERICIUM
NT AMERICIUM ISOTOPES
NT AMERICIUM 241
NT ARGON ISOTOPES
NT BERYLLIUM ISOTOPES
NT BERYLLIUM 7
NT BERYLLIUM 9
NT BERYLLIUM 10
NT BORON 10
NT BROMINE ISOTOPES
NT CALCIUM ISOTOPES
NT CALIFORNIUM ISOTOPES
NT CARBON ISOTOPES
NT CARBON 12
NT CARBON 13
NT CARBON 14
NT CERIUM 144
NT CESIUM ISOTOPES
NT CESIUM 134
NT CESIUM 137
NT CHROMIUM ISOTOPES
NT COBALT 60
NT CURIUM
NT CURIUM 244
NT DEUTERIUM
NT GERMANIUM ISOTOPES
NT HELIUM ISOTOPES
NT HYDROGEN ISOTOPES
NT IODINE ISOTOPES
NT IRON ISOTOPES
NT IRON 59
NT KRYPTON ISOTOPES
NT KRYPTON 85
NT LUTETIUM
NT MAGNESIUM ISOTOPES
NT MANGANESE ISOTOPES
NT METALLIC HYDROGEN
NT NEODYMIUM ISOTOPES
NT NEON ISOTOPES
NT NICKEL ISOTOPES
NT NITROGEN ISOTOPES
NT NITROGEN 15
NT OSMIUM ISOTOPES
NT OXYGEN ISOTOPES
NT PLUTONIUM
NT PLUTONIUM ISOTOPES
NT PLUTONIUM 238
NT PLUTONIUM 239
NT POTASSIUM 40
NT RADIOACTIVE ISOTOPES
NT RADON ISOTOPES
NT RUBIDIUM ISOTOPES
NT SCANDIUM ISOTOPES
NT SILICON ISOTOPES
NT SODIUM ISOTOPES
NT STRONTIUM 90
NT TELLURIUM
NT THORIUM ISOTOPES
NT TRANSURANIUM ELEMENTS
NT TRITIUM
NT URANIUM ISOTOPES
NT URANIUM 235
NT XENON ISOTOPES
NT XENON 129

Magnetohydrodynamic flow of two-component gas analyzed 04 p0491 N85-13133

Isotopic composition of primary cosmic rays H-Fe for ISEE-C
[NASA-CR-175266] 05 p0746 N85-14783

Chemical evolution of the solar nebula: A new model
06 p0887 N85-15631

Chlorine isotopes as environmental tracers in Columbia River basalt groundwaters
[DE85-011392] 19 p3302 N85-30473

Technology for increasing the uranium-235 isotopic abundance in natural uranium feed on a productive scale
[DE85-011252] 19 p3357 N85-30810

NBS (National Bureau of Standards) reactor: Summary of activities Jul. 1983 through Jun. 1984
[PB85-184836] 20 p3522 N85-31907

A Cerenkov-delta E-Cerenkov detector for high energy cosmic ray isotopes and an accelerator study of Ar-40 and Fe-56 fragmentation
[NASA-CR-176028] 20 p3549 N85-32086

Contributions to the 19th International Cosmic Ray Conference
[NASA-CR-176060] 21 p3714 N85-33044

Initial results from the Caltech/DSRI balloon-borne isotope experiment
[OG-4.3-8] 21 p3714 N85-33046

Measurements of Fe and Ar fragmentation cross sections
[PAPER-OG-7.2-20] 21 p3714 N85-33047

Ninteenth International Cosmic Ray Conference. OG sessions, volume 2
[NASA-CP-2376-VOL-2] 22 p3875 N85-34006

Results of a search for deuterium at 25-50 GC/c using a magnetic spectrometer
[OG-4.2-4] 22 p3878 N85-34024

Cosmic ray isotope measurements with a new Cerenkov X total energy telescope
[OG-4.3-4] 22 p3878 N85-34029

A new analysis of cosmic ray isotopes at 3 GeV/n from HEA03-C2 data
[OG-4.3-6] 22 p3879 N85-34031

Initial results from the Caltech/DRSI balloon-borne isotope experiment
[OG-4.3-8] 22 p3879 N85-34033

Abundances of secondary elements among the ultra heavy cosmic rays: Results from HEAO-3
[OG-4.4-6] 22 p3880 N85-34039

High resolution Cherenkov detectors for cosmic ray isotope experiment
[OG-9.1-4] 23 p4023 N85-34930

Mass resolution optimization in a large isotopic composition experiment
[OG-9.1-9] 23 p4023 N85-34935

Measurement of low energy cosmic rays aboard Spacelab-1
[SH-10.1-6] 23 p4053 N85-35137

Stopping relativistic Xe, Ho, Au and U nuclei in nuclear emulsions 24 p4173 N85-35876

ISOTOPIC ENRICHMENT
NT JET MEMBRANE PROCESS

On the connection between the 3HE-enrichment and spectral index of solar energetic particles
[SH-2.2-9] 23 p4001 N85-34804

ISOTOPIC LABELING

Diffusion of Fe-55 in Fe-2O-3 single crystals
[AERE-R-11286] 03 p0333 N85-12147

Isotopes in day to day life
[IAEA/PI/A.6E-84-00924] 03 p0417 N85-12668

Los Alamos MINI-Review: Tracking Antarctic winds
[DE85-004597] 12 p1896 N85-21903

Constraints on the development of the early continental crust from isotopic data 21 p3719 N85-33076

Centrifugal castings of stainless steel spiked with radioactive tracers
[DE85-012003] 22 p3748 N85-33234

Uranium, thorium isotopic analyses and uranium-series ages of calcite and opal and stable isotopic compositions of calcite from drill cores UE25a no. 1, USR G-2 and USW G-3/GU-3, Yucca Mountain, Nevada
[DE85-013039] 23 p3948 N85-34471

ISOTROPIC MEDIA

Compression of a band made of elastic, ideally Coulomb plastic material
[ISSN-0208-5658] 05 p0648 N85-14157

Unified constitutive material models for nonlinear finite-element structural analysis — gas turbine engine blades and vanes
[NASA-TM-86985] 14 p2320 N85-24338

ISOTROPIC TURBULENCE

Decay of a coherent scalar disturbance in a turbulent flow
[NASA-TM-86700] 19 p3264 N85-30244

ISOTROPISM

Trilinear alternating forms on a vector space of dimension 7
[CWI-PM-R8402] 05 p0722 N85-14644

ISOTROPY
NT ISOTROPIC MEDIA

NMR (Nuclear Magnetic Resonance) and macromolecular migration in a melt or in concentrated solutions
[AD-P003906] 01 p0032 N85-10194

Constitutive model development for isotropic materials
02 p0144 N85-10975

Arrival directions of cosmic rays of E .4 EeV
[OG-5.3-4] 22 p3884 N85-34071

ISRAEL

Technology transfer report: Feasibility study for the use of geothermal brine in the Ashdod area, Israel
[DE85-013316] 22 p3810 N85-33596

ISRO

Colloquium about Joint Projects within DFVLR/ISRO Cooperation
[DFVLR-MITT-84-12] 04 p0458 N85-12907

Presentation of Indian Space Research Organization (ISRO)/DFVLR cooperation 04 p0459 N85-12912

ITALY

Examples of environment services: Hydrological and pollution measurements in the Po River (Italy)
[CISE-2299] 11 p1679 N85-20578

ITERATION
NT CONJUGATE GRADIENT METHOD
NT ITERATIVE SOLUTION

A subspace iteration method for determining a dominant span of eigenvectors
[TWISK-329] 01 p0109 N85-10739

The rate of convergence of a class of block Jacobi schemes
[AD-A144736] 01 p0111 N85-10749

Development of a production order release methodology
[AD-A145213] 01 p0124 N85-10852

Generalized linear inversion of 2.5 - dimensional gravity and magnetic anomalies 02 p0226 N85-11460

Parametric analysis for generalized network flow problems
[AD-A145556] 02 p0243 N85-11589

An iterative procedure for obtaining I-projections onto the intersection of convex sets
[AD-A145402] 02 p0251 N85-11639

CHORDS: A new temperature or sound speed profile thinning algorithm
[AD-A145464] 02 p0275 N85-11793

Restoration of multichannel microwave radiometric images
[NASA-CR-174115] 04 p0554 N85-13527

Transformation of two and three-dimensional regions by elliptic systems
[NASA-CR-174176] 04 p0554 N85-13529

Multigrid iteration solution procedure for solving three-dimensional sets of coupled equations
[DE84-016515] 04 p0555 N85-13532

Multigrid iteration solution procedure for solving two-dimensional sets of coupled equations
[DE84-016554] 04 p0555 N85-13533

Iterative method for determining the distortion of elastic-plastic frames
[ISSN-0206-5658] 05 p0647 N85-14156

Very short range statistical forecasting of automated weather observations
[DOT/FAA/PM-84/31] 05 p0679 N85-14359

Interval interation methods for nonlinear equation systems: Theory and comparison on computer
[INTERVALL-BER-84/6] 05 p0719 N85-14612

Mixed defect correction (iteration) for the solution of a singular perturbation problem
[MC-NW-162/83] 05 p0720 N85-14624

An iterative scheme for linear complementarity problems
[AD-A147464] 07 p1032 N85-16555

Distributed asynchronous relaxation methods for convex network flow problems
[AD-A148027] 08 p1211 N85-17622

Signal reconstruction from Fourier transform sign information
[AD-A148039] 08 p1211 N85-17624

A case of a not-so-strange strange attractor
[CWI-AM-R8406] 08 p1214 N85-17643

Designing the profile of turbine blades using an iteration technique 09 p1305 N85-18201

A turbulent closure model for the free atmosphere 09 p1351 N85-18502

Where are the parallel algorithms?
[NASA-CR-172516] 09 p1373 N85-18627

Transonic pressure distribution computations of a flexible wing 11 p1622 N85-20213

Applied mathematics of transport theory
[DE85-000848] 11 p1633 N85-20283

Complex symmetric matrices with strongly stable iterates
[NASA-CR-172542] 11 p1706 N85-20731

A solution method for large deformation contact problems
[AD-A149842] 12 p1866 N85-21707

State dependent priority rules for scheduling
[AD-A149972] 12 p1924 N85-22090

An iteration method for complex scattering problems
[AD-A150038] 12 p1934 N85-22151

On an iterative scheme for the solution of constrained variational equations
[CSIR-TWISK-341] 13 p2149 N85-23342

Iteration of exponential functions 15 p2633 N85-26233

A decomposition procedure for convex quadratic programs
[AD-A151732] 16 p2854 N85-27595

Nonlinear DSA difference schemes for radiative transfer applications
[DE85-005729] 16 p2856 N85-27611

Polynomial iteration for nonsymmetric indefinite linear systems
[AD-A153094] 17 p3019 N85-28671

A study of aerodynamic control in stalled - flight leading-edge vortex formation analysis
[AD-A153758] 18 p3059 N85-28926

Transverse vorticity measurements using an array of four hot-wire probes
[FSFL-R-85-006] 18 p3099 N85-29184

Recent developments in nonlinear normal mode initialization 18 p3142 N85-29451

A robust estimator of location using an adaptive spline model
[AD-A153862] 18 p3174 N85-29676

The origin of the binary-search paradigm
[AD-A154367] 19 p3337 N85-30677

A parallelized point successive over-relaxation method on a multiple instruction multiple data stream computer
[AD-A154377] 19 p3337 N85-30679

Guide on logical database design
[PB85-177970] 19 p3381 N85-30976

Newton's method as a dynamical system: Global convergence and predictability
[AD-A155170] 21 p3632 N85-32564

A practical approach to Karmarkar's algorithm
[AD-A155714] 21 p3673 N85-32818

New developments on the core function for efficient implementation of the difficult residue number system operations
[AD-A154678] 21 p3676 N85-32834

Perturbation-iteration theory for analyzing microwave striplines
[NASA-CR-176189] 24 p4085 N85-35321

ITERATIVE NETWORKS

Analysis and design methodology for VLSI computing networks
[AD-A146030] 03 p0409 N85-12611

ITERATIVE SOLUTION

Augmented weak forms and element-by-element preconditioners: Efficient iterative strategies for structural finite elements. A preliminary study 01 p0058 N85-10384

Parallel, iterative solution of sparse linear systems: Models and architectures
[NASA-CR-172457] 02 p0243 N85-11586

Iterative method of calculating strength of airframe members using finite element method 06 p0775 N85-14955

Use of iterative linear and nonlinear algebraic methods for solving large stiff systems of ODEs
[AD-A148516] 08 p1213 N85-17636

Domain decomposition techniques for solving elliptic partial differential equations on multiprocessors
[DE85-004448] 10 p1549 N85-19769

Some data manipulation requirements for the exploratory analysis of large data sets
[DE85-002541] 10 p1568 N85-19887

On an iterative scheme for the solution of constrained variational equations
[CSIR-TWISK-341] 13 p2149 N85-23342

Solving large linear systems 14 p2396 N85-24759

Synthetic acceleration of coarse-mesh S/sub n/ transport calculations
[DE84-014721] 14 p2409 N85-24855

On the shift parameter in the backward beam method for parabolic problems for preceding times
[CWI-NM-R8411] 14 p2410 N85-24861

Manipulation and simulation of general robots using the zero-position description 15 p2567 N85-25838

Solving the minimal least squares problem subject to bounds on the variables
[TRITA-NA-8215] 16 p2852 N85-27580

Finite elements and the method of conjugate gradients on a concurrent processor
[NASA-CR-175812] 16 p2853 N85-27588

Projected discrete ordinates methods for numerical transport problems
[DE85-005632] 17 p3020 N85-28678

A convolution integral equation solved by Laplace transformation
[CWI-AM-R8409] 17 p3022 N85-28692

Inhomogeneous deformation: The theory and geological application of finite strain compatibility 19 p3312 N85-30532

Multigrid method for multiprocessors
[DE85-007929] 19 p3333 N85-30647

An iterative method for indefinite systems of linear equations
[NASA-CR-172345] 19 p3345 N85-30726

Optimization of a numerical method to calculate elliptic flows
[ESA-TT-889] 20 p3457 N85-31472

On the convergence of an iterative formulation of the electromagnetic scattering from an infinite grating of thin wires 24 p4085 N85-35319

IUE

Constraints to the radiative lifetime of a light neutral fermion in the galactic halo from IUE
[NOTA-INTERNA-817] 02 p0279 N85-11820

Lyman-Alpha aurora 02 p0302 N85-11953

Absorption line studies and the distribution of neutral gas in the local interstellar medium 06 p0873 N85-15544

Synthesis of data on the local interstellar medium 06 p0874 N85-15545

Observations of interstellar HI toward nearby late-type stars 06 p0874 N85-15546

Observations of local interstellar Mg I and Mg II 06 p0874 N85-15547

Mg II spectra of late type stars used to probe the LISM 06 p0874 N85-15548

FeII and MgII in the nearby interstellar medium 06 p0874 N85-15549

Spectroscopic observations of selected stellar systems
[NASA-CR-174288] 08 p1256 N85-17915

Future of Ultraviolet Astronomy Based on Six Years of IUE Research
[NASA-CP-2349] 11 p1743 N85-20961

IUE absorption line studies of highly ionized interstellar gas 11 p1743 N85-20962

Hot stars: Six years of progress 11 p1743 N85-20963

Solar system studies with the IUE: 1982 - 1984 11 p1744 N85-20964

Magellanic cloud objects 11 p1744 N85-20965

Interacting binary systems 11 p1744 N85-20967

Outer atmospheres of cool stars observed with IUE 11 p1744 N85-20968

Future ultraviolet experiments, including FUSE/COLUMBUS 11 p1744 N85-20969

UV observations and results on pre-main sequence stars 11 p1744 N85-20970

White dwarf stars at ultraviolet wavelengths 11 p1744 N85-20971

Supernova remnants and the carbon abundance in M33 11 p1745 N85-20972

Comments on the origins and variations of carbon and nitrogen in the ISM of galaxies as evident from IUE spectroscopy of H 2 regions 11 p1745 N85-20973

IUE spectroscopy of extragalactic H H regions 11 p1745 N85-20974

The usual hot stars in unusual galaxies 11 p1745 N85-20975

Highly ionized gas associated with the small Magellanic cloud 11 p1745 N85-20976

Galactic absorption lines measured from the IUE low dispersion spectra of active galaxies 11 p1745 N85-20977

Self-consistent recalibration of IUE determination of hot DA white dwarf effective temperatures 11 p1751 N85-21016

The fading of R coronae borealis 11 p1753 N85-21029

Observations of RR Lyrae and X Arietis with the IUE satellite 11 p1754 N85-21030

Atmospheric properties of RU Lupi derived from high- and low-resolution IUE spectra 11 p1754 N85-21031

Mg 2 emission of Pop. 2 long-period Cepheids 11 p1754 N85-21032

Blue companions of Cepheids 11 p1754 N85-21033

Ultraviolet observations of Population 2 Cepheids 11 p1754 N85-21034

Ultraviolet analysis of the peculiar F supergiant HD 112374 11 p1754 N85-21035

UV observations of epsilon aurigae during ingress and totality 11 p1755 N85-21038

Egress spectra of the new eclipsing supergiant 22 Vulleculae 11 p1755 N85-21039

The stellar wind in the BO V-type eclipsing binary Y Cygni 11 p1755 N85-21040

Observations of cataclysmic variable star winds 11 p1755 N85-21041

Ultraviolet spectroscopy of the interacting binary U Sagittae 11 p1755 N85-21042

Ultraviolet observations of circumstellar matter in Algol type binary systems 11 p1756 N85-21043

The essence of binary star coalescence: A coordinated ground-based photometric and IUE ultraviolet study of FK Comae 11 p1756 N85-21044

Strange F + Be binary star systems 11 p1756 N85-21045

Multi-year and possibly periodic variations in the UV spectrum of 56 Pegasi 11 p1756 N85-21046

Physical models for the UV continua of symbiotic stars 11 p1756 N85-21048

IUE and optical observations of LMC X-ray binaries 11 p1757 N85-21050

Circumstellar material in Algols and Serpentids 11 p1757 N85-21051

MU Sagittarii and Beta Lyrae: Combined IUE/Voyager observations 11 p1757 N85-21052

A search for the spectroscopic binary companions of Polaris using IUE spectra 11 p1757 N85-21053

The solar stellar connection in the far ultraviolet 11 p1757 N85-21055

Chromospheric activity in M giants 11 p1757 N85-21056

A progress report on the analysis of long exposure high resolution spectra of cool stars 11 p1758 N85-21057

Betelgeuse at maximum luminosity
11 p1758 N85-21061
IUE low-dispersion reference atlas
11 p1760 N85-21073
An IUE high-resolution atlas of O-type spectra
11 p1760 N85-21074
Statistical classification of IUE low-despersion stellar spectra: Progress report 11 p1760 N85-21075
IUE observations of faint standard stars for calibration of the space telescope 11 p1761 N85-21076
Calibrations of wavelengths in SWP echelle spectra
11 p1761 N85-21077
Improved continuum definition in high-background IUE images 11 p1761 N85-21078

IUS
U INERTIAL UPPER STAGE

IZSAK ELLIPSOID
U ELLIPSOIDS
U GEODESY

J

J INTEGRAL
On the treatment of material laws for approximate J-estimation methods
[GKSS-84-E-15] 01 p0062 N85-10414
Eta values for compact geometry specimens to calculate the J integral
[AERE-R-11126] 03 p0374 N85-12385
An experimental evaluation of the J integral in 50% sidegrooved compact geometry specimens
[AERE-R-11202] 03 p0374 N85-12386
Correlation of stable crack growth with the J-integral and the crack tip opening displacement, effects of geometry, size and material: Report on an investigation of the elastic-plastic R-curve methodology
[GKSS-84-E-37] 08 p1173 N85-17395
Direct comparison of unloading compliance and potential drop techniques in J-integral testing
[DE85-001550] 11 p1650 N85-20392
Translational and extensional energy release rates (the J- and M-integrals) for a crack layer in thermoelasticity
[NASA-CR-174872] 12 p1863 N85-21685
The three-dimensional J-integral. An investigation into its use for post-yield fracture safety assessment
[WTHD-167] 20 p3472 N85-31578
A review of path-independent integrals in elastic-plastic fracture mechanics, task 4
[NASA-CR-174956] 22 p3799 N85-33541

J-52 ENGINE
A Q-GERT network simulation model for examining pipeline time in the Navy's J-52 intermediate level jet engine repair cycle
[AD-A147269] 07 p0894 N85-15663

J-85 ENGINE
Problems and possibilities for life extension in gas turbine components 07 p0907 N85-15742

JACKING EQUIPMENT
U JACKS (LIFTS)

JACKS (ELECTRICAL)
U ELECTRIC CONNECTORS

JACKS (LIFTS)
Improvements in linked-spar motion-compensated lifting system
[AD-D011413] 08 p1138 N85-17165
Cargo handling system
[AD-D011569] 14 p2219 N85-23762

JACOBI MATRIX METHOD
On existence and uniqueness of solutions of Hamilton-Jacobi equations
[AD-A147597] 07 p1033 N85-16560

JACOBI POLYNOMIALS
U HYPERGEOMETRIC FUNCTIONS

JAGUAR AIRCRAFT
Experiences obtained from service fatigue monitoring exercises 07 p0895 N85-15672
An update of experience on the fly by wire Jaguar equipped with a full-time digital flight control system
17 p2902 N85-27893

JAMMERS
Noise jammer discrimination by noise modulation bandwidth
[AD-D011473] 10 p1468 N85-19264
Research on adaptive antenna techniques 6
[AD-A149341] 11 p1624 N85-20229

JAMMING
Resistance to HF jamming interference in mobile radio networks by an adaptive, distributed reconfiguration technique
[AD-A145117] 01 p0036 N85-10238
Noise jammer discrimination by noise spectral bandwidth
[AD-D011224] 01 p0038 N85-10242
Reflector antenna having sidelobe suppression elements
[AD-D011227] 01 p0039 N85-10244
Distributed reservation-based code division multiple access
[AD-A147007] 07 p0940 N85-15957
Parallel processor configuration for adaptive antenna arrays
[AD-D011347] 07 p0942 N85-15970
Optimum jamming effects on frequency-hopping M-ary FSK (Frequency-Shift Keying) systems under certain ECCM (Electronic counter-countermeasures) receiver design strategies
[AD-A147768] 08 p1151 N85-17267
Integrated defense communications system antijamming antenna system
[AD-D011423] 08 p1154 N85-17285
Noise jammer discrimination by noise modulation bandwidth
[AD-D011473] 10 p1468 N85-19264
Narrowband spread spectrum systems
10 p1475 N85-19307
Multiple loop sidelobe canceller
[AD-D011533] 12 p1823 N85-21434
The effect of jamming/deception on decision making
[AD-A149740] 12 p1828 N85-21472
FH/MFSK performance in multitone jamming
[NASA-CR-175667] 14 p2290 N85-24197
A survey of radar ECM and ECCM
15 p2536 N85-25653
Margin leveling algorithm for fully saturated satellite transponder with CDMA (Code Division Multiple Access) signalling
[AD-A151710] 15 p2543 N85-25699
Digital RF delay line for ECM (electronic countermeasure) look-through
[AD-A152120] 16 p2774 N85-27120
An analysis of jamming effects on noncoherent digital receivers
[AD-A153791] 18 p3090 N85-29128
Design of a jamming simulator for a binary communication system
[AD-A154617] 21 p3573 N85-32221

JANUS REACTOR
Microdosimetric spectra measurements of JANUS neutrons
[DE85-012108] 22 p3843 N85-33801

JAPAN
Operational precipitation observation system using digitized radar and rain gages 01 p0082 N85-10549
Analysis of radiocobalt in environmental samples
[DRIC-T-7334] 03 p0387 N85-12477
The availability of Japanese scientific and technical information in the United States
[GPO-35-241] 05 p0735 N85-14726
High-technology ceramics in Japan
[TI85-900389] 09 p1299 N85-18157
MAP in Japan: Organization and projects
11 p1655 N85-20425
High-technology ceramics in Japan
[PB85-125029] 12 p1815 N85-21389
The availability of Japanese scientific and technical information in the United States
[GPO-39-478] 12 p1951 N85-22254
Interrelationship of earthquake magnitude and lithospheric-asthenospheric thermodynamic parameters in seismically active zones 13 p2116 N85-23183
General report of the researches of snowpack properties, snowmelt runoff and evapotranspiration in Japan 13 p2124 N85-23225
Snowmelt runoff model in Japan
13 p2124 N85-23227
Application of Martinec-Rango model to river basin in Japan 13 p2124 N85-23228
Analysis of NIMBUS-7 SMMR data — Hokkaido, Japan snow cover 13 p2125 N85-23232
Estimation of regional evapotranspiration using remotely sensed land surface temperature. Part 2: Application of equilibrium evaporation model to estimate evapotranspiration by remote sensing technique — Japan 13 p2125 N85-23234
Results of comparison of long-wave radiation fluxes measured by Soviet and Japanese actinometric radiosounds 14 p2333 N85-24427
The astrometry network of observers in Japan
14 p2436 N85-25028
Welding technology: Japan — Conference
[ISBN-0-85300177-4] 15 p2565 N85-25823
Observation of precipitating clouds by a vertically pointing radar at Morino in the Iburi District, Hokkaido, Japan 15 p2582 N85-25922
Cosmic ray intensity variations observed at Matsushiro (220 M.W.E. in depth)
[SH-4.4-9] 23 p4034 N85-35007
Space activities in the Soviet Union, Japan, and the People's Republic of China 23 p4067 N85-35149

JAPANESE SPACE PROGRAM
Space Research in Japan. National report
01 p0013 N85-10082
Satellite observations 01 p0013 N85-10083
Non-US approaches to space commercialization
02 p0150 N85-11012
NTT unveils satellite communications equipment
10 p1476 N85-19315
Meteorological Satellite Center Technical Note No. 10, 1984
[MSC-TN-10] 12 p1894 N85-21884
History and future views on solar cells of Japanese scientific satellites 13 p2005 N85-22566

JAPANESE SPACECRAFT
Structural aspects of SAR antenna for Japanese Earth Resources Satellite 1 05 p0626 N85-14007
Development of Halley's Comet explorer PLANET-A solar array 13 p2010 N85-22608
Observations of auroras and related plasma phenomena by the Kyokko and Jikiken satellite in IMS — EXOS-A and B satellite 14 p2354 N85-24547

JARRING
U MECHANICAL SHOCK

JEEPS
U AUTOMOBILES

JET AIRCRAFT
NT A-7 AIRCRAFT
NT A-310 AIRCRAFT
NT A-320 AIRCRAFT
NT B-70 AIRCRAFT
NT BOEING 727 AIRCRAFT
NT BOEING 737 AIRCRAFT
NT BOEING 747 AIRCRAFT
NT BOEING 767 AIRCRAFT
NT C-5 AIRCRAFT
NT C-135 AIRCRAFT
NT C-141 AIRCRAFT
NT CL-41 AIRCRAFT
NT CONCORDE AIRCRAFT
NT CV-990 AIRCRAFT
NT DC 8 AIRCRAFT
NT DC 9 AIRCRAFT
NT DC 10 AIRCRAFT
NT DH 115 AIRCRAFT
NT DHC 2 AIRCRAFT
NT EUROPEAN AIRBUS
NT F-8 AIRCRAFT
NT F-14 AIRCRAFT
NT F-15 AIRCRAFT
NT F-16 AIRCRAFT
NT F-17 AIRCRAFT
NT F-18 AIRCRAFT
NT F-27 AIRCRAFT
NT F-104 AIRCRAFT
NT F-106 AIRCRAFT
NT F-111 AIRCRAFT
NT JET PROVOST AIRCRAFT
NT L-1011 AIRCRAFT
NT LEAR JET AIRCRAFT
NT MIRAGE AIRCRAFT
NT MIRAGE 3 AIRCRAFT
NT OV-1 AIRCRAFT
NT P-3 AIRCRAFT
NT T-33 AIRCRAFT
NT TURBOFAN AIRCRAFT
NT TURBOPROP AIRCRAFT
NT U-2 AIRCRAFT
Observations from varying the lift and drag inputs to a noise prediction method for supersonic helical tip speed propellers
[NASA-TM-83797] 01 p0115 N85-10788
Development and flight evaluation of an augmented stability active controls concept: Executive summary
[NASA-CR-166009] 02 p0149 N85-11006
Auditory information systems in military aircraft: Current configurations versus the state of the art
[AD-A145469] 02 p0275 N85-11794
Computer programs to predict induced effects of jets exhausting into a crossflow
[NASA-CR-166591] 05 p0592 N85-13776
Advanced fatigue monitoring on service aircraft
07 p0895 N85-15671
Ground-effect analysis of a jet transport airplane
[NASA-TM-85920] 07 p0897 N85-15687
Analysis of the flow field about a T-45 using PANAIR
[AD-A146811] 07 p0899 N85-15699
The influence on IR emission of engine parameters for an afterburn case. A sensitivity study on NATO infrared air target model (NIRATAM) version: 0.0
[AD-B089311L] 12 p1779 N85-21171
Designer O. K. Antonov on new AN-74 arctic transport
15 p2467 N85-25230
A method for simulating 3-D aircraft flow fields with jet plume effects
[NASA-CR-176802] 18 p2899 N85-26664

Flight trials of a modified gulfstream commander carrying external stores
[AD-A153376] 17 p2896 N85-27859
The AFTI/F16 terrain-aided navigation system
[DE85-008411] 18 p3060 N85-28935

JET AIRCRAFT NOISE
Commercial aircraft noise
[PNR-90206] 03 p0417 N85-12665
Experimental investigation of shock-cell noise reduction for dual-stream nozzles in simulated flight
[NASA-CR-3846] 04 p0557 N85-13549
Computation of noise radiation from a free jet perpendicular to its axis via laser anemometry measurements
[ESA-TT-870] 09 p1379 N85-18889
Fan noise suppression in turbofan engines
[B8580076] 17 p2898 N85-27872

JET AIRSTREAMS
U JET STREAMS (METEOROLOGY)

JET AUGMENTED WING FLAPS
U JET FLAPS
U WING FLAPS

JET BLAST EFFECTS
A study of flow past an airfoil with a jet issuing from its lower surface
[NASA-CR-166610] 04 p0451 N85-12860

JET BOUNDARIES
Buoyant jet entrainment in stratified fluids
19 p3263 N85-30238

JET DAMPING
U DAMPING
U SPIN REDUCTION

JET DRIVE
U JET PROPULSION

JET ENGINE FUELS
NT JP-4 JET FUEL
NT JP-5 JET FUEL
NT JP-8 JET FUEL
Combustion gas properties I-ASTM jet A fuel and dry air
[NASA-TP-2359] 01 p0010 N85-10064
Molecular interactions of high energy fuels and jet fuels with oncogenic viruses and endogenous viruses
[AD-A145484] 02 p0188 N85-11255
Lubricity of well-characterized jet and broad-cut fuels by ball-on-cylinder machine
[NASA-TM-83807] 03 p0339 N85-12183
Compound class quantitation of JP-5 jet fuels by high performance liquid chromatography-differential refractive index detection
[AD-A145754] 03 p0340 N85-12185
Liquid phase products and solid deposit formation from thermally stressed model jet fuels
[NASA-TM-86874] 04 p0481 N85-13066
Method for evaluating petrol products corrosivity using piezoelectric crystals. Part 2: Instruction manual — jet engine corrosion tests
[FOA-C-40198-B4] 04 p0482 N85-13073
Storage stability of jet fuels
[AD-A146360] 06 p0773 N85-14943
Heater block assembly for use in thermal oxidation testing of jet fuel
[AD-D011430] 08 p1123 N85-17077
GC-FTIR (Fourier Transform Infrared Spectrometry) of jet fuels
[AD-A148272] 08 p1135 N85-17155
Atmospheric photochemical modeling of turbine engine fuels. Phase 1: Experimental studies. Volume 2: Environmental chamber data tabulations
[AD-A147786] 08 p1185 N85-17470
Study of advanced fuel system concepts for commercial aircraft and engines
[NASA-CR-174752] 10 p1456 N85-19176
Quantitative determination of compound classes in jet turbine fuels by high performance liquid Chromatography/Differential refractive index detection: Part 2
[AD-A149298] 11 p1613 N85-20144
Oxidation and gum formation in jet fuels
[AD-A149934] 12 p1818 N85-21401
JP-8 and JP-5 as compression ignition engine fuel
[AD-A150796] 14 p2263 N85-24022
Influence of fuel properties on gas turbine combustion performance
[AD-A151464] 15 p2504 N85-25448
Aviation turbine fuels from tar sands bitumen and heavy oils. Part 1: Process analysis
[AD-A151319] 15 p2521 N85-25539
Jet fuel property changes and their effect on producibility and cost in the U.S., Canada, and Europe
[NASA-CR-174840] 16 p2757 N85-27012
Jet fuel instability mechanisms
[NASA-CR-175856] 17 p2936 N85-28127
Research test facility for evaporation and combustion of alternative jet fuels at high air temperatures
[AD-A153830] 18 p3083 N85-29073
The distribution of higher n-alkanes in partially frozen middle distillate fuels
[AD-A153940] 18 p3083 N85-29074
Measurement and correlation of jet fuel viscosities at low temperatures
[NASA-CR-174911] 23 p3921 N85-34295
Nitrogen analysis by chemiluminescence
[AD-A156197] 24 p4083 N85-35308
Biodegradation of jet fuel by aquatic microbial communities
[PB85-191971] 24 p4084 N85-35311

JET ENGINES
NT J-52 ENGINE
NT J-85 ENGINE
NT RAMJET ENGINES
NT SUPERSONIC COMBUSTION RAMJET ENGINES
NT TURBOFAN ENGINES
NT TURBOJET ENGINES
NT TURBOPROP ENGINES
Air force engine repair - Oklahoma City Air Logistics Center, Propulsion Division
[AD-P003999] 03 p0307 N85-11980
Propulsion — jet aircraft engines
[PNR-90208] 03 p0320 N85-12062
The applications of fibre optics in gas turbine engine instrumentation
[PNR-90209] 03 p0420 N85-12687
Air intake efficiency at zero speed and lip suction — jet engines
[BAE-KRS-N-GEN-303] 09 p1272 N85-17996
Oxidation resistant materials for hot gas turbines and jet engines
[AD-B087399L] 13 p1973 N85-22369
Fabrication of ceramic substrate-reinforced and free forms
[NASA-TM-86994] 14 p2247 N85-23926
Fiscal year 1986 technical objective document
[AD-A151039] 14 p2432 N85-25000
Advanced smoke meter development survey and analysis
[NASA-CR-168287] 15 p2560 N85-25792
Alternatives for jet engine control
[NASA-CR-175831] 16 p2709 N85-26713
Alternatives for jet engine control
[NASA-CR-175832] 16 p2709 N85-26714
Alternatives for jet engine control
[NASA-CR-175833] 16 p2709 N85-26715
Testing of materials and coatings for jet engine components under simulated operational conditions
[B8580073] 17 p2899 N85-27873
Opacity control technique for jet engine test cells
[AD-D011668] 19 p3220 N85-29968
Man-vehicle systems research facility advanced aircraft flight simulator throttle mechanism
22 p3798 N85-33527
Component-specific modeling
[NASA-CR-174765] 23 p3897 N85-34140

JET EXHAUST
A 2-dimensional description of potential perturbations to the ozone layer due to NOx and H-2-O aircraft emissions
[AD-A146292] 03 p0392 N85-12511
Opacity control technique for jet engine test cells
[AD-D011668] 19 p3220 N85-29968

JET FLAMES
U FLAMES
U JET FLOW

JET FLAPS
A study of flow past an airfoil with a jet issuing from its lower surface
[NASA-CR-166610] 04 p0451 N85-12860

JET FLIGHT
U JET AIRCRAFT

JET FLOW
NT AIR JETS
NT SUPERSONIC JET FLOW
Characteristics of a turbulent plane offset jet
02 p0196 N85-11310
Tunnel constraint for a jet in crossflow
03 p0314 N85-12027
Study of the velocity-acoustic pressure correlation in a cold jet, centered on the sign and the amplitude of the velocity fluctuations
[ISL-R-124/83] 04 p0501 N85-13193
Laminar jet issuing into stagnant surroundings — PHOENICS code
[PDR/CFDU-IC/15] 04 p0501 N85-13200
Transition and mixing in axisymmetric jets and vortex rings
05 p0591 N85-13769
Transonic jets: A numerical approach in the hodograph plane
05 p0592 N85-13774
Bicomponent flow problems in rheological fluid mechanics
05 p0635 N85-14073
Characterization of jet-contaminant interaction flow in chemical decontamination
[AD-A147298] 08 p1161 N85-17327
Design guide for fluidic laminar proportional amplifiers and laminar jet angular rate sensors
[AD-A147730] 08 p1161 N85-[illegible]
Bipolar flows and X-ray emission from young stellar object
08 p1234 N85-[illegible]
The sensitivity analysis in k-epsilon turbulence modeling applied to jet flows
09 p1318 N85-[illegible]
Notes on compressible flow equations for thermodynamics of hot jets
[BAE-KRS-N-GEN-273] 09 p1318 N85-[illegible]
Supersonic molecular jet study of the liquid state
[AD-A147416] 09 p1379 N85-[illegible]
Flow visualization study of the effect of injection hole geometry on an inclined jet in crossflow
[NASA-TM-86936] 11 p1631 N85-[illegible]
Preliminary analysis of tone-excited two-stream jet velocity decay
[NASA-TM-86951] 12 p1770 N85-21114
An investigation of turbulence mechanisms in V/STOL upwash flow fields
[AD-A149786] 12 p1772 N85-[illegible]
Pseudospectral calculations of two-dimensional transonic flow (Task 1). Numerical investigation of VTOL aerodynamics (Task 2)
[AD-A150123] 12 p1772 N85-[illegible]
Liquid fuel spray processes in high-pressure gas flow
[NASA-TM-86944] 12 p1844 N85-[illegible]
Large amplitude forcing of a high speed 2-dimensional jet
[NASA-CR-175646] 13 p1974 N85-[illegible]
Flow around axisymmetric bodies with uniform-velocity zones
14 p2276 N85-[illegible]
Localization of sources of equivalent noise in fast cold jets, excited and nonexcited
[ISL-CO-201/83] 14 p2416 N85-[illegible]
Numerical calculation of subsonic jets in crossflow with reduced numerical diffusion
[NASA-TM-87003] 15 p2472 N85-[illegible]
Experiments in dilution jet mixing effects of multiple rows and non-circular orifices
[NASA-TM-86996] 15 p2473 N85-[illegible]
An experimental investigation of unexcited and excited elliptic jets
15 p2554 N85-[illegible]
The influence of jet-grid turbulence on heat transfer from the stagnation region of a cylinder in crossflow
[NASA-TM-87011] 15 p2554 N85-[illegible]
An experimental technique for the study of velocity profiles in a laminar jet using a pulsed nitrogen laser
[AD-A151486] 15 p2556 N85-[illegible]
Numerical experiments of jet streak ageostrophic circulations using pseudo-geostrophic initialization and perspectives
15 p2590 N85-[illegible]
Preliminary wind tunnel study of the influence of a jet on the unsteady aerodynamics of a turbojet engine
[ONERA-RT-12/5115-RY-230-R-231G]
16 p2701 N85-[illegible]
Study of the coupling between average, coherent and turbulent fields in a circular excited free jet
[ISL-R-115/83] 16 p2785 N85-[illegible]
Computation model of turbulent free flow: Application to axisymmetric jets
[ISL-R-126/83] 16 p2785 N85-[illegible]
Contribution to the study of equivalent noise source identification in fast cold jets
[ISL-R-114/83] 16 p2861 N85-[illegible]
Analyses of orderly structures in jets and the relationship with emitted noise
[ISL-R-117/83] 16 p2861 N85-[illegible]
Background noise measurements from jet exit vanes designed to reduced flow pulsations in an open-jet wind tunnel
[NASA-TM-86383] 17 p2906 N85-[illegible]
Turbulent transport and length scale measurement experiments with comfined coaxial jets
[NASA-CR-174831] 19 p3265 N85-[illegible]
Density and confinement effects on mixing characteristics of an axisymmetrical CO(2) jet
[AD-A154468] 19 p3267 N85-[illegible]
Hydrodynamic solutions for the diffusion of components in confined media
20 p3456 N85-[illegible]
SCAP: A Shaped Charge Analysis Program. User's manual for SCAP 1.0
[DE85-011182] 20 p3515 N85-[illegible]
Second order modelling in non-constant density flows
22 p3744 N85-[illegible]
Pulsed hydrojet propulsion
[DE85-010771] 22 p3784 N85-[illegible]
The calculation of two-dimensional buoyant surface jets with the k-W model of turbulence — kinetic energy-vorticity fluctuations (k-W)
[CFD/84/21] 22 p3785 N85-[illegible]
Heat transfer characteristics for two-dimensional arrays of impinging jets with initial crossflow
24 p4092 N85-[illegible]

Meteorological data from the OPTOMA (Ocean Prediction Through Observations, Modeling and Analysis) program OPTOMA 2, leg D2. 30 Jun. - 10 Jul. 1984
[AD-A158134] 24 p4123 N85-35560

JET FUELS
U JET ENGINE FUELS

JET IMPINGEMENT
Planar jets impinging on various obstacles and some modes of flow oscillation
[MPIS-MITT-78] 01 p0048 N85-10317
Jet array impingement flow distributions and heat transfer characteristics: Effects of initial crossflow and nonuniform array geometry 02 p0142 N85-10967
An experimental study of jet impingement on a circular cylinder
[AD-A145583] 02 p0198 N85-11326
Analysis of reactor material experiments investigating oxide fuel crust stability and heat transfer in jet impingement flow
[DE85-012097] 24 p4151 N85-35739

JET LAG
Jet lag prevention: Physiological mechanisms and pharmacological therapy
[AD-A145444] 02 p0235 N85-11529
Human performance in continuous/sustained operations and the demands of extended work/rest schedules. An annotated bibliography
[AD-A155819] 21 p3666 N85-32771

JET MEMBRANE PROCESS
Possibilities for studying short-lived nuclei produced at LAMPF
[DE85-010740] 19 p3365 N85-30664

JET MIXING FLOW
Dilution zone mixing studies 02 p0145 N85-10984
Dilution jet mixing 02 p0145 N85-10985
Transition and mixing in axisymmetric jets and vortex rings 05 p0591 N85-13769
Basic studies of multiple free and confined jets
[AD-A149556] 10 p1485 N85-19374
Mixing characteristics of an underexpanded multiple jet ejector
[AD-A149557] 10 p1485 N85-19375
An experimental investigation of an underexpanded rectangular jet ejector
[AD-A149658] 12 p1779 N85-21170
Determination of boundary line between reverse jet and surrounding stream 13 p2043 N85-22789
Development of a temperature measurement system with application to a jet in a cross flow experiment
[NASA-CR-174896] 15 p2472 N85-25262
Experiments in dilution jet mixing effects of multiple rows and non-circular orifices
[NASA-TM-86996] 15 p2473 N85-25266
An experimental investigation of confined, multiple, turbulent jet mixing with recirculation — flow distribution in combustors with injection plates
15 p2555 N85-25764
A theoretical study of two stage thrust augmenting ejectors
[ARL/AERO-R-166] 19 p3218 N85-29954
Buoyant jet entrainment in stratified fluids
19 p3263 N85-30238
Density and confinement effects on mixing characteristics of an axisymmetrical CO(2) jet
[AD-A154468] 19 p3267 N85-30258
An experimental investigation of confined, multiple, turbulent jet mixing with recirculation
20 p3451 N85-31426
Large eddy structures in transitional and turbulent flames
[AD-A154520] 21 p3562 N85-32157

JET NOISE
U JET AIRCRAFT NOISE

JET NOZZLES
Influence of setting angle of jet cooling nozzles on temperature and stress state of a turbine wheel
09 p1306 N85-18206

JET PILOTS
U AIRCRAFT PILOTS

JET PROPULSION
Modeling of propulsive jet plumes--extension of modeling capabilities by utilizing wall curvature effects
[AD-A146262] 03 p0362 N85-12324
Air Force Academy Aeronautics Digest
[AD-A149614] 12 p1769 N85-21104
Fiscal year 1986 technical objective document
[AD-A151039] 14 p2432 N85-25000
A theoretical study of two stage thrust augmenting ejectors
[ARL/AERO-R-166] 19 p3218 N85-29954

JET PROVOST AIRCRAFT
Experiences obtained from service fatigue monitoring exercises 07 p0695 N85-15672

JET PUMPS
Jet pump-drive system for heat removal
[NASA-CASE-NPO-16494-1-CU]
18 p3099 N85-29182

JET STREAMS (METEOROLOGY)
Jet stream errors and tropospheric-stratospheric interactions in the GLAS general circulation model
05 p0683 N85-14392
Small component spectral model of annual course of zonal atmospheric circulation 14 p2337 N85-24453
Role of jet streaks and boundary layer processes in organizing a pre-convective environment
15 p2597 N85-26008
Meso-β scale numerical simulations of the jet streak adjustments which organized the Carolina tornado outbreak and the subsequent explosive coastal cyclogenesis 15 p2598 N85-26011
Great Lakes winter weather and ice conditions for 1982-83
[PB85-165009] 16 p2837 N85-27498
A preliminary intercomparison between numerical upper wind forecasts and research aircraft measurements of jet streams
[NASA-CR-167884] 24 p4120 N85-35539

JET THRUST
Characteristics of a confined jet thrust vector control nozzle
[AD-A153087] 17 p2958 N85-28268

JET VANES
Effect of jet exit vanes on flow pulsations in an open-jet wind tunnel
[NASA-TM-86299] 09 p1273 N85-17999
Background noise measurements from jet exit vanes designed to reduced flow pulsations in an open-jet wind tunnel
[NASA-TM-86383] 17 p2906 N85-27916

JETAVATORS
U GUIDE VANES

JETS
On the interaction of a sound pulse with the shear layer of an axisymmetric jet. Part 3: Nonlinear effects
[NASA-CR-172512] 09 p1378 N85-18663
Exotic interactions among C-jets and Pb-jets
[HE-3.2-6] 24 p4179 N85-35914

JETTISON SYSTEMS
The development of staging mechanisms for the Japanese satellite launcher Mu-3SII
22 p3798 N85-33528

JFET
Method for the fabrication of dielectric isolated junction field effect transistor and PNP transistor
[AD-D011500] 12 p1832 N85-21494

JIGS
Report on high-precision jig-boring machines
01 p0035 N85-10215
Classification of holding jigs for objects of robotized assembly 14 p2266 N85-24039

JIMSPHERE BALLOONS
Atmospheric environment for Space Shuttle (STS-51A) launch
[NASA-TM-86497] 12 p1892 N85-21875

JITTER
U VIBRATION

JOBS
U TASKS

JOINING
Effect of interconnection of the ends of a sliding bearing on film thickness
[AD-A147736] 08 p1132 N85-17135
Effect of interfacial characteristics of metal clad polymeric substrates on electrical high frequency interconnection performance
[NASA-TM-86948] 11 p1624 N85-20223
NASA welding assessment program
[NASA-CR-175682] 15 p2568 N85-25844

JOINTS (ANATOMY)
NT ELBOW (ANATOMY)
NT KNEE (ANATOMY)
NT WRIST
Dynamics of morphological changes in articulation nervous system under hypokinetic conditions as a model of a spaceflight factor 01 p0092 N85-10621

JOINTS (JUNCTIONS)
NT BEAM LEADS
NT BUTT JOINTS
NT LAP JOINTS
NT METAL JOINTS
NT RIVETED JOINTS
NT SEAMS (JOINTS)
NT SOLDERED JOINTS
NT SPOT WELDS
NT WELDED JOINTS
Silicon nitride joining
[AD-A145668] 02 p0187 N85-11248
Storage life of thermal detents
[DE84-016934] 04 p0476 N85-13030
Detection of cracks in a plastics pipe joint by reflection holography
[NPL-DMA(A)-87/MOM-70] 04 p0502 N85-13202
Exploratory study of shear strength of joints for precast segmental bridges
[PB84-235449] 05 p0851 N85-14182
Translational control of a graphically simulated robot arm by kinematic rate equations that overcome elbow joint singularity
[NASA-TP-2376] 06 p0856 N85-15446
Aeroproyekt develops improved runway surfacing
08 p1068 N85-16770
Space shuttle elevon seal panel mechanism
08 p1101 N85-16961
Finite element calculation for a Y-joint and comparison of results with strain measurements
[BLL-RISLEY-TR-4526-(9091.9F)]
08 p1171 N85-17381
Mechanical properties of Shielded Metal Arc (SMA) and Submerged Arc (SA) welded joints for quenched and tempered steel StE 470.
[VTT-319] 09 p1328 N85-18346
Stochastic dynamic analysis of a structure with frictional joints 09 p1337 N85-18408
Long term durability of urea formaldehyde glued joints removed from Vampire aircraft
[AD-A149053] 10 p1424 N85-18985
Adhesive joint formation under field conditions
[AD-D011476] 10 p1453 N85-19153
Excimer laser annealing to fabricate low cost solar cells
[NASA-CR-174394] 11 p1673 N85-20536
Elbow and knee joint for hard space suits and the like
[NASA-CASE-ARC-11610-1] 11 p1697 N85-20686
Characterization of mode 1 and mixed-mode failure of adhesive bonds between composite adherends
[NASA-TM-86355] 12 p1797 N85-21270
Shoulder and hip joint for hard space suits and the like
[NASA-CASE-ARC-11543-1] 12 p1910 N85-21986
Elasticity solution of an adhesively bonded joint
[NASA-CR-175591] 13 p2101 N85-23097
Scattering of elastic waves on fractures randomly distributed in a three-dimensional medium
13 p2111 N85-23151
Overlays for plain jointed concrete pavements
[PB85-156297] 15 p2523 N85-25557
Reflection and transmission of flexural waves at discontinuities 15 p2572 N85-25861
A study of the time dependence in fracture processes relating to service prediction of adhesive joints and advanced composites
[AD-A152064] 15 p2579 N85-25910
Initial quality of advanced joining concepts
[AD-A152241] 16 p2759 N85-27027
An improved torsional method for determining the fracture toughness of stiff materials and of adhesive joints
[AD-A152091] 16 p2800 N85-27267
Elastic equilibrium of composite shells with finite shear rigidity 17 p2942 N85-28163
Further investigations to improve the fatigue life of the Mirage 1110 wing main span
[ARL/STRUC-TM-397] 18 p3061 N85-28938
Self-locking mechanical center joint
[NASA-CASE-LAR-12864-1] 19 p3279 N85-30336
Fundamental studies related to failure of adhesively bonded structures
[AD-A154072] 19 p3285 N85-30374
Elastomers used in aeronautics industry
[SNIAS-851-551-103] 20 p3434 N85-31304
Joining of sintered composite TiC-steel materials by welding
[BLL-M-36253-(5828.4)] 20 p3461 N85-31502
Hubble space telescope: Pointing error effects on nonlinear ball joints
[NASA-TM-86511] 20 p3545 N85-32058
Improved materials for composites and adhesive joints
[AD-A154918] 21 p3561 N85-32152
Improved materials for composite and adhesive joints
[AD-A155065] 21 p3562 N85-32153
Experimental and theoretical assessment of a new technique for the non-destructive evaluation of laminated panels
[AD-A155622] 21 p3562 N85-32155
Resolution of thermal striping issue downstream of a horizontal pipe elbow in stratified pipe flow
[DE85-006195] 21 p3586 N85-32292
Simultaneous junction formation
21 p3610 N85-32426
Pulsed excimer laser processing for cost-effective solar cells 21 p3611 N85-32432
Mechanical connection for a tubular assembly
[DE85-011590] 22 p3792 N85-33497
The stress distribution in pin-loaded orthotropic plates
[NASA-CR-176146] 22 p3800 N85-33547

Three-dimensional finite element failure model for predicting failure in fibre reinforced bolted joints
[BR94778] 23 p3940 N85-34423
Stresses and strains in a plate resulting from two closely-spaced interference-fit fasteners
[ARL/STRUC-TM-409] 23 p3941 N85-34429
Verification of the SRB motor case pin retainer band tips
[NASA-CR-170882] 24 p4070 N85-35220

JORDAN FORM
Contribution of the cup-product of Milnor's fiber with /I/ sup 2 lambda poles 11 p1698 N85-20672
The eigenstructure assignment of deadbeat control systems
[AD-A149761] 12 p1834 N85-21510

JOSEPHSON JUNCTIONS
Transmission line biased coherent array of Josephson oscillators
[AD-D011323] 07 p0944 N85-15979
Coherent array of Josephson oscillators with external bias leads
[AD-D011387] 08 p1156 N85-17293
Resonant activation of a Josephson junction
[DE85-000702] 10 p1583 N85-19857
Thin film technology of high-critical-temperature superconducting electronics
[AD-A150010] 12 p1940 N85-22185
Macroscopic quantum tunnelling in a current biased Josephson junction
[DE85-004603] 13 p2164 N85-23424
Random access memory technologies
[AD-A153089] 17 p3008 N85-28597

JOULE HEATING
U OHMIC DISSIPATION
U RESISTANCE HEATING

JOURNAL BEARINGS
Damping capacity of a sealed squeeze film bearing
05 p0645 N85-14139
Vibration control of rotor shaft
[NASA-TM-87053] 18 p3117 N85-29292

JOURNALS
NBS (National Bureau of Standards) library serial holdings, 1985
[PB85-191948] 22 p3849 N85-33839

JOURNALS (DOCUMENTS)
U PERIODICALS

JOURNALS (SHAFTS)
U SHAFTS (MACHINE ELEMENTS)

JP-4 JET FUEL
Variability of major organic components in aircraft fuels. Volume 3: Sample data package for the reference JP-4 fuel
[AD-A145483] 02 p0188 N85-11254
Variability of major organic components in aircraft fuels. Volume 1: Technical discussion
[AD-A145574] 02 p0188 N85-11256
Variability of major organic components in aircraft fuels. Volume 2: Illustrations
[AD-A145831] 04 p0481 N85-13067
Effects of temperature variation among droplets in an evaporating fuel spray 13 p2004 N85-22562

JP-5 JET FUEL
Variability of major organic components in aircraft fuels. Volume 3: Sample data package for the reference JP-4 fuel
[AD-A145483] 02 p0188 N85-11254
Variability of major organic components in aircraft fuels. Volume 1: Technical discussion
[AD-A145574] 02 p0188 N85-11256
Variability of major organic components in aircraft fuels. Volume 2: Illustrations
[AD-A145831] 04 p0481 N85-13067
Evaluation of jet fuel deposit kinetics. Lot 4
[AD-A147196] 07 p0935 N85-15922

JP-8 JET FUEL
Effects of temperature variation among droplets in an evaporating fuel spray 13 p2004 N85-22562

JUDGMENTS
The effects of feedback and predictability of human judgment
[AD-A145744] 02 p0237 N85-11542
Direction judgement errors in perspective displays
05 p0705 N85-14520
A theory of preference reversals
[AD-A147952] 08 p1216 N85-17661
Task influences in the analytic-intuitive approach to decision making
[AD-A149870] 12 p1950 N85-22250

JUNCTION DIODES
NT MIM DIODES
Buried junction enhanced Schottky barrier device
[AD-D011399] 07 p1044 N85-16635
Diodes in photovoltaic modules and arrays
[NASA-CR-175454] 10 p1508 N85-19513

JUNCTION FIELD EFFECT TRANSISTORS
U JFET

JUNCTION TRANSISTORS
NT JFET
The study of microstrip antenna arrays and related problems
[NASA-CR-174054] 02 p0189 N85-11265
Gamma-induced leakage in junction field-effect transistors
[DE84-014990] 04 p0570 N85-13634
Simulation of solidification in a Bridgman cell
[NASA-CR-175638] 16 p2870 N85-27705
High voltage lateral power transistors: Theory and design 19 p3257 N85-30194
Method of characterizing critical timing paths and analyzing timing related failure modes in very large scale integrated circuits
[AD-D011731] 22 p3759 N85-33298

JUNGLES
U TROPICAL REGIONS

JUPITER (PLANET)
Charged particle erosion of icy satellites: Coronal atmospheres and surface redistribution
03 p0446 N85-12845
Temporal and spatial variations in the intensity of ultraviolet emissions from Jupiter and the Io torus
03 p0448 N85-12846
Measurements of H2O in Jupiter's atmosphere from 5 microns airborne observations 08 p1244 N85-17854
Analysis of Jovian decametric data: Study of radio emission mechanisms
[NASA-CR-174206] 08 p1258 N85-17917
The spatial dependence of the Jovian auroral emissions 11 p1759 N85-21068
Investigations of planetary ring phenomena
13 p2174 N85-23487
Studies of planetary rings 13 p2174 N85-23488
Orbital resonances and planetary accretion in the solar nebula 13 p2179 N85-23523
Analysis of motions of Jupiter's great red spot and white ovals 15 p2670 N85-26472
The asteroid ring 15 p2678 N85-26536
Direct evidence for solar wind control of Jupiter's hectometer-wavelength radio emission
[NASA-TM-86073] 16 p2883 N85-27790
The coorbital hypothesis 22 p3858 N85-33890
The 1986 National Aeronautics and Space Administration authorization
[GPO-47-635] 24 p4166 N85-35829

JUPITER ATMOSPHERE
The Jovian atmospheric window at 2.7 microns: A search for H2S
[NASA-TM-86661] 03 p0445 N85-12836
Lower atmospheric composition of Jupiter from Voyager infrared measurements
[NASA-CR-174196] 05 p0745 N85-14779
Exploration of the solar system by airborne astronomy
08 p1244 N85-17851
Measurements of H2O in Jupiter's atmosphere from 5 microns airborne observations 08 p1244 N85-17854
Near infrared modeling of the equatorial regions of Jupiter and Saturn 09 p1415 N85-18930
Analysis of Jovian low frequency radio emissions
[NASA-CR-174449] 10 p1571 N85-19908
Three dimensional ray tracing of the Jovian magnetosphere in the low frequency range
[NASA-CR-175462] 10 p1571 N85-19909
The Jovian Stratosphere in the ultraviolet
11 p1760 N85-21069
Particle transport in planetary magnetospheres
12 p1954 N85-22275
A Jamin interferometer to determine the helium abundance in the atmosphere of Jupiter
[BONN-IR-83-17] 12 p1961 N85-22329
Analysis of motions of Jupiter's great red spot and white ovals 15 p2670 N85-26472
Dynamics of charged small particles — Jupiter, Saturn magnetospheres 15 p2676 N85-26522
Galileo 15 p2688 N85-26601
Possible period of Jovian activity and possibility of seasons 16 p2723 N85-26810
Monodeurated methane in the outer solar system. 2. Its detection on Uranus at 1.6 microns
[NASA-CR-175762] 16 p2882 N85-27782
The Jovian electron spectrum: 1978-1984
[SH-1.5-19] 23 p3998 N85-34782

JUPITER PROBES
NT GALILEO PROBE
NT GALILEO SPACECRAFT
Galileo 15 p2688 N85-26601

JUPITER RINGS
The Jovian ring 15 p2672 N85-26492
On planetary rings as sources and sinks of magnetospheric plasmas 15 p2677 N85-26526
Future studies of planetary rings by spaceprobes
15 p2679 N85-26541
Jupiter's ring system resolved: Physical properties inferred from the Voyager images
20 p3546 [illegible]

JUPITER SATELLITES
NT CALLISTO
NT EUROPA
NT GALILEAN SATELLITES
NT GANYMEDE
NT IO
Gravity field of the Jovian system from Pioneer and Voyager tracking data 13 p2180 [illegible]
Jupiter/Voyager data analysis
[NASA-CR-175723] 15 p2679 [illegible]
Sixteenth Lunar and Planetary Science Conference. Press abstracts
[NASA-CR-175692] 15 p2680 [illegible]
The energy spectrum of Jovian electrons in interplanetary space
[SH-1.5-18] 21 p3715 [illegible]
The coorbital hypothesis 22 p3858 N85-33890

K

K BAND
U EXTREMELY HIGH FREQUENCIES

K LINES
Variations of the H and K emission lines of singly ionized calcium in the eclipsing binary star system AR Lacertae
02 p0296 N85-11921

K-MESONS
U KAONS

KA BAND
U EXTREMELY HIGH FREQUENCIES

KALMAN FILTERS
Numerical studies in nonlinear filtering
[TWISK-305] 01 p0108 N85-10728
Robust rate control system designs for a submersible
[AD-A144792] 01 p0111 N85-10753
Detection and estimation of image contours
[FUB-35-1983] 01 p0112 N85-10760
Application of modern guidance control theory to a bank-to-turn missile
[AD-A145646] 02 p0166 N85-11123
Improved carrier tracking by smoothing estimators
05 p0623 [illegible]
Algorithm for tracking manuevering object with ambiguous measurements 06 p0791 N85-15057
A semianalytical, artificial satellite orbit propagation procedure based on optimal parameter estimation
[INPE-3301-PRE/613] 10 p1427 [illegible]
Internal variables in the lattice for cholesky factorization. Kalman filtering and model identification
[AD-A149431] 10 p1547 N85-19757
Robust Kalman filtering and its applications
[AD-A149044] 10 p1550 N85-19775
Acta Electronica Sinica (selected articles)
[AD-A148829] 11 p1626 N85-20252
Reference systems for the evaluation of dead-reckoning navigation equipment 13 p1967 [illegible]
Prefiltration in Kalman filter with a priori indeterminacy
13 p2071 [illegible]
Numerical algorithms and software for matrix Riccati equations
[AD-A150148] 13 p2150 N85-23344
Bootstrapping the Kalman filter
[AD-A150509] 13 p2153 N85-23370
Geophysical interpretation of Venus gravity data
13 p2178 N85-23513
Digital computer applications of Kalman filter in target tracking
[AD-A150770] 14 p2404 N85-24421
Investigation of a failure detection/identification system for a tactical aircraft navigation system
[AD-A151846] 15 p2469 [illegible]
Perturbations of Kalman filtering process
15 p2480 [illegible]
Estimation theory applied to improving dynamic structural models
[DE85-004148] 15 p2630 [illegible]
Theory and Applications of State Estimation. NRIMS Summer Seminar Series
[CSIR-SWISK-37] 15 p2635 [illegible]
The Kalman filter 15 p2635 [illegible]
Linear filtering with non-Gaussian initial conditions
15 p2635 [illegible]
Kalman filtering and exponential smoothing in economics 15 p2635 [illegible]
Some aspects of decentralized Kalman filtering
15 p2635 [illegible]
Tracking filters 15 p2635 [illegible]
Applications of Kalman filtering and recursive least-squares in river flow modelling
15 p2636 [illegible]

Formulation and implementation of nonstationary adaptive estimation algorithm with applications to air-data reconstruction [NASA-TM-86727] 16 p2706 N85-26699

Applied Kalman filtering: An overview 17 p2985 N85-28313

Kalman filtering with a two-state clock model 17 p2965 N85-28314

Kalman filter estimates of the NAVSTAR satellite clock parameters 17 p2965 N85-28315

A plan for the development of inertial reconstruction of initial state clock (IRIS) 17 p2966 N85-28317

Proceedings of the Sixteenth Annual Precise Time and Time Interval (PTTI) Applications and Planning Meeting [NASA-TM-87561] 18 p3105 N85-29221

Kalman filter modeling 18 p3107 N85-29237

Relationship between Allan variances and Kalman Filter parameters 18 p3107 N85-29238

Some studies in filtering of atmospheric turbulence [AD-A154042] 19 p3316 N85-30557

A residuals approach to filtering, smoothing and identification for static distributed systems 20 p3418 N85-31213

Parameter estimation in communication system tracking satellite observations [AD-A155137] 21 p3636 N85-32582

Bayesian vs MAP multiple model adaptive estimation for field of view expansion in tracking airborne targets [AD-A155466] 21 p3679 N85-32855

Kalman filter time series analysis of gamma-ray data from NaI(T1) detectors for the ND6620 computer [AD-A154995] 21 p3705 N85-33014

Lectures of a Flight Mechanics Conference — conferences [ESA-TT-831] 24 p4061 N85-35165

Estimation of flight mechanical variables by means of Kalman filters 24 p4062 N85-35171

Recursive partitioning estimation 24 p4141 N85-35670

KANSAS

The application of remote sensing to resource management and environmental quality programs in Kansas [E85-10023] 02 p0218 N85-11436

The influence of the number of ground control points on the scene-to-map registration accuracy — Kansas, Louisiana, Mississipp, and Missouri 07 p0966 N85-16264

Petrography, sedimentology, diagenesis, and reservoir characteristics of some Pennsylvanian phylloid algal limestones: Kansas and Utah, USA 09 p1352 N85-18507

Modeling the backscattering and transmission properties of vegetation canopies [E85-10099] 16 p2809 N85-27320

KAONS

A 1-2 GeV/c beam line for hypernuclear and kaon research [DE85-007623] 16 p2863 N85-27659

AGS broad band neutrino beam [DE85-010954] 19 p3366 N85-30875

K(-) hydrogen bound and continuum states in momentum space [DE85-010429] 22 p3841 N85-33789

KAPITZA RESISTANCE

High specific heat dielectrics and Kapitza resistance at dielectric boundaries [AD-A148476] 08 p1217 N85-17666

KAPTON (TRADEMARK)

Long-term light induced changes in dark conductivity of kapton [AD-A148791] 08 p1224 N85-17706

Laboratory studies of Kapton degradation in an oxygen ion beam 13 p1990 N85-22477

Kapton charging characteristics: Effects of material thickness and electron-energy distribution 13 p1996 N85-22513

Study of Kapton under simulated shuttle environment [NASA-CR-176003] 19 p3225 N85-29997

KARHUNEN-LOEVE EXPANSION

Harmonizable, Cramer, and Karhunen classes of processes [AD-A144984] 01 p0113 N85-10767

KARMAN VORTEX STREET

Velocity and transient measurements in a shock tube using a hot-wire anemometer [AD-A154694] 21 p3589 N85-32305

KC-135 AIRCRAFT

U C-135 AIRCRAFT

KELVIN-HELMHOLTZ INSTABILITY

Magnetohydrodynamic (MHD) turbulence in radio galaxies 12 p1958 N85-22305

Magnetic pulsations recorded in northern Scandinavia during the IMS; a study of Pc 4-5 events 14 p2370 N85-24647

Characteristics of Pc 4,5 pulsations and their source mechanisms 14 p2370 N85-24648

A panel method study of vortex sheets with special emphasis on sheets of axisymmetric geometry [NASA-CR-177365] 21 p3552 N85-32095

KENTUCKY

Image variance and spatial structure in remotely sensed scenes — South Dakota, California, Missouri, Kentucky, Louisiana, Tennessee, District of Columbia, and Oregon 07 p0966 N85-16265

Lithologic and environmental atlas of Berea Sandstone (Mississippian) in the Appalachian Basin [PB85-129039] 11 p1682 N85-20600

KENYA

Evaluation of carrying capacity and landscape damage in northern Kenya by multistage remote sensing [DFVLR-FB-84-47] 14 p2347 N85-24514

KEPLER LAWS

Reduction of nonlinear problems to Schroedinger or heat equations: Formation of Kepler orbits, singular solutions for hydrodynamical equations [REPT-72] 01 p0129 N85-10892

Keplerian and perturbed motion — satellite motion 05 p0598 N85-13808

Spatial mechanics formulas and exercises 05 p0601 N85-13832

Averaging of equations of cometary orbital motion with allowance for nongravitational effects 13 p1978 N85-22411

Nontraditional method for determining unperturbed orbits of unknown space objects using incomplete optical observational data 13 p1979 N85-22417

Using velocity vector in determining Keplerian orbit of geodectic satellite 15 p2478 N85-25297

Diffusion of dust around a central body — Keplerian orbits 15 p2676 N85-26523

KERNEL FUNCTIONS

Small-sample properties of kernel density estimators from randomly right-censored data [AD-A148752] 09 p1374 N85-18634

A kernel type estimator of a quantile function from right-censored data [AD-A148753] 09 p1374 N85-18635

Single integral constitutive equations for viscoelastic fluids [AD-A149410] 10 p1547 N85-19756

On the modified likelihood for density estimation [AD-A149437] 10 p1547 N85-19758

Quantum mechanical and semiclassical approaches to molecular dynamics [DE85-003458] 10 p1555 N85-19803

An asymptotically efficient solution to the bandwidth problem of kernel density estimation, revision [AD-A149600] 12 p1920 N85-22056

Nonparametric estimation of density and hazard rate functions when samples are censored [AD-A150946] 14 p2411 N85-24868

Extent to which least-squares cross-validation minimizes integrated square error in nonparametric density estimation [AD-A153789] 18 p3174 N85-29679

Angle averaged Compton cross sections for degenerate electron gases [AD-A154484] 19 p3371 N85-30908

Memory effects in dynamical many-body systems: The isomnesic (constant-memory) approximation [AD-A154160] 20 p3520 N85-31889

The NAS kernel benchmark program [NASA-TM-86711] 21 p3670 N85-32795

KEROGEN

Comparison of isothermal kerogen decomposition results using reactors with different heat-up rates [DE85-008563] 19 p3237 N85-30068

KEROSENE

Numerical simulations of fuel droplet flows using a Lagrangian triangular mesh [AD-A146087] 03 p0362 N85-12320

Aircraft wing fuel tank environmental simulator tests for evaluation of antimisting fuels [FAA-CT-84-15] 07 p0934 N85-15920

Dependence of combustion of homogeneous kerosene-air mixtures on humidity of air 13 p2051 N85-22835

Practical real-time quality control of antimisting kerosene [DE/FAA/CT-85/1] 18 p3083 N85-29072

Effect of polymer additives on characteristics of direct-current motor with liquid dielectric filler 22 p3772 N85-33376

KETONES

NT ACETONE

NT ACETYLACETONE

Interactions of ketones and hexacarbons [AD-P004019] 06 p0843 N85-15353

Pseudo-p-1,2,2,9,9,10,10-octofluoro (2,2)-p-cyclophane bis-acid chloride [AD-D011393] 07 p0919 N85-15818

Polyaromatic ether-sulfone-keytones with fluoro-substituted-p-cyclophane units as cross-linking sites [AD-D011649] 17 p2933 N85-28105

Spray pyrolysis as a synthetic tool [AD-A153891] 19 p3234 N85-30047

Analysis of aldehydes and ketones in the gas phase [PB85-181865] 20 p3426 N85-31261

KEVLAR (TRADEMARK)

Development of failure criterion for Kevlar-epoxy fabric laminates [NASA-CR-172465] 02 p0170 N85-11138

Chemical modification of the surface of high modulus carbon fibers 04 p0467 N85-12967

Ultrasonic analysis of spherical composite test specimens [DE85-001591] 07 p0976 N85-16197

Comparison of methods for predicting fiber stresses in a cracked Kevlar/epoxy monolayer [DE84-016118] 11 p1593 N85-20022

Ultrasonic analysis of Kevlar-epoxy filament wound spherical test specimens [DE85-005198] 11 p1593 N85-20024

A broadband kevlar radome for shipboard [AD-P004365] 12 p1826 N85-21459

Impurities in Kevlar 49 fibers [DE85-004996] 13 p2036 N85-22767

Development of a field repair technique for mini-sandwich Kevlar/epoxy aircraft skin [AD-A151369] 15 p2503 N85-25439

Effect of low-velocity or ballistic impact damage on the strength of thin composite and aluminum shear panels [NASA-TP-2441] 16 p2742 N85-26924

Flight service evaluation of composite helicopter components [NASA-CR-172562] 23 p3909 N85-34222

KEYING

NT FREQUENCY SHIFT KEYING

NT PHASE SHIFT KEYING

A public key cryptographic algorithm based on a generalization of the knapsack problem [FUB-7-1984] 09 p1313 N85-18250

KIDNEYS

Bioprocessing in space 05 p0690 N85-14439

Distribution of blood flow to brain, kidneys, gut, spleen and posterior extremities in cats in acute hypoxia 07 p1013 N85-16434

Changes in nephron and juxtaglomerular system of primate kidneys under the effect of antiorthostatic hypokinesia 19 p3326 N85-30605

Kidney cell electrophoresis [NASA-CR-171889] 20 p3498 N85-31745

Task description for the 1983 catalog of tasks for the materials processing in space program 20 p3498 N85-31746

Kidney cell electrophoresis, continuing task 20 p3498 N85-31747

Effect of passage number on electrophoretic mobility distributions of cultured human embryonic kidney cells 20 p3501 N85-31762

Density gradient electrophoresis of cultured human embryonic kidney cells 20 p3501 N85-31763

Identification and quantitation of morphological cell types in electrophoretically separated human embryonic kidney cell cultures 20 p3501 N85-31764

Urokinase production by electrophoretically separated cultured human embryonic kidney cells 20 p3501 N85-31765

Summary electrophoretic data base on human embryonic kidney cell strain 8514 20 p3501 N85-31766

A critical synopsis: Continuous growth of proximal tubular kidney epithelial cells in hormone-supplemented serum-free medium 20 p3501 N85-31767

The Fibrin slide assay for detecting urokinase activity in human fetal kidney cells 20 p3502 N85-31768

Results of computer calculations for a simulated distribution of kidney cells 20 p3502 N85-31771

Evaluation of results of cell electrophoresis experiments on space shuttle STS-3 including pre-flight and post-flight laboratory experiments 20 p3502 N85-31772

Pre-flight report on cultured human embryonic kidney cell handling and cell electrophoresis. Prepared prior to continuous-flow electrophoretic separation experiments aboard space shuttle flight STS-8 20 p3503 N85-31775

Properties of electrophoretic fractions of human embryonic kidney cells separated on space shuttle flight STS-8 20 p3503 N85-31776

Detection of internal structure by scattered light intensity: Application to kidney cell sorting 20 p3503 N85-31777

Flow cytometry of human embryonic kidney cells: A light scattering approach 20 p3503 N85-31778

KILOMETRIC WAVES
Theory and computer simulation of auroral kilometric radiation 14 p2365 N85-24617
The IMS advances in understanding terrestrial myriametric radiation 14 p2365 N85-24618
Terrestrial continuum radiation study during the IMS 14 p2365 N85-24619

KIMBERLITE
U BIOTITE
U PERIDOTITE

KINEMATIC EQUATIONS
A triangular finite element for thin plates and shells 01 p0058 N85-10386
Local galactic kinematics 05 p0741 N85-14765
Translational control of a graphically simulated robot arm by kinematic rate equations that overcome elbow joint singularity [NASA-TP-2376] 06 p0856 N85-15446
Equations and algorithms for meteorological applications in air weather service [AD-A148894] 10 p1519 N85-19575
Kinematic dynamo theory for an arbitrary mean flow 14 p2448 N85-25106
The generation of magnetic fields by a flow with chaotic streamlines 14 p2451 N85-25135
Application of quaternions to problems of solid body dynamics in the atmosphere 15 p2481 N85-25313
Kinematic rate control of simulated robot hand at or near wrist singularity [NASA-TP-2440] 16 p2851 N85-27575
Computer methods in manipulator kinematics, dynamics and control: A comparative study 20 p3462 N85-31506
Coordinate transformations and programming for small revolute coordinate robots [RR-273] 20 p3519 N85-31881

KINEMATICS
NT BODY KINEMATICS
Kinematic synthesis of planar cam-link mechanisms for exact path and exact motion generation 03 p0341 N85-12169
Optimization of movements of manipulators with kinematic redundancy 04 p0486 N85-13112
Preliminary grouping in A strong-current linear ion accelerator with a low injection energy [DE84-017192] 04 p0563 N85-13587
Instantaneous kinematics and joint displacement analysis of fully-parallel robotic devices 05 p0641 N85-14113
Proper motions and kinematical properties of Orion trapezium type stellar systems 05 p0739 N85-14755
Kinematics of B and A stars 05 p0741 N85-14766
Anomalous magnetic field in northwestern Pacific Ocean and Pacific Ocean plate kinematics 06 p0820 N85-15210
Observations of highly-ionized interstellar iron 06 p0876 N85-15565
Kinematics of nearby gas and stars 06 p0880 N85-15591
Phase 1-A development kinematic Sterling/Rankine commercial gas-fired heat pump research program [PB85-100931/GAR] 07 p0936 N85-15928
Automatic camera tracking for remote manipulators [DE85-001897] 07 p0974 N85-16187
Modeling of human motion by computer considering measurement errors in initial data 07 p1012 N85-16429
Southern ocean sea-ice morphology and kinematics 08 p1144 N85-17217
The analysis of kinematic restraint and freedom using point contacts [RR-154/03/75/02] 08 p1169 N85-17372
The synthesis of kinematic restraint and freedom using point contacts [RR-154/03/75/03] 08 p1169 N85-17373
A free shear layer prediction of the turbulent wake of a flat plate towed below a free surface [AD-A148699] 09 p1319 N85-18293
Large deformations of a nonlinear elastic solid and the diffusion of an ideal fluid treated as interacting continua 09 p1330 N85-18356
Physics of nonmagnetic relativistic thermal plasmas 09 p1366 N85-18715
The research of driving wheel with movable lugs of the paddy field floating tractor [AD-P004263] 09 p1407 N85-18860
Advanced stress analysis methods applicable to turbine engine structures [NASA-CR-175573] 12 p1778 N85-21165
Mechanical properties for the grasp of a robotic hand [AD-A150062] 12 p1860 N85-21669
Assembly robot control algorithms 13 p2046 N85-22808
On Hybrid and mixed finite element methods [NASA-CR-175551] 13 p2101 N85-23096
New methods for interpreting seismic time fields in media with variable velocities 14 p2343 N85-24490
Practical methods for the compensation and control of multivariable systems [AD-A151047] 14 p2407 N85-24841
Mixing in the solar interior 14 p2446 N85-25095
The kinematic control of redundant manipulators 15 p2566 N85-25836
Manipulation and simulation of general robots using the zero-position description 15 p2567 N85-25838
Optimum rotation of solid body with 1 axis of symmetry 16 p2718 N85-26781
Structural design and kinematic configuration of two-armed robots 16 p2761 N85-27037
A general simulation program for robot manipulator arm dynamics [AD-A152121] 16 p2793 N85-27230
Nonlinear equations for dynamics of pretwisted beams undergoing small strains and large rotations [NASA-TP-2470] 16 p2799 N85-27258
On the accurate representation of large strain non-proportional plastic flow in ductile materials [DE85-007106] 16 p2801 N85-27273
Dynamic creep buckling: Analysis of shell structures subjected to time-dependent mechanical and thermal loading 17 p2913 N85-27959
The position and mobility of the shoulder, spinal column and pelvis in seated subjects [AD-A153751] 18 p3153 N85-29524
Application of the ADAMS program to deployable space truss structures [NASA-CR-177927] 19 p3284 N85-30366
Spiral bevel and circular arc helical gears: Tooth contact analysis and the effect of misalignment on circular arc helical gears [NASA-TM-87013] 20 p3395 N85-31060
Computer methods in manipulator kinematics, dynamics and control: A comparative study 20 p3462 N85-31506
A versatile computer package for mechanism analysis 23 p3924 N85-34314
Calculation of flow kinetics of composite media [BLL-M-35819-(5828.4)] 23 p3929 N85-34348
Generated spiral bevel gears: Optimal machine-tool settings and tooth contact analysis [NASA-TM-87075] 23 p3937 N85-34405
Non-rigid body motion 23 p3964 N85-34576
The kinematic structure of cold frontal rainbands 24 p4119 N85-35531
Kinematic analysis of Hurricane Frederick (1979) using satellite, aircraft and rawinsonde data [NASA-CR-176167] 24 p4119 N85-35533

KINESCOPES
U PICTURE TUBES

KINESTHESIS
U PROPRIOCEPTION

KINETIC ENERGY
Observations of the vertical structure of the eddy field in the Kuroshio extension [AD-A145178] 01 p0089 N85-10599
Laser spectroscopy of combustion intermediates [DE84-016101] 02 p0173 N85-11161
Comparison of wide aperture and short residence time ion lenses [DE84-015274] 03 p0420 N85-12685
Reaction wheels for kinetic energy storage 05 p0607 N85-13874
Comparison of forecast and observed energetics 05 p0683 N85-14389
Motion of heavy symmetric body with flexible bars about stationary point 06 p0780 N85-14989
Measurement of proton autoneutralization potential [DE85-001752] 06 p0865 N85-15501
The influence of deep cumulus convection on large-scale flow during AVE/SESAME 1, 10-11 April 1979 09 p1355 N85-18526
IREB (Intense Relativistic Electron Beam) converter to ac pulses [AD-D011479] 10 p1554 N85-19800
An orthogonal grid technique for studying internal deformation and energy absorption in target penetration [AD-A149989] 12 p1860 N85-21665
Theoretical study of collective ion acceleration in the Luce diode [AD-A150107] 12 p1929 N85-22116
A method for the evaluation of the residual energy of a metallic fragment after perforation of a thin target [ISL-R-113/83] 16 p2794 N85-27233
Applications of Canuto's method to Rayleigh-Taylor-initiated turbulence [DE85-010835] 18 p3102 N85-29202
Comparison of forecast and observed energetics 18 p3143 N85-29459
An implicit finite-difference code for a two-equation turbulence model for three-dimensional flows [NASA-TM-86752] 20 p3454 N85-314
Numerical solutions of turbulent models for flow over a flat plate with angle of attack [DE85-010360] 21 p3585 N85-32
The calculation of two-dimensional buoyant surface jets with the k-W model of turbulence — kinetic energy-vorticity fluctuations (k-W) [CFD/84/21] 22 p3765 N85-33
Dynamics of Mesoscale Weather Systems: 1984 Summer Collogulum [PB85-188266] 22 p3817 N85-33
Parametrized energy spectrum of cosmic-ray protons with kinetic energies down to 1 GeV [OG-4.2-11] 22 p3876 N85-34
SONTRAC: A solar neutron track chamber detector [SH-9.1-12] 23 p4052 N85-35
Prediction of turbulent internal recirculating flows with K-epsilon models 24 p4092 N85-35
Kinematic analysis of Hurricane Frederick (1979) using satellite, aircraft and rawinsonde data [NASA-CR-176167] 24 p4119 N85-35533
Turbulent structure of stably stratified nocturnal slope flows [AD-A155845] 24 p4123 N85-35
Two-point closure study of covariance budgets for turbulent Rayleigh-Benard convection [PB85-169106] 24 p4124 N85-35
Experimental evidence of the decrease of kinetic energy of hadrons in passing through atomic nuclei 24 p4174 N85-35

KINETIC EQUATIONS
NT HELMHOLTZ VORTICITY EQUATION
NT HYDRODYNAMIC EQUATIONS
NT KINEMATIC EQUATIONS
Hamiltonian and Lagrangian theory of gyrokinetic equations 02 p0283 N85-118
Integral of wave kinetic equation of drift waves 02 p0283 N85-118
Interplanetary trajectories 05 p0600 N85-13
A propagator expansion method for solving linearized plasma kinetic equations with collisions [AD-A147524] 07 p1045 N85-16
Theoretical thermodynamics of mixtures at high pressures 13 p2183 N85-22
Analysis of nonlinear parabolic equations modeling plasma diffusion across a magnetic field [DE85-007683] 17 p3040 N85-28
The effects of weak turubience on parametric processes in an unmagnetized plasma 19 p3369 N85-30
Collisional transport for a superthermal ion species in a plasma [DE85-011943] 22 p3845 N85-33
Guiding center distribution function and longitudinal invariant 23 p3978 N85-34

KINETIC FRICTION
NT SLIDING FRICTION
Turbine blade damping study [NASA-CR-171255] 04 p0456 N85-12
Forced vibrations of friction-damped beam structures in two dimensions [UDR-TM-82-08] 04 p0456 N85-12
The effect of frictional forces on fatigue crack growth in lugs [AD-A151994] 15 p2578 N85-25
Kinetic friction coefficient of ice [AD-A155035] 21 p3660 N85-32

KINETIC HEATING
NT AERODYNAMIC HEATING
NT SHOCK HEATING
An experimental investigation and numerical simulation of the thermomechanical phenomena in compressor rotor tip rubbing 03 p0367 N85-12252
An analysis of the feasibility of producing silicon for solar cells by a dichlorosilane/fluidized-bed reactor process [NASA-CR-176036] 20 p3478 N85-31614
High pressure working mode of hollow cathode arc discharges [NASA-TM-77880] 20 p3535 N85-31

KINETIC THEORY
NT CHAPMAN-ENSKOG THEORY
NT MIXING LENGTH FLOW THEORY
NT TRANSPORT THEORY
A propagator expansion method for solving linearized plasma kinetic equations with collisions [AD-A147524] 07 p1045 N85-16
Kinetic Rayleigh-Taylor instability theory in the ionosphere near equator 13 p2067 N85-22011
Kinetic theory and simulation of multi-species plasmas in Tokamaks excited with ICRF microwaves [DE85-008119] 16 p2866 N85-27
Megajoule-class single-pulse KrF laser test facility as a logical step toward inertial fusion commercialization [DE85-009590] 18 p3191 N85-29

The balancing of complex linkage mechanisms
23 p3924 N85-34313

KINETICS
NT ELECTROKINETICS
NT KINETIC ENERGY
NT NEWTON THEORY
NT REACTION KINETICS
NT VARIABLE MASS SYSTEMS

Experiment on nowcasting of heavy rainfall and severe storms in central China in 1979-1981
01 p0081 N85-10545

Kinetics of simple inner- and outer-sphere electrochemical reactions at rotating silver electrodes as examined using surface-enhanced Raman spectroscopy
[AD-A145606] 02 p0172 N85-11154

Surface environmental effects in electrochemical kinetics: Outer-sphere chromium (3) reductions at mercury, gallium, lead, and thallium surfaces
[AD-A145607] 02 p0172 N85-11155

Solvent effects upon electrochemical kinetics: Influences of interfacial solvation and solvent relaxation dynamics
[AD-A145624] 02 p0173 N85-11156

The observation of a single thermoluminescence glow peak described by kinetics more general than the usual 1st and 2nd order kinetics
[DE84-014697] 02 p0173 N85-11160

Critical assessment of low fluence irradiation creep mechanisms
[DE84-015578] 02 p0184 N85-11232

Kinetics of short-range ordering in metallic glasses: Analysis of the crossover effect
[DE84-015524] 02 p0187 N85-11251

Quantum characteristics of kinetic fracturing of solids
02 p0265 N85-11732

Theory of kinetics of impregnation of porous bodies
[BLL-M-35917-(5828.4)] 05 p0616 N85-13942

An analysis of kinetic response variability
05 p0707 N85-14533

Influence of the mechanical and electrochemical characteristics of austenitic and austenoferritic steels on the propagation rate and morphology of stress corrosion cracking
[BLL-RISLEY-TR-4545-(9091.9F)]
06 p0767 N85-14906

Nitriding of titanium and its alloys by N2, NH3 or mixtures of N2 + H2 in a dc arc plasma at low pressures (or = to torr)
[NASA-TM-83803] 06 p0814 N85-15168

Review of the toxicokinetics of n-hexane
[AD-P004018] 06 p0843 N85-15352

Evaluation of jet fuel deposit kinetics. Lot 4
[AD-A147196] 07 p0935 N85-15922

Variation in photosynthesis with light level for model with two photochemical reactions 07 p1012 N85-16430

Effect of disuse on sarcoplasmic reticulum in fast and slow skeletal muscle
[NASA-CR-174337] 08 p1191 N85-17508

Studies of the kinetics and mechanisms of ammonia synthesis and hydrodesulfurization on metal single crystal surfaces
[DE85-001650] 11 p1595 N85-20030

Semiconductor electrochemistry approach to the study of oxide films on nickel electrodes
[DE85-003042] 11 p1630 N85-20264

Saturation kinetics of active medium of oxygen-iodine laser 11 p1716 N85-20807

Shock tube study of the fuel structure effects on the chemical kinetic mechanisms responsible for soot formation, part 2
[NASA-CR-174880] 15 p2504 N85-25444

Kinetics and structure of excited states
[AD-A151902] 15 p2648 N85-26334

Study of the kinetics and thermodynamics of hydrogen in Pd-based alloys
[DE85-007341] 16 p2750 N85-26969

Future fundamental combustion research for aeropropulsion systems
[NASA-TM-87049] 17 p2898 N85-27870

Dynamic creep buckling: Analysis of shell structures subjected to time-dependent mechanical and thermal loading 17 p2913 N85-27959

Research on the kinetics of phase changes in solids
[AD-A152387] 17 p2918 N85-27989

Detailed chemical kinetic study of the effect of molecular structure on autoignition of fuel-air mixtures
[DE85-004424] 17 p2921 N85-28010

Study of the kinetics of hydrogenation using aged catalysts
[DE85-010427] 19 p3230 N85-30025

Kinetics of H-induced stress corrosion cracking. Part 1: Important features of cracking in respect of high strength steels
[BLL-BISI-TRANS-(9022.06)] 19 p3282 N85-30350

Calculation of molecular constants potential energy curves and Franck-Condon factors for lead oxide
[AD-A154521] 21 p3562 N85-32156

The effect of prior parent phase cold work on martensite transformation in Cu-Zn-Al shape memory alloys
[AD-A155140] 21 p3566 N85-32183

Microscopic control of semiconductor surface oxidation
[AD-A154799] 21 p3709 N85-33026

Determination of kinetic parameters of molecular beam epitaxy
[AD-A155222] 21 p3710 N85-33030

KIRCHHOFF LAW OF RADIATION

Toward the theory of acoustic scattering on uneven free surface 21 p3680 N85-32862

Applications of the Kirchoff-Helmholtz integral to problems in body wave seismology
24 p4116 N85-35515

KIRCHHOFF-HELMHOLTZ FLOW
U PIPE FLOW

KIRCHHOFF-HUYGENS PRINCIPLE
U DIFFRACTION
U WAVE PROPAGATION

KITE BALLOONS
U TETHERED BALLOONS

KITS

Robotic order picking
[AD-D011737] 22 p3792 N85-33493

KLYSTRONS

Methods to increase linac efficiency
[DE84-014692] 01 p0118 N85-10809

Quasi-optical harmonic gyrotron and gyroklystron
[AD-D011308] 07 p0947 N85-16001

Multimode harmonic power measurement of 40 MW pulsed S-band klystrons
[DE85-001560] 09 p1316 N85-18272

The effects of mode impurity of Ka-band system performance 10 p1463 N85-19227

Feasibility study for a 34 GHz (Ka band) gyroamplifier
[NASA-CR-174439] 10 p1477 N85-19325

Notes on the RF system for the SLC positron source
[DE85-002628] 11 p1722 N85-20830

Design and testing of gyroklystron amplifiers
[AD-A151026] 14 p2298 N85-24231

VULTURE manual
[DE85-008873] 17 p3013 N85-28631

Coherent X-rays and vacuum-ultraviolet radiation from storage-ring-based undulators and free electron lasers
[DE85-009968] 18 p3183 N85-29738

A collective interaction klystron specification
[AD-D011704] 19 p3255 N85-30186

Los Alamos Free-Electron Laser (FEL) RF system
[DE85-010719] 19 p3278 N85-30329

Quasioptical gyroklystron
[AD-D011666] 19 p3356 N85-30801

Research on gyrotrons
[AD-A154032] 23 p3934 N85-34380

Solid state high power amplifier for driving the SLC injector klystron
[DE85-013063] 24 p4090 N85-35356

SLC Energy Upgrade Program at SLAC
[DE85-014290] 24 p4160 N85-35790

KNEE (ANATOMY)

Elbow and knee joint for hard space suits and the like
[NASA-CASE-ARC-11610-1] 11 p1697 N85-20666

KNIGHT SHIFT
U NUCLEAR MAGNETIC RESONANCE

KNOOP HARDNESS

Surface mechanical properties and wear behavior of ion implanted TiB2
[DE85-001130] 09 p1295 N85-18133

KNOWLEDGE
NT PARADOXES
NT PHILOSOPHY

Knowledge representation and natural-language semantics
[AD-A146025] 03 p0409 N85-12615

Getting mental models and computer models to cooperate 05 p0709 N85-14548

Distributed knowledge base systems for diagnosis and information retrieval
[AD-A146890] 07 p1054 N85-16690

Research on knowledge delivery
[AD-A149565] 10 p1538 N85-19698

Integrating non-semantic knowledge into image segmentation processes
[AD-A149571] 12 p1851 N85-21612

The role of prior knowledge in operating equipment from written instructions
[AD-A151007] 14 p2392 N85-24730

A simple software environment based on objects and relations
[AD-A155704] 21 p3673 N85-32817

Knowledge engineering application in image processing 23 p3965 N85-34583

KNOWLEDGE ENGINEERING
U EXPERT SYSTEMS

KNUDSEN FLOW

Close-spaced high temperature Knudsen flow
[AD-A148477] 08 p1178 N85-17424

KNUDSEN NUMBER
U KNUDSEN FLOW

KOLMOGOROFF THEORY

Closure problem and numerical studies of turbulence
08 p1209 N85-17608

Modeling of shear flow in a stratified fluid
14 p2340 N85-24469

Kolmogorov and scalar spectral regimes in numerical turbulence
[NASA-TM-86699] 17 p2957 N85-28264

KOLMOGOROFF-SMIRNOFF TEST

Kolmogorov-Smirnov goodness-of-fit test: Corrected for use with EEG-like data
[AD-A144711] 01 p0110 N85-10745

A new statistic for the analysis of circular data in gamma-ray astronomy
[OG-9.5-13] 23 p4031 N85-34969

KONDO EFFECT

Green's function solution of the Kondo problems and universality of the thermodynamic properties
[DE85-002739] 12 p1943 N85-22206

Very low temperature studies of hyperfine effects in metals
[DE85-013367] 22 p3749 N85-33236

KOREA

Limited surface observations climatic summary (LISOCS). Camp Casey, Tong Du Chon, Korea
[AD-A147204] 07 p1007 N85-16397

KORTEWEG-DEVRIES EQUATION

Stochastic property of K-dV solitons perturbed by random forces — Korteweg-Devries equation
02 p0283 N85-11843

Lax-pair operators for squared-sum and squared-difference eigenfunctions
[AD-B089083L] 09 p1386 N85-18718

Long nonlinear waves in layers of sudden changes in wind velocity 14 p2340 N85-24470

Internal waves in marine straits
[PREPRINT-415] 18 p3151 N85-29510

Approximate inverse spectral transform for the Korteweg-de Vries equation
[PREPRINT-411] 18 p3172 N85-29656

KOVAR (TRADEMARK)

Sintering and properties of metal-ceramic alloys of the Kovar type
[BLL-BISI-TRANS-21822-(9022.06)]
17 p2927 N85-28060

Slow crack growth in metal reinforced glass composites
[DE85-010094] 18 p3082 N85-29064

KRIGING

Analysis of geohydrologic data by kriging
[AD-P004152] 09 p1349 N85-18488

KRONECKER PRODUCT
U ORTHOGONALITY

KRYPTON
NT KRYPTON ISOTOPES
NT KRYPTON 85

IUE observations of the gaseous component of the local interstellar medium 06 p0674 N85-15553

Optogalvanic measurement of even parity Rydberg levels in krypton gas
[AD-A152113] 16 p2745 N85-26943

Modification of the grain size of sputtered copper with additions of oxygen, krypton, silver, or yttrium
[DE85-010975] 21 p3567 N85-32189

Interactions of heavy nuclei, Kr, Xe and Ho, in light targets
[OG-7.2-21] 23 p4016 N85-34888

KRYPTON FLUORIDE LASERS

An 850 J, 150 ns narrow-band krypton fluoride laser
[DE84-013077] 04 p0506 N85-13226

Investigation of dye lasers pumped by high-power KrF laser radiation 11 p1718 N85-20806

Time-resolved studies of rapid solidification in highly undercooled molten silicon
[DE85-004857] 13 p2038 N85-22765

Design optimization of singlemain-amplifier KrF laser-fusion systems
[DE85-007680] 16 p2791 N85-27215

KrF laser cost/performance model for ICF commercial applications
[DE85-009589] 18 p3182 N85-29728

Megajoule-class single-pulse KrF laser test facility as a logical step toward inertial fusion commercialization
[DE85-009590] 18 p3191 N85-29794

Summary of research for the Inertial Confinement Fusion Program at Los Alamos National Laboratory
[DE85-010330] 19 p3361 N85-30836

Magnetic fields in laser heated plasmas
[DE85-010715] 21 p3707 N85-33022

KRYPTON ISOTOPES
NT KRYPTON 85
Proposed solar neutrino experiment using (81)Br(nu,e(-e)) (81)Kr
[DE85-004802] 15 p2684 N85-26579
KRYPTON 85
The 1984 environmental monitoring report, Sandia National Laboratories, Albuquerque, New Mexico
[DE85-011175] 22 p3811 N85-33607
KU BAND
U SUPERHIGH FREQUENCIES
KUIPER AIRBORNE OBSERVATORY
U C-141 AIRCRAFT
KURILE ISLANDS
Basic structural features and probable mechanism of formation of the Kuril island system
10 p1501 N85-19472

L

L BAND
U ULTRAHIGH FREQUENCIES
L-SAT
Derivation of the Olympus solar array requirements
13 p2009 N85-22598
The Olympus solar array development and test program 13 p2009 N85-22599
Design and qualification testing of the Olympus solar array blanket 13 p2009 N85-22600
The performance of the Olympus power subsystem with its solar array 13 p2009 N85-22601
L-1011 AIRCRAFT
Advanced manufacturing development of a composite empennage component for L-1011 aircraft
[NASA-CR-165665] 02 p0170 N85-11141
Flight service evaluation of advanced composite ailerons on the L-1011 transport aircraft
[NASA-CR-172483] 08 p1118 N85-17049
LABELING (MARKING)
U MARKING
LABOR
New PCB production for robotics application
11 p1617 N85-20169
Cardiorespiratory function and work performance during adaptation to industrial labor in midalpine conditions
22 p3820 N85-33665
LABORATORIES
NT ENVIRONMENTAL LABORATORIES
NT LONG DURATION EXPOSURE FACILITY
NT MANNED ORBITAL LABORATORIES
NT MANNED ORBITAL RESEARCH LABORATORIES
NT SPACE LABORATORIES
NT SPACELAB
NT UNDERWATER RESEARCH LABORATORIES
Spring program summary, 1983
[PB84-222223] 06 p0839 N85-15330
Emerging role of the national laboratory in the development and transfer of materials technology
[DE85-001252] 09 p1288 N85-18086
Robotics in the radiochemical laboratory
[DE85-002824] 10 p1494 N85-19433
The use of small mobile radars to detect, monitor, and quantify bird movements
[AD-P004188] 11 p1580 N85-19951
Personal desktop computing in a research and development laboratory
[DE85-002765] 11 p1705 N85-20728
State measurement laboratories: Program description (part 1). Directory (part 2)
[PB85-137651] 11 p1739 N85-20935
JPL highlights, 1983
[NASA-CR-175556] 12 p1951 N85-22256
Accomplishments of Institute of Cartography summarized 13 p2166 N85-23435
JESS facility modification and environmental/power plans
[NASA-CR-175685] 14 p2227 N85-23807
Fiscal year 1986 technical objective document
[AD-A151039] 14 p2432 N85-25000
AFRPL (Air Force Rocket Propulsion Laboratory) technical objective document FY 85
[AD-A151368] 15 p2495 N85-25389
The human engineering of laboratory data acquisition and control systems
[AD-A151576] 15 p2620 N85-26148
Physics, Computer Science and Mathematics Div.
[DE85-006868] 15 p2642 N85-26298
Design and implementation of the digital engineering laboratory distributed database management system
[AD-A151694] 15 p2665 N85-26450
Guide for the execution of reliability tests in the laboratory — aeronautical equipment
16 p2796 N85-27237
Laboratory research: A question of when, not if
[AD-A153296] 17 p3048 N85-28867
Technical services at NLR
[B8561898] 17 p3049 N85-28871
New technologies to improve laboratory testing
[DE85-006151] 18 p3110 N85-29257
Selected university laboratory needs in support of national security
[AD-A153511] 18 p3197 N85-29833
Current activities and background of technology transfer and exchange program at Lawrence Livermore National Laboratory
[DE85-009526] 18 p3199 N85-29843
Publications of the Jet Propulsion Laboratory 1983
[NASA-CR-175979] 18 p3199 N85-29846
Technical and administrative activities of the Analytical Chemistry Laboratory (ACL)
[DE85-010150] 19 p3236 N85-30063
Clay identification and amount measured by laboratory techniques compared to well log responses: Application to tight gas sands and shales
[DE85-010411] 19 p3362 N85-30843
Computerized Laboratory Analytical and Diagnostic Services (CLADS)
[DE85-010854] 20 p3518 N85-31871
The flow of scientific and technical information in the US Army Research Laboratories
[AD-A155050] 21 p3713 N85-33043
The 1984 effluent and environmental monitoring report for the Bettis Atomic Power Laboratory
[DE85-011533] 22 p3810 N85-33602
Environmental monitoring at Lawrence Livermore National Laboratory: 1984 report
[DE85-011593] 22 p3811 N85-33606
Laboratory evaluation and application of microwave absorption properties under simulated conditions for planetary atmospheres
[NASA-CR-176076] 22 p3651 N85-33647
Procedure for editing the fluxgate magnetometer data of the AFGL (Air Force Geophysics Laboratory) magnetometer network
[AD-A156331] 24 p4117 N85-35523
Progress report on implementing the recommendations of the White House Science Council's Federal Laboratory Review Panel, volume 1
[PB85-185072] 24 p4164 N85-35819
Search for proton decay in the Frejus experiment
[HE-6.2-2] 24 p4210 N85-36138
LABORATORY EQUIPMENT
NT IMAGE FURNACES
An inexpensive microcomputer for laboratory data acquisition and test equipment control
[AD-A146095] 03 p0403 N85-12567
Spacelab mission D1 Frog statolith experiment STATEX: Hardware family and experiment operational sequence
05 p0689 N85-14426
Sampling device
[AD-D011256] 06 p0814 N85-15166
A validated methodology for determination of laboratory instrument computer interface efficacy
[AD-A148338] 10 p1487 N85-19391
Robotics at Savannah River site: Activity report
[DE85-003657] 11 p1648 N85-20363
European Space Tribology Laboratory: Facilities, services, capabilities
[ESA-BR-12] 20 p3398 N85-31080
Recommendations and calculations concerning physical characteristics of the EEVT apparatus
20 p3502 N85-31769
A gel-halo sample pellet: The best of both worlds? Stubby zones without a constricted sample gate
20 p3502 N85-31770
Recommendations for the design and equipping of engineering metrology laboratories
[NPL-MOM-22] 23 p3898 N85-34145
LABRADOR
Drifting buoys on the Labrador shelf
14 p2331 N85-24415
LABYRINTH
NT COCHLEA
NT VESTIBULES
Prediction of seasickness susceptibility
11 p1693 N85-20647
Dissociation of autonomic and sensory vestibular reactions 23 p3953 N85-34501
LABYRINTH SEALS
Theoretical approach to labyrinth seal forces - cross-coupled stiffness of a straight-through labyrinth seal 05 p0643 N85-14127
Experimental investigation of lateral forces induced by flow through model labyrinth glands
05 p0643 N85-14128
Analysis of dynamic characteristics of fluid force induced by labyrinth seal 05 p0643 N85-14129
Prediction of force coefficients for labyrinth seals
05 p0644 N85-14130
An Iwatsubo-based solution for labyrinth seals - comparison with experimental results
05 p0644 N85-14131
Preliminary investigation of labyrinth packing pressure drops at onset of swirl-induced rotor instability
05 p0644 N85-14132
Repair welding and brazing procedures for turbine components and investigation of the brazing behavior of thin filler foils
[MTU-TB-906/84] 07 p0974 N85-[illegible]
Analytical and experimental investigation of rubbing interaction in labyrinth seals for a liquid hydrogen fuel pump — space shuttle main engine
[NASA-CR-174857] 09 p1267 N85-[illegible]
LACQUERS
New air-curing lacquer systems with high solids content
[BMFT-FB-T-85-005] 17 p2936 N85-[illegible]
Oxidation resistant slurry coating for carbon-based materials
[NASA-CASE-LEW-13923-1] 24 p4077 N85-[illegible]
LAG (DELAY)
U TIME LAG
LAGEOS (SATELLITE)
Preliminary processing of laser ranging data from LAGEOS artificial Earth satellite during short merit program observation period 15 p2486 N85-[illegible]
Comparison of gravity field solution techniques
16 p2805 N85-[illegible]
Station coordinates and Earth rotation parameters from Lageos laser ranging 16 p2806 N85-[illegible]
Update on the evolution of the LAGEOS orbit
20 p3401 N85-[illegible]
Effect of solar eclipses on the LAGEOS semimajor axis 20 p3491 N85-[illegible]
Effect of diffusely-reflected sunlight on the orbit of LAGEOS 20 p3491 N85-[illegible]
Ocean tidal parameters from LAGEOS
20 p3493 N85-31716
Earth Albedo and the orbit of LAGEOS
[NASA-TM-86210] 21 p3556 N85-[illegible]
LAGRANGE COORDINATES
Model for high rate gas flows in deformable and reactive porous beds
[DE85-006140] 14 p2253 N85-[illegible]
Users manual for coordinate generation code CRDSRA
[NASA-CR-172584] 17 p2891 N85-[illegible]
Compressible Lagrangian hydrodynamics without Lagrangian cells
[DE85-009597] 20 p3520 N85-[illegible]
Two-dimensional simulation of instability growth due to shocks
[DE85-011869] 22 p3784 N85-[illegible]
Compressible two-phase flow instabilities simulated with a hybrid Lagrange-Euler pseudospectral method
[DE85-009904] 23 p3931 N85-[illegible]
Adaptive rezoner in a two-dimensional Lagrangian hydrodynamic code
[DE85-010108] 24 p4084 N85-[illegible]
LAGRANGE EQUATIONS OF MOTION
U EULER-LAGRANGE EQUATION
LAGRANGE MULTIPLIERS
Fracture, failure, and fragmentation
01 p0059 N85-[illegible]
Some concepts in multi-criteria optimization
[CSIR-TWISK-299] 01 p0108 N85-[illegible]
Numerical simulations of fuel droplet flows using a Lagrangian triangular mesh
[AD-A146087] 03 p0362 N85-[illegible]
Skyrmions and vector mesons: A symmetric approach
[DE84-015297] 04 p0563 N85-[illegible]
Existence, uniqueness and stability conditions for general finite element methods in linear elasticity
09 p1332 N85-[illegible]
Recent advances in hybrid/mixed finite elements
[NASA-CR-175674] 12 p1863 N85-[illegible]
On an iterative scheme for the solution of constrained variational equations
[CSIR-TWISK-341] 13 p2149 N85-[illegible]
The nonlinear analysis of thick composite plates using a cubic spline function
[AD-A152115] 16 p2801 N85-[illegible]
Solving the minimal least squares problem subject to bounds on the variables
[TRITA-NA-8215] 16 p2802 N85-[illegible]
Modern test of chiral anomalies
[DE85-005802] 17 p3080 N85-[illegible]
Computable numerical bounds for Lagrange multipliers of stationary points of nonconvex differentiable nonlinear programs
[AD-A153613] 18 p3169 N85-[illegible]
Numerical methods for the solution of stiff delay differential equations 19 p3334 N85-[illegible]

Model building and practical aspects of nonlinear programming
[AD-A155720] 22 p3829 N85-33711

LAGRANGIAN EQUILIBRIUM POINTS
Lagrangian solutions in photogravitational restricted circular three-body problem 13 p1979 N85-22416
The continuous spectrum of an axisymmetric equilibrium with a mixed poloidal and toroidal magnetic field with gravity included 14 p2450 N85-25129

LAGUERRE FUNCTIONS
Modification of the Week's method for numerical inversion of the Laplace transform
[DE85-006576] 14 p2409 N85-24856
A class of polynomials related to those of Laguerre
[CWI-AM-R8411] 17 p3022 N85-28693

LAKE ICE
NT ICE FLOES
Characteristics of snow cover on sea ice and formation of snow ice II 15 p2582 N85-25924
Great Lakes winter weather and ice conditions for 1982-83
[PB85-165009] 16 p2837 N85-27498

LAKES
NT GREAT LAKES (NORTH AMERICA)
Acid Deposition: Processes of Lake Acidification
[PB84-216175] 01 p0070 N85-10466
Investigation of mineral and thermomineral springs in the Eifel Mountains regarding thermal indications
[BMFT-FB-T-84-019] 02 p0220 N85-11451
Satellite altimetric measurements of lake levels
03 p0383 N85-12447
Late quarterly glaciolacustrine and vegetational history of the Copper River Basin, south-central Alaska
03 p0391 N85-12499
Glacial-lake deposits in the Mount Harper area, Yukon-Tanana Upland 04 p0517 N85-13300
Modeling effects of toxicants on aquatic systems
[DE84-016594] 04 p0531 N85-13396
In-lake water quality management for Lake Eureka: Highlights of third year (1983) operation
[PB85-104149/GAR] 07 p0990 N85-16269
Monitoring approaches for assessing quality of high altitude lakes: Colorado Flat Tops Wilderness Area
[PB85-117232] 11 p1679 N85-20579
Lake ice occurrence as a possible detector of atmospheric CO2 effects on climate
[DE85-002951] 11 p1687 N85-20606
Rationale and basic design for experimental acidification of a lake ecosystem in Northern Wisconsin
[PB85-116077] 12 p1885 N85-21829
A first evaluation of LANDSAT TM data to monitor suspended sediments in lakes — Lake Chicot, Arkansas
13 p2120 N85-23204
Role of natural dissolved organic compounds in determining the concentrations of americium in natural waters
[DE85-010266] 19 p3229 N85-30022
Microwave hydrology: A trilogy
[NASA-CR-176042] 20 p3477 N85-31603
Empirical methods for predicting eutrophication in impoundments. Report 3. Phase 2. Model refinements
[AD-A155463] 21 p3614 N85-32462
Changes in the organic material in lakes in the blast zone of Mount St. Helens, Washington: Hydrologic effects of the eruptions
[GS-CIRC-850-1] 21 p3630 N85-32551
Sulfur cycling in freshwater sediments
21 p3658 N85-32726
Lake ice occurence as a possible detector of atmospheric CO2 effects on climate
[DE85-012967] 23 p3950 N85-34480

LAMB WAVES
Elastic wave gyrometer
[REPT-26/4924/HF] 20 p3459 N85-31484

LAMBERT LAW
U BOUGUER LAW

LAME WAVE EQUATIONS
Spheroidal functions: Properties and tabulation. Application to antenna synthesis
14 p2396 N85-24758

LAMELLA (METALLURGY)
The growth of twins and twin lamellae in synthetic diamond crystals 02 p0181 N85-11213
Determination of local deformation during explosive welding
[BLL-M-36279-(5828.4)] 20 p3462 N85-31503

LAMINA
U LAYERS

LAMINAR BOUNDARY LAYER
Some important problems in unsteady boundary layers including separation. 1: Nature of singularity on oscillating airfoils
[AD-A147887] 07 p0960 N85-16067
Technology developments for laminar boundary layer control on subsonic transport aircraft
08 p1071 N85-16787
Numerical modeling of steady, laminar free-convective boundary layer flow beneath heated or combusting horitzonal surfaces 08 p1160 N85-17318
Aerothermal tests of a 12.5 percent cone at Mach 6.7 for various Reynolds numbers, angles of attack and nose shapes — conducted in Langley 8-foot high temperature tunnel
[NASA-TP-2345] 08 p1161 N85-17322
Leading edge separation criterion for an oscillating airfoil
[AD-P004175] 09 p1267 N85-17960
Numerical approach for the aerodynamic analysis if airfoils with laminar separation
[NASA-CR-172496] 09 p1273 N85-18001
Velocity measurements in a 3D shock wave laminar boundary layer interaction. Part 1: Low speed 2D LDV measurements
[AD-A149533] 10 p1485 N85-19373
Frequency spectra of turbulent pulsations in stability of laminar boundary layer 11 p1716 N85-20795
Re-design of ARL/HLF (Heated Laminar Flow) body nose region
[AD-A150063] 12 p1846 N85-21585
Generation and development of small-amplitude disturbances in a laminar boundary layer in the presence of an acoustic field
[NASA-TM-77826] 14 p2299 N85-24237
Three-dimensional boundary layer research at NLR
15 p2559 N85-25787
Brief review of current work in the UK on three dimensional boundary layers 15 p2559 N85-25788
Proceedings of the 9th US Air Force and the Federal Republic of Germany Data Exchange Agreement Meeting. Viscous and Interacting Flow Field Effects
[AD-A153020] 17 p2958 N85-28266
Experimental observation of transition behavior on a flat plate 20 p3452 N85-31437
Experiments on the influence of active walls on the initial amplitudes and growths of instability waves
[AD-A154630] 21 p3583 N85-32275

LAMINAR BOUNDARY LAYER SEPARATION
U LAMINAR BOUNDARY LAYER

LAMINAR FLAMES
U FLAMES
U LAMINAR FLOW

LAMINAR FLOW
NT BLASIUS FLOW
NT STRATIFIED FLOW
A review and analysis of boundary layer transition data for turbine application
[NASA-TM-86880] 01 p0047 N85-10306
Laminar flow heat exchangers. Viscosity induced non-uniform flow
[AD-A144777] 01 p0047 N85-10307
Analytical modeling of random thermal fluctuations in the NORDA high-frequency sound scattering facility
[AD-A145024] 01 p0116 N85-10790
Hybrid laminar flow control study
[NASA-CR-165930] 02 p0137 N85-10933
Approximate solution of a laminar flow over a flat plate with suction and pressure gradient
[AD-A145482] 02 p0198 N85-11321
Laminar-to-turbulent flow transition under influence of acoustic oscillations 02 p0260 N85-11701
Linear long-wave stability of cylindrical steady laminar flame in rotating medium 02 p0268 N85-11752
Raman and fluorescence spectroscopy in a methane-nitrous oxide laminar flame
[AD-A146092] 03 p0328 N85-12111
Laminar and turbulent boundary layers in a plane of symmetry
[AD-A146261] 03 p0362 N85-12323
Natural laminar flow airfoil design considerations for winglets on low-speed airplanes
[NASA-CR-3853] 04 p0452 N85-12863
Laminar flame propagation/quench for a parallel-wall duct
[DE84-009773] 04 p0470 N85-12993
Laminar jet issuing into stagnant surroundings — PHOENICS code
[PDR/CFDU-IC/15] 04 p0501 N85-13200
Friction and heat exchange in laminar and turbulent boundary layers with axisymmetrical bodies exposed to heterogeneous supersonic flow
05 p0724 N85-14655
Investigation of the local mass transfer of a laminar and turbulent falling liquid film
[BLL-T6368/BG/WH792/84] 06 p0807 N85-15130
Laminar separation bubble with transition: Prediction test with local interaction
[BLL-PNR-90231-(9019.3153)]
06 p0808 N85-15132
Towing tank studies of stratified flow over ridges and valleys
[DE84-011418] 06 p0839 N85-15328
Laminar flow over a backward-facing step
[AD-A147469] 07 p0960 N85-16064
Aircraft drag reduction technology
08 p1070 N85-16782
Design studies of thick laminar flow airfoils for low speed flight employing turbulent boundary layer suction over the rear part 08 p1070 N85-16786
Pneumatic turbulators: A device for drag reduction at Reynolds numbers below 5 million
08 p1071 N85-16791
Design guide for fluidic laminar proportional amplifiers and laminar jet angular rate sensors
[AD-A147730] 08 p1161 N85-17326
Experiments on controlled, unsteady, separated turbulent boundary layers
[AD-P004172] 09 p1266 N85-17957
Laminar separation bubble with transition: Prediction test with local interaction — airfoils
[PNR-90231] 09 p1274 N85-18006
Profile design for wings and propellers
[NASA-TM-77785] 10 p1419 N85-18953
A multistage time-stepping scheme for the Navier-Stokes equations
[NASA-CR-172527] 10 p1463 N85-19365
Research in nonlinear problems of energy: Informal technical report
[DE85-001529] 11 p1595 N85-20031
Pre-turbulence: Transitional Laminar-turbulent flows
11 p1716 N85-20793
Flight-measured laminar boundary-layer transition phenomena including stability theory analysis
[NASA-TP-2417] 12 p1771 N85-21118
Continuous laminar smoke generator
[NASA-CASE-LAR-13014-1] 12 p1781 N85-21178
Kinetics of nitric oxide formation in laminar and turbulent methane combustion
[PB85-149698] 12 p1804 N85-21313
Solution of the three-dimensional Navier-Stokes equations for a steady laminar horseshoe vortex flow
[AD-A149851] 12 p1846 N85-21582
Re-design of ARL/HLF (Heated Laminar Flow) body nose region
[AD-A150063] 12 p1846 N85-21585
Computer-Aided Structural Engineering (CASE) project. Seepage analysis of confined flow problems by the method of fragments (CFRAG)
[AD-A150015] 12 p1875 N85-21762
Hydrodynamic stability problem formulated by numerical solutions of the Navier-Stokes equations
12 p1946 N85-22223
Diffusion deposition in fibrous filters for parallel and transverse flow models
[DE85-006149] 13 p2093 N85-23066
Calibration of sonic valves for the laminar flow control, leading-edge flight test
[NASA-TP-2423] 14 p2210 N85-23707
Calculating boundary layer on profile with laminar and turbulent flow zone 14 p2288 N85-24177
A finite element, Navier-Stokes study of the confined, laminar flow over a downstream facing step
15 p2553 N85-25754
An experimental technique for the study of velocity profiles in a laminar jet using a pulsed nitrogen laser
[AD-A151496] 15 p2556 N85-25771
La Recherche Aerospatiale Bimonthly Bulletin Number 1984-3, 220/May-June
[ESA-TT-882] 16 p2695 N85-26636
Low Reynolds number vehicles
[AGARD-AG-288] 16 p2699 N85-26666
Thermodynamic evaluation of transonic compressor rotors using the finite volume approach
[NASA-CR-175811] 16 p2708 N85-26712
Modeling the role of radicals in the ignition of and flame propagation in hydrogen-air and methane-air mixtures
16 p2744 N85-26935
The overall reaction concept in premixed, laminar, steady-state flames. 2: Initial temperatures and pressures
[AD-A152132] 16 p2746 N85-26944
Boundary layer at moving cylinder surface
16 p2765 N85-27064
Dynamic response of fluid transmission lines
[AD-A151926] 16 p2782 N85-27171
Heat transfer in pipes
[NASA-TM-77838] 17 p2957 N85-28262
A method of determining the suction velocity for laminar flow control of two-dimensional airfoil in incompressible flow
[NAL-TR-845] 18 p3059 N85-29925
A study of aerodynamic control in stalled flight long laminar separation bubble analysis
[AD-A153650] 18 p3059 N85-29930
A model for the combustion of polymethyl methacrylate in air in a laminar diffusion flame
[VTH-LR-439] 18 p3185 N85-29806

Inviscid analysis of two supercritical laminar-flow-control airfoils at design and off-design conditions
[NASA-TM-84657] 19 p3212 N85-29920
Nacelle/pylon/wing integration on a transport model with a natural laminar flow nacelle
[NASA-TP-2439] 19 p3213 N85-29924
Sidewall boundary-layer effects in two-dimensional airfoil testing
[NASA-CR-176034] 20 p3396 N85-31085
Laminar diffusion flames, carbon gasification, and laser diagnostics applied to combustion systems. 1: Laminar diffusion flames with cylindrical symmetry. 2: Diffusion-controlled gasification of carbon particles. 3: Laser diagnostics applied to combustion systems
20 p3423 N85-31243
Transition in a disturbed environment
20 p3452 N85-31438
High Re separated flow solutions using the Navier-Stokes and approximate equations
[AD-A152252] 20 p3454 N85-31451
Vaporization from a heated surface into a saturated stream
[DE85-010484] 20 p3530 N85-31958
Numerical solutions of turbulent models for flow over a flat plate with angle of attack
[DE85-010360] 21 p3585 N85-32286
Theoretical foundations of turbulent flows
21 p3683 N85-32880
Block-implicit calculations of three-dimensional laminar flow in strongly curved ducts
[DE85-003047] 23 p3931 N85-34363
Effects of ambient pressure on the instability of a liquid boiling explosively at the superheat limit
[DE85-009476] 23 p3932 N85-34370

LAMINAR FLOW AIRFOILS
Unsteady Navier-Stokes calculations in an accelerated reference frame
[AD-A151751] 15 p2557 N85-25774
A method of determining the suction velocity for laminar flow control of two-dimensional airfoil in incompressible flow
[NAL-TR-845] 18 p3059 N85-28925

LAMINAR FLOW CONTROL
U BOUNDARY LAYER CONTROL
U LAMINAR BOUNDARY LAYER

LAMINAR HEAT TRANSFER
Laminar heat-transfer distributions on biconics at incidence in hypersonic-hypervelocity flows
[NASA-TP-2213] 07 p0957 N85-16065

LAMINAR JETS
U JET FLOW
U LAMINAR FLOW

LAMINAR WAKES
An experimental study on the instability of a mixing-layer with laminar wake as the initial condition
06 p1076 N85-16824
The mechanisms of flame holding in the wake of a bluff body
[NASA-CR-3866] 12 p1779 N85-21166
A panel method study of vortex sheets with special emphasis on sheets of axisymmetric geometry
[NASA-CR-177365] 21 p3552 N85-32095

LAMINATED MATERIALS
U LAMINATES

LAMINATES
NT PLYWOOD
Development of new and improved polymer matrix resin systems, phase 1
[NASA-CR-166595] 01 p0017 N85-10104
Design sensitivity analysis of an antisymmetric angle-ply laminate
[CSIR-TWISK-318] 01 p0021 N85-10128
Cumulative damage model for advanced composite materials
[AD-A144840] 01 p0022 N85-10135
Composite laminate optimization program suitable for microcomputers 01 p0059 N85-10389
Nonlinear dynamic analysis of sandwich panels
01 p0060 N85-10394
Flight simulation fatigue crack propagation in metal/carbon-epoxy laminates
[NLR-TR-83006-U] 01 p0063 N85-10416
Materials studies for magnetic fusion energy applications at low temperatures, 7
[DE84-013487] 01 p0122 N85-10837
Energy efficient engine. Volume 2. Appendix A: Component development and integration program
[NASA-CR-173085] 02 p0146 N85-10991
Fracture toughness of fibrous composite materials
[NASA-TP-2370] 02 p0170 N85-11136
Investigating compression failure mechanisms in composite laminates with a transparent fiberglass-epoxy birefringent materials
[NASA-TM-86306] 02 p0170 N85-11137
Development of failure criterion for Kevlar-epoxy fabric laminates
[NASA-CR-172465] 02 p0170 N85-11138
The influence of sublaminate cracks on the tension fatigue behavior of a graphite epoxy laminate
[FFA-TN-1984-32] 02 p0210 N85-11386
Calculation of critical temperature for Nb-Cu multilayer film superconductor
[AD-A144321] 02 p0274 N85-11786
Accelerated viscoelastic characterization of T300/5208 graphite-epoxy laminates 03 p0325 N85-12091
Fatigue-impact studies in laminated composites
[AD-A142841] 03 p0326 N85-12097
A digital algorithm for composite laminate analysis: FORTRAN, Revised
[AD-A145633] 03 p0326 N85-12098
Modeling the stress field in laminated composite plates near discontinuities
[PB84-219237] 03 p0327 N85-12103
Evaluation of laterally loaded laminated glass units by theory and experiment
[PB84-216423] 03 p0339 N85-12179
Tensile and crack propagation tests on aluminum alloys of the 2000 and 7000 series in laminated plate and forged products
[M2-678300] 03 p0373 N85-12363
Tough Composite Materials
[NASA-CP-2334] 04 p0463 N85-12941
Characterization of interlaminar crack growth in composites with the double cantilever beam specimen
04 p0463 N85-12942
Characterizing delamination resistance of toughened resin composites 04 p0464 N85-12943
Composite materials characterization and development at AFWAL 04 p0464 N85-12944
Effect of impact damage and open holes on the compression strength of tough resin/high strain fiber laminates 04 p0464 N85-12945
Effects of constituent properties on compression failure mechanisms 04 p0464 N85-12946
The effect of matrix and fiber properties on impact resistance 04 p0464 N85-12947
Development of a heterogeneous laminating resin
04 p0465 N85-12956
Free-edge failures of composite laminates
04 p0467 N85-12971
Flexible matrix composite laminated disk/ring flywheel
05 p0606 N85-13866
Mechanical properties of aligned short carbon fiber reinforced PES and PI laminates
[DFVLR-FB-84-24] 05 p0613 N85-13918
Development of damage in fatigue loaded carbon fiber reinforced plastics 05 p0650 N85-14172
A study of interply layer effects on the free-edge stress field of angleplied laminates
[NASA-TM-86924] 07 p0919 N85-15822
Design procedures for fiber composite structural components: Panels subjected to combined in-plane loads
[NASA-TM-86909] 07 p0919 N85-15823
Modeling localized stress fields in composite laminates
[AD-A148630] 08 p1120 N85-17056
Composite repair of aircraft structures
08 p1120 N85-17059
Contact behavior, impact response and damage in graphite-epoxy laminates subjected to initial stresses
08 p1171 N85-17386
Nonlinear analysis of composite laminates
09 p1288 N85-18087
Delamination growth in graphite epoxy laminates under compressive loads 09 p1288 N85-18088
Development of a heterogeneous laminating resin system
[NASA-CR-172459] 09 p1288 N85-18089
Fracture mechanics analysis and prediction of delamination growth in composite structures
[FFA-TN-1984-45] 09 p1289 N85-18092
Mechanical and transient hygrothermal loading of multilayer orthotropic cylinders 09 p1330 N85-18359
Evaluation of failure criterion for graphite/epoxy fabric laminates
[NASA-CR-172547] 10 p1431 N85-19025
A comprehensive study on sublaminate crack growth stability and its effects on the load-carrying capacity
[AD-A149037] 10 p1432 N85-19028
Impact toughness of composites with layered microstructure of OT4 titanium alloy
10 p1445 N85-19104
Simple higher-order theory for laminated composite plates
[NASA-CR-174421] 10 p1496 N85-19445
Develop and demonstrate manufacturing processes for fabricating graphite filament reinforced polymide (Gr/PI) composite structural elements
[NASA-CR-172497] 11 p1592 N85-20019
New method for studying surface crack growth in laminated polymer composite materials
11 p1598 N85-[illegible]
Method of constructing diagram of bimetal fatigue failure 11 p1599 N85-[illegible]
Bending two-layer metal-polymer plates
11 p1604 N85-[illegible]
Aerostructure nondestructive evaluation by thermal field detection. Phase 2: Technique refinement and quantitative determination of flaw detection capabilities
[AD-A149622] 12 p1777 N85-21[illegible]
Quantitative non-destructive evaluation of damage in composite materials using transmitted and reflected ultrasound
[NASA-CR-175550] 12 p1796 N85-21[illegible]
Accelerated viscoelastic characterization of T300/5208 graphite-epoxy laminates
[NASA-CR-3871] 12 p1797 N85-21[illegible]
Fire and heat resistant laminating resins based on maleimido and citraconimido substituted 1-(diorgano oxyphosphonyl)methyl-2,4- and 2,6-diaminobenzenes
[NASA-CASE-ARC-11533-1] 12 p1812 N85-21[illegible]
Study of laminated dielectric behavior at microwave and millimeter-wave frequencies
[AD-P004358] 12 p1825 N85-214[illegible]
Nonlinear analysis of layered composite plates and shells
[PB85-127181] 12 p1868 N85-217[illegible]
Investigation of the effects of NaOH dopant level on the physical and mechanical properties of carbon/phenolic composite material 12 p1945 N85-22[illegible]
Solid Rocket Motor Case (SRMC) dynamic sensitivity to changes in composite properties
12 p1948 N85-22[illegible]
Directional dependent engineering properties of aluminum-aramid-epoxy laminates
[CCMS-85-02] 13 p2015 N85-22[illegible]
Longitudinal splitting in unidirectional composites, analysis and experiments
[NASA-CR-3881] 13 p2015 N85-22[illegible]
Interlaminar fracture toughness in resin matrix composites
[AD-A150565] 13 p2015 N85-22[illegible]
Mechanical properties and brittle fracture resistance of welded multilayer elements for high pressure vessels
13 p2033 N85-227[illegible]
Fibre composite laminated plate analysis using a card programmable calculator (HP41C/CV)
[NIAST-83/88] 13 p2103 N85-231[illegible]
Some features of the fabrication of multilayer fiber composites by explosive welding
[NASA-TM-77844] 14 p2248 N85-23[illegible]
Monitoring of laminate cure with microdielectrometry
[AD-A150863] 14 p2248 N85-23[illegible]
Reduction of free-edge stress concentration
[AD-A150732] 14 p2321 N85-24[illegible]
Acoustic radiation from bilaminar plates
14 p2415 N85-24[illegible]
Field-induced phenomena in electrical insulation
[AD-A151234] 15 p2547 N85-257[illegible]
Layered composite analysis capability
15 p2573 N85-25[illegible]
Symmetric composite laminate stress analysis
15 p2575 N85-25[illegible]
Design of shear deformable antisymmetric angle-ply laminates to maximize the fundamental frequency and frequency separation
[CSIR-TWISK-333] 15 p2577 N85-25[illegible]
Temperature: Curvature relationships for unsymmetric graphite-epoxy laminates
[VPI-E-85-06] 16 p2743 N85-26[illegible]
The effects of pin elasticity, clearance, and friction on the stresses in a pin-loaded orthotropic plate
[NASA-CR-175816] 16 p2743 N85-26[illegible]
Durability of Aramid reinforced aluminum laminate (ARALL)
[VTH-LR-423] 16 p2744 N85-26[illegible]
The effect of low sheet thicknesses on the fracture toughness of an Al alloy (7075-T6) — Aramid Reinforced Aluminum Laminate (ARALL)
[VTH-LR-425] 16 p2752 N85-26[illegible]
The nonlinear analysis of thick composite plates using a cubic spline function 16 p2798 N85-27[illegible]
The nonlinear analysis of thick composite plates using a cubic spline function
[AD-A152115] 16 p2801 N85-27[illegible]
The application of BRILES rivets for mechanical joining of Aramid Reinforced Aluminum Laminate (ARALL)
[VTH-LR-387] 16 p2802 N85-27[illegible]
Mechanical jointing in Aramid fiber composites: An experimental study
[VTH-LR-371] 16 p2802 N85-27[illegible]
Solution to eigenvalue problems of antisymmetric cross-ply and antisymmetric angle-ply laminated plates using affine transformations
[AD-A153040] 17 p2917 N85-27[illegible]

Strength and failure analysis of composite laminates with holes at room and elevated temperatures
[AD-A153263] 17 p2917 N85-27981
Multiconductor flat cable
[AD-D011685] 17 p2950 N85-28216
Biaxial buckling of specially orthotropic, symmetric composite rectangular plates
[AD-A152969] 17 p2979 N85-28417
Numerical analysis of end effects in symmetric laminated plates
[NAL-TR-850] 18 p3068 N85-28977
The effect of center delamination on the instability of composite cylindrical panels
[AD-A153484] 18 p3069 N85-28979
Crack propagation in unidirectional laminates by the stress intensity factors 18 p3121 N85-29320
Fracture of laminated composite materials
19 p3230 N85-30030
Polymer matrix and graphite fiber interface study
[NASA-CR-177357] 19 p3232 N85-30036
Mesophase mechanisms in the formation of graphitic microstructures
[AD-A154100] 19 p3248 N85-30140
Impact dynamics research on composite transport structures
[NASA-TM-86391] 19 p3264 N85-30367
On design of off-axis specimens
[AD-A154388] 19 p3266 N85-30379
Long-term thermal aging of Celion/V378A composite materials
[NASA-TM-86362] 20 p3421 N85-31236
Delamination micromechanics analysis
[NASA-CR-172596] 20 p3422 N85-31237
Residual thermal and moisture influences on the strain energy release rate analysis of edge delamination
[NASA-TM-86437] 20 p3422 N85-31238
Mechanical properties of aligned short carbon fiber reinforced PES and PI laminates
[ESA-TT-896] 20 p3422 N85-31240
Metallographic preparation of materials with various coatings
[BLL-ORIC-TRANS-7522-(3623.66)]
20 p3433 N85-31299
Development of fracture mechanics maps for composite materials, volume 1
[ESA-CR(P)-2017-VOL-1] 20 p3471 N85-31573
Development of fracture mechanics maps for composite materials, volume 2
[ESA-CR(P)-2017-VOL-2] 20 p3471 N85-31574
Development of fracture mechanics maps for composite materials. Volume 3: Appendices A-E
[ESA-CR(P)-2017-VOL-3] 20 p3472 N85-31575
Development of fracture mechanics maps for composite materials. Volume 4: Appendices F-K
[ESA-CR(P)-2017-VOL-4] 20 p3472 N85-31576
Comparisons of various configurations of the edge delamination test for interlaminar fracture toughness
[NASA-TM-86433] 21 p3561 N85-32151
Experimental and theoretical assessment of a new technique for the non-destructive evaluation of laminated panels
[AD-A155622] 21 p3562 N85-32155
Mechanical characterization and failure modes of fiber reinforced angle-ply composites
24 p4072 N85-35234
Damage induced stress redistribution in composite laminates 24 p4072 N85-35235
Methods for nondestructive tests of CFRP laminates
24 p4074 N85-35248
Damage mechanisms in damaged CFRP laminates
24 p4074 N85-35249

LAMINATIONS
U LAMINATES
LAMPS
U LUMINAIRES
LAND
NT ARID LANDS
NT CASCADE RANGE (CA-OR-WA)
NT COASTAL PLAINS
NT DESERTS
NT FARMLANDS
NT FLOOD PLAINS
NT GOBI DESERT
NT GRASSLANDS
NT MARSHLANDS
NT MOJAVE DESERT (CA)
NT NATIONAL PARKS
NT PLAINS
NT RANGELANDS
NT SAHARA DESERT (AFRICA)
NT TUNDRA
NT WETLANDS
Autoregressive modeling and the classification of land clutter — radar signatures
[ENST-C-84003] 03 p0356 N85-12292
Requirements and special problems of land altimetry — satellite altimetry 03 p0380 N85-12430
Earth observations and the polar platform
[NOAA-TR-NESDIS-18] 11 p1689 N85-20517

LAND ICE
Special difficulties of retrieving surface elevation over continental ice — satellite radar altimetry
03 p0380 N85-12429
Diurnal freeze-thaw frequencies in selected regions of the high latitudes
[AD-A147276] 07 p1007 N85-16400
North Atlantic Deep Water formation: Information from ice cores 15 p2602 N85-26035
Greenland ice sheet mass balance
15 p2603 N85-26043
Potential climatic effects on the Greenland ice sheet
15 p2603 N85-26044
Origin of the Greenland ice sheet
15 p2604 N85-26046

LAND MANAGEMENT
Inventory and monitoring of national park landscapes — remote sensing 05 p0660 N85-14245
HS and E environmental sciences
[DE84-016183] 05 p0672 N85-14314
Landscape management on airports for reduction of bird populations
[AD-P004194] 11 p1581 N85-19980
Inexpensive multipurpose landscaping
11 p1581 N85-19981
Combined analysis of the dynamics of complex ecosystems based on repeated remote measurements
13 p1985 N85-22450
Application of interactive graphic systems in land consolidation. Processing of planning maps
16 p2815 N85-27363
Raster or vector processing. Experience with the application of programs for the construction of thematic maps with boundary design in the Lower Saxony (West Germany) Land Administration for ground research
16 p2815 N85-27365

LAND MOBILE SATELLITE SERVICE
RF characteristics of the hoop column antenna for the land mobile satellite system mission
[NASA-CR-3842] 02 p0189 N85-11264
Propagation measurements for land-mobile satellite services in the 800 MHz band
[CRC-TN-724] 09 p1310 N85-18231
Propagation measurements for land-mobile satellite systems at 1541 MHz
[CRC-TN-723] 09 p1310 N85-18232
Measurements of propagation at 900 MHz in an urban zone for establishing a digital radiomobile system
10 p1472 N85-19288
A comparison of metropolitan and non-metropolitan employment characteristics: Indications of the size of non-metropolitan mobile communication services user classes
[NASA-CR-175648] 13 p2053 N85-22855
NASA mobile satellite program
14 p2229 N85-23814
Mobile antenna and beam pointing studies for satellite mobile communications
[NASA-CR-175736] 15 p2540 N85-25679
Trade-off between land vehicle antenna cost and gain for satellite mobile communications
[NASA-CR-175732] 15 p2540 N85-25681
Land vehicle antennas for satellite mobile communications
[NASA-CR-175735] 15 p2540 N85-25682
Propagation considerations in land mobile satellite transmission
[NASA-CR-175733] 15 p2540 N85-25684
Land mobile satellite transmission measurements at 869 MHz: Selected results from the dedicated stratospheric balloon experiment of November 12 and 13, 1984
[NASA-CR-175734] 15 p2541 N85-25685
Spacecraft configuration study for second generation mobile satellite system
[NASA-CR-175774] 16 p2730 N85-26849
Dynamic performance of several large antenna concepts 20 p3409 N85-31155
Control of large antennas based on electromagnetic performance criteria 20 p3409 N85-31158

LAND USE
NT RURAL LAND USE
Satellite reconnaissance
[AD-B085034] 01 p0015 N85-10094
Estuaries of the Cape. Part 2: Synopses of available information on individual systems. Report 13: Silvermine (CSW 3)
[CSIR-RR-412-PT-2] 01 p0086 N85-10582
Estuaries of the Cape. Part 2: Synopses of available information on individual systems. Report no. 16: Eerste (CSW 6)
[CSIR-RR-415-PT-2] 01 p0087 N85-10585
Estuaries of the Cape. Part 2: Synopses of available information on individual systems. Report no. 19: Groot (WES) (CMS 23) and Sout (CMS 22)
[CSIR-RR-418] 01 p0087 N85-10588
Geographic science: Executive summary
02 p0214 N85-11408
Geographic science 02 p0214 N85-11409
Land use/land cover 02 p0214 N85-11410
Utilization of LANDSAT orbital imagery in the soil survey processes at Rio Grande do Norte state
[E85-10009] 02 p0216 N85-11422
Mapping land use changes in the carboniferous region of Santa Catarina, report 2
[E85-10017] 02 p0217 N85-11430
Assessing erosion on US cropland: Land management and physical features
[PB84-219252] 04 p0528 N85-13366
Modeling long-term changes in forested landscapes and their relation to the Earth's energy balance
05 p0653 N85-14194
Integration of multiple thematic data with LANDSAT data: Some results about the feasibility of Mediterranean land cover inventories 05 p0656 N85-14205
Statistics and mapping of land uses by means of LANDSAT MSS imagery 05 p0657 N85-14219
The use of Thematic Mapper data for land cover survey 05 p0657 N85-14220
Detecting agricultural to urban land use change from multi-temporal MSS digital data — Salt Lake County, Utah
[E85-10049] 07 p0983 N85-16245
Calibration or inverse regression: Which is appropriate for crop surveys using LANDSAT data?
07 p0985 N85-16260
Study of spectral/radiometric characteristics of the Thematic Mapper for land use applications
[E85-10057] 07 p0987 N85-16268
Analysis of data acquired by synthetic aperture radar and LANDSAT Multispectral Scanner over Kershaw County, South Carolina, during the summer season
[E85-10071] 10 p1503 N85-19485
Assessment of LANDSAT for rangeland mapping, Rush Valley, Utah
[E85-10072] 10 p1503 N85-19486
An integrated GIS/remote sensing data base in North Cache soil conservation district, Utah: A pilot project for the Utah Department of Agriculture's RIMS (Resource Inventory and Monitoring System)
[E85-10073] 10 p1504 N85-19487
Anaysis of the quality of image data required by the LANDSAT-4 Thematic Mapper and Multispectral Scanner — agricultural and forest cover types in California
[E85-10074] 10 p1504 N85-19488
Study of spectral/radiometric characteristics of the Thematic Mapper for land use applications
[E85-10075] 10 p1504 N85-19489
Nationwide urban runoff program. Relationship of urban runoff to land use and groundwater resources
[PB85-114692] 10 p1506 N85-19505
Control of mammals at airports
[AD-P004192] 11 p1580 N85-19957
Building a functional, integrated GIS/remote sensing resource analysis and planning system — Utah
[E85-10092] 12 p1874 N85-21754
Characterization of LANDSAT-4 TM and MSS image quality for the interpretation of California's agricultural resources — Central Valley 13 p2118 N85-23190
An initial analysis of LANDSAT-4 Thematic Mapper data for the discrimination of agricultural, forested wetlands, and urban land cover — Poinsett County, Arkansas; and Reelfoot Lake and Union City, Tennessee
13 p2118 N85-23193
Quick look analysis of TM data of the Washington, District of Columbia, area 13 p2119 N85-23197
Thematic Mapper data quality and performance assessment in renewable resources/agriculture/remote sensing 13 p2120 N85-23201
Preliminary comparisons of the information content and utility of TM versus MSS data 13 p2120 N85-23202
The use of Thematic Mapper data for land cover discrimination: Preliminary results from the UK SATMaP programme 13 p2121 N85-23207
Preliminary study of information extraction of LANDSAT TM data for a suburban/regional test site
13 p2121 N85-23208
Comparative techniques used to evaluate Thematic Mapper data for land cover classification in Logan County, West Virginia 13 p2121 N85-23209
Comparison of MSS and TM data for landcover classification in the Chesapeake Bay area: A preliminary report — Taylor's Island, Maryland
13 p2121 N85-23210
Atlas of archived vegetation, land-use and seasonal Albedo data sets
[NASA-TM-86199] 14 p2346 N85-24508

Identifying land use structures of multizonal aerospace photographs using digital data processing
15 p2486 N85-25348

A study of the methods for evaluating the noise impact of a proposed airport on a community
15 p2588 N85-25957

Experience of the Institute of Space Research with the use of remote sensing in urban planning studies
[INPE-3150-PRE/533] 16 p2660 N85-27770

Orphans of the Valley: Abandoned surface mines in the Tennessee Valley. Volume 2: Maps
[DE85-901249] 19 p3301 N85-30465

Microcomputer processing of LANDSAT Thematic Mapper data for the acquisition of military tactical terrain data
[AD-A154781] 21 p3605 N85-32389

Cosmonauts participate in multilevel remote sensing experiment 22 p3731 N85-33130

Resource evaluation and site selection for microalgae production systems
[DE85-008807] 23 p3951 N85-34485

Land Disposal of Hazardous Waste
[PB85-196376] 24 p4113 N85-35500

LANDAU DAMPING

Energy spread in SLC linac with Landau damping
[DE84-016258] 05 p0727 N85-14675

I. F. S. (Institute for Fusion Studies) Newsletter, Volume 4, Number 1
[DE85-007917] 17 p3040 N85-28809

LANDAU FACTOR

Some dynamic electronic properties of semiconductor surfaces and interfaces 20 p3537 N85-32007

Analytical-numerical methods of calculations of energy and three-dimensional particle distributions in electromagnetic cascades
[HE-3.5-13] 24 p4184 N85-35950

Development of electromagnetic cascades in the atmosphere including the Landau-Pomeranchuk-Migdal effect
[HE-4.5-5] 24 p4195 N85-36029

LANDFILLS

Electrical resistivity technique to assess the integrity of geomembrane liners
[PB85-122414/GAR] 09 p1325 N85-18327

Test report for Getty Synthetic Fuels, Inc., Calumet City, Illinois
[PB85-119493] 10 p1459 N85-19191

FAA policy regarding solid waste disposal facilities
[AD-P004196] 11 p1581 N85-19963

Successful control of gulls and other birds at a sanitary landfill
[AD-P004198] 11 p1582 N85-19965

Effectiveness of an overhead wire barrier in deterring gulls from feeding at a sanitary landfill
[AD-P004199] 11 p1582 N85-19966

Effectiveness of an overhead wire barrier system in reducing gull use at the BFI Jedburg sanitary landfill, Berkeley and Dorchester counties, South Carolina
[AD-P004200] 11 p1582 N85-19967

Evaluation of effectiveness of bird scaring operations at a sanitary landfill site near CFB Trenton, Ontario, Canada
[AD-P004201] 11 p1582 N85-19968

High-level waste processing and disposal
[DE85-003564] 11 p1728 N85-20865

Assessment of hazardous waste surface impoundment technology case studies and perspectives of experts
[PB85-117059] 12 p1886 N85-21834

Analysis of leachate production in closed hazardous waste landfills
[DE85-010978] 19 p3310 N85-30520

LANDFORMS
NT ALEUTIAN ISLANDS (US)
NT ALPS MOUNTAINS (EUROPE)
NT ANDES MOUNTAINS (SOUTH AMERICA)
NT APPALACHIAN MOUNTAINS (NORTH AMERICA)
NT BARRIERS (LANDFORMS)
NT BAYOUS
NT BERMUDA
NT BIGHORN MOUNTAINS (MT-WY)
NT BRIDGES (LANDFORMS)
NT CALDERAS
NT CANYONS
NT CAPES (LANDFORMS)
NT CARPATHIAN MOUNTAINS (EUROPE)
NT CASCADE RANGE (CA-OR-WA)
NT COASTAL RANGES (CA)
NT CONES (VOLCANOES)
NT CUBA
NT DELTAS
NT DIVIDES (LANDFORMS)
NT DUNES
NT ESCARPMENTS
NT FLATS (LANDFORMS)
NT GAPS (GEOLOGY)
NT GREENLAND
NT HAWAII
NT HIMALAYAS
NT ICELAND
NT INDONESIA
NT ISLAND ARCS
NT ISLANDS
NT JAPAN
NT KURILE ISLANDS
NT MARS VOLCANOES
NT MASSIFS
NT MISSISSIPPI DELTA (LA)
NT MISSOURI RIVER BASIN (US)
NT MOUNTAINS
NT NEW ZEALAND
NT PACIFIC ISLANDS
NT PIEDMONTS
NT PLATEAUS
NT PUERTO RICO
NT PYRENEES MOUNTAINS (EUROPE)
NT REEFS
NT RIVER BASINS
NT ROCKY MOUNTAINS (NORTH AMERICA)
NT SALT BEDS
NT SIERRA NEVADA MOUNTAINS (CA)
NT STEPPES
NT STRUCTURAL BASINS
NT TASMANIA
NT TERRACES (LANDFORMS)
NT TUNDRA
NT VOLCANOES
NT WATERSHEDS

Terrain analysis procedural guide for surface configuration
[AD-A145637] 02 p0219 N85-11446

Submarine sand ridges: Geology and development, New Jersey, USA 02 p0227 N85-11482

Paleoenvironmental interpretation of the upper cretaceous Point Lookout sandstone: Implications for shoreline progradation and basin tectonic history, San Juan basin, New Mexico 02 p0227 N85-11486

Remote sensing for landforms and soils in the arid southwest United States 03 p0378 N85-12410

Glacier dynamics and the development of glacial landforms in the eastern Puget lowland, Washington
03 p0389 N85-12490

Glacial geology of Barron County, Wisconsin
09 p1351 N85-18500

Newly discovered Martian impact basins
13 p2182 N85-23544

Thickness of ridged plains materials in Hesperia Planum, Mars 13 p2185 N85-23561

Submarine volcanic eruptions and potential analogs for Venus 13 p2187 N85-23573

Transformation of polar ice sublimate residue into Martian circumpolar sand 13 p2189 N85-23580

Potential bedforms on Venus: Wind tunnel simulations
13 p2189 N85-23583

Experiments and analyses of the formation of erosional scour marks with implications to the origin of the Martian outflow channels 13 p2190 N85-23588

Distribution and properties of large symmetric knobs on Mars 13 p2192 N85-23598

Enigmatic hills of the mottled plains, Mare Acidalium quadrangle (MC-4), Mars 13 p2192 N85-23599

Geomorphology and geology of the Southwestern Margaritifer Sinus and Argyre regions of Mars. Part 3: Valley types and distribution 13 p2193 N85-23602

The geomorphology of Rhea
13 p2193 N85-23606

Airphoto interpretation of vegetation and landforms for soil mapping 17 p2963 N85-28436

Mineralogical-geochemical characteristics of ferromanganese formations in Arabian-Indian Ocean Ridge 19 p3293 N85-30416

MELSAR: A mesoscale air quality model for complex terrain. Volume 2: Appendices
[DE85-010991] 19 p3310 N85-30519

Global Mega-Geomorphology
[NASA-CP-2312] 21 p3600 N85-32357

The problem of scale in planetary geomorphology
21 p3603 N85-32375

Global geomorphology: Report of Working Group Number 1 21 p3604 N85-32382

Planetary perspective. Report of Working Group Number 4 21 p3605 N85-32385

Massive sulfide deposits from the southern Juan de Fuca Ridge 24 p4105 N85-35446

LANDING
NT AIRCRAFT LANDING
NT CRASH LANDING
NT DITCHING (LANDING)
NT GLIDE LANDINGS
NT HORIZONTAL SPACECRAFT LANDING
NT MARS LANDING
NT PLANETARY LANDING
NT SKID LANDINGS
NT SPACECRAFT LANDING
NT VERTICAL LANDING
NT WATER LANDING

Wind tunnel results of advanced high speed propfan in the takeoff, climb and landing operating regime
[NASA-TM-87054] 19 p3213 N85-

Ground-based and in-flight simulator studies of flight characteristics of a twin-fuselage passenger transport airplane during approach and landing
[NASA-TP-2451] 23 p3898 N85-3414

LANDING AIDS
NT ALL-WEATHER LANDING SYSTEMS
NT APPROACH INDICATORS
NT ARRESTING GEAR
NT AUTOMATIC LANDING CONTROL
NT INSTRUMENT LANDING SYSTEMS
NT LANDING RADAR
NT MICROWAVE LANDING SYSTEMS
NT RUNWAY LIGHTS

Development and flight test of a helicopter, X-band, portable precision landing system concept
[NASA-TM-86710] 16 p2710 N85-2872

LANDING GEAR

Air force landing gear repair - Ogden Air Logistics Center Industrial Products and Landing Gear Division
[AD-P004001] 03 p0307 N85-11

Determination of parameters of cupped aircraft landing ski 06 p0775 N85-14

Testing solution for IL-76 braking system problem
08 p1067 N85-157

Orbiter wheel and tire certification
08 p1101 N85-16

A literature survey of ground load statistics for landing gear fatigue design purposes
[FFA-TN-1984-39] 09 p1280 N85-183

Deflection model of a CT4-A undercarriage
[AD-A149778] 12 p1777 N85-2115

Safety recommendation(s), A-84-65
[REPT-3908] 14 p2216 N85-2374

Selection of effective arrangement of heavy undercarriage systems for use with concrete runways
14 p2285 N85-24

Active control landing gear for ground loads alleviation
16 p2714 N85-26

Active control landing gear for ground load alleviation
17 p2903 N85-27

LANDING INSTRUMENTS
NT APPROACH INDICATORS

LANDING LOADS

Development of a preliminary ALRS stabilized material pavement analysis system (SPAS)
[AD-A147116] 07 p0910 N85-157

Learjet Model 55 wing analysis with landing loads
15 p2575 N85-2

Active control landing gear for ground load alleviation
17 p2903 N85-27

LANDING RADAR

Landing control centrals
[AD-A149600] 12 p1775 N85-2114

Investigation of imaging and flight guidance concepts for rotorcraft zero visibility approach and landing
[NASA-CR-166571] 17 p2894 N85-278

LANDING SIMULATION

Realistic localizer courses for aircraft instrument landing simulators
[NASA-CR-172333] 04 p0455 N85-12

LANDING SITES

Structural design guidelines for heliports
[FAA-PM-84-23] 02 p0149 N85-110

STS natural environment analysis
[NASA-CR-171221] 03 p0322 N85-12

The search for igneous materials at the Viking landing sites 13 p2194 N85-236

Mars landing sites 22 p3859 N85-3

LANDING SYSTEMS
U LANDING AIDS

LANDMARKS

Potential geological natural landmarks of the East Gulf Coastal Plain
[PB84-230317] 06 p0835 N85-157

Man in Space: National Historic Landmark Theme Study
[PB85-107233/GAR] 07 p0911 N85-157

LANDSAT SATELLITES
NT LANDSAT 1
NT LANDSAT 4
NT LANDSAT 5

Land remote sensing commercialization: A status report 02 p0151 N85-1102

Seminar on Principal Components Analysis in the Atmospheric and Earth Sciences
[CSIR-S-334] 02 p0211 N85-115

The feasibility of satellite remote sensing as a technique for evaluating coal mine surface features
02 p0213 N85-1140

Relationships between grass canopy characteristics and LANDSAT Thematic Mapper bands
02 p0213 N85-11402

The Alaskan mineral resources assessment program: Guide to information contained in the folio of geologic and mineral-resource maps of the Medfra Quadrangle, Alaska
[GS-CIRC-929] 02 p0219 N85-11443

The United States Geological Survey in Alaska: Accomplishments during 1981
[USGS-CIRC-868] 04 p0515 N85-13283

Summary of LANDSAT quadrangle studies in Alaska
04 p0515 N85-13284

LANDSAT instruments characterization
[E85-10032] 04 p0524 N85-13356

LANDSAT instruments characterization
[E85-10029] 05 p0654 N85-14198

Integration of multiple thematic data with LANDSAT data: Some results about the feasibility of Mediterranean land cover inventories 05 p0655 N85-14205

Methodological research in connection with the handling of LANDSAT satellite data for archaeology
05 p0655 N85-14207

A comparison of TIROS-N series satellite data and LANDSAT data over Scotland 05 p0656 N85-14210

Forest cover monitoring by remote sensing in Great Britain 05 p0656 N85-14214

Statistics and mapping of land uses by means of LANDSAT MSS imagery 05 p0657 N85-14219

Landform evaluation through integrated remote sensing methods. A case study in parts of Haryana, India
05 p0657 N85-14221

Combining Heat Capacity Mapping Mission (HCMM) LANDSAT and thematic map information into a unique high precision merged multichannel system — climatology 05 p0660 N85-14239

A multiple approach in remote sensing for structural and lithological mapping by use Modular Optoelectronic Multispectral Scanner (MOMS)/LANDSAT/Heat Capacity Mapping Mission (HCMM) data
05 p0660 N85-14244

An integrated LANDSAT/ancillary data classification of desert rangeland
[E85-10046] 06 p0826 N85-15248

A geographic information system for resource managers based on multi-level remote sensing data
[E85-10047] 06 p0827 N85-15249

The extension of an invertible coniferous forest canopy reflectance model using SIR-B and LANDSAT data
08 p1149 N85-17246

Assessment of LANDSAT for rangeland mapping, Rush Valley, Utah
[E85-10072] 10 p1503 N85-19486

An integrated GIS/remote sensing data base in North Cache soil conservation district, Utah: A pilot project for the Utah Department of Agriculture's RIMS (Resource Inventory and Monitoring System)
[E85-10073] 10 p1504 N85-19487

Thematic Mapper data quality and performance assessment in renewable resources/agriculture/remote sensing 13 p2120 N85-23201

Study of the urban evolution of Brasilia with the use of LANDSAT data
[E85-10101] 16 p2809 N85-27321

Geomorphic classification of Icelandic and Martian volcanoes: Limitations of comparative planetology research from LANDSAT and Viking orbiter images
21 p3603 N85-32372

Use of spaceborne imaging radar in regional geomorphic studies 21 p3603 N85-32377

Quantitative geomorphologic studies from spaceborne platforms 21 p3604 N85-32381

Microcomputer processing of LANDSAT Thematic Mapper data for the acquisition of military tactical terrain data
[AD-A154781] 21 p3605 N85-32389

Satellites and politics: Weather, communications, and earth resources 23 p4057 N85-35144

A comparison of LANDSAT thematic mapper, multispectral scanner and airborne sensors for mapping the distribution of alteration minerals: Examples from the southwestern United States 24 p4106 N85-35452

Processing of LANDSAT imagery to map surface mineral alteration on the Alaska Peninsula, Alaska
24 p4106 N85-35455

LANDSAT 1

Developments in remote sensing
[B8580069] 17 p2984 N85-28441

LANDSAT 4

LANDAT-4/5 image data quality analysis
[E85-10039] 03 p0379 N85-12417

LANDSAT instruments characterization
[E85-10030] 05 p0654 N85-14199

Characterizing the scientific potential of satellite sensors
[E85-10031] 05 p0654 N85-14200

The use of Thematic Mapper data for land cover survey 05 p0657 N85-14220

Study of spectral/radiometric characteristics of the Thematic Mapper for land use applications
[E85-10057] 07 p0987 N85-16268

LANDSAT 4 investigation of Thematic Mapper and Multispectral Scanner applications
[E85-10076] 10 p1504 N85-19490

Thematic Mapper: Design through flight evaluation
[E85-10078] 10 p1504 N85-19492

LANDSAT-4 Science Characterization Early Results. Volume 1: Multispectral Scanner (MSS)
[E85-10067] 11 p1666 N85-20496

Spectral characterization of the LANDAT-4 MSS sensors 11 p1666 N85-20499

Investigation of radiometric properties of LANDSAT-4 MSS — California, North Caroline, South Caroline, and New England 11 p1666 N85-20500

LANDSAT scene-to-scene registration accuracy assessment 11 p1667 N85-20502

Geometric accuracy of LANDSAT-4 MSS image data
11 p1667 N85-20503

Impact of LANDSAT MSS sensor differences on change detection analysis — New Mexico, San Francisco, CA, New Hampshire, and Connecticut
11 p1667 N85-20506

LANDSAT-4 Science Characterization Early Results. Volume 2, part 1: Thematic Mapper (TM)
[E85-10068] 11 p1668 N85-20508

An overview of LANDSAT-4 and the Thematic Mapper
11 p1668 N85-20509

Radiometric calibration and processing procedure for reflective bands on LANDSAT-4 protoflight Thematic Mapper 11 p1668 N85-20510

An overview of the Thematic Mapper geometric correction system 11 p1668 N85-20511

TM digital image products for applications
11 p1668 N85-20512

Spectral characterization of the LANDSAT Thematic Mapper sensors 11 p1669 N85-20514

Prelaunch absolute radiometric calibration of the reflective bands on the LANDSAT-4 protoflight Thematic Mapper 11 p1669 N85-20515

LANDSAT-4 Science Characterization Early Results. Volume 3, part 2: Thematic Mapper (TM)
[E85-10069] 12 p1869 N85-21724

Relative radiometric calibration of LANDSAT TM reflective bands 12 p1869 N85-21725

Evaluation of the radiometric integrity of LANDSAT 4 Thematic Mapper band 6 data 12 p1869 N85-21726

Thermal band characterization of the LANDSAT-4 Thematic Mapper 12 p1869 N85-21727

A preliminary assessment of LANDSAT-4 Thematic Mapper data — Windsor, Ontario and Medicine Hat areas, Canada 12 p1869 N85-21728

Preliminary evaluation of the radiometric calibration of LANDSAT-4 Thematic Mapper data by the Canada Centre for Remote Sensing 12 p1870 N85-21729

A preliminary analysis of LANDSAT-4 Thematic Mapper radiometric performance 12 p1870 N85-21730

TM geometric performance: Line to Line Displacement Analysis (LLDA) — New Mexico
12 p1870 N85-21732

In-progress absolute radiometric inflight calibration of the LANDSAT-4 sensors — New Mexico
12 p1870 N85-21733

LANDSAT-4 Thematic Mapper calibration and atmospheric correction 12 p1870 N85-21734

MTF analysis of LANDSAT-4 Thematic Mapper
12 p1871 N85-21737

Intraband radiometric performance of the LANDSAT 4 Thematic Mapper — Washington, DC, Arkansas, Massachusetts, Virginia, and Arizona
12 p1871 N85-21738

A preliminary evaluation of LANDSAT-4 Thematic Mapper data for their geometric and radiometric accuracies 12 p1871 N85-21739

The use of linear feature detection to investigate Thematic Mapper data performance and processing
12 p1872 N85-21740

An analysis of the high frequency vibrations in early Thematic Mapper scenes 12 p1872 N85-21742

Assessment of Thematic Mapper band-to-band registration by the block correlation method
12 p1872 N85-21743

Tests of low-frequency geometric distortions in LANDSAT 4 images 12 p1872 N85-21744

Investigation of TM band-to-band registration using the JSC registration processor 12 p1872 N85-21745

Geodetic accuracy of LANDSAT 4 Multispectral Scanner and Thematic Mapper data 12 p1873 N85-21746

LANDSAT 4 band 6 data evaluation
[E85-10093] 12 p1874 N85-21755

LANDSAT-4 Science Characterization Early Results. Volume 4: Applications — agriculture, soils land use, geology, hydrology, wetlands, water quality, biomass identification, and snow mapping
[E85-10070] 13 p2117 N85-23186

Overview of TM applications research reports
13 p2117 N85-23187

Impact of Thematic Mapper sensor characteristics on classification accuracy — suburban Washington, D.C., Maryland, and the Chesapeake Bay
13 p2117 N85-23188

Analysis and evaluation of the LANDSAT-4 MSS and TM sensors and ground data processing systems: Early results 13 p2117 N85-23189

Characterization of LANDSAT-4 TM and MSS image quality for the interpretation of California's agricultural resources — Central Valley 13 p2118 N85-23190

Evaluation of Thematic Mapper performance as applied to hydrocarbon exploration — Ontario, Canada; Cement, Oklahoma; and Death Valley, California
13 p2118 N85-23191

An initial analysis of LANDSAT-4 Thematic Mapper data for the discrimination of agricultural, forested wetlands, and urban land cover — Poinsett County, Arkansas; and Reelfoot Lake and Union City, Tennessee
13 p2118 N85-23193

A preliminary comparison of the information content of data from the LANDSAT 4 Thematic Mapper and Multispectral Scanner — Arkansas
13 p2119 N85-23199

Early results of investigations of LANDSAT 4 Thematic Mapper and Multispectral Scanner applications — Washington, D.C. 13 p2119 N85-23200

Preliminary comparisons of the information content and utility of TM versus MSS data 13 p2120 N85-23202

Snow reflectance from Thematic Mapper
13 p2120 N85-23205

The use of Thematic Mapper data for land cover discrimination: Preliminary results from the UK SATMaP programme 13 p2121 N85-23207

Relative accuracy assessment of LANDSAT-4 MSS and TM data for level 1 land cover inventory — Washington, D.C. 13 p2122 N85-23212

NOAA satellite operations: Programs briefing — Environmental satellites, LANDSAT, and space station polar platform 15 p2599 N85-26020

CNPq/INPE LANDSAT system: Report of activities from October 1, 1983 to September 30, 1984 — Brazil
[E85-10097] 16 p2808 N85-27318

LANDSAT-4/5 image data quality analysis
[E85-10105] 24 p4107 N85-35463

Study of spectral/radiometric characteristics of the Thematic Mapper for land use applications
[E85-10106] 24 p4107 N85-35464

LANDSAT 5

LANDAT-4/5 image data quality analysis
[E85-10039] 03 p0379 N85-12417

LANDSAT instruments characterization
[E85-10030] 05 p0654 N85-14199

Study of spectral/radiometric characteristics of the Thematic Mapper for land use applications
[E85-10057] 07 p0987 N85-16268

Thematic Mapper. Volume 1: Calibration report flight model, LANDSAT 5
[E85-10059] 07 p0987 N85-16270

Thematic Mapper. Volume 2: Flight model preshipment review
[E85-10060] 07 p0987 N85-16271

LANDSAT 4 investigation of Thematic Mapper and Multispectral Scanner applications
[E85-10076] 10 p1504 N85-19490

Spectroradiometric calibration of the Thematic Mapper and Multispectral Scanner system
[E85-10077] 10 p1504 N85-19491

Thematic Mapper: Design through flight evaluation
[E85-10078] 10 p1504 N85-19492

An investigation of several aspects of LANDSAT-5 data quality — Palmer County, Shelby, mt; White sands, NM; Great Salt Lake, UT; San Matted Bridge and Sacramento, California
[E85-10096] 13 p2122 N85-23214

Spectroradiometric calibration of the Thematic Mapper and Multispectral Scanner system
[E85-10104] 20 p3476 N85-31601

LANDSAT-4/5 image data quality analysis
[E85-10105] 24 p4107 N85-35463

Study of spectral/radiometric characteristics of the Thematic Mapper for land use applications
[E85-10106] 24 p4107 N85-35464

LANDSCAPE
U TERRAIN
U TOPOGRAPHY

LANGMUIR PROBES
U ELECTROSTATIC PROBES

LANGUAGE PROGRAMMING

Evaluation of PHOENICS as a design analysis tool for SSME 12 p1949 N85-22240

Dataflow computation [CWI-TRACT-6] 14 p2406 N85-24833

The design and analysis of a complete hierarchical interface for the multi-backend database system [AD-A151550] 15 p2629 N85-26203

The effect of communication-language designs on software specifications [AD-A155173] 21 p3672 N85-32609

LANGUAGES

NT ADA (PROGRAMMING LANGUAGE)
NT ASSEMBLY LANGUAGE
NT BASIC (PROGRAMMING LANGUAGE)
NT COBOL
NT COMMAND LANGUAGES
NT ENGLISH LANGUAGE
NT FORTRAN
NT HIGH LEVEL LANGUAGES
NT LISP (PROGRAMMING LANGUAGE)
NT NATURAL LANGUAGE (COMPUTERS)
NT PASCAL (PROGRAMMING LANGUAGE)
NT PL/1
NT PROGRAMMING LANGUAGES
NT QUERY LANGUAGES
NT WORDS (LANGUAGE)

Model theory for infinitely deep languages [ISSN-0355-0087] 01 p0101 N85-10674

Information-theoretic properties of languages and their grammars [AD-A146666] 06 p0799 N85-15106

Spanish language equivalents for a glossary of terms used in the field of space exploration [NASA-TM-87403] 08 p1229 N85-17739

Glossary of the soil sciences [PB85-133452] 12 p1952 N85-22263

Expressiveness and language choice [AD-A153280] 17 p3012 N85-28623

LANTHANIDE SERIES METALS

U RARE EARTH ELEMENTS

LANTHANUM

Kohn anomaly in metastable fcc lanthanum at low temperatures [DE84-015459] 04 p0569 N85-13628

Stability of temporal and energy parameters of picosecond lanthanum beryllate laser 11 p1717 N85-20804

Americium metal preparation on the multigram scale [DE85-003735] 13 p2024 N85-22683

Modified aluminosilicide coating for heat-resistant nickel alloys 15 p2514 N85-25509

LANTHANUM COMPOUNDS

Phonon anomalies in superconducting transition metal compounds — lanthanum and niobium compounds 03 p0426 N85-12718

Magnetic susceptibility, electrical resistivity, and specific heat of single crystal LaFe-4P-12 [DE84-009979] 04 p0570 N85-13633

Strength and failure of ceramic-metallic material 10 p1446 N85-19112

The UFe4P12 and CeFe4P12: Non-metallic isotopes of superconducting LaFe4P12 [DE85-003724] 12 p1942 N85-22195

Development of advanced thermoelectric materials [NASA-CR-175684] 14 p2351 N85-24532

LAP JOINTS

Effect of penetrant on fatigue of aluminum alloy lap joints [NLR-TR-82104-U] 01 p0056 N85-10373

Deformations and strains in adhesive joints by moire interferometry [NASA-CR-172474] 02 p0185 N85-11238

The application of BRILES rivets for mechanical jointing of Aramid Reinforced Aluminum Laminate (ARALL) [VTH-LR-387] 16 p2802 N85-27279

Influence of interface ply orientation on fatigue damage of adhesively bonded composite joints [NASA-TM-86443] 19 p3284 N85-30365

LAPLACE EQUATION

Boundary element methods in potential theory: Four lectures [NPL-DITC-46/84] 05 p0718 N85-14604

Integral equation formulations in two dimensions 05 p0718 N85-14605

Applications of the simple-layer logarithmic potential 05 p0718 N85-14606

Three-dimensional and axisymmetric problems 05 p0718 N85-14608

Simulation of the electrochemical machining process [DE85-003797] 11 p1616 N85-20159

Computation of elliptical functions in problems of celestial mechanics 13 p1979 N85-22418

Applications of the conformal mapping method to the solution of mechanical vibrations problems 13 p2102 N85-23103

Numerical solutions of the potential distribution within the vacuum region of the FEATRON [AD-A153683] 18 p3178 N85-29705

LAPLACE OPERATORS

U LAPLACE TRANSFORMATION

LAPLACE TRANSFORMATION

Fitting aerodynamic forces in the Laplace domain: An application of a nonlinear nongradient technique to multilevel constrained optimization [NASA-TM-86317] 02 p0134 N85-10917

Omni transforms: Applications to renewal theory [AD-A146939] 07 p1029 N85-16534

Numerical solution of semilinear elliptic problems on unbounded domains [AD-A149559] 10 p1549 N85-19767

Three algorithms for parametric frequency domain system identification [DE85-002801] 11 p1706 N85-20735

Application of the system identification technique to goal-directed saccades [AD-A150132] 12 p1906 N85-21967

Time dependent interaction of internal pressure wave with system of two spherical shells 13 p2046 N85-22809

Modification of the Week's method for numerical inversion of the Laplace transform [DE85-006576] 14 p2409 N85-24856

Implementation of Weeks' method for the inverse Laplace transform problem [DE85-005919] 15 p2639 N85-26275

A convolution integral equation solved by Laplace transformation [CWI-AM-R8409] 17 p3022 N85-28692

Numerical solutions of the potential distribution within the vacuum region of the FEATRON [AD-A153683] 18 p3178 N85-29705

An extension to complex-valued functions of an algorithm for numerically inverting the Laplace transform [DE85-010701] 19 p3347 N85-30743

Art of programming programmable microcalculators: Calculation of response from current values of action 22 p3767 N85-33348

Substructure coupling in the frequency domain [NASA-CR-176140] 22 p3800 N85-33543

Characterizations of generalized hyperexponential distributions [AD-A155855] 24 p4142 N85-35680

LARGE SCALE INTEGRATION

Problems in CEMA microelectronic cooperation noted 03 p0341 N85-12196

Functional checking of microprocessors and microprocessor systems 03 p0347 N85-12236

USSR report: Electronics and electrical engineering [JPRS-UEE-84-010] 04 p0485 N85-13095

Practical application of electron beam testing in LSI and VLSI circuits [BMFT-FB-T-84-185] 05 p0633 N85-14061

Fast algorithms and specialized architectures 05 p0714 N85-14579

Electrooptical sensor for automatic detection of objects 06 p0789 N85-15040

Compository speech output (KOSA) with a very large scale integration speech synthesis chip [FI-13-TBR-18] 07 p0942 N85-15974

Development of a 2 micrometer silicon-gate-CMOS-technology for microcomputer oriented VLSI circuits with a supply voltage range between 1.5 and 5 V [BMFT-FB-T-84-203] 07 p0949 N85-16012

Trends in development of software for computer-aided analysis of large-scale integrated circuits 07 p0955 N85-16055

High quality super-large circuits developed 11 p1622 N85-20209

Method of examining microcircuit patterns [NASA-CASE-NPO-16299-1] 11 p1626 N85-20250

Parallel test method for LSI (Large Scale Integration) microprocessors [AD-A150237] 13 p2144 N85-23310

Computer-aided identification of complete constitution model of transistor structure for design of subnanosecond large-scale-integrated circuits 15 p2529 N85-25594

Recent developments 15 p2533 N85-25628

Research in the design of high-performance reconfigurable systems [NASA-CR-175705] 15 p2621 N85-26153

The impact of VLSI on guidance and control system design 16 p2697 N85-26654

Bond test data acquisition and analysis system [DE85-007021] 16 p2780 N85-27158

Efficient VLSI (Very Large Scale Integration) fault simulation [AD-A152661] 17 p2953 N85-28233

High temperature position sensors based on monolithic GaAs Hall IC [BMFT-FB-T-84-266] 17 p2969 N85-28337

Parallel simulation of digital LSI circuits [AD-A154745] 21 p3580 N85-322

Modeling of electronic circuits with high degree of component integration 22 p3786 N85-334

Algorithms and organization of software for computer-aided circuit design 22 p3767 N85-334

Computer simulation of integrated injection logic 22 p3767 N85-334

Synthesis of metrico-topological model for layout of topology of large-scale-integration arrays 22 p3781 N85-334

Laser and electron beam processing of semiconductors [AD-A155914] 24 p4181 N85-357

LARGE SPACE STRUCTURES

Shear deformation plate continua of large double-layered space structures 01 p0059 N85-100

IAC user manual [NASA-CR-175300] 01 p0102 N85-108

Conceptual design and evaluation of selected Space Station concepts: Executive summary [NASA-TM-87382] 02 p0167 N85-111

Conceptual design and evaluation of selected Space Station concepts, volume 1 [NASA-TM-87383] 02 p0168 N85-111

Effects of member imperfections on the behavior of space trusses 02 p0207 N85-113

Qualitative results for distributed systems with discrete damping and stiffness with application to control [AD-A145525] 02 p0209 N85-113

Definition of technology development missions for early space stations: Large space structures [NASA-CR-171209] 03 p0323 N85-120

Definition of technology development missions for early Space Station satellite servicing. Volume 1: Executive summary [NASA-CR-171228] 04 p0460 N85-125

Definition of technology development missions for early Space Station satellite servicing. Volume 2: Technical [NASA-CR-171229] 04 p0461 N85-126

Conceptual design for scaled truss antenna flight experiment [NASA-TM-85804] 04 p0462 N85-126

Experiments in control of flexible structures with uncertain parameters 05 p0602 N85-138

Definition of ground test for verification of large space structure control [NASA-CR-171208] 05 p0602 N85-138

Level of effort 05 p0602 N85-138

Oral presentation of first year final report, appendix A 05 p0602 N85-138

Simplified planar model of ground test verification structure, appendix B 05 p0603 N85-138

Speed test results and hardware/software study of computational speed problem, appendix D 05 p0603 N85-138

Section 1. Method of determining mode shapes and natural frequencies of the NASA unmodified test structure. Section 2. Continuous beam closed from solution to the NASA-LSS astromast torsional vibration, appendix E 05 p0603 N85-138

Definition of ground test for Large Space Structure (LSS) control verification, appendix G 05 p0603 N85-138

Review of technical papers, appendix H 05 p0603 N85-138

Ground test experiment for large space structures, appendix I 05 p0603 N85-138

Environmental interactions working group report 05 p0611 N85-139

Disturbance propagation in structural networks; control of large space structures 06 p0759 N85-148

Broadening the debate 07 p0914 N85-157

Toward a goal-oriented civilian space program 07 p0914 N85-157

Results of principal NASA studies on space station uses and functional requirements 07 p0914 N85-157

Space Station truss structures and construc considerations [NASA-TM-86336] 07 p0916 N85-157

Capillary Pump Loop (CPL) heat pipe developm status report [NASA-CR-175273] 08 p1161 N85-173

The Shock and Vibration Digest, volume 16, no. [AD-A148466] 08 p1171 N85-173

Research and technology highlights of the Lew Research Center [NASA-TM-86899] 08 p1261 N85-178

Modelling and identification of the structural propert of an astromast [CRC-1374] 09 p1329 N85-183

NASA-VCOSS dynamic test facility [NASA-TM-86491] 10 p1427 N85-18

Operational fitness of box truss antennas in response to dynamic slewing
[NASA-CR-172470] 10 p1429 N85-19012

Ground test experiment for large space structures
[NASA-TM-86489] 10 p1429 N85-19013

Active control of large space structures: An introduction and overview
[NASA-TM-86490] 10 p1429 N85-19014

Swing-arm beam erector (SABER) concept for single astronaut assembly of space structure
[NASA-TP-2379] 10 p1429 N85-19015

Develop and demonstrate manufacturing processes for fabricating graphite filament reinforced polymide (Gr/PI) composite structural elements
[NASA-CR-172497] 11 p1592 N85-20019

Compensator development and examination of performance and robustness
[NASA-CR-175470] 11 p1627 N85-20244

Modal control of structural systems
[AD-A149734] 12 p1790 N85-21235

NASA/MSFC ground experiment for large space structure control verification
[NASA-TM-86496] 12 p1792 N85-21248

Definition of ground test for Large Space Structure (LSS) control verification
[NASA-TM-86495] 12 p1792 N85-21249

Space Station
[NASA-EP-211] 12 p1793 N85-21251

ACOSS 17 (Active Control of Space Structures)
[AD-A150007] 12 p1793 N85-21253

Structural sensitivity analysis: Methods, applications and needs
[NASA-TM-85827] 12 p1865 N85-21695

Variable geometry truss concept
[REPT-614] 12 p1865 N85-21697

Report on final recommendations for IMPS engineering-science payload
[NASA-CR-175659] 13 p1988 N85-22464

Spacecraft environmental interactions: A joint Air Force and NASA research and technology program
13 p1997 N85-22517

Interactions measurement payload for Shuttle
13 p1997 N85-22518

A quantitative comparison of active and passive damping for large space structures
[UTIAS-TN-249] 13 p1998 N85-22524

Approximation in optimal control and identification of large space structures
[AD-A150323] 13 p2151 N85-23351

Large Space Antenna Systems Technology, 1984
[NASA-CP-2368-PT-1] 14 p2229 N85-23813

NASA mobile satellite program
14 p2229 N85-23814

Alternatives for satellite sound broadcast systems at HF and VHF 14 p2229 N85-23815

Development concerns for satellite-based air traffic control surveillance systems 14 p2230 N85-23816

Application of pushbroom altimetry from space using large space antennas 14 p2230 N85-23817

Orbiting multi-beam microwave radiometer for soil moisture remote sensing 14 p2230 N85-23818

Low-frequency microwave radiometer for N-ROSS
14 p2230 N85-23819

Large space antenna technology applied to radar-imaging, rain-rate measurements, and ocean wind sensing 14 p2230 N85-23820

Advanced 2-frequency ocean sensing radar using high resolution antenna beams 14 p2230 N85-23821

LDR system concepts and technology
14 p2231 N85-23823

WRAP-RIB antenna technology development
14 p2231 N85-23824

Development of the 15-meter hoop-column antenna system 14 p2231 N85-23825

Box truss development and its application
14 p2231 N85-23826

Synchronously deployable tetrahedral truss reflector
14 p2231 N85-23827

Antenna Technology for QUASAT application --- radio antenna for very long base interferometry missions
14 p2231 N85-23828

Extreme precision antenna reflector study results
14 p2232 N85-23830

NASA space materials research
14 p2232 N85-23831

New concepts in deployable beam structures
14 p2232 N85-23832

Precision space structures 14 p2232 N85-23833

Precision antenna reflector structures
14 p2232 N85-23834

Space Station structures 14 p2232 N85-23835

Verification for large space structures
14 p2232 N85-23836

An optimization study to minimize surface distortions of a hoop-column antenna 14 p2232 N85-23837

Structural dynamics analysis 14 p2233 N85-23838

AFWAL space control technology program
14 p2233 N85-23839

Large Space Antenna Systems Technology, 1984
[NASA-CP-2368-PT-2] 14 p2233 N85-23840

On-orbit systems identification of flexible spacecraft Technol., 1984, Pt. 2 p 465-481
14 p2233 N85-23841

An eigensystem realization algorithm for application to modal testing 14 p2233 N85-23842

MSFC data analysis of the SAFE/DAE experiment
14 p2233 N85-23843

Langley Research Center photogrammetric measurements of solar array dynamics: Preliminary results 14 p2233 N85-23844

Experimental development of a failure detection scheme for large space structures 14 p2234 N85-23846

Dynamic verification of large space structures
14 p2234 N85-23847

Passive and Active Control of Space Structures (PACOSS) 14 p2234 N85-23848

Application of the maximum entropy/optimal projection control design approach for large space structures
14 p2234 N85-23849

Electromagnetic analysis for surface tolerance effects on large space antennas 14 p2234 N85-23850

Application of modern Aperture Integration (AI) and Geometrical Theory of Diffraction (GTD) techniques for analysis of large reflector antennas
14 p2234 N85-23851

Feed system design considerations for large space antenna systems. Part 1: Multiple apertures with non-overlapping feeds 14 p2234 N85-23852

Feed system design considerations for large space antenna systems. Part 2: Single aperture with overlapping feeds 14 p2235 N85-23853

Diffraction analysis of mesh deployable reflector antennas 14 p2235 N85-23854

The space station as a construction base for large space structures 14 p2235 N85-23856

Large Deployable Reflector (LDR) requirements for space station accommodations
14 p2236 N85-23858

Space-based antenna measurement system concepts for space station operation 14 p2236 N85-23860

Solar Array Experiment (SAE) flight experience
14 p2236 N85-23861

Assembly Concept for Construction of Erectible Space Structure (ACCESS) neutral buoyancy testing results
14 p2236 N85-23862

Space Technology Experiments Platform (STEP) status: An in-space test facility 14 p2236 N85-23863

Control Of Flexible Structures (COFS) flight experiment background and description 14 p2236 N85-23864

Shuttle attached antenna Flight Experiment Definition Study (FEDS) 14 p2237 N85-23865

Electro-science requirements for shuttle-attached antenna flight experiments 14 p2237 N85-23866

Model and controller reduction of uncertain systems using covariance equivalent realizations
14 p2243 N85-23902

ACOSS 11 (Active Control Of Space Structures)
[AD-A150639] 14 p2246 N85-23922

Adaptive techniques for control of large space structures
[AD-A150957] 14 p2246 N85-23923

Technology for large space systems: A bibliography with indexes, supplement 11
[NASA-SP-7046(11)] 15 p2475 N85-25277

Definition of technology development missions for early space stations: Large space structures
[NASA-CR-171446] 15 p2476 N85-25281

Construction in space 15 p2484 N85-25328

Construction in space
[NASA-TM-77630] 15 p2492 N85-25374

Definition of ground test for verification of large space structure control
[NASA-CR-171438] 15 p2492 N85-25377

Structures and Dynamics Division research and technology plans for FY 1985 and accomplishments for FY 1984
[NASA-TM-86417] 15 p2577 N85-25895

Model reduction techniques applied to the control of large space structures
[AD-A151784] 16 p2731 N85-26857

The effect of inaccuracies in structural models on the control of large space structures
[AD-A151794] 16 p2732 N85-26858

Incorporating control into the optimal structural design of large flexible space structures
[AD-A152858] 17 p2909 N85-27937

Mathematical modeling and control of a large space structure as applied to a shuttle-antenna configuration
[AD-A153269] 17 p2910 N85-27939

The Shock and Vibration Digest, volume 17, no. 1
[AD-A151051] 17 p2977 N85-28397

On the accuracy of modelling the dynamics of large space structures 19 p3225 N85-29995

The dynamics and control of large flexible space structures, 8
[NASA-CR-175986] 19 p3225 N85-29996

The effect of sensor and actuator errors on static shape control for large space structures
[NASA-TM-86446] 19 p3225 N85-29998

Submillimeter local oscillators for spaceborne heterodyne applications
[NASA-RP-1147] 19 p3226 N85-30005

Self-locking mechanical center joint
[NASA-CASE-LAR-12864-1] 19 p3279 N85-30336

Control system design for lightly coupled large space structures 20 p3399 N85-31086

AFWAL control technology programs
20 p3408 N85-31150

Dynamic performance of several large antenna concepts 20 p3409 N85-31155

Control of large antennas based on electromagnetic performance criteria 20 p3409 N85-31158

Vibration control experiment design for the 15-m hoop/column antenna 20 p3409 N85-31159

A hardware demonstration of distributed control for a flexible offset-feed antenna 20 p3410 N85-31160

Control of flexible structures 20 p3410 N85-31161

Space station configuration and flight dynamics identification 20 p3410 N85-31162

Large space structure flight experiment
20 p3410 N85-31163

Time-optimal bang-bang slew of rigidized SCOLE configuration 20 p3410 N85-31164

Experiments in structural dynamics and control using a grid 20 p3410 N85-31165

The experimental computer control of a two-dimensional hyperbolic system 20 p3411 N85-31166

Rationale for an experimental test for flexible space structure attitude control 20 p3411 N85-31167

Numerical and experimental evaluation for single-axis control of an LSS laboratory model
20 p3411 N85-31168

On the measurement of material damping in a simulated space environment 20 p3411 N85-31169

Proceedings of the Workshop on Identification and Control of Flexible Space Structures, volume 2
[NASA-CR-176052] 20 p3411 N85-31170

Some asymptotic problems in the optimal control of distributed systems 20 p3412 N85-31175

Approximation techniques for parameter estimation and feedback control for distributed models of large flexible structures 20 p3413 N85-31179

Space station parametric models
20 p3413 N85-31180

An integrated control and minimum mass structural optimization algorithm for large space structures
20 p3413 N85-31183

ISAAC (Integrated Structural Analysis and Control) via continuum modeling and distributed frequency domain design techniques 20 p3414 N85-31185

Vibrational stabilization of flexible structures
20 p3414 N85-31188

Stiffness control of large space structures
20 p3414 N85-31189

Sub-optimal control of nonlinear flexible space structures 20 p3414 N85-31190

An overview of latest model reduction and control methods of large flexible space structures
20 p3414 N85-31191

Frequency domain control design of large space structures: A practical approach
20 p3415 N85-31192

A control concept for large flexible spacecraft using order reduction techniques 20 p3415 N85-31193

Proceedings of the Workshop on Identification and Control of Flexible Space Structures, volume 3
[NASA-CR-176053] 20 p3415 N85-31195

Robust control design for large space structures
20 p3416 N85-31200

On the stability of collocated controllers in the presence or uncertain nonlinearities and other perils
20 p3416 N85-31201

Adaptive filtering for large space structures: A closed-form solution 20 p3417 N85-31206

Experimental verification of identification algorithms for control of flexible structures 20 p3418 N85-31211

NASA space station automation: AI-based technology review
[NASA-CR-176094] 21 p3558 N85-32134

NASA space station automation: AI-based technology review. Executive summary
[NASA-CR-176096] 21 p3558 N85-32135

Space station automation study: Autonomous systems and assembly, volume 2
[NASA-CR-176092] 22 p3739 N85-33175

Research and development activities in unified control-structure modeling and design
[NASA-CR-176129] 22 p3740 N85-33179
Research and development activities in unified control-structure modeling and design
[NASA-CR-176111] 22 p3740 N85-33180
Space station rotational equations of motion
[NASA-TP-2511] 23 p3899 N85-34148
Space Station Engineering and Technology Development: Proceedings of the Panel on In-Space Engineering Research and Technology Development
[NASA-CR-176110] 23 p3899 N85-34153
Box truss analysis and technology development. Task 1: Mesh analysis and control
[NASA-CR-172570] 23 p3900 N85-34156
Technology for large space systems: A bibliography with indexes
[NASA-SP-7046(12)] 24 p4066 N85-35209
Identification and control of structures in space
[NASA-CR-176175] 24 p4069 N85-35214
Structural analysis of imperfect three-legged truss columns for large space structures applications
24 p4100 N85-35416

LARGE SPACE TELESCOPE
U HUBBLE SPACE TELESCOPE

LARMOR RADIUS
Theoretical studies of Field-Reversed Configurations (FRC) and experimental study of the FRC during translation
[DE84-016467] 04 p0586 N85-13603
Finite orbit analysis for long wavelength modes in a plasma with a hot component
[DE85-006896] 15 p2658 N85-26404
Stability of high energy particle plasmas to MHD-like modes
[DE85-007879] 17 p3039 N85-28803

LARVAE
The development of the vestibular apparatus under conditions of weightlessness
[NASA-TM-77517] 07 p1011 N85-16422
Chemical composition of Musca domestica L. larval and pupal biomass when developing in organic waste of biological life-support system for man
22 p3824 N85-33691

LARYNX
Metallic aid and technique in fitting voice prosthesis
[AD-D011356] 07 p1014 N85-16442

LASER ANEMOMETERS
Performance evaluation and estimation of a laser time-of-flight velocimeter 03 p0363 N85-12326
Comparative review of laser Doppler and laser two-focus anemometry in turbomachinery applications
[VKI-TM-34] 03 p0367 N85-12350
Computation of noise radiation from a free jet perpendicular to its axis via laser anemometry measurements
[ESA-TT-870] 09 p1379 N85-18669
Determination of the drag of free flying particles in supersonic flow with a pulsed laser
12 p1773 N85-21129
Development of miniature laser Doppler anemometers
[KU-SFB-210/ET/3] 12 p1857 N85-21648
The significance for laser anemometry of particles carried along in a gas flow
[ISL-CO-205/83] 14 p2301 N85-24251
Application of laser anemometry to jets in combustion chambers
[ISL-CO-210/83] 14 p2302 N85-24253
Laser anemometry two dimensional measurement of velocity fluctuations in an excited jet
[ISL-CO-213/83] 14 p2302 N85-24254
Measurements in the flow field of a cylinder with a laser transit anemometer and a drag rake in the Langley 0.3 m transonic cryogenic tunnel
[NASA-TM-86380] 14 p2305 N85-24270
Feasibility study on Laser Doppler Anemometer (LDA) wind velocity measurements using pulsed visible laser light
[ISL-CO-224/83] 16 p2836 N85-27489
An automatic traversing system for Laser Doppler Anemometer (LDA) applications to wind tunnels and to free jets
[ISL-CO-225/83] 16 p2836 N85-27490
Feasibility of mapping velocity flow fields in SSME powerhead by laser anemometry techniques
17 p2915 N85-27971
LDA study of the unburned gas motion induced by nonsteady flame propagation in a constant volume duct
[DE85-009936] 19 p3270 N85-30277
Filter induced errors in laser anemometer measurements using counter processors
[NASA-TM-87047] 19 p3272 N85-30288
The application of laser anemometry to the study of transonic shock boundary-layer interactions
[ISL-CO-204/84] 20 p3396 N85-31067

LASER ANNEALING
Time resolved calorimetry of 30 nm Te-films during laser annealing
[AD-A145047] 01 p0052 N85-10346
Mechanisms of laser annealing of semiconductors
02 p0267 N85-11744
Nonthermal mechanism for laser annealing of semiconductors and formation of super structure
04 p0487 N85-13109
Laser annealing of ion implanted semiconductors
[AD-A146979] 07 p1047 N85-16652
Residual stress after laser processing
11 p1600 N85-20065
Excimer laser annealing to fabricate low cost solar cells
[NASA-CR-174394] 11 p1673 N85-20538
In-orbit laser regeneration of the radiation damaged solar arrays 13 p2008 N85-22588
Thermodynamic and kinetic studies of pulsed laser annealing from transient conductivity measurements
[DE85-003677] 13 p2096 N85-23076
Activation of Si-N modes in silicon by pulsed laser annealing
[DE85-003988] 13 p2097 N85-23082
Specifications of new industrial lasers reviewed
14 p2284 N85-24150
Laser annealing of ion implanted HgCdTe
[AD-A150675] 14 p2427 N85-24966
Excimer laser annealing for fabrication of low-cost solar cells 21 p3611 N85-32433

LASER APPLICATIONS
NT LASER CUTTING
NT LASER FUSION
Flight demonstration of new NRL real-time data acquisition system and laser video waveform sampler
[AD-A145126] 01 p0053 N85-10350
Optical seam tracking of robotic arc welding
[VTT-272] 01 p0055 N85-10368
Achievements in laser development
01 p0115 N85-10784
Investigation of the application of the marginal tension technique to test electronic devices, phase 3
[ESD-11-301] 02 p0206 N85-11360
Dual (GaAl) As-heterostructure based injection laser traveling wave amplifier 02 p0261 N85-11706
Optical recording of information on paper by CO2 and YAG-lasers 02 p0261 N85-11710
Narrowband tunable dye laser with amplifier pumped by powerful nitrogen laser 02 p0262 N85-11716
Laser source of neutral atoms for collective-field particle accelerator 02 p0263 N85-11719
USSR report: Physics and mathematics
[JPRS-UPM-84-004] 02 p0266 N85-11737
Injection lasers based on AlGaAsSb/GaSb and InGaAsSb/GaSb heterostructures
02 p0270 N85-11761
Laser on copper and gold vapors with space diversity media 02 p0270 N85-11762
ONR (Office of Naval Research) Far east Scientific Bulletin, Volume 9, Number 2, April - June 1984
[AD-A145661] 02 p0305 N85-11974
Laser paint removal
[AD-P004009] 03 p0308 N85-11989
Potential application of robotics and state-of-the art end effectors at Letterkenny Army Depot
[AD-P004015] 03 p0309 N85-11994
Optical detection of alkali compounds
[DE84-015505] 03 p0326 N85-12117
Laser and diffusion welding equipment R and D
03 p0352 N85-12265
Laser balancing system for high material removal rates
[NASA-CR-174731] 03 p0365 N85-12341
Three-dimensional photochemical machining with lasers
[AD-A145792] 03 p0365 N85-12342
Bibliography of Soviet laser developments, number 65, May - June 1983
[AD-A146189] 03 p0366 N85-12347
Mapping of mammalian arrhythmias with the cardiac laser scanner 03 p0399 N85-12545
Deceleration, cooling, and trapping of atoms
[AD-A146234] 03 p0418 N85-12672
Formation of superconductive Al(GeSi) alloys by low temperature laser quenching methods
[DE84-016667] 04 p0474 N85-13021
Laser-driven particle accelerators
[DE84-015953] 04 p0506 N85-13227
Laser for determining the ignition conditions of a pyrotechnic mixture
[FOA-C-20542-D1] 04 p0506 N85-13230
Ion beam and laser induced surface modifications
[DE84-016569] 04 p0571 N85-13642
Fundamental equations of the LIF hydroxyl measurements, appendix A 05 p0676 N85-14336
Saturation phenomena in LIF measurements, appendix B 05 p0676 N85-14
Detailed performance calculations: Wayne State University and Ford Motor Company, appendix C
05 p0676 N85-14
Detailed performance calculations: Georgia Institute of Technology Group, appendix E
05 p0676 N85-14
Detailed performance calculations: Portland State Group, appendix F 05 p0676 N85-14
Detailed performance calculations: Harvard Group, appendix G 05 p0676 N85-14
Overview of recent advances in laser applications
05 p0725 N85-14
Formation of reference signals in laser-type gas analyzers with mechanical switching of optical channels
06 p0787 N85-15
Development of a van-portable remote-sensing laser system for selective detection of natural gas leaks
[PB85-101939/GAR] 06 p0811 N85-15
Pulsed electric discharge laser technology. Electron beam window foil material
[AD-A146420] 06 p0813 N85-15
Laser-assisted solar-cell metallization processing
06 p0831 N85-15
Sputtering in thin film technology for optics – laser systems 07 p0868 N85-16
Spacecraft system study: A study to define the impact of laser communication systems on their host spacecraft
[NASA-CR-175272] 07 p0870 N85-16
Noncontact photo-thermal probe-beam deflection measurement of thermal diffusivity in an confined la gas
[AD-A147481] 07 p0971 N85-161
Laser ignition of explosives
[FOA-C-20550-D1] 07 p0972 N85-161
USSR report: Life sciences. Biomedical and behavioral sciences
[JPRS-UBB-84-015] 07 p1010 N85-164
Ion implantation and laser processing of III-V compound semiconductors with applications to the fabrication of microwave devices
[AD-A146846] 07 p1047 N85-166
Laser annealing of ion implanted semiconductors
[AD-A146979] 07 p1047 N85-166
Research and technology, 1984 report
[NASA-TM-83096] 07 p1061 N85-167
Phase-dissipative mechanisms for laser-induced surface desorption-dissociation processes
[AD-A147961] 08 p1121 N85-170
Theoretical and experimental analyses of laser altimeters for barometric measurements over the ocean
08 p1165 N85-173
NASA three-laser airborne differential absorption lidar system electronics
[NASA-CR-174293] 08 p1166 N85-173
The use of lasers in wide-angle visual systems
[AD-P004322] 09 p1269 N85-178
Simulation of repetitively-pulsed laser irradiation of graphite-epoxy composite
[AD-A146696] 09 p1325 N85-182
Feasibility of alpha particle measurement by CO2 laser Thomson scattering
[DE85-001764] 09 p1326 N85-182
USSR report: Life sciences. Biomedical and behavioral sciences
[JPRS-UBB-85-002] 09 p1360 N85-185
Effects of dc electric fields on multiphoton ionization spectra in cesium
[DE85-001542] 09 p1381 N85-186
Recent ICF research by GEKKO 12 glass laser at ILE Osaka 09 p1387 N85-187
Capabilities of laser diagnostics for combustion and flow fields
[DE85-002661] 10 p1438 N85-18
Temperature variation of laser mirror stability criteria
10 p1445 N85-191
Excitation modes and parameters of stress waves in metal exposed to single laser pulses
10 p1446 N85-19
Study of submicron particle size distributions by laser Doppler measurement of Brownian motion
[AD-A149139] 10 p1487 N85-19
Bibliography of Soviet laser developments, Number 66, July-August 1983
[AD-A149113] 10 p1490 N85-19
Laser program annual report 1983
[DE84-017287] 10 p1490 N85-194
Laser air pollution monitoring system planned for Moscow 10 p1500 N85-194
Pulsed excimer laser processing for cost-effective solar cells
[NASA-CR-174429] 10 p1509 N85-195
Pulsed excimer laser processing for cost-effective solar cells
[NASA-CR-175465] 10 p1509 N85-19

Study of microstructure of aluminum and copper alloys after processing with continuous CO2 laser beam
11 p1601 N85-20066
Laser processing of ceramics
[DE85-001184] 11 p1612 N85-20135
Functional system theory in practice
11 p1660 N85-20629
Laser studies of chemical dynamics at the gas-solid interface
[DE84-017580] 11 p1736 N85-20920
Novel photo-thermal technique for flow and spectroscopic measurements in a dense aerosol stream
[AD-A149746] 12 p1800 N85-21287
Two-dimensional measurements of OH concentration and temperature in reactive flows
[AD-A149849] 12 p1800 N85-21292
Portable remote laser sensor for methane leak detection
[NASA-CASE-NPO-15790-1] 12 p1855 N85-21631
Laser clock
[AD-D011513] 12 p1855 N85-21634
Method of and apparatus for measuring temperature and pressure — atmospheric sounding
[NASA-CASE-GSC-12558-1] 12 p1856 N85-21639
Solid propellant combustion diagnostics and automated data retrieval from holograms 13 p1996 N85-22527
A 2 x 6 Back Surface Reflection (BSR) silicon solar cell 13 p2005 N85-22570
Effect of transparent coatings on generation of laser-induced shock waves in metals
13 p2026 N85-22711
China report: Science and technology
[JPRS-CST-85-005] 13 p2052 N85-22843
Laser applications in last 10 years reviewed
13 p2052 N85-22844
Status of and outlook for producing means of transmitting units of plane angle, angular velocity and acceleration with ring lasers 13 p2074 N85-22955
Digital laser platemaker modifications
[AD-A150180] 13 p2096 N85-23074
Computer simulations of rare earth sites in glass: Experimental tests and applications to laser materials
[DE85-008158] 14 p2261 N85-24013
Laser beam shaping system with reduced objective diameter 14 p2275 N85-24095
Sphericity gauge for wavefront of laser radiation
14 p2275 N85-24096
USSR report: Machine tools and metalworking equipment
[JPRS-UMM-85-006] 14 p2283 N85-24146
Specifications of new industrial lasers reviewed
14 p2284 N85-24150
Advanced diagnostics for reacting flows
[AD-A150675] 14 p2301 N85-24246
Applications of lasers in manufacturing
14 p2306 N85-24279
Laser surface treatments 14 p2306 N85-24284
Laser welding in the manufacture of heart pacemakers
14 p2306 N85-24286
Future trends in the use of lasers in manufacturing
14 p2309 N85-24291
Ground-up-to-Space (GUTS) laser propagation code description and manual
[AD-A150783] 14 p2309 N85-24295
Lasers in the domains of ultrashort-time phenomena physics and ballistics
[ISL-CO-236/83] 14 p2310 N85-24299
Laser-assisted solar cell metallization processing
[NASA-CR-175586] 14 p2350 N85-24526
Polar motions measurement study
[AD-A150880] 14 p2372 N85-24664
Producible alternative to CdTe for epitaxy (PACE-2) of LWIR (Long Wave Infrared) HgCdTe
[AD-A150678] 14 p2426 N85-24964
Swedish equipment for automatic docking in space
15 p2480 N85-25363
Optimization of the catalytic oxidation of CO for closed-cycle CO2 laser applications
[NASA-TM-86421] 15 p2504 N85-25445
Corrosion behavior of Al4 aluminum alloy hardened by CO2 laser radiation 15 p2514 N85-25512
An experimental technique for the study of velocity profiles in a laminar jet using a pulsed nitrogen laser
[AD-A151486] 15 p2556 N85-25771
Experimental and theoretical studies of laser cooling and emittance control of neutral beams
[AD-A149215] 15 p2562 N85-25804
Bibliography of Soviet Laser Developments, Number 67, September-October 1983
[AD-A151199] 15 p2562 N85-25805
A plasma initiation-flow chamber to study CW laser beamed energy absorption in light gases
[AD-A151225] 15 p2562 N85-25806
Superfine laser position control using statistically enhanced resolution in real time
[DE85-005643] 15 p2564 N85-25817
Laser-based non-destructive testing techniques for the ultrasonic characterization of sub-surface flaws
[AERE-R-11562] 15 p2572 N85-25856
Dynamics of recrystallization and redistribution of impurities in semiconductors subjected to millisecond laser pulses 15 p2643 N85-26302
Submillimeter-band solid state distributed feedback laser 15 p2644 N85-26307
Industrial laser use expanding in the USSR
15 p2644 N85-26310
Academician Zuyev notes plans for lasers on spacecraft for atmospheric research 16 p2717 N85-26775
Application of space methods in geodesy
16 p2724 N85-26817
Impact of optical inhomogeneity in sintered interface between glasses on laser emission characteristics
16 p2763 N85-27053
USSR report: Machine tools and metalworking equipment
[JPRS-UMM-84-010] 16 p2767 N85-27071
Development, implementation of industrial lasers reviewed 16 p2767 N85-27075
Uses of laser technology described
16 p2768 N85-27080
The utilization of optical fibers in holography
[ISL-R-102/83] 16 p2787 N85-27196
Spectroscopic investigation of materials for frequency agile laser systems
[AD-A151731] 16 p2790 N85-27206
Two-dimensional beat wave acceleration simulation
[DE85-005861] 16 p2791 N85-27214
The copper vapor laser 16 p2824 N85-27417
Research and development of new instruments
16 p2824 N85-27418
Feasibility study on Laser Doppler Anemometer (LDA) wind velocity measurements using pulsed visible laser light
[ISL-CO-224/83] 16 p2836 N85-27489
The development of laser analytical methods for the characterization of solid-liquid and solid-high pressure gas interfaces
[AD-A152382] 17 p2918 N85-27988
Measurement of Franck-Condon factors for the v'=0 progression in the B-X system of PO
[AD-A152734] 17 p2919 N85-27993
X-ray crystallography of steel U8 after pulsed laser hardening
[BLL-BISI-22444-(9022.06)] 17 p2925 N85-28036
Technological apparatus for laser treatment of materials 17 p2944 N85-28174
International time transfer and portable clock evaluation using GPS timing receivers: Preliminary results
17 p2964 N85-28303
Timing of spacecraft data: Time accuracy requirements and timing facilities of the European Space Agency (ESA) 17 p2964 N85-28307
Laser measurements of distances from the ORELA neutron target to experiment stations along flight paths 1 and 6
[DE85-009457] 17 p2971 N85-28352
Presentations at the Tri-Service Cloud Modeling Workshop (2nd), held at the Naval Surface Weapons Center, White Oak, Maryland, 26-27 June 1984, volume 1
[AD-A152735] 17 p2996 N85-28522
Optical system for measuring shadowgraph data
[AD-D011642] 17 p3036 N85-28784
Recent advances in optical measurement methods in physics and chemistry
[DE85-008685] 17 p3037 N85-28792
Philips researches gallium arsenide use for lasers
18 p3087 N85-29106
Laser machining and some applications
[NHK-LABS-NOTE-307] 18 p3112 N85-29266
The application of laser resonance saturation to the development of efficient short wavelength lasers
[AD-A153851] 18 p3113 N85-29270
Definition of requirements for injection locking of pulsed UV lasers
[DE85-010126] 18 p3113 N85-29275
Institute works on modeling thermonuclear plasma processes 19 p3296 N85-30435
Specifics of laser sounding of atmosphere along horizontal and slightly slanting paths over water surface
19 p3297 N85-30441
Development of a technique for in situ detection of stratospheric nitrogen dioxide 19 p3312 N85-30534
EDS operator and control software
[DE85-010470] 19 p3340 N85-30698
Attenuated total reflection method for obtaining optical constants of powders
[AD-A154094] 19 p3367 N85-30881
Laser Schlieren crystal monitor
[NASA-CASE-MFS-26060-1] 19 p3374 N85-30932
Technical and historical overview of the study at Lawrence of porous antireflection coatings
[DE85-010925] 20 p3434 N85-31302
Velocity visualization in gaseous flows
[NASA-CR-174954] 20 p3453 N85-31445
Experimental study of laser produced ions for collective ion acceleration 20 p3460 N85-31494
Improved turbopump dynamics
[NASA-TM-86514] 20 p3462 N85-31509
Ocean tidal parameters from LAGEOS
20 p3493 N85-31716
Electronics Division research and development
[DE85-011887] 20 p3540 N85-32032
East Europe report: Science and technology
[JPRS-ESA-85-023] 21 p3572 N85-32217
Three-dimensional photochemical machining with lasers
[AD-A154711] 21 p3591 N85-32320
Laser-assisted solar-cell metallization processing
21 p3610 N85-32429
Tunable lasers with high conversion efficiency
21 p3687 N85-32906
The sound field of a moving laser-induced acoustic array (theory)
[AD-A154553] 21 p3699 N85-32961
Raman scattering studies in solids
[AD-A155528] 21 p3710 N85-33032
Cryogenic laser calorimetry for impurity analysis
[NASA-CR-176102] 22 p3743 N85-33201
Jet flows: Modelling and experiments
22 p3744 N85-33208
Simultaneous measurement of velocity and density in a turbulent nonpremixed flame 22 p3744 N85-33209
Laser sealed evacuated window glazings
[DE85-000512] 22 p3754 N85-33273
Transparent electrode for optical switch
[DE85-011616] 22 p3761 N85-33310
Electro-optic harmonic conversion to switch a laser beam out of a cavity
[DE85-011619] 22 p3790 N85-33483
Laser effects on opaque targets. Part 2C: Thermal effects of a time-variable beam intensity
[ISL-R-105/84-PT-2C] 22 p3791 N85-33486
Hole cutting in building frames by laser
[FOA-C-20569-D9] 22 p3791 N85-33487
Laser-assisted solar cell metallization processing
[NASA-CR-176124] 22 p3805 N85-33565
Flat-plate solar array project process development area process research of non-CZ silicon material
[NASA-CR-176117] 23 p3945 N85-34445
Observation of mode-converted by ion Bernstein wave by an HCN laser scattering
[IPPJ-724] 23 p3979 N85-34668

LASER BEAM DEFOCUSING
U THERMAL BLOOMING

LASER CAVITIES
Frequency stabilized laser
[AD-D011223] 01 p0053 N85-10351
External cavity diode laser sensor
[AD-D011341] 07 p0969 N85-16152
Halogen mass flow rate detection system
[AD-D011398] 08 p1166 N85-17352
Axial flow laser cavity
[AD-D011506] 12 p1855 N85-21633
Mode control and wavelength tuning in open ended Michelson interferometric semiconductor laser
13 p2095 N85-23073
Scaling blackbody laser to high powers
[NASA-TM-86395] 14 p2309 N85-24292
Internal step-up type higher harmonic light generating device
[DE85-007026] 16 p2790 N85-27213
Design and construction of a CW ND:YAG laser using a single elliptical cavity and water cooled krypton arc lamp pumping
[AD-A152857] 17 p2970 N85-28340
Spatial correlations in the decay from an unstable state in the Malthus Verhulst model — laser cavities
[NOTA-INTERNA-832] 18 p3114 N85-29280
Controlled-linewidth laser source
[AD-D011681] 19 p3274 N85-30306
Optically pumped laser system having extracavity pulse smoother
[AD-D011714] 19 p3276 N85-30319
Grazing incidence beam expander
[DE85-010784] 19 p3368 N85-30889
Generation of single nanosecond high-contrast radiation pules (lambda=10.6 micrometers)
21 p3684 N85-32886
Influence of mirror anisotropy and Brewster window orientation on radiation characteristics of ring lasers
21 p3684 N85-32889
Electro-optic harmonic conversion to switch a laser beam out of a cavity
[DE85-011619] 22 p3790 N85-33483

LASER COMMUNICATION
U OPTICAL COMMUNICATION
LASER CUTTING
Laser Welding, Cutting and Surface Treatment
14 p2308 N85-24278
An analysis of machine tool systems suitable for laser profiling
14 p2308 N85-24282
Laser cutting: A new tool for shipbuilding
14 p2308 N85-24285
Lasers in automobile production
14 p2309 N85-24288
Lasers in the nuclear industry
14 p2309 N85-24289
Laser drilling of aeroengine components
14 p2309 N85-24290
Europe's primary producers of industrial lasers surveyed
18 p3067 N85-29101
Robot, laser tridimensional cutting technology detailed
20 p3438 N85-31335
Applications of laser technology described
21 p3572 N85-32218
LASER DAMAGE
Electronics research at the University of Texas at Austin
[AD-A146900] 07 p0947 N85-15998
Laser rupture of composite materials
10 p1444 N85-19102
Laser Hazards Bibliography, October 1984
[AD-A149534] 10 p1490 N85-19408
Time resolved Raman studies of laser induced damage in TIO2 optical coatings
[DE85-003166] 11 p1640 N85-20332
A study of low-level laser retinal damage
[AD-A150046] 12 p1905 N85-21965
Time-resolved reflectivity measurement of extrinsic silicon during pulsed laser irradiation
[AD-A150350] 13 p2159 N85-23403
Laser induced damage of zinc sulphide
[BAE-BT-13363] 15 p2562 N85-25803
Raman studies of laser damaged single and multi-layer optical coatings
[DE85-009431] 17 p2971 N85-28351
Predamage threshold electron emission from insulator and semiconductor surfaces
[DE85-006968] 19 p3377 N85-30954
Theoretical modeling of laser induced optical degradation
[AD-A155302] 21 p3592 N85-32323
LASER DOPPLER VELOCIMETERS
The development of a diode laser Doppler velocimeter for boundary layer measurements under ice: A feasibility investigation
[AD-A145076] 01 p0053 N85-10348
Hot section laser anemometry
02 p0142 N85-10962
Laser velocimeter measurements and analysis in turbulent flows with combustion. Part 3: A correction lens for laser Doppler measurements in a cylindrical tube
[AD-A146206] 03 p0366 N85-12348
Comparative review of laser Doppler and laser two-focus anemometry in turbomachinery applications
[VKI-TM-34] 03 p0367 N85-12350
Laser anemometer study of separated flow on wing profiles
[ISL-CO-214/83] 04 p0453 N85-12672
An experimental investigation of two-dimensional thrust augmenting ejectors, part 2
[NASA-CR-174110] 04 p0456 N85-12695
Laser Doppler Anemometer (LDA) wind velocity measurements: Possibilities for measurements on windpower units 05 p0666 N85-14300
A scanning laser velocimeter for turbulence research
[NASA-CR-172493] 07 p0897 N85-15686
Combustion dynamics in rockets
[AD-A148478] 08 p1114 N85-17024
Flame propagation and stabilization studies using Rayleigh scattering and laser Doppler velocimetry
[AD-A148802] 09 p1290 N85-18102
The boundary layer on compressor cascade blades
[NASA-CR-174369] 09 p1319 N85-18292
Comparison of two-dimensional laser and hot-wire velocimetry for a supersonic turbulent boundary layer
11 p1576 N85-19927
Velocity and volumetric measurement in free jets
11 p1578 N85-19931
Laser Doppler Anemometry (LDA) signal triggering and effective particle size range
[KU-SFB-210/E/5] 11 p1634 N85-20290
Projection lens scanning laser velocimeter system
[NASA-CASE-ARC-11547-1] 11 p1638 N85-20320
Solid particle receiver experiments: Velocity measurements
[DE85-000257] 12 p1853 N85-21623
Development of miniature laser Doppler anemometers
[KU-SFB-210/ET/3] 12 p1857 N85-21648
Visualization of velocity fields with Doppler images
[ISL-CO-218/83] 14 p2302 N85-24256
Measurement of the expansion velocity of an aerosol cloud during pyrotechnical dispersion
[ISL-R-125/83] 14 p2303 N85-24262
Experimental and theoretical investigation of the motion of particles in a compressible vortex
[ISL-R-129/83] 14 p2303 N85-24264
Application possibilities of laser Doppler anemometry in the investigation of the transonic interaction between shock wave and boundary layer
[ISL-R-131/83] 14 p2304 N85-24265
Interferometric velocity measurements in ballistics
[ISL-CO-239/83] 14 p2306 N85-24276
La Recherche Aerospatiale Bimonthly Bulletin, Number 1984-4, 221/July-August
[ESA-TT-864] 16 p2695 N85-26637
The development of onboard laser velocimeter at the Saint Louis Institute (France) from 1976 to 1982
[ISL-NB-402/83] 16 p2791 N85-27216
Conducting a wind sensing study
[NASA-CR-175782] 16 p2832 N85-27465
An automatic traversing system for Laser Doppler Anemometer (LDA) applications to wind tunnels and to free jets
[ISL-CO-225/83] 16 p2836 N85-27490
Formulation of a coherent light-sheet by means of a cylindrical-spherical optical system
[ISL-R-116/83] 16 p2865 N85-27674
Incident beam polarization for laser Doppler velocimetry employing a sapphire cylindrical window
[NASA-TM-87064] 17 p3037 N85-28786
Vibration-free Raman Doppler velocimeter
[NASA-CASE-LAR-13268-1] 18 p3104 N85-29216
MHD channel development
[DE85-008305] 18 p3192 N85-29796
LDV multiplexer interface
[NASA-CASE-ARC-11536-1] 19 p3258 N85-30202
Recent measurements in turbulent jet flames at Sandia Combustion Research Facility 20 p3424 N85-31254
Velocity visualization in gaseous flows
[NASA-CR-174954] 20 p3453 N85-31445
Development of a new laser Doppler velocimeter for the Ames High Reynolds Channel No. 2
[NASA-TM-86772] 20 p3458 N85-31477
Laser Doppler Anemometer (LDA) measurements in the turbulent near-wake of blunt bodies
[ISL-CO-212/84] 22 p3785 N85-33450
Measurement of velocity and concentration in free jets
[ISL-CO-215/84] 22 p3785 N85-33451
Multiparameter conditionally sampled laser velocimetry measurements during flame propagation in a spark ignition engine
[DE85-009850] 22 p3793 N85-33502
A comparison of laser Doppler anemometry and probe measurements within the boundary layer of an airfoil at subsonic flow
[ISL-CO-219/84] 23 p3895 N85-34127
Study of boundary layer separation on a supercritical profile with a spoiler by means of a laser Doppler velocimeter
[ISL-CO-225/84] 23 p3895 N85-34128
Prediction of the flow-field interference induced by the long-range laser velocimeter in the Ames 40- by 80-foot and the 80- by 120-foot wind tunnels
[NASA-TM-86763] 23 p3898 N85-34146
Nonsimultaneous coupled laser velocimeter measurement technique: Error prediction for spatially noncoincident measurements
[NASA-TM-86718] 23 p3934 N85-34379
The use of a laser Doppler velocimeter in a standard flammability tube
[NASA-CR-174960] 24 p4096 N85-35389
LASER DRILLING
Laser applications in last 10 years reviewed
13 p2052 N85-22844
Specifications of new industrial lasers reviewed
14 p2284 N85-24150
Laser Welding, Cutting and Surface Treatment
14 p2308 N85-24278
Applications of lasers in manufacturing
14 p2308 N85-24279
Laser drilling of aeroengine components
14 p2309 N85-24290
LASER FUSION
Progress in inertial confinement fusion at Lawrence Livermore National Laboratory
[DE84-016227] 04 p0568 N85-13621
Quality assurance in the Antares Laser Fusion Construction Project
[DE84-015493] 05 p0640 N85-14104
Laser program annual report 1983
[DE84-017287] 10 p1490 N85-19412
Raman sidescattering in laser-produced plasmas
[AD-A148905] 10 p1556 N85-19813
Approaches to ultrafast neutron detectors
[DE85-001206] 11 p1636 N85-[illegible]
Modal testing and analysis of NOVA laser structures
[DE84-017569] 11 p1639 N85-[illegible]
Operational characteristics of the OMEGA short-wavelength laser fusion facility
[DE85-002819] 11 p1640 N85-[illegible]
Laser-induced fluorescence of metal-atom impurities in a neutral beam
[DE85-004980] 14 p2310 N85-[illegible]
Laboratory for laser energetics report
[DE85-007235] 15 p2583 N85-[illegible]
Design optimization of single-main-amplifier KrF laser-fusion systems
[DE85-007680] 16 p2791 N85-27215
Sub-nanosecond cinematography in laser fusion research: Current techniques and applications at the Lawrence Livermore Laboratory
[DE85-007252] 17 p2968 N85-[illegible]
Microwave experimental studies of laser fusion
[DE85-006327] 17 p3041 N85-[illegible]
Rapid growth of potassium dihydrogen phosphate crystals
[DE85-007261] 17 p3045 N85-[illegible]
KrF laser cost/performance model for ICF commercial applications
[DE85-009589] 18 p3182 N85-[illegible]
Megajoule-class single-pulse KrF laser test facility as a logical step toward inertial fusion commercialization
[DE85-009590] 18 p3191 N85-29794
Prospects for lasers for fusion energy assessed
21 p3684 N85-[illegible]
Energy and Technology Review
[DE85-011767] 21 p3716 N85-[illegible]
Electro-optic harmonic conversion to switch a laser beam out of a cavity
[DE85-011619] 22 p3790 N85-[illegible]
LASER GEODYNAMIC SATELLITE
U LAGEOS (SATELLITE)
LASER GUIDANCE
East Europe report: Science and technology
[JPRS-ESA-84-045] 06 p0815 N85-15175
Laser-guided measuring system for precisioning device 06 p0816 N85-15176
Optmizing the specifications for an air-surface laser system 16 p2696 N85-[illegible]
LASER GYROSCOPES
Evaluation of the stochastic drift of rate-integrating gyros as preparation for the analysis of laser gyro drift measurements
[ESA-TT-827] 05 p0639 N85-[illegible]
Flight testing of Litton laser gyro strapdown system LTN-90 for general aviation
[DFVLR-MITT-84-16] 07 p0901 N85-15700
Reflectivity measurements of laser gyro mirrors
[ESA-TT-851] 09 p1366 N85-18714
Laser gyroscope random walk determination using a fast filtering technique 16 p2696 N85-[illegible]
Gyrolaser guidance system for medium range missiles
16 p2696 N85-[illegible]
Autofocus motion compensation for synthetic aperture radar and its compatibility with strapdown inertial navigation sensors on highly maneuverable aircraft
[AD-A151940] 16 p2704 N85-[illegible]
Measurements of laser gyro errors as a function of the beam path
[DFVLR-FB-85-02] 17 p2969 N85-[illegible]
Flight testing the Litton LTN 90 laser gyro strapdown system for civil aviation
[ESA-TT-904] 20 p3392 N85-31042
Advanced (unfloated) gyros for satellite control
[ESA-CR(P)-2010] 20 p3419 N85-31222
Development of an active laser gyro for inertial rotation sensing in attitude/heading reference and inertial navigation systems, phase 1
[BMFT-FB-W-85-001] 20 p3460 N85-31480
LASER HEATING
Material degradation in heavy steel plates caused by bending with a laser
[AD-A144784] 01 p0052 N85-10343
Biform resolidification and amorphous phases in a laser and electron beam processed tantalum-iridium alloy
[DE84-013334] 02 p0184 N85-11234
Laser-assisted solar cell metallization processing
[NASA-CR-174213] 06 p0813 N85-15180
Time-resolved studies of ultrarapid solidification of highly undercooled molten silicon formed by pulsed laser irradiation
[DE84-016664] 06 p0813 N85-15184
Analysis of phase composition of products of laser destruction of metallic surfaces
11 p1600 N85-[illegible]
Influence of laser treatment of structure and mechanical properties if MA21 alloy 13 p2029 N85-22713
Specifics of laser heat treatment of high steel tools
13 p2029 N85-22714

Structure of amorphous films of alloys based on Fe, condensed from laser erosion products
13 p2035 N85-22749

Specifications of new industrial lasers reviewed
14 p2284 N85-24150

Laser Welding, Cutting and Surface Treatment
14 p2306 N85-24278

Applications of lasers in manufacturing
14 p2306 N85-24279

Trends in laser equipment 14 p2306 N85-24280

Laser surface treatments 14 p2306 N85-24284

Dopant incorporation in silicon during nonequilibrium solidification: Comparison of 2 processes
[DE85-005566] 14 p2430 N85-24988

Investigation of basic characteristics of laser heating in thermoluminescence and of laser-stimulated luminescence
[AD-A152143] 16 p2790 N85-27212

Limiting processes laser CVD
[DE85-008846] 18 p3114 N85-29279

Development of growth techniques for electromagnetic crystals
[AD-A154069] 19 p3375 N85-30937

Quasi-steady-state melting mode during combined laser irradiation of semiconductor materials
21 p3682 N85-32874

Nonequilibrium kinetics of growth of oxide layer grains during laser heating of metals in air
21 p3689 N85-32919

Coefficient of optical absorption and scattered light capture effect 21 p3695 N85-32959

On one nonlinear problem of laser thermochemistry
21 p3697 N85-32971

Asymptotically stable solutions of some nonlinear equations 21 p3698 N85-32974

Magnetic fields in laser heated plasmas
[DE85-010715] 21 p3707 N85-33022

Laser effects on opaque targets. Part 2C: Thermal effects of a time-variable beam intensity
[ISL-R-105/84-PT-2C] 22 p3791 N85-33486

LASER INTERFEROMETRY

Real time sensing and control of out-of-plane distortion due to line heating by laser
[AD-A144773] 01 p0027 N85-10169

Effect of hydrogen on formation of energy spectrum of multiply charged and copper ions
02 p0263 N85-11720

Improved sensitivities in laser interferometers for the detection of gravitational waves
[MPQ-88] 04 p0506 N85-13232

Modular laser distance measurement system for multiaxis machine tools
[BMFT-FB-T-84-166] 05 p0641 N85-14110

Measuring large amplitudes of mechanical vibrations with laser interferometers 06 p0787 N85-15028

Turbulence measurement interferometer apparatus
[AD-D011377] 07 p0970 N85-16156

High temperature laser interferometric studies of solid electrolytes 09 p1396 N85-18785

CO2 laser interferometer array for Big Dee
[DE85-001718] 10 p1490 N85-19411

Technical support for microwave experiments on the eye lens
[AD-A149702] 12 p1933 N85-22144

Geophysical laser interferometer with 12.5 meter base
13 p2089 N85-23046

System for lower hybrid current startup
15 p2654 N85-26373

One-frequency laser interferometer using the optic fiber as a polarization-independent interference phase detector
[DE85-010544] 19 p3277 N85-30326

Applications of laser technology described
21 p3572 N85-32218

Possibility of measurement of small displacements by ring laser 21 p3687 N85-32904

Practical aspects of laser holographic interferometry in wind tunnels
[NASA-TM-86786] 23 p3933 N85-34378

LASER MATERIALS

Laser diodes for infrared spectroscopy
[BMFT-FB-T-84-131] 05 p0640 N85-14109

Position effects of laser protective materials on simulator tracking performance
[AD-A148297] 08 p1167 N85-17359

Improved solid-state laser sources, volume 2
[DE85-000759] 09 p1325 N85-18330

Picosecond laser pulse interactions with metallic and semiconductor surfaces
[AD-A149112] 10 p1490 N85-19405

Modern solid state laser materials
[DE85-003665] 10 p1490 N85-19410

Advanced crystalline laser materials
[DE85-003142] 12 p1857 N85-21647

Research progress on laser crystals in China
13 p2166 N85-23440

Studies on radiative collisional and ultraviolet lasers
[AD-A151004] 14 p2310 N85-24296

Bibliography of Soviet Laser Developments, Number 67, September-October 1983
[AD-A151199] 15 p2562 N85-25805

Spectroscopic investigation of materials for frequency agile laser systems
[AD-A151731] 16 p2790 N85-27208

Saturation effect in multilevel lasing media
21 p3686 N85-32901

LASER MICROSCOPY

Applications of laser technology described
21 p3572 N85-32218

LASER MODE LOCKING

Microcomputer controlled automatic peak locking of laser circuit 15 p2537 N85-25655

A study of mode-locked argon ion-dye laser systems
16 p2789 N85-27205

Optical injection locking of solid-state oscillators by frequency-multiplexed injection-locked, laser diodes
[AD-D011695] 19 p3275 N85-30307

Dye laser traveling wave amplifier
[NASA-CR-175989] 19 p3275 N85-30308

Choice of optimum saturating absorber for YAG passive mode-locking laser 21 p3685 N85-32893

Dynamics of emission from dye lasers employing synchronous pumping by limited picosecond pulse train
21 p3686 N85-32899

LASER MODES

Linear theory of free-electron lasers with cylindrical interaction space 02 p0262 N85-11718

Laser source of neutral atoms for collective-field particle accelerator 02 p0263 N85-11719

Space-time characteristics of radiation of single-mode injection lasers 02 p0269 N85-11756

Overview of recent advances in laser applications
05 p0725 N85-14660

Electron acceleration by laser fields in a gas
[DE85-000575] 11 p1639 N85-20323

Simplified analytical model for calculation of population inversion in channels of CW gasdynamic lasers operating at various transitions among levels pertaining to coupled upsilon 1 and upsilon 2 modes of CO2
[STN-2] 20 p3461 N85-31496

Self Q-modulation and generation of short pulses in distributed-feedback lasers 21 p3687 N85-32907

LASER OUTPUTS

Extracts from the test plan for in-flight evaluation of the NT-33A peripheral vision display
01 p0009 N85-10055

New type of unique frequency laser communications
[AD-A145128] 01 p0038 N85-10239

Free electron lasers
[AD-A145109] 01 p0053 N85-10349

Achievements in laser development
01 p0115 N85-10784

Laser speckle technique for burner liner strain measurements 02 p0142 N85-10960

High repetition rate nitrogen ion laser
02 p0201 N85-11340

Influence of radiation wavelength on elastic pulse shape during laser excitation 02 p0257 N85-11681

Biaxial-crystal laser with waveguide resonator
02 p0262 N85-11717

Linear theory of free-electron lasers with cylindrical interaction space 02 p0262 N85-11718

Laser source of neutral atoms for collective-field particle accelerator 02 p0263 N85-11719

Nonlinear symmetrization of picosecond pulses in optical fibers 02 p0264 N85-11725

Study of CW injection laser with a dispersive external cavity 02 p0270 N85-11760

Injection lasers based on AlGaAsSb/GaSb and InGaAsSb/GaSb heterostructures
02 p0270 N85-11761

Laser on copper and gold vapors with space diversity media 02 p0270 N85-11762

Efficiency of lasing dye media in pumping high-power radiation with nanosecond pulses
02 p0270 N85-11763

Anomalies in frequency characteristics of solid-state ring laser 02 p0271 N85-11765

Optimizing CW CO2 lasers with respect to output power in different bands 02 p0271 N85-11766

Laser paint removal
[AD-P004009] 03 p0308 N85-11969

Calculation of energy characteristics of double-passage amplifier 03 p0347 N85-12238

Breakdown of porous metals by laser radiation
03 p0349 N85-12249

Heatsink requirements for coherent operation of high-power semiconductor laser arrays
[AD-A146184] 03 p0366 N85-12346

Beam profiling in gigawatt 1064-nm lasers used in research on optical materials at Livermore
[DE84-087228] 04 p0505 N85-13223

Overview of recent advances in laser applications
05 p0725 N85-14660

Storage stability of jet fuels
[AD-A146360] 06 p0773 N85-14943

Device for measuring average power of laser radiation
06 p0786 N85-15026

Laser illuminated nano-second microscope
[DE84-016200] 06 p0811 N85-15152

Laser-assisted solar cell metallization processing
[NASA-CR-174213] 06 p0813 N85-15160

Time-resolved studies of ultrarapid solidification of highly undercooled molten silicon formed by pulsed laser irradiation
[DE84-016664] 06 p0813 N85-15164

Wavelength scaling of laser plasma coupling
[DE84-014637] 06 p0866 N85-15505

RF laser array driver apparatus
[AD-D011375] 07 p0969 N85-16155

Delta wing nozzle assembly for chemical lasers
[AD-D011396] 07 p0970 N85-16158

Design and testing of a refractive laser beam homogenizer
[AD-A146997] 07 p0970 N85-16162

Visible and ultraviolet lasers based on excimer transitions in the homonuclear halogens
[AD-D011311] 07 p0971 N85-16163

Theoretical study of laser-induced surface excitations on a grating
[AD-A147855] 07 p0972 N85-16172

Measurement of high temperature strain by the laser-speckle strain gauge
[NASA-TM-77751] 07 p0977 N85-16207

Longer-scalelength plasma perturbations by an intense laser beam
[AD-A147005] 07 p1045 N85-16638

Construction, testing of 1-MW nitrogen laser
08 p1140 N85-17182

In-situ formation of a grain boundary in field ion microscopy using a laser
[AD-A148225] 08 p1166 N85-17355

Time-resolved studies of free radicals and laser-initiated chain reactions
[DE85-002100] 09 p1326 N85-18332

Laser ablation studies using RIS
[DE85-001118] 09 p1326 N85-18336

Quantum noise effects in single-mode injection lasers
[FUB-11-1984] 09 p1327 N85-18338

Multiphoton ionization of cesium atoms above and below the two-photon ionization threshold
[DE85-000976] 09 p1381 N85-18682

Determination of vapor phase content when metals are struck by laser radiation pulses of various densities
10 p1445 N85-19106

Temperature variation of laser mirror stability criteria
10 p1445 N85-19108

Experimental and theoretical study of condensation in multicomponent vapors
[DE85-000843] 10 p1485 N85-19376

A free electron laser with two-component wiggler
11 p1623 N85-20217

The noise of laser diodes with modulated injection current
[FI-465-TBR-23] 11 p1625 N85-20233

Projection lens scanning laser velocimeter system
[NASA-CASE-ARC-11547-1] 11 p1636 N85-20320

Potential of high-average-power solid state lasers
[DE85-003884] 11 p1639 N85-20329

Model calculations for a CO2 mixing laser with screen nozzle
[ESA-TT-859] 11 p1640 N85-20336

USSR report: Physics and mathematics
[JPRS-UPM-85-001] 11 p1715 N85-20786

Study of light shifts in laser pumped quantum discriminator frequency 11 p1716 N85-20798

Distortion of temporal characteristics during parametric up-conversion of ultrashort laser pulses
11 p1717 N85-20803

Spontaneous diffraction of sequence of supershort light pulses in dye solution 11 p1718 N85-20811

Electron acceleration
[DE85-002337] 11 p1725 N85-20850

Photo-thermal detection of the onset of photo-chemical nucleation (laser-snow) in vapor
[AD-A150111] 12 p1801 N85-21295

Research study of droplet sizing technology leading to the development of an advanced droplet sizing system
[NASA-CR-174639] 12 p1850 N85-21604

Transmission and reflection of laser beams propagating through aerosol clouds in space
[LA-9996-MS] 12 p1856 N85-21638

Dynamics of space charge waves in the laser beat wave accelerator
[AD-A149668] 12 p1936 N85-22163

Adequacy of metal ablation process with laser radiation and a shock-compressed plasma
13 p2028 N85-22706

Neodymium YAG laser pumped with radiation from high frequency electrodeless discharge 13 p2044 N85-22796

Comparison reference etalon of unit laser radiation power 13 p2074 N85-22957

Invariance of probability characteristics of detector to shape of optical pulse signals 13 p2090 N85-23048

Near Field/Far Field (NF/FF) energy loss in Electric Discharge Lasers (EDL's): A mode-medium interaction [AD-A150299] 13 p2096 N85-23075

Chemical stabilization of laser dyes [AD-A150451] 13 p2096 N85-23076

A spatially incoherent and temporally coherent source [AD-A151281] 13 p2157 N85-23390

Ion transport in beam-plasma interactions [AD-A150145] 13 p2161 N85-23410

Laser beam shaping system with reduced objective diameter 14 p2275 N85-24095

Sphericity gauge for wavefront of laser radiation 14 p2275 N85-24096

Trends in laser equipment 14 p2306 N85-24280

Safety with industrial manufacturing lasers 14 p2306 N85-24281

An analysis of machine tool systems suitable for laser profiling 14 p2308 N85-24282

The measurement of laser beam parameters 14 p2308 N85-24283

Laser cutting: A new tool for shipbuilding 14 p2308 N85-24285

Laser spot welding in the electronics industry 14 p2308 N85-24287

Future trends in the use of lasers in manufacturing 14 p2309 N85-24291

Scaling blackbody laser to high powers [NASA-TM-86395] 14 p2309 N85-24292

Active dispersion control for a Doppler broadened laser [AD-D011570] 14 p2310 N85-24297

Calorimeter for measuring high-energy optical pulses [PB85-160695] 15 p2561 N85-25799

Bibliography of Soviet Laser Developments, Number 67, September-October 1983 [AD-A151199] 15 p2562 N85-25805

Method and apparatus for high speed, sustained recording of infrared laser beam patterns [AD-D011585] 15 p2563 N85-25811

Discharge characteristics of high-pressure, fast-discharge XeCl excimer laser 15 p2564 N85-25820

Characteristics of laser emission discharge created by pulsed CO2-laser 15 p2643 N85-26305

Amplification of scattered induced radiation flux in high-gain laser rods 15 p2644 N85-26309

Industrial laser use expanding in the USSR 15 p2644 N85-26310

Method and apparatus for generating a structured light beam array [AD-D011590] 15 p2652 N85-26357

LDA study of non-steady flame propagation in a constant volume duct [DE85-007233] 16 p2746 N85-26948

Population inversion in laser-initiated vacuum arcs [AD-A151858] 16 p2790 N85-27210

Photoionization mass spectrometry with VUV hydrogen laser source [AD-A153362] 17 p2921 N85-28009

Operating characteristics, absorptivity/reflectivity measurements, and pulse system design of the NPS (Naval Postgraduate School) hydrogen fluoride/deuterium fluoride laser [AD-A152712] 17 p2970 N85-28341

Low voltage free electron laser development [AD-A152917] 17 p2970 N85-28342

Instabilities and chaotic behavior of active and passive laser systems [AD-A153366] 17 p2971 N85-28346

Europe's primary producers of industrial lasers surveyed 18 p3087 N85-29101

Magnetically switched power supply systems for lasers [NASA-CASE-NPO-16402-1] 18 p3112 N85-29265

Intense excitation source for high power laser [AD-A153424] 18 p3112 N85-29267

Technique for measuring surface diffusion by laser-beam-localized surface photochemistry [DE85-007885] 18 p3113 N85-29273

Accelerator technology working group summary [DE85-009547] 18 p3180 N85-29717

KrF laser cost/performance model for ICF commercial applications [DE85-009569] 18 p3182 N85-29728

Self-detecting optical sensors [AD-D011657] 18 p3185 N85-29751

All-optical logic gates with external switching by laser and incoherent radiation 18 p3187 N85-29766

Apparatus for non-destructive inspection of blind holes [AD-D011707] 19 p3273 N85-30295

Experiments in plasma initiation and laser absorption in flowing gases [AD-A154303] 19 p3276 N85-30313

Development and application of a high power ND-glass laser instrument [AD-A154366] 19 p3276 N85-30314

Optically pumped laser system having extracavity pulse smoother [AD-D011714] 19 p3276 N85-30319

Phase and amplitude feedback control system for the Los Alamos free-electron laser [DE85-010787] 19 p3277 N85-30325

Research with high-power short-wavelength lasers [DE85-010329] 19 p3278 N85-30332

Clearing of polydisperse aqueous aerosol by laser radiation pulses 19 p3298 N85-30445

Development of a new laser Doppler velocimeter for the Ames High Reynolds Channel No. 2 [NASA-TM-86772] 20 p3458 N85-31477

Z-contrast imaging and electron channeling analysis of dopants in semiconductors [DE85-011410] 21 p3582 N85-32269

The 2-D simulations of the NRL (Naval Research Laboratory) laser experiment [AD-A154915] 21 p3592 N85-32321

Visibility and vertical structure measurements in southern Germany [AD-A154714] 21 p3635 N85-32574

Luminescence and absorption of indium-activated potassium-borate glasses subjected to high-power excitation 21 p3681 N85-32868

Generation and amplification of radiation during stimulated Raman scattering in crystals 21 p3681 N85-32869

Absorption of 10.6 micrometer laser radiation in electron-hole condensate in germanium 21 p3681 N85-32870

Defect formation in amorphous hydrated silicon subjected to laser radiation 21 p3682 N85-32873

Establishment of steady-state power level in pulse-periodic excimer laser 21 p3685 N85-32896

The problem of brightness enhancement during laser frequency doubling 21 p3686 N85-32897

Excimer-laser generator of powerful UV picosecond pulses synchronized with picosecond pulses in visible and IR bands 21 p3686 N85-32903

Investigation of ion-acoustic plasma turbulence in field of powerful electromagnetic wave by CO2-laser radiation scattering 21 p3691 N85-32935

Characteristics of optogalvanic effect in media with inverse populations 21 p3693 N85-32944

Absorption of laser radiation in substance with absorption coefficient depending linearly upon temperature 21 p3694 N85-32953

Optical waveguide along front of exothermic reaction 21 p3694 N85-32954

Coefficient of optical absorption and scattered light capture effect 21 p3695 N85-32959

The sound field of a moving laser-induced acoustic array (theory) [AD-A154553] 21 p3699 N85-32981

Multiphoton production and detection of atoms [AD-A155561] 21 p3702 N85-33000

Method of characterizing critical timing paths and analyzing timing related failure modes in very large scale integrated circuits [AD-D011731] 22 p3759 N85-33298

Sliding discharge in CO2 and excimer lasers 22 p3773 N85-33379

Device for frequency modulation of a laser output spectrum [DE85-011634] 22 p3790 N85-33479

Lasertron simulation with a two-gap output cavity [DE85-011213] 22 p3790 N85-33480

Picosecond-pulse damage studies of diffraction gratings [DE85-010785] 22 p3790 N85-33481

Effects of laser radiation on surfaces and coatings [DE85-010475] 22 p3790 N85-33484

Method and apparatus for measuring areas of photoelectric cells and photoelectric cell performance parameters [DE85-011629] 22 p3810 N85-33599

Microcomputer controlled image processor [AD-D011734] 22 p3833 N85-33735

Time-resolved spectroscopic studies of detonating heterogeneous explosives [DE85-009760] 23 p3921 N85-34297

Thermal transport measurements of UV laser irradiated spherical targets [DE85-011038] 23 p3931 N85-34365

Apparatus and method for the spectrochemical analysis of liquids using the laser spark [DE85-005749] 23 p3935 N85-34387

Ranging system which compares an object reflected component of a light beam to a reference component of the light beam [NASA-CASE-NPO-15885-1] 23 p3973 N85-34

High energy plasma accelerators [DE85-013121] 24 p4155 N85-357

Laser and electron beam processing of semiconductors [AD-A155914] 24 p4161 N85-357

LASER PLASMA INTERACTIONS

Focusing effects of a laser beam in the nonresonant multiphoton ionization (MPI) of gases [LP-207] 04 p0506 N85-132

Role of cavitons in laser-plasma interactions [DE85-001842] 11 p1731 N85-208

Activities report of the Institute of Plasma Research 11 p1733 N85-209

Increased hot-electron production at quarter-critical density in long-scalelength, laser-plasma interactions [AD-A150519] 13 p2161 N85-23411

Ion emission from solid surfaces: Comparison of dust impact with other excitations --- Giotto mission 14 p2244 N85-23912

Direct electron and ion fluid computation of high electrostatic fields in dense inhomogeneous plasma with subsequent nonlinear optical and dynamical laser interaction 15 p2656 N85-26

Progress in inertial fusion at LLNL [DE85-010931] 19 p3277 N85-303

LASER PLASMAS

Optical properties of laser erosion flares in plasma 02 p0270 N85-11784

RF laser plasma measurements [AD-A145936] 03 p0366 N85-12344

Non-LTE considerations in spectral diagnostics of thermal transport and implosion experiments [DE84-015187] 05 p0730 N85-1468

Measurements of X-ray spectra from laser produced plasma 06 p0748 N85-14794

Wavelength scaling of laser plasma coupling [DE84-014637] 06 p0866 N85-1550

Thermal evaporation in blast waves: A model for aneurism formation in the NRL (Naval Research Laboratory) LASER-HANE simulation experiment [AD-A147006] 07 p0978 N85-16210

SWIR and visible atomic emission from laser-produced oxygen and nitrogen plasmas [AD-A147526] 07 p1045 N85-16641

Proceedings on US-Japan Workshop on Tokamak Diagnostics by X-ray, VUV and Optical Radiations [IPPJ-703] 09 p1386 N85-18719

Recent ICF research by GEKKO 12 glass layer at ILE Osaka 09 p1387 N85-18726

Soft X-ray spectroscopy of laser produced plasmas 09 p1387 N85-18727

Electron-hole plasma formation in semiconductors due to the absorption of pulsed CO2 laser light [DE85-001559] 09 p1392 N85-18757

Raman sidescattering in laser-produced plasmas [AD-A148905] 10 p1556 N85-19813

Parametric processes in underdense UV laser-produced plasmas [DE85-002812] 10 p1559 N85-19830

Ion velocity distributions from spherical 1054 nm and 351 nm laser plasmas [DE85-002816] 10 p1559 N85-19833

X-ray line broadening of a diagnostic in laser produced plasma [DE85-001179] 10 p1560 N85-19841

Measurement of hot-electron production and microwave emission by laser-irradiated CH targets [DE85-003139] 11 p1640 N85-20331

Plasma states near surface of metal irradiated by CO2 laser 11 p1719 N85-20815

Influence of shock wave front on nature of luminescence of recombining laser plasma 11 p1719 N85-2081

Coronal spectroscopy in laser plasmas [DE85-002817] 11 p1730 N85-208

Laser-plasma interactions for the deposition and etching of semiconductor materials [DE85-000458] 11 p1731 N85-208

Role of cavitons in laser-plasma interactions [DE85-001842] 11 p1731 N85-208

X-ray spectroscopy of laser-produced plasmas [DE85-002170] 11 p1733 N85-208

Development and application of low energy X-ray an electron physics [AD-A149963] 12 p1926 N85-220

Affect of angle of incidence on plasmas generated duri laser welding [DE85-005724] 15 p2569 N85-258

Characteristics of laser emission discharge created pulsed CO2-laser 15 p2643 N85-263

Soft X-ray diagnostics of laser-produced plasm (HALNA) 15 p2655 N85-263

Laser plasma LINAC
[DE85-006294] 17 p2971 N85-28348
Microwave experimental studies of laser fusion
[DE85-006327] 17 p3041 N85-28614
The application of laser resonance saturation to the development of efficient short wavelength lasers
[AD-A153951] 18 p3113 N85-29270
Research with high-power short-wavelength lasers
[DE85-010329] 19 p3278 N85-30332
Strong coupling effects on bound states in plasmas
[AD-A154353] 19 p3370 N85-30905
Report of near field group
[DE85-010536] 20 p3527 N85-31940
Investigation of plasma processes in electronic transition lasers
[AD-A155598] 21 p3593 N85-32327
Selective population of N = 3 OVIII level during expansion of laser plasma in helium
21 p3688 N85-32914
CCD-based X-ray spectrometry for on-line determination of laser plasma electron temperature
21 p3692 N85-32938
Investigation of space-time structure of glow of laser plasma colliding with flat screen
21 p3693 N85-32947
Magnetic fields in laser heated plasmas
[DE85-010715] 21 p3707 N85-33022
Multiple inner shell vacancies in laser-irradiated Au plasma 23 p3981 N85-34687
Elliptical X-ray analyzer spectrograph application to a laser-produced plasma
[DE85-013790] 24 p4097 N85-35398

LASER PUMPING
Singlet delta oxygen generator
[AD-D011208] 01 p0012 N85-10072
Solar-pumped lasers: A review
02 p0261 N85-11711
Theory of free-electron lasers with focusing pumping field 02 p0262 N85-11714
Narrowband tunable dye laser with amplifier pumped by powerful nitrogen laser 02 p0262 N85-11716
Biaxial-crystal laser with waveguide resonator
02 p0262 N85-11717
Efficiency of lasing dye media in pumping high-power radiation with nanosecond pulses
02 p0270 N85-11763
Transformation of energy spread of laser pumping via phase conjugation 05 p0725 N85-14661
Highly efficient Nd:YAG lasers for free-space optical communications 10 p1463 N85-19229
Improved electron emission by use of a cloth fiber cathode
[AD-A149250] 10 p1480 N85-19340
Electron-oscillatory spectra of yttrium-erbium-aluminum garnet of crystals and their role in laser pumping
11 p1715 N85-20791
Study of light shifts in laser pumped quantum discriminator frequency 11 p1716 N85-20798
Investigation of dye lasers pumped by high-power KrF laser radiation 11 p1718 N85-20806
The effects of surface waves on RF discharge pumped lasers
[AD-A149689] 12 p1856 N85-21643
Scaling blackbody laser to high powers
[NASA-TM-86395] 14 p2309 N85-24292
Population inversion in laser-initiated vacuum arcs
[AD-A151958] 16 p2790 N85-27210
Study on a prismatic dye vat --- laser systems
[CERT-2/6124-04-RO] 16 p2791 N85-27217
Experimental investigation of the pulsed photoacoustic effect produced on a solid surface
[AD-A152114] 16 p2860 N85-27640
Coherently pumped two-frequency laser-type devices
[AD-A154085] 19 p3275 N85-30311
Theoretical modeling of the discharge-pumped XeCl excimer laser 20 p3460 N85-31495
Three-dimensional photochemical machining with lasers
[AD-A154711] 21 p3591 N85-32320
A fast discharge excimer laser with symmetric geometry
[AD-A155294] 21 p3592 N85-32322
Lasing on LiF:F(-)2 - dye centers with transverse pumping 21 p3684 N85-32890
Dynamics of emission from dye lasers employing synchronous pumping by limited picosecond pulse train
21 p3686 N85-32899
Stimulated Mandelstam-Brillouin scattering with distributed feedback 21 p3696 N85-32961
Influence of spatial pumping spectrum on quality of phase conjugate reflection during 4-photon interaction
21 p3696 N85-32964
Photoionization-pumped, Ne 2, X-ray laser studies project
[DE85-012973] 23 p3936 N85-34399

LASER RADAR
U OPTICAL RADAR

LASER RANGE FINDERS
Influence of depolarization of linear polarized radiation on heterodyne detection in laser range finders
[DFVLR-FB-84-31] 10 p1491 N85-19414
Preliminary processing of laser ranging data from LAGEOS artificial Earth satellite during short merit program observation period 15 p2486 N85-25355
Influence of depolarization of linear polarized radiation on the heterodyne detection in laser range finders
[ESA-TT-903] 20 p3461 N85-31500
Contemporary plate motions from LAGEOS
20 p3489 N85-31689
Comparing SLR and VLBI geodetic parameters
20 p3491 N85-31703
Applications of laser technology described
21 p3572 N85-32218

LASER RANGER/TRACKER
Tidal dissipation in the Earth and Moon from lunar laser ranging 04 p0585 N85-13733
Specifics of polarization structure of repeated scattering background in optical laser sounding signals
14 p2342 N85-24485
Station coordinates and Earth rotation parameters from Lageos laser ranging 16 p2806 N85-27299
Theoretical and experimental analyses of the performance of two-color laser ranging systems
[NASA-CR-176159] 23 p3936 N85-34397

LASER SPECTROMETERS
Comparison of flame photometer data with total particle volume calculated from laser spectrometer particle count data
[AD-A151008] 14 p2252 N85-23958
Cryogenic laser calorimetry for impurity analysis
[NASA-CR-176102] 22 p3743 N85-33201

LASER SPECTROSCOPY
NT OPTOGALVANIC SPECTROSCOPY
Laser spectroscopy and gas-phase chemistry in CVD
[DE84-014959] 02 p0173 N85-11158
Laser spectroscopy of combustion intermediates
[DE84-016101] 02 p0173 N85-11161
Laser cooling and trapping of neutral atoms
[AD-A146048] 03 p0366 N85-12345
Bibliography of Soviet laser developments, number 65, May - June 1983
[AD-A146189] 03 p0366 N85-12347
Time-resolved spectroscopy of evanescent-wave excited fluorescence
[DE84-015213] 04 p0473 N85-13013
Intermediate results of a 1-year study of a laser spectrometer in the DOE filter test facilities
[DE84-016478] 04 p0506 N85-13228
Velocity-changing collisional effects in nonlinear atomic spectroscopy and photon echo decay in gases
[NASA-CR-174159] 04 p0559 N85-13559
Laser diodes for infrared spectroscopy
[BMFT-FB-T-84-131] 05 p0640 N85-14109
In situ analysis of corrosive and passive surfaces by laser-excited Raman spectroscopy — lead, galvanized iron, and asbestos-cement pipes
[PB84-229756] 06 p0767 N85-14904
Laser spectroscopy of alkali atom-tetrahaloethylene reactions
[AD-A147431] 07 p0923 N85-15848
Reactions of metal ions and their cluster in the gas phase using laser ionization: ion cyclotron resonance spectroscopy
[DE84-016491] 09 p1293 N85-18120
Developments and applications of laser fluorescence spectroscopy for studies of particle behaviours in fusion plasmas 09 p1389 N85-18735
Measurements of electric fields in plasmas by using beam probe and laser fluorescence techniques
09 p1389 N85-18737
Density measurements of atomic hydrogen in NBT-IM by laser-induced fluorescence spectroscopy
09 p1389 N85-18739
Laser-induced-fluorescence-spectroscopy of atomic processes under a high magnetic field
09 p1389 N85-18740
Capabilities of laser diagnostics for combustion and flow fields
[DE85-002661] 10 p1436 N85-19064
Optical studies of dynamical processes in disordered materials
[DE85-002400] 10 p1453 N85-19156
Fundamental study of catalysts using laser Raman, infrared, auger electron spectroscopy and low energy electron diffraction
[DE85-001813] 11 p1595 N85-20033
Application of Raman, TEM and other ion based techniques to oxidation problems
[AERE-R-11447] 11 p1610 N85-20121
Computer modeling of vibrational energy levels of potential laser candidates (diatomic molecules)
[AD-A151765] 16 p2790 N85-27209
High resolution spectroscopy of C13O16 in gas mixtures
[AD-A152625] 17 p2919 N85-27991
Laser measurement techniques: Laser spectroscopy in semiconductors
[DE85-007887] 17 p2971 N85-28350
Recent advances in optical measurement methods in physics and chemistry
[DE85-008695] 17 p3037 N85-28792
Field measurements with the TAMS-2B and development of methods for measuring HCHO, HC3 and HONO in real air
[PB85-172955] 18 p3135 N85-29419
The development of new techniques in laser spectroscopy 19 p3233 N85-30041
Laser-induced fluorescence measurement of vapor concentration surrounding evaporating droplets
[DE85-009409] 19 p3277 N85-30320
Sensitive detection of tunable diode laser absorption by polarization rotation
[DE85-009621] 19 p3277 N85-30322
Applied Science Division's Environmental Research Program
[DE85-010637] 19 p3308 N85-30510
Reactions of metal ions and their clusters in the gas phase using laser ionization-ion cyclotron resonance spectroscopy
[DE85-009478] 19 p3361 N85-30838
Applications of laser technology described
21 p3572 N85-32218
Activities of the Physics Division
[DE85-000784] 21 p3702 N85-33002
Nonlinear spectroscopy
[AD-A154706] 21 p3704 N85-33010
Rapid analysis of steels using laser-based techniques
[DE85-010747] 22 p3748 N85-33232
Apparatus and method for the spectrochemical analysis of liquids using the laser spark
[DE85-005749] 23 p3935 N85-34387
The detection and study of molecular species using time resolved laser spectroscopy
[AD-A155910] 24 p4075 N85-35256
Infrared generation and wave-mixing studies in cesium
[DE85-012883] 24 p4083 N85-35304
Cryogenic laser calorimetry for impurity analysis
[NASA-CR-176179] 24 p4097 N85-35395
Atmospheric nitrogen oxides: Their detection and chemistry
[PB85-193910] 24 p4114 N85-35502

LASER STABILITY
Measurement of areal mass variation in Rayleigh-Taylor unstable targets
[AD-A145541] 02 p0198 N85-11325
Study of CW injection laser with a dispersive external cavity 02 p0270 N85-11760
Characteristics of unstable resonators in flashlamp-pumped organic-compound lasers
11 p1717 N85-20800
Stability of temporal and energy parameters of picosecond lanthanum beryllate laser
11 p1717 N85-20804
The effects of surface waves on RF discharge pumped lasers
[AD-A149689] 12 p1856 N85-21643

LASER TARGET INTERACTIONS
Measurement of areal mass variation in Rayleigh-Taylor unstable targets
[AD-A145541] 02 p0198 N85-11325
Optical properties of laser erosion flares in plasma
02 p0270 N85-11764
Simulation of the interaction of single-pulsed optical lasers with targets in a vacuum
[DE84-016476] 05 p0640 N85-14107
USSR report: Physics and mathematics
[JPRS-UPM-84-007] 05 p0723 N85-14651
Laser excitation of coupled surface electromagnetic and acoustic waves and of static structures in solids
05 p0723 N85-14652
Transformation of energy spread of laser pumping via phase conjugation 05 p0725 N85-14661
Self-generated magnetic fields and thermal flux inhibition
[AD-A147405] 07 p0971 N85-16166
Bibliography of Soviet laser developments, Number 66, July-August 1983
[AD-A149113] 10 p1490 N85-19406
KMSF X-ray laser experiments, task no. 1
[DE85-001002] 11 p1639 N85-20325
Measurement of hot-electron production and microwave emission by laser-irradiated CH targets
[DE85-003139] 11 p1640 N85-20331

Enhanced thermal coupling by a repetitively pulsed laser
[AD-A154436] 10 p3276 N85-30317

Laser effects on opaque targets. Part 2C: Thermal effects of a time-variable beam intensity
[ISL-R-106/84-PT-2C] 22 p3791 N85-33486

LASER TARGETS

Wavelength scaling of laser plasma coupling
[DE84-014637] 06 p0866 N85-15505

Soft X-ray spectroscopy of laser produced plasmas
09 p1367 N85-18727

A microchannel plate pinhole camera for 20 to 100 keV X-ray imaging
[DE85-001572] 10 p1486 N85-19396

Laser program annual report 1983
[DE84-017267] 10 p1490 N85-19412

Study of opacity effects on line radiation from pellet implosions
[DE85-000390] 10 p1491 N85-19413

Parametric processes in underdense UV laser-produced plasmas
[DE85-002812] 10 p1559 N85-19830

Model testing and analysis of NOVA laser structures
[DE84-017569] 11 p1636 N85-20321

Use of the ORACLE DEMS in determining the response of complex scientific instrumentation
[DE85-001742] 12 p1853 N85-21621

Laboratory for laser energetics report
[DE85-007235] 15 p2563 N85-25614

Autofocus motion compensation for synthetic aperture radar and its compatibility with strapdown inertial navigation sensors on highly maneuverable aircraft
[AD-A151940] 16 p2704 N85-26693

Megajoule-class single-pulse KrF laser test facility as a logical step toward inertial fusion commercialization
[DE85-009590] 18 p3191 N85-29794

Progress in inertial fusion at LLNL
[DE85-010931] 19 p3277 N85-30321

Shifts and widths of hydrogenic ion lines
[DE85-011375] 19 p3277 N85-30323

Hybrid two-dimensional Monte-Carlo electron transport in self-consistent electromagnetic fields
[DE85-010757] 19 p3348 N85-30756

Thermal transport measurements of UV laser irradiated spherical targets
[DE85-011036] 23 p3931 N85-34365

Solid neon sources for plasma and X-ray lasers
[DE85-011347] 24 p4098 N85-35402

LASER WEAPONS

Directed energy missile defense in space
[PB84-210111] 01 p0015 N85-10095

High energy lasers: A primer on directed energy weapons for space use
[AD-A151279] 15 p2582 N85-25807

LASER WELDING

NT BRAZING
NT FUSION WELDING
NT LOW TEMPERATURE BRAZING

Features of laser welding of medium carbon steel through a cadmium coating 01 p0020 N85-10122

Overview of recent advances in laser applications
05 p0725 N85-14660

Two-dimensional modeling of conduction-mode laser welding
[DE85-001604] 09 p1327 N85-18341

Structure and mechanical characteristics of heterogeneous joints produced by laser welding
13 p2034 N85-22742

Specifications of new industrial lasers reviewed
14 p2284 N85-24150

Laser Welding, Cutting and Surface Treatment
14 p2308 N85-24278

Applications of lasers in manufacturing
14 p2308 N85-24279

Trends in laser equipment 14 p2308 N85-24280

Laser welding in the manufacture of heart pacemakers
14 p2308 N85-24286

Laser spot welding in the electronics industry
14 p2308 N85-24287

Lasers in automobile production
14 p2309 N85-24288

Lasers in the nuclear industry
14 p2309 N85-24289

Laser drilling of aeroengine components
14 p2309 N85-24290

Affect of angle of incidence on plasmas generated during laser welding
[DE85-005724] 15 p2569 N85-25652

Laser welder for fabricating neutron tubes
[DE85-009665] 17 p2974 N85-28377

Experimental and theoretical studies on transport processes in laser welding
[DE84-008572] 17 p2975 N85-28378

Laser beam interactions with vapor plumes during Nd:YAG laser welding on aluminum
[DE85-009793] 21 p3593 N85-32326

Laser welding of 6Al-4V titanium alloy
[DE85-012019] 23 p3938 N85-34413

LASER WINDOWS

Pulsed electric discharge laser technology. Electron beam window foil material
[AD-A147486] 07 p0972 N85-16171

Incident beam polarization for laser Doppler velocimetry employing a sapphire cylindrical window
[NASA-TM-87064] 17 p3037 N85-28786

Influence of mirror anisotropy and Brewster window orientation on radiation characteristics of ring lasers
21 p3664 N85-32680

LASERS

NT ARGON LASERS
NT ATMOSPHERIC LASERS
NT CARBON DIOXIDE LASERS
NT CARBON LASERS
NT CARBON MONOXIDE LASERS
NT CHEMICAL LASERS
NT CONTINUOUS WAVE LASERS
NT DF LASERS
NT DYE LASERS
NT EXCIMER LASERS
NT FREE ELECTRON LASERS
NT GALLIUM ARSENIDE LASERS
NT GAS LASERS
NT GASDYNAMIC LASERS
NT GLASS LASERS
NT HCN LASERS
NT HELIUM-NEON LASERS
NT HF LASERS
NT HIGH POWER LASERS
NT INFRARED LASERS
NT INJECTION LASERS
NT IODINE LASERS
NT KRYPTON FLUORIDE LASERS
NT METAL VAPOR LASERS
NT NEODYMIUM LASERS
NT NITROGEN LASERS
NT NOVA LASER SYSTEM
NT NUCLEAR PUMPED LASERS
NT OPTICAL RESONATORS
NT ORGANIC LASERS
NT PLASMADYNAMIC LASERS
NT PULSED LASERS
NT Q SWITCHED LASERS
NT RAMAN LASERS
NT RARE GAS-HALIDE LASERS
NT RING LASERS
NT RUBY LASERS
NT SEMICONDUCTOR LASERS
NT SOLAR-PUMPED LASERS
NT SOLID STATE LASERS
NT TEA LASERS
NT TUNABLE LASERS
NT TWO-WAVELENGTH LASERS
NT ULTRASHORT PULSED LASERS
NT ULTRAVIOLET LASERS
NT WAVEGUIDE LASERS
NT X RAY LASERS
NT XENON CHLORIDE LASERS
NT XENON FLUORIDE LASERS
NT YAG LASERS

Center for Electronics and Electrical Engineering Technical Bulletin covering center programs
[PB84-216056] 01 p0045 N85-10296

The development of a diode laser Doppler velocimeter for boundary layer measurements under ice: A feasibility investigation
[AD-A145076] 01 p0053 N85-10348

East Europe report: Science and technology
[JPRS-ESA-84-029] 01 p0115 N85-10783

Achievements in laser development
01 p0115 N85-10784

Hot section laser anemometry
02 p0142 N85-10962

Laser anemometer optimization
02 p0142 N85-10963

Evaluation of laser profile and deflection measuring system
[FAA-PM-84-24] 02 p0201 N85-11341

Parameters of geometric stability of laser mirror optical surface 02 p0273 N85-11777

Laser paint removal
[AD-P004009] 03 p0308 N85-11969

Calculation of energy characteristics of double-passage amplifier 03 p0347 N85-12238

Beam profiling in gigawatt 1064-nm lasers used in research on optical materials at Livermore
[DE84-067226] 04 p0505 N85-13223

Theory of non-linear index of refraction of compound semiconductors
[DE84-013660] 04 p0589 N85-13626

Dynamic testing of NOVA laser switchyard tower
[DE84-014450] 05 p0640 N85-14103

Quality assurance in the Antares Laser Fusion Construction Project
[DE84-015493] 05 p0640 N85-14104

Cleaning procedures of laser mirror substrates
[DFVLR-MITT-84-06] 05 p0640 N85-14108

China report: Science and technology
[JPRS-CST-84-042] 06 p0747 N85-[illegible]

External cavity diode laser sensor
[AD-D011341] 07 p0959 N85-16112

RF laser array driver apparatus
[AD-D011375] 07 p0959 N85-[illegible]

Laser R and D in the armed services
[AD-A146930] 07 p0970 N85-[illegible]

Bragg cell spectrum analyzer specification
[AD-D011320] 07 p1044 N85-[illegible]

Rayleigh and Raman scattering for density in a swirling flow combustor 08 p1120 N85-[illegible]

In-situ formation of a grain boundary in field ion microscopy using a laser
[AD-A148225] 08 p1166 N85-[illegible]

Theoretical issues involving traps for neutral spin-polarized atoms
[AD-A148035] 08 p1220 N85-[illegible]

Journal of Research of the National Bureau of Standards, Volume 89, Number 1, January-February, 1984
[PB84-235530] 08 p1262 N85-[illegible]

Laser Hazards Bibliography, October 1984
[AD-A149534] 10 p1490 N85-[illegible]

Use of laser flow visualization techniques in reactor component thermal-hydraulic studies
[DE84-014766] 11 p1639 N85-[illegible]

Photoacoustic effect and its applications
12 p1820 N85-21421

Flow measurement by laser Doppler anemometry in a nuclear fuel assembly
[DE85-003260] 12 p1848 N85-[illegible]

Multiple double heterojunction buried laser device
[AD-D011519] 12 p1855 N85-[illegible]

State-selected ion-molecule reaction dynamics
[AD-A150066] 12 p1926 N85-22115

Intensity fluctuations of focused laser beam during reflection in turbulent atmosphere
13 p2078 N85-22975

China report: Science and technology
[JPRS-CST-85-003] 13 p2166 N85-[illegible]

InGaAs/GaAs, Strained-Layer Superlattice (SLS), junction photodetectors, LED's, injection LASER's and FET's for optoelectronic IC applications
[DE85-001940] 14 p2430 N85-[illegible]

China report: Science and technology
[JPRS-CST-85-013] 15 p2536 N85-[illegible]

Modified Landolt C-ring test to measure the effects of laser filters on visual acuity
[AD-A151164] 15 p2617 N85-26127

Internal step-up type higher harmonic light generating device
[DE85-007026] 16 p2700 N85-27213

Lidar ER2 (ozone). Crystal characterization for harmonic conversion --- laser systems
[CERT-2/6129-00] 16 p2672 N85-27717

Photoionization mass spectrometry with VUV hydrogen laser source
[AD-A153362] 17 p2921 N85-[illegible]

High precision materials characterization in the near millimeter wave-length range
[AD-A153267] 17 p2966 N85-[illegible]

Instabilities and chaotic behavior of active and passive laser systems
[AD-A153366] 17 p2971 N85-[illegible]

Support structures for optical components in the Laser Demonstration Facility
[DE85-006679] 17 p2971 N85-[illegible]

Limiting processes laser CVD
[DE85-006646] 18 p3114 N85-[illegible]

Self-detecting optical sensors
[AD-D011657] 18 p3185 N85-28751

Picosecond photoconductive devices for 10 Gbit/s optoelectronic switching 18 p3187 N85-28776

Current activities and background of technology transfer and exchange program at Lawrence Livermore National Laboratory
[DE85-009526] 18 p3199 N85-[illegible]

A laser slope gauge and a spar buoy wave gauge: Tools for the validation of microwave remote sensors
[AD-A154036] 19 p3272 N85-[illegible]

Analog frequency modulated laser using magnetostriction
[AD-D011701] 19 p3276 N85-30318

Four-photon resonant third harmonic generation
[DE85-010070] 19 p3367 N85-[illegible]

USSR report: Life sciences. Biomedical and behavioral sciences
[JPRS-UBB-85-017] 20 p3504 N85-[illegible]

USSR report: Physics and mathematics
[JPRS-UPM-85-004] 21 p3660 N85-[illegible]

Inter-zone auger recombination in GaSb laser structures 21 p3662 N85-32875
The problem of brightness enhancement during laser frequency doubling 21 p3686 N85-32897
Low-threshold injection InGaAsP/GaAs double heterostructure lasers with separate limiting obtained by liquid-phase epitaxy (lambda = 0.78 divided by 0.87 microns, I sub thr = 460 A/cm 2, T = 300 K) 21 p3687 N85-32906
An attempt to detect induced neutron capture in laser radiation field 21 p3690 N85-32928
The sound field of a moving laser-induced acoustic array (theory) [AD-A154553] 21 p3699 N85-32981
Size exclusion chromatography-low angle laser light scattering photometry of lignite macromolecules [DE85-012017] 22 p3745 N85-33215
Pulsed lasers for filming color holographic film images 22 p3781 N85-33426
Metal vapor lasers and their applications [ISL-CO-218/84] 22 p3791 N85-33468
Index of laser program publications and related reports, calendar year 1984 [DE85-011863] 23 p3936 N85-34398
Laser probes of natural gas ignition chemistry [PB85-200210] 24 p4077 N85-35284
Laser and electron beam processing of semiconductors [AD-A155914] 24 p4161 N85-35796
LASING
Space-time characteristics of radiation of single-mode injection lasers 02 p0269 N85-11758
Theoretical analysis of physical processes of lasing medium degradation in semiconductor lasers 02 p0269 N85-11759
Study of CW injection laser with a dispersive external cavity 02 p0270 N85-11760
Injection lasers based on AlGaAsSb/GaSb and InGaAsSb/GaSb heterostructures 02 p0270 N85-11761
Thresholds of optical breakdown in alkali-halide crystals under pulses from CO2-laser 14 p2282 N85-24134
Spectroscopic studies of lasing transitions in the diatomic mercury halides [AD-A151553] 15 p2563 N85-25809
LASV
U F-111 AIRCRAFT
LATCH-UP
Effects of space radiation on advanced semiconductor devices. Part 3: Further cosmic ray simulation studies of single event upsets and latch-up in CMOS memories [AERE-G-3368-PT-3] 22 p3648 N85-33633
LATCHES
Materials properties, loads, and stress analysis, Spartan REM: Appendix A [NASA-CR-171092] 02 p0206 N85-11375
Computer models and output, Spartan REM: Appendix B [NASA-CR-171093] 02 p0208 N85-11376
Hemispherical latching apparatus [NASA-CASE-MFS-25837-1] 19 p3224 N85-29991
Latch assembly [DE85-011660] 22 p3792 N85-33492
LATE STARS
Observations of interstellar HI toward nearby late-type stars 06 p0874 N85-15546
Mg II spectra of late type stars used to probe the LISM 06 p0874 N85-15548
Detection of narrow C 4 and Si 4 absorption features in spectra of stars within 200 pc f the Sun 06 p0876 N85-15564
Spectrophotometry of cool stars from objective prism spectra 07 p0966 N85-16134
The Origin of Nonradiative Heating/Momentum in Hot Stars [NASA-CP-2358] 08 p1231 N85-17755
Far-infrared photometry of low-mass pre-main-sequence stars with broad CO wings 08 p1246 N85-17866
X-ray coronae of late type stars: Theoretical implications 11 p1742 N85-20953
Chromospheric activity in M giants 11 p1757 N85-21056
A progress report on the analysis of long exposure SWP high resolution spectra of cool stars 11 p1758 N85-21057
Precise measurements of radial velocities of emission lines in the far-ultraviolet spectra of late-type stars 11 p1758 N85-21062
Circumstellar shells of late-type stars: A study at millimeter and infrared wavelengths 24 p4167 N85-35836
LATENT HEAT OF FUSION
U HEAT OF FUSION
LATERAL CONTROL
Preliminary airworthiness evaluation of the Rutan Aircraft Factory (RAF), Inc. LONG-EZ airplane with external sight [AD-A145381] 02 p0136 N85-10937
Aileron controls for wind turbine applications [NASA-TM-86867] 02 p0222 N85-11458
The lateral-directional characteristics of a 74-degree Delta wing employing gothic planform vortex flaps [NASA-CR-3848] 03 p0311 N85-12009
Reflection of laterization of sound stimuli in evoked potentials of human brain 04 p0544 N85-13463
Maximum normalized rate as a flying qualities parameter 05 p0702 N85-14503
Flight tests with a new helicopter Force Feel System (FFS) 08 p1075 N85-16818
Leading edge flap system for aircraft control augmentation [NASA-CASE-LAR-12787-2] 11 p1585 N85-19965
Relative control effectiveness technique with application to airplane control coordination [NASA-TP-2416] 14 p2218 N85-23753
Resource allocation in cerebral specialization of function: Behavioral and electrophysiological studies [AD-A155092] 21 p3684 N85-32759
LATERAL OSCILLATION
Clearance flow-generated transverse forces at the rotors of thermal turbomachines [NASA-TM-77292] 07 p0973 N85-16180
Tolerance, fatigue, physiological and performance effects of sustained and oscillating lateral accelerations 10 p1533 N85-19659
LATERAL STABILITY
Experimental investigation of lateral forces induced by flow through model labyrinth glands 05 p0643 N85-14126
Aileron effectiveness for a subsonic transport model with a high-aspect-ratio supercritical wing [NASA-TM-85674] 07 p0986 N85-15695
Operational and developmental experience with the F/A-18A digital flight control system 16 p2713 N85-26742
Experimental and theoretical determination of the wing-induced lateral wind on the tail surfaces in oscillating rolling motion. Part 2: Theoretical investigations for calculation of the lateral wind [IFD-1/84-PT-2] 18 p3061 N85-28940
The lateral distributions of charged particles of energy greater than 0.3 E sub crit in electron-photon cascades in lead and air [HE-3.6-10] 24 p4185 N85-35957
Properties of 10 (18)-10 (19)eV EAS at far core distance [HE-4.7-3] 24 p4198 N85-36054
LATERALITY
U LATERAL STABILITY
LATERALIZATION
U LATERAL CONTROL
LATEX
Preparation of large-particle-size monodisperse latexes in space: The STS-3, STS-4, and STS-7 mission results 02 p0151 N85-11021
Guayule research [GPO-29-562] 04 p0477 N85-13042
Monodisperse Latex Reactor (MLR): A materials processing space shuttle mid-deck payload [NASA-TM-86487] 12 p1782 N85-21187
Preparation of polystryene latex particles in a rotating reactor [NASA-CR-171475] 17 p2933 N85-28108
LATHES
NT TURRET LATHES
Design of a flexible machining system [CETIM-1-3E-140] 04 p0510 N85-13252
Production cells with IR 2SO robot examined 15 p2524 N85-25561
Device for preventing intrusion of a blade during vibration cutting of intermittent cutting with a lathe 16 p2794 N85-27232
Assessing the machinability of gearwheel steels during manufacture [BLL-BISI-TRANS-22343-(9902.06)] 17 p2973 N85-28365
Machining of beryllium with the LLNL precision engineering research lathe [DE85-010632] 19 p3250 N85-30149
LATITUDE
NT GEOMAGNETIC LATITUDE
Space observation of latitudinal changes in vegetation cover 02 p0164 N85-11113
A paleomagnetic study of the Prince William terrane and Nixon Fork terrane, Alaska 02 p0226 N85-11478
Computer-generated latitude and longitude templates for rapid determination of geographic positions in Alaska 04 p0516 N85-13286
Study of factors affecting an HF/VHF direct broadcasting satellite service [PB85-120889/GAR] 09 p1313 N85-18255
Simultaneous determination of the xi and eta components of vertical deflection with a prism astrolabe [SER-B-270-MITT-171] 09 p1343 N85-18450
Tactical military communications by satellite relay at high latitudes 11 p1709 N85-20758
Development of a portable zenith chamber and its use on the 47th parallel [SER-C-287] 11 p1741 N85-20946
Quaternary North Atlantic surface paleoceanography in regions of potential deep-water formation 15 p2602 N85-26036
Some evidence for high energy gamma-ray sources at large galactic latitudes [OG-2.7-5] 22 p3871 N85-33978
Latitude dependence of co-rotating shock acceleration [SH-1.5-14] 23 p3997 N85-34777
Differential measurement of cosmic-ray gradient with respect to interplanetary current sheet [SH-4.2-9] 23 p4007 N85-34847
Determination of galactic cosmic ray latitudinal gradient using Earth based detectors [SH-4.2-13] 23 p4008 N85-34851
Latitudinal gradients of cosmic rays and the polarity reversal of the heliospheric magnetic field: A preliminary evaluation [SH-4.2-16] 23 p4008 N85-34853
Comparative study of the phase of diurnal anisotropy on quiet and disturbed days on a long term basis up to recent period [SH-4.5-9] 23 p4037 N85-35027
Radial and latitudinal gradients of anomalous oxygen during 1977 - 1985 [SH-4.6-4] 23 p4039 N85-35042
LATTICE IMPERFECTIONS
U CRYSTAL DEFECTS
LATTICE PARAMETERS
Neutron scattering on the FRM double crystal spectrometer 03 p0423 N85-12704
EXAFS and Moessbauer study of small metal clusters isolated in rare-gas solids [DE84-015976] 04 p0470 N85-12994
Theory of non-linear index of refraction of compound semiconductors [DE84-013660] 04 p0569 N85-13626
Understanding the high pressure properties of molecular solids and molecular surfaces deposited on hetrogeneous substrates [NASA-CR-174262] 07 p1047 N85-16649
Tracer diffusion in an ordered alloy: Application of the path probability and Monte Carlo methods [DE85-002769] 14 p2257 N85-23986
Relationship between symmetrical tilt, twist, special, and favored grain boundaries [DE85-004024] 14 p2429 N85-24982
Hydrostatic compression of Fe1-chi 0 wustite. 15 p2508 N85-25472
Strained-layer-superlattice optoelectronic devices [DE85-009148] 19 p3377 N85-30953
Z-contrast imaging and electron channeling analysis of dopants in semiconductors [DE85-011410] 21 p3582 N85-32269
Method for preparing Pb-(beta)-aluminum ceramic [DE85-011665] 22 p3752 N85-33256
Changes in lattice cell parameter of film intermetallic compounds RT2 [BLL-M-35874-(5828.4)] 23 p3915 N85-34261
On-line model driven control of the SLC electron Damping Ring [DE85-013377] 24 p4157 N85-35772
Simulation of lattice damage due to dynamic loading [DE85-008468] 24 p4162 N85-35808
LATTICE VIBRATIONS
Anharmonic lattice effects in molecular crystals 03 p0424 N85-12709
Observation of surface vibrational resonances on (110) surfaces of FCC metals [AD-A150469] 13 p2163 N85-23419
Interaction of low energy electrons with surface lattice vibrations [DE85-005475] 14 p2428 N85-24975
The temperature dependence of diffracted beam intensities in atom-surface scattering [AD-A152762] 17 p3029 N85-28736
X-ray diffractometric measurements and calculations of limiting values of discrepancy between lattices and layer thicknesses, preventing generation of dislocations during growth of multilayer heterostructures 21 p3681 N85-32866
Doping superlattices in organometallic VPE InP [AD-A155151] 21 p3710 N85-33029

LATTICES
Aperture studies with PATRICIA and RACETRACK on simple lattices containing SSC dipoles
[DE85-004169] 11 p1724 N85-20942
Combined function lattices for a 6 GeV synchrotron light source
[DE85-010969] 19 p3367 N85-30865
LATTICES (MATHEMATICS)
NT BOOLEAN ALGEBRA
NT BOOLEAN FUNCTIONS
Gauge Theory on a Lattice, 1984: Proceedings
[DE84-014656] 02 p0291 N85-11602
Comparison of analytical and experimental steadyand unsteady-pressure distributions at Mach number 0.78 for a high-aspect-ratio supercritical wing model with oscillating control surfaces
[NASA-TM-84589] 07 p0899 N85-15897
Lattice statistics
[AD-A146862] 07 p1029 N85-16530
Eigenvalue approximation methods for quantum lattice Hamiltonians 16 p2858 N85-27627
Lattice actions improved by block-spin renormalisation group and maximally symmetric lattices
[DE85-007416] 17 p3045 N85-28841
On the definition of topological susceptibility via lattice anomalous Ward identities and its perturbative tail
[PREPRINT-416] 18 p3184 N85-29744
Nested dissection on a mesh-connected processor array
[AD-A154086] 19 p3342 N85-30711
Monte Carlo sampling strategies for lattice gauge calculations
[DE85-010756] 19 p3377 N85-30946
Adaptive identification and control of structural dynamics systems using recursive lattice filters
[NASA-TP-2371] 20 p3407 N85-31142
Lattice theory for nonspecialists, lecture notes
[NIKHEF-H/84-11] 20 p3539 N85-32019
LAUE METHOD
A new high-resolution pickup tube for live X-ray topography
[NHK-LABS-NOTE-309] 18 p3193 N85-29802
LAUNCH COMPLEXES
U LAUNCHING BASES
LAUNCH DATES
Rocket observations 01 p0014 N85-10084
Balloon observations 01 p0014 N85-10086
List of recent Soviet space launches
02 p0165 N85-11120
List of recent Soviet space launches
13 p1985 N85-22457
LAUNCH TIME
U LAUNCH WINDOWS
LAUNCH VEHICLE CONFIGURATIONS
Future launching systems, 3rd prospective phase
[SNIAS-S/DT/Y-25-063] 11 p1589 N85-19999
French CNES official describes Ariane V launcher
15 p2532 N85-25619
LAUNCH VEHICLES
NT ARIANE LAUNCH VEHICLE
NT ATLAS CENTAUR LAUNCH VEHICLE
NT CENTAUR LAUNCH VEHICLE
NT RECOVERABLE LAUNCH VEHICLES
NT REUSABLE LAUNCH VEHICLES
NT TITAN CENTAUR LAUNCH VEHICLE
NT VEGA LAUNCH VEHICLE
Second Symposium on Space Industrialization — space commercialization
[NASA-CP-2313] 02 p0149 N85-11011
Conestoga 2: A low cost commercial space transport system 02 p0153 N85-11033
Comments on the commercialization of expendable launch vehicles 02 p0153 N85-11034
International cooperation and competition in space. Introduction 02 p0295 N85-11912
LOX/LH2 propulsion system for launch vehicle upper stage, test results
[NASA-TM-77727] 03 p0324 N85-12069
Status of Stretched Rohini Satellite System (SROSS) and Augmented Satellite Launch Vehicle Project (ASLV)
04 p0459 N85-12909
The Expendable Launch Vehicle Commercialization Act
[GPO-30-836] 04 p0460 N85-12919
Commercial Space Launch Act
[GPO-39-613] 04 p0578 N85-13690
One rocket multiple satellite launch technology
[AD-A149226] 10 p1427 N85-19002
Commercial space launches
[S-REPT-98-656] 12 p1788 N85-21225
Distance-inertial guidance of launch vehicle described
12 p1820 N85-21417
Estimation of launch vehicle performance parameters
[AD-A151927] 16 p2728 N85-26839
Computer program for prediction of capture maneuver probability for an on-off reaction controlled upper stage
[NASA-CR-165667] 17 p3010 N85-28611
Proceedings of the Workshop on Identification and Control of Flexible Space Structures, volume 1
[NASA-CR-176051] 20 p3408 N85-31146
The development of staging mechanisms for the Japanese satellite launcher Mu-3SII
22 p3798 N85-33526
LAUNCH WINDOWS
The launch window of a geostationary satellite
05 p0600 N85-13822
LAUNCHERS
NT GUN LAUNCHERS
NT HYPERVELOCITY LAUNCHERS
NT MISSILE LAUNCHERS
NT MOBILE MISSILE LAUNCHERS
NT ROCKET LAUNCHERS
A feasibility study on the use of wind profilers to support Space Shuttle launches
[NASA-CR-3861] 04 p0536 N85-13423
Electromagnetic rail launcher as a circuit element
[AD-A150067] 12 p1835 N85-21516
LAUNCHING
NT AIR LAUNCHING
NT ORBITAL LAUNCHING
NT ROCKET LAUNCHING
NT SPACECRAFT LAUNCHING
Voice command weapons launching system
[AD-D011378] 07 p0937 N85-15940
Impact of activation optimization on the Vandenberg Ground Support System using Q-GERT analysis
[AD-A148446] 08 p1105 N85-16986
One rocket multiple satellite launch technology
[AD-A149226] 10 p1427 N85-19002
Guided-mode launching in a slab waveguide by way of diffraction at the edge of a conducting screen residing on one surface of the slab
[AD-A154866] 21 p3575 N85-32232
LAUNCHING BASES
NT CAPE KENNEDY LAUNCH COMPLEX
Sweden's Kiruna may be future launch site for satellites 03 p0310 N85-12000
View of Ariane countdown procedures, Kourou launch facilities 03 p0310 N85-12001
Vandenberg space shuttle launch complex
[S-HRG-98-1075] 05 p0601 N85-13833
Statement of Edward C. Aldridge, Jr., Under Secretary of the Air Force, Department of the Air Force, accompanied by Lieutenant General Robert W. Bazley, Inspector General and Brigadier General Donald J. Kutyna, Director of Space Systems and Command, Control and Communications, Deputy Chief of Staff, Research, Development and Acquisition 05 p0601 N85-13834
Statement of Honorable James M. Beggs, Administrator, National Aeronautics and Space Administration
05 p0601 N85-13835
External tank processing from barge to pad
08 p1096 N85-16927
LAUNCHING DEVICES
U LAUNCHERS
LAUNCHING PADS
Zero adhesion system
[AD-D011237] 01 p0015 N85-10093
Mechanical features of the shuttle rotating service structure 08 p1102 N85-16967
LAUNCHING SITES
NT LAUNCHING PADS
West Europe report: Science and technology
[JPRS-WST-84-004] 03 p0309 N85-11996
Sweden's Kiruna may be future launch site for satellites 03 p0310 N85-12000
Impact of activation optimization on the Vandenberg Ground Support System using Q-GERT analysis
[AD-A148446] 08 p1105 N85-16986
Natural environment analysis
[NASA-CR-171333] 10 p1428 N85-19010
Atmospheric environment for space shuttle (STS-51C) launch
[NASA-TM-86508] 19 p3315 N85-30547
LAVA
Petrology of deep crustal xenoliths from the eastern Snake River Plain, Idaho 02 p0226 N85-11477
Geomorphic classification of lava flows on Io
13 p2173 N85-23480
Characteristics of basaltic lava flows on Venus
13 p2177 N85-23506
Magmas as selective filters of volatiles between planetary mantles and surfaces
13 p2185 N85-23557
Estimates of lava eruption rates at Alba Patera, Mars
13 p2185 N85-23562
Emplacement of long lava flows on Mauna Loa (Hawaii) and Alba (Mars) 13 p2186 N85-23563
Surface structures of Hawaiian lavas
13 p2186 N85-23566
Basaltic pressure ridges: Formation and relationship to flow emplacement 13 p2186 N85-[illegible]
Radar observations of fissure-fed basaltic lava flows, Craters of the Moon, Idaho 13 p2188 N85-[illegible]
Preliminary results of an ALVIN dive program on active hydrothermal vents at the southern Juan de Fuca Ridge
24 p4106 N85-[illegible]
LAW (JURISPRUDENCE)
NT AIR LAW
NT LEGAL LIABILITY
NT LIABILITIES
NT PUBLIC LAW
NT SPACE LAW
Second Symposium on Space Industrialization — space commercialization
[NASA-CP-2313] 02 p0149 N85-11011
Legal considerations and cooperative opportunities for space commercial activities 02 p0150 N85-11013
SAR maritime missions 06 p0751 N85-14813
Effective use of remote sensing products in litigation
[E85-10048] 06 p0827 N85-[illegible]
Government contract contingent liabilities. The anti-deficiency act, and the hobgoblin of little minds
[AD-A147919] 07 p1053 N85-[illegible]
Microcomputers and the electrical engineer
[AD-A150499] 13 p2147 N85-[illegible]
National Aeronautics and Space Administration Authorization Act, 1986
[S-REPT-99-91] 19 p3381 N85-[illegible]
LAWS
NT CHILD-LANGMUIR LAW
NT CLOSURE LAW
NT CONSERVATION LAWS
NT KEPLER LAWS
NT KIRCHHOFF LAW OF RADIATION
NT OHMS LAW
NT SCALING LAWS
NT STOKES LAW OF RADIATION
Some weak and strong laws of large numbers for d(0,1) - valued random variables
[AD-A144845] 01 p0111 N85-10794
LAY-UP
Fracture toughness of fibrous composite materials
[NASA-TP-2370] 02 p0170 N85-11138
LAYERS
Acoustic resonator and method of making same
[DE84-014655] 01 p0116 N85-10792
Propagation of longitudinal elastic waves in multilayered half-space 02 p0273 N85-11770
Elastodynamic stress intensity factors of an interface finite-width crack
[DE84-016908] 06 p0817 N85-15190
Determination of parameters of doped thin semiconductor layers from plasmatic minimum of reflection coefficient for infrared radiation
07 p0954 N85-16047
Antisoiling technology: Theories of surface soiling and performance of antisoiling surface coatings
[NASA-CR-174274] 07 p0981 N85-[illegible]
TEM combined with Al/sub x/Ga/sub 1-x/ as marker layers as a technique for the study of GaAs MBE growth
[DE85-008451] 18 p3194 N85-[illegible]
Tailored vacuum chambers for ac magnets
[DE85-010767] 21 p3591 N85-[illegible]
LAYOUTS
JESS facility modification and environmental/power plans
[NASA-CR-175685] 14 p2227 N85-[illegible]
LDEF
U LONG DURATION EXPOSURE FACILITY
LEACHING
Electrochemical features of the ferric sulfate leaching of CuFeS2/C aggregates
[AD-A148661] 08 p1123 N85-17981
Mod silver metallization for photovoltaics
[NASA-CR-174444] 10 p1509 N85-19518
A comparative evaluation of the effects of acid precipitation, natural acid production and harvesting of cation removal from forests
[DE85-005254] 15 p2589 N85-[illegible]
A comparative evaluation of the effects of acid precipitation, natural acid production and harvesting on cation removal from forests
[DE85-010821] 19 p3309 N85-30511
Source-term considerations for a potential radioactive-waste repository located in unsaturated tuff
[DE85-010090] 20 p3529 N85-[illegible]
Marine environmental quality assessment program, five-year plan (FY 1984 - 1988)
[AD-A154715] 21 p3613 N85-[illegible]
AUTSKED: An addendum
[DE85-010410] 22 p3829 N85-33712
Effects of acid rain on forest nutrient status
[DE85-012486] 23 p3947 N85-[illegible]

LEAD (METAL)

Mechanical properties of a leaded, resulfurized, rephosphorized steel in various thermo/mechanical conditions
[PB84-219494] 03 p0333 N85-12144

Progress in lead/uranium zircon studies of lower paleozoic rocks of the southern Alexander terrane
04 p0618 N85-13304

Behaviour of lead-silver anodes in zinc electrodeposition from sulphuric acid baths
[BLL-MINTEK-TR-1190-(5810.5759)]
06 p0764 N85-14887

Extreme incompatibility of Pb during the crystallization of magmatic iron meteorites 06 p0886 N85-15627

The growth of metastable peritectic compounds
[NASA-CR-171290] 07 p0920 N85-15825

Susceptibility of 2 1/4 Cr-1Mo steel to liquid metal induced embrittlement by lithium-lead solutions
[DE85-000867] 09 p1294 N85-18130

High temperature laser interferometric studies of solid electrolytes 09 p1386 N85-18785

Structure of transient zone in diffusion welding of TsTS-19 piezoceramic with AMg6 alloy
11 p1603 N85-20082

Effect of rhodamine-B on the electrodeposition of lead on copper, revision
[DE85-000674] 11 p1606 N85-20101

EXAFS of monolayers on silver electrodes: SSRL proposal number 717M
[AD-A150823] 13 p2018 N85-22652

Spectral evaluation of irregularity of superconducting coaxial cables 13 p2082 N85-23000

Trends of petroleum fuels
[DE85-000116] 14 p2263 N85-24023

Effects of ion bombardment on the morphology of lead films
[DE85-007232] 15 p2511 N85-25494

Comparative analysis of laboratory and fullscale experimental data for metal flow displacements and speeds
[BLL-M-36266-(5828.4)] 20 p3430 N85-31276

Lead, platinum, and other heavy elements in the primary cosmic radiation: HEAO-3 results sec wg032961 cb052087 20 p3543 N85-32048

Method for preparing Pb-(beta)-aluminum ceramic
[DE85-011685] 22 p3752 N85-33256

Environmental surveillance at Los Alamos during 1984
[DE85-011686] 22 p3811 N85-33605

Germanium and lead: Significant differences between meteoritic and photospheric abundances?
[OG-7.1-2] 23 p4012 N85-34864

Lead and uranium group abundances in cosmic rays
[OG-7.1-3] 23 p4013 N85-34865

Coupling functions for lead and lead-free neutron monitors from the latitudinal measurements performed in 1982 in the research station Academician Kurchatov
[SH-8.1-1] 23 p4044 N85-35076

Sensitivity of single and multiple cosmic ray neutrons to the surrounding medium in a lead-free monitor
[SH-8.1-10] 23 p4051 N85-35125

The neutron moderated detector and groundbased cosmic ray modulation studies
[SH-8.1-13] 23 p4052 N85-35128

The Conterminous United States Mineral Assessment Program 24 p4106 N85-35458

Estimation of the total inelasticity coefficient in interaction of greater than or equal to 20 TeV hadrons with lead
[HE-1.1-8] 24 p4171 N85-35857

LPM effect and primary energy estimations
[HE-3.6-4] 24 p4185 N85-35953

The lateral distributions of charged particles of energy greater than 0.3 E sub crit in electron-photon cascades in lead and air
[HE-3.6-10] 24 p4185 N85-35957

Result of Monte Carlo simulation of electron-photon cascades in lead and layers of lead-scintillator
[HE-3.6-11] 24 p4185 N85-35958

LEAD ACID BATTERIES

Performance of improved lead acid batteries for electric vehicles
[DE84-015845] 04 p0495 N85-13180

Research, development, and demonstration of lead-acid batteries for electric vehicle propulsion
[DE84-017442] 05 p0632 N85-14055

Energy storage with lead acid batteries in photovoltaic systems 05 p0663 N85-14260

Performance on advanced lead-acid batteries for load-leveling applications
[DE84-015817] 06 p0805 N85-15125

Impact of temperature on cycle life of globe ISOA EV-3000 lead-acid batteries
[DE84-015840] 06 p0805 N85-15126

Composite batteries 07 p0936 N85-15932

Prospects for advanced storage battery technologies
[DE84-015706] 09 p1345 N85-18464

Electric vehicle battery test plan and results
[DE84-901072] 09 p1410 N85-18987

Electrical and thermal performance during charging and discharging a Phase 1 gel cell battery
[PB85-114312] 11 p1677 N85-20585

In-vehicle evaluation of the Globe EV 2300 lead-acid, Delco Remy 150 nickel-zinc, and Eagle-Picher NIF 270 nickel-iron battery systems
[NASA-CR-175869] 14 p2349 N85-24521

Lead shortage hastens need for improved storage batteries 15 p2461 N85-25195

Test and evaluation of the Hoppecke Model E240G144/16 electric vehicle battery charger
[DE85-900573] 17 p2955 N85-28253

Transfer of battery technology developed by the US Department of Energy
[DE85-009869] 22 p3808 N85-33589

LEAD ALLOYS

Directional solidification studies of Pb-Bi peritectic alloys
[DE84-015886] 04 p0474 N85-13016

Accuracy of preparation of three-dimensional reference grid
[BLL-M-35921-(5828.4)] 05 p0616 N85-13939

Thermodynamic properties of liquid Li-Pb, Na-Pb and K-Pb]b alloys: Similarities and Differences
[DE85-004074] 18 p3197 N85-29830

Counter current extraction system for tritium recovery from 17Li-83Pb
[DE85-010519] 19 p3240 N85-30090

Comparative analysis of laboratory and fullscale experimental data for metal flow displacements and speeds
[BLL-M-36266-(5828.4)] 20 p3430 N85-31276

LEAD COMPOUNDS

NT LEAD OXIDES
NT LEAD TELLURIDES

Structure of transient zone in diffusion welding of TsTS-19 piezoceramic with AMg6 alloy
11 p1603 N85-20082

Effect of traffic and meteorology on air pollution
16 p2830 N85-27452

LEAD OXIDES

Structural studies on lead dioxides
[DE84-015837] 06 p0805 N85-15127

Spectroscopic studies of lead oxide in a flow tube
[AD-A151849] 15 p2505 N85-25455

Calculation of molecular constants potential energy curves and Franck-Condon factors for lead oxide
[AD-A154521] 21 p3562 N85-32158

LEAD POISONING

Effect of traffic and meteorology on air pollution
16 p2830 N85-27452

Environmental summary for calendar year 1984
[DE85-012020] 22 p3810 N85-33604

Estimating risks of lead-induced hemoglobin decrements under conditions of uncertainty: Methodology, pilot judgments and illustrative calculations
[DE85-012293] 23 p3952 N85-34493

LEAD TELLURIDES

The behavior of Pb(1-x)Sn(x)Te semiconductor laser diodes in a magnetic field
[AD-A145431] 02 p0287 N85-11872

LEAD ZIRCONATE TITANATES

Effect of powder characteristics on microstructure and properties in alkoxide prepared PZT ceramics
[AD-A149082] 10 p1451 N85-19141

Sol-gel processing of lead zirconate titanate films
[ATR-85(8343)-2] 18 p3073 N85-29010

Materials used by industry for the production of piezoelectric transducers. The state of the art of research work performed in the field of PZT ceramics and ferroelectric polymers
[ISL-CO-211/84] 24 p4089 N85-35344

Conduction and aging of piezoelectric PZT ceramics
24 p4089 N85-35346

LEADERSHIP

Conceptual model of critical requirements for effective pilot performance in high performance aircraft
10 p1533 N85-19663

Individual characteristics and unit performance: A review of research and methods
[AD-A153145] 17 p3001 N85-28550

The effects of controversy and concurrence seeking on effective decision making
[AD-A153370] 17 p3002 N85-28555

Central problems in the management of innovation
[AD-A152598] 17 p3047 N85-28852

Symbolic and interactional perspectives on leadership: An integrative framework
[AD-A155247] 21 p3665 N85-32769

LEADING EDGE FLAPS

Leading edge flap system for aircraft control augmentation
[NASA-CASE-LAR-12787-2] 11 p1565 N85-19865

Investigation of the Vortex Tab
[NASA-CR-172566] 15 p2463 N85-25209

Simulator study of the stall departure characteristics of a light general aviation airplane with and without a wing-leading-edge modification
[NASA-TM-86309] 15 p2470 N85-25250

Application of an aerodynamic analysis method including attainable thrust estimates to low speed leading-edge flap design for supersonic cruise vehicles
[NASA-CR-165843] 19 p3212 N85-29916

Aerodynamic characteristics of a distinct wing-body configuration at Mach 6: Experiment, theory, and the hypersonic isolation principle
[NASA-TP-2467] 22 p3727 N85-33107

LEADING EDGE SLATS

Design of an airfoil leading edge slat using an inverse aerodynamic calculation method
08 p1069 N85-16777

Effects of leading-edge devices on the low-speed aerodynamic characteristics of a highly-swept arrow-wing
[NASA-CR-172531] 13 p1968 N85-22365

Pressure distribution data from tests of 2.29 M (7.5 feet) span EET high-lift transport aircraft model in the Ames 12-foot pressure tunnel
[NASA-TM-84517] 19 p3211 N85-29912

Low-speed tests of a high-aspect-ratio, supercritical-wing transport model equipped with a high-lift flap system in the Langley 4- by 7-meter and Ames 12-foot pressure tunnels
[NASA-TP-2097] 20 p3368 N85-31010

Presentation of the acoustic and aerodynamic results of the Aladin 2 concept qualification testing
[NASA-TM-77883] 24 p4060 N85-35161

LEADING EDGES

Prediction of aerodynamic characteristics of fighter wings at high angles of attack
[AD-A145107] 01 p0003 N85-10017

Force and moment measurements on a 74 deg delta wing with an apex flap
[NASA-CR-166081] 02 p0134 N85-10918

Hybrid laminar flow control study
[NASA-CR-165930] 02 p0137 N85-10933

A visual study of a delta wing in steady and unsteady motion
[AD-P004158] 09 p1264 N85-17943

Laminar separation bubble with transition: Prediction test with local interaction --- airfoils
[PNR-90231] 09 p1274 N85-18008

A calculation of slender delta wing with leading-edge separation by quasi-vortex lattice method
12 p1821 N85-21423

Energy losses at leading edge of turbine blade during multirow jet cooling 13 p2049 N85-22826

Interactions of unstable shear layers with leading edges and associated pressure fields 14 p2299 N85-24236

An exploratory study of apex fence flaps on a 74 deg delta wing
[NASA-CR-172463] 15 p2463 N85-25208

Flow past a flat plat with a vortex/sink combination
[JIAA-TR-58] 15 p2464 N85-25215

Some effects of sweep direction and strakes for wings with sharp leading edges
[CA-8421] 17 p2992 N85-27826

On the effect of wing taper and sweep direction on leading edge transition
[CA-8435] 17 p2992 N85-27827

A study of aerodynamic control in stalled flight leading-edge vortex formation analysis
[AD-A153758] 18 p3059 N85-28928

Lee-side flow over delta wings at supersonic speeds
[NASA-TP-2430] 19 p3212 N85-29921

A method for computing the core flow in three-dimensional leading-edge vortices
[NASA-TM-87469] 19 p3214 N85-29932

DC-10 winglet flight evaluation
[NASA-CR-3704] 19 p3217 N85-29949

LEAKAGE

Qualification of noninvasive systems for on-line leak detection in high pressure feed water preheaters
[CISE-2341] 04 p0558 N85-13556

Gamma-induced leakage in junction field-effect transistors
[DE84-014990] 04 p0570 N85-13634

Analysis for leakage and rotordynamic coefficients of surface roughened tapered annular gas seals
05 p0644 N85-14135

Development of a van-portable remote-sensing laser system for selective detection of natural gas leaks
[PB85-101939/GAR] 06 p0811 N85-15156

Identification of leaks: Internal acoustic method, phase 2
[PB85-101947/GAR] 07 p0936 N85-15927

Clearance flow-generated transverse forces at the rotors of thermal turbomachines
[NASA-TM-77292] 07 p0973 N85-16180

A voice-actuated wind tunnel model leak checking system
[NASA-TM-86359] 09 p1263 N85-17936
Leakage-flow induced vibrations of a chimney structure suspended in a liquid flow — nuclear reactors
09 p1339 N85-18420
Theory versus experiment for the rotordynamic coefficients of annular gas seals. Part 2: Constant clearance and convergent-tapered geometry
[NASA-CR-174413] 10 p1491 N85-19416
Theory versus experiment for the rotordynamic coefficients of annular gas seals. Part 1: Test facility and apparatus
[NASA-CR-174409] 10 p1491 N85-19417
Low leakage turbine shaft seals for advanced combined cycle systems
[AD-A149372] 10 p1492 N85-19420
Leak monitoring in high pressure preheaters by a noninvasive ultrasonic method
[CISE-2373] 11 p1650 N85-20394
Leak detection by acoustic emission monitoring in power plant high pressure preheaters
[CISE-2392] 11 p1650 N85-20395
Leakage-flow-induced vibration of a tube-in-tube slip joint
[DE84-007301] 11 p1652 N85-20406
Interactions between F-111 fuselage fuel tank sealants. Part 2: Variation in performance properties of polysulfides after contact with polyester degradation products
[AD-A149777] 12 p1812 N85-21368
Analysis of experimental shaft seal data for high-performance turbomachines, as for Space Shuttle main engines
[NASA-TM-86026] 12 p1844 N85-21569
Carbon granule probe microphone for leak detection — recovery boilers
[NASA-CASE-NPO-16027-1] 12 p1849 N85-21597
Leak detectors for organic Rankine cycle power plants: On-line and manual methods
[DE85-002792] 12 p1852 N85-21617
Portable remote laser sensor for methane leak detection
[NASA-CASE-NPO-15790-1] 12 p1855 N85-21631
Magnetic field interactions with material discontinuities
[AD-A150197] 13 p2154 N85-23373
Effect of apparent fluid masses on natural vibration frequencies of impellers of multistage centrifugal pumps
14 p2277 N85-24106
Effect of diaphragm leakage on turbine stage characteristics 14 p2286 N85-24168
New electronic measurement, control devices
14 p2289 N85-24192
Experimental simulation of the flows in front of and behind a projectile with and without gas slippage
[ISL-CO-232/83] 14 p2302 N85-24258
Hermetic sealing of nonlubricated gas seal and friction characteristics, chapter 7
[DE85-006375] 15 p2569 N85-25851
Physics effects of accidental submersion of space power reactors in water
[DE85-005020] 15 p2650 N85-26344
Management of vacuum leak-detection processes, standards and calibration
[DE85-006705] 16 p2788 N85-27202
Magnetic flux leakage inspection: Principles and applications
[BLL-BISI-TRANS-22248-(9022.06)]
17 p2975 N85-28382
Differential between crack and pseudo-crack indications by means of objective magnetic flux leakage testing
[BLL-BISI-TRANS-22033-(9022.06)]
17 p2976 N85-28386
SSME seal test program: Test results for hole-pattern damper seals
[NASA-CR-171595] 20 p3395 N85-31059
Refrigerated dynamic seal to 6.9 MPa (1000 psi)
[NASA-TM-87108] 23 p3930 N85-34356
Upgrading auxiliary facility outleakage and combustion detection
[DE85-012786] 23 p3934 N85-34386

LEAR JET AIRCRAFT
Aircraft accident report. Central Airlines flight 27, Hughes Charter Air, Gates Learjet model 25 (N51CA) Newark International Airport, Newark, New Jersey, March 30, 1983
[PB84-910411] 02 p0136 N85-10924
Safety recommendation(s), A-84-93 through -95
[REPT-3963/30] 14 p2216 N85-23746
Learjet Model 55 wing analysis with landing loads
15 p2575 N85-25683

LEARNING
NT ASTRONAUT TRAINING
NT CONDITIONING (LEARNING)
NT TRANSFER OF TRAINING
Feature discovery by competitive learning
[AD-A145052] 01 p0097 N85-10646
Memory-based expert systems
[AD-A145612] 02 p0249 N85-11628
The impact of pictorial display on operator learning and performance 05 p0706 N85-14627
Mental models of invisible logical networks
05 p0708 N85-14544
Conjunctive and disjunctive item response functions
[AD-A147815] 07 p1033 N85-16561
Training high performance skills: Fallacies and guidelines
[AD-A148574] 08 p1198 N85-17545
A theorem on the optimal allocation of effort
[AD-A148028] 08 p1211 N85-17623
Toward a model of attention and the development of automatic processing
[AD-A149348] 10 p1567 N85-19882
Learning to search. From weak methods to domain-specific heuristics
[AD-A149949] 12 p1918 N85-22045
Psychophysiological studies. 1: Performance and physiological response in learning, short-term memory and discrimination tasks
[AD-A151016] 14 p2392 N85-24731
The acquisition of procedures from text. A production-system analysis of transfer of training
[AD-A151029] 14 p2392 N85-24732
The impact of group processing on achievement in cooperative learning groups
[AD-A153188] 17 p3001 N85-28551
Oral discussion, group-to-individual transfer and achievement in cooperative learning groups
[AD-A153209] 17 p3001 N85-28552
Biofeedback and performance: An update
[AD-A153228] 17 p3001 N85-28553
Learning and self adaptation applied to the simulation of a human pilot
[ONERA-RT-24/5122-SY] 20 p3511 N85-31828
The International Cometary Explorer (ICE)wallsheet teacher's guide
[NASA-TM-87496] 23 p3968 N85-34727

LEARNING MACHINES
Decentralized control of scheduling in distributed systems
[AD-A147445] 07 p1026 N85-16523
Monte Carlo techniques for analyzing deep penetration problems
[DE85-011426] 23 p3968 N85-34596
Justified generalization: Acquiring procedures from examples
[AD-A156408] 24 p4135 N85-35626

LEARNING THEORY
The design and use of subtasks in part training and their relationship to the whole task
05 p0711 N85-14559
Oral discussion, group-to-individual transfer and achievement in cooperative learning groups
[AD-A153209] 17 p3001 N85-28552
Models for multidimensional tests and hierarchically structured training materials
[AD-A155231] 21 p3665 N85-32766

LEAST SQUARES METHOD
Harmonizable, Cramer, and Karhunen classes of processes
[AD-A144984] 01 p0113 N85-10767
Credibility approximations for Bayesian prediction of second moments
[AD-A144996] 01 p0113 N85-10768
Fast Fourier transform for unequally spaced data
01 p0128 N85-10876
Planning of navigatiun measurements using TD criterion for determination of movement of spacecraft by method of least squares 02 p0159 N85-11061
Determination of nonlinear viscoelasticity parameters for polymeric and composite materials by numerical methods
[AD-A145311] 02 p0186 N85-11240
An algorithm for least squares projections onto the intersection of shifted, convex cones
[AD-A145428] 02 p0251 N85-11640
Estimation in nonlinear time series model II: Some nonstationary series
[AD-A145709] 02 p0255 N85-11668
Local geoid determination in mountain regions
[AD-A145799] 03 p0384 N85-12458
Signal processing algorithms
[AD-A145748] 03 p0406 N85-12590
Least squares estimation of conditionally heteroscedastic autoregressions
[AD-A145994] 03 p0411 N85-12626
Least squares spline regression with block-diagonal variance matrices
[NPL-DITC-40/84] 04 p0554 N85-13523
Satellite orbit determination 05 p0596 N85-13813
Use of least-squares method for estimating errors of turbine blade type parts during fabrication
06 p0776 N85-14963
Parametric estimates of propulsion system
manhours
[AD-A147120] 07 p0984
Optimization of orientation in navigation by two
bodies 07 p0961
Splitting methods for the numerical solution of the incompressible Navier-Stokes equations
[AD-A147463] 07 p1002
Background detection and correction in multicomponent analysis
[AD-A148251] 08 p1212
On the ergodicity of bilinear time series models and some applications
[AD-A148032] 08 p1215
Computer programs for the adjustment of
observation with condition equations between the unknowns
[SER-B-268-MITT-170] 09 p1370
Blunder detection using a sequential least squares adjustment
[AD-A149514] 10 p1548
The inefficiency of least squares: Extensions of Kantorovich inequality
[AD-A149588] 10 p1549
Improved models for increasing wind penetration, economics and operating reliability
[NASA-CR-175536] 11 p1674
Sequential minimization for sum of squares of
functions
[DE85-004162] 11 p1707
New approach for solving large residual nonlinear least squares problems
[DE85-002555] 11 p1707
Influence of individual reflections on the precision of parameter estimates in least squares refinement
[DE85-000830] 11 p1735
Estimation of the impulse response of
channels from digitized waveforms
[CRC-1376] 12 p1822
On the accuracy of least squares methods in the presence of corner singularities
[NASA-CR-172552] 12 p1819
A mixed-basis band structure interpolation scheme applied to the fluorite structure compounds
AuGa2 and AuIn2
[AD-A150131] 12 p1940
Efficiency of algorithms for gas-air channel diagnostics in gas turbine engines based on gas thermodynamic parameters 13 p2048
Consistency of smoothing with running linear fits
[AD-A150232] 13 p2150
Macro for fitting nonlinear models to Poisson distributed data
[DE84-008569] 14 p2412
Least squares reduction technique
14 p2437
Very large least squares problems and supercomputers
[AD-A151270] 15 p2623
Applications of Kalman filtering and recursive least-squares in river flow modelling
15 p2626
Statistical regularization methods in problem of navigational determination of space vehicle orbits
16 p2719
Solving the minimal least squares problem subject to bounds on the variables
[TRITA-NA-8215] 16 p2852
Symbolic Givens reduction in large sparse least squares problems
[DE85-008685] 17 p3021
A multiple regression technique for detecting outliers
[REPT-84-33] 17 p3025
On the condition number of modified moment matrices arising from least squares approximation in the complex plane
[AD-A152353] 17 p3026
Analytical generation of satellite orbits at the RAE (Royal Aircraft Establishment)
[AD-A152855] 17 p3053
Least-squares approximation to minimum chi-square estimators of location and scale parameters and their effect on the Pearson chi-square test
[AD-A153534] 18 p3169
Least squares inversion of Stokes profiles in the presence of velocity gradients 18 p3207
The effect of line damping, magneto-optics and parasitic light on the derivation of sunspot vector magnetic fields
18 p3207
Fast moving average recursive least mean square fit
[DE85-010036] 19 p3348
Description and operation of CHISQMO, INVRTS, VOIGEN, VOIGTV, SMEAR, RUFF, AND POSCAR in the Stokes Analysis Program
[PB85-180626] 19 p3384

Adaptive identification and control of structural dynamics systems using recursive lattice filters
[NASA-TP-2371] 20 p3407 N85-31142
Comparison of ERS-1 scatterometer Monte Carlo performance simulations using a weighted nonlinear least squares and a maximum likelihood estimation method
20 p3420 N85-31224
A guide to the statistical analysis of the results of linear and nonlinear least-squares data fitting
[NPL-DITC-53/84] 20 p3521 N85-31895
Regression metamodel summarization of model behavior
[FEW-120] 20 p3522 N85-31902
A practical approach to Karmarkar's algorithm
[AD-A155714] 21 p3673 N85-32818
On a variational approach to some parameter estimation problems
[NASA-CR-177535] 21 p3675 N85-32829
Kalman filter time series analysis of gamma-ray data from NaI(T1) detectors for the ND6620 computer
[AD-A154895] 21 p3706 N85-33014
Application of nonlinear least squares methods to the analysis of solar spectra
[NASA-CR-176122] 22 p3816 N85-33637
Two-dimensional inversion of resistivity monitoring data from the Cerro Prieto geothermal field
[DE85-012554] 24 p4113 N85-35494

LEAVES
Compilation of elemental concentration data for NBS (National Bureau of Standards) biological, geological and environmental standard reference materials, 1982
[PB84-218338] 01 p0025 N85-10158
Scattering from randomly oriented scatterers of arbitrary shape in the low-frequency limit with application to vegetation 04 p0525 N85-13362
Changes in spectral properties of detached leaves
[E85-10042] 07 p0963 N85-16243
Microwave model prediction and verifications for vegetated terrain
[E85-10182] 16 p2909 N85-27322
Light scattering by leaf layers with application to canopy reflectance modeling: The Scattering by Arbitrarily Inclined Leaves (SAIL) model
[NLR-MP-84011-U] 17 p3038 N85-28796

LECTURES
Eleven lectures on the physics of the quark-gluon plasma
[DE85-004321] 15 p2662 N85-26431

LED (DIODES)
U LIGHT EMITTING DIODES

LEE WAVES
Mesoscale lee cyclogenesis 09 p1355 N85-18527
Kinetic energy and vorticity of lee cyclones
[MITT-40] 17 p2983 N85-28502
The determination of lee circulation during the foehn wind 24 p4122 N85-35554

LEG (ANATOMY)
NT FEET (ANATOMY)
NT KNEE (ANATOMY)
Locomotion research for the analysis of the human gait and for the determination of the maximum loads of the pelvis-leg skeleton. Volume 1: Two-dimensional analysis
[BMFT-FB-T-83-187-VOL-1] 02 p0236 N85-11535
Locomotion research for the analysis of the human gait and for the determination of the maximum loads of the pelvis-leg skeleton. Volume 2: Three-dimensional analysis
[BMFT-FB-T-83-188-VOL-2] 02 p0236 N85-11536
Leg volume changes. Responses to Lower Body Negative Pressure (LBNP) during 7 days of zero-g simulation (6 deg Head-Down Tilt (HDT))
05 p0692 N85-14452
Electromyographic patterns associated with discrete limb movements 05 p0710 N85-14551
Comparison of thermal responses between rest and leg exercise in water
[AD-A148818] 07 p1015 N85-16448
Rat skeletal muscles with simulation of physiological effects of weightlessness (morphological study)
23 p3953 N85-34502
The effect of +Gx acceleration on platelet activation as determined by plasma platelet factor 4 levels
[AD-A155881] 24 p4131 N85-35808

LEGAL LIABILITY
The structures and the role of an international agency for the control of satellites
[NASA-TM-76765] 03 p0441 N85-12806
Microcomputers and the electrical engineer
[AD-A150489] 13 p2147 N85-23325

LEGENDRE CODE
U COMPUTER PROGRAMMING
U NEUTRON SCATTERING

LEGENDRE FUNCTIONS
Boundary conditions in Chebyshev and Legendre methods
[NASA-CR-172489] 02 p0250 N85-11635
Phase function, backscatter, extinction, and absorption for standard radiation atmosphere and El Chichon aerosol models at visible and near-infrared wavelengths
[NASA-TM-86379] 12 p1892 N85-21874
Object identification and manipulation using silhouette moments
[AD-A154755] 21 p3705 N85-33011

LEGENDRE POLYNOMIALS
U LEGENDRE FUNCTIONS

LEGENDRE TRANSFORMATION
U LEGENDRE FUNCTIONS

LEGIBILITY
An exploratory study of the effect of screen size and resolution on the legibility of graphics in automated job performance aids
[AD-A155989] 24 p4136 N85-35832

LEGUMINOUS PLANTS
Mutant peas as probes in the understanding of growth and gravitropism 15 p2611 N85-26098

LEMMAS
U THEOREMS

LENGTH
Estimating number, time and length; a baseline study
05 p0695 N85-14473
Signal propagation delay, wire length distribution and the efficiency of VLSI circuits
[CWI-CS-R8412] 11 p1630 N85-20266
Design of a variable-focal-length optical system
[NASA-CR-175710] 15 p2651 N85-26349
A comparison of methods of least squares adjustment of traverses
[AD-A153612] 18 p3170 N85-29645
Literature survey of discontinuous-fiber-reinforced composites with emphasis on pressure vessels
[DE85-010386] 19 p3232 N85-30036

LENS ANTENNAS
Millimeter wave antenna technology
[AD-A148694] 08 p1155 N85-17291
3-D Dome/Rotman lens antenna breadboard demonstration
[AD-A149809] 12 p1828 N85-21475
Cylindrical lens-array antenna for wideband electronic scanning
[AD-A156085] 24 p4090 N85-35350

LENS DESIGN
Optic's institute's development of equipment for comet probe 15 p2484 N85-25333
Design of a variable-focal-length optical system
[NASA-CR-175710] 15 p2651 N85-26349
Holographic lens for optical correlator
16 p2763 N85-27052
Possibility of developing charged-particle energy analyzer based on hyperboloidal axisymmetrical lens
21 p3691 N85-32933
Electrostatic astigmatic tubular lens
21 p3695 N85-32955
Relaxation lens in inhomogeneous binary mixture
21 p3695 N85-32957
New method for correcting chromatism of mirror-lens objectives 21 p3696 N85-32965

LENSES
NT FRESNEL LENSES
NT GRAVITATIONAL LENSES
NT MAGNETIC LENSES
NT WIDE ANGLE LENSES
Fore-optics systems designed for electronic streak cameras using fiber optics
[DE84-014525] 02 p0281 N85-11830
Laser velocimeter measurements and analysis in turbulent flows with combustion. Part 3: A correction lens for laser Doppler measurements in a cylindrical tube
[AD-A146206] 03 p0366 N85-12348
Comparison of wide aperture and short residence time ion lenses
[DE84-015274] 03 p0420 N85-12685
A low-sidelobe space feed lens
[AD-A147863] 07 p0942 N85-15972
Helmet mounted telescope
[AD-D011355] 07 p1019 N85-16467
Modulation Transfer Function (MTF) measurement techniques for lenses and linear detector arrays
[NASA-TM-86166] 10 p1558 N85-19612
Technical support for microwave experiments on the eye lens
[AD-A149702] 12 p1933 N85-22144
Properties of chirped grating lenses in optical waveguides
[AD-A150023] 12 p1934 N85-22149
Positioning errors of commutating lenses and their influence on characteristics of high speed movie cameras 14 p2273 N85-24085
Laser beam shaping system with reduced objective diameter 14 p2275 N85-24095
Role of fluid lubricant-coolant in fine grinding of optical glass by diamond tool 14 p2280 N85-24125
Applications of compound eye configurations to smart sensor design
[AD-A150731] 14 p2420 N85-24935
Optic's institute's development of equipment for comet probe 15 p2484 N85-25333
Supersonic missile seeker lens system using gradient index material for first element lens
[AD-A151476] 15 p2490 N85-25387
Dall-Null tester for spaceborne applications
[AD-A151772] 16 p2881 N85-27779
Two-degree-of-freedom linear and planar microwave array lenses
[AD-A153701] 18 p3095 N85-29156
Influence of edge effects on performance of electrooptical lens 22 p3770 N85-33366
Automatic sphericity interferometer for testing lens radii
[AD-A155736] 22 p3786 N85-33457
Theoretical and computational research on the focused transport of intense charged particle beams
[DE85-012960] 23 p3972 N85-34621

LEPTONS
NT ANTINEUTRINOS
NT CONDUCTION ELECTRONS
NT ELECTRONS
NT MUONS
NT NEUTRINOS
NT POSITRONS
NT SOLAR NEUTRINOS
Standard model and beyond
[DE85-004269] 14 p2418 N85-24919
Measurements of heavy quark and lepton lifetimes
[DE85-008321] 18 p3181 N85-29724
Deep-inelastic lepton scattering by nuclei: The pion-exchange model
[DE85-010486] 19 p3359 N85-30828
Nuclear structure problems in double beta decay
[DE85-010739] 19 p3364 N85-30859
Toward the question of multi-quark configurations in nuclei 21 p3691 N85-32929
Dependence of the average spatial and energy characteristics of the hadron-lepton cascade on the strong interaction parameters at superhigh energies
24 p4188 N85-35877
Charge 4/3 leptons in cosmic rays
[HE-6.2-14] 24 p4212 N85-36150

LESIONS
NT PULMONARY LESIONS
Neural control of the direction of covert visual orienting
[AD-A145189] 01 p0097 N85-10650
Pathology of organophosphorus-induced delayed neurotoxicity
[AD-P004024] 06 p0844 N85-15358
Application of the isoenergy principle and the A weighting to evaluate lesion risks due to noise in a military environment
[ISL-CO-231/83] 14 p2390 N85-24720
Effects of long-term low-level radiofrequency radiation exposure on rats. Volume 8: Evaluation of longevity, cause of death, and histopathological findings
[AD-A154283] 19 p3327 N85-30610

LETHALITY
Teratogenicity studies of carbaryl and malathion alone and in combination in various laboratory animals
[AD-P004034] 06 p0845 N85-15364
Theory of lethality
[DE85-000457] 11 p1721 N85-20626
Systems vulnerability and lethality in the development phase
[AD-A149737] 12 p1924 N85-22089

LETTERS (SYMBOLS)
U SYMBOLS

LEUKEMIAS
H1-NMR studies on lymphocyte membranes in human lymphoproliferative diseases 20 p3505 N85-31787

LEUKOCYTES
NT LYMPHOCYTES

LEVEL (HORIZONTAL)
NT LIQUID LEVELS
Approximation of difference in water table positions by horizontal stratum in studies of their influence on gravity
10 p1502 N85-19478
Mathematical modeling of results of geometric leveling in variable gravity field 13 p2114 N85-23170

LEVEL (QUANTITY)
NT ATOMIC ENERGY LEVELS
NT EFFECTIVE PERCEIVED NOISE LEVELS
NT ELECTRON STATES
NT ENERGY LEVELS
NT GROUND STATE
NT INTERMOLECULAR FORCES
NT MOLECULAR ENERGY LEVELS
Oscillator development
[AD-A149689] 12 p1834 N85-21509

LEVELING
Margin leveling algorithm for fully saturated satellite transponder with CDMA (Code Division Multiple Access) signalling
[AD-A151710] 15 p2543 N85-25699
Planetary surface processes: A review
22 p3855 N85-33869

LEVERS
The guidelines to design the lever turning gears in articulated vehicles
[AD-P004301] 09 p1409 N85-18878
Axial bearings with lever-type equalizer system
14 p2267 N85-24048

LEVITATION
NT ACOUSTIC LEVITATION
NBS (National Bureau of Standards): Materials measurements
[NASA-CR-174036] 03 p0332 N85-12143
The generation of rolling moments with the superconducting solenoid model
[NASA-CR-172520] 09 p1283 N85-18066
Closed loop electrostatic levitation system
[NASA-CASE-NPO-15553-1] 18 p3092 N85-29142

LEVITATION MELTING
High temperature acoustic levitator
[NASA-CASE-NPO-16022-1] 12 p1927 N85-22105

LIABILITIES
NT LEGAL LIABILITY
Government contract contingent liabilities. The anti-deficiency act, and the hobgoblin of little minds
[AD-A147919] 07 p1053 N85-16684

LIAPUNOV FUNCTIONS
Lyapunov stability of very simple steady solutions of prognostic systems 14 p2333 N85-24429
Optimal open loop and nonlinear feedback control for remote orbital capture
[AD-A151987] 16 p2732 N85-26859
Characterization of intermittency in chaotic systems
[PREPRINT-429] 18 p3173 N85-29669
Sub-optimal control of nonlinear flexible space structures 20 p3414 N85-31190

LIBRARIES
Depository librarians' views on GPO's administration of the depository library program. Report to the Chairman, Joint Committee on Printing
[PB84-212265] 01 p0126 N85-10967
An investigation of the use, cost, perceived value and social context of telecommunications tools in two-year college libraries in the southeastern United States
02 p0293 N85-11901
Collection overlap and coordinated collection development 02 p0293 N85-11902
Evaluation of the National Library of Medicine's programs in the medical behavior sciences. Coverage of the Medical Behavioral Sciences (MBS) literature in monographic databases, study 5
[PB84-230531] 03 p0439 N85-12797
Evaluation of the National Library of Medicine's programs in the medical behavior sciences. Online searchers' reactions to database and vendor capabilities in the Medical Behavioral Sciences (MBS), study 4
[PB84-230523] 03 p0439 N85-12798
Evaluation of the National Library of Medicine's programs in the medical behavior sciences. Quality of indexing: The development and testing of a methodology comparing databases covering the Medical Behavioral Sciences (MBS) literature, study 3
[PB84-230515] 03 p0439 N85-12799
Evaluation of the National Library of Medicine's programs in the medical behavior sciences. Test retrievals in five major databases covering the Medical Behavioral Sciences (MBS) literature, study 2
[PB84-230507] 03 p0440 N85-12800
Evaluation of the National Library of Medicine's programs in the medical behavior sciences. Coverage, overlaps and gaps in bibliographic databases dealing with the Medical Behavioral Sciences (MBS) literature, study 1
[PB84-230499] 03 p0440 N85-12801
Evaluation of the National Library of Medicine's program in the medical behavior sciences. An analysis of the National Library of Medicine's (NLM) handling of Medical Behavioral Sciences (MBS) literatures: Some research tests of methods for evaluating bibliographic databases, executive summary
[PB84-230481] 03 p0440 N85-12802
Automated Library Search System (ALSS) user's manual
[DE84-015852] 04 p0576 N85-13672
Some attributes of online search intermediaries that relate to search outcome 05 p0734 N85-14721
Implementation of a Zilog Z-80 base realization library for the computer systems design environment
[AD-A146359] 06 p0853 N85-15423
The UK Schmidt telescope and the facilities in Edinburgh 07 p0965 N85-16121
Implementation of an Intel 8086 microprocessor-based realization library for the control system design language
[AD-A148506] 08 p1202 N85-17569
Computer center CDC Libraries-PROCFIL (procedures)
[AD-A148633] 08 p1206 N85-17589
Computer center CDC libraries/NSRD (subprograms)
[AD-A148792] 08 p1206 N85-17593
Computer center CDC libraries/utility (programs)
[AD-A148680] 09 p1368 N85-18593
Automation of information services furnished by documentation centers and specialized libraries
[FUB-6-1984] 09 p1402 N85-18827
Computer center CDC libraries
[AD-A149005] 10 p1540 N85-19707
Provision of Federal government publication in electronic format to depository libraries
[S-PRT-98-260] 10 p1567 N85-19880
The integrated library system design concepts for a complete serials control subsystem
[AD-A149379] 10 p1568 N85-19884
Abstract and index collection
[PB85-119501] 10 p1569 N85-19892
Parallel linear algebra library for the Denelcor HEP
[DE85-004685] 12 p1917 N85-22034
Software library: A reusable software issue
[AD-A150722] 14 p2403 N85-24816
Procedures for use in compiling requirements specifications for computerized library systems
[CSTI-76] 15 p2685 N85-26446
List of serials indexed for online users, 1985
[PB85-143220] 15 p2686 N85-26455
Notes for medical catalogers, 1984
[PB85-160206] 18 p3200 N85-29853
National Archives and Records Service (NARS) twenty year preservation plan
[PB85-177640] 18 p3200 N85-29854
Local automation model software benchmarking: Test plan
[AD-A154349] 19 p3337 N85-30676
Performance and library issues for mathematical software on high performance computers
[DE85-010263] 19 p3339 N85-30690
A transportable, machine oriented library of european sky and terrain radiance distributions with contemporary radiometric and meteorological profiles
[AD-A155254] 21 p3637 N85-32590
Lopez Energy Alternatives Project
[DE85-010589] 22 p3849 N85-33837
Technology transfer system automation implementation
[PB85-177335] 22 p3849 N85-33838
NBS (National Bureau of Standards) library serial holdings, 1985
[PB85-191948] 22 p3849 N85-33839
Procedure for editing the fluxgate magnetometer data of the AFGL (Air Force Geophysics Laboratory) magnetometer network
[AD-A156331] 24 p4117 N85-35523
Source header list, supplement 3
[AD-A156100] 24 p4165 N85-35824

LIBRATION
Vibration/libration interaction dynamics during the orbiter based deployment of flexible members
20 p3411 N85-31171

LIBRATIONAL MOTION
Stability of steady motions of dynamically symmetrical solid at a triangular libration point
14 p2279 N85-24120

LICENSING
Commercial space launches
[S-REPT-98-656] 12 p1768 N85-21225
Current regulatory and licensing status for byproduct sources, facilities and applications
[DE85-010967] 22 p3842 N85-33796

LICHENS
Interactive effects of acid rain and gaseous air pollutants on natural terrestrial vegetation
[DE85-005255] 16 p2621 N85-27401

LIDAR
U OPTICAL RADAR

LIE GROUPS
NT SPINOR GROUPS
Lie-transformation action principle for classical plasma dynamics
[DE84-014576] 02 p0285 N85-11858
Unrestricted convergence for generalized Poisson integrals
[CTH-MATH-1984-13] 04 p0556 N85-13540
Covariant lie-transformed plasma action principle
[DE85-000265] 11 p1732 N85-20891
Invariant differential operators on a semisimple symmetric space and finite multiplicities in a Plancherel formula
[CWI-PM-R8409] 12 p1925 N85-22094
Asymptotic behavior of matrix coefficients related to reductive symmetric spaces
[CWI-PM-R8410] 12 p1925 N85-22095
Intertwining functions on compact Lie groups
[CWI-TRACT-5] 14 p2414 N85-24898
A convexity theorem for semisimple symmetric spaces
[CWI-PM-R8414] 14 p2415 N85-24900
Cocycles and magnetic monopole
[DE85-007797] 16 p2556 N85-27012
On the transformation of derivatives of distributions on surfaces
[PREPRINT-434] 18 p3173 N85-29670

LIFE (BIOLOGY)
U LIFE SCIENCES

LIFE (DURABILITY)
NT CARRIER LIFETIME
NT FATIGUE LIFE
NT HALF LIFE
NT SATELLITE LIFETIME
NT SERVICE LIFE
NT STORAGE STABILITY
Effect of scandium on the structure and properties of Al-Zn-Mg alloys 01 p0018 N85-10111
Influence of aluminum metallization coatings on corrosion fatigue properties of steel
01 p0018 N85-10112
Free-piston Stirling engine development
[PB84-237767] 01 p0056 N85-10399
Turbine Engine Hot Section Technology (HOST)
[NASA-TM-83022] 02 p0140 N85-10861
Nonlinear structural and life analyses of a turbine blade 02 p0141 N85-10864
Nonlinear structural and life analyses of a combustor liner 02 p0141 N85-10865
Constitutive model development for isotropic materials
02 p0144 N85-10875
Life prediction and constitutive models for anisotropic materials 02 p0144 N85-10876
Surface protection overview 02 p0144 N85-10878
Effects of surface chemistry on hot corrosion life: Overview 02 p0145 N85-10880
Life distribution properties of devices subject to deterioration
[AD-A145554] 02 p0206 N85-11350
Reliability considerations for the total strain range version of strainrange partitioning
[NASA-CR-174757] 02 p0209 N85-11380
Lifetime of excess charge carriers in weakly doped epitaxial GaAs layers 04 p0487 N85-13108
The monitoring of machines
[CETIM-15-J-041] 04 p0510 N85-13259
Potential of flywheels for spacecraft energy storage
05 p0609 N85-13890
Method for predicting the creep rupture life of nickel-base precipitation-hardened superalloys from their chemical composition
[BLL-PNR-90241-(8019.3153)]
06 p0768 N85-14910
In-flight evalution of LCF life consumption of critical rotor components subjected to high transient thermal stress
07 p0906 N85-15734
Monitoring engine thermal stresses
07 p0906 N85-15735
Accelerated Mission Endurance Testing (AMET)
07 p0906 N85-15736
Inconel 718 alloy resistance to crack propagation
07 p0907 N85-15740
Cumulative damage modeling of fatigue crack growth
07 p0907 N85-15741
Problems and possibilities for life extension in gas turbine components 07 p0907 N85-15742
Engine cyclic durability by analysis and material testing 07 p0907 N85-15744
Life prediction at high temperature under multiaxial loading 07 p0907 N85-15746
Verification of life prediction through component testing 07 p0908 N85-15748
CFM 56-2. Oligocyclic fatigue of the turbofan disk. Dimensionning and tests for verification and improvements 07 p0908 N85-15750
View of future requirements for engine cyclic durability by analysis and testing 07 p0908 N85-15751
Ensuring required metrological reliability of analog instrument channels by parametric compensation
07 p0955 N85-16050
Effective life cycle software support: A study in discipline and versatility 08 p1065 N85-16746
SSME lifetime prediction and verification, integrating environments, structures, materials: The challenge
08 p1095 N85-16918
Ada in mission critical system acquisition: A guidebook
[AD-A149271] 10 p1540 N85-19710
Ada (trademark) Joint Program Office objectives and progress through 1983
[AD-A149436] 10 p1541 N85-19713

A study of interdiffusion in beta + gamma/gamma + gamma prime Ni-Cr-Al [NASA-CR-174852] 11 p1597 N85-20041
Method of constructing diagram of bimetal fatigue failure 11 p1599 N85-20058
Airbus fatigue tests 11 p1618 N85-20186
Emergency Locator Transmitter (ELT) batteries guidance and recommendations [NASA-TM-87436] 11 p1624 N85-20225
Method and apparatus for measuring minority carrier lifetime in a direct band-gap semiconductor [NASA-CASE-NPO-163371-1] 11 p1628 N85-20251
Hyperfine structure and lifetime measurements on electronically excited long-life molecules in a beam experiment [MPIS-11/1984] 11 p1726 N85-20855
Preliminary review of statistical treatment of S-glass/epoxy stress rupture data [AD-A149810] 12 p1797 N85-21275
Plasticizer system for propellant compositions [AD-D011502] 12 p1816 N85-21390
Plasticizer system for propellant compositions [AD-D011508] 12 p1816 N85-21391
Plasticizer system for propellant compositions [AD-D011514] 12 p1817 N85-21393
Plasticizer system for propellant compositions [AD-D011517] 12 p1817 N85-21395
Life study of RF excited Hg arc lamps and CO2 waveguide lasers [AD-A149818] 12 p1856 N85-21640
Technological process effect on the carrier lifetime degradation of silicon solar cell base layer irradiated by 1 MeV electrons (boron doping case) 13 p2007 N85-22585
Low thrust bipropellant engine/redundant seat valve assembly [AD-A150293] 13 p2013 N85-22628
Some specifics of development of fatigue and creep in heat-resistant alloys with asymmetrical multicycle loading 13 p2031 N85-22724
Developing procedures for thermomechanical processing of high-durability VT22 titanium alloy 13 p2031 N85-22726
Durability of VT16 alloy compounds obtained by diffusion welding 13 p2034 N85-22740
A state of the art assessment of turboprop transmission technology and projected needs for the next generation 14 p2220 N85-23770
Fabrication of ceramic substrate-reinforced and free forms [NASA-TM-86994] 14 p2247 N85-23926
Clutchless mechanism for engagement of forging press 14 p2268 N85-24051
Modernization of running gear of crane 14 p2286 N85-24163
Oxygen-hydrogen thrusters for Space Station auxiliary propulsion systems [NASA-CR-175691] 15 p2494 N85-25383
Self-sustaining low-Z coatings for fusion applications 2 - copper-lithium [DE85-002553] 15 p2658 N85-26403
Effects of surface chemistry on hot corrosion life [NASA-CR-174815] 16 p2708 N85-26711
Development of new materials for turbopump bearings 16 p2735 N85-26877
Bearings working group 16 p2735 N85-26878
Material for electrodes of pulsed and arc sources of light [DE85-007453] 16 p2760 N85-27156
Life and reliability modeling of bevel gear reductions [NASA-TM-87006] 16 p2793 N85-27227
Fatigue life analysis of a turboprop reduction gearbox [NASA-TM-87014] 16 p2793 N85-27228
Reexamination of cumulative fatigue damage laws 17 p2914 N85-27962
Optical strain measurement system development 17 p2915 N85-27969
Heat flux sensor calibrator 17 p2915 N85-27970
Feasibility of mapping velocity flow fields in SSME powerhead by laser anemometry techniques 17 p2915 N85-27971
A test methodology for an automated and interactive software development environment [AD-A152857] 17 p3011 N85-28618
Corrosion in civil aircraft structures [SNIAS-851-111-105] 20 p3432 N85-31291
Propellant plasticizer [AD-D011501] 20 p3434 N85-31306
Results of analysis on the design variable cells 20 p3445 N85-31388
Accelerated and real-time geosynchronous life cycling test performance of nickel-hydrogen batteries 20 p3448 N85-31405
Nickel-hydrogen cell test program summary 20 p3448 N85-31407
Micromechanics of high temperature deformation and failure 20 p3486 N85-31534
Improved Nominal Operating Cell Temperature (NOCT) test procedure 21 p3612 N85-32449
Corrosion management strategies for aircraft and related systems 22 p3749 N85-33239
Development of a high-efficiency, gas-fired, heat pipe, warm-air heating system [PB85-199636] 24 p4085 N85-35318

LIFE CYCLE COSTS
Technologies for space station autonomy [NASA-CR-174112] 04 p0458 N85-12906
Accelerated Mission Endurance Testing (AMET) 07 p0906 N85-15736
Concept and cost analysis of an orbiting lunar station [ILR-MITT-138] 07 p0913 N85-15776
Life cycle cost management master plan for the Defense Communications Agency [AD-A146876] 07 p1050 N85-16668
A practical example of reducing life cycle costs and increased availability 08 p1063 N85-16736
Standard Attitude Heading Reference System (SAHRS) full scale development program 08 p1073 N85-16804
Life cycle cost model for very high speed integrated circuits [AD-A147798] 08 p1157 N85-17298
Concept paper for the development of a DOD Ada (trademark) software engineering education and training plan [AD-A148774] 08 p1206 N85-17592
Permanent magnet motors [DE85-000660] 10 p1482 N85-19355
Optimization of a ground coupled heat pump [DE85-000273] 10 p1486 N85-19380
BIT/BITE tradeoff analysis model [AD-A149345] 11 p1701 N85-20697
Life cycle costing in government procurement [AD-A151878] 15 p2666 N85-26456
Some aspects of how to design cost-effective flight control systems 16 p2695 N85-26639
An analysis of the materiel fielding plan for the SINCGARS (Single Channel Ground and Airborne Radio System) radio [AD-A155101] 21 p3576 N85-32238
Development of a high-efficiency, gas-fired, heat pipe, warm-air heating system [PB85-199636] 24 p4085 N85-35318

LIFE RAFTS
Air carrier overwater emergency equipment and procedures [PB85-917006] 21 p3553 N85-32105

LIFE SCIENCES
NT EXTRATERRESTRIAL LIFE
NT MOLECULAR BIOLOGY
National Science Foundation grants and awards for fiscal year 1983, volume 2 [PB84-212323] 01 p0125 N85-10854
Life Sciences Research in Space --- conference [ESA-SP-212] 05 p0689 N85-14425
Space station: New frontier for life sciences in space 05 p0696 N85-14477
USSR report: Life sciences. Biomedical and behavioral sciences [JPRS-UBB-84-027] 07 p1012 N85-16426
Conference on Singlet Molecular Oxygen (COSMO 84), program and abstracts [AD-A147281] 07 p1040 N85-16605
USSR report: Life sciences. Biomedical and behavioral sciences [JPRS-UBB-85-001] 08 p1193 N85-17515
Research and technology, Lyndon B. Johnson Space Center [NASA-TM-58263] 08 p1262 N85-17929
USSR report: Life sciences. Biomedical and behavioral sciences [JPRS-UBB-85-007] 09 p1362 N85-18566
USSR report: Life sciences. Biomedical and behavioral sciences [JPRS-UBB-85-008] 10 p1523 N85-19605
USSR report: Life sciences. Biomedical and behavioral sciences [JPRS-UBB-85-011] 10 p1525 N85-19616
USSR report: Life sciences. Biomedical and behavioral sciences [JPRS-UBB-85-009] 10 p1526 N85-19625
China report: Science and technology [JPRS-CST-84-032] 11 p1621 N85-20202
China report: Science and technology [JPRS-CST-84-040] 11 p1623 N85-20219
China report: Science and technology [JPRS-CST-84-036] 11 p1696 N85-20661
Research and technology activities at Ames Research Center's Biomedical Research Division [NASA-TM-86692] 12 p1899 N85-21925
Aerospace Safety Advisory Panel [NASA-TM-87426] 13 p1970 N85-22373
China report: Science and technology [JPRS-CST-85-003] 13 p2166 N85-23433
USSR report: Life sciences. Biomedical and behavioral sciences [JPRS-UBB-85-012] 14 p2386 N85-24697
Research and technology [NASA-TM-86662] 14 p2456 N85-25166
China report: Science and technology [JPRS-CST-85-009] 15 p2530 N85-25596
China report: Science and technology [JPRS-CST-85-013] 15 p2536 N85-25652
China report: Science and technology [JPRS-CST-85-010] 15 p2564 N85-25819
Structural development and gravity 15 p2606 N85-26071
A search for evidence of large body Earth impacts associated with biological crisis zones in the fossil record 15 p2682 N85-26567
China report: Science and Technology [JPRS-CST-85-012] 16 p2806 N85-27300
Life sciences flight experiments program mission science requirements document. The first life sciences dedicated Spacelab mission, part 1 [NASA-TM-87494] 21 p3559 N85-32137
USSR Space Life Sciences Digest [NASA-CR-3922] 21 p3656 N85-32709
Search for the universal ancestors [NASA-SP-477] 21 p3667 N85-32777
USSR report: Space [JPRS-USP-84-006] 22 p3731 N85-33128
USSR report: Life sciences. Biomedical and behavioral sciences [JPRS-UBB-85-021] 23 p3951 N85-34489
Effect of seeds of heavy charged particles of galactic cosmic radiation 23 p3954 N85-34505

LIFE SPAN
The role of gravity on the reproduction of arabidopsis plants 15 p2607 N85-26069

LIFE SUPPORT SYSTEMS
NT CLOSED ECOLOGICAL SYSTEMS
NT EMERGENCY LIFE SUSTAINING SYSTEMS
Aeronautical systems technology needs: Escape, rescue and survival, test facilities and test equipment and training-simulation equipment [AD-A145059] 01 p0001 N85-10002
Conceptual design and evaluation of selected Space Station concepts, volume 2 [NASA-TM-87384] 02 p0166 N85-11130
The controlled ecological life support system 15 p2688 N85-26603
Controlled Ecological Life Support Systems (CELSS) 15 p2688 N85-26604
Controlled Ecological Life Support System. Life Support Systems in Space Travel [NASA-CP-2378] 18 p3155 N85-29531
BLSS: A contribution to future life support 18 p3155 N85-29534
Advanced regenerative environmental control and life support systems: Air and water regeneration 18 p3155 N85-29535
Dynamic considerations for control of closed life support systems 18 p3155 N85-29537
CELSS transportation analysis 18 p3156 N85-29538
Extended mission life support systems 18 p3157 N85-29547
Space shuttle revitalization system 18 p3157 N85-29548
Space station ECLSS integration analysis: Simplified General Cluster Systems Model, ECLS System Assessment Program enhancements [NASA-CR-176089] 21 p3670 N85-32796
Composition and dynamics of bacteriocenosis associated with algae in human life-support systems 22 p3823 N85-33684
Chemical composition of Musca domestica L. larval and pupal biomass when developing in organic waste of biological life-support system for man 22 p3824 N85-33691

LIFEBOATS
Air carrier overwater emergency equipment and procedures [PB85-917006] 21 p3553 N85-32105

LIFETIME (DURABILITY)
U LIFE (DURABILITY)

LIFT
NT INTERFERENCE LIFT
NT ZERO LIFT
Observations from varying the lift and drag inputs to a noise prediction method for supersonic helical tip speed propellers [NASA-TM-83797] 01 p0115 N85-10788

Lifting surface theory for a helicopter rotor in forward flight
[NASA-TM-86315] 02 p0134 N85-10916
A comparison of Wortmann airfoil computer-generated lift and drag polars with flight and wind tunnel results
[NASA-TM-86036] 04 p0452 N85-12966
A study of lift characteristics of an upper surface blown jetwing with a rectangular nozzle
05 p0591 N85-13767
Improvement of Aerodynamic Performance Through Boundary Layer Control and High Lift Systems
[AGARD-CP-365] 08 p1068 N85-16771
Recent progress of development and understanding of high lift systems 08 p1068 N85-16772
Investigations into the effects of scale and compressibility on lift and drag in the RAE 5m pressurized low-speed wind tunnel 08 p1068 N85-16773
Detailed study of the flow around a multi-element airfoil. Comparison with calculations 08 p1069 N85-16775
Turbulent bubbles behind airfoils and wings at high angle of attack 08 p1069 N85-16779
Aerodynamic issues in the design of high-lift systems for transport aircraft 08 p1069 N85-16780
An update of the Canada/USA augmentor-wing project 08 p1070 N85-16781
Preliminary results from the unsteady airfoil model USTAR2
[AD-P004171] 09 p1266 N85-17956
Icing flight research: Aerodynamic effects of ice and ice shape documentation with stereo photography
[NASA-TM-86906] 09 p1279 N85-18049
Investigations into the effects of scale and compressibility on lift and drag in the RAE 5m pressurised low-speed wind tunnel
[RAE-TM-AERO-2006] 13 p1969 N85-22372
Estimating unsteady aerodynamic forces on a cascade in a three-dimensional turbulence field
[NASA-TM-86701] 14 p2209 N85-23704
A preliminary investigation of the dynamic force-calibration of a magnetic suspension and balance system
[NASA-CR-172580] 14 p2228 N85-23806
Flow past a flat plat with a vortex/sink combination
[JIAA-TR-58] 15 p2464 N85-25215
High specific power aircraft turn maneuvers: Tradeoff of time-to-turn versus change in specific energy
[AD-A151701] 15 p2471 N85-25257
Aerodynamic performance of a wing in ground effect using the PANAIR program
[AD-A153303] 17 p2892 N85-27832
Method of calculating separation flow of subsonic gas stream around wings 17 p2942 N85-28161
A method for computing the core flow in three-dimensional leading-edge vortices
[NASA-TM-87489] 19 p3214 N85-29932
Application of two-dimensional unsteady aerodynamic to a free-tip rotor response analysis
[NASA-CR-177348] 19 p3215 N85-29933
Circulation control lift generation experiment: Hardware development 22 p3799 N85-33535

LIFT AUGMENTATION
Manufacturing report of an augmented lift, variable deflection half wing
[ONERA-RT-25/1736-AY-108-A]
05 p0591 N85-13766
Presentation of the acoustic and aerodynamic results of the Aladin 2 concept qualification testing
[NASA-TM-77883] 24 p4060 N85-35161

LIFT COEFFICIENTS
U AERODYNAMIC COEFFICIENTS
U LIFT

LIFT DEVICES
Incompressible lifting-surface aerodynamics for a rotor-stator combination
[NASA-TM-83767] 03 p0316 N85-12039
Recent progress of development and understanding of high lift systems 08 p1068 N85-16772
Three-dimensional unsteady lifting surface theory in the subsonic range
[NASA-TM-77812] 12 p1770 N85-21111
Auxiliary units for Robots 14 p2285 N85-24161
Wind tunnel wall interference
[AD-A151212] 15 p2474 N85-25273
A computational method for wings of arbitrary planform
[AD-A153788] 18 p3059 N85-28929
Unsteady transonic flow calculations for interfering lifting surface configurations
[NASA-TM-86432] 19 p3214 N85-29931
Trailing edge flow and aerodynamic sound. Part 1: Tonal pressure and velocity fluctuations. Part 2: Random pressure and velocity fluctuations
[AD-A154947] 21 p3552 N85-32097

LIFT DISTRIBUTION
U FORCE DISTRIBUTION
U LIFT

LIFT DRAG RATIO
An experimental study of the transonic equivalence rule with lift, part 2
[AR-LR-614-PT-2] 01 p0001 N85-10004
Low lift-to-drag aero-assisted orbit transfer vehicles
08 p1107 N85-16994
Moderate lift-to-drag aeroassist
08 p1107 N85-16995
Benefits of high aerodynamic efficiency to orbital transfer vehicles 08 p1107 N85-16996
Over the wing propeller
[NASA-CASE-LAR-13134-1] 11 p1584 N85-19980
Aerodynamic performance of a wing in ground effect using the PANAIR program
[AD-A153303] 17 p2892 N85-27832
Study of an efficient long-range Mach 2.7 supersonic transport configuration concept
[NASA-TM-86414] 21 p3554 N85-32110
The influence of helicopter tail shape on drag: An aerodynamic study using a low speed wind tunnel
[AD-A156304] 24 p4082 N85-35174

LIFT FORCES
U LIFT

LIFTING BODIES
NT LIFTING REENTRY VEHICLES
Lifting surface theory for a helicopter rotor in forward flight
[NASA-TM-86315] 02 p0134 N85-10916
An investigation of vortex-induced aerodynamic characteristics of supersonic cruise configurations
[NASA-CR-174299] 07 p0896 N85-15690
Comparison of analytical and experimental steadyand unsteady-pressure distributions at Mach number 0.78 for a high-aspect-ratio supercritical wing model with oscillating control surfaces
[NASA-TM-84580] 07 p0899 N85-15697
Simultaneous flow visualization and unsteady lift measurement on an oscillating lifting surface
[AD-P004157] 09 p1264 N85-17942
Genesis of unsteady separation
[AD-P004173] 09 p1266 N85-17958
Unsteady transonic flow calculations for interfering lifting surface configurations
[NASA-TM-86432] 19 p3214 N85-29931

LIFTING REENTRY VEHICLES
Aerodynamic characteristics of some lifting reentry concepts applicable to transatmospheric vehicle design studies
[NASA-TM-86331] 06 p0747 N85-14787
The application of some lifting-body reentry concepts to missile design
[NASA-TM-86394] 13 p1969 N85-22366

LIFTING ROTORS
NT BEARINGLESS ROTORS
Basic consideration of the lifting capability of stoppable rotors
[AD-A150850] 14 p2219 N85-23750
A new main rotor hub for the AS 332 Super Puma
[SNIAS-851-210-102] 20 p3393 N85-31047

LIFTING SURFACES
U LIFT DEVICES
U LIFTING BODIES
U SURFACES

LIFTS
Hoist
[AD-D011458] 10 p1493 N85-19425

LIGANDS
Chemically modified electrodes and related solution chemistry
[DE84-017110] 05 p0614 N85-13924
Correlation of electronic charge transfer transitions and electrochemical potentials. The Bipyrazine(Tetracarbonyl)Molybdenum(O) system in various solvents
[AD-A147680] 08 p1120 N85-17062
Ligand structural influences upon electrochemical reactivity: Organic substituent effects upon Carboxylatopentaamminecobalt(3) reductions at mercury and gold electrodes
[AD-A150685] 14 p2250 N85-23944
Metal complexes of some heterocyclic ligands
15 p2504 N85-25446
Metal alkoxides: Models for metal oxides. Alkoxide ligands in early transition metal organometallic chemistry
[DE85-011368] 23 p3916 N85-34269

LIGHT (VISIBLE RADIATION)
NT AIRGLOW
NT COHERENT LIGHT
NT GEOCORONAL EMISSIONS
NT LIGHT BEAMS
NT NIGHTGLOW
NT POLARIZED LIGHT
NT SKY RADIATION
NT SUNLIGHT
NT TWILIGHT GLOW
NT ZODIACAL LIGHT
Personal experience with the PVHD and options of situations in which a wide Field Of View (FOV) PVHD might be helpful 01 p0008 N85-
Proton pumping in purple membrane, appendix
[DE84-014601] 01 p0118 N85-
Characteristics of light diffraction by two acoustic waves, one with complex frequency composition
03 p0348 N85-
Improved radiographic viewing system
[AD-A147587] 07 p1016 N85-
Switchable zero order diffraction gratings as light valves
[AD-A147575] 07 p1044 N85-
The relative effectiveness of red and white light for subsequent dark-adaptation
[AD-A148883] 10 p1530 N85-
Optical guiding in a free electron laser
[DE85-003141] 11 p1639 N85-
Study of light shifts in laser pumped quantum discriminator frequency 11 p1716 N85-
Measurement of the configuration of a concave surface by the interference of reflected light
[NASA-TM-77796] 11 p1728 N85-
Acoustooptic cell as space-frequency filter
13 p2080 N85-
Measurement of the nighttime infrared luminosity of Spacelab 1 in the H- and K-bands
[NASA-TM-85972] 14 p2434 N85-
Raman scattering of light in epitaxial films of solid phosphide-gallium arsenide solutions
15 p2643 N85-
Optically triggered transferred-electron device microwave burst and single pulse generators
[AD-D011614] 16 p2776 N85-
Pursuit tracking performance and flash disruption: The effects of training the non-dominant eye on target reacquisition
[AD-A153404] 17 p2998 N85-
The touch panel system: Design and development
[AD-A153014] 17 p3008 N85-
System of white-light density pseudocolor encoding with three primary colors
[AD-D011651] 17 p3037 N85-
Light transmitting window assembly
[NASA-CASE-MSC-18417-1] 18 p3185 N85-
Method for the preparation of photochromic insulating crystals
[DE85-011606] 19 p3262 N85-
Optically pumped laser system having extracavity pulse smoother
[AD-D011714] 19 p3276 N85-
Haze over eastern North America. Part 1: Haze properties
[PB85-181857] 19 p3311 N85-
Quasioptical gyroklystron
[AD-D011686] 19 p3356 N85-
Radioluminescent lighting for Alaskan runway lighting and marking
[DE85-010405] 19 p3368 N85-
Visual phenomena produced by binocularly disparate dynamic visual noise
[AD-A154758] 21 p3663 N85-
Ice fog as an electro-optical obscurant
[AD-A155059] 21 p3705 N85-
Estimating angular position of optical radiation sources when received by array of photodetectors
22 p3776 N85-
Self-study manual on optical radiation measurements. Part 1: Concepts. Chapter 12: Blackbodies, blackbody radiation, and temperature scales
[PB85-195303] 24 p4154 N85-
Study of the shower maximum depth by the method of detection of the EAS Cerenkov light pulse shape
[HE-4.4-15] 24 p4194 N85-
Preliminary results of the Cerenkov EAS flashes in the Crimean Astrophysical Observatory
[HE-4.4-17] 24 p4194 N85-

LIGHT ABSORPTION
U ELECTROMAGNETIC ABSORPTION

LIGHT ADAPTATION
Effect of extreme peripheral light on dark adaptation
[AD-A148923] 10 p1528 N85-
Discovery regarding visual neuron adaptation applicable to robot use 20 p3504 N85-

LIGHT AIRCRAFT
NT CESSNA 402B AIRCRAFT
NT DO-28 AIRCRAFT
Crashworthiness of light aircraft fuselage structures: A numerical and experimental investigation
01 p0060 N85-
Preliminary airworthiness evaluation of the Rutan Aircraft Factory (RAF), Inc. LONG-EZ airplane with external sight
[AD-A145381] 02 p0136 N85-
Low power laminar aircraft structures
04 p0451 N85-

Contribution of the study of light aircraft propeller noise
[ESA-TT-865] 09 p1378 N85-18867
The design of sport and touring aircraft
[NASA-TM-77783] 10 p1423 N85-18875
Development and operation of a measuring data acquisition system for use in light airplanes
24 p4123 N85-35556

LIGHT ALLOYS
NT ALUMINUM ALLOYS
NT BERYLLIUM ALLOYS
NT MAGNESIUM ALLOYS
Influence of recrystallization and solution on the tenacity of the 7010 and 7475 alloys. Oligocyclic fatigue of the 7010 alloy
[ONERA-RT-19/5089-M] 20 p3432 N85-31269

LIGHT AMPLIFIERS
Fiber cable in optical system with brightness amplifier
02 p0263 N85-11724
Optical inhomogeneities in a nanosecond-pulse iodine photodissociation laser with slow UV radiation pumping
21 p3686 N85-32902

LIGHT BEAMS
Fluctuations in parameters of light beam along path with reflection in turbulent atmosphere
02 p0263 N85-11722
Optical computer studies at UK's Heriot-Watt University 09 p1309 N85-18227
Numerical investigation of propagation of radiation pulse at xxx 11 p1718 N85-20809
Spontaneous diffraction of sequence of supershort light pulses in dye solution 11 p1718 N85-20811
Intensity fluctuations of focused laser beam during reflection in turbulent atmosphere
13 p2078 N85-22975
Time spectra of intensity fluctuations along reflecting path 13 p2079 N85-22981
Method and apparatus for generating a structured light beam array
[AD-D011590] 15 p2652 N85-26357
Double window viewing chamber assembly
[NASA-CASE-MFS-28057-1] 18 p3063 N85-28951
Multiport optical detectors 18 p3187 N85-29769
Laser Schlieren crystal monitor
[NASA-CASE-MFS-28060-1] 19 p3374 N85-30932
Influence of coherent light beams on free carriers in semiconductors 21 p3681 N85-32867
Fluctuations in light intensity during backscattering in turbulent medium 21 p3695 N85-32958
Coefficient of optical absorption and scattered light capture effect 21 p3695 N85-32959
Refraction of narrow probing light beam in multilayer optical fiber 22 p3764 N85-33330
Asymmetry of diffraction orders with light diffraction at surface acoustic wave 22 p3782 N85-33431
Ranging system which compares an object reflected component of a light beam to a reference component of the light beam
[NASA-CASE-NPO-15866-1] 23 p3973 N85-34629

LIGHT BULBS
U LUMINAIRES

LIGHT COMMUNICATION
U OPTICAL COMMUNICATION

LIGHT CURVE
One to eight month X-ray light curves for active extragalactic objects 08 p1239 N85-17817
Optical and X-ray observations of 4U2129+47/V1727 CYG in a quiescent state 11 p1742 N85-20950
Recent results on the Crab Pulsar X-ray light curve
11 p1742 N85-20955
Eclipse observations of Epsilon Aurigae
11 p1755 N85-21037
Convex-profile inversion of asteroid lightcurves
13 p2176 N85-23502
Very high energy gamma rays from the Crab Nebula
[OG-2.3-3] 22 p3866 N85-33940
A new approach to evaluate gamma-ray measurements
[OG-9.5-11] 23 p4031 N85-34988
The experimental cascade curves of EAS at E sub 0 10(17) eV obtained by the method of detection of Cherenkov pulse shape
[HE-4.4-16] 24 p4194 N85-36024

LIGHT DURATION
U FLASH
U PULSE DURATION

LIGHT ELEMENTS
Calculation of Si(Li) X-ray detector efficiencies
[DE85-002732] 10 p1489 N85-19400

LIGHT EMISSION
NT BIOLUMINESCENCE
NT CATHODOLUMINESCENCE
NT CHEMILUMINESCENCE
NT ELECTROLUMINESCENCE
NT FLUORESCENCE
NT INCANDESCENCE
NT LUMINESCENCE
NT OPTICAL RESONANCE
NT PHOSPHORESCENCE
NT PHOTOLUMINESCENCE
NT RESONANCE FLUORESCENCE
NT SHOCK WAVE LUMINESCENCE
NT THERMOLUMINESCENCE
NT X RAY FLUORESCENCE
New lighting technologies, their status and impacts on power densities
[DE85-000712] 09 p1315 N85-18266
Formation of optical-line emitting regions in the jets of SS433 12 p1959 N85-22318
Optical monitoring of gamma-ray source fields
[OG-1.1-7] 22 p3861 N85-33908
Search for optical bursts from the gamma ray burst source GBS 0526-66
[OG-1.1-8] 22 p3861 N85-33909

LIGHT EMITTING DIODES
LED multifunction keyboard engineering study
[AD-A145199] 01 p0010 N85-10061
1.5 to 1.7 micrometers LEDs (Light-Emitting Diode)
[AD-A149665] 12 p1834 N85-21506
Transistor-transistor logic microcircuit tester
12 p1842 N85-21556
Focal plane array optical proximity sensor
[NASA-CASE-NPO-15155-1] 12 p1932 N85-22139
AL-124 light-emitting diode in 30 Mbit/s fiber-optic communication line 13 p2069 N85-22925
Optoacoustic receiver with semiconductor-type radiator and photodetector 14 p2274 N85-24086
Error of distance measurement by phase-type optical range finders with photoreceivers of various types
14 p2276 N85-24101
InGaAs/GaAs, Strained-Layer Superlattice (SLS), junction photodetectors, LED's, injection LASER's and FET's for optoelectronic IC applications
[DE85-001940] 14 p2430 N85-24986
Electron irradiation of light emitting diodes
[AD-A154441] 19 p3260 N85-30213
Electrochromic display device
[AD-D011733] 22 p3759 N85-33299
Transceiver test device
[AD-D011728] 22 p3786 N85-33458

LIGHT GAS GUNS
The utilization of a light-gas gun to simulate interior ballistic flow
[ISL-CO-233/83] 14 p2303 N85-24259
Experimental simulation of internal ballistic flows
[ISL-CO-208/84] 20 p3435 N85-31312

LIGHT INTENSITY
U LUMINOUS INTENSITY

LIGHT IONS
Experiments with light ions at CERN super proton synchrotron
[DE85-007625] 17 p3031 N85-28744
Heavy ion medical accelerator options
[DE85-011204] 22 p3841 N85-33784
Light ion sources for ICF
[DE85-011544] 23 p3983 N85-34702
Multidimensional analysis of data obtained in experiments with X-ray emulsion chambers and extensive air showers
[HE-3.6-2] 24 p4184 N85-35951

LIGHT MODULATION
NT ULTRASONIC LIGHT MODULATION
Transfer function of multilayered magnetooptical space-time modulator 02 p0264 N85-11726
Optical waveguide spatial filters
[AD-A145674] 02 p0280 N85-11825
The spectral distribution of field components for a sinusoidal power modulated monofrequency optical carrier source
[FI-44-TBR-94] 04 p0565 N85-13801
A picosecond population modulation study of near interband resonances in semiconductors
09 p1396 N85-18787
An electro-optic spatial light modulator for thermo-elastic generation of programmably focused ultrasound
[AD-A149076] 10 p1553 N85-19794
Switchable zero order diffraction gratings as light valves
[AD-A150129] 12 p1934 N85-22153
Space-time response characteristics of acoustooptic filter for compression of linearly frequency-modulated signal 13 p2071 N85-22937
Theory of diaphragm light modulators with electrical input signal 13 p2082 N85-23002
An electro-optic spatial light modulator for thermoelastic generation of programmably focused ultrasound
[AD-A152086] 15 p2646 N85-26323
Electron-bombarded silicon spatial light modulator
[AD-D011579] 15 p2652 N85-26355
Charge isolation in a spatial light modulator
[AD-D011581] 15 p2652 N85-26356
Construction and analysis of a PRIZ spatial light modulator exhibiting dynamic image selection
[AD-A152318] 17 p3037 N85-28787
Deformable mirror nearest neighbor optical computer
18 p3188 N85-29772
Stokes parameters modulator for birefringent filters
18 p3205 N85-29884
Differentiating spatial light modulator
[AD-D011727] 23 p3973 N85-34632

LIGHT PRESSURE
U ILLUMINANCE

LIGHT PROBES
U LIGHT BEAMS

LIGHT SCATTERING
NT HALOS
Physical-chemical properties of articulated rodlike polymers
[AD-A145549] 02 p0186 N85-11244
Characterization of atmospheric conditions along transmission paths from a remotely piloted vehicle
[AD-A145527] 02 p0232 N85-11511
Structure of vibrational spectrum and selection rules in Raman and hyper-Raman light scattering spectra of inorganic glasses 02 p0271 N85-11769
Extinction by dielectric particles at optical and infrared wavelengths
[AD-A146305] 03 p0413 N85-12640
Brillouin scattering in underdense UV laser-produced plasmas
[DE84-015184] 04 p0567 N85-13814
Storage stability of jet fuels
[AD-A146380] 06 p0773 N85-14943
Investigation of light source and scattering medium related to vapor-screen flow visualization in a supersonic wind tunnel
[NASA-TM-86290] 06 p0810 N85-15144
Research on acoustical and optical scattering, optics of bubbles, diffraction catastrophes, laser generation of sound, and shock induced cavitation
[AD-A146703] 06 p0860 N85-15466
A study of structural phase transitions using light scattering techniques
[AD-A147261] 07 p1048 N85-16654
Light scattered from polished optical surfaces: Wings of the point spread function 08 p1252 N85-17911
Journal of Research of the National Bureau of Standards. Volume 89, Number 1, January-February, 1984
[PB84-235530] 08 p1262 N85-17931
Measurement of drop-size distributions with the aid of a scattered light particle size counting analyser
[BLL-TRANS-WH-620-(9091.9F)]
09 p1317 N85-18278
Application of scattered light particle size counting analysis to the determination of wide drop size distributions
[BLL-TRANS-WH-619-(9091.9F)]
09 p1317 N85-18279
Light scattering studies of lower dimensional colloidal particle and critical fluid systems
[DE85-002067] 09 p1377 N85-18654
Theory of resonant light scattering from a rough surface 09 p1383 N85-18701
Experimental and theoretical study of condensation in multicomponent vapors
[DE85-000843] 10 p1485 N85-19376
Effect of extreme peripheral light on dark adaptation
[AD-A148923] 10 p1528 N85-19636
Experimental investigation of wavefront conjugation during Mandelstam-Brillouin scattering of focused laser beams in condensed media 11 p1716 N85-20796
Spontaneous diffraction of sequence of supershort light pulses in dye solution 11 p1718 N85-20811
Light diffraction with collective, thermal electron density fluctuation in plasmas with several ionic components
[IPF-84-5] 11 p1733 N85-20904
Subnanosecond time-resolved emission study of Cu2O and GaAs
[DE85-002070] 11 p1735 N85-20912
Research study of droplet sizing technology leading to the development of an advanced droplet sizing system
[NASA-CR-174839] 12 p1850 N85-21604
Transmission and reflection of laser beams propagating through aerosol clouds in space
[LA-9998-MS] 12 p1856 N85-21638
On the inversion of the lidar equation
[AD-A149653] 12 p1856 N85-21641
A systematic study of light scattering by irregularly shaped particles
[AD-A150192] 13 p2159 N85-23400
Nonrelativistic Kapitza-Dirac scattering
[AD-A150822] 13 p2159 N85-23405
Scattering properties of a moving dielectric object
[AD-A151974] 15 p2544 N85-25706
Application of scattering methods to the studies of the structure of polymer blends
[IFPP-[illegible]/1984] 17 p2933 N85-28104

Earth observation modeling based on layer scattering matrices
[NLR-MP-84015-U] 17 p2964 N85-26440
Studies of optical-beam phase-conjugation by nonlinear refraction
[AD-A152965] 17 p3037 N85-26786
Light scattering by leaf layers with application to canopy reflectance modeling: The Scattering by Arbitrarily Inclined Leaves (SAIL) model
[NLR-MP-84011-U] 17 p3038 N85-26796
Light scattering and spectroscopic studies of polymerization processes
[AD-A153407] 18 p3069 N85-26964
Technique to reduce scattered light in optical systems
[AD-D011597] 18 p3165 N85-29752
Laser forward and backscattering in particulate media
[AD-A154138] 19 p3275 N85-30312
Detection of internal structure by scattered light intensity: Application to kidney cell sorting
20 p3503 N85-31777
Flow cytometry of human embryonic kidney cells: A light scattering approach 20 p3503 N85-31778
Journal of Research of the National Bureau of Standards, volume 90, number 1, January - February 1985
[PB85-178083] 20 p3522 N85-31906
Phase behavior and QLS (Quasielastic Light Scattering) in potassium linoleate/n-alkanol microemulsions
[AD-A155028] 21 p3563 N85-32153
Temperature measurements on small droplets
21 p3653 N85-32699
Influence on bi-phonon states on Raman scattering of light in molecular crystals 21 p3680 N85-32865
Generation and amplification of radiation during stimulated Raman scattering in crystals
21 p3681 N85-32869
Effective brightness of zero-point fluctuations of the electromagnetic vacuum accompanying parametric scattering of light 21 p3694 N85-32951
Correlation of intensities of different scattering channels 21 p3694 N85-32952
Coefficient of optical absorption and scattered light capture effect 21 p3695 N85-32959
Stimulated Mandelstam-Brillouin scattering with distributed feedback 21 p3696 N85-32961
Influence of phonon interaction on width and form of Mandelstam-Brillouin optical scattering line
21 p3696 N85-32962
Transmission of light by disperse medium of densely packed optically soft particles 21 p3697 N85-32969
Ice fog as an electro-optical obscurant
[AD-A155059] 21 p3706 N85-33015
Calculating solar highlight and shadeless areas for scanning photographs from space and optimizing lighting conditions 22 p3736 N85-33160
Size exclusion chromatography-low angle laser light scattering photometry of lignite macromolecules
[DE85-012017] 22 p3745 N85-33215
Interrelations for the elements of the scattering matrix
22 p3865 N85-33872
High resolution Cherenkov detectors for cosmic ray isotope experiment
[OG-9.1-4] 23 p4023 N85-34930
Energy calibration of the fly's eye detector
[HE-4.4-1] 24 p4192 N85-36011
LIGHT SCATTERING METERS
Apparatus for determining the liquid water content of a gas
[AD-D011297] 07 p0922 N85-15839
Particle sizing from forward scattered light at two angles using a Variable-Focal-Length optical system
[AD-A154164] 20 p3533 N85-31980
LIGHT SOURCES
NT ILLUMINATORS
A limbus-sensing eye movement recorder
[AD-A144772] 01 p0049 N85-10323
An evaluation of flashtube signal characteristics
[AD-A149589] 10 p1423 N85-18974
Formulation of a coherent light-sheet by means of a cylindrical-spherical optical system
[ISL-R-116/83] 16 p2865 N85-27674
Electrodeless HID lamp study
[DE85-010626] 18 p3096 N85-29167
Experience with a high-brightness storage ring: The NSLS 750 MeV VUV ring
[DE85-010547] 18 p3190 N85-29787
Combined function lattices for a 6 GeV synchrotron light source
[DE85-010859] 19 p3367 N85-30895
Radioluminescent lighting for Alaskan runway lighting and marking
[DE85-010405] 19 p3368 N85-30897
Pulsed lasers for filming color holographic film images
22 p3781 N85-33426
Study of composition of cosmic rays with energy .7 E 3 Ee
[OG-6.1-7] 22 p3881 N85-34048
Electronic imaging system and technique
[DE85-005740] 23 p3935 N85-34393
Vacuum system for the Argonne 6 GeV synchrotron light source
[DE85-012286] 24 p4157 N85-35773
Background light measurements at the DUMAND site
[HE-5.2-7] 24 p4203 N85-36084
LIGHT SPEED
On the propagation speed in relativistic quantum mechanics
[CWI-AM-R8410] 17 p3046 N85-26848
Sub-luminal pulses from cosmic ray air showers
[HE-4.7-13] 24 p4200 N85-36063
LIGHT TRANSMISSION
NT HALOS
NT LIGHT SCATTERING
Collapse of cavitation bubbles between two walls in ultrasonic field 02 p0266 N85-11739
Experimental capabilities and prospects for measuring soft X-ray photoabsorption
[DE84-015489] 02 p0278 N85-11813
Atmospheric extinction in critical environments
[AD-A146102] 03 p0396 N85-12527
Free-space propagation of light pulses
[PB84-217108] 03 p0421 N85-12689
Site-specific research conducted in support of the Salton Sea Solar Pond Project, FY 1982 report
[NASA-CR-174182] 05 p0666 N85-14280
Laboratory investigations 05 p0666 N85-14281
Development and analysis of silicon solar cells near 20% efficiency 06 p0829 N85-15267
Long-term light induced changes in dark conductivity of kapton
[AD-A148791] 08 p1224 N85-17706
Development of photoconductive power switch technology
[DE85-001514] 09 p1315 N85-18270
Diffraction diffusion screen with holographically-suppressed zero-order beam
[AD-D011445] 10 p1467 N85-19387
Improvements in glazings: SERI materials research in progress
[DE84-013049] 12 p1614 N85-21378
Transmission and reflection of laser beams propagating through aerosol clouds in space
[LA-9899-MS] 12 p1856 N85-21638
Temperature-insensitive optical fibers
[AD-D011551] 12 p1933 N85-22142
Fine structure of vertical distribution of light attenuation index of sea water 13 p2109 N85-23140
Ways of optimization of light energy transformation in primary stages of photosynthesis. Optimization of lattice structure of uniform photosynthetic unit
14 p2386 N85-24701
Studies of electro-optical attenuation in the vicinity of cloud base
[AD-A151745] 15 p2653 N85-26360
Philips researches gallium arsenide use for lasers
18 p3087 N85-29106
Light transmitting window assembly
[NASA-CASE-MSC-18417-1] 18 p3165 N85-29750
Model computations of light reflection from sea surface 19 p3292 N85-30411
Comparison of 8 to 12 micrometer and 3 to 5 micrometer CVF transmissometer data with LOWTRAN calculations
[AD-A154218] 19 p3350 N85-30763
Switchable zero order diffraction gratings as light valves
[AD-A154471] 20 p3533 N85-31981
Ship-to-ship propagation: Maritime data analyses
[AD-A155484] 21 p3592 N85-32325
Transmission of light by disperse medium of densely packed optically soft particles 21 p3697 N85-32969
Energy calibration of the fly's eye detector
[HE-4.4-1] 24 p4192 N85-36011
The structure of EAS at E 0.1 EeV
[HE-4.4-2] 24 p4193 N85-36012
LIGHT VALVES
Switchable zero order diffraction gratings as light valves
[AD-A147575] 07 p1044 N85-16633
Switchable zero order diffraction gratings as light valves
[AD-A150129] 12 p1934 N85-22153
Electron-bombarded silicon spatial light modulator
[AD-D011579] 15 p2652 N85-26355
Charge isolation in a spatial light modulator
[AD-D011581] 15 p2652 N85-26356
Numerical optical computing at the Ohio State University 18 p3188 N85-29775
Switchable zero order diffraction gratings as light valves
[AD-A154471] 20 p3533 N85-31981
Liquid crystal light valve structures
[NASA-CASE-MSC-20036-1] 22 p3847 N85-33826
LIGHT WATER REACTORS
Neutron detector counting capabilities for (10) B-lined and (235) U fission chambers in high gamma-ray fie
[DE85-011693] 22 p3840 N85-3
Effect of stainless steel weld overlay cladding on the structural integrity of flawed steel plates in bending, serie 1
[TI85-010349] 23 p3939 N85-344
Pressure measurements in a hydrogen combustio environment: Hydrogen-air combustion test series 1 and 2 in the FITS tank, volume 1
[TI85-009899] 24 p4076 N85-35
LIGHTHILL METHOD
Hypersonic flow of mixture around blunt body
06 p0779 N85-14
LIGHTING
U ILLUMINATING
LIGHTING EQUIPMENT
NT AIRCRAFT LIGHTS
NT ARC LAMPS
NT FLASH LAMPS
NT ILLUMINATORS
NT LUMINAIRES
NT MERCURY LAMPS
NT RUNWAY LIGHTS
Brightness comparison of electroluminescent versu incandescent lighting: A photometric validation
[AD-A145395] 02 p0290 N85-118
Development of novel lamps for study of enhanced production of resonance by low-density mercury discharges
[DE84-016889] 06 p0832 N85-14
Evaluation of arctic test of improved titan radioluminescent lighting
[AD-A148215] 08 p1089 N85-18
New lighting technologies, their status and impacts o power densities
[DE85-000712] 09 p1315 N85-18
Lighting controls: The role of advanced technolog past, present and future
[DE84-015977] 09 p1384 N85-187
Astronomy and sodium lighting
[RAND/N-2099-RC] 09 p1413 N85-1891
System of light protection of antenna-mast structure of radio-relay lines 15 p2527 N85-25
LIGHTNING
A lightning detection system in Sweden
01 p0078 N85-105
Nowcasting using lightning location techniques
01 p0084 N85-105
Effects of a lightning strike on a civil defense operatio center
[FOA-A-30035-A3] 02 p0232 N85-1151
Study of effects of lightning on aircraft systems stressed 03 p0310 N85-120
NASA thunderstorm overflight program: Atmospheric electricity research. An overview report on the optical lightning detection experiment for spring and summer 1983
[NASA-TM-86466] 03 p0363 N85-1220
Tests for susceptibility to electromagnetic attack
[SNIAS-842-422-101] 04 p0494 N85-1316
Improvement of lightning arresters energy capability
[SNIAS-842-422-104] 04 p0497 N85-1317
Spring program summary, 1983
[PB84-222223] 06 p0839 N85-155
International Aerospace and Ground Conference on Lightning and Static Electricity. 1984 technical paper Supplement
[NASA-CP-2356] 07 p0999 N85-169
Data and results of a laboratory investigation of microprocessor upset caused by simulated lightning-induced analog transients
07 p0999 N85-169
Lightning research: A user's lament
07 p0999 N85-169
A comparison of lightning and nuclear electromagnetic pulse response of a helicopter 07 p1000 N85-169
A comparison of lightning and nuclear electromagnetic pulse response of tactical shelters
07 p1000 N85-169
Mathematical physics approaches to lightning discharge problems
[NASA-TM-86349] 08 p1187 N85-174
A study of the effects of triggered lightning
[AD-A148296] 08 p1189 N85-174
Direct-strike lightning photographs, swept-fla attachment patterns, and flight conditions for storm hazards 1982
[NASA-TM-86347] 12 p1862 N85-2107
Collection and use of lightning strike data in the western US during summer 1983
[PB85-110534] 12 p1897 N85-210

Preliminary results of associating cloud-to-ground lightning with surface convergence and radar reflectivity at Kennedy Space Center in 1983
[NASA-CR-175543] 12 p1897 N85-21910
Surge strength of symmetric cable with monolithic polyethylene insulation of quads
13 p2082 N85-23001
1981 wC-130 airborne lightning characterization program data review
[AD-A150230] 13 p2139 N85-23275
USSR report: Transportation
[JPRS-UTR-84-017] 15 p2461 N85-25196
Effects of lightning on aircraft studied at Sheremetyevo 15 p2461 N85-25199
Saturn electrostatic discharges
15 p2673 N85-26499
Lightning strikes on aircraft. The TRIP 82 experiment and 3-dimensional electromagnetic interferometry
[ONERA-RF-88/7154-PY] 16 p2703 N85-26690
Lightning-safe carbon fiber composite for Airbus tail unit 18 p3087 N85-29100
Comparison of the electromagnetic properties of lightning and EMP (Electromagnetic pulse): Results of recent lightning studies
[AD-A154325] 19 p3317 N85-30560
Investigation of the lightning vulnerability of nuclear explosive test systems at the Nevada Test Site
[DE85-011761] 24 p4124 N85-35563
Application of pulsed power in the simulation of severe natural lightning
[DE85-012866] 24 p4124 N85-35564

LIGHTS
U LUMINAIRES

LIGNITE
Some principles of plant resources evaluation using remotely sensed data 04 p0543 N85-13459
Alternative anodic reactions in water splitting
[DE85-004159] 12 p1802 N85-21300
Commercial feasibility of underground gasification of Texas lignite to produce synthetic gas
[DE85-001998] 18 p3127 N85-29361
Supercritical solvent extraction of lignite to form carbonaceous chars
[DE85-010159] 19 p3229 N85-30019
Size exclusion chromatography-low angle laser light scattering photometry of lignite macromolecules
[DE85-012017] 22 p3745 N85-33215

LIKELIHOOD RATIO
On the power functions of test statistics in order restricted inference
[AD-A147126] 07 p1035 N85-16566
The asymptotic behavior of the likelihood ratio statistic for testing a shift in mean in a sequence of independent normal variates
[AD-A149329] 10 p1550 N85-19779
Asymptotic expansions of the distribution of test statistics associated with several two parameter exponential distributions
[AD-A151906] 15 p2641 N85-26289

LIMB BRIGHTENING
Comparison of wind derived from the LIMS (Limb Infrared Monitor of the Stratosphere) satellite instrument with rocket observations
[NASA-CR-174083] 04 p0541 N85-13444
Extreme limb profiles of the Sun at far infrared and submillimeter wavelengths 06 p1244 N85-17852

LIMBS (ANATOMY)
NT ARM (ANATOMY)
NT ELBOW (ANATOMY)
NT FEET (ANATOMY)
NT FINGERS
NT HAND (ANATOMY)
NT KNEE (ANATOMY)
NT LEG (ANATOMY)
New uses for sensitivity analysis: How different movement tasks effect limb model parameter sensitivity
05 p0706 N85-14529

LIME
U CALCIUM OXIDES

LIMESTONE
Selection, procurement and description of Salem Limestone samples used to study the effects of acid rain
[PB84-231067] 04 p0484 N85-13088
Paleozoic limestones of the Crazy Mountains and vicinity, Circle quadrangle, east-central Alaska
04 p0517 N85-13296
Petrography, diagenesis and depositional models of the St. Louis limestone, valmeyeran (middle Mississippian), Illinois Basin, USA 09 p1352 N85-18506
Petrography, sedimentology, diagenesis, and reservoir characteristics of some Pennsylvanian phylloid algal limestones: Kansas and Utah, USA
09 p1352 N85-18507
Organogenic structures (submerged reefs) in Silhetian limestone of west Bengal basin
10 p1500 N85-19464
Evaluation of the Santee limestone for use in flue-gas desulfurization systems
[DE85-901277] 19 p3249 N85-30148
Deep-burial diagenesis in carbonates
[DE85-011224] 22 p3602 N85-33554

LIMITATIONS
U CONSTRAINTS

LIMITER AMPLIFIERS
Frequency selective signals-to-noise enhancer/limiter apparatus
[AD-D011583] 15 p2548 N85-25724

LIMITER CIRCUITS
Effects of monolayer converages on substrate sputtering yields
[DE84-016312] 04 p0476 N85-13033

LIMITERS (FUSION REACTORS)
Sources, densities, and transport of impurities in neutral-beam injected Tokamaks
09 p1388 N85-18731
Magnetic divertor design for the compact reversed-field pinch reactor
[DE85-002031] 09 p1391 N85-18753
Extended abstract: Ergodic magnetic limiter experiments on TEXT with a 7/3 resonance
[DE85-001390] 09 p1391 N85-18754
Coupled plasma-neutral transport model for the scrape-off region
[DE85-007559] 16 p2868 N85-27695
New concept for pumping the edge plasma
[DE85-010180] 19 p3371 N85-30909
Limiter
[DE85-011620] 24 p4150 N85-35736
Neutral pumping rates for a next step tokamak ignition device
[DE85-012780] 24 p4157 N85-35776

LIMITS (MATHEMATICS)
Sensitivity analysis of limit state functions for probability-based plastic design
01 p0059 N85-10388
A note on two papers in dependent central limit theory
[CWI-MS-R8410] 05 p0722 N85-14638
On limit of the largest eigenvalue of the large dimensional sample covariance matrix
[AD-A150589] 13 p2151 N85-23358
Statistical techniques for signal processing
[AD-A151231] 15 p2541 N85-25690
Entire functions with spiral limits
15 p2634 N85-26241
Limiting values of stress state index after rupture of metals
[BLL-BISI-TRANS-22293-(9022.06)]
17 p2978 N85-28407

LIMNOLOGY
Automatic hydrological data collection facility using ARGOS 14 p2324 N85-24363
Microwave hydrology: A trilogy
[NASA-CR-176042] 20 p3477 N85-31603

LIMONITE
A comparison of LANDSAT thematic mapper, multispectral scanner and airborne sensors for mapping the distribution of alteration minerals: Examples from the southwestern United States 24 p4106 N85-35452

LINE OF SIGHT
Probe of the nearby interstellar medium by the vacant line of sight to Beta CMa 06 p0874 N85-15551
Kinematics of nearby gas and stars
06 p0880 N85-15591
Solar monochromatic images in magneto-sensitive spectral lines and maps of vector magnetic fields
18 p3207 N85-29897

LINE OF SIGHT COMMUNICATION
Real-time estimation of amplitude and group delay distortion in a PSK line-of-sight communications channel
[AD-A147735] 08 p1151 N85-17266
Influence of propagation in digital wireless beam, microwave links 10 p1470 N85-19277
Wideband line-of-sight channel measurements and simulation: Application to digital radio links
10 p1471 N85-19283
Design criteria for limited scan antennas at digital microwave line of sight links 10 p1471 N85-19284
Some propagation experimental results on protection techniques for line-of-sight digital systems
10 p1472 N85-19286
LOS microwave channel simulation: A survey of models, realizations and new concepts 10 p1472 N85-19291
Theoretical study of a dynamic simulator of selective fading for digital, wireless beam microwave links
10 p1473 N85-19294
A ray trace program for line-of-sight microwave communication links
[AD-A156166] 24 p4087 N85-35336
Microwave propagation studies, measurements and education in Surabaya, Indonesia
[B8464833] 24 p4088 N85-35339

LINE SHAPE
New instabilities in line driven winds
08 p1235 N85-17785
A remote source system for measuring relative positron annihilation line widths in individual slab cylindrical samples
[AERE-R-10549] 12 p1938 N85-22173
A positron annihilation Doppler broadening study of niobium
[DE85-010287] 20 p3527 N85-31936

LINE SPECTRA
NT BALMER SERIES
NT D LINES
NT ELECTRONIC SPECTRA
NT FRAUNHOFER LINES
NT H ALPHA LINE
NT H LINES
NT K LINES
NT LYMAN SPECTRA
NT RYDBERG SERIES
The X-ray spectrum and time variability of narrow emission line galaxies
[NASA-TM-83859] 03 p0446 N85-12842
Absolute transition probabilities of lines in the spectra of astrophysical atoms, molecules, and ions
[NASA-CR-174141] 04 p0580 N85-13705
Search for the radiative decay of a cosmic relic particle with IUE
[PREPRINT-410] 04 p0580 N85-13707
The IRAS galaxy 0421+040P06: An active spiral (?) galaxy with extended radio lobes
[NASA-CR-174208] 06 p0871 N85-15536
A type stars as probes of the local interstellar medium
06 p0874 N85-15550
Probe of the nearby interstellar medium by the vacant line of sight to Beta CMa 06 p0874 N85-15551
Optical emission line studies and the warm, ionized component of the local interstellar medium
06 p0875 N85-15555
A high-resolution study of local interstellar sodium
06 p0875 N85-15556
Degenerate four-wave mixing lineshapes in sodium vapor under pulsed excitation
[AD-A148211] 08 p1222 N85-17698
Departures from LTE populations versus anomalous abundances: The effects of heating
08 p1234 N85-17776
Multiline transfer and the dynamics of stellar winds
08 p1236 N85-17788
Radio Seyferts and the forbidden line region
08 p1236 N85-17793
The ultraviolet spectra of the narrow line active galaxies NGC 3081 and NGC 4507 08 p1237 N85-17799
Duelling winds: A model for broad-line regions — galactic nuclei 08 p1242 N85-17837
Theoretical studies of emission line variability in type 1 Seyfert galaxies 08 p1242 N85-17839
On the stability of broad line clouds in active galactic nuclei 08 p1243 N85-17840
Star formation in globules 08 p1247 N85-17868
Mid-infrared spectroscopy of planetary nebulae
08 p1247 N85-17872
Effect of inner subshell ionization for emission lines of OIV ion 09 p1388 N85-18729
Spectra of highly-ionized atoms for the diagnostics of the new generation of Tokamaks
09 p1388 N85-18730
X-ray line broadening of a diagnostic in laser produced plasma
[DE85-001179] 10 p1560 N85-19841
KMSF X-ray laser experiments, task no. 1
[DE85-001002] 11 p1630 N85-20325
The UV spectra of intermediate redshift quasars
11 p1746 N85-20980
Fluorescent excitation of Fe 2, Mn 2, Ti 2, N 1 lines by V 4, N 5, O 6: Emission lines in the spectra of symbiotic stars and Seyfert galaxies 11 p1746 N85-20984
IUE observations of planetary nebulae in the Magellanic Clouds 11 p1747 N85-20986
1983 observations of the eclipsing nucleus of the bipolar planetary nebula NGC 2346 11 p1747 N85-20987
The changing ultraviolet spectrum of Herbig-Haro object No. 1 11 p1747 N85-20989
Short-wavelength observations of HH-2H and HH-24A
11 p1747 N85-20990
A search for young stellar chromospheres in NGC 2264 11 p1748 N85-20993
Ultraviolet observations of circumstellar matter in Algol type binary systems 11 p1756 N85-21043
Circumstellar material in Algols and Serpentids
11 p1757 N85-21061
Chromospheric emission lines in high-resolution LWR spectra (220 - 3000 alpha) of gamma CRU (M3 3) and alpha ORI (M2 lab) 11 p1758 N85-21068

Precise measurements of radial velocities of emission lines in the far-ultraviolet spectra of late-type stars
11 p1758 N85-21062

Ultraviolet, radio and X-ray observations of hybrid stars
11 p1759 N85-21063

Rotational modulation of chromospheric emission in cool giants and hybrid stars
11 p1759 N85-21064

Magnetospheres and winds in the helium weak stars: Observations of C 5 in upper main sequence CP stars
11 p1759 N85-21066

IUE spectrophotometry of helium weak and silicon stars
11 p1759 N85-21067

Formation of optical-line emitting regions in the jets of SS433
12 p1959 N85-22318

NIMBUS-7 SBUV (Solar Backscatter Ultraviolet) observations of solar UV spectral irradiance variations caused by solar rotation and active-region evolution for the period November 7, 1978 - November 1, 1980
[NASA-CR-175544] 12 p1962 N85-22334

An atlas of nitrogen-broadened water vapor spectra from 500 to 5000 cm(-1), volume 1
[AD-A150527] 13 p2016 N85-22650

Chemical and localization effects in Auger lineshapes of transition metal compounds
[AD-A150865] 14 p2251 N85-23049

Further developments of CCD line array telecine
[BBC-RD-1985/3] 14 p2293 N85-24217

Documentation for the machine-readable version of A Finding List for the Multiplet Tables of NSRDS-NBS 3, Sections 1-10 (Adelman, Adelman, Fischel and Warren 1984)
[NASA-TM-87440] 14 p2438 N85-25048

The Fe XIII 10747 A and Fe XIV 5303 A coronal emission lines polarization
14 p2448 N85-25111

Experience in automation of data processing in interpretation and defining of linear elements from space photographs
15 p2486 N85-25349

Linewidth and bandwidth measurements of the q-branch of h2 using CW coherent anti-Stokes Raman spectroscopy
[AD-A151868] 15 p2506 N85-25456

User manual for IMAGER: The DREO (Defence Research Establishment Ottawa) image processing system
[AD-A151754] 15 p2653 N85-26362

A measurement of the vibrational band strength for the upsilon sub 3 band of the HO2 radical
[NASA-CR-175858] 16 p2744 N85-26936

An atlas of pure water vapor spectra from 500 to 5000/cm, Volume 2
[AD-A151757] 16 p2745 N85-26940

Mirror accessory for line straightening in diffraction spectrometers
16 p2764 N85-27054

Radio observations of comet P/Crommelin
[INPE-3480-PRE/723] 16 p2881 N85-27777

Contribution functions for Zeeman-split lines, and line formation in photospheric faculae
18 p3207 N85-29693

Effect of polarized radiative transfer on the Hanle magnetic field determination in prominences: Analysis of hydrogen H alpha line observations at Pic-du-Midi
18 p3207 N85-29694

The effect of line damping, magneto-optics and parasitic light on the derivation of sunspot vector magnetic fields
18 p3207 N85-29695

The inference of vector magnetic fields from polarization measurements with limited spectral resolution
18 p3207 N85-29696

Solar monochromatic images in magneto-sensitive spectral lines and maps of vector magnetic fields
18 p3207 N85-29697

Controlled-linewidth laser source
[AD-D011681] 19 p3274 N85-30306

Shifts and widths of hydrogenic ion lines
[DE85-011375] 19 p3277 N85-30323

The ultraviolet spectra of intermediate redshift quasars
20 p3544 N85-32056

Voigt line profile computation of infrared lines in the stratosphere and mesosphere
[AERONOMICA-ACTA-A-294-1985]
22 p3813 N85-33622

Detection of gamma-ray lines from the direction of the Crab Nebula
22 p3866 N85-33943

HEAO 3 upper limits to the expected 1634 KeV line from SS 483
[OG-2.4-9] 22 p3868 N85-33954

Search for gamma ray lines from SS433
[OG-2.4-11] 22 p3868 N85-33955

High-resolution spectrum of Cygnus X-1
[OG-2.4-12] 22 p3868 N85-33956

Search for positron annihilation line and continuum radiation from the Galactic Center
[OG-2.5-5] 22 p3869 N85-33962

Abundances from solar-flare gamma-ray line spectroscopy
[SH-2.1-13] 23 p3999 N85-34794

Solar flare gamma-ray line spectroscopy
[SH-2.1-14] 23 p3999 N85-34795

Elliptical X-ray analyzer spectrograph application to a laser-produced plasma
[DE85-013790] 24 p4097 N85-35398

Far-infrared emission lines of CO and OH in the Orion-KL molecular shock
[NASA-TM-86721] 24 p4167 N85-35832

The HEAO-2 Guest Investigator Program: Non-linear growth of instabilities in line-driven stellar winds
[NASA-CR-176168] 24 p4168 N85-35840

The ionization structure of planetary nebulae. Part 4: NGC 7662
[NASA-CR-176151] 24 p4169 N85-35844

LINEAMENT

U STRUCTURAL PROPERTIES (GEOLOGY)

LINEAR ACCELERATORS

NRL (Naval Research Laboratory) FEL (Free Electron Laser) program
[AD-A145057] 01 p0052 N85-10347

Accelerator technology program
[DE84-015052] 01 p0118 N85-10806

Methods to increase linac efficiency
[DE84-014692] 01 p0118 N85-10809

Linac quadrupole connections
[DE84-014694] 01 p0118 N85-10810

Use of magnetic compression based on amorphous alloys as a drive for induction linacs
[DE84-014524] 02 p0277 N85-11805

Use of a first-harmonic RF system in the NSLS booster
[DE84-016432] 02 p0277 N85-11806

Multipurpose 5-MeV linear induction accelerator
[DE84-014523] 02 p0278 N85-11808

Large linear colliders
[DE84-015700] 02 p0278 N85-11811

ATLAS beam properties: Some implications for target making
[DE84-008595] 02 p0278 N85-11812

SLC nomenclature for beamline components
[DE84-014776] 02 p0279 N85-11816

Accelerator development in support of the NRL (Naval research laboratory) beam dynamic program
[AD-A145976] 03 p0417 N85-12669

Cerenkov ring imaging detector development at SLAC
[DE84-015883] 04 p0560 N85-13564

Intense non-relativistic cesium ion beam
[DE84-012575] 04 p0560 N85-13566

Search for neutral, penetrating, metastable particles produced in the SLAC beam dump
[DE84-012468] 04 p0560 N85-13569

LAMPF transmition-region mechanical fabrication
[DE84-017078] 04 p0562 N85-13577

Accelerator Technology Program
[DE84-017083] 04 p0563 N85-13586

Preliminary grouping in A strong-current linear ion accelerator with a low injection energy
[DE84-017192] 04 p0563 N85-13587

Status of beam transport with the ETA and ATA accelerators
[DE84-013205] 05 p0726 N85-14670

Energy spread in SLC linac with Landau damping
[DE84-016259] 05 p0727 N85-14675

Minimizing the energy spread within a single bunch by shaping its charge distribution
[DE84-016172] 05 p0727 N85-14676

ATA probe beam experiment
[DE84-016017] 06 p0862 N85-15477

Calculated parameters for the initial part of an accelerator with high-frequency quadrupole focusing
[RAE-TRANS-2122] 07 p1040 N85-16600

Status of RF superconductivity at Argonne National Laboratory
[DE85-002145] 09 p1312 N85-18245

Experimental investigation of certain beam transport issues in a pulsed transmission line linear accelerator
[DE85-002310] 10 p1555 N85-19805

High power pulsed accelerators with potential industrial applications
[DE85-001710] 11 p1720 N85-20821

Notes on the RF system for the SLC positron source
[DE85-002628] 11 p1722 N85-20830

Low-energy, high-intensity positron beam experiments with a linac
[DE85-001048] 11 p1723 N85-20835

Calculations pertaining to the design of a prebuncher for a 150-MeV electron linear accelerator 3. Comparisons with experimental data
[DE85-002866] 11 p1724 N85-20844

Experiments on ETA comparing wire-conditioned and non-wire-conditioned beam propagation
[DE85-004451] 11 p1725 N85-20848

Look at energy compression as an assist for high power RF production
[DE85-001568] 11 p1725 N85-20851

Operating experience and construction [illegible] ATLAS --- Argonne tandem-linac accelerator
[DE85-002741] 11 p1735 N85-20[illegible]

Enhancing the performance of a high-gain free electron laser operating at millimeter wavelengths
[DE85-000862] 12 p1857 N85-21[illegible]

Single-cavity SLED device
[DE85-002587] 12 p1929 N85-22117

Los Alamos free electron laser: Accelerator performance
[DE85-005722] 13 p2097 N85-2[illegible]

Collective acceleration of ions using high current relativistic electron beams
[DE85-004889] 13 p2157 N85-2[illegible]

Radio frequency quadrupole and alternating phase focusing methods used in proton linear accelerator technology in the USSR
[AD-A150630] 14 p2418 N85-24[illegible]

Two-beam accelerator
[DE85-004662] 15 p2649 N85-2[illegible]

Superconducting traveling wave accelerators
[DE85-006247] 15 p2661 N85-2[illegible]

Generalization of the Child-Langmuir relation for 1-dimensional time-dependent diodes
[DE85-007386] 16 p2779 N85-271[illegible]

Surveying and optical tooling technologies combined to align a skewed beamline at the LAMPF accelerator
[DE85-005902] 16 p2864 N85-27[illegible]

Laser plasma LINAC
[DE85-008294] 17 p2971 N85-2[illegible]

Measurement and interpretation of electron angle at MABE beam stop
[DE85-008583] 17 p3032 N85-2[illegible]

Phase and amplitude considerations for the 2-beam accelerator
[DE85-008455] 18 p3180 N85-29715

Calculations of beam dynamics in Sandia linear electron accelerators, 1984
[DE85-010417] 18 p3180 N85-29719

Plasma wake field accelerator
[DE85-010538] 18 p3191 N85-29701

Preliminary results on open accelerating structures
[DE85-010231] 18 p3191 N85-29703

Accelerator column models for low-current beams
[DE85-010722] 19 p3262 N85-30[illegible]

Los Alamos Free-Electron Laser (FEL) RF system
[DE85-010719] 19 p3278 N85-30[illegible]

Application of GPS in a high precision engineering survey network
[DE85-010556] 19 p3313 N85-30[illegible]

The SLC program
[DE85-011433] 19 p3357 N85-30[illegible]

Beam dynamics in MABE
[DE85-010670] 19 p3356 N85-30[illegible]

Emittance growth caused by current variation in a beam-transport channel
[DE85-010743] 19 p3363 N85-30[illegible]

Mechanical considerations in cw linacs
[DE85-010728] 19 p3363 N85-30[illegible]

Quantum effects in linear collider scaling laws
[DE85-009846] 19 p3363 N85-30[illegible]

Additional muon calculations for the SLC positron source
[DE85-011212] 19 p3363 N85-30[illegible]

Report of near field group
[DE85-010536] 20 p3527 N85-31[illegible]

Requirements for very high energy accelerators
[DE85-011173] 20 p3529 N85-31[illegible]

The 3lambda/4 post coupler for drift-tube linacs
[DE85-010753] 20 p3531 N85-31[illegible]

Lasertron simulation with a two-gap output cavity
[DE85-011213] 22 p3790 N85-33[illegible]

Control technology for radioactive emissions to the atmosphere at US Department of Energy facilities: The Los Alamos Meson Physics Facility
[DE85-011402] 22 p3811 N85-33[illegible]

Determination of DTL configurations
[DE85-010714] 22 p3830 N85-33[illegible]

The cw operation of the FMIT RFQ accelerator
[DE85-012667] 22 p3837 N85-33[illegible]

Transverse emittance of a 2.0-MeV RFQ beam with high brightness
[DE85-012718] 22 p3837 N85-33[illegible]

Proceedings of the 18th LAMPF Users Group Meeting
[DE85-011888] 22 p3839 N85-33[illegible]

Acceleration of polarized H(-) in the BNL 200 MeV linac
[DE85-011836] 22 p3840 N85-33777

Iris tilting and RF steering in the SLAC Linac
[DE85-011704] 22 p3841 N85-33780

Accelerator vibration issues
[DE85-010766] 22 p3842 N85-33[illegible]

New formulation for linear accelerator design
[DE85-011171] 22 p3842 N85-33782

Physics Division annual review, 1 April 1983 - 31 March 1984
[ANL-84-24] 23 p3969 N85-34602
RADLAC technolgy review
[DE85-011995] 23 p3982 N85-34691
Technology of magnetically driven accelerators
[DE85-011957] 23 p3983 N85-34700
Observations of accelerated high current low emittance beams in the SLC Linac
[DE85-013073] 24 p4088 N85-35211
Solid state high power amplifier for driving the SLC injector klystron
[DE85-013063] 24 p4090 N85-35356
ATA upgrade to 150 MeV
[DE85-013174] 24 p4096 N85-35404
Error message recording and reporting in the SLC control system
[DE85-013057] 24 p4140 N85-35664
Time domain reflectometry for SLC BPM system
[DE85-012369] 24 p4155 N85-35758
Four stage HELIA experiment
[DE85-012026] 24 p4156 N85-35766
High resolution beam profile monitors in the SLC
[DE85-013375] 24 p4157 N85-35774
Recent advances in remote handling at LAMPF
[DE85-012725] 24 p4157 N85-35775
SLC Energy Upgrade Program at SLAC
[DE85-014290] 24 p4160 N85-35790
Multi-channel pulser for the SLC thermionic electron source
[DE85-014222] 24 p4160 N85-35792
TOSCA calculations and measurements for the SLAC SLC damping ring dipole magnet
[DE85-014368] 24 p4160 N85-35793

LINEAR ARRAYS
NT MULTISPECTRAL LINEAR ARRAYS
On aircraft antennas and basic scattering studies
[AD-A146017] 03 p0355 N85-12282
A dynamical model for a towed linear sonar antenna
[REPT-6-84] 04 p0512 N85-13263
Synthesis of zeros in radiation pattern of linear antenna array 06 p0784 N85-15015
Modulation Transfer Function (MTF) measurement techniques for lenses and linear detector arrays
[NASA-TM-86166] 10 p1556 N85-19812
Further developments of CCD line array telecine
[BBC-RD-1985/3] 14 p2293 N85-24217
Space processing of acoustic signals in plane-parallel waveguide — antenna arrays 15 p2525 N85-25572
Design and development of a linear Fresnel lens air-cooled photovoltaic module and a stand-alone photovoltaic collector array
[DE85-006854] 16 p2819 N85-27391
The theoretical response of a vertical line array to wind-generated noise in shallow water
[AD-A151730] 16 p2860 N85-27636
Development of a second-generation linear Fresnel Photovoltaic and Thermal (PVT) concentrator array, including fabrication and installation of a 200 square meter collector field
[DE85-008473] 17 p2968 N85-28465
ECM multiple-target retrodirective antenna
[AD-D011528] 20 p3439 N85-31346

LINEAR CIRCUITS
Diakoptic calculation of characteristics for optimization of linear circuits with respect to parameters of individual branches 22 p3767 N85-33346

LINEAR ENERGY TRANSFER (LET)
Inelastic Near-Surface Interactions. Proceedings of the Werner Brandt Workshop on Penetration Phenomena
[DE85-010579] 20 p3526 N85-31926
Hit-size effectiveness theory applied to high doses of low LET radiation for pink mutations in Tradescantia
[DE85-011835] 22 p3819 N85-33657

LINEAR EQUATIONS
NT LINEAR EVOLUTION EQUATIONS
Modular design attitude control system
[NASA-CR-171182] 01 p0016 N85-10096
Parallel, iterative solution of sparse linear systems: Models and architectures
[NASA-CR-172457] 02 p0243 N85-11586
Numerical methods for solving systems of linear equations
[INPE-3240-RPE/463] 02 p0250 N85-11633
United States Air Force on research on algebraic manipulation
[AD-A145737] 02 p0253 N85-11655
Linear theory of free-electron lasers with cylindrical interaction space 02 p0262 N85-11718
Liquid payload moment equations
[AD-A145977] 03 p0362 N85-12319
An integral equation formulation for a boundary value problem of elasticity in the domain exterior to an arc
[PREPRINT-633] 03 p0413 N85-12643
Some implementations of multigrid linear system solvers
[CWI-NM-R8401] 05 p0720 N85-14626
Feedback, adaptivity and A-posterior estimates in finite elements: Aims, theory and experience
[AD-A146869] 07 p1029 N85-16531
First derivatives of flow quantities behind two-dimensional, nonuniform supersonic flow over a convex corner
[NASA-TM-86272] 08 p1077 N85-16628
Signal reconstruction from Fourier transform sign information
[AD-A148039] 08 p1211 N85-17624
A feedback finite element method with a posteriori error estimation. Part 1. The finite element method and some basic properties of the A posteriori error estimator
[AD-A148345] 08 p1212 N85-17631
Use of iterative linear and nonlinear algebraic methods for solving large stiff systems of ODEs
[AD-A148516] 08 p1213 N85-17636
On limits of applicability of linear models to dynamics of gas channels in aircraft engines
09 p1308 N85-18219
Solving large linear systems 14 p2396 N85-24759
The omni-transform in single-channel queues
[AD-A151019] 14 p2409 N85-24852
MATRIX: A program that shows how row and column orderings affect matrix fill-in
[DE85-007522] 15 p2630 N85-26213
A stability analysis of incomplete LU factorizations
[AD-A152058] 15 p2636 N85-26271
Ductility equation for porous metals and its linearization
[BLL-M-36118-(5828.4)] 16 p2746 N85-26958
Solving the minimal least squares problem subject to bounds on the variables
[TRITA-NA-8215] 16 p2852 N85-27580
Numerical methods for the solution of stiff delay differential equations 19 p3334 N85-30653
Numerical algorithms for solving linear algebra problems
[DE85-010310] 19 p3346 N85-30736
A multiple linear regression analysis of hot corrosion attack on a series of nickel base turbine alloys
[NASA-TM-87020] 20 p3431 N85-31284
A new problem in mathematical physics associated with the problem of coherent phase transformation
21 p3696 N85-32976
Implementing linear multistep formulas for solving DAES
[DE85-012400] 22 p3834 N85-33740
Stress analysis of axisymmetric sandwich shells of variable thickness 24 p4101 N85-35419
A new method for boundary value problems
[AD-A155934] 24 p4143 N85-35683

LINEAR EVOLUTION EQUATIONS
Symmetric linear multistep methods for second-order differential equations with periodic solutions
[CWI-NM-R8501] 17 p3022 N85-28698

LINEAR FILTERS
NT KALMAN FILTERS
NT REDUCED ORDER FILTERS
Robust linear filtering for multivariable stationary time series, part 3
[AD-A148169] 08 p1212 N85-17627
Piezoelectric filter with low-Q inductances
13 p2070 N85-22932
Acoustooptic cell as space-frequency filter
13 p2090 N85-23051
Linearization of digital derived rate algorithm for use in linear stability analysis
[NASA-TM-87000] 14 p2243 N85-23904
Theory and Applications of State Estimation. NRIMS Summer Seminar Series
[CSIR-SWISK-37] 15 p2635 N85-26244
The Kalman filter 15 p2635 N85-26246
Linear filtering with non-Gaussian initial conditions
15 p2635 N85-26247
State estimation with interrupted observations
15 p2635 N85-26251
Coupling of the solar wind to measures of magnetic activity
[DE85-002415] 15 p2685 N85-26580
Linear time-invariant, space-variant filters and the WKB approximation with applications to underwater acoustic signal processing
[AD-A154250] 19 p3352 N85-30775
Linear filters as a method of real-time prediction of geomagnetic activity
[DE85-010760] 22 p3660 N85-33899

LINEAR INTEGRATED CIRCUITS
NT OPERATIONAL AMPLIFIERS

LINEAR POLARIZATION
Detection of submillimeter polarization in the Orion Nebula
[NASA-TM-86013] 04 p0579 N85-13700
Polarization of radio molecular lines and mapping of magnetic field direction 06 p0878 N85-15581
Polarization transformation by single-mode fibers — optical fibers
[FI-452-TBR-59] 11 p1729 N85-20876
Coordinated ultraviolet and visual observations of Omega Orionis 1982-1983 11 p1750 N85-21007
Design and performance of etched polarisation transformers for microwave frequencies
[R-NIAS-26] 14 p2297 N85-24218
Magnetic field-vector measurements in quiescent prominences via the Hanle effect: Analysis of prominences observed at Pic-du-Midi and at Sacramento Peak
18 p3206 N85-29686
Influence of depolarization of linear polarized radiation on the heterodyne detection in laser range finders
[ESA-TT-903] 20 p3461 N85-31500

LINEAR PREDICTION
Description of a semiannual selection procedure of vowel parts of the voice signal using a PDP 11/34 computer
[FUB-4-1983] 01 p0039 N85-10250
Coupling of the solar wind to measures of magnetic activity 14 p2357 N85-24585
Environmental background measurement program
[AD-A153880] 19 p3319 N85-30577

LINEAR PROGRAMMING
Interactive graphics nonlinear constrained optimization
01 p0058 N85-10367
A combined logistic regression and Zionts-Wallenius methodology for multiple criteria linear programming
[TWISK-314] 01 p0102 N85-10679
A comparative evaluation of algorithms for generalized network problems
[TWISK-289] 01 p0107 N85-10721
New labeling procedures for the basis graph in generalized networks
[AD-A146217] 03 p0407 N85-12601
A two-segment approximation algorithm for separable convex programming with linear constraints
[AD-A146215] 03 p0412 N85-12634
Boolean approach to zero-one linear programming
[DE84-016654] 04 p0550 N85-13498
Users manual for BRGLM: Interactive general linear model regression, version 3
[DE84-017386] 04 p0550 N85-13501
An iterative scheme for linear complementarity problems
[AD-A147464] 07 p1032 N85-16555
Extracting embedded generalized networks from linear programming problems
[AD-A147565] 07 p1033 N85-16558
Simple approximate variances for b-letter values. A sampling enquiry: Supplement
[DE85-001410] 09 p1376 N85-18647
Efficient algorithm for fuzzy linear programming with multiple objectives
[AD-A149012] 10 p1544 N85-19736
An exact solution to the 2 point OC (Operating-Characteristic) curve determination
[AD-A148120] 11 p1706 N85-20746
Automatic control design procedures for restructurable aircraft control
[NASA-CR-172489] 12 p1780 N85-21173
Parallel linear algebra library for the Denelcor HEP
[DE85-004665] 12 p1917 N85-22034
Needs, opportunities, and options for large scale systems research
[DE85-004642] 12 p1925 N85-22091
Approaches and algorithms for robust signal processing 13 p2062 N85-22878
Optimal allocation of components in parallel-series and series-parallel systems
[AD-A150169] 13 p2144 N85-23309
LEXICON: A structured modeling system for optimization
[AD-A150536] 13 p2147 N85-23329
Minimal cost flow in processing networks: A primal approach
[CWI-TRACT-4] 14 p2432 N85-25001
Solving set covering problems using heuristics with branch and bound
[AD-A151905] 15 p2636 N85-26269
Proposal for an extended set of FORTRAN Basic Linear Algebra subprograms
[DE85-007241] 16 p2848 N85-27562
A decomposition procedure for convex quadratic programs
[AD-A151732] 16 p2854 N85-27595
The interface with decision makers in interactive multiobjective linear programming
[REPT-84-38] 17 p3014 N85-28637
Operations research
[B8561897] 17 p3026 N85-28712
A variable-complexity norm maximization problem
[AD-A153514] 18 p3169 N85-29634

Finding the largest l(p)-ball in a polyhedral set [AD-A153542] 18 p3170 N85-29643

Modeling water resources systems for water quality [AD-A154266] 19 p3300 N85-30457

On the step size in Karmarkar's algorithm [AD-A154040] 19 p3335 N85-30661

Numerical algorithms for solving linear algebra problems [DE85-010310] 19 p3346 N85-30738

An analysis of multi-fingered hands 20 p3462 N85-31504

Symposium on Computational Mathematics-State-of-the-Art: Informal Proceedings [DE85-008122] 20 p3516 N85-31858

Study of an efficient long-range Mach 2.7 supersonic transport configuration concept [NASA-TM-86414] 21 p3554 N85-32110

A practical approach to Karmarkar's algorithm [AD-A155714] 21 p3673 N85-32818

On the problem of linear programming with approximate data 21 p3698 N85-32978

LINEAR RECEIVERS

Liquid cooled, linear focus solar cell receiver [DE84-014446] 01 p0067 N85-10446

LINEAR SYSTEMS

Design of a digital ride quality augmentation system for commuter aircraft [NASA-CR-172419] 01 p0006 N85-10037

The rate of convergence of a class of block Jacobi schemes [AD-A144738] 01 p0111 N85-10749

Credibility approximations for Bayesian prediction of second moments [AD-A144996] 01 p0113 N85-10768

Singular perturbations, coherency and aggregation of dynamic systems [DE84-014166] 01 p0114 N85-10772

Qualitative results for distributed systems with discrete damping and stiffness with application to control [AD-A145525] 02 p0209 N85-11382

On a class of suboptimal controls for infinite-dimensional bilinear systems [RR-259] 02 p0240 N85-11630

Linear intersecting codes — error correction [ENST-C-84002] 03 p0356 N85-12291

Chandrasekhar equations and computational algorithms for distributed parameter systems [NASA-CR-172467] 03 p0402 N85-12564

Maximum likelihood estimation of parameters in linear systems from flight test data: A FORTRAN program [AD-B087198L] 05 p0715 N85-14566

Optimal stochastic LQ control with measurements displaced in time [OUEL-1547/84] 08 p1209 N85-17605

Improved stability and performance bounds using approximate models — control system design [RR-260] 08 p1209 N85-17606

Use of iterative linear and nonlinear algebraic methods for solving large stiff systems of ODEs [AD-A148516] 08 p1213 N85-17636

Dynamics and control of general linear lumped-parameter systems 09 p1372 N85-18623

Chandrasekhar equations for infinite dimensional systems [NASA-CR-172515] 09 p1376 N85-18651

Research in adaptive and decentralized control [AD-A148964] 10 p1543 N85-19728

A note on the disturbance decoupling problem for retarded systems [AD-A149045] 10 p1543 N85-19730

Linear magnetic bearings [NASA-CASE-GSC-12582-2] 11 p1641 N85-20337

Low sidelobe phased array antenna system [AD-D011558] 12 p1823 N85-21435

Methods of progressing waves in turbulent media with applications to acoustics [AD-A149589] 12 p1920 N85-22055

Analysis and design of linear microwave transistor amplifiers 13 p2066 N85-23038

Synthesis of optimal controls for real-time linear digital systems 14 p2270 N85-24062

Transducer of linear displacements 14 p2281 N85-24130

Decomposition in problem of correcting inertial navigation systems 14 p2287 N85-24172

Investigation of the time history and modal responses of some simple linear and nonlinear systems [DE85-002027] 14 p2321 N85-24344

Results of studies of wave field internal structure in prediction of geological cross section 14 p2346 N85-24504

Practical methods for the compensation and control of multivariable systems [AD-A151047] 14 p2407 N85-24841

State estimation with interrupted observations 15 p2635 N85-26251

Fundamental equivalence of generalised state space systems [MATHEMATICS-RESEARCH-182] 15 p2642 N85-26293

Complexity of dense linear system solution on a multiprocessor ring [AD-A151970] 16 n2654 N85-27598

Mathematical modeling and control of a large space structure as applied to a shuttle-antenna configuration [AD-A153269] 17 p2910 N85-27939

Generalised translation invariance and systems theory [CRM-8501] 17 p3017 N85-28657

Efficient parallel solution of linear systems with hyperbolic rotations [AD-A152355] 17 p3018 N85-28661

Efficient parallel solution of linear systems [AD-A152663] 17 p3018 N85-28663

Polynomial iteration for nonsymmetric indefinite linear systems [AD-A153094] 17 p3019 N85-28671

An interactive computer aid for the design and analysis of linear, single input/single output digital and continuous control systems [AD-A153704] 18 p3162 N85-29589

Infinite dimensional linear systems with unbounded control and observation: A functional analytic approach [AD-A153535] 18 p3169 N85-29639

Control and regulation of generalized linear systems 19 p3257 N85-30193

Interactive computer program for the analysis and design of linear time invariant systems [AD-A154076] 19 p3335 N85-30664

An iterative method for indefinite systems of linear equations [NASA-CR-172345] 19 p3345 N85-30728

Profile of a relativistic electron beam propagated through a linear wiggler and an axial guide field [AD-A154403] 19 p3353 N85-30783

A new slab geometry radiation transport differencing scheme [DE85-006681] 19 p3366 N85-30874

New directions in asymptotically stable finite-dimensional adaptive control of linear distributed parameter systems 20 p3412 N85-31177

An overview of latest modal reduction and control methods of large flexible space structures 20 p3414 N85-31191

Frequency domain control design of large space structures: A practical approach 20 p3415 N85-31192

Sensor/actuator selection for the constrained variance control problem 20 p3415 N85-31197

Eigenvalue placement and stabilization by constrained optimization 20 p3416 N85-31198

Stable direct adaptive control of linear infinite-dimensional systems using a command generator tracker approach 20 p3416 N85-31204

Linear system structure and cone containment for bilinear systems [RR-258] 20 p3519 N85-31879

On the choice of parameterization for identification [OUEL-1554/84] 20 p3522 N85-31904

Routing algorithms and stochastic analysis for large communications networks [AD-A154654] 21 p3573 N85-32225

Decomposing the joint distribution of several linear combinations of uniform spacings [AD-A155056] 21 p3677 N85-32645

Design and development of a linear thermal actuator 22 p3796 N85-33516

Substructure coupling in the frequency domain [NASA-CR-176140] 22 p3800 N85-33543

A graph theoretic procedure for the design of feedback patterns [REPT-110] 24 p4142 N85-35673

A new theory for multistep discretizations of stiff ordinary differential equations: Stability with large step sizes [NASA-CR-177941] 24 p4142 N85-35675

Spreading the control complexity in decentralized control of interconnected systems [BU-117] 24 p4144 N85-35688

Decentralized stabilization by high gain feedback [BU-115] 24 p4144 N85-35689

LINEAR TRANSFORMATIONS

Linear associative mapping [ESA-TT-856] 05 p0719 N85-14611

Transformation of electromagnetic waves in plasma with randomly-heterogeneous magnetic field 07 p0953 N85-16039

LINEAR VIBRATION

Nonlinear wave propagation study [AD-A147011] 07 p0996 N85-16329

A pole-free reduced-order characteristic determinant method for linear vibration analysis based on sub-structuring 09 p1338 N85-18412

Dynamics and control of general lumped-parameter systems 09 p1372 N85-

LINEARITY

NT COLLINEARITY

Shift-variant multidimensional systems [AD-A144756] 01 p0111 N85-

Method for calculating linear shrinkage and of metals and alloys [BLL-M-35747-(5826.4)] 02 p0175 N85-

On the rate of mean convergence of finite predictors of multivariate stationary stochastic [AD-A145609] 02 p0254 N85-

Linear conformal gravitation 02 p0265 N85-

A two-segment approximation algorithm for convex programming with linear constraints [AD-A146215] 03 p0412 N85-

Structure of frequency modulated and phase-shift signals reflected from ionosphere at frequencies 07 p0952 N85-

Digital thermometer with linearizer on slide 07 p0954 N85-

Image-to-image correspondence: Linear matching 07 p0986 N85-

SIMM1: A linearized particle code [AD-A148627] 08 p1221 N85-

Effect of scattering on instabilities in line-driven winds 08 p1235 N85-

New instabilities in line driven winds 08 p1236 N85-

On the role played by lines in radiatively driven winds depending on the position of the stars in the diagram 08 p1236 N85-

finite element analysis of bi-material systems applications in hydraulic fracturing 09 p1332 N85-

Existence, uniqueness and stability conditions general finite element methods in linear elasticity 09 p1332 N85-

Improved magnetic bias and delay linearity in a magnetostatic wave delay line [AD-D011441] 10 p1470 N85-

Close-to-convex functions and linear-invariant 10 p1536 N85-

Smoothing with split linear fits [AD-A149032] 10 p1545 N85-

Simulation of the ion-beam-driven drift instability in a magnetic trap, 2 [AD-A149452] 10 p1554 N85-

Method for increasing linearity of load cell 11 p1623 N85-

New results on the PLL false lock phenomenon 12 p1948 N85-

Absolute stability of unsteady movement axisymmetrical rotating flight vehicle 13 p2044 N85-

Approaches and algorithms for robust processing 13 p2062 N85-

Consistency of smoothing with running linear fits [AD-A150232] 13 p2150 N85-

Nonlinear 0-1 programming. 1: Linearization techniques revision [AD-A150960] 14 p2465 N85-

A 4-node bilinear isoparametric element in NASTRAN 15 p2573 N85-

On geoid heights and flexure of the seamounts [AD-A151220] 15 p2604 N85-

An evaluation of discretized conditional probability linear regression threshold techniques in model statistics forecasting of visibility over the north Ocean [AD-A151955] 16 p2657 N85-

Distortion functions [DE85-007511] 16 p2662 N85-

Study on a flexure hinged pendulum [NAL-TR-844] 18 p3104 N85-

Linear motion valve [NASA-CASE-MSC-20148-1] 18 p3115 N85-

Fixed width interval estimation in linear regression [AD-A153633] 18 p3174 N85-

On the characterization of nonnegatively combinations of variance components [AD-A153786] 18 p3174 N85-

Large-time behavior of viscous surface waves [AD-A154805] 21 p3584 N85-

Test evaluation of the Honeywell Single-Degree-of-Freedom (SDF) strapdown [AD-A154766] 21 p3569 N85-

Precision linear ramp function generator [DE85-011647] 22 p3760 N85-

Linear boundary detection using pressure buildup [DE85-009926] 22 p3784 N85-

Instrumentation for sensing moisture content of using a transient thermal pulse [NASA-CASE-NPO-15493-2] 23 p3933 N85-

A new approach to linear quadtrees
23 p3961 N85-34550

Scale separation closure and Alfven wave turbulence
[DE85-013124] 24 p4095 N85-35385

The geostatistical approach to the inverse problem in two-dimensional steady state groundwater modeling
24 p4107 N85-35462

LINEARIZATION

Nonsteady motion of solid sphere in compressible viscous fluid 02 p0269 N85-11753

Quasi-three dimensional modeling of functionally-integrated elements of large-scale integrated circuits 04 p0490 N85-13122

Overview of magnetic bearing control and linearization approaches for annular magnetically suspended devices
05 p0607 N85-13672

Magnetostatic problems in nonlinear media with hysteresis
[DE85-003701] 10 p1482 N85-19358

Elastic-plastic analysis for cyclic loading using a linearized yield condition
[PB85-149607] 14 p2322 N85-24346

Non-linear methods for inertial navigation system alignment
[BAE-ST-12683] 15 p2468 N85-25232

On the equivalent bilinearization of nonlinear controlled delay systems
[RR-272] 20 p3519 N85-31880

Development and validation of a general purpose linearization program for rigid aircraft models
[NASA-TM-86737] 21 p3556 N85-32122

Realization and linearization of a hyperfrequency power amplifier implemented with bipolar transistors in class C polarization — microwave amplifiers
[CNES-NT-114] 23 p3926 N85-34346

Production of initial estimates of photogrammetric variables
[NPL-MOM-66] 23 p3943 N85-34434

LINERS

U LININGS

LINES (GEOMETRY)

NT GEODESIC LINES

A description of the Langley wireframe geometry standard (LaWGS) format
[NASA-TM-85767] 13 p1971 N85-22380

Selection of segment similarity measures for hierarchical picture segmentation 23 p3960 N85-34548

LING-TEMCO-VOUGHT AIRCRAFT

NT A-7 AIRCRAFT

NT F-8 AIRCRAFT

LINGUISTICS

NT MACHINE TRANSLATION

NT PHONEMES

NT PSYCHOLINGUISTICS

NT SEMANTICS

NT SYNTAX

NT WORDS (LANGUAGE)

Neuro-linguistic programming: Eye movements as indicators of representational systems
[AD-A147541] 07 p1016 N85-16454

Toward a principle-based parser
[AD-A147807] 08 p1202 N85-17565

Research on knowledge delivery
[AD-A149565] 10 p1538 N85-19698

Symbiosis between postgraduate training and research projects: A successful experience
[INPE-3216-PRE/569] 16 p2810 N85-27330

Artificial intelligence in Ada (trademark): Pattern-directed processing
[AD-A156230] 24 p4141 N85-35671

LININGS

NT ROCKET LININGS

Nonlinear structural and life analyses of a combustor liner 02 p0141 N85-10955

Heat flux sensors for burner liners and turbine blades and vanes 02 p0142 N85-10961

Burner liner thermal/structural load modelling
02 p0143 N85-10970

Validation of structural analysis methods using the in-house liner cyclic rigs 02 p0146 N85-10987

HOST liner cyclic facilities: Facility description
02 p0146 N85-10988

A study of the Armstrong Whitworth swing beam engine for automotive application 04 p0506 N85-13239

Electrical resistivity technique to assess the integrity of geomembrane liners
[PB85-122414/GAR] 09 p1325 N85-18327

Polymeric liner selection for military waste impoundments
[AD-P004143] 09 p1348 N85-18479

Advanced liner-cooling techniques for gas turbine combustors
[NASA-TM-86952] 12 p1770 N85-21115

Shallow land burial technology: Humid
[DE85-004432] 12 p1932 N85-22136

Determination of wear intensity and resource of crankshafts and cylinder liners of ZIL-130 and ZMZ-53 engines
[BLL-BISI-TRANS-21393-(9022.06)]
17 p2972 N85-26355

Development of carbon based brake lining materials without asbestos content in the form of carbon-carbon composites and carbon-metal or carbon-carbide composites
[BMFT-FB-T-85-014] 18 p3082 N85-29067

Nonlinear analysis of an axisymmetric structure subjected to non-axisymmetric loading
20 p3466 N85-31540

SCAP: A Shaped Charge Analysis Program. User's manual for SCAP 1.0
[DE85-011182] 20 p3515 N85-31854

Elevated temperature crack growth
[NASA-CR-174957] 22 p3799 N85-33540

Prestressed concrete vessel according to the hot liner concept: A critical evaluation of experimental results with a prototype vessel
[OEFZS-4313] 22 p3801 N85-33550

High temperature structural insulating material
[DE85-006361] 23 p3920 N85-34291

Development of advanced high-temperature heat flux sensors. Phase 2: Verification testing
[NASA-CR-174973] 24 p4096 N85-35391

LINKAGES

Kinematic synthesis of planar cam-link mechanisms for exact path and exact motion generation
03 p0341 N85-12189

Burmester theory for 4 precision positions: An extended discourse with application to the dimensional synthesis of arbitrary planar linkages 03 p0367 N85-12351

Second sailplane project: The RP-2
04 p0466 N85-12977

Controlling rotation of elastic manipulator link
04 p0488 N85-13113

Space shuttle elevon seal panel mechanism
08 p1101 N85-16961

Vibrations of rotors connected through couplings with backlash 17 p2940 N85-28147

On the turning lozange of constant side whose vertices alternate between two fixed circles of a ring
[AD-A154803] 21 p3677 N85-32840

The balancing of complex linkage mechanisms
23 p3924 N85-34313

Conjugated symmetrical coupler curves, produced by 4-bar linkages having the same transmission angles
23 p3924 N85-34322

LINKING

U JOINING

LINKS (MATHEMATICS)

On ergodic actions whose self-joinings are graphs
[CWI-PM-R8406] 12 p1925 N85-22093

LIOUVILLE EQUATIONS

Covariant Poisson brackets for classical fields
[DE85-010085] 18 p3171 N85-29654

LIPID METABOLISM

Dynamics of some parameters of carbohydrate and lipid metabolism in recovery period following long-term hypokinesia 01 p0093 N85-10623

Effects of immobilization and high-altitude adaptation on energy metabolism in rats 22 p3820 N85-33663

Lipid hydrolysis in man during antiorthostatic hypokinesia 23 p3953 N85-34500

Lipogenesis in rat liver after flight aboard Cosmos-1129 biosatellite 23 p3954 N85-34506

LIPIDS

NT LIPOPROTEINS

Static and quasiellastic neutron scattering for the investigation of structure, dynamics and transport properties of lipid layers and lipid/protein compounds
03 p0432 N85-12753

The lipid composition and its alteration during the growth stage in pathogenic fungus, epidermophyton floccosum
[NASA-TM-77440] 07 p1011 N85-16421

Liposome-encapsulated hemoglobin for emergency resuscitation
[AD-A146794] 07 p1015 N85-16446

Microalgae culture collection, 1984-1985
[DE84-013035] 11 p1690 N85-20626

Magnetically-localizable, polymerized lipid vesicles and method of disrupting same
[AD-D011686] 19 p3249 N85-30144

Rat blood serum and liver carbohydrates and lipids in recovery period after 15-day hypokinesia
19 p3326 N85-30606

The role of sulfur in osmoregulation and salinity tolerance in cyanobacteria, algae, and plants
21 p3660 N85-32736

LIPOPROTEINS

Distinctive morphological manifestations of acute stress reaction in adrenal cortex of hypokinetic rats
12 p1902 N85-21944

LIPSCHITZ CONDITION

Sensitivity analysis in generalized rational approximation with restricted denominator
[CSIR-TWISK-319] 01 p0109 N85-10734

Domains with Lipschitz mapping functions
10 p1535 N85-19675

Extension of embeddings close to isometries or similarities 15 p2634 N85-26242

Hardy spaces and the L sup P-Neumann problem for Laplace's equation in a Lipschitz domain
[CTH-MATH-1985-02] 22 p3636 N85-33749

LIQUEFACTION

NT COAL LIQUEFACTION

Bench-scale research in biomass direct liquefaction
[DE84-011881] 02 p0223 N85-11460

Biomass thermochemical conversion program
[DE84-017177] 05 p0621 N85-13972

Active cooling requirements for propellant storage
08 p1108 N85-17004

Response of saturated porous nonlinear materials to dynamic loadings
[AD-A148526] 08 p1173 N85-17394

Innovation in earthquake and natural hazards research: Determining soil liquefaction potential
[PB85-149573] 14 p2374 N85-24678

LIQUEFIED GASES

NT LIQUEFIED NATURAL GAS

NT LIQUID AIR

NT LIQUID AMMONIA

NT LIQUID HELIUM

NT LIQUID HELIUM 2

NT LIQUID HYDROGEN

NT LIQUID NITROGEN

NT LIQUID OXYGEN

Status of gaseous fuels for use in highway transportation: A 1983 perspective
[DE84-015205] 01 p0034 N85-10211

Electronics Engineering Department EE Technical Review
[UCRL-50025-84-1] 13 p2083 N85-22887

Liquid membranes for the production of oxygen-enriched air
[DE85-006056] 15 p2506 N85-25460

Hydrocarbon pool and vapor fire data analysis
[DE85-005857] 15 p2523 N85-25550

LIQUEFIED NATURAL GAS

Insulating polymer concrete
[DE84-017239] 04 p0480 N85-13057

Risks in the transport and storage of liquefied natural gas. Sub-project 5-2: Investigation into building damage
[BLL-RISLEY-TR-4606-(9091.9F)]
07 p0935 N85-15926

Penetration of the atmosphere by flammable mixtures as a result of spillage of LNG on the ground
08 p1179 N85-17432

Thermal radiation hazards from Liquified Petroleum Gas (LPG) fireballs
[VTT-304] 09 p1293 N85-18122

Mechanisms of heat and mass transfer across a double-diffusive interface
[PB85-148468] 12 p1848 N85-21594

Facility for large-scale hazardous gas testing
[DE85-011852] 21 p3564 N85-32169

LIQUID AIR

Liquid membranes for the production of oxygen-enriched air
[DE85-006056] 15 p2506 N85-25460

LIQUID ALLOYS

Electronic structure of liquid metal alloys
[DE85-000904] 09 p1295 N85-18136

LIQUID AMMONIA

Two phase discharge of liquefied gases through pipes. Field experiments with ammonia and theoretical model
[FOA-B-40139-C1] 18 p3103 N85-29209

LIQUID ATOMIZATION

Certain optimal parameters of high-velocity Venturi ejection tubes
[BLL-M-35924-(5828.4)] 05 p0634 N85-14066

Injection, atomization, ignition and combustion of liquid fuels in high-speed air streams
[AD-A154056] 19 p3251 N85-30156

LIQUID CHROMATOGRAPHY

Compound class quantitation of JP-5 jet fuels by high performance liquid chromatography-differential refractive index detection
[AD-A145754] 03 p0340 N85-12185

Supercritical fluid chromatography/supersonic jet spectroscopy
[DE84-016199] 04 p0471 N85-12998

Development of acceptance criteria for batches of silane primer for external tank thermal protection system bonding applications
[NASA-CR-171266] 04 p0478 N85-13043

Analysis and characterization of organic carbon compounds in atmospheric particulate matter
[PB84-232636] 06 p0766 N85-14903

Prediction of retention indices of polynuclear aromatic hydrocarbons. Part 1: HPLC on nitrogen containing normal phase packing materials
[DE85-001302] 10 p1436 N85-19051

Quantitative determination of compound classes in jet turbine fuels by high performance liquid Chromatography/Differential refractive index detection: Part 2
[AD-A148298] 11 p1613 N85-20144

Analysis of aldehydes and ketones in the gas phase
[PB85-181666] 20 p3426 N85-31261

Rapid estimation of concentration of aromatic classes in middistillate fuels by high-performance liquid chromatography
[NASA-TP-2485] 20 p3434 N85-31307

LIQUID COOLED REACTORS
NT BOILING WATER REACTORS
NT EXPERIMENTAL BREEDER REACTOR 2
NT LIGHT WATER REACTORS
NT LIQUID METAL COOLED REACTORS
NT PRESSURIZED WATER REACTORS
NT WATER COOLED REACTORS
NT ZERO POWER REACTORS

Thermal hydraulic features of the TMI accident
[DE85-014589] 24 p4152 N85-35747

LIQUID COOLING
NT FILM COOLING

Thermal fluid-structure interaction: A few scaling considerations -- nuclear reactors
[GKSS-84-E-18] 01 p0048 N85-10314

Liquid cooled, linear focus solar cell receiver
[DE84-014446] 01 p0067 N85-10448

Advanced concepts liquid droplet radiator
05 p0610 N85-13899

The liquid droplet radiator - an ultralightweight heat rejection system for efficient energy conversion in space
05 p0610 N85-13900

An evaluation of liquid and two-phase cooling techniques for use in electrical machinery
[AD-A148528] 10 p1484 N85-19372

Method of calculating cooldown process in cryostat of cryogenic electric machine 12 p1843 N85-21567

Thermal state of cooled thin-walled nozzle blade
14 p2270 N85-24066

Role of fluid lubricant-coolant in fine grinding of optical glass by diamond tool 14 p2280 N85-24125

Low gravity exothermic heating/cooling apparatus
[NASA-CASE-MSC-25707-1] 18 p3104 N85-29214

Comparison of the response of shape memory alloy actuators using air-cooling and water-cooling
[AD-A155216] 21 p3567 N85-32185

LIQUID CRYSTALS

Investigation and development of multicolored liquid crystal display systems for automotive dashboard application and large format information boards
[BMFT-FB-T-84-187] 04 p0572 N85-13652

Measurement of parameters defining orientation of liquid crystals in electrooptic cells 06 p0777 N85-14871

Research on submicrometer structures
[AD-A146578] 06 p0867 N85-15508

Synthesis and characterization of unique liquid crystalline block copolyesters. A proposal for a polymer research center at the Atlanta University
[AD-A147280] 07 p0932 N85-15907

Matrix display simulation
[AD-D011371] 07 p1055 N85-16695

Improved real-time ultra-high resolution image projection display using laser-addressed liquid crystal light valve
[AD-D011414] 08 p1223 N85-17705

A brief review of the technology of microemulsions and other micellar systems
[AD-A149759] 12 p1800 N85-21289

Exploratory development of foams from liquid crystal polymers
[NASA-CR-172510] 13 p2036 N85-22754

Interaction of liquid crystals with inhomogeneous surfaces
[AD-A151557] 15 p2680 N85-26413

Nematic liquid crystals for car dashboards
[BMFT-FB-T-84-298] 16 p2872 N85-27718

InP materials
[AD-A152341] 17 p3043 N85-28828

Numerical optical computing at the Ohio State University 18 p3186 N85-29775

Electrochemical studies in liquid crystals
[AD-A154317] 19 p3234 N85-30050

Mesophase mechanisms in the formation of graphitic microstructures
[AD-A154100] 19 p3248 N85-30140

Electrochromic display device
[AD-D011733] 22 p3759 N85-33299

Liquid crystal light valve structures
[NASA-CASE-MSC-20036-1] 22 p3847 N85-33826

Differentiating spatial light modulator
[AD-D011727] 23 p3973 N85-34632

LIQUID DROPS
U DROPS (LIQUIDS)

LIQUID FILLED SHELLS

Moment induced by liquid payload during spin-up without a critical layer
[AD-A145716] 02 p0199 N85-11327

High-frequency asymptotic behavior of reflected and transmitted waves during scattering of sound by hollow elastic sphere filled with fluid 02 p0266 N85-11738

Liquid payload moment equations
[AD-A145977] 03 p0362 N85-12319

A study of the critical layer in a rotating liquid payload
[AD-A146094] 03 p0362 N85-12321

Fluid motion in a rotating and nutating container
[AD-A146175] 03 p0362 N85-12322

Modifications to SOLA-VOF for flow dynamics in spinning cylinders
[AD-A154093] 19 p3265 N85-30250

LIQUID FLOW
NT OPEN CHANNEL FLOW
NT WATER FLOW

Finite element method for a class of viscoelastic flows in deforming domains applied to jet breakup
[DE84-014571] 04 p0500 N85-13186

Magnetic inductive flowmeter for low conducting liquids
[BMFT-FB-T-84-136] 04 p0504 N85-13216

Instability of film boiling of moving liquids
[BLL-WH-603-(9091.9F)] 07 p0956 N85-16056

Leakage-flow induced vibrations of a chimney structure suspended in a liquid flow -- nuclear reactors
09 p1339 N85-18420

Liquid mass flow rate computer
13 p2075 N85-22962

Radiation-dominated snowmelt on Mars
13 p2191 N85-23592

Catalytic hydrotreatment studies with model compounds
[DE85-010187] 19 p3236 N85-30064

Instability and chaotic behavior in a free-surface flow
[AD-A154879] 21 p3584 N85-32279

Detailed validation of a liquid and heat flow code against field performance
[DE85-009901] 23 p3932 N85-34368

LIQUID FUELS
NT AIRCRAFT FUELS
NT AUTOMOBILE FUELS
NT CRYOGENIC ROCKET PROPELLANTS
NT DIESEL FUELS
NT GASOLINE
NT HYDROGEN FUELS
NT HYPERGOLIC ROCKET PROPELLANTS
NT JET ENGINE FUELS
NT JP-4 JET FUEL
NT JP-5 JET FUEL
NT JP-8 JET FUEL
NT KEROGEN
NT KEROSENE
NT LIQUID ROCKET PROPELLANTS
NT MONOPROPELLANTS
NT SLURRY PROPELLANTS

Prospectus of the utilization of leafy spurge (Euphorbia Esula L.) as a source of liquid fuel and biomass
[DE84-015203] 01 p0034 N85-10206

Converting gasoline farm tractors to run efficiently on farm-produced alcohol
[DE84-015796] 02 p0205 N85-11350

Liquid hydrocarbon fuels from syngas
[DE84-015942] 04 p0482 N85-13069

Pressure oscillations in liquid-fueled ramjet engines
05 p0596 N85-13797

Liquid-fueled Ramjet engines
07 p0918 N85-15814

A review of hazard assessment procedures for liquid gun propellants
[AD-A149470] 10 p1457 N85-19182

Numerical simulations of liquid propellant combustion instability: Onset and growth
[DE85-000743] 10 p1458 N85-19186

The influence of fuel quality upon flame-tube temperature and flame radiation in a model gas-turbine primary zone
[K233] 13 p1974 N85-22396

The influence of fuel molecular composition upon flame-tube temperature and flame radiation in a model gas-turbine primary zone
[K234] 13 p2017 N85-22646

Atmospheric dispersion of hypergolic liquid rocket fuels, volume 2
[AD-A150699] 14 p2263 N85-24020

Studies on rocket engines for future European launchers
[SEP-TPRL/K-19572/84] 15 p2495 N85-25393

CON1D: A computer program for calculating spherically symmetric droplet combustion
[DE85-005604] 15 p2507 N85-25464

Improved catalysts for liquid hydrocarbon fuels fro syngas
[DE85-006569] 16 p2746 N85-2

Technical and economic analysis of liquid fuel productio from microalgae
[DE85-002926] 16 p2758 N85-27

Liquid propellants for use in guns: A review
[AD-A153061] 17 p2937 N85-281

Liquid hydrocarbon fuels from syngas
[DE85-009613] 19 p3236 N85-30

Improved catalysts for liquid hydrocarbon fuels fro syngas
[DE85-011062] 20 p3421 N85-312

Biomass thermochemical conversion program
[DE85-011867] 21 p3572 N85-32

Production of liquid fuels and chemicals by microalga
[DE85-006780] 22 p3819 N85-33

LIQUID HELIUM
NT LIQUID HELIUM 2

High specific heat dielectrics and Kapitza resistance a dielectric boundaries
[AD-A148476] 08 p1217 N85-17

Acoustic microscopy at cryogenic temperatures
[AD-A148755] 09 p1364 N85-187

Turbulence in pure superfluid flow
09 p1397 N85-187

Shock compression of liquid helium to 56 GPa (56 kbar 13 p2184 N85-23

A measurement of the intensity of the cosmic background radiation at 3.0 cm
13 p2206 N85-23

NMR manometer for measuring high pressures a liquid-helium temperatures 17 p2944 N85-2817

Balloon-borne, He-cooled Fourier transform spectrometer for far infrared astronomy
[MPE-IR-41] 17 p3053 N85-28

Cooling high intensity atomic hydrogen beams to liquid helium temperatures
[DE85-012515] 24 p4148 N85-3571

LIQUID HELIUM 2

Outlook for realization of proximity effect and Josephson direct current in helium-2 13 p2074 N85-22

Entropy of He 2 and universality near the superfluid in He(4) 19 p3378 N85-30

LIQUID HYDROGEN

Measurement of scattering cross sections of liquid and solid hydrogen deuterium and deuterium hydride fo thermal neutrons
[DE84-014814] 05 p0727 N85-1487

Partial bleed expander cycle for low thrust LOX/LH rocket engine
[NAL-TR-837T] 10 p1430 N85-1901

An air-breathing ballistic space transporter for Europe
[NASA-TM-77645] 12 p1792 N85-2124

Capture of liquid hydrogen boiloff with metal hydride absorbers
[NASA-CR-175677] 14 p2249 N85-23

Ten degree Kelvin hydride refrigerator
[NASA-CASE-NPO-16393-1-CU]
18 p3085 N85-290

Preliminary considerations for the gasdynamic precompression of solid molecular hydrogen
[DE85-013256] 22 p3784 N85-334

LIQUID INJECTION
NT DEEP WELL INJECTION (WASTES)
NT WATER INJECTION

Improvement of gas turbine engine performance by water injection into turbine cooling air
09 p1307 N85-18

Effect of water injection into air for turbine cooling on economy of operation of gas turbine engine with afterburning 13 p2060 N85-22

Vortex generating flow passage design for increased film cooling effectiveness
[NASA-CASE-LEW-14039-1] 22 p3782 N85-334

LIQUID LEVELS

Experimental investigation of the oscillation behavior of a liquid-filled rotor with centrifugal motion
[BLL-DOUNREAY-TR-936-(9091.9F)]
08 p1160 N85-1751

LIQUID LITHIUM

New liquid cathodes for lithium batteries. Part A: Halocarbons
[AD-A148433] 08 p1178 N85-174

LIQUID MERCURY
U MERCURY (METAL)

LIQUID METAL COOLED REACTORS
NT EXPERIMENTAL BREEDER REACTOR 2

Analysis of the natural initiation of vapor explosions
[DE85-000188] 11 p1632 N85-2027

Technical assessment of thermal-hydraulics for high heat flux fusion components
[DE85-013178] 23 p3930 N85-343

LIQUID METAL FAST BREEDER REACTORS

Non-isothermal irradiation creep of nickel alloys Inconel 706 and PE-16
[DE85-000842] 11 p1607 N85-20102

Use of laser flow visualization techniques in reactor component thermal-hydraulic studies
[DE84-014768] 11 p1639 N85-20330

Coolant mixing in LMFBR rod bundles and outlet plenum mixing transients
[DE85-010398] 19 p3268 N85-30268

Loss-of-flow transient characterization in carbide-fueled LMFBRs
[DE85-008552] 19 p3269 N85-30270

Analytical simulation of weld effects in creep range
20 p3468 N85-31550

Resolution of thermal striping issue downstream of a horizontal pipe elbow in stratified pipe flow
[DE85-006195] 21 p3526 N85-32292

LIQUID METALS

NT LIQUID LITHIUM
NT LIQUID POTASSIUM
NT LIQUID SODIUM
NT MERCURY (METAL)

Study of vibrational energy transfer at a liquid tin surface
[AD-A145741] 02 p0277 N85-11804

Emission mechanisms in the liquid metal ion source: A review
[AERE-R-11294] 03 p0418 N85-12675

Reproducibility of readings from oxygen concentration elements
[BLL-M-35920-(5828.4)] 05 p0616 N85-13941

Effects of temperature on the response time of thermocouples and resistance thermometers
[DE84-016855] 06 p0811 N85-15154

Extreme incompatibility of Pb during the crystallization of magnetic iron meteorites 06 p0866 N85-15627

Investigations concerning the magnetic iron meteorites: Static vs. dynamic experiments
06 p0866 N85-15629

Investigation of electric and wear phenomena of liquid metal wetted copper fiber brushes under conditions of high slip ring eccentricity
[AD-A147634] 08 p1156 N85-17295

Susceptibility of 2 1/4 Cr-1Mo steel to liquid metal induced embrittlement by lithium-lead solutions
[DE85-000007] 09 p1294 N85-18130

Electronic structure of liquid metal alloys
[DE85-000804] 09 p1295 N85-18136

Glass corrosion in liquid lithium
[DE85-002086] 09 p1299 N85-18162

Characteristics of the boat inductor for keeping liquid metal in the suspended state
[NASA-TM-77816] 12 p1851 N85-21611

Anomalies of aluminum structure and properties
13 p2026 N85-22693

Division boundary in Al-B composite material with boron in contact with solid and liquid aluminum
13 p2027 N85-22704

Electrodynamic stability of composite liquid-metal contacts 13 p2087 N85-23031

The volume change during solidification
[NASA-TM-77817] 14 p2300 N85-24243

Experimental facility for studying MHD effects in liquid metal cooled blankets
[DE85-000583] 14 p2423 N85-24943

Magneto-fluid-dynamic issues for fusion first wall and blanket systems
[DE85-004022] 14 p2424 N85-24954

Magnetohydrodynamic considerations for the design of self-cooled liquid-metal fusion reactor blankets
[DE85-000242] 14 p2425 N85-24957

Analysis of alkali liquid metal Rankine space power systems
[DE85-005080] 16 p2741 N85-26917

Flat magnetohydrodynamic induction pump
17 p2939 N85-28145

Dependence of characteristics of centrifugal magnetohydrodynamic conduction pump on electrical conductance of end walls. Part 1: Experiment
17 p2939 N85-28146

Liquid-metal transducers for strain measurement during in-pile materials testing 17 p2945 N85-28176

Automatic liquid-metal temperature monitoring with the use of immersed transducers
[BLL-BISI-TRANS-22427-(9022.06)]
18 p3104 N85-29215

Liquid metal thermoelectric converter (LMTEC) for solar applications
[DE85-008405] 18 p3129 N85-29376

Thermodynamic properties of liquid Li-Pb, Na-Pb and K-Pb alloys: Similarities and Differences
[DE85-004074] 18 p3167 N85-29830

Arc spray fabrication of metal matrix composite monotape
[NASA-CASE-LEW-13828-1] 19 p3230 N85-30027

Liquid metal reactor programs: Safeguards and program assurance
[DE85-010621] 19 p3331 N85-30635

Rapid analysis of steels using laser-based techniques
[DE85-010747] 22 p3748 N85-33232

Key issues of fusion nuclear technology development (FINESSE)
[DE85-012599] 22 p3845 N85-33817

Electrically conductive containment vessel for molten aluminum
[DE85-006518] 23 p3939 N85-34415

LIQUID NITROGEN

Wear of anodic oxide films on aluminum alloys in cryogenic liquids
[NAL-TR-818] 06 p0768 N85-14914

New method for heat treatment of metals
10 p1446 N85-19110

Comparison of calculations and measurements of the off-axis radiation dose (Si) in liquid nitrogen as a function of radiation length
[AD-A153676] 18 p3176 N85-29704

A system for the assessment of non-thermal effects of ultrasound on cells at liquid nitrogen temperatures
20 p3523 N85-31915

A liquid nitrogen cooled composite wall hollow cathode — molecular spectroscopy
[USIP-85-07] 20 p3526 N85-31930

Basic cryogenics and materials. Phase 1
[NASA-CR-177932] 21 p3572 N85-32215

Sound speed measurements in liquid oxygen-liquid nitrogen mixtures
[NASA-TP-2464] 24 p4083 N85-35307

LIQUID OXYGEN

Numerical analysis of flow and heat transfer in the VAFB LOX storage Dewar tank
[NASA-CR-171203] 02 p0197 N85-11315

A study on dynamic characteristics of liquid oxygen pumps for rocket engines
[NAL-TR-806] 03 p0324 N85-12088

Ultrasound instrumentation for the 7 inch Mach seven tunnel
[NASA-CR-174277] 07 p1038 N85-16586

Automatic software for controlling cryogenic systems
08 p1097 N85-16932

Partial bleed expander cycle for low thrust LOX/LH2 rocket engine
[NAL-TR-837T] 10 p1430 N85-19018

An air-breathing ballistic space transporter for Europe
[NASA-TM-77645] 12 p1792 N85-21244

Nonlinear rotordynamics analysis
[NASA-CR-171425] 13 p1968 N85-22364

Flow induced vibration of the SSME LOX posts
[NASA-CR-175608] 15 p2495 N85-25391

Studies on rocket engines for future European launchers
[SEP-TPRL/K-19572/84] 15 p2495 N85-25393

Flow-induced vibration of the SSME LOX posts: Additional issues
[DE85-007339] 16 p2741 N85-26916

Flow-induced vibration of SSME main injector liquid-oxygen posts 17 p2912 N85-27951

Ignition characterization of LOX/hydrocarbon propellants
[NASA-CR-171884] 18 p3083 N85-29070

Ignition characterization of LOX/hydrocarbon propellants
[NASA-CR-171882] 18 p3083 N85-29071

Basic cryogenics and materials. Phase 1
[NASA-CR-177932] 21 p3572 N85-32215

Sound speed measurements in liquid oxygen-liquid nitrogen mixtures
[NASA-TP-2464] 24 p4083 N85-35307

LIQUID PHASE EPITAXY

Producing gallium arsenide crystals in space
02 p0151 N85-11023

Effect of liquid phase composition on thickness of epitaxial Ga sub (1-x) Al sub x As films
02 p0257 N85-11683

Symmetry of exchange interaction in crystalline magnetic films 02 p0259 N85-11694

Photoelectric effect in liquid crystals
02 p0259 N85-11695

Current controlled LPE (Liquid Phase Epitaxy) growth of semiconductors
[AD-A145536] 02 p0287 N85-11875

LPE (Liquid phase epitaxy) semiconductor material transfer method
[AD-D011250] 05 p0731 N85-14696

Tunable microwave transversal filters
[AD-A148370] 08 p1158 N85-17304

P-I-N CdTe gamma-ray detectors by Liquid Phase Epitaxy (LPE)
[DE84-012276] 09 p1323 N85-18315

Liquid-phase epitaxial growth of CdTe on HgCdTe
[AD-D011482] 10 p1561 N85-19846

Preparation of crystal growth experiments in Spacelab: Si (FSLP), CdTe (D1), ZnS (D1)
[BMFT-FB-W-84-045] 12 p1788 N85-21227

Development of solid state infrared emitters for gas detection applications
[PB85-148450] 15 p2501 N85-25800

Materials-process interactions in ternary alloy semiconductors
[AD-A153133] 17 p3043 N85-28632

Electron irradiation of light emitting diodes
[AD-A154441] 19 p3260 N85-30213

Design and operation of epitaxial reactor
[DE85-011089] 19 p3306 N85-30491

Low-threshold injection InGaAsP/GaAs double heterostructure lasers with separate limiting obtained by liquid-phase epitaxy (lambda = 0.78 divided by 0.87 microns, I sub thr = 480 A/cm 2, T = 300 K)
21 p3687 N85-32906

LIQUID PHASES

Thermodynamics of decarburization of niobium-bearing high-alloy melts
[BLL-M-35728-(5828.4)] 02 p0175 N85-11169

Deuterium diffusion in a soil-water-ice mixture
[AD-A148457] 08 p1176 N85-17415

Liquid phase methanol process development unit: Installation, operation, and support studies
[DE85-001J11] 09 p1301 N85-18171

Analysis of phase composition of products of laser destruction of metallic surfaces
11 p1600 N85-20064

Densification and deformation in the presence of a liquid phase
[DE85-005101] 13 p2038 N85-22763

Catalyst and reactor development for a liquid phase Fischer-Tropsch process
[DE85-005894] 17 p2922 N85-28014

Electrochemical studies in liquid crystals
[AD-A154317] 19 p3234 N85-30050

Modeling of chemical transformations of SO(x) and NO(x) in the polluted atmosphere: An overview of approaches and current status
[PB85-173169] 20 p3487 N85-31677

Phase behavior and QLS (Quasielastic Light Scattering) in potassium linoleate/n-alkanol microemulsions
[AD-A155028] 21 p3563 N85-32163

Liquid-phase compositions from vapor-phase analyses 2: Adaptation of the Prausnitz program to UF6 and some of its potential impurities
[DE85-011521] 21 p3673 N85-32819

The effect of liquid-liquid phase seperation of glass on the properties and crystallization behavior
[NASA-TM-77890] 23 p3919 N85-34285

Chemistry of ore-forming fluids
24 p4103 N85-35436

LIQUID POTASSIUM

Operating experience with potassium systems — thermal power stations
[OEFZS-4275] 03 p0387 N85-12473

LIQUID PROPELLANT ROCKET ENGINES

NT HYDRAZINE ENGINES
NT HYDROGEN OXYGEN ENGINES
NT RL-10 ENGINES
NT SPACE SHUTTLE MAIN ENGINE

Columbium chamber fabrication study
[AD-A145230] 01 p0017 N85-10102

A study on dynamic characteristics of liquid oxygen pumps for rocket engines
[NAL-TR-806] 03 p0324 N85-12088

A study of air breathing rockets. Part 4: Direct fuel injection into a secondary combustor
[NAL-TR-832] 09 p1287 N85-18083

Partial bleed expander cycle for low thrust LOX/LH2 rocket engine
[NAL-TR-837T] 10 p1430 N85-19018

The 1984 JANNAF Propulsion Systems Hazards Subcommittee Meeting, volume 1
[AD-A148865] 10 p1454 N85-19162

Safety aspects of prepackaged liquid propellant stages for strategic missiles
[AD-P004350] 10 p1456 N85-19174

Low loss injector for liquid propellant rocket engines
[NASA-CASE-MFG-25089-1] 11 p1581 N85-20006

An integral closed loop combustion stability model-status and review 13 p2003 N85-22553

Development of a three-phrase combustion code for modeling liquid rocket engines 13 p2003 N85-22554

Atomization data requirements for rocket combustor modeling 13 p2003 N85-22555

Effect of compliability of hot walls in liquid-propellant engine on low frequency instability
13 p2049 N85-22824

AFRPL (Air Force Rocket Propulsion Laboratory) technical objective document FY 85
[AD-A151368] 15 p2495 N85-25389

Materials for advanced rocket engine turbopump turbine blades 16 p2734 N85-26872

Ignition/combustion processes
16 p2740 N85-26909
A closed loop analysis of POGO instability
[AD-A153121] 17 p2937 N85-28132
Hydrazine and the F-16 20 p3511 N85-31826
Sound speed measurements in liquid oxygen-liquid nitrogen mixtures
[NASA-TP-2464] 24 p4083 N85-35307

LIQUID ROCKET PROPELLANTS
NT CRYOGENIC ROCKET PROPELLANTS
NT HYPERGOLIC ROCKET PROPELLANTS
NT MONOPROPELLANTS
NT SLURRY PROPELLANTS
Safety aspects of prepackaged liquid propellant stages for strategic missiles
[AD-P004300] 10 p1456 N85-19174
Space Transportation System (STS) propellant scavenging system study. Volume 1: Technical report
[NASA-CR-171848-VOL-1] 11 p1589 N85-20000
Fluid slosh dynamics of surface tension tanks in three axis stabilized spacecraft
[MBB-UR-E-739-84-O] 11 p1634 N85-20291
Dynamic investigations of a spherical tank structure filled with liquid using ANSYS three-dimensional fluid elements
[MBB-UR-E-737-83-O] 11 p1654 N85-20418
Feasibility of producing commodities and electricity for space shuttle operations at Vandenberg Air Force Base
[DCN-84-203-001-80-21] 12 p1789 N85-21230
Atomization data requirements for rocket combustor modeling 13 p2003 N85-22555
Low thrust bipropellant engine/redundant seat valve assembly
[AD-A150293] 13 p2013 N85-22626
Atmospheric dispersion of hypergolic liquid rocket fuels, volume 2
[AD-A150699] 14 p2263 N85-24020
Ignition/combustion processes
16 p2740 N85-26909
Application of the hydraulic system frequency response program to propellant feed systems
[AD-A151824] 16 p2741 N85-26914
A closed loop analysis of POGO instability
[AD-A153121] 17 p2937 N85-28132

LIQUID ROTATION
U ROTATING LIQUIDS

LIQUID SLOSHING
In-orbit experiments on IRAS for application to the ISO satellite
[FOK-TR-R-84-057] 03 p0322 N85-12078
Propellant transfer: Tethered depot
08 p1108 N85-17006
Fluid slosh dynamics of surface tension tanks in three axis stabilized spacecraft
[MBB-UR-E-739-84-O] 11 p1634 N85-20291
Analysis of seismic sloshing of reactor tanks considering submerged components and seismic isolation
[DE85-010499] 19 p3269 N85-30273
Further studies on liquid sloshing
[PB85-199695] 24 p4095 N85-35366

LIQUID SODIUM
Induction voidmeter
[DE84-014321] 01 p0050 N85-10329
Study of alternative system conversions for the Solar One pilot plant
[DE85-010026] 22 p3809 N85-33594

LIQUID SURFACES
NT MENISCI
Study of vibrational energy transfer at a liquid tin surface
[AD-A145741] 02 p0277 N85-11804
Free surface effects on the wake of a flat plate
[AD-A146966] 07 p0958 N85-16071
Liquid thickness gage
[NASA-CASE-LAR-13342-1] 11 p1635 N85-20297
Instability and chaotic behavior in a free-surface flow
[AD-A154879] 21 p3584 N85-32279
Surface temperature distribution along a thin liquid layer due to thermocapillary convection
[NASA-TM-87115] 23 p3930 N85-34357

LIQUID WASTES
NT URINE
NT WASTE WATER
Radioactive liquid wastes discharged to ground in the 200 areas during 1984
[DE85-010819] 19 p3310 N85-30517
Review of hazardous waste cleanup and disposal efforts at Tinker Air Force Base
[GPO-43-294] 21 p3613 N85-32457

LIQUID-GAS MIXTURES
NT AEROSOLS
NT FOG
Mathematical-cartographic model for study of distribution of hydrochemical elements in sea water (using dissolved oxygen in the Pacific Ocean as an example)
13 p2109 N85-23138

LIQUID-LIQUID INTERFACES
The behaviour of unstable surfaces: A literature review
[CFD/84/6] 02 p0199 N85-11329
Investigation of the Ostwald ripening of separated particles in liquid-liquid systems under microgravity conditions
[BMFT-FB-W-84-037] 05 p0615 N85-13927
Properties of materials using acoustic waves
[AD-A150465] 13 p2155 N85-23382
Free-surface phenomena under low- and zero-gravity conditions
[NASA-CR-175865] 17 p2907 N85-27922
Computer-aided thermohydraulic design of TEMA type E shell and tube heat exchangers for use in low pressure, liquid-to-liquid, single phase applications
[AD-A153779] 18 p3100 N85-29191
Natural convection experiments in a stratified liquid-saturated porous medium
[DE85-009003] 20 p3455 N85-31457

LIQUID-SOLID INTERFACES
Thermal fluid-structure interaction: A few scaling considerations — nuclear reactors
[GKSS-84-E-18] 01 p0048 N85-10314
Structure and kinetics of physisorption, properties of helium during reduction of the dimension
03 p0432 N85-12749
A similarity analysis of phase change heat conduction in corners 05 p0634 N85-14069
Modulated surface vibrational spectroscopies at electrode/electrolyte interfaces
[AD-A148665] 06 p1123 N85-17083
Linear and nonlinear ultrasonic interaction on liquid-solid boundaries
[AD-A148979] 10 p1553 N85-19793
Time resolved X-ray studies during pulsed laser irradiation of Ge
[DE85-005263] 13 p2097 N85-23083
Surface scattering
[AD-A150252] 13 p2153 N85-23366
The development of laser analytical methods for the characterization of solid-liquid and solid-high pressure gas interfaces
[AD-A152382] 17 p2918 N85-27988
A Navier-Stokes capillary free boundary in open boat crystal growth
[REPT-84-34] 17 p2960 N85-28283
MPS solidification model. Analysis and calculation of macrosegregation in a casting ingot
[NASA-CR-171589] 21 p3566 N85-32178
Polymer-water interaction studies
21 p3609 N85-32411
Approximate determination of the extent of the solid-liquid zone
[BLL-M-35829-(5828.4)] 23 p3914 N85-34251

LIQUID-VAPOR EQUILIBRIUM
Study of the liquid vapor equilibrium in the bromine-hydrobromic acid-water system
[NASA-TM-77767] 07 p0921 N85-15836
A study of liquid-vapor equilibria of the bromine-hydrobromic acid-water system
[NASA-TM-77748] 14 p2249 N85-23940

LIQUID-VAPOR INTERFACES
Surface scattering
[AD-A150252] 13 p2153 N85-23366
Convective instability of horizontal layer of binary mixture 14 p2336 N85-24458
The development of laser analytical methods for the characterization of solid-liquid and solid-high pressure gas interfaces
[AD-A152382] 17 p2918 N85-27988
The polar caps and the climatic evolution of Mars
22 p3854 N85-33866
Effects of ambient pressure on the instability of a liquid boiling explosively at the superheat limit
[DE85-009476] 23 p3932 N85-34370

LIQUIDS
NT CRYOGENIC FLUIDS
NT CRYOGENIC ROCKET PROPELLANTS
NT FERMI LIQUIDS
NT FERROFLUIDS
NT HYDRAULIC FLUIDS
NT HYPERGOLIC ROCKET PROPELLANTS
NT LIQUEFIED GASES
NT LIQUID AMMONIA
NT LIQUID FUELS
NT LIQUID HELIUM
NT LIQUID HYDROGEN
NT LIQUID LITHIUM
NT LIQUID METALS
NT LIQUID NITROGEN
NT LIQUID OXYGEN
NT LIQUID POTASSIUM
NT LIQUID ROCKET PROPELLANTS
NT LIQUID SODIUM
NT MERCURY (METAL)
NT MONOPROPELLANTS
NT ORGANIC LIQUIDS
NT ROTATING LIQUIDS
NT SLURRY PROPELLANTS
The analysis of tank calibration data from several
[DE84-015529] 02 p0200 N85-11
Diffusive combustion of fluids with free surface
02 p0274 N85-117
Nonlinear acoustics
[AD-A145560] 02 p0276 N85-117
Investigation of liquid encapsulation Chochralski growth of InP
[AD-A146096] 03 p0433 N85-127
Separation of metal species by supported liquid membranes
[DE84-014536] 04 p0470 N85-12
Dynamics of liquid filament breakup
[DE84-016006] 04 p0500 N85-131
Bicomponent flow problems in rheological fluid mechanics 05 p0635 N85-14
Motion of electrons in non polar classical liquids
[DE84-013609] 05 p0727 N85-14
Stability of rigid motions and rollers in bicomponent flow of immiscible liquids
[AD-A147302] 07 p0960 N85-16
Convection heat transfer in the critical region of fluid mixtures
[DE85-002118] 07 p0961 N85-16
A virial equation of state option for the TIGER computer program
[AD-A147490] 07 p1025 N85-16
Supersonic molecular jet study of the liquid state
[AD-A147416] 09 p1379 N85-18
Liquid thickness gage
[NASA-CASE-LAR-13342-1] 11 p1635 N85-2029
Influence of pressure on speed of sound in single-phase region of stratifying mixtures 11 p1715 N85-207
Examination of the contact wetting angle in the vicinity of critical temperature
[BLL-T-416/BG/CRS/LR-ST735/84]
13 p2091 N85-2300
Vapor explosions in superheated liquids and fundamental studies of the physics of detonation
[AD-A151362] 15 p2504 N85-2544
Wave propagation in density stratified fluids
16 p2781 N85-2718
Liquid propellants for use in guns: A review
[AD-A153051] 17 p2937 N85-2813
An evaluation and preparation of ferromagnetic liquid composites for use at millimeter wavelengths
[AD-A153939] 18 p3069 N85-29
Liquid sampling system
[DE85-011673] 19 p3265 N85-302
Lost circulation in geothermal wells: Research and development status
[DE85-009836] 19 p3268 N85-302
Seismic analysis of liquid-filled tanks with an eccentric core barrel
[DE85-010249] 19 p3269 N85-3027
Interaction of slow electrons with high-pressure gases (quasi-liquids): Synthesis of our knowledge on slow electron-molecule interactions
[DE85-010061] 19 p3356 N85-30
Weak shock waves propagating in fluid-gas mixtures
[AD-A154759] 21 p3584 N85-3227
Thermophysical properties of fluids for the gas industry
[PB85-198471] 22 p3747 N85-33
Apparatus and method for the spectrochemical analysis of liquids using the laser spark
[DE85-005749] 23 p3835 N85-34
Depletion modeling of liquid dominated geothermal reservoirs
[DE85-009923] 23 p3943 N85-344
Gas analysis of ore-forming fluids
24 p4105 N85-354
Cationic exchange membrane for the zinc-ferricyanide battery
[DE85-013152] 24 p4112 N85-354
Calculation of heavy-ion tracks in liquid water
[DE85-012101] 24 p4149 N85-357

LIQUIDUS
Studies on copper alloys containing chromium on the copper side phase diagram
[NASA-TM-77752] 07 p0927 N85-16

LISP (PROGRAMMING LANGUAGE)
MACSYMA usage at Langley
[NASA-CR-172518] 10 p1537 N85-19
The portable LISP translation tool
[AD-A149765] 12 p1915 N85-20

LISTS
Glossary of landscape and vegetation ecology for Alaska
[PB85-153831] 16 p2616 N85-27

LITERATURE
NT BIOGRAPHY
NT DOCUMENTATION
European Scientific Notes, volume 38, number 12
[AD-A146718] 09 p1418 N85-18846
A network-based approach to text handling for the online scientific community 15 p2664 N85-26444
The next assignment: The state of the literature on space 23 p4057 N85-35146

LITHIUM
NT LIQUID LITHIUM
Method and apparatus for determining the content and distribution of a thermal neutron absorbing material in an object
[DE84-014319] 01 p0117 N85-10801
Lithium battery safety: A fiber-optic application for safe observation of lithium cells under severe tests
[AD-A148846] 06 p0804 N85-15119
Rechargeable lithium cell
[AD-D011302] 07 p0993 N85-16304
Pion inelastic scattering to the first three excited states of Lithium-6
[AD-A147560] 07 p1041 N85-16606
Susceptibility of 2 1/4 Cr-1Mo steel to liquid metal induced embrittlement by lithium-lead solutions
[DE85-000997] 09 p1294 N85-18130
Glass corrosion in liquid lithium
[DE85-002086] 09 p1299 N85-18162
Calculation of Si(Li) X-ray detector efficiencies
[DE85-002732] 10 p1489 N85-19400
Lithium counterdoped silicon solar cell
[NASA-CASE-LEW-14177-1] 11 p1672 N85-20535
Negative lithium emission from a tungsten surface in a plasma
[DE85-003456] 12 p1936 N85-22167
The effects of lithium counterdoping on radiation damage and annealing in n(+)p silicon solar cells
13 p2007 N85-22586
Relationship between topological and magnetic order in small metal clusters
[AD-A150547] 13 p2018 N85-22651
Hartree-Fock interaction between a helium atom and lithium-metal: A test for the effective medium theory
[AD-A150466] 13 p2156 N85-23367
Gigantic lithium deposit discovered in France
14 p2289 N85-24184
Active Magnetospheric Particle Tracing Explorers (AMPTE)
[AD-A151072] 14 p2374 N85-24674
Sodium and lithium corrosion in molybdenum heat pipes
[DE85-005561] 16 p2784 N85-27179
Investigation of the structure and dynamics of electrolytes in solvents used for primary and secondary Li-batteries
[AD-A153099] 17 p2954 N85-28240
Experimental study of dissociative attachment in optically-pumped lithium molecules
[AD-A152800] 17 p3030 N85-28738
Development of reduced activation alloys for fusion service: Draft
[DE85-007464] 18 p3074 N85-29014
British breakthrough in lightweight lithium batteries
18 p3086 N85-29092
Lithium cell reactions
[AD-A154429] 19 p3305 N85-30484
Instrumentation for particle-beams research using excited merging beams
[AD-A154155] 19 p3356 N85-30807
The production and destruction of metastable negative ions
[DE85-011656] 19 p3364 N85-30858
Improvements in safety testing of lithium cells
20 p3444 N85-31379
Design evaluation of high reliability lithium batteries
20 p3444 N85-31380
Safety of Li-SOCl2 cells 20 p3444 N85-31383
Rechargeable lithium-organic electrolyte battery having overcharge protection and method of providing overcharge protection for a lithium-organic electrolyte battery
[AD-D011738] 22 p3606 N85-33575
Evaluation of low-temperature geothermal potential in Utah and Goshen Valleys and adjacent areas, Utah. Part 2: Water temperature and chemistry
[DE85-009344] 23 p3943 N85-34436
Light ion sources for ICF
[DE85-011544] 23 p3983 N85-34702
Thermodynamics of the corrosion of chromium in molten carbonates
[DE85-011407] 24 p4079 N85-35282
Experimental lithium system
[DE85-013252] 24 p4094 N85-35382
The Conterminous United States Mineral Assessment Program 24 p4106 N85-35458

LITHIUM ALLOYS
Sea water rope batteries
[AD-A144775] 01 p0042 N85-10275
Phase equilibria of stored chemical energy reactants
[AD-A146527] 06 p0765 N85-14886
Synergistic sputtering properties of binary alloys
[DE84-017498] 09 p1297 N85-18148
Problem of pore formation mechanism in welded joints of aluminum alloys in the system aluminum-magnesium-lithium 13 p2032 N85-22732
Pechiney strategy includes development of new materials 15 p2531 N85-25807
Performance of a copper-lithium alloy as an impurity control system surface material for a fusion reactor
[DE85-006494] 15 p2657 N85-26396
Self-sustaining low-Z coatings for fusion applications 2 - copper-lithium
[DE85-002553] 15 p2658 N85-26403
Experimental studies of the electronic structure of 1-2 and 1-3 intermetallic compounds
[DE85-006978] 15 p2662 N85-26432
Investigation of the pitting potential of rapidly solidified aluminum-lithium alloys
[VTH-LR-434] 16 p2752 N85-26986
Aluminum-lithium alloys: The answer of the aluminum industry to the threat of advanced fiber-reinforced materials
[VTH-LR-406] 17 p2932 N85-28102
West Europe report: Science and technology
[JPRS-WST-84-035] 18 p3087 N85-29102
Lithium-alloy/iron sulfide battery design studies
[DE85-007991] 18 p3131 N85-29389
Self-sustaining coatings for fusion applications: Copper lithium alloys
[DE85-009740] 18 p3190 N85-29783
Thermodynamic properties of liquid Li-Ph, Na-Pb and K-Pb alloys: Similarities and Differences
[DE85-004074] 18 p3197 N85-29830
Anisotropic electron-impurity scattering in dilute AlLi: (Small) corrections to the local density approximation
[DE85-002946] 19 p3238 N85-30076
Counter current extraction system for tritium recovery from 17Li-83Pb
[DE85-010519] 19 p3240 N85-30090
Molten salt cooling/17Li-83Pb breeding blanket concept
[DE85-010522] 19 p3363 N85-30854
Current state of development and expected performance of copper-lithium alloys as an impurity control system in fusion applications
[DE85-009673] 19 p3372 N85-30917

LITHIUM BORATES
Water absorption and conductivity in poly(ethylene oxide)-lithium tetrafluoroborate films
[AD-A147969] 10 p1450 N85-19138

LITHIUM CHLORIDES
Investigation of the dissolution of CaCrO4 in molten LiCl-KCl eutectic
[DE84-016394] 04 p0469 N85-12965
High capacity inorganic oxyhalide electrochemical cell
[AD-D011321] 07 p0923 N85-15845
Synthesis and properties of Hexachloromolybdates(5) and related species
[AD-A139599] 07 p0924 N85-15852
A safe, high-power-density lithium battery
[AD-A155223] 21 p3613 N85-32454

LITHIUM COMPOUNDS
NT LITHIUM BORATES
NT LITHIUM CHLORIDES
NT LITHIUM FLUORIDES
NT LITHIUM IODATES
NT LITHIUM NIOBATES
NT LITHIUM OXIDES
NT ORGANIC LITHIUM COMPOUNDS
(Vinyloxy)fluorocyclotriphosphazenes
[AD-A147448] 07 p0924 N85-15850
Polymer electrolytes: An investigation of some poly (N-propylaziridine)/lithium salt compositions
[RAE-TR-84036] 08 p1131 N85-17130
Polymer electrolytes: An investigation of some poly (N-propylaziridine)/lithium salt compositions
[AD-A149444] 10 p1452 N85-19146
Neutron scattering studies of graphite intercalation compounds
[DE85-003079] 12 p1942 N85-22196
Ionic conduction and water diffusion in Li (BETA)-alumina
[DE85-007546] 16 p2755 N85-27005
Super hydrides
[AD-A153499] 18 p3070 N85-28986
RAY-O-VAC BR2325 lithium carbon monofluoride cell performance 20 p3444 N85-31382
An update of the JPL program to develop Li-SOCl2 cells 20 p3445 N85-31384

LITHIUM FLUORIDES
Lasing characteristics of YAG: Nd(3+)-laser with LiF passive shutter with F2 color centers
11 p1717 N85-20802
Selective radiative cooling with MgO and/or LiF layers
[DE85-011595] 19 p3282 N85-30228
Lasing on LiF:F(-)2 - dye centers with transverse pumping 21 p3684 N85-32890
In-cavity laser IR spectrum analyzer for investigating non-steady-state processes 21 p3685 N85-32894

LITHIUM IODATES
Design evaluation of high reliability lithium batteries
20 p3444 N85-31380

LITHIUM NIOBATES
Multichannel electrooptical modulators for digital information storage and processing systems
07 p0950 N85-16021

LITHIUM OXIDES
Development of the Cascade inertial-confinement-fusion reactor
[DE85-010933] 19 p3357 N85-30812

LITHIUM SULFUR BATTERIES
Research to explore the feasibility of sulfolanes as electrolytic solvents for rechargeable lithium batteries
[DE85-004345] 12 p1837 N85-21525
Sixth DOE Electrochemical Contractor's Review. Extended abstracts
[DE84-013679] 16 p2779 N85-27151
Lithium-alloy/iron sulfide battery design studies
[DE85-007991] 18 p3131 N85-29389
Lithium cell reactions
[AD-A154429] 19 p3305 N85-30484
Advances in rechargeable lithium molybdenum disulfide batteries 20 p3444 N85-31376
Geosynchronous performance of a lithium-titanium disulfide battery 20 p3444 N85-31377
Development of a lithium secondary battery separator
20 p3444 N85-31378
Transfer of battery technology developed by the US Department of Energy
[DE85-009868] 22 p3808 N85-33588

LITHOGRAPHY
NT PHOTOLITHOGRAPHY
Workshop on the Use of Future Multispectral Imaging Capabilities for Lithologic Mapping: Workshop summary
02 p0214 N85-11413
Ion beam lithography
[BMFT-FB-T-84-182] 04 p0504 N85-13219
Development of short gate FET's
[AD-A147033] 07 p0947 N85-15999
Lithography radiation effects study
[AD-A149552] 10 p1468 N85-19260
China report: Science and technology
[JPRS-CST-85-006] 13 p2052 N85-22843
X-ray lithography and VLSI circuits
13 p2052 N85-22846
Use of optical techniques in studies of wear rates of anodized aluminum and polymer coatings on aluminum
14 p2250 N85-23997
DARPA/TTO program IR binary optics
[AD-A152196] 16 p2865 N85-27672
Communications and logic systems at millimeter wave frequencies, summary 17 p3042 N85-28825

LITHOLOGY
Assessment of computer techniques for processing digital LANDSAT MSS data for lithological discrimination of Serra do Ramalho, State of Bahia
[E85-10033] 03 p0378 N85-12412
Evaluation of criteria for selecting the spectral attributes of digital LANDSAT MSS imagery for discriminating lithological units in the lower Curaca River Valley, Bahia --- Brazil
[E85-10036] 03 p0379 N85-12415
Sedimentary and tectonic evolution of the western Taiwan foredeep 03 p0389 N85-12491
Newly recognized sedimentary environments in the Shelikof Formation, Alaska 04 p0516 N85-13292
A multiple approach in remote sensing for structural and lithological mapping by use Modular Optoelectronic Multispectral Scanner (MOMS)/LANDSAT/Heat Capacity Mapping Mission (HCMM) data
05 p0660 N85-14244
Some methodological aspects of study of layer associations in continents and oceans
06 p0820 N85-15205
Effect of lithology and climate on the morphology of drainage basins in northwestern Colorado
[PB84-226238] 06 p0828 N85-15258
Quantitative use of multiincidence-angle SAR for geologic mapping 08 p1145 N85-17220
Evaluation of the L-band scattering characteristics of volcanic terrain in aid of lithologic identification, assessment of SIR-B calibration, and development of planetary geomorphic analogs 08 p1146 N85-17232
Investigation of SIR-B images for lithologic mapping
08 p1148 N85-17241

Late precambrian to ordovician metamorphism and orogenesis in the Blue Ridge and western Piedmont, Virginia Appalachians 09 p1352 N85-18503

Organogenic structures (submerged reefs) in Silhetian limestone of west Bengal basin 10 p1500 N85-19464

Lithologic and environmental atlas of Berea Sandstone (Mississippian) in the Appalachian Basin
[PB85-129030] 11 p1662 N85-20600

LANDSAT 4 investigations of Thematic Mapper and Multispectral Scanner applications — Drum Mountains, Utah and Tonopath, Nevada
[E85-10095] 12 p1874 N85-21757

Review of problems in lithology 13 p2113 N85-23160

Geologic utility of LANSDAT-4 TM data — Death Valley, California and the Silver Bell area of southern Arizona 13 p2118 N85-23192

Lithologic and structural control on slope morphology in the Valles Marineris 13 p2201 N85-23651

Report on regional groundwater flow modeling for the Palo Duro Basin, Texas
[DE85-007490] 16 p2815 N85-27370

Structural analysis of terrane accretions in the eastern Brooks Range and adjacent areas in central Alaska and Canada
[DE85-008279] 17 p2993 N85-28501

Clay identification and amount measured by laboratory techniques compared to well log responses: Application to tight gas sands and shales
[DE85-010411] 19 p3362 N85-30843

Reduced to pole long-wavelength magnetic anomalies of Africa and Europe 20 p3475 N85-31595

Lithology and stratigraphy of drill holes completed during 1984 in LANL use areas of Yucca Flat, Nevada Test Site, volume 6
[DE85-010695] 22 p3815 N85-33631

Geology and petroleum resources of basins in western China
[DE85-013038] 23 p3948 N85-34469

Some recent deposit modeling efforts 24 p4106 N85-35453

Hydrogeology of the lower Glen Rose Aquifer, south-central Texas 24 p4108 N85-35466

LITHOSPHERE
NT EARTH CORE
NT EARTH CRUST
NT EARTH MANTLE
NT EARTH SURFACE

Lithospheric structure in the Pacific geoid
[NASA-CR-174155] 04 p0526 N85-13365

Oceanic plateaus, anomalous subduction, and the accretion of buoyant features at convergent margins 05 p0688 N85-14422

Stresses and strains in lithosphere caused by Earth's thermoconvective oscillations 06 p0822 N85-15217

Basic structural features and probable mechanism of formation of the Kuril Island system 10 p1501 N85-19472

Thermal conditions and thinning of lithosphere in late cenozoic in southwestern US 10 p1501 N85-19473

Influence of scattering on Q in the lithosphere
[AD-A149318] 10 p1515 N85-19563

Use of paleomagnetic data in tectonic analysis of oceanic structures 13 p2106 N85-23135

Interrelationship of earthquake magnitude and lithospheric-asthenospheric thermodynamic parameters in seismically active zones 13 p2116 N85-23183

Io: Generation of silicate magma by shear melting at the base of a basaltic lithosphere 13 p2172 N85-23476

Formation of bright terrain bands on Ganymede by unstable lithosphere extension 13 p2173 N85-23485

Venus chasmata: A lithosphere stretching model 13 p2178 N85-23516

Elysium region, Mars: Tests of lithospheric loading models for the formation of tectonic features 13 p2200 N85-23650

On geoid heights and flexure of the lithosphere at seamounts
[AD-A151220] 15 p2604 N85-26050

Altimetry data and the elastic stress tensor of subduction zones
[NASA-CR-175796] 16 p2825 N85-27425

Heat flow through ocean floor and its relationship to lithosphere structure and thickness 19 p3294 N85-30422

Geometry, velocity structure and penetration depths of descending slabs in the western Pacific 19 p3319 N85-30574

Euro-African MAGSAT anomaly-tectonic observations 20 p3475 N85-31596

Intraplate crustal deformation due to continental collisions 20 p3490 N85-31693

Satellite-determined stresses in the crust of Europe with particular consideration to the Liege earthquake of November 8, 1983 20 p3490 N85-31694

Conditions during formation of the Earth 21 p3717 N85-33066

Anorthositic oceanic crust in the Archean Earth 21 p3719 N85-33077

A solid-state framework for terrestrial upper mantles 22 p3856 N85-33678

Contrasts in evolution of Venus and Earth 22 p3857 N85-33680

The non-hydrostatic figures of the terrestrial planets 22 p3858 N85-33687

Workshop Proceedings: Interpretation of Seismic Wave Propagation in Laterally Heterogeneous Structures
[BMR-258] 24 p4118 N85-35530

LITTORAL CURRENTS
U COASTAL CURRENTS

LIVER

Biligenic function of white rat liver 01 p0093 N85-10624

Rat blood serum and liver carbohydrates and lipids in recovery period after 15-day hypokinesia 19 p3326 N85-30606

The 1984 environmental monitoring program report for Idaho National Engineering Laboratory site
[DE85-011209] 22 p3812 N85-33611

Effects of immobilization and high-altitude adaptation on energy metabolism in rats 22 p3820 N85-33663

Lipogenesis in rat liver after flight aboard Cosmos-1129 biosatellite 23 p3954 N85-34508

LMCR (REACTORS)
U LIQUID METAL COOLED REACTORS

LMFBR
U LIQUID METAL FAST BREEDER REACTORS

LNG
U LIQUEFIED NATURAL GAS

LOAD DISTRIBUTION (FORCES)

Distributions of fatigue life and fatigue strength in notched specimens of a carbon 8-harness-satin laminate
[NAL-TR-809T] 01 p0061 N85-10407

Design proposals for torsional buckling of stiffeners
[AD-A144783] 01 p0062 N85-10409

Model for non-linear crack growth prediction, taking load sequence (LOSEQ) effects into consideration
[BLL-RAE-TRANS-2114-(5207)] 02 p0206 N85-11371

Fatigue in composite materials 04 p0467 N85-12968

Performance on advanced lead-acid batteries for load-leveling applications
[DE84-015817] 06 p0805 N85-15125

Evaluation of operational loads to verify structural design 07 p0896 N85-15677

Controlled movement of elastic manipulator with distributed parameters 13 p2048 N85-22818

The effect of center delamination on the instability of composite cylindrical panels
[AD-A153494] 18 p3069 N85-28979

LOAD FACTORS
U LOADS (FORCES)

LOAD TESTING MACHINES

Locomotion research for the analysis of the human gait and for the determination of the maximum loads of the pelvis-leg skeleton. Volume 1: Two-dimensional analysis
[BMFT-FB-T-83-187-VOL-1] 02 p0236 N85-11535

Influence of tire on resistance and steering forces of tires
[AD-P004306] 09 p1410 N85-18883

LOAD TESTS

Composite materials characterization and development at AFWAL 04 p0464 N85-12944

Synthesis of load-time histories resulting from statistical analysis 05 p0650 N85-14171

Finite element calculation for a Y-joint and comparison of results with strain measurements
[BLL-RISLEY-TR-4526-(9091.9F)] 08 p1171 N85-17381

A study of spectrum fatigue crack propagation in two aluminum alloys. 1: Spectrum simplification
[NASA-TM-86929] 09 p1293 N85-18124

A study of spectrum fatigue crack propagation in two aluminum alloys. 2: Influence of microstructures
[NASA-TM-86930] 09 p1294 N85-18125

Load carrying capacity of double circular arc gears 14 p2221 N85-23776

Durability calculation of wing panel element 14 p2285 N85-24159

Calibration loading of a strain-gauged diverless helicopter weapon recovery system
[AD-A151486] 15 p2471 N85-25253

An improved torsional method for determining the fracture toughness of stiff materials and of adhesive joints
[AD-A152091] 16 p2800 N85-27267

Composite loads spectra for select space propulsion structural components 17 p2912 N85-27[illegible]

Influence of manganese and heat treatment on structure and properties of Fe-0.1 percent-C-14 percent Cr-based steels
[BLL-BISI-TRANS-22299-(9022.06)] 17 p2928 N85-28[illegible]

LOADING

Magnetic and structural properties of shock-synthesized zinc ferrite
[DE85-000469] 11 p1736 N85-20913

LOADING FORCES
U LOADS (FORCES)

LOADING MOMENTS

Variable loading of elastic-plastic shells of revolution 06 p0779 N85-14881

Stability of hollow shafts under torsion 06 p0780 N85-14882

A literature survey of ground load statistics for landing gear fatigue design purposes
[FFA-TN-1984-39] 09 p1280 N85-18054

Two recent cases of marker load applications on cargo/fighter aircraft fatigue tests 14 p2318 N85-24325

Generation of marker lines on fatigue fracture surfaces 14 p2319 N85-24328

Consolidation theory with consideration of frame plasticity
[REPT-9/1984] 16 p2796 N85-27240

Analysis of elastoplastic grids under conditions of variable loads
[REPT-16/1984] 16 p2797 N85-27242

Calculation of friction at spherical bearing journals in turbomachines 17 p2940 N85-28159

Load-induced rotordynamic instabilities in turbomachinery 19 p3280 N85-30340

Intermittent motion 23 p3925 N85-34323

LOADING OPERATIONS

Mechanical features of the shuttle rotating service structure 08 p1102 N85-16967

STS payload ground handling mechanism at John F. Kennedy Space Center 08 p1103 N85-16971

New applications for robot loaders, unloaders 08 p1139 N85-17175

Hoist
[AD-D011458] 10 p1493 N85-19425

Advanced life analysis methods. Volume 2: Crack growth analysis methods for attachment lugs
[AD-A150420] 13 p2103 N85-23109

Cargo handling system
[AD-D011569] 14 p2219 N85-23762

Calibration loading of a strain-gauged diverless helicopter weapon recovery system
[AD-A151486] 15 p2471 N85-25253

Shuttle car loading system
[NASA-CASE-NPO-15949-1] 23 p3987 N85-34722

LOADING RATE

Constitutive features of solids at shock-wave loading rates
[DE84-015715] 03 p0362 N85-12325

On the use of marker loads and replicas for measuring growth rates for small cracks 14 p2319 N85-24331

Modifications of flight-by-flight load sequences to provide for good fracture surface readability
[NLR-MP-84012-U] 20 p3472 N85-31577

LOADING WAVES
U ELASTIC WAVES
U LOADS (FORCES)

LOADS (FORCES)
NT AERODYNAMIC LOADS
NT AXIAL COMPRESSION LOADS
NT AXIAL LOADS
NT BLAST LOADS
NT COMPRESSION LOADS
NT CRITICAL LOADING
NT CYCLIC LOADS
NT DYNAMIC LOADS
NT EDGE LOADING
NT GUST LOADS
NT IMPACT LOADS
NT LANDING LOADS
NT RANDOM LOADS
NT ROLLING CONTACT LOADS
NT SHOCK LOADS
NT STATIC LOADS
NT THRUST LOADS
NT TRANSIENT LOADS
NT VIBRATORY LOADS
NT WING LOADING

The NBS tri-directional test facility
[PB84-217462] 01 p0051 N85-10334

Three programs for evaluating bending moments, deflections and shear forces in simply-supported uniform bridge decks under South African NA loading: NAB, NAD and NAS. NITRR manual P13
[ISBN-0-7988-2283-X] 01 p0102 N85-10681

Structural analysis 02 p0143 N85-10960

Atmospheric and pressurized low speed wind tunnel performance and cost comparisons
[ARL/AERO-R-160] 02 p0149 N85-11008

A study of environmental characterization of conventional and advanced aluminum alloys for selection and design. Phase 1: Literature review
[NASA-CR-172367-PHASE-1] 02 p0181 N85-11216

Evaluation of laser profile and deflection measuring system
[FAA-PM-84-24] 02 p0201 N85-11341

Materials properties, loads, and stress analysis, Spartan REM: Appendix A
[NASA-CR-171092] 02 p0208 N85-11375

Extended aeroelastic analysis for helicopter rotors with prescribed hub motion and blade appended pendulum vibration absorbers
[NASA-CR-172455] 03 p0315 N85-12038

Evaluation of laterally loaded laminated glass units by theory and experiment
[PB84-216423] 03 p0339 N85-12179

Comparison of predicted and measured friction for a tilt-pad thrust bearing with crown and roughness under hydrodynamic and mixed lubrication
[AD-A145752] 03 p0371 N85-12371

An experimental evaluation of the J integral in 50% sidegrooved compact geometry specimens
[AERE-R-11202] 03 p0374 N85-12386

Application of the ONERA model of dynamic stall
[NASA-TP-2399] 04 p0451 N85-12662

Initial sailplane project: The RP-1 04 p0468 N85-12976

Response of ferritic steels to nonsteady loading at elevated temperatures
[DE84-014280] 04 p0513 N85-13272

Solving equations of movement with variable inertia moment
[BLL-M-35975-(5828.4)] 05 p0641 N85-14111

Analysis of dynamic characteristics of fluid force induced by labyrinth seal 05 p0643 N85-14129

Prediction of force coefficients for labyrinth seals 05 p0644 N85-14130

An iwatsubo-based solution for labyrinth seals - comparison with experimental results 05 p0644 N85-14131

Preliminary investigation of labyrinth packing pressure drops at onset of swirl-induced rotor instability 05 p0644 N85-14132

Identification of dynamic coefficients of annular turbulent seals 05 p0644 N85-14133

Design of electromagnetic bearing for vibration control of flexible transmission shaft 05 p0645 N85-14136

Effects of fluid inertia and turbulence on force coefficients for squeeze film dampers 05 p0645 N85-14137

Conditions for assembling dies for drawing under hydrodynamic friction conditions
[BLL-M-35954-(5828.4)] 05 p0647 N85-14153

An analysis of kinetic response variability 05 p0707 N85-14533

Effects of external loads on human head movement control systems 05 p0707 N85-14534

Experimental investigation and analysis of oscillations of thin-walled spherical shell during pulse loading 05 p0725 N85-14662

Testing the antifriction properties of alloys for heavily loaded bearings 06 p0780 N85-14990

Encapsulation design analysis 06 p0829 N85-15268

Operational Loads Data
[AGARD-CP-375] 07 p0894 N85-15664

Experiences obtained from service fatigue monitoring exercises 07 p0895 N85-15672

CF-5 vertical stabilizer flight load survey 07 p0895 N85-15673

US Army helicopter operational flight loads 07 p0895 N85-15675

Helicopter data acquisition in WHL 07 p0896 N85-15676

Influence of pressure on compaction during compression of powders of iron and 40Kh and 10R6MS steels
[BLL-M-35995-(5828.4)] 07 p0926 N85-15866

Nondestructive measurement of bulk residual stresses
[AD-A147063] 07 p0978 N85-16211

Development of large wind energy power generation system
[NASA-TM-77779] 07 p0992 N85-16301

A theoretical view on the stress analysis of fully inflated parachute canopies
[AD-A148387] 08 p1078 N85-16835

Natural environment analysis
[NASA-CR-174330] 08 p1180 N85-17433

Determination of blade service life under irregular loading conditions 09 p1309 N85-18222

Mechanical and transient hygrothermal loading of multilayer orthotropic cylinders 09 p1330 N85-18359

The Shock and Vibration Bulletin 54. Part 2: Ship shock, shock and blast and ground shock
[AD-A148132] 09 p1334 N85-18386

Direct energy minimization approach to whipping analysis of pressure hulls 09 p1335 N85-18393

Water impact laboratory and flight test results for the space shuttle solid rocket booster aft skirt 09 p1335 N85-18394

Determination of shear coefficient of a general beam cross section by finite element method 09 p1338 N85-18413

A simple prediction model for soil compaction under various wheel loads and geometries as an aid to vehicle design
[AD-P004298] 09 p1409 N85-18875

Forces on undriven, angled wheels
[AD-P004303] 09 p1409 N85-18880

Influence of tire on resistance and steering forces of tires
[AD-P004306] 09 p1410 N85-18883

Detailed pressure distribution measurements obtained on several configurations of an aspect-ratio-7 variable twist wing
[NASA-TM-86308] 10 p1419 N85-18950

Integrated Technology Rotor/Flight Research Rotor (ITR/FRR) concept definition
[NASA-CR-166443] 10 p1423 N85-18978

Estimation of endurance characteristics of heat resistant materials. Report 2: Determination of endurance limit of heat resistant alloys over a broad temperature range 10 p1447 N85-19120

Methodology for stress analysis of heavy metal plate 10 p1460 N85-19203

Design procedure for the new 70-meter antenna subreflector positioner 10 p1463 N85-19232

Elevation bearing maximum load, 70-meter antenna 10 p1464 N85-19239

Hydrostatic bearing pad maximum load and overturning conditions for the 70-meter antenna 10 p1465 N85-19241

Connector/nitinol delta contact force device
[AD-D011467] 10 p1481 N85-19349

Crack problems for bonded nonhomogeneous materials under antiplane shear loading
[NASA-CR-172532] 10 p1495 N85-19438

Interaction between a crack and a soft inclusion
[NASA-CR-172533] 10 p1495 N85-19439

Evaluation of features of reinforcing fibers by testing bundles 11 p1599 N85-20059

Adjustable indicating device for load position
[NASA-CASE-MFS-28008-1] 11 p1635 N85-20300

Tether fundamentals 11 p1643 N85-20345

Techniques to analyze vehicle coastdown data
[DE85-005159] 12 p1772 N85-21127

Characterization of lubricated bearing surfaces operated under high loads
[NASA-TM-86964] 12 p1811 N85-21357

Cost comparison of small gas turbines versus electric motors in a variable load industrial application
[PB85-149763] 12 p1837 N85-21530

Ring-on-ring tests and load capacity of cladding glass
[PB85-106391] 12 p1868 N85-21717

Reliability of structural brittle materials 12 p1946 N85-22222

Study for prediction of rotor/wake/fuselage interference, part 1
[NASA-CR-177340-VOL-1] 13 p1965 N85-22346

Study for prediction of rotor/wake/fuselage interference. Part 2: Program users guide
[NASA-CR-177340-VOL-2] 13 p1966 N85-22347

Prediction of the resistance of structural materials to cavitation erosion
[BLL-DRIC-TRANS-7435-(3623.66)] 13 p2020 N85-22659

Development of a sintered shim
[DE85-006183] 13 p2025 N85-22685

Comparison of dynamic-tension and constant-load strength characteristics of heat-resistant materials 13 p2030 N85-22722

Characteristics of surface crack development in ATtsS aluminum alloy during slow-cycle loading 13 p2034 N85-22745

Steady-state reaction of three-layered cylindrical shell to effect of moving load 13 p2047 N85-22811

Axisymmetrical oscillations of shell systems subjected to impulse loads 13 p2047 N85-22814

Nonlinear behavior and stability of thin spherical shells subjected to non-axisymmetrical loading 13 p2048 N85-22821

Elysium region, Mars: Tests of lithospheric loading models for the formation of tectonic features 13 p2200 N85-23650

Advanced life analysis methods. Volume 4: Tabulated test data for attachment lugs
[AD-A151016] 14 p2219 N85-23760

Load carrying capacity of double circular arc gears 14 p2221 N85-23776

Case depth on flanks of gears for helicopter gearboxes 14 p2222 N85-23780

The observation and interpretation of gear tooth failures 14 p2224 N85-23792

A preliminary investigation of the dynamic force-calibration of a magnetic suspension and balance system
[NASA-CR-172580] 14 p2228 N85-23808

Wave motion of three-component medium under load moving on plane boundary 14 p2277 N85-24105

Computations for segmented radial bearings 14 p2286 N85-24180

Work of axial bearing under dynamic loading 14 p2286 N85-24182

Recent developments in the dynamics of advanced rotor systems
[NASA-TM-86669] 14 p2317 N85-24320

Effect of flight sequences in complex load histories on crack front marking 14 p2318 N85-24326

Generation of marker lines by means of marker loads 14 p2318 N85-24327

Generation of marker lines on fatigue fracture surfaces 14 p2319 N85-24328

Periodic loading sequences for the systematic marking of fatigue crack fracture surfaces 14 p2319 N85-24329

Modifications of flight by flight load sequences to provide for good fracture surface readability 14 p2319 N85-24330

On the use of marker loads and replicas for measuring growth rates for small cracks 14 p2319 N85-24331

On the use of marker loads for fatigue crack growth measurements 14 p2319 N85-24332

Crack propagation under constant and variable stress amplitudes: A comparison of calculations based on the Striation spacing and tests 14 p2320 N85-24336

Finite element model for creep in composite masonry
[PB85-150324] 14 p2322 N85-24347

Comets and nongravitational forces 14 p2437 N85-25038

Unsteady gas dynamics problems related to flight vehicles
[AD-A151187] 15 p2464 N85-25218

Pseudo bipolar nickel-cadmium batteries used as filter elements to pulsed current loads
[AD-A151192] 15 p2547 N85-25717

Structural development and gravity 15 p2608 N85-26071

Finite-difference computations of rotor loads
[NASA-TM-86682] 16 p2700 N85-26669

Automatic flight control modes for the AFTI/F-111 mission adaptive wing aircraft 16 p2714 N85-26756

Rotordynamics 16 p2737 N85-26888

Effects of bearing deadbands on bearing loads and rotor stability 16 p2737 N85-26889

Breakway friction and dynamic friction/wear measurements of various ceramic materials from 25 C (75 F) to 650 C (1200 F)
[NASA-CR-174803] 16 p2754 N85-26994

Experimentally determined distribution of stress around a horizontally loaded model pile in dense sand
[CE-43] 16 p2796 N85-27239

Adaptation of continuous beams and the method of optimizing the flexibility of their elastic supports. Theorem on maximal adaptation loading, supplement
[REPT-10/1984-SUPPL] 16 p2797 N85-27241

Fatigue damage and small crack growth during biaxial loading 16 p2797 N85-27247

Dynamic response of shells and plates subjected to variable magnitude traveling loads 16 p2798 N85-27250

Monitoring of turbo-machines by shaft vibration measurement
[BLL-CE-TRANS-7900-(9022.09)] 16 p2799 N85-27255

Some advances in experimentation supporting development of viscoplastic constitutive models
[NASA-CR-174855] 16 p2799 N85-27260

Structural Integrity and Durability of Reusable Space Propulsion Systems
[NASA-CP-2381] 17 p2910 N85-27941

Composite loads spectra for select space propulsion structural components: Probabilistic load model development 17 p2912 N85-27954

Dynamic creep buckling: Analysis of shell structures subjected to time-dependent mechanical and thermal loading 17 p2913 N85-27959

Overload effects on sustained load crack growth at elevated temperature
[AD-A153223] 17 p2931 N85-28091

The Mises yield condition for thin rotationally symmetric shells
[BLL-BISI-TRANS-22047-(9022.06)] 17 p2978 N85-28409

Finite element thermal-structural analysis of cable-stiffened space structures
[AD-A153822] 18 p3066 N85-28963
B-52B/DTV (Drop Test Vehicle) flight test results: Drop test missions
[NASA-CR-171530] 19 p3215 N85-29934
General Aviation Crashworthiness Project. Phase 2: Impact severity and potential injury prevention in general aviation accidents
[PB85-917002] 19 p3215 N85-29938
Aircraft rotor blade with passive tuned tab
[NASA-CASE-ARC-11444-1] 19 p3217 N85-29947
A study of the stress wave factor technique for the characterization of composite materials
[NASA-CR-174870] 19 p3231 N85-30035
Load-carrying capabilities of refractory alloys for space reactor power applications
[DE85-010566] 19 p3240 N85-30087
Fatigue resistance of VT3-1 titanium alloy related to surface cold working 19 p3245 N85-30120
Temperature and surface damage under lubricated sliding-rolling contacts 19 p3280 N85-30338
Acoustic emission study of fatigue crack extension position in a stress cycle 19 p3283 N85-30355
Residual stress distributions in (plastically) surface deformed two-phase materials 19 p3283 N85-30356
Estimation of dynamic rotor loads for the rotor systems research aircraft: Methodology development and validation
[NASA-CR-177362] 20 p3393 N85-31045
Some advances in experimentation supporting development of viscoplastic constitutive models
20 p3468 N85-31545
A comparison of smooth specimen and analytical simulation techniques for notched members at elevated temperatures 20 p3468 N85-31546
Estimation of power-law creep parameters from bend test data
[PB85-183406] 20 p3472 N85-31579
The effect of stress and hot corrosion on nickel-base superalloys
[AD-A154722] 21 p3566 N85-32181
A comparison of experimental and theoretical results for rotordynamic coefficients of four annular gas seals
[NASA-CR-176086] 21 p3596 N85-32332
Measurement and analysis of critical crack tip processes during fatigue crack growth
[NASA-CR-172597] 21 p3598 N85-32342
Analysis of long bone and vertebral failure patterns
[AD-A154796] 21 p3663 N85-32758
Pressure-shear loading of PBX-9404
[DE85-009982] 23 p3921 N85-34298
Inertial stresses and deformations in mechanisms
23 p3924 N85-34320
Tensile testing apparatus
[NASA-CASE-LAR-13243-1] 23 p3933 N85-34375
The design and analysis of single flank transmission error testor for loaded gears
[NASA-CR-176163] 23 p3937 N85-34404
Further studies on liquid sloshing
[PB85-198695] 24 p4095 N85-35388
Stress-intensity factors for circumferential surface cracks in pipes and rods under tension and bending loads
[NASA-TM-87594] 24 p4101 N85-35424
Prediction of plasticity characteristics for three-dimensional fracture specimens comparison with experiment
[AD-A156425] 24 p4102 N85-35430
Evaluation of the crack plane equilibrium model for predicting plastic fractures
[DE85-005558] 24 p4102 N85-35431
Response of a BWR Mark 2 containment vessel head to loads beyond the design basis
[DE85-010524] 24 p4103 N85-35432
Simulation of lattice damage due to dynamic loading
[DE85-008468] 24 p4162 N85-35806

LOCAL GROUP (ASTRONOMY)
NT ANDROMEDA GALAXIES
NT MILKY WAY GALAXY

LOCALIZATION
U POSITION (LOCATION)

LOCATION
U POSITION (LOCATION)

LOCI
Surfaces with canonical hyperplane sections
[CWI-TRACT-1] 14 p2410 N85-24858
Search for positron annihilation line and continuum radiation from the Galactic Center
[OG-2.5-5] 22 p3860 N85-33962

LOCKHEED AIRCRAFT
NT C-5 AIRCRAFT
NT C-141 AIRCRAFT
NT F-104 AIRCRAFT
NT L-1011 AIRCRAFT
NT P-3 AIRCRAFT
NT T-33 AIRCRAFT
NT U-2 AIRCRAFT

LOCKHEED C-5 AIRCRAFT
U C-5 AIRCRAFT

LOCKHEED U-2 AIRCRAFT
U U-2 AIRCRAFT

LOCKING
NT LASER MODE LOCKING
Storage life of thermal detents
[DE84-016934] 04 p0476 N85-13030
Hydraulic locking boltwork system
[AD-D011299] 06 p0815 N85-15174
A simulator for determining the performance of transaction manager and lock manager combinations in a database
[AD-A147827] 07 p1055 N85-16896
Elbow and knee joint for hard space suits and the like
[NASA-CASE-ARC-11610-1] 11 p1697 N85-20666
Locking of Automative Products hydraulic selector valves
[BAE-EXPER/NOTE-459] 15 p2567 N85-25839
Self-locking mechanical center joint
[NASA-CASE-LAR-12864-1] 19 p3279 N85-30336
Dual optical mechanical position tracker
[AD-D011739] 22 p3844 N85-33811
Variable length strut with longitudinal compliance and locking capability
[NASA-CASE-MFS-25907-1] 23 p3937 N85-34401

LOCKS
An improved servo-controlled inertial clock for laboratory tests of general relativity 19 p3378 N85-30955

LOCKS (FASTENERS)
Connector/nitinol delta contact force device
[AD-D011467] 10 p1481 N85-19349
Mechanical locking between multi-layer printed wiring board conductors and through-hole plating
[AD-D011477] 10 p1481 N85-19352
Code lock with microcircuit 13 p2071 N85-22935

LOCOMOTION
NT WALKING
Influence of simulated weightlessness on the motility of the acellular slime mold Physarum polycephalum
05 p0689 N85-14430
Global optical metrics for self-motion perception
[AD-P004333] 09 p1271 N85-17987
Study of the motion of agricultural vehicles on steep grass-covered slopes
[AD-P004290] 09 p1408 N85-18867
Non-rigid body motion 23 p3964 N85-34576

LOCOMOTIVES
DELTA: An expert system for diesel electric locomotive repair
[AD-P003941] 02 p0248 N85-11621
Antenna matching device tuning for type ZhRU radiostations 06 p0785 N85-15017
Natural gas the new locomotive fuel
[DE84-901824] 09 p1302 N85-18179
Industry review: Locomotive dynamic characterization test-analysis
[NASA-CR-171467] 19 p3362 N85-30981

LOFTING
Semianalytic modeling of aerodynamic shapes
[NASA-TP-2413] 12 p1771 N85-21120

LOG PERIODIC ANTENNAS
Defocusing losses in a log periodic-fed reflector
[AD-A151616] 15 p2547 N85-25722
Frequency independent parabolic phased antenna array of log periodic antennas 22 p3774 N85-33387

LOGARITHMIC RECEIVERS
A multi-channel radar receiver
[AD-A156058] 24 p4087 N85-35333

LOGARITHMS
Applications of the simple-layer logarithmic potential
05 p0718 N85-14606
Generating positively correlated random variables from a sequence of independent random variables with symmetric logarithmically concave densities
[AD-A148438] 08 p1216 N85-17658
Applicability of log-normal model to probabilitistic description of quasi-pulse interference
13 p2084 N85-23014
Parallel update of minimum spanning trees in logarithmic time
[AD-A150497] 13 p2151 N85-23357
Adiabatic thermal models for planetary bodies
22 p3857 N85-33881

LOGIC
Mental models of invisible logical networks
05 p0708 N85-14544

LOGIC CIRCUITS
NT THRESHOLD GATES
Basic EMC (Electromagnetic Compatibility) technology advancement for C3 systems, macromodeling of digital circuits, volume 2B
[AD-A146333] 03 p0359 N85-12306
Restructurable VLSI program
[AD-A148145] 08 p1157 N85-17
Deployment sequence mode selection system fo aircraft ejection seat
[AD-D011484] 10 p1422 N85-1
Development of mass-producible line-focus tracking concentrating solar collectors. Category 2: Trackers
[DE85-002673] 10 p1512 N85-19
Design of explosive logic elements
[DE84-009611] 11 p1614 N85-201
15KW power supply development
[DE86-001057] 11 p1629 N85-2
Transistor-transistor logic microcircuit tester
12 p1842 N85-21
Basic EMC (electromagnetic interference) technology advancement for c3 systems. Volume 3A: Probabilistic analysis of combinational circuits with random delays
[AD-A150349] 13 p2055 N85-22
Development of a planer heterojunction bipolar transistor for very high speed logic
[AD-A150374] 13 p2064 N85-22
Dataflow computation
[CWI-TRACT-6] 14 p2406 N85-24
All-optical logic gates with external switching by laser and incoherent radiation 18 p3187 N85-29
Electro-optic techniques for VLSI interconnect
18 p3188 N85-28774
Electron lithography STAR design guidelines. Part 1: The STAR user design manual
[NASA-CR-170765] 20 p3513 N85-31840
Electron lithography STAR design guidelines. Part 2: The design of a STAR for space applications
[NASA-CR-170766] 20 p3513 N85-31841
Electron lithography STAR design guidelines. Part 3: The mosaic transistor array applied to custom microprocessors. Part 4: Stores logic arrays, SLAs implemented with clocked CMOS
[NASA-CR-170767] 20 p3514 N85-31842
Design of a sixteen-bit pipelined adder using CMOS bulk P-well technology
[AD-A155043] 21 p3580 N85-322
Digital integrated circuits 21 p3609 N85-32787
Method of characterizing critical timing paths and analyzing timing related failure modes in very large scale integrated circuits
[AD-D011731] 22 p3759 N85-33
Hardware realization of digital filters without multipliers
22 p3766 N85-333
Computer simulation of integrated injection logic
22 p3767 N85-333
Research on distributed artificial intelligence
[AD-A155356] 22 p3833 N85-33733

LOGIC DESIGN
Basic EMC (Electromagnetic Compatibility) technology advancement for C3 systems, macromodeling of digital circuits, volume 2B
[AD-A146333] 03 p0359 N85-12306
Knowledge representation and natural-language semantics
[AD-A146025] 03 p0409 N85-12815
Research on introspective systems
[AD-A146406] 06 p0870 N85-15530
Representation and refinement of visual specifications in PegaSys
[AD-A148733] 09 p1368 N85-1859
Dialog system of preparation and presentation of visual information 10 p1526 N85-196
Logic analyzer survey and reviews
[BAE-881/ELO/1645] 15 p2621 N85-26151
Optimal design and use of retry in fault tolerant real-time computer systems
[NASA-CR-175920] 17 p3015 N85-28
Electron lithography STAR design guidelines. Part 1: The STAR user design manual
[NASA-CR-170765] 20 p3513 N85-31840
Electron lithography STAR design guidelines. Part 2: The design of a STAR for space applications
[NASA-CR-170766] 20 p3513 N85-31841
Electron lithography STAR design guidelines. Part 3: The mosaic transistor array applied to custom microprocessors. Part 4: Stores logic arrays, SLAs implemented with clocked CMOS
[NASA-CR-170767] 20 p3514 N85-31842
Modeling of discrete devices with use of multivalued logic and nomograms 22 p3768 N85-33351
Filtration of higher harmonic components in two-level digital computing synthesizers 22 p3778 N85-33410

LOGIC NETWORKS
U LOGIC CIRCUITS

LOGIC PROGRAMMING
TCAS 2 logic performance during phase one operational evaluation
[DOT/FAA/PM-84/20] 05 p0595 N85-1379
A distributed expert system for Space Shuttle flight control 05 p0602 N85-13

Dialog system of preparation and presentation of visual information 10 p1526 N85-19622

Characterizing the parallelism in rule-based expert systems
[DE85-002432] 12 p1919 N85-22047

Evaluation of expert systems
12 p1947 N85-22229

Execution of cellular logic operations in spatially continuous, bit slice processor 14 p2401 N85-24798

Modeling of discrete devices with use of multivalued logic and nomograms 22 p3766 N85-33351

LOGICAL ELEMENTS

Circuit engineering and technological optimization of very high speed LSI logic elements and transistor structures 03 p0347 N85-12237

The automated reasoning system ITP
[ANL-84-27] 12 p1914 N85-22016

Bipolar nonswitching logic arrays: Universal components of function expanders for computation of elementary functions 14 p2400 N85-24797

Execution of cellular logic operations in spatially continuous, bit slice processor 14 p2401 N85-24798

Development of new circuit symbols for binary logic elements
[MBB-Z-38/85-O] 17 p3014 N85-28640

LOGISTICS

NT SPACE LOGISTICS

Software engineering environments for mission critical applications: STARS alternative programmatic approaches
[AD-A145285] 02 p0241 N85-11571

An overview of the Joint Logistics Commanders Automatic Test Equipment Panel
[AD-P003916] 02 p0244 N85-11596

Constraint-based scheduling in an intelligent logistics support system: An artificial intelligence approach
[AD-A145613] 02 p0293 N85-11900

Future robotics program at San Antonio ALC (Air Logistics Center)
[AD-P004011] 03 p0309 N85-11991

Supply center processes
[AD-P004014] 03 p0309 N85-11993

Logistics support costs for the B-1B aircraft can be reduced
[AD-A145846] 03 p0309 N85-11996

Distribution and storage of aviation turbine fuel for military operations in northern Australia
[AD-A147180] 07 p0935 N85-15921

A description of a logistically ideal aircraft
[AD-A148425] 08 p1084 N85-16866

Adapting logistics models to a microcomputer for interface with computer-aided design systems
[AD-A147686] 08 p1202 N85-17566

A preliminary analysis of C-12 aircraft usage by the Navy Air Logistics System
[AD-A151921] 16 p2694 N85-26634

A Dictionary-Directory System (DDS) for the SPLICE system
[AD-A152223] 16 p2878 N85-27759

Bayesian inference and diagnostics for the 3 parameter logistic model
[AD-A153840] 18 p3175 N85-29681

EOQ (Economic Order Quantity) range model
[AD-A153709] 19 p3379 N85-30965

LOGISTICS MANAGEMENT

NT INVENTORY CONTROLS

NT INVENTORY MANAGEMENT

An overview of the Joint Logistics Commanders Automatic Test Equipment Panel
[AD-P003916] 02 p0244 N85-11596

Benefit value to the Air Force of the GIDEP (Government Industry Data Exchange Program) alert
[AD-A145470] 02 p0292 N85-11697

An update of the functional requirements of the Naval Aviation Logistics Command Management Information System (NALCOMIS)
[AD-A146565] 06 p0671 N85-15532

Managing recoverable aircraft components in the PPB and related processes: Executive summary
[AD-A146806] 07 p1050 N85-16667

Feasibility of measuring technical productivity improvements in Air Force Logistics Command depot-level maintenance using the Data Envelopment Analysis (DEA) and Constrained Facet Analysis (CFA) models
[AD-A147329] 07 p1052 N85-16676

Utilization of Increased Airlift Capability (UIAC) study
[AD-A148669] 08 p1081 N85-16847

On maximizing the expected lifetime of replaceable systems
[AD-A150003] 12 p1862 N85-21680

Managing recoverable aircraft components in the PPB (Planning, Programming and Budgeting) and related processes. Technical volume
[AD-A152014] 15 p2457 N85-25169

Improving the defense energy information system (DEIS)
[AD-A153524] 18 p3200 N85-29849

An analysis of the materiel fielding plan for the SINCGARS (Single Channel Ground and Airborne Radio System) radio
[AD-A155101] 21 p3576 N85-32238

Security controls in the Stockpoint Logistics Integrated Communications Environment (SPLICE)
[AD-A155536] 21 p3576 N85-32244

DoD Value Engineering conference report. Value Engineering (VE): A tool that benefits line management. Part 4, Workshop B: VE on spare parts
[AD-A156070] 24 p4163 N85-35813

LONG DURATION EXPOSURE FACILITY

Feasibility of long duration ballooning in Antarctica
[PB84-240571] 04 p0541 N85-13443

The heavy ions in space experiment
[OG-9.1-10] 23 p4023 N85-34936

LONG DURATION SPACE FLIGHT

USSR report: Space Biology and Aerospace Medicine, volume 18, no. 4, July - August 1984
[JPRS-USB-84-006] 01 p0091 N85-10611

Compensatory and adaptive regional hemodynamic reactions to weightlessness during long-term spaceflights 01 p0091 N85-10616

Nutritional models for space travel from chemically defined diets
[NASA-CR-3850] 03 p0402 N85-12561

NASA welding assessment program
[NASA-CR-175512] 12 p1859 N85-21661

Rat tissue opioid peptide content during long-term hypokinesia 12 p1904 N85-21954

Comments on Salyut-7 150-day flight
13 p1977 N85-22406

Research opportunities in human behavior and performances
[NASA-CR-3886] 13 p2142 N85-23299

Nutrition in space flight: Some thoughts
14 p2394 N85-24743

Fluid-electrolyte responses during prolonged space flight: A review and interpretation of significant findings
[NASA-CR-171878] 15 p2617 N85-26124

The controlled ecological life support system
15 p2688 N85-26603

Research on zero-gravity botany apparatus
16 p2723 N85-26811

Construction and functioning of extended orbital systems 16 p2724 N85-26814

BLSS: A contribution to future life support
18 p3155 N85-29534

Advanced regenerative environmental control and life support systems: Air and water regeneration
18 p3155 N85-29535

Extended mission life support systems
18 p3157 N85-29547

Cosmonauts' postural reactions after long-term missions aboard Salyut-6 orbital station 19 p3323 N85-30585

Blood serum enzyme activity following long term spaceflights 19 p3326 N85-30604

Psychological issues relevant to astronaut selection for long-duration space flight: A review of the literature
[AD-A154051] 19 p3330 N85-30627

Air Force Human Resources Laboratory research and development summary
[AD-A154310] 19 p3331 N85-30632

Living aloft: Human requirements for extended spaceflight
[NASA-SP-483] 21 p3666 N85-32772

Cosmonauts' cardiovascular system function during long-term orbital flights aboard Salyut-6 station
22 p3733 N85-33141

Fluid-electrolyte metabolism and renal function in cosmonauts following 185-day spaceflight
23 p3952 N85-34495

LONG RANGE NAVIGATION

U LORAN

LONG RANGE WEATHER FORECASTING

Illinois Climate: Trends, Impacts and Issues
[PB84-211986] 01 p0086 N85-10577

Summary of 1984 Atlantic seasonal tropical cyclone activity and verification of author's forecast
03 p0395 N85-12520

Spectral energetics diagnoses and FGGE spectral observing periods and energetics analyses of forecast experiments with GLAS GCM 05 p0683 N85-14391

Forecasting water temperature decline and freeze-up in rivers
[AD-A147066] 07 p0987 N85-16274

A weather service for agriculture
16 p2830 N85-27450

An appraisal of the duration of the recent drought in northeast Brazil and a forecast for 1985
[INPE-3477-PRE/720] 16 p2834 N85-27478

Accuracy and operational use of medium and extended range numerical atmospheric forecasts: A review
[AD-A155027] 21 p3635 N85-32579

Model projections of time-dependent response to increasing carbon dioxide
[DE85-013326] 22 p3816 N85-33641

LONG TERM EFFECTS

Long-term thermal aging of 2 graphite-polyimide composite materials
[NASA-TP-2369] 03 p0325 N85-12094

Modeling long-term changes in forested landscapes and their relation to the Earth's energy balance
05 p0653 N85-14194

Effects of prolonged hypokinesia on nervous system
08 p1194 N85-17524

Durability and behavior of prestressed concrete beams. Posttensioned concrete beam investigation, supplemental laboratory tests of beams exposed from 1961 to 1982
[AD-A148621] 09 p1304 N85-18191

Evaluation and prediction of long-term environmental effects of nonmetallic materials
[NASA-CR-171353] 10 p1450 N85-19137

Synthetic fuels policy
[GPO-34-227] 11 p1613 N85-20143

Long-range electronics program outlined
11 p1700 N85-20667

Long-term strength and fracture criteria for EI698VD alloy under complex stress conditions
13 p2030 N85-22723

Influence of annealing on cyclic and short-term strength of thin sheets of VT1-0 titanium and OTR4 alloy
13 p2031 N85-22727

Effects of interactive transport and scavenging of smoke on the calculated temperature change resulting from large amounts of smoke
[DE85-006450] 14 p2378 N85-24664

Design and fabrication of a unique electromechanical machine for long-term fatigue testing
[DE85-006524] 15 p2580 N85-25912

Quaternary North Atlantic surface paleoceanography in regions of potential deep-water formation
15 p2602 N85-26036

Effects of long-term low-level radiofrequency radiation exposure on rats. Volume 7: Metabolism, growth and development
[AD-A150829] 15 p2615 N85-26112

Assessing the short- and long-term health effects of decompression sickness among US Navy divers
[AD-A151887] 15 p2618 N85-26132

The cumulative effects of long term exposure to low levels of radiofrequency radiation (RFR)
16 p2776 N85-27132

Acid precipitation in North America: 1980, 1981 and 1982 annual data summaries from acid deposition system data base
[PB85-162477] 16 p2822 N85-27410

Long term exposure of animals to antiorthostatis (-90 deg) as a model of critical homeostatic disturbances
19 p3324 N85-30592

Short term determination of the creep properties of high temperature materials
[CRIF-MT-160] 20 p3432 N85-31268

Predicting photothermal field performance
21 p3608 N85-32404

Topics in electrochemical degradation of photovoltaic modules 21 p3608 N85-32410

Voyager 0.2-lbf thruster valve assembly short pulse test report
[NASA-CR-176121] 22 p3741 N85-33165

Climatic consequences of very high CO2 levels in Earth's early atmosphere 22 p3854 N85-33865

Lipogenesis in rat liver after flight aboard Cosmos-1129 biosatellite 23 p3954 N85-34508

Long-period cosmic ray variations and their altitude dependence
[SH-6.1-19] 23 p4046 N85-35091

High temperature corrosion of ceramics
[DE85-013481] 24 p4083 N85-35303

LONG WAVE RADIATION

The Martian climate: Energy balance models with CO2/H2O atmospheres
[NASA-CR-174073] 03 p0446 N85-12849

Year-to-year variability of components of Earth's radiation budget according to satellite measurement data 16 p2725 N85-26821

Influence of phonon interaction on width and form of Mandelstam-Brillouin optical scattering line
21 p3696 N85-32962

Sporadic radio emission connected with a definite manifestation of solar activity in the near Earth space
[SH-10.1-8] 23 p4053 N85-35139

LONG WAVES (METEOROLOGY)

U PLANETARY WAVES

LONGERONS

Section 1. Method of determining mode shapes and natural frequencies of the NASA unmodified test structure. Section 2. Continuous beam closed from solution to the NASA-LSS astromast torsional vibration, appendix E 05 p0603 N85-13844

Modelling and identification of the structural properties of an astromast [CRC-1374] 08 p1329 N85-18352

Efficient structures for geosynchronous spacecraft solar arrays [NASA-CR-174448] 10 p1426 N85-19004

The residual strength of cracked specimens representing a section of the mirage into wing main spar [ARL/STRUC-R-408] 12 p1865 N85-21699

Definition of ground test for verification of large space structure control [NASA-CR-171438] 15 p2492 N85-25377

Tensile and fracture toughness properties of Mirage III spars [AR-003-019] 15 p2578 N85-25899

Fatigue lives of specimens representing critical locations in Mirage 3 spars under Australian and Swiss test spectra [ARL-STRUC-R-415] 24 p4064 N85-35187

LONGITUDE

Computer-generated latitude and longitude templates for rapid determination of geographic positions in Alaska 04 p0516 N85-13286

Simultaneous determination of the xi and eta components of vertical deflection with a prism astrolabe [SER-B-270-MITT-171] 09 p1343 N85-18450

Longitudinal distribution of cosmic rays in the heliosphere [SH-4.1-14] 23 p4006 N85-34837

LONGITUDE MEASUREMENT

Determination of the longitude differences Munich-Lissabon-San Fernando, Munich-Wettzell, and Munich-Karlsruhe-Niederreiferberg [ASTRON-GEODAET-ARB-44] 04 p0524 N85-13353

Determination of astronomical longitude differences for the European longitude reference system for 1980. Relative right ascension corrections for 125 FK4 and FK4 Sup stars 04 p0524 N85-13354

Determination of astronomical longitude differences: Munich, Karlsruhe, Niederreifenberg in 1974 04 p0524 N85-13355

The longitudinal development of muons in cosmic ray air showers at energies 10(15) - 10(17) eV [HE-4.3-12] 24 p4192 N85-36006

Longitudinal development of muons in large air showers studies from the arrival time distributions measured at 900m above sea level [HE-4.7-4] 24 p4199 N85-36055

LONGITUDINAL CONTROL

Flight tests with a new helicopter Force Feel System (FFS) 08 p1075 N85-16818

A feasibility study of free-tip rotor application as a passive cyclic control device 09 p1279 N85-18046

Remote pivot decoupler pylon: Wing/store suppression [NASA-CASE-LAR-13173-1] 11 p1584 N85-19981

Total energy-rate feedback for automatic glide-slope tracking during wind-shear penetration [NASA-TP-2412] 14 p2226 N85-23801

In-flight investigation of the influence of pitch damping and pitch control effectiveness on landing approach flying qualities of statically unstable transport aircraft [DFVLR-FB-84-12] 17 p2900 N85-27880

Transonic and supersonic wind tunnel tests on control effectiveness on schematic missile configurations [FFA-TN-1983-20] 20 p3389 N85-31020

Transonic and supersonic wind tunnel tests on control effectiveness on schematic missile configurations: Supplement [FFA-TN-1983-20-SUPPL] 20 p3389 N85-31021

Longitudinal tune control in synchrotrons [DE85-010745] 20 p3527 N85-31937

Analysis of flexible aircraft longitudinal dynamics and handling qualities. Volume 1: Analysis methods [NASA-CR-177943-VOL-1] 24 p4066 N85-35202

Analysis of flexible aircraft longitudinal dynamics and handling qualities. Volume 2: Data [NASA-CR-177943-VOL-2] 24 p4067 N85-35203

LONGITUDINAL STABILITY

Approximate neutral point of a subsonic canard aircraft [NASA-TM-86694] 15 p2462 N85-25205

Static longitudinal stability and control characteristics of the Fokker F27 Friendship calculated by simple handbook methods [VTH-LR-394] 16 p2711 N85-26728

Realisation of relaxed static stability on a commercial transport 17 p2903 N85-27899

Active control technology experience with the Space Shuttle in the landing regime 17 p2903 N85-27900

Contributions on the subject of longitudinal movements of aircraft in wind shears [NASA-TM-77637] 18 p3139 N85-29432

LONGITUDINAL WAVES

NT PLANE WAVES

Generation of longitudinal acoustic waves by modulated helicon waves — nonlinear steady state waves in metals 13 p2090 N85-23049

Surface acoustic wave structure and volume waves 15 p2525 N85-25566

The longitudinal thickness of air-shower fronts [OG-9.5-1] 23 p4030 N85-34976

LONGSHORE CURRENTS

U COASTAL CURRENTS

LOOP ANTENNAS

Impedance measurements on a VLF multi-turn loop antenna in a space plasma simulation chamber [AD-A145104] 04 p0492 N85-13141

Tactical HF communication for military helicopters using the NVIS mode 08 p1074 N85-16807

Loop radiating elements [AD-D011409] 08 p1156 N85-17306

Experimental measurements of the ion cyclotron antennas' coupling and RF characteristics [DE85-011569] 23 p3962 N85-34694

LOOPS

Design and performance of sampled data loops for subcarrier and carrier tracking 05 p0623 N85-13988

Wideband phase keyers 12 p1839 N85-21544

New results on the PLL false lock phenomenon 12 p1948 N85-22236

Normal mode calculations for fuselage type intricate structures by regarding them as systems with superposed constraints 13 p2048 N85-22817

Reliability report for communication networks [AD-A153764] 18 p3090 N85-29127

Low-profile fastener [AD-D011667] 19 p3260 N85-30343

Quarter-inch streaming tape drive application with the Serial ASCII Instrumentation Loop (SAIL) system [AD-A155354] 22 p3759 N85-33295

General design principles of high speed frequency synthesizers based on phase synchronization systems 22 p3779 N85-33417

Wide-band phase locked loop amplifier apperatus [AD-D011720] 23 p3927 N85-34337

LORAN

NT LORAN C

Field tests of the real-data acquisiton system for the NASA-LaRC differential absorption lidar [NASA-CR-174020] 01 p0106 N85-10710

LORAN C

National Airspace System Plan: Facilities, equipment and associated development 16 p2704 N85-26692

The time and frequency comparisons via Loran-C and National TV Network in Yugoslavia 18 p3109 N85-29248

Experiments of a LORAN-C aided recovery system and a proposal of its application to rescue system 20 p3404 N85-31121

LORAN-C harbor and harbor entrance survey: Charleston, South Carolina [AD-A154875] 21 p3554 N85-32108

Nonlinear digital phase-locked loops with application to Loran-C receivers 24 p4063 N85-35178

LORENTZ FORCE

Update of thermal conductivity and electrical resistivity of electrolytic iron, tungsten and stainless steel [PB85-115814] 12 p1803 N85-21311

Variations in the small-scale galactic magnetic field and short time-scale intensity variations of extragalactic radio sources 20 p3549 N85-32084

Cerenkov counters for high energy nuclei: Some new developments [OG-9.1-5] 23 p4023 N85-34931

On mini-cluster observed by Chacaltaya emulsion chamber experiment [HE-3.6-12] 24 p4185 N85-35959

LORENTZ GAS

Heat flux in Lorentzian plasma [IPPJ-704] 12 p1935 N85-22158

LORENTZ TRANSFORMATIONS

The solar dynamo and the complex Lorenz equations 14 p2447 N85-25107

Comment on quantum effects on 4-dimensional space-time symmetries [DE85-007780] 16 p2872 N85-27722

Modulation transfer function for two-point and periodic objects using Gaussian and Lorentzian resolution functions [PB85-187557] 19 p3366 N85-30891

Hadron thermodynamics in relativistic nuclear collisions [HE-1.1-8] 24 p4171 N85-35856

LOS ALAMOS TURRET REACTOR

U HIGH TEMPERATURE NUCLEAR REACTORS

LOSSES

Predicted heat transfer loss in the expansion cylinder of a 2 cylinder reciprocating engine [AD-A144831] 01 p0056 N85-10286

Voluntary dehydration and electrolyte losses during prolonged exercise in the heat [AD-A145157] 01 p0095 N85-10589

The effect of temperature on the radiation induced losses of large diameter GPS (Germanium phosphosilicate) and GBS core optical fibers [AD-A145409] 02 p0280 N85-11820

An improved computer model for prediction of axial gas turbine performance losses [NASA-CR-174246] 07 p0904 N85-15724

Age life prediction of nylon 66 parachute materials. Part 1: Mechanical properties [AD-A147698] 08 p1170 N85-17378

Current status of trailing edge loss calculation for a turbine blade [PNR-90244] 09 p1282 N85-18081

Effects of slip on energy distribution between tyre and soil [AD-P004283] 09 p1404 N85-18869

Kinetics of reaction of metals and non-metals during diffusion welding 11 p1602 N85-20076

Hot stars: Six years of progress 11 p1743 N85-20960

The effect of jamming/deception on decision making [AD-A149740] 12 p1828 N85-21472

Reducing electric power losses in discharge chamber of induction plasmatron 12 p1841 N85-21553

Beam loss due to the aperture limitation resulting from intrabeam scattering [DE85-005136] 12 p1930 N85-22124

Optical reflectometer for multimode fiber lightpipes 13 p2075 N85-22961

Effect of diaphragm leakage on turbine stage characteristics 14 p2286 N85-24166

Defocusing losses in a log periodic-fed reflector [AD-A151616] 15 p2547 N85-25722

Finite element prediction of loss factors for structures with frequency-dependent damping treatments 15 p2576 N85-25889

Multi-access fiber optic data bus using FDM/FSK [NASA-CR-175739] 15 p2621 N85-26152

Fuel and oxidizer turbine loss analysis 16 p2739 N85-26900

Histological and compositional responses of bone to immobilization and other experimental conditions [NASA-CR-175837] 16 p2841 N85-27518

Electrochemical and morphological study of the effect of temperature on the restructuring and loss of capacity of alkaline battery electrodes [DE85-006869] 18 p3120 N85-29376

Study of Kapton under simulated shuttle environment [NASA-CR-176003] 19 p3225 N85-29867

Receiver loss study of optimized solar central receiver systems as a function of receiver thermal loss per unit area [DE85-010831] 19 p3266 N85-30265

Important loss mechanisms in high-efficiency solar cells 21 p3610 N85-32424

Kinetic loss experiments on Mite [DE85-012826] 24 p4158 N85-35780

LOSSLESS MATERIALS

Microwave surface resistivity of several materials at ambient temperature 10 p1463 N85-19226

LOSSY MEDIA

Joint services electronics program [AD-A145085] 01 p0042 N85-10276

Impedance of vertical dipoles above a dissipative ground [REPT-S-152] 02 p0192 N85-11287

General image theory for the Sommerfeld problem [REPT-S-154] 02 p0193 N85-11289

Numerical methods for analyzing electromagnetic scattering [NASA-CR-175507] 12 p1823 N85-21438

Normal modes in an overmoded circular waveguide coated with lossy material [NASA-CR-176186] 24 p4065 N85-35320

LOUDNESS

Contribution of tonal components to the overall loudness, annoyance and noisiness of noise: Relation between single tones and noise spectral shape [NASA-CR-3892] 15 p2645 N85-26317

LOUDSPEAKERS

Acoustic scaling: The development of improved instrumentation [BBC-RD-1985/7] 24 p4145 N85-35684

LOUISIANA

The influence of the number of ground control points on the scene-to-map registration accuracy — Kansas, Louisiana, Mississippi, and Missouri 07 p0986 N85-16264

Image variance and spatial structure in remotely sensed scenes — South Dakota, California, Missouri, Kentucky, Louisiana, Tennessee, District of Columbia, and Oregon 07 p0986 N85-16265

Revised Uniform Summary of Surface Weather Observations (RUSSWO). England AFB, Alexandria, Louisiana, parts A-F [AD-A146920] 07 p1006 N85-16391

LOUVERS

Pre-HOST high temperature crack propagation 02 p0141 N85-10956

Vertical solar louver project [DE84-017355] 11 p1676 N85-20558

Fast shutter apperatus [DE85-006501] 23 p3928 N85-34343

LOVE WAVES

Love and Rayleigh waves in irregular ground 04 p0523 N85-13348

Resolution of 2-dimensional seismologic problems by a finite element approximation. Application to the Love wave propagation through the Atlantic border of the Iberic Peninsula 11 p1681 N85-20594

Resolution of 2-dimensional seismologic problems by a finite element approximation. Application to the Love wave propagation through the Atlantic border of the Iberic Peninsula. Appendix: Graphs of results — Lagrange coordinates 11 p1681 N85-20595

LOW ALLOY STEELS

U HIGH STRENGTH STEELS

LOW ALTITUDE

Study of proton and neutron activation of metal samples in low Earth orbit [NASA-CR-171183] 01 p0026 N85-10164

Magnetospheric plasma studies using data from the dynamics high and low altitude plasma instruments [AD-A145751] 03 p0392 N85-12505

Using a limited field of view simulator to instruct high speed, low altitude flying skills [AD-P004309] 09 p1267 N85-17963

Visual perceptual aspects of low level high speed flight and flight simulation [AD-P004310] 09 p1267 N85-17964

Low altitude high speed flight simulation using video disc technology [AD-P004312] 09 p1268 N85-17966

AVTS (Advanced Visual Technology System): A high fidelity visual simulator [AD-P004338] 09 p1271 N85-17992

Personnel protection concepts for advance escape system design 10 p1532 N85-19658

Low altitude texture comparison data base and smooth shaded texture [AD-A150342] 13 p2146 N85-23323

Safety recommendation(s), A-84-82 through -84 [REPT-3957] 14 p2217 N85-23748

Deuteron whistlers at low latitudes in the low altitude topside ionosphere 14 p2366 N85-24625

Low-latitude ducted whistlers observed at Sanya, Hainan, China 14 p2367 N85-24626

Whistler observation at Okinawa, Japan during the IMS 14 p2367 N85-24627

Multistep orbital correction algorithms for an Earth satellite using low thrust engine 15 p2479 N85-25303

Spectral characteristics of protons at low and high altitudes during geomagnetic storm of 29 July 1977 16 p2719 N85-26786

The role of simulation 18 p3058 N85-28919

LOW ASPECT RATIO

Study of controlled diffusion stator blading [NASA-CR-167995] 09 p1281 N85-18058

Calculation of transonic steady and oscillatory pressures on a low aspect ratio model and comparison with experiment [NASA-TM-86449] 21 p3551 N85-32092

LOW ASPECT RATIO WINGS

NT DELTA WINGS

Experimental data base for computers program assessment. Report of the Fluid Dynamics Panel Working Group 04: Addendum [AGARD-AR-138-ADD] 01 p0004 N85-10020

LOW CARBON STEELS

Alloying specially low carbon silicon-bearing steel with nitrogen [BLL-M-35707-(5828.4)] 02 p0175 N85-11170

The influence of aluminum on the qualities of low and medium carbon steel [BLL-M-35754-(5828.4)] 03 p0330 N85-12123

Nondestructive evaluation of residual stress in low-carbon steel [NASA-CR-174157] 04 p0512 N85-13264

Nondestructive evaluation of residual stress in low-carbon steel, introduction 04 p0512 N85-13265

The influence of manganese on intercrystalline internal adsorption of arsenic in low carbon steel [BLL-M-35965-(5828.4)] 05 p0615 N85-13931

Specifics of kinetics of polymorphous conversion upon heating of low carbon steels 13 p2030 N85-22721

The influence of melting practice and of microalloying, with rare earth metals and with boron, on the quality of low-carbon steel [BLL-BISI-22467-(9022.06)] 17 p2925 N85-28036

Multi-phase crystallization of ferrous alloys [BLL-BISI-TRANS-22441-(9022.06)] 17 p2925 N85-28037

Influence of preliminary cold deformation on fineness of pearlite [BLL-BISI-TRANS-22409-(9022.06)] 17 p2927 N85-28054

Influence of thermochemical treatment on properties of low-carbon steel [BLL-BISI-TRANS-22410-(9022.06)] 17 p2927 N85-28055

Preventing the formation of an anomalous structure in chemically sealed low carbon steel [BLL-BISI-TRANS-22373-(9022.06)] 17 p2930 N85-28085

New method for determining stampability of sheet materials [BLL-BISI-22486-(9022.06)] 17 p2972 N85-28380

Tendency of selected low-carbon steels to corrosion cracking in nitrates [BLL-BISI-TRANS-22262-(9022.06)] 18 p3073 N85-29006

Continuous casting of quality steels on billet casters [BMFT-FB-T-84-262] 18 p3078 N85-29041

Microstructure-abrasive wear characteristics of low carbon dual phase steels [DE85-010968] 19 p3239 N85-30083

Production process for steel with decarburized surface adapted for single coating enamelling [BMFT-FB-T-85-022] 20 p3432 N85-31292

Fractographic analysis for nonpropagating conditions of fatigue crack at high stress ratios in mild steel 23 p3905 N85-34194

Crystallographic orientation dependence of fatigue crack propagation in extremely low carbon steel 23 p3906 N85-34195

Safety and reliability of steel structural materials under random service impact loads 23 p3906 N85-34197

LOW CONCENTRATIONS

Model computations of radon, and radon decay product, concentrations in an open system; the Hewlett-Packard 41C program RNSS, version 02 [IRI-190-83-12] 17 p3035 N85-28775

LOW COST

Training effectiveness evaluation and utilization demonstration of a low cost cockpit procedures trainer [AD-A145179] 01 p0013 N85-10078

Low cost gyrocompass [AD-A148295] 08 p1082 N85-16657

Replaceable blade turbine and stationary specimen corrosion testing facility [NASA-TM-86931] 09 p1294 N85-18126

An inexpensive vector thin film magnetometer [AD-A148725] 09 p1323 N85-18310

Low cost, sprayed CuInSe2 solar cell research [DE85-003467] 12 p1881 N85-21799

Aspects of low cost module technology — spacecraft solar arrays 13 p2011 N85-22614

Practical considerations when using water quality and structure monitoring sensors as applied to portable ARGOS satellite transmitter equipment 14 p2330 N85-24405

Development of a low cost drifting buoy 14 p2330 N85-24408

Navigation: Accounting for copy 16 p2695 N85-26641

Iron rich low cost superalloys [NASA-CR-174900] 16 p2748 N85-26962

Performance test results of a low cost GPS time and frequency monitor 18 p3109 N85-29252

Investigation for low-cost permanent magnets [AD-A154387] 19 p3260 N85-30212

A new large-scale, high-resolution multicolor software display concept [AD-A155404] 22 p3827 N85-33703

LOW DENSITY GASES

U RAREFIED GASES

LOW DENSITY MATERIALS

Single-drop impact damage prediction for low density, coated ceramic materials — rain erosion 01 p0061 N85-10402

X-ray gauge measures areal density variations as small as 0.1% [DE85-003774] 12 p1854 N85-21629

French, UK, Swedish research in powder metallurgy, HIP 18 p3088 N85-29109

New form of graphite 19 p3243 N85-30111

Method for making a low density polyethylene waste form for safe disposal of low level radioactive material [DE85-006401] 23 p3920 N85-34292

LOW DENSITY RESEARCH

Nonequilibrium air radiation (Nequair) program: User's manual [NASA-TM-86707] 19 p3353 N85-30780

LOW FREQUENCIES

NT VERY LOW FREQUENCIES

Scattering of plane wave on cylindrical shell in low-frequency region 02 p0256 N85-11677

Low frequency electrical properties of selected dielectrics [DE84-016220] 05 p0632 N85-14052

Study of low-frequency sound with point source in stream with shear 06 p0825 N85-15239

Synoptic observations of the radio noise background in the frequency range 150-180 kHz to provide design data for the low frequency communications designer [AD-A147438] 07 p0941 N85-15965

Detection of low frequency impulsive noise from large wind turbine generators [NASA-CR-172511] 07 p1038 N85-16588

D1 LF wind measurements in the 90 to 100 km height range 08 p1185 N85-17468

Natural unsteadiness of a separation bubble behind a backward-facing step [AD-P004176] 09 p1267 N85-17961

The wobble of the Earth and the low frequency dynamics of the ocean 09 p1358 N85-18546

Design of low loss helix circuits for interference fitted and brazed circuits [NASA-CR-168313] 10 p1478 N85-19328

Simulation of the ion-beam-driven drift instability in a magnetic trap, 2 [AD-A149452] 10 p1554 N85-19798

Analysis of Jovian low frequency radio emissions [NASA-CR-174449] 10 p1571 N85-19906

Autostochastic behavior of solid state ring laser with low frequency periodic loss modulation 11 p1717 N85-20805

L.F. RADIO-DATA: Specification of BBC phase-modulated transmissions on long-wave [BBC-RD-1984/19] 12 p1822 N85-21431

Method of designing digital band-pass filters with infinite memory 12 p1840 N85-21546

Effect of compliability of hot walls in liquid-propellant engine on low frequency instability 13 p2049 N85-22824

Exitation of low-frequency resonance waves by moving conductor in space plasma 13 p2067 N85-22912

The low frequency behaviour of an immersed structure at a standstill in a high density fluid with free surface [TP-1983-31] 13 p2103 N85-23105

Shuttle payload bay dynamic environments: Summary and conclusion report for STS flights 1-5 and 9 [NASA-CR-175656] 14 p2241 N85-23896

Low-frequency oscillations of sea level and group structure of wind waves 14 p2335 N85-24441

Conjugacy of ELF-VHF emissions near L=6 — chorus phenomenon, hiss 14 p2367 N85-24629

Field of point source of low-frequency sound in atmosphere with altitudinally nonuniform wind 15 p2524 N85-25566

Long range downwind propagation of low-frequency sound [NASA-TM-86409] 15 p2645 N85-26318

Evaluation of human exposures to low frequency fields 16 p2776 N85-27135

Biological influences of low-frequency sinusoidal electromagnetic signals alone and superimposed on RF carrier waves [PB85-161248] 16 p2842 N85-27527

Timing accuracy of LF and TV synchronization techniques 17 p2961 N85-28288

Study of sound attenuation in sediments [AD-A153690] 18 p3177 N85-29697

New measurement solutions for low frequency systems 20 p3437 N85-31325

Automated testing of developmental satellite communications systems and subsystems [NASA-TM-87070] 20 p3440 N85-31348

Upward continuation of surface gravity anomalies [AD-A154973] 21 p3631 N85-32560

Influence of phonon interaction on width and form of Mandelstam-Brillouin optical scattering line 21 p3696 N85-32962

RF stabilization of interchange-ballooning modes [DE85-012080] 24 p4090 N85-35353

LOW FREQUENCY BANDS

NT VERY LOW FREQUENCIES

LOW GRAVITY

U REDUCED GRAVITY

LOW GRAVITY MANUFACTURING

Microgravity containerless processing in long drop tubes 02 p0153 N85-11037

Directional solidification of flake and nodular cast iron during KC-135 low-g maneuvers 02 p0154 N85-11040

Project Explorer 02 p0154 N85-11041

Critical point wetting drop tower experiment 02 p0155 N85-11045

Design and implementation of a low-gravity solidification experiment package for the F-104 02 p0156 N85-11053

The feasibility of low-G grey solidification of nodular iron in the F-104 experimental furnace package
[NASA-TM-82527] 10 p1426 N85-18996

Microgravity: A new tool for basic and applied research in space
[EP-212] 16 p2716 N85-26767

Technological experiments on high-altitude rockets 16 p2725 N85-26818

Microgravity silicon zoning investigation
[NASA-CR-171531] 20 p3397 N85-31073

Research study for gel precursors as glass and ceramic starting materials for space processing applications research
[NASA-CR-176113] 22 p3751 N85-33250

LOW LATITUDES
U TROPICAL REGIONS

LOW LEVEL TURBULENCE

Statistics from the operation of the low-level wind shear alert system (LLWAS) during the Joint Airport Weather Studies (JAWS) Project
[DOT/FAA/PM-84/32] 06 p0750 N85-14804

Adding computationally efficient realism to Monte Carlo turbulence simulation
[NASA-TP-2469] 17 p3025 N85-26708

Mean flow and turbulence in complex terrain
[AD-A155138] 21 p3636 N85-32583

LOW MASS
U MASS

LOW NOISE

Low noise multiple crystal-controlled oscillator
[AD-D011401] 07 p0948 N85-16010

Physical electronics of cooled operation of very short compound semiconductor trasnsistors 14 p2297 N85-24223

Cryogenically-cooled, low-noise microwave receivers: Present status and future needs 14 p2298 N85-24226

Low noise polycrystalline semiconductor resistors by hydrogen passivation
[AD-D011721] 23 p3927 N85-34338

LOW PASS FILTERS

China report: Science and technology
[JPRS-CST-84-001] 04 p0557 N85-13545

Present status, future prospects of domestic acoustical instruments 04 p0557 N85-13546

An airborne infrared thermal scanning system for easy use on Navy P-3 aircraft
[AD-A149690] 12 p1933 N85-22143

Synthesis of low-pass filters using coupled lines with unmatched loads 13 p2071 N85-22938

Efficiency of digital compensator of strong non-Gaussian interference 13 p2072 N85-22942

Some studies in filtering of atmospheric turbulence
[AD-A154042] 19 p3316 N85-30557

LOW PRESSURE
NT CYCLOGENESIS
NT HIGH ALTITUDE PRESSURE

Forecasting of polar lows 01 p0075 N85-10495

Energy efficient engine. Low pressure turbine test hardware detailed design report
[NASA-CR-167956] 02 p0147 N85-10994

Semiconductor-type transducer with universal strain gauge for measurement of low pressures 04 p0499 N85-13116

Electrical properties of 10-50 nm TEOS (Tetraethoxysilane) LPCVD (Low Pressure Chemical Vapor Deposition) films
[AD-A146416] 06 p0803 N85-15111

Nitriding of titanium and its alloys by N2, NH3 or mixtures of N2 + H2 in a dc arc plasma at low pressures (or = to torr)
[NASA-TM-83803] 06 p0814 N85-15168

Cut-off lows and their influence on the weather in Switzerland
[REPT-45] 10 p1519 N85-19574

Low loss injector for liquid propellant rocket engines
[NASA-CASE-MFG-25989-1] 11 p1591 N85-20008

Non-self-maintained high-voltage low-pressure discharge 13 p2088 N85-23037

Estimating defectiveness buildup during service in metal of welded runner in low-pressure cylinder of turbine 14 p2271 N85-24070

Measurements in low pressure flow using an electronic beam detector — wind tunnel tests 16 p2701 N85-26676

Experimental testing of cooling by low pressure adsorption in a zeolite
[DE85-007509] 16 p2716 N85-26763

On development mechanisms for polar lows 20 p3496 N85-31727

The nucleation of ice at very low temperatures and pressures 21 p3641 N85-32617

Monitoring dosage of volatile compounds in tests at low barometric pressure 23 p3954 N85-34506

LOW PRESSURE CHAMBERS
U VACUUM CHAMBERS

LOW REYNOLDS NUMBER

Numerical integrations of the Navier-Stokes equations for flow over surface-mounted obstacles 05 p0593 N85-13784

The resistance and mobility functions of two equal spheres in low Reynolds number flow
[AD-A147301] 07 p0959 N85-16080

Low Reynolds number vehicles
[AGARD-AG-288] 16 p2699 N85-26666

Aerodynamic characteristics of a distinct wing-body configuration at Mach 6: Experiment, theory, and the hypersonic isolation principle
[NASA-TP-2467] 22 p3727 N85-33107

LOW SPEED

Results of winglet development studies for DC-10 derivatives
[NASA-CR-3677] 02 p0138 N85-10936

Design studies of thick laminar flow airfoils for low speed flight employing turbulent boundary layer suction over the rear part 08 p1070 N85-16786

Recent methods for calibrating the anemometry of helicopters at low speeds 08 p1074 N85-16809

Air intake efficiency at zero speed and lip suction — jet engines
[BAE-KRS-N-GEN-303] 09 p1272 N85-17996

Effects of leading-edge devices on the low-speed aerodynamic characteristics of a highly-swept arrow-wing
[NASA-CR-172531] 13 p1966 N85-22365

The use of pressure sensing taps on the aircraft wing as sensor for flight control systems 16 p2698 N85-26660

LOW SPEED STABILITY

Application of the ONERA model of dynamic stall
[NASA-TP-2399] 04 p0451 N85-12862

Low-speed stability and control wind-tunnel investigations of effects of spanwise blowing on fighter flight characteristics at high angles of attack — Langely 12-ft low-speed tunnel and 30- by 60-ft tunnel
[NASA-TP-2431] 14 p2210 N85-23706

Low-speed tests of a high-aspect-ratio, supercritical-wing transport model equipped with a high-lift flap system in the Langley 4- by 7-meter and Ames 12-foot pressure tunnels
[NASA-TP-2097] 20 p3388 N85-31010

LOW SPEED WIND TUNNELS
NT SUBSONIC WIND TUNNELS

Atmospheric and pressurized low speed wind tunnel performance and cost comparisons
[ARL/AERO-R-160] 02 p0149 N85-11006

Wall influence corrections in wind tunnels: Blockage correction according to the wall pressure signature method
[FW-FO-1613] 04 p0453 N85-12875

Comparison of options for reduction of noise in the test section of the NASA Langley 4x7m wind tunnel, including reduction of nozzle area
[NASA-CR-172446-VOL-2] 05 p0726 N85-14667

Investigations into the effects of scale and compressibility on lift and drag in the RAE 5m pressurized low-speed wind tunnel 08 p1068 N85-16773

Low-speed wind tunnel tests of the NAL fan-jet STOL research aircraft model with ground simulation by tangential blowing
[NAL-TR-828] 10 p1423 N85-18976

Investigations into the effects of scale and compressibility on lift and drag in the RAE 5m pressurised low-speed wind tunnel
[RAE-TM-AERO-2006] 13 p1969 N85-22372

China report: Science and technology
[JPRS-CST-85-005] 13 p2052 N85-22843

CARD's low-speed wind tunnel described 13 p2052 N85-22849

A numerical simulation of the NFAC (National Full-scale Aerodynamics Complex) open-return wind tunnel inlet flow
[NASA-TM-86724] 16 p2700 N85-26672

Construction 1976-1980: Design, manufacturing, calibration of the German-Dutch wind tunnel (DNW) 17 p2905 N85-27913

Background noise measurements from jet exit vanes designed to reduced flow pulsations in an open-jet wind tunnel
[NASA-TM-86383] 17 p2906 N85-27916

A computer-controlled traverse gear for the Oxford wind engineering research group's 4 metre x 2 metre wind tunnel
[OUEL-1525/84] 20 p3483 N85-31514

The influence of helicopter tail shape on drag: An aerodynamic study using a low speed wind tunnel
[AD-A156304] 24 p4062 N85-35174

LOW TEMPERATURE
NT ULTRALOW TEMPERATURES

Materials studies for magnetic fusion energy applications at low temperatures, 7
[DE84-013487] 01 p0122 N85-10887

Low temperature properties of Mo/Ni superlattices
[DE84-014729] 02 p0288 N85-11881

The extremeness of the cold front of December 31, 1978 over the CSR
[REPT-566] 03 p0377 N85-12400

Diffusion of gases in porous solids: Simulation and measurements
[DE84-016292] 04 p0500 N85-13101

Kohn anomaly in metastable fcc lanthanum at low temperatures
[DE84-015459] 04 p0569 N85-13825

Oxide charge characteristics of low temperature MOS (Metal-Oxide-Silicon) oxide films
[AD-A146447] 06 p0803 N85-15113

Charge trapping in low temperature MOS (Metal-Oxide-Silicon) oxides
[AD-A146450] 06 p0860 N85-15487

Method for making alloy additions to base metals having higher melting points
[AD-D011403] 07 p0928 N85-15884

Effects of low temperatures on the growth and unfrozen water content of an aquatic plant
[AD-A147107] 07 p1011 N85-16424

Carotid baroreceptor influences on peripheral circulatory and thermal responses during cold exposure
[AD-A146806] 07 p1015 N85-16447

Determination of the decomposition behavior of double base propellants at low temperatures 08 p1117 N85-17046

New phases and chemical reactions in solid CO under pressure
[DE85-002033] 09 p1377 N85-18665

Low temperature properties of CeOs2 in the C14 and C15 crystallographic Laves phases
[DE85-003754] 10 p1564 N85-19868

Low-temperature geothermal assessment of the Jordan Valley Salt Lake County, Utah
[DE85-000616] 11 p1670 N85-20524

Low temperature deposition of nickel films
[AD-D011568] 12 p1805 N85-21318

Oscillator development
[AD-A149699] 12 p1834 N85-21508

Experimental studies of low temperature surface interactions of atomic hydrogen using maser technique
[AD-A150216] 13 p2017 N85-22847

Low temperature calibration fixture
[DE85-003969] 13 p2094 N85-23071

Proceedings of the Cold Electronics Workshop
[NASA-CR-175682] 14 p2297 N85-24220

Cold electronics: An overview 14 p2297 N85-24221

Recent developments in semiconductor research 14 p2297 N85-24222

The effects of cooling on delay-time limits in IC's 14 p2297 N85-24224

Si MOS devices at low temperatures 14 p2297 N85-24225

Cryogenically-cooled, low-noise microwave receivers: Present status and future needs 14 p2298 N85-24226

Structural changes with one- and two-stage aging of alloys Ti-Al-Mo-Fe and Ti-Zr-V-Al-Sn 15 p2499 N85-25415

Mechanism of formation of low temperatures in nighttime Venusian thermosphere 16 p2723 N85-26807

Investigation of the requirement for auxiliary heating of Canadian forces personnel
[AD-A151950] 16 p2641 N85-27522

The fatigue properties of welds at low temperature, according to the type of steel
[BLL-BISI-TRANS-22455-(9022.06)] 17 p2978 N85-28410

Hydrogen maser oscillation at 10 K 18 p3108 N85-29241

On the low temperature chemistry preceding end gas autoignition
[DE85-010471] 19 p3252 N85-30182

Physics with low temperature antiproton
[DE85-009627] 19 p3355 N85-30798

Low-temperature positron lifetime and Doppler-broadening measurements for single-crystal nickel oxide containing cation vacancies
[DE85-010236] 19 p3376 N85-30944
Detailed studies of aviation fuel flowability
[NASA-CR-174936] 20 p3435 N85-31306
A comparison of two bench scale tests of fuel low temperature flow properties
[AD-A154477] 20 p3435 N85-31311
Polymer solution-supercritical fluid behavior
[AD-A154514] 21 p3568 N85-32192
Synthesis and properties of arylethersulfone thermoset systems
[AD-A154611] 21 p3569 N85-32196
The nucleation of ice at very low temperatures and pressures 21 p3641 N85-32617
Method for fluorination of actinide fluorides and oxyfluorides using O2F2
[DE85-011646] 22 p3743 N85-33202
Very low temperature studies of hyperfine effects in metals
[DE85-013367] 22 p3749 N85-33236
Low temperature experimental capability for use with gas guns
[DE85-010418] 22 p3801 N85-33548
Measurement and correlation of jet fuel viscosities at low temperatures
[NASA-CR-174911] 23 p3921 N85-34295
Decomposition of martensite in R6M5 and R6AM5 steels after direct immersion in liquid nitrogen
[BLL-M-36305] 24 p4077 N85-35268
Evaluation of low-temperature geothermal potential in north-central Box Elder County, Utah
[DE85-009541] 24 p4112 N85-35490
Energy from low temperature differences
[DE85-008617] 24 p4112 N85-35492

LOW TEMPERATURE BRAZING
Fatigue crack propagation characteristics and fatigue fracture toughness in 780 MPa grade high strength steel weldments at low temperature
[BLL-BISI-TRANS-22369-(9022.06)]
17 p2979 N85-28411

LOW TEMPERATURE ENVIRONMENTS
Evaluation of thermocouple junction temperature
[DE84-015159] 04 p0502 N85-13206
Effects of restricted water intake on performance in a cold environment
[AD-A146904] 07 p1015 N85-16450
Properties of filamentary sublimation residues from dispersions of clay in ice 13 p2197 N85-23629
Low Temperatue Science. Series A: Physical Sciences
[ISSN-0439-3538] 15 p2581 N85-25917

LOW TEMPERATURE PHYSICS
Exothermic processes in solids under low temperatures, their physics and their cryogenic implications
[JUEL-1919] 03 p0414 N85-12651

LOW TEMPERATURE PLASMAS
U COLD PLASMAS

LOW TEMPERATURE TESTS
An evaluation of grease type ball bearing lubricants operating in various environments
[NASA-TM-86480] 02 p0185 N85-11239
Investigation of the production and properties of lattice defects induced by low temperature reactor irradiation
03 p0430 N85-12739
Geomagnetic field dynamics 13 p2116 N85-23182
Mechanical properties of Shielded Metal Arc (SMA) and Submerged Arc (SA) welded joints in a steel Raex 386 P Arctic
[VTT-339] 22 p3801 N85-33551

LOW THRUST
Low thrust bipropellant engine/redundant seat valve assembly
[AD-A150293] 13 p2013 N85-22628

LOW THRUST PROPULSION
NT ELECTROMAGNETIC PROPULSION
NT ELECTROSTATIC PROPULSION
NT ION PROPULSION
NT PLASMA PROPULSION
NT SOLAR PROPULSION
Partial bleed expander cycle for low thrust LOX/LH2 rocket engine
[NAL-TR-837T] 10 p1430 N85-19018
Design and analysis report for the RL10-2B breadboard low thrust engine
[NASA-CR-174857] 10 p1430 N85-19020
Station keeping of geostationary satellites by electric propulsion
[NASA-TM-77820] 14 p2320 N85-24337
Oxygen-hydrogen thrusters for Space Station auxiliary propulsion systems
[NASA-CR-175691] 15 p2494 N85-25383

LOW VELOCITY
U LOW SPEED

LOW VOLTAGE
Optimization of overall dimensions of enclosures for low-voltage devices and equipment
13 p2087 N85-23033
Low voltage free electron laser development
[AD-A152917] 17 p2970 N85-28342

LOW WEIGHT
Free-surface phenomena under low- and zero-gravity conditions
[NASA-CR-175835] 16 p2782 N85-27168

LOWER ATMOSPHERE
NT BIOSPHERE
NT OZONOSPHERE
NT TROPOSPHERE
Exploratory investigation of the need for and feasibility of a Lower Atmosphere Research Satellite (LARS) program
[NASA-CR-171181] 01 p0015 N85-10091
H2O profile in lower atmosphere of Venus based on effective radiation flux measurements
02 p0163 N85-11102
Characteristics of latitude effect on cosmic ray charged component in atmosphere at altitudes 3-5 KM
13 p1978 N85-22413
Influence of bubbles formed upon breaking of waves on gas exchange between ocean and atmosphere
14 p2335 N85-24439
Energy structure of atmospheric boundary layer above waves 14 p2335 N85-24442
The possibility of observing solar neutron events in the lower atmosphere
[NOTA-INTERNA-837] 18 p3209 N85-29906

LOWER BODY NEGATIVE PRESSURE
Leg volume changes. Responses to Lower Body Negative Pressure (LBNP) during 7 days of zero-g simulation (6 deg Head-Down Tilt (HDT))
05 p0692 N85-14452
The influence of angiotensin on the maintenance of venous tone. The effect of Lower Body Negative Pressure (LBNP) and angiotensin blockade
05 p0693 N85-14457
LBNP training of crew members on main missions aboard Salyut-6 orbital station 12 p1901 N85-21936
Oxygenation and regional circulation in gingival mucosa during exposure to lower body negative pressure
23 p3953 N85-34498

LOWER CALIFORNIA (MEXICO)
Stratigraphy, petrology, and tectonic setting of the Alisitos Group, Baja California, Mexico
03 p0389 N85-12488

LOWER IONOSPHERE
NT D REGION
Behavior of charged particles in lower ionosphere with acoustical effects 02 p0161 N85-11089
Experimental results of study of artificial perturbation region in upper and lower ionosphere disturbance by the method of vertical probing 06 p0784 N85-15011
Study of lower ionosphere by pulse cross-modulation method 10 p1500 N85-19467

LOX (OXYGEN)
U LIQUID OXYGEN

LOX-HYDROGEN ENGINES
U HYDROGEN OXYGEN ENGINES

LSI
U LARGE SCALE INTEGRATION

LST
U HUBBLE SPACE TELESCOPE

LUBRICANT TESTS
Performance evaluation of automotive wheel bearing greases
[AD-A145948] 03 p0337 N85-12168
The European Space Tribology Laboratory (ESTL) activities report
[ESA-ESTL-61] 05 p0646 N85-14146
The performance of Fomblin Z25 oil in ball bearings operating in vacuum — spacecraft lubricant
[ESA-ESTL-056] 08 p1134 N85-17150
Locking of Automative Products hydraulic selector valves
[BAE-EXPER/NOTE-459] 15 p2567 N85-25839
European Space Tribology Laboratory: Facilities, services, capabilities
[ESA-BR-12] 20 p3398 N85-31080
Activities report of the European Space Tribology Laboratory
[ESA-ESTL-66] 20 p3484 N85-31653
The use of perfluoroether lubricants in unprotected space environments 22 p3797 N85-33523

LUBRICANTS
NT GAS LUBRICANTS
NT LUBRICATING OILS
NT SOLID LUBRICANTS
An evaluation of grease type ball bearing lubricants operating in various environments
[NASA-TM-86480] 02 p0185 N85-11239
Performance evaluation of automotive wheel bearing greases
[AD-A145948] 03 p0337 N85-12168
Microscopic aspects of the effect of friction reducers at the lubrication limit
[NASA-TM-77413] 03 p0367 N85-12354
Effect of lubricant extreme-pressure additives on surface fatigue life of AISI 9310 spur gears
[NASA-TP-2408] 04 p0507 N85-13234
Fluorinated aliphatic polyalkylether lubricant with an additive composed of an aromatic phosphine substituted with perfluoroalkylether groups
[AD-D011286] 06 p0770 N85-14927
Effects of silver and group 2 fluorides addition to plasma sprayed chromium carbide high temperature solid lubricant for foil gas bearing to 650 deg C
[NASA-TM-86895] 06 p0770 N85-14928
Stability of lubricant film in gas dynamic bearing
06 p0778 N85-14977
Contact angle and surface tension measurements of a five-ring polyphenyl ether
[NASA-TM-86927] 07 p0930 N85-15897
Effect of five lubricants on life of AISI 9310 spur gears
[NASA-TP-2419] 07 p0962 N85-16099
Toxic hazards research
[AD-A147857] 07 p1011 N85-16425
Structure of solids surfaces in wear situations
[AD-A148480] 08 p1168 N85-17366
Tribological properties of graphite-fiber-reinforced, partially fluorinated polyimide composites
[NASA-TM-86926] 09 p1298 N85-18153
Characterization of lubricated bearing surfaces operated under high loads
[NASA-TM-86964] 12 p1811 N85-21357
Formation of high molecular weight products from benzene during boundary lubrication
[NASA-TM-86966] 13 p2017 N85-22644
Use of ferrofluids in machining of metals
13 p2045 N85-22802
Transmission efficiency measurements and correlations with physical characteristics of the lubricant
14 p2222 N85-23781
Chemical-mechanical interaction in gears
14 p2223 N85-23785
Problems regarding the practical evaluation of efficiency of worm gears 14 p2224 N85-23793
Role of fluid lubricant-coolant in fine grinding of optical glass by diamond tool 14 p2260 N85-24125
Model of friction bearing hydrodynamics
14 p2288 N85-24178
Computations for segmented radial bearings
14 p2288 N85-24180
Thermal traction contact performance evaluation under fully flooded and starved conditions
[NASA-CR-168173] 15 p2568 N85-25848
Evaluation of used crankcase oils using computerized infrared spectrometry
[AD-A152993] 17 p2920 N85-27999
Evaluation of used crankcase oils using computerized infrared spectrometry. Appendices
[AD-A152994] 17 p2920 N85-28000
New method for determining stampability of sheet materials
[BLL-BISI-22486-(9022.06)] 17 p2972 N85-28360
Lubricant and additive effects on spur gear fatigue life
[NASA-TM-87044] 17 p2974 N85-28373
Correlation of rheological characteristics of lubricants with transmission efficiency measurements
[NASA-TM-86988] 19 p3260 N85-30342
The design and development of a spacecraft appendage tie down mechanism 22 p3797 N85-33522
The use of perfluoroether lubricants in unprotected space environments 22 p3797 N85-33523

LUBRICATING OILS
Cooperative program evaluation of NATO multigraded diesel engine oils
[AD-A146072] 03 p0337 N85-12171
A simple electronic apparatus for determining the oxidation stability of lubricants and other organic compounds
[AD-A146080] 03 p0338 N85-12172
Effect of two inner-ring oil-flow distribution schemes on the operating characteristics of a 35 millimeter bore ball bearing to 2.5 million DN
[NASA-TP-2404] 04 p0507 N85-13233
Grease versus oil lubrication of wheel bearings in Army equipment
[AD-A147546] 07 p0973 N85-16184
The performance of Fomblin Z25 oil in ball bearings operating in vacuum — spacecraft lubricant
[ESA-ESTL-056] 08 p1134 N85-17150
New technique for fluid feed in simultaneous multisurface grinding 13 p2045 N85-22800
Fine filtration: An attractive route towards lower helicopter operating costs 14 p2221 N85-23774

best copy available

Design of piping for oil drain from turbine bearings
14 p2271 N85-24073
Investigation of reaction layer formation in high-load capacity lubricating oils
[MPA-83-01] 17 p2975 N85-28381
Activities report of the European Space Tribology Laboratory
[ESA-ESTL-66] 20 p3484 N85-31653
LUBRICATION
NT BOUNDARY LUBRICATION
NT SELF LUBRICATION
NT SPACECRAFT LUBRICATION
Performance evaluation of automotive wheel bearing greases
[AD-A145946] 03 p0337 N85-12168
Lubricity of well-characterized jet and broad-cut fuels by ball-on-cylinder machine
[NASA-TM-83807] 03 p0339 N85-12183
Microscopic aspects of the effect of friction reducers at the lubrication limit
[NASA-TM-77413] 03 p0367 N85-12354
Comparison of predicted and measured friction for a tilt-pad thrust bearing with crown and roughness under hydrodynamic and mixed lubrication
[AD-A145752] 03 p0371 N85-12371
Development of gas-lubricated pistons for heavy duty diesel engine technology program
[NASA-CR-174746] 03 p0441 N85-12806
Fundamental tribological properties of ceramics
[NASA-TM-86915] 07 p0930 N85-15893
Grease versus oil lubrication of wheel bearings in Army equipment
[AD-A147546] 07 p0973 N85-16164
Metallographic grinding efficiency
[DE85-001520] 09 p1304 N85-18194
Study of advanced fuel system concepts for commercial aircraft
[NASA-CR-174751] 11 p1584 N85-19978
Tribological systems as applied to aircraft engines
[NASA-TM-86965] 12 p1858 N85-21657
Lubrication and performance of high-speed rolling-element bearings
[NASA-TM-86958] 12 p1859 N85-21658
Development of a multiplane multispeed balancing system for turbine systems
[NASA-CR-174750] 13 p1976 N85-22400
Thermal and thermoelastic effects in rolling/sliding contacts
[AD-A150435] 13 p2165 N85-23429
Gears and Power Transmission Systems for Helicopters and Turboprops
[AGARD-CP-369] 14 p2220 N85-23765
Helicopter transmission lubricants
14 p2220 N85-23768
A state of the art assessment of turboprop transmission technology and projected needs for the next generation
14 p2220 N85-23770
Significant parameters of the behavior and of the surface damage of the lubricated Hertzian contact: An application to gears 14 p2222 N85-23783
Problems of elastic hydrodynamic lubrication of helicopter transmission gears 14 p2222 N85-23784
Wear reduction by lubricants in confined contacts
14 p2223 N85-23786
Experimental study of heat transfer from shaft in cooled radial bearing of GNT-25 gas turbine
14 p2270 N85-24068
Selection of bearing type for large steam turbines
14 p2271 N85-24069
Molybdenum disulphide lubrication: A continuation survey, 1981 - 1983
[REPT-84-549] 18 p3082 N85-29065
Dynamics of thin-film breakup in a constricted pore
[DE85-006442] 18 p3101 N85-29199
Mechanical interactions of rough surfaces
[DE85-005653] 18 p3118 N85-29299
Study of the chemical mechanism in lubrication
[DE85-010788] 19 p3228 N85-30013
Fast approach for calculating film thicknesses and pressures in elastohydrodynamically lubricated contacts at high loads
[NASA-TM-87032] 19 p3264 N85-30242
Temperature and surface damage under lubricated sliding-rolling contacts 19 p3280 N85-30338
Activities report of the European Space Tribology Laboratory
[ESA-ESTL-66] 20 p3484 N85-31653
Surface roughness effects in elastohydrodynamic contacts
[NASA-TP-2468] 21 p3595 N85-32329
Mechanics of a gaseous film barrier to lubricant wetting of elastohydrodynamically lubricated conjunctions
[NASA-TP-2500] 21 p3595 N85-32330
Lubrication and cooling for high speed gears
[NASA-TM-87096] 23 p3938 N85-34407
Elastohydrodynamic lubrication calculations used as a tool to study scuffing
[NASA-TM-87097] 23 p3938 N85-34408
Design and lubrication of high-speed rolling-element bearings
[NASA-TM-87107] 23 p3938 N85-34409
LUBRICATION SYSTEMS
Effect of interconnection of the ends of a sliding bearing on film thickness
[AD-A147736] 06 p1132 N85-17135
Design of piping for oil drain from turbine bearings
14 p2271 N85-24073
Study of axial bearings without oil bath with radial cooling of blocks 14 p2286 N85-24164
LUCITE (TRADEMARK)
U POLYMETHYL METHACRYLATE
LUDER BANDS
U PLASTIC DEFORMATION
U YIELD POINT
LUGS
The research of driving wheel with movable lugs of the paddy field floating tractor
[AD-P004283] 09 p1407 N85-18860
An investigation of the driving wheel thrust of paddy field tractors
[AD-P004284] 09 p1407 N85-18861
Behaviour of soil under a lugged wheel
[AD-P004287] 09 p1407 N85-18864
The analysis on the dynamic performance of a single lug
[AD-P004289] 09 p1408 N85-18866
Advanced life analysis methods. Volume 1: Cracking data survey and NDI (nondestructive inspection) assessment for attachment lugs
[AD-A150419] 13 p2103 N85-23108
Advanced life analysis methods. Volume 2: Crack growth analysis methods for attachment lugs
[AD-A150420] 13 p2103 N85-23109
Advanced life analysis methods. Volume 4: Tabulated test data for attachment lugs
[AD-A151016] 14 p2219 N85-23760
Advanced life analysis methods. Volume 5: Executive summary and damage tolerance criteria recommendations for attachment lugs
[AD-A151017] 14 p2219 N85-23761
Advanced life analysis methods. Volume 3: Experimental evaluation of crack growth analysis methods for attachment lugs
[AD-A151056] 14 p2317 N85-24319
The effect of frictional forces on fatigue crack growth in lugs
[AD-A151994] 15 p2578 N85-25898
Advanced life analysis methods. Volume 6: User's manual for LUGRO computer program to predict crack growth in attachment lugs
[AD-A151235] 15 p2626 N85-26195
LUMBERING AREAS
U FORESTS
LUMINAIRES
NT AIRCRAFT LIGHTS
NT ARC LAMPS
NT FLASH LAMPS
NT MERCURY LAMPS
NT RUNWAY LIGHTS
Determining lamp/ballast system performance with a temperature-controlled integrating chamber
[DE84-014606] 05 p0631 N85-14049
New lighting technologies, their status and impacts on power densities
[DE85-000712] 09 p1315 N85-18266
Evaluation of miniature vacuum ultraviolet lamps for stability and operating characteristics, Lyman-Alpha task
[NASA-CR-171345] 10 p1477 N85-19323
Lifetime and reliability of rubidium discharge lamps for use in atomic frequency standards
[AD-A150787] 14 p2417 N85-24915
Radioluminescent lighting for rural Alaskan runway lighting and marking
[DE85-007022] 16 p2716 N85-26764
Acceptability testing of radioluminescent lights for VFR-night air taxi operations
[DE85-007303] 16 p2716 N85-26765
Material for electrodes of pulsed and arc sources of light
[DE85-007453] 16 p2780 N85-27156
The role of long term lamp fluctuations in the random walk of frequency behavior of the rubidium frequency standard: A case study
[AD-A155338] 21 p3590 N85-32314
LUMINANCE
The Beatrice experiment and the luminance concept in Dante
[NOTA-INTERNA-823] 02 p0281 N85-11831
Approximating true radioluminance distribution from observations on aperture synthesis systems
06 p0783 N85-15003
NBS (National Bureau of Standards) daylight availability database
[PB84-245745] 07 p1054 [illegible]
Astronomy and sodium lighting
[RAND/N-2089-RC] 09 p1413 [illegible]
Electronic displays: Their strengths and weaknesses for advanced high performance aircraft
10 p1533 [illegible]
Television camera video level control system
[NASA-CASE-MSC-18578-1] 12 p1821 [illegible]
Visual simulation requirements for aircraft aspect recognition at real world distances
[AD-A151040] 14 p2228 [illegible]
Issue of sky conditions
[DE85-010590] 19 p3317 [illegible]
Sub-luminal pulses from cosmic ray air showers
[HE-4.7-13] 24 p4200 [illegible]
LUMINESCENCE
NT BIOLUMINESCENCE
NT CATHODOLUMINESCENCE
NT CHEMILUMINESCENCE
NT ELECTROLUMINESCENCE
NT FLUORESCENCE
NT OPTICAL RESONANCE
NT PHOSPHORESCENCE
NT PHOTOLUMINESCENCE
NT RESONANCE FLUORESCENCE
NT SHOCK WAVE LUMINESCENCE
NT THERMOLUMINESCENCE
NT X RAY FLUORESCENCE
Evaluation of arctic test of improved tritium radioluminescent lighting
[DE84-014887] 05 p0587 [illegible]
Photophysical studies of triplet exciton processes in pure polymer films
[DE84-016258] 05 p0620 [illegible]
Processes of smooth increase and dropoff in intensity of glow line lambda' = 5577 A with exposure of ionosphere to electron beam 06 p0822 [illegible]
International Conference on Luminescence
[AD-A148470] 08 p1223 N85-17701
Facilities for studing radiation damage in nonmetals during irradiation
[DE85-000590] 10 p1554 [illegible]
Light your runways and taxiways without electricity
[DE85-000269] 11 p1586 [illegible]
Influence of shock wave front on nature of luminescence of recombining laser plasma 11 p1719 [illegible]
Subnanosecond time-resolved emission study of CdO and GaAs
[DE85-002070] 11 p1735 [illegible]
Examination of the feasibility for demonstration and use of radioluminescent lights for Alaskan remote runway lighting
[DE85-002503] 12 p1762 [illegible]
EXAFS of monolayers on silver electrodes: SSRL proposal number 717M
[AD-A150623] 13 p2018 [illegible]
Glow of ionospheric F-layer in Line 630 nm determined from photographs taken aboard Salyut-6 orbital station: Interpretation of results 16 p2721 [illegible]
Luminescence probe studies of ionomers. 2. Steady-state measurements from sulfonated polyethylene and teflon membranes
[AD-A152233] 16 p2755 [illegible]
Laser measurement techniques: Laser spectroscopy in semiconductors
[DE85-007887] 17 p2971 [illegible]
Luminescence probe studies of ionomers. 1. Steady-state measurements from nafion membrane
[AD-A152475] 17 p3029 [illegible]
Symposium on Luminescent Radiation Receivers and Converters 19 p3295 [illegible]
Radioluminescent lighting for Alaskan runway lighting and marking
[DE85-010405] 19 p3368 [illegible]
The space shuttle glow
[AD-A154937] 21 p3559 [illegible]
Multidimensional luminescence measurements
[AD-A154950] 21 p3563 [illegible]
Luminescence and absorption of indium-activated potassium-borate glasses subjected to high-power excitation 21 p3681 [illegible]
Influence of technological factors on luminescence characteristics of InGaAsP/InP heterolasers (lambda = 1.55 microns) 21 p3686 [illegible]
Spectral-luminescence characteristics and induced emission of Nd-3(+) ion in Gd(2-x)Nd(x)(WO4)3 crystals
21 p3686 [illegible]
Plasmodynamic methods for generating powerful light puses 21 p3693 [illegible]
Optical properties of heterostructures and superlattices
[AD-A156243] 24 p4162 [illegible]
LUMINESCENT INTENSITY
U LUMINOUS INTENSITY

LUMINOSITY

NT STELLAR LUMINOSITY

Considerations regarding the choice of beam parameters and IP configuration for the SSC [DE84-014522] 01 p0118 N85-10803

A search for low luminosity pulsars and its implications for the pulsar luminosity functions 02 p0296 N85-11919

Effects of core mixing on solar oscillation frequencies [DE84-015540] 03 p0449 N85-12853

Continuum distributions of active galactic nuclei 05 p0742 N85-14770

Physical conditions in low-luminosity active galactic nuclei 05 p0742 N85-14771

The correlation between excitation parameter and nebular luminosity for galactic HII regions with application to regions of star formation in M83 05 p0743 N85-14773

Evidence for non-radiative activity in hot stars 06 p1231 N85-17756

Is the ratio of observed X-ray luminosity to bolometric luminosity in early-type stars really a constant? 06 p1234 N85-17777

Non-radiative energy from differential rotation in hot stars 06 p1234 N85-17778

The Orion molecular cloud at far-infrared wavelengths 06 p1245 N85-17860

The 157 micron (C II) luminosity of the galaxy 06 p1248 N85-17877

The structure and dynamics of ringed galaxies 09 p1415 N85-18926

Solid state luminescent light filters for neodymium lasers 11 p1716 N85-20790

STS atmospheric luminosities [NASA-CR-175514] 12 p1791 N85-21240

High energy facilities advanced projects: Intrabeam scattering for a beam of gold ions [DE85-000667] 12 p1941 N85-22192

IRAS observations of Seyfert galaxies [NASA-CR-175557] 12 p1953 N85-22267

Plasma in the clusters of galaxies 12 p1957 N85-22299

The Feinheit method: A phase-independent formulation of the period-luminosity relation for Cephids [NASA-CR-175706] 14 p2440 N85-25056

Atomic physics aspects of a Relativistic Nuclear Collider [DE85-006667] 15 p2650 N85-26342

Electrodes for flash discharge lamps [DE85-006697] 17 p2955 N85-28250

A new luminosity component in 3C48 [NASA-CR-175840] 17 p3052 N85-28894

Evolution of the luminosity function of extragalactic objects [NASA-CR-175977] 18 p3201 N85-29860

Requirements for very high energy accelerators [DE85-011173] 20 p3529 N85-31952

Visibility and vertical structure measurements in southern Germany [AD-A154714] 21 p3635 N85-32574

Solar variability observed through changes in solar figure and mean diameter [DE85-012857] 22 p3860 N85-33900

On gamma and neutrino radiation from Cyg X-3 [OG-2.1-7] 22 p3863 N85-33924

Evidence for long-term variability in the ultra high energy photon flux from Cygnus X-3 [OG-2.1-10] 22 p3863 N85-33926

The universal spectrum of AGNs and QSOs [OG-2.7-9] 22 p3872 N85-33962

X-ray spectra of bursting neutron stars 23 p3961 N85-34686

LUMINOUS FLUX DENSITY

U LUMINOUS INTENSITY

LUMINOUS INTENSITY

NT ILLUMINANCE

NT LUMINANCE

Efficiency of lasing dye media in pumping high-power radiation with nanosecond pulses 02 p0270 N85-11763

Surface coatings for low emittance in the thermal surveillance band [MRL-R-937] 03 p0336 N85-12158

In search of a visual-cortical describing function: A summary of work in progress 05 p0707 N85-14538

Central regulation of sensory flow in human visual system 07 p1013 N85-16435

Individual differences in chromatic brightness matching [AD-A148862] 10 p1529 N85-19641

The relative effectiveness of red and white light for subsequent dark-adaptation [AD-A148863] 10 p1530 N85-19642

Twilight intensity variation of the infrared hydroxyl airglow 11 p1663 N85-20461

EXOSAT observations of the 35d intensity variations of Her X-1 — X ray binary source 11 p1742 N85-20956

Research study of droplet sizing technology leading to the development of an advanced droplet sizing system [NASA-CR-174839] 12 p1850 N85-21604

A posteriori increase of resolving power of optical system forming averaged monochromatic images 13 p2062 N85-23003

Dependence of parameters of silicon photovoltaic cells on temperature and light intensity 14 p2275 N85-24094

Pursuit tracking performance and flash disruption: The effects of training the non-dominant eye on target reacquisition [AD-A153404] 17 p2999 N85-28541

Intense excitation source for high power laser [AD-A153424] 18 p3112 N85-29267

Fluctuations in light intensity during backscattering in turbulent medium 21 p3695 N85-32956

Beam potential measurement of an intense H(-) beam by use of the emissive probe technique [DE85-012671] 24 p4155 N85-35762

Connection between variations of the atmosphere temperature profile and variations of the meson component intensity [HE-3.1-12] 24 p4178 N85-35910

LUMPED PARAMETER SYSTEMS

The analysis by the lumped parameter method of blade platform friction dampers used in the high pressure fuel turbopump on the space shuttle main engine 09 p1338 N85-18417

Basic EMC (Electromagnetic Compatibility) technology advancement for C3 systems. Volume 4E: Modeling of transmission lines. A comparison of lumped-circuit iterative models and the transmission line model [AD-A150652] 14 p2291 N85-24201

LUMPING

Acoustic agglomeration methods and apparatus [NASA-CASE-NPO-15466-1] 12 p1927 N85-22104

LUNA LUNAR PROBES

U LUNIK LUNAR PROBES

LUNAR ATMOSPHERE

Investigation of the daytime lunar atmosphere [NASA-CR-175636] 14 p2440 N85-25057

LUNAR BASES

Lunar nuclear power feasibility study [NASA-CR-171831] 07 p1041 N85-16611

Impact of lunar and planetary missions on the space station [NASA-CR-171832] 08 p1106 N85-16988

Impact of lunar and planetary missions on the space station: Preliminary STS logistics report [NASA-CR-171837] 09 p1285 N85-18072

In-situ rock melting applied to lunar base construction and for exploration drilling and coring on the moon [DE85-006716] 16 p2717 N85-26770

Historical perspective on the Moon base: The British perspective [DE85-005905] 17 p2907 N85-27925

Space ventures and society long-term perspectives [NASA-CR-176012] 19 p3379 N85-30963

LUNAR CINEMATOGRAPHY

U LUNAR PHOTOGRAPHY

LUNAR COMPOSITION

NT LUNAR CORE

Is phosphorus predictably incompatible in igneous processes? 04 p0583 N85-13722

Megaregolith thickness, heat flow, and the bulk composition of the Moon 04 p0583 N85-13723

The bulk-Moon MgO/FeO ratio: A highlands perspective 04 p0583 N85-13724

Bulk composition of the Moon in the context of models for condensation in the solar nebula 04 p0583 N85-13725

Petrologic constraints on the origin of the Moon: Evidence from Apollo 14 04 p0583 N85-13726

Origin of the Moon: Constraints from volatile elements 04 p0584 N85-13727

Tests of the lunar hypothesis 04 p0584 N85-13730

On the origin of the Moon by rotational fission 04 p0587 N85-13746

An integrated dynamical and geochemical approach to lunar origin modelling 04 p0587 N85-13748

A circumterrestrial compositional filter 04 p0588 N85-13753

The origin of the Moon 04 p0588 N85-13754

Remote sensing analyses of localized lunar dark mantle deposits 13 p2195 N85-23616

Spectral reflectance studies of the Orientale basin 13 p2195 N85-23617

Landform identification on radar images 13 p2198 N85-23635

Mineralogical studies of lunar meteorites and their lunar analogs 15 p2683 N85-26572

LUNAR CORE

The size of the lunar core 04 p0581 N85-13713

On the Apollo subsatellite evidence for a lunar core 04 p0581 N85-13714

Implications of lunar palaeomagnetism for the origin of the Moon 04 p0582 N85-13717

Constraints on the origin of the Moon from molybdenum and other siderophile elements 04 p0582 N85-13718

Is phosphorus predictably incompatible in igneous processes? 04 p0583 N85-13722

Cosmogenic Na-22 and Al-26 in Luna-24 lunar drill core soil samples 13 p1981 N85-22427

Implications of convection in the Moon and the terrestrial planets 13 p2183 N85-23548

Modelling equilibrium and fractional crystallization in the system MgO-FeO-CaO-Al2O3-SiO2 13 p2184 N85-23552

Quenching effects on iron site partitioning in the Apollo 17 orange glass composition 13 p2184 N85-23553

LUNAR CRATERS

Physical and mechanical properties of lunar soil as function of specifics of relief and processes in vicinity of operation of Lunokhod-2 02 p0181 N85-11090

Directional properties of circular Maria: Interpretation in the context of a testable gravitational capture model for lunar origin 04 p0586 N85-13743

Moon 09 p1411 N85-18893

Monte Carlo modeling of lunar megaregolith development 13 p2197 N85-23627

Radar observations of fissure-fed basaltic lava flows, Craters of the Moon, Idaho 13 p2199 N85-23640

A comprehensive investigation of the dynamics of micron and submicron lunar ejecta in heliocentric space 19 p3384 N85-30994

Lunar and Martian impact basins: Exposed records of terrestrial bombardment? 21 p3721 N85-33090

LUNAR CRUST

Two lunar global asymmetries 04 p0585 N85-13734

Spectral reflectance studies on the orientale region of the Moon 06 p0888 N85-15639

The deep structure of lunar basins: Clues to the understanding of basin formation and modification 13 p2200 N85-23647

Primordial magmaspheres and their lasting consequences 22 p3857 N85-33882

LUNAR ECHOES

NT LUNAR RADAR ECHOES

LUNAR EFFECTS

NT LUNAR TIDES

Research directions in recent studies of the lunar geomagnetic effects 04 p0520 N85-13320

Daily magnetic variations at Ebro, Spain 04 p0520 N85-13325

Tidal dissipation in the Earth and Moon from lunar laser ranging 04 p0585 N85-13733

Numerical simulations of fission 04 p0585 N85-13737

LUNAR ENVIRONMENT

NT LUNAR ATMOSPHERE

LUNAR EVOLUTION

Conference on the Origin of the Moon [NASA-CR-174088] 04 p0581 N85-13709

Geophysical and geochemical constraints favoring the capture hypothesis 04 p0581 N85-13710

Lunar magma ocean and its implication for origin of the Moon 04 p0581 N85-13711

The initial thermal state of the Moon 04 p0581 N85-13712

Lunar magnetic history 04 p0582 N85-13715

Magnetic constraints on early lunar evolution revisited: Limits on accuracy imposed by methods of paleointensity measurements 04 p0582 N85-13716

Implications of lunar palaeomagnetism for the origin of the Moon 04 p0582 N85-13717

Constraints on the origin of the Moon from molybdenum and other siderophile elements 04 p0582 N85-13718

Nickel-cobalt systematics and their bearing on lunar origin 04 p0582 N85-13719

Ge abundances in the lunar mantle and implications for the origin of the Moon 04 p0582 N85-13721

Megaregolith thickness, heat flow, and the bulk composition of the Moon 04 p0583 N85-13723

The bulk-Moon MgO/FeO ratio: A highlands perspective 04 p0583 N85-13724

Bulk composition of the Moon in the context of models for condensation in the solar nebula 04 p0583 N85-13725

Petrologic constraints on the origin of the Moon: Evidence from Apollo 14 04 p0583 N85-13726

Origin of the Moon: Constraints from volatile elements 04 p0584 N85-13727

Volatile elements in and on lunar volcanic glasses: What do they tell us about lunar genesis?
04 p0584 N85-13728
Tests of the lunar hypothesis
04 p0584 N85-13730
Constraints on lunar origin: Evidence preserved in Precambrian stromatolites 04 p0584 N85-13731
Numerical simulations of fission
04 p0585 N85-13737
The dynamic fission instability and the origin of the Moon 04 p0586 N85-13738
Tidal disruption and the origin of the Moon
04 p0586 N85-13739
A numerical investigation of planetesimal collision trajectories with a Moon accumulating in Earth orbit
04 p0586 N85-13740
Stochastic does not equal ad hoc — theories of lunar origin 04 p0586 N85-13741
A testable gravitational capture model for the origin of the Earth's Moon 04 p0586 N85-13742
Directional properties of circular Maria: Interpretation in the context of a testable gravitational capture model for lunar origin 04 p0586 N85-13743
The problem of iron partition between Earth and Moon during simultaneous formation as a double planet system 04 p0587 N85-13744
Origin of the Moon 04 p0587 N85-13745
On the origin of the Moon by rotational fission
04 p0587 N85-13746
Geochemical evidence for the formation of the Moon by impact induced fission of the proto-Earth
04 p0587 N85-13747
An integrated dynamical and geochemical approach to lunar origin modelling 04 p0587 N85-13748
Lunar origin: role of giant impacts
04 p0587 N85-13749
Models of angular momentum input to a circumterrestrial swarm from encounters with heliocentric planetesimals
04 p0587 N85-13750
Capture of planetesimals into a circumterrestrial swarm 04 p0588 N85-13751
The lunar angular momentum problem
04 p0588 N85-13752
The origin of the Moon 04 p0588 N85-13754
Formation of the prelunar accretion disk
04 p0588 N85-13755
Mechanical models of close approaches and collisions of large protoplanets 04 p0588 N85-13756
Lunar origin from impact on the Earth
04 p0588 N85-13757
Moon 09 p1411 N85-18893
Lunar origin: Role of giant impacts
13 p2179 N85-23519
Implications of convection in the Moon and the terrestrial planets 13 p2183 N85-23546
Modelling equilibrium and fractional crystallization in the system MgO-FeO-CaO-Al2O3-SiO2
13 p2184 N85-23552

LUNAR EXPLORATION
Mission science value-cost savings from the Advanced Imaging Communication System (AICS)
[NASA-CR-174170] 04 p0456 N85-12905
Concept and cost analysis of an orbiting lunar station
[ILR-MITT-138] 07 p0913 N85-15776
A new look at the planets — space probes
[AERONOMICA-ACTA-37-1984]
11 p1765 N85-21096
In-situ rock melting applied to lunar base construction and for exploration drilling and coring on the moon
[DE85-006716] 16 p2717 N85-26770
Surface exploration geophysics applied to the Moon
[DE85-006714] 16 p2884 N85-27793

LUNAR GEOLOGY
NT LUNAR CORE
Physical and mechanical properties of lunar soil as function of specifics of relief and processes in vicinity of operation of Lunokhod-2 02 p0161 N85-11090
Volatile elements in and on lunar volcanic glasses: What do they tell us about lunar genesis?
04 p0584 N85-13728
On the origin of the Moon by rotational fission
04 p0587 N85-13746
Moon 09 p1411 N85-18893
Why not a constant early lunar impact rate?
13 p2181 N85-23536
Correction and geological analysis of lunar 3.8 cm radar data 13 p2198 N85-23634
Closer look at lunar volcanism
[DE85-006663] 15 p2683 N85-26576
Adsorption of Hg on lunar samples
[DE85-007948] 17 p3054 N85-28906

LUNAR IONOSPHERE
U LUNAR ATMOSPHERE

LUNAR MAGNETIC FIELDS
Research directions in recent studies of the lunar geomagnetic effects 04 p0520 N85-13320
Lunar magnetic history 04 p0582 N85-13715
Magnetospheres in the solar system
12 p1954 N85-22274
Magnetic field generation in the cores of terrestrial bodies 22 p3859 N85-33894

LUNAR MANTLE
Nickel-cobalt systematics and their bearing on lunar origin 04 p0582 N85-13719
Abundancies of Ni, Cr, CO and major elements in the silicate portion of the Moon: Constraints from primary lunar magmas 04 p0582 N85-13720
Remote sensing analyses of localized lunar dark mantle deposits 13 p2195 N85-23616
The deep structure of lunar basins: Clues to the understanding of basin formation and modification
13 p2200 N85-23647

LUNAR MAPS
A unified lunar control network
13 p2203 N85-23669

LUNAR MARIA
Two lunar global asymmetries
04 p0585 N85-13734
Directional properties of circular Maria: Interpretation in the context of a testable gravitational capture model for lunar origin 04 p0586 N85-13743
Moon 09 p1411 N85-18893

LUNAR OCCULTATION
NT SOLAR ECLIPSES

LUNAR ORBITS
Implications of lunar palaeomagnetism for the origin of the Moon 04 p0582 N85-13717
Constraints on the origin of viscoelastic bodies
04 p0584 N85-13732
Tidal dissipation in the Earth and Moon from lunar laser ranging 04 p0585 N85-13733
The Moon's orbit history and inferences on its origin
04 p0585 N85-13735
A testable gravitational capture model for the origin of the Earth's Moon 04 p0586 N85-13742
Telescope in lunar orbit 15 p2682 N85-26568

LUNAR PERTURBATION
U LUNAR EFFECTS

LUNAR PHOTOGRAPHY
A unified lunar control network
13 p2203 N85-23669

LUNAR PROBES
NT LUNIK LUNAR PROBES

LUNAR PROGRAMS
NT APOLLO PROJECT

LUNAR RADAR ECHOES
Landform identification on radar images
13 p2198 N85-23635

LUNAR RADIATION
Natural interference phenomena affecting spaceborne receivers
[NASA-CR-174256] 07 p0916 N85-15798

LUNAR ROCKS
Is phosphorus predictably incompatible in igneous processes? 04 p0583 N85-13722
Megaregolith thickness, heat flow, and the bulk composition of the Moon 04 p0583 N85-13723
The bulk-Moon MgO/FeO ratio: A highlands perspective 04 p0583 N85-13724
Petrologic constraints on the origin of the Moon: Evidence from Apollo 14 04 p0583 N85-13726
Origin of the Moon: Constraints from volatile elements 04 p0584 N85-13727
The influence of gravitational body force in meteoritic chondrule and lunar glass formation
06 p0884 N85-15614
Asteroid-meteorite connection: Regolith effects implied by lunar reflectance spectra 06 p0888 N85-15640
Mineralogical investigations of lunar samples and meteorites
[NASA-CR-174291] 08 p1258 N85-17918
Quenching effects on iron site partitioning in the Apollo 17 orange glass composition 13 p2184 N85-23553
Experimental methods for quenching structures in lunar-analog silicate melts: Variations as a function of quench media and composition
13 p2184 N85-23554
Electrolysis of simulated lunar melts
15 p2681 N85-26561
Mineralogical studies of lunar meteorites and their lunar analogs 15 p2683 N85-26572
Microwave processing of lunar materials: Potential applications
[DE85-007223] 16 p2755 N85-27003
Mechanical properties of lunar materials under anhydrous, hard vacuum conditions: Applications of lunar glass structural components
[DE85-006682] 16 p2801 N85-27271

LUNAR ROTATION
The dynamic fission instability and the origin of the Moon 04 p0586 N85-13738

LUNAR ROVING VEHICLES
NT LUNOKHOD LUNAR ROVING VEHICLES

LUNAR SATELLITES
NT IMP
Concept and cost analysis of an orbiting lunar station
[ILR-MITT-138] 07 p0913 N85-15776

LUNAR SCATTERING
U DIFFUSE RADIATION
U LUNAR RADAR ECHOES

LUNAR SHELTERS
In-situ rock melting applied to lunar base construction and for exploration drilling and coring on the moon
[DE85-006716] 16 p2717 N85-26770

LUNAR SOIL
Physical and mechanical properties of lunar soil as function of specifics of relief and processes in vicinity of operation of Lunokhod-2 02 p0161 N85-11090
Constraints on the origin of the Moon from molybdenum and other siderophile elements
04 p0582 N85-13718
Ge abundances in the lunar mantle and implications for the origin of the Moon 04 p0582 N85-13721
The bulk-Moon MgO/FeO ratio: A highlands perspective 04 p0583 N85-13724
Solar cosmic ray produced neon in lunar soils and their implication for gas-rich meteorite studies
06 p0887 N85-15[illegible]
Asteroid-meteorite connection: Regolith effects implied by lunar reflectance spectra 06 p0888 N85-15640
Cosmogenic Na-22 and Al-26 in Luna-24 lunar drill core soil samples 13 p1961 N85-22427
Electrolysis of simulated lunar melts
15 p2681 N85-26561
In-situ rock melting applied to lunar base construction and for exploration drilling and coring on the moon
[DE85-006716] 16 p2717 N85-26770

LUNAR SPACECRAFT
NT APOLLO SPACECRAFT
NT LUNAR SATELLITES
NT LUNIK LUNAR PROBES

LUNAR SURFACE
An error analysis for the use of presently available lunar radio flux data in broadbeam antenna-system measurements
[PB84-218361] 01 p0016 N85-10097
Geophysical and geochemical constraints favoring the capture hypothesis 04 p0581 N85-13710
Lunar magma ocean and its implication for origin of the Moon 04 p0581 N85-13711
The initial thermal state of the Moon
04 p0581 N85-13712
Moon 09 p1411 N85-18893
Why not a constant early lunar impact rate?
13 p2181 N85-23536
Morphology and mechanics of terraces in lunar craters
13 p2182 N85-23543
Quenching effects on iron site partitioning in the Apollo 17 orange glass composition 13 p2184 N85-23553
Remote sensing analyses of localized lunar dark mantle deposits 13 p2195 N85-23616
Spectral reflectance studies of the Orientale basin
13 p2196 N85-23617
Monte Carlo modeling of lunar megaregolith development 13 p2197 N85-23627
Mechanisms of basalt-plains ridge formation
13 p2199 N85-23643
On the absence of strike-slip faults from the planets and satellites 13 p2200 N85-23645
The deep structure of lunar basins: Clues to the understanding of basin formation and modification
13 p2200 N85-23647
Some new photometric data form panoramic pictures taken by Lunokhod-2 15 p2461 N85-25312
Telescope in lunar orbit 15 p2682 N85-26568
Closer look at lunar volcanism
[DE85-006663] 15 p2683 N85-26576
Lunar and Martian impact basins: Exposed records of terrestrial bombardment? 21 p3721 N85-33[illegible]
High-energy neutrinos from a lunar observatory
[HE-5.3-21] 24 p4207 N85-36112

LUNAR SURFACE VEHICLES
NT LUNOKHOD LUNAR ROVING VEHICLES

LUNAR TEMPERATURE
The initial thermal state of the Moon
04 p0581 N85-13712

LUNAR TIDES
Tidal dissipation in the Earth and Moon from lunar laser ranging 04 p0585 N85-13733
The Moon's orbit history and inferences on its origin
04 p0585 N85-13735

LUNAR TOPOGRAPHY
Monte Carlo modeling of lunar megaregolith development 13 p2197 N85-23627

LUNGS
Oxygen delivery during exercise: Limitations to maximum flow 05 p0686 N85-14424

Interaction between lung mechanics and gas exchange by low volume high frequency pulmonary ventilation in patients with respiratory failure
[AD-A146604] 06 p0846 N85-15372
Chemical characterization and toxicologic evaluation of airborne mixtures. Inhalation toxicology of diesel fuel obscurant aerosol in Sprague-Dawley rats. Phase 3. Subchronic exposures
[AD-A150100] 12 p1905 N85-21966
Aerosol deposition along the respiratory tract at zero gravity: A theoretical study
[DE85-006703] 15 p2619 N85-26136
Carcinogenesis of nitrated toluenes and benzenes skin and lung tumor assays in mice
[AD-A155723] 22 p3818 N85-33655
LUNIK LUNAR PROBES
Cosmogenic Na-22 and Al-26 in Luna-24 lunar drill core soil samples 13 p1961 N85-22427
LUNOKHOD LUNAR ROVING VEHICLES
Some new photometric data form panoramic pictures taken by Lunokhod-2 15 p2481 N85-25312
LUTETIUM
Debye temperature and static displacements in LuH sub x single crystals from energy dispersive X-ray diffraction
[DE85-010961] 19 p3376 N85-30946
LUTETIUM COMPOUNDS
Electrochemistry of rare-earth diphthalocyanines
[AD-A145813] 03 p0327 N85-12106
LYAPUNOV FUNCTIONS
U LIAPUNOV FUNCTIONS
LYMAN ALPHA RADIATION
Lyman-Alpha aurora 02 p0302 N85-11953
Temporal and spatial variations in the intensity of ultraviolet emissions from Jupiter and the Io torus
03 p0448 N85-12646
Pioneer 10 and Voyager observations of the interstellar medium in scattered emission of the He 584 A and H Lya 1216 A lines 06 p0673 N85-15541
Changes of LISM characteristics in the heliospheric interface 06 p0673 N85-15542
Observations of interstellar HI toward nearby late-type stars 06 p0674 N85-15546
Radio and UV observations of high latitude HI
06 p0679 N85-15583
Lyman alpha coronagraph research sounding rocket program
[NASA-CR-174376] 09 p1354 N85-18517
MSG-7: Atmospheric penetration of solar radiation in the range of Schumann-Runge bands
11 p1657 N85-20443
Ionospheric absorption on 1539 kHz in relation to solar ionizing radiation 11 p1659 N85-20455
Aeronomical aspects of mesospheric photodissociation: Processes resulting from the solar H Lyman alpha line
[AERONOMICA-ACTA-A-285-1984]
11 p1680 N85-20587
Analysis of white dwarf Lyman alpha profiles
11 p1752 N85-21018
The extent of the local hi halo
[NASA-CR-176115] 23 p3987 N85-34724
On the detectability of key-MeV solar protons through their nonthermal Lyman-alpha emission
[SH-1.3-5] 23 p3993 N85-34752
LYMAN SPECTRA
Lyman-Alpha aurora 02 p0302 N85-11953
Studies of hot B subdwarfs. Part 2: Energy distributions of three bright sdB/sdOB stars in the 950-5500 angstrom range
[NASA-CR-175654] 16 p2881 N85-27775
LYMPH
NT LYMPHOCYTES
LYMPHOCYTES
Experiment 1ES031 on Spacelab 1: Are cells sensitive to gravity? — lymphocyte proliferation
05 p0689 N85-14428
H1-NMR studies on lymphocyte membranes in human lymphoproliferative diseases 20 p3505 N85-31787
The DNA metabolism and poly-(ADP-ribose) synthesis in lymphocytes of persons exposed to low doses of ionizing radiation
[OEFZS-4307] 20 p3507 N85-31800
Sensitivity of human lymphocytes to microgravity in-vitro 20 p3510 N85-31820
Non-rigid body motion 23 p3964 N85-34576
LYOPHILIZATION
U COLLOIDING
LYOPHILS
U COLLOIDS
LYRA CONSTELLATION
Observations of RR Lyrae and X Arietis with the IUE satellite 11 p1754 N85-21030
LYSIMETERS
Field lysimeter facility for evaluating the performance of commercial solidified low-level waste
[DE85-003666] 11 p1727 N85-20863

M

M REGION
The distribution and dynamics of planetary nebulae in M32 and the Andromeda Galaxy
20 p3546 N85-32068
Isotopic overabundances and the energetic particle model of solar flares
[SH-2.2-1] 23 p4000 N85-34796
M STARS
NT FLARE STARS
Theoretical studies of chromospheres and winds in cool stars
[NASA-CR-174204] 06 p0880 N85-15596
Theory tested by means of the stars — viability of the alpha-omega dynamo model 08 p1233 N85-17770
M WINGS
U VARIABLE SWEEP WINGS
MAARS
U CRATERS
MACH NUMBER
Wind tunnel tests on a tube-launched missile configuration with a deflectable nose control and a novel wrap-around fin stabiliser
[AR-003-696] 01 p0001 N85-10003
Effect of upstream sidewall boundary layer removal on an airfoil test — conducted in Langley 0.3-m transonic cryogenic tunnel 03 p0313 N85-12019
Progress in wind tunnel wall interference assessment/correction procedures at the NAE
03 p0314 N85-12025
Space Shuttle Orbiter trimmed center-of-gravity extension study. Volume 8: Effects of configuration modifications on the aerodynamic characteristics of the 140 A/B Orbiter at a Mach number of 5.97
[NASA-TM-72661-VOL-8] 04 p0452 N85-12867
Comparison of analytical and experimental steadyand unsteady-pressure distributions at Mach number 0.78 for a high-aspect-ratio supercritical wing model with oscillating control surfaces
[NASA-TM-84589] 07 p0899 N85-15697
Joined wing transonic design and test validation
[AD-A148355] 08 p1078 N85-16834
Exploratory investigation of the aerodynamic characteristics of a biwing vehicle at Mach 20.3
[NASA-TM-86314] 08 p1113 N85-17021
Unsteady stall penetration of an oscillating swept wing
[AD-P004156] 09 p1264 N85-17941
Mach-10 high Reynolds number development in the NSWC (Naval Surface Weapons Center) hypervelocity facility
[AD-A151241] 15 p2474 N85-25274
Measurements of the symmetric aerodynamic coefficients for flat faced cylinders in the angle of attack regime 0 to 90 deg for transonic and supersonic speeds
[FFA-TN-1984-04] 16 p2700 N85-26675
On power effecient operation of the 2m x 2m transonic wind tunnel at the National Aerospace Laboratory
[NAL-TR-847] 18 p3064 N85-28953
Development of a temperature-compensated hot-film anemometer system for boundary-layer transition detection on high-performance aircraft
[NASA-TM-86732] 22 p3730 N85-33121
An evaluation of three helicopter rotor sections
[NASA-TM-86719] 23 p3893 N85-34115
Unsteady flow in a supersonic cascade with two in-passage shocks
[NASA-CR-3925] 24 p4060 N85-35158
MACH REFLECTION
Experimental study of Mach reflection of weak shock waves 02 p0260 N85-11703
Pseudo-stationery oblique-shock-wave reflections in a polyatomic gas, sulfur hexafluoride
[UTIAS-TN-253] 12 p1845 N85-21577
Tabular and graphical solutions of regular and Mach reflections in pseudo-stationery frozen and vibrational-equilibrium flows, part 1
[UTIAS-283-PT-1] 23 p3893 N85-34117
Tabular and graphical solutions of regular and Mach reflections in pseudo-stationery frozen and vibrational-equilibrium flows, part 2
[UTIAS-283-PT-2] 23 p3894 N85-34118
MACHINE LEARNING
U LEARNING MACHINES
MACHINE LIFE
U SERVICE LIFE
MACHINE RECOGNITION
U ARTIFICIAL INTELLIGENCE
MACHINE STORAGE
U COMPUTER STORAGE DEVICES
MACHINE TOOLS
NT BORING MACHINES
NT GRINDING MACHINES
NT LATHES
NT MILLING MACHINES
NT TURRET LATHES
USSR report: Machine tools and metalworking equipment
[JPRS-UMM-84-019] 01 p0035 N85-10214
Report on high-precision jig-boring machines
01 p0035 N85-10215
The US machine tool industry and the defense industrial base
[PB84-216928] 01 p0036 N85-10225
Use of robotics in heavy machinery, equipment construction industry 04 p0485 N85-13093
USSR report: Machine tools and metalworking equipment
[JPRS-UMM-84-020] 04 p0491 N85-13126
DNC, CNC network for robotized machining cells
04 p0491 N85-13130
Advances of implementing NC machine tools discussed 04 p0491 N85-13131
Thermal shock as a carbide grade development tool
[DE84-016939] 04 p0509 N85-13251
Modular laser distance measurement system for multiaxis machine tools
[BMFT-FB-T-84-166] 05 p0641 N85-14110
Efficiency of programmed motion control systems
06 p0776 N85-14961
East Europe report: Science and technology
[JPRS-ESA-84-045] 06 p0815 N85-15175
New concepts for industrial robots outlined
06 p0815 N85-15176
Machine tools at 1984 Leipzig Spring Fair
06 p0815 N85-15177
NC programming, machine tool information
06 p0816 N85-15178
Laser-guided measuring system for precisioning device 06 p0816 N85-15179
Power of deterministic thinking in machine tool accuracy
[DE85-001751] 07 p0974 N85-16188
USSR report: Machine tools and metalworking equipment
[JPRS-UMM-84-021] 08 p1138 N85-17168
Technology planning for flexible manufacturing systems 08 p1139 N85-17170
USSR report: Machine tools and metalworking equipment
[JPRS-UMM-85-001] 08 p1139 N85-17172
Structure of solids surfaces in wear situations
[AD-A148480] 08 p1168 N85-17366
Airport ground equipment under development at Riga
09 p1278 N85-18038
Scania, ASEA of Sweden use robots for all production phases 09 p1310 N85-18229
The control of manufacturing systems for varying medium-batch production
[PNR-90235] 09 p1371 N85-18616
State and development of the machine-tool industry in Japan. Part 2: Flexible manufacturing systems
[PNR-90236-PT-2] 09 p1371 N85-18617
New method for heat treatment of metals
10 p1446 N85-19110
East Europe report: Science and technology
[JPRS-ESA-85-008] 10 p1460 N85-19200
National Machine Tools Conference slated for 1985: Conference agenda, papers 10 p1460 N85-19202
USSR report: Machine tools and metalworking equipment
[JPRS-UMM-85-003] 10 p1461 N85-19211
Armenia markets new drive motors for machine tools
10 p1461 N85-19212
Dean of Kiev State University on impact of robots
10 p1461 N85-19213
Specifications, applications of gantry robots viewed
10 p1461 N85-19215
Control system of complex CNC machining cell
10 p1462 N85-19218
Productivity gains through CAD of CNC programs
10 p1462 N85-19219
USSR report: Materials science and metallurgy
[JPRS-UMS-84-005] 11 p1597 N85-20044
East Europe report: Science and technology
[JPRS-ESA-85-009] 11 p1616 N85-20165
Institute director surveys industrial automation drive
11 p1617 N85-20167
Increased use of CNC in machine tool construction
11 p1617 N85-20170
New CNC systems described
11 p1617 N85-20172
Technological and economic assessment of advanced ceramic materials: Volume 4: A case study of integrated optic devices
[PB85-113116] 12 p1815 N85-21385
Technological and economic assessment of advanced ceramic materials. Volume 6: A case study of ceramic cutting tools
[PB85-113132] 12 p1815 N85-21387
Development of a sintered shim
[DE85-006183] 13 p2025 N85-22685

Rational use of tatanium in nonferrous metallurgy
13 p2031 N85-22728

New technique for fluid feed in simultaneous multisurface grinding 13 p2045 N85-22800

USSR report: Machine tools and metalworking equipment
[JPRS-UMM-85-005] 13 p2051 N85-22839

Diamond cutters' grinders 13 p2051 N85-22841

Machine tool vibrations: A review
13 p2102 N85-23104

USSR report: Engineering and equipment
[JPRS-UEQ-84-001] 14 p2266 N85-24034

Small-size measuring gauges for metal cutting machine tools 14 p2267 N85-24045

Fabrication of turbine parts with transportable tools
14 p2267 N85-24046

Novel drives for machine tools
14 p2268 N85-24053

Use of program controlled machine tools to automate and mechanize production processes in pipe manufacture 14 p2269 N85-24059

USSR report: Machine tools and metalworking equipment
[JPRS-UMM-85-006] 14 p2283 N85-24146

Metal waste in machine tool industry examined
14 p2283 N85-24147

New CNC turning centers described
14 p2284 N85-24148

Large CNC machining center for turbine production
14 p2284 N85-24149

Minister B. V. Balmont on status of automation drive
14 p2284 N85-24151

USSR report: Machine tools and metalworking equipment
[JPRS-UMM-85-004] 14 p2284 N85-24152

Integrated control system for FMS components
14 p2285 N85-24156

Cutting structural materials in vacuum
14 p2286 N85-24165

Automating the study of error in discrete aerodynamic fairing design 14 p2288 N85-24176

An analysis of machine tool systems suitable for laser profiling 14 p2306 N85-24282

Robotic deburring. Part 2: Evaluation of cutters and noncompliant tooling
[DE85-006182] 14 p2311 N85-24308

Electrical features of new DNC, CNC system viewed — direct numerical control 15 p2524 N85-25562

Flexible machining systems described
15 p2524 N85-25563

USSR report: Machine tools and metalworking equipment
[JPRS-UMM-84-010] 16 p2767 N85-27071

Status, prospects of computer-aided design discussed
16 p2767 N85-27073

New robotized, vertical broaching machine featured
16 p2767 N85-27074

Guidelines for optimization of robotized machining cells 16 p2767 N85-27076

East Europe report: Science and technology
[JPRS-ESA-85-019] 16 p2767 N85-27077

Extreme evaluation of reliability indices for components of metallurgical equipment
[BLL-M-36070-(5828.4)] 16 p2786 N85-27234

Steels with improved machinability
[BLL-BISI-22341-(9022.06)] 17 p2927 N85-28061

USSR report: Machine tools and metalworking equipment
[JPRS-UMM-84-014] 17 p2946 N85-28186

Applications of robots in machine tool industry reviewed 17 p2946 N85-28189

Manufacturing information system
[AD-A152715] 17 p3011 N85-28616

Spiral bevel and circular arc helical gears: Tooth contact analysis and the effect of misalignment on circular arc helical gears
[NASA-TM-87013] 20 p3395 N85-31060

USSR report: Machine tools and metalworking equipment
[JPRS-UMM-85-008] 20 p3437 N85-31329

Standard series of direct-current motors for regulated electric drives 22 p3772 N85-33375

Generation of round bores in composite structure railguns
[DE85-011672] 22 p3793 N85-33501

Properties of tungsten-free steel for cutting tools
[BLL-M-36606-(5828.4)] 23 p3915 N85-34259

Generated spiral bevel gears: Optimal machine-tool settings and tooth contact analysis
[NASA-TM-87075] 23 p3937 N85-34405

MACHINE TRANSLATION

An operational system for subject switching between controlled vocabularies: A computational linguistics approach
[NASA-CR-3838] 02 p0293 N85-11903

Graphics translators for computer-aided drafting and design: Interface alternatives for the A/E community
[AD-A148892] 10 p1540 N85-19706

Developing an automated technique for translating a relational database into an equivalent network one
[AD-A151844] 15 p2666 N85-26451

Expressiveness and language choice
[AD-A153280] 17 p3012 N85-28623

Local automation model software benchmarking: Test plan
[AD-A154349] 19 p3337 N85-30676

MACHINE-INDEPENDENT PROGRAMS

Machine computation of delay and capacitance of transistor structures of subnanosecond large integrated circuits 04 p0490 N85-13120

MACHINING

NT CHEMICAL MACHINING
NT ELECTROCHEMICAL MACHINING
NT MILLING (MACHINING)
NT SPARK MACHINING

Three-dimensional photochemical machining with lasers
[AD-A145792] 03 p0365 N85-12342

DNC, CNC network for robotized machining cells
04 p0491 N85-13130

Design of a flexible machining system
[CETIM-1-3E-140] 04 p0510 N85-13252

USSR report: Machine tools and metalworking equipment
[JPRS-UMM-84-021] 08 p1138 N85-17168

Survey of the finish characteristics of machined optical surfaces
[DE85-001343] 09 p1365 N85-18708

National Machine Tools Conference slated for 1985: Conference agenda, papers 10 p1460 N85-19202

Production turret lathe retrofitted with robot
10 p1461 N85-19214

Evaluation of machining damage in brittle materials
[DE85-001794] 11 p1612 N85-20136

Nondestructive method for detecting machine damage in beryllium
[DE85-001074] 12 p1862 N85-21681

Use of ferrofluids in machining of metals
13 p2045 N85-22802

USSR report: Machine tools and metalworking equipment
[JPRS-UMM-85-005] 13 p2051 N85-22839

T700 cutter life improvement program
[AD-A150450] 13 p2099 N85-23089

Technology for pressure-instrumented thin airfoil models, phase 1
[NASA-CR-3891] 14 p2227 N85-23804

Group technology for working turbine drive wheel disks 14 p2269 N85-24061

An analysis of machine tool systems suitable for laser profiling 14 p2306 N85-24282

Influence of phosphorus content and heat treatment on the machinability of electroless nickel deposits
[DE85-007250] 15 p2522 N85-25548

Steels with improved machinability
[BLL-BISI-22341-(9022.06)] 17 p2927 N85-28061

Study of a simulated test for assessing the machinability of steels
[BLL-BISI-TRANS-22344-(9022.06)]
17 p2972 N85-28357

Study of a test method for assessing machinability in gear cutting operations
[BLL-BISI-TRANS-22345-(9022.06)]
17 p2972 N85-28359

Examples of application of machinability tests
[BLL-BISI-TRANS-22346-(9022.06)]
17 p2973 N85-28363

Assessing the machinability of gearwheel steels during manufacture
[BLL-BISI-TRANS-22343-(9902.06)]
17 p2973 N85-28365

Europe's primary producers of industrial lasers surveyed 18 p3087 N85-29101

Laser machining and some applications
[NHK-LABS-NOTE-307] 18 p3112 N85-29266

Machining of beryllium with the LLNL precision engineering research lathe
[DE85-010632] 19 p3250 N85-30149

Metallographic preparation of materials with various coatings
[BLL-DRIC-TRANS-7522-(3623.66)]
20 p3433 N85-31299

Machining-induced deformation in stepped specimens of PH 13-8 Mo, 18 nickel maraging steel grade 200T1 and grain-refined HP 9-4-20
[NASA-CR-172450] 21 p3565 N85-32177

Method of precisely modifying predetermined surface layers of a workpiece by cluster ion impact therewith
[DE85-006519] 23 p3984 N85-34710

Single-point diamond crushing of Zerodur with in polishing and metrology on a diamond turning machi
[DE85-012918] 24 p4083 N85-

MACROCLIMATE

U CLIMATE

MACROMOLECULES

U MOLECULES

MACULAR VISION

U VISION

MAGELLANIC CLOUDS

Studies of extragalactic RR Lyrae stars
03 p0444 N85-1

On the scale of distances of the galaxy
05 p0737 N85-147

Optical studies of X-ray selected Active Galactic Nucl (AGN) in the direction of the Large Magellanic Clo (LMC) 08 p1237 N85-177

Far IR observations of the Magellanic clouds
08 p1248 N85-178

Magellanic cloud objects 11 p1744 N85-20

Highly ionized gas associated with the small Magellanic cloud 11 p1745 N85-20

Galactic absorption lines measured from the IUE low dispersion spectra of active galaxies
11 p1745 N85-20

IUE observations of planetary nebulae in the Magellanic Clouds 11 p1747 N85-20

The UV extinction laws in two very young clusters, NGC 6530 in the galaxy and NGC 2100 in the LMC
11 p1748 N85-20

Ultraviolet studies of the young populous cluster NGC 2100 in the LMC 11 p1748 N85-20

All-Union conference of radio astronomers
13 p1977 N85-224

Optical pulsar in the Large Magellanic Cloud remnant 0540-69.3
[DE85-006707] 16 p2883 N85-277

MAGMA

Lunar magma ocean and its implication for origin of the Moon 04 p0581 N85-13711

Abundancies of Ni, Cr, CO and major elements in the silicate portion of the Moon: Constraints from primary lunar magmas 04 p0582 N85-13726

Two lunar global asymmetries
04 p0585 N85-13734

Petrology and petrogenesis of Batholitic rocks, San Jacinto Mountains, southern California
05 p0673 N85-1432

Extreme incompatibility of Pb during the crystallization of magmatic iron meteorites 06 p0886 N85-1582

Correlation and petrological interpretation of abyssal and terrestrial tephra layers 09 p1353 N85-1861

Physical characterization of magma
[DE85-000566] 09 p1354 N85-1861

Vertical movements and structure formation within island systems of northeast Asia 10 p1501 N85-1947

Mesozoic magmatism of Mongolian-Okhotsk Belt and its possible geodynamic interpretation
10 p1502 N85-194

High-resolution microseismicity study of possible magmatic intrusion in the Long Valley Caldera
[DE85-001076] 11 p1681 N85-205

Shallow magma targets in the western US
[DE85-003274] 12 p1881 N85-216

Magmatism in continent-ocean transition zone (development of ideas of A. N. Zavaritskiy)
13 p2113 N85-231

Thermohydrodynamic model: Hydrothermal system, shallowly seated magma chamber
13 p2115 N85-231

Io: Generation of silicate magma by shear melting at the base of a basaltic lithosphere
13 p2172 N85-234

Characteristics of basaltic lava flows on Venus
13 p2177 N85-235

Modelling equilibrium and fractional crystallization in the system MgO-FeO-CaO-Al2O3-SiO2
13 p2184 N85-235

Magmas as selective filters of volatiles between planetary mantles and surfaces
13 p2185 N85-235

Volcanism of the Colorado Plateau (basin and range transition): Implications for crustal processes
13 p2187 N85-235

A silicic shield volcano in Bolivia
13 p2187 N85-235

Hydrovolcanism 13 p2188 N85-235

What we know about Mars (but otherwise wouldn't) if it is the shergottite parent body
15 p2582 N85-25

Selection of promising sites for magma energy experiments
[DE85-006832] 16 p2820 N85-27

Melt zones beneath five volcanic complexes in California: An assessment of shallow magma occurrences
[DE85-010844] 19 p3305 N85-30489
Anorthositic oceanic crust in the Archean Earth
21 p3719 N85-33077
Earth's primordial differentiation, and its after-effects
21 p3722 N85-33092
Primordial magmaspheres and their lasting consequences 22 p3857 N85-33882
Geochemical confirmation of the lunar magmasphere hypothesis 22 p3859 N85-33895
Heat transfer and brine evolution in magma-hydrothermal systems 24 p4104 N85-35441
Ore genesis at the Monterrosas deposit in the Coastal Batholith, Ica, Peru 24 p4115 N85-35510

MAGNESIUM
NT MAGNESIUM ISOTOPES
Universal binding energy relations in metallic adhesion
[NASA-TM-86869] 03 p0331 N85-12132
Strong-coupling superconductivity of Mg in proximity to Ta
[DE84-015462] 04 p0569 N85-13627
Testing of production of silicon-titanium-magnesium alloying composition
[BLL-M-35904-(5828.4)] 05 p0616 N85-13937
Observations of local interstellar Mg I and Mg II
06 p0874 N85-15547
Mg II spectra of late type stars used to probe the LISM 06 p0874 N85-15548
FeII and MgII in the nearby interstellar medium
06 p0874 N85-15549
Minor elements and cathodoluminescence of Mg-rich olivines from Murchison and Allende carbonaceous meteorites 06 p0884 N85-15619
Combustion properties of fuel-rich magnesium propellants with HTPB as binder
[FOA-C-20555-D1] 07 p0935 N85-15924
Structure of transient zone in diffusion welding of TsTS-19 piezoceramic with AMg6 alloy
11 p1603 N85-20082
Observations of Mg 1 and Mg 2 in the local ISM
11 p1748 N85-20997
Mg 2 emission of Pop. 2 long-period Cepheids
11 p1754 N85-21032
Ultraviolet, radio and X-ray observations of hybrid stars 11 p1759 N85-21063
Structural strenght of strip D16T aluminum alloy with low copper and magnesium content
13 p2025 N85-22691
New deformable secondary aluminum alloys
13 p2026 N85-22694
The effect of microalloying with calcium and magnesium on the plasticity of Poldi AKN 20 Ni-based alloy
[BLL-BISI-TRANS-2174-(9022.06)]
17 p2929 N85-28075
Effect of periodic accelerations on physiochemical properties and Ca2+ reactivity of actomyosin in white rat myocardium and skeletal muscles
19 p3324 N85-30594
Measurements of Fe and Ar fragmentation cross sections
[PAPER-OG-7.2-20] 21 p3714 N85-33047
Photoionization of alkali and alkaline earth atoms: Na and Mg
[DE85-011812] 22 p3837 N85-33755
Radiation measurements on magnesium flames
[BLL-CE-TRANS-8110-(9022.09)]
24 p4075 N85-35254

MAGNESIUM ALLOYS
Relationships between electronic structure and stability of metallic glasses
[AD-A145606] 02 p0287 N85-11874
Application of the diffraction model to amorphous magnesium zinc alloys
[AD-A147369] 07 p0928 N85-15883
Influence of excess phases on fracture toughness of cast alumin-magnesium-zinc alloy
10 p1442 N85-19091
Computation of thermal shock-free straightening conditions for aluminum-magnesium alloy welded structures 10 p1449 N85-19131
Rapid solidification processing of magnesium alloys
[AD-A150270] 13 p2022 N85-22668
Influence of laser treatment of structure and mechanical properties if MA21 alloy 13 p2029 N85-22713
Problem of pore formation mechanism in welded joints of aluminum alloys in the system aluminum-magnesium-lithium 13 p2032 N85-22732
The role of hydrogen in the stress corrosion failure of high strength Al-Zn-Mg alloys
[AD-A150691] 14 p2256 N85-23976
Temperature variation of resistivity of certain alloys based on transition and simple metals in amorphous and crystalline states 15 p2496 N85-25399
Superplasticity in a thermo-mechanically processed Aluminum-10.2%Mg-0.52%Mn alloy
[AD-A152016] 15 p2510 N85-25465
Special features of the one-sided automatic welding of structures of Al-Mg alloys 16 p2792 N85-27222
Thermal expansion effects in electrical transport in amorphous metals
[AD-A152477] 17 p2930 N85-28069
Study of phase equilibria and crystallization processes in Al-Zn-Mg alloy systems 19 p3241 N85-30096
Influence of type of processing of AK4 alloy on its surface state and strength of bonding of plasma coatings
19 p3242 N85-30103
Resistance to corrosion fatigue in aluminum alloy 1561 in sea water 19 p3243 N85-30108
Atomized magnetism-aluminum protective coatings
19 p3244 N85-30116
The effect of alloy additions on superplasticity in thermomechanically processed high magnesium aluminum-magnesium alloys
[AD-A155142] 21 p3567 N85-32184

MAGNESIUM CHLORIDES
Coexistence of antiferromagnetism and spin-glass ordering in the Ising system FeO 55MgO 45Cl2
[DE85-004164] 12 p1942 N85-22197

MAGNESIUM COMPOUNDS
NT CHLOROPHYLLS
NT DOLOMITE (MINERAL)
NT ENSTATITE
NT MAGNESIUM CHLORIDES
NT MAGNESIUM FLUORIDES
NT MAGNESIUM OXIDES
Fracture toughness of MgCr(sub)2O(sub)4-ZrO(sub)2
[DE85-007945] 17 p2917 N85-27982

MAGNESIUM FLUORIDES
Peculiarities of MgF2 film formation and optimization of MgF2 film deposition process 14 p2281 N85-24132

MAGNESIUM ISOTOPES
A 200-MeV pi(+) induced nucleon removal from 24Mg
17 p3042 N85-28821

MAGNESIUM OXIDES
The bulk-Moon MgO/FeO ratio: A highlands perspective 04 p0583 N85-13724
Surface effects of corrosive media on hardness, friction, and wear of materials
[NASA-TM-83711] 07 p0930 N85-15896
Special purpose materials for fusion application
[DE85-005346] 14 p2424 N85-24950
Selective radiative cooling with MgO and/or LiF layers
[DE85-011595] 19 p3262 N85-30228
Method for the preparation of photochromic insulating crystals
[DE85-011606] 19 p3262 N85-30229

MAGNESYN (TRADEMARK)
U SERVOMOTORS

MAGNET COILS
NT FIELD COILS
Design, construction, and operational results of an 800-A, 10-kV hot deck amplifier
[DE84-014044] 04 p0496 N85-13162
Positron flux concentrator: An update
[DE84-016260] 04 p0561 N85-13576
Two-rotor alternators with superconductor field winding 06 p0795 N85-15082
Design and test of a four channel motor for electromechanical flight control actuation
[NASA-CR-171838] 08 p1156 N85-17294
Design and construction details of the FRX-C/T device: A compact toroid plasma translation experiment
[DE85-001527] 09 p1390 N85-18749
Transient voltage oscillations in coils
[DE85-006715] 15 p2550 N85-25738
Magnetics calculations for an ELMO Bumpy Square
[DE85-011436] 21 p3707 N85-33021
Series-counterpulse repetitive-pulse inductive storage circuit
[DE85-006436] 23 p3926 N85-34342

MAGNETIC ABSORPTION
U ELECTROMAGNETIC ABSORPTION

MAGNETIC ANNULAR ARC
Development of theory of high-current high-pressure pulsed arc 15 p2645 N85-26314

MAGNETIC ANOMALIES
NT GEOMAGNETIC HOLLOW
The south-central United States magnetic anomaly
[E85-10025] 02 p0218 N85-11436
Continental and oceanic crustal magnetization modelling
[E85-10034] 03 p0378 N85-12413
Phonon anomalies in superconducting transition metal compounds -- lanthanum and niobium compounds
03 p0426 N85-12718
Petrologic model of the northern Mississippi embayment based on satellite magnetic and ground based geophysical data
[NASA-TM-85075] 04 p0533 N85-13406
Measurements of electric fields obtained by stratospheric balloons in the region of the South Atlantic anomaly
[INPE-3216-PRE/571] 05 p0675 N85-14335
Anomalous magnetic field in northwestern Pacific Ocean and Pacific Ocean plate kinematics
06 p0820 N85-15210
Correlation radius of gravitational and magnetic anomalies and methods of its determination
06 p0821 N85-15213
The mineralogy of global magnetic anomalies
[E85-10061] 07 p0987 N85-16272
Prospects and means for development of theory and practice of interpretation of gravitational and magnetic anomalies 10 p1501 N85-19474
Geological reasons for change in intensity of linear magnetic anomalies of the Kursk magnetic anomaly
[NASA-TM-77824] 10 p1514 N85-19552
Precursors for Brazilian magnetic anomalies from 1922 to 1969
[INPE-3283-PRE/605] 11 p1681 N85-20590
Structure of Iceland and ocean floor spreading
13 p2112 N85-23159
MAGSAT anomaly field data of the crustal properties of Australia
[E85-10100] 13 p2122 N85-23215
An investigation of the crustal properties of Australia and surrounding regions derived from interpretation of MAGSAT anomaly field data 13 p2122 N85-23216
Remanent magnetization model for the broken ridge satellite magnetic anomaly 13 p2123 N85-23219
System of interpretation of remote sensing data when hydrocarbons are present, volume 2
[INPE-3087-TDL/162-VOL-2] 16 p2810 N85-27326
X-ray intensification at balloon altitudes of the South Atlantic magnetic anomaly in association with geomagnetic activity
[INPE-3469-PRE/712] 16 p2827 N85-27437
Structure of Reykjanes Ridge rift zone and Icelandic thermal anomaly 19 p3289 N85-30395
Improving the geological interpretation of magnetic and gravity satellite anomalies
[E85-10103] 20 p3473 N85-31585
MAGSAT scalar anomaly map of South America
20 p3473 N85-31586
MAGSAT satellite magnetic anomaly map over South America 20 p3474 N85-31587
Geologic analysis of averaged magnetic satellite anomalies 20 p3474 N85-31588
Statistical magnetic anomalies from satellite measurements for geologic analysis
20 p3474 N85-31589
Binning of satellite magnetic anomalies
20 p3474 N85-31590
The south-central United States magnetic anomaly
20 p3474 N85-31591
The south-central United States magnetic anomaly
20 p3475 N85-31592
A comparative study of spherical and flat-Earth geopotential modeling at satellite elevations
20 p3475 N85-31593
A comparative study of spherical and flat-Earth geopotential modeling at satellite elevations
20 p3475 N85-31594
Reduced to pole long-wavelength magnetic anomalies of Africa and Europe 20 p3475 N85-31595
Euro-African MAGSAT anomaly-tectonic observations
20 p3475 N85-31596
Long-wavelength magnetic and gravity anomaly correlations on Africa and Europe
20 p3476 N85-31597
Continental and oceanic magnetic anomalies: Enhancement through GRM 20 p3476 N85-31598
Continental magnetic anomaly constraints on continental reconstruction 20 p3476 N85-31599
Regional magnetic anomaly constraints on continental rifting 20 p3476 N85-31600
A real time index of geomagnetic background noise for the MAD (Magnetic Anomaly Detection) frequency band
[AD-A155717] 22 p3814 N85-33627
Solar cycle variations of the anaomalous cosmic ray component
[SH-4.6-2] 23 p4039 N85-35040
Temporal variations of the anomalous oxygen component, 1977 - 1984
[SH-4.6-3] 23 p4039 N85-35041

MAGNETIC BEARINGS
Overview of magnetic bearing control and linearization approaches for annular magnetically suspended devices
05 p0607 N85-13872
Europeans active in magnetic bearing industry
08 p1141 N85-17196
Linear magnetic bearings
[NASA-CASE-GSC-12582-2] 11 p1641 N85-20337
A theoretical model for the study of nonlinear dynamics of magnetic bearings 20 p3482 N85-31505

MAGNETIC CHARGE DENSITY
New types of power supplies for ultrasonic processing equipment 12 p1843 N85-21566
MAGNETIC CIRCUITS
Lightweight cladding for magnetic circuits
[AD-D011409] 10 p1481 N85-19350
MAGNETIC COILS
NT FIELD COILS
Results of prototype field measurements on SM4
[NAC-83-01] 01 p0117 N85-10797
Magnetic spin reduction system for free spinning objects
[NASA-CASE-MFS-25966-1] 02 p0166 N85-11122
High-performance TF coil design for the Toroidal Fusion Core Experiment (TFCX)
[DE85-001127] 08 p1159 N85-17315
Extended abstract: Ergodic magnetic limiter experiments on TEXT with a 7/3 resonance
[DE85-001390] 09 p1391 N85-18754
Mathematical model of electromagnetic suspension device with two control windings
13 p2074 N85-22954
Outline of alternative design of R-Tokamak
15 p2654 N85-26371
Simultaneous phase and frequency control of a three-phase inductor-convertor bridge
[DE85-006197] 18 p3096 N85-29164
Physics-magnetics trade studies for tandem mirror reactors
[DE85-010043] 18 p3182 N85-29732
Recent progress in stellarator reactor conceptual design
[DE85-009592] 18 p3189 N85-29780
Magnetics calculations for an ELMO Bumpy Square
[DE85-010442] 18 p3191 N85-29782
Plasma engineering models of tandem mirror devices with high-field test-cell inserts
[DE85-010046] 18 p3192 N85-29797
TFCX shielding optimization
[DE85-010503] 19 p3359 N85-30626
MIG: MCNP Input Generator for EFFI magnet geometrics
[DE85-010494] 20 p3515 N85-31857
Assessment of magnetic field asymmetries in ELMO Bumpy square
[DE85-011905] 22 p3846 N85-33619
High-field launch electron cyclotron heating experiments in the ELMO Bumpy Torus
[DE85-012068] 22 p3846 N85-33625
Design improvements and cost reductions for a 5000 MWh superconducting Magnetic Energy Storage plant
[DE85-010572] 22 p3847 N85-33630
Reversing-counterpulse repetitive-pulse inductive storage circuit
[DE85-006409] 23 p3928 N85-34344
Apparatus for unilateral generation of a homogeneous magnetic field
[DE85-006001] 23 p3928 N85-34345
Assessment of magnetic field asymmetries in ELMO Bumpy square
[DE85-011559] 23 p3964 N85-34705
Analysis of a pulsed power system containing rotating machine
[DE85-014128] 24 p4159 N85-35786
Effect of Cu4Ti compound formation on the characteristics of NbTi accelerator magnet wire
[DE85-014226] 24 p4159 N85-35788
MAGNETIC COMPASSES
Impact of magnetic isolation on pointing system performance in the presence of structural flexibility
[NASA-CR-172481] 16 p2732 N85-26861
MAGNETIC COMPRESSION
Use of magnetic compression based on amorphous alloys as a drive for induction linacs
[DE84-014524] 02 p0277 N85-11805
Los Alamos Spheromak Program
[DE85-010748] 20 p3398 N85-31077
Magnetics calculations for an ELMO Bumpy Square
[DE85-011438] 21 p3707 N85-33021
MAGNETIC CONTROL
Magnetic spin reduction system for free spinning objects
[NASA-CASE-MFS-25966-1] 02 p0166 N85-11122
MAGNETIC COOLING
Deceleration, cooling, and trapping of atoms
[AD-A146234] 03 p0418 N85-12672
Magnetic refrigeration and heat pumping design options
[DE85-003405] 13 p2092 N85-23064
MAGNETIC DIPOLES
General image theory for the Sommerfeld problem
[REPT-S-154] 02 p0193 N85-11289
Comparisons of secular variation in two-dipole and spherical harmonic models with observatory data in Eurasia, 1935-1975 04 p0521 N85-13330
Advanced artificial dielectric materials for millimeter wavelength applications
[AD-A148960] 10 p1431 N85-19027
Aperture studies with PATRICIA and RACETRACK on simple lattices containing SSC dipoles
[DE85-004163] 11 p1724 N85-20842
The ULF/ELF/VLF electromagnetic fields generated in a sea of finite depth by elevated dipole sources
[AD-A149838] 12 p1626 N85-21470
Orientation and strength of Martian magnetic dipole
16 p2723 N85-26808
Possible configuration of Martian magnetosphere
16 p2723 N85-26809
Ion-acoustic double layer in a magnetic picket fence configuration
[INPE-3552-PRE/764] 19 p3369 N85-30698
Numerical modeling of subsurface communication
[DE85-012818] 21 p3577 N85-32249
On the influence of the heliomagnetospheric periphery on the galactic cosmic rays
[SH-4.2-19] 23 p4009 N85-34856
Pulsars as cosmic ray particle accelerators: Dynamics of electrons
[OG-6.2-23] 23 p4021 N85-34919
Event parameters: Fixed targets
24 p4146 N85-35702
High energy cosmic ray signature of quark nuggets
[HE-6.2-11] 24 p4212 N85-36147
MAGNETIC DISKS
ADAM: An abstract database machine
[RSRE-84007] 02 p0293 N85-11904
Analog disc recorder system: Operator's reference manual
[DE84-016026] 04 p0503 N85-13209
MOM peripherals 08 p1141 N85-17189
Television animation store: Recording pictures on a parallel transfer magnetic disc
[BBC-RD-1984/17] 10 p1462 N85-19220
Recovery of lost files from VAX/WMS disk structures: A case study
[DE85-010652] 19 p3333 N85-30650
Performance and electric field limitations in inflow disk MHD generators 20 p3534 N85-31967
Conferences of quantum-radiooptics section
22 p3773 N85-33360
MAGNETIC DISPERSION
Comments on the paper by F. Pegoraro, L. Sugiyama: Spatial diffusion of charged high-energy fusion products by shear Alfven perturbations
[INPE-3291-PRE/606] 16 p2586 N85-27675
A method of solving the dispersion equation for electrostatic electron waves in magnetized plasma
[KGI-PREPRINT-071] 16 p2589 N85-27697
High harmonic rectangular gyrotron
19 p3256 N85-30189
MAGNETIC DISTURBANCES
NT MAGNETIC STORMS
National solar-terrestrial research program
[PB84-216183] 01 p0072 N85-10479
Plans for Interbol satellite experiment
13 p1977 N85-22407
Substorms in energetic radiation belt particles according to data from Meteor artificial Earth satellite
16 p2719 N85-26788
Magnetic and thermodynamic structure of the solar corona during sunspot minimum
18 p3203 N85-29673
Study of spectral exponent on quiet and disturbed days
[SH-4.5-10] 23 p4037 N85-35028
The cosmic ray differential diurnal variation dependences on the zenith angle and the geomagnetic disturbance
[SH-4.5-16] 23 p4038 N85-35033
MAGNETIC DOMAINS
Investigation of domain structures and walls using neutron diffraction 03 p0423 N85-12702
Neutron scattering on structural phase transitions with domain building 03 p0425 N85-12711
SEM (Scanning Electron Microscopy) studies of magnetic domains in amorphous metals
[AD-A150963] 14 p2256 N85-23979
MAGNETIC EFFECTS
NT MAGNETIC RIGIDITY
Induction voidmeter
[DE84-014321] 01 p0050 N85-10329
Magnetic interaction in low-dimensional systems
03 p0426 N85-12717
Effect of external magnetic field on characteristics of current-carrying steel tape 06 p0786 N85-15034
The determination of vertical sintering speed of sinter charges
[BLL-M-36033-(5828.4)] 07 p0926 N85-15869
Influence of geomagnetic disturbances on cardiovascular function of athletes
08 p1193 N85-17516
Calculation of secondary-electron escape currents from inclined-spacecraft surfaces in a magnetic field
13 p1992 [illegible]
Magnetovolume effects in some Y-Ni intermetallic compounds
[ISSN-0066-2003] 13 p2021 [illegible]
Mechanisms of magnetic heating of the solar corona
14 p2446 [illegible]
On the role of mother-planet magnetic field in spiral structure explanation of formation of spokes — Saturn rings 15 p2676 [illegible]
Very low temperature studies of hyperfine effects in metals
[DE85-013367] 22 p3749 [illegible]
Relativistic electron in curved magnetic fields
[OG-6.2-11] 22 p3880 [illegible]
Summary of activities, 1983
[LBL-18500] 23 p3969 [illegible]
Heavy cosmic ray measurement aboard Spacelab-1
[SH-10.1-7] 23 p4053 [illegible]
Injector losses on Mite
[DE85-012356] 24 p4090 [illegible]
MAGNETIC ENERGY STORAGE
Repetitive pulse generation with inductive energy storage: A new technology for defense
[DE84-017090] 06 p0806 [illegible]
Plasma erosion opening switch
[DE85-011384] 20 p3535 [illegible]
Design improvements and cost reductions for a 5000 MWh superconducting Magnetic Energy Storage plant
[DE85-010572] 22 p3847 [illegible]
Superconducting magnetic energy storage for asynchronous electrical systems
[DE85-005986] 22 p3847 [illegible]
MAGNETIC EQUATOR
Magnetosonic waves and their relationship with energetic protons 14 p2306 [illegible]
Experimental check of ion transport mechanism in Earth's radiation belt with exposure to nonsteady-state electric fields 15 p2480 [illegible]
Spatial variation of cosmic rays near the heliospheric current sheet
[SH-4.2-10] 23 p4007 [illegible]
Effects of a wavy neutral sheet on cosmic ray anisotropies
[SH-4.2-11] 23 p4008 [illegible]
Determination of galactic cosmic ray latitudinal gradient using Earth based detectors
[SH-4.2-13] 23 p4008 [illegible]
MAGNETIC FIELD CONFIGURATIONS
Plasma drift equilibrium (gyration) in toroidal systems with complex magnetic-field geometry
[DE84-015627] 01 p0122 [illegible]
Elimination of stochasticity in stellarators
02 p0282 [illegible]
Relaxation of plasma rotation in a Tokamak in the presence of extraneous forces and corrugation of the magnetic field
[DE84-015628] 02 p0284 [illegible]
On the annual and semiannual variation of S sub R at l'Aquila — geomagnetism 04 p0520 [illegible]
On some new features of semiannual variation of the geomagnetic field 04 p0520 [illegible]
Experimental observation of plasma neoclassical currents
[DE84-015706] 04 p0586 [illegible]
Zero-current, high beta stelleration equilibria with rotational transform profile control
[DE84-016635] 04 p0588 [illegible]
Compact torroidal development: Activity plan for field reversed configurations
[DE84-017145] 05 p0730 [illegible]
High frequency plasma generator for ion thrusters
[NASA-CR-174772] 08 p1114 [illegible]
Diffusion of particles in a slowly modulated wave
[DE85-000729] 09 p1391 [illegible]
A free electron laser with a rotating quadrupole wiggler
[AD-A149052] 10 p1489 [illegible]
Physical aspects of the prediction of solar flares
[NASA-CR-175487] 10 p1572 [illegible]
Proposal for hollow cathode electron gun for electron cooling
[DE85-002721] 11 p1630 [illegible]
Magnetic fluctuations, field reversal maintenance, and anomalous thermal transport in the reversed field pinch
[DE85-003604] 11 p1732 [illegible]
Dynamics of space charge waves in the laser beat wave accelerator
[AD-A149666] 12 p1936 [illegible]
Forced recognition by nonlinear MHD waves and sequential triggering of solar flares
12 p1956 [illegible]
The continuous spectrum of an axisymmetric self-gravitating equilibrium in the presence of a poloidal magnetic field 12 p1959 [illegible]

Magnetostatic-wave propagation in a finite YIG-Loaded rectangular waveguide
[AD-A150332] 13 p2055 N85-22865
The structure and dynamics of the magnetosphere: Progress in the IMS 14 p2355 N85-24550
Magnetic field in the Earth's outer magnetosphere: Prognoz-6, -7 data 14 p2356 N85-24556
Structure of the boundary layer for steady-state magnetopause reconnection 14 p2356 N85-24561
Spline techniques for magnetic fields
[DE85-004919] 14 p2415 N85-24902
On the structure of magnetic fields in the solar convection zone 14 p2447 N85-25103
Amplification and maintenance of thin magnetic flux tubes by compressible convection — solar magnetism
14 p2447 N85-25104
A numerical simulation of the formation of solar prominences 14 p2448 N85-25112
Linear incompressible magnetoconvection in a planar layer with a nonuniform horizontal magnetic field
14 p2450 N85-25127
The continuous spectrum of an axisymmetric equilibrium with a mixed poloidal and toroidal magnetic field with gravity included 14 p2450 N85-25128
A study of the material motion into an eruptive prominence — solar prominence
14 p2453 N85-25146
Magnetic field structures of hard X-ray flares observed by HINOTORI spacecraft — solar flares
14 p2455 N85-25161
Internal field probing of translating FRCs
[DE85-003732] 15 p2657 N85-26394
On the role of mother-planet magnetic field in spiral structure explanation of formation of spokes — Saturn rings 15 p2676 N85-26525
TOKASTAR: A Tokamak stellarator hybrid with possible bean-shaped operation
[IPPJ-718] 16 p2866 N85-27680
Inherent magnetic field error measurements in ELMO Bumpy Torus
[DE85-005855] 16 p2867 N85-27685
Charge uncovering effects on flute instabilities in hot electron plasmas
[DE85-006957] 16 p2867 N85-27686
Spherical torus, compact fusion at low field
[DE85-006963] 16 p2867 N85-27689
I. F. S. (Institute for Fusion Studies) Newsletter, Volume 4, Number 1
[DE85-007917] 17 p3040 N85-28809
Theoretical and numerical studies of magnetic field line displacements in an Elmo Bumpy Torus
[DE85-008757] 17 p3041 N85-28816
Physics-magnetics trade studies for tandem mirror reactors
[DE85-010043] 18 p3182 N85-29732
Magnetics calculations for an ELMO Bumpy Square
[DE85-010442] 18 p3191 N85-29792
Plasma engineering models of tandem mirror devices with high-field test-cell inserts
[DE85-010046] 18 p3192 N85-29797
Toroidal viscosity and ambipolarity in the neoclassical transport theory of axisymmetric tori
[DE85-010622] 19 p3358 N85-30820
Magnetic probing of the solar interior
[NASA-CR-176025] 19 p3385 N85-30998
MIG: MCNP Input Generator for EFFI magnet geometrics
[DE85-010494] 20 p3515 N85-31857
Magnetics calculations for an ELMO Bumpy Square
[DE85-011436] 21 p3707 N85-33021
Magnetic shielding with superconductors based on niobium-tin compounds 22 p3771 N85-33370
Electron and ion cyclotron heating calculations in the tandem-mirror
[DE85-011858] 22 p3842 N85-33797
Method and apparatus for maintaining equilibrium in a helical axis stellarator
[DE85-011626] 22 p3845 N85-33815
Elmo bumpy square plasma confinement device
[DE85-011628] 22 p3845 N85-33816
Assessment of magnetic field asymmetries in ELMO Bumpy square
[DE85-011905] 22 p3846 N85-33819
Spectral measurements of magnetic energy and magnetic helicity between 0.29 and 0.97 AU
[IFSI-85-2] 22 p3850 N85-33844
Potential effect in transport due to non-axisymmetric confining field 23 p3975 N85-34645
Activities of the RF Section 23 p3975 N85-34646
Radial transport caused by collision
23 p3976 N85-34652
Assessment of magnetic field asymmetries in ELMO Bumpy square
[DE85-011559] 23 p3984 N85-34705

MAGNETIC FIELD INTENSITY
U MAGNETIC FLUX

MAGNETIC FIELD INVERSIONS
Reversals of the Earth's magnetic field
04 p0521 N85-13332
Effects of solar magnetic field on cosmic rays
[SH-4.2-12] 23 p4008 N85-34850
On the influence of the heliomagnetospheric periphery on the galactic cosmic rays
[SH-4.2-19] 23 p4009 N85-34856
An update on the correlation between the cosmic radiation intensity and the geomagnetic AA index
[SH-4.2-24] 23 p4009 N85-34861

MAGNETIC FIELDS
NT BIOMAGNETISM
NT FORCE-FREE MAGNETIC FIELDS
NT GEOMAGNETISM
NT INTERPLANETARY MAGNETIC FIELDS
NT INTERSTELLAR MAGNETIC FIELDS
NT LUNAR MAGNETIC FIELDS
NT NONUNIFORM MAGNETIC FIELDS
NT PALEOMAGNETISM
NT PLANETARY MAGNETIC FIELDS
NT SOLAR MAGNETIC FIELD
NT STELLAR MAGNETIC FIELDS
NT TRAPPED MAGNETIC FIELDS
Natural environment design criteria for the Advanced X-ray Astrophysics Facility (AXAF) definition and preliminary design
[NASA-TM-86481] 01 p0014 N85-10089
Induction voltmeter
[DE84-014321] 01 p0050 N85-10329
NASA Geodynamics Program
[NASA-TM-87359] 01 p0063 N85-10418
Investigation of current setting procedures for sector magnets
[CSIR-NAC-83-03] 01 p0117 N85-10795
Final magnetic shimming of vacuum chamber suspension holes on the sector magnets
[CSIR-NAC-83-02] 01 p0117 N85-10796
Results of prototype field measurements on SM4
[NAC-83-01] 01 p0117 N85-10797
Magnetic spin reduction system for free spinning objects
[NASA-CASE-MFS-25966-1] 02 p0166 N85-11122
Generalized linear inversion of 2.5 - dimensional gravity and magnetic anomalies 02 p0226 N85-11480
Plane wave (EMP) incidence on a finitely conducting plane Earth with the magnetic field intensity parallel to the Earth's surface
[DE84-015364] 02 p0228 N85-11493
Polarization of ultrasound transmitted through boundary of magnetically inactive and equatorially magnetized media 02 p0257 N85-11682
Excitation of quasi-static magnetic fields with axial structure 02 p0259 N85-11696
Random processes and magnetohydrodynamic turbulence 02 p0271 N85-11767
Destruction of magnetic surfaces in three-dimensional MHD equilibria 02 p0282 N85-11838
Elimination of stochasticity in stellarators
02 p0282 N85-11839
The behavior of Pb(1-x)Sn(x)Te semiconductor laser diodes in a magnetic field
[AD-A145431] 02 p0287 N85-11872
Theory of the double critical state in type-2 superconductors
[DE84-015461] 02 p0289 N85-11886
Nonlinear electromagnetic waves in ferromagnetic conducting media 03 p0346 N85-12232
Magnetic characteristics of some volcanic rocks of the west Carpathians
[REPT-557] 03 p0376 N85-12400
Magnetospheric plasma studies using data from the dynamics high and low altitude plasma instruments
[AD-A145751] 03 p0392 N85-12505
On the cause of X-line formation in the near-Earth plasma sheet: Results of adiabatic convection of Plasma-Sheet-Plasma
[AD-A145835] 03 p0396 N85-12525
Electrical parameters in 60-Hz biological exposure systems and their measurement: A primer
[PB84-217793] 03 p0400 N85-12548
Charged particle erosion of icy satellites: Coronal atmospheres and surface redistribution
03 p0448 N85-12845
Vector magnetic field analysis of Lorentz forces acting in the solar atmosphere
[AD-A145941] 03 p0449 N85-12852
Ion thruster performance model
[NASA-CR-174810] 04 p0462 N85-12935
EXAFS and Moessbauer study of small metal clusters isolated in rare-gas solids
[DE84-015976] 04 p0470 N85-12994
Superconducting magnet for probing eddy currents in dynamic models 04 p0489 N85-13117
Human reactions to ELF (Extremely Low Frequency) electric and magnetic fields. An annotated bibliography of current literature, fourth edition
[PB84-230356] 04 p0545 N85-13472
Oscillating field current drive for reversed field pinch discharges
[DE84-015090] 04 p0567 N85-13610
Monte Carlo studies of transport in stellarators
[DE84-017633] 04 p0568 N85-13625
Magnetic constraints on early lunar evolution revisited: Limits on accuracy imposed by methods of paleointensity measurements 04 p0582 N85-13716
Magnetohydrodynamic and gasdynamic theories for planetary bow waves
[NASA-CR-174135] 04 p0589 N85-13760
The determination of eddy current losses in electrical equipment
[DE84-016340] 05 p0632 N85-14050
Particle physics
[DE84-013634] 05 p0727 N85-14673
Equations of plasma transport in a curved magnetic field
[DE84-015625] 05 p0730 N85-14690
Magnetic field calculation for ideal conductors by method of equivalent currents 06 p0768 N85-15035
Birkeland currents correlated with dc-electric fields observed during the CENTAUR BBX rocket experiments
[DRI-6-84] 06 p0834 N85-15311
A warm magnetoactive plasma in a large volume of space 06 p0878 N85-15579
Axisymmetric electromagnetic field influence on the characteristic velocity of an arc-jet
[NASA-TM-77475] 07 p0938 N85-15942
Slow surface magnetoplasma waves in oblique magnetic field 07 p0952 N85-16034
Transformation of electromagnetic waves in plasma with randomly-heterogeneous magnetic field
07 p0953 N85-16039
Amplitude mode magnetic sensors
[AD-D011335] 07 p0961 N85-16094
Self-generated magnetic fields and thermal flux inhibition
[AD-A147405] 07 p0971 N85-16166
Thermal evaporation in blast waves: A model for aneurism formation in the NRL (Naval Research Laboratory) LASER-HANE simulation experiment
[AD-A147006] 07 p0978 N85-16210
Ionospheric turbulence: Interchange instabilities and chaotic fluid behavior
[AD-A147810] 07 p0998 N85-16337
A low perturbation electron injector for cyclic accelerators
[AD-D011312] 07 p1040 N85-16604
Disclinations in carbon-carbon composites
[AD-A148290] 08 p1119 N85-17052
Evaluation of interstitial gas contamination in titanium alloys using induced magnetic field analysis
[AD-P004130] 08 p1127 N85-17105
Electromagnetic inspection of wire ropes using sensor arrays
[AD-A148317] 08 p1170 N85-17379
Estimate of sound absorption due to magnetoelastic interactions
[AD-A148216] 08 p1216 N85-17671
Evidence for non-radiative activity in stars with T sub eff 10000 K 08 p1231 N85-17757
Winds from rotating, magnetic, hot stars
08 p1234 N85-17775
Current measurements by Faraday rotation in single mode optical fibers
[DE85-002025] 09 p1384 N85-18707
Beam probe spectroscopic technique for ion temperature and magnetic field measurements
09 p1389 N85-18738
Laser-induced-fluorescence-spectroscopy of atomic processes under a high magnetic field
09 p1389 N85-18740
Brief outline of analytic stability studies of magnetically insulated systems — bibliciographies
[DE85-000212] 09 p1393 N85-18765
Advanced ion thruster research
[NASA-CR-174862] 10 p1430 N85-19021
Electromagnetic braking of a metallic projectile in flight
[AD-A149424] 10 p1480 N85-19345
Experience highlights from the design and manufacture of US LCT coils
[DE84-017504] 10 p1482 N85-19354
Role of multiple helicity nonlinear interaction of tearing modes in dynamo and anomalous thermal transport in the Reversed Pitch Field
[DE85-002176] 10 p1560 N85-19839
Resistive evolution of general plasma configuration
[DE85-002340] 10 p1561 N85-19843

Magnetization of very thin Ni films in epitaxial metal film sandwiches of Cu
[DE85-001840] 10 p1563 N85-19660

Development of high field Nb-Ti accelerator dipoles
[DE85-000621] 11 p1714 N85-20782

Aperture studies with PATRICIA and RACETRACK on simple attices containing SSC dipoles
[DE85-004163] 11 p1724 N85-20842

Stability of superconducting composites in a magnetic field
[DE85-002731] 11 p1734 N85-20907

Multifrequency observations of BL LAC objects and violently variable quasars 11 p1746 N85-20981

Magnetically-induced luminescence of (Ir(2=phos)(2)C10(4)
[AD-A149659] 12 p1799 N85-21286

Magentically actuated compressor
[NASA-CASE-GSC-12799-1] 12 p1816 N85-21404

Magnetic field in main gap of seperator
12 p1843 N85-21563

Behavior of small ferromagnetic particles in traveling magnetic field 12 p1843 N85-21564

Rotating squid magnetometers and gradiometers
[AD-D011529] 12 p1849 N85-21600

Betatron-synchrotron detrapping in a tapered wiggler free electron laser
[AD-A149686] 12 p1856 N85-21642

Effect of long-term repeated exposure to high-intensity stationary magnetic field on adrenomedullary activity
12 p1904 N85-21955

Effect of stationary magnetic field on bleeding time
12 p1904 N85-21956

Superconducting magnet technology for accelerators
[DE85-004192] 12 p1926 N85-22102

Strong iron accelerating by collisionless magnetosonic shock wave propagating perpendicular to a magnetic field
[IPPJ-709] 12 p1935 N85-22161

Use of ferrofluids in machining of metals
13 p2045 N85-22802

Exitation of low-frequency resonance waves by moving conductor in space plasma 13 p2067 N85-22912

Magnetic noise in single-machine rotating frequency converters 13 p2077 N85-22969

Study of resolution of deep MT soundings by means of physical model 13 p2112 N85-23155

Discrimination of normal and anomalous magnetic and electric fields in geoelectromagnetic variations
13 p2114 N85-23166

1981 wC-130 airborne lightning characterization program data review
[AD-A150230] 13 p2136 N85-23275

High-field dipoles for future accelerators
[DE85-002315] 13 p2157 N85-23391

Improvement in magnetic field properties of vanadium-gallium superconductors by enhancement of spin-orbit scattering
[DE85-002893] 13 p2164 N85-23422

Design, theoretical innovations in Tokamaks systems
14 p2289 N85-24190

Applications of eddy currents
14 p2316 N85-24315

Spreading of greatly extended inhomogeneities in upper ionosphere 14 p2339 N85-24462

Experimental investigation of neutral plasma beam propagation across a magnetic field
[AD-A150944] 14 p2423 N85-24947

Cosmic ray environment model for Earth orbit
[NASA-CR-175866] 14 p2455 N85-25165

Magnetic field penetration into cometary ionosphere
15 p2477 N85-25290

Resonant rotations of satellite in polar orbit in magnetic and gravitational fields 15 p2479 N85-25302

Two interactive graphics postprocessors for NASTRAN 15 p2574 N85-25871

Forced MHD turbulence in a uniform external magnetic field
[NASA-CR-172576] 15 p2654 N85-26368

High energy beam experiment
15 p2654 N85-26376

Effects of magnetic shear on lower hybrid waves in the supraauroral region
[AD-A151960] 15 p2656 N85-26392

Evaluation of human exposures to low frequency fields 16 p2776 N85-27135

Electric field and energy transfer by magnetopause reconnection
[INPE-3446-PRE/701] 16 p2826 N85-27432

A multipole model of the observed cerebral cortex magnetic field
[AD-A152237] 16 p2842 N85-27526

High energy particle acceleration by coherent electromagnetic waves propagating across the magnetic field
[IPPJ-717] 16 p2866 N85-27679

Prospects for developing attractive magnetic fusion concepts
[DE85-006925] 16 p2867 N85-27684

Thermal and magnetic properties of neutron stars
16 p2880 N85-27774

The state of martensite after quenching in a magnetic field
[BLL-BISI-TRANS-22297-(9022.06)]
17 p2926 N85-28051

Magnetic monopoles
[DE85-006176] 17 p3027 N85-28719

Effects of level broadening on the magnetothermal oscillations in two-dimensional electron systems
[AD-A152639] 17 p3029 N85-28732

I. F. S. (Institute for Fusion Studies) Newsletter, Volume 4, Number 1
[DE85-007917] 17 p3040 N85-28809

Theoretical and numerical studies of magnetic field line displacements in an Elmo Bumpy Torus
[DE85-008757] 17 p3041 N85-28816

Central limit theorems in the area of large deviations for some dependent random variables
[AD-A153125] 17 p3043 N85-28831

Experimental research on electrical propulsion
[NASA-TM-77876] 18 p3067 N85-28969

Reciprocating magnetic refrigerator employing tandem porous matrices within a reciprocating displacer
[NASA-CASE-NPO-16257-1] 18 p3085 N85-29082

Swedish space program includes research satellites
18 p3086 N85-29113

Maser cavity servo-tuning system
[NASA-CASE-NPO-15890-1-CU]
18 p3093 N85-29143

Effects of Formvar coating and copper-nickel outer sheath on the ac losses of multi-strand subsize cables
[DE85-010413] 18 p3096 N85-29166

Optical fiber magnetic field sensor with nanosecond response time
[DE85-008409] 18 p3110 N85-29259

Intense ion beam diode diagnostics using a tunable dye laser
[DE85-008079] 18 p3113 N85-29272

Auroral zone electric fields from DE-1 and -2 at magnetic conjunctions
[NASA-CR-175974] 18 p3136 N85-29421

Wide-angle optics with strong magnetic fields for efficient generation of secondary-particle beams
[DE85-007727] 18 p3179 N85-29713

3d calculations of a fixed field alternating gradient synchrotron magnet
[DE85-002742] 18 p3183 N85-29739

Electromagnetic solitary waves in magnetized plasmas
[DE85-010064] 18 p3190 N85-29788

Inertial fusion reactors and magnetic fields
[DE85-009571] 18 p3191 N85-29789

MHD channel development
[DE85-008305] 18 p3192 N85-29796

Magnetic impurities in superconductors
[DE85-008372] 18 p3196 N85-29825

The vector structure of active magnetic fields
18 p3203 N85-29870

The Hanle effect applied to magnetic field measurements 18 p3204 N85-29878

Some design considerations for a satellite-borne magnetograph 18 p3204 N85-29879

Analysis of the new polarimeter for the Marshall Space Flight Center vector magnetograph
18 p3205 N85-29881

Inferred flows of electric currents in solar active regions 18 p3206 N85-29899

Comparisons of simultaneous vector magnetograms
18 p3206 N85-29900

Ephemeral regions versus pseudo ephemeral regions
18 p3206 N85-29901

Cosmic ray modulation and turbulent interaction regions near 11 AU
[NASA-TM-86193] 18 p3209 N85-29909

Magnetically-localizable, polymerized lipid vesicles and method of disrupting same
[AD-D011686] 19 p3249 N85-30144

An experimental study of the magnetoelastic bending of thin plates made of soft ferromagnetic material
19 p3282 N85-30352

Functions of Prognoz-10: Intercosmos' station explained 19 p3296 N85-30433

Effect of triphthasine and elenium on changes in evoked bioelectrical activity of the brain exposed to stationary magnetic field 19 p3325 N85-30601

Profile of a relativistic electron beam propagated through a linear wiggler and an axial guide field
[AD-A154403] 19 p3353 N85-30763

Trajectories of charged particles traversing a plasma sheath in an oblique magnetic field
[DE85-011070] 19 p3371 N85-30911

Fractional statistics and fractional quantized Hall effect
[DE85-007833] 19 p3375 N85-[illegible]

Design of aggressive superconducting TFCX magnet systems
[DE85-010003] 19 p3376 N85-[illegible]

Stability of a hot symmetric tandem mirror with thermal barrier
[DE85-010539] 19 p3377 N85-[illegible]

Structure of the distant geotail: ISEE-3 observations
20 p3486 N85-[illegible]

The temporal evolution of a small auroral substorm as viewed from high altitudes with Dynamics Explorer 1
[NASA-CR-176064] 20 p3493 N85-[illegible]

Guide to the Main Ring DO overpass
[DE85-011722] 20 p3531 N85-[illegible]

Alternating current OHMIC heating in a toroidal stellarator 20 p3534 N85-[illegible]

Slow tearing modes: Transitions to instability
20 p3534 N85-[illegible]

Simulating the effects of plasma disruption with a 1 MA current pulse in a coaxial test fixture
[DE85-010491] 20 p3535 N85-[illegible]

On the role of the magnetic field strength in critical ionization velocity interaction
[TRITA-EPP-85-01] 20 p3536 N85-[illegible]

Electrodeposition of chromium and copper in magnetic fields
[AD-A154648] 21 p3568 N85-[illegible]

Magnetic materials
[AD-A154679] 21 p3580 N85-[illegible]

Analysis of spacecraft data
[NASA-CR-171567] 21 p3660 N85-[illegible]

Investigation of reproducibility of emission wavelength of helium-neon laser with external neon absorption cell (0.63 micrometers) 21 p3663 N85-[illegible]

Solution of problem of equilibrium confinement of plasma by magnetic field in an infinite circular cylinder
21 p3692 N85-[illegible]

The Faraday effect in ruby and corundum in strong magnetic fields 21 p3697 N85-[illegible]

Magnetic fields in laser heated plasmas
[DE85-010715] 21 p3707 N85-[illegible]

Very low temperature studies of hyperfine effects in metals
[DE85-013367] 22 p3749 N85-[illegible]

Analysis of solution of Bloch's equations in time domain 22 p3771 N85-33371

Calculation of external magnetic field of a shielded transformer 22 p3771 N85-33373

Magnetic field and equivalent circuit of induction motors with shielded poles 22 p3772 N85-[illegible]

Electron trajectories in a combined wiggler and alternating gradient quadrupole field
[DE85-010727] 22 p3842 N85-[illegible]

Collisional transport for a superthermal ion species in a plasma
[DE85-011943] 22 p3845 N85-[illegible]

Striation free doped silicon
[AD-A155730] 22 p3847 N85-[illegible]

Magnetotails of the terrestrial planets: A comparative study 22 p3856 N85-[illegible]

Virgo cluster as a high energy cosmic rays source
[OG-5.4-6] 22 p3866 N85-[illegible]

Theoretical and Experimental Beam Plasma Physics (TEBPP) 23 p3901 N85-[illegible]

Improved negative ion source
[DE85-006445] 23 p3912 N85-[illegible]

Apparatus for unilateral generation of a homogeneous magnetic field
[DE85-006001] 23 p3926 N85-[illegible]

Some physical differences between sheet plasma and multicusp plasma as volume produced H- or D- ion sources
[IPPJ-728] 23 p3974 N85-[illegible]

Size effects of vacuum chamber for H- (D-) ion volume production by sheet plasma 1
[IPPJ-731] 23 p3974 N85-[illegible]

Magnetohydrodynamic equilibrium and stability of spheromak with spheroidal plasma-vacuum interface
[IPPJ-732] 23 p3974 N85-[illegible]

Radial transport phenomena for TMX-upgrade
23 p3976 N85-[illegible]

RF induced radial diffusion in tandem mirrors
23 p3976 N85-[illegible]

Induced azimuthal electric field effects on tandem transport and ambipolarity 23 p3976 N85-[illegible]

Low frequency instability in a mirror field
23 p3977 N85-[illegible]

Azimuthal uniformity and current balance study of ICRH-produced plasma in RFC-XXM
23 p3977 N85-[illegible]

Breakdown of intrinsic ambipolarity for the radial diffusion due to a rotating RF field 23 p3977 N85-[illegible]

Guiding center distribution function and longitudinal invariant 23 p3978 N85-[illegible]

Simulation studies on stability of hot electron plasma
23 p3978 N85-34664
Behavior of helically-trapped fast ion orbits in heliotron E
23 p3978 N85-34666
Neoclassical diffusion including ellipticity in a heliotron-like configuration 23 p3978 N85-34667
Technology of magnetically driven accelerators
[DE85-011867] 23 p3983 N85-34700
Acceleration of ions and electrons to near-cosmic ray energies in a perpendicular shock: The January 6, 1978 event
[SH-1.5-4] 23 p3996 N85-34773
Isotopic overabundances and the energetic particle model of solar flares
[SH-2.2-1] 23 p4000 N85-34796
The dispersive evolution of charged-particle bunches in random magnetic fields
[SH-4.1-2] 23 p4004 N85-34828
Numerical descriptions of cosmic-ray transport
[SH-4.1-3] 23 p4004 N85-34829
Latitudinal gradients of cosmic rays and the polarity reversal of the heliospheric magnetic field: A preliminary evaluation
[SH-4.2-16] 23 p4008 N85-34853
Alfven wave scattering and the secondary to primary ratio
[OG-7.2-9] 23 p4015 N85-34878
The role of cosmic rays in magnetic hydrodynamics of interstellar medium
[OG-7.2-15] 23 p4015 N85-34882
On magnetic pair production above fast pulsar polar caps
[OG-8.2-13] 23 p4020 N85-34909
Cosmic rays 10Be biennal data and their relationship to auroras and sunspots
[SH-7.1-1] 23 p4047 N85-35094
Long-time asymptotics of a system for plasma diffusion
[NASA-CR-177947] 24 p4093 N85-35375
Aeromagnetic and gravity models of the pluton below the Lake City caldera, Colorado
24 p4104 N85-35442
SLC arc transport system: Magnet design and construction
[DE85-014289] 24 p4159 N85-35789
TOSCA calculations and measurements for the SLAC SLC damping ring dipole magnet
[DE85-014366] 24 p4160 N85-35793
A new study of muons in air showers by NBU air shower array 24 p4190 N85-35997
Radio wave emitted by an extensive air showers in 100Hz to 1MHz region
[HE-4.6-15] 24 p4196 N85-36051

MAGNETIC FILMS
Symmetry of exchange interaction in crystalline magnetic films 02 p0259 N85-11694
Twisted domain wall in very thin magnetic films with perpendicular anisotropy 03 p0350 N85-12252
Development of wide band recording materials
[AD-A154861] 21 p3589 N85-32309
Changes in lattice cell parameter of film intermetallic compounds RT2
[BLL-M-35874-(5828.4)] 23 p3915 N85-34261

MAGNETIC FLUX
Induction voltmeter
[DE84-014321] 01 p0050 N85-10329
Free electron lasers
[AD-A145109] 01 p0053 N85-10349
Plane wave (EMP) incidence on a finitely conducting plane Earth with the magnetic field intensity parallel to the Earth's surface
[DE84-015364] 02 p0226 N85-11493
Flux-line pinning by the grain boundary in niobium bicrystals
[DE84-016688] 04 p0570 N85-13638
ATA probe beam experiment
[DE84-016017] 06 p0862 N85-15477
Magnetic fusion energy plasma interactive and high heat flux components. Volume 2: Technical assessment of the critical issues and problem areas in high heat flux materials and component development
[DE85-001155] 09 p1393 N85-18764
Electromagnetic inspection of wire ropes using sensor arrays
[AD-A149016] 10 p1495 N85-19436
Fermi surface study of CeSb
[DE85-002532] 10 p1564 N85-19862
Convergent spectral representation for 3-dimensional inverse MHD equilibria
[DE85-000666] 11 p1733 N85-20900
Magnetic field in main gap of separator
12 p1843 N85-21563
Ultrasensitive measuring devices
[DE85-000672] 12 p1853 N85-21622
Non-contacting electromagnetic de-spin system for Earth orbiting satellites 12 p1946 N85-22225
Equilibrium model of thin magnetic flux tubes — solar atmosphere 12 p1958 N85-22310
Observation of cosmic ray flux variations in stratosphere 13 p1961 N85-22430
Method of separately determining electrophysical properties of bulky conductor 13 p2073 N85-22951
Magnetic buoyancy instabilities in the convective overshoot zone — Sun 14 p2447 N85-25101
The photospheric temperature structure of magnetic flux tubes 14 p2447 N85-25102
On the structure of magnetic fields in the solar convection zone 14 p2447 N85-25103
Amplification and maintenance of thin magnetic flux tubes by compressible convection — solar magnetism
14 p2447 N85-25104
Nonlinear time-evolution of kink-unstable magnetic flux tubes in the convection zone of the Sun
14 p2447 N85-25105
A consideration of the solar cycle in the light of the behavior of the large active regions
14 p2452 N85-25140
Approximate closed-form expression for the electron-scattering-induced interaction between magnetic flux lines and grain boundaries
[DE85-004699] 15 p2660 N85-26417
Magnetic flux leakage inspection: Principles and applications
[BLL-BISI-TRANS-22248-(9022.06)]
17 p2975 N85-28382
Differential between crack and pseudo-crack indications by means of objective magnetic flux leakage testing
[BLL-BISI-TRANS-22033-(9022.06)]
17 p2976 N85-28386
Induction heating gun
[NASA-CASE-LAR-13181-1] 18 p3085 N85-29083
Measurements of Solar Vector Magnetic Fields
[NASA-CP-2374] 18 p3203 N85-29869
Current evolution in a numerical emerging-magnetic-flux model 18 p3204 N85-29875
Evidence for submergencew of magnetic flux in a growing active region 18 p3208 N85-29902
Ballooning instabilities on a magnetic separatrix
[DE85-010855] 19 p3372 N85-30915
Flux pinning and flux flow studies in superconductors using flux flow noise techniques
[DE85-010814] 19 p3376 N85-30945
Fractal structure of the interplanetary magnetic field
[NASA-TM-86212] 19 p3383 N85-30987
Structure of the distant geotail: ISEE-3 observations
20 p3488 N85-31678
Alternating current OHMIC heating in a toroidal stellarator 20 p3534 N85-31988
Spectral measurements of magnetic energy and magnetic helicity between 0.29 and 0.97 AU
[IFSI-85-2] 22 p3850 N85-33844
Neutral particle beam intensity controller
[DE85-008411] 23 p3969 N85-34604
Effect of ECH and ICH on ambipciar potential in NBT-1M 23 p3978 N85-34661
Stellarator approach to fusion plasma confinement
[DE85-011420] 23 p3984 N85-34704
Interstellar turbulence, random density variations, and scintillation measurements
[OG-7.2-13] 23 p4015 N85-34880
System expectations for Pioneer 1 foil implosion experiments
[DE85-014129] 24 p4091 N85-35359
Proposed FRX-D experiment
[DE85-012766] 24 p4158 N85-35778
The structure of Herbig-Haro object 43 and Orion dark cloud extinction
[NASA-TM-87503] 24 p4166 N85-35831

MAGNETIC FORMING
Major facility overhauls at LAMPF
[DE85-012724] 24 p4156 N85-35765

MAGNETIC INDUCTION
Multipurpose 5-MeV linear induction accelerator
[DE84-014523] 02 p0278 N85-11806
In-line beam current monitor
[DE84-014054] 04 p0560 N85-13567
Magnetic flux leakage inspection: Principles and applications
[BLL-BISI-TRANS-22248-(9022.06)]
17 p2975 N85-28382
Magnetic field and equivalent circuit of induction motors with shielded poles 22 p3772 N85-33378

MAGNETIC INDUCTION PROBES
U MAGNETIC PROBES

MAGNETIC LENSES
Fast and precise processing of material by means of an intensive electron beam
[BMFT-FB-T-84-123] 03 p0342 N85-12201

MAGNETIC MATERIALS
NT FERROFLUIDS
NT FERROMAGNETIC FILMS
NT FERROMAGNETIC MATERIALS
NT MAGNETITE
Metamagnetic systems 03 p0423 N85-12701
Anisotropy and microstructure of rare earth permanent magnet materials
[AD-A146549] 06 p0859 N85-15460
Selection of regenerator geometry for magnetic refrigerator applications
[DE84-012637] 11 p1616 N85-20160
Magnetic X-ray scattering studies of the rare Earth metal holmium
[DE85-003608] 12 p1807 N85-21336
Metrology for Electronic Technology: A bibliography of NBS (National Bureau of Standards)
[PB85-112895] 12 p1830 N85-21486
Green's function solution of the Kondo problems and universality of the thermodynamic properties
[DE85-002739] 12 p1943 N85-22206
Relationship between topological and magnetic order in small metal clusters
[AD-A150547] 13 p2018 N85-22651
SEM (Scanning Electron Microscopy) studies of magnetic domains in amorphous metals
[AD-A150963] 14 p2256 N85-23979
Practical surface methods 14 p2316 N85-24314
Tunneling in magnetic superconducting systems
[AD-A150677] 14 p2426 N85-24963
Magnetic steels with the lowest specific total losses
[BMFT-FB-T-84-263] 18 p3078 N85-29042
Magnetic materials
[AD-A154679] 21 p3580 N85-32256
Metallic glass composition
[DE85-011594] 22 p3751 N85-33253
Induction motors with minimum waste of magnetic iron
22 p3772 N85-33377

MAGNETIC MEASUREMENT
Results of prototype field measurements on SM4
[NAC-83-01] 01 p0117 N85-10797
Magnetic properties of the cobalt matrix in WC-Co compacts 02 p0177 N85-11186
Present practice for the recording of the Earth magnetic field — geophysical observatories
04 p0519 N85-13317
Analysis of the daily geomagnetic variation with the use of MAGSAT data — MAGSAT satellites
04 p0520 N85-13319
Contributions to the error analysis in the relativity gyroscope experiment 05 p0638 N85-14095
Amplitude mode magnetic sensors
[AD-D011335] 07 p0981 N85-16094
External cavity diode laser sensor
[AD-D011341] 07 p0989 N85-16152
Low power microprocessor based measurements system for determining the integrity of coatings on buried pipelines
[ERS-E.380] 09 p1324 N85-18323
Magnetization of very thin Ni films in epitaxial metal film sandwiches of Cu
[DE85-001840] 10 p1583 N85-19980
Magnetic measurements, calibrations, and standards: Report on a survey
[PB85-127827] 11 p1698 N85-20317
Solution of direct magnetometric problem on spherical Earth 13 p2116 N85-23179
Rapid advances in geological work
13 p2166 N85-23437
Metal complexes of some heterocyclic ligands
15 p2504 N85-25446
Overview of applications of SQUIDS
[DE85-009942] 20 p3458 N85-31480
A real time index of geomagnetic background noise for the MAD (Magnetic Anomaly Detection) frequency band
[AD-A155717] 22 p3814 N85-33627
Absolute measurement of Declination (D) by means of a proton magnetometer
[DMI-GEOPHYS-PAPERS-R-68]
22 p3836 N85-33751
Interplanetary magnetic field control of high-latitude electric fields and currents determined from Greenland magnetometer data
[DMI-GEOPHYS-PAPERS-R-69]
22 p3850 N85-33845

MAGNETIC METALS
U MAGNETIC MATERIALS
U METALS

MAGNETIC MIRRORS
Small, octopole-stabilized tandem mirror reactor
[DE85-002144] 10 p1559 N85-19632
Monte Carlo studies of tandem mirror plasmas interacting with waves in the Ion Cyclotron Range of Frequencies (ICRF)
[DE85-002968] 11 p1731 N85-20863

Efficient heating and confinement of ions in an axisymmetric magnetic mirror supplemented with dc electric field [IPPJ-707] 12 p1935 N85-22160

Spectroscopic study of sources and control of impurities in TMX-U: Revision 1 [DE85-004423] 12 p1937 N85-22170

Stability of high energy particle plasmas to MHD-like modes [DE85-007879] 17 p3039 N85-26803

Physics-magnetics trade studies for tandem mirror reactors [DE85-010043] 18 p3182 N85-29732

Plasma engineering models of tandem mirror devices with high-field test-cell inserts [DE85-010046] 18 p3192 N85-29797

Tritium system design for the mirror reactors FPD-1, FPD-2 and FPD-3 [DE85-010490] 19 p3363 N85-30852

Stability of a hot symmetric tandem mirror with thermal barrier [DE85-010539] 19 p3377 N85-30952

Neutronics activities for next generation devices [DE85-010488] 20 p3527 N85-31930

Simulation of automatic control of MFTF-B neutral beams [DE85-010640] 20 p3530 N85-31960

Proton ring trapping in a magnetic mirror 20 p3534 N85-31990

Energy and Technology Review [DE85-011767] 21 p3716 N85-33061

Elmo bumpy square plasma confinement device [DE85-011628] 22 p3845 N85-33816

Proceedings of the US-Japan Workshop on Transport in Open-Ended Systems [IPPJ-727] 23 p3975 N85-34644

Electron dynamics and transport in a mirror field 23 p3977 N85-34656

RF stabilization of interchange-ballooning modes [DE85-012060] 24 p4090 N85-35353

Analysis of a pulsed power system containing rotating machine [DE85-014128] 24 p4159 N85-35786

MAGNETIC MOMENTS

Electronic structure and properties of magnetic defects in Co(1+x)Al(1-x) and Fe(1+x)Al(1-x) alloys [NASA-TM-77498] 07 p1047 N85-16648

Stochastic methods for the description of multiparticle production [DE84-009981] 10 p1556 N85-19810

Magnetization of very thin Ni films in epitaxial metal film sandwiches of Cu [DE85-001840] 10 p1563 N85-19860

Measurement of the induced moment magnetic form factor of a heavy fermion superconductor [DE85-004165] 12 p1942 N85-22194

Microscopic magnetic structure of multiple bilayers of thin films of Fe and Ge [DE85-004188] 13 p2024 N85-22882

Theoretical studies of high energy phenomenon: Analysis of models of CP and T violation [DE85-007455] 17 p3036 N85-26782

Excited leptons contribution to muon g-2 [PREPRINT-432] 18 p3184 N85-29745

Physics with low temperature antiproton [DE85-009627] 19 p3355 N85-30798

MAGNETIC MONOPOLES

Study for a large area underground detector made with organic scintillators for searching for magnetic monopoles [NOTA-INTERNA-814] 02 p0201 N85-11339

An underground search for massive slow particles (hunting Grand Unified Theory (GUT) monopoles) [NOTA-INTERNA-821] 02 p0292 N85-11894

Renewal request for high energy physics at Texas A and M University [DE85-004469] 11 p1724 N85-20843

Superheavy magnetic monopoles and the standard cosmology [DE85-003922] 15 p2666 N85-26587

Cocycles and magnetic monopole [DE85-007797] 16 p2856 N85-27612

Magnetic monopoles [DE85-006176] 17 p3027 N85-28719

A possible digital circuit able to recognize magnetic monopoles crossing a thick scintillator counter [NOTA-INTERNA-826] 18 p3097 N85-29173

Study for a large area acrylic scintillator detector — magnetic monopoles [NOTA-INTERNA-827] 18 p3097 N85-29174

Measurement of the attenuation length of an acrylic scintillator — magnetic monopoles [NOTA-INTERNA-828] 18 p3097 N85-29175

Experimental performance of a digital circuit able to recognize magnetic monopole events [NOTA-INTERNA-838] 18 p3097 N85-29176

The dimensional reduction transition [DE85-003948] 19 p3383 N85-30990

Nineteenth International Cosmic Ray Conference. HE sessions, volume 8 [NASA-CP-2376-VOL-8] 24 p4200 N85-36066

Search for magnetic monopoles using proportional counters filled with helium gas [HE-6.1-1] 24 p4209 N85-36127

Magnetic monopole search by 130 m(2)sr He gas proportional counter [HE-6.1-2] 24 p4209 N85-36128

Results of a search for monopoles and tachyons in horizontal cosmic ray flux [HE-6.1-3] 24 p4209 N85-36129

Monopole, astrophysics and cosmic ray observatory at Gran Sasso [HE-6.1-4] 24 p4209 N85-36130

Monopole search below the Parker limit with the MACRO detector at Gran Sasso [HE-6.1-5] 24 p4209 N85-36131

Limits on monopole fluxes from KFG experiment [HE-6.1-6] 24 p4209 N85-36132

An experiment to detect gut monopoles [HE-6.1-7] 24 p4210 N85-36133

Search for supermassive magnetic monopoles using mica crystals [HE-6.1-8] 24 p4210 N85-36134

The homestake surface-underground scintillations: Description [HE-6.1-9] 24 p4210 N85-36135

Upper limit on magnetic monopole flux from Baksan experiment [HE-6.1-11] 24 p4210 N85-36136

Results from the UCSD magnetic monopole search [HE-6.1-12] 24 p4210 N85-36137

MAGNETIC PERMEABILITY

Theory of near-field phased arrays for electromagnetic susceptibility testing [PB84-217836] 01 p0042 N85-10273

Effect of annealing in transverse magnetic field on magnetic permeability of amorphous Fe5Co70Si15B10 alloy 03 p0349 N85-12247

Magnetic susceptibility, electrical resistivity, and specific heat of single crystal LaFe-4P-12 [DE84-009979] 04 p0570 N85-13633

Electronic structure and properties of magnetic defects in Co(1+x)Al(1-x) and Fe(1+x)Al(1-x) alloys [NASA-TM-77498] 07 p1047 N85-16648

Magnetism of californium metal [DE85-001141] 09 p1377 N85-18657

Effects of hydrogen on magnetic properties of amorphous zirconium alloys [DE85-003303] 11 p1607 N85-20107

Investigation of electric and magnetic properties of intercalated graphite [AD-A149601] 12 p1797 N85-21274

Method of separately determining electrophysical properties of bulky conductor 13 p2073 N85-22951

Optimum dimensions of power solenoids for magnetic suspension [NASA-TM-77864] 17 p3026 N85-28716

Linear motion valve [NASA-CASE-MSC-20145-1] 18 p3115 N85-29284

Advanced detectors and signal processing [NASA-CR-176193] 24 p4088 N85-35343

MAGNETIC POLES

Magnetosphere, rings, and moons of Uranus 02 p0301 N85-11951

Development of high field Nb-Ti accelerator dipoles [DE85-000621] 11 p1714 N85-20762

Preliminary documentation for the polar code [AD-A154125] 19 p3336 N85-30667

Magnetic field and equivalent circuit of induction motors with shielded poles 22 p3772 N85-33378

MAGNETIC PROBES

Internal field probing of translating FRCs [DE85-003732] 15 p2657 N85-26394

Magnetic flux leakage inspection: Principles and applications [BLL-BISI-TRANS-22248-(9022.06)] 17 p2975 N85-28382

Magnetic probing of the solar interior [NASA-CR-176025] 19 p3385 N85-30996

MAGNETIC PROPERTIES

NT ANTIFERROMAGNETISM
NT BIOMAGNETISM
NT CURIE TEMPERATURE
NT DIAMAGNETISM
NT FERROMAGNETISM
NT GEOMAGNETISM
NT GYROMAGNETISM
NT MAGNETIC EFFECTS
NT MAGNETIC INDUCTION
NT MAGNETIC MOMENTS
NT MAGNETIC PERMEABILITY
NT MAGNETIC RELAXATION
NT MAGNETIC RIGIDITY
NT MAGNETIC SUSPENSION
NT MAGNETOACOUSTICS
NT MAGNETOACTIVITY
NT MAGNETORESISTIVITY
NT MAGNETOSTRICTION
NT PALEOMAGNETISM
NT PARAMAGNETISM
NT POLARIZATION CHARACTERISTICS
NT SPIN-LATTICE RELAXATION
NT THERMOMAGNETIC EFFECTS

Preparation and properties of single crystals of hydrogen bis(phthalocyaninato) neodymium(3) [AD-A144933] 01 p0123 N85-10699

Input-output stability analysis with magnetic hysteresis non-linearity: A class of multipliers [AD-A145729] 02 p0253 N85-11684

Magnetic properties of and superfine interactions in amorphous Fe-Cr-Co-Si-B alloys 03 p0349 N85-12246

Magnetic characteristics of some volcanic rocks of the west Carpathians [REPT-557] 03 p0376 N85-12400

Report on research results in solid state nuclear physics, 1980-1982 [JUEL-SPEZ-250] 03 p0422 N85-12696

Magnetic properties of intermetallic phases and simple systems — neutron diffraction 03 p0422 N85-12697

Investigations of magnetic phase transitions with neutron scattering 03 p0423 N85-12700

Metamagnetic systems 03 p0423 N85-12701

Neutron scattering on magnetic structures and at magnetic phase transitions 03 p0424 N85-12706

Magnetism of the rare earth compounds — intermetallic compounds 03 p0424 N85-12707

Growth and magnetic investigations of single crystals of intermetallic compounds of rare earths and uranium — magnetic properties 03 p0425 N85-12712

Magnetic interaction in low-dimensional systems 03 p0426 N85-12717

USSR report: Physics and mathematics [JPRS-UPM-84-007] 05 p0723 N85-14651

Actinides, the narrowest bands [DE84-016463] 05 p0733 N85-14710

Electronic and magnetic properties of transition-metal surfaces, interfaces and overlayers [DE84-016886] 05 p0733 N85-14713

The growth of metastable peritectic compounds [NASA-CR-171289] 07 p0920 N85-15624

Structure-property relationships in intercalated graphite [AD-A147949] 08 p1219 N85-17690

Study of the physical properties of crystalline rocks in the southeast Voronezh anteclise [NASA-TM-77823] 10 p1514 N85-19651

Study of magnetism at surfaces by scattering of neutrons at grazing incidence [DE84-015850] 10 p1564 N85-19865

Magnetic measurements, calibrations, and standards: Report on a survey [PB85-127827] 11 p1636 N85-20317

Theoretical determination of surface magnetism [DE85-003224] 11 p1714 N85-20763

Magnetic and structural properties of shock-synthesized zinc ferrite [DE85-000469] 11 p1736 N85-20915

Electric and magnetic properties of intercalated graphite [AD-A149848] 12 p1798 N85-21276

Magnetic studies of Ni3Al(Fe) compounds [DE85-005262] 13 p2025 N85-22886

Primary processing of experimental magnetovariation sounding data using spline functions 13 p2115 N85-23175

Improvement in magnetic field properties of vanadium-gallium superconductors by enhancement of spin-orbit scattering [DE85-002893] 13 p2164 N85-23422

Mixed valence materials [AD-A151009] 14 p2252 N85-23959

Parameters of magnetically active layers of Indian Ocean determined from deep drilling data and magnetic surveys 14 p2337 N85-24481

Transient analysis of a magnetic heat pump 15 p2576 N85-25891

Effect of nickel addition on the thermal, magnetic and magnetomechanical properties of Fe(80)B(15)Si(5) [AD-A152281] 16 p2749 N85-26867

Paramagnetic form factors from itinerant electron theory [DE85-005272] 16 p2750 N85-26873

Effects of wear on structure-sensitive magnetic properties of ceramic ferrite in contact with magnetic tape [NASA-TM-87007] 16 p2753 N85-26891

Magnetic impurities in superconductors
[DE85-008372] 18 p3196 N85-29825

Flux pinning and flux flow studies in superconductors using flux flow noise techniques
[DE85-010814] 19 p3376 N85-30945

A dual spin space station design
20 p3408 N85-31152

Magnitude and range of the RKKy interaction in SmRh4B4
[DE85-012284] 23 p3985 N85-34712

ATA upgrade to 150 MeV
[DE85-013174] 24 p4098 N85-35404

MAGNETIC RECORDING

Television animation store: Recording pictures on a parallel transfer magnetic disc
[BBC-RD-1984/17] 10 p1462 N85-19220

Remote self-contained undersea monitor
[AD-D011520] 12 p1849 N85-21599

GSFC specification electronic data processing magnetic recording tape
[NASA-TM-80599] 12 p1851 N85-21609

Video animation system
[DE85-005494] 14 p2405 N85-24831

Operation of autotracking system in various video playback modes 16 p2764 N85-27055

Balloon-borne video cassette recorders for digital data storage
[OG-9.3-11] 21 p3715 N85-33050

Quarter-inch streaming tape drive application with the Serial ASCII Instrumentation Loop (SAIL) system
[AD-A155354] 22 p3759 N85-33295

Module for interfacing microprocessors and microcomputer 22 p3774 N85-33390

MAGNETIC RELAXATION

NT SPIN-LATTICE RELAXATION

Nuclear Magnetic Resonance of Polymeric Materials
[AD-A145078] 01 p0032 N85-10192

Theory of nuclear magnetic relaxation
[AD-P003911] 01 p0032 N85-10197

Anisotropy and relaxation effects of Co2+ ions in LiTi ferrite
[AD-A146550] 06 p0861 N85-15469

MAGNETIC RESONANCE

NT ELECTRON PARAMAGNETIC RESONANCE

NT FERROMAGNETIC RESONANCE

NT NUCLEAR MAGNETIC RESONANCE

NT PROTON RESONANCE

Analysis of glow discharges for understanding the process of film formation
[NASA-TM-83750] 01 p0022 N85-10138

Magnetic resonance studies of transient radicals and radical ions
[DE84-011699] 03 p0328 N85-12116

Analysis of spin echo signals in multi-pulse experiment
06 p0792 N85-15065

High switching speed electrically tuned microwave magnetic resonance devices
[AD-D011699] 19 p3260 N85-30217

MAGNETIC RIGIDITY

Absolute rigidity spectrum of protons and helium nuclei above 10 GV/c
[OG-4.1-1] 22 p3875 N85-34007

Observation of cosmic ray positrons from 5 to 25 GeV
[OG-6.2-5] 22 p3889 N85-34104

An observation of cosmic ray positrons from 10-20 GeV
[OG-6.2-6] 22 p3889 N85-34105

Diurnal effect in cosmic rays at middle latitudes according to stratospheric measurements
[SH-4.5-6] 23 p4036 N85-35026

Anomalous increase of solar anisotropy above 150GV in 1981-1983
[SH-4.5-18] 23 p4038 N85-35035

Re-evaluation of cosmic ray cutoff terminology
[SH-6.1-11] 23 p4045 N85-35084

The use of the McIlwain L-parameter to estimate cosmic ray vertical cutoff rigidities for different epochs of the geomagnetic field
[SH-6.1-12] 23 p4045 N85-35085

MAGNETIC SHIELDING

Magnetic shielding with superconductors based on niobium-tin compounds 22 p3771 N85-33370

MAGNETIC SIGNALS

The magneto-optical filter, working principles and recent progress 14 p2442 N85-25066

Fluxgate magnetometer (SSM) for the defense meteorological satellite program (DMSP) block 5D-2, flight 7
[AD-A155229] 21 p3560 N85-32143

A real time index of geomagnetic background noise for the MAD (Magnetic Anomaly Detection) frequency band
[AD-A155717] 22 p3614 N85-33627

MAGNETIC SIGNATURES

Orientation and strength of Martian magnetic dipole
16 p2723 N85-26808

Possible configuration of Martian magnetosphere
16 p2723 N85-26809

Analysis of the new polarimeter for the Marshall Space Flight Center vector magnetograph
18 p3205 N85-29881

The San Fernando Observatory video Stokes polarimeter 18 p3205 N85-29885

The new solar magnetograph for the Canary Islands Observatory THEMIS 18 p3205 N85-29886

The vector magnetograph of the Sayan Solar Observatory 18 p3206 N85-29887

Diagnostics of vector magnetic fields
18 p3206 N85-29889

Comparisons of simultaneous vector magnetograms
18 p3208 N85-29900

Ephemeral regions versus pseudo ephemeral regions
18 p3208 N85-29901

Evidence for submergencew of magnetic flux in a growing active region 18 p3208 N85-29902

Graphic displays of vector magnetograph data
18 p3209 N85-29904

Solar cycle variation of ephemeral regions
[AD-A154967] 21 p3723 N85-33097

Aeromagnetic and radiometric signatures of a possible porphyry system in the western Tushar Mountains, Utah
24 p4103 N85-35437

MAGNETIC SPECTROSCOPY

Mixed valence materials
[AD-A151009] 14 p2252 N85-23959

NMR in the 80 s: New nuclei, new pulses — nuclear magnetic resonance (NMR)
[DRIC-T-7487] 22 p3836 N85-33754

Improved negative ion source
[DE85-006445] 23 p3912 N85-34241

MAGNETIC STARS

High energy cosmic ray signature of quark nuggets
[HE-6.2-11] 24 p4212 N85-36147

MAGNETIC STORAGE

NT BUBBLE MEMORY DEVICES

NT MAGNETIC DISKS

MAGNETIC STORMS

Precipitation of protons with E sub p approximately 1 MeV near plasmopause 02 p0161 N85-11093

Behavior of the ionospheric F region in low latitudes and in the equatorial region of Brazil during strong magnetic storms in the 1978 to 1983 period
[INPE-3231-PRE/581] 05 p0675 N85-14333

Nocturnal increases of ionization in the ionospheric F region in the low latitude of Brazil during magnetic storms
[INPE-3271-PRE/596] 05 p0675 N85-14334

Hot plasma particles in the Earth's outer magnetosphere: New understandings during the IMS
[DE84-016826] 05 p0677 N85-14348

Repulsive force of magnetic clouds during solar flares and magnetospheric substorms
06 p0824 N85-15233

Influence of geomagnetic disturbances on cardiovascular function of athletes
08 p1193 N85-17516

Observation of a westward travelling surge from satellites at low, medium and high altitudes
[NASA-TM-87434] 09 p1342 N85-18442

High energy particle effects in the D region during and after geomagnetic storms 11 p1664 N85-20485

Dependence of the high latitude middle atmosphere ionization on structures in interplanetary space
11 p1664 N85-20487

Solar terrestrial influences on the D region as shown by the level of atmospheric radio noise
11 p1664 N85-20488

Latitudinal dependence of the energy input into the mesosphere by high energy electrons
11 p1664 N85-20489

Geomagnetic disturbances caused by internal atmospheric dynamics 11 p1665 N85-20491

Substorms in the Earth's atmosphere
[DE85-000654] 12 p1890 N85-21861

Periodic substorm activity in the geomagnetic tail
[NASA-CR-175629] 13 p2161 N85-23409

Diagram of nonstationary rejoining of magnetic force lines 14 p2344 N85-24492

Excitation of geomagnetic Pcl-2 and pulsations with decreasing period during microsubstorms
14 p2344 N85-24494

Observations of energetic electron and ion distributions near the magnetopause at geosynchronous orbit and related ground effects 14 p2356 N85-24560

Response of magnetospheric substorm activity to changes in the interplanetary magnetized plasma
14 p2357 N85-24563

Timing between particle injections at the geostationary orbit and particle flux decreases in the distant geomagnetic tail during substorms 14 p2358 N85-24569

Plasma sheet dynamics deduced from ISEE-1 and -2 energetic particle flux data 14 p2358 N85-24570

Streaming reversal of energetic particles in the magnetotail during a substorm 14 p2358 N85-24571

Ring current dynamics and plasma sheet sources — magnetic storms 14 p2359 N85-24577

Electrodynamics of magnetosphere-ionosphere coupling 14 p2359 N85-24579

Electron and proton precipitation in magnetic substorms — auroral substorms
14 p2360 N85-24585

Development of an auroral absorption substorm
14 p2360 N85-24586

Coordinated balloon-satellite studies of energetic electron precipitation mechanisms
14 p2360 N85-24587

Observations during a magnetosphere substorm triggered by a Storm Sudden Commencement (SSC): A case study 14 p2361 N85-24588

SAMBO-GEOS: Substorm trapped particle particle boundary movements, particle precipitation and acceleration 14 p2361 N85-24589

Auroral X-rays and equatorial electrons in the morning sector — substorm 14 p2361 N85-24590

On the location of the source for X-ray microbursts
14 p2361 N85-24591

Disturbance of midlatitude electrodynamic parameters due to the magnetospheric convection
14 p2362 N85-24593

Testing of some substorm features by multiple balloon observations 14 p2363 N85-24600

Characteristics of the electrodynamics of auroral arcs as inferred from rocket and ground-base observations during IMS 14 p2363 N85-24601

On the dynamics of the westward traveling surge
14 p2364 N85-24607

Theory and computer simulation of auroral kilometric radiation 14 p2365 N85-24617

Short-period magnetic pulsations during substorms
14 p2368 N85-24636

Substorm associated Pc 1 emission in the morning sub-cleft latitudes 14 p2368 N85-24637

Pi2 pulsations and the substorm current wedge - ground observations 14 p2370 N85-24650

Ground-satellite observations of substorm related Pi 2 pulsations and current systems
14 p2370 N85-24651

Observation of polar aurora from the Salyut-6 space station during the great geomagnetic storm of 11-13 Apr. 1981 15 p2477 N85-25291

Spectral characteristics of protons at low and high altitudes during geomagnetic storm of 29 July 1977
16 p2719 N85-26786

Correlated fluctuations of charged particle fluxes and magnetic field according to data from Intercosmos-10 satellite 16 p2722 N85-26802

Effects of Birkeland current limitation on high latitude convection patterns
[TRITA-EPP-84-10] 20 p3494 N85-31725

The longitudinal asymmetry of the interplanetary perturbation producing Forbush decreases
[IFSI-84-18] 20 p3546 N85-32065

Interplanetary disturbances during Forbush decreases
[IFSI-84-10] 20 p3547 N85-32075

Transient cosmic ray increase associated with a geomagnetic storm
[SH-5.1-8] 23 p4042 N85-35062

Study of dominating parameters of high speed solar plasma streams in relation to cosmic ray and geomagnetic storms
[SH-5.1-11] 23 p4042 N85-35064

Dynamics of the penetration boundaries of solar protons during a strong magnetic storm
[SH-6.1-16] 23 p4046 N85-35089

MAGNETIC SUBSTORMS

U MAGNETIC STORMS

MAGNETIC SURVEYS

Geological effectiveness of automated processing of highly precise aeromagnetic surveys in Caspian region
06 p0821 N85-15216

GADB: A database facility for modelling naturally occurring geophysical fields 13 p2122 N85-23217

Data selection techniques in the interpretation of MAGSAT data over Australia 13 p2123 N85-23218

Parameters of magnetically active layers of Indian Ocean determined from deep drilling data and magnetic surveys
14 p2337 N85-24451

Interpretation of directional magnetotelluric soundings by analytical continuation method
14 p2343 N85-24488

Directional analysis of wave packets of magnetotelluric field 14 p2344 N85-24495

Method for determining depth and shape of a sub-surface conductive object
[DE85-008502] 23 p3935 N85-34389

Magnetic search system
[PB85-185108] 23 p3949 N85-34477

MAGNETIC SUSCEPTIBILITY
U MAGNETIC PERMEABILITY
MAGNETIC SUSPENSION
Optimum dimensions of power solenoids for magnetic suspension 04 p0489 N85-13118
European development experience on energy storage wheels for space 05 p0606 N85-13656
Magnetically suspended reaction wheel assembly 05 p0607 N85-13670
Magnetic suspension options for spacecraft inertia-wheel applications 05 p0607 N85-13671
Overview of magnetic bearing control and linearization approaches for annular magnetically suspended devices 05 p0607 N85-13672
Magnetically suspended flywheel system study 05 p0607 N85-13673
The generation of rolling moments with the superconducting solenoid model
[NASA-CR-172520] 09 p1283 N85-18066
Characteristics of the boat inductor for keeping liquid metal in the suspended state
[NASA-TM-77816] 12 p1851 N85-21611
Mathematical model of electromagnetic suspension device with two control windings 13 p2074 N85-22954
A preliminary investigation of the dynamic force-calibration of a magnetic suspension and balance system
[NASA-CR-172580] 14 p2228 N85-23808
Study on needs for a magnetic suspension system operating with a transonic wind tunnel
[NASA-CR-3900] 16 p2715 N85-26759
Effect of superconducting solenoid model cores on spanwise iron magnet roll control
[NASA-TM-86378] 17 p2905 N85-27915
Optimum dimensions of power solenoids for magnetic suspension
[NASA-TM-77864] 17 p3026 N85-28716
An improved servo-controlled inertial clock for laboratory tests of general relativity 19 p3378 N85-30955
A theoretical model for the study of nonlinear dynamics of magnetic bearings 20 p3462 N85-31505
Optimization of design parameters for alternating current stabilizer based on magnetic suspension 22 p3772 N85-33374

MAGNETIC TAPE RECORDERS
U MAGNETIC RECORDING
U TAPE RECORDERS
MAGNETIC TAPES
NT COMPUTER COMPATIBLE TAPES
Documentation for the machine-readable version of A Catalogue of Extragalactic Radio Source Identifications (Veron-Cetty and Veron 1983)
[NASA-TM-87373] 03 p0405 N85-12587
Documentation for the machine-readable version of The Revised AFGL Infrared Sky Survey Catalog (Price and Murdock 1983)
[NASA-TM-87377] 03 p0405 N85-12538
Documentation for the machine-readable version of the MK classification extension catalogue Morris-Kennedy (1983)
[NASA-TM-87372] 04 p0549 N85-13491
Effect of external magnetic field on characteristics of current-carrying steel tape 06 p0788 N85-15034
High speed magnetic tape interface for a microcomputer
[CSIRO-TP-7] 06 p0847 N85-15377
Beginner's guide to blocked records on magnetic tape
[DE85-001691] 06 p0855 N85-15433
EDP computer tapes described 08 p1142 N85-17203
The care and feeding of magnetic tapes
[AD-A145653] 09 p1366 N85-18585
Satellite support to the Sierra Cooperative Pilot Project: 1979/80 and 1980/81
[PB85-115079] 10 p1520 N85-19583
Humidity effects on adhesion of nickel-zinc ferrite in elastic contact with magnetic tape and itself
[NASA-TP-2449] 12 p1811 N85-21359
The 20:16 block code for digital recording and transmission channels
[BBC-RD-1985/1] 12 p1824 N85-21443
Atmospheric handbook: Atmospheric data tables available on computer tape
[PB85-108512] 12 p1891 N85-21867
Simple detonation meter 13 p2077 N85-22971
Prediction of the long term stability of polyester-based recording media
[PB85-160133] 14 p2262 N85-24019
Documentation for the machine-readable version of A Finding List for the Multiplet Tables of NSRDS-NBS 3, Sections 1-10 (Adelman, Adelman, Fischel and Warren 1984)
[NASA-TM-87440] 14 p2438 N85-25048
Documentation for the machine-readable version of the Cordoba Durchmusterung (CD)
[NASA-TM-87441] 14 p2439 N85-25049
Catalog of the National Energy Software Center
[TI85-900521] 15 p2630 N85-26209
Effects of wear on structure-sensitive magnetic properties of ceramic ferrite in contact with magnetic tape
[NASA-TM-87007] 16 p2753 N85-26991
A transportable, machine oriented library of european sky and terrain radiance distributions with contemporary radiometric and meteorological profiles
[AD-A155254] 21 p3637 N85-32590
Quarter-inch streaming tape drive application with the Serial ASCII Instrumentation Loop (SAIL) system
[AD-A155354] 22 p3759 N85-33295
Relaxation techniques
[AD-A156248] 24 p4133 N85-35621
Using an LSI-11/23 and RT-11 to digitize analog tapes
[DE85-012736] 24 p4139 N85-35656
Aeronautical Systems Division Manufacturing/Quality assurance orientation
[AD-A156128] 24 p4164 N85-35817
MAGNETIC TRANSDUCERS
Electromagnetic Acoustic Transducers (EMATs) for erosion monitoring
[DE85-004834] 12 p1654 N85-21628
A literature review of EMATs, with stress calculations for simple EMAT geometries
[AERE-R-11415] 15 p2642 N85-26295
Geomagnetic velocimeter
[AD-D011672] 19 p3218 N85-29953
MAGNETIC VARIATIONS
NT GEOMAGNETIC PULSATIONS
NT NOCTURNAL VARIATIONS
Analysis of the daily geomagnetic variation with the use of MAGSAT data — MAGSAT satellites 04 p0520 N85-13319
Research directions in recent studies of the lunar geomagnetic effects 04 p0520 N85-13320
On derivation and significance of geomagnetic equivalent amplitude indices 04 p0520 N85-13321
A directly obtained geomagnetic activity measure, J3 04 p0520 N85-13322
Daily magnetic variations at Ebro, Spain 04 p0520 N85-13325
Geomagnetic secular variation at Ebro Observatory during the past 70 years 04 p0521 N85-13331
Spectrum of geomagnetic field variations in the range of periods between 1 and 10 years 06 p0821 N85-15215
Artificial ionospheric disturbances caused by powerful radio waves
[AD-A148077] 08 p1186 N85-17473
Dynamic spectra of mean monthly values of geomagnetic field elements based on spectral-time analysis data 14 p2344 N85-24496
Report of the geomagnetic and geoelectric observations, 1983 (rapid variations)
[REPT-24] 15 p2591 N85-25975
Poloidal rotation of magnetic fluctuations in reversed field pinch plasma
[IPPJ-715] 16 p2866 N85-27677
A study of the cyclical variations of coronal holes and their relation to open magnetic fields
[AD-A155251] 21 p3723 N85-33099
Diurnal variations from muon data at Takeyama underground station
[SH-4.5-13] 23 p4037 N85-35030
Long term changes in cosmic ray diurnal variations observed by ion chambers in Hong Kong and Japan
[SH-4.5-14] 23 p4037 N85-35031
The modulation features of the long-period cosmic ray variations in connection with the sign change of the general magnetic field of the Sun
[SH-4.5-15] 23 p4037 N85-35032
Change of cosmic ray anisotropy with solar activity
[SH-4.5-20] 23 p4038 N85-35037
Magnetic fluctuation and cosmic ray diurnal variations
[SH-4.5-21] 23 p4038 N85-35038
Solar cycle variations of the anaomalous cosmic ray component
[SH-4.6-2] 23 p4039 N85-35040
MAGNETICALLY TRAPPED PARTICLES
NT INNER RADIATION BELT
NT OUTER RADIATION BELT
NT PROTON BELTS
NT RADIATION BELTS
Asymptotic orbit theory for trapped electrons in inhomogeneous Whistler field
[AD-A146178] 03 p0392 N85-12510
Longitude and pitch-angle distributions of streams of high-energy electrons under Earth's radiation belts 13 p1978 N85-22415
Correlated fluctuations of charged particle fluxes and magnetic field according to data from Intercosmos-10 satellite 16 p2722 N85-[illegible]
System and method of operating toroidal magnetic confinement devices
[DE85-011670] 22 p3845 N85-[illegible]
MAGNETITE
Evolutionary history of CI and CM chondrites 06 p0884 N85-1[illegible]
Structure and property formation mechanism in magnetite alloy-binder composite 10 p1444 N85-1[illegible]
Some recent deposit modeling efforts 24 p4106 N85-3[illegible]
MAGNETIZATION
Determination of optimum Curie point as a function of source and sink temperatures for magnetic heat pumps
[DE84-016995] 04 p0489 N85-131[illegible]
Petrologic model of the northern Mississippi embayment based on satellite magnetic and ground based geophysical data
[NASA-TM-85075] 04 p0533 N85-134[illegible]
Electronic structure and properties of magnetic defects in Co(1+x)Al(1-x) and Fe(1+x)Al(1-x) alloys
[NASA-TM-77486] 07 p1047 N85-16[illegible]
Replacement of Fe-3+ ions in nickel ferrites by nonmagnetic Al-3+ and Sc-3+ ions
[BLL-WH-594-(9091.9F)] 08 p1125 N85-170[illegible]
Cobalt-free permanent magnet alloys
[AD-A149272] 10 p1441 N85-1907[illegible]
Magnetization of very thin Ni films in epitaxial metal film sandwiches of Cu
[DE85-001840] 10 p1563 N85-19[illegible]
Application of hysteresis modelling to the non-destructive inspection of stress
[DE85-003081] 11 p1650 N85-20[illegible]
Theoretical determination of surface magnetism
[DE85-003224] 11 p1714 N85-207[illegible]
Magnetization measurements on multifilamentary Nb3Sn and NbTi conductors
[DE85-001237] 11 p1737 N85-20[illegible]
Measurement of the induced moment magnetic form factor of a heavy fermion superconductor
[DE85-004165] 12 p1942 N85-2218[illegible]
Remanent magnetization model for the broken ridge satellite magnetic anomaly 13 p2123 N85-2321[illegible]
Standing of industrial radiography in South Africa 14 p2316 N85-24311
Study of amorphous strips and microconductors by ferromagnetic resonance method 15 p2497 N85-2540[illegible]
Magnetic steels with the lowest specific total losses
[BMFT-FB-T-84-263] 18 p3076 N85-2804[illegible]
Diffusion of strongly magnetized cosmic ray particles in a turbulent medium
[OG-7.2-16] 23 p4015 N85-34[illegible]
MAGNETO-OPTICS
Guided-wave optic devices for integrated optic information processing
[AD-A145695] 02 p0280 N85-1162[illegible]
Characterization of III-V compound semiconductor device materials
[AD-A148203] 08 p1228 N85-1771[illegible]
Evaluation of a magneto-optical filter and a Fabry-Perot interferometer for the measurement of solar velocity fields from space 14 p2442 N85-250[illegible]
Optical fiber magnetic field sensor with nanosecond response time
[DE85-006409] 18 p3110 N85-29[illegible]
Diagnostics of vector magnetic fields 18 p3206 N85-29[illegible]
The inference of vector magnetic fields from polarization measurements with limited spectral resolution 18 p3207 N85-29[illegible]
Magnetic materials
[AD-A154679] 21 p3580 N85-322[illegible]
Development of wide band recording materials
[AD-A154961] 21 p3589 N85-32[illegible]
MAGNETOACOUSTIC WAVES
Magnetosonic waves and their relationship with energetic protons 14 p2368 N85-24[illegible]
Oscillatory convection in sunspots 14 p2446 N85-250[illegible]
On running penumbral waves 14 p2453 N85-25150
MAGNETOACOUSTICS
Squid detection of acoustomagnetic effects 19 p3373 N85-30[illegible]
MAGNETOACTIVITY
NT MAGNETORESISTIVITY
Diamagnetic instability of cyclotron waves in plasma 21 p3693 N85-32[illegible]
MAGNETOELASTIC VIBRATIONS
U MAGNETOELASTIC WAVES
MAGNETOELASTIC WAVES
NT MAGNETOACOUSTIC WAVES

Influence of axial shaft load on operation of magnetoelastic torque transducer
14 p2270 N85-24065
Cyclotron absorption of fast magnetosonic wave in stellarator
21 p3693 N85-32945
Resonant ion acceleration by oblique magnetosonic shock wave in a collisionless plasma
[IPPJ-736] 23 p3975 N85-34643

MAGNETOELASTICITY
U MAGNETOSTRICTION

MAGNETOGASDYNAMICS
U MAGNETOHYDRODYNAMICS

MAGNETOGRAMS
U MAGNETIC SIGNATURES

MAGNETOHYDRODYNAMIC ACCELERATION
U PLASMA ACCELERATION

MAGNETOHYDRODYNAMIC FLOW
Solar flares and laboratory experiments on magnetic reconnection in current sheaths
02 p0162 N85-11099
Electric field and plasma energization in computer simulations of magnetotail reconnection
[DE84-014023] 02 p0265 N85-11859
The solar wind at 20-30 AU 02 p0301 N85-11950
Magnetohydrodynamic and gasdynamic theories for planetary bow waves
[NASA-CR-174132] 03 p0448 N85-12850
China report: Science and technology
[JPRS-CST-84-003] 04 p0491 N85-13132
Magnetohydrodynamic flow of two-component gas analyzed 04 p0491 N85-13133
Plasma flow in the near and distant geomagnetic tail
[DE84-014029] 04 p0534 N85-13415
Magnetohydrodynamic and gasdynamic theories for planetary bow waves
[NASA-CR-174135] 04 p0589 N85-13760
Application of the energy problem to the problem of plasma flow stability
[DE84-013359] 05 p0730 N85-14691
Magnetic effects in the heating and modification of flows in the outer stellar atmospheres with application to early type star case 08 p1235 N85-17783
On the hydrodynamical equations of astrophysical jets — active galactic nuclei 08 p1241 N85-17831
Centrifugally driven magnetohydrodynamic (MHD) winds and the nonthermal emission regions in Active Galactic Nuclei (AGN) 08 p1242 N85-17835
Macroscopic currents and wind perturbations in the frame of the wind and shock model — galactic nuclei
08 p1242 N85-17836
Simulation of thermal and electromagnetic processes in induction plasmatrons 12 p1841 N85-21552
Pressure-gradient-driven Tokamak resistive MHD instability in the banana-plateau collisionality regime
[DE85-004568] 12 p1937 N85-22171
Wakes and differential charging of large bodies in low Earth orbit 13 p1992 N85-22488
Efficiency of electric field transfer at Earth's magnetopause and flow amplitudes related to reconnection 14 p2356 N85-24557
Hydromagnetic vortices: An interpretation for dawnside events as on December 11, 1977 — magnetotail
14 p2371 N85-24653
Kinematic dynamo theory for an arbitrary mean flow
14 p2448 N85-25108
A siphon flow model for Evershed motion — sunspot regions 14 p2453 N85-25147
An interplanetary magnetic field ensemble at 1 AU
[NASA-TM-86209] 16 p2862 N85-27784
Flat magnetohydrodynamic induction pump
17 p2939 N85-28145
Dependence of characteristics of centrifugal magnetohydrodynamic conduction pump on electrical conductance of end walls. Part 1: Experiment
17 p2939 N85-28146
Reversed field pinch dynamics and transport studies
[DE85-007553] 18 p3189 N85-29778
Screening phase transitions in two-dimensional Coulomb gas
[NOTA-INTERNA-830] 18 p3192 N85-29798
Current evolution in a numerical emerging-magnetic-flux model 18 p3204 N85-29875
Thermal contraction of current flow through electrode turbulent boundary layer 21 p3690 N85-32926
Modeling the exhaust of the pulsed plasma thruster
[AD-A155344] 21 p3707 N85-33018
Time-dependent nonlinear cosmic ray shocks confirming abstract
[OG-8.1-3] 23 p4017 N85-34893
Efficiency of regular acceleration of particles by a shock wave at different injection regimes
[OG-8.1-13] 23 p4019 N85-34902

MAGNETOHYDRODYNAMIC GENERATORS
Khibiny experiment described
07 p0981 N85-16230
MHD performance demonstration experiment, FY 1974 to FY 1984
[DE85-000854] 08 p1224 N85-17709
Development of materials for open-cycle MHD
[DE84-017283] 09 p1393 N85-18770
Three-dimensional analysis of heat transfer and gas flow in a radiant furnace
[DE84-011732] 11 p1633 N85-20284
Performance of solar thermal systems with liquid metal MHD conversion
[DE85-002758] 11 p1675 N85-20555
Experimental investigations of thermal radiation from potassium atoms in magnetohydrodynamic system: Preliminary report
[DE85-003715] 12 p1936 N85-22169
Radiation heat transfer within an open-cycle MHD generator channel — mathematical models
[NLR-TR-83066-U] 14 p2304 N85-24267
Parametric study of potential early commercial power plants Task 3-A MHD cost analysis
[NASA-CR-175839] 16 p2817 N85-27377
MHD channel development
[DE85-008305] 18 p3192 N85-29796
Performance and electric field limitations in inflow disk MHD generators 20 p3534 N85-31987
MHD generator CDIF
[DE85-011369] 20 p3536 N85-32001
Thermal contraction of current flow through electrode turbulent boundary layer 21 p3690 N85-32926
Study to assess the effects of magnetohydrodynamic electromagnetic pulse on electric power systems, phase 1, volume 3
[DE85-011301] 24 p4156 N85-35771

MAGNETOHYDRODYNAMIC STABILITY
NT WEIBEL INSTABILITY
MHD instabilities in simple plasma configuration
[AD-A144936] 01 p0121 N85-10829
Experimental observation of neoclassical currents
[DE84-015113] 01 p0122 N85-10834
Means of varying conditions in the expanded boundary divertor without affecting energy confinement
[DE84-013840] 01 p0122 N85-10836
Plasma drift equilibrium (gyration) in toroidal systems with complex magnetic-field geometry
[DE84-015627] 01 p0122 N85-10839
Studies of solar flares and coronal loops
[AD-A145009] 01 p0130 N85-10898
Bremsstrahlung radiation from longitudinal plasma waves caused by subthermal electrons in plasma
02 p0264 N85-11730
Neutral beam interactions with materials
[AD-A145636] 02 p0285 N85-11857
Physics of reversed-field pinch profile sustainment
[DE84-014024] 04 p0565 N85-13602
Theoretical studies in tandem mirror physics
[DE84-015634] 04 p0566 N85-13604
Theory of resistive ballooning modes in Tokamaks
[DE84-015626] 04 p0566 N85-13606
Internal helical mode m = 1 of a Tokamak in the plateau and banana regimes
[DE84-015623] 04 p0566 N85-13607
Fusion plasma theory. Task 1: Magnetic confinement fusion plasma theory
[DE84-014941] 04 p0566 N85-13608
Fusion plasma theory. Task 3: Auxiliary heating in Tokamaks and tandem mirrors
[DE84-014940] 04 p0566 N85-13609
High-Beta Tokamak research
[DE84-016470] 04 p0568 N85-13618
High-Beta plasma theory
[DE84-016471] 04 p0568 N85-13619
Proceedings of the US-Japan Theory Workshop on 3-D MHD Studies
[DE84-012019] 04 p0568 N85-13620
Application of the energy problem to the problem of plasma flow stability
[DE84-013359] 05 p0730 N85-14691
Stabilization of the hot electron precessional mode in a symmetric tandem mirror by the axial variation of radial electric field
[DE84-016389] 05 p0730 N85-14692
Passive stabilization of vertical instability in Tokamak reactor 06 p0775 N85-14958
Limits of possible operation of the R-Tokamak due to ideal MHD instabilities
[IPPJ-694] 06 p0863 N85-15486
Theoretical investigations relevant to magnetic fusion research, April 1, 1983 - March 31, 1984
[DE85-001778] 06 p0865 N85-15498
Shear-Alfven dynamics of toroidally confined plasmas, part A
[DE85-001590] 06 p0866 N85-15502
Shear-Alfven dynamics of toroidally confined plasmas, part B
[DE85-001787] 06 p0866 N85-15504
The role of finite parallel length on the stability of barium clouds
[AD-A146972] 07 p0996 N85-16328
Asymptotic behaviour of the plasma equation
[AD-A147242] 07 p1031 N85-16549
Experimental results on Tokamak beta limits from ISX-B
[DE84-015372] 07 p1046 N85-16644
Radiatively driven winds and what they imply: A review of radiative driven instabilities and their importance in hot stars 08 p1235 N85-17782
Impurity control by additional current rise and gas puffing during ICRF heating in JIPP T-IIU Tokamak
09 p1387 N85-18725
Impact of atomic data on Tokamak modeling
09 p1390 N85-18743
The plasma assisted modified betatron
[AD-A148729] 09 p1390 N85-18746
MHD equilibrium and stability for stellarator/torsatron configurations
[DE85-001139] 09 p1391 N85-18750
Effect of alpha particles on the stability of Elmo Bumpy Torus (EBT) reactor
[DE84-017266] 09 p1392 N85-18759
Brief outline of analytic stability studies of magnetically insulated systems — biblioliographies
[DE85-000212] 09 p1393 N85-18765
Effects of q and high beta on Tokamak stability
[DE84-016850] 09 p1393 N85-18767
Four phase model for turbulent instabilities calculation in plasma jets
[IPF-84-2] 09 p1394 N85-18776
Experimental investigation of certain beam transport issues in a pulsed transmission line linear accelerator
[DE85-002310] 10 p1555 N85-19805
Small, octopole-stabilized tandem mirror reactor
[DE85-002144] 10 p1559 N85-19832
Finite-(beta) optimization of tandem mirrors
[DE85-002658] 10 p1560 N85-19835
Role of multiple helicity nonlinear interaction of tearing modes in dynamo and anomalous thermal transport in the Reversed Pitch Field
[DE85-002176] 10 p1560 N85-19839
Electrodynamic interactions 11 p1643 N85-20348
Explosive instability of strong electromagnetic wave in plasma 11 p1719 N85-20817
Coronal spectroscopy in laser plasmas
[DE85-002817] 11 p1730 N85-20880
Observations of low frequency plasma fluctuations in ELMC Bumpy Torus
[DE85-003796] 11 p1732 N85-20895
Theory of resistivity-gradient-driven turbulence
[DE85-002175] 11 p1733 N85-20898
Activation of solar flares 12 p1954 N85-22276
Signatures of the coalescence instability in solar flares
12 p1956 N85-22293
Discharges on a negatively biased solar cell array in a charged-particle environment 13 p1994 N85-22499
Increased hot-electron production at quarter-critical density in long-scalelength, laser-plasma interactions
[AD-A150519] 13 p2161 N85-23411
Lower hybrid heating and current drive, and ion cyclotron heating experiments on the Alcator C and the Versator II Tokamaks
[DE85-004918] 13 p2161 N85-23412
Theoretical and observational studies of stellar activity
13 p2171 N85-23468
Magnetic instabilities — solar magnetism
14 p2449 N85-25117
Energy balance in resistive instabilities — solar prominences 14 p2454 N85-25155
Asymmetric flux generation and its relaxation in reversed field pinch
[IPPJ-712] 15 p2656 N85-26387
Effects of finite current channel width on the current convective instability
[AD-A151414] 15 p2656 N85-26389
Stability and vibrations of internal windings of high-current superconducting solenoid magnets
[AD-A151465] 15 p2656 N85-26390
Effects of magnetic shear on lower hybrid waves in the suprauroral region
[AD-A151960] 15 p2656 N85-26392
MHD fluctuations in ISX-B
[DE85-004800] 15 p2657 N85-26395
Plasma-wall interactions in tandem mirror machines
[DE85-006387] 15 p2657 N85-26399
Toroidal equilibrium with low frequency wave driven currents
[DE85-005790] 15 p2658 N85-26401
Theoretical studies of Elmo Bumpy Torus
[DE85-007202] 15 p2658 N85-26402
Finite orbit analysis for long wavelength modes in a plasma with a hot component
[DE85-006896] 15 p2658 N85-26404

Optimal control theory applied to fusion plasma thermal stabilization
[DE85-007599] 15 p2658 N85-26405
Ballooning beta limits of dee and bean shaped Tokamaks
[IPPJ-713] 16 p2866 N85-27676
Magnetohydrodynamic stability of spheromak plasma in toroidal flux conserver with rectangular cross section
[IPPJ-716] 16 p2866 N85-27678
Geophysical plasmas and atmospheric modeling
[AD-A152605] 17 p2993 N85-28487
Application of the MHD energy principle to magnetostatic atmospheres
[NASA-CR-175967] 18 p3136 N85-29420
Millimeter wave generation by relativistic electron beams
[AD-A153960] 18 p3179 N85-29706
Research with high-power short-wavelength lasers
[DE85-010329] 19 p3276 N85-30332
Two-point theory of current-driven ion-cyclotron turbulence
[DE85-010114] 19 p3372 N85-30918
Stability of a hot symmetric tandem mirror with thermal barrier
[DE85-010539] 19 p3377 N85-30952
Effects of coronal disturbances on the ionization state of the solar wind
[NASA-CR-175967] 19 p3385 N85-31000
Nuclear responses in INTOR plasma stabilization elements
[DE85-010489] 20 p3535 N85-31995
Drift anisotropy instability of a finite Beta magnetospheric plasma
[IFSI-84-12] 20 p3536 N85-32005
Diamagnetic instability of cyclotron waves in plasma
21 p3663 N85-32948
Low frequency instabilities driven by an ion temperature anisotropy
[AD-A154902] 21 p3707 N85-33016
User's manual for the FLORA equilibrium and stability code
[DE85-013182] 23 p3966 N85-34590
Magnetohydrodynamic equilibrium and stability of spheromak with spheroidal plasma-vacuum interface
[IPPJ-732] 23 p3974 N85-34640
Low frequency instability in a mirror field
23 p3977 N85-34657
ECH tokamak
[DE85-012074] 23 p3984 N85-34707
Onset of solar flares as predicted by two-dimensional MHD-models of quiescent prominences
[SH-1.3-1] 23 p3992 N85-34750
A cosmic ray driven instability
[OG-8.1-5] 23 p4018 N85-34895

MAGNETOHYDRODYNAMIC TURBULENCE
NT PLASMA TURBULENCE
Random processes and magnetohydrodynamic turbulence 02 p0271 N85-11767
Magnetohydrodynamic (MHD) turbulence in radio galaxies 12 p1958 N85-22305
Forced MHD turbulence in a uniform external magnetic field
[NASA-CR-172576] 15 p2654 N85-26368
An interplanetary magnetic field ensemble at 1 AU
[NASA-TM-86209] 16 p2882 N85-27784
Cosmic ray modulation and turbulent interaction regions near 11 AU
[NASA-TM-86193] 18 p3209 N85-29909
Fractal structure of the interplanetary magnetic field
[NASA-TM-86212] 19 p3383 N85-30987
Prompt acceleration of ions by oblique turbulent shocks in solar flares
[SH-1.1-6] 23 p3989 N85-34733
Isotopic overabundances and the energetic particle model of solar flares
[SH-2.2-1] 23 p4000 N85-34796
Diffusion of strongly magnetized cosmic ray particles in a turbulent medium
[OG-7.2-16] 23 p4015 N85-34883

MAGNETOHYDRODYNAMIC WAVES
NT ELECTROSTATIC WAVES
NT PLASMA WAVES
Precipitation of protons with E sub p approximately 1 MeV near plasmopause 02 p0161 N85-11093
Fine structure of Alfven maser radiation
06 p0824 N85-15232
Shear-Alfven dynamics of toroidally confined plasmas, part A
[DE85-001590] 06 p0866 N85-15502
A leaky waveguide model for MHD wave driven winds from coronal holes 08 p1235 N85-17781
Generation of Alfven waves due to thermal modulation of the electrical conductivity
[AD-A148369] 10 p1558 N85-19626
Driven global Alfven eigenmodes
[DE85-001056] 11 p1732 N85-20890
Forced recognition by nonlinear MHD waves and sequential triggering of solar flares
12 p1956 N85-22291
Nonlinear evolution of astrophysical Alfven waves
12 p1956 N85-22294
Hydromagnetic precursors of interplanetary plasma burst 13 p1976 N85-22414
Excitation of low-frequency plasma waves by a conducting, tethered satellite 13 p2171 N85-23470
Anisoptropy of Alfven wave absorption in ionosphere
14 p2339 N85-24484
Diagram of nonstationary rejoining of magnetic force lines 14 p2344 N85-24492
Magnetosphere-ionosphere interaction through hydromagnetic waves 14 p2364 N85-24610
Contribution of the Scandinavian Twin Auroral Radar Experiment (STARE) radar to the understanding of the physical mechanisms associated with Pc5 pulsations
14 p2364 N85-24613
Propagation and amplification of Ion Cyclotron Waves (ICW's) in a multicomponent plasma. The Earth magnetosphere as a giant maser for Alfven waves
14 p2368 N85-24634
Results of ULF-wave investigations in the USSR
14 p2369 N85-24644
Magnetic pulsations recorded in northern Scandinavia during the IMS; a study of Pc 4-5 events
14 p2370 N85-24647
Implications of the global appearance of Pi2 and Pc 3 bursts 14 p2371 N85-24652
Magnetospheric wave characteristics derived from cross-spectral analysis 14 p2371 N85-24650
Nonlinear dynamos — solar activity
14 p2447 N85-25106
Observational constraints on heating processes — solar corona 14 p2449 N85-25115
Waves in inhomogeneous media — magnetohydrodynamic waves; solar atmosphere
14 p2448 N85-25116
Dynamo action of magnetostrophic waves — solar atmosphere 14 p2451 N85-25136
Coronal heating by turbulent phase mixed MHD waves — solar corona 14 p2453 N85-25148
Effects of atmospheric stratification on dissipative acoustic and Alfven waves — solar atmosphere
14 p2453 N85-25149
On running penumbral waves
14 p2453 N85-25150
Comments on the paper by F. Pegoraro, L. Sugiyama: Spatial diffusion of charged high-energy fusion products by shear Alfven perturbations
[INPE-3291-PRE/606] 16 p2866 N85-27675
Solar wind observations associated with a slow forward shock wave at 0.31 AU
[MPAE-W-79-84-46] 17 p3055 N85-28909
Stability of a hot symmetric tandem mirror with thermal barrier
[DE85-010539] 19 p3377 N85-30952
Stochastic particle acceleration in solar flares
[SH-1.1-4] 23 p3989 N85-34731
Alfven wave scattering and the secondary to primary ratio
[OG-7.2-9] 23 p4015 N85-34878
Diffusion of strongly magnetized cosmic ray particles in a turbulent medium
[OG-7.2-16] 23 p4015 N85-34883
The role of cosmic rays and Alfven waves in the structure of the galactic halo
[OG-7.2-13] 23 p4016 N85-34885
A cosmic ray driven instability
[OG-8.1-5] 23 p4018 N85-34895
Relativistic transport theory for cosmic-rays
[OG-8.3-8] 23 p4022 N85-34926
Scale separation closure and Alfven wave turbulence
[DE85-013124] 24 p4095 N85-35385
Parallel fast-forward shock within 1 AU: Helios-1 and 2 observations
[MPAE-W-79-84-27] 24 p4169 N85-35847

MAGNETOHYDRODYNAMICS
NT CYLINDRICAL PLASMAS
Fluctuation spectrum for linear gyroviscous MHD
[IPP-6/237] 01 p0121 N85-10828
MHD instabilities in simple plasma configuration
[AD-A144936] 01 p0121 N85-10829
Ceramic materials for MHD electrodes
[DE84-015580] 02 p0187 N85-11250
Destruction of magnetic surfaces in three-dimensional MHD equilibria 02 p0282 N85-11838
Electric field and plasma energization in computer simulations of magnetotail reconnection
[DE84-014023] 02 p0285 N85-11850
Magnetohydrodynamic and gasdynamic theories for planetary bow waves
[NASA-CR-174132] 03 p0448 N85-12850
High-Beta plasma theory
[DE84-016471] 04 p0568 N85-13619
Proceedings of the US-Japan Theory Workshop on 3-D MHD Studies
[DE84-012016] 04 p0568 N85-1
Special topics reports for the reference tandem mirror fusion breeder: Liquid metal MHD pressure drop effects in the packet bed blanket, volume 1
[DE85-002142] 06 p0865 N85-1
Spicules and surges
[AD-A146785] 07 p1061 N85-1
MHD performance demonstration experiment, FY 19 to FY 1984
[DE85-000854] 08 p1224 N85-1
Electromagnetic pulse (EMP) interaction with electric power systems. Power Systems Technology Program
[DE85-000166] 09 p1312 N85-1
Normal mode analysis for linear resistive magnetohydrodynamics
[IPP-6/235] 11 p1730 N85-2
Convergent spectral representation for 3-dimensional inverse MBD equilibria
[DE85-000666] 11 p1733 N85-2
Strong iron accelerating by collisionless magnetosonic shock wave propagating perpendicular to a magnetic field
[IPPJ-709] 12 p1935 N85-2
Hydrodynamics of astrophysical jets — active galactic nuclei 12 p1958 N85-2
An analytic model for hydromagnetospheres — stellar winds; pulsars; cosmic jets 12 p1959 N85-2
Development of a Global 3-D magnetohydrodynamic computational model for solar wind-cometary and planetary studies
[NASA-CR-175490] 12 p1962 N85-2
Physics of the inner heliosphere: Mechanisms, models and observational signatures
[NASA-CR-175632] 13 p2205 N85-2
Dynamics of solid body with ellipsoidal cavity containing magnetic fluid 14 p2279 N85-241
Electromagnetic field of currents and its use to estimate total conductivity of sedimentary deposits in Western Black Sea 14 p2334 N85-24
Experimental facility for studying MHD effects in liquid metal cooled blankets
[DE85-000583] 14 p2423 N85-24
Magneto-fluid-dynamic issues for fusion first wall and blanket systems
[DE85-004022] 14 p2424 N85-24
Magnetohydrodynamic considerations for the design of self-cooled liquid-metal fusion reactor blankets
[DE85-000242] 14 p2425 N85-24
Numerical simulations of convectively excited gravity waves 14 p2444 N85-25
The hydromagnetics of the Sun — conference
[ESA-SP-220] 14 p2445 N85-25
Magnetoconvection: The interaction of convection and small scale magnetic fields — photosphere
14 p2446 N85-25
Nonlinear dynamos — solar activity
14 p2447 N85-251
A numerical simulation of the formation of solar prominences 14 p2448 N85-2511
The possible role of electrical currents in coronal phenomena 14 p2453 N85-2515
Solar magnetohydrodynamics: Symposium review
14 p2455 N85-25
Magnetohydrodynamics of Earth's bow shock
15 p2461 N85-25
Development of a global 3-D magnetohydrodynamic computational model for solar wind/cometary and planetary studies
[NASA-CR-175724] 15 p2684 N85-26
Stream dynamics between 1 AU and 2 AU: A detailed comparison of observations and theory
[NASA-TM-86086] 15 p2684 N85-26
Asymptotic solutions of MHD equations with finite conductivity
[REPT-12/1984] 16 p2852 N85-27
A four-field model for Tokamak plasma dynamics
[DE85-007111] 16 p2868 N85-27
Fluid modeling of magnetized plasmas
[DE85-007679] 17 p3039 N85-28
Electromagnetic solitary waves in magnetized plasma
[DE85-010064] 18 p3190 N85-29
Coal-Fired MHD Combustor Development Project, Phase 3D
[DE85-008822] 18 p3192 N85-29
MHD channel development
[DE85-008305] 18 p3192 N85-29
The effects of alpha particle production on the stability of an Elmo Bumpy Torus (EBT) reactor
19 p3369 N85-30
Solar-wind magnetosphere energy input functions
[NASA-CR-176021] 19 p3385 N85-31
Magnetohydrodynamics and the National Coal Science, Technology, and Engineering Development Acts
[S-HRG-98-1179] 20 p3535 N85-31

Planetary Dynamics
[NASA-CR-176001] 21 p3679 N85-32857
Plasmadynamic methods for generating powerful light pulses 21 p3693 N85-32943
A system of magnetohydrodynamic-type equations
21 p3693 N85-32946
Method and apparatus for maintaining equilibrium in a helical axis stellarator
[DE85-011626] 22 p3845 N85-33815
Linear filters as a method of real-time prediction of geomagnetic activity
[DE85-010760] 22 p3860 N85-33899
Moving finite element method for ICF target implosion
23 p3880 N85-34675
Instrument to synchronize Thomson scattering diagnostic measurements with MHD activity in a Tokamak
[DE85-012082] 23 p3884 N85-34708
Onset of solar flares as predicted by two-dimensional MHD-models of quiescent prominences
[SH-1.3-1] 23 p3892 N85-34750
The role of cosmic rays in magnetic hydrodynamics of interstellar medium
[OG-7.2-15] 23 p4015 N85-34882
Some rigorous results concerning spectral theory for ideal MHD
[DE85-013427] 24 p4156 N85-35770

MAGNETOIONIC PLASMA
U PLASMAS (PHYSICS)

MAGNETOMECHANICS (PHYSICS)
Contributions to the 7th International Acoustic Emission Symposium
[AD-A148368] 02 p0275 N85-11792
Moessbauer study of amorphous Fe(67)Co(18)B(14)S(1)
[AERE-R-11526] 11 p1737 N85-20928

MAGNETOMETERS
NT VARIOMETERS
Magnetic properties of the cobalt matrix in WC-Co compacts 02 p0177 N85-11186
Present practice for the recording of the Earth magnetic field — geophysical observatories
04 p0519 N85-13317
Amplitude mode magnetic sensors
[AD-D011335] 07 p0961 N85-16094
Investigation of dynamic noise affecting geodynamics information in a tethered subsatellite
[NASA-CR-174292] 08 p1174 N85-17405
An inexpensive vector thin film magnetometer
[AD-A148725] 09 p1323 N85-18310
A preliminary study of a cryogenic equivalence principle experiment on Shuttle
[NASA-CR-171300] 10 p1426 N85-18994
Note of the dynamic behavior of a magnet system suspended by a thin fiber, with special reference to the Quartz Horizontal Magnetometer (QHM)
[DMI-GEOPHYS-PAPERS-R-70]
11 p1714 N85-20785
Rotating squid magnetometers and gradiometers
[AD-D011529] 12 p1849 N85-21600
Satellite, auroral radar and ground magnometer observations of transient ULF pulsations
14 p2369 N85-24645
Ground magnetic observations of high-latitude Pi2 pulsations: Scandinavian magnetometer array results
14 p2370 N85-24649
The use of a self-compensated magnetometer in an economical navigation system for the helicopter
16 p2697 N85-26650
A method of estimating aircraft attitude from fly by wire flight control system data 16 p2697 N85-26653
On the use of a sunward-libration-point orbiting spacecraft as an IMF monitor for magnetospheric studies
[NASA-CR-175809] 16 p2825 N85-27426
Results of the magnetic field experiments E2 and E4 onboard Helios 1 and Helios 2 — magnetometer development 16 p2885 N85-27799
Rome/Goddard Space Flight Center (GSFC) magnetic field experiment: A summary of results — flux gate magnetometer 16 p2885 N85-27800
Research relative to the development of a cryogenic microwave cavity gradiometer for orbital use
[NASA-CR-176002] 19 p3222 N85-29980
Overview of applications of SQUIDS
[DE85-009942] 20 p3456 N85-31480
Spaceborne gradiometer error analysis
20 p3492 N85-31707
Fluxgate magnetometer (SSM) for the defense meteorological satellite program (DMSP) block 5D-2, flight 7
[AD-A150229] 21 p3560 N85-32143
The Galileo spacecraft magnetometer boom
22 p3796 N85-33513
Magnetic search system
[PB85-186109] 23 p3949 N85-34477
Procedure for editing the fluxgate magnetometer data of the AFGL (Air Force Geophysics Laboratory) magnetometer network
[AD-A156331] 24 p4117 N85-35523

MAGNETOMETRY
U MAGNETIC MEASUREMENT

MAGNETOPAUSE
Magnetohydrodynamic and gasdynamic theories for planetary bow waves
[NASA-CR-174132] 03 p0448 N85-12850
Reduction and analysis of data from the plasma wave instruments on the IMP-6 and IMP-8 spacecraft
[NASA-CR-175127] 04 p0480 N85-12918
The Earth magnetosphere: A charged particle accelerator 04 p0519 N85-13315
Research relative to plasma transport across the magnetopause
[NASA-CR-174300] 07 p1045 N85-16636
Research study of space plasma boundary processes
[NASA-CR-174351] 10 p1586 N85-19623
The Earth's magnetopause — International Magnetospheric Study 14 p2355 N85-24549
Electric field and plasma observations near the magnetopause and bow shock during a rapid compression 14 p2355 N85-24553
Magnetic field observations at the dayside magnetopause: ISEE-1 and -2 contributions during the IMS 14 p2356 N85-24555
Efficiency of electric field transfer at Earth's magnetopause and flow amplitudes related to reconnection 14 p2356 N85-24557
Satellite-borne electric field measurements with spherical double probes — ISEE satellites
14 p2356 N85-24558
Energetic particle sounding at the magnetopause and implications for magnetic reconnection
14 p2356 N85-24559
Observations of energetic electron and ion distributions near the magnetopause at geosynchronous orbit and related ground effects 14 p2356 N85-24560
Structure of the boundary layer for steady-state magnetopause reconnection 14 p2356 N85-24561
Characteristics of Pc 4,5 pulsations and their source mechanisms 14 p2370 N85-24646
The structure, stability, wave transmission and energy transfer at the Earth's magnetopause
14 p2372 N85-24661
Bursts of relativistic electrons in magnetopause and in outer radiation belt 16 p2722 N85-26801

MAGNETOPLASMADYNAMICS
Convection of plasma in polar ionosphere, comparison of measurements from Cosmos-184 with model dependent on interplanetary magnetic field vector
02 p0160 N85-11066
The Earth's magnetopause — International Magnetospheric Study 14 p2355 N85-24549
The structure and dynamics of the magnetosphere: Progress in the IMS 14 p2355 N85-24550
Plasma sheet dynamics deduced from ISEE-1 and -2 energetic particle flux data 14 p2358 N85-24570

MAGNETOPLASMAS
U PLASMAS (PHYSICS)

MAGNETORESISTIVITY
Magnetoconductance in aluminum films, wires, and cylinders 19 p3374 N85-30928
Development of position sensors for microcomputer-oriented sensor systems
[BMFT-FB-T-85-021] 24 p4091 N85-35361

MAGNETOSONIC RESONANCE
Cyclotron absorption of fast magnetosonic wave in stellarator 21 p3693 N85-32945

MAGNETOSPHERE
NT GEOMAGNETIC TAIL
NT MAGNETOPAUSE
The propagation and growth of whistler mode waves generated by electron beams in Earth's bow shock
[AD-A145572] 02 p0226 N85-11492
Uranus and Neptune
[NASA-CP-2330] 02 p0298 N85-11927
Magnetospheric structures: Uranus and Neptune
02 p0301 N85-11949
Magnetosphere, rings, and moons of Uranus
02 p0301 N85-11951
Do the satellites of Uranus control its magnetosphere?
02 p0301 N85-11952
Magnetospheric plasma studies using data from the dynamics high and low altitude plasma instruments
[AD-A145751] 03 p0392 N85-12505
On the cause of X-line formation in the near-Earth plasma sheet: Results of adiabatic convection of Plasma-Sheet-Plasma
[AD-A145835] 03 p0398 N85-12525
The Earth magnetosphere: A charged particle accelerator 04 p0519 N85-13315
Hot plasma particles in the Earth's outer magnetosphere: New understandings during the IMS
[DE84-016826] 05 p0677 N85-14348
Summaries of physical research in the geosciences
[DE85-001882] 06 p0818 N85-15194
Observation of natural noise near upper hybrid resonance in terrestrial magnetosphere by Prognoz-5 satellite 06 p0822 N85-15221
Electric field in plasma layer of magnetosphere during preliminary substorm phase 06 p0824 N85-15231
Fine structure of Alfven maser radiation
06 p0824 N85-15232
Birkeland currents correlated with dc-electric fields observed during the CENTAUR BBX rocket experiments
[DRI-6-84] 06 p0834 N85-15311
Electric fields in Earth orbital space
[AD-A146448] 06 p0835 N85-15313
Region 1 birkeland currents from a global MHD simulation of the magnetosphere
[AD-A147435] 07 p0997 N85-16335
Earth's radiation belts
[AD-A147927] 07 p0998 N85-16339
Ionospheric and magnetospheric modifications caused by VLF waves
[AD-A146210] 08 p1186 N85-17475
Current carriers for the field-aligned current system
[NASA-TM-86161] 08 p1260 N85-17925
Morphology of keV-electrons in the Earth's magnetosphere as observed by GEOS 1
[DRI-3-84] 09 p1350 N85-18496
Partial penetration of IMF B(sub y) into the magnetosphere
[DRI-5-84] 10 p1514 N85-19554
Recent investigations at INPE in magnetospheric physics and geomagnetism
[INPE-3280-PRE/603] 10 p1514 N85-19555
Ionospheric research at INPE
[INPE-3279-PRE/602] 10 p1514 N85-19556
A modeling analysis program for the JPL table mountain Io sodium cloud data
[NASA-CR-175474] 10 p1572 N85-19910
High energy particle effects in the D region during and after geomagnetic storms 11 p1664 N85-20485
Application of dimensional analysis to the problem of solar wind-magnetosphere energy coupling
[DE85-002414] 11 p1674 N85-20551
A modeling analysis program for the JPL Table Mountain Io sodium cloud data
[NASA-CR-175493] 11 p1681 N85-20589
Magnetospheres and winds in the helium weak stars: Observations of C 5 in upper main sequence CP stars
11 p1759 N85-21066
Substorms in the Earth's atmosphere
[DE85-000654] 12 p1890 N85-21861
Space research and the new approach to the mechanics of fluid media in cosmos 12 p1953 N85-22271
Magnetospheres in the solar system
12 p1954 N85-22274
Particle transport in planetary magnetospheres
12 p1954 N85-22275
The axisymmetric pulsar magnetosphere
12 p1955 N85-22279
Nonlinear waves in the magnetosphere of pulsars
12 p1955 N85-22281
About static and dynamic solutions of the aligned rotator model — pulsar magnetospheres
12 p1958 N85-22306
An analytic model for hydromagnetospheres — stellar winds; pulsars; cosmic jets 12 p1959 N85-22313
Plans for interbol satellite experiment
13 p1977 N85-22407
Aerospace spacecraft-charging guidelines document
13 p1994 N85-22501
Argon ion pollution of the magnetosphere
13 p1996 N85-22523
Excitation of low-frequency plasma waves by a conducting, tethered satellite 13 p2171 N85-23470
Interaction of the magnetospheric ions with the surfaces of the icy satellites of Saturn 13 p2174 N85-23491
Diurnal variations in terrestrial magnetic field and structure of magnetosphere 14 p2344 N85-24493
Excitation of geomagnetic Pci-2 and pulsations with decreasing period during microsubstorms
14 p2344 N85-24494
Plasma and magnetospheric research
[NASA-CR-175675] 14 p2354 N85-24543
Achievements of the International Magnetospheric Study (IMS) — conference
[ESA-SP-217] 14 p2354 N85-24544
Some contributions to knowledge of the magnetospheric plasma by ISEE-1 investigators
14 p2354 N85-24546
The structure and dynamics of the magnetosphere: Progress in the IMS 14 p2355 N85-24550

Observations of the magnetospheric boundary layers — International Magnetospheric Study
14 p2356 N85-24551
Hot plasma and energetic particles in the Earth's outer magnetosphere: New understandings during the IMS
14 p2356 N85-24552
The keV electrons and 80 keV protons in the vicinity of the high latitude magnetosphere and at the bow shock 14 p2356 N85-24554
Magnetic field in the Earth's outer magnetosphere: Prognoz-6, -7 data 14 p2356 N85-24556
The application of dimensional analysis to the problem of solar wind-magnetosphere energy coupling
14 p2357 N85-24564
Coupling of the solar wind to measures of magnetic activity 14 p2357 N85-24565
Entry of solar energetic protons into the distant plasma sheet dependence on distance from the neutral sheet
14 p2357 N85-24567
Particle sources, transport, storage and precipitation — magnetosphere 14 p2359 N85-24576
IMS advances in studies of field-aligned currents and their related electrodynamics 14 p2359 N85-24578
Electrodynamics of magnetosphere-ionosphere coupling 14 p2359 N85-24579
Achievements of the plasma composition experiment on ISEE-1 during the IMS 14 p2360 N85-24583
Observations during a magnetosphere substorm triggered by a Storm Sudden Commencement (SSC): A case study 14 p2361 N85-24588
Disturbance of midlatitude electrodynamic parameters due to the magnetospheric convection
14 p2362 N85-24593
The magnetospheric convection electric field at ionospheric altitudes: A case study based on STARE and Saint-Santin data 14 p2362 N85-24594
Results of the Langmuir-probe experiment on board Intercosmos-18 — ionosphere-magnetosphere interaction 14 p2362 N85-24596
Comparison of magnetospheric and ionospheric electric fields using different empirical mapping factors
14 p2362 N85-24597
Solar wind control of electric fields and currents in the magnetosphere and ionosphere
14 p2364 N85-24608
Ionosphere-magnetosphere coupling and convection
14 p2364 N85-24609
Magnetosphere-ionosphere interaction through hydromagnetic waves 14 p2364 N85-24610
Pc 1-2 pulsations and related phenomena: A review — geomagnetic pulsations 14 p2364 N85-24611
An evaluation of the contributions of the IMS to experimental and theoretical studies of ULF plasma
14 p2365 N85-24614
Solar wind control of magnetospheric convection
14 p2365 N85-24615
Magnetospheric effects on the upper atmosphere
14 p2365 N85-24616
ELF chorus in the Earth's outer magnetosphere
14 p2366 N85-24624
Contribution of relaxation sounding experiments to the understanding of magnetospheric processes
14 p2371 N85-24655
Contribution of mutual impedance experiments to the understanding of magnetospheric processes — GEOS satellites 14 p2371 N85-24656
The use of the spectral matrix in analyzing the propagation characteristics of electromagnetic emissions — magnetosphere 14 p2371 N85-24658
Magnetospheric wave characteristics derived from cross-spectral analysis 14 p2371 N85-24659
Advances in magnetospheric plasma-wave research during the IMS 14 p2372 N85-24662
Active Magnetospheric Particle Tracing Explorers (AMPTE)
[AD-A151072] 14 p2374 N85-24674
Dynamo action of magnetostrophic waves — solar atmosphere 14 p2451 N85-25136
Space-time features of solar cosmic ray penetration into high latitude regions of Earth's magnetosphere based on Intercosmos-19 satellite data 15 p2481 N85-25310
Modeling longitudinal motions of thermal O+ and H+ ions in magnetic field tube convective through daytime polar cusp 15 p2481 N85-25314
Plasma and magnetospheric research
[NASA-CR-171447] 15 p2591 N85-25976
Dynamics of charged small particles — Jupiter, Saturn magnetospheres 15 p2676 N85-26522
On planetary rings as sources and sinks of magnetospheric plasmas 15 p2677 N85-26526
Electrons and cosmic ray produced protons in Saturn's inner magnetosphere
[NASA-TM-87469] 15 p2679 N85-26546
Coupling of the solar wind to measures of magnetic activity
[DE85-002415] 15 p2685 N85-26580
Substorms in energetic radiation belt particles according to data from Meteor artificial Earth satellite
16 p2719 N85-26788
Modeling plasma mantle of Earth's magnetosphere
16 p2720 N85-26790
Orientation and strength of Martian magnetic dipole
16 p2723 N85-26808
Possible configuration of Martian magnetosphere
16 p2723 N85-26809
Electric field and energy transfer by magnetopause reconnection
[INPE-3448-PRE/701] 16 p2826 N85-27432
Solar activity monitoring satellite (SAMSAT): Impact on space environment services
[PB85-165066] 16 p2868 N85-27818
IMS (International Magnetospheric Study) contributions to the understanding of auroral precipitation, transport, and particle sources
[AD-A152320] 17 p2992 N85-28492
The boundary layers as the primary transport regions of the Earth's magnetotail
[AD-A152714] 17 p2992 N85-28496
More on shock-wave studies with Prognoz-10 satellite
19 p3296 N85-30432
Functions of Prognoz-10: Intercosmos' station explained 19 p3296 N85-30433
Prognoz-10 Intercosmos' station launched to study shock waves 19 p3296 N85-30434
Magnetospheres of the outer planets
[AD-A154354] 19 p3384 N85-30996
Solar-wind magnetosphere energy input functions
[NASA-CR-176021] 19 p3385 N85-31001
The role of scientific ballooning for exploration of the magnetosphere
[TRITA-EPP-84-07] 20 p3494 N85-31724
Observations of low energy magnetospheric plasma outside the plasmasphere
[KGI-PREPRINT-075] 20 p3536 N85-32004
Drift anisotropy instability of a finite Beta magnetospheric plasma
[IFSI-84-12] 20 p3536 N85-32005
Magnetospheric response to solar wind variations
[DE85-010762] 20 p3547 N85-32074
Interaction between an interplanetary shock and the Earth's magnetosphere on 27 August 1978: ISEE-1 electric field and ISEE-2 plasma observations
[IFSI-84-15] 20 p3548 N85-32078
The radiation of the Vela pulsar
20 p3548 N85-32080
A model of pulsed radiation from the Crab pulsar
20 p3548 N85-32081
ISEE-1 data reduction and analysis plasma composition experiment
[NASA-CR-175306] 21 p3630 N85-32552
Statistical analyses in the study of solar wind-magnetosphere coupling
[DE85-009596] 22 p3859 N85-33898
Linear filters as a method of real-time prediction of geomagnetic activity
[DE85-010760] 22 p3860 N85-33899
On the emission region of gamma ray bursts
[OG-1.1-4] 22 p3861 N85-33906
Waves in Space Plasmas (WISP)
23 p3901 N85-34164
Cosmic-ray transport in the galactic magnetosphere
[OG-7.2-17] 23 p4016 N85-34884
The influence of quiet asymmetric magnetosphere on the cutoff rigidities of the main cone
[SH-6.1-10] 23 p4045 N85-35083
Penetration of solar protons into the Earth's magnetosphere on November 22, 1977
[SH-6.1-15] 23 p4046 N85-35086
Dynamics of the penetration boundaries of solar protons during a strong magnetic storm
[SH-6.1-16] 23 p4046 N85-35089
The influence of the Earth's magnetosphere on the high-energy solar protons
[SH-6.1-22] 23 p4046 N85-35093
A suggested standardized format for cosmic ray ground-level event data
[SH-9.1-15] 23 p4052 N85-35130
Observation of nuclei with energies 8-30 MeV per nucleon in the Earth's magnetosphere at the altitudes 350 KM
[SH-10.1-5] 23 p4053 N85-35136
Two-dimensional quasineutral description of particles and fields above discrete auroral arcs
[NASA-CR-176170] 24 p4116 N85-35517
High energy radiation from neutron stars
[DE85-014353] 24 p4169 N85-35843

MAGNETOSPHERIC ELECTRON DENSITY
Energetic particle sounding at the magnetopause and implications for magnetic reconnection
14 p2356 N85-24559
Morphology of 2keV-electrons observed by GEOS 1
14 p2360 N85-24581
Coordinated balloon-satellite studies of energe electron precipitation mechanisms
14 p2360 N85-24
Contribution of relaxation sounding experiments to the understanding of magnetospheric processes
14 p2371 N85-24
Ionospheric electron density profile and relat studies
[AD-A155257] 21 p3632 N85-32

MAGNETOSPHERIC INSTABILITY
Cold streams of ionospheric oxygen in the plasma she during the CDAW-6 event of March 22, 1979
[NASA-CR-174064] 03 p0393 N85-1261
Repulsive force of magnetic clouds during solar fla and magnetospheric substorms
06 p0824 N85-152
Long-period magnetospheric pulsations observed wi an electric field experiment in the magnetosphere
14 p2369 N85-24
Magnetospheric pulsations observed by ISEE 1 and 2 satellites 14 p2369 N85-24
Characteristics of Pc 4,5 pulsations and their sourc mechanisms 14 p2370 N85-24
Ionospheric electron density profile and relat studies
[AD-A155257] 21 p3632 N85-32
Robinson instability and beam loading
[DE85-013301] 24 p4151 N85-357

MAGNETOSPHERIC ION DENSITY
NT MAGNETOSPHERIC PROTON DENSITY
Achievements of the plasma composition experim on ISEE-1 during the IMS 14 p2360 N85-245

MAGNETOSPHERIC PROTON DENSITY
Energetic particle sounding at the magnetopause and implications for magnetic reconnection
14 p2356 N85-245
Magnetotail current sheet and energetic particles observed on ISEE-1 14 p2357 N85-245
Magnetosonic waves and their relationship wi energetic protons 14 p2368 N85-246

MAGNETOSTATICS
Magnetostatic wave frequency analyzer apparatus
[AD-D011249] 05 p0631 N85-1404
Improved magnetic bias and delay linearity in a magnetostatic wave delay line
[AD-D011441] 10 p1479 N85-1903
Magnetostatic problems in nonlinear media wi hysteresis
[DE85-003701] 10 p1482 N85-1935
Magnetostatic-wave propagation in a finite YIG-Loaded rectangular waveguide
[AD-A150332] 13 p2055 N85-228
Axisymmetric magnetofluidistatic (MFS) equilibria of solar coronal loops: An integral equation approach
14 p2449 N85-2511

MAGNETOSTRICTION
Estimate of sound absorption due to magnetoelastic interactions
[AD-A148216] 08 p1216 N85-1787
Analog frequency modulated laser using magnetostriction
[AD-D011701] 19 p3276 N85-3031
An experimental study of the magnetoelastic bending of thin plates made of soft ferromagnetic material
19 p3282 N85-3035

MAGNETOTELLURIC PROFILING
U MAGNETIC SURVEYS
MAGNETOVARIOGRAPHS
U VARIOMETERS
MAGNETRON SPUTTERING
Compensation of dangling bonds in A-Si, Ga:H alloys
[DE85-002905] 15 p2662 N85-264
MAGNETRONS
Rippled-field magnetron apparatus
[AD-D011354] 07 p0969 N85-1615
Experimental and theoretical investigation of microwave and millimeter wave radiation from hollow, rotating electron beams
[AD-A153827] 18 p3179 N85-2979
Improved negative ion source
[DE85-006445] 23 p3912 N85-342
MAGNETS
NT CRYOGENIC MAGNETS
NT ELECTROMAGNETS
NT FERRIMAGNETS
NT SUPERCONDUCTING MAGNETS
NT WIGGLER MAGNETS
On the calculating models of permanent magnets
[AD-A145111] 01 p0115 N85-1078
Shock electromechanical energy converter wi permanent magnet
[AD-D011228] 01 p0115 N85-1078
Calibration of hall probes
[CSIR-NAC-83-04] 01 p0116 N85-1078
Results of prototype field measurements on SM4
[NAC-83-01] 01 p0117 N85-1078

LAMPF transition-region mechanical fabrication
[DE84-017078] 04 p0562 N85-13577
Anisotropy and microstructure of rare earth permanent magnet materials
[AD-A146649] 06 p0859 N85-15460
Rotary magnetic heat pump
[DE84-017017] 09 p1320 N85-18303
Cobalt-free permanent magnet alloys
[AD-A148272] 10 p1441 N85-19079
Permanent magnet motors
[DE85-000860] 10 p1482 N85-19355
Non-contacting electromagnetic de-spin system for Earth orbiting satellites 12 p1946 N85-22225
The ferrite permanent magnet AC motor: A technical and economical assessment
[DE85-002480] 13 p2086 N85-22903
Mechanization and automation of production processes in turbine building 14 p2269 N85-24057
Linear motion valve
[NASA-CASE-MSC-20148-1] 18 p3115 N85-29264
3d calculations of a fixed field alternating gradient synchrotron magnet
[DE85-002742] 18 p3183 N85-29739
Investigation for low-cost permanent magnets
[AD-A154367] 19 p3260 N85-30212
Combined function lattices for a 6 GeV synchrotron light source
[DE85-010959] 19 p3367 N85-30685
Hot isostatically pressed Sm(2)(TM)17 magnets
[AD-A155479] 21 p3582 N85-32267
Tailored vacuum chambers for ac magnets
[DE85-010767] 21 p3591 N85-32319
SLC arc transport system: Magnet design and construction
[DE85-014289] 24 p4159 N85-35789

MAGNIFICATION
Investigation into the use of the TV magnifier in the Netherlands
[HSE-TRANS-11142] 20 p3533 N85-31986

MAGNIFIERS
U MAGNIFICATION

MAGNITUDE
NT STELLAR MAGNITUDE
On the error of typhoon intensity estimation by means of IR Dvorak technique occurring when the eye is very small 12 p1894 N85-21886

MAGNONS
Symmetry of exchange interaction in crystalline magnetic films 02 p0259 N85-11694
Observation of standing spinwaves in thin Fe-films by means of Raman spectroscopy
[DE85-003036] 11 p1735 N85-20913

MAGSAT SATELLITES
Analysis of the daily geomagnetic variation with the use of MAGSAT data — MAGSAT satellites
04 p0520 N85-13319
Science Applications, part 2 11 p1643 N85-20347

MAIN SEQUENCE STARS
NT PRE-MAIN SEQUENCE STARS
Theoretical studies of chromospheres and winds in cool stars
[NASA-CR-174204] 06 p0880 N85-15596
Theory tested by means of the stars — viability of the alpha-omega dynamo model 08 p1233 N85-17770
A survey for photometric variability from space
08 p1251 N85-17897
On the progenitors of white dwarfs
[NASA-CR-174378] 09 p1413 N85-18913
Interstellar extinction in the nucleus of H PER
11 p1749 N85-21001
Main sequence B stars with strong winds
11 p1750 N85-21005
A search for the spectroscopic binary companions of Polaris using IUE spectra 11 p1757 N85-21053
The solar stellar connection in the far ultraviolet
11 p1757 N85-21055
Magnetospheres and winds in the helium weak stars: Observations of C 5 in upper main sequence CP stars
11 p1759 N85-21066

MAINE
Peat resources of Maine. Volume 1: Aroostook County
[DE85-004196] 11 p1669 N85-20519
Peat resources of Maine. Volume 4: Southern and western Maine
[DE85-004198] 11 p1670 N85-20520
Peat resources of Maine. Volume 2: Penobscot County
[DE85-004195] 11 p1670 N85-20522
Peat resources of Maine. Volume 5: Washington County
[DE85-004197] 11 p1670 N85-20523

MAINTAINABILITY
Ada (trademark) training curriculum. Software engineering for managers m101 teacher's exercise guide
[AD-A145094] 01 p0104 N85-10695
Artificial intelligence approaches to monitoring system integrity
[AD-P003930] 02 p0246 N85-11610
Design for Tactical Avionics Maintainability
[AGARD-CP-361] 08 p1063 N85-16731
Objectives in studying the maintainability of aircraft systems 08 p1063 N85-16732
Joint service design for testability program
08 p1063 N85-16733
The embedded test (BIT): Impact on the total cost of possession 08 p1063 N85-16734
ATE user's view on design for maintainability
08 p1064 N85-16737
Maintainability: An ILS effort to manipulate LCC
08 p1064 N85-16743
The production of maintainable, trustworthy, and portable software 08 p1064 N85-16744
A description of a logistically ideal aircraft
[AD-A148425] 08 p1084 N85-16866
Computer aided of maintainability design: A feasibility study
[AD-A149293] 11 p1738 N85-20932
Maintainability time standards for electronic equipment
[AD-A149684] 12 p1834 N85-21507
Reliability analysis of automatic systems
[VTT-301] 12 p1863 N85-21682
A summary and assessment of historical reliability and maintainability data for solar hot water and space conditioning systems
[DE84-004521] 12 p1876 N85-21770
Design for tactical avionics maintainability, technical evaluation report
[AGARD-AR-204] 14 p2225 N85-23798
Statistical aspects of reliability, maintainability and availability
[AD-A151228] 15 p2640 N85-26282
Space Station Engineering and Technology Development
[NASA-CR-175806] 16 p2731 N85-26851
A framework for software development
[AD-A152067] 16 p2847 N85-27551
Maintenance of long life space systems, volume 1
[MATRA-0316/DX60-VOL-1] 18 p3066 N85-28964
Maintenance of long life space systems, volume 2
[MATRA-0350/DX60-VOL-2] 18 p3066 N85-28965
Los Alamos optical materials reliability, maintainability, and exposure testing program
[DE85-011894] 21 p3613 N85-32456
Air university commander's and supervisor's guide on substance abuse
[AD-A156336] 24 p4133 N85-35622

MAINTENANCE
NT AIRCRAFT MAINTENANCE
NT FILE MAINTENANCE (COMPUTERS)
NT SPACE MAINTENANCE
NT SPACECRAFT MAINTENANCE
Hot-gas cleanup for molten carbonate fuel cells-dechlorination and soot formation
[DE84-003072] 01 p0068 N85-10450
Stochastic properties of a sequence of interfailure times under minimal repair and under revival
[AD-A145003] 01 p0113 N85-10769
Updating logical databases
[AD-A144937] 01 p0125 N85-10860
Air Force Human Resources Laboratory report: Fiscal year, 1983
[AD-A145647] 02 p0238 N85-11548
Artificial Intelligence in Maintenance: Proceedings of the Joint Services Workshop
[AD-A145349] 02 p0244 N85-11592
The need for improvements in weapon system maintenance: What can AI (Artificial Intelligence) contribute?
[AD-P003913] 02 p0244 N85-11593
Artificial intelligence applications to maintenance
[AD-P003914] 02 p0244 N85-11594
On applying AI (Artificial Intelligence) to maintenance and troubleshooting
[AD-P003915] 02 p0244 N85-11595
Overview of training and aiding
[AD-P003917] 02 p0245 N85-11597
AI (Artificial Intelligence) approaches to troubleshooting
[AD-P003918] 02 p0245 N85-11598
Diagnosis based on description of structure and function
[AD-P003919] 02 p0245 N85-11599
Designing an expert system for training automotive electrical troubleshooting
[AD-P003926] 02 p0246 N85-11606
Models of natural intelligence in fault diagnosis tasks: Implications for training and aiding of maintenance personnel
[AD-P003927] 02 p0246 N85-11607
A generalized model of fault-isolation performance
[AD-P003928] 02 p0246 N85-11608
Expert systems in maintenance diagnostics for self-repair of digital flight control systems
[AD-P003933] 02 p0247 N85-11613
Model-based probabilistic reasoning for electronics troubleshooting
[AD-P003937] 02 p0247 N85-11617
Knowledge based tools for electronic equipment maintenance
[AD-P003940] 02 p0248 N85-11620
DELTA: An expert system for diesel electric locomotive repair
[AD-P003941] 02 p0248 N85-11621
LES: (Lockheed Expert System): A model-based expert system for electronic maintenance
[AD-P003944] 02 p0248 N85-11624
The application of artificial intelligence to a maintenance and diagnostic information system
[AD-P003945] 02 p0249 N85-11625
Future robotics program at San Antonio ALC (Air Logistics Center)
[AD-P004011] 03 p0309 N85-11991
Logistics support costs for the B-1B aircraft can be reduced
[AD-A145646] 03 p0309 N85-11996
Development of a pavement maintenance management system. Volume 10: Summary of development from 1974 through 1983
[AD-A146035] 03 p0320 N85-12067
Materials for emergency repair of runways
[AD-A146139] 03 p0320 N85-12068
Development of a pavement maintenance management system. Volume 9: Development of airfield pavement performance prediction models
[AD-A146150] 03 p0321 N85-12069
Correlation and reassessment of the OTEC plant power cycle
[DE84-015467] 04 p0529 N85-13362
Minimal cut-set methodology for artificial intelligence applications
[DE84-016674] 04 p0553 N85-13518
Electric vehicle maintenance
[PB84-233352] 04 p0579 N85-13693
Prefabricated panels for rapidly runway repair and expedient airfield surfacing
[AD-D011277] 05 p0597 N85-13804
Situational interactive micro/graphic simulator system for improving maintenance performance
[AD-A146677] 06 p0757 N85-14846
Analyses to develop models to project failure rates and repair costs of electronic modules and subassemblies
[AD-A146509] 06 p0816 N85-15180
National airspace system configuration management interface control document. Maintenance processor subsystem to remote monitoring subsystems and remote monitoring subsystem concentrators
[NAS-MD-790] 07 p0900 N85-15705
System for rapid repair of damaged airfield runways
[AD-D011325] 07 p0909 N85-15754
An analysis of the technical training of enlisted minuteman missile maintenance personnel
[AD-A147076] 07 p0912 N85-15775
Grease versus oil lubrication of wheel bearings in Army equipment
[AD-A147546] 07 p0973 N85-16184
Managing recoverable aircraft components in the PPB and related processes: Executive summary
[AD-A146806] 07 p1050 N85-16667
A simulation model for Air Launched Cruise Missile engine management
[AD-A147018] 07 p1051 N85-16672
Feasibility of measuring technical productivity improvements in Air Force Logistics Command depot-level maintenance using the Data Envelopment Analysis (DEA) and Constrained Facet Analysis (CFA) models
[AD-A147329] 07 p1052 N85-16676
Maintainability: An ILS effort to manipulate LCC
08 p1064 N85-16743
A weapon system design approach to diagnostics
08 p1066 N85-16752
Planning for the on-orbit servicing of military spacecraft
[AD-A148447] 08 p1104 N85-16963
Flight service evaluation of advanced composite ailerons on the L-1011 transport aircraft
[NASA-CR-172463] 08 p1118 N85-17049
Repair of composites 08 p1120 N85-17058
Operating and maintenance guidelines for the kinergetics (trade name) environmental control system. Carbon dioxide scrubber model DH-10 and heat exchanger model CCU-01
[AD-A148107] 08 p1200 N85-17557
Performance management system enhancement and maintenance
[NASA-CR-175271] 08 p1202 N85-17564

Prematurely terminated sequential tests for MIL-STD 781C
[AD-A149417] 08 p1216 N85-17857
Liquid phase methanol process development unit: Installation, operation, and support studies
[DE85-001311] 09 p1301 N85-18171
Control and electronic subsystems for the advanced servomanipulator
[DE85-001900] 09 p1327 N85-18343
The care and feeding of magnetic tapes
[AD-A145853] 09 p1366 N85-18585
Material flow in the manufacturing system: Fault-diagnosis systems as support for the maintenance of highly automated manufacturing systems
[PNR-90236] 09 p1371 N85-18618
In situ washing procedures for the UKIRT 3.8 meter primary mirror — United Kingdom Infrared Telescope (UKIRT)
[UKIRT-20] 09 p1414 N85-18918
Adhesive joint formation under field conditions
[AD-D011478] 10 p1453 N85-19153
Monitoring the execution of plans in SIPE (System for Interactive Planning and Execution) monitoring
[AD-A149138] 10 p1544 N85-19731
Fiat introduces 1000-CC engine
11 p1618 N85-20185
Corrosion and coatings review of specifications and drawings of facilities for the Oman Military Construction Program at Masirah Island, Oman
[AD-A149738] 12 p1812 N85-21368
Operation and maintenance requirements of the Army Remotely Piloted Vehicle (RPV)
[NASA-CR-175714] 14 p2218 N85-23755
Establishment and maintenance of certification standards for helicopter and turboprop power transmission systems 14 p2224 N85-23796
Mini-Seminar on Non-Destructive Testing
[CSIR-TSD-0009/83] 14 p2316 N85-24306
Lead shortage hastens need for improved storage batteries 15 p2461 N85-25195
Pavement-marking materials: New York's experience
[PB85-153294] 15 p2523 N85-25558
Automation of servicibility of radio-relay station equipment 15 p2527 N85-25582
Installation, maintenance and operating manual for the Lucas-type fuel injection system of the 3 B rotary engine
[NASA-TM-77872] 15 p2568 N85-25846
Graphic simulation of a machine-repairman model
[AD-A151761] 16 p2694 N85-26633
Maintaining consistency and accommodating network repair in a self-regenerative distributed database management system (a discussion of the means and cost) 16 p2698 N85-26656
Management aspects of software maintenance
[AD-A152035] 16 p2847 N85-27550
Inspection evaluation and repair of the flawed feedwater nozzle of the 50 MWe Dodewaard GKN boiling water reactor
[ISBN-90-353-0017-3] 17 p2977 N85-28394
Tokamak fusion core experiment maintenance study
[DE85-008040] 17 p3040 N85-28813
The use of flight simulators in measuring and improving training effectiveness
[AD-A153817] 18 p3064 N85-28954
Automated maintenance system test program increment VI production scheduling
[AD-A153694] 18 p3198 N85-29838
Touch-off: A method to determine the position of an object by means of a sensor-driven robot
[DE85-011178] 19 p3339 N85-30691
Fusion Power Demonstration (FPD) maintenance and disassembly considerations
[DE85-011413] 22 p3846 N85-33620
Upgrading auxiliary facility outleakage and combustion detection
[DE85-012796] 23 p3934 N85-34386
Maintenance port system
[AD-D011724] 23 p3967 N85-34594
Dissected motors-propellants motor number STM-012. Phase 15: Surveillance report, stage 1
[AD-A156088] 24 p4071 N85-35226
Quality assurance considerations for the implementation of a pulsed power R and D project
[DE85-012357] 24 p4148 N85-35720
Time domain reflectometry for SLC BPM system
[DE85-012389] 24 p4155 N85-35758

MAINTENANCE TRAINING
The psychology of technical devices and technical discourse
[AD-P003929] 02 p0246 N85-11609
AFHRL (Air Force Human Resources Laboratory) program for artificial intelligence applications to maintenance and training
[AD-P003931] 02 p0247 N85-11611
Artificial intelligence contributions to training and maintenance
[AD-P003934] 02 p0247 N85-11614
An analysis of the technical training of enlisted minuteman missile maintenance personnel
[AD-A147078] 07 p0912 N85-15775
Maintenance training simulators prime item development specification. Model specification and handbook
[AD-A154106] 19 p3330 N85-30628

MALEATES
Stabilized unsaturated polyesters
[NASA-CASE-NPO-16103-1] 18 p3078 N85-29043
Condensation of anhydrides or dicarboxylic acids with compounds containing active methylene groups. Part 1: Condensation of phthalic anhydride with acetoacetic and malonic ester
[NASA-TM-77886] 19 p3227 N85-30010

MALES
Anthropometric cockpit compatibility assessment of US Army aircraft for large and small personnel wearing a training, warm-weather clothing configuration
[AD-A145206] 01 p0099 N85-10656
Skeletal muscle metabolism during exercise is influenced by heat acclimation
[AD-A148845] 10 p1527 N85-19632
Assessment of muscle strength and prediction of lifting capacity in US Army personnel
[AD-A148846] 10 p1527 N85-19633
Hemodynamics responses to upright tilt at sea level and high altitude
[AD-A148848] 10 p1527 N85-19634
Dynamics of quantitative and qualitative changes in conditionally pathogenic microflora of the human intestine during long-term hypokinesia 12 p1903 N85-21953
Aerobic and anaerobic exercise tolerance in the heat: Effect and acclimatization 14 p2388 N85-24707
Comparative anaerobic power of males and females
[AD-A151960] 16 p2842 N85-27523
Positive Gz accelerations tolerance of individuals 41 to 58 years of age 19 p3323 N85-30586
Investigation of some aspects of amino acid metabolism in man during brief exposure to antiorthostatic hypokinesia combined with ultraviolet radiation
22 p3822 N85-33678

MALFUNCTIONS
Safety recommendation(s), A-84-65
[REPT-3908] 14 p2216 N85-23743
General Aviation Airworthiness Alerts, no. 85
[FAA-AC-43-16] 22 p3729 N85-33117

MALLEABILITY
Assessing the machinability of gearwheel steels during manufacture
[BLL-BISI-TRANS-22343-(9902.06)]
17 p2973 N85-28365

MAMMALS
NT BABOONS
NT BEARS
NT CATS
NT DEER
NT DOGS
NT DOLPHINS
NT GUINEA PIGS
NT HUMAN BEINGS
NT MICE
NT MONKEYS
NT PRIMATES
NT RABBITS
NT RATS
NT SEALS (ANIMALS)
NT SHEEP
NT WHALES
Genetic effects of microwave exposure on mammalian cells in vitro. Volume 2, Appendix A: Cytogenetics and growth kinetics data, 850 MHz
[AD-A148866] 10 p1522 N85-19599
Genetic effects of microwave exposure on mammalian cells in vitro. Volume 2, Appendix B: Cytogenetics and growth kinetics data, 1.2 GHz
[AD-A148867] 10 p1522 N85-19600
Control of mammals at airports
[AD-P004192] 11 p1580 N85-19957
Mammalian gravity receptors: Structure and metabolism 15 p2605 N85-26055
Gravitational effects on reproduction, growth and development of mammals 15 p2612 N85-26097
Quantitation of Na+, K+-ATPase enzyme activity in tissues of the mammalian vestibular system
15 p2613 N85-26102
A communications link for an implantable electrode array
[AD-A152238] 16 p2640 N85-27510
Effects of method of detachment on electrophoretic mobility of mammalian cells grown in monolayer culture
20 p3500 N85-31757
Vertebrate development in space: Gravity is a drag (and has been for eons and eons) 24 p4126 N85-35560
Report of the NASA Mammalian Developmental Biology Working Group 24 p4128 N85-3

MAN
U HUMAN BEINGS

MAN ENVIRONMENT INTERACTIONS
The SANCOR programme on coastal processes, April 1982 - March 1986
[REPT-68] 01 p0069 N85-10
Modeling long-term changes in forested landscapes and their relation to the Earth's energy balance
05 p0653 N85-1
Education and training for the climate related activities in Latin America and the Caribbean
07 p1004 N85-1
Ozone and temperature trends due to the injection of trace species in the atmosphere
[AERONOMICA-ACTA-A-288-1984]
18 p3132 N85-2
Applied climatology — regional planning
18 p3147 N85-2
Ozone in the 21st century: Increase or decrease
[AERONOMICA-ACTA-A-291-1984]
20 p3489 N85-31
Meteorology and Society: Statements presented at the 9th congress under agenda item 12 — World Meteorological Organization
[WMO-643] 22 p3817 N85-3
Agents and effects of ozone trends in the atmosphere
[AERONOMICA-ACTA-A-287-1984]
23 p3948 N85-34

MAN MACHINE SYSTEMS
Nowcasting with Doppler radar: The forecaster-computer relationship
01 p0077 N85-10514
FRONTIERS: Progress with a system for nowcasting rain — Forecasting Rain Optimized using New Techniques of Interactively Enhanced Radar and Satellite (FRONTIERS) 01 p0082 N85-10552
Nowcasting: Advances with McIDAS 3 — Man-computer Interactive Data System System (McIDAS)
01 p0082 N85-10553
Development of nowcasting in China
01 p0083 N85-10554
Interactive computer display systems in nowcasting
01 p0083 N85-10557
MERIT: A man/computer data management and enhancement system for upper air nowcasting/forecasting in the United States — Minimum Energy Routes using Interactive Techniques (MERIT)
01 p0083 N85-10
PROMIS 600: The pilot project for the future Swedish weather service 01 p0083 N85-10
Robust rate control system designs for a submersible
[AD-A144792] 01 p0111 N85-10
Effects of alternative chromatic mixed graphics displays in decision support systems
[AD-A145561] 02 p0242 N85-11
An effective graphics user interface for rules and inference mechanisms
[AD-P003942] 02 p0248 N85-11
Decision Support System (DSS): A survey
[NRIMS-TWISK-317] 02 p0292 N85-11
A management workstation concept
[AD-A145617] 02 p0294 N85-11
Use of prototyping for man-machine interface requirements definition on the AWDS (Automated Weather Distribution System) program
[AD-A146033] 03 p0396 N85-12
Preserving the time dimension in information systems
03 p0437 N85-12
Developments in Soviet robot technology viewed
04 p0491 N85-13127
Development, new application of Soviet robots
04 p0491 N85-13129
Rech-1 speech synthesizer for man-machine dialog
04 p0543 N85-13
The human role in space. Volume 1: Executive summary
[NASA-CR-171223] 04 p0546 N85-13
The Interactive Planetary Image Processing System (IPIPS): A major facility for research and teaching in remote sensing 05 p0655 N85-14
An interactive technique for satellite-improved rainfall monitoring 05 p0658 N85-14
A methodology for an integrated spatial data model and its application to image classification
05 p0659 N85-14
Twentieth Annual Conference on Manual Control, volume 1
[NASA-CP-2341-VOL-1] 05 p0699 N85-14
Time series modeling of human operator dynamics in manual control tasks 05 p0699 N85-14
Statistical time series models of pilot control with applications to instrument discrimination
05 p0700 N85-14

Utilization of historic information in an optimization task
05 p0700 N85-14490

Six degrees of freedom control with each hand?
05 p0700 N85-14492

A model for the effectiveness of aircraft alerting and warning systems
05 p0702 N85-14506

Evaluation of fuzzy rulemaking for expert systems for failure detection
05 p0703 N85-14508

Psychological issues in online adaptive task allocation
05 p0704 N85-14516

Suppression of biodynamic interference by adaptive filtering
05 p0706 N85-14530

Twentieth Annual Conference on Manual Control, volume 2
[NASA-CP-2341-VOL-2] 05 p0707 N85-14535

Representing multidimensional systems using visual displays
05 p0711 N85-14560

Performance measures for aircraft landings as a function of aircraft dynamics
05 p0712 N85-14565

Measuring pilot workload in a moving-base simulator. Part 2: Building levels of workload
05 p0712 N85-14566

Multi-crew model analytic assessment of landing performance and decision-making demands
05 p0712 N85-14567

A framework for research on adaptive decision aids
[AD-A138331] 05 p0734 N85-14719

Technical Workshop: Advanced Helicopter Cockpit Design
[NASA-CP-2351] 06 p0750 N85-14806

Superaugmented rotorcraft program
06 p0750 N85-14807

Helicopter human factors programs and plans
06 p0751 N85-14808

Guidance and navigation programs and plans
06 p0751 N85-14809

Integrated cockpit design for the Army helicopter improvement program
06 p0751 N85-14816

Man-machine interface requirements - advanced technology
06 p0753 N85-14825

Design and analysis of an SQL (Structured Query Language) interface for a multi-backend database system
[AD-A146534] 06 p0856 N85-15447

Mental status in relation to special conditions of activity
07 p1011 N85-16420

Interaction of human cognitive models and computer based models in supervisory control
[AD-A142547] 07 p1020 N85-16474

Mental models and cooperative problem solving with expert systems
[AD-A147843] 07 p1021 N85-16479

International aviation (selected articles)
[AD-A148704] 08 p1067 N85-16762

Integrated control and display systems for helicopter battlefield mission management
08 p1073 N85-16805

A review of US Army aircrew-aircraft integration research programs
08 p1075 N85-16814

Time series analysis of closed-loop pilot vehicle dynamics
08 p1087 N85-16876

Ground man-machine interfaces for orbiter checkout
08 p1091 N85-16897

East Europe report: Science and technology
[JPRS-ESA-84-046] 08 p1139 N85-17176

Man-machine communication research for robotics reported
08 p1139 N85-17177

Automatic speech recognition in severe environments
[AD-A148461] 08 p1153 N85-17280

A computer aided Multi-Man-Machine Work Area Design and Evaluation System (MAWADES)
[AD-A147950] 08 p1199 N85-17554

Steps towards parsing of query sequences to a database
[AD-A145769] 08 p1206 N85-17590

The effects of time delay in man-machine control systems: Implications for design of flight simulator Visual-Display-Delay compensation
[AD-P004329] 09 p1270 N85-17983

Role of engineering psychology
09 p1361 N85-18561

Problems of psychological support of automated organization control systems
09 p1362 N85-18571

Material flow in the manufacturing system: Fault-diagnosis systems as support for the maintenance of highly automated manufacturing systems
[PNR-90238] 09 p1371 N85-18618

Dean of Kiev State University on impact of robots
10 p1461 N85-19213

Production turret lathe retrofitted with robot
10 p1461 N85-19214

Control system of complex CNC machining cell
10 p1462 N85-19218

Health standards for general vibration
10 p1523 N85-19607

Sector suite man-machine functional capabilities and performance requirements
[AD-A148881] 10 p1531 N85-19647

Man-machine interaction: Operator
[AD-A149075] 10 p1531 N85-19648

Human Factors Considerations in High Performance Aircraft
[AGARD-CP-371] 10 p1532 N85-19653

Military pilot ergonomics 10 p1532 N85-19655

Grasp of information by the pilot in future combat aircraft
10 p1533 N85-19662

The cockpit of the year 2000: How big a step?
10 p1534 N85-19667

The multiple resources model of human performance: Implications for display design 10 p1534 N85-19669

French plans for fifth generation computer systems
[AD-A149435] 10 p1544 N85-19732

Reliability of DNC system examined
11 p1617 N85-20171

Man/machine interface for a nuclear cask remote handling control station: System design requirements
[DE85-000256] 11 p1697 N85-20667

Parallel input and feedback in dialogue cells
[CWI-CS-R8413] 11 p1703 N85-20706

Data and information systems and decision making in large public organizations: Research agenda
[DE85-003639] 11 p1738 N85-20931

Operations concept for the advanced automation system man-machine interface
[AD-A149797] 12 p1774 N85-21139

Automatic speech recognition in severe environments
[PB85-121697] 12 p1830 N85-21490

The man-machine interface
[AD-A149971] 12 p1910 N85-21989

An interactive environment for the development of an expert system in ZOG
[AD-A149954] 12 p1915 N85-22025

Design of graphic displays in computerized systems
[AD-A150071] 12 p1916 N85-22027

Research and Modeling of Supervisory Control Behavior, report of a workshop
[AD-A149621] 12 p1950 N85-22248

USSR report: Space
[JPRS-USP-85-001] 13 p1977 N85-22403

TASS update on unmanned flight of Salyut-7
13 p1977 N85-22404

A design analysis and implementation of a user-friendly interface for the UNIX operating system
[AD-A150558] 13 p2145 N85-23312

Investigation of transport operations of ergatic robot
14 p2266 N85-24166

Interference effects of vocalization on dual task performance
[AD-A150687] 14 p2291 N85-24203

The acquisition of procedures from text. A production-system analysis of transfer of training
[AD-A151029] 14 p2392 N85-24732

Programmer/analyst workstation evaluation report
[NASA-CR-175289] 14 p2394 N85-24749

Dual-task timesharing using a projected attitude display (Malcolm horizon)
[AD-A150789] 14 p2395 N85-24750

Robotic arc welding 15 p2586 N85-25830

Biotechnology in Japan
[PB85-169464] 15 p2615 N85-26113

Computerized biophysical data acquisition system for motion sickness studies
[AD-A151691] 15 p2618 N85-26131

Proceedings of the BAe human factors seminar
[BAE-BT-11873] 15 p2620 N85-26145

Human factors department 1981 publications
[BAE-BT-12685] 15 p2620 N85-26147

Activities report for FOA 53: Laboratory for man and information systems
[FOA-C-53019-H] 15 p2621 N85-26150

Extension of the software development workbench to include microcomputer workstations
[AD-A151903] 15 p2630 N85-26207

A description of the process of elaborating man-machine dialog in an aircraft equipped with cathode tubes: Roles and specifications of piloted simulation methods
16 p2696 N85-26658

A comparison of pictorial and speech warning messages in the modern cockpit
[AD-A151917] 16 p2707 N85-26706

Fujian forges ahead in electronic production
16 p2806 N85-27301

Automation of the reporting and tracking requirements of architect-engineering type contracts
[AD-A152218] 16 p2876 N85-27745

Controller requirements for uncoupled aircraft motion, volume 2
[AD-A153300] 17 p2900 N85-27879

Hand controllers for teleoperation. A state-of-the-art technology survey and evaluation
[NASA-CR-175890] 17 p3002 N85-28559

Mechanizing of handling operations in drop forging with hammers and presses (conducted ergonomical examinations)
[BMFT-FB-HA-84-051] 17 p3002 N85-28561

Efforts at office automation and information systems utilization at Martin Marietta Energy Systems, Incorporated
[DE85-008154] 17 p3013 N85-28833

The interface with decision makers in interactive multiobjective linear programming
[REPT-84-38] 17 p3014 N85-28837

General laws of development of technology
17 p3049 N85-28875

A study of user-defined searching requirements for the on-line version of the directory of DOD-sponsored R and D data bases on the Defense Gateway computer system
[AD-A153000] 17 p3050 N85-28878

Man-machine tradeoff study 18 p3156 N85-29561

Some ideas and questions regarding space station design for human use 18 p3158 N85-29562

Space station automation study-satellite servicing. Volume 1: Executive summary
[NASA-CR-171512] 19 p3226 N85-29999

Space station automation study-satellite servicing, volume 2
[NASA-CR-171513] 19 p3226 N85-30000

Adaptive aiding for symbiotic human-computer control: Conceptual model and experimental approach
[AD-A153870] 19 p3332 N85-30644

ZOG-Vinson technology demonstration project. Volume 2: System description
[AD-A153871] 19 p3333 N85-30645

ZOG/VINSON technology demonstration project system description. Volume 1
[AD-A154211] 19 p3342 N85-30713

Space Station man-machine automation trade-off analysis
[NASA-CR-176046] 20 p3408 N85-31147

Manipulators in teleoperation
[DE85-010563] 20 p3512 N85-31833

The blind and the paralyzed. The notion of the tool revealed and integrated in a different organization environment
[SNIAS-851-422-104] 20 p3513 N85-31835

Program Manager: The journal of the defense systems management college, volume 14, number 2, March-April 1985
[AD-A154219] 20 p3540 N85-32031

Myoelectric control of a computer based expert system for flight control
[AD-A154961] 21 p3557 N85-32126

Importance of automation, robotization in economy
21 p3572 N85-32219

Design guidelines for user-system interface software
[AD-A154907] 21 p3671 N85-32807

A PASCAL interpreter for the functional programming language ELC (Extended lambda calculus)
[AD-A155218] 21 p3672 N85-32810

Space station automation and robotics study. Operator-systems interface
[NASA-CR-176095] 22 p3738 N85-33172

Space station automation study: Autonomous systems and assembly, volume 2
[NASA-CR-176092] 22 p3739 N85-33175

Machine intelligence for robotics applications
[DE85-011430] 22 p3793 N85-33503

Man-vehicle systems research facility advanced aircraft flight simulator throttle mechanism
22 p3796 N85-33527

The CADME approach to the interface of solid modellers 23 p3961 N85-34554

Designing a graphics application interface
23 p3964 N85-34574

Development of NATOPS performance software for the SH-3D and SH-3H helicopters
[AD-A156140] 24 p4065 N85-35192

The integrated manual and automatic control of complex flight systems
[NASA-CR-176166] 24 p4066 N85-35201

An exploratory study of the effect of screen size and resolution on the legibility of graphics in automated job performance aids
[AD-A155969] 24 p4136 N85-35632

MANAGEMENT
NT CONFIGURATION MANAGEMENT
NT CONTRACT MANAGEMENT
NT DATA MANAGEMENT
NT ENGINEERING MANAGEMENT
NT ENVIRONMENT MANAGEMENT
NT FINANCIAL MANAGEMENT
NT FOREST MANAGEMENT
NT INDUSTRIAL MANAGEMENT
NT INFORMATION MANAGEMENT
NT INVENTORY CONTROLS
NT INVENTORY MANAGEMENT
NT LAND MANAGEMENT

NT LOGISTICS MANAGEMENT
NT PERSONNEL MANAGEMENT
NT PROCUREMENT MANAGEMENT
NT PRODUCTION MANAGEMENT
NT PROJECT MANAGEMENT
NT RESEARCH MANAGEMENT
NT RESOURCES MANAGEMENT
NT SAFETY MANAGEMENT
NT SYSTEMS MANAGEMENT
NT WATER MANAGEMENT
Synopsis of the OTA Workshop on Cost Containment of Civilian Infrastructure (Civilian Space Station) Elements 07 p0915 N85-15790
Distribution and storage of aviation turbine fuel for military operations in northern Australia
[AD-A147180] 07 p0935 N85-15821
Principles of multiobjective optimization
[AD-A147520] 07 p1052 N85-16679
Technical order managers handbook: Utilization assessment
[AD-A147579] 07 p1055 N85-16694
Flight Training Technology for Regional/Commuter Airline Operations: Regional Airline Association/NASA Workshop Proceedings
[NASA-CP-2346] 09 p1275 N85-18009
Management training for cockpit crews at Piedmont flight 09 p1276 N85-18013
Video concepts in CRM training
09 p1276 N85-18015
Use of simplifier scenarios for CRM training
09 p1276 N85-18016
Management: A bibliography for NASA managers
[NASA-SP-7500(19)] 15 p2664 N85-26439
Central problems in the management of innovation
[AD-A152596] 17 p3047 N85-26652
Management of Corrosion
[AGARD-LS-141] 22 p3749 N85-33236
DOD Value Engineering Conference report. Value Engineering (VE): A tool that benefits line management held at Leesburg, Virginia on 1-2 November 1984. Part 1. Executive summary
[AD-A156067] 24 p4163 N85-35810
DOD Value Engineering Conference report. Value Engineering (VE): A tool that benefits line management held at Leesburg, Virginia on 1-2 November 1984. Part 2. Plenary session
[AD-A156068] 24 p4163 N85-35811
DoD Value Engineering conference report. Value Engineering (VE): A tool that benefits line management. Part 5, Workshop C: VEP/VECP administration, negotiation, and implementation
[AD-A156071] 24 p4163 N85-35814

MANAGEMENT ANALYSIS
Doing business in space: How to get there from here
02 p0156 N85-11057
An overview of the Joint Logistics Commanders Automatic Test Equipment Panel
[AD-P003916] 02 p0244 N85-11596
Planning for the on-orbit servicing of military spacecraft
[AD-A148447] 06 p1104 N85-16983
Performance management system enhancement and maintenance
[NASA-CR-175271] 08 p1202 N85-17564
Aviation maintenance computerized management information systems: Perspective for the future
[AD-A150637] 13 p1966 N85-22349
Food service management 14 p2393 N85-24736
Guide on workload forecasting
[PB85-177632] 19 p3341 N85-30704
Program Manager: The journal of the defense systems management college, volume 14, number 2, March-April 1985
[AD-A154219] 20 p3540 N85-32031

MANAGEMENT INFORMATION SYSTEMS
Data dictionary systems and their role in information resource management
[AD-A144905] 01 p0125 N85-10859
Effects of alternative chromatic mixed graphics displays in decision support systems
[AD-A145561] 02 p0242 N85-11578
A management workstation concept
[AD-A145617] 02 p0294 N85-11906
Primer on the registration of technical information in industry 03 p0436 N85-12786
Maintenance Management Information and Control System (MMICS): Administrative boon or burden
[AD-A145762] 03 p0436 N85-12790
Executive information system
[DE84-015355] 04 p0576 N85-13675
Introduction to software packages
[PB84-217843] 06 p0856 N85-15441
An update of the functional requirements of the Naval Aviation Logistics Command Management Information System (NALCOMIS)
[AD-A146565] 06 p0871 N85-15532
The effects of software quality control and baseline management on the acquisition of computer programs
[AD-A147051] 07 p1024 N85-16502
A study of the relationship between user attitudes and the success of the MAJCOM and AFRCE work information management system
[AD-A146856] 07 p1051 N85-16671
A validated methodology for determination of laboratory instrument computer interface efficacy
[AD-A148338] 10 p1487 N85-19391
The evolution from data processing to information resource management
[AD-A149429] 10 p1567 N85-19678
An interactive environment for the development of an expert system in ZOG
[AD-A149654] 12 p1915 N85-22025
Aviation maintenance computerized management information systems: Perspective for the future
[AD-A150637] 13 p1966 N85-22349
General design considerations of an Air Force information system
[AD-A150611] 13 p2156 N85-23449
The design and analysis of a complete hierarchical interface for the multi-backend database system
[AD-A151550] 15 p2629 N85-26203
An analysis of data dictionaries and their role in information resource management
[AD-A152134] 16 p2774 N85-27121
Implementation and analysis of a microcomputer based relational database system
[AD-A151770] 16 p2845 N85-27536
Data dictionary design as a stepping-stone to DBMS (Data Base Management System) implementation in the Indonesian Army Data Collecting and Processing Service
[AD-A152101] 16 p2877 N85-27752
Manufacturing information system
[AD-A152715] 17 p3011 N85-28616
DLA: Data/data base administration analysis
[AD-A153031] 17 p3050 N85-28679
Improving the defense energy information system (DEIS)
[AD-A153524] 18 p3200 N85-29849
Test and Evaluation Master Plan (TEMP) for the Navy Occupational Health Information Management System (NOHIMS). Phase 1: Appendix A through appendix U
[AD-A154179] 19 p3360 N85-30967
The Human Resource Management Information Network (HRMIN): A cost comparison in accordance with Office of Management and Budget (OMB) Circular no. A-76, 5 April 1979
[AD-A154583] 21 p3713 N85-33039
Integration of office automation within computing
[DE85-010021] 22 p3833 N85-33736

MANAGEMENT METHODS
NT DELPHI METHOD (FORECASTING)
NT PATTERN METHOD (FORECASTING)
NT PROFILE METHOD (FORECASTING)
Artificial Intelligence in Maintenance: Proceedings of the Joint Services Workshop
[AD-A145349] 02 p0244 N85-11592
Diagnosis based on description of structure and function
[AD-P003919] 02 p0245 N85-11599
Decision Support System (DSS): A survey
[NRIMS-TWISK-317] 02 p0292 N85-11896
Maintenance Management Information and Control System (MMICS): Administrative boon or burden
[AD-A145762] 03 p0436 N85-12790
Design of a scientific information collation and dissemination system, volumes 1 thru 3
[AD-A146002] 03 p0436 N85-12791
International comparative study of systems for the government advancement of research and development
[NASA-TM-77589] 04 p0578 N85-13689
Performance evaluation of A-10 aircraft mainteance units and aircraft using constrained facet analysis
[AD-A146955] 07 p0893 N85-15660
A Q-GERT network simulation model for examining pipeline time in the Navy's J-52 intermediate level jet engine repair cycle
[AD-A147269] 07 p0894 N85-15663
Feasibility of measuring technical productivity improvements in Air Force Logistics Command depot-level maintenance using the Data Envelopment Analysis (DEA) and Constrained Facet Analysis (CFA) models
[AD-A147329] 07 p1052 N85-16676
Effective life cycle software support: A study in discipline and versatility 08 p1065 N85-16746
Manufacturing costs, equipment needs and technological opportunities among small and medium-size manufacturers
[DE85-000479] 09 p1304 N85-18193
Management challenges encountered in CAD implementation
[DE85-002072] 10 p1541 N85-19716
Security of personal computer systems: A management guide
[PB85-161040] 14 p2400 N85-
The development and implementation of advanced welding technology 15 p2585 N85-
Welding techniques in pressure part technology
15 p2586 N85-
Future information technology, 1984 telecommunications
[PB85-165650] 15 p2624 N85-
Management communication and financial modeling
15 p2627 N85-
Management: A bibliography for NASA managers
[NASA-SP-7500(19)] 15 p2664 N85-
Management aspects of software maintenance
[AD-A152035] 16 p2647 N85-27
The significance of Helios for Europe
16 p2686 N85-27
Managerial benefits of Helios for the European industry 16 p2687 N85-27
Helios project support 16 p2687 N85-2761
Integrating quality assurance and research and development
[DE85-007974] 17 p2976 N85-
Future directions in operations research
[REPT-84-24] 17 p3026 N85-28711
Multicriteria decision analysis as an aid to strategic planning of energy research and development
[REPT-84-02] 17 p3049 N85-28
Direct digital control study
[AD-A153685] 18 p3167 N85-2
Automated maintenance system test program increment VI production scheduling
[AD-A153694] 18 p3196 N85-
CMP: Code Maintenance Package reference manual, version 2.0
[DE85-011396] 19 p3340 N85-30
Guide on workload forecasting
[PB85-177632] 19 p3341 N85-30704
Discrete simulation models - their role in the design, development and management of inventory control systems
[PNR-90249] 23 p3966 N85-34719
Fire service emergency management handbook
[AD-A155780] 24 p4084 N85-35
DoD Value Engineering conference report. Value Engineering (VE): A tool that benefits line management. Part 6, Workshop D: VE training-orientation
[AD-A156072] 24 p4164 N85-35815
Aeronautical Systems Division Manufacturing/Quality assurance orientation
[AD-A156128] 24 p4164 N85-35817

MANAGEMENT PLANNING
NT PRODUCTION PLANNING
NT PROJECT PLANNING
Hydrologic and economic models for watershed evaluation and research
[PB84-222371] 01 p0066 N85-104
Development of a production order release methodology
[AD-A145213] 01 p0124 N85-10
System engineering and integration contract for implementation of the National Airspace System plan, volume 1, sections 1.0-4.0, 6.0
[AD-A145783] 03 p0317 N85-1204
Matrix organizations: Overcoming the disadvantages
[AD-A145318] 03 p0436 N85-12772
Five-year plan for meeting the automatic data processing and telecommunications needs of the Federal Government. Volume 2: Major information technology systems acquisition plans of Federal executive agencies, 1984-1989
[PB84-214519] 03 p0436 N85-1277
IRM (Information Resources Management) long-range plan: Fiscal year 1984-1988 (update). Volume 2: ADP and telecommunications acquisition plan
[PB84-229244] 03 p0439 N85-127
USSR report: Machine tools and metalworking equipment
[JPRS-UMM-84-020] 04 p0491 N85-1312
Development, new application of Soviet robots
04 p0491 N85-13129
Advances of implementing NC machine tools discussed 04 p0491 N85-13131
Survey relating to the implementation of cost/schedule control systems criteria within the Department of Defense and industry
[AD-A146664] 06 p0670 N85-15
Decentralized control of scheduling in distributed systems
[AD-A147446] 07 p1022 N85-1648
The effects of software quality control and baseline management on the acquisition of computer programs
[AD-A147051] 07 p1024 N85-165

The management of research institutions: A look at government laboratories
[NASA-SP-481] 07 p1050 N85-16665

Life cycle cost management master plan for the Defense Communications Agency
[AD-A146876] 07 p1050 N85-16668

Acquisition planning at the Defense Communications Agency
[AD-A146877] 07 p1051 N85-16669

A study of the relationship between user attitudes and the success of the MAJCOM and AFRCE work information management system
[AD-A146886] 07 p1051 N85-16671

An evaluation of the effect of establishing a minimum Economic Order Quantity (EOQ) on the Air Force EOQ item management system
[AD-A147121] 07 p1051 N85-16673

Project manager's handbook for special projects
[AD-A147913] 07 p1053 N85-16683

Commerce Lab: Mission analysis. Payload integration study
[NASA-CR-171265] 08 p1104 N85-16982

Decentralized control of scheduling in distributed systems
[AD-A147686] 08 p1228 N85-17731

Strategic management for organizational effectiveness. The effect of human resource planning on retention and related issues, volume 1
[AD-A149398] 10 p1566 N85-19874

Strategic management for organizational effectiveness. The effect of human resource planning on retention and related issues, volume 2
[AD-A149399] 10 p1566 N85-19875

Strategic management for organizational effectiveness. The effect of human resource planning on retention and related issues, volume 3
[AD-A149400] 10 p1566 N85-19876

Strategic management for organizational effectiveness. The effect of human resource planning on retention and related issues: Methodological appendix
[AD-A149401] 10 p1566 N85-19877

Siemens, Philips megaproject to yield superchip in 5 years 11 p1592 N85-20018

Environmental Monitoring Improvement Act
[GPO-39-742] 11 p1677 N85-20568

Software management issues — space station software development 11 p1700 N85-20690

Program manager: The Journal of the Defense Systems Management College. Volume 13, Number 6, November-December 1984
[AD-A149546] 11 p1739 N85-20933

Air Force satellite position management
12 p1787 N85-21217

Computing Division two-year operational plan, FY 1984 - 1985
[LA-9978-MS] 12 p1913 N85-22006

Response to NAS plan audit report recommendations
[FAA-ES-85-1] 15 p2468 N85-25235

Manufacturing methods and technology CAD/CAM (Computer-Aided Design/Computer-Aided Manufacturing) related efforts (FY 1980 - 1986)
[AD-A151817] 16 p2846 N85-27547

Personal computer aided decision analysis
[AD-A151911] 16 p2875 N85-27743

Navy program manager's guide, 1985 edition
[AD-A151925] 16 p2876 N85-27744

Management control systems and interdependencies: An empirical study
[AD-A152260] 16 p2876 N85-27746

An examination of alternative forms of fit in contingency theory
[AD-A152602] 17 p3047 N85-28853

The concept of fit in contingency theory
[AD-A152603] 17 p3047 N85-28854

Documentation for the West German Federal Cabinet's space policy decision 17 p3051 N85-28886

Evaluation and Validation (E/V) team public report, volume 1
[AD-A153609] 18 p3161 N85-29584

Overhead management guide for aerospace procurements
[AD-A153626] 18 p3198 N85-29835

Guide on workload forecasting
[PB85-177632] 19 p3341 N85-30704

Assessment of computer resource management plan for division support weapon system
[AD-A154142] 19 p3342 N85-30712

EOQ (Economic Order Quantity) range model
[AD-A153709] 19 p3379 N85-30965

Producibility Engineering and Planning (PEP): Program management guidelines
[AD-A153730] 19 p3379 N85-30966

Quality analysis 21 p3668 N85-32785

Study to encourage and facilitate industrial investment and involvement in space
[NASA-CR-176152] 23 p3898 N85-34147

Analyzing performance of small projects using URS and PMAS, information pamphlet
[DE85-011964] 23 p3986 N85-34718

Aeronautical Systems Division Manufacturing/Quality assurance orientation
[AD-A156128] 24 p4164 N85-35817

MANAGEMENT SYSTEMS
NT FLIGHT MANAGEMENT SYSTEMS
NT MANAGEMENT INFORMATION SYSTEMS

Report of the Department of Aerospace Engineering
03 p0307 N85-11977

Development of a pavement maintenance management system. Volume 10: Summary of development from 1974 through 1983
[AD-A146035] 03 p0320 N85-12067

Development of a pavement maintenance management system. Volume 9: Development of airfield pavement performance prediction models
[AD-A146150] 03 p0321 N85-12069

An evaluation of the effect of establishing a minimum Economic Order Quantity (EOQ) on the Air Force EOQ item management system
[AD-A147121] 07 p1051 N85-16673

Technology planning for flexible manufacturing systems 08 p1139 N85-17170

Automated plant, production management system
08 p1139 N85-17171

Kernel Ada Programming Support Environment (KAPSE) interface team public report, volume 4
[AD-A147648] 08 p1205 N85-17581

GIDEP representative interaction
[DE84-016792] 09 p1401 N85-18820

Biotechnology in Japan
[PB85-169464] 15 p2615 N85-26113

National Airspace System Plan: Facilities, equipment and associated development 16 p2704 N85-26692

Management control systems and interdependencies: An empirical study
[AD-A152260] 16 p2876 N85-27746

West European report: Science and technology
[JPRS-WST-84-036] 18 p3066 N85-28960

Interactive graphics for a data analysis management system
[DE85-010977] 19 p3334 N85-30651

The economics of private sector R and D decisionmaking in aeronautics
[NASA-CR-176007] 19 p3379 N85-30962

NASA Space controls research and technology program 20 p3406 N85-31149

Evaluative report on the Institute for Computer Sciences and Technology, National Bureau of Standards, fiscal year 1984
[PB85-176097] 20 p3514 N85-31848

Determining functional requirements for NASA Goddard's command management system software design using expert systems 20 p3539 N85-32020

Symbolic and interactional perspectives on leadership: An integrative framework
[AD-A155247] 21 p3665 N85-32769

DOD Value Engineering Conference report. Value Engineering (VE): A tool that benefits line management held at Leesburg, Virginia on 1-2 November 1984. Part 1. Executive summary
[AD-A156067] 24 p4163 N85-35810

DOD Value Engineering Conference report. Value Engineering (VE): A tool that benefits line management held at Leesburg, Virginia on 1-2 November 1984. Part 2. Plenary session
[AD-A156068] 24 p4163 N85-35811

MANDELSTAM REPRESENTATION

Experimental investigation of wavefront conjugation during Mandelstam-Brillouin scattering of focused laser beams in condensed media 11 p1716 N85-20796

Stimulated Mandelstam-Brillouin scattering with distributed feedback 21 p3696 N85-32961

MANEUVERABILITY

A generalized mathematical soluation for transient off tracking of single vehicles and truck combinations
[DM-2] 01 p0107 N85-10719

Performance capabilities of the C-5 and C-17 cargo aircraft
[AD-A145518] 02 p0138 N85-10939

Robotics in nondestructive inspection at Sacramento Air Logistics Center
[AD-P004012] 03 p0309 N85-11992

Details of export A-5 close-support aircraft given — Qiang-5 aircraft 06 p0748 N85-14793

Supermaneuverability
[AD-P004153] 09 p1263 N85-17936

Thrust vectoring apparatus for maneuvering missile in flight
[AD-D011693] 19 p3226 N85-30004

MANEUVERABLE SPACECRAFT
NT APOLLO SPACECRAFT
NT LIFTING REENTRY VEHICLES
NT RENDEZVOUS SPACECRAFT

MANEUVERS
NT AIRCRAFT MANEUVERS
NT EVASIVE ACTIONS
NT HOVERING
NT ORBITAL MANEUVERS
NT ORBITAL RENDEZVOUS
NT SIDESLIP
NT SPACECRAFT DOCKING
NT SPACECRAFT MANEUVERS

Helicopter pilot performance for discrete-maneuver flight tasks 05 p0702 N85-14502

Translational control of a graphically simulated robot arm by kinematic rate equations that overcome elbow joint singularity
[NASA-TP-2376] 06 p0856 N85-15446

Bifurcation theory applied to aircraft motions
[NASA-TM-86704] 14 p2210 N85-23705

Harrier 15 p2687 N85-26595

Design of robust controllers for a multiple input-multiple output control system with uncertain parameters application to the lateral and longitudinal modes of the KC-135 transport aircraft
[AD-A153100] 17 p2900 N85-27877

MANGANESE
NT MANGANESE ISOTOPES

International strategic minerals inventory. Summary report: Manganese
[GS-CIRC-930-A] 02 p0219 N85-11442

Weld metal solidification cracking in a carbon-manganese steel 03 p0330 N85-12126

The influence of manganese on intercrystalline internal adsorption of arsenic in low carbon steel
[BLL-M-35965-(5828.4)] 05 p0615 N85-13931

Manganese in recent sediments of Ukrainian SSR Black Sea shelf 06 p0819 N85-15200

The growth of metastable peritectic compounds
[NASA-CR-171289] 07 p0920 N85-15824

SPAR X technical report for experiment 76-22 directional solidification of magnetic composites
[NASA-CR-171271] 07 p0927 N85-15880

Analysis of diffusion in an ion-implanted alloy using a phenomenological model
[AERE-R-11527] 11 p1609 N85-20120

Investigation of manganese dioxide as an improved solid desiccant
[DE85-004034] 13 p2018 N85-22654

Technical and cost analyses of manganese nodule processing techniques and their significant variations
[PB85-148815] 14 p2258 N85-23992

Measurements of radiation-induced segregation and diffusion in ion irradiated alloy using implanted manganese
[AERE-R-11528] 14 p2258 N85-23994

Influence of manganese and heat treatment on structure and properties of Fe-0.1 percent-C-14 percent Cr-based steels
[BLL-BISI-TRANS-22299-(9022.06)]
17 p2928 N85-28071

Part played by non-metallic inclusions during deformation and fracture of steel with different grain sizes
[BLL-BISI-TRANS-22321-(9022.06)]
17 p2928 N85-28072

Temperature and manganese content dependences of tensile deformation in iron-high manganese binary alloys
[DE85-007656] 17 p2932 N85-28098

Solid phase reactions among manganese, potassium perchlorate and barium chromate
[HSE-TRANS-11166] 19 p3237 N85-30071

Geochemistry of manganese in ocean
19 p3291 N85-30406

Mineralogical-geochemical characteristics of ferromanganese formations in Arabian-Indian Ocean Ridge 19 p3293 N85-30416

Analysis of ferrates and ferrites of three transition metals using Moessbauer effects
[BLL-CE-TRANS-8019-(9022.09)]
20 p3430 N85-31273

Physical and chemical aerosol characteristics in extremely clean air masses at Cape Grim, Tasmania
21 p3646 N85-32655

Possible roles of manganese redox chemistry in the sulfur cycle 21 p3659 N85-32731

Precision measurements of solar energetic particle elemental composition
[PAPER-SH-2.1-4] 21 p3715 N85-33052

Environmental surveillance at Los Alamos during 1984
[DE85-011886] 22 p3811 N85-33605

Cobalt-rich ferromanganese crusts in the oceans
24 p4104 N85-35444

Applications of the mineral resources data system and the international strategic minerals inventory in mineral-resource assessments by region and commodity
24 p4105 N85-35451

MANGANESE ALLOYS
Rapid solidification of steels: Model and commercial alloys 02 p0176 N85-11184
Metallurgy Institute's developments for alloy and aircraft producers 03 p0353 N85-12268
Thermal diffusivity and conductivity of chromium-manganese alloying compositions
[BLL-M-35025-(5828.4)] 05 p0613 N85-13938
Study of high performance alloy electroforming
[NASA-CR-174276] 07 p0927 N85-15875
Magnetic excitation in CuMn spin glass alloy
[DE85-002584] 10 p1453 N85-19159
Study of high performance alloy electroforming
[NASA-CR-175741] 15 p2506 N85-25473
Superplasticity in a thermo-mechanically processed Aluminum-10.2%Mg-0.52%Mn alloy
[AD-A152016] 15 p2510 N85-25485
Swelling behavior of manganese-bearing AISI 216 steel
[DE85-005712] 15 p2512 N85-25495
Mechanical stabilization of austenite against epsilon martensite and its effect on deformation behavior in high manganese steels
[DE85-007654] 17 p2932 N85-28097
Strength versus toughness relation in Fe-high manganese alloys
[DE85-007682] 18 p3074 N85-29013
Directional solidification of an eutectic Bi-MnBi alloy
[BLL-M-36270-(5828.4)] 20 p3430 N85-31275
Dynamics of the melting of chromium-manganese alloys in molten steel
[BLL-M-35850-(5828.4)] 23 p3914 N85-34252
MANGANESE COMPOUNDS
NT MANGANESE OXIDES
Unsinkability of ferromanganese nodules
06 p0819 N85-15202
MANGANESE ISOTOPES
Cosmogenic Mn-53 in meteorites
[SH-7.1-17] 23 p4049 N85-35107
MANGANESE OXIDES
Influence of eutectic silicate inclusions on micro-processes during deformation and fracture of 12GS steel
[BLL-BISI-TRANS-22296-(9022.06)]
17 p2929 N85-28073
Carbon reduction of mixtures of MnO(2) and Fe(2)O(3)
[BLL-M-36260-(5828.4)] 20 p3422 N85-31241
Iron and manganese in oxide minerals and in glasses: Preliminary consideration of Eh buffering potential at Yucca Mountain, Nevada
[DE85-011692] 23 p3916 N85-34271
MANGANESE 53
U MANGANESE ISOTOPES
MANGANESE 54
U MANGANESE ISOTOPES
MANGANESE 56
U MANGANESE ISOTOPES
MANIFOLDS
Manifold insulated with knitted impregnated sleeve
[AD-D011270] 06 p0814 N85-15167
Calculation of flow about posts and powerhead model — space shuttle main engine
[NASA-CR-171344] 10 p1483 N85-19362
Experimental evaluation of an advanced Space Shuttle main engine hot-gas manifold design concept
16 p2736 N85-26898
Numerical analysis of flow non-uniformity in the hot gas manifold of the Space Shuttle main engine
16 p2738 N85-26899
Investigation of the behavior of fuel in the intake manifold and its relation to SI engines, 1980 - 1983
19 p3279 N85-30337
MANIFOLDS (MATHEMATICS)
NT RIEMANN MANIFOLD
A continuous Helson surface in R3
11 p1696 N85-20674
Supermanifolds and Berezin's new integral
[DE85-001633] 11 p1706 N85-20732
Using semigroups and the Trotter product formula to solve quasi-linear systems
[DE85-002041] 11 p1706 N85-20736
Special relativity of Kaluza-Klein
[DE85-007636] 17 p3046 N85-28847
MANIPULATION
U MANIPULATORS
MANIPULATORS
NT REMOTE MANIPULATOR SYSTEM
Portable slotting device
[AD-D011213] 01 p0033 N85-10206
United States Air Force on research on algebraic manipulation
[AD-A145737] 02 p0253 N85-11655
Industrial robots and transmanipulations: Important link in setup of automated production lines
03 p0345 N85-12222
Test-bed for programmable automation research. Phase 1
[AD-A145872] 03 p0409 N85-12614
Optimization of movements of manipulators with kinematic redundancy 04 p0488 N85-13112
Controlling rotation of elastic manipulator link
04 p0488 N85-13113
USSR report: Machine tools and metalworking equipment
[JPRS-UMM-84-020] 04 p0491 N85-13126
Soviet robot exhibition reviewed
04 p0491 N85-13128
Improved robotic equipment for radiological emergencies
[DE84-017637] 04 p0509 N85-13249
Evaluation of automated decisionmaking methodologies and development of an integrated robotic system simulation
[NASA-CR-172401] 04 p0552 N85-13516
Instantaneous kinematics and joint displacement analysis of fully-parallel robotic devices
05 p0641 N85-14113
Application of robotics in remote fuel fabrication operations
[DE84-011481] 05 p0646 N85-14144
Review of teleoperator research
05 p0703 N85-14511
Translational control of a graphically simulated robot arm by kinematic rate equations that overcome elbow joint singularity
[NASA-TP-2376] 06 p0856 N85-15446
Precise control of flexible manipulators
[NASA-CR-174210] 07 p0973 N85-16178
Automatic camera tracking for remote manipulators
[DE85-001897] 07 p0974 N85-16187
Design features, applications of new robots
08 p1139 N85-17174
The optimal control and design of a flexible manipulator arm 09 p1327 N85-18340
Control and electronic subsystems for the advanced servomanipulator
[DE85-001900] 09 p1327 N85-18343
Dual arm master controller concept
[DE85-001901] 09 p1327 N85-18344
Advanced remotely maintainable force-reflecting servomanipulator concept
[DE85-001902] 09 p1328 N85-18345
Parallel algorithms for robot dynamics
[DE84-016563] 09 p1369 N85-18605
Dean of Kiev State University on impact of robots
10 p1461 N85-19213
Planning of minimum-time trajectories for robot arms
[AD-A148956] 10 p1492 N85-19416
Simplified grasping and manipulation with dextrous robot hands
[AD-A148962] 10 p1492 N85-19419
Some data manipulation requirements for the exploratory analysis of large data sets
[DE85-002541] 10 p1568 N85-19887
Real time algorithms for robotic control of teleoperations
[DE85-001137] 11 p1647 N85-20380
A remotely controlled orbiting retriever
12 p1786 N85-21212
Impacts of robotic and flexible manufacturing technologies on manufacturing costs and employment
[AD-A150060] 12 p1860 N85-21668
Mechanical properties for the grasp of a robotic hand
[AD-A150062] 12 p1860 N85-21669
Sensor control of robot arc welding
12 p1948 N85-22233
Cyclic industrial robots with mechanical energy storing devices: Multipositional system with one or several degrees of freedom 13 p2045 N85-22803
Design of tightening device and calculation of forces in manipulator transmissions with base-drive mounted
13 p2046 N85-22804
Hydraulic brakes for industrial robots
13 p2046 N85-22806
Controlled movement of elastic manipulator with distributed parameters 13 p2048 N85-22818
Investigation of dynamics of manipulator with elastic sections 13 p2048 N85-22819
Optimum design of electrical motors for multilink manipulators and automated manufacturing systems
13 p2062 N85-22880
Controllable movements of elastic manipulator with three degrees of freedom 14 p2266 N85-24040
Modular design, versatility of robots viewed
14 p2284 N85-24155
Integrated control system for FMS components
14 p2285 N85-24156
Investigation of transport operations of ergatic robot
14 p2286 N85-24166
Plans, developments in robotics
14 p2289 N85-24191
Study of experimental robotized system for arc welding based on Universal-15 manipulator
15 p2500 N85-254
Italy's Fiat uses Sweden's Asea seeing robot
15 p2536 N85-
Applicability of modular versus universal robots discussed 15 p2536 N85-
Robotic arc welding 15 p2566 N85-
The kinematic control of redundant manipulators
15 p2566 N85-
Manipulation and simulation of general robots using the zero-position description 15 p2567 N85-
Structural design and kinematic configuration of two-armed robots 16 p2761 N85-27
Experience of sheet stamping robotic complexes
16 p2761 N85-27
Automatic manipulators for forging rollers
16 p2762 N85-27
Updating model RPD-1.25 industrial robot
16 p2762 N85-27
Industrial robots and automatic manipulators for forging and pressing operations at Second International Exhibition 16 p2762 N85-27
Control of motion of manipulator robots on basis of first-order kinematic algorithms
16 p2762 N85-27
Guidelines for optimization of robotized machining cells 16 p2767 N85-27
A general simulation program for robot manipulator arm dynamics
[AD-A152121] 16 p2793 N85-27
Kinematic rate control of simulated robot hand at or near wrist singularity
[NASA-TP-2440] 16 p2851 N85-27575
Positioning of a robotic manipulator through the use of visual feedback
[AD-A151933] 16 p2851 N85-27577
Precision manipulator heating and cooling apparatus for use in UHV systems with sample transfer capability
[NASA-CASE-LAR-13040-1] 18 p3116 N85-
HERMIES-1: A mobile robot for navigation and manipulation experiments
[DE85-008652] 18 p3118 N85-
Analysis of remote operating systems for space-based servicing operations, volume 1
[NASA-CR-171885] 19 p3225 N85-
Analysis of remote operating systems for space-based servicing operations. Volume 2: Study results
[NASA-CR-171886] 19 p3225 N85-
Space station automation study-satellite servicing. Volume 1: Executive summary
[NASA-CR-171512] 19 p3226 N85-
Space station automation study-satellite servicing, volume 2
[NASA-CR-171513] 19 p3226 N85-30
A remote-operated manipulator vehicle
[HSE-TRANS-11133] 19 p3281 N85-3
Computer methods in manipulator kinematics, dynamics and control: A comparative study
20 p3462 N85-31
Manipulators in teleoperation
[DE85-010563] 20 p3512 N85-31
Ultrasonic position reference systems for an autonomous sentry robot and a robot manipulator arm
[AD-A155481] 21 p3596 N85-
East Europe report: Science and technology. Selections on CSSR computer technology
[JPRS-ESA-84-017] 21 p3665 N85-32
Robots, Manipulators 21 p3668 N85-32
Space robot simulator vehicle
[NASA-CR-176133] 22 p3739 N85-33
Future of robots in nuclear plants and processes
[DE85-011505] 22 p3793 N85-
Dual arm master controller development
22 p3797 N85-
The compliance of end effector force sensors for robot manipulator control 24 p4098 N85-
Testbed for sensory control of intelligent machines
[DE85-012355] 24 p4099 N85-35412
MANNED ORBITAL LABORATORIES
NT MANNED ORBITAL RESEARCH LABORATORIES
NT SPACELAB
Manned space station solar array study
[ESA-CR(P)-1941] 09 p1287 N85-1
Identification and control of structures in space
[NASA-CR-175790] 16 p2731 N85-
European utilization aspects of a US manned space station, volume 1
[ESA-CR(P)-1987-VOL-1] 17 p2907 N85-27
European utilization aspects of a US manned space station, volume 2
[ESA-CR(P)-1987-VOL-2] 17 p2907 N85-27
USSR report: Space
[JPRS-USP-84-006] 22 p3731 N85-33

Space Station Polar Platform: Integrating research and operational missions
[PB85-195270] 24 p4069 N85-35218

MANNED ORBITAL RESEARCH LABORATORIES
NT SPACELAB
Concept for a commercial space station laboratory
02 p0153 N85-11035
Role of Space Station: The how of space industrialization 02 p0153 N85-11036

MANNED ORBITAL SPACE STATIONS
U ORBITAL SPACE STATIONS

MANNED SPACE FLIGHT
NT SPACE SHUTTLE MISSION 31-C
NT SPACE SHUTTLE MISSION 41-B
NT SPACE SHUTTLE MISSION 41-C
NT SPACE SHUTTLE MISSION 41-G
NT SPACE SHUTTLE MISSION 51-A
NT SPACE SHUTTLE MISSION 51-C
Bone structure and microgravity
05 p0694 N85-14463
Man in Space: National Historic Landmark Theme Study
[PB85-107233/GAR] 07 p0911 N85-15768
25th anniversary of the Gagarin Cosmonaut Training Center
[NASA-TM-77644] 09 p1286 N85-18076
Biomechanics finds practical applications in aerospace research 11 p1621 N85-20205
The space flight of the Soviet-Indian crew
[NASA-TM-77615] 12 p1768 N85-21226
USSR report: Space
[JPRS-USP-85-001] 13 p1977 N85-22403
TASS update on unmanned flight of Salyut-7
13 p1977 N85-22404
Feoktistov recalls period leading to Gagarin spaceflight 13 p1985 N85-22451
Feoktistov says manned lunar, Mars flights lack justification 13 p1985 N85-22452
Research opportunities in human behavior and performances
[NASA-CR-3886] 13 p2142 N85-23299
USSR report: Space
[JPRS-USP-85-004] 16 p2717 N85-26772
Tass reports program for Salyut-7 fully completed
16 p2717 N85-26773
Living aloft: Human requirements for extended spaceflight
[NASA-SP-483] 21 p3666 N85-32772
USSR report: Space
[JPRS-USP-84-006] 22 p3731 N85-33128
Proceedings of a Scientific Meeting on the Occasion of the Inauguration of New Buildings for the DFVLR Institute for Aerospace Medicine
[ESA-TT-857] 24 p4129 N85-35595
Biophysical research in space — radiation effects
24 p4130 N85-35603

MANNED SPACECRAFT
NT APOLLO SPACECRAFT
NT LONG DURATION EXPOSURE FACILITY
NT MANNED ORBITAL LABORATORIES
NT MANNED ORBITAL RESEARCH LABORATORIES
NT ORBITAL SPACE STATIONS
NT SALYUT SPACE STATION
NT SHUTTLE DERIVED VEHICLES
NT SKYLAB 3
NT SKYLAB 4
NT SOYUZ SPACECRAFT
NT SPACE SHUTTLES
NT SPACE STATIONS
Features and uses of progress cargo ships
02 p0157 N85-11061
Tass reports launch of Progress-22
02 p0157 N85-11063
Progress-22 docks with Salyut-7
02 p0157 N85-11064
Tass reports launch of Soyuz T-12
02 p0158 N85-11070
Dynamics and controls working group summary
05 p0604 N85-13854
A historical overview of the electrical power systems in the US manned and some US unmanned spacecraft
[NASA-CR-174806] 05 p0612 N85-13910
Manned space station solar array study
[ESA-CR(P)-1941] 09 p1287 N85-18081
Keynote address 09 p1333 N85-18378
Approaches to radiation guidelines for space travel
[DE85-001248] 09 p1363 N85-18576
Space Station
[NASA-EP-211] 12 p1793 N85-21251
Descent vehicles
[NASA-TM-77654] 17 p2909 N85-27933
Some Europeans voice opposition to space station participation 18 p3066 N85-28961

MANOMETERS
NMR manometer for measuring high pressures at liquid-helium temperatures 17 p2944 N85-28171

MANPOWER
NT SCIENTISTS
Parametric estimates of propulsion system maintenance manhours
[AD-A147120] 07 p0894 N85-15662
Application of the HARDMAN methodology to the single channel ground-airborne radio system (SINCGARS)
[NASA-CR-175486] 10 p1467 N85-19259

MANTLE (EARTH STRUCTURE)
U EARTH MANTLE

MANUAL
Standard analytical procedures of the NOAA National Analytical Facility, 1984-85: Extractable toxic organic compounds
[PB86-126282] 12 p1887 N85-21840
Outside users payload model
[NASA-CR-176011] 19 p3223 N85-29986

MANUAL CONTROL
NT VISUAL CONTROL
Twentieth Annual Conference on Manual Control, volume 1
[NASA-CP-2341-VOL-1] 05 p0699 N85-14487
Time series modeling of human operator dynamics in manual control tasks 05 p0699 N85-14488
A nonlinear filter for compensating for time delays in manual control systems 05 p0700 N85-14493
Model estimation and identification of manual controller objectives in complex tracking tasks
05 p0700 N85-14494
A method for measuring the effective throughput time delay in simulated displays involving manual control
05 p0701 N85-14497
Effects of transport delays of manual control system performance 05 p0701 N85-14498
Multiloop manual control of dynamic systems
05 p0702 N85-14505
The effect of part-simulation of weightlessness on human control of bilateral teleoperation: Neuromotor considerations 05 p0703 N85-14510
Suppression of biodynamic interference by adaptive filtering 05 p0706 N85-14530
Active sticks: A new dimension in controller design
05 p0706 N85-14531
Twentieth Annual Conference on Manual Control, volume 2
[NASA-CP-2341-VOL-2] 05 p0707 N85-14535
On looking into the black box: Prospects and limits in the search for mental models 05 p0709 N85-14546
A manual control test for the detection and deterrence of impaired drivers 05 p0709 N85-14550
Manual-control analysis applied to the money-supply control task 05 p0710 N85-14553
Types of tracking errors induced by concurrent secondary manual task 05 p0711 N85-14561
Low-speed longitudinal orbiter qualities
08 p1092 N85-16905
Order picking in an aisle
[AD-A149553] 10 p1548 N85-19766
The effect of strategy in second order manual control on resource competition with a sternberg memory search task
[AD-A150965] 14 p2391 N85-24727
Docking simulation analysis of range data requirements for the orbital maneuvering vehicle
[NASA-TM-86510] 20 p3407 N85-31143
The integrated manual and automatic control of complex flight systems
[NASA-CR-176166] 24 p4066 N85-35201

MANUALS
NT INSTALLATION MANUALS
NT USER MANUALS (COMPUTER PROGRAMS)
Manual for Raman cells
[NASA-TM-77756] 01 p0052 N85-10342
Ada (trademark) training curriculum. Real-time concepts l303 teacher's guide
[AD-A145093] 01 p0104 N85-10694
Ada (trademark) training curriculum. Software engineering for managers m101 teacher's exercise guide
[AD-A145094] 01 p0104 N85-10695
Intelligent information retrieval from on-line technical documentation
[AD-P003946] 02 p0249 N85-11626
Method for evaluating petrol products corrosivity using piezoelectric crystals. Part 2: Instruction manual — jet engine corrosion tests
[FOA-C-40196-B4] 04 p0462 N85-13073
Performance management system enhancement and maintenance
[NASA-CR-175271] 08 p1202 N85-17564
NATO AC/310 activities report on NATO STANAG 4170 and Allied Ordnance Publication 7 (Manual of Tests for Qualification of Explosive Materials for Military Use)
[AD-P004341] 10 p1454 N85-19165
User's guide for the Photochemical Box Model (PBM)
[PB85-137164] 11 p1682 N85-20602
Review of US manual of clinical aviation medicine
12 p1904 N85-21057
A strain gauge manual
[AD-A151602] 16 p2767 N85-27197
DoD manual for standard data elements, part 2
[AD-A152202] 16 p2878 N85-27755
DoD manual for standard data elements, part 3
[AD-A152203] 16 p2878 N85-27756
DoD manual for standard data elements, part 4
[AD-A152204] 16 p2878 N85-27757
DoD manual for standard data elements, part 5
[AD-A152205] 16 p2878 N85-27758
Technical instructions for a control operating system of the gas flow installation for the solid fuel combustion chamber
[VTH-LR-410] 18 p3118 N85-29302
A retarding ion mass spectrometer for the Dynamics Explorer-1
[NASA-CR-171588] 21 p3589 N85-32303
Ada (trademark) training curriculum. Advanced Ada topics L305 teacher's guide exercises
[AD-A154621] 21 p3670 N85-32798
A manual of methods for the continuous flow determination of ammonia, nitrate-nitrite, phosphate and silicate in seawater
[IOS-177] 23 p3913 N85-34243
Master Fit users' guide, version 1.0
[DE85-014199] 24 p4140 N85-35667
Comet Halley returns: A teachers' guide 1985-1986
[NASA-EP-197] 24 p4168 N85-35839

MANUFACTURING
NT COMPUTER AIDED MANUFACTURING
NT LOW GRAVITY MANUFACTURING
NT SPACE MANUFACTURING
Fluorinated diamond particles bonded in a filled fluorocarbon resin matrix
[DE84-014444] 01 p0022 N85-10136
Report on high-precision jig-boring machines
01 p0035 N85-10215
Publications of Center for Manufacturing Engineering (of the National Bureau of Standards), 1978-1983
[PB84-224526] 01 p0036 N85-10228
Manufacturing methods for microwave circuits
[AD-A145237] 01 p0043 N85-10278
Microminiature coaxial cable and methods of manufacture
[DE84-014228] 01 p0044 N85-10284
RADC/NBS (Rome Air Development Center/National Bureau of Standards) Workshop. Moisture Measurement and Control for Semiconductor Devices, 3
[PB84-219559] 01 p0051 N85-10337
Advanced manufacturing development of a composite empennage component for L-1011 aircraft
[NASA-CR-165885] 02 p0170 N85-11141
Manufacturing Methods and Technology (MM/T) specifications for miniature cathode ray tube
[AD-A145597] 02 p0194 N85-11298
Industrial robots and transmanipulations: Important link in setup of automated production lines
03 p0345 N85-12222
Newer carbon fibers and their properties
04 p0465 N85-12955
Quality organization — quality control
[CNES-NT-106] 04 p0511 N85-13257
Manufacturing report of an augmented lift, variable deflection half wing
[ONERA-RT-25/1736-AY-106-A]
05 p0591 N85-13766
Influence of residual stresses resulting from manufacturing on the fatigue strength of welded joints
05 p0650 N85-14177
The relationship between radiation sensitivity and redox equilibria — glass processing variables
[AD-A147216] 07 p0932 N85-15906
Fiat, Peugeot introduce integrated robotized engine: CAD used 07 p0936 N85-15933
Flexible manufacturing system for the production of aircraft parts
[BLL-PNR-90237-(8018.3153)]
08 p1137 N85-17159
The effects of manufacturing automation on the surge and mobilization capabilities of the gas turbine engine industry
[AD-A147295] 08 p1137 N85-17162
Control systems for robotic production lines
08 p1138 N85-17169
Technology planning for flexible manufacturing systems 08 p1139 N85-17170
Summaries of press automation conference presented
08 p1139 N85-17173
New applications for robot loaders, unloaders
08 p1139 N85-17175
Specifications of bloc floppy disk drives
08 p1141 N85-17188
MOM peripherals 08 p1141 N85-17189

Europeans active in magnetic bearing industry
08 p1141 N85-17195
Ultrasonic transducers, performance variability, design, and manufacturing procedures
[AD-A148575] 08 p1156 N85-17306
Production of concentrated nitric acid
[DE84-017191] 09 p1293 N85-18121
Manufacturing costs, equipment needs and technological opportunities among small and medium-size manufacturers
[DE85-000479] 09 p1304 N85-18193
Evaluating the variability of ceramics with X-ray fluorescence
[DE85-002028] 10 p1453 N85-19155
Experience highlights from the design and manufacture of US LCT coils
[DE84-017504] 10 p1482 N85-19354
Develop and demonstrate manufacturing processes for fabricating graphite filament reinforced polymide (Gr/PI) composite structural elements
[NASA-CR-172497] 11 p1592 N85-20019
Robot production lines in operation
11 p1617 N85-20166
New PCB production for robotics application
11 p1617 N85-20169
Reliability of DNC system examined
11 p1617 N85-20171
Report of the Technology and Test Panel
11 p1646 N85-20370
Exploratory assessment of second generation robotics and sensor-based systems
[PB85-132793] 11 p1648 N85-20388
Technological and economic assessment of advanced ceramic materials. Volume 5: A case study of ceramic toxic and combustible gas sensors
[PB85-113124] 12 p1815 N85-21386
Speed and accuracy in automated manufacture
[DE85-003913] 12 p1819 N85-21410
Computer integration of engineering design and production: A national opportunity
[NASA-CR-175483] 12 p1820 N85-21414
Impacts of robotic and flexible manufacturing technologies on manufacturing costs and employment
[AD-A150060] 12 p1860 N85-21668
A 2 x 6 Back Surface Reflection (BSR) silicon solar cell 13 p2005 N85-22570
Optimum design of electrical motors for multilink manipulators and automated manufacturing systems
13 p2062 N85-22880
Use of program controlled machine tools to automate and mechanize production processes in pipe manufacture 14 p2269 N85-24059
USSR report: Machine tools and metalworking equipment
[JPRS-UMM-85-006] 14 p2283 N85-24146
Metal waste in machine tool industry examined
14 p2283 N85-24147
Specifications of new industrial lasers reviewed
14 p2284 N85-24150
Minister B. V. Balmont on status of automation drive
14 p2284 N85-24151
West Europe report: Science and technology
[JPRS-WST-85-013] 14 p2289 N85-24183
Laser Welding, Cutting and Surface Treatment
14 p2308 N85-24278
Lasers in automobile production
14 p2309 N85-24288
Future trends in the use of lasers in manufacturing
14 p2309 N85-24291
Status of the U.K. N.D.T. industry today
14 p2316 N85-24309
Fiber optics applications for MIL-STD-1760
[AD-A151113] 15 p2470 N85-25251
Powder metallurgy production problems
15 p2497 N85-25406
French robotics research at Grenoble labs
15 p2523 N85-25555
Status of French research in plastic batteries
15 p2530 N85-25603
France develops new continuous vacuum treatment method 15 p2531 N85-25611
Criteria for qualifying for FRG federal CAD/CAM subsidies 15 p2536 N85-25651
ONR (Office of Naval Research) Far East Scientific Bulletin, Volume 9, Number 4, October-December 1984
[AD-A151274] 15 p2665 N85-26448
Manufacturing and producibility technology
16 p2733 N85-26866
USSR report: Engineering and equipment
[JPRS-UEQ-84-006] 16 p2760 N85-27035
Experience with introduction of Finish perforation of precision parts for optical instruments
16 p2761 N85-27038
Calculating reliability and productivity of cold stamping robot complex as queuing system
16 p2761 N85-27039
Estimates of errors of a gyroscope stabilized platform
16 p2763 N85-27050
Physio-chemical mechanisms of the processes of the formation of globular inclusions in ball-bearing metal
[BLL-BISI-TRANS-22235-(9022.06)]
17 p2924 N85-28030
Uses of, experiences in production of custom designed IC's 17 p2945 N85-28180
Modern equipment for manufacture of IC's in Hungary
17 p2945 N85-28181
Robots, automatic devices inside VW's Wolfsburg plant 17 p2946 N85-28186
Future directions of robotics, automation in Italy
17 p2946 N85-28187
Application of 4-wire submerged arc method to welding UOE pipe
[BLL-BISI-TRANS-22417-(9022.06)]
17 p2972 N85-28356
Production of electrically welded tubes with removed internal flash
[BLL-BISI-TRANS-22382-(9022.06)]
17 p2973 N85-28367
Future of ceramic turbochargers: Promises and pitfalls
[DE85-006209] 17 p2975 N85-28380
Principal quality assurance measures in the manufacture of HF-welded high-pressure linepipe
[BLL-BISI-TRANS-21690-(9022.06)]
17 p2976 N85-28389
Component problems plague French robotics industry
18 p3085 N85-29088
Crystallization of aluminum-based alloys in weightlessness 19 p3242 N85-30101
Producibility Engineering and Planning (PEP): Program management guidelines
[AD-A153730] 19 p3379 N85-30966
Improved turbopump dynamics
[NASA-TM-86514] 20 p3462 N85-31509
Encapsulation processing and manufacturing yield analysis 21 p3611 N85-32434
GDR semiconductor parts 21 p3669 N85-32788
Structure and functions of ultra-thin films of organic compounds
[DRIC-T-7481] 22 p3741 N85-33188
Centralized surveillance of flexible workshops for the manufacturing of composite materials
[SNIAS-851-430-103] 23 p3910 N85-34227
Manufacturing process to reduce large grain growth in zirconium alloys
[DE85-011649] 23 p3915 N85-34267
A rational approach to cam design
23 p3923 N85-34311

MANY BODY PROBLEM
Capture of planetesimals into a circumterrestrial swarm 04 p0586 N85-13751
The restricted problem of 2 + N bodies
09 p1414 N85-18925
Capture of planetesimals into a circumterrestrial swarm 13 p2179 N85-23522
Ionization equilibrium and equation of state in the solar interior 14 p2445 N85-25088
Boson degrees of freedom in Fermion many-body systems
[DE85-006997] 16 p2863 N85-27660
Mutli-particle quantum mechanics obeying fractional statistics
[DE85-007630] 16 p2873 N85-27723
Quantized Hall conductance as a topological invariant
[DE85-007796] 18 p3193 N85-29606
Quasiparticle excitations in valence-fluctuation materials: Effects of band structure and crystal fields
[DE85-010783] 19 p3359 N85-30824
Memory effects in dynamical many-body systems: The isomnesic (constant-memory) approximation
[AD-A154160] 20 p3520 N85-31889
Ab initio calculations of materials properties
[DE85-011167] 20 p3531 N85-31964

MANY ELECTRON EFFECTS
Many-electron effects in electron impact ionization of multiply charged ions
[DE85-005570] 15 p2649 N85-26340

MANY PARTICLE THEORY
U MANY BODY PROBLEM

MAP MATCHING GUIDANCE
SIR-B cartography and stereo topographic mapping
08 p1147 N85-17234

MAPPING
NT CADASTRAL MAPPING
NT COMPUTER AIDED MAPPING
NT ICE MAPPING
NT PHOTOMAPPING
NT PLANETARY MAPPING
NT SOIL MAPPING
NT THEMATIC MAPPING
NT THERMAL MAPPING

The inferring of preferences from indifferences in multicriteria decision analysis
[CSIR-TWISK-306] 01 p0108 N85-10
Model diagnosis in two-way tables by means of row and column Euclidean maps
[CSIR-TWISK-307] 01 p0109 N85-10
On Bezout domains, elementary divisor rings, and pole assignability
[CSIR-TWISK-330] 01 p0110 N85-10
Range-residuated mappings
[AD-A145148] 01 p0112 N85-10
LANDSAT data and interactive computer mapping
02 p0152 N85-11
Commentary on cosmonauts geological mapping photography 02 p0158 N85-11
Workshop on the Use of Future Multispectral Imaging Capabilities for Lithologic Mapping: Workshop summary
02 p0214 N85-11
A preliminary study of the feasibility of detecting the floating macrophytes by means of digital processing of MSS/LANDSAT data
[E85-10005] 02 p0215 N85-114
On complementary and independent mappings on databases
[AD-A145557] 03 p0438 N85-127
Summary of LANDSAT quadrangle studies in Alaska
04 p0515 N85-12
Digital elevation models improve processing of Alaskan gravity data 04 p0515 N85-12
Cretaceous plutonic rocks, Mitkof and Kupreanof Islands, Petersburg quadrangle, southeastern Alaska
04 p0518 N85-12
A review of seismicity in peninsular Spain
04 p0523 N85-13
Blind zones and aspect ratio bias in acquisition of discontinuity orientation data
[DE84-002718] 04 p0533 N85-13
An integrated LANDSAT/ancillary data classification of desert rangeland
[E85-10046] 06 p0626 N85-15
Computer vision research and its applications to automated cartography
[AD-A146668] 06 p0628 N85-15
AFOS (Automation of Field Operations and Services) display of MDR (Manually Digitized Radar) data on local map backgrounds
[PB84-220797] 06 p0640 N85-15
HEAO-1 diffuse soft X-ray sky maps
06 p0677 N85-15
Manual and automated line generalization and feature displacement: Appendixes
[AD-A143251] 07 p1054 N85-16
Map display for helicopters 08 p1073 N85-16
Quantitative use of multiincidence-angle SAR for geologic mapping 08 p1145 N85-172
SIR-B cartography and stereo topographic mapping
08 p1147 N85-172
Application and calibration of the subsurface mapping capability of SIR-B in desert regions
08 p1148 N85-172
Analysis of SIR-B radar illumination of geometry for depth of penetration and surface feature and vegetation detection, Nevada and California
08 p1149 N85-172
Color visual simulation applications at the Defense Mapping Agency
[AD-P004315] 09 p1268 N85-17
Symbol structure, information content and visual icons: A carto-seniotic theory of map signs
09 p1342 N85-18
An analysis of the seasonal variations in the water vapor transport fields over the Southern Hemisphere
09 p1356 N85-18
Application of SLF (Standard Linear Format) to digital hydrographic products
[AD-A149509] 10 p1522 N85-19
Retinal information mapping system
[AD-D011531] 12 p1649 N85-21
Hybrid method of mapping and photogeodetic control network densification
[PB85-133775] 12 p1676 N85-21
Implementation of the computer program-system MOSS (Map Overlay and Statistical System) on a VAX-11 series computer under VMS
[AD-A149612] 12 p1914 N85-22
Geological remote sensing develops rapidly, finds broad applications 13 p2052 N85-22
Possibility of mapping active tectonic structures from mercury gas aureoles over sea surface
13 p2113 N85-23
Possibilities of aerial electric prospecting by long cable method for detecting poorly conducting strata
13 p2115 N85-23
China report: Science and technology
[JPRS-CST-85-003] 13 p2166 N85-23

Development, achievements in China's cartography work 13 p2166 N85-23434
Accomplishments of Institute of Cartography summarized 13 p2166 N85-23435
Geophysical interpretation of Venus gravity data 13 p2178 N85-23513
Newly discovered Martian impact basins 13 p2182 N85-23544
Mapping and geological analysis of Mercury and Venus radar ranging data 13 p2196 N85-23633
Mars radar catalog 13 p2196 N85-23636
Late Tertiary and Quaternary river systems of the eastern Sahara as mapped on shuttle radar and LANDSAT images 13 p2199 N85-23641
Map design for computer processing: Literature review and DMA product critique
[AD-A151081] 14 p2347 N85-24513
Comparison of magnetospheric and ionospheric electric fields using different empirical mapping factors 14 p2362 N85-24597
Commercial data base management system for geonames data base
[AD-A150835] 14 p2433 N85-25007
Measurement of ocean surface currents from space with multi-frequency microwave radars 15 p2539 N85-25672
Contamination of the fetch-limited directional wave spectrum by waves emanating from an embayment
[NASA-TM-84441] 15 p2604 N85-26046
The design and analysis of a complete hierarchical interface for the multi-backend database system
[AD-A151560] 15 p2629 N85-26203
The Mars ancient cratered terrain, smooth plains boundary: Implications of Viking color data for evolution of the Amenthes Region 15 p2682 N85-26564
Study and mapping of anthropogenic effect on environment in different regions of USSR on basis of space photographs 16 p2726 N85-26824
Creating a Mobile Autonomous Robot Research System (MARRS)
[AD-A151963] 16 p2793 N85-27229
Acid precipitation in North America: 1980, 1981 and 1982 annual data summaries from acid deposition system data base
[PB85-162477] 16 p2822 N85-27410
Circulation statistics from January and July: Simulation with the NCAR (National Center for Atmospheric Research) community climate model (CCMOB)
[PB85-165637] 16 p2837 N85-27497
Comparative study of the digital analysis of areas of the Earth's surface prepared for planting using different classification algorithms
[INPE-3359-PRE/637] 16 p2846 N85-27545
Microwave responses of the western North Atlantic
[NASA-CR-175888] 17 p2946 N85-28191
Evaluation of Defense Mapping Agency level 1 second edition digital data for training simulator applications
[AD-A152444] 17 p2983 N85-28437
Boundary to constructive solid geometry mappings: A focus on 2-D issues 17 p3004 N85-28570
German contributions to the cartography of Antarctica by means of photogrammetry and remote sensing 18 p3124 N85-29342
Reports on cartography and geodesy. Series 1: Original reports, number 93
[ISSN-0469-4236] 18 p3124 N85-29343
On approximating a set-valued function locally
[AD-A153540] 18 p3170 N85-29641
Diagnostics of vector magnetic fields 18 p3206 N85-29889
A constant altitude flight survey method for mapping atmospheric ambient pressures and systematic radar errors
[NASA-TM-86733] 19 p3217 N85-29951
Discovery in earthquake forecasting and seismic zoning recorded 19 p3295 N85-30426
Space methods for geological research 19 p3295 N85-30429
Fracture detection and mapping for geothermal reservoir definition: An assessment of current technology, research, and research needs
[DE85-010827] 19 p3301 N85-30464
Defense Mapping Agency (DMA) raster-to-Vector analysis
[AD-A154153] 19 p3336 N85-30668
Defense Mapping Agency (DMA) raster-to-Vector benchmark testing
[AD-A154152] 19 p3336 N85-30683
Combined finite element meshing techniques using SUPERTAB
[DE85-011383] 19 p3340 N85-30696
Single-dish high sensitivity determination of solar limb emission at 22 and 44 GHz
[INPE-3545-PRE/758] 19 p3365 N85-30999
Video discs - what are they and where do they fit in?
[AD-A154166] 20 p3458 N85-31479
SEASAT altimetry for surface height of inland seas 20 p3493 N85-31714
Correlation analysis of 1 to 30 MeV celestial gamma rays 20 p3549 N85-32083
Mapping with QUASAT (quasar satellite) using short observation times
[AD-A155155] 21 p3559 N85-32141
The measurement of strain fields by X-ray topographic contour mapping
[AD-A154570] 21 p3599 N85-32348
Use of the synoptic view: Examples from Earth and other planets 21 p3602 N85-32371
Techniques, problems and uses of mega-geomorphological mapping 21 p3604 N85-32378
Planetary perspective. Report of Working Group Number 4 21 p3605 N85-32385
Realizing the full potential of the video disc for mapping applications
[AD-A154986] 21 p3606 N85-32391
Optical storage technology for mapping
[AD-A154989] 21 p3606 N85-32392
Fracture detection and characterization for geothermal reservoir definition
[DE85-008677] 22 p3815 N85-33630
Graph-theoretical exorcism
[DE85-011916] 23 p3955 N85-34512
A comparison of LANDSAT thematic mapper, multispectral scanner and airborne sensors for mapping the distribution of alteration minerals: Examples from the southwestern United States 24 p4106 N85-35452
Evaluation: Close-range photogrammetry for slope inventory and monitoring
[PB85-192755] 24 p4108 N85-35470

MAPS
NT ASTRONOMICAL MAPS
NT LUNAR MAPS
NT METEOROLOGICAL CHARTS
NT PHOTOMAPS
NT RADAR MAPS
NT RELIEF MAPS
Requirements and specifications for cartographic video discs
[AD-A144906] 01 p0049 N85-10325
Environmental geologic atlas of the North Carolina coastal zone: Dare, Hyde, Tyrrell and Washington Counties
[PB84-222975] 01 p0066 N85-10439
Birkhoff orbits for non-monotone twist maps
[AD-A144718] 01 p0110 N85-10747
Range-residuated mappings
[AD-A145148] 01 p0112 N85-10759
The Alaskan mineral resources assessment program: Guide to information contained in the folio of geologic and mineral-resource maps of the Medfra Quadrangle, Alaska
[GS-CIRC-926] 02 p0219 N85-11443
Diffusion and intermittency in an extended one-dimensional maps 02 p0282 N85-11834
Long time correlation and stochastic diffusion in the standard map 02 p0282 N85-11835
Mars-Earth geographical comparisons: A pictorial view
[NASA-TM-86166] 02 p0302 N85-11957
Two-dimensional modeling for lineal and areal probabilities of weather conditions
[AD-A147970] 08 p1168 N85-17486
NGC 2024: Multi-wavelength infrared and radio observations 08 p1246 N85-17865
Far-infrared photometry of low-mass pre-main-sequence stars with broad CO wings 08 p1246 N85-17866
Automatic land vehicle navigation using road map data
[DE84-017178] 09 p1278 N85-18043
Automatic map name placement system 09 p1341 N85-18438
Ground-water level data and preliminary potentiometric-surface maps, Yucca Mountain and vicinity, Nye County, Nevada
[DE85-001771] 09 p1343 N85-18448
Monthly and Seasonal Weather Outlook for November, 1984, Volume 38, Number 27, October 30, 1984
[PB85-118800] 10 p1521 N85-19588
Index to published geologic maps in the region around the potential Yucca Mountain nuclear waste repository site, southern Nye County, Nevada
[DE85-000260] 11 p1669 N85-20518
Digital and color energy maps for graphic display of hourly data
[DE85-000526] 11 p1673 N85-20543
Monthly and seasonal weather outlook for mid-October to mid-November 1984, volume 38, number 20, 13 October 1984
[PB85-113546] 11 p1687 N85-20611
Digital laser platemaker modifications
[AD-A150190] 13 p2096 N85-23074
An investigation of the crustal properties of Australia and surrounding regions derived from interpretation of MAGSAT anomaly field data 13 p2122 N85-23216
Development, achievements in China's cartography work 13 p2166 N85-23434
Accomplishments of Institute of Cartography summarized 13 p2166 N85-23435
Hexagonal data base study
[AD-A150176] 13 p2167 N85-23448
Mars geologic mapping: A review and new concepts 13 p2202 N85-23663
The Galilean Satellite Geological Mapping Program, 1984 13 p2203 N85-23664
Map design for computer processing: Literature review and DMA product critique
[AD-A151081] 14 p2347 N85-24513
Testing of scanner-assisted revision of the topographic map 1:25,000 (TK 25) 16 p2814 N85-27359
Circulation statistics from January and July: Simulation with the NCAR (National Center for Atmospheric Research) community climate model (CCMOB)
[PB85-165637] 16 p2837 N85-27497
UTM (Universal Transverse Mercator) determinations from geographical data
[AD-A152293] 16 p2856 N85-27610
Orphans of the Valley: Abandoned surface mines in the Tennessee Valley. Volume 2: Maps
[DE85-901249] 19 p3301 N85-30465
Defense Mapping Agency (DMA) raster-to-Vector analysis
[AD-A154153] 19 p3336 N85-30668
Defense Mapping Agency (DMA) raster-to-Vector benchmark testing
[AD-A154152] 19 p3338 N85-30683
MAGSAT scalar anomaly map of South America 20 p3473 N85-31586
MAGSAT satellite magnetic anomaly map over South America 20 p3474 N85-31587
Planetary perspective. Report of Working Group Number 4 21 p3605 N85-32385
The automatic labeling of geographic maps: A problem in computer aesthetics 23 p3962 N85-34561
An experimental study of dielectric rod antennas for millimeter-wave imaging applications
[AD-A155832] 24 p4086 N85-35328
New silver resource map of the United States: Potential for increased domestic silver production 24 p4105 N85-35445
Early and middle Cenozoic volcanic synthesis 24 p4105 N85-35449
Applications of the mineral resources data system and the international strategic minerals inventory in mineral-resource assessments by region and commodity 24 p4105 N85-35451

MARAGING STEELS
A study of vacuum melting to increase the toughness of maraging steels
[AD-A145017] 01 p0028 N85-10175
Maraging steels: Structure, properties and applications 02 p0177 N85-11191
Near-threshold fatigue crack growth and crack closure in 17-4 precipitation hardening steel and 2043-T3 aluminum alloy
[FFA-TN-1984-16] 02 p0210 N85-11385
Machining-induced deformation in stepped specimens of PH 13-8 Mo, 18 nickel maraging steel grade 200T1 and grain-refined HP 9-4-20
[NASA-CR-172450] 21 p3565 N85-32177

MARANGONI CONVECTION
High Marangoni number convection in a square cavity
[NASA-CR-174283] 07 p0959 N85-16078

MARGINS
Margin leveling algorithm for fully saturated satellite transponder with CDMA (Code Division Multiple Access) signalling
[AD-A151710] 15 p2543 N85-25690

MARIA
NT LUNAR MARIA

MARINE BIOLOGY
Activities of the Coastal Research Center
[PB84-231323] 05 p0672 N85-14320
USSR report: Life sciences. Biomedical and behavioral sciences
[JPRS-UBB-84-015] 07 p1010 N85-16416
Extremely Low Frequency (ELF) Communications System Ecological Monitoring Program: Summary of 1983 progress
[AD-A147704] 08 p1151 N85-17265
Bibliography of venomous and poisonous marine animals and their toxins
[AD-A148409] 08 p1192 N85-17514
An assessment of biological processes close to the sea bed in a slope region and its significance to the assessment of sea-bed disposal of radioactive waste
[IOS-185] 09 p1360 N85-18554

Microplankton species assemblages at the Scripps Pier from March to November 1983 during the 1982-1984 El Nino event
[NASA-CR-175663] 12 p1899 N85-21926

Production and turnover of suspended organic detritus in the coastal water of the southeastern continental shelf
[DE85-003977] 13 p2140 N85-23290

An analysis of issues concerning acid rain, report to the Congress of the United States
[TI85-901070] 15 p2589 N85-25959

MARMAP survey of the continental shelf from Cape Hatteras, North Carolina to Cape Sable, Nova Scotia (1977 - 1983). Atlas 1: Summary of operations
[PB85-150965] 16 p2839 N85-27506

Towards a study of synoptic-scale variability of the California current system
[NASA-CR-175871] 17 p2997 N85-28529

Chemical, biological, and physical measurements from the subtropical western North Atlantic Ocean. Summer 1982, USNS Lynch, cruise 710-82
[AD-A153823] 18 p3201 N85-29857

Use of a two-dimensional flow model to quantify aquatic habitat
[AD-A154287] 19 p3266 N85-30253

Marine environmental quality assessment program, five-year plan (FY 1984 - 1988)
[AD-A154715] 21 p3613 N85-32459

MARINE CHEMISTRY

The marine geochemistry of the rare earth elements
[AD-A145132] 01 p0088 N85-10598

Activities of the Coastal Research Center
[PB84-231323] 05 p0672 N85-14320

Gas-liquid chemistry of natural waters, volume 1
[DE85-002603] 12 p1884 N85-21822

Operation guiding light-scientific program and field plan. The pilot field experiment for NORDA project chemical dynamics in ocean frontal areas
[AD-A153765] 18 p3150 N85-29507

Chemical, biological, and physical measurements from the subtropical western North Atlantic Ocean. Summer 1982, USNS Lynch, cruise 710-82
[AD-A153823] 18 p3201 N85-29857

Dispersal From Deep Ocean Sources: Physical and Related Scientific Processes
[DE85-010420] 20 p3497 N85-31740

MARINE ENVIRONMENTS

Mineral nutrients in Mediterranean ecosystems
[REPT-71] 01 p0069 N85-10456

Radiotracer studies of the dispersion of solid pollutants in marine and estuarial environment: Measurement of diffusion coefficients and the phenomenon of dispersion by currents
[BLL-DRIC-TRANS-7104-(3623.66)]
02 p0224 N85-11468

Evaluation of an aerosol prediction model for coastal regions using marine aerosol generation and transport data
[AD-A145443] 02 p0231 N85-11510

Experiences with a high-blockage model tested in the NASA Ames 12-foot pressure wind tunnel
03 p0315 N85-12032

Icing rate on stationary structures under marine conditions
[AD-A145795] 03 p0395 N85-12524

Newly recognized sedimentary environments in the Shelikof Formation, Alaska 04 p0516 N85-13292

Interactions of the marine phosphorus and carbon cycles 05 p0653 N85-14190

Multi-property modeling of the marine biosphere in relation to global climate and carbon cycles
05 p0678 N85-14355

An investigation of the marine boundary layer during cold air outbreak 05 p0680 N85-14368

Structure and growth of the marine boundary layer
05 p0680 N85-14369

Marine helicopter missions 06 p0751 N85-14811

SAR maritime missions 06 p0751 N85-14813

Mariners weather log, volume 28, no. 3, July-August-September 1984
[PB85-107266] 06 p0840 N85-15334

Environmental research laboratories (of the National Oceanic and Atmospheric Administration) programs and plans: FY 1983 programs and FY 1984 plans
[PB84-226729] 06 p0840 N85-15336

Experiments in forecasting atmospheric marine horizontal visibility using model output statistics with conditional probabilities of discretized parameters
[AD-A147574] 07 p1008 N85-16404

Bibliography of venomous and poisonous marine animals and their toxins
[AD-A148409] 08 p1192 N85-17514

Special features of computations of vertical distribution of concentration of suspended sediments under marine conditions 13 p2106 N85-23125

Contribution to theory of ocean-atmosphere gas exchange 13 p2108 N85-23134

The relationship between marine aerosol particles and satellite-detected radiance 13 p2131 N85-23263

Variability in constant-load-amplitude fatigue crack growth rates in marine environments
[AD-A150786] 14 p2255 N85-23975

Statistical/Trend analysis of the marine atmospheric boundary layer model
[AD-A151053] 14 p2374 N85-24673

Geophysical Fluid Dynamics Laboratory activities, FY84, plans, FY85
[PB85-147601] 15 p2558 N85-25783

The physics of the marine stratocumulus-capped mixed layer 15 p2593 N85-25979

Monitoring of marine environment
16 p2812 N85-27341

An evaluation of discretized conditional probability and linear regression threshold techniques in model output statistics forecasting of visibility over the north Atlantic Ocean
[AD-A151955] 16 p2857 N85-27619

Fatigue of synthetic fibers for marine rope applications
[MIT-R84-2] 17 p2979 N85-28414

Environmental Research Laboratories publication abstracts, FY 1984
[PB85-180594] 19 p3313 N85-30540

Environmental background measurement program
[AD-A153860] 19 p3319 N85-30577

Optimisation of MCr Al coating compositions for marine gas turbines
[BR91159] 20 p3394 N85-31056

The U.S. Geological Survey in Alaska: Accomplishments during 1982
[US-GEOL-SURV-CIRC-939] 20 p3493 N85-31719

Understanding and laboratory prediction of the atmospheric corrosion behavior of steels and of non-ferrous metals and alloys
[AD-A154642] 21 p3566 N85-32179

Using ship wake patterns to evaluate SAR (Synthetic Aperture Radar) ocean wave imaging mechanisms. Joint US-Canadian Ocean Wave Investigation Project
[AD-A154633] 21 p3573 N85-32223

Marine environmental quality assessment program, five-year plan (FY 1984 - 1988)
[AD-A154715] 21 p3613 N85-32459

Forecasting atmospheric visibility over the summer north Atlantic using the principal discriminant method
[AD-A155537] 21 p3637 N85-32593

Bacterial ice nuclei of marine origin: Some recent observations 21 p3640 N85-32611

Marine aerosols at the Dutch North Sea coast: Size distributions and fractionation of trace elements
21 p3648 N85-32664

Sulfates in marine aerosols over the tropical Western Pacific Ocean 21 p3651 N85-32690

Granulometric study of the acidity and sulfate excess in marine aerosols 21 p3652 N85-32691

Sulfur diagenesis in marine sediments
21 p3658 N85-32721

Sulfur reduction in sediments of marine and evaporite environments 21 p3661 N85-32742

Submarine hydrothermal environments as sites for the origin and evolution of life 21 p3719 N85-33074

Corrosion management strategies for aircraft and related systems 22 p3749 N85-33239

Current requirements for the design and maintenance against corrosion of UK military aircraft
22 p3750 N85-33244

The development and evaluation of the creep and corrosion resistant alloy IN6201
[PNR-90253] 23 p3917 N85-34278

MARINE GEOLOGY

U HYDROGEOLOGY

MARINE METEOROLOGY

Operational use of shipboard numerical aid programs
01 p0062 N85-10546

Energy-active zones in north Atlantic as manifestation of interannual variability of radiation balance
02 p0164 N85-11108

Bibliography of climate textbooks and studies
[WCP-84] 02 p0231 N85-11505

Observational-numerical study of maritime extratropical cyclones using FGGE data 05 p0685 N85-14400

Air-sea interaction during cold air outbreaks
05 p0685 N85-14401

Mariners weather log, volume 28, no. 3, July-August-September 1984
[PB85-107266] 06 p0840 N85-15334

MIZEX. A program for mesoscale Air-Ice-Ocean interaction experiments in arctic marginal ice zones. 4: Initial results and analysis from MIZEX 83
[AD-A148255] 08 p1173 N85-17399

Development of guidance forecasts at the Royal Netherlands Meteorological Institute (KNMI). Part 2 Extreme wind speed at IJmuiden
[KNMI-TR-54-PT-2] 08 p1190 N85-17

Annual data and verification tabulation for Eastern North Pacific tropical storms and hurricanes, 1983
[PB85-109635] 10 p1520 N85-1

Science opportunities using the NASA scatterometer on N-ROSS
[NASA-CR-175639] 13 p2123 N85-2

The BALSAMINE experiment
14 p2238 N85-2

Automatic weather stations in Antarctica
14 p2324 N85-24

The 1981 transatlantic boat race contribution for marine meteorological measurements 14 p2324 N85-24

The development of an automated marine meteorological data system 14 p2324 N85-24

Intermediate results of the NORDSEE experiment
[AD-A151363] 15 p2542 N85-2

Report of the Hydrographic Service Royal Australian Navy for the year ended 30th june 1984, issue number 20
[AD-A151460] 15 p2583 N85-2

Diagnostic verification of the GLAS (Goddard Laboratory for Atmospheric Sciences) general circulation model as applied to a case of extratropical maritime explosive cyclogenesis
[AD-A153686] 18 p3148 N85-29

Mariners weather log, volume 29, number 1, winter 1985
[PB85-177483] 19 p3318 N85-30

Mariners weather log, volume 28, number 4, fall 1984
[PB85-178406] 19 p3318 N85-30

Commission for Marine Meteorology
[WMO-640] 20 p3496 N85-31

MARINE NAVIGATION

U SURFACE NAVIGATION

MARINE PROPULSION

An analytic model of gas turbine engine installations
[AD-A148708] 09 p1281 N85-18

USSR report: Engineering and equipment
[JPRS-UEQ-85-004] 17 p2939 N85-28

MARINE RESOURCES

Cultivation and conversion of marine macroalgae – biomass energy production
[DE84-004522] 04 p0544 N85-13

The use of hydrometeorological data in explaining shrimp cycles in Guyana 07 p1004 N85-16

Contribution of the NOAA-7 and 8 and ARGOS partnership to white tuna fishing in the northeast Atlantic
16 p2813 N85-27

MARINE TECHNOLOGY

Design proposals for torsional buckling of stiffeners
[AD-A144783] 01 p0062 N85-10

Evaluation of an integrated mixed-layer model for single station prediction in a marine regime
01 p0080 N85-10

Ultrafiltration as pretreatment for the preparation of drinking water by reverse osmosis onboard ships
[PML-1984-32] 01 p0098 N85-10

High-data-rate wide-angle underwater acoustic telemetry system
[DE84-015696] 02 p0233 N85-11

NAVAIR's (Naval air systems command) AI (Artificial Intelligence) program for ATE (Automated Test Equipment)
[AD-P003935] 02 p0247 N85-11

Navy programs on ion implantation for materials modification
[AD-P003952] 02 p0286 N85-11

ONR (Office of Naval Research) Far east Scientific Bulletin, Volume 9, Number 2, April - June 1984
[AD-A145681] 02 p0305 N85-11

The Lindstrom-Madden method for series systems with repeated components
[AD-A146265] 03 p0412 N85-12

Protective coverings for fiber reinforced epoxy composites
[PB84-231069] 04 p0480 N85-13

Naval surface weapons center technology transfer report (FY83)
[AD-A146501] 06 p0671 N85-15

USC (University of Southern California) Sea Grant Program Directory, 1984-1985
[PB85-135051] 12 p1899 N85-21

Research needs for artificial intelligence applications in support of C3 (Command, Control, and Communications)
[AD-A150667] 14 p2292 N85-24

Miscellaneous ARGOS maritime applications — yacht races 14 p2327 N85-24

A summary of the Naval Postgraduate School research program
[AD-A151721] 16 p2875 N85-27

Recent Naval Postgraduate School publications
[AD-A151723] 16 p2875 N85-27

The dynamics of slack marine cables
[AD-A155022] 21 p3599 N85-32348
Physical oceanography program science abstracts
[AD-A154637] 21 p3654 N85-32701
High powered epicyclic gears: Some recent development 23 p3924 N85-34316

MARINE TRANSPORTATION
USSR report: Transportation
[JPRS-UTR-85-006] 15 p2460 N85-25189
USSR report: Transportation
[JPRS-UTR-84-017] 15 p2461 N85-25196
USSR report: Transportation
[JPRS-UTR-84-014] 15 p2467 N85-25229
Review and evaluation of plans to incorporate NAVSTAR global positioning system user equipment on military sealift command ships
[AD-A153799] 18 p3060 N85-28934
The international organization of maritime search and rescue 20 p3400 N85-31089

MARINER SPACE PROBES
NT MARINER 5 SPACE PROBE
NT MARINER 9 SPACE PROBE

MARINER 5 SPACE PROBE
Evaluation of semiconductor devices for Electric and Hybrid Vehicle (EHV) ac-drive applications, volume 2
[NASA-CR-176103] 22 p3759 N85-33294

MARINER 9 SPACE PROBE
Participation in the Mars Data Analysis Program: Analysis of cloud forms in Viking and Mariner 9 images
[NASA-CR-175604] 13 p2204 N85-23673

MARISAT SATELLITES
INMARSAT: An overview 20 p3400 N85-31091
Existing and potential INMARSAT capabilities for the Future Global Maritime Distress and Safety System
20 p3402 N85-31110
The International Radio Consultative Committee (CCIR) recommended satellite Emergency Position Indicating Radio Beacon (EPIRB) system operating through geostationary satellites at 1.6 GHz
20 p3402 N85-31112
UK experience with COSPAS-SARSAT and INMARSAT distress systems 20 p3406 N85-31132
INMARSAT distress and safety communication
20 p3406 N85-31134
Future prospects for a combined INMARSAT polar communication and search and rescue satellite system
20 p3406 N85-31137

MARITIME SATELLITES
NT ERS-1 (ESA SATELLITE)
INMARSAT marine satellite organization
13 p1985 N85-22456
INMARSAT: An overview 20 p3400 N85-31091
Maritime mobile satellite techniques as an integral part of the Future Global Maritime Distress and Safety System (FGMDSS): The position of the Federal Republic of Germany 20 p3406 N85-31136
Future prospects for a combined INMARSAT polar communication and search and rescue satellite system
20 p3406 N85-31137

MARKERS
TEM combined with Al/sub x/Ga/sub 1-x/ as marker layers as a technique for the study of GaAs MBE growth
[DE85-008451] 18 p3194 N85-29809

MARKET RESEARCH
Abrasive products study
[PB84-223635] 01 p0033 N85-10205
User requirements for very-short-range weather forecasts: Some key issues 01 p0084 N85-10562
Use of short-range weather forecasts at construction sites: Some results from a user and a market test
01 p0084 N85-10563
Foreign civil aviation competition: 1976 summary and implications
[NASA-TM-X-73907] 02 p0133 N85-10907
The future of satellite remote sensing: A worldwide assessment and prediction 02 p0151 N85-11025
German domestic scheduled air transport in the year 2000
[ESA-TT-828] 05 p0595 N85-13792
Telecommunication market research processing
[ENST-83E018] 23 p3926 N85-34331

MARKETING
Abrasive products study
[PB84-223635] 01 p0033 N85-10205
Financial issues for commercial space ventures: Paying for the dreams 02 p0150 N85-11014
Subliminal communication technology
[GPO-38-833] 05 p0622 N85-13979
UK, FRG, France: R and D in sensors, related fields
08 p1142 N85-17197
French panel makes specific proposals for robotics research. Current state of French robotics
11 p1618 N85-20180
Development of computer centers, equipment described: Problems of computer centers
11 p1700 N85-20686
High-technology ceramics in Japan
[PB85-125029] 12 p1815 N85-21389
MBB cost-reduction plan for Airbus construction described 15 p2532 N85-25616
FRG journal analyzes state, prospects of airbus programs: General analysis 15 p2535 N85-25638
French firm plans recapture of domestic CAD/CAM market 15 p2535 N85-25641
Air quality benefit analysis for Los Angeles and San Francisco based on housing values and visibility
[PB85-166049] 16 p2822 N85-27409
The Ariane launch vehicle is the key of the Europeans to the space market 17 p2906 N85-27931

MARKING
NT ISOTOPIC LABELING
New labeling procedures for the basis graph in generalized networks
[AD-A146217] 03 p0407 N85-12601
Simultaneous determination of cerebral blood flow and partition coefficient with a freely diffusable tracer
[DE85-001226] 11 p1690 N85-20625
On the use of marker loads for fatigue crack growth measurements 14 p2319 N85-24332
Pavement-marking materials: New York's experience
[PB85-153294] 15 p2523 N85-25558
On the use of marker loads for fatigue crack growth measurements
[FFA-TN-1984-52] 16 p2802 N85-27277
Resource management for the tagged token dataflow architecture
[AD-A154773] 21 p3667 N85-32779

MARKOV CHAINS
Numerical studies in nonlinear filtering
[TWISK-305] 01 p0108 N85-10728
The growth and composition of supercritical branching populations on general type spaces
[CTH-MATH-1984-18] 05 p0721 N85-14631
Limiting distributions of functionals of Markov chains
[AD-A147832] 07 p1036 N85-16577
Regenerative structure of Markov chains simulated via common random numbers
[AD-A149092] 10 p1550 N85-19777
Algebraic decay in self-similar Markov chains
[DE85-003162] 11 p1707 N85-20740
Reliability bounds for fault-tolerant systems with competing responses to component failures
[NASA-TP-2409] 13 p2100 N85-23090
Regenerative simulation of non-Markovian stochastic systems
[AD-A150344] 13 p2153 N85-23367
Automatic symbolic solution of Markov chains
[AD-A150476] 13 p2153 N85-23369
Ergodicity and Steady-State-Equilibrium conditions for Markov chains
[AD-A151038] 14 p2409 N85-24854
Sensitivity of conditions for lumping finite Markov chains
[AD-A152122] 16 p2655 N85-27604
Sensitivity of the stationary distribution vector for an ergodic Markov chain
[DE85-006979] 16 p2857 N85-27621
Limit behaviour for stochastic monotonicity and applications
[AD-A153814] 18 p3170 N85-29648
Tunisian climate seen through a Markov process
[CT-585] 23 p3950 N85-34482

MARKOV PROCESSES
NT MARKOV CHAINS
Markovian control problems: Functional equations and algorithms
[MCTH-97] 01 p0107 N85-10717
Optimum replacement of a system subject to shocks
[AD-A145811] 03 p0372 N85-12374
Regenerative simulation methods for local area computer networks
[AD-A146197] 03 p0409 N85-12612
Very short range statistical forecasting of automated weather observations
[DOT/FAA/PM-84/31] 05 p0679 N85-14359
Power spectral ensity of markov texture fields
07 p0986 N85-16262
On modeling the performance and reliability of multi-mode computer systems
[AD-A148444] 08 p1208 N85-17599
A unified model for performance and reliability of Fault-Tolerant/Multi-Mode systems
[AD-A148789] 08 p1208 N85-17601
Extended Stochastic Petri Nets: Applications and analysis
[AD-A148439] 08 p1213 N85-17633
Convergence of quasi-stationary to stationary distributions for stochastically monotone Markov processes
[AD-A148041] 08 p1215 N85-17652
State estimation with interrupted observations
15 p2635 N85-26251
Inference and state estimation for stochastic point processes
[AD-A151216] 15 p2640 N85-26281
Bayesian estimation of one dimensional discrete markov random fields
[AD-A151503] 15 p2640 N85-26284
A Markov method for simulating non-Gaussian wind speed time series
[DE85-007131] 16 p2835 N85-27485
Sensitivity of conditions for lumping finite Markov chains
[AD-A152122] 16 p2655 N85-27604
An abstract specification language for Markov reliability models
[NASA-TM-86423] 16 p2857 N85-27616
An application of Markov chains to the problem of migration in inventory systems
[AD-A151954] 16 p2857 N85-27618
Theory of laser-stimulated surface process. 2: A generalized-master-equation approach to energy transfer between an IR laser, an aspecties and phonons
[AD-A153083] 17 p2970 N85-28344
On estimating transition intensities of a Markov process with aggregate data of a certain type
[CWI-MS-R8411] 17 p3025 N85-28707
Maximum flow in planar networks with exponentially distributed arc capacities
[AD-A153158] 17 p3026 N85-28710
Quantum model of dephasing-enhanced laser desorption: Master equation approach
[AD-A153769] 18 p3112 N85-29269
The completion time of a job on multi-mode systems
[AD-A154113] 19 p3336 N85-30666
Memory effects in dynamical many-body systems: The isomnesic (constant-memory) approximation
[AD-A154160] 20 p3520 N85-31869
Comprehensive radio direction finder with electronically stabilized radiation pattern 22 p3762 N85-33318
Optimal complex nonlinear processing of continuous and pulsed signals 22 p3763 N85-33323
Synthesis of optimum receiver and processor for interfering radio pulse signals 22 p3769 N85-33361
Optimal Bayesian estimators for image segmentation and surface reconstruction
[AD-A155732] 22 p3827 N85-33704

MARROW
Effect of spaceflight factors on rat bone marrow cells
01 p0092 N85-10620

MARS
Volcanic debris flows in the Elysium region of Mars
13 p2185 N85-23560
Estimates of lava eruption rates at Alba Patera, Mars
13 p2185 N85-23562

MARS (PLANET)
Mars exploration, Venus swingby and conjunction class mission modes, time period 2000 to 2045
[NASA-TM-86477] 02 p0303 N85-11961
Martian impact basins: Morphology differences and tectonic provinces
[NASA-CR-174074] 03 p0448 N85-12847
The Martian climate: Energy balance models with CO2/H2O atmospheres
[NASA-CR-174073] 03 p0448 N85-12849
A Mars dust sample return mission
[CNES-CT/PMF/APS/EMS-177]
04 p0459 N85-12915
Mars polar volatiles: Topographic and geologic setting
[NASA-CR-174069] 04 p0581 N85-13706
An autonomous roving vehicle for the planet Mars: A summary of over 15 years of research
[RPI-TR-MP-83] 07 p0973 N85-16179
The geology of the terrestrial planets
[NASA-SP-469] 09 p1410 N85-18888
Mars 09 p1411 N85-18894
A model for the climatic behavior of water on Mars
09 p1415 N85-18931
Conclusion of Viking Lander Imaging Investigation: Picture catalog of experiment data record
[NASA-RP-1137] 11 p1763 N85-21099
Viking radio science data analysis and synthesis
[NASA-CR-175631] 13 p2171 N85-23471
Study and estimation of planet-crossing asteroid populations: Discoveries and analysis
13 p2175 N85-23496
Viking radio science data analysis and synthesis
13 p2180 N85-23528
Estimates of lava eruption rates at Alba Patera, Mars
13 p2185 N85-23562
Observed changes at Viking Lander 1
13 p2188 N85-23575
Seasonal and secular variation of the Solis Lacus albedo feature: Relation to the Martian dust-transport cycle
13 p2188 N85-23576
Eolian erosion on Mars: Three scales
13 p2186 N85-23577

The origin of regional dust deposits on Mars 13 p2188 N85-23578
On the latitudinal distribution of debris in the Northern Hemisphere of Mars 13 p2188 N85-23579
Transformation of polar ice sublimate residue into Martian circumpolar sand 13 p2189 N85-23580
The effect of particle density on aeolian transport 13 p2189 N85-23581
Paleohydrologic implications of valley networks of Mars 13 p2190 N85-23585
Fluvial drainage basins and valley networks: Eastern Margaritifer Sinus, Mars 13 p2190 N85-23586
Catastrophic-flood features in Swedish Lapland as a terrestrial analog for Martian channel flows 13 p2190 N85-23587
Experiments and analyses of the formation of erosional scour marks with implications to the origin of the Martian outflow channels 13 p2190 N85-23588
Relative time-scale for channeling events within chaotic terrains, Margaritifer Sinus, Mars 13 p2190 N85-23589
Terrestrial analog studies for Martian patterned ground 13 p2190 N85-23590
Origin of Martian polygonal terrain: Preliminary results 13 p2191 N85-23591
Radiation-dominated snowmelt on Mars 13 p2191 N85-23592
Chemical weathering of soils from the dry valleys of Antarctica: A terrestrial analog of Martian weathering processes 13 p2197 N85-23626
Mars radar catalog 13 p2198 N85-23636
Statistics of Aeolian surface of Mars 13 p2199 N85-23637
Radar and the detection of liquid water on Mars 13 p2199 N85-23638
Planetary interior modeling and tectonic implications 13 p2200 N85-23649
Elysium region, Mars: Tests of lithospheric loading models for the formation of tectonic features 13 p2200 N85-23650
Mars: Stratigraphy of western highlands and polar regions 13 p2201 N85-23653
Participation in the Mars Data Analysis Program: Analysis of cloud forms in Viking and Mariner 9 images [NASA-CR-175604] 13 p2204 N85-23673
Structure and origin of Martian satellites 15 p2483 N85-25323
Distribution of gravity and plumb line deflection at Martian surface 15 p2483 N85-25324
Sixteenth Lunar and Planetary Science Conference. Press abstracts [NASA-CR-175692] 15 p2680 N85-26546
Identification of the youngest meteorites and a discussion of the possibility that they came from Mars 15 p2681 N85-26559
What we know about Mars (but otherwise wouldn't) if it is the shergottite parent body 15 p2682 N85-26565
Orientation and strength of Martian magnetic dipole 16 p2723 N85-26808
Possible configuration of Martian magnetosphere 16 p2723 N85-26809
The influence of global dust storms on the mean seasonal daily insolations at the Martian surface [AERONOMICA-ACTA-A-289-1984] 18 p3203 N85-29868
Space ventures and society long-term perspectives [NASA-CR-176012] 19 p3379 N85-30963
Mega-geomorphology: Mars vis a vis Earth 21 p3601 N85-32360
The polar caps and the climatic evolution of Mars 22 p3854 N85-33866
Volatiles on satellites of the outer solar system 22 p3854 N85-33868
Permafrost features on Earth and Mars: Similarities, differences 22 p3855 N85-33870
Venus, Earth and Mars: Present bounds on similarities and differences in bulk composition 22 p3856 N85-33876
Planning for VRM: Radar and sonar studies of volcanic terrains on Earth, Venus and Mars 22 p3857 N85-33884
What we have learned about the magnetic field of Mars 22 p3858 N85-33892
Comparisons of the North Polar Cap of Mars and the Earth's Northern Hemisphere snow cover [NASA-TM-86191] 23 p3989 N85-34728

MARS ATMOSPHERE
Clouds above the Martin Limb: Viking observations [NASA-CR-174027] 02 p0296 N85-11922
The Martian climate: Energy balance models with CO2/H2O atmospheres [NASA-CR-174073] 03 p0446 N85-12849
A Mars dust sample return mission [CNES-CT/PMF/APS/EMS-177] 04 p0459 N85-12915
Construction of a superheterodyne receiver for 10 micron waves to be put on a Cassegrain optics telescope for spectroscopic research on the Mars and Venus atmospheres [MPE-183] 06 p0872 N85-15536
Exploration of the solar system by airborne astronomy 08 p1244 N85-17851
Mars 09 p1411 N85-18694
The effect of particle density on aeolian transport 13 p2189 N85-23581
Mars: Long term changes in the state and distribution of H2O 13 p2191 N85-23593
Water-ice clouds on Mars: Location and seasonal variation 13 p2194 N85-23611
The Martian climate: Energy balance models with CO2/H2O atmospheres [NASA-CR-175722] 15 p2679 N85-26547
Dust devils on Mars 15 p2683 N85-26573
The influence of global dust storms on the mean seasonal daily insolations at the Martian surface [AERONOMICA-ACTA-A-289-1984] 18 p3203 N85-29868
Noble gas patterns in the atmospheres of Mars and Earth: A comparison via the SNC meteorites 22 p3852 N85-33853

MARS CRATERS
Martian impact basins: Morphology differences and tectonic provinces [NASA-CR-174074] 03 p0448 N85-12847
Mars 09 p1411 N85-18694
The nature of Martian flow ejecta craters 13 p2183 N85-23545
Paleohydrologic implications of valley networks of Mars 13 p2190 N85-23585
Geomorphology and geology of the Southwestern Margaritifer Sinus and Argyre regions of Mars. Part 2: Crater size-frequency distribution curves and geomorphic unit ages 13 p2192 N85-23601
Geomorphology and geology of the Southwestern Margaritifer Sinus and Argyre regions of Mars. Part 4: Flow ejecta crater distribution 13 p2193 N85-23603
Identification of the youngest meteorites and a discussion of the possibility that they came from Mars 15 p2681 N85-26559
Lunar and Martian impact basins: Exposed records of terrestrial bombardment? 21 p3721 N85-33090

MARS ENVIRONMENT
NT MARS ATMOSPHERE
Properties of filamentary sublimation residues from dispersions of clay in ice 13 p2197 N85-23629
Statistics of Aeolian surface of Mars 13 p2199 N85-23637

MARS LANDING
Mars landing sites 22 p3859 N85-33893

MARS PHOTOGRAPHS
Mars-Earth geographical comparisons: A pictorial view [NASA-TM-86166] 02 p0302 N85-11957
Conclusion of Viking Lander Imaging Investigation: Picture catalog of experiment data record [NASA-RP-1137] 11 p1765 N85-21099
Viking Lander mosaics of Mars 13 p2203 N85-23667
The control network of Mars: October 1984 13 p2203 N85-23670

MARS PROBES
NT VIKING LANDER SPACECRAFT
NT VIKING LANDER 1
NT VIKING MARS PROGRAM
NT VIKING ORBITER SPACECRAFT
NT VIKING SPACECRAFT
A Mars dust sample return mission [CNES-CT/PMF/APS/EMS-177] 04 p0459 N85-12915
Mars landing sites 22 p3859 N85-33893

MARS SURFACE
Mars-Earth geographical comparisons: A pictorial view [NASA-TM-86166] 02 p0302 N85-11957
Martian impact basins: Morphology differences and tectonic provinces [NASA-CR-174074] 03 p0448 N85-12847
The Martian climate: Energy balance models with CO2/H2O atmospheres [NASA-CR-174073] 03 p0446 N85-12849
Growth of soil bacteria in presence of Martian soil analog, carbon dioxide and hydrogen peroxide 09 p1361 N85-18560
Mars 09 p1411 N85-18694
Conclusion of Viking Lander Imaging Investigation: Picture catalog of experiment data record [NASA-RP-1137] 11 p1765 N85-21099
Physiography of the Martian west equatorial uplift 12 p1961 N85-22325
The origin and evolution of terrestrial and Martian labyrinths [NASA-CR-175511] 12 p1961 N85-
Viking radio science data analysis and synthesis 13 p2180 N85-
Martian terrain ages 13 p2181 N85-
The evolution of CO2 on Mars 13 p2185 N85-
Ridged plains of Lunae Planum: Thickness revised 13 p2185 N85-
Thickness of ridged plains materials in Hesperia Planum, Mars 13 p2185 N85-
Observed changes at Viking Lander 1 13 p2188 N85-
Seasonal and secular variation of the Solis Lacus feature: Relation to the Martian dust-transport cycle 13 p2188 N85-
Eolian erosion on Mars: Three scales 13 p2188 N85-
The origin of regional dust deposits on Mars 13 p2188 N85-
On the latitudinal distribution of debris in the Hemisphere of Mars 13 p2188 N85-
Transformation of polar ice sublimate Martian circumpolar sand 13 p2189 N85-
Paleohydrologic implications of valley networks of Mars 13 p2190 N85-
Fluvial drainage basins and valley networks: Margaritifer Sinus, Mars 13 p2190 N85-
Catastrophic-flood features in Swedish Lapland terrestrial analog for Martian channel flows 13 p2190 N85-
Experiments and analyses of the formation of scour marks with implications to the origin of the outflow channels 13 p2190 N85-
Mars: Long term changes in the state and of H2O 13 p2191 N85-
Mapping structures characteristic of the highland boundary scarp on Mars 13 p2191 N85-
Investigations of the Mars cratered terrain: plains boundary in the eastern equatorial region 13 p2191 N85-
Martian fretted terrain morphometry interpreted principal components analysis 13 p2192 N85-
Distribution and properties of large symmetric knobs Mars 13 p2192 N85-
Enigmatic hills of the mottled plains, Mare quadrangle (MC-4), Mars 13 p2192 N85-
Geomorphology and geology of the Southwestern Margaritifer Sinus and Argyre regions of Mars. Part 1: Geological and geomorphological overview 13 p2192 N85-
Geomorphology and geology of the Margaritifer Sinus and Argyre regions of Mars. Part 2 Crater size-frequency distribution curves and unit ages 13 p2192 N85-
Geomorphology and geology of the Southwestern Margaritifer Sinus and Argyre regions of Mars. Part 3 Valley types and distribution 13 p2193 N85-
Geomorphology and geology of the Margaritifer Sinus and Argyre regions of Mars. Part 4 Flow ejecta crater distribution 13 p2193 N85-
Planetary analogs in Antarctica: Mars 13 p2193 N85-
Multispectral analysis of the Kasei Vallis-Lunae region of Mars 13 p2193 N85-
Geologic interpretation of remote sensing data for the Martian volcano, Ascraeus Mons 13 p2194 N85-
The search for igneous materials at the Viking landing sites 13 p2194 N85-
Basalts of Mars: Constraints on volatile evolution 13 p2194 N85-
First direct detection of clay minerals on Mars 13 p2194 N85-
Iron oxides of Mars: Evidence for contemporary weathering 13 p2195 N85-
Reassignment of the iron (3) absorption bands in the spectra of Mars 13 p2195 N85-
Zeolites on Mars: Prospects for remote sensing 13 p2195 N85-
Mars radar catalog 13 p2198 N85-
Statistics of Aeolian surface of Mars 13 p2199 N85-
Radar and the detection of liquid water on Mars 13 p2199 N85-
Mechanisms of basalt-plains ridge formation 13 p2199 N85-
On the absence of strike-slip faults from the planets and satellites 13 p2200 N85-
Lithologic and structural control on slope morphology in the Valles Marineris 13 p2201 N85-
Valles Marineris basin beds: A complex story 13 p2201 N85-
Kasei Vallis of Mars: Dating the interplay of tectonics and geomorphology 13 p2201 N85-

Mars geologic mapping: A review and new concepts
13 p2202 N85-23663
Mars planimetric mapping 13 p2203 N85-23666
The Mars ancient cratered terrain, smooth plains boundary: Implications of Viking color data for evolution of the Amenthes Region 15 p2682 N85-26564
Mars: Seasonally variable radar reflectivity
15 p2683 N85-26570
Dust devils on Mars 15 p2683 N85-26573
Geological analyses of the surface of Venus and Mars from lander spacecraft images and orbital radar observations 19 p3364 N85-30993
Lunar and Martian impact basins: Exposed records of terrestrial bombardment? 21 p3721 N85-33090

MARS VOLCANOES
Mars 09 p1411 N85-18894
Emplacement of long lava flows on Mauna Loa (Hawaii) and Alba (Mars) 13 p2186 N85-23563
Geologic interpretation of remote sensing data for the Martian volcano, Ascraeus Mons
13 p2194 N85-23608
Geologic interpretation of remote sensing data for the Martian volcano Ascraeus Mons
19 p3384 N85-30992
Geomorphic classification of Icelandic and Martian volcanoes: Limitations of comparative planetology research from LANDSAT and Viking orbiter images
21 p3603 N85-32372

MARSHES
U MARSHLANDS

MARSHLANDS
Remote sensing of coastal wetlands biomass using Thematic Mapper wavebands — Lewes, Delaware
13 p2119 N85-23196

MARTENSITE
Structural changes with one- and two-stage aging of alloys Ti-Al-Mo-Fe and Ti-Zr-V-Al-Sn
15 p2499 N85-25415
The state of martensite after quenching in a magnetic field
[BLL-BISI-TRANS-22297-(9022.06)]
17 p2926 N85-28051
The structure of carbon martensite analyzed with Moessbauer spectra
[BLL-BISI-TRANS-22402-(9022.06)]
17 p2927 N85-28062
Mechanical stabilization of austenite against epsilon martensite and its effect on deformation behavior in high manganese steels
[DE85-007654] 17 p2932 N85-28097
Fatigue crack propagation characteristics and fatigue fracture toughness in 780 MPa grade high strength steel weldments at low temperature
[BLL-BISI-TRANS-22369-(9022.06)]
17 p2979 N85-28411
Shape memory effect in uranium-niobium alloys below room temperature
[DE85-012984] 23 p3916 N85-34268
Decomposition of martensite in R6M5 and R6AM5 steels after direct immersion in liquid nitrogen
[BLL-M-36305] 24 p4077 N85-35268

MARTENSITIC STAINLESS STEELS
Microstructure and deformation aspects of some specialty steels and hard metals
02 p0176 N85-11182
Maraging steels: Structure, properties and applications 02 p0177 N85-11191
Metallurgy of a 12 percent chromium stainless steel
02 p0178 N85-11195
Mechanism of titanium impact on brittle tendency in delayed deformation of martensite-aging steels
11 p1604 N85-20087
The role of void nucleation in the swelling resistance of ferritic steel
[AERE-R-11525] 11 p1610 N85-20122

MARTENSITIC TRANSFORMATION
Fatigue crack propagation in metastable titanium alloys
[AD-A145824] 03 p0372 N85-12376
Effect of phase state of TiC-NiTi powder composite materials on nature of failure and mechanical properties
13 p2027 N85-22702
Mechanical properties of cast Martensitic high-strength multicomponent titanium alloys
15 p2514 N85-25514
Textural transformations taking place during heat and mechanical treatment in triplex steels
[BLL-BISI-TRANS-22404-(9022.06)]
17 p2927 N85-28063
Influence of structural state and alloy content of austenite on formation of martensitic phases in steels
[BLL-BISI-TRANS-22386-(9022.06)]
17 p2928 N85-28068
The mechanics of internal stress and microcrack toughening mechanisms in ceramics
[AD-A154049] 19 p3248 N85-30139
The effect of prior parent phase cold work on martensite transformation in Cu-Zn-Al shape memory alloys
[AD-A155140] 21 p3566 N85-32183
Electrical resistivity and hysteresis of the equiatomic nickel-titanium alloy near the martensitic transformation temperature 23 p3904 N85-34181
Decomposition of martensite in R6M5 and R6AM5 steels after direct immersion in liquid nitrogen
[BLL-M-36305] 24 p4077 N85-35268

MARTINGALES
Applications of functional analytic and Martingale methods
[AD-A145555] 02 p0255 N85-11672
The growth and composition of supercritical branching populations on general type spaces
[CTH-MATH-1984-18] 05 p0721 N85-14631
An on-line parameter estimation algorithm for counting process observations
[CWI-OS-R8406] 05 p0721 N85-14632
A note on two papers in dependent central limit theory
[CWI-MS-R8410] 05 p0722 N85-14638
A martingale approach to supercritical (C-M-J) branching processes
[CTH-MATH-1984-25] 05 p0722 N85-14643

MARYLAND
Erosion and sedimentation chronology of three watersheds in Maryland
[PB84-207356] 01 p0071 N85-10467

MASCONS
The non-hydrostatic figures of the terrestrial planets
22 p3858 N85-33887

MASER OUTPUTS
Software for Crimea-Pushchino radiointerferometer
06 p0783 N85-15007
Fine structure of Alfven maser radiation
06 p0824 N85-15232
Electron-cyclotron maser emission during solar and stellar flares
[NASA-CR-175883] 17 p3054 N85-28907
Hydrogen maser oscillation at 10 K
18 p3106 N85-29241

MASER RESONATORS
U MASERS

MASERS
NT HYDROGEN MASERS
NT INTERSTELLAR MASERS
NT TRAVELING WAVE MASERS
NT WATER MASERS
A new maser effect in plasma turbulence
02 p0284 N85-11852
Passive maser using timesharing for control of the cavity and control of the oscillator on the line of stimulated emission
[AD-D011326] 07 p0959 N85-16151
Technology for satellite power conversion
[NASA-CR-174335] 09 p1343 N85-18451
The superconducting cavity stability ruby maser oscillator 17 p2967 N85-28324
Maser cavity servo-tuning system
[NASA-CASE-NPO-15890-1-CU]
18 p3093 N85-29143
The system design of a rubidium maser frequency standard 18 p3106 N85-29232
Operation of a quasioptical electron cyclotron maser
[DE85-008450] 18 p3113 N85-29276
Turbulence and wave particle interactions in solar-terrestrial plasmas
[NASA-CR-175970] 18 p3209 N85-29906
Cerenkov maser and Cerenkov laser devices
[AD-A155443] 21 p3592 N85-32324
USSR report: Physics and mathematics
[JPRS-UPM-85-004] 21 p3680 N85-32860

MASKING
Spatial and temporal visual masking and visibility
[AD-A151968] 16 p2842 N85-27524
Low defect, high purity crystalline layers grown by selective deposition
[NASA-CASE-NPO-15813-1] 19 p3373 N85-30922
Basic development of a 1.5 micrometer very large scale integrated technique, part 1-4
[BMFT-FB-T-85-032-PT-1-4] 20 p3449 N85-31417
SONTRAC: A solar neutron track chamber detector
[SH-9.1-12] 23 p4052 N85-35127

MASKS
Computerized circuit designs: Realization of masks to manufacture microwave circuits
[CNES-NT-107] 04 p0496 N85-13168
Hydrogen-oxygen (hydrox) breathing at 1.3MPa
[FOA-C-58015-H1] 09 p1364 N85-18577
Lithography radiation effects study
[AD-A149552] 10 p1468 N85-19260
DARPA/TTO program IR binary optics
[AD-A152196] 16 p2865 N85-27672
A prototype test chamber for fit testing of protective masks in the field
[FOA-C-40206-C1(C2)] 20 p3512 N85-31834

MASONRY
Finite element model for creep in composite masonry
[PB85-150324] 14 p2322 N85-24347

MASS
NT CENTER OF MASS
NT CRITICAL MASS
NT ELECTRON MASS
NT PARTICLE MASS
NT STELLAR MASS
Searching for top, Higgs, and supersymmetry: The minimum invariant mass technique
[DE84-014539] 01 p0119 N85-10813
Measurement of areal mass variation in Rayleigh-Taylor unstable targets
[AD-A145541] 02 p0198 N85-11325
A method for automatic water mass classification
[AD-D011405] 08 p1191 N85-17505
Hot stars: Six years of progress
11 p1743 N85-20963
Histological and compositional responses of bone to immobilization and other experimental conditions
[NASA-CR-175837] 16 p2841 N85-27518
The role of thermal motions of air particles for fireballs
[PUBL-59] 17 p3053 N85-28900
One mechanism for generation of wave disturbances in spectra of turbulent flows near ocean surface
19 p3289 N85-30397
Physics with low temperature antiproton
[DE85-009627] 19 p3355 N85-30798
Mass-discrimination during prolonged weightlessness
20 p3509 N85-31814
Plasma mass and effective inductance in a small railgun
[AD-A154644] 21 p3589 N85-32304

MASS DISTRIBUTION
Measurement of the inertial constants of a rigid or flexible structure of arbitrary share through a vibration test
[NASA-TM-77557] 02 p0209 N85-11381
The origin and evolution of Uranus and Neptune
02 p0298 N85-11928
Satellite masses in the Uranus and Neptune systems
[PSI-CONTRIB-198] 02 p0301 N85-11947
The influence of stellar luminosity and temperature calibration on the determination of the initial mass function 05 p0740 N85-14760
Far infrared spectroscopy of (O III) in M82
08 p1249 N85-17883
Primer for mass metrology
[PB85-121424/GAR] 09 p1305 N85-18199
Effect of hitch positions on the performance of track-grouser systems
[AD-P004277] 09 p1406 N85-18853
Mass distribution and evolutionary scheme for central stars of planetary nebulae 11 p1751 N85-21012
Dynamics of gas disks in triaxial galaxies
13 p2171 N85-23469
Greenland ice sheet mass balance
15 p2603 N85-26043
Potential climatic effects on the Greenland ice sheet
15 p2603 N85-26044
Aluminum-air power cell: The M3-3 experiment
[DE85-008878] 18 p3096 N85-29168
Design of helicopter rotor blades for optimum dynamic characteristics
[NASA-CR-176076] 20 p3393 N85-31044

MASS DRIVERS (PAYLOAD DELIVERY)
Possibilities and limits of electromagnetic acceleration in space applications
[ILR-MITT-136] 02 p0193 N85-11292

MASS FILTERS
U FLUID FILTERS

MASS FLOW
Comparison of options for reduction of noise in the test section of the NASA Langley 4x7m wind tunnel, including reduction of nozzle area
[NASA-CR-172446-VOL-2] 05 p0726 N85-14667
Flow measurement device
[AD-D011432] 08 p1168 N85-17369
Methanol vaporization: Effects on volumetric efficiency and on determination of optimum fuel delivery system
[PB84-243914] 09 p1302 N85-18181
Field validation of statistically-based acceptance plan for bituminous airport pavements. Volume 2: Statistical analysis of Marshall properties of plant-produced bituminous materials
[FAA-PM-84-12-VOL-2] 12 p1781 N85-21181
Mathematical modeling of transient performance of gas turbine engine 13 p2050 N85-22634
Turbulence measurements in shock induced flows
13 p2091 N85-23055
Effective specific impulse of secondary flow injected into a rocket nozzle
[NAL-TR-848T] 18 p3067 N85-28970

Quasi non-intrusive sampling and analysis of gases associated with the boundary layer on the tethered satellite and similar supersonic and hypersonic research vehicles
[NASA-CR-176075] 20 p3407 N85-31140
Free zone electrophoresis simulation of static column electrophoresis in microgravity on shuttle flight STS-3
20 p3502 N85-31773
Microgravity electrophoresis: A study of the factors that affect free-fluid separation 20 p3502 N85-31774
Pre-flight report on cultured human embryonic kidney cell handling and cell electrophoresis. Prepared prior to continuous-flow electrophoretic separation experiments aboard space shuttle flight STS-8
20 p3503 N85-31775
Properties of electrophoretic fractions of human embryonic kidney cells separated on space shuttle flight STS-8 20 p3503 N85-31776
Flow cytometry of human embryonic kidney cells: A light scattering approach 20 p3503 N85-31778
Heat-mass flow enhancement system for a metal hydride assembly
[DE85-010696] 22 p3783 N85-33441
The balancing of complex linkage mechanisms
23 p3924 N85-34313

MASS FLOW RATE
Finite element method for a class of viscoelastic flows in deforming domains applied to jet breakup
[DE84-014571] 04 p0500 N85-13186
Surge transient simulation in turbo-jet engine
05 p0596 N85-13796
Halogen mass flow rate detection system
[AD-D011396] 08 p1166 N85-17352
An episodic red-wing structure of SiIV, lambda 1394A, in gamma Cas 11 p1750 N85-21009
Calibration of sonic valves for the laminar flow control, leading-edge flight test
[NASA-TP-2423] 14 p2210 N85-23707
Deep water formation 15 p2601 N85-26030
Density and confinement effects on mixing characteristics of an axisymmetrical CO(2) jet
[AD-A154468] 19 p3267 N85-30258

MASS RATIOS
NT MASS TO LIGHT RATIOS
Satellite physical and orbital characteristics
16 p2604 N85-27287

MASS SPECTRA
Experimental medium energy physics
[DE84-014625] 02 p0278 N85-11807
Nitriding of titanium and its alloys by N2, NH3 or mixtures of N2 + H2 in a dc arc plasma at low pressures (or = to torr)
[NASA-TM-83803] 06 p0814 N85-15168
Mass analysis of neutral particles and ions released during electrical breakdowns on spacecraft surfaces
[NASA-CR-175585] 12 p1793 N85-21250
Analysis of biological particles by mass spectrometry
[AD-A149952] 13 p2141 N85-23291
The muon content of EAS as a function of primary energy
[OG-5.1-8] 22 p3881 N85-34050
Mass resolution optimization in a large isotopic composition experiment
[OG-9.1-9] 23 p4023 N85-34935

MASS SPECTROMETERS
Advanced mass spectrometers for hydrogen isotope analyses
[DE85-000716] 06 p0811 N85-15150
The design of an ion-neutral mass spectrometer to be used in the Shuttle environment
[AD-A148093] 08 p1114 N85-17022
A cometary ion mass spectrometer
[NASA-CR-174328] 08 p1164 N85-17343
Laser ablation studies using RIS
[DE85-001118] 09 p1326 N85-18336
Documentation for an instrument database system
[DE84-017392] 09 p1402 N85-18826
A GC/MS (Gas Chromatograph/Mass Spectrometer) data management process. Part 1: User's guide, version 1.0
[PB85-116051] 12 p1803 N85-21309
Analyses via automated mass spectrometry (MS/DS)
12 p1947 N85-22227
A computer controlled mass spectrometer system for investigating the decomposition of non-metallic materials under atmospheric conditions 12 p1948 N85-22237
Mass spectra of neutral particles released during electrical breakdown of thin polymer films
13 p1996 N85-22511
Plasma environment effects on the Giotto Ion Mass Spectrometer 14 p2245 N85-23919
Extraction of ions from solutions at atmospheric pressure, mass spectrometric analysis of bioorganic substances 14 p2387 N85-24706
Galileo 15 p2688 N85-26601
An investigation of tropospheric ions
16 p2823 N85-27412
Mass spectrometry technology at the Jet Propulsion Laboratory (JPL) 18 p3157 N85-29552
Mass spectrometer based gas permeation apparatus
[DE85-011176] 19 p3273 N85-30299
Reactions of metal ions and their clusters in the gas phase using laser ionization-ion cyclotron resonance spectroscopy
[DE85-009476] 19 p3361 N85-30638
A retarding ion mass spectrometer for the Dynamics Explorer-1
[NASA-CR-171588] 21 p3589 N85-32303
Fabrication and test of modified quadrupole mass spectrometer
[AD-A155186] 21 p3590 N85-32312
Analysis of spacecraft data
[NASA-CR-171587] 21 p3669 N85-32789
Ion composition measurements of the disturbed and quiet D-region in 1980 - 1981
[AD-A156055] 24 p4117 N85-35521

MASS SPECTROMETRY
U MASS SPECTROSCOPY

MASS SPECTROSCOPY
Supercritical fluid chromatography/supersonic jet spectroscopy
[DE84-016199] 04 p0471 N85-12996
Cardiac output measured by mass spectroscopy
05 p0692 N85-14449
Advanced mass spectrometers for hydrogen isotope analyses
[DE85-000716] 06 p0811 N85-15150
An optical and mass spectrometric study of the aluminum-oxygen flame
[AD-A147434] 07 p0923 N85-15649
Nondestructive evaluation of titanium alloys. ESCA (Electron Spectroscopy for Chemical Analysis), ISS (Ion Scattering Spectroscopy), and SIMS (Secondary Ion Mass Spectrometry) examination of titanium alloy solid surfaces
[AD-P004135] 08 p1128 N85-17110
Analysis of middle distillate fuels by high resolution field ionization mass spectrometry
[AD-A147724] 08 p1135 N85-17153
Mass spectrometry/mass spectrometry as a screening method for detecting explosive vapors
[DE85-001276] 09 p1292 N85-18110
Supersonic molecular jet study of the liquid state
[AD-A147416] 09 p1379 N85-18671
Comparative evaluation of GC/MS (Gas Chromatography/Mass Spectrometry) data analysis processing
[PB85-125664] 11 p1596 N85-20037
Instrumentation for Application Number 1: Mass spectrometric analysis of the boundary layer associated with the tethered satellite 11 p1646 N85-20372
A GC/MS (Gas Chromatograph/Mass Spectrometer) data management process. Part 2: Program documentation, version 1.0
[PB85-116069] 12 p1803 N85-21310
New high resolution scanning ion microprobe and focused ion beam applications
[AD-A149992] 12 p1852 N85-21616
Analyses via automated mass spectrometry (MS/DS)
12 p1947 N85-22227
Analysis of biological particles by mass spectrometry
[AD-A149952] 13 p2141 N85-23291
Collaborative shock tube studies of benzene pyrolysis
[DE85-006347] 14 p2253 N85-23962
Glueball candidates
[DE85-003627] 14 p2418 N85-24921
Secondary ion mass spectrometry studies of solids and surfaces
[AD-A151744] 16 p2745 N85-26939
Photoionization mass spectrometry with VUV hydrogen laser source
[AD-A153362] 17 p2921 N85-28009
Resonance ionization mass spectrometry of carbon
[DE85-009040] 17 p2923 N85-28018
Morphological stability and fluid dynamics of vapor crystal growth
[NASA-CR-175879] 17 p3042 N85-28822
Mass spectrometry technology at the Jet Propulsion Laboratory (JPL) 18 p3157 N85-29552
Selective detection of species in complex matrices by SIMS (Secondary Ion Mass Spectrometry)
[AD-D011685] 19 p3235 N85-30053
Measurement of combustion species by electron impact fluorescence
[DE85-011163] 19 p3236 N85-30065
Identification and quantification of nitropolynuclear aromatic hydrocarbons in ambient and indoor air particulate samples
[PB85-176790] 19 p3311 N85-30525
Quasi non-intrusive sampling and analysis of gases associated with the boundary layer on the tethered satellite and similar supersonic and hypersonic research vehicles
[NASA-CR-176075] 20 p3407 N85-31140
Micro-scale methods for characterization of [illegible] fluid extraction and fractionation processes
[DE85-010966] 20 p3455 N85-[illegible]
Compositional analysis of silicon
20 p3460 N85-[illegible]
Aerosol analysis and emission spectrometry with [illegible] jets
[DE85-010576] 21 p3564 N85-[illegible]
Determination of organobromide compounds in [illegible] by gas chromatography-negative ion chemical [illegible] mass spectrometry
[DRIC-T-7411] 22 p3748 N85-[illegible]
Gas composition and molecule velocity in the [illegible] products of pentaerythritol tetranitrate (PETN) in [illegible] in a high vacuum container. Analysis by mass [illegible] and time of flight spectrometry
[ISL-R-109/84] 22 p3747 N85-[illegible]
Improved negative ion source
[DE85-006445] 23 p3912 N85-[illegible]
Real time analysis of PETN detonation products
[DE85-009581] 23 p3922 N85-[illegible]
Heats of formation of gas phase organosulfur [illegible] radicals and ions measured by PEPICO and [illegible] of (17)O and (33)S NMR spectroscopy to [illegible] determination of organosulfur compounds
[DE85-010558] 24 p4071 N85-[illegible]
Gas analysis of ore-forming fluids
24 p4105 N85-[illegible]
Ion composition measurements of the disturbed and quiet D-region in 1980 - 1981
[AD-A156055] 24 p4117 N85-[illegible]

MASS TO LIGHT RATIOS
Calculation of Si(Li) X-ray detector efficiencies
[DE85-002732] 10 p1489 N85-[illegible]
The muon content of EAS as a function of primary energy
[OG-5.1-8] 22 p3881 N85-[illegible]

MASS TRANSFER
Second All-Union Seminar on Hydromechanics and Heat and Mass Exchange in Weightlessness, summaries of reports
[NASA-TM-77590] 01 p0047 N85-[illegible]
The inducement of planetary boundary layer mass convergence associated with varying vorticity beneath tropospheric wind maximum 01 p0074 N85-10494
Bibliography of US patents on augmentation of convective heat and mass transfer, part 2
[DE84-014865] 04 p0498 N85-1317
Similarity considerations in 1-component 2-phase flow
[DE84-016370] 04 p0499 N85-13184
Investigation of an ejector heat pump by analytical methods
[DE84-016675] 04 p0500 N85-1318
Proposal for wall function for friction and heat transfer in the presence of roughness and mass transfer
[CFD/84/12] 04 p0501 N85-1319
Mass and momentum transport in a turbulent buoyant vertical axisymmetric jet 05 p0635 N85-1407
Development of a mass transfer machine for gas/liquid operations in the absence of gravity
[BMFT-FB-W-84-027] 05 p0637 N85-14081
Variability of short-term eddy-correlation estimates of mass exchange
[DE84-007271] 05 p0677 N85-1434
Investigation of the local mass transfer of a laminar and turbulent falling liquid film
[BLL-T6368/BG/WH792/84] 06 p0807 N85-15130
On the role played by lines in radiatively driven stellar winds depending on the position of the stars in the HR diagram 08 p1236 N85-17787
Multiline transfer and the dynamics of stellar winds
08 p1236 N85-1778
A one dimensional dynamical model of ocean/atmosphere interactions
09 p1358 N85-1854
Heat and mass exchange in a partially stratified fluid
[DE85-000528] 10 p1486 N85-1908
Formaldehyde and tracer gas transfer between airstreams in enthalpy-type air-to-air heat exchangers
[DE84-016951] 11 p1631 N85-2027
The eclipsing binary U Sagittae: Evidence for CNO processing and mass exchange in the past
11 p1757 N85-2134
Mechanisms of heat and mass transfer across a double-diffusive interface
[PB85-148468] 12 p1848 N85-2159
A survey for galactic plane ultraviolet-excess objects: Space densities for white dwarfs, subdwarfs, and cataclysmic variables 13 p2169 N85-234
Seasonal and secular variation of the Solis Lacus albedo feature: Relation to the Martian dust-transport cycle
13 p2188 N85-2357
Eolian erosion on Mars: Three scales
13 p2188 N85-2357
The effect of particle density on aeolian transport
13 p2189 N85-2358

A comparison of terrestrial saltation flux in the laboratory and the field 13 p2169 N85-23582

Mass and heat transfer in reflux condensers of absorption heat pumps
[DFVLR-FB-83-43] 14 p2304 N85-24266

Dissolution of solid solutions in absence of internal mass transfer
[BLL-M-38092-(5828.4)] 16 p2748 N85-26959

Stefan-Maxwell relations for plasma diffusion currents in magnetic field 17 p2942 N85-28160

Transport in aqueous battery systems
[DE85-007246] 17 p2955 N85-28251

CALTECH-DOE program on numerical analysis, computing and fundamental studies of motion, energy and mass transfer in fluids
[DE85-008106] 17 p2959 N85-28274

Molten carbonate fuel cell performance model update
[DE85-003356] 17 p2986 N85-28454

Variability of short term eddy-correlation estimates of mass exchange
[PB85-172641] 18 p3138 N85-29431

Effect of multi-functional inhibitors on the electrochemistry within corrosion crack
19 p3238 N85-30075

Turbulent transport and length scale measurement experiments with confined coaxial jets
[NASA-CR-174631] 19 p3265 N85-30245

Thermomigration in porous media. Study of the development of a drying zone 20 p3456 N85-31482

Influence of spatial variability of hydraulic characteristics of soils on surface parameters obtained from remote sensing data in infrared and microwaves
[NASA-TM-77902] 20 p3477 N85-31604

Vaporization from a heated surface into a saturated stream
[DE85-010484] 20 p3530 N85-31958

New estimating procedures for surface runoff, sediment yield, and contaminant transport in Los Alamos County, New Mexico
[DE85-011890] 21 p3606 N85-32393

Vertical transport in the atmosphere: Measurement capabilities and requirements of VHF radars, part 1.6A
21 p3617 N85-32476

A new hypothesis for the observed vertical distribution of atmospheric aerosols 21 p3645 N85-32646

Size spectra for the source-enhanced coagulation with the turbulent mass transfer 21 p3645 N85-32649

Study of molecular diffusivity influence on mass transfer rate at a water-atmosphere interface
22 p3747 N85-33222

Advances in open-cycle solid desiccant cooling
[DE85-006797] 22 p3806 N85-33590

Determination of properties of zeolite/refrigerant combinations for solar refrigeration systems
[DE85-012009] 23 p3945 N85-34448

Studies in thermo-hydro-chemical transport in porous and fractured media
[DE85-012555] 23 p3949 N85-34473

Molecular and macromolecular sieving by asymmetric ultrafiltration membranes
[PB85-157766] 24 p4077 N85-35266

MASSACHUSETTS

Intraband radiometric performance of the LANDSAT 4 Thematic Mapper — Washington, DC, Arkansas, Massachusetts, Virginia, and Arizona
12 p1871 N85-21738

MASSIFS

Thematic mapping of likely target areas for the occurence of cassiterite in the Serra do Mocambo (GO) granitic massifs using LANDSAT 2 digital imaging
[E85-10027] 02 p0219 N85-11440

Earthquake activity in the Bohemian massif and in the western Carpathians
[REPT-547] 03 p0375 N85-12390

Geomorphology and geology of the Southwestern Margaritifer Sinus and Argyre regions of Mars. Part 1: Geological and geomorphological overview
13 p2192 N85-23600

MASTICATION

Characteristics of human masseter under conditions of hypokinesia 11 p1691 N85-20630

MATCHED FILTERS

Optical implementation of the synthetic discriminant function
[AD-A149582] 10 p1557 N85-19817

Fundamental limits to synchronization and tracking
[AD-A149623] 12 p1833 N85-21504

Acousto-optically addressed Fourier transform matched filters
[AD-A150298] 13 p2063 N85-22889

An investigation into generalised matched filter techniques
[BAE-BR-12971] 15 p2651 N85-26348

Rayleigh criteria resolution of optical correlations
[AD-A151711] 15 p2652 N85-26359

Compression of spread spectrum signals on an excessively dispersive channel
[AD-A155184] 21 p3576 N85-32240

Matched filtering of visual evoked potentials to detect acceleration (+Gz) induced blackout
[AD-A155912] 24 p4131 N85-35609

MATCHING

Antenna matching device tuning for type ZhRU radiostations 06 p0785 N85-15017

The combinatorics of local constraints in model-based recognition and localization
[AD-A148338] 08 p1230 N85-17746

A generalized ordering constraint for stereo correspondence
[AD-A149182] 10 p1487 N85-19390

Individual differences in chromatic brightness matching
[AD-A148862] 10 p1529 N85-19641

Some facets of the tri-index assignment polytope
[AD-A149195] 10 p1547 N85-19753

On large matchings and cycles in sparse random graphs
[AD-A149194] 10 p1550 N85-19778

Multichannel digital processing of wideband signals
12 p1840 N85-21548

Dimensions of smooth mating parts with protective coatings 14 p2260 N85-24124

The effect of set size on color matching
[AD-A150899] 14 p2386 N85-24713

On matchings and Hamiltonian cycles in random graphs
[AD-A151015] 14 p2409 N85-24851

Further study of digital matching of dissimilar images
[AD-A153112] 17 p3019 N85-28672

Generalized planar matching
[AD-A154809] 21 p3677 N85-32842

Digital matched filter 22 p3765 N85-33339

Hierarchical chamfer matching
[FOA-C-30387-E1] 22 p3802 N85-33558

MATERIAL ABSORPTION

Characterization and selection of polymer materials for binary munitions storage. Part 2: Characterization of LLDPE resins
[AD-A148324] 08 p1133 N85-17144

Influence of chemical form, feeding regimen, and animal species on the gastrointestinal absorption of plutonium
[DE85-010291] 21 p3662 N85-32751

MATERIAL BALANCE

NT WATER BALANCE

Aluminum-air power cell: The M3-3 experiment
[DE85-008878] 18 p3096 N85-29168

Measurement of uranium enrichment for gaseous uranium at low pressure
[DE85-012697] 24 p4150 N85-35733

MATERIAL REMOVAL (MACHINING)

U MACHINING

MATERIALS

Thermodynamic calculations and the chemical vapour deposition of hard materials 02 p0179 N85-11200

Electrochemical investigations of novel electrode materials
[DE84-014352] 04 p0495 N85-13158

Online directory of databases for material properties
[DE84-016511] 09 p1402 N85-18824

A DOE directory of databases for material properties
[UCAR-10124] 11 p1739 N85-20937

Topics in optical materials and device research, 3. Volume 2
[AD-A149727] 12 p1911 N85-21996

Electrostatic forming and testing of polymer films on a 16-foot diameter test fixture
[NASA-TM-86328] 13 p2063 N85-22885

Low gravity exothermic heating/cooling apparatus
[NASA-CASE-MSC-25707-1] 18 p3104 N85-29214

MATERIALS HANDLING

NT GROUND HANDLING

NT PROPELLANT TRANSFER

NT REMOTE HANDLING

DoD Robotics Application Workshop Proceedings
[AD-A145867] 03 p0307 N85-11978

Depot modernization at the Defense Logistics Agency
[AD-P004008] 03 p0308 N85-11988

Future robotics program at San Antonio ALC (Air Logistics Center)
[AD-P004011] 03 p0309 N85-11991

Supply center processes
[AD-P004014] 03 p0309 N85-11993

Field applications for robotic materiel handling
[AD-P004016] 03 p0309 N85-11995

Testing the antifriction properties of alloys for heavily loaded bearings 06 p0780 N85-14990

Multi-directional straddle-lift carrier
[AD-D011315] 07 p0973 N85-16183

Improvements in linked-spar motion-compensated lifting system
[AD-D011413] 08 p1138 N85-17165

BI-PAC F-15 external fuel tank container modification
[AD-A148838] 09 p1280 N85-18053

Control of the manufacturing process and material flow in flexible manufacturing systems
[PNR-90234] 09 p1371 N85-18615

Material flow in the manufacturing system: Fault-diagnosis systems as support for the maintenance of highly automated manufacturing systems
[PNR-90238] 09 p1371 N85-18618

A review of hazard assessment procedures for liquid gun propellants
[AD-A149470] 10 p1457 N85-19182

Simplified grasping and manipulation with dextrous robot hands
[AD-A148962] 10 p1492 N85-19419

Hoist
[AD-D011458] 10 p1493 N85-19425

Automated parts storage and retrieval system positioning device and method
[AD-D011494] 11 p1647 N85-20379

Methods/materials matrix of ultimate disposal techniques for spilled hazardous materials
[PB85-116853] 12 p1885 N85-21833

Cargo handling system
[AD-D011569] 14 p2219 N85-23762

Auxiliary units for Robots 14 p2265 N85-24161

MI-8 helicopter cargo loading experiment for Arctic shipping 14 p2332 N85-24425

Development of molten carbonate fuel cell power plant technology
[DE84-016839] 14 p2352 N85-24536

West Europe report: Science and technology
[JPRS-WST-84-014] 15 p2536 N85-25647

Technological experiments on high-altitude rockets
16 p2725 N85-26818

Technological apparatus for laser treatment of materials 17 p2944 N85-28174

West Europe report: Science and technology
[JPRS-WST-84-037] 18 p3088 N85-29108

French, UK, Swedish research in powder metallurgy, HIP 18 p3088 N85-29109

Qualitative comparison of fusion reactor materials for waste handling and disposal
[DE85-010473] 19 p3360 N85-30830

Oil tank electrostatic charging report
[DRIC-T-6967] 20 p3436 N85-31319

A systematic plan for the continued study of dimensional stability of metallic alloys considered for the fabrication of cryogenic wind tunnel models
[NASA-CR-172449] 21 p3565 N85-32172

TNT equivalency of EAK explosive
[AD-A155737] 21 p3571 N85-32211

Basic cryogenics and materials. Phase 1
[NASA-CR-177932] 21 p3572 N85-32215

Monosilane and disilane, 1984 report
[DE85-008776] 22 p3752 N85-33262

Corrosion resistant storage container for radioactive material
[DE85-011686] 22 p3838 N85-33765

Office of Civilian Radioactive Waste Management
[DE85-012585] 22 p3839 N85-33774

Container for radioactive materials
[DE85-005757] 23 p3972 N85-34626

Laboratory vibration schedules
[AD-A155856] 24 p4064 N85-35186

Radiation safety problems in handling highly active tritium targets
[DE85-014268] 24 p4151 N85-35742

MATERIALS RECOVERY

NT NUCLEAR FUEL REPROCESSING

NT WATER RECLAMATION

Research and development work on a single cation specific membrane for the recovery of raw materials with electrodialysis
[BMFT-FB-T-84-163] 03 p0329 N85-12120

Investigation of internal fields and motions, radiation damages and recovery processes using beta and gamma active probe nuclei 03 p0427 N85-12726

Flow-based analyses of metal deformation processes: An overview 06 p0796 N85-15067

Microbiological method for the desiliconization of high-silica bauxites
[BLL-MINTEK-TR-1168-(5810.5759)]
07 p0925 N85-15864

Research and development work concerning liquid membranes
[BMFT-FB-T-84-227] 08 p1124 N85-17067

Adaptation of remelting procedures for the use of recycled metal in nickel-base superalloy castings
[PNR-90232] 09 p1297 N85-18149

Treatment of wastewater (red water) resulting from TNT (trinitrotoluene) purification
[AD-P004146] 09 p1348 N85-18482

Hydrolysis of plastic wastes with the aim of recovering and reprocessing the starting components (recycling)
[BMFT-FB-T-84-250] 12 p1685 N85-21828

Lead shortage hastens need for improved storage batteries 15 p2461 N85-25195
Microwave processing of lunar materials: Potential applications
[DE85-007223] 16 p2755 N85-27003
Michelle-derived catalysts for extended Schulz-Flory
[DE85-005656] 17 p2922 N85-28012
Conservation and substitution technology for critical metals in bearings and related components for industrial equipment and opportunities for improved bearing performance
[PB85-176248] 18 p3082 N85-29069
Counter current extraction system for tritium recovery from 17Li-83Pb
[DE85-010619] 19 p3240 N85-30090
Development of processes for the inclusion of radioactive waste in glass-metal compounds and ceramic materials
[BLL-CE-TRANS-8014-(9022.09)]
20 p3526 N85-31931
Measurement of uranium enrichment for gaseous uranium at low pressure
[DE85-012697] 24 p4150 N85-35733

MATERIALS SCIENCE
Non-oxide ceramics: A new class of engineering materials 02 p0179 N85-11199
USSR report: Engineering and equipment
[JPRS-UEQ-84-007] 06 p0775 N85-14954
Encapsulation materials and processing
06 p0830 N85-15269
West Europe report: Science and technology
[JPRS-WST-84-039] 07 p0936 N85-15929
Research and technology highlights of the Lewis Research Center
[NASA-TM-86899] 08 p1261 N85-17926
USSR report: Materials science and metallurgy
[JPRS-UMS-84-008] 10 p1442 N85-19086
Metals and Ceramics Division Materials Science Program
[DE85-003795] 11 p1592 N85-20012
USSR report: Materials science and metallurgy
[JPRS-UMS-84-005] 11 p1597 N85-20044
Research in surface sciences, disordered materials, and solidification and growth
[PB85-132140] 11 p1737 N85-20927
Technological and economic assessment of advanced ceramic materials. Volume 1: Summary and conclusions
[PB85-113082] 12 p1815 N85-21383
Thermal response of aircraft cabin ceiling materials during a post-crash, external fuel-spill, fire scenario
[PB85-145647] 14 p2220 N85-23764
Material research in microgravity
[NASA-TM-77628] 14 p2226 N85-23811
USSR report: Engineering and equipment
[JPRS-UEQ-84-005] 14 p2285 N85-24157
West Europe report: Science and technology
[JPRS-WST-84-020] 15 p2534 N85-25633
Activities of Istituto Elettrotecnico Nazionale Galileo Ferraris 18 p3199 N85-29845
USSR report: Materials Science and Metallurgy
[JPRS-UMS-85-005] 19 p3241 N85-30095
Proceedings of the Twentyseventh Japan Congress on Materials Research
[ISSN-0368-3141] 23 p3903 N85-34180

MATERIALS TESTING REACTORS
U NUCLEAR RESEARCH AND TEST REACTORS

MATERIALS TESTS
Measurement of material properties to Mbar pressures using time-resolved shock wave techniques
[DE85-007319] 15 p2558 N85-25780
Evaluation methods of ceramic fiber reinforced metal matrix composite 23 p3907 N85-34206

MATHEMATICAL ANALYSIS
U APPLICATIONS OF MATHEMATICS

MATHEMATICAL LOGIC
NT ALGORITHMS
NT BOOLEAN ALGEBRA
NT BOOLEAN FUNCTIONS
NT BOREL SETS
NT EQUIVALENCE
NT FORMULAS (MATHEMATICS)
NT LATTICES (MATHEMATICS)
NT PARSING ALGORITHMS
NT SET THEORY
NT SIMPLEX METHOD
NT THRESHOLD LOGIC
Model theory for infinitely deep languages
[ISSN-0355-0087] 01 p0101 N85-10674
Research topics: Multiprocessing algorithms for computational logic
[DE84-015500] 02 p0242 N85-11583
Belief structures
[AD-A147526] 07 p1036 N85-16575
Polylith and environments for mathematical computation
[DE85-002967] 11 p1702 N85-20704
Universal file processing program for field programmable integrated circuits
[DE85-004384] 12 p1837 N85-21526
System of microprocessor instructions
22 p3770 N85-33362

MATHEMATICAL MODELS
NT ANALOG SIMULATION
NT BIOLOGICAL MODELS (MATHEMATICS)
NT DIGITAL SIMULATION
NT PETRI NETS
NT THOMAS-FERMI MODEL
Implementation of the supersonic triplet singularity into the USTORE computer code
[CSIR-NIAST-83/47] 01 p0001 N85-10006
Prediction of aerodynamic characteristics of fighter wings at high angles of attack
[AD-A145107] 01 p0003 N85-10017
Aerodynamics of airfoils subject to 3-dimensional periodic gusts
[AD-A145149] 01 p0003 N85-10018
Modular design attitude control system
[NASA-CR-171182] 01 p0016 N85-10098
Singular asymptotic expansions in nonlinear rotordynamics
[NASA-CR-174012] 01 p0017 N85-10100
Cumulative damage model for advanced composite materials
[AD-A144840] 01 p0022 N85-10135
Computer simulation of the shock initiation of detonation in solid explosives
[PML-1984-23] 01 p0033 N85-10207
A model for grain misalignment in cylindrical port motors
[AD-A144856] 01 p0034 N85-10210
Modelling the demand for construction
[CSIR-TWISK-322] 01 p0035 N85-10218
Predictor model for seasonal variations in skid resistance. Volume 2: Comprehensive report
[PB84-226820] 01 p0037 N85-10230
Battery optimization considerations
[DE84-014759] 01 p0044 N85-10288
DYNKIN: A computer program for the description of detailed gas reactions in interaction with gas dynamics
[AD-B085364] 01 p0046 N85-10296
Single viewpoint self calibration: A contribution to field calibration of recording chambers
[SER-C-289] 01 p0049 N85-10320
Economic model of calibration improvements for automatic test equipment
[PB84-217827] 01 p0051 N85-10335
Combustion modeling of a 2 cylinder cycle reciprocating engine
[AD-A144782] 01 p0055 N85-10364
Estimation of the threshold in fatigue crack initiation models: A Bayesian approach
[AD-A144847] 01 p0062 N85-10410
Development of advanced constitutive model for reinforced concrete
[AD-A145050] 01 p0062 N85-10411
A generalized mathematical soluation for transient off tracking of single vehicles and truck combinations
[DM-2] 01 p0107 N85-10719
On the calculating models of permanent magnets
[AD-A145111] 01 p0115 N85-10780
KrCl lasers for fusion
[DE84-012210] 01 p0122 N85-10835
Reduction of nonlinear problems to Schroedinger or heat equations: Formation of Kepler orbits, singular solutions for hydrodynamical equations
[REPT-72] 01 p0129 N85-10892
Structure and evolution of the large scale solar and heliospheric magnetic fields
[NASA-CR-175268] 01 p0130 N85-10897
Enhanced TCAS 2/CDTI traffic Sensor digital simulation model and program description
[NASA-CR-172445] 02 p0136 N85-10927
Advanced composite stabilizer for Boeing 737 aircraft
[NASA-CR-168451] 02 p0137 N85-10934
Quasi-steady analysis of aircraft panel flammability
[AD-A145461] 02 p0138 N85-10938
Advances in electrophoretic seperations
02 p0156 N85-11054
Satellite servicing: A business opportunity?
02 p0156 N85-11056
Cumulative damage model for advanced composite materials
[AD-A145441] 02 p0171 N85-11142
A study of environmental characterization of conventional and advanced aluminum alloys for selection and design. Phase 2: The breaking load test method
[NASA-CR-172387-PHASE-2] 02 p0182 N85-11219
Direct numerical simulation of curved turbulent
flow
[NASA-TM-85974] 02 p0187 N85-11
A constitutive modeling technique based on a generalized rheological model to predict the response
materials 02 p0207 N85-11
Computer models and output, Spartan REM: Append
B
[NASA-CR-171093] 02 p0208 N85-11
Biophysical and spectral modeling for crop identifica
and assessment
[E85-10006] 02 p0215 N85-114
Study on spectral/radiometric characteristics of the Thematic Mapper for land use applications
[E85-10021] 02 p0218 N85-114
Theoretical development of Monte Carlo codes for modeling cumulus cloud fields
[NASA-CR-174063] 02 p0230 N85-11
Northern Hemisphere atlas of 1-minute rainfall
[AD-A145411] 02 p0231 N85-11
Southern Hemisphere atlas of 1-minute rainfall
[AD-A145421] 02 p0231 N85-11
Description of the software acquisition process
model
[AD-A145413] 02 p0241 N85-115
Parallel searching and merging on ZMOB
[AD-A145424] 02 p0241 N85-115
Trajectory estimation using combined time-of-arrival
velocity measurements
[DE84-015872] 02 p0242 N85-115
Diagnosis based on description of structure and function
[AD-P003919] 02 p0245 N85-11
Weighted distributions arising out of methods of ascertainment
[AD-A145615] 02 p0252 N85-11
Likelihood estimation for generalized mixed exponential distributions
[AD-A145675] 02 p0252 N85-11
Dynamics of symmetry breaking: Phase coherence in finite and random systems
[NOTA-INTERNA-813] 02 p0253 N85-11
Unified approach to sensitivity and uncertainty analysis
[DE84-014049] 02 p0255 N85-11
A mathematical theory of command and control structures
[AD-A145608] 02 p0256 N85-11
Method of splitting for solution of problems in semiconductor physics 02 p0265 N85-117
A simple transport model 02 p0284 N85-11
Fractals: From snow flakes to galactic clusters
[NOTA-INTERNA-796] 02 p0298 N85-11
Determination of equivalent model geometry for tunnel wall interference assessment/correction
03 p0314 N85-12
Estimation of helicopter performance using a program based on blade element analysis
[AD-A146341] 03 p0318 N85-12
Damping synthesis for a spacecraft using substructure and component data
[CRC-1365] 03 p0323 N85-12
Chemoviscosity modeling for thermosetting resins
[NASA-CR-172443] 03 p0326 N85-12
Kinematic synthesis of planar cam-link mechanisms for exact path and exact motion generation
03 p0341 N85-12
Autoregressive modeling and the classification of land clutter — radar signatures
[ENST-C-84003] 03 p0356 N85-12
Second order modeling of scalar turbulent flows
03 p0360 N85-12311
Comparison of predicted and measured friction for a tilt-pad thrust bearing with crown and roughness under hydrodynamic and mixed lubrication
[AD-A145752] 03 p0371 N85-12
Numerical simulations of compliant material response to turbulent flow, revision 1
[AD-A145801] 03 p0372 N85-12
A decomposable algorithm for contour surface display generation
[AD-A145783] 03 p0410 N85-12
Least squares estimation of conditionally heteroscedastic autoregressions
[AD-A145994] 03 p0411 N85-12
Prediction and modeling of helicopter noise
[AD-A145764] 03 p0415 N85-12
Ways to improve management of Federal funded computerized models
[LCD-75-111] 03 p0435 N85-12
A methodology for comparing the variable costs of the continuous and periodic review models
[AD-A146351] 03 p0436 N85-12
A stochastic model for optimizing the consumption and exploration of nonrenewable natural resources
[INPE-2770-PRE/343] 03 p0440 N85-12

Dynamical models for radio jets
03 p0449 N85-12654

Modelling viscous flow in turbomachinery
[PNR-90220] 04 p0457 N85-12898

Review of the attributes and performance of six urban diffusion models
[PB84-226650] 04 p0484 N85-13087

Mathematical modeling of assembly processes involving use of sensitized robots 04 p0488 N85-13111

A preliminary study of numerical simulation of thermosolutal convection of interest to crystal growth
[NASA-TP-2384] 04 p0498 N85-13175

Numerical modelling of the drying of porous materials
[DE84-013056] 04 p0499 N85-13181

Comparisons of secular variation in two-dipole and spherical harmonic models with observatory data in Eurasia, 1965-1975 04 p0521 N85-13330

Reversals of the Earth's magnetic field
04 p0521 N85-13332

Scattering models in the microwave regime
[NASA-CR-174001] 04 p0525 N85-13361

Outline of a new emissions model for military and civilian aircraft facilities
[DE84-016455] 04 p0531 N85-13394

Urban aerosol modeling
[PB84-233469] 04 p0532 N85-13401

Relationship between model complexity and data base quality for complex terrain tracer experiments
[DE84-015022] 04 p0539 N85-13429

Operational numerical forecasts: Survey and verification over the period 1978-1983
[KNMI-TR-49] 04 p0540 N85-13435

Computational models of crystals
[DE84-016831] 04 p0572 N85-13647

Model reduction for control system design
05 p0596 N85-13799

Theory of kinetics of impregnation of porous bodies
[BLL-M-35917-(5828.4)] 05 p0616 N85-13942

Parametric models for signal processing: Autoregressive (AR), Moving Average (MA) and mixed autoregressive with moving average (ARMA)
[ENST-84D001] 05 p0628 N85-14028

Damping capacity of a sealed squeeze film bearing
05 p0645 N85-14139

Theoretical analysis of the dynamic behavior of structures with a passenger car as example
05 p0649 N85-14170

The upwind power plant Manzanares
05 p0669 N85-14305

Structure and growth of the marine boundary layer
05 p0680 N85-14369

Implicit numerical methods in meteorology
05 p0686 N85-14408

Statistical time series models of pilot control with applications to instrument discrimination
05 p0700 N85-14489

Model estimation and identification of manual controller objectives in complex tracking tasks
05 p0700 N85-14494

Structure errors in system identification
05 p0700 N85-14495

Use of artificial intelligence and simple mathematics to analyze a physiological model 05 p0717 N85-14597

Mathematical models for the brightness temperature of object and environment in the microwave region
[ESA-TT-829] 05 p0718 N85-14610

Some error estimates for the p-version of the finite element method
[CTH-MATH-1984-21] 05 p0719 N85-14614

A comment on Rosen's comments on activation and inhibition
[CTH-MATH-1984-24] 05 p0719 N85-14617

Relaxation times for queueing systems
[CWI-OS-R8407] 05 p0719 N85-14618

Construction of a confidence region for linear functions with unknown parameters
[CTH-MATH-1984-17] 05 p0721 N85-14630

A martingale approach to supercritical (C-M-J) branching processes
[CTH-MATH-1984-25] 05 p0722 N85-14643

Molarity principle: Foundation for parallel digital signal processes 05 p0725 N85-14663

Analysis of flat finite antenna consisting of waveguide radiators 06 p0790 N85-15048

Individual geopotential coefficients of order 15 and 30, from resonant satellite orbits
[AD-A146687] 06 p0828 N85-15256

Summary of photovoltaic performance models
06 p0832 N85-15296

Practical application of IREPS (Integrated Refractive Effects Prediction System)
[AD-A146526] 06 p0838 N85-15323

Toward an improved FIPS cost-benefit methodology. Phase 2: Descriptive models, general purpose application software development and maintenance
[PB84-226843] 06 p0870 N85-15527

Tristatic tracking filter used by the multistatic measurement system
[AD-A146885] 07 p0911 N85-15769

Efficient computation of reflector antenna aperture distributions and far field patterns
[AD-A147367] 07 p0940 N85-15962

An asymptotic analysis of a transient p-n junction model
[AD-A147270] 07 p0947 N85-16004

Ensuring required metrological reliability of analog instrument channels by parametric compensation
07 p0955 N85-16050

Trends in development of software for computer-aided analysis of large-scale integrated circuits
07 p0955 N85-16055

Analysis of the heating process of a body in a melt
[BLL-M-36014-(5828.4)] 07 p0956 N85-16057

Numerical reconstruction of part of an actual blast-wave flow field to agree with available experimental data
[UTIAS-TN-251] 07 p0956 N85-16061

Numerical studies of interacting vortices
[NASA-TM-86325] 07 p0957 N85-16062

Growth/reflectance model interface for wheat and corresponding model
[E85-10058] 07 p0987 N85-16269

Forecasting water temperature decline and freeze-up in rivers
[AD-A147066] 07 p0987 N85-16274

Water and climate, study of one case
07 p1002 N85-16369

Experiments in forecasting atmospheric marine horizontal visibility using model output statistics with conditional probabilities of discretized parameters
[AD-A147574] 07 p1006 N85-16404

Model robust response surface designs: Scaling 2-level factorials
[AD-A147494] 07 p1033 N85-16556

Conjunctive and disjunctive item response functions
[AD-A147615] 07 p1033 N85-16561

Response surface designs
[AD-A147202] 07 p1035 N85-16569

Current and current shear effects in the parabolic approximation for underwater sound channels
[AD-A147833] 07 p1039 N85-16597

Austrian contributions to fuel rod failure models shown at the International Standard Problem (ISP)-14
[OEFZS-4276] 07 p1041 N85-16613

A simulation model for Air Launched Cruise Missile engine management
[AD-A147018] 07 p1051 N85-16672

A Generalized Escape System Simulation (GESS) computer program. Volume 2: GESS programmer's manual, version 2
[AD-A146363] 08 p1081 N85-16845

Mathematical models for space shuttle ground systems 08 p1097 N85-16933

Modeling techniques used in the communications link analysis and simulation system (CLASS)
08 p1100 N85-16953

Numerical simulation of the shock detonation transition 08 p1116 N85-17039

Modelling the thermal explosion phenomenon in solid propellants: The case of fixed and variable temperatures 08 p1117 N85-17044

Numerical modeling of steady, laminar free-convective boundary layer flow beneath heated or combusting horitzonal surfaces 08 p1160 N85-17318

A study of Reynolds-stress closure model
[NASA-CR-174342] 08 p1161 N85-17324

Evolution of nonlinear wave groups on water of slowly-varying depth
[AD-A147947] 08 p1162 N85-17329

Papers of the 15th International Society for Photogrammetry and Remote Sensing (ISPRS) Congress — conferences
[TRITA-FMI-9] 08 p1175 N85-17406

Mathematical aspects of digital terrain information; Report from International Society for Photogrammetry and Remote Sensing (ISPRS) working group 3:3, 1980 - 1984 — photogrammetry 08 p1175 N85-17407

A comparative test of photogrammetrically sampled digital elevation models 08 p1175 N85-17408

Multimodels increase accuracy: Summary of an experiment — photogrammetry
08 p1175 N85-17409

Sequential data processing for photogrammetric acquisition of digital elevation models
08 p1176 N85-17413

Advanced development of an active neuromusculature response to mechanical stress
[AD-A148436] 08 p1196 N85-17536

Adapting logistics models to a microcomputer for interface with computer-aided design systems
[AD-A147666] 08 p1202 N85-17566

Improved stability and performance bounds using approximate models — control system design
[RR-260] 08 p1209 N85-17606

The EM algorithm for censored data
[AD-A148136] 08 p1212 N85-17626

Background detection and correction in multicomponent analysis
[AD-A148251] 08 p1212 N85-17628

Multicomponent calibration and quantitation methods
[AD-A148252] 08 p1212 N85-17629

On the ergodicity of bilinear time series models and some applications
[AD-A148032] 08 p1215 N85-17651

Production rate variations cost models
[AD-A147706] 08 p1228 N85-17732

The calculation of theoretical chromospheric models and the interpretation of solar spectra from rockets and spacecraft
[NASA-CR-174289] 08 p1259 N85-17922

Modeling of aircraft performance from flight test results using quasi steady-state test techniques
09 p1279 N85-18047

Battery response to pulse loads: A mathematical model
[DE85-001149] 09 p1316 N85-18277

The sensitivity analysis in k-epsilon turbulence modeling applied to jet flows 09 p1318 N85-18288

Three-dimensional vortex methods
[DE85-000391] 09 p1320 N85-18299

Two-dimensional modeling of conduction-mode laser welding
[DE85-001804] 09 p1327 N85-18341

Models for shock damage to marine structural materials 09 p1336 N85-18400

Structural modifications by viscoelastic elements
09 p1337 N85-18407

World Geodetic System, 1984
[AD-A147409] 09 p1342 N85-18445

Models for mixture experiments when the response depends on the total amount
[DE85-000370] 09 p1374 N85-18637

Study of mathematical models of mutation and selection in multi-locus systems
[DE85-000873] 09 p1376 N85-18648

Control of tractors on sloping ground
[AD-P004292] 09 p1408 N85-18869

A simple prediction model for soil compaction under various wheel loads and geometries as an aid to vehicle design
[AD-P004296] 09 p1409 N85-18875

Modeling and simulation of a fin actuation system
[AD-A149443] 10 p1428 N85-19005

Mathematical modeling of wave fields by superimposition of boundary waves in reflected earthquake waves method 10 p1501 N85-19476

Predicting the performance of distributed knowledge-based systems: A modeling approach
[AD-A149021] 10 p1545 N85-19738

Modelling and residual analysis of nonlinear auto-regressive time series in exponential variables
[AD-A149047] 10 p1550 N85-19776

Rock mechanics: Issues and research needs in the disposal of wastes in hydraulic fractures
[DE85-001399] 10 p1556 N85-19809

Thermodynamics of the reactive flow model
[DE85-004405] 10 p1565 N85-19870

Compensator development and examination of performance and robustness
[NASA-CR-175470] 11 p1627 N85-20244

Theoretical and experimental analysis of vertical, concentric-tube ground-coupled heat exchangers
[DE85-000474] 11 p1633 N85-20286

The use of analytical models to interpret data properly
[ERS-E.341] 11 p1651 N85-20399

The use of analytical models to interpret measured data properly. 1. General background theory
11 p1651 N85-20400

The use of analytical models to interpret measured data properly. 2. The application to modal analysis of structures 11 p1651 N85-20401

A three-dimensional geometric-physical model for conventional geodetic observations-observables, parameter estimation, and deformation analysis
[SER-C-296] 11 p1665 N85-20493

Performance of the SERI parallel-passage dehumidifier
[DE85-000509] 11 p1672 N85-20536

Research on the basic understanding of high efficiency in silicon solar cells
[DE85-000507] 11 p1672 N85-20537

Continued research in mesoscale air pollution simulation modeling. Volume 7. Mathematical modeling of urban aerosol dynamics
[PB85-137388] 11 p1679 N85-20584

Precursors for Brazilian magnetic anomalies from 1922 to 1969
[INPE-3283-PRE/605] 11 p1681 N85-20590

Resolution of 2-dimensional seismologic problems by a finite element approximation. Application to the Love wave propagation through the Atlantic border of the Iberic Peninsula 11 p1681 N85-20594

Resolution of 2-dimensional seismologic problems by a finite element approximation. Application to the Love wave propagation through the Atlantic border of the Iberic Peninsula. Appendix: Graphs of results — Lagrange coordinates 11 p1681 N85-20595

User's guide for the Photochemical Box Model (PBM)
[PB85-137164] 11 p1682 N85-20602

A method for reduction of ambiguity in segmentation of images
[INPE-3394-TDL/186] 11 p1697 N85-20684

Digital imaging processing
[INPE-3325-PRE/624] 11 p1701 N85-20696

Investigation of the output parameters of the pulsed neutron generator NGI-5
[DE85-001623] 11 p1725 N85-20849

Theory of resistivity-gradient-driven turbulence
[DE85-00[illegible]] 11 p1733 N85-20898

Cometary atmospheres: Modeling the spatial distribution of observed neutral radicals
[NASA-CR-175485] 11 p1765 N85-21098

Deflection model of a CT4-A undercarriage
[AD-A149778] 12 p1777 N85-21156

The influence on IR emission of engine parameters for an afterburn case. A sensitivity study on NATO infrared air target model (NIRATAM) version: 0.0
[AD-B089311L] 12 p1779 N85-21171

ACOSS 17 (Active Control of Space Structures)
[AD-A150007] 12 p1793 N85-21253

A computer analysis of the RF performance of a ground-mounted, air-supported radome
[AD-P004352] 12 p1824 N85-21446

Simulation of thermal and electromagnetic processes in induction plasmatrons 12 p1841 N85-21552

An investigation of compressible flows over open cavities including shear layer thickness effects
[AD-A150086] 12 p1847 N85-21588

A new model for thin plates with rapidly varying thickness. Part 3: Comparison of different scalings
[AD-A149748] 12 p1866 N85-21704

Numerical simulation of static and dynamic shadow patterns using an atomistic description of crack initiation and propagation
[DE85-003226] 12 p1867 N85-21715

User's guide to the TAMW wheat model as implemented on the IBM 360/195 computer
[E85-10084] 12 p1873 N85-21749

Local behavior of solutions of an elliptic-parabolic equation
[AD-A149624] 12 p1920 N85-22057

Ordinary and proper location M-estimates for ARMA models, revised
[AD-A149705] 12 p1920 N85-22061

A review of some aspects of robust inference for time series
[AD-A149706] 12 p1923 N85-22062

A note on validity generalization procedures
[AD-A150065] 12 p1924 N85-22085

Surface forward scattering and reflection
[AD-A150115] 12 p1928 N85-22112

Singular asymptotic expansions in nonlinear rotordynamics 12 p1945 N85-22218

A mathematical formulation of the problem of optimal use of ground resources for future space missions
12 p1947 N85-22232

Computational mechanics: A perspective on problems and opportunities for increasing productivity and quality of engineering
[PB85-128106] 12 p1950 N85-22252

Simple theoretical models for composite rotor blades
[NASA-CR-175620] 13 p1971 N85-22382

Model reduction for control system design
[NASA-CR-170417] 13 p1975 N85-22398

Expansion of functions describing planetary surface and gravity field 13 p1978 N85-22410

Nontraditional method for determining unperturbed orbits of unknown space objects using incomplete optical observational data 13 p1979 N85-22417

An integral closed loop combustion stability model-status and review 13 p2003 N85-22553

Improved modeling of the open circuit voltage of solar cells 13 p2011 N85-22619

Some unique features of isentrophic flow of gas under high pressures 13 p2043 N85-22786

Mathematical modeling of transient performance of gas turbine engine 13 p2050 N85-22834

Research efforts in support of resonance extraction studies. Volume 1: Improvement and validation of TWFD (Thin-Wire Frequency-Domain): A thin-wire frequency-domain scattering code
[AD-A150296] 13 p2054 N85-22864

Mathematical model of discriminator for signals with fluctuations and thermal noise 13 p2072 N85-22943

Mathematical model of electromagnetic suspension device with two control windings
13 p2074 N85-22954

Problem of diffraction by wavy surface: Comparison of numerical methods of solution
13 p2079 N85-22985

Mathematical modeling of two-frequency laser sounding of scattering media 13 p2089 N85-23045

Investigation of parabolic computational techniques for internal high-speed viscous flows
[NASA-CR-172555] 13 p2091 N85-23056

Numerical experiments with simple model of ocean climate 13 p2106 N85-23123

Numerical modeling of plane stick-slip fault
13 p2111 N85-23150

Mathematical modeling of results of geometric leveling in variable gravity field 13 p2114 N85-23170

The microwave propagation and backscattering characteristics of vegetation — wheat, sorghum, soybeans and corn fields in Kansas
[E85-10088] 13 p2122 N85-23213

Remanent magnetization model for the broken ridge satellite magnetic anomaly 13 p2123 N85-23219

Estimation of regional evapotranspiration using remotely sensed land surface temperature. Part 1: Measurement of evapotranspiration at the Environmental Research Center and determination of Priestley-Taylor parameter
13 p2125 N85-23233

Estimation of regional evapotranspiration using remotely sensed land surface temperature. Part 2: Application of equilibrium evaporation model to estimate evapotranspiration by remote sensing technique — Japan 13 p2125 N85-23234

Testing an energy balance model for estimating actual evapotranspiration using remotely sensed data — Hannover, West Germany barley and wheat fields
13 p2125 N85-23236

ROSS: An object-oriented language for constructing simulations
[AD-A150556] 13 p2147 N85-23330

On a mathematical structure for an image algebra
[AD-A150226] 13 p2150 N85-23348

The design of a unified package for the solution of stochastic petri net models
[AD-A150326] 13 p2151 N85-23354

Magnetic field interactions with material discontinuities
[AD-A150197] 13 p2154 N85-23373

A model for eclipsing cataclysmic variables
13 p2171 N85-23467

Impact crater scaling laws 13 p2181 N85-23532

Planetary interior modeling and tectonic implications
13 p2200 N85-23649

Elysium region, Mars: Tests of lithospheric loading models for the formation of tectonic features
13 p2200 N85-23650

An eigensystem realization algorithm for application to modal testing 14 p2233 N85-23842

Adaptive techniques for control of large space structures
[AD-A150957] 14 p2246 N85-23923

Model of normal and erosive burning of composite propellants
[ONERA-NT-1984-3] 14 p2263 N85-24024

Determining optimum service conditions for concentrator mirrors by methods of mathematically planned experiment 14 p2274 N85-24090

Basic EMC (Electromagnetic Compatibility) technology advancement for C3 systems. Volume 4E: Modeling of transmission lines. A comparison of lumped-circuit iterative models and the transmission line model
[AD-A150652] 14 p2291 N85-24201

Radiation heat transfer within an open-cycle MHD generator channel — mathematical models
[NLR-TR-83066-U] 14 p2304 N85-24267

Developement of a theoretical model to describe the interaction between electric discharge and supersonic flow of a pulsed CO laser
[DFVLR-FB-84-45] 14 p2310 N85-24301

Seismic analysis of rotating mechanical systems
[PB85-149599] 14 p2311 N85-24307

Interpretation of directional magnetotelluric soundings by analytical continuation method
14 p2343 N85-24488

Determination of crust and upper mantle density based on deep seismic sounding and gravimetry data, part 1
14 p2345 N85-24498

Modelling of photodegradation in solar cell modules of substrate and superstrate design made with ethylene-vinyl acetate as pottant material
[NASA-CR-175690] 14 p2350 [illegible]

Adjustment of the national dispersion model for air pollution from elevated sources
[KNMI-TR-57] 14 p2353 [illegible]

The dawn-dusk asymmetry of particles near the neutral sheet of geomagnetotail 14 p2358 [illegible]

A study of terrain reductions, density anomalies and geophysical inversion methods in gravity field modeling
[AD-A150786] 14 p2373 [illegible]

Visual recognition of simple objects by a connection network
[AD-A151043] 14 p2389 [illegible]

Potential models — Earth gravity
14 p2396 [illegible]

Orbit reconstitution — satellite orbits
14 p2396 [illegible]

The generation of three-dimensional body-fitted coordinate systems for viscous flow problems
[AD-A150861] 14 p2408 [illegible]

Macro for fitting nonlinear models to Poisson distributed data
[DE84-008569] 14 p2412 [illegible]

Application of far-field models to the disposal of nuclear waste in geologic formations
[DE85-005489] 14 p2420 [illegible]

A fast ray tracing routine for laterally inhomogeneous media
[AD-A150984] 14 p2421 [illegible]

A system-level mathematical model for evaluation of power train performance of load-leveled electric-vehicles
[NASA-CR-175652] 14 p2434 [illegible]

Solar inverse theory 14 p2441 [illegible]

Numerical simulations of convectively excited gravity waves 14 p2444 [illegible]

Cosmic ray environment model for Earth orbit
[NASA-CR-175666] 14 p2455 [illegible]

Automatic Dynamic Aircraft Modeler (ADAM), volume 1
[AD-A151410] 15 p2471 [illegible]

Multi-rate digital autopilot modeling methodology
[AD-A152044] 15 p2474 N85-25272

Mathematical modeling of the AEDC (Arnold Engineering Development Center) propulsion wind tunnel (16T)
[AD-A151293] 15 p2475 N85-25275

Mathematical model for rollout of planet roving vehicle from landing craft 15 p2484 N85-25334

Local elastoplastic fracture of fibrous composite materials 15 p2497 N85-25405

The accuracy of approximate solutions in the analysis of fracture of composites
[NASA-CR-175738] 15 p2503 N85-25437

Mathematical aspect of welding technology research discussed 15 p2538 [illegible]

CSMP (Continuous System Modeling Program) modeling of brushless DC motors
[AD-A152043] 15 p2549 N85-25731

On coupling factors of explosion
15 p2551 N85-25747

A critical evaluation of various turbulence models as applied to internal fluid flows
[NASA-TP-2474] 15 p2554 N85-25757

Turbulence effects on a glow discharge as derived from continuity and energy considerations
[AD-A151838] 15 p2557 N85-25775

NPLOT: An interactive plotting program for NASTRAN finite element models 15 p2573 [illegible]

Ritz procedure for COSMIC/NASTRAN
15 p2575 N85-25877

Analysis of shell type structures subjected to time dependent mechanical and thermal loading
[NASA-CR-175747] 15 p2577 [illegible]

Modeling and optimization of a multiple-cell photovoltaic converter system 15 p2585 [illegible]

Operational methods for calculating atmospheric dispersion
[BLL-CE-TRANS-8040-(9022.09)]
15 p2588 [illegible]

Field validation of 6-particle puff model
[DE85-004073] 15 p2589 [illegible]

Numerical experiments of jet streak ageostrophic circulations using pseudo-geostrophic initialization and perspectives 15 p2590 [illegible]

A simulation experiment on the impact of geostationary temperature retrievals in numerical models
15 p2597 N85-26005

Numerical simulation of North Atlantic Sea ice variability, 1951 - 1980 15 p2603 N85-26040

Origin of the Greenland ice sheet
15 p2604 N85-26046

On geoid heights and flexure of the lithosphere at seamounts
[AD-A151220] 15 p2604 N85-26050

Description, validation, and modification of the Guyton model for space-flight applications. Part A. Guyton model of circulatory, fluid and electrolyte control. Part B. Modification of the Guyton model for circulatory, fluid and electrolyte control
[NASA-CR-171676] 15 p2616 N85-26122

Mathematical models relating to human thermoregulation: Basic assumptions, validation, and application. Parts A and B
[AD-A151556] 15 p2618 N85-26130

An MRTD-compatible bar pattern response model for TV and direct view sighting systems
[BAE-BT-12090] 15 p2620 N85-26146

The modeling and simulation of feedback control systems
[NASA-CR-171875] 15 p2632 N85-26225

On failure modeling, revised
[AD-A151411] 15 p2637 N85-26263

Lectures on probability and statistics
[DE85-007079] 15 p2641 N85-26291

Numerical modeling of gas dynamic phenomena during supersonic flow of viscous gas in channel with electrical flow discharge 15 p2643 N85-26304

Fundamental studies of structure borne noise for advanced turboprop applications
[NASA-CR-175737] 15 p2646 N85-26320

An application of the Rayleigh distribution to contract cost data
[AD-A151551] 15 p2664 N85-26441

The investigation of tethered satellite system dynamics
[NASA-CR-175855] 16 p2731 N85-26854

The effect of inaccuracies in structural models on the control of large space structures
[AD-A151794] 16 p2732 N85-26858

Evaluation of human exposures to low frequency fields 16 p2776 N85-27135

Theoretical and experimental comparisons of nearfield electrogalvanic fields due to nonlinear polarization layers
[AD-A152065] 16 p2779 N85-27149

Studies of structure and modeling in turbulent shear flows
[AD-A151807] 16 p2782 N85-27170

Two-d heat transfer through porous media with heat generation
[AD-A151965] 16 p2783 N85-27173

The development of a computational model for a two-dimensional turbulent flow. Part 1: Mathematical background — solid fuel combustion
[VTH-LR-436-PT-1] 16 p2785 N85-27188

Optimal modeling with a minimum of local distortion
[REPT-16/1984] 16 p2797 N85-27243

Topex Gravity Model Development Team activities during fiscal year 1984
[NASA-TM-86208] 16 p2804 N85-27285

Atmospheric density model 16 p2805 N85-27297

Use of forest modeling to project acid rain effects
[DE85-005251] 16 p2821 N85-27400

Fluid-dynamic model of a downburst
[UTIAS-271] 16 p2829 N85-27441

General continuous formulations of atmospheric energy laws 16 p2830 N85-27448

A modeling analysis program for the JPL table mountain Io sodium cloud
[NASA-CR-175851] 16 p2833 N85-27466

Intercomparison of Radiation Codes in Climate Models (ICRCCM)
[DE85-007251] 16 p2835 N85-27487

Comparison of a diffusion model with dye dispersion measurements to study turbulence in coastal waters
[INPE-3492-PRE/729] 16 p2838 N85-27504

Sensitivity of conditions for lumping finite Markov chains
[AD-A152122] 16 p2855 N85-27604

An application of Markov chains to the problem of migration in inventory systems
[AD-A151954] 16 p2857 N85-27618

Sensitivity of the stationary distribution vector for an ergodic Markov chain
[DE85-006979] 16 p2857 N85-27621

Refinements in the computation of collision probabilities
[DE85-006118] 16 p2864 N85-27663

Kinetic theory and simulation of multi-species plasmas in Tokamaks excited with ICRF microwaves
[DE85-008119] 16 p2866 N85-27691

Polycrystalline semiconductor heterojunction modelling (CdS/CuInSe(sub)2)
[DE85-002913] 16 p2871 N85-27713

Inflation from extra dimensions
[DE85-007634] 16 p2883 N85-27787

An introduction to vortex breakdown and vortex core bursting
[NAE-AN-28] 17 p2892 N85-27829

Parameter identification results of tests in nonsteady symmetric flight with the Hawker Hunter Mk 7
[NLR-TR-83042-U] 17 p2897 N85-27860

Mathematical modeling and control of a large space structure as applied to a shuttle-antenna configuration
[AD-A153269] 17 p2910 N85-27939

Composite loads spectra for select space propulsion structural components: Probabilistic load model development 17 p2912 N85-27954

Hydrogen embrittlement of high-strength steel
[B8580075] 17 p2933 N85-28103

Navier-Stokes computational study of axisymmetric transonic turbulent flows with a two-equation model of turbulence
[AD-A152653] 17 p2958 N85-28265

Coherent structure reflective turbulent viscous flow modeling
[AD-A153066] 17 p2958 N85-28267

Statistical models used in analyzing the quality of welded tubes
[BLL-BISI-TRANS-22232-(9022.06)]
17 p2976 N85-28384

Earth observation modeling based on layer scattering matrices
[NLR-MP-84015-U] 17 p2984 N85-28440

Simplified analysis of Stirling engines and heat pumps
[DE85-006753] 17 p2986 N85-28457

Two-dimensional inverse kinematic problem: Application to the Saudi Arabian refraction profile
17 p2990 N85-28478

Crustal structure of the Red Sea-Arabian Shield transition 17 p2990 N85-28479

A crustal section for the Arabian Shield and adjacent Red Sea margin derived from first-arrival data
17 p2990 N85-28480

A seismic refraction profile across the Arabian Shield
17 p2990 N85-28481

A preliminary examination of the 1978 refraction profiles in Saudi Arabia 17 p2990 N85-28482

A comparison of crustal sections: Arabian Shield to the Red Sea 17 p2992 N85-28491

Solar radiance models for determination of ERBE scanner filter factor
[NASA-CR-172595] 17 p2995 N85-28513

Presentations at the Tri-Service Cloud Modeling Workshop (2nd), held at the Naval Surface Weapons Center, White Oak, Maryland, 26-27 June 1984, volume 1
[AD-A152735] 17 p2996 N85-28522

Parameterization of subgrid-scale fluxes in mesoscale meteorological models
[AD-A153016] 17 p2996 N85-28523

Mathematical modeling and simulation of climate and climatic change
[DE85-008974] 17 p2997 N85-28526

A new technique for system-to-system transfer of surface data 17 p3007 N85-28589

Optical phenomena in computer vision
[AD-A152970] 17 p3008 N85-28595

A discussion of adaptive grids and their applicability in numerical hydrodynamic modeling
[AD-A151843] 17 p3017 N85-28659

Deconvolution methods for multi-sensors
[AD-A152351] 17 p3018 N85-28660

Echo-response from crack-like two-dimensional reflectors in focused ultrasonic fields
17 p3027 N85-28724

Kirchhoff modeling via wave equation datuming
[AD-A152399] 17 p3028 N85-28727

Light scattering by leaf layers with application to canopy reflectance modeling: The Scattering by Arbitrarily Inclined Leaves (SAIL) model
[NLR-MP-84011-U] 17 p3038 N85-28796

Analysis of nonlinear parabolic equations modeling plasma diffusion across a magnetic field
[DE85-007683] 17 p3040 N85-28807

Continous chemical reaction chromatography
[DE85-009612] 18 p3072 N85-28998

Time-averaged and time-dependent computations of isothermal flowfields in a centerbody combustor
[AD-A153682] 18 p3100 N85-29189

Kalman filter modeling 18 p3107 N85-29237

Relationship between Allan variances and Kalman Filter parameters 18 p3107 N85-29238

Description and illustration of the use of CRACKS IV
[AD-A153543] 18 p3121 N85-29325

Conceptual hydrologic model of flow in the unsaturated zone, Yucca Mountain, Nevada
[DE85-008346] 18 p3125 N85-29350

F-cell: The Aspen fuel cell model
[DE85-001975] 18 p3131 N85-29393

Thermal performance testing and mathematically modeling of integral collector storage solar hot water systems
[PB85-186908] 18 p3132 N85-29398

Vertical redistribution of a pollutant tracer due to cumulus convection
[PB85-172971] 18 p3134 N85-29415

Wave-theoretical approach to seismic modeling problems (WELMOD)
[BMFT-FB-T-84-258] 18 p3137 N85-29429

High-latitude filtering in a global grid-point model using model normal modes 18 p3140 N85-29442

A numerical study of the Pacific polar low
[AD-A153777] 18 p3149 N85-29495

Utilization of the SEASAT scatterometer winds for ocean mixed layer modeling
[AD-A153748] 18 p3150 N85-29506

Image processing: Mathematics, engineering or art
[DE85-007666] 18 p3154 N85-29527

Atmosphere behavior in gas-closed mouse-algal systems: An experimental and modelling study
18 p3155 N85-29536

Distribution of mathematical software via electronic mail
[DE85-009664] 18 p3166 N85-29617

The role of ellipticity and normality assumptions in formulating live-boundary conditions in elasticity
[AD-A153475] 18 p3168 N85-29630

Bayesian full rank marginalization for 2-way contingency tables
[AD-A153641] 18 p3171 N85-29649

Monotonicity preserving bicubic interpolation
[DE85-004206] 18 p3172 N85-29657

Nonparametric renewal function estimation
[AD-A153474] 18 p3173 N85-29672

A robust estimator of location using an adaptive spline model
[AD-A153662] 18 p3174 N85-29676

An extended two-target differential game model for medium-range air combat game analysis
[NASA-CR-175968] 18 p3175 N85-29687

Further studies of the NRL collective particle accelerator via numerical modeling with the MAGIC code
[AD-A153583] 18 p3178 N85-29703

Electron multiple, plural and single scattering
[DE85-010325] 18 p3181 N85-29721

Plasma engineering models of tandem mirror devices with high-field test-cell inserts
[DE85-010046] 18 p3192 N85-29797

Numerical simulations of the effect of floor and ceiling venting on fire and smoke spread in aircraft cabins
[PB85-178333] 19 p3216 N85-29939

Outside users payload model
[NASA-CR-176011] 19 p3223 N85-29986

On the accuracy of modelling the dynamics of large space structures 19 p3225 N85-29995

Accelerator column models for low-current beams
[DE85-010722] 19 p3262 N85-30226

Turbulent transport and length scale measurement experiments with comfined coaxial jets
[NASA-CR-174831] 19 p3265 N85-30245

Use of a two-dimensional flow model to quantify aquatic habitat
[AD-A154287] 19 p3266 N85-30253

A method for predicting additive drag reduction from small-diameter pipe flows
[AD-A154411] 19 p3266 N85-30254

Thermal performance and design of a solid particle cavity receiver
[DE85-010830] 19 p3274 N85-30300

Laser forward and backscattering in particulate media
[AD-A154138] 19 p3275 N85-30312

A mathematical model of reciprocating combustion engine dynamics for the diagnosis of deficient energy conversion 19 p3280 N85-30339

Computational methods in advanced stress and durability analyses
[AD-A154119] 19 p3286 N85-30375

Plane Tsunami wave caused by elastic oscillations of ocean floor 19 p3290 N85-30403

Model computations of light reflection from sea surface 19 p3292 N85-30411

Method for computing evolution of random hydropdynamic fields on basis of adjoint equations
19 p3292 N85-30412

Mathematical model of global processes in the biosphere 19 p3295 N85-30431

Institute works on modeling thermonuclear plasma processes 19 p3296 N85-30435

Using PVFORM, a systems performance model, to determine optimum mounting configurations for flat-plate photovoltaic modules
[DE85-011191] 19 p3306 N85-30495

F-CAP documentation
[DE85-003369] 19 p3307 N85-30503

Qualitative and quantitative examination of the performance of regional air quality models representing different modeling approaches
[DE85-010508] 19 p3310 N85-30518

MELSAR: A mesoscale air quality model for complex terrain. Volume 2: Appendices
[DE85-010991] 19 p3310 N85-30519
Analysis of leachate production in closed hazardous waste landfills
[DE85-010978] 19 p3310 N85-30520
Synthetic rainfall and its use in hydrologic modeling
19 p3314 N85-30542
A probabilistic forecasting model of tropical cyclone-generated storm surge for a straight coastline
19 p3314 N85-30544
Atmospheric planetary wave responses to external forcing
[NASA-CR-176000] 19 p3315 N85-30548
A global low order spectral model designed for climate sensitivity studies
[NASA-CR-175999] 19 p3315 N85-30549
Effects of relative humidity gradients on the evaluation of submicron aerosol flux measurements in the atmospheric surface layer
[DE85-010510] 19 p3316 N85-30555
Effect of vertical shear on regional-scale trajectories in near-frontal conditions
[DE85-007554] 19 p3317 N85-30561
Examination of the time and spatial scales appropriate for the carbon dioxide climate change issue
[DE85-009852] 19 p3317 N85-30563
Geometry, velocity structure and penetration depths of descending slabs in the western Pacific
19 p3319 N85-30574
Evolution of the oceanic upper mantle and effects on sea floor subsidence geoid height and heat flow
19 p3319 N85-30575
An approach to modeling database activity
19 p3332 N85-30642
Estimating ability with the wrong model
[AD-A154071] 19 p3335 N85-30663
High gain adaptive control of decentralized systems
[DE85-010040] 19 p3339 N85-30688
Performance and library issues for mathematical software on high performance computers
[DE85-010263] 19 p3339 N85-30690
Identification of a mathematical model 1: Goodness of fit criterion
[HSE-TRANS-11109] 19 p3341 N85-30703
Expending expertise by use of an expert system
[DE85-010759] 19 p3344 N85-30723
One-dimensional hybrid code for FRM dynamics
[DE85-010687] 19 p3361 N85-30840
Modulation transfer function for two-point and periodic objects using Gaussian and Lorentzian resolution functions
[PB85-187557] 19 p3368 N85-30891
Perspectives of nonlinear dynamics
[IPPJ-723] 19 p3370 N85-30902
Plasma radiation sources. Quasi-adiabatic theory and numerical modeling in the electro-diffusive approximation
[AD-A154375] 19 p3370 N85-30906
Steady-state spheromak reactor studies
[DE85-009585] 19 p3372 N85-30916
A study on the control of third generation spacecraft
20 p3415 N85-31196
An Eigensystem Realization Algorithm (ERA) for model parameter identification and model reduction
20 p3418 N85-31212
Ion thruster performance model
20 p3420 N85-31226
Conditional modelling in turbulent shear flows
20 p3424 N85-31250
Computer-controlled carburizing
[BLL-OA-TRANS-3204-(6196.300)]
20 p3429 N85-31268
Scattering models in signal processing
20 p3439 N85-31339
Modeling taper charge with a non-linear equation
20 p3445 N85-31390
Informatics Division 20 p3449 N85-31416
Numerical and experimental investigation of turbomachinery rotor flow fields
20 p3451 N85-31429
Turbulence modeling in a two-dimensional wake
20 p3452 N85-31431
Natural convection experiments in a stratified liquid-saturated porous medium
[DE85-008003] 20 p3455 N85-31457
Intermittent gas-liquid flow modeling in horizontal or weakly inclined pipes
[EME-132] 20 p3456 N85-31465
A theoretical model for the study of nonlinear dynamics of magnetic bearings 20 p3482 N85-31505
Theoretical modelling of the electro-chemistry in a corrosion fatigue crack. Part 2: Mathematical aspects of associated unsteady reaction equations
[NPL-DMA(A)-100-PT-2] 20 p3485 N85-31529
Numerical considerations in the development and implementation of constitutive models
20 p3467 N85-31541
On numerical integration and computer implementation of viscoplastic models 20 p3467 N85-31542
Numerical study of tensile fracture in plane stress
[ONERA-RT-22/7169-RY-070-R]
20 p3470 N85-31563
Mathematical model of the nitrogen cycle in a nonsaturated area of cultivated soil
20 p3478 N85-31610
Current status of one- and two-dimensional numerical models: Successes and limitations
20 p3482 N85-31636
Update on the evolution of the LAGEOS orbit
20 p3491 N85-31698
Error spectrum of Goddard satellite models for the gravity field 20 p3491 N85-31704
On development mechanisms for polar lows
20 p3495 N85-31727
Benthic boundary layer modelling studies
[IOS-181] 20 p3497 N85-31742
A systems analysis of the erythropoietic responses to weightlessness. Volume 1: Mathematical model simulations of the erythropoietic responses to weightlessness
[NASA-CR-171890] 20 p3506 N85-31794
A systems analysis of the erythropoietic responses to weightlessness. Volume 2: Description of the model of erythropoiesis regulation. Part A: Model for regulation of erythropoiesis. Part B: Detailed description of the model for regulation of erythropoiesis
[NASA-CR-171891] 20 p3506 N85-31795
Distributed implementation of functional program evaluation
[DE85-009573] 20 p3514 N85-31844
Exponential order statistic models of software reliability growth
[NASA-CR-3909] 20 p3515 N85-31852
SCAP: A Shaped Charge Analysis Program. User's manual for SCAP 1.0
[DE85-011182] 20 p3515 N85-31854
Time-implicit Monte-Carlo collision algorithm for particle-in-cell electron transport models
[DE85-010758] 20 p3521 N85-31900
Propagation and reflection of a finite amplitude ultrasonic beam including harmonic content: A numeric model
20 p3523 N85-31914
Source-term considerations for a potential radioactive-waste repository located in unsaturated tuff
[DE85-010090] 20 p3529 N85-31953
Aerodynamic characteristics of the standard dynamics model in coning motion at Mach 0.6
[NASA-TM-86717] 21 p3552 N85-32094
Development of reduced order models for control system design using the OPTSYSX program
[AD-A154552] 21 p3556 N85-32124
Injection of drag reducing additives into turbulent water flows: Two-component velocity measurements and mixing length model predictions
[AD-A154604] 21 p3583 N85-32274
Theoretical modeling of laser induced optical degradation
[AD-A155302] 21 p3592 N85-32323
A continuous damage model based on stepwise-stress creep rupture tests
[NASA-CR-174941] 21 p3597 N85-32341
Modelling and parameter estimation for distributed vibratory systems
[AD-A154518] 21 p3598 N85-32344
Development of improved dynamic failure models
[AD-A155586] 21 p3600 N85-32354
A new global geomorphology?
21 p3601 N85-32358
Modeling of the silane FBR system
21 p3609 N85-32415
Comprehensive silicon solar-cell computer modeling
21 p3609 N85-32421
Emergency modeling of hazardous air pollutants
[AD-A155441] 21 p3614 N85-32461
The Norwegian seismic array (NORSAR)
[AD-A154751] 21 p3631 N85-32555
The diurnal variation of the neutral sodium species in the upper atmosphere: A model study
[AD-A154988] 21 p3631 N85-32561
Development of ultrasonic modeling techniques for the study of crustal inhomogeneities
[AD-A155206] 21 p3632 N85-32565
Diagnostics of severe convection and subsynoptic scale ageostrophic circulations
[NASA-CR-171581] 21 p3634 N85-32571
Scavenging of submicron aerosol particles by snow crystals: Theory and experiments
21 p3648 N85-32667
A probabilistic method for particle size analysis of aerosols 21 p3648 N85-32669
A simple model to investigate the activation process in waterclouds 21 p3649 N85-[illegible]
Numerical modeling of sea ice dynamics and ice thickness characteristics
[AD-A154600] 21 p3654 N85-[illegible]
Carbon and sulfur cycling through geologic time
21 p3658 N85-[illegible]
An error-dependent model of instrument-scanning behavior in commercial airline pilots
[NASA-CR-3908] 21 p3665 N85-[illegible]
Optimal low thrust transfer using a first-order perturbation model
[AD-A154761] 21 p3676 N85-[illegible]
Theory of soliton waves
[AD-A154784] 21 p3676 N85-[illegible]
Identification of unsteady aerodynamics and aeroelastic integro-differential systems
[NASA-TM-86749] 21 p3678 N85-[illegible]
Diamagnetic instability of cyclotron waves in plasma
21 p3693 N85-[illegible]
Asymptotically stable solutions of some nonlinear equations 21 p3696 N85-[illegible]
Iteration solution for a submerged force-driven finite cylinder
[AD-A154587] 21 p3699 N85-[illegible]
Overground Excess Sound Attenuation (ESA). Volume 3: Application of ESA data in NOISEFILE
[AD-A154820] 21 p3699 N85-[illegible]
Lateral attenuation of aircraft flight noise
[AD-A154958] 21 p3700 N85-[illegible]
Modeling the exhaust of the pulsed plasma thruster
[AD-A155344] 21 p3707 N85-[illegible]
Feasibility of applications of Competition Decision Assist Package (CDAP) to spare parts
[AD-A154716] 21 p3712 N85-[illegible]
Discrimination of linear contour elements of space photographs based on visual perception model
22 p3736 N85-33181
Modeling granular explosive detonations with shear band concepts
[DE85-011823] 22 p3754 N85-33271
Model that predicts pulse charged gas switching breakdown phenomena
[DE85-013119] 22 p3761 N85-33313
Method of estimating convergence of Haar coefficients in message compression problems
22 p3769 N85-[illegible]
Analysis of crosstalk in nonhomogeneous multiconductor lines 22 p3769 N85-[illegible]
Estimating optimum technical and economic indicators of data transmission systems 22 p3777 N85-[illegible]
Pulsed hydrojet propulsion
[DE85-010771] 22 p3784 N85-[illegible]
The calculation of two-dimensional buoyant surface jets with the k-W model of turbulence — kinetic energy-vorticity fluctuations (k-W)
[CFD/84/21] 22 p3785 N85-33448
Current internal-dosimetry practices at US Department of Energy facilities
[DE85-011718] 22 p3787 N85-[illegible]
Numerical experiment of elastic wave propagation by framework model
[DRIC-T-7462] 22 p3796 N85-33511
Stochastic groundwater flow modeling using the second-order method
[DE85-011250] 22 p3802 N85-[illegible]
Theory of cellwise optimization for solar central receiver system
[DE85-012586] 22 p3807 N85-33579
Estimation of Sr90 and Cs137 activity introduced and accumulation in the Po basin until 1983
[CISE-2515] 22 p3813 N85-33617
Model projections of time-dependent response to increasing carbon dioxide
[DE85-013326] 22 p3816 N85-33641
Data Base Workshop: Availability-Reliability Modeling
[DE85-011570] 22 p3829 N85-33713
Presentation of numerical simulation work in terminal ballistics using a few examples. Applications of the calculation model Program for Elastoplastic Simulation of Impacts (PEPSI) of the Franco-German Research Institute Saint Louis (ISL)
[ISL-CO-209/84] 22 p3834 N85-33741
A formulation and analysis of combat games
[NASA-TP-2487] 22 p3835 N85-33745
New formulation for linear accelerator design
[DE85-011171] 22 p3842 N85-[illegible]
Late-stage planetesimals: How big?
22 p3852 N85-[illegible]
Component-specific modeling
[NASA-CR-174765] 23 p3897 N85-34140
On high strain rate fragmentation of a closed vessel
23 p3904 N85-[illegible]

Experimental evaluation of the thermodynamic properties of concentrated aqueous potassium hydroxide solutions
[DE85-010626] 23 p3912 N85-34238

Pressure-shear loading of PBX-9404
[DE85-009962] 23 p3921 N85-34298

Modeling heterogeneous high explosive burn with an explicit hot-spot process
[DE85-009593] 23 p3922 N85-34300

Three-dimensional hydrodynamic hot-spot model
[DE85-008587] 23 p3922 N85-34301

Detonation of condensed explosives: Evolution of knowledge in the last 40 years
[ISL-CO-226/84] 23 p3923 N85-34307

Finding the roots of the transcendental equations in problems in determining the thermal conductivity of spheres with heterogeneous boundary conditions
[BLL-M-35678-(5828.4)] 23 p3929 N85-34347

Preliminary SPR thermal model description and results for WH-11 and BM-4
[DE85-013171] 23 p3931 N85-34360

Detailed validation of a liquid and heat flow code against field performance
[DE85-009901] 23 p3932 N85-34368

Mathematical modeling of ultimate heat sink cooling ponds
[TI85-009747] 23 p3932 N85-34369

Modeling of geothermal systems
[DE85-012553] 23 p3943 N85-34439

Ocean thermal energy conversion
[DE85-012291] 23 p3946 N85-34456

Evaluation of source strength and dispersion model predications with data from large nitrogen tetroxide field experiments
[DE85-011855] 23 p3947 N85-34465

Graph-theoretical exorcism
[DE85-011916] 23 p3955 N85-34512

Computer analysis techniques for the temporal evaluation of cardiac wall motion
23 p3958 N85-34530

A user-friendly computer-aided construction of boundaries 23 p3962 N85-34564

Numerical solutions of the Vlasov equation
23 p3979 N85-34672

Cubic interpolated pseudo-particle method (CIP) for solving hyperbolic-type equation
23 p3979 N85-34673

Numerical simulation in astrophysics: Smoothed particle methods 23 p3979 N85-34674

Moving finite element method for ICF target implosion
23 p3980 N85-34675

Dissipation terms in one-dimensional hydrodynamic code for ICF target 23 p3980 N85-34677

Simulation of instability of cylindrically converging shock waves 23 p3980 N85-34679

On the heat flux derived by the moment method in Lorentzian plasma between hot and cold walls
23 p3980 N85-34682

Observation of helical sawtooth oscillations in a tokamak
[DE85-012062] 23 p3983 N85-34703

The 1973-1984 solar modulation of cosmic ray nuclei
[SH-4.1-16] 23 p4006 N85-34836

Evidence for regions of negligible cosmic-ray modulation in the inner heliosphere (10 AU)
[SH-4.1-21] 23 p4006 N85-34840

Drift and observations in cosmic-ray modulation, 2
[SH-4.2-5] 23 p4007 N85-34843

Electron capture decay of cosmic rays: A model of the inhomogeneous interstellar medium
[OG-7.1-10] 23 p4014 N85-34871

The model-independence of cosmic ray source determinations
[OG-7.2-1] 23 p4014 N85-34873

Explanation of the secondary to primary ratio within the continuous Fermi accelerator model
[OG-8.3-2] 23 p4021 N85-34921

Empirical model for the Earth's cosmic ray shadow at 400 KM: Prohibited cosmic ray access
[SH-6.1-14] 23 p4046 N85-35087

Chemoviscosity modeling for thermosetting resins, 2
[NASA-CR-177958] 24 p4073 N85-35243

An analytical and numerical model of radiation heat transfer in direct injection-type diesel combustion
24 p4092 N85-35368

Studies on effects of boundary conditions in confined turbulent flow predictions
[NASA-CR-3929] 24 p4093 N85-35371

Transient three-phase three-component systems. Part 1: Formulation of the system of differential equations
[DE85-013267] 24 p4095 N85-35384

Development of a mathematical model for predicting the percentage fatigue life increase resulting from shot peened components
[AD-A155774] 24 p4101 N85-35425

An atmospheric boundary layer model forced by the operational ECMWV-model
[WSR-3] 24 p4120 N85-35541

A mechanical model of the human body and its application 24 p4129 N85-35598

Benchmark evaluation of PC simscript
[AD-A156133] 24 p4138 N85-35651

Algorithmic approaches in sets of good answers in inverse problems
[PM/84/18] 24 p4142 N85-35677

Constrained stiffness matrix adjustment using mode data
[AD-A155988] 24 p4143 N85-35685

Model robust response surface designs: Scaling two-level factorials
[AD-A156218] 24 p4143 N85-35686

Acoustic resonances in cylinder bundles oscillating in a compressible fluid
[DE85-004086] 24 p4145 N85-35699

A lead glass tubing drift calorimeter
24 p4147 N85-35711

Use of a minimum-ellipse criterion in the study of ion-beam extraction systems
[DE85-012670] 24 p4148 N85-35721

Applications and misapplications of the channel-capture formalism of direct neutron capture
[DE85-013992] 24 p4152 N85-35748

On-line model driven control of the SLC electron Damping Ring
[DE85-013377] 24 p4157 N85-35772

MATHEMATICAL PROGRAMMING
NT DYNAMIC PROGRAMMING
NT LINEAR PROGRAMMING
NT NONLINEAR PROGRAMMING
NT QUADRATIC PROGRAMMING

Sensitivity analysis in generalized rational approximation with restricted denominator
[CSIR-TWISK-319] 01 p0109 N85-10734

On the formal development of graph theoretical algorithms by transformation
[TUM-I8403] 04 p0553 N85-13522

Monotone operators in mathematical programming
[AD-A147309] 07 p1025 N85-16506

Fast arithmetic for microcomputers
08 p1140 N85-17180

Relative performance of micro and mainframe computers
[AD-A149281] 10 p1538 N85-19695

Description of 8048 microcomputer operation published 11 p1700 N85-20685

An approach for user controlled reinforced concrete design optimization 15 p2627 N85-26187

Mathematical software for hyperbolic equations and two point boundary value problems
[AD-A151982] 15 p2638 N85-26270

Mathematical programming in computer network design
[AD-A152275] 16 p2848 N85-27558

H-sets, convex programming and constrained approximation
[TRITA-NA-8306] 16 p2853 N85-27587

The essence of invexity
[CSIR-TWISK-321] 16 p2858 N85-27626

A global optimization algorithm using stochastic differential equations
[AD-A153526] 18 p3161 N85-29583

The origin of the binary-search paradigm
[AD-A154367] 19 p3337 N85-30677

Mathematical programming in the Netherlands
[REPT-ARW-03-THE-BDK/ORS/83/10]
20 p3517 N85-31866

New developments on the core function for efficient implementation of the difficult residue number system operations
[AD-A154678] 21 p3676 N85-32834

Necessary and sufficient conditions for single-extremum and convex problems of mathematical programming
21 p3698 N85-32977

A geometric modeller for turbomachinery applications
23 p3962 N85-34556

MATHEMATICAL TABLES

Log linear model applications
[AD-A146620] 06 p0858 N85-15457

Tables for distributions of quadratic forms
[AD-A154064] 19 p3347 N85-30745

MATHEMATICS

USSR report: Physics and mathematics
[JPRS-UPM-84-006] 02 p0256 N85-11676

Emergency Mathematics and Science Education Act
[GPO-29-561] 03 p0435 N85-12770

Experimental mathematics
[CWI-PM-R8411] 12 p1925 N85-22096

Ada (trademark) training curriculum. Advanced Ada topics L305 teacher's guide exercises
[AD-A154621] 21 p3670 N85-32798

MATRICES (CIRCUITS)

A study of reflex optoelectronic switching matrices and their derivatives
[CRC-TN-720] 19 p3253 N85-30169

Charge Injection Device (CID) used as a photodector: Implementation and performance. Application to light source tracking (stars, lasers)
[CNES-83/CT/DRT/TIT/OE/146]
20 p3533 N85-31983

MATRICES (MATHEMATICS)
NT ADJOINTS
NT CANONICAL FORMS
NT EIGENVALUES
NT EIGENVECTORS
NT JORDAN FORM
NT STIFFNESS MATRIX

Calculations of optical properties of transition metals
[BLL-M-35744-(5828.4)] 02 p0175 N85-11175

Seminar on Principal Components Analysis in the Atmospheric and Earth Sciences
[CSIR-S-334] 02 p0211 N85-11388

Principal components: A review
02 p0211 N85-11390

Description of a data matrix structure and model diagnosis by means of row and column Euclidean maps
02 p0211 N85-11392

A fast, compact assignment algorithm
[NRIMS-TWISK-331] 02 p0250 N85-11632

Numerical methods for solving systems of linear equations
[INPE-3240-RPE/463] 02 p0250 N85-11633

Pointwise iterations of finite element modeling of advection-diffusion equations
[DE84-015284] 02 p0253 N85-11656

Evaluating A(T) *D*A for sparse matrices: Analysis
[AD-A145916] 03 p0411 N85-12625

Bulletin of the Faculty of Engineering, Hokkaido University, no. 123
[ISSN-0385-602-X] 04 p0482 N85-13075

Implication structures for generalized implication matrix in ISM 04 p0483 N85-13079

Least squares spline regression with block-diagonal variance matrices
[NPL-DITC-40/84] 04 p0554 N85-13523

Effects of changing the signs of rows and columns of a matrix and the hyperbolic transpose
[DE84-014651] 04 p0555 N85-13530

Electrooptical matrix multiplication using the twos complement arithmetic for improved accuracy
[AD-D011252] 05 p0728 N85-14682

Advanced cube processor
[AD-D011262] 05 p0729 N85-14683

Algebraic techniques in systolic array design
[AD-A146417] 06 p0857 N85-15451

On a random difference equation for matrices and a characterization of the gamma distribution
[AD-A146858] 07 p1029 N85-16529

Lattice statistics
[AD-A146862] 07 p1029 N85-16530

Continuity of the null space basis and constrained optimization
[AD-A147038] 07 p1030 N85-16538

A complete characterization of triply balanced matrices with applications to survey sampling
[AD-A147083] 07 p1031 N85-16542

Extracting embedded generalized networks from linear programming problems
[AD-A147565] 07 p1033 N85-16558

Sequential and parallel matrix computations
[AD-A147871] 07 p1034 N85-16562

Structural optimization and other large-scale processes
[AD-A147895] 07 p1034 N85-16564

An optimal parallel processing method for inverting sparse matrices 09 p1367 N85-18588

Modeling relationships using groups and items
09 p1367 N85-18591

On the connection between multigrid and cyclic reduction
[NASA-TM-86020] 09 p1373 N85-18629

Investigation of three-dimensional mesh generation with precise controls
[AD-A148759] 09 p1374 N85-18636

Methods of computer-aided analysis of non-Gaussian noise and application to robust adaptive detection, part 2
[AD-A148879] 10 p1539 N85-19704

The inefficiency of least squares: Extensions of Kantorovich inequality
[AD-A149568] 10 p1549 N85-19768

On the probability density of signal-to-noise ratio in an improved adaptive detector, part 1
[AD-A148856] 10 p1550 N85-19772

Triple matrix product optical processors using combined time-and-space integration
[AD-D011483] 10 p1557 N85-19820

Complex symmetric matrices with strongly stable iterates
[NASA-CR-172542] 11 p1706 N85-20731
Differentiating matrices for arbitrarily spaced grid points
[NASA-CR-172556] 12 p1919 N85-22051
On the limiting empirical distribution function of the eigenvalues of a multivariate F matrix
[AD-A149818] 12 p1921 N85-22065
Direct secant updates of sparse matrix factors
[DE85-004006] 12 p1922 N85-22073
Asymptotic behavior of matrix coefficients related to reductive symmetric spaces
[CWI-PM-R8410] 12 p1925 N85-22095
Implementation of some concurrent algorithms
[DE85-004687] 13 p2148 N85-23334
On limit of the largest eigenvalue of the large dimensional sample covariance matrix
[AD-A150589] 13 p2151 N85-23358
Algorithm for singular decomposition
[DE85-016488] 13 p2152 N85-23361
Sparse matrix computations
[DE85-004780] 13 p2152 N85-23362
Model synthesis of multidimensional PI-regulators for objects with inertial sections 14 p2270 N85-24064
On positive vectors, positive matrices and the specialization ordering
[CWI-PM-R8407] 14 p2414 N85-24899
MATRIX: A program that shows how row and column orderings affect matrix fill-in
[DE85-007522] 15 p2630 N85-26213
Investigation of the numerical method of moments for digital computer determination of differential equations
[AD-A151886] 15 p2638 N85-26268
Explicit construction of contractivity matrices
[TRITA-NA-8309] 16 p2852 N85-27586
Finite elements and the method of conjugate gradients on a concurrent processor
[NASA-CR-175812] 16 p2853 N85-27588
Formulas for updating the generalized inverse of a symmetric matrix perturbed by a symmetric rank 2 matrix composed of 2 nonsymmetric DYADS
[AD-A151736] 16 p2858 N85-27629
Computing the singular value decomposition of a product of two matrices
[DE85-006977] 16 p2859 N85-27631
A method to calculate the parameters of wings of arbitrary planform
[AD-A152689] 17 p2892 N85-27831
Discrete mathematics for communications systems
[AD-A152814] 17 p3018 N85-28664
Robust tests of mean vector in symmetrical multivariate distributions
[AD-A153116] 17 p3020 N85-28674
Symbolic Givens reduction in large sparse least squares problems
[DE85-008685] 17 p3021 N85-28681
On the condition number of modified moment matrices arising from least squares approximation in the complex plane
[AD-A152353] 17 p3026 N85-28714
Kalman filter modeling 18 p3107 N85-29237
Studies in quality improvement. Part 1: Dispersion effects from fractional designs, revised
[AD-A153516] 18 p3119 N85-29308
Pipelined Givens method for computing the QR factorization of a sparse matrix
[DE85-009772] 18 p3171 N85-29653
High accuracy digital acousto-optic matrix computer
[AD-D011692] 19 p3343 N85-30716
An iterative method for indefinite systems of linear equations
[NASA-CR-172345] 19 p3345 N85-30728
Monte Carlo sampling strategies for lattice gauge calculations
[DE85-010756] 19 p3377 N85-30948
Matrix transfer function design for flexible structures: An application 20 p3416 N85-31199
Fast eigenvector methods for digital signal processing
20 p3439 N85-31341
Method to render second order beam optics programs symplectic
[DE85-010631] 20 p3515 N85-31855
Detection of and search for faults in programmable logic arrays 22 p3778 N85-33409
Determination of low chloride values in Rocky Flats scrub alloy solutions and other complex matrices
[DE85-011506] 23 p3911 N85-34234
Invariant tests and likelihood ratio tests for multivariate elliptically contoured distributions
[AD-A155844] 24 p4142 N85-35679
MATRIX ANALYSIS
U MATRICES (MATHEMATICS)
MATRIX MATERIALS
High performance fibers for structurally reliable metal and ceramic composites — advanced gas turbine engine materials
[NASA-TM-86878] 03 p0325 N85-12095
Matrix resin characterization in cured graphite composites using diffuse reflectance-FTIR
04 p0466 N85-12959
Solvent resistant thermoplastic composite matrices
04 p0466 N85-12960
Aliphatic-aromatic heterocyclics as potential thermoplastics for composite matrices
04 p0466 N85-12962
Constituent properties and interrelationships
04 p0467 N85-12964
Matrix synthesis and characterization
04 p0467 N85-12965
Work hardening of simple two phase composites
[DE84-014629] 04 p0468 N85-12978
Carbon fibre reinforced aluminum matrix composites: A critical review
[AD-A146367] 06 p0764 N85-14883
Fine-grained millimeter-sized objects in type 3 ordinary chondrites and their relation to chondrules and matrix
06 p0882 N85-15603
Chondrule rims and interchondrule matrix in UOC
06 p0882 N85-15604
The influence of porosity on the deformation and fracture of alloys
[AD-A146766] 08 p1130 N85-17124
Development of a heterogeneous laminating resin system
[NASA-CR-172459] 09 p1288 N85-18089
Proceedings of Colloquium/Workshop on Composite Materials and Structures, Standardization, Qualification, Certification held at washington, D.C. on 8-10 May 1984
[AD-A149039] 10 p1432 N85-19029
Quantitative estimate of compatibility of fiber composite material components 10 p1444 N85-19099
Structure and property formation mechanism in magnetite alloy-binder composite
10 p1444 N85-19103
Fiber composite materials with titanium matrix
10 p1445 N85-19105
Chemical approach for controlling nadimide cure temperature and rate with maleimide
[NASA-CASE-LEW-13770-3] 12 p1809 N85-21350
Chemical approach for controlling nadimide cure temperature and rate with maleimide
[NASA-CASE-LEW-13770-4] 12 p1810 N85-21351
Method and apparatus for detecting acoustic emissions from metal matrix wire
[AD-D011556] 12 p1927 N85-22107
Development of epoxy matrices for filament-wound graphite structures
[DE85-003674] 13 p2015 N85-22642
Monitoring of laminate cure with microdielectrometry
[AD-A150863] 14 p2248 N85-23934
In-plane shear properties of graphite Fibre/Epoxy composites for aerospace applications: Evaluation of test methods by the decision analysis technique
[AD-A151599] 15 p2503 N85-25440
Mechanics of polymers and composites: Research opportunities
[DE85-007052] 15 p2503 N85-25442
Development of a new faster process for the fabrication of ceramic fiber-reinforced ceramic composites by chemical vapor infiltration
[DE85-007560] 16 p2756 N85-27007
Polymer matrix and graphite fiber interface study
[NASA-CR-177357] 19 p3232 N85-30036
Chemical approach for controlling nadimide cure temperature and rate
[NASA-CASE-LEW-13770-6] 19 p3232 N85-30039
Features of the interaction between fibers and matrix in production of aluminum-boron composite material
19 p3244 N85-30117
Matrix fracture in fiber-reinforced ceramics
[AD-A154704] 21 p3569 N85-32197
Apparatus and method for identification of matrix materials in which transuranic elements are embedded using thermal neutron capture gamma-ray emission
[DE85-011659] 22 p3766 N85-33454
Development of solid thorium-232 reference materials
[DE85-011459] 22 p3641 N85-33785
Impact fracture mechanism of polymer plates containing a heavy inner material 23 p3906 N85-34215
Mechanical properties of SiC fiber-reinforced reaction-bonded Si3N4 composites
[NASA-TM-87086] 23 p3909 N85-34223
Viscoelastic behavior of short-fiber composite materials
[DE85-011293] 23 p3910 N85-34225
MATRIX METHODS
A routine to find the lowest few eigenvalues and vectors for the generalised sparse symmetric eigenproblem
[NPL-DITC-43/84] 05 p0722 N85-14
The use of analytical models to interpret measured data property. 1. General background theory
11 p1651 N85-20
The use of analytical models to interpret measured data property. 2. The application to modal analysis of structures 11 p1651 N85-20
Adaptive filtering for large space structures: A closed-form solution 20 p3417 N85-31
MATRIX STRESS CALCULATION
U MATRIX METHODS
MATRIX THEORY
A T-matrix theory of galactic heavy-ion fragmentation
[NASA-TP-2363] 08 p1221 N85-17
MATTER (PHYSICS)
Galaxy and cluster formation in a universe dominated by cold dark matter
[DE84-015879] 04 p0580 N85-13
Space charge, interfacial kinetics, and electrical response of condensed matter
[AD-A146364] 06 p0765 N85-14
Theoretical studies relating to the interaction of radiation with matter: Atomic collision processes occurring in the presence of radiation fields
[AD-A146654] 07 p1040 N85-16
Propagation of sound in matter
[AD-A151052] 14 p2416 N85-24
Particle physics: Recent successes and future prospects
[DE85-008175] 17 p3033 N85-28
Proceedings of the 1984 Workshop on High-Energy Excitations in Condensed Matter, volume 2
[DE85-007395] 19 p3357 N85-30
Characterization of the optical and thermal properties of matter by photothermal techniques
[DE85-012807] 24 p4076 N85-35
MATTS (SYSTEMS)
User's manual of the BNDSCO computer program for solving constrained optimal control problems
[DFVLR-MITT-85-05] 20 p3516 N85-31
MATURING
U GROWTH
MAXIMA
Attainable rates of convergence of maxima
[AD-A150636] 14 p2408 N85-24
Large deviations for the maxima of some random fields
[AD-A155909] 24 p4143 N85-35
MAXIMUM ENTROPY METHOD
Autoregressive modeling and the classification of land clutter — radar signatures
[ENST-C-84003] 03 p0356 N85-12
On maximum entropy signal analysis
[AD-A144374] 03 p0410 N85-12
Fundamental limitations in antenna resolution by maximum entropy methods
[DE84-017052] 04 p0493 N85-13
Local geomagnetic characteristics of solar activity (Dourbes 1960-1978) 04 p0521 N85-13
Relative-entropy minimization with uncertain constraints–theory and application to spectrum analysis
[AD-A149192] 10 p1546 N85-19
Space and time variations and turbopause dynamical structure 11 p1663 N85-20
Simulation of estimating periodicity of seasonally stationary time series
[DE85-003517] 11 p1708 N85-20
Determination of experimental Tokamak plasma properties using maximum entropy analysis
[DE85-001723] 12 p1936 N85-22
Application of the maximum entropy/optimal projection control design approach for large space structures
14 p2234 N85-23
Maximum entropy spectral analysis
[LEOK-TR-1984-06] 14 p2299 N85-24
MAXIMUM LIKELIHOOD ESTIMATES
A Monte Carlo comparison of the recovery of winds near upwind and downwind from the SASS-1 model function by means of the sum of squares algorithm and a maximum likelihood estimator
[NASA-CR-3839] 01 p0064 N85-10
Nonparametric maximum penalized likelihood estimation of a density from arbitrarily right-censored observations
[AD-A145569] 02 p0251 N85-11
Likelihood estimation for generalized mixed exponential distributions
[AD-A145675] 02 p0252 N85-11
Maximum likelihood estimation of the survival functions of N stochastically ordered random variables
[AD-A145429] 02 p0254 N85-11
The ML (Maximum Likelihood) method for frequency estimation of real sinusoids in noise
[AD-A146053] 03 p0411 N85-12

Maximum likelihood and Bayesian parameter estimation in item response theory
[AD-A145776] 03 p0413 N85-12644

A very efficient transfer function bounding technique on bit error rate for Viterbi decoded, rate 1/N convolutional codes 05 p0624 N85-13991

Maximum likelihood estimation of parameters in linear systems from flight test data: A FORTRAN program
[AD-B087196L] 05 p0715 N85-14588

Estimating a monotone density
[CWI-MS-R8403] 05 p0721 N85-14533

More than you want to know about maximum likelihood estimation
[NASA-TM-85905] 07 p0909 N85-15752

Improved digital baseband transmission by application of maximum likelihood decoding to an 8-level signal generated by convolution and block coding
[R-44-TBR-93] 07 p0942 N85-15973

Bayesian estimation of normal mixture parameters 07 p0965 N85-16255

Local likelihood estimation
[AD-A147317] 07 p1035 N85-16571

Improved estimation procedures for item response functions
[AD-A147677] 08 p1215 N85-17648

Statistical aspects of shear fracture propagation
[ERS-E.366] 09 p1341 N85-18434

User's guide to MIX: A computer code for fitting mixture distributions to data
[DE85-001451] 09 p1369 N85-18603

Estimating the scale parameter of an exponential distribution from a sample of time-censored r-th order statistics
[AD-A148060] 09 p1375 N85-18644

Adaptive signal processing for radio communications 10 p1473 N85-19295

The likelihood displacement: A unifying principle for influence measures
[AD-A149456] 10 p1551 N85-19783

Identification of dynamic systems, theory and formulation
[NASA-RP-1138] 10 p1551 N85-19784

On the application of compatibility checking techniques to dynamic flight test data
[ARL/AERO-R-161] 12 p1776 N85-21151

Ordinary and proper location M-estimates for ARMA models, revised
[AD-A149705] 12 p1920 N85-22061

Accuracy of approximation of Bayes estimates in presence of noninformative parameters 13 p2064 N85-23015

Reception of signal with unknown amplitude and duration submerged in white noise 13 p2064 N85-23016

Why do noninvertible estimated moving averages occur?
[AD-A150368] 13 p2153 N85-23368

Better bootstrap confidence intervals
[AD-A150796] 14 p2406 N85-24846

Nonparametric estimation of density and hazard rate functions when samples are censored
[AD-A150946] 14 p2411 N85-24868

Censored observations, repeated measures and mixed effects models: An approach using the EM algorithm and normal errors
[MATHEMATICS-RESEARCH-183] 15 p2636 N85-26256

Validation of the ERBE scanner scene identification methodology: Analysis with Nimbus-7 ERB data
[NASA-CR-172596] 16 p2832 N85-27466

Topics in time delay estimation
[AD-A152231] 16 p2855 N85-27607

Multivariable statistical modelling and its application 16 p2857 N85-27617

Local likelihood estimation
[DE85-007238] 16 p2857 N85-27620

Nonsmooth analysis and Frechet differentiability of M-functionals
[AD-A152932] 17 p3019 N85-28668

Extraction of aerodynamic parameters for aircraft at extreme flight conditions
[NASA-TM-86730] 18 p3175 N85-29686

Maximum likelihood estimation with emphasis on aircraft flight data 20 p3417 N85-31208

A residuals approach to filtering, smoothing and identification for static distributed systems 20 p3418 N85-31213

Numerical experimentation with maximum likelihood identification in static distributed systems 20 p3418 N85-31214

Comparison of ERS-1 scatterometer Monte Carlo performance simulations using a weighted nonlinear least squares and a maximum likelihood estimation method 20 p3420 N85-31224

On the confidence limits for Weibull reliability and quantiles: The case of maximum likelihood estimation from small size censored samples
[REPT-84-RR-345] 20 p3521 N85-31898

Robust detection and classification of regional seismic signals using a two mode/two stage cascaded adaptive arma (CAARMA) model
[AD-A154710] 21 p3630 N85-32554

On a variational approach to some parameter estimation problems
[NASA-CR-177935] 21 p3675 N85-32829

Weibull distribution based on maximum likelihood with interval inspection data
[NASA-TM-86515] 21 p3678 N85-32847

Invariant tests and likelihood ratio tests for multivariate elliptically contoured distributions
[AD-A155844] 24 p4142 N85-35679

A new method of differential structural analysis of gamma-family basic parameters
[HE-3.6-3] 24 p4184 N85-35952

Study of the time-differentiated particle flux density at various distances from EAS axis
[HE-4.7-15] 24 p4200 N85-36065

MAXWELL EQUATION

Theoretical study of laser-induced surface excitations on a grating
[AD-A147855] 07 p0972 N85-16172

The liner package: An incipient MHD capability for CCUBE
[LA-9969-MS] 12 p1913 N85-22007

An iteration method for complex scattering problems
[AD-A150038] 12 p1934 N85-22151

Nonlinear waves in the magnetosphere of pulsars 12 p1955 N85-22281

Explosive transverse electric field and particle acceleration during magnetic collapse — cosmic plasma 12 p1956 N85-22292

Solutions of field equations in General Relativity with spinor connection 15 p2663 N85-26436

Cavityless optical bistability in systems of two-level atoms 18 p3186 N85-29764

Modeling solar magnetic structures 18 p3203 N85-29872

Trends in measurement of solar vector magnetic fields using the Zeeman effect 18 p3204 N85-29877

Laser forward and backscattering in particulate media
[AD-A154138] 19 p3275 N85-30312

Equations of motion for electromagnetic waves in 4-dimensional Euclidian space 21 p3697 N85-32970

Analysis of the nonlinear equations describing the elastic, thermal, and electromagnetic behavior of solids: Existence of solutions of semi-inverse problems 24 p4100 N85-35415

Relation between field energy and RMS emittance in intense particle beams
[DE85-012655] 24 p4159 N85-35784

MAXWELL FLUIDS

Dynamics of liquid filament breakup
[DE84-016008] 04 p0500 N85-13187

Existence of slow steady flows of viscoelastic fluids with differential constitutive equations
[AD-A147240] 07 p0959 N85-16077

MAXWELL-BOLTZMANN DENSITY FUNCTION

High resolution hard X-ray spectra of solar and cosmic sources 14 p2455 N85-25163

Attenuated total reflection method for obtaining optical constants of powders
[AD-A154094] 19 p3367 N85-30881

The electric current densities beneath thunderstorms 20 p3494 N85-31726

Effect of ECH and ICH on ambipolar potential in NBT-1M 23 p3978 N85-34861

MAXWELLIAN DISTRIBUTION (DENSITY)
U MAXWELL-BOLTZMANN DENSITY FUNCTION

MAYPOLE ANTENNAS

Combined state and parameter estimation for a static model of the Maypole (Hoop-Column) antenna suface 20 p3417 N85-31210

MCDONNELL AIRCRAFT
NT DC 10 AIRCRAFT
NT RF-4 AIRCRAFT

MCDONNELL DOUGLAS AIRCRAFT
NT DC 8 AIRCRAFT
NT DC 9 AIRCRAFT
NT DC 10 AIRCRAFT
NT F-18 AIRCRAFT
NT RF-4 AIRCRAFT

MEADOWLANDS
U GRASSLANDS

MEAN

On the rate of mean convergence of finite linear predictors of multivariate stationary stochastic processes
[AD-A145609] 02 p0254 N85-11664

Estimating the scale parameter of an exponential distribution from a sample of time-censored r-th order statistics
[AD-A148060] 09 p1375 N85-18644

The asymptotic behavior of the likelihood ratio statistic for testing a shift in mean in a sequence of independent normal variates
[AD-A149329] 10 p1550 N85-19779

Asymptotic distributions of the sample mean, autocovariances and autocorrelations of long-memory time series
[AD-A149409] 10 p1551 N85-19781

Motion of symmetrical satellite with flexible viscoelastic rods about center of mass in circular orbit 13 p1979 N85-22420

Microcomputer: Controlled statistics analyzer
[BLL-CE-TRANS-7971-(9022.09)] 13 p2144 N85-23306

The worldwide distribution of the seasonal cycle of mean sea level
[IOS-190] 20 p3497 N85-31743

The mean ionic charge of silicon in 3HE-rich solar flares
[SH-2.2-8] 23 p4000 N85-34803

MEAN FREE PATH

Anomalon search — heavy cosmic ray interactions
[NOTA-INTERNA-825] 02 p0305 N85-11970

Arc-evaporated carbon films: Optical properties and electron mean free paths
[DE85-001246] 06 p0867 N85-15510

Statistical theory of fragmentation processes
[DE85-002206] 11 p1653 N85-20414

Mean free paths, viscosity, and the limitations of perfect fluid hydrodynamics in the description of the quark-gluon plasma
[DE85-005501] 15 p2649 N85-26339

Monte Carlo techniques for analyzing deep penetration problems
[DE85-011426] 23 p3866 N85-34598

Calculation of heavy-ion tracks in liquid water
[DE85-012101] 24 p4149 N85-35725

Penetrative nature of high energy showers observed in Chacaltaya emulsion chamber
[HE-3.3-5] 24 p4180 N85-35923

On mini-cluster observed by Chacaltaya emulsion chamber experiment
[HE-3.6-12] 24 p4185 N85-35969

Search for anomalons using plastic nuclear track detectors
[HE-6.2-12] 24 p4212 N85-36148

Search for acoustic signals from high energy cascades
[HE-7.1-1] 24 p4213 N85-36155

MEAN SQUARE VALUES

A complete characterization of triply balanced matrices with applications to survey sampling
[AD-A147083] 07 p1031 N85-16542

A note on the prediction error for small time lags into the future
[AD-A148221] 08 p1216 N85-17654

Fast moving average recursive least mean square fit
[DE85-010036] 19 p3348 N85-30752

MEANDERS

The gulf stream deflection and meander energetics experiment. Current meter and bottom pressure gauge data report for the September, 1981 to April, 1982 mooring period
[AD-A144977] 01 p0068 N85-10595

MEASURE AND INTEGRATION
NT BOREL SETS
NT INTEGRAL CALCULUS
NT J INTEGRAL
NT NUMERICAL INTEGRATION
NT RUNGE-KUTTA METHOD
NT WEIGHTING FUNCTIONS

Measure determining classes of balls in Banach space
[CTH-MATH-1984-14] 04 p0556 N85-13541

A limit theorem for the superposition of renewal processes
[CWI-MS-R8406] 05 p0722 N85-14636

Generalized predictor-corrector methods of high order for the time integration of parabolic differential equations
[CWI-NM-R8402] 08 p1214 N85-17644

A conformal mapping suitable for problems involving interaction between given geometries and known far fields
[AD-A149060] 10 p1545 N85-19744

Developments in microelectronics: Past and future 15 p2530 N85-25597

Relaxation methods for hyperbolic equations
[REPT-84-20] 17 p3021 N85-28687

State Weights and Measures Laboratories: Program handbook
[PB85-183358] 18 p3111 N85-29263

Some properties of Loeb-Sobolev spaces
[CTH-MATH-1985-01] 22 p3835 N85-33748

MEASURE THEORY
U MEASURE AND INTEGRATION
MEASUREMENT
Measurement assurance programs. Part 2: Development and implementation
[PB84-217876] 01 p0051 N85-10338
Measurement assurance programs. Part 1: General introduction
[PB84-217868] 01 p0051 N85-10339
Water resources data for Michigan, water year 1983
[PB84-225176] 01 p0066 N85-10442
Method for measuring haze in transparencies
[AD-D011233] 01 p0120 N85-10823
Quantization study for ERS-1 wave mode
[DFVLR-FB-84-39] 11 p1625 N85-20234
State measurement laboratories: Program description (part 1). Directory (part 2)
[PB85-137651] 11 p1739 N85-20935
In situ thin film measurements
[AD-A151379] 15 p2652 N85-26353
Principles of quality assurance of chemical measurements
[PB85-177947] 18 p3072 N85-28997
Use of the VAD technique and measurements of momentum flux in the stratosphere at Arecibo, part 4.3A
21 p3622 N85-32505
Measurement control for plutonium isotopic measurements using gamma-ray spectrometry
[DE85-013394] 24 p4097 N85-35397
MEASURES
Invariant measures and the equicontinuous structure relation 1
[CWI-PM-R8403] 05 p0723 N85-14645
Invariant measures and the equicontinuous structure relation 2: The relative case
[CWI-PM-R8404] 05 p0723 N85-14646
MEASURING
U MEASUREMENT
MEASURING INSTRUMENTS
NT ACCELEROMETERS
NT ACTINOMETERS
NT ALTIMETERS
NT AMMETERS
NT ANALYZERS
NT ANEMOMETERS
NT APPROACH INDICATORS
NT ASTROLABES
NT ATOMIC CLOCKS
NT ATTITUDE INDICATORS
NT AUTONOMOUS SPACECRAFT CLOCKS
NT BALLOON-BORNE INSTRUMENTS
NT BAROMETERS
NT BATHYMETERS
NT BATHYTHERMOGRAPHS
NT BOLOMETERS
NT CALORIMETERS
NT CERENKOV COUNTERS
NT CHRONOMETERS
NT CLOCKS
NT CLOUD HEIGHT INDICATORS
NT COMPARATORS
NT COMPASSES
NT COULOMETERS
NT COUNTERS
NT CYCLOTRON RESONANCE DEVICES
NT DENSIMETERS
NT DENSITOMETERS
NT DIFFRACTOMETERS
NT DISTANCE MEASURING EQUIPMENT
NT DOSIMETERS
NT DYNAMOMETERS
NT ELECTRICAL CONDUCTIVITY METERS
NT ELECTROMETERS
NT ELECTRON PROBES
NT ELECTROPHOTOMETERS
NT ELECTROSTATIC PROBES
NT ELLIPSOMETERS
NT ENGINE ANALYZERS
NT ENGINE MONITORING INSTRUMENTS
NT ERGOMETERS
NT EXTENSOMETERS
NT FABRY-PEROT INTERFEROMETERS
NT FABRY-PEROT SPECTROMETERS
NT FIELD INTENSITY METERS
NT FLAME PROBES
NT FLIGHT LOAD RECORDERS
NT FLIR DETECTORS
NT FLOW DIRECTION INDICATORS
NT FLOWMETERS
NT FUEL GAGES
NT GALVANOMETERS
NT GAMMA RAY SPECTROMETERS
NT GAS METERS
NT GONIOMETERS
NT GRAVITY GRADIOMETERS
NT GYRO HORIZONS
NT GYROCOMPASSES
NT HELIOMETERS
NT HODOSCOPES
NT HOT-FILM ANEMOMETERS
NT HOT-WIRE ANEMOMETERS
NT HOT-WIRE FLOWMETERS
NT HYGROMETERS
NT IMPEDANCE PROBES
NT INDICATING INSTRUMENTS
NT INFRARED DETECTORS
NT INFRARED INSTRUMENTS
NT INFRARED INTERFEROMETERS
NT INFRARED RADIOMETERS
NT INFRARED SCANNERS
NT INFRARED SPECTROMETERS
NT INFRARED SPECTROPHOTOMETERS
NT INTERFEROMETERS
NT ION PROBES
NT IONIZATION GAGES
NT IONOSONDES
NT LASER ANEMOMETERS
NT LASER DOPPLER VELOCIMETERS
NT LASER RANGE FINDERS
NT LASER SPECTROMETERS
NT LIGHT SCATTERING METERS
NT MAGNETIC PROBES
NT MAGNETOMETERS
NT MANOMETERS
NT MASS SPECTROMETERS
NT METEOROLOGICAL INSTRUMENTS
NT MICHELSON INTERFEROMETERS
NT MICROBALANCES
NT MICRODENSITOMETERS
NT MICROWAVE INTERFEROMETERS
NT MICROWAVE PROBES
NT MICROWAVE RADIOMETERS
NT MICROWAVE REFLECTOMETERS
NT MICROWAVE SENSORS
NT MICROWAVE SPECTROMETERS
NT MOISTURE METERS
NT MONOCHROMATORS
NT MULTISPECTRAL BAND SCANNERS
NT NEPHELOMETERS
NT NEUTRON COUNTERS
NT NEUTRON SPECTROMETERS
NT OCULOMETERS
NT OMEGA NAVIGATION SYSTEM
NT OPTICAL MEASURING INSTRUMENTS
NT OPTICAL RANGE FINDERS
NT OPTICAL SCANNERS
NT OSCILLOGRAPHS
NT OXYGEN ANALYZERS
NT PARTICLE TELESCOPES
NT PASSIVE L-BAND RADIOMETERS
NT PENETROMETERS
NT PHOTOGONIOMETERS
NT PHOTOMETERS
NT PIEZOELECTRIC GAGES
NT PLAN POSITION INDICATORS
NT PLASMA PROBES
NT POLARIMETERS
NT POSITION INDICATORS
NT POTENTIOMETERS (INSTRUMENTS)
NT PRESSURE GAGES
NT PROFILOMETERS
NT PROPORTIONAL COUNTERS
NT PYRANOMETERS
NT PYROHELIOMETERS
NT PYROMETERS
NT QUANTUM COUNTERS
NT RADIATION COUNTERS
NT RADIATION DETECTORS
NT RADIATION MEASURING INSTRUMENTS
NT RADIO ALTIMETERS
NT RADIO DIRECTION FINDERS
NT RADIO INTERFEROMETERS
NT RADIOMETERS
NT RADIOSONDES
NT RAIN GAGES
NT RANGE FINDERS
NT RAWINSONDES
NT REFLECTOMETERS
NT RESISTANCE THERMOMETERS
NT RESONANCE PROBES
NT RHEOMETERS
NT RIOMETERS
NT SATELLITE-BORNE INSTRUMENTS
NT SCATTEROMETERS
NT SCINTILLATION COUNTERS
NT SEISMOGRAPHS
NT SIGNAL ANALYZERS
NT SILICON RADIATION DETECTORS
NT SMOKE DETECTORS
NT SOLAR SPECTROMETERS
NT SONDES
NT SPACECRAFT POSITION INDICATORS
NT SPARK CHAMBERS
NT SPECTROHELIOGRAPHS
NT SPECTROMETERS
NT SPECTROPHOTOMETERS
NT SPECTRORADIOMETERS
NT SPEED INDICATORS
NT SPUTTERING GAGES
NT STRAIN GAGE ACCELEROMETERS
NT STRAIN GAGES
NT TACHOMETERS
NT TEMPERATURE MEASURING INSTRUMENTS
NT TEMPERATURE PROBES
NT TENSIOMETERS
NT THEODOLITES
NT THERMOCOUPLE PYROMETERS
NT THERMOMETERS
NT THRESHOLD DETECTORS (DOSIMETERS)
NT TILTMETERS
NT TIME MEASURING INSTRUMENTS
NT TIME OF FLIGHT SPECTROMETERS
NT TIMING DEVICES
NT TORQUEMETERS
NT TRANSMISSOMETERS
NT TURBULENCE METERS
NT ULTRAVIOLET SPECTROMETERS
NT ULTRAVIOLET SPECTROPHOTOMETERS
NT VARIOMETERS
NT VIBRATION METERS
NT VOLTMETERS
NT WATTMETERS
NT WEATHER DATA RECORDERS
NT WEIGHT INDICATORS
NT WIND VANES
Pavement friction measurements on nontangent sections of roadways, vol. 1
[PB84-219732] 01 p0036 N85-10227
Aspects and applications of SAR (Synthetic Aperture Radar) imagery for mensuration
[AD-A146301] 03 p0356 N85-12290
Method for evaluating petrol products corrosivity using piezoelectric crystals. Part 2: Instruction manual -- jet engine corrosion tests
[FOA-C-40198-B4] 04 p0482 N85-13073
Portable instrument for the detection and identification of air pollutants
[DE84-014767] 05 p0672 N85-14316
Assessment of Techniques for Measuring Tropospheric H sub x O sub y
[NASA-CP-2332] 05 p0675 N85-14336
Assessment of Techniques for Measuring Tropospheric H sub x O sub y: Summary 05 p0675 N85-14337
Experimentation and measurement
[PB84-233659] 06 p0812 N85-15157
East Europe report: Science and technology
[JPRS-ESA-84-045] 06 p0815 N85-15175
Laser-guided measuring system for precisioning device 06 p0816 N85-15179
Advanced fatigue monitoring on service aircraft
07 p0895 N85-15671
The determination of vertical sintering speed of sinter charges
[BLL-M-36033-(5828.4)] 07 p0928 N85-15899
Gallium arsenide compounds tested nondestructively with X-rays 07 p0936 N85-15884
Performance characteristics of a battery charger and state-of-charge indicator
[NASA-CR-174273] 07 p0946 N85-15982
Ensuring required metrological reliability of analog instrument channels by parametric compensation
07 p0955 N85-16050
High temperature thermocouple and heat flux gauge using a unique thin film-hardware hot juncture
[NASA-TM-86898] 07 p0962 N85-16096
A narrow band pulsed eddy current instrument for materials testing
[AERE-R-11229] 07 p0968 N85-16149
Data acquisition, measurement devices at 1984 Leipzig Spring Fair 09 p1378 N85-18881
Radiation response of optical fibers in a nuclear reactor
[DE84-017221] 09 p1385 N85-18710
Electromagnetic compatibility of measurement and control equipment in nuclear installations
[BLL-WH-607-(9091.9F)] 11 p1623 N85-20222
Liquid thickness gage
[NASA-CASE-LAR-13342-1] 11 p1635 N85-20297
Precision volume measuring system
[DE85-002569] 11 p1636 N85-20305
In-situ detection of micron-sized dust particles in near-Earth space 12 p1765 N85-21225
Transistor-transistor logic microcircuit tester
12 p1842 N85-21558
Program for controlling electrical measuring contact instrument on glow-discharge indicator panel
12 p1842 N85-21559

Self-charging metering and dispensing device for fluids
[NASA-CASE-MSC-20275-1] 12 p1846 N85-21595
Dielectric measurements in infralow-frequency band
13 p2067 N85-23034
Proceedings of the Geoscience Instrumentation Workshop
[DE85-004359] 13 p2132 N85-23268
Monitoring of laminate cure with microdielectrometry
[AD-A150863] 14 p2248 N85-23934
New electronic measurement, control devices
14 p2289 N85-24192
An atlas of pure water vapor spectra from 500 to 5000/cm, volume 1
[AD-A151756] 15 p2505 N85-25454
Instrument for measuring dispersional distortions in optical fibers and cables 15 p2530 N85-25595
Advanced smoke meter development survey and analysis
[NASA-CR-168287] 15 p2560 N85-25792
Development and diffusion of automated clinical chemistry analyzers
[PB85-150696] 15 p2561 N85-25796
Three new fiber-optic components
[DE85-008269] 15 p2653 N85-26364
Study of acceptance criteria for joint densities in bituminous airport pavements
[FAA-PM-85-5] 16 p2715 N85-26761
Free-surface phenomena under low- and zero-gravity conditions
[NASA-CR-175835] 16 p2782 N85-27166
A transduction path method of solid state sensor analysis and investigation
[AD-A152123] 16 p2870 N85-27707
Uniaxial angular accelerometers
17 p2944 N85-28173
Apparatus for measuring velocity of sound in fluids
17 p2944 N85-28175
Technique for measuring the effective source reflection coefficient of 2-resistor power splitters
[DE85-009964] 17 p2956 N85-28256
Theoretical and experimental studies of the mechanics of viscoelastic liquids
[AD-A153505] 18 p3070 N85-28987
Oscillating pressure device for dynamic calibration of pressure transducers
[NASA-CASE-LAR-13094-1] 18 p3104 N85-29217
State Weights and Measures Laboratories: Program handbook
[PB85-183358] 18 p3111 N85-29263
A simple power meter for high energy pulsed lasers
[AD-D011661] 18 p3113 N85-29271
Ultrasonic testing of tubes
[BLL-BISI-TRANS-22337-(9022.06)]
18 p3119 N85-29304
Electrodynamic transducers for ultrasonic reception
18 p3119 N85-29306
Rapid rate-kinetic turbidometric assay for quantitation of antiviral complement-fixing antibodies
[AD-A153644] 18 p3152 N85-29518
Multiport optical detectors 18 p3187 N85-29769
A laser slope gauge and a spar buoy wave gauge: Tools for the validation of microwave remote sensors
[AD-A154038] 19 p3272 N85-30290
Transport and relaxation processes in supercritical fluids
[DE85-010554] 19 p3356 N85-30816
Proceedings of the Electronic Test Equipment Division's Annual Program Review of Electronic Test Equipment Industry Response to Emerging Defense Requirements
[AD-A154455] 20 p3436 N85-31320
New measurement solutions in the microwave industry
20 p3437 N85-31324
An overview of measurement solutions for digital systems 20 p3437 N85-31326
Solid surface characterization by contact angle measurements
[FOA-C-40209-C,B2] 20 p3459 N85-31483
Improved coordinate measuring machine calibration and control
[DE85-012053] 21 p3590 N85-32315
Digital tachometer 22 p3779 N85-33416
Capacitance measuring device
[DE85-011643] 22 p3787 N85-33460
Electrochemical methane sensor
[DE85-011663] 22 p3787 N85-33464
On-line temperature sensor
[DE85-011641] 22 p3787 N85-33465
Evaluation of coordinate measuring machines
[DE85-011712] 22 p3788 N85-33467
Development of a prototype energy meter
[PB85-186430] 22 p3789 N85-33476
Instrumentation for sensing moisture content of material using a transient thermal pulse
[NASA-CASE-NPO-15493-2] 23 p3933 N85-34373
Apparatus and method for the spectrochemical analysis of liquids using the laser spark
[DE85-005749] 23 p3935 N85-34387
Improved flow cytometer measurement of binding assays
[DE85-006407] 23 p3935 N85-34390
Hydrology
[PB85-182964] 23 p3944 N85-34440
Measurement of low energy cosmic rays aboard Spacelab-1
[SH-10.1-6] 23 p4053 N85-35137
Analyzer, flight line
[AD-A155777] 24 p4067 N85-35207
Development of advanced high-temperature heat flux sensors. Phase 2: Verification testing
[NASA-CR-174973] 24 p4096 N85-35391
Atmospheric nitrogen oxides: Their detection and chemistry
[PB85-193910] 24 p4114 N85-35502
Development of an NBS (National Bureau of Standards) polymer gage for dynamic soil stress measurement
[PB85-208494] 24 p4116 N85-35526

MECHANICAL DEVICES
Stimulus factors in motion perception and spatial orientation 01 p0006 N85-10049
On the computer analysis of structures and mechanical systems 01 p0061 N85-10404
Materials properties, loads, and stress analysis, Spartan REM: Appendix A
[NASA-CR-171092] 02 p0208 N85-11375
Computer models and output, Spartan REM: Appendix B
[NASA-CR-171093] 02 p0208 N85-11376
Kinematic synthesis of planar cam-link mechanisms for exact path and exact motion generation
03 p0341 N85-12169
Soviet robot exhibition reviewed
04 p0491 N85-13128
Swing-arm beam erector (SABER) concept for single astronaut assembly of space structure
[NASA-TP-2379] 10 p1429 N85-19015
Planning of minimum-time trajectories for robot arms
[AD-A148956] 10 p1492 N85-19418
Hoist
[AD-D011458] 10 p1493 N85-19425
Extended moment arm anti-spin device
[NASA-CASE-LAR-12979-1] 12 p1776 N85-21147
Maintainability time standards for electronic equipment
[AD-A149684] 12 p1834 N85-21507
Connection system — insuring against loss of a tool component without using multiple tethers
[NASA-CASE-MSC-20319-1] 12 p1857 N85-21649
Mechanical properties for the grasp of a robotic hand
[AD-A150062] 12 p1860 N85-21669
Cyclic industrial robots with mechanical energy storing devices: Principles of drive design
13 p2046 N85-22807
Optimum design and automated dynamic analysis of flexible mechanisms
[AD-A150152] 13 p2099 N85-23088
Stabilization of steady motion of mechanical systems
14 p2280 N85-24122
Auxiliary units for Robots 14 p2285 N85-24161
Preliminary technology utilization assessment of the robotic fruit harvester
[NASA-CR-175634] 16 p2844 N85-27532
Apparatus for mounting a field emission cathode
[NASA-CASE-LEW-14108-1] 18 p3094 N85-29149
Hoop/column antenna deployment mechanism overview 22 p3796 N85-33514
The properties of thin-section, four-point-contact ball bearings in space 22 p3797 N85-33521
The design and development of a spacecraft appendage tie down mechanism 22 p3797 N85-33522
The balancing of complex linkage mechanisms
23 p3924 N85-34313
A versatile computer package for mechanism analysis
23 p3924 N85-34314
A versatile computer package for mechanism analysis, part 2: Dynamics and balance
23 p3924 N85-34315

MECHANICAL DRAWINGS
U ENGINEERING DRAWINGS

MECHANICAL DRIVES
NT HELICOPTER PROPELLER DRIVE
NT TRANSMISSIONS (MACHINE ELEMENTS)
Vibrational power transmission of an idealised gearbox
[ISVR-TR-124] 02 p0204 N85-11346
Nitinol devices, phase 2, integration of slip ring system and tracking mechanism with memory drive
[BMFT-FB-W-84-032] 05 p0619 N85-13959
Torque sensor
[AD-D011276] 05 p0639 N85-14096
Space shuttle rudder/speedbrake actuation subsystem
08 p1102 N85-16965
Specifications of bloc floppy disk drives
08 p1141 N85-17188
MOM peripherals 08 p1141 N85-17189
Acoustic radiation from single and double ribbed circular cylindrical shells
[AD-A148771] 08 p1219 N85-17676
Precision measurement of torsional oscillations induced by gear errors 09 p1338 N85-18416
Adjustment structure
[AD-D011461] 10 p1459 N85-19193
Armenia markets new drive motors for machine tools
10 p1461 N85-19212
Antenna axle drive torques for the 70-meter antenna
10 p1464 N85-19237
Characteristics of the elevation drive suspension of the 64-meter antennas 10 p1464 N85-19240
Seven-year thermal-vacuum real-life test of a solar array drive mechanism manufactured by Marconi Space and Defence Systems (Model No. 002)
[ESA-ESTL-62] 11 p1616 N85-20161
Design of tightening device and calculation of forces in manipulator transmissions with base-drive mounted
13 p2046 N85-22804
Cyclic industrial robots with mechanical energy storing devices: Principles of drive design
13 p2046 N85-22807
Assembly robot control algorithms
13 p2046 N85-22808
Summary of drive-train component technology in helicopters 14 p2220 N85-23766
Special power train requirements for the next generation of rotary-wing aircraft 14 p2220 N85-23769
Pneumohydraulic drive 14 p2268 N85-24050
Novel drives for machine tools
14 p2268 N85-24053
Manufacture of drive wheel vanes for hydraulic turbines on program controlled machine tools
14 p2269 N85-24056
Solid state compressor
[AD-A150790] 14 p2311 N85-24302
Thermal traction contact performance evaluation under fully flooded and starved conditions
[NASA-CR-168173] 15 p2568 N85-25848
A description of the 64-meter antenna elevation drive gears and their strange wear 16 p2771 N85-27107
AC powertrain for an electric vehicle, phase 2 and phase 3
[NASA-CR-175780] 16 p2880 N85-27771
Vibrations of rotors connected through couplings with backlash 17 p2940 N85-28147
Remotely operable peristaltic pump
[NASA-CASE-MFS-28059-1] 18 p3116 N85-29288
Study of meshing of beveled gears with normally decreasing arc teeth
[NASA-TM-77866] 18 p3117 N85-29293
Improvement of conditions for meshing spiral bevel gears
[NASA-TM-77867] 18 p3117 N85-29294
Observations of high resistance on slip-rings employing Ag/MoS2/Cu brushes — solar array drives
[ESA-ESTL-70] 18 p3123 N85-29333
Department of Energy gear drive unit final prototype testing and design evaluation
[DE85-003296] 22 p3793 N85-33499
Ninteenth Aerospace Mechanisms Symposium
[NASA-CP-2371] 22 p3795 N85-33512
Drag-compensated, precision-powered hinge system
22 p3796 N85-33517
The design and development of a constant-speed solar array drive 22 p3796 N85-33519
Application of traction drives as servo mechanisms
22 p3797 N85-33520
Features of the solar array drive mechanism for the space telescope 22 p3798 N85-33532
Dual optical mechanical position tracker
[AD-D011739] 22 p3844 N85-33811
High powered epicyclic gears: Some recent development 23 p3924 N85-34316
State-of-the-art of solid-state motor controllers
[TI85-006674] 24 p4162 N85-35806

MECHANICAL ENGINEERING
National Science Foundation grants and awards for fiscal year 1983, volume 2
[PB84-212323] 01 p0125 N85-10854
Activities report of the Department of Engineering
03 p0342 N85-12202
Heavy duty precision pan and tilt head
[AD-A148669] 04 p0509 N85-13246
Activities report in technology
[ISBN-951-38-1998-1] 04 p0577 N85-13681
BAe antenna hardware technology for current satellite projects 05 p0626 N85-14011
Hemispherical antenna pointing mechanism — satellite antennas 05 p0627 N85-14021
Machine tools at 1984 Leipzig Spring Fair
06 p0815 N85-15177

A summary of the foundation research program
[AD-A146524] 06 p0691 N85-15856
Research and technology, 1984 report
[NASA-TM-83096] 07 p1061 N85-16730
Eigenvalues of rotating machinery
08 p1167 N85-17361
The analysis of kinematic restraint and freedom using point contacts
[RR-154/03/75/02] 08 p1169 N85-17372
The synthesis of kinematic restraint and freedom using point contacts
[RR-154/03/75/03] 08 p1169 N85-17373
Technical data on new engineering products
10 p1460 N85-19201
Flexible applications robot used in Moscow training course 10 p1462 N85-19217
Design and qualification testing of the Olympus solar array blanket 13 p2009 N85-22600
The Olympus solar array structure and mechanisms
13 p2012 N85-22623
Advances in cutting tool technology surveyed
13 p2051 N85-22840
The design and validation of software for dimensional metrology
[NPL-DITC-50/84] 15 p2521 N85-25542
Compilation of abstracts of theses submitted by candidates for degrees
[AD-A151722] 16 p2875 N85-27730
Micro-CAE mechanical engineering software development at Lawrence Livermore National Laboratory and participating universities and technology transfer
[DE85-008660] 18 p3163 N85-29597
Special tools used by cosmonauts in EVA
22 p3731 N85-33129
Proceedings of the Mechanisms Conference, volume 1 23 p3923 N85-34309
Proceedings of the Mechanisms Conference, volume 2 23 p3924 N85-34318
An introduction to finite elements
23 p3924 N85-34319
Inertial stresses and deformations in mechanisms
23 p3924 N85-34320
Optimisation in the computer aided design of mechanisms 23 p3924 N85-34321

MECHANICAL MEASUREMENT
NT DISPLACEMENT MEASUREMENT
NT DRAG MEASUREMENT
NT FLOW MEASUREMENT
NT FRICTION MEASUREMENT
NT PRESSURE MEASUREMENT
NT STRESS MEASUREMENT
NT THRUST MEASUREMENT
NT VELOCITY MEASUREMENT
NT VIBRATION MEASUREMENT
NT WIND MEASUREMENT
NT WIND VELOCITY MEASUREMENT
Measuring and control tasks in OPTIWA
05 p0669 N85-14304
Viscosity measurements for thick-film pastes
06 p0831 N85-15280
Application of the unloading compliance methods in fracture toughness measurements of a quenched and tempered steel
[BLL-CE-TRANS-7953-(9022.09)]
20 p3465 N85-31523
A versatile computer package for mechanism analysis
23 p3924 N85-34314

MECHANICAL OSCILLATORS
NT PENDULUMS
Measurement of blood and plasma density with the mechanical oscillator technique
05 p0693 N85-14456
Quality control in soil compaction by behaviours of exciter
[AD-P004295] 09 p1408 N85-18872
Precise bearing support ditherer
[AD-D011470] 10 p1493 N85-19426
Investigation of the time history and modal responses of some simple linear and nonlinear systems
[DE85-002027] 14 p2321 N85-24344
Method for controlling the viscosity of siloxane oils
[DE85-011586] 23 p3909 N85-34221

MECHANICAL PROPERTIES
NT ABRASION RESISTANCE
NT AEROELASTICITY
NT BRITTLENESS
NT BULK MODULUS
NT COMPRESSIBILITY
NT COMPRESSIVE STRENGTH
NT CREEP PROPERTIES
NT CREEP RUPTURE STRENGTH
NT CREEP STRENGTH
NT DIMENSIONAL STABILITY
NT DUCTILITY
NT DYNAMIC MODULUS OF ELASTICITY
NT EARTHQUAKE RESISTANCE
NT ELASTIC PROPERTIES
NT ELASTOPLASTICITY
NT ELECTROSTRICTION
NT FATIGUE LIFE
NT FIBER STRENGTH
NT FLEXIBILITY
NT FRACTURE STRENGTH
NT HARDNESS
NT HIGH STRENGTH
NT HYDROELASTICITY
NT IMPACT STRENGTH
NT KNOOP HARDNESS
NT MAGNETOSTRICTION
NT MALLEABILITY
NT MICROHARDNESS
NT MICROYIELD STRENGTH
NT MODULAR RATIOS
NT MODULUS OF ELASTICITY
NT NOTCH SENSITIVITY
NT NOTCH STRENGTH
NT PHOTOELASTICITY
NT PHOTOPLASTICITY
NT PHOTOVISCOELASTICITY
NT PIEZOELECTRICITY
NT PLASTIC PROPERTIES
NT POISSON RATIO
NT PROPORTIONAL LIMIT
NT RESILIENCE
NT SHEAR CREEP
NT SHEAR PROPERTIES
NT SHEAR STRENGTH
NT SHELL STABILITY
NT STEADY STATE CREEP
NT STIFFNESS
NT STRESS CYCLES
NT STRESS RATIO
NT STRESS RELAXATION
NT STRUCTURAL STABILITY
NT SUPERPLASTICITY
NT TENSILE CREEP
NT TENSILE PROPERTIES
NT TENSILE STRENGTH
NT THERMAL RESISTANCE
NT THERMOELASTICITY
NT THERMOPLASTICITY
NT THERMOVISCOELASTICITY
NT TOUGHNESS
NT VISCOELASTICITY
NT VISCOPLASTICITY
NT WELD STRENGTH
NT YIELD POINT
NT YIELD STRENGTH
Development of new and improved polymer matrix resin systems, phase 1
[NASA-CR-166595] 01 p0017 N85-10104
Effect of scandium on the structure and properties of Al-Zn-Mg alloys 01 p0018 N85-10111
Heat treatment of welded joints in OT4 and VT20 titanium alloys 01 p0020 N85-10119
Influence of nitrogen on the sensitization, corrosion, mechanical, and microstructural properties of austenitic stainless steels
[DE84-015134] 01 p0028 N85-10177
Fabrication and characterization of Si3N4 ceramics without additives by high pressure hot pressing
[NASA-TM-77724] 01 p0031 N85-10189
Diblock copolymers of polystyrene/1,2 polybutadiene and polystyrene/polybutene-1: Molecular structure, morphology and mechanical properties
[AD-A144960] 01 p0033 N85-10201
Electrically conductive rigid polyurethane foam
[DE84-014490] 01 p0033 N85-10203
Broadband transverse field interaction continuous beam amplifier
[AD-D011229] 01 p0043 N85-10279
Ultrasonic nondestructive evaluation, microstructure, and mechanical property interrelations
[NASA-TM-86876] 01 p0056 N85-10371
Materials studies for magnetic fusion energy applications at low temperatures, 7
[DE84-013487] 01 p0122 N85-10837
Laser speckle technique for burner liner strain measurements 02 p0142 N85-10960
Microstructural design in low alloy steels
02 p0176 N85-11179
Toughness in high speed steels and hard metals
02 p0176 N85-11181
The constitution as the basis for recent and future developments of wear resistant materials
02 p0179 N85-11205
Physical-chemical properties of articulated rodlike polymers
[AD-A145549] 02 p0186 N85-11244
Silicon nitride joining
[AD-A145668] 02 p0187 N85-11248
Method of making a porous carbon cathode: A poro carbon cathode so made, and electrochemical including the porous carbon cathode
[AD-D011243] 02 p0195 N85-11
Materials properties, loads, and stress analysis, Spa REM: Appendix A
[NASA-CR-171092] 02 p0206 N85-11
Use of magnetic compression based on amorpho alloys as a drive for induction linacs
[DE84-014524] 02 p0277 N85-11
Optical waveguide spatial filters
[AD-A145674] 02 p0280 N85-11
Materials modification by ion beam mixing
[AD-P003948] 02 p0286 N85-11
Review of the University of Manchester Ion Implanta Conference
[AD-P003950] 02 p0286 N85-11
Mechanical properties of a leaded, resulfurized, rephosphorized steel in various thermo/mechanical conditions
[PB84-216464] 03 p0333 N85-12
Guide to the selection of rubbers
[AMTE(N)-TM-84301] 03 p0336 N85-12
USSR report: Materials science and metallurgy
[JPRS-UMS-84-007] 03 p0348 N85-12
Causes of strength reduction in welded titanium-stee joints 03 p0352 N85-12
Reinforcement of molybdenum disilicide with nema crystals of aluminum oxide 03 p0353 N85-12
Constitutive features of solids at shock-wave loadin rates
[DE84-015715] 03 p0362 N85-12
Static and dynamic characteristics of materials wit beam-microstructure 03 p0370 N85-12
Review: Role of refractory metal alloys in fusion reacto applications
[AERE-R-11317] 03 p0422 N85-12
Morphology and dynamic mechanical properties o diglycidyl ether of bisphenol-A toughened wit carboxyl-terminated butadiene-acrylonitrile
04 p0466 N85-12
Matrix synthesis and characterization
04 p0467 N85-12
Experimental and theoretical studies of moisture an temperature effects on the mechanical properties o graphite/epoxy laminates and neat resins
04 p0467 N85-12
High temperature mechanical properties of ceramic
[DE84-016492] 04 p0480 N85-13
Nondestructive determination of mechanical propertie — aluminum alloys 04 p0512 N85-13
Arctic ice island and sea ice movements and mechanical properties
[DE84-016323] 04 p0542 N85-13
Investigation of the relations between neat resin and advanced composite mechanical properties. Volume 1: Results
[NASA-CR-172303] 05 p0612 N85-13
Characterization of stressed metals using acoustic shear waves 05 p0648 N85-14
Theoretical methods for the study of transition metals in crystals
[DE84-015606] 05 p0732 N85-14
Investigation of the relations between resin and advanced composite mechanical properties. Volume 2: Appendices
[NASA-CR-172303-VOL-2] 06 p0763 N85-14
The metallurgical processes during the soft soldering of copper and copper alloys and the strength characteristics of soldered joints
[BLL-T6388/BG/WH803/84] 06 p0767 N85-14
Effect of substituted phenylnadimides on processing and properties of PMR polyimide composites
[NASA-TM-86902] 06 p0770 N85-14
Effects of surface interactions and mechanical properties of PBXs (plastic bonded explosives) o explosive sensitivity
[AD-A146368] 06 p0773 N85-14
A nonnoble front metallization process
06 p0830 N85-15
Size dependence of chondrule textural types
06 p0862 N85-15
Titanium Matrix/Continuous Fiber/Continuous fiber composite interface interactions and their influence o mechanical properties
[AD-A147504] 07 p0920 N85-15
Austenitic stainless steel for high temperature and pressure applications
[BLL-RISLEY-TR-4527-(9091.9F)]
07 p0925 N85-15
Design of ordered intermetallic alloys fo high-temperature structural use
[DE85-000697] 07 p0926 N85-15
Gradient polymers
[AD-A146836] 07 p0931 N85-15

Thermal and mechanical properties of polyurethane foams and a survey of insulating concretes at cryogenic temperatures
[PB85-100949/GAR] 07 p0934 N85-15918

Determination of the decomposition behavior of double base propellants at low temperatures
08 p1117 N85-17045

Effects of high energy radiation on the mechanical properties of epoxy-graphite fiber reinforced composites
[NASA-CR-174314] 08 p1118 N85-17047

ESR (Electroslag Refining) technology in Australia: Laboratory research and industrial development
[AD-A147770] 08 p1129 N85-17114

Mechanical properties and microstructure of centrifugally cast alloy 718
[AD-A147800] 08 p1129 N85-17116

Review of the mechanical properties of SMC and GRP materials
[NPL-DMA(A)-86] 08 p1131 N85-17128

Field test results of experimental EPDM (Ethylene Propylene Diene Monomer) and PUF (Polyurethane Foam) roofing
[AD-A147697] 08 p1132 N85-17133

Process development for the production of technically high quality monocrystalline diamond grits
[BMFT-FB-T-84-204] 08 p1138 N85-17186

Effect of iron on the performance of IN 625 weld deposits
[BR91456] 08 p1169 N85-17376

Age life prediction of nylon 66 parachute materials. Part 1: Mechanical properties
[AD-A147696] 08 p1170 N85-17378

The Shock and Vibration Digest, volume 16, no. 10
[AD-A147566] 09 p1331 N85-18361

Physical characterization of magma
[DE85-000568] 09 p1354 N85-18519

Magnetic fusion energy plasma interactive and high heat flux components. Volume 2: Technical assessment of the critical issues and problem areas in high heat flux materials and component development
[DE85-001155] 09 p1393 N85-18764

Online directory of databases for material properties
[DE84-016511] 09 p1402 N85-18824

Mechanics of composite materials
[DE85-003611] 10 p1432 N85-19031

Mechanical properties of Be-Al composite
10 p1443 N85-19094

Quantitative estimate of compatibility of fiber composite material components 10 p1444 N85-19099

Influence of laser hardening on mechanical properties of type 45 steel with various preliminary heat treatments
10 p1446 N85-19111

Kinetics of joint formation during diffusion welding of VT5 titanium alloys 10 p1448 N85-19125

Modern solid state laser materials
[DE85-003665] 10 p1490 N85-19410

Mechanical interactions of rough surfaces
[DE85-000814] 10 p1494 N85-19434

Study of the physical properties of crystalline rocks in the southeast Voronezh anteclise
[NASA-TM-77823] 10 p1514 N85-19551

Strength properties of unidirectionally reinforced hybrid composites 11 p1599 N85-20056

Effect of silicon and titanium properties on Ni18Co9Mb5Ti steel 11 p1601 N85-20069

Dependence of mechanical properties of large VT3-1 alloy forgings on microstructure parameters
11 p1602 N85-20072

Effect of macrostructure on durability of polycrystalline graphite 11 p1605 N85-20091

Method for increasing linearity of load cell
11 p1623 N85-20221

Report of the Technology and Test Panel
11 p1646 N85-20370

Requirements of quantitative NDE in developing fracture control plans
[DE85-003147] 11 p1654 N85-20415

Magnetic and structural properties of shock-synthesized zinc ferrite
[DE85-000469] 11 p1736 N85-20915

A DOE directory of databases for material properties
[UCAR-10124] 11 p1739 N85-20937

Composite structural materials
[NASA-CR-175515] 12 p1796 N85-21268

Effect of reduction of strategic Columbium addition in 718 Alloy on the structure and properties
[NASA-CR-174841] 12 p1805 N85-21320

Effects of chromium and aluminum on mechanical and oxidation properties of iron-nickel-base superalloys based on CG-27
[NASA-TP-2443] 12 p1805 N85-21323

Elastomer toughened polyimide adhesives --- bonding metal and composite material structures for aircraft and spacecraft
[NASA-CASE-LAR-12775-2] 12 p1809 N85-21349

Broadband thermoplastic radomes
[AD-P004369] 12 p1827 N85-21483

A new model for thin plates with rapidly varying thickness. Part 3: Comparison of different scalings
[AD-A149748] 12 p1866 N85-21704

Summary of recent research on mechanical behavior of polycrystalline solids
[DE85-004601] 12 p1942 N85-22199

Research Reports: 1984 NASA/ASEE Summer Faculty Fellowship Program
[NASA-CR-171317] 12 p1944 N85-22210

Investigation of the effects of NaOH dopant level on the physical and mechanical properties of carbon/phenolic composite material 12 p1945 N85-22213

Solid Rocket Motor Case (SRMC) dynamic sensitivity to changes in composite properties
12 p1948 N85-22238

Kapton charging characteristics: Effects of material thickness and electron-energy distribution
13 p1996 N85-22513

Influence of external electric field on structural-mechanical properties of powdered materials
13 p2013 N85-22630

Rapid solidification processing of magnesium alloys
[AD-A150270] 13 p2022 N85-22668

Mechanical properties of electrodeposited nickel and copper
[DE85-005321] 13 p2023 N85-22677

Influence of laser treatment of structure and mechanical properties if MA21 alloy 13 p2029 N85-22713

Influence of annealing on cyclic and short-term strength of thin sheets of VT1-0 titanium and OTR4 alloy
13 p2031 N85-22727

Method of calculating strength of joint produced by cold welding of aluminum under discrete loading
13 p2034 N85-22743

Effect of moisture in inert gases on density of seam metal and on mechanical characteristics of welded joints of aluminum and aluminum alloys
13 p2034 N85-22744

Characteristics of surface crack development in ATtaS aluminum alloy during slow-cycle loading
13 p2034 N85-22745

Research program on the effect of pressure on the mechanical properties of polymers, part 2
[DE85-000995] 13 p2037 N85-22761

Diamond cutters' grinders 13 p2051 N85-22841

The ferrite permanent magnet AC motor: A technical and economical assessment
[DE85-002480] 13 p2066 N85-22903

The Shock and Vibration Digest, volume 16, no. 12
[AD-A150594] 13 p2102 N85-23102

Significant parameters of the behavior and of the surface damage of the lubricated Hertzian contact: An application to gears 14 p2222 N85-23783

Extreme precision antenna reflector study results
14 p2232 N85-23830

NASA space materials research
14 p2232 N85-23831

Fracture toughness of HY-130 steel weld metals
[AD-A150841] 14 p2255 N85-23976

Outlook for polymer composite materials
15 p2497 N85-25403

Research, development of composite materials described 15 p2497 N85-25404

Local elastoplastic fracture of fibrous composite materials 15 p2497 N85-25405

Ways of improving level and stability of mechanical characteristics of diffusion-welded joints of OT4 titanium alloy 15 p2499 N85-25417

Structure and mechanical properties of dispersion-hardened nickel alloy joints welded by diffusion 15 p2500 N85-25422

Influence of oxygen traces on the properties of tungsten heavy metals
[BLL-RARDE-TR-1177-(7291.7965)]
15 p2506 N85-25470

Mechanical properties of TiN deposits obtained by PVD and TiN, TiC, TiC + TiN obtained by CVD
[BLL-RISLEY-TR-5097-(9091.9F)]
15 p2506 N85-25471

Study of high performance alloy electroforming
[NASA-CR-175741] 15 p2506 N85-25473

Summary of recent investigations of the mechanical properties of polycrystalline solids
[DE85-006776] 15 p2511 N85-25492

Oxidation of nickel-aluminum and iron-aluminum alloys
[DE85-006930] 15 p2512 N85-25497

USSR report: Materials science and metallurgy
[JPRS-UMS-85-004] 15 p2513 N85-25503

Hardening of titanium alloy electric-arc welded joints
15 p2514 N85-25513

Mechanical properties of cast Martensitic high-strength multicomponent titanium alloys
15 p2514 N85-25514

Thermal stability of titanium alloys after cold plastic deformation 15 p2515 N85-25515

Structure and properties of VT20L titanium alloy with 0.1-0.3 percent content 15 p2515 N85-25517

Effect of initial structure on texture of pressed titanium alloy bars 15 p2515 N85-25518

Mechanical aspects of interfaces and surfaces in ceramic containing systems
[AD-A151978] 15 p2519 N85-25530

Titanium alloys, products, standards listed
15 p2533 N85-25626

A Gimbal sizing analysis for an IPACS rotating assembly
[NASA-CR-172524] 16 p2741 N85-26913

Pulsed electrodeposition
[DE85-007057] 16 p2747 N85-26950

Effect of nickel addition on the thermal, magnetic and magnetomechanical properties of Fe(80)B(15)Si(5)
[AD-A152281] 16 p2749 N85-26967

New materials and techniques for aircraft structures
[B8580074] 17 p2897 N85-27861

Mechanical properties of polycrystalline alpa titanium
[BLL-BISI-TRANS-21923-(9022.06)]
17 p2924 N85-28029

Thermomechanical treatment aimed at the protection of type 316 stainless steel from IGC and IGSCC
[BLL-BISI-TRANS-22498-(9022.06)]
17 p2925 N85-28040

The synergistic actions of stress corrosion cracking and corrosion fatigue
[BLL-BISI-TRANS-22334-(9022.06)]
17 p2926 N85-28045

Improving the properties of copper and copper alloys through heat treatment and alloying
[BLL-BISI-TRANS-21939-(9022.06)]
17 p2926 N85-28047

Steels with improved machinability
[BLL-BISI-22341-(9022.06)] 17 p2927 N85-28061

Microstructure and mechanical properties of rare-earths-microalloyed high-speed tool steel
[BLL-BISI-TRANS-22043-(9022.06)]
17 p2928 N85-28064

Physical properties of steels and their temperature dependence
[BLL-BISI-TRANS-22285-(9022.06)]
17 p2928 N85-28065

Influence of composition on the microstructural evolution and mechanical properties of irradiated Fe-Ni-Cr ternaries
[DE85-007462] 17 p2931 N85-28094

USSR report: Engineering and equipment
[JPRS-UEQ-85-004] 17 p2939 N85-28142

Conformational and mechanical properties at high strain rates
[AD-A153401] 17 p2959 N85-28272

Examination of the regions of the joint of sheets bonded by the explosive welding technique
[BLL-BISI-TRANS-22352-(9022.06)]
17 p2973 N85-28370

Tests of low-cycle fatigue of elected steels of class 11
[BLL-BISI-TRANS-22039-(9022.06)]
17 p2978 N85-28404

Radiation damage experiments and lifetime estimates for beryllium components in fusion systems
[DE85-006038] 17 p3040 N85-28811

Mechanical properties of adhesively bonded aluminum structures protected with hydration inhibitors
[AD-A153755] 18 p3079 N85-29047

Statistical fracture theories for brittle materials
[AD-A153530] 18 p3121 N85-29324

Measurement and calculation of the mechanical response of a highly fractured rock
[DE85-008421] 18 p3127 N85-29362

Influence of microstructure on mechanical properties in cemented tungsten-carbides 19 p3230 N85-30029

Possible causes of modification and strengthening of aluminum by scandium 19 p3241 N85-30099

Properties of heat resistant Ni-Al-Nb alloys with unidirectional eutectic structure
19 p3247 N85-30133

Mechanical protection of DLC films on fused silica slides
[NASA-TM-87056] 19 p3248 N85-30138

On design of off-axis specimens
[AD-A154328] 19 p3286 N85-30379

Numerical simulation of chemical and physical properties of cumulus clouds
[DE85-009744] 19 p3317 N85-30564

Special materials: Carbons
[SNIAS-851-551-104] 20 p3421 N85-31235

Activities report of the Laboratory of Mechanics and Energetics 20 p3437 N85-31328

Improved materials for composite and adhesive joints
[AD-A155065] 21 p3562 N85-32153

Basic cryogenics and materials. Phase 1
[NASA-CR-177932] 21 p3572 N85-32215

Effects of environment on spacecraft materials
22 p3733 N85-33144
Filament wound structures in PSP carbon composite
[RV10/84424] 22 p3743 N85-33198
Rationale in the selection of corrosion protective coating systems 22 p3750 N85-33242
Geologic, technical, and economic sensitivity analysis in support of the GRI (Gase Research Institute) tight gas reservoirs project area
[PB85-192276] 22 p3802 N85-33550
Mechanical properties of SiC fiber-reinforced reaction-bonded Si3N4 composites
[NASA-TM-87085] 23 p3909 N85-34223
Proceedings of the Mechanisms Conference, volume 1 23 p3923 N85-34309
A versatile computer package for mechanism analysis, part 2: Dynamics and balance
23 p3924 N85-34315
Proceedings of the Mechanisms Conference, volume 2 23 p3924 N85-34318
Generated spiral bevel gears: Optimal machine-tool settings and tooth contact analysis
[NASA-TM-87075] 23 p3937 N85-34405
Contribution to the properties of carbon fiber reinforced composites — structural mechanics
[ESA-TT-849] 24 p4074 N85-35246
Interaction of trace elements and welding parameters on GTA weld shape
[DE85-004046] 24 p4080 N85-35264
Development and characterization of carbon-bonded carbon fiber insulation for radioisotope space power systems
[DE85-013365] 24 p4082 N85-35299
User's guide: A computer program for strength analysis of non-hydraulic concrute structural elements. Report 1. Concrete General Strength Investigation (CGSI)
[AD-A156392] 24 p4102 N85-35428

MECHANICAL RESONANCE
U RESONANT VIBRATION

MECHANICAL SHOCK
NT HYDRAULIC SHOCK
Shock capturing finite difference algorithms for supersonic flow past fighter and missile type configurations
[NASA-CR-174051] 02 p0134 N85-10913
The Shock and Vibration Digest, volume 16, no. 9
[AD-A146779] 07 p0976 N85-16200
Reflections on trends in dynamics: The Navy's perspective 09 p1334 N85-18382
Acceleration responses of typical LRU's subjected to bench handling and installation shock
09 p1334 N85-18385
The Shock and Vibration Bulletin 54. Part 2: Ship shock, shock and blast and ground shock
[AD-A148132] 09 p1334 N85-18388
Two-dimensional shock response of a mass on energy-absorbing shock mounts
09 p1334 N85-18389
Optimum design for nonlinear shock mounts for transient inputs 09 p1334 N85-18390
Alternative shock characterizations for consistent shock test specifications 09 p1335 N85-18396
Shock response analysis by personal computer using the extended IFT algorithm 09 p1335 N85-18397
A study of the effect of mass loading on the shock environment 09 p1336 N85-18401
The Shock and Vibration Bulletin 54. Part 3: Structural dynamics, machinery dynamics and vibration problems
[AD-A148133] 09 p1337 N85-18406
The Shock and Vibration Digest, volume 16, no. 12
[AD-A150594] 13 p2102 N85-23102
Recovery of pyroshock data from distorted acceleration records
[NASA-TP-2494] 20 p3407 N85-31141
Short-time spectroscopic measurement of the temperature of solids
[ISL-CO-202/84] 20 p3459 N85-31486
A mechanical model of the human body and its application 24 p4129 N85-35598

MECHANICS (PHYSICS)
USSR report: Physics and mathematics
[JPRS-UPM-84-006] 02 p0256 N85-11676
Computational mechanics: A perspective on problems and opportunities for increasing productivity and quality of engineering
[PB85-128106] 12 p1950 N85-22252
User's and programmer's guide to the mechanics of moving finite element code
[DE85-006165] 13 p2152 N85-23335

MECHANIZATION
Economic model of calibration improvements for automatic test equipment
[PB84-217827] 01 p0051 N85-10335
Automation of assembly of electrical products
03 p0346 N85-12228
Automation and robotics in welding
15 p2566 N85-25631
USSR report: Science and technology policy
[JPRS-UST-85-008] 17 p3049 N85-28872
Importance of automation, robotization in economy
21 p3572 N85-32219
Re-designing a mechanism for higher speed: A case history from textile machinery 23 p3923 N85-34310

MECHANORECEPTORS
Effects of tasks on responses of human skin mechanoreceptors 11 p1691 N85-20635
Gravity perception in a Cladoceran-Zooplankter: Anatomy of antennal socket setae of Daphnia magna
15 p2605 N85-26057

MEDIA
NT ANISOTROPIC MEDIA
NT ELASTIC MEDIA
NT INTERGALACTIC MEDIA
NT INTERPLANETARY DUST
NT INTERPLANETARY MEDIUM
NT ZODIACAL DUST
Thermomechanical cracking in layered media from moving friction load
[AD-A146022] 03 p0373 N85-12379
Localization of waves in a disordered medium
19 p3373 N85-30926
Toward the propagation of waves in unsteady media
21 p3683 N85-32881

MEDIAN (STATISTICS)
A multiple regression technique for detecting outliers
[REPT-84-33] 17 p3025 N85-28706

MEDICAL ELECTRONICS
Bioengineering and rehabilitation: Windows of opportunity past, present and future
[NASA-EP-216] 16 p2841 N85-27516

MEDICAL EQUIPMENT
NT PROSTHETIC DEVICES
NT RESPIRATORS
NT X RAY APPARATUS
NT X RAY TUBES
Military vital sign monitor
[AD-A147257] 07 p1016 N85-16452
Improved radiographic viewing system
[AD-A147587] 07 p1016 N85-16456
Functional system theory in practice
11 p1690 N85-20629
Medical planning criteria for implementation of clinical hyperbaric facilities
[AD-A151001] 14 p2389 N85-24715
Bioengineering and rehabilitation: Windows of opportunity past, present and future
[NASA-EP-216] 16 p2841 N85-27516
Gas analysis techniques for human physiological measurements in space — Spacelab
[A/6537] 20 p3507 N85-31803
Heavy ion medical accelerator options
[DE85-011204] 22 p3841 N85-33784
New technologies at the forefront of industrial developments 24 p4061 N85-35168
Dental multi-purpose slowspeed handpieces test and evaluation
[AD-A155764] 24 p4130 N85-35606

MEDICAL PERSONNEL
Efforts to improve aviation medical examiner performance through continuing medical education and annual performance reports
[AD-A148078] 08 p1195 N85-17531

MEDICAL SCIENCE
NT ANESTHESIOLOGY
NT DENTISTRY
NT ENDOCRINOLOGY
NT EPIDEMIOLOGY
NT HISTOLOGY
NT HUMAN PATHOLOGY
NT IMMUNOLOGY
NT NEUROLOGY
NT NEUROPSYCHIATRY
NT NUCLEAR MEDICINE
NT OPHTHALMOLOGY
NT PATHOLOGY
NT RADIOBIOLOGY
NT RADIOLOGY
Evaluation of the National Library of Medicine's programs in the medical behavior sciences. Coverage of the Medical Behavioral Sciences (MBS) literature in monographic databases, study 5
[PB84-230531] 03 p0439 N85-12797
Evaluation of the National Library of Medicine's programs in the medical behavior sciences. Online searchers' reactions to database and vendor capabilities in the Medical Behavioral Sciences (MBS), study 4
[PB84-230523] 03 p0439 N85-12798
Evaluation of the National Library of Medicine's programs in the medical behavior sciences. Quality of indexing: The development and testing of a methodology comparing databases covering the Medical Behavioral Sciences (MBS) literature, study 3
[PB84-230515] 03 p0439 N85-127
Evaluation of the National Library of Medicine's programs in the medical behavior sciences. Test retrievals in five major databases covering the Medical Behavioral Sciences (MBS) literature, study 2
[PB84-230507] 03 p0440 N85-12
Evaluation of the National Library of Medicine's programs in the medical behavior sciences. Coverage, overlaps and gaps in bibliographic databases dealing with the Medical Behavioral Sciences (MBS) literature, study 1
[PB84-230499] 03 p0440 N85-12
Evaluation of the National Library of Medicine's programs in the medical behavior sciences. An analysis of the National Library of Medicine's (NLM) handling of Medical Behavioral Sciences (MBS) literatures: Some research tests of methods for evaluating bibliographic databases, executive summary
[PB84-230481] 03 p0440 N85-12
The application of basic control laws to human medicine
[DFVLR-MITT-84-13] 05 p0697 N85-14
USSR report: Life sciences. Biomedical and behavioral sciences
[JPRS-UBB-85-001] 08 p1193 N85-175
USSR report: Life sciences. Biomedical and behavioral sciences
[JPRS-UBB-85-007] 09 p1362 N85-18
USSR report: Life sciences. Biomedical and behavioral sciences
[JPRS-UBB-85-008] 10 p1523 N85-19
USSR report: Life sciences. Biomedical and behavioral sciences
[JPRS-UBB-85-010] 11 p1690 N85-20
Symposium on Military Aviation Medicine summarized
11 p1696 N85-20
Research and technology activities at Ames Research Center's Biomedical Research Division
[NASA-TM-86692] 12 p1899 N85-21
Armed forces special Symposium on Medicine at Altitudes 13 p2166 N85-23
China report: Science and technology
[JPRS-CST-84-012] 14 p2263 N85-24
Advances in study of cold injury in Army
14 p2263 N85-24
China report: Science and technology
[JPRS-CST-85-011] 15 p2551 N85-25
Alterations/corrections to the BRASS Program
[NASA-CR-171874] 15 p2616 N85-26
New technologies to improve laboratory testing
[DE85-008151] 18 p3110 N85-29
Applications of aerospace technology in biology and medicine
[NASA-CR-166100] 19 p3328 N85-30
USSR Space Life Sciences Digest
[NASA-CR-3922] 21 p3656 N85-32
Structural changes in thyroid due to high-altitude adaptation in Kirghizia 22 p3820 N85-33
Electroanesthesia as a means of controlling cold stress of local hypothermia 22 p3823 N85-33
USSR report: Life sciences. Biomedical and behavioral sciences
[JPRS-UBB-85-021] 23 p3951 N85-34
USSR report: Space Biology and Aerospace Medicine, vol. 19, no. 3, May - June 1985
[JPRS-USB-85-005] 23 p3952 N85-34
Tolerance to +Gz and +Gx accelerations of individuals in older age groups in good health and with early signs of arteriosclerosis 23 p3952 N85-34
Proceedings of the 14th Army Science Conference. Volume 2: Principal authors I through O
[AD-A149201] 24 p4144 N85-35

MEDICAL SERVICES
Bioengineering and rehabilitation: Windows of opportunity past, present and future
[NASA-EP-216] 16 p2841 N85-27
Test and Evaluation Master Plan (TEMP) for the Navy Occupational Health Information Management System (NOHIMS). Phase 1: Appendix A through appendix U
[AD-A154179] 19 p3380 N85-30

MEDITERRANEAN SEA
Mineral nutrients in Mediterranean ecosystems
[REPT-71] 01 p0089 N85-10
SEASAT altimeter data over the Mediterranean: Implications for ERS-1 03 p0382 N85-12
The altimeter as a support to the scatterometer in the representation of winds and derived wave fields in coastal waters and enclosed seas: A research at its onset
03 p0383 N85-12
Hydrologic characteristics of the Mediterranean and Black Sea 07 p0981 N85-16

Bio-optical variability in the Alboran Sea as assessed by Nimbus-7 coastal zone color scanner
[AD-A147909] 07 p0969 N85-16281
Preliminary report on the results of hydrological measurements in the southern Tyrrhenian Sea, in the Messina strait and in the western Ionian sea
[PREPRINT-433] 14 p2362 N85-24693
Variability of air humidity profiles over ocean determined by lidar sounding 19 p3296 N85-30436
Seasonal variability and spatial non-uniformity of bioluminescence in the Mediterranean Sea
[DRIC-T-7545] 24 p4125 N85-35572

MEETINGS
U CONFERENCES

MEISSNER EFFECT
U DIAMAGNETISM
U SUPERCONDUCTIVITY

MELT SPINNING
Rapidly solidified NiAl and FeAl
[NASA-TM-86941] 11 p1597 N85-20042
Rapid solidification processing of magnesium alloys
[AD-A150270] 13 p2022 N85-22668
Apparatus for producing amorphous and microcrystalline metal powders 13 p2030 N85-22720
Microstructures in rapidly solidified Ni-Mo alloys
[NASA-TM-87100] 23 p3915 N85-34266

MELTING
NT FUSION (MELTING)
NT LEVITATION MELTING
NT VACUUM MELTING
Time resolved calorimetry of 30 nm Te-films during laser annealing
[AD-A145047] 01 p0052 N85-10346
Design and implementation of a low-gravity solidification experiment package for the F-104
02 p0156 N85-11053
Studies of laser melting and rapid solidification using amorphous silicon
[DE84-014737] 02 p0202 N85-11345
Abundancies of Ni, Cr, CO and major elements in the silicate portion of the Moon: Constraints from primary lunar magmas 04 p0582 N85-13720
Fractionation of siderophiles in cosmic spherules and its implications 06 p0884 N85-15613
Influence of temperatures of reactants on nature of product of solid-phase reactions
[BLL-M-36019-(5828.4)] 07 p0921 N85-15832
Procedure for investigating high-temperature properties of iron-ore materials
[BLL-M-36020-(5828.4)] 07 p0926 N85-15868
Diurnal freeze-thaw frequencies in selected regions of the high latitudes
[AD-A147276] 07 p1007 N85-16400
Adaptation of remelting procedures for the use of recycled metal in nickel-base superalloy castings
[PNR-90232] 09 p1297 N85-18149
Comparison of property regeneration techniques and life prediction procedures applied to laboratory tested and service exposed Ni-Cr alloys
[NPL-DMA(A)-91] 09 p1333 N85-18374
Stabilization of contaminated soils by in situ vitrification
[AD-P004144] 09 p1348 N85-18480
Influence of melting conditions on strength of transition zone between steel and composite material
10 p1450 N85-19133
Development of media for dynamic latent heat storage for the low-temperature range. Part 1: Thermal analyses of selected salt hydrate systems
[NASA-TM-77776] 10 p1507 N85-19510
Analysis of phase composition of products of laser destruction of metallic surfaces
11 p1600 N85-20064
Hot melt adhesive attachment pad
[NASA-CASE-LAR-12894-1] 11 p1610 N85-20125
Initial velocity of the emerging free boundary in a two-phase Stefan problem with imposed flux
[DE85-003813] 11 p1631 N85-20272
Si-on-insulator formation using a line-source electron beam
[DE85-003449] 11 p1737 N85-20925
Experimental and numerical analysis of electric currents and electromagnetic blunting of cracks in thin plates
[AD-A150418] 13 p2022 N85-22669
Determining degree of partial melting of asthenosphere from seismic data 13 p2107 N85-23127
Hydrovolcanism 13 p2188 N85-23574
Radiation-dominated snowmelt on Mars
13 p2191 N85-23592
North Atlantic Deep Water formation: Information from ice cores 15 p2602 N85-26035
In-situ rock melting applied to lunar base construction and for exploration drilling and coring on the moon
[DE85-006716] 16 p2717 N85-26770
The influence of melting practice and of microalloying, with rare earth metals and with boron, on the quality of low-carbon steel
[BLL-BISI-22467-(9022.06)] 17 p2925 N85-28036
Influence of temperature in melting and casting on quality of medium-alloy steel
[BLL-BISI-TRANS-22310-(9902.06)]
17 p2938 N85-28137
Modern sedimentation in the northern Barents Sea: Input, dispersal and deposition of suspended sediments from glacial meltwater
[AD-A152520] 17 p2997 N85-28530
Preparation of heavy metal fluoride glasses in the bulk form
[AD-A153784] 18 p3079 N85-29049
Feasibility of melt casting strontium fluoride to produce high-density heat sources
[DE85-009429] 18 p3130 N85-29381
Determination of the vacancy formation enthalpy in chromium by positron annihilation
[DE85-010288] 19 p3239 N85-30084
A study of freezing and melting with eutectic interactions 19 p3378 N85-30956
The nature of the anomalies on the polytherms of the properties of molten metallic alloys
[BLL-M-36265-(5828.4)] 20 p3430 N85-31277
Method for determining Wagner parameters of interaction of first and second orders
[BLL-M-36261-(5828.4)] 20 p3430 N85-31278
Quasi-steady-state melting mode during combined laser irradiation of semiconductor materials
21 p3662 N85-32874
Experimental studies of glass refining
[NASA-CR-176130] 22 p3751 N85-33248
Laser effects on opaque targets. Part 2C: Thermal effects of a time-variable beam intensity
[ISL-R-105/84-PT-2C] 22 p3791 N85-33486
Technology of off-gas treatment for liquid-fed ceramic melters
[DE85-012467] 22 p3812 N85-33610
Dynamic compaction of a monosized spherical tungsten powder
[DE85-014806] 24 p4080 N85-35289
Analysis of reactor material experiments investigating oxide fuel crust stability and heat transfer in jet impingement flow
[DE85-012097] 24 p4151 N85-35739

MELTING POINTS
Sealing ceramic material in low melting point glass
[NASA-TM-77599] 01 p0031 N85-10190
Evaluation of thermocouple junction temperature
[DE84-015159] 04 p0502 N85-13206
Kinetics of saturation of porous titanium with low melting point metals 10 p1446 N85-19114
Study of advanced fuel system concepts for commercial aircraft and engines
[NASA-CR-174752] 10 p1456 N85-19176
Jet fuel property changes and their effect on producibility and cost in the U.S., Canada, and Europe
[NASA-CR-174840] 16 p2757 N85-27012
Fuel freeze point investigations
[AD-A152801] 17 p2937 N85-28129
Radar study of the melting layer
[ESA-CR(P)-1974] 17 p2997 N85-28527
High performance mixed bisimide resins and composites based thereon
[NASA-CASE-ARC-11538-1-SB]
19 p3231 N85-30033
Processable and stable conductive polymers
[AD-D011684] 19 p3249 N85-30143
Development of low-melting fused salts 8: Formation of molybdenum film from molten ammonium formate bath
[BLL-OA-TRANS-3195-(6196.300)]
20 p3429 N85-31264
Ice-forming efficiency of the soluble and insoluble portions of dust contained in snow
21 p3643 N85-32631
Measurement and correlation of jet fuel viscosities at low temperatures
[NASA-CR-174911] 23 p3921 N85-34295

MELTS (CRYSTAL GROWTH)
NT CONTAINERLESS MELTS
NT IMPACT MELTS
NT MELT SPINNING
New metallurgical processes based on high-speed crystallization and diffusion of metals
01 p0021 N85-10126
Nuclear Magnetic Resonance of Polymeric Materials
[AD-A145078] 01 p0032 N85-10192
Dynamics of polymers in solution and melts
[AD-P003907] 01 p0032 N85-10193
NMR (Nuclear Magnetic Resonance) and macromolecular migration in a melt or in concentrated solutions
[AD-P003908] 01 p0032 N85-10194
Producing semiconductor materials by superfast cooling of melt 03 p0354 N85-12274
Neutron scattering on macromolecular solid state materials, solutions and melts 03 p0431 N85-12747
Dynamic crystallization of silicate melts
[NASA-CR-174103] 06 p0743 N85-14774
Calculation of energy of atomization in silicate tetrahedron Si4(4-)
[BLL-M-36000-(5828.4)] 07 p1040 N85-16599
The growth of large diameter single crystals by vertical solidification of the melt
[AD-A148756] 09 p1397 N85-18792
Method for synthesizing indium phosphide
[AD-D011475] 10 p1563 N85-19855
Total immersion crystal growth
[NASA-CASE-NPO-15800-2] 12 p1939 N85-22178
Experimental methods for quenching structures in lunar-analog silicate melts: Variations as a function of quench media and composition
13 p2184 N85-23554
The volume change during solidification
[NASA-TM-77617] 14 p2300 N85-24243
Impurity studies
[DE85-006235] 15 p2661 N85-26423
A Navier-Stokes capillary free boundary in open boat crystal growth
[REPT-84-34] 17 p2960 N85-28283
Crystallization of aluminum-based alloys in weightlessness 19 p3242 N85-30101
Conditions for formation of parageneses containing kyanite-orthoclase in region of Mount Provender and Pratt Peak (Shackleton Range, Antarctica)
19 p3298 N85-30447
Ribbon growing method and apparatus
[NASA-CASE-NPO-16306-1-CU]
19 p3375 N85-30934
Temperature field around a spherical, cylindrical, and needle-shaped crystal, growing in a pre-cooled melt
[NASA-TM-77889] 20 p3537 N85-32011
Silicon dendritic web growth 21 p3611 N85-32435
Temperature-stress modeling
21 p3611 N85-32436
Silicon ribbon stress-strain activities
21 p3611 N85-32437

MEMBRANE ANALOGY
U MEMBRANE STRUCTURES
U STRUCTURAL ANALYSIS

MEMBRANE STRUCTURES
NT SKIN (STRUCTURAL MEMBER)
Development of a preprototype times wastewater recovery subsystem, addendum
[NASA-CR-171823] 07 p1019 N85-16468
Ion transporting composite membranes. 1: Nafion impregnated gore-tex
[AD-A151020] 14 p2252 N85-23980
Evaluation of developmental membranes for the mixed reactant iron-chromium redox system
[NASA-TM-87074] 23 p3944 N85-34443

MEMBRANE THEORY
U STRUCTURAL ANALYSIS

MEMBRANES
NT ION EXCHANGE MEMBRANE ELECTROLYTES
NT MEMBRANE STRUCTURES
NT SKIN (STRUCTURAL MEMBER)
Operating experiences of reverse osmosis plants treating Rand Water Board (RWB) water: Pitfalls and problems 01 p0023 N85-10142
Control of the dynamic response of a damped membrane by distributed forces
[CSIR-TWISK-312] 01 p0061 N85-10406
Proton pumping in purple membrane, appendix 1
[DE84-014601] 01 p0118 N85-10811
Neutron small angle scattering of the free and membrane-bound ATPase — adenosine triphosphate (ATP) 03 p0431 N85-12746
Separation of metal species by supported liquid membranes
[DE84-014536] 04 p0470 N85-12902
Field/cell interaction model
[DE84-011914] 04 p0544 N85-13465
DOE supported research in alcohol fuel technology development
[DE84-007686] 06 p0774 N85-14948
Data appendix: F-number = 1.0 EMR with a flexible back electrode
[NASA-CR-172477] 07 p0946 N85-15994
Workshop on membrane biophysics
[AD-A148238] 08 p1192 N85-17512
Mechanisms of gas permeation through polymer membranes
[DE84-017423] 09 p1293 N85-18117
The Shock and Vibration Digest, volume 16, no. 10
[AD-A147588] 09 p1331 N85-18361
A review of approximate methods for determining the vibrational modes of membranes
09 p1331 N85-18363

Effect of air cavity on the vibration analysis of loaded drums 09 p1339 N85-18422
ECUT, Energy Conversion and Utilization Technologies program: Isothermal separation processes update
[NASA-CR-175463] 10 p1433 N85-19033
Bioelectrochemistry 2: Membrane phenomena
[AD-A149132] 10 p1522 N85-19602
The effect of inert gases on ion transport across the erythrocyte membrane
[AD-A148669] 10 p1527 N85-19635
Investigation of structure-permeability relationships of silicone polymer membranes
[PB85-148476] 11 p1596 N85-20036
Supported liquid membrane battery separators
[DE85-001031] 12 p1836 N85-21519
Interaction of metals and metalloids with biomembranes
[DE85-004802] 13 p2141 N85-23293
Ion transporting composite membranes. 1: Nafion impregnated gore-tex
[AD-A151020] 14 p2252 N85-23960
Liquid membranes for the production of oxygen-enriched air
[DE85-006056] 15 p2506 N85-25460
Luminescence probe studies of ionomers. 2. Steady-state measurements from sulfonated polyethylene and teflon membranes
[AD-A152233] 16 p2755 N85-27000
Interactions between electromagnetic fields
[AD-A153796] 18 p3091 N85-29129
Threshold effects and cellular recognition
[DE85-010616] 19 p3327 N85-30614
A system for the assessment of non-thermal effects of ultrasound on cells at liquid nitrogen temperatures
20 p3523 N85-31915
Silicon dendritic web growth 21 p3611 N85-32435
Temperature-stress modeling
21 p3611 N85-32436
Silicon ribbon stress-strain activities
21 p3611 N85-32437
Analysis of stress-strain relationships in silicon ribbon
21 p3611 N85-32438
Stress and buckling analysis 21 p3611 N85-32439
Stress and efficiency studies in EFG
21 p3611 N85-32440
Silicon sheet surface studies
21 p3611 N85-32441
Edge-defined film-fed growth of thin silicon sheets
21 p3612 N85-32443
The investigation of natural and artificial ice nuclei by the improved membrane filter method
21 p3642 N85-32626
Development and demonstration of a spiral-wound thin-film composite membrane system for the economical production of oxygen-enriched air, phase 4
[DE85-012360] 23 p3920 N85-34268
Membrane reinforcement in concrete shells: Design versus nonlinear behavior 24 p4084 N85-35312
Development and evaluation of sulfonated polysulfone membranes for the zinc-ferricyanide battery
[DE85-009104] 24 p4090 N85-35357
Cationic exchange membrane for the zinc-ferricyanide battery
[DE85-013152] 24 p4112 N85-35489

MEMORY
The effects of feedback and predictability of human judgment
[AD-A145744] 02 p0237 N85-11542
Measuring workload differences between short-term memory and long-term memory scenarios in a simulated flight environment 05 p0703 N85-14513
Visual attention to radar displays
05 p0704 N85-14514
Subjective workload assessment and voluntary control of effort in a tracking task 05 p0706 N85-14540
The representation of action plans in long term memory 05 p0709 N85-14545
Effects of individual mnemonic characteristics on problem solving 07 p1010 N85-16419
Problems of psychological support of automated organization control systems 09 p1362 N85-18570
Stereotype traits can be processed automatically
[AD-A150947] 14 p2391 N85-24725
The effect of strategy in second order manual control on resource competition with a sternberg memory search task
[AD-A150985] 14 p2391 N85-24727
The role of prior knowledge in operating equipment from written instructions
[AD-A151007] 14 p2392 N85-24730
Psychophysiological studies. 1: Performance and physiological response in learning, short-term memory and discrimination tasks
[AD-A151018] 14 p2392 N85-24731
Skilled memory
[AD-A152063] 15 p2620 N85-26143
The levels of processing conceptualization of human memory: Some empirical and theoretical issues
[AD-A152321] 17 p3000 N85-28544
Distributed memory
[AD-A153364] 17 p3001 N85-28554
The effect of set size on time to recall color coded information
[AD-A155013] 21 p3665 N85-32767

MEMORY (COMPUTERS)
Microcomputers in Hungary 01 p0115 N85-10786
Analysis of dynamic characteristics and ways of development of bipolar main memory with miniaturization of integrated circuit elements 04 p0490 N85-13123
Memory hierarchies for Directly Executed Language microprocessors 05 p0713 N85-14570
Improving the Spacelab mass memory unit tape layout with a simulation model
[NASA-TM-86483] 05 p0713 N85-14571
Electrical characterization of VLSI (Very Large Scale Integration) memories
[AD-A147657] 08 p1156 N85-17296
Programmable realtime interface between a block floating point processor and memory
[AD-D011431] 08 p1203 N85-17571
Vector computer memory bank contention
[NASA-CR-177342] 09 p1376 N85-18649
Automatic multi-banking of memory for microprocessors
[NASA-CASE-NPO-15295-1] 12 p1911 N85-21992
Trends in computational capabilities for fluid dynamics
15 p2457 N85-25172
Signal flow model for sequential logic built from combinational logic elements and its implementation in Prolog
[DE85-005792] 15 p2549 N85-25734
Microstore: The Stanford analog memory unit
[DE85-005534] 18 p3095 N85-29160
Performance of the butterfly processor-memory interconnection in a vector environment
[DE85-007931] 19 p3261 N85-30224
Development and evaluation of a fault-tolerant multiprocessor (FTMP) computer. Volume 1: FTMP principles of operation
[NASA-CR-166071] 19 p3341 N85-30705
Fault-tolerant computing research
[AD-A154082] 19 p3342 N85-30710
Digital matched filter 22 p3765 N85-33339
Basic features of personal computers
22 p3766 N85-33344
Design of digital bandpass filters with finite memory
22 p3775 N85-33392
Spatial trees: A fast access method for unstructured graphical data 23 p3958 N85-34533
Analysis of transient radiation upset in a 16K SRAM
[DE85-009442] 23 p3965 N85-34586
Error-correcting codes for computer memories
24 p4136 N85-35636

MENISCI
Advanced radiator concepts
[NASA-TM-87008] 14 p2300 N85-24245
Effects of thermal fluctuations on systems with small surface tension
[PREPRINT-437] 18 p3152 N85-29520

MENTAL HEALTH
Job and family stress as predictors of pilot health, job satisfaction and performance
[AD-A142176] 07 p1018 N85-16464

MENTAL PERFORMANCE
Primate equilibrium performance and diazepam: A behavioral tolerance effect
[AD-A145156] 01 p0094 N85-10634
A representation for the functioning of devices that supports compilation of expert problem solving structures: An extended summary
[AD-P003921] 02 p0245 N85-11601
Cognitive coordinate systems: Accounts of mental rotation and individual differences in spatial ability
[AD-A146149] 03 p0401 N85-12557
The role of knowledge structures in fault diagnosis
05 p0703 N85-14509
POPCORN: A supervisory control simulation for workload and performance research
05 p0704 N85-14515
ERPS to monitor non-conscious mentation
05 p0707 N85-14536
Decision tree rating scales for workload estimation: Theme and variations 05 p0708 N85-14541
Mental models of invisible logical networks
05 p0708 N85-14544
The Sternberg task as a workload metric in flight handling qualities research 05 p0712 N85-14566
Mental status in relation to special conditions of activity 07 p1011 N85-16420
Cognitive performance during successive sustained physical work episodes
[AD-A146061] 08 p1200 N85-17556
Methods of monitoring mental work efficiency, emotional activity 10 p1526 N85-[illegible]
Improvement of workload estimation techniques in piloting tasks
[NASA-CR-174374] 10 p1531 N85-[illegible]
Qualitative process theory
[AD-A148987] 10 p1543 N85-[illegible]
Human cognition and intelligence: Towards an integrated theoretical perspective
[CSIR-SR-PERS-350] 13 p2143 N85-[illegible]
Perceived heterogeneity and its effect on various types of tasks
[AD-A151003] 14 p2382 N85-[illegible]
Space brain research in China reported
15 p2537 N85-[illegible]
A portable battery for objective, non-obtrusive measures of human performances
[NASA-CR-171868] 15 p2586 N85-[illegible]
Skilled memory
[AD-A152063] 15 p2620 N85-[illegible]
Effects of dehydration or cold exposure and restricted fluid intake upon cognitive performance
[AD-A151973] 16 p2842 N85-[illegible]
Performance Evaluation Tests for Environmental Research (PETER) evaluation of 112 measures
[AD-A152317] 17 p2999 N85-[illegible]
The levels of processing conceptualization of human memory: Some empirical and theoretical issues
[AD-A152321] 17 p3000 N85-28544
Oral discussion, group-to-individual transfer and achievement in cooperative learning groups
[AD-A153209] 17 p3001 N85-[illegible]
A task battery for applied human performance assessment research
[AD-A153677] 18 p3154 N85-[illegible]
Equipercentile test equating: The effects of presmoothing and postsmoothing on the magnitude of sample-dependent errors
[AD-A154110] 19 p3347 N85-[illegible]
Design and implementation of an intelligence database
[AD-A154095] 19 p3361 N85-[illegible]
Manual and computer-aided sequential diagnostic inference
[AD-A156229] 24 p4133 N85-[illegible]

MENTAL STRESS
U STRESS (PSYCHOLOGY)

MERCAPTAN
U THIOLS

MERCAPTO COMPOUNDS
U THIOLS

MERCATOR PROJECTION
UTM (Universal Transverse Mercator) determinations from geographical data
[AD-A152293] 16 p2856 N85-27610

MERCURY (METAL)
Measurement of magnetic sublevel differential scattering cross sections for potassium and mercury
[MPIS-10/1983] 01 p0119 N85-10815
Mercury health effects update: Health issue assessment
[PB85-123925] 10 p1526 N85-[illegible]
Ligand structural influences upon electrochemical reactivity: Organic substituent effects upon Carboxylatopentaamminecobalt(3) reductions at mercury and gold electrodes
[AD-A150685] 14 p2250 N85-23844
Intramolecular electron transfer at metal surfaces. Part 5: Pendant substituent effects upon thiocarboxylate-bridged Cobalt (3) reduction kinetics at mercury and gold electrodes
[AD-A150647] 14 p2254 N85-23871
Spectroscopic studies of lasing transitions in the diatomic mercury halides
[AD-A151553] 15 p2563 N85-[illegible]
Adsorption of Hg on lunar samples
[DE85-007946] 17 p3054 N85-[illegible]
Environmental surveillance at Los Alamos during 1984
[DE85-011866] 22 p3811 N85-[illegible]

MERCURY (PLANET)
The geology of the terrestrial planets
[NASA-SP-469] 09 p1410 N85-[illegible]
Mercury 09 p1411 N85-[illegible]
Mercury radar altimetry: A preliminary analysis
13 p2198 N85-[illegible]
Mapping and geological analysis of Mercury and Venus radar ranging data 13 p2198 N85-[illegible]
Mechanisms of basalt-plains ridge formation
13 p2199 N85-[illegible]
Questions about Mercury's role in comparative planetary geophysics 22 p3853 N85-[illegible]

MERCURY ARCS
Investigation of light source and scattering medium related to vapor-screen flow visualization in a supersonic wind tunnel
[NASA-TM-86290] 06 p0810 N85-15144

MERCURY CADMIUM TELLURIDES

Effect of an underlayer of cadmium telluride on the reflection-reducing properties of zinc sulfide on mercury cadmium telluride
[AD-A146195] 03 p0414 N85-12649

HgCdTe surface and defect study program
[AD-A146343] 03 p0434 N85-12764

Liquid-phase epitaxial growth of CdTe on HgCdTe
[AD-D011482] 10 p1561 N85-19846

Method for the preparation of epitaxial films of mercury cadmium telluride
[AD-D011532] 12 p1938 N85-22175

Theoretical interpretation of thermal arrest data from differential thermal analysis measurements
12 p1949 N85-22241

Producible alternative to CdTe for epitaxy (PACE-2) of LWIR (Long Wave Infrared) HgCdTe
[AD-A150676] 14 p2426 N85-24964

Laser annealing of ion implanted HgCdTe
[AD-A150675] 14 p2427 N85-24966

Properties of defects in Hg(1-x)Cd(x)Te
[AD-A153243] 17 p3044 N85-28835

Interface chemistry of Hg(1-x)Cd(x)Te
[AD-A154876] 21 p3583 N85-32161

Mosaic Infrared Sensor for Space Astronomy (MIRSSA)
[NASA-CR-176154] 22 p3786 N85-33456

HgCdTe surface and defect study program
[AD-A156079] 24 p4161 N85-35799

MERCURY COMPOUNDS

NT MERCURY TELLURIDES

Mercuric iodide photodetectors for scintillation spectroscopy
[DE85-001437] 10 p1437 N85-19056

New and revised methods of purifying mercuric iodide
[DE85-011664] 22 p3749 N85-33237

MERCURY ION ENGINES

Development of the Engineering Test Satellite-3 (ETS-3) ion engine system
[NASA-TM-77538] 01 p0017 N85-10101

Ion thruster system (8-cm) cyclic endurance test
[NASA-CR-174745] 04 p0463 N85-12937

Ion thruster project
[NASA-TM-77726] 07 p0917 N85-15805

Analysis of orbit transfer vehicles for GPS Block 3 satellites
[AD-A152021] 16 p2732 N85-26860

MERCURY LAMPS

Optical radiation emissions from selected sources. Part 2: High intensity discharge lamps
[PB85-149136] 15 p2523 N85-25551

Electrodeless HID lamp study
[DE85-010626] 18 p3096 N85-29167

MERCURY TELLURIDES

Quaternary narrow-band semiconductors (HgTe)x (InSb)1-x for far-infrared detectors
[AD-A148350] 10 p1562 N85-19852

MERIDIONAL FLOW

Global scale diagnoses of FGGE data
[NASA-CR-174356] 09 p1356 N85-18533

The modelling of latitudinal gradients in the solar wind in the outer solar system 12 p1947 N85-22231

Azimuthal and meridional asymmetries of the solar wind and quasiperiodic variations of intensity of Galactic Cosmic Rays (GCR)
[SH-4.4-20] 23 p4035 N85-35016

MEROMORPHIC FUNCTIONS

NT ELLIPTIC FUNCTIONS

Annals of the Finnish Academy of Sciences, series A. 1: Mathematics, volume 8, part 2
[ISSN-0066-1953] 10 p1535 N85-19673

On the spherical derivative of a meromorphic function with a Nevanlinna deficient value
10 p1535 N85-19676

Locally univalent functions in the unit disk
10 p1536 N85-19680

Contribution of the cup-product of Milnor's fiber with /I/ sup 2 lambda poles 11 p1698 N85-20672

Annals of the Scientific Academy of Finland, series A. 1: Mathematics, volume 9
[ISSN-0066-1953] 15 p2633 N85-26229

On meromorphic functions continuous on the Stoilow boundary 15 p2633 N85-26232

On the length of asymptotic paths of meromorphic functions of order zero 15 p2633 N85-26234

MESFETS

U FIELD EFFECT TRANSISTORS

MESH

Image theory for a vertical electric dipole above a wire grid with square cells
[REPT-S-150] 02 p0192 N85-11286

Numerical simulations of fuel droplet flows using a Lagrangian triangular mesh
[AD-A146087] 03 p0362 N85-12320

Diffraction diffusion screen with holographically-suppressed zero-order beam
[AD-D011445] 10 p1487 N85-19367

WRAP-RIB antenna technology development
14 p2231 N85-23824

Diffraction analysis of mesh deployable reflector antennas 14 p2235 N85-23854

Determination of electromagnetic properties of mesh material using advanced radiometer techniques
14 p2235 N85-23855

Synthetic acceleration of coarse-mesh S/sub n/ transport calculations
[DE84-014721] 14 p2409 N85-24855

Flow through very porous inclined screens
[NASA-TM-86979] 15 p2555 N85-25761

Isoparametric 3-D finite element mesh generation using interactive computer graphics 15 p2574 N85-25873

On the interconnection of incompatible solid finite element meshes using multipoint constraints
15 p2575 N85-25879

Use of COSMIC NASTRAN in a design department
15 p2575 N85-25881

An incremental multigrid strategy for the fluid dynamics equations
[AD-A151953] 16 p2783 N85-27172

Montonicity preserving bicubic interpolation, revision 1
[DE85-007978] 17 p3021 N85-28683

Study of meshing of beveled gears with normally decreasing arc teeth
[NASA-TM-77866] 18 p3117 N85-29293

Application of closed-form solutions to a mesh point field in silicon solar cells 20 p3482 N85-31637

Adaptive rezoner in a two-dimensional Lagrangian hydrodynamic code
[DE85-010108] 24 p4094 N85-35381

MESH (MATHEMATICS)

U COMPUTATIONAL GRIDS

MESOMETEOROLOGY

Rocket measurements of mesospheric ionization irregularities
[NASA-CR-176056] 20 p3494 N85-31721

MESONS

NT HYPERONS
NT KAONS
NT MUONS
NT PIONS
NT VECTOR MESONS

Searching for top, Higgs, and supersymmetry: The minimum invariant mass technique
[DE84-014539] 01 p0119 N85-10613

Proposal for the systematic naming of mesons and baryons
[DE85-008453] 17 p3035 N85-28773

A comprehensive study of psi meson production
[DE85-008094] 18 p3180 N85-29718

Control technology for radioactive emissions to the atmosphere at US Department of Energy facilities: The Los Alamos Meson Physics Facility
[DE85-011402] 22 p3611 N85-33609

Proceedings of the 18th LAMPF Users Group Meeting
[DE85-011888] 22 p3639 N85-33773

The SCR flare of 16 February 1984 as recorded by the Sayan spectrograph
[SH-1.3-17] 23 p3994 N85-34761

The phi-meson and Chiral-mass-meson production in heavy-ion collisions as potential probes of quark-gluon-plasma and Chiral symmetry transitions
24 p4175 N85-35884

Forward particle production in inelastic Ne-22 inteVractions in emulsion at 4.1 A Ge/c
[HE-1.4-7] 24 p4176 N85-35895

Meson multiplicity in nucleus-nucleus collisions above 4 GeV/amu
[HE-1.4-10] 24 p4177 N85-35897

Connection between variations of the atmosphere temperature profile and variations of the meson component intensity
[HE-3.1-12] 24 p4178 N85-35910

MESOPAUSE

Radiation transport in the Earth atmosphere
04 p0522 N85-13341

Cold Arctic Mesopause Project (CAMP): Scientific objectives 11 p1656 N85-20433

Large scale winter time disturbances in meteor winds over central and eastern Europe
11 p1661 N85-20467

Coupling between the thermosphere and the stratosphere: The role of nitric oxide
11 p1662 N85-20472

Meteor wind results from Atlanta, USA, and Ramey, Puerto Rico 11 p1662 N85-20474

Basic features of global circulation in the mesopause lower thermosphere region 11 p1662 N85-20475

The nucleation of ice at very low temperatures and pressures 21 p3641 N85-32617

MESOSCALE PHENOMENA

NT JET STREAMS (METEOROLOGY)

Nowcasting 2. Mesoscale Observations and Very-Short-Range Weather Forecasting — conferences
[ESA-SP-208] 01 p0073 N85-10487

The mesoscale-beta-scale evolution of mid-latitude meso-alpha-scale convective complexes
01 p0073 N85-10488

Generation of deep convective clouds along mesoscale storm outflow boundaries 01 p0074 N85-10490

Automated analysis and nowcasting of mesoscale convective systems 01 p0074 N85-10492

Three-dimensional mesoscale analysis of serial soundings 01 p0074 N85-10493

Layered sloping mesoscale structures and rainbands in atmospheric frontal regions and their relation to symmetric instability 01 p0075 N85-10497

About the influence of nonadiabatic processes on frontogenesis near the ground 01 p0075 N85-10498

Some mesoscale weather effects and the very short-range forecasting impact of variable snow cover
01 p0075 N85-10499

Detailed analysis of the structure of local wind systems in Canterbury, New Zealand 01 p0075 N85-10501

Test results from RAINSAT 01 p0076 N85-10508

VHF/UHF radar and its application in nowcasting
01 p0078 N85-10516

Analysis strategies for field dependent estimation and network design — mesoscale modeling
01 p0078 N85-10520

Evaluation of surface sensible heat flux effects on the generation and modification of mesoscale circulations
01 p0079 N85-10527

Predicability of mesoscale phenomena
01 p0079 N85-10528

The initialization of mesoscale models
01 p0079 N85-10529

Applications of a finite-element regional model to very-short-range forecasting 01 p0080 N85-10531

Application of mesoscale numerical model to local weather prediction 01 p0080 N85-10532

The United Kingdom Meteorological Office mesoscale forecasting system 01 p0080 N85-10533

A local dynamical interpretation method of numerical weather forecasting 01 p0080 N85-10536

A one-level mesoscale model suitable for nowcasting and short-term forecasting in regions of complex terrain
01 p0081 N85-10541

Short-term forecasting using a REMOS approach — regime model output statistics (REMOS)
01 p0081 N85-10544

Experiment on nowcasting of heavy rainfall and severe storms in central China in 1979-1981
01 p0081 N85-10545

Simple methods in very short-range forecasting based on data from a mesoscale network of automatic stations (ANETZ) and from satellite (Meteosat) and radar — Swiss Alps 01 p0082 N85-10548

Development of an operational system for Very-Short-Range Forecasting (VSRF) at Swedish Meteorological and Hydrological Institute (SMHI)
01 p0083 N85-10559

Use of short-range weather forecasts at construction sites: Some results from a user and a market test
01 p0084 N85-10563

Benefits resulting from tailored very-short-range forecasts in Sweden 01 p0084 N85-10564

The arc cloud complex: A case study
[AD-A145384] 02 p0231 N85-11507

Mesoscale and convective-scale characteristics of mature hurricanes 03 p0394 N85-12516

Recent examples of mesoscale numerical forecasts of severe weather events along the east coast
[NASA-TM-86172] 03 p0395 N85-12523

Investigations of severe/tornadic thunderstorm development and evolution based on satellite and AVE/SESAME/VAS data
[NASA-CR-174154] 04 p0538 N85-13424

Weather research program report; FY 1983
[PB84-236694] 04 p0541 N85-13440

Dynamics of coupled ice-ocean system in the marginal ice zone: Study of the mesoscale processes and of constitutive equations for sea ice
[NASA-CR-174171] 04 p0542 N85-13448

Conditional symmetric instability and mesoscale rainbands 05 p0678 N85-14356

An investigation of the marine boundary layer during cold air outbreak 05 p0680 N85-14368

Convective scale weather analysis and forecasting
[NASA-CR-174185] 06 p0838 N85-15320

Simple mesoscale models for operational use in regions of topographic and thermal forcing: Development and evaluation
[AD-A146667] 06 p0839 N85-15325

Precipitation characteristics of a dual mesoscale convective complex
[PB84-226711] 06 p0840 N85-15337

An evaluation of an advection fog prediction model
[AD-A147436] 07 p1006 N85-16403

Interactions between mean flow and finite-amplitude mesoscale eddies in a barotropic ocean
[AD-A147249] 07 p1009 N85-16413

Studies of coastal mesoscale winds using SIR-B
08 p1147 N85-17236

The use of principal components analysis techniques Nimbus-7 coastal zone color scanner data to define mesoscale ocean features through a warm humid atmosphere
[AD-A148567] 08 p1176 N85-17416

Sea breeze-induced mesoscale systems and severe weather
[NASA-CR-174317] 08 p1187 N85-17480

A method for determining mesoscale dynamic topography
[AD-D011412] 08 p1191 N85-17506

Mesoscale lee cyclogenesis 09 p1355 N85-18527

The rationale and suggested approaches for research geosynchronous satellite measurements for severe storm and mesoscale investigations
[NASA-TM-86185] 09 p1356 N85-18532

The influence of soil moisture distribution on the severe-storm environment of the southern Great Plains: A numerical study of the SESAME 4 case
09 p1357 N85-18534

Mesoscale storm and dry period parameters from hourly precipitation data: Program documentation
[DE85-001366] 09 p1357 N85-18538

Rain volume estimation over areas using satellite and radar data
[NASA-CR-174434] 10 p1518 N85-19568

Continued research in mesoscale air pollution simulation modeling. Volume 5: Refinements in numerical analysis, transport, chemistry, and pollutant removal
[PB85-137362] 11 p1680 N85-20585

Mesoscale studies of flow regimes and fluxes of particulate matter in coastal waters
[DE85-003825] 11 p1689 N85-20620

Continued research in mesoscale air pollution simulation modeling. Volume 6. Further studies in the modeling of microscale phenomena
[PB85-137370] 12 p1887 N85-21844

Digital processing of mesoscale analysis and space sensor data
[NASA-CR-171429] 13 p2146 N85-23319

Mountain barrier baroclinity effects on surface winds along the Alaskan Arctic coast 14 p2238 N85-23877

Variational mesoscale satellite data assimilation and initialization
[NASA-CR-175704] 14 p2378 N85-24880

Mesoscale Atmospheric Processes Research Program Science Review
[NASA-TM-87465] 15 p2594 N85-25967

Modeling of midwest severe thunderstorms
15 p2596 N85-25995

Satellite detection of severe thunderstorms
15 p2596 N85-25996

Mesoscale analysis and modeling group
15 p2596 N85-26001

Recent VAS imaging/sounding research
15 p2597 N85-26004

A simulation experiment on the impact of geostationary temperature retrievals in numerical models
15 p2597 N85-26005

VAS/model impact study 15 p2597 N85-26006

Role of jet streaks and boundary layer processes in organizing a pre-convective environment
15 p2597 N85-26008

Role of frontal circulations and gravity waves in initiating convective storm systems 15 p2598 N85-26010

Sea breeze-induced mesoscale systems and severe weather 15 p2598 N85-26012

The sensitivity of mesoscale cyclogenesis forecasts to detailed three-dimensional isentropic initial analyses and varied vertical model resolution
15 p2598 N85-26015

Influence of coherent mesoscale structures on satellite-based Doppler lidar wind measurements
[NASA-CR-175853] 16 p2833 N85-27467

MARMAP survey of the continental shelf from Cape Hatteras, North Carolina to Cape Sable, Nova Scotia (1977 - 1983). Atlas 1: Summary of operations
[PB85-150985] 16 p2839 N85-27506

Convective storm downdraft outflows detected by NASA/MSFC's Airborne 10.6 micron pulsed Doppler Lidar System
[NASA-CR-3898] 17 p2995 N85-28511

Arctic mixed layer dynamics
[AD-A153582] 18 p3150 N85-29505

MELSAR: A mesoscale air quality model for complex terrain. Volume 2: Appendices
[DE85-010991] 19 p3310 N85-30519

Approximate factorization method for computation of nonhydrostatic mesoscale flows
[DE85-007259] 19 p3313 N85-30537

System enhancements of Mesoscale Analysis and Space Sensor (MASS) computer system
[NASA-CR-171463] 19 p3342 N85-30708

Global mean sea surface based upon a combination of the GEOS-3 and SEASAT altimeter data
20 p3492 N85-31710

Diagnostics of severe convection and subsynoptic scale ageostrophic circulations
[NASA-CR-171581] 21 p3634 N85-32571

Dynamics of Mesoscale Weather Systems: 1984 Summer Colloquium
[PB85-188266] 22 p3817 N85-33649

Airborne Investigations of Mesoscale Convective Systems (AIMCS), 1984: Operational summary and data inventory
[PB85-187904] 24 p4125 N85-35571

MESOSPHERE

Ground-based measurements of mesosphere temperatures by optical means
08 p1183 N85-17453

Incoherent scatter radar studies of the mesosphere
08 p1184 N85-17463

PMP-2: Equatorial wave dynamics
11 p1655 N85-20422

Variation of derived mesospheric nitric oxide in relation to wind and temperature in winter
11 p1658 N85-20452

Seasonal characteristics of mesospheric plasma and their transitions 11 p1660 N85-20464

VHF radar observations in the stratosphere and mesosphere during a stratospheric warming
11 p1661 N85-20468

Latitudinal dependence of the energy input into the mesosphere by high energy electrons
11 p1664 N85-20489

Aeronomical aspects of mesospheric photodissociation: Processes resulting from the solar H Lyman alpha line
[AERONOMICA-ACTA-A-285-1984]
11 p1680 N85-20587

Experiment for measuring electric fields within the sounding rocket project Energy Budget
[BMFT-FB-W-84-048] 12 p1891 N85-21866

Wave dynamics and transport in the stratosphere
[NASA-CR-175789] 16 p2823 N85-27413

Circulation and transport in the middle atmosphere: Mesosphere and lower thermosphere
18 p3148 N85-29492

Gravity waves from the stratosphere to the mesosphere, part 1.3B 21 p3616 N85-32471

A numerical analysis of transient planetary waves and the vertical structure in a meso-strato-troposphere model, part 1.4A 21 p3617 N85-32473

Morphology of the scattering targets: Fresnel and turbulent mechanisms, part 2.1A
21 p3618 N85-32481

Observations of mesospheric turbulence by rocket probe and VHF radar, part 2.4A 21 p3619 N85-32484

Interpretation of radar returns from the mesosphere, part 2.3A 21 p3619 N85-32485

Radar echoes at 2.66 and 40.92 MHz from the mesosphere, part 2.6A 21 p3619 N85-32486

Antenna induced range smearing in MST radars
21 p3620 N85-32495

Effects of line-of-sight velocity on spaced-antenna measurements, part 3.5A 21 p3621 N85-32496

Mesospheric measurements of irregularity patches using a 3-antenna interferometer, part 3.6B
21 p3621 N85-32498

Spectral measurements of turbulence and gravity waves, part 4.2A 21 p3622 N85-32501

Relationship of isolated turbulent regions to the general turbulent background, part 4.4A
21 p3623 N85-32506

Estimation of vertical diffusion from observations of Atmospheric turbulence layers, part 4.4B
21 p3623 N85-32507

Momentum flux measurements: Techniques and needs, part 4.5A 21 p3623 N85-32508

Sample interchange of MST radar data from the Urbana radar 21 p3627 N85-32531

Urbana radar systems: Possibilities and limitations
21 p3628 N85-32540

Progress and plans for the Colorado Wind Profiler Network 21 p3628 N85-32542

Voigt line profile computation of infrared lines in the stratosphere and mesosphere
[AERONOMICA-ACTA-A-294-1985]
22 p3813 N85-33622

MESSAGE PROCESSING

Reserve and authentication in Integrated Services Distributed Networks (ISDN) networks
[FUB-37-1983] 01 p0041 N85-1

Pluribus satellite IMP (Interface Message Processor) development mobile access terminal network
[AD-A145348] 02 p0190 N85-11

Real-time Ada (trademark)
[AD-A146258] 03 p0407 N85-12

Crew communication as a factor in aviation accidents
05 p0710 N85-14

Selecting a leader in a clique in O(N log N) messages
[AD-A146581] 06 p0857 N85-154

Implementation of a constraint machine for prism - A parallel problem solver
[AD-A147844] 07 p1026 N85-16612

Benchmarking database systems in multiple backend configurations
[AD-A148191] 08 p1202 N85-175

EGP (Exterior Gateway Protocol) gateway under Berkeley UNIX 4.2
[AD-A148056] 08 p1206 N85-17

Performance evaluation of a database system in multiple backend configurations
[AD-A148192] 08 p1229 N85-1774

Extracting digital data from a bus and multiplexing it with a video signal
[AD-D011491] 11 p1636 N85-20

Distributed asynchronous deterministic and stochastic gradient optimization algorithms: Revision
[AD-A149997] 12 p1921 N85-22

A perspective on multiaccess channels
[AD-A150183] 13 p2146 N85-23322

Orphan detection in the Argus system
[AD-A150562] 13 p2148 N85-23331

Distributed matchmaking for processes in computer networks
[CWI-CS-R8421] 17 p3016 N85-28

Assured information flow capping architecture
[AD-A155392] 22 p3756 N85-33

Pluribus satellite IMP (Interface Message Processors) development mobile access terminal network
[AD-A155754] 24 p4069 N85-35216

MESSAGES

Comparative review of single-line and multiline optical character readers used in mail processing
[PB84-234624] 04 p0548 N85-134

Selecting a leader in a clique in O(N log N) messages
[AD-A146581] 06 p0857 N85-15453

Experimental satellite system for determining coordinates of maritime distress
09 p1308 N85-18

Study of terrestrial mobile systems for personal communications
[MCS-8436] 20 p3441 N85-31357

METABOLIC WASTES
NT FECES
NT HUMAN WASTES
NT URINE

BLSS: A contribution to future life support
18 p3155 N85-2953

METABOLISM
NT ADRENAL METABOLISM
NT CALCIUM METABOLISM
NT CARBOHYDRATE METABOLISM
NT ELECTROLYTE METABOLISM
NT ENZYME ACTIVITY
NT FERMENTATION
NT HORMONE METABOLISMS
NT LIPID METABOLISM
NT MINERAL METABOLISM
NT NITROGEN METABOLISM
NT OXYGEN METABOLISM
NT PHOSPHORUS METABOLISM
NT PROTEIN METABOLISM

Vitamin metabolism in cosmonauts following short-term flights 01 p0091 N85-10615

Functional capacities of elderly subjects exposed to simulated spaceflight factors 01 p0091 N85-10617

Skeletal muscle metabolism in hypokinetic rats
[NASA-CR-174059] 02 p0233 N85-11520

Toxicology and metabolism of nickel compounds
[DE84-014919] 05 p0696 N85-1447

Chemistry and metabolism of delayed neurotoxic organophosphorus esters
[AD-P004023] 06 p0844 N85-15357

Comparison of thermal responses between rest and leg exercise in water
[AD-A146818] 07 p1015 N85-16448

Influence of hyperthermia on body temperature and content of catecholamines in white rat hypothalamus
10 p1524 N85-196

Skeletal muscle metabolism during exercise is influenced by heat acclimation
[AD-A148845] 10 p1527 N85-19

Effects of hyperthermia on free amino acids in rat brain and in subcellular fractions 11 p1691 N85-20631

Effects of hypothermia on brain metabolism
11 p1692 N85-20636

USSR report: Space Biology and Aerospace Medicine, volume 18, no. 6, November - December 1984
[JPRS-USB-85-002] 12 p1900 N85-21931

Cosmonauts' blood plasma free amino acid levels during preflight training 12 p1901 N85-21937

Fluid metabolism of monkeys during two-week antiorthostatic hypokinesia 12 p1902 N85-21943

NASA Space Biology Program: 9th Annual Symposium
[NASA-CP-2336] 15 p2605 N85-26054

Constant fiber number during skeletal muscle atrophy and modified arachidonate metabolism during hypertrophy 15 p2609 N85-26078

Gravity, body mass and composition, and metabolic rate 15 p2610 N85-26084

Differential effect of denervation on free radical scavenging enzymes in slow and fast muscle of rat
[NASA-CR-175719] 15 p2614 N85-26110

Research opportunities in loss of red blood cell mass in space flight
[NASA-CR-175808] 16 p2841 N85-27517

Changes in pentose and glucuronate pathway dehydrogenases in rat brains following single or multiple hypothermic episodes 20 p3505 N85-31790

The role of sulfur in osmoregulation and salinity tolerance in cyanobacteria, algae, and plants
21 p3660 N85-32736

Sulfur cycling and metabolism of phototrophic and filamentous sulfur bacteria 21 p3660 N85-32737

Anaerobic reduction of elemental sulfur by Chromatium vinosum and Beggiatoa alba 21 p3660 N85-32739

Interactions among sulfide-oxidizing bacteria
21 p3661 N85-32741

Studies of circulatory and metabolic changes during ketamine narcosis
[AD-A154512] 21 p3663 N85-32756

Microwave radiation and thermoregulation
[AD-A155718] 22 p3818 N85-33654

Investigation of some aspects of amino acid metabolism in man during brief exposure to antiorthostatic hypokinesia combined with ultraviolet radiation
22 p3822 N85-33678

Response of amino acids in hindlimb muscles to recovery from hypogravity and unloading by tail-cast suspension
[NASA-CR-176183] 24 p4128 N85-35589

METABOLITES

Effect of 1,25-dihydroxycholecalciferol and 24,25 dihydroxycholecalciferol on growth and alteration of rat bones during hypokinesa (histomorphometric study)
01 p0092 N85-10622

METAGALAXY
U UNIVERSE

METAL BONDING
NT METAL-METAL BONDING

Bondability of Al-Si thin film in thermosonic gold wire bonding — integrated circuits
[NASA-TM-77795] 10 p1439 N85-19071

Study of character of adhesive interaction and breaking of polyimid-aluminum foil junction during process of hardening 13 p2014 N85-22637

Technology for pressure-instrumented thin airfoil models, phase 1
[NASA-CR-3891] 14 p2227 N85-23804

Diffusion vacuum welding 15 p2499 N85-25416

Fracture surface analysis in composite and titanium bonding: Part 1: Titanium bonding
[NASA-CR-175750] 15 p2502 N85-25434

Development of acceptance criteria for batches of silane primer for external tank thermal protection system bonding applications
[NASA-CR-175850] 16 p2754 N85-26995

New process for production of bimetal with corrosion-resistant cladding layer
[BLL-BISI-TRANS-22371-(9022.06)]
17 p2927 N85-28056

Fatigue resistance of homogeneous and heterogeneous welded joints of TS5 titanium alloy
19 p3246 N85-30126

Advanced thermal barrier system bond coatings for use on Ni, Co-, and Fe-base alloy substrates
[NASA-TM-87062] 20 p3431 N85-31283

Determination of deformation speed during high-speed deformation of cylindrical shells
[BLL-M-36280-(5828.4)] 20 p3465 N85-31527

Study of an ultrasonic detection method to inspect bonding effects in light alloy bonded structures, test report no. 43-954/F — aircraft structures
[PV-43-954/F] 22 p3795 N85-33510

METAL COATINGS
NT ALUMINUM COATINGS
NT GOLD COATINGS
NT NICKEL COATINGS
NT ZINC COATINGS

Features of laser welding of medium carbon steel through a cadmium coating 01 p0020 N85-10122

Methods for producing platinum-group metal coatings from molten alkali cyanides
[PB84-225994] 01 p0029 N85-10181

USSR report: Materials science and metallurgy
[JPRS-UMS-84-007] 03 p0348 N85-12244

Electrochemical behaviour of TiCl4 solutions in low melting point organic media
[BLL-OA-TRANS-3174-(6196.3)]
06 p0764 N85-14888

Plasma deposition of amorphous metal alloys
[DE85-000768] 09 p1295 N85-18132

Effects of MAR-M247 substrate (modified) composition on coating oxidation coating/substrate interdiffusion — protective coatings for hot section components of gas turbine engines
[NASA-CR-174851] 10 p1440 N85-19073

The role of silver in self-lubricating coatings for use at extreme temperatures
[NASA-TM-86943] 11 p1611 N85-20127

Low temperature deposition of nickel films
[AD-D011568] 12 p1805 N85-21319

Metallic and metalloceramic coating by thermal decomposition
[NASA-TM-86992] 13 p2036 N85-22755

Film and interstitial formation of metals in plasma-sprayed ceramics
[NASA-TM-86993] 13 p2036 N85-22756

Gear-cutting tools made of ultra high speed steel coated with TiN
[BLL-RISLEY-TR-5109-(9091.9F)]
15 p2567 N85-25837

Self-sustaining low-Z coatings for fusion applications 2 - copper-lithium
[DE85-002553] 15 p2656 N85-26403

Effects of surface chemistry on hot corrosion life
[NASA-CR-174915] 16 p2706 N85-26711

Vacuum plasma coatings for turbine blades
16 p2734 N85-26869

Solid state hydrogen pumping and storage material
[AD-D011610] 16 p2757 N85-27011

Forming of coating protection system: Mechanism of paint-coating anti-corrosion protection of steel
[BLL-BISI-TRANS-22081-(9022.06)]
17 p2925 N85-28033

Corrosion resistant coating
[NASA-CASE-NPO-15928-1] 18 p3073 N85-29005

Atomized magnetism-aluminum protective coatings
19 p3244 N85-30116

East Europe report: Science and technology
[JPRS-ESA-85-021] 21 p3568 N85-32190

Tests on zirconium nitride coatings applied to SW 18 steel using the chemical vapor deposition method
24 p4078 N85-35271

METAL COMBUSTION

Status of boron combustion research
13 p1996 N85-22526

Ignition phenomena of bulk aluminum alloy as a function of oxygen pressure 13 p1999 N85-22531

Review of zirconium-zircaloy pyrophoricity
[DE85-011169] 23 p3916 N85-34270

METAL COMPOUNDS

Macrocyclic poly(tertiary) phosphines for the attachment of metals to surfaces of photodevices
[DE84-015552] 05 p0617 N85-13946

Structure-property relationships in intercalated graphite
[AD-A147949] 08 p1219 N85-17680

Metal-support interactions: The effect of catalyst preparation on catalytic activity
[DE84-017425] 09 p1293 N85-18118

Phthalocyanine polymers
[NASA-CASE-ARC-11413-1] 12 p1809 N85-21348

METAL CORROSION
U CORROSION

METAL CRYSTALS

New metallurgical processes based on high-speed crystallization and diffusion of metals
01 p0021 N85-10126

Raman scattering from metastable GaSb(1-x) Ge(2x) alloys
[AD-A145897] 03 p0327 N85-12108

Back stress in dislocation creep. Part 1: Basic concepts and measuring techniques
[NASA-TM-77773] 07 p0977 N85-16206

Magnetism of californium metal
[DE85-001141] 09 p1377 N85-18657

Studies of the kinetics and mechanisms of ammonia synthesis and hydrodesulfurization on metal single crystal surfaces
[DE85-001650] 11 p1595 N85-20030

Summary of recent research on mechanical behavior of polycrystalline solids
[DE85-004601] 12 p1942 N85-22199

Observation of surface vibrational resonances on (110) surfaces of FCC metals
[AD-A150469] 13 p2163 N85-23419

Measurements of radiation-induced segregation and diffusion in ion irradiated alloy using implanted manganese
[AERE-R-11528] 14 p2258 N85-23994

Summary of recent investigations of the mechanical properties of polycrystalline solids
[DE85-006776] 15 p2511 N85-25492

The precipitation mechanism in a metallic solid solution crystal: Case of the aluminum-copper and aluminum-silver systems
[DE85-009061] 18 p3077 N85-29032

METAL CUTTING

New titanium carbide grade for metal cutting
02 p0181 N85-11214

Specifications, applications of gantry robots viewed
10 p1461 N85-19215

Productivity gains through CAD of CNC programs
10 p1462 N85-19219

Small-size measuring gauges for metal cutting machine tools 14 p2267 N85-24045

Group technology for working turbine drive wheel disks 14 p2269 N85-24061

USSR report: Machine tools and metalworking equipment
[JPRS-UMM-85-006] 14 p2283 N85-24146

Large CNC machining center for turbine production
14 p2284 N85-24149

Laser cutting: A new tool for shipbuilding
14 p2306 N85-24285

USSR report: Machine tools and metalworking equipment
[JPRS-UMM-84-010] 16 p2767 N85-27071

New robotized, vertical broaching machine featured
16 p2767 N85-27074

Development, implementation of industrial lasers reviewed 16 p2767 N85-27075

Study of a test method for assessing machinability in gear cutting operations
[BLL-BISI-TRANS-22345-(9022.06)]
17 p2972 N85-28359

Very high speed lap with negative lift effect
[AD-D011711] 19 p3261 N85-30345

Mechanical properties of plasma arc cut steel
23 p3905 N85-34188

METAL DRAWING

Prediction of forming limit diagrams for deep drawing
06 p0796 N85-15089

Gel drawn fibers of poly(vinyl alcohol)
[AD-A149062] 10 p1435 N85-19040

New method for determining stampability of sheet materials
[BLL-BISI-22486-(9022.06)] 17 p2972 N85-28360

Durability of reinforced hard-alloy draw plates
[BLL-M-36278-(5828.4)] 20 p3465 N85-31526

METAL FATIGUE

The inter-relation of microstructure, toughness and fatigue crack growth behaviour in WC-Co hardmetals
02 p0177 N85-11188

New titanium carbide grade for metal cutting
02 p0181 N85-11214

Reliability considerations for the total strain range version of strainrange partitioning
[NASA-CR-174757] 02 p0209 N85-11380

Near-threshold fatigue crack growth and crack closure in 17-4 precipitation hardening steel and 2043-T3 aluminum alloy
[FFA-TN-1984-16] 02 p0210 N85-11385

Acoustic emission monitoring of fatigue in 7010 aluminum alloys
[AERE-R-11167] 03 p0334 N85-12152

Fatigue crack propagation in metastable titanium alloys
[AD-A145824] 03 p0372 N85-12376

Constitutive modeling of engine materials
[AD-A146630] 06 p0817 N85-15189

Modelling of deformation and fracture in high-temperature structural materials
[DE84-016906] 06 p0818 N85-15191

Cumulative damage modeling of fatigue crack growth
07 p0907 N85-15741

Thermal-mechanical fatigue crack growth in Inconel X-750
[NASA-CR-174740] 07 p0927 N85-15877

A study of spectrum fatigue crack propagation in two aluminum alloys. 1: Spectrum simplification
[NASA-TM-86929] 09 p1293 N85-18124

A study of spectrum fatigue crack propagation in two aluminum alloys. 2: Influence of microstructures
[NASA-TM-86930] 09 p1294 N85-18125

Ti-6Al-4V alloy castings prepared in zircon sand molds and the effect of hot isostatic pressing
[PB85-109932/GAR] 09 p1296 N85-18150

Development of surface cracks in AMg6 alloy under low-cycle loading conditions 10 p1442 N85-19089

Fractographic features of titanium alloy fatigue failure under repeated static stress and high frequency vibration 11 p1601 N85-20070

Effect of hydrogen on fatigue of VT6 alloy
11 p1601 N85-20071

Effect of stress concentration fatigue resistance of refractory nickel alloys under asymmetrical multicycle loading, communication 1 11 p1604 N85-20086

Fatigue crack growth in Aramid Reinforced Aluminum Laminates (ARALL): Mechanisms and predictions
[DFVLR-FB-84-37] 11 p1609 N85-20118

Structural strenght of strip D16T aluminum alloy with low copper and magnesium content
13 p2025 N85-22691

Fatigue life, crack initiation, and propagation of 304 stainless steel with non-proportional axialtorsional strain-paths 13 p2101 N85-23094

A study of fatigue crack growth in 2 1/4 Cr1Mo steel. Part 1: The influences of environment and material condition
[AERE-R-11472] 14 p2259 N85-23993

Study of fatigue strength of shafts with segmented channels 14 p2282 N85-24138

Fatigue crack propagation and fracture in 7050 and 7091 aluminum alloy forgings 14 p2318 N85-24324

Fatigue crack topography and crack growth analysis — wrought and cast aluminum 14 p2319 N85-24333

Crack propagation under constant and variable stress amplitudes: A comparison of calculations based on the Striation spacing and tests 14 p2320 N85-24336

Fatigue strength of alpha-titanium alloys under cophasal action of variable normal and tangential stresses
15 p2406 N85-25407

On the use of marker loads for fatigue crack growth measurements
[FFA-TN-1984-52] 16 p2802 N85-27277

Reaction-bonded and fiber-reinforced SiC static and dynamic gas turbine components
[BMFT-FB-T-84-302] 17 p2899 N85-27874

Role of hydrogen and structure on CMSX-2
17 p2915 N85-27967

The synergistic actions of stress corrosion cracking and corrosion fatigue
[BLL-BISI-TRANS-22334-(9022.06)]
17 p2926 N85-28045

X-ray diffraction study of changes in stress-strain distributions during fatigue of a 2-phase alloy
[AD-A152367] 17 p2930 N85-28087

Development of high temperature resistant, noncorrosible, non-metallic ceramic materials, especially silicon nitride in gas turbine application
[BMFT-FB-T-85-015] 17 p2936 N85-28125

Development of high temperature resistant noncorrodible silicon carbide components for gas turbine applications, follow-up report
[BMFT-FB-T-85-016] 17 p2936 N85-28126

The fatigue properties of welds at low temperature, according to the type of steel
[BLL-BISI-TRANS-22455-(9022.06)]
17 p2978 N85-28410

Fractographic analysis for nonpropagating conditions of fatigue crack at high stress ratios in mild steel
23 p3905 N85-34194

Crystallographic orientation dependence of fatigue crack propagation in extremely low carbon steel
23 p3906 N85-34195

Fatigue crack retardation phenomenon caused by single-multiple overloads in 2017-T3 aluminum allow
23 p3906 N85-34196

The stress pattern analysis of coarse grain titanium specimens
[PNR-90250] 23 p3942 N85-34433

METAL FIBERS

Investigation of electric and wear phenomena of liquid metal wetted copper fiber brushes under conditions of high slip ring eccentricity
[AD-A147634] 08 p1156 N85-17295

Influence of volumetric fiber content on some matrix damage factors during thermal cycling of tungsten-EI 765 composite 10 p1443 N85-19097

Theoretical and experimental investigation of mechanically fastened composites
[AD-A150961] 14 p2246 N85-23935

Production and compaction of amorphous metal powders
[BLL-BISI-TRANS-22387-(9022.06)]
17 p2929 N85-28080

Research on design of cryotransformers and its prospects for the future
[AD-A152400] 17 p2952 N85-28230

METAL FILMS

Research on large, highly accurate, inflatable reflectors
[AD-A145080] 01 p0016 N85-10099

Platinum thin film resistors as accurate and stable temperature sensors
[NASA-TM-77728] 01 p0049 N85-10322

Composition of metal films on gallium arsenide surface 02 p0257 N85-11685

Calculation of critical temperature for Nb-Cu multilayer film superconductor
[AD-A144321] 02 p0274 N85-11786

Formation of subsurface Al2O3 layers in aluminum by oxygen ion implantation
[DE84-015599] 04 p0474 N85-13020

Effects of monolayer coverages on substrate sputtering yields 06 p0865 N85-15496

Synergestic sputtering properties of binary alloys
06 p0865 N85-15497

Method for bonding insulator to insulator
[AD-D011340] 07 p0929 N85-15691

Structural studies of amorphous Mo-Ge alloys using synchrotron radiation
[DE85-002061] 08 p1131 N85-17125

Short range order-long range order in superconducting materials
[AD-A148764] 08 p1227 N85-17724

Bondability of Al-Si thin film in thermosonic gold wire bonding — integrated circuits
[NASA-TM-77795] 10 p1439 N85-19071

Picosecond laser pulse interactions with metallic and semiconductor surfaces
[AD-A149112] 10 p1490 N85-19405

Magnetization of very thin Ni films in epitaxial metal film sandwiches of Cu
[DE85-001640] 10 p1563 N85-19860

Quasi-thermodynamic prediction of hydrogen reemission behavior from titanium films
[DE85-003667] 10 p1564 N85-19864

Structural studies of sputtered Ni-As-O films
[DE85-003229] 11 p1605 N85-20095

Effect of interfacial characteristics of metal clad polymeric substrates on electrical high frequency interconnection performance
[NASA-TM-86948] 11 p1624 N85-20223

Observation of standing spinwaves in thin Fe-films by means of Raman spectroscopy
[DE85-003036] 11 p1735 N85-20913

Reaction of amorphous NiNb films with crystalline metal overlayers
[DE85-005483] 13 p2024 N85-22680

Study of 1/f noise in solids
[AD-A151069] 14 p2428 N85-24972

Effects of ion bombardment on the morphology of lead films
[DE85-007232] 15 p2511 N85-25494

The replacement of precious metal thick film inks using conductive polymer technology
[AD-A152002] 16 p2749 N85-26965

Sol-gel processing of lead zirconate titanate films
[ATR-85(8343)-2] 18 p3073 N85-29010

The determination of optical constants of thin metal films by surface plasma techniques 19 p3373 N85-30925

Amorphous metallic films in silicon metallization systems 21 p3610 N85-32427

METAL FINISHING
NT ELECTROPOLISHING
NT SHOT PEENING

Advanced high-efficiency concentrator cells
[DE84-013020] 09 p1344 N85-18459

Kinetics of the formation of a complex alloyed boride coating on iron and its properties
[BLL-BISI-TRANS-22303-(9022.06)]
17 p2930 N85-28084

METAL FLUORIDES
NT BERYLLIUM FLUORIDES
NT CADMIUM FLUORIDES
NT CALCIUM FLUORIDES
NT LITHIUM FLUORIDES
NT MAGNESIUM FLUORIDES
NT STRONTIUM FLUORIDES
NT URANIUM FLUORIDES

Preparation of heavy metal fluoride glasses in the bulk form
[AD-A153784] 18 p3079 N85-29049

METAL FOILS

Zero adhesion system
[AD-D011237] 01 p0015 N85-10093

Formation of subsurface Al2O3 layers in aluminum by oxygen ion implantation
[DE84-015599] 04 p0474 N85-13020

Pulsed electric discharge laser technology. Electron beam window foil material
[AD-A147486] 07 p0972 N85-161

Confinement of low-energy electrons near metallic surfaces for plasmon generation
[DE85-001119] 09 p1381 N85-18

Study of character of adhesive interaction and breaking of polyimid-aluminum foil junction during process of hardening 13 p2014 N85-22

Conversions in amorphous zirconium-vanadium alloy
15 p2496 N85-25

The effects of water and hydrogen on materials used in integrated circuit packages
[AD-A151893] 15 p2518 N85-25

Determination of local deformation during explosive welding
[BLL-M-36279-(5828.4)] 20 p3482 N85-31

METAL FORGING
U FORGING

METAL FORMING
U FORMING TECHNIQUES
U METAL WORKING

METAL GRINDING

Very high speed lap with negative lift effect
[AD-D011711] 19 p3281 N85-30

Study on the correlation between grinding conditions and residual stresses in ground surface of steel by the X-ray method 23 p3907 N85-34

METAL HALIDES
NT ALKALI HALIDES
NT ALUMINUM CHLORIDES
NT BERYLLIUM FLUORIDES
NT CADMIUM FLUORIDES
NT CALCIUM CHLORIDES
NT CALCIUM FLUORIDES
NT CESIUM IODIDES
NT COPPER CHLORIDES
NT IRON CHLORIDES
NT LITHIUM CHLORIDES
NT LITHIUM FLUORIDES
NT MAGNESIUM FLUORIDES
NT POTASSIUM CHLORIDES
NT SILVER CHLORIDES
NT SILVER HALIDES
NT SILVER IODIDES
NT SODIUM CHLORIDES
NT SODIUM IODIDES
NT STRONTIUM FLUORIDES
NT TITANIUM CHLORIDES
NT URANIUM FLUORIDES
NT ZINC CHLORIDES

Combustion kinetics of metal oxide and halide radicals
[AD-A150924] 14 p2251 N85-23

METAL HARDENING
U HARDENING (MATERIALS)

METAL HYDRIDES

Gas chromatographic separation of hydrogen isotopes using metal hydrides
[DE84-014455] 04 p0469 N85-12

Paramagnetic impurity effects in NMR determinations of hydrogen diffusion and electronic structure in metal hydrides. Cerium in YH-2 and LaH-2.25
[DE84-014127] 04 p0472 N85-13

Thermodynamical characteristics of heat storage reactors using metal hydrides
[NAL-TR-822] 06 p0869 N85-155

Properties and thermal stabilities of amorphous transition metal hydrides
[DE85-002117] 11 p1607 N85-201

Capture of liquid hydrogen boiloff with metal hydride absorbers
[NASA-CR-175677] 14 p2249 N85-23

Heat-mass flow enhancement system for a metal hydride assembly
[DE85-010698] 22 p3763 N85-33441

METAL INSULATOR SEMICONDUCTORS
U MIS (SEMICONDUCTORS)

METAL IONS
NT FERRIC IONS

Repetitively pulsed metal ion beams for ion implantation
[DE84-014065] 05 p0732 N85-147

Anisotropy and relaxation effects of Co2+ ions in LiTi ferrite
[AD-A146550] 06 p0861 N85-154

Homogeneous reaction involving components of different redox couples. 1: Theoretical considerations and digital simulation
[AD-A148666] 08 p1124 N85-170

Research and development work concerning liquid membranes
[BMFT-FB-T-84-227] 08 p1124 N85-170

Reactions of metal ions and their cluster in the gas phase using laser ionization: Ion cyclotron resonance spectroscopy
[DE84-016491] 09 p1293 N85-181

Negative lithium emission from a tungsten surface in a plasma
[DE85-003456] 12 p1936 N85-22167
International Conference on Coordination Chemistry (23rd) held at Boulder, Colorado on 29 July - 3 August, 1984
[AD-A150960] 14 p2252 N85-23956
Laser-induced fluorescence of metal-atom impurities in a neutral beam
[DE85-004960] 14 p2310 N85-24296
Reactions of metal ions and their clusters in the gas phase using laser ionization-ion cyclotron resonance spectroscopy
[DE85-009478] 19 p3361 N85-30838
Interpretation of 119 Sn isomer shifts and 3d 5/2-core-level shifts based on Dirac-Slater calculations on a number of ionic states
[USIP-85-06] 20 p3532 N85-31973

METAL JOINTS
NT SOLDERED JOINTS
NT SPOT WELDS
NT WELDED JOINTS
Fatigue behavior of bolted joints made of carbon fiber reinforced epoxy resins 05 p0650 N85-14173
Recommended aluminum pipe welding procedures for corps of engineers construction
[AD-A146712] 06 p0815 N85-15172
Durability calculation of wing panel element
14 p2285 N85-24159
Joining of sintered composite TiC-steel materials by welding
[BLL-M-36253-(5828.4)] 20 p3461 N85-31502
Moire interferometric measurement of relative displacements in dovetail joints
[OUEL-1563/85] 20 p3471 N85-31566
Negative flexural behavior of precase composite slabs with steel joint 23 p3904 N85-34183

METAL MATRIX COMPOSITES
High performance fibers for structurally reliable metal and ceramic composites — advanced gas turbine engine materials
[NASA-TM-86878] 03 p0325 N85-12095
Composite structural materials
[NASA-CR-174077] 04 p0467 N85-12966
Fatigue behavior of continuous fiber silicon-carbide-aluminum composites
[NASA-TM-86332] 06 p0763 N85-14879
Titanium Matrix/Continuous Fiber/Continuous fiber composite interface interactions and their influence on mechanical properties
[AD-A147504] 07 p0920 N85-15829
The response of metallic structures to dynamic loading 08 p1172 N85-17389
Spreading upon compacting of fiber composite materials with porous metal matrix 10 p1443 N85-19096
Structure and property formation mechanism in magnetite alloy-binder composite
10 p1444 N85-19103
Evaluation and prediction of long-term environmental effects of nonmetallic materials
[NASA-CR-171353] 10 p1450 N85-19137
Effect of operating medium on cyclic durability of AD33-W composite 13 p2029 N85-22716
MMCIAC (Metal Matrix Composites Information Analysis Center)
[AD-A150654] 14 p2248 N85-23933
The effect of notch acuity on the fracture toughness of silicon carbide/aluminum metal matrix composites
[AD-A150970] 14 p2248 N85-23936
Localized corrosion currents from graphite/aluminum and welded SiC/Al metal matrix composites
[AD-A150988] 14 p2256 N85-23980
Mechanical aspects of interfaces and surfaces in ceramic containing systems
[AD-A151978] 15 p2519 N85-25530
On residual stresses and stress intensity factors in composite materials 15 p2572 N85-25859
Nonlinear structural analysis for fiber-reinforced superalloy turbine blades 16 p2737 N85-26887
Microscopic study of the influence of impurities on interface bonding
[AD-A151725] 16 p2743 N85-26928
Titanium metal-matrix composites
[AD-D011643] 17 p2930 N85-28086
Localized ionic currents from a corroding iron-copper galvanic couple
[AD-A153627] 18 p3074 N85-29011
Development of carbon based brake lining materials without asbestos content in the form of carbon-carbon composites and carbon-metal or carbon-carbide composites
[BMFT-FB-T-85-014] 18 p3082 N85-29067
Fatigue behavior of unidirectional FP-Al composites with circular holes
[AD-A153466] 18 p3121 N85-29322
Arc spray fabrication of metal matrix composite monotape
[NASA-CASE-LEW-13828-1] 19 p3230 N85-30027
Effect of matrix composition on steel fiber reinforced concrete properties 19 p3230 N85-30028
Three body abrasive wear in various metal combinations 23 p3906 N85-34200
X-ray measurement of thermal stresses in tungsten fiber-copper composites 23 p3907 N85-34205
Evaluation methods of ceramic fiber reinforced metal matrix composite 23 p3907 N85-34206
Fracture behavior of aluminum composites reinforced with fiber 23 p3907 N85-34207
Rotating bending fatigue strength of silicon carbide and alumina-fiber reinforced aluminum
23 p3907 N85-34208

METAL OXIDE SEMICONDUCTORS
NT CHARGE COUPLED DEVICES
NT CHARGE INJECTION DEVICES
NT CHARGE TRANSFER DEVICES
NT CMOS
Metal oxide semiconductors power transistors
[CNES-84/QPE/FT/190] 04 p0496 N85-13166
NMOS test chip for a course in semiconductor parameter measurements
[PB84-216506] 04 p0497 N85-13174
Power MOS fast switching techniques
[DE84-015046] 05 p0732 N85-14707
Optics of solids (surface related) and effect of surface roughness on MOS
[AD-A146883] 07 p0946 N85-15996
Design of self-checking N-MOS (H-MOS) integrated circuits 08 p1064 N85-16742
Silicon superlattices. 2: Si-Ge heterostructures and MOS systems
[NASA-CR-174267] 08 p1224 N85-17711
Comparison of ionizing radiation and hot electron effects in MOS structures
[DE84-016766] 09 p1400 N85-18609
The Si/SiO2 intrinsic states and interface charges. Chapter 1: Origin, properties, models, impact
[HMI-B-413] 09 p1400 N85-18812
Qualitative of analysis of MOS circuits
[AD-A149267] 10 p1480 N85-19341
Variational calculation of the 2D H2 molecule
[INPE-3304-PRE/615] 10 p1554 N85-19796
Study of metal oxide semiconductor structures by capacitive transient spectroscopy
[ENST-84E011] 11 p1737 N85-20926
Factors affecting SOS (Silicon-On-Sapphire) yield and reliability
[AD-A150004] 12 p1835 N85-21515
Metal-semiconductor phase transition and its application
[DRIC-T-7149] 13 p2021 N85-22665
Electrical overstress protection of submicron devices
[AD-A150334] 13 p2064 N85-22892
Algorithm in Walsh function basis for analysis of integrated microcircuits on MOS-structures
13 p2083 N85-23006
Si MOS devices at low temperatures
14 p2297 N85-24225
Studies in electron phenomena in MOS structures: The pulsed C-V method 15 p2659 N85-26407
Completely consumed carbide: A new process for dielectric isolation
[AD-A152379] 17 p2916 N85-27987
Self-scanning MDS-integrated photosensor strip
17 p2940 N85-28151
Goals, achievements of microelectronics program
17 p2945 N85-28179
VLSI workshop and project: February - November 1982
[WSRL-0374-TR] 17 p2951 N85-28223
Random access memory technologies
[AD-A153089] 17 p3006 N85-28597
System design of multi-layer (3-dimensional) integrated circuits
[AD-A153468] 18 p3094 N85-29154
Microstore: The Stanford analog memory unit
[DE85-005534] 18 p3095 N85-29160
Electronic states in silicon and on its interfaces
[AD-A153864] 18 p3193 N85-29807
Electron spin resonance study of interface states induced by electron injection in metal-oxide-semiconductor devices
[DE85-009502] 18 p3195 N85-29817
Photoeffects of semiconductor electrolyte interfaces
[AD-A154163] 20 p3449 N85-31411
Electron lithography STAR design guidelines. Part 1: The STAR user design manual
[NASA-CR-170765] 20 p3513 N85-31840
Electron lithography STAR design guidelines. Part 2: The design of a STAR for space applications
[NASA-CR-170766] 20 p3513 N85-31841
Electron lithography STAR design guidelines. Part 3: The mosaic transistor array applied to custom microprocessors. Part 4: Stores logic arrays, SLAs implemented with clocked CMOS
[NASA-CR-170767] 20 p3514 N85-31842
Synthesis of tests for programmable logic arrays
22 p3777 N85-33408

METAL OXIDES
NT ALKALINE EARTH OXIDES
NT ALUMINUM OXIDES
NT BARIUM OXIDES
NT BERYLLIUM OXIDES
NT BISMUTH OXIDES
NT CALCIUM OXIDES
NT CERIUM OXIDES
NT CHROMITES
NT CHROMIUM OXIDES
NT COBALT OXIDES
NT COPPER OXIDES
NT IRON OXIDES
NT LEAD OXIDES
NT LITHIUM OXIDES
NT MAGNESIUM OXIDES
NT MAGNETITE
NT MANGANESE OXIDES
NT MOLYBDENUM OXIDES
NT NICKEL OXIDES
NT NIOBIUM OXIDES
NT PLUTONIUM OXIDES
NT POTASSIUM OXIDES
NT RUTILE
NT SAPPHIRE
NT TIN OXIDES
NT TITANIUM OXIDES
NT VANADIUM OXIDES
NT YTTRIUM OXIDES
NT ZINC OXIDES
NT ZIRCONIUM OXIDES
An investigation of the role of sintering in gas-solid interactions
[DE84-015481] 02 p0288 N85-11884
The electrochemical deoxidation of molten oxide substances
[BLL-M-35962-(5828.4)] 05 p0614 N85-13920
Charge trapping in low temperature MOS (Metal-Oxide-Silicon) oxides
[AD-A146450] 06 p0860 N85-15467
Combustion kinetics of metal oxide and halide radicals
[AD-A148521] 08 p1122 N85-17076
Adhesive joint formation under field conditions
[AD-D011478] 10 p1453 N85-19153
Thermal barrier coating system
[NASA-CASE-LEW-13324-2] 12 p1796 N85-21266
Characterization of high temperature electrically conducting oxides
[DE85-004296] 12 p1803 N85-21307
Combustion kinetics of metal oxide and halide radicals
[AD-A150924] 14 p2251 N85-23952
High-temperature oxidation of reaction-roasted silicon nitride with various additives 19 p3244 N85-30114
Molecular orbital studies in oxidation: Sulfate formation and metal-metal oxide adhesion
[NASA-CR-176070] 21 p3565 N85-32174
A study of adherent oxide scales
[AD-A155554] 21 p3567 N85-32188
Long-term research in Japan: Amorphous metals, metal oxide varistors, high-power semiconductors and superconducting generators
[DE85-010827] 22 p3748 N85-33230
Composite desiccant structure
[DE85-006400] 23 p3910 N85-34226
Metal alkoxides: Models for metal oxides. Alkoxide ligands in early transition metal organometallic chemistry
[DE85-011368] 23 p3916 N85-34269

METAL PARTICLES
NT METAL POWDER
NT POWDERED ALUMINUM
Breakdown of porous metals by laser radiation
03 p0349 N85-12249
Sample introduction methods for improving the particle detection capability of the spectrometric oil analysis program
[AD-A150139] 13 p2158 N85-23399
Particulate and whisker toughened alumina composites
[DE85-005239] 16 p2743 N85-26930
The enhancement of molecular fluorescence and photochemistry by small metal particles
[AD-A152740] 17 p2919 N85-27994
Spectral characteristics of grinding sparks used for identification of scrap metals
[PB85-196570] 24 p4080 N85-35290

METAL PLATES
Material degradation in heavy steel plates caused by bending with a laser
[AD-A144764] 01 p0052 N85-10343

Characterization of aluminum alloy 7010 in moderate width plate and T651 and T7651 metallurgical states
[REPT-44-806/F] 05 p0619 N85-13961

Copper-nickel sheathing study, phase 2. Two-year service performance of test panels on the ARCO TEXAS
[PB84-242411] 06 p0775 N85-14952

NDE (Nondestructive Evaluation) of oxygen contaminated titanium alloys and weldments
[AD-P004121] 08 p1126 N85-17096

Feasibility study to demonstrate detection of low levels of oxygen contaminant in titanium using eddy current and ultrasonic NDE (Nondestructive Evaluation) techniques
[AD-P004129] 08 p1127 N85-17104

East Europe report: Science and technology
[JPRS-ESA-85-006] 10 p1480 N85-19200

Methodology for stress analysis of heavy metal plate
10 p1480 N85-19203

Bending two-layer metal-polymer plates
11 p1604 N85-20085

Numerical results of acoustic radiation, transmission and reflection of steel plate in water
[AMTE(N)-TM-84037] 13 p2155 N85-23378

Ultrasonic SH wave velocity in textured aluminum plates
[AERE-R-11516] 15 p2509 N85-25475

Angular dependence of the Rayleigh-surface wave velocity in polycrystalline metals with small anisotropy
[AERE-R-11595] 15 p2509 N85-25476

Compositional control of plate steels
16 p2585 N85-25826

Ultrafast holography using optical fibers
[ISL-CO-238/83] 16 p2788 N85-27204

Formation of a fine structure during shock wave welding
[BLL-BISI-TRANS-22401-(9022.06)]
17 p2973 N85-28368

Brittle fracture behaviour of cold formed, welded 10mm to 20 mm thick plate manufactured from plain carbon structural steels
[BLL-BISI-TRANS-21678-(9022.06)]
18 p3120 N85-29311

A clamped rectangular plate containing a crack
[NASA-CR-177925] 20 p3469 N85-31552

Stresses and strains in a plate resulting from two closely-spaced interference-fit fasteners
[ARL/STRUC-TM-409] 23 p3941 N85-34429

Strain measurement using point recognition picture processing
[DRIC-T-7407] 24 p4101 N85-35421

METAL POLISHING

NT ELECTROPOLISHING

Metallographic preparation of materials with various coatings
[BLL-DRIC-TRANS-7522-(3623.66)]
20 p3433 N85-31299

METAL POWDER

NT POWDERED ALUMINUM

Silicon carbide ceramic production
[NASA-TM-77598] 01 p0035 N85-10220

Mechanochemical reactions of elastomers with metals
[AD-A145657] 02 p0186 N85-11246

Tests and modeling for sintering theory
[DE84-015110] 04 p0473 N85-13012

Influence of pressure on compaction during compression of powders of iron and 40Kh and 10R6MS steels
[BLL-M-35995-(5828.4)] 07 p0926 N85-15666

Application of diffusion welding of nickel based metals and application of electron beam welding of hot isostatically pressed nickel based powdered metals
08 p1169 N85-17375

Improving operational properties of titanium alloys by diffusion siliciding 11 p1602 N85-20075

Preparation and study of highly reactive metal powders
[AD-A150026] 12 p1806 N85-21331

Slip casting and nitridation of silicon powder
[NASA-TM-77809] 12 p1818 N85-21406

Structural distortions of ultra-dispersed titanium nitride powders 13 p2029 N85-22717

Degassification of silicon nitride powders of various origins 13 p2030 N85-22718

Apperatus for producing amorphous and microcrystalline metal powders 13 p2030 N85-22720

Research on products obtained by powder metallurgy
16 p2768 N85-27081

Electrodes for flash discharge lamps
[DE85-008897] 17 p2955 N85-28250

Powder metallurgy forged gear development
[NASA-TM-87483] 18 p3117 N85-29295

Distribution of density in closed-impression die forging of axisymmetrical products from metal powders
19 p3245 N85-30118

Sintering studies project
[AD-A154750] 21 p3572 N85-32216

Influence of technology of atomization of naturally alloyed iron on grain-size characteristics of powder material
[BLL-M-35810-(5828.4)] 23 p3914 N85-34257

Chromium-base powder alloys for welding cladding layer of bimetal
[BLL-M-35776-(5828.4)] 23 p3915 N85-34260

Synthesis of ultrafine ceramic and metallic powders in a thermal argon rf plasma
[DE85-009634] 23 p3983 N85-34696

METAL SHEETS

Prediction of forming limit diagrams for deep drawing
06 p0796 N85-15089

Study of superplastic alloys based on Al-Zn-Ca
10 p1442 N85-19092

Method for continuously casting
[AD-D011481] 10 p1459 N85-19195

High strength steel sheet with dual phase structure
[BMFT-FB-T-84-219] 12 p1808 N85-21342

Auxiliary units for Robots 14 p2265 N85-24161

Effectiveness of use of heat-dissipating clamps to reduce deformation during argon arc welding of thin sheets of AMg6 alloy 15 p2501 N85-25427

Experience of sheet stamping robotic complexes
16 p2761 N85-27041

Examination of the regions of the joint of sheets bonded by the explosive welding technique
[BLL-BISI-TRANS-22352-(9022.06)]
17 p2973 N85-28370

Inhibited anticorrosion protection of automotive steel strip in the NLMK
[BLL-M-36250-(5828.4)] 20 p3430 N85-31274

A theory of electromagnetic shielding with applications to MIL-STD-285, IEEE-299, and EMP simulation
[AD-A154905] 21 p3575 N85-32233

METAL SHELLS

Dynamic creep buckling: Analysis of shell structures subjected to time-dependent mechanical and thermal loading 17 p2913 N85-27959

METAL SPINNING

Microstructural and electronic characteristics of metallic spin glasses
[AD-A149959] 12 p1813 N85-21371

METAL SPRAYING

Conversions in amorphous zirconium-vanadium alloy
15 p2496 N85-25400

METAL STRIPS

High strength steel sheet with dual phase structure
[BMFT-FB-T-84-219] 12 p1808 N85-21342

High tensile strength, punchable, hot rolled strips with good plasticity
[BMFT-FB-T-84-256] 18 p3078 N85-29040

METAL SURFACES

Metrological consequences of the hard optical boundary assumption
[PB84-223577] 01 p0121 N85-10827

Erosion of sintered WC-Co alloys
02 p0179 N85-11201

Parameters of geometric stability of laser mirror optical surface 02 p0273 N85-11777

The modification of metallic corrosion by ion implantation: Engineering applications and fundamentals studies
[AD-P003954] 02 p0286 N85-11870

Intramolecular electron transfer at metal surfaces. 4: Dependence of tunneling probability upon donor-acceptor separation distance
[AD-A145611] 02 p0287 N85-11876

Characterization of amorphous surface layers in Fe implanted with Ti and C
[DE84-014960] 02 p0289 N85-11885

Fast and precise processing of material by means of an intensive electron beam
[BMFT-FB-T-84-123] 03 p0342 N85-12201

Dispersion forces of solids under stress. Chemisorption under stress
[AD-A146171] 03 p0373 N85-12380

Electronic and magnetic properties of transition-metal surfaces, interfaces and overlayers
[DE84-016666] 05 p0733 N85-14713

A review of metallic surface treatments for corrosion mitigation
[AD-A146701] 06 p0769 N85-14916

Surface effects of corrosive media on hardness, friction, and wear of materials
[NASA-TM-83711] 07 p0930 N85-15896

Cryogenic glass-to-metal seal
[AD-D011370] 07 p0933 N85-15911

Arc erosion of metal in current interval of 1-10 amperes 07 p0953 N85-16042

Low and moderate temperature oxidation of atomically clean nickel, chromium and Ni-Cr alloys
[DE84-017350] 09 p1295 N85-18131

Ion beam studies of hydrogen in metals
[DE84-017422] 09 p1297 N85-18145

Fundamental aspects on ion-beam surface modification: Defect production and migration processes
[DE85-000093] 09 p1399 N85-18[illegible]

Characterization of erosion of metallic materials under cavitation attack in a mineral oil
[NASA-TM-86934] 10 p1440 N85-19[illegible]

Role of hydrogen in processes of deformation and fracture of metals 10 p1448 N85-191[illegible]

Influence of melting conditions on strength of transition zone between steel and composite material
10 p1450 N85-19[illegible]

Picosecond laser pulse interactions with metallic and semiconductor surfaces
[AD-A149112] 10 p1490 N85-194[illegible]

Effect of implantation species on the tribological response of stainless steel surfaces
[DE85-003530] 10 p1493 N85-194[illegible]

Analysis of phase composition of products of laser destruction of metallic surfaces
11 p1600 N85-20[illegible]

Study of microstructure of aluminum and copper alloys after processing with continuous CO2 laser beam
11 p1601 N85-20[illegible]

Theoretical determination of surface magnetism
[DE85-003224] 11 p1714 N85-207[illegible]

Plasma states near surface of metal irradiated by CO2 laser 11 p1719 N85-2081[illegible]

Classical rainbow scattering of alkali ions on metal surfaces. Application to the investigation of unknown surface structures
[MPIS-10/1984] 11 p1726 N85-2085[illegible]

Mass analysis of neutral particles and ions released during electrical breakdowns on spacecraft surfaces
[NASA-CR-175585] 12 p1793 N85-212[illegible]

Adsorption thermodynamics and surface transport of metal catalyst poisons
[DE85-003750] 12 p1802 N85-21301

Ion-beam nitriding of steels
[NASA-CASE-LEW-14104-1] 12 p1805 N85-2132[illegible]

Effects of B, Ti and Ta implantation on the wear resistance of Fe and Ni-plated Fe
[AD-A149947] 12 p1806 N85-21330

Chemisorption theory: Adsorption on copper-nickel alloys and titanium surface embrittlement
[DE85-001815] 12 p1807 N85-21334

Evaluation of Epoxo 300-C nonskid coating for use on bridge decks
[PB85-108843] 12 p1819 N85-21412

Formation of alumina layers on iron-base alloys
[BLL-T6418/BG/LRS/LRST737/84]
13 p2020 N85-22657

Study of the effects of implantation on the high Fe-Ni-Cr and Ni-Cr-Al alloys
[NASA-CR-175625] 13 p2021 N85-22661

Hydrogen on impurity-covered iron surfaces
14 p2254 N85-239[illegible]

Intramolecular electron transfer at metal surfaces. Part 5: Pendant substituent effects upon thiocarboxylate-bridged Cobalt (3) reduction kinetics at mercury and gold electrodes
[AD-A150647] 14 p2254 N85-23971

Electroreflectance spectroscopy as a probe of the electronic structure at the metal-electronic interface
[DE85-003541] 14 p2428 N85-2497[illegible]

Material for protection of metal surfaces against corrosion by molten salts
[DE85-007714] 16 p2750 N85-259[illegible]

Characteristics of polyacrylic acid-complexed zinc phosphate conversion films deposited on metal surfaces
[DE85-004057] 16 p2750 N85-25974

Surface degradation of ductile metal in elevated temperature gas-particle streams
[DE85-006428] 18 p3074 N85-29017

Micro-reactions of metal contacts on various types of GaAs surfaces
[AD-A153650] 18 p3193 N85-29[illegible]

Resolvability of defect ensembles with positron annihilation studies
[DE85-010041] 18 p3196 N85-299[illegible]

Mechanical modification of friction surfaces of aluminum alloys by friction transfer 19 p3241 N85-300[illegible]

Machining of beryllium with the LLNL precision engineering research lathe
[DE85-010832] 19 p3250 N85-3014[illegible]

Spontaneous emission by two atoms with different resonance frequencies near a metal surface
[AD-A154115] 19 p3353 N85-3078[illegible]

Fluorescence quenching by metal semiconductor and insulator surfaces 19 p3374 N85-309[illegible]

An investigation of cementation and carbonitriding by means of ionic bombardment
[BLL-OA-TRANS-3203-(6196.300)]
20 p3429 N85-312[illegible]

Why CO bonds side-on at low coverage and both side-on and upright at high coverage on the Cr(110) surface
[NASA-CR-176071] 21 p3565 N85-3217[illegible]

Nonradiative damping of molecular electronic excited states by metal surfaces
[AD-A154619] 21 p3701 N85-32994
The effect of metal overlayers of thermionic dispenser cathodes
[AD-A154795] 21 p3701 N85-32995
Materials characterization with intense positron beams
[DE85-011650] 22 p3839 N85-33769
Study on the correlation between grinding conditions and residual stresses in ground surface of steel by the X-ray method 23 p3907 N85-34203
Method for preparing hydride configurations and reactive metal surface
[DE85-006443] 23 p3917 N85-34274
Electronic structure and lattice dynamics of dimensionally constrained and disordered solids
[AD-A155927] 24 p4161 N85-35797

METAL VAPOR LASERS
Numerical analysis of parameters of self-heating copper vapor lasers 02 p0260 N85-11704
High power metal vapor laser
[AD-D011271] 06 p0813 N85-15159
Measurement of elements in the stratosphere
[NASA-CR-175891] 16 p2823 N85-27414
High efficiency transverse dc electron beams
[AD-A152036] 16 p2862 N85-27651
Infrared generation and wave-mixing studies in cesium
[DE85-012663] 24 p4083 N85-35304

METAL VAPORS
NT SODIUM VAPOR
Laser on copper and gold vapors with space diversity media 02 p0270 N85-11762
Metal vapor arc switch electromagnetic accelerator technology
[NASA-CR-174380] 09 p1314 N85-18259
Analysis of the dissipation mechanism within an instationary cathode spot of metal vapor arcs
[AD-A149256] 10 p1558 N85-19825
Combustion kinetics of metal atoms and metallic radicals over wide temperature ranges 13 p1999 N85-22530
Response of steam-water mixtures to pressure transients
[DE85-010796] 19 p3267 N85-30262
Passive Q-modulation of optical cavities by KCl crystals containing OH(-) -ions 21 p3688 N85-32915
Metal vapor lasers and their applications
[ISL-CO-218/84] 22 p3791 N85-33488

METAL WHISKER REINFORCEMENT
U WHISKER COMPOSITES

METAL WORKING
NT CLADDING
NT EXPLOSIVE FORMING
NT FORGING
NT MAGNETIC FORMING
NT METAL DRAWING
NT METAL SPINNING
NT SIZING (SHAPING)
USSR report: Machine tools and metalworking equipment
[JPRS-UMM-84-019] 01 p0035 N85-10214
Microstructural design in low alloy steels
02 p0176 N85-11179
USSR report: Machine tools and metalworking equipment
[JPRS-UMM-84-020] 04 p0491 N85-13126
Process Modeling Applied to Metal Forming and Thermomechanical Processing
[AGARD-LS-137] 06 p0796 N85-15086
Flow-based analyses of metal deformation processes: An overview 06 p0796 N85-15087
Prediction of forming limit diagrams for deep drawing
06 p0796 N85-15089
Numerical methods in metalforming
06 p0797 N85-15092
Finite element simulation of forging processes
06 p0797 N85-15093
Computer-aided design of extrusion dies by metal-flow simulation 06 p0797 N85-15094
Modeling microstructural changes during hot rolling of steels 06 p0798 N85-15096
Heliostat tested 07 p0994 N85-16318
Materials of the fourth scientific-technical Conference on Questions of the Extrusion of Metals (Selected articles)
[AD-A148578] 08 p1130 N85-17121
USSR report: Machine tools and metalworking equipment
[JPRS-UMM-84-021] 08 p1138 N85-17168
Control systems for robotic production lines
08 p1138 N85-17169
USSR report: Machine tools and metalworking equipment
[JPRS-UMM-85-001] 08 p1139 N85-17172
USSR report: Machine tools and metalworking equipment
[JPRS-UMM-85-003] 10 p1461 N85-19211
Developments in GDR metal forming technology assessed 11 p1617 N85-20168
Use of ferrofluids in machining of metals
13 p2045 N85-22802
USSR report: Machine tools and metalworking equipment
[JPRS-UMM-85-005] 13 p2051 N85-22839
Advances in cutting tool technology surveyed
13 p2051 N85-22840
New tooling for plasma cutting technology
13 p2051 N85-22842
Metal waste in machine tool industry examined
14 p2283 N85-24147
USSR report: Machine tools and metalworking equipment
[JPRS-UMM-85-004] 14 p2284 N85-24152
Powder metallurgy production problems
15 p2497 N85-25406
Optimizing hot workability and controlling microstructures in difficult to process high strength and high temperature materials
[AD-D011586] 15 p2510 N85-25482
Production of shaped parts of NITINOL alloys by solid-state sintering
[AD-A152069] 16 p2749 N85-26966
Experience with introduction of Finish perforation of precision parts for optical instruments
16 p2761 N85-27038
USSR report: Machine tools and metalworking equipment
[JPRS-UMM-84-010] 16 p2767 N85-27071
New robotized, vertical broaching machine featured
16 p2767 N85-27074
Development, implementation of industrial lasers reviewed 16 p2767 N85-27075
USSR report: Machine tools and metalworking equipment
[JPRS-UMM-84-014] 17 p2946 N85-28188
New method for determining stampability of sheet materials
[BLL-BISI-22486-(9022.06)] 17 p2972 N85-28360
State of stress and penetration of plastic deformation in forming
[BLL-BISI-22199-(9022.06)] 17 p2977 N85-28398
Strain fields for aluminum at different tooling temperatures and extrusion ratios
[DE85-008257] 18 p3075 N85-29020
The fabrication, microstructure, and strengthening behavior of heavily cold-worked in situ composites
19 p3231 N85-30031
USSR report: Machine tools and metalworking equipment
[JPRS-UMM-85-008] 20 p3437 N85-31329
Thermomechanical deformation in the presence of metallurgical changes 20 p3466 N85-31533
Study on the correlation between grinding conditions and residual stresses in ground surface of steel by the X-ray method 23 p3907 N85-34203
Algorithm for calculation of strain state from measurements of node coordinates of arbitrary curvilinear grid
[BLL-M-36304-(5828.4)] 23 p3940 N85-34422

METAL-INSULATOR-METAL DIODES
U MIM DIODES

METAL-INSULATOR-METAL SEMICONDUCTORS
U MIM (SEMICONDUCTORS)

METAL-METAL BONDING
Influence of aluminum oxide film on thermocompression bonding of gold wire to evaporated aluminum film
[NASA-TM-77503] 03 p0330 N85-12127
Causes of strength reduction in welded titanium-steel joints 03 p0352 N85-12262
Investigation of the creep behaviour of soft soldered joints with solder L-SnAg5 at ambient temperature
[BLL-T6383/BG/WH796/84] 07 p0926 N85-15865
Comparative studies on the electronic structures of W2(O2CH)4 and W2(O2CH)4-(CH3)2 by the relativistic X Alpha-SW method: A d3-d3 metal dimer with a quadruple metal-metal bond?
[AD-A148814] 09 p1397 N85-18793
Microscopic study of the influence of impurities on interface bonding
[AD-A151725] 16 p2743 N85-26926
Solid state bonding of molybdenum and TZM
[BLL-T6439/BG/LRS/LRST751/85]
16 p2792 N85-27220
New examples of clusters, extended metal-metal bonding and interstitial derivatives
[DE85-005926] 17 p3044 N85-28837
Molecular orbital studies in oxidation: Sulfate formation and metal-metal oxide adhesion
[NASA-CR-176070] 21 p3565 N85-32174
Anti wear property of two phasic metal composite
23 p3906 N85-34199

METALLIC GLASSES
Relationships between electronic structure and stability of metallic glasses
[AD-A145141] 01 p0028 N85-10176
Kinetics of short-range ordering in metallic glasses: Analysis of the crossover effect
[DE84-015524] 02 p0187 N85-11251
Use of magnetic compression based on amorphous alloys as a drive for induction linacs
[DE84-014524] 02 p0277 N85-11805
Relationships between electronic structure and stability of metallic glasses
[AD-A145506] 02 p0287 N85-11874
Re-evaluation of phase separation in Ti-Zr-Be metallic glasses
[DE84-015803] 03 p0338 N85-12176
Evidence for d-band conduction in metallic glasses containing transition metal elements
[DE84-014822] 04 p0570 N85-13635
Structural relaxation and isoconfigurational flow of a metallic glass near equilibrium
[AD-A147888] 07 p0933 N85-15915
Electronic properties of intercalated graphite and amorphous metals
[AD-A147664] 08 p1225 N85-17716
Electrical resistivity and structural changes upon relaxation and crystallization of (Mo/sub 0.6/Ru/sub 0.4)sub 100-x/B/sub x/ metallic glasses
[DE84-017261] 09 p1299 N85-18160
Study of the mechanism for annealing embrittlement of an iron-based metallic glass
[DE84-016856] 09 p1300 N85-18164
Amorphous Ni-Ti alloys: A new method of synthesis
[DE85-002744] 11 p1605 N85-20094
Properties and thermal stabilities of amorphous transition metal hydrides
[DE85-002117] 11 p1607 N85-20104
Effects of hydrogen on magnetic properties of amorphous zirconium alloys
[DE85-003303] 11 p1607 N85-20107
Microstructural and electronic characteristics of metallic spin glasses
[AD-A149959] 12 p1813 N85-21371
Quenching effects on iron site partitioning in the Apollo 17 orange glass composition 13 p2184 N85-23553
Surface composition, properties and thermal stability of massive and fine metallic glasses
15 p2513 N85-25506
Effect of nickel addition on the thermal, magnetic and magnetomechanical properties of Fe(80)B(15)Si(5)
[AD-A152261] 16 p2749 N85-26967
Vibrational spectra of a-Fe(.78)P(.22) by inelastic neutron scattering
[DE85-008298] 17 p2922 N85-28016
Theoretical studies on the structures of insulating and metallic glasses
[DE85-010022] 18 p3194 N85-29814
Metallic glass composition
[DE85-011594] 22 p3751 N85-33253

METALLIC HYDROGEN
Experiments with phase transitions at very high pressure
[NASA-CR-174029] 02 p0172 N85-11148

METALLIC PLASMAS
Synthesis of ultrafine ceramic and metallic powders in a thermal argon rf plasma
[DE85-009634] 23 p3983 N85-34896

METALLIC STARS
Lessons from the globular cluster NGC 5466
05 p0739 N85-14749
Ultraviolet observations of Population 2 Cepheids
11 p1754 N85-21034

METALLIZING
Influence of aluminum metallization coatings on corrosion fatigue properties of steel
01 p0018 N85-10112
MOD silver metallization for photovoltaics
[NASA-CR-174011] 01 p0026 N85-10163
Laser-assisted solar cell metallization processing
[NASA-CR-174213] 06 p0813 N85-15160
Amorphous metallic layers in Si metallization systems
06 p0830 N85-15277
A nonnoble front metallization process
06 p0830 N85-15279
Laser-assisted solar-cell metallization processing
06 p0831 N85-15282
Ion cluster beam deposition research
06 p0831 N85-15283
Mod silver metallization for photovoltaics
[NASA-CR-174444] 10 p1509 N85-19518
MOD silver metallization for photovoltaics
[NASA-CR-175460] 10 p1510 N85-19526
A process to produce fine line metallic collection patterns on semiconductors devices
[NASA-CASE-NPO-16413-1] 12 p1805 N85-21325

Electrostatic forming and testing of polymer films on a 16-foot diameter test fixture
[NASA-TM-86326] 13 p2063 N85-22885
Laser-assisted solar cell metallization processing
[NASA-CR-175686] 14 p2350 N85-24528
Structure of condensed aluminum thin film metallizations 15 p2512 N85-25501
Ink jet printing of silver metallization for photovoltaics
[NASA-CR-175798] 15 p2586 N85-25943
Metallurgical means of preventing the corrosion of metal
[BLL-BISI-TRANS-22320-(9022.06)]
17 p2929 N85-28082
Micro-reactions of metal contacts on various types of GaAs surfaces
[AD-A153650] 18 p3193 N85-29606
Metallographic preparation of materials with various coatings
[BLL-DRIC-TRANS-7522-(3623.66)]
20 p3433 N85-31299
High reflective surfaces for millimeter RF waves, phase A — satellite antenna reflectors
[HRS-FR-01] 20 p3442 N85-31366
High temperature electronics technology: Life test report
[AD-A154681] 21 p3580 N85-32257
Amorphous metallic films in silicon metallization systems 21 p3610 N85-32427
Laser-assisted solar-cell metallization processing
21 p3610 N85-32429
A non-noble front metallization process
21 p3611 N85-32430
Pulsed excimer laser processing for cost-effective solar cells 21 p3611 N85-32432
Laser-assisted solar cell metallization processing
[NASA-CR-176124] 22 p3805 N85-33565
Ink jet printing of silver metallization for photovoltaics
[NASA-CR-176054] 22 p3805 N85-33569
Development of metallization process: FSA project, cells and module formation research area
[NASA-CR-176136] 23 p3945 N85-34447

METALLOGRAPHY
Electrolytic lapping technique for vanadium
[DE84-014710] 02 p0183 N85-11227
Biform resolidification and amorphous phases in a laser and electron beam processed tantalum-iridium alloy
[DE84-013334] 02 p0184 N85-11234
Metallography of Kovar/glass/thermite interfaces
[DE84-015247] 02 p0195 N85-11302
A metallographic investigation of rotating bands for 7.5 cm artillery projectiles
[FOA-C-20551-D2] 07 p0929 N85-15888
Metallographic grinding efficiency
[DE85-001520] 09 p1304 N85-18194
Properties and microstructures for dual alloy combinations of three superalloys with alloy 901
[NASA-TM-86987] 16 p2749 N85-26963
Ca-Ga, Sr-Ga and Ba-Ga binary systems
[DE85-006454] 16 p2751 N85-26980
Full statistical characteristics of microdeformation
[BLL-M-36076-(5828.4)] 16 p2798 N85-27254
Physio-chemical mechanisms of the processes of the formation of globular inclusions in ball-bearing metal
[BLL-BISI-TRANS-22235-(9022.06)]
17 p2924 N85-28030
Quality testing to the specifications of the Stahl-Eisen-Pruefblatt 1570/71 using an automatic image analysis system
[BLL-BISI-TRANS-22253-(9022.06)]
17 p2976 N85-28385
Metallographic preparation of materials with various coatings
[BLL-DRIC-TRANS-7522-(3623.66)]
20 p3433 N85-31299
The effect of stress and hot corrosion on nickel-base superalloys
[AD-A154722] 21 p3566 N85-32181
Proceedings of the Twentyseventh Japan Congress on Materials Research
[ISSN-0368-3141] 23 p3903 N85-34160
Characterization of modified 9 r-1 Mo steel sand castings
[DE85-012057] 24 p4080 N85-35287

METALLOIDS
NT ANTIMONY
NT ARSENIC
NT BORON
NT BORON 10
NT GERMANIUM
NT GERMANIUM ISOTOPES
NT SILICON
NT SILICON ISOTOPES
NT TELLURIUM
Measurement of state and dynamic solid state properties in nonmetals using excited probe nuclei on the Erlanger 12 MeV tandem accelerator 03 p0428 N85-12730
Interaction of metals and metalloids with biomembranes
[DE85-004902] 13 p2141 N85-23293
Pressure-dependence of TiS(2) and TiSe(2) bandstructures
[AD-A151200] 15 p2659 N85-26410
Method of production of metals by cathodic solution of their compounds in electrolytic cells
[BLL-OA-TRANS-3207-(6196.300)]
20 p3429 N85-31266

METALLORGANIC COMPOUNDS
U ORGANOMETALLIC COMPOUNDS

METALLURGY
Metalurgy of a 12 percent chromium stainless steel
02 p0178 N85-11195
The metallurgical processes during the soft soldering of copper and copper alloys and the strength characteristics of soldered joints
[BLL-T6366/BG/WH603/84] 06 p0767 N85-14906
Machine tools at 1984 Leipzig Spring Fair
06 p0815 N85-15177
Method for making alloy additions to base metals having higher melting points
[AD-D011403] 07 p0928 N85-15884
USSR report: Materials science and metallurgy
[JPRS-UMS-84-008] 10 p1442 N85-19068
USSR report: Materials science and metallurgy
[JPRS-UMS-84-005] 11 p1597 N85-20044
USSR report: Materials science and metallurgy
[JPRS-UMS-85-001] 15 p2496 N85-25395
Estimation of the depth of a spherical cap in an hydraulic drawing test for some simple conditions of loss of stability
[REPT-4/1984] 16 p2748 N85-26956
Extreme evaluation of reliability indices for components of metallurgical equipment
[BLL-M-36070-(5828.4)] 16 p2796 N85-27234
Metallurgical means of preventing the corrosion of metal
[BLL-BISI-TRANS-22320-(9022.06)]
17 p2929 N85-28082
The thermal calculation of opaque heat screens
[BLL-M-36273-(5828.4)] 20 p3450 N85-31421

METALS
NT ACTINIDE SERIES
NT ALKALI METALS
NT ALKALINE EARTH METALS
NT ALUMINUM
NT ALUMINUM COATINGS
NT ALUMINUM ISOTOPES
NT ALUMINUM 26
NT AMERICIUM
NT AMERICIUM ISOTOPES
NT AMERICIUM 241
NT BARIUM
NT BERYLLIUM
NT BERYLLIUM ISOTOPES
NT BERYLLIUM 7
NT BERYLLIUM 9
NT BERYLLIUM 10
NT BISMUTH
NT CADMIUM
NT CALCIUM
NT CALCIUM ISOTOPES
NT CALIFORNIUM ISOTOPES
NT CERIUM
NT CERIUM 144
NT CESIUM
NT CESIUM ISOTOPES
NT CESIUM 134
NT CESIUM 137
NT CHROMIUM
NT CHROMIUM ISOTOPES
NT COBALT
NT COBALT 60
NT CURIUM
NT CURIUM 244
NT ERBIUM
NT FERROUS METALS
NT GADOLINIUM
NT GALLIUM
NT GOLD
NT GOLD COATINGS
NT HAFNIUM
NT HOLMIUM
NT INDIUM
NT IRIDIUM
NT IRON
NT IRON ISOTOPES
NT IRON 59
NT LANTHANUM
NT LEAD (METAL)
NT LIQUID LITHIUM
NT LIQUID METALS
NT LIQUID POTASSIUM
NT LIQUID SODIUM
NT LITHIUM
NT LUTETIUM
NT MAGNESIUM
NT MAGNESIUM ISOTOPES
NT MANGANESE
NT MANGANESE ISOTOPES
NT MERCURY (METAL)
NT METAL COATINGS
NT METAL CRYSTALS
NT METAL FILMS
NT METAL FOILS
NT METAL MATRIX COMPOSITES
NT METAL POWDER
NT METAL VAPORS
NT MOLYBDENUM
NT NEODYMIUM
NT NEODYMIUM ISOTOPES
NT NICKEL
NT NICKEL COATINGS
NT NICKEL ISOTOPES
NT NIOBIUM
NT NOBLE METALS
NT NONFERROUS METALS
NT OSMIUM
NT OSMIUM ISOTOPES
NT PALLADIUM
NT PLATINUM
NT PLUTONIUM
NT PLUTONIUM ISOTOPES
NT PLUTONIUM 238
NT PLUTONIUM 239
NT POTASSIUM
NT POTASSIUM 40
NT POWDERED ALUMINUM
NT PRASEODYMIUM
NT RADIUM
NT RARE EARTH ELEMENTS
NT REFRACTORY METALS
NT RHENIUM
NT RHODIUM
NT RUBIDIUM
NT RUBIDIUM ISOTOPES
NT RUTHENIUM
NT SAMARIUM
NT SCANDIUM
NT SCANDIUM ISOTOPES
NT SILVER
NT SINTERED ALUMINUM POWDER
NT SODIUM
NT SODIUM ISOTOPES
NT SODIUM VAPOR
NT STRONTIUM 90
NT TANTALUM
NT TECHNETIUM
NT THALLIUM
NT THORIUM
NT THORIUM ISOTOPES
NT TIN
NT TITANIUM
NT TRANSITION METALS
NT TRANSURANIUM ELEMENTS
NT TUNGSTEN
NT URANIUM
NT URANIUM ISOTOPES
NT URANIUM 235
NT VANADIUM
NT YTTERBIUM
NT YTTRIUM
NT ZINC
NT ZINC COATINGS
NT ZIRCONIUM
Study of proton and neutron activation of metal samples in low Earth orbit
[NASA-CR-171183] 01 p0026 N85-10164
The driving-force dependence of electrochemical rate parameters: Origins of anodic-cathodic asymmetries for metal aquo redox couples
[AD-A145605] 02 p0172 N85-11153
Method for calculating linear shrinkage and expansion of metals and alloys
[BLL-M-35747-(5828.4)] 02 p0175 N85-11173
Microstructural basis of strength and toughness in hardmetals 02 p0177 N85-11185
The constitution as the basis for recent and future developments of wear resistant materials
02 p0179 N85-11205
Application of positron annihilation in materials science
[DE84-014733] 02 p0268 N85-11883
Universal binding energy relations in metallic adhesion
[NASA-TM-86869] 03 p0331 N85-12132
Structure and properties of titanium alloys after isothermal deformation at low speeds
03 p0351 N85-12280

Photoelectrochemistry with chemically modified electrodes
[DE84-016798] 04 p0471 N85-12997
A bibliography of publications on corrosion and oxidation from UK government laboratories at Teddington, 1924 - 1983
[NPL-DMA(A)-82] 04 p0472 N85-13004
Effect of humidity on fretting wear of several pure metals
[NASA-TP-2403] 04 p0472 N85-13006
Effect of barrier height on friction behavior of the semiconductors silicon and gallium arsenide in contact with pure metals
[NASA-TP-2405] 04 p0476 N85-13044
Structure and properties of grain boundaries
[DE84-014388] 04 p0570 N85-13636
Distribution of oxygen between metal and basic slags
[BLL-M-35932-(5828.4)] 05 p0616 N85-13935
Characterization of stressed metals using acoustic shear waves 05 p0648 N85-14159
Modelling of deformation and fracture in high-temperature structural materials
[DE84-016906] 06 p0818 N85-15191
Inclined dislocation emission at a shielded crack tip
[DE84-016703] 06 p0818 N85-15192
Polymer-metal interface bond stability
06 p0830 N85-15272
JPL in-house fluidized-bed reactor research
06 p0832 N85-15291
Analysis of the heating process of a body in a melt
[BLL-M-36014-(5828.4)] 07 p0956 N85-16057
Measurement of high temperature strain by the laser-speckle strain gauge
[NASA-TM-77751] 07 p0977 N85-16207
Ion microscopy of metals and semiconductors
[AD-A147118] 07 p1043 N85-16626
Application of electricity to the reheating of metals prior to forming. Forging, lamination, induction
[BLL-TR-T6399/BG/MRS14903/84]
08 p1137 N85-17160
Lider studies of the alkali metals
08 p1184 N85-17460
Electronic properties of intercalated graphite and amorphous metals
[AD-A147664] 08 p1225 N85-17716
Metal-support interactions: Their effects upon adsorption, electronics, and activity/selectivity properties of cobalt in hydrogenation
[DE85-003316] 09 p1292 N85-18113
Resistivity of alloys
[DE85-000906] 09 p1296 N85-18138
Ion beam studies of hydrogen in metals
[DE84-017422] 09 p1297 N85-18145
A metal-catalyzed rearrangement of alkene-alkynes and the stereochemistry of metallacyclobutene ring opening
[AD-A149084] 10 p1435 N85-19042
Characterization of erosion of metallic materials under cavitation attack in a mineral oil
[NASA-TM-86934] 10 p1440 N85-19075
Determination of vapor phase content when metals are struck by laser radiation pulses of various densities
10 p1445 N85-19106
Excitation modes and parameters of stress waves in metal exposed to single laser pulses
10 p1446 N85-19109
Removal of heavy metals by artificial wetlands
[PB85-116127] 10 p1513 N85-19548
Kinetics of reaction of metals and non-metals during diffusion welding 11 p1602 N85-20076
Electron-plastic effect in metals
11 p1605 N85-20089
Insulation bonding test system
[NASA-CASE-MFS-25862-1] 11 p1610 N85-20126
Computer simulation of grain-boundary properties in ionic crystals and metals
[DE85-000577] 11 p1734 N85-20908
Studies of silicon-refractory metal interfaces: Photoemission study of interface formation and compound nucleation
[AD-A150075] 12 p1800 N85-21293
Properties of supported metal catalysts
[DE85-003927] 12 p1802 N85-21303
Method and apparatus for detecting acoustic emissions from metal matrix wire
[AD-D011556] 12 p1927 N85-22107
Effects of scatterer spacing statistics on ultrasonic backscatter signal spectra
[DE85-003259] 12 p1928 N85-22114
Experimental determination of systems suitable for study as monotectic binary metallic alloy solidification models
12 p1948 N85-22235
Characteristics of EMI generated by negative metal-positive dielectric voltage stresses due to spacecraft charging 13 p1995 N85-22505
Adequacy of metal ablation process with laser radiation and a shock-compressed plasma
13 p2028 N85-22708
Effect of transparent coatings on generation of laser-induced shock waves in metals
13 p2028 N85-22711
Generation of longitudinal acoustic waves by modulated helicon waves — nonlinear steady state waves in metals
13 p2090 N85-23049
Characterization of atomic defects and their aggregates using positron annihilation spectroscopy
[DE85-006206] 14 p2418 N85-24918
Monte Carlo lattice models for adsorbed polymer conformation
[NASA-TP-2453] 14 p2426 N85-24981
USSR report: Materials science and metallurgy
[JPRS-UMS-85-001] 15 p2496 N85-25395
Study of amorphous strips and microconductors by ferromagnetic resonance method
15 p2497 N85-25402
C2H(n) fragments on metal surfaces
[AD-A151474] 15 p2505 N85-25449
Sweden develops new rapid solidification process
15 p2531 N85-25610
Electronic properties of new organic conductors
[DE85-005590] 15 p2549 N85-25736
Experimental and theoretical study of the infrared reflectance of thin oxide films on metals
[DE85-005799] 15 p2653 N85-26366
Pressure-dependence of TiS(2) and TiSe(2) bandstructures
[AD-A151200] 15 p2659 N85-26410
Ignition of metals in high pressure oxygen
16 p2735 N85-26874
Ductility equation for porous metals and its linearization
[BLL-M-36118-(5828.4)] 16 p2748 N85-26958
Electrical resistivity in amorphous metals: Consequences of phonon ineffectiveness in the diffraction model
[AD-A152130] 16 p2779 N85-27150
Thermal expansion effects in electrical transport in amorphous metals
[AD-A152477] 17 p2930 N85-28089
Electrons and grain boundary energies in metals
[DE85-009530] 17 p2932 N85-28099
Limiting values of stress state index after rupture of metals
[BLL-BISI-TRANS-22293-(9022.06)]
17 p2978 N85-28407
The effect of ion-bombardment-induced atomic mixing on depth-profiling of interfaces
[AD-A153199] 17 p3044 N85-28834
Thermodynamic calculations of equilibrium states in metal-carbon-hydrogen-oxygen system
[BLL-BISI-TRANS-22092-(9022.06)]
17 p3045 N85-28844
Field theory of the metal-insulator transitions in restricted symmetries
[NOTA-INTERNA-829] 18 p3196 N85-29826
Multiaxial fatigue and fracture: A literature review
[ARL/STRUC-R-410] 19 p3285 N85-30370
Polyethylene imine-metal salt solid electrolyte
[AD-D011678] 19 p3305 N85-30485
Spectrographic investigation of low-voltage arc discharge in argon atmosphere
[BLL-M-36276-(5828.4)] 20 p3422 N85-31242
Study of solute segregation at interfaces using Auger electron spectroscopy
[DE85-005709] 20 p3423 N85-31247
Method of production of metals by cathodic solution of their compounds in electrolytic cells
[BLL-OA-TRANS-3207-(6196.300)]
20 p3429 N85-31266
The nature of the anomalies on the polytherms of the properties of molten metallic alloys
[BLL-M-36265-(5828.4)] 20 p3430 N85-31277
Influence of error of determination of moire isotach orders on the stability of their approximation
[BLL-M-36277-(5828.4)] 20 p3450 N85-31423
Viscoplasticity based on overstress with a differential growth law for the equilibrium stress
20 p3466 N85-31532
On the use of internal state variables in thermoviscoplastic constitutive equations
20 p3466 N85-31536
On numerical integration and computer implementation of viscoplastic models 20 p3467 N85-31542
Simulation model of acoustic emission due to microscopic fracture in metals
[BLL-BISI-TRANS-22367-(9022.06)]
20 p3523 N85-31909
Development of processes for the inclusion of radioactive waste in glass-metal compounds and ceramic materials
[BLL-CE-TRANS-8014-(9022.09)]
20 p3526 N85-31931
Metal-insulator-metal models of tunneling
20 p3536 N85-32006
Study of proton and neutron activation of metal samples in low Earth orbit
[NASA-CR-171596] 21 p3558 N85-32130
High-frequency furnace
[DE85-011210] 21 p3586 N85-32291
On one nonlinear problem of laser thermochemistry
21 p3697 N85-32971
The effect of metal overlayers of thermionic dispenser cathodes
[AD-A154795] 21 p3701 N85-32995
Long-term research in Japan: Amorphous metals, metal oxide varistors, high-power semiconductors and superconducting generators
[DE85-010827] 22 p3748 N85-33230
Proceedings of the Twentyseventh Japan Congress on Materials Research
[ISSN-0368-3141] 23 p3903 N85-34180
Method for extracting lanthanides and actinides from acid solutions by modification of Purex solvent
[DE85-005763] 23 p3909 N85-34220
Direct determination of metals in organic matrices by Inductively Coupled Plasma-Atomic Emission Spectrometry (ICP-AES)
[DE85-012015] 23 p3911 N85-34233

METAMORPHISM (GEOLOGY)
Petrology of deep crustal xenoliths from the eastern Snake River Plain, Idaho 02 p0226 N85-11477
Geology and geochemistry of early Tertiary submarine volcanic rocks of the Aleutian Islands, and their bearing on the development of the Aleutian Island Arc
03 p0389 N85-12493
Metamorphic petrology of the Table Mountain area, Circle quadrangle, Alaska 04 p0516 N85-13295
Structural observations in the Circle quadrangle, Yukon-Tanana Upland, Alaska 04 p0517 N85-13298
The northern coast plutonic-metamorphic complex, southeastern Alaska and northwestern British Columbia
04 p0518 N85-13305
Cretaceous plutonic rocks, Mitkof and Kupreanof Islands, Petersburg quadrangle, southeastern Alaska
04 p0518 N85-13306
Late oligocene gabbro near Ketchikan, southeastern Alaska 04 p0518 N85-13307
A tectonic and metamorphic history of the north-central Klamath Mountains, California 05 p0673 N85-14323
Late precambrian to ordovician metamorphism and orogenesis in the Blue Ridge and western Piedmont, Virginia Appalachians 09 p1352 N85-18503
Conditions for formation of parageneses containing kyanite-orthoclase in region of Mount Provender and Pratt Peak (Shackleton Range, Antarctica)
19 p3296 N85-30447
Hydrothermal alteration in the 3.5 b.y. old Onverwacht Group of South Africa 21 p3718 N85-33071
The 3.5 b.y. old Onverwacht Group: A remnant of ancient oceanic crust 21 p3718 N85-33073
Bedrock geology of the Brattleboro Quadrangle, Vermont-New Hampshire
[DE85-011027] 22 p3815 N85-33634
Structural development of the west-central Grant Range, Nye County, Nevada 24 p4115 N85-35506

METASTABILITY
U METASTABLE STATE

METASTABLE ATOMS
Infrared emission and atomic transitions
[AD-A147840] 07 p1041 N85-16607

METASTABLE STATE
Metastable phase formation in ion implanted metals
[DE84-014945] 02 p0183 N85-11229
Raman scattering from metastable GaSb(1-x) Ge(2x) alloys
[AD-A145897] 03 p0327 N85-12108
Fatigue crack propagation in metastable titanium alloys
[AD-A145824] 03 p0372 N85-12376
Formation of superconductive Al(GeSi) alloys by low temperature laser quenching methods
[DE84-016667] 04 p0474 N85-13021
Search for neutral, penetrating, metastable particles produced in the SLAC beam dump
[DE84-012468] 04 p0560 N85-13569
Kohn anomaly in metastable fcc lanthanum at low temperatures
[DE84-015459] 04 p0569 N85-13628
Electron spin polarization effects in low energy electron diffraction. ion neutralization and metastable atom deexcitation at solid surfaces
[DE84-016550] 04 p0572 N85-13649

The growth of metastable peritectic compounds
[NASA-CR-171289] 07 p0920 N85-15824
The growth of metastable peritectic compounds
[NASA-CR-171290] 07 p0920 N85-15825
An experimental and theoretical investigation of optogalvanic effects
[AD-A148456] 08 p1223 N85-17700
Effect of inner subshell ionization for emission lines of OIV ion 09 p1388 N85-18729
Alloy development, processing and characterization of devitrified titanium base microcrystalline alloys
[AD-A149609] 12 p1806 N85-21327
Specifics of structure and mechanical properties of metastable beta-titanium alloys after deformation and aging 13 p2032 N85-22731
Theoretical and experimental studies of stabilized metastable helium
[AD-A150706] 14 p2417 N85-24913
Effect of inner subshell ionization on emission lines OIV ions
[IPPJ-719] 19 p3370 N85-30903
Theoretical investigation of material characteristics of semiconductor superlattices
[AD-A154126] 19 p3375 N85-30938
Globally-asynchronous locally-synchronous systems
[AD-A154624] 21 p3573 N85-32222
Detection of excited states by laser-induced fluorescence
[AD-A155558] 21 p3592 N85-32326
Modulated voltage metastable ionization detector
[NASA-CASE-ARC-11503-1] 23 p3933 N85-34374

METAZOA
U ANIMALS

METEOR BURSTS
U METEOROID SHOWERS

METEOR CRATERS
U CRATERS

METEOR HAZARDS
U METEOROID HAZARDS

METEOR TRAILS
Scattering of radio waves on magnitized meteor trail
03 p0344 N85-12221
Discovery of nuclear tracks in interplanetary dust
06 p0689 N85-15647
Influence of Faraday effect in ionosphere on nonmutuality of meteor radio channel
07 p0952 N85-16037
MWR, Meteor Wind Radars 08 p1184 N85-17462
Calculation of amplitude-phase characteristics of signal scattered obliquely on meteor trail
13 p2073 N85-22948
Ionization coefficient for atomic collisions in meteor trail 16 p2720 N85-26792
Interpolation problems in meteor radar analysis, part 7.6A 21 p3626 N85-32528
MENTOR: Adding an outlying receiver to an ST radar for meteor-wind measurement 21 p3628 N85-32538

METEORITE COLLISIONS
Impact phenomena as factors in the evolution of the Earth
[NASA-CR-174015] 01 p0072 N85-10474

METEORITE COMPRESSION TESTS
U COMPRESSION TESTS
U MECHANICAL PROPERTIES
U METEORITES

METEORITE CRATERS
Martian terrain ages 13 p2181 N85-23537
Interaction of Martian flow ejecta blankets with pre-existing impact craters: Morphological observations
13 p2183 N85-23546
The Mars ancient cratered terrain, smooth plains boundary: Implications of Viking color data for evolution of the Amenthes Region 15 p2682 N85-26564
A search for evidence of large body Earth impacts associated with biological crisis zones in the fossil record 15 p2682 N85-26567
Large arcuate scars: A geological legacy of the Earth's accretionary past 21 p3721 N85-33089

METEORITES
NT ALLENDE METEORITE
NT CARBONACEOUS CHONDRITES
NT CARBONACEOUS METEORITES
NT CHONDRITES
NT IRON METEORITES
NT MICROMETEORITES
NT PANTAR CHONDRITES
NT STONY METEORITES
NT TEKTITES
The origin of the Moon 04 p0588 N85-13754
Atmospheric heating of meteorites: Results from nuclear track studies 06 p0882 N85-15607
Solar cosmic ray produced neon in lunar soils and their implication for gas-rich meteorite studies
06 p0887 N85-15636
Meteorite concentrations in Antarctica: How complete is the picture? 06 p0889 N85-15644
Discovery of nuclear tracks in interplanetary dust
06 p0889 N85-15647
Mineralogical investigations of lunar samples and meteorites
[NASA-CR-174291] 08 p1256 N85-17918
Lunar sample analysis — Allende meteorite
[NASA-CR-171851] 10 p1572 N85-19911
Antarctic Meteorite Newsletter, volume 8, number 1
[NASA-CR-175587] 12 p1961 N85-22328
Sixteenth Lunar and Planetary Science Conference. Press abstracts
[NASA-CR-175692] 15 p2680 N85-26548
Evidence in meteorites for an active early Sun
15 p2680 N85-26550
Nd-isotopic evidence for the origin of the Sudbury complex by meteoritic impact 15 p2680 N85-26554
Identification of the youngest meteorites and a discussion of the possibility that they came from Mars
15 p2681 N85-26559
What we know about Mars (but otherwise wouldn't) if it is the shergottite parent body
15 p2682 N85-26565
The impact ejection of living organisms into space
15 p2682 N85-26566
Mineralogical studies of lunar meteorites and their lunar analogs 15 p2683 N85-26572
The role of thermal motions of air particles for fireballs
[PUBL-59] 17 p3053 N85-28900
MENTOR: Adding an outlying receiver to an ST radar for meteor-wind measurement 21 p3628 N85-32538
Explosion in flight 21 p3683 N85-32883
Terrestrial Planets: Comparative Planetology
[NASA-CR-176093] 22 p3851 N85-33849
Noble gas patterns in the atmospheres of Mars and Earth: A comparison via the SNC meteorites
22 p3852 N85-33853
Ultraheavy cosmic ray tracks in meteorites: A reappraisal, based on calibrations with relativistic ions
[OG-4.4-10] 22 p3860 N85-34041
Cosmic-ray exposure records and origins of meteorites
[SH-7.1-7] 23 p4047 N85-35099
Depth and size effects on cosmogenic nuclide production in meteorites
[SH-7.1-9] 23 p4048 N85-35101
Clusters and cycles in the cosmic ray age distributions of meteorites
[SH-7.1-11] 23 p4048 N85-35103
The read-out system of spatial distribution of thermoluminescence in meteorites
[SH-9.1-16] 23 p4052 N85-35131

METEORITIC COMPOSITION
Size dependence of chondrule textural types
06 p0882 N85-15606
Neutron activation analysis of stoney spherules from a marine sediment sample 06 p0883 N85-15608
Oxygen isotopes in deep sea spherules
06 p0883 N85-15609
Minor elements in relict olivine grains of deep-sea spheres: Match with Mg-rich olivines from C2 meteorites 06 p0883 N85-15610
The Colony meteorite and the possible existence of a new chemical subgroup of CO3 chondrites
06 p0885 N85-15621
X-radiography of slices of the Allende Meteorite
06 p0885 N85-15622
A study of tetrataenite 06 p0885 N85-15623
Mossbauer spectroscopy and X-ray diffraction of samples from the Santa Catharina iron meteorite
06 p0885 N85-15624
Structural development in the Santa Catharina meteorite 06 p0886 N85-15625
Low temperature diffusion coefficients in the Fe-Ni and FeNiP systems: Application to meteorite cooling rates
06 p0886 N85-15626
Extreme incompatibility of Pb during the crystallization of magmatic iron meteorites 06 p0886 N85-15627
Experimental and theoretical study of the formation of the 2AB, 3AB, and 9A meteorite chemical groups from the parent liquid 06 p0886 N85-15628
Investigations concerning the magmatic iron meteorites: Static vs. dynamic experiments
06 p0886 N85-15629
Boron cosmochemistry 06 p0888 N85-15642
Differentiated meteorites and the components of chondrites
[NASA-CR-174201] 06 p0890 N85-15649
Hibonite: Crystal chemistry and origin of blue coloration in meteoritic assemblages 13 p2184 N85-23555
Crystal chemistry of meteoritic hibonites
13 p2185 N85-23556
Evidence in meteorites for an active early Sun
15 p2680 N85-26550
A spectacular nitrogen isotope anomaly in Bencubbin
15 p2683 N85-26569
Origin and evolution of ordinary chondrite meteorites
15 p2683 N85-26571
Mineralogical studies of lunar meteorites and their lunar analogs 15 p2683 N85-26572
Origin of mesosiderites as a natural consequence of planet formation 15 p2683 N85-26574
Ionization coefficient for atomic collisions in meteor trail 16 p2720 N85-26792
Cosmic-ray exposure records and origins of meteorites
[SH-7.1-7] 23 p4047 N85-35099
Accelerator experiments on the contribution of secondary particles to the production of cosmogenic nuclides in meteorites
[SH-7.1-8] 23 p4048 N85-35100
Depth and size effects on cosmogenic nuclide production in meteorites
[SH-7.1-9] 23 p4048 N85-35101
Spallogenic origin of nuclei in meteorites
[SH-7.1-10] 23 p4048 N85-35102

METEORITIC DAMAGE
Directional properties of circular Maria: Interpretation in the context of a testable gravitational capture model for lunar origin 04 p0586 N85-13743
Origin of the Moon 04 p0587 N85-13745
Grainsize evolution and differential comminution in an experimental regolith 06 p0888 N85-15658
Spectral reflectance studies on the orientale region of the Moon 06 p0888 N85-15659
Periodic cometary showers: Real or imaginary?
15 p2680 N85-26555
A search for evidence of large body Earth impacts associated with biological crisis zones in the fossil record 15 p2682 N85-26567

METEORITIC DUST
U MICROMETEOROIDS

METEORITIC IONIZATION
U ATMOSPHERIC IONIZATION
U METEOR TRAILS

METEORITIC MICROSTRUCTURES
X-radiography of slices of the Allende Meteorite
06 p0885 N85-15622
Mossbauer spectroscopy and X-ray diffraction of samples from the Santa Catharina iron meteorite
06 p0885 N85-15624
Speculations on the formation of metallic meteorite phases 06 p0889 N85-15646
Antarctic Meteorite Newsletter, volume 8, number 1
[NASA-CR-175587] 12 p1961 N85-22328
Crystal chemistry of meteoritic hibonites
13 p2185 N85-23556
Evidence in meteorites for an active early Sun
15 p2680 N85-26550

METEOROID CRATERS
U METEORITE CRATERS

METEOROID DUST CLOUDS
NT ZODIACAL DUST

METEOROID HAZARDS
Manmade orbital debris studies at NASA Langley
12 p1783 N85-21192
Periodic cometary showers: Real or imaginary?
15 p2680 N85-26555

METEOROID PROTECTION
Manmade orbital debris studies at NASA Langley
12 p1783 N85-21192
Hypervelocity impact investigations and meteoroid shielding experience related to Apollo and Skylab
12 p1785 N85-21206
Space debris protection for a reusable orbital transfer vehicle 12 p1786 N85-21208
Parametric analysis: SOC meteoroid and debris protection 12 p1786 N85-21209

METEOROID SHOWERS
NT ARIETID METEOROIDS
NT ORIONID METEOROIDS
Periodic cometary showers: Real or imaginary?
15 p2680 N85-26555

METEOROID TECHNOLOGY SATELLITE
U EXPLORER 46 SATELLITE

METEOROIDS
NT ARIETID METEOROIDS
NT MICROMETEOROIDS
NT ORIONID METEOROIDS
NT RADIO METEORS
NT ZODIACAL DUST
Natural environment design criteria for the Advanced X-ray Astrophysics Facility (AXAF) definition and preliminary design
[NASA-TM-86481] 01 p0014 N85-10068
Interaction of large meteoroids with the atmosphere
11 p1656 N85-20431
The global meteor observation system (GLOBMET)
11 p1656 N85-20432
Middle Atmosphere Program. Handbook for MAP, volume 7
[NASA-CR-175479] 11 p1656 N85-20457

Global meteor observation system (GLOBMET)
11 p1656 N85-20436

Atmospheric profile imprint in firewall ablation coefficient
11 p1662 N85-20473

Survivable propagation
[AD-A150070] 12 p1829 N85-21478

Improvement of VHF(MB) model
[AD-A150087] 12 p1829 N85-21480

Plasma production by meteoroid impact
13 p2174 N85-23492

The evolution of meteor streams
15 p2678 N85-26539

Examination of returned solar-max surfaces for impacting orbital debris and meteoroids
15 p2681 N85-26560

A study of the chemistry of alkali metals in the upper atmosphere
[AD-A156349] 24 p4117 N85-35524

METEOROLOGICAL BALLOONS

NT JIMSPHERE BALLOONS

Feasibility of long duration ballooning in Antarctica
[PB84-240571] 04 p0541 N85-13443

Meteorological Sounding System (MSS) standard operating procedures
[AD-A149513] 10 p1519 N85-19578

Location and data collection for long stratospheric balloon flights 14 p2328 N85-24377

Development of an adjustable buoyancy balloon tracer of atmospheric motion. Phase 1: Systems design and demonstration of feasibility
[PB85-185817] 22 p3817 N85-33648

METEOROLOGICAL CHARTS

The 500 millibar sign frequency teleconnection charts: Winter
[PB85-108276/GAR] 07 p1009 N85-16410

Use and interpretation of isentropic analyses
[PB85-132694] 11 p1668 N85-20618

Investigations of micro-turbulence in the bottom of the boundary layer
[AD-A149823] 12 p1896 N85-21897

Digital processing of mesoscale analysis and space sensor data
[NASA-CR-171429] 13 p2146 N85-23319

Development of a graphic system: Example using the outline of synoptic charts
[INPE-3296-PRE/611] 16 p2810 N85-27327

A graphic system for drawing synoptic maps by computer
[INPE-3215-PRE/568] 16 p2834 N85-27474

SINOGRAFO: A system for influencing and forecasting weather
[INPE-3349-PRE/626] 16 p2834 N85-27475

Monthly and seasonal weather outlook for mid-February to mid-March 1985, volume 39, number 4, February 14, 1985
[PB85-164580] 18 p3149 N85-29500

METEOROLOGICAL FLIGHT

Airborne research meteorological data collected by the National Hurricane Research Laboratory (Hurricane Research Division/AOML) during the 1982-1983 hurricane seasons: Inventory and availability
[PB85-163681] 17 p2997 N85-28528

Proceedings of Meteorological Motor Glider (MEMO) Workshop '84
[DFVLR-MITT-85-04] 24 p4121 N85-35542

Motor glider meteorology 24 p4121 N85-35543

Typical and historical aspects of motor gliders as meteorological measuring aircraft
24 p4121 N85-35544

Determination of vertical air velocity using measurements of the aircraft motion
24 p4121 N85-35545

A comparison between Falcon data and motor glider data 24 p4121 N85-35547

Case studies for flux measurements along a low-flying route to the south of Munich 24 p4121 N85-35548

Environmental-physical measurements and determination of atmospheric turbulence with the ASK-16 motor glider 24 p4122 N85-35549

Partitioning of the vertical turbulent energy transport into positive and negative contributions — meteorology
24 p4122 N85-35551

Aircraft measurements during the Bonn Experiment (BONEX 1) — meteorology 24 p4122 N85-35552

Meteorological measurements with motor gliders in Poland 24 p4122 N85-35555

The principles of wind measurement with the help of aircraft 24 p4123 N85-35558

METEOROLOGICAL INSTRUMENTS

NT BAROMETERS
NT CLOUD HEIGHT INDICATORS
NT IONOSONDES
NT RADIOSONDES
NT RAIN GAGES
NT RAWINSONDES
NT WEATHER DATA RECORDERS
NT WIND VANES

An evaluation of wind measurements by four Doppler sodars
[PB85-115301] 10 p1520 N85-19586

ADAPS (Airborne Data Acquisition and Processing System) operation and maintenance manual
[AD-A149297] 11 p1585 N85-19983

Instructor's handbook on meteorological instrumentation
[PB85-105930] 11 p1688 N85-20615

Cabauw (Netherlands) meteorological data tapes 1973-1984: Description of instrumentation and data processing for continuous measurements
[KNMI-WR-84-6] 14 p2379 N85-24685

SCPP (Sierra Cooperative Pilot Project) Forecasting Support 16 p2837 N85-27493

Snow Scale/Rate meter
[AD-D011648] 17 p2994 N85-28505

Notes on atmospheric stability, turbulence, and its measurements
[AD-A155230] 21 p3637 N85-32588

Verification of Doppler sodar measurements — atmospheric boundary layer
[KNMI-WR-85-2] 22 p3817 N85-33645

METEOROLOGICAL PARAMETERS

Pavement friction measurements on nontangent sections of roadways, vol. 1
[PB84-219732] 01 p0036 N85-10227

The SANCOR programme on coastal processes, April 1982 - March 1988
[REPT-68] 01 p0069 N85-10455

The development of objective forecast techniques based on advection of surface weather parameters
01 p0078 N85-10522

Synthesis of current measurements in Puget Sound, Washington. Volume 1: Index to current measurements made in Puget Sound from 1908-1980 with daily and record averages for selected measurements
[PB84-214105] 01 p0089 N85-10603

A principal component analysis of eastern Transvaal seasonal rainfall, 1950 to 1981
02 p0212 N85-11395

Arctic haze: Meteorological aspects of long-range transport 02 p0230 N85-11499

Southern Hemisphere atlas of 1-minute rainfall rates
[AD-A145421] 02 p0231 N85-11509

STS natural environment analysis
[NASA-CR-171221] 03 p0322 N85-12079

Achievements in development of space meteorology
03 p0343 N85-12212

GASP cloud- and particle-encounter statistics and their application to LFC aircraft studies. Volume 2: Appendixes
[NASA-TM-85835-VOL-2] 03 p0395 N85-12522

Closely spaced independent parallel runway simulation
[DOT/FAA/CT-84/45] 04 p0457 N85-12902

Acquisition and storage of Cabauw measurements: A system proposal
[KNMI-TR-48] 04 p0540 N85-13434

Operational numerical forecasts: Survey and verification over the period 1978-1983
[KNMI-TR-49] 04 p0540 N85-13435

Atmospheric environment for Space Shuttle (STS-41D) launch
[NASA-TM-86484] 05 p0679 N85-14358

Investigation of satellite measurements in the presence of clouds, forcing influences on clouds and feedback to the large scale following convection
05 p0682 N85-14381

ECMWF/NMC/GLAS joint simulation study
05 p0682 N85-14385

Epidemiologic methods applied to the study of the relationship between climate and human health
05 p0687 N85-14418

Spring program summary, 1983
[PB84-222223] 06 p0839 N85-15330

Climate applications: General
07 p1001 N85-16355

Meteorological aspects of the 1982-83 El Nino/southern oscillation episode 07 p1001 N85-16356

Climate and water quality 07 p1002 N85-16368

Revised Uniform Summary of Surface Weather Observations (RUSSWO). Shemya AFB, Alaska, parts A-F
[AD-A146917] 07 p1005 N85-16388

Revised Uniform Summary of Surface Weather Observations (RUSSWO). Pope AFB, Fayetteville, North Carolina, parts A-F
[AD-A146918] 07 p1005 N85-16389

Revised Uniform Summary of Surface Weather Observations (RUSSWO). Sondestrom AB, Greenland, parts A-F
[AD-A146919] 07 p1005 N85-16390

Revised Uniform Summary of Surface Weather Observations (RUSSWO). England AFB, Alexandria, Louisiana, parts A-F
[AD-A146920] 07 p1006 N85-16391

Revised Uniform Summary of Surface Weather Observations (RUSSWO). Parts A-F: Homestead AFB, Florida
[AD-A147203] 07 p1007 N85-16396

Limited surface observations climatic summary (LISOCS). Camp Casey, Tong Du Chon, Korea
[AD-A147204] 07 p1007 N85-16397

Limited surface observatins climatic summary (LISOCS). Ansback AHP, Germany
[AD-A147205] 07 p1007 N85-16398

Revised Uniform Summary of Surface Weather Observations (RUSSWO). O'Hare International Airport, Chicago, parts A-F
[AD-A147206] 07 p1007 N85-16399

Interrelationship of atmospheric parameters in Honduras
[AD-A147371] 07 p1007 N85-16401

Guidelines for atmospheric measurements in support of electro-optical systems testing
[AD-A148090] 08 p1186 N85-17474

The visibility climatology of McMurdo Sound-Williams Field, Antarctica
[AD-A148108] 08 p1189 N85-17492

An automatic weather station network for low-altitude wind shear investigations
[AD-A148139] 08 p1189 N85-17493

Meteorological factors responsible for high CO (carbon monoxide) levels in Alaskan cities
[PB85-115137/GAR] 09 p1350 N85-18493

Mesoscale storm and dry period parameters from hourly precipitation data: Program documentation
[DE85-001366] 09 p1357 N85-18536

Weather data for simplified energy calculation methods. Volume 4: United States, WYEC data
[DE85-000491] 09 p1357 N85-18539

Weather data for simplified energy calculation methods. Volume 3. Western United States: TRY data
[DE85-000495] 09 p1358 N85-18540

Weather data for simplified energy calculation methods. Volume 1. Eastern United States: TRY data
[DE85-000493] 09 p1358 N85-18541

PATHFINDER: A trajectory prediction system for the Great Lakes
[PB85-115335] 10 p1506 N85-19506

Equations and algorithms for meteorological applications in air weather service
[AD-A148894] 10 p1519 N85-19575

Meteorological Sounding System (MSS) standard operating procedures
[AD-A149513] 10 p1519 N85-19578

MIZEX (Marginal Ice Zone Program): A program for mesoscale air-ice-ocean interaction experiments in Arctic marginal ice zones. 5. MIZEX 84. Summer experiment PI (Principal Investigator) preliminary reports
[AD-A148986] 10 p1521 N85-19594

Middle Atmosphere Program. Handbook for MAP. Volume 12: Coordinated Study of the Behavior of the Middle Atmosphere in Winter (PMP-1) Workshops
[NASA-CR-175475] 11 p1685 N85-20492

Weather data for simplified energy calculation methods. Volume 2: Middle United States. TRY data
[DE85-000494] 11 p1687 N85-20606

International list of selected, supplementary and auxiliary ships — WMO
[WMO-47-ED-84] 11 p1687 N85-20609

Instructor's handbook on meteorological instrumentation
[PB85-105930] 11 p1688 N85-20615

Use and interpretation of isentropic analyses
[PB85-132694] 11 p1688 N85-20618

Civil weather satellite systems
11 p1711 N85-20768

Meteorological and oceanographic support during the Falklands conflict 11 p1712 N85-20769

Practical applications of satellite-derived meteorological and oceanographic data in Naval operations
11 p1712 N85-20771

Sector analysis of relevant meteorological parameters for long range transport of air pollutants
[NR-27] 12 p1893 N85-21862

Navy tactical applications guide. Volume 4. Part 1. Eastern North Pacific weather analysis and forecast applications
[AD-A150097] 12 p1896 N85-21900

Slow motions in the tropical troposphere
13 p2131 N85-23262

Summary of Meteorological Observations, Surface (SMOS) Camp Pendleton, California
[AD-A150482] 13 p2138 N85-23277

Summary of Meteorological Observations, Surface (SMOS), Bermuda
[AD-A150537] 13 p2138 N85-23278

Summary of Meteorological Observations Surface (SMOS), Sigonella, Sicily/Navy [AD-A150539] 13 p2138 N85-23280

Summary of Meteorological Observations, Surface (SMOS), Alameda, California [AD-A150609] 13 p2138 N85-23281

The experience of the Swedish Meteorological and Hydrological Institute (SMHI) with the ARGOS system [PM-U1/81] 14 p2240 N85-23892

Meteorological buoys developed at the EERM laboratory 14 p2326 N85-24374

The Tropical Ocean and Global Atmosphere program (TOGA) 14 p2330 N85-24411

An overview of NDBC drifting buoy development programs — NOAA Data Buoy Center (DBC) 14 p2332 N85-24422

Cabauw (Netherlands) meteorological data tapes 1973-1984: Description of instrumentation and data processing for continuous measurements [KNMI-WR-84-6] 14 p2379 N85-24665

Meteorological conditions affecting electromagnetic propagation on the Arabian Peninsula [AD-A152019] 15 p2544 N85-25708

East coast snowstorm survey 15 p2598 N85-26013

Model sensitivity studies of major east coast storms 15 p2598 N85-26016

Three-dimensional/perspective display techniques for meteorological data sets 15 p2599 N85-26018

General meteorological package (GEMPAK) 15 p2599 N85-26019

Meteorological factors in Earth-Satellite propagation [NASA-CR-175764] 16 p2769 N85-27069

EHF attenuation derived from emission temperatures in light rain [AD-A151166] 16 p2772 N85-27110

Routine wave and meteorological measurements in offshore areas using ARGOS data surveillance 16 p2812 N85-27344

Forecast of Atlantic seasonal hurricane activity for 1985 16 p2833 N85-27470

Summary of Meteorological Observations, Surface (SMOS), Dallas, Texas [AD-A150599] 16 p2835 N85-27480

Hurricane Research Division, fiscal year 1984 programs, fiscal year 1985 projections 16 p2836 N85-27491

Investigation of air pollution impact in Eastern Bavaria: Measurement results from August and September, 1984 [DFVLR-FB-85-03] 17 p2988 N85-28471

Functional and performance requirements of the next NOAA-Kasas City computer system 17 p2994 N85-28510

Air Weather Service (AWS) climatic briefs: Europe [AD-A152528] 17 p2996 N85-28519

Radar study of the melting layer [ESA-CR(P)-1974] 17 p2997 N85-28527

Contributions on the subject of longitudinal movements of aircraft in wind shears [NASA-TM-77637] 18 p3139 N85-29432

Environmental Research Laboratories publication abstracts, FY 1984 [PB85-180594] 19 p3313 N85-30540

Atmospheric environment for space shuttle (STS-51C) launch [NASA-TM-86508] 19 p3315 N85-30547

Workshop on objective analysis: Analysis strategies for field-dependent estimation [PB85-179901] 19 p3318 N85-30569

Experimental investigation of properties of ice-forming reagents 21 p3639 N85-32602

Solar energy meteorological research and training program: Region 4 [DE85-011783] 22 p3816 N85-33640

Development of an adjustable buoyancy balloon tracer of atmospheric motion. Phase 1: Systems design and demonstration of feasibility [PB85-185817] 22 p3817 N85-33648

Description of a test site for large-scale heavy gas dispersion and combustion experiments [DE85-004987] 23 p3911 N85-34231

Incorporating meteorological data into receptor analysis: RAPS (Regional Air Pollution Study) revisited [PB85-188944] 24 p4114 N85-35503

An atmospheric boundary layer model forced by the operational ECMWV-model [WSR-3] 24 p4120 N85-35541

Meteorological data from the OPTOMA (Ocean Prediction Through Observations, Modeling and Analysis) program OPTOMA 2, leg D2. 30 Jun. - 10 Jul. 1984 [AD-A156134] 24 p4123 N85-35560

METEOROLOGICAL PROBES

U SONDES

METEOROLOGICAL RADAR

Operational evaluation of 5 cm Doppler radar. Two contributions: Review of WSR-74C Doppler radar operations at WSO Montgomery, Alabama (April 1982 - August 1983). The Johnson-Effect resolving ambiguous Doppler velocities [PB84-207521] 01 p0041 N85-10269

Combining radar and satellite data for the localization and identification of summer convection 01 p0077 N85-10509

A multipurpose weather radar network 01 p0077 N85-10510

Remote sensing of atmospheric particulates: Technological innovation and physical limitations in applications to short-range weather prediction [NSF ATM-82-09684] 01 p0077 N85-10511

The use of dual polarisation radar for observing and predicting convective activity 01 p0077 N85-10512

The PROMIS Doppler radar system; design and operational experience 01 p0077 N85-10513

Nowcasting with Doppler radar: The forecaster-computer relationship 01 p0077 N85-10514

Doppler radar analysis of a frontal zone prior to convective development 01 p0077 N85-10515

VHF/UHF radar and its application in nowcasting 01 p0078 N85-10516

The potential use of atmospheric profilers in short-range prediction 01 p0078 N85-10518

Preliminary assessment of very short term forecasting of rain from single radar data 01 p0078 N85-10523

Optimum parameters for determining the motion of radar field by cross-correlation method 01 p0079 N85-10524

Digital radar data as an aid in nowcasting in Hong Kong 01 p0079 N85-10525

Simple methods in very short-range forecasting based on data from a mesoscale network of automatic stations (ANETZ) and from satellite (Meteosat) and radar — Swiss Alps 01 p0082 N85-10548

Operational precipitation observation system using digitized radar and rain gages 01 p0082 N85-10549

The French weather radar network: A status report 01 p0082 N85-10550

PROMIS 600: The pilot project for the future Swedish weather service 01 p0083 N85-10560

Project COST 72 (The European weather radar project) today 01 p0084 N85-10561

Utilization of SAGE aerosol profiles in the analysis of Mauna Loa stratospheric lidar data [NASA-CR-174198] 05 p0675 N85-14332

Rain volume estimation over areas using satellite and radar data 05 p0686 N85-14406

Simultaneous ocean cross-section and rainfall measurements from space with a nadir-pointing radar [NASA-TM-86167] 07 p0987 N85-16273

MWR, Meteor Wind Radars 08 p1184 N85-17462

The potential of the NEXRAD radar system for warning of bird hazards [AD-P004210] 11 p1583 N85-19977

Digital controller for the Wave Propagation Laboratory's VHF and UHF wind-profiling radars [PB85-112142] 11 p1626 N85-20236

Prospective investigations with DFVLR radar of possible relevance in the assessment of radio interference due to scattering from precipitations — meteorological radar [DFVLR-FB-84-42] 12 p1830 N85-21485

Radiosodar system for remote synchronous measurements of wind speed, temperature and its fluctuations 13 p2110 N85-23145

Experimental study of anisotropy of scattering of radar signals by clouds and precipitation 14 p2340 N85-24473

Observation of precipitating clouds by a vertically pointing radar at Morino in the Iburi District, Hokkaido, Japan 15 p2582 N85-25922

Hurricane structure and dynamics from stereoscopic and infrared satellite observations and radar data 15 p2594 N85-25988

Contamination of the fetch-limited directional wave spectrum by waves emanating from an embayment [NASA-TM-84441] 15 p2604 N85-26046

The development and application of volume scan and cell tracking capabilities for the analysis of convective cloud systems 16 p2830 N85-27451

The use of radar in determining precipitation processes in the BEWMEX area 16 p2831 N85-27455

Conducting a wind sensing study [NASA-CR-175782] 16 p2832 N85-27465

Statistical comparison of radar echoes of convective precipitation between the northern Alps and its foreland [DFVLR-FB-85-07] 17 p2950 N85-28215

Weather radar studies [AD-A152563] 17 p2996 N85-28521

Radar study of the melting layer [ESA-CR(P)-1974] 17 p2997 N85-28527

Progress in radar meteorology 18 p3148 N85-29[illegible]

Use of radar with frequency modulation for studying atmospheric boundary layer 19 p3296 N85-30[illegible]

Middle Atmosphere Program. Handbook for MAP. Volume 14: URSI/SCOSTEP Workshop on Technical Aspects of MST Radar [NASA-CR-176066] 21 p3615 N85-32466

Meteorological and aeronomical requirements for MST radar networks (keynote paper), part 1 21 p3615 N85-32467

Tropospheric-stratospheric exchange, part 1.1A 21 p3615 N85-32468

Gravity waves from the stratosphere to the mesosphere, part 1.3B 21 p3616 N85-32471

The suppression of convective wavebreaking by radiative transfer processes, part 1.3C 21 p3616 N85-32472

General circulation of the middle atmosphere, part 1.4B 21 p3617 N85-32474

Performance of the Colorado wind-profiling network, part 1.5A 21 p3617 N85-32475

Vertical transport in the atmosphere: Measurement capabilities and requirements of VHF radars, part 1.6A 21 p3617 N85-32476

Comparison of tropopause altitude determination by the Platteville Radar, Sunset Radar and the NWS Rawinsonde 21 p3617 N85-32477

Synoptic-scale dynamics with vertical velocity, part 1.8A 21 p3617 N85-32478

Practical use of a tropopause height determination algorithm on an MST radar data set, part 1.8B 21 p3618 N85-32479

Morphology of the scattering targets: Fresnel and turbulent mechanisms, part 2.1A 21 p3618 N85-32481

Usefulness of multifrequency MST radar measurements, part 2.6B 21 p3619 N85-32487

Anisotropy of the permittivity field inferred from aspect-sensitive radar echoes 21 p3620 N85-32492

Accuracy of velocity and power determination by the Doppler method 21 p3620 N85-32493

Determination of billows and other turbulent structures, part 4.1A 21 p3621 N85-32500

Spectral measurements of turbulence and gravity waves, part 4.2A 21 p3622 N85-32501

Gravity-wave spectra in the atmosphere observed by MST radar, part 4.2B 21 p3622 N85-32502

Momentum flux measurements: Techniques and needs, part 4.5A 21 p3623 N85-32508

Tropospheric gravity waves observed by three closely spaced ST radars 21 p3623 N85-32509

Determination of horizontal and vertical wavelengths of gravity waves in the mesosphere by spaced wind measurements 21 p3623 N85-32510

Criteria for site selection and frequency allocation (keynote paper), part 5 21 p3623 N85-32511

Frequency and site selection criteria for MST radars, part 5.1A 21 p3624 N85-32512

Summary of session on optimum transmitter and antenna configuration for MST radar, part 6 21 p3624 N85-32514

Practicality of electronic beam steering for MST/ST radars, part 6.2A 21 p3624 N85-32516

Testing and optimizing MST coaxial collinear arrays, part 6.4A 21 p3625 N85-32518

Overview of on-line data processing for MST radars (keynote paper), part 7 21 p3625 N85-32519

Coding schemes for improving MST radar performance, part 7.1A 21 p3625 N85-32520

Elimination of range-aliased echoes in the VHF radars 21 p3625 N85-32521

Sidelobe reduction of Barker codes, part 7.1C 21 p3625 N85-32522

A high-speed digital signal processor for atmospheric radar, part 7.3A 21 p3626 N85-32525

Hardware schemes for fast Fourier transform, part 7.4A 21 p3626 N85-32526

Criteria and algorithms for spectrum parameterization of MST radar signals 21 p3626 N85-32527

Interpolation problems in meteor radar analysis, part 7.6A 21 p3626 N85-32528

Data base management: MSTRAC (keynote paper), part 8 21 p3626 N85-32530

Sample interchange of MST radar data from the Urbana radar 21 p3627 N85-32531

MST radar data management 21 p3627 N85-32532

Data base for the Colorado profiling network 21 p3627 N85-32533

Further developments of EISCAT as an MST radar 21 p3627 N85-32534

Status of the Jicamarca radar 21 p3627 N85-32535

Recent results at the Sunset radar 21 p3627 N85-32536

The Boot Lake MF imaging radar
21 p3628 N85-32537
MENTOR: Adding an outlying receiver to an ST radar for meteor-wind measurement 21 p3628 N85-32538
Summary of progress at the Poker Flat Observatory in Alaska 21 p3628 N85-32539
Urbana radar systems: Possibilities and limitations
21 p3628 N85-32540
The Sondrestrom radar: Progress and proposed upgrades for ST work 21 p3629 N85-32541
Progress and plans for the Colorado Wind Profiler Network 21 p3628 N85-32542
The MU radar now partly in operation
21 p3628 N85-32543
Network ST radar and related measurements at Pennsylvania State University 21 p3629 N85-32544
A note on the proposed UK VHF radar
21 p3629 N85-32545
The Adelaide VHF radar: Capabilities and future plans
21 p3629 N85-32546
The Proust radar 21 p3629 N85-32547
Millstone Hill radar: Capabilities for S/T observations
21 p3629 N85-32548
The Ponape ST radar 21 p3629 N85-32549
Measurements of vertical velocity over flat terrain by ST radar and other related uses of the radar data set
21 p3630 N85-32550
Automated cell detection as a mesocyclone precursor tool
[AD-A154952] 21 p3635 N85-32577
Method and apparatus for four-beam radar
[PB85-181477] 22 p3757 N85-33289
A multi-channel radar receiver
[AD-A156058] 24 p4087 N85-35333
Polarization diversity addition to the 10 centimeter Doppler weather radar
[AD-A156062] 24 p4087 N85-35334

METEOROLOGICAL RESEARCH AIRCRAFT
NOAA (National Oceanic and Atmospheric Administration) Aircraft Satellite Data Link (ASDL)
[PB84-243773] 07 p0942 N85-15976
Three powered sailplanes as meteorological instrumentation for atmospheric boundary layer studies at DFVLR
[DFVLR-FB-84-50] 17 p2897 N85-27862
DFVLR measuring system for the determination of the spatial distribution of environmental parameters of the atmosphere by means of mobile instrumented platforms
[DFVLR-FB-85-09] 17 p2969 N85-28472
Airborne research meteorological data collected by the National Hurricane Research Laboratory (Hurricane Research Division/AOML) during the 1982-1983 hurricane seasons: Inventory and availability
[PB85-163681] 17 p2997 N85-28528
A preliminary intercomparison between numerical upper wind forecasts and research aircraft measurements of jet streams
[NASA-CR-167884] 24 p4120 N85-35539

METEOROLOGICAL ROCKETS
U SOUNDING ROCKETS

METEOROLOGICAL SATELLITES
NT AEROS SATELLITE
NT ARC CLOUDS
NT DMSP SATELLITES
NT METEOSAT SATELLITE
NT NIMBUS SATELLITES
NT NIMBUS 5 SATELLITE
NT NIMBUS 7 SATELLITE
NT NOAA SATELLITES
NT NOAA 6 SATELLITE
NT NOAA 7 SATELLITE
NT NOAA 8 SATELLITE
NT SIRS B SATELLITE
NT TIROS N SERIES SATELLITES
NT TIROS SATELLITES
Satellite reconnaissance
[AD-B085034] 01 p0015 N85-10094
The past, present, and anticipated future contributions of geosynchronous satellites to short range prediction
01 p0076 N85-10503
A system for meteorological satellite, radar, conventional data and model analysis 01 p0082 N85-10551
Atlas of polar cap energetic particle observations. Volume 1: TIROS-N, 1 January 1979 - 28 February 1981
[PB84-233402] 04 p0535 N85-13419
Frost nowcasting in the agricultural area of Valencia (Spain) — meteorological satellites
05 p0658 N85-14225
Use of photographs of meteorologic satellites in synoptic analysis
[BESIT-5] 05 p0679 N85-14357
Applications of sequential estimation to numerical weather prediction 05 p0681 N85-14374
Weather and climate parameters from Tiros-N
05 p0681 N85-14377
Weather satellite products in the Flight Service Automation System (FSAS)
[AD-A146520] 06 p0759 N85-14855
Satellite definition of the bio-optical and thermal variation of coastal eddies associated with the African current
[AD-A147910] 07 p0989 N85-16282
An auroral X-ray imaging spectrometer
[AD-A147756] 08 p1185 N85-17469
The rationale and suggested approaches for research geosynchronous satellite measurements for severe storm and mesoscale investigations
[NASA-TM-86185] 09 p1356 N85-18532
Technical evaluation report on the 48th Symposium of the Avionics Panel on Space System Applications to Tactical Operations
[AGARD-AR-203] 10 p1425 N85-18988
Processing of Global Area Coverage (GAC) data of the TIROS-N/NOAA series polar orbiters
[AD-A148992] 10 p1519 N85-19576
Defense Meteorological Satellite Program (DMSP)
11 p1711 N85-20766
Military applications of meteorological satellite (METSAT) data 11 p1711 N85-20767
Development of satellite data presentation for environmental forecasting 11 p1712 N85-20770
Meteorological Satellite Center Technical Note No. 10, 1984
[MSC-TN-10] 12 p1894 N85-21884
An analysis of the data obtained by a simultaneous observation of GMS and GMS-2: A study of the difference between the brightness temperatures by GMS and those by GMS-2 12 p1894 N85-21888
GMS operational calibration procedure and status
12 p1895 N85-21893
Remote sensing used for study of forest resources
13 p1963 N85-22440
Research on atmospheric dust formations using satellite observation data 15 p2485 N85-25339
NOAA satellite operations: Programs briefing — Environmental satellites, LANDSAT, and space station polar platform 15 p2599 N85-26020
Recent failures of weather satellites
[S-HRG-98-1070] 16 p2731 N85-26855
Aerospace technology determines forest-fire danger
19 p3295 N85-30427
Six mechanisms used on the SSM/1 radiometer
22 p3798 N85-33534

METEOROLOGICAL SERVICES
A summary of operational developments in nowcasting and short-range forecasting techniques on the Canadian West Coast 01 p0082 N85-10547
The French weather radar network: A status report
01 p0082 N85-10550
Development of nowcasting in China
01 p0083 N85-10554
PROFS: An approach to improved operational weather services — Program for Regional Observing and Forecasting Services (PROFS) 01 p0083 N85-10555
A subjective evaluation of the PROFS operational workstation based upon a real-time forecasting experiment in summer 1983 — Program for Regional Observing and Forecasting Services (PROFS) 01 p0083 N85-10556
PROMIS 600: The pilot project for the future Swedish weather service 01 p0083 N85-10560
Use of short-range weather forecasts at construction sites: Some results from a user and a market test
01 p0084 N85-10563
Benefits resulting from tailored very-short-range forecasts in Sweden 01 p0084 N85-10564
Some aspects of matching nowcasting and Very-Short-Range Forecasting (VSRF) products with the need of a multilingual community of a mountainous country — Swiss Alps 01 p0084 N85-10566
Videotex and weather services: Finnish applications
01 p0084 N85-10567
Acquisition and storage of Cabauw measurements: A system proposal
[KNMI-TR-48] 04 p0540 N85-13434
Weather satellite products in the Flight Service Automation System (FSAS)
[AD-A146520] 06 p0759 N85-14855
Climate and climate data. Report on the workshop held in Brasilia (Argentina) from 11-15 April 1983
07 p1001 N85-16357
Requirements for training in climate-related subjects
07 p1004 N85-16378
Equations and algorithms for meteorological applications in air weather service
[AD-A148894] 10 p1519 N85-19575
AFOS (Automation of Field Operations and Services)-ERA forecast verification, September 1984
[PB85-137578] 12 p1897 N85-21912
Project PAPA: The integration of drifting buoy data into an operational meteorological service
14 p2238 N85-23874
The ARGOS communications performance trials
14 p2326 N85-24376
Collecting meteorological reports with the ARGOS system 14 p2329 N85-24398
A weather service for agriculture
16 p2830 N85-27450
Meteorology and food production: The theme of the 16 meteorology day
[AD-A152372] 17 p2996 N85-28518
J. P. Finley: The first severe storms forecaster
[PB85-17453] 19 p3318 N85-30566
150 years of meteorology in Belgium
22 p3817 N85-33642

METEOROLOGICAL STATIONS
U WEATHER STATIONS

METEOROLOGY
NT AEROLOGY
NT AGROMETEOROLOGY
NT ALPINE METEOROLOGY
NT BIOMETEOROLOGY
NT HYDROMETEOROLOGY
NT LONG RANGE WEATHER FORECASTING
NT MARINE METEOROLOGY
NT MESOMETEOROLOGY
NT MICROMETEOROLOGY
NT NOWCASTING
NT NUMERICAL WEATHER FORECASTING
NT POLAR METEOROLOGY
NT RADIO METEOROLOGY
NT STATISTICAL WEATHER FORECASTING
NT SYNOPTIC METEOROLOGY
NT TROPICAL METEOROLOGY
NT WEATHER FORECASTING
Research study: Studies in atmospheric processes from Space Platforms
[NASA-CR-171176] 01 p0072 N85-10473
The climate of Denmark. Summaries of observations from light vessels. 3: Sea temperature
[ISBN-87-7478-215-0] 01 p0073 N85-10481
Photon and electron dosimetry at the Physikalische-Technische Bundesanstalt in Brunswick
[PTB-DOS-9] 01 p0119 N85-10814
Seminar on Principal Components Analysis in the Atmospheric and Earth Sciences
[CSIR-S-334] 02 p0211 N85-11388
Application of correspondence analysis to meteorological data 02 p0211 N85-11393
Statistical interpretation of NWP model output: An overview of techniques used and results achieved
[REPT-551.509.313] 02 p0231 N85-11503
Bibliography of climate textbooks and studies
[WCP-84] 02 p0231 N85-11505
Southern Hemisphere atlas of 1-minute rainfall rates
[AD-A145421] 02 p0231 N85-11509
Atmospheric tracer experiments in a deep narrow valley
[PB84-234590] 04 p0532 N85-13402
Report on United States Antarctic research activities, February 1983 - October 1984 and United States Antarctic research activities planned for October 1984 - September 1985
[PB84-231265] 05 p0677 N85-14352
Atmospheric environment for Space Shuttle (STS-41D) launch
[NASA-TM-86484] 05 p0679 N85-14358
Implicit numerical methods in meteorology
05 p0666 N85-14408
A comparison of evaporation duct models for IREPS (Integrated Refractive Effects Prediction System)
[AD-A146471] 06 p0799 N85-15103
USSR report: Earth sciences
[JPRS-UES-84-007] 06 p0819 N85-15196
The 47th Annual Meteoritical Society Meeting
[NASA-CR-174071] 06 p0881 N85-15599
A summary of the foundation research program
[AD-A146524] 06 p0891 N85-15656
USSR report: Earth sciences
[JPRS-UES-84-008] 07 p0980 N85-16223
Atmospheric acidification chemistry: A review
[PB84-215490] 09 p1350 N85-18495
Natural environment analysis
[NASA-CR-171333] 10 p1426 N85-19010
USSR report: Earth sciences
[JPRS-UES-85-003] 10 p1497 N85-19446
Frozen precipitation and concurrent weather: A case study for Munchen-Riem, West Germany
[AD-A149227] 10 p1519 N85-19577
Instructor's handbook on meteorological instrumentation
[PB85-105930] 11 p1688 N85-20615
Isentropic objective analysis
[PB85-112167] 11 p1688 N85-20617
Use and interpretation of isentropic analyses
[PB85-132694] 11 p1688 N85-20618

Communications software for Olympics Micromation Computer System
[PB85-108610] 11 p1704 N85-20723
Space Shuttle interactive meteorological data system study
[NASA-CR-171418] 12 p1892 N85-21876
On the relative motion of typhoons: In the case of Typhoon 8306 and Typhoons 8306 and 8307
12 p1894 N85-21885
On the error of typhoon intensity estimation by means of IR Dvorak technique occurring when the eye is very small 12 p1894 N85-21886
SAOSUM: A short summary of observations
[PB85-120384] 12 p1897 N85-21909
Earth radiation budget experiment software development
[NASA-CR-172567] 12 p1912 N85-22002
USSR report: Earth sciences
[JPRS-UES-85-002] 13 p2105 N85-23116
Mean flow and turbulence in complex terrain NPS (Naval Postgraduate School)/Vandenberg measurement system
[AD-A150184] 13 p2138 N85-23274
Environmental satellites 14 p2328 N85-24392
USSR report: Earth sciences
[JPRS-UES-85-004] 14 p2332 N85-24424
Possible multiple atmospheric thermal modes with time scale on order of one month 14 p2333 N85-24430
Variational mesoscale satellite data assimilation and initialization
[NASA-CR-175704] 14 p2378 N85-24680
An introduction to USAFETAC (USAF Environmental Technical Applications Center)
[AD-A150971] 14 p2378 N85-24682
Geophysical Fluid Dynamics Laboratory activities, FY84, plans, FY85
[PB85-147601] 15 p2558 N85-25783
Low Temperature Science. Series A: Physical Sciences
[ISSN-0439-3538] 15 p2581 N85-25917
Operational methods for calculating atmospheric dispersion
[BLL-CE-TRANS-8040-(9022.09)]
15 p2588 N85-25955
General meteorological package (GEMPAK)
15 p2589 N85-26019
Oceanographic variations in recent decades and their impact on the fertility of the Iceland Sea
15 p2602 N85-26034
USSR report: Earth sciences
[JPRS-UES-85-005] 16 p2807 N85-27307
Review and annotated bibliography of benthic studies in coastal and estuarine areas of Florida with a selected compilation of worldwide benthic methodological references and southeastern United States benthic taxonomic references
[PB85-151041] 16 p2822 N85-27405
Study of the functions of similarity of the planetary boundary layer. Part 1: Theory
[INPE-3129-PRE/520-PT-1] 16 p2826 N85-27426
Symposium on Atmospheric Sciences in South Africa
[CSIR-S-331] 16 p2829 N85-27442
Hurricane Research Division, fiscal year 1984 programs, fiscal year 1985 projections 16 p2836 N85-27491
Comparison of circulation statistics based on FGGE (First GARP Global Experiment) level 3-B analyses produced by GFDL (Geophysics Fluid Dynamics Laboratory) and ECMWF (European Centre for Medium Range Weather Forecasts) for special observing periods
[PB85-153948] 16 p2836 N85-27492
Compilation of abstracts of theses submitted by candidates for degrees
[AD-A151722] 16 p2875 N85-27739
Developments in the area of air traffic control systems and the relation with meteorology
[NLR-MP-84029-U] 17 p2895 N85-27848
Air Weather Service (AWS) climatic briefs: Europe
[AD-A152528] 17 p2996 N85-28519
Airborne research meteorological data collected by the National Hurricane Research Laboratory (Hurricane Research Division/AOML) during the 1982-1983 hurricane seasons: Inventory and availability
[PB85-163681] 17 p2997 N85-28526
Improved cloud and surface fields derived from HIRS2/MSU 18 p3140 N85-29439
Hellmut Berg issue — meteorology
[MITT-39] 18 p3147 N85-29463
Numerical meteorology 18 p3147 N85-29464
Regional meteorology of the Bering Sea during MIZEX-West, February and March 1983
[PB85-173699] 18 p3150 N85-29503
Middle Atmosphere Program. Handbook for MAP. Volume 14: URSI/SCOSTEP Workshop on Technical Aspects of MST Radar
[NASA-CR-176065] 21 p3615 N85-32466
Generation of available potential energy and the energy cycle during the global weather experiment
[NASA-CR-175301] 21 p3634 N85-32572
Meteorological weapons
[AD-A154735] 21 p3635 N85-32575
A transportable, machine oriented library of european sky and terrain radiance distributions with contemporary radiometric and meteorological profiles
[AD-A155254] 21 p3637 N85-32590
Medium range atmospheric forecast system: Evaluation plan
[AD-A155823] 21 p3638 N85-32595
Meteorology and Society: Statements presented at the 9th congress under agenda item 12 — World Meteorological Organization
[WMO-643] 22 p3817 N85-33644

METEORS
U METEOROIDS

METEOSAT SATELLITE
Short period forecasts in West Africa using Meteosat data 01 p0079 N85-10526
The METEOSAT exploitation project, operational use of a remote sensing system 05 p0658 N85-14223
Conceptual ideas for a second generation METEOSAT system 05 p0658 N85-14226

METERS
U MEASURING INSTRUMENTS

METHACRYLATE RESINS
U ACRYLIC RESINS

METHANATION
An infrared study of isotopic exchange during methanation over supported rhodium catalysts; an inverse spillover effect
[AD-A149390] 10 p1435 N85-19046
An infrared study of the hydrogenation of carbon dioxide on supported rhodium catalysts
[AD-A149477] 10 p1436 N85-19049
Characterization of supported metal catalysts by imaging, microdiffraction and microanalysis techniques
[DE85-005567] 14 p2253 N85-23961

METHANE
Plasma deposited diamondlike carbon on GaAs and InP
[NASA-TM-86870] 01 p0123 N85-10844
Raman and fluorescence spectroscopy in a methane-nitrous oxide laminar flame
[AD-A146092] 03 p0326 N85-12111
Methane heat transfer investigation
[NASA-CR-171199] 03 p0362 N85-12318
Study of catalysts and mechanisms in synthesis reactions
[DE84-015025] 04 p0470 N85-12990
Methane-fueled vehicle RD and D
[GPO-37-926] 04 p0481 N85-13064
Diffusion of gases in porous solids: Simulation and measurements
[DE84-016292] 04 p0500 N85-13191
Biomass thermochemical conversion program
[DE84-017177] 06 p0621 N85-13972
The structure of dilute combusting sprays
[NASA-CR-174838] 07 p0905 N85-15728
The abundance of deuterium in the outer solar system from ground-based measurements of monodeuterated methane 07 p1060 N85-16725
Liquid phase methanol process development unit: Installation, operation, and support studies
[DE85-001311] 09 p1301 N85-18171
Mechanisms and reaction dynamics related to methane combustion
[PB85-129690] 10 p1438 N85-19065
Dissociated methanol citation
[DE85-000505] 10 p1458 N85-19188
Test report for Getty Synthetic Fuels, Inc., Calumet City, Illinois
[PB85-119493] 10 p1459 N85-19191
Kinetics of nitric oxide formation in laminar and turbulent methane combustion
[PB85-149696] 12 p1804 N85-21313
Mechanisms of heat and mass transfer across a double-diffusive interface
[PB85-148488] 12 p1848 N85-21594
Portable remote laser sensor for methane leak detection
[NASA-CASE-NPO-15790-1] 12 p1855 N85-21631
Ignition of mixtures of SiH sub 4, CH sub 4, O sub 2, and Ar or N sub 2 behind reflected shock waves
[NASA-TP-2415] 13 p1974 N85-22395
Anaerobic digestion of biomass: status summary and research development needs, 1983
[PB85-161925] 13 p2040 N85-22772
Optical properties of hydrogenated amorphous carbon films grown from methane plasma
[NASA-TM-86995] 15 p2656 N85-26406
Modeling the role of radicals in the ignition of and flame propagation in hydrogen-air and methane-air mixtures
16 p2744 N85-26935
Low pressure storage of methane on inter
for potential vehicular applications
[DE85-006949] 16 p2758 N85-
Studies related to the deep Earth gas: 198
[PB85-171114] 16 p2816 N85-
Monodeuterated methane in the outer solar system. 2
Its detection on Uranus at 1.6 microns
[NASA-CR-175762] 16 p2862 N85-
Fatty and aromatic acid catabolizing bacteria for methanogenic ecosystems
[DE85-008133] 17 p2908 N85-
Heat of mixing experiments for liquified gases
[PB85-183697] 18 p3084 N85-
Optical waveguide sensor for methane gas
[AD-D011691] 19 p3273 N85-
Flash pyrolysis of biomass with reactive and non
gases
[DE85-010962] 19 p3306 N85-
Atmospheric chlorofluromethanes as tracers of oce
circulation and mixing: Measurement and calibra
techniques and studies in the Greenland and Norweg
Seas 19 p3319 N85-
Rayleigh scattering for density measurements i
premixed flames: One point, time series data
20 p3424 N85-
Mechanistic and kinetic studies of the elementary processes in catalytic combustion of methane
[PB85-188308] 20 p3435 N85-31
Elementary processes in the catalytic combustion of methane (mechanism, intermediates, and controlling reactions)
[PB85-188357] 20 p3438 N85-31
Electrochemical methane sensor
[DE85-011683] 22 p3767 N85-
Measurements of the fragmentation of (40)Ar, (56)Fe and
(12)C in CH2C and H targets between 300 and 18
MeV/nuc at the Bevalac
[OG-7.2-19] 23 p4016 N85-
Microbiological and biochemical studies towards optimization of substrate utilization by methanogenic bacteria
[PB85-188332] 24 p4084 N85-

METHIONINE
Blood amino acids of cosmonauts before and after 211-day spaceflight 12 p1900 N85-21

METHOD OF CHARACTERISTICS
Modeling of propulsive jet plumes--extension of modeling capabilities by utilizing wall curvature effects
[AD-A146262] 03 p0362 N85-12
High altitude chemically reacting gas particle mixtures. Volume 1: A theoretical analysis and development of the numerical solution — rocket nozzle and orbital plume flow fields
[NASA-CR-171826] 07 p0916 N85-15
The split-coefficient matrix method for supersonic three dimensional flow 12 p1821 N85-21

METHOD OF MOMENTS
Variational and moment method solutions of the fields in a parallel-plate waveguide-aperture system
[DE85-006288] 13 p2057 N85-22
Analysis of waveguide discontinuities by the method of moments
[AD-A151499] 15 p2547 N85-25
Investigation of the numerical method of moments for digital computer determination of differential equations
[AD-A151896] 15 p2638 N85-26
Analysis of systems of waveguide discontinuities by the method of moments 19 p3253 N85-30
Random vibration of nonlinear, parametrically excited systems 19 p3262 N85-30
Calculation of mixed depth for some metal-Si systems
[DE85-011907] 23 p3971 N85-34

METHODOLOGY
Method for making alloy additions to base metals having higher melting points
[AD-D011403] 07 p0928 N85-15
Use of iterative linear and nonlinear algebraic methods for solving large stiff systems of ODEs
[AD-A148516] 08 p1213 N85-17
Software and its relationship to methods
[DE85-004784] 14 p2405 N85-24

METHODS
U METHODOLOGY
U PROCEDURES

METHOXY SYSTEMS
Preparations of methoxynitrophenazines and their photoconductivities
[NASA-TM-77775] 14 p2247 N85-23

METHYL ALCOHOLS
Advanced concepts for methanol fuel vehicles
[DE84-013612] 04 p0482 N85-13071
Dissociated methanol vehicle test results
[DE84-004507] 04 p0509 N85-13
Impact of alcohol fuels on urban air pollution: Methanol photochemistry study
[DE84-012950] 04 p0531 N85-13

Methanol vaporization: Effects on volumetric efficiency and on determination of optimum fuel delivery system
[PB84-243914] 09 p1302 N85-18181
Volatility of in-use gasoline and gasoline-methanol blends
[PB85-117976] 10 p1459 N85-19189
Engine wear and cold startability of methanol fueled engines.
[DE85-001208] 11 p1647 N85-20381
Methanol adsorption on Pt(111)
[DE85-006602] 17 p2923 N85-28017
Conversion of methanol to gasoline: Engineering and construction of the demonstration plant
[DE85-003257] 17 p2937 N85-28133
Investigation of the flame speeds of propane/methanol gas mixtures
[DE85-012617] 23 p3912 N85-34239

METHYL CHLORIDE
The synthesis and characterization of Poly(Oxy(2-Methyl-1,3-Phenylene) Methyl-1,3 -Phenylene) Oxyterephthaloyl)Oxy
[AD-A148269] 08 p1133 N85-17143

METHYL COMPOUNDS
NT METHYL POLYSILOXANE
Interactions of ketones and hexacarbons
[AD-P004019] 06 p0843 N85-15353
Characterization and selection of polymer materials for binary munitions storage. Part 2: Characterization of LLDPE resins
[AD-A148324] 08 p1133 N85-17144
Properties of ultra-violet cured poly(dimethylsiloxane)-urea acrylates
[AD-A148570] 08 p1134 N85-17146
Poly(dimethylsiloxane)-polyurethane elastomers: Synthesis and properties of segmented copolymers and related zwitterionomers
[AD-A148571] 08 p1134 N85-17147
Crystallization behavior of poly(3,3-bis(Ethoxymethyl) oxetane) and poly(3,3-bis(Azidomethyl) oxetane)
[AD-A148271] 08 p1226 N85-17720
Improved lithium-intercalation cathode material
[AD-A149319] 10 p1435 N85-19043
Stable polymeric carbon radicals. Part 2: Attempts at the preparation of polyradicals of the triphenylmethyl type linked by P-phenylene units
[NASA-TM-77799] 10 p1450 N85-19134
Process for producing tris s(n-methylamino) methylsilane
[NASA-CASE-MFS-25721-1] 12 p1799 N85-21260
Electrochemical reduction of titanium in dimethyl sulphoxide
[BLL-OA-TRANS-3225-(6196.300))
20 p3429 N85-31267

METHYL POLYSILOXANE
Neutron scattering on polysiloxanes
03 p0432 N85-12751

METHYLENE
Electrically conducting complexes of poly(3,6-n-methylcarbazolyl methylene)
[AD-A147884] 07 p0933 N85-15914
The effect of occupational exposure and the body weight to height ratio on exhaled methylene chloride breath concentration in females at one, eighteen and sixty-six hours post exposure 14 p2368 N85-24708
Mechanical properties of adhesively bonded aluminum structures protected with hydration inhibitors
[AD-A153755] 18 p3079 N85-29047
Condensation of anhydrides or dicarboxylic acids with compounds containing active methylene groups. Part 1: Condensation of phthalic anhydride with acetoacetic and malonic ester
[NASA-TM-77866] 19 p3227 N85-30010

METHYLENE BLUE
The electrochemistry of azine, oxazine and thiazine dyes
[AD-A152394] 17 p2918 N85-27990

METRIC CONVERSION
U METRICATION

METRIC PHOTOGRAPHY
Metric camera experiment: Spacelab 1 mission
05 p0658 N85-14229
The photogrammetric camera experiment on Spacelab 1
05 p0658 N85-14230
Metric evaluation of SAR-580 optical images for cartographic purposes 05 p0659 N85-14231

METRIC SPACE
NT HILBERT SPACE
On two concepts of fundamental matching
[CBR-TWISK-335] 01 p0110 N85-10743
Extension of embeddings close to isometries or similarities 15 p2634 N85-26242
The definition and computation of a metric on plane curves. The meaning of a face on a geometric model
17 p3004 N85-28571
Performance measurement of OSI (Open System Interconnection) class 4 transport implementations
[PB85-177657] 18 p3161 N85-29582
Synthesis of metrico-topological model for layout of topology of large-scale-integration arrays
22 p3781 N85-33427

METRICATION
Performance measurement of OSI (Open System Interconnection) class 4 transport implementations
[PB85-177657] 18 p3161 N85-29582

METROLOGY
Force standard machines of the National Institutes for Metrology, vol. 2
[PTB-ME-62-VOL-2] 01 p0036 N85-10224
Center for Electronics and Electrical Engineering Technical Bulletin covering center programs with 1984 CEEE events calendar
[PB84-223684] 01 p0045 N85-10293
Center for Electronics and Electrical Engineering Technical Bulletin covering center programs
[PB84-219716] 01 p0045 N85-10295
Metrological consequences of the hard optical boundary assumption
[PB84-223577] 01 p0121 N85-10827
Center for Electronic and Electrical Engineering Technical Progress Bulletin, January - March 1983, no. 2
[PB84-231224] 03 p0360 N85-12306
Error and uncertainty — metrology
[NPL-DPMA-2] 08 p1137 N85-17161
Guidelines for atmospheric measurements in support of electro-optical systems testing
[AD-A148090] 08 p1186 N85-17474
Primer for mass metrology
[PB85-121424/GAR] 09 p1305 N85-18199
Modeling turbulent flow in compressible fluids: Metrological aspects — conferences
11 p1575 N85-19926
Metrology for Electronic Technology: A bibliography of NBS (National Bureau of Standards)
[PB85-112895] 12 p1830 N85-21486
The design and validation of software for dimensional metrology
[NPL-DITC-50/84] 15 p2521 N85-25542
New sensor for industrial metrology developed
15 p2538 N85-25665
Measurement capabilities of the Bendix Metrology Organization
[DE85-005795] 16 p2760 N85-27029
NBS physical measurement services
[NBSIR-84-2875] 16 p2859 N85-27633
Methods for optimal recursive estimation of non-stationary time series, applications to atomic time and frequency metrology 17 p2965 N85-28312
Activities of Istituto Elettrotecnico Nazionale Galileo Ferraris 18 p3199 N85-29845
Activities report in energy technology
[OEFZS-4302] 18 p3199 N85-29846
The 1982 National Measurement Requirements Survey
[NMRC-83-01-SUMM] 20 p3436 N85-31321
Recommendations for the design and equipping of engineering metrology laboratories
[NPL-MOM-22] 23 p3898 N85-34145

METROPOLITAN AREAS
U CITIES

MEXICO
Socio-economic impact of climate — Mexico
07 p1003 N85-16372
Geology of the Batopilas mining district, Chihuahua, Mexico, volumes 1 and 2 09 p1351 N85-18498
SIR-A imagery in geologic studies of the Sierra Madre Oriental, northeastern Mexico. Part 1 (Regional stratigraphy): The use of morphostratigraphic units in remote sensing mapping
[NASA-CR-175457] 10 p1505 N85-19497
Analysis of the Gran Desierto, Pinacte Region, Sonora, Mexico, via shuttle imaging radar
[NASA-CR-175711] 15 p2582 N85-25927

MICA
NT BIOTITE
Structural morphology and associated strain within parts of the US section of the Kootenay Arc, NE, Washington
09 p1352 N85-18505
Search for supermassive magnetic monopoles using mica crystals
[HE-6.1-8] 24 p4210 N85-36134

MICE
Effects of simulated weightlessness on mammalian development. Part 2: Meiotic maturation of mouse oocytes during clinostat rotation 15 p2612 N85-26094
Effects on in vivo and in vitro exposure to excess gravity on growth and differentiation of mammalian embryos
15 p2612 N85-26095
The controlled ecological life support system
15 p2688 N85-29603
Radioprotective efficacy of ATP and adenosine with exposure to high energy protons
19 p3325 N85-30602
Mouse oocyte killing by neutrons: Target considerations
[DE85-011362] 19 p3328 N85-30624
Differences in susceptibility of inbred mice to bacillus anthracis
[AD-A155646] 21 p3662 N85-32750

MICHELSON INTERFEROMETERS
Development of a measuring procedure for the automatic evaluation of the flatness of reflective surfaces
[BMFT-FB-T-84-168] 03 p0421 N85-12688
Improved sensitivities in laser interferometers for the detection of gravitational waves
[MPQ-88] 04 p0506 N85-13232
Geophysical laser interferometer with 12.5 meter base
13 p2069 N85-23046
Mode control and wavelength tuning in open ended Michelson interferometric semiconductor laser
13 p2095 N85-23073
Special topics in infrared interferometry — Michelson interferometer development
[NASA-TM-87472] 17 p3036 N85-28794
Wide Angle Michelson Doppler Imaging Interferometer (WAMDII) 23 p3902 N85-34172

MICHIGAN
Water resources data for Michigan, water year 1983
[PB84-225176] 01 p0066 N85-10442
Compilation of annual reports of the Navy ELF (Extremely Low Frequency) communications system ecological monitoring program. Volume 1: Tabs A-E
[AD-A148326] 08 p1152 N85-17272
Compilation of annual reports of the Navy ELF (Extremely Low Frequency) communications system ecological monitoring program (1983). Volume 2: Tabs F-J
[AD-A148327] 08 p1152 N85-17273
Diagenesis of niagaran (middle silurian) pinnacle reefs, northwest Michigan 09 p1352 N85-18508

MICROANALYSIS
Secondary fluorescence effects on X-ray microanalysis
[DE84-016600] 05 p0618 N85-13951
Transmission electron microscopy of inorganic materials
[DE85-000708] 09 p1291 N85-18107
K and L-shell cross-sections for X-ray microanalysis in an AEM
[DE85-002733] 11 p1721 N85-20822
Characterization of supported metal catalysts by imaging, microdiffraction and microanalysis techniques
[DE85-005567] 14 p2253 N85-23961
Secondary fluorescence effects on X-ray microanalysis
[DE85-005565] 15 p2506 N85-25457
Z-contrast imaging and electron channeling analysis of dopants in semiconductors
[DE85-011410] 21 p3582 N85-32269
Cyanobacterial mats: Microanalysis of community metabolism 21 p3661 N85-32743
Microanalysis of dissolved iron and phosphate in pore waters of hypersaline sediment
21 p3661 N85-32744

MICROBALANCES
Data analysis for lidar and quartz crystal microbalance systems
[NASA-CR-172601] 21 p3615 N85-32484

MICROBALLOONS
Microshell (trademark)-tipped optical fibers as sensors of high-pressure pulses in adverse environments
[DE84-015520] 03 p0365 N85-12336
Development of the sonic pump levitator
[NASA-CR-171382] 12 p1782 N85-21186

MICROBE
U MICROORGANISMS

MICROBIOLOGY
NT BACTERIOLOGY
Evaluation of survival straws (pocket purifier)
[AD-A148240] 03 p0328 N85-12114
Microbiological method for the desiliconization of high-silica bauxites
[BLL-MINTEK-TR-1168-(5810.5759)]
07 p0925 N85-15864
USSR report: Life sciences. Biomedical and behavioral sciences
[JPRS-UBB-84-015] 07 p1010 N85-16416
USSR report: Life sciences. Biomedical and behavioral sciences
[JPRS-UBB-85-002] 09 p1380 N85-18559
USSR report: Space Biology and Aerospace Medicine, volume 18, no. 6, November - December 1984
[JPRS-USB-85-002] 12 p1900 N85-21931
Results of sanitary-microbiological studies aboard Cosmos-1129 biosatellites 12 p1903 N85-21952

Dynamics of quantitative and qualitative changes in conditionally pathogenic microflora of the human intestine during long-term hypokinesia 12 p1903 N85-21953
USSR report: Life sciences. Biomedical and behavioral sciences
[JPRS-UBB-85-012] 14 p2386 N85-24697
Flow through bacteria detection system
[NASA-CASE-LAR-12871-1] 18 p3104 N85-29218
Development anmd testing of electrophoresis solutions. Task I.1: Development of optimal buffer system
20 p3500 N85-31755
The global sulfur cycle
[NASA-TM-87570] 21 p3656 N85-32710
Results of microbiological studies conducted during operation of Salyut-6 orbital station
22 p3823 N85-33682
USSR report: Space Biology and Aerospace Medicine, vol. 19, no. 3, May - June 1985
[JPRS-USB-85-005] 23 p3952 N85-34494
Microbiological and biochemical studies towards optimization of substrate utilization by methanogenic bacteria
[PB85-186332] 24 p4064 N85-35310
Literature search for new physical methods for biological aerosol detection
[AD-A155883] 24 p4126 N85-35592

MICROCALORIMETERS
U CALORIMETERS

MICROCHANNEL PLATES
Fine grained hodoscopes based on scintillating optical fibers
[DE84-014849] 01 p0120 N85-10625
A microchannel plate streak camera
[DE84-016536] 06 p0811 N85-15153
Photometry with Multi-Anode Microchannel Arrays (MAMAs) and Charge Injection Devices (CIDs)
08 p1252 N85-17909
Improved performance for large area triple layer microchannel plate detector for a neutral spectrometer in Doublet III
[DE85-001719] 10 p1488 N85-19395
Development of high resolution imaging detectors for X-ray astronomy
[NASA-CR-175505] 12 p1953 N85-22266
Utilization of microchannel plates in the flash X-ray technique
[ISL-CO-229/83] 14 p2306 N85-24275
Microchannel plate streak camera
[DE85-011604] 20 p3458 N85-31481

MICROCHANNELS
The development and test of ultra-large-format multi-anode microchannel array detector systems
[NASA-CR-174247] 07 p1043 N85-16622

MICROCIRCUITS
U MICROELECTRONICS

MICROCLIMATOLOGY
Bibliography of climate textbooks and studies
[WCP-84] 02 p0231 N85-11505

MICROCOMPUTERS
NT PERSONAL COMPUTERS
Composite laminate optimization program suitable for microcomputers 01 p0059 N85-10389
A microcomputer aided measurement equipment for monitoring performance in digital radio relay systems
[FUB-4-1984] 01 p0101 N85-10668
Floating-point function generation routines for 16-bit microcomputers
[NASA-TM-83783] 01 p0102 N85-10683
Microcomputer management guidelines
[PB84-212174] 01 p0105 N85-10704
Analysis of three database system architectures using benchmarks
[PB84-217512] 01 p0105 N85-10706
Microcomputers in Hungary 01 p0115 N85-10786
Systems analysis for microcomputer acquisitions
[AD-A145447] 02 p0230 N85-11556
East Europe report, science and technology. Czechoslovakia: System of small electronic computers
[JPRS-ESA-84-040] 02 p0230 N85-11558
Development of a microcomputer coupled atmospheric and oceanic boundary layer prediction model
[AD-A146334] 03 p0397 N85-12530
An inexpensive microcomputer for laboratory data acquisition and test equipment control
[AD-A146095] 03 p0403 N85-12567
Information Center handbook
[PB84-211341] 03 p0439 N85-12795
A control scheme for microcomputers being used in multiprocessor arrays
[DE84-014680] 04 p0547 N85-13479
Microcomputer control of a residential photovoltaic power conditioning system
[DE84-013867] 04 p0547 N85-13480
Hardware multiplier processor
[DE84-006174] 05 p0713 N85-14574
How to implement the welcome program in compatible microcomputers such as Apple 2
[INPE-3114-PRE/511] 05 p0715 N85-14586
Machine tools at 1984 Leipzig Spring Fair
06 p0815 N85-15177
High speed magnetic tape interface for a microcomputer
[CSIRO-TP-7] 06 p0847 N85-15377
A standard operating system interface for microcomputer software development
[AD-A146584] 06 p0854 N85-15428
Control system design language implementation of a gas turbine starting controller
[AD-A147896] 07 p0905 N85-15732
Development of a 2 micrometer silicon-gate-CMOS-technology for microcomputer oriented VLSI circuits with a supply voltage range between 1.5 and 5 V
[BMFT-FB-T-84-203] 07 p0949 N85-16012
Microcomputer control of a residential photovoltaic power conditioning system
[DE84-014774] 07 p1022 N85-16488
Possibilities and impossibilities of microcomputer systems
[AD-1984-904] 07 p1029 N85-16522
Ultrasound instrumentation for the 7 inch Mach seven tunnel
[NASA-CR-174277] 07 p1038 N85-16586
Fast arithmetic for microcomputers
08 p1140 N85-17180
Specifications of bloc floppy disk drives
08 p1141 N85-17188
Adapting logistics models to a microcomputer for interface with computer-aided design systems
[AD-A147686] 08 p1202 N85-17566
MINDS: A microcomputer interactive data system for 8086-based controllers
[NASA-TP-2378] 08 p1204 N85-17576
Guide to personal desktop computing at ANL
[DE85-001436] 08 p1206 N85-17594
Data acquisition, measurement devices at 1984 Leipzig Spring Fair 09 p1378 N85-18661
Linear, position-sensitive X-ray detector used for real-time calculations of small-angle scattering parameters with submillisecond resolution
[DE85-002530] 10 p1489 N85-19401
A decision model for selection of microcomputers and operating systems
[AD-A149076] 10 p1538 N85-19694
Relative performance of micro and mainframe computers
[AD-A149261] 10 p1538 N85-19695
Microcomputers in transit: A hardware handbook
[PB85-113660] 10 p1538 N85-19700
Order picking in an aisle
[AD-A149553] 10 p1548 N85-19766
ESOP expert system model described
11 p1619 N85-20187
Guidepost routing algorithm for distributed computer networks 11 p1622 N85-20210
East Europe report: Scientific affairs
[JPRS-ESA-84-006] 11 p1700 N85-20684
Description of 8048 microcomputer operation published 11 p1700 N85-20685
A functional vehicle for autonomous mobile robot research
[AD-A150052] 12 p1860 N85-21686
Selection and use of general-purpose programming-language: Program examples, volume 2
[PB85-122000] 12 p1917 N85-22039
Selection and use of general-purpose programming language: Overview, volume 1
[PB85-122018] 12 p1917 N85-22040
Microcomputers in transit: A software handbook
[PB85-136414] 12 p1918 N85-22042
Microcomputer: Controlled statistics analyzer
[BLL-CE-TRANS-7971-(9022.09)]
13 p2144 N85-23306
Exploiting parallel computing with limited program changes using a network of microcomputers
[NASA-TM-86387] 13 p2146 N85-23318
Microcomputers and the electrical engineer
[AD-A150499] 13 p2147 N85-23325
An improved battery state-of-charge indicator
[NASA-CR-175701] 14 p2298 N85-24227
Arithmetic and elementary functions on mini and microcomputers 14 p2396 N85-24761
Evaluating the appropriateness of microcomputers for litigation document management using the analytic hierarchy process 14 p2399 N85-24786
USSR report: Cybernetics, computers, and automation technology
[JPRS-UCC-85-002] 14 p2400 N85-24794
The problem of creating a standardized series of personal computers 14 p2400 N85-24795
Automation of development of software for [illegible] units that are implemented in the form of multiprocessor systems on a microcomputer base
14 p2401 N85-[illegible]
Microcomputer application of aerospace asset surface search planning
[AD-A151833] 15 p2487 N85-[illegible]
Czech institute develops microcomputer for [illegible]
15 p2494 N85-[illegible]
Using a single-board computer to maintain constant voltage, current sources 15 p2551 N85-[illegible]
Recent advances in arc welding equipment and their application 15 p2586 N85-[illegible]
The design and implementation of a syntax directed editor for a space constrained microcomputer
[AD-A151313] 15 p2623 N85-[illegible]
An extension of a microcomputer based system for analysis of line drawing quantization schemes
[AD-A152006] 15 p2624 N85-[illegible]
Mini- and microcomputer local control network architecture and design principles
15 p2625 N85-[illegible]
Extension of the software development workbench to include microcomputer workstations
[AD-A151903] 15 p2630 N85-[illegible]
Investigation of the numerical method of moments for digital computer determination of differential equations
[AD-A151896] 15 p2638 N85-[illegible]
System design of automated VLSI (Very Large Scale Integrated) test station and implementation of selected system aspects
[AD-A151961] 16 p2778 N85-27147
Design and construction of a computer controlled mirothermocouple probe for the study of buoyant jets
[AD-A152224] 16 p2788 N85-[illegible]
China report: Science and Technology
[JPRS-CST-85-012] 16 p2806 N85-27300
Implementation and analysis of a microcomputer based relational database system
[AD-A151770] 16 p2845 N85-27538
Detailed design of an object oriented, multiprogramming, multitasking operating system for sixteen-bit microcomputers
[AD-A152086] 16 p2847 N85-27552
Numerical optimization algorithm for engineering problems using microcomputer
[AD-A152135] 16 p2847 N85-27554
Computer assisted flight schedule optimization
[AD-A151689] 16 p2858 N85-[illegible]
A portable pulse analyzer for nuclear geophysics using a Sinclair-TK microcomputer
[INPE-3278-PRE/601] 16 p2864 N85-[illegible]
Automation of the reporting and tracking requirements of architect-engineering type contracts
[AD-A152218] 16 p2876 N85-27716
Design of an interface to an information retrieval network 16 p2877 N85-[illegible]
Ultrasonic flaw detector with microcomputer interpretation
[BMFT-FB-T-84-272] 17 p2977 N85-[illegible]
Microcomputer-controlled system for measuring atmospheric particle fluxes
[DE85-007910] 17 p2986 N85-[illegible]
Microprocessor controlled temperature chassis
[DE85-008392] 17 p3009 N85-[illegible]
A programming system for a modular flexible multimicrocomputer system for the automatic control of automated test equipment
[JUEL-1962] 17 p3014 N85-[illegible]
A task battery for applied human performance assessment research
[AD-A153677] 18 p3154 N85-[illegible]
Safety system with microcomputer
[OEFZS-4294] 18 p3166 N85-[illegible]
Deployable Core Automated Maintenance System (DCAMS)
[AD-A153695] 18 p3196 N85-[illegible]
Fracture mechanics formulas on microcomputers
[NASA-TM-77850] 19 p3294 N85-[illegible]
Graceful fault tolerance in large networks of microcomputers 19 p3332 N85-[illegible]
ZOG-Vinson technology demonstration project. Volume 2: System description
[AD-A153871] 19 p3333 N85-[illegible]
Demonstration project: Putting the bioastronautics data book on line
[NASA-CR-176424] 19 p3335 N85-[illegible]
ZOG/VINSON technology demonstration project system description. Volume 1
[AD-A154211] 19 p3342 N85-30713
Implementation of a serial communication process for a fault tolerant, real time, multitransputer operating system
[AD-A154237] 19 p3343 N85-30714

Forth system for coherent-scatter radar data acquisition and processing
[NASA-CR-176055] 20 p3494 N85-31720
Visualization of computation results. Definition of a graphics satellite computer
[ONERA-RT-2/3587-CY] 20 p3514 N85-31845
PIPE-1000: An implementation of piping on an HP-1000 minicomputer
[PB85-191955] 20 p3514 N85-31847
DHC: A diurnal heat capacity program for microcomputers
[DE85-009645] 20 p3516 N85-31859
Microcomputers in transportation: Software and source book, February 1985
[PB85-181022] 20 p3517 N85-31866
Microcomputer processing of LANDSAT Thematic Mapper data for the acquisition of military tactical terrain data
[AD-A154781] 21 p3605 N85-32389
Robots, Manipulators 21 p3666 N85-32786
An automated quality assurance surveillance plan for ADP (Automated Data Processing) operations under the Navy's commercial activities program
[AD-A154767] 21 p3671 N85-32802
A comparison and analysis of Vintr's global routing algorithm with the Lee routing algorithm in two-layer printed circuit boards
[AD-A155800] 21 p3673 N85-32816
Development of a dedicated speech work station
[AD-A155465] 21 p3674 N85-32824
Microcomputer network: Investigation and implementation
[AD-A155631] 21 p3674 N85-32826
Art of programming programmable microcalculators: Calculation of response from current values of action
22 p3767 N85-33348
Module for interfacing microprpcessors and microcomputer 22 p3774 N85-33390
Art of programming programmable microcalculators, part 4: errors of calculations 22 p3778 N85-33411
Microcomputer controlled image processor
[AD-D011734] 22 p3833 N85-33735
An innovative user interface for microcomputer-based computer-aided design 23 p3961 N85-34555
Recording system for the solar neutron monitoring at Mt. Norikura
[SH-8.1-6] 23 p4051 N85-35123
Development of position sensors for microcomputer-oriented sensor systems
[BMFT-FB-T-85-021] 24 p4091 N85-35361
Materials and process development for microcomputer-compatible pressure, temperature, and position sensors
[BMFT-FB-T-85-024] 24 p4097 N85-35399
Expert systems research in regional resource evaluation: Experiences in the application of microcomputer technologies 24 p4105 N85-35450
DSS/MIS (Decision Support Systems/Management Information Systems) design and implementation for LAMPS Mk 3 utilizing a microcomputer and a maintenance personnel assignment program
[AD-A155852] 24 p4135 N85-35629
A quickly tested Pascal random number generator for microcomputers
[AD-A156059] 24 p4136 N85-35633
A research program to reduce the interior noise in general aviation aircraft, index and summary
[NASA-CR-176178] 24 p4145 N85-35695
Application of thermoluminescence for detection of cascade shower 1: Hardware and software of reader system
[HE-7.1-6] 24 p4213 N85-36160
Spatial distribution read-out system for thermoluminescence sheets
[HE-7.1-7] 24 p4213 N85-36161

MICROCRACKS
Salt action on concrete
[AD-A147812] 07 p0833 N85-15912
Fundamentals of microcrack nucleation mechanics
[NASA-CR-3851] 07 p0975 N85-16195
Influence of constant amplitude and variable amplitude loading on crack initiation and micro crack propagation in Al 2024-T3
[DFVLR-FB-84-29] 07 p0979 N85-16220
Experimental and analytical study of ceramic-coated turbine-tip shroud seals for small turbine engines
[NASA-TM-86881] 09 p1261 N85-18057
Evaluation of machining damage in brittle materials
[DE85-001794] 11 p1612 N85-20136
Change in microstructure of heat-resistant nickel alloys upon thermal cycling in a current of gas
13 p2031 N85-22725
On Rayleigh waves and Rayleigh wave extension of surface micro-cracks 15 p2572 N85-25860
Mechanical properties of high performance carbon fibers
16 p2742 N85-26922
The mechanics of internal stress and microcrack toughening mechanisms in ceramics
[AD-A154049] 19 p3248 N85-30139
Mechanics of near tip microcracking in brittle material
[AD-A154684] 21 p3598 N85-32346

MICROCRYSTALS
Basic ice nucleation mechanisms on mono and microcrystals and ice forming nuclei. Theoretical analysis and experimental results achieved in the laboratory over the past ten years: Review paper
21 p3642 N85-32629
Size and shape dependence of CO adsorption sites on sapphire supported Fe microcrystals
[NASA-CR-176171] 24 p4160 N85-35794

MICRODENSITOMETERS
Recent developments on the COSMOS plate-scanning machine — microdensitometer 07 p0966 N85-16128
Plate measurements and reductions at Muenster — astronomical photography 07 p0966 N85-16129
First tests on the astrometric performance of the new PDS1010G at Hamburg Observatory — granite microdensitometer 07 p0966 N85-16135
Astrometric applications of the Mt. Stromlo PDS 1010A — microdensitometer 07 p0967 N85-16136

MICROELECTRONICS
NT LARGE SCALE INTEGRATION
Manufacturing methods for microwave circuits
[AD-A145237] 01 p0043 N85-10278
Moving object detection system using infrared scanning
[AD-D011222] 01 p0120 N85-10822
Energy deposition in microvolumes of silicon from high energy proton reactions
[AD-A144713] 01 p0123 N85-10845
Cosmic ray effects on microelectronics. Part 3: Propagation of cosmic rays in the atmosphere
[AD-A145026] 01 p0131 N85-10902
Fundamental electronic properties of donor-type graphite intercalated compounds
[AD-A146148] 03 p0326 N85-12099
West Europe report: Science and technology, no. 166
[JPRS-84845] 03 p0341 N85-12190
French firms develop artificial intelligence robot
03 p0341 N85-12192
Swiss firm improves method for soldering printed circuits 03 p0341 N85-12193
Integrated circuits, MBM's, form focus of work at French LETI 03 p0341 N85-12194
East Europe report: Scientific affairs, no. 791
[JPRS-84624] 03 p0341 N85-12195
Problems in CEMA microelectronic cooperation noted
03 p0341 N85-12196
East Europe report: Science and technology
[JPRS-ESA-84-038] 03 p0343 N85-12210
USSR report: Electronics and electrical engineering
[JPRS-UEE-84-014] 03 p0344 N85-12215
Chemical derivatization of an array of three gold microelectrodes with polypyrrole: Fabrication of a molecule-based transistor
[AD-A146221] 03 p0359 N85-12304
Contamination problems during surface cleaning for thermocompression bonding
[DE84-013066] 04 p0475 N85-13023
Procedures for precap visual inspection
[NASA-RP-1122] 04 p0495 N85-13156
The effect of aircraft generated electromagnetic interference (EMI) on future avionics systems: A compendium
[AD-A148380] 06 p0799 N85-15101
East Europe report: Science and technology
[JPRS-ESA-84-045] 06 p0815 N85-15175
Facility safety study
[NASA-CR-174280] 07 p0910 N85-15759
Improvement of electromechanical systems by utilization of microelectronic technology 07 p0955 N85-16053
Solid state research
[NASA-CR-174285] 07 p1048 N85-16656
The construction and behaviour of ultramicroelectrodes: Investigations of novel electrochemical systems
[AD-A148658] 08 p1123 N85-17079
Robotics application in construction industry assessed
08 p1139 N85-17178
Telecommunications equipment at 1984 Leipzig Spring Fair 08 p1140 N85-17179
Electronics component R and D, production capability reviewed 08 p1140 N85-17181
Researchers on third generation robotics development
08 p1140 N85-17184
Flexible manufacturing system concept features cache memory 08 p1140 N85-17186
West Europe report: Science and technology
[JPRS-WST-85-001] 08 p1141 N85-17190
East Europe report: Science and technology
[JPRS-ESA-84-043] 08 p1142 N85-17198
Chemical, material electronics studies established
08 p1142 N85-17200
General assessment of GDR microelectronics industry, applications 08 p1142 N85-17202
Solid state research
[AD-A147640] 08 p1225 N85-17714
Gallium arsenide/AlGaAs multilayer structures with special doping profiles for microwave and optoelectronic devices
[BMFT-FB-T-84-207] 08 p1227 N85-17725
The planned expansion of microelectronics capability at Sandia National Laboratory
[TI85-004326] 09 p1314 N85-18260
Semiconductors at Leipzig Spring Fair
09 p1377 N85-18660
West Europe report: Science and technology
[JPRS-WST-85-004] 10 p1460 N85-19204
Researchers, projects at French intelligent machine center 10 p1460 N85-19207
MOD silver metallization for photovoltaics
[NASA-CR-175460] 10 p1510 N85-19526
East Europe report: Science and technology
[JPRS-ESA-85-009] 11 p1616 N85-20165
Institute director surveys industrial automation drive
11 p1617 N85-20167
New CNC systems described
11 p1617 N85-20172
West Europe report: Science and technology
[JPRS-WST-85-008] 11 p1617 N85-20174
CAD/CAM systems for printed circuit design, manufacture 11 p1619 N85-20188
Electronics Engineering Department: EE technical review
[DE85-004360] 11 p1629 N85-20259
Description of 8048 microcomputer operation published 11 p1700 N85-20685
Long-range electronics program outlined
11 p1700 N85-20687
USSR report: Electronics and electrical engineering
[JPRS-UEE-85-004] 12 p1837 N85-21531
Transistor-transistor logic microcircuit tester
12 p1842 N85-21556
Redundancy of codes for detection and correction of unidirectional errors 12 p1842 N85-21557
New high resolution scanning ion microprobe and focused ion beam applications
[AD-A149992] 12 p1852 N85-21616
Investigation of device and electronic interactions in GaAs device processing
[AD-A149747] 12 p1840 N85-22182
Electrical overstress protection of submicron devices
[AD-A150334] 13 p2064 N85-22892
Code lock with microcircuit 13 p2071 N85-22935
Recommendation on use of series K157UL1 microcircuits 13 p2071 N85-22936
Application of K176-series microcircuits
13 p2077 N85-22973
Parallel test method for LSI (Large Scale Integration) microprocessors
[AD-A150237] 13 p2144 N85-23310
USSR report: Machine tools and metalworking equipment
[JPRS-UMM-85-004] 14 p2284 N85-24152
China report: Science and technology
[JPRS-CST-85-009] 15 p2530 N85-25596
Developments in microelectronics: Past and future
15 p2530 N85-25597
West Europe report: Science and technology
[JPRS-WST-84-007] 15 p2530 N85-25600
Phase-locked loop design with MH84046
15 p2534 N85-25631
West Europe report: Science and technology
[JPRS-WST-84-009] 15 p2535 N85-25639
West Europe report: Science and technology
[JPRS-WST-84-010] 15 p2536 N85-25644
West Europe report: Science and technology
[JPRS-WST-84-014] 15 p2536 N85-25647
CaD systems for electronic component design reviewed 15 p2537 N85-25660
New designs from electronics R and D center
15 p2538 N85-25668
Recent advances in arc welding equipment and their application 15 p2566 N85-25832
East Europe report: Science and technology
[JPRS-ESA-85-019] 16 p2767 N85-27077
Bond test data acquisition and analysis system
[DE85-007021] 16 p2780 N85-27158
China report: Science and Technology
[JPRS-CST-85-012] 16 p2806 N85-27300
NBS (National Bureau of Standards) research reports
[PB85-127421] 16 p2879 N85-27764
East Europe report: Science and technology
[JPRS-ESA-85-017] 17 p2945 N85-28177
Goals, achievements of microelectronics program
17 p2945 N85-28179
West Europe report: Science and technology
[JPRS-WST-84-024] 17 p2945 N85-28183

Present status of physics research in Spain: Some impressionistic remarks
[AD-A152455] 17 p3027 N85-28718
West European report: Science and technology
[JPRS-WST-84-036] 18 p3086 N85-28960
West Europe report: Science and technology
[JPRS-WST-84-031] 18 p3086 N85-29089
West Europe report: Science and technology
[JPRS-WST-84-032] 18 p3086 N85-29095
West Europe report: Science and technology
[JPRS-WST-84-035] 18 p3087 N85-29102
Method for ultrasonic bonding to soft microelectronic substrates
[NASA-CASE-NPO-16087-1] 18 p3094 N85-29151
Laser machining and some applications
[NHK-LABS-NOTE-307] 18 p3112 N85-29266
West Europe report: Science and technology
[JPRS-WST-85-020] 20 p3438 N85-31333
France's LETI reports 1983 electronic components research 20 p3438 N85-31336
Leading-edge microelectronics research at Sweden's Chalmers 20 p3438 N85-31337
Swedish program for sensor research, development
20 p3438 N85-31338
Resistance of polyaniline films as a function of electrochemical potential and the fabrication of polyaniline-based microelectronic devices
[AD-A154899] 21 p3569 N85-32201
East Europe report: Science and technology
[JPRS-ESA-85-023] 21 p3572 N85-32217
High temperature electronics technology: Life test report
[AD-A154661] 21 p3580 N85-32257
Selections on CSSR computer technology
21 p3668 N85-32782
GDR semiconductor parts 21 p3669 N85-32788
Prospects for a new kind of synthesis: Assembly of molecular components to achieve functions
[AD-A155023] 21 p3702 N85-32997
Solid state research
[AD-A154783] 21 p3709 N85-33025
Electrotransport in thin films
[AD-A155584] 21 p3710 N85-33034
Space station automation study. Automation requirements derived from space manufacturing concepts. Volume 1: Executive summary
[NASA-CR-176099] 22 p3736 N85-33170
Space Station automation study. Automation requirements derived from space manufacturing concepts. Volume 2: Technical report
[NASA-CR-176100] 22 p3736 N85-33171
Photothyristor optrons and optron microcircuits, part 1
22 p3781 N85-33424

MICROFILMS
Facsimile transmission of microforms
[AD-A144855] 01 p0038 N85-10236

MICROGRAPHY
U PHOTOMICROGRAPHY

MICROGRAVITY
U REDUCED GRAVITY

MICROGRAVITY APPLICATIONS
Monodisperse Latex Reactor (MLR): A materials processing space shuttle mid-deck payload
[NASA-TM-86487] 12 p1782 N85-21187

MICROHARDNESS
Study of deformation and fracture of AMg6N weldable aluminum alloy by method of acoustic emission
03 p0352 N85-12266
Nitriding of titanium and its alloys by N2, NH3 or mixtures of N2 + H2 in a dc arc plasma at low pressures (or = to torr)
[NASA-TM-83803] 06 p0814 N85-15168
Surface effects of corrosive media on hardness, friction, and wear of materials
[NASA-TM-83711] 07 p0930 N85-15896
Estimation of endurance characteristics of heat resistant materials. Report 2: Determination of endurance limit of heat resistant alloys over a broad temperature range
10 p1447 N85-19120
Ion-beam nitriding of steels
[NASA-CASE-LEW-14104-1] 12 p1805 N85-21324
Structure and mechanical characteristics of heterogeneous joints produced by laser welding
13 p2034 N85-22742
Frictional and structural characterization of ion-nitrided low and high chromium steels
[NASA-TM-86991] 13 p2098 N85-23085
Pulsed electrodeposition
[DE85-007067] 16 p2747 N85-26960

MICROINDENTATION
U MICROHARDNESS

MICROMANOMETERS
U MANOMETERS

MICROMECHANICS
Investigation of toughened neat resins and their relations to advanced composite mechanical properties
04 p0464 N85-12949
Numerical investigation of the micromechanics of composite fracture 04 p0467 N85-12970
Investigation of the relations between resin and advanced composite mechanical properties. Volume 2: Appendices
[NASA-CR-172303-VOL-2] 06 p0763 N85-14880
Some aspects of the micromechanics of hot spot formation in energetic materials
[AD-P004348] 10 p1456 N85-19172
Delamination micromechanics analysis
[NASA-CR-172598] 20 p3422 N85-31237
Micromechanics of high temperature deformation and failure 20 p3486 N85-31534

MICROMETEORITES
The micrometeorite experiment on Helios — inner solar system 16 p2885 N85-27797

MICROMETEOROIDS
NT ZODIACAL DUST
Hypervelocity impacts on Skylab 4/Apollo windows
12 p1785 N85-21202
Survey of probable micrometer-sized Earth-orbital debris fragments in the NASA-JSC cosmic dust sample collection 12 p1785 N85-21203
Impacts on Explorer 46 from an Earth orbiting population 12 p1785 N85-21204
In-situ detection of micron-sized dust particles in near-Earth space 12 p1785 N85-21205
The Jovian ring 15 p2672 N85-26492
The gravito-electrodynamics of charged dust in planetary ring systems 15 p2677 N85-26531

MICROMETEOROLOGY
Bibliography of climate textbooks and studies
[WCP-84] 02 p0231 N85-11506
Eddy correlation measurements of energy partition for Amazonian forest
[INPE-3195-PRE/559] 06 p0827 N85-15252
The micrometeorology of an Amazonian rainforest
[INPE-3515-PRE/740] 19 p3315 N85-30551
Investigations of micro-turbulence in the bottom of the boundary layer
[AD-A155148] 21 p3636 N85-32585

MICROMETEORS
U MICROMETEOROIDS

MICROMINIATURIZATION
NT LARGE SCALE INTEGRATION
Qualitative of analysis of MOS circuits
[AD-A149267] 10 p1480 N85-19341
Checking microcode algebraically
[AD-A149441] 10 p1547 N85-19759
The use of ultrasound to monitor incipient failure of rolling element bearings 23 p3924 N85-34317

MICROMOTORS
Semiconductors at Leipzig Spring Fair
09 p1377 N85-18660

MICROORGANISMS
NT AEROBES
NT ANAEROBES
NT BACILLUS
NT BACTERIA
NT CLOSTRIDIUM BOTULINUM
NT ESCHERICHIA
NT PROTOZOA
NT PSEUDOMONAS
NT STAPHYLOCOCCUS
NT VIRUSES
Lagging development of biotechnology described
01 p0115 N85-10787
Spacelab 1 experiment: Microorganisms in space hard environment 05 p0691 N85-14443
DOE supported research in alcohol fuel technology development
[DE84-007686] 06 p0774 N85-14948
A biological sensor for the detection of toxicants
[AD-D011304] 07 p0967 N85-16141
Distinctions of SPF rats used in experiments aboard biosatellites 07 p1012 N85-16427
Growth of soil bacteria in presence of Martian soil analog, carbon dioxide and hydrogen peroxide
09 p1361 N85-18580
Dynamics of quantitative and qualitative changes in conditionally pathogenic microflora of the human intestine during long-term hypokinesia 12 p1903 N85-21953
Analysis of biological particles by mass spectrometry
[AD-A149952] 13 p2141 N85-23291
The impact ejection of living organisms into space
15 p2662 N85-26566
Flow through bacteria detection system
[NASA-CASE-LAR-12871-1] 18 p3104 N85-29216
Equipment development for rapid detection of microorganisms in air and water
[FOA-A-40046-B2] 18 p3134 N85-29410
A basic study to assess the potential usefulness of resonance Raman spectroscopy as a means of rapidly detecting and identifying bacteria and other microorganisms
[AD-A153549] 18 p3152 N85-[illegible]
Influence of underwater volcanic mountains of Atlantic on microplankton distribution 19 p3294 N85-[illegible]
Microbial ecology of extreme environments: Antarctic yeasts and growth in substrate-limited habitats
[NASA-CR-176005] 19 p3326 N85-[illegible]
Biocatalysis project
[NASA-CR-176044] 20 p3498 N85-3174[illegible]
Efficiency tests of samplers for microbiological aerosols, a review
[FOA-C-40199-B1] 20 p3504 N85-317[illegible]
Protocyanobacteria: Oxygenic and Anoxygenic photosynthesis in mat-forming bacteria
21 p3657 N85-3271[illegible]
Sulfur transformations at the hydrogen sulfide/oxygen interface in stratified waters and in cyanobacterial mats
21 p3657 N85-3271[illegible]
Microbiology of solar salt ponds
21 p3658 N85-327[illegible]
Some thoughts on GAIA and the sulfur cycle
21 p3658 N85-327[illegible]
From microbial communities to cells
21 p3659 N85-327[illegible]
Microbial colonization and growth on metal sulfides and other mineral surfaces 21 p3662 N85-3274[illegible]
Sulfur Cycle 21 p3662 N85-3274[illegible]
Results of microbiological studies conducted during operation of Salyut-6 orbital station
22 p3823 N85-33[illegible]
Distinctions in formation of microflora on construction materials used in habitable pressurized compartments
22 p3823 N85-33[illegible]
Screening and characterizing oleaginous microalgal species from the southeastern United States
[DE85-008767] 23 p3951 N85-34[illegible]
Microorganisms in space flight
23 p3951 N85-34[illegible]
Production of butanol by fermentation in the presence of cocultures of clostridium
[NASA-CASE-NPO-16203-1] 24 p4071 N85-35[illegible]
Biodegradation of jet fuel by aquatic microbial communities
[PB85-191971] 24 p4084 N85-3531[illegible]
Report of the Microbial Development Working Group
24 p4127 N85-35[illegible]

MICROPARTICLES
Monodisperse Latex Reactor (MLR): A materials processing space shuttle mid-deck payload
[NASA-TM-86487] 12 p1782 N85-2118[illegible]

MICROPHONES
Determination of the pressure sensitivity of 1 inch condenser microphones
[PTB-AK-26] 05 p0633 N85-140[illegible]
Carbon granule probe microphone for leak detection – recovery boilers
[NASA-CASE-NPO-16027-1] 12 p1649 N85-2159[illegible]
Recording of acoustic wave in gaseous medium with thin-film pyroelectric transducers
15 p2525 N85-2557[illegible]
Spectral methods for the estimation of acoustic intensity, energy density, and surface velocity using a multimicrophone probe 20 p3524 N85-319[illegible]
A theoretical appraisal of the use of ground-plane microphones for aircraft noise measurements
[NPL-AC-103] 22 p3836 N85-337[illegible]
Acoustic scaling: The development of improved instrumentation
[BBC-RD-1985/7] 24 p4145 N85-35[illegible]

MICROPHOTOMETERS
U PHOTOMETERS

MICROPOROSITY
Design and use of nonstandard tensile specimens for irradiated materials testing
[DE85-001071] 11 p1652 N85-204[illegible]
Predicting microfracture in ceramics via a microcontinuum model
[DE85-005654] 18 p3061 N85-290[illegible]

MICROPROCESSORS
A relational approach to the development of expert diagnostic systems
[NASA-TM-86286] 01 p0009 N85-105[illegible]
Evaluating a scientific workstation computer
[DE84-014764] 01 p0100 N85-106[illegible]
The application of microprocessors in the command and control of satellites by the MECB stations
[INPE-3262-RPE/466] 02 p0239 N85-115[illegible]
The microprocessor control of a motor-alternator
[RAE-TM-NAV-ENG-1023(L)] 02 p0244 N85-115[illegible]
Functional checking of microprocessors and microprocessor systems 03 p0347 N85-12[illegible]
Microprocessor implementation of algorithms of nonlinear filtration 04 p0486 N85-13104

Revision of signal and interference space-time processing algorithms for implementation by microprocessors 04 p0487 N85-13105

Portable microprocessor-controlled instrument for sensing, identifying and monitoring gaseous chemicals
[DE84-013431] 04 p0504 N85-13214

Fiber optic, Fabry-Perot high temperature sensor
[NASA-CR-174712] 04 p0564 N85-13594

A new physical Lagrangian tracer
[DE84-016212] 05 p0687 N85-14419

Memory hierarchies for Directly Executed Language microprocessors 05 p0713 N85-14570

Hardware multiplier processor
[DE84-008174] 05 p0713 N85-14574

Internal structure of microprocessor
06 p0785 N85-15020

Peculiarities of microprocessor implementation of algorithms for processing radio signals and noise in large antenna arrays 06 p0792 N85-15059

Workshop on Computer Architecture
[AD-A146455] 06 p0847 N85-15378

Implementation of a Zilog Z-80 base realization library for the computer systems design environment
[AD-A146369] 06 p0853 N85-15423

Control system design language implementation of a gas turbine starting controller
[AD-A147896] 07 p0905 N85-15732

A microprocessor data system for developing countries — climatology 07 p1003 N85-16377

Functional built-in-test in a pipelined image processor
08 p1064 N85-16740

Data stimulated on-line-checking (IROLD)
08 p1066 N85-16754

Automatic error detection and recovery techniques in onboard intelligent units for space and avionic application 08 p1066 N85-16756

Microprocessors in geophysical instruments discussed
08 p1142 N85-17199

Implementation of an Intel 8086 microprocessor-based realization library for the control system design language
[AD-A148506] 08 p1202 N85-17569

MC68CRX cross-assembler users manual
[AD-A148031] 08 p1205 N85-17584

Design description of a microprocessor based Engine Monitoring and Control unit (EMAC) for small turboshaft
[NASA-TM-86860] 09 p1263 N85-17935

Software for event oriented processing on multiprocessor systems
[DE84-016720] 09 p1370 N85-18607

Computer equipment at 1984 Leipzig Spring Fair
09 p1378 N85-18662

A microprocessor controlled parallel model with FDPSK 10 p1475 N85-19304

Advanced inverter technology
[AD-A149335] 10 p1480 N85-19343

Linear, position-sensitive X-ray detector used for real-time calculations of small-angle scattering parameters with submillisecond resolution
[DE85-002530] 10 p1489 N85-19401

Microprocessor-based monitoring and control project, phase 1
[DE84-901874] 10 p1538 N85-19699

Personal desktop computing in a research and development laboratory
[DE85-002765] 11 p1705 N85-20728

Synthesis of digital control for object with lag
12 p1843 N85-21582

Remote self-contained undersea monitor
[AD-D011520] 12 p1849 N85-21599

Microprocessor-controlled anodic stripping voltammeter for trace metal analysis in tap water
[DE85-002781] 12 p1852 N85-21619

Microprocessor-controlled rotating shadowband radiometer
[DE85-003833] 12 p1854 N85-21630

Second generation USAFSAM (United States Air Force School of Aerospace Medicine) microprocessor audiometer
[AD-A149938] 12 p1905 N85-21963

Automatic multi-banking of memory for microprocessors
[NASA-CASE-NPO-15295-1] 12 p1911 N85-21992

Variable data base generator apparatus
[AD-D011518] 12 p1911 N85-21993

NDE methods for green ceramics
[DE85-004019] 13 p2036 N85-22766

The audiomat: An automatic audiometer for use in occupational audiometry
[DRIC-T-7136] 13 p2142 N85-23294

Research on CAD/CAM support for microprocessor development surveyed 14 p2280 N85-24193

Automatic hydrological data collection facility using ARGOS 14 p2324 N85-24363

Bipolar nonswitching logic arrays: Universal components of function expanders for computation of elementary functions 14 p2400 N85-24797

Systems design and application of computers with flexible architecture 14 p2401 N85-24800

Implementation of an inertial navigation algorithm using a limited wordlength microprocessor for a strapdown navigation computer
[BAE-ST-12792] 15 p2468 N85-25234

Structurization of programs for real-time microprocessor arrays 15 p2529 N85-25592

China report: Science and technology
[JPRS-CST-85-007] 15 p2533 N85-25621

Microprocessor controlled storage sampling oscilloscope 15 p2533 N85-25622

Effective microinstruction pipeline organization in a high-capacity microprocessor 15 p2625 N85-26176

Optimal control of electric drive with simultaneous control inputs for motor current and flux
16 p2763 N85-27049

Creating a Mobile Autonomous Robot Research System (MARRS)
[AD-A151983] 16 p2793 N85-27229

Development of a microprocessor controlled communication system for ships
[BMFT-FB-T-84-275] 17 p2950 N85-28216

VLSI (Very large scale integrated circuits) device reliability models
[AD-A153268] 17 p2954 N85-28245

Microprocessor controlled temperature chassis
[DE85-006392] 17 p3009 N85-28602

Development of a multiprocessor system, using the MOTORLA microprocessor 6809, with the aim of providing maximum flexibility in the design of individual control devices
[BMFT-FB-T-84-270] 17 p3010 N85-28607

The AFTI/F16 terrain-aided navigation system
[DE85-008411] 18 p3060 N85-28935

Development of a butterfly multiprocessor test bed description of butterfly components
[AD-A153692] 18 p3095 N85-29155

A variable frequency control for three-phase induction motors 19 p3258 N85-30190

Development and evaluation of a fault-tolerant multiprocessor (FTMP) computer. Volume 1: FTMP principles of operation
[NASA-CR-166071] 19 p3341 N85-30705

Apollo multiplexer operations manual
[DE85-011293] 19 p3343 N85-30719

Control system for parabolic dish concentrator No. 1
[NASA-CR-176045] 20 p3463 N85-31510

Production verification of the acoustic emission weld monitor
[AD-A154166] 20 p3464 N85-31519

Microprocessor AirborneData Acquisition and Replay (MADAR) system
[AD-A151728] 20 p3514 N85-31843

A miroprocessor based multiscaling data acquisition system for Mossbauer spectroscopy
[USIP-85-01] 20 p3518 N85-31875

Microprocessor control design for a low-head crossflow turbine
[AD-A155477] 21 p3556 N85-32121

A microprocessor-controlled, multichannel fluorimeter for analysis of sea water
[AD-A154986] 21 p3590 N85-32310

Ultrasonic position reference systems for an autonomous sentry robot and a robot manipulator arm
[AD-A155481] 21 p3596 N85-32336

The 8080 emulator 21 p3668 N85-32783

Basic features of personal computers
22 p3766 N85-33344

System of microprocessor instructions
22 p3770 N85-33362

Module for interfacing microprocessors and microcomputer 22 p3774 N85-33390

Developmental trends in radio receiver design
22 p3777 N85-33407

Optical-fiber/microprocessor-based remote velocity sensor
[DE85-010071] 22 p3788 N85-33470

Magnetic search system
[PB85-185108] 23 p3949 N85-34477

Hardware math for the 6502 microprocessor
[NASA-TM-86517] 23 p3955 N85-34511

New technologies at the forefront of industrial developments 24 p4061 N85-35166

Design for MISP: A multiple instruction stream shared pipeline processor
[AD-A158314] 24 p4136 N85-35635

Error message recording and reporting in the SLC control system
[DE85-013057] 24 p4140 N85-35664

Report on the SLC control system
[DE85-013076] 24 p4148 N85-35722

Investigation of cosmic rays in very short time scales
[HE-4.6-7] 24 p4197 N85-36044

Microprocessor-based single particle calibration of scintillation counter
[HE-4.6-13] 24 p4198 N85-36049

A mini-array for large air showers
[HE-4.7-1 24 p4199 N85-36061

Study of the time-differentiated particle flux density at various distances from EAS axis
[HE-4.7-15] 24 p4200 N85-36065

MICROPROGRAMMING

S-MICRO: A system for simulating a microprogrammed control unit
[INPE-3224-PRE/575] 05 p0715 N85-14585

Data stimulated on-line-checking (IROLD)
08 p1066 N85-16754

Development and analysis of a global compaction technique of microprograms 19 p3334 N85-30654

Implementation of a proposed system for automated microcode generation
[AD-A154235] 19 p3336 N85-30671

Evaluation and implementation of a functional microprogram generator
[AD-A155164] 21 p3674 N85-32823

Design of a microprogram control unit with concurrent error detection
[AD-A156447] 24 p4139 N85-35655

MICROROCKET ENGINES
NT ORBIT MANEUVERING ENGINE (SPACE SHUTTLE)

The highly underexpanded exhaust plume from nozzles with boundary layers
[DFVLR-FB-85-10] 20 p3421 N85-31230

MICROSCALES
U MICROBALANCES

MICROSCOPES
NT ACOUSTIC MICROSCOPES
NT ELECTRON MICROSCOPES
NT ION MICROSCOPES
NT OPTICAL MICROSCOPES

Laser illuminated nano-second microscope
[DE84-016200] 06 p0811 N85-15152

Photoacoustic microscopy of oxygen contaminated titanium alloys
[AD-P004127] 08 p1127 N85-17102

Microscopic identification of feathers in order to improve birdstrike statistics
[AD-P004187] 11 p1579 N85-19950

Method of examining microcircuit patterns
[NASA-CASE-NPO-16299-1] 11 p1628 N85-20250

Operation of the Zeiss cytopherometer with Zn/ZnSO4 electrode system of Tenforde et al
20 p3499 N85-31752

MICROSCOPY
NT ELECTRON MICROSCOPY
NT LASER MICROSCOPY
NT ULTRAVIOLET MICROSCOPY

Ion contrasting chamber for discrimination of grains and textures
[BMFT-FB-T-84-151] 04 p0477 N85-13036

Acoustic microscopy at cryogenic temperatures
[AD-A148756] 09 p1384 N85-18704

Application of optical and electron microscopic techniques in the fractographic determination of fatigue crack growth rates 14 p2320 N85-24334

Measuring: The quantifying art
14 p2437 N85-25035

A micrographic and gravimetric study of intercalation and deintercalation of graphite fibers
[NASA-TM-87026] 17 p2934 N85-28110

Modification of the grain size of sputtered copper with additions of oxygen, krypton, silver, or yttrium
[DE85-010975] 21 p3567 N85-32189

MICROSEISMS

Wave-wave interactions, microseisms, and infrasonic ambient noise in the ocean
[AD-A146529] 06 p0859 N85-15463

Microseism level, time variations at Turkmen seismic stations studied 07 p0981 N85-16231

A seismic ARGOS data collection platform
16 p2813 N85-27350

MICROSTRIP TRANSMISSION LINES

The study of microstrip antenna arrays and related problems
[NASA-CR-174054] 02 p0189 N85-11266

Microstrip directional filters
[INPE-3127-PRE/518] 02 p0194 N85-11293

Green function in theory of microstrip antennas
06 p0790 N85-15050

A transistor oscillator-doubler
[AD-D011409] 08 p1156 N85-17307

Effect of interfacial characteristics of metal clad polymeric substrates on electrical high frequency interconnection performance
[NASA-TM-86946] 11 p1624 N85-20223

An experimental investigation of microstrip properties on soft substrates from 2 to 40 GHz
[NASA-TM-86961] 11 p1624 N85-20224

Distributed Gunn effect devices; a numerical analysis of microstrip circuits on thin active GaAs substrates
[FOA-C-30383-E] 12 p1837 N85-21527
A generalized solution to a class of printed circuit antennas 13 p2062 N85-22862
Synthesis of optimum smooth transition in microstrip through line on microwave integrated circuit
13 p2089 N85-23041
Microstrip comb array design
[R-NIAS-24] 14 p2290 N85-24195
A study of computational techniques for noncanonical microstrip antennas and arrays
[AD-A152216] 16 p2774 N85-27123
Mutual coupling analysis for conformal microstrip antennas
[AD-A154282] 19 p3259 N85-30210
Dielectric resonator stabilized microstrip oscillator
[AD-D011706] 19 p3261 N85-30219
Mutual coupling analysis for conformal microstrip antennas 20 p3439 N85-31343
Calculating dominant (quasi-t) mode group velocity in shielded microstrip line 22 p3780 N85-33422
Multidiode integrated-circuit protective device
22 p3781 N85-33425
Perturbation-iteration theory for analyzing microwave striplines
[NASA-CR-176189] 24 p4085 N85-35321
Characterization of microstrip discontinuities in the time and frequency domains
[NASA-CR-176190] 24 p4088 N85-35342

MICROSTRUCTURE
NT METEORITIC MICROSTRUCTURES
Results of the technical exchange agreement between NASA and DuPont on the containerless drop tube solidification of NiAl3
[NASA-TM-86473] 01 p0014 N85-10087
Effects of cobalt, boron, and zirconium on the microstructure of Udimet 738
[NASA-CR-174762] 01 p0027 N85-10166
The effects of seven alloying elements on the microstructure and stress-rupture behavior of nickle-base superalloys
[NASA-TM-83791] 01 p0027 N85-10168
Influence of nitrogen on the sensitization, corrosion, mechanical, and microstructural properties of austenitic stainless steels
[DE84-015134] 01 p0028 N85-10177
Ceramic microstructure and adhesion
[NASA-TM-83804] 01 p0031 N85-10186
Ultrasonic nondestructive evaluation, microstructure, and mechanical property interrelations
[NASA-TM-86876] 01 p0056 N85-10371
The effect of overload on three different kinds of steel
02 p0174 N85-11165
Effect of microstructure and trapping on the hydrogen embrittlement susceptibility of a titanium bearing HSLA steel 02 p0174 N85-11166
International Conference on Recent Developments in Specialty Steels and Hard Materials. Conference abstracts
[CSIR-S-256] 02 p0176 N85-11177
Microstructural design and control of sintered hard materials 02 p0176 N85-11180
Microstructure and deformation aspects of some specialty steels and hard metals
02 p0176 N85-11182
Rapid solidification of steels: Model and commercial alloys 02 p0176 N85-11184
Microstructural basis of strength and toughness in hardmetals 02 p0177 N85-11185
The inter-relation of microstructure, toughness and fatigue crack growth behaviour in WC-Co hardmetals
02 p0177 N85-11188
An investigation into the superhardening effect in molybdenum-free steel with specific reference to alloy substitution 02 p0180 N85-11209
The structure of rapidly solidified nickel-base alloys
02 p0181 N85-11215
Microstructure and creep behaviour at elevated temperature of unidirectionally solidified eutectic nickel base superalloys 02 p0181 N85-11216
Metastable phase formation in ion implanted metals
[DE84-014945] 02 p0183 N85-11229
Review: The influence of short circuit diffusion on the oxidation of nickel, chromium and nickel/chromium alloys
[AERE-R-11311] 02 p0185 N85-11237
Plastic deformation and microstructural transformations of metals under shock waves 02 p0272 N85-11775
Internal friction, microstructure and radiation effects
[DE84-013905] 02 p0288 N85-11880
Application of positron annihilation in materials science
[DE84-014733] 02 p0288 N85-11883
Characterization of amorphous surface layers in Fe implanted with Ti and C
[DE84-014960] 02 p0289 N85-11885
Structure of silane coupling agents adsorbed on silicon powder
[AD-A145803] 03 p0327 N85-12105
Effect of rhenium on the structure and properties of the weld metal of a molybdenum alloy
[NASA-TM-77491] 03 p0330 N85-12128
Effects of tin on microstructure and mechanical behavior of Inconel 718
[NASA-TM-86866] 03 p0330 N85-12129
Application of solidification theory to rapid solidification processing
[AD-A145953] 03 p0331 N85-12136
Effects of prior austenite and ferrite grain size on fracture properties of a plain carbon steel
[AD-A146276] 03 p0332 N85-12138
The effects of microstructure on the temper embrittlement susceptibility of a Cr-2-1/4 1Mo forging
[AERE-R-11110] 03 p0334 N85-12151
A study of precipitation and boron distribution in 20 Cr 25Ni base stainless steels
[AERE-M-3353] 03 p0334 N85-12154
Microstructure and properties of ceramics
[NASA-TM-77416] 03 p0335 N85-12155
Microstructure of ceramics fabricated by unidirectional solidification
[NASA-TM-77423] 03 p0336 N85-12157
Ceramic powder for sintering materials
[NASA-TM-77434] 03 p0336 N85-12160
Ceramic microstructure development
[AD-A145753] 03 p0337 N85-12166
Microstructure development in polymers
[AD-A145960] 03 p0337 N85-12170
Structure of two-phase titanium alloys with different microstructures 03 p0351 N85-12257
Constitutive features of solids at shock-wave loading rates
[DE84-015715] 03 p0362 N85-12325
Static and dynamic characteristics of materials with beam-microstructure 03 p0370 N85-12361
Stress relief cracking studies of 2 1/4Cr1Mo steel
[AERE-R-11111] 03 p0374 N85-12386
Effect of a thermal gradient applied to a sinusoidal surface profile
[DE84-015649] 03 p0434 N85-12765
Development and fabrication of refractory bodies for gas turbine engines
[BMFT-FB-T-84-180] 04 p0457 N85-12899
The chemical nature of the fiber/resin interface in composite materials 04 p0465 N85-12953
Subgrains, dislocations and the elevated-temperature strength of type 304 stainless steel
[DE84-001233] 04 p0473 N85-13014
The Al-Be system: The effects of RSP on structure and phase relating
[DE84-015604] 04 p0474 N85-13019
Ion contrasting chamber for discrimination of grains and textures
[BMFT-FB-T-84-151] 04 p0477 N85-13036
Microstructural effects in abrasive wear
[DE84-016155] 04 p0509 N85-13247
Nondestructive determination of mechanical properties — aluminum alloys 04 p0512 N85-13266
Imaging of surfaces and defects of crystals
[DE84-016449] 04 p0570 N85-13632
Study of the reactive-element effect in oxidation of Fe-Cr alloys using transverse section analytical electron microscopy
[DE84-016237] 04 p0571 N85-13641
The microstructural characteristics of revert superalloys — for turbine blades
05 p0617 N85-13945
Application of solidification theory to rapid solidification processing
[AD-A146619] 06 p0769 N85-14917
Microstructure of rapidly quenched type 308 stainless steel weld filler metal and its implications on rapid solidification processes
[DE85-000930] 06 p0769 N85-14920
Development and characterization of ductile Long-Range-Ordered (LRO) alloys (Fe,Co, Ni)3V for high-temperature structural use
[DE84-016750] 06 p0769 N85-14921
Microstructural origins of hot spots in RDX explosive and a reference inert material
[AD-A146685] 06 p0774 N85-14947
Process Modeling Applied to Metal Forming and Thermomechanical Processing
[AGARD-LS-137] 06 p0796 N85-15086
Microstructure, texture and formability of thin aluminium sheets 06 p0796 N85-15088
The role of microstructure in the modelling of plastic flow in P/M superalloys at forging temperatures and strain rate 06 p0796 N85-15090
Control of microstructure during hot working of Ti-6242 06 p0797 N85-15091
Modeling microstructural changes during hot rolling of steels 06 p0798 N85-15094
Structural studies on lead dioxides
[DE84-015837] 06 p0805 N85-15107
Investigation of structural and electrical properties of low-angle silicon sheet 06 p0831 N85-15284
Anisotropy and microstructure of rare earth permanent magnet materials
[AD-A146549] 06 p0859 N85-15480
Oxygen isotopes in deep sea spherules
06 p0863 N85-15609
Aqueous alteration of meteorite parent bodies: Possible role of unfrozen water and the Antarctic meteorite analogy 06 p0864 N85-15617
The growth of metastable peritectic compounds
[NASA-CR-171289] 07 p0920 N85-15824
The formation of isolated phase precipitates during the decomposition of high-coercive force Fe-Cr-Co alloys
[BLL-M-36028-(5828.4)] 07 p0924 N85-15865
Studies on copper alloys containing chromium on the copper side phase diagram
[NASA-TM-77752] 07 p0927 N85-15878
Fundamentals of microcrack nucleation mechanics
[NASA-CR-3851] 07 p0975 N85-16195
Effects of oxygen on the microstructure and properties of titanium 6211 alloys
[AD-P004122] 08 p1126 N85-17097
Effects of oxygen-contamination-induced microstructural changes on the reverberation of ultrasound in Ti-6211 alloys
[AD-P004124] 08 p1126 N85-17099
Ultrasonic evaluation of titanium contamination with correlation techniques
[AD-P004126] 08 p1126 N85-17101
High resolution acoustic microstructural characterization of titanium with interstitial contamination
[AD-P004128] 08 p1127 N85-17108
Grain refining and microstructural modification during solidification
[AD-A147705] 08 p1128 N85-17111
Mechanical properties and microstructure of centrifugally cast alloy 718
[AD-A147800] 08 p1129 N85-17116
Rapid solidification processing and powder metallurgy of Al alloys
[AD-A148427] 08 p1130 N85-17120
Effect of microstructure and trapping on the hydrogen embrittlement susceptibility of a ti-bearing HSLA steel
[AD-A148610] 08 p1130 N85-17122
Structural studies of amorphous Mo-Ge alloys using synchrotron radiation
[DE85-002061] 08 p1131 N85-17125
Research on nondestructive testing
[AD-A148375] 08 p1171 N85-17380
A study of spectrum fatigue crack propagation in two aluminum alloys. 2: Influence of microstructures
[NASA-TM-86930] 09 p1294 N85-18125
The effect of tantalum on the structure/properties of two polycrystalline nickel-base superalloys: B-1900 + Hf MAR-M247
[NASA-CR-174847] 09 p1294 N85-18127
Alloying effects and microstructure of iron aluminides
[DE85-000903] 09 p1295 N85-18137
Ti-6Al-4V alloy castings prepared in zircon sand molds and the effect of hot isostatic pressing
[PB85-109932/GAR] 09 p1298 N85-18150
Mechanisms of elevated temperature rupture in single phase ceramics
[DE85-000697] 09 p1299 N85-18156
The feasibility of low-G grey solidification of nodular iron in the F-104 experimental furnace package
[NASA-TM-82527] 10 p1426 N85-18996
Mechanics of composite materials
[DE85-003611] 10 p1432 N85-19031
Creep-rupture behavior of iron superalloys in high-pressure hydrogen
[NASA-CR-174411] 10 p1441 N85-19078
Impact toughness of composites with layered microstructure of OT4 titanium alloy
10 p1445 N85-19104
Effect of powder characteristics on microstructure and properties in alkoxide prepared PZT ceramics
[AD-A149082] 10 p1451 N85-19141
Microstructural analysis of ion containing polymers
[DE85-001594] 10 p1453 N85-19157
Reliability studies of ceramic capacitors
[AD-A149126] 10 p1479 N85-19338
The effect of filler wire and flux compositions on the microstructure and properties of microalloyed steel weld metal
[AD-A149529] 10 p1492 N85-19423

Internal Gravity Waves and Small-Scale Turbulence: Proceedings of the 2nd 'Aha Huliko'a Hawaiian Winter Workshop
[AD-A149510] 10 p1522 N85-19597
Application of layered synthetic microstructures to high temperature plasma diagnostics
[DE85-002035] 10 p1559 N85-19828
Effect of ingot structure of failure ductility of pressed semifinished products of high-durability aluminum alloys
11 p1597 N85-20045
Study of microstructure of aluminum and copper alloys after processing with continuous CO2 laser beam
11 p1601 N85-20066
Dependence of mechanical properties of large VT3-1 alloy forgings on microstructure parameters
11 p1602 N85-20072
Electron-diffraction structural examination of amorphous iron-tin alloys 11 p1604 N85-20084
Effect of microstructure on solid particle erosion in multiphase materials
[DE85-000426] 11 p1608 N85-20109
Weldability and mechanical property characterization of weld clad alloy 800H tubesheet forging
[DE85-001737] 11 p1609 N85-20116
The role of void nucleation in the swelling resistance of ferritic steel
[AERE-R-11525] 11 p1610 N85-20122
Design and use of nonstandard tensile specimens for irradiated materials testing
[DE85-001071] 11 p1652 N85-20408
Transverse microstructure of an oxide scale formed on a 20 % Cr/25 % Ni niobium stabilized stainless steel
[AERE-R-11034] 12 p1804 N85-21315
Method for refining microstructures of cast titanium articles
[AD-D011518] 12 p1804 N85-21318
Effect of reduction of strategic Columbium addition in 718 Alloy on the structure and properties
[NASA-CR-174841] 12 p1805 N85-21320
Stress corrosion cracking and oxidation characteristics of boride-strengthened microcrystalline iron and nickel based alloys
[AD-A149605] 12 p1806 N85-21326
Microstructural and electronic characteristics of metallic spin glasses
[AD-A149959] 12 p1813 N85-21371
Micromechanical modeling of microstructural damage in creeping alloys
[DE85-003925] 13 p2022 N85-22671
TEM/FIM study of modulated microstructures in the Fe-Be system
[DE85-005379] 13 p2023 N85-22676
Influence of laser treatment of structure and mechanical properties if MA21 alloy 13 p2029 N85-22713
Electrodynamic stability of composite liquid-metal contacts 13 p2067 N85-23031
Microstructural study on the processing and properties of high-field A15 superconducting materials
[DE85-004652] 13 p2184 N85-23423
Non-steady combustion of composite solid propellants
[AD-A150827] 14 p2250 N85-23947
Synthesis and properties of elevated temperature P/M aluminum alloys
[AD-A151031] 14 p2256 N85-23981
Microstructure and properties of ferrous alloy weldments
[DE85-005582] 14 p2257 N85-23987
Laser surface treatments 14 p2308 N85-24284
Investigation of the MBE growth of InSb and novel quantum well structures
[AD-A151014] 14 p2427 N85-24969
Study of amorphous strips and microconductors by ferromagnetic resonance method
15 p2497 N85-25402
Effect of aluminum on nature of titanium alloy failure
15 p2498 N85-25411
Hydrogen resistance of VT1-0 titanium under 150 MPa pressure at room temperature 15 p2499 N85-25414
Structural changes with one- and two-stage aging of alloys Ti-Al-Mo-Fe and Ti-Zr-V-Al-Sn
15 p2499 N85-25415
Ways of improving level and stability of mechanical characteristics of diffusion-welded joints of OT4 titanium alloy 15 p2499 N85-25417
Microstructural characteristics during the controlled solidification of a binary system
[DE85-005200] 15 p2507 N85-25481
Application of solidification theory to rapid solidification processing
[AD-A151251] 15 p2509 N85-25480
Optimizing hot workability and controlling microstructures in difficult to process high strength and high temperature materials
[AD-D011586] 15 p2510 N85-25482
Mossbauer spectrometry: Testing of a new computer based system and its application to a study of an aluminum-iron-cerium alloy
[AD-A151626] 15 p2510 N85-25483
Metallurgical characterization of aluminum powder consolidation
[AD-A151990] 15 p2510 N85-25484
Structure of condensed aluminum thin film metallizations 15 p2512 N85-25501
Dependence of plasticity of VT1-00 titanium alloy on microstructure 15 p2515 N85-25516
Transformation toughened ceramics: A potential material for light diesel engine application
[AD-A151421] 15 p2518 N85-25526
Mammalian gravity receptors: Structure and metabolism 15 p2605 N85-26055
Radiation effects on structural materials
[DE85-007032] 15 p2649 N85-26338
Relationships between microstructure and microfissuring in alloy 718 16 p2735 N85-26876
Microstructures and properties of rapidly solidified alloys
[NASA-CR-172377] 16 p2748 N85-26961
Properties and microstructures for dual alloy combinations of three superalloys with alloy 901
[NASA-TM-86967] 16 p2749 N85-26963
Hydrogen induced crack growth in Grade-12 Titanium
[BNL-NUREG-35598] 16 p2751 N85-26976
Microwave processing of lunar materials: Potential applications
[DE85-007223] 16 p2755 N85-27003
Multiple scattering of electromagnetic waves in discrete random media
[AD-A151766] 16 p2772 N85-27112
Full statistical characteristics of microdeformation
[BLL-M-36076-(5828.4)] 16 p2798 N85-27254
Constitutive cyclic deformation behavior in single-crystal and directionally solidified SSME high-pressure fuel turbopump airfoil materials 17 p2914 N85-27965
Study of self-propagating condensed phase reactions TiB(2) synthesis
[AD-A153198] 17 p2921 N85-28006
Powder-metallurgy alloys and steels
[BLL-BISI-TRANS-22239-(9022.06)]
17 p2926 N85-28050
Textural transformations taking place during heat and mechanical treatment in triplex steels
[BLL-BISI-TRANS-22404-(9022.06)]
17 p2927 N85-28063
Microstructure and mechanical properties of rare-earths-microalloyed high-speed tool steel
[BLL-BISI-TRANS-22043-(9022.06)]
17 p2928 N85-28064
Preventing the formation of an anomalous structure in chemically sealed low carbon steel
[BLL-BISI-TRANS-22373-(9022.06)]
17 p2930 N85-28085
Influence of composition on the microstructural evolution and mechanical properties of irradiated Fe-Ni-Cr ternaries
[DE85-007462] 17 p2931 N85-28094
Properties of nitrogen containing stainless alloy designed for high resistance to pitting
[DE85-008282] 17 p2931 N85-28095
Mechanical stabilization of austenite against epsilon martensite and its effect on deformation behavior in high manganese steels
[DE85-007654] 17 p2932 N85-28097
Microstructure-mechanical property relationships in transformation-toughened ceramics
[DE85-009722] 17 p2935 N85-28117
Submerged arc welding of new Czechoslovak micro-alloy steels
[BLL-BISI-TRANS-22193-(9022.06)]
17 p2972 N85-28356
Formation of a fine structure during shock wave welding
[BLL-BISI-TRANS-22401-(9022.06)]
17 p2973 N85-28368
Preliminary results of the Inconel 617 optimization program. Advanced gas cooled reactor materials program
[DE85-008235] 18 p3075 N85-29024
Sintering reactions, structure and properties of a cobalt free nonconventional hard material
[DE85-007704] 18 p3076 N85-29025
Evaluation of 7XXX-series aluminum alloys for the W87 aft support ring
[DE85-009987] 18 p3076 N85-29027
Predicting microfracture in ceramics via a microcontract model
[DE85-005654] 18 p3081 N85-29060
Study of the influence of metallurgical factors on fatigue and fracture of aerospace structural materials
[AD-A153913] 18 p3122 N85-29328
Influence of microstructure on mechanical properties in cemented tungsten-carbides 19 p3230 N85-30029
The fabrication, microstructure, and strengthening behavior of heavily cold-worked in situ composites
19 p3231 N85-30031
The physical and mechanical properties of near-equiatomic titanium-nickel
19 p3237 N85-30072
Internal structure of GP zones in dilute Al-Cu alloys
19 p3238 N85-30073
Microstructures and mechanical properties of microalloyed medium carbon steels
19 p3238 N85-30074
Microstructure-abrasive wear characteristics of low carbon dual phase steels
[DE85-010988] 19 p3239 N85-30083
The microstructural state of Nb3Sn in a multifilamentary titanium doped bronze-process wire
[DE85-010979] 19 p3240 N85-30089
Weldability/microstructure relationships of high nickel alloys for header applications
[DE85-009337] 19 p3241 N85-30094
Specifics of fine structure of pressed aluminum alloys manufactured by plasma atomization
19 p3242 N85-30102
Effect of matrix plasticity on durability of fibrous composition materials 19 p3243 N85-30107
Mesophase mechanisms in the formation of graphitic microstructures
[AD-A154100] 19 p3248 N85-30140
Superconducting electronic film structures
[AD-A154196] 19 p3259 N85-30207
Investigation for low-cost permanent magnets
[AD-A154387] 19 p3260 N85-30212
Microstructural analysis of Pacific Ocean and Indian Ocean ultrabasites 19 p3291 N85-30405
Grain structure identification by ultrasound frequency averaging and deconvolution
[AD-A154332] 19 p3352 N85-30777
The microstructure approach to conserved scalar pdf models 20 p3424 N85-31251
Phase size distribution in WC/Co hardmetal
[NPL-DMA(A)-93] 20 p3431 N85-31281
Structure and chemistry of sol-gel derived transparent silica aerogel
[DE85-009902] 20 p3434 N85-31303
Metallurgical origins of fracture toughness and microstructure and fracture toughness of an HSLA (High-Strength/Low-Alloy) steel
[AD-A155530] 21 p3567 N85-32187
Fundamental investigations of failure during superplastic forming process
[AD-A154647] 21 p3588 N85-32194
The variability of aerosol microstructure in continental and oceanic surface layers of the atmosphere in anticyclones 21 p3647 N85-32660
Variation of the submicron aerosol structure
21 p3647 N85-32661
Microstructure-mechanical property relationships in the transformation-toughened ceramics
[DE85-011946] 22 p3752 N85-33261
Investigation of the microstructure and photovoltaic properties of semicrystalline silicon
22 p3806 N85-33573
Manufacturing process to reduce large grain growth in zirconium alloys
[DE85-011649] 23 p3915 N85-34267
Experimental attempt to achieve microstructure variations through temperature/time permutations for a nonwrought powder metallurgy uranium-6 niobium alloy
[DE85-013166] 23 p3916 N85-34272
Influence of particle erosion on the microstructural changes in metals and alloys
[TI85-901384] 23 p3917 N85-34276
High resolution electron microscopic characterization of interfaces in ceramics
[DE85-011207] 23 p3920 N85-34289
Near-threshold fatigue: An overview of the role of microstructure and environment
[DE85-009903] 23 p3941 N85-34431
Analytical ultrasonics for structural materials
[TI85-008132] 23 p3968 N85-34600
Effect of thermal ageing on the mechanical properties of PWR pressure vessel steels and weldments
[AERE-R-11460] 24 p4078 N85-35275
Effect of prior warm rolling on the retained austenite content and hardening response of VIM-VAR (vacuum-induction melted-vacuum-arc remelted) AISI M-50 steel
[AD-A156145] 24 p4079 N85-35281
Effect of microstructure on the fatigue behavior of Fe-C-X alloys
[DE85-011749] 24 p4080 N85-35285

MICROTRONS
Performance of an RF beam monitor on the NBS-Los Alamos racetrack microtron
[DE85-010725] 19 p3262 N85-30232
MICROWAVE AMPLIFIERS
NT CYCLOTRON RESONANCE DEVICES
Linear wideband microwave amplifiers for monolithic integrated microcircuits 07 p0955 N85-16051
Combined microwave parallel amplifier-RF attenuator/modulator
[AD-D011535] 12 p1833 N85-21499
Analysis and design of linear microwave transistor amplifiers 13 p2088 N85-23036
Proceedings of the Cold Electronics Workshop
[NASA-CR-175662] 14 p2297 N85-24220
Cryogenically-cooled, low-noise microwave receivers: Present status and future needs
14 p2298 N85-24226
Design and testing of gyroklystron amplifiers
[AD-A151026] 14 p2298 N85-24231
The design of megawatt gyrotrons
[DE85-007892] 17 p3032 N85-28754
Proposal for continuation of research on megawatt gyrotrons for the period January 1, 1985 through December 31, 1986
[DE85-009962] 18 p3110 N85-29260
Design and fabrication of monolithic broadband microwave GaAs low noise FET amplifiers
20 p3443 N85-31370
Thirty GHz low noise GaAs FET amplifiers — satellite-ground communication
[CD.6500686] 20 p3449 N85-31413
140 GHz gyrotron development program
[DE85-010348] 20 p3537 N85-32013
Clarke Stations and mercurian mass-drivers: Energy for large-scale transportation systems
[DE85-009607] 21 p3560 N85-32145
High-power solid-state rf source for accelerator cavities
[DE85-012672] 22 p3761 N85-33309
Study of nonlinear distortion in microwave amplifiers using Schottky gate field effect transistors
22 p3780 N85-33423
Realization and linearization of a hyperfrequency power amplifier implemented with bipolar transistors in class C polarization — microwave amplifiers
[CNES-NT-114] 23 p3928 N85-34346
MICROWAVE ANTENNAS
NT HORN ANTENNAS
NT LENS ANTENNAS
NT RECTENNAS
NT SLOT ANTENNAS
NT SPACETENNAS
Mark IVA DSN 26-meter subnet
05 p0624 N85-13995
64-meter to 70-meter antenna extension
05 p0624 N85-13996
Antenna microwave subsystem
05 p0625 N85-13997
Characterization of MMIC devices for active array antennas
[NASA-TM-86907] 07 p0913 N85-15779
The 20 GHz proof-of-concept test model results for a multiple scan beam dual reflector antenna
[NASA-CR-174268] 07 p0938 N85-15944
A low-sidelobe space feed lens
[AD-A147883] 07 p0942 N85-15972
Power transfer from natural emitters to collection apertures at microwave wavelengths
[NASA-CR-174275] 07 p0945 N85-15989
Microwave surface resistivity of several materials at ambient temperature 10 p1463 N85-19226
The effects of mode impurity of Ka-band system performance 10 p1463 N85-19227
Comparison of measured and calculated mutual coupling in the near field between microwave antennas
[PB85-105963] 11 p1625 N85-20237
Orbiting multi-beam microwave radiometer for soil moisture remote sensing 14 p2230 N85-23818
Low-frequency microwave radiometer for N-ROSS
14 p2230 N85-23819
Development of the microwave antenna range of the national antenna test facility at Paardefontein
[R-NIAS-21] 15 p2539 N85-25669
ECM multiple-target retrodirective antenna
[AD-D011528] 20 p3439 N85-31346
MICROWAVE ATTENUATION
Attenuation experimental data bank in the COST 205 project. Structure and management of the final supports
[FUB-5-1983] 01 p0126 N85-10865
Absorption of radiation by water vapor in windows of relative transparency of 95-145 micrometer range
13 p2076 N85-22968
The microwave propagation and backscattering characteristics of vegetation — wheat, sorghum, soybeans and corn fields in Kansas
[E85-10088] 13 p2122 N85-23213
Precision microwave attenuation measurement by time interval ratio
[RSRE-85005] 22 p3755 N85-33260
MICROWAVE CIRCUITS
Manufacturing methods for microwave circuits
[AD-A145237] 01 p0043 N85-10278
Computerized circuit designs: Realization of masks to manufacture microwave circuits
[CNES-NT-107] 04 p0496 N85-13168
Interface structures for millimeter-wave circuits
[AD-A146557] 06 p0804 N85-15118
Characterization of MMIC devices for active array antennas
[NASA-TM-86907] 07 p0913 N85-15779
Slow wave circuit with shaped dielectric substrate
[AD-D011385] 07 p0945 N85-15986
Investigation of planar waveguides and components for millimeter-wave integrated circuits
[AD-A147360] 07 p0948 N85-16005
Configuration study for a 30 GHz monolithic receive array, volume 1
[NASA-CR-174697-VOL-1] 09 p1311 N85-18239
Monolithic thin film SAW (Surface Acoustic Wave) structures
[AD-A149782] 12 p1835 N85-21511
Reduction of amplitude-phase distortions of movable microwave coupling circuit for antenna field measurements 13 p2068 N85-22920
Measurement methods for accurate microwave characterization and modeling of MESFET chips
[AD-A152360] 17 p2952 N85-28227
Communications and logic systems at millimeter wave frequencies
[NASA-CR-175859] 17 p3042 N85-28824
Microwave semiconductor research: Materials, devices and circuits and gallium arsenide ballistic electron transistors
[AD-A154698] 21 p3709 N85-33024
Software for frequency analysis of microwave circuits
22 p3768 N85-33352
MICROWAVE COUPLING
NT COUPLING CIRCUITS
A transistor oscillator-doubler
[AD-D011406] 08 p1158 N85-17307
Effect of resonant microwave power on a PIG ion source
[DE85-001396] 09 p1379 N85-18673
Phenomenology of microwave coupling, part 1
[DE85-003097] 11 p1624 N85-20229
Reduction of amplitude-phase distortions of movable microwave coupling circuit for antenna field measurements 13 p2068 N85-22920
Synthesis of multistep directional couplers with nonminimum-phase characteristics
13 p2079 N85-22986
Maser cavity servo-tuning system
[NASA-CASE-NPO-15890-1-CU]
18 p3093 N85-29143
Mutual coupling analysis for conformal microstrip antennas 20 p3439 N85-31343
MICROWAVE EMISSION
Power transfer from natural emitters to collection apertures at microwave wavelengths
[NASA-CR-174275] 07 p0945 N85-15989
Microwave emissions from snow
[E85-10065] 08 p1174 N85-17403
Data report on variations in the composition of sea ice during MIZEX/East'83 with the Nimbus-7 SMMR
[NASA-TM-86170] 09 p1342 N85-18443
Measurement of hot-electron production and microwave emission by laser-irradiated CH targets
[DE85-003139] 11 p1640 N85-20331
Remote Sensing of Snow and Evapotranspiration
[NASA-CP-2363] 13 p2123 N85-23223
Microwave radiometer observations of snowpack properties and comparison of U.S. Japanese results — Hokkaido, Japan and Vermont and North Dakota test sites 13 p2125 N85-23230
Microwave remote sensing of soil moisture
13 p2125 N85-23235
Modeling of radiothermal radiation of rain by Monte-Carlo method 14 p2341 N85-24476
Technical development to improve satellite sounding over radiatively complex terrain
[NASA-CR-175746] 15 p2583 N85-25929
Microwave emission from relativistic electron beams
[AD-A151472] 15 p2648 N85-26333
Microwave emission from Saturn's rings
15 p2670 N85-26475
Experiments in microwave exposure in the rat: Body temperature, serum chemistry and the use of chemical restraint
[PB85-156834] 16 p2840 N85-2731
MICROWAVE EQUIPMENT
NT COLD CATHODE TUBES
NT GYRATORS
NT HELITRONS
NT HORN ANTENNAS
NT KLYSTRONS
NT LENS ANTENNAS
NT MAGNETRONS
NT MICROWAVE AMPLIFIERS
NT MICROWAVE ANTENNAS
NT MICROWAVE FILTERS
NT MICROWAVE INTERFEROMETERS
NT MICROWAVE OSCILLATORS
NT MICROWAVE PROBES
NT MICROWAVE RADIOMETERS
NT MICROWAVE TUBES
NT PHOTOMULTIPLIER TUBES
NT RECTENNAS
NT SLOT ANTENNAS
NT SPACETENNAS
NT THERMICONS
NT THYRATRONS
NT TRAVELING WAVE TUBES
NT VIDICONS
Linear theory of free-electron lasers with cylindrical interaction space 02 p0262 N85-11718
Target detection using microwave irradiances from natural sources: A passive, local and global surveillance system
[NASA-CR-174260] 07 p0946 N85-1599
USSR report: Electronics and electrical engineering
[JPRS-UEE-84-017] 07 p0951 N85-1602
Investigation of the ice dynamics in the marginal ice zone
[AD-A146729] 07 p1009 N85-16411
Microwave resonator using lateral excitation
[AD-D011374] 07 p1039 N85-1659
Transient response of a small-signal microwave GaAs FET to X-rays
[DE85-000066] 09 p1315 N85-1808
The impact of propagation effects on the design of high capacity digital microwave links in the 18 GHz frequency band 10 p1470 N85-1927
Improved electron emission by use of a cloth fiber cathode
[AD-A149250] 10 p1480 N85-1994
Planar ferroelectric microcapacitors for microwave devices 13 p2087 N85-2300
Demonstration of feasibility of depositing semiconductor layers using microwave enhanced plasma techniques
[NASA-CR-174392] 13 p2163 N85-23421
Equipment for hot-to-serve foods
14 p2393 N85-24741
Study of 1/f noise in solids
[AD-A151069] 14 p2428 N85-24872
Future prospects of China's microwave semiconductor technology 15 p2530 N85-2589
In situ microwave measurements of dielectric properties and moisture in materials
[DE85-003622] 16 p2747 N85-2685
Microwave processing of lunar materials: Potential applications
[DE85-007223] 16 p2755 N85-2700
Hardware test program for evaluation of baseline range-range rate sensor concept
[NASA-CR-175794] 16 p2787 N85-2719
An inexpensive radar-responding relocation device for drifting oceanographic instruments
[AD-A152170] 16 p2836 N85-2750
Design of the waveguide for microwave heating of solid lithium ceramic blankets
[DE85-009776] 17 p2935 N85-28120
Technique for measuring the effective source reflection coefficient of 2-resistor power splitters
[DE85-009964] 17 p2956 N85-2825
VULTURE manual
[DE85-008873] 17 p3013 N85-2860
Research relative to the development of a cryogenic microwave cavity gradiometer for orbital use
[NASA-CR-176002] 19 p3222 N85-2988
New measurement solutions in the microwave industry
20 p3437 N85-3132
Microwave semiconductor research: Materials, devices and circuits and gallium arsenide ballistic electron transistors
[AD-A154698] 21 p3709 N85-3302
USSR report: Electronics and electrical engineering
[JPRS-UEE-84-003] 22 p3773 N85-3308
Instrumentation for sensing moisture content of material using a transient thermal pulse
[NASA-CASE-NPO-15493-2] 23 p3933 N85-34073

MICROWAVE FILTERS
Microstrip directional filters
[INPE-3127-PRE/516] 02 p0194 N85-11293
Dual mode directionally coupled band reject filter apparatus
[AD-D011359] 07 p0945 N85-15984
Tunable microwave transversal filters
[AD-A146370] 08 p1158 N85-17304
Synthesis of low-pass filters using coupled lines with unmatched loads 13 p2071 N85-22938
Investigation of bimodal paramagnetic filter
13 p2083 N85-23007
Microwave bandstop filter
[AD-D011716] 19 p3261 N85-30222
Receive shaping filter manufacture — QPSK uplinks
[ESA-CR(P)-1996] 20 p3449 N85-31412
MICROWAVE FREQUENCIES
NT C BAND
NT EXTREMELY HIGH FREQUENCIES
NT SUPERHIGH FREQUENCIES
Spectral noise density and random errors of pulse frequency characteristic meters
03 p0346 N85-12231
Improvement of the accuracy of reflection factor measurements by a computer 05 p0629 N85-14033
Realization of noise power in the microwave range by thermal noise standards 05 p0629 N85-14034
Calculations of high-current characteristics of silicon diodes at microwave frequencies
[AD-A147406] 09 p1314 N85-18261
Spectrum resource assessment of the frequency bands from 17.7-40.5 GHz
[PB85-125748] 10 p1469 N85-19267
Spectrum resource assessment of the 1530-1660.5 MHz band
[NTIA/REPT-84/160] 10 p1469 N85-19268
Spectrum resource assessment of the fixed and mobile services in the 947-17,700 MHz band, phase 1
[PB85-128288] 11 p1626 N85-20243
Study of laminated dielectric behavior at microwave and millimeter-wave frequencies
[AD-P004358] 12 p1825 N85-21452
Process for making a heterojunction source-drain insulated gate field-effect transistors utilizing diffusion to form the lattice
[AD-D011536] 12 p1939 N85-22176
Design and performance of etched polarisation transformers for microwave frequencies
[R-NIAS-26] 14 p2297 N85-24216
Frequency and time standards based on stored ions
18 p3105 N85-29223
Effects of hydrometeors on electromagnetic wave propagation
[AD-A155379] 22 p3759 N85-33297
Recording small frequency drifts of microwave oscillators 22 p3771 N85-33372
Strongly coupled millimeter-band waveguide directional couplers 22 p3779 N85-33418
Microwave properties of a quiet sea
[NASA-CR-176199] 24 p4085 N85-35322
MICROWAVE HOLOGRAPHY
Detection of cracks in a plastics pipe joint by reflection holography
[NPL-DMA(A)-87/MOM-70] 04 p0502 N85-13202
MICROWAVE IMAGERY
The interpretation of SIR-B imagery of surface waves and other oceanographic features using in-situ, meteorological satellite and infrared satellite data
08 p1143 N85-17212
Microwave and optical remote sensing of forest vegetation 08 p1146 N85-17228
Development and evaluation of techniques for using combined microwave and optical image data for vegetation studies 08 p1148 N85-17240
Automatic terrain elevation mapping and registration
08 p1148 N85-17242
Resolution enhancement of multichannel microwave imagery from the Nimbus-7 SMMR for maritime rainfall analysis
[NASA-CR-174367] 10 p1462 N85-19221
Earth resources research using the Shuttle Imaging Radar system 11 p1713 N85-20779
Digital processing of passive Ka-band microwave images for sea-ice classification
[AD-A150686] 14 p2347 N85-24511
Microwave responses of the western North Atlantic
[NASA-CR-175886] 17 p2946 N85-28191
Microwave hydrology: A trilogy
[NASA-CR-176042] 20 p3477 N85-31603
MICROWAVE INTERFEROMETERS
Direct reading fast microwave interferometer for EBT
[DE85-000183] 11 p1636 N85-20306
System for lower hybrid current startup
15 p2654 N85-26373
MICROWAVE LANDING SYSTEMS
Flight tests of the Digital Integrated Automatic Landing System (DIALS)
[NASA-CR-3859] 04 p0457 N85-12900
Developments in the area of air traffic control systems and the relation with meteorology
[NLR-MP-84029-U] 17 p2895 N85-27848
Evaluation of a fault tolerant system for an integrated avionics sensor configuration with TSRV flight data
[NASA-CR-172589] 18 p3062 N85-28941
Microwave landing systems for heliport operators, owners and users
[FAA-PM-85-7] 19 p3216 N85-29940
MICROWAVE OSCILLATORS
Planning of hybrid integrated circuits for microwave-band oscillators 04 p0490 N85-13124
Low frequency noise in oscillator with limited space-charge accumulation 06 p0786 N85-15024
Device for frequency stabilization of microwave oscillators 06 p0788 N85-15033
Coherent array of Josephson oscillators with external bias leads
[AD-D011367] 08 p1156 N85-17293
An integrated varactor tuned coaxial gunn oscillator for 60 GHz operation
[AD-D011439] 10 p1479 N85-19335
Filter reflection image guide oscillator and solid state line scanning device
[AD-D011440] 10 p1479 N85-19336
The 60 GHz gyrotron development program
[DE85-000599] 12 p1836 N85-21522
Effect of space-charge field on output characteristics of O-type oscillators with distributed interaction
13 p2089 N85-23043
Dielectric resonator
[AD-D011573] 14 p2299 N85-24233
Deterministic and random phase noise of oscillators — synthetic aperture radar
[ESA-TT-845] 20 p3449 N85-31415
Recording small frequency drifts of microwave oscillators 22 p3771 N85-33372
MICROWAVE PROBES
Mutiple reflection theory for microwave measurement of solid propellant burning rates
13 p2002 N85-22549
MICROWAVE RADIATION
U MICROWAVES
MICROWAVE RADIOMETERS
Use of ground based microwave radiometers for nowcasting 01 p0078 N85-10517
The potential use of atmospheric profilers in short-range prediction 01 p0078 N85-10518
Multispectral passive microwave correlations with an antecedent precipitation index using the Nimbus 7 SMMR
[AD-A145419] 02 p0200 N85-11334
Feasibility study of a satellite-borne 90 GHz radiometer 04 p0459 N85-12914
Restoration of multichannel microwave radiometric images
[NASA-CR-174115] 04 p0554 N85-13527
Basic investigation concerning the applicability of multispectral radiation data from microwave radiometry measurements to geoscientific objectives of remote sensing
[ESA-TT-846] 05 p0628 N85-14027
Studies of atmospheric water in storms with the Nimbus 7 scanning multichannel microwave radiometer
05 p0682 N85-14382
Mathematical models for the brightness temperature of object and environment in the microwave region
[ESA-TT-829] 05 p0718 N85-14610
Microstrip antenna for multichannel radiometer
06 p0791 N85-15056
Support for the Naval Research Laboratory Passive Microwave Clutter Analysis Program
[AD-A146771] 07 p0939 N85-15951
Spaceborne receivers: Basic principles
[NASA-CR-174269] 07 p0946 N85-15990
Spaceborne microwave radiometers: Background and technology requirements
[LD-R-267] 08 p1165 N85-17350
Microwave radiometric studies of composition and structure 08 p1183 N85-17456
The 13.9 GHz radiometer design
[AD-A149637] 12 p1851 N85-21613
Studies on physical properties of snow based on multi channel microwave radiometer
13 p2125 N85-23231
Orbiting multi-beam microwave radiometer for soil moisture remote sensing 14 p2230 N85-23818
Low-frequency microwave radiometer for N-ROSS
14 p2230 N85-23819
Determination of electromagnetic properties of mesh material using advanced radiometer techniques
14 p2235 N85-23855
Determination of temperature and degree of roughness of sea and land surfaces by microwave radiometric polarization measurements 14 p2334 N85-24432
Aerospace technology determines forest-fire danger
19 p3295 N85-30427
MIZEX, 1984, NASA CV-990 flight report
[NASA-TM-86216] 19 p3299 N85-30451
Radiometry: A useful prediction tool — atmospheric attenuation
[ESA-SP-1071] 20 p3399 N85-31084
Preliminary investigations concerning a 90 GHz radiometer satellite experiment
[ESA-TT-860] 20 p3420 N85-31225
High reflective surfaces for millimeter RF waves, phase A — satellite antenna reflectors
[HRS-FR-01] 20 p3442 N85-31366
Network ST radar and related measurements at Pennsylvania State University 21 p3629 N85-32544
Six mechanisms used on the SSM/1 radiometer
22 p3798 N85-33534
MICROWAVE REFLECTOMETERS
Implementing waveguide bandwidth six-port reflectometer circuits at millimetric wavelengths
[RSRE-MEMO-3678] 04 p0495 N85-13155
Comparing different theoretical designs of six-port reflectometer junctions
[AD-A149419] 13 p2054 N85-22861
MICROWAVE RESONANCE
High switching speed electrically tuned microwave magnetic resonance devices
[AD-D011699] 19 p3260 N85-30217
Laboratory evaluation and application of microwave absorption properties under simulated conditions for planetary atmospheres
[NASA-CR-176078] 22 p3851 N85-33847
MICROWAVE SCATTERING
Numerical investigation of diffraction models of microwave integrated circuits 03 p0347 N85-12233
Scattering models in the microwave regime
[NASA-CR-174001] 04 p0525 N85-13361
Scattering of H10-mode wave by narrow conducting plate inside rectangular waveguide
06 p0788 N85-15036
Research in image understanding as applied to 3-D tomographic imaging with near optical resolution
[AD-A150098] 12 p1829 N85-21483
The microwave propagation and backscattering characteristics of vegetation — wheat, sorghum, soybeans and corn fields in Kansas
[E85-10066] 13 p2122 N85-23213
Modeling the backscattering and transmission properties of vegetation canopies
[E85-10099] 16 p2609 N85-27320
Microwave model prediction and verifications for vegetated terrain
[E85-10102] 16 p2609 N85-27322
MICROWAVE SENSORS
The investigation of selected oceanographic applications of spaceborne synthetic-aperture radar
08 p1146 N85-17233
Passive microwave remote sensing for sea ice research
[NASA-CR-175570] 12 p1874 N85-21758
Evaluation of OMV ranging and docking systems
12 p1947 N85-22230
Short-range radiotechnical point sensor
13 p2061 N85-22996
Cryogenically-cooled, low-noise microwave receivers: Present status and future needs
14 p2298 N85-24226
Ion sensor signal fluctuations during operation of spacecraft reaction engines 16 p2724 N85-26815
Wideband disturbance accomodation in precision flexible space structures 20 p3415 N85-31194
Influence of spatial variability of hydraulic characteristics of soils on surface parameters obtained from remote sensing data in infrared and microwaves
[NASA-TM-77902] 20 p3477 N85-31604
MICROWAVE SOUNDING
Research relative to high spatial resolution passive microwave sounding systems 05 p0681 N85-14380
Investigation of satellite measurements in the presence of clouds, forcing influences on clouds and feedback to the large scale following convection
05 p0682 N85-14381
Experimental results of temperature-wind soundings of the atmosphere by the radio acoustical method
14 p2340 N85-24471
MICROWAVE SPECTRA
A review of the millimeter and centimeter observations of Uranus 02 p0299 N85-11935
Cosmology 07 p1056 N85-16701
Laboratory evaluation and application of microwave absorption properties under simulated conditions for planetary atmospheres
[NASA-CR-176078] 22 p3851 N85-33847

MICROWAVE SPECTROMETERS
Virtual cathode oscillator study
[AD-A149266] 10 p1460 N85-19342
MICROWAVE SWITCHING
Wave guide branchings (n-port) types of representation of linear, time-independent and sourceless n-ports
[NASA-TM-77770] 01 p0037 N85-10233
MICROWAVE TRANSMISSION
NT MANDELSTAM REPRESENTATION
Interference experiment with the Sirio-OTS satellites
[FUB-17-1983] 01 p0040 N85-10254
The pluviometric recording stations in the 11 GHz radio link at Inviolatella Monte S. Pancrazio — Italy
[FUB-6-1983] 01 p0066 N85-10575
Real-time estimation of amplitude and group delay distortion in a PSK line-of-sight communications channel
09 p1311 N85-18237
Digital data communications over microwave radio channels 10 p1469 N85-19272
Influence of propagation in digital wireless beam, microwave links 10 p1470 N85-19277
Theoretical study of a dynamic simulator of selective fading for digital, wireless beam microwave links
10 p1473 N85-19294
Millimeter-wave range masers: A review
13 p2069 N85-23042
High switching speed electrically tuned microwave magnetic resonance devices
[AD-D011699] 19 p3260 N85-30217
Study of the interferences of 2 GHz radio beams with a DORIS system — precise low orbit determination system (DORIS)
[CNES-CT/DRT/TIT/RL-84/140-T]
20 p3442 N85-31362
Utilization of microwave measuring systems for the automation of composite materials manufacturing
[SNIAS-851-430-102] 22 p3742 N85-33197
New directional couplers for multimode circular waveguides applied to intense pulsed microwave systems
[DE85-011753] 23 p3926 N85-34330
Perturbation-iteration theory for analyzing microwave striplines
[NASA-CR-176189] 24 p4085 N85-35321
Microwave propagation studies, measurements and education in Surabaya, Indonesia
[B8464633] 24 p4088 N85-35339
MICROWAVE TUBES
NT COLD CATHODE TUBES
NT HELITRONS
NT KLYSTRONS
NT MAGNETRONS
NT MICROWAVE OSCILLATORS
NT PHOTOMULTIPLIER TUBES
NT THERMICONS
NT THYRATRONS
NT TRAVELING WAVE TUBES
Millimeter-wave travelling-wave IMPATT diode
[AD-A146545] 06 p0804 N85-15117
Research relative to the development of a cryogenic microwave cavity gradiometer for orbital use
[NASA-CR-174249] 07 p0962 N85-16095
Microwave tubes: Literature survey no. 5 comprising year 1983
[FOA-C-30377-E] 15 p2550 N85-25739
MICROWAVES
NT CENTIMETER WAVES
NT DECIMETER WAVES
NT MICROWAVE EMISSION
NT MILLIMETER WAVES
A coaxial noise standard for the 1 GHz to 12.4 GHz frequency range
[PB84-217694] 01 p0042 N85-10272
Transverse field interaction multibeam amplifier
[AD-D011241] 01 p0043 N85-10282
Conversion of microwave signals by superconducting films in the resistive state
[NASA-TM-77595] 01 p0123 N85-10843
The Bellkt experiment 02 p0159 N85-11079
Radiofrequency and microwave radiation
[AD-A145492] 02 p0191 N85-11274
Microwave susceptibility experiments
[DE84-016186] 02 p0192 N85-11281
Harmonic emission from high power gyrotron oscillators
[AD-A145621] 02 p0200 N85-11335
Active microwave measurements of sea ice under fall conditions: The RADARSAT/FIREX fall experiment — in the Canadian Arctic
[E85-10019] 02 p0217 N85-11432
Laboratory evaluation of microwave absorption properties under simulated conditions for planetary atmospheres
[NASA-CR-174060] 02 p0303 N85-11960
Numerical investigation of diffraction models of microwave integrated circuits 03 p0347 N85-12233
Generation of superpowerful microsecond electromagnetic radiation pulses
03 p0347 N85-12234
Determination of bound water in biological tissue and energy dissipated in bound water by low level microwaves
[AD-A143101] 03 p0399 N85-12547
Research activities of the Illinois University Coordinated Science Laboratory
[AD-A145589] 03 p0449 N85-12856
Ceramic/ceramic seals by microwave heating
[DE84-007486] 04 p0479 N85-13050
Microwave measurement of the complex dielectric tensor at anisotropic slab materials
[DE84-017050] 04 p0493 N85-13144
Thermoregulatory consequences of long-term microwave exposure at controlled ambient temperatures
[PB84-236603] 05 p0697 N85-14484
New measurements of the spectrum of the cosmic microwave background
[DE84-016055] 05 p0746 N85-14785
A new leaky wave antenna for millimeter waves based on the groove guide
[AD-A146428] 06 p0799 N85-15102
Natural interference phenomena affecting spaceborne receivers
[NASA-CR-174256] 07 p0916 N85-15796
Support for the Naval Research Laboratory Passive Microwave Clutter Analysis Program
[AD-A146771] 07 p0939 N85-15951
Micro-waveguide transformers of coherent optical signals 07 p0950 N85-16022
Effect of microwave radiation on local blood circulation and oxygenation of brain tissue
07 p1012 N85-16431
Electromagnetic processing of materials
[AD-A148604] 09 p1311 N85-18241
Microwave discharge in a supersonic flow for the excitation of a gas dynamic CO laser
[ESA-TT-833] 09 p1326 N85-18337
Resonant activation of a Josephson junction
[DE85-000702] 10 p1563 N85-19857
Effect of interfacial characteristics of metal clad polymeric substrates on electrical high frequency interconnection performance
[NASA-TM-86948] 11 p1624 N85-20223
Precision tunable resonant microwave cavity
[NASA-CASE-LEW-13935-1] 11 p1626 N85-20248
Evaluation of resonant modes in isolated dielectric resonators using a surface integral equation formulation
[PB85-110831] 12 p1837 N85-21528
Analysis and computations of microwave-atmospheric interactions
[AD-A149666] 12 p1889 N85-21854
Technical support for microwave experiments on the eye lens
[AD-A149702] 12 p1933 N85-22144
Microwave blackbodies for spaceborne receivers
[NASA-CR-175647] 13 p2094 N85-23068
Calculations of microwave brightness temperature of rough soil surfaces: Bare field
[NASA-TM-86200] 13 p2123 N85-23221
Design considerations for high-altitude, long-endurance, microwave-powered aircraft
[NASA-TM-86403] 14 p2218 N85-23751
Microwave methods for paving
[DE85-004194] 14 p2265 N85-24032
Determining atmosphere moisture content from differences in two-frequency microwave radiation measurements 14 p2341 N85-24474
A survey of radar ECM and ECCM
15 p2536 N85-25653
Measurement of ocean surface currents from space with multi-frequency microwave radars
15 p2539 N85-25672
Microwave tubes: Literature survey no. 5 comprising year 1983
[FOA-C-30377-E] 15 p2550 N85-25739
Effects of long-term low-level radiofrequency radiation exposure on rats. Volume 7: Metabolism, growth and development
[AD-A150829] 15 p2615 N85-26112
Thermal consequences of localized SAR from RFR exposures 16 p2775 N85-27130
The medical results of human exposures to radio frequency radiation 16 p2776 N85-27133
Development and application of new radiofrequency radiation safety standards 16 p2777 N85-27137
Active and passive remote sensing of ice
[AD-A151741] 16 p2815 N85-27369
Hydrogen recovery from extraterrestrial materials using microwave energy
[DE85-006717] 16 p2883 N85-27789
A synchrotron/inverse Compton interpretation of a solar burst producing fast pulses at lambda 3 mm and hard X-rays 16 p2887 N85-27815
Microwaves and hard X-rays ultrafast time structures at the impulsive phase of solar bursts
[INPE-3479-PRE/721] 16 p2888 N85-27816
Microwave responses of the western North Atlantic
[NASA-CR-175886] 17 p2946 N85-28191
Microwave experimental studies of laser fusion
[DE85-008327] 17 p3041 N85-28814
Low density inorganic foams fabricated using microwaves
[DE85-007708] 18 p3080 N85-29051
Beam forming network
[NASA-CASE-NPO-15743-1] 18 p3089 N85-29118
Two-degree-of-freedom linear and planar microwave array lenses
[AD-A153701] 18 p3095 N85-29158
Measurement of permittivity and permeability of microwave materials
[AD-D011656] 18 p3176 N85-29699
Experimental and theoretical investigation of microwave and millimeter wave radiation from hollow, rotating electron beams
[AD-A153827] 18 p3179 N85-29708
Multiport optical detectors 18 p3187 N85-29769
Preliminary results on open accelerating structures
[DE85-010231] 18 p3191 N85-29795
High switching speed electrically tuned microwave magnetic resonance devices
[AD-D011699] 19 p3260 N85-30217
Use of Omega radio navigation system in geophysical work in Antarctica 19 p3296 N85-30448
Effects of long-term low-level radiofrequency radiation exposure on rats. Volume 8: Evaluation of longevity, cause of death, and histopathological findings
[AD-A154263] 19 p3327 N85-30610
New measurement solutions in the microwave industry
20 p3437 N85-31324
New concepts in free electron lasers
20 p3460 N85-31490
Microwave SAW (Surface Acoustic Wave) monochromator
[AD-D011718] 21 p3590 N85-32311
Microwave-enhanced thin-film deposition
21 p3611 N85-32431
Form factor effects on microwave Cerenkov radiation
[AD-A154577] 21 p3701 N85-32988
Sodium nitrate containing mixture for producing ceramic-glass-ceramic seal by microwave heating
[DE85-011610] 22 p3751 N85-33254
Vacuum ultraviolet laser
[DE85-011632] 22 p3790 N85-33478
Six mechanisms used on the SSM/1 radiometer
22 p3796 N85-33534
Microwave radiation and thermoregulation
[AD-A155718] 22 p3818 N85-33664
Quantitative analysis of flare accelerated electrons through their hard X-ray and microwave radiation
[SH-1.2-7] 23 p3991 N85-34742
Feasibility study of radar-transmitting materials
[AD-A155839] 24 p4067 N85-35229
A ray trace program for line-of-sight microwave communication links
[AD-A156168] 24 p4087 N85-35339
Literature search for new physical methods for biological aerosol detection
[AD-A155883] 24 p4128 N85-35582
Electromagnetic compatibility conference features biological interactions
[AD-A155813] 24 p4144 N85-35682
MICROWEIGHING
U WEIGHT MEASUREMENT
MICROYIELD STRENGTH
Dependence of microplasticity of beryllium on grain size and heat treatment 03 p0353 N85-12273
MIDAIR COLLISIONS
NT BIRD-AIRCRAFT COLLISIONS
TCAS II: Design and validation of the high-traffic-density surveillance subsystem
[DOT/FAA/PM-84/5] 13 p1970 N85-22275
MIDDLE ATMOSPHERE
NT MESOPAUSE
NT MESOSPHERE
NT OZONOSPHERE
NT STRATOSPHERE
National solar-terrestrial research program
[PB84-216183] 01 p0072 N85-10479
Middle atmospheric ionization. Observations and chemistry 04 p0622 N85-13049
Middle Atmosphere program. Handbook for MAP. Volume 13: Ground-based techniques
[NASA-CR-174345] 08 p1183 N85-17452
Microwave radiometric studies of composition and structure 08 p1183 N85-17459
Lidar systems for aerosol studies: An outline
08 p1183 N85-17457

Active optical sounding of ozone and minor constituents in the middle atmosphere: A review of ground-based lidar measurements 08 p1183 N85-17458
Lidar studies of temperature and density using Rayleigh scattering 08 p1184 N85-17459
Middle Atmosphere Program. Handbook for MAP, volume 4
[NASA-CR-175482] 11 p1654 N85-20420
PMP-1: A coordinated study of the behavior of the middle atmosphere in winter 11 p1654 N85-20421
French activities relevant to middle atmosphere research 11 p1655 N85-20423
MAP in India 11 p1655 N85-20424
MAP in Japan: Organization and projects
11 p1655 N85-20425
UK participation in the Middle Atmosphere Programme
11 p1655 N85-20426
MAP-related activities in the United States
11 p1655 N85-20427
Soviet National Middle Atmosphere Program
11 p1655 N85-20428
The Middle Atmosphere Program: Winter in Northern Europe (MAP/WINE) 11 p1655 N85-20429
The Middle Atmosphere Program: A special project for the Antarctic Middle Atmosphere (AMA)
11 p1656 N85-20430
Interaction of large meteoroids with the atmosphere
11 p1656 N85-20431
Middle Atmosphere Program. Handbook for MAP, volume 6
[NASA-CR-175480] 11 p1656 N85-20436
Winter in Northern Europe (WINE) project
11 p1657 N85-20439
MAP activities in Hungary 11 p1657 N85-20440
PMP-2 report: Equatorial wave dynamics
11 p1657 N85-20442
MSG-7: Atmospheric penetration of solar radiation in the range of Schumann-Runge bands
11 p1657 N85-20443
Middle Atmosphere Program. Handbook for MAP, volume 8
[NASA-CR-175478] 11 p1657 N85-20445
The first winter of MAP-dynamics, 1982-1983: A winter with three different warming periods
11 p1657 N85-20446
MSG-7: Molecular absorption processes related to the penetration of ultraviolet solar radiation into the middle atmosphere 11 p1658 N85-20449
Middle Atmosphere Program. Handbook for MAP, volume 10
[NASA-CR-175477] 11 p1658 N85-20450
Neutral atmosphere properties determining D-region electron densities 11 p1658 N85-20451
Middle atmosphere temperature and dynamics as revealed from D-region observations
11 p1659 N85-20453
A model of the influence of neutral air dynamics on the seasonal variation in the low ionosphere
11 p1660 N85-20462
Midwinter disturbances in the middle atmosphere
11 p1661 N85-20465
Spring changeover of the middle atmosphere circulation compared with rocket wind data up to 80 km
11 p1661 N85-20466
Some aspects of general circulation and tides in the middle atmosphere 11 p1661 N85-20470
Atmospheric profile imprint in firewall ablation coefficient 11 p1662 N85-20473
Winds and waves (4 min - 11 yrs) in the upper middle atmosphere (60-110 km) at Saskatoon, Canada (52 deg N, 107 deg W): MF radar (2.2 MHz) soundings 1973 - 1983 11 p1662 N85-20476
Dependence of the high latitude middle atmosphere ionization on structures in interplanetary space
11 p1664 N85-20487
Middle Atmosphere Program. Handbook for MAP. Volume 12: Coordinated Study of the Behavior of the Middle Atmosphere in Winter (PMP-1) Workshops
[NASA-CR-175475] 11 p1665 N85-20492
Middle atmosphere NO and NO2 observed by means of the Spacelab one grille spectrometer
[AERONOMICA-ACTA-A-293-1984]
11 p1680 N85-20588
An improved rocket-borne electric field meter for the middle atmosphere
[NASA-CR-175510] 12 p1888 N85-21851
Middle Atmosphere Program. Handbook for MAP. Volume 14: URSI/SCOSTEP Workshop on Technical Aspects of MST Radar
[NASA-CR-176085] 21 p3615 N85-32466
Excerpts from the paper: Research Status and Recommendation from the Alaska Workshop on Gravity Waves and Turbulence in the Middle Atmosphere, part 1.3A 21 p3616 N85-32470
General circulation of the middle atmosphere, part 1.4B 21 p3617 N85-32474
Sample interchange of MST radar data from the Urbana radar 21 p3627 N85-32531
The MU radar now partly in operation
21 p3628 N85-32543
Middle Atmosphere Program. Handbook for MAP, volume 11
[NASA-CR-176107] 22 p3814 N85-33625

MIDLATITUDE ATMOSPHERE
The mesoscale-beta-scale evolution of mid-latitude meso-alpha-scale convective complexes
01 p0073 N85-10486
Model of atmospheric ozone for middle latitudes
02 p0161 N85-11091
Medium- and large-scale wave disturbances and heterogeneities of electron concentration in outer ionosphere in middle and low latitudes
06 p0825 N85-15241
Winter anomaly of the lower ionosphere and its possible causes 11 p1660 N85-20459
Structure and energetics of medium-scale atmospheric waves in the Southern Hemisphere
20 p3489 N85-31685

MIDLATITUDES
U TEMPERATE REGIONS

MIE SCATTERING
NT RAYLEIGH SCATTERING
Investigation of light source and scattering medium related to vapor-screen flow visualization in a supersonic wind tunnel
[NASA-TM-86290] 06 p0810 N85-15144
Novel photo-thermal technique for flow and spectroscopic measurements in a dense aerosol stream
[AD-A149745] 12 p1800 N85-21287
A systematic study of light scattering by irregularly shaped particles
[AD-A150192] 13 p2159 N85-23400
Macrostructure and microphysics of Saturn's E-ring
15 p2677 N85-26526
A comprehensive investigation of the dynamics of micron and submicron lunar ejecta in heliocentric space
19 p3384 N85-30994
Journal of Research of the National Bureau of Standards, volume 90, number 1, January - February 1985
[PB85-179083] 20 p3522 N85-31908
Ice fog as an electro-optical obscurant
[AD-A155059] 21 p3705 N85-33015
Calculation of the diffusion of light by aerosols: Description of the MIELOR software and results obtained
[REPT-80] 24 p4137 N85-35638

MIE THEORY
U MIE SCATTERING

MIG AIRCRAFT
China has developed a new version of fighter aircraft
[AD-A155293] 21 p3555 N85-32118

MIGRATION
The use of small mobile radars to detect, monitor, and quantify bird movements
[AD-P004188] 11 p1580 N85-19951
Plasticizer system for propellant compositions
[AD-D011514] 12 p1817 N85-21393
Transatlantic migration study of the leathery turtle using the ARGOS system. Transatlantic turtle race
14 p2326 N85-24379
An application of Markov chains to the problem of migration in inventory systems
[AD-A151954] 16 p2857 N85-27618
Propellant plasticizer
[AD-D011501] 20 p3434 N85-31306
Microgravity electrophoresis: A study of the factors that affect free-fluid separation 20 p3502 N85-31774
Thermally induced chemical migration: A natural analog approach
[DE85-012308] 23 p3949 N85-34474

MILANKOVITCH THEORY
U CLIMATOLOGY

MILITARY AIR FACILITIES
DoD Robotics Application Workshop Proceedings
[AD-A145867] 03 p0307 N85-11978
Air force engine repair - Oklahoma City Air Logistics Center, Propulsion Division
[AD-P003999] 03 p0307 N85-11980
Air force landing gear repair - Ogden Air Logistics Center Industrial Products and Landing Gear Division
[AD-P004001] 03 p0307 N85-11982
Depot modernization at the Defense Logistics Agency
[AD-P004006] 03 p0308 N85-11988
Future robotics program at San Antonio ALC (Air Logistics Center)
[AD-P004011] 03 p0309 N85-11991
Supply center processes
[AD-P004014] 03 p0309 N85-11993
Development of a pavement maintenance management system. Volume 9: Development of airfield pavement performance prediction models
[AD-A146150] 03 p0321 N85-12069
Visibility monitoring in the southern California desert for the Department of Defense: Research on operations-limiting visual extinction, RESOLVE protocol
[AD-A146817] 06 p0835 N85-15315
Installation restoration program. Phase 2: Stage 1 problem confirmation study, Duluth International Airport Duluth, Minnesota
[AD-A148318] 08 p1069 N85-16665
Environmental and energy audits of Air Force government owned-contractor operated installations
[AD-P004137] 09 p1347 N85-18474
Staff assistance to bases for bird hazards
[AD-P004205] 11 p1583 N85-19972
Bird strike avoidance system for Dover AFB, Delaware
[AD-P004206] 11 p1583 N85-19973
Mean conditions and turbulence statistics at Vandenberg AFB, California
[AD-A151386] 15 p2665 N85-26449
Review of hazardous waste cleanup and disposal efforts at Tinker Air Force Base
[GPO-43-294] 21 p3613 N85-32457

MILITARY AIRCRAFT
Determining training device requirements in Army aviation systems 05 p0711 N85-14558
The Air Force stock fund and aircraft availability
[AD-A148653] 08 p1067 N85-16761
Mission-oriented requirements for updating MIL-H-8501. Volume 1: STI proposed structure — military rotorcraft
[NASA-CR-177331-VOL-1] 08 p1068 N85-16877
Mission-oriented requirements for updating MIL-H-8501. Volume 2: STI background and rationale — military rotorcraft
[NASA-CR-177331-VOL-2] 08 p1068 N85-16878
Using the control system design environment in the design of a data link receiver unit for the Coast Guard HH-65A helicopter
[AD-A148624] 08 p1068 N85-16880
Reliability predictions for military avionics. Royal Signals and Radar Establishment reliability prediction method no. 250
[BR69221] 13 p1973 N85-22388
High specific power aircraft turn maneuvers: Tradeoff of time-to-turn versus change in specific energy
[AD-A151701] 15 p2471 N85-25257
Generation of flight paths using heuristic search
[AD-A151949] 16 p2704 N85-26694
Operations research
[B8561897] 17 p3026 N85-28712

MILITARY AVIATION
Determining training device requirements in Army aviation systems 05 p0711 N85-14558
Keeping up with operational loads in the French Air Force: Defining new equipment
07 p0896 N85-15661
Development of NATOPS (Naval Air Training and Operating Procedure Standardization) performance software for the H-46D helicopter
[AD-A156069] 24 p4064 N85-35190

MILITARY HELICOPTERS
NT CH-47 HELICOPTER
NT UH-1 HELICOPTER
NT UH-60A HELICOPTER
Airworthiness and flight characteristics test of the JOH-6A light combat helicopter configured with a wire strike protection system
[AD-A144880] 01 p0006 N85-10036
Airworthiness and Flight Characteristics (A and FC) test of the EH - 1X/EH - 1H helicopter configurations
[AD-A144861] 01 p0007 N85-10039
US Army helicopter operational flight loads
07 p0895 N85-15675
Speed benefits of tilt-rotor designs for LHX
[NASA-CR-166437] 07 p0902 N85-15717
A digital piloting system for the combat helicopter
08 p1074 N85-16806
Tactical HF communication for military helicopters using the NVIS mode 08 p1074 N85-16807
Evaluation of nose, roof, and mast mounted sensor platforms for piloting and sighting, integrated in future combat helicopters 08 p1074 N85-16808
The design and development of an integrated core system for battlefield helicopters
08 p1074 N85-16811
Evolution toward a multi-bus architecture for Army helicopter avionic systems 08 p1074 N85-16812
A review of US Army aircrew-aircraft integration research programs 08 p1075 N85-16814
A simulator for studying helicopter weapons systems
08 p1075 N85-16816
Preliminary airworthiness evaluation AH-1S (MC) helicopter with external fuel tanks installed
[AD-A148091] 08 p1084 N85-16865
Aircrew-aircraft integration issues in future US Army helicopters 10 p1535 N85-19672

Proceedings of the 14th Army Science Conference. Volume 1: Principal Authors A through H
[AD-A149200] 10 p1573 N85-19920
Cost-estimating relationships for tactical combat aircraft
[AD-A151575] 15 p2471 N85-25255
Piloted simulation of one-on-one helicopter air combat at NOE flight levels
[NASA-TM-86686] 16 p2710 N85-26720
A new main rotor hub for the AS 332 Super Puma
[SNIAS-851-210-102] 20 p3393 N85-31047
Research Flight Simulator for Helicopters (RFSH): Description and application to fire control system design
[SNIAS-851-210-106] 20 p3393 N85-31050

MILITARY OPERATIONS
NT COMBAT
NT ELECTRONIC WARFARE
Command control group behaviors. Objective 1: A methodology for and identification of command control group behaviors
[AD-A145690] 02 p0191 N85-11279
On applying AI (Artificial Intelligence) to maintenance and troubleshooting
[AD-P003915] 02 p0244 N85-11595
Overview of training and aiding
[AD-P003917] 02 p0245 N85-11597
AFHRL (Air Force Human Resources Laboratory) program for artificial intelligence applications to maintenance and training
[AD-P003931] 02 p0247 N85-11611
Artificial intelligence applications to automatic test equipment
[AD-P003936] 02 p0247 N85-11616
Model-based probabilistic reasoning for electronics troubleshooting
[AD-P003937] 02 p0247 N85-11617
The structures and the role of an international agency for the control of satellites
[NASA-TM-76765] 03 p0441 N85-12806
Army aviation today and tomorrow
06 p0751 N85-14810
Marine helicopter missions 06 p0751 N85-14811
Attack helicopter (AH-1T) cockpit systems integration
06 p0753 N85-14826
Distribution and storage of aviation turbine fuel for military operations in northern Australia
[AD-A147180] 07 p0935 N85-15921
The Air Force can improve its forecasts of aircraft spare parts requirements
[AD-A147911] 07 p1053 N85-16682
Estimating wartime support resource requirements. Statistical and related policy issues
[AD-A147923] 07 p1053 N85-16685
Operational requirements versus technological capabilities 08 p1072 N85-16798
Automatic briefing and mission management systems for battlefield support 08 p1073 N85-16799
Standard Attitude Heading Reference System (SAHRS) full scale development program
08 p1073 N85-16804
Integrated control and display systems for helicopter battlefield mission management
08 p1073 N85-16805
Evaluation of nose, roof, and mast mounted sensor platforms for piloting and sighting, integrated in future combat helicopters 08 p1074 N85-16806
Design of an evaluation system to measure performance degradation due to continuous operations
[AD-A148186] 08 p1200 N85-17556
Military applications of the Singer Link-Miles IMAGE visual system
[AD-P004337] 09 p1271 N85-17991
Assessment of environmental costs at ordnance activities
[AD-P004140] 09 p1347 N85-18476
Personnel protection concepts for advance escape system design 10 p1532 N85-19858
Space System Applications to Tactical Operations
[AGARD-CP-344] 11 p1709 N85-20751
Tactical operations and space applications
11 p1709 N85-20752
EHF MILSATCOM systems for tactical users
11 p1709 N85-20755
Tactical military communications by satellite relay at high latitudes 11 p1709 N85-20756
The Ferranti Tactical SHF SATCOM station (MANSAT) 11 p1710 N85-20759
Tactical satellite terminals for land and airborne C3 applications 11 p1710 N85-20760
The Global Positioning System (GPS): Program status update 11 p1710 N85-20761
Potential impact of Navstar GPS on NATO tactical operations 11 p1711 N85-20763
Tactical applications of GPS user equipment
11 p1711 N85-20765
Practical applications of satellite-derived meteorological and oceanographic data in Naval operations
11 p1712 N85-20771
Dual band radome wall design
[AD-P004357] 12 p1825 N85-21451
Base communications issues for the 1980s
[AD-A149764] 12 p1828 N85-21474
Statistics of french Armee de l'air ejections 1970 - 1980 12 p1906 N85-21971
Testing of the digital flight control system of the German CCV fighter experimental aircraft
13 p1968 N85-22361
SPARTEN (Scientific Program of Aerobic and Resistance Training Exercise in the Navy): A total body fitness program for health and physical readiness
[AD-A150669] 14 p2386 N85-24711
Exercise-heat strain during hypohydration: Interaction with heat acclimation and aerobic fitness
[AD-A151023] 14 p2389 N85-24717
Nutritional criteria for military rations and effects of prolonged feeding on acceptability
14 p2394 N85-24742
Fiber optics applications for MIL-STD-1760
[AD-A151113] 15 p2470 N85-25251
A database design for the Brazilian Air Force Flying Unit Operational Control System
[AD-A151848] 15 p2666 N85-26452
The evolution of active control technology systems for the 1990's helicopter 16 p2715 N85-26758
US said to seek military advantage in space
16 p2727 N85-26831
Military journal on US intelligence satellites
16 p2727 N85-26832
Development of a persistent chemical agent simulation system
[NASA-CR-175760] 16 p2745 N85-26937
The NAVTAG (Naval Tactical Game) system and its modification to include the SH-60B helicopter
[AD-A152004] 16 p2858 N85-27624
A Dictionary-Directory System (DDS) for the SPLICE system
[AD-A152223] 16 p2878 N85-27759
Soviet space programs, 1976-1980 (with supplementary data through 1983). Part 3: Unmanned space activities
[S-PRT-98-235-PT-3] 16 p2879 N85-27765
Future of V/STOL aircraft systems: A survey of opinions
[NASA-TM-86689] 18 p3061 N85-28937
US restrictions on technology transfer reviewed
18 p3088 N85-29115
Introduction to European air traffic control
[AD-A156328] 24 p4062 N85-35176
A guide to USAF helicopter instrument flight procedures
[AD-A156102] 24 p4063 N85-35182
RAFTS: A T-38 replacement for the 21st century
[AD-A156103] 24 p4065 N85-35191
Next generation gunship
[AD-A156361] 24 p4065 N85-35193
Air university commander's and supervisor's guide on substance abuse
[AD-A156336] 24 p4133 N85-35622

MILITARY SPACECRAFT
NT DMSP SATELLITES
NT RECONNAISSANCE SPACECRAFT
NT VELA SATELLITES
Autonomous navigation of USAF spacecraft
03 p0321 N85-12074
Planning for the on-orbit servicing of military spacecraft
[AD-A148447] 08 p1104 N85-16983
US MILSATCOM: Present and future
11 p1709 N85-20753
UK Skynet 4 communications satellites
11 p1710 N85-20757
Minimization of system vulnerability in Naval satellite communication networks 11 p1710 N85-20758
Militarization of space activity in United States
15 p2456 N85-25360
New ESA director on space station, military space
18 p3066 N85-28962

MILITARY TECHNOLOGY
Directed energy missile defense in space
[PB84-210111] 01 p0015 N85-10095
Frequency stabilized laser
[AD-D011223] 01 p0053 N85-10351
The application of artificial intelligence to a maintenance and diagnostic information system
[AD-P003945] 02 p0249 N85-11625
Air Force Materials Laboratory plans/projects
[AD-P004010] 03 p0308 N85-11990
Field applications for robotic materiel handling
[AD-P004016] 03 p0309 N85-11995
Wideband integrated voice/data technology
[AD-A146054] 03 p0355 N85-12283
Naval surface weapons center technology transfer report (FY83)
[AD-A146501] 06 p0871 N85-
Laser R and D in the armed services
[AD-A146930] 07 p0970 N85-
Documentation and separate test program development is most important for test/maintenance
08 p1066 N85-
Helicopter Guidance and Control Systems for Battlefield Support
[AGARD-CP-359] 08 p1072 N85-
The changing vibration simulation for military ground vehicles 09 p1334 N85-
A rig for testing the soft soil performance of track systems
[AD-P004272] 09 p1405 N85-
Technical evaluation report on the 48th Symposium of the Avionics Panel on Space System Applications to Tactical Operations
[AGARD-AR-203] 10 p1425 N85-
Narrowband spread spectrum systems
10 p1475 N85-
Tire deflation mechanism
[AD-D011480] 10 p1483 N85-
Phenomenology of microwave coupling, part 1
[DE85-003097] 11 p1624 N85-
Symposium on Military Aviation Medicine summarized
11 p1696 N85-
U.S., Soviet space program aims contrasted
13 p1986 N85-
Low-bit rate speech encoders based on Line-Spectrum Frequencies (LSF)
[AD-A150518] 13 p2056 N85-
Current approaches for the biophysical and physiological evaluation of combat clothing for environmental extremes
[AD-A151012] 14 p2395 N85-
Some critical factors that limit the effectiveness of machine intelligence technology in military systems applications
[AD-A150684] 14 p2407 N85-
Artificial intelligence applications to testability
[AD-A150694] 14 p2407 N85-
Personal computer aided decision analysis
[AD-A151911] 16 p2675 N85-
Science and Technology in the Soviet Union
[AD-A152828] 17 p3047 N85-
Soviet weapons development and the scientific community
[AD-P004562] 17 p3047 N85-
Technology and technical efficiency in the Soviet Union: Dominant patterns of constrained optimization in a noncompetitive economic regime
[AD-P004567] 17 p3048 N85-
The revolution in military affairs and the Soviet system
[AD-P004568] 17 p3048 N85-
Program Manager: The journal of the defense systems management college, volume 14, number 2, March-April 1985
[AD-A154219] 20 p3540 N85-
Meteorological weapons
[AD-A154735] 21 p3636 N85-
Air Force Office of Scientific Research (AFOSR) Technical report summaries: First quarter (CY)
[AD-A154757] 21 p3713 N85-
Military hydrology. Report 9: State-of-the-art review and annotated bibliography of dam-breach flood forecasting
[AD-A155383] 22 p3801 N85-
Proceedings of the 14th Army Science Conference. Volume 2: Principal authors I through O
[AD-A149201] 24 p4144 N85-
Proceedings of the 14th Army Science Conference. Volume 3: Principal authors P through Z
[AD-A149202] 24 p4144 N85-

MILKY WAY GALAXY
Constraints to the radiative lifetime of a light neutral fermion in the galactic halo from IUE
[NOTA-INTERNA-617] 02 p0279 N85-
Distribution and properties of molecular clouds in the galaxy 03 p0442 N85-12810
The number and distribution of molecular clouds in the inner galaxy 03 p0442 N85-12811
IRAS observations of galactic star formation
03 p0442 N85-12813
A large scale height galactic component of the diffuse 2-60 keV background
[NASA-TM-83837] 03 p0446 N85-12841
Cosmic ray propagation in the local superbubble
[NASA-TM-85030] 03 p0449 N85-
Far-infrared line emission from the galaxy
[NASA-CR-174166] 04 p0560 N85-13702
Local galactic kinematics 05 p0741 N85-
Molecular clouds within 100 pc
06 p0877 N85-

A wide latitude CO survey of molecular clouds in the northern Milky Way 06 p0877 N85-15574

Dark cloud and globule distribution for galactic longitudes 230 to 360 degrees 06 p0878 N85-15575

The z-dependence of the spin temperature of HI 06 p0878 N85-15580

The galaxy scene and QUASAT — VLBI satellite 07 p1056 N85-16703

Airborne Astronomy Symposium. A symposium commemorating the tenth anniversary of operations of the Kuiper Airborne Observatory [NASA-CP-2353] 08 p1244 N85-17848

Far infrared observations of molecular clouds in the outer galaxy 08 p1247 N85-17869

Far infrared continuum emission from the galactic center 08 p1248 N85-17876

The 157 micron (C II) luminosity of the galaxy 08 p1248 N85-17877

Variation of oxygen and nitrogen abundances in the galaxy 08 p1248 N85-17878

The color excesses of classical cepheids and the structure of our galaxy 13 p2169 N85-23469

The structure of galactic HI in directions of low total column density [NASA-CR-175709] 16 p2882 N85-27765

A high energy X-ray study of the galactic center [AD-A153652] 18 p3202 N85-29662

The 8.3 and 12.4 micron imaging of the Galactic Center source complex with the Goddard infrared array camera [NASA-TM-86225] 19 p3362 N85-30962

Cosmic-ray transport in the galactic magnetosphere [OG-7.2-17] 23 p4016 N85-34884

MILLIMETER WAVES

Atmospheric channel performance measurements at 10 to 100 GHz [PB84-211325] 01 p0042 N85-10271

Scattering from snow backgrounds at 35, 98, and 140 GHz [AD-A145796] 03 p0355 N85-12280

Modeling rain polarization effects to millimeter wave frequencies [PB84-231042] 03 p0357 N85-12296

Millimeter-wave propagation and remote sensing of the atmosphere [AD-A146339] 03 p0393 N85-12512

Anglo-German millimeter wave backscatter measurements on snow, environmental data report [REPT-7-84] 04 p0492 N85-13136

Implementing waveguide bandwidth six-port reflectometer circuits at millimetric wavelengths [RSRE-MEMO-3678] 04 p0495 N85-13155

The UK and Netherlands millimetre-wave telescope — Netherlands (NL) 05 p0625 N85-14003

A new leaky wave antenna for millimeter waves based on the groove guide [AD-A146426] 06 p0799 N85-15102

Millimeter-wave travelling-wave IMPATT diode [AD-A146545] 06 p0804 N85-15117

Interface structures for millimeter-wave circuits [AD-A146557] 06 p0804 N85-15118

MMIC devices for active phased array antennas [NASA-CR-174281] 07 p0938 N85-15943

A quasi-optical method for measuring the complex permittivity of materials [AD-A147483] 07 p0941 N85-15966

Investigation of planar waveguides and components for millimeter-wave integrated circuits [AD-A147380] 07 p0948 N85-16005

Low-loss flexible dielectric waveguide for millimeter-wave transmission and its application to devices [AD-A147848] 07 p0948 N85-16006

Development of a 30 GHz/1 kW broadband traveling wave tube with suppression of band edge oscillations [BMFT-FB-W-84-035] 07 p0948 N85-16011

Rippled-field magnetron apparatus [AD-D011364] 07 p0969 N85-16154

A new free electron laser using a relativistic beam with spiralling electron [AD-D011318] 07 p0971 N85-16165

Millimeter wave antenna technology [AD-A148694] 08 p1155 N85-17291

Multi-spectral observations of the star formation: The role of far infrared photometry 08 p1245 N85-17859

Instrumentation for submillimeter polarimetry 08 p1250 N85-17889

High power millimeter-wave mode converters in overmoded circular waveguides using periodic wall perturbations [IPF-84-6] 09 p1395 N85-18780

Advanced artificial dielectric materials for millimeter wavelength applications [AD-A148600] 10 p1431 N85-19027

An electronically controlled array for simulation of passive target/background signatures at millimeter wavelengths [AD-D011456] 10 p1466 N85-19263

Effective millimeter wave transmission under severe multipath conditions 10 p1475 N85-19306

Image line voltage controlled oscillator with replaceable components [AD-D011436] 10 p1479 N85-19333

An integrated varactor tuned coaxial gunn oscillator for 60 GHz operation [AD-D011439] 10 p1479 N85-19335

Virtual cathode oscillator study [AD-A149266] 10 p1480 N85-19342

Millimeter wave dielectric property measurement of gyrotron window materials [DE85-004430] 12 p1802 N85-21304

Study of laminated dielectric behavior at microwave and millimeter-wave frequencies [AD-P004358] 12 p1825 N85-21452

A millimeter wave apparatus for free-space measurement of dielectric constants at high temperature [AD-P004361] 12 p1826 N85-21455

Design and calibration of a 35GHz dielectrometer [AD-P004363] 12 p1826 N85-21457

Exploration of new methods to produce efficient sources of coherent near millimeter wave radiation [AD-A150094] 12 p1829 N85-21481

Effect of space-charge field on output characteristics of O-type oscillators with distributed interaction 13 p2089 N85-23043

Millimeter-wave diffraction devices and materials [AD-A150676] 14 p2418 N85-24917

Monolithic planar doped barrier limiter [AD-D011576] 15 p2548 N85-25723

Microwave emission from relativistic electron beams [AD-A151472] 15 p2646 N85-26333

EHF attenuation derived from emission temperatures in light rain [AD-A151166] 16 p2772 N85-27110

Calibration methods in millimeter-wave radioastronomy [INPE-3481-PRE/724] 16 p2881 N85-27778

Radiometer integrated into a communication terminal [AD-A151746] 17 p2947 N85-28195

A transport theory of millimeter wave propagation in woods and forests [AD-A151663] 17 p2947 N85-28196

High precision materials characterization in the near millimeter wave-length range [AD-A153267] 17 p2968 N85-28331

Communications and logic systems at millimeter wave frequencies [NASA-CR-175859] 17 p3042 N85-28824

An evaluation and preparation of ferromagnetic liquid composites for use at millimeter wavelengths [AD-A153939] 18 p3069 N85-28980

Some further aspects of the influence of raindrop-size distributions on millimeter-wave propagation [PB85-168334] 18 p3092 N85-29136

Two-degree-of-freedom linear and planar microwave array lenses [AD-A153701] 18 p3095 N85-29156

Atmospheric probing by active millimeter wave system [AD-A153550] 18 p3136 N85-29422

Experimental and theoretical investigation of microwave and millimeter wave radiation from hollow, rotating electron beams [AD-A153627] 18 p3179 N85-29706

Millimeter wave generation by relativistic electron beams [AD-A153980] 18 p3179 N85-29708

A comparison of millimeter wave, direct detect and heterodyne laser intersatellite links [AD-A151064] 20 p3461 N85-31496

Millimetre wave pulse technology — satellite mapping [ESA-CR(P)-2004] 20 p3478 N85-31611

A multiplying slot array [AD-A155570] 21 p3576 N85-32245

Effects of hydrometeors on electromagnetic wave propagation [AD-A155379] 22 p3759 N85-33297

Examination of anisotropic films by resonance method 22 p3778 N85-33412

Strongly coupled millimeter-band waveguide directional couplers 22 p3779 N85-33418

Waveguide dielectric millimeter band filter with enhanced selectivity 22 p3780 N85-33421

An experimental study of dielectric rod antennas for millimeter-wave imaging applications [AD-A155832] 24 p4086 N85-35328

Millimeter-wave propagation in moist air: Model versus path data [AD-A156040] 24 p4087 N85-35331

MILLING (MACHINING)

Manufacturing methods for microwave circuits [AD-A145237] 01 p0043 N85-10278

Structural changes during milling of aluminum oxide powders [NASA-TM-77486] 04 p0472 N85-13008

Electropulse chemical machining [DE84-016693] 04 p0484 N85-13084

Inclusion formation during solidification of steels with improved machinability [BMFT-FB-T-84-160] 05 p0619 N85-13957

Technology reports of the Yamaguchi University, volume 3, no. 3 [ISSN-0386-3433] 09 p1302 N85-18182

Method of testing carbide inserts for premature fracture by face milling of cylindrical workpieces 09 p1303 N85-18183

Flexible manufacturing system for machining axially symmetric workpieces [PNR-90229] 09 p1305 N85-18196

Factors influencing the ball milling of Si3N4 in water [NASA-TM-86932] 10 p1450 N85-19136

Parametric evaluation of ball milling of SiC in water [NASA-TM-86974] 12 p1811 N85-21356

Milling of spherical zones in parts 14 p2266 N85-24041

Milling machine with numerical programmed control for cutting teeth 14 p2268 N85-24052

Re-designing a mechanism for higher speed: A case history from textile machinery 23 p3923 N85-34310

Method for measuring surface activity of silicon nitride powder [NASA-TM-77806] 24 p4073 N85-35242

MILLING (MIXING)

U COMPOUNDING

MILLING MACHINES

New tooling for plasma cutting technology 13 p2051 N85-22842

T700 cutter life improvement program [AD-A150450] 13 p2099 N85-23069

Microstructure and mechanical properties of rare-earths-microalloyed high-speed tool steel [BLL-BISI-TRANS-22043-(9022.06)] 17 p2926 N85-28064

The application of numerical control (NC) in manufacturing wind tunnel models [B8560078] 17 p2939 N85-28140

MIM (SEMICONDUCTORS)

EMC (Electromagnetic compatibility) spec criteria in Volterra systems [AD-A147659] 08 p1151 N85-17263

MIM DIODES

Research and developmental study on MIS thin film solar cells of amorphous hydrogenated silicon, part 2 [BMFT-FB-T-84-290] 17 p2966 N85-28467

MINE DETECTORS

The PINGUIN B3: A remotely piloted vehicle for mine identification and disposal [MBB-UM-1/84-O] 16 p2874 N85-27736

MINERAL DEPOSITS

International strategic minerals inventory. Summary report: Manganese [GS-CIRC-930-A] 02 p0219 N85-11442

Petrology and genesis of carbonate-hosted Pb-Zn-Ag, San Cristobal District, Department of Junin, Peru 03 p0369 N85-12467

Lacustrine and eolian deposits of Wisconsin age at Riverside Bluff in the upper Tanana River valley, Alaska 04 p0517 N85-13299

Geology and geochemical evolution of the Lost River, Alaska, tin deposit 04 p0533 N85-13405

Alabama Tin Belt: Metallogenesis and mineral resource evaluation. Year-end report [DE84-901335] 07 p0969 N85-16283

Geology of the Batopilas mining district, Chihuahua, Mexico, volumes 1 and 2 09 p1351 N85-18496

Types of placer formation of eastern Arctic shelf 10 p1496 N85-19452

Silver metallogeny in Earth's Pacific Ocean segment 10 p1496 N85-19455

Relationship of gold content to gravity fields in Far East 10 p1501 N85-19475

Geological reasons for change in intensity of linear magnetic anomalies of the Kursk magnetic anomaly [NASA-TM-77624] 10 p1514 N85-19552

Radioactive waste isolation in salt: Peer review of the Office of Nuclear Waste Isolation's report on the organic geochemistry of deep groundwaters from the Palo Duro Basin, Texas [DE85-001439] 10 p1556 N85-19811

LANDSAT 4 investigations of Thematic Mapper and Multispectral Scanner applications — Drum Mountains, Utah and Tonopath, Nevada [E85-10095] 12 p1874 N85-21757

Geologic utility of LANSDAT-4 TM data — Death Valley, California and the Silver Bell area of southern Arizona 13 p2118 N85-23192

Characteristics of alunyte deposits discussed 13 p2166 N85-23438

Technical and cost analyses of manganese nodule processing techniques and their significant variations
[PB85-148615] 14 p2256 N85-23992

Gigantic lithium deposit discovered in France
14 p2289 N85-24184

Influence of phosphorus content and heat treatment on the machinability of electroless nickel deposits
[DE85-007250] 15 p2522 N85-25548

Nd-isotopic evidence for the origin of the Sudbury complex by meteoritic impact 15 p2660 N85-26554

Yearbook of the Bureau of Mineral Resources, Geology and Physics: Geoscientific research, resource assessment, and database development, 1 Jul. 1983 to 30 Jun. 1984
[BMR-84] 17 p2969 N85-28474

Ash contents of Costa Rican peat deposits
[DE85-010734] 19 p3301 N85-30462

Orphans of the Valley: Abandoned surface mines in the Tennessee Valley. Volume 2: Maps
[DE85-901249] 19 p3301 N85-30465

Petroleum and mineral resources of Antarctica
[US-GEOL-SURV-CIRC-909] 20 p3477 N85-31605

Comparative study of fracture planes computed from topography and lineaments from imagery with structures and mineralization in the magnetic belt of Washington State
[DE85-010972] 20 p3477 N85-31608

The U.S. Geological Survey in Alaska: Accomplishments during 1982
[US-GEOL-SURV-CIRC-939] 20 p3493 N85-31719

Geomorphology, tectonics, and exploration
21 p3601 N85-32365

Sulfur reduction in sediments of marine and evaporite environments 21 p3661 N85-32742

The United States Geological Survey in Alaska: Accomplishments during 1983
[USGS-CIRC-945] 23 p3948 N85-34468

USGS research on mineral resources, 1985
[CIRC-949] 24 p4103 N85-35435

Chemistry of ore-forming fluids
24 p4103 N85-35436

Aeromagnetic and radiometric signatures of a possible porphyry system in the western Tushar Mountains, Utah
24 p4103 N85-35437

Some geophysical guides to ore in southern and southwestern Alaska 24 p4103 N85-35438

Marine phosphorite deposits model for exploration, with emphasis on deposits in the US Atlantic coastal plain
24 p4104 N85-35439

The role of regional subsurface geochemistry in resource assessment in the central United States
24 p4104 N85-35440

Aeromagnetic and gravity models of the pluton below the Lake City caldera, Colorado
24 p4104 N85-35442

Origin of sedimentary humic acids, potential carriers of ore-forming elements 24 p4104 N85-35443

Cobalt-rich ferromanganese crusts in the oceans
24 p4104 N85-35444

New silver resource map of the United States: Potential for increased domestic silver production
24 p4105 N85-35445

Massive sulfide deposits from the southern Juan de Fuca Ridge 24 p4105 N85-35446

Gas analysis of ore-forming fluids
24 p4105 N85-35447

Mineral deposit models: Theory and practice
24 p4105 N85-35448

Expert systems research in regional resource evaluation: Experiences in the application of microcomputer technologies 24 p4105 N85-35450

Applications of the mineral resources data system and the international strategic minerals inventory in mineral-resource assessments by region and commodity
24 p4105 N85-35451

A comparison of LANDSAT thematic mapper, multispectral scanner and airborne sensors for mapping the distribution of alteration minerals: Examples from the southwestern United States 24 p4106 N85-35452

Some recent deposit modeling efforts
24 p4106 N85-35453

Processing of LANDSAT imagery to map surface mineral alteration on the Alaska Peninsula, Alaska
24 p4106 N85-35455

Mineral resources programs 24 p4106 N85-35456

The development of assessment techniques program
24 p4106 N85-35457

The Conterminous United States Mineral Assessment Program 24 p4106 N85-35458

Federal Mineral Land Information System
24 p4106 N85-35459

The Alaska Mineral Resources Assessment Program
24 p4107 N85-35460

Hydrogeology of the lower Glen Rose Aquifer, south-central Texas 24 p4108 N85-35466

Ore genesis at the Monterrosas deposit in the Coastal Batholith, Ica, Peru 24 p4115 N85-35510

MINERAL EXPLORATION

The feasibility of satellite remote sensing as a technique for evaluating coal mine surface features
02 p0213 N85-11401

Remote sensing as a mineral prospecting technique
[E85-10010] 02 p0216 N85-11423

Thematic mapping of likely target areas for the occurence of cassiterite in the Serra do Mocambo (GO) granitic massifs using LANDSAT 2 digital imaging
[E85-10027] 02 p0219 N85-11440

Development of a method for exploring low-reflectance areas through the combined use of different geophysical methods taking the north-west German basin as an example
[BMFT-FB-T-83-180] 02 p0220 N85-11450

Methods for correlating geological, geochemical and geophysical data with satellite imagery in central Ireland
05 p0655 N85-14206

USSR report: Earth sciences
[JPRS-UES-84-003] 07 p0980 N85-16223

Maritime prospecting, mining discussed
07 p0980 N85-16226

Exploring ocean's mineral wealth
07 p0980 N85-16227

Microprocessors in geophysical instruments discussed
08 p1142 N85-17199

Analysis of SIR-B radar illumination of geometry for depth of penetration and surface feature and vegetation detection, Nevada and California
08 p1149 N85-17248

Depositional modeling of tetrahedrite in the Coeur d'Alene district, Idaho 08 p1152 N85-17448

Deep seabed stable reference areas
[PB84-241470] 09 p1360 N85-18555

Arctic-North Atlantic rift megasystem
13 p2105 N85-23117

Possibilities of aerial electric prospecting by long cable method for detecting poorly conducting strata
13 p2115 N85-23177

Evaluation of Thematic Mapper performance as applied to hydrocarbon exploration — Ontario, Canada; Cement, Oklahoma; and Death Valley, California
13 p2118 N85-23191

China report: Science and technology
[JPRS-CST-84-012] 14 p2283 N85-24140

Investigative report on using geological research to promote prospecting 14 p2283 N85-24142

Organizing geological work tasks for 1985 outlined
16 p2806 N85-27303

Comparative study of fracture planes computed from topography and lineaments from imagery with structures and mineralization in the magnetic belt of Washington State
[DE85-010972] 20 p3477 N85-31608

Geomorphology, tectonics, and exploration
21 p3601 N85-32365

Use of space photographs for analysis of structural and dynamic conditions of formation of ancient phlogopite and apatite deposits 22 p3735 N85-33153

USGS research on mineral resources, 1985
[CIRC-949] 24 p4103 N85-35435

Aeromagnetic and radiometric signatures of a possible porphyry system in the western Tushar Mountains Utah
24 p4103 N85-35437

Some geophysical guides to ore in southern and southwestern Alaska 24 p4103 N85-35438

Marine phosphorite deposits model for exploration, with emphasis on deposits in the US Atlantic coastal plain
24 p4104 N85-35439

The role of regional subsurface geochemistry in resource assessment in the central United States
24 p4104 N85-35440

Aeromagnetic and gravity models of the pluton below the Lake City caldera, Colorado
24 p4104 N85-35442

Massive sulfide deposits from the southern Juan de Fuca Ridge 24 p4105 N85-35446

Gas analysis of ore-forming fluids
24 p4105 N85-35447

Mineral deposit models: Theory and practice
24 p4105 N85-35448

Early and middle Cenozoic volcanic synthesis
24 p4105 N85-35449

Mineral resources programs 24 p4106 N85-35456

The Conterminous United States Mineral Assessment Program 24 p4106 N85-35458

Federal Mineral Land Information System
24 p4106 N85-35459

The Alaska Mineral Resources Assessment Program
24 p4107 N85-35460

MINERAL METABOLISM

Effect of 1,25-dihydroxycholecalciferol and 24,2 dihydroxycholecalciferol on growth and alteration of r bones during hypokinesia (histomorphometric study)
01 p0062 N85-

Alterations in gut transport of minerals and in bind proteins during simulated weightlessness
[NASA-CR-175637] 14 p2266 N85-

The role of vitamin D in the bone changes associat with simulated weightlessness 15 p2506 N85-

Changes in bone structure and metabolism durin simulated weightlessness: Endocrine and dietary facto
[NASA-CR-175961] 18 p3153 N85-

Fluid-electrolyte metabolism and renal function i cosmonauts following 185-day spaceflight
23 p3952 N85-

MINERAL OILS

Characterization of erosion of metallic materials und cavitation attack in a mineral oil
[NASA-TM-86934] 10 p1440 N85-

MINERALOGY

Petrology and genesis of carbonate-hosted Pb-Zn-Ag San Cristobal District, Department of Junin, Peru
03 p0389 N85-

Peculiar spherules from Antarctica and their origi
06 p0863 N85-

Hydrothermal alteration of CM carbonaceo chondrites: Implications of the identification of tochili as one type of meteoritic PCP 06 p0864 N85-

The mineralogy of global magnetic anomalies
[E85-10061] 07 p0987 N85-

Alabama Tin Belt: Metallogenesis and mineral resour evaluation. Year-end report
[DE84-901335] 07 p0989 N85-

A wind-tunnel study of the saltation of heterogeneo (size, density) sands 08 p1182 N85-17

Mineralogical investigations of lunar samples and meteorites
[NASA-CR-174291] 08 p1258 N85-17

Diagenesis of niagaran (middle silurian) pinnacle reef northwest Michigan 09 p1352 N85-

Research and development related to the Nevad nuclear waste storage investigations
[DE85-002303] 12 p1932 N85-

Characteristics of alumyte deposits discussed
13 p2166 N85-

The olivine asteroids: Discovery, mineralogy, and relationship to pallasites 13 p2175 N85-

Crystal chemistry of meteoritic hibonites
13 p2185 N85-

Determining mineral types and abundances fro reflectance measurements 13 p2196 N85-

Determination of mineral type, abundance, and gra size with remotely obtained reflectance spectra
13 p2196 N85-

Quantitative analyses of planetary reflectance spectr
13 p2197 N85-

Analysis of SMIRR data for volcanic and sedimenta terrains of the trans-Pecos region, Texas
13 p2197 N85-

Mineralogical-geochemical characteristics ferromanganese formations in Arabian-Indian Ocea Ridge 19 p3293 N85-

Petrologic and geochemical characterization of th Topopah Spring Member of the Paintbrush Tuff: Outc samples used in waste package experiments
[DE85-010449] 19 p3302 N85-

Physical and chemical changes to rock near electric heated boreholes at Spent Fuel Test-Climax
[DE85-010834] 19 p3302 N85-

Mineralogy and chemistry of the Earth
22 p3856 N85-

MINERALS

NT ASBESTOS
NT BERYL
NT BIOTITE
NT CALCITE
NT CHROMITES
NT DOLOMITE (MINERAL)
NT ENSTATITE
NT FELDSPARS
NT FLUORITE
NT GARNETS
NT GRAPHITE
NT IRON ORES
NT LIMONITE
NT MAGNETITE
NT MICA
NT OLIVINE
NT PEROVSKITES
NT PYRITES
NT PYROXENES
NT QUARTZ
NT SERPENTINE

NT SIDERITES
NT SPINEL
NT TROILITE
Operating experiences of reverse osmosis plants treating Rand Water Board (RWB) water: Pitfalls and problems 01 p0023 N85-10142
Compilation of elemental concentration data for NBS (National Bureau of Standards) biological, geological and environmental standard reference materials, 1982
[PB84-216338] 01 p0025 N85-10158
Mineral nutrients in Mediterranean ecosystems
[REPT-71] 01 p0069 N85-10456
Middle infrared spectral studies of geologic materials in their natural state using photothermal beam deflection spectroscopy
[AD-A144884] 01 p0120 N85-10820
The Alaskan mineral resources assessment program: Guide to information contained in the folio of geologic and mineral-resource maps of the Medfra Quadrangle, Alaska
[GS-CIRC-909] 02 p0219 N85-11443
Late oligocene gabbro near Ketchikan, southeastern Alaska 04 p0518 N85-13307
Atmospheric heating of meteorites: Results from nuclear track studies 06 p0882 N85-15607
A study of tetrataenite 06 p0885 N85-15623
Structural development in the Santa Catharina meteorite 06 p0886 N85-15625
New data on presence of ores in salt dome structures of Dnieper-Donets Basin 07 p0961 N85-16234
Geostatistics for resource and reserve estimation
[PB85-105781/GAR] 07 p0989 N85-16286
A study of structural phase transitions using light scattering techniques
[AD-A147261] 07 p1048 N85-16654
Depositional modeling of tetrahedrite in the Coeur d'Alene district, Idaho 08 p1182 N85-17448
Impact and collisional processes in the solar system
[NASA-CR-174297] 08 p1255 N85-17914
Evaluating the variability of ceramics with X-ray fluorescence
[DE85-002028] 10 p1453 N85-19155
Review of problems in lithology
13 p2113 N85-23160
Rapid advances in geological work
13 p2166 N85-23437
Characteristics of alumyte deposits discussed
13 p2166 N85-23438
Impact and collisional processes in the solar system
13 p2180 N85-23530
First direct detection of clay minerals on Mars
13 p2194 N85-23612
Iron oxides of Mars: Evidence for contemporary weathering 13 p2195 N85-23613
Zeolites on Mars: Prospects for remote sensing
13 p2195 N85-23615
Temperature anomalies above ore bodies
14 p2345 N85-24500
Hydrostatic compression of Fe1-chi 0 wuestite.
15 p2506 N85-25472
Spectral reflectance of carbonate minerals and rocks in the visible and near infrared (0.35 - 2.55 microns) and its applications in carbonate petrology
[NASA-CR-175763] 15 p2591 N85-25973
Effects of temperature on remotely sensed mafic mineral absorption features 16 p2809 N85-27323
Review of national emission standards for mercury
[PB85-153906] 16 p2822 N85-27406
Process for clarification of water
[DE85-007864] 17 p2923 N85-28023
Space-flight simulations of calcium metabolism using a mathematical model of calcium regulation
[NASA-CR-171883] 19 p3328 N85-30621
Mineral aerosols and source identification
21 p3646 N85-32654
Microbial colonization and growth on metal sulfides and other mineral surfaces 21 p3662 N85-32747
The effects of prolonged feeding meal, ready-to-eat (MRE) operational rations
[AD-A154763] 21 p3666 N85-32773
Quantitative determination of mineral composition by powder X-ray diffraction
[DE85-011654] 22 p3760 N85-33301
Chemistry of ore-forming fluids
24 p4103 N85-35436
MINES (EXCAVATIONS)
Land use/land cover 02 p0214 N85-11410
Mapping land use changes in the carboniferous region of Santa Catarina, report 2
[E85-10017] 02 p0217 N85-11430
Interactive system for the interpretation of coal deposit data as a basis of future mine planning systems
[BMFT-FB-T-83-115] 02 p0220 N85-11449
Effect of lithology and climate on the morphology of drainage basins in northwestern Colorado
[PB84-228238] 06 p0828 N85-15258
Geology of the Batopilas mining district, Chihuahua, Mexico, volumes 1 and 2 09 p1351 N85-18496
Stability indicators for front end loaders
[AD-P004293] 09 p1408 N85-18870
Effect of water vapor and water droplets on the RAM-1 (Real-Time Aerosol Monitor): Preliminary results
[PB85-109429] 11 p1637 N85-20313
China report: Science and technology
[JPRS-CST-84-038] 11 p1686 N85-20661
Comparative techniques used to evaluate Thematic Mapper data for land cover classification in Logan County, West Virginia 13 p2121 N85-23209
Rapid advances in geological work
13 p2166 N85-23437
Development of a stationary carbon monoxide detector
[BMFT-FB-T-84-253] 18 p3134 N85-29413
Orphans of the Valley: Abandoned surface mines in the Tennessee Valley. Volume 2: Maps
[DE85-901249] 19 p3301 N85-30485
New silver resource map of the United States: Potential for increased domestic silver production
24 p4105 N85-35445
Federal Mineral Land Information System
24 p4106 N85-35459
The homestake surface-underground scintillations: Description
[HE-6.1-9] 24 p4210 N85-36135
MINIATURE ELECTRONIC EQUIPMENT
A miniature urethane molded acoustic transducer
[AD-A146459] 06 p0804 N85-15114
Miniature electrooptical air flow sensor
[NASA-CASE-LAR-13065-1] 11 p1635 N85-20295
A miniature tactical Rb frequency standard
18 p3106 N85-29229
Miniature infra-red data acquisition and telemetry system
[NASA-CR-177953] 24 p4096 N85-35390
MINIATURIZATION
NT MICROMINIATURIZATION
Microminiature coaxial cable and methods of manufacture
[DE84-014228] 01 p0044 N85-10284
Manufacturing Methods and Technology (MM/T) specifications for miniature cathode ray tube
[AD-A145597] 02 p0194 N85-11298
Guided-wave optic devices for integrated optic information processing
[AD-A145695] 02 p0280 N85-11827
Development of miniature laser Doppler anemometers
[KU-SFB-210/ET/3] 12 p1857 N85-21648
Miniature two-mode filters 22 p3775 N85-33394
MINICOMPUTERS
East Europe report: Science and technology
[JPRS-ESA-84-030] 01 p0101 N85-10670
Analysis of three database system architectures using benchmarks
[PB84-217512] 01 p0105 N85-10706
East Europe report, science and technology. Czechoslovakia: System of small electronic computers
[JPRS-ESA-84-040] 02 p0239 N85-11558
Use of minicomputers for the formation of hydrological data banks 07 p1001 N85-16358
Specifications of bloc floppy disk drives
08 p1141 N85-17188
Design and analysis of an access control system for a multi-backend database system
[AD-A148750] 09 p1367 N85-18586
Proposal for a small scheme implementation
[AD-A148707] 09 p1368 N85-18595
The integrated library system design concepts for a complete serials control subsystem
[AD-A149379] 10 p1568 N85-19684
Arithmetic and elementary functions on mini and microcomputers 14 p2396 N85-24761
Computer technology advances exhibited
15 p2625 N85-26175
Mini- and microcomputer local control network architecture and design principles
15 p2625 N85-26179
Management considerations for an information center
[AD-A151774] 16 p2875 N85-27742
Program DISAS: A computer program to obtain hard-copy plots of an image displayed on a vector graphics device in a local-area-network
[AD-A153643] 18 p3162 N85-29586
Visualization of computation results. Definition of a graphics satellite computer
[ONERA-RT-2/3587-CY] 20 p3514 N85-31845
Electronic file system on an SM 90 minicomputer: The SARDE project
[ENST-84E018] 22 p3828 N85-33705
User's operating procedures. Volume 3: Projects directorate information programs
[NASA-CR-177950] 23 p3956 N85-34520
Procedure for editing the fluxgate magnetometer data of the AFGL (Air Force Geophysics Laboratory) magnetometer network
[AD-A156331] 24 p4117 N85-35523
Optimize computer throughput using array processors
[AD-A155843] 24 p4135 N85-35628
MINIMAL SURFACES
Lectures on generalized solutions to the minimal surface equation
[DE84-016662] 05 p0722 N85-14642
MINIMAX TECHNIQUE
Minimax optimal control in the reentry of a space glider 02 p0167 N85-11124
Nonlinear regression with emphasis on spline methods
[AD-A146192] 03 p0412 N85-12633
An H-infinity-minimax approach to the design of robust control systems
[OUEL-1537/84] 05 p0717 N85-14600
Minimax multiple t-tests for comparing k normal populations with a control
[AD-A148306] 08 p1215 N85-17656
On maximizing the expected lifetime of replaceable systems
[AD-A150003] 12 p1862 N85-21680
Regular synthesis of pairs of phase-keyed binary minimax signals 13 p2069 N85-22923
Minimax problem of estimating trajectory parameters in continuous formulation 15 p2479 N85-25301
Topics in time delay estimation
[AD-A152231] 16 p2855 N85-27607
Robust tests of mean vector in symmetrical multivariate distributions
[AD-A153116] 17 p3020 N85-28674
MINIMIZATION
U OPTIMIZATION
MINIMUM ENTROPY METHOD
An overview of latest model reduction and control methods of large flexible space structures
20 p3414 N85-31191
MINIMUM VARIANCE ORBIT DETERMINATION
Satellite orbit determination 05 p0598 N85-13813
Heliosynchronism and phasing. Application to the SPOT orbit 05 p0600 N85-13826
Orbit reconstitution --- satellite orbits
14 p2396 N85-24765
MINING
Geostatistics for resource and reserve estimation
[PB85-105781/GAR] 07 p0989 N85-16286
China report: Science and technology
[JPRS-CST-85-003] 13 p2166 N85-23433
Rapid advances in geological work
13 p2166 N85-23437
Technical and cost analyses of manganese nodule processing techniques and their significant variations
[PB85-148815] 14 p2258 N85-23992
Gigantic lithium deposit discovered in France
14 p2289 N85-24184
Mining cosmic dust from the blue ice lakes of Greenland 15 p2682 N85-26563
An analysis of alternate hydrogen sources for lunar manufacture
[DE85-007234] 16 p2884 N85-27792
Shuttle car loading system
[NASA-CASE-NPO-15949-1] 23 p3987 N85-34722
MINIVAR ORBIT DETERMINATION
U MINIMUM VARIANCE ORBIT DETERMINATION
MINKOWSKI SPACE
Special relativity of Kaluza-Klein
[DE85-007836] 17 p3046 N85-28847
MINOR PLANET 1221
U AMOR ASTEROID
MINORITIES
Companies participating in the Department of Defense Subcontracting Program, first three quarters fiscal year 1984
[AD-A146137] 03 p0436 N85-12775
NASA iniuatives with historically black colleges and universities
[NASA-EP-210] 19 p3379 N85-30960
MINORITY CARRIERS
Studies in electron phenomena in MOS structures: The pulsed C-V method 15 p2659 N85-26407
High efficiency large area polysilicon solar cells
20 p3482 N85-31639
High-purity silicon crystal growth
21 p3612 N85-32444
MINUTEMAN ICBM
An analysis of the technical training of enlisted minuteman missile maintenance personnel
[AD-A147076] 07 p0912 N85-15775
MINUTEMAN MISSILES
U MINUTEMAN ICBM
MIRAGE AIRCRAFT
NT MIRAGE 3 AIRCRAFT
Aeroelastic analysis and the identification of flight loads --- Mirage 2000 aircraft 07 p0896 N85-15679

Map display for helicopters 08 p1073 N85-16801
A comparison of fatigue lives under a complex and a much simplified flight-by-flight testing sequence --- Mirage 3 aircraft
[ARL/STRUC-TM-386] 09 p1280 N85-18052
Unsteady aerodynamic characterization of a military aircraft in vertical gusts
[NASA-TM-77810] 12 p1770 N85-21110
Calculation of unsteady transonic flow around a high swept wing 15 p2459 N85-25184

MIRAGE 3 AIRCRAFT
Fatigue crack propagation in mirage 1110 wing main spar specimens and the effects of spectrum truncation on life
[ARL/STRUC-R-405] 12 p1776 N85-21152
Tensile and fracture toughness properties of Mirage III spars
[AR-003-019] 15 p2578 N85-25899
Further investigations to improve the fatigue life of the Mirage 1110 wing main span
[ARL/STRUC-TM-397] 16 p3061 N85-26936

MIRANDA SATELLITE
Satellite masses in the Uranus and Neptune systems
[PSI-CONTRIB-198] 02 p0301 N85-11947

MIRROR FUSION
Theoretical studies in tandem mirror physics
[DE84-016834] 04 p0566 N85-13604
Fusion plasma theory. Task 3: ECRH and transport modeling in tandem mirrors and divertor physics
[DE84-014939] 04 p0567 N85-13612
EBT electron energy confinement experiments
[DE84-015402] 04 p0567 N85-13613
Stabilization of the hot electron precessional mode in a symmetric tandem mirror by the axial variation of radial electric field
[DE84-016369] 05 p0730 N85-14692
Theoretical investigations relevant to magnetic fusion research, April 1, 1983 - March 31, 1984
[DE85-001776] 06 p0865 N85-15496
Special topics reports for the reference tandem mirror fusion breeder: Liquid metal MHD pressure drop effects in the packet bed blanket, volume 1
[DE85-002142] 06 p0866 N85-15500
Long-pulse beamlines for the mirror fusion test facility
[DE84-017091] 09 p1392 N85-18760
Heat transfer and mechanical interactions in fusion nuclear systems
[DE84-016233] 09 p1392 N85-18761
Electronics Engineering Department: EE technical review
[DE85-004360] 11 p1629 N85-20259
Mirror fusion progress
[DE85-001187] 11 p1731 N85-20888
Plasma-wall interactions in tandem mirror machines
[DE85-006367] 15 p2657 N85-26399
Stability of high energy particle plasmas to MHD-like modes
[DE85-007879] 17 p3039 N85-28803
An Impurity Control Test Facility (ICTF) for the study of fusion reactor/plasma edge materials
[DE85-007846] 17 p3040 N85-28810
Energy and Technology Review
[DE85-004358] 17 p3049 N85-28888
Physics-magnetics trade studies for tandem mirror reactors
[DE85-010043] 18 p3182 N85-29732
Test cell modeling and optimization for FPD-2
[DE85-010836] 19 p3358 N85-30821
Stability of a hot symmetric tandem mirror with thermal barrier
[DE85-010539] 19 p3377 N85-30952
Neutronics activities for next generation devices
[DE85-010486] 20 p3527 N85-31939
Modeling and optimization of a test-cell upgrade for MFTF-B operating in the high neutron wall loading mode
[DE85-008807] 20 p3528 N85-31946
Simulation of automatic control of MFTF-B neutral beams
[DE85-010540] 20 p3530 N85-31960
Energy and Technology Review
[DE85-011767] 21 p3716 N85-33061
Proceedings of the US-Japan Workshop on Transport in Open-Ended Systems
[IPPJ-727] 23 p3975 N85-34644
Plug and thermal barrier potential formation in Gamma 10 23 p3976 N85-34648
RF induced radial diffusion in tandem mirrors
23 p3976 N85-34649
Induced azimuthal electric field effects on tandem transport and ambipolarity 23 p3976 N85-34650
Recent experiments in Gamma-10
23 p3976 N85-34651
Radial transport caused by collision
23 p3976 N85-34652
Transport issues in Phaedrus-type plasmas
23 p3976 N85-34653
Possibility of potential generation by lower hybrid wave 23 p3977 N85-34654
Bounce resonance heating and radial transport of electrons 23 p3977 N85-34655
Electron dynamics and transport in a mirror field
23 p3977 N85-34656
Low frequency instability in a mirror field
23 p3977 N85-34657
Model of azimuthal non-uniformities induced by RF heating in RFC-XXM 23 p3977 N85-34658
Azimuthal uniformity and current balance study of ICRH-produced plasma in RFC-XXM
23 p3977 N85-34659
Advanced Toroidal Facility (ATF)
[DE85-011567] 23 p3983 N85-34690
Perspective on the next ten years in plasma physics
[DE85-011849] 23 p3984 N85-34706
Analysis of a pulsed power system containing rotating machine
[DE85-014129] 24 p4150 N85-35786

MIRRORS
NT FRESNEL REFLECTORS
NT MAGNETIC MIRRORS
NT PARABOLOID MIRRORS
NT ROTATING MIRRORS
Parameters of geometric stability of laser mirror optical surface 02 p0273 N85-11777
Development of a measuring procedure for the automatic evaluation of the flatness of reflective surfaces
[BMFT-FB-T-84-169] 03 p0421 N85-12698
Dynamic testing of NOVA laser switchyard tower
[DE84-014450] 05 p0640 N85-14103
Cleaning procedures of laser mirror substrates
[DFVLR-MITT-84-06] 05 p0640 N85-14106
Design of two-mirror scanner with axes of rotation not in plane of mirrors 06 p0777 N85-14969
High energy laser mirror
[AD-D011255] 06 p0812 N85-15158
Dual-secondary mirror Cassegrain optical system
[AD-D011273] 06 p0862 N85-15478
Plasma-surface interactions in large tandem mirror devices, MFTF-B
[DE85-001753] 06 p0865 N85-15490
Theoretical investigations relevant to magnetic fusion research
[DE85-001777] 06 p0866 N85-15503
Evaluation of colorless polyimide film for thermal control coating applications
[NASA-TM-86341] 07 p0930 N85-15894
Reverse wave suppression in unstable ring resonator
[AD-A146825] 07 p0939 N85-15952
Unstable optical resonator with canceling edge waves
[AD-D011379] 07 p1042 N85-16618
Mirror actuator control system
[AD-D011383] 07 p1042 N85-16619
Light scattered from polished optical surfaces: Wings of the point spread function 08 p1252 N85-17911
Calculation and computer simulation of the Paraboloidal Mirror Analyzer (PMA)
[DE85-001417] 09 p1384 N85-18705
Reflectivity measurements of laser gyro mirrors
[ESA-TT-851] 09 p1386 N85-18714
Procedures for the bonding of the E.M.C. mirror onto its INVAR mirror flange --- United Kingdom Infrared Telescope
[UKIRT-19] 09 p1414 N85-18917
In situ washing procedures for the UKIRT 3.8 meter primary mirror --- United Kingdom Infrared Telescope (UKIRT)
[UKIRT-20] 09 p1414 N85-18918
Temperature variation of laser mirror stability criteria
10 p1445 N85-19106
Fine figuring actuator
[AD-D011476] 10 p1557 N85-19819
Solar optical telescope primary mirror controller
[NASA-CR-174416] 10 p1570 N85-19903
Characteristics of unstable resonators in flashlamp-pumped organic-compound lasers
11 p1717 N85-20800
Four-wave hypersonic reversing mirrors in saturated mode 11 p1719 N85-20812
Optimization of piezoceramic optical deflector
11 p1719 N85-20813
Wide-angle flat field telescope
[NASA-CASE-GSC-12825-1] 11 p1728 N85-20868
An analysis of the high frequency vibrations in early Thematic Mapper scenes 12 p1872 N85-21742
Three-mirror open resonator for millimeter wave band
13 p2077 N85-22972
ROSA: A computer model for optical power ratio calculations
[DE85-006174] 13 p2129 N85-23251
Innovative research in the design and operation of large telescopes for space: Aspects of giant telescopes in space
[NASA-CR-175626] 13 p2170 N85-
Measurement of sensitivity of shadowgraph instruments with spherical autocollimating mirror
14 p2274 N85-
Multilayer reflecting systems based on glassy chalcogenides for infrared lasers
14 p2274 N85-
Determining optimum service conditions for concentrator mirrors by methods of mathematically planned experiment 14 p2274 N85-
Vibration isolator actuator
[AD-D011574] 14 p2321 N85-
Angular error of position of RATAN-600 screens during radial displacement 15 p2476 N85-
Mirror accessory for line straightening in diffraction spectrometers 16 p2764 N85-
Software for reflectivity calculations of X-ray mirrors, revision 1
[DE85-006642] 16 p2867 N85-
Downdraw extrusion of ULE(TM) glass
[AD-A153783] 18 p3079 N85-
Thin layered interference mirrors to reduce radiation damage
[DE85-009763] 18 p3185 N85-
Optically bistable devices using InSb
18 p3186 N85-
Deformable mirror nearest neighbor optical computer
18 p3186 N85-
Optically pumped laser system having intracavity pulse smoother
[AD-D011714] 19 p3276 N85-
Measurements of folded path optical scintillation using a corner cube, a cat's eye and a flat mirror reflector
[AD-A154044] 19 p3367 N85-
Silicon nitride protective coatings for silvered glass mirrors
[DE85-011637] 20 p3433 N85-
Influence of mirror anisotropy and Brewster window orientation on radiation characteristics of ring lasers
21 p3684 N85-
Mirror reflection of charged particles from + amorphous and polycrystalline surfaces 21 p3686 N85-
Comparison of findings of theories describing reflection from real surface with experiments in region of ultrasoft X-radiation 21 p3694 N85-
Dielectric mirror with ferromagnetic substrate
21 p3696 N85-
Mean intensity of wave reflected by wavefront reversing mirror in turbulent medium 22 p3782 N85-
Method of bonding silver to glass and mirrors produced according to this method
[DE85-011642] 22 p3792 N85-
Electron and ion cyclotron heating calculations in the tandem-mirror
[DE85-011856] 22 p3842 N85-
Role of ECRH in potential formation for tandem mirrors
[DE85-011859] 22 p3848 N85-
Effect of ECH and ICH on ambipolar potential in NBT-1M 23 p3978 N85-
Fokker-Planck calculation of hot electron formation in the thermal barrier region of tandem mirror Gamma-10
[IPPJ-726] 23 p3979 N85-
A method to improve observations of gamma-ray sources near 10 (15) eV
[OG-9.5-5] 23 p4030 N85-
Single-point diamond crushing of Zerodur with in-situ polishing and metrology on a diamond turning machine
[DE85-012916] 24 p4083 N85-
A normal incidence X-ray telescope sounding rocket payload
[NASA-CR-176169] 24 p4153 N85-

MIS (SEMICONDUCTORS)
Novel techniques for the fabricating and characterization of GaAs MIS (Metal Insulator Semiconductor) structures
[AD-A145766] 03 p0358 N85-
Aluminum nitride insulator for 3-5 MIS (Metal-Insulator-Semiconductor) applications
[AD-A147842] 07 p1049 N85-

MISALIGNMENT
Gyrodynamic fixture for measuring thrust line components
[AD-D011256] 06 p0760 N85-
Study of energy versus misorientation for grain boundaries in gold by crystallite rotation method. 1: 001 twist boundaries
[DE85-004596] 12 p1943 N85-
Dependence of properties of optical cavity on misalignment 14 p2276 N85-

MISCIBILITY
U SOLUBILITY

MISFETS
U FIELD EFFECT TRANSISTORS

MISMATCH (ELECTRICAL)
Nonlinearity and spectral mismatch problems of solar cells 13 p2010 N85-22805
MISORIENTATION
U MISALIGNMENT
MISS DISTANCE
Methodology improvement program for the second generation miss distance radar (MIDI 2)
[AD-A148467] 08 p1153 N85-17261
MISSILE ANTENNAS
Hardwire missile receiver coupler
[AD-D011350] 07 p0937 N85-15936
Dual mode radio frequency-infrared frequency system
[AD-D011402] 08 p1081 N85-16850
MISSILE BODIES
Empirical formulas for the prediction of the base pressure of missile bodies at subsonic velocities
[DFVLR-FB-84-23] 03 p0316 N85-12044
Empirical formulas for the prediction of the base pressure of missile bodies at subsonic velocities
[ESA-TT-893] 20 p3399 N85-31082
Flow modeling at the base region of missiles
[SNIAS-851-320-101] 20 p3420 N85-31228
MISSILE CASES
U MISSILE BODIES
MISSILE COMPONENTS
NT MISSILE ANTENNAS
NT MISSILE BODIES
Zero adhesion system
[AD-D011237] 01 p0015 N85-10093
Hardwire missile receiver coupler
[AD-D011350] 07 p0937 N85-15936
Modeling and simulation of a fin actuation system
[AD-A149443] 10 p1428 N85-19005
Dual band radome wall design
[AD-P004357] 12 p1825 N85-21451
Hot radome boresight error measurements
[AD-P004364] 12 p1826 N85-21458
Supersonic missile seeker lens system using gradient index material for first element lens
[AD-A151476] 15 p2490 N85-25367
MISSILE CONFIGURATIONS
Wind tunnel tests on a tube-launched missile configuration with a deflectable nose control and a novel wrap-around fin stabiliser
[AR-003-896] 01 p0001 N85-10003
Shock capturing finite difference algorithms for supersonic flow past fighter and missile type configurations
[NASA-CR-174051] 02 p0134 N85-10913
An overview of some monoplaner missile programs
[NASA-TM-86330] 06 p0747 N85-14786
MISSILE CONTROL
Application of modern guidance control theory to a bank-to-turn missile
[AD-A145848] 02 p0166 N85-11123
Polaris guidance system
[AD-D011324] 07 p0900 N85-15704
Prediction of cruciform all-movable control characteristics at transonic speeds
[AD-A147291] 08 p1078 N85-16832
Optical data processing for missile guidance
[AD-A149346] 10 p1422 N85-18972
Space interception guidance with uncertain factors
13 p2042 N85-22781
Multi-rate digital autopilot modeling methodology
[AD-A152044] 15 p2474 N85-25272
Optical flow-patterns of image velocity and their potential use in guidance and image interpretation
[BAE-BT-12091] 15 p2651 N85-26347
Cost-effective missile guidance through distributed architecture and standard processes
16 p2698 N85-26862
Computer simulation of a cruise missile using brushless dc motor fin control
[AD-A156935] 24 p4089 N85-35349
MISSILE DEFENSE
Directed energy missile defense in space
[PB84-210111] 01 p0015 N85-10095
About ambiguity and Q-functions
[AD-A145293] 02 p0250 N85-11636
MISSILE DESIGN
Tactical missiles technologies. Research and prospectives
[SNIAS-841-320-101] 04 p0461 N85-12925
Proceedings of the 17th Symposium on Electromagnetic Windows, part 1
[AD-A149185] 10 p1486 N85-19253
The application of some lifting-body reentry concepts to missile design
[NASA-TM-86304] 13 p1969 N85-22366
Simulation: A tool for cost-effective systems design and live test reduction 16 p2698 N85-26857
Cost-effective missile guidance through distributed architecture and standard processes
16 p2698 N85-26862
Flow modeling at the base region of missiles
[SNIAS-851-320-101] 20 p3420 N85-31228
MISSILE DETECTION
NT RADAR DETECTION
MISSILE ENGINE CASES
U ROCKET ENGINE CASES
MISSILE GUIDANCE
U MISSILE CONTROL
MISSILE LAUNCHERS
NT MOBILE MISSILE LAUNCHERS
Wind tunnel tests on a tube-launched missile configuration with a deflectable nose control and a novel wrap-around fin stabiliser
[AR-003-896] 01 p0001 N85-10003
Zero adhesion system
[AD-D011237] 01 p0015 N85-10093
Hardwire missile receiver coupler
[AD-D011350] 07 p0937 N85-15936
Lateral support system for canister-launched missile
[AD-D011369] 08 p1106 N85-16987
Missile launcher integral shock isolation and running gear system
[AD-D011490] 11 p1589 N85-19998
MISSILE SILOS
Invited papers: DNA ICBM technical R and D program 09 p1333 N85-18379
Empirical development of ground acceleration, velocity and displacement for accidental explosions at J5 or the proposed large altitude rocket cell at Arnold Engineering Development Center
[DE85-008324] 16 p2758 N85-27020
MISSILE STABILIZATION
U MISSILE CONTROL
U STABILIZATION
MISSILE STORAGE
Safety aspects of prepackaged liquid propellant stages for strategic missiles
[AD-P004350] 10 p1456 N85-19174
MISSILE SYSTEMS
Tactical missiles technologies. Research and prospectives
[SNIAS-841-320-101] 04 p0461 N85-12925
Some dynamical aspects of Army missile systems
09 p1333 N85-18380
Simulation: A tool for cost-effective systems design and live test reduction 16 p2698 N85-26857
MISSILE TRAJECTORIES
Fast response impulse generator
[AD-D011283] 06 p0759 N85-14853
Technical manual: Description and operation Slaved Tracking System
[DE85-004807] 13 p2094 N85-23070
Estimation of launch vehicle performance parameters
[AD-A151927] 16 p2728 N85-26839
MISSILE VIBRATION
Some dynamical aspects of Army missile systems
09 p1333 N85-18380
MISSILES
NT AIR TO SURFACE MISSILES
NT ANTIMISSILE MISSILES
NT BALLISTIC MISSILES
NT CRUISE MISSILES
NT INTERCONTINENTAL BALLISTIC MISSILES
NT MINUTEMAN ICBM
NT POLARIS MISSILES
NT RAMJET MISSILES
NT SIDEWINDER MISSILES
NT SURFACE TO SURFACE MISSILES
Ramjet and Ramrocket Propulsion Systems for Missiles
[AGARD-LS-136] 07 p0917 N85-15809
Some aspects of engine and airframe integration for Ramjet and Ramrocket powered missiles
07 p0918 N85-15812
Special problems of Ramjet with solid fuel
07 p0918 N85-15815
Solid propellant Ramrockets 07 p0918 N85-15816
Air Force space technology center space technology: Emphasis 84 09 p1333 N85-18381
The 1984 JANNAF Propulsion Systems Hazards Subcommittee Meeting, volume 1
[AD-A148865] 10 p1454 N85-19162
Preventing explosive propagation in racks or containers of tactical missiles
[AD-P004342] 10 p1455 N85-19166
Fiscal year 1986 technical objective document
[AD-A151039] 14 p2432 N85-25000
Gyrolaser guidance system for medium range missiles
16 p2698 N85-26849
A simulation study of jammer nulling trade-offs in a reactively steered adaptive array
[AD-A153461] 18 p3090 N85-29124
An extended two-target differential game model for medium-range air combat game analysis
[NASA-CR-175088] 18 p3175 N85-29687
Thrust vectoring apparatus for maneuvering missile in flight
[AD-D011693] 19 p3226 N85-30004
Transonic and supersonic wind tunnel tests on control effectiveness on schematic missile configurations
[FFA-TN-1983-20] 20 p3389 N85-31020
Transonic and supersonic wind tunnel tests on control effectiveness on schematic missile configurations: Supplement
[FFA-TN-1983-20-SUPPL] 20 p3389 N85-31021
MISSION PLANNING
Information Science Panel joint meeting with Imaging Science Panel 02 p0214 N85-11415
Mars exploration, Venus swingby and conjunction class mission modes, time period 2000 to 2045
[NASA-TM-86477] 02 p0303 N85-11961
Proceedings of a Workshop on Applications of Tethers in Space, Executive Summary
[NASA-CR-171195] 03 p0322 N85-12075
Lessons from the SEASAT and GEOS-3 altimeters data projects 03 p0384 N85-12457
Status of Stretched Rohini Satellite System (SROSS) and Augmented Satellite Launch Vehicle Project (ASLV)
04 p0459 N85-12909
A Mars dust sample return mission
[CNES-CT/PMF/APS/EMS-177]
04 p0459 N85-12915
Interstellar mission 04 p0459 N85-12916
Definition of technology development missions for early Space Station satellite servicing. Volume 2: Technical
[NASA-CR-171229] 04 p0461 N85-12923
The human role in space. Volume 1: Executive summary
[NASA-CR-171223] 04 p0546 N85-13473
The satellite maneuvers determination department
05 p0590 N85-13820
Missions/planning panel 05 p0609 N85-13886
Sample return from a comet flyby
06 p0889 N85-15646
Commerce Laboratory: Mission analysis payload integration study
[NASA-CR-171298] 07 p0911 N85-15784
Results of principal NASA studies on space station uses and functional requirements 07 p0914 N85-15787
Acquisition planning at the Defense Communications Agency
[AD-A146877] 07 p1051 N85-16669
QUASAT: A VLBI observatory in space -- conferences
[ESA-SP-213] 07 p1056 N85-16700
Automatic briefing and mission management systems for battlefield support 08 p1073 N85-16799
A Computer-generated topographic display system for navigation and mission planning in helicopters
08 p1073 N85-16800
Descent guidance and mission planning for space shuttle 08 p1092 N85-16902
Commerce Lab: Mission analysis and payload integration study
[NASA-CR-171272] 08 p1104 N85-16981
Commerce Lab: Mission analysis. Payload integration study
[NASA-CR-171285] 08 p1104 N85-16982
Impact of lunar and planetary missions on the space station
[NASA-CR-171832] 08 p1106 N85-16988
Space Station needs, attributes, and architectural option study
[NASA-CR-174316] 08 p1109 N85-17011
The SIR-B science investigations plan
[NASA-CR-174282] 08 p1143 N85-17208
Space Station engineering and technology development
[NASA-CR-174393] 09 p1287 N85-18079
Air Force space technology center space technology: Emphasis 84 09 p1333 N85-18381
Data Requirement (DR) MA-03: Payload missions integration — Spacelab payloads
[NASA-CR-171331] 10 p1428 N85-19009
CNES, INRA do joint remote-sensing research
10 p1477 N85-19321
Human Factors Considerations in High Performance Aircraft
[AGARD-CP-371] 10 p1532 N85-19853
Satellite module design 11 p1642 N85-20344
A mathematical formulation of the problem of optimal use of ground resources for future space missions
12 p1947 N85-22232
Activities of the Jet Propulsion Laboratory, 1 January - 31 December 1983
[NASA-CR-175665] 13 p2167 N85-23447
National Space Transportation Systems Program mission report
[NASA-TM-87454] 14 p2242 N85-23699
NASA plans for a space station
14 p2393 N85-24735

Shuttle operational test and scientific investigations
14 p2394 N85-24748

Mission analysis and orbit control of the heliosynchronous satellite SPOT
14 p2397 N85-24773

Towards the Halley Comet 14 p2399 N85-24783

The development of a performance and mission planning program for the A-7E aircraft
[AD-A151717] 15 p2471 N85-25258

Definition of technology development missions for early space stations: Large space structures
[NASA-CR-171448] 15 p2476 N85-25281

Automatic rendezvous and docking systems functional and performance requirements
[NASA-CR-171886] 15 p2492 N85-25376

Calendar of Ariane launches 1984 - 1987
15 p2523 N85-25554

European space science horizon 2000
[ESA-SP-1070] 16 p2717 N85-26771

A SLAM II simulation model for analyzing space station mission processing requirements
[NASA-CR-175664] 16 p2731 N85-26853

Tethered nuclear power for the Space Station
[NASA-TM-87023] 16 p2740 N85-26912

Component-specific modeling
[NASA-CR-174766] 16 p2799 N85-27261

Shuttle-tethered satellite system definition study extension
[NASA-CR-171473] 17 p2907 N85-27923

Mission requirements and handling qualities
18 p3057 N85-28918

Customer and mission influence on space station architecture 18 p3159 N85-29567

Space station automation study. Volume 2: Technical report. Autonomous systems and assembly
[NASA-CR-171515] 19 p3226 N85-30001

An artificial intelligence based framework for planning air launched cruise missile missions
[AD-A154466] 19 p3344 N85-30722

Mission analysis of solar powered aircraft
[NASA-CR-172583] 20 p3397 N85-31072

Maritime search and rescue cooperation and planning
20 p3400 N85-31093

X-ray satellite
[NASA-TM-77882] 20 p3407 N85-31145

Space Station reference configuration description
[NASA-TM-87493] 20 p3408 N85-31146

Studies toward a manned space station: Participation of European industry in NASA space station (MSS)
[SNIAS-S/DT-Y-25-212] 20 p3418 N85-31217

Life sciences flight experiments program mission science requirements document. The first life sciences dedicated Spacelab mission, part 1
[NASA-TM-87494] 21 p3559 N85-32137

Space station automation study. Automation requirements derived from space manufacturing concepts. Volume 1: Executive summary
[NASA-CR-176099] 22 p3736 N85-33170

Space Station automation study. Automation requirements derived from space manufacturing concepts. Volume 2: Technical report
[NASA-CR-176100] 22 p3736 N85-33171

Space Station Engineering and Technology Development: Proceedings of the Panel on In-Space Engineering Research and Technology Development
[NASA-CR-176110] 23 p3899 N85-34153

MISSIONS

Search for proton decay in the Frejus experiment
[HE-6.2-2] 24 p4210 N85-36138

Data acquisition system for phase-2 KGF proton decay experiment
[HE-6.2-4] 24 p4211 N85-36140

MISSISSIPPI

Water resources data, Mississippi, water year 1982
[PB84-224559] 01 p0065 N85-10434

Remote sensing applications program
[E85-10022] 02 p0218 N85-11435

Petrologic model of the northern Mississippi embayment based on satellite magnetic and ground based geophysical data
[NASA-TM-86075] 04 p0533 N85-13406

The influence of the number of ground control points on the scene-to-map registration accuracy — Kansas, Louisiana, Mississippi, and Missouri
07 p0966 N85-16264

MISSISSIPPI DELTA (LA)

Geological, structural, and geomorphological analyses from SIR-B 08 p1145 N85-17226

MISSISSIPPI RIVER (US)

Use of a two-dimensional flow model to quantify aquatic habitat
[AD-A154287] 19 p3286 N85-30253

MISSOURI

The influence of the number of ground control points on the scene-to-map registration accuracy — Kansas, Louisiana, Mississippi, and Missouri
07 p0966 N85-16264

Image variance and spatial structure in remotely sensed scenes — South Dakota, California, Missouri, Kentucky, Louisiana, Tennessee, District of Columbia, and Oregon
07 p0966 N85-16265

MISSOURI RIVER BASIN (US)

Water resources data for Colorado, water year 1983. Volume 1: Missouri River Basin, Arkansas River Basin and Rio Grande Basin
[PB85-123859] 11 p1671 N85-20526

MIST

Mist flammability studies of candidate fire-resistant hydraulic fluids
[AD-A148572] 08 p1134 N85-17146

Description of a technique to measure spray distribution in an air stream
[AD-A149780] 12 p1771 N85-21122

MITOCHONDRIA

Effects of hyperthermia on free amino acids in rat brain and in subcellular fractions 11 p1691 N85-20631

Effects of immobilization and high-altitude adaptation on energy metabolism in rats 22 p3620 N85-33663

MIXED CRYSTALS

Structural phase transitions in doped hexahalogen metallates 03 p0426 N85-12721

MIXED FLOW

U MULTIPHASE FLOW

MIXERS

On selecting bypass mixers for turbofan engines
09 p1306 N85-18207

Flameholder with integrated air mixer
[AD-D011549] 12 p1776 N85-21161

Switching mixer
[AD-D011602] 16 p2777 N85-27139

MIXING

NT COLLOIDING
NT COMPOUNDING
NT DISSOLVING
NT HOMOGENIZING
NT SIGNAL MIXING
NT TURBULENT MIXING

Materials modification by ion beam mixing
[AD-P003948] 02 p0286 N85-11864

Nonlinear optical studies of rydberg atoms using degenerate four-wave mixing
[AD-A148827] 07 p1043 N85-16623

An experimental study on the instability of a mixing-layer with laminar wake as the initial condition
08 p1076 N85-16824

Effects of a periodic disturbance on structure and mixing in turbulent shear layers and wakes
[AD-A140278] 10 p1484 N85-19370

Convergence rates in the strong law for bounded mixing sequences
[CWI-MS-R8412] 12 p1922 N85-22076

Constraints of observations of solar oscillations on solar models with mixing by turbulent diffusion
[DE85-003741] 13 p2205 N85-23678

Influences of thermal spikes in ion beam mixing
[DE85-006130] 14 p2419 N85-24924

Mixing in the solar interior 14 p2446 N85-25095

Ion beam mixing of marker layers in Al and Si
[DE85-006227] 15 p2511 N85-25490

North Atlantic Deep Water Formation
[NASA-CP-2367] 15 p2601 N85-26026

North Atlantic Deep Water and the world ocean
15 p2602 N85-26033

Glacial-to-interglacial changes in NADW fluxes?
15 p2602 N85-26037

Evaluation of experimental epoxy monomers
[NASA-TM-87476] 16 p2754 N85-26996

Holoswitch, phase 1
[AD-A152212] 16 p2787 N85-27196

The seasonal cycle of atmospheric CO in the Southern Hemisphere 16 p2830 N85-27447

Surface modification of solids
[DE85-007543] 16 p2871 N85-27715

A bilaterally deterministic rho-mixing stationary random sequence
[AD-A152856] 17 p3019 N85-28686

The effect of ion-bombardment-induced atomic mixing on depth-profiling of interfaces
[AD-A153199] 17 p3044 N85-28834

Experimental determination of the mixing frequency parameter for coalescence/dispersion modeling of turbulent combustion
[DE85-011488] 19 p3270 N85-30280

Large eddy structures in transitional and turbulent flames
[AD-A154520] 21 p3562 N85-32157

Numerical solution of the Navier-Stokes equations in 3-D internal flows: An emerging capability
21 p3589 N85-

Survey of mixing in metal/insulator systems
[DE85-011838] 23 p3866 N85-347

Holoswitch
[AD-A155841] 24 p4096 N85-

MIXING CIRCUITS

Conversion of microwave signals by superconducting films in the resistive state
[NASA-TM-77595] 01 p0123 N85-

Coherent receiver phase and amplitude alignment circuit
[AD-D011487] 10 p1486 N85-1

Detection of angular modulated electromagnetic signals
[AD-D011563] 12 p1823 N85-214

High-speed digital baseband mixer
16 p2771 N85-271

Switching mixer
[AD-D011602] 16 p2777 N85-271

Communications and logic systems at millimeter wave frequencies, summary 17 p3042 N85-28

Multiport optical detectors 18 p3187 N85-29

MIXING DEPTH

U MIXING HEIGHT

MIXING HEIGHT

Mean maximum mixing heights for northern Asia for the winter of 1978
[DE84-015960] 05 p0672 N85-1431

MIXING LENGTH FLOW THEORY

Model calculations for a CO2 mixing laser with screen nozzle
[ESA-TT-859] 11 p1640 N85-203

Contribution to the theory of stationary separation areas
[NASA-TM-77825] 14 p2300 N85-242

MIXTURES

NT ADMIXTURES
NT AEROSOLS
NT AQUEOUS SOLUTIONS
NT BINARY MIXTURES
NT COLLOIDS
NT DISPERSIONS
NT EMULSIONS
NT EUTECTIC ALLOYS
NT EUTECTICS
NT EXPIRED AIR
NT FOG
NT GAS MIXTURES
NT LIQUID-GAS MIXTURES
NT METAL MATRIX COMPOSITES
NT NUCLEAR EMULSIONS
NT PHOTOGRAPHIC EMULSIONS
NT SIALON
NT SLURRIES
NT SMOKE
NT SOLID SOLUTIONS
NT SOLID SUSPENSIONS
NT SOLUTIONS

Equation of state study for polar fluids
[PB84-222601] 01 p0025 N85-1015

Factor analysis applied to a silane coupling agent on E-glass fiber system
[AD-A145667] 02 p0187 N85-113

Small angle neutron scattering (SANS) on polymer-oligomer mixtures and on deformed polyethylene melts 03 p0432 N85-12

Thermite and Fe/KClO4: Some thermodynamic calculations
[DE84-016845] 04 p0573 N85-13

Pharmacokinetic interactions of mixtures
[AD-P004032] 06 p0844 N85-150

The toxicity of complex mixtures
[AD-P004033] 06 p0844 N85-150

Aspects of solvent toxicity in mixtures
[AD-P004036] 06 p0845 N85-150

Properties of miscible polymer blends
[AD-A147090] 07 p0931 N85-159

Convection heat transfer in the critical region of fluid mixtures
[DE85-002118] 07 p0961 N85-16

Background detection and correction in multicomponent analysis
[AD-A148251] 08 p1212 N85-17

Compressive strength-maturity relationships of mortar containing fly ash
[AD-A148705] 09 p1338 N85-18

User's guide to MIX: A computer code for fitting mixture distributions to data
[DE85-001451] 09 p1369 N85-18

Models for mixture experiments when the response depends on the total amount
[DE85-000370] 09 p1374 N85-18

User's manual for GRIZZLY
[DE85-001405] 11 p1702 N85-20

Influence of pressure on speed of sound in single-phase region of stratifying mixtures 11 p1715 N85-20788
Wavecode constitutive models: Nonhomogeneous mixtures
[DE85-000636] 12 p1796 N85-21278
Process for producing tris s(n-methylamino) methylsilane
[NASA-CASE-MFS-25721-1] 12 p1799 N85-21280
PSA, Renault work on all fuel automobile engine
15 p2531 N85-25604
Modeling the role of radicals in the ignition of and flame propagation in hydrogen-air and methane-air mixtures
16 p2744 N85-26935
Equation of state and two-body correlations for fluids of non-spherical molecules
[AD-A151969] 16 p2783 N85-27174
Application of scattering methods to the studies of the structure of polymer blends
[IFPR-13/1984] 17 p2933 N85-28104
High performance mixed bisimide resins and composites based thereon
[NASA-CASE-ARC-11538-1-SB]
19 p3231 N85-30033
An experimental apparatus to study nucleate pool boiling of R-114 and oil mixtures
[AD-A154077] 19 p3265 N85-30249
Antistarshapedness, dispersiveness and mixtures
[AD-A155583] 21 p3678 N85-32849
Sodium nitrate containing mixture for producing ceramic-glass-ceramic seal by microwave heating
[DE85-011810] 22 p3751 N85-33254
Development of a prototype energy meter
[PB85-199430] 22 p3789 N85-33476
Equation of state study for polar fluids
[PB85-204345] 24 p4076 N85-35262
Nitrogen analysis by chemiluminescence
[AD-A156197] 24 p4083 N85-35308
MLA
U MULTISPECTRAL LINEAR ARRAYS
MMS
U MULTIMISSION MODULAR SPACECRAFT
MNEMONICS
Effects of individual mnemonic characteristics on problem solving 07 p1010 N85-16419
MOBILE COMMUNICATION SYSTEMS
NT LAND MOBILE SATELLITE SERVICE
Defense Meteorological Satellite Program (DMSP)
11 p1711 N85-20766
Spread spectrum mobile radio communications
[AD-A149836] 12 p1829 N85-21477
Concepts and cost trade-offs for land vehicle antennas in satellite mobile communications
[NASA-CR-175731] 15 p2540 N85-25880
Measurement results from a balloon experiment simulating land mobile satellite transmissions
[NASA-CR-175740] 15 p2540 N85-25883
Moon bounce communications to small terminals
[AD-A153297] 17 p2950 N85-28212
Personal mobile communications by satellite
[REPT-15-4572] 18 p3091 N85-29135
Preliminary investigation of the performance of repeater technology for satellite sound broadcasting
[SSP/017/82] 18 p3092 N85-29137
Study of terrestrial mobile systems for personal communications
[MCS-8436] 20 p3441 N85-31357
Pluribus satellite IMP (Interface Message Processors) development mobile access terminal network
[AD-A155754] 24 p4060 N85-35216
MOBILE MISSILE LAUNCHERS
Invited papers: DNA ICBM technical R and D program 09 p1333 N85-18379
MOBILITY
NT CARRIER MOBILITY
NT ELECTRON MOBILITY
NT HOLE MOBILITY
NT IONIC MOBILITY
Diffusion mechanisms and point defects in transition-metal oxides
[DE84-016236] 04 p0571 N85-13639
Electron distribution function and mobility in 3-5 compounds for high and low fields
[AD-A147447] 07 p1048 N85-16658
Grouser effect studies
[AD-P004276] 09 p1406 N85-18854
Mobility of the small combine (track type) on soft ground-relationship between the position of the center of gravity and the mobility
[AD-P004285] 09 p1407 N85-18862
Determination of functional mobility of human nervous system with the PNN-3 instrument
10 p1525 N85-19618
Robotics at Savannah River site: Activity report
[DE85-003657] 11 p1648 N85-20383
Hall mobility in fluid argon
[DE85-007266] 17 p3045 N85-28840
The position and mobility of the shoulder, spinal column and pelvis in seated subjects
[AD-A153751] 18 p3153 N85-29524
Effects of coating rectangular microscopic electrophoresis chamber with methylcellulose
20 p3498 N85-31748
Theoretical prediction of stationary positions in the rectangular chamber during asymmetric electroosmotic flow 20 p3499 N85-31750
Summary electrophoretic data base on human embryonic kidney cell strain 8514
20 p3501 N85-31766
MODAL RESPONSE
The Shock and Vibration Digest, volume 16, no. 8
[AD-A146663] 02 p0208 N85-11372
Hardware and software selection for experimental modal analysis 02 p0208 N85-11373
F-8 refueling boom ground vibration test
[NASA-TM-84914] 07 p0902 N85-15713
Elias Klein memorial lecture: Modal testing, a critical review 09 p1334 N85-18383
The use of analytical models to interpret data properly
[ERS-E.341] 11 p1651 N85-20399
The use of analytical models to interpret measured data properly. 1. General background theory
11 p1651 N85-20400
The use of analytical models to interpret measured data properly. 2. The application to modal analysis of structures 11 p1651 N85-20401
Multishaker modal testing
[NASA-CR-176139] 22 p3800 N85-33544
A model parameter extraction procedure applicable to linear time-invariant dynamic systems
[NASA-CR-176120] 22 p3835 N85-33747
Automated dynamic analytical model improvement for damped structures
[NASA-CR-177945] 23 p3941 N85-34425
MODE (STATISTICS)
Normal mode analysis for linear resistive magnetohydrodynamics
[IPP-6/235] 11 p1730 N85-20878
MODE COUPLING
U COUPLED MODES
MODE OF VIBRATION
U VIBRATION MODE
MODE SHAPES
U MODAL RESPONSE
MODE TRANSFORMERS
Design and construction of a mode converter from rectangular TE 10 to circular TE 11
[REPT-84-158] 05 p0633 N85-14064
Transformation of mode composition of circular optical waveguide 07 p0950 N85-16023
High power millimeter-wave mode converters in overmoded circular waveguides using periodic wall perturbations
[IPF-84-6] 09 p1395 N85-18780
Design of mode converters from TE circular om modes in circular waveguides to TE rectangular mo modes in rectangular waveguides for high power applications in the frequency range 1 to 30 GHz
[IPF-84-7] 09 p1395 N85-18781
MODELS
NT AIRCRAFT MODELS
NT ANALOG SIMULATION
NT ASTRONOMICAL MODELS
NT ATMOSPHERIC MODELS
NT BIOLOGICAL MODELS (MATHEMATICS)
NT BREADBOARD MODELS
NT DENSITY WAVE MODEL
NT DIGITAL SIMULATION
NT DYNAMIC MODELS
NT ENVIRONMENT MODELS
NT HYDROLOGY MODELS
NT MATHEMATICAL MODELS
NT NUCLEAR MODELS
NT OCEAN MODELS
NT REFERENCE ATMOSPHERES
NT SCALE MODELS
NT SPACECRAFT MODELS
NT STELLAR MODELS
NT THOMAS-FERMI MODEL
NT WIND TUNNEL MODELS
Development of the Antares electron gun
[DE84-014043] 01 p0053 N85-10352
Retardation analytical model to extend service life
[NASA-CR-171177] 01 p0057 N85-10376
Effects of surface chemistry on hot corrosion life: Overview 02 p0145 N85-10980
Simulation study of a new inverse-pinch high Coulomb transfer switch
[NASA-CR-172420] 02 p0194 N85-11294
Evaluation of an aerosol prediction model for coastal regions using marine aerosol generation and transport data
[AD-A145443] 02 p0231 N85-11510
SMP: A solid modeling program
[NASA-CR-172473] 02 p0241 N85-11570
Models of natural intelligence in fault diagnosis tasks: Implications for training and aiding of maintenance personnel
[AD-P003927] 02 p0246 N85-11607
A generalized model of fault-isolation performance
[AD-P003928] 02 p0246 N85-11608
Estimation in nonlinear time series model II: Some nonstationary series
[AD-A145709] 02 p0255 N85-11669
Numerical investigation of diffraction models of microwave integrated circuits 03 p0347 N85-12233
A topological approach to database theory
03 p0437 N85-12781
Digital elevation models improve processing of Alaskan gravity data 04 p0515 N85-13285
Resonance model of Pc3 in subtropical regions --- geomagnetism 04 p0520 N85-13323
Models of angular momentum input to a circumterrestrial swarm from encounters with heliocentric planetesimals
04 p0587 N85-13750
Mechanical models of close approaches and collisions of large protoplanets 04 p0588 N85-13756
Analytical modeling of spacecraft power systems
05 p0610 N85-13897
Modelling the aerodynamics in a system of continuous channels and experimentation procedure
[BLL-M-35923-(5828.4)] 05 p0634 N85-14067
Mental models of invisible logical networks
05 p0706 N85-14544
On looking into the black box: Prospects and limits in the search for mental models 05 p0709 N85-14546
A comparison of evaporation duct models for IREPS (Integrated Refractive Effects Prediction System)
[AD-A146471] 06 p0799 N85-15103
A hydrogen partitioning model for hydrogen assisted crack growth
[AD-A147365] 07 p0978 N85-16214
General model of earthquakes and the place of warnings in it 07 p0981 N85-16232
Model of team organization and behavior and team description method
[AD-A147540] 07 p1053 N85-16680
Ballistic/detonic transition of propellants
08 p1117 N85-17041
Depositional modeling of tetrahedrite in the Coeur d'Alene district, Idaho 08 p1182 N85-17448
Crystalline structure of urea ice sheets used in modeling experiments in the CRREL test basin
[AD-A148434] 08 p1226 N85-17722
Designing off-road vehicles with good ride behaviour
[AD-P004267] 09 p1405 N85-18843
A decision model for selection of microcomputers and operating systems
[AD-A149076] 10 p1536 N85-19694
LSS 2018: A double-lined spectroscopic binary central star with an extremely large reflection effect
[NASA-CR-175503] 11 p1762 N85-21082
A study of transonic flutter of a two-dimensional airfoil using the U-g and p-k methods
[LR-615] 12 p1771 N85-21121
Modeling of transient heat pipe operation
[NASA-CR-175496] 12 p1844 N85-21571
Flow measurement by laser Doppler anemometry in a nuclear fuel assembly
[DE85-003260] 12 p1848 N85-21592
Evaluation of complex terrain air quality simulation models
[PB85-119485] 12 p1866 N85-21836
Protons with energies above 30 KeV in Earth's radiation belt at low altitudes during magnetically quiet time close to geomagnetic equator 13 p1980 N85-22423
Auroral-polar cap environment and its impact on spacecraft plasma interactions 13 p1991 N85-22484
Three-dimensional calculation of shuttle charging in polar orbit 13 p1992 N85-22486
Acoustic energy balance method
13 p2000 N85-22537
Measurement requirements for the detection of ozone trends 13 p2105 N85-23115
Study of resolution of deep MT soundings by means of physical model 13 p2112 N85-23155
LEXICON: A structured modeling system for optimization
[AD-A150536] 13 p2147 N85-23329
Monte Carlo modeling of lunar megaregolith development 13 p2197 N85-23627
Analyses of radar images of small craters
13 p2199 N85-23642
Terrestrial analogs for planetary wrinkle ridges
13 p2199 N85-23644
Mixing, chemical reaction and flow field development in ducted rockets
[DE85-004063] 14 p2247 N85-23926

A model for the compressive buckling of extended chain polymers [AD-A151025] 14 p2280 N85-24008

Thermocouple modeling [DE85-005172] 14 p2306 N85-24273

The retrieval expert model of information retrieval 14 p2433 N85-25003

Near-nucleus studies of Comet Halley 14 p2435 N85-25016

Temperature, velocity, and species mapping in an induction plasma [DE85-004005] 15 p2512 N85-25499

Heavy doping effects in high efficiency silicon solar cells [NASA-CR-175661] 15 p2586 N85-25940

Management communication and financial modeling 15 p2627 N85-26190

Harnessing computional powe. Distributed combinator reduction [DE85-005867] 15 p2631 N85-26216

Feasibility analysis of moving bank multiple model adaptive estimation and control algorithms [AD-A152015] 15 p2641 N85-26292

SU(N,1) inflation [DE85-003652] 15 p2669 N85-26469

Study of longitudinal landing flying qualities evaluation using pilot model theory [AD-A152194] 16 p2706 N85-26702

Metal armatures for railguns [AD-A152129] 16 p2728 N85-26836

Model reduction techniques applied to the control of large space structures [AD-A151784] 16 p2731 N85-26857

Liquid rocket combustor computer code development 16 p2740 N85-26910

Laser Schlieren and ultraviolet diagnostics of rocket combustion 16 p2740 N85-26911

Mechanical properties of high performance carbon fibers 16 p2742 N85-26922

Optical best arc RMS test results 16 p2804 N85-27290

The selection of the starting field: General versus tailored model 16 p2805 N85-27294

A wind-bivane/microprocessor system for on-line prediction and display of pollutant distributions 16 p2830 N85-27449

A multipole model of the observed cerebral cortex magnetic field [AD-A152237] 16 p2842 N85-27526

A general purpose scatter storage subsystem and a comparison of hashing methods [NASA-CR-175814] 16 p2845 N85-27542

Multivariable statistical modelling and its application 16 p2857 N85-27617

Airport and airway system cost allocation model. Volume 7: User's manual [AD-A152877] 17 p2906 N85-27917

Composite loads spectra for select space propulsion structural components 17 p2912 N85-27953

One-dimensional velocity-depth functions determined for the Arabian Shield and the southwestern Red Sea: A comparison of models 17 p2992 N85-28490

The definition and computation of a metric on plane curves. The meaning of a face on a geometric model 17 p3004 N85-28571

Improving the effectiveness of integral property calculation in a CSG solid modeling system by exploiting predictability 17 p3006 N85-28586

Generation and display apparatus [AD-D011639] 17 p3008 N85-28599

The design of megawatt gyrotrons [DE85-007992] 17 p3032 N85-28754

Experimental methods of heavy quark detection [DE85-006316] 17 p3036 N85-28781

Mockups and human productivity studies 18 p3159 N85-29570

The fabrication, microstructure, and strengthening behavior of heavily cold-worked in situ composites 19 p3231 N85-30031

Pressure recovery in a cylindrical heat pipe at high radial Reynolds numbers and at high Mach numbers [DE85-010718] 19 p3269 N85-30274

Optimization of single and multi-component analytical techniques [HSE-TRANS-10967] 19 p3347 N85-30744

Experimental level-structure determination in odd-odd actinide nuclei [DE85-010476] 19 p3360 N85-30835

Primordial inflation and supergravity [DE85-009536] 19 p3383 N85-30989

Venus thermospheric circulation [PB85-180420] 19 p3384 N85-30997

An overview of latest model reduction and control methods of large flexible space structures 20 p3414 N85-31191

New adatom model for Si(111) 7X7 and Si(111)Ge 5X5 reconstructed surfaces 20 p3480 N85-31625

Modeling of chemical transformations of SO(x) and NO(x) in the polluted atmosphere: An overview of approaches and current status [PB85-173169] 20 p3487 N85-31677

MPS solidification model. Analysis and calculation of macrosegregation in a casting ingot [NASA-CR-171589] 21 p3566 N85-32178

Numerical modeling of subsurface communication [DE85-012818] 21 p3577 N85-32249

Numerical solutions of turbulent models for flow over a flat plate with angle of attack [DE85-010360] 21 p3585 N85-32286

A modified Fresnel scattering model for the parameterization of Fresnel returns, part 2.3A 21 p3618 N85-32483

Review of the psychological issues relating to the effectiveness of structured programming [AD-A154593] 21 p3665 N85-32766

On the dependence of the convergence of Gummel's algorithm on the regularity of the solution [AD-A154628] 21 p3675 N85-32832

Cosmic ray He3 measurements [OG-4.2-3] 21 p3714 N85-33045

Sandia Cooperative Group on the Aerothermochemistry of Turbulent Combustion. Discussion record of the second meeting [DE85-007493] 22 p3743 N85-33203

Second order modelling in non-constant density flows 22 p3744 N85-33206

Jet flows: Modelling and experiments 22 p3744 N85-33208

A model for predicting propagation-related DSCS (Defense Communications Engineering Center) margin requirements [AD-A155355] 22 p3756 N85-33281

Development of a chemical kinetic mechanism for the US EPA (Environmental Protection Agency) regional oxidant model [PB85-185858] 22 p3813 N85-33618

Modeling of auto exhaust smog chamber data for EKMA development [PB85-186492] 22 p3813 N85-33619

Model building and practical aspects of nonlinear programming [AD-A155720] 22 p3829 N85-33711

Role of ECRH in potential formation for tandem mirrors [DE85-011859] 22 p3848 N85-33834

Models of planetary structure and evolution: The case of Io 22 p3855 N85-33874

On galactic origin of cosmic rays with energy up to 10(19) eV [OG-5.4-15] 22 p3887 N85-34091

Halo of NGC 4631 and models of cosmic-ray transport [OG-6.2-3] 22 p3889 N85-34103

Detonation in tungsten-loaded HMX [DE85-009606] 23 p3922 N85-34299

Mathematical modeling of ultimate heat sink cooling ponds [TI85-009747] 23 p3932 N85-34369

The impact of supercomputers on experimentation: A view from a national laboratory [NASA-TM-86822] 23 p3955 N85-34510

Spatial trees: A fast access method for unstructured graphical data 23 p3958 N85-34533

3D computer animation: More an evolution problem than a motion problem 23 p3959 N85-34536

Using dynamic analysis to animate articulated bodies such as humans and robots 23 p3959 N85-34537

Simulation studies on stability of hot electron plasma 23 p3978 N85-34664

Perspective on the next ten years in plasma physics [DE85-011849] 23 p3984 N85-34706

The influence of nonstationarity of the solar activity and general solar field on modulation of cosmic rays [SH-4.2-17] 23 p4006 N85-34854

Spatial distribution of cosmic rays in magnetic cycles of the Sun [SH-4.2-20] 23 p4009 N85-34867

Diurnal anisotropy during solar activity cycle twenty and diffusion-convection model [SH-4.5-7] 23 p4036 N85-35025

FAA requirements for model to support capacity, delay, noise and energy programs [AD-A155815] 24 p4063 N85-35179

Elliptical X-ray analyzer spectrograph application to a laser-produced plasma [DE85-013790] 24 p4097 N85-35396

Linear absorption and scattering of laser beams [AD-A156167] 24 p4098 N85-35401

Investment justification of robotic technology in aerospace manufacturing. User's manual [AD-A156193] 24 p4099 N85-35410

Expert systems research in regional resource evaluation: Experiences in the application of microcomputer technologies 24 p4105 N85-[illegible]

The development of assessment techniques program 24 p4106 N85-[illegible]

Comparative analysis of operational forecasts versus actual weather conditions in airline flight planning, volume 2 [NASA-CR-167863] 24 p4119 N85-[illegible]

Comparative analysis of operational forecasts versus actual weather conditions in airline flight planning: Summary report [NASA-CR-167866] 24 p4120 N85-[illegible]

On-line model driven control of the SLC electron Damping Ring [DE85-013377] 24 p4157 N85-[illegible]

Circumstellar shells of late-type stars: A study at millimeter and infrared wavelengths 24 p4167 N85-[illegible]

Gamma-hadron families and scaling violation [HE-3.4-7] 24 p4182 N85-[illegible]

On the halo events observed by Mount Fuji and Mount Kanbala Emulsion Chamber Experiments [HE-3.4-9] 24 p4182 N85-[illegible]

Multidimensional analysis of data obtained in experiments with X-ray emulsion chambers and extensive air showers [HE-3.6-2] 24 p4184 N85-[illegible]

Experimental basis for the models of cascade propagation in atmosphere [HE-3.6-6] 24 p4185 N85-[illegible]

Relation between gamma-ray family and EAS core: Monte-Carlo simulation of EAS core [HE-3.6-7] 24 p4185 N85-[illegible]

A comparative analysis of gamma and hadron families at the superhigh energies recorded in experiment Pamir [HE-3.7-1] 24 p4185 N85-[illegible]

Electrons, muons and hadrons in extensive air showers and how do they depend on nuclear interaction model, part 2 24 p4187 N85-[illegible]

The maximum depth of shower with E sub 0 larger than 10(17) eV on average characteristics of EAS different components 24 p4188 N85-[illegible]

Sensitivity of depth of maximum and absorption depth of EAS to hadron production mechanism 24 p4188 N85-[illegible]

The capability of the existing network of installations for detecting the antineutrino burst from collapsing stars [HE-5.3-13] 24 p4206 N85-36107

A search for cosmic sources of high energy neutrinos with small underground detectors [HE-5.3-16] 24 p4206 N85-36110

MODEMS

Adaptive signal processing for radio communications 10 p1473 N85-19895

Fast synchronization model for UHF spread-spectrum communication system 10 p1473 N85-19896

A modem with pseudo-orthoganal codes: Experimental results 10 p1474 N85-19902

Error correction coding for a self-adaptive modem: Theoretical and experimental results 10 p1474 N85-19903

A microprocessor controlled parallel model with FDPSK 10 p1475 N85-19904

Serial data transmission with large output on the HF channel 10 p1475 N85-19905

Comparative architectures for a multiple function speech processor [AD-A150873] 14 p2292 N85-24211

MODERATION (ENERGY ABSORPTION)

NT THERMALIZATION (ENERGY ABSORPTION)

MODERATORS

Radiation damage experiments and lifetime estimates for beryllium components in fusion systems [DE85-008036] 17 p3040 N85-28811

MODES

NT AXIAL MODES
NT BALLOONING MODES
NT COUPLED MODES
NT FAILURE MODES
NT LASER MODES
NT MODES (STANDING WAVES)
NT PROPAGATION MODES
NT PUSHBROOM SENSOR MODES
NT VIBRATION MODE

Resonant frequencies and mode shapes for single and double cylindrical shells [AD-A144778] 01 p0062 N85-10408

MHD instabilities in simple plasma configuration [AD-A144936] 01 p0121 N85-10820

Influence of mode noise suppression in multimode fiber optic light guides 03 p0348 N85-12242

Normal mode initialization 05 p0680 N85-14372

Buildup of oscillations in two-mode gyrotron 06 p0766 N85-15037

Nonlocal and nonlinear effects on solar oscillations
09 p1416 N85-18934
Calculation of mode field in electron beam welding of VT6 titanium alloy
10 p1449 N85-19129
The effects of internal waves on acoustic normal modes
[AD-A150235] 13 p2155 N85-23379
Development and application of a unified balancing approach with multiple constraints
16 p2737 N85-26891
Miniature two-mode filters 22 p3775 N85-33394

MODES (STANDING WAVES)
Implications of observed frequencies of solar P modes
14 p2443 N85-25073
The vertical structure of global rotational normal modes
18 p3144 N85-29464

MODIFICATION
U REVISIONS

MODULAR RATIOS
Modular photovoltaic array field
[SAND-83-7028] 02 p0222 N85-11454

MODULARITY
Modular design, versatility of robots viewed
14 p2284 N85-24155
A modular dissimilar redundant computer designed for high integrity control 17 p2904 N85-27904

MODULATED CONTINUOUS RADIATION
Dynamics of growth of surface periodic structures when intense light acts on condensed media
02 p0268 N85-11748

MODULATION
NT AMPLITUDE MODULATION
NT FREQUENCY MODULATION
NT FREQUENCY SHIFT KEYING
NT INTERMODULATION
NT LIGHT MODULATION
NT PHASE MODULATION
NT PHASE SHIFT KEYING
NT PULSE AMPLITUDE MODULATION
NT PULSE CODE MODULATION
NT PULSE DURATION MODULATION
NT PULSE FREQUENCY MODULATION
NT PULSE MODULATION
NT PULSE POSITION MODULATION
NT PULSE TIME MODULATION
NT TRAVELING WAVE MODULATION
NT ULTRASONIC LIGHT MODULATION
NT VELOCITY MODULATION
Investigation of several aspects of LANDSAT 4/5 data quality
[E85-10038] 04 p0525 N85-13357
Reduction of signal modulation caused by polarization in visible optical scanning systems
[AD-D011369] 07 p1042 N85-16620
Noise jammer discrimination by noise modulation bandwidth
[AD-D011473] 10 p1468 N85-19264
Infrared modulation of photoluminescence in glow discharge amorphous silicon
[DE85-016993] 11 p1737 N85-20922
Fundamental limits to synchronization and tracking
[AD-A149623] 12 p1833 N85-21504
Generation of longitudinal acoustic waves by modulated helicon waves — nonlinear steady state waves in metals
13 p2090 N85-23049
Modulation of light energy transduction in photosynthesis
[DE85-004711] 13 p2141 N85-23292
Rational pulse-shaping filters for almost MSK-like modulation
[AD-A153065] 17 p2949 N85-26208
Moon bounce communications to small terminals
[AD-A153297] 17 p2950 N85-26212
Cosmic ray modulation and turbulent interaction regions near 11 AU
[NASA-TM-86193] 18 p3209 N85-29909
Modulated voltage metastable ionization detector
[NASA-CASE-ARC-11503-1] 23 p3933 N85-34374
Longitudinal distribution of cosmic rays in the heliosphere
[SH-4.1-14] 23 p4006 N85-34837
Effects of solar magnetic field on cosmic rays
[SH-4.2-12] 23 p4006 N85-34850
The influence of nonstationarity of the solar activity and general solar field on modulation of cosmic rays
[SH-4.2-17] 23 p4008 N85-34854
The effect of the neutral sheet structure of the interplanetary magnetic field on cosmic ray distribution in space
[SH-4.2-18] 23 p4008 N85-34855
On the influence of the heliomagnetospheric periphery on the galactic cosmic rays
[SH-4.2-19] 23 p4009 N85-34856
Spatial distribution of cosmic rays in magnetic cycles of the Sun
[SH-4.2-20] 23 p4009 N85-34857
11- and 22-year variations of the cosmic ray density and of the solar wind speed
[SH-4.2-21] 23 p4009 N85-34858
The dependence of solar modulation on the sign of the cosmic ray particle charge
[SH-4.2-23] 23 p4009 N85-34860
An update on the correlation between the cosmic radiation intensity and the geomagnetic AA index
[SH-4.2-24] 23 p4009 N85-34861
Long-term modulation of cosmic rays during solar cycle 21
[SH-4.4-10] 23 p4034 N85-35008
Role of solar flare index in long term modulation of cosmic ray intensity
[SH-4.4-12] 23 p4034 N85-35009
A study of periodicities and recurrences in solar activity and cosmic ray modulation
[SH-4.4-14] 23 p4034 N85-35010

MODULATION TRANSFER FUNCTION
The spectral distribution of field components for a sinusoidal power modulated monofrequency optical carrier source
[FI-44-TBR-94] 04 p0585 N85-13601
Spaceborne receivers: Basic principles
[NASA-CR-174269] 07 p0946 N85-15990
LANDSAT-4 Thematic Mapper Modulation Transfer Function (MFT) evaluation — California and New Mexico
[E85-10055] 07 p0964 N85-16250
Modulation Transfer Function (MTF) measurement techniques for lenses and linear detector arrays
[NASA-TM-86168] 10 p1556 N85-19812
Infrared material optical damage by rain
[AD-P004372] 12 p1827 N85-21466
MTF analysis of LANDSAT-4 Thematic Mapper
12 p1871 N85-21737
An investigation of several aspects of LANDSAT-5 data quality — Palmer County, Shelby, mt; White sands, NM; Great Salt Lake, UT; San Matted Bridge and Sacramento, California
[E85-10096] 13 p2122 N85-23214
Modulation transfer function for two-point and periodic objects using Gaussian and Lorentzian resolution functions
[PB85-187557] 19 p3368 N85-30691

MODULATORS
NT MODEMS
Frequency shifting in multimode fiber optic phase modulation devices 03 p0347 N85-12239
Advanced infrared laser modulator development
[NASA-CR-172479] 06 p0862 N85-15479
Multichannel electrooptical modulators for digital information storage and processing systems
07 p0950 N85-16021
Miniature high performance pulsed modulator apparatus
[AD-D011427] 08 p1158 N85-17310
Battery charger
[AD-D011420] 08 p1178 N85-17425
Multiplex gas chromatography for use in space craft
[NASA-TM-86668] 09 p1290 N85-18097
An electro-optic spatial light modulator for thermo-elastic generation of programmably focused ultrasound
[AD-A149078] 10 p1553 N85-19794
Development of a 20 GHz modulator for the payload of a satellite for propagation and transmission experiments, including the required converters of the test equipment
[BMFT-FB-W-84-044] 11 p1590 N85-20004
Detection of angular modulated electromagnetic signals
[AD-D011563] 12 p1823 N85-21437
An electro-optic spatial light modulator for thermoelastic generation of programmably focused ultrasound
[AD-A152066] 15 p2646 N85-26323
Spatial light modulator having a capacitively coupled photoconductor
[AD-D011646] 17 p3037 N85-28790
Optical modulators and bistable devices using molecular gases 18 p3186 N85-29761
Stokes parameters modulator for birefringent filters
18 p3205 N85-29884
SLC Energy Upgrade Program at SLAC
[DE85-014290] 24 p4160 N85-35790

MODULATORS-DEMODULATORS
U MODEMS

MODULES
NT CHEMICAL RELEASE MODULES
NT ELECTRONIC MODULES
NT SPACECRAFT MODULES
Modular detonator device
[AD-D011232] 03 p0340 N85-12184
Thermal characterization of photovoltaic modules in natural environments 06 p0832 N85-15296
Demonstration of transparent solar array module design
[NASA-CR-174257] 07 p0992 N85-16302
Application of large eddy interaction model to channel flow
[NASA-TM-86691] 12 p1844 N85-21572
Test results of an organic Rankine-cycle power module for a small community solar thermal power experiment
[NASA-CR-175696] 14 p2350 N85-24524
Intermediate load modules for test and evaluation
[NASA-CR-175697] 14 p2350 N85-24526
On localization of injective modules
[CSIR-TWISK-342] 14 p2413 N85-24878
Module performance and failure analysis area: Flat-plate solar array project
[NASA-CR-175689] 15 p2565 N85-25936
Operating characteristics of a 0.87 kW-hr flywheel energy storage module
[NASA-TM-87036] 17 p2974 N85-28371
CAMAC 488 module: 68000 based GPIB interface module
[DE85-009367] 17 p3014 N85-28635

MODULUS OF ELASTICITY
NT DYNAMIC MODULUS OF ELASTICITY
The theory of elastic modulus of fabric composites and its examination by experiments
[NAL-TR-806] 01 p0022 N85-10133
Detection of hydrogen assisted crack growth by measurement of modulus changes and acoustic emission
[DE84-015752] 02 p0184 N85-11236
Effective moduli of elasticity of unidirectional fibrous composite 02 p0265 N85-11733
Evaluation of moduli and thicknesses of pavement systems by spectral-analysis-of-surface-waves method
[PB84-219112] 03 p0342 N85-12205
Transformation toughened ceramics for the heavy duty diesel engine technology program
[NASA-CR-174669] 07 p1055 N85-16696
Solid Rocket Motor Case (SRMC) dynamic sensitivity to changes in composite properties
12 p1948 N85-22238
Development and study of two-matrix glass fiber composite with increased transverse deformation
13 p2027 N85-22700
Fracture mechanics evaluation of GaAs
[NASA-CR-175657] 13 p2102 N85-23101
High resistance and raised modulus carbon fibers
[NASA-TM-76684] 15 p2502 N85-25436
Compressive strength of epoxy resin chocks subjected to elevated temperatures
[AD-A152018] 15 p2519 N85-25532
Natural vibrations of reinforced spherical shells
17 p2943 N85-28165
A concept for the intrinsic dielectric strength of electrical insulation materials
[NASA-CR-176040] 20 p3448 N85-31410
Rolling, slip and traction measurements on low modulus materials
[NASA-CR-174909] 22 p3791 N85-33491
Effects of temperature on the tensile strength and elastic modulus of composite material
[AD-A156112] 24 p4075 N85-35251

MOHAWK AIRCRAFT
U OV-1 AIRCRAFT

MOHR CIRCLES
U FRACTURE MECHANICS

MOIRE EFFECTS
A comparison of electronic heterodyne moire deflectometry and electronic heterodyne holographic interferometry for flow measurements
[NASA-TM-87071] 21 p3586 N85-32302

MOIRE FRINGES
Holographic FLI for detection of defects
[AD-A148339] 08 p1164 N85-17345
Influence of error of determination of moire isotach orders on the stability of their approximation
[BLL-M-36277-(5828.4)] 20 p3450 N85-31423
Modular digital holographic fringe data processing system
[NASA-CR-177952] 23 p3933 N85-34376
Experiments and discussions on the analysis of interferograms with closed-loop fringes
[NPL-MOM-68] 23 p3956 N85-34515

MOIRE INTERFEROMETRY
Holographic FLI for detection of defects
[AD-A148339] 08 p1164 N85-17345
Moire interferometric measurement of relative displacements in dovetail joints
[OUEL-1563/85] 20 p3471 N85-31566
Experiments and discussions on the analysis of interferograms with closed-loop fringes
[NPL-MOM-68] 23 p3956 N85-34515

MOISTURE
NT SOIL MOISTURE
Experimental and theoretical studies of moisture and temperature effects on the mechanical properties of graphite/epoxy laminates and neat resins
04 p0467 N85-12969

Thermal properties of soils and soils testing
[DE84-015312] 04 p0525 N85-13360
An evaluation and comparison of vertical profile data from the VISSR Atmospheric Sounder (VAS)
[NASA-TP-2425] 07 p1000 N85-16351
Thermal stress-dependent dilation of concrete
[DE84-014688] 11 p1653 N85-20412
The evolution of CO2 on Mars
13 p2185 N85-23558
Wave motion of three-component medium under load moving on plane boundary 14 p2277 N85-24105
Experimental study of the effect of moist environments on epoxy resin chocks
[AD-A152052] 15 p2568 N85-25849
Bound and free moisture studies of solid materials by FTNMR
[DE85-003227] 16 p2747 N85-26952
In situ microwave measurements of dielectric properties and moisture in materials
[DE85-003622] 16 p2747 N85-26953
Trace water sensor
[NASA-CASE-NPO-15722-1] 18 p3103 N85-29212
Flight-service program for advanced composite rudders on transport aircraft
[NASA-CR-174537] 19 p3217 N85-29950
Metabolic mechanisms of plant growth at low water potentials 19 p3327 N85-30612
Upgrading auxiliary facility outleakage and combustion detection
[DE85-012796] 23 p3934 N85-34388

MOISTURE CONTENT
NT ATMOSPHERIC MOISTURE
Surface soil moisture measurements of the White Sands, New Mexico
[NOAA-TM-NESDIS-7] 02 p0219 N85-11441
Determination of the conservation state of long conservation agricultural products by means of capacitive sensors
[NOTA-INTERNA-799] 02 p0220 N85-11447
Operational test of three instruments for measuring liquid water content in laboratory and from aircraft
[DFVLR-MITT-84-08] 03 p0397 N85-12531
The areal pattern of latent and sensible heat fluxes: The combination of soil physics and remotely sensed data 05 p0656 N85-14213
Apparatus for determining the liquid water content of a gas
[AD-D011297] 07 p0922 N85-15839
Effects of low temperatures on the growth and unfrozen water content of an aquatic plant
[AD-A147107] 07 p1011 N85-16424
The effects of soil moisture on bistatic clutter power
[AD-A147636] 08 p1150 N85-17261
LX-10 and LX-17 moisture content and release
[DE84-016579] 09 p1301 N85-18173
Development and evaluation of a procedure for the rapid analysis of fresh concrete
[AD-A149741] 12 p1666 N85-21703
Human lung fluid content during 7-day head-down tilt
12 p1902 N85-21941
Effect of moisture in inert gases on density of seam metal and on mechanical characteristics of welded joints of aluminum and aluminum alloys
13 p2034 N85-22744
Dependence of combustion of homogeneous kerosene-air mixtures on humidity of air
13 p2051 N85-22835
Distribution of snow and maximum snow water equivalent obtained by LANDSAT data and degree day method 13 p2124 N85-23229
Microwave radiometer observations of snowpack properties and comparison of U.S. Japanese results — Hokkaido, Japan and Vermont and North Dakota test sites 13 p2125 N85-23230
Studies on physical properties of snow based on multi channel microwave radiometer
13 p2125 N85-23231
Determination of electromagnetic properties of mesh material using advanced radiometer techniques
14 p2235 N85-23655
Measurement of water equivalent of mountain snow cover — ARGOS system 14 p2327 N85-24386
Determination of total moisture content in cloud-free atmosphere by relative radio emission measurements
14 p2340 N85-24472
Determining atmosphere moisture content from differences in two-frequency microwave radiation measurements 14 p2341 N85-24474
High-frequency microwave observations of convective precipitation 15 p2596 N85-26000
Recent VAS imaging/sounding research
15 p2597 N85-26004
Impact of soil moisture in organizing a severe storm outbreak 15 p2597 N85-26009
Luminescence probe studies of ionomers. 2. Steady-state measurements from sulfonated polyethylene and teflon membranes
[AD-A152233] 16 p2755 N85-27000
Moisture content and gas sampling device
[NASA-CASE-MSC-18866-1] 18 p3103 N85-29213
Aerospace technology determines forest-fire danger
19 p3295 N85-30427
Fiber optic moisture sensor
[DE85-011651] 22 p3787 N85-33462
Effect of substrate moisture on growth and structure of corn leaf 22 p3624 N85-33692
Instrumentation for sensing moisture content of material using a transient thermal pulse
[NASA-CASE-NPO-15493-2] 23 p3933 N85-34373

MOISTURE DETECTORS
U MOISTURE METERS

MOISTURE METERS
NT HYGROMETERS
Determination of the conservation state of long conservation agricultural products by means of capacitive sensors
[NOTA-INTERNA-799] 02 p0220 N85-11447
Operational test of three instruments for measuring liquid water content in laboratory and from aircraft
[DFVLR-MITT-84-08] 03 p0397 N85-12531
Microstrip antenna for multichannel radiometer
06 p0791 N85-15056
Fiber optic moisture sensor
[DE85-011651] 22 p3787 N85-33462
Instrumentation for sensing moisture content of material using a transient thermal pulse
[NASA-CASE-NPO-15493-2] 23 p3933 N85-34373

MOISTURE RESISTANCE
The water vapor resistances of some clothing assemblies used by flying personnel of the Swedish Armed Forces: A series of model studies
[FOA-C-59011-H1] 02 p0238 N85-11551
Process for improving moisture resistance of epoxy resins by addition of chromium ions
[NASA-CASE-LAR-13226-1] 23 p3919 N85-34282

MOJAVE DESERT (CA)
Visibility monitoring in the southern California desert for the Department of Defense: Research on operations-limiting visual extinction, RESOLVE protocol
[AD-A146617] 06 p0835 N85-15315

MOL (ORBITAL LABORATORIES)
U MANNED ORBITAL LABORATORIES

MOLDING MATERIALS
Sealing ceramic material in low melting point glass
[NASA-TM-77599] 01 p0031 N85-10190
General studies on composite materials. Evaluation of auxiliary products of national origin
[SNIAS-2500/DCI-PR/84] 03 p0326 N85-12101
Review of the mechanical properties of SMC and GRP materials
[NPL-DMA(A)-88] 08 p1131 N85-17128
Exploratory development of foams from liquid crystal polymers
[NASA-CR-172510] 13 p2036 N85-22754
New material, process spins off from Volvo LCP 2000 program 15 p2536 N85-25646

MOLDS
Sintered silicon carbide molded body and method for its production
[NASA-TM-77646] 14 p2259 N85-23999
Method and apparatus for casting conductive and semi-conductive materials
[DE85-011655] 22 p3792 N85-33494

MOLECULAR ABSORPTION
Middle Atmosphere Program. Handbook for MAP, volume 8
[NASA-CR-175478] 11 p1657 N85-20445
MSG-7: Molecular absorption processes related to the penetration of ultraviolet solar radiation into the middle atmosphere 11 p1658 N85-20449
Absorption of ozone molecules in strong field of tea CO2 injection laser 11 p1718 N85-20808
Carbon monoxide adsorption on a platinum electrode studied by polarization modulated FT-IRRAS (Fourier Transform-IR Reflections Adsorption Spectroscopy). Part 1: CO adsorbed in the double layer potential region and its oxidation in acids
[AD-A149751] 12 p1800 N85-21288

MOLECULAR BEAM EPITAXY
Silicon sheet with molecular beam epitaxy for high efficiency solar cells
[NASA-CR-174022] 02 p0222 N85-11459
Pulsed irradiation of optimized, MBE grown, AlGaAs/GaAs radiation hardened photodiodes
[DE84-014984] 04 p0569 N85-13831
High-efficiency silicon solar cell research
06 p0829 N85-15261
MBE growth for high-efficiency silicon solar cells
06 p0829 N85-15265
Strained-layer superlattice emitter and detector structures using modulation-doped active regions
[DE85-000064] 06 p0867 N85-15511
Development of short gate FET's
[AD-A147033] 07 p0947 N85-15889
Aluminum nitride insulator for 3-5 MIS (Metal-Insulator-Semiconductor) applications
[AD-A147842] 07 p1049 N85-16662
Gallium arsenide/AlGaAs multilayer structures with special doping profiles for microwave and optoelectronic devices
[BMFT-FB-T-84-207] 08 p1227 N85-17725
Some investigations of molecular beam epitaxial growth of 3-5 semiconductor films via Monte-Carlo computer simulations, carrier tunneling and spectroscopic ellipsometry
[AD-A149465] 10 p1563 N85-19854
Characterization of high purity Si-doped molecular beam epitaxial GaAs
[AD-A149651] 12 p1939 N85-22181
AlN insulator for 3-5 MIS applications
[AD-A150674] 14 p2426 N85-24982
Producible alternative to CdTe for epitaxy (PACE-2) of LWIR (Long Wave Infrared) HgCdTe
[AD-A150678] 14 p2426 N85-24984
Investigation of the MBE growth of InSb and novel quantum well structures
[AD-A151014] 14 p2427 N85-24989
Fabrication and I-V characterization of AlGaAs/GaAs MODFETs with P-type surface layers grown by molecular beam epitaxy
[AD-A151695] 15 p2680 N85-26415
A study of Ga(.47)In(.53)As and Al(.48)In(.52)As for very high frequency device applications
[AD-A151995] 16 p2870 N85-27708
TEM investigation of polar-on-nonpolar epitaxy: GaAs-AlGaAs on (100) Ge
[DE85-007613] 16 p2871 N85-27714
Communications and logic systems at millimeter wave frequencies, summary 17 p3042 N85-28825
Leading-edge microelectronics research at Sweden's Chalmers 20 p3438 N85-31337
Determination of kinetic parameters of molecular beam epitaxy
[AD-A155222] 21 p3710 N85-33030
Sixty GHz IMPATT diode development
[NASA-CR-174969] 22 p3758 N85-33293
Investigations of the molecular beam epitaxial growth and characteristics of external excitation induced non-equilibrium phases of immiscible 3-5 compound semiconductors
[AD-A156325] 24 p4162 N85-35804

MOLECULAR BEAMS
Molecular beam scattering 03 p0417 N85-12666
Instrumentation for particle-beams research using laser excited merging beams
[AD-A147968] 08 p1220 N85-17681
Hyperfine structure and lifetime measurements on electronically excited long-life molecules in a beam experiment
[MPIS-11/1984] 11 p1726 N85-20865
Measurements of integral yields of charged secondary particles using neutral beams simulating a cometary fly-by — Giotto mission 14 p2244 N85-23960
Development of an apparatus for obtaining molecular beams in the energy range from 2 to 200 eV
[NASA-TM-77835] 15 p2647 N85-26326
TEM combined with Al/sub x/Ga/sub 1-x/ as marker layers as a technique for the study of GaAs MBE growth
[DE85-008451] 18 p3194 N85-29863
Measurement of combustion species by electron impact fluorescence
[DE85-011163] 19 p3236 N85-30085
Instrumentation for particle-beams research using excited merging beams
[AD-A154155] 19 p3356 N85-30807
Shuttle Molecular Gun: Smog. Potential experiment for the electrodynamic Tethered Satellite System (TSS) mission
[IFSI-84-17] 20 p3419 N85-31221
Interrelations for the elements of the scattering matrix
22 p3855 N85-33872
High-resolution spectroscopy and dynamics of multiphoton processes in atoms and molecules
[AD-A155862] 24 p4147 N85-35714
Investigations of the molecular beam epitaxial growth and characteristics of external excitation induced non-equilibrium phases of immiscible 3-5 compound semiconductors
[AD-A156325] 24 p4162 N85-35804

MOLECULAR BIOLOGY
The cosmic history of the biogenic elements and compounds
[NASA-SP-476] 17 p3003 N85-28562
Institute works on modeling thermonuclear plasma processes 19 p3296 N85-30435

Molecular biology of environmental aromatic hydrocarbons
[DE85-015036] 24 p4128 N85-35593

MOLECULAR BONDS
U CHEMICAL BONDS

MOLECULAR CHAINS
Nuclear Magnetic Resonance of Polymeric Materials
[AD-A145078] 01 p0032 N85-10192
NMR (Nuclear Magnetic Resonance) and macromolecular migration in a melt or in concentrated solutions
[AD-P003908] 01 p0032 N85-10194
Deuteron NMR (Nuclear Magnetic Resonance) in relation to the glass transition in polymers
[AD-P003910] 01 p0032 N85-10196

MOLECULAR CLOUDS
Star Formation Workshop
[ROE-OR-13] 03 p0441 N85-12809
Distribution and properties of molecular clouds in the galaxy 03 p0442 N85-12810
The number and distribution of molecular clouds in the inner galaxy 03 p0442 N85-12811
Far-infrared observations of some regions of star formation 03 p0442 N85-12814
Relation of core structure to high velocity outflow in G35.2-0.74 and other molecular clouds
03 p0443 N85-12818
Time-dependent chemistry of molecular clouds
03 p0443 N85-12822
The significance of comets for star formation
03 p0443 N85-12824
Molecules in external galaxies
03 p0444 N85-12828
Future theoretical needs in studies of star formation
03 p0444 N85-12829
The fragmentation of molecular clouds and the IMF
05 p0740 N85-14759
Molecular clouds within 100 pc
06 p0877 N85-15573
A wide latitude CO survey of molecular clouds in the northern Milky Way 06 p0877 N85-15574
The Draco Nebula, a molecular cloud associated with a high velocity cloud? 06 p0878 N85-15577
Nearby molecular hydrogen 06 p0879 N85-15582
The Orion molecular cloud at far-infrared wavelengths
08 p1245 N85-17860
First results of submillimeter polarimetry
08 p1246 N85-17861
Far-infrared photometry of low-mass pre-main-sequence stars with broad CO wings 08 p1246 N85-17866
Star formation in globules 08 p1247 N85-17868
Far infrared observations of molecular clouds in the outer galaxy 08 p1247 N85-17869
Boundary conditions for the paleoenvironment: Chemical and physical processes in the pre-solar nebula -- molecular clouds, interstellar matter, and abundance
[NASA-CR-174370] 10 p1570 N85-19901
Mechanical energy release by protostars to molecular clouds 12 p1957 N85-22302
The Formation of preplanetary disks from the collapse of rotating molecular cloud cores
13 p2180 N85-23526
Radio counterparts of galactic gamma-ray sources
20 p3549 N85-32085
Galactic gamma-ray sources, SNOBs, and giant H2 regions
[OG-2.5-4] 22 p3869 N85-33861
The galactic gamma-ray distribution and the radial cosmic ray gradient
[OG-3.1-4] 22 p3873 N85-33892
Cosmic ray secondary nuclei and the structure of the galaxy
[OG-7.2-4] 23 p4014 N85-34876
Alfven wave scattering and the secondary to primary ratio
[OG-7.2-6] 23 p4015 N85-34878
Giant molecular clouds as regions of particle acceleration 23 p4020 N85-34913
Far-infrared emission lines of CO and OH in the Orion-KL molecular shock
[NASA-TM-86721] 24 p4167 N85-35832

MOLECULAR COLLISIONS
Collisional excitation cross sections
[AD-A145198] 01 p0117 N85-10800
Energy transfer in atom-molecule scattering experiments in the 1eV region with SF6-Ar, CF4-Ne and Xe-CO2 systems as examples
[REPT-11/1983] 04 p0563 N85-13586
Rotational inelastic scattering of He-atoms at HF-, HCl-, CF4-, SF6-, C2H6- and C2F6-molecules
[MPIS-9/1984] 04 p0564 N85-13590
Laboratory studies of atomic collision processes of importance in planetary atmospheres
[NASA-CR-174142] 04 p0569 N85-13758
Chaos near the Coulomb Barrier: Nuclear molecules
[DE85-001280] 07 p1041 N85-16608
Collisional energy exchange in polyatomic molecules
[AD-A147710] 08 p1219 N85-17679
Atomic and molecular collision processes
[DE85-001604] 09 p1382 N85-18690
Quantum mechanical and semiclassical approaches to molecular dynamics
[DE85-003458] 10 p1555 N85-19803
Studies of collisional and nonlinear radiative process for development of coherent UV and XUV sources
[AD-A152001] 16 p2865 N85-27670
Large, energetic cluster impacts on surfaces
[DE85-006559] 17 p3034 N85-28769
Interaction of slow electrons with high-pressure gases (quasi-liquids): Synthesis of our knowledge on slow electron-molecule interactions
[DE85-010061] 19 p3355 N85-30800
Inelastic Near-Surface Interactions. Proceedings of the Werner Brandt Workshop on Penetration Phenomena
[DE85-010579] 20 p3526 N85-31928

MOLECULAR DIFFUSION
The role of molecular diffusion in the adhesion of elastomers
[AD-A145576] 02 p0186 N85-11245
Contribution to theory of ocean-atmosphere gas exchange 13 p2108 N85-23134
Current understanding of point defects and diffusion processes in silicon 20 p3481 N85-31632
Vortex dynamics simulation of conserved scalar dissipation 22 p3745 N85-33210

MOLECULAR DISSOCIATION
U DISSOCIATION

MOLECULAR ELECTRONICS
NT LARGE SCALE INTEGRATION
Investigation of several low-lying levels of X doublet pi state of NCO using argon laser excited fluorescence
[AD-A153893] 18 p3071 N85-28994

MOLECULAR ENERGY LEVELS
NT INTERMOLECULAR FORCES
Electronic and redox properties of stacked-ring silicon phthalocyanines from molecular orbital theory
[AD-A147161] 07 p0922 N85-15844
Pion inelastic scattering to the first three excited states of Lithium-6
[AD-A147560] 07 p1041 N85-16606
Sequential excitation preparation of molecular energy levels with special structural and chemical properties
[AD-A150301] 13 p2156 N85-23386
Noncontinuum solvent effects upon the intrinsic free-energy barrier for electron-transfer reactions
[AD-A150662] 14 p2250 N85-23943
Intermolecular energy transfer between the individual zero-field levels of triplet traps in an orientationally disordered solid
[AD-A150751] 14 p2417 N85-24914
Computer modeling of vibrational energy levels of potential laser candidates (diatomic molecules)
[AD-A151765] 16 p2790 N85-27209
A method to estimate the self-consistency effects on electronic structure calculations
[INPE-3536-PRE/752] 19 p3375 N85-30936

MOLECULAR EXCITATION
Collisional excitation cross sections
[AD-A145198] 01 p0117 N85-10800
Electronic-to-vibrational energy transfer studies of singlet molecular oxygen and hydrogen halides
[AD-A145587] 02 p0277 N85-11802
Theoretical studies in molecular fragmentation: Processes, energetics and diagnostics
[AD-A146310] 03 p0418 N85-12673
Quantum Monte Carlo for molecules
[AD-A148158] 08 p1227 N85-17727
Photoionization of excited molecular states
[DE84-017454] 09 p1291 N85-18103
Hyperfine structure and lifetime measurements on electronically excited long-life molecules in a beam experiment
[MPIS-11/1984] 11 p1726 N85-20855
Direct measurement of the temperature dependence of the velocity of the reaction of deuterium atoms with vibration-excited hydrogen molecules
[MPIS-12/1984] 11 p1726 N85-20856
Threshold double photoionization of argon with synchrotron radiation
[AD-A150615] 13 p2157 N85-23389
Transverse periodic boundary conditions in molecular dynamics with uniaxial strain shock waves
[DE85-006497] 16 p2863 N85-27656
Studies of collisional and nonlinear radiative process for development of coherent UV and XUV sources
[AD-A152001] 16 p2865 N85-27670
Electronically excited alkaline earth oxides: Chemical production and collisional energy transfer processes
[AD-A153172] 17 p3044 N85-28833
Nonradiative damping of molecular electronic excited states by metal surfaces
[AD-A154619] 21 p3701 N85-32994
The detection and study of molecular species using time resolved laser spectroscopy
[AD-A155910] 24 p4075 N85-35256
High-resolution spectroscopy and dynamics of multiphoton processes in atoms and molecules
[AD-A156862] 24 p4147 N85-35714

MOLECULAR FLOW
NT TRANSITION FLOW
Bipolar molecular outflows: T Tauri stars and Herbig-Haro objects 03 p0446 N85-12837
Structure of amorphous films of alloys based on Fe, condensed from laser erosion products
13 p2035 N85-22749
Cone drag in the transition from continuum to free molecular flow
[OUEL-1538/84] 20 p3390 N85-31023
Variations in the small-scale galactic magnetic field and short time-scale intensity variations of extragalactic radio sources 20 p3549 N85-32084

MOLECULAR GASES
NT DIATOMIC GASES
NT POLAR GASES
Electron collision processes in molecular gases
[AD-A146078] 03 p0418 N85-12671
Conference on Singlet Molecular Oxygen (COSMO 84), program and abstracts
[AD-A147281] 07 p1040 N85-16605
Understanding the high pressure properties of molecular solids and molecular surfaces deposited on hetrogeneous substrates
[NASA-CR-174262] 07 p1047 N85-16649
Optical modulators and bistable devices using molecular gases 18 p3186 N85-29761
Participation of singlet oxygen in photodestruction of air-saturated solutions of coumarin dyes
21 p3685 N85-32891
The possibilities of remote analysis of atmospheric gases based on Raman scattering spectroscopy
21 p3685 N85-32892
Preliminary considerations for the gasdynamic precompression of solid molecular hydrogen
[DE85-013256] 22 p3784 N85-33445
Far-infrared observations of young clusters embedded in the R Coronae Austrinae and RHO Ophiuchi dark clouds
[NASA-TM-86681] 24 p4167 N85-35834

MOLECULAR INTERACTIONS
NT INTERSTELLAR CHEMISTRY
NT MOLECULAR COLLISIONS
Molecular mechanisms of n-hexane neurotoxicity
[AD-P004020] 06 p0843 N85-15354
Vibrational spectroscopy of chemisorption phenomena on model catalyst surfaces
[AD-A146753] 07 p0922 N85-15840
Applications of molecular dynamics to the study of shock-induced chemistry
[AD-A148017] 08 p1121 N85-17066
USSR report: Physics and mathematics
[JPRS-UPM-85-001] 11 p1715 N85-20786
In situ monitoring of electrochemical reactions by surface enhanced Raman scattering
[PB85-149789] 12 p1803 N85-21312
Bibliography of atomic and molecular processes, 1983
[DE85-000662] 12 p1929 N85-22121
Theoretical study of near-threshold electron-molecule scattering
[DE85-004530] 12 p1930 N85-22126
Combustion kinetics of metal atoms and metallic radicals over wide temperature ranges 13 p1999 N85-22530
Molecular dynamics of propellant gases, part 2
13 p2002 N85-22552
Molecular dynamics studies of energy transfer processes in crystal systems
[AD-A150161] 13 p2163 N85-23416
Intermolecular energy transfer between the individual zero-field levels of triplet traps in an orientationally disordered solid
[AD-A150751] 14 p2417 N85-24914
USSR report: Physics and mathematics
[JPRS-UPM-85-003] 15 p2642 N85-26300
Finite-perturbation intermediate neglect of differential overlap molecular orbital calculations of nuclear magnetic resonance spin-spin coupling constants for polycyclic aromatic hydrocarbons and aromatic nitrogen heterocyclics
[NASA-TM-87486] 20 p3525 N85-31927
USSR report: Physics and mathematics
[JPRS-UPM-85-004] 21 p3680 N85-32860
Intermolecular explosives
[DE85-009609] 23 p3921 N85-34296

MOLECULAR IONS
Electronics research at the University of Texas at Austin
[AD-A146900] 07 p0947 N85-15998
State-selected ion-molecule reaction dynamics
[AD-A150068] 12 p1328 N85-22115

Multiparticle 3D imaging technique to study the structure of molecular ions
[DE85-001843] 12 p1929 N85-22122

Extraction of ions from solutions at atmospheric pressure, mass spectrometric analysis of bioorganic substances 14 p2367 N85-24706

Hydrogen vibrational population distributions and negative ion generation in tandem high-density hydrogen discharges
[DE85-006764] 16 p2863 N85-27657

Imaging Spectrometric Observatory (ISO)
23 p3902 N85-34169

Negative ion sources equipped with continuous annular and spherical geometry surface ionizers
[DE85-011939] 23 p3971 N85-34619

MOLECULAR ORBITALS

Application of quantum chemistry of atmospheric chemistry
[AD-A147035] 07 p0922 N85-15843

Electronic and redox properties of stacked-ring silicon phthalocyanines from molecular orbital theory
[AD-A147161] 07 p0922 N85-15844

Why CO bonds side-on at low coverage and both side-on and upright at high coverage on the Cr(110) surface
[NASA-CR-176071] 21 p3565 N85-32173

Molecular orbital studies in oxidation: Sulfate formation and metal-metal oxide adhesion
[NASA-CR-176070] 21 p3565 N85-32174

MOLECULAR OSCILLATIONS

Electronic-to-vibrational energy transfer studies of singlet molecular oxygen and hydrogen halides
[AD-A145567] 02 p0277 N85-11602

High temperature gas energy transfer
[AD-A146134] 03 p0328 N85-12113

Phase-dissipative mechanisms for laser-induced surface desorption-dissociation processes
[AD-A147961] 08 p1121 N85-17065

Supersonic molecular jet study of the liquid state
[AD-A147416] 09 p1379 N85-18671

Sequential excitation preparation of molecular energy levels with special structural and chemical properties
[AD-A150301] 13 p2156 N85-23386

Rotational energy transfer in highly vibrationally excited hydrogen fluoride and deuterium fluoride
[AD-A152003] 16 p2862 N85-27650

Vibrationally enhanced dissociation of diatomic molecules
[AD-A154627] 21 p3701 N85-32996

MOLECULAR OSCILLATORS

Construction techniques of a molecular hydrogen laser
[AD-A152928] 17 p2970 N85-28343

MOLECULAR PHYSICS

The 2nd European Conference on Atomic and Molecular Physics
[AD-A155663] 24 p4148 N85-35715

MOLECULAR PUMPS

Optimum geometry of interblade passages in impellers of thermomolecular vacuum pump
16 p2764 N85-27058

Impurity and particle control systems for tokamak reactor experiments
[DE85-006124] 19 p3366 N85-30873

MOLECULAR RELAXATION

Collisional excitation cross sections
[AD-A145108] 01 p0117 N85-10900

Anomalies in frequency characteristics of solid-state ring laser 02 p0271 N85-11765

Low-frequency sound absorption measurements in air
[NASA-RP-1128] 02 p0275 N85-11789

Phase-dissipative mechanisms for laser-induced surface desorption-dissociation processes
[AD-A147961] 08 p1121 N85-17065

Transport relaxation processes in supercritical fluids
[DE85-002076] 09 p1398 N85-18798

Saturation kinetics of active medium of oxygen-iodine laser 11 p1718 N85-20807

Vibrational relaxation in H-2 molecules by wall collisions: Applications to negative ion source processes
[DE85-000852] 11 p1721 N85-20828

Theory of relaxation processes in decomposing polymer materials during high-intensity convective heating
13 p2028 N85-22710

Quantum statistical theory of vibrational dynamics in a laser-driven admolecule-surface system
[AD-A152022] 16 p2872 N85-27719

Some amplification by relaxation processes in nitrogen and mixtures of nitrogen with helium and hydrogen
[AD-A153620] 18 p3071 N85-28992

Laser-stimulated vibrational excitation of an adspecies studied by a generalized master equation: Neutral atomic hydrogen on hydrated KCl(001)
[AD-A153665] 18 p3112 N85-29266

Theoretical modeling of the discharge-pumped XeCl excimer laser 20 p3460 N85-31495

MOLECULAR ROTATION

Calculation of the scattering function of rotating molecules with emphasis on the tunnel spectra of absorbed molecules 03 p0427 N85-12725

Rotational inelastic scattering of He-atoms at HF-, HCl-, CF4-, SF6-, C2H6- and C2F6-molecules
[MPIS-9/1984] 04 p0564 N85-13590

Detection of the J-10 manifold of the pure rotational band of phosphine on Saturn 06 p1245 N85-17855

Far-infrared spectroscopy of interstellar gas
06 p1245 N85-17858

Photoionization of excited molecular states
[DE84-017464] 09 p1291 N85-18103

Two-dimensional measurements of OH concentration and temperature in reactive flows
[AD-A149649] 12 p1800 N85-21292

Rotational energy transfer in highly vibrationally excited hydrogen fluoride and deuterium fluoride
[AD-A152003] 16 p2862 N85-27650

Rotational relaxation studies of hydrogen fluoride
[AD-A152711] 17 p3029 N85-28734

MOLECULAR SIEVES

U ABSORBENTS

MOLECULAR SPECTRA

NT ELECTRONIC SPECTRA
NT RAMAN SPECTRA
NT VIBRATIONAL SPECTRA

On the content of nitrogen in atmospheres of late giants derived from molecular bands on NH in the UV spectral range 05 p0740 N85-14761

Starbursts in galaxies: Implications of molecular and far-infrared observations 06 p1248 N85-17881

The fluorescence of cometary OH and CN
09 p1411 N85-18896

Mass analysis of neutral particles and ions released during electrical breakdowns on spacecraft surfaces
[NASA-CR-175585] 12 p1793 N85-21250

MOLECULAR SPECTROSCOPY

NT RAMAN SPECTROSCOPY

The 248 nm - new short wavelength for pumping lasers employing vapors of complex molecules
02 p0261 N85-11705

Vibrational spectroscopy of chemisorption phenomena on model catalyst surfaces
[AD-A146753] 07 p0922 N85-15840

Development of an airborne measuring system for remote sensing of Earth surface and atmosphere, spectroscopic investigations
[BMFT-FB-W-84-029] 08 p1176 N85-17420

Study of metal oxide semiconductor structures by capacitive transient spectroscopy
[ENST-84E011] 11 p1737 N85-20926

A liquid nitrogen cooled composite wall hollow cathode — molecular spectroscopy
[USIP-85-07] 20 p3526 N85-31930

MOLECULAR STRUCTURE

Diblock copolymers of polystyrene/1,2 polybutadiene and polystyrene/polybutene-1: Molecular structure, morphology and mechanical properties
[AD-A144980] 01 p0033 N85-10201

Proton pumping in purple membrane, appendix 1
[DE84-014801] 01 p0118 N85-10811

Physical-chemical properties of articulated rodlike polymers
[AD-A145549] 02 p0186 N85-11244

Computer molecular dynamics of 2-D water (ice) structures under shock
[AD-A145818] 03 p0372 N85-12375

Stable isotope studies
[DE84-016752] 04 p0562 N85-13583

Structure and properties of grain boundaries
[DE84-014368] 04 p0570 N85-13636

Synthesis of film-forming electron-accepting polymers
[AD-A146430] 05 p0771 N85-14931

Structure and functions of fungal cell surfaces
[NASA-TM-77439] 06 p0842 N85-15347

Structure determination of molecular adsorbates with dynamical LEED and HREELS
[DE85-002007] 06 p0861 N85-15473

Catalytic oxidation by transition metal ions in zeolites
[AD-A146826] 07 p0922 N85-15842

Quantum Monte Carlo for molecules
[AD-A148159] 08 p1227 N85-17727

Isomer enumeration in polytertiary phosphines and related compounds
[AD-A148058] 09 p1290 N85-18099

Supersonic molecular jet study of the liquid state
[AD-A147416] 09 p1379 N85-18671

Metal atom diffusion in amorphous silica and at the silica surface
[DE84-017351] 09 p1380 N85-18674

Compilation of atomic data for diagnostics of Tokamak
09 p1390 N85-18744

Compositional, structural, and physical studies of some graphite hexafluoroarsenates and their relatives
[DE85-000655] 10 p1432 N85-19030

On shrinkage and molecular extension
[AD-A149100] 10 p1451 N85-19144

Characterization of acetylene-terminated resin cure states
[AD-A149463] 10 p1452 N85-19148

Application of Monte Carlo and molecular dynamics methods to the calculation of thermodynamic properties of molten salts
[AD-A148897] 10 p1566 N85-[illegible]

Characterization of the network structure of a hardened epoxy resin (TGMDA/DDS system)
[ONERA-RT-3/3346-M] 11 p1613 N85-[illegible]

Multiparticle 3D imaging technique to study the structure of molecular ions
[DE85-001843] 12 p1929 N85-22122

The crystal and molecular structure of a new propellant compound: Triaminoguanidium Azide Nitrate (TAZN)
13 p2002 N85-22551

The chemistry of RDX and HMX cluster ions
13 p2004 N85-22561

The influence of fuel molecular composition upon flame-tube temperature and flame radiation in a model gas-turbine primary zone
[K234] 13 p2017 N85-22848

Sequential excitation preparation of molecular energy levels with special structural and chemical properties
[AD-A150301] 13 p2156 N85-23386

Bonding information from Auger spectroscopy
[AD-A150664] 14 p2251 N85-23948

Extraction of ions from solutions at atmospheric pressure, mass spectrometric analysis of bioorganic substances 14 p2367 N85-24706

Metal complexes of some heterocyclic ligands
15 p2504 N85-25448

Studies of photosynthetic Energy Conversion
[DE85-005973] 15 p2586 N85-25944

Equation of state and two-body correlations for fluids of non-spherical molecules
[AD-A151969] 16 p2783 N85-27174

Periodic cluster simulation of a disordered impurity system
[INPE-3453-PRE/705] 16 p2858 N85-27628

An investigation of molecular structure of copolymers using positron annihilation spectroscopy
[NASA-TM-86431] 17 p2916 N85-27977

Detailed chemical kinetic study of the effect of molecular structure on autoignition of fuel-air mixtures
[DE85-004424] 17 p2921 N85-28010

Electroweak interactions in nuclei
[DE85-007811] 17 p3033 N85-[illegible]

Exploratory study of coal conversion chemistry
[DE85-010393] 19 p3229 N85-30018

Molecular toxicology of chromatin: The role of Poly(ADP-Ribose) in gene control
[AD-A154415] 19 p3327 N85-30811

Activities of Rutgers - The State University Department of Mathematics
[AD-A154158] 19 p3370 N85-30904

A method to estimate the self-consistency effects on electronic structure calculations
[INPE-3536-PRE/752] 19 p3375 N85-30938

Interaction of solutes with stretched polymers
[AD-A154662] 21 p3589 N85-32196

Polymerizable ultraviolet stabilizers
21 p3606 N85-32408

Insights into the phylogenetic positions of photosynthetic bacteria obtained from 5S rRNA and 16S rRNA sequence data 21 p3658 N85-32719

X-ray diffractometric measurements and calculations of limiting values of discrepancy between lattices and layer thicknesses, preventing generation of dislocations during growth of multilayer heterostructures
21 p3661 N85-[illegible]

Three-dimensional reconstruction and data display of chromosome structure studied by electron microscope tomography
[DE85-011562] 22 p3825 N85-33667

On the potential link equation of a spot centre with relative deformation for a semi-infinite molecular crystal
[BLL-M-35795-(5828.4)] 23 p3985 N85-34711

The detection and study of molecular species using time resolved laser spectroscopy
[AD-A155910] 24 p4075 N85-35258

MOLECULAR THEORY

Flow and plasticity via nonequilibrium molecular dynamics
[DE85-001011] 10 p1555 N85-[illegible]

Simulation of brittle fracture via molecular dynamics
[DE85-001061] 11 p1653 N85-20410

Atomic, Molecular and Solid-State Theory, and Computational Quantum Chemistry, part 1
[DE85-009401] 20 p3526 N85-31929

Equation of state study for polar fluids
[PB85-204345] 24 p4076 N85-35262

MOLECULAR WEIGHT

Physical-chemical properties of articulated rodlike polymers [AD-A145549] 02 p0186 N85-11244

Thermoplastic/melt-processable polyimides 04 p0466 N85-12961

Determination of the decomposition behavior of double base propellants at low temperatures 08 p1117 N85-17045

Characterization and adhesive bonding of poly(etheretherketone) resins and composites [DE85-002526] 11 p1593 N85-20023

Structural basis for the mechanical properties of polyethlenes [PB85-148771] 11 p1613 N85-20142

Synthesis and thermomechanical properties of new AT-Phenylene R systems [AD-A149961] 12 p1813 N85-21372

Extraction of ions from solutions at atmospheric pressure, mass spectrometric analysis of bioorganic substances 14 p2387 N85-24706

High performance size exclusion chromatography (IX) bulk and component analysis of silanol groups in polydimethylsiloxanes: Process development endeavor [DE85-008853] 15 p2506 N85-25458

A soluble linear Schiff-base coordination polymer containing eight-coordinate zirconium(4) [AD-A151446] 15 p2518 N85-25527

Formulation/cure technology for ultrahigh molecular weight silphenylene-siloxane polymers [NASA-TP-2476] 16 p2753 N85-26990

Relationship of isolated turbulent regions to the general turbulent background, part 4.4A 21 p3623 N85-32506

Size exclusion chromatography-low angle laser light scattering photometry of lignite macromolecules [DE85-012017] 22 p3745 N85-33215

Molecular and macromolecular sieving by asymmetric ultrafiltration membranes [PB85-157766] 24 p4077 N85-35266

MOLECULES

NT DIATOMIC MOLECULES

NT POLYATOMIC MOLECULES

Spectrophotometric studies of iodine complexes in an aluminum chloride - butylpyridinium chloride ionic liquid [AD-A145074] 01 p0024 N85-10150

Nuclear Magnetic Resonance of Polymeric Materials [AD-A145078] 01 p0032 N85-10192

Theory of nuclear magnetic relaxation [AD-P003911] 01 p0032 N85-10197

A perturbation solution for rigid dumbbell suspensions in steady shear flow [AD-A144876] 01 p0111 N85-10755

Chemical derivatization of an array of three gold microelectrodes with polypyrrole: Fabrication of a molecule-based transistor [AD-A146221] 03 p0359 N85-12304

Neutron scattering on macromolecular solid state materials, solutions and melts 03 p0431 N85-12747

Physico-chemical investigation of some areas of fundamental significance to biophysics [DE84-016385] 04 p0471 N85-12999

Loeb solutions of the Boltzmann equation with initial boundary values and external forces [CTH-MATH-1984-23] 05 p0719 N85-14616

Electronically excited atomic and molecular oxygen [AD-A147732] 06 p1121 N85-17064

Time-of-flight spectroscopy of ionic and metastable fragments from dissociating molecules [AD-A146068] 06 p1220 N85-17683

Quantum Monte Carlo for molecules [AD-A146159] 06 p1227 N85-17727

Microscopic study of fluid flow 09 p1317 N85-18280

Supersonic molecular jet study of the liquid state [AD-A147416] 09 p1379 N85-18671

Molecular hydrogen and thermal phases in astrophysics 09 p1414 N85-18922

Polymers and macromolecules [DE85-003176] 10 p1454 N85-19160

Dynamical studies of molecular systems [DE85-003053] 11 p1594 N85-20028

Electrostatic potentials: A new method for interpreting and predicting molecular reactivities and for designing synthetic pathways. Applications to nitroaromatics, nitramines and nitrated [AD-A150120] 12 p1801 N85-21298

Some unique aspects of fouling on copper as compared to titanium or nickel [AD-A150072] 12 p1806 N85-21332

Mean delta-ray energies in ion molecule collisions [DE85-005524] 13 p2157 N85-23395

O. F. Mossotti and the physics of molecules [NOTA-INTERNA-822] 14 p2420 N85-24031

Spectroscopy of quasimolecular X-rays with H-like decelerated ions [DE85-006565] 15 p2649 N85-26337

Experimental study of dissociative attachment in optically-pumped lithium molecules [AD-A152900] 17 p3030 N85-28736

Spectroscopy of surface adsorbed molecules [DE85-009452] 17 p3034 N85-28768

Space shuttle molecular and wake vacuum measurements [NASA-TM-86500] 19 p3222 N85-29978

Determining partial molar volume of hydrogen in titanium alloys 19 p3245 N85-30119

Activities of Rutgers - The State University Department of Mathematics [AD-A154158] 19 p3370 N85-30904

Photoabsorption and photodissociation of molecules important in the interstellar medium [NASA-CR-175918] 19 p3383 N85-30986

Size exclusion chromatography-low angle laser light scattering photometry of lignite macromolecules [DE85-012017] 22 p3745 N85-33215

Preparation and use of very pure o-D2 [DE85-009415] 22 p3843 N85-33800

Electron density distribution analysis for nitroguanidine [DE85-009598] 23 p3969 N85-34603

Solar modulation of cosmic ray intensity and solar flare events inferred from (14)C contents in dated tree rings [SH-7.1-2] 23 p4047 N85-35095

MOLIERE FORMULA

U COSMIC RAY SHOWERS

U SECONDARY COSMIC RAYS

U SPATIAL DISTRIBUTION

MOLTEN SALT ELECTROLYTES

Hot-gas cleanup for molten carbonate fuel cells-dechlorination and soot formation [DE84-003072] 01 p0068 N85-10450

Physico-chemical investigations on the electronic partial conductivity of molten electrolytes, especially of the eutectic mixture LiCl-KCl [BMFT-FB-T-84-205] 05 p0633 N85-14063

Polymer electrolytes: An investigation of some poly (N-propylaziridine)/lithium salt compositions [RAE-TR-84036] 06 p1131 N85-17130

Electrolyte resevoir for carbonate fuel cells [DE85-005736] 23 p3947 N85-34460

MOLTEN SALTS

Effects of H2S on molten carbonate fuel cells [DE84-015166] 02 p0195 N85-11307

Thermal energy storage at 900 deg C [DE84-004589] 04 p0530 N85-13387

Measurement of oxide ion concentration in NaCl-ZnCl2 molten salt and several applications [BLL-AWRE-TRANS-74-(9091.9F)] 06 p0764 N85-14886

Electrochemical behaviour of TiCl4 solutions in low melting point organic media [BLL-OA-TRANS-3174-(6196.3)] 06 p0764 N85-14888

Advanced latent heat storage media for high-temperature industrial applications [DE85-000907] 09 p1345 N85-18461

Application of Monte Carlo and molecular dynamics methods to the calculation of thermodynamic properties of molten salts [AD-A148897] 10 p1565 N85-19869

Direct contact heat recovery from molten salt [DE85-002830] 11 p1674 N85-20550

Electrochemistry and electrochemical methodology in molten salts [AD-A149613] 12 p1799 N85-21284

Cathode materials for molten carbonate fuel cells [DE85-004078] 13 p2130 N85-23254

Exploratory corrosion tests on alloys in molten salts at 900(0)C [DE85-000511] 14 p2257 N85-23983

Exploratory corrosion tests on materials and fluids for advanced high-temperature molten-salt storage [DE85-002911] 14 p2258 N85-23991

Material for protection of metal surfaces against corrosion by molten salts [DE85-007714] 16 p2750 N85-26966

High temperature sensible heat storage options [DE85-000534] 18 p3129 N85-29375

Development of molten carbonate fuel cell power plant, volume 1 [DE85-008743] 18 p3131 N85-29394

Mechanism of strength degradation for hot corrosion of alpha-SiC [NASA-TM-87052] 19 p3248 N85-30135

Molten salt cooling/17Li-83Pb breeding blanket concept [DE85-010522] 19 p3363 N85-30854

Development of low-melting fused salts 8: Formation of molybdenum film from molten ammonium formate bath [BLL-OA-TRANS-3195-(6196.300)] 20 p3429 N85-31264

Design of a helium-cooled molten salt fusion breeder [DE85-010474] 20 p3526 N85-31943

The effect of stress and hot corrosion on nickel-base superalloys [AD-A154722] 21 p3566 N85-32181

Recent advances in d-c relaxation techniques for the measurement of kinetics of fast electrode reactions [DE85-005029] 22 p3745 N85-33216

Molten carbonate fuel cell separator [DE85-011615] 22 p3806 N85-33577

Study of alternative system conversions for the Solar One pilot plant [DE85-010026] 22 p3809 N85-33594

Thermodynamics of the corrosion of chromium in molten carbonates [DE85-011407] 24 p4079 N85-35282

MOLYBDATES

Additives for heat engine coal slurry fuels [DE84-016434] 05 p0621 N85-13971

Synthesis and properties of Hexachloromolybdates(5) and related species [AD-A139599] 07 p0924 N85-15852

MOLYBDENUM

The effect of replacing molybdenum with vanadium on the corrosion resistant properties of stainless steels 02 p0178 N85-11197

Recent developments on the role of molybdenum in irons and steels 02 p0180 N85-11206

Swaged Mo-5 percent W alloy and recrystallized commercially pure molybdenum 02 p0180 N85-11208

The influence of rare Earth elements on the temper embrittlement behaviour and mechanical properties of a low alloy steel 02 p0180 N85-11210

The role of molybdenum as an alloy element in adhesive wear resistance 02 p0181 N85-11212

Corrosion in alkali metal/molybdenum heat pipes [DE84-014039] 02 p0184 N85-11233

Review: Role of refractory metal alloys in fusion reactor applications [AERE-R-11317] 03 p0422 N85-12695

Constraints on the origin of the Moon from molybdenum and other siderophile elements 04 p0582 N85-13718

Autenite transformation in powder-compacted chromium-nickel-molybdenum steels during continuous cooling [BLL-M-35981-(5828.4)] 05 p0615 N85-13933

Special features of the deformation of molybdenum at high temperatures [BLL-M-36027-(5828.4)] 07 p0924 N85-15856

Investigation of granules of molybdenum-base alloys obtained with pulsed discharges [BLL-M-36012-(5828.4)] 07 p0926 N85-15871

Identification of spectra of highly ionized Mo, Nb, Zr and Y atoms 09 p1390 N85-18745

WRAP-RIB antenna technology development 14 p2231 N85-23824

Molybdenum solar neutrino experiment [DE85-003747] 14 p2445 N85-25090

Corrosion inhibitor formulation for molybdenum, tungsten and other metals [AD-D011593] 15 p2510 N85-25486

Electronic transport in Mo/Ni superlattice [DE85-006835] 15 p2661 N85-26425

Sodium and lithium corrosion in molybedenum heat pipes [DE85-005561] 16 p2784 N85-27179

Solid state bonding of molybdenum and TZM [BLL-T6439/BG/LRS/LRST751/85] 16 p2792 N85-27220

Influence of heat treatment parameters on the properties of induction hardened Ni-Cr-Mo steels [BLL-BISI-TRANS-2499-(9022.06)] 17 p2926 N85-28053

Influence of temperature in melting and casting on quality of medium-alloy steel [BLL-BISI-TRANS-22310-(9902.06)] 17 p2938 N85-28137

Study of a simulated test for assessing the machinability of steels [BLL-BISI-TRANS-22344-(9022.06)] 17 p2972 N85-28357

Elevated temperature erosion corrosion of 9Cr1Mo steel [DE85-008445] 18 p3074 N85-29016

Surface degradation of ductile metal in elevated temperature gas-particle streams [DE85-008428] 18 p3074 N85-29017

The effect of temperature on the corrosion-erosion of 9Cr1Mo steel
[DE85-008507] 18 p3076 N85-29030
Structural transformation of a 9% Cr - 2%Mo steel (type Z10CDNbV 09-02) for use in steam generators for fast neutron reactors
[BLL-CE-TRANS-7943-(9022.09)]
20 p3430 N85-31271
The effect of pre-heating on the structure and properties of chromium-molybdenum steels
[BLL-M-35897-(5828.4)] 23 p3914 N85-34255
Development of metallization process: FSA project, cells and module formation research area
[NASA-CR-176136] 23 p3945 N85-34447
Some recent deposit modeling efforts
24 p4106 N85-35453
The Conterminous United States Mineral Assessment Program 24 p4106 N85-35458

MOLYBDENUM ALLOYS
NT RENE 95
Effect of rhenium on the structure and properties of the weld metal of a molybdenum alloy
[NASA-TM-77491] 03 p0330 N85-12128
The formation of isolated phase precipitates during the decomposition of high-coercive force Fe-Cr-Co alloys
[BLL-M-36028-(5828.4)] 07 p0924 N85-15855
Susceptibility of 2 1/4 Cr-1Mo steel to liquid metal induced embrittlement by lithium-lead solutions
[DE85-000997] 09 p1294 N85-18130
Effect of tempering on the strength and toughness of 2 1/4 Cr-1 Mo steel weldments
[DE85-003818] 09 p1296 N85-18140
Electrical resistivity and structural changes upon relaxation and crystallization of (Mo/sub 0.6/Ru/sub 0.4)sub 100-x/B/sub x/ metallic glasses
[DE84-017281] 09 p1299 N85-18160
Assessment of the need for an advanced high-strength chromium-molybdenum steel for construction of third-generation gasifier pressure vessels
[DE85-002865] 11 p1606 N85-20097
Ferromagnetic resonance in a Ni-Mo superlattice
[DE85-003039] 11 p1735 N85-20911
Partial replacement of chromium in austenitic stainless steels by molybdenum, copper, and vanadium, report of investigations 1984
[PB85-116506] 12 p1809 N85-21346
Solution softening in molybdenum-rhenium alloys
[DE85-006706] 16 p2750 N85-26972
Study to optimize Cr-Mo steels to resist hydrogen and temper embrittlement
[DE85-005492] 17 p2932 N85-28096
Corrosion-erosion rates/mechanisms of 9Cr1Mo steel
[DE85-008506] 18 p3076 N85-29029
Fatigue behavior of HY-130 steel weldments containing fabrication discontinuities
[AD-A153630] 18 p3122 N85-29326
Fatigue-crack growth and ductile fracture toughness behavior of ASTM A387 Grade 91 steel
[DE85-008495] 20 p3431 N85-31286
Reliability of welds to repair defects in cast components made from CrMoV steel
[BLL-CE-TRANS-8054-(9022.09)]
20 p3461 N85-31501
Application of the unloading compliance methods in fracture toughness measurements of a quenched and tempered steel
[BLL-CE-TRANS-7953-(9022.09)]
20 p3465 N85-31523
Fatigue behavior of chromium-containing ferritic steels at elevated temperature
[DE85-012309] 22 p3748 N85-33231
Microstructures in rapidly solidified Ni-Mo alloys
[NASA-TM-87100] 23 p3915 N85-34266
Characterization of modified 9 Cr Mo steel extruded pipe
[DE85-012056] 23 p3941 N85-34430
Characterization of modified 9 r-1 Mo steel sand castings
[DE85-012057] 24 p4080 N85-35287

MOLYBDENUM COMPOUNDS
NT MOLYBDATES
NT MOLYBDENUM DISULFIDES
NT MOLYBDENUM OXIDES
Reinforcement of molybdenum disilicide with nematic crystals of aluminum oxide 03 p0353 N85-12269
Preparation and electronic properties of MoS(2) and WS(2) single crystals grown in the presence of cobalt
[AD-A146508] 06 p0866 N85-15506
The mechanisms of phenylacetylene polymerization by molybdenum and titanium initiators
[AD-A150993] 14 p2260 N85-24007

MOLYBDENUM DISULFIDES
Structural studies of sputtered MOS(2) films by angle-resolved photoelectron spectroscopy
[AD-A146052] 03 p0433 N85-12759
Molybdenum disulphide lubrication: A continuation survey, 1981 - 1983
[REPT-84-549] 18 p3082 N85-29065
Advances in rechargeable lithium molybdenum disulfide batteries 20 p3444 N85-31376

MOLYBDENUM OXIDES
Butene oxidation by molybdenum crystalographic shear compounds
[DE84-013910] 05 p0614 N85-13923
Correlation of electronic charge transfer transitions and electrochemical potentials. The Bipyrazine(Tetracarbonyl)Molybdenum(O) system in various solvents
[AD-A147680] 08 p1120 N85-17062
Development of low-melting fused salts 8: Formation of molybdenum film from molten ammonium formate bath
[BLL-OA-TRANS-3195-(6196.300)]
20 p3429 N85-31264

MOLYBDENUM SULFIDES
NT MOLYBDENUM DISULFIDES

MOMENT DISTRIBUTION
Force and moment measurements on a 74 deg delta wing with an apex flap
[NASA-CR-166081] 02 p0134 N85-10918
Mathematical modeling of assembly processes involving use of sensitized robots 04 p0488 N85-13111
Experimentally determined distribution of stress around a horizontally loaded model pile in dense sand
[CE-43] 16 p2796 N85-27239
Moment-method formulation of the cavity-probe aperture antenna
[DE85-013264] 24 p4086 N85-35336

MOMENTS
NT BENDING MOMENTS
NT DIPOLE MOMENTS
NT DISTRIBUTION MOMENTS
NT ELECTRIC MOMENTS
NT LOADING MOMENTS
NT MAGNETIC MOMENTS
NT MEAN
NT MOMENTS OF INERTIA
NT ORTHOGONALITY
NT PITCHING MOMENTS
NT ROLLING MOMENTS
NT STABILITY DERIVATIVES
NT STANDARD DEVIATION
NT TORQUE
NT YAWING MOMENTS
Experimental trim drag values and flow-field measurements for a wide-body transport model with conventional and supercritical wings
[NASA-TP-2071] 02 p0135 N85-10920
Determination of moments of initial estimate during linear approximation of distribution of ejected impurity
07 p0954 N85-16045
Magnetic and structural properties of shock-synthesized zinc ferrite
[DE85-000469] 11 p1736 N85-20915
A moment solution for an arbitrary configuration of partly shielded wires above a ground plane
[AD-A149762] 12 p1828 N85-21473
Stability of functionals determined by moment conditions
[TRITA-NA-8310] 16 p2852 N85-27585
Moments in particle-in-cell simulations
[DE85-010792] 19 p3356 N85-30803
The use of moments of momentum to account for crystal habits
[NASA-CR-3907] 20 p3421 N85-31232
Object identification and manipulation using silhouette moments
[AD-A154756] 21 p3705 N85-33011

MOMENTS OF INERTIA
Solving equations of movement with variable inertia moment
[BLL-M-35975-(5828.4)] 05 p0641 N85-14111
Inertial analysis of the Charpy test
[OUEL-1571/85] 20 p3471 N85-31570
Inertial stresses and deformations in mechanisms
23 p3924 N85-34320

MOMENTUM
NT ANGULAR MOMENTUM
Turbulent boundary layers over rough surfaces hypersonic flow
[AD-A145040] 01 p0003 N85-10016
Review of some vortex relations
[NASA-CR-172452] 01 p0046 N85-10302
Searching for top, Higgs, and supersymmetry: The minimum invariant mass technique
[DE84-014539] 01 p0119 N85-10813
Autonomous momentum management for space station, exhibit A
[NASA-CR-171256] 04 p0462 N85-12933
Turbulent drag reduction research
08 p1071 N85-16788
The Origin of Nonradiative Heating/Momentum in Hot Stars
[NASA-CP-2358] 08 p1231 N85-17759
Theoretical investigation of dynamic stall using a momentum integral method
[AD-P004170] 09 p1256 N85-17985
The Fermi surface and momentum space densities of ferromagnetic Gd using the Positron technique
09 p1396 N85-18780
Aspects of planetary wave transports in the middle atmosphere 11 p1661 N85-20471
Mathematical modeling of transient performance of gas turbine engine 13 p2050 N85-22804
Investigation of potential and viscous flow effects contributing to dynamic stall
[AD-A151696] 15 p2557 N85-25773
Coherent state description of non-topological solitons and momentum projection
[DE85-007814] 17 p3033 N85-28701
Multiple equilibria of the barotropic vorticity equation on a sphere 18 p3146 N85-29475
An experimental investigation of curvature and freestream turbulence effects on heat transfer and fluid mechanics in transitional boundary layer flows
19 p3264 N85-30246
The use of moments of momentum to account for crystal habits
[NASA-CR-3907] 20 p3421 N85-31232
Techniques for the study of gravity waves and turbulence (keynote paper), part 4 21 p3621 N85-32499
Momentum flux measurements: Techniques and needs, part 4.5A 21 p3623 N85-32509
Electron loss process and cross section of multiply charged ions by neutral atoms 23 p3961 N85-34665
1Single particle momentum and angular distributions in hadron-hadron collisions at ultrahigh energies
[HE-1.2-1] 24 p4171 N85-35880

MOMENTUM ENERGY
U KINETIC ENERGY

MOMENTUM THEORY
Phase space factors in multiparticle processes
24 p4175 N85-35889

MOMENTUM TRANSFER
Mass and momentum transport in a turbulent buoyant vertical axisymmetric jet 05 p0636 N85-14070
Analysis of diabatic heating during FGGE
05 p0683 N85-14383
Momentum distributions in superfluid helium: Bose condensate fraction
[DE84-014676] 05 p0731 N85-14700
Corotating interaction regions in stellar winds: Particle acceleration and non-thermal radio emission in hot stars
08 p1234 N85-17773
Synchrotron emission from chaotic stellar winds
08 p1234 N85-17774
A one dimensional dynamical model of ocean/atmosphere interactions
09 p1358 N85-18545
Studies of P-shell nuclei by large momentum transfer electron scattering
[DE84-016803] 09 p1361 N85-18686
Momentum and heat transfers in a complex, but well-defined turbulent fluid flow
[DE85-002857] 10 p1466 N85-19081
UK participation in the Middle Atmosphere Programme
11 p1655 N85-20426
Recent progress in electron scattering at SLAC
[DE85-002718] 11 p1723 N85-20840
Physics of the inner heliosphere: Mechanisms, models and observational signatures
[NASA-CR-175632] 13 p2205 N85-23677
Circulation and transport in the middle atmosphere: Troposphere and lower atmosphere
18 p3148 N85-29481
Circulation and transport in the middle atmosphere: Mesosphere and lower thermosphere
18 p3148 N85-29482
Magnetic scattering and polarized neutrons
[DE85-009823] 19 p3355 N85-30794
Transverse momentum distribution of pion deg in the fragmentation region of super high energy interactions
24 p4180 N85-35821

MONEL (TRADEMARK)
The use of austenitic stainless steel versus monel (Ni-cu) alloy in pressurized Gaseous Oxygen (GOX) life support systems
[AD-A156305] 24 p4134 N85-35825

MONGE-AMPERE EQUATION
New methods for numerical solution of one class of strongly nonlinear partial differential equations with applications in hydrodynamics
[AD-A149026] 10 p1545 N85-19739

MONITORS
NT INFRARED RADIOMETERS

User experience of existing corrosion monitoring techniques and the development of Thin Layer Activation (TLA) for corrosion monitoring
[AERE-R-11248] 01 p0029 N85-10183
A microcomputer aided measurement equipment for monitoring performance in digital radio relay systems
[FUB-4-1984] 01 p0101 N85-10668
The structures and the role of an international agency for the control of satellites
[NASA-TM-76765] 03 p0441 N85-12806
System status display information
[NASA-CR-172347] 04 p0455 N85-12889
Comparison of wind derived from the LIMS (Limb Infrared Monitor of the Stratosphere) satellite instrument with rocket observations
[NASA-CR-174083] 04 p0541 N85-13444
Qualification of noninvasive systems for on-line leak detection in high pressure feed water preheaters
[CISE-2341] 04 p0558 N85-13555
In-line beam current monitor
[DE84-014054] 04 p0560 N85-13567
Use of monitors in FORTRAN: A tutorial on the barrier, self-scheduling DO-loop and Askfor monitors
[DE84-016506] 05 p0715 N85-14587
Tornado: Structural Usage Monitoring System (SUMS) 07 p0696 N85-15660
Battery control and fault detection method
[AD-D011384] 07 p0993 N85-16307
Military vital sign monitor
[AD-A147257] 07 p1016 N85-16452
Interactive color-graphics interface for energy monitoring and control systems
[AD-A147536] 07 p1025 N85-16509
Monitoring cure of epoxy resins using a microdielectrometer
[AD-A148618] 08 p1119 N85-17054
The use of microdielectrometry in monitoring the cure of resins and composites
[AD-A148619] 08 p1119 N85-17055
Battery chargur
[AD-D011420] 08 p1178 N85-17425
Design description of a microprocessor based Engine Monitoring and Control unit (EMAC) for small turboshaft
[NASA-TM-86860] 09 p1263 N85-17935
Effect of water vapor and water droplets on the RAM-1 (Real-Time Aerosol Monitor): Preliminary results
[PB85-109429] 11 p1637 N85-20313
Development of a low cost electrochemical CO monitor based on anodic scanning voltammetry in nonaqueous electrolyte
[PB85-113488] 11 p1637 N85-20314
Continuous measurement of zircaloy corrosion in air with an ultrasonic corrosion monitor
[DE85-003663] 12 p1807 N85-21337
Remote self-contained undersea monitor
[AD-D011520] 12 p1849 N85-21599
Applications of vibration analysis to the condition monitoring of rolling element bearings
[ARL/AERO-R-163] 12 p1859 N85-21663
Focal plane array optical proximity sensor
[NASA-CASE-NPO-15155-1] 12 p1932 N85-22139
Invariant system of technological preparation of production 14 p2268 N85-24056
An improved battery state-of-charge indicator
[NASA-CR-175701] 14 p2298 N85-24227
Computer controlled acquistion of corrosion rate data from multiple sensors
[PB85-157378] 15 p2524 N85-25559
Continued development of a data base management system performance monitor, volume 2
[AD-A151714] 15 p2623 N85-26167
Signal analysis techniques for incipient failure detection in turbomachinery 16 p2736 N85-26884
Reusable rocket engine turbopump condition monitoring 16 p2740 N85-26907
Equipment for monitoring low concentrations of volatile substances in gases or liquid metals
[BLL-DOUNREAY-TR-949-(9091.9F)]
16 p2786 N85-27190
Results from radiation monitoring equipment experiment on STS-8
[AD-A153241] 17 p3055 N85-28911
Retinally stabilized differential resolution television display
[NASA-CASE-NPO-15432-1] 18 p3089 N85-29117
Laser Schlieren crystal monitor
[NASA-CASE-MFS-28060-1] 19 p3374 N85-30932
Heat transfer monitor for measurements of fouling of industrial heat exchangers
[DE85-010257] 20 p3455 N85-31455
Production verification of the acoustic emission weld monitor
[AD-A154168] 20 p3464 N85-31519
Results from radiation monitoring equipment experiments on STS-41C, 41D, 41G and 51A
[AD-A154676] 21 p3580 N85-32142
Monitoring dosage of volatile compounds in tests at low barometric pressure 23 p3954 N85-34506
Evaluation: Close-range photogrammetry for slope inventory and monitoring
[PB85-192755] 24 p4108 N85-35470

MONKEYS
Primate equilibrium performance and diazepam: A behavioral tolerance effect
[AD-A145156] 01 p0094 N85-10634
Specific absorption rate in a sitting rhesus model at 225, 1290, and 5950 MHz for E, H, and K polarizations
[AD-A145435] 02 p0234 N85-11524
Susceptibility of cat and squirrel monkey to motion sickness induced by visual stimulation: Correlation with susceptibility to vestibular stimulation
11 p1694 N85-20850
Histological and compositional responses of bone to immobilization and other experimental conditions
[NASA-CR-175637] 16 p2841 N85-27518
Encapsulation and packaging of a semiconductor multielectrode array for cortical implantation
[AD-A153180] 17 p2996 N85-28535
Primate adrenal reactions to antiorthostatic hypokinesia 19 p3324 N85-30591
Analysis of long bone and vertebral failure patterns
[AD-A154796] 21 p3663 N85-32758
Morphological study of antiorthostatic hypokinesia in monkeys 22 p3822 N85-33680

MONOCHROMATIC RADIATION
Analysis of data entry performance: Chromatic versus monochromatic
[AD-A145568] 03 p0438 N85-12789
Application of tunable monochromatic synchrotron radiation to the quantitative determination of trace elements
[DE85-001271] 09 p1291 N85-18106
Design of VUV monochromator systems
09 p1388 N85-18733
Kinetic energies of fragment ions produced by dissociative photoionization of NO
[NASA-CR-175721] 15 p2647 N85-26327

MONOCHROMATIZATION
A posteriori increase of resolving power of optical system forming averaged monochromatic images
13 p2082 N85-23003

MONOCHROMATORS
A normal-incidence monochromator branch line on the FEL-undulator for experimental studies in the 5 to 30 eV region
[DE84-014379] 04 p0505 N85-13225
Design of VUV monochromator systems
09 p1388 N85-18733
In situ thin film measurement
[AD-A151365] 15 p2659 N85-26411
Optical 3-D signature device for detecting chemical agents
[AD-D011669] 19 p3272 N85-30293
Microwave SAW (Surface Acoustic Wave) monochromator
[AD-D011718] 21 p3590 N85-32311

MONOCRYSTALS
U SINGLE CRYSTALS

MONOLITHIC CIRCUITS
U INTEGRATED CIRCUITS

MONOMERS
Implantation of ionized monomer into aluminum alloy 6061 for marine corrosion protection
[AD-A144874] 01 p0028 N85-10172
Vinyl citrates from citric acid as new monomers
[BMFT-FB-T-83-256] 03 p0336 N85-12178
Chemical modification of the surface of high modulus carbon fibers 04 p0467 N85-12967
Conduction in polymerized polyfunctional diacetylenes
[AD-A149104] 10 p1451 N85-19145
Process for preparing highly optically transparent-colorless armomatic polyimide film
[NASA-CASE-LAR-13351-1] 12 p1811 N85-21360
Chiral polymers
[AD-A150366] 13 p2037 N85-22760
Evaluation of experimental epoxy monomers
[NASA-TM-87476] 16 p2754 N85-26996
Light scattering and spectroscopic studies of polymerization processes
[AD-A153407] 18 p3069 N85-28984
Processable and stable conductive polymers
[AD-D011684] 19 p3249 N85-30143
Graphite/PMR polyimide composites with improved toughness
[NASA-TM-87081] 21 p3561 N85-32148

MONOMOLECULAR FILMS
Interaction of UV-laser radiation with molecular surface-films
[AD-A146311] 03 p0366 N85-12349

MONOPLANES
NT A-7 AIRCRAFT
NT B-70 AIRCRAFT
NT BOEING 737 AIRCRAFT
NT BOEING 767 AIRCRAFT
NT C-135 AIRCRAFT
NT C-141 AIRCRAFT
NT CESSNA 402B AIRCRAFT
NT CL-41 AIRCRAFT
NT CV-990 AIRCRAFT
NT DC 8 AIRCRAFT
NT DH 115 AIRCRAFT
NT DHC 2 AIRCRAFT
NT DO-28 AIRCRAFT
NT F-8 AIRCRAFT
NT F-17 AIRCRAFT
NT F-27 AIRCRAFT
NT F-104 AIRCRAFT
NT F-106 AIRCRAFT
NT JET PROVOST AIRCRAFT
NT MIRAGE AIRCRAFT
NT MIRAGE 3 AIRCRAFT
NT OV-1 AIRCRAFT
NT P-3 AIRCRAFT
NT RF-4 AIRCRAFT
NT T-33 AIRCRAFT
NT U-2 AIRCRAFT
An overview of some monoplaner missile programs
[NASA-TM-86330] 06 p0747 N85-14786

MONOPOLE ANTENNAS
NT WHIP ANTENNAS
Compact wideband multiple conductor monopole antenna
[AD-D011331] 07 p0944 N85-15081
Surface wave excitation study
[DE85-005301] 13 p2056 N85-22875
Parameterization of a transient electromagnetic facility and test antennas from transient data
[DE85-006231] 15 p2545 N85-25710

MONOPOLES
NT MAGNETIC MONOPOLES
Slowly rotating pulsed radiation source
02 p0256 N85-11678

MONOPROPELLANTS
Liquid propellants for use in guns: A review
[AD-A153051] 17 p2937 N85-28131

MONOPULSE ANTENNAS
Phase only adaptive nulling in a monopulse antenna
[AD-D011289] 05 p0628 N85-14026
Inherent angular tracking error in an amplitude comparison monopulse radar
[AD-A154212] 19 p3255 N85-30185

MONOPULSE RADAR
Phase only adaptive nulling in a monopulse antenna
[AD-D011289] 05 p0628 N85-14026
Conformal phased array antenna pattern corrector
[AD-D011489] 10 p1468 N85-19266
A radome for air traffic control SSR radar systems
[AD-P004373] 12 p1827 N85-21467
Ziv-Zakai bound applied to an amplitude-comparison monopulse radar
[AD-A151937] 16 p2773 N85-27118
Angular tracking error in A phase comparison monopulse tracking radar: A critical review and extension of the phase front distortion approach
[AD-A152628] 17 p2949 N85-28205
Inherent angular tracking error in an amplitude comparison monopulse radar
[AD-A154212] 19 p3255 N85-30185

MONOSACCHARIDES
NT RIBOSE

MONOTONE FUNCTIONS
Estimating a monotone density
[CWI-MS-R8403] 05 p0721 N85-14633
A monotonicity property of the power function of multivariate tests
[CWI-MS-R8406] 05 p0721 N85-14635
Stable monotone variational inequalities
[AD-A147123] 07 p1031 N85-16544
Convergence of quasi-stationary to stationary distributions for stochastically monotone Markov processes
[AD-A148041] 08 p1215 N85-17652
On functions with a finite or locally bounded Dirichlet integral 15 p2635 N85-2624
When is a Bernstein-Bezier curve the graph of a function? 17 p3003 N85-28568
Limit behaviour for stochastic monotonicity and applications
[AD-A153814] 18 p3170 N85-29648

MONSOONS
Investigation of satellite measurements in the presence of clouds, forcing influences on clouds and feedback to the large scale following convection
05 p0882 N85-14381

Relationship of Indian monsoon intensity to time of onset 13 p2106 N85-23120
The BALSAMINE experiment
14 p2238 N85-23876
Radiative forcing of the southwest summer monsoon (a satellite perspective) 15 p2593 N85-25961
Influence of land surface processes on the Indian monsoon: A numerical study 18 p3146 N85-29478
On the interannual variability of the Indian monsoon and the Southern Oscillation 20 p3495 N85-31726

MONTANA
Geology of selected migmatite zones within the bitterroot lobe of the Idaho batholith, Idaho and Montana
03 p0389 N85-12489
Chronologic and climatic control on soil development, northern Bighorn Basin, Wyoming and Montana
08 p1181 N85-17443
Depositional systems and coal occurrence in the Fort Union Formation (Paleocene), Powder River Basin, Wyoming and Montana 24 p4114 N85-35505

MONTE CARLO METHOD
A Monte Carlo comparison of the recovery of winds near upwind and downwind from the SASS-1 model function by means of the sum of squares algorithm and a maximum likelihood estimator
[NASA-CR-3839] 01 p0064 N85-10421
SANDYL radiation transport code at the Naval Research Laboratory
[AD-A144890] 01 p0117 N85-10799
Theoretical development of Monte Carlo codes for modeling cumulus cloud fields
[NASA-CR-174063] 02 p0230 N85-11500
Design and implementation of a moduler program system for statistical analyses
[IKE-4-114] 04 p0551 N85-13503
Risk analysis without Monte Carlo methods
04 p0556 N85-13537
Approximating the percentage points of Greenwood's statistic with Cornish-Fisher expansions
[CWI-MS-R8405] 05 p0721 N85-14634
Binaries and evolution of globular clusters
05 p0738 N85-14744
Efficient scores, variance decompositions and Monte Carlo swindles
[AD-A146673] 06 p0858 N85-15458
The effect of assumptions about cost element probability distributions on operating and support cost risk analysis
[AD-A147553] 07 p1036 N85-16576
Validation of the communications link analysis and simulation system (CLASS) 08 p1100 N85-16954
The extension of an invertible coniferous forest canopy reflectance model using SIR-B and LANDSAT data
08 p1149 N85-17246
Two-dimensional modeling for lineal and areal probabilities of weather conditions
[AD-A147970] 08 p1188 N85-17486
A modified Monte-Carlo technique for the simulation of satellite communication systems
[AD-A148689] 08 p1214 N85-17641
Quantum Monte Carlo for molecules
[AD-A148159] 08 p1227 N85-17727
Multiline transfer and the dynamics of stellar winds
08 p1236 N85-17788
Turbulent premixed flame study
[DE85-003220] 09 p1292 N85-18112
Generation of radiation transport geometry from computer-generated design data — monte carlo solution of the neutron transport equation
[DE84-017380] 09 p1370 N85-18606
Small-sample properties of kernel density estimators from randomly right-censored data
[AD-A148752] 09 p1374 N85-18634
A kernel type estimator of a quantile function from right-censored data
[AD-A148753] 09 p1374 N85-18635
Monte Carlo simulation of electron thermalization in rare gases
[NAL-TR-834T] 09 p1375 N85-18643
Monte Carlo simulation of gas Cerenkov detectors
[DE85-002422] 10 p1488 N85-19394
Some investigations of molecular beam epitaxial growth of 3-5 semiconductor films via Monte-Carlo computer simulations, carrier tunneling and spectroscopic ellipsometry
[AD-A149485] 10 p1563 N85-19854
Application of Monte Carlo and molecular dynamics methods to the calculation of thermodynamic properties of molten salts
[AD-A148897] 10 p1565 N85-19869
MCNP code
[DE85-002565] 11 p1702 N85-20706
ITS: The Integrated TIGER Series of coupled electron/photon Monte Carlo transport codes
[DE85-003719] 11 p1725 N85-20847
Monte Carlo studies of tandem mirror plasmas interacting with waves in the Ion Cyclotron Range of Frequencies (ICRF)
[DE85-002968] 11 p1731 N85-20883
Simulating supersymmetry at the SSC
[DE85-000699] 11 p1736 N85-20917
Cometary atmospheres: Modeling the spatial distribution of observed neutral radicals
[NASA-CR-175491] 11 p1765 N85-21097
A model for the evolution of on-orbit manmade debris environment 12 p1784 N85-21196
Ordinary and proper location M-estimates for ARMA models, revised
[AD-A149705] 12 p1920 N85-22061
Jet topologies in hadron-hadron collisions
[DE85-001328] 12 p1929 N85-22119
A Monte Carlo sampling plan for estimating network reliability
[AD-A150511] 13 p2065 N85-22898
Introduction to combinatorial geometry
[DE85-003266] 13 p2152 N85-23364
Problems in recovering crater production functions
13 p2182 N85-23539
Monte Carlo modeling of lunar megaregolith development 13 p2197 N85-23627
Tracer diffusion in an ordered alloy: Application of the path probability and Monte Carlo methods
[DE85-002768] 14 p2257 N85-23986
Modeling of radiothermal radiation of rain by Monte-Carlo method 14 p2341 N85-24476
Research in theoretical nuclear physics
[DE85-006172] 14 p2418 N85-24920
Monte Carlo lattice models for adsorbed polymer conformation
[NASA-TP-2453] 14 p2426 N85-24961
Soliton energetics in extended Peierls-Hubbard models: A quantum Monte Carlo study
[DE85-005409] 14 p2429 N85-24981
Lattice Monte Carlo calculations of finite temperature QCD
[DE85-004035] 14 p2431 N85-24992
Multiple scattering of electromagnetic waves in discrete random media
[AD-A151766] 16 p2772 N85-27112
A mathematical model for calculating detection probability of a diffusion target
[AD-A152026] 16 p2854 N85-27601
An overview of stochastic signal modeling
[AD-A152144] 16 p2855 N85-27605
The statistical analysis of initial imperfection measurements — shell profiles
[VTH-LR-442] 16 p2857 N85-27622
Energy reflection coefficient for H+ ions at energies between 10 and 80 keV
[DE85-007547] 16 p2863 N85-27662
LIGHT: A ray tracing code to simulate light collection in scintillation spectrometers and light pipes
[DE85-007213] 16 p2865 N85-27673
Adding computationally efficient realism to Monte Carlo turbulence simulation
[NASA-TP-2469] 17 p3025 N85-28708
Incorporation of Monte Carlo electron interface studies into photon general cavity theory
[DE85-007674] 17 p3034 N85-28772
Lattice actions improved by block-spin renormalisation group and maximally symmetric lattices
[DE85-007416] 17 p3045 N85-28841
Diffusion of gases in porous solids: Simulation and measurements
[DE85-008870] 18 p3101 N85-29196
Fast electromagnetic (EM) shower simulation
[NOTA-INTERNA-831] 18 p3175 N85-29683
Monte Carlo simulation of thermalization of subexcitation electrons in He, Ne, Ar, Kr and Xe
[NAL-TR-843T] 18 p3178 N85-29702
Comparison of calculations and measurements of the off-axis radiation dose (SI) in liquid nitrogen as a function of radiation length
[AD-A153676] 18 p3178 N85-29704
SPECTER: Neutron damage calculations for materials irradiations
[DE85-005791] 18 p3180 N85-29716
Mathematics of oil production
[DE85-011235] 19 p3267 N85-30261
SABRINA: An interactive solid geometry modeling program for Monte Carlo
[DE85-010796] 19 p3339 N85-30692
MECA: A multiprocessor concept specialized to Monte Carlo
[DE85-010791] 19 p3346 N85-30737
MCNP variance reduction overview
[DE85-010765] 19 p3346 N85-30741
A comparison of four Monte Carlo methods for estimating the probability OF S=T connectedness
[AD-A154264] 19 p3348 N85-30749
MCNP: A general Monte Carlo code for neutron and photon transport
[DE85-010764] 19 p3348 N85-30750
Low-discrepancy point sets in transport codes
[DE85-010786] 19 p3348 N85-30755
Hybrid two-dimensional Monte-Carlo electron transport in self-consistent electromagnetic fields
[DE85-010757] 19 p3348 N85-30756
Monte Carlo alpha calculation
[DE85-010720] 19 p3349 N85-30758
Surface effects on sputtered atoms and their angular and energy dependence
[DE85-010506] 19 p3354 N85-30789
High-energy particle Monte Carlo at Los Alamos
[DE85-010716] 19 p3363 N85-30856
Monte Carlo electron/photon transport
[DE85-010799] 19 p3364 N85-30861
Monte Carlo simulations of fermion systems: The determinant method
[DE85-010708] 19 p3376 N85-30947
Monte Carlo sampling strategies for lattice gauge calculations
[DE85-010756] 19 p3377 N85-30948
Comparison of ERS-1 scatterometer Monte Carlo performance simulations using a weighted nonlinear least squares and a maximum likelihood estimation method
20 p3420 N85-31224
Direct simulation techniques for the Boltzmann equation
[DFVLR-FB-85-13] 20 p3457 N85-31470
MIG: MCNP Input Generator for EFFI magnet geometrics
[DE85-010494] 20 p3515 N85-31857
Monte Carlo: In the beginning and some great expectations
[DE85-010789] 20 p3518 N85-31872
Monte-Carlo treatment of nonlinear collisional effects in charged-particle transport
[DE85-010755] 20 p3521 N85-31887
Methods of Monte Carlo electron transport in particle-in-cell codes
[DE85-010702] 20 p3521 N85-31888
Time-implicit Monte-Carlo collision algorithm for particle-in-cell electron transport models
[DE85-010758] 20 p3521 N85-31890
Forecasting of tropical cyclone motion using an EOF (Empirical Orthogonal Function) representation of wind forcing
[AD-A155034] 21 p3636 N85-32580
Monte Carlo studies of H2O layers adsorbed on a model basal face of AgI 21 p3643 N85-32633
Radiation transport
[DE85-010333] 21 p3703 N85-33005
Power density and threshold control strategies for radar track initiation
[AD-A155357] 22 p3756 N85-33292
MORSE-CGA: A Monte Carlo radiation transport code with array geometry capability
[DE85-012063] 22 p3830 N85-33718
Monte Carlo learning-biasing experiment with intelligent random numbers
[DE85-010713] 22 p3834 N85-33742
Implicit Monte Carlo methods and non-equilibrium Marshak wave radiative transport
[DE85-010711] 22 p3835 N85-33743
Nuclear data for MCNP
[DE85-010794] 22 p3840 N85-33782
Digital characterization of particle tracks for microdosimetry
[DE85-012898] 22 p3846 N85-33822
Energy spectrum of extragalactic gamma-ray sources
[OG-2.7-13] 22 p3872 N85-33988
Long term variability of the cosmic ray intensity
[OG-3.1-11] 22 p3874 N85-33990
Arrival directions of cosmic rays of E .4 EeV
[OG-5.3-4] 22 p3884 N85-34071
Coupled electron-photon transport calculations using the method of discrete ordinates
[DE85-009444] 23 p3967 N85-34597
Monte Carlo techniques for analyzing deep penetration problems
[DE85-011426] 23 p3968 N85-34598
CYLTRAN calculations of electron effects on XD detectors
[LA-10264-MS] 23 p3969 N85-34601
Low-energy sputterings with the Monte Carlo Program ACAT
[IPPJ-AM-40] 23 p3982 N85-34680
Monte Carlo calculations of relativistic solar proton propagation in interplanetary space
[SH-3.2-11] 23 p4004 N85-34836
Modeling a high energy gamma-ray telescope
[OG-9.2-5] 23 p4025 N85-34944
A position sensitive phoswich hard X-ray detector system
[OG-9.3-12] 23 p4028 N85-34967

On the statistical significance of excess events: Remarks of caution and the need for a standard method of calculation
[OG-9.5-10] 23 p4031 N85-34987
Additional flux of particles and albedo-electrons in upper atmosphere
[SH-8.1-6] 23 p4045 N85-35080
Monte Carlo calibration of the SMM gamma ray spectrometer for high energy gamma rays and neutrons
[SH-8.1-8] 23 p4051 N85-35121
Two-dimensional numerical modeling of ion implanted GaAs MESFET devices 24 p4086 N85-35341
Calculation of heavy-ion tracks in liquid water
[DE85-012101] 24 p4149 N85-35725
EAS accompanied by gamma-families at Mt. Norikura and comparison with Monte Carlo simulation
[HE-3.3-10] 24 p4181 N85-35928
Relation between gamma-ray family and EAS core: Monte-Carlo simulation of EAS core
[HE-3.5-7] 24 p4185 N85-35955
The lateral distributions of charged particles of energy greater than 0.3 E sub crit in electron-photon cascades in lead and air
[HE-3.6-10] 24 p4185 N85-35957
Result of Monte-Carlo simulation of electron-photon cascades in lead and layers of lead-scintillator
[HE-3.6-11] 24 p4185 N85-35958
Hadrons registration in emulsion chamber with carbon block
[HE-3.7-3] 24 p4186 N85-35962
New analysis of nuclear interaction observed by Mt. Kanbara emulsion chamber experiment
[HE-3.7-4] 24 p4186 N85-35963
Intensities of high-energy cosmic rays at Mount Kanbala
[HE-3.7-5] 24 p4186 N85-35964
Ultra high energy events in ECHOS series and primary energy spectrum
[HE-3.7-9] 24 p4186 N85-35966
Theoretical study of EAS hadronic structure
24 p4189 N85-35991
Particle distributions in approximately 10(13) - 10(16) eV air shower cores at mountain altitude and comparison with Monte Carlo simulations
[HE-4.2-18] 24 p4190 N85-35994
The longitudinal development of muons in cosmic ray air showers at energies 10(15) - 10(17) eV
[HE-4.3-12] 24 p4192 N85-36006
Topological aspects of age parameter
[HE-4.3-13] 24 p4192 N85-36007
Monte Carlo simulation of EAS generated by 10(14) - 10(16) eV protons
[HE-4.3-14] 24 p4192 N85-36008
A three-dimensional Monte Carlo calculation of the photon initiated showers and Kiel result
[HE-4.5-13] 24 p4196 N85-36035
Multimuons events and primary composition
[HE-5.1-5] 24 p4201 N85-36070
The spectrum of cosmic ray muons obtained with 100-ton scintillation detector underground and the analysis of recent experimental data
[HE-5.1-6] 24 p4201 N85-36071
A new world survey expression for cosmic ray vertical intensity vs. depth in standard rock
[HE-5.1-10] 24 p4201 N85-36073
Muon groups and primary composition at 10 to the 13th power to 10 to the 15th power eV
[HE-5.1-12] 24 p4201 N85-36074

MONTEREY BAY (CA)
Coastal erosion along Monterey Bay
[AD-A155610] 21 p3655 N85-32707

MOON
Magnetosphere, rings, and moons of Uranus
02 p0301 N85-11951
Conference on the Origin of the Moon
[NASA-CR-174068] 04 p0581 N85-13709
Geophysical and geochemical constraints favoring the capture hypothesis 04 p0581 N85-13710
Lunar magma ocean and its implication for origin of the Moon 04 p0581 N85-13711
The initial thermal state of the Moon
04 p0581 N85-13712
Lunar magnetic history 04 p0582 N85-13715
The I-Pu-Xe age of the Moon
04 p0584 N85-13729
Constraints on the origin of viscoelastic bodies
04 p0584 N85-13732
Tidal disruption and the origin of the Moon
04 p0586 N85-13739
A numerical investigation of planetesimal collision trajectories with a Moon accumulating in Earth orbit
04 p0586 N85-13740
Stochastic does not equal ad hoc --- theories of lunar origin 04 p0586 N85-13741
A testable gravitational capture model for the origin of the Earth's Moon 04 p0586 N85-13742
Directional properties of circular Maria: Interpretation in the context of a testable gravitational capture model for lunar origin 04 p0586 N85-13743
The problem of iron partition between Earth and Moon during simultaneous formation as a double planet system 04 p0587 N85-13744
Origin of the Moon 04 p0587 N85-13745
Geochemical evidence for the formation of the Moon by impact induced fission of the proto-Earth
04 p0587 N85-13747
Catalogue of observations of total occultations of stars by the Moon for the years 1972 to 1980 and of grazing occultations for the years 1963 to 1980
[BULL-192] 05 p0741 N85-14768
Spectral reflectance studies on the orientale region of the Moon 06 p0888 N85-15639
The geology of the terrestrial planets
[NASA-SP-469] 09 p1410 N85-18888
Moon 09 p1411 N85-18893
Herstmonceux observations of the Sun, planets and Moon, 1957 - 1982
[BULL-193] 11 p1762 N85-21067
A new look at the planets --- space probes
[AERONOMICA-ACTA-37-1984]
11 p1765 N85-21096
Giant planets and their satellites: Cosmochemistry, evolution and structure 13 p2175 N85-23494
A circum-terrestrial compositional filter
13 p2179 N85-23520
Models of angular momentum input to a circum-terrestrial swarm from encounters with heliocentric planetesimals 13 p2179 N85-23521
Landform identification on radar images
13 p2198 N85-23635
Radar observations of fissure-fed basaltic lava flows, Craters of the Moon, Idaho 13 p2199 N85-23640
Relationship between seismic status of Earth and relative position of bodies in sun-earth-moon system
14 p2345 N85-24499
Neutrino measurements on the Moon
[DE85-007700] 16 p2884 N85-27791
An analysis of alternate hydrogen sources for lunar manufacture
[DE85-007234] 16 p2884 N85-27792
Surface exploration geophysics applied to the Moon
[DE85-006714] 16 p2884 N85-27793
Moon bounce communications to small terminals
[AD-A153297] 17 p2950 N85-28212
Analytical generation of satellite orbits at the RAE (Royal Aircraft Establishment)
[AD-A152655] 17 p3053 N85-28901
Adsorption of Hg on lunar samples
[DE85-007948] 17 p3054 N85-28906
Geochemical confirmation of the lunar magmasphere hypothesis 22 p3859 N85-33895

MOORING
The long term upper ocean study (LOTUS). Cruise summary and hydrographic data report, OCEANUS 154, May 1984
[AD-A147906] 07 p1009 N85-16414
The body burden of organic vapors in artificial air trial measurements aboard a moored submarine
[AD-A149698] 12 p1910 N85-21988

MOORINGS
U MOORING

MORAINES
U GLACIAL DRIFT

MORL
U MANNED ORBITAL RESEARCH LABORATORIES

MORNING
Substorm associated Pc 1 emission in the morning sub-cleft latitudes 14 p2368 N85-24637

MORPHOLOGY
NT GEOMORPHOLOGY
NT ISOMORPHISM
NT POLYMORPHISM
Morphological changes of gamma prime precipitates in nickel-base superalloy single crystals
[NASA-TM-83698] 01 p0026 N85-10165
Morphology and dynamic mechanical properties of diglycidyl ether of bisphenol-A toughened with carboxyl-terminated butadiene-acrylonitrile
04 p0466 N85-12958
Effect of lithology and climate on the morphology of drainage basins in northwestern Colorado
[PB84-228236] 06 p0828 N85-15258
Structure and functions of fungal cell surfaces
[NASA-TM-77439] 06 p0842 N85-15347
Rubber-modified epoxies. 1: Cure, transitions, and morphology
[AD-A147377] 07 p0932 N85-15908
Effects of body mass and morphology on thermal responses in water
[AD-A147568] 07 p1016 N85-16455
Rubber-modified epoxies. Part 2: Morphology, transitions, and mechanical properties
[AD-A147962] 08 p1132 N85-17137
Australian Multiexperimental Assessment of SIR-B (AMAS) 08 p1148 N85-17243
Morphology and optical polarization of the 3C 273 jet --- radio jet 08 p1238 N85-17803
Tribological properties of graphite-fiber-reinforced, partially fluorinated polyimide composites
[NASA-TM-86926] 09 p1298 N85-18153
Influence of the amorphous-crystalline interface morphology on dislocation nucleation in pre-amorphized silicon
[DE85-002068] 09 p1398 N85-18800
Microstructural analysis of ion containing polymers
[DE85-001594] 10 p1453 N85-19157
Mechanism and pattern of fatigue crack growth in aluminum alloys 11 p1597 N85-20047
Morphological study of monkeys submitted to antiorthostatic hypokinesia 12 p1902 N85-21942
Effect of long-term repeated exposure to high-intensity stationary magnetic field on adrenomedullary activity
12 p1904 N85-21955
On the morphology of spiral modes --- disk galaxies
12 p1955 N85-22283
Origin of Martian polygonal terrain: Preliminary results
13 p2191 N85-23591
Morphology of 2keV-electrons observed by GEOS 1
14 p2360 N85-24581
Effects of ion bombardment on the morphology of lead films
[DE85-007232] 15 p2511 N85-25494
Induced changes in the cholinergic system of sciatic nerve and slow and fast twitch muscle of rats
15 p2609 N85-26061
Percutaneous connectors
[NASA-CR-175627] 16 p2839 N85-27506
The state of martensite after quenching in a magnetic field
[BLL-BISI-TRANS-22297-(9022.06)]
17 p2926 N85-28051
Application of scattering methods to the studies of the structure of polymer blends
[IFPR-13/1984] 17 p2933 N85-28104
Morphological stability and fluid dynamics of vapor crystal growth
[NASA-CR-175879] 17 p3042 N85-28822
Morphological stability and fluid dynamics of vapor crystal growth
[NASA-CR-175880] 17 p3042 N85-28823
The structure of ion plated films in relation to coating properties
[NASA-TM-87055] 18 p3085 N85-29065
Electrochemical and morphological study of the effect of temperature on the restructuring and loss of capacity of alkaline battery electrodes
[DE85-006869] 18 p3129 N85-29378
Method for growth of crystals by pressure reduction of supercritical or subcritical solution
[NASA-CASE-NPO-15772-1] 18 p3192 N85-29800
Morphological study of primate hypothalamus and hypophysis after experiment with antiorthostatic hypokinesia 19 p3325 N85-30603
A study of freezing and melting with eutectic interactions 19 p3378 N85-30956
Measurement and analysis of two-phase flow through low permeability media, task 3
[PB85-188373] 20 p3435 N85-31313
Identification and quantitation of morphological cell types in electrophoretically separated human embryonic kidney cell cultures 20 p3501 N85-31764
Milliarcsecond morphology of the twin quasar 0957 + 56A,B: The view through a gravitational lens
20 p3544 N85-32054
Understanding and laboratory prediction of the atmospheric corrosion behavior of steels and of non-ferrous metals and alloys
[AD-A154642] 21 p3568 N85-32179
Enrichments for phototrophic bacteria and characterization by morphology and pigment analysis
21 p3660 N85-32738

MORPHOTROPISM
U ISOMORPHISM

MORTALITY
Morbidity and mortality associated with exposure to Otto Fuel II in the U.S. Navy 1966-1979
[AD-A148726] 09 p1363 N85-18574
Response of unmanaged forests to CO2-induced climate change: Available information, initial tests and data requirements
[DOE/NSB-0053] 12 p1883 N85-21817

MORTARS (MATERIAL)
Compressive strength-maturity relationships of mortar containing fly ash
[AD-A148705] 09 p1339 N85-18423

Experimental characterization and stability of salt- and nonsalt-containing grouts and mortars (BCT-1F- and BCT-1FF-related)
[DE85-012339] 22 p3753 N85-33263

MOS (JAPANESE SPACECRAFT)
U JAPANESE SPACECRAFT

MOS (SEMICONDUCTORS)
U METAL OXIDE SEMICONDUCTORS

MOSAICS
Viking Lander mosaics of Mars
13 p2203 N85-23667
Voyager cartography 13 p2203 N85-23668
Mosaic Infrared Sensor for Space Astronomy (MIRSSA)
[NASA-CR-176154] 22 p3786 N85-33456

MOSCOW
Laser air pollution monitoring system planned for Moscow 10 p1500 N85-19465

MOSFET
U FIELD EFFECT TRANSISTORS

MOSS (SPACE STATIONS)
U ORBITAL SPACE STATIONS

MOSSBAUER EFFECT
Mossbauer spectroscopic investigations of the diffusion and correlation of lattice defects (complementary to neutron spectroscopic investigations)
03 p0429 N85-12736
Mossbauer effect and contactless conductivity studies of superconducting actinides intermetallics and hydrides. Mossbauer high pressure studies
03 p0430 N85-12743
Mossbauer spectroscopy and X-ray diffraction of samples from the Santa Catharina iron meteorite
06 p0885 N85-15624
Theoretical determination of surface magnetism
[DE85-003224] 11 p1714 N85-20783
Moessbauer study of amorphous Fe(67)Co(18)B(14)S(1)
[AERE-R-11526] 11 p1737 N85-20928
Inelastic scattering in condensed matter with high intensity Moessbauer radiation
[DE85-003531] 12 p1854 N85-21627
Quenching effects on iron site partitioning in the Apollo 17 orange glass composition 13 p2184 N85-23553
Hibonite: Crystal chemistry and origin of blue coloration in meteoritic assemblages 13 p2184 N85-23555
Mossbauer spectrometry: Testing of a new computer based system and its application to a study of an aluminum-iron-cerium alloy
[AD-A151826] 15 p2510 N85-25483
The structure of carbon martensite analyzed with Moessbauer spectra
[BLL-BISI-TRANS-22402-(9022.06)]
17 p2927 N85-28062
Highly dispersed metal atoms in zeolites
[DE85-010515] 19 p3354 N85-30792
Analysis of ferrates and ferrites of three transition metals using Moessbauer effects
[BLL-CE-TRANS-8019-(9022.09)]
20 p3430 N85-31273
In situ Moessbauer investigation of bimetallic catalysts on a base: FeRu, FeRh, FePd, FeIr, and FePt on SiO2
[B8563200] 20 p3432 N85-31293
A miroprocessor based multiscaling data acquisition system for Mossbauer spectroscopy
[USIP-85-01] 20 p3518 N85-31875
Noble metals as incipient transition metals
[DE85-013283] 24 p4080 N85-35286

MOTILITY
U LOCOMOTION

MOTION
A control model: Interpretation of Fitts' law
05 p0706 N85-14526
Modeling of human motion by computer considering measurement errors in initial data
07 p1012 N85-16429
More limit theory for the sample correlation function of moving averages
[AD-A148975] 10 p1550 N85-19773
Television animation store: Digital chroma, key and mixer units
[BBC-RD-1984/16] 12 p1824 N85-21442
3D computer animation: More an evolution problem than a motion problem 23 p3959 N85-34536
Using dynamic analysis to animate articulated bodies such as humans and robots 23 p3959 N85-34537
Towards an integrated view of 3-D computer character animation 23 p3959 N85-34538
Research issues in generating graphical explanations
23 p3959 N85-34539

MOTION AFTEREFFECTS
Thresholds for detection of linear oscillation following prolonged weightlessness 20 p3508 N85-31810

MOTION EQUATIONS
U EQUATIONS OF MOTION

MOTION PERCEPTION
Theory underlying the peripheral vision horizon device
01 p0008 N85-10048
Stimulus factors in motion perception and spatial orientation 01 p0008 N85-10049
The peripheral visual cue assessment facility at Ames Research Center 01 p0008 N85-10050
Evaluation of the Malcolm horizon in a moving-base flight simulator 01 p0008 N85-10051
Thresholds of perception of whole body linear oscillation: Modification by spaceflight 05 p0694 N85-14467
Visual-vestibular interaction in human motion perception 05 p0695 N85-14471
Use of linear perspective scene cues in a simulated height regulation task 05 p0704 N85-14517
Mean and random errors of visual roll rate perception from central and peripheral visual displays
05 p0704 N85-14519
Direction judgement errors in perspective displays
05 p0705 N85-14520
The interaction of focused attention with flow-field sensitivity 05 p0705 N85-14521
Accuracy of system step response roll magnitude estimation from central and peripheral visual displays and simulator cockpit motion 05 p0705 N85-14522
Automatic determination of motion in an image sequence. The interest for interpretation
[ENST-84E012] 05 p0716 N85-14592
Spatiotemporal characteristics of visual localization
[AD-A148013] 08 p1200 N85-17555
Optical flow and texture variables useful in detecting decelerating and accelerating self-motion
[AD-A148718] 09 p1384 N85-18703

MOTION PICTURES
Positioning errors of commutating lenses and their influence on characteristics of high speed movie cameras 14 p2273 N85-24085
Pulsed lasers for filming color holographic film images
22 p3781 N85-33426

MOTION SICKNESS
The adaptation of vestibulo-spinal reflexes as a function of spaceflight and their relationship to space motion sickness 05 p0694 N85-14468
Proceedings of a Workshop on Research Issues in Simulator Sickness
[AD-A148543] 08 p1196 N85-17538
Simulator sickness: Sensorimotor disturbances induced in flight simulators
[AD-P004334] 09 p1271 N85-17988
Management of vibration sickness in coal mines by hyperbaric oxygenation 10 p1523 N85-19609
Comparative assessment of different treatment modalities in miners with vibration- and noise-induced disease 10 p1524 N85-19610
Modulated sinusoidal currents in management of vibration sickness 10 p1524 N85-19612
Motion Sickness: Mechanisms, Prediction, Prevention and Treatment
[AGARD-CP-372] 11 p1693 N85-20642
Neurophysiological correlates of motion sickness: Role of vestibulocerebellum and 'vomiting center' reanalyzed
11 p1693 N85-20643
Influence of gravitoinertial force level on apparent magnitude of coriolis cross-coupled angular accelerations and motion sickness 11 p1693 N85-20644
Vestibular and oculomotor function during Gz variations 11 p1693 N85-20645
Prediction of the space adaptation syndrome
11 p1693 N85-20646
Prediction of seasickness susceptibility
11 p1693 N85-20647
Laboratory tests of motion sickness susceptibility
11 p1694 N85-20648
Results of a longitudinal study of airsickness incidence during Naval flight officer training
11 p1694 N85-20649
Susceptibility of cat and squirrel monkey to motion sickness induced by visual stimulation: Correlation with susceptibility to vestibular stimulation
11 p1694 N85-20650
Susceptability to kinetoses and the amplitude perceived from sensory illusions 11 p1694 N85-20651
Preflight and postflight motion sickness testing of the Spacelab 1 crew 11 p1694 N85-20652
Simulator sickness: Reaction to a transformed perceptual world. 6: Preliminary site surveys
11 p1694 N85-20653
Space motion sickness monitoring experiment: Spacelab 1 11 p1695 N85-20654
Space adaptation syndrome: Incidence and operational implications for the space transportation system program
11 p1695 N85-20655
Analysis of head motion during simulated, rough water operation of a 2200 ton surface effect ship
11 p1695 N85-20656
A double blind comparative trial of powdered ginger root, hyosine hydrobromide, and cinnarizine in the prophylaxis of motion sickness induced by cross coupled stimulation
11 p1695 N85-20657
The current status of the RAF programme of desensitisation for motion sick aircrew
11 p1695 N85-20658
Psychological components in the development and prevention of air sickness 11 p1696 N85-20659
Biofeedback treatment of airsickness: A review
11 p1696 N85-20660
Results of a longitudinal study of airsickness during naval flight officer training: Executive summary
[AD-A150887] 14 p2388 N85-24712
Shuttle operational test and scientific investigations
14 p2394 N85-24746
Sensory and motor properties of the cerebellar uvula and modulus 15 p2613 N85-26104
Anatomy of the vestibulo-automatic outflow to the gut
15 p2614 N85-26108
Airsickness control using biofeedback to self-regulate psychophysiological responses
[AD-A151167] 15 p2617 N85-26128
Computerized biophysical data acquisition system for motion sickness studies
[AD-A151691] 15 p2618 N85-26131
What is being done to control motion sickness?
15 p2687 N85-26699
Mission operations requirements document for D-1 Experiment 102, Vestibular Experiments in Spacelab
[NASA-TM-87495] 21 p3557 N85-32129
USSR report: Space Biology and Aerospace Medicine, volume 19, no. 2, March - April 1985
[JPRS-USB-85-004] 22 p3820 N85-33687
Labyrinthine and extralabyrinthine mechanisms of development of motion sickness in weightlessness
22 p3821 N85-33688
Effect of experimental motion sickness on postrotary nystagmus and counterrotation illusion
22 p3824 N85-33690
A review of motion sickness with special reference to simulator sickness
[AD-A155975] 24 p4131 N85-35611

MOTION SICKNESS DRUGS
Management of microcirculatory disorders in vibration sickness 10 p1524 N85-19611
A double blind comparative trial of powdered ginger root, hyosine hydrobromide, and cinnarizine in the prophylaxis of motion sickness induced by cross coupled stimulation
11 p1695 N85-20657

MOTION SIMULATION
Motion sensor evaluation using simulation
[DE84-014989] 01 p0050 N85-10331
Models for the effects of G-seat cuing on roll-axis tracking performance 05 p0707 N85-14532
Method for prompt modeling of quasiperiodic movement of solid near-axisymmetrical body in atmosphere
13 p2043 N85-22790
A systematic determination of skill and simulator requirements for airline transport pilot certification
[AD-A154135] 19 p3330 N85-30630
Docking simulation analysis of range data requirements for the orbital maneuvering vehicle
[NASA-TM-86510] 20 p3407 N85-31143

MOTION SIMULATORS
Suppression of biodynamic interference by adaptive filtering 05 p0706 N85-14530

MOTION STABILITY
NT AERODYNAMIC STABILITY
NT AIRCRAFT STABILITY
NT ATTITUDE STABILITY
NT BOUNDARY LAYER STABILITY
NT DIRECTIONAL STABILITY
NT FLAME STABILITY
NT FLOW STABILITY
NT GYROSCOPIC STABILITY
NT LATERAL STABILITY
NT LONGITUDINAL STABILITY
NT LOW SPEED STABILITY
NT MAGNETOHYDRODYNAMIC STABILITY
NT ROTARY STABILITY
NT SPACECRAFT STABILITY
NT WEIBEL INSTABILITY
Improvements in linked-spar motion-compensated lifting system
[AD-D011413] 08 p1136 N85-17165
Translating rudder pedal system
[AD-D011510] 12 p1780 N85-21172
Absolute stability of unsteady movement of axisymmetrical rotating flight vehicle
13 p2044 N85-22793
Electronics Engineering Department EE Technical Review
[UCRL-50025-84-1] 13 p2063 N85-22887

Linearization of digital derived rate algorithm for use in linear stability analysis
[NASA-TM-87000] 14 p2243 N85-23904
Stability of steady modes of motion by axis of rotating wheel in nonlinear bearings 14 p2279 N85-24117
Stability of steady motions of dynamically symmetrical solid at a triangular libration point
14 p2279 N85-24120
Investigation of dynamic noise affecting geodynamics information in a tethered subsatellite
[NASA-CR-176031] 20 p3476 N85-31602
MOTIVATION
NT CONTRACT INCENTIVES
Analysis of team performance in a programmed environment
[NASA-CR-175634] 14 p2392 N85-24728
Effect of triphthasine and elenium on changes in evoked bioelectrical activity of the brain exposed to stationary magnetic field 19 p3325 N85-30601
Air university commander's and supervisor's guide on substance abuse
[AD-A158336] 24 p4133 N85-35622
MOTOR SYSTEMS (BIOLOGY)
U EFFERENT NERVOUS SYSTEMS
MOTOR VEHICLES
NT AUTOMOBILES
NT ELECTRIC AUTOMOBILES
NT ELECTRIC MOTOR VEHICLES
NT TANK TRUCKS
NT TRACKED VEHICLES
NT TRACTORS
NT TRUCKS
Size specific total particulate emission factors for mobile sources
[PB84-226653] 01 p0071 N85-10471
Vehicle-to-vehicle connection mechanism
[AD-D011267] 05 p0645 N85-14142
The changing vibration simulation for military ground vehicles 09 p1334 N85-18387
Study of the motion of agricultural vehicles on steep grass-covered slopes
[AD-P004290] 09 p1408 N85-18867
Alternative fuels for buses: Current assessment and future perspectives
[PB85-116325] 10 p1459 N85-19190
USSR report: Transportation
[JPRS-UTR-84-008] 14 p2208 N85-23694
USSR report: Transportation
[JPRS-UTR-84-015] 15 p2460 N85-25192
USSR report: Transportation
[JPRS-UTR-84-014] 15 p2467 N85-25229
An electron microscopic study of urban aerosol
21 p3651 N85-32689
MOTORS
NT ASYNCHRONOUS MOTORS
NT ELECTRIC MOTORS
NT INDUCTION MOTORS
NT MICROMOTORS
NT SERVOMOTORS
NT SYNCHRONOUS MOTORS
NT TORQUE MOTORS
Solving equations of movement with variable inertia moment
[BLL-M-35975-(5828.4)] 05 p0641 N85-14111
Dual optical mechanical position tracker
[AD-D011739] 22 p3844 N85-33611
MOUNTAINS
NT ALPS MOUNTAINS (EUROPE)
NT ANDES MOUNTAINS (SOUTH AMERICA)
NT APPALACHIAN MOUNTAINS (NORTH AMERICA)
NT BIGHORN MOUNTAINS (MT-WY)
NT CARPATHIAN MOUNTAINS (EUROPE)
NT CASCADE RANGE (CA-OR-WA)
NT COASTAL RANGES (CA)
NT HIMALAYAS
NT PYRENEES MOUNTAINS (EUROPE)
NT ROCKY MOUNTAINS (NORTH AMERICA)
NT SIERRA NEVADA MOUNTAINS (CA)
Fungi of Mt. Babia Gora. 2: Indicative value of macromycetes in forest associations. A: Initial considerations
[NASA-TM-77485] 01 p0094 N85-10632
Fungi of Mount Babia Gora. 3: The indicating value of macromycetes in the forest associations
[NASA-TM-77486] 01 p0094 N85-10633
The effect of naproxen on acute mountain sickness and vascular responses to hypoxia
[AD-A145144] 01 p0095 N85-10638
Local geoid determination in mountain regions
[AD-A145799] 03 p0384 N85-12458
Stratigraphy, petrology, and structure of the Pingston terrane, Mount Hayes C-5 and C-6 quadrangles, eastern Alaska Range, Alaska 04 p0517 N85-13301
Paleogene volcanic rocks of the Matanuska Valley area and the displacement history of the Castle Mountain fault 04 p0518 N85-13303
Effect of mountain wave dynamics on orographic storms
[DE84-014713] 04 p0540 N85-13433
A tectonic and metamorphic history of the north-central Klamath Mountains, California 05 p0673 N85-14323
Petrology and structure of Pwemain to Jurassic rocks near Yreka, Klamath Mountains, California
05 p0673 N85-14325
Sedimentation, structure and tectonics of the Umpqua group (paleocene to early eocene), southwestern Oregon 05 p0678 N85-14354
Tectonic, volcanic, and climatic geomorphology study of the Sierras Pampeanas Andes, northwestern Argentina 08 p1144 N85-17215
Post-Laramide history of North Central Wyoming
08 p1181 N85-17444
Sedimentary petrology and provenance of the upper Jackforth Sandstone (Morrowan) Quachita Mountains, Arkansas, USA 08 p1182 N85-17447
Stratigraphy of early ordovician El Paso group of the southern Hueco Mountains, Hudspeth County, Texas
09 p1353 N85-18510
Preliminary photomaps of Venus surface in the Maxwell Mountains and adjacent areas 13 p1982 N85-22438
The geology of Mt. Hope, a silicic volcanic center in West Central Arizona 13 p2187 N85-23571
Geomorphology and geology of the Southwestern Margaritifer Sinus and Argyre regions of Mars. Part 1: Geological and geomorphological overview
13 p2192 N85-23600
Mountain barrier baroclinity effects on surface winds along the Alaskan Arctic coast 14 p2238 N85-23877
Hydrological data collection from Swedish mountain areas 14 p2327 N85-24388
Structural analysis of terrane accretions in the eastern Brooks Range and adjacent areas in central Alaska and Canada
[DE85-008279] 17 p2993 N85-28501
Implications about in situ stress at Yucca Mountain
[DE85-008068] 18 p3126 N85-29356
Influence of underwater volcanic mountains of Atlantic on microplankton distribution 19 p3294 N85-30424
The Terrain-Responsive Atmospheric Code (TRAC) for plume growth and dispersion in complex terrain
[DE85-010541] 19 p3309 N85-30513
Possible use of the COSPAS/SARSAT system within the Swedish mountain rescue organization
20 p3401 N85-31100
The 1984 biotic studies of Yucca Mountain, Nevada test site, Nye County, Nevada
[DE85-011715] 23 p3951 N85-34487
Aeromagnetic and radiometric signatures of a possible porphyry system in the western Tushar Mountains, Utah
24 p4103 N85-35437
MOUNTING
NT RIGID MOUNTING
Mounting construction for turbine vane assembly
[AD-D011395] 07 p0904 N85-15723
Recommended improvements for second generation 121.5/243 MHz ELT's
[NASA-CR-175274] 08 p1080 N85-16841
Gear case vibration isolation in a geared turbine generator 09 p1338 N85-18414
Advanced life analysis methods. Volume 1: Cracking data survey and NDI (nondestructive inspection) assessment for attachment lugs
[AD-A150419] 13 p2103 N85-23108
Advanced life analysis methods. Volume 2: Crack growth analysis methods for attachment lugs
[AD-A150420] 13 p2103 N85-23109
Precise mounting of instruments in universal suspension with skewed axes 14 p2273 N85-24083
Support structures for optical components in the Laser Demonstration Facility
[DE85-008879] 17 p2971 N85-28349
Using PVFORM, a systems performance model, to determine optimum mounting configurations for flat-plate photovoltaic modules
[DE85-011191] 19 p3306 N85-30495
MOUNTS
U SUPPORTS
MOVEMENT
U MOTION
MOVING TARGET INDICATORS
Moving object detection system using infrared scanning
[AD-D011222] 01 p0120 N85-10822
Optimization of moving-target selection radar devices for nonGaussian signals for stationary targets
06 p0789 N85-15043
Algorithm for tracking manuevering object with ambiguous measurements 06 p0791 N85-15057
Adaptive MTI (Moving Target Indicator) system
[AD-D011361] 07 p0937 N85-15937
Dual mode scanner-tracker
[AD-D011417] 08 p1113 N85-17018
Hybrid state estimation approach to multiobject tracking for airborne surveillance radars
[AD-A148459] 08 p1153 N85-17279
Pulse heterodyne equipment for measurements of range and velocity of moving targets-pulse radar
[ESA-TT-845] 09 p1312 N85-18246
MTI system simulation and clutter output statistics
[AD-A149193] 10 p1467 N85-19255
Method and means for providing frequency agile operation of MTI (Moving Target Indicator) radar
[AD-D011561] 12 p1823 N85-21436
Moving target detection 13 p2067 N85-22915
Eye movement in response to single and multiple targets
[AD-A151115] 15 p2617 N85-26126
Interference suppressor for radar MTI
[AD-D011606] 16 p2769 N85-27086
Techniques for operating Charge Coupled Devices (CCD's) in very high speed framing mode
[AD-A152878] 17 p2953 N85-28238
Atmospheric probing by active millimeter wave system
[AD-A153550] 18 p3138 N85-29422
Characteristics of digital range finder with stroboscopic discretization 22 p3762 N85-33319
MRCA AIRCRAFT
Tornado: Structural Usage Monitoring System (SUMS) 07 p0896 N85-15680
Flight parameters recording for structure fatigue life monitoring 07 p0896 N85-15682
Study and realisation of a 3rd level maintenance center based on ATE systems utilization
08 p1063 N85-16735
MSAT
Propagation considerations in land mobile satellite transmission
[NASA-CR-175733] 15 p2540 N85-25684
Combined trellis coding with asymmetric MPSK modulation: An MSAT-X report
[NASA-CR-176039] 20 p3440 N85-31347
Second-generation mobile satellite system. A conceptual design and trade-off study
[NASA-CR-176195] 24 p4086 N85-35325
MTF
U MODULATION TRANSFER FUNCTION
MTI RADAR
U MOVING TARGET INDICATORS
MUBIS (SCANNERS)
U MULTIPLE BEAM INTERVAL SCANNERS
MUFFLERS
Technology reports of the Yamaguchi University, volume 3, no. 3
[ISSN-0386-3433] 09 p1302 N85-18182
Studies on reactive mufflers. Part 2: Mufflers with air flow 09 p1303 N85-18184
MULLITES
Transformation toughened ceramics for the heavy duty diesel engine technology program
[NASA-CR-174689] 07 p1055 N85-16698
MULTI-ANODE MICROCHANNEL ARRAYS
The multi-anode microchannel array detector system: Current status and future prospects
11 p1761 N85-21080
MULTI-ROLE COMBAT AIRCRAFT
U MRCA AIRCRAFT
MULTIBEAM ANTENNAS
Configuration study for a 30 GHz monolithic receive array: Technical assessment
[NASA-CR-174697] 09 p1311 N85-18238
Configuration study for a 30 GHz monolithic receive array, volume 1
[NASA-CR-174697-VOL-1] 09 p1311 N85-18239
Shuttle S-band high gain switched beam breadboard antennas
[NASA-CR-171852] 10 p1478 N85-19327
3-D Dome/Rotman lens antenna breadboard demonstration
[AD-A149809] 12 p1826 N85-21475
Synthesis of multistep directional couplers with nonminimum-phase characteristics
13 p2079 N85-22986
Orbiting multi-beam microwave radiometer for soil moisture remote sensing 14 p2230 N85-23818
Design, fabrication and testing of a multibeam forming network
[NASA-CR-175695] 14 p2298 N85-24228
MULTICHANNEL COMMUNICATION
Guided-wave optic devices for integrated optic information processing
[AD-A145695] 02 p0280 N85-11827
Analysis of a coded, M-ary orthogonal input optical channel with random-gain photomultiplier detection
05 p0624 N85-13990
Synthesis of systems for coherent weighted signal processing against background of correlated interference 06 p0790 N85-15045

Multiwavelength bidirectional coupler-decouplers
[AD-A147009] 07 p1043 N85-16625
Equipment for multiplexing multichannel radio-relay lines of communication
[AD-A148402] 08 p1153 N85-17276
Error probability during optimal noncoherent reception of binary signals in multibeam channel
13 p2068 N85-22922
Asymptotically optimum multialternative sequential procedures for discernment of processes minimizing average length of observations
13 p2084 N85-23012
A perspective on multiaccess channels
[AD-A150183] 13 p2146 N85-23322

MULTICHANNEL PLATES
U MICROCHANNEL PLATES

MULTILAYER INSULATION
System design of multi-layer (3-dimensional) integrated circuits
[AD-A153468] 18 p3094 N85-29154

MULTILAYER STRUCTURES
U LAMINATES

MULTILOOP SYSTEMS
U CASCADE CONTROL

MULTIMISSION MODULAR SPACECRAFT
Satellite module design 11 p1642 N85-20344
Multimission advanced configurations study — telecommunication satellites
[MATRA-DM.51/CC/FL/0151.83]
12 p1790 N85-21237

MULTIMODE RESONATORS
Transformation of mode composition of circular optical waveguide 07 p0950 N85-16023
Coupled-cavity gyrotrons with mode conversion
13 p2076 N85-22967
Investigation of generation of oscillations using anomalous Doppler effect 13 p2079 N85-22980

MULTIPATH TRANSMISSION
Digital radio link: Comparison of the resistance of two different 4-phase modulation forms to multipath propagation
[FOA-C-30362-E] 02 p0193 N85-11291
Limits of the propagation medium with respect to digital signal transmission 10 p1469 N85-19270
Propagation influences on the performance of a reduced bandwidth quadrature phase shift keyed digital radio system 10 p1470 N85-19274
A review of atmospheric multipath measurements and digital system performance 10 p1470 N85-19279
Multipath and Doppler observations during transatlantic digital HF propagation experiments
10 p1471 N85-19281
An ionospheric mode detection system for HF communications application 10 p1471 N85-19282
Wideband line-of-sight channel measurements and simulation: Application to digital radio links
10 p1471 N85-19283
Design criteria for limited scan antennas at digital microwave line of sight links 10 p1471 N85-19284
Measurements and predictions of multipath dispersion for troposcatter links 10 p1472 N85-19289
Asynchronous transmission with strong spectral spread 10 p1474 N85-19300
Fast data and voice transmission for mobile services with high immunity against multipath and co-channel interference 10 p1475 N85-19306
Effective millimeter wave transmission under severe multipath conditions 10 p1475 N85-19308
Accurate baseline determination by radio interferometry on NAVSTAR GPS satellite transmissions
[AD-A150881] 14 p2291 N85-24202
Distributed control of circuits in multiuser communication networks with circuit precedence and path suitability criteria using failsafe routing concepts
[AD-A151825] 16 p2772 N85-27113
Development of a modified time delay spectrometry technique for underwater acoustic measurements in a multipath environment
[AD-A152111] 16 p2860 N85-27639
A comparison of multipath arrival structures observed in the presence of a surface duct with predictions obtained using classical ray techniques and the parabolic equation method
[AD-A156024] 24 p4145 N85-35696

MULTIPHASE FLOW
NT TWO PHASE FLOW
Investigation of phase separation models in RELAP 4/MOD 6
[OEFZS-4286] 05 p0636 N85-14093
Modelling the local interstellar medium as a supernova remnant in a multiphase gas 06 p0879 N85-15585
Combustion in high speed air flows
[AD-A148371] 08 p1122 N85-17070
Investigation of condensing, three-phase, two-component, flow through porous media
09 p1317 N85-18283
Development of a three-phrase combustion code for modeling liquid rocket engines 13 p2003 N85-22554
The physics of the marine stratocumulus-capped mixed layer 15 p2593 N85-25979
An experimental study of plane mixing layer development
[NASA-TM-86696] 19 p3221 N85-29971
An investigation of hydraulic transients in combination free surface and pressurized flows
19 p3264 N85-30239
Mathematics of oil production
[DE85-011235] 19 p3267 N85-30261
PHOENICS 84: A multi-dimensional multi-phase general-purpose computer simulator for fluid flow, heat transfer and combustion: 36 lecture panels
[CFD/84/18] 20 p3457 N85-31468
Progress in the development of a two-fluid model of turbulence: A set of 42 lecture panels
[CFD/84/20] 20 p3457 N85-31469
Experimental study of free and mixed convective flow of air in a heated cavity
[DE85-012538] 24 p4094 N85-35360

MULTIPHOTON ABSORPTION
Laser ablation studies using RIS
[DE85-001118] 09 p1326 N85-18336
Generation of stimulated emission in the soft X-ray range by nonlinear processes with excimer lasers
[DE85-012465] 24 p4096 N85-35403

MULTIPLE ACCESS
NT CODE DIVISION MULTIPLE ACCESS
NT DEMAND ASSIGNMENT MULTIPLE ACCESS
NT FREQUENCY DIVISION MULTIPLE ACCESS
NT TIME DIVISION MULTIPLE ACCESS
Throughput characteristics of Carrier Sense Multiple Access (CSMA) networks
[FUB-25-1983] 01 p0106 N85-10713
A perspective on multiaccess channels
[AD-A146606] 06 p0799 N85-15105
Analysis of the performance of multiaccess networks of the bus type
[FUB-47-1983] 09 p1313 N85-18249
A perspective on multiaccess channels
[AD-A150183] 13 p2146 N85-23322
On the throughput of channel access algorithms with limited sensing
[AD-A151984] 15 p2630 N85-26208
High performance asynchronous limited sensing algorithms for CSMA and CSMA-CD channels
[AD-A153919] 18 p3171 N85-29650

MULTIPLE BEAM INTERVAL SCANNERS
The 20 GHz proof-of-concept test model results for a multiple scan beam dual reflector antenna
[NASA-CR-174268] 07 p0938 N85-15944
Digital controller for the Wave Propagation Laboratory's VHF and UHF wind-profiling radars
[PB85-112142] 11 p1626 N85-20238
Feed system design considerations for large space antenna systems. Part 1: Multiple apertures with non-overlapping feeds 14 p2234 N85-23852
Feed system design considerations for large space antenna systems. Part 2: Single aperture with overlapping feeds 14 p2235 N85-23853
Offset reflector with horn feed array, used as an experimental sensor for radiometric measurements
[ESA-TT-830] 20 p3443 N85-31369
Method and apparatus for four-beam radar
[PB85-181477] 22 p3757 N85-33289

MULTIPLE TARGET TRAJECTORY SYSTEMS
U MATTS (SYSTEMS)

MULTIPLETS
U FINE STRUCTURE

MULTIPLEX TRANSMISSION
U MULTIPLEXING

MULTIPLEXERS
U MULTIPLEXING

MULTIPLEXING
NT FREQUENCY DIVISION MULTIPLEXING
NT TIME DIVISION MULTIPLEXING
NT WAVELENGTH DIVISION MULTIPLEXING
A total dose characterization of five commercial analog multiplexers
[AD-A146886] 07 p0946 N85-15997
Electro-optical target detection
[AD-D011366] 07 p1042 N85-16617
Equipment for multiplexing multichannel radio-relay lines of communication
[AD-A148402] 08 p1153 N85-17276
Integrated digital networks
[AD-A150605] 13 p2056 N85-22873
Interference immunity of fiber-optic communication lines with spectral multiplexing of channels
13 p2069 N85-22924
Interactive communication channel
[AD-D011580] 15 p2542 N85-25695
Wavelength multiplexer-demultiplexer
[AD-D011606] 16 p2777 N85-27140
Channel multiplexers for broadcast satellite transponders in the 12 GHz band
[NHK-LABS-NOTE-310] 18 p3090 N85-29132
LDV multiplexer interface
[NASA-CASE-ARC-11536-1] 19 p3258 N85-30202
Apollo multiplexer operations manual
[DE85-011293] 19 p3343 N85-30710

MULTIPLICATION
VLSI architectures for the multiplication of integers modulo a Fermat number 05 p0624 N85-13660
Electrooptical matrix multiplication using the twos complement arithmetic for improved accuracy
[AD-D011252] 05 p0728 N85-14662
Advanced cube processor
[AD-D011262] 05 p0729 N85-14663
Triple matrix product optical processors using combined time-and-space integration
[AD-D011483] 10 p1557 N85-19620
High accuracy digital acousto-optic matrix computer
[AD-D011692] 19 p3343 N85-30716

MULTIPLIER PHOTOTUBES
U PHOTOMULTIPLIER TUBES

MULTIPLIERS
NT CHANNEL MULTIPLIERS
Input-output stability analysis with magnetic hysteresis non-linearity: A class of multipliers
[AD-A145729] 02 p0253 N85-11664
Application of a silicon compiler to VLSI (Very Large Scale Integrated circuits) design of digital pipelined multipliers
[AD-A146328] 03 p0403 N85-12599
Developments of optical fast-gated imaging systems
[DE84-016170] 04 p0502 N85-13204
Hardware multiplier processor
[DE84-006174] 05 p0713 N85-14574
Efficiency of digital compensator of strong non-Gaussian interference 13 p2072 N85-22942
Numerical optical computing at the Ohio State University 18 p3188 N85-29775
Hardware realization of digital filters without multipliers
22 p3766 N85-33340

MULTIPOLAR FIELDS
Small, octopole-stabilized tandem mirror reactor
[DE85-002144] 10 p1559 N85-19632

MULTIPOLES
Structures of ordered linear dislocation multipoles in Cu-Al alloys
[ISSN-0379-6906] 13 p2021 N85-22684
A multipole model of the observed cerebral cortex magnetic field
[AD-A152237] 16 p2642 N85-27526

MULTIPROCESSING (COMPUTERS)
NT PIPELINING (COMPUTERS)
The FLEX/32 multicomputing environment
01 p0057 N85-10378
Application of concurrent processing to structural dynamic response computations
01 p0057 N85-10380
Hardware for a real-time multiprocessor simulator
[NASA-TM-83805] 01 p0099 N85-10659
Activities of the MIT Laboratory for Computer Science
[AD-A145134] 01 p0100 N85-10661
DISCUS multiprocessor enhancements — Distributed Control Microprocessor System (DISCUS)
[RSRE-MEMO-3591] 02 p0239 N85-11554
Criteria for the optimization of processing flow in a model of an incremental computer with multiprocessing resources
[INPE-3046-TDL/156] 02 p0240 N85-11560
Parallel searching and merging on ZMOB
[AD-A145424] 02 p0241 N85-11574
Research topics: Multiprocessing algorithms for computational logic
[DE84-015500] 02 p0242 N85-11583
Fault tolerant computing research
[AD-A145640] 02 p0244 N85-11590
The design and performance analysis of an arbiter for a multi-processor shared-memory system
[AD-A146074] 03 p0403 N85-12596
A building blocks approach to statistical databases
03 p0437 N85-12762
A control scheme for microcomputers being used in multiprocessor arrays
[DE84-014590] 04 p0547 N85-13479
Development of the NLTSS operating system
[DE84-013702] 05 p0714 N85-14576
Concurrency in parallel processing systems
05 p0714 N85-14581
Local area network evaluation by MICROSS extensions
[AD-A146773] 07 p1027 N85-16521
Evolution toward a multi-bus architecture for Army helicopter avionic systems 08 p1074 N85-16612
Operating system for a real-time multiprocessor propulsion system simulator. User's manual
[NASA-TP-2426] 08 p1207 N85-17596

Software for event oriented processing on multiprocessor systems
[DE84-016720] 09 p1370 N85-18607

Multitasking kernel for the C and FORTRAN programming languages
[DE85-001799] 09 p1370 N85-18609

Where are the parallel algorithms?
[NASA-CR-172516] 09 p1373 N85-18627

The feasibility of a multiprocessor architecture for real-time contour surface display generation
[AD-A149427] 10 p1538 N85-19697

Methodology investigation software testing of multiprocessor systems
[AD-A149446] 10 p1541 N85-19714

Domain decomposition techniques for solving elliptic partial differential equations on multiprocessors
[DE85-004448] 10 p1549 N85-19769

A quality control experiment in a real time multiprocessor operating system: The Mara 880 --- software testing
11 p1702 N85-20707

Solving partial differential equations on multiprocessors
[DE85-000745] 11 p1706 N85-20734

RAPIDbus: Design of an extensible multiprocessor structure
[AD-A150061] 12 p1912 N85-21998

Exploiting multiprocessors: Issues and options
[DE85-003144] 13 p2145 N85-23313

Synthesis of tree-structured computing systems through use of closures
[AD-A150502] 13 p2147 N85-23326

Use of function processors in multiprocessor systems
14 p2400 N85-24796

Organization of conveyor processing of vector commands in multiprocessor computer systems with a reorganizable structure 14 p2401 N85-24799

Automation of development of software for switching units that are implemented in the form of multiprocessor systems on a microcomputer base
14 p2401 N85-24802

The EGPA multiprocessor system and its possible application for pattern recognition tasks --- computer architecture 15 p2622 N85-26156

Backend control processor for a multi-processor relational database computer system
[AD-A151692] 15 p2624 N85-26169

ADA (trademark) tasking and exceptions: A formal definition
[AD-A151618] 15 p2629 N85-26204

Reentrancy and multitasking on CRAY computers
[DE85-007256] 15 p2630 N85-26211

Communication complexity of the Gaussian elimination algorithm on multiprocessors
[AD-A151691] 15 p2638 N85-26267

A moduler dissimilar redundant computer designed for high integrity control 16 p2714 N85-26751

Reports on cartography and geodesy. Series 1: Original reports, no. 94
[ISSN-0469-4236] 16 p2814 N85-27357

Realization of cartographic tasks on the multiprocessor system EGPA --- image processing
16 p2814 N85-27360

Multigrid algorithms on the hypercube multiprocessor
[AD-A152200] 16 p2847 N85-27556

Parallel computation of multiple-scale problems
[DE85-007230] 16 p2849 N85-27563

Local uniform mesh refinement on loosely-coupled parallel processors
[AD-A152199] 16 p2850 N85-27571

Complexity of dense linear system solution on a multiprocessor ring
[AD-A151970] 16 p2854 N85-27598

Multiple array processors for ocean acoustic problems
[AD-A152174] 16 p2860 N85-27641

A moduler dissimilar redundant computer designed for high integrity control 17 p2904 N85-27904

Development of a multiprocessor system, using the MOTORLA microprocessor 6809, with the aim of providing maximum flexibility in the design of individual control devices
[BMFT-FB-T-84-270] 17 p3010 N85-28607

Real-Time Multiprocessor Programming Language (RTMPL) user's manual
[NASA-TP-2422] 17 p3010 N85-28610

Parallel Cholesky factorization on a multiprocessor
[DE85-006762] 17 p3021 N85-28682

Development of a butterfly multiprocessor test bed description of butterfly components
[AD-A153692] 18 p3096 N85-29155

Tradeoffs among portability, complexity, and efficiency in multiprocessing environments
[DE85-007699] 18 p3161 N85-29580

Performance measurement of OSI (Open System Interconnection) class 4 transport implementations
[PB85-177657] 18 p3161 N85-29582

Introduction to programming multiple-processor computers
[DE85-010274] 18 p3164 N85-29599

The multiple processor machine for image processing, volume 5
[ESA-CR(P)-1976-VOL-5] 18 p3164 N85-29603

Solving elliptic partial differential equations on the hypercube multiprocessor
[AD-A153464] 18 p3168 N85-29629

Performance of the butterfly processor-memory interconnection in a vector environment
[DE85-007931] 19 p3261 N85-30224

Multigrid method for multiprocessors
[DE85-007929] 19 p3333 N85-30647

The BLAZE language: A parallel language for scientific programming
[NASA-CR-172615] 19 p3334 N85-30656

A parallelized point successive over-relaxation method on a multiple instruction multiple data stream computer
[AD-A154377] 19 p3337 N85-30679

Development and evaluation of a fault-tolerant multiprocessor (FTMP) computer. Volume 1: FTMP principles of operation
[NASA-CR-166071] 19 p3341 N85-30705

Development and evaluation of a Fault-Tolerant Multiprocessor (FTMP) computer. Volume 2: FTMP software
[NASA-CR-166072] 19 p3341 N85-30706

Development and evaluation of a Fault-Tolerant Multiprocessor (FTMP) computer. Volume 3: FTMP test and evaluation
[NASA-CR-166073] 19 p3341 N85-30707

Proceedings of the Argonne Workshop on Programming the Next Generation of Supercomputers
[DE85-008348] 19 p3343 N85-30718

MECA: A multiprocessor concept specialized to Monte Carlo
[DE85-010791] 19 p3346 N85-30737

Work in Amsterdam on local intelligence --- artificial intelligence
[NIKHEF-H/84-9] 20 p3518 N85-31877

Performance and evaluation of real-time multicomputer control systems
[NASA-CR-176098] 21 p3673 N85-32821

Concurrent implementation of the Crank-Nicolson method for heat transfer analysis
[NASA-TM-86448] 21 p3674 N85-32822

Use of monitors in Pascal on the Lemur: A tutorial on the barrier, self-scheduling FOR-loop, and askfor monitors
[ANL-84-53] 22 p3828 N85-33706

Parallel Cholesky factorization in message-passing multiprocessor environments
[DE85-012079] 22 p3830 N85-33717

Modeling and measurement of fault-tolerant multiprocessors
[NASA-CR-3920] 22 p3833 N85-33732

Some ideas for decomposing the domain of elliptic partial differential equations in the Schwarz process
[DE85-011844] 22 p3834 N85-33739

MULTIPROGRAMMING

PROGEN: An incremental programming environment
[NRIMS-TWISK-315] 02 p0241 N85-11568

ES devices at fair 08 p1141 N85-17187

Exploiting multiprocessors: Issues and options
[DE85-003144] 13 p2145 N85-23313

Structurization of programs for real-time microprocessor arrays 15 p2529 N85-25592

Detailed design of an object oriented, multiprogramming, multitasking operating system for sixteen-bit microcomputers
[AD-A152086] 16 p2847 N85-27552

Research in computer science
[NASA-CR-175922] 17 p3010 N85-28612

MULTIPROPELLANTS

U ROCKET PROPELLANTS

MULTIRADAR TRACKING

U RADAR NETWORKS

MULTISENSOR APPLICATIONS

Multisensor satellite data integration for sea surface wind speed and direction determination
[NASA-CR-174162] 04 p0542 N85-13446

MULTISPECTRAL BAND CAMERAS

An overview of Multispectral Electro-Optical Stereo Scanner (MEOSS) mission 04 p0458 N85-12908

Modular Optoelektronischer Multispektraler Scanner (MOMS), interpretation and evaluation of the MOMS image Arica, West Coast of South America --- STS-7 flight
05 p0657 N85-14222

The Brasex multispectral camera: Preliminary characteristics
[INPE-3424-PRE/687] 16 p2787 N85-27195

MULTISPECTRAL BAND SCANNERS

Direction dependent radiation behavior in the classification of multispectral aircraft remote sensing data
[SER-C-290] 01 p0063 N85-10419

The application of principal components analysis to LANDSAT MSS data 02 p0212 N85-11398

The feasibility of satellite remote sensing as a technique for evaluating coal mine surface features
02 p0213 N85-11401

Imaging Science Panel. Multispectral Imaging Science Working Group joint meeting with Information Science Panel: Introduction 02 p0213 N85-11406

The Monocular Electro-Optical Stereo Scanner Experiment (MEOSS) 04 p0459 N85-12910

LANDSAT instruments characterization
[E85-10032] 04 p0524 N85-13356

Investigation of several aspects of LANDSAT 4/5 data quality
[E85-10036] 04 p0525 N85-13357

Basic investigation concerning the applicability of multispectral radiation data from microwave radiometry measurements to geoscientific objectives of remote sensing
[ESA-TT-846] 05 p0628 N85-14027

LANDSAT instruments characterization
[E85-10030] 05 p0654 N85-14199

Characterizing the scientific potential of satellite sensors
[E85-10031] 05 p0654 N85-14200

Integrative investigation on forest damage detection based on airborne Multispectral Scanner data
05 p0656 N85-14215

Integration of multispectral data obtained at different view angles for vegetation analysis
05 p0657 N85-14218

The use of Thematic Mapper data for land cover survey 05 p0657 N85-14220

Multispectral remote sensing of inland wetlands in South Carolina: Selecting the appropriate sensor
[DE84-013951] 05 p0661 N85-14247

Electronic satellite imaging system MOMS-ESA
[BMFT-FB-W-84-033] 05 p0661 N85-14248

Studies of atmospheric water in storms with the Nimbus 7 scanning multichannel microwave radiometer
05 p0682 N85-14382

Characterizing the scientific potential of satellite sensors --- San Francisco, California
[E85-10053] 07 p0984 N85-16249

Study of spectral/radiometric characteristics of the Thematic Mapper for land use applications
[E85-10057] 07 p0987 N85-16268

Thematic Mapper. Volume 1: Calibration report flight model, LANDSAT 5
[E85-10059] 07 p0987 N85-16270

Thematic Mapper. Volume 2: Flight model preshipment review
[E85-10060] 07 p0987 N85-16271

Enhancement of multispectral scanner images by digital filtering
[ESA-TT-624] 07 p0989 N85-16284

Forest area estimates from LANDSAT MSS and forest inventory plot data
[PB85-105617/GAR] 07 p0990 N85-16290

Spectroradiometric calibration of the Thematic Mapper and Multispectral Scanner system
[E85-10077] 10 p1504 N85-19491

LANDSAT-4 Science Characterization Early Results. Volume 1: Multispectral Scanner (MSS)
[E85-10067] 11 p1666 N85-20496

Spectral characterization of the LANDAT-4 MSS sensors 11 p1666 N85-20499

Investigation of radiometric properties of LANDSAT-4 MSS --- California, North Carolina, South Carolina, and New England 11 p1666 N85-20500

LANDSAT scene-to-scene registration accuracy assessment 11 p1667 N85-20502

Geometric accuracy of LANDSAT-4 MSS image data
11 p1667 N85-20503

Impact of LANDSAT MSS sensor differences on change detection analysis --- New Mexico, San Francisco, CA, New Hampshire, and Connecticut
11 p1667 N85-20506

Spectral characterization of the LANDSAT Thematic Mapper sensors 11 p1669 N85-20514

Prelaunch absolute radiometric calibration of the reflective bands on the LANDSAT-4 protoflight Thematic Mapper 11 p1669 N85-20515

The spot operational remote sensing satellite system: Current status and perspectives
11 p1713 N85-20776

In-progress absolute radiometric inflight calibration of the LANDSAT-4 sensors --- New Mexico
12 p1870 N85-21733

LANDSAT-4 Thematic Mapper calibration and atmospheric correction 12 p1870 N85-21734

Thematic Mapper spectral dimensionality and data structure 12 p1871 N85-21736

Intraband radiometric performance of the LANDSAT 4 Thematic Mapper — Washington, DC, Arkansas, Massachusetts, Virginia, and Arizona 12 p1871 N85-21738

The use of linear feature detection to investigate Thematic Mapper data performance and processing 12 p1872 N85-21740

Geodetic accuracy of LANDSAT 4 Multispectral Scanner and Thematic Mapper data 12 p1873 N85-21746

Preliminary comparisons of the information content and utility of TM versus MSS data 13 p2120 N85-23202

The use of Thematic Mapper data for land cover discrimination: Preliminary results from the UK SATMaP programme 13 p2121 N85-23207

Calculation of image shift in panoramic photography 15 p2488 N85-25357

Modular Optoelectronic Multispectral Scanner (MOMS) for Earth observation. First results of STS-7 mission [MBB-UR-717/83-O] 16 p2874 N85-27732

Thermal Infrared Multispectral Scanner (TIMS): An investigator's guide to TIMS data [NASA-CR-175875] 17 p2961 N85-28286

An assessment of the potential role of multispectral imagery in bathymetric charting [AD-A152460] 17 p2984 N85-28438

Dynamic rectification of airborne scanner digital image recordings 18 p3124 N85-29344

Nimbus 7 Coastal Zone Color Scanner (CZCS). Level 2 data product users' guide [NASA-TM-86202] 19 p3299 N85-30452

Nimbus 7 Coastal Zone Color Scanner (CZCS). Level 1 data product users' guide [NASA-TM-86203] 19 p3299 N85-30453

Spectroradiometric calibration of the Thematic Mapper and Multispectral Scanner system [E85-10104] 20 p3476 N85-31601

Stripe filters on multispectral linear arrays [NASA-CR-175305] 21 p3579 N85-32252

Use of spaceborne imaging radar in regional geomorphic studies 21 p3603 N85-32377

Quantitative geomorphologic studies from spaceborne platforms 21 p3604 N85-32381

Calculating solar highlight and shadeless areas for scanning photographs from space and optimizing lighting conditions 22 p3736 N85-33160

Comprehensive mapping of arid territories of Arizona using space photography 22 p3737 N85-33164

MULTISPECTRAL LINEAR ARRAYS

Imaging Science Panel. Multispectral Imaging Science Working Group joint meeting with Information Science Panel: Introduction 02 p0213 N85-11406

An overview of Multispectral Electro-Optical Stereo Scanner (MEOSS) mission 04 p0458 N85-12906

Chemometric analysis of multisensor arrays [AD-A153605] 18 p3174 N85-29680

Nimbus 7 Coastal Zone Color Scanner (CZCS). Level 1 data product users' guide [NASA-TM-86203] 19 p3299 N85-30453

Stripe filters on multispectral linear arrays [NASA-CR-175305] 21 p3579 N85-32252

The application of bispectral analyses to aeroelastic phenomena 24 p4060 N85-35157

MULTISPECTRAL PHOTOGRAPHY

NT COLOR INFRARED PHOTOGRAPHY

NT INFRARED PHOTOGRAPHY

NT RADAR PHOTOGRAPHY

Space observation of latitudinal changes in vegetation cover 02 p0164 N85-11113

The Multispectral Imaging Science Working Group. Volume 1: Executive summary [E85-10001] 02 p0213 N85-11404

The Multispectral Imaging Science Working Group. Volume 2: Working group reports [E85-10002] 02 p0213 N85-11405

Botanical sciences team 02 p0214 N85-11407

Noise removal in multichannel images [NASA-CR-174116] 04 p0554 N85-13526

Evaluation of SPOT simulation data of the S GEOS campaign of the EEC by data of the test sites Freiburg and Staubing (West Germany) 05 p0659 N85-14237

Combining Heat Capacity Mapping Mission (HCMM) LANDSAT and thematic map information into a unique high precision merged multichannel system — climatology 05 p0660 N85-14239

Microwave and optical remote sensing of forest vegetation 08 p1146 N85-17228

Feature extraction assessment study [AD-A150189] 13 p2126 N85-23239

Comprehensive, integrated, remote sensing at DOE sites [DE85-004867] 13 p2126 N85-23240

Multispectral analysis of the Kasei Vallis-Lanae Planum region of Mars 13 p2193 N85-23607

Studies in parallel image processing 14 p2399 N85-24789

Efficient contextual measures for classification of multispectral image data 14 p2433 N85-25005

Relative geological information yield from small-scale multizonal space images (example of Fergama depression and its mountainous margins) 15 p2485 N85-25343

Identifying land use structures of multizonal aerospace photographs using digital data processing 15 p2486 N85-25348

Lidar and radiometer observations of thunderstorm tops 15 p2595 N85-25994

Interpretation of multiband photographs made during Telefoto-80 experiment for the purpose of discriminating agricultural crops 22 p3735 N85-33152

Cataloging the spectral brightness coefficients of the forested region of the European territory of the USSR 22 p3735 N85-33155

Regression analysis of aircraft and ground measurement data on vegetation cover 22 p3735 N85-33156

Direct regression analysis of remote sensing data (using example of grass cover) 22 p3736 N85-33157

MULTISPECTRAL RADAR

Multispectral (X and C band) crop classification with synthetic aperture radar (SAR-580) optical data 05 p0657 N85-14217

Digital controller for the Wave Propagation Laboratory's VHF and UHF wind-profiling radars [PB85-112142] 11 p1626 N85-20238

MULTISPECTRAL RESOURCE SAMPLER

A comparison of LANDSAT thematic mapper, multispectral scanner and airborne sensors for mapping the distribution of alteration minerals: Examples from the southwestern United States 24 p4106 N85-35452

MULTISTAGE COMPRESSORS

U TURBOCOMPRESSORS

MULTISTAGE ROCKET VEHICLES

NT ARIANE LAUNCH VEHICLE

NT ATLAS CENTAUR LAUNCH VEHICLE

NT VEGA LAUNCH VEHICLE

Conestoga 2: A low cost commercial space transport system 02 p0153 N85-11033

An experimental study on the induced normal force on tail-fins due to wing-tail interference [NAL-TR-814] 03 p0318 N85-12051

The development of staging mechanisms for the Japanese satellite launcher Mu-3SII 22 p3798 N85-33528

MULTISTATIC RADAR

Tristatic tracking filter used by the multistatic measurement system [AD-A146885] 07 p0911 N85-15769

Bistatic coherent radar receiving system [AD-D011447] 10 p1466 N85-19252

High time-resolution studies of the auroral ionosphere [AD-A150945] 14 p2409 N85-24850

Multi-bistatic radar for short range surveillance [BAE-BT-10603] 15 p2539 N85-25673

Phase synchronizing large antenna arrays using the spatial correlation properties of radar clutter 20 p3439 N85-31344

Potential coordinate estimate accuracy estimation accuracy by multiposition radar systems 22 p3763 N85-33322

MULTITEMPORAL ANALYSIS

U TEMPORAL RESOLUTION

MULTIVARIATE STATISTICAL ANALYSIS

NT BIVARIATE ANALYSIS

NT COVARIANCE

NT DISCRETE FUNCTIONS

NT ORTHOGONALITY

NT REGRESSION ANALYSIS

MICROSCOPE: A software system for multivariate analysis [AD-A144720] 01 p0103 N85-10688

Testing of inequality hypotheses in linear models using the Bayes method [SER-C-292] 01 p0112 N85-10761

Total positivity. A review [AD-A145205] 01 p0114 N85-10771

The information in the minor principal components 02 p0211 N85-11391

Asymptotically optimal adaptive control [AD-A145666] 02 p0249 N85-11629

On the rate of mean convergence of finite linear predictors of multivariate stationary stochastic processes [AD-A145609] 02 p0254 N85-11664

Computer equipment for research in statistics [AD-A145755] 03 p0406 N85-12591

Return difference feedback design for robust uncertainty tolerance in stochastic multivariable control systems [AD-A145861] 03 p0411 N85-12624

Multivariate analyses of sedimentological data at two early Bronze age sites, Bab edh-Dhra and Numeira, southeast Dead Sea Graben, Jordan 05 p0674 N85-14326

A monotonicity property of the power function of multivariate tests [CWI-MS-R8406] 05 p0721 N85-14695

Asymptotic distributions of estimators for posterior probabilities in a classification model with both continuous and discrete variables [CWI-MS-R8409] 05 p0722 N85-14697

Log linear model applications [AD-A146620] 06 p0858 N85-15457

The stable evaluation of multivariate b-splines [AD-A147386] 07 p1032 N85-16551

The symmetry group and exponents of operator stable probability measures [AD-A147187] 07 p1035 N85-16569

A factor analysis for time series [AD-A147495] 07 p1036 N85-16574

Tail behaviour for suprema of empirical processes [AD-A147629] 08 p1210 N85-17613

Robust linear filtering for multivariable stationary time series, part 3 [AD-A148169] 08 p1212 N85-17627

Multicomponent calibration and quantitation methods [AD-A148252] 08 p1212 N85-17629

Methods and applications of time series analysis. Part 2: Linear stochastic models [AD-A147292] 08 p1214 N85-17646

Generating positively correlated random variables from a sequence of independent random variables with symmetric logarithmically concave densities [AD-A148438] 08 p1216 N85-17659

Methods of computer-aided analysis of non-Gaussian noise and application to robust adaptive detection, part 2 [AD-A148879] 10 p1539 N85-19704

Dual adaptive control based upon sensitivity functions [NASA-CR-169331] 10 p1543 N85-19727

Controlled approximation and a characterization of the local approximation order [AD-A149095] 10 p1546 N85-19750

Looking at multivariate data through fuzzy sets [DE85-000684] 11 p1702 N85-20706

On the limiting empirical distribution function of the eigenvalues of a multivariate F matrix [AD-A149818] 12 p1921 N85-22065

An asymptotically optimal subclass of BTIB designs for comparisons with a control [AD-A149819] 12 p1921 N85-22068

Draftsman displays: A graphical technique for exploratory data analysis [AD-A150515] 13 p2041 N85-22775

Effects of assuming independent component failure times, if they are actually dependent, in a series system [AD-A150582] 13 p2101 N85-23092

Multivariate analysis and its applications [AD-A150324] 13 p2151 N85-23352

On limit of the largest eigenvalue of the large dimensional sample covariance matrix [AD-A150589] 13 p2151 N85-23358

The integration of information from an analog-visual display: The role of dimensional integrality [AD-A150756] 14 p2404 N85-24820

Practical methods for the compensation and control of multivariable systems [AD-A151047] 14 p2407 N85-24841

Ergodicity and Steady-State-Equilibrium conditions for Markov chains [AD-A151038] 14 p2409 N85-24854

Classification and multiple regression through projection pursuit [AD-A150797] 14 p2411 N85-24867

Convolution of the IFRA (Increasing Failure Rate Average) scaled-mins class [AD-A151070] 14 p2411 N85-24870

Construction of efficient algorithms for the estimation of multivariate probability densities [AD-A151509] 15 p2640 N85-26285

On limiting empirical distribution function of the eigenvalues of a multivariate F matrix, revised [AD-A151885] 15 p2641 N85-26288

On asymptotic joint distribution of the eigenvalues of the noncentral manova matrix for nonnormal populations [AD-A151886] 15 p2642 N85-26294

The statistical analysis of initial imperfection measurements — shell profiles [VTH-LR-442] 16 p2857 N85-27622

Analysis of control system from a viewpoint of desired pole placement and desired degree of robustness [AD-A152627] 17 p2899 N85-27876

An empirical comparison of the accuracy of univariate and multivariate corrections for range restriction [AD-A153071] 17 p3019 N85-28670

Detection of multivariate outliers with dispersion slippage in elliptically symmetric distributions [AD-A153785] 18 p3174 N85-29677

Robust control of multivariable and large space systems
[AD-A155117] 21 p3559 N85-32140
Computer graphics for multivariate data
23 p3958 N85-34528
Invariant tests and likelihood ratio tests for multivariate elliptically contoured distributions
[AD-A155844] 24 p4142 N85-35679

MULTIVIBRATORS
NT FLIP-FLOPS

MUON SPIN ROTATION
Spin dynamics of rare Earth ions in crystal fields probed by muon spin rotation
[DE84-013805] 02 p0278 N85-11610
Activities of the Solid State Physics Research Institute
[NASA-CR-175899] 17 p3042 N85-28818
Muon spin rotation studies 17 p3042 N85-28819
Proportional drift tubes for large area muon detectors
[HE-5.2-11] 24 p4203 N85-36087

MUONS
Uniaxial stress induced symmetry breaking for muon sites in Fe 17 p3042 N85-28820
Early study of muons and muon decay
[NOTA-INTERNA-835] 18 p3184 N85-29742
Excited leptons contribution to muon g-2
[PREPRINT-432] 18 p3184 N85-29745
Additional muon calculations for the SLC positron source
[DE85-011212] 19 p3363 N85-30855
Search for gamma rays of energy 10(15) eV from Cygnus X-3
[OG-2.1-1] 22 p3862 N85-33919
Observation of an excess of cosmic ray muons of energies 2 TeV from the direction of Cygnus X-3
[OG-2.1-3] 22 p3863 N85-33920
Muon content of gamma ray induced EAS from Cygnus X-3
[OG-2.1-4] 22 p3863 N85-33921
Observations of Cygnus X-3 above 10(15) eV from 1979 - 1984
[OG-2.1-6] 22 p3863 N85-33923
Evidence for long-term variability in the ultra high energy photon flux from Cygnus X-3
[OG-2.1-10] 22 p3863 N85-33926
Constraints on cosmic-ray observation of Cygnus X-3
[OG-2.2-3] 22 p3864 N85-33930
Search for excess showers from Crab Nebula
[OG-2.3-2] 22 p3866 N85-33939
Search for ultra high energy gamma-rays from various sources
[OG-2.6-7] 22 p3870 N85-33960
The muon content of EAS as a function of primary energy
[OG-5.1-8] 22 p3881 N85-34050
Estimation of composition of cosmic rays with E sub zero approximately equals 10(17) - 10(18) eV
[OG-5.1-14] 22 p3882 N85-34055
All particle energy spectrum of cosmic rays in 10 to the 15th power - 10 to the 20th power eV region
[OG-5.1-15] 22 p3882 N85-34056
Composition of primary cosmic rays near the bend from a study of hadrons in air showers at sea level
[OG-5.2-2] 22 p3883 N85-34059
The composition of cosmic rays near the Bend (10 to the 15th power eV) from a study of muons in air showers at sea level
[OG-5.2-3] 22 p3883 N85-34060
EAS fluctuation approach to primary mass composition investigation
[OG-5.2-5] 22 p3883 N85-34062
The primary composition beyond 10 to the 5th power GeV as deduced from high energy hadrons and muons in air showers
[OG-5.2-6] 22 p3883 N85-34063
High-energy multiple muons and heavy primary cosmic-rays
[OG-5.2-9] 22 p3883 N85-34065
Composition of primary cosmic rays near the knee
[OG-5.2-10] 22 p3884 N85-34066
Anisotropy of cosmic rays of energy 10 (15) eV to 10 (17) eV observed at Akeno
[OG-5.3-3] 22 p3884 N85-34070
The sidereal anisotropy of cosmic rays around 3 x 10 (15) eV observed at a middle north latitude
[OG-5.3-6] 22 p3884 N85-34072
Cosmic ray intensity variations at primary rigidities near 1900 GV
[OG-5.3-0] 22 p3885 N85-34075
Corrected sidereal anisotropy for underground moons
[SH-4.4-7] 23 p4033 N85-35005
Long-term modulation of galactic cosmic rays in high-energy region
[SH 4.4-22] 23 p4035 N85-35018
The cosmic ray differential diurnal variation dependences on the zenith angle and the geomagnetic disturbance
[SH-4.5-16] 23 p4038 N85-35033
Anomalous increase of solar anisotropy above 150GV in 1981-1983
[SH-4.5-18] 23 p4038 N85-35035
Atmospheric effects on the underground muon intensity
[SH-6.1-3] 23 p4044 N85-35078
Burst size distributions in the digitized data of the ion chambers t Mt. Norikura and sea level stations
[SH-9.1-9] 23 p4051 N85-35124
Plastic scintillators in coincidence for the study of multi-particle production of sea level cosmic rays in dense medium
[SH-9.1-11] 23 p4052 N85-35126
New Matsushiro underground cosmic ray station (220 M.W.E. in depth)
[SH-9.1-14] 23 p4052 N85-35129
Neutrino production of like sign dimuons
[DE85-013594] 24 p4151 N85-35741
Electrons, muons and hadrons in extensive air showers and how do they depend on nuclear interaction model, part 2 24 p4187 N85-35969
Analysis of equi-intensity curves and NU distribution of EAS 24 p4187 N85-35970
A new study of shower age distribution in near vertical showers by EAS air shower array
24 p4190 N85-35996
A new study of muons in air showers by NBU air shower array 24 p4190 N85-35997
Study of muons near shower cores at sea level using the E594 neutrino detector 24 p4191 N85-36000
Correlation of high energy muons with primary composition in extensive air shower
[HE-4.3-7] 24 p4191 N85-36001
Measurement of energy muons in EAS at energy region larger thean 10(17) eV
[HE-4.3-8] 24 p4191 N85-36002
Muon fluctuation studies of EAS 10(17) eV
[HE-4.3-9] 24 p4191 N85-36003
Average features of the muon component of EAS or = 10(17) eV
[HE-4.3-10] 24 p4191 N85-36004
Measurement of shower electrons and muons using a small air shower array
[HE-4.3-11] 24 p4192 N85-36005
The longitudinal development of muons in cosmic ray air showers at energies 10(15) - 10(17) eV
[HE-4.3-12] 24 p4192 N85-36006
Lateral distribution of high energy muons in EAS of sizes Ne approximately equals 10(5) and Ne approximately equals 10(6)
[HE-4.3-16] 24 p4192 N85-36010
The identification of gamma ray induced EAS
[HE-4.5-1] 24 p4195 N85-36026
Muons in gamma showers
[HE-4.5-3] 24 p4195 N85-36027
Muon spectrum in air showers initiated by gamma rays
[HE-4.5-4] 24 p4195 N85-36028
Development of electromagnetic cascades in the atmosphere including the Landau-Pomeranchuk-Migdal effect
[HE-4.5-5] 24 p4195 N85-36029
Electromagnetic and muonic structure of showers initiated by gamma-rays and by hadrons
[HE-4.5-6] 24 p4195 N85-36030
The muon content of gamma-ray showers
[HE-4.5-7] 24 p4195 N85-36031
Simulation of gamma-initiated showers
[HE-4.5-10] 24 p4195 N85-36033
An underground cosmic ray muon telescope for observation of cosmic ray anisotropy
24 p4196 N85-36037
Nuclear cascades in electromagnetic showers produced by primary gamma-quanta in the atmosphere
[HE-4.5-16] 24 p4196 N85-36038
On the possibilities of large-scale radio and fiber optics detectors in cosmic rays
[HE-4.6-2] 24 p4196 N85-36039
A possible EAS array above the Souden 2 detector
[HE-4.6-9] 24 p4197 N85-36046
Samarkand complex setup for investigation of cosmic ray variation in the energy range of 7 10 (9) - 10 (15) eV
[HE-4.6-14] 24 p4198 N85-36050
Longitudinal development of muons in large air showers studies from the arrival time distributions measured at 900m above sea level
[HE-4.7-4] 24 p4199 N85-36055
Arrival time distributions of electrons in air showers with primary energies above 10 (18)eV observed at 900m above sea level
[HE-4.7-5] 24 p4199 N85-36056
A note on some statistical properties of rise time parameters used in muon arrival time measurements
[HE-4.7-12] 24 p4199 N85-36062
Sub-luminal pulses from cosmic ray air showers
[HE-4.7-13] 24 p4200 N85-36063
Nineteenth International Cosmic Ray Conference. HE sessions, volume 8
[NASA-CP-2376-VOL-8] 24 p4200 N85-36066
Preliminary results on underground muon bundles observed in the Frejus proton-decay detector
[HE-5.1-1] 24 p4200 N85-36067
Muon and neutrino results from KGF experiment at a depth of 7000 hg/square cm
[HE-5.1-2] 24 p4200 N85-36068
Relevance of multiple muons detected underground to the mass composition of primary cosmic rays
[HE-5.1-4] 24 p4201 N85-36069
Multimuons events and primary composition
[HE-5.1-5] 24 p4201 N85-36070
The spectrum of cosmic ray muons obtained with 100-ton scintillation detector underground and the analysis of recent experimental data
[HE-5.1-6] 24 p4201 N85-36071
A large area cosmic muon detector located at Ohya stone mine
[HE-5.1-7] 24 p4201 N85-36072
A new world survey expression for cosmic ray vertical intensity vs. depth in standard rock
[HE-5.1-10] 24 p4201 N85-36073
Muon groups and primary composition at 10 to the 13th power to 10 to the 15th power eV
[HE-5.1-12] 24 p4201 N85-36074
On muon energy spectrum in muon groups underground
[HE-5.1-14] 24 p4201 N85-36076
Energy spectrum of cascades generated by muons in Baksan underground scintillation telescope
[HE-5.1-15] 24 p4202 N85-36077
Underwater measurements of muon intensity
[HE-5.1-16] 24 p4202 N85-36078
Multiple muons in MACRO
[HE-5.2-1] 24 p4202 N85-36079
The Nagoya cosmic-ray muon spectrometer 3, part 1: Preliminary observations
[HE-5.2-2] 24 p4202 N85-36080
The Nagoya cosmic-ray muon spectrometer 3, part 2: Track detector
[HE-5.2-3] 24 p4202 N85-36081
The Nagoya cosmic-ray muon spectrometer 3, part 3: Automatic film scanning equipment
[HE-5.2-4] 24 p4202 N85-36082
The Nagoya cosmic-ray muon spectrometer 3, part 4: Track reconstruction method
[HE-5.2-5] 24 p4202 N85-36083
Background light measurements at the DUMAND site
[HE-5.2-7] 24 p4203 N85-36084
Hybrid TLC-pair meter for the Sphinx Project
[HE-5.2-10] 24 p4203 N85-36086
Proportional drift tubes for large area muon detectors
[HE-5.2-11] 24 p4203 N85-36087
An upper limit of muon flux of energies above 100 TeV determined from horizontal air showers observed at Akeno
[HE-5.2-12] 24 p4203 N85-36088
Comments on the measurements of multiple muon phenomena
[HE-5.2-13] 24 p4203 N85-36089
Energy spectrum of cascade showers induced by cosmic ray muons in the range from 50 GeV to 5 TeV
[HE-5.2-14] 24 p4203 N85-36090
Measurement of muon intensity by Cerenkov method
[HE-5.2-15] 24 p4204 N85-36091
Analytical calculation of muon intensities under deep sea-water
[HE-5.2-16] 24 p4204 N85-36092
Photo nuclear energy loss term for muon-nucleus interactions based on xi scaling model of QCD
[HE-5.2-17] 24 p4204 N85-36093
On method of muon spectrum measurements by the scintillation detectors of a large thickness T4t sub o
[HE-5.2-18] 24 p4204 N85-36094
Range fluctuations of high energy muons passing through matter
[HE-5.2-19] 24 p4204 N85-36095
The research program of the Liquid Scintillation Detector (LSD) in the Mont Blanc Laboratory
[HE-5.3-6] 24 p4205 N85-36100
Atmospheric neutrinos observed in underground detectors
[HE-5.3-8] 24 p4205 N85-36102
Measurement of neutrino oscillations in MACRO experiment
[HE-5.3-10] 24 p4206 N85-36104
High energy neutrino astronomy with MACRO
[HE-5.3-12] 24 p4206 N85-36106

Angular distribution of muons produced by cosmic ray neutrinos in rock
[HE-5.3-24] 24 p4207 N85-36115
Multiple muons of conventional and exotic origin in DUMAND
[HE-5.4-4] 24 p4207 N85-36117
Atmospheric muons and neutrinos, and the neutrino-induced muon flux underground
[HE-5.4-7] 24 p4207 N85-36118
Analysis of the electron component of EAS at observational level 700 g x cm(-2) with a scale breaking interaction model and gammaisation hypothesis
[HE-5.4-8] 24 p4208 N85-36119
Relationship of sea level muon charge ratio to primary composition including nuclear target effects
[HE-5.4-10] 24 p4208 N85-36121
Study of photonuclear muon interactions at Baksan underground scintillation telescope
[HE-5.4-10] 24 p4208 N85-36122
Calculation of intensity of high energy muon groups observed deep underground
[HE-5.4-13] 24 p4208 N85-36123
Modular detector for deep underwater registration of muons and muon groups
[HE-5.4-15] 24 p4208 N85-36125
Results of investigation of muon fluxes of superhigh energy cosmic rays with X-ray emulsion chambers
[HE-5.4-16] 24 p4208 N85-36126
Energetic delayed hadrons in large air showers observed at 5200m above sea level
[HE-6.2-9] 24 p4211 N85-36145
Muon and neutrino fluxes
[HE-6.2-18] 24 p4213 N85-36154

MUSCLE RELAXANTS
Smith predictor and self-tuning control of muscle relaxant drug administration
[RR-257] 02 p0235 N85-11534

MUSCLES
NT MYOCARDIUM
Skeletal muscle metabolism in hypokinetic rats
[NASA-CR-174059] 02 p0233 N85-11520
Modulation of the cytosolic androgen receptor in striated muscle by sex steroids
[NASA-CR-174173] 04 p0545 N85-13468
An analysis of kinetic response variability
05 p0707 N85-14533
Electromyographic patterns associated with discrete limb movements 05 p0710 N85-14551
Alterations in skeletal muscle with disuse atrophy
[NASA-CR-174195] 06 p0843 N85-15349
Effect of disuse on sarcoplasmic reticulum in fast and slow skeletal muscle
[NASA-CR-174337] 08 p1191 N85-17508
Acid phosphatase and protease activities in immobilized rat skeletal muscles
[NASA-CR-174340] 08 p1192 N85-17509
A comparison of rat myosin from fast and slow skeletal muscle and the effect of disuse
[NASA-CR-174339] 08 p1192 N85-17510
Neural compensation, muscle load distribution and muscle function in control of biped models
09 p1314 N85-18257
Application of the system identification technique to goal-directed saccades
[AD-A150132] 12 p1906 N85-21967
Aerobic and anaerobic exercise tolerance in the heat: Effect and acclimatization 14 p2388 N85-24707
SPARTEN (Scientific Program of Aerobic and Resistance Training Exercise in the Navy): A total body fitness program for health and physical readiness
[AD-A150869] 14 p2388 N85-24711
Is fast fiber innervation responsible for increased acetylcholinesterase activity in reinnervating soleus muscles?
[NASA-CR-175716] 15 p2614 N85-26108
Differential effect of denervation on free radical scavenging enzymes in slow and fast muscle of rat
[NASA-CR-175719] 15 p2614 N85-26110
Effect of periodic accelerations on physiochemical properties and Ca2+ reactivity of actomyosin in white rat myocardium and skeletal muscles
19 p3324 N85-30594
The 1984 environmental monitoring program report for Idaho National Engineering Laboratory site
[DE85-011209] 22 p3812 N85-33611
Response of amino acids in hindlimb muscles to recovery from hypogravity and unloading by tail-cast suspension
[NASA-CR-176183] 24 p4128 N85-35589
Relaxation techniques
[AD-A156248] 24 p4133 N85-35621

MUSCULAR FATIGUE
The effects of helicopter vibration on the spinal system
[AD-A146274] 03 p0402 N85-12562
Responses of skeletal muscle to unloading, a review
[NASA-CR-176177] 24 p4128 N85-35594

MUSCULAR FUNCTION
USSR report: Space Biology and Aerospace Medicine, volume 18, no. 4, July - August 1984
[JPRS-USB-84-006] 01 p0091 N85-10611
Change in energetics of muscular contraction as a result of hyperoxia 01 p0093 N85-10629
Effects of muscle atrophy on motor control: Cage size effects 15 p2609 N85-26080
Induced changes in the cholinergic system of sciatic nerve and slow and fast twitch muscle of rats
15 p2609 N85-26081
Regional circulation during testing on isokinetic dynamometer following 14-day bedrest
19 p3323 N85-30590
Postural adjustments associated with arm movements in weightlessness 20 p3509 N85-31813
Muscle protein and glycogen responses to recovery from hypogravity and unloading by tail-cast suspension
[NASA-CR-176181] 24 p4128 N85-35591

MUSCULAR STRENGTH
Assessment of muscle strength and prediction of lifting capacity in US Army personnel
[AD-A148846] 10 p1527 N85-19633
Comparative analysis of effects of weightlessness and its models on velocity and strength properties and tone of human skeletal muscles 12 p1901 N85-21936
Use and disuse and the control of acetylcholinesterase activity in fast and slow twitch muscle of rat
[NASA-CR-175717] 15 p2614 N85-26109
Rat skeletal muscles with simulation of physiological effects of weightlessness (morphological study)
23 p3953 N85-34502
Responses of skeletal muscle to unloading, a review
[NASA-CR-176177] 24 p4128 N85-35594

MUSCULAR TONUS
Comparative analysis of effects of weightlessness and its models on velocity and strength properties and tone of human skeletal muscles 12 p1901 N85-21936

MUSCULOSKELETAL SYSTEM
NT BONES
NT CEREBRUM
NT ELBOW (ANATOMY)
NT FEMUR
NT JOINTS (ANATOMY)
NT KNEE (ANATOMY)
NT MARROW
NT PELVIS
NT SCIATIC REGION
NT SKULL
NT VERTEBRAE
NT VERTEBRAL COLUMN
NT WRIST
Non-invasive techniques for determining musculoskeleton body composition
[DE84-015718] 04 p0545 N85-13470
Evaluation of the musculoskeletal diseases program
[PB84-230648] 07 p1017 N85-16461
Skeletal muscle metabolism during exercise is influenced by heat acclimation
[AD-A148845] 10 p1527 N85-19632
Characteristics of human masseter under conditions of hypokinesia 11 p1691 N85-20630
Alterations in gut transport of minerals and in binding proteins during simulated weightlessness
[NASA-CR-175637] 14 p2388 N85-24709
Nutrition in space flight: Some thoughts
14 p2394 N85-24743
Constant fiber number during skeletal muscle atrophy and modified arachidonate metabolism during hypertrophy 15 p2609 N85-26078
Gravity, body mass and composition, and metabolic rate 15 p2610 N85-26084
Changes in bone structure and metabolism during simulated weightlessness: Endocrine and dietary factors
[NASA-CR-175961] 18 p3153 N85-29521
Results and prospects of physiological research during spaceflights 22 p3732 N85-33139
Formation of new microvessels in skeletal muscles of rats exposed to hypobaric hypoxia for one week
22 p3820 N85-33662
Morphological study of antiorthostatic hypokinesia in monkeys 22 p3822 N85-33680
Fluid-electrolyte metabolism and renal function in cosmonauts following 185-day spaceflight
23 p3952 N85-34495
Responses of skeletal muscle to unloading, a review
[NASA-CR-176177] 24 p4128 N85-35594

MUTAGENS
Toxicology of natural and man-made toxicants in drinking water
[AD-P004035] 06 p0845 N85-15365

MUTATIONS
Effect of spaceflight factors on rat bone marrow cells
01 p0092 N85-10620
Study of mathematical models of mutation and selection in multi-locus systems
[DE85-000873] 09 p1376 N85-18646
Toxicity, mutagenesis and aging due to endogenous oxygen radicals
[AD-A150121] 12 p1900 N85-21928
Mutant peas as probes in the understanding of growth and gravitropism 15 p2611 N85-26086
Genetics in methylotrophic bacteria
[DE85-011460] 19 p3327 N85-30815
Mouse oocyte killing by neutrons: Target considerations
[DE85-011362] 19 p3328 N85-30824
Organization of the R region in maize
[DE85-011273] 20 p3504 N85-31780
Hit-size effectiveness theory applied to high doses of low LET radiation for pink mutations in Tradescantia
[DE85-011835] 22 p3819 N85-33657

MYOCARDIAL INFARCTION
Morbidity and mortality associated with exposure to Otto Fuel II in the U.S. Navy 1966-1979
[AD-A148726] 09 p1363 N85-18574
Longitudinal study of cardiovascular disease in US Navy pilots
[AD-A154331] 19 p3328 N85-30823

MYOCARDIUM
Morphological study of monkeys submitted to antiorthostatic hypokinesia 12 p1902 N85-21942
Preventive effect of acute heat factors during hypokinesia 12 p1902 N85-21945
Effects of blood volume overload on myocardial ultrastructure in relation to adaptation to high altitude hypoxia 22 p3820 N85-33664

MYOPIA
Test and evaluation of the 2.4-micron photorefractor ocular screening system
[NASA-TM-86492] 15 p2615 N85-26115

N

N-P JUNCTIONS
U P-N JUNCTIONS

N-TYPE SEMICONDUCTORS
Composition of metal films on gallium arsenide surface 02 p0257 N85-11685
Novel transport and recombination processes in semiconductors
[AD-A145969] 03 p0433 N85-12757
High temperature thermoelectric energy conversion
05 p0610 N85-13894
Photoluminescent and electroluminescent properties of Cd sub 0.95 Mn sub 0.05 Se electrodes
[AD-A146775] 07 p0946 N85-15995
Diffusion barrier for long wavelength laser diodes
[AD-D011390] 07 p0970 N85-16157
Surface and interfacial properties of Ga(0.47) In(0.53)As alloys
[AD-A148891] 10 p1562 N85-19840
Multiple double heterojunction buried laser device
[AD-D011519] 12 p1855 N85-21635
Thermally stimulated conductivity in semi-insulating gallium arsenide 13 p2088 N85-23036
Fabrication and I-V characterization of AlGaAs/GaAs MODFETs with P-type surface layers grown by molecular beam epitaxy
[AD-A151695] 15 p2660 N85-26415
Electrical properties of bulk grown nitrogen doped silicon
[AD-A155471] 21 p3581 N85-32266
TEMO and TEB thermoelectronic devices
22 p3779 N85-33415

NACELLES
Energy efficient engine ICLS Nacelle detail design report
[NASA-CR-167870] 02 p0146 N85-10903
Installed nacelle drag-improvement tests of an M = 0.8 turboprop transport configuration
[NASA-TM-84302] 07 p0902 N85-15716
Some aspects of engine and airframe integration for Ramjet and Ramrocket powered missiles
07 p0918 N85-15812
Over the wing propeller
[NASA-CASE-LAR-13134-1] 11 p1584 N85-19980
Hover test results of a small-scale twin-tilt nacelle model
[NASA-TM-86665] 14 p2210 N85-23706
Low-speed wind-tunnel tests of an advanced eight-bladed propeller
[NASA-TM-86364] 19 p3214 N85-29928
Calculation of transonic flows around an aircraft configuration with motorized nacelle
[SNIAS-851-111-106] 20 p3387 N85-31008

An experimental investigation of propfan installations on an upswept supercritical wing at transonic Mach numbers
[NASA-CR-172605] 20 p3388 N85-31013
Design of the nacelle for the A-320 aircraft
[SNIAS-851-111-111] 20 p3393 N85-31046
NAMIBIA
An evaluation of the electrodialysis reversal process (Edr) for the desalination of brackish water from the Omaruru delta (SWA/Namibia)
01 p0023 N85-10141
NAMING
NT NORMS
Commercial data base management system for geonames data base
[AD-A150635] 14 p2433 N85-25007
Proposal for the systematic naming of mesons and baryons
[DE85-006453] 17 p3035 N85-28773
Distributed name management
[AD-A154765] 21 p3712 N85-33037
The automatic labeling of geographic maps: A problem in computer aesthetics 23 p3962 N85-34561
NAP-OF-THE-EARTH NAVIGATION
Guidance and navigation programs and plans
06 p0751 N85-14809
Integrated cockpit design for the Army helicopter improvement program 06 p0751 N85-14816
Assessment of simulation fidelity using measurements of piloting technique in flight 08 p1075 N85-16817
Ground evaluation of helicopter air-to-air warfare
13 p1967 N85-22360
Piloted simulation of one-on-one helicopter air combat at NOE flight levels
[NASA-TM-86686] 16 p2710 N85-26720
NAPHTHALENE
Supercritical fluid chromatography/supersonic jet spectroscopy
[DE84-016199] 04 p0471 N85-12998
Intermolecular energy transfer between the individual zero-field levels of triplet traps in an orientationally disordered solid
[AD-A150751] 14 p2417 N85-24914
Transport and relaxation processes in supercritical fluids
[DE85-010554] 19 p3358 N85-30816
NAPPES
U FOLDS (GEOLOGY)
NARROWBAND
Improvement of the narrowband linear predictive coder. Part 2: Synthesis improvements
[AD-A145031] 01 p0038 N85-10237
Digital radio receivers and problems of analog-to-digital conversion of narrow-band signals
04 p0486 N85-13101
The adaptive spectrum analyser
05 p0622 N85-13978
A narrow band pulsed eddy current instrument for materials testing
[AERE-R-11229] 07 p0968 N85-18149
Survey of narrow band vocoder technology
[AD-A151919] 16 p2773 N85-27114
NASA PROGRAMS
NT ACEE PROGRAM
NT APOLLO APPLICATIONS PROGRAM
NT APOLLO PROJECT
NT EARTH RESOURCES PROGRAM
NT GALILEO PROJECT
NT HELIOS PROJECT
NT NASTRAN
NT PROJECT SETI
NT SCOUT PROJECT
NT SKYLAB PROGRAM
NT SUPERSONIC CRUISE AIRCRAFT RESEARCH
NT TIROS PROJECT
NT VIKING MARS PROGRAM
NT VOYAGER PROJECT
Department of Housing and Urban Development, and certain independent agencies appropriations for fiscal year 1985, part 2
[S-REPT-98-889-PT-2] 01 p0127 N85-10870
National Aeronautics and Space Administration
01 p0127 N85-10871
Workshop on Automated Space Station
01 p0127 N85-10873
Project Explorer 02 p0154 N85-11041
Initiatives to promote space commercialization
[GPO-37-551] 02 p0156 N85-11058
Statement of Hon. James M. Beggs, Administrator, NASA, Washington, DC 02 p0156 N85-11059
Research and technology
[NASA-TM-86321] 02 p0305 N85-11973
Proceedings of a Workshop on Applications of Tethers in Space, Executive Summary
[NASA-CR-171195] 03 p0322 N85-12075
Proceedings of a Workshop on the Applications of Tethers in Space, Volume 1
[NASA-CR-171196] 03 p0322 N85-12076
Review of Space Shuttle requirements, operations, and future plans
[GPO-39-101] 04 p0461 N85-12927
The 1984 NASA/ASEE summer faculty fellowship program
[NASA-TM-87392] 04 p0574 N85-13662
The 1984 ASEE-NASA summer faculty fellowship program (aeronautics and research)
[NASA-TM-87393] 04 p0575 N85-13664
NASA-Ames vertical gun 04 p0579 N85-13696
NASA's SESAC report on research and analysis in space and Earth sciences 04 p0579 N85-13697
Space telescope cost, schedule, and performance review, 1984
[GPO-39-065] 04 p0579 N85-13698
Resident research associateships. Postdoctoral and senior research awards
[NASA-TM-87399] 05 p0734 N85-14717
Issues and findings 07 p0914 N85-15782
Financing considerations and Federal budget impacts
07 p0915 N85-15792
A research in support of NASA's space science
[NASA-CR-174267] 08 p1227 N85-17728
Summary of activities of Aeronautics and Space Engineering Board
[NASA-CR-174294] 08 p1228 N85-17729
Scientific and technical information output of the Langley Research Center for calendar year 1984
[NASA-TM-86336] 08 p1229 N85-17740
United Kingdom report on space research
08 p1231 N85-17752
Chronology of KSC and KSC related events for 1983
[NASA-TM-87400] 08 p1261 N85-17927
Manned space station solar array study
[ESA-CR(P)-1941] 09 p1287 N85-18081
NASA new technology identification and evaluation
[NASA-CR-174368] 09 p1403 N85-18832
Resident research associateships. Postdoctoral and senior research awards: Opportunities for research at the Jet Propulsion Laboratory
[NASA-CR-174343] 09 p1418 N85-18945
Aerospace Safety Advisory Panel
[NASA-TM-87428] 12 p1774 N85-21135
NASA/MSFC ground experiment for large space structure control verification
[NASA-TM-86496] 12 p1792 N85-21248
Bibliography of Lewis Research Center technical publications announced in 1983
[NASA-TM-83693] 12 p1951 N85-22255
Summary of activities of the Committee on Science and Technology
[H-REPT-98-1189] 12 p1964 N85-22341
U.S., Soviet space program aims contrasted
13 p1985 N85-22455
NASA photovoltaic research and technology development program for space applications
13 p2011 N85-22617
NASA's land remote sensing plans for the 1980's
13 p2124 N85-23224
Small business innovation research: Abstracts of 1984. Phase 1 awards
[NASA-TM-87427] 13 p2165 N85-23431
NASA Patent Abstracts Bibliography. A continuing bibliography. Section 2: Indexes
[NASA-SP-7039(26)] 13 p2167 N85-23445
Authorizing appropriations to the National Aeronautics and Space Administration for fiscal year 1986
[H-REPT-99-32] 13 p2188 N85-23452
NASA space materials research
14 p2232 N85-23831
Precision space structures 14 p2232 N85-23833
NASA Thesaurus supplement, a three part cumulative supplement to the 1982 edition of the NASA Thesaurus
[NASA-SP-7051(SUPPL-3)] 14 p2432 N85-25002
Technology for large space systems: A bibliography with indexes, supplement 11
[NASA-SP-7046(11)] 15 p2475 N85-25277
Militarization of space activity in United States
15 p2488 N85-25360
Study on the extension of experiment resources in the MAUS project
[BMFT-FB-W-84-051] 15 p2650 N85-26343
Management: A bibliography for NASA managers
[NASA-SP-7500(19)] 15 p2664 N85-26439
The 1985 long-range program plan
[NASA-TM-87464] 15 p2664 N85-26440
NASA photography index
[NASA-TM-87457] 15 p2665 N85-26445
NASA Ames Summer High School Apprenticeship Research Program
[NASA-TM-86006] 15 p2686 N85-26590
The search for extraterrestrial intelligence
15 p2689 N85-26609
Activities of the Aeronautics and Space Engineering Board
[NASA-CR-175825] 16 p2691 N85-26610
Spacestation: The next logical step
[NASA-EP-213] 16 p2730 N85-26847
Bioengineering and rehabilitation: Windows of opportunity past, present and future
[NASA-EP-216] 16 p2841 N85-27516
Department of Housing and Urban Development-independent agencies appropriations for 1986. Part 6: National Aeronautics and Space Administration
[GPO-47-235] 16 p2879 N85-27768
European utilization aspects of a US manned space station, volume 1
[ESA-CR(P)-1987-VOL-1] 17 p2907 N85-27926
European utilization aspects of a US manned space station, volume 2
[ESA-CR(P)-1987-VOL-2] 17 p2907 N85-27927
Summer High School Apprenticeship Research Program (SHARP) of the National Aeronautics and Space Administration
[NASA-CR-175791] 17 p3046 N85-28849
National Aeronautics and Space Administration Authorization Act, 1986
[S-REPT-99-91] 17 p3051 N85-28885
Space station study
[BL-6167] 18 p3066 N85-28959
NASA initiatives with historically black colleges and universities
[NASA-EP-210] 19 p3379 N85-30960
National Aeronautics and Space Administration Authorization Act, 1986
[S-REPT-99-91] 19 p3381 N85-30978
Studies toward a manned space station: Participation of European industry in NASA space station (MSS)
[SNIAS-S/DT-Y-25-212] 20 p3418 N85-31217
NASA authorization, 1986, volume 1
[GPO-46-365] 20 p3541 N85-32039
Life sciences flight experiments program mission science requirements document. The first life sciences dedicated Spacelab mission, part 1
[NASA-TM-87494] 21 p3559 N85-32137
Testimony of Robert A. Frosch before the Subcommittee on HUD and Independent Agencies of the Senate Committee on Appropriations
[NASA-TM-87496] 22 p3738 N85-33173
NASA patent abstracts bibliography: A continuing bibliography. Section 1: Abstracts (supplement 27)
[NASA-SP-7039(27)-SECTION-1]
22 p3849 N85-33840
Department of Housing and Urban Development Independent Agencies Appropriation Bill, 1986
[S-REPT-99-129] 23 p3987 N85-34720
National Aeronautics and Space Administration research and development: Program description
23 p3987 N85-34721
A spacefaring people: Perspectives on early spaceflight
[NASA-SP-4405] 23 p4056 N85-35142
Management of large-scale technology
23 p4057 N85-35145
NASA patent abstracts bibliography, a continuing bibliography. Section 2: Indexes (supplement 27)
[NASA-SP-7039(27)-SECTION-2]
24 p4164 N85-35820
NASA SPACE PROGRAMS
NT APOLLO APPLICATIONS PROGRAM
NT APOLLO PROJECT
NT EARTH RESOURCES PROGRAM
NT GALILEO PROJECT
NT HELIOS PROJECT
NT PROJECT SETI
NT SCOUT PROJECT
NT SKYLAB PROGRAM
NT TIROS PROJECT
NT VOYAGER PROJECT
NASA STRUCTURAL ANALYSIS PROGRAM
U NASTRAN
NASTRAN
Comparison of free component mode synthesis techniques using MSC/NASTRAN
[DE84-014451] 04 p0514 N85-13278
Investigation of the HPFTP first stage impeller crack
[NASA-CR-171281] 07 p0977 N85-16208
Thirteenth NASTRAN Users' Colloquium
[NASA-CP-2373] 15 p2573 N85-25863
New enhancements in April 85 NASTRAN release
15 p2573 N85-25864
Improved accuracy in solid isoparametric elements using selectively reduced integration 15 p2573 N85-25865
Crack elements for COSMIC/NASTRAN
15 p2573 N85-25866
A 4-node bilinear isoparametric element in Rockwell NASTRAN 15 p2573 N85-25867

best copy available

Layered composite analysis capability
15 p2573 N85-25868
NPLOT: An interactive plotting program for NASTRAN finite element models 15 p2573 N85-25869
COSMIC/NASTRAN-PATRAN interface
15 p2574 N85-25870
Two interactive graphics postprocessors for NASTRAN 15 p2574 N85-25871
An unusual application of NASTRAN contour plotting capability 15 p2574 N85-25872
A new NASTRAN capability for data reduction
15 p2574 N85-25874
Automatic Dynamic Aircraft Modeler (ADAM) for the computer program NASTRAN 15 p2574 N85-25875
Ritz procedure for COSMIC/NASTRAN
15 p2575 N85-25877
Symmetric composite laminate stress analysis
15 p2575 N85-25878
NASTRAN's application in agricultural engineering
15 p2575 N85-25880
Use of COSMIC NASTRAN in a design department
15 p2575 N85-25881
An elastic analysis of a plated bone to determine fracture gap motion 15 p2575 N85-25882
Learjet Model 55 wing analysis with landing loads
15 p2575 N85-25883
Fillet weld stress using finite element methods
15 p2576 N85-25884
The structural finite element model of the C-5A
15 p2576 N85-25885
Using NASTRAN to model missile inertia loads
15 p2576 N85-25886
Experience with free bodies 15 p2576 N85-25887
NASTRAN analysis comparison to shock tube tests used to simulate nuclear overpressures
15 p2576 N85-25888
Finite element prediction of loss factors for structures with frequency-dependent damping treatments
15 p2576 N85-25889
Direct transient analysis of a fuze assembly by axisymmetric solid elements 15 p2576 N85-25890
Transient analysis of a magnetic heat pump
15 p2576 N85-25891
NASTRAN-based software for the structural dynamic analysis of vertical and horizontal axis wind turbines
[DE85-001712] 15 p2580 N85-25911
Structural analysis of electronic assembly housing
[DE85-005794] 15 p2580 N85-25913

NATIONAL AIRSPACE SYSTEM
National airspace review 02 p0136 N85-10926
System engineering and integration contract for implementation of the National Airspace System Plan. Volume 2: Section 5.0
[AD-A145710] 02 p0137 N85-10929
System engineering and integration contract for implementation of the National Airspace System plan, volume 1, sections 1.0-4.0, 6.0
[AD-A145763] 03 p0317 N85-12048
National airspace system configuration management interface control document. Maintenance processor subsystem to remote monitoring subsystems and remote monitoring subsystem concentrators
[NAS-MD-790] 07 p0900 N85-15705
National airspace review: Airport radar service area operational confirmation report
[DOT/FAA/AT-84/2] 07 p0901 N85-15707
National airspace review enhancement plan, revision 3
[AD-A150743] 08 p1082 N85-16852
National airspace system: Operational requirements
[AD-A149349] 10 p1422 N85-18973
Response to NAS plan audit report recommendations
[FAA-ES-85-1] 15 p2468 N85-25235
National Airspace System Plan: Facilities, equipment and associated development 16 p2704 N85-26692
National airspace review, change 1
[AD-A152369] 17 p2894 N85-27844

NATIONAL AIRSPACE UTILIZATION SYSTEM
National airspace review 02 p0136 N85-10926
National airspace system configuration management interface control document. Maintenance processor subsystem to remote monitoring subsystems and remote monitoring subsystem concentrators
[NAS-MD-790] 07 p0900 N85-15705

NATIONAL AVIATION SYSTEM
Satellite navigation
[S-HRG-98-656] 08 p1082 N85-16851
Thirty years' activities for aircraft safety
20 p3391 N85-31033

NATIONAL OCEANIC SATELLITE SYSTEM
Ocean services user needs assessment. Volume 1: Survey results, conclusions and recommendations
[NASA-CR-174104] 04 p0541 N85-13445

NATIONAL PARKS
Inventory and monitoring of national park landscapes — remote sensing 05 p0660 N85-14245

NATIONS
NT ALABAMA
NT ALASKA
NT ARGENTINA
NT ARIZONA
NT ARKANSAS
NT AUSTRALIA
NT AUSTRIA
NT BANGLADESH
NT BELGIUM
NT BOLIVIA
NT BRAZIL
NT BRITISH COLUMBIA
NT BULGARIA
NT CALIFORNIA
NT CANADA
NT CHILE
NT CHINA
NT COLOMBIA
NT COLORADO
NT CONNECTICUT
NT COSTA RICA
NT CUBA
NT CZECHOSLOVAKIA
NT DELAWARE
NT DENMARK
NT EAST GERMANY
NT EGYPT
NT ENGLAND
NT FINLAND
NT FLORIDA
NT FRANCE
NT GEORGIA
NT GUATEMALA
NT GUYANA
NT HAWAII
NT HONDURAS
NT HUNGARY
NT ICELAND
NT IDAHO
NT ILLINOIS
NT INDIA
NT INDIANA
NT INDONESIA
NT IOWA
NT IRAN
NT ISRAEL
NT ITALY
NT JAPAN
NT KANSAS
NT KENTUCKY
NT KENYA
NT LOUISIANA
NT MAINE
NT MARYLAND
NT MASSACHUSETTS
NT MEXICO
NT MICHIGAN
NT MISSISSIPPI
NT MISSOURI
NT MONTANA
NT NEBRASKA
NT NETHERLANDS
NT NEVADA
NT NEW HAMPSHIRE
NT NEW JERSEY
NT NEW MEXICO
NT NEW YORK
NT NEW ZEALAND
NT NIGERIA
NT NORTH CAROLINA
NT NORTH DAKOTA
NT NORWAY
NT OHIO
NT OKLAHOMA
NT OREGON
NT PENNSYLVANIA
NT PERU
NT POLAND
NT REPUBLIC OF SOUTH AFRICA
NT SAUDI ARABIA
NT SOUTH CAROLINA
NT SOUTH DAKOTA
NT SPAIN
NT SUDAN
NT SWEDEN
NT SWITZERLAND
NT TAIWAN
NT TENNESSEE
NT TEXAS
NT THAILAND
NT TUNISIA
NT TURKEY
NT U.S.S.R.
NT UNITED KINGDOM
NT UNITED STATES
NT UTAH
NT VIRGINIA
NT WASHINGTON
NT WEST GERMANY
NT WISCONSIN
NT WYOMING
NT YUGOSLAVIA

NATURAL FREQUENCIES
U RESONANT FREQUENCIES

NATURAL GAS
NT LIQUEFIED NATURAL GAS
Status of gaseous fuels for use in highway transportation: A 1983 perspective
[DE84-015205] 01 p0034 N85-10211
State of knowledge of environmental concerns related to natural gas-fueled vehicles
[DE84-015894] 01 p0070 N85-10461
US energy for the rest of the century, 1984 edition
[PB84-207406] 04 p0531 N85-13200
Development of a van-portable remote-sensing laser system for selective detection of natural gas leaks
[PB85-101939/GAR] 06 p0811 N85-15158
Analysis of gases in the Earth's crust
[PB85-113397/GAR] 07 p0990 N85-16087
USSR report: Energy
[JPRS-UEN-84-036] 07 p0994 N85-16012
Natural gas the new locomotive fuel
[DE84-901824] 09 p1302 N85-18179
The influence of modern control techniques on the gas industry
[ERS-E.395] 09 p1325 N85-18026
Measurement of gas compressibility factor data for natural gas and synthetic gas components and their mixtures
[PB85-129047] 11 p1614 N85-20151
Solar-gas systems impact analysis study
[PB85-129068] 11 p1616 N85-20163
Combustion gas properties. 2: Natural gas fuel and dry air
[NASA-TP-2435] 12 p1779 N85-21108
New method of reconstructing conditions of recent differentiation of oil and gas in the Amudarya Basin (based on results of interpretation of space photographs)
13 p1984 N85-22446
Low pressure storage of methane on interlayered clays for potential vehicular applications
[DE85-006949] 16 p2758 N85-27017
Deep source gas
[DE85-001984] 18 p3126 N85-29359
Natural gas anomaly in bottom waters of South China Sea 19 p3290 N85-30388
Development of improved capabilities for computation of gas supercompressibility factors and other properties
[PB85-188316] 20 p3436 N85-31315
Ultrasonic flowmetering with reflected pulses
[PB85-179885] 20 p3460 N85-31482
Environmental concerns related to natural gas vehicles
[DE85-010246] 20 p3486 N85-31666
State of knowledge of environmental concerns related to natural-gas-fueled vehicles
[DE85-009746] 20 p3486 N85-31667
Development of a prototype energy meter
[PB85-198430] 22 p3769 N85-33476
Geologic, technical, and economic sensitivity analysis in support of the GRI (Gase Research Institute) tight gas reservoirs project area
[PB85-192276] 22 p3802 N85-33559
Laser probes of natural gas ignition chemistry
[PB85-200210] 24 p4077 N85-35284
Assessment of metal heating technologies for ferrous forging: A pilot study of the form value of natural gas
[PB85-204394] 24 p4084 N85-35314
High Temperature Heating System (HTHS)
[PB85-188340] 24 p4084 N85-35316

NATURAL GAS EXPLORATION
New method of reconstructing conditions of recent differentiation of oil and gas in the Amudarya Basin (based on results of interpretation of space photographs)
13 p1984 N85-22446
Evaluation of Thematic Mapper performance as applied to hydrocarbon exploration --- Ontario, Canada; Cement, Oklahoma; and Death Valley, California
13 p2118 N85-23191
Western gas sands
[DE85-001985] 18 p3126 N85-29360
Pacific index, April 1963 - October 1984
[TI85-901335] 19 p3320 N85-30582
Using remote photographs in prospecting for hydrocarbons on the Kerch Peninsula
22 p3735 N85-33154

NATURAL LANGUAGE (COMPUTERS)
On the requirements of expert systems for fault isolation
[AD-P003947] 02 p0249 N85-11627

Research in knowledge representation for natural language understanding
[AD-A145807] 03 p0409 N85-12613

Knowledge representation and natural-language semantics
[AD-A146025] 03 p0409 N85-12615

Interpretation of natural language database queries using optimization methods 05 p0735 N85-14723

Toward a principle-based parser
[AD-A147637] 08 p1202 N85-17565

Ada (trademark) Joint Program Office objectives and progress through 1983
[AD-A149436] 10 p1541 N85-19713

French plans for fifth generation computer systems
[AD-A149435] 10 p1544 N85-19732

The four forms of omega
[AD-A149694] 12 p1915 N85-22020

Infinite computing
[AD-A151437] 15 p2628 N85-26197

Research in knowledge representation for natural language understanding
[AD-A152260] 16 p2851 N85-27579

Language design, computers and brains
[AD-A152819] 17 p3008 N85-28594

Experience with omega: Implementation of a prototype programming environment: Part 1
[AD-A155438] 21 p3672 N85-32811

Research on distributed artificial intelligence
[AD-A155356] 22 p3833 N85-33733

EPALIT: A data management system applied to the control and retrieval of technical reports
[PB85-193068] 24 p4166 N85-35828

NATURAL LASERS

U LASERS

NATURAL SATELLITES

NT CALLISTO
NT CHARON
NT DEIMOS
NT ENCELADUS
NT EUROPA
NT GALILEAN SATELLITES
NT GANYMEDE
NT IO
NT JUPITER SATELLITES
NT MOON
NT SATURN SATELLITES
NT TITAN
NT TRITON

Origin and evolution of the Uranian and Neptunian satellites: Some dynamical considerations
02 p0300 N85-11943

Composition, structure and evolution of Uranian and Neptunian satellites 02 p0300 N85-11944

Physical properties of the Uranian satellites
02 p0300 N85-11946

Do the satellites of Uranus control its magnetosphere?
02 p0301 N85-11952

The rheology of icy satellites
[NASA-CR-174024] 02 p0302 N85-11959

Charged particle erosion of icy satellites: Coronal atmospheres and surface redistribution
03 p0448 N85-12845

Impact and collisional processes in the solar system
[NASA-CR-174297] 08 p1255 N85-17914

Interaction of the magnetospheric ions with the surfaces of the icy satellites of Saturn 13 p2174 N85-23491

Origin and evolution of the Saturn system
13 p2175 N85-23493

Studies of icy bodies: Uranian satellites and cometary nuclei 13 p2175 N85-23496

Small solar system bodies 13 p2175 N85-23499

Impact and collisional processes in the solar system
13 p2180 N85-23530

How a shepherd guides a sheep herd --- satellite-planetary ring interaction
15 p2674 N85-26503

Effects of shepherd conjunctions on Saturn's F-ring
15 p2675 N85-26511

Applications of three-body resonances to satellites and planetary rings 15 p2676 N85-26518

Extended atmospheres of outer planet satellites and comets
[NASA-CR-176137] 22 p3851 N85-33848

What determines the location of satellites and planets? 22 p3853 N85-33856

Volatiles on satellites of the outer solar system
22 p3854 N85-33868

Interpretation of photometric measurements of airless bodies 22 p3855 N85-33871

NAUTICAL CHARTS

Advanced technology for hydrographic mapping
[FOA-C-30371-E1] 08 p1176 N85-17418

NAVIER-STOKES EQUATION

Accelerated convergence for incompressible flow calculations
[NASA-TM-86863] 02 p0140 N85-10949

The CMC/3DPNS computer program for prediction of three-dimensional, subsonic, turbulent aerodynamic juncture region flow. Volume 3: Programmers' manual
[NASA-CR-165998] 02 p0197 N85-11318

Further development of a transonic cascade analysis
[AD-A145410] 02 p0198 N85-11319

Moment induced by liquid payload during spin-up without a critical layer
[AD-A145716] 02 p0199 N85-11327

Navier-Stokes solution of 3-dimensional hypersonic afterbody flowfields over capsule-type vehicles
[NAL-TR-819] 03 p0311 N85-12010

Model equation for simulating flows in multistage turbomachinery
[NASA-TM-86869] 03 p0315 N85-12036

Physics on aircraft wakes
[NASA-CR-174105] 04 p0453 N85-12871

Numerical integrations of the Navier-Stokes equations for flow over surface-mounted obstacles
05 p0593 N85-13784

Navier-Stokes computational study of axisymmetric transonic turbulent flows with a two-equation model of turbulence 05 p0634 N85-14068

Numerical investigations into the parabolized Navier-Stokes equations 05 p0635 N85-14075

Reducing numerical diffusion for incompressible flow calculations
[NASA-TM-83621] 06 p0756 N85-14840

A second-order accurate parabolized Navier-Stokes algorithm for internal flows
[NASA-CR-174258] 07 p0956 N85-16059

Computational analysis of scramjet dual mode operation
[NASA-CR-174250] 07 p0956 N85-16060

Numerical studies of interacting vortices
[NASA-TM-86325] 07 p0957 N85-16062

Development of a Navier-Stokes rotor and stator analysis
[AD-A146967] 07 p0958 N85-16070

Splitting methods for the numerical solution of the incompressible Navier-Stokes equations
[AD-A147463] 07 p1032 N85-16554

Analysis of a penalty finite element approximation of the Navier Stokes equations 08 p1161 N85-17321

Numerical solution of the Navier-Stokes equations for unsteady separated flows
[AD-P004161] 09 p1265 N85-17946

A Navier-Stokes calculation of the airfoil dynamic stall process
[AD-P004163] 09 p1265 N85-17948

Researched applied to transonic compressors in numerical fluid mechanics of inviscid flow and viscous flow
[NASA-CR-174353] 09 p1319 N85-18291

A free shear layer prediction of the turbulent wake of a flat plate towed below a free surface
[AD-A148699] 09 p1319 N85-18293

A series expansion study of the Navier-Stokes equations
[DFVLR-FB-84-34] 09 p1321 N85-18306

Evaluation of inviscid/boundary layer and parabolized Navier-Stokes solutions for design of reentry vehicles
[DE84-014329] 10 p1428 N85-19006

Thrust chamber performance using Navier-Stokes solution --- space shuttle main engine viscous nozzle calculation
[NASA-CR-171346] 10 p1430 N85-19019

A multistage time-stepping scheme for the Navier-Stokes equations
[NASA-CR-172527] 10 p1483 N85-19365

Algorithms for the Euler and Navier-Stokes equations for supercomputers
[NASA-CR-172543] 10 p1539 N85-19701

Experimental approach to terms within grids --- turbulent flow calculations 11 p1576 N85-19930

A new method for calculating the flow field in a dump combustor
[AD-A149305] 11 p1631 N85-20271

Pseudospectral calculations of two-dimensional transonic flow (Task 1). Numerical investigation of VTOL aerodynamics (Task 2)
[AD-A150123] 12 p1772 N85-21126

Numerical study of large-eddy breakup and its effect on the drag characteristics of boundary layers
[NASA-CR-3884] 12 p1797 N85-21272

Surface-slip equations for multicomponent nonequilibrium air flow
[NASA-TM-85820] 12 p1845 N85-21573

Solution of the three-dimensional Navier-Stokes equations for a steady laminar horseshoe vortex flow
[AD-A149851] 12 p1846 N85-21582

Hydrodynamic stability problem formulated by numerical solutions of the Navier-Stokes equations
12 p1946 N85-22223

Internal fluid mechanism of solid propellant rocket motors 13 p2001 N85-22544

Liquid moment on a filled coning cylinder during spin-up: Ad hoc model
[AD-A150280] 13 p2092 N85-23060

Significance of the thin-layer Navier-Stokes approximation
[DE85-002630] 13 p2092 N85-23063

Wave motion of three-component medium under load moving on plane boundary 14 p2277 N85-24105

Block-implicit multigrid solution of Navier-Stokes equations in primitive variables
[DE85-004071] 14 p2301 N85-24250

A 3-dimensional Navier-Stokes-Euler code for blunt-body flow computations
[NASA-TM-58266] 15 p2463 N85-25211

A finite element, Navier-Stokes study of the confined, laminar flow over a downstream facing step
15 p2553 N85-25754

Numerical simulation of boundary layer excitation by surface heating/cooling
[NASA-CR-172575] 15 p2554 N85-25756

Computational models of the viscous sublayer and limiting behavior of turbulence near a wall
[AD-A151198] 15 p2556 N85-25767

Unsteady Navier-Stokes calculations in an accelerated reference frame
[AD-A151751] 15 p2557 N85-25774

Flow over a biconic configuration with an afterbody compression flap
[AD-A151882] 15 p2557 N85-25778

Viscous effects on blast wave flowfields
[AD-A152013] 15 p2558 N85-25779

Numerical solutions of 3-dimensional Navier-Stokes equations for closed bluff-bodies
[NASA-CR-175755] 15 p2636 N85-26255

Numerical analyses in aerodynamic design of aero-engine fan 16 p2692 N85-26618

Navier-Stokes solution of hypersonic blunt-nosed body flowfields 16 p2693 N85-26624

Recent progress in computational aerodynamics
16 p2693 N85-26626

LU methods for the compressible Navier-Stokes equations 16 p2781 N85-27160

Theoretical investigation of three-dimensional shock wave turbulent boundary layer interactions. Part 3
[AD-A152251] 16 p2783 N85-27177

Users manual for coordinate generation code CRDSRA
[NASA-CR-172584] 17 p2891 N85-27824

User's manual for airfoil flow field computer code SRAIR
[NASA-CR-172585] 17 p2891 N85-27825

Use of quaternions in flight mechanics
[AD-A152616] 17 p2899 N85-27875

Navier-Stokes computational study of axisymmetric transonic turbulent flows with a two-equation model of turbulence
[AD-A152653] 17 p2958 N85-28265

Proceedings of the 9th US Air Force and the Federal Republic of Germany Data Exchange Agreement Meeting, Viscous and Interacting Flow Field Effects
[AD-A153020] 17 p2958 N85-28266

A Navier-Stokes capillary free boundary in open boat crystal growth
[REPT-84-34] 17 p2960 N85-28283

Numerical computation of space shuttle orbiter flow field
[NASA-CR-175912] 18 p3058 N85-28921

Numerical simulation of unsteady motion in a turbulent mixing layer
[NAL-TR-849T] 18 p3099 N85-29183

Two approaches for the prediction of plume-induced separation
[AD-A154098] 19 p3215 N85-29935

Application of computational fluid dynamics to complex inlet ducts
[NASA-TM-87060] 19 p3265 N85-30247

A numerical solution of a nonisothermal wall using the two-dimensional Navier-Stokes equations
[AD-A154467] 19 p3266 N85-30257

On spectral multigrid methods for the time-dependent Navier-Stokes equations
[NASA-CR-172613] 19 p3344 N85-30725

Superconvergence of finite element approximation for Navier-Stokes equations 19 p3345 N85-30732

Turbulent solutions of equations of fluid motion
20 p3453 N85-31441

An implicit finite-difference code for a two-equation turbulence model for three-dimensional flows
[NASA-TM-86752] 20 p3454 N85-31448

High Re separated flow solutions using the Navier-Stokes and approximate equations
[AD-A152252] 20 p3454 N85-31451

The calculation of fully three dimensional flow through any type of turbomachine blade row
21 p3567 N85-32294

Performance evaluation of flow in turbomachinery blade rows 21 p3587 N85-32299
Calculation of steady and unsteady airfoil flow fields via the Navier-Stokes equations
[NASA-CR-3699] 22 p3727 N85-33105
Jet flows: Modelling and experiments
22 p3744 N85-33208
A mixed pseudospectral/finite difference method for a thermally driven fluid in a nonuniform gravitational field
[NASA-TM-87581] 22 p3763 N85-33436
A three-dimensional viscous flow analysis for the helicopter tip vortex generation problem
[NASA-CR-3906] 23 p3893 N85-34114
Comments on the prediction of dynamic stall
[GU-AERO-8501] 23 p3894 N85-34125
A curvilinear coordinate method for the solutions of initial value problems using the third-order upwind differencing scheme
[IPPJ-734] 23 p3975 N85-34642

NAVIGATION
NT AIR NAVIGATION
NT ALL-WEATHER AIR NAVIGATION
NT AREA NAVIGATION
NT ASTRONAVIGATION
NT CELESTIAL NAVIGATION
NT DEAD RECKONING
NT DIGITAL NAVIGATION
NT DOPPLER NAVIGATION
NT HYBRID NAVIGATION SYSTEMS
NT INERTIAL NAVIGATION
NT INTERPLANETARY NAVIGATION
NT LORAN
NT LORAN C
NT NAP-OF-THE-EARTH NAVIGATION
NT OMEGA NAVIGATION SYSTEM
NT RADAR NAVIGATION
NT RADIO NAVIGATION
NT SPACE NAVIGATION
NT SURFACE NAVIGATION
NT TACAN
NT VHF OMNIRANGE NAVIGATION
Operational requirements - system concepts
06 p0752 N85-14823
Certification of advanced systems
06 p0753 N85-14829
Integrated navigation systems: Where are we headed?
[AD-A146425] 06 p0753 N85-14832
Map display for helicopters 08 p1073 N85-16801
Development of a Helicopter integrated navigation system 08 p1073 N85-16802
High accuracy Doppler navigation employing optimum integrated position fix information
08 p1073 N85-16803
Standard Attitude Heading Reference System (SAHRS) full scale development program
08 p1073 N85-16804
Integrated control and display systems for helicopter battlefield mission management
08 p1073 N85-16805
Shuttle navigation status 08 p1092 N85-16901
Space Shuttle Technical Conference, part 2
[NASA-CP-2342-PT-2] 08 p1096 N85-16937
Three position estimation procedures
[AD-A148748] 09 p1278 N85-18042
Automatic land vehicle navigation using road map data
[DE84-017178] 09 p1278 N85-18043
USSR report: Engineering and equipment
[JPRS-UEQ-85-001] 09 p1305 N85-18200
Using the global positioning system (GPS) phase observable for relative geodesy: Modeling, processing, and results 09 p1341 N85-18437
The use of synthetic aperture radar imagery to detect hazards to navigation
[AD-A149324] 10 p1422 N85-18971
The Telecommunications and Data Acquisition Report
[NASA-CR-174366] 10 p1462 N85-19224
Space System Applications to Tactical Operations
[AGARD-CP-344] 11 p1709 N85-20751
Dynamic world modeling for an intelligent mobile robot using a rotating ultra-sonic ranging device
[AD-A149979] 12 p1775 N85-21143
Investigation of a failure detection/identification system for a tactical aircraft navigation system
[AD-A151848] 15 p2469 N85-25240
A cost-efficient control procedure for the benefit of all airspace users 16 p2697 N85-26651
Avionics data base
[AD-A152415] 17 p2897 N85-27863
Time transfer techniques: Historical overview, current practices and future capabilities
18 p3106 N85-29245
HERMIES-1: A mobile robot for navigation and manipulation experiments
[DE85-006652] 18 p3118 N85-29301
LORAN-C harbor and harbor entrance survey: Charleston, South Carolina
[AD-A154875] 21 p3554 N85-32108
The potential of the NAVSTAR global positioning system for the Corps of Engineers, civil works
[AD-A154913] 21 p3554 N85-32109
Nonlinear digital phase-locked loops with application to Loran-C receivers 24 p4063 N85-35178

NAVIGATION AIDS
NT COMPASSES
NT GYROCOMPASSES
NT MAGNETIC COMPASSES
NT NAVIGATION INSTRUMENTS
NT RADAR BEACONS
NT RADIO BEACONS
NT RADIO DIRECTION FINDERS
Peripheral vision displays: The future
01 p0009 N85-10058
A production peripheral vision display system
01 p0010 N85-10059
Use of microprocessor techniques and new antenna systems to improve the navigation aids very high frequency omnidirectional radar (VOR), Doppler VOR and Instrument Landing System (ILS)
[BMFT-FB-W-84-026] 02 p0137 N85-10930
Autonomous navigation of USAF spacecraft
03 p0321 N85-12074
Integrated navigation systems: Where are we headed?
[AD-A146425] 06 p0753 N85-14832
Technology development for unmanned untethered submersible vehicle systems
[AD-A148794] 09 p1304 N85-18190
The susceptibility of aeronautical navigational aids to interference from adjacent-band broadcast transmissions
[BBC-RD-1984/12] 09 p1311 N85-18234
An evaluation of flashtube signal characteristics
[AD-A149569] 10 p1423 N85-18974
Navigation for an intelligent mobile robot
[AD-A150051] 12 p1775 N85-21144
Reference systems for the evaluation of dead-reckoning navigation equipment 13 p1967 N85-22358
Operational experience with ion concentration sensors in orientation systems 13 p1980 N85-22422
USSR report: Engineering and equipment
[JPRS-UEQ-84-001] 14 p2265 N85-24034
Combinatorial performance/cost analysis of an autonomous navigation system for aircraft
16 p2695 N85-26640
Preguidance and piloting with the aid of composite inertial sensors 16 p2696 N85-26646
The use of a self-compensated magnetometer in an economical navigation system for the helicopter
16 p2697 N85-26650
A method of estimating aircraft attitude from fly by wire flight control system data 16 p2697 N85-26653
Terrain following without use of forward looking sensors 16 p2698 N85-26659
Low cost two gimbal inertial platform and its system integration 16 p2698 N85-26661
Navigation and flight director guidance for the NASA/FAA helicopter MLS curved approach flight test program
[NASA-CR-177350] 16 p2704 N85-26691
Observability in problem of correction of inertial navigation systems using additional information from artificial Earth satellite 16 p2719 N85-26785
Avionics data base
[AD-A152415] 17 p2897 N85-27863
The AFTI/F16 terrain-aided navigation system
[DE85-008411] 18 p3060 N85-28935
The DREO (Defence Research Establishment Ottawa) Inertial Navigation Laboratory: Development and test capabilities
[AD-A154425] 19 p3216 N85-29945
LORAN-C harbor and harbor entrance survey: Charleston, South Carolina
[AD-A154875] 21 p3554 N85-32108

NAVIGATION INSTRUMENTS
NT ATTITUDE INDICATORS
NT COMPASSES
NT GYRO HORIZONS
NT GYROCOMPASSES
NT MAGNETIC COMPASSES
NT RADIO ALTIMETERS
NT RADIO DIRECTION FINDERS
Evaluation of air and ground launched cruise missile navigational element containers
[AD-A149854] 12 p1774 N85-21138
Reference systems for the evaluation of dead-reckoning navigation equipment 13 p1967 N85-22358
Navigation and flight director guidance for the NASA/FAA helicopter MLS curved approach flight test program
[NASA-CR-177350] 16 p2704 N85-26691

NAVIGATION SATELLITES
NT NAVSTAR SATELLITES
NT TRANSIT SATELLITES
The motion of the Earth by Doppler observing campaign (MEDOC) 05 p0601 N85-13601
A replenishment phase study for the NAVSTAR global positioning system
[AD-A152030] 16 p2704 N85-[illegible]
Observability in problem of correction of inertial navigation systems using additional information from artificial Earth satellite 16 p2719 N85-26785
Analysis of orbit transfer vehicles for GPS Block I satellites
[AD-A152021] 16 p2732 N85-[illegible]
Scintillation using NNSS satellites
[AD-A152804] 17 p2949 N85-28227
Rescue satellite COSPAS 20 p3401 N85-31108

NAVIGATORS
International flight planning handbook
[AD-A156330] 24 p4062 N85-35177

NAVSTAR SATELLITES
Simulation of the performance of adaptively controlled Navstar antennas in battlefield scenarios
10 p1472 N85-19282
Potential impact of Navstar GPS on NATO tactical operations 11 p1711 N85-20763
Coverage and buildup of the Navstar constellation
11 p1711 N85-20764
Optimization of guidance and control using function minimization and NAVSTAR/GPS
[AD-A149956] 12 p1775 N85-21141
Program INNAVSAT: Global Positioning System (GPS): Test and demonstration program
[BMFT-FB-W-84-047] 12 p1775 N85-21145
Accurate baseline determination by radio interferometry on NAVSTAR GPS satellite transmissions
[AD-A150681] 14 p2291 N85-24292
Real-time position determinations using the GPS TI4100/GEOSTAR receiver
[AD-A152551] 17 p2694 N85-27845
Kalman filter estimates of the NAVSTAR satellite clock parameters 17 p2965 N85-28315
Review and evaluation of plans to incorporate NAVSTAR global positioning system user equipment on military sealift command ships
[AD-A153799] 18 p3060 N85-28904
On-orbit frequency stability analysis of the GPS NAVSTAR-1 quartz clock and the NAVSTARs-6 and -8 rubidium clocks 18 p3105 N85-29227
Rubidium and cesium frequency standards status and performance on the GPS program
18 p3106 N85-29228
The NAVSTAR Global Positioning System (GPS) receiver development program, phase 1
[BMFT-FB-W-85-002] 20 p3399 N85-31085

NAVY
Don't fowl out
[AD-P004179] 11 p1578 N85-19941
Practical applications of satellite-derived meteorological and oceanographic data in Naval operations
11 p1712 N85-20771
Navy tactical applications guide. Volume 4. Part 1. Eastern North Pacific weather analysis and forecast applications
[AD-A150097] 12 p1896 N85-21900
A review of neck injury and impaired consciousness associated with US Navy ejections 1 January 1969 - 31 December 1979 12 p1906 N85-21973
An airborne infrared thermal scanning system for easy use on Navy P-3 aircraft
[AD-A149690] 12 p1933 N85-22143
SPARTEN (Scientific Program of Aerobic and Resistance Training Exercise in the Navy): A total body fitness program for health and physical readiness
[AD-A150669] 14 p2388 N85-24711
A preliminary analysis of C-12 aircraft usage by the Navy Air Logistics System
[AD-A151921] 16 p2694 N85-26634
Recent Naval Postgraduate School publications
[AD-A151723] 16 p2875 N85-27740
Navy program manager's guide, 1985 edition
[AD-A151925] 16 p2876 N85-27744
Navy geothermal plan
[AD-A152478] 17 p2985 N85-28450
Test and Evaluation Master Plan (TEMP) for the Navy Occupational Health Information Management System (NOHIMS). Phase 1: Appendix A through appendix U
[AD-A154179] 19 p3380 N85-30967
Development of NATOPS (Naval Air Training and Operating Procedure Standardization) performance software for the H-46D helicopter
[AD-A156069] 24 p4064 N85-35190
Solar pond technology for Navy applications
[AD-A155877] 24 p4112 N85-35488

NEAR FIELDS
Case study of sample spacing in planar near-field measurement of high gain antennas
[NASA-TM-86672] 01 p0037 N85-10234
System of equations for finding antenna radiation pattern from near-field samples 06 p0791 N85-15054
Comparison of measured and calculated mutual coupling in the near field between microwave antennas
[PB85-105863] 11 p1625 N85-20237
Near Field/Far Field (NF/FF) energy loss in Electric Discharge Lasers (EDL's): A mode-medium interaction
[AD-A150299] 13 p2096 N85-23075
Analytical studies and experimental measurements of amplitude and phase of near-field range antenna probes
[AD-A150922] 14 p2293 N85-24212
Theoretical and experimental comparisons of nearfield electrogalvanic fields due to nonlinear polarization layers
[AD-A152085] 16 p2779 N85-27149
High precision materials characterization in the near millimeter wave-length range
[AD-A153267] 17 p2968 N85-28331
An experimental study of plane mixing layer development
[NASA-TM-86698] 19 p3221 N85-29971
Transient dynamic solutions of some half space problems by the boundary element method
19 p3283 N85-30360
Report of near field group
[DE85-010536] 20 p3527 N85-31940
NEAR INFRARED RADIATION
A high resolution spectroscopic study of the oxygen molecule
[NASA-CR-174061] 02 p0172 N85-11150
Variation in spectral response of soybeans with respect to illumination, view, and canopy geometry
[E85-10040] 07 p0982 N85-16241
Detection of the J-10 manifold of the pure rotational band of phosphine on Saturn 08 p1245 N85-17855
The 1.5 - 3.5 micron spectroscopy of the Orion H2 source 08 p1246 N85-17864
The BRESEX multispectral camera: Preliminary characteristics
[INPE-3357-PRE/635] 10 p1487 N85-19386
The Feinheit method: A phase-independent formulation of the period-luminosity relation for Cephids
[NASA-CR-175708] 14 p2440 N85-25056
Space methods in oceanology
[NASA-TM-77652] 15 p2604 N85-26047
In situ thin film measurements
[AD-A151379] 15 p2652 N85-26353
INPE's line imaging camera: Preliminary results
[INPE-3476-PRE/719] 16 p2787 N85-27194
The ISAVF opto-mechanical test bed
[NASA-TM-87505] 24 p4067 N85-35206
NEAR WAKES
A study of the effect of wake-passing on turbine blades
[OUEL-1515/84] 03 p0363 N85-12326
Wake flow behind bluff bodies
05 p0593 N85-13783
Unsteady flow characteristics in the near-wake of a two-dimensional obstacle
[NASA-TM-77762] 07 p0897 N85-15684
Free surface effects on the wake of a flat plate
[AD-A146988] 07 p0958 N85-16071
Giotto plasmasheath and wake charging near Halley's Comet: Revised parameters 14 p2245 N85-23915
Experimental investigations of prismatic cylinders in flow with harmonic pulsations
[KU-SFB-210/E/4] 16 p2785 N85-27186
Wake effects of the aerodynamic performance of horizontal axis wind turbines 19 p3211 N85-29915
Laser Doppler Anemometer (LDA) measurements in the turbulent near-wake of blunt bodies
[ISL-CO-212/84] 22 p3785 N85-33450
NEARSHORE WATER
NT COASTAL WATER
Activities of the Coastal Research Center
[PB84-231323] 05 p0672 N85-14320
Slope water intrusions within the nearshore waters off Long Island, New York
[DE85-001386] 09 p1359 N85-18549
NEBRASKA
Revised Uniform Summary of Surface Weather Observations (RUSSWO). Offutt AFB, Nebraska, parts A-F
[AD-A147183] 07 p1006 N85-16394
NEBULAE
NT CASSIOPEIA A
NT CRAB NEBULA
NT ORION NEBULA
NT PLANETARY NEBULAE
Far-infrared observations of some regions of star formation 03 p0442 N85-12814
Open cluster formation — stellar evolution
03 p0442 N85-12815
An infrared study of the bi-polar outflow region GGD 12-15
[NASA-TM-86655] 03 p0445 N85-12835
Bulk composition of the Moon in the context of models for condensation in the solar nebula
04 p0583 N85-13725
The distribution of dust in the region of the Rosette Nebula and MON OB2 association
05 p0739 N85-14753
The correlation between excitation parameter and nebular luminosity for galactic HII regions with application to regions of star formation in M83
05 p0743 N85-14773
Dark cloud and globule distribution for galactic longitudes 230 to 360 degrees 06 p0878 N85-15575
A neutral gas jet in a low velocity shock front at the boundary of the Draco Nebula 06 p0878 N85-15576
The Draco Nebula, a molecular cloud associated with a high velocity cloud? 06 p0878 N85-15577
Bipolar ejection of matter from hot stars
08 p1233 N85-17767
Fragmentation and turbulence in collapsing gas clouds
[DE85-003745] 11 p1633 N85-20282
Future of Ultraviolet Astronomy Based on Six Years of IUE Research
[NASA-CP-2349] 11 p1743 N85-20961
IUE spectroscopy of extragalactic H H regions
11 p1745 N85-20974
Structure of the Seyfert broad line region and absorption region of NGC 4151 11 p1746 N85-20978
A model for the variable continuum of the Seyfert 1 galaxy NGC 5548 11 p1747 N85-20985
Dust in the region of Herbig-Haro objects: The case of NGC 1999 11 p1747 N85-20991
Ultraviolet studies of the young populous cluster NGC 2100 in the LMC 11 p1748 N85-20995
IUE and ESO observations of the P Cyg star AG Carinae and its ring nebula 11 p1750 N85-21006
The electron spectra in the synchrotron nebula of the supernova remnant G 29.7-0.3
[OG-6.2-10] 22 p3689 N85-34109
Far-infrared observations of young clusters embedded in the R Coronae Austrinae and RHO Ophiuchi dark clouds
[NASA-TM-86681] 24 p4167 N85-35834
The nature and geometry of infrared reflection nebulae 24 p4167 N85-35835
NECK (ANATOMY)
The clinical and radiological assessment of cervical injury, Annex A 12 p1907 N85-21976
NEEL TEMPERATURE
Coexistence of antiferromagnetism and spin-glass ordering in the Ising system FeO 55MgO 45Cl2
[DE85-004164] 12 p1942 N85-22197
NEGATIVE CONDUCTANCE
Circuit transients due to negative bias arcs on a high-voltage solar array in low Earth orbit
[NASA-TP-2407] 06 p0760 N85-14858
NEGATIVE FEEDBACK
Playback amplifier with high interference immunity
13 p2077 N85-22970
NEGATIVE IONS
Surface production of negative hydrogen ions
[AD-A145437] 02 p0277 N85-11801
Vibrational relaxation in H-2 molecules by wall collisions: Applications to negative ion source processes
[DE85-000852] 11 p1721 N85-20828
Hydrogen vibrational population distributions and negative ion generation in tandem high density hydrogen discharges
[DE85-001207] 11 p1722 N85-20834
Reconsideration of sheath related to negative ion extraction
[IPPJ-706] 12 p1935 N85-22159
Negative lithium emission from a tungsten surface in a plasma
[DE85-003456] 12 p1936 N85-22167
Theoretical studies of kinetic mechanisms of negative ion formation in plasmas
[AD-A150820] 14 p2423 N85-24946
A study of excitations during collisionally-induced electron detachment of negative ions
[AD-A152879] 17 p3030 N85-28739
Generation of intense negative ion beams
[NASA-CASE-NPO-16061-1-CU]
18 p3178 N85-29701
Maximum current densities from tandem high density systems
[DE85-008968] 18 p3180 N85-29720
One- and two-electron transfer processes in ion-surface scattering
[AD-A154208] 19 p3353 N85-30782
The production and destruction of metastable negative ions
[DE85-011056] 19 p3364 N85-30858
Improved negative ion source
[DE85-006445] 23 p3912 N85-34241
Negative ion sources equipped with continuous annular and spherical geometry surface ionizers
[DE85-011939] 23 p3971 N85-34619
NEGATRONS
An observation of cosmic ray positrons from 10-20 GeV
[OG-6.2-6] 22 p3689 N85-34105
NEODYMIUM
Structural, morphological and optical characteristics of KGd(WO4)2 crystals 14 p2260 N85-24126
Investigation for low-cost permanent magnets
[AD-A154387] 19 p3260 N85-30212
Spectral-luminescence characteristics and induced emission of Nd-3(+) ion in Gd(2-x)Nd(x)(WO4)3 crystals
21 p3688 N85-32912
NEODYMIUM ALLOYS
Anisotropy and microstructure of rare earth permanent magnet materials
[AD-A146549] 06 p0859 N85-15460
NEODYMIUM COMPOUNDS
Preparation and properties of single crystals of hydrogen bis(phthalocyaninato) neodymium(3)
[AD-A144933] 01 p0123 N85-10846
NEODYMIUM ISOTOPES
Constraints on the development of the early continental crust from isotopic data 21 p3719 N85-33076
NEODYMIUM LASERS
Pulsed neodymium glass laser system for investigating nonlinear optical phenomena in gases
03 p0348 N85-12241
Laser balancing system for high material removal rates
[NASA-CR-174731] 03 p0365 N85-123[illegible]
Design and testing of a refractive laser beam homogenizer
[AD-A146997] 07 p0970 N85-16162
Highly efficient Nd:YAG lasers for free-space optical communications 10 p1463 N85-19229
Solid state luminescent light filters for neodymium lasers 11 p1716 N85-20799
Lasing charactertistics of YAG: Nd(3+)-laser with LiF passive shutter with F2 color centers
11 p1717 N85-20802
Stability of temporal and energy parameters of picosecond lanthanum berylate laser
11 p1717 N85-20804
Autostochastic behavior of solid state ring laser with low frequency periodic loss modulation
11 p1717 N85-20805
Neodymium YAG laser pumped with radiation from high frequency electrodeless discharge
13 p2044 N85-22796
Research, development of laser glasses in China
13 p2166 N85-23439
Amplification of scattered induced radiation flux in high-gain laser rods 15 p2644 N85-26309
Conducting a wind sensing study
[NASA-CR-175782] 16 p2832 N85-27465
Development and application of a high power ND-glass laser instrument
[AD-A154366] 19 p3276 N85-30314
Laser beam interactions with vapor plumes during Nd:YAG laser welding on aluminum
[DE85-009793] 21 p3593 N85-32328
Luminescence and absorption of indium-activated potassium-borate glasses subjected to high-power excitation 21 p3681 N85-32868
Defect formation in amorphous hydrated silicon subjected to laser radiation 21 p3682 N85-32873
Selective population of N = 3 OVIII level during expansion of laser plasma in helium
21 p3688 N85-32914
Passive Q-modulation of optical cavities by KCl crystals containing OH(-) -ions 21 p3688 N85-32915
Switching power supply
[DE85-005993] 22 p3761 N85-33312
Infrared generation and wave-mixing studies in cesium
[DE85-012883] 24 p4083 N85-35304
Elliptical X-ray analyzer spectrograph application to a laser-produced plasma
[DE85-013790] 24 p4097 N85-35398
NEON
NT NEON ISOTOPES
Study of opacity effects on line radiation from pellet implosions
[DE85-000380] 10 p1491 N85-19413
Time dependent Hartree-Fock theory of ion-atom collisions: Application to F(9+) + Ne
[DE85-003083] 11 p1723 N85-20836
Hydrogen maser oscillation at 10 K
18 p3108 N85-29241
Initial results from the Caltech/DSRI balloon-borne isotope experiment
[OG-4.3-8] 21 p3714 N85-33046

Solar cycle variations of the anomalous cosmic ray component
[PAPER-SH-4.6-2] 21 p3715 N85-33057
Recombination and ionization in a nitrogen plasma
[AD-A155426] 22 p3845 N85-33813
A new analysis of cosmic ray isotopes at 3 GeV/n from HEA03-C2 data
[OG-4.3-6] 22 p3879 N85-34031
Photoionization-pumped, Ne 2, X-ray laser studies project
[DE85-012973] 23 p3936 N85-34399

NEON ISOTOPES
Solar cosmic ray produced neon in lunar soils and their implication for gas-rich meteorite studies
06 p0867 N85-15636
The (20)Ne interaction in extended matter
[NASA-TM-86312] 07 p1061 N85-16728
The energy dependence of the neon-22 excess in the cosmic radiation
[OG-4.3-7] 22 p3879 N85-34032
Forward particle production in inelastic Ne-22 inteVractions in emulsion at 4.1 A Ge/c
[HE-1.4-7] 24 p4176 N85-35895

NEON 19
U NEON ISOTOPES

NEOPLASMS
NT CANCER
NT LEUKEMIAS

NEOPRENES
U CHLOROPRENE RESINS

NEPHANALYSIS
A new NASA/MSFC mission analysis global cloud cover data base
[NASA-TP-2448] 12 p1893 N85-21878

NEPHELOMETERS
Chemical, biological, and physical measurements from the subtropical western North Atlantic Ocean. Summer 1982, USNS Lynch, cruise 710-82
[AD-A153823] 18 p3201 N85-29857

NEPTUNE (PLANET)
Uranus and Neptune
[NASA-CP-2330] 02 p0298 N85-11927
The origin and evolution of Uranus and Neptune
02 p0298 N85-11928
Atmospheres of Uranus and Neptune
02 p0298 N85-11929
Aeronomy 02 p0298 N85-11930
Temperature structures and infrared-derived properties of the atmosphere of Uranus and Neptune
02 p0298 N85-11931
Rotational properties of Uranus and Neptune
02 p0299 N85-11940
Oblatenesses of Uranus and Neptune
02 p0300 N85-11941
Physical properties of Neptune and Triton inferred from the Orbit of Triton 02 p0300 N85-11942
Origin and evolution of the Uranian and Neptunian satellites: Some dynamical considerations
02 p0300 N85-11943
Composition, structure and evolution of Uranian and Neptunian satellites 02 p0300 N85-11944
Physical properties of the satellites of Neptune
02 p0300 N85-11945
Satellite masses in the Uranus and Neptune systems
[PSI-CONTRIB-196] 02 p0301 N85-11947
Magnetospheric structures: Uranus and Neptune
02 p0301 N85-11949
The structure of the Uranian rings and the search for rings around Neptune 02 p0302 N85-11954
The structure and composition of Uranus and Neptune
13 p2175 N85-23495
Rings around Neptune? 15 p2672 N85-26491
Sixteenth Lunar and Planetary Science Conference. Press abstracts
[NASA-CR-175692] 15 p2680 N85-26548
Occultation detection of a Neptune ring segment
15 p2681 N85-26558
The 1986 National Aeronautics and Space Administration authorization
[GPO-47-635] 24 p4166 N85-35829

NEPTUNE ATMOSPHERE
Properties of the upper tropospheres of Uranus and Neptune derived from observations at visible to near-infrared wavelengths 02 p0298 N85-11933
Near infrared imaging of Uranus and Neptune
02 p0299 N85-11934
Atmospheric dynamics of Uranus and Neptune: Theoretical considerations 02 p0299 N85-11936
Variability of Neptune 02 p0299 N85-11938
Ultraviolet observations of Uranus and Neptune below 3000 A 11 p1760 N85-21071
Possible period of Jovian activity and possibility of seasons 16 p2723 N85-26810

NEPTUNIUM COMPOUNDS
Volume compressibilities of transuranium elements compounds, especially of neptunium compounds
03 p0431 N85-12744

NERNST HEAT THEOREM
U NERNST-ETTINGSHAUSEN EFFECT

NERNST-ETTINGSHAUSEN EFFECT
Magnetic fields in laser heated plasmas
[DE85-010715] 21 p3707 N85-33022

NERVES
Dynamics of morphological changes in articulation nervous system under hypokinetic conditions as a model of a spaceflight factor 01 p0092 N85-10621
Pathology of organophosphorus-induced delayed neurotoxicity
[AD-P004024] 06 p0844 N85-15358
Natural electrical activity of human sympathetic nerve fibers, recorded from body surface
07 p1013 N85-16433
Is fast fiber innervation responsible for increased acetylcholinesterase activity in reinnervating soleus muscles?
[NASA-CR-175716] 15 p2614 N85-26108
Differential effect of denervation on free radical scavenging enzymes in slow and fast muscle of rat
[NASA-CR-175719] 15 p2614 N85-26110

NERVOUS SYSTEM
NT AUTONOMIC NERVOUS SYSTEM
NT BRAIN
NT BRAIN STEM
NT CENTRAL NERVOUS SYSTEM
NT CEREBELLUM
NT CEREBRAL CORTEX
NT CEREBRAL VENTRICLES
NT CEREBRUM
NT EFFERENT NERVOUS SYSTEMS
NT NERVES
NT NEURONS
NT PERIPHERAL NERVOUS SYSTEM
NT SPINAL CORD
NT SPINE
NT SYMPATHETIC NERVOUS SYSTEM
NT SYNAPSES
NT THALAMUS
Effects of prolonged hypokinesia on nervous system
08 p1194 N85-17524
Neural compensation, muscle load distribution and muscle function in control of biped models
09 p1314 N85-18257
Determination of functional mobility of human nervous system with the PNN-3 instrument
10 p1525 N85-19618
Mercury health effects update: Health issue assessment
[illegible]85-123925] 10 p1528 N85-19639
Selecting one among the many: A simple network implementing shifts in selective visual attention
[AD-A148969] 10 p1530 N85-19644

NETHERLANDS
Fokker wants to start new Netherlands space program
03 p0310 N85-11999
Synoptical observations of snow depths at Dutch meteorological stations, 1956 - 1977
[KNMI-TR-51] 07 p1006 N85-16407
On the altitudinal distribution of birds and bird strikes in the Netherlands
[AD-P004189] 11 p1580 N85-19952
Task and future of the Large Institutes of Technology (LIT)
[B8474720] 11 p1741 N85-20945
Wind observation station description for Den Helder (period 1843-1972) and De Kooy (period 1955-1980)
[KNMI-TR-42] 14 p2379 N85-24686
Rotterdam Airport and the Common Market
17 p2894 N85-27840
Water quantity and quality research for the Rhine Meuse estuary
[PUBL-325] 17 p2968 N85-28470
Observations of surface water temperature in the Netherlands since 1860: Statistics
[KNMI-WR-84-3] 17 p2997 N85-28531
Observations of surface water temperature in the Netherlands since 1860: Tables for light vessels
[KNMI-WR-84-4] 17 p2998 N85-28532
Observations of surface water temperature in the Netherlands since 1860: Series from KNMI-RWS
[KNMI-WR-84-5] 17 p2998 N85-28533
OWEMA report: A project study concerning the possibilities and the desirability of a east-west runway for Maastricht Airport (Netherlands) as a Euro-regional air freight center
[B8476490] 18 p3064 N85-28955
Climatological data of stations in the Netherlands No. 11: Frequency tables and tables with runs according to measurements at principal climatological stations 1961-1980, sunshine stations 1956-1980, precipitation stations 1951-1980
[KNMI-150-11] 18 p3149 N85-29489
Wind energy in the north Netherlands region
20 p3485 N85-31681
Wind turbines and environment management
[CP-MEMO-1983-11] 20 p3485 N85-31682
Mathematical programming in the Netherlands
[REPT-ARW-03-THE-BDK/ORS/83/10]
20 p3517 N85-31688
Microwave propagation studies, measurements and education in Surabaya, Indonesia
[B8464633] 24 p4068 N85-35339

NETS
NT NEURAL NETS
NT PETRI NETS
Spline curves, wire frames and B-value
17 p3006 N85-29587

NETWORK ANALYSIS
NT CRITICAL PATH METHOD
Interaction of voice and data traffic in a packet switching communication network and virtual circuit
[FUB-63-1982] 01 p0039 N85-10249
Broadband local distribution networks: Problems and prospects in Italy
[FUB-18-1983] 01 p0040 N85-10255
End-to-end performance in local area networks of interconnected token rings
[FUB-42-1983] 01 p0107 N85-10714
A comparative evaluation of algorithms for generalized network problems
[TWISK-289] 01 p0107 N85-10721
Parametric analysis for generalized network flow problems
[AD-A145558] 02 p0243 N85-11589
Study on the conversion and test of protocols
[ENST-84E005] 03 p0356 N85-12290
The application of queueing theory to communications networks: A review
[AD-A146880] 04 p0492 N85-13140
Relaxation times for queueing systems
[CWI-OS-R8407] 05 p0719 N85-14616
The transient behavior of networks with infinite server nodes
[CWI-OS-R8406] 05 p0722 N85-14640
Local area network evaluation by MICROSS extensions
[AD-A146773] 07 p1027 N85-16521
EGP (Exterior Gateway Protocol) gateway under Berkeley UNIX 4.2
[AD-A148056] 08 p1208 N85-17587
Distributed asynchronous relaxation methods for convex network flow problems
[AD-A148027] 08 p1211 N85-17622
Beyond fault trees to fault graphs
[DE84-017022] 09 p1370 N85-18606
Coordination in a distributed problem solving network
[AD-A148925] 10 p1565 N85-19872
Vertical solar louver project
[DE84-017335] 11 p1676 N85-20558
A fully distributed approach to the design of a 16 K bit/sec VHF packet radio network
[AD-A141282] 13 p2054 N85-22859
Research using a DISCUS based network emulator
[AD-A141294] 13 p2149 N85-23338
Evaluating computer-communication networks with simulation techniques
[AD-A151852] 15 p2632 N85-26222
Developing an automated technique for translating a relational database into an equivalent network one
[AD-A151844] 15 p2686 N85-26451
Algebra of communicating processes
[CWI-CS-R8421] 17 p2950 N85-28214
Defense data network support concept analysis
[AD-A153214] 17 p3016 N85-28649
Numerical methods for stiff ordinary and elliptic partial differential equations
[AD-A153247] 17 p3020 N85-29675
Maximum flow in planar networks with exponentially distributed arc capacities
[AD-A153158] 17 p3026 N85-28710
Harold Hazen and the theory and design of servomechanism
[RR-270] 22 p3794 N85-33508

NETWORK CONTROL
Communications protocols for a fault tolerant, integrated local area network for Space Station applications
[NASA-TM-86304] 01 p0106 N85-10711
Proceedings of the 5th LAN-Transport Workshop
[PB84-232667] 01 p0107 N85-10715
Performance evaluation and control of distributed computer communication networks
[AD-A148103] 08 p1206 N85-17596

Process algebra with asynchronous communication mechanisms [CWI-CS-R8410] 11 p1625 N85-20235

System dynamics and network control [AD-A149420] 13 p2054 N85-22863

Distributed control of circuits in multiuser communication networks with circuit precedence and path suitability criteria using failsafe routing concepts [AD-A151825] 16 p2772 N85-27113

Distributed elections in a ring of processors using Archimedean time [CWI-CS-R8416] 17 p3016 N85-28653

LAN (Local Area Network) interoperability study of protocols needed for distributed command and control [AD-A154033] 19 p3255 N85-30182

A study of the ESA-NAVSAT control segment [ESA-CR(P)-2000] 20 p3398 N85-31079

NETWORK SYNTHESIS

Stuttgart Interconnection Network Project from PIX to NICS [NASA-TM-77802] 06 p0670 N85-15528

Design, fabrication and testing of a multibeam forming network [NASA-CR-175695] 14 p2298 N85-24228

Regional seismic wave propagation [AD-A150801] 14 p2373 N85-24671

Corrective-predictive systems [BLL-M-36063-(5828.4)] 16 p2851 N85-27573

NETWORKS

Extracting embedded generalized networks from linear programming problems [AD-A147565] 07 p1033 N85-16558

Selecting one among the many: A simple network implementing shifts in selective visual attention [AD-A148989] 10 p1530 N85-19644

Design of the National Trends Network for monitoring the chemistry of atmospheric precipitation [GS-CIRC-964] 20 p3486 N85-31664

Procedure for editing the fluxgate magnetometer data of the AFGL (Air Force Geophysics Laboratory) magnetometer network [AD-A156331] 24 p4117 N85-35523

NEUMANN PROBLEM

Integral equation formulations in two dimensions 05 p0718 N85-14605

Three-dimensional, direct and vectorized elliptic solvers for various boundary conditions [AD-B088266L] 08 p1206 N85-17595

On the connection between multigrid and cyclic reduction [NASA-TM-86020] 09 p1373 N85-18629

Neumann type boundary conditions for Hamilton-Jacobi equations [AD-A149069] 10 p1546 N85-19746

The low frequency behaviour of an immersed structure at a standstill in a high density fluid with free surface [TP-1983-31] 13 p2103 N85-23105

Adaptive detection of noise signal according to Neumann-Pearson criterion 15 p2527 N85-25580

Sobolev-Poincare's inequality and the Neumann problem for u sub t = divergence of the absolute value of the gradient u to the p-2 power x the gradient u [AD-A154788] 21 p3676 N85-32839

Hardy spaces and the L sup P-Neumann problem for Laplace's equation in a Lipschitz domain [CTH-MATH-1985-02] 22 p3836 N85-33749

NEURAL NETS

Feature discovery by competitive learning [AD-A145052] 01 p0097 N85-10646

Direct assessment of synaptic modification rules [AD-A148376] 08 p1196 N85-17534

Biological investigations of adaptive networks. Neuronal control of conditioned responding [AD-A150959] 14 p2385 N85-24695

Semantic networks and neural nets [AD-A150750] 14 p2407 N85-24840

Distributed memory [AD-A153364] 17 p3001 N85-28554

NEUROLOGY

Cognitive science program. A framework for relating cognitive to neural systems [AD-A145185] 01 p0097 N85-10649

Neural control of the direction of covert visual orienting [AD-A145189] 01 p0097 N85-10650

Inhibition of return: Neural basis and function [AD-A145242] 01 p0098 N85-10652

Proceedings of the 14th Conference on Environmental Toxicology [AD-A146400] 06 p0843 N85-15350

Neurotoxicology: A new scientific challenge [AD-P004017] 06 p0843 N85-15351

Interactions of ketones and hexacarbons [AD-P004019] 06 p0843 N85-15353

Molecular mechanisms of n-hexane neurotoxicity [AD-P004020] 06 p0843 N85-15354

Pathology and axonal transport in hexacarbon neuropathies [AD-P004021] 06 p0843 N85-15355

Organophosphorus-induced delayed neurotoxicity: Syndrome and experimental models [AD-P004022] 06 p0844 N85-15356

Chemistry and metabolism of delayed neurotoxic organophosphorus esters [AD-P004023] 06 p0844 N85-15357

Pathology of organophosphorus-induced delayed neurotoxicity [AD-P004024] 06 p0844 N85-15358

Electrophysiologic changes in organophosphorus-induced delayed neurotoxicity [AD-P004025] 06 p0844 N85-15359

Biochemistry and pathogenic hypotheses of organophosphorus-induced delayed neurotoxicity [AD-P004026] 06 p0844 N85-15360

Multiple resources and brain laterality [AD-A148912] 10 p1530 N85-19643

USSR report: Life sciences. Biomedical and behavioral sciences [JPRS-UBB-85-010] 11 p1690 N85-20628

Biological investigations of adaptive networks. Neuronal control of conditioned responding [AD-A150959] 14 p2385 N85-24695

A model for generalization and specification by single neurons [AD-A150871] 14 p2391 N85-24724

Neural mechanism by which gravitational stimulus and stress affect the secretion of renin and other hormones 15 p2610 N85-26083

Academician Ovchinnikov on future of bioorganic chemistry 17 p3049 N85-28874

NEUROMUSCULAR TRANSMISSION

The effect of part-simulation of weightlessness on human control of bilateral teleoperation: Neuromotor considerations 05 p0703 N85-14510

Advanced development of an active neuromusculature response to mechanical stress [AD-A148436] 08 p1196 N85-17536

Neural compensation, muscle load distribution and muscle function in control of biped models 09 p1314 N85-18257

Investigation of adaptive distinctions of mechanism of controlled glycemia in Macaca rhesus monkeys 12 p1902 N85-21946

Application of the system identification technique to goal-directed saccades [AD-A150132] 12 p1906 N85-21967

Induced changes in the cholinergic system of sciatic nerve and slow and fast twitch muscle of rats 15 p2609 N85-26081

Changes in the cholinergic system of rat sciatic nerve and skeletal muscle following suspension induced disuse [NASA-CR-175718] 15 p2615 N85-26111

Physical chemical state of water in living cells [AD-A154566] 21 p3662 N85-32749

NEURON TRANSMISSION
U BIOELECTRICITY

NEURONS

Cognitive science program. A framework for relating cognitive to neural systems [AD-A145185] 01 p0097 N85-10649

Biological investigations of adaptive networks. Neuronal control of conditioned responding [AD-A150959] 14 p2385 N85-24695

A model for generalization and specification by single neurons [AD-A150871] 14 p2391 N85-24724

Cell death, neuronal plasticity and functional loading in the development of the central nervous system 15 p2612 N85-26096

Sensory and motor properties of the cerebellar uvula and modulus 15 p2613 N85-26104

Anatomy of the vestibulo-automatic outflow to the gut 15 p2614 N85-26106

Discovery regarding visual neuron adaptation applicable to robot use 20 p3504 N85-31786

NEUROPHYSIOLOGY

Dynamics of morphological changes in articulation nervous system under hypokinetic conditions as a model of a spaceflight factor 01 p0092 N85-10621

Organophosphorus-induced delayed neurotoxicity: Syndrome and experimental models [AD-P004022] 06 p0844 N85-15356

Aspects of solvent toxicity in mixtures [AD-P004036] 06 p0845 N85-15366

Lateral specifics of visual perception 07 p1013 N85-16436

Change in relationship of biopotentials of brain zones for various levels of working capacity 07 p1013 N85-16438

Vision by man and machine: How the brain processes visual information may be suggested by studies in computer vision (and vice versa) [AD-A147890] 07 p1017 N85-16458

Effects of partial deprivation of slow-wave sleep on sleep-wakefulness cycles 10 p1524 N85-19613

USSR report: Life sciences. Biomedical and behavioral sciences [JPRS-UBB-85-010] 11 p1690 N85-20628

Characteristics of human masseter under conditions of hypokinesia 11 p1691 N85-20630

Topography of human brain electric potentials and dominance 11 p1691 N85-20633

Functional significance of some EEG parameters and dominant principle 11 p1691 N85-20634

Neurophysiological correlates of motion sickness: Role of vestibulocerebellum and 'vomiting center' reanalyzed 11 p1693 N85-20643

Circadian rhythm control: Neurophysiological investigations 15 p2612 N85-26099

Airsickness control using biofeedback to self-regulate psychophysiological responses [AD-A151167] 15 p2617 N85-26128

Functional impairment and structural cervical injuries in human surrogates [PB85-167436] 15 p2619 N85-26137

NEUROPSYCHIATRY

Toward a computational neuropsychology of high-level vision [AD-A145711] 02 p0236 N85-11540

Psychometric evaluation of head injury among fliers referred to the AF School of Aerospace Medicine [AD-A151479] 15 p2617 N85-26129

NEUROSCIENCE
U NEUROLOGY

NEUROTRANSMITTERS

USSR report: Life sciences. Biomedical and behavioral sciences [JPRS-UBB-85-010] 11 p1690 N85-20628

Use and disuse and the control of acetylcholinesterase activity in fast and slow twitch muscle of rat [NASA-CR-175717] 15 p2614 N85-26109

NEUTRAL ATMOSPHERES

Neutral atmosphere properties determining D-region electron densities 11 p1658 N85-20451

A model of the influence of neutral air dynamics on the seasonal variation in the low ionosphere 11 p1660 N85-20462

The diurnal variation of the neutral sodium species in the upper atmosphere: A model study [AD-A154988] 21 p3631 N85-32561

NEUTRAL ATOMS

Plasma surface interactions in magnetic fusion systems [DE84-015255] 01 p0123 N85-10842

Laser cooling and trapping of neutral atoms [AD-A146046] 03 p0366 N85-12345

Forces on neutral atoms due to electromagnetic fields [AD-A146984] 07 p1040 N85-16603

Theoretical issues involving traps for neutral spin-polarized atoms [AD-A148035] 08 p1220 N85-17682

Numerical model for swirl cooling in high-heat-flux particle beam targets and the design of a swirl-flow-based plasma limiter [DE85-003824] 11 p1732 N85-20894

Secondary ion mass spectrometry studies of solids and surfaces [AD-A151744] 16 p2745 N85-26939

NEUTRAL BEAMS
NT MOLECULAR BEAMS
NT NEUTRON BEAMS

Neutral beam interactions with materials [AD-A145636] 02 p0285 N85-11857

Low energy ion-molecule reaction dynamics and chemiionization kinetics [DE84-015881] 04 p0559 N85-13562

Alpha-particle diagnostics with high energy neutral beams [IPPJ-695] 06 p0863 N85-15485

The role of fast electrons for the performance characteristics of hydrogen ion sources 09 p1303 N85-18189

Sources, densities, and transport of impurities in neutral-beam injected Tokamaks 09 p1388 N85-18731

Beam probe spectroscopic technique for ion temperature and magnetic field measurements 09 p1389 N85-18738

Long-pulse beamlines for the mirror fusion test facility [DE84-017091] 09 p1392 N85-18760

All solid state high voltage power supply for neutral beam sources [DE85-002531] 11 p1629 N85-20257

Collisional pumping for the production of intense spin-polarized, neutral beams: Target considerations
[DE85-003459] 11 p1723 N85-20841
Neutral beam injector oxygen impurity measurements and concentration reduction via gettering processes
[DE85-000661] 12 p1836 N85-21521
Spectroscopic study of sources and control of impurities in TMX-U: Revision 1
[DE85-004423] 12 p1937 N85-22170
Measurements of integral yields of charged secondary particles using neutral beams simulating a cometary fly-by — Giotto mission 14 p2244 N85-23908
Laser-induced fluorescence of metal-atom impurities in a neutral beam
[DE85-004960] 14 p2310 N85-24298
Experimental and theoretical studies of laser cooling and emittance control of neutral beams
[AD-A149215] 15 p2562 N85-25804
Development of an apparatus for obtaining molecular beams in the energy range from 2 to 200 eV
[NASA-TM-77835] 15 p2647 N85-26326
Development of RF plasma generators for neutral beams
[DE85-004125] 15 p2658 N85-26400
Simulation of automatic control of MFTF-B neutral beams
[DE85-010640] 20 p3530 N85-31960
Recent experiments in Gamma-10
23 p3976 N85-34651
Considerations on collective ion aceleration as an intense ion injector
[DE85-012706] 24 p4155 N85-35757

NEUTRAL CURRENTS
Neutral-current x-distributions
[DE84-016522] 09 p1382 N85-18691
Plasma waves at and near the neutral sheet
14 p2358 N85-24572

NEUTRAL GASES
Absorption line studies and the distribution of neutral gas in the local interstellar medium
06 p0873 N85-15544
Synthesis of data on the local interstellar medium
06 p0874 N85-15545
A neutral gas jet in a low velocity shock front at the boundary of the Draco Nebula 06 p0878 N85-15576
Radio and UV observations of high latitude HI
06 p0879 N85-15583
Seasonal characteristics of mesospheric plasma and their transitions 11 p1660 N85-20464
Electrostatic charging of the Giotto spacecraft due to neutral gas impact 14 p2244 N85-23913
Digital image analysis of four-frame holographic plasma and neutral gas interferograms
[DE85-008397] 16 p2786 N85-27200
The structure of galactic HI in directions of low total column density
[NASA-CR-175709] 16 p2882 N85-27785
On the anomalous component
[SH-4.6-6] 23 p4039 N85-35044

NEUTRAL PARTICLES
NT COLD NEUTRONS
NT FAST NEUTRONS
NT NEUTRONS
NT THERMAL NEUTRONS
Emission mechanisms in the liquid metal ion source: A review
[AERE-R-11294] 03 p0418 N85-12675
Search for neutral, penetrating, metastable particles produced in the SLAC beam dump
[DE84-012466] 04 p0560 N85-13569
Gas pressure and electron density in the active zone level of hollow cathode arc discharges
[NASA-TM-77468] 07 p0945 N85-15988
Improved performance for large area triple layer microchannel plate detector for a neutral spectrometer in Doublet III
[DE85-001719] 10 p1488 N85-19395
Mass analysis of neutral particles and ions released during electrical breakdowns on spacecraft surfaces
[NASA-CR-175585] 12 p1793 N85-21250
User's guide for TWOHEX: A code package for two-dimensional, neutral-particle transport in equilateral triangular meshes
[DE85-004482] 12 p1930 N85-22125
Mass spectra of neutral particles released during electrical breakdown of thin polymer films
13 p1996 N85-22511
Measurement of charged secondary particle emission under ion and neutral impact — Giotto mission
14 p2243 N85-23906
Cometary atmospheres: Modeling the spatial distribution of observed neutral radicals
[NASA-CR-175852] 16 p2882 N85-27781
Neutral particle beam intensity controller
[DE85-006411] 23 p3969 N85-34604
Behavior of helically-trapped fast ion orbits in heliotron E 23 p3978 N85-34666
Neutral pion production in solar flares
[SH-1.4-7] 23 p3995 N85-34767
Strategic defense initiative
[DE85-012778] 24 p4150 N85-35735

NEUTRAL SHEETS
Cosmic ray intensity and the tilt of the neutral sheet
[SH-4.2-8] 23 p4007 N85-34846
Effects of a wavy neutral sheet on cosmic ray anisotropies
[SH-4.2-11] 23 p4008 N85-34849
Difference between even and odd 11-year cycles in cosmic ray intensity
[SH-4.2-22] 23 p4009 N85-34859
Influence of the neutral sheet on the Swinson's type north-south anisotropy of cosmic rays
[SH-4.3-10] 23 p4032 N85-34995
The sidereal semi-diurnal variation observed at high zenith angles at Mawson, 1968-1984, and the polarity of the solar main field
[SH-4.4-6] 23 p4033 N85-35004

NEUTRALIZERS
Development anmd te'ting of electrophoresis solutions. Task I.1: Development of optimal buffer system
20 p3500 N85-31755

NEUTRINO BEAMS
AGS broad band neutrino beam
[DE85-010954] 19 p3366 N85-30875
On gamma and neutrino radiation from Cyg X-3
[OG-2.1-7] 22 p3863 N85-33924

NEUTRINOS
NT SOLAR NEUTRINOS
Results on weak current from CHARM collaboration — neutrino interactions
[NOTA-INTERNA-810] 02 p0279 N85-11817
Search for the radiative decay of a cosmic relic particle with IUE
[PREPRINT-410] 04 p0580 N85-13707
Iron core collapse models of Type 2 supernovae
[DE84-013909] 05 p0743 N85-14775
Neutrino measurements on the Moon
[DE85-007700] 16 p2884 N85-27791
Did bosonic sneutrino stars ever exist
[PREPRINT-421] 18 p3202 N85-29867
Search for proton decay
[DE85-008283] 19 p3353 N85-30786
Search for neutrino oscillations at the Brookhaven AGS
[DE85-009766] 20 p3530 N85-31957
Neutrino-antineutrino annihilation around collapsing star
[OG-1.1-10] 22 p3861 N85-33911
Detection of 10 (1) GeV cosmic neutrinos with a space station
[OG-9.4-10] 23 p4030 N85-34977
Neutrino production from the solar atmosphere
[SH-8.1-9] 23 p4050 N85-35114
Solar cosmic ray bursts and solar neutrino fluxes
[SH-8.1-10] 23 p4050 N85-35115
Three dimensional calculation of flux of low energy atmospheric neutrinos
[SH-8.1-11] 23 p4050 N85-35116
Neutrino production of like sign dimuons
[DE85-013594] 24 p4151 N85-35741
High energy physics at Tufts University
[DOE/ER-40085/7] 24 p4152 N85-35744
Nineteenth International Cosmic Ray Conference. HE sessions, volume 8
[NASA-CP-2376-VOL-8] 24 p4200 N85-36066
Muon and neutrino results from KGF experiment at a depth of 7000 hg/square cm
[HE-5.1-2] 24 p4200 N85-36068
Background light measurements at the DUMAND site
[HE-5.2-7] 24 p4203 N85-36084
Hybrid TLC-pair meter for the Sphinx Project
[HE-5.2-10] 24 p4203 N85-36086
A study of atmospheric neutrinos with the IMB detector
[HE-5.3-7] 24 p4205 N85-36101
Atmospheric neutrinos observed in underground detectors
[HE-5.3-8] 24 p4205 N85-36102
Geophysical searches for three-neutrino oscillations
[HE-5.3-9] 24 p4205 N85-36103
Measurement of neutrino oscillations in MACRO experiment
[HE-5.3-10] 24 p4206 N85-36104
The capability of the existing network of installations for detecting the antineutrino burst from collapsing stars
[HE-5.3-13] 24 p4206 N85-36107
Energy spectra of high energy atmospheric neutrinos
[HE-5.3-14] 24 p4206 N85-36108
A standard source for high energy neutrino astronomy
[HE-5.3-15] 24 p4206 N85-36109
A search for cosmic sources of high energy neutrinos with small underground detectors
[HE-5.3-16] 24 p4206 N85-36110
Neutrino astronomy and the atmospheric background
[HE-5.3-17] 24 p4207 N85-36111
High-energy neutrinos from a lunar observatory
[HE-5.3-21] 24 p4207 N85-36112
Characteristics of slow particles emitted in the charged current interactions of neutrinos with emulsion nuclei
[HE-5.3-22] 24 p4207 N85-36113
QCD analysis of neutrino charged current structure function F2 in deep inelastic scattering
[HE-5.3-23] 24 p4207 N85-36114
Angular distribution of muons produced by cosmic ray neutrinos in rock
[HE-5.3-24] 24 p4207 N85-36115
Atmospheric muons and neutrinos, and the neutrino-induced muon flux underground
[HE-5.4-7] 24 p4207 N85-36116
Nucleon decay and atmospheric neutrinos in the Mont Blanc experiment
[HE-6.2-6] 24 p4211 N85-36142
Muon and neutrino fluxes
[HE-6.2-18] 24 p4213 N85-36154
Experimental investigation of radiative-acoustic effects in the water by the thermodynamical conditions of Dumand
[HE-7.1-2] 24 p4213 N85-36158

NEUTRON ABSORBERS
Method and apparatus for determining the content and distribution of a thermal neutron absorbing material in an object
[DE84-014319] 01 p0117 N85-10861
Time-integrated yield for the Joint European Torus (JET), April - September 1984
[AERE-M-3449] 17 p3038 N85-28797

NEUTRON ACTIVATION ANALYSIS
In vivo neutron activation analysis: Body composition studies in health and disease
[DE84-014092] 05 p0696 N85-14480
JPL in-house fluidized-bed reactor research
06 p0832 N85-15291
Neutron activation analysis of stoney spherules from a marine sediment sample 06 p0883 N85-15606
Proceedings of the 2nd Workshop on Nondestructive Evaluation (NDE) of Titanium Alloys
[AD-A147626] 08 p1125 N85-17095
Measurement of oxygen contamination in titanium alloy ingots by fast neutron activation analysis
[AD-P004133] 08 p1128 N85-17108
Neutron activation analysis of titanium with oxygen contamination
[AD-P004134] 08 p1128 N85-17109
Investigation of the output parameters of the pulsed neutron generator NGI-5
[DE85-001823] 11 p1725 N85-20849
Multiple element neutron-activation analysis of atmospheric aerosols with X-ray and gamma-spectrometric recording of radionuclides formed
13 p2013 N85-22631
Time-integrated yield for the Joint European Torus (JET), April - September 1984
[AERE-M-3449] 17 p3038 N85-28797
Quantitative analysis of defects in silicon-characterization of UCP, HAMCO, and microcrystalline material
[NASA-CR-175968] 18 p3079 N85-29046
Proceedings of the Fifth International Conference on Nuclear Methods in Environmental and Energy Research
[DE84-017348] 19 p3310 N85-30521
Sulfur activation at the Little Boy-Comet Critical Assembly: A replica of the Hiroshima bomb
[DE85-010261] 20 p3527 N85-31906
Determination of the average neutron activation cross section with an annular-shaped 241 Am/Be neutron source and a NaI(T1) detector for the 27 Al (n,p)27 Mg-reaction
[REPT-4/1984] 20 p3532 N85-31975
Activation analysis of natural water using neutrons of various energies 21 p3690 N85-32924
Rhodium-103 and Indium-115 inelastic scattering reactions for fission neutron dosimetry
21 p3703 N85-33004

NEUTRON BEAMS
Performing (p vector,)ic)n), (d vector, n) and (n vector, n) measurements with a rotating magnet beam swinger
[DE84-017003] 04 p0562 N85-13582
Paramagnetic scattering from Ni
[DE85-004207] 12 p1942 N85-22198
Magnetic scattering and polarized neutrons
[DE85-009823] 19 p3355 N85-30794
Measurement and evaluation of selected 14-MeV neutron cross sections for fusion
[DE85-010295] 19 p3365 N85-30867
Cosmic ray north-south anisotropy 1961 - 1983
[SH-4.2-6] 23 p4007 N85-34844

NEUTRON COUNTERS
NT NEUTRON SPECTROMETERS
Method and apparatus for determining the content and distribution of a thermal neutron absorbing material in an object
[DE84-014319] 01 p0117 N85-10801
Approaches to ultrafast neutron detectors
[DE85-001206] 11 p1636 N85-20307
Ultrahigh-sensitivity threshold neutron detector for plasma diagnostics
[DE85-005270] 13 p2161 N85-23413
Neutron detector counting capabilities for (10) B-lined and (235) U fission chambers in high gamma-ray fluxes
[DE85-011693] 22 p3840 N85-33780
Spectra of solar proton ground level events using neutron monitor and neutron moderated detector recordings
[SH-1.3-14] 23 p3994 N85-34759
Determination of galactic cosmic ray latitudinal gradient using Earth based detectors
[SH-4.2-13] 23 p4008 N85-34851
An update on the correlation between the cosmic radiation intensity and the geomagnetic AA index
[SH-4.2-24] 23 p4009 N85-34861
Cosmic ray sidereal diurnal variation of galactic origin observed by neutron monitors
[SH-4.4-2] 23 p4033 N85-35000
Observations of cosmic-ray modulations in the fall, 1984
[SH-5.1-16] 23 p4043 N85-35069
Frequency spectra of short-period variations of cosmic ray
[SH-5.1-17] 23 p4043 N85-35070
Coupling functions for lead and lead-free neutron monitors from the latitudinal measurements performed in 1982 in the research station Academician Kurchatov
[SH-6.1-1] 23 p4044 N85-35076
On the solar cycle variation in the barometer coefficients of high latitude neutron monitors
[SH-6.1-2] 23 p4044 N85-35077
Recording system for the solar neutron monitoring at Mt. Norikura
[SH-9.1-8] 23 p4051 N85-35123
Sensitivity of single and multiple cosmic ray neutrons to the surrounding medium in a lead-free monitor
[SH-9.1-10] 23 p4051 N85-35125
SONTRAC: A solar neutron track chamber detector
[SH-9.1-12] 23 p4052 N85-35127
The neutron moderated detector and groundbased cosmic ray modulation studies
[SH-9.1-13] 23 p4052 N85-35128
New Matsushiro underground cosmic ray station (220 M.W.E. in depth)
[SH-9.1-14] 23 p4052 N85-35129
A suggested standardized format for cosmic ray ground-level event data
[SH-9.1-15] 23 p4052 N85-35130
The influences of the galactic cosmic ray on the atmospheric ozone
[SH-10.1-1] 23 p4053 N85-35133
NEUTRON CROSS SECTIONS
SPECTER: Neutron damage calculations for materials irradiations
[DE85-005791] 18 p3180 N85-29716
Chemical spectroscopy
[DE85-009594] 18 p3191 N85-29790
Measurement and evaluation of selected 14-MeV neutron cross sections for fusion
[DE85-010295] 19 p3365 N85-30867
An attempt to detect induced neutron capture in laser radiation field 21 p3690 N85-32928
Rhodium-103 and Indium-115 inelastic scattering reactions for fission neutron dosimetry
21 p3703 N85-33004
Radiation transport
[DE85-010333] 21 p3703 N85-33005
The effects of newly measured cross sections in hydrogen on the production of secondary nuclei during the propagation of cosmic rays through interstellar H
[OG-7.2-2] 23 p4014 N85-34874
(NAT)Fe(n,n'x) spectra at 65.5 MeV
[AD-A156776] 24 p4150 N85-35730
NEUTRON DECAY
High energy neutron and gamma-radiation generated during the solar flares
[SH-1.4-8] 23 p3995 N85-34768
NEUTRON DETECTORS
U NEUTRON COUNTERS
NEUTRON DIFFRACTION
Diffraction by the time-of-flight technique at pulsed neutron sources
[DE84-015839] 03 p0418 N85-12674
Magnetic properties of intermetallic phases and simple systems — neutron diffraction 03 p0422 N85-12697
Fine structure analysis with thermal neutrons and development and construction of a multidetector system
03 p0422 N85-12698
Investigation of domain structures and walls using neutron diffraction 03 p0423 N85-12702
Construction of a neutron single crystal diffractometer
03 p0427 N85-12723
Measurement of scattering cross sections of liquid and solid hydrogen deuterium and deuterium hydride for thermal neutrons
[DE84-014814] 05 p0727 N85-14671
Momentum distributions in superfluid helium: Bose condensate fraction
[DE84-014676] 05 p0731 N85-14700
Neutron diffraction studies of the hydrogen bonding and water molecules in zeolites
[DE84-016431] 06 p0766 N85-14900
SANS and TEM studies of carbide precipitation and creep damage in type 304 stainless steel
[DE85-000933] 09 p1206 N85-18139
Study of magnetism at surfaces by scattering of neutrons at grazing incidence
[DE84-015650] 10 p1564 N85-19865
Microscopic magnetic structure of multiple bilayers of thin films of Fe and Ge
[DE85-004168] 13 p2024 N85-22682
Ultrasonic SH wave velocity in textured aluminum plates
[AERE-R-11516] 15 p2509 N85-25475
High resolution powder diffraction
[DE85-006287] 17 p2922 N85-28015
Magnetism at interfaces and surfaces, as probed by neutron scattering
[DE85-007967] 18 p3176 N85-29690
Structural and physical studies on a new class of low-dimensional conducting material: FeOCl intercalated with TTF and related molecules
[DE85-009701] 18 p3196 N85-29824
Magnetic scattering and polarized neutrons
[DE85-009823] 19 p3355 N85-30794
Determination of the intramolecular potential flow from a neutron diffraction experiment
[B8563199] 20 p3532 N85-31978
NEUTRON EMISSION
Nuclear moments and nuclear structure
[DE84-015847] 04 p0561 N85-13573
Performing (p vector,]lc]n), (d vector, n) and (n vector, n) measurements with a rotating magnet beam swinger
[DE84-017003] 04 p0562 N85-13582
Neutron and gamma-ray signatures for particle acceleration in solar flares 12 p1954 N85-22278
Refinements in the computation of collision probabilities
[DE85-006118] 16 p2864 N85-27663
Fast-neutron-spectrum measurements for the thick-target (9)Be(d/ = 7 MeV
[DE85-010481] 18 p3183 N85-29735
Investigation of thick-target neutron emission from Be-9(d,n)B-10 at E(d) = 7 MeV for angles other than zero degrees
[DE85-010254] 20 p3528 N85-31947
Methodology for evaluating P sub nu distributions: Results to date
[DE85-007286] 20 p3530 N85-31956
Magnetically insulated diode for generating pulsed neutron and gamma ray emissions
[DE85-011658] 22 p3760 N85-33306
Apparatus and method for identification of matrix materials in which transuranic elements are embedded using thermal neutron capture gamma-ray emission
[DE85-011659] 22 p3786 N85-33454
Measurement of radionuclides in waste packages
[DE85-011674] 22 p3838 N85-33766
Calculated neutron-induced cross sections for /sup 63,65/Cu/sup 58,60/Ni and (52) Cr from 1 to 20 MeV and comparisons with experiments
[DE85-011928] 22 p3844 N85-33806
Helios 1 energetic particle observations of the solar gamma ray flare events of 7, 21 June 1980 and 3 June 1982
[SH-1.3-8] 23 p3993 N85-34755
Source energy spectra from demodulation of solar particle data by interplanetary and coronal transport
[SH-1.3-13] 23 p3994 N85-34758
On the angular and energy distribution of solar neutrons generated in P-P reactions
[SH-1.4-9] 23 p3995 N85-34769
Recording system for the solar neutron monitoring at Mt. Norikura
[SH-9.1-8] 23 p4051 N85-35123
Sensitivity of single and multiple cosmic ray neutrons to the surrounding medium in a lead-free monitor
[SH-9.1-10] 23 p4051 N85-35125
The neutron moderated detector and groundbased cosmic ray modulation studies
[SH-9.1-13] 23 p4052 N85-35128
Neutron production by Ne and Si ions on a thick Cu target at 670 MeV/A with application to radiation protection
[DE85-014526] 24 p4152 N85-35746
NEUTRON FLUX
U FLUX (RATE)
NEUTRON FLUX DENSITY
Monte Carlo alpha calculation
[DE85-010720] 19 p3349 N85-30758
Study of proton and neutron activation of metal samples in low Earth orbit
[NASA-CR-171596] 21 p3558 N85-32130
Neutron flux, spectrum and dose equivalent measurements for a 4500-W(th) 238 PuO2 general purpose heat source
[DE85-011361] 22 p3841 N85-33786
Solar modulation of cosmic ray intensity and solar flare events inferred from (14)C contents in dated tree rings
[SH-7.1-2] 23 p4047 N85-35095
Neutronic calculations for a new high flux reactor
[DE85-011551] 24 p4150 N85-35734
Samarkand complex setup for investigation of cosmic ray variation in the energy range of 7 10 (9) - 10 (15) eV
[HE-4.6-14] 24 p4198 N85-36050
NEUTRON IRRADIATION
Review: Role of refractory metal alloys in fusion reactor applications
[AERE-R-11317] 03 p0422 N85-12695
Neutron irradiation of semiconductors — lattice defects, electron irradiation 03 p0428 N85-12732
Sputtering of gold irradiated with thermal neutrons
03 p0429 N85-12738
Investigation of the production and properties of lattice defects induced by low temperature reactor irradiation
03 p0430 N85-12739
Spectroscopic investigations on neutron induced impurity atoms and radiation defects
03 p0430 N85-12742
Evaluation of ferritic alloy Fe-2 1/4Cr-1Mo after neutron irradiation: Irradiation creep and swelling
[DE84-014647] 04 p0474 N85-13022
Effect of neutron irradiation on the high temperature operation of injection laser diodes
[DE85-000068] 09 p1326 N85-18333
Radiation effects in Straind-Layer Superlattice (SLS) structures
[DE85-001713] 09 p1398 N85-18799
Major facilities for materials research and related disciplines
[PB85-108850] 11 p1739 N85-20934
Effects of neutron irradiation on the fracture properties of HT-9 weld
[DE85-001068] 12 p1807 N85-21339
Effects of neutron irradiation at 450(0)C and 16 dpa on the properties of various commercial copper alloys
[DE85-005716] 13 p2024 N85-22684
Effect of elevated-temperature neutron irradiation on fracture toughness of ceramics
[DE85-000652] 14 p2261 N85-24010
Measurement and evaluation of selected 14-MeV neutron cross sections for fusion
[DE85-010295] 19 p3365 N85-30867
Study of proton and neutron activation of metal samples in low Earth orbit
[NASA-CR-171596] 21 p3558 N85-32130
The 1983 international intercomparison of nuclear accident dosimetry systems at Oak Ridge National Laboratory
[DE85-011303] 23 p3934 N85-34362
Rapid annealing of temperature-compensated, precision voltage references following fast-neutron irradiation
[DE85-009821] 23 p3970 N85-34609
NEUTRON PHYSICS
Neutronics activities for next generation devices
[DE85-010488] 20 p3527 N85-31939
Nuclear data for MCNP
[DE85-010794] 22 p3840 N85-33782
NEUTRON RADIOGRAPHY
Tomographic reconstruction of neutron radiograph images
[AD-A145882] 02 p0280 N85-11826
Robotics in nondestructive inspection at Sacramento Air Logistics Center
[AD-P004012] 03 p0309 N85-11992
Mobile accelerator neutron radiography system
[AD-A146808] 09 p1323 N85-18311
NBS (National Bureau of Standards) reactor: Summary of activities Jul. 1983 through Jun. 1984
[PB85-184836] 20 p3522 N85-31907
NEUTRON SCATTERING
Report on research results in solid state nuclear physics, 1980-1982
[JUEL-SPEZ-250] 03 p0422 N85-12696
Investigations of magnetic phase transitions with neutron scattering 03 p0423 N85-12700

Crystal chemistry and real structure of crystals
03 p0423 N85-12703
Neutron scattering on the FRM double crystal spectrometer 03 p0423 N85-12704
Neutron interferometry and double diffractometer for condensed matter 03 p0424 N85-12705
Neutron scattering on magnetic structures and at magnetic phase transitions 03 p0424 N85-12706
Diffuse elastic and inelastic neutron scattering of disorder transitions and boundaries. Phase determination of structure factors 03 p0424 N85-12708
Development and utilization of advanced methods of neutron scattering 03 p0424 N85-12710
Neutron scattering on structural phase transitions with domain building 03 p0425 N85-12711
Inelastic neutron scattering on crystals for the clarification of structure and semiconductor properties
03 p0425 N85-12714
Measurements on the triple axis spectrometer UNIDAS for the investigation of dynamic processes in crystals using inelastic neutron scattering 03 p0426 N85-12716
Quasielastic neutron scattering on single crystals of solid ionic conductor 03 p0426 N85-12719
X-ray and neutron scattering and X-ray spectroscopy for the study of defects in solid state materials
03 p0430 N85-12741
Neutron small angle scattering of the free and membrane-bound ATPase — adenosine triphosphate (ATP) 03 p0431 N85-12746
Neutron scattering on macromolecular solid state materials, solutions and melts 03 p0431 N85-12747
Description and characterization of deuterated polymers for the analysis with neutron scattering
03 p0431 N85-12748
Small angle neutron scattering (SANS) on polymer-oligomer mixtures and on deformed polyethylene melts 03 p0432 N85-12750
Neutron scattering on polysiloxanes
03 p0432 N85-12751
Neutron scattering for the investigation of solid state materials, utilization in chemical structures
03 p0432 N85-12752
Static and quasielastic neutron scattering for the investigation of structure, dynamics and transport properties of lipid layers and lipid/protein compounds
03 p0432 N85-12753
Performing (p vector,]ic)n), (d vector, n) and (n vector, n) measurements with a rotating magnet beam swinger
[DE84-017003] 04 p0562 N85-13582
Journal of Research of the National Bureau of Standards, Volume 89, Number 1, January-February, 1984
[PB84-235530] 08 p1262 N85-17931
The Fermi surface and momentum space densities of ferromagnetic Gd using the Positron technique
09 p1396 N85-18788
On shrinkage and molecular extension
[AD-A149100] 10 p1451 N85-19144
Study of magnetism at surfaces by scattering of neutrons at grazing incidence
[DE84-015850] 10 p1564 N85-19865
SANS studies of polymers
[DE85-002471] 11 p1612 N85-20134
Major facilities for materials research and related disciplines
[PB85-108850] 11 p1739 N85-20934
Neutron scattering studies of graphite intercalation compounds
[DE85-003079] 12 p1942 N85-22196
Paramagnetic form factors from itinerant electron theory
[DE85-005272] 16 p2750 N85-26973
Discrete foundation for physics and experience
[DE85-008172] 16 p2872 N85-27720
Vibrational spectra of a-Fe(.78)P(.22) by inelastic neutron scattering
[DE85-008298] 17 p2922 N85-28016
Neutron scattering and reactions on 59Co from 1 to 20 MeV
[AERE-R-11439] 17 p3028 N85-28729
An examination of the use of wave packets for the calculation of atom diffraction by surface
[AD-A152760] 17 p3029 N85-28735
Magnetism at interfaces and surfaces, as probed by neutron scattering
[DE85-007987] 18 p3176 N85-29690
Chemical spectroscopy
[DE85-009594] 18 p3191 N85-29790
Magnetic scattering and polarized neutrons
[DE85-009823] 19 p3355 N85-30794
Neutron scattering study of the heavy fermion system UBe-13
[DE85-010955] 19 p3356 N85-30804
Investigation of thick-target neutron emission from Be-9(d,n)B-10 at E(d) = 7 MeV for angles other than zero degrees
[DE85-010254] 20 p3528 N85-31947
Toward a theory of excitation of atoms during nuclear and magnetic neutron scattering
21 p3689 N85-32918
Scientific Opportunities with Advanced Facilities for Neutron Scattering
[DE85-012113] 22 p3839 N85-33770
Capture in the 1.15-keV iron resonance
[DE85-011913] 23 p3970 N85-34612
Some nuclear data needs in astrophysics
[DE85-012916] 24 p4166 N85-35842

NEUTRON SOURCES
Diffraction by the time-of-flight technique at pulsed neutron sources
[DE84-015839] 03 p0418 N85-12674
Construction of a cold neutron source at FRM, Munich
03 p0427 N85-12722
Investigation of special facilities for a spallation neutron source 03 p0427 N85-12724
Fast neutron capture with a white neutron source
[DE84-016799] 04 p0562 N85-13580
Preliminary grouping in A strong-current linear ion accelerator with a low injection energy
[DE84-017192] 04 p0563 N85-13587
Investigation of the output parameters of the pulsed neutron generator NGI-5
[DE85-001823] 11 p1725 N85-20849
3d calculations of a fixed field alternating gradient synchrotron magnet
[DE85-002742] 18 p3183 N85-29739
High-energy particle Monte Carlo at Los Alamos
[DE85-010716] 19 p3363 N85-30856
Determination of the average neutron activation cross section with an annular-shaped 241 Am/Be neutron source and a NaI(T1) detector for the 27 Al (n,p)27 Mg-reaction
[REPT-4/1984] 20 p3532 N85-31975
Radiation transport
[DE85-010333] 21 p3703 N85-33005
Scientific Opportunities with Advanced Facilities for Neutron Scattering
[DE85-012113] 22 p3839 N85-33770
Nuclear physics in the 10 to 300 MeV energy range using a pulsed white neutron source
[DE85-003713] 22 p3839 N85-33775
Time extended production of neutrons during a solar flare
[SH-1.4-1] 23 p3994 N85-34762
Pulsed-neutron-source models for the astrophysical s-process
[DE85-012927] 24 p4151 N85-35740
Los Alamos high-current proton storage ring
[DE85-012684] 24 p4158 N85-35779

NEUTRON SPECTRA
Nuclear moments and nuclear structure
[DE84-015847] 04 p0561 N85-13573
The effect of the choice or response matrix on unfolded bonner sphere spectra
[AD-A150462] 13 p2159 N85-23404
Fast-neutron-spectrum measurements for the thick-target (9)Be(d/ = 7 MeV
[DE85-010481] 18 p3183 N85-29735
High-energy particle Monte Carlo at Los Alamos
[DE85-010716] 19 p3363 N85-30856
Paired ion chamber constants for fission gamma-neutron fields
[AD-A155069] 21 p3702 N85-32999
Neutron flux, spectrum and dose equivalent measurements for a 4500-W(th) 238 PuO2 general purpose heat source
[DE85-011361] 22 p3841 N85-33786
Microdosimetric spectra measurements of JANUS neutrons
[DE85-012108] 22 p3843 N85-33801
SONTRAC: A solar neutron track chamber detector
[SH-9.1-12] 23 p4052 N85-35127
The neutron moderated detector and groundbased cosmic ray modulation studies
[SH-9.1-13] 23 p4052 N85-35128

NEUTRON SPECTROMETERS
Neutron scattering on the FRM double crystal spectrometer 03 p0423 N85-12704
Development and utilization of advanced methods of neutron scattering 03 p0424 N85-12710
Construction, putting into operation, and utilization of a triple axis neutron spectrometer
03 p0425 N85-12715
Measurements on the triple axis spectrometer UNIDAS for the investigation of dynamic processes in crystals using inelastic neutron scattering 03 p0426 N85-12716
The effect of the choice or response matrix on unfolded bonner sphere spectra
[AD-A150462] 13 p2159 N85-23404
Observations on (3)He neutron spectrometry
[DE85-010731] 23 p3970 N85-34608

NEUTRON STARS
NT PULSARS
Transport properties of the outer crust of magnetic neutron stars 09 p1415 N85-18927
A spectroscopic study of LMC X-4
[NASA-CR-174414] 10 p1571 N85-19866
X-ray bursts: Observation versus theory
[NASA-CR-174415] 10 p1573 N85-19868
Old and new neutron stars
[DE85-002716] 11 p1762 N85-21095
Cooling of neutron stars with hyperons
[DE85-004641] 13 p2171 N85-23472
Extragalactic origin or gamma-ray bursts, revision 1
[DE85-005622] 15 p2666 N85-26588
Thermal and magnetic properties of neutron stars
16 p2880 N85-27774
Axion mass limits from pulsar X-rays
[DE85-010634] 18 p3202 N85-29865
Annihilation radiation in cosmic gamma-ray bursts
[OG-1.1-3] 22 p3861 N85-33905
On the emission region of gamma ray bursts
[OG-1.1-4] 22 p3861 N85-33906
Observations of Cygnus X-3 above 10(15) eV from 1976 - 1984
[OG-2.1-6] 22 p3863 N85-33923
On gamma and neutrino radiation from Cyg X-3
[OG-2.1-7] 22 p3863 N85-33924
500 TeV gamma rays from Hercules X-1
[OG-2.2-7] 22 p3865 N85-33933
A model for the UHE gamma-rays from Hercules X-1
[OG-2.2-8] 22 p3865 N85-33934
High-resolution spectroscopic observation of Vela X-1 in the hard X-ray energy range
[OG-2.2-10] 22 p3865 N85-33936
Observation of gamma-rays from LMC X-4 above 10(16) eV
[OG-2.6-10] 22 p3870 N85-33972
Investigations of the cyclotron resonance effects in the X ray spectrum of the neutron star Hercules X-1
[MPE-191] 22 p3890 N85-34112
X-ray spectra of bursting neutron stars
23 p3981 N85-34686
Quasiperiodic oscillations in bright galactic-bulge X-ray sources
[NASA-CR-176138] 23 p3987 N85-34723
A very important process of nucleosynthesis in stars
[OG-7.1-11] 23 p4014 N85-34872
High energy radiation from neutron stars
[DE85-014353] 24 p4169 N85-35843
High energy cosmic ray signature of quark nuggets
[HE-6.2-11] 24 p4212 N85-36147

NEUTRON TRANSMUTATION
U NUCLEAR REACTIONS

NEUTRONS
NT COLD NEUTRONS
NT FAST NEUTRONS
NT THERMAL NEUTRONS
Study of proton and neutron activation of metal samples in low Earth orbit
[NASA-CR-171183] 01 p0026 N85-10184
Study of structure of nuclei with neutrons and nuclear data measurements for MFE
[DE84-015128] 01 p0117 N85-10882
Effects of irradiation fluence and creep on fracture toughness of 347/348 stainless steel
[DE84-016091] 05 p0618 N85-13953
Generation of radiation transport geometry from computer-generated design data — monte carlo solution of the neutron transport equation
[DE84-017380] 09 p1370 N85-18606
Instrumental background in balloon-borne gamma-ray spectrometers and techniques for its reduction
[NASA-TM-86162] 09 p1413 N85-18911
MCNP code
[DE85-002565] 11 p1702 N85-20705
Finite element method for solving neutron transport problems
[DE85-001075] 11 p1722 N85-20829
A linear characteristic-nodal transport method for the two-dimensional (X,Y)-geometry multigroup discrete ordinates equations over an arbitrary triangle mesh
[LA-10092-T] 12 p1913 N85-22008
Cyclic changes in barometric coefficient of cosmic ray neutron component 15 p2478 N85-25293
Space radiation monitor observations from Salyut-4 orbital station 15 p2482 N85-25317
Nuclear radiation induced absorption in optical materials
[DE85-007128] 15 p2649 N85-26336
Physics effects of accidental submersion of space power reactors in water
[DE85-005020] 15 p2650 N85-26344
Nonlinear DSA difference schemes for radiative transfer applications
[DE85-005729] 16 p2856 N85-27611
Laser welder for fabricating neutron tubes
[DE85-009965] 17 p2974 N85-28377

Axion mass limits from pulsar X-rays
[DE85-010634] 18 p3202 N85-29865

The possibility of observing solar neutron events in the lower atmosphere
[NOTA-INTERNA-837] 18 p3209 N85-29906

Mouse oocyte killing by neutrons: Target considerations
[DE85-011362] 19 p3328 N85-30624

MCNP: A general Monte Carlo code for neutron and photon transport
[DE85-010764] 19 p3348 N85-30753

Low-discrepancy point sets in transport codes
[DE85-010786] 19 p3348 N85-30755

Modeling and optimization of a test-cell upgrade for MFTF-B operating in the high neutron wall loading mode
[DE85-009997] 20 p3528 N85-31946

Solid-state track recorder neutron dosimetry in the Three-Mile Island Unit-2 reactor cavity
[DE85-011360] 20 p3531 N85-31966

Detection of solar neutrons by ground based neutron monitors
[IFSI-84-11] 20 p3547 N85-32076

Multiple collision solutions for time-dependent neutron transport in slabs of finite thickness
[OEFZS-4312] 22 p3838 N85-33762

Novette diagnostic support
[DE85-012937] 23 p3934 N85-34363

Application of evaluated fission-product delayed-neutron precursor data in reactor kinetics calculations
[DE85-012728] 23 p3972 N85-34624

The SCR flare of 16 February 1984 as recorded by the Sayan spectrograph
[SH-1.3-17] 23 p3994 N85-34761

Further observations of protons resulting from the decay of neutrons ejected by solar flares
[SH-1.4-2] 23 p3994 N85-34763

Suggestions for improving the efficiency of ground-based neutron monitors for detecting solar neutrons
[SH-1.4-3] 23 p3995 N85-34764

Search for solar neutrons using NM-64 equipment
[SH-1.4-5] 23 p3995 N85-34765

A search for solar neutrons on a long duration balloon flight
[SH-1.4-6] 23 p3995 N85-34766

High energy neutron and gamma-radiation generated during the solar flares
[SH-1.4-8] 23 p3995 N85-34768

Energetic particle observations of the solar-gamma ray/neutron flare events of 3 Jun 1982 and 21 June 1980 isotopic and chemical composition
[SH-2.1-3] 23 p3998 N85-34784

Exponential anisotropy of solar cosmic rays
[SH-3.2-1] 23 p4002 N85-34817

Neutron-rich nuclei in cosmic rays and Wolf-Rayet stars
[OG-8.2-6] 23 p4019 N85-34906

An approach of reducing the background induced by neutrons
[OG-9.3-5] 23 p4027 N85-34960

Neutron-induced 2.2 MeV background in gamma ray telescopes
[OG-9.3-6] 23 p4027 N85-34961

Characteristics of cosmic ray pole-equator anisotropy derived from spherical harmonic analysis of neutron monitor data
[SH-4.3-12] 23 p4032 N85-34996

First zonal harmonic component of cosmic ray neutron intensity
[SH-4.3-13] 23 p4032 N85-34997

Monte Carlo calibration of the SMM gamma ray spectrometer for high energy gamma rays and neutrons
[SH-9.1-6] 23 p4051 N85-35121

Comparisons of monthly mean cosmic ray counting rates observes from worldwide network of neutron monitors
[SH-9.1-7] 23 p4051 N85-35122

(NAT)Fe(n,n'x) spectra at 65.5 MeV
[AD-A155776] 24 p4150 N85-35730

Neutron production by Ne and Si ions on a thick Cu target at 670 MeV/A with application to radiation protection
[DE85-014526] 24 p4152 N85-35746

Applications and misapplications of the channel-capture formalism of direct neutron capture
[DE85-013992] 24 p4152 N85-35748

Los Alamos high-current proton storage ring
[DE85-012664] 24 p4158 N85-35779

Some nuclear data needs in astrophysics
[DE85-012916] 24 p4168 N85-35842

Determination of the cross section of the proton, pion and neutron inelastic interaction with lead and carbon nuclei at 0.5 - 5.0 TeV energies (PION experiment)
[HE-1.1-6] 24 p4170 N85-35853

The spectrum of neutrons at 60 hg m(-2)
[HE-5.2-20] 24 p4204 N85-36096

NEVADA

Hydrogeochemical investigation of thermal springs in the Black Canyon-Hoover Dam area, Nevada and Arizona
[PB84-202472] 01 p0064 N85-10428

Post-Sonoman conodont biofacies of the Triassic of northwestern Nevada 03 p0390 N85-12497

Classification of vegetation communities in the Battle Mountain SE quadrangle, Nevada with MSS digital data
[E85-10043] 06 p0826 N85-15246

Analysis of SIR-B radar illumination of geometry for depth of penetration and surface feature and vegetation detection, Nevada and California
08 p1149 N85-17248

Index to published geologic maps in the region around the potential Yucca Mountain nuclear waste repository site, southern Nye County, Nevada
[DE85-000260] 11 p1669 N85-20518

Research and development related to the Nevada nuclear waste storage investigations
[DE85-002303] 12 p1932 N85-22138

Summary of Meteorological Observations, Surface (SMOS), Fallon, Nevada
[AD-A150481] 13 p2138 N85-23276

Preliminary assessment of climatic change during late Wisconsin time, southwest Great Basin and vicinity, Arizona, California and Nevada
[DE85-008343] 16 p2836 N85-27488

Analysis of the elastic and strength properties of Yucca Mountain tuff, Nevada
[DE85-006975] 19 p3300 N85-30460

Petrologic and geochemical characterization of the Topopah Spring Member of the Paintbrush Tuff: Outcrop samples used in waste package experiments
[DE85-010449] 19 p3302 N85-30470

Structural and tectonic history of the Golconda allochton, southern Toiyabe Range, Nevada
19 p3312 N85-30529

Comparison of survey and photogrammetry methods to position gravity data, Yucca Mountain, Nevada
[DE85-011685] 21 p3590 N85-32316

A 1984 environmental summary: Sandia National Laboratories Tonopah Test Range, Tonopah, Nevada
[DE85-011145] 22 p3812 N85-33612

Iron and manganese in oxide minerals and in glasses: Preliminary consideration of Eh buffering potential at Yucca Mountain, Nevada
[DE85-011892] 23 p3916 N85-34271

Simulated effects of increased recharge on the ground-water flow system of Yucca Mountain and vicinity, Nevada-California
[DE85-012985] 24 p4106 N85-35469

NEW ENGLAND (US)

Investigation of radiometric properties of LANDSAT-4 MSS — California, North Carolina, South Carolina, and New England 11 p1666 N85-20500

East coast snowstorm survey
15 p2598 N85-26013

Model sensitivity studies of major east coast storms
15 p2598 N85-26016

Justification and plan for participation in GALE
15 p2599 N85-26017

NEW HAMPSHIRE

Potential for acidification of six remote ponds in the White Mountains of New Hampshire
[PB84-207349] 02 p0225 N85-11475

Climate at CRREL (Cold Regions Research and Engineering Laboratory) Hanover, New Hampshire
[AD-A148400] 08 p1189 N85-17495

Impact of LANDSAT MSS sensor differences on change detection analysis — New Mexico, San Francisco, CA, New Hampshire, and Connecticut
11 p1667 N85-20506

NEW JERSEY

Soil formation on tertiary landsurfaces of the New Jersey coastal plain 08 p1181 N85-17441

NEW MEXICO

Spectroradiometric calibration of the Thematic Mapper and Multispectral Scanner system
[E85-10026] 02 p0218 N85-11439

Surface soil moisture measurements of the White Sands, New Mexico
[NOAA-TM-NESDIS-7] 02 p0219 N85-11441

Solar energy resource assessment in Eastern New Mexico and solar and wind energy resource assessment in Eastern New Mexico
[DE84-901511] 04 p0527 N85-13370

LANDSAT instruments characterization
[E85-10028] 05 p0654 N85-14197

LANDSAT-4 Thematic Mapper Modulation Transfer Function (MFT) evaluation — California and New Mexico
[E85-10055] 07 p0984 N85-16250

Spectroradiometric calibration of the Thematic Mapper and Multispectral Scanner system
[E85-10077] 10 p1504 N85-19491

Impact of LANDSAT MSS sensor differences on change detection analysis — New Mexico, San Francisco, CA, New Hampshire, and Connecticut
11 p1667 N85-20506

In-progress absolute radiometric inflight calibration of the LANDSAT-4 sensors — New Mexico
12 p1870 N85-21733

Evaluation of geothermal potential of Rio Grande rift and Basin and Range province, New Mexico
[DE85-901360] 19 p3301 N85-30466

Remote sensing of hydrologic transport processes using spot simulation data
[DE85-012412] 24 p4108 N85-35467

NEW YORK

Major institutional arrangements affecting ground water in New York state
[PB84-202506] 01 p0065 N85-10429

Slope water intrusions within the nearshore waters off Long Island, New York
[DE85-001386] 09 p1359 N85-18549

Analysis of flow within the coastal boundary layer off Long Island, New York
[DE85-001384] 09 p1359 N85-18550

Pavement-marking materials: New York's experience
[PB85-153294] 15 p2523 N85-25558

NEW ZEALAND

Detailed analysis of the structure of local wind systems in Canterbury, New Zealand 01 p0075 N85-10501

New Zealand SIR-B science investigations
08 p1144 N85-17218

NEWS MEDIA

Origin, processing, and dissemination of scientific news, with examples from 20 research institutes
[JUEL-1940] 17 p3050 N85-28882

NEWTON THEORY

Quasi-three dimensional modeling of functionally-integrated elements of large-scale integrated circuits 04 p0490 N85-13122

Elements of celestial mechanics
14 p2396 N85-24762

Finite axisymmetric deformation of a thin shell of revolution 16 p2798 N85-27251

NEWTON-RAPHSON METHOD

A solution method for large deformation contact problems
[AD-A149842] 12 p1866 N85-21707

Direct secant updates of sparse matrix factors
[DE85-004008] 12 p1922 N85-22073

A numerical procedure on three-dimensional parabolic flow in duct 16 p2692 N85-26620

X-ray spectra of bursting neutron stars
23 p3961 N85-34686

NEWTONIAN FLUIDS

Trapping for Newtonian diffusion processes
[REPT-73] 01 p0130 N85-10893

Dynamics of liquid filament breakup
[DE84-016008] 04 p0500 N85-13187

Numerical experiments and theoretical analysis of the flow of an elastic liquid of the Maxwell-Oldroyd type in the presence of geometrical singularities
[WTHD-164] 08 p1163 N85-17340

Practical real-time quality control of antimisting kerosene
[DE/FAA/CT-85/1] 18 p3083 N85-29072

On the importance of viscous dissipation in Io
22 p3855 N85-33873

NICKEL

NT NICKEL ISOTOPES

The effects of seven alloying elements on the microstructure and stress-rupture behavior of nickle-base superalloys
[NASA-TM-83791] 01 p0027 N85-10168

Thermodynamics of reactions of deoxidation of nickel melts
[BLL-M-35729-(5826.4)] 02 p0175 N85-11168

The reactions of cobalt, iron and nickel in SO-2 atmospheres: Similarities and differences
[NASA-TM-86868] 02 p0181 N85-11217

Environment-induced embrittlement: Effect of impurity segregation and state of stress
[DE84-015436] 02 p0184 N85-11235

Review: The influence of short circuit diffusion on the oxidation of nickel, chromium and nickel/chromium alloys
[AERE-R-11311] 02 p0185 N85-11237

Characterization of ion implanted deuterium traps in nickel by equilibration with deuterium gas
[DE84-014958] 02 p0286 N85-11879

Electroforming of nickel
[SNIAS-841-501-101] 04 p0484 N85-13085

Nickel-cobalt systematics and their bearing on lunar origin 04 p0582 N85-13719

Abundancies of Ni, Cr, CO and major elements in the silicate portion of the Moon: Constraints from primary lunar magmas 04 p0582 N85-13720

Autenite transformation in powder-compacted chromium-nickel-molybdenum steels during continuous cooling
[BLL-M-35981-(5828.4)] 05 p0615 N85-13933
Mechanisms of impurity diffusion in rutile
[DE84-014741] 06 p0786 N85-14902
Comparison between the properties of conventional wrought and powder metallurgical alloys for turbine disc applications 07 p0906 N85-15739
Optimization of the NiCrAl-Y/ZrO-Y2O3 thermal barrier system
[NASA-TM-86905] 07 p0927 N85-15878
Surface effects of corrosive media on hardness, friction, and wear of materials
[NASA-TM-83711] 07 p0930 N85-15896
Defective nature of the crystalline lattice of nickel ferrite-based solid solutions
[BLL-WH-595-(9091.9F)] 07 p1046 N85-16645
Hydrogen embrittlement of nickel
[AD-A148322] 08 p1129 N35-17119
The influence of strain rate and porosity on the deformation and fracture of titanium and nickel
[AD-A148670] 08 p1130 N85-17123
Stability of amorphous metals on semiconductor substrates
[DE84-017256] 09 p1295 N85-18134
Production method of nickel electrode
[NASA-TM-76946] 10 p1439 N85-19069
Method of producing nickel electrode
[NASA-TM-76944] 10 p1440 N85-19077
Radiation-induced compositional redistribution and local phase transformation in irradiated alloys
[DE85-000080] 10 p1441 N85-19082
Antifriction properties of gas thermal coatings of clad carbine powders 10 p1447 N85-19115
Magnetization of very thin Ni films in epitaxial metal film sandwiches of Cu
[DE85-001840] 10 p1563 N85-19860
Analysis of diffusion in an ion-implanted alloy using a phenomenological model
[AERE-R-11527] 11 p1609 N85-20120
Semiconductor electrochemistry approach to the study of oxide films on nickel electrodes
[DE85-003042] 11 p1630 N85-20264
Low temperature deposition of nickel films
[AD-D011566] 12 p1805 N85-21319
Humidity effects on adhesion of nickel-zinc ferrite in elastic contact with magnetic tape and itself
[NASA-TP-2449] 12 p1811 N85-21359
Paramagnetic scattering from Ni
[DE85-004207] 12 p1942 N85-22196
Mechanical properties of electrodeposited nickel and copper
[DE85-005321] 13 p2023 N85-22677
Role of segregated P and S in intergranular stress corrosion cracking of nickel
[DE85-004547] 13 p2024 N85-22679
Apparatus for producing amorphous and microcrystalline metal powders 13 p2030 N85-22720
Molten carbonate fuel cell performance model update, draft
[DE85-005423] 13 p2129 N85-23252
Adsorption site, adsorption energy and normal vibration frequency of H/Ni(100) via total energy calculations
[AD-A150555] 13 p2156 N85-23368
Observation of surface vibrational resonances on (110) surfaces of FCC metals
[AD-A150469] 13 p2163 N85-23419
Dipole active surface vibrational resonances on clean and hydrogen covered Ni(110)
[AD-A150546] 13 p2163 N85-23420
Characterization of supported metal catalysts by imaging, microdiffraction and microanalysis techniques
[DE85-005567] 14 p2253 N85-23961
Microstructure and properties of ferrous alloy weldments
[DE85-005582] 14 p2257 N85-23987
The effects of water and hydrogen on materials used in integrated circuit packages
[AD-A151893] 15 p2518 N85-25529
Influence of phosphorus content and heat treatment on the machinability of electroless nickel deposits
[DE85-007250] 15 p2522 N85-25548
Crack closure characteristics considering center cracked and compact tension specimens
[AD-A151702] 15 p2579 N85-25907
Electronic transport in Mo/Ni superlattice
[DE85-006835] 15 p2661 N85-26425
Nd-isotopic evidence for the origin of the Sudbury complex by meteoritic impact 15 p2680 N85-26554
Effect of nickel addition on the thermal, magnetic and magnetomechanical properties of Fe(80)B(15)Si(5)
[AD-A152281] 16 p2749 N85-26967
Low dose irradiation creep of pure nickel
[DE85-006320] 16 p2751 N85-26975
Influence of manganese and heat treatment on structure and properties of Fe-0.1 percent-C-14 percent Cr-based steels
[BLL-BISI-TRANS-22299-(9022.06)]
17 p2928 N85-28071
The physical and mechanical properties of near-equiatomic titanium-nickel
19 p3237 N85-30072
State variable theories based on Hart's formulation
[DE85-009474] 19 p3239 N85-30082
Thermodynamics of high temperature materials
[AD-A154269] 19 p3378 N85-30958
Analysis of ferrates and ferrites of three transition metals using Moessbauer effects
[BLL-CE-TRANS-8019-(9022.09)]
20 p3430 N85-31273
Defect production and recovery in FCC metals irradiated at 4.2 K
[DE85-010477] 20 p3538 N85-32014
The effect of diffusive hydrogen segregation on fracture of polycrystalline nickel
[AD-A155238] 21 p3567 N85-32186
Relative abundances of sub-iron to iron nuclei in low energy (50-250 MeV/N) cosmic rays as observed in the Skylab experiment
[OG-4.1-4] 22 p3876 N85-34010
Calculating the interatomic pair potential allowing for resonance interaction in titanium, nickel and vanadium
[BLL-M-35843-(5828.4)] 23 p3913 N85-34249
Metal (2) 4,4',4',4'' phthalocyanine tetraamines as curing agents for epoxy resins
[NASA-CASE-ARC-11424-1] 23 p3919 N85-34261
Oxidation resistant slurry coating for carbon-based materials
[NASA-CASE-LEW-13923-1] 24 p4077 N85-35267
X-ray fluorescence analysis of 304L stainless steel
[DE85-013254] 24 p4080 N85-35288
Applications of the mineral resources data system and the international strategic minerals inventory in mineral-resource assessments by region and commodity
24 p4105 N85-35451
The Conterminous United States Mineral Assessment Program 24 p4106 N85-35458

NICKEL ALLOYS
NT HASTELLOY (TRADEMARK)
NT INCONEL (TRADEMARK)
NT MONEL (TRADEMARK)
NT NITINOL ALLOYS
NT RENE 95
NT UDIMET ALLOYS
NT WASPALOY
Results of the technical exchange agreement between NASA and DuPont on the containerless drop tube solidification of NiAl3
[NASA-TM-86473] 01 p0014 N85-10087
Weldability of aged heat resistant nickel alloys
01 p0021 N85-10125
Morphological changes of gamma prime precipitates in nickel-base superalloy single crystals
[NASA-TM-83698] 01 p0026 N85-10165
Containerless drop tube solidification and grain refinement of NiAl3 02 p0154 N85-11042
Determining the optimum heating parameters for precision alloys --- iron-nickel alloys
[BLL-M-35718-(5824.4)] 02 p0174 N85-11167
Thermodynamics of decarburization of niobium-bearing high-alloy melts
[BLL-M-35728-(5828.4)] 02 p0175 N85-11169
Rapid solidification of steels: Model and commercial alloys 02 p0178 N85-11184
The structure of rapidly solidified nickel-base alloys
02 p0181 N85-11215
Microstructure and creep behaviour at elevated temperature of unidirectionally solidified eutectic nickel base superalloys 02 p0181 N85-11216
The transient oxidation of single crystal NiAl+Zr
[NASA-CR-174756] 02 p0182 N85-11221
The effect of tantalum and carbon on the structure/properties of a single crystal nickel-base superalloy
[NASA-CR-174779] 02 p0182 N85-11223
Studies on the hot corrosion of a nickel-base superalloy, Udimet 700
[NASA-TM-86882] 02 p0183 N85-11224
Review: The influence of short circuit diffusion on the oxidation of nickel, chromium and nickel/chromium alloys
[AERE-R-11311] 02 p0185 N85-11237
Plastic strain localization in superalloy single crystals
[AD-A145705] 02 p0288 N85-11878
The effects of Cr, Co, Al, Mo and Ta on the cyclic oxidation behavior of a prototype cast Ni-base superalloy based on a 2(5) composite statistically designed experiment
[NASA-TM-83784] 03 p0331 N85-12131
The effect of orientation on fatigue growth in a nickel-based single crystal superalloy
[PNR-90207] 03 p0332 N85-12141
Structural stability of nickel heat resistant alloys at high temperatures 03 p0350 N85-12251
Radiation effects in amorphous metallic alloys
[DE84-014302] 04 p0475 N85-13035
The effect of trace elements on the properties at high temperature of a Ni-Cr-base alloy
05 p0617 N85-13844
Method for predicting the creep rupture life of nickel-base precipitation-hardened superalloys from their chemical composition
[BLL-PNR-90241-(8019.3153)]
06 p0766 N85-14810
Application of solidification theory to rapid solidification processing
[AD-A146619] 06 p0769 N85-14817
Metallographic evaluation of the reactions between boronated graphite and Fe-Ni-Cr alloys
[DE84-015374] 06 p0769 N85-14822
A study of tetrataenite 06 p0885 N85-15623
Low temperature diffusion coefficients in the Fe-Ni and FeNiP systems: Application to meteorite cooling rates
06 p0886 N85-15628
Speculations on the formation of metallic meteorite phases 06 p0889 N85-15646
Problems and possibilities for life extension in gas turbine components 07 p0907 N85-15742
Study of high performance alloy electroforming
[NASA-CR-174276] 07 p0927 N85-15875
Design of ordered intermetallic alloys for high-temperature structural use
[DE85-000697] 07 p0928 N85-15885
Recommendations for the use of Ni-Cr-base alloy extensometers for measurement of creep strain
[NPL-DMA(A)-81] 08 p1164 N85-17342
The effect of tantalum on the structure/properties of two polycrystalline nickel-base superalloys: B-1900 + Hf MAR-M247
[NASA-CR-174847] 09 p1294 N85-18127
Low and moderate temperature oxidation of atomically clean nickel, chromium and Ni-Cr alloys
[DE84-017350] 09 p1295 N85-18131
Plasma deposition of amorphous metal alloys
[DE85-000768] 09 p1295 N85-18132
Adaptation of remelting procedures for the use of recycled metal in nickel-base superalloy castings
[PNR-90232] 09 p1297 N85-18149
Laser-intiated combustion studies on metallic alloys in pressurized oxygen
[PB85-128114] 10 p1438 N85-19066
Low cycle fatigue of MAR-M 200 single crystals at 760 and 870 deg C
[NASA-TM-86933] 10 p1440 N85-19074
Influence of volumetric fiber content on some matrix damage factors during thermal cycling of tungsten-EI 765 composite 10 p1443 N85-19097
Influence of gaseous hydrogen on strength and ductility of nickel heat-resistant alloys 10 p1447 N85-19119
Diffusion welding with forced deformation of heat-resistant nickel-based dispersion hardened alloy
10 p1449 N85-19130
Effect of stress concentration fatigue resistance of refractory nickel alloys under asymmetrical multicycle loading, communication 1 11 p1604 N85-20086
Effect of form memory in alloys based on Cu-Al systems 11 p1604 N85-20089
Amorphous Ni-Ti alloys: A new method of synthesis
[DE85-002744] 11 p1605 N85-20094
Structural studies of sputtered Ni-As-O films
[DE85-003229] 11 p1605 N85-20095
Heavy ion induced crystallization in amorphous phases
[DE85-003114] 11 p1606 N85-20098
Non-isothermal irradiation creep of nickel alloys Inconel 706 and PE-16
[DE85-000842] 11 p1607 N85-20102
Initial development of nickel and nickel-iron aluminides for structural uses
[DE84-016641] 11 p1608 N85-20108
Ferromagnetic resonance in a Ni-Mo superlattice
[DE85-003039] 11 p1735 N85-20811
Stress corrosion cracking and oxidation characteristics of boride-strengthened microcrystalline iron and nickel based alloys
[AD-A149605] 12 p1806 N85-21329
Sputter-induced compositional modifications in a Ni-Au alloy
[DE85-002771] 12 p1807 N85-21333
Chemisorption theory: Adsorption on copper-nickel alloys and titanium surface embrittlement
[DE85-001815] 12 p1807 N85-21334

Performance of Chromel versus Alumel and Nicrosil versus Nisil thermocouple assemblies in vacuum and argon between 1000 deg C and 1200 deg C
[DE85-000810] 12 p1853 N85-21624

Study of the effects of implantation on the high Fe-Ni-Cr and Ni-Cr-Al alloys
[NASA-CR-175625] 13 p2021 N85-22661

Thermodynamics of copper-nickel alloys containing aluminum, silicon, titanium, and chromium relative to their use in ceramic brazing
[DE85-004787] 13 p2023 N85-22674

Reaction of amorphous NiNb films with crystalline metal overlayers
[DE85-005483] 13 p2024 N85-22680

Effect of phase state of TiC-NiTi powder composite materials on nature of failure and mechanical properties
13 p2027 N85-22702

Long-term strength and fracture criteria for EI698VD alloy under complex stress conditions
13 p2030 N85-22723

Change in microstructure of heat-resistant nickel alloys upon thermal cycling in a current of gas
13 p2031 N85-22725

The cyclic stress-strain behavior of nickel-base superalloy poly- and single crystals
14 p2254 N85-23969

Local phase transformation in alloys during charged-particle irradiation
[DE85-005012] 14 p2258 N85-23990

Structure and mechanical properties of dispersion-hardened nickel alloy joints welded by diffusion
15 p2500 N85-25422

Contact point and seam welding of heat-resistant alloys
15 p2501 N85-25429

Study of high performance alloy electroforming
[NASA-CR-175741] 15 p2508 N85-25473

Effects of primary recoil energy on the production rate of mobile defects during elevated temperature irradiation
[DE85-006218] 15 p2511 N85-25489

Design of ductile polycrystaline Ni3Al alloys
[DE85-005572] 15 p2511 N85-25491

Weldability of Ni3Al-type aluminide alloys
[DE85-006932] 15 p2512 N85-25496

Studies of ferritic filler metals for welding 9 percent nickel steel
15 p2565 N85-25825

Fatigue life extension 16 p2733 N85-26864

Ignition of metals in high pressure oxygen
16 p2735 N85-26874

Relationships between microstructure and microfissuring in alloy 718 16 p2735 N85-26876

Structural inhomogeneities in amorphous nickel-phosphorus alloy
[BLL-M-36103-(5828.4)] 16 p2748 N85-26960

Role of hydrogen and structure on CMSX-2
17 p2915 N85-27967

The behaviour of nitride inclusions in nickel-base alloys
[BLL-BISI-TRANS-22396-(9022.06)]
17 p2927 N85-28058

The effect of microalloying with calcium and magnesium on the plasticity of Poldi AKN 20 Ni-based alloy
[BLL-BISI-TRANS-2174-(9022.06)]
17 p2929 N85-28075

Kinetics of the formation of a complex alloyed boride coating on iron and its properties
[BLL-BISI-TRANS-22303-(9022.06)]
17 p2930 N85-28084

Sintering reactions, structure and properties of a cobalt free nonconventional hard material
[DE85-007704] 18 p3076 N85-29025

Study of the influence of metallurgical factors on fatigue and fracture of aerospace structural materials
[AD-A153913] 18 p3122 N85-29328

Weldability/microstructure relationships of high nickel alloys for header applications
[DE85-009337] 19 p3241 N85-30094

Effect of prolonged high temperature on durability of coated high-temperature nickel alloys
19 p3243 N85-30105

On compounding nickel alloys as defense against sulfide-oxide corrosion 19 p3243 N85-30109

Properties of heat resistant Ni-Al-Nb alloys with unidirectional eutectic structure
19 p3247 N85-30133

concentration variation of work function of alloys in the system nickel-titanium-aluminum
19 p3247 N85-30134

Investigation for low-cost permanent magnets
[AD-A154387] 19 p3260 N85-30212

A study of the effect of a mismatch in gamma and gamma prime phase lattice spacings on the high temperature strength characteristics of dispersion-hardened nickel alloys
[BLL-CE-TRANS-8048-(9022.09)]
20 p3430 N85-31279

Mechanical behavior of Ni-Cr-base superalloys in forms and conditions representative of service
[NPL-DMA(A)-94] 20 p3431 N85-31282

A multiple linear regression analysis of hot corrosion attack on a series of nickel base turbine alloys
[NASA-TM-87020] 20 p3431 N85-31284

Long range ordered alloys modified by addition of niobium and cerium
[DE85-011661] 20 p3431 N85-31285

Experimental studies of the geometric and electronic structure of chemisorption bonding
[PB85-192250] 22 p3747 N85-33228

Metallic glass composition
[DE85-011594] 22 p3751 N85-33253

Electrical resistivity and hysteresis of the equiatomic nickel-titanium alloy near the martensitic transformation temperature 23 p3904 N85-34181

Microstructures in rapidly solidified Ni-Mo alloys
[NASA-TM-87100] 23 p3915 N85-34266

The development and evaluation of the creep and corrosion resistant alloy IN6201
[PNR-90253] 23 p3917 N85-34278

Microshrink, tensile properties, and the detection of microshrink
[AD-A155875] 24 p4079 N85-35278

Deposition of nickel-cobalt alloys by controlled-potential electrolysis
[PB85-198562] 24 p4081 N85-35291

NICKEL CADMIUM BATTERIES

Positive electrodes of nickel-cadmium batteries
[NASA-TM-77808] 10 p1478 N85-19330

Nickel-cadmium battery cell reversal from resistive network effects
[AD-A149626] 12 p1834 N85-21505

Pseudo bipolar nickel-cadmium batteries used as filter elements to pulsed current loads
[AD-A151192] 15 p2547 N85-25717

Analysis and testing of the thermal properties of space battery cells, phase B, draft
[ESA-CR(P)-1971] 15 p2550 N85-25741

Proposed energy systems for the Brazilian data collection satellite
[INPE-3393-PRE/664] 16 p2731 N85-26856

Investigation of pseudo bi-polar nickel cadmium batteries as filter elements for pulsed power loads
[AD-A152112] 16 p2819 N85-27389

Nickel-cadmium cell design variable program data analysis
[NASA-TM-86196] 19 p3258 N85-30203

The 1984 Goddard Space Flight Center Battery Workshop
[NASA-CP-2382] 20 p3443 N85-31371

RCA's planned test program to compare the performance and life of NiCd cells containing Pellon 2536 in contrast with Pellon 2505 separator material
20 p3445 N85-31385

Failure modes experienced on spacecraft NiCd batteries 20 p3445 N85-31386

Nickel cadmium cell design variable program data analysis 20 p3445 N85-31387

Results of analysis on the design variable cells
20 p3445 N85-31388

Fundamental algorithms of the Goddard battery model
20 p3445 N85-31389

Modeling taper charge with a non-linear equation
20 p3445 N85-31390

High discharge rate characteristics of nickel-cadmium batteries for pulse load filtering
20 p3446 N85-31391

Nickel-cadmium battery cell reversal from resistive network effects 20 p3446 N85-31392

LEO life testing with different charge control
20 p3446 N85-31393

A 34 ampere-hour nickel-cadmium minimum trickle charge testing 20 p3446 N85-31394

AUSSAT battery life test program
20 p3446 N85-31395

Flight experience of Solar Mesosphere Explorer's two nickel-cadmium batteries 20 p3446 N85-31396

Deep reconditioning of batteries during DSCS 3 flight operations 20 p3446 N85-31397

NICKEL COATINGS

USSR report: Materials Science and Metallurgy
[JPRS-UMS-85-005] 19 p3241 N85-30095

NICKEL COMPOUNDS

NT NICKEL OXIDES

The alpha-form of the hydroxides of bivalent metals
[NASA-TM-77508] 04 p0473 N85-13009

Toxicology and metabolism of nickel compounds
[DE84-014919] 05 p0696 N85-14478

Vaporization behavior, phase equilibria, and thermodynamic stabilities of nickel phosphides
[AD-A146663] 06 p0765 N85-14897

Replacement of Fe-3+ ions in nickel ferrites by nonmagnetic Al-3+ and Sc-3+ ions
[BLL-WH-594-(9091.9F)] 08 p1125 N85-17090

Liquid phase methanol process development unit: Installation, operation, and support studies
[DE85-001311] 09 p1301 N85-18171

Defective nature of the crystalline lattice of nickel ferrite-based solid solutions
[BLL-TRANS-WH-595-(9091.9F)]
10 p1439 N85-19068

Alloys based on NiAl for high temperature applications
[NASA-TM-86976] 12 p1805 N85-21322

Magnetovolume effects in some Y-Ni intermetallic compounds
[ISSN-0066-2003] 13 p2021 N85-22663

Raman structural studies of the nickel electrode
[NASA-CR-175619] 13 p2162 N85-23414

NICKEL HYDROGEN BATTERIES

Advanced nickel-hydrogen cell configuration study
[NASA-CR-174775] 01 p0067 N85-10444

Design and development of a sealed 100-Ah nickel-hydrogen battery
[DE84-016935] 06 p0805 N85-15128

Prospects for advanced storage battery technologies
[DE84-015706] 09 p1345 N85-18464

Multikilowatt hydrogen-nickel oxide battery system
[DE85-003339] 15 p2550 N85-25737

Analysis and testing of the thermal properties of space battery cells, phase B, draft
[ESA-CR(P)-1971] 15 p2550 N85-25741

Initial performance of advanced designs for IPV nickel-hydrogen cells
[NASA-TM-87029] 17 p2984 N85-28444

Life cycle test results of a bipolar nickel hydrogen battery
[NASA-TM-87046] 19 p3304 N85-30480

The 1984 Goddard Space Flight Center Battery Workshop
[NASA-CP-2382] 20 p3443 N85-31371

Multikilowatt hydrogen-nickel oxide battery system
20 p3443 N85-31373

Design principles for nickel hydrogen cells and batteries 20 p3447 N85-31398

Improved specific energy Ni-H2 cell
20 p3447 N85-31399

Bipolar nickel-hydrogen battery design
20 p3447 N85-31400

Nickel-hydrogen spacecraft module configurations study 20 p3447 N85-31401

Nickel hydrogen bipolar battery electrode design
20 p3447 N85-31402

Nickel-cadmium cell life test 20 p3447 N85-31403

Initial performance of advanced designs for IPV nickel-hydrogen cells 20 p3448 N85-31404

Accelerated and real-time geosynchronous life cycling test performance of nickel-hydrogen batteries
20 p3448 N85-31405

Life cycle test results of a bipolar nickel hydrogen battery 20 p3448 N85-31406

Nickel-hydrogen cell test program summary
20 p3448 N85-31407

The failure mechanism of a nickel electrode in a nickel-hydrogen cell 20 p3448 N85-31408

An industry and government survey: A nickel-hydrogen testing data base 20 p3448 N85-31409

Design principles for nickel-hydrogun cells and batteries
[NASA-TM-87037] 20 p3483 N85-31646

NICKEL ISOTOPES

Fusion reactions at low energy
[DE85-010561] 20 p3528 N85-31944

NICKEL OXIDES

Design and development of a sealed 100-Ah nickel-hydrogen battery
[DE84-016935] 06 p0805 N85-15128

Grain boundary structure in NiO
[DE84-016242] 06 p0868 N85-15519

Semiconductor electrochemistry approach to the study of oxide films on nickel electrodes
[DE85-003042] 11 p1630 N85-20264

Grain boundaries in NiO
[DE85-006129] 13 p2025 N85-22667

Tilt grain boundaries in NiO
[DE85-006839] 16 p2751 N85-26978

Low-temperature positron lifetime and Doppler-broadening measurements for single-crystal nickel oxide containing cation vacancies
[DE85-010238] 19 p3376 N85-30944

Multikilowatt hydrogen-nickel oxide battery system
20 p3443 N85-31373

Adsorption of O2, SO2, and SO3 on nickel oxide. Mechanism for sulfate formation
[NASA-CR-176072] 21 p3565 N85-32175

NICKEL STEELS

A study of precipitation and boron distribution in 20 Cr 25Ni base stainless steels
[AERE-M-3353] 03 p0334 N85-12154

The corrosion resistance of chromium-nickel steel containing rare-earth metals
[BLL-BISI-TRANS-22477-(9022.06)]
17 p2925 N85-28041
Influence of heat treatment parameters on the properties of induction hardened Ni-Cr-Mo steels
[BLL-BISI-TRANS-2499-(9022.06)]
17 p2926 N85-28053
Obtaining oxide films on surface of tubes of chromium-nickel steels
[BLL-BISI-TRANS-22478-(9022.06)]
17 p2929 N85-28076
Influence of temperature in melting and casting on quality of medium-alloy steel
[BLL-BISI-TRANS-22310-(9902.06)]
17 p2938 N85-28137
The fatigue properties of welds at low temperature, according to the type of steel
[BLL-BISI-TRANS-22455-(9022.06)]
17 p2978 N85-28410
Fatigue behavior of HY-130 steel weldments containing fabrication discontinuities
[AD-A153630] 18 p3122 N85-29326
Application of the unloading compliance methods in fracture toughness measurements of a quenched and tempered steel
[BLL-CE-TRANS-7953-(9022.09)]
20 p3465 N85-31523
Effects of residual stresses and distortion on the nickel 200 and stainless steel 304 weldments
[DE85-011868] 22 p3748 N85-33233

NICKEL ZINC BATTERIES
Research, development, and demonstration of nickel-iron batteries for electric vehicle propulsion
[DE84-017430] 05 p0632 N85-14054
Supported liquid membrane battery separators
[DE85-001031] 12 p1836 N85-21519
In-vehicle evaluation of the Globe EV 2300 lead-acid, Delco Remy 150 nickel-zinc, and Eagle-Picher NIF 270 nickel-iron battery systems
[NASA-CR-175653] 14 p2349 N85-24521
Transfer of battery technology developed by the US Department of Energy
[DE85-009668] 22 p3808 N85-33586

NIGERIA
Geophysical investigations of the central part of Niger State, Nigeria 03 p0390 N85-12496

NIGHT
Two-level model for formation of night ionosphere of Venus from radio occulation experiments
02 p0162 N85-11100
HH-60D night hawk helicopter
06 p0752 N85-14817
Mechanism of formation of low temperatures in nighttime Venusian thermosphere 16 p2723 N85-26807
Turbulent structure of stably stratified nocturnal slope flows
[AD-A155845] 24 p4123 N85-35559

NIGHT AIRGLOW
U NIGHTGLOW

NIGHT E LAYER
U E REGION
U NIGHT SKY

NIGHT F LAYER
U F REGION
U NIGHT SKY

NIGHT FLIGHTS (AIRCRAFT)
Peripheral vision horizon display on the single seat night attack A-10 01 p0008 N85-10053
Civil law enforcement missions
06 p0751 N85-14812
Some thoughts on the implementation of pilot night vision devices for helicopters 06 p0751 N85-14814
Flight research on visual aids and navigation equipment for helicopter low-level flight at night
08 p1076 N85-16820

NIGHT SKY
Inference of equatorial field-line integrated electron density values using whistlers
[AD-A145822] 03 p0392 N85-12507
The Malin effect in stellar photography
07 p0966 N85-16131

NIGHT VISION
Dark focus: Intersubject variation, intrasubject stability, and relationship to near retinoscopy
[AD-A145489] 02 p0235 N85-11530
Some thoughts on the implementation of pilot night vision devices for helicopters 06 p0751 N85-14814
Effect of extreme peripheral light on dark adaptation
[AD-A146923] 10 p1526 N85-19636
The relative effectiveness of red and white light for subsequent dark-adaptation
[AD-A146883] 10 p1530 N85-19642
Immediate visibility after red and white adaptation
[AD-A156271] 24 p4132 N85-35616

NIGHTGLOW
Upper atmosphere research at INPE
[INPE-3281-PRE/604] 10 p1515 N85-19557
First sodium nightglow results for Natal
[INPE-3397-PRE/666] 10 p1515 N85-19560
Increase in hydrogen emission of upper atmosphere following launches of space vehicles
13 p1981 N85-22431
Fabry-Perot interferometer and skymapping photometer determinations of midlatitude f-region neutral winds and temperatures and airglow enhancement/depletions
[AD-A150730] 14 p2373 N85-24666

NIMBUS SATELLITES
NT NIMBUS 5 SATELLITE
NT NIMBUS 7 SATELLITE
Severe storm detection with passive 37 GHz observations 15 p2596 N85-25997
Satellites and politics: Weather, communications, and earth resources 23 p4057 N85-35144

NIMBUS 5 SATELLITE
Analysis of selective chopper radiometer data
[NASA-CR-175157] 12 p1895 N85-21894

NIMBUS 7 SATELLITE
Coastal Zone Color Scanner (CZCS): Imagery of near-surface phytoplankton pigment concentrations from the first coastal ocean dynamics experiment (CODE-1), March - July 1981
[NASA-CR-174169] 04 p0542 N85-13447
Bio-optical variability in the Alboran Sea as assessed by Nimbus-7 coastal zone color scanner
[AD-A147909] 07 p0989 N85-16281
Data report on variations in the composition of sea ice during MIZEX/East'83 with the Nimbus-7 SMMR
[NASA-TM-86170] 09 p1342 N85-18443
Atlas of relectance patterns for uniform earth and cloud surfaces (NIMBUS-7ERB-61 days)
[PB85-116382] 12 p1891 N85-21870
NIMBUS-7 SBUV (Solar Backscatter Ultraviolet) observations of solar UV spectral irradiance variations caused by solar rotation and active-region evolution for the period November 7, 1978 - November 1, 1980
[NASA-CR-175544] 12 p1962 N85-22334
Validation of the ERBE scanner scene identification methodology: Analysis with Nimbus-7 ERB data
[NASA-CR-172596] 16 p2632 N85-27466
MIZEX, 1984, NASA CV-990 flight report
[NASA-TM-86216] 19 p3299 N85-30451

NIMPHE (ENGINE)
U HYDRAZINE ENGINES

NIOBATES
NT LITHIUM NIOBATES

NIOBIUM
Columbium chamber fabrication study
[AD-A145230] 01 p0017 N85-10102
The oxidation behaviour of a 20 percent Cr/25 percent Ni/Nb stabilized stainless steel in carbon dioxide at high temperatures and its improvement by cerium and yttrium
[AERE-R-11228] 01 p0029 N85-10182
Review: Role of refractory metal alloys in fusion reactor applications
[AERE-R-11317] 03 p0422 N85-12695
Flux-line pinning by the grain boundary in niobium bicrystals
[DE84-016668] 04 p0570 N85-13638
Surface studies of Nb, its compounds, and coatings
[DE84-017353] 06 p0866 N85-15516
Stability of amorphous metals on semiconductor substrates
[DE84-017256] 09 p1295 N85-18134
Transverse microstructure of an oxide scale formed on a 20 % Cr/25 % Ni niobium stabilized stainless steel
[AERE-R-11034] 12 p1804 N85-21315
Spectral evaluation of irregularity of superconducting coaxial cables 13 p2082 N85-23000
Studies of deformation in niobium by X-ray topographic methods
[AD-A150726] 14 p2427 N85-24965
Positron annihilation studies of vacancy formation in tungsten, chromium, and niobium
[DE85-006837] 16 p2871 N85-27710
Submerged arc welding of new Czechoslovak micro-alloy steels
[BLL-BISI-TRANS-22193-(9022.06)]
17 p2972 N85-28356
Microstructures and mechanical properties of microalloyed medium carbon steels
19 p3238 N85-30074
Long range ordered alloys modified by addition of niobium and cerium
[DE85-011661] 20 p3431 N85-31285
A positron annihilation Doppler broadening study of niobium
[DE85-010287] 20 p3527 N85-31936
Evaluated nuclear-data file for niobium
[DE85-012095] 21 p3704 N85-33009
Shape memory effect in uranium-niobium alloys below room temperature
[DE85-012964] 23 p3916 N85-342
Fast-neutron interaction with niobium
[DE85-011471] 24 p4150 N85-357

NIOBIUM ALLOYS
Thermodynamics of decarburization of niobium-bearing high-alloy melts
[BLL-M-35728-(5828.4)] 02 p0175 N85-111
Calculation of critical temperature for Nb-Cu multilayer film superconductor
[AD-A144321] 02 p0274 N85-117
Characterization of Nb-8 wt % Al wires by analytical electron microscopy
[DE85-002726] 10 p1442 N85-190
Effect of reduction of strategic Columbium addition in 718 Alloy on the structure and properties
[NASA-CR-174841] 12 p1805 N85-213
Reaction of amorphous NiNb films with crystalline metal overlayers
[DE85-005483] 13 p2024 N85-22
Decomposition of VTAN alloy solid solution upon irradiation and thermal aging 13 p2029 N85-22712
High temperature antifriction properties of Ti sub 1-sub xNb sub x C sub 0.5N sub 0.5 alloys
13 p2029 N85-22715
Effect of oxygen on mechanical properties of Nb-V alloy
[DE85-002681] 14 p2256 N85-2
Special purpose materials for fusion application
[DE85-005346] 14 p2424 N85-24
Effect of protective atmosphere composition on durability of welded joints of niobium alloys
15 p2502 N85-254
The microstructural state of Nb3Sn in a multifilamentary titanium doped bronze-process wire
[DE85-010979] 19 p3240 N85-30
Critical current density and microstructural state of an internal tin multifilamentary superconducting wire
[DE85-009966] 22 p3761 N85-33
Experimental attempt to achieve microstructure variations through temperature/time permutations for a nonwrought powder metallurgy uranium-6 niobium alloy
[DE85-013166] 23 p3916 N85-34272

NIOBIUM CARBIDES
Possibility of producing monolithic composite materials based on niobium carbide 13 p2028 N85-22707

NIOBIUM COMPOUNDS
NT NIOBIUM CARBIDES
NT NIOBIUM OXIDES
NT NIOBIUM STANNIDES
Phonon anomalies in superconducting transition metal compounds — lanthanum and niobium compounds
03 p0426 N85-12718
Surface studies of Nb, its compounds, and coatings
[DE84-017353] 06 p0866 N85-15516
Short range order-long range order in superconducting materials
[AD-A148764] 08 p1227 N85-17724
Application of NbN films to the development of very high field superconducting magnets
[DE85-002729] 10 p1565 N85-19
Magnetization measurements on multifilamentary Nb3Sn and NbTi conductors
[DE85-001237] 11 p1737 N85-20
Critical current measurements on an NbTi superconducting wire standard reference material
[PB85-118594] 13 p2066 N85-22
Thin films properties of sputtered niobium silicide on SiO2, Si3N4 and on n+ poly-Si
[AD-A152378] 17 p2952 N85-28

NIOBIUM OXIDES
Electrochromic and thermochromic materials for solar energy applications with emphasis on niobium and vanadium oxides
[DE85-010630] 19 p3249 N85-30147

NIOBIUM STANNIDES
Properties of Ti alloyed multifilamentary Nb3Sn wires by internal tin process
[DE85-003212] 12 p1941 N85-22191

NITINOL ALLOYS
Nitinol devices, phase 2, integration of slip ring system and tracking mechanism with memory drive
[BMFT-FB-W-84-032] 05 p0619 N85-13
Production of shaped parts of NITINOL alloys by solid-state sintering
[AD-A152089] 16 p2749 N85-26

NITRAMINE PROPELLANTS
Transition to detonation from rapid-compression (ramp-waves) generated in a burning porous bed
[AD-P004345] 10 p1455 N85-19
Chemical kinetics of gas phase decomposition products of nitramine propellants 13 p2003 N85-22558
Kinetics of mechanism of the thermal decomposition of dimethylnitramine and dimethylnitrosamine
13 p2004 N85-22559

Study on the combustion of nitramine propulsion powder up to 1500 MPa and comparison of the performance with that of classical propulsion powders
[ISL-CO-203/83] 14 p2264 N85-24025
Analysis of deflagration to detonation transition in high-energy solid propellants 16 p2757 N85-27010

NITRATE ESTERS
Morbidity and mortality associated with exposure to Otto Fuel II in the U.S. Navy 1966-1979
[AD-A148726] 09 p1363 N85-18574

NITRATES
NT AMMONIUM NITRATES
NT CELLULOSE NITRATE
NT DINITRATES
NT HYDRAZINE NITRATE
NT PETN
NT SODIUM NITRATES
Denitrification-efficiencies of alternate carbon sources
[AD-A148029] 08 p1119 N85-17050
Meteorological support for the 1983 Deep Creek, Maryland experiment
[DE85-002616] 11 p1678 N85-20575
Applicability of laboratory kinetics studies to the evaluation of aqueous phase atmospheric oxidation of sulfur-4
[DE85-000586] 12 p1883 N85-21819
The crystal and molecular structure of a new propellant compound: Triaminoguanidium Azide Nitrate (TAZN)
13 p2002 N85-22551
Geographic variation in the relationships of temperature, salinity or sigma sub t versus plant nutrient concentrations in the world ocean -- silicic acid, nitrate, and phosphate concentration
[NASA-CR-175621] 13 p2140 N85-23287
Influence of preliminary thermomechanical treatment on depth and hardness of nitrided layers
[BLL-BISI-TRANS-22488-(9022.06)]
17 p2929 N85-26078
Tendency of selected low-carbon steels to corrosion cracking in nitrates
[BLL-BISI-TRANS-22262-(9022.06)]
18 p3073 N85-29006
Environmental surveillance at Los Alamos during 1984
[DE85-011886] 22 p3811 N85-33605
Throughfall rate and chemistry studies: Whiteface Mountain
[DE85-012407] 23 p3947 N85-34464

NITRATION
The nitrogen cycle: Atmosphere interactions
05 p0653 N85-14191
Mononitration of durene
[NASA-TM-77774] 06 p0765 N85-14892
Nitrolysis of the CN single bond and related chemistry of nitro and nitroso groups
[AD-A151753] 15 p2505 N85-25453

NITRIC ACID
Production of concentrated nitric acid
[DE84-017191] 09 p1293 N85-18121
Stratospheric concentration of nitric acid, ozone and carbonyl sulfide: Measurement of nitric acid absorption in the Q branch of the V4 band as a function of temperature
[ESA-TT-864] 09 p1355 N85-18524
Meteorological support for the 1983 Deep Creek, Maryland experiment
[DE85-002616] 11 p1678 N85-20575
Studies of the mechanisms and rates with which nitrogen species are incorporated into cloud water and precipitation
[PB85-144350] 12 p1898 N85-21914
An analysis of issues concerning acid rain, report to the Congress of the United States
[TI85-901070] 15 p2589 N85-25959
Analysis and model/data comparisons of large-scale releases of nitrogen tetroxide
[DE85-009989] 18 p3133 N85-29406
Determination of the association constant for pertechnetic acid
[DE85-010224] 19 p3235 N85-30057

NITRIC OXIDE
Stability evaluation of sulfur dioxide nitric oxide and carbon monoxide gases in cylinders
11 p1648 N85-20387
Variation of derived mesospheric nitric oxide in relation to wind and temperature in winter
11 p1658 N85-20452
Coupling between the thermosphere and the stratosphere: The role of nitric oxide
11 p1662 N85-20472
Middle atmosphere NO and NO2 observed by means of the Spacelab one grille spectrometer
[AERONOMICA-ACTA-A-293-1984]
11 p1680 N85-20588
Laser studies of chemical dynamics at the gas-solid interface
[DE84-017590] 11 p1736 N85-20920
Kinetics of nitric oxide formation in laminar and turbulent methane combustion
[PB85-149698] 12 p1804 N85-21313
The source of stratospheric NO and N2O
[NASA-CR-175713] 15 p2588 N85-25956
An analysis of issues concerning acid rain, report to the Congress of the United States
[TI85-901070] 15 p2589 N85-25959
Slow chemistry effects in a turbulent mixing layer
20 p3424 N85-31252
Static high pressure study of nitric oxide chemistry: Proposed mechanism for nitric oxide detonation
[DE85-010795] 22 p3746 N85-33220
The 1984 environmental monitoring program report for Idaho National Engineering Laboratory site
[DE85-011209] 22 p3812 N85-33611
Dissociative and double photoionization cross sections of NO from threshold to 120 A
[NASA-CR-176185] 24 p4147 N85-35713

NITRIDES
NT ALUMINUM NITRIDES
NT BORON NITRIDES
NT SILICON NITRIDES
NT TITANIUM NITRIDES
NT ZIRCONIUM NITRIDES
Corrosion resistance of nitrided low-alloy steels
[PB84-235027] 04 p0477 N85-13040
Application of NbN films to the development of very high field superconducting magnets
[DE85-002729] 10 p1565 N85-19867
The behaviour of nitride inclusions in nickel-base alloys
[BLL-BISI-TRANS-22396-(9022.06)]
17 p2927 N85-28058
Technological apparatus for laser treatment of materials 17 p2944 N85-28174
Thermodynamic data for mineral technology
[PB85-184331] 22 p3803 N85-33560

NITRIDING
Change in the nitrogen content when nitrided alloys are heated
[BLL-M-35946-(5828.4)] 05 p0615 N85-13929
Nitriding of titanium and its alloys by N2, NH3 or mixtures of N2 + H2 in a dc arc plasma at low pressures (or = to torr)
[NASA-TM-83803] 06 p0814 N85-15168
Ion-beam nitriding of steels
[NASA-CASE-LEW-14104-1] 12 p1805 N85-21324
Slip casting and nitridation of silicon powder
[NASA-TM-77809] 12 p1818 N85-21406
Thermodynamic analysis of the plasma nitriding of ferrovanadium
[BLL-BISI-TRANS-22237-(9022.06)]
17 p2924 N85-28032
An investigation of cementation and carbonitriding by means of ionic bombardment
[BLL-OA-TRANS-3203-(6196.300)]
20 p3429 N85-31265
Nitridation of SiO2 for surface passivation
20 p3480 N85-31627
Nitriding of super alloys for enhancing physical properties
[DE85-005762] 23 p3917 N85-34275

NITRILES
NT ACRYLONITRILES
Development of nitrile rubbers and foams having a high static modulus and low creep
[BR91465] 14 p2259 N85-24001
Microstructural characteristics during the controlled solidification of a binary system
[DE85-005200] 15 p2507 N85-25461
Processable and stable conductive polymers
[AD-D011684] 19 p3249 N85-30143

NITRO COMPOUNDS
NT NITROBENZENES
NT NITROGUANIDINE
NT NITROPROPANE
NT TRINITROTOLUENE
Acute oral toxicity (LD50) of 4-nitrophenyl monochloromethyl (Phenyl) phosphinate (TA009) in male rats
[AD-A148337] 08 p1192 N85-17513
Preparations of methoxynitrophenazines and their photoconductivities
[NASA-TM-77775] 14 p2247 N85-23929
Electrochemistry of Hexanitroazobenzene (HNAB)
[DE85-010807] 21 p3565 N85-32171
Sensitivity and performance characterization of DINGU
[DE85-010750] 22 p3754 N85-33269
Experimental studies of chemical reactivity during shock initiation of hexanitrostilbene
[DE85-011726] 22 p3754 N85-33270
Ethylenediamine salt of 5-nitrotetrazole and preparation
[DE85-005736] 23 p3923 N85-34306

NITROBENZENES
NT TRINITROTOLUENE
Hazardous air pollutants: Wet removal rates and mechanisms
[PB85-138626] 12 p1887 N85-21842
Single-pulse Raman and photoacoustic spectroscopy studies of Triaminotrinitrobenzene (TATB) and related compounds
[DE85-010072] 18 p3064 N85-29078
Electrochemistry of Hexanitroazobenzene (HNAB)
[DE85-010807] 21 p3565 N85-32171

NITROCELLULOSE
U CELLULOSE NITRATE

NITROGEN
NT LIQUID NITROGEN
NT NITROGEN IONS
NT NITROGEN ISOTOPES
NT NITROGEN 15
Treating silicon carbide sinter by heating in nitrogen
[NASA-TM-77601] 01 p0021 N85-10130
Influence of nitrogen on the sensitization, corrosion, mechanical, and microstructural properties of austenitic stainless steels
[DE84-015134] 01 p0026 N85-10177
Electron energy loss rates in N-2, O-2 and air
[AD-A145156] 01 p0072 N85-10476
Feasibility of the electrochemical method of determining nitrogen content in metallic melts
[BLL-M-35730-(5828.4)] 03 p0330 N85-12124
Lubricity of well-characterized jet and broad-cut fuels by ball-on-cylinder machine
[NASA-TM-83807] 03 p0339 N85-12183
Diffusion of gases in porous solids: Simulation and measurements
[DE84-016292] 04 p0500 N85-13191
Effects of acid rain on plant microbial associations in California
[PB84-242122] 04 p0532 N85-13404
Change in the nitrogen content when nitrided alloys are heated
[BLL-M-35946-(5828.4)] 05 p0615 N85-13929
The nitrogen cycle: Atmosphere interactions
05 p0653 N85-14191
Terrestrial nitrogen cycles: Some unanswered questions 05 p0653 N85-14192
Recent studies of the ocean nitrogen cycle
05 p0653 N85-14193
Shock testing of a nitrogen tank (Cryo diffusion type 220 VLR) on the middle weight shock stand
[NASA-TM-77747] 06 p0817 N85-15183
The low-energy secondary cosmic ray flux: Detectors in iron meteorites 06 p0887 N85-15635
Flow of nitrogen-pressurized Halon 1301 in fire extinguishing systems
[NASA-CR-174271] 07 p0900 N85-15701
Nitrogen flushing during exposure of large Schmidt telescope plates 07 p0963 N85-16109
Variation of oxygen and nitrogen abundances in the galaxy 08 p1248 N85-17878
Effects of heteroatom substituents on the properties of 1,2-dioxetanes
[AD-A148727] 09 p1290 N85-18100
The reaction of oxygen-nitrogen mixtures with granular activated carbons below the spontaneous ignition temperature
[AD-A149041] 10 p1434 N85-19039
Growth and reflectance characteristics of winter wheat canopies
[E85-10080] 10 p1505 N85-19494
Role of nitrogen in improving resistance to localized corrosion in austenitic stainless steels
11 p1609 N85-20115
Stability evaluation of sulfur dioxide nitric oxide and carbon monoxide gases in cylinders
11 p1648 N85-20387
Nitrogen control of photosynthetic protein synthesis
[DE85-003513] 11 p1690 N85-20623
Comments on the origins and variations of carbon and nitrogen in the ISM of galaxies as evident from IUE spectroscopy of H 2 regions 11 p1745 N85-20973
Molecular dynamics of propellant gases, part 2
13 p2002 N85-22552
An atlas of nitrogen-broadened water vapor spectra from 500 to 5000 cm(-1), volume 1
[AD-A150527] 13 p2018 N85-22650
Statistical comparison of pooled nitrogen washout data of various altitude decompression response groups
[NASA-TM-58265] 15 p2639 N85-26278
A comprehensive strategy for saturation decompression with nitrogen-oxygen
[AD-A151800] 16 p2841 N85-27520
Systematic nomenclature of the nitrogen, oxygen and sulfur functional polycyclic aromatic hydrocarbons
[DE85-007426] 17 p2916 N85-27974

Some amplification by relaxation processes in nitrogen and mixtures of nitrogen with helium and hydrogen
[AD-A153620] 18 p3071 N85-28992
Heat of mixing experiments for liquified gases
[PB85-183697] 18 p3084 N85-29081
Screening Prosopis (mesquite) species for biofuel production on semi-arid lands
[DE85-010048] 19 p3302 N85-30471
Flash pyrolysis of biomass with reactive and non-reactive gases
[DE85-010962] 19 p3306 N85-30496
Calculation of the propagation constant in a rectangular waveguide containing an inhomogeneous longitudinally magnetized plasma
[DE85-012072] 21 p3577 N85-32250
Biogeochemical cycling and remote sensing
21 p3659 N85-32733
Solar cycle variations of the anomalous cosmic ray component
[PAPER-SH-4.6-2] 21 p3715 N85-33057
Carbon and nitrogen in the deep Earth
21 p3721 N85-33085
Electrode erosion in arc discharges at atmospheric pressure
[NASA-TM-87087] 23 p3903 N85-34178
Oxygen analyzer
[DE85-006002] 23 p3935 N85-34392
Determination of individual tolerance in hyperbaric oxygen 23 p3954 N85-34507
Nitrogen analysis by chemiluminescence
[AD-A156197] 24 p4063 N85-35306
Detection threshold energy of high energy cascade showers using thermoluminescence PTFE-sheet and hot-gas reader
[HE-7.1-5] 24 p4213 N85-36159

NITROGEN COMPOUNDS
NT ALUMINUM NITRIDES
NT AMIDES
NT AMMONIA
NT AMMONIUM NITRATES
NT ATROPINE
NT AZIDES (INORGANIC)
NT AZIDES (ORGANIC)
NT AZO COMPOUNDS
NT BORON NITRIDES
NT CELLULOSE NITRATE
NT CYANO COMPOUNDS
NT DIISOCYANATES
NT DINITRATES
NT HYDRAZINE NITRATE
NT IMIDES
NT IMINES
NT ISOCYANATES
NT LIQUID AMMONIA
NT NITRATE ESTERS
NT NITRATES
NT NITRIC ACID
NT NITRIC OXIDE
NT NITRIDES
NT NITRO COMPOUNDS
NT NITROBENZENES
NT NITROGEN DIOXIDE
NT NITROGEN OXIDES
NT NITROGEN TETROXIDE
NT NITROGUANIDINE
NT NITROPROPANE
NT NITROSO COMPOUNDS
NT NITROUS OXIDES
NT PETN
NT POLYIMIDES
NT QUINOLINE
NT RDX
NT SILICON NITRIDES
NT SODIUM NITRATES
NT THIAZINE (TRADEMARK)
NT TITANIUM NITRIDES
NT TRIAMINOGUANIDINIUM AZIDE
NT TRINITROTOLUENE
NT TRYPTOPHAN
NT UREAS
NT ZIRCONIUM NITRIDES
Theoretical studies in molecular fragmentation: Processes, energetics and diagnostics
[AD-A146310] 03 p0416 N85-12673
Boron-nitrogen polymers. 1: Mechanistic studies of borazine pyrolyses
[AD-A146470] 06 p0771 N85-14933
Non-photochemical interactions of sulfur and nitrogen compounds in acid deposition
[DE84-016141] 10 p1513 N85-19546
Electrostatic potentials: A new method for interpreting and predicting molecular reactivities and for designing synthetic pathways. Applications to nitroaromatics, nitramines and nitrated
[AD-A150120] 12 p1801 N85-21296
Gas-liquid chemistry of natural waters, volume 2
[DE85-002457] 12 p1884 N85-21823
Adsorption behaviour of nitrogen compounds on to porous polymer beads and applications to atmospheric sampling
[BLL-DRIC-TRANS-7399-(3623.66)]
13 p2036 N85-22753
Preparation of nitrocompounds
[AD-A153687] 18 p3071 N85-28993
Mathematical model of the nitrogen cycle in a nonsaturated area of cultivated soil
20 p3478 N85-31610
Synthesis of energetic materials
[AD-A154867] 21 p3571 N85-32210

NITROGEN DIOXIDE
Short-term human respiratory effects of nitrogen dioxide: Determination of quantitative dose-response profiles. Phase 2: Exposure of asthmatic volunteers to 4 PPM NO2
[PB85-104388/GAR] 07 p1017 N85-16462
National Performance Audit Program ambient air audits of analytical proficiency
[PB85-138204] 11 p1680 N85-20586
Middle atmosphere NO and NO2 observed by means of the Spacelab one grille spectrometer
[AERONOMICA-ACTA-A-293-1984]
11 p1680 N85-20588
Research and development of new instruments
16 p2824 N85-27418
Lidar system using polarization discrimination techniques for molecular air pollution monitoring
19 p3308 N85-30504
Development of a technique for in situ detection of stratospheric nitrogen dioxide 19 p3312 N85-30534
Facility for large-scale hazardous gas testing
[DE85-011852] 21 p3564 N85-32169
The 1984 environmental monitoring program report for Idaho National Engineering Laboratory site
[DE85-011209] 22 p3812 N85-33611

NITROGEN FIXATION
U NITROGENATION

NITROGEN IONS
Oxygen-nitrogen interactions in ion-implanted silicon
[DE85-010091] 18 p3195 N85-29819
Electrical properties of bulk grown nitrogen doped silicon
[AD-A155471] 21 p3581 N85-32266

NITROGEN ISOTOPES
NT NITROGEN 15
Evidence for pairing of implanted nitrogen in silicon
[DE84-015622] 06 p0868 N85-15517
A spectacular nitrogen isotope anomaly in Bencubbin
15 p2663 N85-26569
Control technology for radioactive emissions to the atmosphere at US Department of Energy facilities: The Los Alamos Meson Physics Facility
[DE85-011402] 22 p3811 N85-33609
Implications of new measurements of O-16 + p + C-12,13, N-14,15 for the abundances of C, N isotopes at the cosmic ray source
[OG-4.3-2] 22 p3878 N85-34027

NITROGEN LASERS
High repetition rate nitrogen ion laser
02 p0201 N85-11340
Formation of lattice defects by nitrogen laser exposure in A2B6 semiconductors with wide forbidden band
02 p0258 N85-11692
Construction, testing of 1-MW nitrogen laser
08 p1140 N85-17182
An experimental technique for the study of velocity profiles in a laminar jet using a pulsed nitrogen laser
[AD-A151496] 15 p2556 N85-25771
Investigation of influence of gas exit modes on characteristics of N2O - N2 - He discharge laser
21 p3684 N85-32886

NITROGEN METABOLISM
Effect of high ammonia content in closed environment on some parameters of human nitrogen and carbohydrate metabolism against background of a controlled diet
12 p1903 N85-21948

NITROGEN OXIDES
NT NITRIC OXIDE
NT NITROGEN DIOXIDE
NT NITROGEN TETROXIDE
NT NITROUS OXIDES
Future scenarios and ozone change
[DE84-014781] 01 p0085 N85-10573
Estimation of the potential and probable source regions for acid precipitation
[DE84-015119] 02 p0225 N85-11472
A 2-dimensional description of potential perturbations to the ozone layer due to NOx and H-2-O aircraft emissions
[AD-A146292] 03 p0392 N85-12511
Direct measurements of nitrous acid, nitrogen dioxi and formaldehyde in auto exhaust by differential optic absorption spectroscopy
[PB84-226269] 06 p0767 N85-14
NOx emissions near a heat pump with gas motor
[BLL-WH-782-(9091.9F)] 07 p0995 N85-16
Impact of aircraft emissions on air quality in the vicin of airports. Volume 4. Nitrogen dioxide an hydrocarbons
[AD-A148253] 08 p1180 N85-174
Optical studies of nitrogen oxides in the stratospher
08 p1183 N85-174
Evaluation of the particulate levels occuring whil 1.0/1.2 g/mi nitrogen oxide standards for light duty dies vehicles and light duty diesel trucks
[PB85-115939/GAR] 09 p1350 N85-184
MAP/GLOBUS campaign 1983
11 p1658 N85-204
Evaluation of recent SO/sub x/and NO/sub x/ emissio inventories
[DE85-002649] 11 p1677 N85-205
National Acid Precipitation Assessment Program. Report to the President and Congress (1983)
[PB85-116713] 11 p1679 N85-208
Results of recent large-scale NH3 and N2O4 dispersion experiments
[DE85-004988] 15 p2589 N85-25
Kinetic energies of fragment ions produced by dissociative photoionization of NO
[NASA-CR-175721] 15 p2647 N85-26
Is there more than one steady state for NOx?
15 p2687 N85-26
Transformation of nitrogen oxides while sampling combustion products
[AD-A152184] 16 p2746 N85-26
Absolute calibrations of SO2 and NO analyzers by photographic methods
[DFVLR-MITT-85-02] 17 p2994 N85-28
Analysis and model/data comparisons of large-scale releases of nitrogen tetroxide
[DE85-008989] 18 p3133 N85-294
Investigation of the reaction system NOX/ClOX/HOX under tropospheric and stratospheric conditions
[BPT-11/84] 18 p3137 N85-294
Assessment of the role of nitrogen oxides in nonurban ozone formation
[PB85-173680] 19 p3311 N85-305
Historic emissions of sulfur and nitrogen oxides in the U.S. from 1900 to 1980. Volume 1: Results
[PB85-191195] 20 p3487 N85-3167
Historic emissions of sulfur and nitrogen oxides in the U.S. from 1900 to 1980. Volume 2: Data
[PB85-191203] 20 p3487 N85-3167
Emergency modeling of hazardous air pollutants
[AD-A155441] 21 p3614 N85-324
Technology of off-gas treatment for liquid-fed ceramic melters
[DE85-012467] 22 p3812 N85-3361
Atmospheric reaction products from hazardous air pollutant degradation
[PB85-185841] 22 p3813 N85-336
Forecasting future industrial SO2 and NO/sub x/ emissions, revised 23 p3947 N85-344
Review of US NOx abatement technology
[PB85-193522] 24 p4114 N85-355
Atmospheric nitrogen oxides: Their detection and chemistry
[PB85-193910] 24 p4114 N85-355
The measurement of nitrogen oxide (NO, NO2) exchange over plant/soil surfaces
[CSIRO-DAR-TP-8] 24 p4127 N85-355

NITROGEN PLASMA
SWIR and visible atomic emission from laser-produced oxygen and nitrogen plasmas
[AD-A147528] 07 p1045 N85-168
A 50-kW electric-discharge CO2 laser
[AD-A149779] 12 p1857 N85-216
Frictional and structural characterization of ion-nitrided low and high chromium steels
[NASA-TM-86991] 13 p2098 N85-22
Thermodynamic analysis of the plasma nitriding of ferrovanadium
[BLL-BISI-TRANS-22237-(9022.06)]
17 p2924 N85-28
Recombination and ionization in a nitrogen plasma
[AD-A155426] 22 p3845 N85-33

NITROGEN TETROXIDE
Atmospheric dispersion of hypergolic liquid rocket fuels, volume 1
[AD-A149597] 12 p1817 N85-21
Evaluation of source strength and dispersion model predications with data from large nitrogen tetroxide field experiments
[DE85-011855] 23 p3947 N85-344

NITROGEN 15
Stable isotope studies
[DE84-016752] 04 p0582 N85-13583
Evidence for pairing of implanted nitrogen in silicon
[DE84-015822] 06 p0868 N85-15517
NITROGENATION
Alloying specially low carbon silicon-bearing steel with nitrogen
[BLL-M-35707-(5828.4)] 02 p0175 N85-11170
Recent studies of the ocean nitrogen cycle
05 p0653 N85-14193
Effects of acid rain on forest nutrient status
[DE85-012486] 23 p3947 N85-34483
NITROGUANIDINE
Electron density distribution analysis for nitroguanidine
[DE85-009690] 23 p3969 N85-34603
NITROLYSIS
Nitrolysis of the CN single bond and related chemistry of nitro and nitroso groups
[AD-A151753] 15 p2505 N85-25453
NITROPROPANE
Multiple product channels in the collision free UV photodissociation of 2-nitropropane
[AD-A150688] 14 p2251 N85-23951
NITROSO COMPOUNDS
Nitrolysis of the CN single bond and related chemistry of nitro and nitroso groups
[AD-A151753] 15 p2505 N85-25453
NITROUS OXIDES
Raman and fluorescence spectroscopy in a methane-nitrous oxide laminar flame
[AD-A148092] 03 p0328 N85-12111
Continued research in mesoscale air pollution simulation modeling. Volume 5: Refinements in numerical analysis, transport, chemistry, and pollutant removal
[PB85-137362] 11 p1680 N85-20585
Non-precipitating cumulus cloud study
[DE85-002352] 12 p1896 N85-21902
Modeling of chemical transformations of SO(x) and NO(x) in the polluted atmosphere: An overview of approaches and current status
[PB85-173169] 20 p3487 N85-31677
Review of US NOx abatement technology
[PB85-193522] 24 p4114 N85-35501
The measurement of nitrogen oxide (NO, NO2) exchange over plant/soil surfaces
[CSIRO-DAR-TP-8] 24 p4127 N85-35587
NMR
U NUCLEAR MAGNETIC RESONANCE
NOAA E
U NOAA 8 SATELLITE
NOAA SATELLITES
NT NOAA 6 SATELLITE
NT NOAA 7 SATELLITE
NT NOAA 8 SATELLITE
Report of the First Session of the International Working Group on Data Management for the International Satellite Cloud Climatology Project (ISCCP)
[WCP-42] 01 p0073 N85-10483
Cloud cover sampling capability of various satellite combinations for ISCCP 01 p0073 N85-10484
Monitoring and mapping global vegetation cover using data from meteorological satellites
05 p0656 N85-14211
An interactive technique for satellite-improved rainfall monitoring 05 p0658 N85-14224
Environmental data inventory for the antarctic area
[PB85-107944] 06 p0819 N85-15195
Civil weather satellite systems
11 p1711 N85-20768
The development of image processing of NOAA AVHRR data and its application to sea surface temperature
12 p1895 N85-21891
Scientific requirements for ozone measurements
13 p2105 N85-23113
The ARGOS system status report after 2 years operation 14 p2237 N85-23870
System performance, data distribution and technical files — ARGOS project 14 p2237 N85-23871
The ARGOS system status report
14 p2239 N85-23884
Automatic weather stations in Antarctica
14 p2324 N85-24360
The ARGOS system after 3 years operation
14 p2325 N85-24368
The use of TOMS data in evaluating and improving the total ozone from TOVS measurements
[NOAA-TR-NESDIS-23] 22 p3814 N85-33626
NOAA 6 SATELLITE
Image texture study for the operational meteorological satellites NOAA 6 and NOAA 7 and its variation with time. Application to the Beauce region
[ENST-84E009] 05 p0661 N85-14249
Observation of a westward travelling surge from satellites at low, medium and high altitudes
[NASA-TM-87434] 09 p1342 N85-18442
The ARGOS system main characteristics — satellite based localization 14 p2325 N85-24367
The ARGOS program — satellite based localization
14 p2397 N85-24775
Location and data collection satellite system ARGOS. User's guide — satellite based localization
16 p2816 N85-27371
First results of oceanography utilization of infrared high resolution picture transmission images
[KNMI-TR-59] 18 p3151 N85-29511
NOAA 7 SATELLITE
Image texture study for the operational meteorological satellites NOAA 6 and NOAA 7 and its variation with time. Application to the Beauce region
[ENST-84E009] 05 p0661 N85-14249
The ARGOS system main characteristics — satellite based localization 14 p2325 N85-24367
The ARGOS program — satellite based localization
14 p2397 N85-24775
Availability of the ARGOS system based on the orbital characteristics of the TIROS-N satellites — oceanographic/meteorological data
16 p2813 N85-27352
Contribution of the NOAA-7 and 8 and ARGOS partnership to white tuna fishing in the northeast Atlantic
16 p2813 N85-27355
Location and data collection satellite system ARGOS. User's guide — satellite based localization
16 p2816 N85-27371
Information relative to cartography and geodesy. Series 2: Translations, number 42, volume 1
[ISSN-0469-4244] 18 p3123 N85-29338
Digital image mapping of Antarctica using NOAA-7 AVHRR imagery 18 p3124 N85-29340
First results of oceanography utilization of infrared high resolution picture transmission images
[KNMI-TR-59] 18 p3151 N85-29511
NOAA 8 SATELLITE
Availability of the ARGOS system based on the orbital characteristics of the TIROS-N satellites — oceanographic/meteorological data
16 p2813 N85-27352
Contribution of the NOAA-7 and 8 and ARGOS partnership to white tuna fishing in the northeast Atlantic
16 p2813 N85-27355
First results of oceanography utilization of infrared high resolution picture transmission images
[KNMI-TR-59] 18 p3151 N85-29511
SARSAT 121.5/243 MHz technical evaluation
20 p3405 N85-31126

NOBLE GASES
U RARE GASES
NOBLE METALS
NT GOLD
NT RUTHENIUM
NT SILVER
Conductor structure for thick film electrical device
[AD-D011240] 01 p0043 N85-10281
The replacement of precious metal thick film inks using conductive polymer technology. Phase 1: Feasibility study
[AD-A147814] 07 p0933 N85-15913
Comparisons between computed and observed grain boundary structures and properties in metals
[DE85-002596] 10 p1442 N85-19085
Noble metals as incipient transition metals
[DE85-013283] 24 p4080 N85-35286
NOCTILUCENCE
U LUMINESCENCE
NOCTILUCENT CLOUDS
Interaction of large meteoroids with the atmosphere
11 p1656 N85-20431
Cold Arctic Mesopause Project (CAMP): Scientific objectives 11 p1656 N85-20433
NOCTURNAL VARIATIONS
Relationship between model complexity and data base quality for complex terrain tracer experiments
[DE84-015022] 04 p0539 N85-13429
Comparison between tracer measurements and model calculations for nighttime drainage flows in complex terrain
[DE84-014709] 04 p0539 N85-13431
Atmospheric studies in complex terrain
[DE84-008553] 05 p0676 N85-14345
Statistical relationships between meteorological data stations and implications to diagnostic models in complex terrain
[DE84-014380] 06 p0839 N85-15328
On the formation of the nocturnal coastal surface wind speed maximum 09 p1356 N85-18528
Categorization of nocturnal drainage flows within the Brush Creek valley in western Colorado and the variability of sigma theta in complex terrain
[DE85-011291] 19 p3300 N85-30461
VALMET: A valley air pollution model
[DE85-010820] 21 p3614 N85-32463
NODULES
Unsinkability of ferromanganese nodules
06 p0819 N85-15202
Exploring ocean's mineral wealth
07 p0980 N85-16227
NOE NAVIGATION
U NAP-OF-THE-EARTH NAVIGATION
NOISE
Study on spectral/radiometric characteristics of the Thematic Mapper for land use applications
[E85-10021] 02 p0216 N85-11434
NBS (National Bureau of Standards) and WR62 and WR90 reference noise standards
[PB84-235704] 07 p0942 N85-15977
Investigation of dynamic noise affecting geodynamics information in a tethered subsatellite
[NASA-CR-176031] 20 p3476 N85-31602
Visual phenomena produced by binocularly disparate dynamic visual noise
[AD-A154758] 21 p3663 N85-32757
NOISE (SOUND)
NT AERODYNAMIC NOISE
NT AIRCRAFT NOISE
NT ENGINE NOISE
NT JET AIRCRAFT NOISE
NT SONIC BOOMS
NT THERMAL NOISE
Study of annoyance due to urban automobile traffic
[NASA-TM-77514] 01 p0089 N85-10458
Response measurements for two building structures excited by noise from a large horizontal axis wind turbine generator
[NASA-CR-172482] 04 p0558 N85-13552
Wave-wave interactions, microseisms, and infrasonic ambient noise in the ocean
[AD-A146529] 06 p0859 N85-15463
Detection of low frequency impulsive noise from large wind turbine generators
[NASA-CR-172511] 07 p1038 N85-16588
Investigation of dynamic noise affecting geodynamics information in a tethered subsatellite
[NASA-CR-174292] 08 p1174 N85-17405
Computation of noise radiation from a free jet perpendicular to its axis via laser anemometry measurements
[ESA-TT-870] 09 p1379 N85-18669
Effects of overall vibration and noise on operational personnel 10 p1523 N85-19608
Further comparison of wind tunnel and airplane acoustic data for advanced design high speed propeller models
[NASA-TM-86935] 12 p1927 N85-22108
Machine tool vibrations: A review
13 p2102 N85-23104
Transmission of gear noise to aircraft interiors prediction methods 14 p2223 N85-23788
Several specific and nonspecific responses of the human and animal body to ship noise
[NASA-TM-77483] 15 p2615 N85-26116
Contribution of tonal components to the overall loudness, annoyance and noisiness of noise: Relation between single tones and noise spectral shape
[NASA-CR-3892] 15 p2645 N85-26317
Vortex studies relating to boundary layer turbulence and noise
[NASA-TM-87475] 16 p2782 N85-27169
The theoretical response of a vertical line array to wind-generated noise in shallow water
[AD-A151730] 16 p2860 N85-27638
Acoustic noise associated with the MOD-1 wind turbine: Its source, impact, and control
[DE85-002947] 18 p3176 N85-29700
A study of interior noise levels, noise sources and transmission paths in light aircraft
[NASA-CR-172152] 19 p3350 N85-30766
Operational noise data for the LACV-30 air cushion vehicle
[AD-A154063] 19 p3351 N85-30773
Aviation noise effects
[AD-A154319] 19 p3352 N85-30776
Noise in stages and in interstage couplings of various transistor circuits 22 p3765 N85-33334
Some problems in high speed gears and gearing
23 p3923 N85-34312
Generated spiral bevel gears: Optimal machine-tool settings and tooth contact analysis
[NASA-TM-87075] 23 p3937 N85-34405
NOISE ATTENUATION
U NOISE REDUCTION
NOISE ELIMINATION
U NOISE REDUCTION
NOISE GENERATORS
Calibration of noise power transfer standards, measurement uncertainties and long term stability
05 p0630 N85-14035

The development of a 90 GHz solid state noise source
[CD.6500695] 05 p0733 N85-14715

NOISE HAZARDS
U HAZARDS
U NOISE (SOUND)

NOISE INJURIES

Application of the isoenergy principle and the A weighting to evaluate lesion risks due to noise in a military environment
[ISL-CO-231/83] 14 p2390 N85-24720

Auditory impairment and the onset of disability and handicap in noise-induced hearing loss
[ISVR-TR-126] 20 p3507 N85-31801

Noise reduction in the automotive test cell of the Motor Institute of Naples
[REPT-85-RR-361] 20 p3524 N85-31917

NOISE INTENSITY

Human response to vibroacoustic environments of space vehicles
[NASA-TM-86316] 01 p0116 N85-10789

Rules for post-detector detection of weak signals in non-Gaussian noise of unknown power
03 p0344 N85-12218

Investigation on experimental techniques to detect, locate and quantify gear noise in helicopter transmissions
[NASA-CR-3847] 08 p1217 N85-17667

Noise in stages and in interstage couplings of various transistor circuits 22 p3765 N85-33334

NOISE MEASUREMENT

Analysis of noise measured from a propeller in a wake
[NASA-TP-2358] 02 p0274 N85-11788

Airport noise impact prediction and measurement
03 p0387 N85-12476

Study of annoyance due to urban automobile traffic. Annex 4: A catalog of the characteristics of noise at different measuring points
[NASA-TM-77516] 03 p0387 N85-12478

Patterns of behavior in lodgings exposed to traffic noise
[NASA-TM-77750] 03 p0387 N85-12479

Total area of diffusion elements in a reverberation chamber and measured degree of sound absorption
[NRC/CNR-TT-2110] 03 p0415 N85-12653

Evaluation of the Langley 4- by 7-meter tunnel for propeller noise measurements
[NASA-TM-85721] 04 p0558 N85-13553

Coaxial noise measurement circuits
05 p0630 N85-14036

Helicopter noise survey performed at Las Vegas, Nevada, 19-21 January, 1984
[AD-A147392] 07 p1039 N85-16593

Noise measurement flight test: Data-analyses aerospatiale AS-355F TwinStar helicopter
[AD-A147497] 07 p1039 N85-16595

Noise measurement flight test for Boeing Vertol 234/CH 47-d helicopter: Data/analyses
[AD-A148172] 08 p1218 N85-17670

Noise measurement flight test: Data-analyses Aerospatiale AS 350D AStar helicopter
[AD-A148496] 08 p1218 N85-17672

Noise measurement flight test: Data-analyses, Sikorsky S-76A helicopter
[AD-A148525] 08 p1218 N85-17673

A preliminary assessment of environmental noise from large Wind Energy Conversion Systems (WECS) based on experiences from Swedish prototypes
[FFA-TN-1984-48] 09 p1379 N85-18668

Statistical study of anthropogenic seismic noise with IVK-7 computer system 10 p1503 N85-19483

Noise measurement flight test: Data/Analyses, hughes 500 D/E helicopter
[AD-A148110] 14 p2219 N85-23758

Transmission error measurements in gearbox development 14 p2224 N85-23794

Sound propagation studies for a large horizontal axis wind turbine
[NASA-CR-172564] 14 p2415 N85-24904

An experimental study of the noise generated by vaporous cavitation in turbulent shear flows produced by confined orifice plates 15 p2645 N85-26316

Contribution of tonal components to the overall loudness, annoyance and noisiness of noise: Relation between single tones and noise spectral shape
[NASA-CR-3892] 15 p2645 N85-26317

Contribution to the study of equivalent noise source identification in fast cold jets
[ISL-R-114/83] 16 p2861 N85-27645

Analyses of orderly structures in jets and the relationship with emitted noise
[ISL-R-117/83] 16 p2861 N85-27646

Prediction of free-field noise levels from aircraft flyover measurements
[VTH-LR-427] 16 p2861 N85-27647

Measured noise performance of a new method of frequency hopping
[AD-A152679] 17 p2953 N85-28234

A study of interior noise levels, noise sources and transmission paths in light aircraft
[NASA-CR-172152] 19 p3350 N85-30766

Design of a freestanding noise measurement and recording system to predict the intensity and location of electromagnetic radiation from earthquakes
[AD-A155070] 21 p3632 N85-32563

FAA/GAMA (Federal Aviation Administration/General Aviation Manufacturer's Association) propeller aircraft noise test program, Salina Municipal Airport, Salina, Kansas
[AD-A154818] 21 p3699 N85-32983

Overground Excess Sound Attenuation (ESA). Volume 3: Application of ESA data in NOISEFILE
[AD-A154820] 21 p3699 N85-32984

Helicopter noise survey for selected cities in the contiguous US
[AD-A154893] 21 p3699 N85-32985

A theoretical appraisal of the use of ground-plane microphones for aircraft noise measurements
[NPL-AC-103] 22 p3836 N85-33752

A Programmable Automatic Noise Data and Other Related parameter Acquisition system (PANDORA) — wind energy converters 24 p4111 N85-35479

NOISE POLLUTION

Study of annoyance due to urban automobile traffic
[NASA-TM-77514] 01 p0069 N85-10458

Study of annoyance due to urban automobile traffic. Annex 4: A catalog of the characteristics of noise at different measuring points
[NASA-TM-77516] 03 p0387 N85-12478

Patterns of behavior in lodgings exposed to traffic noise
[NASA-TM-77750] 03 p0387 N85-12479

NOISEMAP 4.4 computer program update, operator's manual, addendum 1
[AD-A147091] 07 p1025 N85-16503

Construction and application of a questionnaire for the social scientific investigation of environmental noise effects
[NASA-TM-75492] 10 p1512 N85-19544

Development of guidelines for setting physiological and hygienic standards for noise levels in aerospace medicine 19 p3323 N85-30584

The timing of noise-sensitive activities in residential areas
[NASA-CR-177937] 20 p3524 N85-31918

Statistical methods for efficient design of community surveys of response to noise: Random coefficients regression models
[NASA-CR-177933] 21 p3698 N85-32979

GROWIAN: First observations of the environmental impact at the GROWIAN site — wind energy converter
24 p4110 N85-35476

NOISE PREDICTION

On the application of a hairpin vortex model of wall turbulence to trailing edge noise prediction
[NASA-CR-177938] 22 p3728 N85-33109

Wind turbine noise: Prediction tools and design parameter dependence 24 p4110 N85-35477

NOISE PREDICTION (AIRCRAFT)

Observations from varying the lift and drag inputs to a noise prediction method for supersonic helical tip speed propellers
[NASA-TM-83797] 01 p0115 N85-10786

Airport noise impact prediction and measurement
03 p0387 N85-12476

Prediction and modeling of helicopter noise
[AD-A145764] 03 p0415 N85-12656

Contribution of the study of light aircraft propeller noise
[ESA-TT-885] 09 p1378 N85-18667

Wind tunnel acoustic study of a propeller installed behind an airplane empennage: Data report
[NASA-CR-177335] 13 p2154 N85-23377

Transmission of gear noise to aircraft interiors prediction methods 14 p2223 N85-23786

A study of the methods for evaluating the noise impact of a proposed airport on a community
15 p2588 N85-25957

Prediction of free-field noise levels from aircraft flyover measurements
[VTH-LR-427] 16 p2861 N85-27647

Design of sidewall treatment of cabin noise control of a twin engine turboprop aircraft
[NASA-CR-172245] 19 p3351 N85-30771

Some problems in high speed gears and gearing
23 p3923 N85-34312

Optimally designed propellers constrained by noise
24 p4065 N85-35196

NOISE PROPAGATION

A preliminary assessment of environmental noise from large Wind Energy Conversion Systems (WECS) based on experiences from Swedish prototypes
[FFA-TN-1984-48] 09 p1379 N85-18668

Computation of noise radiation from a free jet perpendicular to its axis via laser anemometry measurements
[ESA-TT-870] 09 p1379 N85-18669

Noise transmission loss of a rectangular plate in an infinite baffle
[NASA-TP-2398] 12 p1927 [illegible]

Gear noise origins 14 p2224 N85-23791

Long range downwind propagation of low-frequency sound
[NASA-TM-86409] 15 p2645 N85-26318

An evaluation of proposed acoustic treatments for the NASA LaRC 4 x 7 meter wind tunnel
[NASA-CR-172577] 15 p2646 N85-26319

Interaction of finite-amplitude sound with air-filled porous materials
[NASA-CR-174885] 16 p2860 N85-27637

Aircraft cabin noise prediction and optimization
[NASA-CR-175962] 19 p3350 N85-30769

Design of sidewall treatment of cabin noise control of a twin engine turboprop aircraft
[NASA-CR-172245] 19 p3351 N85-30771

Overground Excess Sound Attenuation (ESA). Volume 3: Application of ESA data in NOISEFILE
[AD-A154820] 21 p3699 N85-32984

Some problems in high speed gears and gearing
23 p3923 N85-34312

NOISE REDUCTION

Noise isolation system for high-speed circuits
[DE84-014229] 01 p0043 N85-10280

Conversion of microwave signals by superconducting films in the resistive state
[NASA-TM-77595] 01 p0123 N85-10843

Highlights of the Institute of Sound and Vibration Research 01 p0131 N85-10905

Jet noise suppression by porous plug nozzles
[NASA-CR-3613] 02 p0275 N85-11790

Noise reduction of the exhaust from pneumatic tools
[BMFT-FB-HA-83-021] 02 p0276 N85-11799

Influence of mode noise suppression in multimode fiber optic light guides 03 p0348 N85-12242

Numerical simulations of compliant material response to turbulent flow, revision 1
[AD-A145801] 03 p0372 N85-12373

Commercial aircraft noise
[PNR-90206] 03 p0417 N85-12665

Tap noise-pressure fluctuations. Study of the acoustic behavior of hydraulic equipment in buildings as a function of the temperature
[CETIM-11-H-337] 04 p0502 N85-13201

A.A.D. engine noise evaluation
04 p0508 N85-13241

Experimental investigation of shock-cell noise reduction for dual-stream nozzles in simulated flight
[NASA-CR-3846] 04 p0557 N85-13549

Experimental investigation of shock-cell noise reduction for single stream nozzles in simulated flight
[NASA-CR-3845] 04 p0557 N85-13550

Noise in small portable motocompressors. Experiments on limited-cost acoustic treatments to obtain progressive improvements
[CETIM-11-H-445] 04 p0558 N85-13557

Vibroacoustic control diagnostics of selected machines based on research on the slide bearing of an automobile engine and the alternator
[ISSN-0208-5658] 05 p0641 N85-14112

LANDSAT instruments characterization
[E85-10029] 05 p0654 N85-14136

Detailed performance calculations: Goddard Group appendix D 05 p0676 N85-14341

Sources, paths, and concepts for reduction of noise in the test section of the NASA Langley 4x7m wind tunnel
[NASA-CR-172446-VOL-1] 05 p0726 N85-14866

Comparison of options for reduction of noise in the test section of the NASA Langley 4x7m wind tunnel, including reduction of nozzle area
[NASA-CR-172446-VOL-2] 05 p0726 N85-14867

Studies on reactive mufflers. Part 2: Mufflers with air flow 09 p1303 N85-18184

Acoustic tomographic reconstrution of anomalies in three-dimensional bodies
[DE84-017035] 09 p1378 N85-18666

One-dimensional processing for adaptive image restoration
[AD-A149314] 10 p1557 N85-19815

Noise constraints effecting optimal propeller designs
[NASA-TM-86967] 11 p1575 N85-19823

Comparator with noise suppression
[NASA-CASE-LAR-13151-1] 11 p1627 N85-20247

Abatement of noise and vibration in pipelines of hydro systems 14 p2276 N85-24102

A study of the methods for evaluating the noise impact of a proposed airport on a community
15 p2588 N85-25957
An evaluation of proposed acoustic treatments for the NASA LeRC 4 x 7 meter wind tunnel
[NASA-CR-172577] 15 p2646 N85-26319
Interaction of finite-amplitude sound with air-filled porous materials
[NASA-CR-174885] 16 p2860 N85-27637
Fan noise suppression in turbofan engines
[B8580076] 17 p2898 N85-27872
A simplified GPS C/A reciever front end with low noise performance 18 p3109 N85-29251
Reports on cartography and geodesy. Series 1: Original reports, number 93
[ISSN-0469-4236] 18 p3124 N85-29343
An information theoretical method for automatic noise elimination in digital image processing
18 p3124 N85-29345
Effects of propeller rotation direction on airplane interior noise levels
[NASA-TP-2444] 19 p3350 N85-30767
Aircraft cabin noise prediction and optimization
[NASA-CR-175982] 19 p3350 N85-30768
Design of sidewall treatment of cabin noise control of a twin engine turboprop aircraft
[NASA-CR-172245] 19 p3351 N85-30771
Noise reduction in the automotive test cell of the Motor Institute of Naples
[REPT-85-RR-361] 20 p3524 N85-31917
Models for describing active noise control in ducts
[ISVR-TR-127] 20 p3525 N85-31922
Sound-insulating enclosures — machine noise
[BMFT-FB-HA-85-005] 20 p3525 N85-31925
FAA/GAMA (Federal Aviation Administration/General Aviation Manufacturer's Association) propeller aircraft noise test program, Salina Municipal Airport, Salina, Kansas
[AD-A154818] 21 p3699 N85-32983
Discussion of the paper, Some Aspects of Propulsion for the Augmenter-Wing Concept, by D. C. Whittley
[NASA-TM-77884] 22 p3727 N85-33108
Some problems in high speed gears and gearing
23 p3923 N85-34312
Langley aeronautics and space test highlights, 1984
[NASA-TM-87585] 23 p4057 N85-35151
Optimally designed propellers constrained by noise
24 p4065 N85-35196
A research program to reduce the interior noise in general aviation aircraft, index and summary
[NASA-CR-176178] 24 p4145 N85-35695
NOISE SPECTRA
Noise jammer discrimination by noise spectral bandwidth
[AD-D011224] 01 p0038 N85-10242
Noise analysis of the Coarse Optical Power Spectrum Estimator (COPSE) data acquisition system
[AD-A145918] 03 p0419 N85-12677
Study of the velocity-acoustic pressure correlation in a cold jet, centered on the sign and the amplitude of the velocity fluctuations
[ISL-R-124/83] 04 p0501 N85-13193
Detection of low frequency impulsive noise from large wind turbine generators
[NASA-CR-172511] 07 p1038 N85-16588
Quantum noise effects in single-mode injection lasers
[FUB-11-1984] 09 p1327 N85-18338
Effects of vane/blade ratio and spacing on fan noise, volume 1
[NASA-CR-174664] 10 p1553 N85-19791
Effects of vane/blade ratio and spacing on fan noise. Volume 2: Data supplement
[NASA-CR-174665] 10 p1553 N85-19792
Shuttle electrical environment
13 p1990 N85-22475
Noise characteristics of sulfur-doped silicon diodes
13 p2073 N85-22952
Flux pinning and flux flow studies in superconductors using flux flow noise techniques
[DE85-010814] 19 p3376 N85-30945
Overview of applications of SQUIDS
[DE85-009942] 20 p3458 N85-31480
Overground Excess Sound Attenuation (ESA). Volume 3: Application of ESA data in NOISEFILE
[AD-A154820] 21 p3699 N85-32984
Lateral attenuation of aircraft flight noise
[AD-A154958] 21 p3700 N85-32986
A comparison of calculated and measured background noise rates in hard X-ray telescopes at balloon altitude
[OG-9.3-7] 23 p4028 N85-34962
NOISE SUPPRESSORS
U NOISE REDUCTION
NOISE TEMPERATURE
A coaxial noise standard for the 1 GHz to 12.4 GHz frequency range
[PB84-217884] 01 p0042 N85-10272
Superconducting NbTi and Pb(Cu) bandpass filters
05 p0623 N85-13966
The dc SQUID as a tuned radiofrequency amplifier
[DE85-000701] 06 p0805 N85-15123
Preliminary investigation into using the sun as a source for G/T (Gain to System Noise Temperature) measurements
[PB85-128148] 12 p1952 N85-22265
NOISE THRESHOLD
Robust detection of fading narrow-band signals in non-Gaussian noise
[AD-A152262] 16 p2774 N85-27124
NOISE TOLERANCE
Study of annoyance due to urban automobile traffic
[NASA-TM-77514] 01 p0069 N85-10458
Airport noise impact prediction and measurement
03 p0387 N85-12476
NOISEMAP 4.4 computer program update, operator's manual, addendum 1
[AD-A147091] 07 p1025 N85-16503
Construction and application of a questionnaire for the social scientific investigation of environmental noise effects
[NASA-TM-75492] 10 p1512 N85-19544
Investigation of influence of communications link and synchronization error on noise tolerence of group transmission of binary information based on orthogonal Walsh function 13 p2086 N85-23026
A community survey of helicopter noise annoyance conducted under controlled noise exposure conditions
[NASA-TM-86400] 13 p2154 N85-23374
Disturbance to the population due to flight operations at landing fields. Questionnaire on community reaction to non-commercial and sporting aviation
[NASA-TM-76531] 14 p2353 N85-24537
Effect of broad-band constant noise on some systems of animal body 14 p2387 N85-24705
NOMENCLATURES
Fungi of Mt. Babia Gora. 1: Mycoflora of forests
[NASA-TM-77484] 02 p0234 N85-11522
SLC nomenclature for beamline components
[DE84-014776] 02 p0279 N85-11816
DoD manual for standard data elements, part 2
[AD-A152202] 16 p2878 N85-27755
DoD manual for standard data elements, part 3
[AD-A152203] 16 p2878 N85-27756
DoD manual for standard data elements, part 4
[AD-A152204] 16 p2878 N85-27757
DoD manual for standard data elements, part 5
[AD-A152205] 16 p2878 N85-27758
Systematic nomenclature of the nitrogen, oxygen and sulfur functional polycyclic aromatic hydrocarbons
[DE85-007426] 17 p2916 N85-27974
Coping with computer terminology
[DE85-006076] 18 p3161 N85-29579
NOMINAL VALUES
U APPROXIMATION
NOMOGRAMS
U NOMOGRAPHS
NOMOGRAPHS
Nomographs for estimating the levelized cost of energy from flat-plate and concentrator photovoltaic systems
[NASA-CR-176048] 20 p3483 N85-31645
Modeling of discrete devices with use of multivalued logic and nomograms 22 p3768 N85-33351
NONADIABATIC PROCESSES
U HEAT TRANSFER
NONADIABATIC THEORY
Nonlocal and nonadiabatic expression for the ponderomotive force near cyclotron resonance
[IPPJ-736] 23 p3974 N85-34636
NONAQUEOUS ELECTROLYTES
Voltammetry and coulometry with immersed thin layer electrodes. Part 1: Model for effects of solution resistivity in linear sweep voltammetry
[AD-A148655] 08 p1159 N85-17313
Development of a low cost electrochemical CO monitor based on anodic scanning voltammetry in nonaqueous electrolyte
[PB85-113488] 11 p1637 N85-20314
Electrochemical reduction of titanium in dimethyl sulphoxide
[BLL-OA-TRANS-3225-(6196.300)]
20 p3429 N85-31267
NONCONDENSABLE GASES
Theoretical analysis of condensation in the presence of noncondensable gases as applied to open cycle OTEC condensers
[DE84-015809] 11 p1675 N85-20556
NONCONDUCTORS
U ELECTRICAL INSULATION
NONCONSERVATIVE FORCES
Satellite physical and orbital characteristics
16 p2804 N85-27287
NONDESTRUCTIVE TESTS
NT NEUTRON RADIOGRAPHY
NT STATIC FIRING
Nonlinear ultrasonic characterization of oxygen impurities in titanium, 2
[AD-A144857] 01 p0027 N85-10171
Electromagnetic-acoustic-transducer
e system for thick-weld inspection
[PB84-219492] 01 p0051 N85-10336
Ultrasonic nondestructive evaluation, microstructure, and mechanical property interrelations
[NASA-TM-86876] 01 p0056 N85-10371
Evaluation of interfacial stresses from the amplitude of reflected ultrasonic signal
[DE84-015472] 02 p0276 N85-11798
Robotics in nondestructive inspection at Sacramento Air Logistics Center
[AD-P004012] 03 p0309 N85-11992
Acoustic emission monitoring of fatigue in 7010 aluminum alloys
[AERE-R-11167] 03 p0334 N85-12152
Evaluation of moduli and thicknesses of pavement systems by spectral-analysis-of-surface-waves method
[PB84-219112] 03 p0342 N85-12205
Research in quantitative NDE techniques
[AD-A145990] 03 p0369 N85-12358
Technical activities 1983, Office of Nondestructive Evaluation
[PB84-217074] 03 p0370 N85-12360
Microwave measurement of the complex dielectric tensor at anisotropic slab materials
[DE84-017050] 04 p0493 N85-13144
Defect detection threshold in riveted joints, test report no.44-833/F — in aircraft 04 p0511 N85-13260
Nondestructive evaluation of residual stress in low-carbon steel
[NASA-CR-174157] 04 p0512 N85-13264
Nondestructive evaluation of residual stress in low-carbon steel, introduction 04 p0512 N85-13265
Nondestructive determination of mechanical properties — aluminum alloys 04 p0512 N85-13266
CuInSe2-based photoelectrochemical cells: Their use in characterization of thin CuInSe2 films, and as photovoltaic cells per se
[DE84-004514] 04 p0529 N85-13379
Impact of NDE unreliability on pressure vessel fracture predictions
[DE84-015586] 05 p0647 N85-14151
Measuring the corrosion rate of reinforcing steel in concrete
[PB84-244532] 06 p0770 N85-14925
Synthesis study of nondestructive testing devices for use in overlay thickness design of flexible pavements
[PB84-218080] 06 p0774 N85-14950
Pulse-echo method for flaw detection in concrete
[PB84-234509] 06 p0775 N85-14953
Nondestructive deceleration of a rocket sled — target penetration tests
[FOA-C-20548-D3] 07 p0912 N85-15771
Gallium arsenide compounds tested nondestructively with X-rays 07 p0936 N85-15934
A narrow band pulsed eddy current instrument for materials testing
[AERE-R-11229] 07 p0968 N85-16149
Comparison of the sensitivities of ultrasonic, radiographic and acoustic emission test methods for the examination of a thick weld
[BLL-RISLEY-TR-4547-(9091.9F)]
07 p0975 N85-16194
Nondestructive inspection: Improved capabilities of technicians
[AD-A147388] 07 p0975 N85-16196
Nondestructive tests and fracture mechanics investigations in the Component Integrity Research Programme
[BLL-RISLEY-TR-4541-(9091.9F)]
07 p0976 N85-16199
Nondestructive measurement of bulk residual stresses
[AD-A147063] 07 p0978 N85-16211
Ultrasonic measurements, X-ray photographs and image processing
[BLL-RISLEY-TR-4586-(9091.9F)]
07 p1037 N85-16583
Proceedings of the 2nd Workshop on Nondestructive Evaluation (NDE) of Titanium Alloys
[AD-A147626] 08 p1125 N85-17095
NDE (Nondestructive Evaluation) of oxygen contaminated titanium alloys and weldments
[AD-P004121] 08 p1126 N85-17096
Effects of oxygen-contamination-induced microstructural changes on the reverberation of ultrasound in Ti-6211 alloys
[AD-P004124] 08 p1126 N85-17099
Acoustical characterization of Ti-6211 weldments and oxygen contamination Ti-6211 plate
[AD-P004125] 08 p1126 N85-17100

Feasibility study to demonstrate detection of low levels of oxygen contaminant in titanium using eddy current and ultrasonic NDE (Nondestructive Evaluation) techniques
[AD-P004129] 06 p1127 N85-17104
Electromagnetic NDE of interstitial contamination in titanium alloy weldments
[AD-P004131] 06 p1127 N85-17106
Evaluation of the thermoelectric method for determination of interstitial gases in titanium
[AD-P004132] 06 p1127 N85-17107
Measurement of oxygen contamination in titanium alloy ingots by fast neutron activation analysis
[AD-P004133] 06 p1128 N85-17108
Neutron activation analysis of titanium with oxygen contamination
[AD-P004134] 06 p1128 N85-17109
Nondestructive evaluation of titanium alloys. ESCA (Electron Spectroscopy for Chemical Analysis), ISS (Ion Scattering Spectroscopy), and SIMS (Secondary Ion Mass Spectrometry) examination of titanium alloy solid surfaces
[AD-P004135] 06 p1128 N85-17110
Ultrasonic transducers, performance variability, design, and manufacturing procedures
[AD-A148575] 06 p1158 N85-17306
Research on nondestructive testing
[AD-A148375] 06 p1171 N85-17380
Exploratory development of advanced surface flaw detection methods
[AD-A148757] 09 p1281 N85-18060
Evaluation of laterally loaded laminated glass units by theory and experiment
[PB85-111532/GAR] 09 p1300 N85-18166
Nondestructive characterization of semiconductor surfaces and interfaces 09 p1329 N85-18349
Experimental verification of eddy-current flaw theory
[DE85-001288] 09 p1329 N85-18350
Emerging technology of synthetic aperture focusing for ultrasonic testing
[DE85-000373] 09 p1378 N85-18664
Develop and demonstrate manufacturing processes for fabricating graphite filament reinforced polymide (Gr/PI) composite structural elements
[NASA-CR-172497] 11 p1592 N85-20019
Insulation bonding test system
[NASA-CASE-MFS-25862-1] 11 p1610 N85-20126
Method and apparatus for measuring minority carrier lifetime in a direct band-gap semiconductor
[NASA-CASE-NPO-163371-1] 11 p1628 N85-20251
NDE for heat engine ceramics
[NASA-TM-86949] 11 p1649 N85-20389
Stress waves in an isotropic elastic plate excited by a circular transducer
[NASA-CR-3877] 11 p1650 N85-20390
Infrared-thermal wave scanner for NDE of naval thermal spray coatings
[DE85-002237] 11 p1650 N85-20391
Application of hysteresis modelling to the non-destructive inspection of stress
[DE85-003081] 11 p1650 N85-20393
Aerostructure nondestructive evaluation by thermal field detection. Phase 2: Technique refinement and quantitative determination of flaw detection capabilities
[AD-A149622] 12 p1777 N85-21155
Quantitative non-destructive evaluation of damage in composite materials using transmitted and reflected ultrasound
[NASA-CR-175550] 12 p1796 N85-21269
Method and apparatus for mapping the distribution of chemical elements in an extended medium
[NASA-CASE-GSC-12808-1] 12 p1798 N85-21279
The role of dislocations in ultrasonic attenuation
[AERE-R-11384] 12 p1804 N85-21317
Nondestructive testing of stainless steel to improve quality and output efficiency of the processing of ingot and continuous casting
[BMFT-FB-T-84-240] 12 p1808 N85-21345
Eddy current test probe with circumferential segments and method of testing material surrounding fastener holes
[AD-D011554] 12 p1850 N85-21603
A new NDE (Non-Destructive Evaluation) capability for thin-shelled structures
[AD-A149625] 12 p1862 N85-21678
Nondestructive method for detecting machine damage in beryllium
[DE85-001074] 12 p1862 N85-21681
Defect characterisation and monitoring by acoustic emission
[AERE-R-11409] 12 p1863 N85-21683
The measurement of residual stresses using ultrasonics
[AERE-R-11415] 12 p1868 N85-21722
Investigation of steel structures using ultrasonic waves
[BR0/8258] 13 p2101 N85-22691
Magnetic field interactions with material discontinuities
[AD-A150197] 13 p2154 N85-23373
Mini-Seminar on Non-Destructive Testing
[CSIR-TSD-0009/83] 14 p2316 N85-24308
Status of the U.K. N.D.T. industry today
14 p2316 N85-24309
Ultrasonic non-destructive testing technique
14 p2316 N85-24313
Applications of eddy currents
14 p2316 N85-24315
Flash radiography 14 p2317 N85-24316
New developments in industrial radiography
14 p2317 N85-24317
Acoustic emission of semiconductor devices
15 p2529 N85-25593
Nondestructive equipment study
[NASA-CR-171865] 15 p2571 N85-25853
Laser-based non-destructive testing techniques for the ultrasonic characterization of sub-surface flaws
[AERE-R-11562] 15 p2572 N85-25856
System for NDH of thermal spray coating bonds
[DE85-007463] 15 p2572 N85-25858
Spectral reflectance of carbonate minerals and rocks in the visible and near infrared (0.35 - 2.55 microns) and its applications in carbonate petrology
[NASA-CR-175763] 15 p2591 N85-25973
An electro-optic spatial light modulator for thermoelastic generation of programmably focused ultrasound
[AD-A152066] 15 p2646 N85-26323
Ultrasonic characterization of porosity: Theory
[DE85-005922] 15 p2646 N85-26325
Optical monitoring of photo-acoustic pulse propagation in silicon wafers
[AD-A151333] 15 p2651 N85-26352
Nondestructive tests of ceramic components for aircraft turbines 16 p2709 N85-26718
Initial quality of advanced joining concepts
[AD-A152241] 16 p2759 N85-27027
Echo-response from crack-like two-dimensional reflectors in focused ultrasonic fields. Ultrasonic crack tip method for the determination of crack depth
[BLL-BISI-22062-(9022.06)] 16 p2796 N85-27236
Structural Integrity and Durability of Reusable Space Propulsion Systems
[NASA-CP-2381] 17 p2910 N85-27941
Differential between crack and pseudo-crack indications by means of objective magnetic flux leakage testing
[BLL-BISI-TRANS-22033-(9022.06)]
17 p2976 N85-28386
Non-destructive testing of HF-welded pipe
[BLL-BISI-TRANS-22182-(9022.06)]
17 p2976 N85-28388
Detecting and analyzing crack defects
[BLL-BISI-TRANS-22062-(9022.06)]
17 p3027 N85-28723
Echo-response from crack-like two-dimensional reflectors in focused ultrasonic fields
17 p3027 N85-28724
Compact L-edge densitometer for uranium concentration assay
[DE85-010344] 18 p3110 N85-29261
Investigation on the application of the pulsed eddy current method of non-destructive testing using controlled signals (CS-technique)
[BLL-BISI-TRANS-22249-(9022.06)]
18 p3119 N85-29303
Ultrasonic testing of plates containing edge cracks
[NASA-CR-3904] 18 p3119 N85-29307
A study of the stress wave factor technique for the characterization of composite materials
[NASA-CR-174870] 19 p3231 N85-30035
Apparatus for non-destructive inspection of blind holes
[AD-D011707] 19 p3273 N85-30295
Optical beam deflection detection of thermal waves in opaque solids 19 p3374 N85-30927
Production verification of the acoustic emission weld monitor
[AD-A154168] 20 p3464 N85-31519
Description of an holographic interferometry nondestructive test installation: Application to bond tests
[SNIAS-851-430-101] 20 p3464 N85-31521
Philosophy of nondestructive control in aeronautics quality control. Knowledge of and improvements to nondestructive test safety
[SNIAS-851-551-101] 20 p3465 N85-31522
Modifications of flight-by-flight load sequences to provide for good fracture surface readability
[NLR-MP-84012-U] 20 p3472 N85-31577
NBS (National Bureau of Standards) reactor: Summary of activities Jul. 1983 through Jun. 1984
[PB85-184836] 20 p3522 N85-31907
Solid-state track recorder neutron dosimetry in the Three-Mile Island Unit-2 reactor cavity
[DE85-011360] 20 p3531 N85-31966
Experimental and theoretical assessment of a new technique for the non-destructive evaluation of laminated panels
[AD-A155622] 21 p3562 N85-32
Reliability of void detection in structural ceramics using scanning laser acoustic microscopy
[NASA-TM-87035] 21 p3597 N85-32
Acoustic emission during transformation of austenite in 38KhN3MF steel
[BLL-M-35825-(5828.4)] 23 p3914 N85-34
Quantitative non-destructive evaluation of composite materials based on ultrasonic wave propagation
[NASA-CR-176176] 24 p4074 N85-35
Ultrasonic inspection of carbon fiber reinforced plastic by means of sample-recognition methods
[NASA-TM-77896] 24 p4074 N85-35
Methods for nondestructive tests of CFRP laminates
24 p4074 N85-35
Fatigue damage detection in steels by optical correlation
[AD-A155830] 24 p4079 N85-35
Subcritical fracture propagation in rocks: An examination using the methods of fracture mechanics and non-destructive testing 24 p4116 N85-35
NONEQUILIBRIUM CONDITIONS
Nonequilibrium air radiation (Nequair) program: User's manual
[NASA-TM-86707] 19 p3353 N85-30
Non-equilibrium effects in turbulent diffusion flames
20 p3425 N85-31
Implicit Monte Carlo methods and non-equilibrium Marshak wave radiative transport
[DE85-010711] 22 p3835 N85-33
Calculations of heavy ion charge state distributions for nonequilibrium conditions
[SH-2.1-12] 23 p3999 N85-34
NONEQUILIBRIUM DRAG
U FRICTION DRAG
NONEQUILIBRIUM FLOW
Computation of the nonequilibrium flow in a gasdynamic laser
[AD-A141022] 04 p0505 N85-13224
Flow and plasticity via nonequilibrium molecular dynamics
[DE85-001011] 10 p1555 N85-19
Hypersonic nonequilibrium gas flow past zero-aspect wing 16 p2765 N85-27
Some amplification by relaxation processes in nitrogen and mixtures of nitrogen with helium and hydrogen
[AD-A153620] 18 p3071 N85-28
Transient three-phase three-component systems. Part 1: Formulation of the system of differential equations
[DE85-013267] 24 p4095 N85-35
NONEQUILIBRIUM IONIZATION
Non equilibrium ionization in the local hot bubble
06 p0879 N85-15
Stromgren trails of hot white dwarfs
06 p0879 N85-15
NONEQUILIBRIUM PLASMAS
Excitation of impurities by heavy particles and radiative losses of thermonuclear plasma
11 p1719 N85-20
Plasma processing of materials
[AD-A152398] 17 p3039 N85-28
NONEQUILIBRIUM RADIATION
Nonequilibrium air radiation (Nequair) program: User's manual
[NASA-TM-86707] 19 p3353 N85-30
NONEUCLIDIAN GEOMETRY
U DIFFERENTIAL GEOMETRY
NONFERROUS METALS
Testing the antifriction properties of alloys for heavily loaded bearings 06 p0780 N85-14
A computer controlled mass spectrometer system for investigating the decomposition of non-metallic materials under atmospheric conditions 12 p1946 N85-22
Rational use of tatanium in nonferrous metallurgy
13 p2031 N85-22
Inoculation of non-metallic inclusions in steel
[BLL-BISI-TRANS-22431-(9022.06)]
17 p2925 N85-28
NONFLAMMABLE MATERIALS
Flame-resistant materials for use in pyrotechnic safety clothing
[AD-A148857] 07 p0931 N85-1
(Vinyloxy)chlorocyclotriphosphazenes
[AD-D011471] 10 p1453 N85-1
High performance mixed bisimide resins and composites based thereon
[NASA-CASE-ARC-11538-1-SB]
19 p3231 N85-30
Investigation of experimental lightweight [illegible] materials for A/C engine bay applications
[AD-A155765] 24 p4062 N85-35
NONHOMOGENEITY
U INHOMOGENEITY

ONISOTHERMAL PROCESSES
A numerical solution of a nonisothermal wall using the wo-dimensional Navier-Stokes equations
[AD-A154467] 19 p3266 N85-30257
Thermomechanical deformation in the presence of metallurgical changes 20 p3466 N85-31533
ONISOTROPIC PLATES
U ANISOTROPIC PLATES
ONISOTROPY
U ANISOTROPY
ONLIFTING VEHICLES
U BALLISTIC VEHICLES
ONLINEAR EQUATIONS
NT MONGE-AMPERE EQUATION
NT NONLINEAR EVOLUTION EQUATIONS
NT QUADRATIC EQUATIONS
Quasi-Newton algorithms for large scale nonlinear systems 02 p0208 N85-11370
Inverse problems, optimization and algorithms
[AD-A145397] 02 p0250 N85-11636
Supersymmetric Yang-Mills fields as an integrable system and connections with other non-linear systems
[DE84-013231] 04 p0556 N85-13539
A lumped mass finite element method with quadrature for a nonlinear parabolic problem
[CTH-MATH-1984-22] 05 p0719 N85-14615
Trust region methods for minimization
[AD-A147073] 07 p1030 N85-16540
Self similar solutions for a degenerate Cauchy problem
[AD-A147241] 07 p1031 N85-16548
Nonlinear wave propagation
[AD-A148114] 08 p1152 N85-17269
On solving nonlinear problems of aircraft structural mechanical design 09 p1309 N85-18223
Nonlocal and nonlinear effects on solar oscillations
09 p1416 N85-18934
New methods for numerical solution of one class of strongly nonlinear partial differential equations with applications in hydrodynamics
[AD-A149026] 10 p1545 N85-19739
Hamilton-Jacobi equations in infinite dimensions. Part 1. Uniqueness of viscosity solutions
[AD-A149094] 10 p1546 N85-19749
Construction of solutions for two-dimensional Riemann problems
[DE85-003136] 10 p1549 N85-19770
Triple layer system for numerical integration of equations of gas dynamics and nonlinear heat conduction equation
[DE85-000297] 11 p1632 N85-20277
Local strain redistribution corrections for a simplified inelastic analysis procedure based on an elastic finite-element analysis
[NASA-TP-2421] 11 p1651 N85-20396
Algebraic decay in self-similar Markov chains
[DE85-003162] 11 p1707 N85-20740
Time marching numerical solution of the dynamic response of nonlinear systems
[NAF-AN-25] 12 p1865 N85-21696
Local behavior of solutions of an elliptic-parabolic equation
[AD-A149624] 12 p1920 N85-22057
A method of calculating periodic solutions of second order dynamical systems
[AD-A149634] 12 p1920 N85-22058
Nonlinear partial differential equations and related problems of Pade approximations
[AD-A149650] 12 p1920 N85-22059
Nonlinear sigma-models and integration methods
[DE85-004447] 12 p1922 N85-22071
Direct secant updates of sparse matrix factors
[DE85-004008] 12 p1922 N85-22073
Influence of internal gravity waves on F layer
14 p2338 N85-24460
Solution of coupled system of PDE by the transistorized multigrid method
[DE85-006377] 15 p2639 N85-26276
An approximation theory for nonlinear evolution equations and single conservation laws
16 p2691 N85-26614
Internal resonance in nonlinear vibrating systems
[REPT-15/1984] 16 p2797 N85-27245
A split explicit model for short-term numerical weather prediction 16 p2831 N85-27460
Fundamentals of plasma simulation
[DE85-007699] 16 p2867 N85-27683
Large scale electricity production scheduling via nonlinear optimization
[REPT-84-07] 17 p3017 N85-28655
Convergence of Newton's method for a single real equation
[NASA-TP-2489] 17 p3017 N85-28656
On the algebraic equations in implicit Runge-Kutta methods
[CWI-NM-R8413] 17 p3022 N85-28696
Coherent state description of non-topological solitons and momentum projection
[DE85-007814] 17 p3033 N85-28761
Sensitivity analysis of initial value problems with mixed ode's and algebraic equations
[AD-A153528] 18 p3169 N85-29637
Quantized Hall effect in two-dimensional electron systems
[AD-A154347] 19 p3259 N85-30211
Large deflections of a cantilever beam under arbitrarily directed tip load
[NASA-TM-86442] 19 p3264 N85-30363
Use of adjoint equations in problems of evaluating state of random hydrodynamic fields
19 p3289 N85-30398
A global low order spectral model designed for climate sensitivity studies
[NASA-CR-175999] 19 p3315 N85-30549
Perspectives of nonlinear dynamics
[IPPJ-723] 19 p3370 N85-30902
Automatic assembly of space stations
20 p3409 N85-31153
Modeling taper charge with a non-linear equation
20 p3445 N85-31390
Approximate solution to the problem of heating massive bodies by radiation
[BLL-M-36272-(5828.4)] 20 p3450 N85-31422
Construction of constraint equation for stresses and strains
[BLL-M-36239-(5828.4)] 20 p3465 N85-31524
Viscoplasticity based on overstress with a differential growth law for the equilibrium stress
20 p3466 N85-31532
Constitutive modeling of superalloy single crystals and directionally solidified materials
20 p3466 N85-31535
Non-model based estimation with applications to sensor calibration using multiple sensors
[AD-A154736] 21 p3589 N85-32306
Numerical model of a pulse combustor
[DE85-011717] 23 p3912 N85-34240
A review of spectral methods
[NASA-CR-172502] 23 p3929 N85-34350
Nonlinear flap-lag-extensional vibrations of rotating, pretwisted, preconed beams including Coriolis effects
[NASA-TM-87102] 23 p3941 N85-34427
DISPL1: A software package for one and two spatially dimensioned kinetics-diffusion problems
[ANL-84-56] 23 p3956 N85-34516
Identification and control of structures in space
[NASA-CR-176175] 24 p4069 N85-35214
Long-time asymptotics of a system for plasma diffusion
[NASA-CR-177947] 24 p4093 N85-35375
Analysis of the nonlinear equations describing the elastic, thermal, and electromagnetic behavior of solids: Existence of solutions of semi-inverse problems
24 p4100 N85-35415
NONLINEAR EVOLUTION EQUATIONS
Step-by-step stability in the numerical solution of partial differential equations
[CWI-NW-161/83] 05 p0720 N85-14623
Lax-pair operators for squared-sum and squared-difference eigenfunctions
[AD-B089083L] 09 p1386 N85-18718
Recent developments and open problems in the mathematical theory of viscoelasticity
[AD-A149043] 10 p1545 N85-19742
Nonlinear evolution of astrophysical Alfven waves
12 p1956 N85-22294
A fast implementation of explicit time stepping algorithms with the finite element method for a class of nonlinear evolution problems
[REPT-84-03] 17 p3021 N85-28686
Spectral transform approach to Backlund transformations
[PREPRINT-420] 18 p3172 N85-29663
Reduction techniques for infinite-dimensional Hamiltonian systems: Some ideas and applications
[PREPRINT-424] 18 p3173 N85-29666
NONLINEAR FEEDBACK
Optimal open loop and nonlinear feedback control for remote orbital capture
[AD-A151967] 16 p2732 N85-26859
NONLINEAR FILTERS
Numerical studies in nonlinear filtering
[TWISK-306] 01 p0108 N85-10729
Microprocessor implementation of algorithms of nonlinear filtration 04 p0486 N85-13104
A nonlinear filter for compensating for time delays in manual control systems 05 p0700 N85-14493
Numerical methods and approximation and modelling problems in stochastic control theory
[AD-A146827] 07 p1029 N85-16533
Digital imaging processing
[INPE-3325-PRE/624] 11 p1701 N85-20696
Synthesis of optimum receiver and processor for signal packet of radio pulses 12 p1839 N85-21541
Prefiltration in Kalman filter with a priori indeterminacy
13 p2071 N85-22939
Assessment of a nonlinear method of INS alignment — inertial navigation systems (INS)
[BAE-BT-12684] 15 p2466 N85-25233
Theory and Applications of State Estimation. NRIMS Summer Seminar Series
[CSIR-SWISK-37] 15 p2635 N85-26244
Nonlinear estimation 15 p2635 N85-26245
Truncated nonlinear filters 15 p2635 N85-26249
Recursive nonlinear filtering through complete linearization
[AD-A155029] 21 p3677 N85-32844
Comprehensive radio direction finder with electronically stabilized radiation pattern 22 p3762 N85-33318
Optimal complex nonlinear processing of continuous and pulsed signals 22 p3763 N85-33323
Nonlinear filtration of clutter 22 p3777 N85-33404
NONLINEAR OPTICS
Self-induced nonlinear effects in optical fibers: A unified approach
[FUB-67-1982] 09 p1385 N85-18713
Chaos and order in an optical ring cavity
[CWI-AM-R8416] 17 p3038 N85-28795
Optically nonlinear and bistable behaviour of direct gap semiconductors 18 p3186 N85-29759
An experimental nonlinear optical waveguide device
18 p3186 N85-29762
Prospects for parallel nonlinear optical signal processing using GaAs etalons and ZnS interference filters
18 p3187 N85-29765
Applications and investigations of second harmonic generation 19 p3367 N85-30878
Edge detection and geometric methods in computer vision
[AD-A155873] 24 p4135 N85-35630
NONLINEAR PROGRAMMING
Composite laminate optimization program suitable for microcomputers 01 p0059 N85-10369
ADS: A FORTRAN program for automated design synthesis, version 1.00
[NASA-CR-172460] 01 p0102 N85-10684
A sequential quadratic programming algorithm for solving large, sparse nonlinear programs
[AD-A145854] 03 p0407 N85-12597
Optimization of moving-target selection radar devices for nonGaussian signals for stationary targets
06 p0789 N85-15043
Generalized convex functions: Properties, optimality and duality
[DE85-001553] 09 p1376 N85-18652
Large scale electricity production scheduling via nonlinear optimization
[REPT-84-07] 17 p3017 N85-28655
Recent developments in nonlinear normal mode initialization 18 p3142 N85-29451
Computable numerical bounds for Lagrange multipliers of stationary points of nonconvex differentiable nonlinear programs
[AD-A153513] 18 p3169 N85-29633
Expected utility, penalty functions, and duality in stochastic nonlinear programming, revised
[AD-A154034] 19 p3335 N85-30660
User's manual of the BNDSCO computer program for solving constrained optimal control problems
[DFVLR-MITT-85-05] 20 p3516 N85-31865
Local epi-continuity and local optimization
[AD-A154812] 21 p3677 N85-32843
Optimization of design parameters for alternating current stabilizer based on magnetic suspension
22 p3772 N85-33374
Model building and practical aspects of nonlinear programming
[AD-A155720] 22 p3829 N85-33711
NONLINEAR SYSTEMS
Non-Gaussian approach for parametric random vibration of non-linear structures 01 p0060 N85-10396
Development of advanced constitutive model for reinforced concrete
[AD-A145050] 01 p0062 N85-10411
Determination of the input-output characteristics of time-invariant memoryless nonlinear devices
[FUB-41-1983] 01 p0100 N85-10667
Time invariant memoryless nonlinear systems identification method
[FUB-9-1983] 01 p0114 N85-10773
Aeroelastic stability analysis with interacting structural nonlinearities 02 p0207 N85-11364
Linear and bilinear infinite-dimensional representations of finite-dimensional nonlinear systems
[RR-259] 02 p0254 N85-11681
Nonlinear acoustics
[AD-A145580] 02 p0276 N85-11796

N-frequency quasiperiodicity and chaos in dissipative dynamical systems 02 p0282 N85-11840

Nonlinear system identification methodology development based on F-4S flight test data analysis
[AD-A146289] 03 p0318 N85-12053

Forced oscillations theory for resonant extended interaction electron devices
[PR-206] 03 p0358 N85-12298

Non-linear systems in infinite dimensional state spaces
[AD-A145828] 03 p0410 N85-12623

Filtering and prediction performance for a class of systems with uncertain parameters
[AD-A146145] 03 p0411 N85-12630

Formulation and solution methods for classical problems of static buckling
[CETIM-101010] 04 p0514 N85-13280

Nonlinear deformation and static linear buckling of structures under pressure
[CETIM-11-E-350] 04 p0514 N85-13281

Fly's eye sensor nonlinear signal processing
[AD-D011290] 05 p0729 N85-14684

Iterative method of calculating strength of airframe members using finite element method
06 p0775 N85-14955

Techniques for nonlinear random vibration problems
07 p0977 N85-16201

Nonlinear ultrasonic characterization of oxygen impurities in titanium
[AD-P004123] 08 p1126 N85-17098

EMC (Electromagnetic compatibility) spec criteria in Volterra systems
[AD-A147659] 08 p1151 N85-17263

On a general nonlinear theory of plates and shells: Formulation and applications 08 p1172 N85-17387

A nonlinear technique for high-resolution data processing
[AD-D011415] 08 p1203 N85-17570

On the global asymptotic stabilization of nonlinear systems
[PREPRINT-838] 08 p1209 N85-17604

The practical identification of systems with nonlinearities
[RR-264] 08 p1209 N85-17607

Use of iterative linear and nonlinear algebraic methods for solving large stiff systems of ODEs
[AD-A148516] 08 p1213 N85-17636

Research in stochastic processes
[AD-A148622] 08 p1216 N85-17660

Nonlinear real-time optical signal processing
[AD-A148293] 08 p1222 N85-17699

Nonlinear analysis of composite laminates
09 p1268 N85-18087

Modal analysis of structural systems involving nonlinear coupling 09 p1337 N85-18409

A program design for an adaptive, non-linear finite element solver
[AD-A148880] 10 p1539 N85-19705

On the application of compatibility checking techniques to dynamic flight test data
[ARL/AERO-R-161] 12 p1776 N85-21151

Time marching numerical solution of the dynamic response of nonlinear systems
[NAF-AN-25] 12 p1865 N85-21696

Nonlinear rotordynamics analysis
[NASA-CR-171425] 13 p1968 N85-22364

Nonlinear interactions between vortices and acoustic waves in a rocket combustion chamber
13 p1999 N85-22533

A model for large sparse contingency tables
[AD-A150320] 13 p2151 N85-23350

Investigation of the time history and modal responses of some simple linear and nonlinear systems
[DE85-002027] 14 p2321 N85-24344

System theoretic description of physical systems
[CWI-TRACT-3] 14 p2414 N85-24894

Statistical techniques for signal processing
[AD-A151231] 15 p2541 N85-25690

Effect of internal pressure on flexibility and stress intensification factors for pipe elbows analyzed by the finite element method
[AD-A151161] 15 p2578 N85-25901

Computer program TRAMP: Inclusion of state space facilities and the analysis of non-linear elements
[BAE-BT-12643] 15 p2626 N85-26181

Application of CFD techniques toward the validation of nonlinear aerodynamic models
[NASA-TM-86715] 16 p2700 N85-26671

Alternatives for jet engine control
[NASA-CR-175831] 16 p2709 N85-26713

Alternatives for jet engine control
[NASA-CR-175832] 16 p2709 N85-26714

Alternatives for jet engine control
[NASA-CR-175833] 16 p2709 N85-26715

Observations, theoretical ideas and modeling of turbulent flows: Past, present and future
[NASA-TM-86679] 16 p2782 N85-27167

An analytical investigation of dynamic coupling in nonlinear, geared rotor systems
16 p2792 N85-27218

Numerical methods for stiff ordinary and elliptic partial differential equations
[AD-A153247] 17 p3020 N85-28675

Scalar modal control of a nonlinear system using time varying gain
[AD-A153252] 17 p3020 N85-28676

Estimating random integrals from noisy observations: Sampling designs and their performance
[AD-A152926] 17 p3025 N85-28702

Evaluation of a fault tolerant system for an integrated avionics sensor configuration with TSRV flight data
[NASA-CR-172589] 18 p3062 N85-28941

A numerical study of the Pacific polar low
[AD-A153777] 18 p3149 N85-29495

On design of off-axis specimens
[AD-A154328] 19 p3286 N85-30379

Excitation of turbulence by density waves
[NASA-CR-3905] 19 p3314 N85-30546

Sub-optimal control of nonlinear flexible space structures 20 p3414 N85-31190

A nonlinear dual-adaptive control strategy for identification and control of flexible structures
20 p3416 N85-31203

A theoretical model for the study of nonlinear dynamics of magnetic bearings 20 p3462 N85-31505

Dynamical study of flat plates by nonlinear elasticity theory
[STN-8] 20 p3471 N85-31572

On the equivalent bilinearization of nonlinear controlled delay systems
[RR-272] 20 p3519 N85-31880

An overview of nonlinear systems identification
[RR-271] 20 p3520 N85-31894

Aerodynamic characteristics of the standard dynamics model in coning motion at Mach 0.6
[NASA-TM-86717] 21 p3552 N85-32094

On the dependence of the convergence of Gummel's algorithm on the regularity of the solution
[AD-A154628] 21 p3675 N85-32832

Theory of soliton waves
[AD-A154784] 21 p3676 N85-32837

The application of bispectral analyses to aeroelastic phenomena 24 p4060 N85-35157

NONLINEARITY

Nonlinear propagation in a depth-dependent ocean
[AD-A145079] 01 p0116 N85-10791

Nonlinear oscillations of 2 body system relative to center of mass in elliptical orbit 02 p0159 N85-11082

Optimal nonlinear feedback control of spacecraft attitude maneuvers 02 p0167 N85-11126

Determination of nonlinear viscoelasticity parameters for polymeric and composite materials by numerical methods
[AD-A145311] 02 p0185 N85-11240

A nonlinear theory for gyro-devices
[AD-A145297] 02 p0200 N85-11333

Model for non-linear crack growth prediction, taking load sequence (LOSEQ) effects into consideration
[BLL-RAE-TRANS-2114-(5207)]
02 p0208 N85-11371

Weak shocks and steady waves in a nonlinear elastic rod or granular material
[AD-A145715] 02 p0209 N85-11383

Statistical Plasma Physics. Proceedings of the Workshop of the US-Japan Joint Institute for Fusion Theory Program
[IPPJ-689] 02 p0282 N85-11832

Stochasticity and transport in Hamiltonian systems
02 p0282 N85-11836

Pulsed neodymium glass laser system for investigating nonlinear optical phenomena in gases
03 p0348 N85-12241

Self-study manual on optical radiation measurements. Part 1: Concepts. Chapter 11: Linearity considerations and calibrations
[PB84-218346] 03 p0421 N85-12690

Simulation of a transmission circuit composed of slightly nonlinear elements. Computation of the intermodulation on signals composed of N carriers
[CNES-NT-105] 04 p0496 N85-13167

Numerical improvement of asymptotic solutions and nonlinear shell analysis 05 p0648 N85-14156

PROGRAM VSAERO: A computer program for calculating the non-linear aerodynamic characteristics of arbitrary configurations: User's manual
[NASA-CR-166476] 06 p0749 N85-14802

Perceptibility of nonlinear distortions in power amplifier
06 p0789 N85-15041

Supersonic nonlinear potential analysis
[NASA-CR-172456] 07 p0897 N85-15685

An investigation of vortex-induced aerodynamic characteristics of supersonic cruise configurations
[NASA-CR-174299] 07 p0898 N85-1

Nonlinear semigroups and evolution governed by accretive operators
[AD-A147556] 07 p1033 N85-1

Nonlinear optical studies of rydberg atoms using degenerate four-wave mixing
[AD-A146827] 07 p1043 N85-1

Prediction of dynamic stall characteristics using advanced non-linear panel methods
[AD-A148453] 08 p1076 N85-1

The pressure deflagration limit of solid rocket propellants 08 p1117 N85-17

Nonlinear finite element analysis of elastic and elastic-plastic buckling of cylinders under complex combined loads 09 p1332 N85-18

Generation and evolution of diabatic planetary waves in continuously stratified atmosphere with Ekman dissipation 09 p1354 N85-18515

On the interaction of a sound pulse with the shear layer of an axisymmetric jet. Part 3: Nonlinear effects
[NASA-CR-172512] 09 p1378 N85-18

Magnetostatic problems in nonlinear media with hysteresis
[DE85-003701] 10 p1482 N85-19

Finite element analysis of nonlinear oscillations and flutter of shells of revolution
[AD-A149071] 10 p1496 N85-19440

Nonlinear seismology 10 p1503 N85-19482

Symmetry breaking for a class of semi-linear elliptic problems
[AD-A149093] 10 p1546 N85-19748

Modelling and residual analysis of nonlinear auto-regressive time series in exponential variables
[AD-A148047] 10 p1550 N85-19776

New approach for solving large residual nonlinear least squares problems
[DE85-002555] 11 p1707 N85-20742

Nonlinear analysis for high-temperature multilayered fiber composite structures --- turbine blades
[NASA-TM-83754] 12 p1797 N85-21273

Control of nonlinear objects 12 p1842 N85-21561

On local total strain redistribution using a simplified cyclic inelastic analysis based on an elastic solution
[NASA-TM-86913] 12 p1864 N85-21

Nonlinear analysis of layered composite plates and shells
[PB85-127161] 12 p1868 N85-21718

Mesh effects on the computation of non-linear gravity waves of arbitrary discharge
[COLL-AERON-8501] 12 p1888 N85-21

Seismic waves and dispersion relations
13 p2116 N85-23181

Bifurcation theory applied to aircraft motions
[NASA-TM-86704] 14 p2210 N85-23705

Macro for fitting nonlinear models to Poisson distributed data
[DE84-006569] 14 p2412 N85-24871

Nonlinear problems in flight dynamics involving aerodynamic bifurcations
[NASA-TM-86706] 15 p2462 N85-25

Uniqueness and stability in nonlinear elasticity and viscoelasticity
[AD-A151470] 15 p2637 N85-26

The nonlinear analysis of thick composite plates using a cubic spline function 16 p2798 N85-27

Studies of collisional and nonlinear radiative process for development of coherent UV and XUV sources
[AD-A152001] 16 p2865 N85-27670

Method of calculating separation flow of subsonic gas stream around wings 17 p2942 N85-28161

Numerical solution of one-dimensional nonlinear problems of statics for elastic beams and shells under rigid constraints 17 p2943 N85-28

How a swing behaves
[DE85-008280] 17 p3027 N85-28

Nonlinear problems in continuum mechanics
[AD-A153367] 17 p3046 N85-28

Hyperbolic phenomena in the flow of viscoelastic fluids
[AD-A153533] 18 p3099 N85-29

Nonlinear plasma reactions on the antenna impedance of high transmission power satellites
[BMFT-FB-W-84-053] 18 p3192 N85-29

The stability and dynamics of elastic structures and fluid flows
[AD-A154188] 19 p3266 N85-30

On the stability of collocated controllers in the presence or uncertain nonlinearities and other perils
20 p3416 N85-312

Basic EMC (Electromagnetic Compatibility) technology advancement for C3 systems. Volume 1B: Demodulation radio frequency interference effects in operational amplifier circuits
[AD-A154121] 20 p3440 N85-31

Nonlinear Constitutive Relations for High Temperature Application, 1984
[NASA-CP-2369] 20 p3465 N85-31530
Nonlinear analysis of an axisymmetric structure subjected to non-axisymmetric loading
20 p3468 N85-31549
Strongly nonlinear dynamics of baroclinic waves
20 p3488 N85-31681
Nonlinear dynamics: A personal perspective
[DE85-010982] 20 p3521 N85-31899
Hubble space telescope: Pointing error effects on nonlinear ball joints
[NASA-TM-86511] 20 p3545 N85-32058
New approximations and findings of theory of nonlinear acoustic beams 21 p3680 N85-32863
Toward the propagation of waves in unsteady media
21 p3683 N85-32881
Nonlinear spectroscopy
[AD-A154708] 21 p3704 N85-33010
Study of nonlinear distortion in microwave amplifiers using Schottky gate field effect transistors
22 p3780 N85-33423
Nonlinear response and failure characteristics of internally pressurized composite cylindrical panels
[NASA-CR-176148] 22 p3800 N85-33546
Application of nonlinear least squares methods to the analysis of solar spectra
[NASA-CR-176122] 22 p3816 N85-33637
Refractive indices and thermo-optic coefficients of nonlinear crystals isomorphic to KH2PO4
[DE85-012988] 22 p3847 N85-33831
Elastohydrodynamic lubrication calculations used as a tool to study scuffing
[NASA-TM-87097] 23 p3938 N85-34408
Nonlinear adhesive behavior effects in a cracked orthotropic sheet stiffened by a semi-infinite orthotropic sheet
[NASA-TM-87584] 23 p3941 N85-34426
Nonlinear digital phase-locked loops with application to Loran-C receivers 24 p4063 N85-35178
Membrane reinforcement in concrete shells: Design versus nonlinear behavior 24 p4084 N85-35312
Generation of stimulated emission in the soft X-ray range by nonlinear processes with excimer lasers
[DE85-012465] 24 p4096 N85-35403
Analysis of the nonlinear equations describing the elastic, thermal, and electromagnetic behavior of solids: Existence of solutions of semi-inverse problems
24 p4100 N85-35415
Width of nonlinear difference resonances
[DE85-013026] 24 p4148 N85-35719
The HEAO-2 Guest Investigator Program: Non-linear growth of instabilities in line-driven stellar winds
[NASA-CR-176168] 24 p4168 N85-35840
NONNEWTONIAN FLOW
A two phase flow model at the level of a narrowing section — blood flow 20 p3507 N85-31799
NONNEWTONIAN FLUIDS
Vertical channel free convection for a power law fluid with a constant heat flux
[DE84-014551] 01 p0047 N85-10311
Nonnewtonian, unsteady flow in a convergent divergent duct 20 p3456 N85-31463
NONOSCILLATORY ACTION
Uniformly high-order accurate non-oscillatory schemes, 1
[NASA-CR-175768] 16 p2853 N85-27589
NONPARAMETRIC STATISTICS
Nonparametric maximum penalized likelihood estimation of a density from arbitrarily right-censored observations
[AD-A145569] 02 p0251 N85-11644
Nonparametric analysis of Minnesota spruce and aspen tree data and LANDSAT data 07 p0984 N85-16253
Bootstrap confidence intervals
[AD-A147572] 07 p1033 N85-16559
A kernel type estimator of a quantile function from right-censored data
[AD-A148753] 09 p1374 N85-18635
Nonparametric estimation of density and hazard rate functions when samples are censored
[AD-A150946] 14 p2411 N85-24868
Generation and termination of binary decision trees for nonparametric multiclass classification
[AD-A151361] 15 p2640 N85-26283
Construction of efficient algorithms for the estimation of multivariate probability densities
[AD-A151509] 15 p2640 N85-26285
A non-parametric probability density estimator and some applications
[AD-A151653] 15 p2641 N85-26287
Confidence intervals based on interpolated order statistics
[AD-A152807] 17 p3025 N85-28701
Nonparametric renewal function estimation
[AD-A153474] 18 p3173 N85-29672
Nonparametric estimation of the probability of ruin
[AD-A153523] 18 p3174 N85-29674
A new approach to evaluate gamma-ray measurements
[OG-9.5-11] 23 p4031 N85-34988
Multidimensional analysis of data obtained in experiments with X-ray emulsion chambers and extensive air showers
[HE-3.6-2] 24 p4184 N85-35951
NONPOINT SOURCES
Algorithm for astronomical, extended source, signal-to-noise radio calculations
[NASA-TP-2396] 03 p0445 N85-12833
NONREFLECTION
U ENERGY ABSORPTION
NONRELATIVISTIC ELECTRONS
U ELECTRONS
NONRIGIDITY
U FLEXIBILITY
NONSTABILIZED OSCILLATION
Coupled acoustic and hydrodynamic wave instabilities
13 p2000 N85-22538
Nonlinear problems in flight dynamics involving aerodynamic bifurcations
[NASA-TM-86706] 15 p2462 N85-25206
NONUNIFORM FLOW
Laminar flow heat exchangers. Viscosity induced non-uniform flow
[AD-A144777] 01 p0047 N85-10307
First derivatives of flow quantities behind two-dimensional, nonuniform supersonic flow over a convex corner
[NASA-TM-86272] 08 p1077 N85-16828
Studies on the interference of wings and propeller slipstreams
[NASA-CR-175753] 15 p2463 N85-25210
Effect of nonuniform size on internal stresses in a rapid, simple shear flow of granular materials. Part 1: Two grain sizes
[AD-A154045] 19 p3285 N85-30372
NONUNIFORM MAGNETIC FIELDS
Geological reasons for change in intensity of linear magnetic anomalies of the Kursk magnetic anomaly
[NASA-TM-77824] 10 p1514 N85-19552
Fermi surface study of CeSb
[DE85-002532] 10 p1564 N85-19862
Velocity space diffusion of high energy ions induced by a lower hybrid wave in a nonuniform magnetic field
[IPPJ-714] 16 p2866 N85-27681
Electrostatic ion cyclotron instability due to a nonuniform electric field perpendicular to the external magnetic field
[AD-A155474] 21 p3707 N85-33019
NONUNIFORM PLASMAS
Diffraction of plane TM-wave on continuously irregular elliptical plasma 13 p2067 N85-22914
NONUNIFORMITY
Spectral evaluation of irregularity of superconducting coaxial cables 13 p2082 N85-23000
Gradient scaling for nonuniform meshes
[DE85-009625] 22 p3784 N85-33443
NONVISCOUS FLOW
U INVISCID FLOW
NOREPINEPHRINE
Does a 50-cycle alternating field have central nervous effects?
[BLL-CE-TRANS-8083-(9022.09)]
16 p2839 N85-27507
NORMAL DENSITY FUNCTIONS
The performance of variable sampling plans when the normal distribution is truncated
[AD-A147717] 08 p1215 N85-17649
A new method of approximating normal and t-tail areas
[AD-A149457] 10 p1548 N85-19761
Comparison of MESOI atmospheric dispersion estimates with data and estimates from other models
[DE85-002372] 11 p1678 N85-20572
Full statistical characteristics of microdeformation
[BLL-M-36076-(5828.4)] 16 p2798 N85-27254
Analysis and model/data comparisons of large-scale releases of nitrogen tetroxide
[DE85-008989] 18 p3133 N85-29406
A robust estimator of location using an adaptive spline model
[AD-A153662] 18 p3174 N85-29676
Bayesian inference and diagnostics for the 3 parameter logistic model
[AD-A153840] 18 p3175 N85-29681
Evaluation of densities and distributions via hermite and generalized laguerre series employing high-order expansion coefficients determined recursively via moments or cumulants
[AD-A153950] 18 p3175 N85-29682
Decay of a coherent scalar disturbance in a turbulent flow
[NASA-TM-86700] 19 p3264 N85-30244
Bayesian factor analysis
[AD-A154184] 19 p3347 N85-30747
Comments on estimating quantiles for Gaussian functionals by simulation
[AD-A154302] 19 p3348 N85-30750
The distribution of the number of empty cells in a generalized random allocation scheme
[AD-A154806] 21 p3677 N85-32841
The dispersive evolution of charged-particle bunches in random magnetic fields
[SH-4.1-2] 23 p4004 N85-34828
On the statistical significance of excess events: Remarks of caution and the need for a standard method of calculation
[OG-9.5-10] 23 p4031 N85-34987
Large deviations for the maxima of some random fields
[AD-A155909] 24 p4143 N85-35681
NORMAL DISTRIBUTIONS
U NORMAL DENSITY FUNCTIONS
NORMAL FORCE DISTRIBUTION
U FORCE DISTRIBUTION
NORMAL SHOCK WAVES
Effect of the Basset term on particle relaxation behind normal shock waves
[AD-A145446] 02 p0196 N85-11320
Dispersion curves for normal waves in cylindrical shell and conditions for spatial coincidence in vicinity of critical frequencies 06 p0778 N85-14973
Calculation of an unsteady transonic flow with shock waves and separation in Laval nozzles
[MPIS-14/1984] 14 p2213 N85-23728
Parallel fast-forward shock within 1 AU: Helios-1 and 2 observations
[MPAE-W-79-84-27] 24 p4169 N85-35847
NORMALITY
More limit theory for the sample correlation function of moving averages
[AD-A148975] 10 p1550 N85-19773
NORMALIZING (STATISTICS)
Renormalization theory in four dimensional scalar fields
[NOTA-INTERNA-824] 02 p0292 N85-11895
Probability distribution density of normalized radar range 04 p0485 N85-13098
Development of computer aided database design and maintenance tools
[AD-A151782] 16 p2845 N85-27537
The distribution and dynamics of planetary nebulae in M32 and the Andromeda Galaxy
20 p3546 N85-32068
NORMS
On the distribution of integral and prime divisors with equal norms 11 p1698 N85-20669
A variable-complexity norm maximization problem
[AD-A153514] 18 p3169 N85-29634
Dosimetry and limit values for internal contamination with radionuclides: From (International Commission on Radioactive Protection) ICRP-2 to ICRP-30
[IRI-190-84-03] 20 p3507 N85-31804
NORTH AMERICA
Tectonic history of a continent: Island arc boundary, west-central Idaho 05 p0673 N85-14324
Simulating responses to expected climate change in eastern North America: Applications to decision-making in the forest industry
[DE85-001272] 07 p1008 N85-16406
North American vegetation patterns observed with the NOAA-7 advanced very high resolution radiometer — North America
[E85-10062] 08 p1174 N85-17400
Monthly and seasonal weather outlook for January 1985, volume 39, number 1
[PB85-148799] 12 p1898 N85-21915
Arctic-North Atlantic rift megasystem
13 p2105 N85-23117
El Nino, the capricious child 13 p2106 N85-23121
Acid precipitation in North America: 1980, 1981 and 1982 annual data summaries from acid deposition system data base
[PB85-162477] 16 p2822 N85-27410
Monthly and seasonal weather outlook for mid-January to mid-February 1985, volume 39, number 2, January 15, 1985
[PB85-164572] 16 p2837 N85-27500
Monthly and seasonal weather outlook for February 1985, volume 39, number 3, January 30, 1985
[PB85-159424] 16 p2838 N85-27502
Monthly and seasonal weather outlook for mid-February to mid-March 1985, volume 39, number 4, February 14, 1985
[PB85-164580] 18 p3149 N85-29500
Use of 121.5/243.0 MHz COSPAS-SARSAT data by North American SAR agencies — search and rescue (SAR) 20 p3405 N85-31127

NORTH AMERICAN AIRCRAFT
NT B-1 AIRCRAFT
NT B-70 AIRCRAFT
NT X-15 AIRCRAFT
NORTH ATLANTIC TREATY ORGANIZATION (NATO)
Hazard Studies for Solid Propellant Rocket Motors
[AGARD-CP-367] 08 p1114 N85-17025
Aims and requirements of NATO group AC/310
08 p1114 N85-17026
NORTH CAROLINA
Environmental geologic atlas of the North Carolina coastal zone: Dare, Hyde, Tyrrell and Washington Counties
[PB84-222975] 01 p0066 N85-10439
Revised Uniform Summary of Surface Weather Observations (RUSSWO). Pope AFB, Fayetteville, North Caroline, parts A-F
[AD-A146918] 07 p1005 N85-16369
Control technology for fiber reinforced plastics industry at AMF Hatteras Yachts, New Bern Division, New Bern, North Caroline
[PB85-109015] 10 p1460 N85-19198
Investigation of radiometric properties of LANDSAT-4 MSS — California, North Carolina, South Carolina, and New England 11 p1686 N85-20500
NORTH DAKOTA
Geothermal resource assessment for North Dakota
[DE84-016128] 04 p0526 N85-13367
NORTH POLAR SPUR (ASTRONOMY)
The nature of the soft X-ray emitting region in the direction of the North Polar spur
06 p0877 N85-15568
Excess gamma rays from the Loop I supernova remnant
[OG-3.1-10] 22 p3874 N85-33998
NORTH SEA
Effects of the oceans on polar motion: Continued investigations
[E85-10037] 03 p0379 N85-12416
Impact of ERS-1 observations on wave forecasting in the North Sea 03 p0381 N85-12437
Determination of the altimetric geoid and gravity anomalies in the North Sea: Implications for a solution of the general circulation problem using ERS-1 data
03 p0382 N85-12446
The structure of the Iceland-Faeroe ridge, derived from geophysical measurements
[DRIC-T-7255] 03 p0397 N85-12535
Measurements on the diffusion of hydrogen chloride in the waste gas plume of incineration ships in the North Sea. Part 1: Methodology, instrumentation and presentation of data
[GKSS-84-E-23-PT-1] 05 p0672 N85-14319
Intrusion of radioactive industrially polluted water from North Sea into central Baltic Sea
10 p1498 N85-19454
NORTHERN HEMISPHERE
NT ARCTIC REGIONS
Climate of the Northern Hemisphere, 1851 - 1900 compared to contemporary climate
[DE84-016368] 04 p0539 N85-13426
Interannual variations of the winter circulation in the Northern Hemisphere and in the southern oscillation (meridian) and their possible connections with the climate of Northeast Brazil
[INPE-3333-TDL/182] 10 p1519 N85-19573
Middle Atmosphere Program. Handbook for MAP, volume 5
[NASA-CR-175481] 11 p1656 N85-20434
A catalogue of dynamic parameters describing the variability of the middle stratosphere during the northern winters 11 p1656 N85-20435
Middle Atmosphere Program. Handbook for MAP, volume 7
[NASA-CR-175479] 11 p1656 N85-20437
Workshop on Comparison of Data and Derived Dynamical Quantities During Northern Hemisphere (PMP-1) Winters 11 p1657 N85-20444
Middle Atmosphere Program. Handbook for MAP. Volume 12: Coordinated Study of the Behavior of the Middle Atmosphere in Winter (PMP-1) Workshops
[NASA-CR-175475] 11 p1665 N85-20492
The 500 millibar sign frequency teleconnection charts: Fall
[PB85-110930] 11 p1687 N85-20612
The 500 millibar sign frequency teleconnection charts: Summer
[PB85-111359] 11 p1688 N85-20613
The 500 millibar sign frequency teleconnection charts: Spring
[PB85-111367] 11 p1688 N85-20614
A new NASA/MSFC mission analysis global cloud cover data base
[NASA-TP-2448] 12 p1893 N85-21878
Moisture variation in northern hemisphere temperate latitudes 13 p2105 N85-23119
Optimization of system for observing Northern Hemisphere atmospheric pressure field
15 p2485 N85-25338
Numerical simulation of North Atlantic Sea ice variability, 1951 - 1980 15 p2603 N85-26040
Climatic impact of a change in North Atlantic Deep Water formation 15 p2603 N85-26045
Full shadow phenomenon in Earth's upper atmosphere 16 p2608 N85-27316
A climatic data bank for Northern Hemisphere land areas, 1851-1980
[DE85-007863] 16 p2635 N85-27486
The contrasting Northern Hemisphere winters of 1980-81 and 1981-82 18 p3144 N85-29468
On the global distribution of three-dimensional Eliassen-Palm fluxes by stationary waves
18 p3145 N85-29469
Transient eddies in the UCLA GCM
18 p3145 N85-29470
Troposphere-stratosphere (surface-55 km) monthly general circulation statistics for the Northern Hemisphere-four year averages
[NASA-TM-86182] 20 p3495 N85-31730
All sky Northern Hemisphere 10(15) EV gamma-ray survey
[OG-2.6-3] 22 p3870 N85-33968
NORTHERN SKY
The structure of galactic HI in directions of low total column density
[NASA-CR-175709] 16 p2882 N85-27785
All sky Northern Hemisphere 10(15) EV gamma-ray survey
[OG-2.6-3] 22 p3870 N85-33968
NORTHROP AIRCRAFT
NT F-18 AIRCRAFT
NORWAY
Space research in Norway
[SAD-110-T] 03 p0321 N85-12072
Deployment of a regional array in Norway
[AD-A147032] 07 p0997 N85-16330
Finnair, LOT, SAS reps in USSR on present operations, plans 09 p1278 N85-18035
The national Search and Rescue (SAR) needs and organization in Norway 20 p3401 N85-31099
The COSPAS/SARSAT local user terminal in Tromso, Norway. Special considerations and experience with high latitude location (69 deg, 43 min N)
20 p3402 N85-31109
The COSPAS-SARSAT system evaluation in Norway
20 p3406 N85-31133
NOSE
Re-design of ARL/HLF (Heated Laminar Flow) body nose region
[AD-A150063] 12 p1846 N85-21585
NOSE CAPS
U NOSE CONES
NOSE CONES
Laminar heat-transfer distributions on biconics at incidence in hypersonic-hypervelocity flows
[NASA-TP-2213] 07 p0957 N85-16065
Structure of SYLDA double launch system for Ariane
17 p2946 N85-28185
Applied research and development for falling-sphere air density measuring systems
[AD-A155227] 21 p3552 N85-32099
The development of staging mechanisms for the Japanese satellite launcher Mu-3SII
22 p3798 N85-33528
NOSE FINS
Wind tunnel tests on a tube-launched missile configuration with a deflectable nose control and a novel wrap-around fin stabiliser
[AR-003-696] 01 p0001 N85-10003
NOSES (FOREBODIES)
NT NOSE CONES
Automated radome testing
[AD-P004362] 12 p1826 N85-21456
Development of the F-20 nose radome
[AD-P004374] 12 p1827 N85-21468
Nose and inlet duct radomes for the firebolt aerial target
[AD-P004375] 12 p1827 N85-21469
Transonic merging separated flows
[AD-A150667] 14 p2213 N85-23724
Development of a fuselage forward section in Carbon Fiber Reinforced Plastic (CFRP) type of construction
[MBB/LFA34/CFK/PUB/006] 17 p2895 N85-27851
Wind tunnel drag evaluations of helicopter nose sections
[AD-A155489] 21 p3553 N85-32100
NOTATION
U CODING
NOTCH SENSITIVITY
The effect of notch acuity on the fracture toughness of silicon carbide/aluminum metal matrix composites
[AD-A150970] 14 p2248 N85-23936
Creep-fatigue interaction of notched 304 stainless steel bars 16 p2798 N85-2724
Initiation, growth and coalescence of small fatigue cracks
[AD-A151799] 16 p2800 N85-2725
NOTCH STRENGTH
Preliminary report on tests of tensile specimens with a part-through surface notch for a filament wound graphite/epoxy material
[NASA-CR-172545] 10 p1431 N85-1903
Tendency of selected low-carbon steels to corrosion cracking in nitrates
[BLL-BISI-TRANS-22262-(9022.06)]
18 p3073 N85-2900
Finite element analysis of notch behavior using a state variable constitutive equation 20 p3468 N85-3154
Damage mechanisms in damaged CFRP laminates
24 p4074 N85-3524
NOTCH TESTS
NT CHARPY IMPACT TEST
A discussion of problems encountered in the dynamic fracture toughness testing of materials
[OUEL-1524/84] 06 p1173 N85-1778
Effect of tempering on the strength and toughness of 2 1/4 Cr-1 Mo steel weldments
[DE85-003818] 09 p1296 N85-1814
Finite element analysis of notch behavior using a state variable constitutive equation 20 p3468 N85-3154
Effect of strain rate on the initial failure of notched GRP laminates 23 p3908 N85-3421
NOTCHED METALS
U NOTCH TESTS
NOTCHES
Weldability of micro-alloy steels as reaction of structure and inclusions
[BLL-BISI-TRANS-22196-(9022.06)]
17 p2924 N85-2802
NOVA LASER SYSTEM
Modal testing and analysis of NOVA laser structures
[DE84-017569] 11 p1636 N85-2032
Technical and historical overview of the study at Lawrence of porous antireflection coatings
[DE85-010925] 20 p3434 N85-3130
NOVAE
NT DWARF NOVAE
NT HERCULES NOVA
The abundances of the elements -carbon to silicon- in Nova Corona Austrina 1981 11 p1753 N85-21024
Hydrodynamic simulations of recurrent novae
11 p1753 N85-21025
Strong earthquakes, novae and cosmic ray environment
[SH-10.1-3] 23 p4053 N85-3513
NOWCASTING
Nowcasting 2. Mesoscale Observations and Very-Short-Range Weather Forecasting — conference
[ESA-SP-208] 01 p0073 N85-10487
On the nowcasting of mountain-generated thunderstorm systems 01 p0074 N85-10489
Generation of deep convective clouds along mesoscale storm outflow boundaries 01 p0074 N85-10490
Automated analysis and nowcasting of mesoscale convective systems 01 p0074 N85-10492
Forecasting of polar lows 01 p0075 N85-10495
Rain bands and symmetric instability
01 p0075 N85-10496
Some mesoscale weather effects and the very short-range forecasting impact of variable snow cover
01 p0075 N85-10499
Frontal motion in mountainous terrain: Analysis and implications for 0 to 12 hour forecasts
01 p0076 N85-10502
The past, present, and anticipated future contributions of geosynchronous satellites to short range prediction
01 p0076 N85-10503
Use of satellite soundings and imagery for nowcasting and very-short-range forecasting
01 p0076 N85-10504
NESDIS operational precipitation estimation techniques 01 p0076 N85-10505
A scheme for the delineation and extrapolation of thunderstorms from GOES satellite data
01 p0076 N85-10507
Test results from RAINSAT 01 p0076 N85-10508
The use of dual polarisation radar for observing and predicting convective activity 01 p0077 N85-10512
The PROMIS Doppler radar system; design and operational experience 01 p0077 N85-10513
Nowcasting with Doppler radar: The forecaster-computer relationship
01 p0077 N85-10514
Doppler radar analysis of a frontal zone prior to convective development 01 p0077 N85-10515
VHF/UHF radar and its application in nowcasting
01 p0078 N85-10516

Use of ground based microwave radiometers for nowcasting 01 p0078 N85-10517
The potential use of atmospheric profilers in short-range prediction 01 p0078 N85-10518
Analysis strategies for field dependent estimation and network design — mesoscale modeling 01 p0078 N85-10520
Application of automatic pattern methods in very-short-range forecasting 01 p0078 N85-10521
The development of objective forecast techniques based on advection of surface weather parameters 01 p0078 N85-10522
Preliminary assessment of very short term forecasting of rain from single radar data 01 p0078 N85-10523
Optimum parameters for determining the motion of radar field by cross-correlation method 01 p0079 N85-10524
Digital radar data as an aid in nowcasting in Hong Kong 01 p0079 N85-10525
Short period forecasts in West Africa using Meteosat data 01 p0079 N85-10526
Predicability of mesoscale phenomena 01 p0079 N85-10528
The initialization of mesoscale models 01 p0079 N85-10529
Applications of a finite-element regional model to very-short-range forecasting 01 p0080 N85-10531
Application of mesoscale numerical model to local weather prediction 01 p0080 N85-10532
The United Kingdom Meteorological Office mesoscale forecasting system 01 p0080 N85-10533
An operational forecasting system for stratus and fog with sodar 01 p0081 N85-10539
Preparation steps for the use of one-dimensional interpretation models for nowcasting purposes in the German weather net 01 p0081 N85-10540
A one-level mesoscale model suitable for nowcasting and short-term forecasting in regions of complex terrain 01 p0081 N85-10541
A short-term forecast model for thunderstorm rotation 01 p0081 N85-10542
Experiment on nowcasting of heavy rainfall and severe storms in central China in 1979-1981 01 p0081 N85-10545
A summary of operational developments in nowcasting and short-range forecasting techniques on the Canadian West Coast 01 p0082 N85-10547
Simple methods in very short-range forecasting based on data from a mesoscale network of automatic stations (ANETZ) and from satellite (Meteosat) and radar — Swiss Alps 01 p0082 N85-10548
FRONTIERS: Progress with a system for nowcasting rain — Forecasting Rain Optimized using New Techniques of Interactively Enhanced Radar and Satellite (FRONTIERS) 01 p0082 N85-10552
Nowcasting: Advances with McIDAS 3 — Man-computer Interactive Data System System (McIDAS) 01 p0082 N85-10553
Development of nowcasting in China 01 p0083 N85-10554
Interactive computer display systems in nowcasting 01 p0083 N85-10557
MERIT: A man/computer data management and enhancement system for upper air nowcasting/forecasting in the United States — Minimum Energy Routes using Interactive Techniques (MERIT) 01 p0083 N85-10558
Development of an operational system for Very-Short-Range Forecasting (VSRF) at Swedish Meteorological and Hydrological Institute (SMHI) 01 p0083 N85-10559
PROMIS 600: The pilot project for the future Swedish weather service 01 p0083 N85-10560
User requirements for very-short-range weather forecasts: Some key issues 01 p0084 N85-10562
Use of short-range weather forecasts at construction sites: Some results from a user and a market test 01 p0084 N85-10563
Benefits resulting from tailored very-short-range forecasts in Sweden 01 p0084 N85-10564
Some aspects of matching nowcasting and Very-Short-Range Forecasting (VSRF) products with the need of a multilingual community of a mountainous country — Swiss Alps 01 p0084 N85-10566
Nowcasting using lightning location techniques 01 p0084 N85-10568
Frost nowcasting in the agricultural area of Valencia (Spain) — meteorological satellites 05 p0658 N85-14225
TAF verification (airport weather forecasts) [GEOPHYSBDBW-FM-205] 05 p0687 N85-14420
Agricultural weather report for the Ijsselmeer polders in the 1984 summer season; a verification report [KNMI-TR-61] 20 p3496 N85-31737

NOXIOUS MATERIALS
U CONTAMINANTS

NOZZLE COEFFICIENT
U NOZZLE FLOW

NOZZLE DESIGN
Jet noise suppression by porous plug nozzles [NASA-CR-3613] 02 p0275 N85-11790
Experimental investigation of shock-cell noise reduction for single stream nozzles in simulated flight [NASA-CR-3845] 04 p0557 N85-13550
Delta wing nozzle assembly for chemical lasers [AD-D011396] 07 p0970 N85-16158
Some aspects of the design of a fly-by-wire flying control system for a supersonic V/STOL fighter aircraft [COLL-AERON-8413] 12 p1780 N85-21175
Characteristics of a confined jet thrust vector control nozzle [AD-A153067] 17 p2958 N85-28268
Convoluted nozzle design for the RL10 derivative 2B engine [NASA-CR-174953] 19 p3220 N85-29965
Analytical simulation of weld effects in creep range 20 p3468 N85-31550

NOZZLE EFFICIENCY
Static internal performance of single-expansion-ramp nozzles with various combinations of internal geometric parameters [NASA-TM-86270] 06 p0749 N85-14797
Advanced OTV engine concepts 08 p1108 N85-17001
Mixing characteristics of an underexpanded multiple jet ejector [AD-A149557] 10 p1485 N85-19375
Modifications to the nozzle test chamber to extend nozzle static-test capability [NASA-TM-86368] 15 p2484 N85-25216

NOZZLE FLOW
Local stability analysis for a planar shock wave [NASA-TP-2387] 04 p0452 N85-12864
Experimental investigation of shock-cell noise reduction for single stream nozzles in simulated flight [NASA-CR-3845] 04 p0557 N85-13550
Transonic jets: A numerical approach in the hodograph plane 05 p0592 N85-13774
Flow of nitrogen-pressurized Halon 1301 in fire extinguishing systems [NASA-CR-174271] 07 p0900 N85-15701
A computer program for the performance analysis of scarfed nozzles [AD-A147370] 07 p0905 N85-15730
Delta wing nozzle assembly for chemical lasers [AD-D011396] 07 p0970 N85-16158
Critical flashing flow of subcooled fluids in nozzles with contour discontinuities [DE84-017229] 09 p1319 N85-18296
Static internal performance of a two-dimensional convergent nozzle with thrust-vectoring capability up to 60 deg [NASA-TP-2391] 10 p1419 N85-18951
SSME thrust chamber simulation using Navier-Stokes equations [NASA-CR-171349] 10 p1430 N85-19017
Preliminary analysis of selected gas dynamic problems — space shuttle main engine main combustion transients and IUS nozzle flow [NASA-CR-171343] 10 p1483 N85-19361
Mixing characteristics of an underexpanded multiple jet ejector [AD-A149557] 10 p1485 N85-19375
Characteristics of flow of oscillatory-relaxing gas in nozzles with constant cross-sections in throat region 11 p1716 N85-20794
An experimental study of spray thruster [REPT-613] 12 p1845 N85-21578
Calculation of an unsteady transonic flow with shock waves and separation in Laval nozzles [MPIS-14/1984] 14 p2213 N85-23728
Thermal state of cooled thin-walled nozzle blade 14 p2270 N85-24066
Effect of drag behind nozzle array on its force and energy characteristics 14 p2277 N85-24107
Modifications to the nozzle test chamber to extend nozzle static-test capability [NASA-TM-86368] 15 p2484 N85-25216
An experimental study of clustered, two-dimensional rocket nozzles [AD-A151889] 15 p2495 N85-25390
Nozzle wall roughness effects on free-stream noise and transition in the pilot low-disturbance tunnel [NASA-TM-86389] 23 p3930 N85-34355

NOZZLE GEOMETRY
Density distribution in supersonic jet discharged into vacuum from nozzle with bevel tip 02 p0269 N85-11757
An experimental investigation of two-dimensional thrust augmenting ejectors, part 1 [NASA-CR-174111] 04 p0456 N85-12894
A study of lift characteristics of an upper surface blown jetwing with a rectangular nozzle 05 p0591 N85-13767
Certain optimal parameters of high-velocity Venturi ejection tubes [BLL-M-35924-(5828.4)] 05 p0634 N85-14086
Comparison of options for reduction of noise in the test section of the NASA Langley 4x7m wind tunnel, including reduction of nozzle area [NASA-CR-172446-VOL-2] 05 p0726 N85-14667
Multiple steady states for characteristic initial value problems [NASA-CR-172486] 06 p0749 N85-14800
Preliminary analysis of tone-excited two-stream jet velocity decay [NASA-TM-86951] 12 p1770 N85-21114
Some unique features of isentrophic flow of gas under high pressures 13 p2043 N85-22788
Thermal state of cooled thin-walled nozzle blade 14 p2270 N85-24066
Effect of drag behind nozzle array on its force and energy characteristics 14 p2277 N85-24107
Nonnewtonian, unsteady flow in a convergent divergent duct 20 p3456 N85-31463
Investigation of influence of gas exit modes on characteristics of N2O - N2 - He discharge laser 21 p3684 N85-32688

NOZZLE INSERTS
Thermal state of cooled thin-walled nozzle blade 14 p2270 N85-24066

NOZZLE THRUST COEFFICIENTS
Static internal performance of a two-dimensional convergent nozzle with thrust-vectoring capability up to 60 deg [NASA-TP-2391] 10 p1419 N85-18951

NOZZLE WALLS
A curved test section for research on transonic shock wave-boundary layer interaction [VTH-LR-414] 16 p2701 N85-26682

NOZZLES
Turbine test report, addendum [DE84-015130] 02 p0205 N85-11353
Investigation of an ejector heat pump by analytical methods [DE84-016675] 04 p0500 N85-13189
Pressure drop and coefficients of internal heat transfer necessary for transpiration cooling 13 p2050 N85-22831
Discussion of the paper, Some Aspects of Propulsion for the Augmenter-Wing Concept, by D. C. Whittley [NASA-TM-77884] 22 p3727 N85-33108

NUCLEAR AUXILIARY POWER UNITS
NT SNAP
NT SPACE POWER REACTORS
NT SPACE POWER UNIT REACTORS
Spaceborne power systems preference analyses. Volume 1: Summary [NASA-CR-175644] 14 p2349 N85-24517
Spaceborne power systems preference analyses. Volume 2: Decision analysis [NASA-CR-175645] 14 p2349 N85-24518

NUCLEAR CAPTURE
NT ELECTRON CAPTURE
Activities of the Solid State Physics Research Institute [NASA-CR-175699] 17 p3042 N85-28818
A 200-MeV pi(+) induced nucleon removal from 24Mg 17 p3042 N85-28821
An attempt to detect induced neutron capture in laser radiation field 21 p3690 N85-32928
Evaluated nuclear-data file for niobium [DE85-012095] 21 p3704 N85-33009
Applications and misapplications of the channel-capture formalism of direct neutron capture [DE85-013992] 24 p4152 N85-35748

NUCLEAR CHEMISTRY
Fundamental molecular physics and chemistry, part 1 [DE84-009127] 04 p0561 N85-13571
Activities in nuclear physics and high energy physics 11 p1728 N85-20866

NUCLEAR DEFORMATION
Trapping model analysis of annihilation line narrowing in some plastically deformed metals and alloys [AERE-R-10593] 14 p2258 N85-23995

NUCLEAR ELECTRIC POWER GENERATION
NT NUCLEAR AUXILIARY POWER UNITS
NT NUCLEAR POWER PLANTS
NT NUCLEAR POWER REACTORS
NT SNAP
NT SPACE POWER REACTORS
NT SPACE POWER UNIT REACTORS
NT THERMONUCLEAR POWER GENERATION
USSR report: Engineering and equipment [JPRS-UEQ-84-007] 06 p0775 N85-14954
Technology transfer to the Middle East [PB85-127744] 12 p1952 N85-22264

USSR report: Engineering and equipment
[JPRS-UEQ-85-004] 17 p2939 N85-28142
East Europe report: Science and technology
[JPRS-ESA-85-023] 21 p3572 N85-32217
Magnetic Fusion Program plan
[DE85-009861] 22 p3846 N85-33823

NUCLEAR ELECTRIC PROPULSION
Rendezvous with Saturn's rings
15 p2679 N85-26543
Tethered nuclear power for the Space Station
[NASA-TM-87023] 16 p2740 N85-26912
An evaluation of oxygen-hydrogen propulsion systems for the Space Station
[NASA-TM-87059] 18 p3067 N85-28971

NUCLEAR EMULSIONS
The inner granulometric density of the tracks in nuclear emulsions and its application to determine the chemical spectrum of primary cosmic ray nuclidi
[OG-4.3-9] 22 p3879 N85-34034
Abundance of low energy (50-150 MeV) antiprotons in cosmic rays
[OG-6.1-1] 22 p3887 N85-34092
A survey of multiplicities and rapidity densities from existing emission data on hadron-nucleus nucleus-nucleus collisions 24 p4146 N85-35706
On a possibility of inelasticity partial coefficient K sub gamma determination in pi C and pi Pb interactions at 10 to the 14th power eV (experiment PAMIR 1)
[HE-1.1-12] 24 p4171 N85-35859
Anuglar distribution of shower particles produced in the collisions of 20-GeV/c and 300-GeV negative pions with emulsion nuclei 24 p4172 N85-35868
Stopping relativistic Xe, Ho, Au and U nuclei in nuclear emulsions 24 p4173 N85-35876
Heavy nucleus collisions between 20 and 60 GeV/nucleon
[HE-1.4-2] 24 p4175 N85-35890
Characteristics of central collision events in Fe-nucleus interactions for 20 - 60 GeV/nucleon
[HE-1.4-3] 24 p4176 N85-35891
Nucleus-nucleus interaction above several hundred GeV/n
[HE-1.4-4] 24 p4176 N85-35892
Observation of direct hadronic pairs in nucleus-nucleus collisions in JACEE emulsion chambers
[HE-1.4-5] 24 p4176 N85-35893
Excessive production of electron pairs by soft photons in low multiplicity ion interactions
[HE-1.4-6] 24 p4176 N85-35894
On the mechanism of anomalous nucleus-nucleus interactions at energies above 1 TeV/nucleon
[HE-1.4-8] 24 p4177 N85-35896
Meson multiplicity in nucleus-nucleus collisions above 4 GeV/amu
[HE-1.4-10] 24 p4177 N85-35897
Inclusive angular distribution of alpha and Li fragments produced in the Fe-C and Fe-Pb collisions at 1.88 GeV/u
[HE-1.4-11] 24 p4177 N85-35898
Experiment Pamir-3. Coplanar emission of high energy gamma-quanta at interaction of hadrons with nuclei of air atoms at energies above 10 to the 7th power GeV
[HE-1.4-12] 24 p4177 N85-35899
The effect of the relative nuclear size on the nucleus-nucleus interactions
[HE-1.4-13] 24 p4177 N85-35900
Japan - USSR joint emulsion chamber experiment at Pamir
[HE-3.1-1] 24 p4177 N85-35901
Intensities of high-energy cosmic rays at Mount Kanbala
[HE-3.1-2] 24 p4177 N85-35902
High energy gamma-rays and hadrons at Mount Fuji
[HE-3.1-3] 24 p4177 N85-35903
On the characteristics of emulsion chamber family events produced in low heights
[HE-3.1-6] 24 p4178 N85-35904
Some characteristic cosmic ray events and an attempt at their explanation
[HE-3.1-8] 24 p4178 N85-35906
Energy spectra of proton and nuclei of primary cosmic rays in energy region 10 TeV/particle
[HE-3.1-10] 24 p4178 N85-35908
Jets in air-jet family
[HE-3.2-1] 24 p4179 N85-35912
Search for anomalous C-jets in Chacaltaya emulsion chamber experiment
[HE-3.2-5] 24 p4179 N85-35913
Exotic interactions among C-jets and Pb-jets
[HE-3.2-6] 24 p4179 N85-35914
Characteristics of anomalously high multiplicity cosmic ray interactions
[HE-3.3-1] 24 p4180 N85-35920
Transverse momentum distribution of pion deg in the fragmentation region of super high energy interactions
24 p4180 N85-35921
Study of hadron bundles observed in Chacaltaya two-story emulsion chamber
[HE-3.3-4] 24 p4180 N85-35922
Atmospheric interactions detected in both the upper and the lower chambers at Chacaltaya
[HE-3.3-7] 24 p4180 N85-35925

NUCLEAR ENERGY
Advancement of remote technology: Past perspectives and future plans
[DE85-000934] 09 p1327 N85-18342
Proceedings of the Fifth International Conference on Nuclear Methods in Environmental and Energy Research
[DE84-017348] 19 p3310 N85-30521

NUCLEAR EXPLOSION EFFECT
EMP injection on conduit entries, type Brattberg -- electromagnetic pulse (EMP) injection
[FOA-E-30001-A3] 02 p0193 N85-11280
Electromagnetic pulse and the electric power network
[DE84-015403] 04 p0493 N85-13143
Tests for susceptibility to electromagnetic attack
[SNIAS-842-422-101] 04 p0494 N85-13154
Evaluation of nuclear detonation location capability under high attack scenario
[AD-A155761] 24 p4149 N85-35729

NUCLEAR EXPLOSIONS
NT THERMONUCLEAR EXPLOSIONS
Seismology 1983: Nuclear test ban verification, earthquake and Earth resource investigation
[FOA-C-20537-T1] 02 p0229 N85-11495
Theoretical and observed dispersion of acoustic-gravity waves in atmosphere 04 p0557 N85-13547
High-bandwidth multichannel fiber optic system for measuring gamma rays
[DE84-014526] 04 p0564 N85-13596
China report: Science and technology
[JPRS-CST-84-025] 11 p1620 N85-20197
Micro-deformation of quartz under dynamic action and its applications 11 p1620 N85-20201
Attenuation of seismic waves at regional distances
[AD-A150198] 13 p2132 N85-23267
NASTRAN analysis comparison to shock tube tests used to simulate nuclear overpressures
15 p2576 N85-25888
Elastic-workhardening SDF (Single-Degree-of-Freedom) system subjected to random blast excitations
[AD-A151866] 15 p2579 N85-25909
Three new fiber-optic components
[DE85-006269] 15 p2653 N85-26364
A multiphase continuum model to describe dynamic loading effects in nonlinear porous media
[DE85-010102] 19 p3301 N85-30463
Seismic discrimination
[AD-A154167] 20 p3494 N85-31722
Marine Sample Exploitation Project: Estimates regarding the sensitivity and technology for the detection of nuclear explosion debris in the marine environment
[DE85-013176] 23 p3947 N85-34462
Investigation of the lightning vulnerability of nuclear explosive test systems at the Nevada Test Site
[DE85-011761] 24 p4124 N85-35563
Evaluation of nuclear detonation location capability under high attack scenario
[AD-A155761] 24 p4149 N85-35729
Ground motion measurements for the QUESO nuclear event
[DE85-014806] 24 p4151 N85-35743
Heavy flavours production in quark-gluon plasma formed in high energy nuclear reactions
24 p4175 N85-35886

NUCLEAR FISSION
Energy-advanced nuclear data: Measurements and physical interpretations
[DE85-006198] 19 p3366 N85-30872
Design of a helium-cooled molten salt fusion breeder
[DE85-010474] 20 p3528 N85-31943
Liquid uranium alloy-helium fission reactor
[DE85-006511] 23 p3970 N85-34607
A very important process of nucleosynthesis in stars
[OG-7.1-11] 23 p4014 N85-34872
Neutronic calculations for a new high flux reactor
[DE85-011551] 24 p4150 N85-35734

NUCLEAR FUEL ELEMENTS
Technology status of thermionic fuel elements for space nuclear power 05 p0610 N85-13893
Austrian contributions to fuel rod failure models shown at the International Standard Problem (ISP)-14
[OEFZS-4276] 07 p1041 N85-16613
Evacuate and backfill apparatus and method
[DE85-008018] 23 p3938 N85-34411
Thermal hydraulic features of the TMI accident
[DE85-014569] 24 p4152 N85-35747

NUCLEAR FUEL REPROCESSING
Advancement of remote systems technology: Past perspectives and future plans
[DE84-016710] 04 p0509 N85-13250
Inquiry into disintegration control of irradiated low enrichment uranium for high temperature gas cooled reactors
[OEFZS-7281] 07 p1042 N85-16815
Advancement of remote technology: Past perspectives and future plans
[DE85-000934] 09 p1327 N85-18342
Control and electronic subsystems for the advanced servomanipulator
[DE85-001900] 09 p1327 N85-18343
Dual arm master controller concept
[DE85-001901] 09 p1327 N85-18344
Advanced remotely maintainable force-reflecting servomanipulator concept
[DE85-001902] 09 p1328 N85-18345
Flow measurement by laser Doppler anemometry in a nuclear fuel assembly
[DE85-003260] 12 p1848 N85-21892
Consolidated fuel reprocessing program
[DE85-010591] 19 p3358 N85-30818
Analytical methods in the purex process
[BLL-DOUNREAY-TR-952(9091.9F)]
24 p4149 N85-35727

NUCLEAR FUELS
NT CERAMIC NUCLEAR FUELS
NT SPENT FUELS
USSR report: Energy
[JPRS-UEN-84-036] 07 p0994 N85-16312
Irradiation effects on fuels for space reactors
[DE84-016460] 12 p1931 N85-22134
Tritium catalyzed deuterium Tokamaks
[DE85-004825] 12 p1936 N85-22166
Feasibility study of a fission-suppressed Tokamak fusion breeder
[DE85-009099] 18 p3190 N85-29798
Experimental program to determine maximum temperatures for dry storage of spent fuel
[DE85-010307] 19 p3236 N85-30080
Mixtures experiment where the amount of the mixture is a factor under study
[DE85-010974] 19 p3250 N85-30153
Response of steam-water mixtures to pressure transients
[DE85-010798] 19 p3267 N85-30262
A review of the SIMMER-2 analyses of liquid-metal-cooled fast breeder reactor core-disruptive accident fuel escape
[DE85-010803] 19 p3366 N85-30876
Solid-state track recorder neutron dosimetry in the Three-Mile Island Unit-2 reactor cavity
[DE85-011360] 20 p3531 N85-31868
East Europe report: Science and technology
[JPRS-ESA-85-021] 21 p3588 N85-32190
Reaction of uranium and the fluorocarbon FC-75
[DE85-012322] 22 p3843 N85-33802
Liquid uranium alloy-helium fission reactor
[DE85-006511] 23 p3970 N85-34607
Seperation of uranium from technetium in recovery of spent nuclear fuel
[DE85-006499] 23 p3972 N85-34627

NUCLEAR FUSION
NT CONTROLLED FUSION
Study of structure of nuclei with neutrons and nuclear data measurements for MFE
[DE84-015128] 01 p0117 N85-10802
Fusion and its future in Illinois
[DE84-014686] 01 p0122 N85-10830
Materials studies for magnetic fusion energy applications at low temperatures, 7
[DE84-013487] 01 p0122 N85-10837
Report on solar neutrino experiments
[DE84-014567] 01 p0131 N85-10899
Statistical Plasma Physics. Proceedings of the Workshop of the US-Japan Joint Institute for Fusion Theory Program
[IPPJ-689] 02 p0282 N85-11832
Chlorine and bromine solar neutrino experiments
[DE84-015720] 02 p0304 N85-11909
Fusion plasma theory. Task 3: Auxiliary heating in Tokamaks and tandem mirrors
[DE84-014940] 04 p0566 N85-13609
Theoretical investigations relevant to magnetic fusion research
[DE85-001777] 06 p0866 N85-15503
Multihole couplers for overmoded waveguide systems
[IPF-83-8] 09 p1394 N85-18773
Short mode selective directional couplers
[IPF-83-9] 09 p1394 N85-18774
Improved directional couplers for overmoded waveguide systems
[IPF-84-1] 09 p1394 N85-18775
Lidar-Thomson scattering — Joint European Torus
[IPF-84-3] 09 p1394 N85-18777
Two phases of neutron production in the POSEIDON plasma focus
[IPF-84-10] 09 p1395 N85-18783

A proposed method for fast determination of plasma parameters
11 p1730 N85-20877
[IPP-1/228]

Light diffraction with collective, thermal electron density fluctuation in plasmas with several ionic components
11 p1733 N85-20904
[IPF-84-5]

Plasma and nuclear processes in solar matter
12 p1954 N85-22277

Opacity determinations for Inertial Confinement Fusion (ICF) materials using an average atom model
12 p1957 N85-22295

Slowing down of charged particles by the bound electrons in a plasma — ion beams, nuclear fusion
14 p2419 N85-24929
[LP-209]

Glossary of fusion energy
[DE84-017180] 14 p2425 N85-24958

A new approach to queer differential equations
[AD-A149321] 15 p2638 N85-26272

Plasma theory and computations
15 p2655 N85-26384

Prospects for developing attractive magnetic fusion concepts
[DE85-006925] 16 p2867 N85-27684

Fusion-power-core design of a Compact Reversed-Field Pinch Reactor (CRFPR)
[DE85-007710] 16 p2868 N85-27692

Experimental plasma research: Plasma summaries
[DE85-008116] 17 p3039 N85-28805

Tokamak fusion core experiment maintenance study
[DE85-008040] 17 p3040 N85-28813

Current activities and background of technology transfer and exchange program at Lawrence Livermore National Laboratory
[DE85-009526] 18 p3199 N85-29843

LINE: A code which simulates spectral line shapes for fusion reaction products generated by various speed distributions
[DE85-010633] 19 p3341 N85-30702

Magnetic fusion 1985: What next?
[DE85-009953] 19 p3365 N85-30868

Energy-advanced nuclear data: Measurements and physical interpretations
[DE85-006198] 19 p3366 N85-30872

Fusion reactions at low energy
[DE85-010561] 20 p3528 N85-31944

Nuclear responses in INTOR plasma stabilization elements
[DE85-010489] 20 p3535 N85-31995

Nuclear data needs for fusion energy development
[DE85-010445] 20 p3536 N85-32000

Prospects for lasers for fusion energy assessed
21 p3684 N85-32885

Infrared laser holography used in fusion plasma studies 21 p3687 N85-32905

Tritium technology review
[DE85-010504] 21 p3703 N85-33006

Gamma-ray line emission from Al-26 produced by Wolf-Rayet stars
[OG-3.2-5] 22 p3875 N85-34003

Diffuse galactic annihilation radiation from supernova nucleosynthesis
[OG-3.2-8] 22 p3875 N85-34004

Numerical solutions of the Vlasov equation
23 p3979 N85-34672

Dissipation terms in one-dimensional hydrodynamic code for ICF target 23 p3980 N85-34677

Stability of implosion dynamics
23 p3980 N85-34680

Nucleosynthesis in the terrestrial and solar atmospheres
[SH-2.2-2] 23 p4000 N85-34797

Propagation and nucleosynthesis of ultraheavy cosmic rays
[OG-7.1-6] 23 p4013 N85-34867

A very important process of nucleosynthesis in stars
[OG-7.1-11] 23 p4014 N85-34872

Results of ultra-low level 71ge counting for application in the Gallex-solar neutrino experiment at the Gran Sasso Underground Physics Laboratory
[SH-8.1-2] 23 p4049 N85-35106

Gamma-ray production cross sections for alpha-particle induced reactions on F-19 and Na-23
[DE85-012603] 24 p4150 N85-35732

Operations considerations in designing a high speed multi-channel data acquisition system
[DE85-012840] 24 p4154 N85-35756

Some nuclear data needs in astrophysics
[DE85-012916] 24 p4168 N85-35842

NUCLEAR INTERACTIONS
NT ELECTRON CAPTURE
NT NUCLEAR CAPTURE
NT SPIN-ORBIT INTERACTIONS
NT STRONG INTERACTIONS (FIELD THEORY)
NT WEAK INTERACTIONS (FIELD THEORY)

Chaos near the Coulomb Barrier: Nuclear molecules
[DC85-001280] 07 p1041 N85-16608

Workshop on Nuclear Dynamics 3
[INC-40007-24] 12 p1931 N85-22130

Theoretical aspects of electroweak and other interactions in medium-energy nuclear physics
[DE85-003821] 13 p2157 N85-23392

Nuclear spectroscopic studies
[DE85-006894] 16 p2862 N85-27652

Study of proton and neutron activation of metal samples in low Earth orbit
[NASA-CR-171596] 21 p3556 N85-32130

Contributions to the 19th International Cosmic Ray Conference
[NASA-CR-176060] 21 p3714 N85-33044

Gamma ray line production from cosmic ray spallation reactions 22 p3875 N85-34005

Abundance of low energy (50-150 MeV) antiprotons in cosmic rays
[OG-6.1-1] 22 p3887 N85-34092

Search for heavy antinuclei in the cosmic radiation
[OG-6.1-2] 22 p3887 N85-34093

Ninteenth International Cosmic Ray Conference. OG sessions, volume 3
[NASA-CP-2376-VOL-3] 23 p4012 N85-34862

Cosmic ray secondary nuclei and the structure of the galaxy
[OG-7.2-4] 23 p4014 N85-34876

Observations of accelerated high current low emittance beams in the SLC Linac
[DE85-013073] 24 p4068 N85-35211

Proceedings of the Workshop on Detectors for Relativistic Nuclear Collisions
[LBL-18225] 24 p4146 N85-35700

Detectors for relativistic nuclear collisions (report from the Fixed-Target Hadron Group)
24 p4146 N85-35701

Event parameters: Fixed targets
24 p4146 N85-35702

Working group on penetrating probes at fixed target facilities 24 p4146 N85-35703

A survey of multiplicities and rapidity densities from existing emission data on hadron-nucleus nucleus-nucleus collisions 24 p4146 N85-35706

A simulation of ultra-relativistic nucleus-nucleus collisions 24 p4146 N85-35707

Some remarks about simulation of cosmic ray phenomena with use of nuclear interaction models based on the current SPS proton-antiproton data
[HE-1.2-6] 24 p4172 N85-35864

Low P sub T hadron-nucleus interactions
[HE-1.2-7] 24 p4172 N85-35865

The response of a scintillation counter below an emulsion chamber to heavy nucleus interactions in the chamber 24 p4175 N85-35889

Characteristics of central collision events in Fe-nucleus interactions for 20 - 60 GeV/nucleon
[HE-1.4-3] 24 p4176 N85-35891

Nucleus-nucleus interaction above several hundred GeV/n
[HE-1.4-4] 24 p4176 N85-35892

Observation of direct hadronic pairs in nucleus-nucleus collisions in JACEE emulsion chambers
[HE-1.4-5] 24 p4176 N85-35893

Excessive production of electron pairs by soft photons in low multiplicity ion interactions
[HE-1.4-6] 24 p4176 N85-35894

Meson multiplicity in nucleus-nucleus collisions above 4 GeV/amu
[HE-1.4-10] 24 p4177 N85-35897

Inclusive angular distribution of alpha and Li fragments produced in the Fe-C and Fe-Pb collisions at 1.88 GeV/u
[HE-1.4-11] 24 p4177 N85-35898

The effect of the relative nuclear size on the nucleus-nucleus interactions
[HE-1.4-13] 24 p4177 N85-35900

Japan - USSR joint emulsion chamber experiment at Pamir
[HE-3.1-1] 24 p4177 N85-35901

On the characteristics of emulsion chamber family events produced in low heights
[HE-3.1-6] 24 p4178 N85-35904

Search for anomalous C-jets in Chacaltaya emulsion chamber experiment
[HE-3.2-5] 24 p4179 N85-35913

Exotic interactions among C-jets and Pb-jets
[HE-3.2-6] 24 p4179 N85-35914

Scaling violation in hadron-nucleus interaction
[HE-3.2-8] 24 p4179 N85-35916

The model of independent particles emission in the multiparticle production theory
[HE-3.2-10] 24 p4179 N85-35918

Study of hadron bundles observed in Chacaltaya two-story emulsion chamber
[HE-3.3-4] 24 p4180 N85-35922

Anomalous correlation between hadron and electromagnetic particles in hadron and gamma-ray families
[HE-3.3-6] 24 p4180 N85-35924

Atmospheric interactions detected in both the upper and the lower chambers at Chacaltaya
[HE-3.3-7] 24 p4180 N85-35925

Lateral distribution of high energy hadrons and gamma ray in air shower cores observed with emulsion chambers
[HE-3.3-8] 24 p4180 N85-35926

Size distributions of air showers accompanied with high energy gamma ray bundles observed at Mt. Chacaltaya
[HE-3.3-9] 24 p4181 N85-35927

A halo event created at 200 m above the Chacaltaya emulsion chamber
[HE-3.4-5] 24 p4182 N85-35933

A binocular-type atmospheric interaction generating sequential exotic features
[HE-3.4-6] 24 p4182 N85-35934

Gamma-hadron families and scaling violation
[HE-3.4-7] 24 p4182 N85-35935

Super-family P2 C-96-125 observed by Japan-URSS Joint Emulsion Chamber Experiment
[HE-3.4-8] 24 p4182 N85-35936

On the halo events observed by Mount Fuji and Mount Kanbala Emulsion Chamber Experiments
[HE-3.4-9] 24 p4182 N85-35937

Experiment Pamir-2. Fianit: A giant super-family with halo (Epsilon sub 0 at approximately 10(17) eV)
[HE-3.4-10] 24 p4182 N85-35938

Experiment Pamir-4: Analysis of superfamily with halo of electromagnetic nature detected in deep XEC
[HE-3.4-11] 24 p4183 N85-35939

Particle interactions at energies over 1000 TeV inferred from gamma-families observed at Mount Fuji
[HE-3.5-1] 24 p4183 N85-35940

A search for mini-clusters in Japan-USSR Joint Experiment at Pamir
[HE-3.5-2] 24 p4183 N85-35941

Mini-clusters
[HE-3.5-3] 24 p4183 N85-35942

Structure of super-families
[HE-3.5-7] 24 p4183 N85-35944

Extremely high energy hadron and gamma-ray families(3). Core structure of the halo of superfamily
[HE-3.5-8] 24 p4183 N85-35945

Numerical analysis of electromagnetic cascades in emulsion chambers
[HE-3.5-9] 24 p4184 N85-35946

New analysis of nuclear interaction observed by Mt. Kanbara emulsion chamber experiment
[HE-3.7-4] 24 p4186 N85-35963

Structured events in Pamir carbon X-ray chambers
[HE-3.7-7] 24 p4186 N85-35965

Electrons, muons and hadrons in extensive air showers and how do they depend on nuclear interaction model, part 2 24 p4187 N85-35969

Electrons, muons and hadrons in extensive air showers and how do they depend on nuclear interaction model, part 1 24 p4187 N85-35972

Tskhra-Tskaro complex intended for the investigations of EAS spatial characteristics near axis
24 p4190 N85-35995

Correlation of high energy muons with primary composition in extensive air shower
[HE-4.3-7] 24 p4191 N85-36001

The longitudinal development of muons in cosmic ray air showers at energies 10(15) - 10(17) eV
[HE-4.3-12] 24 p4192 N85-36006

Simulation of gamma-initiated showers
[HE-4.5-10] 24 p4195 N85-36033

Delayed particles in EAS at Akeno
[HE-6.2-8] 24 p4211 N85-36144

NUCLEAR MAGNETIC RESONANCE
NT PROTON RESONANCE

Studies of hydrogenated amorphous silicon
[DE84-013038] 01 p0067 N85-10443

Electronic structure and lattice dynamics of solid state substances from gamma nuclear resonance absorption and angular correlation measurements
03 p0427 N85-12728

Paramagnetic impurity effects in NMR determinations of hydrogen diffusion and electronic structure in metal hydrides. Cerium in YH-2 and LaH-2.25
[DE84-014127] 04 p0472 N85-13005

Development program: Nuclear magnetic resonance gyroscope (NMR-gyro). Phase 1: Development of an experimental model
[BMFT-FB-W-84-041] 05 p0639 N85-14101

Polarization in chemically doped hydrogen-rich glasses
[DE84-017486] 06 p0771 N85-14936

The 13C nuclear magnetic resonance in graphite intercalation compounds
[NASA-CR-174261] 07 p1040 N85-16601

NMR study on rotational fluctuation in solid hydrogen and deuterium 09 p1289 N85-18093
Advanced NMR characterization of zeolite catalysts
[DE85-000456] 09 p1291 N85-18104
Transport and relaxation processes in supercritical fluids
[DE85-002079] 09 p1396 N85-18797
Theoretical determination of surface magnetism
[DE85-003224] 11 p1714 N85-20783
Proton NMR and susceptibility measurements in TiCoH/sub x
[DE85-003309] 12 p1807 N85-21336
Synthesis and thermomechanical properties of new AT-Phenylene R systems
[AD-A149961] 12 p1813 N85-21372
Phase separation in polyurethanes: A deuterium NMR study
[AD-A151515] 15 p2505 N85-25451
Electronic properties of new organic conductors
[DE85-005590] 15 p2549 N85-25736
Bound and free moisture studies of solid materials by FTNMR
[DE85-003227] 16 p2747 N85-26952
Ion and polymer chain motion in a superionic sodium-poly(ethylene oxide) complex
[AD-A152290] 16 p2755 N85-27001
NMR manometer for measuring high pressures at liquid-helium temperatures 17 p2944 N85-28171
Characteristics of charge transfer in the dispersed phase of electrorheological suspensions
[RAE-TRANS-2125] 19 p3233 N85-30040
Biology and Medicine Division
[DE85-010638] 19 p3327 N85-30613
NMR investigation of crystalline electric field effect on spin-spin relaxation in (Y(1-x)RE(x))Rh4B4
[DE85-010512] 19 p3357 N85-30814
Advanced NMR characterization of zeolite catalysts
[DE85-010143] 19 p3363 N85-30853
H1-NMR studies on lymphocyte membranes in human lymphoproliferative diseases 20 p3505 N85-31787
An EPR (Electron-Paramagnetic-Resonance) and ENDOR (Electron-Nuclear-Double-Resonance) study of ferroelectric ammonium sulfate
[AD-A155580] 21 p3710 N85-33033
NMR in the 80 s: New nuclei, new pulses — nuclear magnetic resonance (NMR)
[DRIC-T-7467] 22 p3836 N85-33754
Nuclear magnetic resonance study of the intramolecular rearrangement of 2-(5-cyanotetrazolato)pentaammine cobalt (III) perchlorate
[DE85-010610] 22 p3839 N85-33772
Apparatus for unilateral generation of a homogeneous magnetic field
[DE85-006001] 23 p3928 N85-34345

NUCLEAR MEDICINE
NT RADIOBIOLOGY
Isotopes in day to day life
[IAEA/PI/A.6E-84-00924] 03 p0417 N85-12668
Applications of CdTe to nuclear medicine
[DE85-011877] 23 p3952 N85-34492

NUCLEAR MODELS
Particle physics: Recent successes and future prospects
[DE85-008175] 17 p3033 N85-28765
Many-body processes in atomic and molecular physics
[DE85-009750] 19 p3354 N85-30791
Proceedings of the 1984 Workshop on High-Energy Excitations in Condensed Matter, volume 2
[DE85-007395] 19 p3357 N85-30809
Soliton matter as a model of dense nuclear matter
[DE85-009937] 19 p3359 N85-30825
Heavy quarks and CP: Moriond 1985
[DE85-010553] 22 p3841 N85-33790
Quark structure of nuclei
[DE85-010781] 22 p3842 N85-33795

NUCLEAR PARTICLES
NT ALPHA PARTICLES
NT ANTINEUTRINOS
NT ANTINUCLEONS
NT ANTIPARTICLES
NT ANTIPROTONS
NT BETA PARTICLES
NT BOSONS
NT HYPERONS
NT KAONS
NT MESONS
NT MUONS
NT NUCLEONS
NT PHOTOELECTRONS
NT PHOTONS
NT PIONS
NT POSITRONS
NT VECTOR MESONS
A numerical study of the mean trajectory approximation in a non-adiabatic process
[AD-A152763] 17 p3030 N85-28737
Possibilities for studying short-lived nuclei produced at LAMPF
[DE85-010740] 19 p3365 N85-30864
Plastic scintillator detectors for the study of transfer and breakup reactions at intermediate energies
[DE85-009945] 20 p3528 N85-31945
Abundances from solar-flare gamma-ray line spectroscopy
[SH-2.1-13] 23 p3999 N85-34794
The heavy ions in space experiment
[OG-9.1-10] 23 p4023 N85-34936
Cherenkov-dE/dx-range measurements on cosmic ray iron group nuclei
[OG-9.1-12] 23 p4024 N85-34937
The response of ionization chambers to relativistic heavy nuclei
[OG-9.1-13] 23 p4024 N85-34938

NUCLEAR PHYSICS
NT REACTOR PHYSICS
USSR report: Physics and mathematics
[JPRS-UPM-84-006] 02 p0256 N85-11676
Experimental medium energy physics
[DE84-014625] 02 p0278 N85-11807
ATLAS beam properties: Some implications for target making
[DE84-006595] 02 p0278 N85-11812
Solid state investigations with nuclear physics methods 03 p0428 N85-12731
Activities report in nuclear physics
05 p0726 N85-14680
Experimental investigations in particle physics at intermediate energies
[DE85-001481] 11 p1722 N85-20832
Renewal request for high energy physics at Texas A and M University
[DE85-004469] 11 p1724 N85-20843
Activities in nuclear physics and high energy physics
11 p1728 N85-20866
Theoretical nuclear physics
[DE85-003466] 12 p1932 N85-22135
Research in theoretical nuclear physics
[DE85-004349] 12 p1932 N85-22137
Theoretical aspects of electroweak and other interactions in medium-energy nuclear physics
[DE85-003621] 13 p2157 N85-23392
Research in theoretical nuclear physics
[DE85-006172] 14 p2418 N85-24920
Breakthrough in container confinement of ultracold neutrons 15 p2644 N85-26311
Heavy ion physics at BNL, the AGS and RHIC
[DE85-005951] 17 p3033 N85-28760
High energy gamma rays from complex particle collisions
[DE85-007671] 17 p3036 N85-28783
Research activities of the Physics Division
[DE85-006958] 19 p3357 N85-30811
Work in Amsterdam on local intelligence — artificial intelligence
[NIKHEF-H/84-9] 20 p3518 N85-31877
Current experiments in elementary particle physics, revision 1-85
[DE85-011513] 20 p3529 N85-31950
Activities report in nuclear physics and particle acceleration 20 p3532 N85-31977
USSR report: Physics and mathematics
[JPRS-UPM-85-004] 21 p3680 N85-32860
High-energy Physics Institute building 3-trillion-ev accelerator 21 p3691 N85-32934
Activities of the Physics Division
[DE85-000784] 21 p3702 N85-33002
Proceedings of the 18th LAMPF Users Group Meeting
[DE85-011888] 22 p3839 N85-33773
Nuclear physics in the 10 to 300 MeV energy range using a pulsed white neutron source
[DE85-003713] 22 p3839 N85-33775
Physics Division annual review, 1 April 1983 - 31 March 1984
[ANL-84-24] 23 p3969 N85-34602
Forty-five years of e(+)e(-) annihilation physics: 1956 to 2001
[DE85-013052] 24 p4149 N85-35723

NUCLEAR POTENTIAL
K(-) hydrogen bound and continuum states in momentum space
[DE85-010429] 22 p3841 N85-33789

NUCLEAR POWER GENERATION
U NUCLEAR ELECTRIC POWER GENERATION

NUCLEAR POWER PLANTS
A pilot study of future research on seismic hazards in Sweden
[FOA-C-20544-T1] 02 p0229 N85-11496
Control and electronic subsystems for the advanced servomanipulator
[DE85-001900] 09 p1327 N85-18343
Electromagnetic compatibility of measurement and control equipment in nuclear installations
[BLL-WH-607-(9091.9F)] 11 p1623 N85-2022
Assuring structural integrity in Army systems
[NASA-CR-175492] 11 p1651 N85-20
Computer-generated display system guidelines. Volume 1: Display design
[DE85-000679] 11 p1701 N85-20
Lasers in the nuclear industry
14 p2309 N85-24
Application of new welding technology in the fabrication of nuclear power plant 15 p2566 N85-25
Information presentation in power plant control rooms
[VTT-320] 16 p2864 N85-27
Corrosion test on high-alloy steels
[BLL-BISI-TRANS-21627-(9022.06)]
17 p2926 N85-28
Investigation on the application of the pulsed eddy current method of non-destructive testing using controlled signals (CS-technique)
[BLL-BISI-TRANS-22249-(9022.06)]
18 p3119 N85-29
A remote-operated manipulator vehicle
[HSE-TRANS-11133] 19 p3281 N85-30
Seismic pipe support construction practices
[DE85-901315] 19 p3287 N85-30
Advanced ultrasonic imaging of piping in Dresden and Vermont Yankee reactors
[TI85-010049] 20 p3464 N85-3152
Airborne cloud tracking measurements during the Three Mile Island nuclear station accident, Middletown, Pennsylvania. Date of survey: March - June 1979
[DE85-012060] 22 p3816 N85-33
SMACS: A system of computer programs for probabilistic seismic analysis of structures and subsystems. Volume 1: User's manual
[DE85-011853] 22 p3830 N85-3372
State-of-the-art of solid-state motor controllers
[TI85-008674] 24 p4162 N85-35

NUCLEAR POWER REACTORS
NT SPACE POWER REACTORS
NT SPACE POWER UNIT REACTORS
Acoustic imaging in a water filled metallic pipe – monitoring heat exchangers in nuclear power reactors
[DE84-016051] 09 p1378 N85-18
Graphic display development program, volume 1
[DE85-011076] 19 p3333 N85-30
ASME performance test on TVA Sequoyah unit 1
[DE85-901316] 19 p3358 N85-3081
Magnetic fusion 1985: What next?
[DE85-009953] 19 p3385 N85-30
Applicability of 100kWe-class of space reactor power systems to NASA manned space station missions
[NASA-CR-174696] 24 p4149 N85-357

NUCLEAR PROPULSION
NT NUCLEAR ELECTRIC PROPULSION

NUCLEAR PUMPED LASERS
Estimate of nuclear-pumped X-ray laser mechanism
06 p0748 N85-147

NUCLEAR RADIATION
NT BETA PARTICLES
NT FAST NEUTRONS
NT GAMMA RAY BEAMS
NT GAMMA RAY BURSTS
NT GAMMA RAYS
NT NEUTRON BEAMS
NT SPALLATION
NT THERMAL NEUTRONS
Inquiry into disintegration control of irradiated low enrichment uranium for high temperature gas cooled reactors
[OEFZS-7281] 07 p1042 N85-1661
Nuclear radiation induced absorption in optical materials
[DE85-007128] 15 p2649 N85-25
Space radiation studies — Spacelab 2 Payload
[NASA-CR-171410] 15 p2685 N85-25
MATADOR (Methods for the Analysis of Transport And Deposition Of Radionuclides) code description and user's manual
[TI85-901402] 23 p3966 N85-34
Abundances from solar-flare gamma-ray lin
spectroscopy
[SH-2.1-13] 23 p3999 N85-347

NUCLEAR RADIATION SPECTROSCOPY
Investigations of vacuum ultraviolet and soft X-ra
lasers
[AD-A148277] 08 p1167 N85-17
Moessbauer study of amorpho
Fe(67)Co(18)B(14)S(1)
[AERE-R-11528] 11 p1737 N85-2
NMR in the 80 s: New nuclei, new pulses — nucle
magnetic resonance (NMR)
[DRIC-T-7467] 22 p3836 N85-3

NUCLEAR REACTIONS
NT ALPHA DECAY
NT ANNIHILATION REACTIONS
NT CONTROLLED FUSION
NT ELECTRON CAPTURE
NT ELECTRON SCATTERING
NT HIGH ENERGY INTERACTIONS
NT NEUTRON EMISSION
NT NEUTRON SCATTERING
NT NUCLEAR CAPTURE
NT NUCLEAR FISSION
NT NUCLEAR FUSION
NT NUCLEAR INTERACTIONS
NT NUCLEAR SCATTERING
NT PHOTONUCLEAR REACTIONS
NT PHOTOPRODUCTION
NT POSITRON ANNIHILATION
NT PROTON SCATTERING
NT PROTON-PROTON REACTIONS
NT RADIOACTIVE DECAY
NT RESONANCE SCATTERING
NT SPALLATION
NT SPIN-ORBIT INTERACTIONS
NT THERMONUCLEAR REACTIONS
Engineering Physics Division
[DE84-007778] 02 p0274 N85-11787
Solar neutrino spectroscopy
[DE84-015518] 02 p0304 N85-11968
A study of defects in neutron transmutation doped silicon: Gallium by hall effect analysis
[AD-A146047] 03 p0433 N85-12758
Tables of nuclear cross sections for galactic cosmic rays: Absorption cross sections
[NASA-RP-1134] 16 p2864 N85-27665
Activities report in nuclear physics and high energy physics
[JF40026] 17 p3035 N85-28777
New approaches to functionalized fluorocarbons
[AD-A154205] 19 p3248 N85-30141
Multiple collision solutions for time-dependent neutron transport in slabs of finite thickness
[OEFZS-4312] 22 p3838 N85-33762
Bibliography and index for nuclear reactions among light charged particles, volume 26
[DE85-011482] 22 p3838 N85-33768
Pairing correction of particle-hole state densities for two kinds of fermions
[DE85-011549] 23 p3971 N85-34620
Some nuclear data needs in astrophysics
[DE85-012916] 24 p4168 N85-35842
Heavy flavours production in quark-gluon plasma formed in high energy nuclear reactions
24 p4175 N85-35886
Preliminary results on underground muon bundles observed in the Frejus proton-decay detector
[HE-5.1-1] 24 p4200 N85-36067

NUCLEAR REACTOR CONTROL
Instrumentation and controls evaluation for space nuclear power systems
[DE85-000983] 09 p1383 N85-18895
Tritium technology review
[DE85-010504] 21 p3703 N85-33006

NUCLEAR REACTORS
NT BOILING WATER REACTORS
NT BREEDER REACTORS
NT EXPERIMENTAL BREEDER REACTOR 2
NT FAST NUCLEAR REACTORS
NT FAST TEST REACTORS
NT FUSION REACTORS
NT GAS COOLED REACTORS
NT HEALTH PHYSICS RESEARCH REACTOR
NT HIGH TEMPERATURE GAS COOLED REACTORS
NT HIGH TEMPERATURE NUCLEAR REACTORS
NT JANUS REACTOR
NT LIGHT WATER REACTORS
NT LIQUID COOLED REACTORS
NT LIQUID METAL COOLED REACTORS
NT LIQUID METAL FAST BREEDER REACTORS
NT NUCLEAR POWER REACTORS
NT NUCLEAR RESEARCH AND TEST REACTORS
NT PRESSURIZED WATER REACTORS
NT SPACE POWER REACTORS
NT SPACE POWER UNIT REACTORS
NT SPHEROMAKS
NT TOKAMAK DEVICES
NT WATER COOLED REACTORS
NT ZERO POWER REACTORS
The reactor dynamic code RETRANS: Structure and users guide
[OEFZS-4287] 07 p1041 N85-16614
Something in the air at Windscale --- radioactive contaminants from the Sellafield nuclear Complex for reprocessing and storing irradiated fuel
[BLL-RISLEY-TR-4996-(9091.9F)]
08 p1179 N85-17429
Leakage-flow induced vibrations of a chimney structure suspended in a liquid flow --- nuclear reactors
09 p1339 N85-18420
Radiation response of optical fibers in a nuclear reactor
[DE84-017221] 09 p1385 N85-18710
Proceedings of the 1984 DOE Nuclear Reactor and Facility Safety Conference, volume 1
[DE84-012130] 12 p1931 N85-22132
Proceedings of the DOE Nuclear Reactor and Facility Safety Conference, volume 2
[DE84-012694] 12 p1931 N85-22133
Comprehensive, integrated, remote sensing at DOE sites
[DE85-004867] 13 p2126 N85-23240
USSR report: Engineering and equipment
[JPRS-UEQ-84-001] 14 p2265 N85-24034
The gamma thermometer: A new type of fixed internal instrumentation developed by EDF
[BLL-CE-TRANS-8080-(9022.09)]
15 p2560 N85-25791
Analysis of orbit transfer vehicles for GPS Block 3 satellites
[AD-A152021] 16 p2732 N85-26860
High thermal power density heat transfer apparatus providing electrical isolation at high temperature using heat pipes
[NASA-CASE-LEW-12950-2] 18 p3098 N85-29179
Jet pump-drive system for heat removal
[NASA-CASE-NPO-16494-1-CU]
18 p3099 N85-29182
Flow visualization study of inverted annular flow of post dryout heat transfer region
[DE85-010482] 19 p3289 N85-30275
Development of the Cascade inertial-confinement-fusion reactor
[DE85-010933] 19 p3357 N85-30812
Simulation and operation of the EBR-2 automatic control rod drive system
[DE85-010262] 19 p3360 N85-30832
Source Term Experiments Project (STEP): Aerosol characterization system
[DE85-010248] 19 p3361 N85-30839
Solid-state track recorder neutron dosimetry in the Three-Mile Island Unit-2 reactor cavity
[DE85-011380] 20 p3531 N85-31966
Experimental method for measuring positronium reflection from surfaces
[DE85-010949] 20 p3531 N85-31967
Operation of solid state lasers exposed to electron beam 21 p3685 N85-32895
On-line temperature sensor
[DE85-011641] 22 p3787 N85-33465
Data Base Workshop: Availability-Reliability Modeling
[DE85-011570] 22 p3829 N85-33713
Neutronic calculations for a new high flux reactor
[DE85-011551] 24 p4150 N85-35734

NUCLEAR RELAXATION
Nuclear Magnetic Resonance of Polymeric Materials
[AD-A145078] 01 p0032 N85-10192
Theory of nuclear magnetic relaxation
[AD-P003911] 01 p0032 N85-10197

NUCLEAR RESEARCH
Engineering Physics Division
[DE84-007778] 02 p0274 N85-11787
China report: Science and technology
[JPRS-CST-84-025] 11 p1620 N85-20197
USSR report: Engineering and equipment
[JPRS-UEQ-85-004] 17 p2939 N85-28142

NUCLEAR RESEARCH AND TEST REACTORS
NT EXPERIMENTAL BREEDER REACTOR 2
NT HEALTH PHYSICS RESEARCH REACTOR
NT HIGH TEMPERATURE NUCLEAR REACTORS
NT JANUS REACTOR
Lidar-Thomson scattering --- nuclear fusion
[IPP-1/299] 08 p1221 N85-17693
Lidar-Thomson scattering --- Joint European Torus
[IPF-84-3] 09 p1394 N85-18777
NBS (National Bureau of Standards) reactor: Summary of activities Jul. 1983 through Jun. 1984
[PB85-184836] 20 p3522 N85-31907
Scientific Opportunities with Advanced Facilities for Neutron Scattering
[DE85-012113] 22 p3639 N85-33770

NUCLEAR SCATTERING
NT NEUTRON SCATTERING
NT RESONANCE SCATTERING
Bremsstrahlung from nuclear scattering at low energy near a resonance
[DE84-014852] 04 p0561 N85-13572
Toward the question of multi-quark configurations in nuclei 21 p3691 N85-32929
A unification of the interactions and the diffractive processes 24 p4173 N85-35870
On mini-cluster observed by Chacaltaya emulsion chamber experiment
[HE-3.6-12] 24 p4185 N85-35959

NUCLEAR SHIELDING
U RADIATION SHIELDING

NUCLEAR SPIN
Nuclear Magnetic Resonance of Polymeric Materials
[AD-A145078] 01 p0032 N85-10192
NMR (Nuclear Magnetic Resonance) and macromolecular migration in a melt or in concentrated solutions
[AD-P003908] 01 p0032 N85-10194
Collisional pumping for the production of intense spin-polarized, neutral beams: Target considerations
[DE85-003459] 11 p1723 N85-20841
Remarks on nucleon-nucleon hard scattering
[NIKHEF-H/84-14] 20 p3532 N85-31979

NUCLEAR STRUCTURE
Comment on the validity of an L2 treatment of the center of mass problem
[CSIR-TWISK-324] 01 p0114 N85-10779
Study of structure of nuclei with neutrons and nuclear data measurements for MFE
[DE84-015128] 01 p0117 N85-10802
Dirac single particle wave functions in inelastic electron scattering
[DE84-015129] 02 p0279 N85-11814
Studies of P-shell nuclei by large momentum transfer electron scattering
[DE84-016803] 09 p1381 N85-18686
Investigations of the structure and electromagnetic interactions of few-body systems
[DE85-002854] 11 p1721 N85-20824
Nuclear spectroscopic studies
[DE85-006894] 16 p2862 N85-27652
Extension of the consistent Q formalism to odd-A nuclei in the W-Pt region
[DE85-008284] 17 p3034 N85-28770
High energy gamma rays from complex particle collisions
[DE85-007871] 17 p3036 N85-28783
A 200-MeV pi(+) induced nucleon removal from 24Mg
17 p3042 N85-28821
S-matrix theory of nuclear forces
[DE85-007633] 18 p3179 N85-29710
Boson-fermion symmetries in the W-Pt region
[DE85-009755] 19 p3362 N85-30845
Nuclear structure problems in double beta decay
[DE85-010739] 19 p3364 N85-30859

NUCLEAR TEST REACTORS
U NUCLEAR RESEARCH AND TEST REACTORS

NUCLEAR WASTES
U RADIOACTIVE WASTES

NUCLEAR WEAPONS
Directed energy missile defense in space
[PB84-210111] 01 p0015 N85-10095
US said to seek military advantage in space
16 p2727 N85-26831
Military journal on US intelligence satellites
16 p2727 N85-26832
Surveillance program for the dissection and analysis of explosive and pyrotechnic components
[DE85-006105] 16 p2757 N85-27016
Nuclear thermal transmittance in the atmosphere using LOWTRAN-6 computer code
[AD-A154669] 21 p3630 N85-32553
Evaluation of nuclear detonation location capability under high attack scenario
[AD-A155761] 24 p4149 N85-35729

NUCLEATE BOILING
Subcooled flow boiling at high heat flux
[OUEL-1540/84] 08 p1163 N85-17338
An experimental apparatus to study nucleate pool boiling of R-114 and oil mixtures
[AD-A154077] 19 p3265 N85-30249

NUCLEATION
NT CLOUD SEEDING
Experimental and theoretical study of condensation in multicomponent vapors
[DE84-015610] 02 p0174 N85-11164
Dynamic crystallization of silicate melts
[NASA-CR-174103] 05 p0743 N85-14774
Homogeneous condensation of gaseous mixtures of Si, Fe, O, N, and C in relative cosmic abundance and implications for astronomical condensation
06 p0867 N85-15632
Fundamentals of microcrack nucleation mechanics
[NASA-CR-3851] 07 p0975 N85-16195
Influence of the amorphous-crystalline interface morphology on dislocation nucleation in pre-amorphized silicon
[DE85-002068] 09 p1398 N85-18800
Experimental and theoretical study of condensation in multicomponent vapors
[DE85-000843] 10 p1485 N85-19376

The role of void nucleation in the swelling resistance of ferritic steel
[AERE-R-11525] 11 p1610 N85-20122

A computer simulation of thin film nucleation and growth: The Volmer-Weber case
[NASA-TM-86068] 12 p1796 N85-21264

Photo-thermal detection of the onset of photo-chemical nucleation (laser-snow) in vapor
[AD-A150111] 12 p1801 N85-21295

Ionic mechanisms of soot formation in flames
[AD-A150119] 12 p1801 N85-21297

Nucleation of phase transitions in the vicinity of phase boundary. Part 1: Comparison of various idolated mechanisms. Part 2: Coupled cluster growth processes
[N-0208-5658] 12 p1938 N85-22174

Theory of oriented nucleation with asymmetric single elements. 2: Effects of rotational diffusion
[IFTR-32/1984] 12 p1939 N85-22179

Research on the kinetics of phase changes in solids
[AD-A152387] 17 p2918 N85-27989

Experimental and theoretical study of condensation in multicomponent vapors
[DE85-009357] 17 p2923 N85-28021

Interfacial segregation and fracture
[DE85-009779] 18 p3075 N85-29019

Flow field effects on nucleation in a reacting mixing layer
[ARL/AERO-R-165] 19 p3263 N85-30237

Amorphous alloys of ion-implanted Fe-Ti-C
[DE85-010656] 19 p3360 N85-30834

Ice nucleation by silver iodine particles with nearly critical sizes 21 p3636 N85-32600

The nucleation of ice crystals during the freezing of large supercooled drops 21 p3640 N85-32606

Concentrations of ice nuclei of different modes of activities 21 p3641 N85-32616

The nucleation of ice at very low temperatures and pressures 21 p3641 N85-32617

Ice nucleating characteristics of Capparis Aphylla, an Indian herb 21 p3641 N85-32619

The capture of ice nucleating and non ice-nucleating aerosols by ice phase precipitation
21 p3641 N85-32620

Supersaturation obtained in a condensation nucleus counter 21 p3642 N85-32624

Basic ice nucleation mechanisms on mono and microcrystals and ice forming nuclei. Theoretical analysis and experimental results achieved in the laboratory over the past ten years: Review paper
21 p3642 N85-32629

Ice nucleation of single water droplet by silver iodide: A laboratory observation 21 p3643 N85-32630

Ice-forming efficiency of the soluble and insoluble portions of dust contained in snow
21 p3643 N85-32631

Critical supersaturations with respect to water for fast condensation-freezing ice nucleation
21 p3643 N85-32632

Concentration and source areas of ice nuclei in the Alaskan atmosphere 21 p3643 N85-32634

Cloud droplet nucleation and initial growth derived from lidar depolarization studies 21 p3644 N85-32635

Eleventh International Conference on Atmospheric Aerosols, Condensation and Ice Nuclei, volume 1
[PB85-182400] 21 p3644 N85-32636

The first condensation nucleus conference
21 p3644 N85-32637

The influence of Brownian coagulation on the size distributions of atmospheric aerosols
21 p3645 N85-32643

Measurements of giant salt nuclei from inland in east China 21 p3648 N85-32668

Cloud condensation on insoluble particles
21 p3648 N85-32670

The measured rate of condensation nucleation to droplets using the techniques of chemical kinetics
21 p3652 N85-32694

Effect of ions on cloud formation and its role in solar terrestrial relationship 21 p3653 N85-32697

Modeling granular explosive detonations with shear band concepts
[DE85-011823] 22 p3754 N85-33271

Interrelationships among the terrestrial planets
22 p3853 N85-33859

The effect of liquid-liquid phase separation of glass on the properties and crystallization behavior
[NASA-TM-77690] 23 p3919 N85-34285

Size and shape dependence of CO adsorption sites on sapphire supported Fe microcrystals
[NASA-CR-176171] 24 p4160 N85-35794

NUCLEI

Arcsecond positions for milliarcsecond VLBI nuclei of extragalactic radio sources. Part 3: 74 sources
10 p1483 N85-19225

A thermal diffusion chamber for the measurement of cloud condensation nuclei 21 p3642 N85-32627

Breakdown of helium nuclei in matter processed near black holes
[OG-8.2-20] 23 p4021 N85-34916

NUCLEI (NUCLEAR PHYSICS)

NT ALPHA PARTICLES
NT DEUTERONS
NT EVEN-EVEN NUCLEI
NT HEAVY NUCLEI
NT HYPERNUCLEI
NT ODD-EVEN NUCLEI
NT ODD-ODD NUCLEI

Study of structure of nuclei with neutrons and nuclear data measurements for MFE
[DE84-015126] 01 p0117 N85-10802

Energy deposition in microvolumes of silicon from high energy proton reactions
[AD-A144713] 01 p0123 N85-10845

Investigations of the structure and electromagnetic interactions of few-body systems
[DE85-002854] 11 p1721 N85-20824

Recent progress in electron scattering at SLAC
[DE85-002718] 11 p1723 N85-20840

Shell-model Lanczos-method studies of the Gamow-Teller strength function in astrophysics
[DE85-004205] 11 p1763 N85-21093

Solar cycle variations of the anomalous cosmic ray component
[PAPER-SH-4.6-2] 21 p3715 N85-33057

Radial and latitudinal gradients of anomalous oxygen during 1977 - 1985
[PAPER-SH-4.6-4] 21 p3716 N85-33058

NMR in the 80 s: New nuclei, new pulses — nuclear magnetic resonance (NMR)
[DRIC-T-7467] 22 p3836 N85-33754

Ninteenth International Cosmic Ray Conference. OG sessions, volume 2
[NASA-CP-2376-VOL-2] 22 p3875 N85-34006

Absolute rigidity spectrum of protons and helium nuclei above 10 GV/c
[OG-4.1-1] 22 p3875 N85-34007

Charge and energy dependence of the residence time of cosmic ray nuclei below 15 GeV/nucleon
[OG-4.1-3] 22 p3876 N85-34009

Relative abundances of sub-iron to iron nuclei in low energy (50-250 MeV/N) cosmic rays as observed in the Skylab experiment
[OG-4.1-4] 22 p3876 N85-34010

Cosmic ray charge and energy spectrum measurements using a new large area Cerenkov x dE/dx telescope
[OG-4.1-5] 22 p3876 N85-34011

Energy spectrum of cosmic-ray iron nucleus observed with emulsion chamber
[OG-4.1-10] 22 p3877 N85-34016

Measurement of the iron spectrum from 60 to 200 GeV per nucleon
[OG-4.1-11] 22 p3877 N85-34017

Cosmic ray nuclei of energy 50 GeV/NUC
[OG-4.1-12] 22 p3877 N85-34018

Composition and energy spectra of cosmic ray nuclei above 500 GeV/nucleon from the JACEE emulsion chambers
[OG-4.1-13] 22 p3877 N85-34019

Charge composition and energy spectral of cosmic ray primary particles for energies higher than 1 TeV
[OG-4.1-14] 22 p3877 N85-34020

Measurements of galactic hydrogen and helium isotopes from 1978 through 1983
[OG-4.2-2] 22 p3877 N85-34022

Primary cosmic ray spectrum in the 10 to the 12th power - 10 to the 16th power eV energy range from the NUSEX experiment
[OG-5.1-5] 22 p3881 N85-34047

Observation of arrival times of EAS with energies or = 6 x 10 (14) eV
[OG-5.3-8] 22 p3885 N85-34074

Search for heavy antinuclei in the cosmic radiation
[OG-6.1-2] 22 p3887 N85-34093

Analysis of experimental data on interstellar antiprotons in the light of measurements of high-energy electrons and He-3 nuclei
[OG-6.1-6] 22 p3888 N85-34097

Study of photon emission by electron capture during solar nuclei acceleration, 1: Temperature-dependent cross section for charge changing processes
[SH-1.1-8] 23 p3990 N85-34735

Study of photon emission by electron capture during solar nuclei acceleration. 2: Delimitation of conditions for charge transfert establishment
[SH-1.1-9] 23 p3990 N85-34736

Observation of the fluxes of nuclei with energies 10-20 MEV per nucleon during the solar flare of April 26, 1984
[SH-2.1-1] 23 p3996 N85-34783

Measurements of the fragmentation of (40)Ar, (28)Si and (12)C in CH2C and H targets between 300 and 1500 MeV/nuc at the Bevalac
[OG-7.2-19] 23 p4016 N85-34866

Cross sections for the production of fragments with Z greater than or equal to 8 by fragmentation of Z greater than or equal to 9 and less than or equal to 28 nuclei
[OG-7.2-22] 23 p4016 N85-[illegible]

Calculation of improved spallation cross sections
[OG-7.2-23] 23 p4017 N85-[illegible]

Cerenkov counters for high energy nuclei: Some new developments
[OG-9.1-5] 23 p4023 N85-[illegible]

Detector calibration of the Indian cosmic ray experiment (IONS) in Space-Shuttle Spacelab-13
[SH-9.1-2] 23 p4050 N85-35117

Observation of nuclei with energies 8-30 MeV per nucleon in the Earth's magnetosphere at the altitudes 350 KM
[SH-10.1-5] 23 p4053 N85-3513[illegible]

Nineteenth International Cosmic Ray Conference. HE Sessions, volume 6
[NASA-CP-2376-VOL-6] 24 p4170 N85-358[illegible]

On total cross sections and slopes at superhigh energies
[HE-1.1-4] 24 p4170 N85-358[illegible]

Measurement of interaction cross section of cosmic ray Fe nuclei (E4 GeV/N) with Al target
[HE-1.1-7] 24 p4170 N85-358[illegible]

Empirical description of the hadron-hadron and hadron-nucleus interaction at the accelerator energy range
[HE-1.2-4] 24 p4171 N85-358[illegible]

Low P sub T hadron-nucleus interactions
[HE-1.2-7] 24 p4172 N85-358[illegible]

Anuglar distribution of shower particles produced in the collisions of 20-GeV/c and 300-GeV negative pions with emulsion nuclei 24 p4172 N85-358[illegible]

Determination of primary energy in nucleus-nucleus collisions and the high P(sub)T tail of alpha-particles
24 p4173 N85-35875

Stopping relativistic Xe, Ho, Au and U nuclei in nuclear emulsions 24 p4173 N85-35876

Physical meaning of the multiplicities of emitted nucleons in hadron-nucleus collisions 24 p4174 N85-35877

How are particle production, nucleon emission and target fragment evaporation processes interrelated in hadron-nucleus collisions? 24 p4174 N85-35878

Experimental evidence of the decrease of kinetic energy of hadrons in passing through atomic nuclei
24 p4174 N85-35880

Energy-range relations for hadrons in nuclear matter
24 p4174 N85-35881

Scattering and stopping of hadrons in nuclear matter
24 p4174 N85-35882

Measurements of hadron mean free path for the particle-producing collisions in nuclear matter
24 p4174 N85-35883

The phi-meson and Chiral-mass-meson production in heavy-ion collisions as potential probes of quark-gluon-plasma and Chiral symmetry transitions
24 p4175 N85-35884

Experimental basis for the models of cascade propagation in atmosphere
[HE-3.6-6] 24 p4185 N85-35954

A study of gamma-families generated in nucleon-nucleus (NA) and pion-nucleus (pi A) interactions
[HE-3.7-2] 24 p4186 N85-35961

Dependence of the average spatial and energy characteristics of the hadron-lepton cascade on the strong interaction parameters at superhigh energies
24 p4188 N85-35977

A facility for investigation of multiple hadrons at cosmic-ray energies
[HE-4.6-8] 24 p4197 N85-36045

Photo nuclear energy loss term for muon-nucleus interactions based on xi scaling model of QCD
[HE-5.2-17] 24 p4204 N85-36090

NUCLEIC ACIDS

NT DEOXYRIBONUCLEIC ACID
NT RIBONUCLEIC ACIDS

NUCLEON-NUCLEON INTERACTIONS

Theoretical aspects of the nucleon-nucleon workshop
[DE85-003740] 14 p2420 N85-24933

Nonrelativistic theory of heavy-ion collisions
[DE85-007538] 17 p3031 N85-28747

Nucleon-nucleon program at TRIUMF
[DE85-900430] 17 p3032 N85-28756

S-matrix theory of nuclear forces
[DE85-007633] 18 p3179 N85-29710

Development of the relativistic impulse approximation
[DE85-008505] 18 p3179 N85-29711

Intermediate energy nuclear theory
[DE85-010440] 18 p3182 N85-29731

Summary of the discussion of the theory of radiative processes
[DE85-007812] 19 p3371 N85-30914

Antiproton-nucleus inelastic scattering and the spin-isospin dependence of the N anti N interaction
[DE85-010546] 20 p3526 N85-31935

The nucleon intensity in the atmosphere and the Pt distribution
[HE-3.1-9] 24 p4178 N85-35907
New aspects in nucleon-nucleus collisions and EAS properties around 10(6) GeV 24 p4187 N85-35974
Small air showers and collider physics
[HE-4.1-9] 24 p4187 N85-35975
Primary chemical composition from simultaneous recording of muons induced cascades and accompanying muon group underground
[HE-5.1-13] 24 p4201 N85-36075
NUCLEON-NUCLEON SCATTERING
Remarks on nucleon-nucleon hard scattering
[NIKHEF-H/84-14] 20 p3532 N85-31979
Comparison of big event with calculations of the air shower development
[HE-3.6-6] 24 p4185 N85-35956
NUCLEONS
Bremsstrahlung from nuclear scattering at low energy near a resonance
[DE84-014862] 04 p0561 N85-13572
Solar He-3-rich events and non-relativistic electron events: A new association
[NASA-TM-86179] 06 p0690 N85-15652
Neutral-current x-distributions
[DE84-016522] 09 p1382 N85-18891
A 200-MeV pi(+) induced nucleon removal from 24Mg 17 p3042 N85-28621
Soliton matter as a model of dense nuclear matter
[DE85-009937] 19 p3359 N85-30825
Deep-inelastic lepton scattering by nuclei: The pion-exchange model
[DE85-010498] 19 p3359 N85-30828
Discussion session: Nucleon- and antinucleon-nucleus inelastic scattering and charge exchange
[DE85-010723] 19 p3364 N85-30860
Cosmic ray He3 measurements
[OG-4.2-3] 21 p3714 N85-33045
Initial results from the Caltech/DSRI balloon-borne isotope experiment
[OG-4.3-8] 21 p3714 N85-33046
K(-) hydrogen bound and continuum states in momentum space
[DE85-010429] 22 p3841 N85-33789
New calorimetric all-particle energy spectrum
[OG-5.1-4] 22 p3881 N85-34046
Observation of nuclei with energies 8-30 MeV per nucleon in the Earth's magnetosphere at the altitudes 350 KM
[SH-10.1-5] 23 p4053 N85-35136
Heavy cosmic ray measurement aboard Spacelab-1
[SH-10.1-7] 23 p4053 N85-35138
Proceedings of the Workshop on Detectors for Relativistic Nuclear Collisions
[LBL-18225] 24 p4146 N85-35700
High energy physics at Tufts University
[DOE/ER-40085/7] 24 p4152 N85-35744
Nucleon-nucleus interactions from JACEE 24 p4173 N85-35869
Is the inelastic charge-exchange contribution constant at the large X and superhigh energies? Qaut 01Kuchin, I. A. 24 p4173 N85-35871
Propagation of cosmic rays through the atmosphere in the quark-gluon strings model 24 p4173 N85-35873
Scaling violation in the fragmentation region of inclusive nucleon spektrum 24 p4173 N85-35874
Physical meaning of the multiplicities of emitted nucleons in hadron-nucleus collisions 24 p4174 N85-35877
How are particle production, nucleon emission and target fragment evaporation processes interrelated in hadron-nucleus collisions? 24 p4174 N85-35878
Experimental study of the space-time development of the particle production process in hadron-nucleon collisions, using massive target nucleus as a detector 24 p4174 N85-35879
Measurements of hadron mean free path for the particle-producing collisions in nuclear matter 24 p4174 N85-35883
Ringlike inelastic events in cosmic rays and accelerators 24 p4175 N85-35887
Experimental basis for the models of cascade propagation in atmosphere
[HE-3.6-6] 24 p4185 N85-35954
On mini-cluster observed by Chacaltaya emulsion chamber experiment
[HE-3.6-12] 24 p4185 N85-35959
A study of gamma-families generated in nucleon-nucleus (NA) and pion-nucleus (pi A) interactions
[HE-3.7-2] 24 p4186 N85-35961
New aspects in nucleon-nucleus collisions and EAS properties around 10(6) GeV 24 p4187 N85-35974
Small air showers and collider physics
[HE-4.1-9] 24 p4187 N85-35975
Sub-luminal pulses from cosmic ray air showers
[HE-4.7-13] 24 p4200 N85-36063
A study of atmospheric neutrinos with the IMB detector
[HE-5.3-7] 24 p4205 N85-36101
Limits on monopole fluxes from KFG experiment
[HE-6.1-6] 24 p4209 N85-36132
Search for proton decay in the Frejus experiment
[HE-6.2-2] 24 p4210 N85-36138
Results on nucleon life-time from the Kolar gold field experiment
[HE-6.2-3] 24 p4211 N85-36139
Construction of the Soudan 2 detector
[HE-6.2-5] 24 p4211 N85-36141
Nucleon decay and atmospheric neutrinos in the Mont Blanc experiment
[HE-6.2-6] 24 p4211 N85-36142
Energetic delayed hadrons in large air showers observed at 5200m above sea level
[HE-6.2-9] 24 p4211 N85-36145
NUCLEOSIDES
NT ADENOSINE DIPHOSPHATE
NT ADENOSINE TRIPHOSPHATE
NT ADENOSINES
The DNA metabolism and poly-(ADP-ribose) synthesis in lymphocytes of persons exposed to low doses of ionizing radiation
[OEFZS-4307] 20 p3507 N85-31800
NUCLEOSYNTHESIS
U NUCLEAR FUSION
NUCLEOTIDES
NT ADENOSINE DIPHOSPHATE
NT ADENOSINE TRIPHOSPHATE
NT ADENOSINES
NUCLIDES
NT ALUMINUM ISOTOPES
NT ALUMINUM 26
NT AMERICIUM
NT AMERICIUM ISOTOPES
NT AMERICIUM 241
NT ARGON ISOTOPES
NT BERYLLIUM ISOTOPES
NT BERYLLIUM 7
NT BERYLLIUM 9
NT BERYLLIUM 10
NT BORON 10
NT BROMINE ISOTOPES
NT CALCIUM ISOTOPES
NT CALIFORNIUM ISOTOPES
NT CARBON ISOTOPES
NT CARBON 12
NT CARBON 13
NT CARBON 14
NT CERIUM 144
NT CESIUM ISOTOPES
NT CESIUM 134
NT CESIUM 137
NT CHROMIUM ISOTOPES
NT COBALT 60
NT CURIUM
NT CURIUM 244
NT DEUTERIUM
NT GERMANIUM ISOTOPES
NT HELIUM ISOTOPES
NT HYDROGEN ISOTOPES
NT IODINE ISOTOPES
NT IRON ISOTOPES
NT IRON 59
NT ISOTOPES
NT KRYPTON ISOTOPES
NT KRYPTON 85
NT LUTETIUM
NT MANGANESE ISOTOPES
NT NEODYMIUM ISOTOPES
NT NEON ISOTOPES
NT NICKEL ISOTOPES
NT NITROGEN ISOTOPES
NT NITROGEN 15
NT OXYGEN ISOTOPES
NT PLUTONIUM
NT PLUTONIUM ISOTOPES
NT PLUTONIUM 238
NT PLUTONIUM 239
NT POTASSIUM 40
NT RADIOACTIVE ISOTOPES
NT RADON ISOTOPES
NT RUBIDIUM ISOTOPES
NT SCANDIUM ISOTOPES
NT SODIUM ISOTOPES
NT STRONTIUM 90
NT TELLURIUM
NT THORIUM ISOTOPES
NT TRANSURANIUM ELEMENTS
NT TRITIUM
NT URANIUM ISOTOPES
NT URANIUM 235
NT XENON ISOTOPES
NT XENON 129
The low-energy secondary cosmic ray flux: Detectors in iron meteorites 06 p0687 N85-15635
International program to improve decay data for transactinium nuclides
[DE85-011258] 20 p3529 N85-31954
The isotopic composition of cosmic ray chlorine
[OG-4.3-3] 22 p3878 N85-34028
Cosmic ray isotope measurements with a new Cerenkov X total energy telescope
[OG-4.3-4] 22 p3878 N85-34029
The inner granulometric density of the tracks in nuclear emulsions and its application to determine the chemical spectrum of primary cosmic ray nuclidi
[OG-4.3-9] 22 p3879 N85-34034
Variations in the propagation of UH-nuclei
[OG-7.1-1] 23 p4012 N85-34863
Cosmogenic-nuclide production by primary cosmic-ray protons
[SH-7.1-6] 23 p4047 N85-35098
The detection and study of molecular species using time resolved laser spectroscopy
[AD-A155910] 24 p4075 N85-35256
NULL HYPOTHESIS
Continuity of the null space basis and constrained optimization
[AD-A147038] 07 p1030 N85-16538
On the power functions of test statistics in order restricted inference
[AD-A147126] 07 p1035 N85-16566
A new approach to evaluate gamma-ray measurements
[OG-9.5-11] 23 p4031 N85-34988
NULL ZONES
Parallel processor configuration for adaptive antenna arrays
[AD-D011347] 07 p0942 N85-15970
Null generation using discs on a reflector
[AD-A151897] 15 p2544 N85-25703
Adaptive nulling at HF using a compact array of active parasitic antennas
[AD-A152582] 17 p2948 N85-28203
Effect of some estimators on a large sample approximation to the non-null distribution of the pearson chi-square statistic
[AD-A153515] 18 p3173 N85-29673
Null synthesis with phase and amplitude controls at the subarray outputs
[AD-A155187] 21 p3576 N85-32241
Reconciling Bayesian and frequentist evidence in the one-sided testing program
[AD-A155603] 21 p3678 N85-32950
A planar version of a 4.0 gigahertz reactively steered adaptive array
[AD-A156029] 24 p4087 N85-35330
NUMBER THEORY
NT ARITHMETIC
NT CONGRUENCES
NT DIVIDING (MATHEMATICS)
NT FIXED POINT ARITHMETIC
NT FLOATING POINT ARITHMETIC
NT INDUCTION (MATHEMATICS)
NT INTEGERS
NT MULTIPLICATION
Disproof of the Mertens conjecture
[CWI-NM-R8412] 14 p2414 N85-24896
A convexity theorem for semisimple symmetric spaces
[CWI-PM-R8414] 14 p2415 N85-24900
NUMERICAL ANALYSIS
NT APPROXIMATION
NT BORN APPROXIMATION
NT CHEBYSHEV APPROXIMATION
NT COMPUTATIONAL CHEMISTRY
NT COMPUTATIONAL FLUID DYNAMICS
NT CONJUGATE GRADIENT METHOD
NT DIFFERENCE EQUATIONS
NT EDDINGTON APPROXIMATION
NT ERROR ANALYSIS
NT FINITE DIFFERENCE THEORY
NT FINITE ELEMENT METHOD
NT FINITE VOLUME METHOD
NT HARTREE APPROXIMATION
NT INTERPOLATION
NT ITERATION
NT ITERATIVE SOLUTION
NT LEAST SQUARES METHOD
NT MEAN SQUARE VALUES
NT MONTE CARLO METHOD
NT NEWTON-RAPHSON METHOD
NT NOMOGRAPHS
NT NUMERICAL DIFFERENTIATION
NT NUMERICAL INTEGRATION
NT PADE APPROXIMATION
NT PARTICLE IN CELL TECHNIQUE
NT RELAXATION METHOD (MATHEMATICS)

NT RITZ AVERAGING METHOD
NT RUNGE-KUTTA METHOD
NT TRUNCATION ERRORS

Numerical analysis of the 3-dimensional inviscid hypersonic flow around capsule-type bodies by the alternate directional implicit method
[NAL-TR-799] 01 p0002 N85-10012

Comparison of numerical techniques for integration of stiff ordinary differential equations arising in combustion chemistry
[NASA-TP-2372] 01 p0011 N85-10065

Radiation effects on structural materials
[DE84-014771] 01 p0029 N85-10178

Numerical analysis of some problems related to the mechanics of pneumatic tires: Finite deformation/rolling contact of a viscoelastic cylinder and finite deformation of cord-reinforced rubber composites
01 p0060 N85-10397

Effect of the Basset term on particle relaxation behind normal shock waves
[AD-A145446] 02 p0198 N85-11320

Numerical analysis of parameters of self-heating copper vapor lasers 02 p0260 N85-11704

Difference schemes for equations of Schrodinger type
[AD-A145812] 03 p0410 N85-12622

Application of summability methods to Jackson theorems for splines
[AD-A146256] 03 p0412 N85-12635

The Lindstrom-Madden method for series systems with repeated components
[AD-A146265] 03 p0412 N85-12636

The development of new methods for solving the target identification or inverse scattering problem for time-harmonic acoustic and electromagnetic waves
[AD-A145821] 03 p0415 N85-12657

Analyses of energy extraction efficiency of unstable resonators
[AD-A148301] 06 p0813 N85-15161

Research in applied mathematics, numerical analysis, and computer science
[NASA-CR-172505] 07 p1021 N85-16480

Use of coordinate functions to calculate deformation fields
[BLL-M-36010-(5828.4)] 07 p1028 N85-16524

An efficient numerical solution technique for wave propagation in horizontally stratified ocean environments
[AD-A148537] 08 p1190 N85-17502

Utilization of numerical optimization techniques in the design of robust multi-input, multi-output control systems
[AD-A148289] 08 p1212 N85-17830

A numerical study of several supersonic flows
09 p1272 N85-17995

The analysis by the lumped parameter method of blade platform friction dampers used in the high pressure fuel turbopump on the space shuttle main engine
09 p1338 N85-18417

Exact simultaneous confidence intervals for pairwise comparisons of three normal means
[AD-A146751] 09 p1375 N85-18645

Study on steerability of articulated tracked vehicles
[AD-P004306] 09 p1410 N85-18885

Computable real analysis
[AD-A149079] 10 p1546 N85-19747

A new method of approximating normal and t-tail areas
[AD-A149457] 10 p1548 N85-19761

Numerical simulation of turbulent reacting flows
[DE84-016777] 11 p1632 N85-20276

Numerical investigation of propagation of radiation pulse at xxx 11 p1718 N85-20809

Measurement of the configuration of a concave surface by the interference of reflected light
[NASA-TM-77796] 11 p1726 N85-20867

Evaluation of resonant modes in isolated dielectric resonators using a surface integral equation formulation
[PB85-110831] 12 p1837 N85-21526

Interaction of part-through cracks in a flat plate
[NASA-CR-175588] 12 p1864 N85-21692

Intensification of tropical instabilities
[AD-A149985] 12 p1896 N85-21899

Cumulative reports and publications through December 31, 1984
[NASA-CR-172569] 12 p1911 N85-21991

A linear characteristic-nodal transport method for the two-dimensional (X,Y)-geometry multigroup discrete ordinates equations over an arbitrary triangle mesh
[LA-10092-T] 12 p1913 N85-22006

A method of calculating periodic solutions of second order dynamical systems
[AD-A149634] 12 p1920 N85-22058

Statistics for the maximum of several positive random variables with application to networking
[AD-A150005] 12 p1922 N85-22069

Approximation order from certain spaces of smooth bivariate splines on a 3-direction mesh
[AD-A149633] 12 p1925 N85-22092

Hydrodynamic stability problem formulated by numerical solutions of the Navier-Stokes equations
12 p1946 N85-22223

China report: Science and technology
[JPRS-CST-84-008] 13 p1972 N85-22384

Elasticity solution of an adhesively bonded joint
[NASA-CR-175591] 13 p2101 N85-23097

Evolution of set of Rossby waves toward anisotropic equilibrium state 13 p2109 N85-23141

Two-dimensional numerical model of sensible and latent heat transport in an irrigated field under advective conditions 13 p2131 N85-23261

Second thoughts on the mathematical software effort: A perspective
[DE85-004831] 13 p2146 N85-23333

Computations of two-dimensional airfoil-vortex interactions — helicopter rotor flowfields
[NASA-CR-3885] 14 p2210 N85-23709

Analysis of slabs-on-grade for a variety of loading and support conditions
[AD-A150965] 14 p2264 N85-24030

Flow around axisymmetric bodies with uniform-velocity zones 14 p2276 N85-24103

An analytical and numerical study of the interaction of rarefaction waves with area changes in ducts. Part 2: Area enlargements
[UTIAS-273] 14 p2300 N85-24242

On the influence of turbulent motions on non-radial oscillations 14 p2444 N85-25083

Mathematical aspect of welding technology research discussed 15 p2536 N85-25663

Unsteady Navier-Stokes calculations in an accelerated reference frame
[AD-A151751] 15 p2557 N85-25774

Frequency/period estimation and adaptive rejection of periodic disturbances
[AD-A149229] 15 p2632 N85-26226

Numerical analysis of supersonic reactive flow in wake of reverse step 15 p2643 N85-26303

Forced MHD turbulence in a uniform external magnetic field
[NASA-CR-172576] 15 p2654 N85-26368

Proceedings of the NAL Symposium on Aircraft Computational Aerodynamics
[NAL-SP-1] 16 p2691 N85-26611

Progress of computational fluid dynamics in the world
16 p2691 N85-26612

Numerical analyses in aerodynamic design of aero-engine fan 16 p2692 N85-26618

Numerical simulation of inviscid compressible flow through three-dimensional cascade
16 p2692 N85-26619

A numerical procedure on three-dimensional parabolic flow in duct 16 p2692 N85-26620

Nonlinear structural analysis for fiber-reinforced superalloy turbine blades 16 p2737 N85-26887

Numerical analysis of flow non-uniformity in the hot gas manifold of the Space Shuttle main engine
16 p2738 N85-26899

A study of computational techniques for noncanonical microstrip antennas and arrays
[AD-A152216] 16 p2774 N85-27123

An incremental multigrid strategy for the fluid dynamics equations
[AD-A151953] 16 p2783 N85-27172

In plane stress analysis
[NASA-CR-175775] 16 p2799 N85-27259

A decomposition procedure for convex quadratic programs
[AD-A151732] 16 p2854 N85-27595

Evaluation of an algorithm for the solution of the time-dependent Euler equations
[AD-A151993] 16 p2854 N85-27600

Multiple array processors for ocean acoustic problems
[AD-A152174] 16 p2860 N85-27641

Kinetic theory and simulation of multi-species plasmas in Tokamaks excited with ICRF microwaves
[DE85-008119] 16 p2868 N85-27691

On the choice of coordinates for semiconductor simulation
[AD-A152214] 16 p2870 N85-27706

Numerical solution of one-dimensional nonlinear problems of statics for elastic beams and shells under rigid constraints 17 p2943 N85-28166

Kolmogorov and scalar spectral regimes in numerical turbulence
[NASA-TM-86699] 17 p2957 N85-28264

CALTECH-DOE program on numerical analysis, computing and fundamental studies of motion, energy and mass transfer in fluids
[DE85-008106] 17 p2959 N85-28274

Spectral decomposition and verification of NOGAPS 500MB medium-range forecasts
[AD-A152550] 17 p2996 N85-28520

Software for estimating sparse Hessian matrices
[DE85-008121] 17 p3013 N85-28629

A discussion of adaptive grids and their applicability in numerical hydrodynamic modeling
[AD-A151843] 17 p3017 N85-28669

Numerical methods for stiff ordinary and elliptic partial differential equations
[AD-A153247] 17 p3020 N85-28675

Numerical evaluation of low frequency sound propagation in layered media
[AD-A152690] 17 p3028 N85-28728

Fluid modeling of magnetized plasmas
[DE85-007679] 17 p3039 N85-28804

Numerical analysis of end effects in symmetric laminated plates
[NAL-TR-850] 18 p3068 N85-28977

Time-averaged and time-dependent computations of isothermal flowfields in a centerbody combustor
[AD-A153682] 18 p3100 N85-29189

Laser-stimulated vibrational excitation of an adspecies studied by a generalized master equation: Neutral atomic hydrogen on hydrated KCl(001)
[AD-A153665] 18 p3112 N85-29289

A numerical study of the Pacific polar low
[AD-A153777] 18 p3149 N85-29495

Computable numerical bounds for Lagrange multipliers of stationary points of nonconvex differentiable nonlinear programs
[AD-A153513] 18 p3169 N85-29633

Numerical solutions of the potential distribution within the vacuum region of the FEATRON
[AD-A153683] 18 p3176 N85-29705

Evaluation of the eigenvalue method in the solution of transient heat conduction problems
[AD-A154434] 19 p3266 N85-30258

Computational methods in advanced stress and durability analyses
[AD-A154119] 19 p3286 N85-30375

Foundations of data envelopment analysis for Pareto-Koopmans efficient empirical production functions
[AD-A154244] 19 p3346 N85-30735

Mathematics of surfaces
[DE85-010439] 19 p3346 N85-30742

Effect of diffusely-reflected sunlight on the orbit of LAGEOS 20 p3491 N85-31700

Compressible Lagrangian hydrodynamics without Lagrangian cells
[DE85-009597] 20 p3520 N85-31891

Numerical modeling of subsurface communication
[DE85-012818] 21 p3577 N85-32249

Numerical solutions of turbulent models for flow over a flat plate with angle of attack
[DE85-010380] 21 p3585 N85-32296

A numerical analysis of transient planetary waves and the vertical structure in a meso-strato-troposphere model, part 1.4A 21 p3617 N85-32473

Circulation analysis of two snowstorms during the SNOW-TWO program
[AD-A155225] 21 p3637 N85-32587

Numerical simulations of the response of intense ocean currents to atmospheric forcing
[AD-A155161] 21 p3655 N85-32704

Overlap integrals for atom-metal surface interactions
[AD-A155038] 21 p3702 N85-32988

Method of and apparatus for generating an interstitial point in a data stream having an even number of data points
[NASA-CASE-MFS-25319-1] 22 p3827 N85-33701

QKPLT users guide, version 2.0
[L-10094-M] 22 p3828 N85-33707

Implementing linear multistep formulas for solving DAES
[DE85-012400] 22 p3834 N85-33740

Three-dimensional hydrodynamic hot-spot model
[DE85-009587] 23 p3922 N85-34301

Modeling of geothermal systems
[DE85-012553] 23 p3943 N85-34439

The impact of supercomputers on experimentation: A view from a national laboratory
[NASA-TM-86822] 23 p3955 N85-34510

Analytic and numerical calculations of the ambipolar electric field in a stellarator 23 p3978 N85-34665

Numerical simulation in astrophysics: Smoothed particle methods 23 p3979 N85-34674

Numerical calculations on shock loaded materials
23 p3980 N85-34676

Two-dimensional simulation of LIB target implosion
23 p3980 N85-34678

Effects of a wavy neutral sheet on cosmic ray anisotropies
[SH-4.2-11] 23 p4006 N85-34846

The influence of nonstationarity of the solar activity and general solar field on modulation of cosmic rays
[SH-4.2-17] 23 p4006 N85-34854

Time-dependent nonlinear cosmic ray shocks confirming abstract
[OG-8.1-3] 23 p4017 N85-34890

Algorithmic approaches in sets of good answers in inverse problems
[PM/84/16] 24 p4142 N85-35677

Invariant tests and likelihood ratio tests for multivariate elliptically contoured distributions
[AD-A158844] 24 p4142 N85-35679

Constrained stiffness matrix adjustment using mode data
[AD-A155868] 24 p4143 N85-35685

Relation between field energy and RMS emittance in intense particle beams
[DE85-012665] 24 p4159 N85-35784

Analytical-numerical methods of calculations of energy and three-dimensional particle distributions in electromagnetic cascades
[IE-3.5-13] 24 p4184 N85-35950

NUMERICAL CONTROL

Publications of Center for Manufacturing Engineering (of the National Bureau of Standards), 1978-1983
[PB84-224526] 01 p0036 N85-10228

The NBS tri-directional test facility
[PB84-217462] 01 p0051 N85-10334

Autonomous Attitude Determination System (AADS). Volume 1: System description
[NASA-TM-87365] 02 p0240 N85-11559

Experimental study with parameter variations on a hydraulic positioning servo with computer implemented observer
[FOA-C-20545-E3] 02 p0256 N85-11673

Development of a modular multicoordinate measuring system with continuous-path microprocessor control
[BMFT-FB-T-84-158] 03 p0406 N85-12608

Advances of implementing NC machine tools discussed 04 p0491 N85-13131

Portable microprocessor-controlled instrument for sensing, identifying and monitoring gaseous chemicals
[DE84-013431] 04 p0504 N85-13214

Design of a flexible machining system
[CETIM-1-3E-140] 04 p0510 N85-13252

A unified method for evaluating real-time computer controllers: A case study — aircraft control
[NASA-CR-174168] 04 p0547 N85-13478

Optical characterization of radiation-resistant fibers
[DE84-015246] 05 p0620 N85-13964

Programming and application of numerical controlled measuring machines (NCMES)
[BMFT-FB-T-84-153] 05 p0717 N85-14599

Efficiency of programmed motion control systems
06 p0776 N85-14961

NC programming, machine tool information
06 p0816 N85-15178

Performance characteristics of a battery charger and state-of-charge indicator
[NASA-CR-174273] 07 p0946 N85-15992

Passive maser using timesharing for control of the cavity and control of the oscillator on the line of stimulated emission
[AD-D011326] 07 p0969 N85-16151

Shuttle avionics software trials, tribulations and success 08 p1090 N85-16891

Man-machine interface and control of the shuttle digital flight system 08 p1091 N85-16894

Space shuttle main engine hardware simulation
08 p1091 N85-16895

Flexible manufacturing system for the production of aircraft parts
[BLL-PNR-90237-(8019.3153)]
08 p1137 N85-17159

New applications for robot loaders, unloaders
08 p1139 N85-17175

Utilization of numerical optimization techniques in the design of robust multi-input, multi-output control systems
[AD-A148289] 08 p1212 N85-17630

Design description of a microprocessor based Engine Monitoring and Control unit (EMAC) for small turboshaft
[NASA-TM-86660] 09 p1263 N85-17935

Design and realization of a multiradar tracking system for air traffic control
[ENST-84E010] 09 p1279 N85-18044

Flexible manufacturing system for machining axially symmetric workpieces
[PNR-90229] 09 p1305 N85-18196

The control of manufacturing systems for varying medium-batch production
[PNR-90235] 09 p1371 N85-18616

Strategy planning by an intelligent machine
[DE84-016609] 09 p1372 N85-18624

Electric vehicle battery test plan and results
[DE84-901972] 09 p1410 N85-18887

Armenia markets new drive motors for machine tools
10 p1481 N85-19212

Productivity gains through CAD of CNC programs
10 p1482 N85-19219

A microprocessor controlled parallel model with FDPSK 10 p1475 N85-19304

The F-18: A new era for human factors
10 p1534 N85-19671

Reliability of DNC system examined
11 p1617 N85-20171

New CNC systems described
11 p1617 N85-20172

Digital temperature and velocity control of mach 0.3 atmospheric pressure durability testing burner rigs in long time, unattended cyclic testing
[NASA-TM-86959] 12 p1805 N85-21321

Synthesis of digital control for object with lag
12 p1843 N85-21562

SIMULA: Digital controller simulation package
[PB85-134492] 12 p1917 N85-22041

Sensor control of robot arc welding
12 p1948 N85-22233

A computer controlled mass spectrometer system for investigating the decomposition of non-metallic materials under atmospheric conditions 12 p1948 N85-22237

Research and Modeling of Supervisory Control Behavior, report of a workshop
[AD-A149621] 12 p1950 N85-22248

Reliability of robotized welding apparatus
13 p2034 N85-22741

Assembly robot control algorithms
13 p2046 N85-22806

Manufacturing perspective in the design of bevel gearing 14 p2221 N85-23777

Milling machine with numerical programmed control for cutting teeth 14 p2268 N85-24052

Mechanization and automation of production processes in turbine building 14 p2269 N85-24057

Manufacture of drive wheel vanes for hydraulic turbines on program controlled machine tools
14 p2269 N85-24058

Use of program controlled machine tools to automate and mechanize production processes in pipe manufacture 14 p2269 N85-24059

USSR report: Machine tools and metalworking equipment
[JPRS-UMM-85-006] 14 p2283 N85-24146

New CNC turning centers described
14 p2284 N85-24148

Large CNC machining center for turbine production
14 p2284 N85-24149

Minister B. V. Balmont on status of automation drive
14 p2284 N85-24151

Robots for application in forge-press operation
14 p2284 N85-24154

Integrated control system for FMS components
14 p2285 N85-24156

Automating the study of error in discrete aerodynamic fairing design 14 p2288 N85-24176

French work toward flexible software workshops
14 p2289 N85-24187

Investigation of doubly-fed machine in variable speed application
[DE85-004378] 14 p2299 N85-24234

Czech institute develops microcomputer for satellites
15 p2484 N85-25331

Selection of optimal control program for solar cell panels of Earth satellites 15 p2484 N85-25335

Electrical features of new DNC, CNC system viewed — direct numerical control 15 p2524 N85-25562

Microcomputer controlled image acquisition system
15 p2537 N85-25654

Microcomputer controlled automatic peak locking of laser circuit 15 p2537 N85-25655

Using a single-board computer to maintain constant voltage, current sources 15 p2551 N85-25749

Development of robots and application to industrial processes
[NASA-CR-175754] 15 p2567 N85-25840

Application of AFTI/F-16 task-tailored control modes in advanced multirole fighters 16 p2712 N85-26735

X-29A digital flight control system design
16 p2712 N85-26736

Some flight test results with redundant digital flight control systems 16 p2712 N85-26739

An update on experience on the fly by wire Jaguar equipped with a full-time digital flight control system
16 p2712 N85-26740

Optimal control of electric drive with simultaneous control inputs for motor current and flux
16 p2763 N85-27049

Development, implementation of industrial lasers reviewed 16 p2767 N85-27075

Guidelines for optimization of robotized machining cells 16 p2767 N85-27076

The development and application of volume scan and cell tracking capabilities for the analysis of convective cloud systems 16 p2830 N85-27451

Corrective-predictive systems
[BLL-M-36063-(5828.4)] 16 p2851 N85-27573

The application of numerical control (NC) in manufacturing wind tunnel models
[B8580078] 17 p2939 N85-28140

Automation of Precise Time Reference Stations (PTRS) 17 p2962 N85-28291

Adapting shape parameters for cubic Bezier curves
17 p3004 N85-28576

Triangular Berstein-Bezier patches, a survey and new results 17 p3005 N85-28577

A uniform subdivision method for triangular Bezier patches 17 p3005 N85-28578

Microprocessor controlled temperature chassis
[DE85-008392] 17 p3009 N85-28602

Automatic volume calibration system
[DE85-008955] 18 p3102 N85-29204

An interactive computer aid for the design and analysis of linear, single input/single output digital and continuous control systems
[AD-A153704] 18 p3162 N85-29589

Space station automation study. Volume 1: Executive summary. Autonomous systems and assembly
[NASA-CR-171514] 19 p3226 N85-30002

MELCOR Accident Consequence Code System (MACCS)
[DE85-009712] 19 p3339 N85-30689

Computer-controlled carburizing
[BLL-OA-TRANS-3204-(6196.300)]
20 p3429 N85-31268

Drag soldering process control
[DE85-010853] 20 p3433 N85-31301

Flight control system for a computer controlled aircraft with limited sensors
[AD-A155107] 21 p3555 N85-32115

Speech understanding research
[AD-A155462] 21 p3700 N85-32990

Standard series of direct-current motors for regulated electric drives 22 p3772 N85-33375

Project management using graphics
23 p3962 N85-34560

The automatic labeling of geographic maps: A problem in computer aesthetics 23 p3962 N85-34561

Design and construction of an advanced power conditioning subsystem for small photovoltaic applications
[DE85-013940] 24 p4113 N85-35496

Optimizing data access in the LAMPF control system
[DE85-012653] 24 p4140 N85-35663

Distribution of computer functionality for accelerator control at the Brookhaven AGS
[DE85-012520] 24 p4141 N85-35669

On-line model driven control of the SLC electron Damping Ring
[DE85-013377] 24 p4157 N85-35772

NUMERICAL DIFFERENTIATION

Methods for numerical differentiation
[AD-A145058] 01 p0112 N85-10756

On edge detection
[AD-A148573] 08 p1223 N85-17703

NUMERICAL FLOW VISUALIZATION

Numerical methods for bluff body aerodynamics
05 p0593 N85-13762

Developments in the simulation of compressible inviscid and viscous flow on supercomputers
[NASA-TM-86674] 11 p1575 N85-19924

Calculation of an unsteady transonic flow with shock waves and separation in Laval nozzles
[MPIS-14/1984] 14 p2213 N85-23728

Calculation of transonic flows around an aircraft configuration with motorized nacelle
[SNIAS-851-111-106] 20 p3387 N85-31009

NUMERICAL INTEGRATION

NT RUNGE-KUTTA METHOD

Oscillatory integrals by Hermite interpolatory rules
[CSIR-TWISK-301] 01 p0108 N85-10725

Conservation laws and the numerical solution of ODEs
[DE84-016206] 04 p0555 N85-13531

Orbit extrapolation — satellite orbits
05 p0596 N85-13811

Calculation of cumulative distributions and detection probabilities in communications and optics
[AD-A147781] 08 p1215 N85-17650

Contribution to the study of a numerical implicit method for solving the Euler equations
[ESA-TT-872] 10 p1549 N85-19771

Triple layer system for numerical integration of equations of gas dynamics and nonlinear heat conduction equation
[DE85-000297] 11 p1632 N85-20277

Evaluation of two numerical integrator schemes
[PB85-138196] 11 p1683 N85-20603

A comparison of the efficiency of numerical methods for integrating chemical kinetic rate equations
[NASA-TM-83590] 12 p1778 N85-21162

Nonlinear sigma-models and integration methods
[DE85-004447] 12 p1922 N85-22071

Problem of diffraction by wavy surface: Comparison of numerical methods of solution
13 p2079 N85-22965
Improved accuracy in solid isoparametric elements using selectively reduced integration 15 p2573 N85-25865
Numerical integration through force discontinuities: Solar radiation pressure 16 p2805 N85-27298
Sensitivity analysis of initial value problems with mixed ode's and algebraic equations
[AD-A153528] 18 p3169 N85-29637
Bayesian inference and diagnostics for the 3 parameter logistic model
[AD-A153840] 18 p3175 N85-29681
Numerical optical computing at the Ohio State University 18 p3188 N85-29775
Application of closed-form solutions to a mesh point field in silicon solar cells 20 p3482 N85-31637
Reliability prediction of the series system with spares subject to Weibull failure 24 p4100 N85-35413

NUMERICAL STABILITY
On explicit difference schemes for hyperbolic systems with variable coefficient 2
[PREPRINT-808] 03 p0413 N85-12641
Convergence of method of lines approximations to partial differential equations
[CWI-NM-R8404] 05 p0720 N85-14627
Stability results for discrete Volterra equations: Numerical experiments
[CWI-NM-R8409] 11 p1707 N85-20743
Lyapunov stability of very simple steady solutions of prognostic systems 14 p2333 N85-24429
On the stability of predictor-corrector methods for parabolic equations with delay
[CWI-NM-R8410] 14 p2410 N85-24860
A stability analysis of incomplete LU factorizations
[AD-A152058] 15 p2638 N85-26271
Squeezing the most out of Eigenvalue solvers on high-performance computers
[DE85-007569] 16 p2849 N85-27565
Stability of functionals determined by moment conditions
[TRITA-NA-8310] 16 p2852 N85-27585
Compressor and turbine models - numerical stability and other aspects
[AD-A153811] 18 p3063 N85-28948
Evaluation of the eigenvalue method in the solution of transient heat conduction problems
[AD-A154434] 19 p3266 N85-30256
A numerical and analytical investigation of lee cyclogenesis
[AD-A155607] 21 p3638 N85-32594

NUMERICAL WEATHER FORECASTING
Rain bands and symmetric instability
01 p0075 N85-10496
Test results from RAINSAT 01 p0076 N85-10506
The potential use of atmospheric profilers in short-range prediction 01 p0078 N85-10518
A simulation experiment of a rapidly developed medium scale cyclone 01 p0079 N85-10530
Application of mesoscale numerical model to local weather prediction 01 p0080 N85-10532
The United Kingdom Meteorological Office mesoscale forecasting system 01 p0080 N85-10533
Numerical forecast of pressure field by considering the mutual influence of orography, thermal nonhomogeneity and surface friction 01 p0080 N85-10534
Evaluation of an integrated mixed-layer model for single station prediction in a marine regime
01 p0080 N85-10535
A local dynamical interpretation method of numerical weather forecasting 01 p0080 N85-10536
An operational numerical model for prediction of fog and stratus 01 p0080 N85-10537
Operational use of shipboard numerical aid programs
01 p0082 N85-10546
A system for meteorological satellite, radar, conventional data and model analysis 01 p0082 N85-10551
Development of an operational system for Very-Short-Range Forecasting (VSRF) at Swedish Meteorological and Hydrological Institute (SMHI)
01 p0083 N85-10559
The extremeness of the cold front of December 31, 1978 over the CSR
[REPT-568] 03 p0377 N85-12409
Impact of ERS-1 observations on wave forecasting in the North Sea 03 p0381 N85-12437
Recent examples of mesoscale numerical forecasts of severe weather events along the east coast
[NASA-TM-86172] 03 p0395 N85-12523
Operational numerical forecasts: Survey and verification over the period 1978-1983
[KNMI-TR-49] 04 p0540 N85-13435
Orographic effects in atmospheric circulation
05 p0679 N85-14362
Spectral general circulation model development
05 p0679 N85-14363
Numerical modeling of the atmosphere
05 p0680 N85-14370
Comparison of optimum interpolation and Cressman analyses 05 p0680 N85-14371
Normal mode initialization 05 p0680 N85-14372
Forecast impact of components of the FGGE observing system 05 p0681 N85-14373
Applications of sequential estimation to numerical weather prediction 05 p0681 N85-14374
Some new mathematical methods for variational objective analysis 05 p0681 N85-14375
Extended range forecasting 05 p0681 N85-14376
Weather and climate parameters from Tiros-N
05 p0681 N85-14377
Applications of TOMS ozone data and clustering techniques in satellite soundings
05 p0681 N85-14379
Research relative to high spatial resolution passive microwave sounding systems 05 p0681 N85-14380
ECMWF/NMC/GLAS joint simulation study
05 p0682 N85-14385
The use of available potential energy to evaluate two GLAS FGGE data sets 05 p0682 N85-14387
Comparison of forecast and observed energetics
05 p0683 N85-14389
Energy diagnostics and impact studies of FGGE global data sets and GLAS GCM simulations
05 p0683 N85-14390
Spectral energetics diagnoses and FGGE spectral observing periods and energetics analyses of forecast experiments with GLAS GCM 05 p0683 N85-14391
Jet stream errors and tropospheric-stratospheric interactions in the GLAS general circulation model
05 p0683 N85-14392
Theoretical modeling for numerical weather prediction
05 p0684 N85-14395
Numerical prediction of the president's day cyclone
05 p0684 N85-14399
Development of guidance forecasts at the Royal Netherlands Metorological Institute (KNMI). Part 1: General information
[KNMI-TR-54-PT-1] 08 p1190 N85-17499
Velocity inversion using a stratified reference
[AD-A150082] 12 p1889 N85-21858
Summary of Meteorological Observations, Surface (SMOS), Bermuda
[AD-A150537] 13 p2138 N85-23278
Summary of Meteorological Observations, Surface (SMOS), Beaufort, South Carolina
[AD-A150538] 13 p2138 N85-23279
Lyapunov stability of very simple steady solutions of prognostic systems 14 p2333 N85-24429
Utilization of satellite data in mesoscale modeling of severe weather 15 p2597 N85-26007
Meso-B scale numerical simulations of the jet streak adjustments which organized the Carolina tornado outbreak and the subsequent explosive coastal cyclogenesis 15 p2598 N85-26011
Numerical studies of frontal dynamics
15 p2598 N85-26014
Wind modelling for increased aircraft operational efficiency 16 p2697 N85-26652
Data from BOC-yachts: A significant input to Southern Hemisphere analysis 16 p2814 N85-27356
A split explicit model for short-term numerical weather prediction 16 p2831 N85-27460
Statistical interpretation of the ECMWF model using MOS to predict surface wind and temperature
[WSR-2] 17 p2995 N85-28515
The impact of scatterometer data on limited-area model predictions of the QE 2 storm 18 p3139 N85-29436
A factored implicit scheme for numerical weather prediction with small factorization error
18 p3141 N85-29447
Comparison of optimum interpolation and Cressman analyses 18 p3141 N85-29448
Recent developments in nonlinear normal mode initialization 18 p3142 N85-29451
Comparison of two orographical data sets for the GLAS Fourth Order GCM 18 p3142 N85-29452
Development and testing of the variable vertical resolution Fourth Order GCM 18 p3142 N85-29453
Developement of an optimum interpolation analysis method for the CYBER 205 18 p3143 N85-29456
Model development highlight for 1984: The GLA Fourth Order GCM 18 p3143 N85-29457
Response of winter forecasts made with the GLA Fourth Order GCM to Changes in the horizontal grid resolution
18 p3143 N85-29458
Comparison of forecast and observed energetics
18 p3143 N85-29459
Error growth in operational 10-day forecasts
18 p3143 N85-29460
Numerical meteorology 18 p3147 N85-29484
A numerical study of the Pacific polar low
[AD-A153777] 18 p3149 N85-29495
Monthly and seasonal weather outlook for mid-February to mid-March 1985, volume 39, number 4, February 14, 1985
[PB85-164580] 18 p3149 N85-
A probabilistic forecasting model of tropical cyclone-generated storm surge for a straight coastline
19 p3314 N85-3054
Utilization of satellite data and regional scale numerical models in short range weather forecasting
[NASA-CR-175980] 19 p3314 N85-3054
Examination of the time and spatial scales appropriate for the carbon dioxide climate change issue
[DE85-009852] 19 p3317 N85-305
AEV local verification for aviation, precipitation, and temperature programs: AV, REL, TEM
[PB85-179125] 19 p3318 N85-3055
Accuracy and operational use of medium and extended range numerical atmospheric forecasts: A review
[AD-A155027] 21 p3635 N85-3257
Medium range atmospheric forecast system: Evaluation plan
[AD-A155623] 21 p3638 N85-3259

NUSSELT NUMBER
Numerical solutions of turbulent models for flow over a flat plate with angle of attack
[DE85-010380] 21 p3585 N85-3228

NUTATION
Transient optical nutation in CO2 laser
02 p0261 N85-1170
Active nutation control of spacecraft using a magnetic bearing momentum wheel with Vernier gimbaling capability
[NAL-TR-8201] 06 p0759 N85-1465
Attitude data consistence check of rocket payloads
[BMFT-FB-W-84-049] 12 p1790 N85-2122
Earth rotation and polar wandering
14 p2399 N85-2478
The Earth's wobble and associated ocean motions
20 p3490 N85-3169

NUTATIONAL OSCILLATION
U NUTATION

NUTRIENTS
Characterization of heat transfer in nutrient materials — space flight feeding
[NASA-CR-171841] 08 p1199 N85-17551
Effects of acid rain on forest nutrient status
[DE85-012486] 23 p3947 N85-3446

NUTRITION
Nutritional models for space travel from chemically defined diets
[NASA-CR-3850] 03 p0402 N85-12581
Feasibility of producing a range of food products from a limited range of undifferenitiated major food components
[NASA-CR-177329] 07 p1020 N85-16473
Food Service and Nutrition for the Space Station
[NASA-CP-2370] 14 p2393 N85-24730
The context for food service and nutrition in the space station 14 p2393 N85-24734
Preparation methods: Past and potential methods of food preparation for space 14 p2393 N85-24738
Nutritional criteria for military rations and effects of prolonged feeding on acceptability
14 p2394 N85-24742
Nutrition in space flight: Some thoughts
14 p2394 N85-24743
Food service and nutritional needs
14 p2394 N85-24744
Psychobiology and food perception
14 p2394 N85-24745
Diet of first Soviet expedition on Mount Everest
19 p3323 N85-30586
Chemolithotrophy and physiology of bacterial nutrient limitation 21 p3659 N85-32730
Influence of chemical form, feeding regimen, and animal species on the gastrointestinal absorption of plutonium
[DE85-010291] 21 p3662 N85-32751

NUTRITIONAL REQUIREMENTS
NT CALORIC REQUIREMENTS
Mineral nutrients in Mediterranean ecosystems
[REPT-71] 01 p0069 N85-10456
Problems associated with the utilization of algae in bioregenerative life support systems
[NASA-CR-166615] 07 p1019 N85-1646
Diet of first Soviet expedition on Mount Everest
19 p3323 N85-30586

NUTS (FASTENERS)
Tube coupling device
[NASA-CASE-MFS-25964-1] 11 p1647 N85-2097

NYLON (TRADEMARK)
Temperature dependence of the crystal structures of Nylon 11
[AD-A147563] 07 p1049 N85-1686
Piezoelectric transducer using electrically poled gamma-phase Nylon 11
[AD-D011552] 12 p1850 N85-2160

The effects of sea water and concentrated salt solutions on the fatigue of nylon 6,6 fibers
17 p2979 N85-28416

Solid-state co-extrusion of nylon 6 gel
[AD-A156187] 24 p4082 N85-35298

NYLON RESINS
U POLYAMIDE RESINS

NYQUIST DIAGRAM
On the relationship between Lehtomaki's robustness test and an inverse Nyquist based test
[QUEL-1526/84] 03 p0409 N85-12616

Approximate models in multivariable process control: An inverse Nyquist array and robust tuning regulator interpretation
[RR-261] 08 p1216 N85-17663

NYSTAGMUS
NT VESTIBULAR NYSTAGMUS
Stimulus factors in motion perception and spatial orientation 01 p0008 N85-10049
Influence of limboreticular complex on some reactions of rabbits 19 p3326 N85-30607
The European vestibular experiments of the Spacelab-1 mission 20 p3508 N85-31808
Some results of the European vestibular experiments in the Spacelab-1 mission 20 p3508 N85-31809

O

O RING SEALS
Analysis of experimental shaft seal data for high-performance turbomachines, as for Space Shuttle main engines
[NASA-TM-86928] 12 p1844 N85-21569
Experimental stiffness of tapered bore seals
[NASA-TM-86978] 15 p2568 N85-25847

O STARS
Observations of the O-type subdwarf eclipsing binary system LB 3459 (AA Dor) 01 p0128 N85-10881
Spectroscopic observations of selected stellar systems
[NASA-CR-174288] 08 p1255 N85-17915
A spectroscopic study of LMC X-4
[NASA-CR-174414] 10 p1571 N85-19905
UV observations and results on pre-main sequence stars 11 p1744 N85-20970
Stellar winds in the young galactic cluster NGC 6530
11 p1750 N85-21004

IUE and Voyager observations of very hot O-type subdwarfs 11 p1751 N85-21010
Statistical classification of IUE low-despersion stellar spectra: Progress report 11 p1760 N85-21075
Possible origin of the anomalous component of cosmic rays
[SH-4.6-7] 23 p4039 N85-35045

OAO
NT OAO 3

OAO 3
Absorption line studies and the distribution of neutral gas in the local interstellar medium
06 p0873 N85-15544

Synthesis of data on the local interstellar medium
06 p0874 N85-15545

Observations of interstellar HI toward nearby late-type stars 06 p0874 N85-15546
Observations of local interstellar Mg I and Mg II
06 p0874 N85-15547

IUE absorption line studies of highly ionized interstellar gas 11 p1743 N85-20962
MU Sagittarii and Beta Lyrae: Combined IUE/Voyager observations 11 p1757 N85-21052

OAO-C
U OAO 3

OATS
Multi crop area estimation in Idaho using EDITOR
[E85-10054] 06 p0827 N85-15251

OBLATE SPHEROIDS
Oblatenesses of Uranus and Neptune
02 p0300 N85-11941

OBLIQUE SHOCK WAVES
Oblique shock wave-turbulent boundary layer interaction on a porous wall with suction 08 p1072 N85-16794
Tabular and graphical solutions of regular and Mach reflections in pseudo-stationary frozen and vibrational-equilibrium flows, part 1
[UTIAS-283-PT-1] 23 p3893 N85-34117
Tabular and graphical solutions of regular and Mach reflections in pseudo-stationary frozen and vibrational-equilibrium flows, part 2
[UTIAS-283-PT-2] 23 p3894 N85-34118

OBSCURATION
U OCCULTATION

OBSERVABILITY (SYSTEMS)
A three-dimensional geometric-physical model for conventional geodetic observations-observables, parameter estimation, and deformation analysis
[SER-C-298] 11 p1665 N85-20493
State estimation with interrupted observations
15 p2635 N85-26251

Observability in problem of correction of inertial navigation systems using additional information from artificial Earth satellite 16 p2719 N85-26785

OBSERVATION
NT EARTH OBSERVATIONS (FROM SPACE)
NT SATELLITE OBSERVATION
NT SPACE OBSERVATIONS (FROM EARTH)
NT SPOT (FRENCH SATELLITE)
NT VISUAL OBSERVATION
Exploring the solar system with stellar occultations
08 p1245 N85-17857

Observations of mesospheric turbulence by rocket probe and VHF radar, part 2.4A 21 p3619 N85-32484
Analysis of unreplicated factorials allowing for possibly faulty observations
[AD-A154813] 21 p3678 N85-32848

OBSERVATION AIRCRAFT
NT MIRAGE AIRCRAFT
NT MIRAGE 3 AIRCRAFT
NT OV-1 AIRCRAFT
NT RF-4 AIRCRAFT
NT U-2 AIRCRAFT
Investigation of air pollution impact in Eastern Bavaria: Measurement results from August and September, 1984
[DFVLR-FB-85-03] 17 p2988 N85-28471
Motor glider meteorology 24 p4121 N85-35543

OBSERVATORIES
NT ASTRONOMICAL OBSERVATORIES
NT ASTRONOMICAL SATELLITES
NT GAMMA RAY OBSERVATORY
NT GEOPHYSICAL OBSERVATORIES
NT HEAO
NT HEAO 1
NT HEAO 2
NT HEAO 3
NT HUBBLE SPACE TELESCOPE
NT INFRARED ASTRONOMY SATELLITE
NT IUE
NT OAO 3
NT OGO
NT QUASAT
NT ROSAT MISSION
NT SOLAR OBSERVATORIES
NT SPACE INFRARED TELESCOPE FACILITY
NT SPARTAN SATELLITES
Recent results on the Crab Pulsar X-ray light curve
11 p1742 N85-20955

Monopole, astrophysics and cosmic ray observatory at Gran Sasso
[HE-6.1-4] 24 p4209 N85-36130

OBSTACLE AVOIDANCE
LPI-radar for helicopter obstacle warning
08 p1074 N85-16810

OBSTACLES
U BARRIERS

OBSTRUCTING
U BLOCKING

OCCLUSION
Reaction of cerebral ventricles to antiorthostatic position and occlusion of jugular veins 01 p0093 N85-10626
Dynamic occlusion analysis in optical flow fields
[AD-A145805] 03 p0406 N85-12594

OCCULTATION
NT RADIO OCCULTATION
NT SOLAR ECLIPSES
NT STELLAR OCCULTATION
The structure of the Uranian rings and the search for rings around Neptune 02 p0302 N85-11954
Ice fog as an electro-optical obscurant
[AD-A155059] 21 p3705 N85-33015
Application of nonlinear least squares methods to the analysis of solar spectra
[NASA-CR-176122] 22 p3816 N85-33637

OCCUPATION
Cognitive asymmetry and occupation. Computer programmers, students, and bank personnel, part 1 and part 2
[AD-A147125] 08 p1197 N85-17540
Success in learning occupation of chemical production technician as function of certain personality traits and development of psychophysiological functions
09 p1362 N85-18568

OCEAN BOTTOM
Seafloor geosciences division: Missions, technical specialties, accomplishments, and activities, calendar year 1983
[AD-A144849] 01 p0087 N85-10592
The gulf stream deflection and meander energetics experiment. Current meter and bottom pressure gauge data report for the September, 1981 to April, 1982 mooring period
[AD-A144977] 01 p0088 N85-10595
Marine geological and geophysical investigations of the Antarctic Continental Margin, 1984
[GS-CIRC-935] 02 p0212 N85-11400
On gravity from SST, geoid from Seasat, and plate age and fracture zones in the Pacific
[E85-10020] 02 p0217 N85-11433
A comparison of seismic properties of young and mature oceanic crust 02 p0226 N85-11479
Submarine sand ridges: Geology and development, New Jersey, USA 02 p0227 N85-11482
A study of highly energetic near-bottom ocean flow at the base of the Scotian Rise 02 p0233 N85-11515
One-year records of current and bottom pressure in the strait between Nordaustlandet and Kvitoeya and Svalbard, 1980 - 1981
[AD-A145594] 02 p0233 N85-11518
Continental and oceanic crustal magnetization modelling
[E85-10034] 03 p0378 N85-12413
The structure of the Iceland-Faeroe ridge, derived from geophysical measurements
[DRIC-T-7255] 03 p0397 N85-12535
Unsinkability of ferromanganese nodules
06 p0819 N85-15202

Some methodological aspects of study of layer associations in continents and oceans
06 p0820 N85-15205

Some trends in the modern Earth sciences — plate tectonics and Earth's crust 06 p0820 N85-15207
Boundary velocities of mohorovicic discontinuity and upper mantle structure of Pacific Ocean bed
06 p0821 N85-15211

Platinum group nuggets in deep sea sediments
06 p0883 N85-15611

Exploring ocean's mineral wealth
07 p0980 N85-16227

Satellite photographs suggest arctic volcano
07 p0982 N85-16239

Research of inverse methods to describe the structure of the earth and ocean bottom
[AD-A147082] 07 p1030 N85-16541
Ocean acoustics
[AD-A147062] 07 p1038 N85-16591
Arctic marine acoustics
[AD-A147492] 07 p1039 N85-16594
Late Quaternary deep-water paleoceanography of the eastern equatorial Indian Ocean: Evidence from Bethnic foraminifera, carbonate dissolution, and stable isotopes
08 p1182 N85-17446

Detailed oceanic crustal modeling
[AD-A148589] 08 p1191 N85-17507
A broadband matching network
[AD-D011406] 08 p1219 N85-17675
Preliminary post-emplacement safety analysis of the subseabed disposal of high-level nuclear waste
[DE84-011162] 08 p1221 N85-17692
Technology development for unmanned untethered submersible vehicle systems
[AD-A148794] 09 p1304 N85-18190
Measurements of sediment temperatures, conductivity and heat flow in the North Atlantic and their relevance to radioactive waste disposal
[IOS-172] 09 p1359 N85-18551
Benthic boundary layer, IOS observational programme: Discovery Gap measurements, March 1984 — Institute of Oceanographic Sciences (IOS)
[ISO-180] 09 p1359 N85-18552
The use of in-situ photography in studies of the deep-sea benthos at IOS — Institute of Oceanographic Sciences (IOS)
[IOS-182] 09 p1360 N85-18553
An assessement of biological processes close to the sea bed in a slope region and its significance to the assessment of sea-bed disposal of radioactive waste
[IOS-185] 09 p1360 N85-18554
Deep seabed stable reference areas
[PB84-241470] 09 p1360 N85-18555
Propagation of electromagnetic fields along the sea/sea-bed interface
[AD-A149523] 10 p1467 N85-19257
New data on structure of Shirshov Ridge (Bering Sea)
10 p1498 N85-19456

Specifics of backscattering of sound by bottom of bank in open sea 10 p1499 N85-19460
Aluminum in biogenic cycle and forms of its occurence in ocean 10 p1499 N85-19463
Research on ocean floor electrical surveys
[AD-A149631] 12 p1899 N85-21920
Determining degree of partial melting of asthenosphere from seismic data 13 p2107 N85-23127

Determining adsorption of surface-active substances by sea bottom deposits 13 p2107 N85-23126
Use of paleomagnetic data in tectonic analysis of oceanic structures 13 p2108 N85-23135
More precise curve of dependence between density and velocity of longitudinal waves in consolidated crust and top of mantle in oceanic structures
13 p2110 N85-23143
Crustal and upper mantle density model of Owen fault zone 13 p2110 N85-23144
Structure of Iceland and ocean floor spreading
13 p2112 N85-23159
Assessing LANDSAT TM and MSS data for detecting submerged plant communities 13 p2120 N85-23203
Remanent magnetization model for the broken ridge satellite magnetic anomaly 13 p2123 N85-23219
Submarine volcanic eruptions and potential analogs for Venus 13 p2187 N85-23573
The Deep Drifter Program — deep ocean sensors
14 p2329 N85-24400
Automation of radiometric measurements in nuclear oceanology 14 p2337 N85-24452
Most important geochemical barrier zones in ocean (with example of Atlantic Ocean basin)
14 p2343 N85-24491
Water wave propagation over uneven bottoms
[AD-A151450] 15 p2556 N85-25769
The effect of the Benthic Boundary Layer on the physics of intense mesoscale eddies
[AD-A153193] 17 p2958 N85-28270
Geoacoustic models: Washington state continental margin
[AD-A153781] 18 p3177 N85-29699
Concretization of high level radioactive source in marine sediment
[AD-D011703] 19 p3249 N85-30146
Natural gas anomaly in bottom waters of South China Sea 19 p3290 N85-30399
Ultramicroscopic study of structure of phosphorites from Sea of Japan floor 19 p3290 N85-30400
Plane Tsunami wave caused by elastic oscillations of ocean floor 19 p3290 N85-30403
Heat flow through ocean floor and its relationship to lithosphere structure and thickness
19 p3294 N85-30422
Density characteristics of asthenosphere in Atlantic Ocean 19 p3294 N85-30423
Influence of underwater volcanic mountains of Atlantic on microplankton distribution 19 p3294 N85-30424
Evolution of the oceanic upper mantle and effects on sea floor subsidence geoid height and heat flow
19 p3319 N85-30575
Environmental background measurement program
[AD-A153660] 19 p3319 N85-30577
Dispersal From Deep Ocean Sources: Physical and Related Scientific Processes
[DE85-010420] 20 p3497 N85-31740
Benthic boundary layer modelling studies
[IOS-181] 20 p3497 N85-31742
Global geomorphology 21 p3601 N85-32359
Deep sea mega-geomorphology: Progress and problems 21 p3602 N85-32369
Sulfur and carbon cycling in organic-rich marine sediments 21 p3659 N85-32729
A random layer model for reflection from ocean bottom sediments
[AD-A155019] 21 p3700 N85-32988
Understanding coherence losses incurred by bottom-retained signals
[AD-A155559] 21 p3701 N85-32992
The 3.5 b.y. old Onverwacht Group: A remnant of ancient oceanic crust 21 p3718 N85-33073
Anorthositic oceanic crust in the Archean Earth
21 p3719 N85-33077
Subduction zone tectonic studies to develop concepts for the occurrence of sediment subduction
[DE85-011794] 22 p3815 N85-33632
Arctic and offshore research
[DE85-001995] 22 p3818 N85-33653
Research at the Institute of Oceanographic Sciences related to the possible disposal of radioactive waste on or beneath the seafloor
[IOS-204] 23 p3973 N85-34628
Marine phosphorite deposits model for exploration, with emphasis on deposits in the US Atlantic coastal plain
24 p4104 N85-35439
Massive sulfide deposits from the southern Juan de Fuca Ridge 24 p4105 N85-35446
Background light measurements at the DUMAND site
[HE-5.2-7] 24 p4203 N85-36084
Measurements of light background at large depth in the ocean
[HE-5.2-8] 24 p4203 N85-36085

OCEAN COLOR SCANNER
Characteristic vector analysis of inflection ratio spectra: New technique for analysis of ocean color data
[NASA-TP-2426] 13 p2126 N85-23237

OCEAN CURRENTS
NT COASTAL CURRENTS
NT EL NINO
NT GULF STREAM
An improved analytical theory of Rossby wave driven Eulerian and Lagrangian mean flows along non-zonal barriers with application to the Hawaiian Ridge
[AD-A144951] 01 p0086 N85-10593
The gulf stream deflection and meander energetics experiment. Current meter and bottom pressure gauge data report for the September, 1981 to April, 1982 mooring period
[AD-A144977] 01 p0088 N85-10595
A description and discussion of FREDDEX oceanographic measurements
[AD-A145032] 01 p0088 N85-10596
Observations of the vertical structure of the eddy field in the Kuroshio extension
[AD-A145178] 01 p0089 N85-10599
Analysis and interpretation of current measurements from the Beaufort Sea
[AD-A145197] 01 p0089 N85-10600
Numerical studies of mesoscale eddies using quasigeostrophic and primitive equation ocean models
[PB84-214048] 01 p0089 N85-10602
Radiotracer studies of the dispersion of solid pollutants in marine and estuarial environment: Measurement of diffusion coefficients and the phenomenon of dispersion by currents
[BLL-DRIC-TRANS-7104-(3623.66)]
02 p0224 N85-11468
A study of highly energetic near-bottom ocean flow at the base of the Scotian Rise 02 p0233 N85-11515
One-year records of current and bottom pressure in the strait between Nordaustlandet and Kvitoeya and Svalbard, 1980 - 1981
[AD-A145594] 02 p0233 N85-11518
Eddy detection in the Norwegian, Greenland, and Barents Seas with a radar altimeter
03 p0382 N85-12442
Determination of the altimetric geoid and gravity anomalies in the North Sea: Implications for a solution of the general circulation problem using ERS-1 data
03 p0382 N85-12446
The POSEIDON altimeter description
03 p0383 N85-12454
The Long Term Upper Ocean Study (LOTUS). Cruise summary
[AD-A145767] 03 p0397 N85-12536
Dynamics of coupled ice-ocean system in the marginal ice zone: Study of the mesoscale processes and of constitutive equations for sea ice
[NASA-CR-174171] 04 p0542 N85-13448
Tide tables 1985, high and low water predictions, central and western Pacific Ocean and Indian Ocean
[PB84-238393] 04 p0542 N85-13451
Recent observations of tides and tidal currents from the northeastern Bering Sea shelf
[PB84-241785] 04 p0543 N85-13452
Sigma code testing
[AD-A146548] 06 p0841 N85-15340
Bio-optical variability in the Alboran Sea as assessed by Nimbus-7 coastal zone color scanner
[AD-A147909] 07 p0989 N85-16281
Satellite definition of the bio-optical and thermal variation of coastal eddies associated with the African current
[AD-A147910] 07 p0989 N85-16282
The problem of climate and climate variation
07 p1001 N85-16353
Meteorological aspects of the 1982-83 El Nino/southern oscillation episode 07 p1001 N85-16356
Ocean and climate, an example. The interannual variability of the tropical Pacific Ocean
07 p1002 N85-16365
The El Nino phenomenon and its agrometeorological implications 07 p1004 N85-16382
A compilation of moored current meter and wind recorder data. Volume 35: Long-Term Upper Ocean Study (LOTUS) (Moorings 764, 765, 766, 767, 770), May 1982 - April 1983
[AD-A147103] 07 p1009 N85-16412
The long term upper ocean study (LOTUS). Cruise summary and hydrographic data report, OCEANUS 154, May 1984
[AD-A147906] 07 p1009 N85-16414
Current and current shear effects in the parabolic approximation for underwater sound channels
[AD-A147833] 07 p1039 N85-16597
Use of SIR-B multiincidence-angle imagery to study iceberg detectability and offshore ocean feature extraction 08 p1145 N85-17225

MIZEX. A program for mesoscale Air-Ice-Ocean interaction experiments in arctic marginal ice zones. 4: Initial results and analysis from MIZEX 83
[AD-A148255] 08 p1173 N85-17
Bibliography update on the California current system and related mesoscale ocean modeling
[AD-A148546] 08 p1190 N85-17
Deep water mass circulation in the Western Alboran Basin: Measurements in July and September 198 (Alboran I experiment)
[AD-A148566] 08 p1191 N85-170
Surface currents of the Indian Ocean (to 25 deg S, 100 deg E.)
[IOS-187] 10 p1521 N85-19
Atlas of the Beaufort Sea
[AD-A149545] 11 p1669 N85-20
Intensification of tropical instabilities
[AD-A149985] 12 p1896 N85-21
Circulation and internal waves in a cold Gulf Stream waves
[AD-A149704] 12 p1896 N85-21
Preliminary results of the oceanographic cruise of USCGC NORTHWIND to the Greenland Sea
[AD-A149802] 12 p1896 N85-21
Microplankton species assemblages at the Scripps Pier from March to November 1983 during the 1982-1984 El Nino event
[NASA-CR-175553] 12 p1899 N85-21
Calculation of level surface in problems of large-scale ocean circulation 13 p2108 N85-2
Double and inverse Taylor-Hogg vortices in a stratified ocean 13 p2108 N85-23137
Circulation pattern of the North Atlantic, part of the warmwater sphere research effort at Kiel University
14 p2239 N85-23
Surface currents in the tropical Pacific during 1979-1980 using drifting buoys 14 p2323 N85-2436
The Indian Ocean surface dynamics experiment (SINODE) 14 p2325 N85-24370
The ARGOS contribution to the First GARP Global Experiment (FGGE) study of drifting buoys
14 p2325 N85-24371
Main features of Antarctic Ocean circulation as revealed by satellite tracking of icebergs
14 p2325 N85-24372
The Deep Drifter Program — deep ocean sensors
14 p2329 N85-24400
Frontal nature of Cromwell Current
14 p2336 N85-24445
Local mechanism of equatorial countercurrents
14 p2336 N85-24446
Modeling evolution of unstable geostropic eddies in barotropic ocean 14 p2336 N85-24447
A study of the turbulent layer in the water at an air-water interface 14 p2378 N85-24679
Observations of the California countercurrent
[AD-A150781] 14 p2382 N85-24691
Some preliminary results concerning deep northern-boundary currents in the North Pacific
[AD-A151021] 14 p2382 N85-24692
Measurement of ocean surface currents from space with multi-frequency microwave radars
15 p2539 N85-25672
Chemical signatures associated with the freshening of Northern Atlantic waters between 1972 and 1981
15 p2601 N85-26032
North Atlantic Deep Water and the world ocean
15 p2602 N85-26033
Glacial-to-interglacial changes in NADW fluxes?
15 p2602 N85-26037
Changes in the high-latitude ocean as possible causes of atmosphere CO2 variations 15 p2602 N85-26038
Possible sea ice impacts on oceanic deep convection
15 p2603 N85-26041
Development of a Lagrangian drifting buoy
16 p2811 N85-27338
Long term drifting float for measuring mean oceanic circulation using ARGOS system
16 p2811 N85-27339
ARGOS-tracked drifters in the Rockall Trough
16 p2812 N85-27340
Results of an initial trial of a satellite telemetering buoy measuring near surface current
16 p2812 N85-2734
Towards a study of synoptic-scale variability of the California current system
[NASA-CR-175871] 17 p2997 N85-2852
Rip in White Sea 19 p3290 N85-3040
Study of drift currents in initial stage of generation of wind waves by laser Doppler anemometer
19 p3291 N85-3040
Dynamic theory of polar tide 19 p3292 N85-3041
Sand dispersion from an ephemeral river delta on the wave-dominated central California coast
[AD-A154352] 19 p3300 N85-304

Northeast Brazil droughts and Atlantic SST anomalies
[INPE-3538-PRE/754] 19 p3316 N85-30553

Atmospheric chlorofluromethanes as tracers of ocean circulation and mixing: Measurement and calibration techniques and studies in the Greenland and Norwegian Seas 19 p3319 N85-30573

Experiments using atmospheric forcing from a FGGE analysis to drive an upper ocean model
[INPE-3503-PRE/738] 19 p3319 N85-30576

Error spectrum of Goddard satellite models for the gravity field 20 p3491 N85-31704

Ocean circulation studies 20 p3492 N85-31712

Dispersal From Deep Ocean Sources: Physical and Related Scientific Processes
[DE85-010420] 20 p3497 N85-31740

Horizontal and vertical structure of velocity, potential vorticity and energy in the gulf stream
[AD-A154753] 21 p3655 N85-32702

Hydrographic data from the OPTOMA (Ocean Prediction Through Observations, Modeling and Analysis) program: OPTOMA15, 24 January to 23 February 1985
[AD-A155012] 21 p3655 N85-32703

Numerical simulations of the response of intense ocean currents to atmospheric forcing
[AD-A155161] 21 p3655 N85-32704

Method and apparatus for Delta Kappa synthetic aperture radar measurement of ocean current
[NASA-CASE-NPO-15704-1] 23 p3925 N85-34327

Meteorological data from the OPTOMA (Ocean Prediction Through Observations, Modeling and Analysis) program OPTOMA 2, leg D2. 30 Jun. - 10 Jul. 1984
[AD-A158134] 24 p4123 N85-35560

OCEAN DATA ACQUISITIONS SYSTEMS

Sea ice data buoys in the Weddell Sea
[AD-A144953] 01 p0086 N85-10594

High-data-rate wide-angle underwater acoustic telemetry system
[DE84-015696] 02 p0233 N85-11519

Ocean wave parameters extraction using satellite short-pulse radar altimeters 03 p0380 N85-12425

The impact of satellite altimeter data on wave research 03 p0380 N85-12427

The NASA/JPL pilot ocean data system 03 p0381 N85-12433

NODC/1983: National Oceanographic Data Center report
[PB84-222231] 04 p0542 N85-13449

Advanced technology for hydrographic mapping
[FOA-C-30371-E1] 08 p1176 N85-17418

The use of in-situ photography in studies of the deep-sea benthos at IOS — Institute of Oceanographic Sciences (IOS)
[IOS-182] 09 p1360 N85-18553

International list of selected, supplementary and auxiliary ships — WMO
[WMO-47-ED-84] 11 p1687 N85-20609

Remote self-contained undersea monitor
[AD-D011520] 12 p1849 N85-21599

Method of measuring sea surface water temperature with a satellite including wideband passive synthetic-aperture multichannel receiver
[NASA-CASE-NPO-15651-1] 12 p1869 N85-21723

Project PAPA: The integration of drifting buoy data into an operational meteorological service 14 p2238 N85-23874

Automatic buoys to assist the tuna fishery off the Azores 14 p2238 N85-23879

Operational experiences with the ARGOS system in oceanography and oil spill emergency planning. Future plans for the use of the ARGOS system as a component in offshore data collection system 14 p2239 N85-23887

Some experience from ARGOS stations in the open sea 14 p2240 N85-23891

Proceedings of the ARGOS Users Conference on Data Collection and Location by Satellite 14 p2322 N85-24348

The development of Platform Transmitter Terminal (PTT) and its application for drifting buoys 14 p2323 N85-24353

US programs using the ARGOS data collection and platform location system 14 p2323 N85-24355

Inferences of future operations drawn from past and present applications of drifting buoys 14 p2323 N85-24356

US program in anchored data buoy and the other fixed observation platforms 14 p2324 N85-24358

One thousand days in the brine — platform transmitter terminals 14 p2324 N85-24359

Data Collection and Platform Location by Satellite: ARGOS Users' Conference 14 p2325 N85-24366

The ARGOS system main characteristics — satellite based localization 14 p2325 N85-24367

Meteorological buoys developed at the EERM laboratory 14 p2326 N85-24374

The ARGOS contribution to the successful dredging of a deep moored current meter 14 p2327 N85-24381

Data Collection and Platform Location by Satellite: ARGOS users' Conference 14 p2329 N85-24391

Collecting meteorological reports with the ARGOS system 14 p2329 N85-24398

The French Ocean Climate in Equatorial Atlantic (FOCAL) Drifter Program, 1983-1984 14 p2329 N85-24399

The Deep Drifter Program — deep ocean sensors 14 p2329 N85-24400

US programs using the ARGOS data collection and platform location system 14 p2329 N85-24401

Telemetered meteorological and engineering data from a deep sea moored body in the Long Term Upper Ocean Study (LOTUS) 14 p2329 N85-24402

Practical considerations when using water quality and structure monitoring sensors as applied to portable ARGOS satellite transmitter equipment 14 p2330 N85-24405

Drifting buoy development and future programs — Japanese ARGOS program 14 p2330 N85-24406

Development of a low cost drifting buoy 14 p2330 N85-24408

Data Collection and Platform Location by Satellite: ARGOS Users' Conference 14 p2330 N85-24409

US program using the ARGOS data collection and platform location system 14 p2330 N85-24410

A report on the DRIFTERS program — buoys 14 p2331 N85-24413

Drifting buoys on the Labrador shelf 14 p2331 N85-24415

A new versatile ARGOS PTT for oceanographic applications — Platform Transmit Terminal (PTT) 14 p2331 N85-24417

Overview of data processing at AES local user terminals — Canadian Atmospheric Environment Service (AES) 14 p2331 N85-24418

An overview of NDBC drifting buoy development programs — NOAA Data Buoy Center (DBC) 14 p2332 N85-24422

Preliminary report on the results of hydrological measurements in the southern Tyrrhenian Sea, in the Messina strait and in the western Ionian sea
[PREPRINT-433] 14 p2382 N85-24693

Survey of remote sensing techniques for wave measurement
[NASA-TM-84429] 15 p2583 N85-25928

Ocean circulation and meteorology off the Georgia coast. Part 1: Real-time telemetry system for data collection
[PB85-155935] 15 p2605 N85-26052

Data Collection and Platform Location by Satellite: ARGOS Users' Conference 16 p2811 N85-27333

DB2 and DB3: The next generation — buoys 16 p2811 N85-27337

Development of a Lagrangian drifting buoy 16 p2811 N85-27338

Long term drifting float for measuring mean oceanic circulation using ARGOS system 16 p2811 N85-27339

Monitoring of marine environment 16 p2812 N85-27341

Routine wave and meteorological measurements in offshore areas using ARGOS data surveillance 16 p2812 N85-27344

Results of an initial trial of a satellite telemetering buoy measuring near surface current 16 p2812 N85-27345

An operational buoy network collecting meteorological data 16 p2813 N85-27351

Availability of the ARGOS system based on the orbital characteristics of the TIROS-N satellites — oceanographic/meteorological data 16 p2813 N85-27352

Contribution of the NOAA-7 and 8 and ARGOS partnership to white tuna fishing in the northeast Atlantic 16 p2813 N85-27355

First results of oceanography utilization of infrared high resolution picture transmission images
[KNMI-TR-59] 18 p3151 N85-29511

ERS economic impace study
[ESA-CR(P)-1979] 18 p3199 N85-29847

Chemical, biological, and physical measurements from the subtropical western North Atlantic Ocean. Summer 1982, USNS Lynch, cruise 710-82
[AD-A153823] 18 p3201 N85-29857

Tropical Ocean and Global Atmosphere (TOGA) heat exchange project: A summary report
[NASA-CR-176038] 20 p3496 N85-31738

Large-scale sea surface temperature variability from satellite and shipboard measurements
[NASA-CR-176123] 22 p3818 N85-33651

OCEAN DATA PLATFORMS

U OCEAN DATA ACQUISITIONS SYSTEMS

OCEAN DATA STATIONS

U OCEAN DATA ACQUISITIONS SYSTEMS

OCEAN DYNAMICS

Large-scale ocean-atmosphere interactions in the mid-latitudes and equatorial regions: A literature review
[CSIR-T/SEA-8302] 01 p0073 N85-10482

Observations of the vertical structure of the eddy field in the Kuroshio extension
[AD-A145178] 01 p0089 N85-10599

Return wave heights off South Uist estimated from seven years of data
[IOS-164] 01 p0089 N85-10601

Numerical studies of mesoscale eddies using quasigeostrophic and primitive equation ocean models
[PB84-214048] 01 p0089 N85-10602

Synthesis of current measurements in Puget Sound, Washington. Volume 1: Index to current measurements made in Puget Sound from 1908-1980 with daily and record averages for selected measurements
[PB84-214105] 01 p0089 N85-10603

A study of highly energetic near-bottom ocean flow at the base of the Scotian Rise 02 p0233 N85-11515

Monitoring of the tidal dynamics of the Dutch Waddensea by SIR-B 08 p1147 N85-17235

A one dimensional dynamical model of ocean/atmosphere interactions 09 p1358 N85-18545

Characteristic vector analysis of inflection ratio spectra: New technique for analysis of ocean color data
[NASA-TP-2428] 13 p2126 N85-23237

The Indian Ocean surface dynamics experiment (SINODE) 14 p2325 N85-24370

The ARGOS contribution to the First GARP Global Experiment (FGGE) study of drifting buoys 14 p2325 N85-24371

A large-scale air sea interaction project over the Pacific basin 14 p2326 N85-24373

Review of North Atlantic source waters 15 p2601 N85-26029

Deep water formation 15 p2601 N85-26030

Temporal and spatial scales of Labrador Sea water formation 15 p2601 N85-26031

Chemical signatures associated with the freshening of Northern Atlantic waters between 1972 and 1981 15 p2601 N85-26032

North Atlantic Deep Water and the world ocean 15 p2602 N85-26033

Oceanographic variations in recent decades and their impact on the fertility of the Iceland Sea 15 p2602 N85-26034

Quaternary North Atlantic surface paleoceanography in regions of potential deep-water formation 15 p2602 N85-26036

First results of oceanography utilization of infrared high resolution picture transmission images
[KNMI-TR-59] 18 p3151 N85-29511

Destruction of density jumps in ocean by turbulence 19 p3291 N85-30407

Study of drift currents in initial stage of generation of wind waves by laser Doppler anemometer 19 p3291 N85-30408

Frequency of recurrence and critical conditions for generation of Langmuir circulations 19 p3291 N85-30409

Dynamic theory of polar tide 19 p3292 N85-30414

Atmospheric chlorofluromethanes as tracers of ocean circulation and mixing: Measurement and calibration techniques and studies in the Greenland and Norwegian Seas 19 p3319 N85-30573

Research, progress and the mark A box model for physical, biological and chemical transports
[DE85-010574] 19 p3320 N85-30581

Physical oceanography program science abstracts
[AD-A154637] 21 p3654 N85-32701

Air-sea interaction with SSM/I and altimeter
[NASA-CR-176105] 22 p3818 N85-33650

Large-scale sea surface temperature variability from satellite and shipboard measurements
[NASA-CR-176123] 22 p3818 N85-33651

OCEAN MODELS

Numerical studies of mesoscale eddies using quasigeostrophic and primitive equation ocean models
[PB84-214048] 01 p0089 N85-10602

MIZEX. A program for mesoscale air-ice-ocean interaction experiments in arctic marginal ice zones. III: Modeling the marginal ice zone
[AD-A145351] 02 p0233 N85-11517

Intercomparison of GEOS 3/SEASAT wave data and wave model data 03 p0381 N85-12438

Simulation of wavefronts returned by realistic surfaces 03 p0383 N85-12448

Parameterizing extreme still water levels and waves in design level studies
[IOS-183] 03 p0398 N85-12542

NUTSATSEA: An on line data reduction program linking a Chemlab continuous flow analyser to a Commodore PET microcomputer
[IOS-176] 03 p0403 N85-12570
Sigma code testing
[AD-A146548] 06 p0841 N85-15340
Interactions between mean flow and finite-amplitude mesoscale eddies in a barotropic ocean
[AD-A147249] 07 p1009 N85-16413
Research of inverse methods to describe the structure of the earth and ocean bottom
[AD-A147082] 07 p1030 N85-16541
Bibliography update on the California current system and related mesoscale ocean modeling
[AD-A148546] 08 p1190 N85-17503
A critical analysis of ocean thermal analysis models in operation at FNOC (Fleet Numerical Oceanography Centers)
[AD-A148731] 09 p1359 N85-18547
Stochastic convective-dispersive transport model for wastes disposed at the 106-mile ocean disposal site
[PB85-116176] 12 p1865 N85-21831
Intensification of tropical instabilities
[AD-A149965] 12 p1896 N85-21899
Calculation of level surface in problems of large-scale ocean circulation 13 p2108 N85-23136
Mathematical-cartographic model for study of distribution of hydrochemical elements in sea water (using dissolved oxygen in the Pacific Ocean as an example)
13 p2109 N85-23138
Sea-ice motion in response to geostrophic winds
14 p2323 N85-24357
Influence of bubbles formed upon breaking of waves on gas exchange between ocean and atmosphere
14 p2335 N85-24439
Representation of temperature and salinity fields using statisticallyt orthogonal functions (in example of polymode data) 14 p2337 N85-24449
Sensitivity analysis of a coupled atmospheric-oceanic boundary layer model
[AD-A150760] 14 p2382 N85-24690
Ocean modeling of the North Atlantic
15 p2602 N85-26039
Ocean tide models for Topex analysis
16 p2805 N85-27291
Tropical Oceans-Global Atmosphere (TOGA) experiment planning for the Brazilian participation in TOGA global climate program
[INPE-3499-PRE/735] 16 p2834 N85-27477
Comparison of a diffusion model with dye dispersion measurements to study turbulence in coastal waters
[INPE-3492-PRE/729] 16 p2838 N85-27504
Research Review, 1983
[NASA-TM-86219] 18 p3139 N85-29433
On Fofonoff's mode 18 p3145 N85-29471
Utilization of the SEASAT scatterometer winds for ocean mixed layer modeling
[AD-A153748] 18 p3150 N85-29506
Parametric description of cold film on ocean surface
19 p3292 N85-30410
Dynamic theory of polar tide 19 p3292 N85-30414
Experiments using atmospheric forcing from a FGGE analysis to drive an upper ocean model
[INPE-3503-PRE/738] 19 p3319 N85-30576
One-dimensional model hindcasts of warm anomalies in the North Pacific Ocean
[AD-A154128] 19 p3320 N85-30579
Research, progress and the mark A box model for physical, biological and chemical transports
[DE85-010574] 19 p3320 N85-30581
Dispersal From Deep Ocean Sources: Physical and Related Scientific Processes
[DE85-010420] 20 p3497 N85-31740
Benthic boundary layer modelling studies
[IOS-181] 20 p3497 N85-31742
Anorthositic oceanic crust in the Archean Earth
21 p3719 N85-33077

OCEAN SURFACE
Large-scale ocean-atmosphere interactions in the mid-latitudes and equatorial regions: A literature review
[CSIR-T/SEA-8302] 01 p0073 N85-10482
The Marine Resources Experiment Program (MAREX)
[NASA-TM-87368] 01 p0066 N85-10580
Return wave heights off South Uist estimated from seven years of data
[IOS-164] 01 p0069 N85-10601
Energy-active zones in north Atlantic as manifestation of interannual variability of radiation balance
02 p0164 N85-11108
A radar sea clutter model for atmospheric ducting conditions
[AD-A145321] 02 p0190 N85-11268
Theory of radio wave propagation over the ocean
02 p0259 N85-11698
SEASAT altimeter data over the Mediterranean: Implications for ERS-1 03 p0382 N85-12443
Satellite altimetry for sea-surfacing topography determination and geoid improvement
03 p0382 N85-12444
Development of a microcomputer coupled atmospheric and oceanic boundary layer prediction model
[AD-A146334] 03 p0397 N85-12530
Simple prediction of convergence zone propagation in waters around australia
[AD-A145986] 03 p0416 N85-12659
Multisensor satellite data integration for sea surface wind speed and direction determination
[NASA-CR-174162] 04 p0542 N85-13446
Components of the time variation of sea surface height from SEASAT altimeter data 05 p0658 N85-14227
Statistical analysis of visual wave observations and gage/radar measurements
[AD-A146358] 06 p0798 N85-15100
Energy active areas of ocean
06 p0820 N85-15204
Studies of the ocean surface and the coupling between the sea and the atmosphere
[AD-A146546] 06 [illegible] N85-15339
The interpretation of SIR-B imagery of surface waves and other oceanographic features using in-situ, meteorological satellite, and infrared satellite data
08 p1143 N85-17212
Remote sensing of rice fields and sea pollution by SIR-B 08 p1145 N85-17222
The investigation of selected oceanographic applications of spaceborne synthetic-aperture radar
08 p1146 N85-17233
The use of synthetic aperture radar imagery to detect hazards to navigation
[AD-A149324] 10 p1422 N85-18971
Surface currents of the Indian Ocean (to 25 deg S., 100 deg E.)
[IOS-187] 10 p1521 N85-19593
Drifting buoy data from equatorial Pacific Ocean, 31 Aug. 1980 - 30 Apr. 1982
[PB85-120046] 10 p1522 N85-19598
[illegible]graphic and meteorological research based on the data produced by SEASAT
[E85-10091] [illegible] p1874 N85-21753
Calculation of level surface in problems of large-scale ocean circulation 13 p2108 N85-23136
Possibility of mapping active tectonic structures from mercury gas aureoles over sea surface
13 p2113 N85-23162
Surface currents in the tropical Pacific during 1979-1980 using drifting buoys 14 p2323 N85-24354
The Indian Ocean surface dynamics experiment (SINODE) 14 p2325 N85-24370
Possible multiple atmospheric thermal modes with time scale on order of one month 14 p2333 N85-24430
Influence of bubbles formed upon breaking of waves on gas exchange between ocean and atmosphere
14 p2335 N85-24439
Low-frequency oscillations of sea level and group structure of wind waves 14 p2335 N85-24441
Energy structure of atmospheric boundary layer above waves 14 p2335 N85-24442
Frontal nature of Cromwell Current
14 p2336 N85-24445
Parameterization of apparent and latent heat fluxes above water surface in calm weather under natural conditions 14 p2337 N85-24454
Measurement of ocean surface currents from space with multi-frequency microwave radars
15 p2539 N85-25672
Survey of remote sensing techniques for wave measurement
[NASA-TM-84429] 15 p2583 N85-25928
Quaternary North Atlantic surface paleoceanography in regions of potential deep-water formation
15 p2602 N85-26036
Changes in the high-latitude ocean as possible causes of atmosphere CO2 variations 15 p2602 N85-26038
Sea ice, climate and Fram Strait
15 p2603 N85-26042
Ocean circulation and meteorology off the Georgia coast. Part 1: Real-time telemetry system for data collection
[PB85-155935] 15 p2605 N85-26052
Sound propagation through directional internal wave fields
[AD-A151168] 15 p2646 N85-26321
Topex Gravity Model Development Team activities during fiscal year 1984
[NASA-TM-86208] 16 p2804 N85-27285
Results of an initial trial of a satellite telemetering buoy measuring near surface current
16 p2812 N85-27345
Atmospheric frontal zone studies
[NASA-CR-175293] 16 p2833 N85-27469
On the 1983 drought in northeast Brazil
[INPE-3412-PRE/678] 16 p2834 N85-27476
Simulation of a synchronously coupled atmosphere-ocean prediction model
[AD-A152020] 16 p2835 N85-274
Analysis of ocean surface wind fields using SEASAT-A scatterometer data 18 p3139 N85-294
Intercomparison of sea-surface temperature anomaly fields 18 p3140 N85-294
A GCM study of the atmospheric response to tropical SST anomalies 18 p3146 N85-294
One mechanism for generation of wave disturbances in spectra of turbulent flows near ocean surface
19 p3289 N85-30
Study of drift currents in initial stage of generation of wind waves by laser Doppler anemometer
19 p3291 N85-304
Frequency of recurrence and critical conditions for generation of Langmuir circulations
19 p3291 N85-304
Parametric description of cold film on ocean surface
19 p3292 N85-304
Model computations of light reflection from sea surface 19 p3292 N85-3041
Sea surface radio emission at wavelengths 0.8 and 1.3 cm near Brewster angle 19 p3293 N85-304
Specifics of laser sounding of atmosphere along horizontal and slightly slanting paths over water surface
19 p3297 N85-3044
A survey of the turbulence in the marine surface layer for the operation of low-Reynolds number aircraft
[AD-A154133] 19 p3316 N85-305
A study of the turbulent layer in the water at an air-water interface
[AD-A154117] 19 p3319 N85-305
One-dimensional model hindcasts of warm anomalies in the North Pacific Ocean
[AD-A154128] 19 p3320 N85-3057
Geodynamics Branch research program
[NASA-TM-86223] 20 p3489 N85-316
Global mean sea surface based upon a combination of the GEOS-3 and SEASAT altimeter data
20 p3492 N85-3171
Using ship wake patterns to evaluate SAR (Synthetic Aperture Radar) ocean wave imaging mechanisms. Joint US-Canadian Ocean Wave Investigation Project
[AD-A154633] 21 p3573 N85-3222
Numerical simulations of the response of intense ocean currents to atmospheric forcing
[AD-A155161] 21 p3655 N85-3270
Simulation of the coupled atmospheric and oceanic boundary layer model during MILDEX
[AD-A155166] 21 p3655 N85-3270
Basic properties and interpretation of synthesized radar images of sea waves with long synthetization time
22 p3773 N85-333
Large-scale sea surface temperature variability from satellite and shipboard measurements
[NASA-CR-176123] 22 p3818 N85-3365
Microwave properties of a quiet sea
[NASA-CR-176199] 24 p4085 N85-3532
Sea surface and remotely sensed temperatures off Cape Mendocino, California
[NASA-TM-86712] 24 p4125 N85-3557

OCEAN TEMPERATURE
NT SEA SURFACE TEMPERATURE
The gulf stream deflection and meander energetics experiment. Current meter and bottom pressure gauge data report for the September, 1981 to April, 1982 mooring period
[AD-A144977] 01 p0068 N85-105
Ocean and climate, an example. The interannual variability of the tropical Pacific Ocean
07 p1002 N85-163
The ocean and the dynamics of the tropical atmosphere; its possible predicability 07 p1002 N85-163
A compilation of moored current meter and wind recorder data. Volume 35: Long-Term Upper Ocean Study (LOTUS) (Moorings 764, 765, 766, 767, 770). May 1982 - April 1983
[AD-A147103] 07 p1009 N85-1641
Measurements of sediment temperatures, conductivity and heat flow in the North Atlantic and their relevance to radioactive waste disposal
[IOS-172] 09 p1359 N85-1855
Drifting buoy data from equatorial Pacific Ocean, 31 Aug. 1980 - 30 Apr. 1982
[PB85-120046] 10 p1522 N85-195
Hydrographic data collected in 1982 and 1983 for EPOCS (Equatorial Pacific Ocean Climate Studies)
[PB85-110799] 12 p1876 N85-217
Oceanic role in terrestrial climate
[DE85-004422] 12 p1896 N85-2190
Horizontal coherence of temperature microstructure in upper ocean layer 13 p2109 N85-2313

Geographic variation in the relationships of temperature, salinity or sigma sub t versus plant nutrient concentrations in the world ocean — silicic acid, nitrate, and phosphate concentration
[NASA-CR-175621] 13 p2140 N85-23297

Dynamic stochastic model of long-period variability of ocean surface temperature 14 p2334 N85-24437

Representation of temperature and salinity fields using statisticallyt orthogonal functions (in example of polymode data)
14 p2337 N85-24440

North Atlantic Deep Water Formation
[NASA-CP-2367] 15 p2601 N85-26028

Review of North Atlantic source waters
15 p2601 N85-26029

Deep water formation 15 p2601 N85-26030

Temporal and spatial scales of Labrador Sea water formation
15 p2601 N85-26031

North Atlantic Deep Water and the world ocean
15 p2602 N85-26033

Oceanographic variations in recent decades and their impact on the fertility of the Iceland Sea
15 p2602 N85-26034

Quaternary North Atlantic surface paleoceanography in regions of potential deep-water formation
15 p2602 N85-26036

Glacial-to-interglacial changes in NADW fluxes?
15 p2602 N85-26037

Real-time enhancement of a climatology or forecast of ocean thermal structure using observed ocean temperatures
[AD-A151118] 15 p2604 N85-26049

Ocean circulation and meteorology off the Georgia coast. Part 1: Real-time telemetry system for data collection
[PB85-158935] 15 p2605 N85-26052

On the 1983 drought in northeast Brazil
[INPE-3412-PRE/678] 16 p2834 N85-27476

Intercomparison of sea-surface temperature anomaly fields 18 p3140 N85-29440

A GCM study of the atmospheric response to tropical SST anomalies 18 p3146 N85-29477

Publications of the Jet Propulsion Laboratory 1983
[NASA-CR-175979] 18 p3199 N85-29848

Parametric description of cold film on ocean surface
19 p3292 N85-30410

Air-sea interaction with SSM/I and altimeter
[NASA-CR-176105] 22 p3818 N85-33650

Large-scale sea surface temperature variability from satellite and shipboard measurements
[NASA-CR-176123] 22 p3818 N85-33651

OCEAN THERMAL ENERGY CONVERSION

Biofouling and corrosion studies at the Seacoast Test Facility in Hawaii
[DE84-014643] 01 p0029 N85-10180

Ocean energy systems at the Johns Hopkins University Applied Physics Laboratory
[PB84-225705] 03 p0387 N85-12474

Research approaches to qualify aluminum for Ocean Thermal Energy Conversion (OTEC) systems
[DE84-013007] 04 p0476 N85-13034

Correlation and reassessment of the OTEC plant power cycle
[DE84-015467] 04 p0529 N85-13382

Open cycle OTEC thermal-hydraulic systems analysis and parametric studies
[DE84-013011] 04 p0530 N85-13391

NOAA OTEC CWP (National Oceanic and Atmospheric Administration Ocean Thermal Energy Conversion Cold Water Pipe) at-sea test. Volume 3, part 1: Tabulation of the power spectra for selected channels
[PB84-238955] 09 p1346 N85-18467

NOAA OTEC CWP (National Oceanic and Atmospheric Administration Ocean Thermal Energy Conversion Cold Water Pipe) at-sea test. Volume 3: Additional tabulation of the power spectra, part 2
[PB84-238997] 09 p1346 N85-18468

Conceptual design of a 10 MW shore-based OTEC plant
[DE84-015808] 10 p1511 N85-19532

OTEC (Ocean Thermal Energy Conversion) Cold Water Pipe At-Sea Test Program. Phase 2: Suspended pipe test
[PB85-119931] 10 p1512 N85-19542

Theoretical analysis of condensation in the presence of noncondensable gases as applied to open cycle OTEC condensers
[DE84-015809] 11 p1675 N85-20556

Ocean energy systems
[PB85-110856] 11 p1676 N85-20564

Experimental study of steam condensation on water in countercurrent flow in presence of inert gases
[DE84-013028] 12 p1861 N85-21800

Temperature sensors for OTEC applications
[DE85-009807] 18 p3110 N85-29254

Numerical techniques for steady two-dimensional transcritical stratified flow problems, with an application to the intermediate field dynamics of ocean thermal energy conversion plants
[DE85-008347] 18 p3151 N85-29509

Renewable technologies program summaries
[DE85-001509] 19 p3307 N85-30500

Heat transfer monitor for measurements of fouling of industrial heat exchangers
[DE85-010257] 20 p3455 N85-31455

Solar energy education. Renewable energy: A background text
[DE85-010365] 23 p3946 N85-34452

Ocean thermal energy conversion
[DE85-012291] 23 p3946 N85-34456

Energy from low temperature differences
[DE85-008817] 24 p4112 N85-35492

OCEANOGRAPHIC PARAMETERS

NT OCEAN TEMPERATURE

Sea ice data buoys in the Weddell Sea
[AD-A144953] 01 p0088 N85-10594

A description and discussion of FREDDEX oceanographic measurements
[AD-A145032] 01 p0088 N85-10596

Analysis and interpretation of current measurements from the Beaufort Sea
[AD-A145197] 01 p0089 N85-10600

Active remote sensing of ocean parameters, an engineering study 02 p0213 N85-11403

One-year records of current and bottom pressure in the strait between Nordaustlandet and Kvitoeya and Svalbard, 1980 - 1981
[AD-A145594] 02 p0233 N85-11518

Archiving and exchange of a computerized marine seismic database: The ROSE (Rivera Ocean Seismic Experiment) data archive system
[AD-A145658] 02 p0294 N85-11906

Ocean wave parameters extraction using satellite short-pulse radar altimeters 03 p0380 N85-12425

Physical oceanography report. Helicopter-based STD data from MIZEX 83 (Marginal ice zone experiment)
[AD-A145848] 03 p0398 N85-12538

An introduction to the MIAS conversion system
[IOS-184] 03 p0403 N85-12571

Multisensor satellite data integration for sea surface wind speed and direction determination
[NASA-CR-174162] 04 p0542 N85-13446

The long term upper ocean study (LOTUS). Cruise summary and hydrographic data report, OCEANUS 154, May 1984
[AD-A147908] 07 p1009 N85-16414

Smoothing with split linear fits
[AD-A149032] 10 p1545 N85-19740

Atlas of the Beaufort Sea
[AD-A149545] 11 p1689 N85-20619

Advanced 2-frequency ocean sensing radar using high resolution antenna beams 14 p2230 N85-23821

The Tropical Ocean and Global Atmosphere program (TOGA) 14 p2330 N85-24411

Observations of the California countercurrent
[AD-A150781] 14 p2382 N85-24891

Ocean modeling of the North Atlantic
15 p2602 N85-26039

Space methods in oceanology
[NASA-TM-77652] 15 p2604 N85-26047

Tenth Conference of Working Group of Socialist Countries on Remote Sensing of Earth under Intercosmos Program 16 p2725 N85-26820

Function of remote sensing in Brazil
[INPE-3314-PRE/621] 16 p2810 N85-27329

Diffusion coefficients for coastal water determined from aerial photographs
[INPE-3413-PRE/679] 16 p2810 N85-27331

Symposium on Atmospheric Sciences in South Africa
[CSIR-S-331] 16 p2829 N85-27442

Air flow of the western coastal boundary of South Africa and its influence on the ocean 16 p2831 N85-27459

NASA Oceanic Processes Program annual review
[NASA-TM-87565] 16 p2838 N85-27503

Towards a study of synoptic-scale variability of the California current system
[NASA-CR-175871] 17 p2997 N85-28529

Intercomparison of sea-surface temperature anomaly fields 18 p3140 N85-29440

Geological-geophysical and gas-biochemical studies in Bering Sea 19 p3291 N85-30404

Geochemistry of manganese in ocean
19 p3291 N85-30406

Environmental background measurement program
[AD-A153860] 19 p3319 N85-30577

Research, progress and the mark A box model for physical, biological and chemical transports
[DE85-010574] 19 p3320 N85-30581

Tropical Ocean and Global Atmosphere (TOGA) heat exchange project: A summary report
[NASA-CR-176036] 20 p3496 N85-31738

The worldwide distribution of the seasonal cycle of mean sea level
[IOS-190] 20 p3497 N85-31743

Hydrographic data from the OPTOMA (Ocean Prediction Through Observations, Modeling and Analysis) program: OPTOMA15, 24 January to 23 February 1985
[AD-A155012] 21 p3655 N85-32703

Basic properties and interpretation of synthesized radar images of sea waves with long synthetization time
22 p3773 N85-33384

Salinity driven oceanographic upwelling
[DE85-011664] 22 p3818 N85-33652

OCEANOGRAPHY

Satellite reconnaissance
[AD-B085034] 01 p0015 N85-10094

The development of a diode laser Doppler velocimeter for boundary layer measurements under ice: A feasibility investigation
[AD-A145076] 01 p0053 N85-10348

Estuaries of the Cape. Part 2: Synopses of available information on individual systems. Report no. 17: Lourens (CSW 7)
[CSIR-RR-416-PT-2] 01 p0087 N85-10586

Estuaries of the Cape. Part 2: Synposes of available information on individual systems. Report no. 19: Groot (WES) (CMS 23) and Sout (CMS 22)
[CSIR-RR-418] 01 p0087 N85-10588

Sea-level in the world ocean. Part 6: The South Atlantic and South Pacific Oceans, a catalogue of measurements
[CSIR-T/SEA-8303-6] 01 p0087 N85-10590

Sea-level in the world ocean. Part 7: The Indian Ocean, a catalogue of measurements
[CSIR-T/SEA-8303-7] 01 p0087 N85-10591

Seafloor geosciences division: Missions, technical specialties, accomplishments, and activities, calendar year 1983
[AD-A144849] 01 p0087 N85-10592

Applications of remote sensing techniques to oceanography and sea ice
[FOA-B-60004-M7] 02 p0220 N85-11446

Radiotracer studies of the dispersion of solid pollutants in marine and estuarial environment: Measurement of diffusion coefficients and the phenomenon of dispersion by currents
[BLL-DRIC-TRANS-7104-(3623.66)]
02 p0224 N85-11468

Bibliography of climate textbooks and studies
[WCP-84] 02 p0231 N85-11505

A study of highly energetic near-bottom ocean flow at the base of the Scotian Rise 02 p0233 N85-11515

Physical oceanography report. Helicopter-based STD data from MIZEX 83 (Marginal ice zone experiment)
[AD-A145848] 03 p0398 N85-12538

Abstracts of papers submitted in 1983 for publication
[PB84-217579] 03 p0398 N85-12543

Coastal Zone Color Scanner (CZCS): Imagery of near-surface phytoplankton pigment concentrations from the first coastal ocean dynamics experiment (CODE-1), March - July 1981
[NASA-CR-174169] 04 p0542 N85-13447

Contributions to remote sensing : Applications of thermal infrared
[COMMUN-34/1984] 05 p0654 N85-14196

Activities of the Coastal Research Center
[PB84-231323] 05 p0672 N85-14320

USSR report: Earth sciences
[JPRS-UES-84-007] 06 p0819 N85-15196

A summary of the foundation research program
[AD-A146524] 06 p0891 N85-15656

USSR report: Earth sciences
[JPRS-UES-84-008] 07 p0960 N85-16223

Exploring ocean's mineral wealth
07 p0960 N85-16227

Ocean and climate, an example. The interannual variability of the tropical Pacific Ocean
07 p1002 N85-16365

Oceanographic data for development of the US exclusive economic zone
[PB85-106458/GAR] 07 p1010 N85-16415

The interpretation of SIR-B imagery of surface waves and other oceanographic features using in-situ, meteorological satellite, and infrared satellite data
08 p1143 N85-17212

The spatial evolution of the directional wave spectrum in the Southern Ocean: Its relation to extreme waves in Agulhas Current 08 p1144 N85-17213

Evaluation of SIR-B imagery for geologic and geomorphic mapping, hydrology, and oceanography in Australia 08 p1148 N85-17229

SEASAT 3 and 4
[AD-A148343] 08 p1152 N85-17274

Altimetry, orbits and tides
[E85-10066] 08 p1174 N85-17404

The use of principal components analysis techniques Nimbus-7 coastal zone color scanner data to define mesoscale ocean features through a warm humid atmosphere
[AD-A148567] 08 p1176 N85-17416

Late Quaternary deep-water paleoceanography of the eastern equatorial Indian Ocean: Evidence from Bethnic foraminifera, carbonate dissolution, and stable isotopes
08 p1182 N85-17446

Bibliography update on the California current system and related mesoscale ocean modeling
[AD-A148546] 08 p1190 N85-17503

A critical analysis of ocean thermal analysis models in operation at FNOC (Fleet Numerical Oceanography Centers)
[AD-A148731] 09 p1359 N85-18547

USSR report: Earth sciences
[JPRS-UES-85-003] 10 p1497 N85-19446

Nautical charting with remotely sensed imagery, volume 1
[AD-A149361] 10 p1506 N85-19503

Practical applications of satellite-derived meteorological and oceanographic data in Naval operations
11 p1712 N85-20771

Hydrographic data collected in 1982 and 1983 for EPOCS (Equatorial Pacific Ocean Climate Studies)
[PB85-110799] 12 p1876 N85-21765

USC (University of Southern California) Sea Grant Program Directory, 1984-1985
[PB85-135051] 12 p1899 N85-21922

Biological processes in the water column of the South Atlantic Bight. Volume 1: Published manuscripts
[DE85-004610] 12 p1900 N85-21929

An airborne infrared thermal scanning system for easy use on Navy P-3 aircraft
[AD-A149690] 12 p1933 N85-22143

USSR report: Earth sciences
[JPRS-UES-85-002] 13 p2105 N85-23116

World ocean level oscillations and their relationship to change in inflow of continental waters
13 p2108 N85-23133

Fine structure of vertical distribution of light attenuation index of sea water 13 p2109 N85-23140

Science opportunities using the NASA scatterometer on N-ROSS
[NASA-CR-175839] 13 p2123 N85-23222

USSR report: Earth sciences
[JPRS-UES-85-004] 14 p2332 N85-24424

Determination of temperature and degree of roughness of sea and land surfaces by microwave radiometric polarization measurements 14 p2334 N85-24432

One physical mechanism of formation of fine structure of ocean waters 14 p2334 N85-24436

Two-cycle mechanism of dissipation of tidal energy in ocean 14 p2335 N85-24438

Automation of radiometric measurements in nuclear oceanology 14 p2337 N85-24452

Most important geochemical barrier zones in ocean (with example of Atlantic Ocean basin)
14 p2343 N85-24491

Remote sensing of directional wave spectra using the surface contour radar
[NASA-TM-84440] 14 p2347 N85-24510

Preliminary report on the results of hydrological measurements in the southern Tyrrhenian Sea, in the Messina strait and in the western Ionian sea
[PREPRINT-433] 14 p2382 N85-24693

Geophysical Fluid Dynamics Laboratory activities, FY84, plans, FY85
[PB85-147801] 15 p2558 N85-25783

Real-time enhancement of a climatology or forecast of ocean thermal structure using observed ocean temperatures
[AD-A151116] 15 p2604 N85-26049

ONR (Office of Naval Research) Far East Scientific Bulletin, Volume 9, Number 4, October-December 1984
[AD-A151274] 15 p2665 N85-26448

China's integrated circuit production
16 p2806 N85-27302

USSR report: Earth sciences
[JPRS-UES-85-005] 16 p2807 N85-27307

An inexpensive radar-responding relocation device for drifting oceanographic instruments
[AD-A152170] 16 p2838 N85-27505

The effect of the Benthic Boundary Layer on the physics of intense mesoscale eddies
[AD-A153193] 17 p2958 N85-28270

Low-rate discharge of various electrochemical batteries for use with oceanographic instruments
[AD-A153965] 18 p3095 N85-29159

Environmental Research Laboratories (of the National Oceanic and Atmospheric Administration) programs and plans: FY 1984 programs and FY 1985 plans
[PB85-171494] 18 p3149 N85-29501

Arctic mixed layer dynamics
[AD-A153582] 18 p3150 N85-29505

Utilization of the SEASAT scatterometer winds for ocean mixed layer modeling
[AD-A153748] 18 p3150 N85-29506

Metrology and Oceanology Institutes' underwater acoustics R and D 19 p3289 N85-30394

Geological-geophysical and gas-biochemical studies in Bering Sea 19 p3291 N85-30404

Sixth All-Union Marine Geology School
19 p3294 N85-30420

Environmental Research Laboratories publication abstracts, FY 1984
[PB85-180594] 19 p3313 N85-30540

Environmental background measurement program
[AD-A153860] 19 p3319 N85-30577

The application of computer imaging techniques to ocean topography and geophysical data
20 p3492 N85-31711

Ocean circulation studies 20 p3492 N85-31712

The time averaged circulation of the oceans from satellite altimetry 20 p3493 N85-31713

Ocean tidal parameters from LAGEOS
20 p3493 N85-31716

Offshore oceanographic and environmental monitoring services for the Strategic Petroleum Reserve, volume 3
[DE85-009907] 20 p3497 N85-31741

Physical oceanography program science abstracts
[AD-A154637] 21 p3654 N85-32701

Climate modeling: A retrospective-prospective view with consideration for the atmospheric carbon dioxide-climate issue
[DE85-011532] 23 p3950 N85-34481

Noiseless coding for the Gamma Ray spectrometer
[NASA-CR-176201] 24 p4069 N85-35219

Microwave properties of a quiet sea
[NASA-CR-176199] 24 p4085 N85-35322

Sea surface and remotely sensed temperatures off Cape Mendocino, California
[NASA-TM-86712] 24 p4125 N85-35573

OCEANS
NT ARCTIC OCEAN
NT ATLANTIC OCEAN
NT INDIAN OCEAN
NT PACIFIC OCEAN

The Marine Resources Experiment Program (MAREX)
[NASA-TM-87368] 01 p0086 N85-10580

Nonlinear propagation in a depth-dependent ocean
[AD-A145079] 01 p0116 N85-10791

Prediction of wave height of wind-generated seas in finite water depth
[AD-A145996] 03 p0398 N85-12539

Plans for the NRL/NORDA (Naval Research Laboratory-Naval Ocean Research and Development Activity) fine-scale variability experiment - 1984 (FVX-84)
[AD-A146041] 03 p0398 N85-12540

Recent studies of the ocean nitrogen cycle
05 p0653 N85-14193

Energy diagnostics and impact studies of FGGE global data sets and GLAS GCM simulations
05 p0683 N85-14390

Internal waves in ocean 06 p0819 N85-15201

Wave-wave interactions, microseisms, and infrasonic ambient noise in the ocean
[AD-A146529] 06 p0859 N85-15463

Interactions between mean flow and finite-amplitude mesoscale eddies in a barotropic ocean
[AD-A147249] 07 p1009 N85-16413

New Zealand SIR-B science investigations
08 p1144 N85-17218

Theoretical and experimental analyses of laser altimeters for barometric measurements over the ocean
08 p1165 N85-17351

An efficient numerical solution technique for wave propagation in horizontally stratified ocean environments
[AD-A148537] 08 p1190 N85-17502

ONR (Office of Naval Research) Far East Scientific Bulletin, volume 9, number 3, July to September 1984
[AD-A147282] 08 p1262 N85-17930

The wobble of the Earth and the low frequency dynamics of the ocean 09 p1358 N85-18546

Field studies of run-up generated by wind waves on dissipative beaches
[AD-A148793] 09 p1359 N85-18548

Evolution of sedimentation basins in Earth's history
10 p1497 N85-19451

Tectonic position and formation of young alkaline provinces of continents and oceans
10 p1502 N85-19480

Mercury health effects update: Health issue assessment
[PB85-123925] 10 p1528 N85-19639

Earth observations and the polar platform
[NOAA-TR-NESDIS-18] 11 p1669 N85-20517

Along-track deflection of the vertical from SEASAT: GEBCO (General Bathymetric Chart of the Oceans) overlays
[PB85-129641] 12 p1876 N85-21767

Carbonate chemistry of the Weddell Sea
[DOE/EV-110611/4] 12 p1898 N85-21816

Numerical experiments with simple model of ocean climate 13 p2106 N85-23123

Boundary velocities of longitudinal seismic waves and lateral inhomogeneities of upper ocean mantle
13 p2113 N85-23165

Assessing LANDSAT TM and MSS data for detecting submerged plant communities 13 p2120 N85-2320

Luminescence in the ocean
[AD-B089136L] 13 p2140 N85-2329

Internal waves in layers of Earth's upper mantle
16 p2807 N85-27312

Reconstruction of past atmospheric CO/sub 2/ contents from the chemistry of the contemporary ocean: An evaluation
[DE85-008426] 18 p3133 N85-29401

Specification of surface roughness over oceans in the GLAS Fourth Order GCM 18 p3142 N85-29455

Environmental Research Laboratories (of the National Oceanic and Atmospheric Administration) programs and plans: FY 1984 programs and FY 1985 plans
[PB85-171494] 18 p3149 N85-29501

Operation guiding light-scientific program and field plan. The pilot field experiment for NORDA project chemical dynamics in ocean frontal areas
[AD-A153765] 18 p3150 N85-29507

Sixth All-Union Marine Geology School
19 p3294 N85-30420

Use of stereographic projection in marine geodesy
19 p3294 N85-30421

MIZEX, 1984, NASA CV-990 flight report
[NASA-TM-86216] 19 p3299 N85-30451

Satellite measurements of atmospheric aerosols
[AD-A153807] 19 p3316 N85-30558

Linear time-invariant, space-variant filters and the WKB approximation with applications to underwater acoustic signal processing
[AD-A154250] 19 p3352 N85-30775

Maritime search and rescue cooperation and planning
20 p3400 N85-31083

Continental and oceanic magnetic anomalies: Enhancement through GRM 20 p3476 N85-31598

Global Mega-Geomorphology
[NASA-CP-2312] 21 p3600 N85-32267

The variability of aerosol microstructure in continental and oceanic surface layers of the atmosphere in anticyclones 21 p3647 N85-32680

Some thoughts on GAIA and the sulfur cycle
21 p3658 N85-32727

Global environmental transport models for tritium
[DE85-011437] 22 p3816 N85-33636

Two dimensional CO2-ocean model including the biological processes
[DE85-012341] 23 p3950 N85-3448

Cobalt-rich ferromanganese crusts in the oceans
24 p4104 N85-3544

OCTANE NUMBER

Trends of petroleum fuels
[DE85-000116] 14 p2263 N85-2402

OCULOMETERS

Eye movement in response to single and multip
targets
[AD-A151115] 15 p2617 N85-2612

Electrooculographic measurement, fatigue an
variability of performance in simulated aircraft flight
19 p3217 N85-2094

OCULOMOTOR NERVES

Sensory and motor properties of the cerebellar un
and modulus 15 p2613 N85-261

ODAS
U OCEAN DATA ACQUISITIONS SYSTEMS

ODD-EVEN NUCLEI

Extension of the consistent Q formalism to odd-A nu
in the W-Pt region
[DE85-008284] 17 p3034 N85-287

Boson-fermion symmetries in the W-Pt region
[DE85-009755] 19 p3362 N85-308

ODD-ODD NUCLEI

Experimental level-structure determination in odd-
actinide nuclei
[DE85-010476] 19 p3360 N85-30

OFF-ON CONTROL

Time-optimal bang-bang slew of rigidized SCO
configuration 20 p3410 N85-31

OFFGASSING

Technology of off-gas treatment for liquid-fed cer
melters
[DE85-012467] 22 p3812 N85-33

OFFSHORE PLATFORMS

High-data-rate wide-angle underwater aco
telemetry system
[DE84-015696] 02 p0233 N85-1

Icing rate on stationary structures under m
conditions
[AD-A145795] 03 p0395 N85-1

Full load testing in the platform module prior to tow-out: A case history of subsynchronous instability
05 p0642 N85-14117

A crew exposure study. Volume 1: Offshore
[AD-A146664] 07 p1015 N85-16449

Defect tolerance in pipeline girth welds
[ERS-E.353] 09 p1328 N85-18347

OFT
U SPACE TRANSPORTATION SYSTEM FLIGHTS

OFT 1
U SPACE TRANSPORTATION SYSTEM 1 FLIGHT

OFT 3
U SPACE TRANSPORTATION SYSTEM 3 FLIGHT

OFT 4
U SPACE TRANSPORTATION SYSTEM 4 FLIGHT

OGEE WINGS
U VARIABLE SWEEP WINGS

OGO

The downshift of electron plasma oscillations in the electron foreshock region
[NASA-CR-175633] 14 p2423 N85-24945

OHIO

Interlobate comparison of glacial-depositional style as evidenced by small-relief glacial landscape features in Illinois, Indiana, and Ohio, utilizing SIR-B
08 p1146 N85-17231

Lithologic and environmental atlas of Berea Sandstone (Mississippian) in the Appalachian Basin
[PB85-129039] 11 p1682 N85-20600

OHMIC DISSIPATION

Alternating current OHMIC heating in a toroidal stellarator 20 p3534 N85-31968

OHMS LAW

Mathematical physics approaches to lightning discharge problems
[NASA-TM-86349] 08 p1187 N85-17482

OIL EXPLORATION

A stochastic model for optimizing the consumption and exploration of nonrenewable natural resources
[INPE-2770-PRE/343] 03 p0440 N85-12604

Geological effectiveness of automated processing of highly precise aeromagnetic surveys in Caspian region
06 p0821 N85-15216

New method of reconstructing conditions of recent differentiation of oil and gas in the Amudarya Basin (based on results of interpretation of space photographs)
13 p1984 N85-22446

Evaluation of Thematic Mapper performance as applied to hydrocarbon exploration — Ontario, Canada; Cement, Oklahoma; and Death Valley, California
13 p2118 N85-23191

Use of space information in petroleum- and gas-prospecting work (example of Southern Mangyshlak)
15 p2485 N85-25341

Pacific index, April 1983 - October 1984
[TI85-901335] 19 p3320 N85-30582

Using remote photographs in prospecting for hydrocarbons on the Kerch Peninsula
22 p3735 N85-33154

The transient electromagnetic depth sounding technique applied to hydrocarbons and geothermal exploration
[MITT-42] 23 p3949 N85-34476

OIL FIELDS

New method of reconstructing conditions of recent differentiation of oil and gas in the Amudarya Basin (based on results of interpretation of space photographs)
13 p1984 N85-22446

Steamflood pilots in the O'Connell Ranch field and the T-4 Ranch field
[DE85-901363] 24 p4108 N85-35468

OIL POLLUTION

Drifting ice as mechanical factor in purifying and polluting hydrosphere 13 p2108 N85-23132

Operational experiences with the ARGOS system in oceanography and oil spill emergency planning. Future plans for the use of the ARGOS system as a component in offshore data collection system
14 p2239 N85-23887

Arabian gulf circulation — pollution monitoring
14 p2331 N85-24412

OIL RECOVERY

Investigation of condensing, three-phase, two-component, flow through porous media
09 p1317 N85-18283

Synthesis and characterization of novel polymers from non-petroleum sources for use in enhanced oil recovery
[DE85-010922] 19 p3250 N85-30151

OIL SLICKS

Internal waves in ocean 06 p0819 N85-15201

OILS
NT CRUDE OIL
NT FUEL OILS
NT LUBRICATING OILS
NT MINERAL OILS
NT SHALE OIL

Computations for segmented radial bearings
14 p2288 N85-24180

Aviation turbine fuels from tar sands bitumen and heavy oils. Part 1: Process analysis
[AD-A151319] 15 p2521 N85-25539

Oil resistant silicone elastomers
[AD-131523] 16 p2753 N85-26987

Combustion and micro-explosion of water/oil emulsions in high pressure environments
[AD-A152960] 17 p2919 N85-27997

An experimental apparatus to study nucleate pool boiling of R-114 and oil mixtures
[AD-A154077] 19 p3265 N85-30249

Mathematics of oil production
[DE85-011235] 19 p3267 N85-30261

The influence of oil contamination on the nucleate pool-boiling behavior of R-114 from a structured surface
[AD-A155609] 21 p3585 N85-32284

Method of distributing liquefaction catalysts in solid carbonaceous material
[DE85-005759] 23 p3909 N85-34218

Method for controlling the viscosity of siloxane oils
[DE85-011586] 23 p3909 N85-34221

Further studies on liquid sloshing
[PB85-198695] 24 p4095 N85-35388

Steamflood pilots in the O'Connell Ranch field and the T-4 Ranch field
[DE85-901363] 24 p4108 N85-35468

OKLAHOMA

Post-carboniferous tectonics in the Anadarko Basin, Oklahoma: Evidence from side-looking radar imagery
[NASA-CR-175458] 10 p1506 N85-19498

OLEFINS
U ALKENES

OLIVINE

Mechanisms of electrical conductivity in olivine
[DE84-014333] 04 p0495 N85-13159

Is phosphorus predictably incompatible in igneous processes? 04 p0583 N85-13722

Minor elements in relict olivine grains of deep-sea spheres: Match with Mg-rich olivines from C2 meteorites 06 p0883 N85-15610

Minor elements and cathodoluminescence of Mg-rich olivines from Murchison and Allende carbonaceous meteorites 06 p0884 N85-15619

Strain analysis of the Leoville chondrite and conditions in asteroidal interiors 06 p0885 N85-15620

The olivine asteroids: Discovery, mineralogy, and relationship to palasites 13 p2175 N85-23500

OME
U ORBIT MANEUVERING ENGINE (SPACE SHUTTLE)

OMEGA NAVIGATION SYSTEM

Error analysis of wind determined using a VLF Omega sonde
[WSRL-0361-TM] 06 p0838 N85-15321

Use of three omega radionavigation system position lines for solving problems in marine geodesy
13 p2107 N85-23131

OMNIDIRECTIONAL ANTENNAS
NT MONOPOLE ANTENNAS
NT WHIP ANTENNAS

OMNIRANGE NAVIGATION
U VHF OMNIRANGE NAVIGATION

ON-LINE SYSTEMS

On line digitizer software
[AD-A146249] 03 p0403 N85-12568

Maintenance Management Information and Control System (MMICS): Administrative boon or burden
[AD-A145762] 03 p0438 N85-12790

User behavior upon introduction of a network help system
[DE84-016466] 04 p0552 N85-13515

International information networks for material properties
[DE84-013336] 04 p0576 N85-13676

Some attributes of online search intermediaries that relate to search outcome 05 p0734 N85-14721

Electrooptical sensor for automatic detection of objects 06 p0789 N85-15040

Workshop on Computer Architecture
[AD-A146455] 06 p0847 N85-15378

Research activities of the Norwegian seismic array (NORSAR)
[AD-A146778] 07 p0996 N85-16326

Data stimulated on-line-checking (IROLD)
08 p1066 N85-16754

Real-time estimation of amplitude and group delay distortion in a PSK line-of-sight communications channel
[AD-A147735] 08 p1151 N85-17266

Pilot climate data system
[NASA-CR-174321] 08 p1187 N85-17481

CIG (Computer image generation) data bases in an instance: Bits and pieces
[AD-P004318] 09 p1269 N85-17972

Online database search strategies and thesaural relationship models 09 p1402 N85-18822

Commentary on start of scientific data transmissions with USSR 10 p1476 N85-19319

Provision of Federal government publication in electronic format to depository libraries
[S-PRT-98-260] 10 p1567 N85-19880

A DOE directory of databases for material properties
[UCAR-10124] 11 p1739 N85-20937

Base communications issues for the 1980s
[AD-A149764] 12 p1828 N85-21474

Calculation and display of stack departure times for aircraft inbound to Heathrow Airport
[AD-A151991] 15 p2469 N85-25241

A network-based approach to text handling for the online scientific community 15 p2664 N85-26444

Document retrieval from a relational database management system: An investigation of multiple-line query formulation using SEQUEL
15 p2665 N85-26447

List of serials indexed for online users, 1985
[PB85-143220] 15 p2666 N85-26455

Retrieval performance in a full text journal article database 16 p2877 N85-27747

A study of user-defined searching requirements for the on-line version of the directory of DOD-sponsored R and D data bases on the Defense Gateway computer system
[AD-A153000] 17 p3050 N85-28878

Distribution of mathematical software via electronic mail
[DE85-009664] 18 p3166 N85-29617

SAFEORD: Safety of explosive ordnance databank
[AD-A154058] 19 p3380 N85-30972

Individual differences in online search behavior: The effect of learning styles and cognitive abilities on process and outcome 20 p3541 N85-32037

Interactive on-line conferences
[AD-A154723] 21 p3574 N85-32227

Overview of on-line data processing for MST radars (keynote paper), part 7 21 p3625 N85-32519

On-line model driven control of the SLC electron Damping Ring
[DE85-013377] 24 p4157 N85-35772

ONBOARD COMPUTERS
U AIRBORNE/SPACEBORNE COMPUTERS

ONBOARD DATA PROCESSING

Overview of Autonomous Payload Control Experiment
04 p0459 N85-12911

Keeping up with operational loads in the French Air Force: Defining new equipment
07 p0896 N85-15881

Automatic error detection and recovery techniques in onboard intelligent units for space and avionic application 08 p1066 N85-16756

Designer on Aeroflot automated COMMO system development 08 p1067 N85-16765

On-board processing for linescan sensors in miniature unmanned aircraft
[RAE-TM-SPACE-327] 08 p1085 N85-16870

Integration of ground and on-board system for terminal count 08 p1092 N85-16898

Automation of checkout for the shuttle operations era
08 p1092 N85-16900

Air Force space technology center space technology: Emphasis 84 09 p1333 N85-18381

Spaceborne automatic data processing
14 p2397 N85-24769

DORIS: Prediction in Doppler measurement — satellite onboard measurement
[CNES-CT/DTI/MS/AE/170] 16 p2729 N85-26843

Piloted simulation of an algorithm for onboard control of time-optimal intercept
[NASA-TP-2445] 18 p3063 N85-28949

In orbit infrastructure
[DM-51/CC-FL-044-83] 18 p3066 N85-28966

Investigation and construction of the Mini Remote Terminal Unit (mRTU-M) Analog Processor Module (AP-M), volume 1
[MR-DS-01-VOL-1] 18 p3166 N85-29619

Investigation and construction of the Mini Remote Terminal Unit (mRTU-M), Analog Processor Module (AP-M), volume 2
[MR-DS-01-VOL-2] 18 p3166 N85-29620

Standard Generic approach for Spacecraft Autonomy and Automation, phase 2 (SGASA-2). Volume 1: Executive summary
[ESA053-1-VOL-1] 18 p3167 N85-29623

Standard Generic Approach for Spacecraft Autonomy and Automation, phase 2 (SGASA-2). Volume 2: Technical report
[ESA053-1-VOL-2] 18 p3167 N85-29624

Standard Generic Approach for Spacecraft Autonomy and Automation, phase 2 (SGASA-2). Volume 3: Appendices
[ESA053-1-VOL-3] 18 p3167 N85-29625

Evolution of 406 MHz Search and Rescue (SAR) processor 20 p3403 N85-31116
Study of the applicability of higher order languages for on-board satellite software production
[ESA-CR(P)-2024] 20 p3516 N85-31864
Implications of artificial intelligence on the design of future onboard systems
[SFENA-DPS/C/S3/84252A] 23 p3967 N85-34596
ONBOARD EQUIPMENT
NT AIRBORNE EQUIPMENT
NT AIRBORNE/SPACEBORNE COMPUTERS
NT AIRCRAFT EQUIPMENT
NT BOMBING EQUIPMENT
NT SPACECRAFT ELECTRONIC EQUIPMENT
NT SPACECRAFT EQUIPMENT
Study of effects of lightning on aircraft systems stressed 03 p0310 N85-12005
Improvements in linked-spar motion-compensated lifting system
[AD-D011413] 08 p1138 N85-17165
The value and utility of inflight onboard simulation
[AD-A148033] 08 p1196 N85-17543
On-board Computer Image Generator (CIG) applications
[AD-P004335] 09 p1271 N85-17989
Dynamic training devices in CRM training 09 p1276 N85-18018
Use of airplanes for loft training 09 p1276 N85-18019
Cockpit resources management and the theory of the situation 09 p1276 N85-18022
Cockpit resource management training 09 p1276 N85-18023
Telemetry systems of Interkosmos satellites 11 p1617 N85-20173
Adaptive control of airborne radar antennas 13 p2060 N85-22989
The development of onboard laser velocimeter at the Saint Louis Institute (France) from 1976 to 1982
[ISL-NB-402/83] 16 p2791 N85-27216
Data from BOC-yachts: A significant input to Southern Hemisphere analysis 16 p2814 N85-27358
Results of the magnetic field experiments E2 and E4 onboard Helios 1 and Helios 2 — magnetometer development 16 p2885 N85-27799
Rome/Goddard Space Flight Center (GSFC) magnetic field experiment: A summary of results — flux gate magnetometer 16 p2885 N85-27800
Flight control system for a computer controlled aircraft with limited sensors
[AD-A155107] 21 p3555 N85-32115
SCRIBE data of October 23, 1983 flight
[AD-A154864] 21 p3705 N85-33012
Comprehensive radio direction finder with electronically stabilized radiation pattern 22 p3762 N85-33318
ONE DIMENSIONAL FLOW
ICARUS: A general one-dimensional heat conduction code
[DE84-016125] 01 p0047 N85-10310
One-dimensional two-phase constant lag flow in combustion chamber of solid propellant rocket motors
[AD-A145679] 02 p0173 N85-11157
The overall reaction concept in premixed, laminar, steady-state flames. 2: Initial temperatures cnd pressures
[AD-A152132] 16 p2746 N85-26944
Evaluation of an algorithm for the solution of the time-dependent Euler equations
[AD-A151993] 16 p2854 N85-27600
Explosion in flight 21 p3683 N85-32883
Unsteady flow in a supersonic cascade with two in-passage shocks
[NASA-CR-3925] 24 p4060 N85-35158
ONISOTROPY
U ANISOTROPY
ONTOGENESIS
U ONTOGENY
ONTOGENY
General description of experiment dealing with rat ontogenesis aboard Cosmos-1514 biosatellite 22 p3822 N85-33679
NASA Developmental Biology Workshop: A summary
[NASA-TM-86756] 24 p4126 N85-35578
OOCYTES
U GAMETOCYTES
OPACITY
The smallest sizes of diffuse interstellar clouds 06 p0878 N85-15578
Study of opacity effects on line radiation from pellet implosions
[DE85-000380] 10 p1491 N85-19413
X-ray line broadening of a diagnostic in laser produced plasma
[DE85-001179] 10 p1560 N85-19841
Opacity determinations for Inertial Confinement Fusion (ICF) materials using an average atom model 12 p1957 N85-22295
Opacity control technique for jet engine test cells
[AD-D011688] 19 p3220 N85-29968
Frequent observations of extragalactic compact sources at 24 GHz 19 p3386 N85-31003
Implicit Monte Carlo methods and non-equilibrium Marshak wave radiative transport
[DE85-010711] 22 p3835 N85-33743
X-ray spectra of bursting neutron stars 23 p3981 N85-34686
OPEN CHANNEL FLOW
Technology reports of the Yamaguchi University, volume 3, no. 3
[ISSN-0386-3433] 09 p1302 N85-18182
On the virtual wall height in open channel flow with large relative roughness 09 p1303 N85-18188
Calculation of oscillating turbulent flows in open channels
[KU-SFB-80/T/228] 11 p1633 N85-20289
Behavior of turbulent gas jets in an axisymmetric confinement
[NASA-CR-174829] 15 p2473 N85-25265
Monogroove heat pipe design: Insulated liquid channel with bridging wick
[NASA-CASE-MSC-20497-1] 18 p3096 N85-29180
OPEN CIRCUIT VOLTAGE
Avalanche photodiode statistics in triggered-avalanche detection mode 05 p0623 N85-13987
Improved modeling of the open circuit voltage of solar cells 13 p2011 N85-22619
New high-efficiency silicon solar cells
[NASA-CR-175643] 13 p2128 N85-23244
OPENINGS
NT APERTURES
NT PORTS (OPENINGS)
NT SLITS
NT SYNTHETIC APERTURES
A buckling analysis for rectangular orthotropic plates with centrally located cutouts
[NASA-TM-86263] 04 p0513 N85-13268
Optimum geometry of interblade passages in impellers of thermomolecular vacuum pump 16 p2764 N85-27058
Strength and failure analysis of composite laminates with holes at room and elevated temperatures
[AD-A153263] 17 p2917 N85-27981
OPERATING COSTS
Energy efficient engine flight propulsion system preliminary analysis and design report
[NASA-CR-174701] 02 p0140 N85-10947
Energy efficient engine component development and integration program
[NASA-CR-169496] 02 p0146 N85-10989
Energy efficient engine. Volume 1: Component development and integration program
[NASA-CR-173084] 02 p0146 N85-10992
Activities report of the aerospace industry in West Germany
[ISSN-0722-3838] 07 p1053 N85-16686
Activities report of the aerospace industry in West Germany
[ISSN-0722-3838] 07 p1054 N85-16687
OPERATING SYSTEMS (COMPUTERS)
New YeS 1056 unified system computer model described 04 p0485 N85-13092
Development of the NLTSS operating system
[DE84-013702] 05 p0714 N85-14576
Requirements and overview of the LINCS distributed operating system architecture
[DE84-013721] 05 p0714 N85-14577
Operating system versus programming environment, for example the UNIX
[SWA-84/037] 07 p1027 N85-16516
EGP (Exterior Gateway Protocol) gateway under Berkeley UNIX 4.2
[AD-A148056] 08 p1206 N85-17597
A unified model for performance and reliability of Fault-Tolerant/Multi-Mode systems
[AD-A148789] 08 p1208 N85-17601
A decision model for selection of microcomputers and operating systems
[AD-A149076] 10 p1538 N85-19694
Structurization of programs for real-time microprocessor arrays 15 p2529 N85-25592
Detailed design of an object oriented, multiprogramming, multitasking operating system for sixteen-bit microcomputers
[AD-A152086] 16 p2847 N85-27552
Multicomputer operating systems and applications
[AD-A153205] 17 p3016 N85-28648
The design of a capability-based distributed operating system
[CWI-CS-R8418] 17 p3016 N85-28650
Distributed systems management in wide area networks
[CWI-CS-R8419] 17 p3016 N85-28651
A new taxonomy for distributed computer systems based upon operating system structure
[NASA-TM-86438] 19 p3342 N85-30709
A distributed real-time operating system
[NIKHEF-H/84-8] 20 p3518 N85-31876
User's operating procedures. Volume 1: Scout project information programs
[NASA-CR-177948] 23 p3956 N85-34613
OPERATING TEMPERATURE
Electromagnetic Acoustic Transducers (EMATs) for erosion monitoring
[DE85-004834] 12 p1854 N85-21629
Proceedings of the Cold Electronics Workshop
[NASA-CR-175662] 14 p2297 N85-24220
Cold electronics: An overview 14 p2297 N85-24221
Si MOS devices at low temperatures 14 p2297 N85-24225
Stressed-strained state of tightening buckles in sectional runners of gas turbines 17 p2940 N85-28149
Status of high-efficiency module design and fabrication 21 p3612 N85-32446
OPERATIONAL AMPLIFIERS
Semiconductors at Leipzig Spring Fair 09 p1377 N85-18880
A circuit grammar for operational amplifier design
[AD-A149566] 10 p1481 N85-19346
Development of thin film hybrid IC active filter for video band use
[NHK-LABS-NOTE-312] 18 p3094 N85-29153
OPERATIONAL HAZARDS
Radio Frequency Radiation (RFR) measurements in operational settings 16 p2777 N85-27139
OPERATIONAL PROBLEMS
Results of Space Shuttle Flight 41-C
[GPO-36-092] 04 p0461 N85-12928
Statement of Captain Robert L. Crippen, USN, Commander of Space Shuttle Flight 41-C; Francis R. Scobee, pilot; Doctor George D. Nelson, Mission Specialist; Terry J. Hart, Mission Specialist; and Doctor James D. Van Hoften, Mission Specialist; accompanied by Frank Cepollina, Solar Maximum Repair Mission Project Manager, Goddard Space Flight Center 04 p0461 N85-12929
Statement of Frank Cepollina, Solar Maximum Repair Mission Project Manager, Goddard Space Flight Center 04 p0461 N85-12930
Operational problems with radiation survey meters: The university and accelerator
[DE84-015703] 06 p0811 N85-15151
Electric and hybrid vehicle demonstration project
[DE84-014622] 06 p0871 N85-15535
Design evolution of the orbiter reaction control subsystem 08 p1099 N85-16844
Electric and hybrid vehicle demonstration project
[DE85-003939] 13 p2169 N85-23455
Gas turbines: Operating conditions, material selection and development
[NLR-MP-83046-U] 20 p3395 N85-3106
OPERATIONS
Optimum performance parameters for ski-jum operations of USAF fighter aircraft
[AD-A148532] 08 p1084 N85-1686
OPERATIONS RESEARCH
NT DYNAMIC PROGRAMMING
NT LINEAR PROGRAMMING
NT MATHEMATICAL PROGRAMMING
NT NONLINEAR PROGRAMMING
NT QUADRATIC PROGRAMMING
Interactive graphics nonlinear constrained optimizatio 01 p0058 N85-103
Optimizing search with positive information feedbac
[CSIR-TWISK-313] 01 p0125 N85-108
A summary of the foundation research program
[AD-A146524] 06 p0891 N85-156
Principles of multiobjective optimization
[AD-A147520] 07 p1052 N85-166
Distributed asynchronous relaxation methods for conv network flow problems
[AD-A148027] 08 p1211 N85-176
European scientific notes. Volume 38, number 11
[AD-A148228] 08 p1230 N85-177
European Scientific Notes, volume 38, number 12
[AD-A148713] 09 p1418 N85-18
A proposed integration among organizatio information requirements, media richness and structu design
[AD-A149317] 10 p1567 N85-19
European Scientific Notes. Volume 39, number 2
[AD-A148994] 10 p1573 N85-19
Control of nonlinear objects 12 p1842 N85-21

Statistics for the maximum of several positive random variables with application to networking
[AD-A150005] 12 p1922 N85-22069

A decision support methodology for space technology advocacy
[AD-A151695] 15 p2476 N85-25283

Management control systems and interdependencies: An empirical study
[AD-A152280] 16 p2876 N85-27746

A greedy algorithm for the transhipment along a single road problem
[AD-A152343] 17 p3025 N85-28709

Future directions in operations research
[REPT-84-24] 17 p3026 N85-28711

Operations research
[B8561897] 17 p3026 N85-28712

A new taxonomy for distributed computer systems based upon operating system structure
[NASA-TM-86438] 19 p3342 N85-30709

The priming effect in task design research
[AD-A154589] 21 p3679 N85-32852

Necessary and sufficient conditions for single-extremum and convex problems of mathematical programming
21 p3698 N85-32977

Design and implementation of an interactive route editor 23 p3962 N85-34559

OPERATOR PERFORMANCE

Human engineering data base for design and selection of cathode ray tube and other display systems
[AD-A145704] 02 p0236 N85-11549

The human operator and system effectiveness
[AD-A146326] 03 p0402 N85-12563

Analysis of data entry performance: Chromatic versus monochromatic
[AD-A145568] 03 p0438 N85-12789

Defect detection threshold in riveted joints, test report no.44-833/F — in aircraft 04 p0511 N85-13260

Six degrees of freedom control with each hand?
05 p0700 N85-14492

Effects of control stick parameters on human controller response 05 p0701 N85-14496

Effects of transport delays of manual control system performance 05 p0701 N85-14498

The effect of part-simulation of weightlessness on human control of bilateral teleoperation: Neuromotor considerations 05 p0703 N85-14510

Visual attention to radar displays
05 p0704 N85-14514

POPCORN: A supervisory control simulation for workload and performance research
05 p0704 N85-14515

Psychological issues in online adaptive task allocation
05 p0704 N85-14516

The impact of pictorial display on operator learning and performance 05 p0706 N85-14527

A manual control test for the detection and deterrence of impaired drivers 05 p0709 N85-14550

The effects of task structure on time-sharing efficiency and resource allocation optimality
05 p0711 N85-14562

Multi-crew model analytic assessment of landing performance and decision-making demands
05 p0712 N85-14567

Speech-action interrelationships in operational work
07 p1010 N85-16418

Work physiology of operating personnel at power plants in arid regions 10 p1523 N85-19606

The effect of jamming/deception on decision making
[AD-A149740] 12 p1828 N85-21472

The role of prior knowledge in operating equipment from written instructions
[AD-A151007] 14 p2392 N85-24730

Shape with and without redundant colour as coding mechanism for simulated radar displays in a time-extended simple vigilance task
[AD-A151683] 16 p2844 N85-27533

Operator's functional comfort zone when controlling moving object 22 p3821 N85-33670

Manual and computer-aided sequential diagnostic inference
[AD-A156229] 24 p4133 N85-35620

OPERATORS (MATHEMATICS)

Scattering theory by Enss' method for operator valued matrices: Dirac operator in an electric field
[REPT-84] 01 p0045 N85-10290

On the commutant of an irreducible set of operators in real Hilbert space
[TUM-M8316] 01 p0114 N85-10774

Quasistable parametric optimization without compact level sets
[AD-A144716] 01 p0114 N85-10776

Boundary conditions in Chebyshev and Legendre methods
[NASA-CR-172469] 02 p0250 N85-11635

Linear and bilinear infinite-dimensional representations of finite-dimensional nonlinear systems
[RR-259] 02 p0254 N85-11661

An introduction to multilinear formula score theory
[AD-A145696] 02 p0254 N85-11667

Model equation for simulating flows in multistage turbomachinery
[NASA-TM-86869] 03 p0315 N85-12036

Application of summability methods to Jackson theorems for splines
[AD-A146256] 03 p0412 N85-12635

On the theory of coercitive linear partial differential operators
[ISSN-0355-0087] 03 p0414 N85-12646

Molarity principle: Foundation for parallel digital signal processes 05 p0725 N85-14663

Monotone operators in mathematical programming
[AD-A147309] 07 p1025 N85-16506

An operator method for computing the asymptotics of a collision resolution interval
[AD-A146837] 07 p1028 N85-16528

Nonlinear semigroups and evolution governed by accretive operators
[AD-A147556] 07 p1033 N85-16557

The symmetry group and exponents of operator stable probability measures
[AD-A147187] 07 p1035 N85-16566

Boundary conditions for artificial dissipation operators — convection
[FFA-TN-1984-53] 09 p1375 N85-18642

Lax-pair operators for squared-sum and squared-difference eigenfunctions
[AD-B089063L] 09 p1386 N85-18718

Annuals of the Finnish Academy of Sciences, series A. 1: Mathematics, volume 8, part 2
[ISSN-0066-1953] 10 p1535 N85-19673

Towards the construction of periodic solutions of pseudodifferential equations with the aid of algebraic operators 10 p1535 N85-19674

A non-hypoelliptic Dirichlet problem from stochastics
10 p1537 N85-19687

Annals of the Fourier Institute, volume 34, no. 4
11 p1698 N85-20668

Classic Fourier microdistributions in the real analytic case 11 p1698 N85-20673

The eigenvalues of the pseudospectral Fourier approximation to the operator sin (2x) d/dx
[NASA-CR-172538] 11 p1706 N85-20729

Normal mode analysis for linear resistive magnetohydrodynamics
[IPP-6/235] 11 p1730 N85-20878

Invariant differential operators on a semisimple symmetric space and finite multiplicities in a Plancherel formula
[CWI-PM-R8409] 12 p1925 N85-22094

Asymptotic construction of a procedure for plane-wave synthesis and migration
[AD-A150969] 14 p2374 N85-24672

On an assymetric choice for a cluster expansion of the three-body problem
[CSIR-TWISK-339] 14 p2408 N85-24844

A new implicit plus minus splitting method for the solution of the Euler equations in the transonic flow regime
15 p2461 N85-25200

Analysis of spectral operators in one-dimensional domains
[NASA-CR-172573] 15 p2633 N85-26228

Deconvolution methods for multi-sensors
[AD-A152351] 17 p3018 N85-28660

A note on integral operators
[REPT-83-26] 17 p3021 N85-28668

About product formulas with variable step-size
[AD-A153527] 18 p3169 N85-29636

Infinite dimensional linear systems with unbounded control and observation: A functional analytic approach
[AD-A153535] 18 p3169 N85-29639

Some applications of a convenient finite-dimensional matrix representation of the differential operator
[PREPRINT-416] 18 p3172 N85-29661

Numerical tests of a novel technique to compute the eigenvalues of differential operators
[PREPRINT-427] 18 p3173 N85-29667

Spectral Theory of Sturm-Liouville Differential Operators: Proceedings of the 1984 Workshop
[DE85-009893] 20 p3520 N85-31890

Aspects of SAR image segmentation
[AD-A154965] 21 p3575 N85-32236

Edge detection and geometric methods in computer vision
[AD-A155873] 24 p4135 N85-35630

Some rigorous results concerning spectral theory for ideal MHD
[DE85-013427] 24 p4156 N85-35770

OPERATORS (PERSONNEL)
NT AIRCRAFT PILOTS
NT PILOTS (PERSONNEL)

Random pattern tracking acceleration tolerance tester
[AD-D011404] 07 p1017 N85-16459

Work capacity of heat and electric power plant operations working 12 hour day and night shifts
09 p1362 N85-18567

Study of bodily functional status and quality of controlling action of power unit operators with various intensities of labor 09 p1362 N85-18569

Ride comfort of off-road vehicles
[AD-P004279] 09 p1406 N85-18855

Man-machine interaction: Operator
[AD-A149075] 10 p1531 N85-19648

Research and Modeling of Supervisory Control Behavior, report of a workshop
[AD-A149621] 12 p1950 N85-22248

Streamlined Test Reporting And Planning (STRAP): Computerized human factors questionnaire
[AD-A150811] 14 p2395 N85-24751

A comparison of numeric data entry with touch-sensitive and conventional numeric keypads
[AD-A153276] 17 p3008 N85-28598

Adaptive aiding for symbiotic human-computer control: Conceptual model and experimental approach
[AD-A153870] 19 p3332 N85-30644

Computer center policy
[AD-A154416] 19 p3338 N85-30681

Robot environment expert system
[NASA-CR-3915] 23 p3967 N85-34593

OPHTHALMOLOGY

Investigation into the use of the TV magnifier in the Netherlands
[HSE-TRANS-11142] 20 p3533 N85-31986

OPIK THEORY

The study of the physics of cometary nuclei
[NASA-CR-175917] 17 p3054 N85-28905

OPTICAL ABSORPTION
U ELECTROMAGNETIC ABSORPTION
U LIGHT TRANSMISSION

OPTICAL AMPLIFIERS
U LIGHT AMPLIFIERS

OPTICAL BISTABILITY

Digital Optical Circuit Technology
[AGARD-CP-362] 18 p3185 N85-29757

Optically bistable devices using InSb
18 p3186 N85-29758

Optically nonlinear and bistable behaviour of direct gap semiconductors 18 p3186 N85-29759

Optical bistability in Cd(x)Hg(1-x)Te
18 p3186 N85-29760

Optical modulators and bistable devices using molecular gases 18 p3186 N85-29761

An experimental nonlinear optical waveguide device
18 p3186 N85-29762

Stationary properties and switching characteristics of dispersive optical bistability in CuCl
18 p3186 N85-29763

Cavityless optical bistability in systems of two-level atoms 18 p3186 N85-29764

All-optical logic gates with external switching by laser and incoherent radiation 18 p3187 N85-29766

OPTICAL COMMUNICATION

New type of unique frequency laser communications
[AD-A145128] 01 p0038 N85-10239

Timing performance of phase-locked loops in optical pulse position modulation communication systems
[AD-A145403] 02 p0190 N85-11271

Low-threshold injection lasers on grown GaInPAs/InP heterostructures (1.2-1.6 micrometers wavelengths)
02 p0258 N85-11693

Optical recording of information on paper by CO2 and YAG-lasers 02 p0261 N85-11710

Regenerators of binary pulses for optical communication systems 04 p0485 N85-13099

Simulation of optical configurations and signal processing methods in Anger-type neutron-position scintillation detector
[DE84-012095] 04 p0503 N85-13210

Analysis of a coded, M-ary orthogonal input optical channel with random-gain photomultiplier detection
05 p0624 N85-13990

A single optical fiber telephone system
[AD-D011293] 06 p0799 N85-15107

Holographic directional coupler for fiber optic systems
[AD-D011365] 07 p0937 N85-15939

Micro-waveguide transformers of coherent optical signals 07 p0950 N85-16022

Nonlinear processing of optical pulse signals
07 p0951 N85-16026

Analysis of threshold effects during estimation of arrival time of optical signals 07 p0951 N85-16030

Potential effectiveness of spatial processing in detecting signals against background of interfering reflections
07 p0952 N85-16032

Spacecraft system study: A study to define the impact of laser communication systems on their host spacecraft
[NASA-CR-175272] 07 p0970 N85-16159

RF fiber optic link
[AD-A148679] 08 p1155 N85-17290
Two-photon coherent state light - its generation and potential applications
[AD-A148245] 08 p1166 N85-17356
Optical wave propagation and imaging in the atmosphere 08 p1222 N85-17694
Matrix-matrix multiplication using an electrooptical systolic-engagement array processing architecture
[AD-D011410] 08 p1223 N85-17704
Quantum noise effects in single-mode injection lasers
[FUB-11-1984] 09 p1327 N85-18338
The Telecommunications and Data Acquisition Report
[NASA-CR-174366] 10 p1462 N85-19224
Detection and symbol synchronization for multiple-bit per photon optical communications
10 p1463 N85-19226
Highly efficient Nd:YAG lasers for free-space optical communications 10 p1463 N85-19229
Optical fiber communications link design in compliance with systems performance standards
[PB85-111037] 12 p1830 N85-21489
The future of lightwave technology
[PB85-109759] 12 p1935 N85-22155
Optimization of number of pulses in detection of fluctuating optical signals 13 p2081 N85-22993
Technical Digest: Symposium on Optical Fiber measurements, 1984
[PB85-114700] 13 p2160 N85-23407
Spatial acquisition algorithms and systems for intersatellite optical communication links
[AD-A150794] 14 p2292 N85-24207
The effects of atmospheric turbulence on an air-to-air optical communication link
[AD-A151840] 15 p2543 N85-25700
Length dependent, optical time delay/filter device for electrical signals
[AD-D011594] 15 p2549 N85-25732
Mode dependent, optical time delay system for electrical signals
[AD-D011596] 15 p2653 N85-26363
Optical non-line-of-sight covert, secure high data communication system
[AD-D011607] 16 p2769 N85-27087
Photon detection with cooled avalanche photodiodes: Theory and preliminary experimental results
16 p2770 N85-27096
The development and implementation of an optical communications laboratory
[AD-A151682] 16 p2772 N85-27111
The weighting function for scintillation on a folded path
[AD-A152659] 17 p2949 N85-28206
Philips researches gallium arsenide use for lasers
18 p3087 N85-29106
Rifa of Sweden conducts research in 3-5 materials
18 p3088 N85-29107
Multiport optical detectors 18 p3187 N85-29769
Picosecond photoconductive devices for 10 Gbit/s optoelectronic switching 18 p3187 N85-29770
Optical techniques for signal distribution and control in advanced radar and communication systems
18 p3188 N85-29773
A study of reflex optoelectronic switching matrices and their derivatives
[CRC-TN-720] 19 p3253 N85-30169
Thin film phase transition materials development program
[AD-A154260] 19 p3259 N85-30209
Fiber optic expanded beam connector
[AD-A154057] 19 p3367 N85-30880
Phase-locked loops for optical homodyne detection, volume 1 — spaceborne receivers
[ESA-CR(P)-2029-VOL-1] 20 p3442 N85-31367
Phase locked loops for optical homodyne detection, volume 2 — spaceborne receivers
[ESA-CR(P)-2029-VOL-2] 20 p3442 N85-31368
A comparison of millimeter wave, direct detect and heterodyne laser intersatellite links
[AD-A151964] 20 p3461 N85-31496
Intersatellite optical links: The point ahead angle
[CNES-83/DRT/TIT/TR/150] 20 p3533 N85-31984
Optical receivers using rough reflectors
[NASA-CR-176200] 24 p4154 N85-35750

OPTICAL COMPUTERS
West Europe report: Science and technology
[JPRS-WST-85-003] 09 p1309 N85-18224
Optical computer studies at UK's Heriot-Watt University 09 p1309 N85-18227
Triple matrix product optical processors using combined time-and-space integration
[AD-D011483] 10 p1557 N85-19820
Technical evaluation report on Avionics Panel Specialists' Meeting on Digital Optical Circuit Technology
[AGARD-AR-202] 15 p2653 N85-26367
Methods for the optical processing of signals
[DRIC-T-7439] 22 p3844 N85-33609

OPTICAL CORRECTION PROCEDURE
Fast Hartmann method for problems in astronomical adaptive optics 02 p0161 N85-11094
Holographic corrector in objective with compound main mirror 17 p2941 N85-28153
New method for correcting chromatism of mirror-lens objectives 21 p3696 N85-32965

OPTICAL COUPLING
Multiwavelength bidirectional coupler-decouplers
[AD-A147009] 07 p1043 N85-16625
Dimensions of smooth mating parts with protective coatings 14 p2280 N85-24124
Multi-access fiber optic data bus using FDM/FSK
[NASA-CR-175739] 15 p2621 N85-26152
Spatial light modulator having a capacitively coupled photoconductor
[AD-D011646] 17 p3037 N85-28790
Optical fiber coupling method and apparatus
[NASA-CASE-NPO-15464-1] 18 p3184 N85-29749

OPTICAL DATA PROCESSING
NT SCENE ANALYSIS
Standards for commercially emerging technologies: A preliminary cost-benefit assessment for the Optical Digital data disk (OD3) technology for mass data storage applications
[PB84-223593] 01 p0101 N85-10669
Guided-wave optic devices for integrated optic information processing
[AD-A145695] 02 p0280 N85-11827
LANDAT-4/5 image data quality analysis
[E85-10039] 03 p0379 N85-12417
Multi-disciplinary techniques for understanding time-varying space-based imagery
[AD-A144357] 05 p0728 N85-14681
Electrooptical matrix multiplication using the twos complement arithmetic for improved accuracy
[AD-D011252] 05 p0728 N85-14682
Advanced cube processor
[AD-D011262] 05 p0729 N85-14683
Wavelength coded image transmission and holographic optical elements
[AD-A146490] 06 p0810 N85-15147
Two-dimensional signal processing and storage and theory and applications of electromagnetic measurements. Supplemental appendix
[AD-A146848] 07 p0939 N85-15953
Modern signal processing and reconnaissance — conferences
[FOA-C-30374-E1] 07 p0942 N85-15975
White-light optical information processing and holography
[AD-A146938] 07 p0967 N85-16138
Development and evaluation of techniques for using combined microwave and optical image data for vegetation studies 08 p1148 N85-17240
Nonlinear real-time optical signal processing
[AD-A148293] 08 p1222 N85-17699
Optical data processing for missile guidance
[AD-A149346] 10 p1422 N85-18972
Optical implementation of the synthetic discriminant function
[AD-A149562] 10 p1557 N85-19817
Triple matrix product optical processors using combined time-and-space integration
[AD-D011483] 10 p1557 N85-19820
Optical eigenvector
[AD-A149550] 11 p1729 N85-20871
Topics in optical materials and device research, 3: Volume 1
[AD-A149726] 12 p1933 N85-22145
Switchable zero order diffraction gratings as light valves
[AD-A150129] 12 p1934 N85-22153
Electronic generation of text for television
[BBC-RD-1984/14] 13 p2053 N85-22856
Two-dimensional signal processing and storage and theory and applications of electromagnetic measurements
[AD-A150590] 13 p2065 N85-22899
Optical memory research and its application to digital optical processing 13 p2158 N85-23397
Optical processing in radon space
[AD-A150289] 13 p2159 N85-23402
Space-variant optical systems
[AD-A151032] 14 p2421 N85-24939
Evaluating radiation distortions of optical image of Earth's surface in horizontally inhomogeneous atmosphere 15 p2486 N85-25345
Optical flow-patterns of image velocity and their potential use in guidance and image interpretation
[BAE-BT-12091] 15 p2651 N85-26347
An investigation into generalised matched filter techniques
[BAE-BR-12971] 15 p2651 N85-26348
Feasibility studies of optical processing of image bandwidth compression schemes
[AD-A151254] 15 p2651 [illegible]
Electron-bombarded silicon spatial light modulator
[AD-D011579] 15 p2652 [illegible]
Technical evaluation report on Avionics Panel Specialists' Meeting on Digital Optical Circuit Technology
[AGARD-AR-202] 15 p2653 [illegible]
La Recherche Aerospatiale Bimonthly Bulletin, Number 1984-4, 221/July-August
[ESA-TT-884] 16 p2695 [illegible]
SVIT complex for analysis of space photography
16 p2725 [illegible]
China's integrated circuit production
16 p2806 N85-27702
Optical phenomena in computer vision
[AD-A152970] 17 p3008 [illegible]
Studies of optical-beam phase-conjugation by nonlinear refraction
[AD-A152865] 17 p3037 [illegible]
Spatial light modulator having a capacitively coupled photoconductor
[AD-D011646] 17 p3037 [illegible]
The prospects of the digital optical computer
18 p3186 N85-29771
Deformable mirror nearest neighbor optical computer
18 p3188 N85-29772
Numerical optical computing at the Ohio State University 18 p3186 N85-29775
Thin film phase transition materials development program
[AD-A154260] 19 p3259 N85-30209
High accuracy digital acousto-optic matrix computer
[AD-D011692] 19 p3343 N85-30718
Digital holographic sythesis of pattern-forming transparencies for ring antenna arrays
22 p3763 N85-33326
Characteristics of optical information-measurement channels with utilization of scattering effects
22 p3781 N85-33425
A general purpose image processing package
23 p3961 N85-34549

OPTICAL DATA STORAGE MATERIALS
Proceedings of the National Bureau of Standards and National Security Agency Workshop on Standardization Issues for Optical Data Disk (OD3) Technology
[PB84-217785] 06 p0848 N85-15380
Multichannel electrooptical modulators for digital information storage and processing systems
07 p0950 N85-16021
West Europe report: Science and technology
[JPRS-WST-84-026] 15 p2532 N85-25817
Philips tested new materials for optical data storage
15 p2532 N85-25820
Conferences of quantum-radiooptics section
22 p3773 N85-33390

OPTICAL DENSITY
The calibration of photographic and spectroscopic films: A densitometric analysis of IIaO film flown aboard the Space Shuttle 3
[NASA-CR-174278] 07 p0962 N85-16101
NGC 2024: Multi-wavelength infrared and radio observations 08 p1246 N85-17685
SAM 2 measurements of the polar stratospheric aerosol, volume 5
[NASA-RP-1140] 15 p2590 N85-25870
Use of Goudrian model in studying laws of reflection in vegetation-soil system in optical range. 2: Influence of illumination conditions on spectral brightness coefficients 16 p2726 N85-26827
Projections of plasma cloud structures and their spectra
[AD-A153608] 18 p3189 N85-29776
Laser Schlieren crystal monitor
[NASA-CASE-MFS-28060-1] 19 p3374 N85-30832
Hadrons registration in emulsion chamber with carbon block
[HE-3.7-3] 24 p4186 N85-35982
Structured events in Pamir carbon X-ray chambers
[HE-3.7-7] 24 p4186 N85-35985

OPTICAL DEPOLARIZATION
Influence of depolarization of linear polarized radiation on heterodyne detection in laser range finders
[DFVLR-FB-84-31] 10 p1491 N85-19414

OPTICAL DISKS
Role of optical disk at computing centers
[DE85-005124] 13 p2145 N85-23314
Conferences of quantum-radiooptics section
22 p3773 N85-33390

OPTICAL EMISSION
U LIGHT EMISSION

OPTICAL EMISSION SPECTROSCOPY
NT LASER SPECTROSCOPY
Optical and UV emission of active galactic nuclei
08 p1236 N85-17781

Optical studies of X-ray selected Active Galactic Nuclei (AGN) in the direction of the Large Magellanic Cloud (LMC)
08 p1237 N85-17797
Spatially resolved optical spectroscopy of the radio jet of the X-ray galaxy NGC 2110 08 p1238 N85-17804
Observational constraints on heating processes — solar corona
14 p2449 N85-25115

OPTICAL EQUIPMENT
NT ASTRONOMICAL TELESCOPES
NT BALLISTIC CAMERAS
NT CAMERAS
NT COLLIMATORS
NT DIFFRACTOMETERS
NT ELECTROPHOTOMETERS
NT ELLIPSOMETERS
NT FRAMING CAMERAS
NT HELIOMETERS
NT HIGH SPEED CAMERAS
NT IMAGE CONVERTERS
NT INFRARED SPECTROMETERS
NT INFRARED SPECTROPHOTOMETERS
NT LASER DOPPLER VELOCIMETERS
NT LIGHT SCATTERING METERS
NT MICRODENSITOMETERS
NT MICROWAVE REFLECTOMETERS
NT MULTISPECTRAL BAND CAMERAS
NT MULTISPECTRAL BAND SCANNERS
NT NEPHELOMETERS
NT OPTICAL GYROSCOPES
NT OPTICAL MEASURING INSTRUMENTS
NT OPTICAL MICROSCOPES
NT OPTICAL RADAR
NT OPTICAL RANGE FINDERS
NT OPTICAL SCANNERS
NT PANORAMIC CAMERAS
NT PERISCOPES
NT PHOTOGONIOMETERS
NT PHOTOMETERS
NT PINHOLE CAMERAS
NT POLARIMETERS
NT PRISMATIC BARS
NT PRISMS
NT PYRHELIOMETERS
NT REFLECTOMETERS
NT SCHMIDT CAMERAS
NT SPECTROHELIOGRAPHS
NT SPECTROPHOTOMETERS
NT SPECTROSCOPIC TELESCOPES
NT STREAK CAMERAS
NT STROBOSCOPES
NT TELEVISION CAMERAS
NT THEODOLITES
NT THERMICONS
NT TRANSMISSOMETERS
NT ULTRAVIOLET SPECTROMETERS
NT ULTRAVIOLET SPECTROPHOTOMETERS
NT WIDE ANGLE LENSES
NT X RAY TELESCOPES
Programmable optical sensor
[AD-D011244] 02 p0281 N85-11829
Direct view helmet mounted telescope
[AD-D011291] 06 p0755 N85-14839
Effect of aberration in optical system on illuminance distribution over image of strip in semicoherent light
06 p0777 N85-14970
Optics and opto-electronic systems
[AD-A147277] 07 p1044 N85-16630
LPI-radar for helicopter obstacle warning
08 p1074 N85-16810
Air combat visual simulation using a head slaved projector
[AD-P004327] 09 p1270 N85-17981
Survey of the finish characteristics of machined optical surfaces
[DE85-001343] 09 p1365 N85-18708
Monte Carlo simulation of gas Carenkov detectors
[DE85-002422] 10 p1488 N85-19394
Optical mark reader
[AD-D011462] 10 p1557 N85-19818
Airborne remote sensing CCD imaging system
11 p1623 N85-20220
Topics in optical materials and device research, 3. Volume 2
[AD-A149727] 12 p1911 N85-21996
High resolution diffraction grating
[AD-D011541] 12 p1933 N85-22141
Topics in optical materials and device research, 3: Volume 1
[AD-A149726] 12 p1933 N85-22145
Optical system
[NASA-CASE-NPO-15601-1] 13 p2158 N85-23396
Equipment for performing surfaces of optical parts
14 p2266 N85-24043
Color-selective coating for viewfinder in optical instruments 14 p2276 N85-24098
Transducer of linear displacements
14 p2281 N85-24130
Three-dimensional sensing and interpretation
[AD-A150890] 14 p2311 N85-24304
Space-variant optical systems
[AD-A151032] 14 p2421 N85-24939
Instrument for measuring dispersional distortions in optical fibers and cables 15 p2530 N85-25595
ACT applied to helicopter flight control
16 p2712 N85-26738
USSR report: Engineering and equipment
[JPRS-UEQ-84-006] 16 p2760 N85-27035
Experience with introduction of Finish perforation of precision parts for optical instruments
16 p2761 N85-27036
The utilization of optical fibers in holography
[ISL-R-102/83] 16 p2787 N85-27196
Formulation of a coherent light-sheet by means of a cylindrical-spherical optical system
[ISL-R-116/83] 16 p2865 N85-27674
Acoustooptic pulse-echo transducer system
[NASA-CR-175919] 17 p2951 N85-28224
Instabilities and chaotic behavior of active and passive laser systems
[AD-A153366] 17 p2971 N85-28346
Support structures for optical components in the Laser Demonstration Facility
[DE85-006879] 17 p2971 N85-28349
Spatial light modulator having a capacitively coupled photoconductor
[AD-D011646] 17 p3037 N85-28790
Technique to reduce scattered light in optical systems
[AD-D011597] 18 p3185 N85-29752
High-pressure optical cell
[AD-A153639] 18 p3185 N85-29754
Digital Optical Circuit Technology
[AGARD-CP-362] 18 p3185 N85-29757
Optically bistable devices using InSb
18 p3186 N85-29758
An experimental nonlinear optical waveguide device
18 p3186 N85-29762
Multiport optical detectors 18 p3187 N85-29769
Optical 3-D signature device for detecting chemical agents
[AD-D011689] 19 p3272 N85-30293
Optical multiplexing on monomode fibers
[ENST-83E016] 20 p3533 N85-31982
Space optics
[CNES-84/105/T/CT/DRT/TIT/10]
20 p3533 N85-31985
Optical storage technology for mapping
[AD-A154969] 21 p3606 N85-32392
Microwave semiconductor research: Materials, devices and circuits and gallium arsenide ballistic electron transistors
[AD-A154698] 21 p3709 N85-33024
Conferences of quantum-radiooptics section
22 p3773 N85-33380
Fundamentals of radio optical theory of resonant and directional quasi-optical devices
22 p3780 N85-33420
Single-point diamond crushing of Zerodur with in-situ polishing and metrology on a diamond turning machine
[DE85-012918] 24 p4083 N85-35305

OPTICAL FILTERS
NT BIREFRINGENT FILTERS
Single crystal semiconductor multilayers for electrically active optical interference filters
[DE84-015614] 04 p0571 N85-13640
Position effects of laser protective materials on simulator tracking performance
[AD-A148297] 08 p1167 N85-17359
Filter and passband problems
08 p1252 N85-17910
Solid state luminescent light filters for neodymium lasers 11 p1716 N85-20799
Lasing characertistics of YAG: Nd(3+)-laser with LiF passive shutter with F2 color centers
11 p1717 N85-20802
Imaging apparatus for transverse electrode electro-optic tunable filter
[AD-D011524] 12 p1832 N85-21497
The magneto-optical filter, working principles and recent progress 14 p2442 N85-25066
Length dependent, optical time delay/filter device for electrical signals
[AD-D011594] 15 p2549 N85-25732
Modified Landolt C-ring test to measure the effects of laser filters on visual acuity
[AD-A151164] 15 p2617 N85-26127
Mode dependent, optical time delay system for electrical signals
[AD-D011596] 15 p2653 N85-26363
Three new fiber-optic components
[DE85-006269] 15 p2653 N85-26364
Prospects for parallel nonlinear optical signal processing using GaAs etalons and ZnS interference filters
18 p3187 N85-29765
Filter induced errors in laser anemometer measurements using counter processors
[NASA-TM-87047] 19 p3272 N85-30286

OPTICAL GENERATORS
U LASER CAVITIES

OPTICAL GYROSCOPES
Analysis of fiber-gyroscopes discussed
13 p2052 N85-22845

OPTICAL HETERODYNING
Measuring large amplitudes of mechanical vibrations with laser interferometers 06 p0787 N85-15026
A 150 micron heterodyne spectrometer for airborne astronomy 08 p1249 N85-17887
Tunable heterodyne receiver from 100 micron to 1,000 micron for airborne observations
08 p1249 N85-17888
Influence of depolarization of linear polarized radiation on heterodyne detection in laser range finders
[DFVLR-FB-84-31] 10 p1491 N85-19414
Multiport optical detectors 18 p3187 N85-29769
Phase locked loops for optical homodyne detection, volume 2 --- spaceborne receivers
[ESA-CR(P)-2029-VOL-2] 20 p3442 N85-31368
A comparison of millimeter wave, direct detect and heterodyne laser intersatellite links
[AD-A151964] 20 p3461 N85-31496
Influence of depolarization of linear polarized radiation on the heterodyne detection in laser range finders
[ESA-TT-903] 20 p3461 N85-31500

OPTICAL IMAGES
U IMAGES

OPTICAL MASER MODULATION
U LIGHT MODULATION

OPTICAL MASERS
U LASERS

OPTICAL MEASUREMENT
NT ASTRONOMICAL PHOTOMETRY
NT COLORIMETRY
NT ELECTROPHOTOMETRY
NT INFRARED PHOTOMETRY
NT PHOTOMETRY
NT POLARIMETRY
NT SPECTROPHOTOMETRY
NT STELLAR SPECTROPHOTOMETRY
NT ULTRAVIOLET PHOTOMETRY
NT VISUAL PHOTOMETRY
Model study of the interaction of a blast wave with the superstructure of ships. Part 5: Application of optical measurement methods to the study of blast interaction
[PML-1984-12-PT-5] 01 p0057 N85-10375
Metrological consequences of the hard optical boundary assumption
[PB84-223577] 01 p0121 N85-10827
Predicting optical image displacement velocity in survey of Earth's surface 02 p0165 N85-11116
Methods for determining atmospheric optical parameters using results of space survey of Earth's surface
02 p0165 N85-11117
Checking optical-polarization measurements at interfaces 02 p0271 N85-11770
Development of optical techniques for Earth rotational measurements
[AD-A145859] 03 p0364 N85-12333
Energy parameters of optical radiation space research systems 06 p0791 N85-15058
Channel constructed to provide well defined boundary layers for vorticity optical probe measurements
[AD-A146679] 06 p0809 N85-15140
An experimental and theoretical investigation of optogalvanic effects
[AD-A148456] 08 p1223 N85-17700
S-11 and S-20 photocathode research activity, revision 1
[DE84-017164] 09 p1326 N85-18335
Modulation Transfer Function (MTF) measurement techniques for lenses and linear detector arrays
[NASA-TM-86168] 10 p1556 N85-19812
Preliminary design of an Earth-based debris detection system using current technology and existing installations 12 p1784 N85-21199
Parameters of amplitude-modulated signal upon reflections 13 p2076 N85-22966
In situ thin film measurement
[AD-A151385] 15 p2659 N85-26411
Recent advances in optical measurement methods in physics and chemistry
[DE85-008695] 17 p3037 N85-28792
Remote Sensing Technology: Symposium Proceedings
[DE85-010212] 20 p3477 N85-31606
New optical satellite data 20 p3492 N85-31705
Optical best arc RMS test results
20 p3492 N85-31706

Simulation model of acoustic emission due to microscopic fracture in metals
[BLL-BISI-TRANS-22367-(9022.06)]
20 p3523 N85-31909
SCRIBE data of October 23, 1983 flight
[AD-A154864] 21 p3705 N85-33012
The ISAVF opto-mechanical test bed
[NASA-TM-87505] 24 p4067 N85-35206
Self-study manual on optical radiation measurements. Part 1: Concepts. Chapter 12: Blackbodies, blackbody radiation, and temperature scales
[PB85-195303] 24 p4154 N85-35754
Energy calibration of the fly's eye detector
[HE-4.4-1] 24 p4192 N85-36011

OPTICAL MEASURING INSTRUMENTS
NT DIFFRACTOMETERS
NT ELECTROPHOTOMETERS
NT ELLIPSOMETERS
NT INFRARED SPECTROMETERS
NT INFRARED SPECTROPHOTOMETERS
NT LIGHT SCATTERING METERS
NT MICRODENSITOMETERS
NT MICROWAVE REFLECTOMETERS
NT MULTISPECTRAL BAND SCANNERS
NT NEPHELOMETERS
NT OCULOMETERS
NT OPTICAL RANGE FINDERS
NT OPTICAL SCANNERS
NT PHOTOGONIOMETERS
NT PHOTOMETERS
NT POLARIMETERS
NT REFLECTOMETERS
NT SPECTROPHOTOMETERS
NT THEODOLITES
NT TRANSMISSOMETERS
NT ULTRAVIOLET SPECTROMETERS
NT ULTRAVIOLET SPECTROPHOTOMETERS
Programmable optical sensor
[AD-D011244] 02 p0261 N85-11829
Sensor technology for second, third generation industrial robots. Optical sensor applications
03 p0342 N85-12196
Formation of reference signals in laser-type gas analyzers with mechanical switching of optical channels
06 p0787 N85-15027
Optical method of measuring velocity of shear waves
06 p0787 N85-15029
Facilities for studing radiation damage in nonmetals during irradiation
[DE85-000590] 10 p1554 N85-19601
Operating time meter for tape recorder
12 p1836 N85-21537
Design of an optical proximity sensor using multiple cones of light for measuring surface shape — application to a robot manipulator
[AD-A150050] 12 p1934 N85-22152
Small-size measuring gauges for metal cutting machine tools 14 p2267 N85-24045
OMEGA: An optronic device to measure the incidence angle of a projectile
[ISL-CO-207/83] 14 p2306 N85-24274
First- and second-order charged particle optics
[DE85-006310] 14 p2421 N85-24940
Application of infrared radiometers for airborne detection of clear air turbulence and low level wind shear, airborne infrared low level wind shear detection test
[NASA-CR-175725] 15 p2594 N85-25965
Method and apparatus for generating a structured light beam array
[AD-D011590] 15 p2652 N85-26357
Surveying and optical tooling technologies combined to align a skewed beamline at the LAMPF accelerator
[DE85-005902] 16 p2864 N85-27664
Optical strain measurement system development
17 p2915 N85-27969
Optical system for measuring shadowgraph data
[AD-D011642] 17 p3036 N85-28784
Vibration-free Raman Doppler velocimeter
[NASA-CASE-LAR-13268-1] 18 p3104 N85-29216
Optical fiber magnetic field sensor with nanosecond response time
[DE85-008409] 18 p3110 N85-29259
Self-detecting optical sensors
[AD-D011657] 18 p3185 N85-29751
Fiber optic sensors operating at dc
[AD-D011674] 19 p3271 N85-30283
Apparatus for non-destructive inspection of blind holes
[AD-D011707] 19 p3273 N85-30295
Method of measuring spherical aberration and apparatus therefor
[AD-D011706] 19 p3367 N85-30862
Wideband disturbance accomodation in precision flexible space structures 20 p3415 N85-31194
A simple optical extensometer achieving high accuracy
[NPL-DMA(A)-95] 20 p3458 N85-31474
New method for compensating and measuring any motion of three-dimensional objects in holographic interferometry
[ISL-CO-216/84] 22 p3789 N85-33474
Redefining the scratch standards
[PB85-194736] 24 p4154 N85-35755

OPTICAL MEMORY (DATA STORAGE)
Acousto-optically addressed Fourier transform matched filters
[AD-A150296] 13 p2063 N85-22889
Two-dimensional signal processing and storage and theory and applications of electromagnetic measurements
[AD-A150590] 13 p2065 N85-22899
Realizing the full potential of the video disc for mapping applications
[AD-A154966] 21 p3606 N85-32391
Optical storage technology for mapping
[AD-A154989] 21 p3606 N85-32392

OPTICAL METHODS
U OPTICS

OPTICAL MICROSCOPES
Polarisation insensitive achromatic cube beamsplitter — binocular microscopes
[NPL-MOM-72] 23 p3973 N85-34630

OPTICAL MODULATION
U LIGHT MODULATION

OPTICAL PATHS
Measurement of the configuration of a concave surface by the interference of reflected light
[NASA-TM-77796] 11 p1728 N85-20867
Time spectra of intensity fluctuations along reflecting path 13 p2079 N85-22981
Mean free path lenght of photons with broken cloud cover 14 p2336 N85-24455
Arctic acoustic tomography MIZEX 84
[AD-A154426] 19 p3320 N85-30580
Microcomputer controlled image processor
[AD-D011734] 22 p3833 N85-33735

OPTICAL POLARIZATION
Morphology and optical polarization of the 3C 273 jet — radio jet 08 p1236 N85-17803
Research in image understanding as applied to 3-D tomographic imaging with near optical resolution
[AD-A150096] 12 p1829 N85-21463
The Saturn ring particles from optical reflectance polarimetry 15 p2671 N85-26484

OPTICAL PROPERTIES
NT ABSORPTANCE
NT ABSORPTIVITY
NT BIREFRINGENCE
NT BRIGHTNESS
NT BRIGHTNESS DISTRIBUTION
NT COLOR
NT DICHROISM
NT LUMINOSITY
NT OPACITY
NT OPTICAL BISTABILITY
NT OPTICAL REFLECTION
NT PHOSPHORESCENCE
NT PHOTOCONDUCTIVITY
NT PHOTOELECTRIC EFFECT
NT PHOTOELECTRIC EMISSION
NT PHOTOIONIZATION
NT PHOTOVISCOELASTICITY
NT PHOTOVOLTAIC EFFECT
NT RADIANCE
NT REFLECTANCE
NT REFRACTIVITY
NT SKY BRIGHTNESS
NT SOLAR GRANULATION
NT SPECTRAL REFLECTANCE
NT STELLAR LUMINOSITY
NT STIGMATISM
NT TRANSLUCENCE
NT TRANSMISSIVITY
NT TRANSMITTANCE
NT TRANSPARENCE
NT TURBIDITY
NT WATER COLOR
The two modes of visual processing: Implications for spatial orientation 01 p0008 N85-10047
Investigating compression failure mechanisms in composite laminates with a transparent fiberglass-epoxy birefringent materials
[NASA-TM-86306] 02 p0170 N85-11137
Trivalent ion exchange in beta alumina
[AD-A145373] 02 p0172 N85-11151
Calculations of optical properties of transition metals
[BLL-M-35744-(5828.4)] 02 p0175 N85-11175
Optical properties of laser erosion flares in plasma
02 p0270 N85-11764
Checking optical-polarization measurements at interfaces 02 p0271 N85-11770
Using fiber-optics light guides in diagnosing intense shock waves 02 p0272 N85-11773
Pulsed neodymium glass laser system for investigating nonlinear optical phenomena in gases
03 p0348 N85-12241
NASA thunderstorm overflight program: Atmospheric electricity research. An overview report on the optical lightning detection experiment for spring and summer 1983
[NASA-TM-86468] 03 p0363 N85-12330
Dynamic occlusion analysis in optical flow fields
[AD-A145805] 03 p0406 N85-12584
Dielectric and optical properties of sputtered thin films
[AD-A146210] 03 p0420 N85-12861
Self-study manual on optical radiation measurements. Part 1: Concepts. Chapter 11: Linearity considerations and calibrations
[PB84-218346] 03 p0421 N85-12880
Concentrator optical characterization using computer mathematical modelling and point source testing
[NASA-CR-174109] 04 p0528 N85-13375
Optical characterization of radiation-resistant fibers
[DE84-015248] 05 p0620 N85-13984
Photoluminescence studies of Ga(As,P) strained-layer superlattices
[DE84-015709] 05 p0731 N85-14701
Analysis of optical and electrical performance of a TCP-coated solar cell 06 p0832 N85-15259
Optical polarization as a probe of the local interstellar medium 06 p0875 N85-15580
Optical properties of composite materials
[AD-A146768] 07 p0920 N85-15929
Multiple scattering effects on transmission through the atmosphere
[AD-A147527] 07 p0941 N85-15989
Comparison measurements on optical particle counters
[BLL-DOUNREAY-TR-934-(9091.9F)]
07 p0961 N85-16092
Bio-optical variability in the Alboran Sea as assessed by Nimbus-7 coastal zone color scanner
[AD-A147909] 07 p0989 N85-16281
Optical RF downconverter
[AD-D011336] 07 p1042 N85-16916
Nonlinear optical studies of rydberg atoms using degenerate four-wave mixing
[AD-A146827] 07 p1043 N85-16923
Multiwavelength bidirectional coupler-decouplers
[AD-A147009] 07 p1043 N85-16925
Quantum noise and excess noise in optical homodyne and heterodyne receivers
[AD-A148296] 08 p1157 N85-17389
International Conference on Luminescence
[AD-A148470] 08 p1223 N85-17701
Optical computer studies at UK's Heriot-Watt University 09 p1309 N85-18227
Survey of the finish characteristics of machined optical surfaces
[DE85-001343] 09 p1385 N85-18708
Effective antireflection coatings of transparent polymeric materials by gas-phase surface fluorination
[DE84-013027] 09 p1385 N85-18711
High temperature laser interferometric studies of solid electrolytes 09 p1396 N85-18785
Infrared horizon sensor modeling for attitude determination and control: Analysis and mission experience
[NASA-TM-86181] 10 p1429 N85-19018
Calculation of optical characteristics of shell ecological system based on its mathematical model
10 p1496 N85-19453
Ab initio calculations of the optical properties of ions in glass
[DE85-001008] 11 p1612 N85-20133
Optically bistable devices using semiconductor materials
[AD-A149551] 11 p1628 N85-20253
Subnanosecond time-resolved emission study of Cu2O and GaAs
[DE85-002070] 11 p1735 N85-20912
Novel photo-thermal technique for flow and spectroscopic measurements in a dense aerosol stream
[AD-A149745] 12 p1800 N85-21287
Control of electronic, magnetic and optical properties of doped polyacetylene conductors
[AD-A150117] 12 p1814 N85-21375
Investigation of the optical properties of solar elements 12 p1879 N85-21786
Multiple resolution representation and probabilistic matching of 2-D gray-scale shape
[AD-A149981] 12 p1933 N85-22147
Time-resolved ellipsometry and reflectivity measurements of the optical properties of silicon during pulsed excimer laser irradiation
[DE85-005091] 13 p2096 N85-23079
Assessing LANDSAT TM and MSS data for detecting submerged plant communities 13 p2120 N85-23203

Research in the optical sciences
[AD-A150196] 13 p2159 N85-23401
Power control of induction equipment for founding optical glass in array of platinum crucibles
14 p2267 N85-24044
Dependence of properties of optical cavity on misalignment 14 p2276 N85-24099
Water-resistance and some other properties of polyalkali fluorophosphate glasses 14 p2281 N85-24133
Thresholds of optical breakdown in alkali-halide crystals under pulses from CO2-laser 14 p2282 N85-24134
Classification of atmospheric aerosol for evaluation of its effect on climate 14 p2333 N85-24428
Stress and efficiency studies
[NASA-CR-175668] 14 p2351 N85-24531
First- and second-order charged particle optics
[DE85-006310] 14 p2421 N85-24940
Particle curtain generator for optical property measurements of solid particles
[DE85-005784] 15 p2560 N85-25797
Optical monitoring of photo-acoustic pulse propagation in silicon wafers
[AD-A151333] 15 p2651 N85-26352
In situ thin film measurements
[AD-A151379] 15 p2652 N85-26353
Experimental and theoretical study of the infrared reflectance of thin oxide films on metals
[DE85-005799] 15 p2653 N85-26366
Optical properties of hydrogenated amorphous carbon films grown from methane plasma
[NASA-TM-86995] 15 p2658 N85-26406
Interaction of liquid crystals with inhomogeneous surfaces
[AD-A151557] 15 p2660 N85-26413
Optical pulsar in the Large Magellanic Cloud remnant 0540-69.3
[DE85-006707] 16 p2883 N85-27788
USSR report: Engineering and equipment
[JPRS-UEQ-85-004] 17 p2939 N85-28142
Materials-process interactions in ternary alloy semiconductors
[AD-A153133] 17 p3043 N85-28632
Electrochromic and thermochromic materials for solar energy applications with emphasis on niobium and vanadium oxides
[DE85-010630] 19 p3249 N85-30147
Machining of beryllium with the LLNL precision engineering research lathe
[DE85-010832] 19 p3250 N85-30149
Optical effects of thin film adhesives in multijunction solar cells
[DE85-010120] 19 p3305 N85-30488
Opticals constant at X-ray wavelengths
[DE85-009743] 19 p3355 N85-30795
Application of single and multiple scattering techniques to optical properties of dielectric media
19 p3366 N85-30877
Failure analysis of thin-film amorphous-silicon solar-cell modules 21 p3613 N85-32452
Properties of aerosol particles detected by satellites in coastal regions 21 p3641 N85-32622
Radiative-collision generation of sound in gases subjected to single-pulse optical excitation
21 p3689 N85-32920
Nonlinear spectroscopy
[AD-A154706] 21 p3704 N85-33010
Optical output stabilization method for direct current arc lamps
[AD-A154987] 21 p3705 N85-33013
Impact of fluctuations in optical properties of atmosphere on the ratio of spectral brightness from remote sensing of agricultural land 22 p3734 N85-33149
Hercules X-1: Pulsed gamma-rays detected above 150 GeV
[OG-2.2-9] 22 p3865 N85-33935
Theoretical and experimental analyses of the performance of two-color laser ranging systems
[NASA-CR-176159] 23 p3936 N85-34397
Characterization of the optical and thermal properties of matter by photothermal techniques
[DE85-012607] 24 p4076 N85-35260
Los Alamos free-electron laser
[DE85-012666] 24 p4098 N85-35405
Optical properties of heterostructures and superlattices
[AD-A156243] 24 p4162 N85-35802
Ionic crystals
[DE85-009482] 24 p4163 N85-35809

OPTICAL PUMPING
NT LASER PUMPING
Synchronously pumped mode-locked semiconductor platelet laser
[AD-D011214] 01 p0051 N85-10340
Tunable CW semiconductor platelet laser
[AD-D011215] 01 p0052 N85-10341
Intense excitation source of blue-green laser
[AD-A147450] 07 p0971 N85-16168
High-power radiating plasma
[NASA-TM-77784] 07 p1045 N85-16637
Optical studies of dynamical processes in disordered materials
[DE85-002400] 10 p1453 N85-19158
Optically pumped iodine monofluoride laser
[AD-D011555] 12 p1855 N85-21637
High precision materials characterization in the near millimeter wave-length range
[AD-A153267] 17 p2968 N85-28331
Design and construction of a CW ND:YAG laser using a single elliptical cavity and water cooled krypton arc lamp pumping
[AD-A152657] 17 p2970 N85-28340
Experimental study of dissociative attachment in optically-pumped lithium molecules
[AD-A152800] 17 p3030 N85-28738
Diode laser 87Rb optical pumping in an evacuated wall-coated cell 18 p3105 N85-29226
Optically pumped laser system having extracavity pulse smoother
[AD-D011714] 19 p3276 N85-30319
Electron-atom collision studies using optically state selected beams
[DE85-010848] 19 p3368 N85-30886
Fiber optics interface for a dye laser oscillator and method
[DE85-005765] 23 p3973 N85-34633
Infrared generation and wave-mixing studies in cesium
[DE85-012883] 24 p4063 N85-35304
Generation of stimulated emission in the soft X-ray range by nonlinear processes with excimer lasers
[DE85-012465] 24 p4096 N85-35403

OPTICAL RADAR
Shipboard measurement of cloud bases and average surface visibility with an eye-safe lidar
[AD-A144889] 01 p0052 N85-10345
Field tests of the real-data acquisiton system for the NASA-LaRC differential absorption lidar
[NASA-CR-174020] 01 p0106 N85-10710
Multifrequency lidar based on dye laser
02 p0262 N85-11715
Measurement of range-resolved water vapor concentration by coherent CO2 differential absorption lidar
[PB84-236892] 04 p0535 N85-13420
Utilization of SAGE aerosol profiles in the analysis of Mauna Loa stratospheric lidar data
[NASA-CR-174198] 05 p0675 N85-14332
Detailed performance calculations: Wayne State University and Ford Motor Company, appendix C
05 p0676 N85-14340
Lidar measurements of structural characteristics of atmospheric turbulence 06 p0824 N85-15229
Dual mode scanner-tracker
[AD-D011417] 08 p1113 N85-17018
NASA three-laser airborne differential absorption lidar system electronics
[NASA-CR-174293] 08 p1166 N85-17353
Lidar systems for aerosol studies: An outline
08 p1183 N85-17457
Active optical sounding of ozone and minor constituents in the middle atmosphere: A review of ground-based lidar measurements 08 p1183 N85-17458
Lidar studies of temperature and density using Rayleigh scattering 08 p1184 N85-17459
Lidar studies of the alkali metals
08 p1184 N85-17460
Lidar-Thomson scattering — nuclear fusion
[IPP-1/299] 08 p1221 N85-17693
Pulse heterodyne equipment for measurements of range and velocity of moving targets-pulse radar
[ESA-TT-845] 09 p1312 N85-18246
Carbon dioxide laser radar for monitoring atmospheric transmittance and atmospheric aerosol
09 p1354 N85-18516
Development and operation of a real-time data acquisition system for the NASA-LaRC differential absorption lidar
[NASA-CR-174384] 09 p1366 N85-18583
Investigations relating to the simultaneous use of Combined Optical Adaptive Techniques (COAT) and angle-tracking
[ESA-TT-844] 09 p1385 N85-18712
Lidar-Thomson scattering — Joint European Torus
[IPF-84-3] 09 p1394 N85-18777
Airborne lidar measurements of El Chichon stratospheric aerosols, October 1982 to November 1982
[NASA-RP-1136] 10 p1514 N85-19550
Lidar observations of stratospheric aerosol over Mauna Loa Observatory, 1974 - 1981
[PB85-115061] 11 p1682 N85-20597
In situ orbital debris experiment concepts
12 p1784 N85-21198
On the inversion of the lidar equation
[AD-A149653] 12 p1856 N85-21641
Observational study of transport in the free troposphere
[PB85-144145] 12 p1887 N85-21845
Analysis of the NASA/MSFC Airborne Doppler Lidar results from San Gorgonio Pass, California
[NASA-CR-171355] 12 p1892 N85-21873
Time spectra of intensity fluctuations along reflecting path 13 p2079 N85-22981
Picosecond lidar techniques in laboratory and field diagnostics
[AD-A150755] 14 p2309 N85-24294
3D (Three-Dimensional) sensor for adaptive suspension vehicle
[AD-A150921] 14 p2311 N85-24305
Specifics of polarization structure of repeated scattering background in optical laser sounding signals
14 p2342 N85-24485
Interference immunity of optical radar system with phased antenna array 15 p2526 N85-25575
Lidar and radiometer observations of thunderstorm tops 15 p2595 N85-25994
High-frequency microwave observations of convective precipitation 15 p2596 N85-26000
Utilization of remote sensing data in the evaluation of air pollution characteristics in the south coast/Southeast Desert Air Basin
[PB85-162063] 16 p2822 N85-27407
Analysis of the NASA/MSFC airborne Doppler lidar results from San Gorgonio Pass, California
[NASA-CR-3901] 16 p2832 N85-27463
Conducting a wind sensing study
[NASA-CR-175782] 16 p2832 N85-27465
Influence of coherent mesoscale structures on satellite-based Doppler lidar wind measurements
[NASA-CR-175853] 16 p2833 N85-27467
Geophysical monitoring for climatic change, number 12
[PB85-172278] 16 p2837 N85-27496
Test of lidar inversion algorithm sensitivity to atmospheric backscatter and extinction parameters, revision A
[AD-A152082] 16 p2865 N85-27671
Lidar ER2 (ozone). Crystal characterization for harmonic conversion — laser systems
[CERT-2/6129-00] 16 p2872 N85-27717
Convective storm downdraft outflows detected by NASA/MSFC's Airborne 10.6 micron pulsed Doppler Lidar System
[NASA-CR-3898] 17 p2995 N85-28511
Thin film phase transition materials development program
[AD-A154260] 19 p3259 N85-30209
Technology assessment of high pulse energy CO(2) lasers for remote sensing from satellites
[NASA-TM-86415] 19 p3275 N85-30309
Lidar techniques for search and rescue
[DE85-009586] 19 p3278 N85-30327
Variability of air humidity profiles over ocean determined by lidar sounding 19 p3296 N85-30436
Specifics of laser sounding of atmosphere along horizontal and slightly slanting paths over water surface
19 p3297 N85-30441
Lidar system using polarization discrimination techniques for molecular air pollution monitoring
19 p3308 N85-30504
Comparison of wind and turbulence measurements from Doppler lidar and instrumented aircraft
[NASA-CR-171535] 20 p3495 N85-31729
Data analysis for lidar and quartz crystal microbalance systems
[NASA-CR-172601] 21 p3615 N85-32464
Visibility and vertical structure measurements in southern Germany
[AD-A154714] 21 p3335 N85-32574
Cloud droplet nucleation and initial growth derived from lidar depolarization studies 21 p3644 N85-32635
Laser Elektronika-01 for air pollution control lidar
21 p3684 N85-32887
Participation of singlet oxygen in photodestruction of air-saturated solutions of coumarin dyes
21 p3685 N85-32891

OPTICAL RANGE FINDERS
NT LASER RANGE FINDERS
Error of distance measurement by phase-type optical range finders with photoreceivers of various types
14 p2276 N85-24101

OPTICAL REFLECTION
Metrological consequences of the hard optical boundary assumption
[PB84-223577] 01 p0121 N85-10827
Polarized electron cyclotron emission in the Tokapole 2 Tokamak
[DE84-014953] 01 p0122 N85-10838

Space environment simulation to test satellite thermal control coatings, volume 1
[CERT-4128-VOL-1] 08 p1109 N85-17012
Space environment simulation to test satellite thermal control coatings. Volume 2: Annex 1
[ESA-CR(P)-1870-VOL-2] 08 p1109 N85-17013
Space environment simulation to test satellite thermal control coatings. Volume 2: Annexes 2, 3, 4
[ESA-CR(P)-1870-VOL-3] 08 p1109 N85-17014
Transmission and reflection of laser beams propagating through aerosol clouds in space
[LA-9996-MS] 12 p1856 N85-21638
Parameters of amplitude-modulated signal upon reflections 13 p2076 N85-22966
Time spectra of intensity fluctuations along reflecting path 13 p2079 N85-22981
Performance estimate of a reflecting light pipe for infrared detectors
[AD-A141269] 13 p2158 N85-23398
Diffuse reflection of light from turbid conservative medium of finite thickness with incidence of beam on surface of scattering glancing 14 p2342 N85-24481
Determining characteristics of optical radiation reflectors based on results of remote sensing
15 p2488 N85-25358
Apparatus for non-destructive inspection of blind holes
[AD-D011707] 19 p3273 N85-30295
Model computations of light reflection from sea surface 19 p3292 N85-30411
Attenuated total reflection method for obtaining optical constants of powders
[AD-A154094] 19 p3367 N85-30881
Influence of spatial pumping spectrum on quality of phase conjugate reflection during 4-photon interaction
21 p3696 N85-32964

OPTICAL RELAY SYSTEMS
Facilities for studing radiation damage in nonmetals during irradiation
[DE85-000590] 10 p1554 N85-19801
Experimental demonstration of an optoelectronic switch matrix for satellite-switched TDMA signals in the 0.3-4.0 GHz band
[CRC-TN-717] 19 p3253 N85-30170

OPTICAL RESONANCE
Optical studies of dynamical processes in disordered materials
[DE85-002400] 10 p1453 N85-19158
Resonance identifications in Saturn's rings
15 p2674 N85-26504
Saturation effect in multilevel lasing media
21 p3686 N85-32901

OPTICAL RESONATORS
Unstable optical resonator with cancelling edge waves
[AD-D011379] 07 p1042 N85-16618
Reflectivity measurements of laser gyro mirrors
[ESA-TT-851] 09 p1386 N85-18714
Characteristics of unstable resonators in flashlamp-pumped organic-compound lasers
11 p1717 N85-20800
Resonator optical designs for free electron lasers
[DE85-007678] 17 p2971 N85-28347
Optical modulators and bistable devices using molecular gases 18 p3186 N85-29761

OPTICAL SCANNERS
NT MULTISPECTRAL BAND SCANNERS
Moving object detection system using infrared scanning
[AD-D011222] 01 p0120 N85-10622
DoD Robotics Application Workshop Proceedings
[AD-A145867] 03 p0307 N85-11978
Air Force honeycomb shaping at SM-ALC (Sacramento Air Logistics Center)
[AD-P004005] 03 p0308 N85-11985
Mapping of mammalian arrhythmias with the cardiac laser scanner 03 p0399 N85-12545
Design of two-mirror scanner with axes of rotation not in plane of mirrors 06 p0777 N85-14969
Electrooptical sensor for automatic detection of objects 06 p0789 N85-15040
Reduction of signal modulation caused by polarization in visible optical scanning systems
[AD-D011389] 07 p1042 N85-16620
Dual mode scanner-tracker
[AD-D011417] 08 p1113 N85-17018
Design and analysis of airborne scanning optical systems 11 p1623 N85-20218
A scanning optical microprobe for infrared detector measurement
[AD-A151748] 15 p2653 N85-26361
Testing of scanner-assisted revision of the topographic map 1:25,000 (TK 25) 16 p2814 N85-27359
Applied computer graphics in a geographic information system: Problems and successes
23 p3962 N85-34563

OPTICAL SENSORS
U OPTICAL MEASURING INSTRUMENTS

OPTICAL SIGNALS
U OPTICAL COMMUNICATION

OPTICAL SPECTRUM
U LIGHT (VISIBLE RADIATION)
U SPECTRA

OPTICAL THICKNESS
Some statistical characteristics of atmospheric optical thickness in visible spectral range
02 p0164 N85-11109
Pair production at moderate optical depths — galactic nuclei X ray spectra 08 p1241 N85-17830
Saturn's rings resolved by the VLA — Very Larg Array (VLA) 15 p2670 N85-26476
Impact of fluctuations in optical properties of atmosphere on the ratio of spectral brightness from remote sensing of agricultural land 22 p3734 N85-33149

OPTICAL TRACKING
Optical seam tracking of robotic arc welding
[VTT-272] 01 p0055 N85-10368
Positior: effects of laser protective materials on simulator tracking performance
[AD-A148297] 08 p1167 N85-17359
Optical flow and texture variables useful in detecting decelerating and accelerating self-motion
[AD-A148718] 09 p1384 N85-18703
Investigations relating to the simultaneous use of Combined Optical Adaptive Techniques (COAT) and angle-tracking
[ESA-TT-844] 09 p1385 N85-18712
NORAD operational system 12 p1783 N85-21189
History of satellite break-ups in space
12 p1783 N85-21190
Modified Landolt C-ring test to measure the effects of laser filters on visual acuity
[AD-A151164] 15 p2617 N85-26127
Optical flow-patterns of image velocity and their potential use in guidance and image interpretation
[BAE-BT-12091] 15 p2651 N85-26347
Rayleigh criteria resolution of optical correlations
[AD-A151711] 15 p2652 N85-26359
An automatic traversing system for Laser Doppler Anemometer (LDA) applications to wind tunnels and to free jets
[ISL-CO-225/83] 16 p2836 N85-27490
M-BLASER: A device to study pursuit tracking in the rhesus monkey
[AD-A152986] 17 p2998 N85-28534
Pursuit tracking performance and flash disruption: The effects of training the non-dominant eye on target reacquisition
[AD-A153404] 17 p2999 N85-28541
Retinally stabilized differential resolution television display
[NASA-CASE-NPO-15432-1] 18 p3089 N85-29117

OPTICAL TRANSFER FUNCTION
Infrared material optical damage by rain
[AD-P004372] 12 p1827 N85-21466
DARPA/TTO program IR binary optics
[AD-A152196] 16 p2865 N85-27672

OPTICAL WAVEGUIDES
Guided-wave optic devices for integrated optic information processing
[AD-A145695] 02 p0260 N85-11827
Influence of mode noise suppression in multimode fiber optic light guides 03 p0348 N85-12242
Integration of detectors with optical waveguide structures
[AD-A146278] 03 p0420 N85-12682
Qualitative and quantitative compositional analysis of shale derived by gas chromatography and combined gas Chromatography/Mass spectrometry. Executive summary
[AD-A148369] 07 p0924 N85-15851
Precision electrooptical deflector based on corrugated light guide 07 p0950 N85-16020
Transformation of mode composition of circular optical waveguide 07 p0950 N85-16023
General theory and design considerations for optical waveguide chemical vapor sensors
[AD-A148505] 08 p1223 N85-17702
Self-induced nonlinear effects in optical fibers: A unified approach
[FUB-67-1982] 09 p1385 N85-18713
Betegeuse at maximum luminosity
11 p1758 N85-21061
Properties of chirped grating lenses in optical waveguides
[AD-A150023] 12 p1934 N85-22149
Dispersion characteristics of small-mode gradient optical fibers 13 p2082 N85-23004
Integrated optical components utilizing acoustooptic and electrooptic diffraction in micro-waveguides
13 p2089 N85-23044
Acoustooptic demodulation of frequency-modulated signals 13 p2090 N85-23050
Technical Digest: Symposium on Optical Fiber measurements, 1984
[PB85-114700] 13 p2160 N85-23
Investigation of semiconductor clad optical waveguides
[NASA-CR-175870] 17 p3036 N85-28
Optical waveguide characterization using grating couplers
[AD-A153063] 17 p3037 N85-28
An experimental nonlinear optical waveguide device
18 p3186 N85-29
The potential of semiconductors for optical integrated circuits 18 p3187 N85-29
A study of reflex optoelectronic switching matrices and their derivatives
[CRC-TN-720] 19 p3253 N85-30
Optical waveguide sensor for methane gas
[AD-D011691] 19 p3273 N85-30
Optical waveguide along front of exothermic reaction
21 p3694 N85-32
Methods for measuring and analyzing dispersion properties of multimode fiber optic lightpipes (a review)
21 p3695 N85-32
Photothyristor optrons and optron microcircuits, part 1
22 p3781 N85-33

OPTICS
Technical activities 1983, Office of Nondestructive Evaluation
[PB84-217074] 03 p0370 N85-12
Focussing and confinement
[DE84-016181] 05 p0640 N85-14
The use of an optical data acquisition system for bladed disk vibration analysis
[NASA-TM-86891] 06 p0817 N85-15
Theory and applications of two-photon quantum optics
[AD-A147382] 07 p1044 N85-16
Ill-posed problems and regularization analysis in early vision
[AD-A147753] 08 p1222 N85-17
High-pressure optical cell
[AD-A153639] 18 p3185 N85-29
Wideband disturbance accomodation in precision flexible space structures 20 p3415 N85-31
Summary of activities, 1983
[LBL-18500] 23 p3969 N85-34

OPTIMAL CONTROL
NT TIME OPTIMAL CONTROL
On the Pontryagin principle for stochastic optimal control
[TWISK-328] 01 p0112 N85-10
Application of modern guidance control theory to a bank-to-turn missile
[AD-A145646] 02 p0166 N85-11
Minimax optimal control in the reentry of a space glider 02 p0167 N85-11124
Asymptotically optimal adaptive control
[AD-A145666] 02 p0249 N85-11629
On a class of suboptimal controls for infinite-dimensional bilinear systems
[RR-258] 02 p0249 N85-11630
Control and performance of a photovoltaic-thermal energy system 03 p0387 N85-12475
Chandrasekhar equations and computational algorithms for distributed parameter systems
[NASA-CR-172467] 03 p0402 N85-12584
Utilization of historic information in an optimization task 05 p0700 N85-14
Algorithm for tracking manuevering object with ambiguous measurements 06 p0791 N85-15057
Research on optimal control, stabilization and computational algorithms for aerospace applications
[NASA-CR-174318] 08 p1209 N85-17603
Optimal stochastic LQ control with measurements displaced in time
[OUEL-1547/84] 08 p1209 N85-17605
SUBOPT: A CAD program for suboptimal linear regulators
[NASA-CR-172536] 10 p1539 N85-19702
Optimal symmetric flight studies
[NASA-CR-172508] 12 p1760 N85-21178
An asymptotically optimal subclass of BTIB designs for comparisons with a control
[AD-A149819] 12 p1921 N85-22066
Synthesis of quasi-optimum two-level signal discriminator with level changing at unknown point
13 p2063 N85-23010
Approximation in optimal control and identification of large space structures
[AD-A150323] 13 p2151 N85-23351
Optimal designs for comparisons between two sets of treatments
[AD-A150621] 13 p2152 N85-23360
Total energy-rate feedback for automatic glide-slope tracking during wind-shear penetration
[NASA-TP-2412] 14 p2226 N85-23801

Application of the maximum entropy/optimal projection control design approach for large space structures
14 p2234 N85-23849

Synthesis of optimal controls for real-time linear digital systems
14 p2270 N85-24062

Optimal space trajectories 14 p2396 N85-24756

Selection of optimal control program for solar cell panels of Earth satellites
15 p2484 N85-25335

Optimal control theory applied to fusion plasma thermal stabilization
[DE85-007599] 15 p2658 N85-26405

Application of linear optimal control theory to the design of the elevator control system of the DHC-2 Beaver experimental aircraft
[VTH-LR-411] 16 p2711 N85-26729

The effect of inaccuracies in structural models on the control of large space structures
[AD-A151794] 16 p2732 N85-26858

Optimal control of electric drive with simultaneous control inputs for motor current and flux
16 p2763 N85-27049

Development of graphical pole-zero, root-locus, Bode, Nyquist, and Nichols responses using the OPTSYSX program
[AD-A152148] 16 p2847 N85-27555

Development of graphical time response using the OPTSYSX program
[AD-A152221] 16 p2848 N85-27557

Some new results on the discrete-time Riccati Equation and their use in the design of optimal regulators and observer-estimators
[AD-A151934] 16 p2854 N85-27597

Research on optimal control, stabilization and computational algorithms for aerospace applications
[NASA-CR-172528] 19 p3221 N85-29970

Some asymptotic problems in the optimal control of distributed systems 20 p3412 N85-31175

A factorization approach to the linear regulator quadratic cost problem 20 p3413 N85-31178

An integrated control and minimum mass structural optimization algorithm for large space structures
20 p3413 N85-31183

Optimization of controlled structures
20 p3414 N85-31186

Robust control design for large space structures
20 p3416 N85-31200

User's manual of the BNDSCO computer program for solving constrained optimal control problems
[DFVLR-MITT-85-05] 20 p3516 N85-31865

OPTIMIZATION
NT FLIGHT OPTIMIZATION
NT OPTIMAL CONTROL
NT TIME OPTIMAL CONTROL
NT TRAJECTORY OPTIMIZATION

Study to optimize Cr-Mo steels to resist hydrogen and temper embrittlement. A study of carbides formed in low alloy Cr-Mo steels
[DE84-015208] 01 p0029 N85-10179

Combustion modeling of a 2 cylinder cycle reciprocating engine
[AD-A144782] 01 p0055 N85-10364

Interactive graphics nonlinear constrained optimization
01 p0058 N85-10387

Composite laminate optimization program suitable for microcomputers 01 p0059 N85-10389

Hydrologic and economic models for watershed evaluation and research
[PB84-222371] 01 p0066 N85-10438

Manual of phosphoric acid fuel cell power plant optimization model and computer program
[NASA-CR-174721] 01 p0067 N85-10445

ADS: A FORTRAN program for automated design synthesis, version 1.00
[NASA-CR-172460] 01 p0102 N85-10684

Some concepts in multi-criteria optimization
[CSIR-TWISK-299] 01 p0108 N85-10722

On the commutant of an irreducible set of operators in real Hilbert space
[TUM-M8316] 01 p0114 N85-10774

Quasistable parametric optimization without compact level sets
[AD-A144716] 01 p0114 N85-10776

Optimizing search with positive information feedback
[CSIR-TWISK-313] 01 p0125 N85-10855

Fitting aerodynamic forces in the Laplace domain: An application of a nonlinear nongradient technique to multilevel constrained optimization
[NASA-TM-86317] 02 p0134 N85-10917

Energy efficient engine. High pressure compressor detail design report
[NASA-CR-165558] 02 p0147 N85-10998

Asymptotically optimal adaptive control
[AD-A145666] 02 p0249 N85-11629

Inverse problems, optimization and algorithms
[AD-A145397] 02 p0250 N85-11636

Constrained optimization using iterated partial Kuhn-Tucker vectors
[AD-A145476] 02 p0251 N85-11641

Rapidly convergent algorithms for nonsmooth optimization
[AD-A145556] 02 p0251 N85-11643

Minimization of anomalous errors in measuring systems employing search and testing devices
03 p0344 N85-12219

Circuit engineering and technological optimization of very high speed LSI logic elements and transistor structures 03 p0347 N85-12237

Evaluating A(T) *D*A for sparse matrices: Analysis
[AD-A145916] 03 p0411 N85-12625

The Lindstrom-Madden method for series systems with repeated components
[AD-A146265] 03 p0412 N85-12636

A methodology for supporting views in relational databases 03 p0437 N85-12783

Optimization of movements of manipulators with kinematic redundancy 04 p0488 N85-13112

Boolean approach to zero-one linear programming
[DE84-016654] 04 p0550 N85-13498

Utilization of historic information in an optimisation task 05 p0700 N85-14490

Interpretation of natural language database queries using optimization methods 05 p0735 N85-14723

A self-organizing database system: A different approach to query optimization 05 p0735 N85-14725

Optimization of the die entrance shape for polymeric extrusion
[DE85-001588] 06 p0772 N85-14937

Optimization of moving-target selection radar devices for nonGaussian signals for stationary targets
06 p0789 N85-15043

A nonnoble front metallization process
06 p0830 N85-15279

Performance of Bayes-optimal angle-of-arrival estimators
[AD-A146594] 06 p0858 N85-15454

An improved computer model for prediction of axial gas turbine performance losses
[NASA-CR-174246] 07 p0904 N85-15724

Predicted performance benefits of an adaptive digital engine control system of an F-15 airplane
[NASA-TM-85916] 07 p0905 N85-15729

Optimization of the NiCrAl-Y/ZrO-Y2O3 thermal barrier system
[NASA-TM-86905] 07 p0927 N85-15878

Charge domain filters for enhanced monolithic signal processing
[AD-A147428] 07 p0941 N85-15964

Analysis of effectiveness of partial optimization of spatial processing systems 07 p0952 N85-16031

Reduction method for thermal analysis of complex aerospace structures
[NASA-TP-2373] 07 p0957 N85-16066

Continuity of the null space basis and constrained optimization
[AD-A147038] 07 p1030 N85-16538

Trust region methods for minimization
[AD-A147073] 07 p1030 N85-16540

Some applications of penalty functions in mathematical programming
[AD-A147443] 07 p1032 N85-16552

Structural optimization and other large-scale processes
[AD-A147895] 07 p1034 N85-16564

Pari-mutuel as a system of aggregation of information
[AD-A147210] 07 p1035 N85-16570

Principles of multiobjective optimization
[AD-A147520] 07 p1052 N85-16679

Efficient computation of optimal time for transaction processing in a database system
[AD-A147568] 07 p1054 N85-16693

An optimization method for the preliminary design of interplanetary aerobraking missions
08 p1076 N85-16822

Impact of activation optimization on the Vandenberg Ground Support System using Q-GERT analysis
[AD-A148448] 08 p1105 N85-16986

Finite element computation of structural design sensitivity analysis 09 p1330 N85-18353

Design oriented identification of critical points in transient response 09 p1330 N85-18357

Treatment of general boundary conditions and point-wise state variable constraints in optimum design for static and dynamic response
09 p1330 N85-18358

Optimization of vibrating beams including the effects of coupled bending and torsional modes
09 p1331 N85-18364

Optimization of design and control strategies for geothermal space heating systems
[DE85-000496] 09 p1344 N85-18458

Partial evaluation as a means of language extensibility
[AD-A148730] 09 p1368 N85-18596

Generalized convex functions: Properties, optimality and duality
[DE85-001553] 09 p1376 N85-18652

GaAlAs Sb APD optimization
[AD-A149406] 10 p1480 N85-19344

Optimization of a ground coupled heat pump
[DE85-000273] 10 p1486 N85-19380

Identification of dynamic systems, theory and formulation
[NASA-RP-1138] 10 p1551 N85-19784

Improving engineering system design by formal decomposition, sensitivity analysis, and optimization
[NASA-TM-86377] 10 p1551 N85-19785

Finite-(beta) optimization of tandem mirrors
[DE85-002658] 10 p1560 N85-19835

Noise constraints effecting optimal propeller designs
[NASA-TM-86967] 11 p1575 N85-19923

Sequential minimization for sum of squares of unknown functions
[DE85-004162] 11 p1707 N85-20738

Space nuclear-power reactor design based on combined neutronic and thermal-fluid analyses
[DE85-002433] 11 p1727 N85-20864

On maximizing the expected lifetime of replaceable systems
[AD-A150003] 12 p1862 N85-21680

Towards the generation of efficient code from verified programs
[TR-40] 12 p1914 N85-22017

Rates of convergence of semistochastic approximation procedures for solving stochastic optimization problems
12 p1924 N85-22088

A mathematical formulation of the problem of optimal use of ground resources for future space missions
12 p1947 N85-22232

Preliminary development of an approximation procedure for supercritical wing design optimization applications
[AD-A150177] 13 p1972 N85-22383

China report: Science and technology
[JPRS-CST-84-008] 13 p1972 N85-22384

Optimal design efforts in Shanghai described
13 p1972 N85-22386

Model reduction for control system design
[NASA-CR-170417] 13 p1975 N85-22398

Analysis and optimization of parameters of fanned surface acoustic wave transducers
13 p2070 N85-22934

Optimization of number of pulses in detection of fluctuating optical signals 13 p2081 N85-22993

Asymptotically optimum multialternative sequential procedures for discernment of processes minimizing average length of observations
13 p2084 N85-23012

Shape optimization for minimal stress concentration
13 p2101 N85-23093

Optimal allocation of components in parallel-series and series-parallel systems
[AD-A150169] 13 p2144 N85-23309

Relative control effectiveness technique with application to airplane control coordination
[NASA-TP-2416] 14 p2218 N85-23753

Software for designing teeth for reduction gears and transmissions 14 p2221 N85-23773

Manufacturing perspective in the design of bevel gearing 14 p2221 N85-23777

An optimization study to minimize surface distortions of a hoop-column antenna 14 p2232 N85-23837

Some optimization problems in static aeroelasticity for wings made of composite materials
14 p2277 N85-24104

Some problems in optimally designing shells of revolution 14 p2278 N85-24114

Ways of optimization of light energy transformation in primary stages of photosynthesis. Optimization of lattice structure of uniform photosynthetic unit
14 p2386 N85-24701

Optimal control and optimization
14 p2395 N85-24755

An expert system for choosing the best combination of options in a general-purpose program for automated design synthesis
[NASA-TM-86329] 14 p2402 N85-24807

Software and its relationship to methods
[DE85-004784] 14 p2405 N85-24829

Optimization of the catalytic oxidation of CO for closed-cycle CO2 laser applications
[NASA-TM-86421] 15 p2504 N85-25445

Mercedes-Benz auto 2000 achieves low drag coefficient 15 p2530 N85-25602

Receiver optimization for detection in doubly spread communication channels
[AD-A151226] 15 p2541 N85-25689

Design of shear deformable antisymmetric angle-ply laminates to maximize the fundamental frenquency and frequency separation
[CSIR-TWISK-333] 15 p2577 N85-25892

Solving set covering problems using heuristics with branch and bound
[AD-A151905] 15 p2638 N85-26269

Design and implementation of the digital engineering laboratory distributed database management system
[AD-A151694] 15 p2665 N85-26450

Optmizing the specifications for an air-surface laser system 16 p2696 N85-26644

Alternatives for jet engine control
[NASA-CR-175831] 16 p2709 N85-26713

Alternatives for jet engine control
[NASA-CR-175833] 16 p2709 N85-26715

ESP (External-Stores Program): A pilot computer program for determining flutter-critical external-store configurations. Volume 1: User's manual
[AD-A152268] 16 p2710 N85-26725

Probabilistic computer model of optimal runway turnoffs
[NASA-CR-172549] 16 p2715 N85-26760

Optimum rotation of solid body with 1 axis of symmetry 16 p2718 N85-26781

Hybrid bearings for LH2 and LO2 turbopumps
16 p2736 N85-26880

Rotordynamics 16 p2737 N85-26888

Advanced energy storage systems
[AD-A152244] 16 p2741 N85-26915

Adaptation of continuous beams and the method of optimizing the flexibility of their elastic supports. Theorem on maximal adaptation loading, supplement
[REPT-10/1984-SUPPL] 16 p2797 N85-27241

Development and application of optimum sensitivity analysis of structures
[NASA-CR-175857] 16 p2799 N85-27257

Parallel computing in optimization
[AD-A151812] 16 p2850 N85-27568

H-sets, convex programming and constrained approximation
[TRITA-NA-8308] 16 p2853 N85-27587

The essence of invexity
[CSIR-TWISK-321] 16 p2858 N85-27626

Incorporating control into the optimal structural design of large flexible space structures
[AD-A152858] 17 p2909 N85-27937

Digital methods of the optimum processing of radar signals
[AD-A152469] 17 p2948 N85-28202

Optimally robust redundancy relations for failure in uncertain systems
[NASA-CR-175953] 17 p2976 N85-28391

The construction of curves and surfaces using numerical optimization techniques 17 p3003 N85-28565

Large scale electricity production scheduling via nonlinear optimization
[REPT-84-07] 17 p3017 N85-28655

The role of duality in optimization problems involving entropy functionals, with applications to information theory
[AD-A152336] 17 p3026 N85-28713

Optimum dimensions of power solenoids for magnetic suspension
[NASA-TM-77864] 17 p3026 N85-28716

The method of residual minimization in compressible steady flows
[AD-A153924] 18 p3100 N85-29193

Optimization of axially compressed carbon fiber reinforced plastic (CFRP) cylinders
18 p3121 N85-29318

Comparison of optimum interpolation and Cressman analyses 18 p3141 N85-29448

A global optimization algorithm using stochastic differential equations
[AD-A153526] 18 p3161 N85-29583

A quadratic programming algorithm
[AD-A153476] 18 p3166 N85-29631

Detection of multivariate outliers with dispersion slippage in elliptically symmetric distributions
[AD-A153785] 18 p3174 N85-29677

Adaptive signal detection and other topics in real time signal processing
[AD-A154139] 19 p3255 N85-30184

Receiver loss study of optimized solar central receiver systems as a function of receiver thermal loss per unit area
[DE85-010831] 19 p3268 N85-30265

High-efficiency, low-cost, passively-cooled PV concentrator module
[DE85-010013] 19 p3305 N85-30490

Identification of a mathematical model 1: Goodness of fit criterion
[HSE-TRANS-11109] 19 p3341 N85-30703

Optimization of single and multi-component analytical techniques
[HSE-TRANS-10987] 19 p3347 N85-30744

Evaluation of curve-smoothing techniques
[HSE-TRANS-11108] 19 p3349 N85-30759

TFCK shielding optimization
[DE85-010503] 19 p3359 N85-30826

Design of helicopter rotor blades for optimum dynamic characteristics
[NASA-CR-176076] 20 p3393 N85-31044

Interactive aircraft flight control and aeroelastic stabilization
[NASA-CR-176035] 20 p3396 N85-31064

An integrated control and minimum mass structural optimization algorithm for large space structures
20 p3413 N85-31183

Characteristic elastic systems of time-limited optimal maneuvers 20 p3413 N85-31184

A control concept for large flexible spacecraft using order reduction techniques 20 p3415 N85-31193

Wideband disturbance accomodation in precision flexible space structures 20 p3415 N85-31194

Sensor/actuator selection for the constrained variance control problem 20 p3415 N85-31197

Eigenvalue placement and stabilization by constrained optimization 20 p3416 N85-31198

Optimal sensor locations for structural identification
20 p3417 N85-31209

An Eigensystem Realization Algorithm (ERA) for modal parameter identification and model reduction
20 p3418 N85-31212

Drag soldering process control
[DE85-010653] 20 p3433 N85-31301

The design of Direct Injection (DI) diesel engines. Injection system by a numerical optimization technique
[REPT-84-RR-346] 20 p3462 N85-31506

Design of simulation experiments
[FEW-123] 20 p3519 N85-31865

Modeling and optimization of a test-cell upgrade for MFTF-B operating in the high neutron wall loading mode
[DE85-009997] 20 p3528 N85-31946

Globally-asynchronous locally-synchronous systems
[AD-A154624] 21 p3573 N85-32222

Application of adaptive noise cancellation to Coast Guard voice communications
[AD-A154796] 21 p3574 N85-32230

Testing and optimizing MST coaxial collinear arrays, part 6.4A 21 p3625 N85-32518

The Norwegian seismic array (NORSAR)
[AD-A154751] 21 p3631 N85-32555

New developments on the core function for efficient implementation of the difficult residue number system operations
[AD-A154678] 21 p3676 N85-32834

Optimal low thrust transfer using a first-order perturbation model
[AD-A154761] 21 p3676 N85-32835

Generalized planar matching
[AD-A154809] 21 p3677 N85-32842

Local epi-continuity and local optimization
[AD-A154812] 21 p3677 N85-32843

Optimization of sampling in statistical physics experiments 21 p3698 N85-32975

Necessary and sufficient conditions for single-extremum and convex problems of mathematical programming
21 p3698 N85-32977

Diakoptic calculation of characteristics for optimization of linear circuits with respect to parameters of individual branches 22 p3767 N85-33346

Optimization of radioelectronic circuits with software for modeling of integrated circuits on unified system computer 22 p3768 N85-33354

Determination of sensitivity functions for discrete dynamic systems from results of function modeling on digital computer 22 p3769 N85-33359

Synthesis of optimum receiver and processor for interfering radio pulse signals 22 p3769 N85-33361

Optimization of design parameters for alternating current stabilizer based on magnetic suspension
22 p3772 N85-33374

Gradiental adaptive corrector with optimum tuning step 22 p3776 N85-33403

Synthesis of system with nonideal components for optimal processing of radio signal
22 p3777 N85-33405

Estimating optimum technical and economic indicators of data transmission systems 22 p3777 N85-33406

Theory of cellwise optimization for solar central receiver system
[DE85-012586] 22 p3807 N85-33579

Blanket optimization studies for Cascade
[DE85-010002] 22 p3846 N85-33824

High pressure compressor component performance report
[NASA-CR-168245] 23 p3897 N85-34138

Re-designing a mechanism for higher speed: A ca history from textile machinery 23 p3923 N85-34

Optimisation in the computer aided design o mechanisms 23 p3924 N85-34

Mass resolution optimization in a large isotop composition experiment
[OG-9.1-9] 23 p4023 N85-34

An automated technique for encasing specific payloads with low-drag fairings 24 p4063 N85-35

Energy management of three-dimensional minimum-time intercept
[NASA-CR-176174] 24 p4064 N85-35

An evaluation of a class of practical optimization techniques for structural dynamics applications
[PB85-195766] 24 p4103 N85-35

Optimizing data access in the LAMPF control system
[DE85-012653] 24 p4140 N85-35

Two methods of global data assimilation
[AD-A155981] 24 p4143 N85-35

Beryllium production
[DE85-013360] 24 p4148 N85-35

OPTIMUM CONTROL
U OPTIMAL CONTROL

OPTOGALVANIC SPECTROSCOPY
An experimental and theoretical investigation of optogalvanic effects
[AD-A146456] 08 p1223 N85-1770

OR-GATES
U GATES (CIRCUITS)

ORBIT CALCULATION
NT MINIMUM VARIANCE ORBIT DETERMINATION

Satellite motion: Lectures and exercises on space mechanics
[ISBN-2-85428-114-4] 05 p0596 N85-1380

Orbit extrapolation — satellite orbits
05 p0598 N85-13811

Measurements in satellite orbit tracing
05 p0598 N85-13812

Spatial mechanics formulas and exercises
05 p0601 N85-1382

On the origin of Triton and Pluto
13 p2175 N85-2340

Location and synchronization — space-time coordinates 14 p2397 N85-2470

The work on Comet Halley's orbit at ESOC
14 p2438 N85-25041

Use of atmospheric models in predicting artificial Earth satellite motion 15 p2478 N85-2529

Using velocity vector in determining Keplerian orbit of geodectic satellite 15 p2478 N85-2529

Autonomous state determination for an Earth orbiting satellite using horizon and star sensors
[AD-A151827] 15 p2493 N85-2537

Flight Experiment Demonstration System (FEDS) functional description and interface document
[NASA-CR-175290] 16 p2717 N85-2676

Accuracy in predicting orbital motion of artificial Earth satellite 16 p2720 N85-2678

DORIS: Prediction in Doppler measurement — satellite onboard measurement
[CNES-CT/DTI/MS/AE/170] 16 p2729 N85-2684

Topex Gravity Model Development Team activities during fiscal year 1984
[NASA-TM-86208] 16 p2804 N85-2728

Satellite physical and orbital characteristics
16 p2804 N85-2728

Gravity model development software status
16 p2804 N85-2728

Radial orbit error spectrum for Topex
16 p2805 N85-2729

An algorithm for the influence numbers in the expansion of the lumped gravitational potential coefficients in the presence of resonant inclination variation
[AD-A154229] 19 p3336 N85-3068

Study of the interferences of 2 GHz radio beams with a DORIS system — precise low orbit determination system (DORIS)
[CNES-CT/DRT/TIT/RL-84/140-T]
20 p3442 N85-313

Effect of solar eclipses on the LAGEOS semimajo axis 20 p3491 N85-316

Geodyn systems development
20 p3492 N85-317

ORBIT DECAY
Natural atmospheric reentry — satellite orbit decay
05 p0600 N85-1382

Orbital Debris
[NASA-CP-2360] 12 p1783 N85-211

History of satellite break-ups in space
12 p1783 N85-211

Manmade orbital debris studies at NASA Langley
12 p1783 N85-211

NASA/JSC orbital debris study: Debris model
12 p1783 N85-211

Proposed preliminary design criteria model environme for the 1990's 12 p1784 N85-211

The long term behaviour of Earth orbits and the implications for debris control 12 p1786 N85-21213
Natural reentry of satellites 14 p2397 N85-24774
Examination of returned solar-max surfaces for impacting orbital debris and meteoroids
15 p2681 N85-26560
Update on the evolution of the LAGEOS orbit
20 p3491 N85-31698

ORBIT EQUATIONS
U ORBITAL MECHANICS

ORBIT MANEUVERING ENGINE (SPACE SHUTTLE)
Orbital Maneuvering system design evolution
08 p1098 N85-16943
Space station systems technology study (add-on task). Volume 1: Executive summary
[NASA-CR-171415] 13 p1986 N85-22459
Selected tether applications in space: Phase 2. Executive summary
[NASA-CR-171421] 13 p1987 N85-22462
Selected tether applications in space: Phase 2
[NASA-CR-171422] 13 p1987 N85-22463

ORBIT PERTURBATION
NT SATELLITE PERTURBATION
Deformations of two-dimensional dissipative maps — orbit perturbation
[REPT-69] 01 p0129 N85-10691
Theory of the orbital motion of an artificial Earth satellite
[NAL-TR-807] 06 p0758 N85-14847
SIMM1: A linearized particle code
[AD-A148627] 08 p1221 N85-17689
A semianalytical, artificial satellite orbit propagation procedure based on optimal parameter estimation
[INPE-3301-PRE/613] 10 p1427 N85-18997
Selection of a model of Earth's albedo radiation, practical calculation of its effect on the trajectory of a satellite
[NASA-TM-77870] 15 p2591 N85-25972
The 6 pi-periodic solutions of plane restricted elliptical 3-body problem in neighborhood of libration points
16 p2718 N85-26779
Stability of periodic satellite motions relative to center of mass in circular orbit 16 p2718 N85-26780
Simulation of a low orbit restitution. Covariance analysis of the position-velocity by Doppler and accelerometer measurements
[CNES-CT/DTI/MS/AE/166] 16 p2728 N85-26836
Analytical generation of satellite orbits at the RAE (Royal Aircraft Establishment)
[AD-A152655] 17 p3053 N85-28901
Effect of solar eclipses on the LAGEOS semimajor axis 20 p3491 N85-31699
Effect of diffusely-reflected sunlight on the orbit of LAGEOS 20 p3491 N85-31700
Optical best arc RMS test results
20 p3492 N85-31706

ORBIT SPECTRUM UTILIZATION
The international environment UNISPACE '82 and the ITU: A relationship between orbit-spectrum resource allocation and orbital debris 12 p1787 N85-21215
Transmission and orbital constraints in space-related programs: Briefing summary 12 p1787 N85-21216
Engineering calculations for communications satellite systems planning
[NASA-CR-175552] 12 p1789 N85-21233

ORBIT TRANSFER VEHICLES
Possibilities and limits of electromagnetic acceleration in space applications
[ILR-MITT-136] 02 p0193 N85-11292
Boundary layer simulator improvement
[NASA-CR-174199] 05 p0597 N85-13802
Advanced concepts liquid droplet radiator
05 p0610 N85-13899
Impact of lunar and planetary missions on the space station
[NASA-CR-171832] 08 p1106 N85-16988
OTV Propulsion Issues
[NASA-CP-2347] 08 p1106 N85-16989
NASA OAST perspective 08 p1106 N85-16990
Space station task force perspective
08 p1106 N85-16992
Performance assessment of aero-assisted orbital transfer vehicles 08 p1106 N85-16993
Low lift-to-drag aero-assisted orbit transfer vehicles
08 p1107 N85-16994
Moderate lift-to-drag aeroassist
08 p1107 N85-16995
Benefits of high aerodynamic efficiency to orbital transfer vehicles 08 p1107 N85-16996
OTV propulsion tecnology programmatic overview
08 p1107 N85-16997
Drives and benefits overview
08 p1107 N85-16998
Aerojet advanced engine concept
08 p1107 N85-16999
Advanced OTV engines and issues
08 p1108 N85-17000
Advanced OTV engine concepts
08 p1108 N85-17001
Earth-to-orbit propellant transportation overview
08 p1108 N85-17002
Active cooling requirements for propellant storage
08 p1108 N85-17004
Propellant transfer: Attached depot
08 p1108 N85-17005
Propellant transfer: Tethered depot
08 p1108 N85-17006
OTV fluid mangement systems
08 p1108 N85-17007
Vehicle/engine integration — orbit transfer vehicles
08 p1109 N85-17008
Orbital transfer vehicle propulsion issues
08 p1109 N85-17009
Space based OTV servicing 08 p1109 N85-17010
Design and analysis report for the RL10-2B breadboard low thrust engine
[NASA-CR-174857] 10 p1430 N85-19020
The servicing vehicle of Columbus
[MBB-UR-E-750-84-O] 11 p1588 N85-19997
Orbital Debris
[NASA-CP-2360] 12 p1783 N85-21188
Environment definition, small particles, diameter less than or equal to 1 MM 12 p1788 N85-21223
Design study of an integrated aerobraking orbital transfer vehicle
[NASA-TM-58264] 12 p1795 N85-21262
Space station systems technology study (add-on task). Volume 1: Executive summary
[NASA-CR-171415] 13 p1986 N85-22459
Selected tether applications in space: Phase 2. Executive summary
[NASA-CR-171421] 13 p1987 N85-22462
Selected tether applications in space: Phase 2
[NASA-CR-171422] 13 p1987 N85-22463
Space Station technology planning
13 p1989 N85-22471
Space station systems technology study (add-on task). Volume 2: Trade study and technology selection
[NASA-CR-171416] 15 p2475 N85-25279
Analysis of orbit transfer vehicles for GPS Block 3 satellites
[AD-A152021] 16 p2732 N85-26860
Convoluted nozzle design for the RL10 derivative 2B engine
[NASA-CR-174953] 19 p3220 N85-29965
Nonequilibrium air radiation (Nequair) program: User's manual
[NASA-TM-86707] 19 p3353 N85-30780
A review of shock waves around aeroassisted orbital transfer vehicles
[NASA-TM-86769] 22 p3739 N85-33177
A dual, fault-tolerant aerospace actuator
22 p3798 N85-33530
Design of a dual fault tolerant space shuttle payload deployment actuator 22 p3798 N85-33531
Status of advanced orbital transfer propulsion
[NASA-TM-87069] 24 p4071 N85-35225

ORBITAL ASSEMBLY
Swing-arm beam erector (SABER) concept for single astronaut assembly of space structure
[NASA-TP-2379] 10 p1429 N85-19015
Verification for large space structures
14 p2232 N85-23836
Assembly Concept for Construction of Erectible Space Structure (ACCESS) neutral buoyancy testing results
14 p2236 N85-23862
Construction in space
[NASA-TM-77630] 15 p2492 N85-25374
Construction and functioning of extended orbital systems 16 p2724 N85-26814
NASA space station automation: AI-based technology review
[NASA-CR-176094] 21 p3558 N85-32134
NASA space station automation: AI-based technology review. Executive summary
[NASA-CR-176096] 21 p3558 N85-32135
A modular docking mechanism for in-orbit assembly and spacecraft servicing 22 p3796 N85-33516

ORBITAL ELEMENTS
Theory of the orbital motion of an artificial Earth Satellite
[NAL-TR-807] 09 p1285 N85-18075
History of satellite break-ups in space
12 p1783 N85-21190
Some numerical estimates of perturbation of orbital elements of artificial Earth satellite with total dynamic symmetry about rotating aspherical Earth
15 p2478 N85-25294
Systematic and random deformations of orbits of long-period comets 15 p2479 N85-25299
Multistep orbital correction algorithms for an Earth satellite using low thrust engine
15 p2479 N85-25303
Orbital elements of Saturn's F ring and its shepherding satellites 15 p2675 N85-26515
Gravity model development software status
16 p2804 N85-27289
Optical best arc RMS test results
16 p2804 N85-27290
An algorithm for the influence numbers in the expansion of the lumped gravitational potential coefficients in the presence of resonant inclination variation
[AD-A154228] 19 p3336 N85-30669
An introduction to satellite orbits
[RAE-TM-SPACE-344] 20 p3397 N85-31076
Geodyn systems development
20 p3492 N85-31708
Insolation changes on Pluto caused by orbital element variations
[AERONOMICA-ACTA-A-290-1984]
20 p3546 N85-32070

ORBITAL FLIGHT TEST 1 (SHUTTLE)
U SPACE TRANSPORTATION SYSTEM 1 FLIGHT

ORBITAL FLIGHT TEST 3 (SHUTTLE)
U SPACE TRANSPORTATION SYSTEM 3 FLIGHT

ORBITAL FLIGHT TEST 4 (SHUTTLE)
U SPACE TRANSPORTATION SYSTEM 4 FLIGHT

ORBITAL FLIGHT TESTS (SHUTTLE)
U SPACE TRANSPORTATION SYSTEM FLIGHTS

ORBITAL LAUNCHING
Analysis of orbit transfer vehicles for GPS Block 3 satellites
[AD-A152021] 16 p2732 N85-26860

ORBITAL LIFETIME
Natural atmospheric reentry — satellite orbit decay
05 p0600 N85-13829
The long term behaviour of Earth orbits and the implications for debris control 12 p1786 N85-21213
Natural reentry of satellites 14 p2397 N85-24774

ORBITAL MANEUVERING VEHICLES
The servicing vehicle of Columbus
[MBB-UR-E-750-84-O] 11 p1588 N85-19997
Evaluation of OMV ranging and docking systems
12 p1947 N85-22230
Space station systems technology study (add-on task). Volume 2: Trade study and technology selection
[NASA-CR-171416] 15 p2475 N85-25279
Automatic rendezvous and docking systems functional and performance requirements
[NASA-CR-171866] 15 p2492 N85-25376
Docking simulation analysis of range data requirements for the orbital maneuvering vehicle
[NASA-TM-86510] 20 p3407 N85-31143
NASA space station automation: AI-based technology review
[NASA-CR-176094] 21 p3558 N85-32134
NASA space station automation: AI-based technology review. Executive summary
[NASA-CR-176096] 21 p3558 N85-32135
Space station automation and robotics study. Operator-systems interface
[NASA-CR-176095] 22 p3738 N85-33172
Hardware test program for evaluation of basline range-range rate sensor concept
[NASA-CR-176143] 23 p3933 N85-34377
Status of advanced orbital transfer propulsion
[NASA-TM-87069] 24 p4071 N85-35225

ORBITAL MANEUVERS
USSR report: Space
[JPRS-USP-84-005] 02 p0156 N85-11060
Features and uses of progress cargo ships
02 p0157 N85-11061
Orbital maneuvers with finite thrust. Volume 1: Mathematical formulation, numerical methods, catalog concept
[ESA-CR(P)-1910-VOL-1] 06 p0758 N85-14848
Orbit maneuvers with finite thrust. Volume 2: Reference manual, part 1
[ESA-CR(P)-1910-VOL-2-PT-1]
06 p0758 N85-14849
Orbit maneuvers with finite thrust. Volume 3: User's guide, part 2
[ESA-CR(P)-1910-VOL-3-PT-2]
06 p0758 N85-14850
Orbit maneuvers with finite thrust. Volume 3: Reference catalog, parts 1 and 2
[ESA-CR(P)-1910-VOL-3-PT-1/2]
06 p0758 N85-14851
Orbit maneuvers with finite thrust. Volume 3: Reference catalog, part 3
[ESA-CR(P)-1910-VOL-3-PT-3]
06 p0758 N85-14852
Shuttle-tethered satellite system definition study extension
[NASA-CR-171473] 17 p2907 N85-27923
Docking simulation analysis of range data requirements for the orbital maneuvering vehicle
[NASA-TM-86510] 20 p3407 N85-31143

ORBITAL MECHANICS
NT KEPLER LAWS
NT MINIMUM VARIANCE ORBIT DETERMINATION
Deformations of two-dimensional dissipative maps — orbit perturbation
[REPT-69] 01 p0129 N85-10691
USSR report: Space
[JPRS-USP-84-005] 02 p0156 N85-11060
Tass reports launch of Soyuz T-12
02 p0158 N85-11070
Some considerations on elliptic heliocentric orbits
[INPE-3217-PRE/570] 02 p0297 N85-11926
A testable gravitational capture model for the origin of the Earth's Moon 04 p0586 N85-13742
Satellite motion: Lectures and exercises on space mechanics
[ISBN-2-85428-114-4] 05 p0596 N85-13807
Orbit perturbation — satellites
05 p0598 N85-13810
Orbit extrapolation — satellite orbits
05 p0598 N85-13811
The CDC: Facilities on offer from the CNES computing center for space mathematics (a look at the capacities of CDC computers) 05 p0599 N85-13818
JPL highlights
[NASA-CR-175517] 11 p1767 N85-21102
Orbital Debris
[NASA-CP-2360] 12 p1783 N85-21188
History of satellite break-ups in space
12 p1783 N85-21190
NORAD's PARCS small satellite tests (1976 and 1978) 12 p1783 N85-21191
NASA/JSC orbital debris study: Debris model
12 p1783 N85-21193
The long term behuviour of Earth orbits and the implications for debris control 12 p1786 N85-21213
Debris in the geostationary orbit ring, the endless shooting gallery: The necessity for a disposal policy
12 p1786 N85-21214
Algorithm for determining optimal three impulse point-to-orbit transfer with limited transfer time
13 p1979 N85-22419
Satellite oscillations in elliptical orbit
13 p1981 N85-22429
Satellite-to-satellite orbit determination using minimum, discrete range and range-rate data only
13 p1985 N85-22458
Halley's Comet, a bibliography
[LC-84-600109] 13 p2204 N85-23674
Motion of satellite with total dynamic symmetry around rotating aspherical Earth 14 p2287 N85-24174
Orbit perturbation. Extrapolation of perturbed orbits
14 p2396 N85-24763
Modeling needed for the design and definition of spacecraft attitude and orbit control systems
14 p2397 N85-24766
Attitude measurements and determination
14 p2397 N85-24767
Mission analysis and orbit control of the heliosynchronous satellite SPOT
14 p2397 N85-24773
Some numerical estimates of perturbation of orbital elements of artificial Earth satellite with total dynamic symmetry about rotating aspherical Earth
15 p2478 N85-25294
Using velocity vector in determining Keplerian orbit of geodectic satellite 15 p2478 N85-25297
Resonance identifications in Saturn's rings
15 p2674 N85-26504
Dense but collisionless orbiting rings — Saturn rings
15 p2675 N85-26517
The asteroid ring 15 p2678 N85-26536
Integrable cases of restricted doubly averaged 3-body problem 16 p2718 N85-26778
Optimal relative data weights
16 p2805 N85-27296
Numerical integration through force discontinuities: Solar radiation pressure 16 p2805 N85-27298
Shuttle-tethered satellite system definition study extension
[NASA-CR-171473] 17 p2907 N85-27923
Maximizing the semi-major axis for a freely coning solar sailcraft
[AD-A153175] 17 p2909 N85-27938
How a swing behaves
[DE85-008280] 17 p3027 N85-28720
An introduction to satellite orbits
[RAE-TM-SPACE-344] 20 p3397 N85-31076
Effect of diffusely-reflected sunlight on the orbit of LAGEOS 20 p3491 N85-31700
Structural dynamics model and response of the deployable reference configuration space station
[NASA-TM-86386] 22 p3799 N85-33539
Target observability for satellite-based sensors
[AD-A156139] 24 p4069 N85-35217

ORBITAL MOTION
U ORBITS

ORBITAL POSITION ESTIMATION
Planning of navigation measurements using TD criterion for determination of movement of spacecraft by method of least squares 02 p0159 N85-11081
Satellite orbit determination 05 p0598 N85-13813
The performance of differential VLBI delay during interplanetary cruise 05 p0623 N85-13984
Shuttle navigation status 08 p1062 N85-16901
A semianalytical, artificial satellite orbit propagation procedure based on optimal parameter estimation
[INPE-3301-PRE/613] 10 p1427 N85-18997
Air Force satellite position management
12 p1787 N85-21217
Use of atmospheric models in predicting artificial Earth satellite motion 15 p2478 N85-25296
Minimax problem of estimating trajectory parameters in continuous formulation 15 p2479 N85-25301
Inference and state estimation for stochastic point processes
[AD-A151216] 15 p2640 N85-26281
Accuracy in predicting orbital motion of artificial Earth satellite 16 p2720 N85-26793
Simulation of a low orbit restitution. Covariance analysis of the position-velocity by Doppler and accelerometer measurements
[CNES-CT/DTI/MS/AE/166] 16 p2728 N85-26836
Optical best arc RMS test results
16 p2804 N85-27290
Self-tuning adaptive-controller using online frequency identification 20 p3417 N85-31205
Combined state and parameter estimation for a static model of the Maypole (Hoop-Column) antenna suface
20 p3417 N85-31210

ORBITAL RENDEZVOUS
Optimal multiple-impulse nonlinear orbital rendezvous
08 p1105 N85-16984
Docking simulation analysis of range data requirements for the orbital maneuvering vehicle
[NASA-TM-86510] 20 p3407 N85-31143

ORBITAL SERVICING
Tass reports launch of Soyuz T-12
02 p0158 N85-11070
Magnetic spin reduction system for free spinning objects
[NASA-CASE-MFS-25966-1] 02 p0166 N85-11122
Definition of technology development missions for early Space Station satellite servicing. Volume 1: Executive summary
[NASA-CR-171228] 04 p0460 N85-12922
Definition of technology development missions for early Space Station satellite servicing. Volume 2: Technical
[NASA-CR-171229] 04 p0461 N85-12923
OTV propulsion tecnology programmatic overview
08 p1107 N85-16997
Space based OTV servicing 08 p1109 N85-17010
The servicing vehicle of Columbus
[MBB-UR-E-750-84-O] 11 p1588 N85-19997
Applications of Tethers in Space, volume 1
[NASA-CP-2364] 11 p1642 N85-20339
Orbital Debris
[NASA-CP-2360] 12 p1783 N85-21188
Satellite services and orbital retrieval
12 p1786 N85-21211
Utilization of space station by the large deployment reflector 14 p2235 N85-23857
Analysis of remote operating systems for space-based servicing operations, volume 1
[NASA-CR-171885] 19 p3225 N85-29993
Analysis of remote operating systems for space-based servicing operations. Volume 2: Study results
[NASA-CR-171886] 19 p3225 N85-29994
Space station automation study-satellite servicing. Volume 1: Executive summary
[NASA-CR-171512] 19 p3226 N85-29999
Space station automation study-satellite servicing, volume 2
[NASA-CR-171513] 19 p3226 N85-30000
A modular docking mechanism for in-orbit assembly and spacecraft servicing 22 p3796 N85-33516

ORBITAL SIMULATORS
U SPACE SIMULATORS

ORBITAL SPACE STATIONS
NT EOSS
NT LONG DURATION EXPOSURE FACILITY
NT ORBITING LUNAR STATIONS
NT SALYUT SPACE STATION
NT SKYLAB 3
NT SKYLAB 4
Definition of technology development missions for early space stations: Large space structures
[NASA-CR-171209] 03 p0323 N85-12084
Definition of technology development missions for early Space Station satellite servicing. Volume 1: Executive summary
[NASA-CR-171228] 04 p0460 N85-12922
Advanced and nontraditional concepts working group report 05 p0612 N85-13[illegible]
Space station: New frontier for life sciences in space
05 p0696 N85-1447[illegible]
Engineering model system study for a regenerative fuel cell: Study report
[NASA-CR-174801] 07 p0991 N85-16[illegible]
Drives and benefits overview
08 p1107 N85-16[illegible]
Manned space station solar array study
[ESA-CR(P)-1941] 09 p1287 N85-18[illegible]
Preliminary concepts of candidate elements for a potential European participation in a manned space station
[MBB-UR-E-749-84-O] 11 p1587 N85-199[illegible]
The servicing vehicle of Columbus
[MBB-UR-E-750-84-O] 11 p1588 N85-19997
Earth observations and the polar platform
[NOAA-TR-NESDIS-18] 11 p1669 N85-20[illegible]
Space Station Software Issues
[NASA-CP-2361] 11 p1700 N85-20[illegible]
Software management issues — space station software development 11 p1700 N85-20[illegible]
Software development environment issues — space station software development 11 p1700 N85-20[illegible]
Software standards issues — space station software development 11 p1701 N85-20[illegible]
Information systems issues 11 p1701 N85-20[illegible]
Parametric analysis: SOC meteoroid and debris protection 12 p1786 N85-212[illegible]
Natural environment design criteria for the Space Station definition and preliminary design
[NASA-TM-86498] 12 p1789 N85-212[illegible]
Computer integration of engineering design and production: A national opportunity
[NASA-CR-175483] 12 p1820 N85-21414
Debris impact on Earth-orbiting spacecraft
12 p1948 N85-22[illegible]
The intelligent database machine
12 p1949 N85-22[illegible]
Concentrator technologies evaluation for large solar arrays and their application for space stations/platforms
13 p2010 N85-226[illegible]
Space Station solar array 13 p2010 N85-22610
Analysis of space station operations in the space debris environment
[AD-A151872] 15 p2493 N85-253[illegible]
Manrating orbital transfer vehicle propulsion
[NASA-TM-87019] 15 p2494 N85-253[illegible]
Space methods in oceanology
[NASA-TM-77652] 15 p2604 N85-26047
European utilization aspects of a US manned space station, volume 1
[ESA-CR(P)-1987-VOL-1] 17 p2907 N85-27[illegible]
European utilization aspects of a US manned space station, volume 2
[ESA-CR(P)-1987-VOL-2] 17 p2907 N85-27[illegible]
Space station study
[BL-6167] 18 p3066 N85-28[illegible]
Some Europeans voice opposition to space station participation 18 p3066 N85-28[illegible]
New ESA director on space station, military space
18 p3066 N85-28[illegible]
ESA presents plans for European manned space station 18 p3085 N85-28[illegible]
Space station automation study-satellite servicing. Volume 1: Executive summary
[NASA-CR-171512] 19 p3226 N85-29999
Space station automation study-satellite servicing. volume 2
[NASA-CR-171513] 19 p3226 N85-30000
Space ventures and society long-term perspectives
[NASA-CR-176012] 19 p3379 N85-30[illegible]
Multivariable control of a soft coupled space station
20 p3408 N85-3115[illegible]
Studies toward a manned space station: Participation of European industry in NASA space station (MSS)
[SNIAS-S/DT-Y-25-212] 20 p3418 N85-31217
Comparative study on data system architectures — spacecraft data processing
[ESA-CR(P)-2015] 21 p3675 N85-33[illegible]
Applicability of 100kWe-class of space reactor power systems to NASA manned space station missions
[NASA-CR-174696] 24 p4149 N85-357[illegible]

ORBITAL TEST SATELLITE (ESA)
U OTS (ESA)

ORBITAL TRANSFER
U TRANSFER ORBITS

ORBITAL VELOCITY
Using velocity vector in determining Keplerian orbit of geodectic satellite 15 p2478 N85-25297

Simulation of a low orbit restitution. Covariance analysis of the position-velocity by Doppler and accelerometer measurements
[CNES-CT/DTI/MS/AE/166] 16 p2728 N85-26836
ORBITALS
NT ELECTRON ORBITALS
NT MOLECULAR ORBITALS
Vacancy-rearrangement theory in the first Magnus approximation
[DE85-004435] 12 p1930 N85-22123
ORBITING GEOPHYSICAL OBSERVATORY
U OGO
ORBITING LUNAR STATIONS
Concept and cost analysis of an orbiting lunar station
[ILR-MITT-136] 07 p0913 N85-15776
ORBITING SATELLITES
U ARTIFICIAL SATELLITES
ORBITS
NT CIRCULAR ORBITS
NT EARTH ORBITS
NT ECCENTRIC ORBITS
NT ELLIPTICAL ORBITS
NT GEOSYNCHRONOUS ORBITS
NT INTERPLANETARY TRANSFER ORBITS
NT LUNAR ORBITS
NT PARKING ORBITS
NT PERIGEES
NT PERIHELIONS
NT PLANETARY ORBITS
NT POLAR ORBITS
NT SATELLITE ORBITS
NT SOLAR ORBITS
NT SPACECRAFT ORBITS
NT STATIONARY ORBITS
NT TRANSFER ORBITS
Birkhoff orbits for non-monotone twist maps
[AD-A144718] 01 p0110 N85-10747
Shape of power spectrum of intermittent chaos
02 p0263 N85-11841
Physical properties of Neptune and Triton inferred from the Orbit of Triton 02 p0300 N85-11942
Origin and evolution of the Uranian and Neptunian satellites: Some dynamical considerations
02 p0300 N85-11943
The asteroidal source region of ordinary chondrites
06 p0881 N85-15600
An optimization method for the preliminary design of interplanetary aerobraking missions
08 p1076 N85-16822
Improvement in magnetic field properties of vanadium-gallium superconductors by enhancement of spin-orbit scattering
[DE85-002893] 13 p2164 N85-23422
The orbits of Comets Halley and Giocobini-Zinner
14 p2437 N85-25039
The orbital motion of Comet Halley
14 p2437 N85-25040
Systematic and random deformations of orbits of long-period comets 15 p2479 N85-25299
Indications of twist in the Epsilon rings of Uranus
15 p2672 N85-26490
Construction and functioning of extended orbital systems 16 p2724 N85-26814
Multiple time-scale methods in particle simulations of plasmas
[DE85-007519] 17 p3040 N85-28808
Tenth-order expansion formulae for the orbital eccentricity function K (sub lpq)(e) obtained using a symbolic algebraic manipulation system
[AD-A153754] 18 p3170 N85-29647
An algorithm for the influence numbers in the expansion of the lumped gravitational potential coefficients in the presence of resonant inclination variation
[AD-A154229] 19 p3336 N85-30669
Guide to the Main Ring DO overpass
[DE85-011722] 20 p3531 N85-31963
Estimating the change in asymptotic direction due to secular changes in the geomagnetic field
[SH-6.1-13] 23 p4045 N85-35086
ORDER-DISORDER TRANSFORMATIONS
Static and dynamic disordering in amorphous magnets and crystals 03 p0422 N85-12699
Diffuse elastic and inelastic neutron scattering of disorder transitions and boundaries. Phase determination of structure factors 03 p0424 N85-12708
The disordering process in an L1sub2 ordered alloy
[DE84-016599] 04 p0475 N85-13028
Development and characterization of ductile Long-Range-Ordered (LRO) alloys (Fe,Co, Ni)3V for high-temperature structural use
[DE84-016750] 06 p0769 N85-14921
Phase diagram of polymer blends containing block copolymers
[AD-A147706] 08 p1132 N85-17134
Phase formation and stability in the pseudobinary Ni3Al-Ni3V alloy system
[DE85-001117] 09 p1296 N85-18143
First principles theory of Fermi-surface driven concentration waves in Cu/sub c/Pd/sub 1-c/ alloys
[DE85-005367] 13 p2024 N85-22681
On the feasibility of Ab Initio calculations of ordering alloy phase diagrams
[DE85-007073] 16 p2751 N85-26979
The disordering process in an L12 ordered alloy
[DE85-008152] 17 p2931 N85-28093
Local density theory of heats of formation and short-range order parameters in substitutionally disordered alloys
[DE85-009811] 18 p3075 N85-29021
Electronic structure and lattice dynamics of dimensionally constrained and disordered solids
[AD-A155927] 24 p4161 N85-35797
ORDNANCE
Evolution of the NWC (Naval Weapons Center) thermal standard. Part 5: Thermal standard development and applications
[AD-A146173] 03 p0364 N85-12334
Safing and arming mechanism
[AD-D011261] 05 p0621 N85-13969
Assessment of environmental costs at ordnance activities
[AD-P004140] 09 p1347 N85-18476
The remote detection of polynuclear aromatic hydrocarbons using laser-induced fluorescence
[AD-A152294] 16 p2757 N85-27013
Voltammetric analysis of ordnance materials. Part 2: A portable digital voltammeter for use with a silver wire working electrode
[AD-A152480] 17 p2967 N85-28325
SAFEORD: Safety of explosive ordnance databank
[AD-A154058] 19 p3380 N85-30972
Development of improved dynamic failure models
[AD-A155586] 21 p3600 N85-32354
OREGON
Image variance and spatial structure in remotely sensed scenes -- South Dakota, California, Missouri, Kentucky, Louisiana, Tennessee, District of Columbia, and Oregon
07 p0986 N85-16265
Mesoscale studies of flow regimes and fluxes of particulate matter in coastal waters
[DE85-003625] 11 p1689 N85-20620
ORES
U MINERALS
ORGANIC CHARGE TRANSFER SALTS
Synthesis of film-forming electron-accepting polymers
[AD-A146430] 06 p0771 N85-14931
ORGANIC CHEMISTRY
Biocatalyzed processes for production of commodity chemicals: Assessment of future research advances for N-butanol production
[NASA-CR-174264] 07 p0919 N85-15819
A study of organic chemical reactions in microemulsions
[AD-A150063] 12 p1796 N85-21265
Abstracts of the 36th Southeastern Regional Meeting of the American Chemical Society
[AD-A151506] 15 p2496 N85-25394
Systematic nomenclature of the nitrogen, oxygen and sulfur functional polycyclic aromatic hydrocarbons
[DE85-007426] 17 p2916 N85-27974
Academician Ovchinnikov on future of bioorganic chemistry 17 p3049 N85-28874
Biocatalysis project
[NASA-CR-176044] 20 p3498 N85-31744
Studies in photochemical smog chemistry. 1: Atmospheric chemistry of toulene. 2: Analysis of chemical reaction mechanisms for photochemical smog
24 p4113 N85-35497
ORGANIC COMPOUNDS
NT ADENOSINE DIPHOSPHATE
NT ADENOSINE TRIPHOSPHATE
NT ADENOSINES
NT ALANINE
NT AMINO ACIDS
NT ASPARTATES
NT ASPARTIC ACID
NT CARBON TETRAFLUORIDE
NT CHOLINE
NT CYCLIC COMPOUNDS
NT FATS
NT FATTY ACIDS
NT FLUORINE ORGANIC COMPOUNDS
NT FLUOROCARBONS
NT FLUOROHYDROCARBONS
NT GLUTAMINE
NT GLUTATHIONE
NT GLYCINE
NT METHIONINE
NT ORGANIC CHARGE TRANSFER SALTS
NT ORGANIC LIQUIDS
NT ORGANIC SULFUR COMPOUNDS
NT OXIDASE
NT PEPTIDES
NT PERFLUOROALKANE
NT PHOSPHAZENE
NT POLYNUCLEAR ORGANIC COMPOUNDS
NT POLYPEPTIDES
NT PROPARGYL GROUPS
NT QUINOLINE
NT TETRAHYDROFURAN
NT TRYPTOPHAN
A simple electronic apparatus for determining the oxidation stability of lubricants and other organic compounds
[AD-A146080] 03 p0338 N85-12172
Organic aerosol formation: OH(hydroxyl radical) versus ozone oxidation pathways
[PB84-219880] 03 p0388 N85-12484
Time-resolved spectroscopy of evanescent-wave excited fluorescence
[DE84-015213] 04 p0473 N85-13013
VOC emissions from volatile organic liquid storage tanks: Background information for proposed standards
[PB84-237320] 04 p0532 N85-13403
Determination of halogens and sulfur in organic compounds and polymers by combustion-ion chromatography
[DE84-016186] 05 p0614 N85-13921
Gas chromatographic determination of content of harmful substances in air of industrial locations
06 p0761 N85-14866
Study of effectiveness of fire-resistant activity of antipyrenes for fibers of aromatic polyamides
06 p0762 N85-14874
Electrochemical behaviour of TiCl4 solutions in low melting point organic media
[BLL-OA-TRANS-3174-(6196.3)]
06 p0764 N85-14888
Pathology and axonal transport in hexacarbon neuropathies
[AD-P004021] 06 p0843 N85-15355
Solar wind and cosmic ray irradiation of grains and ices - application to erosion and synthesis of organic compounds in the solar system
06 p0866 N85-15637
Continuous organic electrochemical synthesis
[DE85-001400] 10 p1437 N85-19057
A study of organic chemical reactions in microemulsions
[AD-A150063] 12 p1796 N85-21265
Gas-liquid chemistry of natural waters, volume 1
[DE85-002603] 12 p1884 N85-21822
Standard analytical procedures of the NOAA National Analytical Facility, 1984-85: Extractable toxic organic compounds
[PB85-126262] 12 p1887 N85-21840
The body burden of organic vapors in artificial air trial measurements aboard a moored submarine
[AD-A149698] 12 p1910 N85-21968
One mechanism of formation of organic fraction in atmospheric aerosol 13 p2014 N85-22632
Analysis of biological particles by mass spectrometry
[AD-A149952] 13 p2141 N85-23291
Literature review for development of the master analytical scheme for organic compounds in water
[PB85-152874] 15 p2507 N85-25488
Thermally modulated electron affinity detector for priority pollutant analysis
[PB85-158145] 15 p2508 N85-25469
Procedure for certifying quantity of volatile organic compounds emitted by paint, ink and other coatings
[PB85-159044] 15 p2520 N85-25537
Philips tested new materials for optical data storage
15 p2532 N85-25620
Electronic properties of new organic conductors
[DE85-005590] 15 p2549 N85-25736
Carbon isotopes in bulk carbonaceous chondrites
15 p2681 N85-26557
Analytical methods for determination of POHC (Principal Organic Hazardous Constituents) in combustion products
[PB85-161578] 16 p2747 N85-26955
Role of natural dissolved organic compounds in determining the concentrations of americium in natural waters
[DE85-010266] 19 p3229 N85-30022
Technical and administrative activities of the Analytical Chemistry Laboratory (ACL)
[DE85-010150] 19 p3236 N85-30063
Thermodynamic study of CO2-organic compound interaction at high pressures and temperatures
[DE85-010999] 19 p3268 N85-30266
Sea water photoluminescence
19 p3292 N85-30415

Speciation of hazardous inorganic compounds by Fourier transform infrared (FTIR) spectroscopy
[PB85-188969] 20 p3426 N85-31262

Aerosol analysis and emission spectrometry with free jets
[DE85-010576] 21 p3564 N85-32168

Distribution and abundance of organic thiols
21 p3657 N85-32717

Development of a chemical kinetic mechanism for the US EPA (Environmental Protection Agency) regional oxidant model
[PB85-185858] 22 p3813 N85-33618

Anaerobic microbial transformations in subsurface environments
[DE85-012790] 22 p3819 N85-33659

Atmospheric modeling of organics for risk assessment: A Chemist's view
[DE85-009770] 23 p3909 N85-34217

Aspects of high-resolution gas chromatography as applied to the analysis of hydrocarbon fuels and other complex organic mixtures. Volume 1
[AD-A156154] 24 p4076 N85-35257

ORGANIC FLUORINE COMPOUNDS
U FLUORINE ORGANIC COMPOUNDS

ORGANIC LASERS
NT DYE LASERS

Characteristics of unstable resonators in flashlamp-pumped organic-compound lasers
11 p1717 N85-20600

ORGANIC LIQUIDS

Turbulent shear fields for dispersion of aqueous drops in organic liquids and application to gel-sphere processes
[DE84-016562] 06 p0809 N85-15141

ORGANIC LITHIUM COMPOUNDS

(Vinyloxy)chlorocyclotriphosphazenes
[AD-D011471] 10 p1453 N85-19152

ORGANIC MATERIALS
NT PEAT

Production and turnover of suspended organic detritus in the coastal water of the southeastern continental shelf
[DE85-003977] 13 p2140 N85-23290

West Europe report: Science and technology
[JPRS-WST-85-013] 14 p2289 N85-24183

Corrosion control through a better understanding of the metallic substrate-organic coating-interface
[AD-A151238] 15 p2509 N85-25479

Comparison of TT-F-1098 solvent-thinned block fillers with water-thinnable block fillers
[AD-A154207] 19 p3249 N85-30142

Changes in the organic material in lakes in the blast zone of Mount St. Helens, Washington: Hydrologic effects of the eruptions
[GS-CIRC-850-1] 21 p3630 N85-32551

Rechargeable lithium-organic electrolyte battery having overcharge protection and method of providing overcharge protection for a lithium-organic electrolyte battery
[AD-D011738] 22 p3806 N85-33575

ORGANIC NITRATES
NT CELLULOSE NITRATE
NT PETN

ORGANIC PEROXIDES

Chemical transformation in acid rain. Volume 1: New methodologies for sampling and analysis of gas-phase peroxide
[PB85-173425] 19 p3311 N85-30527

ORGANIC PHOSPHORUS COMPOUNDS
NT PHOSPHAZENE

Macrocyclic poly(tertiary) phosphines for the attachment of metals to surfaces of photodevices
[DE84-015552] 06 p0617 N85-13946

Proceedings of the 14th Conference on Environmental Toxicology
[AD-A148400] 06 p0843 N85-15350

Organophosphorus-induced delayed neurotoxicity: Syndrome and experimental models
[AD-P004022] 06 p0844 N85-15356

Chemistry and metabolism of delayed neurotoxic organophosphorus esters
[AD-P004023] 06 p0844 N85-15357

Pathology of organophosphorus-induced delayed neurotoxicity
[AD-P004024] 06 p0844 N85-15358

Electrophysiologic changes in organophosphorus-induced delayed neurotoxicity
[AD-P004025] 06 p0844 N85-15359

Biochemistry and pathogenic hypotheses of organophosphorus-induced delayed neurotoxicity
[AD-P004026] 06 p0844 N85-15360

Critical overview of hexacarbons and organophosphates
[AD-P004027] 06 p0844 N85-15361

Isolation, concentration and subsequent analysis by capillary gas chromatography of trace amounts of organophosphorus compounds from aqueous samples
[AD-B088301L] 12 p1803 N85-21308

USSR report: Chemistry
[JPRS-UCH-85-001] 13 p2013 N85-22629

Measurement of Franck-Condon factors for the $v'=0$ progression in the B-X system of PO
[AD-A152734] 17 p2919 N85-27993

TRU decontamination of high-level PUREX waste by solvent extraction using a mixed octyl(phenyl)-N,N-diisobutyl-carbamoyl methylphosphine oxide/TBP/NPH (TRUEX) solvent
[DE85-010251] 19 p3235 N85-30054

ORGANIC SEMICONDUCTORS

Study of application of organic semiconductors to electronic components
[BMFT-FB-T-84-142] 02 p0289 N85-11890

Optimizing conductive polymer compounds
[BMFT-FB-T-84-145] 03 p0336 N85-12177

Research on submicrometer structures
[AD-A146578] 06 p0867 N85-15508

Studies on organic semiconductors. 15: Effects of the substituents on the photoconductivities of substituted anthracenes
[NASA-TM-77788] 08 p1225 N85-17712

Transport studies of several novel organic conductors
[DE85-003950] 14 p2429 N85-24979

Structure and functions of ultra-thin films of organic compounds
[DRIC-T-7481] 22 p3741 N85-33188

ORGANIC SILICON COMPOUNDS

Structural and synthetic organosilicon chemistry
[AD-A147101] 07 p0919 N85-15820

Preparation of silicon carbide-silicon nitride fibers by the pyrolysis of polycarbosilazane precursors
[NASA-TM-86505] 17 p2933 N85-28107

ORGANIC SULFUR COMPOUNDS

Heats of formation of gas phase organosulfur molecules, radicals and ions measured by PEPICO and application of (17)O and (33)S NMR spectroscopy to structure determination of organosulfur compounds
[DE85-010558] 24 p4071 N85-35229

ORGANISMS

Recent studies of the ocean nitrogen cycle
05 p0653 N85-14193

Aluminum in biogenic cycle and forms of its occurence in ocean 10 p1499 N85-19463

ORGANIZATIONS
NT EUROPEAN SPACE AGENCY
NT ISRO
NT NORTH ATLANTIC TREATY ORGANIZATION (NATO)
NT WORLD METEOROLOGICAL ORGANIZATION

National Science Foundation, fiscal year 1983, volume 1
[PB84-212315] 01 p0124 N85-10853

EPA (Environmental Protection Agency) environmental data base and model directory, volume 1
[PB84-207562] 01 p0126 N85-10868

A mathematical theory of command and control structures
[AD-A145608] 02 p0256 N85-11675

Matrix organizations: Overcoming the disadvantages
[AD-A145318] 03 p0436 N85-12772

International coordination in scientific research
04 p0519 N85-13311

Sunset of the Civil Aeronautics Board
[S-HRG-98-940] 09 p1403 N85-18829

Strategic management for organizational effectiveness. The effect of human resource planning on retention and related issues, volume 1
[AD-A149398] 10 p1566 N85-19874

Strategic management for organizational effectiveness. The effect of human resource planning on retention and related issues, volume 2
[AD-A149399] 10 p1566 N85-19875

Strategic management for organizational effectiveness. The effect of human resource planning on retention and related issues, volume 3
[AD-A149400] 10 p1566 N85-19876

Strategic management for organizational effectiveness. The effect of human resource planning on retention and related issues: Methodological appendix
[AD-A149401] 10 p1566 N85-19877

A proposed integration among organizational information requirements, media richness and structural design
[AD-A149317] 10 p1567 N85-19881

Calender of selected aeronautical and space meetings
[AGARD-CAL-84/2] 10 p1573 N85-19917

MAP-related activities in the United States
11 p1655 N85-20427

Model research: The National Advisory Committee for Aeronautics, 1915-1958, volume 1
[NASA-SP-4103-VOL-1] 14 p2207 N85-23683

Model research, the National Advisory Committee for Aeronautics, 1915-1958, volume 2
[NASA-SP-4103-VOL-2] 14 p2207 N85-

Measurement capabilities of the Bendix Metrology Organization
[DE85-005795] 16 p2760 N85-27

SELPER (Latin American Society of Remote Sensing Specialists)
[INPE-3315-PRE/622] 16 p2810 N85-27

National Telecommunications and Information Administration authorization
[GPO-38-660] 16 p2679 N85-27

An examination of alternative forms of fit in contingency theory
[AD-A152602] 17 p3047 N85-2

The concept of fit in contingency theory
[AD-A152603] 17 p3047 N85-2

Worldwide directory of national Earth-science agencies and related international organizations
[GS-CIRC-934] 21 p3605 N85-32

The flow of scientific and technical information in the US Army Research Laboratories
[AD-A155050] 21 p3713 N85-3

ORGANIZING

Quality organization — quality control
[CNES-NT-106] 04 p0511 N85-13

A self-organizing database system: A different approach to query optimization 05 p0735 N85-147

Model of team organization and behavior and team description method
[AD-A147540] 07 p1053 N85-1

Automation of information services furnished by documentation centers and specialized libraries
[FUB-6-1984] 09 p1402 N85-18

Navy information systems: Planning, policy, organization, and management
[PB85-176113] 20 p3541 N85-3

ORGANOMETALLIC COMPOUNDS
NT CHLOROPHYLLS
NT HEMOGLOBIN
NT ORGANIC LITHIUM COMPOUNDS
NT OXYHEMOGLOBIN

USSR report: Chemistry
[JPRS-UCH-84-012] 06 p0761 N85-14

Metallo-Organic Decomposition (MOD) silver metallization for photovoltaics 06 p0830 N85-152

Mod silver metallization for photovoltaics
[NASA-CR-174444] 10 p1509 N85-1951

Preparation and study of highly reactive metal powders
[AD-A150026] 12 p1806 N85-2133

Synthesis, static and reactive characterization of supported organometallics
[DE85-004285] 12 p1808 N85-2134

Synthesis of phenols from metal-carbynes and dynes
[AD-A151913] 16 p2754 N85-26

The spectroscopy and reaction kinetics of coordinatively unsaturated metal carbonyls
[AD-A153079] 17 p2920 N85-2800

Metallophthalocyanine dimers incorporating five atom covalent bridges
[AD-A154365] 19 p3234 N85-3005

New approaches to functionalized fluorocarbons
[AD-A154205] 19 p3248 N85-3014

Multilayer capacitor dielectrics produced from metallo-organic precursors
[AD-A154592] 21 p3580 N85-3225

Marine environmental quality assessment program five-year plan (FY 1984 - 1988)
[AD-A154715] 21 p3613 N85-324

Doping superlattices in organometallic VPE InP
[AD-A155151] 21 p3710 N85-330

Research study for gel precursors as glass and ceramic starting materials for space processing application research
[NASA-CR-176113] 22 p3751 N85-33

Metal alkoxides: Models for metal oxides. Alkoxide ligands in early transition metal organometallic chemistry
[DE85-011368] 23 p3916 N85-34

ORGANOMETALLIC POLYMERS

(Vinyloxy)chlorocyclotriphosphazenes
[AD-D011471] 10 p1453 N85-191

ORGANS
NT BLADDER
NT KIDNEYS
NT LIVER
NT LUNGS
NT PITUITARY GLAND
NT SPLEEN

Gravity, body mass and composition, and metabolic rate 15 p2610 N85-2

ORIENTATION

Determining object orientation from a single image or multiple information sources
[AD-A149980] 12 p1933 N85-2

Parametric stability of analytical close-range photogrammetry 24 p4107 N85-35461

ORIFICE FLOW
Calibration and use of filter test facility orifice plates [DE84-016851] 04 p0500 N85-13190
Buckling and eccentricity effects on orifice metering accuracy — gas meters [ERS-E.360] 09 p1324 N85-18321
Experiments in dilution jet mixing effects of multiple rows and non-circular orifices [NASA-TM-86996] 15 p2473 N85-25266
An experimental study of the noise generated by vaporous cavitation in turbulent shear flows produced by confined orifice plates 15 p2645 N85-26316
Flow rate and pressure profiles for 1 to 4 axially alined orifice inlets [NASA-TP-2460] 16 p2782 N85-27165

ORIFICES
Flow rate and pressure profiles for 1 to 4 axially alined orifice inlets [NASA-TP-2460] 16 p2782 N85-27165

ORION AIRCRAFT
U P-3 AIRCRAFT

ORION CONSTELLATION
NT ORION NEBULA
The unidentified emission features: A study of the Orion Bar and planetary nebulae 08 p1246 N85-17862
The 1.5 - 3.5 micron spectroscopy of the Orion H2 source 08 p1246 N85-17864

ORION NEBULA
Detection of submillimeter polarization in the Orion Nebula [NASA-TM-86013] 04 p0579 N85-13700
Proper motions and kinematical properties of Orion trapezium type stellar systems 05 p0739 N85-14755
Water maser outburst 07 p1058 N85-16720
The Orion molecular cloud at far-infrared wavelengths 08 p1245 N85-17860
First results of submillimeter polarimetry 08 p1246 N85-17861
Photoionization structure of the Orion Nebula 08 p1246 N85-17863
Molecular spectroscopy from the Kuiper Airborne Observatory [NASA-CR-175748] 16 p2882 N85-27783
The structure of Herbig-Haro object 43 and Orion dark cloud extinction [NASA-TM-87503] 24 p4166 N85-35831
Far-infrared emission lines of CO and OH in the Orion-KL molecular shock [NASA-TM-86721] 24 p4167 N85-35832
Observations of far-infrared transitions between excited states of OH [NASA-TM-86722] 24 p4167 N85-35833

ORIONID METEOROIDS
Refractory inclusions in the Ornans C30 chondrite 15 p2680 N85-26553

ORNITHOPTER AIRCRAFT
U RESEARCH AIRCRAFT

OROGRAPHIC CLOUDS
U CAP CLOUDS

OROGRAPHY
Numerical forecast of pressure field by considering the mutual influence of orography, thermal nonhomogeneity and surface friction 01 p0080 N85-10534
Sedimentary and tectonic evolution of the western Taiwan foredeep 03 p0380 N85-12491
Effect of mountain wave dynamics on orographic storms [DE84-014713] 04 p0540 N85-13433
Orographic effects in atmospheric circulation 05 p0679 N85-14362
Fully implicit numerical methods for the baroclinic primitive equations 05 p0679 N85-14365
Ground-based snow and ice crystal observation system used in Sierra Nevada winter orographic storms [PB85-115343] 10 p1520 N85-19564
Orographic disturbances of upper atmosphere emissions 11 p1663 N85-20480
Comparison of observations of orographic disturbances in the troposphere and upper atmosphere 14 p2341 N85-24479
Theory and modeling of the interaction between subgrid scale orography and large scale flow [DM-43] 16 p2827 N85-27440
Statistical comparison of radar echoes of convective precipitation between the northern Alps and its foreland [DFVLR-FB-85-07] 17 p2950 N85-28215
On Long's solution to hydrostatic flow over mountains [DFVLR-MITT-84-02] 17 p2994 N85-28503
Comparison of two orographical data sets for the GLAS Fourth Order GCM 18 p3142 N85-29452
Some recent developments in numerical modelling at ECMWF 18 p3147 N85-29481
Project Skywater, 1983-84 SCPP (Sierra Cooperative Pilot Project) data inventory [PB85-167052] 24 p4124 N85-35565

ORRERIES
U ASTRONOMICAL MODELS

ORTHOGONAL FUNCTIONS
NT WALSH FUNCTION
Application of large eddy interaction model to channel flow [NASA-TM-86691] 12 p1844 N85-21572
Noise tolerance of digital demodulator for complex signal system employing binary quantization 13 p2070 N85-22929
Representation of temperature and salinity fields using statisticallyt orthogonal functions (in example of polymode data) 14 p2337 N85-24449
Natural vibrations of reinforced spherical shells 17 p2943 N85-28165
Symbolic Givens reduction in large sparse least squares problems [DE85-006685] 17 p3021 N85-28681

ORTHOGONAL MULTIPLEXING THEORY
A modem with pseudo-orthoganal codes: Experimental results 10 p1474 N85-19302

ORTHOGONALITY
Orthogonal polynomials and rigged Hilbert space [TUM-M8313] 03 p0414 N85-12647
Multiple channel adaptive filtering using a fast orthogonalization network: An application to efficient pulsed Doppler radar processing [AD-A147929] 08 p1211 N85-17619
Numerical generation of orthogonal and nonorthogonal coordinates in two dimensional simply and doubly connected regions [VKI-TN-151] 08 p1216 N85-17662
Initial fracture stages of orthogonally reinforced composite material 11 p1599 N85-20055
Orthogonalizer for inphase and quadrature digital data [AD-D011679] 19 p3254 N85-30174
Generation of three-dimensional body-fitted coordinates using hyperbolic partial differential equations [NASA-TM-86753] 20 p3519 N85-31887

ORTHONORMAL FUNCTIONS
Some families of near-orthonormal analytic and harmonic functions [AD-A144722] 01 p0110 N85-10748
Effects of changing the signs of rows and columns of a matrix and the hyperbolic transpose [DE84-014651] 04 p0555 N85-13530
Canonical analysis of the fermion sector in higher-derivative supergravity [DE85-007628] 16 p2859 N85-27635

ORTHOPHOTOGRAPHY
What does digital image processing perform in the production of orthophotomaps 16 p2815 N85-27368
The significance of orthophoto maps for developing countries 18 p3124 N85-29341

ORTHOSTATIC TOLERANCE
Circulatory orthostatic instability: Role of deconditioning of resistive vessels 01 p0091 N85-10612
Aviation-related cardiorespiratory effects of blood donation in female pilots [AD-A148045] 08 p1195 N85-17529
Investigation of adaptive distinctions of mechanism of controlled glycemia in Macaca rheseus monkeys 12 p1902 N85-21946
Computer simulation studies in fluid and calcium regulation and orthostatic intolerance [NASA-CR-171869] 15 p2616 N85-26117
Analysis of head-down tilt as an analog of weightlessness using a mathematical simulation model [NASA-CR-171870] 15 p2616 N85-26118
Predictions of cardiovascular responses during STS reentry using mathematical models [NASA-CR-171871] 15 p2616 N85-26119
Effect of 120-day antiorthostatic bedrest on gas exchange and pulmonary circulation in man 19 p3323 N85-30589
Primate adrenal reactions to antiorthostatic hypokinesia 19 p3324 N85-30591
Long term exposure of animals to antiorthostatis (-90 deg) as a model of critical homeostatic disturbances 19 p3324 N85-30592
Changes in nephron and juxtaglomerular system of primate kidneys under the effect of antiorthostatic hypokinesia 19 p3326 N85-30605
Typological characteristics of hemodynamic states of healthy subjects in orthostatic position 22 p3821 N85-33673
Cardiovascular responses to orthostatism and weightlessness 24 p4130 N85-35601

ORTHOTROPIC CYLINDERS
Mechanical and transient hygrothermal loading of multilayer orthotropic cylinders 09 p1330 N85-18359
Stability of anisotropic cylindrical sandwich shells 16 p2766 N85-27065

ORTHOTROPIC PLATES
Stress analysis of pin-loaded orthotropic plates using orthotropic photoelasticity 02 p0207 N85-11366
A buckling analysis for rectangular orthotropic plates with centrally located cutouts [NASA-TM-86263] 04 p0513 N85-13288
Stresses in pin-loaded orthotropic plates using photoelasticity [NASA-CR-172498] 07 p0977 N85-16204
Fracture analysis of notched composites [NASA-CR-172563] 11 p1593 N85-20020
The effects of pin elasticity, clearance, and friction on the stresses in a pin-loaded orthotropic plate [NASA-CR-175816] 16 p2743 N85-26927
An approximation to the problem of a pin-loaded hole in an orthothropic plate [VTH-LR-386] 16 p2802 N85-27278
Biaxial buckling of specially orthotropic, symmetric composite rectangular plates [AD-A152958] 17 p2979 N85-28417
A cracked orthotropic sheet stiffened by a semi-infinite orthotropic sheet [NASA-TP-2455] 21 p3597 N85-32339
The stress distribution in pin-loaded orthotropic plates [NASA-CR-176146] 22 p3800 N85-33547
Nonlinear adhesive behavior effects in a cracked orthotropic sheet stiffened by a semi-infinite orthotropic sheet [NASA-TM-87584] 23 p3941 N85-34426

ORTHOTROPIC SHELLS
An analysis for axially compressed orthotropic shells with a multimode imperfection representation [VTH-LR-422] 16 p2803 N85-27281
Stress analysis of axisymmetric sandwich shells of variable thickness 24 p4101 N85-35419

ORTHOTROPISM
Stress analysis of pin-loaded orthotropic plates using orthotropic photoelasticity 02 p0207 N85-11366
Shear-stress distribution and shear stiffness in the case represented by a non-homogeneous cross-section, of any shape, but composed of an orthotropic material, when subjected to a shear force [DRIC-T-7430] 20 p3469 N85-31554

OSCILLATING CYLINDERS
Some important problems in unsteady boundary layers including separation. 1: Nature of singularity on oscillating airfoils [AD-A147897] 07 p0960 N85-16087

OSCILLATING FLOW
Development and applications of algorithms for calculating the transonic flow about harmonically oscillating wings [NASA-CR-172376] 01 p0002 N85-10007
Planar jets impinging on various obstacles and some modes of flow oscillation [MPIS-MITT-78] 01 p0048 N85-10317
Numerical studies of unsteady transonic flow over an oscillating airfoil [NASA-TM-86011] 03 p0361 N85-12316
An organ-pipe oscillation — PHOENICS code [PDR/CFDU-IC/14] 04 p0501 N85-13199
Float zone experiments in space [NASA-CR-171284] 07 p0911 N85-15766
Calculation of oscillating turbulent flows in open channels [KU-SFB-80/T/228] 11 p1633 N85-20289
Large amplitude forcing of a high speed 2-dimensional jet [NASA-CR-175646] 13 p1974 N85-22393
The role of convective perturbations in supercritical inlet oscillations 13 p2004 N85-22563
Stability of an oscillating boundary layer [NASA-TM-77827] 14 p2299 N85-24238
Numerical studies of unsteady transonic flow over oscillating airfoil 15 p2458 N85-25174
A supersonic potential gradient method for the calculation of unsteady aerodynamic pressures on harmonically oscillating wings [DFVLR-FB-85-11] 20 p3390 N85-31026
Development of artificially produced perturbations in supersonic boundary layer 21 p3683 N85-32879

OSCILLATION DAMPERS
Control of the dynamic response of a damped membrane by distributed forces [CSIR-TWISK-312] 01 p0061 N85-10406
Investigation of current setting procedures for sector magnets [CSIR-NAC-83-03] 01 p0117 N85-10795
Controlled movement of elastic manipulator with distributed parameters 13 p2048 N85-22813
A study of transonic flutter of a two-dimensional airfoil using the U-g and p-k methods [AD-A151463] 15 p2473 N85-25268
Variable force, eddy-current or magnetic damper [NASA-CASE-LEW-13717-1] 19 p3279 N85-30333

OSCILLATIONS
NT ELECTRON OSCILLATIONS
NT HARMONIC OSCILLATION
NT MOLECULAR OSCILLATIONS
NT NONOSCILLATORY ACTION
NT NONSTABILIZED OSCILLATION
NT PLASMA OSCILLATIONS
NT PRESSURE OSCILLATIONS
NT SELF OSCILLATION
NT SOLAR OSCILLATIONS
NT STABLE OSCILLATIONS
NT STELLAR OSCILLATIONS
NT TRANSIENT OSCILLATIONS
NT TRANSVERSE OSCILLATION
NT WING OSCILLATIONS
Oscillatory integrals by Hermite interpolatory rules
[CSIR-TWISK-301] 01 p0108 N85-10725
Upwind compact finite difference schemes
[CSIR-TWISK-334] 01 p0110 N85-10742
Periodic oscillation of gyrostat-satellite about its center of mass in an elliptical orbit 02 p0159 N85-11080
Laminar-to-turbulent flow transition under influence of acoustic oscillations 02 p0260 N85-11701
Forced oscillations theory for resonant extended interaction electron devices
[PR-206] 03 p0358 N85-12298
Wear and corrosion of components under stress and subjected to motion
[AD-A145781] 03 p0372 N85-12372
Experimental investigation and analysis of oscillations of thin-walled spherical shell during pulse loading
05 p0725 N85-14662
Limits of applicability of long wave theory in studies of oscillations of n-layer fluid 06 p0824 N85-15234
Studies of the wall shear stress in a turbulent pulsating pipe flow
[AD-A146772] 07 p0957 N85-16068
Experimental investigation of the oscillation behaviour of a liquid-filled rotor with centrifugal motion
[BLL-DOUNREAY-TR-936-(9091.9F)]
08 p1160 N85-17317
Electronic properties of intercalated graphite and amorphous metals
[AD-A147664] 08 p1225 N85-17716
A Navier-Stokes calculation of the airfoil dynamic stall process
[AD-P004163] 09 p1265 N85-17948
Leading edge separation criterion for an oscillating airfoil
[AD-P004175] 09 p1267 N85-17960
Combustion driven oscillation of ducted diffusion flame
09 p1289 N85-18094
Thermal striping downstream of a horizontal elbow under thermally stratified transient flow conditions
[DE84-014687] 09 p1320 N85-18302
One-electron capture processes by highly charged ions from helium: Present status of HICE-IPP
09 p1369 N85-18736
Vacuum ultraviolet electronic properties of liquids
[DE85-000305] 10 p1563 N85-19858
PMP-2: Equatorial wave dynamics
11 p1655 N85-20422
Resonance between betatron and synchrotron oscillations in a free electron laser: A 3-D numerical study
[AD-A150059] 12 p1857 N85-21645
Space shuttle pilot-induced-oscillation research testing
13 p1966 N85-22351
Satellite oscillations in elliptical orbit
13 p1981 N85-22429
Measurements of distributed combustion
13 p2001 N85-22542
Distributed combustion: A mechanism of acoustic suppression 13 p2001 N85-22543
Interaction of cylindrical shell with concentrated mass moving along its inner surface 13 p2047 N85-22810
Stereo decoder without subcarrier restoration
13 p2068 N85-22921
Machine analysis of resonance characteristics of plate-type radio electronic equipment constructions
13 p2085 N85-23018
Regions of propagation of short-wave perturbations in spherical layer of rotating fluid 13 p2107 N85-23130
Observation of long-period oscillations of Earth
13 p2110 N85-23149
Nature of seismic images with amplitude and time fluctuations of recorded oscillations
13 p2112 N85-23156
Oscillations of gas turbine installation rotors under operating conditions 14 p2272 N85-24077
Study of dynamic characteristics of prefabricated gas turbine compressor rotor 14 p2272 N85-24078
Considering zonal wind in semidiurnal tide problem
14 p2335 N85-24440
Low-frequency oscillations of sea level and group structure of wind waves 14 p2335 N85-24441
Determining geometrical divergence using seismic observation data 14 p2343 N85-24489
Chaotic dynamics of instabilities in solids
[DE85-004909] 14 p2429 N85-24978
Frequency/period estimation and adaptive rejection of periodic disturbances
[AD-A149229] 15 p2632 N85-26226
Application of the hydraulic system frequency response program to propellant feed systems
[AD-A151824] 16 p2741 N85-26914
Analysis of combustion oscillations in heterogeneous systems
[AD-A151999] 16 p2745 N85-26942
Internal resonance in nonlinear vibrating systems
[REPT-15/1984] 16 p2797 N85-27245
Wing tunnel investigation of dynamic stall of an NACA 0016 airfoil oscillating in pitch
[NAE-AN-27] 17 p2892 N85-27830
Buildup of oscillation of bodies in stratified fluid
17 p2941 N85-28157
Acoustic oscillations of rods and plates
17 p2944 N85-28170
Effects of level broadening on the magnetothermal oscillations in two-dimensional electron systems
[AD-A152639] 17 p3029 N85-28732
Turbulence structure in the boundary layers of an oscillating airfoil
[AD-A153631] 18 p3059 N85-28926
Calculations of beam dynamics in Sandia linear electron accelerators, 1984
[DE85-010417] 18 p3180 N85-29719
Gyrotron traveling-wave device including quarter wavelength anti-reflective dielectric layer to enhance microwave absorption
[AD-D011690] 19 p3271 N85-30265
Ballooning instabilities on a magnetic separatrix
[DE85-010855] 19 p3372 N85-30915
Data set 8: ZKP wing, oscillating aileron
20 p3390 N85-31029
Frequency domain control design of large space structures: A practical approach
20 p3415 N85-31192
An examination of the Southern Oscillation in the upper troposheric tropical and subtopical wind field
20 p3488 N85-31680
Thresholds for detection of linear oscillation following prolonged weightlessness 20 p3508 N85-31810
Search for neutrino oscillations at the Brookhaven AGS
[DE85-009766] 20 p3530 N85-31957
A simple model for testing the effects of gravity-wave-produced vertical oscillations of scattering irregularities on spaced-antenna, horizontal drift measurements 21 p3619 N85-32489
Saturation of a longitudinal instability due to nonlinearity of the wake field
[DE85-012514] 22 p3837 N85-33761
Robinson instability and beam loading
[DE85-013301] 24 p4151 N85-35737
Relation between field energy and RMS emittance in intense particle beams
[DE85-012655] 24 p4159 N85-35784
Geophysical searches for three-neutrino oscillations
[HE-5.3-9] 24 p4205 N85-36103
Measurement of neutrino oscillations in MACRO experiment
[HE-5.3-10] 24 p4206 N85-36104

OSCILLATOR STRENGTHS
What formulas are good for representing dipole and generalized oscillator-strength spectra
[DE84-014641] 02 p0278 N85-11809
Notes for lectures in China: The Bethe theory of inelastic collisions of fast charged particles with atoms and molecules
[DE84-017487] 09 p1380 N85-18676
Applications and investigations of second harmonic generation 19 p3367 N85-30876

OSCILLATORS
NT CATHODE RAY TUBES
NT CRYSTAL OSCILLATORS
NT GAS DISCHARGE TUBES
NT HARMONIC OSCILLATORS
NT HELITRONS
NT MAGNETRONS
NT MECHANICAL OSCILLATORS
NT MICROWAVE OSCILLATORS
NT MICROWAVE TUBES
NT MOLECULAR OSCILLATORS
NT PENDULUMS
NT PICTURE TUBES
NT VOLTAGE CONTROLLED OSCILLATORS
Isolated load switching with surge suppression
[AD-D011218] 01 p0042 N85-10274
Power flow between non-conservatively coupled oscillators
[ISVR-TR-125] 02 p0209 N85-11377
Behavior orbits of two coupled oscillators
02 p0282 N85-11830
Oscillator strengths for OII ions
[NASA-CR-174153] 04 p0559 N85-13556
Transmission line biased coherent array of Josephson oscillators
[AD-D011323] 07 p0944 N85-15979
Low noise multiple crystal-controlled oscillator
[AD-D011401] 07 p0948 N85-16010
New construction principles for oscillator power summing devices 07 p0949 N85-16016
Silent discharge carbon dioxide gas laser machining facility
[BLL-CTO-2267-(9091.9F)] 07 p0969 N85-16150
Passive maser using timesharing for control of the cavity and control of the oscillator on the line of stimulated emission
[AD-D011326] 07 p0969 N85-16151
Phased locked array laser systems
[AD-D011317] 07 p0971 N85-16184
NBS frequency measurement system from a user's viewpoint
[DE84-016782] 09 p1315 N85-18268
A coaxial cavity gunn oscillator using probe coupled microstrip
[AD-D011437] 10 p1479 N85-19334
Integrated circuit tunable cavity oscillator
[AD-D011474] 10 p1481 N85-19351
Oscillator development
[AD-A149699] 12 p1834 N85-21509
Design considerations for a 100 kW CW, 140 GHz gyrotron oscillator
[DE85-005282] 13 p2066 N85-22904
Square-pulse generator 13 p2075 N85-22959
Experimental study of high-stability oscillator with surface-acoustic-wave resonator in feedback loop
13 p2090 N85-23053
Injection controlled laser transmitter with twin local oscillators
[AD-D011577] 15 p2563 N85-25810
The measurement of linear frequency drift in oscillators 17 p2966 N85-28316
The superconducting cavity stability ruby maser oscillator 17 p2967 N85-28324
VULTURE manual
[DE85-006873] 17 p3013 N85-28631
How a swing behaves
[DE85-008280] 17 p3027 N85-28720
Submillimeter local oscillators for spaceborne heterodyne applications
[NASA-RP-1147] 19 p3226 N85-30005
Temperature sensitive oscillator
[NASA-CASE-GSC-12956-1] 19 p3258 N85-30201
Dielectric resonator stabilized microstrip oscillator
[AD-D011708] 19 p3261 N85-30219
Development and application of a high power ND-glass laser instrument
[AD-A154366] 19 p3276 N85-30314
High-brightness photoemitter development for electron accelerator injectors
[DE85-009546] 19 p3355 N85-30796
A multiplying slot array
[AD-A155570] 21 p3576 N85-32245
Generation of single nanosecond high-contrast radiation pules (lambda = 10.6 micrometers)
21 p3684 N85-32888
Fiber optics interface for a dye laser oscillator and method
[DE85-005765] 23 p3973 N85-34833
Los Alamos free-electron laser
[DE85-012666] 24 p4098 N85-35405

OSCILLOGRAMS
U OSCILLOGRAPHS

OSCILLOGRAPHS
Automatic correction of static characteristics of measurement channel of digital oscillograph
06 p0795 N85-15063

OSCILLOSCOPES
An optically coupled sampling system with 4 GHz bandwith
[AD-A148057] 09 p1384 N85-18702
China report: Science and technology
[JPRS-CST-85-007] 15 p2533 N85-25621
Microprocessor controlled storage sampling oscilloscope 15 p2533 N85-25622
The structure of the shower disk observed at Mt. Norikura
[HE-4.7-1] 24 p4198 N85-36052
Sub-luminal pulses from cosmic ray air showers
[HE-4.7-13] 24 p4200 N85-36063

OSMIUM
NT OSMIUM ISOTOPES
Low temperature properties of CeOs2 in the C14 and C15 crystallographic Laves phases
[DE85-003754] 10 p1564 N85-19866

Current status of the Os-191 yields Ir-191m generator
[DE85-008306] 23 p3971 N85-34614
OSMIUM ISOTOPES
Identification of vibrational-rotational transitions of Os-192O4 within frequency tuning limits of high pressure CO2 waveguide laser 21 p3689 N85-32917
OSMOSIS
NT REVERSE OSMOSIS
Evaluation of hollow fiber ultrafiltration as a pretreatment for reverse osmosis desalination of seawater
[PB84-212406] 01 p0026 N85-10160
GAMPHI: A database of activity and osmotic coefficients for aqueous electrolyte solutions
[PB85-183390] 18 p3072 N85-29002
Kidney cell electrophoresis
[NASA-CR-171889] 20 p3496 N85-31745
A gel-halo sample pellet: The best of both worlds? Stubby zones without a constricted sample gate
20 p3502 N85-31770
Results of computer calculations for a simulated distribution of kidney cells 20 p3502 N85-31771
Evaluation of results of cell electrophoresis experiments on space shuttle STS-3 including pre-flight and post-flight laboratory experiments 20 p3502 N85-31772
Condensation properties of atmospheric aerosol
21 p3649 N85-32672
The role of sulfur in osmoregulation and salinity tolerance in cyanobacteria, algae, and plants
21 p3660 N85-32736
OSMOTIC PRESSURE
U OSMOSIS
OSS-1 PAYLOAD
Vibroacoustic study of the NASA Goddard Space Flight Center OSS-1 payload
[NASA-CR-175320] 13 p1988 N85-22465
Vehicle charging on STS-3 Mission
13 p1989 N85-22473
OSTEOPOROSIS
Actual and simulated weightlessness inhibit osteogenesis in long bone metaphysis by different mechanisms 15 p2608 N85-26074
Mechanisms of osteodystrophy in weightlessness
22 p3733 N85-33143
OTF
U OPTICAL TRANSFER FUNCTION
OTOLITH ORGANS
The adaptation of vestibulo-spinal reflexes as a function of spaceflight and their relationship to space motion sickness 05 p0694 N85-14468
Problems of space biology. Volume 50: Nystagmometry for evaluation of the status of the vestibular function
[NASA-TM-77616] 14 p2385 N85-24694
Reinterpretation of otolith input as a primary factor in space motion sickness 20 p3509 N85-31812
Effect of experimental motion sickness on postrotory nystagmus and counterrotation illusion
22 p3824 N85-33690
OTS (ESA)
Interference experiment with the Sirio-OTS satellites
[FUB-17-1983] 01 p0040 N85-10254
OTTO CYCLE
Analysis and simulation of the I C engine Otto cycle using the second law of thermodynamics
02 p0291 N85-11891
OTV
U ORBIT TRANSFER VEHICLES
OUTCROPS
Concordant bands of augen gneiss within metasedimentary rocks in the Big Delta C-2 quadrangle, east-central Alaska 04 p0516 N85-13294
Paleozoic limestones of the Crazy Mountains and vicinity, Circle quadrangle, east-central Alaska
04 p0517 N85-13296
Petrology and petrogenesis of Batholitic rocks, San Jacinto Mountains, southern California
05 p0673 N85-14322
OUTER RADIATION BELT
Electron flux with electron energies above 40 MeV at altitudes of about 500 km in region where capture is possible and outside it when L is 3 or greater
15 p2481 N85-25315
Bursts of relativistic electrons in magnetopause and in outer radiation belt 16 p2722 N85-26801
OUTER SPACE TREATY
The structures and the role of an international agency for the control of satellites
[NASA-TM-76765] 03 p0441 N85-12806
U.S., Soviet space program aims contrasted
13 p1985 N85-22455
OUTGASSING
Where is the Earth's missing xenon?
06 p0888 N85-15641
Ambient air contamination: Characterization and detection techniques 18 p3157 N85-29546
OUTLET FLOW
Continuous laminar smoke generator
[NASA-CASE-LAR-13014-1] 12 p1781 N85-21178
effect of gas stream sweeping past the effluent of a perforated plate on heat transfer inside the perforations
13 p2051 N85-22636
Development of an artificial boundary layer for different outlet flows 14 p2212 N85-23719
OUTLETS
NT VENTS
Heat exchanger
[DE84-014299] 01 p0047 N85-10309
Investigation of influence of gas exit modes on characteristics of N2O - N2 - He discharge laser
21 p3684 N85-32888
OUTLETS (GEOLOGY)
U ESTUARIES
OUTLIERS (STATISTICS)
The information in the minor principal components
[CSIR-TWISK-320] 01 p0109 N85-10735
Influential observations in time series
[AD-A144719] 01 p0112 N85-10763
Some new estimation methods for weighted regression when there are possible outliers
[AD-A152104] 16 p2854 N85-27602
A multiple regression technique for detecting outliers
[REPT-84-33] 17 p3025 N85-28706
OUTPUT
NT LASER OUTPUTS
NT MASER OUTPUTS
A limbus-sensing eye movement recorder
[AD-A144772] 01 p0049 N85-10323
Determination of the input-output characteristics of time-invariant memoryless nonlinear devices
[FUB-41-1983] 01 p0100 N85-10867
Cardiac output measured by mass spectroscopy
05 p0692 N85-14449
Cardiac output measurement with soluble gases
05 p0692 N85-14450
Experiments in forecasting atmospheric marine horizontal visibility using model output statistics with conditional probabilities of discretized parameters
[AD-A147574] 07 p1008 N85-16404
MTI system simulation and clutter output statistics
[AD-A149193] 10 p1467 N85-19255
Adaptive regulation of transmitter radiation power in radio lines during delays of control signals
12 p1841 N85-21551
Confidence intervals using the regenerative method for simulation output analysis
[AD-A150147] 13 p2149 N85-23343
Design and testing of gyroklystron amplifiers
[AD-A151026] 14 p2298 N85-24231
Multivariable statistical modelling and its application
16 p2857 N85-27617
Semicrystalline casting process development and verification
[DE85-007695] 18 p3081 N85-29058
Probabilistic analysis of combinational circuits with random delays 19 p3257 N85-30192
Microwave SAW (Surface Acoustic Wave) monochromator
[AD-D011718] 21 p3590 N85-32311
Optical output stabilization method for direct current arc lamps
[AD-A154987] 21 p3705 N85-33013
Raster functionality for a VDI
[DE85-006734] 24 p4097 N85-35396
Optimize computer throughput using array processors
[AD-A155843] 24 p4135 N85-35628
Software maintenance relating to the input translator and z-80 realization volume of the computer systems design environment
[AD-A155849] 24 p4138 N85-35646
Beryllium production
[DE85-013360] 24 p4148 N85-35716
OV-1 AIRCRAFT
Preliminary airworthiness evaluation of a National Aeronautics and Space Administration automated stall warning system for an OV-1 aircraft
[AD-A152010] 16 p2707 N85-26708
OVER-THE-HORIZON RADAR
Skywave radar detectability of volcanic aersols
[AD-A151448] 15 p2542 N85-25694
OVERCAST
U CLOUD COVER
OVERPRESSURE
Experimental investigation of the electric breakdown in SF6
[BLL-CE-TRANS-7987-(9022.09)]
15 p2546 N85-25714
NASTRAN analysis comparison to shock tube tests used to simulate nuclear overpressures
15 p2576 N85-25888
TNT equivalency of EAK explosive
[AD-A155737] 21 p3571 N85-32211
BLAF: A blast field reconstruction program from pressure histories
[AD-A155300] 21 p3585 N85-32263
OVERTONES
U HARMONICS
OVERVOLTAGE
Advanced metal oxide varistor concepts
[DE84-016677] 09 p1316 N85-18276
Power quality and protection of electric distribution systems with small, dispersed generation devices
[DE85-000990] 09 p1344 N85-18453
Stability of highly nonlinear oxide-zinc resistors under continuous voltage of industrial frequency
13 p2067 N85-23030
Requirements placed on information processing equipment
[BLL-CE-TRANS-7983-(9022.09)]
13 p2144 N85-23307
OXAZOLE
Infrared spectroscopy study of the SP-250 epoxy resin system
[AD-A145660] 03 p0337 N85-12167
Chiral polymers
[AD-A150366] 13 p2037 N85-22760
OXIDASE
Galactose oxidase in stereospecific oxidation of primary alcohols
[AD-A154059] 19 p3234 N85-30048
OXIDATION
NT ELECTROCHEMICAL OXIDATION
NT PHOTOOXIDATION
NT RUSTING
The oxidation behaviour of a 20 percent Cr/25 percent Ni/Nb stabilized stainless steel in carbon dioxide at high temperatures and its improvement by cerium and yttrium
[AERE-R-11228] 01 p0029 N85-10182
Determining the optimum heating parameters for precision alloys — iron-nickel alloys
[BLL-M-35718-(5824.4)] 02 p0174 N85-11167
The transient oxidation of single crystal NiAl+Zr
[NASA-CR-174756] 02 p0182 N85-11221
Review: The influence of short circuit diffusion on the oxidation of nickel, chromium and nickel/chromium alloys
[AERE-R-11311] 02 p0185 N85-11237
Analysis techniques for tracer studies of oxidation
[NASA-CR-174796] 03 p0336 N85-12162
A simple electronic apparatus for determining the oxidation stability of lubricants and other organic compounds
[AD-A146080] 03 p0336 N85-12172
Effect of oxidizing medium and heat treatment on stoichiometry of ZnSe crystal surface
03 p0353 N85-12272
Organic aerosol formation: OH(hydroxyl radical) versus ozone oxidation pathways
[PB84-219680] 03 p0388 N85-12484
Structural studies of sputtered MOS(2) films by angle-resolved photoelectron spectroscopy
[AD-A146052] 03 p0433 N85-12759
A bibliography of publications on corrosion and oxidation from UK government laboratories at Teddington, 1924 - 1983
[NPL-DMA(A)-82] 04 p0472 N85-13004
Study of the reactive-element effect in oxidation of Fe-Cr alloys using transverse section analytical electron microscopy
[DE84-016237] 04 p0571 N85-13641
Butene oxidation by molybdenum crystalographic shear compounds
[DE84-013910] 05 p0614 N85-13923
Distribution of oxygen between metal and basic slags
[BLL-M-35932-(5828.4)] 05 p0616 N85-13935
Solid state, surface and catalytic properties of oxides
[DE85-002096] 06 p0867 N85-15512
Platinum group nuggets in deep sea sediments
06 p0883 N85-15611
Corrosion study on zirconium refractory coatings. 1: Oxidation of zirconium nitride coatings by oxygen
[BLL-RISLEY-TR-5044-(9091.9F)]
07 p0925 N85-15857
Optimization of the NiCrAl-Y/ZrO-Y2O3 thermal barrier system
[NASA-TM-86905] 07 p0927 N85-15878
The mineralogy of global magnetic anomalies
[E85-10061] 07 p0987 N85-16272
Biochemical evaluation of bodily influence of high and low temperatures 07 p1014 N85-16441
Low and moderate temperature oxidation of atomically clean nickel, chromium and Ni-Cr alloys
[DE84-017350] 09 p1295 N85-18131
An infrared study of the oxidation of carbon monoxide over supported rhodium catalysts
[AD-A149478] 10 p1436 N85-19050
Continuous organic electrochemical synthesis
[DE85-001400] 10 p1437 N85-19057

Kinetics of oxidation of titanium alloy upon heating to 1000 deg C 10 p1448 N85-19122
Fuels combustion research
[AD-A149106] 10 p1457 N85-19178
Electron oxidation of graphite by fluorospecies
[DE85-001196] 11 p1595 N85-20034
Structure-phase state and properties of high-durability VAL8 alloy 11 p1597 N85-20046
Weldability of alloy ABM1 to alloy 1201
11 p1603 N85-20080
Initial development of nickel and nickel-iron aluminides for structural uses
[DE84-016641] 11 p1606 N85-20108
Application of Raman, TEM and other ion based techniques to oxidation problems
[AERE-R-11447] 11 p1610 N85-20121
Effects of chromium and aluminum on mechanical and oxidation properties of iron-nickel-base superalloys based on CG-27
[NASA-TP-2443] 12 p1805 N85-21323
Stress corrosion cracking and oxidation characteristics of boride-strengthened microcrystalline iron and nickel based alloys
[AD-A149805] 12 p1806 N85-21326
Oxidation and hot corrosion of hot-pressed Si3N4 at 1000 deg C
[NASA-TM-86977] 12 p1811 N85-21358
The use of hydrazine as an alternate source of energy
[NASA-CR-175535] 12 p1817 N85-21397
Oxidation and gum formation in jet fuels
[AD-A149934] 12 p1818 N85-21401
Applicability of laboratory kinetics studies to the evaluation of aqueous phase atmospheric oxidation of sulfur-4
[DE85-000586] 12 p1883 N85-21819
Combustion kinetics of metal atoms and metallic radicals over wide temperature ranges 13 p1999 N85-22530
Combustion of zirconium carbide
13 p1999 N85-22532
Interaction of metals and metalloids with biomembranes
[DE85-004902] 13 p2141 N85-23293
Improvement by cerium and yttrium ion implantation of oxidation behaviour of stabilised stainless steel in carbon dioxide
[AERE-R-11523] 14 p2259 N85-23996
Study of oxidized surface coating on titanium after annealing 15 p2498 N85-25412
Shock tube study of the fuel structure effects on the chemical kinetic mechanisms responsible for soot formation, part 2
[NASA-CR-174880] 15 p2504 N85-25444
Optimization of the catalytic oxidation of CO for closed-cycle CO2 laser applications
[NASA-TM-86421] 15 p2504 N85-25445
Oxidation of nickel-aluminum and iron-aluminum alloys
[DE85-006930] 15 p2512 N85-25497
Effects of surface chemistry on hot corrosion life
[NASA-CR-174915] 16 p2708 N85-26711
Elementary reactions of importance in oxidation, combustion ignition and flame inhibitions
[AD-A153139] 17 p2921 N85-28004
Oxygen isotopic study of the oxidation of SO2 by H2O2 in the atmosphere
[DE85-004017] 17 p2988 N85-28468
Chemical transformation modules for Eulerian acid deposition models. Volume 1: The gas-phase chemistry
[PB85-173714] 18 p3072 N85-29001
Corrosion Research Center of the University of Minnesota
[DE85-009418] 18 p3075 N85-29022
Corrosion-erosion rates/mechanisms of 9Cr1Mo steel
[DE85-008506] 18 p3076 N85-29029
High-temperature oxidation of alloys in mixed oxidants
[DE85-009706] 18 p3077 N85-29035
Methods for simulating gas phase SO2 oxidation in atmospheric models
[PB85-173110] 18 p3135 N85-29418
Burner rig corrosion of SiC at 1000 deg C
[NASA-TM-87061] 19 p3227 N85-30011
Novel analytical approaches to coal beneficiation
[DE85-010437] 19 p3229 N85-30021
Galactose oxidase in stereospecific oxidation of primary alcohols
[AD-A154059] 19 p3234 N85-30048
Experimental program to determine maximum temperatures for dry storage of spent fuel
[DE85-010307] 19 p3236 N85-30060
Physical-mechanical characteristics and wear resistance of coatings applied by microarc oxidation
19 p3242 N85-30104
Changes of structure of EP648-VI alloy as a result of high-temperature gas corrosion
19 p3243 N85-30110
Effect of thermochemical processing on fatigue resistance of titanium alloys 19 p3244 N85-30112
Ion beam sputter-deposited thin film coatings for protection of spacecraft polymers in low Earth orbit
[NASA-TM-87051] 19 p3248 N85-30137
Fuel-rich catalytic combustion: A soot-free technique for in situ hydrogen-like enrichment
[NASA-TP-2498] 20 p3423 N85-31244
Current understanding of point defects and diffusion processes in silicon 20 p3481 N85-31632
Shock tube measurements of growth constants in the branched-chain ethane-carbon monoxide-oxygen system
[NASA-TM-87068] 21 p3562 N85-32156
Basic research in novel inorganic reagents and fluorocarbon chemistry
[AD-A155340] 21 p3564 N85-32165
Molecular orbital studies in oxidation: Sulfate formation and metal-metal oxide adhesion
[NASA-CR-176070] 21 p3565 N85-32174
A study of adherent oxide scales
[AD-A155554] 21 p3567 N85-32188
Aerobic sulfur-oxidizing bacteria: Environmental selection and diversification 21 p3656 N85-32712
Some thoughts on GAIA and the sulfur cycle
21 p3658 N85-32727
Possible roles of manganese redox chemistry in the sulfur cycle 21 p3659 N85-32731
Sulfate-reducing bacteria: Microbiology and physiology 21 p3659 N85-32732
Structure and physiology of Beggiatoa and Thiothrix
21 p3659 N85-32734
Interactions among sulfide-oxidizing bacteria
21 p3661 N85-32741
Nonequilibrium kinetics of growth of oxide layer grains during laser heating of metals in air
21 p3689 N85-32919
Raman scattering studies in solids
[AD-A155528] 21 p3710 N85-33032
Method for removing chlorine compounds from hydrocarbon mixtures
[DE85-011608] 22 p3742 N85-33191
Oxidation of formaldehyde solutions used for the preservation of reverse osmosis membranes
[PB85-185585] 22 p3742 N85-33194
Rechargeable lithium-organic electrolyte battery having overcharge protection and method of providing overcharge protection for a lithium-organic electrolyte battery
[AD-D011738] 22 p3806 N85-33575
Effects of immobilization and high-altitude adaptation on energy metabolism in rats 22 p3820 N85-33663
Process for improving the quality of epitaxial silicon films grown on insulating substrates
[AD-D011730] 22 p3847 N85-33828
Oxidation states of iron in the terrestrial planets: Evidence and implications for accretion models
22 p3852 N85-33854
Electrolytic synthesis of colored eta alumina film
23 p3906 N85-34201
An X-ray diffraction study of titanium oxidation
[NASA-CR-176263] 23 p3915 N85-34264
Aluminum work function: Effect of oxidation, mechanical scraping and ion bombardment
[NASA-TM-87079] 23 p3915 N85-34265
Gas shielding apparatus
[DE85-005992] 23 p3939 N85-34416
The preparation of TEM specimens showing oxide scales in transverse cross-section
[AERE-R-11579] 24 p4078 N85-35276
High temperature corrosion of ceramics
[DE85-013481] 24 p4083 N85-35303
Development and evaluation of sulfonated polysulfone membranes for the zinc-ferricyanide battery
[DE85-009104] 24 p4090 N85-35357

OXIDATION RESISTANCE
The effects of Cr, Co, Al, Mo and Ta on the cyclic oxidation behavior of a prototype cast Ni-base superalloy based on a 2(5) composite statistically designed experiment
[NASA-TM-83784] 03 p0331 N85-12131
Oxidation resistance of silicon ceramics
[NASA-TM-77429] 07 p0931 N85-15898
Effects of MAR-M247 substrate (modified) composition on coating oxidation coating/substrate interdiffusion — protective coatings for hot section components of gas turbine engines
[NASA-CR-174851] 10 p1440 N85-19073
Oxidation of PT-7M and OT4-1 titanium alloys in air
11 p1600 N85-20063
Investigation of the development possibilities of a ferritic creep and oxidation-resistant steel for application under creep conditions above 650 deg C
[BMFT-FB-T-84-244] 12 p1808 N85-21344
Oxidation resistant materials for hot gas turbines and jet engines
[AD-B087399L] 13 p1973 N85-22389
High-temperature oxidation of reaction-roasted silicon nitride with various additives 19 p3244 N85-30114
Thermal barrier coating system
[NASA-CASE-LEW-14057-1] 24 p4072 N85-[illegible]

OXIDATION-REDUCTION REACTIONS
The driving-force dependence of electrochemical rate parameters: Origins of anodic-cathodic asymmetries for metal aquo redox couples
[AD-A145805] 02 p0172 N85-11130
The oxidation of transition-metal ions by molecular oxygen
[BLL-M-29593-(5828.4)] 02 p0175 N85-11172
Electrochemistry of rare-earth diphthalocyanines
[AD-A145813] 03 p0327 N85-12106
NASA Redox Storage System Development Project
[NASA-TM-83677] 03 p0365 N85-12465
Chemically modified electrodes and related solution chemistry
[DE84-017110] 05 p0614 N85-13604
Catalytic oxidation by transition metal ions in zeolites
[AD-A146826] 07 p0922 N85-15642
Correlation of electronic charge transfer transitions and electrochemical potentials. The Bipyrazine(Tetracarbonyl)Molybdenum(O) system in various solvents
[AD-A147660] 08 p1120 N85-17062
Preparation and study of highly reactive metal powders
[AD-A150026] 12 p1806 N85-21331
Intramolecular electron transfer at metal surfaces. Part 5: Pendant substituent effects upon thiocarboxylate-bridged Cobalt (3) reduction kinetics at mercury and gold electrodes
[AD-A150647] 14 p2254 N85-23971
Cycling performance of the iron-chromium redox energy storage system
[NASA-TM-87034] 16 p2619 N85-27387
The electronic spectra of phthalocyanine radical anions and cations
[AD-A152328] 17 p2918 N85-27986
Electrochemical studies in liquid crystals
[AD-A154317] 19 p3234 N85-30060
Diffusion welding of incompatible materials
19 p3245 N85-30121
Anaerobic reduction of elemental sulfur by Chromatium vinosum and Beggiatoa alba 21 p3660 N85-32739
Microscopic control of semiconductor surface oxidation
[AD-A154799] 21 p3709 N85-33026
Isotopic Biogeochemistry
[NASA-CR-176128] 22 p3741 N85-33189
A kinetic model for predicting oxidative degradation rates in combined radiation-thermal environments
[TI85-002629] 24 p4100 N85-35414

OXIDE FILMS
Influence of parameters of alumimun alloy anodizing process on oxide coating thickness
01 p0018 N85-10113
Non-oxide ceramics: A new class of engineering materials 02 p0179 N85-11186
Optimized conditions for the formation of buried insulating layers in Si by high dose implantation of oxygen
[DE84-015369] 02 p0266 N85-11662
Electrochemistry of rare-earth diphthalocyanines
[AD-A145813] 03 p0327 N85-12106
Influence of aluminum oxide film on thermocompression bonding of gold wire to evaporated aluminum film
[NASA-TM-77503] 03 p0330 N85-12127
Transport processes during the growth of oxide films at elevated temperature
[AERE-R-11293] 03 p0434 N85-12766
Oxygen diffusion from anodic surface oxide films on titanium subhydride studies by auger electron spectroscopy and electron energy loss spectroscopy
[DE84-016942] 04 p0572 N85-13646
Anti-reflection coatings materials and models
05 p0665 N85-14276
Hydrogen production employing high-temperature solid oxide cells
[DE84-014559] 06 p0766 N85-14661
Wear of anodic oxide films on aluminum alloys in cryogenic liquids
[NAL-TR-818] 06 p0768 N85-14814
Recording holograms on thin films of titanium dioxide
06 p0789 N85-15039
Electrical properties of 10-50 nm TEOS (Tetraethoxysilane) LPCVD (Low Pressure Chemical Vapor Deposition) films
[AD-A146416] 06 p0803 N85-15111
Oxide charge characteristics of low temperature MOS (Metal-Oxide-Silicon) oxide films
[AD-A146447] 06 p0803 N85-15113
Charge trapping in low temperature MOS (Metal-Oxide-Silicon) oxides
[AD-A146450] 06 p0860 N85-15467

Characterization of thermally treated gallium arsenide by laser-Raman and Auger spectroscopy
[AD-A148414] 06 p1226 N85-17721
Photon scattering and interaction analysis of interfacial corrosion and catalysis
[DE85-002534] 11 p1606 N85-20114
Semiconductor electrochemistry approach to the study of oxide films on nickel electrodes
[DE85-003042] 11 p1630 N85-20264
Time resolved Raman studies of laser induced damage in TiO2 optical coatings
[DE85-003166] 11 p1640 N85-20332
The characterisation of oxide films on treated aluminium alloys
[MOAD-R-849] 13 p2022 N85-22667
Experimental and theoretical study of the infrared reflectance of thin oxide films on metals
[DE85-005799] 15 p2653 N85-26366
Obtaining oxide films on surface of tubes of chromium-nickel steels
[BLL-BISI-TRANS-22476-(9022.06)]
17 p2929 N85-28076
Technology development for thin-film-trace humidity sensors
[BMFT-FB-T-84-268] 17 p2969 N85-28338
Influence of type of processing of AK4 alloy on its surface state and strength of bonding of plasma coatings
19 p3242 N85-30103
Ion beam sputter-deposited thin film coatings for protection of spacecraft polymers in low Earth orbit
[NASA-TM-87051] 19 p3248 N85-30137
Development of low-melting fused salts 8: Formation of molybdenum film from molten ammonium formate bath
[BLL-OA-TRANS-3195-(6196.300)]
20 p3429 N85-31264
Electrolytic synthesis of colored eta alumina film
23 p3906 N85-34201
Features of behavior of gas bubbles in molten oxide films during enamelling: Communication 2
[BLL-M-35781-(5828.4)] 23 p3919 N85-34283
Thermal barrier coating system
[NASA-CASE-LEW-14057-1] 24 p4072 N85-35233

OXIDES
NT ALKALINE EARTH OXIDES
NT ALUMINUM OXIDES
NT ANHYDRIDES
NT BARIUM OXIDES
NT BERYLLIUM OXIDES
NT BISMUTH OXIDES
NT BORON OXIDES
NT CALCIUM OXIDES
NT CARBON DIOXIDE
NT CARBON MONOXIDE
NT CERIUM OXIDES
NT CHLORINE OXIDES
NT CHROMITES
NT CHROMIUM OXIDES
NT COBALT OXIDES
NT COPPER OXIDES
NT DIOXIDES
NT ENSTATITE
NT GERMANIUM OXIDES
NT HYDROGEN PEROXIDE
NT INORGANIC PEROXIDES
NT IRON OXIDES
NT LEAD OXIDES
NT LITHIUM OXIDES
NT MAGNESIUM OXIDES
NT MAGNETITE
NT MANGANESE OXIDES
NT METAL OXIDES
NT MOLYBDENUM OXIDES
NT NICKEL OXIDES
NT NIOBIUM OXIDES
NT NITRIC OXIDE
NT NITROGEN DIOXIDE
NT NITROGEN OXIDES
NT NITROGEN TETROXIDE
NT NITROUS OXIDES
NT ORGANIC PEROXIDES
NT PEROXIDES
NT PLUTONIUM OXIDES
NT POTASSIUM OXIDES
NT PYROXENES
NT QUARTZ
NT RUTILE
NT SAPPHIRE
NT SILICON DIOXIDE
NT SILICON OXIDES
NT SULFUR DIOXIDES
NT SULFUR OXIDES
NT TIN OXIDES
NT TITANIUM OXIDES
NT VANADIUM OXIDES
NT YTTRIUM OXIDES
NT ZINC OXIDES
NT ZIRCONIUM OXIDES
Observation of oxide skin in powder metallurgy aluminum alloys
[AD-A145919] 03 p0331 N85-12135
Effect of oxide coated thickness on thermal ignition of titanium-based pyrotechnics
[DE84-013061] 04 p0481 N85-13065
Measurement of oxide ion concentration in NaCl-ZnCl2 molten salt and several applications
[BLL-AWRE-TRANS-74-(9091.9F)]
06 p0764 N85-14886
Effects of heteroatom substituents on the properties of 1,2-dioxetanes
[AD-A148727] 09 p1290 N85-18100
Transverse microstructure of an oxide scale formed on a 20 % Cr/25 % Ni niobium stabilized stainless steel
[AERE-R-11034] 12 p1804 N85-21315
Gasification of boron oxide drops and boron slurry agglomerates in combustion gases
13 p1999 N85-22529
Electrical and thermal transport property studies of high-temperature thermoelectric materials
[AD-A150167] 13 p2163 N85-23417
An investigation of the structure and high temperature mechanical properties of oxide dispersion strengthened alloys
[AD-A151107] 15 p2509 N85-25477
Quality testing to the specifications of the Stahl-Eisen-Pruefblatt 1570/71 using an automatic image analysis system
[BLL-BISI-TRANS-22253-(9022.06)]
17 p2976 N85-28385
Chemical transformation modules for Eulerian acid deposition models. Volume 1: The gas-phase chemistry
[PB85-173714] 18 p3072 N85-29001
Thermodynamic systematics of oxides of americium, curium and neighboring elements
[DE85-009704] 18 p3197 N85-29831
Effect of heating temperature in a vacuum on state of surface layers of welded OT4 titanium alloy
19 p3245 N85-30123
Method for production of ceramic oxide and carbide bodies by polymer inclusion and decomposition
[DE85-011668] 19 p3250 N85-30152
Process and design considerations for high-efficiency solar cells 20 p3482 N85-31641
The effect of stress and hot corrosion on nickel-base superalloys
[AD-A154722] 21 p3566 N85-32181
The diurnal variation of the neutral sodium species in the upper atmosphere: A model study
[AD-A154988] 21 p3631 N85-32561
Thermodynamic data for mineral technology
[PB85-184331] 22 p3803 N85-33560

OXIDIZERS
NT LIQUID OXYGEN
NT PHOTOCHEMICAL OXIDANTS
Atmospheric dispersion of hypergolic liquid rocket fuels, volume 1
[AD-A149597] 12 p1817 N85-21399
Process for improving the quality of epitaxial silicon films grown on insulating substrates
[AD-D011730] 22 p3847 N85-33828

OXIMETRY
Oxygen uptake as an indicator of animal adaptation to altitude hypoxia 19 p3324 N85-30595

OXYALKYLATION
U ALKYLATION

OXYFLUORIDES
Method for fluorination of actinide fluorides and oxyfluorides using O2F2
[DE85-011646] 22 p3743 N85-33202

OXYGEN
NT LIQUID OXYGEN
NT OXYGEN ATOMS
NT OXYGEN IONS
NT OXYGEN ISOTOPES
NT OXYGEN PLASMA
NT OZONE
Singlet delta oxygen generator
[AD-D011208] 01 p0012 N85-10072
Nonlinear ultrasonic characterization of oxygen impurities in titanium, 2
[AD-A144657] 01 p0027 N85-10171
Electron energy loss rates in N-2, O-2 and air
[AD-A145158] 01 p0072 N85-10476
Effect of maximum physical load on oxygen-transport properties of blood 01 p0093 N85-10627
Change in energetics of muscular contraction as a result of hyperoxia 01 p0093 N85-10629
A high resolution spectroscopic study of the oxygen molecule
[NASA-CR-174061] 02 p0172 N85-11150
Electrocatalysis of fuel cell reactions: Investigation of alternate electrolytes
[NASA-CR-174753] 02 p0222 N85-11455
Electronic-to-vibrational energy transfer studies of singlet molecular oxygen and hydrogen halides
[AD-A145587] 02 p0277 N85-11802
The rheology of icy satellites
[NASA-CR-174024] 02 p0302 N85-11959
Study of singlet oxygen-pentavalent phosphorus reactions
[AD-A145696] 03 p0327 N85-12107
Oscillator strengths for OII ions
[NASA-CR-174153] 04 p0559 N85-13558
Oxygen diffusion from anodic surface oxide films on titanium subhydride studies by auger electron spectroscopy and electron energy loss spectroscopy
[DE84-016942] 04 p0572 N85-13648
Reproducibility of readings from oxygen concentration elements
[BLL-M-35920-(5828.4)] 05 p0616 N85-13941
Oxygen delivery during exercise: Limitations to maximum flow 05 p0666 N85-14424
Measuring EUV line emission from the hot interstellar medium 06 p0860 N85-15595
Conference on Singlet Molecular Oxygen (COSMO 84), program and abstracts
[AD-A147281] 07 p1040 N85-16605
Proceedings of the 2nd Workshop on Nondestructive Evaluation (NDE) of Titanium Alloys
[AD-A147626] 08 p1125 N85-17095
Effects of oxygen on the microstructure and properties of titanium 6211 alloys
[AD-P004122] 08 p1126 N85-17097
Nonlinear ultrasonic characterization of oxygen impurities in titanium
[AD-P004123] 08 p1126 N85-17098
Effects of oxygen-contamination-induced microstructural changes on the reverberation of ultrasound in Ti-6211 alloys
[AD-P004124] 08 p1126 N85-17099
Acoustical characterization of Ti-6211 weldments and oxygen contamination Ti-6211 plate
[AD-P004125] 08 p1126 N85-17100
Ultrasonic evaluation of titanium contamination with correlation techniques
[AD-P004126] 08 p1126 N85-17101
Photoacoustic microscopy of oxygen contaminated titanium alloys
[AD-P004127] 08 p1127 N85-17102
High resolution acoustic microstructural characterization of titanium with interstitial contamination
[AD-P004128] 08 p1127 N85-17103
Feasibility study to demonstrate detection of low levels of oxygen contaminant in titanium using eddy current and ultrasonic NDE (Nondestructive Evaluation) techniques
[AD-P004129] 08 p1127 N85-17104
Evaluation of interstitial gas contamination in titanium alloys using induced magnetic field analysis
[AD-P004130] 08 p1127 N85-17105
Electromagnetic NDE of interstitial contamination in titanium alloy weldments
[AD-P004131] 08 p1127 N85-17106
Neutron activation analysis of titanium with oxygen contamination
[AD-P004134] 08 p1128 N85-17109
Nondestructive evaluation of titanium alloys. ESCA (Electron Spectroscopy for Chemical Analysis), ISS (Ion Scattering Spectroscopy), and SIMS (Secondary Ion Mass Spectrometry) examination of titanium alloy solid surfaces
[AD-P004135] 08 p1128 N85-17110
Variation of oxygen and nitrogen abundances in the galaxy 08 p1248 N85-17878
Blood viscosity responses to acute exercise and aerobic conditioning in women 09 p1363 N85-18573
Hydrogen-oxygen (hydrox) breathing at 1.3MPa
[FOA-C-58015-H1] 09 p1364 N85-18577
Metal atom diffusion in amorphous silica and at the silica surface
[DE84-017351] 09 p1380 N85-18674
The reaction of oxygen-nitrogen mixtures with granular activated carbons below the spontaneous ignition temperature
[AD-A149041] 10 p1434 N85-19039
Artificial photosynthesis with algal and reconstituted systems
[DE85-002557] 10 p1523 N85-19604
Orographic disturbances of upper atmosphere emissions 11 p1663 N85-20480
Saturation kinetics of active medium of oxygen-iodine laser 11 p1718 N85-20807
Comments on the origins and variations of carbon and nitrogen in the ISM of galaxies as evident from IUE spectroscopy of H 2 regions 11 p1745 N85-20973
Carbon, silicon, and oxygen in the white dwarf star GD 40 11 p1752 N85-21017

Toxicity, mutagenesis and aging due to endogenous oxygen radicals
[AD-A150121] 12 p1900 N85-21928
Characterization of material surfaces exposed to atomic oxygen on space shuttle missions
12 p1946 N85-22220
Ignition phenomena of bulk aluminum alloy as a function of oxygen pressure 13 p1999 N85-22531
Sulfur oxygen processes on Io
13 p2173 N85-23481
Diagrams of chemical and electrochemical equilibria in the presence of oxygen and sulphur
[AD-A150929] 14 p2251 N85-23953
Effect of oxygen on mechanical properties of Nb-V alloy
[DE85-002661] 14 p2256 N85-23982
Study of oxidized surface coating on titanium after annealing 15 p2496 N85-25412
Ignition of metals in high pressure oxygen
16 p2735 N85-26874
Hazards in welding due to oxygen changes in the workplace atmosphere
[BLL-WI-TRANS-684-(9312.57)]
16 p2792 N85-27224
Systematic nomenclature of the nitrogen, oxygen and sulfur functional polycyclic aromatic hydrocarbons
[DE85-007426] 17 p2916 N85-27874
Oxygen evolution on NiCo2O4 electrodes
17 p2924 N85-28026
Thermodynamic calculations of equilibrium states in metal-carbon-hydrogen-oxygen system
[BLL-BISI-TRANS-22092-(9022.06)]
17 p3045 N85-28844
Chemical, biological, and physical measurements from the subtropical western North Atlantic Ocean. Summer 1982, USNS Lynch, cruise 710-82
[AD-A153823] 18 p3201 N85-29857
Study of Kapton under simulated shuttle environment
[NASA-CR-176003] 19 p3225 N85-29997
Light-weight oxygen delivery hood assembly for hyperbaric chamber
[AD-D011709] 19 p3331 N85-30634
Oxygen and carbon impurities and related defects in silicon 20 p3481 N85-31631
Infrared absorption of oxygen complexes in electron-irradiated silicon
[FOA-C-30379-E1,E2,E3,E4] 20 p3538 N85-32015
Shock tube measurements of growth constants in the branched-chain ethane-carbon monoxide-oxygen system
[NASA-TM-87066] 21 p3562 N85-32156
Modification of the grain size of sputtered copper with additions of oxygen, krypton, silver, or yttrium
[DE85-010975] 21 p3567 N85-32189
Studies of oxygen- and carbon-related defects in high-efficiency silicon solar cells
21 p3609 N85-32420
Sulfur transformations at the hydrogen sulfide/oxygen interface in stratified waters and in cyanobacterial mats
21 p3657 N85-32715
Distribution and abundance of organic thiols
21 p3657 N85-32717
Evolution of the atmosphere 21 p3658 N85-32725
Microbial communities and microprofiles of sulfide and oxygen of alum rock sulfur springs
21 p3661 N85-32746
Changes in the energy spectrum of anomalous oxygen and helium during 1977 - 1985
[PAPER-SH-4.6-1] 21 p3715 N85-33056
Solar cycle variations of the anomalous cosmic ray component
[PAPER-SH-4.6-2] 21 p3715 N85-33057
Radial and latitudinal gradients of anomalous oxygen during 1977 - 1985
[PAPER-SH-4.6-4] 21 p3716 N85-33058
Stress and efficiency studies in EFG
[NASA-CR-176125] 22 p3751 N85-33251
Durability of oxygen sensors
[PB85-183093] 22 p3789 N85-33477
Oxygen analyzer
[DE85-006002] 23 p3935 N85-34392
Increase of total CO2 in the World ocean
[DE85-007756] 23 p3950 N85-34484
Determination of individual tolerance in hyperbaric oxygen 23 p3954 N85-34507
Changes in the energy spectrum of anomalous oxygen and helium during 1977-1985
[SH-4.6-1] 23 p4039 N85-35039
Temporal variations of the anomalous oxygen component, 1977 - 1984
[SH-4.6-3] 23 p4039 N85-35041
Radial and latitudinal gradients of anomalous oxygen during 1977 - 1985
[SH-4.6-4] 23 p4039 N85-35042
Thermodynamics of the corrosion of chromium in molten carbonates
[DE85-011407] 24 p4079 N85-35282

OXYGEN ANALYZERS
Halogen mass flow rate detection system
[AD-D011398] 08 p1166 N85-17352
OXYGEN ATOMS
Electronically excited atomic and molecular oxygen
[AD-A147732] 08 p1121 N85-17064
The source of stratospheric NO and N2O
[NASA-CR-175713] 15 p2586 N85-25956
Adsorption of O2, SO2, and SO3 on nickel oxide. Mechanism for sulfate formation
[NASA-CR-176072] 21 p3565 N85-32175
OXYGEN COMPOUNDS
Gas phase ion-molecule chemistry of carbon, nitrogen and oxygen compounds
[AD-A152676] 17 p2919 N85-27996
OXYGEN CONSUMPTION
Manned testing of two closed-circuit oxygen underwater breathing apparatus: US Navy Emerson Rig and Fenzy PO.68
[AD-A148300] 08 p1200 N85-17560
The energy cost of women walking and running in shoes and boots
[AD-A151022] 14 p2389 N85-24716
Relationship between the Army two mile run test and maximal oxygen uptake
[AD-A153914] 18 p3154 N85-29526
Oxygen uptake as an indicator of animal adaptation to altitude hypoxia 19 p3324 N85-30595
An analysis of aerobic capacity in a large United States population
[AD-A156200] 24 p4132 N85-35614
OXYGEN DEFICIENCY
U HYPOXIA
OXYGEN DETECTORS
U OXYGEN ANALYZERS
OXYGEN IONS
Optimized conditions for the formation of buried insulating layers in Si by high dose implantation of oxygen
[DE84-015389] 02 p0288 N85-11882
Cold streams of ionospheric oxygen in the plasma sheet during the CDAW-6 event of March 22, 1979
[NASA-CR-174064] 03 p0393 N85-12513
Studies of the chemistry of vibrationally and electronically excited species in planetary upper atmospheres
[NASA-CR-174134] 03 p0449 N85-12851
Effect of inner subshell ionization for emission lines of OIV ion 09 p1388 N85-18729
Neutral beam injector oxygen impurity measurements and concentration reduction via gettering processes
[DE85-000861] 12 p1836 N85-21521
Three-dimensional calculation of shuttle charging in polar orbit 13 p1992 N85-22486
The ionospheric O+ streams in the magnetotail between 22 RE and 6 RE 14 p2360 N85-24582
Oxygen-nitrogen interactions in ion-implanted silicon
[DE85-010091] 18 p3195 N85-29819
ISEE-1 data reduction and analysis plasma composition experiment
[NASA-CR-175306] 21 p3630 N85-32552
Observation of nuclei with energies 8-30 MeV per nucleon in the Earth's magnetosphere at the altitudes 350 KM
[SH-10.1-5] 23 p4053 N85-35136
OXYGEN ISOTOPES
Size dependence of chondrule textural types
06 p0682 N85-15606
Oxygen isotopes in deep sea spherules
06 p0683 N85-15609
Control technology for radioactive emissions to the atmosphere at US Department of Energy facilities: The Los Alamos Meson Physics Facility
[DE85-011402] 22 p3811 N85-33609
Implications of new measurements of O-16 + p + C-12,13, N-14,15 for the abundances of C, N isotopes at the cosmic ray source
[OG-4.3-2] 22 p3678 N85-34027
Nucleosynthesis in the terrestrial and solar atmospheres
[SH-2.2-2] 23 p4000 N85-34797
OXYGEN METABOLISM
Respiratory chain of alkalophilic bacteria
[DE84-012558] 09 p1360 N85-18556
OXYGEN PLASMA
SWIR and visible atomic emission from laser-produced oxygen and nitrogen plasmas
[AD-A147528] 07 p1045 N85-16641
OXYGEN PRODUCTION
Development and demonstration of a spiral-wound thin-film composite membrane system for the economical production of oxygen-enriched air, phase 4
[DE85-012380] 23 p3920 N85-34288
OXYGEN RECOMBINATION
Electronically excited atomic and molecular oxygen
[AD-A147732] 08 p1121 N85-17064

OXYGEN SPECTRA
Forbidden lines of oxygen in comet spectra
02 p0163 N85-11106
OXYGEN SUPPLY EQUIPMENT
Ultralightweight oxygen container
[PB84-220730] 01 p0036 N85-10236
Slow opening valve — valve design for shuttle portable oxygen system
[NASA-CASE-MSC-20112-1] 11 p1642 N85-20038
Light-weight oxygen delivery hood assembly for hyperbaric chamber
[AD-D011709] 19 p3331 N85-30634
Improved oxygen sources for breathing apparatus
[NASA-TM-86671] 24 p4134 N85-35620
OXYGEN SYSTEMS
U OXYGEN SUPPLY EQUIPMENT
OXYGEN TENSION
NT HYPOXEMIA
Effect of microwave radiation on local blood circulation and oxygenation of brain tissue
07 p1012 N85-16431
OXYGEN TOXICITY
U HYPEROXIA
OXYGENATION
Pulmonary blood flow and oxygenation of arterial blood in a healthy subject upon 7 days hypokinesia
07 p1014 N85-16439
Management of vibration sickness in coal mines by hyperbaric oxygenation 10 p1523 N85-19809
Hydrographic data collected in 1982 and 1983 for EPOCS (Equatorial Pacific Ocean Climate Studies)
[PB85-110799] 12 p1676 N85-21765
Mathematical-cartographic model for study of distribution of hydrochemical elements in sea water (using dissolved oxygen in the Pacific Ocean as an example)
13 p2109 N85-23136
Chemical signatures associated with the freshening of Northern Atlantic waters between 1972 and 1981
15 p2601 N85-26022
Jet fuel instability mechanisms
[NASA-CR-175856] 17 p2936 N85-28127
Modeling of auto exhaust smog chamber data for EKMA development
[PB85-186492] 22 p3613 N85-33619
Biological modulation of planetary atmospheres: The early Earth scenario 22 p3654 N85-33667
Oxygenation and regional circulation in gingival mucosa during exposure to lower body negative pressure
23 p3953 N85-34498
OXYHALIDES
High capacity inorganic oxyhalide electrochemical cell
[AD-D011321] 07 p0923 N85-15845
OXYHEMOGLOBIN
Liposome-encapsulated hemoglobin for emergency resuscitation
[AD-A146794] 07 p1015 N85-16446
OZONE
Future scenarios and ozone change
[DE84-014781] 01 p0065 N85-10573
Organic aerosol formation: OH(hydroxyl radical) versus ozone oxidation pathways
[PB84-219880] 03 p0388 N85-12484
Analysis of Santa Barbara oxidant study
[PB84-229277] 03 p0388 N85-12486
A 2-dimensional description of potential perturbations to the ozone layer due to NOx and H-2-O aircraft emissions
[AD-A146292] 03 p0392 N85-12511
Trends in ozone and temperature structure: Comparison of theory and measurements
[DE84-016201] 04 p0539 N85-13429
Aspects of the comparison of stratospheric trace species measurements with photochemical models
[DE84-017028] 05 p0672 N85-14317
Detailed performance calculations: Wayne State University and Ford Motor Company, appendix C
05 p0676 N85-14340
Applications of TOMS ozone data and clustering techniques in satellite soundings
05 p0681 N85-14379
Active optical sounding of ozone and minor constituents in the middle atmosphere: A review of ground-based lidar measurements 08 p1183 N85-17458
Stratospheric concentration of nitric acid, ozone and carbonyl sulfide: Measurement of nitric acid absorption in the Q branch of the V4 band as a function of temperature
[ESA-TT-864] 09 p1355 N85-18524
Upper atmosphere research at INPE
[INPE-3281-PRE/604] 10 p1515 N85-19857
Aerosol limb absorption — stratosphere
[NASA-TM-77733] 10 p1515 N85-19862
Health assessment document for carbon tetrachloride
[PB85-124196] 10 p1528 N85-19659
Soviet National Middle Atmosphere Program
11 p1655 N85-20426

MAP/GLOBUS campaign 1983
11 p1658 N85-20447

MSG-7: Molecular absorption processes related to the penetration of ultraviolet solar radiation into the middle atmosphere
11 p1658 N85-20449

Changes in the ozone content over central Europe during reversals of stratospheric circulation in late winter
11 p1661 N85-20469

Ozone measurements in the mesosphere during a solar proton event
11 p1665 N85-20490

Air quality for ozone and other photochemical oxidants. External review draft, volume 1
[PB85-126035] 11 p1679 N85-20582

Air quality criteria for ozone and other photochemical oxidants. External review draft, volume 5
[PB85-126076-VOL-5] 11 p1679 N85-20583

Continued research in mesoscale air pollution simulation modeling. Volume 5: Refinements in numerical analysis, transport, chemistry, and pollutant removal
[PB85-137362] 11 p1680 N85-20585

Absorption of ozone molecules in strong field of tea CO2 injection laser
11 p1718 N85-20808

Gas-liquid chemistry of natural waters, volume 1
[DE85-002603] 12 p1884 N85-21822

Gas-liquid chemistry of natural waters, volume 2
[DE85-002457] 12 p1884 N85-21823

Air quality criteria for ozone and other photochemical oxidants. External review draft, volume 2
[PB85-126043] 12 p1886 N85-21836

Air quality criteria for ozone and other photochemical oxidants, external review draft, volume 3
[PB85-126050] 12 p1886 N85-21837

Air quality criteria for ozone and other photochemical oxidants. External review draft, volume 4
[PB85-126068] 12 p1886 N85-21838

Simultaneous cabin and ambient ozone measurements on two Boeing 747 airplanes. Volume 3: October 1978 - July 1979
[NASA-TM-86883] 12 p1892 N85-21872

Non-precipitating cumulus cloud study
[DE85-002352] 12 p1896 N85-21902

Ozone Correlative Measurements Workshop
[NASA-CP-2362] 13 p2105 N85-23112

Scientific requirements for ozone measurements
13 p2105 N85-23113

Method for determining the number of correlative measurements required to validate the SBUV/2 ozone retrievals
13 p2105 N85-23114

Measurement requirements for the detection of ozone trends
13 p21C5 N85-23115

A theoretical study of the ozone quasi-biennial oscillation in the tropical stratosphere
13 p2132 N85-23264

Cumulus cloud venting of mixed layer ozone
[NASA-TM-87429] 13 p2132 N85-23269

Study of integral and spectral direct solar radiation over Atlantic
14 p2341 N85-24475

Development of algorithms for using satellite meteorological data sets to study global transport of stratospheric aerosols and ozone
[NASA-CR-172540] 15 p2591 N85-25974

Impact of ozone on vegetation
[PB85-159937] 16 p2821 N85-27403

Free radicals in the stratosphere: A new observational technique
16 p2824 N85-27415

Research and development of new instruments
16 p2824 N85-27418

In-situ stratospheric ozone measurements: Recent results and their implications
16 p2824 N85-27419

Role and fate of ozone in the atmosphere
16 p2824 N85-27421

Geophysical monitoring for climatic change, number 12
[PB85-172278] 16 p2837 N85-27496

Ozone and temperature trends due to the injection of trace species in the atmosphere
[AERONOMICA-ACTA-A-288-1984]
18 p3132 N85-29399

Impact of alcohol fuels on urban air pollution: Methanol photochemistry study
[DE85-009539] 18 p3133 N85-29403

Conceptual Design for a Gulf Coast Oxidant Transport and Transformation Experiment: Workshop proceedings and recommendations
[PB85-173789] 18 p3135 N85-29417

Improvement of the basic knowledge of the climatology of the vertical ozone layer by enhanced balloon sounding
[BPT-6/84] 18 p3137 N85-29426

Photochemical processes in the lower stratosphere (ozone layer)
18 p3148 N85-29490

Assessment of the role of nitrogen oxides in nonurban ozone formation
[PB85-173680] 19 p3311 N85-30524

Chemical transformation in acid rain. Volume 1: New methodologies for sampling and analysis of gas-phase peroxide
[PB85-173425] 19 p3311 N85-30527

Development of a technique for in situ detection of stratospheric nitrogen dioxide
19 p3312 N85-30534

Tropical ozone: Seasonal variations in the troposphere at 6 deg S
[INPE-3555-PRE/766] 19 p3313 N85-30535

Annual environmental monitoring report, January-December 1984
[DE85-011669] 20 p3486 N85-31665

Ozone in the 21st century: Increase or decrease
[AERONOMICA-ACTA-A-291-1984]
20 p3489 N85-31687

Modeling of auto exhaust smog chamber data for EKMA development
[PB85-186492] 22 p3813 N85-33619

Atmospheric reaction products from hazardous air pollutant degradation
[PB85-185841] 22 p3813 N85-33620

The use of TOMS data in evaluating and improving the total ozone from TOVS measurements
[NOAA-TR-NESDIS-23] 22 p3814 N85-33626

Agents and effects of ozone trends in the atmosphere
[AERONOMICA-ACTA-A-287-1984]
23 p3948 N85-34486

The influences of the galactic cosmic ray on the atmospheric ozone
[SH-10.1-1] 23 p4053 N85-35133

Space Station Polar Platform: Integrating research and operational missions
[PB85-195279] 24 p4069 N85-35218

A study of the chemistry of alkali metals in the upper atmosphere
[AD-A156349] 24 p4117 N85-35524

OZONOMETRY

Model of atmospheric ozone for middle latitudes
02 p0161 N85-11091

One approach to remote sensing of total ozone content
16 p2725 N85-26822

Improvement of the basic knowledge of the climatology of the vertical ozone layer by enhanced balloon sounding
[BPT-6/84] 18 p3137 N85-29426

Ozone during sudden stratospheric warming: A three-dimensional simulation
[AERONOMICA-ACTA-A-292-1984]
22 p3813 N85-33621

OZONOSPHERE

Solar radiation in the ozone layer
04 p0522 N85-13342

Plant responses to solar UV-B radiation
05 p0690 N85-14436

Photochemical processes in the lower stratosphere (ozone layer)
18 p3148 N85-29490

P

P WAVES

Transport properties of Topopah Spring tuff
[DE85-010448] 19 p3270 N85-30278

P-I-N DIODES

U DIODES
U P-I-N JUNCTIONS

P-I-N JUNCTIONS

Allowable surge currents and failure mechanisms in semiconductor power devices in various modes of operation
06 p0795 N85-15080

EMC enhanced constant Z modulator
[AD-A147715] 08 p1157 N85-17297

P-I-N CdTe gamma-ray detectors by Liquid Phase Epitaxy (LPE)
[DE84-012276] 09 p1323 N85-18315

Radiation effects induced in pin photodiodes by 40- and 85-MeV protons
[NASA-CR-175678] 14 p2426 N85-24960

P-N JUNCTIONS

Radiation measuring system using transistor flux sensors
[AD-D011239] 01 p0050 N85-10326

Spectral distribution of radiation in n junctions of GaAs during avalanche breakdown
02 p0258 N85-11668

Novel transport and recombination processes in semiconductors
[AD-A145969] 03 p0433 N85-12757

An asymptotic analysis of a transient p-n junction model
[AD-A147270] 07 p0947 N85-16004

Dependence of breakdown voltage for p-n junction on parameters of ion implantation and semiconductor heat treatment
07 p0954 N85-16046

Improved modeling of the open circuit voltage of solar cells
13 p2011 N85-22619

A second order difference scheme for transient semiconductor device simulation
[AD-A154824] 21 p3709 N85-33027

A review of the physics and response models for burnout of semiconductor devices
[AD-A155031] 21 p3709 N85-33028

P-N-P JUNCTIONS

Method for the fabrication of dielectric isolated junction field effect transistor and PNP transistor
[AD-D011500] 12 p1832 N85-21494

KT3127A, KT3128A transistors
22 p3779 N85-33414

P-N-P-N JUNCTIONS

Integrated power devices with three-dimensional connection for automation systems
06 p0794 N85-15077

Dependence of parameters of silicon photovoltaic cells on temperature and light intensity
14 p2275 N85-24094

P-TYPE SEMICONDUCTORS

Novel transport and recombination processes in semiconductors
[AD-A145969] 03 p0433 N85-12757

A study of defects in neutron transmutation doped silicon: Gallium by hall effect analysis
[AD-A146047] 03 p0433 N85-12758

High temperature thermoelectric energy conversion
05 p0610 N85-13894

Electrically conducting complexes of poly(3,6-n-methylcarbazolyl methylene)
[AD-A147884] 07 p0933 N85-15914

Photoelectrochemical reduction of carbon dioxide
[PB85-129054] 11 p1596 N85-20036

Multiple double heterojunction buried laser device
[AD-D011519] 12 p1855 N85-21635

Thin film cadmium telluride and zinc phosphide solar cells
[DE85-002904] 15 p2587 N85-25950

Fabrication and I-V characterization of AlGaAs/GaAs MODFETs with P-type surface layers grown by molecular beam epitaxy
[AD-A151695] 15 p2660 N85-26415

TEMO and TEB thermoelectronic devices
22 p3779 N85-33415

P-84 AIRCRAFT

U JET PROVOST AIRCRAFT

P-3 AIRCRAFT

An analysis of constraints to coordinated tactical crew interaction in the P-3C aircraft
[AD-A147220] 07 p1021 N85-16478

An airborne infrared thermal scanning system for easy use on Navy P-3 aircraft
[AD-A149690] 12 p1933 N85-22143

P-531 HELICOPTER

Wind-tunnel evaluation of a 21-percent-scale powered model of a prototype advanced scout helicopter
[NASA-TP-2420] 18 p3058 N85-28923

PACIFIC ISLANDS

NT JAPAN
NT KURILE ISLANDS
NT NEW ZEALAND

Vertical movements and structure formation within island systems of northeast Asia
10 p1501 N85-19471

PACIFIC NORTHWEST (US)

Ecology of estuarine channels of the pacific northwest coast: A community profile
[PB84-209709] 01 p0070 N85-10464

Pacific Northwest and Alaska bioenergy program glossary
[DE85-011740] 22 p3008 N85-33591

PACIFIC OCEAN

Sea-level in the world ocean. Part 5: The North-East Pacific and Arctic Oceans, a catalogue of measurements
[CSIR-T/SEA-8303-5] 01 p0087 N85-10589

Sea-level in the world ocean. Part 6: The South Atlantic and South Pacific Oceans, a catalogue of measurements
[CSIR-T/SEA-8303-6] 01 p0087 N85-10590

On gravity from SST, geoid from Seasat, and plate age and fracture zones in the Pacific
[E85-10020] 02 p0217 N85-11433

A comparison of seismic properties of young and mature oceanic crust
02 p0226 N85-11479

Lithospheric structure in the Pacific geoid
[NASA-CR-174155] 04 p0526 N85-13365

Tide tables 1985, high and low water predictions, central and western Pacific Ocean and Indian Ocean
[PB84-236393] 04 p0542 N85-13451

Archiving and exchange of a computerized marine seismic database: The ROSE data archive system
[DE84-901453] 04 p0576 N85-13677

Earthquakes and tectonics of Pacific Ocean margins
06 p0820 N85-15206

Anomalous magnetic field in northwestern Pacific Ocean and Pacific Ocean plate kinematics
06 p0820 N85-15210

Boundary velocities of mohorovicic discontinuity and upper mantle structure of Pacific Ocean bed
06 p0821 N85-15211

Tides and tidal currents of the inland waters of Western Washington
[PB84-237379] 06 p0842 N85-15346

Ocean and climate, an example. The interannual variability of the tropical Pacific Ocean
07 p1002 N85-16365

Oceanographic data for development of the US exclusive economic zone
[PB85-106458/GAR] 07 p1010 N85-16415

The spatial evolution of t he directional wave spectrum in the Southern Ocean: Its relation to extreme waves in Agulhas Current 08 p1144 N85-17213

Bibliography update on the California current system and related mesoscale ocean modeling
[AD-A148546] 08 p1190 N85-17503

Preliminary post-emplacement safety analysis of the subseabed disposal of high-level nuclear waste
[DE84-011162] 08 p1221 N85-17692

Silver metallogeny in Earth's Pacific Ocean segment
10 p1498 N85-19455

Annual data and verification tabulation for Eastern North Pacific tropical storms and hurricanes, 1983
[PB85-109635] 10 p1520 N85-19580

Tropical cyclone data tape for the Eastern and Central North Pacific Basins, 1949-1983: Contents, limitations and uses
[PB85-110054] 10 p1520 N85-19585

Drifting buoy data from equatorial Pacific Ocean, 31 Aug. 1980 - 30 Apr. 1982
[PB85-120046] 10 p1522 N85-19596

Mesoscale studies of flow regimes and fluxes of particulate matter in coastal waters
[DE85-003825] 11 p1689 N85-20620

Hydrographic data collected in 1982 and 1983 for EPOCS (Equatorial Pacific Ocean Climate Studies)
[PB85-110799] 12 p1876 N85-21765

Varying structure and intensity change characteristics of 4 Western North Pacific tropical cyclones
[AD-A149628] 12 p1895 N85-21895

Microplankton species assemblages at the Scripps Pier from March to November 1983 during the 1982-1984 El Nino event
[NASA-CR-175553] 12 p1899 N85-21926

El Nino, the capricious child 13 p2106 N85-23121

Absolute movement of Pacific Ocean plate during last 120 million years 13 p2107 N85-23126

Mathematical-cartographic model for study of distribution of hydrochemical elements in sea water (using dissolved oxygen in the Pacific Ocean as an example)
13 p2109 N85-23136

Surface currents in the tropical Pacific during 1979-1980 using drifting buoys 14 p2323 N85-24354

A large-scale air sea interaction project over the Pacific basin 14 p2326 N85-24373

The transpacific experimental sailing by YASEIGO 3
14 p2327 N85-24380

Applications of ARGOS measurements in equatorial Pacific Ocean-atmosphere interaction studies
14 p2331 N85-24414

Absolute movement of Pacific Ocean plate based on paleoclimatic and paleomagnetic data and trajectory of hot spots during last 120 million years
14 p2334 N85-24435

Some preliminary results concerning deep northern-boundary currents in the North Pacific
[AD-A151021] 14 p2382 N85-24692

Glacial-to-interglacial changes in NADW fluxes?
15 p2602 N85-26037

The ARGOS system used for tracking gray whales
16 p2812 N85-27347

Tectonic structure features of some deep faults in Atlantic and Pacific Oceans (according to deep seismic sounding-reflected waves method data)
19 p3295 N85-30428

Mariners weather log, volume 28, number 4, fall 1984
[PB85-176408] 19 p3318 N85-30571

One-dimensional model hindcasts of warm anomalies in the North Pacific Ocean
[AD-A154128] 19 p3320 N85-30579

Pacific index, April 1983 - October 1984
[TI85-901335] 19 p3320 N85-30582

Sulfates in marine aerosols over the tropical Western Pacific Ocean 21 p3651 N85-32690

Meteorological data from the OPTOMA (Ocean Prediction Through Observations, Modeling and Analysis) program OPTOMA 2, leg D2. 30 Jun. - 10 Jul. 1984
[AD-A156134] 24 p4123 N85-35560

PACKAGES
NT INSTRUMENT PACKAGES

PACKAGING
NT ELECTRONIC PACKAGING

Safety aspects of prepackaged liquid propellant stages for strategic missiles
[AD-P004350] 10 p1456 N85-19174

Evaluation of air and ground launched cruise missile navigational element containers
[AD-A149654] 12 p1774 N85-21138

Synchronously deployable tetrahedral truss reflector
14 p2231 N85-23827

Packaging's contribution for the effectiveness of the space station's food service operation
14 p2394 N85-24746

Packaging for food service 14 p2394 N85-24747

Encapsulation and packaging of a semiconductor multielectrode array for cortical implantation
[AD-A153180] 17 p2998 N85-28535

Sintering studies project
[AD-A154750] 21 p3572 N85-32216

PACKET SWITCHING

Interaction of voice and data traffic in a packet switching communication network and virtual circuit
[FUB-63-1982] 01 p0039 N85-10249

Voice communication handling in X 25 packet switching networks
[FUB-30-1983] 01 p0040 N85-10260

Throughput characteristics of Carrier Sense Multiple Access (CSMA) networks
[FUB-25-1983] 01 p0106 N85-10713

Contribution to the study and realization of the CARTHAGE multiservice local network
[ENST-84E006] 05 p0716 N85-14595

Voice data procuesing in packet switching modes
[FUB-44-1983] 09 p1312 N85-18248

Analysis of the performance of multiaccess networks of the bus type
[FUB-47-1983] 09 p1313 N85-18249

Asymptotic analysis of Markovian access control computer communication networks
09 p1372 N85-18619

A concatenated coding scheme for error control
[NASA-CR-175504] 12 p1912 N85-22001

Satellite channels in packet-switching networks
13 p2067 N85-22909

Onboard demand scheduling of a multibeam SS/TDMA satellite with integrated circuit and packet switching
14 p2229 N85-23812

Mathematical programming in computer network design
[AD-A152275] 16 p2848 N85-27558

A study of topologies and protocols for fiber optic local area network
[NASA-CR-175771] 16 p2864 N85-27669

High performance asynchronous limited sensing algorithms for CSMA and CSMA-CD channels
[AD-A153919] 18 p3171 N85-29650

A graphics interface for interactive simulation of packet-switched networks 23 p3962 N85-34558

PACKET TRANSMISSION
NT PACKET SWITCHING

Asymptotic analysis of Markovian access control computer communication networks
09 p1372 N85-18619

Multicomputer communication system
[NASA-CASE-NPO-15433-1] 12 p1822 N85-21428

Spread spectrum mobile radio communications
[AD-A149936] 12 p1829 N85-21477

A fully distributed approach to the design of a 16 K bit/sec VHF packet radio network
[AD-A141282] 13 p2054 N85-22859

Wideband integrated voice/data technology
[AD-A152329] 17 p2947 N85-28197

PACKETS (COMMUNICATION)

Throughput increase in frequency hopped multiple access channels by means of discrimination against partially overlapping interference
[AD-A145540] 02 p0191 N85-11275

Transmission scheduling to reduce convex delay costs in packet networks
[AD-A148451] 08 p1153 N85-17278

Synthesis of optimum receiver and processor for signal packet of radio pulses 12 p1839 N85-21541

Satellite channels in packet-switching networks
13 p2067 N85-22909

PACKING DENSITY

System design of multi-layer (3-dimensional) integrated circuits
[AD-A153468] 18 p3094 N85-29154

PACKINGS (SEALS)

Inhibited anticorrosion protection of automotive steel strip in the NLMK
[BLL-M-36250-(5828.4)] 20 p3430 N85-31274

PAD

Factor analysis applied to a silane coupling agent on E-glass fiber system
[AD-A145887] 02 p0187 N85-11249

PADE APPROXIMATION

Mesh effects on the computation of non-linear gravity waves of arbitrary discharge
[COLL-AERON-8501] 12 p1866 N85-21

Nonlinear partial differential equations and related problems of Pade approximations
[AD-A149650] 12 p1920 N85-2

Pade tables of a class of entire functions
[CSIR-TWISK-337] 14 p2413 N85-24

Approximate inverse spectral transform for the Korteweg-de Vries equation
[PREPRINT-411] 18 p3172 N85-29

Well-posedness of one-way wave equations and absorbing boundary conditions
[NASA-CR-172619] 19 p3345 N85-30

PAINTS

Laser paint removal
[AD-P004009] 03 p0306 N85-11

Progress on solar absorber selective paint research
[DE84-015536] 04 p0480 N85-12

Application of electrochemical engineering methods and theory to solving corrosion and adhesion problems with organic coatings
[AD-A147799] 08 p1129 N85-17115

East Europe report: Science and technology
[JPRS-ESA-85-006] 10 p1460 N85-19

Hydrogen embrittlement of cadmium-plated ultra-high strength steels in paint strippers
[ARL/MAT-R-117] 12 p1806 N85-21

Contactless determination of the conductivity of the white paint PCB-Z — Giotto spacecraft thermal control coating 14 p2243 N85-2

Impact ionization from gold, aluminum and PCB-Z – Giotto spacecraft paint PCB-Z 14 p2244 N85-2

Investigation of the influence of some paint systems and water displacing corrosion inhibitors on anodic undermining corrosion of aluminum 2024 clad alloy – aircraft structures
[VTH-LR-443] 16 p2756 N85-27

Forming of coating protection system: Mechanism of paint-coating anti-corrosion protection of steel
[BLL-BISI-TRANS-22061-(9022.06)]
17 p2925 N85-2

Diffusely reflecting paints including polytetrafluoroethylene and method of manufacture
[NASA-CASE-GSC-12883-1] 18 p3079 N85-29

Comparison of TT-F-1098 solvent-thinned block fillers with water-thinnable block fillers
[AD-A154207] 19 p3249 N85-30142

Thickness-insensitive selective surface paint
[DE85-010568] 19 p3250 N85-30150

Working with flammable solvents, thinners, paints and adhesives
[HSE-TRANS-11086] 19 p3250 N85-30154

Land vehicle corrosion management
22 p3750 N85-33

Space shuttle SRB TPS protective paint test and evaluation in NASA Hot Gas Facility and AEDC Tunnel C
[NASA-CR-170884] 24 p4061 N85-35

PAIR PRODUCTION

Power law X- and gamma-ray emission from relativistic thermal plasmas 08 p1241 N85-17

Pair production at moderate optical depths — galactic nuclei X ray spectra 08 p1241 N85-17

Electron-positron pair equilibrium in strongly magnetized plasmas 12 p1957 N85-22

Electron-positron pairs in a mildly relativistic plasma in active galactic nuclei 12 p1957 N85-22

Atomic physics aspects of a Relativistic Nuclear Collider
[DE85-006867] 15 p2550 N85-2

Photon-photon collisions
[DE85-008056] 17 p3030 N85-2

Physics of (very) high energy e(+)-e(-) colliders
[DE85-008177] 17 p3036 N85-2

Measurements of heavy quark and lepton lifetimes
[DE85-008321] 18 p3181 N85-29

The radiation of the Vela pulsar
20 p3548 N85-3

Paired ion chamber constants for fission gamma-neutron fields
[AD-A155069] 21 p3702 N85-3

Secondary antiproton production in relativistic plasmas
[OG-6.1-4] 22 p3886 N85-34

Calculating the interatomic pair potential allowing for resonance interaction in titanium, nickel and vanadium
[BLL-M-35843-(5828.4)] 23 p3913 N85-34

Neutral pion production in solar flares
[SH-1.4-7] 23 p3995 N85-34

On magnetic pair production above fast pulsar polar caps
[OG-8.2-13] 23 p4020 N85-34

Neutron-induced 2.2 MeV background in gamma ray telescopes
[OG-9.3-6] 23 p4027 N85-34

Observation of direct hadronic pairs in nucleus-nucleus collisions in JACEE emulsion chambers
[HE-1.4-5] 24 p4176 N85-35893
Excessive production of electron pairs by soft photons in low multiplicity ion interactions
[HE-1.4-6] 24 p4176 N85-35894
LPM effect and primary energy estimations
[HE-3.8-4] 24 p4185 N85-35953
Result of Monte-Carlo simulation of electron-photon cascades in lead and layers of lead-scintillator
[HE-3.8-11] 24 p4185 N85-35958
Missing energies at pair creation
[HE-4.4-8] 24 p4193 N85-36018

PALEOBIOLOGY
Constraints on lunar origin: Evidence preserved in Precambrian stromatolites 04 p0584 N85-13731
Paleoclimatologists use past to predict weather patterns 06 p0819 N85-15197
Precambrian evolution and the rock record
21 p3656 N85-32711

PALEOMAGNETISM
A paleomagnetic study of the Prince William terrane and Nixon Fork terrane, Alaska 02 p0226 N85-11478
Paleomagnetic latitude of paleocene volcanic rocks of the Cantwell Formation, central Alaska
04 p0517 N85-13302
Implications of lunar paleomagnetism for the origin of the Moon 04 p0582 N85-13717
Use of paleomagnetic data in tectonic analysis of oceanic structures 13 p2108 N85-23135
Geomagnetic field dynamics 13 p2116 N85-23182
Absolute movement of Pacific Ocean plate based on paleoclimatic and paleomagnetic data and trajectory of hot spots during last 120 million years
14 p2334 N85-24435

PALEONTOLOGY
Paleohydrology and geomorphology of selected reaches of the upper Wabash Valley, Indiana
02 p0226 N85-11481
Paleoenvironmental interpretation of the upper cretaceous Point Lookout sandstone: Implications for shoreline progradation and basin tectonic history, San Juan basin, New Mexico 02 p0227 N85-11486
Post-Sonoman conodont biofacies of the Triassic of northwestern Nevada 03 p0390 N85-12497
Geographic and stratigraphic distribution of Miocene palynomorphs in north Idaho 03 p0390 N85-12498
Metamorphic petrology of the Table Mountain area, Circle quadrangle, Alaska 04 p0516 N85-13295
Late Paleozoic and early Mesozoic radiolarians in the Circle quadrangle, east-central Alaska
04 p0517 N85-13297
Magnetic constraints on early lunar evolution revisited: Limits on accuracy imposed by methods of paleointensity measurements 04 p0582 N85-13716
Late Quaternary deep-water paleoceanography of the eastern equatorial Indian Ocean: Evidence from Bethnic foraminifera, carbonate dissolution, and stable isotopes
08 p1182 N85-17446
Global paleoclimatic data base for 6000 years BP
[DE85-008828] 15 p2600 N85-26024
Global Mega-Geomorphology
[NASA-CP-2312] 21 p3600 N85-32357
Some observations on paleogeomorphology
21 p3601 N85-32363
Paleoenvironmental investigations at seed cave (Windust cave H-45FR46), Franklin County, Washington
[AD-A154777] 21 p3635 N85-32576
Precambrian evolution and the rock record
21 p3656 N85-32711

PALLADIUM
Surface chemistry of palladium
[DE84-014572] 02 p0173 N85-11163
Electron energy loss investigation of the electronic and structural properties of palladium
[NOTA-INTERNA-803] 02 p0289 N85-11888
Study of catalysts and mechanisms in synthesis reactions
[DE84-015025] 04 p0470 N85-12990
Transition metal catalyzed transformations of unsaturated molecules
[DE85-008531] 18 p3080 N85-29055
FTIR studies of hydrocarbon synthesis on Pd/ZSM5 catalysts
[DE85-012430] 24 p4071 N85-35230
Characterization of catalysts with metal-support effects and of the species adsorbed on their surfaces
[DE85-012254] 24 p4086 N85-35394

PALLADIUM ALLOYS
Surface segregation of sulfur during oscillatory pin-on-plate wear studies of precious metal electrical contact alloys. 1: Friction and electrical contact resistance
[DE84-008962] 02 p0195 N85-11303
First principles theory of Fermi-surface driven concentration waves in Cu/sub c/Pd/sub 1-c/ alloys
[DE85-005367] 13 p2024 N85-22681
Study of the kinetics and thermodynamics of hydrogen in Pd-based alloys
[DE85-007341] 16 p2750 N85-26869
Electrical conductivity and phase diagram of binary alloys. 21: The system palladium-chromium
[NASA-TM-77863] 18 p3073 N85-29009

PALLADIUM COMPOUNDS
Electrical conductivity and phase diagram of binary alloys. 21: The system palladium-chromium
[NASA-TM-77863] 18 p3073 N85-29009

PAM (MODULATION)
U PULSE AMPLITUDE MODULATION

PANCREAS
Endocrine responses to hypotensive gravitational stress: Catecholamines, pancreatic polypeptide, and vasopressin 05 p0693 N85-14460
Lipid hydrolysis in man during antiorthostatic hypokinesia 23 p3953 N85-34500

PANEL METHOD (FLUID DYNAMICS)
PAN AIR: A computer program for predicting subsonic or supersonic linear potential flows about arbitrary configurations using a higher order panel method. Volume 3: Case manual (version 1.0)
[NASA-CR-3253] 02 p0135 N85-10922
Viscous-inviscid aerodynamic analysis of two-dimensional thrust augmentors
[NASA-CR-177321] 04 p0451 N85-12861
Prediction of dynamic stall characteristics using advanced non-linear panel methods
[AD-A148453] 08 p1078 N85-16836
Application of the vortex-lattice concept to flows with smooth-surface separation 08 p1160 N85-17320
Numerical approach for the aerodynamic analysis if airfoils with laminar separation
[NASA-CR-172496] 09 p1273 N85-18001
Calculation of the flow around thick wings with separation vortices 12 p1821 N85-21424
Application of time-linearized methods to oscillating wings in transonic flow and flutter
15 p2459 N85-25182
A study of aerodynamic control in stalled flight leading-edge vortex formation analysis
[AD-A153758] 18 p3059 N85-28928
Shock waves in adjacent engine inlets
[ISL-R-104/84] 20 p3396 N85-31066
A panel method study of vortex sheets with special emphasis on sheets of axisymmetric geometry
[NASA-CR-177365] 21 p3552 N85-32095
Calculation of compressible flow about three-dimensional inlets with auxiliary inlets, slats and vanes by means of a panel method
[NASA-CR-174975] 24 p4060 N85-35162

PANELS
NT CURVED PANELS
NT RECTANGULAR PANELS
NT WING PANELS
Composite laminate optimization program suitable for microcomputers 01 p0059 N85-10389
Quasi-steady analysis of aircraft panel flammability
[AD-A145461] 02 p0138 N85-10936
Features of new solar panels on Salyut-7
02 p0157 N85-11062
Tensile strength of composite sheets with unidirectional stringers and crack-like damage: A brief report
[NASA-TM-86310] 02 p0170 N85-11139
Effect of stress concentrations in composite structures
[NASA-CR-173976] 02 p0170 N85-11140
Performance of two transonic airfoil wind tunnels utilizing limited ventilation 03 p0313 N85-12020
Long-term thermal aging of 2 graphite-polyimide composite materials
[NASA-TP-2369] 03 p0325 N85-12094
Prefabricated panels for rapidly runway repair and expedient airfield surfacing
[AD-D011277] 05 p0597 N85-13804
Design procedures for fiber composite structural components: Panels subjected to combined in-plane loads
[NASA-TM-86909] 07 p0919 N85-15823
Preliminary evaluation of an improved flammability test method for aircraft materials
[FAA-CT-84-22] 08 p1080 N85-16840
Challenges in the development of the orbiter radiator system 08 p1096 N85-16925
Space shuttle elevon seal panel mechanism
08 p1101 N85-16961
Composite repair of aircraft structures
08 p1120 N85-17059
A simple engineering treatment of center cracked tension panels in the regime of nonlinear fracture mechanics under plane stress conditions
[GKSS-84-E-38] 08 p1173 N85-17396
A safety evaluation of the relocation of the ACM (Air Combat Maneuver) panel in the F-14 ( )/AIP (Avionics Integration Program)
[AD-A149596] 12 p1777 N85-21158
Temperature responses of composite panels
[AD-A150053] 12 p1796 N85-21277
Power from the Sun: Light at night
[PB85-124097] 12 p1883 N85-21814
Aircraft safety improvement 15 p2689 N85-26602
The touch panel system: Design and development
[AD-A153014] 17 p3008 N85-28596
Resistance to corrosion fatigue in aluminum alloy 1561 in sea water 19 p3243 N85-30108
The thermal calculation of opaque heat screens
[BLL-M-36273-(5828.4)] 20 p3450 N85-31421
Experimental and theoretical assessment of a new technique for the non-destructive evaluation of laminated panels
[AD-A155622] 21 p3582 N85-32155
An investigation into the comparisons of the underwater shock effects on a stiffened flat plate to the predictive nature of a computer model
[AD-A155612] 21 p3600 N85-32355
Joint design for improved fatigue life of diffusion-bonded box-stiffened panels
[NASA-TP-2480] 22 p3799 N85-33537
Nonlinear response and failure characteristics of internally pressurized composite cylindrical panels
[NASA-CR-176148] 22 p3800 N85-33546
A new large-scale, high-resolution multicolor software display concept
[AD-A155404] 22 p3827 N85-33703
Removable cleanable antireflection shield
[AD-D011735] 22 p3844 N85-33810
A research program to reduce the interior noise in general aviation aircraft, index and summary
[NASA-CR-176178] 24 p4145 N85-35695

PANORAMIC CAMERAS
Calculation of image shift in panoramic photography
15 p2488 N85-25357

PANTAR CHONDRITES
Solar cosmic ray produced neon in lunar soils and their implication for gas-rich meteorite studies
06 p0887 N85-15636

PAPER (MATERIAL)
Optical mark reader
[AD-D011462] 10 p1557 N85-19818

PARABOLAS
Constrained parabolic approximation of curves in the finite element method
[CSIR-TWISK-340] 14 p2406 N85-24843
The nonlinear analysis of thick composite plates using a cubic spline function
[AD-A152115] 16 p2801 N85-27268
Curved finite elements and curve approximation
17 p3007 N85-28590

PARABOLIC ANTENNAS
Parabolic tapers for overmoded waveguides
[DE84-014237] 01 p0039 N85-10247
Dual offset reflector antenna systems with rotationally symmetric aperture distributions
[AD-A147346] 07 p0940 N85-15961
Efficient computation of reflector antenna aperture distributions and far field patterns
[AD-A147367] 07 p0940 N85-15962
Image lobe analysis for large radomes
[AD-P004359] 12 p1825 N85-21453
Experimental verification of beam deflection from hybrid reflector antenna within wide-angle sector
13 p2079 N85-22964
Null generation using discs on a reflector
[AD-A151897] 15 p2544 N85-25703
Frequency independent parabolic phased antenna array of log periodic antennas 22 p3774 N85-33387

PARABOLIC BODIES
Scattering by a parabolic cylinder: A uniform asymptotic expansion
[AD-A145880] 02 p0252 N85-11652
Progress in solar thermal distributed receiver technology
[DE85-008086] 18 p3128 N85-29372

PARABOLIC DIFFERENTIAL EQUATIONS
Time discretization of parabolic problems by the discontinuous Galerkin method
[CTH-MATH-1984-16] 04 p0556 N85-13543
Numerical investigations into the parabolized Navier-Stokes equations 05 p0635 N85-14075
A lumped mass finite element method with quadrature for a nonlinear parabolic problem
[CTH-MATH-1984-22] 05 p0719 N85-14615
Generalized predictor-corrector methods of high order for the time integration of parabolic differential equations
[CWI-NM-R8402] 08 p1214 N85-17644
On the local behaviour of solutions of degenerate parabolic equations with measurable coefficients
[AD-A147412] 09 p1373 N85-18631

Spectral methods in time for parabolic problems
[NASA-CR-172539] 11 p1706 N85-20730
Local behavior of solutions of an elliptic-parabolic equation
[AD-A149824] 12 p1920 N85-22057
Brownian motion with a parabolic drift and Airy functions
[CWI-MS-R8413] 12 p1925 N85-22097
On the stability of predictor-corrector methods for parabolic equations with delay
[CWI-NM-R8410] 14 p2410 N85-24860
On the shift parameter in the backward beam method for parabolic problems for preceding times
[CWI-NM-R8411] 14 p2410 N85-24861
Water wave propagation over uneven bottoms
[AD-A151450] 15 p2556 N85-25769
Recent progress in the development and application of the parabolic equation
[AD-A151475] 15 p2637 N85-26265
Analysis of nonlinear parabolic equations modeling plasma diffusion across a magnetic field
[DE85-007663] 17 p3040 N85-28807
Numerical and experimental investigation of turbomachinery rotor flow fields
20 p3451 N85-31429
Sobolev-Poincare's inequality and the Neumann problem for u sub t = divergence of the absolute value of the gradient u to the p-2 power x the gradient u
[AD-A154788] 21 p3676 N85-32839
FEMALE: Finite Element Method for Arbitrary Lagrangian and Eulerian elements
23 p3979 N85-34671
Long-time asymptotics of a system for plasma diffusion
[NASA-CR-177947] 24 p4093 N85-35375

PARABOLIC REFLECTORS
NT PARABOLOID MIRRORS
Liquid cooled, linear focus solar cell receiver
[DE84-014446] 01 p0067 N85-10448
RF characteristics of the hoop column antenna for the land mobile satellite system mission
[NASA-CR-3842] 02 p018 N85-11264
Analytical thermal formulations for antenna dishes — satellite antennas 05 p0627 N85-14017
Joint Indo-German program on solar energy: Parabolic dish program, step 1
[BMFT-FB-T-84-175] 05 p0670 N85-14312
Efficient computation of reflector antenna aperture distributions and far field patterns
[AD-A147367] 07 p0940 N85-15962
BBC receiving terminal for the European orbital test satellite
[BBC-RD-1984/15] 08 p1142 N85-17205
Calculation and computer simulation of the Paraboloidal Mirror Analyzer (PMA)
[DE85-001417] 09 p1384 N85-18705
Innovative solar thermal dish technology development
[DE85-002787] 11 p1673 N85-20539
Value of PV systems experiments. Volume 1: A preliminary assessment of the lessons learned from nine intermediate-size systems
[DE85-001494] 11 p1674 N85-20546
Axial focusing of signal from distant point radiator reflected twice in deep paraboloid
13 p2078 N85-22979
Synchronously deployable tetrahedral truss reflector
14 p2231 N85-23827
Electromagnetic analysis for surface tolerance effects on large space antennas 14 p2234 N85-23850
Prime-focus parabolic reflector antenna: Theory and measurement
[R-NIAS-20] 14 p2291 N85-24199
Development and testing of Parabolic Dish Concentrator No. 1
[NASA-CR-175651] 14 p2350 N85-24522
A study of structural concepts for ultralightweight spacecraft
[NASA-CR-175765] 16 p2730 N85-26848
A bibliography of reports of the Sandia solar thermal distributed receiver systems project
[SAND-84-0313] 16 p2817 N85-27378
Manufacturing cost analysis of a parabolic dish concentrator (General Electric design) for solar thermal electric power systems in selected production volumes
[NASA-CR-175772] 16 p2818 N85-27380
Activity and accomplishments of dish/Stirling electric power system development
[NASA-CR-175841] 17 p2985 N85-28445
Parabolic dish test site: History and operating experience
[NASA-CR-175892] 17 p2985 N85-28447
A program for the calculation of paraboloidal-dish solar thermal power plant performance
[NASA-CR-175874] 17 p2985 N85-28449
Shenandoah parabolic dish solar collector
[DE85-008326] 17 p2987 N85-28460
DOE/Sandia point-focus concentrator program, draft
[DE85-006209] 17 p3038 N85-28793
Progress in solar thermal distributed receiver technology
[DE85-008066] 18 p3128 N85-29372
Liquid metal thermoelectric converter (LMTEC) for solar applications
[DE85-008405] 18 p3129 N85-29376
High reflective surfaces for millimeter RF waves, phase A — satellite antenna reflectors
[HRS-FR-01] 20 p3442 N85-31366
View-limiting shrouds for insolation radiometers
[NASA-CR-176041] 20 p3458 N85-31476
Control system for parabolic dish concentrator No. 1
[NASA-CR-176045] 20 p3463 N85-31510
Optical analysis of parabolic dish concentrators for solar dynamic power systems in space
[NASA-TM-87080] 23 p3903 N85-34176

PARABOLOID MIRRORS
Influence of strut cross-section on strut radiation of reflector antennas
[FI-455-TBR-39] 03 p0357 N85-12295
Holographic corrector in objective with compound main mirror 17 p2941 N85-28153

PARABOLOIDS
U PARABOLIC BODIES

PARACHUTE DESCENT
Parachute expedition to Arctic
07 p0962 N85-16240
Tactical deployment of satellite-reporting drifting data buoys for environmental data acquisition
14 p2332 N85-24423
Processing methods of rawinsonde measurements at the descent by parachute
[KNMI-WR-84-7] 18 p3149 N85-29498

PARACHUTE FABRICS
Age life prediction of nylon 66 parachute materials. Part 1: Mechanical properties
[AD-A147698] 08 p1170 N85-17378

PARACHUTES
NT DRAG CHUTES
NT RECOVERY PARACHUTES
60,000 pound capacity extraction system
[AD-A145841] 03 p0318 N85-12052
A theoretical view on the stress analysis of fully inflated parachute canopies
[AD-A148367] 08 p1078 N85-16835
Deployment sequence mode selection system for aircraft ejection seat
[AD-D011464] 10 p1422 N85-18968
Airspeed sensing pressure valve system
[AD-D011472] 10 p1425 N85-18987
Parachute inflation dynamics
11 p1715 N85-20792
Parachute extraction device for ultralight gliders
[CH-643499-A5] 16 p2699 N85-26663
Dual towline spin-recovery device
[NASA-CASE-LAR-13076-1] 24 p4066 N85-35200

PARACHUTING
U PARACHUTE DESCENT

PARADOXES
The automated reasoning system ITP
[ANL-84-27] 12 p1914 N85-22016

PARAFFINS
Catalytic conversion of C3-C4 paraffins to gasoline
[DE85-004181] 10 p1458 N85-19187

PARAGLIDERS
NT FLEXIBLE WINGS

PARALLAX
NT STELLAR PARALLAX
Measurement of pulsar parallax by Very Long Baseline Interferometry 03 p0444 N85-12830
The parallax of pulsar 0950+08 and the local free electron density 06 p0879 N85-15584
Ranging system which compares an object reflected component of a light beam to a reference component of the light beam
[NASA-CASE-NPO-15865-1] 23 p3973 N85-34629

PARALLEL COMPUTERS
Workshop on Computer Architecture
[AD-A146455] 06 p0847 N85-15378
Solution of partial differential equations on vector and parallel computers
[NASA-CR-172500] 07 p1028 N85-16525

PARALLEL FLOW
NT PIPE FLOW
NT THREE DIMENSIONAL FLOW
Parallel flow diffusion battery
[DE84-005964] 05 p0631 N85-14047
Long range effect of turbulent pressure pulsations in plane-parallel flows at different velocities with various flame fronts 09 p1308 N85-18220
Diffusion deposition in fibrous filters for parallel and transverse flow models
[DE85-006149] 13 p2093 N85-23066
On spectral multigrid methods for the time-dependen Navier-Stokes equations
[NASA-CR-172613] 19 p3344 N85-

PARALLEL PLATES
Diffraction of plane electromagnetic wave in semiinfinite grid of parallel conductors arranged at ang to its edge 03 p0344 N85-1217
An indirect measure of below-ground electric fiel conductivity, and dielectric constant
[AD-A146518] 06 p0804 N85-1
Variational and moment method solutions of the fie in a parallel-plate waveguide-aperture system
[DE85-006288] 13 p2057 N85-
Aberration characteristics of plane-parallel compensat plate 14 p2276 N85-
Analysis of the electromagnetic scattering from an inl geometry with lossy walls
[NASA-CR-175743] 15 p2541 N85-
Collodial particle transport with simultaneous lim growth and capture
[DE85-010368] 19 p3235 N85-
Nickel cadmium cell design variable program da analysis 20 p3445 N85-

PARALLEL PROCESSING (COMPUTERS)
Aerospatiale's experimentations of vectorization o supercomputers for aircraft structural problems
01 p0007 N85-1
Initial experience with distributing structural calculation among computers operating in parallel
01 p0058 N85-1
Hardware for a real-time multiprocessor simulator
[NASA-TM-83805] 01 p0099 N85-1
Function algorithms for MPP scientific subroutines, volume 1
[NASA-CR-175246] 01 p0102 N85-1
Numerical algorithms and parallel tasking
[AD-A145090] 01 p0104 N85-1
Design and descriptive tools for systolic architecture
[DE84-015521] 02 p0239 N85-1155
Criteria for the optimization of processing flow in a model of an incremental computer with multiprocessing resources
[INPE-3046-TDL/158] 02 p0240 N85-115
Parallel triangularization of substructured finite element problems
[NASA-CR-172466] 02 p0241 N85-115
Parallel, iterative solution of sparse linear systems Models and architectures
[NASA-CR-172457] 02 p0243 N85-115
Intelligent information retrieval from on-line technica documentation
[AD-P003946] 02 p0249 N85-116
Real-time Ada (trademark)
[AD-A146258] 03 p0407 N85-126
Analysis and design methodology for VLSI computin networks
[AD-A146030] 03 p0409 N85-1261
A decomposable algorithm for contour surface disp generation
[AD-A145783] 03 p0410 N85-1261
Automatic recognition and turbuling objects
[AD-A145908] 03 p0419 N85-126
Comparison analysis of algorithm for construction functional tests for combined large-scale integrat circuits 04 p0490 N85-131
Parallel processing of numerical transport algorith
[DE84-016825] 04 p0555 N85-13
Instantaneous kinematics and joint displaceme analysis of fully-parallel robotic devices
05 p0641 N85-141
Massively parallel processor 05 p0660 N85-14
Research in computer science
[NASA-CR-174086] 05 p0713 N85-14
Concurrency in parallel processing systems
06 p0714 N85-14
Workshop on Computer Architecture
[AD-A146455] 06 p0847 N85-15
Parallel processor configuration for adaptive an arrays
[AD-D011347] 07 p0942 N85-15
Future database machine architectures
[AD-A146786] 07 p1022 N85-1
Implementation of a constraint machine for prim parallel problem solver
[AD-A147844] 07 p1026 N85-1
What a parallel programming language has to l say
[AD-A147854] 07 p1026 N85-1
Sequential and parallel matrix computations
[AD-A147871] 07 p1034 N85-1
An optimal parallel processing method for inve sparse matrices 09 p1367 N85-1
Parallel algorithms for robot dynamics
[DE84-016563] 09 p1369 N85-1
System software for the finite element machine
[NASA-CR-3870] 09 p1372 N85-1

Where are the parallel algorithms?
[NASA-CR-172516] 09 p1373 N85-18627
Domain decomposition techniques for solving elliptic partial differential equations on multiprocessors
[DE85-004448] 10 p1549 N85-19769
Parallel processing experiences on the Denelcor HEP computer
[DE85-000853] 11 p1702 N85-20703
PISCES: An environment for parallel scientific computation
[NASA-CR-172544] 12 p1913 N85-22004
Interface specifications for SCR (Software Cost Reduction) (A-7E) extended computer module, revised
[AD-A149848] 12 p1915 N85-22024
Very-high level concurrent programming
[AD-A150060] 12 p1916 N85-22026
Characterizing the parallelism in rule-based expert systems
[DE85-002432] 12 p1919 N85-22047
Parallel processing of encoded bit strings
[AD-A149812] 12 p1921 N85-22064
Optimal allocation of components in parallel-series and series-parallel systems
[AD-A150169] 13 p2144 N85-23309
Exploiting parallel computing with limited program changes using a network of microcomputers
[NASA-TM-86387] 13 p2146 N85-23318
Parallel processing for computational continuum dynamics
[AD-A150613] 13 p2147 N85-23327
Studies in parallel image processing
14 p2399 N85-24789
The enhancement of concurrent processing through functional programming languages
[AD-A150771] 14 p2404 N85-24822
Workshop on Parallel Computer Architectures in Pattern Recognition and Image Processing
[BMFT-FB-DV-84-006] 15 p2622 N85-26154
Posing of the problem, status, and future of parallel computer architecture for image processing
15 p2622 N85-26155
Recognition of objects in their natural environment — parallel processing 15 p2622 N85-26156
ADA (trademark) tasking and exceptions: A formal definition
[AD-A151618] 15 p2629 N85-26204
Harnessing computional power: Distributed combinator reduction
[DE85-005967] 15 p2631 N85-26216
Parallel time 0(log N) acceptance of deterministic CFLs
[AD-A152255] 16 p2845 N85-27539
Parallel computation of multiple-scale problems
[DE85-007230] 16 p2849 N85-27563
Parallel computing in optimization
[AD-A151812] 16 p2850 N85-27568
Local uniform mesh refinement on loosely-coupled parallel processors
[AD-A152199] 16 p2850 N85-27571
Complexity of dense linear system solution on a multiprocessor ring
[AD-A151970] 16 p2854 N85-27598
Computational plasma physics and supercomputers, revision 1
[DE85-007228] 16 p2867 N85-27687
Language design, computers and brains
[AD-A152619] 17 p3006 N85-28594
Introduction to the IEEE-488 bus
[INPE-3316-NTE/227] 17 p3010 N85-28613
Efficient parallel solution of linear systems with hyperbolic rotations
[AD-A152355] 17 p3018 N85-28661
Efficient parallel solution of linear systems
[AD-A152663] 17 p3018 N85-28663
Torus data flow for parallel computation of missized matrix problems
[DE85-008761] 17 p3026 N85-28715
Development of a butterfly multiprocessor test bed description of butterfly components
[AD-A153692] 18 p3095 N85-29155
Tradeoffs among portability, complexity, and efficiency in multiprocessing environments
[DE85-007899] 18 p3161 N85-29580
Parallel computation of multiple-scale problems, revision 1
[DE85-009447] 18 p3164 N85-29598
The prospects of the digital optical computer
18 p3186 N85-29771
A parallelized point successive over-relaxation method on a multiple instruction multiple data stream computer
[AD-A154377] 19 p3337 N85-30679
VLSI structures for numerical and digital signal processing computations 20 p3439 N85-31340
Methods for design and evaluation of integrated hardware-software systems for concurrent computation
[NASA-CR-176066] 20 p3515 N85-31851
Study of new computing algorithms for supercomputers. Application to parallel processing computation
[SNIAS-440-070/84] 20 p3516 N85-31860
Parallel simulation of digital LSI circuits
[AD-A154745] 21 p3580 N85-32258
Tight bounds on the complexity of parallel sorting
[AD-A154726] 21 p3667 N85-32778
Optimum predistortion of digital signals for transmission over parallel channels 22 p3776 N85-33397
Parallel processing on the Livermore VAX 11/780-4 parallel processor system with compatability to Cray Research, Inc. (CRI) multitasking, version 1
[DE85-011856] 23 p3967 N85-34595

PARALLEL PROGRAMMING
On the formal description and derivation of temporal proof rules for program properties
[TUM-I8405] 01 p0101 N85-10675
What a parallel programming language has to let you say
[AD-A147854] 07 p1026 N85-16513
Parallel input and feedback in dialogue cells
[CWI-CS-R8413] 11 p1703 N85-20706
PASLIB programmer's guide for the finite element machine, revision 2.1-A
[NASA-CR-172281] 11 p1705 N85-20727
Parallel linear algebra library for the Denelcor HEP
[DE85-004685] 12 p1917 N85-22034
Implementation of some concurrent algorithms
[DE85-004687] 13 p2148 N85-23334
Optical memory research and its application to digital optical processing 13 p2158 N85-23397
Use of function processors in multiprocessor systems
14 p2400 N85-24796
Dataflow computation
[CWI-TRACT-6] 14 p2406 N85-24833
Parallel programmable charge domain device
[AD-D011599] 15 p2549 N85-25733
Recent trends in software technology for vector processors 16 p2691 N85-26615
Recent advances in supercomputers
16 p2693 N85-26625
Reliability models for dataflow computer systems
[NASA-CR-175813] 16 p2848 N85-27543
Research in computer science
[NASA-CR-175922] 17 p3010 N85-28612
Tradeoffs among portability, complexity, and efficiency in multiprocessing environments
[DE85-007899] 18 p3161 N85-29580
The BLAZE language: A parallel language for scientific programming
[NASA-CR-172615] 19 p3334 N85-30656
Parallel Cholesky factorization in message-passing multiprocessor environments
[DE85-012079] 22 p3830 N85-33717
Reordering computations for parallel execution
[NASA-CR-177961] 23 p3957 N85-34522

PARALLEL STRIP LINES
U MICROSTRIP TRANSMISSION LINES

PARALLELEPIPEDS
Closely spaced independent parallel runway simulation
[DOT/FAA/CT-84/45] 04 p0457 N85-12902
Building an octree from a set of parallelepipeds
23 p3964 N85-34572

PARAMAGNETIC AMPLIFIERS
U MASERS

PARAMAGNETIC RESONANCE
NT ELECTRON PARAMAGNETIC RESONANCE

PARAMAGNETISM
High specific heat dielectrics and Kapitza resistance at dielectric boundaries
[AD-A148476] 08 p1217 N85-17686
Paramagnetic scattering from Ni
[DE85-004207] 12 p1942 N85-22196
Investigation of bimodal paramagnetic filter
13 p2083 N85-23007
Paramagnetic form factors from itinerant electron theory
[DE85-006272] 16 p2750 N85-26973
An EPR (Electron-Paramagnetic-Resonance) and ENDOR (Electron-Nuclear-Double-Resonance) study of ferroelectric ammonium sulfate
[AD-A155580] 21 p3710 N85-33033

PARAMETER IDENTIFICATION
Optimum parameters for determining the motion of radar field by cross-correlation method
01 p0079 N85-10524
List of recent Soviet space launches
02 p0165 N85-11120
Simulation study of a new inverse-pinch high Coulomb transfer switch
[NASA-CR-172420] 02 p0194 N85-11294
Control and identification of time varying systems
[AD-A145638] 02 p0252 N85-11649
CVD parameter study using strategy of experimentation
[DE84-015900] 04 p0473 N85-13011
Parametric models for signal processing: Autoregressive (AR), Moving Average (MA) and mixed autoregressive with moving average (ARMA)
[ENST-84D001] 05 p0626 N85-14028
Model estimation and identification of manual controller objectives in complex tracking tasks
05 p0700 N85-14494
Effects of control stick parameters on human controller response 05 p0701 N85-14496
A search for possible members of open clusters among known Ap stars 05 p0737 N85-14740
The Lund catalogue of open cluster parameters
05 p0738 N85-14742
Quality control of integrated circuits by parametric identification methods 06 p0796 N85-15085
Aeroelastic analysis and the identification of flight loads — Mirage 2000 aircraft 07 p0896 N85-15679
More than you want to know about maximum likelihood estimation
[NASA-TM-85905] 07 p0909 N85-15752
Estimating location parameters in a mixture
07 p0984 N85-16252
Bayesian estimation of normal mixture parameters
07 p0985 N85-16255
Snow characterization measurements from SNOW-TWO/Smoke Week 6
[AD-A147423] 07 p1008 N85-16402
Identification and parameter estimation of phosphate balance models in drinking water reservoirs
[PUBL-313] 08 p1181 N85-17439
Identification of vibration parameters of flexible structures 09 p1331 N85-18360
Dynamics and control of general linear lumped-parameter systems 09 p1372 N85-18623
Initialization of Thompson-Pisarenko's algorithm — sinusoidal signal parameter estimation
[FUB-46-1983] 09 p1375 N85-18641
A method for estimating the rolling moment due to spin rate for arbitrary planform wings
[NASA-TM-86365] 10 p1425 N85-18990
A semianalytical, artificial satellite orbit propagation procedure based on optimal parameter estimation
[INPE-3301-PRE/613] 10 p1427 N85-18997
Measurements of propagation at 900 MHz in an urban zone for establishing a digital radiomobile system
10 p1472 N85-19288
Identification of dynamic systems, theory and formulation
[NASA-RP-1138] 10 p1551 N85-19784
A three-dimensional geometric-physical model for conventional geodetic observations-observables, parameter estimation, and deformation analysis
[SER-C-298] 11 p1665 N85-20493
A proposed method for fast determination of plasma parameters
[IPP-1/228] 11 p1730 N85-20877
Determination of physical parameters of jets in radio galaxies 12 p1958 N85-22304
Air combat simulation: Methods, models, trends
13 p1967 N85-22359
Determination of aerodynamic and propulsion parameters of general aviation aircraft using steady state flight test data 13 p1971 N85-22377
Use of Walsh functions for calculating characteristics of digital filters with impulse response of finite duration
13 p2083 N85-23011
An eigensystem realization algorithm for application to modal testing 14 p2233 N85-23842
Peculiarities of MgF2 film formation and optimization of MgF2 film deposition process 14 p2281 N85-24132
Determination of directional gyro parameters
14 p2287 N85-24171
Results of studies of wave field internal structure in prediction of geological cross section
14 p2346 N85-24504
Observation model and parameter partials for the JPL VLBI parameter estimation software MASTERFIT-F 2.0
[NASA-CR-175840] 14 p2347 N85-24509
Parameter estimation in stochastic dynamic systems
14 p2395 N85-24754
Identification of dynamic systems
[AGARD-AG-300-VOL-2] 15 p2470 N85-25249
Minimax problem of estimating trajectory parameters in continuous formulation 15 p2479 N85-25301
Predischarge parameters of SF6-CO2 determined by laser 15 p2564 N85-25821
Estimation theory applied to improving dynamic structural models
[DE85-004148] 15 p2630 N85-26210
Theoretical investigation of lasing in 4.3 micron region in CO2 laser 15 p2643 N85-26306
Optimum parameters of aerogyroscopic satellite orientation system 16 p2718 N85-26782
Development and application of optimum sensitivity analysis of structures
[NASA-CR-175857] 16 p2799 N85-27257

Parameter identification results of tests in nonsteady symmetric flight with the Hawker Hunter Mk 7
[NLR-TR-83042-U] 17 p2897 N85-27860

Identification of gust input and gust response characteristics from Do 28 TNT flight test data
[DFVLR-FB-84-48] 17 p2900 N85-27861

Heating parameter estimation using coaxial thermocouple gages in wind tunnel test articles
[AD-A153039] 17 p2968 N85-28326

Robust regression through robust covariances
[AD-A153301] 17 p3020 N85-28677

Thermophysical properties correlations and pseudocomponent characterization parameter estimation for fossil fluids
[DE85-009297] 19 p3230 N85-30024

Expending expertise by use of an expert system
[DE85-010759] 19 p3344 N85-30723

Vibration control experiment design for the 15-m hoop/column antenna 20 p3409 N85-31159

A nonlinear dual-adaptive control strategy for identification and control of flexible structures
20 p3416 N85-31203

Stable direct adaptive control of linear infinite-dimensional systems using a command generator tracker approach 20 p3416 N85-31204

Maximum likelihood estimation with emphasis on aircraft flight data 20 p3417 N85-31208

Optimal sensor locations for structural identification
20 p3417 N85-31209

Combined state and parameter estimation for a static model of the Maypole (Hoop-Column) antenna suface
20 p3417 N85-31210

Experimental verification of identification algorithms for control of flexible structures 20 p3418 N85-31211

An Eigensystem Realization Algorithm (ERA) for modal parameter identification and model reduction
20 p3418 N85-31212

A residuals approach to filtering, smoothing and identification for static distributed systems
20 p3418 N85-31213

Numerical experimentation with maximum likelihood identification in static distributed systems
20 p3418 N85-31214

Geodyn systems development
20 p3492 N85-31708

An overview of nonlinear systems identification
[RR-271] 20 p3520 N85-31894

On the choice of parameterization for identification
[OUEL-1554/84] 20 p3522 N85-31904

Modelling and parameter estimation for distributed vibratory systems
[AD-A154518] 21 p3596 N85-32344

Physics of heavily doped silicon and solar-cell parameter measurement 21 p3609 N85-32418

Measuring bulk recombination rates and boundary recombination velocities 21 p3609 N85-32419

Synthesis of adaptive filters for tracking radio systems
22 p3763 N85-33325

Real-time multiparameter pulse processing with decision tables
[DE85-011663] 23 p3966 N85-34589

The effect of instrumentation system parameters on the results of a flight mechanical system identification
24 p4061 N85-35170

Aspects of input signal design for order and parameter estimation in linear dynamical systems
[ER-83/05] 24 p4091 N85-35362

A strategy for calibrating atmospheric transport models
[CSIRO-DAR-TP-9] 24 p4116 N85-35518

Recursive partitioning estimation
24 p4141 N85-35670

PARAMETERIZATION
NT PARAMETER IDENTIFICATION

Qualitative results for distributed systems with discrete damping and stiffness with application to control
[AD-A145525] 02 p0209 N85-11382

Parametric analysis for generalized network flow problems
[AD-A145558] 02 p0243 N85-11589

Asymptotically optimal adaptive control
[AD-A145666] 02 p0249 N85-11629

Fluctuations in parameters of light beam along path with reflection in turbulent atmosphere
02 p0263 N85-11722

Parameterizing extreme still water levels and waves in design level studies
[IOS-183] 03 p0398 N85-12542

Maximum likelihood and Bayesian parameter estimation in item response theory
[AD-A145775] 03 p0413 N85-12644

Priority rewrite systems — computer programming
[CWI-CS-R8407] 05 p0720 N85-14621

Construction of a confidence region for linear functions with unknown parameters
[CTH-MATH-1984-17] 05 p0721 N85-14630

An on-line parameter estimation algorithm for counting process observations
[CWI-OS-R8406] 05 p0721 N85-14632

The effects of long-periodic forcing in a zero-dimensional climate model 07 p1002 N85-16363

Development of a mixed scanning interactive system for decision support
[AD-A146695] 07 p1051 N85-16670

Radiation parameterization programs for use in general circulation models
[AD-A148015] 08 p1188 N85-17486

On the ergodicity of bilinear time series models and some applications
[AD-A148032] 08 p1215 N85-17651

Speech analysis by parametric methods: A survey
[ENST-84C004] 09 p1313 N85-18251

Stress waves in an isotropic elastic plate excited by a circular transducer
[NASA-CR-3877] 11 p1650 N85-20390

The use of analytical models to interpret measured data properly. 1. General background theory
11 p1651 N85-20400

Contribution to the study of perturbational stabilization
[ONERA-NT-1984-1] 11 p1714 N85-20781

A proposed method for fast determination of plasma parameters
[IPP-1/228] 11 p1730 N85-20877

Spatial resolution estimation of LANDSAT-4 Thematic Mapper data 12 p1872 N85-21741

Statistics for the maximum of several positive random variables with application to networking
[AD-A150005] 12 p1922 N85-22069

Polynomial parameterization in inverse gravimetric problem 13 p2115 N85-23174

Parameterization of a transient electromagnetic facility and test antennas from transient data
[DE85-006231] 15 p2545 N85-25710

Parameterization of subgrid-scale fluxes in mesoscale meteorological models
[AD-A153016] 17 p2996 N85-28523

Free-form design in solid modelling
17 p3004 N85-28569

Adapting shape parameters for cubic Bezier curves
17 p3004 N85-28576

Parameterization in grid generation
17 p3005 N85-28581

The static aeroelasticity of a composite wing
18 p3121 N85-29321

Parameterization of surface fluxes in the VVR Fourth Order GCM 18 p3142 N85-29454

Error growth in operational 10-day forecasts
18 p3143 N85-29460

Preliminary GCM results with a new radiation parameterization 18 p3145 N85-29474

A new CO2 transmittance parameterization and its impact on the GLA GCM 18 p3146 N85-29476

Control and regulation of generalized linear systems
19 p3257 N85-30193

Approximation techniques for parameter estimation and feedback control for distributed models of large flexible structures 20 p3413 N85-31179

Robust control design for large space structures
20 p3416 N85-31200

Errors and parameterizations of sub-grid scale processes in regional-scale atmospheric models
20 p3488 N85-31682

On the choice of parameterization for identification
[OUEL-1554/84] 20 p3522 N85-31904

Assessment of the performance of an in-field Gaussian plume/puff model for overwater use
[AD-A155435] 21 p3614 N85-32460

A modified Fresnel scattering model for the parameterization of Fresnel returns, part 2.3A
21 p3618 N85-32483

Criteria and algorithms for spectrum parameterization of MST radar signals 21 p3626 N85-32527

On a variational approach to some parameter estimation problems
[NASA-CR-177935] 21 p3675 N85-32829

A modal parameter extraction procedure applicable to linear time-invariant dynamic systems
[NASA-CR-176120] 22 p3835 N85-33747

Parametrized energy spectrum of cosmic-ray protons with kinetic energies down to 1 GeV
[OG-4.2-11] 22 p3678 N85-34025

Application of a turbulent closure model to the parameterization of the vertical diffusion of heat, momentum, and humidity in the ECMWF model — European Center for Medium Term Weather Forecasting (ECMWF)
[MITT-41] 24 p4095 N85-35367

A new method of differential structural analysis of gamma-family basic parameters
[HE-3.6-3] 24 p4184 N85-35952

Multiple muons in MACRO
[HE-5.2-1] 24 p4202 N85-36079

PARAMETERS
U INDEPENDENT VARIABLES

PARAMETRIC AMPLIFIERS

Millimeter-wave range masers: A review
13 p2089 N85-220

PARAMETRIC FREQUENCY CONVERTERS

Principles of designing digital compensatin accelerometers 17 p2944 N85-281

PARAMETRIC OSCILLATORS
U PARAMETRIC AMPLIFIERS

PARATHYROID GLAND

The salutary effect of dietary calcium on bone mass i a rat model of simulated weightlessness
15 p2808 N85-280

PARITY

Spurious center of mass effects in a dynamical determined basis
[CSIR-TWISK-310] 01 p0109 N85-107

Parity and time-reversal non-conversation in atom
[DE84-016924] 04 p0562 N85-135

Selected topics from J/psi decays
[DE85-010537] 18 p3183 N85-297

Spatial parity violation in elastic neutron-nucl interaction channel 21 p3691 N85-328

PARKING ORBITS

The international environment UNISPACE '82 and th ITU: A relationship between orbit-spectrum resource allocation and orbital debris 12 p1787 N85-212

PARKINSON DISEASE

Influence of activation of ASFS-2 on human emotional status 08 p1194 N85-175

PARKS
NT NATIONAL PARKS

PARSING ALGORITHMS

Toward a principle-based parser
[AD-A147637] 08 p1202 N85-175

Steps towards parsing of query sequences to a database
[AD-A148769] 08 p1206 N85-175

An algorithm for generating abstract syntax trees
[NASA-CR-172541] 12 p1912 N85-220

Construction of a menu-based system
[NASA-CR-172560] 13 p2146 N85-232

Evaluating syntactic constraints to speech recognitio in a fighter aircraft environment
[AD-A152117] 16 p2773 N85-271

Speech understanding research
[AD-A155462] 21 p3700 N85-329

Project management using graphics
23 p3962 N85-345

Artificial intelligence in Ada (trademark): Pattern-directed processing
[AD-A156230] 24 p4141 N85-356

PARTIAL DIFFERENTIAL EQUATIONS
NT BIHARMONIC EQUATIONS
NT BURGER EQUATION
NT ELLIPTIC DIFFERENTIAL EQUATIONS
NT EULER-CAUCHY EQUATIONS
NT FOKKER-PLANCK EQUATION
NT GAUSS EQUATION
NT HELMHOLTZ VORTICITY EQUATION
NT LIOUVILLE EQUATIONS
NT MONGE-AMPERE EQUATION
NT PARABOLIC DIFFERENTIAL EQUATIONS
NT VLASOV EQUATIONS

The approximation of nonsmooth solutions of hyperbolic partial differential equations
[CSIR-TWISK-297] 01 p0108 N85-107

Qualitative results for distributed systems with discrete damping and stiffness with application to control
[AD-A145525] 02 p0209 N85-113

Approximation of discontinuous solutions of hyperbolic partial differential equations
[NRIMS-TWISK-302] 02 p0250 N85-116

Numerical methods for singularly perturbed differential equations with applications
[AD-A145639] 02 p0252 N85-116

A pseudospectral Legendre method for hyperbolic equations with an improved stability condition
[NASA-CR-172475] 03 p0410 N85-126

Convergence of SIP (Strongly Implicit Procedure)
[AD-A145810] 03 p0410 N85-126

Moving finite elements in 2-D
[AD-A146266] 03 p0412 N85-126

Solution generating technique for the Einste equations 03 p0435 N85-127

Step-by-step stability in the numerical solution of partial differential equations
[CWI-NW-161/83] 05 p0720 N85-148

Convergence of method of lines approximations to partial differential equations
[CWI-NM-R8404] 05 p0720 N85-145

Viscosity solutions of Hamilton-Jacobi equations at the boundary
[AD-A147444] 07 p1032 N85-160

Splitting methods for the numerical solution of the incompressible Navier-Stokes equations
[AD-A147463] 07 p1032 N85-16554

On existence and uniqueness of solutions of Hamilton-Jacobi equations
[AD-A147597] 07 p1033 N85-16560

Composites with a periodic structure, mathematical analysis and numerical treatment
[AD-A148301] 08 p1119 N85-17063

Thermal-stress analysis for a wood composite blade
[NASA-CR-174794] 08 p1178 N85-17421

Three-dimensional, direct and vectorized elliptic solvers for various boundary conditions
[AD-B088266L] 08 p1206 N85-17595

A moving finite element method for time dependent partial differential equations with error estimation and refinement
[AD-A147719] 08 p1210 N85-17617

A local refinement finite element method for time dependent partial differential equations
[AD-A147943] 08 p1211 N85-17620

A feedback finite element method with a posteriori error estimation. Part 1. The finite element method and some basic properties of the A posteriori error estimator
[AD-A148345] 08 p1212 N85-17631

Generation of 3-dimensional body fitted coordinates using hyperbolic partial differential equations
[AD-A148059] 09 p1274 N85-18006

Designing the profile of turbine blades using an iteration technique
09 p1305 N85-18201

Accuracy of the finite analytic method for scalar transport calculations
[DE85-001474] 09 p1320 N85-18300

The implementation of irregular grid systems for the finite difference solution of partial differential equations
[LU-MATH-RES-161] 09 p1373 N85-18630

Solution of the h-equation for a single point source excitation of magnitude K
[DE84-017574] 09 p1374 N85-18636

Annals of the Finnish Academy of Sciences, series A. 1: Mathematics, volume 8, part 2
[ISSN-0066-1953] 10 p1535 N85-19673

Towards the construction of periodic solutions of pseudodifferential equations with the aid of algebraic operators
10 p1535 N85-19674

Analytical foundations of the theory of quasiconformal mappings in Rn
10 p1536 N85-19679

A non-hypoelliptic Dirichlet problem from stochastics
10 p1537 N85-19687

New methods for numerical solution of one class of strongly nonlinear partial differential equations with applications in hydrodynamics
[AD-A149028] 10 p1545 N85-19739

Vectorization and implementation of an efficient multigrid algorithm for the solution of elliptic partial differential equations
[AD-A149049] 10 p1545 N85-19743

Neumann type boundary conditions for Hamilton-Jacobi equations
[AD-A149069] 10 p1546 N85-19746

Symmetry breaking for a class of semi-linear elliptic problems
[AD-A149093] 10 p1546 N85-19748

Hamilton-Jacobi equations in infinite dimensions. Part 1. Uniqueness of viscosity solutions
[AD-A149094] 10 p1546 N85-19749

Evaluation of time integrators for the shallow water equations
[CWI-NM-R8406] 11 p1634 N85-20292

Solving partial differential equations on multiprocessors
[DE85-000745] 11 p1706 N85-20734

Transverse vibration and buckling of a cantilevered beam with tip body under constant axial base acceleration
[NASA-CR-175567] 12 p1864 N85-21694

Numerical methods for tracking interfaces
[LA-9917-MS] 12 p1919 N85-22052

Effect of compliability of hot walls in liquid-propellant engine on low frequency instability
13 p2049 N85-22824

Models of discontinous random fields
13 p2079 N85-22983

A mathematical formulation of the Scole control problem, part 1
[NASA-CR-172581] 14 p2243 N85-23903

Implementation of a C1 triangular element based on the p-version of the finite element method
[AD-A150904] 14 p2404 N85-24825

The generation of three-dimensional body-fitted coordinate systems for viscous flow problems
[AD-A150861] 14 p2408 N85-24848

Application of adaptive grids in solving the partial differential equations governing fluid flow
[AD-A151175] 15 p2555 N85-25766

Pseudo-unsteady systems for steady inviscid flows
[ESA-TT-877] 15 p2556 N85-25782

Very large least squares problems and supercomputers
[AD-A151270] 15 p2623 N85-26162

Analysis of spectral operators in one-dimensional domains
[NASA-CR-172573] 15 p2633 N85-26228

Solution of coupled system of PDE by the transistorized multigrid method
[DE85-006377] 15 p2639 N85-26276

Analysis of combustion oscillations in heterogeneous systems
[AD-A151999] 16 p2745 N85-26942

A split explicit model for short-term numerical weather prediction
16 p2831 N85-27460

Local uniform mesh refinement on loosely-coupled parallel processors
[AD-A152199] 16 p2850 N85-27571

Uniformly high-order accurate non-oscillatory schemes, 1
[NASA-CR-175766] 16 p2853 N85-27589

On the choice of coordinates for semiconductor simulation
[AD-A152214] 16 p2870 N85-27708

Natural vibrations of reinforced spherical shells
17 p2943 N85-28165

Parameterization in grid generation
17 p3005 N85-28581

A survey of composite grid generation for general three-dimensional sections
17 p3006 N85-28584

Solving elliptic partial differential equations on the hypercube multiprocessor
[AD-A153464] 18 p3168 N85-29629

The Cauchy problem for u sub t = Delta u(m) when O m 1
[AD-/.153521] 18 p3169 N85-29635

Well-posedness of one-way wave equations and absorbing boundary conditions
[NASA-CR-172619] 19 p3345 N85-30727

An iterative method for indefinite systems of linear equations
[NASA-CR-172345] 19 p3345 N85-30728

Finite control in underdamped distributed parameter systems
20 p3412 N85-31176

Proceedings of the 1st Workshop for the Design of Expert System Partial Differential Equation Solvers
[AD-A154192] 20 p3515 N85-31853

Generation of three-dimensional body-fitted coordinates using hyperbolic partial differential equations
[NASA-TM-86753] 20 p3519 N85-31887

A derivation of relativistic effects in satellite tracking
[AD-A154620] 21 p3558 N85-32132

A variable node finite element method applied to the gas dynamics equations
[AD-A155211] 21 p3584 N85-32281

On a variational approach to some parameter estimation problems
[NASA-CR-177935] 21 p3675 N85-32829

A review of spectral methods
[NASA-CR-172502] 23 p3929 N85-34350

Transient three-phase three-component systems. Part 1: Formulation of the system of differential equations
[DE85-013267] 24 p4095 N85-35384

Analysis of the nonlinear equations describing the elastic, thermal, and electromagnetic behavior of solids: Existence of solutions of semi-inverse problems
24 p4100 N85-35415

Stress analysis of axisymmetric sandwich shells of variable thickness
24 p4101 N85-35419

PARTIAL PRESSURE

NT HYPOXEMIA
NT OXYGEN TENSION

Variations with time of the carbon dioxide partial pressure in central and south Atlantic surface waters
[AD-A145825] 03 p0398 N85-12537

Reconstruction of past atmospheric CO/sub 2/ contents from the chemistry of the contemporary ocean: An evaluation
[DE85-008426] 18 p3133 N85-29401

Determination of kinetic parameters of molecular beam epitaxy
[AD-A156222] 21 p3710 N85-33030

Thermodynamics of the corrosion of chromium in molten carbonates
[DE85-011407] 24 p4079 N85-35282

PARTICLE ACCELERATION

High energy-resolution inelastic X-ray scattering
[DE84-014565] 01 p0118 N85-10804

Notes on NAC report NAC-83-05: Beam Pulse Length Determination by Spectral Analysis
[CSIR-NAC-83-06] 01 p0119 N85-10816

Long time correlation and stochastic diffusion in the standard map
02 p0282 N85-11835

Electric field and plasma energization in computer simulations of magnetotail reconnection
[DE84-014023] 02 p0285 N85-11859

Particle acceleration in two-ribbon flares — solar flares
04 p0519 N85-13314

The Earth magnetosphere: A charged particle accelerator
04 p0519 N85-13315

Particle physics
[DE84-013834] 05 p0727 N85-14673

Electromagnetic acceleration of macroparticles to hypervelocities in axisymmetric geometry
[IPPJ-696] 06 p0863 N85-15484

Corotating interaction regions in stellar winds: Particle acceleration and non-thermal radio emission in hot stars
08 p1234 N85-17773

Synchrotron emission from chaotic stellar winds
08 p1234 N85-17774

Collimated winds from active galactic nuclei
08 p1241 N85-17832

Observation of a westward travelling surge from satellites at low, medium and high altitudes
[NASA-TM-87434] 09 p1342 N85-18442

Review of polarized proton beam techniques and a report on the workshop on polarized beams
[DE85-004390] 12 p1930 N85-22127

Strong iron accelerating by collisionless magnnetosonic shock wave propagating perpendicular to a magnetic field
[IPPJ-709] 12 p1935 N85-22161

Neutron and gamma-ray signatures for particle acceleration in solar flares
12 p1954 N85-22278

Self-similar modified shock structures — cosmic rays
12 p1956 N85-22290

Explosive transverse electric field and particle acceleration during magnetic collapse — cosmic plasma
12 p1956 N85-22292

Signatures of the coalescence instability in solar flares
12 p1956 N85-22293

Hydrodynamics of astrophysical jets — active galactic nuclei
12 p1958 N85-22307

Streaming reversal of energetic particles in the magnetotail during a substorm
14 p2358 N85-24571

SAMBO-GEOS: Substorm trapped particle particle boundary movements, particle precipitation and acceleration
14 p2361 N85-24589

High energy particle acceleration by coherent electromagnetic waves propagating across the magnetic field
[IPPJ-717] 16 p2866 N85-27679

Fundamentals of plasma simulation
[DE85-007699] 16 p2867 N85-27683

IMS (International Magnetospheric Study) contributions to the understanding of auroral precipitation, transport, and particle sources
[AD-A152320] 17 p2992 N85-28492

Wide-angle optics with strong magnetic fields for efficient generation of secondary-particle beams
[DE85-007727] 18 p3179 N85-29713

Activities report of the Werner-Heisenberg Institute for Physics
[ISSN-0173-6256] 18 p3184 N85-29748

Time-resolved energy spectrum of the ion beam generated in the plasma focus
19 p3369 N85-30892

Experimental study of laser produced ions for collective ion acceleration
20 p3460 N85-31494

Publications from the Department of Plasma Physics and the Unit of Accelerator Technology, index and abstracts, 1984
[TRITA-EPP-84-13] 20 p3534 N85-31991

500 TeV gamma rays from Hercules X-1
[OG-2.2-7] 22 p3865 N85-33933

Physics Division annual review, 1 April 1983 - 31 March 1984
[ANL-84-24] 23 p3969 N85-34602

Ninteenth International Cosmic Ray Conference. SH sessions, volume 4
[NASA-CP-2376-VOL-4] 23 p3989 N85-34729

Stochastic particle acceleration in solar flares
[SH-1.1-4] 23 p3989 N85-34731

First-order shock acceleration in solar flares
[SH-1.1-5] 23 p3989 N85-34732

Prompt acceleration of ions by oblique turbulent shocks in solar flares
[SH-1.1-6] 23 p3989 N85-34733

Study of photon emission by electron capture during solar nuclei acceleration, 1: Temperature-dependent cross section for charge changing processes
[SH-1.1-8] 23 p3990 N85-34735

Study of photon emission by electron capture during solar nuclei acceleration. 2: Delimitation of conditions for charge transfert establishment
[SH-1.1-9] 23 p3990 N85-34736

Study of non-thermal photon production under different scenarios in solar flares. 2: The Compton inverse and Bremsstrahlung models and fittings
[SH-1.2-3] 23 p3991 N85-34739

Quantitative analysis of flare accelerated electrons through their hard X-ray and microwave radiation
[SH-1.2-7] 23 p3991 N85-34742

Two classes of solar energetic particle events associated with impulsive and long duration soft X-ray flares
[SH-1.2-12] 23 p3992 N85-34747

The energy spectra of solar flare electrons
[SH-1.2-14] 23 p3992 N85-34749

The starting conditions for an optically small solar gamma ray flare
[SH-1.3-2] 23 p3993 N85-34751

Observations of solar flare gamma-rays and protons
[SH-1.3-6] 23 p3993 N85-34753

Energetic protons from a disappearing solar filament
[SH-1.3-7] 23 p3993 N85-34754

Helios 1 energetic particle observations of the solar gamma ray flare events of 7, 21 June 1980 and 3 June 1982
[SH-1.3-8] 23 p3993 N85-34755

Shock and statistical acceleration of energetic particles in the interplanetary medium
[SH-1.5-1] 23 p3996 N85-34771

Particle acceleration due to shocks in the interplanetary field: High time resolution data and simulation results
[SH-1.5-5] 23 p3996 N85-34774

Spatial dependence of the local diffusion coefficient measured upstream of the November 12, 1978 interplanetary traveling shock
[SH-1.5-12] 23 p3996 N85-34776

Latitude dependence of co-rotating shock acceleration
[SH-1.5-14] 23 p3997 N85-34777

Elemental abundences in corotating events
[SH-1.5-15] 23 p3997 N85-34778

Cosmic ray acceleration by stellar wind. Simulation for heliosphere
[SH-1.5-17] 23 p3997 N85-34780

On the retention of high-energy protons and nuclei with charges Z or equal to 2 in large solar flares after the process of their acceleration
[SH-2.1-8] 23 p3998 N85-34789

Type 3 solar radio bursts and 3HE-rich events
[SH-2.2-3] 23 p4000 N85-34798

Elemental abundance differences between nuclei acclerated in CIR shocks and solar flares
[SH-2.2-6] 23 p4000 N85-34801

On the connection between the 3HE-enrichment and spectral index of solar energetic particles
[SH-2.2-9] 23 p4001 N85-34804

The plasma mechanism for preferential acceleration of heavy ions
[SH-2.2-10] 23 p4001 N85-34805

Nineteenth International Cosmic Ray Conference. OG sessions, volume 3
[NASA-CP-2376-VOL-3] 23 p4012 N85-34862

Sources of the ultraheavy cosmic rays
[OG-7.1-7] 23 p4013 N85-34868

Selfsimilar time dependent shock structures
[OG-8.1-4] 23 p4017 N85-34894

The central engine of quasars and AGNs: A relativistic proton radiative shock
[OG-8.1-7] 23 p4018 N85-34897

A model for the origin of high-energy cosmic rays
[OG-8.1-8] 23 p4018 N85-34898

Onion-shell model for cosmic ray electrons and radio synchrotron emission in supernova remnants
[OG-8.1-10] 23 p4018 N85-34900

Approximate supernova remnant dynamics with cosmic ray production
[OG-8.1-12] 23 p4019 N85-34901

Efficiency of regular acceleration of particles by a shock wave at different injection regimes
[OG-8.1-13] 23 p4019 N85-34902

The nucleosynthesis of deterium and helium-3
[OG-8.2-18] 23 p4020 N85-34914

Pulsars as cosmic ray particle accelerators: Proton orbits
[OG-8.2-21] 23 p4021 N85-34917

Pulsars as cosmic ray accelerators: Energy development of protons
[OG-8.2-22] 23 p4021 N85-34918

Propagation of injected cosmic rays under distributed reacceleration
[OG-8.3-3] 23 p4021 N85-34922

Secondary to primary ratio and the continuous acceleration
[OG-8.3-4] 23 p4022 N85-34923

Propagation of cosmic rays and new evidence for distributed acceleration
[OG-8.3-5] 23 p4022 N85-34924

Exact solutions for sporadic acceleration of cosmic rays
[OG-8.3-7] 23 p4022 N85-34925

Stochastic particle acceleration in flaring stars
[OG-8.3-9] 23 p4022 N85-34927

On the anomalous component
[SH-4.6-6] 23 p4039 N85-35044

Possible origin of the anomalous component of cosmic rays
[SH-4.6-7] 23 p4039 N85-35045

PARTICLE ACCELERATOR TARGETS

Experimental medium energy physics
[DE84-014625] 02 p0276 N85-11807

ATLAS beam properties: Some implications for target making
[DE84-006595] 02 p0278 N85-11812

Long-pulse beamlines for the mirror fusion test facility
[DE84-017091] 09 p1392 N85-18760

Proceedings of the Workshop on Polarized Targets in Storage Rings
[DE85-002704] 16 p2862 N85-27653

Laser measurements of distances from the ORELA neutron target to experiment stations along flight paths 1 and 6
[DE85-009457] 17 p2971 N85-28352

Mouse oocyte killing by neutrons: Target considerations
[DE85-011362] 19 p3328 N85-30624

Fixed-target physics at Fermilab
[DE85-010141] 20 p3528 N85-31942

Nuclear physics in the 10 to 300 MeV energy range using a pulsed white neutron source
[DE85-003713] 22 p3839 N85-33775

Light ion sources for ICF
[DE85-011544] 23 p3983 N85-34702

Interactions of heavy nuclei, Kr, Xe and Ho, in light targets
[OG-7.2-21] 23 p4016 N85-34888

Event parameters: Fixed targets
24 p4146 N85-35702

Working group on penetrating probes at fixed target facilities 24 p4146 N85-35703

Summary of the working group on penetrating probes in collider experiments. 1: The collider environment
24 p4146 N85-35704

(NAT)Fe(n,n'x) spectra at 65.5 MeV
[AD-A155776] 24 p4150 N85-35730

Radiation safety problems in handling highly active tritium targets
[DE85-014268] 24 p4151 N85-35742

Neutron production by Ne and Si ions on a thick Cu target at 670 MeV/A with application to radiation protection
[DE85-014526] 24 p4152 N85-35746

Major facility overhauls at LAMPF
[DE85-012724] 24 p4156 N85-35765

Recent advances in remote handling at LAMPF
[DE85-012725] 24 p4157 N85-35775

How are particle production, nucleon emission and target fragment evaporation processes interrelated in hadron-nucleus collisions? 24 p4174 N85-35878

PARTICLE ACCELERATORS

NT BETATRONS
NT CYCLIC ACCELERATORS
NT CYCLOTRONS
NT ELECTRON ACCELERATORS
NT ION ACCELERATORS
NT LINEAR ACCELERATORS
NT MICROTRONS
NT STORAGE RINGS (PARTICLE ACCELERATORS)
NT SYNCHROTRONS

Accelerator technology program
[DE84-015052] 01 p0118 N85-10806

Engineering Physics Division
[DE84-007778] 02 p0274 N85-11787

Diffraction by the time-of-flight technique at pulsed neutron sources
[DE84-015839] 03 p0418 N85-12674

Utilization of a tandem accelerator for the investigation of solid state properties by means of heavy ions
03 p0429 N85-12733

Laser-driven particle accelerators
[DE84-015953] 04 p0506 N85-13227

Fast neutron capture with a white neutron source
[DE84-016799] 04 p0562 N85-13580

Accelerator Technology Program
[DE84-017083] 04 p0563 N85-13586

A proton laser accelerator by means of the inverse free electron laser mechanism
[DE85-000231] 06 p0813 N85-15163

Electron beam propagation along charged foils
[DE85-002137] 06 p0861 N85-15472

Fermilab research program workbook
[DE84-012568] 06 p0862 N85-15476

Bunch coalescing in the main ring to form intense proton and antiproton bunches without RF counterphasing
[DE85-001364] 09 p1382 N85-18692

High energy pulsed particle accelerator
[AD-A149247] 10 p1554 N85-19797

IREB (Intense Relativistic Electron Beam) converter to ac pulses
[AD-D011479] 10 p1554 N85-19800

Simulation of space charge effects in particle accelerators
[DE85-001828] 12 p1929 N85-22120

Variable flexing device for targets in internal beams of charged particle accelerators 13 p2044 N85-22797

Experimental studies of elementary particle interactions at high energies
[DE85-004795] 13 p2157 N85-23094

Explosive emission cathode plasmas in intense relativistic electron beam diodes
[AD-A150669] 14 p2417 N85-24912

Radio frequency quadrupole and alternating phase focusing methods used in proton linear accelerator technology in the USSR
[AD-A150830] 14 p2418 N85-24916

Standard model and beyond
[DE85-004269] 14 p2418 N85-24919

Summaries of FY 1984 research in high energy physics
[DE85-005641] 14 p2420 N85-24934

Beam trapping in high current cyclic accelerators with strong focusing fields
[AD-A151392] 15 p2648 N85-26331

Modified betatron accelerator studies
[AD-A151420] 15 p2648 N85-26332

Development of RF plasma generators for neutral beams
[DE85-004125] 15 p2658 N85-26400

Space station as quark matter factory
[DE85-004606] 15 p2685 N85-26586

Two-dimensional beat wave acceleration simulation
[DE85-005961] 16 p2791 N85-27214

Experiments and detectors for high energy heavy ion colliders
[DE85-007927] 17 p3031 N85-28748

Report of the Working Group on Other Acceleration Schemes
[DE85-008447] 17 p3033 N85-28764

Activities report in nuclear physics and high energy physics
[JF40026] 17 p3035 N85-28777

Accelerator technology working group summary
[DE85-009547] 18 p3180 N85-29717

A collective interaction klystron specification
[AD-D011704] 19 p3255 N85-30186

Research activities of the Physics Division
[DE85-006958] 19 p3357 N85-30611

Possibilities for studying short-lived nuclei produced at LAMPF
[DE85-010740] 19 p3365 N85-30664

Development of a resistive load for PBFA 2 rimfire gas switch simultaneity and laser triggering tests
[DE85-011080] 19 p3365 N85-30669

Method to render second order beam optics programs symplectic
[DE85-010631] 20 p3515 N85-31855

Fixed-target physics at Fermilab
[DE85-010141] 20 p3528 N85-31942

Plastic scintillator detectors for the study of transfer and breakup reactions at intermediate energies
[DE85-009945] 20 p3528 N85-31945

Current experiments in elementary particle physics, revision 1-85
[DE85-011513] 20 p3529 N85-31950

Activities report in nuclear physics and particle acceleration 20 p3532 N85-31977

An absolute calibration of the solid state detectors in the narrow band neutrino beam at CERN
[NIKHEF-H/84-10] 20 p3538 N85-32017

Vacuum interface flashover with bipolar electric fields
[DE85-012027] 22 p3753 N85-33275

Model that predicts pulse charged gas switching breakdown phenomena
[DE85-013119] 22 p3761 N85-33313

PMEXA: Diagnostic filtering program for the PBFA-1 performance monitoring and evaluation system
[DE85-013179] 22 p3831 N85-33725

Supermite vacuum interface design
[DE85-012861] 22 p3837 N85-33759

Rf program for LAMPF 2
[DE85-012693] 22 p3837 N85-33760

Summary of activities, 1983
[LBL-18500] 23 p3969 N85-34605

Repetitive pulse accelerator technology for light ion inertial confinement fusion
[DE85-012030] 23 p3982 N85-34693

Distribution of computer functionality for accelerator control at the Brookhaven AGS
[DE85-012520] 24 p4141 N85-35669

Width of nonlinear difference resonances
[DE85-013026] 24 p4148 N85-35719

Quality assurance considerations for the implementation of a pulsed power R and D project
[DE85-012357] 24 p4148 N85-35720

Operations considerations in designing a high speed multi-channel data acquisition system
[DE85-012840] 24 p4154 N85-35756

High vacuum portable pumping station suitable for accelerator use
[DE85-011840] 24 p4155 N85-35759

Ion source development for the Los Alamos heavy ion fusion injector
[DE85-012682] 24 p4156 N85-35766

Surface discharges as intense photon sources in the extreme ultraviolet
[DE85-012593] 24 p4158 N85-35782

SLC arc transport system: Magnet design and construction
[DE85-014289] 24 p4159 N85-35789

PARTICLE BEAMS

NT ATOMIC BEAMS
NT ELECTRON BEAMS
NT ION BEAMS
NT MOLECULAR BEAMS
NT NEUTRAL BEAMS
NT NEUTRINO BEAMS
NT NEUTRON BEAMS
NT PION BEAMS
NT PROTON BEAMS
NT RELATIVISTIC ELECTRON BEAMS

Visible wavelength interferometer for high speed electron density diagnostics
[AD-A145686] 02 p0277 N85-11803

Antiproton source beam position system
[DE84-016716] 09 p1380 N85-18679

Force balance limiting current for charged particle beams
[DE84-016976] 09 p1381 N85-18685

Computerized study of several electrostatic, surface-ionization ion-source configurations
[DE85-001512] 11 p1721 N85-20823

Theory of lethality
[DE85-000457] 11 p1721 N85-20826

Low-energy, high-intensity positron beam experiments with a linac
[DE85-001048] 11 p1723 N85-20835

Numerical model for swirl cooling in high-heat-flux particle beam targets and the design of a swirl-flow-based plasma limiter
[DE85-003824] 11 p1732 N85-20894

Statistical phenomena in particle beams
[DE85-001050] 12 p1929 N85-22118

Suppression of tilting instability of a compact torus by energetic particle beams
[IPPJ-705] 12 p1935 N85-22157

High energy facilities advanced projects: Intrabeam scattering for a beam of gold ions
[DE85-000887] 12 p1941 N85-22192

Experimental investigation of neutral plasma beam propagation across a magnetic field
[AD-A150944] 14 p2423 N85-24947

Noninductive current drive in Tokamaks
[DE85-005427] 14 p2424 N85-24951

Sound emission by particle beam passing through hole in rigid shield 15 p2525 N85-25570

Modified betatron accelerator studies
[AD-A151420] 15 p2648 N85-26332

A proportional-plus-integral controller for a particle beam weapon
[AD-A153213] 17 p3035 N85-28778

Comparison of simulation with experiment in an RFQ
[DE85-010770] 19 p3349 N85-30757

Optical beam deflection detection of thermal waves in opaque solids 19 p3374 N85-30927

Permanent magnets for production and use of high energy particle beams
[DE85-009934] 20 p3522 N85-31905

Fixed-target physics at Fermilab
[DE85-010141] 20 p3528 N85-31942

Current experiments in elementary particle physics, revision 1-85
[DE85-011513] 20 p3529 N85-31950

Requirements for very high energy accelerators
[DE85-011173] 20 p3529 N85-31952

Studies in mixed species charged particle beam dynamics
[OUEL-1545/84] 20 p3531 N85-31969

Injection of hydrogen macroparticles into T-10 tokamak 21 p3692 N85-32937

Model that predicts pulse charged gas switching breakdown phenomena
[DE85-013119] 22 p3761 N85-33313

PMEXA: Diagnostic filtering program for the PBFA-1 performance monitoring and evaluation system
[DE85-013179] 22 p3831 N85-33725

Rf program for LAMPF 2
[DE85-012693] 22 p3837 N85-33760

Polarization of fast particle beams by collisional pumping
[DE85-011621] 22 p3838 N85-33764

Accelerator vibration issues
[DE85-010766] 22 p3842 N85-33791

Interrelations for the elements of the scattering matrix
22 p3855 N85-33872

Space Experiments with Particle Accelerators (SEPAC) 23 p3901 N85-34165

Recoverable Plasma Diagnostics Package (RPDP)
23 p3902 N85-34167

Neutral particle beam intensity controller
[DE85-006411] 23 p3969 N85-34604

Theoretical and computational research on the focused transport of intense charged particle beams
[DE85-012980] 23 p3972 N85-34621

Depth and size effects on cosmogenic nuclide production in meteorites
[SH-7.1-9] 23 p4046 N85-35101

Observations of accelerated high current low emittance beams in the SLC Linac
[DE85-013073] 24 p4068 N85-35211

Operations considerations in designing a high speed multi-channel data acquisition system
[DE85-012840] 24 p4154 N85-35756

Synchronous timing of multi-energy fast beam extraction during a single AGS cycle
[DE85-011829] 24 p4158 N85-35781

Relation between field energy and RMS emittance in intense particle beams
[DE85-012655] 24 p4159 N85-35784

Accelerator physics measurements at the damping ring
[DE85-013373] 24 p4159 N85-35785

PARTICLE COLLISIONS

Large linear colliders
[DE84-015700] 02 p0278 N85-11811

Report of the reference designs study group on the superconducting super collider
[DE84-015567] 04 p0569 N85-13630

Waves and instabilities in collisionless shocks
[AD-A146689] 06 p0881 N85-15597

Theoretical studies relating to the interaction of radiation with matter: Atomic collision processes occurring in the presence of radiation fields
[AD-A146854] 07 p1040 N85-16602

SU(2) x U(1) vacuum and the Centauro events
[NASA-TM-86082] 08 p1260 N85-17926

Very high energy probes of the quark-gluon plasma
[DE84-016992] 09 p1392 N85-18763

Quantum mechanical and semiclassical approaches to molecular dynamics
[DE85-003458] 10 p1555 N85-19803

Correlated 2 electron effects in collisions of multiply charged Au ions with He
[DE85-003064] 11 p1723 N85-20837

Simulating supersymmetry at the SSC
[DE85-000699] 11 p1736 N85-20917

Theoretical study of near-threshold electron-molecule scattering
[DE85-004530] 12 p1930 N85-22126

Adequacy of metal ablation process with laser radiation and a shock-compressed plasma
13 p2028 N85-22706

Future accelerator studies of high energy heavy ion collisions
[DE85-005885] 15 p2650 N85-26346

Evolution of collisional systems — planetary disks
15 p2674 N85-26505

Size distribution in collisional systems — planetary rings 15 p2674 N85-26506

Comments on collision mechanics in ring systems — planetary rings
[PSI-CONTRIB-186] 15 p2675 N85-26510

Tables of nuclear cross sections for galactic cosmic rays: Absorption cross sections
[NASA-RP-1134] 16 p2864 N85-27665

Measuring structure functions at SSC energies
[DE85-007515] 17 p3031 N85-28746

Cluster production and entropy
[DE85-007626] 17 p3032 N85-28752

New experimental results in two photon physics
[NIKHEF-H/84-16] 17 p3035 N85-28776

Physics of (very) high energy e(+)-e(-) colliders
[DE85-008177] 17 p3036 N85-28780

High energy gamma rays from complex particle collisions
[DE85-007871] 17 p3036 N85-28783

Excited state populations and charge-exchange of fast ions in solids
[DE85-009362] 18 p3180 N85-29714

Present and future directions of atomic physics research with multiply-charged ions at Brookhaven National Laboratory
[DE85-010960] 19 p3354 N85-30788

Proceedings of the 1984 Workshop on High-Energy Excitations in Condensed Matter, volume 2
[DE85-007395] 19 p3357 N85-30800

Pion production and the nuclear equation of state
[DE85-009941] 19 p3365 N85-30870

Multiple collision solutions for time-dependent neutron transport in slabs of finite thickness
[OEFZS-4312] 22 p3838 N85-33762

Gamma ray line production from cosmic ray spallation reactions 22 p3875 N85-34005

Radial transport caused by collision
23 p3976 N85-34652

Electron loss process and cross section of multiply charged ions by neutral atoms 23 p3981 N85-34685

Low-energy sputterings with the Monte Carlo Program ACAT
[IPPJ-AM-40] 23 p3982 N85-34690

Cross sections for the production of fragments with Z greater than or equal to 8 by fragmentation of Z greater than or equal to 9 and less than or equal to 26 nuclei
[OG-7.2-22] 23 p4016 N85-34889

The response of ionization chambers to relativistic heavy nuclei
[OG-9.1-13] 23 p4024 N85-34939

Plastic scintillators in coincidence for the study of multi-particle production of sea level cosmic rays in dense medium
[SH-9.1-11] 23 p4052 N85-35126

The use of austenitic stainless steel versus monel (Ni-cu) alloy in pressurized Gaseous Oxygen (GOX) life support systems
[AD-A156305] 24 p4134 N85-35625

Working group on penetrating probes at fixed target facilities 24 p4146 N85-35703

Summary of the working group on penetrating probes in collider experiments. 1: The collider environment
24 p4146 N85-35704

Report of working group on detectors for hadrons and event parameters at colliders 24 p4146 N85-35705

A survey of multiplicities and rapidity densities from existing emission data on hadron-nucleus nucleus-nucleus collisions 24 p4146 N85-35706

A simulation of ultra-relativistic nucleus-nucleus collisions 24 p4146 N85-35707

Very high energy probes of the quark-gluon plasma
24 p4147 N85-35708

A holographic streamer chamber for relativistic nucleus-nucleus collision experiments
24 p4147 N85-35710

SLC arc transport system: Magnet design and construction
[DE85-014289] 24 p4159 N85-35789

Design considerations for personnel access penetrations for the superconducting super collider
[DE85-013027] 24 p4162 N85-35807

Measurement of interaction cross section of cosmic ray Fe nuclei (E4 GeV/N) with Al target
[HE-1.1-7] 24 p4170 N85-35855

Hadron thermodynamics in relativistic nuclear collisions
[HE-1.1-8] 24 p4171 N85-35856

1Single particle momentum and angular distributions in hadron-hadron collisions at ultrahigh energies
[HE-1.2-1] 24 p4171 N85-35860

Low P sub T hadron-nucleus interactions
[HE-1.2-7] 24 p4172 N85-35865

A test of the Feynman scaling in the fragmentation region
[HE-1.2-9] 24 p4172 N85-35867

Anuglar distribution of shower particles produced in the collisions of 20-GeV/c and 300-GeV negative pions with emulsion nuclei 24 p4172 N85-35868

Determination of primary energy in nucleus-nucleus collisions and the high P(sub)T tail of alpha-particles
24 p4173 N85-35875

Physical meaning of the multiplicities of emitted nucleons in hadron-nucleus collisions 24 p4174 N85-35877

How are particle production, nucleon emission and target fragment evaporation processes interrelated in hadron-nucleus collisions? 24 p4174 N85-35878

Experimental study of the space-time development of the particle production process in hadron-nucleon collisions, using massive target nucleus as a detector
24 p4174 N85-35879

Energy-range relations for hadrons in nuclear matter
24 p4174 N85-35881

Scattering and stopping of hadrons in nuclear matter
24 p4174 N85-35882

Measurements of hadron mean free path for the particle-producing collisions in nuclear matter
24 p4174 N85-35883

SU(2) x U(1) vacuum and the Centauro events
24 p4175 N85-35885

The multiplicity and the spectra of secondaries correlated with the leading particle energy
[HE-3.2-11] 24 p4179 N85-35919

A study of gamma-families generated in nucleon-nucleus (NA) and pion-nucleus (pi A) interactions
[HE-3.7-2] 24 p4186 N85-35981

The muon content of gamma-ray showers
[HE-4.5-7] 24 p4195 N85-36031
Fast scintillation counter preamplifier for the observation of Linsley effect
[HE-4.7-9] 24 p4199 N85-36060
A mini-array for large air showers
[HE-4.7-10] 24 p4199 N85-36061
A note on some statistical properties of rise time parameters used in muon arrival time measurements
[HE-4.7-12] 24 p4199 N85-36062

PARTICLE COUNTERS
U RADIATION COUNTERS

PARTICLE DECAY
U RADIOACTIVE DECAY

PARTICLE DENSITY (CONCENTRATION)
NT CARRIER DENSITY (SOLID STATE)
NT ELECTRON DENSITY (CONCENTRATION)
NT ELECTRON DENSITY PROFILES
NT ELECTRON DISTRIBUTION
NT ION DENSITY (CONCENTRATION)
NT IONOSPHERIC ELECTRON DENSITY
NT IONOSPHERIC ION DENSITY
NT MAGNETOSPHERIC ELECTRON DENSITY
NT MAGNETOSPHERIC ION DENSITY
NT MAGNETOSPHERIC PROTON DENSITY
NT PLASMA DENSITY
NT PROTON DENSITY (CONCENTRATION)
Dynamics of the Uranian rings
02 p0302 N85-11956
Mesoscale studies of flow regimes and fluxes of particulate matter in coastal waters
[DE85-003825] 11 p1669 N85-20620
Properties of materials using acoustic waves
[AD-A150465] 13 p2155 N85-23382
Electrophoretic mobilities of cultured human embryonic kidney cells in various buffers 20 p3501 N85-31761
The composition of cosmic rays near the Bend (10 to the 15th power eV) from a study of muons in air showers at sea level
[OG-5.2-3] 22 p3883 N85-34060
Composition of primary cosmic rays at energies 10(15) to approximately 10(16) eV
[OG-5.2-4] 22 p3883 N85-34061
Observation of cosmic ray positrons from 5 to 25 GeV
[OG-6.2-5] 22 p3889 N85-34104
Second-order Compton-Getting effect on arbitrary intensity distribution
[SH-3.1-10] 23 p4002 N85-34814
The expected cosmic ray density and stream distributions at the heliolatitudinal asymmetry of solar wind
[SH-4.2-14] 23 p4008 N85-34852
Angular resolution of air-shower array-telescopes
[OG-9.5-8] 23 p4030 N85-34983
Hadrons registration in emulsion chamber with carbon block
[HE-3.7-3] 24 p4186 N85-35962
Peculiarities of gamma-quanta distribution at 20 TeV energy
[HE-3.7-10] 24 p4186 N85-35967
Core structure of EAS in 10(15) to 10(17) eV
24 p4189 N85-35989
Particle distributions in approximately 10(14) 10(16) eV air shower cores at sea level 24 p4189 N85-35990
Monte Carlo simulations of electron lateral distributions in the core region of 10(13) - 10(16) eV air showers
24 p4190 N85-35992
Comparison of simulation results with sea-level experimental data on 10(14) - 10(16) air shower cores
24 p4190 N85-35993
A new study of shower age distribution in near vertical showers by EAS air shower array
24 p4190 N85-35996
A new study of muons in air showers by NBU air shower array 24 p4190 N85-35997
Lateral distribution of electrons of air showers
24 p4191 N85-35998
Detailed studies of the electron lateral distribution in extensive air showers with energies around 10(16) eV
24 p4191 N85-35999
Measurement of energy muons in EAS at energy region larger thean 10(17) eV
[HE-4.3-8] 24 p4191 N85-36002
Muon fluctuation studies of EAS 10(17) eV
[HE-4.3-9] 24 p4191 N85-36003
Measurement of shower electrons and muons using a small air shower array
[HE-4.3-11] 24 p4192 N85-36005
The system of EAS time analysis
[HE-4.4-10] 24 p4193 N85-36018
Properties of 10 (18)-10 (19)eV EAS at far core distance
[HE-4.7-3] 24 p4198 N85-36054
The thickness of the shower disc as observed in showers produced by primaries above 10 (19)eV
[HE-4.7-6] 24 p4199 N85-36057
Expected rates with mini-arrays for air showers
[HE-4.7-8] 24 p4199 N85-36059
Thickness of the particle swarm in cosmic ray air showers
[HE-4.7-14] 24 p4200 N85-36064
Progress report on a new search for free e/3 quarks in the cores of 10(15) - 10(16) eV air showers
[HE-6.2-15] 24 p4212 N85-36151

PARTICLE DETECTORS
U RADIATION COUNTERS

PARTICLE DIFFUSION
NT ELECTRON DIFFUSION
NT IONIC DIFFUSION
Performance deterioration of cascades exposed to solid particles 03 p0319 N85-12057
Paramagnetic impurity effects in NMR determinations of hydrogen diffusion and electronic structure in metal hydrides. Cerium in YH-2 and LaH-2.25
[DE84-014127] 04 p0472 N85-13005
Synergisms in hydrogen recycling, session summary
06 p0864 N85-15491
Steady state hydrogen transport in solids
06 p0864 N85-15492
Synergistic effects related to surface composition, session summary 06 p0865 N85-15495
Theory of oriented nucleation with asymmetric single elements. 2: Effects of rotational diffusion
[IFTR-32/1984] 12 p1939 N85-22179
Boundary of modulation diffusion and stochastic instability of high energy protons in inner radiation belt
15 p2482 N85-25316
Diffusion of dust around a central body — Keplerian orbits 15 p2676 N85-26523
Nonlinear DSA difference schemes for radiative transfer applications
[DE85-005729] 16 p2856 N85-27611
Collodial particle transport with simultaneous birth, growth and capture
[DE85-010388] 19 p3235 N85-30055
Propagation and secondary production of low energy antiprotons in the atmosphere
[OG-6.1-3] 22 p3887 N85-34094
Guiding center distribution function and longitudinal invariant 23 p3978 N85-34663
Diffusion in the chromosphere and the composition of the solar corona and energetic particles
[SH-2.1-9] 23 p3999 N85-34790
Coronal propagation of solar flare particles observed by satellite
[SH-3.1-2] 23 p4001 N85-34807
Investigation of cosmic ray propagation in interplanetary space
[SH-3.2-9] 23 p4004 N85-34824
Diffusion-convection function of cosmic rays
[SH-3.2-10] 23 p4004 N85-34825
Numerical descriptions of cosmic-ray transport
[SH-4.1-3] 23 p4004 N85-34829
Numerical and analytic descriptions of cosmic-ray transport
[SH-4.1-4] 23 p4005 N85-34830
Diffusion of strongly magnetized cosmic ray particles in a turbulent medium
[OG-7.2-16] 23 p4015 N85-34883
Calculation of the diffusion of light by aerosols: Description of the MIELOR software and results obtained
[REPT-80] 24 p4137 N85-35638
Atmospheric muons and neutrinos, and the neutrino-induced muon flux underground
[HE-5.4-7] 24 p4207 N85-36118

PARTICLE EMISSION
NT ELECTRON EMISSION
NT FIELD EMISSION
NT ION EMISSION
NT NEUTRON EMISSION
NT PHOTOELECTRIC EMISSION
NT SECONDARY EMISSION
NT THERMIONIC EMISSION
Centrifugally driven magnetohydrodynamic (MHD) winds and the nonthermal emission regions in Active Galactic Nuclei (AGN) 08 p1242 N85-17835
Theoretical studies of high energy phenomenon: Analysis of models of CP and T violation
[DE85-007455] 17 p3036 N85-28782
Production of stable embryo particles in dense ion tracks of alpha particle emissions in the atmosphere
21 p3644 N85-32638
Application of Particle Induced X-ray Emission analysis (PIXE) to aerosol long range transport studies
21 p3648 N85-32665
On some problems of gamma-astronomy
[OG-2.7-15] 22 p3873 N85-33988
Multicomponent analysis of total COS-B gamma-ray data at intermediate lattitudes
[OG-3.1-3] 22 p3873 N85-33991
Forecasting future industrial SO2 and NC/sub x/ emissions, revised 23 p3947 N85-34461
Study of photon emission by electron capture during solar nuclei acceleration, 1: Temperature-dependent cross section for charge changing processes
[SH-1.1-8] 23 p3990 N85-34735
Study of photon emission by electron capture during solar nuclei acceleration. 2: Delimitation of conditions for charge transfert establishment
[SH-1.1-9] 23 p3990 N85-34736
Study of photon emission by electron capture during solar nuclei acceleration. 3: Photon production evaluations
[SH-1.1-10] 23 p3990 N85-34737
Solar neutrinos, solar flares, solar activity cycle and the proton decay
[SH-8.1-8] 23 p4049 N85-35113
Physical meaning of the multiplicities of emitted nucleons in hadron-nucleus collisions 24 p4174 N85-35877
How are particle production, nucleon emission and target fragment evaporation processes interrelated in hadron-nucleus collisions? 24 p4174 N85-35878
Experimental evidence of the decrease of kinetic energy of hadrons in passing through atomic nuclei
24 p4174 N85-35880
Energy-range relations for hadrons in nuclear matter
24 p4174 N85-35881
The model of independent particles emission in the multiparticle production theory
[HE-3.2-10] 24 p4179 N85-35918
A study of atmospheric neutrinos with the IMB detector
[HE-5.3-7] 24 p4205 N85-36101
Study of photonuclear muon interactions at Baksan underground scintillation telescope
[HE-5.4-10] 24 p4208 N85-36122
Collimated groups of particles as possible manifestation of heavy meson production
[HE-5.4-14] 24 p4208 N85-36124
Limits on monopole fluxes from KFG experiment
[HE-6.1-6] 24 p4209 N85-36132
An experiment to detect gut monopoles
[HE-6.1-7] 24 p4210 N85-36133
Construction of the Soudan 2 detector
[HE-6.2-5] 24 p4211 N85-36141
Nucleon decay and atmospheric neutrinos in the Mont Blanc experiment
[HE-6.2-6] 24 p4211 N85-36142

PARTICLE ENERGY
NT ELECTRON ENERGY
NT ELECTRON STATES
NT PROTON ENERGY
Dynamics of the Uranian rings
02 p0302 N85-11956
Calculation of energy of atomization in silicate tetrahedron Si4(4-)
[BLL-M-36000-(5828.4)] 07 p1040 N85-16599
Experimental investigations in particle physics at intermediate energies
[DE85-001481] 11 p1722 N85-20832
Development of an apparatus for obtaining molecular beams in the energy range from 2 to 200 eV
[NASA-TM-77835] 15 p2647 N85-26326
Secondary ion mass spectrometry studies of solids and surfaces
[AD-A151744] 16 p2745 N85-26930
Particle physics: Recent successes and future prospects
[DE85-008175] 17 p3033 N85-28765
On some problems of gamma-astronomy
[OG-2.7-15] 22 p3873 N85-3398
All particle energy spectrum of cosmic rays in 10 to the 15th power - 10 to the 20th power eV region
[OG-5.1-15] 22 p3882 N85-3405
Abundance of low energy (50-150 MeV) antiprotons in cosmic rays
[OG-6.1-1] 22 p3887 N85-3409
Evidence for a dynamical halo around the edge-on gala NGC 4631
[OG-6.2-1] 22 p3889 N85-3410
Source energy spectra from demodulation of sola particle data by interplanetary and coronal transport
[SH-1.3-13] 23 p3994 N85-3475
the role of shock waves in modulation of galactic cosm rays
[SH-4.1-7] 23 p4005 N85-3483
SONTRAC: A solar neutron track chamber detect
[SH-9.1-12] 23 p4052 N85-3512
The model of independent particles emission in th multiparticle production theory
[HE-3.2-10] 24 p4179 N85-359
The multiplicity and the spectra of secondar correlated with the leading particle energy
[HE-3.2-11] 24 p4179 N85-359

PARTICLE FLUX
U FLUX (RATE)

PARTICLE FLUX DENSITY
NT ELECTRON FLUX DENSITY
NT NEUTRON FLUX DENSITY
NT PROTON FLUX DENSITY

SCATHA (spacecraft charging at high altitudes) plasma interaction experiment: SC-3 high energy particle spectrometer; SC-8 energetic ion composition experiment
[AD-A149726] 12 p1793 N85-21252

Rocket observations of the ionosphere during the eclipse of 26 February 1979
[NASA-CR-175513] 12 p1886 N85-21850

Timing between particle injections at the geostationary orbit and particle flux decreases in the distant geomagnetic tail during substorms 14 p2358 N85-24569

Plasma sheet dynamics deduced from ISEE-1 and -2 energetic particle flux data 14 p2358 N85-24570

Correlated fluctuations of charged particle fluxes and magnetic field according to data from Intercosmos-10 satellite 16 p2722 N85-26802

Helios 1 energetic particle observations of the solar gamma ray flare events of 7, 21 June 1980 and 3 June 1982
[SH-1.3-8] 23 p3993 N85-34755

The dispersive evolution of charged-particle bunches in random magnetic fields
[SH-4.1-2] 23 p4004 N85-34828

Observation of pick-up ions in the solar wind: Evidence for the source of the anomalous cosmic ray component?
[SH-4.6-5] 23 p4039 N85-35043

Cosmogenic-nuclide production by primary cosmic-ray protons
[SH-7.1-6] 23 p4047 N85-35098

Accelerator experiments on the contribution of secondary particles to the production of cosmogenic nuclides in meteorites
[SH-7.1-8] 23 p4048 N85-35100

Spallogenic origin of nuclei in meteorites
[SH-7.1-10] 23 p4048 N85-35102

The 4He1H ratios in the chemical compositions of solar flare particles and the primordial solar nebula
[SH-7.1-12] 23 p4048 N85-35104

A mini-array for large air showers
[HE-4.7-10] 24 p4199 N85-36061

A note on some statistical properties of rise time parameters used in muon arrival time measurements
[HE-4.7-12] 24 p4199 N85-36062

Study of the time-differentiated particle flux density at various distances from EAS axis
[HE-4.7-15] 24 p4200 N85-36065

The capability of the existing network of installations for detecting the antineutrino burst from collapsing stars
[HE-5.3-13] 24 p4206 N85-36107

PARTICLE IN CELL TECHNIQUE

Simulations of satellite-plasma interaction, including electron space charges — Giotto mission
14 p2245 N85-23916

Time-implicit Monte-Carlo collision algorithm for particle-in-cell electron transport models
[DE85-010758] 20 p3521 N85-31900

PARTICLE INTERACTIONS
NT ELECTRON CAPTURE
NT ELEMENTARY PARTICLE INTERACTIONS
NT INTERSTELLAR CHEMISTRY
NT ION ATOM INTERACTIONS
NT MOLECULAR COLLISIONS
NT MOLECULAR INTERACTIONS
NT NUCLEAR CAPTURE
NT NUCLEAR INTERACTIONS
NT NUCLEON-NUCLEON INTERACTIONS
NT PLASMA-PARTICLE INTERACTIONS
NT SPIN-ORBIT INTERACTIONS
NT STRONG INTERACTIONS (FIELD THEORY)
NT WEAK ENERGY INTERACTIONS
NT WEAK INTERACTIONS (FIELD THEORY)

Measurement of magnetic sublevel differential scattering cross sections for potassium and mercury
[MPIS-10/1983] 01 p0119 N85-10815

Energy deposition in microvolumes of silicon from high energy proton reactions
[AD-A144713] 01 p0123 N85-10845

On the co-variant formulation of the law of motion of passive particles in a field of turbulence
[REPT-564] 03 p0377 N85-12407

Tune shifts for coasting beams crossing at small angles
[DE84-017174] 04 p0562 N85-13579

Fermilab research program workbook
[DE84-012568] 06 p0862 N85-15476

Calculation of energy of atomization in silicate tetrahedron Si4(4-)
[BLL-M-36000-(5828.4)] 07 p1040 N85-16599

Theoretical studies relating to the interaction of radiation with matter: Atomic collision processes occurring in the presence of radiation fields
[AD-A148854] 07 p1040 N85-16602

Stochastic methods for the description of multiparticle production
[DE84-009981] 10 p1556 N85-19810

Bibliography of atomic and molecular processes, 1983
[DE85-000862] 12 p1929 N85-22121

Ion transport in beam-plasma interactions
[AD-A150145] 13 p2161 N85-23410

Summaries of FY 1984 research in high energy physics
[DE85-005641] 14 p2420 N85-24934

Introduction to LINE: A Feynman diagram graphic operator
[DE85-009299] 17 p3013 N85-28632

Implications for supersymmetry of the CERN monojets
[DE85-008178] 17 p3030 N85-28741

Photon-photon collisions
[DE85-008056] 17 p3030 N85-28742

Measuring structure functions at SSC energies
[DE85-007515] 17 p3031 N85-28746

Electroweak interactions in nuclei
[DE85-007811] 17 p3033 N85-28762

Possible indication of an A-dependence of R in deep-inelastic electron scattering from nuclei
[DE85-008174] 17 p3033 N85-28763

Physics of (very) high energy e(+)-e(-) colliders
[DE85-008177] 17 p3036 N85-28780

Oxygen-nitrogen interactions in ion-implanted silicon
[DE85-010091] 18 p3195 N85-29819

Gravitational properties of antimatter
[DE85-009601] 18 p3197 N85-29832

One- and two-electron transfer processes in ion-surface scattering
[AD-A154208] 19 p3353 N85-30782

Theory of high energy collision processes
[DE85-010183] 19 p3362 N85-30846

Free-zone electrophoresis of animal cells. 1: Experiments on cell-cell interactions
20 p3499 N85-31754

Plastic scintillator detectors for the study of transfer and breakup reactions at intermediate energies
[DE85-009945] 20 p3525 N85-31945

Current experiments in elementary particle physics, revision 1-85
[DE85-011513] 20 p3529 N85-31950

Interactions of heavy nuclei, Kr, Xe and Ho, in light targets 20 p3544 N85-32050

Wave/particle interactions in the plasma sheet
[NASA-CR-171537] 20 p3547 N85-32072

Interacting Boson approximation
[DE85-003016] 22 p3837 N85-33756

Polarization of fast particle beams by collisional pumping
[DE85-011621] 22 p3838 N85-33764

Proceedings of the 18th LAMPF Users Group Meeting
[DE85-011886] 22 p3839 N85-33773

Cosmic ray composition between 10 to the 15th power - 10 to the 17th power eV obtained by air shower experiments
[OG-5.1-12] 22 p3882 N85-34053

Space Experiments with Particle Accelerators (SEPAC) 23 p3901 N85-34165

Electron loss process and cross section of multiply charged ions by neutral atoms 23 p3981 N85-34685

Multiple inner shell vacancies in laser-irradiated Au plasma 23 p3981 N85-34687

Cosmic ray modulation in a random anisotropic magnetic field
[SH-4.1-20] 23 p4006 N85-34839

Interactions of heavy nuclei, Kr, Xe and Ho, in light targets
[OG-7.2-21] 23 p4016 N85-34888

A cosmic ray driven instability
[OG-8.1-5] 23 p4018 N85-34895

Plastic scintillators in coincidence for the study of multi-particle production of sea level cosmic rays in dense medium
[SH-9.1-11] 23 p4052 N85-35126

A suggested standardized format for cosmic ray ground-level event data
[SH-9.1-15] 23 p4052 N85-35130

Detector requirements for intensity interferometry measurements 24 p4147 N85-35709

A holographic streamer chamber for relativistic nucleus-nucleus collision experiments
24 p4147 N85-35710

Fractional charge resolution in music
24 p4147 N85-35712

Neutrino production of like sign dimuons
[DE85-013594] 24 p4151 N85-35741

High energy physics at Tufts University
[DOE/ER-40085/7] 24 p4152 N85-35744

Studies of relativistic heavy ion collisions
[DE85-014686] 24 p4152 N85-35745

Resonance localization in tokamaks excited with ICRF waves
[DE85-014559] 24 p4160 N85-35791

Some nuclear data needs in astrophysics
[DE85-012916] 24 p4168 N85-35842

Nineteenth International Cosmic Ray Conference. HE Sessions, volume 6
[NASA-CP-2376-VOL-6] 24 p4170 N85-35848

On total cross sections and slopes at superhigh energies
[HE-1.1-4] 24 p4170 N85-35852

Determination of the cross section of the proton, pion and neutron inelastic interaction with lead and carbon nuclei at 0.5 - 5.0 TeV energies (PION experiment)
[HE-1.1-5] 24 p4170 N85-35853

Measurement of interaction cross section of cosmic ray Fe nuclei (E4 GeV/N) with Al target
[HE-1.1-7] 24 p4170 N85-35855

QCD-motivated description of very high energy particle interactions
[HE-1.2-2] 24 p4171 N85-35861

Empirical description of the hadron-hadron and hadron-nucleus interaction at the accelerator energy range
[HE-1.2-4] 24 p4171 N85-35862

Low P sub T hadron-nucleus interactions
[HE-1.2-7] 24 p4172 N85-35865

Angular distribution and multiplicity of backward hadrons in hFe interactions at 0.5-5.0 TeV energies (PION Experiment)
[HE-1.2-8] 24 p4172 N85-35866

A test of the Feynman scaling in the fragmentation region
[HE-1.2-9] 24 p4172 N85-35867

A unification of the interactions and the diffractive processes 24 p4173 N85-35870

Propagation of cosmic rays through the atmosphere in the quark-gluon strings model 24 p4173 N85-35873

Experimental evidence of the decrease of kinetic energy of hadrons in passing through atomic nuclei
24 p4174 N85-35880

The phi-meson and Chiral-mass-meson production in heavy-ion collisions as potential probes of quark-gluon-plasma and Chiral symmetry transitions
24 p4175 N85-35884

Ringlike inelastic events in cosmic rays and accelerators 24 p4175 N85-35887

Few-particles generation channels in inelastic hadron-nuclear interactions at energy approximately equals 400 GeV
[HE-3.2-9] 24 p4179 N85-35917

The multiplicity and the spectra of secondaries correlated with the leading particle energy
[HE-3.2-11] 24 p4179 N85-35919

Characteristics of anomalously high multiplicity cosmic ray interactions
[HE-3.3-1] 24 p4180 N85-35920

Analytical-numerical methods of calculations of energy and three-dimensional particle distributions in electromagnetic cascades
[HE-3.5-13] 24 p4184 N85-35950

Relation between gamma-ray family and EAS core: Monte-Carlo simulation of EAS core
[HE-3.6-7] 24 p4185 N85-35955

A study of gamma-families generated in nucleon-nucleus (NA) and pion-nucleus (pi A) interactions
[HE-3.7-2] 24 p4186 N85-35961

High energy hadrons in extensive air showers
24 p4187 N85-35976

Electromagnetic and muonic structure of showers initiated by gamma-rays and by hadrons
[HE-4.5-6] 24 p4195 N85-36030

A facility for investigation of multiple hadrons at cosmic-ray energies
[HE-4.6-8] 24 p4197 N85-36045

Arrival time distributions of electrons in air showers with primary energies above 10 (18)eV observed at 900m above sea level
[HE-4.7-5] 24 p4199 N85-36056

Methods for roof-top mini-arrays
[HE-4.7-7] 24 p4199 N85-36058

Photo nuclear energy loss term for muon-nucleus interactions based on xi scaling model of QCD
[HE-5.2-17] 24 p4204 N85-36093

The spectrum of neutrons at 60 hg m(-2)
[HE-5.2-20] 24 p4204 N85-36096

Limits on deeply penetrating particles in the 10(17) eV cosmic ray flux
[HE-5.3-1] 24 p4205 N85-36098

A study of atmospheric neutrinos with the IMB detector
[HE-5.3-7] 24 p4205 N85-36101

Atmospheric neutrinos observed in underground detectors
[HE-5.3-8] 24 p4205 N85-36102

High energy neutrino astronomy with MACRO
[HE-5.3-12] 24 p4206 N85-36106

Characteristics of slow particles emitted in the charged current interactions of neutrinos with emulsion nuclei
[HE-5.3-22] 24 p4207 N85-36113
Nucleon decay and atmospheric neutrinos in the Mont Blanc experiment
[HE-6.2-6] 24 p4211 N85-36142
Energetic delayed hadrons in large air showers observed at 5200m above sea level
[HE-6.2-9] 24 p4211 N85-36145
Search for long-lived massive particles in extensive air showers
[HE-6.2-10] 24 p4212 N85-36146
Search for anomalons using plastic nuclear track detectors
[HE-6.2-12] 24 p4212 N85-36148
Observation of genetic relation among new phenomena Geminion, Chiron and mini-Centauro
[HE-6.2-16] 24 p4212 N85-36152
Tien-Shan effect and charmed particles
[HE-6.2-17] 24 p4212 N85-36153
Muon and neutrino fluxes
[HE-6.2-18] 24 p4213 N85-36154

PARTICLE LADEN JETS
Influence of turbulence on erosion by a particle-laden fluid jet
[DE84-014365] 09 p1320 N85-18301
Jets in air-jet family
[HE-3.2-1] 24 p4179 N85-35912
Search for anomalous C-jets in Chacaltaya emulsion chamber experiment
[HE-3.2-5] 24 p4179 N85-35913
Exotic interactions among C-jets and Pb-jets
[HE-3.2-6] 24 p4179 N85-35914

PARTICLE MASS
NT ELECTRON MASS
Free energy and effective mass of the polaron at finite temperatures
[TUM-M8401] 03 p0417 N85-12667
Search for neutrino oscillations at the Brookhaven AGS
[DE85-009766] 20 p3530 N85-31957
Systematics of quark mass matrices in the Standard Electroweak Model
[USIP-85-05] 20 p3532 N85-31972
Aerosol analysis and emission spectrometry with free jets
[DE85-010576] 21 p3564 N85-32168
Does low-energy physics depend on the potential of a heavy Higgs-particle
[NIKHEF-H/85-1] 22 p3838 N85-33763
Observation of cosmic ray positrons from 5 to 25 GeV
[OG-6.2-5] 22 p3889 N85-34104

PARTICLE MOTION
A covariant derivation of the ponderomotive force
[AD-A145054] 01 p0121 N85-10830
Response of propellants to high dynamic stresses: The uses of gun launch techniques
[DE84-013223] 02 p0188 N85-11259
Green River air quality model development: Meteorological and tracer data, July/August 1982. Field study in Brush Valley, Colorado
[DE84-014975] 02 p0225 N85-11474
Long-time tail in the two-wave model
02 p0282 N85-11837
Stable distribution and Levy process in fractal turbulence 02 p0283 N85-11846
Lie-transformation action principle for classical plasma dynamics
[DE84-014576] 02 p0285 N85-11858
Wall effects on the slow steady motion of a particle in a viscous incompressible fluid
[PREPRINT-828] 03 p0363 N85-12327
Dynamic compression and volatile release of carbonates
[NASA-CR-174076] 03 p0391 N85-12504
Particle entrainment in a compressible vortex
[ISL-CO-230/83] 04 p0500 N85-13192
MC2969 escapement study
[DE84-014542] 05 p0645 N85-14143
Surging as a potential response of ice sheets to CO2-induced changes in the polar environment (SPICAE)
[DE84-016472] 06 p0841 N85-15341
Earth's radiation belts
[AD-A147927] 07 p0998 N85-16339
Simulation of the ion-beam-driven drift instability in a magnetic trap, 1
[AD-A149451] 10 p1452 N85-19147
Dynamical studies of molecular systems
[DE85-003053] 11 p1594 N85-20028
Determination of the drag of free flying particles in supersonic flow with a pulsed laser
12 p1773 N85-21129
Particle transport in planetary magnetospheres
12 p1954 N85-22275
Experimental and theoretical investigation of the motion of particles in a compressible vortex
[ISL-R-129/83] 14 p2303 N85-24264
Dynamics of charged small particles — Jupiter, Saturn magnetospheres 15 p2676 N85-26522
CALTECH-DOE program on numerical analysis, computing and fundamental studies of motion, energy and mass transfer in fluids
[DE85-008106] 17 p2959 N85-28274
Stability in dynamical systems
[DE85-006698] 17 p3034 N85-28766
Forced structural response using component mode synthesis
[DE85-008479] 19 p3267 N85-30383
Electrophoretic mobility of cells in a vertical Ficoll gradient 20 p3499 N85-31753
Free-zone electrophoresis of animal cells. 1: Experiments on cell-cell interactions
20 p3499 N85-31754
Development anmd testing of electrophoresis solutions. Task I.1: Development of optimal buffer system
20 p3500 N85-31755
Electrophoretic mobilities of erythrocytes in various buffers 20 p3500 N85-31756
Effects of method of detachment on electrophoretic mobility of mammalian cells grown in monolayer culture
20 p3500 N85-31757
Preparative electrophoresis of cultured human cells: Effect of cell cycle phase 20 p3500 N85-31758
The role of cell size in density gradient electrophoretic separation of mouse leukemia cells according to position in the cell cycle 20 p3500 N85-31760
Electrophoretic mobilities of cultured human embryonic kidney cells in various buffers 20 p3501 N85-31761
Effect of passage number on electrophoretic mobility distributions of cultured human embryonic kidney cells
20 p3501 N85-31762
Monte-Carlo treatment of nonlinear collisional effects in charged-particle transport
[DE85-010755] 20 p3521 N85-31897
Longitudinal tune control in synchrotrons
[DE85-010745] 20 p3527 N85-31937
Properties of the reflected beams from the Earth's bow shock: A simple model
[IFSI-84-14] 20 p3549 N85-32088
Relativistic electron in curved magnetic fields
[OG-6.2-11] 22 p3890 N85-34110
Pulsars as cosmic ray particle accelerators: Proton orbits
[OG-8.2-21] 23 p4021 N85-34917
Mini and super mini arrays for the study of highest energy cosmic rays
[OG-9.4-9] 23 p4029 N85-34976
The cosmic ray differential diurnal variation dependences on the zenith angle and the geomagnetic disturbance
[SH-4.5-16] 23 p4038 N85-35033
Changes in the energy spectrum of anomalous oxygen and helium during 1977-1985
[SH-4.6-1] 23 p4039 N85-35039
Two-dimensional quasineutral description of particles and fields above discrete auroral arcs
[NASA-CR-176170] 24 p4116 N85-35517
Peculiarities of gamma-quanta distribution at 20 TeV energy
[HE-3.7-10] 24 p4186 N85-35967

PARTICLE PRECIPITATION
NT ELECTRON PRECIPITATION
NT PROTON PRECIPITATION
Relations between the particle precipitation events in mid-latitudes, the ring current intensity and the polarity of the interplanetary magnetic field
04 p0519 N85-13316
Current carriers for the field-aligned current system
[NASA-TM-86161] 08 p1260 N85-17925
Ionospheric research at INPE
[INPE-3279-PRE/602] 10 p1514 N85-19556
Upper atmosphere research at INPE
[INPE-3281-PRE/604] 10 p1515 N85-19557
Ozone measurements in the mesosphere during a solar proton event 11 p1665 N85-20490
Particle sources, transport, storage and precipitation — magnetosphere 14 p2359 N85-24576
SAMBO-GEOS: Substorm trapped particle particle boundary movements, particle precipitation and acceleration 14 p2361 N85-24589
The IMS contributions to the understanding of auroral precipitation, transport and particle sources
14 p2372 N85-24660
A study of the generation mechanisms of high latitude and equatorial F-region irregularities using DE-2 data
[NASA-CR-175745] 16 p2825 N85-27423
IMS (International Magnetospheric Study) contributions to the understanding of auroral precipitation, transport, and particle sources
[AD-A152320] 17 p2992 N85-28492
Characteristics and sources of E-region ionization in the continuous aurora
[AD-A155016] 21 p3632 N85-32582
Helios 1 energetic particle observations of the solar gamma ray flare events of 7, 21 June 1980 and 3 June 1982
[SH-1.3-8] 23 p3993 N85-34785

PARTICLE PRODUCTION
NT PAIR PRODUCTION
Emission mechanisms in the liquid metal ion source: A review
[AERE-R-11294] 03 p0418 N85-12675
Nuclear moments and nuclear structure
[DE84-015847] 04 p0561 N85-12573
Two phases of neutron production in the POSEIDON plasma focus
[IPF-84-10] 09 p1395 N85-18783
Stochastic methods for the description of multiparticle production
[DE84-009961] 10 p1556 N85-19810
Simulating supersymmetry at the SSC
[DE85-000699] 11 p1736 N85-20817
The IMS contributions to the understanding of auroral precipitation, transport and particle sources
14 p2372 N85-24660
Resonances in photon-photon scattering
[DE85-004607] 14 p2419 N85-24926
Preparation of polystryene latex particles in a rotating reactor
[NASA-CR-171475] 17 p2933 N85-28108
Implications for supersymmetry of the CERN monojets
[DE85-008178] 17 p3030 N85-28741
Photon-photon collisions
[DE85-008056] 17 p3030 N85-28742
Experiments with light ions at CERN super proton synchrotron
[DE85-007625] 17 p3031 N85-28744
Cluster production and entropy
[DE85-007626] 17 p3032 N85-28752
Heavy quark production processes in QCD
[DE85-007240] 17 p3036 N85-28779
Experimental methods of heavy quark detection
[DE85-006316] 17 p3036 N85-28781
Some comments on SSC physics
[DE85-008444] 18 p3179 N85-29712
A comprehensive study of psi meson production
[DE85-008094] 18 p3180 N85-29718
Intermediate energy nuclear theory
[DE85-010440] 18 p3182 N85-29731
Selected topics from J/psi decays
[DE85-010537] 18 p3183 N85-29736
Topics in intermediate vector boson physics
[NOTA-INTERNA-841] 18 p3184 N85-29743
Pion production and the nuclear equation of state
[DE85-009941] 19 p3365 N85-30870
The dimensional reduction transition
[DE85-003948] 19 p3383 N85-30990
A model of pulsed radiation from the Crab pulsar
20 p3548 N85-32081
Formation of particles in the air of the humid tropical forests 21 p3644 N85-32639
Some evidence for large gravitational redshift in Seyfert galaxy NGC 4151
[OG-2.7-11] 22 p3872 N85-33884
Inverse-Compton gamma rays in the galaxy
[OG-3.1-2] 22 p3873 N85-33890
Propagation and secondary production of low energy antiprotons in the atmosphere
[OG-6.1-3] 22 p3887 N85-34094
Observed antiprotons and energy dependent confinement of cosmic rays: A conflict?
[OG-6.1-7] 22 p3888 N85-34098
Reestimation of the production spectra of cosmic ray secondary positrons and electrons in the ISM
[OG-6.2-8] 22 p3889 N85-34107
Study of non-thermal photon production under different scenarios in solar flares. 1: Scenarios and formulations
[SH-1.2-2] 23 p3991 N85-34736
Study of non-thermal photon production under different scenarios in solar flares. 2: The Compton inverse an Bremsstrahlung models and fittings
[SH-1.2-3] 23 p3991 N85-3473
The starting conditions for an optically small sola gamma ray flare
[SH-1.3-2] 23 p3993 N85-3475
Time extended production of neutrons during a so flare
[SH-1.4-1] 23 p3994 N85-3476
Relativistic cosmic ray spectra in the full non-line theory of shock acceleration
[OG-8.1-6] 23 p4018 N85-348
Secondary gamma-ray production in a coded apertu mask
[OG-9.2-6] 23 p4025 N85-349
Spallogenic origin of nuclei in meteorites
[SH-7.1-10] 23 p4048 N85-351

Neutrino production from the solar atmosphere
23 p4050 N85-35114
[SH-8.1-8]

Solar cosmic ray bursts and solar neutrino fluxes
23 p4050 N85-35115
[SH-8.1-10]

High energy physics at Tufts University
24 p4152 N85-35744
[DOE/ER-40085/7]

Studies of relativistic heavy ion collisions
24 p4152 N85-35745
[DE85-014686]

Nineteenth International Cosmic Ray Conference. HE Sessions, volume 6
24 p4170 N85-35848
[NASA-CP-2376-VOL-6]

QCD-motivated description of very high energy particle interactions
24 p4171 N85-35861
[HE-1.2-2]

Multiplicity distributions in interaction models used for cascade simulations
24 p4172 N85-35863
[HE-1.2-5]

Is the inelastic charge-exchange contribution constant at the large X and superhigh energies? Qaut 01Kuchin, I. A.
24 p4173 N85-35871

General consequences of the violated Feynman scaling
24 p4173 N85-35872

How are particle production, nucleon emission and target fragment evaporation processes interrelated in hadron-nucleus collisions?
24 p4174 N85-35876

Experimental study of the space-time development of the particle production process in hadron-nucleon collisions, using massive target nucleus as a detector
24 p4174 N85-35879

Energy-range relations for hadrons in nuclear matter
24 p4174 N85-35881

Scattering and stopping of hadrons in nuclear matter
24 p4174 N85-35882

Measurements of hadron mean free path for the particle-producing collisions in nuclear matter
24 p4174 N85-35883

The phi-meson and Chiral-mass-meson production in heavy-ion collisions as potential probes of quark-gluon-plasma and Chiral symmetry transitions
24 p4175 N85-35884

Heavy flavours production in quark-gluon plasma formed in high energy nuclear reactions
24 p4175 N85-35886

Forward particle production in inelastic Ne-22 inteVractions in emulsion at 4.1 A Ge/c
24 p4176 N85-35895
[HE-1.4-7]

High energy gamma-rays and hadrons at Mount Fuji
24 p4177 N85-35903
[HE-3.1-3]

Some characteristic cosmic ray events and an attempt at their explanation
24 p4178 N85-35906
[HE-3.1-8]

The model of independent particles emission in the multiparticle production theory
24 p4179 N85-35918
[HE-3.2-10]

Experimental basis for the models of cascade propagation in atmosphere
24 p4185 N85-35954
[HE-3.6-6]

Atmospheric neutrinos observed in underground detectors
24 p4205 N85-36102
[HE-5.3-8]

Collimated groups of particles as possible manifestation of heavy meson production
24 p4208 N85-36124
[HE-5.4-14]

PARTICLE SIZE DISTRIBUTION

Milling of Si3N4 with Si3N4 hardware
[NASA-TM-86864] 01 p0031 N85-10191

Preparation of large-particle-size monodisperse latexes in space: The STS-3, STS-4, and STS-7 mission results
02 p0151 N85-11021

Aerosol sampling bias from differential electrostatic charge and particle size 02 p0224 N85-11467

Particle size distribution on surfaces in clean rooms
[AD-A146057] 03 p0328 N85-12109

Characteristics of aerosol volume distributions measured at Meppen, W. Germany
[AD-A146138] 03 p0396 N85-12528

Intermediate results of a 1-year study of a laser spectrometer in the DOE filter test facilities
[DE84-016478] 04 p0506 N85-13228

Parallel flow diffusion battery
[DE84-005964] 05 p0631 N85-14047

Influence of grain size distribution on the undrained dynamic properties of saturated sand
[PB85-102382/GAR] 09 p1305 N85-18197

Investigation of fuel additive effects on sooting flames
[AD-A149154] 10 p1457 N85-19179

Study of submicron particle size distributions by laser Doppler measurement of Brownian motion
[AD-A149130] 10 p1487 N85-19388

Condensational transformation of atmospheric aerosol particle distribution functions 10 p1500 N85-19466

Solar fuel synthesis based on colloidal and particulate semiconductors
[PB85-129104] 11 p1614 N85-20152

Laser Doppler Anemometry (LDA) signal triggering and effective particle size range
[KU-SFB-210/E/5] 11 p1634 N85-20290

Particle size, number, composition and velocity from solid rocket motors 12 p1785 N85-21201

Environment definition, large particles
12 p1787 N85-21220

Measurements 12 p1787 N85-21222

Environment definition, small particles, diameter less than or equal to 1 MM 12 p1788 N85-21223

Research study of droplet sizing technology leading to the development of an advanced droplet sizing system
[NASA-CR-174839] 12 p1850 N85-21604

Microstructure of Venus cloud layer based on spectrophotometric data from Venera-11 spacecraft
13 p1982 N85-22436

Solid propellant combustion diagnostics and automated data retrieval from holograms 13 p1998 N85-22527

Characterization of heterogeneity of composite propellants and its effects on combustion behavior
13 p2000 N85-22539

Recent trends in particle size analysis techniques
[NASA-TM-77735] 13 p2017 N85-22645

Size and velocity distributions of particles and droplets in spray combustion systems
[AD-A150355] 13 p2017 N85-22648

Laser diagnostic analyses of sooting flames
[AD-A150478] 13 p2017 N85-22649

Infrared aerosol absorption index
13 p2110 N85-23147

Potential bedforms on Venus: Wind tunnel simulations
13 p2189 N85-23583

Quantitative analyses of planetary reflectance spectra
13 p2197 N85-23625

Qualification of the T2 wind tunnel in cryogenic operation. B: Flow fluctuations, particle detection and qualification
[NASA-TM-77782] 14 p2227 N85-23806

Comparison of flame photometer data with total particle volume calculated from laser spectrometer particle count data
[AD-A151006] 14 p2252 N85-23958

Characterization of supported metal catalysts by imaging, microdiffraction and microanalysis techniques
[DE85-005567] 14 p2253 N85-23961

An apparatus for sizing particulate matter in solid rocket motors
[AD-A151282] 15 p2495 N85-25388

Particle shape characterization
[AD-A151961] 15 p2544 N85-25707

Particle curtain generator for optical property measurements of solid particles
[DE85-005784] 15 p2560 N85-25797

Case studies of snow clouds by means of snow crystal sondes 15 p2581 N85-25921

Size distributions of elemental carbon in atmospheric aerosols
[PB85-153534] 15 p2589 N85-25963

Physical properties of Saturn's rings
15 p2672 N85-26493

A simple model of Saturn's rings revisited
15 p2674 N85-26506

Size distribution in collisional systems — planetary rings 15 p2674 N85-26508

Diffusion instability in a bimodal disc — planetary rings
15 p2675 N85-26513

Macrostructure and microphysics of Saturn's E-ring
15 p2677 N85-26528

Ultrasonic dispersion of soils for routine particle size analysis: Recommended procedures
[DE85-005530] 16 p2861 ''35-27643

An investigation into the soot production processes in a gas turbine engine
[AD-A152710] 17 p2919 N85-27992

Effect of nonuniform size on internal stresses in a rapid, simple shear flow of granular materials. Part 1: Two grain sizes
[AD-A154045] 19 p3285 N85-30372

Effect of nonuniform size on internal stresses in a rapid, simple shear flow of granular materials. Part 2: Multiple grain sizes
[AD-A154046] 19 p3285 N85-30373

Phase size distribution in WC/Co hardmetal
[NPL-DMA(A)-93] 20 p3431 N85-31261

Size and DNA distributions of electrophoretically separated cultured human kidney cells
20 p3500 N85-31759

The role of cell size in density gradient electrophoretic separation of mouse leukemia cells according to position in the cell cycle 20 p3500 N85-31760

Journal of Research of the National Bureau of Standards, volume 90, number 1, January - February 1985
[PB85-179063] 20 p3522 N85-31908

Particle sizing from forward scattered light at two angles using a Variable-Focal-Length optical system
[AD-A154164] 20 p3533 N85-31980

Large eddy structures in transitional and turbulent flames
[AD-A154520] 21 p3582 N85-32157

Photoinduced active sites on ice nucleating aerosol of silver iodide 21 p3639 N85-32601

Experimental investigation of properties of ice-forming reagents 21 p3639 N85-32602

The effect of supersaturation, temperature and particle size on ice-nucleating ability of atmospheric aerosol
21 p3639 N85-32604

Multi-channel electric aerosol spectrometer
21 p3642 N85-32623

Formation of particles in the air of the humid tropical forests 21 p3644 N85-32639

The influence of Brownian coagulation on the size distributions of atmospheric aerosols
21 p3645 N85-32643

A new hypothesis for the observed vertical distribution of atmospheric aerosols 21 p3645 N85-32646

On the mechanisms responsible for the formation of typical size spectra and vertical distribution of tropospheric aerosol particles 21 p3645 N85-32647

Our knowledge about the atmospheric aerosol
21 p3646 N85-32650

Characteristics of aerosol composition in a nonurban area, north China 21 p3646 N85-32651

Variation of the submicron aerosol structure
21 p3647 N85-32661

Variability of rural aerosols under stable weather conditions 21 p3647 N85-32663

Marine aerosols at the Dutch North Sea coast: Size distributions and fractionation of trace elements
21 p3648 N85-32664

A probabilistic method for particle size analysis of aerosols 21 p3648 N85-32669

An electron microscopic study of urban aerosol
21 p3651 N85-32689

Composition of primary cosmic rays near the knee
[OG-5.2-10] 22 p3864 N85-34066

Review of zirconium-zircaloy pyrophoricity
[DE85-011169] 23 p3916 N85-34270

Synthesis of ultrafine ceramic and metallic powders in a thermal argon rf plasma
[DE85-009634] 23 p3963 N85-34696

Size distributions of air showers accompanied with high energy gamma ray bundles observed at Mt. Chacaltaya
[HE-3.3-9] 24 p4181 N85-35927

Comparison of absolute intensity between EAS with gamma-families and general EAS at Mount Norikura
[HE-3.3-11] 24 p4181 N85-35929

Photo nuclear energy loss term for muon-nucleus interactions based on xi scaling model of QCD
[HE-5.2-17] 24 p4204 N85-36093

PARTICLE SPIN

NT ELECTRON SPIN

NT NUCLEAR SPIN

Spin dynamics of rare Earth ions in crystal fields probed by muon spin rotation
[DE84-013805] 02 p0278 N85-11810

A geometrical theory of spin motion
[DE84-016537] 04 p0574 N85-13658

Muon spin rotation studies 17 p3042 N85-28819

Spin physics at BNL
[DE85-009768] 20 p3529 N85-31955

Cooling high intensity atomic hydrogen beams to liquid helium temperatures
[DE85-012515] 24 p4148 N85-35716

PARTICLE TELESCOPES

Plastic scintillator detectors for the study of transfer and breakup reactions at intermediate energies
[DE85-009945] 20 p3528 N85-31945

The energy spectrum of Jovian electrons in interplanetary space
[SH-1.5-18] 21 p3715 N85-33051

Secondary gamma-ray production in a coded aperture mask
[OG-9.2-6] 23 p4025 N85-34945

Operating characteristics of a prototype high energy gamma-ray telescope
[OG-9.2-7] 23 p4025 N85-34946

High energy gamma ray balloon instrument
[OG-9.2-12] 23 p4026 N85-34951

Results of a study to build a gamma-ray telescope in an external tank
[OG-9.3-3] 23 p4027 N85-34958

An approach of reducing the background induced by neutrons
[OG-9.3-5] 23 p4027 N85-34960

Astrophysical applications of high angular resolution array-telescopes
[OG-9.5-7] 23 p4031 N85-34984

Sidereal variations deep underground in Tasmania
[SH-4.4-4] 23 p4033 N85-35002

Corrected sidereal anisotropy for underground muons
[SH-4.4-7] 23 p4033 N85-35005

Cosmic ray intensity variations observed at Matsushiro (220 M.W.E. in depth)
23 p4034 N85-35007
[SH-4.4-9]

Study of cosmic ray scintillations from 5-minute data of the scintillations telescope Izmran and world-wide network stations
23 p4043 N85-35071
[SH-5.1-18]

Coupling functions for lead and lead-free neutron monitors from the latitudinal measurements performed in 1982 in the research station Academician Kurchatov
23 p4044 N85-35076
[SH-6.1-1]

Atmospheric effects on the underground muon intensity
23 p4044 N85-35078
[SH-6.1-3]

Observation of energy spectrum of electron albedo in low latitude region at Hyderabad, India
23 p4045 N85-35081
[SH-6.1-7]

A silicon surface barrier telescope for solar particles identification
23 p4050 N85-35118
[SH-9.1-3]

A bi-directional charged particle telescope to observe flux, energy spectrum and angular distribution of relativistic and non-relativistic particles
23 p4050 N85-35119
[SH-9.1-4]

An underground cosmic ray muon telescope for observation of cosmic ray anisotropy
24 p4196 N85-36037

PARTICLE THEORY

The search for proton decay: Introduction
01 p0131 N85-10904
[DE84-014349]

Solar neutrino spectroscopy
02 p0304 N85-11968
[DE84-015513]

Parity and time-reversal non-conversation in atoms
04 p0562 N85-13581
[DE84-016924]

Toward unification of elementary particle physics and cosmology in 10-dimensions
05 p0727 N85-14674
[DE84-013950]

On the nature of the baryon asymmetry
05 p0746 N85-14784
[NASA-TM-86156]

Ultraviolet divergences and supersymmetric theories
11 p1729 N85-20875
[DE85-001649]

A systematic study of light scattering by irregularly shaped particles
13 p2159 N85-23400
[AD-A150192]

Particle sources, transport, storage and precipitation — magnetosphere
14 p2359 N85-24576

Inflation from extra dimensions
16 p2683 N85-27787
[DE85-007834]

Spectrographic investigation of low-voltage arc discharge in argon atmosphere
20 p3422 N85-31242
[BLL-M-36276-(5828.4)]

Vector calculation of particle code
23 p3981 N85-34688

Relativistic cosmic ray spectra in the full non-linear theory of shock acceleration
23 p4018 N85-34896
[OG-8.1-6]

PARTICLE TRACKS

Green River air quality model development: Meteorological and tracer data, July/August 1982. Field study in Brush Valley, Colorado
02 p0225 N85-11474
[DE84-014975]

Climatological variability in modeling of long-term regional transport and deposition of air pollutants
04 p0539 N85-13430
[DE84-014726]

Scintillator-fiber charged particle track-imaging detector
04 p0559 N85-13560
[NASA-CR-174160]

Aspects of the comparison of stratospheric trace species measurements with photochemical models
05 p0672 N85-14317
[DE84-017028]

Use of ground radar to detect reentering debris
12 p1784 N85-21200

Digital characterization of particle tracks for microdosimetry
22 p3646 N85-33822
[DE85-012898]

Ultraheavy cosmic ray tracks in meteorites: A reappraisal, based on calibrations with relativistic ions
22 p3680 N85-34041
[OG-4.4-10]

Cross sections for the production of fragments with Z greater than or equal to 5 by fragmentation of Z greater than or equal to 9 and less than or equal to 26 nuclei
23 p4016 N85-34880
[OG-7.2-22]

SONTRAC: A solar neutron track chamber detector
23 p4052 N85-35127
[SH-9.1-12]

Observation of nuclei with energies 8-30 MeV per nucleon in the Earth's magnetosphere at the altitudes 350 KM
23 p4053 N85-35136
[SH-10.1-5]

Measurement of low energy cosmic rays aboard Spacelab-1
23 p4053 N85-35137
[SH-10.1-6]

Heavy cosmic ray measurement aboard Spacelab-1
23 p4053 N85-35138
[SH-10.1-7]

Elemental tracers of source regions of contaminants in precipitation
24 p4113 N85-35499
[DE85-012858]

Calculation of heavy-ion tracks in liquid water
24 p4149 N85-35725
[DE85-012101]

Experimental basis for the models of cascade propagation in atmosphere
24 p4185 N85-35954
[HE-3.6-6]

Search for supermassive magnetic monopoles using mica crystals
24 p4210 N85-36134
[HE-6.1-8]

Spatial distribution read-out system for thermoluminescence sheets
24 p4213 N85-36161
[HE-7.1-7]

PARTICLE TRAJECTORIES
NT ELECTRON TRAJECTORIES

Focusing beam of 1-GeV protons with volumetric capture to the mode of channeling by bent single crystal
02 p0268 N85-11750

Performance deterioration of cascades exposed to solid particles
03 p0319 N85-12057

Averaging effects in models of three-dimensional two-phase flows
10 p1484 N85-19371
[AD-A149313]

A free electron laser with a rotating quadrupole wiggler
10 p1489 N85-19404
[AD-A149052]

PATHFINDER: A trajectory prediction system for the Great Lakes
10 p1506 N85-19506
[PB85-115335]

Cometary atmospheres: Modeling the spatial distribution of observed neutral radicals
11 p1785 N85-21097
[NASA-CR-175491]

The dawn-dusk asymmetry of particles near the neutral sheet of geomagnetotail
14 p2358 N85-24574

Development and validation of a new fallout transport method using variable spectral winds
15 p2599 N85-26022
[AD-A151871]

A numerical study of the mean trajectory approximation in a non-adiabatic process
17 p3030 N85-28737
[AD-A152763]

Trajectories of charged particles traversing a plasma sheath in an oblique magnetic field
19 p3371 N85-30911
[DE85-011070]

Observation of cosmic ray positrons from 5 to 25 GeV
22 p3889 N85-34104
[OG-6.2-5]

Pulsars as cosmic ray particle accelerators: Proton orbits
23 p4021 N85-34917
[OG-8.2-21]

Bevalac calibration of the SOFIE range and hodoscope detectors
23 p4023 N85-34933
[OG-9.1-7]

Cherenkov-dE/dx-range measurements on cosmic ray iron group nuclei
23 p4024 N85-34937
[OG-9.1-12]

The response of ionization chambers to relativistic heavy nuclei
23 p4024 N85-34939
[OG-9.1-13]

Twenty-two-year cycle of the upper limiting rigidity of Daly waves
23 p4036 N85-35023
[SH-4.5-5]

Re-evaluation of cosmic ray cutoff terminology
23 p4045 N85-35084
[SH-6.1-11]

Estimating the change in asymptotic direction due to secular changes in the geomagnetic field
23 p4045 N85-35086
[SH-6.1-13]

Strategic defense initiative
24 p4150 N85-35735
[DE85-012778]

The structure of EAS at E 0.1 EeV
24 p4193 N85-36012
[HE-4.4-2]

Transition effect of air shower particles in plastic scintillators
24 p4193 N85-36017
[HE-4.4-9]

The Nagoya cosmic-ray muon spectrometer 3, part 4: Track reconstruction method
24 p4202 N85-36083
[HE-5.2-5]

Comments on the measurements of multiple muon phenomena
24 p4203 N85-36089
[HE-5.2-13]

PARTICLES
NT AEROSOLS
NT ALPHA PARTICLES
NT ANIONS
NT ANTINEUTRINOS
NT ANTINUCLEONS
NT ANTIPARTICLES
NT ANTIPROTONS
NT ARGON PLASMA
NT BARYONS
NT BETA PARTICLES
NT BOSONS
NT BOUNDARY LAYER PLASMAS
NT CATIONS
NT CHARGED PARTICLES
NT COLD NEUTRONS
NT COLD PLASMAS
NT COLLISIONAL PLASMAS
NT COLLISIONLESS PLASMAS
NT CONDUCTION ELECTRONS
NT CORPUSCULAR RADIATION
NT COSMIC PLASMA
NT CYCLOTRON RADIATION
NT CYLINDRICAL PLASMAS
NT DENSE PLASMAS
NT DEUTERIUM PLASMA
NT DEUTERONS
NT DROPS (LIQUIDS)
NT ELECTRON BEAMS
NT ELECTRON PLASMA
NT ELECTRON PRECIPITATION
NT ELECTRON RADIATION
NT ELECTRONS
NT ELEMENTARY PARTICLES
NT ELLIPTICAL PLASMAS
NT ENERGETIC PARTICLES
NT EVEN-EVEN NUCLEI
NT FAST NEUTRONS
NT FERMIONS
NT FERRIC IONS
NT FINES
NT FOG
NT FREE ELECTRONS
NT GLUONS
NT HADRONS
NT HEAVY NUCLEI
NT HELIUM PLASMA
NT HIGH ENERGY ELECTRONS
NT HIGH TEMPERATURE PLASMAS
NT HOT ELECTRONS
NT HYDROGEN PLASMA
NT HYPERNUCLEI
NT HYPERONS
NT INNER RADIATION BELT
NT ION CYCLOTRON RADIATION
NT KAONS
NT LASER PLASMAS
NT LEPTONS
NT LIGHT BEAMS
NT MAGNETIC MONOPOLES
NT MAGNETICALLY TRAPPED PARTICLES
NT MESONS
NT METAL IONS
NT METAL PARTICLES
NT METALLIC PLASMAS
NT MICROPARTICLES
NT MIST
NT MUONS
NT NEGATIVE IONS
NT NEGATRONS
NT NEUTRAL PARTICLES
NT NEUTRINOS
NT NEUTRONS
NT NITROGEN PLASMA
NT NONEQUILIBRIUM PLASMAS
NT NONUNIFORM PLASMAS
NT NUCLEAR PARTICLES
NT NUCLEI (NUCLEAR PHYSICS)
NT NUCLEONS
NT ODD-EVEN NUCLEI
NT ODD-ODD NUCLEI
NT OUTER RADIATION BELT
NT OXYGEN PLASMA
NT PHOTOELECTRONS
NT PHOTONS
NT PIONS
NT PLASMA CLOUDS
NT PLASMA FOCUS
NT PLASMA JETS
NT PLASMA LAYERS
NT PLASMA SHEATHS
NT PLASMAS (PHYSICS)
NT POLARONS
NT POLLEN
NT POSITRONS
NT POWDER (PARTICLES)
NT POWDERED ALUMINUM
NT PRIMARY COSMIC RAYS
NT PROTON BELTS
NT PROTONS
NT QUARKS
NT RADIATION BELTS
NT RELATIVISTIC ELECTRON BEAMS
NT RELATIVISTIC PARTICLES
NT RELATIVISTIC PLASMAS
NT ROTATING PLASMAS
NT SEMICONDUCTOR PLASMAS
NT SOLAR CORPUSCULAR RADIATION
NT SOLAR COSMIC RAYS
NT SOLAR ELECTRONS
NT SOLAR NEUTRINOS
NT SOLAR PROTONS
NT SOLAR WIND
NT SOOT
NT SPACE PLASMAS
NT SPHERICAL PLASMAS

NT STELLAR WINDS
NT STRONGLY COUPLED PLASMAS
NT TACHYONS
NT THERMAL NEUTRONS
NT THERMAL PLASMAS
NT TOROIDAL PLASMAS
NT TRAPPED PARTICLES
NT VECTOR MESONS

Fluorinated diamond particles bonded in a filled fluorocarbon resin matrix
[DE84-014444] 01 p0022 N85-10136

Technical Review of the Solid Particle Receiver Program
[DE84-015181] 01 p0066 N85-10451

Size specific total particulate emission factors for mobile sources
[PB84-226653] 01 p0071 N85-10471

Effect of the Basset term on particle relaxation behind normal shock waves
[AD-A145446] 02 p0198 N85-11320

A finite element projection method for the solution of particle transport problems with anisotropic scattering
[AD-A145362] 02 p0250 N85-11637

Algebra of hydrodynamic flows of an ideal fluid and the prediction of the behaviour of a system of particles of a passive admixture on Riemann surfaces with a variable curvature
[REPT-555] 03 p0377 N85-12406

Extinction by dielectric particles at optical and infrared wavelengths
[AD-A146306] 03 p0413 N85-12640

Recent heavy particle decay in a matter dominated universe
[NASA-CR-175501] 11 p1764 N85-21095

Solid particle environment and protection for the Galileo Orbiter 12 p1786 N85-21207

A method for determining in situ the absorption coefficient of particulate media using pulsed laser technique
[AD-D011546] 12 p1799 N85-21281

Improved silicon grinding method and apparatus
[NASA-CASE-NPO-16336-1-CU] 12 p1819 N85-21407

Solid particle receiver experiments: Velocity measurements
[DE85-000257] 12 p1853 N85-21623

The orientation distribution of nonspherical aerosol particles within a cloud
[AD-A150800] 13 p2092 N85-23061

Sample introduction methods for improving the particle detection capability of the spectrometric oil analysis program
[AD-A150139] 13 p2158 N85-23399

The effect of particle density on aeolian transport 13 p2189 N85-23581

A review of radar observations of Saturn's rings 15 p2670 N85-26474

Saturn's E ring 15 p2671 N85-26481

The Saturn ring particles from optical reflectance polarimetry 15 p2671 N85-26484

Solved und unsolved problems in planetary ring dynamics 15 p2674 N85-26502

Physical and geological nature of Saturn's larger ring particles 15 p2674 N85-26509

Dynamics of neutral small particles --- in the solar system 15 p2676 N85-26521

Multivalued electrostatic potentials; chance or necessity for the charge of solid particles near Saturn? 15 p2677 N85-26523

Preparation of polystryene latex particles in a rotating reactor
[NASA-CR-171475] 17 p2933 N85-28108

Surface degradation of ductile metal in elevated temperature gas-particle streams
[DE85-008426] 18 p3074 N85-29017

Chemical, biological, and physical measurements from the subtropical western North Atlantic Ocean. Summer 1982, USNS Lynch, cruise 710-82
[AD-A153623] 18 p3201 N85-29857

Collodial particle transport with simultaneous birth, growth and capture
[DE85-010388] 19 p3235 N85-30055

Scattering by distributions of small thin particles 19 p3253 N85-30172

Thermal performance and design of a solid particle cavity receiver
[DE85-010830] 19 p3274 N85-30300

Acoustic particle separation
[NASA-CASE-NPO-155559-1] 19 p3350 N85-30765

Wall effect on lateral migration of spherical particles in a linear shear flow 20 p3452 N85-31432

Absorption and scattering properties of aerosols of aggregated particles in the infrared spectral region
[AD-A155475] 21 p3637 N85-32591

Ice-forming efficiency of the soluble and insoluble portions of dust contained in snow 21 p3643 N85-32631

Study of the formation of particles from natural hydrocarbons released by vegetation 21 p3644 N85-32640

A study of time transformation of natural photochemical aerosols 21 p3645 N85-32644

Measurements of the critical supersaturation of 0.029 to 0.035 micron radius particles at Washington, District of Columbia 21 p3649 N85-32676

Integrated current collector and catalyst support
[DE85-011616] 22 p3761 N85-33311

Drying of pulverized material with heated condensible vapor
[DE85-011656] 22 p3783 N85-33438

Influence of particle erosion on the microstructural changes in metals and alloys
[TI85-901384] 23 p3917 N85-34276

Acoustic cross-correlation flowmeter for solid-gas flow
[DE85-005988] 23 p3935 N85-34391

The influence of nonstationarity of the solar activity and general solar field on modulation of cosmic rays
[SH-4.2-17] 23 p4008 N85-34854

Search for proton decay in the Frejus experiment
[HE-6.2-2] 24 p4210 N85-36136

Results on nucleon life-time from the Kolar gold field experiment
[HE-6.2-3] 24 p4211 N85-36139

Data acquisition system for phase-2 KGF proton decay experiment
[HE-6.2-4] 24 p4211 N85-36140

Search for long-lived massive particles in extensive air showers
[HE-6.2-10] 24 p4212 N85-36146

PARTICULATE FILTERS
U FLUID FILTERS

PARTICULATE SAMPLING

Remote sensing of atmospheric particulates: Technological innovation and physical limitations in applications to short-range weather prediction
[NSF ATM-82-09684] 01 p0077 N85-10511

Aerosol sampling bias from differential electrostatic charge and particle size 02 p0224 N85-11467

Analysis and characterization of organic carbon compounds in atmospheric particulate matter
[PB84-232636] 06 p0766 N85-14903

Sample return from a comet flyby 06 p0889 N85-15646

Evaluation of the particulate levels occurring under 1.0/1.2 g/mi nitrogen oxide standards for light duty diesel vehicles and light duty diesel trucks
[PB85-115939/GAR] 09 p1350 N85-18494

Solar fuel synthesis based on colloidal and particulate semiconductors
[PB85-129104] 11 p1614 N85-20152

National Performance Audit Program ambient air audits of analytical proficiency
[PB85-136204] 11 p1680 N85-20586

Diesel engine emissions of particulates and associated organic matter
[PB85-154425] 15 p2590 N85-25964

Microcomputer-controlled system for measuring atmospheric particle fluxes
[DE85-007910] 17 p2988 N85-28469

Role of natural dissolved organic compounds in determining the concentrations of americium in natural waters
[DE85-010266] 19 p3229 N85-30022

Sources of copper air emissions
[PB85-191136] 19 p3310 N85-30523

Identification and quantification of nitropolynuclear aromatic hydrocarbons in ambient and indoor air particulate samples
[PB85-176790] 19 p3311 N85-30525

Fuel-rich catalytic combustion: A soot-free technique for in situ hydrogen-like enrichment
[NASA-TP-2498] 20 p3423 N85-31244

Particulate contamination control in clean rooms by particle fallout (PFO) measurements
[ESA-PSS-01-204-ISSUE-1] 20 p3467 N85-31673

Physical and chemical aerosol characteristics in extremely clean air masses at Cape Grim, Tasmania 21 p3646 N85-32655

Technology of off-gas treatment for liquid-fed ceramic melters
[DE85-012467] 22 p3812 N85-33610

A study of the control of particulate emissions from turbine engine test cells 24 p4067 N85-35205

PARTITIONS (MATHEMATICS)

Parallel triangularization of substructured finite element problems
[NASA-CR-172466] 02 p0241 N85-11569

Some facets of the tri-index assignment polytope
[AD-A149195] 10 p1547 N85-19753

PASCAL (PROGRAMMING LANGUAGE)

PASCAL-MP algebraic and numerical manipulator for polynomials
[INPE-3229-TDL/176] 02 p0240 N85-11562

Programmer's guide for ASKF 77: A tool for programming of dialogs in FORTRAN and PASCAL
[FOA-C-30366-E1] 02 p0243 N85-11585

The automated reasoning system ITP
[ANL-84-27] 12 p1914 N85-22016

Computer Performance Modeling Tool (CPMT)
[AD-A154436] 19 p3338 N85-30682

A PASCAL interpreter for the functional programming language ELC (Extended lambda calculus)
[AD-A155218] 21 p3672 N85-32810

Use of monitors in Pascal on the Lemur: A tutorial on the barrier, self-scheduling FOR-loop, and askfor monitors
[ANL-84-53] 22 p3828 N85-33706

A prototype PASCAL program validation system
[NPL-DITC-57/85] 23 p3956 N85-34513

A quickly tested Pascal random number generator for microcomputers
[AD-A156059] 24 p4136 N85-35633

PASSAGEWAYS
NT STRAITS

Vortex-generating coolant-flow-passage design for increased film-cooling effectiveness and surface coverage
[NASA-TP-2388] 03 p0361 N85-12314

PASSENGER AIRCRAFT
NT A-310 AIRCRAFT
NT A-320 AIRCRAFT
NT BO-105 HELICOPTER
NT BOEING 727 AIRCRAFT
NT BOEING 737 AIRCRAFT
NT BOEING 747 AIRCRAFT
NT BOEING 767 AIRCRAFT
NT CESSNA 402B AIRCRAFT
NT CH-47 HELICOPTER
NT CV-990 AIRCRAFT
NT DC 8 AIRCRAFT
NT DC 10 AIRCRAFT
NT DO-28 AIRCRAFT
NT EUROPEAN AIRBUS
NT F-27 AIRCRAFT
NT L-1011 AIRCRAFT

Aircraft accident report, Scandinavian Airlines System, Flight 901, McDonnell Douglas DC-10-30, John F. Kennedy International Airport, Jamaica, New York, February 28, 1984
[PB84-910415] 05 p0594 N85-13786

A preliminary analysis of C-12 aircraft usage by the Navy Air Logistics System
[AD-A151921] 16 p2694 N85-26634

FAA regulation of 9-seat and under passenger aircraft
[GPO-42-703] 20 p3391 N85-31032

MBB demonstrates new research aircraft ATTAS 20 p3436 N85-31334

PASSENGERS

High-speed intercity rail passenger service
[GPO-35-896] 10 p1570 N85-19897

Air traffic: Instruments, airports, companies, post, cargo and passengers 18 p3060 N85-28932

Aviation safety (aircraft passenger survivability and cabin safety)
[GPO-39-847] 23 p3895 N85-34130

PASSES
U GAPS (GEOLOGY)

PASSIVATION
U PASSIVITY

PASSIVE L-BAND RADIOMETERS

Study of the improvement in analyzing passive microwave remote sensing data by integrated use of ground data 05 p0658 N85-14226

PASSIVE SATELLITES
NT LAGEOS (SATELLITE)

Tactical applications of GPS user equipment 11 p1711 N85-20765

A study of structural concepts for ultralightweight spacecraft
[NASA-CR-175765] 16 p2730 N85-26848

PASSIVITY

Hydrogen passivation of electrically active defects in crystalline silicon solar cells
[DE84-004590] 02 p0223 N85-11461

Research relative to high spatial resolution passive microwave sounding systems 05 p0681 N85-14380

Influence of the mechanical and electrochemical characteristics of austenitic and austenoferritic steels on the propagation rate and morphology of stress corrosion cracking
[BLL-RISLEY-TR-4545-(9091.9F)] 06 p0767 N85-14906

Passive storage technologies 08 p1108 N85-17003

Surface and allied studies in silicon solar cells
[NASA-CR-174447] 11 p1671 N85-20531
Role of passive surface films on corrosion fatigue crack initiation
[DE85-000438] 14 p2257 N85-23985
Investigation of silicon surface passivation by silicon nitride film deposition
[NASA-CR-175693] 15 p2585 N85-25936
Corrosion characteristics of some steels produced through a self-cleaning rotating electrode
[BLL-BISI-TRANS-22046-(9022.08)] 17 p2925 N85-28034
Passivation on high Q acoustic strain sensor for accelerometer
[AD-A153665] 18 p3177 N85-29695
Nitridation of SiO2 for surface passivation 20 p3480 N85-31627
Surface passivation and junction formation using low energy hydrogen implants 20 p3480 N85-31628
EBIC characterization and hydrogen passivation in silicon sheet 20 p3481 N85-31634
Silicon surface passivation by silicon nitride deposition 21 p3610 N85-32423
The development and evaluation of point defect models for the growth of passive films on single crystal, polycrystalline, and amorphous metal surfaces
[AD-A154685] 21 p3709 N85-33023
Low noise polycrystalline semiconductor resistors by hydrogen passivation
[AD-D011721] 23 p3927 N85-34338

PASTE (CONSISTENCY)
Development of metallization process: FSA project, cells and module formation research area
[NASA-CR-176136] 23 p3945 N85-34447

PASTES
Viscosity measurements for thick-film pastes 06 p0831 N85-15280

PATENT APPLICATIONS
Charge depletion meter
[AD-D011484] 10 p1488 N85-19393
Flying objects
[CH-634516-A5] 15 p2469 N85-25242
Airfoil wing with flap
[CH-634787-A5] 15 p2469 N85-25243
Helicopter rotor
[CH-637890-A5] 15 p2470 N85-25245
Aircraft
[CH-642598-A5] 15 p2470 N85-25246
Satellite structure
[CH-642922-A5] 15 p2492 N85-25373
Dual optical mechanical position tracker
[AD-D011739] 22 p3844 N85-33811
NASA patent abstracts bibliography: A continuing bibliography. Section 1: Abstracts (supplement 27)
[NASA-SP-7039(27)-SECTION-1] 22 p3849 N85-33840

PATENT POLICY
NASA Patent Abstracts Bibliography. A continuing bibliography. Section 2: Indexes
[NASA-SP-7039(26)] 13 p2167 N85-23445
NASA patent abstracts bibliography, a continuing bibliography. Section 2: Indexes (supplement 27)
[NASA-SP-7039(27)-SECTION-2] 24 p4164 N85-35820

PATENTS
Summary of trends in photovoltaic patent activity
[DE84-015757] 01 p0066 N85-10452
Bibliography of US patents on augmentation of convective heat and mass transfer, part 2
[DE84-014665] 04 p0498 N85-13178
The Uniform Science and Technology Research and Development Utilization Act
[GPO-36-327] 04 p0577 N85-13685
Uniform Science and Technology Research and Development Utilization Act
[H-REPT-98-963-PT-1] 04 p0577 N85-13686
Flying objects
[CH-634516-A5] 15 p2469 N85-25242
Airfoil wing with flap
[CH-634787-A5] 15 p2469 N85-25243
Aircraft structure for application to training aircraft
[CH-635286-A5] 15 p2469 N85-25244
Aircraft
[CH-642598-A5] 15 p2470 N85-25246
System for radio remote control of dropping bombs
[CH-639335-A5] 15 p2491 N85-25371
Jinc-trap resonator
[AD-D011650] 17 p2970 N85-28339
Orthogonalizer for inphase and quadrature digital data
[AD-D011679] 19 p3254 N85-30174
NASA patent abstracts bibliography: A continuing bibliography. Section 1: Abstracts (supplement 27)
[NASA-SP-7039(27)-SECTION-1] 22 p3849 N85-33840

PATHOGENESIS
Pathogenesis and treatment of cerebral air embolism and associated disorders
[AD-A146723] 07 p1014 N85-16443
Distinctions in formation of microflora on construction materials used in habitable pressurized compartments 22 p3823 N85-33683

PATHOLOGICAL EFFECTS
Pathophysiological study of poisoning due to thermal degradation of materials — aircraft cabins
[CERMA-84-15] 11 p1692 N85-20640

PATHOLOGY
NT HUMAN PATHOLOGY
Pathology and axonal transport in hexacarbon neuropathies
[AD-P004021] 06 p0843 N85-15355
Pathology of organophosphorus-induced delayed neurotoxicity
[AD-P004024] 06 p0844 N85-15358
Effects of long-term low-level radiofrequency radiation exposure on rats. Volume 8: Evaluation of longevity, cause of death, and histopathological findings
[AD-A154283] 19 p3327 N85-30610

PATIENTS
Interaction between lung mechanics and gas exchange by low volume high frequency pulmonary ventilation in patients with respiratory failure
[AD-A146604] 06 p0846 N85-15372

PATTERN DISTRIBUTION
U DISTRIBUTION (PROPERTY)

PATTERN METHOD (FORECASTING)
Quasi stationary states in the Southern Hemisphere 18 p3144 N85-29465

PATTERN RECOGNITION
NT CHARACTER RECOGNITION
Content, variety, and augmentation of simulated visual scenes for teaching air-to-ground attack
[AD-A145218] 01 p0013 N85-10060
Application of automatic pattern methods in very-short-range forecasting 01 p0078 N85-10521
Fundamental remote sensing science research program. Part 1: Status report of the mathematical pattern recognition and image analysis project
[E85-10004] 02 p0215 N85-11417
Hypothesis on the origin of lineaments in the LANDSAT and SLAR images of precambrian soil in the low Contas River Valley (southern Bahia)
[E85-10007] 02 p0215 N85-11420
Failure detection processes by pattern recognition and expert systems
[AD-P003924] 02 p0246 N85-11604
An investigation into fuzzy clustering and classification
[AD-A145571] 02 p0251 N85-11645
Design of edge detectors for reduced images
[AD-A145700] 02 p0252 N85-11653
Automatic recognition and turbuling objects
[AD-A145908] 03 p0419 N85-12676
Fidelity of satellite soundings 05 p0682 N85-14383
Experiences with digital processing of images at INPE
[E85-10045] 06 p0826 N85-15247
Proceedings of the Second Annual Symposium on Mathematical Pattern Recognition and Image Analysis Program
[E85-10056] 07 p0984 N85-16251
Multivariate spline methods in surface fitting 07 p0985 N85-16257
Calibration or inverse regression: Which is appropriate for crop surveys using LANDSAT data? 07 p0985 N85-16260
Power spectral ensity of markov texture fields 07 p0986 N85-16262
Rectification of single and multiple frames of satellite scanner imagery using points and edges as control 07 p0986 N85-16263
The influence of the number of ground control points on the scene-to-map registration accuracy — Kansas, Louisiana, Mississipp, and Missouri 07 p0986 N85-16264
Image variance and spatial structure in remotely sensed scenes — South Dakota, California, Missouri, Kentucky, Louisiana, Tennessee, District of Columbia, and Oregon 07 p0986 N85-16265
Image-to-image correspondence: Linear structure matching 07 p0986 N85-16266
Analysis of subpixel registration 07 p0986 N85-16267
An automatic pattern recognition apparatus
[AD-D011319] 07 p1043 N85-16628
Rule-based evidence accrual system for image understanding
[AD-A147835] 07 p1044 N85-16634
Analysis of terrestrial conditions and dynamics
[E85-10063] 08 p1174 N85-17401
Direct assessment of synaptic modification rules
[AD-A148376] 08 p1196 N85-17534
Discriminability of signals from noise in a dynamic stereoscopic space
[AD-A148406] 08 p1196 N85-175
Extraction of feature information from 3-dimensional CAD data 08 p1203 N85-175
Recognition of complex 3-dimensional objects using 3-dimensional moment invariants
[AD-A148119] 08 p1212 N85-176
Neurocognitive pattern analysis of an auditory and visual numeric motor control task. Part 1: Development of methods
[AD-A148809] 09 p1364 N85-1857
Optical data processing for missile guidance
[AD-A149346] 10 p1422 N85-1897
Multi target tracking by dynamic scene analysis
[AD-A148922] 10 p1466 N85-1925
Application of SIMCA (Soft Independent Modeling of Class Analogy) pattern recognition to air pollutant analytical data
[PB85-124683] 10 p1513 N85-1954
Image Understanding: Proceedings of the 15th Workshop
[AD-A149496] 10 p1557 N85-19816
Optical implementation of the synthetic discriminant function
[AD-A149582] 10 p1557 N85-19817
Method of multivariant intraclass pattern recognition
[AD-D011546] 12 p1818 N85-21405
Assessment of Thematic Mapper band-to-band registration by the block correlation method 12 p1872 N85-21740
A computer-based gaming system for assessing recognition performance (RECOG)
[AD-A149752] 12 p1915 N85-2202
Technical support for creating an artificial intelligence system for feature extraction and experimental design
[NASA-CR-175298] 12 p1918 N85-22044
Multiple resolution representation and probabilistic matching of 2-D gray-scale shape
[AD-A149981] 12 p1933 N85-22147
Acousto-optically addressed Fourier transform matched filters
[AD-A150298] 13 p2063 N85-22
Electroacoustical imaging technique for encoding incoherent radiance fields as Gabor elementary signals
[NASA-TM-86372] 13 p2094 N85-2306
Preliminary evaluation of Thematic Mapper image data quality 13 p2118 N85-23194
Comparative techniques used to evaluate Thematic Mapper data for land cover classification in Logan County, West Virginia 13 p2121 N85-23209
Relative accuracy assessment of LANDSAT-4 MSS and TM data for level 1 land cover inventory — Washington, D.C. 13 p2122 N85-23212
Feature extraction assessment study
[AD-A150189] 13 p2126 N85-232
Multivariate analysis and its applications
[AD-A150324] 13 p2151 N85-233
Terrestrial analog studies for Martian patterned ground 13 p2190 N85-23
Basic research in electronics (JSEP)
[AD-A151002] 14 p2298 N85-242
Three-dimensional sensing and interpretation
[AD-A150890] 14 p2311 N85-2430
Geological information content of reflected wave record form 14 p2345 N85-2450
Visual recognition of simple objects by a connection network
[AD-A151043] 14 p2389 N85-2471
Perceptual organization and visual recognition
[AD-A150826] 14 p2391 N85-2472
Feasibility of optical instruments based on multiaperture optics
[AD-A150866] 14 p2421 N85-24
Evaluating identifiability in remote sensing problems 15 p2486 N85-2534
Identifying land use structures of multizonal aerospace photographs using digital data processing 15 p2486 N85-253
Interpretation of space photolineaments 15 p2487 N85-253
Vision algorithms and psychophysics
[AD-A151886] 15 p2620 N85-2614
Workshop on Parallel Computer Architectures in Pattern Recognition and Image Processing
[BMFT-FB-DV-84-006] 15 p2622 N85-2615
The EGPA multiprocessor system and its possi application for pattern recognition tasks — comput architecture 15 p2622 N85-2615
Industrial applications of pattern recognition and ima processing 15 p2622 N85-261
Recognition of objects in their natural environment parallel processing 15 p2622 N85-261
Influence and possibilities of Very Large Sc Integration (VLSI) in pattern recognition and ima processing 15 p2622 N85-26

Computer architecture for image processing and pattern recognition in the Federal Republic of Germany. Status 1983, a review
15 p2623 N85-26161

Scene analysis using recursive frequency domain correlation with energy normalization
[AD-A151777] 16 p2854 N85-27596

An IKBS approach to image understanding
[AD-A151962] 16 p2854 N85-27599

Ultrasonic testing of carbon fiber reinforced plastics (CFRP) using pattern recognition methods
[MBB-BS-563/84-0] 16 p2873 N85-27726

Pattern selection and instability in nonlinear wave equation: An aspect of soliton and chaos
[DE85-008578] 18 p3101 N85-29197

Air photo analysis, photo interpretation logic, and feature extraction
[AD-A153926] 18 p3124 N85-29347

Applications of fuzzy set theory to satellite soundings
18 p3141 N85-29445

Approaches to digital image registration and recognition
19 p3257 N85-30197

Adaptive aiding for symbiotic human-computer control: Conceptual model and experimental approach
[AD-A153870] 19 p3332 N85-30644

Texture perception and shape from texture
[AD-A154276] 19 p3336 N85-30672

Target discrimination using infrared techniques: Theoretical considerations
[AD-A154070] 19 p3350 N85-30762

A cluster analysis method for identification of subpopulations of cells in flow cytometric list-mode arrays
20 p3503 N85-31779

Automated cell detection as a mesocyclone precursor tool
[AD-A154952] 21 p3635 N85-32577

Object identification and manipulation using silhouette moments
[AD-A154755] 21 p3705 N85-33011

Recognition and clear representation of handwritten electronic diagrams 23 p3960 N85-34541

A star camera aspect system suitable for use in balloon experiments
[OG-9.3-10] 23 p4028 N85-34965

Artificial intelligence in Ada (trademark): Pattern-directed processing
[AD-A156230] 24 p4141 N85-35671

A holographic streamer chamber for relativistic nucleus-nucleus collision experiments
24 p4147 N85-35710

PATTERN REGISTRATION

Multi-disciplinary techniques for understanding time-varying space-based imagery
[AD-A144357] 05 p0728 N85-14681

The influence of the number of ground control points on the scene-to-map registration accuracy — Kansas, Louisiana, Mississipp, and Missouri
07 p0986 N85-16264

Analysis of subpixel registration
07 p0986 N85-16267

The use of image registration technique in Brasilia's urban growth monitoring
[INPE-3302-PRE/614] 10 p1569 N85-19896

Investigation of TM band-to-band registration using the JSC registration processor 12 p1872 N85-21745

Geodetic accuracy of LANDSAT 4 Multispectral Scanner and Thematic Mapper data 12 p1873 N85-21746

Technical support for creating an artificial intelligence system for feature extraction and experimental design
[NASA-CR-175286] 12 p1918 N85-22044

Study of the urban evolution of Brasilia with the use of LANDSAT data
[E85-10101] 16 p2809 N85-27321

Approaches to digital image registration and recognition 19 p3257 N85-30197

Repetition of dense cloud cover above Indian Ocean from generalized satellite data 22 p3737 N85-33165

The design, development, testing, fabrication, calibration and integration of a High Resolution Imager (HRI) for the Roentgen Satellite (ROSAT)
[NASA-CR-175302] 22 p3741 N85-33184

Depth dimension compression of 3-D images
22 p3764 N85-33332

PATTERNS

Multiple resolution representation and probabilistic matching of 2-D gray-scale shape
[AD-A149981] 12 p1933 N85-22147

Multi-robot assembly of IC's 23 p3964 N85-34577

PAVEMENTS

Pavement friction measurements on nontangent sections of roadways, vol. 1
[PB84-219732] 01 p0036 N85-10227

Predictor model for seasonal variations in skid resistance. Volume 2: Comprehensive report
[PB84-228820] 01 p0037 N85-10230

A study of bituminous pavements to determine a correlation between pavement structure designs and tripping of asphalt cement
[PB84-217751] 01 p0037 N85-10231

Evaluation of laser profile and deflection measuring system
[FAA-PM-84-24] 02 p0201 N85-11341

Development of a pavement maintenance management system. Volume 10: Summary of development from 1974 through 1983
[AD-A146035] 03 p0320 N85-12067

Development of a pavement maintenance management system. Volume 9: Development of airfield pavement performance prediction models
[AD-A146150] 03 p0321 N85-12069

Experimental AC (Asphalt Concrete) overlays of PCC pavement
[PB84-218171] 03 p0342 N85-12203

Evaluation of moduli and thicknesses of pavement systems by spectral-analysis-of-surface-waves method
[PB84-219112] 03 p0342 N85-12205

Skid resistance of bituminous surfaces in Ohio
[PB84-234491] 04 p0484 N85-13086

Prefabricated panels for rapidly runway repair and expedient airfield surfacing
[AD-D011277] 05 p0597 N85-13804

Synthesis study of nondestructive testing devices for use in overlay thickness design of flexible pavements
[PB84-216080] 06 p0774 N85-14950

System for rapid repair of damaged airfield runways
[AD-D011325] 07 p0909 N85-15754

Development of a preliminary ALRS stabilized material pavement analysis system (SPAS)
[AD-A147116] 07 p0910 N85-15760

Aeroproyekt develops improved runway surfacing
08 p1068 N85-16770

Runway rubber removal specification development field evaluation procedures development
[FAA-PM-84-27] 12 p1781 N85-21179

Field validation of statistically-based acceptance plan for bituminous airport pavements. Volume 1: Correlation analysis of Marshall properties of laboratory-compacted specimens
[FAA-PM-84-12-VOL-1] 12 p1781 N85-21180

Field validation of statistically-based acceptance plan for bituminous airport pavements. Volume 2: Statistical analysis of Marshall properties of plant-produced bituminous materials
[FAA-PM-84-12-VOL-2] 12 p1781 N85-21181

Field validation of statistically-based acceptance plan for bituminous airport pavements. Volume 3: Statistical analysis of 3 methods for determining maximum specific gravity of bituminous concrete mixtures
[FAA-PM-84-12-VOL-3] 12 p1781 N85-21182

Field validation of statistically-based acceptance plan for bituminous airport pavements. Volume 4: Computer simulation of multiple acceptance criteria
[FAA-PM-84-12-VOL-4] 12 p1782 N85-21183

Field validation of statistically-based acceptance plan for bituminous airport pavements. Volume 5: Summary of validation studies
[FAA-PM-84-12-VOL-5] 12 p1782 N85-21184

Evaluation of Epoxo 300-C nonskid coating for use on bridge decks
[PB85-108843] 12 p1819 N85-21412

Stress-relieving interlayers for bituminous resurfacings
[PB85-136885] 12 p1820 N85-21415

Analysis of slabs-on-grade for a variety of loading and support conditions
[AD-A150965] 14 p2264 N85-24030

Microwave methods for paving
[DE85-004194] 14 p2265 N85-24032

Overlays for plain jointed concrete pavements
[PB85-156297] 15 p2523 N85-25557

Pavement-marking materials: New York's experience
[PB85-153294] 15 p2523 N85-25558

Study of acceptance criteria for joint densities in bituminous airport pavements
[FAA-PM-85-5] 16 p2715 N85-26761

Review of rigid pavement design for vehicular parking areas
[AD-A154284] 19 p3222 N85-29975

PAYLOAD CONTROL

Commerce Laboratory: Mission analysis payload integration study
[NASA-CR-171298] 07 p0911 N85-15764

Sounding rocket program Aeronomie. The payload M-I in the project MAP-WINE
[BMFT-FB-W-84-046] 12 p1790 N85-21238

A normal incidence X-ray telescope sounding rocket payload
[NASA-CR-176169] 24 p4153 N85-35749

PAYLOAD DELIVERY (STS)

Selected tether applications in space: An analysis of five selected concepts
[NASA-CR-171222] 04 p0460 N85-12921

Advanced OTV engine concepts
08 p1106 N85-17001

Satellite services and orbital retrieval
12 p1786 N85-21211

A dual, fault-tolerant aerospace actuator
22 p3798 N85-33530

Design of a dual fault tolerant space shuttle payload deployment actuator 22 p3798 N85-33531

PAYLOAD DEPLOYMENT & RETRIEVAL SYSTEM

NT REMOTE MANIPULATOR SYSTEM

Tethers open new space options
11 p1642 N85-20340

Tethered satellite system project overview
11 p1642 N85-20341

Shuttle tethered satellite system program overview
11 p1642 N85-20342

Transportation applications, part 1
11 p1643 N85-20349

Space science and applications
11 p1644 N85-20362

Report of the Transportation Panel
11 p1645 N85-20364

Report of the Artificial Gravity Panel
11 p1645 N85-20365

Satellite services and orbital retrieval
12 p1786 N85-21211

A dual, fault-tolerant aerospace actuator
22 p3798 N85-33530

Design of a dual fault tolerant space shuttle payload deployment actuator 22 p3798 N85-33531

Appendange deployment mechanism for the Hubble Space Telescope program 22 p3798 N85-33533

The role of tethers on space station
[NASA-TM-86519] 23 p3900 N85-34154

PAYLOAD INTEGRATION

Commerce Laboratory: Mission analysis payload integration study
[NASA-CR-171298] 07 p0911 N85-15764

Commerce Lab: Mission analysis and payload integration study
[NASA-CR-171272] 08 p1104 N85-16981

Commerce Lab: Mission analysis. Payload integration study
[NASA-CR-171285] 08 p1104 N85-16982

Commerce lab: Mission analysis and payload integration study
[NASA-CR-174381] 10 p1426 N85-18993

Commerce Lab: Mission analysis payload integration study. Appendix A: Data bases
[NASA-CR-176016] 19 p3224 N85-29988

PAYLOAD INTEGRATION PLAN

Commerce Laboratory: Mission analysis payload integration study
[NASA-CR-171298] 07 p0911 N85-15764

Data Requirement (DR) MA-03: Payload missions integration — Spacelab payloads
[NASA-CR-171331] 10 p1428 N85-19009

PAYLOAD RETRIEVAL (STS)

Satellite services and orbital retrieval
12 p1786 N85-21211

A remotely controlled orbiting retriever
12 p1786 N85-21212

The investigation of tethered satellite system dynamics
[NASA-CR-175855] 16 p2731 N85-26854

PAYLOAD STATIONS

Small Payload Flight Systems (SPFS)
02 p0152 N85-11030

PAYLOAD TRANSFER

Transportation applications, part 2
11 p1643 N85-20350

Satellite services and orbital retrieval
12 p1786 N85-21211

Ignition, separation of boosters, stages in Ariane 3
14 p2289 N85-24185

PAYLOADS

NT ATMOSPHERIC GENERAL CIRCULATION EXPERIMENT
NT EARTH RADIATION BUDGET EXPERIMENT
NT OSS-1 PAYLOAD
NT PLASMA INTERACTION EXPERIMENT
NT SHUTTLE IMAGING RADAR
NT SPACE SHUTTLE PAYLOADS
NT SPACEBORNE EXPERIMENTS
NT SPACELAB
NT SPACELAB PAYLOADS
NT STARLAB
NT X RAY ASTROPHYSICS FACILITY

A study of the critical layer in a rotating liquid payload
[AD-A146094] 03 p0362 N85-12321

A normal incidence, high resolution X-ray telescope for solar coronal observations
[NASA-CR-174145] 04 p0579 N85-13899

On-orbit support of DARPA-301 payload
[AD-A146897] 07 p0911 N85-15767

Artificial gravity: Tethers and containers
11 p1645 N85-20367
Rail accelerator technology and applications
[NASA-TM-86947] 12 p1794 N85-21258
Assessment of candidate-expendable launch vehicles for large payloads
[NASA-CR-175540] 14 p2237 N85-23867
Get Away Special (GAS) thermal design summary
[X-732-83-8] 15 p2475 N85-25278
Costs, payload of Ariane, US Space Shuttle compared
15 p2530 N85-25601
Space station trace contaminent control
18 p3157 N85-29550
Outside users payload model
[NASA-CR-176011] 19 p3223 N85-29986
German payloads for EURECA 1
[BMFT-FB-W-85-003] 20 p3419 N85-31223
Brush and commutator segment torquer motor
[AD-D011726] 23 p3927 N85-34340
Research of advanced techniques for X-ray detectors and telescopes with applications to rockets and the LAMAR facility
[NASA-CR-176161] 23 p4054 N85-35141
An automated technique for encasing specific payloads with low-drag fairings 24 p4063 N85-35183

PCB
U POLYCHLORINATED BIPHENYLS

PCM (MATERIALS)
U PHASE CHANGE MATERIALS

PCM (MODULATION)
U PULSE CODE MODULATION

PCM TELEMETRY
Telemetry (TM)/telecommand (TC) processor study
[ESA-CR(P)-1915] 03 p0323 N85-12061

PDM (MODULATION)
U PULSE DURATION MODULATION

PDP COMPUTERS
NT PDP 11 COMPUTER
NT PDP 11/70 COMPUTER

PDP 11 COMPUTER
A procedure for communications with PDP-10 and PDP-11 (IS/1 UNIX) type computers through use of CPT word processing equipment, revision 1
[DE85-007596] 16 p2845 N85-27540
Data processing on the rotor test stand at DFVLR in Brunswick: Microprogrammable interfaces and array processor as key components in a PDP 11 real time data acquisition and processing system
[DFVLR-MITT-85-03] 17 p2906 N85-27921

PDP 11/70 COMPUTER
Specification of a transport protocol for computer communications. Volume 1: Overview and Services. Volume 2: Class 2 protocol. Volume 3: Class 4 protocol
[PB84-222650] 06 p0846 N85-15380
Specification of a transport protocol for computer communications. Volume 4: Service specifications. Volume 5: Guidance for the implementor. Volume 6: Guidance for implementation selection
[PB84-222668] 06 p0848 N85-15385
Specification of a transport protocol for computer communications. Volume 7: Testing OSL protocols, a compendium of papers. Volume 8: User's guide to the testing system for implementations of the ICST transport protocol. Volume 9: A test suite for implementations of the ICST transport protocol. Volume 10: Specification of a remote scenario interpreter for implementations of the ICST transport protocol
[PB84-222676] 06 p0846 N85-15386

PEARLITE
Influence of preliminary cold deformation on fineness of pearlite
[BLL-BISI-TRANS-22409-(9022.08)]
17 p2927 N85-28054
Effects of hot deformation on the kinetics of the pearlite transformation in eutectoid steel
[BLL-M-35844-(5828.4)] 23 p3913 N85-34250

PEARSON DISTRIBUTIONS
Adaptive detection of noise signal according to Neumann-Pearson criterion 15 p2527 N85-25580
Least-squares approximation to minimum chi-square estimators of location and scale parameters and their effect on the Pearson chi-square test
[AD-A153534] 18 p3169 N85-29636
Effect of some estimators on a large sample approximation to the non-null distribution of the pearson chi-square statistic
[AD-A153515] 18 p3173 N85-29673

PEAT
Versatility of peat emphasized
07 p0994 N85-16316
Peat resources of Maine. Volume 1: Aroostook County
[DE85-004196] 11 p1669 N85-20519
Peat resources of Maine. Volume 4: Southern and western Maine
[DE85-004198] 11 p1670 N85-20520
Peat resources of Maine. Volume 2: Penobscot County
[DE85-004195] 11 p1670 N85-20522
Peat resources of Maine. Volume 5: Washington County
[DE85-004197] 11 p1670 N85-20523
Ash contents of Costa Rican peat deposits
[DE85-010734] 19 p3301 N85-30462

PECULIAR STARS
NT SYMBIOTIC STARS
The spectroscopic antics of S 18/SMC
11 p1750 N85-21008

PEDIMENTS
U PIEDMONTS

PEDIPLAINS
U PIEDMONTS

PEDOLOGY
U SOIL SCIENCE

PEELING
A study of bituminous pavements to determine a correlation between pavement structure designs and tripping of asphalt cement
[PB84-217751] 01 p0037 N85-10231
Finger materials for air cushion vehicles. Volume 2: Base fabrics for finger materials
[AD-A149701] 12 p1819 N85-21408

PEENING
NT SHOT PEENING

PELLETS
Thermal conductivity of iron/potassium perchlorate heat powder
[DE84-017071] 04 p0476 N85-13035
Study of opacity effects on line radiation from pellet implosions
[DE85-000380] 10 p1491 N85-19413
Robotic thermal battery pellet fabrication
[DE85-007755] 16 p2779 N85-27154
Ion beam-plasma interactions
[DE85-010202] 19 p3371 N85-30913
A gel-halo sample pellet: The best of both worlds? Stubby zones without a constricted sample gate
20 p3502 N85-31770
Burn front velocity as a function of pellet density in iron-potassium perchlorate heat powders
[DE85-011448] 21 p3572 N85-32214

PELTIER EFFECTS
Peltier heat of a small polaron in a magnetic semiconductor
[DE85-000470] 14 p2430 N85-24963

PELVIS
Locomotion research for the analysis of the human gait and for the determination of the maximum loads of the pelvis-leg skeleton. Volume 1: Two-dimensional analysis
[BMFT-FB-T-83-187-VOL-1] 02 p0236 N85-11535
Locomotion research for the analysis of the human gait and for the determination of the maximum loads of the pelvis-leg skeleton. Volume 2: Three-dimensional analysis
[BMFT-FB-T-83-188-VOL-2] 02 p0236 N85-11536
The position and mobility of the shoulder, spinal column and pelvis in seated subjects
[AD-A153751] 18 p3153 N85-29524

PENALTY FUNCTION
Some applications of penalty functions in mathematical programming
[AD-A147443] 07 p1032 N85-16552
Analysis of a penalty finite element approximation of the Navier Stokes equations 08 p1161 N85-17321

PENDULUMS
Soil tilt measurement: First results of the comparative analysis of the response of two different tiltmeters
[NOTA-INTERNA-818] 02 p0228 N85-11494
Structure-property relationships in polymeric matrix materials
[AD-A153929] 18 p3080 N85-29050
Study on a flexure hinged pendulum accelerometer
[NAL-TR-844] 18 p3104 N85-29220

PENETRANTS
Technical activities 1983, Office of Nondestructive Evaluation
[PB84-217074] 03 p0370 N85-12360

PENETRATING PARTICLES
U CORPUSCULAR RADIATION

PENETRATION
Penetrator/armour interactions: Background to Australian work
[MRL-R-936] 03 p0367 N85-12353
Application and calibration of the subsurface mapping capability of SIR-B in desert regions
08 p1148 N85-17244
Ground truth for SIR-B images obtained by SIR system 8 impulse radar 08 p1149 N85-17251
Tractor power selection with compaction constraints
[AD-P004300] 09 p1409 N85-19877
Evaluation of the birdstrike threat to the F-15 present fleet, rapid deployment force, and dual role fighter transparencies
[AD-A148954] 10 p1421 N85-19886
Aircraft skin penetrator and agent applicator. Volume 1: Working model development and construction
[AD-A150498] 13 p1970 N85-22074
Aircraft skin penetrator and agent applicator. Volume 2: Test and evaluation
[AD-A151609] 15 p2486 N85-25225
Magnetic field penetration into cometary ionosphere
15 p2477 N85-25280
Study of intermediate velocity penetration of steel spheres into deep aluminum targets
[DE85-010419] 19 p3287 N85-30386
Geometry, velocity structure and penetration depths of descending slabs in the western Pacific
19 p3319 N85-30574
The effect of stress and hot corrosion on nickel-base superalloys
[AD-A154722] 21 p3566 N85-32181
Ice fog as an electro-optical obscurant
[AD-A155059] 21 p3705 N85-33015
Multiaxial stress analysis taking account of penetration depth of X-rays. A solution by means of polynomial approximation 23 p3907 N85-34204
Monte Carlo techniques for analyzing deep penetration problems
[DE85-011426] 23 p3968 N85-34506
Dynamics of the penetration boundaries of solar protons during a strong magnetic storm
[SH-6.1-16] 23 p4046 N85-35086
Experimental data for characterizing perforating impacts: Fragmentation processes
[AD-A156370] 24 p4102 N85-35427

PENETRATION BALLISTICS
U TERMINAL BALLISTICS

PENETROMETERS
Physical and mechanical properties of lunar soil as function of specifics of relief and processes in vicinity of operation of Lunokhod-2 02 p0161 N85-11090

PENNSYLVANIA
LANDSAT instruments characterization
[E85-10026] 05 p0654 N85-14197
Remote sensing of hydrologic transport processes using spot simulation data
[DE85-012412] 24 p4108 N85-35487

PENTACHLORIDES
U CHLORIDES

PENTAERYTHRITOL TETRANITRATE
U PETN

PENTANES
Thermodynamic properties of isobutane-isopentane mixtures from -40 to +600(0)F and up to 1000 psia
[DE84-015137] 01 p0124 N85-10850
Multiphoton ionization of benzene in solution
[DE85-000893] 06 p0766 N85-14089
Thermophysical properties of working fluids for binary geothermal cycles
[DE85-000385] 12 p1881 N85-21904

PENTOSE
NT RIBOSE
Changes in pentose and glucuronate pathway dehydrogenases in rat brains following single or multiple hypothermic episodes 20 p3505 N85-31700

PENUMBRAS
On running penumbral waves
14 p2453 N85-25150

PEOPLES DEMOCRATIC REPUBLIC OF GERMANY
U EAST GERMANY

PEPTIDES
NT POLYPEPTIDES
Effect of short-term hypokinesia on rat opioid system reaction 01 p0093 N85-10825
Rat tissue opioid peptide content during long-term hypokinesia 12 p1904 N85-21954

PERCENTAGE
U RATIOS

PERCEPTION
NT AUDITORY PERCEPTION
NT BINAURAL HEARING
NT CONSCIOUSNESS
NT MOTION PERCEPTION
NT PROPRIOCEPTION
NT SENSORY PERCEPTION
NT SOUND LOCALIZATION
NT SPACE PERCEPTION
NT TACTILE DISCRIMINATION
NT TOUCH
NT VERTICAL PERCEPTION
NT VISUAL DISCRIMINATION
NT VISUAL PERCEPTION

The psychology of technical devices and technical discourse
[AD-P003829] 02 p0246 N85-11609
Subliminal communication technology
[GPO-38-893] 06 p0622 N85-13979
Experiment 1ES031 on Spacelab 1: Are cells sensitive to gravity? — lymphocyte proliferation
05 p0689 N85-14428
Observation of the contractile vacuolar system of Paramecium caudatum on the fast running clinostat
05 p0689 N85-14431
Gravity and cell differentiation in lentil roots
05 p0690 N85-14433
The use of horizontal clinostats in studies of plant statocyte development 05 p0690 N85-14435
Twentieth Annual Conference on Manual Control, volume 1
[NASA-CP-2341-VOL-1] 06 p0699 N85-14487
Subjective workload assessment and voluntary control of effort in a tracking task 05 p0708 N85-14540
Assessing the subjective workload of directional orientation tasks 05 p0708 N85-14542
Classification systems for individual differences in multiple-task performance and subjective estimates of workload 05 p0708 N85-14543
Military pilot ergonomics 10 p1532 N85-19655
Grasp of information by the pilot in future combat aircraft 10 p1533 N85-19662
Annals of the New York Academy of Sciences, Volume 423 — timing and time perception
[AD-A150031] 12 p1909 N85-21961
Mass-discrimination during prolonged weightlessness
20 p3509 N85-31814
Resource allocation in cerebral specialization of function: Behavioral and electrophysiological studies
[AD-A155092] 21 p3664 N85-32759
The effects of prolonged feeding meal, ready-to-eat (MRE) operational rations
[AD-A154763] 21 p3666 N85-32773
PERCEPTRONS
U SELF ORGANIZING SYSTEMS
PERCHLORATES
NT AMMONIUM PERCHLORATES
NT POTASSIUM PERCHLORATES
CP DDT detonators. 4: Thermal aging
[DE85-011172] 19 p3251 N85-30160
Nuclear magnetic resonance study of the intramolecular rearrangement of 2-(5-cyanotetrazolato)pentaammine cobalt (III) perchlorate
[DE85-010810] 22 p3639 N85-33772
PERCOLATION
Determining deep heat flow and rate of horizontal percolation from temperature measurements in aquifer
13 p2116 N85-23180
Non-equilibrium effects in turbulent diffusion flames
20 p3425 N85-31258
PERCUSSION
Effect of air cavity on the vibration analysis of loaded drums 09 p1339 N85-18422
PERFECT GAS
U IDEAL GAS
PERFLUORO COMPOUNDS
NT PERFLUOROALKANE
Cross-Appalachian Tracer Experiment (CAPTEX '83)
[PB84-236641] 06 p0834 N85-15307
The use of perfluoroether lubricants in unprotected space environments 22 p3797 N85-33523
PERFLUOROALKANE
Design and chemical synthesis of iodine-containing molecules for application to solar-pumped I* lasers
[NASA-CR-176010] 19 p3275 N85-30310
PERFORATED PLATES
Stresses in pin-loaded orthotropic plates using photoelasticity
[NASA-CR-172498] 07 p0977 N85-16204
Mechanical locking between multi-layer printed wiring board conductors and through-hole plating
[AD-D011477] 10 p1481 N85-19352
Stresses in a half-plane containing either a pressurized hole or an interference-fit disc
[ARL/STRUC-R-409] 12 p1865 N85-21700
Elastic response of a half-plane to a bonded interference-fit disc of the same material
[ARL/STRUC-R-406] 12 p1865 N85-21701
effect of gas stream sweeping past the effluent of a perforated plate on heat transfer inside the perforations
13 p2051 N85-22836
Sound emission by particle beam passing through hole in rigid shield 15 p2525 N85-25570
PERFORATING
Experience with introduction of Finish perforation of precision parts for optical instruments
16 p2761 N85-27038
Some asymptotic problems in the optimal control of distributed systems 20 p3412 N85-31175
PERFORATION
Wind tunnel wall interference
[AD-A151212] 15 p2474 N85-25273
PERFORMANCE
A generalized model of fault-isolation performance
[AD-P003926] 02 p0246 N85-11606
Optimum performance parameters for ski-jump operations of USAF fighter aircraft
[AD-A148532] 08 p1084 N85-16867
Electric vehicle demonstration project
[DE85-003124] 11 p1741 N85-20944
Experimental and theoretical study of fatigue crack initiation in metals 19 p3283 N85-30357
Life cycle test results of a bipolar nickel hydrogen battery
[NASA-TM-87046] 19 p3304 N85-30430
PERFORMANCE PREDICTION
NT PREDICTION ANALYSIS TECHNIQUES
Primate equilibrium performance and diazepam: A behavioral tolerance effect
[AD-A145156] 01 p0094 N85-10634
End-to-end performance in local area networks of interconnected token rings
[FUB-42-1983] 01 p0107 N85-10714
Phosphoric acid fuel cell power plant system performance model and computer program
[NASA-CR-174638] 02 p0222 N85-11456
Individual differences in automatic and controlled information processing
[AD-A146245] 03 p0401 N85-12559
Design and off-design performance prediction of high pressure ratio centrifugal compressors
05 p0636 N85-14082
Synthesis of load-time histories resulting from statistical analysis 05 p0650 N85-14171
Measurement-technical problems in the investigation of wind energy units 05 p0668 N85-14295
Hollings hungry mantid model for the invertebrate functional response considered as a Markov process. Part 3: Mathematical elaborations
[CWI-AM-R8407-PT-3] 05 p0722 N85-14639
Predicting changes in reliability characteristics of gas turbine engines during operation
06 p0776 N85-14964
The influence of fastener flexibility on load transfer and fatigue life predictions for multirow bolted and riveted joints — aircraft structures
[LBF-FB-172/84] 07 p0979 N85-16219
What should DOE do to help establish voluntary consensus standards for measuring and rating the performance of PV modules?
[NASA-CR-174265] 07 p0992 N85-16297
Technical performance measurement handbook
[AD-A147314] 07 p1052 N85-16675
Performance prediction of pneumatic tyres on sand
[AD-P004262] 09 p1404 N85-18838
Sample size and precision in communication performance measurements
[PB85-1143270] 12 p1830 N85-21488
Aerodynamic research efforts at SERI Wind Energy Research Center at Rocky Flats
[DE85-000529] 12 p1881 N85-21805
Surface wave excitation study
[DE85-005301] 13 p2056 N85-22875
Investigations of the high frequency performance of impact avalanche transit-time diodes
13 p2063 N85-22664
Boundary layer control by transition fixing — conference
[DFVLR-MITT-84-17] 14 p2211 N85-23712
Parameters of symmetric rhombic drive mechanism for single-cylinder Stirling engine 14 p2271 N85-24072
Introduction to methods of evaluating the operational reliability of complex systems: Application to satellite control ground support 14 p2307 N85-24771
A system-level mathematical model for evaluation of power train performance of load-leveled electric-vehicles
[NASA-CR-175652] 14 p2434 N85-25009
Performance of a copper-lithium alloy as an impurity control system surface material for a fusion reactor
[DE85-006494] 15 p2657 N85-26398
Simulation: A tool for cost-effective systems design and live test reduction 16 p2696 N85-26657
Analytical fuel property effects--small combustors
[NASA-CR-174736] 16 p2708 N85-26709
Technical overview structural dynamics
16 p2736 N85-26883
Solar elements with distributed parameters
16 p2760 N85-27036
Calculation of viscous compressible flows in small gas turbines 17 p2912 N85-27950
Flat magnetohydrodynamic induction pump
17 p2939 N85-28145
A program for the calculation of paraboloidal-dish solar thermal power plant performance
[NASA-CR-175874] 17 p2965 N85-28449
Mission requirements and handling qualities
18 p3057 N85-28918
Establishment of a methodology for predicting lifetimes in active solar systems
[DE85-008829] 18 p3130 N85-29383
Aerodynamic analysis of a horizontal axis wind turbine by use of helical vortex theory. Volume 1: Theory
[NASA-CR-168054] 19 p3212 N85-29916
Onset of freezing in residential air-to-air heat exchangers
[DE85-009960] 19 p3267 N85-30259
Analytical model for predicting emergency shutdown of a two-bladed horizontal axis wind turbine
[NASA-TM-83472] 19 p3303 N85-30476
Performance comparison between NACA 23024 and NACA 64(3)-618 airfoil configurated rotors for horizontal-axis wind turbines
[NASA-TM-83471] 19 p3303 N85-30477
Ion thruster performance model
20 p3420 N85-31226
Galileo battery testing and the impact of test automation 20 p3444 N85-31381
Fundamental algorithms of the Goddard battery model
20 p3445 N85-31389
Environmental factors in corrosion and deterioration of materials 22 p3750 N85-33241
Design and development of a linear thermal actuator
22 p3796 N85-33518
PMEXA: Diagnostic filtering program for the PBFA-1 performance monitoring and evaluation system
[DE85-013179] 22 p3831 N85-33725
Assessment of metal heating technologies for ferrous forging: A pilot study of the form value of natural gas
[PB85-204394] 24 p4084 N85-35314
Wind turbine noise: Prediction tools and design parameter dependence 24 p4110 N85-35477
PERFORMANCE TESTS
Evaluation of the Malcolm horizon in a moving-base flight simulator 01 p0008 N85-10051
Peripheral vision horizon display testing in RF-4C aircraft 01 p0009 N85-10054
A preliminary flight evaluation of the peripheral vision display using the NT-33A aircraft
[AD-A145123] 01 p0010 N85-10060
Cylinder power fault diagnosis in military diesel engines
[TT-8405] 01 p0053 N85-10354
Rotordynamic analysis of the SSME turbopumps using reduced models
[NASA-CR-171170] 01 p0054 N85-10355
Performance of the h, p and h-p versions
01 p0058 N85-10383
Advanced blade tip seal system, volume 2
[NASA-CR-167851] 02 p0147 N85-10999
The Palmqvist test and its applications in WC-Co alloys 02 p0177 N85-11187
Alternate fuels combustion research
[AD-A145691] 02 p0188 N85-11258
Radar, target and ranging
[AD-A145407] 02 p0190 N85-11272
15 kW general purpose frequency changer performance improvement
[AD-A145503] 02 p0194 N85-11297
The IMX double direct process
[AD-A146250] 03 p0340 N85-12188
Construction, putting into operation, and utilization of a triple axis neutron spectrometer
03 p0425 N85-12715
Performance of improved lead acid batteries for electric vehicles
[DE84-015845] 04 p0495 N85-13160
Space telescope cost, schedule, and performance review, 1984
[GPO-39-065] 04 p0579 N85-13698
Technical support services for space and terrestrial systems programs
[DE84-009031] 05 p0597 N85-13806
Test signal generator for coherent air-to-ground radars
[AD-D011278] 05 p0628 N85-14025
Realized field tests — solar generators
05 p0664 N85-14271
Implementation assessment of a network service. The test responder exerciser specification
[NPL-DITC-44/84] 05 p0716 N85-14594
Procedural aspects of testing aerodynamic models with combustion in high-enthalpy transient-mode installations
05 p0725 N85-14658
Choice of criteria for rejection of insulating components in high-voltage surge equipment
06 p0765 N85-15021
Encapsulation design analysis
06 p0829 N85-15268
Qualification of an electrothermal hydrazine thruster with a vacuum thrust of 0.5 to 2.0 N
[BMFT-FB-W-84-043] 07 p0917 N85-15808

PERFORMANCE TESTS

Special problems of Ramjet with solid fuel
07 p0918 N85-15815

Bearing tester fit analysis
[NASA-CR-171282] 07 p0973 N85-16161

Demonstration of transparent solar array module design
[NASA-CR-174257] 07 p0992 N85-16302

Evaluation of the measured energy performance of four solar systems
[AD-A147912] 07 p0993 N85-16306

Comparative investigation of three commercial radiosonde systems
[KNMI-TR-53] 07 p1009 N85-16409

Design of self-checking N-MOS (H-MOS) integrated circuits
08 p1064 N85-16742

Construction, testing of 1-MW nitrogen laser
08 p1140 N85-17182

Ultrasonic transducers, performance variability, design, and manufacturing procedures
[AD-A148575] 08 p1158 N85-17306

Ceramic fabric material testing
[DE84-012014] 09 p1300 N85-18165

FORTRAN 77 computer program for test procedure calculations of vented heaters
[PB85-109627/GAR] 09 p1305 N85-18198

Operational characteristics of a 1000 MVA superconducting power transmission system
[DE85-000232] 09 p1314 N85-18263

Fiat introduces 1000-CC engine
11 p1618 N85-20185

Spectral characterization of the LANDAT-4 MSS sensors
11 p1666 N85-20499

A system simulator for the solar generator of artificial satellites
[INPE-3320-TDL/180] 11 p1672 N85-20534

Wind generator for Solar Office Complex, Luna Vocational Technical Institute, Las Vegas, New Mexico
[DE85-900103] 11 p1674 N85-20547

Electrical and thermal performance during charging and discharging a Phase 1 gel cell battery
[PB85-114312] 11 p1677 N85-20565

BIT/BITE tradeoff analysis model
[AD-A149345] 11 p1701 N85-20697

GPS system field testing 11 p1711 N85-20762

Coverage and buildup of the Navstar constellation
11 p1711 N85-20764

Tailored airfoils for vertical axis wind turbines
[DE85-004626] 12 p1772 N85-21129

Landing control centrals
[AD-A149800] 12 p1775 N85-21140

Field validation of statistically-based acceptance plan for bituminous airport pavements. Volume 4: Computer simulation of multiple acceptance criteria
[FAA-PM-84-12-VOL-4] 12 p1782 N85-21183

Performance assessment of Class 1E pressure transmitters subjected to environmental stresses
[DE85-001623] 12 p1854 N85-21626

The Olympus solar array development and test program
13 p2009 N85-22599

Surge strength of symmetric cable with monolithic polyethylene insulation of quads
13 p2082 N85-23001

Algorithm in Walsh function basis for analysis of integrated microcircuits on MOS-structures
13 p2083 N85-23006

Laboratory tests of reciprocating internal combustion engines
[AD-A150143] 13 p2098 N85-23067

Thermal state of cooled thin-walled nozzle blade
14 p2270 N85-24066

Optimization of combined convective and film cooling of perforated baffle blades in gas turbines
14 p2270 N85-24067

Selection of bearing type for large steam turbines
14 p2271 N85-24069

Work of axial bearing under dynamic loading
14 p2288 N85-24182

Advanced life analysis methods. Volume 3: Experimental evaluation of crack growth analysis methods for attachment lugs
[AD-A151058] 14 p2317 N85-24319

Experimental report on a fiber optic light guide made by Galileo Electro-Optics Corporation
[DE85-006161] 14 p2421 N85-24941

Performance testing and system characterization. DOE hybrid test vehicle, phase 3
[NASA-CR-175668] 14 p2434 N85-25010

US Army Aviation Engineering Flight Activity (USAAEFA) report bibliography update 1983 - 1984
[AD-A151381] 15 p2457 N85-25166

Space station propulsion: The advanced development program at Lewis
[NASA-TM-86999] 15 p2494 N85-25386

Evaluation of adequacy pf JP54 protection level for large electric machines
15 p2528 N85-25586

France develops new continuous vacuum treatment method
15 p2531 N85-25611

Space reactor ground tests, assessment of facility needs
[DE85-008814] 15 p2650 N85-26345

Field use of electric vehicles compared to prototype tests
[DE85-006887] 15 p2667 N85-26456

The series 2000: A miniature gas bearing DTG for low cost strapdown guidance and control
16 p2696 N85-26648

High-pressure hydrogen testing of single crystal superalloys for advanced rocket engine turbopump turbine blades
16 p2735 N85-26875

Instrumentation technology overview
16 p2739 N85-26903

Operational test results of a prototype superconducting power transmission system and their extrapolation to the performance of a large system
[DE85-006731] 16 p2779 N85-27153

Management of vacuum leak-detection processes, standards and calibration
[DE85-006705] 16 p2788 N85-27202

Documentation and solar cell modules
[NASA-CR-175769] 16 p2818 N85-27384

Effect of precipitation on wind turbine performance
[NASA-TM-86986] 16 p2818 N85-27385

Shape with and without redundent colour as coding mechanism for simulated radar displays in a time-extended simple vigilance task
[AD-A151683] 16 p2844 N85-27533

Distance Measuring Equipment (DME), general
[AD-A152585] 17 p2895 N85-27846

An assessment of the suitability of the BHGA structural test rig for aerodynamic testing of hang gliders
[CA-8505] 17 p2896 N85-27853

Rotorcraft research testing in the National Full-Scale Aerodynamics Complex at NASA Ames Research Center
[NASA-TM-86687] 17 p2896 N85-27854

Testing of materials and coatings for jet engine components under simulated operational conditions
[B8580073] 17 p2899 N85-27873

Evaluation of used crankcase oils using computerized infrared spectrometry. Appendices
[AD-A152994] 17 p2920 N85-28000

MM2 LRSLA testing stage 3 propellant
[AD-A152540] 17 p2937 N85-28128

Performance evaluation of fiber-optic converters
17 p2941 N85-28154

Performance analysis of the DSN baseband assembly (Bba) Real-Time Combiner (RTC)
[NASA-CR-175878] 17 p2946 N85-28190

Baseline cycle testing of a 500-kWh zinc chloride battery at the Battery Energy Storage Test (BEST) Facility
[DE85-006948] 17 p2955 N85-28249

Test and evaluation of the Hoppecke Model E240G144/16 electric vehicle battery charger
[DE85-900573] 17 p2955 N85-28253

International time transfer and portable clock evaluation using GPS timing receivers: Preliminary results
17 p2964 N85-28303

Field test report of the Department of Energy's 100-kW vertical axis wind turbine
[DE85-008475] 17 p2987 N85-28458

Shenandoah parabolic dish solar collector
[DE85-008326] 17 p2987 N85-28460

Test plan for acceptance, verification and performance testing of the Bedford Lucas Chloride Electric Van. Part 1: Acceptance and verification testing at EG and G Automotive Research. Part 2: INEL performance testing, revision 1
[DE85-005157] 17 p3051 N85-28888

The attitude control model tests for the Infrared Astronomical Satellite (IRAS)
[B8580071] 18 p3067 N85-28967

A simplified GPS C/A reciever front end with low noise performance
18 p3109 N85-29251

Performance test results of a low cost GPS time and frequency monitor
18 p3109 N85-29252

Thermal performance testing and mathematically modeling of integral collector storage solar hot water systems
[PB85-186906] 18 p3132 N85-29398

Automated Weather Observing System (AWOS) demonstration program
[AD-A153463] 18 p3148 N85-29493

A task battery for applied human performance assessment research
[AD-A153677] 18 p3154 N85-29530

Specification of software quality attributes. Volume 3: Software quality evaluation guidebook
[AD-A153990] 18 p3163 N85-29595

Performance evaluation of stochastic timed decision-free Petri Nets
[AD-A153987] 18 p3171 N85-29652

Operation of HFTF to test the MIT 12 T coil
[DE85-010409] 18 p3195 N85-29821

Low-speed wind-tunnel tests of an advanced eight-bladed propeller
[NASA-TM-86364] 19 p3214 N85-29839

Traffic alert and collision avoidance system: Operational simulation
[FAA-PM-85-10] 19 p3216 N85-29841

Inertial navigation system - LAS II for SGT YORK testing
[AD-A154204] 19 p3216 N85-29844

The DREO (Defence Research Establishment Ottawa) Inertial Navigation Laboratory: Development and test capabilities
[AD-A154425] 19 p3216 N85-29845

Split-cross-bridge resistor for testing for proper fabrication of integrated circuits
[NASA-CASE-NPO-16021-1] 19 p3256 N85-30187

Recent results of the Los Alamos free-electron laser oscillator experiment
[DE85-010736] 19 p3277 N85-30324

Free-piston Stirling engine/linear alternator 1000-hour endurance test
[NASA-CR-174771] 19 p3304 N85-30481

Develop and test fuel cell powered on-site integrated total energy systems. Phase 3: Full-scale power plant development
[NASA-CR-168338] 19 p3304 N85-30483

Performance envelopes and optimal appropriateness measurement
[AD-A154129] 19 p3330 N85-30629

Ada compiler validation summary report: University of Karlsruhe-GMD/German MOD VAX 11 compiler, version v1.0
[AD-A154370] 19 p3337 N85-30676

The CCIR satellite EPIRB coordinated trials programme --- Emergency Position Indicating Radio Beacon (EPIRB); International Radio Consultative Committee (CCIR) 20 p3402 N85-31111

A 406 MHz geostationary satellite SARSAT experiment 20 p3403 N85-31113

SARSAT 121.5/243 MHz technical evaluation
20 p3405 N85-31128

RCA's planned test program to compare the performance and life of NiCd cells containing Pellion 2536 in contrast with Pellion 2505 seperator material
20 p3445 N85-31386

A 34 ampere-hour nickel-cadmium minimum trickle charge testing 20 p3446 N85-31394

Nickel-hydrogen cell test program summary
20 p3448 N85-31407

An industry and government survey: A nickel-hydrogen testing data base 20 p3448 N85-31409

Recommendations and calculations concerning physical characteristics of the EEVT apparatus
20 p3502 N85-31799

MHD generator CDIF
[DE85-011389] 20 p3536 N85-32001

Fin-line horn antennas
[AD-A154597] 21 p3560 N85-32255

Fabrication and test of modified quadrupole mass spectrometer
[AD-A155186] 21 p3590 N85-32312

Module Hipot and ground continuity test results
21 p3612 N85-32447

Sensitivity and performance characterization of DINGU
[DE85-010750] 22 p3754 N85-33289

Partial discharges in and electric strength of high-voltage polymer insulation at cryogenic temperatures
22 p3770 N85-33364

Beta response of selected instruments
[DE85-013278] 22 p3788 N85-33489

Rolling, slip and traction measurements on low modulus materials
[NASA-CR-174809] 22 p3791 N85-33491

Failure testing of active solar energy system components
[DE84-013024] 22 p3804 N85-33581

Block 5 documentation and solar modules
[NASA-CR-176134] 22 p3805 N85-33584

Method and apparatus for measuring areas of photoelectric cells and photoelectric cell performance parameters
[DE85-011629] 22 p3810 N85-33599

Effect of interference on the performance of a minimum TCAS 2
[FAA-PM-84-33] 23 p3895 N85-34131

Test plan for performance testing of the Eaton AC- electric vehicle
[DE85-011954] 23 p3927 N85-343

Circuit approaches to increasing SRAM performance total dose environments
[DE85-009441] 23 p3966 N85-34

Planetary-gear-support bearing test rig design
[NASA-CR-174927] 24 p4064 N85-35

Development of NATOPS (Naval Air Training and Operating Procedure Standardization) performance software for the H-46D helicopter
[AD-A156069] 24 p4064 N85-35180
Dissected motors-propellants motor number STM-012. Phase 15: Surveillance report, stage 1
[AD-A156066] 24 p4071 N85-35226
Solid state high power amplifier for driving the SLC injector klystron
[DE85-013063] 24 p4090 N85-35356
Dental multi-purpose slowspeed handpieces test and evaluation
[AD-A155764] 24 p4130 N85-35606
Four stage HELIA experiment
[DE85-012026] 24 p4158 N85-35788

PERFUSION
U DIFFUSION

PERIDOTITE
The mineralogy of global magnetic anomalies
[E85-10061] 07 p0967 N85-16272

PERIGEES
The long term behaviour of Earth orbits and the implications for debris control 12 p1786 N85-21213

PERIHELIONS
Comet thermal modeling 13 p2176 N85-23505
Photometric study of Pluto near perihelion. Part 2: Refinement of rotation period: Color indices
15 p2483 N85-25325

PERIOD EQUATIONS
U PERIODIC FUNCTIONS

PERIODIC FUNCTIONS
NT TANGENTS
Dynamics of growth of surface periodic structures when intense light acts on condensed media
02 p0268 N85-11748
Propagation of acoustic shear waves through active periodic structure 04 p0490 N85-13125
An analytical model of periodic waves in shallow water
[AD-A147501] 07 p0960 N85-16085
An analytical model of periodic waves in shallow water
[AD-A147502] 07 p0960 N85-16086
Periodic solutions of prescribed energy for a class of Hamiltonian systems
[AD-A149487] 10 p1548 N85-19764
Application of perturbation theory to problem in orbital theory 15 p2537 N85-25856
On the accuracy of the Poincare-Lindstedt method
[REPT-84-37] 17 p3022 N85-28690
Symmetric linear multistep methods for second-order differential equations with periodic solutions
[CWI-NM-R8501] 17 p3022 N85-28698
Interpolation and differentiation for periodic functions
[PREPRINT-419] 18 p3172 N85-29662
On the convergence of an iterative formulation of the electromagnetic scattering from an infinite grating of thin wires 24 p4085 N85-35319

PERIODIC ORBITS
U ORBITS

PERIODIC PROCESSES
U CYCLES

PERIODIC VARIATIONS
NT ANNUAL VARIATIONS
NT DIURNAL VARIATIONS
NT NOCTURNAL VARIATIONS
NT SECULAR VARIATIONS
Periodic oscillation of gyrostat-satellite about its center of mass in an elliptical orbit 02 p0159 N85-11080
Analysis of the Frascati and Geneva gravitational wave antenna background exhibiting the one half sideral day period
[NOTA-INTERNA-801] 02 p0192 N85-11283
N-frequency quasiperiodicity and chaos in dissipative dynamical systems 02 p0282 N85-11840
Thermal effects in stellar pulsations
02 p0297 N85-11925
Extraction of wave period from altimeter data
03 p0382 N85-12439
Global maps of foF2 derived from observations and theoretical values
[AD-A145866] 03 p0392 N85-12509
Variations with time of the carbon dioxide partial pressure in central and south Atlantic surface waters
[AD-A145825] 03 p0398 N85-12537
On derivation and significance of geomagnetic equivalent amplitude indices 04 p0520 N85-13321
Atlas of polar cap energetic particle observations. Volume 1: TIROS-N, 1 January 1979 - 28 February 1981
[PB84-233402] 04 p0535 N85-13419
Generation of available potential energy and other diagnostic studies during FGGE
05 p0683 N85-14388
A modified unit commitment and generation control for utilities with large wind generation penetrations
[DE84-015382] 06 p0806 N85-15129
Nature of short-period variations of cosmic rays in stratosphere 06 p0823 N85-15224
Microseism level, time variations at Turkmen seismic stations studied 07 p0981 N85-16231
The effects of long-periodic forcing in a zero-dimensional climate model 07 p1002 N85-16363
Composites with a periodic structure, mathematical analysis and numerical treatment
[AD-A148301] 08 p1119 N85-17053
Potential applications of forced unsteady flows
[AD-P004155] 09 p1264 N85-17940
Gamma-ray burster recurrence timescales
[NASA-TM-86157] 09 p1417 N85-18942
Effects of a periodic disturbance on structure and mixing in turbulent shear layers and wakes
[AD-A149278] 10 p1484 N85-19370
Simulation of estimating periodicity of seasonally stationary time series
[DE85-003517] 11 p1706 N85-20748
Search for millisecond rotational periods in some low-mass X-ray binaries observed by EXOSAT
11 p1741 N85-20949
EXOSAT observations of the galactic bulge X-ray source GX17+2 — X ray binary star 11 p1742 N85-20951
An episodic red-wing structure of SiIV, lambda 1394A, in gamma Cas 11 p1750 N85-21009
Multi-year and possibly periodic variations in the UV spectrum of 56 Pegasi 11 p1756 N85-21046
Observations of current pulsations of characteristics in atmosphere with period of about 1.5 hours
14 p2341 N85-24480
Relationship between seismic status of Earth and relative position of bodies in sun-earth-moon system
14 p2345 N85-24499
Ten years observations of long-period oscillations of the Sun 14 p2450 N85-25123
Variability of the quiet photospheric network
14 p2452 N85-25144
Elementary sunspot energy model
15 p2476 N85-25287
Cyclic changes in barometric coefficient of cosmic ray neutron component 15 p2478 N85-25293
Annual cycle. Part 1: The annual variation of surface temperatures over the United States and Canada
[PB85-147676] 15 p2600 N85-26026
North Atlantic Deep Water Formation
[NASA-CP-2367] 15 p2601 N85-26028
Changes in the high-latitude ocean as possible causes of atmosphere CO2 variations 15 p2602 N85-26036
The 6 pi-periodic solutions of plane restricted elliptical 3-body problem in neighborhood of libration points
16 p2718 N85-26779
Stability of periodic satellite motions relative to center of mass in circular orbit 16 p2718 N85-26780
Periodicity of variations in galactic cosmic ray fluxes and solar activity parameters near 20th cycle minimum
16 p2720 N85-26791
Variations in intensity of secondary cosmic radiation observed on 10-11 August 1981
16 p2721 N85-26796
Possible period of Jovian activity and possibility of seasons 16 p2723 N85-26810
Precipitable water in the atmosphere, determined from surface dewpoint values 16 p2831 N85-27457
Influence of coherent mesoscale structures on satellite-based Doppler lidar wind measurements
[NASA-CR-175853] 16 p2833 N85-27467
Qualitative and quantitative examination of the performance of regional air quality models representing different modeling approaches
[DE85-010508] 19 p3310 N85-30518
Southern oscillation/El Nino excitation of the Earth's Chandler wobble 20 p3490 N85-31695
Solar-geophysical data no. 485, January 1985. Part 1 (prompt reports): Data for December 1984, November 1984 and late data
[PB85-181360] 20 p3548 N85-32079
On gamma and neutrino radiation from Cyg X-3
[OG-2.1-7] 22 p3863 N85-33924
1000 GeV gamma rays from Cygnus X-3: An update
[OG-2.1-8] 22 p3863 N85-33925
Secondary periodicities of microbursts of TeV gamma rays from the Crab pulsar
[OG-2.3-5] 22 p3866 N85-33942
The 1000 GeV gamma rays from ms pulsars
[OG-2.3-12] 22 p3867 N85-33948
Periodic gamma-ray emissions from Geminga at or = 10(12) eV
[OG-2.4-2] 22 p3867 N85-33949
Search for periodicities near 59 s in the COS-B gamma-ray data of 2CG195+04 (Geminga)
[OG-2.4-3] 22 p3867 N85-33950
Search for gamma-rays above 400 GeV from Geminga
[OG-2.4-4] 22 p3867 N85-33951
Observations on TeV gamma rays from Geminga and PSR 0950+08
[OG-2.4-6] 22 p3868 N85-33953
Search for gamma ray lines from SS433
[OG-2.4-11] 22 p3868 N85-33955
Propagation of the phase of solar modulation
[SH-4.1-12] 23 p4006 N85-34835
Ninteenth International Cosmic Ray Conference. SH sessions, volume 5
[NASA-CP-2376-VOL-5] 23 p4031 N85-34991
Cosmic ray power spectral variations. 3: Solar rotation periodicities
[SH-4.4-16] 23 p4034 N85-35012
Variations of the cosmic ray general component in Antarctica
[SH-4.4-17] 23 p4035 N85-35013
Cosmic ray variations with the period close to 27 days and their connection with solar activity longitudinal distribution
[SH-4.4-19] 23 p4035 N85-35015
Azimuthal and meridional asymmetries of the solar wind and quasiperiodic variations of intensity of Galactic Cosmic Rays (GCR)
[SH-4.4-20] 23 p4035 N85-35016
Dynamics of two-year cosmic ray variations inferred from the data of spacecraft and stratospheric measurements and from the neutron monitor data in 1959-1981
[SH-4.4-21] 23 p4035 N85-35017
Formulation of cosmic-ray solar daily variation and its seasonal variation, produced from generalized stationary anisotropy of solar origin
[SH-4.5-2] 23 p4036 N85-35020
Temporal variations of the anomalous oxygen component, 1977 - 1984
[SH-4.6-3] 23 p4039 N85-35041
A relation between the short time variations of cosmic rays and geomagnetic field change
[SH-5.1-14] 23 p4043 N85-35067
Observations of cosmic-ray modulations in the fall, 1984
[SH-5.1-16] 23 p4043 N85-35069
Frequency spectra of short-period variations of cosmic ray
[SH-5.1-17] 23 p4043 N85-35070
Long-period cosmic ray variations and their altitude dependence
[SH-6.1-19] 23 p4046 N85-35091
Solar modulation of cosmic ray intensity and solar flare events inferred from (14)C contents in dated tree rings
[SH-7.1-2] 23 p4047 N85-35095
When did the average cosmic ray flux increase?
[SH-7.1-4] 23 p4047 N85-35097
Radiocarbon content in the annual tree rings during last 150 years and time variation of cosmic rays
[SH-7.1-15] 23 p4048 N85-35106

PERIODICALS
Center for Electronics and Electrical Engineering Technical Bulletin covering center programs
[PB84-218056] 01 p0045 N85-10296
The integrated library system design concepts for a complete serials control subsystem
[AD-A149379] 10 p1568 N85-19884
Sourcebook: Gaining access to US government information on the environment and natural resources
[DE84-017419] 11 p1740 N85-20941
D-1 report: The first German spacelab mission
[NASA-TM-77637] 13 p1977 N85-22402
Lopez Energy Alternatives Project
[DE85-010589] 22 p3849 N85-33837
NBS (National Bureau of Standards) library serial holdings, 1985
[PB85-191948] 22 p3849 N85-33839

PERIODICITY
U PERIODIC VARIATIONS

PERIODICITY (BIOLOGY)
U RHYTHM (BIOLOGY)

PERIPHERAL EQUIPMENT (COMPUTERS)
NT BUFFER STORAGE
NT COMPUTER COMPATIBLE TAPES
NT COMPUTER STORAGE DEVICES
NT MAGNETIC TAPES
NT OPTICAL DISKS
NT RANDOM ACCESS MEMORY
NT READ-ONLY MEMORY DEVICES
NT REGISTERS (COMPUTERS)
FCC (Federal Communication Commission) methods of measurement of radio noise emissions from computing devices
[PB84-243591] 06 p0849 N85-15367
Generation and display apparatus
[AD-D011639] 17 p3006 N85-28599

PERIPHERAL NERVOUS SYSTEM
Is fast fiber innervation responsible for increased acetylcholinesterase activity in reinnervating soleus muscles?
[NASA-CR-175716] 15 p2614 N85-26108

PERIPHERAL VISION
Peripheral Vision Horizon Display (PVHD) [NASA-CP-2306] 01 p0006 N85-10044
Personal experience with the PVHD and opinion of situations in which a wide Field Of View (FOV) PVHD might be helpful 01 p0006 N85-10045
The two modes of visual processing: Implications for spatial orientation 01 p0006 N85-10047
Theory underlying the peripheral vision horizon device 01 p0006 N85-10048
The peripheral visual cue assessment facility at Ames Research Center 01 p0006 N85-10050
Evaluation of the Malcolm horizon in a moving-base flight simulator 01 p0006 N85-10051
Peripheral vision horizon display on the single seat night attack A-10 01 p0009 N85-10053
Peripheral vision horizon display testing in RF-4C aircraft 01 p0009 N85-10054
Extracts from the test plan for in-flight evaluation of the NT-33A peripheral vision display 01 p0009 N85-10055
NASA Ames-Dryden T-37 demonstration comments 01 p0009 N85-10056
Early Air Force Flight Test Center (AFFTC) experience with Peripheral Vision Horizon Displays (PVHD) 01 p0009 N85-10057
Peripheral vision displays: The future 01 p0009 N85-10058
A production peripheral vision display system 01 p0010 N85-10059
A preliminary flight evaluation of the peripheral vision display using the NT-33A aircraft [AD-A145123] 01 p0010 N85-10060
Bulletin of the Faculty of Engineering, Hokkaido University, no. 123 [ISSN-0385-602-X] 04 p0482 N85-13075
A mathematical model of visual perception regarding peripheral vision and its application to the Hermann's illusion 04 p0483 N85-13080
Mean and random errors of visual roll rate perception from central and peripheral visual displays 05 p0704 N85-14519
Accuracy of system step response roll magnitude estimation from central and peripheral visual displays and simulator cockpit motion 05 p0705 N85-14522
Dual-task timesharing using a projected attitude display (Malcolm horizon) [AD-A150789] 14 p2395 N85-24750
Perception of roll rate from an artificial horizon and peripheral displays [VTH-LR-403] 17 p3002 N85-28557

PERIPHERIES
U BOUNDARIES

PERISCOPES
Immediate visibility after red and white adaptation [AD-A156271] 24 p4132 N85-35616

PERMAFROST
Geothermal studies in Alaska: Conditions at Prudhoe Bay 04 p0516 N85-13290
Pulse transmission through frozen silt [AD-A147108] 07 p0940 N85-15958
Deuterium diffusion in a soil-water-ice mixture [AD-A148457] 08 p1176 N85-17415
Permafrost and subsurface ice in the solar system 13 p2191 N85-23594
Permafrost, seasonally frozen ground, snow cover and vegetation in the USSR [AD-A153626] 18 p3124 N85-29346
Permafrost features on Earth and Mars: Similarities, differences 22 p3855 N85-33870

PERMEABILITY
NT DIELECTRIC PERMEABILITY
Separation of metal species by supported liquid membranes [DE84-014536] 04 p0470 N85-12992
Influence of inter-layer effect on charge gas-permeability [BLL-M-35919-(5828.4)] 05 p0616 N85-13940
Effect of water on hydrogen permeability — Stirling engines [NASA-TM-86904] 06 p0761 N85-14864
Influence of size grading of sintering ore on the sintering process [BLL-M-36004-(5828.4)] 07 p0924 N85-15854
Investigation of structure-permeability relationships of silicone polymer membranes [PB85-148476] 11 p1596 N85-20038
Effect of host-rock dissolution and precipitation on permeability in a nuclear waste repository in tuff [DE85-000675] 11 p1727 N85-20860
Practical surface methods 14 p2316 N85-24314
Applications of eddy currents 14 p2316 N85-24315
Variational bounds on Darcy's constant [DE85-006636] 15 p2580 N85-25916
An experimental study of brine upward migration in thin sea ice 15 p2582 N85-25923
Ionic conduction and water diffusion in Li (BETA)-alumina [DE85-007548] 16 p2755 N85-27005
Variational bounds on Darcy's constant [DE85-006959] 18 p3101 N85-29195
Measurement of permittivity and permeability of microwave materials [AD-D011656] 18 p3176 N85-29688
Mass spectrometer based gas permeation apparatus [DE85-011176] 19 p3273 N85-30299
Tables of generalized hydrogen diffusion profiles and permeating fluxes for fusion applications [DE85-008876] 19 p3372 N85-30919
Measurement and analysis of two-phase flow through low permeability media, task 3 [PB85-188373] 20 p3435 N85-31313
Permeation of mixed penetrants through glassy polymer membranes [AD-A155605] 21 p3570 N85-32207
WIPP horizon in situ permeability measurements [DE85-012687] 22 p3802 N85-33557
Geologic, technical, and economic sensitivity analysis in support of the GRI (Gase Research Institute) tight gas reservoirs project area [PB85-192276] 22 p3802 N85-33559
Organic solvent alteration of hydraulic properties of sedimentary rocks of low permeability: A review [DE85-012537] 22 p3815 N85-33635
Development and evaluation of sulfonated polysulfone membranes for the zinc-ferricyanide battery [DE85-009104] 24 p4090 N85-35357

PERMEATING
Theory of kinetics of impregnation of porous bodies [BLL-M-35917-(5828.4)] 05 p0616 N85-13942
Steady state hydrogen transport in solids 06 p0864 N85-15492
Mechanisms of gas permeation through polymer membranes [DE84-017423] 09 p1293 N85-18117

PERMITTIVITY
Calculations of optical properties of transition metals [BLL-M-35744-(5828.4)] 02 p0175 N85-11175
Plane wave (EMP) incidence on a finitely conducting plane Earth with the magnetic field intensity parallel to the Earth's surface [DE84-015364] 02 p0226 N85-11493
Apparatus for measuring dielectric characteristics of polymer materials in millimetric range of wavelengths at 4.2-300 K temperatures 06 p0788 N85-15032
An indirect measure of below-ground electric field, conductivity, and dielectric constant [AD-A146516] 06 p0804 N85-15115
A quasi-optical method for measuring the complex permittivity of materials [AD-A147483] 07 p0941 N85-15966
The effects of soil moisture on bistatic clutter power [AD-A147636] 08 p1150 N85-17261
An experimental investigation of microstrip properties on soft substrates from 2 to 40 GHz [NASA-TM-86961] 11 p1624 N85-20224
Study of laminated dielectric behavior at microwave and millimeter-wave frequencies [AD-P004358] 12 p1825 N85-21452
A millimeter wave apparatus for free-space measurement of dielectric constants at high temperature [AD-P004361] 12 p1826 N85-21455
Determining distribution of complex dielectric permittivity over cylindrical body of intricate cross section from electromagnetic field measurement 12 p1842 N85-21559
Electric field effects on ion currents in satellite wakes 13 p1991 N85-22485
Extraction of surface-wave energy from plasma waveguide 13 p2077 N85-22974
Change of electrical characteristics of radio-frequency cables under thermal effect 13 p2081 N85-22999
Dielectric measurements in infralow-frequency band 13 p2087 N85-23034
Microwave remote sensing of soil moisture 13 p2125 N85-23235
Mars radar catalog 13 p2198 N85-23636
Chemical interpretation of the relaxed permittivity during epoxy resin cure [AD-A150955] 14 p2260 N85-24005
Determination of temperature and degree of roughness of sea and land surfaces by microwave radiometric polarization measurements 14 p2334 N85-24432
Measurement of permittivity and permeability of microwave materials [AD-D011656] 18 p3176 N85-29688
Transversely reinforced piezoelectric composites [AD-D011676] 19 p3260 N85-30214
The determination of optical constants of thin metal films by surface plasma techniques 19 p3373 N85-30925
Examination of anisotropic films by resonance method 22 p3778 N85-33412

PEROVSKITES
Piezoelectric and electrostrictive materials for transducer applications [AD-A145115] 01 p0043 N85-10277
Peculiar spherules from Antarctica and their origin 06 p0883 N85-15612
Integrated current collector and catalyst support [DE85-011616] 22 p3761 N85-33311

PEROXIDES
NT HYDROGEN PEROXIDE
NT INORGANIC PEROXIDES
NT ORGANIC PEROXIDES
Evaluation of the alkaline peroxide pre-bond surface treatment for titanium [AD-A147352] 07 p0926 N85-15881
Chemical transformations in acid rain. Volume 2: Investigation of kinetics and mechanism of aqueous-phase peroxide formation [PB85-173433] 18 p3135 N85-29416

PERSONAL COMPUTERS
How to implement the welcome program in compatible microcomputers such as Apple 2 [INPE-3114-PRE/511] 05 p0715 N85-14998
Possibilities and impossibilities of microcomputer systems [AD-1984-904] 07 p1028 N85-16522
Guide to personal desktop computing at ANL [DE85-001438] 08 p1206 N85-17594
Personal desktop computing in a research and development laboratory [DE85-002765] 11 p1705 N85-20728
ZTL: A subroutine package for the IBM personal computer to support the Ziatech ZT1488 IEEE-488 controller [LA-10141-MS] 12 p1913 N85-22010
HGRAPH: A subroutine package for the IBM personal computer to support the Hercules Graphic Card [LA-10144-MS] 12 p1914 N85-22013
ZTLCK: A subroutine package for the IBM personal computer to support the Ziatech ZT1488 real time clock [LA-10146-MS] 12 p1914 N85-22014
TRANIO: A subroutine package for the IBM personal computer to support the transfer 6002 CAMAC crate controller [LA-10145-MS] 12 p1914 N85-22015
The performance of a type-insensitive Runge-Kutta code on a personal computer [TUM-I8410] 12 p1919 N85-22048
Two degree-of-freedom flutter solution for a personal computer [NASA-TM-86381] 13 p1971 N85-22379
Personal computer aided decision analysis [AD-A151911] 16 p2875 N85-27740
Benchmark evaluation of PC simscript [AD-A156133] 24 p4138 N85-35851

PERSONALITY
The Reports of Aeromedical Laboratory, volume 25, no. 1/2 [ISSN-0023-2858] 01 p0090 N85-10605
The relationship between emotional tension scale and psychological uneasiness of JASDF pilots in flying situations 01 p0090 N85-10606
Classification systems for individual differences in multiple-task performance and subjective estimates of workload 05 p0706 N85-14543
Success in learning occupation of chemical production technician as function of certain personality traits and development of psychophysiological functions 09 p1362 N85-18588
Individual characteristics and unit performance: A review of research and methods [AD-A153145] 17 p3001 N85-28550
The relationship between personality and performance 24 p4129 N85-35800

PERSONALITY TESTS
Psychological testing on the computer [R/PERS-618] 01 p0097 N85-10645
Rapid determination of cadet discipline by projective tests 22 p3821 N85-33871

PERSONNEL
NT AIR TRAFFIC CONTROLLERS (PERSONNEL)
NT AIRCRAFT PILOTS
NT ASTRONAUTS
NT COSMONAUTS
NT CREWS
NT FLIGHT CREWS
NT FLYING PERSONNEL
NT INSTRUCTORS
NT MEDICAL PERSONNEL
NT NAVIGATORS
NT OPERATORS (PERSONNEL)
NT PILOTS (PERSONNEL)
NT POLICE

NT PROGRAMMERS
NT SCIENTISTS
NT SPACECREWS

Models of natural intelligence in fault diagnosis tasks: Implications for training and aiding of maintenance personnel
[AD-P003927] 02 p0246 N85-11607

The role of physical and physiological capacities and their modification on the tolerance to various stress experienced by Air Force personnel
[AD-A145779] 03 p0400 N85-12550

Cardiovascular disease among U.S. Navy pilots
[AD-A145871] 03 p0400 N85 12552

Maintenance Management Information and Control System (MMICS): Administrative boon or burden
[AD-A145762] 03 p0438 N85-12790

The human role in space. Volume 2: Research analysis and technology report
[NASA-CR-171224] 04 p0546 N85-13474

An analysis of the technical training of enlisted minuteman missile maintenance personnel
[AD-A147078] 07 p0912 N85-15775

Model of team organization and behavior and team description method
[AD-A147540] 07 p1053 N85-16680

Project manager's handbook for special projects
[AD-A147913] 07 p1053 N85-16683

Solid rocket booster retrieval operations
08 p1096 N85-16928

Interagency program on space nuclear power: Directory of participants in the SP-100 program
[DE85-026339] 08 p1221 N85-17691

Success in learning occupation of chemical production technician as function of certain personality traits and development of psychophysiological functions
09 p1362 N85-18568

European Scientific Notes, volume 38, number 12
[AD-A148713] 09 p1418 N85-18946

Robotic safety
[DE85-002314] 10 p1493 N85-19431

Application of the Hardman methodology to the Single Channel Ground-Airborne Radio System (SINCGARS)
[NASA-CR-175694] 14 p2218 N85-23756

SPARTEN (Scientific Program of Aerobic and Resistance Training Exercise in the Navy): A total body fitness program for health and physical readiness
[AD-A150869] 14 p2388 N85-24711

Investigation of the requirement for auxiliary heating of Canadian forces personnel
[AD-A151950] 16 p2841 N85-27522

Summary of Research, Academic Departments, 1983 - 1984
[AD-A151724] 16 p2875 N85-27741

Predictors of transfer adjustment: A longitudinal study
[AD-A152462] 17 p3000 N85-28548

An empirical comparison of the accuracy of univariate and multivariate corrections for range restriction
[AD-A153071] 17 p3019 N85-28670

Evaluation and Validation (E/V) team public report, volume 1
[AD-A153609] 18 p3161 N85-29584

Assessment of computer resource management plan for division support weapon system
[AD-A154142] 19 p3342 N85-30712

U.S. Civil airmen statistics for calendar year 1984
[AD-A156326] 24 p4059 N85-35153

Data processing professionals and DP application users' perceptions and expectations of operational roles of persons working in a DP/application user interface group 24 p4165 N85-35821

PERSONNEL DEVELOPMENT

Nondestructive inspection: Improved capabilities of technicians
[AD-A147388] 07 p0975 N85-16196

Efforts to improve aviation medical examiner performance through continuing medical education and annual performance reports
[AD-A148078] 08 p1195 N85-17531

Training guide for scientific and engineering trainees 1984
[AD-A147963] 08 p1198 N85-17542

Improvements in personnel needed for better flight safety 14 p2208 N85-23693

Administration chief on air traffic control improvements
15 p2460 N85-25193

Guidelines of the Federal Minister of Transportation for the formation and examination of airline personnel, part 4
17 p3002 N85-28556

PERSONNEL MANAGEMENT

Air Force Human Resources Laboratory report: Fiscal year, 1983
[AD-A145647] 02 p0238 N85-11548

Performance evaluation of A-10 aircraft mainteance units and aircraft using constrained facet analysis
[AD-A146955] 07 p0893 N85-15660

Interaction of human cognitive models and computer based models in supervisory control
[AD-A142547] 07 p1020 N85-16474

Communications skills for CRM training
09 p1276 N85-18017

Bibliography of unclassified reports, FY 1984
[AD-A148838] 09 p1401 N85-18819

Strategic management for organizational effectiveness. The effect of human resource planning on retention and related issues, volume 1
[AD-A149398] 10 p1566 N85-19874

Strategic management for organizational effectiveness. The effect of human resource planning on retention and related issues, volume 2
[AD-A149399] 10 p1566 N85-19875

Strategic management for organizational effectiveness. The effect of human resource planning on retention and related issues, volume 3
[AD-A149400] 10 p1566 N85-19876

Strategic management for organizational effectiveness. The effect of human resource planning on retention and related issues: Methodological appendix
[AD-A149401] 10 p1566 N85-19877

PERSONNEL SELECTION

NT PILOT SELECTION

The construction of auditive tests of attention and spatial orientation and their factorial structure
[DFVLR-FB-84-21] 05 p0699 N85-14485

Cognitive asymmetry and occupation. Computer programmers, students, and bank personnel, part 1 and part 2
[AD-A147125] 08 p1197 N85-17540

Automated CPX support system preliminary design phase
[NASA-CR-175784] 16 p2769 N85-27091

Construction of a job-oriented test for the selection of air traffic controllers
[DFVLR-FB-84-51] 17 p3002 N85-28558

Psychological issues relevant to astronaut selection for long-duration space flight: A review of the literature
[AD-A154051] 19 p3330 N85-30627

PERSPIRATION

Peripheral changes in regional sweating responses to exercise in hypobaric environments
[AD-A150757] 14 p2388 N85-24710

Preparing Alberto Salazar for the heat of the 1984 Olympic Marathon
[AD-A150942] 14 p2389 N85-24714

PERT

Statistics for the maximum of several positive random variables with application to networking
[AD-A150005] 12 p1922 N85-22069

PERTURBATION

NT ORBIT PERTURBATION
NT SATELLITE PERTURBATION

N-frequency quasiperiodicity and chaos in dissipative dynamical systems 02 p0282 N85-11840

Chaotic behavior induced by solitons in perturbed integrable systems 02 p0283 N85-11844

Two- and three-dimensional model and wall data from a flexible-walled transonic test section
03 p0312 N85-12015

Investigations of flow field perturbations induced on slotted transonic-tunnel walls 03 p0312 N85-12018

A study of the critical layer in a rotating liquid payload
[AD-A146094] 03 p0362 N85-12321

A 2-dimensional description of potential perturbations to the ozone layer due to NOx and H-2-O aircraft emissions
[AD-A146292] 03 p0392 N85-12511

Dynamic stiffness characteristics of high eccentricity ratio bearings and seals by perturbation testing
05 p0645 N85-14141

Some aspects of understanding changes in the global carbon cycle 05 p0652 N85-14186

Artificial defocusing lens in ionosphere
05 p0724 N85-14654

Excitation of spiral patterns in responsible density wave theory 05 p0740 N85-14764

Comparison of uniform perturbation solutions and numerical solutions for some potential flows past slender bodies
[NASA-CR-172485] 06 p0749 N85-14799

Phase problem in aperture synthesis systems
06 p0782 N85-15002

Analysis of spin echo signals in multi-pulse experiment
06 p0792 N85-15065

Longer-scalelength plasma perturbations by an intense laser beam
[AD-A147005] 07 p1045 N85-16638

Tropospheric and ionospheric phase perturbations and Doppler frequency shift effects
[AD-A148579] 08 p1154 N85-17283

Exploratory development of advanced surface flaw detection methods
[AD-A148757] 09 p1261 N85-18060

Perturbation of a multiple eigenvalue in the Benard problem for two fluid layers
[AD-A149068] 10 p1546 N85-19745

Resonant activation of a Josephson junction
[DE85-000702] 10 p1563 N85-19857

Geomagnetic disturbances caused by internal atmospheric dynamics 11 p1665 N85-20491

Three-dimensional baroclinic instability of a Hadley cell for small Richardson number
[NASA-TP-2450] 11 p1687 N85-20605

21 Layer troposphere-stratosphere climate model
[NASA-TM-86183] 12 p1892 N85-21871

Pressure-gradient-driven Tokamak resistive MHD instability in the banana-plateau collisionality regime
[DE85-004566] 12 p1937 N85-22171

A study of the compatibility of an existing CFD package with a broader class of material constitutions
12 p1945 N85-22219

Flutter taming: A new tool for the aeroelastic designer
[AD-A150834] 14 p2228 N85-23802

Investigation and optimization of fuel production using dye-based transition metal complexes as charge-transfer intermediates
[PB85-161941] 14 p2264 N85-24029

Flow around axisymmetric bodies with uniform-velocity zones 14 p2276 N85-24103

Improvement and extension of a numerical procedure for the three dimensional unsteady transonic flows
15 p2459 N85-25181

Turbulence effects on a glow discharge as derived from continuity and energy considerations
[AD-A151838] 15 p2557 N85-25775

Method for evaluating perturbation in algorithms for solving navigational problems 16 p2718 N85-26783

Identification and control of structures in space
[NASA-CR-175790] 16 p2731 N85-26850

Formulas for updating the generalized inverse of a symmetric matrix perturbed by a symmetric rank 2 matrix composed of 2 nonsymmetric DYADS
[AD-A151736] 16 p2858 N85-27629

Analysis of control system from a viewpoint of desired pole placement and desired degree of robustness
[AD-A152627] 17 p2899 N85-27876

Maximizing the semi-major axis for a freely coning solar sailcraft
[AD-A153175] 17 p2909 N85-27938

Experiments on sorption characteristics of solid desiccant materials for solar desiccant cooling systems
[DE85-000542] 17 p2923 N85-28019

Supersonic flow around blunt wedge
17 p2942 N85-28158

The polar caps and the climatic evolution of Mars
22 p3654 N85-33866

Longitudinal dependence of the interplanetary perturbation produced by energetic type 4 solar flares and of the associated cosmic ray modulation
[SH-5.1-5] 23 p4042 N85-35059

Short perturbations of cosmic ray intensity and electric field in atmosphere
[SH-6.1-18] 23 p4046 N85-35090

DEPTH-CHARGE static and time-dependent perturbation/sensitivity system for nuclear reactor core analysis, revision 1
[DE85-013103] 24 p4139 N85-35659

Acoustic resonances in cylinder bundles oscillating in a compressibile fluid
[DE85-004066] 24 p4145 N85-35699

PERTURBATION THEORY

A perturbation solution for rigid dumbbell suspensions in steady shear flow
[AD-A144876] 01 p0111 N85-10755

Singular perturbations, coherency and aggregation of dynamic systems
[DE84-014165] 01 p0114 N85-10772

Quasistable parametric optimization without compact level sets
[AD-A144716] 01 p0114 N85-10776

Numerical methods for singularly perturbed differential equations with applications
[AD-A145639] 02 p0252 N85-11650

Random processes and magnetohydrodynamic turbulence 02 p0271 N85-11767

Electrons in a disordered medium
[NOTA-INTERNA-816] 02 p0279 N85-11819

Mixed defect correction (iteration) for the solution of a singular perturbation problem
[MC-NW-162/83] 05 p0720 N85-14624

Scattering of electromagnetic waves by surface with small asperities 06 p0784 N85-15013

Theory of the orbital motion of an artificial Earth Satellite
[NAL-TR-807] 09 p1285 N85-18075

Geometric Hamiltonian structures and perturbation theory
[DE85-002005] 11 p1707 N85-20737

Velocity inversion using a stratified reference
[AD-A150082] 12 p1889 N85-21858
Thermal stability of static coronal loops: Part 1: Effects of boundary conditions
[NASA-CR-175495] 12 p1981 N85-22330
Surface scattering
[AD-A150252] 13 p2153 N85-23366
Nonrelativistic Kapitza-Dirac scattering
[AD-A150622] 13 p2159 N85-23405
Parton dynamics in hadronic processes
[DE85-006072] 14 p2418 N85-24922
Resonances in photon-photon scattering
[DE85-004607] 14 p2419 N85-24928
Perturbations of Kalman filtering process
15 p2480 N85-25305
Application of perturbation theory to problem in orbital theory 15 p2537 N85-25656
Lattice overview
[DE85-007282] 15 p2662 N85-26427
Eleven lectures on the physics of the quark-gluon plasma
[DE85-004321] 15 p2662 N85-26431
Sensitivity of the stationary distribution vector for an ergodic Markov chain
[DE85-006979] 16 p2857 N85-27621
The temperature dependence of diffracted beam intensities in atom-surface scattering
[AD-A152762] 17 p3029 N85-28736
Photon structure function: Theory
[DE85-006064] 17 p3031 N85-28745
Stability in dynamical systems
[DE85-006698] 17 p3034 N85-28766
Theoretical and numerical studies of magnetic field line displacements in an Elmo Bumpy Torus
[DE85-008757] 17 p3041 N85-28816
Numerical simulation of the transient by the unstable state in a Lotka-Volterra model
[NOTA-INTERNA-833] 18 p3175 N85-29684
Perturbative treatment of quasi-resonant proton neutralization at alkali-halide surfaces
[AD-A154143] 19 p3356 N85-30806
A theory of quasi-conical solutions of noninteger degree — flow fields on supersonic wings
[UTH-LR-420] 20 p3390 N85-31024
An overview of latest model reduction and control methods of large flexible space structures
20 p3414 N85-31191
Wave propagation and methods of solution of the wave equation for moving disturbances sources
[ESA-TT-824] 20 p3522 N85-31906
Finite-perturbation intermediate neglect of differential overlap molecular orbital calculations of nuclear magnetic resonance spin-spin coupling constants for polycyclic aromatic hydrocarbons and aromatic nitrogen heterocyclics
[NASA-TM-87486] 20 p3525 N85-31927
Some dynamic electronic properties of semiconductor surfaces and interfaces 20 p3537 N85-32007
Calculation of the propagation constant in a rectangular waveguide containing an inhomogeneous longitudinally magnetized plasma
[DE85-012072] 21 p3577 N85-32250
Reflection of acoustic beam from inhomogeneous boundary 21 p3680 N85-32864
Identification and control of structures in space
[NASA-CR-176175] 24 p4069 N85-35214
Perturbation-iteration theory for analyzing microwave striplines
[NASA-CR-176180] 24 p4085 N85-35321
Two-point closure study of covariance budgets for turbulent Rayleigh-Benard convection
[PB85-189108] 24 p4124 N85-35568
Multiple vacancy production by high energy heavy ions
[DE85-004428] 24 p4162 N85-35805

PERU
Petrology and genesis of carbonate-hosted Pb-Zn-Ag, San Cristobal District, Department of Junin, Peru
03 p0389 N85-12487
Climate and fisheries: A Peruvian case study
07 p1003 N85-16373
The El Nino phenomenon and its agrometeorological implications 07 p1004 N85-16382

PESTICIDES
USSR report: Chemistry
[JPRS-UCH-84-012] 06 p0761 N85-14865
Teratogenicity studies of carbaryl and malathion alone and in combination in various laboratory animals
[AD-P004034] 06 p0845 N85-15364
Installation restoration program. Phase 2: Stage 1 problem confirmation study, Duluth International Airport Duluth, Minnesota
[AD-A148318] 08 p1069 N85-16885
EPA (Environmental Protection Agency) research program guide, FY-1985, October 1, 1984 - September 30, 1985
[PB85-181881] 20 p3487 N85-31676

PETN
Deformation, fracture and explosive properties of reactive materials
[AD-A146396] 06 p0774 N85-14945
Development of a PETN DDT detonator
[DE84-016944] 09 p1302 N85-18178
Nonprimary-explosive, hot-wire detonator
[DE85-005195] 12 p1818 N85-21403
X-ray photoelectron spectroscopy study of the compatibility of the explosive PETN with candidate plastic bonding materials
[DE85-010804] 19 p3251 N85-30161
Static high pressure study of nitric oxide chemistry: Proposed mechanism for nitric oxide detonation
[DE85-010795] 22 p3746 N85-33220
Gas composition and molecule velocity in the detonation products of pentaerythritol tetranitrate (PETN) in expansion in a high vacuum container. Analysis by mass spectroscopy and time of flight spectrometry
[ISL-R-109/84] 22 p3747 N85-33226
Time-resolved spectroscopic studies of detonating heterogeneous explosives
[DE85-009760] 23 p3921 N85-34297
Effect of precipitation variables on the specific surface and explosion characteristics of pentaerythritol tetranitrate
[DE85-009620] 23 p3922 N85-34302
Real time analysis of PETN detonation products
[DE85-009581] 23 p3922 N85-34303
Friction, impact, and electrostatic discharge sensitivities of energetic materials
[DE85-013321] 24 p4083 N85-35309

PETRI NETS
Extended Stochastic Petri Nets: Applications and analysis
[AD-A148439] 08 p1213 N85-17633
The design of a unified package for the solution of stochastic petri net models
[AD-A150326] 13 p2151 N85-23354
Regenerative stochastic Petri nets
[AD-A150343] 13 p2151 N85-23355
Performance evaluation of stochastic timed decision-free Petri Nets
[AD-A153987] 18 p3171 N85-29652
Petcom: A software instrument for the analysis of Petri networks, oriented towards communication protocols
[FUB-50-1983] 22 p3756 N85-33286

PETROGRAPHY
Petrography, diagenesis and depositional models of the St. Louis limestone, valmeyeran (middle Mississippian), Illinois Basin, USA 09 p1352 N85-18506
Study of the physical properties of crystalline rocks in the southeast Voronezh anteclise
[NASA-TM-77823] 10 p1514 N85-19551
Assessment of computer based geologic mapping of rock units in the LANDSAT-4 scene of northern Death Valley, California 13 p2119 N85-23195
Geological information content of reflected wave record form 14 p2345 N85-24502
Location of continental Permian volcanites of central Asia and its tectonic interpretation
14 p2346 N85-24505
Structural analysis of terrane accretions in the eastern Brooks Range and adjacent areas in central Alaska and Canada
[DE85-008279] 17 p2993 N85-28501
Clay identification and amount measured by laboratory techniques compared to well log responses: Application to tight gas sands and shales
[DE85-010411] 19 p3362 N85-30843
Chemistry of ore-forming fluids
24 p4103 N85-35436

PETROLEUM
U CRUDE OIL

PETROLEUM PRODUCTS
NT ASPHALT
NT BUTANES
NT DIESEL FUELS
NT GASOLINE
NT GREASES
NT LUBRICATING OILS
NT NATURAL GAS
User experience of existing corrosion monitoring techniques and the development of Thin Layer Activation (TLA) for corrosion monitoring
[AERE-R-11248] 01 p0029 N85-10183
Studies related to the deep Earth gas: 1983
[PB85-171114] 16 p2616 N85-27373
Improving the defense energy information system (DEIS)
[AD-A153524] 18 p3200 N85-29849
Influence of surface films of petroleum products on conditions for absorption of solar radiation by upper water layer 19 p3289 N85-30396
Protection products for the conductors of high voltage overhead lines
[BLL-OA-TRANS-3219-(6196.300)]
20 p3429 N85-31289
Biodegradation of jet fuel by aquatic microbial communities
[PB85-191071] 24 p4084 N85-35311

PETROLOGY
NT PETROGRAPHY
Petrology of deep crustal xenoliths from the eastern Snake River Plain, Idaho 02 p0226 N85-11477
The petrology and geochemistry of high cascade volcanics in southern Washington: Mount Saint Helens volcano and the Indian Heaven basalt field
02 p0227 N85-11487
Petrology and genesis of carbonate-hosted Pb-Zn-Ag, San Cristobal District, Department of Junin, Peru
03 p0389 N85-12487
Stratigraphy, petrology, and tectonic setting of the Alisitos Group, Baja California, Mexico
03 p0389 N85-12488
Geology of selected migmatite zones within the bitterroot lobe of the Idaho batholith, Idaho and Montana
03 p0389 N85-12489
Geology and geochemistry of early Tertiary submarine volcanic rocks of the Aleutian Islands, and their bearing on the development of the Aleutian Island Arc
03 p0389 N85-12493
Franciscan and related rocks of southern Humbolt County, northern California coast ranges: Analysis of structure, tectonics, sedimentary petrology, paleogeography, depositional histroy, and thermal maturity 03 p0390 N85-12495
Metamorphic petrology of the Table Mountain area, Circle quadrangle, Alaska 04 p0516 N85-13296
Stratigraphy, petrology, and structure of the Pingston terrane, Mount Hayes C-5 and C-6 quadrangles, eastern Alaska Range, Alaska 04 p0517 N85-13301
Report of the field work performed in the Basins of the Quebra Osso and Tanque Petro Rivers in the Catas Altas quadrangle, Minas Gerais
[INPE-3268-NTE/225] 04 p0525 N85-13359
Petrologic model of the northern Mississippi embayment based on satellite magnetic and ground based geophysical data
[NASA-TM-85075] 04 p0533 N85-13406
Petrologic constraints on the origin of the Moon: Evidence from Apollo 14 04 p0563 N85-13726
Petrology and petrogenesis of Batholitic rocks, San Jacinto Mountains, southern California
05 p0673 N85-14322
Petrology and structure of Pwemain to Jurassic rocks near Yreka, Klamath Mountains, California
05 p0673 N85-14325
Geology, petrology, and tectonic setting of the Mafic rocks of the 1480 Ma old granite-rhyolite terrane of Missouri, USA 05 p0674 N85-14327
Evolutionary history of CI and CM chondrites
06 p0884 N85-15615
Aqueous alteration of meteorite parent bodies: Possible role of unfrozen water and the Antarctic meteorite analogy 06 p0884 N85-15617
High pressure physics research focusing on composite materials 08 p1140 N85-17185
Sedimentary petrology and provenance of the upper Jackforth Sandstone (Morrowan) Quachita Mountains, Arkansas, USA 08 p1182 N85-17447
Part 1. Stratigraphy, structure and petrology of the Peterborough 1.5-minute quadrangle, New Hampshire and part 2. Graphite textural and isotropic variations in plutonic rocks, south-central New Hampshire
09 p1353 N85-18511
Correlation and petrological interpretation of abyssal and terrestrial tephra layers 09 p1353 N85-18512
Research and development related to the Nevada nuclear waste storage investigations
[DE85-002303] 12 p1932 N85-22138
Antarctic Meteorite Newsletter, volume 8, number 1
[NASA-CR-175587] 12 p1961 N85-22328
Reports of the Planetary Geology and Geophysics Program, 1984
[NASA-TM-87563] 13 p2172 N85-23474
Io: Generation of silicate magma by shear melting at the base of a basaltic lithosphere
13 p2172 N85-23476
Modeling equilibrium and fractional crystallization in the system MgO-FeO-CaO-Al2O3-SiO2
13 p2184 N85-23552
Quenching effects on iron site partitioning in the Apollo 17 orange glass composition 13 p2184 N85-23553
Petrologic and geochemical characterization of the Topopah Spring Member of the Paintbrush Tuff: Outcrop samples used in waste package experiments
[DE85-010449] 19 p3302 N85-30470

Some relations among directions of curves at an ariant point on a thermodynamic phase diagram
19 p3312 N85-30530
Dating Archean zircon by ion microprobe: New light an old problem 21 p3722 N85-33094
Bedrock geology of the Brattleboro Quadrangle, rmont-New Hampshire
E85-011027] 22 p3815 N85-33634
(MODULATION)
PULSE FREQUENCY MODULATION

Potential for acidification of six remote ponds in the White ountains of New Hampshire
B84-207349] 02 p0225 N85-11475
Sequential precipitation chemistry sampling program at rookhaven National Laboratory with an analytical ummary of 1976-1982 data
E85-002786] 10 p1513 N85-19545
Acid rain: Towards automated monitoring
16 p2829 N85-27444
Evaluation of methods used for the determination of cidity in acid rain samples
PB85-178309] 19 p3237 N85-30070
Increase of total CO2 in the World ocean
DE85-007756] 23 p3950 N85-34484
FACTOR
Investigation of chemical durability mechanisms in luoride glasses
AD-A145420] 02 p0186 N85-11241
A biological sensor for the detection of toxicants
AD-D011304] 07 p0967 N85-16141
Respiratory chain of alkalophilic bacteria
[DE84-012556] 09 p1360 N85-18556
Physiochemically controlled scour jet array system
[AD-D011688] 19 p3308 N85-30505
Method for determining the point of zero zeta potential of semiconductor
[NASA-CASE-LAR-12893-1] 19 p3373 N85-30923
Environmental surveillance at Los Alamos during 1984
[DE85-011866] 22 p3611 N85-33605
Throughfall rate and chemistry studies: Whiteface Mountain
[DE85-012407] 23 p3947 N85-34464
Increase of total CO2 in the World ocean
[DE85-007756] 23 p3950 N85-34484

HARMACOLOGY
East Europe report: Science and technology
[JPRS-ESA-84-029] 01 p0115 N85-10783
Jet lag prevention: Physiological mechanisms and pharmacological therapy
[AD-A145444] 02 p0235 N85-11529
Bioprocessing in space 05 p0690 N85-14438
Pharmacokinetic interactions of mixtures
[AD-P004032] 06 p0844 N85-15362
USSR report: Life sciences. Biomedical and behavioral sciences
[JPRS-UBB-84-015] 07 p1010 N85-16416
An atropinized heat-stressed rat model: Dose response effects and pharmacokinetics
[AD-A146851] 07 p1011 N85-16423
Review of US guide on medication and flying
12 p1904 N85-21958
East Europe report: Science and technology
[JPRS-ESA-85-023] 21 p3572 N85-32217
Interaction of opiate and phencyclidine derivatives with the acetylcholine receptor
[AD-A155119] 21 p3664 N85-32761
USSR report: Life sciences. Biomedical and behavioral sciences
[JPRS-UBB-85-018] 22 p3819 N85-33860
Effect of dibazol on parameters of nonspecific resistance of subjects in pressurized cabins
23 p3954 N85-34504

HASE ANGLE
U PHASE SHIFT

HASE CHANGE MATERIALS
Investigation of the Ostwald ripening of separated particles in liquid-liquid systems under microgravity conditions
[BMFT-FB-W-84-037] 05 p0615 N85-13927
Numerical investigation of phase change heat transfer in a horizontal cylinder including effects of natural convection 09 p1318 N85-18286
Advanced latent heat storage media for high-temperature industrial applications
[DE85-000907] 09 p1345 N85-18461
Development of media for dynamic latent heat storage for the low-temperature range. Part 1: Thermal analyses of selected salt hydrate systems
[NASA-TM-77778] 10 p1507 N85-19510
Evaluation of ettringite and related compounds for use in solar energy storage
[DE85-003249] 12 p1882 N85-21809
Natural convection during heat accumulation by substances with change of aggregate state
13 p2043 N85-22787
Latent heat storage in cooling systems
[DE85-005355] 13 p2129 N85-23248
Overview of latent storage for passive solar applications
[DE85-005354] 13 p2129 N85-23249
Effects of the phase compositions of cast low-pearlite steels micro-alloyed with vanadium and titanium of their structure and properties
[BLL-BISI-TRANS-22301-(9022.06)]
17 p2928 N85-28067
High temperature composite thermal storage systems
[DE85-005073] 17 p2986 N85-28455
Materials research for passive solar systems: Solid-state phase-change materials
[DE85-008779] 18 p3132 N85-29395
The interactions of composition and stress in crystalline solids
[PB85-179075] 20 p3473 N85-31583

PHASE COHERENCE
Dynamics of symmetry breaking: Phase coherence in finite and random systems
[NOTA-INTERNA-813] 02 p0253 N85-11658
Coherent array of Josephson oscillators with external bias leads
[AD-D011367] 08 p1156 N85-17293
Comparative analysis of noise tolerance of quasi-coherent phase shift keying signal demodulators
13 p2072 N85-22946
Reception noise immunity of multiposition signals
13 p2085 N85-23023
Study of the coupling between average, coherent and turbulent fields in a circular excited free jet
[ISL-R-115/83] 16 p2785 N85-27184

PHASE CONJUGATION
Two novel plasma diagnostic tools: Fiber sensors and phase conjugation
[DE84-014033] 01 p0123 N85-10840
Influence of spatial pumping spectrum on quality of phase conjugate reflection during 4-photon interaction
21 p3696 N85-32964

PHASE CONTRAST
Ion contrasting chamber for discrimination of grains and textures
[BMFT-FB-T-84-151] 04 p0477 N85-13036
Synthesis of multistep directional couplers with nonminimum-phase characteristics
13 p2079 N85-22986
Resolution at its current limit: Applications of the Berkeley ARM
[DE85-009959] 19 p3274 N85-30301

PHASE CONTROL
Determination of row-and-column control principle of phase antenna array from amplitude-phase distribution of field in aperture 07 p0952 N85-16033
Coherent receiver phase and amplitude alignment circuit
[AD-D011487] 10 p1468 N85-19265
Method and apparatus for self-calibration and phasing of array antenna
[NASA-CASE-NPO-15920-1] 12 p1832 N85-21493
Transient processes in tuned amplifier during phase-shift keying with smooth phase variation
15 p2527 N85-25581
Simultaneous phase and frequency control of a three-phase inductor-convertor bridge
[DE85-006197] 18 p3096 N85-29164
Wide-band phase locked loop amplifier apparatus
[AD-D011720] 23 p3927 N85-34337

PHASE DEMODULATORS
Interference immunity of binary systems with second-order phase-difference modulation in various reception modes 13 p2072 N85-22944
Comparative analysis of noise tolerance of quasi-coherent phase shift keying signal demodulators
13 p2072 N85-22946

PHASE DETECTORS
Double reference pulsed phase locked loop (DRP-2L-2)
[NASA-CASE-LAR-13310-1] 12 p1824 N85-21441
Wideband phase keyers 12 p1839 N85-21544
Maser cavity servo-tuning system
[NASA-CASE-NPO-15890-1-CU]
18 p3093 N85-29143
Fiber optic gyroscope with alternating output signal
[AD-D011689] 19 p3271 N85-30284
One-frequency laser interferometer using the optic fiber as a polarization-independent interference phase detector
[DE85-010544] 19 p3277 N85-30326

PHASE DEVIATION
Error in compensating phase fluctuations of wave field by means of adaptive reflectors with continuous or compound surface 13 p2080 N85-22988
Investigation of bimodal paramagnetic filter
13 p2083 N85-23007

PHASE DIAGRAMS
An investigation of the solubility and diffusivity of chromium in gallium arsenide
[AD-A144949] 01 p0024 N85-10148
Metamagnetic systems 03 p0423 N85-12701
Neutron scattering on magnetic structures and at magnetic phase transitions 03 p0424 N85-12706
Thermodynamics and phase equilibria in the vandium-silicon system
[AD-A145870] 03 p0435 N85-12769
Critical evaluation of binary rare Earth diagrams
[DE84-014880] 04 p0470 N85-12991
Mathematical models for the boiling diagram of the ideal two-component mixture
[DFVLR-FB-84-22] 04 p0471 N85-13000
Critical evaluation of binary rare earth phase diagrams
[DE84-015057] 05 p0614 N85-13922
Phase diagrams of organic superconductors
[DE84-016219] 05 p0731 N85-14609
Phase equilibria of stored chemical energy reactants
[AD-A146527] 06 p0785 N85-14696
Phase diagram of polymer blends containing block copolymers
[AD-A147706] 08 p1132 N85-17134
Application of computer methods for calculation of multicomponent phase diagrams of high temperature structural ceramics
[AD-A148138] 08 p1133 N85-17140
Electronic structure of liquid metal alloys
[DE85-000904] 09 p1295 N85-18136
New phases and chemical reactions in solid CO under pressure
[DE85-002033] 09 p1377 N85-18655
Quasi-thermodynamic prediction of hydrogen reemission behavior from titanium films
[DE85-003667] 10 p1564 N85-19864
Research on microemulsions for storage and conversion of solar energy
[DE85-000181] 12 p1882 N85-21807
Separating polymer solutions using high pressure LCST Lower Critical Solution Temperature) phenomena
[AD-A151538] 15 p2518 N85-25528
High pressure cosmochemistry applied to major planetary interiors: Experimental studies
[NASA-CR-175715] 15 p2679 N85-26544
On the feasibility of Ab Initio calculations of ordering alloy phase diagrams
[DE85-007073] 16 p2751 N85-26979
Ca-Ga, Sr-Ga and Ba-Ga binary systems
[DE85-006454] 16 p2751 N85-26980
Activities report of the Institute of Astronomy and Astrophysics 17 p3052 N85-28892
Electrical conductivity and phase diagram of binary alloys. 21: The system palladium-chromium
[NASA-TM-77863] 18 p3073 N85-29009
Local density theory of heats of formation and short-range order parameters in substitutionally disordered alloys
[DE85-009811] 18 p3075 N85-29021
Binary phase diagram determinations
[DE85-010856] 19 p3235 N85-30056
Some relations among directions of curves at an invariant point on a thermodynamic phase diagram
19 p3312 N85-30530
Phase behavior and QLS (Quasielastic Light Scattering) in potassium linoleate/n-alkanol microemulsions
[AD-A155026] 21 p3563 N85-32163
Cluster variation study of coherent ordering in FCC and BCC solid solutions
[AD-A156039] 24 p4079 N85-35280

PHASE ERROR
The Statistical Loop Analyzer (SLA)
08 p1100 N85-16955
Analytical studies and experimental measurements of amplitude and phase of near-field range antenna probes
[AD-A150922] 14 p2293 N85-24212
Angular tracking error in A phase comparison monopulse tracking radar: A critical review and extension of the phase front distortion approach
[AD-A152628] 17 p2919 N85-28205
Modulation using four phase levels. Theoretical study of the degradation caused by a spurious phase modulation
[CNES-83/219/CT/DRT/TIT/TR]
20 p3441 N85-31360

PHASE LOCK DEMODULATORS
Phase-locked loops for optical homodyne detection, volume 1 — spaceborne receivers
[ESA-CR(P)-2029-VOL-1] 20 p3442 N85-31367
Phase locked loops for optical homodyne detection, volume 2 — spaceborne receivers
[ESA-CR(P)-2029-VOL-2] 20 p3442 N85-31368

PHASE LOCKED SYSTEMS
Timing performance of phase-locked loops in optical pulse position modulation communication systems
[AD-A145403] 02 p0190 N85-11271

Design and performance of sampled data loops for subcarrier and carrier tracking 05 p0623 N85-13966
Device for frequency stabilization of microwave oscillators 06 p0788 N85-15033
Transmission line biased coherent array of Josephson oscillators
[AD-D011323] 07 p0944 N85-15979
Phased locked array laser systems
[AD-D011317] 07 p0971 N85-16164
Processing circuit with asymmetry corrector and convolutional encoder for digital data
[NASA-CASE-MSC-20187-1] 11 p1626 N85-20249
Double reference pulsed phase locked loop (DRP-2L-2)
[NASA-CASE-LAR-13310-1] 12 p1824 N85-21441
Phase function, backscatter, extinction, and absorption for standard radiation atmosphere and El Chichon aerosol models at visible and near-infrared wavelengths
[NASA-TM-86379] 12 p1892 N85-21874
New results on the PLL false lock phenomenon
12 p1948 N85-22236
Stereo decoder without subcarrier restoration
13 p2068 N85-22921
Study of phase radiogeodetic systems with phase-locked loops 13 p2115 N85-23172
System of phase-lock automatic frequency control with acoustoelectronic convolver 15 p2526 N85-25573
MHB4046 phase-lock circuit 15 p2533 N85-25629
Phase-locked loop design with MHB4046
15 p2534 N85-25631
Additional PLL designs 15 p2534 N85-25632
Digital filters for digital phase-locked loops
16 p2771 N85-27104
Phase-lock fiber optic interferometer
[AD-D011603] 16 p2786 N85-27191
Experimental performance of a frequency measurement circuit
[AD-A152951] 17 p2953 N85-28239
Atmospheric probing by active millimeter wave system
[AD-A153550] 18 p3136 N85-29422
Phase locked loop synchronization for direct detection optical PPM communication systems
[NASA-CR-176026] 19 p3254 N85-30178
Dielectric resonator stabilized microstrip oscillator
[AD-D011706] 19 p3261 N85-30219
Phase-locked loops for optical homodyne detection, volume 1 — spaceborne receivers
[ESA-CR(P)-2029-VOL-1] 20 p3442 N85-31367
Phase locked loops for optical homodyne detection, volume 2 — spaceborne receivers
[ESA-CR(P)-2029-VOL-2] 20 p3442 N85-31368
A phase-locked frequency multiplier for the signal averaging of the vibration of the Wessex helicopter input spiral bevel pinion
[AD-A154914] 21 p3555 N85-32113
Practicality of electronic beam steering for MST/ST radars, part 6.2A 21 p3624 N85-32516
General design principles of high speed frequency synthesizers based on phase synchronization systems
22 p3779 N85-33417
Wide-band phase locked loop amplifier apparatus
[AD-D011720] 23 p3927 N85-34337
Nonlinear digital phase-locked loops with application to Loran-C receivers 24 p4063 N85-35178

PHASE MATCHING
Huffman-coded pulse compression waveforms
[AD-A155322] 21 p3576 N85-32243

PHASE MODULATION
NT PHASE SHIFT KEYING
Digital radio link: Comparison of the resistance of two different 4-phase modulation forms to multipath propagation
[FOA-C-30362-E] 02 p0193 N85-11291
Visible wavelength interferometer for high speed electron density diagnostics
[AD-A145686] 02 p0277 N85-11803
Frequency shifting in multimode fiber optic phase modulation devices 03 p0347 N85-12239
Influence of mode noise suppression in multimode fiber optic light guides 03 p0348 N85-12242
Micro-waveguide transformers of coherent optical signals 07 p0950 N85-16022
L.F. RADIO-DATA: Specification of BBC phase-modulated transmissions on long-wave
[BBC-RD-1984/19] 12 p1822 N85-21431
Interference immunity of binary systems with second-order phase-difference modulation in various reception modes 13 p2072 N85-22944
Synthesis of optimum single-channel discrete signals and filters 13 p2080 N85-22990
Reception noise immunity of multiposition signals
13 p2085 N85-23023
The latitudinal variation of geomagnetic pulsation amplitude and phase 14 p2370 N85-24646
A phase modulation evaluation procedure for an ARGOS type signal 16 p2811 N85-27336
Experimental evaluation of a new form of M-ary (M = 8) phase shift keying including design of the transmitter and receiver
[AD-A155103] 21 p3576 N85-32239
A new description of combined trellis coding with asymmetric modulation
[NASA-CR-176197] 24 p4086 N85-35323

PHASE SHIFT
High frequency phase-noise in semiconductor lasers
[FUB-20-1983] 01 p0053 N85-10353
Metrological consequences of the hard optical boundary assumption
[PB84-223577] 01 p0121 N85-10827
Dynamics of growth of surface periodic structures when intense light acts on condensed media
02 p0268 N85-11748
Dust properties determined from backscattering in the interplanetary and interstellar medium
03 p0446 N85-12838
Extended X-ray absorption fine structure (Exafs) studies of the actinides
[DE84-015633] 04 p0559 N85-13561
Infralow-frequency digital phase meter
06 p0787 N85-15031
Tropospheric and ionospheric phase perturbations and Doppler frequency shift effects
[AD-A148579] 08 p1154 N85-17283
CO_2 laser interferometer array for Big Dee
[DE85-001718] 10 p1490 N85-19411
Method and apparatus for measuring minority carrier lifetime in a direct band-gap semiconductor
[NASA-CASE-NPO-163371-1] 11 p1628 N85-20251
Double reference pulsed phase locked loop (DRP-2L-2)
[NASA-CASE-LAR-13310-1] 12 p1824 N85-21441
Combined microwave parallel amplifier-RF attenuator/modulator
[AD-D011535] 12 p1833 N85-21499
Wideband phase keyers 12 p1839 N85-21544
Use of electronic coding-frequency meters to measure parameters of pulsed radio signals
13 p2076 N85-22964
Change of electrical characteristics of radio-frequency cables under thermal effect 13 p2081 N85-22999
Calculation of image shift in panoramic photography
15 p2486 N85-25357
Relationship between Allan variances and Kalman Filter parameters 18 p3107 N85-29238
Thin film phase transition materials development program
[AD-A154260] 19 p3259 N85-30209
High switching speed electrically tuned microwave magnetic resonance devices
[AD-D011699] 19 p3260 N85-30217
Design of a jamming simulator for a binary communication system
[AD-A154617] 21 p3573 N85-32221
Solid state high power amplifier for driving the SLC injector klystron
[DE85-013063] 24 p4090 N85-35356
Analysis of two-parameter constant background born inversion for acoustic synthetic data
[AD-A156394] 24 p4145 N85-35696

PHASE SHIFT CIRCUITS
NT CIRCULATORS (PHASE SHIFT CIRCUITS)
Coplanar Schottky variable phase shifter
[AD-A146304] 03 p0359 N85-12305
Phase only adaptive nulling in a monopulse antenna
[AD-D011289] 05 p0628 N85-14026
Fast switching driver for inductive load, such as a phase shifter
[AD-D011368] 08 p1143 N85-17207
Low sidelobe phased array antenna system
[AD-D011556] 12 p1823 N85-21435
USSR report: Electronics and electrical engineering
[JPRS-UEE-85-002] 13 p2066 N85-22907
Wavelength multiplexer-demultiplexer
[AD-D011606] 16 p2777 N85-27140
High switching speed electrically tuned microwave magnetic resonance devices
[AD-D011699] 19 p3260 N85-30217
Dielectric resonator oscillators with digital temperature compensation
[AD-D011715] 19 p3261 N85-30221
East Europe report: Science and technology
[JPRS-ESA-85-021] 21 p3568 N85-32190

PHASE SHIFT KEYING
A transmission analysis for the use of 2-4 PSK modulation in satellite broadcasting
[ESA-STM-231] 04 p0494 N85-13151
Structure of frequency modulated and phase-shift keyed signals reflected from ionosphere at near-critical frequencies 07 p0952 N85-16035
AWQPSK: An optimum modulation technique for spread spectrum communication 09 p1311 N85-18235
A microprocessor controlled parallel model wi
FDPSK 10 p1475 N85-1800
Development of a 20 GHz modulator for the payload of a satellite for propagation and transmission experiments, including the required converters of the test equipment
[BMFT-FB-W-84-044] 11 p1590 N85-2000
Wideband phase keyers 12 p1839 N85-2154
Optimal discrete filtration of intricate phase-keyed signals 12 p1840 N85-2155
Regular synthesis of pairs of phase-keyed binary minimax signals 13 p2069 N85-2288
Dispersion of phase-shift keyed systems with fixed number of blocks 13 p2070 N85-2288
Analysis of characteristics of digital discriminators for phase-shift keyed signals 13 p2070 N85-2289
Combined processing method and matched filter for discrete composite frequency phase-shift keyed signal
13 p2070 N85-2289
Ionospheric distortions of digital signals with wideband modulation 13 p2072 N85-22945
Comparative analysis of noise tolerance of quasi-coherent phase shift keying signal demodulators
13 p2072 N85-22946
Transient processes in tuned amplifier during phase-shift keying with smooth phase variation
15 p2527 N85-2598
Analysis of space diversity techniques for EHF (Extremely High Frequency) satellite downlinks
[AD-A151900] 15 p2544 N85-25705
Bit error rate of coherent M-ary PSK
16 p2770 N85-2709
Serial Minimum Shift Keying (SMSK) follow-on study – spacecraft communication
[ESA-CR(P)-2026] 20 p3399 N85-3108
Modulation using four phase levels. Theoretical study of the degradation caused by a spurious phase modulation
[CNES-83/219/CT/DRT/TIT/TR]
20 p3441 N85-31360
Study of a limited band signal transmission chain
[CNES-CT/DRT/TIT/TR-83/221]
20 p3442 N85-31361
Receive shaping filter manufacture — QPSK uplinks
[ESA-CR(P)-1998] 20 p3449 N85-31412
Experimental evaluation of a new form of M-ary (M = 8) phase shift keying including design of the transmitter and receiver
[AD-A155103] 21 p3576 N85-32239
Transformation of spectrum of phase-code keyed signal for scanning in time 22 p3765 N85-3333
A new description of combined trellis coding with asymmetric modulation
[NASA-CR-176197] 24 p4086 N85-35323
DMSK: A practical 2400-bps receiver for the mobile satellite service: An MSAT-X Report
[NASA-CR-176194] 24 p4086 N85-35324
Necessary bandwidth and spectral properties of digital modulation
[PB85-185367] 24 p4088 N85-35340

PHASE TRANSFORMATIONS
NT BOILING
NT COAL LIQUEFACTION
NT EVAPORATION
NT EVAPOTRANSPIRATION
NT FILM BOILING
NT FLASHING (VAPORIZING)
NT FREEZING
NT FUSION (MELTING)
NT LEVITATION MELTING
NT LIQUEFACTION
NT MARTENSITIC TRANSFORMATION
NT MELTING
NT NUCLEATE BOILING
NT PROPELLANT EVAPORATION
NT SUBLIMATION
NT TRANSPIRATION
NT VACUUM MELTING
NT VAPORIZING
NT ZONE MELTING
Fabrication and characterization of Si_3N_4 ceramic without additives by high pressure hot pressing
[NASA-TM-77724] 01 p0031 N85-1018
Fundamental studies of structure property relationship in transformation toughened ceramics
[DE84-015344] 01 p0033 N85-1020
ICARUS: A general one-dimensional heat conduction code
[DE84-016125] 01 p0047 N85-1031
Influence of 5f electrons on structures and bonding the actinide-hydrogen intermetallics
[DE84-013693] 01 p0118 N85-1080
Research program in theoretical high-energy phys
[DE84-013717] 01 p0119 N85-108
Experiments with phase transitions at very hi pressure
[NASA-CR-174029] 02 p0172 N85-111

Alloying effects of reactive elements in ferritic stainless steels 02 p0178 N85-11198

The role of molybdenum as an alloy element in adhesive wear resistance 02 p0181 N85-11212

Metastable phase formation in ion implanted metals [DE84-014945] 02 p0183 N85-11229

Kinetics of short-range ordering in metallic glasses: Analysis of the crossover effect [DE84-015524] 02 p0187 N85-11251

Phase transition which exhibits 1/omega-spectrum: A rigorous result 02 p0283 N85-11842

High pressure cosmochemistry applied to major planetary interiors: Experimental studies [NASA-CR-174032] 02 p0302 N85-11958

Synthesis of stereoisomeric - metal complexes using phase-transfer catalysis and photochemical transforms [AD-A145787] 03 p0331 N85-12134

Microstructure development in polymers [AD-A145980] 03 p0337 N85-12170

Re-evaluation of phase separation in Ti-Zr-Be metallic glasses [DE84-015603] 03 p0338 N85-12176

Effect of heat treatment on phase composition and crystal structure of thin WSi2 films on silicon substrates 03 p0350 N85-12253

Structural recrystallization in titanium 03 p0351 N85-12258

Constitutive features of solids at shock-wave loading rates [DE84-015715] 03 p0362 N85-12325

Non-linear systems in infinite dimensional state spaces [AD-A145828] 03 p0410 N85-12623

Investigations of magnetic phase transitions with neutron scattering 03 p0423 N85-12700

Neutron scattering on structural phase transitions with domain building 03 p0425 N85-12711

Phase transformations of AlPO4 with SiO2 structures 03 p0425 N85-12713

Structural phase transitions in doped hexahalogen metallates 03 p0426 N85-12721

Center for dielectric studies [AD-A146183] 03 p0434 N85-12761

The 6th International Summer Institute in Surface Science 1983) [AD-A146253] 03 p0434 N85-12762

Thermodynamics and phase equilibria in the vandium-silicon system [AD-A145670] 03 p0435 N85-12769

CVD parameter study using strategy of experimentation [DE84-015900] 04 p0473 N85-13011

Nonthermal mechanism for laser annealing of semiconductors and formation of super structure 04 p0487 N85-13109

Deterministic sensitivity analysis of two-phase flow systems: Forward and adjoint methods [DE84-016276] 04 p0499 N85-13185

Geology and geochemical evolution of the Lost River, Alaska, tin deposit 04 p0533 N85-13405

Zero-flux planes and flux reversals in multicomponent diffusion [DE84-015212] 05 p0618 N85-13950

A similarity analysis of phase change heat conduction in corners 05 p0634 N85-14069

Electrochemistry in near-critical and supercritical fluids. I. Ammonia [AD-A146429] 06 p0765 N85-14894

Phase equilibria of stored chemical energy reactants [AD-A146527] 06 p0765 N85-14896

Control of microstructure during hot working of Ti-6242 06 p0797 N85-15091

Reciprocal solubility of phases in multi-component systems [BLL-M-36003-(5828.4)] 07 p0926 N85-15870

A study of structural phase transitions using light scattering techniques [AD-A147261] 07 p1048 N85-16654

Passive storage technologies 08 p1106 N85-17003

Transient combustion: An important consideration in deflagration-to-detonation transition 08 p1116 N85-17037

The DDT process for high energy propellants 08 p1116 N85-17038

Phase-dissipative mechanisms for laser-induced surface desorption-dissociation processes [AD-A147961] 08 p1121 N85-17065

Research in phase transfer catalysis [AD-A148266] 08 p1121 N85-17068

Grain refining and microstructural modification during solidification [AD-A147705] 08 p1128 N85-17111

Phase diagram of polymer blends containing block copolymers [AD-A147706] 08 p1132 N85-17134

Structure-property relationships in thermoplastic elastomers. Part 1: Segmented polyether-polyurethanes [AD-A148043] 08 p1133 N85-17138

Structure-property relationships in intercalated graphite [AD-A147949] 08 p1219 N85-17680

Phase formation and stability in the pseudobinary Ni3Al-Ni3V alloy system [DE85-001117] 09 p1296 N85-18143

Radiation-induced compositional redistribution and local phase transformation in irradiated alloys [DE85-000080] 10 p1441 N85-19082

Determination of vapor phase content when metals are struck by laser radiation pulses of various densities 10 p1445 N85-19106

Study of the volumetric changes in VT23 alloy upon heating 10 p1448 N85-19123

Metal-nonmetal transitions in N-doped many-valley Si and Ge [INPE-3358-PRE/636] 10 p1562 N85-19848

A study of interdiffusion in beta + gamma/gamma + gamma prime Ni-Cr-Al [NASA-CR-174852] 11 p1597 N85-20041

Structure-phase state and properties of high-durability VAL8 alloy 11 p1597 N85-20046

Study of phase composition of Al-B plasma coatings 11 p1598 N85-20050

Phase transformations in vanadium alloys of titanium during quenching and tempering 11 p1602 N85-20073

Electric and magnetic properties of intercalated graphite [AD-A149848] 12 p1798 N85-21276

Hydrogen flame acceleration and transition to detonation [DE85-000611] 12 p1802 N85-21299

Alloy development, processing and characterization of devitrified titanium base microcrystalline alloys [AD-A149609] 12 p1806 N85-21327

Generalized radome BSE (radome boresight error) characterization using superposition techniques [AD-P004354] 12 p1825 N85-21448

Phase change thermal energy storage and the model building codes [PB85-111201] 12 p1883 N85-21813

Experimental determination of systems suitable for study as monotectic binary metallic alloy solidification models 12 p1948 N85-22235

Metal-semiconductor phase transition and its application [DRIC-T-7149] 13 p2021 N85-22665

Influence of hydrogen bonding in block copolymers and their blends 13 p2036 N85-22752

Local phase transformation in alloys during charged-particle irradiation [DE85-005012] 14 p2258 N85-23990

Dynamic shock studies of PZT 95/5 ferroelectric ceramic [DE85-006137] 14 p2261 N85-24015

The volume change during solidification [NASA-TM-77817] 14 p2300 N85-24243

Conversions in amorphous zirconium-vanadium alloy 15 p2496 N85-25400

Phase separation in polyurethanes: A deuterium NMR study [AD-A151515] 15 p2505 N85-25451

Eleven lectures on the physics of the quark-gluon plasma [DE85-004321] 15 p2662 N85-26431

Transformation of nitrogen oxides while sampling combustion products [AD-A152184] 16 p2746 N85-26945

Models of long-period superstructure [DE85-007659] 16 p2751 N85-26981

Research on the kinetics of phase changes in solids [AD-A152387] 17 p2918 N85-27989

Study of self-propagating condensed phase reactions TiB(2) synthesis [AD-A153198] 17 p2921 N85-28006

Microstructure-mechanical property relationships in transformation-toughened ceramics [DE85-009722] 17 p2935 N85-28117

Preparation of nitrocompounds [AD-A153687] 18 p3071 N85-28993

Chemical transformation modules for Eulerian acid deposition models. Volume 1: The gas-phase chemistry [PB85-173714] 18 p3072 N85-29001

Ten degree Kelvin hydride refrigerator [NASA-CASE-NPO-16393-1-CU] 18 p3085 N85-29084

Screening phase transitions in two-dimensional Coulomb gas [NOTA-INTERNA-830] 18 p3192 N85-29798

Pseudopotentials and total energy calculations: Applications to crystal stability, vibrational properties, phase transformations, and surface structures [DE85-007657] 18 p3194 N85-29810

Solid phase reactions among manganese, potassium perchlorate and barium chromate [HSE-TRANS-11166] 19 p3237 N85-30071

Fundamental studies of beta phase decomposition modes in titanium alloys [AD-A154122] 19 p3238 N85-30078

Study of phase equilibria and crystallization processes in Al-Zn-Mg alloy systems 19 p3241 N85-30098

High temperature Raman studies of phase transitions in thin film dielectrics [DE85-010973] 19 p3263 N85-30234

Clearing of polydisperse aqueous aerosol by laser radiation pulses 19 p3298 N85-30445

Comparison of the response of shape memory alloy actuators using air-cooling and water-cooling [AD-A155216] 21 p3567 N85-32185

The shearing contribution in transformation toughening of brittle materials [AD-A154656] 21 p3568 N85-32195

Aerobic sulfur-oxidizing bacteria: Environmental selection and diversification 21 p3656 N85-32712

Sulfur transformations at the hydrogen sulfide/oxygen interface in stratified waters and in cyanobacterial mats 21 p3657 N85-32715

The Konstantinov effect and absorption of sound in inhomogeneous media 21 p3680 N85-32861

An EPR (Electron-Paramagnetic-Resonance) and ENDOR (Electron-Nuclear-Double-Resonance) study of ferroelectric ammonium sulfate [AD-A155580] 21 p3710 N85-33033

Microstructure-mechanical property relationships in the transformation-toughened ceramics [DE85-011946] 22 p3752 N85-33261

Phase transformations taking place in austenitic steel during deformation at different rates [BLL-M-35875-(5828.4)] 23 p3914 N85-34254

Shape memory effect in uranium-niobium alloys below room temperature [DE85-012964] 23 p3916 N85-34268

Transient three-phase three-component systems. Part 1: Formulation of the system of differential equations [DE85-013267] 24 p4096 N85-35384

PHASE VELOCITY

Wave phase velocity in a wind gradient — gravity waves 04 p0523 N85-13343

Experimental determination of propagation rate of ELF signals employed by Omega radio navigation system for phase measurements 06 p0793 N85-15066

The development of a transducer system for the accurate measurement of ultrasonic phase delay of SH plate waves [AERE-R-11596] 15 p2559 N85-25790

PHASE-SPACE INTEGRAL

Phase space factors in multiparticle processes 24 p4175 N85-35888

PHASED ARRAYS

Reflector antenna having sidelobe suppression elements [AD-D011227] 01 p0039 N85-10244

Theory of near-field phased arrays for electromagnetic susceptibility testing [PB84-217836] 01 p0042 N85-10273

Phase only adaptive nulling in a monopulse antenna [AD-D011289] 05 p0626 N85-14026

Characteristics of circular-polarized printed radiators in planar phased antenna array 06 p0790 N85-15049

Investigation of characteristics of phased antenna array considering interaction between radiators and properties of power divider 06 p0790 N85-15051

MMIC devices for active phased array antennas [NASA-CR-174281] 07 p0936 N85-15943

Determination of row-and-column control principle of phase antenna array from amplitude-phase distribution of field in aperture 07 p0952 N85-16033

Short period guided waves over oceanic and continental paths [AD-A147053] 07 p0997 N85-16331

Configuration study for a 30 GHz monolithic receive array: Technical assessment [NASA-CR-174697] 09 p1311 N85-18238

Configuration study for a 30 GHz monolithic receive array, volume 1 [NASA-CR-174697-VOL-1] 09 p1311 N85-18239

Conformal phased array antenna pattern corrector [AD-D011459] 10 p1468 N85-19266

Design criteria for limited scan antennas at digital microwave line of sight links 10 p1471 N85-19284

Use of ground radar to detect reentering debris 12 p1784 N85-21200

Low sidelobe phased array antenna system [AD-D011558] 12 p1823 N85-21435

Method and apparatus for self-calibration and phasing of array antenna
[NASA-CASE-NPO-15920-1] 12 p1832 N85-21493
Wide angle phased array dome lens antenna with a reflection/transmission switch
[AD-D011562] 12 p1833 N85-21502
Phased antenna array for wind profiling applications
[PB85-132684] 12 p1837 N85-21529
Design considerations for high-altitude, long-endurance, microwave-powered aircraft
[NASA-TM-86403] 14 p2216 N85-23751
Interference immunity of optical radar system with phased antenna array 15 p2526 N85-25575
Cophasal horizontal wideband array antennas for transmitting with asymmetric output
15 p2526 N85-25576
Optical techniques for signal distribution and control in advanced radar and communication systems
18 p3166 N85-29773
Dual sense, circularly polarized helical antenna
[AD-D011660] 19 p3254 N85-30175
MMIC devices for active phased array antennas
[NASA-CR-176015] 19 p3254 N85-30177
New concepts in free electron lasers
20 p3460 N85-31493
Null synthesis with phase and amplitude controls at the subarray outputs
[AD-A155187] 21 p3576 N85-32241
Evaluation of the effects of roll angle on the natural convection heat transfer from an array of cylindrical spines
[AD-A154694] 21 p3583 N85-32273
Most desirable terrain, e.g., flat vs valley location, part 5.1B 21 p3624 N85-32513
Adaptive synthesis of antennas with separation of signals by direction of arrival 22 p3764 N85-33326
Frequency independent parabolic phased antenna array of log periodic antennas 22 p3774 N85-33387

PHENOLIC RESINS
Investigation of the effects of NaOH dopant level on the physical and mechanical properties of carbon/phenolic composite material 12 p1945 N85-22213
Mechanical modification of friction surfaces of aluminum alloys by friction transfer 19 p3241 N85-30097
Long-term strength of glass fibre/phenolic resin composites
[NPL-DMA(A)-98] 22 p3742 N85-33195
Poly-functional building material from fiberglass (its fabrication and properties) 23 p3906 N85-34209

PHENOLOGY
NOAA-AISC user's guide for implementing CERES maize model for large area yield estimation
[E85-10083] 12 p1873 N85-21748
User's guide to the TAMW wheat model as implemented on the IBM 360/195 computer
[E85-10084] 12 p1873 N85-21749
NOAA-AISC user's guide for implementing CERES wheat model for large area yield estimation
[E85-10085] 12 p1873 N85-21750
Estimating solar radiation for plant simulation models
[E85-10089] 12 p1873 N85-21751

PHENOLS
Preliminary evaluation of an improved flammability test method for aircraft materials
[FAA-CT-84-22] 08 p1080 N85-16840
Synthesis of phenols from metal-carbynes and diynes
[AD-A151913] 16 p2754 N85-26997
SRB attach ring phenolic TPS fishtail seal evaluation tests
[NASA-CR-170867] 24 p4098 N85-35407

PHENOMENOLOGY
NT MESOSCALE PHENOMENA
NT PHENOLOGY
An internally consistent gamma ray burst time history phenomenology
[OG-1.2-6] 22 p3862 N85-33916

PHENYLS
NT POLYCHLORINATED BIPHENYLS
NT POLYPHENYLS
NT TRIPHENYLS
Effect of substituted phenylnadimides on processing and properties of PMR polyimide composites
[NASA-TM-86902] 06 p0770 N85-14929
Polymerization and halogen scrambling behavior of phenyl-substituted cyclotriphosphazenes
[AD-A146366] 06 p0771 N85-14930
The synthesis and characterization of Poly(Oxy(2-Methyl-1,3-Phenylene) Methyl-1,3 -Phenylene) Oxyterephthaloyl)Oxy
[AD-A148269] 08 p1133 N85-17143
Acute oral toxicity (LD50) of 4-nitrophenyl monochloromethyl (Phenyl) phosphinate (TA009) in male rats
[AD-A148337] 08 p1192 N85-17513
Ideal gas thermodynamic properties for the phenyl, phenoxy, and o-biphenyl radicals
[NASA-TM-83800] 12 p1943 N85-22204
Preparations of methoxynitrophenazines and their photoconductivities
[NASA-TM-77775] 14 p2247 N85-23929
Substituent effects on the electrical conductivities of the phenazine derivatives
[NASA-TM-77792] 14 p2249 N85-23938

PHILOSOPHY
NT PARADOXES
Outer space law: A problem of astronautics
[NASA-TM-77760] 07 p1055 N85-16697
Discovery refutation and verification refutation: The proposals of Von Neumann and Wiener in the development of 20th century physics
[NOTA-INTERNA-840] 14 p2431 N85-24993
The Impact of Science on Society
[NASA-SP-482] 14 p2431 N85-24994
The legacy of science 14 p2432 N85-24995

PHOBIAS
NT FEAR OF FLYING

PHOBOS
Structure and origin of Martian satellites
15 p2483 N85-25323

PHONEMES
Vowel phoneme identification in speech
[FUB-26-1983] 01 p0040 N85-10257
Comparative analysis of the clustering of the LPC coefficients in phoneme recognition
[FUB-30-1983] 01 p0041 N85-10264
Research in continuous speech recognition
[AD-A150474] 13 p2055 N85-22868
Implementation of a real-time, interactive, continuous speech recognition system
[AD-A151936] 16 p2773 N85-27117
Evaluating syntactic constraints to speech recognition in a fighter aircraft environment
[AD-A152117] 16 p2773 N85-27119
Study to determine potential flight applications and human factors design guidelines for voice recognition and synthesis systems
[NASA-CR-172590] 20 p3440 N85-31349
Phonetic transcription statistics: Constitution and statistical utilization
[ENST-85D001] 22 p3756 N85-33285

PHONETICS
Voice phonetic coding and decoding processes
[FUB-29-1983] 01 p0040 N85-10259
Research in continuous speech recognition
[AD-A150474] 13 p2055 N85-22868
Automation of the process of speech signal segmentation in an analogic-numeric system
[REPT-5/1984] 16 p2766 N85-27082
Phonetic transcription statistics: Constitution and statistical utilization
[ENST-85D001] 22 p3756 N85-33285

PHONOCARDIOGRAPHY
NT ECHOCARDIOGRAPHY

PHONONS
Phonon anomalies in superconducting transition metal compounds — lanthanum and niobium compounds
03 p0426 N85-12718
Folded acoustic and quantized optic phonons in semiconductor superlattices
[AD-A145935] 03 p0433 N85-12756
Phonon-impurity relaxation and acoustic wave absorption in yttrium-aluminum garnet crystals with impurities 11 p1715 N85-20790
Effect of impurities on absorption in semiconductors and lasing of semiconductor lasers 11 p1716 N85-20797
Electrical and thermal transport property studies of high-temperature thermoelectric materials
[AD-A150900] 14 p2427 N85-24967
Infrared nonlinear processes in semiconductors
[AD-A150966] 14 p2427 N85-24968
Raman studies of surface temperature in laser-heated semiconductors
[AD-A151377] 15 p2650 N85-26412
Theory of laser-stimulated surface process. 2: A generalized-master-equation approach to energy transfer between an IR laser, an aspecties and phonons
[AD-A153063] 17 p2970 N85-28344
Localization of waves in a disordered medium
19 p3373 N85-30926
Influence on bi-phonon states on Raman scattering of light in molecular crystals 21 p3680 N85-32865
Influence of phonon interaction on width and form of Mandelstam-Brillouin optical scattering line
21 p3696 N85-32962
Calculating the interatomic pair potential allowing for resonance interaction in titanium, nickel and vanadium
[BLL-M-35843-(5828.4)] 23 p3913 N85-34249

PHOSPHATES
NT ADENOSINE DIPHOSPHATE
NT ADENOSINE TRIPHOSPHATE
NT CALCIUM PHOSPHATES
NT INDIUM PHOSPHATES
NT POTASSIUM PHOSPHATES
Identification and parameter estimation of phosphate balance models in drinking water reservoirs
[PUBL-313] 08 p1181 N85-17439
Geographic variation in the relationships of temperature, salinity or sigma sub t versus plant nutrient concentrations in the world ocean — silicic acid, nitrate, and phosphate concentration
[NASA-CR-175621] 13 p2140 N85-23287
Water-resistance and some other properties of polyalkali fluorophosphate glasses 14 p2261 N85-24130
Addendum to the STCAL and LTCAL user's guide
[NASA-CR-171880] 15 p2626 N85-26194
Characteristics of polyacrylic acid-complexed zinc phosphate conversion films deposited on metal surfaces
[DE85-004057] 16 p2750 N85-26974
Characteristics of charge transfer in the dispersed phase of electrorheological suspensions
[RAE-TRANS-2125] 19 p3233 N85-30040
Design of micelles as dephosphorylating agents
[AD-A155589] 21 p3564 N85-32186
Microanalysis of dissolved iron and phosphate in pore waters of hypersaline sediment
21 p3661 N85-32744
Applications of the mineral resources data system and the international strategic minerals inventory in mineral-resource assessments by region and commodity
24 p4105 N85-35451

PHOSPHAZENE
Polymerization and halogen scrambling behavior of phenyl-substituted cyclotriphosphazenes
[AD-A146366] 06 p0771 N85-14930
(Vinyloxy)fluorocyclotriphosphazenes
[AD-A147448] 07 p0924 N85-15850
Polyphosphazene solid electrolytes
[AD-A147008] 07 p0931 N85-15902
New synthesis of phosphazene polymers
[AD-A147567] 07 p0933 N85-15910
(Vinyloxy)chlorocyclotriphosphazenes
[AD-D011471] 10 p1453 N85-19152
The synthesis and structure of polyphosphazenes
[AD-A153134] 17 p2934 N85-28112

PHOSPHIDES
NT GALLIUM PHOSPHIDES
NT INDIUM PHOSPHIDES
Vaporization behavior of chromium phosphides. The solid 2-phase regions CrP-Cr12P7, Cr12P7-Cr3P, and Cr3P-Cr
[AD-A145481] 02 p0172 N85-11152
Magnetic susceptibility, electrical resistivity, and specific heat of single crystal LaFe-4P-12
[DE84-009979] 04 p0570 N85-13833
Vaporization behavior, phase equilibria, and thermodynamic stabilities of nickel phosphides
[AD-A146683] 06 p0765 N85-14897
The UFe4P12 and CeFe4P12: Non-metallic isotopes of superconducting LaFe4P12
[DE85-003724] 12 p1942 N85-22195
Thin film cadmium telluride and zinc phosphide solar cells
[DE85-002904] 15 p2587 N85-25950
Photoelectronic properties of zinc phosphide crystals and heterojunctions
[DE85-008777] 19 p3307 N85-30501

PHOSPHINES
Macrocyclic poly(tertiary) phosphines for the attachment of metals to surfaces of photodevices
[DE84-015552] 05 p0617 N85-13946
Fluorinated aliphatic polyalkylether lubricant with an additive composed of an aromatic phosphine substituted with perfluoroalkylether groups
[AD-D011286] 06 p0770 N85-14927
New synthesis of phosphazene polymers
[AD-A147567] 07 p0933 N85-15910
Detection of the J-10 manifold of the pure rotational band of phosphine on Saturn 08 p1245 N85-17855
Isomer enumeration in polytertiary phosphines and related compounds
[AD-A148058] 09 p1290 N85-18089
Phosphorus-containing imide resins
[NASA-CASE-ARC-11368-2] 12 p1809 N85-21347

PHOSPHORESCENCE
Intermolecular energy transfer between the individual zero-field levels of triplet traps in an orientationally disordered solid
[AD-A150751] 14 p2417 N85-24914
Photophysical studies of triplet exciton processes in pure polymer films
[DE85-006571] 18 p3060 N85-29058
Beam tests of phosphorescent screens
[DE85-009843] 18 p3097 N85-29170

PHOSPHORIC ACID

Electrochemical behavior of amorphous alloys based on iron, cobalt and nickel in H3PO4 solutions alone and mixed with HF 15 p2513 N85-25505

Mechanical properties of adhesively bonded aluminum structures protected with hydration inhibitors
[AD-A153755] 18 p3079 N85-29047

Improved acid electrolytes for fuel cells
[PB85-176053] 18 p3132 N85-29397

System for the continuous generation of phosphorous aerosols from red phosphorus-butyl rubber
[DE85-013527] 24 p4072 N85-35232

PHOSPHORIC ACID FUEL CELLS

Manual of phosphoric acid fuel cell power plant optimization model and computer program
[NASA-CR-174721] 01 p0067 N85-10445

Manual of phosphoric acid fuel cell stack three-dimensional model and computer program
[NASA-CR-174722] 01 p0067 N85-10447

Electrocatalysis of fuel cell reactions: Investigation of alternate electrolytes
[NASA-CR-174753] 02 p0222 N85-11455

Phosphoric acid fuel cell power plant system performance model and computer program
[NASA-CR-174638] 02 p0222 N85-11456

Gas cooled fuel cell systems technology development
[NASA-CR-174732] 07 p0991 N85-16291

Electric utility acid fuel cell stack technology advancement
[NASA-CR-174804] 08 p1178 N85-17422

Preparation and evaluation of advanced catalysts for phosphoric acid fuel cells
[NASA-CR-168223] 10 p1508 N85-19511

Develop and test fuel cell powered on-site integrated total energy systems. Phase 3: Full-scale power plant development
[NASA-CR-174887] 15 p2586 N85-25941

F-cell: The Aspen fuel cell model
[DE85-001975] 18 p3131 N85-29393

New catalysts and new electrolytes for acid fuel cells
[DE85-009940] 19 p3307 N85-30498

PHOSPHORS

Research on electroluminescence in thin film yttrium oxysulfide
[AD-A146909] 07 p1037 N85-16582

Applications of pulsed-laser techniques and thermographic phosphors to dynamic thermometry of rotating surfaces
[DE85-000403] 11 p1630 N85-20328

Investigation of basic characteristics of laser heating in thermoluminescence and of laser-stimulated luminescence
[AD-A152143] 16 p2790 N85-27212

Streak tube characterization
[DE85-009674] 17 p2956 N85-28255

PHOSPHORUS

Mechanical properties of a leaded, resulfurized, rephosphorized steel in various thermo/mechanical conditions
[PB84-216404] 03 p0333 N85-12144

Is phosphorus predictably incompatible in igneous processes? 04 p0583 N85-13722

Global carbon - nitrogen - phosphorus cycle interactions: A key to solving the atmospheric CO2 balance problem? 05 p0652 N85-14188

Interactions of the marine phosphorus and carbon cycles 05 p0653 N85-14190

Plasma deposition of amorphous metal alloys
[DE85-000768] 09 p1295 N85-18132

Study of processes of modification of Al-Si alloys 13 p2026 N85-22695

Determination of symmetry of immediate surroundings in amorphous Co-P alloys 15 p2496 N85-25398

Influence of phosphorus content and heat treatment on the machinability of electroless nickel deposits
[DE85-007250] 15 p2522 N85-25548

Addendum to the STCAL and LTCAL user's guide
[NASA-CR-171880] 15 p2628 N85-26194

Multiphoton production and detection of atoms
[AD-A155561] 21 p3702 N85-33000

Precision measurements of solar energetic particle elemental composition
[PAPER-SH-2.1-4] 21 p3715 N85-33052

Fire-resistant phosphorus containing polyimides and copolyimides
[NASA-CASE-ARC-11522-2] 23 p3918 N85-34280

Marine phosphorite deposits model for exploration, with emphasis on deposits in the US Atlantic coastal plain 24 p4104 N85-35439

PHOSPHORUS COMPOUNDS
NT ADENOSINE DIPHOSPHATE
NT ADENOSINE TRIPHOSPHATE
NT CALCIUM PHOSPHATES
NT GALLIUM PHOSPHIDES
NT INDIUM PHOSPHATES
NT INDIUM PHOSPHIDES
NT ORGANIC PHOSPHORUS COMPOUNDS
NT PHOSPHATES
NT PHOSPHIDES
NT PHOSPHINES
NT PHOSPHORIC ACID
NT PHOSPHORUS POLYMERS
NT POTASSIUM PHOSPHATES

The effect of temperature on the radiation induced losses of large diameter GPS (Germanium phosphosilicate) and GBS core optical fibers
[AD-A145409] 02 p0280 N85-11823

Study of singlet oxygen-pentavalent phosphorus reactions
[AD-A145896] 03 p0327 N85-12107

USSR report: Chemistry
[JPRS-UCH-84-012] 06 p0761 N85-14865

Magnetically-induced luminescence of (Ir(2=phos)(2)C10(4)
[AD-A149659] 12 p1799 N85-21286

Structural inhomogeneities in amorphous nickel-phosphorus alloy
[BLL-M-36103-(5828.4)] 16 p2748 N85-26960

Zn3P2 as an improved semiconductor for photovoltaic solar cells
[DE85-008772] 18 p3097 N85-29171

Improved acid electrolytes for fuel cells
[PB85-176053] 18 p3132 N85-29397

PHOSPHORUS METABOLISM

The role of 1,25-dihydroxyvitamin D in the inhibition of bone formation induced by skeletal unloading
[NASA-TM-87480] 18 p3153 N85-29522

PHOSPHORUS POLYMERS

Phosphorus-containing imide resins
[NASA-CASE-ARC-11368-2] 12 p1809 N85-21347

PHOSPHORYLATION

Design of micelles as dephosphorylating agents
[AD-A155589] 21 p3564 N85-32166

PHOTOABSORPTION

Experimental capabilities and prospects for measuring soft X-ray photoabsorption
[DE84-015488] 02 p0278 N85-11813

Electron-hole plasma formation in semiconductors due to the absorption of pulsed CO2 laser light
[DE85-001559] 09 p1392 N85-18757

Workshop report on new directions in soft X-ray photoabsorption
[DE85-006150] 14 p2419 N85-24923

Heliocentric sail problem with variable gravity field reduction 16 p2724 N85-26816

Quantitative studies for photoabsorption and fluorescence of HCl
[NASA-CR-175965] 19 p3233 N85-30043

Photoabsorption and photodissociation of molecules important in the interstellar medium
[NASA-CR-175918] 19 p3383 N85-30986

High-resolution spectroscopy and dynamics of multiphoton processes in atoms and molecules
[AD-A155862] 24 p4147 N85-35714

PHOTOACOUSTIC MICROSCOPY

Photoacoustic microscopy of oxygen contaminated titanium alloys
[AD-P004127] 08 p1127 N85-17102

Photoacoustic imaging
[AD-A150823] 14 p2416 N85-24905

PHOTOACOUSTIC SPECTROSCOPY

Optoacoustic spectroscopy
[AD-A145995] 03 p0419 N85-12679

Physico-chemical investigation of some areas of fundamental significance to biophysics
[DE84-016385] 04 p0471 N85-12999

High resolution photoacoustic and photothermal imaging 05 p0723 N85-14649

Investigations of photochemistry using holography and photoacoustic spectroscopy
[AD-A146637] 06 p0810 N85-15149

A study of the chemical interaction of gases with activated carbon
[AD-A147342] 07 p0923 N85-15846

Photoacoustic microscopy of oxygen contaminated titanium alloys
[AD-P004127] 08 p1127 N85-17102

Photoacoustic spectroscopy at electrode-solution interface
[DE85-001872] 09 p1292 N85-18111

Photoacoustic effect and its applications 12 p1820 N85-21421

Experimental investigation of the pulsed photoacoustic effect produced on a solid surface
[AD-A152114] 16 p2860 N85-27640

Single-pulse Raman and photoacoustic spectroscopy studies of Triaminotrinitrobenzene (TATB) and related compounds
[DE85-010072] 13 p3084 N85-29078

Photo-acoustic effect in finite-dimensional semiconductors 21 p3682 N85-32876

PHOTOCATHODES

Programmable optical sensor
[AD-D011244] 02 p0281 N85-11829

Fore-optics systems designed for electronic streak cameras using fiber optics
[DE84-014525] 02 p0281 N85-11830

A microchannel plate streak camera
[DE84-016536] 06 p0811 N85-15153

S-11 and S-20 photocathode research activity, revision 1
[DE84-017164] 09 p1326 N85-18335

Development and application of low energy X-ray and electron physics
[AD-A149963] 12 p1926 N85-22099

High-resolution SIT TV tube for subnanosecond image shuttering
[DE85-005189] 13 p2095 N85-23072

Streak tube characterization
[DE85-009674] 17 p2956 N85-28255

Microchannel plate streak camera
[DE85-011604] 20 p3458 N85-31481

On the possibilities of large-scale radio and fiber optics detectors in cosmic rays
[HE-4.6-2] 24 p4196 N85-36039

PHOTOCELLS
U PHOTOELECTRIC CELLS

PHOTOCHEMICAL OXIDANTS

Air quality for ozone and other photochemical oxidants. External review draft, volume 1
[PB85-126035] 11 p1679 N85-20582

Air quality criteria for ozone and other photochemical oxidants. External review draft, volume 5
[PB85-126076-VOL-5] 11 p1679 N85-20583

Air quality criteria for ozone and other photochemical oxidants. External review draft, volume 2
[PB85-126043] 12 p1886 N85-21836

Air quality criteria for ozone and other photochemical oxidants, external review draft, volume 3
[PB85-126050] 12 p1886 N85-21837

Evaluation of chemical reaction mechanisms for photochemical smog. Part 2: Quantitative evaluation of the mechanisms, revised
[PB85-166060] 16 p2822 N85-27406

Development of a chemical kinetic mechanism for the US EPA (Environmental Protection Agency) regional oxidant model
[PB85-185858] 22 p3813 N85-33618

PHOTOCHEMICAL REACTIONS
NT PHOTOCHROMISM
NT PHOTODECOMPOSITION
NT PHOTOLYSIS
NT PHOTOSYNTHESIS
NT RADIOLYSIS

A determination of the photochemical quantum yields from 2 excited triplet states of biacetyl using holography
[AD-A145091] 01 p0050 N85-10326

Research on photoelectrochemical cells based on CdSe, CdSe/sub 1-x/te/sub x and other photoelectrode materials
[DE84-004527] 02 p0224 N85-11466

Aeronomy 02 p0298 N85-11930

Synthesis of stereoisomeric - metal complexes using phase-transfer catalysis and photochemical transforms
[AD-A145787] 03 p0331 N85-12134

Three-dimensional photochemical machining with lasers
[AD-A145792] 03 p0365 N85-12342

Interaction of UV-laser radiation with molecular surface-films
[AD-A146311] 03 p0366 N85-12349

A 2-dimensional description of potential perturbations to the ozone layer due to NOx and H-2-O aircraft emissions
[AD-A146292] 03 p0392 N85-12511

Regional-scale (1000 KM) model of photochemical air pollution. Part 2: Input processor network design
[PB84-232651] 04 p0532 N85-13400

The nitrogen cycle: Atmosphere interactions 05 p0653 N85-14191

Aspects of the comparison of stratospheric trace species measurements with photochemical models
[DE84-017026] 05 p0672 N85-14317

Determination of Toluene's degradation products under simulated atmospheric conditions 05 p0674 N85-14331

Investigations of photochemistry using holography and photoacoustic spectroscopy
[AD-A146637] 06 p0810 N85-15149

Production of hydrogen by cyanobacteria
[PB85-113421/GAR] 07 p0935 N85-15925

Photochemistry and kinetics of the O*2-HI system
[AD-A147433] 07 p0971 N85-16167

Variation in photosynthesis with light level for model with two photochemical reactions 07 p1012 N85-16430

Conference on Singlet Molecular Oxygen (COSMO 84), program and abstracts
[AD-A147281] 07 p1040 N85-16605
Atmospheric photochemical modeling of turbine engine fuels. Phase 1: Experimental studies. Volume 2: Environmental chamber data tabulations
[AD-A147786] 08 p1165 N85-17470
Dynamics and mechanisms of catalytic processes and hot chemistry
[DE85-002899] 09 p1292 N85-18114
Hydrogen from solar energy
[DE85-001914] 10 p1437 N85-19055
Non-photochemical interactions of sulfur and nitrogen compounds in acid deposition
[DE84-016141] 10 p1513 N85-19546
Photosynthesis of ammonia
[DE85-001462] 11 p1595 N85-20029
Middle Atmosphere Program. Handbook for MAP, volume 4
[NASA-CR-175482] 11 p1654 N85-20420
The Middle Atmosphere Program: Winter In Northern Europe (MAP/WINE) 11 p1655 N85-20429
Energy transfer and photochemistry in biomimetic solar conversion
[PB85-129112] 11 p1677 N85-20566
User's guide for the Photochemical Box Model (PBM)
[PB85-137164] 11 p1682 N85-20602
Primary light harvesting system: The relationship of phycobilisomes to photosystem 1 and 2
[DE85-003075] 11 p1689 N85-20622
Photo-thermal detection of the onset of photo-chemical nucleation (laser-snow) in vapor
[AD-A150111] 12 p1801 N85-21295
Gas-liquid chemistry of natural waters, volume 1
[DE85-002603] 12 p1884 N85-21822
Gas-liquid chemistry of natural waters, volume 2
[DE85-002457] 12 p1884 N85-21823
Air quality criteria for ozone and other photochemical oxidants. External review draft, volume 4
[PB85-126068] 12 p1886 N85-21838
Chemical kinetics and photochemical data for use in stratospheric modeling. Evaluation number 6
[NASA-CR-175564] 12 p1888 N85-21849
Chemical stabilization of laser dyes
[AD-A150451] 13 p2096 N85-23076
Composition and photochemical reactivity of turbine engine exhaust
[AD-A150559] 13 p2130 N85-23256
A theoretical study of the ozone quasi-biennial oscillation in the tropical stratosphere 13 p2132 N85-23264
Investigation and optimization of fuel production using dye-based transition metal complexes as charge-transfer intermediates
[PB85-161941] 14 p2264 N85-24029
One-dimensional nonstationary model of photochemical transformations of gas impurities in stratosphere
14 p2342 N85-24484
Sensitization and quenching in the conversion of light energy into chemical energy
[DE85-006301] 14 p2351 N85-24535
Applications of photoinduced electron transfer and hydrogen abstraction reactions to chemical and electrochemical conversion processes
[DE85-006068] 15 p2506 N85-25459
Eight DOE Solar Photochemistry Research Conference: Proceedings
[DE85-005094] 15 p2587 N85-25948
Measurement of elements in the stratosphere
[NASA-CR-175891] 16 p2823 N85-27414
Free radicals in the stratosphere: A new observational technique 16 p2824 N85-27415
Effect of traffic and meteorology on air pollution
16 p2830 N85-27452
The enhancement of molecular fluorescence and photochemistry by small metal particles
[AD-A152740] 17 p2919 N85-27994
Photochemical ignition studies. 1: Laser ignition of flowing premixed gases
[AD-A153048] 17 p2920 N85-28002
Photochemistry of coordination complexes: The phthalocyanines
[DE85-007693] 17 p2923 N85-28022
Technique for measuring surface diffusion by laser-beam-localized surface photochemistry
[DE85-007865] 18 p3113 N85-29273
Impact of alcohol fuels on urban air pollution: Methanol photochemistry study
[DE85-009539] 18 p3133 N85-29403
Kinetics and intensity of photochemical processes in the atmosphere
[BPT-10/84] 18 p3134 N85-29411
Investigation of the reaction system NOX/ClOX/HOX under tropospheric and stratospheric conditions
[BPT-11/84] 18 p3137 N85-29427
Photochemical processes in the lower stratosphere (ozone layer) 18 p3148 N85-29490
Radiation damage and repair in cells and cell components. Part 2: Physical radiations and biological significance
[DE85-008934] 18 p3152 N85-29518
The diurnal variation of the neutral sodium species in the upper atmosphere: A model study
[AD-A154986] 21 p3631 N85-32561
Photochemical aerosol formation in polluted atmosphere 21 p3644 N85-32642
A study of time transformation of natural photochemical aerosols 21 p3645 N85-32644
Process for functionalizing alkanes
[DE85-006420] 23 p3909 N85-34219
Electron photoejection in carbanions
[DE85-011747] 23 p3911 N85-34230
Electron photoejection in carbanions
[DE85-011748] 23 p3912 N85-34237
The photodissociation of acetylene at 193.3 NM
[AD-A155775] 24 p4075 N85-35255
Vectorial electron transfer on designed surfaces
[PB85-204600] 24 p4076 N85-35263
Studies in photochemical smog chemistry. 1: Atmospheric chemistry of toulene. 2: Analysis of chemical reaction mechanisms for photochemical smog
24 p4113 N85-35497

PHOTOCHEMISTRY
U PHOTOCHEMICAL REACTIONS

PHOTOCHROMISM
Method for the preparation of photochromic insulating crystals
[DE85-011606] 19 p3262 N85-30229

PHOTOCLINOMETRY
U PHOTOGRAMMETRY

PHOTOCONDUCTIVE CELLS
Magnetic and photoconductive repetitive rail-gun opening switches
[DE84-017080] 04 p0496 N85-13163
A general purpose image processing package
23 p3961 N85-34549

PHOTOCONDUCTIVITY
Effect of light pulses on film of chalcogenide vitreous semiconductors 02 p0258 N85-11687
Photoconductivity and emission from the impurity excited states in silicon
[DE84-015563] 04 p0479 N85-13052
Advanced amorphous materials for photovoltaic conversion
[DE84-017198] 04 p0529 N85-13384
Real-time analysis of space characteristics of microwave electromagnetic pulse fields by means of controllable layer structures 07 p0955 N85-16052
Density of states and recombination in amorphous silicon (a-Si:H)
[BMFT-FB-T-84-216] 08 p1135 N85-17151
Studies on organic semiconductors. 15: Effects of the substituents on the photoconductivities of substituted anthracenes
[NASA-TM-77788] 08 p1225 N85-17712
Development of photoconductive power switch technology
[DE85-001514] 09 p1315 N85-18270
Optical memory research and its application to digital optical processing 13 p2158 N85-23397
Preparations of methoxynitrophenazines and their photoconductivities
[NASA-TM-77775] 14 p2247 N85-23929
Substituent effects on the electrical conductivities of the phenazine derivatives
[NASA-TM-77792] 14 p2249 N85-23938
Investigation of the MBE growth of InSb and novel quantum well structures
[AD-A151014] 14 p2427 N85-24969
Properties of defects in Hg(1-x)Cd(x)Te
[AD-A153243] 17 p3044 N85-28835
Picosecond photoconductive devices for 10 Gbit/s optoelectronic switching 18 p3187 N85-29770
Drift mobilities by time-of-flight methods and time-dependent phototransport in the nanosecond regime in amorphous semiconductors
[DE85-008729] 18 p3194 N85-29815
A study of Co and Mn in ZnO varistors
[DE85-011193] 19 p3263 N85-30233
Photoeffects of semiconductor electrolyte interfaces
[AD-A154163] 20 p3449 N85-31411
Electron irradiation of N type cadmium telluride
[AD-A156117] 24 p4161 N85-35801

PHOTOCONDUCTORS
Photocopiers: Do they pose a health hazard?
[P83-1E] 02 p0234 N85-11527
Effect of an underlayer of cadmium telluride on the reflection-reducing properties of zinc sulfide on mercury cadmium telluride
[AD-A146195] 03 p0414 N85-12649
Physics and design of advanced infrared bolometers and photoconductors
[DE84-016883] 04 p0503 N85-13213
Development of high responsivity GeGa photoconductors
[DE84-016902] 04 p0571 N85-13640
Development of photoconductive power switch technology
[DE85-001514] 09 p1315 N85-18270
Picosecond photoconductive devices for 10 Gbit/s optoelectronic switching 18 p3187 N85-29770
Photoconductive pulse power switches: A review
[DE85-014125] 24 p4091 N85-35360

PHOTOCURRENTS
U ELECTRIC CURRENT
U PHOTOELECTRIC EMISSION

PHOTODECOMPOSITION
The detection and study of molecular species using time resolved laser spectroscopy
[AD-A155910] 24 p4075 N85-35250

PHOTODETACHMENT
Characterization of multiphoton ionization processes in the ultraviolet
[AD-A151427] 15 p2652 N85-26054

PHOTODETECTORS
U PHOTOMETERS

PHOTODIODES
A concept for a hadron calorimeter with photodiode readout
[MPI-PAE/EXP-E1-130] 01 p0050 N85-10032
Improvements in photodiode readout for small CsI (Tl) crystals
[MPI-PAE/EXP-E1-131] 01 p0051 N85-10033
Fine grained hodoscopes based on scintillating optical fibers
[DE84-014649] 01 p0120 N85-10825
Pulsed irradiation of optimized, MBE grown, AlGaAs/GaAs radiation hardened photodiodes
[DE84-014984] 04 p0569 N85-13631
Avalanche photodiode statistics in triggered-avalanche detection mode 05 p0623 N85-13987
Study in spurious sensitivity of electronics in space
[AD-A148386] 08 p1158 N85-17305
The use of self-scanned silicon photodiode arrays for astronomical spectrophotometry
08 p1252 N85-17907
Photodiodes for astronomical stellar radiometry
08 p1252 N85-17908
GaAlAs Sb APD optimization
[AD-A149406] 10 p1480 N85-19344
Linear, position-sensitive X-ray detector used for real-time calculations of small-angle scattering parameters with submillisecond resolution
[DE85-002530] 10 p1489 N85-19401
Focal plane array optical proximity sensor
[NASA-CASE-NPO-15155-1] 12 p1932 N85-22130
Optoacoustic receiver with semiconductor-type radiator and photodetector 14 p2274 N85-24086
OMEGA: An optronic device to measure the incidence angle of a projectile
[ISL-CO-207/83] 14 p2306 N85-24274
Photon detection with cooled avalanche photodiodes: Theory and preliminary experimental results
16 p2770 N85-27096
Self-scanning MDS-integrated photosensor strip
17 p2940 N85-28151
Rifa of Sweden conducts research in 3-5 materials
18 p3066 N85-29107
Development of photodetectors
[AD-A153773] 18 p3095 N85-29158
Summary of recent studies on AlGaAs/GaAs radiation hardened photodiodes
[DE85-009501] 18 p3194 N85-29812
Noise characteristics of an avalanche photodiode
[AD-A154096] 19 p3258 N85-30205
Particle sizing from forward scattered light at two angles using a Variable-Focal-Length optical system
[AD-A154164] 20 p3533 N85-31980
Application of photodiodes to the detection of electromagnetic bursts 24 p4189 N85-35986

PHOTODISSOCIATION
Solar radiation in the ozone layer
04 p0522 N85-13342
Theoretical studies of highly ionized species
[DE84-016797] 04 p0561 N85-13574
Laboratory studies of atomic collision processes of importance in planetary atmospheres
[NASA-CR-174142] 04 p0589 N85-13759
Excimer laser photofragmentation of organophosphonates. 1: Detection of the PO radical from dimethyl methyl phosphonate (DMMP)
[AD-A149471] 10 p1490 N85-19407
Aeronomical aspects of mesospheric photodissociation: Processes resulting from the solar H Lyman alpha line
[AERONOMICA-ACTA-A-285-1984]
11 p1660 N85-20587
Multiple product channels in the collision free UV photodissociation of 2-nitropropane
[AD-A150886] 14 p2251 N85-23951

The source of stratospheric NO and N2O
[NASA-CR-175713] 15 p2588 N85-25956
Atmospheric chemistry
[INPE-3190-PRE/554] 16 p2626 N85-27430
Cometary atmospheres: Modeling the spatial distribution of observed neutral radicals
[NASA-CR-175852] 16 p2882 N85-27781
Crossed molecular beam studies of the reactions of oxygen and fluorine atoms
[AD-A153302] 17 p2921 N85-28006
Adiabatic approach in the theory of polyatomic photodissociation: Application to C2N2
[DE85-006515] 18 p3071 N85-28996
Quantitative studies for photoabsorption and fluorescence of HCl
[NASA-CR-175965] 19 p3233 N85-30043
Photoabsorption and photodissociation of molecules important in the interstellar medium
[NASA-CR-175918] 19 p3383 N85-30986
Radiative augmented combustion
[AD-A154137] 20 p3423 N85-31246
Optical inhomogeneities in a nanosecond-pulse iodine photodissociation laser with slow UV radiation pumping
21 p3686 N85-32902
Multiphoton production and detection of atoms
[AD-A155561] 21 p3702 N85-33000
Photofragment fluorescence as a sensitive probe for gas-phase alkali compounds and their photochemistry
[DE85-010707] 22 p3746 N85-33219
The photodissociation of acetylene at 193.3 NM
[AD-A155775] 24 p4075 N85-35255
High-resolution spectroscopy and dynamics of multiphoton processes in atoms and molecules
[AD-A155862] 24 p4147 N85-35714

PHOTOELASTICITY
NT PHOTOVISCOELASTICITY
Stress analysis of pin-loaded orthotropic plates using orthotropic photoelasticity 02 p0207 N85-11366
CFM 56-2. Oligocyclic fatigue of the turbofan disk: Dimensionning and tests for verification and improvements 07 p0908 N85-15750
Stresses in pin-loaded orthotropic plates using photoelasticity
[NASA-CR-172498] 07 p0977 N85-16204
Stress concentration due to axial tension of loaded nonsymmetric-shaped grooves
[AD-A149425] 10 p1496 N85-19442
Root stresses in conformal gears-strain gauge and photoelastic investigations 14 p2223 N85-23787
Stress concentration in the elastoplastic state and residual stress after unloading
[AD-A155628] 21 p3600 N85-32356

PHOTOELECTRIC CELLS
NT PHOTOCONDUCTIVE CELLS
NT PHOTOVOLTAIC CELLS
Photoelectric effect in liquid crystals
02 p0259 N85-11695
Efficiency of photoelectric conversion of short radiation pulses 03 p0348 N85-12240
CuInSe2-based photoelectrochemical cells: Their use in characterization of thin CuInSe2 films, and as photovoltaic cells per se
[DE84-004514] 04 p0529 N85-13379
A two photoelectrode solid-state photoelectrochemical cell
[AD-A148982] 10 p1434 N85-19038
Small aperture analysis of the dual TEM (transverse electromagnetic) cell and an investigation of test object scattering in a single TEM cell
[PB85-159952] 14 p2306 N85-24277
Applications of photoinduced electron transfer and hydrogen abstraction reactions to chemical and electrochemical conversion processes
[DE85-006068] 15 p2506 N85-25459
Performance evaluation of fiber-optic converters
17 p2941 N85-28154
High-pressure optical cell
[AD-A153639] 18 p3185 N85-29754
Polymer blends for use in photoelectrochemical cells for conversion of solar energy to electricity
[DE85-011602] 22 p3752 N85-33258
Method and apparatus for measuring areas of photoelectric cells and photoelectric cell performance parameters
[DE85-011629] 22 p3810 N85-33599

PHOTOELECTRIC EFFECT
NT PHOTOIONIZATION
Photoelectric effect in liquid crystals
02 p0259 N85-11695
Determining composition in surface region of semiconductor crystals by method of sudden changes in X-ray photoelectric effect 02 p0267 N85-11746
Fundamental molecular physics and chemistry, part 1
[DE84-009127] 04 p0561 N85-13571
Test results from a comparative evaluation of a condensation nuclei fire detector
[NASA-CR-3874] 12 p1862 N85-21675
Transducer of linear displacements
14 p2281 N85-24130

PHOTOELECTRIC EMISSION
Photocurrent oscillations in Bi12GeO20 metal-semiconductor-metal structures
02 p0266 N85-11741
Investigation of effect of photocurrent amplification in meta-dielectric-semiconductor structures based on silicon 04 p0488 N85-13110
Surface structure determination with ARPEFS
[DE84-016904] 04 p0571 N85-13644
Supercell band structure calculations of the two peak photo-and inverse photoemission spectra in Ce and Pr compounds
[DE84-017485] 06 p0867 N85-15513
Study in molecular lasers
[AD-A148246] 08 p1166 N85-17357
Photoemission, vibrational and stimulated desorption studies of metal-semiconductor interfaces and of chemisorbed atoms and molecules
[AD-A147709] 08 p1225 N85-17717
A statistical evaluation of the limitations of single-channel intermediate-band photoelectric stellar photometry 08 p1251 N85-17900
S-11 and S-20 photocathode research activity, revision 1
[DE84-017164] 09 p1326 N85-18335
Temperature-dependent surface states and transitions of Si(111)-7x7
[AD-A149156] 10 p1562 N85-19850
Ion implanted lateral in 2Ga 8As/GaAs strained-layer superlattice photodector
[DE85-001365] 10 p1563 N85-19859
Operating time meter for tape recorder
12 p1836 N85-21537
Angle-resolved photoemission study of AuGa2 and AuIn2 intermetallic compounds
[AD-A150000] 12 p1940 N85-22183
Multiport optical detectors 18 p3187 N85-29769
Dual optical mechanical position tracker
[AD-D011739] 22 p3844 N85-33811
Noble metals as incipient transition metals
[DE85-013283] 24 p4080 N85-35286
Exit channels of autoionization resonances in atoms
[DE85-012299] 24 p4149 N85-35726
Ionic crystals
[DE85-009482] 24 p4163 N85-35809

PHOTOELECTRIC GENERATORS
Space power plants 16 p2724 N85-26813

PHOTOELECTRIC MATERIALS
Increased voltage photovoltaic cell
[NASA-CASE-NPO-16155-1] 19 p3303 N85-30475
High-brightness photoemitter development for electron accelerator injectors
[DE85-009548] 19 p3355 N85-30796
Practical aspects of photovoltaic technology, applications and cost (revised)
[NASA-CR-174963] 24 p4110 N85-35472

PHOTOELECTRIC PHOTOMETERS
U ELECTROPHOTOMETERS

PHOTOELECTROCHEMICAL DEVICES
Research on photoelectrochemical cells based on CdSe, CdSe/sub 1-x/te/sub x and other photoelectrode materials
[DE84-004527] 02 p0224 N85-11466
CuInSe2-based photoelectrochemical cells: Their use in characterization of thin CuInSe2 films, and as photovoltaic cells per se
[DE84-004514] 04 p0529 N85-13379
Method for determining the point of zero zeta potential of semiconductor
[NASA-CASE-LAR-12893-1] 19 p3373 N85-30923

PHOTOELECTROCHEMISTRY
Research on photoelectrochemical cells based on CdSe, CdSe/sub 1-x/te/sub x and other photoelectrode materials
[DE84-004527] 02 p0224 N85-11466
Photoelectrochemistry with chemically modified electrodes
[DE84-016796] 04 p0471 N85-12997
Luminescent properties of graded cadmium sulfoselenide electrodes prepared from cadmium sulfide substrates
[AD-A146710] 06 p0766 N85-14898
A two photoelectrode solid-state photoelectrochemical cell
[AD-A148982] 10 p1434 N85-19038
Photoelectrochemical reduction of carbon dioxide
[PB85-129054] 11 p1596 N85-20036
Solar-assisted hydrogen generation by photoelectrocatalysis
[PB85-149706] 12 p1804 N85-21314
The electrochemistry of azine, oxazine and thiazine dyes
[AD-A152394] 17 p2918 N85-27990
Photoeffects of semiconductor electrolyte interfaces
[AD-A154163] 20 p3449 N85-31411

PHOTOELECTROMAGNETIC DETECTORS
U PHOTOELECTROMAGNETIC EFFECTS
U RADIATION MEASURING INSTRUMENTS

PHOTOELECTROMAGNETIC EFFECTS
Photoelectric effect in liquid crystals
02 p0259 N85-11695

PHOTOELECTRON SPECTROSCOPY
The effect of thin-film growth mode on XPS/UPS/AES intensities
[AD-A146264] 03 p0434 N85-12763
Electron spectrometry experiments with the use of synchrotron radiation
[DE85-001286] 07 p1041 N85-16610
Photoionization of excited molecular states
[DE84-017454] 09 p1291 N85-18103
Characterization of CO binding sites on Rh(111) and Rh(331) surfaces by XPS and LEED (Low Energy Electron Diffraction): Comparison to EELS (Electron Energy Loss Spectroscopy) results
[AD-A149331] 10 p1435 N85-19044
Studies of silicon-refractory metal interfaces: Photoemission study of interface formation and compound nucleation
[AD-A150075] 12 p1800 N85-21293
Some unique aspects of fouling on copper as compared to titanium or nickel
[AD-A150072] 12 p1806 N85-21332
The Valence- and conduction-band structure of the sapphire (1102) surface
[AD-A150001] 12 p1940 N85-22184
Workshop report on new directions in soft X-ray photoabsorption
[DE85-006150] 14 p2419 N85-24923
Spectroscopy of surface adsorbed molecules
[DE85-009452] 17 p3034 N85-28768
Materials-process interactions in ternary alloy semiconductors
[AD-A153133] 17 p3043 N85-28832
The photochemical oxidation of GaAs
[AD-A153689] 19 p3233 N85-30045
Chemical structure of interfaces
20 p3480 N85-31629
Photoelectron studies of autoionizing Rydberg states in HCl
[DE85-011813] 21 p3702 N85-33001
Experimental studies of the geometric and electronic structure of chemisorption bonding
[PB85-192250] 22 p3747 N85-33228
Heats of formation of gas phase organosulfur molecules, radicals and ions measured by PEPICO and application of (17)O and (33)S NMR spectroscopy to structure determination of organosulfur compounds
[DE85-010558] 24 p4071 N85-35229

PHOTOELECTRONICS
U ELECTRONICS

PHOTOELECTRONS
Ionospheric electron density profile and related studies
[AD-A155257] 21 p3632 N85-32567

PHOTOEMISSION
U PHOTOELECTRIC EMISSION

PHOTOEMISSIVITY
U EMISSIVITY
U PHOTOELECTRIC EMISSION

PHOTOEMITTERS
U PHOTOELECTRIC MATERIALS

PHOTOGEOLOGY
Seismotectonic nature of some annular photoanomalies registered by remote methods 02 p0164 N85-11110
Predicting fracturing zones in Caspian depression subsalt deposits on basis of space information and geological-geophysical data 02 p0164 N85-11111
Assessment of computer techniques for processing digital LANDSAT MSS data for lithological discrimination of Serra do Ramalho, State of Bahia
[E85-10033] 03 p0378 N85-12412
Report of the field work performed in the Basins of the Quebra Osso and Tanque Petro Rivers in the Catas Altas quadrangle, Minas Gerais
[INPE-3268-NTE/225] 04 p0525 N85-13359
A preliminary evaluation of LANDSAT-4 Thematic Mapper data for their geometric and radiometric accuracies 12 p1871 N85-21739
LANDSAT 4 investigations of Thematic Mapper and Multispectral Scanner applications -- Drum Mountains, Utah and Tonopath, Nevada
[E85-10095] 12 p1874 N85-21757
Evaluation of Thematic Mapper performance as applied to hydrocarbon exploration -- Ontario, Canada; Cement, Oklahoma; and Death Valley, California
13 p2118 N85-23191

Geologic utility of LANSDAT-4 TM data --- Death Valley, California and the Silver Bell area of southern Arizona
13 p2118 N85-23192

Assessment of computer based geologic mapping of rock units in the LANDSAT-4 scene of northern Death Valley, California 13 p2119 N85-23195

Geologic interpretation of remote sensing data for the Martian volcano, Ascraeus Mons
13 p2194 N85-23606

The deep structure of lunar basins: Clues to the understanding of basin formation and modification
13 p2200 N85-23647

Mars geologic mapping: A review and new concepts
13 p2202 N85-23663

Example of joint use of data from surface studies and space photographs in investigating dynamics of zone of North Zeravshan seismogenic faults
15 p2485 N85-25342

Relative geological information yield from small-scale multizonal space images (example of Fergama depression and its mountainous margins) 15 p2485 N85-25343

Function of remote sensing in Brazil
[INPE-3314-PRE/621] 16 p2810 N85-27329

Space methods for geological research
19 p3295 N85-30429

Geologic interpretation of remote sensing data for the Martian volcano Ascraeus Mons
19 p3384 N85-30992

Quantitative geomorphologic studies from spaceborne platforms 21 p3604 N85-32381

Use of space photographs for analysis of structural and dynamic conditions of formation of ancient phlogopite and apatite deposits 22 p3736 N85-33153

Using remote photographs in prospecting for hydrocarbons on the Kerch Peninsula
22 p3735 N85-33154

Geology and geomorphology of the Roraima group, southeastern Venezuela 24 p4115 N85-35511

PHOTOGONIOMETERS

Influence of geometric conditions on the indicatrix of reflection of the perfect reflecting diffuser
[PTB-OPT-16] 03 p0420 N85-12686

Status of and outlook for producing means of transmitting units of plane angle, angular velocity and acceleration with ring lasers 13 p2074 N85-22955

PHOTOGRAMMETRY

Single viewpoint self calibration: A contribution to field calibration of recording chambers
[SER-C-289] 01 p0049 N85-10320

Initial feasibility ground test of a proposed photogrammetric system for measuring the shapes of ice accretions on helicopter rotor blades during forward flight
[NASA-TM-87391] 04 p0455 N85-12887

The photogrammetric camera experiment on Spacelab 1 05 p0658 N85-14230

Papers of the 15th International Society for Photogrammetry and Remote Sensing (ISPRS) Congress --- conferences
[TRITA-FMI-9] 08 p1175 N85-17406

Mathematical aspects of digital terrain information; Report from International Society for Photogrammetry and Remote Sensing (ISPRS) working group 3:3, 1980 - 1984 --- photogrammetry 08 p1175 N85-17407

A comparative test of photogrammetrically sampled digital elevation models 08 p1175 N85-17408

Multimodels increase accuracy: Summary of an experiment --- photogrammetry
08 p1175 N85-17409

Hierarchical data structures and algorithms for digital stereoscopical mensuration 08 p1175 N85-17410

An efficient algorithm for the computation of the inverse in bundle adjustment systems --- photogrammetry
08 p1175 N85-17411

Digital elevation model computation using fast Poisson solutions 08 p1175 N85-17412

Sequential data processing for photogrammetric acquisition of digital elevation models
08 p1176 N85-17413

Processing of underwater photographs
10 p1499 N85-19462

Earth resources: A continuing bibliography with indexes
[NASA-SP-7041(44)] 10 p1503 N85-19484

Radar calibration using direct measurement equipment and oblique photometry
[AD-D011530] 12 p1822 N85-21433

Hybrid method of mapping and photogeodetic control network densification
[PB85-133775] 12 p1876 N85-21766

Evaluating accuracy in orientation of topographic photograph and satellite-centered direction from star photograph 13 p1983 N85-22442

A unified lunar control network
13 p2203 N85-23669

The control network of Mars: October 1984
13 p2203 N85-23670

The control networks of the satellites of Jupiter and Saturn 13 p2204 N85-23671

Shape of Io 13 p2204 N85-23672

One aspect of determination of direction of space survey base from photographs of planetary surface and star sky
15 p2487 N85-25352

Minimizing influence of Earth's curvature in projective rectification of space photographs into photoplans and photomaps 16 p2727 N85-26829

Use of vector processors in cartographic raster data processing, with special regard to the AP-120B vector processor 16 p2814 N85-27358

Standards and specifications for geodetic control networks
[PB85-166478] 16 p2816 N85-27374

Investigations of the accuracy of the Digital Photogrammetry System (DPS), a rigorous three-dimensional compilation process for pushbroom imagery
[MBB-UA-753/83-O] 16 p2874 N85-27734

German contributions to the cartography of Antarctica by means of photogrammetry and remote sensing
18 p3124 N85-29342

Comparison of survey and photogrammetry methods to position gravity data, Yucca Mountain, Nevada
[DE85-011685] 21 p3590 N85-32316

Coastal erosion along Monterey Bay
[AD-A155610] 21 p3655 N85-32707

Production of initial estimates of photogrammetric variables
[NPL-MOM-66] 23 p3943 N85-34434

Parametric stability of analytical close-range photogrammetry 24 p4107 N85-35461

Evaluation: Close-range photogrammetry for slope inventory and monitoring
[PB85-192755] 24 p4108 N85-35470

PHOTOGRAPH INTERPRETATION
U PHOTOINTERPRETATION

PHOTOGRAPHIC EMULSIONS
NT NUCLEAR EMULSIONS

Astronomical photography 1984 --- conferences
[ROE-OR-14] 07 p0962 N85-16102

A spectrosensitometer with an absolute calibration
07 p0963 N85-16106

Comparison of the fine grain compensation hypersensitization (FAH) process with gas hypersensitizing techniques --- astronomical photography plates
07 p0963 N85-16107

The results of hydrogen hypersensitization of photoemulsions --- astronomical photography
07 p0963 N85-16108

The most effective astronomical photographic emulsions for recording of faint and low-contrast objects
07 p0963 N85-16110

Astronomical applications of new infrared films
07 p0964 N85-16111

The 3a-F emulsion and the quasar redshift cut-off
07 p0964 N85-16112

Microspots on spectroscopic plates --- astronomical photography 07 p0964 N85-16113

Where to next in astronomical photography? --- tabular grain emulsions 07 p0964 N85-16114

What do we want: Increased speed, resolution, contrast or DOE? --- astronomical photography
07 p0964 N85-16115

The Malin effect in stellar photography
07 p0966 N85-16131

A quantitative image evaluation study of a concurrent photon amplification treated emulsion
[AD-A151831] 15 p2560 N85-25796

PHOTOGRAPHIC EQUIPMENT
NT BALLISTIC CAMERAS
NT CAMERAS
NT FRAMING CAMERAS
NT HIGH SPEED CAMERAS
NT MULTISPECTRAL BAND CAMERAS
NT PANORAMIC CAMERAS
NT PHOTOGRAPHIC PROCESSING EQUIPMENT
NT PINHOLE CAMERAS
NT SCHMIDT CAMERAS
NT STREAK CAMERAS
NT TELEVISION CAMERAS

Vapor-screen technique for flow visualization in the Langley Unitary Plan Wind Tunnel
[NASA-TM-86384] 19 p3214 N85-29929

PHOTOGRAPHIC FILM
NT MICROFILMS

The calibration of photographic and spectroscopic films: A densitometric analysis of IIaC film flown aboard the Space Shuttle 3
[NASA-CR-174278] 07 p0962 N85-16101

FLACS: A new sensitometer for measurement of extreme low intensity reciprocity in a controlled environment --- X-ray films 07 p0963 N85-16104

Astronomical applications of new infrared films
07 p0964 N85-16111

Infrared presensitization photography
[AD-A146968] 07 p0967 N85-16139

S-11 and S-20 photocathode research activity, revision 1
[DE84-017164] 09 p1326 N85-18306

Development and application of low energy X-ray and electron physics
[AD-A149963] 12 p1926 N85-22090

Prediction of the long term stability of polyester-based recording media
[PB85-160133] 14 p2262 N85-24019

Astrometry of comets using hypersensitized type 2415 film 14 p2435 N85-25021

Electronic detection and concealment of film dirt
[BBC-RD-1985/4] 15 p2538 N85-25967

Method and apparatus for high speed, sustained recording of infrared laser beam patterns
[AD-D011585] 15 p2563 N85-25811

Infrared presensitization photography
16 p2786 N85-27180

High sensitive X-ray films to detect electron showers in 100 GeV region
[HE-3.1-13] 24 p4178 N85-35911

X-ray film chamber with carbon target of Tien-Shan complex array 24 p4179 N85-35915

The Nagoya cosmic-ray muon spectrometer 3, part 3: Automatic film scanning equipment
[HE-5.2-4] 24 p4202 N85-36082

PHOTOGRAPHIC MEASUREMENT
NT PHOTOGRAMMETRY

Spectroscopic data for globular cluster giants. 1: Stars of the red giant tip 01 p0128 N85-10965

Variability of Neptune 02 p0299 N85-11938

Holographic assembly for measuring velocity fields of supersonic ballistic splinters at a large distance
[ISL-CO-203/84] 20 p3459 N85-31487

PHOTOGRAPHIC PLATES

SENSIT.FOR: A program for sensitometric reduction
07 p0963 N85-16105

Nitrogen flushing during exposure of large Schmidt telescope plates 07 p0963 N85-16109

Microspots on spectroscopic plates --- astronomical photography 07 p0964 N85-16113

Using a Gossen light meter to produce enlarged interpositive film copies from glass plates --- astronomical photography 07 p0964 N85-16118

Processing of photographic observing material at the National Astronomical Observatory Rozhen
07 p0965 N85-16120

The UK Schmidt telescope and the facilities in Edinburgh 07 p0965 N85-16121

An investigation into the fidelity of reproduction of UKST original objective prism plates on to film --- United Kingdom Schmidt Telescope (UKST) 07 p0965 N85-16123

Extending magnitude standards to faint stars with a sub-beam prism 07 p0965 N85-16124

Astronomers' problems with the calibration of Schmidt plates 07 p0965 N85-16126

Power spectrum analysis of astronomical photographs digitised with small apertures 07 p0965 N85-16127

Plate measurements and reductions at Muenster --- astronomical photography 07 p0966 N85-16129

The Malin effect in stellar photography
07 p0966 N85-16131

Stellar photographic photometry using a double wedge technique with a focal reducer system
07 p0966 N85-16133

Spectrophotometry of cool stars from objective prism spectra 07 p0966 N85-16134

Digital laser platemaker modifications
[AD-A150190] 13 p2096 N85-23074

Astrometric plates obtained at the primary focus of large aperture reflectors 14 p2436 N85-25022

The astrometry network of observers in USSR
14 p2436 N85-25029

Least squares reduction technique
14 p2437 N85-25036

Reduction of astrometric plates
14 p2437 N85-25037

PHOTOGRAPHIC PROCESSING

Comparison of the fine grain compensation hypersensitization (FAH) process with gas hypersensitizing techniques --- astronomical photography plates
07 p0963 N85-16107

The results of hydrogen hypersensitization of photoemulsions --- astronomical photography
07 p0963 N85-16108

Nitrogen flushing during exposure of large Schmidt telescope plates 07 p0963 N85-16109

Some aspects of photography with a small Schmidt camera --- astronomical photography
07 p0964 N85-16116

Using a Gossen light meter to produce enlarged interpositive film copies from glass plates --- astronomical photography
07 p0964 N85-16118

Unsharp masking at the enlarger --- astronomical photography
07 p0964 N85-16119

Processing of photographic observing material at the National Astronomical Observatory Rozhen
07 p0965 N85-16120

The work of the photolabs at the Royal Observatory, Edinburgh --- astronomical photography
07 p0965 N85-16122

Cometary astrometry with Schmidt cameras
14 p2435 N85-25020

PHOTOGRAPHIC PROCESSING EQUIPMENT

Photo-reconnaissance system
[AD-D011287] 06 p0826 N85-15245

Processing of photographic observing material at the National Astronomical Observatory Rozhen
07 p0965 N85-16120

The work of the photolabs at the Royal Observatory, Edinburgh --- astronomical photography
07 p0965 N85-16122

PHOTOGRAPHIC RECORDING

Single viewpoint self calibration: A contribution to field calibration of recording chambers
[SER-C-289] 01 p0049 N85-10320

Preliminary results using a rapid photographic wake traverse system --- in a wind tunnel
[RAE-TM-AERO-1987] 02 p0200 N85-11332

Recording holograms on thin films of titanium dioxide
06 p0789 N85-15039

PHOTOGRAPHS

NT MARS PHOTOGRAPHS
NT MOTION PICTURES
NT PHOTOMICROGRAPHS

Problem of determining highly accurate coordinates of artificial satellites by photographic methods
02 p0162 N85-11096

Initial feasibility ground test of a proposed photogrammetric system for measuring the shapes of ice accretions on helicopter rotor blades during forward flight
[NASA-TM-87391] 04 p0455 N85-12887

Direct-strike lightning photographs, swept-flash attachment patterns, and flight conditions for storm hazards 1982
[NASA-TM-86347] 12 p1892 N85-21877

Near-nucleus studies of Comet Halley
14 p2435 N85-25018

NASA photography index
[NASA-TM-87457] 15 p2665 N85-26445

Vapor-screen technique for flow visualization in the Langley Unitary Plan Wind Tunnel
[NASA-TM-86384] 19 p3214 N85-29929

Cultural data base implementation study and computer-aided scene modeling system users manual
[AD-A154232] 19 p3333 N85-30646

PHOTOGRAPHY

NT ACOUSTICAL HOLOGRAPHY
NT AERIAL PHOTOGRAPHY
NT ALL SKY PHOTOGRAPHY
NT ASTRONOMICAL PHOTOGRAPHY
NT AUTORADIOGRAPHY
NT BLACK AND WHITE PHOTOGRAPHY
NT CINEMATOGRAPHY
NT CLOUD PHOTOGRAPHY
NT COLOR INFRARED PHOTOGRAPHY
NT COLOR PHOTOGRAPHY
NT ELECTRO-OPTICAL PHOTOGRAPHY
NT FRACTOGRAPHY
NT HIGH SPEED PHOTOGRAPHY
NT HOLOGRAPHY
NT INFRARED IMAGERY
NT INFRARED PHOTOGRAPHY
NT LUNAR PHOTOGRAPHY
NT METRIC PHOTOGRAPHY
NT MICROWAVE HOLOGRAPHY
NT MULTISPECTRAL PHOTOGRAPHY
NT ORTHOPHOTOGRAPHY
NT PHOTOMICROGRAPHY
NT RADAR PHOTOGRAPHY
NT SATELLITE-BORNE PHOTOGRAPHY
NT SCHLIEREN PHOTOGRAPHY
NT SHADOWGRAPH PHOTOGRAPHY
NT SPACEBORNE PHOTOGRAPHY
NT STEREOPHOTOGRAPHY
NT STEREOSCOPY
NT STREAK PHOTOGRAPHY
NT ULTRAVIOLET PHOTOMETRY
NT UNDERWATER PHOTOGRAPHY
NT WHITE LIGHT HOLOGRAPHY

Geophysical experiments, photography aboard Salyut-7
02 p0157 N85-11066

Commentary on cosmonauts geological mapping, photography
02 p0158 N85-11069

Study of delamination cracking under static and cyclic loads of carbon-epoxy composite materials
[REPT-42-727/F] 03 p0327 N85-12102

Studies of ignition and combustion wave propagation in exothermic systems using high-speed photography
[DE84-016482] 04 p0471 N85-12995

Chemical and photographic evaluation of rigid explosive transfer lines
[AD-A149303] 11 p1613 N85-20145

Photorefractor ocular screening system
[NASA-CASE-MFS-28011-1SB]
11 p1692 N85-20639

Relationship between brightness spectrum of photographic image and spectrum of rises on a water surface with waves
13 p2115 N85-23171

Some new photometric data form panoramic pictures taken by Lunokhod-2
15 p2481 N85-25312

Test and evaluation of the 2.4-micron photorefractor ocular screening system
[NASA-TM-86492] 15 p2615 N85-26115

USSR report: Engineering and equipment
[JPRS-UEQ-85-004] 17 p2939 N85-28142

PHOTOINTERPRETATION

Method for interpreting soil cover of flowed fields using spectral brightnesses measured from space photographs
02 p0164 N85-11112

Utilization of LANDSAT orbital imagery in the soil survey processes at Rio Grande do Norte state
[E85-10009] 02 p0216 N85-11422

Executive report: Results of the IRGA-CNPq/INPE experimental project
[E85-10011] 02 p0216 N85-11424

Development and testing of a rural credit supervision system at the level of counties and rural properties utilizing remote sensing techniqes
[E85-10016] 02 p0217 N85-11431

Remote sensing for landforms and soils in the arid southwest United States
03 p0378 N85-12410

Integrated analysis of remote sensing products from basic geological surveys --- Brazil
[E85-10052] 07 p0984 N85-16248

Evidence accumulation for spatial reasoning
07 p0985 N85-16261

Forest area estimates from LANDSAT MSS and forest inventory plot data
[PB85-105617/GAR] 07 p0990 N85-16290

Assessment of LANDSAT for rangeland mapping, Rush Valley, Utah
[E85-10072] 10 p1503 N85-19486

LANDSAT 4 investigation of Thematic Mapper and Multispectral Scanner applications
[E85-10076] 10 p1504 N85-19490

Method for approximating autocorrelation functions for describing areal photoimage features
13 p1983 N85-22443

Experience in automated interpretation of aerospace photographs
13 p1983 N85-22444

Geoindication method for interpreting aerial and space photographs: Status and prospects
13 p1984 N85-22445

Experience in combined special mapping using space information
13 p1984 N85-22449

Combined analysis of the dynamics of complex ecosystems based on repeated remote measurements
13 p1985 N85-22450

Overview of TM applications research reports
13 p2117 N85-23187

Preliminary study of information extraction of LANDSAT TM data for a suburban/regional test site
13 p2121 N85-23208

Identifying land use structures of multizonal aerospace photographs using digital data processing
15 p2486 N85-25348

Interpretation of space photolineaments
15 p2487 N85-25353

Shuttle imaging radar-B (SIR-B) data analysis for identifying rainfall event occurrence and intensity
[NASA-CR-175712] 15 p2594 N85-25986

Documentation of PHOTO: A user's manual for the analysis of photographic and X-ray negatives
[AD-A152988] 17 p2967 N85-28327

Airphoto interpretation of vegetation and landforms for soil mapping
17 p2983 N85-28436

Air photo analysis, photo interpretation logic, and feature extraction
[AD-A153926] 18 p3124 N85-29347

Geologic interpretation of remote sensing data for the Martian volcano Ascraeus Mons
19 p3384 N85-30992

Handbook for obtaining and using aerial photography to map aquatic plant distribution
[AD-A154584] 21 p3605 N85-32368

PHOTOIONIZATION

Magnetic resonance studies of transient radicals and radical ions
[DE84-011699] 03 p0328 N85-12116

Physico-chemical investigation of some areas of fundamental significance to biophysics
[DE84-016385] 04 p0471 N85-12999

Multiphoton ionization of benzene in solution
[DE85-000893] 06 p0786 N85-14899

Photoionization structure of the Orion Nebula
08 p1246 N85-17863

Photoionization of excited molecular states
[DE84-017454] 09 p1291 N85-18103

Time-resolved studies of free radicals and laser-initiated chain reactions
[DE85-002100] 09 p1326 N85-18332

Multiphoton ionization of atomic cesium
[DE85-001266] 09 p1380 N85-18678

Multiphoton ionization of cesium atoms above and below the two-photon ionization threshold
[DE85-000976] 09 p1381 N85-18682

Effects of dc electric fields on multiphoton ionization spectra in cesium
[DE85-001542] 09 p1381 N85-18684

State-selected ion-molecule reaction dynamics
[AD-A150068] 12 p1928 N85-22115

Threshold double photoionization of argon with synchrotron radiation
[AD-A150615] 13 p2157 N85-23389

Workshop report on new directions in soft X-ray photoabsorption
[DE85-006150] 14 p2419 N85-24923

Experimental and theoretical studies of laser cooling and emittance control of neutral beams
[AD-A149215] 15 p2562 N85-25804

Kinetic energies of fragment ions produced by dissociative photoionization of NO
[NASA-CR-175721] 15 p2647 N85-26327

Characterization of multiphoton ionization processes in the ultraviolet
[AD-A151427] 15 p2652 N85-26354

Photoionization mass spectrometry with VUV hydrogen laser source
[AD-A153382] 17 p2921 N85-28009

An ultrasensitive and element specific photoionization detection system for environmental analysis
[AD-A153365] 17 p2968 N85-28332

Experimental study of dissociative attachment in optically-pumped lithium molecules
[AD-A152800] 17 p3030 N85-28738

Development of a technique for in situ detection of stratospheric nitrogen dioxide
19 p3312 N85-30534

Many-body processes in atomic and molecular physics
[DE85-009750] 19 p3354 N85-30791

Ionospheric electron density profile and related studies
[AD-A155257] 21 p3632 N85-32567

Activities of the Physics Division
[DE85-000784] 21 p3702 N85-33002

Photoionization of alkali and alkaline earth atoms: Na and Mg
[DE85-011812] 22 p3837 N85-33755

Photoionization-pumped, Ne 2, X-ray laser studies project
[DE85-012973] 23 p3936 N85-34399

Heats of formation of gas phase organosulfur molecules, radicals and ions measured by PEPICO and application of (17)O and (33)S NMR spectroscopy to structure determination of organosulfur compounds
[DE85-010556] 24 p4071 N85-35229

Dissociative and double photoionization cross sections of NO from threshold to 120 A
[NASA-CR-176185] 24 p4147 N85-35713

High-resolution spectroscopy and dynamics of multiphoton processes in atoms and molecules
[AD-A155862] 24 p4147 N85-35714

Exit channels of autoionization resonances in atoms
[DE85-012299] 24 p4149 N85-35726

PHOTOLITHOGRAPHY

Low-threshold injection lasers on grown GaInPAs/InP heterostructures (1.2-1.6 micrometers wavelengths)
02 p0258 N85-11693

Exposure modelling of particle beam lithography
[AD-A147849] 08 p1219 N85-17678

Thin film transistors for addressing flat panel displays
[BMFT-FB-T-84-210] 08 p1227 N85-17726

Basic development of a 1.5 micrometer very large scale integrated technique, part 1-4
[BMFT-FB-T-85-032-PT-1-4] 20 p3449 N85-31417

PHOTOLUMINESCENCE

NT X RAY FLUORESCENCE

Photoluminescent properties of epitaxial p-GaSb
02 p0267 N85-11745

Advanced amorphous materials for photovoltaic conversion
[DE84-017198] 04 p0529 N85-13384

Photoluminescence studies of Ga(As,P) strained-layer superlattices
[DE84-015709] 05 p0731 N85-14701

Luminescent properties of graded cadmium sulfoselenide electrodes prepared from cadmium sulfide substrates
[AD-A146710] 06 p0766 N85-14896
Characterization of III-V compound semiconductor device materials
[AD-A148205] 08 p1226 N85-17719
Infrared modulation of photoluminescence in glow discharge amorphous silicon
[DE85-016993] 11 p1737 N85-20922
Investigation of the MBE growth of InSb and novel quantum well structures
[AD-A151014] 14 p2427 N85-24969
Electrogenerated chemiluminescence
[AD-A153547] 18 p3070 N85-28990
Sea water photoluminescence
19 p3292 N85-30415
A theory of exciton photoluminescence for two types of neutral acceptors in silicon. A study of the systems Si:(B, IN), Si:(Al), (Si), Si:(Ga, In), Si:(B, Al), Si:(B, Ga), and Si:(Al, GA)
[AD-A155452] 21 p3710 N85-33031

PHOTOLUMINESCENT BANDS
Formation of lattice defects by nitrogen laser exposure in A2B6 semiconductors with wide forbidden band
02 p0258 N85-11692

PHOTOLYSIS
NT RADIOLYSIS
Laser-assisted solar-cell metallization processing
06 p0831 N85-15282
Synthesis, static and reactive characterization of supported organometallics
[DE85-004285] 12 p1808 N85-21340
Multiple product channels in the collision free UV photodissociation of 2-nitropropene
[AD-A150666] 14 p2251 N85-23951
The source of stratospheric NO and N2O
[NASA-CR-175713] 15 p2588 N85-25956
In-situ stratospheric ozone measurements: Recent results and their implications 16 p2824 N85-27419
Water vapor 16 p2824 N85-27420
Photochemical ignition studies. 1: Laser ignition of flowing premixed gases
[AD-A153046] 17 p2920 N85-28002
The spectroscopy and reaction kinetics of coordinated unsaturated metal carbonyls
[AD-A153079] 17 p2920 N85-28003
Kinetics of hydrolysis and products of hydrolysis and photolysis of tetryl
[AD-A153144] 17 p2921 N85-28005
Study of the formation of sulfuric acid aerosols
[DE85-006102] 17 p2922 N85-28011
Kinetics and intensity of photochemical processes in the atmosphere
[BPT-10/84] 18 p3134 N85-29411
Lifetime and quenching measurements of C2H emission produced by vacuum ultraviolet photolysis of C2H2
[DE85-010769] 19 p3278 N85-30330
Photofragment fluorescence as a sensitive probe for gas-phase alkali compounds and their photochemistry
[DE85-010707] 22 p3746 N85-33219

PHOTOMAPPING
Choice of cartographic projection for space system data bank used in studying natural resources
02 p0165 N85-11119
Study of Volga river delta using space photosurvey materials 15 p2485 N85-25340
Use of space photographic information to map plant cover 15 p2486 N85-25359
Minimizing influence of Earth's curvature in projective rectification of space photographs into photoplans and photomaps 16 p2727 N85-26829
Information relative to cartography and geodesy. Series 2: Translations, number 42, volume 1
[ISSN-0469-4244] 18 p3123 N85-29338
Two satellite image maps of Central Europe
18 p3123 N85-29339
Digital image mapping of Antarctica using NOAA-7 AVHRR imagery 18 p3124 N85-29340
The significance of orthophoto maps for developing countries 18 p3124 N85-29341
Mapping of dynamics of deltas by space photography
22 p3737 N85-33163
Comprehensive mapping of arid territories of Arizona using space photography 22 p3737 N85-33164

PHOTOMAPS
Preliminary photomaps of Venus surface in the Maxwell Mountains and adjacent areas 13 p1982 N85-22438
What does digital image processing perform in the production of orthophotomaps 16 p2615 N85-27368
Information relative to cartography and geodesy. Series 2: Translations, Number 42, Volume 2 — maps
[ISSN-0469-4244] 18 p3123 N85-29337

PHOTOMASKS
Unsharp masking at the enlarger — astronomical photography 07 p0964 N85-16119
Mask aligner for solar cell fabrication
[AD-D011450] 10 p1510 N85-19529
Basic development of a 1.5 micrometer very large scale integrated technique, part 1-4
[BMFT-FB-T-85-032-PT-1-4] 20 p3449 N85-31417

PHOTOMETERS
NT ELECTROPHOTOMETERS
NT ULTRAVIOLET SPECTROMETERS
NT ULTRAVIOLET SPECTROPHOTOMETERS
Integration of detectors with optical waveguide structures
[AD-A146278] 03 p0420 N85-12662
Electrooptical matrix multiplication using the twos complement arithmetic for improved accuracy
[AD-D011252] 05 p0728 N85-14682
Energy parameters of optical radiation space research systems 06 p0791 N85-15058
Apparatus for determining the liquid water content of a gas
[AD-D011297] 07 p0922 N85-15839
Using a Gossen light meter to produce enlarged interpositive film copies from glass plates — astronomical photography 07 p0964 N85-16118
Two-photon coherent state light - its generation and potential applications
[AD-A148245] 08 p1166 N85-17356
Semiconductor superlattice photodetectors
[NASA-CR-174347] 09 p1397 N85-18791
Mercuric iodide photodetectors for scintillation spectroscopy
[DE85-001437] 10 p1437 N85-19056
Ion implanted lateral in 2Ga 8As/GaAs strained-layer superlattice photodector
[DE85-001365] 10 p1563 N85-19859
Effect of variance of photoreceiver frequency characteristics on characteristics of measuring instruments 13 p2076 N85-22965
Invariance of probability characteristics of detector to shape of optical pulse signals 13 p2090 N85-23048
Fabry-Perot interferometer and skymapping photometer determinations of midlatitude f-region neutral winds and temperatures and airglow enhancement/depletions
[AD-A150730] 14 p2373 N85-24666
Measurements with an auroral spectrometer in the Energy Budget Campaign
[BMFT-FB-W-84-050] 14 p2374 N85-24677
InGaAs/GaAs, Strained-Layer Superlattice (SLS), junction photodetectors, LED's, injection LASER's and FET's for optoelectronic IC applications
[DE85-001940] 14 p2430 N85-24986
Research and development of new instruments
16 p2824 N85-27418
The vector magnetograph of the Sayan Solar Observatory 18 p3206 N85-29887
Phase locked loop synchronization for direct detection optical PPM communication systems
[NASA-CR-176026] 19 p3254 N85-30178
The temporal evolution of a small auroral substorm as viewed from high altitudes with Dynamics Explorer 1
[NASA-CR-176064] 20 p3493 N85-31718
Charge Injection Device (CID) used as a photodector: Implementation and performance. Application to light source tracking (stars, lasers)
[CNES-83/CT/DRT/TIT/OE/146]
20 p3533 N85-31983
Color evolution in high redshift galaxies
20 p3544 N85-32055
Sahara Desert dust transport to the south
21 p3648 N85-32666
Comparative characteristics of optical multiposition pulse signals with intersymbol distortion
22 p3764 N85-33329
Estimating angular position of optical radiation source when received by array of photodetectors
22 p3778 N85-33413
Hadrons registration in emulsion chamber with carbon block
[HE-3.7-3] 24 p4186 N85-35962

PHOTOMETRY
NT ASTRONOMICAL PHOTOMETRY
NT ELECTROPHOTOMETRY
NT INFRARED PHOTOMETRY
NT SPECTROPHOTOMETRY
NT STELLAR SPECTROPHOTOMETRY
NT ULTRAVIOLET PHOTOMETRY
NT VISUAL PHOTOMETRY
UBV photometry of E region stars: Some intercomparisons 01 p0128 N85-10880
Theoretical elements of photometry
[BLL-RISLEY-TR-5022-(9091.9F)]
02 p0279 N85-11821
The present state of the International Star Cluster Photometry Programme 05 p0737 N85-14741
On the most probable number of flare stars in the Pleiades field 05 p0739 N85-14756
Determining grasp points using photometric stereo and the PRISM binocular stereo system
[AD-A147782] 08 p1222 N85-17867
Far infrared and submillimeter observations of the giant planets 08 p1245 N85-17888
Multi-spectral observations of the star formation: The role of far infrared photometry 08 p1245 N85-17889
Far-infrared photometry of low-mass pre-main-sequence stars with broad CO wings 08 p1246 N85-17890
High sensitivity, high angular resolution far-infrared photometry from the KAO 08 p1248 N85-17891
Proceedings of the Workshop on Improvements to Photometry
[NASA-CP-2350] 08 p1250 N85-17892
History of photometric precision
08 p1250 N85-17893
Photometric precision needed for planetary detection
08 p1250 N85-17894
A survey for photometric variability from space
08 p1251 N85-17897
The ground based photometric limitations to the search for light variations due to 5-minute solar-type oscillations in other stars 08 p1251 N85-17898
Atmospheric limitations in stellar seismology: Should one measure radial velocity or brightness fluctuations?
08 p1251 N85-17899
The atmospheric extinction problem
08 p1251 N85-17901
Gain instabilities in photomultipliers: How accurate are photon counting measurements?
08 p1251 N85-17903
CCDs: Their cause and cure
08 p1252 N85-17905
Astronomy and sodium lighting
[RAND/N-2089-RC] 09 p1413 N85-18814
Individual differences in chromatic brightness matching
[AD-A148862] 10 p1529 N85-19841
Physical models for the UV continua of symbiotic stars
11 p1756 N85-21048
Planetary cartography in the next decade (1984 - 1994)
[NASA-SP-475] 12 p1960 N85-22323
Photometric analysis of Jupiter-illuminated images of Io 13 p2196 N85-23620
Comparison of flame photometer data with total particle volume calculated from laser spectrometer particle count data
[AD-A151008] 14 p2252 N85-23958
Some new photometric data form panoramic pictures taken by Lunokhod-2 15 p2461 N85-25312
Jupiter/Voyager data analysis
[NASA-CR-175723] 15 p2679 N85-26545
Absolute calibrations of SO2 and NO analyzers by photographic methods
[DFVLR-MITT-85-02] 17 p2994 N85-28504
Activities of Istituto Elettrotecnico Nazionale Galileo Ferraris 18 p3199 N85-29845
Size exclusion chromatography-low angle laser light scattering photometry of lignite macromolecules
[DE85-012017] 22 p3745 N85-33215
Interpretation of photometric measurements of airless bodies 22 p3855 N85-33871
A cosmic ray super high multicore family event. 1: Experiment and general features
[HE-3.4-1] 24 p4181 N85-35930

PHOTOMICROGRAPHS
Automatic analysis of speckle photographs by microcomputer
[NPL-DITC-47/84] 09 p1322 N85-18308

PHOTOMICROGRAPHY
Micrographic and fractographic examination of alloys 2214 and 2024 for conditions which would cause burning of the metal on being put into solution, trial 17/175
[DGT-23.419] 11 p1609 N85-20117
Method of examining microcircuit patterns
[NASA-CASE-NPO-16299-1] 11 p1628 N85-20250

PHOTOMULTIPLIER TUBES
Fine grained hodoscopes based on scintillating optical fibers
[DE84-014849] 01 p0120 N85-10825
Preliminary evaluation of RCA C83036E prototype photomultiplier
[DE84-016894] 04 p0496 N85-13165
Simulation of optical configurations and signal processing methods in Anger-type neutron-position scintillation detector
[DE84-012095] 04 p0503 N85-13210
Analysis of a coded, M-ary orthogonal input optical channel with random-gain photomultiplier detection
05 p0624 N85-13880
Study in spurious sensitivity of electronics in space
[AD-A148366] 08 p1156 N85-17305
Gain instabilities in photomultipliers: How accurate are photon counting measurements?
08 p1251 N85-17903

Improved Gonda's circuit described
15 p2551 N85-25748

Microchannel plate streak camera
[DE85-011604] 20 p3458 N85-31481

Evidence for long-term variability in the ultra high energy photon flux from Cygnus X-3
[OG-2.1-10] 22 p3863 N85-33926

Improved method for the stabilization of NaI-photomultiplier gamma detectors against thermal and other drift
[DE85-011830] 23 p3970 N85-34613

The angular resolution of air shower gamma ray telescopes
[OG-9.5-14] 23 p4031 N85-34990

The read-out system of spatial distribution of thermoluminescence in meteorites
[SH-8.1-16] 23 p4052 N85-35131

Air fluorescence detection of large air showers below the horizon
[HE-4.6-6] 24 p4197 N85-36043

The structure of the shower disk observed at Mt. Norikura
[HE-4.7-1] 24 p4198 N85-36052

Structure of air shower disc near the core
[HE-4.7-2] 24 p4198 N85-36053

Arrival time distributions of electrons in air showers with primary energies above 10 (18)eV observed at 900m above sea level
[HE-4.7-5] 24 p4199 N85-36056

Methods for roof-top mini-arrays
[HE-4.7-7] 24 p4199 N85-36058

Fast scintillation counter preamplifier for the observation of Linsley effect
[HE-4.7-9] 24 p4199 N85-36060

A mini-array for large air showers
[HE-4.7-10] 24 p4199 N85-36061

Detection threshold energy of high energy cascade showers using thermoluminescence PTFE-sheet and hot-gas reader
[HE-7.1-5] 24 p4213 N85-36159

PHOTON ABSORPTIOMETRY

Experimental capabilities and prospects for measuring soft X-ray photoabsorption
[DE84-015466] 02 p0278 N85-11813

Techniques for measuring intercepted and absorbed PAR in corn canopies
[E85-10061] 10 p1505 N85-19495

PHOTON BEAMS

NT LIGHT BEAMS

Photon and electron dosimetry at the Physikalische-Technische Bundesanstalt in Brunswick
[PTB-DOS-9] 01 p0119 N85-10814

Stationary properties and switching characteristics of dispersive optical bistability in CuCl
18 p3186 N85-29763

Evidence for long-term variability in the ultra high energy photon flux from Cygnus X-3
[OG-2.1-10] 22 p3863 N85-33926

X-ray spectra of bursting neutron stars
23 p3961 N85-34686

Breeding new light into old machines (and new)
[DE85-013055] 24 p4155 N85-35763

PHOTON DENSITY

Low-energy gamma rays from Cygnus X-1
[OG-2.4-13] 22 p3866 N85-33957

Some evidence for large gravitational redshift in Seyfert galaxy NGC 4151
[OG-2.7-11] 22 p3872 N85-33984

A new measurement of the cosmic ray energy spectrum between 3 x 10 to the 15th power eV and 3 x 10 to the 16th power eV
[OG-5.1-6] 22 p3881 N85-34048

PHOTON-ELECTRON INTERACTION

An inverse Compton model of the X-ray emission in Seyfert galaxies
08 p1241 N85-17827

CYLTRAN calculations of electron effects on XD detectors
[LA-10264-MS] 23 p3960 N85-34601

A new method of differential structural analysis of gamma-family basic parameters
[HE-3.6-3] 24 p4184 N85-35952

Samarkand complex setup for investigation of cosmic ray variation in the energy range of 7 10 (9) - 10 (15) eV
[HE-4.6-14] 24 p4198 N85-36050

PHOTONICS

Influence of spatial pumping spectrum on quality of phase conjugate reflection during 4-photon interaction
21 p3696 N85-32964

PHOTONS

NT LIGHT BEAMS

Avalanche photodiode statistics in triggered-avalanche detection mode
05 p0623 N85-13987

Theory and applications of two-photon quantum optics
[AD-A147382] 07 p1044 N85-16631

Two-photon coherent state light - its generation and potential applications
[AD-A148245] 08 p1166 N85-17356

Gain instabilities in photomultipliers: How accurate are photon counting measurements?
08 p1251 N85-17903

CCDs: Their cause and cure
08 p1252 N85-17905

Multiphoton ionization of cesium atoms above and below the two-photon ionization threshold
[DE85-000976] 09 p1361 N85-18682

Physics of nonmagnetic relativistic thermal plasmas
09 p1366 N85-18715

Detection and symbol synchronization for multiple-bit per photon optical communications
10 p1463 N85-19226

Photonic methods of high speed analog data recording
[DE84-016723] 11 p1637 N85-20308

MCNP code
[DE85-002565] 11 p1702 N85-20705

ITS: The Integrated TIGER Series of coupled electron/photon Monte Carlo transport codes
[DE85-003719] 11 p1725 N85-20847

Exploration of new methods to produce efficient sources of coherent near millimeter wave radiation
[AD-A150094] 12 p1829 N85-21481

Mean free path lenght of photons with broken cloud cover
14 p2338 N85-24455

A quantitative image evaluation study of a concurrent photon amplification treated emulsion
[AD-A151831] 15 p2560 N85-25796

Characterization of multiphoton ionization processes in the ultraviolet
[AD-A151427] 15 p2652 N85-26354

Photon detection with cooled avalanche photodiodes: Theory and preliminary experimental results
16 p2770 N85-27096

Photon-photon collisions
[DE85-008056] 17 p3030 N85-28742

Photon structure function: Theory
[DE85-008064] 17 p3031 N85-28745

Incorporation of Monte Carlo electron interface studies into photon general cavity theory
[DE85-007674] 17 p3034 N85-28772

New experimental results in two photon physics
[NIKHEF-H/84-16] 17 p3035 N85-28776

Adiatatic approach in the theory of polyatomic photodissociation: Application to C2N2
[DE85-008515] 18 p3071 N85-28996

The prospects of the digital optical computer
18 p3188 N85-29771

Method of reducing impurity and antisite defects in semiconductor crystal materials, and device and apparatus respectively produced from and utilizing same
[AD-D011696] 19 p3260 N85-30216

Coherently pumped two-frequency laser-type devices
[AD-A154085] 19 p3275 N85-30311

MCNP: A general Monte Carlo code for neutron and photon transport
[DE85-010764] 19 p3348 N85-30753

Double photon excitation of high-Rydberg atoms as a long-lived submillimeter detector
[NASA-CASE-NPO-16372-1] 19 p3352 N85-30779

Monte Carlo electron/photon transport
[DE85-010799] 19 p3364 N85-30861

Four-photon resonant third harmonic generation
[DE85-010070] 19 p3367 N85-30883

Photon-counting image sensors for the ultraviolet
[NASA-CR-176062] 20 p3458 N85-31478

The possibility of observing and exploiting the generation of high-energy photons by electrons in the field of an intense electromagnetic wave 21 p3691 N85-32931

Influence of spatial pumping spectrum on quality of phase conjugate reflection during 4-photon interaction
21 p3696 N85-32964

Implicit Monte Carlo methods and non-equilibrium Marshak wave radiative transport
[DE85-010711] 22 p3835 N85-33743

Reduction of reabsorption effects in scintillators by employing solutes with large Stokes shifts
[DE85-011645] 22 p3838 N85-33767

Unthermalized plasma in bursts sources
[OG-1.1-5] 22 p3861 N85-33907

A search in the COS-B data base for correlated time variability in regions containing objects of interest
[OG-2.5-9] 22 p3869 N85-33964

Search for ultra high energy gamma-rays from various sources
[OG-2.6-7] 22 p3870 N85-33969

The universal spectrum of AGNs and QSOs
[OG-2.7-9] 22 p3872 N85-33982

Low-excitation Herbig-Haro objects and interstellar extinction
[NASA-CR-176142] 23 p3988 N85-34726

Study of photon emission by electron capture during solar nuclei acceleration, 1: Temperature-dependent cross section for charge changing processes
[SH-1.1-8] 23 p3990 N85-34735

Study of photon emission by electron capture during solar nuclei acceleration. 2: Delimitation of conditions for charge transfert establishment
[SH-1.1-9] 23 p3990 N85-34736

Study of photon emission by electron capture during solar nuclei acceleration. 3: Photon production evaluations
[SH-1.1-10] 23 p3990 N85-34737

Study of non-thermal photon production under different scenarios in solar flares. 1: Scenarios and formulations
[SH-1.2-2] 23 p3991 N85-34738

Study of non-thermal photon production under different scenarios in solar flares. 2: The Compton inverse and Bremsstrahlung models and fittings
[SH-1.2-3] 23 p3991 N85-34739

Observations of solar flare photon energy spectra from 20 keV to 7 MeV
[SH-1.2-9] 23 p3992 N85-34744

On the detectability of key-MeV solar protons through their nonthermal Lyman-alpha emission
[SH-1.3-5] 23 p3993 N85-34752

A coded aperture imaging system optimized for hard X-ray and gamma ray astronomy
[OG-9.2-3] 23 p4024 N85-34942

Secondary gamma-ray production in a coded aperture mask
[OG-9.2-6] 23 p4025 N85-34945

The final COS-B database now publicly available
[OG-9.3-8] 23 p4028 N85-34963

Generation of stimulated emission in the soft X-ray range by nonlinear processes with excimer lasers
[DE85-012465] 24 p4098 N85-35403

Status of the zeta(8.3)
[DE85-013070] 24 p4149 N85-35724

Calibration of a high-level photon irradiation
[DE85-013044] 24 p4151 N85-35738

Surface discharges as intense photon sources in the extreme ultraviolet
[DE85-012593] 24 p4158 N85-35782

Circumstellar shells of late-type stars: A study at millimeter and infrared wavelengths
24 p4167 N85-35836

Nucleon-nucleus interactions from JACEE
24 p4173 N85-35869

An experimental study of correlations in the development of the electron-photon cascades
[HE-3.5-10] 24 p4184 N85-35947

Electrons, muons and hadrons in extensive air showers and how do they depend on nuclear interaction model, part 1
24 p4187 N85-35972

The identification of gamma ray induced EAS
[HE-4.5-1] 24 p4195 N85-36026

Electromagnetic and muonic structure of showers initiated by gamma-rays and by hadrons
[HE-4.5-6] 24 p4195 N85-36030

The hump in the Cerenkov lateral distribution of gamma ray showers
[HE-4.5-9] 24 p4195 N85-36032

A three-dimensional Monte Carlo calculation of the photon initiated showers and Kiel result
[HE-4.5-13] 24 p4196 N85-36035

Study of photonuclear muon interactions at Baksan underground scintillation telescope
[HE-5.4-10] 24 p4208 N85-36122

PHOTONUCLEAR REACTIONS

Investigations of the structure and electromagnetic interactions of few-body systems
[DE85-002854] 11 p1721 N85-20824

Reduction of reabsorption effects in scintillators by employing solutes with large Stokes shifts
[DE85-011645] 22 p3838 N85-33767

Nuclear data for MCNP
[DE85-010794] 22 p3840 N85-33782

Longitudinal development of muons in large air showers studies from the arrival time distributions measured at 900m above sea level
[HE-4.7-4] 24 p4199 N85-36055

Study of the time-differentiated particle flux density at various distances from EAS axis
[HE-4.7-15] 24 p4200 N85-36065

PHOTOOXIDATION

Determination of Toluene's degradation products under simulated atmospheric conditions
05 p0674 N85-14331

Modelling of photodegradation in solar cell modules of substrate and superstrate design made with ethylene-vinyl acetate as pottant material
[NASA-CR-175690] 14 p2350 N85-24527

Formation and fate of toxic chemicals in California's atmosphere
[PB85-172609] 16 p3134 N85-29414

The photochemical oxidation of GaAs
[AD-A153689] 19 p3233 N85-30045
Atmospheric nitrogen oxides: Their detection and chemistry
[PB85-193910] 24 p4114 N85-35502

PHOTOPEAK
Intercomparison of the calculated absolute efficiency values between true coaxial and true closed-end coaxial Ge (Li) and NaI detectors
[REPT-5-1984] 20 p3532 N85-31976

PHOTOPLASTICITY
State of stress and penetration of plastic deformation in forming
[BLL-BISI-22199-(9022.06)] 17 p2977 N85-28396

PHOTOPRODUCTION
Muons in gamma showers
[HE-4.5-3] 24 p4195 N85-36027

PHOTORECEPTORS
Gravistimulus production in roots of corn
15 p2607 N85-26066
Mutant peas as probes in the understanding of growth and gravitropism 15 p2611 N85-26088
Differentiating spatial light modulator
[AD-D011727] 23 p3973 N85-34632

PHOTORECONNAISSANCE
Photo-reconnaissance system
[AD-D011267] 06 p0826 N85-15245

PHOTOREDUCTION
U PHOTOCHEMICAL REACTIONS

PHOTORESISTIVITY
U PHOTOCONDUCTIVITY

PHOTORESISTORS
U PHOTOCONDUCTORS

PHOTOSENSITIVITY
NT LIGHT ADAPTATION
NT PHOTOTROPISM
Cerenkov ring imaging detector development at SLAC
[DE84-015663] 04 p0560 N85-13564
FLACS: A new sensitometer for measurement of extreme low intensity reciprocity in a controlled environment --- X-ray films 07 p0963 N85-16104
Comparison of the fine grain compensation hypersensitization (FAH) process with gas hypersensitizing techniques --- astronomical photography plates
07 p0963 N85-16107
Investigation and optimization of fuel production using dye-based transition metal complexes as charge-transfer intermediates
[PB85-161941] 14 p2264 N85-24029
The electrochemistry of azine, oxazine and thiazine dyes
[AD-A152394] 17 p2918 N85-27990
Three-dimensional photochemical machining with lasers
[AD-A154711] 21 p3591 N85-32320
An enhanced photoresponse at dislocation subgrain boundaries revealed by X-ray topography of polysilicon solar cells 22 p3806 N85-33572
Liquid crystal light valve structures
[NASA-CASE-MSC-20036-1] 22 p3847 N85-33826
Electron photoejection in carbanions
[DE85-011747] 23 p3911 N85-34230
Screening and characterizing oleaginous microalgal species from the southeastern United States
[DE85-008787] 23 p3951 N85-34488
High sensitive X-ray films to detect electron showers in 100 GeV region
[HE-3.1-13] 24 p4178 N85-35911

PHOTOSENSORS
U RADIATION MEASURING INSTRUMENTS

PHOTOSPHERE
NT SOLAR GRANULATION
Structure and evolution of the large scale solar and heliospheric magnetic fields
[NASA-CR-175268] 01 p0130 N85-10697
Vector magnetic field analysis of Lorentz forces acting in the solar atmosphere
[AD-A145941] 03 p0449 N85-12852
Elemental abundances of mercury-manganese stars and the population 2 type star HD 109995
[NASA-CR-174296] 08 p1255 N85-17913
Energy release in solar flares
[NASA-CR-174302] 08 p1259 N85-17924
Ultraviolet spectroscopy of the interacting binary U Sagittae 11 p1755 N85-21042
Betegeuse at maximum luminosity
11 p1758 N85-21061
Sensitivity of inferred subphotospheric velocity field to mode selection, analysis technique and noise
14 p2442 N85-25065
Magnetoconvection: The interaction of convection and small scale magnetic fields --- photosphere
14 p2446 N85-25098
The photospheric temperature structure of magnetic flux tubes 14 p2447 N85-25102
A model for the dynamics of the deep photosphere
14 p2450 N85-25129
Solar cycle variations of sunspot temperatures
14 p2452 N85-25141
Solar cycle variation of ephemeral active regions
14 p2452 N85-25142
Variability of the quiet photospheric network
14 p2452 N85-25144
Measurements of Solar Vector Magnetic Fields
[NASA-CP-2374] 18 p3203 N85-29869
The vector structure of active magnetic fields
18 p3203 N85-29870
Current evolution in a numerical emerging-magnetic-flux model 18 p3204 N85-29875
Stokes parameters modulator for birefringent filters
18 p3205 N85-29884
Magnetic probing of the solar interior
[NASA-CR-176025] 19 p3385 N85-30998
Single-dish high sensitivity determination of solar limb emission at 22 and 44 GHz
[INPE-3545-PRE/758] 19 p3385 N85-30999
Solar photospheric and coronal abundances from solar energetic particle measurements
[NASA-CR-176029] 20 p3547 N85-32073
Contributions to the 19th International Cosmic Ray Conference
[NASA-CR-176060] 21 p3714 N85-33044
Solar coronal and photospheric abundances from solar energetic particle measurements
[PAPER-SH-2.1-5] 21 p3715 N85-33053
Heating of the deep chromosphere during solar flares
[AD-A155256] 21 p3723 N85-33100
Helios 1 energetic particle observations of the solar gamma ray flare events of 7, 21 June 1980 and 3 June 1982
[SH-1.3-8] 23 p3993 N85-34755
Precision measurements of solar energetic particle elemental composition
[SH-2.1-4] 23 p3998 N85-34785
Solar Coronal and photospheric abundances from solar energetic particle measurements
[SH-2.1-5] 23 p3998 N85-34786
Diffusion in the chromosphere and the composition of the solar corona and energetic particles
[SH-2.1-9] 23 p3999 N85-34790
Abundances from solar-flare gamma-ray line spectroscopy
[SH-2.1-13] 23 p3999 N85-34794
The HEAO-2 Guest Investigator Program: Non-linear growth of instabilities in line-driven stellar winds
[NASA-CR-176168] 24 p4166 N85-35840

PHOTOSYNTHESIS
The Marine Resources Experiment Program (MAREX)
[NASA-TM-87366] 01 p0086 N85-10580
Proton pumping in purple membrane, appendix 1
[DE84-014601] 01 p0118 N85-10811
Terrestrial nitrogen cycles: Some unanswered questions 05 p0653 N85-14192
Spectral estimators of absorbed photosynthetically active radiation in corn canopies
[E85-10041] 07 p0983 N85-16242
Variation in photosynthesis with light level for model with two photochemical reactions 07 p1012 N85-16430
Workshop on membrane biophysics
[AD-A148238] 08 p1192 N85-17512
Techniques for measuring intercepted and absorbed PAR in corn canopies
[E85-10081] 10 p1505 N85-19495
Artificial photosynthesis with algal and reconstituted systems
[DE85-002557] 10 p1523 N85-19604
Photosynthesis of ammonia
[DE85-001482] 11 p1595 N85-20029
Energy transfer and photochemistry in biomimetic solar conversion
[PB85-129112] 11 p1677 N85-20566
Effect of elevated atmospheric CO2 on plant communities
[DE85-001810] 11 p1678 N85-20576
Primary light harvesting system: The relationship of phycobilisomes to photosystem 1 and 2
[DE85-003075] 11 p1689 N85-20622
Nitrogen control of photosynthetic protein synthesis
[DE85-003513] 11 p1690 N85-20623
Photosynthetic water splitting
[DE85-002460] 11 p1690 N85-20627
Modulation of light energy transduction in photosynthesis
[DE85-004711] 13 p2141 N85-23292
Ways of optimization of light energy transformation in primary stages of photosynthesis. Necessity of optimization of photosynthetic unit structure and method for calculating efficiency 14 p2386 N85-24700
Ways of optimization of light energy transformation in primary stages of photosynthesis. Optimization of lattice structure of uniform photosynthetic unit
14 p2386 N85-24701
Bioenergy, solar biotech research in France, Europe
15 p2536 N85-25646
Studies of photosynthetic Energy Conversion
[DE85-005973] 15 p2586 N85-25944
Eight DOE Solar Photochemistry Research Conference Proceedings
[DE85-005094] 15 p2587 N85-25946
Photosynthetic acclimation of Acer saccharum
[DE85-008247] 17 p2998 N85-28536
Atmosphere behavior in gas-closed mouse-algal systems: An experimental and modelling study
18 p3155 N85-29636
Metabolic mechanisms of plant growth at low water potentials 19 p3327 N85-30612
Protocyanobacteria: Oxygenic and Anoxygenic photosynthesis in mat-forming bacteria
21 p3657 N85-32714
Cytochromes and iron sulfur proteins in sulfur metabolism of phototrophic bacteria
21 p3657 N85-32718
Insights into the phylogenetic positions of photosynthetic bacteria obtained from 5S rRNA and 16S rRNA sequence data 21 p3658 N85-32719
Ecophysiology of phototrophic sulfur bacteria in lakes: Vertical distribution of planktonic populations
21 p3658 N85-32722
Anaerobic reduction of elemental sulfur by Chromatium vinosum and Beggiatoa alba 21 p3660 N85-32739
Interactions among sulfide-oxidizing bacteria
21 p3661 N85-32741
Cyanobacterial mats: Microanalysis of community metabolism 21 p3661 N85-32743
Microanalysis of dissolved iron and phosphate in pore waters of hypersaline sediment
21 p3661 N85-32744
Glutathione in cyanobacteria
21 p3661 N85-32745
Microbial communities and microprofiles of sulfide and oxygen of alum rock sulfur springs
21 p3661 N85-32746
Biological modulation of planetary atmospheres: The early Earth scenario 22 p3354 N85-33667

PHOTOTHERMAL CONVERSION
Control and performance of a photovoltaic-thermal energy system 03 p0387 N85-12475
High resolution photoacoustic and photothermal imaging 05 p0723 N85-14849
Photothermal degradation of encapsulants
06 p0830 N85-15270
Short duration winter-time performances of different passive solar systems
[DE85-000650] 11 p1675 N85-20557
Photoacoustic imaging
[AD-A150823] 14 p2416 N85-24905
High-altitude testing of selective optical coatings for solar radiators and collectors 17 p2939 N85-28143
Selective coatings for solar heat converters
17 p2939 N85-28144
Characterization of the optical and thermal properties of matter by photothermal techniques
[DE85-012607] 24 p4076 N85-35260

PHOTOTHERMOTROPISM
U ANISOTROPY
U PHOTOTROPISM
U TEMPERATURE EFFECTS

PHOTOTRANSISTORS
High-temperature optically activated GaAs power switching for aircraft digital electronic control
[NASA-CR-174711] 04 p0457 N85-12901
The touch panel system: Design and development
[AD-A153014] 17 p3008 N85-28596

PHOTOTROPISM
The global sulfur cycle
[NASA-TM-87570] 21 p3656 N85-32710
Phototrophic bacteria and their role in the biogeochemical sulfur cycle 21 p3660 N85-32735
Sulfur cycling and metabolism of phototrophic and filamentous sulfur bacteria 21 p3660 N85-32737
Enrichments for phototrophic bacteria and characterization by morphology and pigment analysis
21 p3660 N85-32738
Buoyant densities of phototrophic sulfur bacteria and cyanobacteria 21 p3660 N85-32740
Interactions among sulfide-oxidizing bacteria
21 p3661 N85-32741
Cyanobacterial mats: Microanalysis of community metabolism 21 p3661 N85-32743
Glutathione in cyanobacteria
21 p3661 N85-32745

PHOTOTUBES
NT PHOTOMULTIPLIER TUBES

PHOTOVISCOELASTICITY
Influence of cyclic thermal loading on internal stress in casted epoxy resin
23 p3906 N85-34211
PHOTOVOLTAGES
Safety requirements for wiring systems and connectors for photovoltaic systems
[NASA-CR-174431] 10 p1477 N85-18324
PHOTOVOLTAIC CELLS
MOD silver metallization for photovoltaics
[NASA-CR-174011] 01 p0026 N85-10163
Summary of trends in photovoltaic patent activity
[DE84-015757] 01 p0066 N85-10452
DOE/SERI polycrystalline thin-film photovoltaic research
[DE84-004516] 02 p0223 N85-11464
Cascaded solar photovoltaic cells based on InP-GaInPAs and InP-CdS heterostructures
02 p0268 N85-11749
Control aspects of the Schuchuli Village stand-alone photovoltaic power system
[NASA-TM-83790] 04 p0495 N85-13157
Evaluation of some photovoltaic concentrator solar cell-heat sink coupling materials
[DE84-016027] 04 p0529 N85-13378
Silicon for solar cells
[DE84-004503] 04 p0529 N85-13381
Microcomputer control of a residential photovoltaic power conditioning system
[DE84-013667] 04 p0547 N85-13480
Trends in space photovoltaic technology
05 p0609 N85-13886
Information package on photovoltaics
05 p0661 N85-14250
Material models and device structures for GaAs solar cells, introduction
05 p0665 N85-14276
Comparison of SCAPID/GaAs to experiment
05 p0665 N85-14279
Encapsulation design analysis
06 p0829 N85-15266
Photothermal degradation of encapsulants
06 p0630 N85-15270
Polymer-polymer interface bond stability
06 p0630 N85-15271
Predicting electrochemical breakdown in terrestrial photovoltaic modules
06 p0830 N85-15273
Module flammability research
06 p0830 N85-15274
Process research of non-Cz silicon material
06 p0830 N85-15275
Thermal characterization of photovoltaic modules in natural environments
06 p0832 N85-15296
Summary of photovoltaic performance models
06 p0832 N85-15298
Characterization of bicrystal grain boundary properties using device structures
[DE84-004509] 06 p0869 N85-15523
Antisoiling technology: Theories of surface soiling and performance of antisoiling surface coatings
[NASA-CR-174274] 07 p0991 N85-16296
What should DOE do to help establish voluntary consensus standards for measuring and rating the performance of PV modules?
[NASA-CR-174265] 07 p0992 N85-16297
Microcomputer control of a residential photovoltaic power conditioning system
[DE84-014774] 07 p1022 N85-16488
Compilation of Sandia papers contributed to the 17th IEEE Photovoltaic Specialists Conference
[DE84-017456] 09 p1315 N85-18267
Signal Hill solar-powered repeater report and recommendations
[DE85-000487] 09 p1316 N85-18273
Diodes in photovoltaic modules and arrays
[NASA-CR-175454] 10 p1508 N85-19513
Mod silver metallization for photovoltaics
[NASA-CR-174444] 10 p1509 N85-19518
Investigation of accelerated stress factors and failure/degradation mechanisms in terrestrial solar cells
[NASA-CR-175469] 10 p1510 N85-19524
Analysis of inverter models and harmonic propagation. Part 3. Transient processes in inverter models
[DE85-000191] 10 p1510 N85-19530
Overview of photovoltaic concentrator technology
[DE84-016790] 10 p1512 N85-19539
Surface and allied studies in silicon solar cells
[NASA-CR-174447] 11 p1671 N85-20531
Research on the basic understanding of high efficiency in silicon solar cells
[DE85-000507] 11 p1672 N85-20537
GaAs and 3-5 compound solar cells status and prospects for use in space
[NASA-TM-86960] 12 p1796 N85-21261
Power from the Sun: Light at night
[PB85-124097] 12 p1883 N85-21814
History and future views on solar cells of Japanese scientific satellites
13 p2005 N85-22566
Thin and ultrathin silicon solar cells for space use
13 p2005 N85-22567
Space solar cells: Adjusting to new demands
13 p2005 N85-22568
The high voltage silicon cell: A comparative analysis
13 p2005 N85-22569
A 2 x 6 Back Surface Reflection (BSR) silicon solar cell
13 p2005 N85-22570
Experiences with implanted Back Surface Field (BSF) solar cells
13 p2005 N85-22571
A low cost approach with larger diameter silicon wafer — solar cells
13 p2006 N85-22572
Bifacial light sensitive space solar cell
13 p2006 N85-22573
Gallium arsenide arrays versus silicon arrays for space application
13 p2006 N85-22574
Space qualified AlGaAs/GaAs solar cells
13 p2006 N85-22575
Availability of AlGaAs/GaAs solar cells in space
13 p2006 N85-22576
Comparative study of GaAs solar cell potentialities for space applications
13 p2006 N85-22577
Investigation of high output gallium arsenide solar cells
13 p2006 N85-22578
Development of very thin large area GaAs solar cells for space application
13 p2006 N85-22579
GaAs and 3-5 compound solar cells status and prospects for use in space
13 p2007 N85-22580
GaAlAs-GaAs solar cell development: Prospective for space applications under concentration
13 p2007 N85-22581
Investigation of the degradation of GaAs photovoltaic cells by proton and electron irradiation
13 p2008 N85-22587
Electrical design of the Intelsat 6 solar generator
13 p2008 N85-22592
Survival testing of silicon solar modules
13 p2009 N85-22602
Calibration of solar cells outside the atmosphere
13 p2009 N85-22603
Inverse behavior of silicon photovoltaic cells
13 p2010 N85-22604
NASA photovoltaic research and technology development program for space applications
13 p2011 N85-22617
High output photovoltaic conversion: The quadrispectral project --- spacecraft power supplies
13 p2012 N85-22626
Operational performance of the photovoltaic-powered grain mill and water pump at Tangaye, Burkina Faso (formerly Upper Volta)
[NASA-TM-86970] 13 p2128 N85-23243
Photovoltaic cells of InP-CdS heterojunction type and their temperature characteristics under A-M illumination
14 p2275 N85-24092
Dependence of parameters of silicon photovoltaic cells on temperature and light intensity
14 p2275 N85-24094
Silicon-sheet and thin-film cell and module technology potential: Issue study
[NASA-CR-175654] 14 p2349 N85-24520
Intermediate load modules for test and evaluation
[NASA-CR-175697] 14 p2350 N85-24526
Modeling and optimization of a multiple-cell photovoltaic converter system
15 p2585 N85-25934
Electrical research on solar cells and photovoltaic materials
[NASA-CR-175699] 15 p2585 N85-25935
Ink jet printing of silver metallization for photovoltaics
[NASA-CR-175798] 15 p2586 N85-25943
Solar elements with distributed parameters
16 p2760 N85-27036
Photovoltaic cell reliability research: Investigation of accelerated stress factors and failure-degradation mechanisms in terrestrial solar cells
[NASA-CR-175815] 16 p2819 N85-27388
Design and development of a linear Fresnel lens air-cooled photovoltaic module and a stand-alone photovoltaic collector array
[DE85-006854] 16 p2819 N85-27391
Electrical research on solar cells and photovoltaic materials
[NASA-CR-175897] 17 p2986 N85-28452
Terrestrial photovoltaic power systems with sunlight concentration
[DE85-008396] 17 p2987 N85-28464
SERI photovoltaic advanced research and development project: FY 1984 accomplishments
[DE85-002939] 18 p3126 N85-29368
Airport solar photovoltaic concentrator phase 3
[DE85-006773] 18 p3128 N85-29370
Dynamic simulation of dispersed, grid-connected photovoltaic power systems: System studies
[DE85-011179] 19 p3262 N85-30231
Increased voltage photovoltaic cell
[NASA-CASE-NPO-16155-1] 19 p3303 N85-30475
Current status of silicon materials research for photovoltaic applications
[DE85-006799] 19 p3304 N85-30482
Block 5 documentation and solar modules
[NASA-CR-176009] 19 p3306 N85-30494
Using PVFORM, a systems performance model, to determine optimum mounting configurations for flat-plate photovoltaic modules
[DE85-011191] 19 p3306 N85-30495
Electricity from sunlight: The emergence of photovoltaics, revised edition
[DE85-002920] 19 p3307 N85-30502
Historical perspective of barriers to achieving high-efficiency silicon solar cells
20 p3479 N85-31616
User handbook for block 5 silicon solar cell modules
[NASA-CR-176043] 20 p3483 N85-31644
Photovoltaic concentrator research status
[DE85-010119] 20 p3483 N85-31647
Gallium arsenide arrays versus silicon arrays for space application
[SNIAS-851-440-104] 20 p3485 N85-31657
Photovoltaic solar devices
[BMFT-FB-T-84-288] 20 p3485 N85-31660
High-efficiency crystalline silicon technology development
21 p3607 N85-32395
Flat-plate module efficiency versus cost tradeoffs
21 p3607 N85-32398
Georgetown University Photovoltaic Higher Education National Exemplar Facility (PHENEF)
21 p3607 N85-32400
Photothermal degradation studies of encapsulants
21 p3608 N85-32403
Topics in electrochemical degradation of photovoltaic modules
21 p3608 N85-32410
Polymer-water interaction studies
21 p3609 N85-32411
Encapsulation processing and manufacturing yield analysis
21 p3611 N85-32434
Photovoltaic module spread-of-flame testing
21 p3612 N85-32446
Development of high-efficiency solar cells on silicon web
[NASA-CR-176101] 22 p3805 N85-33566
Photovoltaics technical information guide
[DE85-002924] 22 p3808 N85-33585
Photovoltaic industry progress through 1984
[DE85-013029] 22 p3809 N85-33596
Federal export assistance programs applicable to the US photovoltaic industry
[NASA-CR-176114] 22 p3849 N85-33841
Thermionic photovoltaic energy converter
[NASA-CASE-LEW-14077-1] 23 p3944 N85-34441
Practical aspects of photovoltaic technology, applications and cost (revised)
[NASA-CR-174963] 24 p4110 N85-35472
Monolithic photovoltaic series array for an energy coupler
[BMFT-FB-T-85-023] 24 p4113 N85-35496
PHOTOVOLTAIC CONVERSION
Control and performance of a photovoltaic-thermal energy system
03 p0387 N85-12475
Advanced amorphous materials for photovoltaic conversion
[DE84-017198] 04 p0529 N85-13384
National Photovoltaics Program Annual Review Meeting, abstracts
[DE84-013003] 04 p0530 N85-13390
Health and environmental effects document for photovoltaic energy systems, 1983
[DE84-017179] 04 p0532 N85-13399
Photovoltaic working group report
05 p0611 N85-13902
Information package on photovoltaics
05 p0661 N85-14250
Stimulation of technologies towards photovoltaic energy conversion
05 p0661 N85-14251
Photovoltaic power supply units
05 p0662 N85-14252
Development and construction of a prototype photovoltaic energy supply unit
05 p0662 N85-14254
Fundamentals of solar energy conversion based on fluorescence collectors
05 p0662 N85-14258
Energy storage with lead acid batteries in photovoltaic systems
05 p0663 N85-14260
The 15 photovoltaic pilot projects of the European Communities
05 p0663 N85-14263
Photovoltaic 100 kWp pilot plant on the Greek island Kythnos
05 p0664 N85-14266
Mains-connected photovoltaic system for a house
05 p0664 N85-14267
Photovoltaic pump systems 05 p0664 N85-14269
Utilization possibilities of photovoltaics in the private sector
05 p0664 N85-14272

Considerations on the dimensioning of photovoltaic supply systems in the low power range
05 p0665 N85-14273

Solar energy conversion based on the principle of fluorescent collectors. Installation of a test collector to deliver several Watts power
[BMFT-FB-T-84-192] 07 p0993 N85-16308

Solar energy conversion based on the principle of fluorescent collectors
[BMFT-FB-T-84-193] 07 p0994 N85-16309

MOD silver metallization for photovoltaics
[NASA-CR-175460] 10 p1510 N85-19526

Photovoltaic Systems Development and Evaluation Projects Integration Meeting
[DE84-008530] 11 p1673 N85-20542

International Congress Centrum Berlin report on photovoltaics 12 p1677 N85-21773

Crystallization methods for solar cell silicon
12 p1877 N85-21774

Development and prototype construction of photovoltaic energy supply units 12 p1878 N85-21781

Photovoltaic solar components
12 p1878 N85-21782

Photovoltaic roofing tile systems
12 p1878 N85-21783

Investigation of the optical properties of solar elements 12 p1879 N85-21786

Development of high-efficiency economic systems for photovoltaics 12 p1880 N85-21795

Photovoltaic Generators in Space — conferences
[ESA-SP-210] 13 p2005 N85-22565

NASA photovoltaic research and technology development program for space applications
13 p2011 N85-22617

Study of concentration for space photovoltaic generators 13 p2011 N85-22618

High output photovoltaic conversion: The quadrispectral project — spacecraft power supplies
13 p2012 N85-22626

Module performance and failure analysis area: Flat-plate solar array project
[NASA-CR-175689] 15 p2565 N85-25936

Documents of the JPL Photovoltaics Program Analysis and Integration Center: An annotated bibliography
[NASA-CR-175873] 17 p2985 N85-28448

Development of a second-generation linear Fresnel Photovoltaic and Thermal (PVT) concentrator array, including fabrication and installation of a 200 square meter collector field
[DE85-008473] 17 p2988 N85-28465

Investigation of a Si and related semiconductors as materials for photovoltaic conversion
[DE85-002932] 18 p3096 N85-29163

Research recommendations for ac interfacing between electric utility transmission and distribution systems and wind, photovoltaics, and OTEC energy systems
[DE85-002942] 18 p3096 N85-29169

Photovoltaic Systems Development Project: An activity summary
[DE85-009994] 18 p3129 N85-29379

Electricity from sunlight: The emergence of photovoltaics, revised edition
[DE85-002920] 19 p3307 N85-30502

Nomographs for estimating the levelized cost of energy from flat-plate and concentrator photovoltaic systems
[NASA-CR-176048] 20 p3483 N85-31645

Study of concentration for space photovoltaic generators
[SNIAS-851-440-105] 20 p3485 N85-31658

Investigation of the microstructure and photovoltaic properties of semicrystalline silicon
22 p3806 N85-33573

Photovoltaic energy systems
[DE85-011630] 22 p3807 N85-33581

Photovoltaics technology program summary
[DE85-013098] 24 p4112 N85-35493

Design and construction of an advanced power conditioning subsystem for small photovoltaic applications
[DE85-013940] 24 p4113 N85-35495

PHOTOVOLTAIC EFFECT

MOD silver metallization for photovoltaics
[NASA-CR-174011] 01 p0026 N85-10163

Automated installation methods for photovoltaic arrays 2
[SAND-84-7035] 02 p0222 N85-11453

Modular photovoltaic array field
[SAND-83-7026] 02 p0222 N85-11454

Research on gallium arsenide diffused junction solar cells
[NASA-CR-174057] 02 p0222 N85-11457

Research directions and progress in the SERI advanced high efficiency concept program
[DE84-004592] 02 p0223 N85-11462

Five year research plan, 1984-1988. Photovoltaics: Electricity from sunlight
[DE84-013009] 04 p0528 N85-13377

Trends in space photovoltaic technology
05 p0609 N85-13888

Information package on photovoltaics
05 p0661 N85-14250

What should DOE do to help establish voluntary consensus standards for measuring and rating the performance of PV modules?
[NASA-CR-174265] 07 p0992 N85-16297

The 35 kilowatt peak power photovoltaic system
[DE85-000189] 10 p1511 N85-19537

Study of low energy density photovoltaic applications under varying rate structures
[DE85-000165] 10 p1511 N85-19538

Value of PV systems experiments. Volume 1: A preliminary assessment of the lessons learned from nine intermediate-size systems
[DE85-001494] 11 p1674 N85-20546

Abstracts of 6th Annual Review Meeting on Photovoltaic Advanced Research and Development
[DE84-013047] 13 p2128 N85-23246

MOD silver metallization for photovoltaics
[NASA-CR-175773] 16 p2818 N85-27381

Maintenance of photovoltaic power systems
[AD-A152299] 16 p2819 N85-27390

Study of the degradation of short-circuit current and the open-circuit tension of spatial solar cells as a function of the fluency of 1MeV electrons
[INPE-3356-PRE/634] 16 p2867 N85-27814

Relative potentials of concentrating and two-axis tracking flat-plate photovoltaic arrays for central-station applications
[NASA-CR-175889] 17 p2985 N85-28446

Research recommendations for ac interfacing between electric utility transmission and distribution systems and wind, photovoltaics, and OTEC energy systems
[DE85-002942] 18 p3096 N85-29169

Photovoltaic Systems Development Project: An activity summary
[DE85-009994] 18 p3129 N85-29379

Some practical considerations for economical back contact formation on high efficiency solar cells
20 p3479 N85-31620

High efficiency solar cell research for space applications 20 p3480 N85-31624

Structural defects in crystalline silicon
20 p3481 N85-31630

Air Force Federal Photovoltaic Utilization Program
[DE85-010812] 20 p3484 N85-31648

Predicting photothermal field performance
21 p3606 N85-32404

Micromolecular modeling 21 p3608 N85-32405

Silicon refinement by chemical vapor transport
21 p3609 N85-32412

MOD silver metallization for photovoltaics
21 p3610 N85-32428

Ink jet printing of silver metallization for photovoltaics
[NASA-CR-176054] 22 p3805 N85-33569

Investigation of the microstructure and photovoltaic properties of semicrystalline silicon
22 p3806 N85-33573

Photovoltaic industry progress through 1984
[DE85-013029] 22 p3809 N85-33596

Thermionic photovoltaic energy converter
[NASA-CASE-LEW-14077-1] 23 p3944 N85-34441

Investigation of test methods, material properties, and processes for solar cell encapsulants
[NASA-CR-176132] 23 p3945 N85-34446

PHTHALATES

The synthesis and characterization of Poly(Oxy(2-Methyl-1,3-Phenylene) Methyl-1,3 -Phenylene) Oxyterephthaloyl)Oxy
[AD-A148269] 08 p1133 N85-17143

Crystallization behavior of poly(3,3-bis(Ethoxymethyl) oxentane) and poly(3,3-bis(Azidomethyl) oxetane)
[AD-A148271] 08 p1226 N85-17720

Stabilized unsaturated polyesters
[NASA-CASE-NPO-16103-1] 18 p3078 N85-29043

Condensation of anhydrides or dicarboxylic acids with compounds containing active methylene groups. Part 19: Condensation of phthalic and substituted phthalic anhydrides with benzoylacetic ester
[NASA-TM-77885] 19 p3227 N85-30009

Condensation of anhydrides or dicarboxylic acids with compounds containing active methylene groups. Part 1: Condensation of phthalic anhydride with acetoacetic and malonic ester
[NASA-TM-77886] 19 p3227 N85-30010

Processable and stable conductive polymers
[AD-D011684] 19 p3249 N85-30143

PHTHALOCYANIN

Two silicon phthalocyanines and a silicon naphthalocyanine: Synthesis, electrochemistry and electrogenerated chemiluminescence
[AD-A144760] 01 p0023 N85-10146

A silicon phthalocyanine and a silicon naphthalocyanine: Synthesis, electrochemistry, and electrogenerated chemiluminescence
[AD-A146441] 06 p0765 N85-14865

Electronic and redox properties of stacked-ring silicon phthalocyanines from molecular orbital theory
[AD-A147161] 07 p0922 N85-15844

Phthalocyanine polymers
[NASA-CASE-ARC-11413-1] 12 p1809 N85-21348

The production of copper phthalocyanine and/or its derivatives
[NASA-TM-77629] 17 p2917 N85-27983

The electronic spectra of phthalocyanine radical anions and cations
[AD-A152328] 17 p2918 N85-27986

Photochemistry of coordination complexes: The phthalocyanines
[DE85-007693] 17 p2923 N85-28022

Metallophthalocyanine dimers incorporating five atom covalent bridges
[AD-A154365] 19 p3234 N85-30051

Metal (2) 4,4',4',4'' phthalocyanine tetraamines as curing agents for epoxy resins
[NASA-CASE-ARC-11424-1] 23 p3919 N85-34281

PHUGOID OSCILLATIONS
U OSCILLATIONS
U OSCILLATORS
U PITCH (INCLINATION)

PHYLLOQUINONE

Vitamin K and the metabolic state of bone
05 p0694 N85-14485

PHYSICAL CHEMISTRY
NT QUANTUM CHEMISTRY

National Science Foundation grants and awards for fiscal year 1983, volume 2
[PB84-212323] 01 p0125 N85-10854

Physico-chemical investigation of some areas of fundamental significance to biophysics
[DE84-016385] 04 p0471 N85-12980

Surface physics instrumentation
[AD-A149304] 11 p1728 N85-20860

Physical-chemical investigations of copper sulfides for use in CdS/Cu2S solar cells 12 p1880 N85-21794

Estimating degree of development of physical-chemical interaction among components in Al-B fiber composite material 13 p2027 N85-22705

Physical chemistry of exothermic gas-aerosol calorimetry
[AD-A150872] 14 p2251 N85-23950

Abstracts of the 36th Southeastern Regional Meeting of the American Chemical Society
[AD-A151506] 15 p2496 N85-25394

Atmosphere behavior in gas-closed mouse-algal systems: An experimental and modelling study
18 p3155 N85-29636

Chemistry division report
[DE85-010586] 24 p4071 N85-35228

PHYSICAL CONSTANTS TESTING REACTOR
U NUCLEAR RESEARCH AND TEST REACTORS
U WATER COOLED REACTORS

PHYSICAL ENDURANCE
U PHYSICAL FITNESS

PHYSICAL EXAMINATIONS

Health examination findings among active civil airmen
[AD-A148325] 08 p1195 N85-17533

PHYSICAL EXERCISE
NT HYPERKINESIA

The Reports of Aeromedical Laboratory, volume 25, no. 1/2
[ISSN-0023-2858] 01 p0090 N85-10605

The effects of isotonic training on +Gz tolerance
01 p0090 N85-10607

Effect of maximum physical load on oxygen-transport properties of blood 01 p0093 N85-10627

Oxygen delivery during exercise: Limitations to maximum flow 05 p0688 N85-14424

The effect of propranolol on the training response to endurance exercise in normal human adults
05 p0696 N85-14479

A machine for weight-lift testing
[AD-A146816] 07 p0973 N85-16182

Change in relationship of biopotentials of brain zones for various levels of working capacity
07 p1013 N85-16438

Encephalographic correlates of autogenous change in human functional state 08 p1193 N85-17518

Effect of prolonged hunger during experimental hikes
11 p1692 N85-20637

Sleep deprivation and exercise tolerance
[AD-A150180] 13 p2142 N85-23295

Sleep deprivation and exercise tolerance
[AD-A150566] 13 p2142 N85-23296

Sleep deprivation and exercise tolerance
[AD-A150626] 13 p2142 N85-23297

Peripheral changes in regional sweating responses to exercise in hypobaric environments
[AD-A150757] 14 p2368 N85-24710

Heat injury: Prevention is the key
[AD-A153734] 19 p3328 N85-30622

Cosmonauts' cardiovascular system function during long-term orbital flights aboard Salyut-6 station
22 p3733 N85-33141

Cardiorespiratory function and work performance during adaptation to industrial labor in midalpine conditions
22 p3820 N85-33665

PHYSICAL FACTORS

Critical assessment of low fluence irradiation creep mechanisms
[DE84-015578] 02 p0184 N85-11232

Glucose tolerance in trained and untrained subjects during head-down tilt (6 deg) 05 p0693 N85-14461

Physical dimensions of humans, values, envelope curves in different postures
[HSE-TRANS-10869] 20 p3513 N85-31838

PHYSICAL FITNESS

A machine for weight-lift testing
[AD-A146816] 07 p0973 N85-16182

Human factors and training research in military organizations and systems
[AD-A146832] 07 p1020 N85-16475

Assessment of muscle strength and prediction of lifting capacity in US Army personnel
[AD-A146846] 10 p1527 N85-19633

SPARTEN (Scientific Program of Aerobic and Resistance Training Exercise in the Navy): A total body fitness program for health and physical readiness
[AD-A150669] 14 p2388 N85-24711

Relationship between the Army two mile run test and maximal oxygen uptake
[AD-A153914] 18 p3154 N85-29526

Physical training and G tolerance
20 p3511 N85-31824

Centrifuge operations and training in the Royal Netherlands Air Force 20 p3511 N85-31825

An analysis of aerobic capacity in a large United States population
[AD-A156200] 24 p4132 N85-35614

Relaxation techniques
[AD-A156248] 24 p4133 N85-35621

PHYSICAL OPTICS

An analysis of physical optics models for rough surface scattering
[AD-A154960] 21 p3575 N85-32235

PHYSICAL PROPERTIES

Properties of polycaproamide fibers modified by grafted polyacrylonitrile 06 p0761 N85-14867

Special soft solder TK-3 (L-SnCu 3 - DIN 1707)
[BLL-T6334/BG/WH799/84(9022.46)]
06 p0767 N85-14907

Online directory of databases for material properties
[DE84-016511] 09 p1402 N85-18824

Study of the physical properties of crystalline rocks in the southeast Voronezh anteclise
[NASA-TM-77823] 10 p1514 N85-19551

The physical and mechanical properties of near-equiatomic titanium-nickel
19 p3237 N85-30072

PHYSICAL SCIENCES

National Science Foundation grants and awards for fiscal year 1983, volume 2
[PB84-212323] 01 p0125 N85-10854

Effect of physical work and sleep loss on recovery sleep
[AD-A146082] 03 p0401 N85-12554

PHYSICAL WORK

Psychological issues in the design of expert systems
[AD-A146081] 03 p0438 N85-12792

Factors determining effectiveness of voluntary decrease in ventilation during muscular work using instrumented feedback 08 p1193 N85-17520

Cognitive performance during successive sustained physical work episodes
[AD-A149061] 08 p1200 N85-17556

PHYSICS

Overview of the physics issues at the SSC
[DE85-007074] 16 p2859 N85-27634

Proceedings of the 19th Annual Conference of the Finnish Physical Society
[REPT-104] 20 p3532 N85-31974

Solar energy education: Renewable energy activities for chemistry and physics
[DE85-010371] 23 p3946 N85-34455

PHYSIOCHEMISTRY

Review on physiological and medical problems related to climates ranging from altitude to sub-tropics
05 p0687 N85-14417

Physio-chemical mechanisms of the processes of the formation of globular inclusions in ball-bearing metal
[BLL-BISI-TRANS-22235-(9022.06)]
17 p2924 N85-26030

Physical-chemical model for the mechanism of glass corrosion with particular consideration of simulated radioactive waste glasses
[DE85-007713] 17 p2935 N85-28121

Effect of heating temperature in a vacuum on state of surface layers of welded OT4 titanium alloy
19 p3245 N85-30123

Physiochemically controlled scour jet array system
[AD-D011688] 19 p3308 N85-30505

Zinc: Biological effects. Facts and fiction
[USIP-84-12] 20 p3507 N85-31798

Activities report in nuclear physics and particle acceleration 20 p3532 N85-31977

Ecophysiology of phototrophic sulfur bacteria in lakes: Vertical distribution of planktonic populations
21 p3658 N85-32722

Tests on zirconium nitride coatings applied to SW 16 steel using the chemical vapor deposition method
24 p4076 N85-35271

PHYSIOGRAPHY

U GEOMORPHOLOGY

PHYSIOLOGICAL ACCELERATION

Problems of aviation and space medicine and psychology discussed at 14th Gagarin lectures
23 p3954 N85-34509

PHYSIOLOGICAL EFFECTS

NT HEMODYNAMIC RESPONSES

NT PHYSIOLOGICAL RESPONSES

A study of fatigue of shiftworkers in air traffic control and weather service groups in JASDF
01 p0090 N85-10610

Circulatory orthostatic instability: Role of deconditioning of resistive vessels 01 p0091 N85-10612

Hemopoiesis in rats submitted to weightlessness
01 p0091 N85-10613

Frequency and nature of electrocardiographic disturbances in dogs during single and repeated exposure to +G sub z accelerations 01 p0092 N85-10619

Dynamics of morphological changes in articulation nervous system under hypokinetic conditions as a model of a spaceflight factor 01 p0092 N85-10621

Effect of 1,25-dihydroxycholecalciferol and 24,25 dihydroxycholecalciferol on growth and alteration of rat bones during hypokinesa (histomorphometric study)
01 p0092 N85-10622

Dynamics of some parameters of carbohydrate and lipid metabolism in recovery period following long-term hypokinesa 01 p0093 N85-10623

Biligenic function of white rat liver
01 p0093 N85-10624

Effect of short-term hypokinesia on rat opioid system reaction 01 p0093 N85-10625

Reaction of cerebral ventricles to antiorthostatic position and occlusion of jugular veins 01 p0093 N85-10626

Effect of maximum physical load on oxygen-transport properties of blood 01 p0093 N85-10627

Effect of hyperoxia and increased gas atmosphere density on contractile function of the right ventricle
01 p0093 N85-10628

Change in energetics of muscular contraction as a result of hyperoxia 01 p0093 N85-10629

Hemodynamics and neurodynamics of the human brain during exposure to moderate hypoxic hypoxia
01 p0094 N85-10630

Proton pumping in purple membrane, appendix 1
[DE84-014601] 01 p0116 N85-10811

The effect of sleep loss on the human visual event-related potential
[AD-A145364] 02 p0234 N85-11528

Mechanisms of oxygen toxicity and methods of protection
[AD-A145830] 03 p0400 N85-12551

The effects of helicopter vibration on the spinal system
[AD-A146274] 03 p0402 N85-12562

A survey of space biology and space medicine
[ESA-BR-17] 04 p0545 N85-13466

Review on physiological and medical problems related to climates ranging from altitude to sub-tropics
05 p0687 N85-14417

Pharmacokinetic interactions of mixtures
[AD-P004032] 06 p0844 N85-15362

Aspects of solvent toxicity in mixtures
[AD-P004036] 06 p0845 N85-15366

The epidemiology and toxicology of Agent Orange
[AD-P004038] 06 p0845 N85-15368

Human reactions to transient electric currents, volume 12
[PB84-231463] 06 p0846 N85-15374

Pulmonary blood flow and oxygenation of arterial blood in a healthy subject upon 7 days hypokinesia
07 p1014 N85-16439

Testing changes in visual function due to orbital environment
[AD-A147259] 07 p1016 N85-16453

Tolerance endpoint for evaluating the effects of heat stress in dogs
[AD-A148104] 08 p1192 N85-17511

Encephalographic correlates of autogenous change in human functional state 08 p1193 N85-17518

Dynamics of external respiration and gas metabolism under combined effect of hypoxia and hypercapnia
08 p1193 N85-17519

Influence of activation of ASFS-2 on human emotional status 08 p1194 N85-17522

Effects of prolonged hypokinesia on nervous system
08 p1194 N85-17524

The effect of beta adrenergic blockade on ratings of perceived exertion
[AD-A148053] 08 p1195 N85-17530

Effects of pyridostigmine on psychomotor and visual performance
[AD-A148553] 08 p1196 N85-17539

Gravity and biological systems: Emphasis on human physiology
[ESA-BR-21] 09 p1360 N85-18558

Effect of modulated ultrahigh frequency field on behavior and hormone level in female rats under emotional stress
09 p1361 N85-18562

Study of bodily functional status and quality of controlling action of power unit operators with various intensities of labor 09 p1362 N85-18569

Construction and application of a questionnaire for the social scientific investigation of environmental noise effects
[NASA-TM-75492] 10 p1512 N85-19544

Genetic effects of microwave exposure on mammalian cells in vitro, volume 2
[AD-A149347] 10 p1523 N85-19603

Work physiology of operating personnel at power plants in arid regions 10 p1523 N85-19606

Effects of overall vibration and noise on operational personnel 10 p1523 N85-19608

Management of vibration sickness in coal mines by hyperbaric oxygenation 10 p1523 N85-19609

Influence of hyperthermia on body temperature and content of catecholamines in white rat hypothalamus
10 p1524 N85-19615

Aircraft noise effects: An interdisciplinary study of the effects of aircraft noise on man. Part 1: Basic report
[NASA-TM-75819] 10 p1526 N85-19629

Aircraft noise effects: An interdisciplinary study of the effect of aircraft noise on man. Part 2: Appendix
[NASA-TM-75818] 10 p1527 N85-19630

Aircraft noise effects: An inter-disciplinary study of the effect of aircraft noise on man. Part 3: Supplementary analyses of the social-scientific portion of the study on aircraft noise conducted by the DFG
[NASA-TM-75802] 10 p1527 N85-19631

Health assessment document for carbon tetrachloride
[PB85-124196] 10 p1528 N85-19638

Mercury health effects update: Health issue assessment
[PB85-123925] 10 p1528 N85-19639

Heat stress and personal protective equipment
[DE85-003552] 10 p1532 N85-19652

Observations of physiological and psychological effects of terrain following flight based on in-flight test experience 10 p1532 N85-19657

Tolerance, fatigue, physiological and performance effects of sustained and oscillating lateral accelerations
10 p1533 N85-19659

Biomechanics finds practical applications in aerospace research 11 p1621 N85-20205

Physiological considerations of artificial gravity
11 p1643 N85-20351

Physiological considerations of artificial gravity
11 p1645 N85-20366

USSR report: Life sciences. Biomedical and behavioral sciences
[JPRS-UBB-85-010] 11 p1690 N85-20628

Functional system theory in practice
11 p1690 N85-20629

Effects of hyperthermia on free amino acids in rat brain and in subcellular fractions 11 p1691 N85-20631

Effects of hypothermia on brain metabolism
11 p1692 N85-20636

Effect of prolonged hunger during experimental hikes
11 p1692 N85-20637

Laboratory tests of motion sickness susceptibility
11 p1694 N85-20648

Simulator sickness: Reaction to a transformed perceptual world. 6: Preliminary site surveys
11 p1694 N85-20653

Analysis of head motion during simulated, rough water operation of a 2200 ton surface effect ship
11 p1695 N85-20656

best copy available

The current status of the RAF programme of desensitisation for motion sick aircrew
11 p1695 N85-20656
Symposium on Military Aviation Medicine summarized
11 p1696 N85-20663
Air quality criteria for ozone and other photochemical oxidants. External review draft, volume 2
[PB85-126043] 12 p1886 N85-21836
Research and technology activities at Ames Research Center's Biomedical Research Division
[NASA-TM-86692] 12 p1899 N85-21925
USSR report: Space Biology and Aerospace Medicine, volume 18, no. 6, November - December 1984
[JPRS-USB-85-002] 12 p1900 N85-21931
Distinctive morphological manifestations of acute stress reaction in adrenal cortex of hypokinetic rats
12 p1902 N85-21944
Multiple regression method used to assess animal adaptation to hypoxic hypoxia 12 p1902 N85-21947
Results of sanitary-microbiological studies aboard Cosmos-1129 biosatellites 12 p1903 N85-21952
Rat tissue opioid peptide content during long-term hypokinesia 12 p1904 N85-21954
Effect of long-term repeated exposure to high-intensity stationary magnetic field on adrenomedullary activity
12 p1904 N85-21955
Effect of stationary magnetic field on bleeding time
12 p1904 N85-21956
High pressure environmental conditioning systems and chamber rehabilitation
[AD-A150039] 12 p1905 N85-21964
Effect of broad-band constant noise on some systems of animal body 14 p2387 N85-24705
Aerobic and anaerobic exercise tolerance in the heat: Effect and acclimatization 14 p2388 N85-24707
Effects of muscle atrophy on motor control: Cage size effects 15 p2609 N85-26080
Neural mechanism by which gravitational stimulus and stress affect the secretion of renin and other hormones
15 p2610 N85-26083
Homeostasis in primates in the hyperdynamic environment — circadian timekeeping and effects of lower body positive pressure on sleep
15 p2610 N85-26085
Predictions of cardiovascular responses during STS reentry using mathematical models
[NASA-CR-171871] 15 p2616 N85-26119
Description, validation, and modification of the Guyton model for space-flight applications. Part A. Guyton model of circulatory, fluid and electrolyte control. Part B. Modification of the Guyton model for circulatory, fluid and electrolyte control
[NASA-CR-171876] 15 p2616 N85-26122
Mathematical modeling of fluid-electrolyte alterations during weightlessness
[NASA-CR-171881] 15 p2617 N85-26125
Assessing the short- and long-term health effects of decompression sickness among US Navy divers
[AD-A151887] 15 p2618 N85-26132
A brief description of the two primate experiments to be carried out on SL-4 15 p2687 N85-26597
Cardiovascular effects of weightlessness
15 p2688 N85-26607
Percutaneous connectors
[NASA-CR-175627] 16 p2839 N85-27506
Biological and human health effects of extremely low frequency electromagnetic fields. Post-1977 literature review
[AD-A152731] 17 p2999 N85-28539
Mechanizing of handling operations in drop forging with hammers and presses (conducted ergonomical examinations)
[BMFT-FB-HA-84-0[illegible]] 17 p3002 N85-28561
Internal contamination issues
18 p3156 N85-29543
Ambient air contamination: Characterization and detection techniques 18 p3157 N85-29546
Internal contamination in the space station
18 p3157 N85-29549
Alloy development for irradiation performance
[DE85-010454] 19 p3240 N85-30091
Cosmonauts' postural reactions after long-term missions aboard Salyut-6 orbital station 19 p3323 N85-30585
Effect of triphthasine and elenium on changes in evoked bioelectrical activity of the brain exposed to stationary magnetic field 19 p3325 N85-30601
Aviation noise effects
[AD-A154319] 19 p3352 N85-30776
Phenomenon of universal rosette-forming cell stimulation by extreme stress 20 p3505 N85-31789
Changes in pentose and glucuronate pathway dehydrogenases in rat brains following single or multiple hypothermic episodes 20 p3505 N85-31790
Anatomy of stress 20 p3505 N85-31791
Zinc: Biological effects. Facts and fiction
[USIP-84-12] 20 p3507 N85-31798
Gas analysis techniques for human physiological measurements in space — Spacelab
[A/8537] 20 p3507 N85-31803
Results of Space Experiments in Physiology and Medicine and Informal Briefings by the F-16 Medical Working Group
[AGARD-CP-377] 20 p3507 N85-31805
Evaluation of Results of Space Experiments in Physiology and Medicine and Informal Briefings by the F-16 Medical Working Group 20 p3508 N85-31806
Postural adjustments associated with arm movements in weightlessness 20 p3509 N85-31813
Cardiovascular research in space: Problems and results 20 p3510 N85-31817
G-induced Loss of Consciousness (GLC)
20 p3510 N85-31823
Study of requirements for and method of multidimensional acoustic imaging — spaceborne experiments
[ESA-CR(P)-2020] 20 p3525 N85-31924
Results and prospects of physiological research during spaceflights 22 p3732 N85-33139
Antihypertensive neutral lipid
[DE85-011625] 22 p3819 N85-33656
Effects of immobilization and high-altitude adaptation on energy metabolism in rats 22 p3820 N85-33663
Mammalian tissue sensitivity to long-term exposure to high-intensity stationary magnetic fields
22 p3823 N85-33686
Rat skeletal muscles with simulation of physiological effects of weightlessness (morphological study)
23 p3953 N85-34502
Proceedings of a Scientic Meeting on the Occasion of the Inauguration of New Buildings for the DFVLR Institute for Aerospace Medicine
[ESA-TT-857] 24 p4129 N85-35595
The deep diving simulator TITAN: Physiological problems associated with staying in great depths of water 24 p4130 N85-35604
Genetic and physiological control of protective antigen synthesis by bacillus anthracis
[AD-A156324] 24 p4133 N85-35617
PHYSIOLOGICAL FACTORS
NT PHYSICAL FACTORS
Experiments with hydrox at 1.3 MPa (13 atm) — for divers
[FOA-C-58014-H1] 04 p0545 N85-13471
Use of artificial intelligence and simple mathematics to analyze a physiological model 05 p0717 N85-14597
Results of the carbon monoxide study in Washington, D.C. and Denver, Colorado, in the winter of 1982-83
[PB84-230069] 06 p0834 N85-15309
Psychological and physiological basis of stereophonic effect 15 p2526 N85-25574
Selection procedures for F-16 pilots in the Belgian Air Force 20 p3510 N85-31822
Electroanesthesia as a means of controlling cold stress of local hypothermia 22 p3823 N85-33687
PHYSIOLOGICAL RESPONSES
NT HEMODYNAMIC RESPONSES
Jet lag prevention: Physiological mechanisms and pharmacological therapy
[AD-A145444] 02 p0235 N85-11529
An investigation of the use of steady-state evoked potentials for human performance and workload assessment and control
[AD-A145727] 02 p0237 N85-11541
Visually evoked responses from non-occipital areas of the human cortex
[AD-A146079] 03 p0400 N85-12553
Evidence for multiple areas in the human auditory cortex
[AD-A146086] 03 p0401 N85-12555
Proceedings of the 14th Conference on Environmental Toxicology
[AD-A146400] 06 p0843 N85-15350
Distinctions of SPF rats used in experiments aboard biosatellites 07 p1012 N85-16427
Effect of microwave radiation on local blood circulation and oxygenation of brain tissue
07 p1012 N85-16431
Carotid baroreceptor influences on peripheral circulatory and thermal responses during cold exposure
[AD-A146806] 07 p1015 N85-16447
Neuro-linguistic programming: Eye movements as indicators of representational systems
[AD-A147541] 07 p1016 N85-16454
Effect of disuse on sarcoplasmic reticulum in fast and slow skeletal muscle
[NASA-CR-174337] 08 p1191 N85-17508
Acid phosphatase and protease activities in immobilized rat skeletal muscles
[NASA-CR-174340] 08 p1192 N85-17509
A comparison of rat myosin from fast and slow skeletal muscle and the effect of disuse
[NASA-CR-174339] 08 p1192 N85-17510
Workshop on membrane biophysics
[AD-A148238] 08 p1192 N85-17512
Thermoregulatory responses during exercise at graded hypohydration levels
[AD-A147733] 08 p1195 N85-17529
Advanced development of an active neuromusculature response to mechanical stress
[AD-A148436] 08 p1196 N85-17536
The physiology of ultradian rhythms and their role in affecting disease resistance
[AD-A148842] 09 p1363 N85-18575
Hemodynamics responses to upright tilt at sea level and high altitude
[AD-A148846] 10 p1527 N85-19804
Multiple resources and brain laterality
[AD-A148912] 10 p1530 N85-19843
Chemical characterization and toxicologic evaluation of airborne mixtures. Inhalation toxicology of diesel fuel obscurant aerosol in Sprague-Dawley rats. Phase 3. Subchronic exposures
[AD-A150100] 12 p1905 N85-21966
Sleep deprivation and exercise tolerance
[AD-A150180] 13 p2142 N85-23295
Sleep deprivation and exercise tolerance
[AD-A150568] 13 p2142 N85-23296
Sleep deprivation and exercise tolerance
[AD-A150626] 13 p2142 N85-23297
Effect of broad-band constant noise on some systems of animal body 14 p2387 N85-24705
A model for generalization and specification by single neurons
[AD-A150871] 14 p2391 N85-24724
Psychophysiological studies. 1: Performance and physiological response in learning, short-term memory and discrimination tasks
[AD-A151018] 14 p2392 N85-24731
Current approaches for the biophysical and physiological evaluation of combat clothing for environmental extremes
[AD-A151012] 14 p2395 N85-24752
Several specific and nonspecific responses of the human and animal body to ship noise
[NASA-TM-77483] 15 p2615 N85-26116
Eye movement in response to single and multiple targets
[AD-A151115] 15 p2617 N85-26128
Physiological differences between men and women in exercise-heat tolerance and heat acclimation
[AD-A152048] 15 p2618 N85-26135
Plasma hormonal responses at graded hypohydration levels during exercise/heat stress
[AD-A153681] 18 p3153 N85-29523
An integrated analysis of the physiological effects of space flight: Executive summary
[NASA-CR-171892] 20 p3506 N85-31796
Empirical methods for predicting eutrophication in impoundments. Report 3. Phase 2. Model refinements
[AD-A155483] 21 p3614 N85-32462
USAFSAM review and analysis of radiofrequency radiation bioeffects literature
[AD-A155113] 21 p3664 N85-32760
Microwave radiation and thermoregulation
[AD-A155718] 22 p3818 N85-33654
Cardiovascular responses to orthostatism and weightlessness 24 p4130 N85-35601
Physiological responses to unvarying (steady) and 2-2-1 shifts: Miami International Flight Service Station
[AD-A155751] 24 p4133 N85-35619
PHYSIOLOGICAL TESTS
NT BODY SWAY TEST
NT VESTIBULAR TESTS
Variability of cardiac rhythm during information loading
10 p1525 N85-19619
Space motion sickness monitoring experiment: Spacelab 1 11 p1695 N85-20654
Chemical characterization and toxicologic evaluation of airborne mixtures. Inhalation toxicology of diesel fuel obscurant aerosol in Sprague-Dawley rats. Phase 3. Subchronic exposures
[AD-A150100] 12 p1905 N85-21966
PHYSIOLOGY
NT AUDIOLOGY
NT ELECTROPHYSIOLOGY
NT EXERCISE PHYSIOLOGY
NT GRAVITATIONAL PHYSIOLOGY
NT HEMATOPOIETIC SYSTEM
NT NEUROPHYSIOLOGY
NT PSYCHOPHYSIOLOGY
NT RESPIRATORY PHYSIOLOGY
NT UNDERWATER PHYSIOLOGY
NT WORKLOADS (PSYCHOPHYSIOLOGY)
USSR report: Life sciences. Biomedical and behavioral sciences
[JPRS-UBB-85-008] 10 p1523 N85-19605
Morphological study of monkeys submitted to antiorthostatic hypokinesia 12 p1902 N85-21942

Problems of space biology. Volume 50: Nystagmometry for evaluation of the status of the vestibular function
[NASA-TM-77616] 14 p2385 N85-24694
Principal patterns of functional changes of human respiratory system in adaptation to high pressure
14 p2387 N85-24704
Development of guidelines for setting physiological and hygienic standards for noise levels in aerospace medicine 19 p3323 N85-30584
Chemolithotrophy and physiology of bacterial nutrient limitation 21 p3659 N85-32730
Structure and physiology of Beggiatoa and Thiothrix
21 p3659 N85-32734
Sulfur cycling and metabolism of phototrophic and filamentous sulfur bacteria 21 p3660 N85-32737
USSR report: Life sciences. Biomedical and behavioral sciences
[JPRS-UBB-85-018] 22 p3819 N85-33660
PHYTOTRONS
Plant growth in space 05 p0691 N85-14444
PICKLING (METALLURGY)
Pickling of stainless steels: A review
[PB85-111979] 10 p1442 N85-19087
PICKOFFS
U SENSORS
PICKUPS
U SENSORS
PICOSECOND PULSES
Nonlinear symmetrization of picosecond pulses in optical fibers 02 p0264 N85-11725
Coherent amplification of ultrasonic pulses in activated crystals 05 p0724 N85-14653
Transformation of energy spread of laser pumping via phase conjugation 05 p0725 N85-14661
Optically induced intervalence-band transitions in germanium by the absorption of 1.06 micrometers picosecond pulses
[DE85-000946] 09 p1399 N85-18803
Picosecond laser pulse interactions with metallic and semiconductor surfaces
[AD-A149112] 10 p1490 N85-19405
Picosecond photoconductive devices for 10 Gbit/s optoelectronic switching 18 p3187 N85-29770
Dynamics of emission from dye lasers employing synchronous pumping by limited picosecond pulse train
21 p3686 N85-32899
PICTURE TUBES
Plans, developments in robotics
14 p2289 N85-24191
PIEDMONTS
Late precambrian to ordovician metamorphism and orogenesis in the Blue Ridge and western Piedmont, Virginia Appalachians 09 p1352 N85-18503
PIEZOELECTRIC CERAMICS
NT LEAD ZIRCONATE TITANATES
Optimization of piezoceramic optical deflector
11 p1719 N85-20813
Elasticity formulas for thin-walled shells with piezoceramic layers 13 p2047 N85-22816
Reaction of piezoceramic shell to concentrated forces
14 p2279 N85-24115
Effect of axisymmetric vibration modes on sensitivity and directivity characteristics of piezoceramic sphere — hydrophones 15 p2525 N85-25569
Scattering of sounds by piezoceramic cylindrical shell near rigid surface 17 p2943 N85-28168
Experiments on the influence of active walls on the initial amplitudes and growths of instability waves
[AD-A154630] 21 p3583 N85-32275
Materials used by industry for the production of piezoelectric transducers. The state of the art of research work performed in the field of PZT ceramics and ferroelectric polymers
[ISL-CO-211/84] 24 p4089 N85-35344
Piezoelectric transducers, state of research
24 p4089 N85-35345
Conduction and aging of piezoelectric PZT ceramics
24 p4089 N85-35346
PIEZOELECTRIC CRYSTALS
Piezoelectric and electrostrictive materials for transducer applications
[AD-A145115] 01 p0043 N85-10277
Method for evaluating petrol products corrosivity using piezoelectric crystals. Part 2: Instruction manual — jet engine corrosion tests
[FOA-C-40199-B4] 04 p0482 N85-13073
Microwave resonator using lateral excitation
[AD-D011374] 07 p1039 N85-16596
Normal coordinate monolithic crystal filter
[AD-D011496] 12 p1941 N85-22188
Stress compensation crystal device
[AD-D011497] 12 p1941 N85-22189
Adjustment of the frequency-temperature characteristics of crystal oscillators
[AD-D011588] 15 p2548 N85-25726
Suppression of vibration effects on piezoelectric crystal resonators
[AD-D011625] 16 p2778 N85-27142
Acceleration resistant combination of opposite-handed piezoelectric crystals
[AD-D011626] 16 p2778 N85-27143
Dual species ion implantation of ternary compounds based on In-Ga-As
[AD-D011617] 16 p2869 N85-27698
Power generation efficiency of piezoelectric crystals
20 p3537 N85-32008
Materials used by industry for the production of piezoelectric transducers. The state of the art of research work performed in the field of PZT ceramics and ferroelectric polymers
[ISL-CO-211/84] 24 p4089 N85-35344
PIEZOELECTRIC GAGES
Development of components for micro-C oriented sensor systems
[BMFT-FB-T-84-126] 04 p0504 N85-13215
PIEZOELECTRIC TRANSDUCERS
NT PIEZOELECTRIC GAGES
Piezoelectric and electrostrictive materials for transducer applications
[AD-A145115] 01 p0043 N85-10277
An automated immittance measuring system for electroacoustic transducers
[AD-A145701] 02 p0200 N85-11336
Development of a polymer pressure gage with temperature compensation 03 p0365 N85-12340
Analysis of piezoelectric disks and cylinders using finite element method
[AD-A146323] 03 p0414 N85-12650
Optimization piezoelectric transducer width of acousto-optical devices 07 p0950 N85-16024
Lightweight, broadband Rayleigh wave transducer
[AD-D011345] 07 p1037 N85-16584
Piezoelectric stress transducer used for measurements of explosions in hard rock 11 p1638 N85-20316
Piezoelectric transducer using electrically poled gamma-phase Nylon 11
[AD-D011552] 12 p1850 N85-21602
Piezoelectric filter with low-Q inductances
13 p2070 N85-22932
Piezoelectric and electrostatic polymeric transducers for acoustic emission detection
[AD-A150883] 14 p2306 N85-24272
Recording of acoustic wave in gaseous medium with thin-film pyroelectric transducers
15 p2525 N85-25571
The development of a transducer system for the accurate measurement of ultrasonic phase delay of SH plate waves
[AERE-R-11598] 15 p2559 N85-25790
A study of gas solid reactions using coated piezoelectric detectors
[AD-A153047] 17 p2920 N85-28001
Microwave SAW (Surface Acoustic Wave) monochromator
[AD-D011718] 21 p3590 N85-32311
Materials used by industry for the production of piezoelectric transducers. The state of the art of research work performed in the field of PZT ceramics and ferroelectric polymers
[ISL-CO-211/84] 24 p4089 N85-35344
Piezoelectric transducers, state of research
24 p4089 N85-35345
Ferroelectric homopolymer PVF2 and P (VDF-TrFe) copolymers 24 p4089 N85-35347
PIEZOELECTRICITY
Piezoelectric and electrostrictive materials for transducer applications
[AD-A145115] 01 p0043 N85-10277
Acoustic emission linear pulse holography
[DE84-014519] 01 p0050 N85-10330
Saint Venant conditions in theory of piezoelastic shells
06 p0780 N85-14967
Switchable zero order diffraction gratings as light valves
[AD-A147575] 07 p1044 N85-16633
Switchable zero order diffraction gratings as light valves
[AD-A150129] 12 p1934 N85-22153
Piezoelectric plastics — polyvinyl fluoride
[ISL-CO-202/83] 14 p2262 N85-24017
Compensation of acoustic wave devices
[AD-D011582] 15 p2646 N85-26322
Applications of piezoelectric and pyroelectric thin films: Opportunities for Langmuir-Blodgett technology
[AD-A149239] 15 p2659 N85-26408
Piezoelectric and pyroelectric polymers
16 p2756 N85-27008
Transversely reinforced piezoelectric composites
[AD-D011676] 19 p3260 N85-30214
Microwave bandstop filter
[AD-D011716] 19 p3261 N85-30222
Some dynamic electronic properties of semiconductor surfaces and interfaces 20 p3537 N85-32007
Power generation efficiency of piezoelectric crystals
20 p3537 N85-32008
Device for frequency modulation of a laser output spectrum
[DE85-011634] 22 p3790 N85-33479
Non-bonded ultrasonic transducer
[DE85-011006] 22 p3794 N85-33504
PIEZORESISTIVE TRANSDUCERS
NT PIEZOELECTRIC GAGES
Technology of thin silicon foils for the fabrication of monolithic integrated sensors
[BMFT-FB-T-84-209] 12 p1943 N85-22202
An advanced solid state pressure transducer for high reliability SSME application 16 p2739 N85-26905
Research pressure instrumentation for NASA space shuttle main engine
[NASA-CR-176014] 19 p3227 N85-30006
PIGMENTS
NT CAROTENE
NT CHLOROPHYLLS
NT CYTOCHROMES
Proton pumping in purple membrane, appendix 1
[DE84-014601] 01 p0118 N85-10811
The structure and function of fungal cells
[NASA-TM-77443] 06 p0842 N85-15348
Process for preparation of crosslinked poly(tri-n-butyltin) methacrylate with simultaneous particle size reduction
[AD-D011313] 07 p0932 N85-15905
Primary light harvesting system: The relationship of phycobilisomes to photosystem 1 and 2
[DE85-003075] 11 p1689 N85-20622
PILE FOUNDATIONS
Experimentally determined distribution of stress around a horizontally loaded model pile in dense sand
[CE-43] 16 p2796 N85-27239
PILOT ERROR
A model for the effectiveness of aircraft alerting and warning systems 05 p0702 N85-14506
Direction judgement errors in perspective displays
05 p0705 N85-14520
Safety recommendation(s), A-84-93 through -95
[REPT-3983/33] 14 p2216 N85-23746
Investigation of technology needs for avoiding helicopter pilot error related accidents
[NASA-CR-3895] 15 p2465 N85-25220
Safety recommendation(s), A-84-96
[REPT-3983A/217] 15 p2466 N85-25223
PILOT PERFORMANCE
A mathematical simulation model of the CH-47B helicopter, volume 1
[NASA-TM-84351-VOL-1] 01 p0006 N85-10033
The Malcolm horizon: History and future
01 p0008 N85-10046
Content, variety, and augmentation of simulated visual scenes for teaching air-to-ground attack
[AD-A145218] 01 p0013 N85-10080
Workload demand and CNS depressant stressor efffects on spatial orientation information processing
[AD-A145211] 01 p0098 N85-10651
Aircraft accident report. Central Airlines flight 27, Hughes Charter Air, Gates Learjet model 25 (N51CA) Newark International Airport, Newark, New Jersey, March 30, 1983
[PB84-910411] 02 p0136 N85-10924
Integrated Application of Active Controls (IAAC) technology to an advanced subsonic transport project-longitudinal handling qualities study of a relaxed-stability airplane
[NASA-CR-3660] 02 p0148 N85-11005
An in-flight investigation of a twin fuselage configuration in approach and landing
[NASA-CR-172366] 05 p0596 N85-13601
Investigation of pilot behavior in flight tests with a rate command/attitude hold control system
[DFVLR-FB-84-25] 05 p0699 N85-14486
Statistical time series models of pilot control with applications to instrument discrimination
05 p0700 N85-14489
Measurements of pilot time delay as influenced by controller characteristics and vehicles time delays
05 p0701 N85-14500
Helicopter pilot performance for discrete-maneuver flight tasks 05 p0702 N85-14502
Measuring workload differences between short-term memory and long-term memory scenarios in a simulated flight environment 05 p0703 N85-14513
Use of linear perspective scene cues in a simulated height regulation task 05 p0704 N85-14517
Cockpit window edge proximity effects on judgements of horizon vertical displacement
05 p0704 N85-14518
Mean and random errors of visual roll rate perception from central and peripheral visual displays
05 p0704 N85-14519

Accuracy of system step response roll magnitude estimation from central and peripheral visual displays and simulator cockpit motion 05 p0705 N85-14522
Twentieth Annual Conference on Manual Control, volume 2
[NASA-CP-2341-VOL-2] 05 p0707 N85-14535
Assessing the subjective workload of directional orientation tasks 05 p0708 N85-14542
A full mission simulator study of aircrew performances: The measurement of crew coordination and decisionmaking factors and their relationships to flight task performances 05 p0710 N85-14556
Measuring pilot workload in a moving-base simulator. Part 2: Building levels of workload
05 p0712 N85-14566
The Sternberg task as a workload metric in flight handling qualities research 05 p0712 N85-14568
Superaugmented rotorcraft program
06 p0750 N85-14807
Some thoughts on the implementation of pilot night vision devices for helicopters 06 p0751 N85-14814
Intelligent interfaces for tactical airborne platforms
06 p0752 N85-14820
Operational requirements - system concepts
06 p0752 N85-14823
Mental status in relation to special conditions of activity 07 p1011 N85-16420
Job and family stress as predictors of pilot health, job satisfaction and performance
[AD-A142176] 07 p1018 N85-16484
Practice makes perfect
[AD-A147124] 07 p1019 N85-16486
Assessment of simulation fidelity using measurements of piloting technique in flight 08 p1075 N85-16817
Effects of pyridostigmine on psychomotor and visual performance
[AD-A148553] 08 p1196 N85-17539
Improvement of workload estimation techniques in piloting tasks
[NASA-CR-174374] 10 p1531 N85-19646
Tolerance, fatigue, physiological and performance effects of sustained and oscillating lateral accelerations
10 p1533 N85-19659
Impact of future aircombat characteristics on pilot performance and cockpit design
10 p1533 N85-19661
Conceptual model of critical requirements for effective pilot performance in high performance aircraft
10 p1533 N85-19663
The cockpit of the year 2000: How big a step?
10 p1534 N85-19667
Pilot workload, performance and aircraft control automation 10 p1534 N85-19670
Aviation medicine's role in modern airforce discussed
11 p1686 N85-20662
Close air support mission: Development of a unitary measure of pilot performance
[AD-A149285] 11 p1697 N85-20665
Space shuttle pilot-induced-oscillation research testing
13 p1966 N85-22351
Air combat simulation: Methods, models, trends
13 p1967 N85-22359
Complex program of ergonomic studies Pilot described 14 p2386 N85-24698
Mental workload measurement: Event-related potentials and ratings of workload and fatigue
[NASA-CR-177354] 15 p2619 N85-26139
Correlations between selection ratings and success as army aviators
[FOA-C-53020-H2] 15 p2620 N85-26144
A comparison of pictorial and speech warning messages in the modern cockpit
[AD-A151917] 16 p2707 N85-26706
Development factors and field dependence-independence
[AD-A152337] 17 p3000 N85-28545
Technical evaluation of the Naval Automated Pilot Aptitude Measurement System (NAPAMS)
[AD-A152361] 17 p3000 N85-28547
Stabilizing force feedback in bio-actuated control systems
[AD-D011634] 17 p3002 N85-28560
The use of flight simulators in measuring and improving training effectiveness
[AD-A153817] 18 p3064 N85-28954
Electrooculographic measurement, fatigue and variability of performance in simulated aircraft flight
19 p3217 N85-29948
Psychophysiological nature of aircraft feel
19 p3323 N85-30587
The value of DMT in the selection of pilots
[RAE-TRANS-2127] 19 p3330 N85-30626
A systematic determination of skill and simulator requirements for airline transport pilot certification
[AD-A154135] 19 p3330 N85-30630
Selection procedures for F-16 pilots in the Belgian Air Force 20 p3510 N85-31822
G-induced Loss of Consciousness (GLC)
20 p3510 N85-31823
Physical training and G tolerance
20 p3511 N85-31824
An error-dependent model of instrument-scanning behavior in commercial airline pilots
[NASA-CR-3908] 21 p3665 N85-32765
Human performance in continuous/sustained operations and the demands of extended work/rest schedules. An annotated bibliography
[AD-A155619] 21 p3666 N85-32771

PILOT PLANTS
The 15 photovoltaic pilot projects of the European Communities 05 p0663 N85-14263
Photovoltaic 100 kWp pilot plant on the Greek island Kythnos 05 p0664 N85-14266
Development and prototype construction of photovoltaic energy supply units 12 p1878 N85-21781
10 MWe Solar Thermal Central Receiver Pilot Plant total capitol costs
[DE85-009113] 18 p3131 N85-29390
Study of alternative system conversions for the Solar One pilot plant
[DE85-010026] 22 p3809 N85-33594

PILOT SELECTION
Correlations between selection ratings and success as army aviators
[FOA-C-53020-H2] 15 p2620 N85-26144
Selection procedures for F-16 pilots in the Belgian Air Force 20 p3510 N85-31822
Rapid determination of cadet discipline by projective tests 22 p3821 N85-33671

PILOT TRAINING
Training effectiveness evaluation and utilization demonstration of a low cost cockpit procedures trainer
[AD-A145179] 01 p0013 N85-10078
Content, variety, and augmentation of simulated visual scenes for teaching air-to-ground attack
[AD-A145218] 01 p0013 N85-10080
Determining training device requirements in Army aviation systems 05 p0711 N85-14558
Analysis of the flow field about a T-45 using PANAIR
[AD-A146811] 07 p0899 N85-15699
Directions of the West German Ministry of Transport for education and control of airline personnel (section 3, chapters 2 and 12) 08 p1081 N85-16848
Directions of the West German Ministry of Transport for education and control or airline personnel, Report 6; chapters 3/A and 3/B 08 p1081 N85-16849
Using a limited field of view simulator to instruct high speed, low altitude flying skills
[AD-P004309] 09 p1267 N85-17963
Visual perceptual aspects of low level high speed flight and flight simulation
[AD-P004310] 09 p1267 N85-17964
On-board Computer Image Generator (CIG) applications
[AD-P004335] 09 p1271 N85-17989
CIG (Computer Image Generator) goes to war: The tactical illusion
[AD-P004336] 09 p1271 N85-17990
Flight Training Technology for Regional/Commuter Airline Operations: Regional Airline Association/NASA Workshop Proceedings
[NASA-CP-2348] 09 p1275 N85-18009
Flight crew training technology: A review
09 p1275 N85-18010
Low-cost training technology
09 p1275 N85-18011
Captain development training at US Air
09 p1275 N85-18012
Management training for cockpit crews at Piedmont flight 09 p1276 N85-18013
Use of simplifier scenarios for CRM training
09 p1276 N85-18016
Safety awareness, pilot education, and incident reporting programs 09 p1276 N85-18020
The aviation safety reporting system
09 p1276 N85-18021
Simulation of aircraft behaviour on and close to the ground
[NASA-TM-87460] 14 p2218 N85-23754
Visual simulation requirements for aircraft aspect recognition at real world distances
[AD-A151040] 14 p2228 N85-23810
Technical evaluation of the Naval Automated Pilot Aptitude Measurement System (NAPAMS)
[AD-A152361] 17 p3000 N85-28547
Guidelines of the Federal Minister of Transportation for the formation and examination of airline personnel, part 4 17 p3002 N85-28556
Human factors in cockpit automation: A field study of flight crew transition
[NASA-CR-177333] 19 p3215 N85-29937
The value of DMT in the selection of pilots
[RAE-TRANS-2127] 19 p3330 N85-30626
Selection procedures for F-16 pilots in the Belgian Air Force 20 p3510 N85-31822
G-induced Loss of Consciousness (GLC)
20 p3510 N85-31823
Physical training and G tolerance
20 p3511 N85-31824
Centrifuge operations and training in the Royal Netherlands Air Force 20 p3511 N85-31825
Advanced simulator for pilot training and helmet-mounted visual display configuration comparisons
[AD-A155326] 21 p3667 N85-32776
Rapid determination of cadet discipline by projective tests 22 p3821 N85-33671
RAFTS: A T-38 replacement for the 21st century
[AD-A156103] 24 p4065 N85-35191

PILOTED CENTRIFUGES
U HUMAN CENTRIFUGES

PILOTLESS AIRCRAFT
Visual systems for remotely controlled vehicles
05 p0703 N85-14512
On-board processing for linescan sensors in miniature unmanned aircraft
[RAE-TM-SPACE-327] 08 p1065 N85-16870

PILOTS (PERSONNEL)
NT AIRCRAFT PILOTS
Anthropometric cockpit compatibility assessment of US Army aircraft for large and small personnel wearing a training, warm-weather clothing configuration
[AD-A145206] 01 p0099 N85-10656
Decision tree rating scales for workload estimation: Theme and variations
[NASA-CR-174062] 02 p0237 N85-11544
Cardiovascular disease among U.S. Navy pilots
[AD-A145871] 03 p0400 N85-12552
Differences in health risks by aircraft model among US Navy pilots
[AD-A146147] 03 p0401 N85-12556
Measurements of pilot time delay as influenced by controller characteristics and vehicles time delays
05 p0701 N85-14500
Multiloop manual control of dynamic systems
05 p0702 N85-14505
A model for the effectiveness of aircraft alerting and warning systems 05 p0702 N85-14506
Human factors survey: C-5 pilots
[AD-A147106] 07 p1020 N85-16477
Evaluation of arctic test of improved tritium radioluminescent lighting
[AD-A148215] 08 p1089 N85-16884
Aviation-related cardiorespiratory effects of blood donation in female pilots
[AD-A148045] 08 p1195 N85-17529
Health examination findings among active civil airmen
[AD-A148325] 08 p1195 N85-17533
An investigation of spinal injury potential from the use of the ACES 2 ejection seat by lower weight female pilots
[AD-A148449] 08 p1196 N85-17537
Development of an electro-pneumatic anti-G valve for high performance fighter aircraft
[AD-A148488] 08 p1201 N85-17561
Global optical metrics for self-motion perception
[AD-P004333] 09 p1271 N85-17987
Simulator sickness: Sensorimotor disturbances induced in flight simulators
[AD-P004334] 09 p1271 N85-17988
Communications skills for CRM training
09 p1276 N85-18017
Pilot education and safety awareness programs
09 p1277 N85-18026
Innovative approaches to recurrent training
09 p1277 N85-18028
Medically disqualified airline pilots
[AD-A149454] 10 p1528 N85-19607
Crewstation assessment of reach as applied to the OH-58A helicopter
[AD-A149413] 10 p1531 N85-19650
Military pilot ergonomics 10 p1532 N85-19655
Biofeedback treatment of airsickness: A review
11 p1696 N85-20660
US Army Aviation Engineering Flight Activity (USAAEFA) report bibliography update 1983 - 1984
[AD-A151361] 15 p2457 N85-25188
Airsickness control using biofeedback to self-regulate psychophysiological responses
[AD-A151167] 15 p2617 N85-26128
Psychometric evaluation of head injury among fliers referred to the AF School of Aerospace Medicine
[AD-A151479] 15 p2617 N85-26129
Aspects of application of ACT systems for pilot workload alleviation 16 p2712 N85-26734
Aspects of application of ACT systems for pilot workload alleviation 17 p2901 N85-27987

Development factors and field dependence-independence [AD-A152337] 17 p3000 N85-28545

Operation guiding light-scientific program and field plan. The pilot field experiment for NORDA project chemical dynamics in ocean frontal areas [AD-A153765] 18 p3150 N85-29507

Longitudinal study of cardiovascular disease in US Navy pilots [AD-A154331] 19 p3328 N85-30623

The value of DMT in the selection of pilots [RAE-TRANS-2127] 19 p3330 N85-30626

U.S. Civil airmen statistics for calendar year 1984 [AD-A156326] 24 p4059 N85-35153

International flight planning handbook [AD-A156330] 24 p4062 N85-35177

PINCH EFFECT

NT PLASMA PINCH
NT REVERSE FIELD PINCH
NT THETA PINCH
NT ZETA PINCH

PINHOLE CAMERAS

A microchannel plate pinhole camera for 20 to 100 keV X-ray imaging [DE85-001572] 10 p1488 N85-19396

Sequentially-framing soft X-ray pinhole camera for Tokamak plasma studies [DE85-001717] 10 p1489 N85-19399

Three-dimensional and tomographic imaging device for X-ray and gamma-ray emitting objects [NASA-CASE-GSC-12851-1] 19 p3271 N85-30281

PINHOLES

Double pinhole spatial phase correlator apparatus [AD-D011495] 11 p1729 N85-20872

PINNING

NT FLUX PINNING

PINS

Extractor for spring-lock pin connectors [AD-D011235] 01 p0043 N85-10280

Stress analysis of pin-loaded orthotropic plates using orthotropic photoelasticity 02 p0207 N85-11366

Connector/nitinol delta contact force device [AD-D011467] 10 p1481 N85-19349

The effects of pin elasticity, clearance, and friction on the stresses in a pin-loaded orthotropic plate [NASA-CR-175816] 16 p2743 N85-26927

An approximation to the problem of a pin-loaded hole in an orthothropic plate [VTH-LR-386] 16 p2802 N85-27278

Printed wiring board circuit isolator tool [AD-D011636] 17 p2968 N85-28333

The stress distribution in pin-loaded orthotropic plates [NASA-CR-176146] 22 p3800 N85-33547

Evacuate and backfill apparatus and method [DE85-006018] 23 p3938 N85-34411

Verification of the SRB motor case pin retainer band tips [NASA-CR-170882] 24 p4070 N85-35220

PION BEAMS

Study of hadron bundles observed in Chacaltaya two-story emulsion chamber [HE-3.3-4] 24 p4180 N85-35922

Experimental basis for the models of cascade propagation in atmosphere [HE-3.6-6] 24 p4185 N85-35954

PIONEER F SPACE PROBE

U PIONEER 10 SPACE PROBE

PIONEER G SPACE PROBE

U PIONEER 11 SPACE PROBE

PIONEER SATURN SPACECRAFT

U PIONEER 11 SPACE PROBE

PIONEER SPACE PROBES

NT PIONEER 10 SPACE PROBE
NT PIONEER 11 SPACE PROBE

Charged particle erosion of icy satellites: Coronal atmospheres and surface redistribution 03 p0448 N85-12845

Interpretation of Venus gravitational anomalies 15 p2483 N85-25322

PIONEER VENUS SPACECRAFT

Analysis and interpretation of observations of airglow at 297 nm in the Venus thermosphere 13 p2172 N85-23473

Venus gravity: Global field results 13 p2177 N85-23512

Geophysical interpretation of Venus gravity data 13 p2178 N85-23513

Venus chasmata: A lithosphere stretching model 13 p2178 N85-23516

Programming for Pioneer 12 15 p2686 N85-26606

PIONEER 12 SPACE PROBE

U PIONEER VENUS SPACECRAFT

PIONEER 10 SPACE PROBE

Pioneer 10 and Voyager observations of the interstellar medium in scattered emission of the He 584 A and H Lya 1216 A lines 06 p0873 N85-15541

PIONEER 11 SPACE PROBE

Investigations of planetary ring phenomena 13 p2174 N85-23487

Electrons and cosmic ray produced protons in Saturn's inner magnetosphere [NASA-TM-87469] 15 p2679 N85-26546

PIONS

Experimental medium energy physics [DE84-014625] 02 p0278 N85-11807

Skyrmions and vector mesons: A symmetric approach [DE84-015297] 04 p0563 N85-13584

Pion inelastic scattering to the first three excited states of Lithium-6 [AD-A147560] 07 p1041 N85-16606

A 1-2 GeV/c beam line for hypernuclear and kaon research [DE85-007623] 16 p2863 N85-27659

Deep-inelastic lepton scattering by nuclei: The pion-exchange model [DE85-010496] 19 p3359 N85-30828

Pion production and the nuclear equation of state [DE85-009941] 19 p3365 N85-30870

AGS broad band neutrino beam [DE85-010954] 19 p3366 N85-30875

Neutral pion production in solar flares [SH-1.4-7] 23 p3995 N85-34767

Determination of the cross section of the proton, pion and neutron inelastic interaction with lead and carbon nuclei at 0.5 - 5.0 TeV energies (PION experiment) [HE-1.1-6] 24 p4170 N85-35853

Angular distribution and multiplicity of backward hadrons in hFe interactions at 0.5-5.0 TeV energies (PION Experiment) [HE-1.2-8] 24 p4172 N85-35866

Anuglar distribution of shower particles produced in the collisions of 20-GeV/c and 300-GeV negative pions with emulsion nuclei 24 p4172 N85-35868

Is the inelastic charge-exchange contribution constant at the large X and superhigh energies? Qaut 01Kuchin, I. A. 24 p4173 N85-35871

Energy-range relations for hadrons in nuclear matter 24 p4174 N85-35881

Measurements of hadron mean free path for the particle-producing collisions in nuclear matter 24 p4174 N85-35883

On mini-cluster observed by Chacaltaya emulsion chamber experiment [HE-3.6-12] 24 p4185 N85-35959

A study of gamma-families generated in nucleon-nucleus (NA) and pion-nucleus (pi A) interactions [HE-3.7-2] 24 p4186 N85-35961

Study of photonuclear muon interactions at Baksan underground scintillation telescope [HE-5.4-10] 24 p4208 N85-36122

Observation of genetic relation among new phenomena Geminion, Chiron and mini-Centauro [HE-6.2-16] 24 p4212 N85-36152

Tien-Shan effect and charmed particles [HE-6.2-17] 24 p4212 N85-36153

PIPE FLOW

Classical free-streamline flow over a polygonal obstacle [NASA-CR-172448] 01 p0046 N85-10301

Thermal fluid-structure interaction: A few scaling considerations --- nuclear reactors [GKSS-84-E-18] 01 p0048 N85-10314

Void fraction measurements performed in a vertical large diameter tube compared to different predicting correlations [GKSS-84-E-24] 01 p0048 N85-10315

Visualization of the diverging two-phase flow pattern in a horizontal T-junction with vertical branch [GKSS-84-E-25] 01 p0048 N85-10316

Fluid layer between infinite elastic plates II. Distribution of power flow [AD-A146690] 03 p0361 N85-12312

An organ-pipe oscillation --- PHOENICS code [PDR/CFDU-IC/14] 04 p0501 N85-13199

Wave propagation in compliant tubes containing a heat-conducting viscous fluid [WTHD-163] 05 p0636 N85-14094

Flow of nitrogen-pressurized Halon 1301 in fire extinguishing systems [NASA-CR-174271] 07 p0900 N85-15701

Studies of the wall shear stress in a turbulent pulsating pipe flow [AD-A146772] 07 p0957 N85-16068

The stability of an infinite elastic pipe with uniform mean flow [AD-A146686] 08 p1161 N85-17326

Computation of flow and heat transfer in flow around a 180 deg bend [AD-A148065] 08 p1162 N85-17330

Thermal striping downstream of a horizontal elbow under thermally stratified transient flow conditions [DE84-014687] 09 p1320 N85-18302

The influence of modern control techniques on the gas industry [ERS-E.395] 09 p1325 N85-18326

Design of piping for oil drain from turbine bearings 14 p2271 N85-24073

Unsteady flows in a tube with combustion reaction [ISL-R-118/83] 14 p2303 N85-24261

Behavior of turbulent gas jets in an axisymmetric confinement [NASA-CR-174829] 15 p2473 N85-25265

Heat transfer in pipes [NASA-TM-77838] 17 p2957 N85-28262

Steady, incompressible, inviscid flow through a finite collapsible tube under longitudinal tension [REPT-84-01] 17 p2959 N85-28278

Flow through finite collapsible tubes: A branching problem [REPT-84-29] 17 p2960 N85-28281

Monogroove heat pipe design: Insulated liquid channel with bridging wick [NASA-CASE-MSC-20497-1] 18 p3098 N85-29180

Transport characteristics of slurries in pipelines: Flow regimes and pressure drop [DE85-009453] 18 p3101 N85-29198

Dynamic stability of a spinning tube conveying a flowing fluid [DE85-007583] 18 p3102 N85-29207

Experimental investigations of the unsteady turbulent friction behavior with pressure impulses in a circular pipe [IWAWI-MITT-102] 18 p3103 N85-29210

A method for predicting additive drag reduction from small-diameter pipe flows [AD-A154411] 19 p3266 N85-30254

Droplet deposition in vertical two-phase flow [CFD/84/22] 20 p3456 N85-31460

Intermittent gas-liquid flow modeling in horizontal or weakly inclined pipes [EME-132] 20 p3456 N85-31465

Resolution of thermal striping issue downstream of a horizontal pipe elbow in stratified pipe flow [DE85-006195] 21 p3586 N85-32292

Computer and water-model simulation of flow through poppet valves [CFD/85/2] 22 p3785 N85-33449

Experimental simulation of in-bore flows using a high pressure shock tube [ISL-CO-217/84] 22 p3785 N85-33452

PIPELINES

NT SEWERS

Low power microprocessor based measurements system for determining the integrity of coatings on buried pipelines [ERS-E.380] 09 p1324 N85-18323

Defect tolerance in pipeline girth welds [ERS-E.353] 09 p1328 N85-18347

Hydrogen induced cracking in pipeline steels [ERS-E.327] 09 p1340 N85-18429

Mechanism of hydrogen induced cracking in pipeline steels [ERS-E.349] 09 p1340 N85-18430

The influence of mechanical damage on transmission pipeline integrity [ERS-E.351] 09 p1340 N85-18431

Recent studies of the significance of mechanical damage in pipelines [ERS-E.367] 09 p1341 N85-18433

Statistical aspects of shear fracture propagation [ERS-E.368] 09 p1341 N85-18434

The effect of an elastic foundation and of dissipative forces on the stability of fluid conveying pipes [TAE-563] 12 p1863 N85-21688

Abatement of noise and vibration in pipelines of hydro systems 14 p2276 N85-24102

Underwater pipeline: Welding by high frequency induction [BLL-WI-TRANS-682-(9312.57)] 16 p2792 N85-27221

Effect of the agressive action of soil on metallic pipelines. New possibilities for the passive and active corrosion protection [BLL-BISI-TRANS-21630-(9022.06)] 17 p2928 N85-28070

Hydrogen degradation of pipeline steels [DE85-008930] 17 p2932 N85-28101

Model documentation of the gas analysis modeling system. Volume 1: Model overview [DE85-010952] 20 p3515 N85-31856

PIPELINING (COMPUTERS)

Solution of partial differential equations on vector and parallel computers [NASA-CR-172500] 07 p1028 N85-16525

Siemens introduces fast computer with pipeline architecture 11 p1618 N85-20176

Exploiting multiprocessors: Issues and options [DE85-003144] 13 p2145 N85-23313

Implementation of some concurrent algorithms
[DE85-004667] 13 p2148 N85-23334

Effective microinstruction pipeline organization in a high-capacity microprocessor 15 p2625 N85-26176

Squeezing the most out of Eigenvalue solvers on high-performance computers
[DE85-007569] 16 p2849 N85-27565

Pipelined programmable charge domain device
[AD-D011598] 17 p2951 N85-28225

Pipelined Givens method for computing the QR factorization of a sparse matrix
[DE85-009772] 18 p3171 N85-29653

VLSI structures for numerical and digital signal processing computations 20 p3439 N85-31340

PIPES (TUBES)

NT GAS PIPES

Lightweight composite launcher pod
[AD-D011236] 01 p0015 N85-10092

Bifouling and corrosion studies at the Seacoast Test Facility in Hawaii
[DE84-014643] 01 p0029 N85-10180

Heat exchanger
[DE84-014299] 01 p0047 N85-10309

Void fraction measurements performed in a vertical large diameter tube compared to different predicting correlations
[GKSS-84-E-24] 01 p0048 N85-10315

Method and apparatus for determining the content and distribution of a thermal neutron absorbing material in an object
[DE84-014319] 01 p0117 N85-10601

Directional nature of strengthening during thermomechanical treatment
[BLL-M-35746-(5828.4)] 02 p0175 N85-11174

Recent developments on the role of molybdenum in irons and steels 02 p0180 N85-11206

Modernization of IDTs-6 ultrasonic installation
[BLL-M-35716-(5828.4)] 02 p0206 N85-11356

Polycyclic aromatic hydrocarbons on the inner surfaces of copper tubing
[AD-A145979] 03 p0337 N85-12169

Corrosion of brass in potable water service
[CETIM-100390] 04 p0477 N85-13037

Detection of cracks in a plastics pipe joint by reflection holography
[NPL-DMA(A)-87/MOM-70] 04 p0502 N85-13202

Field installed brazed thermocouple feedthroughs for high vacuum experiments
[DE84-013556] 04 p0503 N85-13207

Ultrasonic and metallurgical examination of a cracked type 304 stainless steel BWR pipe weldment
[TI84-014968] 04 p0511 N85-13254

Wave propagation in compliant tubes containing a heat-conducting viscous fluid
[WTHD-163] 05 p0638 N85-14094

In situ analysis of corrosive and passive surfaces by laser-excited Raman spectroscopy — lead, galvanized iron, and asbestos-cement pipes
[PB84-229756] 06 p0767 N85-14904

Recommended aluminum pipe welding procedures for corps of engineers construction
[AD-A146712] 06 p0815 N85-15172

Identification of leaks: Internal acoustic method, phase 2
[PB85-101947/GAR] 07 p0936 N85-15927

Studies of the wall shear stress in a turbulent pulsating pipe flow
[AD-A146772] 07 p0957 N85-16068

Heat transfer due to film condensation on vertical fluted tubes
[AD-A147258] 07 p0959 N85-16079

Method for non contacting gauging of the wall thickness of tubes by backscattering radiation
[OEFZS-4274] 07 p0968 N85-16144

Improvement of gas-tightness of OTTG and TBO-5 threaded pipe couplings
[BLL-M-35993-(5828.4)] 07 p0972 N85-16175

Damping capacity of multilayer tube during torsion
[BLL-M-36011-(5828.4)] 07 p0977 N85-16202

Convective heat transfer coefficients for pipe flow with curvature induced secondary motion
09 p1318 N85-18285

Development of the GASCOPACT (R) pipe and cable tracer
[ERS-E.340] 09 p1324 N85-18320

GASCOPACT: A new approach to pipe and cable location
[ERS-E.383] 09 p1325 N85-18324

NOAA OTEC CWP (National Oceanic and Atmospheric Administration Ocean Thermal Energy Conversion Cold Water Pipe) at-sea test. Volume 3, part 1: Tabulation of the power spectra for selected channels
[PB84-238955] 09 p1346 N85-18467

NOAA OTEC CWP (National Oceanic and Atmospheric Administration Ocean Thermal Energy Conversion Cold Water Pipe) at-sea test. Volume 3: Additional tabulation of the power spectra, part 2
[PB84-238997] 09 p1346 N85-18468

Acoustic imaging in a water filled metallic pipe — monitoring heat exchangers in nuclear power reactors
[DE84-016051] 09 p1378 N85-18665

Conceptual design of a 10 MW shore-based OTEC plant
[DE84-015806] 10 p1511 N85-19532

OTEC (Ocean Thermal Energy Conversion) Cold Water Pipe At-Sea Test Program. Phase 2: Suspended pipe test
[PB85-119931] 10 p1512 N85-19542

Evaluation of 7010 aluminium alloy extruded tube in the T76 condition
[BR92019] 11 p1596 N85-20039

Ultrasonic large-diameter pipe weld testing installations 11 p1603 N85-20081

Structural basis for the mechanical properties of polyethylenes
[PB85-149771] 11 p1613 N85-20142

Leakage-flow-induced vibration of a tube-in-tube slip joint
[DE84-007301] 11 p1652 N85-20406

Simplified theory for the behaviour of buried flexible cylinders under the influence of uniform hoop compression
[PB85-116531] 11 p1654 N85-20419

Characterization and optimization of polyethylene resins and gas pipe
[PB85-118511] 12 p1815 N85-21382

The effect of an elastic foundation and of dissipative forces on the stability of fluid conveying pipes
[TAE-563] 12 p1863 N85-21688

Steam generator tube vibration tests
[DE85-003599] 12 p1867 N85-21712

Behavior of buried flexible cylinders under the influence of nonuniform hoop compression
[PB85-116523] 12 p1868 N85-21718

Influence of welding defects at melting boundary on static strength of welded joint in large-diameter pipe
13 p2033 N85-22735

Cooling performance improvement of a horizontal ground coupled heat pump
[DE85-002470] 13 p2093 N85-23065

Measurement of damping of graphite epoxy materials
[NASA-CR-175663] 14 p2248 N85-23931

Use of program controlled machine tools to automate and mechanize production processes in pipe manufacture 14 p2269 N85-24059

Problem of reduction to ideal tube in experimental aerodynamics 14 p2288 N85-24179

Fluid mechanics and heat transfer spirally fluted tubing
[AD-A150774] 14 p2301 N85-24247

Flow induced vibration of the SSME LOX posts
[NASA-CR-175606] 15 p2495 N85-25391

Pressure welding of corrosion-resistant steel with AMg6 aluminum 15 p2501 N85-25426

Soviet Institute director on GDR-USSR welding technology 15 p2538 N85-25662

Effect of internal pressure on flexibility and stress intensification factors for pipe elbows analyzed by the finite element method
[AD-A151161] 15 p2578 N85-25901

Filmwise condensation of steam on low integral-finned tubes
[AD-A152220] 16 p2783 N85-27176

Magnetic method of inspecting mechanical properties of general purpose tubes
[BLL-M-36084-(5828.4)] 16 p2796 N85-27235

Local heat treatment of welded joints of pipes and rotary vessels 17 p2924 N85-28028

Obtaining oxide films on surface of tubes of chromium-nickel steels
[BLL-BISI-TRANS-22478-(9022.06)]
17 p2929 N85-28076

Removal of longitudinal internal flash from electrically welded tubes
[BLL-BISI-TRANS-22380-(9022.06)]
17 p2938 N85-28136

Local heat treatment of welded joints of pipes and rotary vessels
[BLL-BISI-TRANS-22197-(9022.06)]
17 p2972 N85-28354

Application of 4-wire submerged arc method to welding UOE pipe
[BLL-BISI-TRANS-22417-(9022.06)]
17 p2972 N85-28358

Production of thin-walled electricity welded tubes with reduced internal flash
[BLL-BISI-TRANS-22381-(9022.06)]
17 p2973 N85-28364

High-speed longitudinal welding of pipes by automatic submerged arc process
[BLL-BISI-TRANS-22340-(9902.06)]
17 p2973 N85-28366

Production of electrically welded tubes with removed internal flash
[BLL-BISI-TRANS-22382-(9022.06)]
17 p2973 N85-28367

Steel Tubes
[BLL-BISI-TRANS-22064-(9022.06)]
17 p2973 N85-28369

Statistical models used in analyzing the quality of welded tubes
[BLL-BISI-TRANS-22232-(9022.06)]
17 p2976 N85-28384

Non-destructive testing of HF-welded pipe
[BLL-BISI-TRANS-22182-(9022.06)]
17 p2976 N85-28388

Principal quality assurance measures in the manufacture of HF-welded high-pressure linepipe
[BLL-BISI-TRANS-21690-(9022.06)]
17 p2976 N85-28389

DOE/ANL/HTRI heat exchanger tube vibration data bank: Addendum 5
[DE85-007730] 17 p2980 N85-28425

Properties of polyethylene gas piping materials
[PB85-187045] 18 p3062 N85-29068

Dynamic stability of a spinning tube conveying a flowing fluid
[DE85-007583] 18 p3102 N85-29207

Ultrasonic testing of tubes
[BLL-BISI-TRANS-22337-(9022.06)]
18 p3119 N85-29304

Characteristic features of testing equipment: Application to the ultrasonic inspection of tubes
18 p3119 N85-29305

Measurement of turbofan-turbojet thrust from tailpipe static pressure
[AD-A154036] 19 p3220 N85-29967

A method for predicting additive drag reduction from small-diameter pipe flows
[AD-A154411] 19 p3266 N85-30254

Improved fluid flow meter for measuring the rate of fluid flow in a conduit
[NASA-CASE-MFS-28030-1] 19 p3271 N85-30286

Seismic pipe support construction practices
[DE85-901315] 19 p3287 N85-30386

SHAPS-2: A three-dimensional computer program for linear/non-linear, static/dynamic analyses of piping systems
[DE85-010500] 19 p3335 N85-30658

Elastomers used in aeronautics industry
[SNIAS-851-551-103] 20 p3434 N85-31304

Viscous flows in rotating pipes with internal cavities and related vortex breakdowns
[NASA-TM-86761] 20 p3454 N85-31447

Film condensation of steam on externally finned horizontal tubes
[AD-A155642] 21 p3585 N85-32285

Resolution of thermal striping issue downstream of a horizontal pipe elbow in stratified pipe flow
[DE85-006195] 21 p3586 N85-32292

Process and device for forming imprints on ceramic tubes
[DE85-013137] 22 p3753 N85-33284

Stresses and deformations in cross-ply composite tubes subjected to a uniform temperature change: Elasticity and Approximate Solutions
[NASA-CR-176147] 22 p3800 N85-33545

Mechanical ratcheting behaviors of a steel pipe under combined cyclic axial load and internal pressure
23 p3904 N85-34184

Experimental study of collapse of thick-walled tube under external pressure and axial force
23 p3904 N85-34186

Forced convective, nonequilibrium, post-CHF heat transfer experiment data and correlation comparison report
[TI85-009331] 23 p3932 N85-34371

Calculations on the feasibility of ultrasonic inspection of steam generator tubing in pressurized water reactors
[AERE-R-10960] 23 p3940 N85-34419

Characterization of modified 9 Cr Mo steel extruded pipe
[DE85-012056] 23 p3941 N85-34430

Stress-intensity factors for circumferential surface cracks in pipes and rods under tension and bending loads
[NASA-TM-87594] 24 p4101 N85-35424

Evaluation of the crack plane equilibrium model for predicting plastic fractures
[DE85-005558] 24 p4102 N85-35431

PISTON ENGINES

NT DIESEL ENGINES

Predicted heat transfer loss in the expansion cylinder of a 2 cylinder reciprocating engine
[AD-A144831] 01 p0055 N85-10366
The KZD-85 engine test. Engine type: 1 cylinder, 2 stroke motor 2100 Husquarna
[FWE-FO-1717] 02 p0205 N85-11354
A study of the Armstrong Whitworth swing beam engine for automotive application 04 p0506 N85-13239
Long term technology development program
04 p0506 N85-13244
Evaluation of heat engine for hybrid vehicle application
[NASA-CR-174163] 04 p0506 N85-13245
Linear harmonic analysis of Stirling engine thermodynamics
[DE84-016646] 04 p0574 N85-13657
Stirling engine development, state of the art, possible engine applications and suitability in comparison to established plants and systems
[BMFT-FB-T-84-196] 05 p0646 N85-14149
Some characteristics of automotive gasolines and their performance in a light aircraft engine
[FAA-CT-84-12] 07 p0934 N85-15919
Birds and aviation
[AD-P004177] 11 p1578 N85-19939
Gas-fired duplex free-piston Stirling refrigerator
12 p1819 N85-21413
Overview of the 1985 NASA Lewis Research Center SP-100 free-piston Stirling engine activities
[NASA-TM-87028] 16 p2680 N85-27769
A mathematical model of reciprocating combustion engine dynamics for the diagnosis of deficient energy conversion 19 p3260 N85-30339
Reciprocating Brayton cycle motor
[REPT-84-RR-336] 20 p3462 N85-31507

PISTONS
Cylinder power fault diagnosis in military diesel engines
[TT-8405] 01 p0053 N85-10354
Liquid-piston Stirling machines
[DE84-014255] 02 p0205 N85-11351
Development of gas-lubricated pistons for heavy duty diesel engine technology program
[NASA-CR-174746] 03 p0441 N85-12808
Laminar flame propagation/quench for a parallel-wall duct
[DE84-009773] 04 p0470 N85-12993
Roller crosshead analysis 04 p0507 N85-13238
Improved apparatus and techniques for high temperature and pressure deformation of crystalline materials
[DE84-016049] 04 p0569 N85-13629
Pneumatic clamping device
[AD-D011544] 12 p1856 N85-21656
Sliding seal materials for adiabatic engines
[NASA-CR-174893] 13 p2037 N85-22757
Effect of form and clearance of a piston launched in a tube on the boundary layer and the heat transfer
[ISL-CO-216/83] 14 p2302 N85-24255
Compression waves in front of and behind a piston launched in a shock tube
[ISL-R-101/83] 14 p2303 N85-24260
Active control landing gear for ground loads alleviation
16 p2714 N85-26749
Lightweight piston
[NASA-CASE-LAR-13150-1] 18 p3068 N85-28975
Thermo-electric valve
[AD-D011682] 19 p3252 N85-30165
A device to detect Top Dead Center (TDC) position in motored engines
[REPT-84-RR-347] 20 p3458 N85-31475
Fast shutter apparatus
[DE85-006501] 23 p3928 N95-34343

PITCH (INCLINATION)
Development and flight evaluation of an augmented stability active controls concept: Executive summary
[NASA-CR-166009] 02 p0149 N85-11006
Cockpit window edge proximity effects on judgements of horizon vertical displacement
05 p0704 N85-14518
Integrated Application of Active Controls (IAAC) technology to an advanced subsonic transport project. ACT/Control/Guidance System study, volume 1
[NASA-CR-165963-VOL-1] 06 p0754 N85-14837
Integrated Application of Active Controls (IAAC) technology to an advanced subsonic transport project. ACT/Control/Guidance System study. Volume 2: Appendices
[NASA-CR-165963-VOL-2] 06 p0754 N85-14838
Pitch angle scattering and particle precipitation in a pulsating aurora: An experimental study
[KGI-185] 09 p1355 N85-18523
Inviscid analysis of unsteady blade tip flow correlation studies
[NASA-CR-172506] 10 p1420 N85-18958
Some effects of display format variables on the perception of aircraft spatial orientation
10 p1534 N85-19666
Directivity of Bremsstrahlung radiation from relativistic beams and the Gamma-Rays from solar flares
[NASA-CR-174433] 10 p1572 N85-19913
Generation of a pair of symmetric eddies behind a slender axisymmetric body with pitch angle
[ISL-R-121/83] 11 p1577 N85-19934
Protons with energies above 30 KeV in Earth's radiation belt at low altitudes during magnetically quiet time close to geomagnetic equator 13 p1980 N85-22423
Investigation of potential and viscous flow effects contributing to dynamic stall
[AD-A151696] 15 p2557 N85-25773
Inclinations of the Uranian rings
15 p2672 N85-26487
Wing tunnel investigation of dynamic stall of an NACA 0018 airfoil oscillating in pitch
[NAE-AN-27] 17 p2892 N85-27830
Proposals for the determination of necessary elevator handling characteristics of sailplanes in high speed range
[DFVLR-FB-84-52] 17 p2900 N85-27882
Conceptual design of a fixed-pitch wind turbine generator system rated at 400 kilowatts
[NASA-CR-174877] 18 p3127 N85-29363
New concept for a wall detector for alpha particles
[DE85-009037] 18 p3183 N85-29740
Compendum of unsteady aerodynamic measurements, addendum 1
[AGARD-R-702-ADD-1] 20 p3390 N85-31028
Data set 9: LANN wing. Pitching oscillation
20 p3390 N85-31030
In-flight evaluation of pure time delays in pitch and roll
[NASA-TM-86744] 21 p3556 N85-32123
Fokker-Planck calculation of hot electron formation in the thermal barrier region of tandem mirror Gamma-10
[IPPJ-726] 23 p3979 N85-34669
Pitch angle distributions of 35-1000 keV protons at quasi-perpendicular interplanetary shocks
[SH-1.5-6] 23 p3996 N85-34775
Diagnostic of electromagnetic conditions in space using cosmic rays
[SH-4.5-19] 23 p4038 N85-35036
Magnetic fluctuation and cosmic ray diurnal variations
[SH-4.5-21] 23 p4038 N85-35038

PITCH ANGLES
U PITCH (INCLINATION)

PITCH ATTITUDE CONTROL
U LONGITUDINAL CONTROL

PITCHING MOMENTS
An evaluation of three helicopter rotor sections
[NASA-TM-86719] 23 p3893 N85-34115

PITOT TUBES
Mixing characteristics of an underexpanded multiple jet ejector
[AD-A149557] 10 p1485 N85-19375
A comparison of laser Doppler anemometry and probe measurements within the boundary layer of an airfoil at subsonic flow
[ISL-CO-219/84] 23 p3895 N85-34127

PITTING
The influence of metallurgical aspects on the pitting corrosion behaviour of high alloy stainless steels
02 p0179 N85-11202
Electrochemical pitting evaluation of aluminum alloy 7075 in machining coolant
[DE84-016844] 04 p0475 N85-13026
Stochastic models of pitting corrosion of stainless steels. Part 1: Modelling of the initiation and growth of pits at constant potential
[AERE-R-11146-PT-1] 09 p1298 N85-18151
Local electrochemistry of pitting corrosion in stainless steels
[DE85-005207] 13 p2023 N85-22673
Studies of the initiation of pitting corrosion on stainless steels
[AERE-M-3400] 14 p2254 N85-23967
The design and construction of a flow channel and rig for corrosion studies
[AERE-M-3455] 15 p2506 N85-25474
Investigation of the pitting potential of rapidly solidified aluminum-lithium alloys
[VTH-LR-434] 16 p2752 N85-26986
Effects of gamma-ray irradiation on dislocations in sodium nitrate single crystals
[DE85-008291] 18 p3195 N85-29818
Mechanism of strength degradation for hot corrosion of alpha-SiC
[NASA-TM-87052] 19 p3248 N85-30135
Pitting corrosion of ferrous alloys
[AERE-R-11490] 24 p4078 N85-35273

PITUITARY GLAND
Regulation of physical activity in antiorthostatic position by acting on adrenosympathetic and hypophyseo-adrenocortical systems
22 p3824 N85-33689

PITUITARY HORMONES
NT ADRENOCORTICOTROPIN (ACTH)

PIX
U PLASMA INTERACTION EXPERIMENT

PL/1
Selection and use of general-purpose programming-language: Program examples, volume 2
[PB85-122000] 12 p1917 N85-22039
Selection and use of general-purpose programming language: Overview, volume 1
[PB85-122018] 12 p1917 N85-22040

PLAGES (FACULAE)
U FACULAE

PLAINS
NT COASTAL PLAINS
NT FLOOD PLAINS
NT TUNDRA
Petrology of deep crustal xenoliths from the eastern Snake River Plain, Idaho 02 p0226 N85-11477
Thickness of ridged plains materials in Hesperia Planum, Mars 13 p2185 N85-23561
Investigations of the Mars cratered terrain: Smooth plains boundary in the eastern equatorial region
13 p2191 N85-23596
Enigmatic hills of the mottled plains, Mare Acidalium quadrangle (MC-4), Mars 13 p2192 N85-23599
Geomorphology and geology of the Southwestern Margaritifer Sinus and Argyre regions of Mars. Part 1: Geological and geomorphological overview
13 p2192 N85-23600
Mechanisms of basalt-plains ridge formation
13 p2199 N85-23643

PLAN POSITION INDICATORS
Influence of a perspective cockpit traffic display format on pilot avoidance maneuvers 10 p1534 N85-19668

PLANAR STRUCTURES
Burmester theory for 4 precision positions: An extended discourse with application to the dimensional synthesis of arbitrary planar linkages 03 p0367 N85-12351
Autonomous momentum management for space station
[NASA-CR-174065] 04 p0462 N85-12931
Axial representations of shape
[AD-A150387] 13 p2151 N85-23356
The structure and composition of Uranus and Neptune
13 p2175 N85-23495
Linear incompressible magnetoconvection in a planar layer with a nonuniform horizontal magnetic field
14 p2450 N85-25127
Two-degree-of-freedom linear and planar microwave array lenses
[AD-A153701] 18 p3095 N85-29156
LSI/VLSI ion implanted planar GaAs IC processing
[AD-A155110] 21 p3581 N85-32262
Generalized planar matching
[AD-A154809] 21 p3677 N85-32842
A planar version of a 4.0 gigahertz reactively steered adaptive array
[AD-A156029] 24 p4067 N85-35330

PLANCKS CONSTANT
X-ray spectra of bursting neutron stars
23 p3981 N85-34686

PLANE STRAIN
Crack tip opening displacement for work hardening materials
[GKSS-84-E-26] 01 p0063 N85-10415
Free-edge failures of composite laminates
04 p0467 N85-12971
Multiaxial yield behavior of 1100 aluminum following various magnitudes of prestrain
[DE84-013904] 05 p0617 N85-13949
Fundamentals of microcrack nucleation mechanics
[NASA-CR-3851] 07 p0975 N85-16195
Modeling of large-scale accretionary wedge and thin-skinned trust-and-fold belt mechanics
08 p1161 N85-17442
Strain-controlled creep rupture in non-isothermal materials 09 p1332 N85-18368
Elastic wave scattering from an interface crack in a layered half space 13 p2101 N85-23095
Elasticity solution of an adhesively bonded joint
[NASA-CR-175591] 13 p2101 N85-23097
Numerical study of ductile rupture in plane deformations
[ONERA-RT-23/7169-RY-072-R]
20 p3469 N85-31557
Numerical study of tensile fracture in plane stress
[ONERA-RT-22/7169-RY-070-R]
20 p3470 N85-31563

A cracked orthotropic sheet stiffened by a semi-infinite orthotropic sheet
[NASA-TP-2455] 21 p3597 N85-32339

PLANE WAVES

Theory of near-field phased arrays for electromagnetic susceptibility testing
[PB84-217836] 01 p0042 N85-10273

Finitely conducting, infinitely long, cylindrical wire in the presence of a plane wave (EMP)
[DE84-015363] 02 p0192 N85-11282

Plane wave (EMP) incidence on a finitely conducting plane Earth with the magnetic field intensity parallel to the Earth's surface
[DE84-015364] 02 p0228 N85-11493

Scattering of plane wave on cylindrical shell in low-frequency region 02 p0256 N85-11677

Parameters of detonation waves excited in gas during concentrated release of energy
02 p0268 N85-11751

Diffraction of plane polarized waves by noncircular cylindrical cavity 02 p0269 N85-11754

Dispersion curves for normal waves in cylindrical shell and conditions for spatial coincidence in vicinity of critical frequencies 06 p0778 N85-14973

Bulk cavitation caused by a plane shock wave
[AD-A147031] 07 p0958 N85-16072

Multiple parallel wires above a finitely conducting plane earth in the presence of a plane wave (EMP)
[DE85-001116] 11 p1625 N85-20231

A mixed-basis band structure interpolation scheme applied to the fluorite structure compounds NiSi2, AuAl2, AuGa2 and AuIn2
[AD-A150131] 12 p1940 N85-22187

Interpretation of directional magnetotelluric soundings by analytical continuation method
14 p2343 N85-24468

Asymptotic construction of a procedure for plane-wave synthesis and migration
[AD-A150969] 14 p2374 N85-24672

Analysis of the electromagnetic scattering from an inlet geometry with lossy walls
[NASA-CR-175743] 15 p2541 N85-25686

Kirchhoff modeling via wave equation datuming
[AD-A152399] 17 p3028 N85-28727

Guided-mode launching in a slab waveguide by way of diffraction at the edge of a conducting screen residing on one surface of the slab
[AD-A154886] 21 p3575 N85-32232

Transient analysis of electromagnetic reflection from dispersive materials
[PB85-200186] 24 p4154 N85-35753

PLANET EPHEMERIDES

Relating the planetary ephemerides and the radio reference frame 16 p2770 N85-27095

PLANET ORIGINS

U PLANETARY EVOLUTION

PLANETARY ATMOSPHERES

NT HELIUM HYDROGEN ATMOSPHERES
NT JUPITER ATMOSPHERE
NT MARS ATMOSPHERE
NT NEPTUNE ATMOSPHERE
NT SATURN ATMOSPHERE
NT URANUS ATMOSPHERE
NT VENUS ATMOSPHERE

Atmospheres of Uranus and Neptune
02 p0298 N85-11929

Temperature structures and infrared-derived properties of the atmosphere of Uranus and Neptune
02 p0298 N85-11931

Laboratory studies of atomic collision processes of importance in planetary atmospheres
[NASA-CR-174142] 04 p0589 N85-13758

Effects of the solar and extraterrestrial environments on space power systems 05 p0610 N85-13898

The Interactive Planetary Image Processing System (IPIPS): A major facility for research and teaching in remote sensing 05 p0655 N85-14203

Shock-induced CO2 loss from CaCO3: Implications for early planetary atmospheres
[NASA-CR-174197] 05 p0745 N85-14777

Studies of radiative transfer in planetary atmospheres
[NASA-CR-174194] 05 p0745 N85-14778

Far infrared and submillimeter observations of the giant planets 08 p1245 N85-17856

Exploring the solar system with stellar occultations
08 p1245 N85-17857

Impact and collisional processes in the solar system
[NASA-CR-174297] 08 p1255 N85-17914

A modeling analysis program for the JPL table mountain Io sodium cloud data
[NASA-CR-175474] 10 p1572 N85-19910

Solar system studies with the IUE: 1982 - 1984
11 p1744 N85-20964

Radio scintillations observed during atmospheric occultations of Voyager: Internal gravity waves at Titan and magnetic field orientations at Jupiter and Saturn
[NASA-CR-175554] 12 p1961 N85-22327

Impact and collisional processes in the solar system
13 p2180 N85-23530

Magmas as selective filters of volatiles between planetary mantles and surfaces
13 p2185 N85-23557

Approximate analytic method of calculating trajectories of movement of a flight vehicle in the atmosphere
14 p2279 N85-24121

Development of a global 3-D magnetohydrodynamic computational model for solar wind/cometary and planetary studies
[NASA-CR-175724] 15 p2684 N85-26577

An experimental investigation of the angular scattering and backscattering behaviors of the simulated clouds of the outer planets
[NASA-CR-175909] 17 p3052 N85-28896

Magnetospheres of the outer planets
[AD-A154354] 19 p3384 N85-30996

Hadley circulation in planetary atmospheres
20 p3546 N85-32067

Aeolian geomorphology from the global perspective
21 p3603 N85-32373

Impact processes and their implications for planetary formation and early evolution 22 p3853 N85-33860

Origin of the atmosphere and hydrosphere of the terrestrial planets 22 p3853 N85-33863

An impact-induced terrestrial atmosphere and iron-water reactions during accretion of the Earth
22 p3854 N85-33864

Biological modulation of planetary atmospheres: The early Earth scenario 22 p3854 N85-33867

Volatiles on satellites of the outer solar system
22 p3854 N85-33868

Interrelations for the elements of the scattering matrix
22 p3855 N85-33872

PLANETARY BASES

Impact of lunar and planetary missions on the space station: Preliminary STS logistics report
[NASA-CR-171837] 09 p1285 N85-18072

PLANETARY BOUNDARY LAYER

The inducement of planetary boundary layer mass convergence associated with varying vorticity beneath tropospheric wind maximum 01 p0074 N85-10494

Numerical forecast of pressure field by considering the mutual influence of orography, thermal nonhomogeneity and surface friction 01 p0080 N85-10534

A diagnostic approach to obtaining planetary boundary layer winds using satellite-derived thermal data
05 p0674 N85-14330

A vertically resolved planetary boundary layer
05 p0680 N85-14367

Large-eddy simulation. Guidelines for its application to planetary boundary layer research
[AD-A146381] 06 p0890 N85-15651

Observations of the magnetospheric boundary layers — International Magnetospheric Study
14 p2355 N85-24551

The behavior of the atmosphere in the desert planetary boundary layer
[AD-A151286] 15 p2592 N85-25977

Study of the functions of similarity of the planetary boundary layer. Part 1: Theory
[INPE-3129-PRE/520-PT-1] 16 p2826 N85-27426

Study of the functions of similarity of the planetary boundary layer. Part 2: Results
[INPE-3130-PRE/521-VOL-2] 16 p2826 N85-27429

Large-eddy simulation in planetary boundary-layer research 18 p3147 N85-29482

Reports from the German Meteorological Service. No. 167: Results of aerological soundings in the model area upper Rhine: Heat release project upper Rhine area, part 3
[ISBN-3-88148-216-4] 23 p3950 N85-34479

Application of a turbulent closure model to the parameterization of the vertical diffusion of heat, momentum, and humidity in the ECMWF model — European Center for Medium Term Weather Forecasting (ECMWF)
[MITT-41] 24 p4095 N85-35387

PLANETARY COMPOSITION

High pressure cosmochemistry applied to major planetary interiors: Experimental studies
[NASA-CR-174032] 02 p0302 N85-11958

Detection of the J-10 manifold of the pure rotational band of phosphine on Saturn 08 p1245 N85-17855

Venus 09 p1411 N85-18891

Near infrared modeling of the equatorial regions of Jupiter and Saturn 09 p1415 N85-18930

Multispectral analysis of the Kasei Vallis-Lanae Planum region of Mars 13 p2193 N85-23607

The search for igneous materials at the Viking landing sites 13 p2194 N85-23609

Basalts of Mars: Constraints on volatile evolution
13 p2194 N85-23610

First direct detection of clay minerals on Mars
13 p2194 N85-23612

Iron oxides of Mars: Evidence for contemporary weathering 13 p2195 N85-23613

Reassignment of the iron (3) absorption bands in the spectra of Mars 13 p2195 N85-23614

Zeolites on Mars: Prospects for remote sensing
13 p2195 N85-23615

High pressure cosmochemistry applied to major planetary interiors: Experimental studies
[NASA-CR-175715] 15 p2679 N85-26544

Workshop on the Early Earth: The Interval from Accretion to the Older Archean
[NASA-CR-176037] 21 p3717 N85-33062

Conditions during formation of the Earth
21 p3717 N85-33066

Early evolution of the crust-mantle system
21 p3717 N85-33067

Was core formation violent enough to homogenize the early mantle? 21 p3718 N85-33068

The problem of the Earth's CO2 content and the iron core 21 p3718 N85-33069

A review of noble gas geochemistry in relation to early Earth history 21 p3720 N85-33081

Carbon and nitrogen in the deep Earth
21 p3721 N85-33085

Chemical evolution of the Earth: Equilibrium or disequilibrium process? 21 p3721 N85-33088

Thermal, dynamic and compositional aspects of the core-forming Earth 21 p3722 N85-33091

Earth's primordial differentiation, and its after-effects
21 p3722 N85-33092

Terrestrial Planets: Comparative Planetology
[NASA-CR-176093] 22 p3851 N85-33849

Noble gas patterns in the atmospheres of Mars and Earth: A comparison via the SNC meteorites
22 p3852 N85-33853

Venus, Earth and Mars: Present bounds on similarities and differences in bulk composition
22 p3856 N85-33876

Mineralogy and chemistry of the Earth
22 p3856 N85-33877

PLANETARY CORES

NT EARTH CORE

Interior structure of Uranus 02 p0299 N85-11939

Planetary reorientation by surface loads
22 p3858 N85-33886

Geochemical confirmation of the lunar magmasphere hypothesis 22 p3859 N85-33895

PLANETARY CRATERS

NT MARS CRATERS

Geological, structural, and geomorphological analyses from SIR-B 08 p1145 N85-17226

Mercury 09 p1411 N85-18890

Impact cratering calculation 13 p2180 N85-23531

Impact crater scaling laws 13 p2181 N85-23532

Problems in recovering crater production functions
13 p2182 N85-23539

Examination of returned solar-max surfaces for impacting orbital debris and meteoroids
15 p2681 N85-26550

Considerations of large scale impact and the early Earth 21 p3718 N85-33070

PLANETARY ENTRY

U ATMOSPHERIC ENTRY

PLANETARY ENVIRONMENTS

NT HELIUM HYDROGEN ATMOSPHERES
NT JUPITER ATMOSPHERE
NT MARS ATMOSPHERE
NT MARS ENVIRONMENT
NT NEPTUNE ATMOSPHERE
NT PLANETARY ATMOSPHERES
NT SATURN ATMOSPHERE
NT URANUS ATMOSPHERE
NT VENUS ATMOSPHERE

The dynamic fission instability and the origin of the Moon 04 p0586 N85-13739

Far infrared and submillimeter observations of the giant planets 08 p1245 N85-17856

Exploring the solar system with stellar occultations
08 p1245 N85-17857

Ganymede and Callisto: Beauty is only skin deep
15 p2680 N85-26552

Activities at the Lunar and Planetary Institute
[NASA-CR-175914] 18 p3201 N85-29859

Microbial ecology of extreme environments: Antarctic yeasts and growth in substrate-limited habitats
[NASA-CR-176005] 19 p3326 N85-30609

Activities report of the Laboratory of Stellar and Planetary Physics
[G-127] 20 p3544 N85-32052

The global sulfur cycle
[NASA-TM-87570] 21 p3656 N85-32719

Impact processes and their implications for planetary formation and early evolution 22 p3853 N85-33860
Questions about Mercury's role in comparative planetary geophysics 22 p3853 N85-33861
PLANETARY EVOLUTION
Impact phenomena as factors in the evolution of the Earth
[NASA-CR-174015] 01 p0072 N85-10474
The origin and evolution of Uranus and Neptune 02 p0298 N85-11928
Interior structure of Uranus 02 p0299 N85-11939
The problem of iron partition between Earth and Moon during simultaneous formation as a double planet system 04 p0587 N85-13744
The geology of the terrestrial planets
[NASA-SP-469] 09 p1410 N85-18888
Asteroids, comets and planet formation 09 p1410 N85-18889
Mercury 09 p1411 N85-18890
Earth 09 p1411 N85-18892
Evolution of sedimentation basins in Earth's history 10 p1497 N85-19451
Planetary geology in the 1980s
[NASA-SP-467] 13 p2169 N85-23457
Studies of planetary rings 13 p2174 N85-23488
Origin and evolution of the Saturn system 13 p2175 N85-23493
Giant planets and their satellites: Cosmochemistry, evolution and structure 13 p2175 N85-23494
The structure and composition of Uranus and Neptune 13 p2175 N85-23495
On the origin of Triton and Pluto 13 p2175 N85-23497
The Formation of preplanetary disks from the collapse of rotating molecular cloud cores 13 p2180 N85-23526
The evolution of CO2 on Mars 13 p2185 N85-23558
Three-layer generic Ganymedes: Structure and evolution 13 p2202 N85-23657
Structure and origin of Martian satellites 15 p2483 N85-25323
Evolution of collisional systems — planetary disks 15 p2674 N85-26505
The formation of spokes in Saturn's rings 15 p2676 N85-26524
The E-ring of Saturn 15 p2677 N85-26527
Formation of the solar system 15 p2677 N85-26532
The formation of the terrestrial planets from lunar sized planetesimals 15 p2678 N85-26533
Statistical theory of planet growth 15 p2678 N85-26534
Tidal breakup and origin of the Uranian ring system 15 p2678 N85-26535
Asteroid compositional rings: Clues to the compositions of primordial planetesimals in the middle solar system 15 p2678 N85-26537
Sixteenth Lunar and Planetary Science Conference. Press abstracts
[NASA-CR-175692] 15 p2680 N85-26548
Chondrule-like particles provide evidence of early Archean meteorite impacts, South Africa and western Australia 15 p2682 N85-26562
What we know about Mars (but otherwise wouldn't) if it is the shergottite parent body 15 p2682 N85-26565
Geologic interpretation of remote sensing data for the Martian volcano Ascraeus Mons 19 p3384 N85-30992
Global geomorphology: Report of Working Group Number 1 21 p3604 N85-32382
Landscape inheritance: Report of Working Group Number 2 21 p3604 N85-32383
Protocyanobacteria: Oxygenic and Anoxygenic photosynthesis in mat-forming bacteria 21 p3657 N85-32714
Workshop on the Early Earth: The Interval from Accretion to the Older Archean
[NASA-CR-176037] 21 p3717 N85-33062
Conditions during formation of the Earth 21 p3717 N85-33066
Early evolution of the crust-mantle system 21 p3717 N85-33067
Was core formation violent enough to homogenize the early mantle? 21 p3718 N85-33068
Considerations of large scale impact and the early Earth 21 p3718 N85-33070
Noble gases and the early history of the Earth: Inappropriate paradigms and assumptions inhibit research and communication 21 p3719 N85-33075
A review of noble gas geochemistry in relation to early Earth history 21 p3720 N85-33081
Archean sedimentary systems and crustal evolution 21 p3720 N85-33082
Crustal radiogenic heat production and the selective survival of ancient continental crust 21 p3721 N85-33086
Large arcuate scars: A geological legacy of the Earth's accretionary past 21 p3721 N85-33089
Thermal, dynamic and compositional aspects of the core-forming Earth 21 p3722 N85-33091
Comments on RS-17 X-ray telescope 22 p3731 N85-33132
Terrestrial Planets: Comparative Planetology
[NASA-CR-176093] 22 p3851 N85-33849
Relationships between chondritic meteorites and planets 22 p3851 N85-33851
Interrelationships among the terrestrial planets 22 p3853 N85-33859
Questions about Mercury's role in comparative planetary geophysics 22 p3853 N85-33861
Volatile loss following very large impacts 22 p3853 N85-33862
Origin of the atmosphere and hydrosphere of the terrestrial planets 22 p3853 N85-33863
An impact-induced terrestrial atmosphere and iron-water reactions during accretion of the Earth 22 p3854 N85-33864
Climatic consequences of very high CO2 levels in Earth's early atmosphere 22 p3854 N85-33865
The polar caps and the climatic evolution of Mars 22 p3854 N85-33866
Biological modulation of planetary atmospheres: The early Earth scenario 22 p3854 N85-33867
Volatiles on satellites of the outer solar system 22 p3854 N85-33868
Planetary surface processes: A review 22 p3855 N85-33869
Interpretation of photometric measurements of airless bodies 22 p3855 N85-33871
Models of planetary structure and evolution: The case of Io 22 p3855 N85-33874
Mineralogy and chemistry of the Earth 22 p3856 N85-33877
Crustal development in the terrestrial planets 22 p3856 N85-33879
Contrasts in evolution of Venus and Earth 22 p3857 N85-33880
Primordial magmaspheres and their lasting consequences 22 p3857 N85-33882
Thermal evolution of coastal California with implications for hydrocarbon maturation 24 p4115 N85-35509
The ionization structure of planetary nebulae. Part 4: NGC 7662
[NASA-CR-176151] 24 p4169 N85-35844
PLANETARY EXPLORATION
U SPACE EXPLORATION
PLANETARY GEOLOGY
NT MARS VOLCANOES
A bibliography of planetary geology and geophysics principal investigators and their associates, 1983 - 1984
[NASA-TM-87361] 01 p0127 N85-10874
Mars-Earth geographical comparisons: A pictorial view
[NASA-TM-86166] 02 p0302 N85-11957
The geology of the terrestrial planets
[NASA-SP-469] 09 p1410 N85-18888
Mars 09 p1411 N85-18894
The origin and evolution of terrestrial and Martian rock labyrinths
[NASA-CR-175511] 12 p1961 N85-22326
Planetary geology in the 1980s
[NASA-SP-467] 13 p2169 N85-23457
Reports of the Planetary Geology and Geophysics Program, 1984
[NASA-TM-87563] 13 p2172 N85-23474
A statistical treatment of the regional slope characteristics of Venus and Earth 13 p2178 N85-23517
Centrifuge impact cratering experiments 13 p2181 N85-23533
Progress on Experimental impact studies 13 p2181 N85-23534
Progress on studies of early intense cratering 13 p2181 N85-23535
Why not a constant early lunar impact rate? 13 p2181 N85-23536
Martian terrain ages 13 p2181 N85-23537
Impacts in ice: Commissions of solar system crater population 13 p2181 N85-23538
Problems in recovering crater production functions 13 p2182 N85-23539
A parmetric study of crater-saturation simulation 13 p2182 N85-23540
Average spacing for rings of individual multi-ring basins is 2.0(0.5)D 13 p2182 N85-23541
Ring-diameter ratios for multi-ring basins average 2.0(0.5)D 13 p2182 N85-23542
Morphology and mechanics of terraces in lunar craters 13 p2182 N85-23543
Newly discovered Martian impact basins 13 p2182 N85-23544
The nature of Martian flow ejecta craters 13 p2183 N85-23545
Interaction of Martian flow ejecta blankets with pre-existing impact craters: Morphological observations 13 p2183 N85-23546
Ripple ring basins on Ganymede and Callisto 13 p2183 N85-23547
Implications of convection in the Moon and the terrestrial planets 13 p2183 N85-23548
High pressure cosmochemistry of major planetary interiors: Laboratory studies of the water-rich region of the system ammonia-water 13 p2183 N85-23549
Modelling equilibrium and fractional crystallization in the system MgO-FeO-CaO-Al2O3-SiO2 13 p2184 N85-23552
Ridged plains of Lunae Planum: Thickness distribution revised 13 p2185 N85-23559
Volcanic debris flows in the Elysium region of Mars 13 p2185 N85-23560
Thickness of ridged plains materials in Hesperia Planum, Mars 13 p2185 N85-23561
Mapping structures characteristic of the highland boundary scarp on Mars 13 p2191 N85-23595
Investigations of the Mars cratered terrain: Smooth plains boundary in the eastern equatorial region 13 p2191 N85-23596
Martian fretted terrain morphometry interpreted using principal components analysis 13 p2192 N85-23597
Enigmatic hills of the mottled plains, Mare Acidalium quadrangle (MC-4), Mars 13 p2192 N85-23599
Geomorphology and geology of the Southwestern Margaritifer Sinus and Argyre regions of Mars. Part 1: Geological and geomorphological overview 13 p2192 N85-23600
Geomorphology and geology of the Southwestern Margaritifer Sinus and Argyre regions of Mars. Part 2: Crater size-frequency distribution curves and geomorphic unit ages 13 p2192 N85-23601
Geomorphology and geology of the Southwestern Margaritifer Sinus and Argyre regions of Mars. Part 3: Valley types and distribution 13 p2193 N85-23602
Geomorphology and geology of the Southwestern Margaritifer Sinus and Argyre regions of Mars. Part 4: Flow ejecta crater distribution 13 p2193 N85-23603
Multispectral analysis of the Kasei Vallis-Lanae Planum region of Mars 13 p2193 N85-23607
Io: Precise comparison of Voyager spectral curves with laboratory measurements 13 p2196 N85-23619
Determining mineral types and abundances from reflectance measurements 13 p2196 N85-23622
Determination of mineral type, abundance, and grain size with remotely obtained reflectance spectra 13 p2196 N85-23623
Quantitative analyses of planetary reflectance spectra 13 p2197 N85-23625
Terrestrial analogs for planetary wrinkle ridges 13 p2199 N85-23644
On the absence of strike-slip faults from the planets and satellites 13 p2200 N85-23645
Lunar mascon loading: An example of the importance of fault initiation depth on fault type predictions from stresses on planetary surfaces 13 p2200 N85-23646
Planetary interior modeling and tectonic implications 13 p2200 N85-23649
Elysium region, Mars: Tests of lithospheric loading models for the formation of tectonic features 13 p2200 N85-23650
Lithologic and structural control on slope morphology in the Valles Marineris 13 p2201 N85-23651
Valles Marineris basin beds: A complex story 13 p2201 N85-23652
Mars: Stratigraphy of western highlands and polar regions 13 p2201 N85-23653
Kasei Vallis of Mars: Dating the interplay of tectonics and geomorphology 13 p2201 N85-23654
Creep of ice: Further studies 13 p2201 N85-23655
Fault offsets and lateral crustal movement on Europa 13 p2201 N85-23656
Three-layer generic Ganymedes: Structure and evolution 13 p2202 N85-23657
Lineaments on Ganymede: New evidence for late tectonic activity 13 p2202 N85-23658
Global tectonics on Ganymede 13 p2202 N85-23659
Tectonics of the Galileo Regio on Ganymede 13 p2202 N85-23660
Importance of the tectonic motions on Ganymede 13 p2202 N85-23661
Tectonics of the Valhalla structure on Callisto 13 p2202 N85-23662
Mars geologic mapping: A review and new concepts 13 p2202 N85-23663

Physical and geological nature of Saturn's larger ring particles 15 p2674 N85-26509

Ganymede and Callisto: Beauty is only skin deep 15 p2680 N85-26552

Geologic interpretation of remote sensing data for the Martian volcano Ascraeus Mons 19 p3384 N85-30992

Geological analyses of the surface of Venus and Mars from lander spacecraft images and orbital radar observations 19 p3384 N85-30993

The problem of scale in planetary geomorphology 21 p3603 N85-32375

Landscape inheritance: Report of Working Group Number 2 21 p3604 N85-32383

Questions about Mercury's role in comparative planetary geophysics 22 p3853 N85-33861

PLANETARY GRAVITATION

Rotational properties of Uranus and Neptune 02 p0299 N85-11940

Research relative to the development of a cryogenic microwave cavity gradiometer for orbital use [NASA-CR-174249] 07 p0962 N85-16095

Gravity anomaly map of Mars and Moon and analysis of Venus gravity field: New analysis procedures [NASA-CR-174295] 08 p1258 N85-17919

Expansion of functions describing planetary surface and gravity field 13 p1978 N85-22410

Viking radio science data analysis and synthesis 13 p2180 N85-23528

Gravity field of the Jovian system from Pioneer and Voyager tracking data 13 p2180 N85-23529

Evolution of collisional systems — planetary disks 15 p2674 N85-26505

The non-hydrostatic figures of the terrestrial planets 22 p3858 N85-33887

Admittance functions from Venus vertical gravity and modes of topographic support 22 p3858 N85-33889

PLANETARY LANDING

Mathematical model for rollout of planet roving vehicle from landing craft 15 p2484 N85-25334

PLANETARY LIMB

Clouds above the Martin Limb: Viking observations [NASA-CR-174027] 02 p0296 N85-11922

PLANETARY MAGNETIC FIELDS

Magnetospheric structures: Uranus and Neptune 02 p0301 N85-11949

Effects of the solar and extraterrestrial environments on space power systems 05 p0610 N85-13898

Magnetospheres in the solar system 12 p1954 N85-22274

Particle transport in planetary magnetospheres 12 p1954 N85-22275

Hydromagnetic precursors of interplanetary plasma burst 13 p1978 N85-22414

Dynamics of charged small particles — Jupiter, Saturn magnetospheres 15 p2676 N85-26522

On the role of mother-planet magnetic field in spiral structure explanation of formation of spokes — Saturn rings 15 p2676 N85-26525

The gravito-electrodynamics of charged dust in planetary ring systems 15 p2677 N85-26531

What we know about Mars (but otherwise wouldn't) if it is the shergottite parent body 15 p2682 N85-26565

Orientation and strength of Martian magnetic dipole 16 p2723 N85-26808

Possible configuration of Martian magnetosphere 16 p2723 N85-26809

Planetary Dynamos [NASA-CR-176001] 21 p3679 N85-32857

The magnetic field of planets 22 p3858 N85-33891

What we have learned about the magnetic field of Mars 22 p3858 N85-33892

Magnetic field generation in the cores of terrestrial bodies 22 p3859 N85-33894

PLANETARY MANTLES

NT EARTH MANTLE

Magmas as selective filters of volatiles between planetary mantles and surfaces 13 p2185 N85-23557

A solid-state framework for terrestrial upper mantles 22 p3856 N85-33878

Crustal development in the terrestrial planets 22 p3856 N85-33879

The non-hydrostatic figures of the terrestrial planets 22 p3858 N85-33887

Dynamic compensation of Venus's geoid: A comparison with Earth 22 p3856 N85-33888

PLANETARY MAPPING

Planetary cartography in the next decade (1984 - 1994) [NASA-SP-475] 12 p1960 N85-22323

Visualization of radar altimetry data for Venus 13 p1982 N85-22437

Mapping structures characteristic of the highland boundary scarp on Mars 13 p2191 N85-23595

Tectonics of the Galileo Regio on Ganymede 13 p2202 N85-23660

Mars geologic mapping: A review and new concepts 13 p2202 N85-23663

The Galilean Satellite Geological Mapping Program, 1984 13 p2203 N85-23664

Geology of the Ganymede quadrangle Jg7 13 p2203 N85-23665

Mars planimetric mapping 13 p2203 N85-23666

Viking Lander mosaics of Mars 13 p2203 N85-23667

Voyager cartography 13 p2203 N85-23668

The control network of Mars: October 1984 13 p2203 N85-23670

The control networks of the satellites of Jupiter and Saturn 13 p2204 N85-23671

Distribution of gravity and plumb line deflection at Martian surface 15 p2483 N85-25324

PLANETARY MOTION

U SOLAR ORBITS

PLANETARY NEBULAE

The unidentified emission features: A study of the Orion Bar and planetary nebulae 08 p1246 N85-17862

Mid-infrared spectroscopy of planetary nebulae 08 p1247 N85-17872

Spectral characteristics of dust in planetary nebulae 08 p1247 N85-17873

Variation of oxygen and nitrogen abundances in the galaxy 08 p1248 N85-17878

Ultraviolet spectroscopy of selected astronomical sources [NASA-CR-174379] 09 p1413 N85-18912

On the progenitors of white dwarfs [NASA-CR-174378] 09 p1413 N85-18913

Far-infrared line observations of planetary nebulae. 1: The O 3 spectrum [NASA-TM-86670] 10 p1570 N85-19900

IUE observations of planetary nebulae in the Magellanic Clouds 11 p1747 N85-20986

1983 observations of the eclipsing nucleus of the bipolar planetary nebula NGC 2346 11 p1747 N85-20987

Mass distribution and evolutionary scheme for central stars of planetary nebulae 11 p1751 N85-21012

The central star of NGC 40 11 p1751 N85-21013

LSS 2018: A double-lined spectroscopic binary central star with an extremely large reflection effect [NASA-CR-175503] 11 p1762 N85-21082

The distribution and dynamics of planetary nebulae in M32 and the Andromeda Galaxy 20 p3546 N85-32068

The ionization structure of planetary nebulae. Part 4: NGC 7662 [NASA-CR-176151] 24 p4169 N85-35844

PLANETARY ORBITS

Some considerations on elliptic heliocentric orbits [INPE-3217-PRE/570] 02 p0297 N85-11926

Venus 09 p1411 N85-18891

Small solar system bodies 13 p2175 N85-23499

The coorbital hypothesis 22 p3858 N85-33890

PLANETARY RADIATION

Infrared thermal radiation of Venus 02 p0163 N85-11101

Ultraviolet observations of Uranus and Neptune below 3000 Angstrom 02 p0298 N85-11932

Properties of the upper tropospheres of Uranus and Neptune derived from observations at visible to near-infrared wavelengths 02 p0298 N85-11933

Microwave emission from Saturn's rings 15 p2670 N85-26475

Saturn's E-ring in the red spectral region 15 p2671 N85-26480

PLANETARY RINGS

NT JUPITER RINGS

NT SATURN RINGS

NT URANUS RINGS

Uranus and Neptune [NASA-CP-2330] 02 p0298 N85-11927

The origin and evolution of Uranus and Neptune 02 p0298 N85-11928

Exploration of the solar system by airborne astronomy 08 p1244 N85-17851

Investigations of planetary ring phenomena 13 p2174 N85-23487

Studies of planetary rings 13 p2174 N85-23488

Dynamical studies of Saturn's rings 13 p2174 N85-23489

Meteoroidal impacts, plasma, fine structure of ringlets and spokes on Saturn's ring B 13 p2174 N85-23490

Plasma production by meteoroid impact 13 p2174 N85-23492

Origin and evolution of the Saturn system 13 p2175 N85-23493

Planetary Rings. Colloquium 75 — conferences [ISBN-2-85426-100-4] 15 p2670 N85-26473

Rings around Neptune? 15 p2672 N85-26491

How a shepherd guides a sheep hard — satellite-planetary ring interaction 15 p2674 N85-26503

Evolution of collisional systems — planetary disks 15 p2674 N85-26505

Size distribution in collisional systems — planetary rings 15 p2674 N85-26509

Comments on collision mechanics in ring systems — planetary rings [PSI-CONTRIB-186] 15 p2675 N85-26510

On the radial structure of planetary rings 15 p2675 N85-26512

Diffusion instability in a bimodal disc — planetary rings 15 p2675 N85-26513

Stochastic modeling of planetary ring systems 15 p2675 N85-26516

Applications of three-body resonances to satellites and planetary rings 15 p2676 N85-26518

Dynamics of neutral small particles — in the solar system 15 p2676 N85-26521

Diffusion of dust around a central body — Keplerian orbits 15 p2676 N85-26523

On the electric charge carried by dust grain excitation of violent discharge — planetary rings 15 p2677 N85-26530

The gravito-electrodynamics of charged dust in planetary ring systems 15 p2677 N85-26531

Future observations of planetary rings from ground-based observatories and Earth-orbiting satellites 15 p2678 N85-26540

Occultation detection of a Neptune ring segment 15 p2681 N85-26558

PLANETARY ROTATION

The origin and evolution of Uranus and Neptune 02 p0298 N85-11928

Rotational properties of Uranus and Neptune 02 p0299 N85-11940

On the origin of the Moon by rotational fission 04 p0587 N85-13746

Venus 09 p1411 N85-18881

Viking radio science data analysis and synthesis [NASA-CR-175631] 13 p2171 N85-23471

Viking radio science data analysis and synthesis 13 p2180 N85-23528

Motion of satellite with total dynamic symmetry around rotating aspherical Earth 14 p2287 N85-24174

Construction of conditionally periodic solutions of problem of reciprocating motion of axially symmetric satellite of triaxial planet 15 p2480 N85-25304

Photometric study of Pluto near perihelion. Part 2: Refinement of rotation period: Color indices 15 p2483 N85-25325

The vertical structure of global rotational normal modes 18 p3144 N85-29484

PLANETARY SATELLITES

U NATURAL SATELLITES

PLANETARY SPACE FLIGHT

U INTERPLANETARY FLIGHT

PLANETARY SPACECRAFT

U INTERPLANETARY SPACECRAFT

PLANETARY STRUCTURE

Atmospheres of Uranus and Neptune 02 p0298 N85-11923

Oblatenesses of Uranus and Neptune 02 p0300 N85-11941

Giant planets and their satellites: Cosmochemistry, evolution and structure 13 p2175 N85-23494

Studies of icy bodies: Uranian satellites and cometary nuclei 13 p2175 N85-23496

Viking radio science data analysis and synthesis 13 p2180 N85-23528

Planetary surface processes: A review 22 p3855 N85-33869

Models of planetary structure and evolution: The case of Io 22 p3855 N85-33874

Planetary reorientation by surface loads 22 p3856 N85-33886

The non-hydrostatic figures of the terrestrial planets 22 p3858 N85-33887

Dynamic compensation of Venus's geoid: A comparison with Earth 22 p3856 N85-33888

Applications of the Galerkin formalism in the coupling of the earth's free oscillations 24 p4116 N85-35514

PLANETARY SURFACES

NT MARS SURFACE

NT VENUS SURFACE

Grainsize evolution and differential comminution in a experimental regolith 06 p0888 N85-1563

Mercury 09 p1411 N85-188

Expansion of functions describing planetary surface an gravity field 13 p1978 N85-2241

Evaluating accuracy in orientation of topograph photograph and satellite-centered direction from sta photograph 13 p1963 N85-2244

Planetary geology in the 1980s
[NASA-SP-467] 13 p2169 N85-23457
A parmetric study of crater-saturation simulation
13 p2182 N85-23540
Relative time-scale for channeling events within chaotic terrains, Margaritifer Sinus, Mars
13 p2190 N85-23589
Permafrost and subsurface ice in the solar system
13 p2191 N85-23594
Terrestrial analogs for planetary wrinkle ridges
13 p2199 N85-23644
Lunar mascon loading: An example of the importance of fault initiation depth on fault type predictions from stresses on planetary surfaces
13 p2200 N85-23646
Results on volcanism, surface geology from Venera-15, -16 15 p2482 N85-25321
Distribution of gravity and plumb line deflection at Martian surface 15 p2483 N85-25324
One aspect of determination of direction of space survey base from photographs of planetary surface and star sky
15 p2487 N85-25352
Ganymede and Callisto: Beauty is only skin deep
15 p2660 N85-26552
Considerations of large scale impact and the early Earth 21 p3718 N85-33070
Origin of the atmosphere and hydrosphere of the terrestrial planets 22 p3853 N85-33863
An impact-induced terrestrial atmosphere and iron-water reactions during accretion of the Earth
22 p3854 N85-33864
Biological modulation of planetary atmospheres: The early Earth scenario 22 p3854 N85-33867
Planetary surface processes: A review
22 p3855 N85-33869
Permafrost features on Earth and Mars: Similarities, differences 22 p3855 N85-33870
Interpretation of photometric measurements of airless bodies 22 p3855 N85-33871
Planetary reorientation by surface loads
22 p3858 N85-33886

PLANETARY TEMPERATURE
Seasonal variations in Triton's atmospheric mass and composition 02 p0301 N85-11946
Planetary fluids He and NH3 at high shock pressures and temperatures
[DE85-011851] 22 p3859 N85-33896

PLANETARY WAVES
An improved analytical theory of Rossby wave driven Eulerian and Lagrangian mean flows along non-zonal barriers with application to the Hawaiian Ridge
[AD-A144951] 01 p0068 N85-10593
Quasi-stationary atmospheric responses to large-scale forcing 02 p0227 N85-11484
Global Scale Atmospheric Processes Research Program Review
[NASA-CP-2344] 05 p0679 N85-14360
Global scale diagnosis of FGGE data
05 p0683 N85-14394
Large scale rossby waves during FGGE
05 p0684 N85-14396
Limits of applicability of long wave theory in studies of oscillations of n-layer fluid 06 p0824 N85-15234
Interactions between mean flow and finite-amplitude mesoscale eddies in a barotropic ocean
[AD-A147249] 07 p1009 N85-16413
Generation and evolution of diabatic planetary waves in continuously stratified atmosphere with Ekman dissipation 09 p1354 N85-18515
Global scale diagnoses of FGGE data
[NASA-CR-174356] 09 p1356 N85-18533
Combined effects of baroclinic and barotropic instability in a nonlinear low order model
[DM-41] 09 p1358 N85-18544
PMP-2 report: Equatorial wave dynamics
11 p1657 N85-20442
Midwinter disturbances in the middle atmosphere
11 p1661 N85-20465
Aspects of planetary wave transports in the middle atmosphere 11 p1661 N85-20471
Winds and waves (4 min - 11 yrs) in the upper middle atmosphere (60-110 km) at Saskatoon, Canada (52 deg N, 107 deg W): MF radar (2.2 MHz) soundings 1973 - 1983 11 p1662 N85-20476
21 Layer troposphere-stratosphere climate model
[NASA-TM-86163] 12 p1892 N85-21871
Numerical investigation of evolution of energy spectrum of slightly nonlinear Rossby waves
13 p2106 N85-23124
Long nonlinear waves in layers of sudden changes in wind velocity 14 p2340 N85-24470
Forced MHD turbulence in a uniform external magnetic field
[NASA-CR-172576] 15 p2654 N85-26368
Wave dynamics and transport in the stratosphere
[NASA-CR-175789] 16 p2823 N85-27413
Mechanistic experiments to determine the origin of Southern Hemisphere stationary waves
18 p3143 N85-29461
Quasi stationary states in the Southern Hemisphere
18 p3144 N85-29465
On the global distribution of three-dimensional Eliassen-Palm fluxes by stationary waves
18 p3145 N85-29469
Finite amplitude stability of a Rossby wave in a channel 19 p3314 N85-30543
Atmospheric planetary wave response to external forcing
[NASA-CR-176000] 19 p3315 N85-30548
Sensitivity of planetary waves to initial conditions and forcing
[AD-A154111] 19 p3345 N85-30734
A numerical analysis of transient planetary waves and the vertical structure in a meso-strato-troposphere model, part 1.4A 21 p3617 N85-32473

PLANETISMALS
U PROTOPLANETS

PLANETOCENTRIC COORDINATES
NT GEOCENTRIC COORDINATES

PLANETOLOGY
Activities at the Lunar and Planetary Institute
[NASA-CR-174069] 04 p0579 N85-13694
Activities at the Lunar and Planetary Institute, introduction 04 p0579 N85-13695
A new look at the planets --- space probes
[AERONOMICA-ACTA-37-1984]
11 p1765 N85-21096
USSR report: Space
[JPRS-USP-85-003] 15 p2476 N85-25284
Jupiter's ring system resolved: Physical properties inferred from the Voyager images
20 p3546 N85-32069
Geomorphic classification of Icelandic and Martian volcanoes: Limitations of comparative planetology research from LANDSAT and Viking orbiter images
21 p3603 N85-32372
Spacecraft-aided research discussed at geology Congress 22 p3734 N85-33147
Terrestrial Planets: Comparative Planetology
[NASA-CR-176093] 22 p3851 N85-33849

PLANETS
NT EARTH (PLANET)
NT GAS GIANT PLANETS
NT JUPITER (PLANET)
NT MARS (PLANET)
NT MERCURY (PLANET)
NT NEPTUNE (PLANET)
NT PLUTO (PLANET)
NT SATURN (PLANET)
NT TERRESTRIAL PLANETS
NT URANUS (PLANET)
NT URANUS RINGS
NT VENUS (PLANET)
High pressure cosmochemistry applied to major planetary interiors: Experimental studies
[NASA-CR-174032] 02 p0302 N85-11958
Magnetohydrodynamic and gasdynamic theories for planetary bow waves
[NASA-CR-174135] 04 p0589 N85-13780
Astrometric applications of the Mt. Stromlo PDS 1010A — microdensitometer 07 p0967 N85-16136
Photometric precision needed for planetary detection
08 p1250 N85-17894
Impact and collisional processes in the solar system
[NASA-CR-174297] 08 p1255 N85-17914
Herstmonceux observations of the Sun, planets and Moon, 1957 - 1982
[BULL-193] 11 p1762 N85-21067
A new look at the planets --- space probes
[AERONOMICA-ACTA-37-1984]
11 p1765 N85-21096
Impact and collisional processes in the solar system
13 p2180 N85-23530
Astometry at La Silla 14 p2436 N85-25025
Activities at the Lunar and Planetary Institute
[NASA-CR-175914] 18 p3201 N85-29859

PLANFORMS
NT DELTA WINGS
NT RECTANGULAR PANELS
NT RECTANGULAR PLANFORMS
NT RECTANGULAR PLATES
NT RECTANGULAR WINGS
NT SWEPT FORWARD WINGS
NT SWEPTBACK WINGS
NT VARIABLE SWEEP WINGS
NT WING PLANFORMS

PLANIGRAPHY
U TOMOGRAPHY

PLANKTON
Calculation of optical characteristics of shelf ecological system based on its mathematical model
10 p1498 N85-19453
Microplankton species assemblages at the Scripps Pier from March to November 1983 during the 1982-1984 El Nino event
[NASA-CR-175553] 12 p1899 N85-21926
Biological processes in the water column of the South Atlantic Bight. Volume 1: Published manuscripts
[DE85-004610] 12 p1900 N85-21929
Possible role of ocean biota in global carbon balance — phytoplankton production 13 p2107 N85-23129
Geographic variation in the relationships of temperature, salinity or sigma sub t versus plant nutrient concentrations in the world ocean — silicic acid, nitrate, and phosphate concentration
[NASA-CR-175621] 13 p2140 N85-23287
Production and turnover of suspended organic detritus in the coastal water of the southeastern continental shelf
[DE85-003977] 13 p2140 N85-23290
Global paleoclimatic data base for 6000 years BP
[DE85-006628] 15 p2600 N85-26024
Ecology of Pamlico River, North Carolina: An estuarine profile
[PB85-155703] 16 p2822 N85-27404
MARMAP survey of the continental shelf from Cape Hatteras, North Carolina to Cape Sable, Nova Scotia (1977 - 1983). Atlas 1: Summary of operations
[PB85-150965] 16 p2839 N85-27506
Influence of underwater volcanic mountains of Atlantic on microplankton distribution 19 p3294 N85-30424
Properties of forest derived cloud condensation nuclei
21 p3650 N85-32682
Ecophysiology of phototrophic sulfur bacteria in lakes: Vertical distribution of planktonic populations
21 p3658 N85-32722
Marine Sample Exploitation Project: Estimates regarding the sensitivity and technology for the detection of nuclear explosion debris in the marine environment
[DE85-013176] 23 p3947 N85-34462
Seasonal variability and spatial non-uniformity of bioluminescence in the Mediterranean Sea
[DRIC-T-7545] 24 p4125 N85-35572

PLANKTON BLOOM
U PLANKTON

PLANNING
NT AIRPORT PLANNING
NT MANAGEMENT PLANNING
NT MISSION PLANNING
NT PRODUCTION PLANNING
NT PROJECT PLANNING
NT REGIONAL PLANNING
NT URBAN PLANNING
Air Force Materials Laboratory plans/projects
[AD-P004010] 03 p0306 N85-11990
The Air Force can improve its forecasts of aircraft spare parts requirements
[AD-A147911] 07 p1053 N85-16682
Developing double sampling plans for attributes to meet sample size criteria
[AD-A148144] 08 p1205 N85-17587
Strategy planning by an intelligent machine
[DE84-016609] 09 p1372 N85-18624
On motion planning with uncertainty: Revised
[AD-A149521] 10 p1492 N85-19421
A computer system for generating single and double sampling plans for attributes data
[AD-A149548] 11 p1701 N85-20698
FAA aviation forecasts: Fiscal years 1985-1996
[AD-A151050] 14 p2216 N85-23747
An approach to planning in the inflight emergency domain
[AD-A151869] 15 p2467 N85-25228
Artificial intelligence based control of a sensor-driven machine
[DE85-006972] 15 p2633 N85-26227
Historical perspective on the Moon base: The British perspective
[DE85-005905] 17 p2907 N85-27925
Experiments with stored heavy ions
[DE85-009976] 19 p3356 N85-30802
Report to the Working Group on Technology, Growth and Employment
[DE85-010320] 19 p3372 N85-30920
Navy information systems: Planning, policy, organization, and management
[PB85-176113] 20 p3541 N85-32036
Quality assurance considerations for the implementation of a pulsed power R and D project
[DE85-012357] 24 p4148 N85-35720

PLANOTRONS
NT HELITRONS
NT THERMICONS
NT THYRATRONS

PLANT DESIGN
Conceptual design of a 10 MW shore-based OTEC plant
[DE84-015806] 10 p1511 N85-19532

Some plant location problems — computer networks
[FUB-14-1984] 22 p3835 N85-33746

PLANT ROOTS
Gravity and cell differentiation in lentil roots
05 p0690 N85-14433
Comparative effects of auxin and abscisic acid on growth, hydrogen ion efflux and gravitropism in primary roots of maize
[NASA-CR-174355] 09 p1342 N85-18444
Amyloplast sedimentation kinetics in corn roots
15 p2606 N85-26059
Calcium and calmodulin localization in gravitropically-responding plant organs
15 p2606 N85-26061
The interaction of calcium and auxin in the gravitropic response of roots 15 p2606 N85-26062
Transduction of the root gravitropic stimulus: Can apical calcium regulate auxin distribution?
15 p2606 N85-26063
Role of Ca++ in shoot gravitropism — avena
15 p2607 N85-26065
Gravistimulus production in roots of corn
15 p2607 N85-26066
Differential wall growth in gravistimulated corn roots: Its timing and regulation 15 p2614 N85-26105

PLANT STRESS
Remote sensing of plant stress and diseases
05 p0657 N85-14216
Attempts to localize and identify the gravity sensing device of plant seedlings 15 p2607 N85-26064
The role of gravity on the reproduction of arabidopsis plants 15 p2607 N85-26069
Importance of gravity for plant growth and behavior
15 p2608 N85-26070

PLANTS (BOTANY)
NT ALFALFA
NT AQUATIC PLANTS
NT BARLEY
NT BRUSH (BOTANY)
NT CONIFERS
NT CORN
NT DECIDUOUS TREES
NT FOLIAGE
NT GRASSES
NT GUAYULE
NT LEAVES
NT LICHENS
NT OATS
NT SUGAR CANE
NT TOBACCO
NT TREES (PLANTS)
Prospectus of the utilization of leafy spurge (Euphorbia Esula L.) as a source of liquid fuel and biomass
[DE84-015203] 01 p0034 N85-10208
Estuaries of the Cape. Part 2: Synopses of available information on individual systems. Report 13: Silvermine (CSW 3)
[CSIR-RR-412-PT-2] 01 p0086 N85-10582
Estuaries of the Cape. Part 2: Synopses of available information on individual systems. Report no. 17: Lourens (CSW 7)
[CSIR-RR-416-PT-2] 01 p0087 N85-10586
A preliminary study of the feasibility of detecting the floating macrophytes by means of digital processing of MSS/LANDSAT data
[E85-10005] 02 p0215 N85-11418
Effects of acid rain on plant microbial associations in California
[PB84-242122] 04 p0532 N85-13404
Some principles of plant resources evaluation using remotely sensed data 04 p0543 N85-13459
Carbon cycle: Terrestrial interactions
05 p0652 N85-14187
The use of horizontal clinostats in studies of plant statocyte development 05 p0690 N85-14435
Plant responses to solar UV-B radiation
05 p0690 N85-14436
Preliminary results of advanced Biostack experiments with plant seeds and spores — cosmic ray effects
05 p0691 N85-14441
Plant growth in space 05 p0691 N85-14444
Controlled ecological life support system higher plant flight experiments
[NASA-CR-177323] 07 p1020 N85-16471
Calculation of optical characteristics of shelf ecological system based on its mathematical model
10 p1498 N85-19453
Vegetation analysis for arid lands geobotany
[NASA-CR-175455] 10 p1506 N85-19500
Effect of elevated atmospheric CO2 on plant communities
[DE85-001810] 11 p1676 N85-20576
Process development for commercial production of natural rubber from Guayule
[PB85-124956] 12 p1815 N85-21388
Estimating solar radiation for plant simulation models
[E85-10089] 12 p1873 N85-21751
Assessing LANDSAT TM and MSS data for detecting submerged plant communities 13 p2120 N85-23203
NASA Space Biology Program: 9th Annual Symposium
[NASA-CP-2336] 15 p2605 N85-26054
Polyamines as possible modulators of gravity induced calcium transport in plants 15 p2606 N85-26060
A possible explanation of why gravitropic growth is detected earlier than straight growth
15 p2607 N85-26067
Daylily as a system to study effects of space flight on plant development 15 p2607 N85-26068
The role of gravity on the reproduction of arabidopsis plants 15 p2607 N85-26069
Importance of gravity for plant growth and behavior
15 p2608 N85-26070
Gravitropism in leafy dicot stems
15 p2610 N85-26086
Mechanical stress regulation of plant growth and development 15 p2610 N85-26087
Plant growth biophysics: The basis for growth asymmetry induced by gravity 15 p2611 N85-26089
An indirect role for ethylene in shoot-inversion release of apical dominance in Pharbitis nil
15 p2611 N85-26090
Participation of ethylene in two modes of gravistimulation of shoots 15 p2613 N85-26101
Isolation of hybridomas for golgi-associated proteins and a plant calmodulin 15 p2613 N85-26103
A search for evidence of large body Earth impacts associated with biological crisis zones in the fossil record 15 p2682 N85-26567
The controlled ecological life support system
15 p2688 N85-26603
Research on zero-gravity botany apparatus
16 p2723 N85-26811
Ecology of Pamlico River, North Carolina: An estuarine profile
[PB85-155703] 16 p2822 N85-27404
Genetic engineering of plants: Agricultural research opportunities and policy concerns
[DE85-006771] 16 p2840 N85-27513
Photosynthetic acclimation of Acer saccharum
[DE85-008247] 17 p2998 N85-28536
Organization of the R region in maize
[DE85-011273] 20 p3504 N85-31780
Ice nucleating characteristics of Capparis Aphylla, an Indian herb 21 p3641 N85-32619
The role of sulfur in osmoregulation and salinity tolerance in cyanobacteria, algae, and plants
21 p3660 N85-32736
Hydroponics developments for spaceship garden
21 p3663 N85-32754
The 1984 environmental monitoring report, Sandia National Laboratories, Albuquerque, New Mexico
[DE85-011175] 22 p3611 N85-33607
Effect of substrate moisture on growth and structure of corn leaf 22 p3624 N85-33692
The 1984 biotic studies of Yucca Mountain, Nevada test site, Nye County, Nevada
[DE85-011715] 23 p3951 N85-34487
Mineral deposit models: Theory and practice
24 p4105 N85-35448
The measurement of nitrogen oxide (NO, NO2) exchange over plant/soil surfaces
[CSIRO-DAR-TP-8] 24 p4127 N85-35587

PLANTS (INDUSTRIES)
U INDUSTRIAL PLANTS

PLASMA ACCELERATION
Transverse electron resonance accelerator
[DE85-008289] 17 p3032 N85-28758
Report of the Working Group on Other Acceleration Schemes
[DE85-008447] 17 p3033 N85-28764
High energy plasma accelerators
[DE85-013121] 24 p4155 N85-35760

PLASMA ACCELERATORS
NT COAXIAL PLASMA ACCELERATORS
Electromagnetic acceleration of macroparticles to hypervelocities in axisymmetric geometry
[IPPJ-696] 06 p0863 N85-15484
Explosive emission cathode plasmas in intensive relativistic electron beam diodes
[AD-A147917] 07 p1046 N85-16642
Space Experiments with Particle Accelerators (SEPAC) 23 p3901 N85-34165
High energy plasma accelerators
[DE85-013121] 24 p4155 N85-35760

PLASMA ARC CUTTING
USSR report: Machine tools and metalworking equipment
[JPRS-UMM-85-005] 13 p2051 N85-22839
New tooling for plasma cutting technology
13 p2051 N85-22842
Mechanical properties of plasma arc cut steel
23 p3905 N85-34186

PLASMA ARC SPRAYING
U ARC SPRAYING

PLASMA ARC WELDING
The variable polarity plasma arc welding process: Its application to the Space Shuttle external tank
[NASA-TM-86482] 05 p0641 N85-14116
Cobalt-free permanent magnet alloys
[AD-A149272] 10 p1441 N85-19079
The strength and characteristics of VPPA welded 2219-T87 aluminum alloy 12 p1946 N85-22224
Weldability/microstructure relationships of high nickel alloys for header applications
[DE85-009337] 19 p3241 N85-30094
Plasma arc welding, equipment, installation and process control
[DE85-008481] 19 p3373 N85-30921
Mechanical properties of Shielded Metal Arc (SMA) and Submerged Arc (SA) welded joints in a steel Raex 386 P Arctic
[VTT-339] 22 p3801 N85-33551

PLASMA ARCS
U PLASMA JETS

PLASMA BUBBLES
Irregularity decay in an isolated plasma bubble
[AD-A145782] 03 p0392 N85-12506
Observations of plasma bubbles and their zonal drift using polarimeters
[INPE-3219-PRE/572] 05 p0729 N85-14698

PLASMA CHEMISTRY
The plasma assisted modified betatron
[AD-A148728] 09 p1390 N85-18748
Spatial resolution of small particles in silane discharge
[AD-A150953] 14 p2423 N85-24548

PLASMA CLOUDS
Repulsive force of magnetic clouds during solar flares and magnetospheric substorms
06 p0824 N85-15233
The role of finite parallel length on the stability of barium clouds
[AD-A146972] 07 p0996 N85-16328
Giotto residual ionization 14 p2244 N85-23909
A model of plasma cloud expansion generated by a dust particle impact — Giotto mission
14 p2245 N85-23914
Dependence of equatorial F-region plasma bubble rise velocity and dynamo electric field on solar cycle
[INPE-3439-PRE/696] 16 p2826 N85-27434
Projections of plasma cloud structures and their spectra
[AD-A153608] 18 p3189 N85-29776
Influence of magnetic clouds on cosmic ray intensity variations
[SH-5.1-12] 23 p4042 N85-35065

PLASMA COMPOSITION
ISEE-1 data reduction and analysis plasma composition experiment
[NASA-CR-175306] 21 p3630 N85-32552
Diffusion in the chromosphere and the composition of the solar corona and energetic particles
[SH-2.1-9] 23 p3999 N85-34790

PLASMA COMPRESSION
Adequacy of metal ablation process with laser radiation and a shock-compressed plasma
13 p2028 N85-22708
Electric field and plasma observations near the magnetopause and bow shock during a rapid compression 14 p2355 N85-24553
Strong coupling effects on bound states in plasmas
[AD-A154353] 19 p3370 N85-30905
Numerical studies of high current beam compression in heavy ion fusion
[DE85-011874] 24 p4158 N85-35783

PLASMA CONDUCTIVITY
Impact of atomic data on Tokamak modeling
09 p1390 N85-18743
Exitation of low-frequency resonance waves by moving conductor in space plasma 13 p2067 N85-22912
Asymmetric flux generation and its relaxation in reversed field pinch
[IPPJ-712] 15 p2656 N85-26387
Current enhancement in a conducting channel
[AD-A155418] 22 p3845 N85-33812

PLASMA CONFINEMENT
U PLASMA CONTROL

PLASMA CONTROL
Means of varying conditions in the expanded boundary divertor without affecting energy confinement
[DE84-013840] 01 p0122 N85-10836
Study of plasma convection and wall interactions in magnetic confinement systems
[DE84-013959] 03 p0421 N85-12692
Fusion plasma theory. Task 1: Magnetic confinement fusion plasma theory
[DE84-014941] 04 p0566 N85-13809

EBT electron energy confinement experiments
[DE84-015402] 04 p0567 N85-13613

Application of the energy problem to the problem of plasma flow stability
[DE84-013369] 05 p0730 N85-14691

Compact toroidal development: Activity plan for field reversed configurations
[DE84-017145] 05 p0730 N85-14695

Passive stabilization of vertical instability in Tokamak reactor 06 p0775 N85-14958

The origin of plasma rotation in the early phase of an FRC produced by a reversed field theta pinch
[IPPJ-698] 06 p0863 N85-15482

Theoretical investigations relevant to magnetic fusion research, April 1, 1983 - March 31, 1984
[DE85-001776] 06 p0865 N85-15498

Plasma-surface interactions in large tandem mirror devices, MFTF-B
[DE85-001753] 06 p0865 N85-15499

Shear-Alfven dynamics of toroidally confined plasmas, part A
[DE85-001590] 06 p0866 N85-15502

Shear-Alfven dynamics of toroidally confined plasmas, part B
[DE85-001767] 06 p0866 N85-15504

A propagator expansion method for solving linearized plasma kinetic equations with collisions
[AD-A147524] 07 p1045 N85-16640

Sources, densities, and transport of impurities in neutral-beam injected Tokamaks
09 p1388 N85-18731

Effect of alpha particles on the stability of Elmo Bumpy Torus (EBT) reactor
[DE84-017266] 09 p1392 N85-18759

CTR plasma engineering studies
[DE84-017447] 09 p1392 N85-18762

Small, octopole-stabilized tandem mirror reactor
[DE85-002144] 10 p1559 N85-19832

Finite-(beta) optimization of tandem mirrors
[DE85-002658] 10 p1560 N85-19835

Entrop production determination of the ambipolar solution nearest equilibrium
[DE85-003049] 10 p1560 N85-19836

FRC translation dynamics and plasma confinement properties in FRX-C/T
[DE85-002366] 10 p1560 N85-19842

Thermal barrier confinement experiments in TMX-U tandem mirror, revision 1
[DE84-017029] 10 p1561 N85-19844

TMX-U neutral pressure measurement diagnostic systems
[DE85-000746] 11 p1730 N85-20881

Mirror fusion progress
[DE85-001187] 11 p1731 N85-20888

Observations of low frequency plasma fluctuations in ELMC Bumpy Torus
[DE85-003796] 11 p1732 N85-20895

Plasma performance of TFCX and jet with sawtoothing
[DE85-003335] 12 p1936 N85-22168

Opacity determinations for Inertial Confinement Fusion (ICF) materials using an average atom model
12 p1957 N85-22295

Winding insulation in electromagnetic systems for Tokamak reactor plants 13 p2087 N85-23035

Confinement properties of high energy density plasmas in the Wisconsin levitated octupole
13 p2161 N85-23408

Lower hybrid heating and current drive, and ion cyclotron heating experiments on the Alcator C and the Versator II Tokamaks
[DE85-004918] 13 p2161 N85-23412

Breakthrough in container confinement of ultracold neutrons 15 p2644 N85-26311

Nagoya bumpy torus 15 p2655 N85-26377

High beta pinch plasma (STP-L)
15 p2655 N85-26381

Plasma theory and computations
15 p2655 N85-26384

Heavy ion beam study of potential formation in bumpy torus plasma
[IPPJ-711] 15 p2656 N85-26386

Internal field probing of translating FRCs
[DE85-003732] 15 p2657 N85-26394

MHD fluctuations in ISX-B
[DE85-004800] 15 p2657 N85-26395

Plasma-wall interactions in tandem mirror machines
[DE85-006387] 15 p2657 N85-26399

Magnetohydrodynamic stability of spheromak plasma in toroidal flux conserver with rectangular cross section
[IPPJ-716] 16 p2866 N85-27678

TOKASTAR: A Tokamak stellarator hybrid with possible bean-shaped operation
[IPPJ-718] 16 p2866 N85-27680

Spherical torus, compact fusion at low field
[DE85-006983] 16 p2867 N85-27689

Time-resolving electron temperature diagnostic for ALCATOR C
[DE85-004916] 16 p2868 N85-27690

Stability of high energy particle plasmas to MHD-like modes
[DE85-007679] 17 p3039 N85-28803

An Impurity Control Test Facility (ICTF) for the study of fusion reactor/plasma edge materials
[DE85-007946] 17 p3040 N85-28810

Comparison study of toroidal-field divertors for a compact reversed-field pinch reactor
[DE85-009591] 18 p3189 N85-29781

Whist code calculations of ignition margin in an ignition Tokamak
[DE85-009507] 18 p3190 N85-29784

Radiation-cooled helicity-injecting reversed field pinch formed with relativistic electrons
[IPPJ-721] 19 p3370 N85-30901

New concept for pumping the edge plasma
[DE85-010160] 19 p3371 N85-30909

Los Alamos Spheromak Program
[DE85-010748] 20 p3398 N85-31077

System and method of operating toroidal magnetic confinement devices
[DE85-011670] 22 p3845 N85-33814

Method and apparatus for maintaining equilibrium in a helical axis stellarator
[DE85-011626] 22 p3845 N85-33815

Elmo bumpy square plasma confinement device
[DE85-011628] 22 p3845 N85-33816

Confinement and heating of high beta plasma with emphasis on compact toroids. Compact toroid research
[DE85-011463] 22 p3846 N85-33821

Collisional relaxation of electron tail distribution
[IPPJ-729] 23 p3974 N85-34635

Proceedings of the US-Japan Workshop on Transport in Open-Ended Systems
[IPPJ-727] 23 p3975 N85-34644

Potential effect in transport due to non-axisymmetric confining field 23 p3975 N85-34645

Activities of the RF Section 23 p3975 N85-34646

Radial transport phenomena for TMX-upgrade
23 p3976 N85-34647

Plug and thermal barrier potential formation in Gamma 10 23 p3976 N85-34648

Induced azimuthal electric field effects on tandem transport and ambipolarity 23 p3976 N85-34650

Recent experiments in Gamma-10
23 p3976 N85-34651

Azimuthal uniformity and current balance study of ICRH-produced plasma in RFC-XXM
23 p3977 N85-34659

Moving finite element method for ICF target implosion
23 p3980 N85-34675

Stability of implosion dynamics
23 p3980 N85-34680

On the heat flux derived by the moment method in Lorentzian plasma between hot and cold walls
23 p3980 N85-34682

Integral representation for nonlinear heat transport
23 p3981 N85-34683

Advanced Toroidal Facility (ATF)
[DE85-011567] 23 p3983 N85-34699

Stellarator approach to fusion plasma confinement
[DE85-011420] 23 p3984 N85-34704

Limiter
[DE85-011620] 24 p4150 N85-35736

Confinement and heating of high beta plasmas with emphasis on compact toroids
[DE85-011459] 24 p4155 N85-35761

Analysis of a pulsed power system containing rotating machine
[DE85-014128] 24 p4159 N85-35786

Diagnostics for Pioneer 1 imploding plasma experiments
[DE85-014120] 24 p4159 N85-35787

PLASMA CURRENTS

Fast waves near the lower hybrid frequency
[DE84-015217] 01 p0123 N85-10841

Numerical investigation of characteristics of current flow for different methods of obtaining discharge in high speed lasers. Mechanism underlying current flow in positive glow discharge column 02 p0264 N85-11728

Experimental observation of plasma neoclassical currents
[DE84-015706] 04 p0566 N85-13605

Generation of suprathermal electrons during plasma current startup by lower hybrid waves in a Tokamak
[IPPJ-697] 06 p0863 N85-15483

The anode mechanism of a thermal argon arc
[NASA-TM-77754] 07 p0921 N85-15835

Current measurements by Faraday rotation in single mode optical fibers
[DE85-002025] 09 p1384 N85-18707

Diffusion driven plasma current with turbulent dynamo
[IPPJ-700] 09 p1386 N85-18716

Wave absorption and transport studies on Electron Cyclotron Resonance (ECR) heated stellarator plasmas in W 7-A
[IPF-84-9] 09 p1395 N85-18782

Observations of bulk electron heating due to return current in a tokamak discharge started up by lower hybrid waves
[IPPJ-706] 12 p1937 N85-22172

Direct measurements of severe spacecraft charging in auroral ionosphere 13 p1991 N85-22480

Ram-wake effects on plasma current collection of the PIX 2 Langmuir probe 13 p1993 N85-22496

Entry of solar energetic protons into the distant plasma sheet dependence on distance from the neutral sheet
14 p2357 N85-24567

Estimate of the amplitude of transient electric fields in the magnetotail 14 p2358 N85-24568

Plasma sheet dynamics deduced from ISEE-1 and -2 energetic particle flux data 14 p2358 N85-24570

Current distribution in a plasma erosion opening switch
[AD-A150987] 14 p2424 N85-24949

Noninductive current drive in Tokamaks
[DE85-005427] 14 p2424 N85-24951

The possible role of electrical currents in coronal phenomena 14 p2453 N85-25151

High energy beam experiment
15 p2654 N85-26376

High beta pinch plasma (STP-3(M))
15 p2655 N85-26380

Alternating current OHMIC heating in a toroidal stellarator 20 p3534 N85-31988

Simulating the effects of plasma disruption with a 1 MA current pulse in a coaxial test fixture
[DE85-010491] 20 p3536 N85-31996

Current enhancement in a conducting channel
[AD-A155418] 22 p3845 N85-33812

Size effects of vacuum chamber for H- (D-) ion volume production by sheet plasma 1
[IPPJ-731] 23 p3974 N85-34639

Langmuir probe on ISX-B
[DE85-012066] 23 p3983 N85-34697

PLASMA CYLINDERS

NT CYLINDRICAL PLASMAS

Scattering of radio waves on magnitized meteor trail
03 p0344 N85-12221

Diffraction of plane TM-wave on continuously irregular elliptical plasma 13 p2087 N85-22014

PLASMA DENSITY

Precipitation of protons with E sub p approximately 1 MeV near plasmopause 02 p0161 N85-11093

The solar wind at 20-30 AU 02 p0301 N85-11950

Irregularity decay in an isolated plasma bubble
[AD-A145782] 03 p0392 N85-12506

Overview of recent advances in laser applications
05 p0725 N85-14660

Longer-scalelength plasma perturbations by an intense laser beam
[AD-A147005] 07 p1045 N85-16638

Electrostatic wave observation during a space simulation Beam-Plasma-Discharge (BPD)
[NASA-CR-174286] 07 p1045 N85-16639

Far-infrared laser diagnostic on EBT and extreme far-forward laser scattering on ISX
[DE85-001788] 07 p1046 N85-16643

Artificial ionospheric disturbances caused by powerful radio waves
[AD-A146077] 08 p1186 N85-17473

Far-infrared interferometry/polarimetry on the ISX-B Tokamak
[DE84-015401] 10 p1558 N85-19827

Ion quadrupole effects in spectral line broadening
[DE85-001504] 11 p1730 N85-20879

Transient waveform acquisition system for the ELMO Bumpy Torus
[DE85-000154] 11 p1733 N85-20901

Hollow cathode apperatus
[NASA-CASE-NPO-15560-1] 12 p1832 N85-21491

Plasmachemical evaporation and doping of amorphous silicon 12 p1879 N85-21790

Electrostatic confinement in a bumpy torus
[DE85-003794] 12 p1936 N85-22164

Determination of experimental Tokamak plasma properties using maximum entropy analysis
[DE85-001723] 12 p1936 N85-22165

Vehicle charging on STS-3 Mission
13 p1989 N85-22473

Ram-wake effects on plasma current collection of the PIX 2 Langmuir probe 13 p1993 N85-22496

NASCAP simulation of PIX 2 experiments
13 p1993 N85-22497

Confinement properties of high energy density plasmas in the Wisconsin levitated octupole
13 p2161 N85-23408

Increased hot-electron production at quarter-critical density in long-scalelength, laser-plasma interactions
[AD-A150519] 13 p2161 N85-23411

Theoretical studies of kinetic mechanisms of negative ion formation in plasmas
[AD-A150820] 14 p2423 N85-24946

Chaotic dynamics of instabilities in solids
[DE85-004909] 14 p2429 N85-24978

Affect of angle of incidence on plasmas generated during laser welding
[DE85-005724] 15 p2569 N85-25852

Internal field probing of translating FRCs
[DE85-003732] 15 p2657 N85-26394

Direct evidence for solar wind control of Jupiter's hectometer-wavelength radio emission
[NASA-TM-86073] 16 p2883 N85-27790

Heating of electrons in a high density tokamak by a micro-wave near second harmonic frequency
[DE85-010682] 19 p3359 N85-30822

Effects of a radial electric field on tokamak edge turbulence
[DE85-010401] 19 p3371 N85-30910

Thermal ion heating in the vicinity of the plasmapause
[NASA-CR-176030] 20 p3535 N85-31993

Theoretical and Experimental Beam Plasma Physics (TEBPP) 23 p3901 N85-34166

Breakdown of intrinsic ambipolarity for the radial diffusion due to a rotating RF field 23 p3977 N85-34660

Simulation studies on stability of hot electron plasma
23 p3978 N85-34664

Current interruption by density depression
[DE85-013120] 24 p4169 N85-35846

PLASMA DIAGNOSTICS

Rocket observations 01 p0014 N85-10064

SEPAC (space experiments with particle accelerators)
01 p0014 N85-10065

Analysis of glow discharges for understanding the process of film formation
[NASA-TM-83750] 01 p0022 N85-10136

Fluctuation spectrum for linear gyroviscous MHD
[IPP-6/237] 01 p0121 N85-10828

Experimental observation of neoclassical currents
[DE84-015113] 01 p0122 N85-10834

Two novel plasma diagnostic tools: Fiber sensors and phase conjugation
[DE84-014033] 01 p0123 N85-10840

Physics of the inner heliosphere 1-10R sub O plasma diagnostics and models
[NASA-CR-174010] 02 p0304 N85-11964

A high transmission, 20 channel polychromator for the Thomson scattering diagnostic of TORTUR 3 — plasma diagnostics
[REPT-84-156] 03 p0422 N85-12694

High-Beta Tokamak research
[DE84-016470] 04 p0568 N85-13618

Non-LTE considerations in spectral diagnostics of thermal transport and implosion experiments
[DE84-015187] 05 p0730 N85-14689

Imaging polarimeter-interferometer arrays for Tokamak measurements
[DE84-015916] 05 p0730 N85-14693

Nitriding of titanium and its alloys by N2, NH3 or mixtures of N2 + H2 in a dc arc plasma at low pressures (or = to torr)
[NASA-TM-83803] 06 p0814 N85-15168

Alpha-particle diagnostics with high energy neutral beams
[IPPJ-695] 06 p0863 N85-15485

Measurement of proton autoneutralization potential
[DE85-001752] 06 p0865 N85-15501

Far-infrared laser diagnostic on EBT and extreme far-forward laser scattering on ISX
[DE85-001788] 07 p1046 N85-16643

Advanced diagnostics for reacting flows
[AD-A148479] 08 p1162 N85-17334

Feasibility of alpha particle measurement by CO2 laser Thomson scattering
[DE85-001764] 09 p1326 N85-18334

Current measurements by Faraday rotation in single mode optical fibers
[DE85-002025] 09 p1384 N85-18707

Proceedings on US-Japan Workshop on Tokamak Diagnostics by X-ray, VUV and Optical Radiations
[IPPJ-703] 09 p1386 N85-18719

X-rays spectroscopy on the PLT and TFTR Tokamaks
09 p1386 N85-18720

Present status of Heliotron E experiment
09 p1387 N85-18721

Spectroscopic measurement on Heliotron E
09 p1387 N85-18722

Radial profiles of high resolution X-ray spectra from the Alcator C Tokamak 09 p1387 N85-18723

Recent activities on JIPP T-IIU Tokamak
09 p1387 N85-18724

Spectroscopic instrumentation for Tokamak diagnostics 09 p1388 N85-18732

Determination of ion temperature and rotation velocity profiles by visible, UV and X-ray spectroscopy on Doublet 3 09 p1388 N85-18734

Measurements of electric fields in plasmas by using beam probe and laser fluorescence techniques
09 p1389 N85-18737

Beam probe spectroscopic technique for ion temperature and magnetic field measurements
09 p1389 N85-18738

Compilation of atomic data for diagnostics of Tokamak
09 p1390 N85-18744

The coordinated research program at IAEA on atomic collision data for plasma diagnostics
09 p1390 N85-18747

Cookbook for determining essential transmission characteristics of spherical section electrostatic analyzers
[DE85-001404] 09 p1391 N85-18751

Experimental investigations of driven Alfven wave resonances in a Tokamak plasma using carbon dioxide laser interferometry
[DE85-001049] 09 p1392 N85-18758

Background calculations for the measurement of the ion temperature in a deuterium plasma
[DE84-016546] 09 p1393 N85-18768

Lidar-Thomson scattering — Joint European Torus
[IPF-84-3] 09 p1394 N85-18777

Improved performance for large area triple layer microchannel plate detector for a neutral spectrometer in Doublet III
[DE85-001719] 10 p1488 N85-19395

Sequentially-framing soft X-ray pinhole camera for Tokamak plasma studies
[DE85-001717] 10 p1489 N85-19399

Bibliography of Soviet laser developments, Number 66, July-August 1983
[AD-A149113] 10 p1490 N85-19406

CO2 laser interferometer array for Big Dee
[DE85-001718] 10 p1490 N85-19411

Far-infrared interferometry/polarimetry on the ISX-B Tokamak
[DE84-015401] 10 p1558 N85-19827

Application of layered synthetic microstructures to high temperature plasma diagnostics
[DE85-002035] 10 p1559 N85-19828

Space-time statistics of the turbulence in a Tokamak edge plasma
[DE85-002667] 10 p1559 N85-19834

X-ray line broadening of a diagnostic in laser produced plasma
[DE85-001179] 10 p1560 N85-19841

Direct reading fast microwave interferometer for EBT
[DE85-000183] 11 p1636 N85-20306

Electrodynamic interactions 11 p1643 N85-20348

Applications of Tethers in Space, volume 2
[NASA-CP-2365] 11 p1644 N85-20361

Novel probe for determining the size and position of a relativistic electron beam
[DE85-001044] 11 p1723 N85-20836

A proposed method for fast determination of plasma parameters
[IPP-1/228] 11 p1730 N85-20877

Ion quadrupole effects in spectral line broadening
[DE85-001504] 11 p1730 N85-20879

TMX-U neutral pressure measurement diagnostic systems
[DE85-000746] 11 p1730 N85-20881

Mirror fusion progress
[DE85-001187] 11 p1731 N85-20888

X-ray spectroscopy of laser-produced plasmas
[DE85-002170] 11 p1733 N85-20897

Transient waveform acquisition system for the ELMO Bumpy Torus
[DE85-000154] 11 p1733 N85-20901

Edge diagnostics for tandem mirror machines
[DE85-001209] 11 p1733 N85-20902

Activities report of the Institute of Plasma Research
11 p1733 N85-20903

Intensified CCD camera system for plasma diagnostics
[DE85-002252] 12 p1853 N95-21620

Arc-driven rail gun research
[NASA-CR-174816] 12 p1859 N85-21662

Determination of experimental Tokamak plasma properties using maximum entropy analysis
[DE85-001723] 12 p1936 N85-22165

X-ray astronomy and plasma astrophysics
12 p1953 N85-22288

Plans for Interbol satellite experiment
13 p1977 N85-22407

Suprathermal plasma observed on STS-3 Mission by plasma diagnostics package 13 p1989 N85-22472

Vehicle charging on STS-3 Mission
13 p1989 N85-22473

Electron and ion density depletions measured in the STS-3 orbiter wake 13 p1989 N85-22474

Measured electron contribution to Shuttle plasma environment: Abbreviated update
13 p1990 N85-22476

Ram-wake effects on plasma current collection of the PIX 2 Langmuir probe 13 p1993 N85-22496

Feasibility of alpha particle measurement by CO2 laser Thomson scattering
[DE85-004936] 13 p2097 N85-23061

Confinement properties of high energy density plasma in the Wisconsin levitated octupole
13 p2161 N85-23408

Ion transport in beam-plasma interactions
[AD-A150145] 13 p2161 N85-23410

Ultrahigh-sensitivity threshold neutron detector for plasma diagnostics
[DE85-005270] 13 p2161 N85-23413

Physics of the inner heliosphere: Mechanisms, models and observational signatures
[NASA-CR-175632] 13 p2205 N85-23877

An impact plasma monitor for cometary missions — Giotto , VEGA 14 p2245 N85-23916

Advanced diagnostics for reacting flows
[AD-A150675] 14 p2301 N85-24246

Advances in magnetospheric plasma diagnosis by active experiments --- IMS satellites 14 p2371 N85-24654

Contribution of mutual impedance experiments to the understanding of magnetospheric processes --- GEOS satellites 14 p2371 N85-24656

Plasma-edge studies using carbon resistance probes
[DE85-005589] 14 p2424 N85-24955

Annual Review, April 1983 - March 1984
[ISSN-0547-1567] 15 p2654 N85-26369

System for lower hybrid current startup
15 p2654 N85-26373

Preparatory experiments. 1: JIPP T-IIU
15 p2654 N85-26374

Nagoya bumpy torus 15 p2655 N85-26377

Soft X-ray diagnostics of laser-produced plasmas (HALNA) 15 p2655 N85-26382

Diagnostics of a glow discharge used to produce hydrogenated amorphous silicon films
[DE85-002914] 15 p2661 N85-26420

Sub-nanosecond cinematography in laser fusion research: Current techniques and applications at the Lawrence Livermore Laboratory
[DE85-007252] 17 p2968 N85-28334

Experimental plasma research: Plasma summaries
[DE85-008116] 17 p3039 N85-28805

Accelerator-based plasma-wall interaction studies on the TEXTOR Tokamak
[DE85-007540] 17 p3040 N85-28806

Electron temperature measurements from induced toroidal current in ELMO Bumpy Torus scale
[DE85-008549] 18 p3189 N85-29779

Experiments in plasma initiation and laser absorption in flowing gases
[AD-A154303] 19 p3276 N85-30313

Research activities of the Physics Division
[DE85-006958] 19 p3357 N85-30811

Research support for plasma diagnostics on Elmo Bumpy Torus: Diamagnetic measurements and data analysis and development of ring models for realistic representation of fields near the plasma
[DE85-010035] 19 p3371 N85-30912

Thomson scattering on Elmo Bumpy Torus
[DE85-010584] 20 p3527 N85-31941

Global effects of double layers --- plasma layers
[TRITA-EPP-84-12] 20 p3536 N85-32002

Observations of low energy magnetospheric plasma outside the plasmasphere
[KGI-PREPRINT-075] 20 p3536 N85-32004

Space Experiments with Particle Accelerators (SEPAC) 23 p3901 N85-34165

Recoverable Plasma Diagnostics Package (RPDP)
23 p3902 N85-34167

Magnetospheric multiprobes: MMP/CHEMSAT
23 p3902 N85-34171

Novette diagnostic support
[DE85-012937] 23 p3934 N85-34389

Langmuir probe on ISX-B
[DE85-012066] 23 p3983 N85-34697

Instrument to synchronize Thomson scattering diagnostic measurements with MHD activity in a Tokamak
[DE85-012082] 23 p3984 N95-34708

Diagnostics for Pioneer 1 imploding plasma experiments
[DE85-014120] 24 p4159 N85-35787

PLASMA DIFFUSION

Asymptotic behaviour of the plasma equation
[AD-A147242] 07 p1031 N85-16549

Velocity space diffusion of high energy ions induced by a lower hybrid wave in a nonuniform magnetic field
[IPPJ-714] 16 p2866 N85-27681

Stefan-Maxwell relations for plasma diffusion currents in magnetic field 17 p2942 N85-28160

Influence of type of processing of AK4 alloy on its surface state and strength of bonding of plasma coatings
19 p3242 N85-30103
Plasma radiation sources. Quasi-adiabatic theory and numerical modeling in the electro-diffusive approximation
[AD-A154375] 19 p3370 N85-30906
Schottky theory of three component plasmas
[AD-A154461] 19 p3371 N85-30907
RF induced radial diffusion in tandem mirrors
23 p3976 N85-34649
Guiding center distribution function and longitudinal invariant 23 p3978 N85-34663
The plasma mechanism for preferential acceleration of heavy ions
[SH-2.2-10] 23 p4001 N85-34805
Long-time asymptotics of a system for plasma diffusion
[NASA-CR-177947] 24 p4093 N85-35375

PLASMA DIODES
Explosive emission cathode plasmas in intensive relativistic electron beam diodes
[AD-A147917] 07 p1046 N85-16642
Theoretical study of collective ion acceleration in the Luce diode
[AD-A150107] 12 p1929 N85-22116
Electrochromic display device
[AD-D011733] 22 p3759 N85-33299

PLASMA DISCHARGES
U PLASMA JETS

PLASMA DISPERSION
U PLASMA DIFFUSION

PLASMA DISPLAY DEVICES
Frictional and structural characterization of ion-nitrided low and high chromium steels
[NASA-TM-86991] 13 p2098 N85-23085
Electrochromic display device
[AD-D011733] 22 p3759 N85-33299

PLASMA DRIFT
Plasma drift equilibrium (gyration) in toroidal systems with complex magnetic-field geometry
[DE84-015827] 01 p0122 N85-10839
Integral of wave kinetic equation of drift waves
02 p0283 N85-11848
Plasma drift towards a plane equipotential surface
[TRITA-EPP-84-01] 02 p0285 N85-11860
Fusion plasma theory. Task 3: ECRH and transport modeling in tandem mirrors and divertor physics
[DE84-014939] 04 p0567 N85-13612
Observations of plasma bubbles and their zonal drift using polarimeters
[INPE-3219-PRE/572] 05 p0729 N85-14888
The role of finite parallel length on the stability of barium clouds
[AD-A146972] 07 p0996 N85-16328
Ionospheric turbulence: Interchange instabilities and chaotic fluid behavior
[AD-A147810] 07 p0998 N85-16337
Fusion Energy Division
[DE85-001701] 11 p1731 N85-20884
Electrostatic confinement in a bumpy torus
[DE85-003794] 12 p1936 N85-22164
Heavy ion beam study of potential formation in bumpy torus plasma
[IPPJ-711] 15 p2656 N85-26388
Coupled plasma-neutral transport model for the scrape-off region
[DE85-007559] 16 p2868 N85-27695
Drift anisotropy instability of a finite Beta magnetospheric plasma
[IFSI-84-12] 20 p3536 N85-32005

PLASMA DYNAMICS
Long-time tail in the two-wave model
02 p0282 N85-11837
Lie-transformation action principle for classical plasma dynamics
[DE84-014576] 02 p0285 N85-11858
Magnetospheric plasma studies using data from the dynamics high and low altitude plasma instruments
[AD-A145751] 03 p0392 N85-12505
Solar wind dynamics at small distances from the sun
06 p0823 N85-15227
Shear-Alfven dynamics of toroidally confined plasmas, part B
[DE85-001787] 06 p0866 N85-15504
Spark column plasma dynamics model (a first principles model for laser triggered spart gaps)
[AD-A147954] 08 p1166 N85-17354
Four-fluid description of turbulent plasma focus dynamics
[IPF-84-4] 09 p1395 N85-18778
Ionospheric research at INPE
[INPE-3279-PRE/602] 10 p1514 N85-19556
Rail accelerator technology and applications
[NASA-TM-86947] 12 p1794 N85-21258
Theoretical study of collective ion acceleration in the Luce diode
[AD-A150107] 12 p1929 N85-22116
Ring current dynamics and plasma sheet sources — magnetic storms 14 p2359 N85-24577
The structure, stability, wave transmission and energy transfer at the Earth's magnetopause
14 p2372 N85-24681
Laboratory for laser energetics report
[DE85-007235] 15 p2563 N85-25814
Poloidal rotation of magnetic fluctuations in reversed field pinch plasma
[IPPJ-715] 16 p2866 N85-27677
A four-field model for Tokamak plasma dynamics
[DE85-007111] 16 p2868 N85-27694
Application of the MHD energy principle to magnetostatic atmospheres
[NASA-CR-175967] 18 p3136 N85-29420
Projections of plasma cloud structures and their spectra
[AD-A153608] 18 p3188 N85-29776
Plasmodynamic methods for generating powerful light puses 21 p3693 N85-32943
Workshop report on Simulation Techniques for Shock Wave Phenomena and Characteristics of Plasmas in Inertial Confinement Fusion
[IPPJ-725] 23 p3979 N85-34670

PLASMA ELECTRODES
Space-time characteristics of field in longitudinal pulse-period discharge typical in pumping of self-terminating lasers 21 p3887 N85-32909

PLASMA ENGINES
Modeling the exhaust of the pulsed plasma thruster
[AD-A155344] 21 p3707 N85-33018

PLASMA EQUILIBRIUM
Plasma drift equilibrium (gyration) in toroidal systems with complex magnetic-field geometry
[DE84-015827] 01 p0122 N85-10839
Destruction of magnetic surfaces in three-dimensional MHD equilibria 02 p0282 N85-11838
Zero-current, high beta stelleration equilibria with rotational transform profile control
[DE84-016835] 04 p0568 N85-13624
Electric field in plasma layer of magnetosphere during preliminary substorm phase 06 p0824 N85-15231
Resistive evolution of general plasma configuration
[DE85-002340] 10 p1561 N85-19843
Monte Carlo studies of tandem mirror plasmas interacting with waves in the Ion Cyclotron Range of Frequencies (ICRF)
[DE85-002988] 11 p1731 N85-20883
Convergent spectral representation for 3-dimensional inverse MBD equilibria
[DE85-000866] 11 p1733 N85-20900
The continuous spectrum of an axisymmetric, self-gravitating equilibrium in the presence of a poloidal magnetic field 12 p1959 N85-22315
Modified betatron accelerator studies
[AD-A151420] 15 p2648 N85-26332
Toroidal equilibrium with low frequency wave driven currents
[DE85-005790] 15 p2658 N85-26401
Reversed field pinch dynamics and transport studies
[DE85-007553] 18 p3189 N85-29778
Solution of problem of equilibrium confinement of plasma by magnetic field in an infinite circular cylinder
21 p3692 N85-32936
Recombination and ionization in a nitrogen plasma
[AD-A155426] 22 p3845 N85-33813
User's manual for the FLORA equilibrium and stability code
[DE85-013182] 23 p3966 N85-34590
Magnetohydrodynamic equilibrium and stability of spheromak with spheroidal plasma-vacuum interface
[IPPJ-732] 23 p3974 N85-34640

PLASMA ETCHING
Basic development of a 1.5 micrometer very large scale integrated technique, part 1-4
[BMFT-FB-T-85-032-PT-1-4] 20 p3449 N85-31417

PLASMA FLOW
U MAGNETOHYDRODYNAMIC FLOW

PLASMA FLUX MEASUREMENT
Confinement and heating of high beta plasmas with emphasis on compact toroids
[DE85-011459] 24 p4155 N85-35761

PLASMA FOCUS
Intense excitation source of blue-green laser
[AD-A147450] 07 p0971 N85-16166
Four-fluid description of turbulent plasma focus dynamics
[IPF-84-4] 09 p1395 N85-18778
Two phases of neutron production in the POSEIDON plasma focus
[IPF-84-10] 09 p1395 N85-18783
Activities report of the Institute of Plasma Research
11 p1733 N85-20903
Restrike particle beam experiments on a dense plasma focus. Opening switch research on a dense plasma focus
[AD-A152891] 17 p3039 N85-28802
Time-resolved energy spectrum of the ion beam generated in the plasma focus 19 p3369 N85-30892
Plasmodynamic methods for generating powerful light puses 21 p3693 N85-32943
The electromagnetic ram action of the plasma focus as a paradigm for the generation of cosmic rays and the gigantic jets in active galaxies
[OG-8.2-14] 23 p4020 N85-34910

PLASMA FREQUENCIES
Spatial resolution of small particles in silane discharge
[AD-A150953] 14 p2423 N85-24948
Experimental measurements of the ion cyclotron antennas' coupling and RF characteristics
[DE85-011569] 23 p3982 N85-34694

PLASMA GENERATION
U PLASMA GENERATORS

PLASMA GENERATORS
NT PLASMA GUNS
NT PLASMATRONS
NT TOKAMAK DEVICES
K-shell yield scaling law for conventional PRS loads
[AD-A145155] 01 p0121 N85-10831
High frequency plasma generator for ion thrusters
[NASA-CR-174772] 08 p1114 N85-17023
Bibliography of Soviet laser developments, Number 66, July-August 1983
[AD-A149113] 10 p1490 N85-19406
Characteristics of multiarc plasma devices
12 p1841 N85-21554
EMI characteristics of a potential control system
13 p1994 N85-22502
Explosive emission cathode plasmas in intense relativistic electron beam diodes
[AD-A150669] 14 p2417 N85-24912
Experimental investigation of neutral plasma beam propagation across a magnetic field
[AD-A150944] 14 p2423 N85-24947
Radio frequency containment
15 p2654 N85-26375
Basic studies. 1: Basic experiments in plasma physics 15 p2655 N85-26378
Development of RF plasma generators for neutral beams
[DE85-004125] 15 p2658 N85-26400
Experimental research on electrical propulsion. Note 2: Experimental research on a plasma jet with vortex type stabilization for propulsion
[NASA-TM-77874] 18 p3067 N85-28968
Time-resolved energy spectrum of the ion beam generated in the plasma focus 19 p3369 N85-30892

PLASMA GUNS
Hot hollow cathode gun assembly
[DE84-014312] 01 p0121 N85-10632
Steady-state spheromak reactor studies
[DE85-009585] 19 p3372 N85-30916

PLASMA HEATING
NT ELECTRON CYCLOTRON HEATING
Fast waves near the lower hybrid frequency
[DE84-015217] 01 p0123 N85-10841
Fusion plasma theory. Task 3: Auxiliary heating in Tokamaks and tandem mirrors
[DE84-014940] 04 p0566 N85-13609
Oscillating field current drive for reversed field pinch discharges
[DE84-015090] 04 p0567 N85-13610
Elma Bumpy Torus physics
[DE84-013909] 05 p0730 N85-14694
High frequency plasma generator for ion thrusters
[NASA-CR-174772] 08 p1114 N85-17023
Heating in the solar mantle 08 p1233 N85-17769
The role of fast electrons for the performance characteristics of hydrogen ion sources
09 p1303 N85-18189
Slow wave antenna coupling to ion Bernstein waves for plasma heating in ICRF
[AD-B089084L] 09 p1386 N85-18717
Impurity control by additional current rise and gas puffing during ICRF heating in JIPP T-IIU Tokamak
09 p1387 N85-18725
Long-pulse beamlines for the mirror fusion test facility
[DE84-017091] 09 p1392 N85-18760
The energy spectra of slowed-down neutrals from the heating beams in ASDEX — tokamak
[REPT-84-157] 09 p1394 N85-18772
Improved directional couplers for overmoded waveguide systems
[IPF-84-1] 09 p1394 N85-18775
Design of mode converters from TE circular om modes in circular waveguides to TE rectangular mo modes in rectangular waveguides for high power applications in the frequency range 1 to 30 GHz
[IPF-84-7] 09 p1395 N85-18781

Generation of Alfven waves due to thermal modulation of the electrical conductivity
[AD-A149389] 10 p1558 N85-19826
Thermal barrier confinement experiments in TMX-U tandem mirror, revision 1
[DE84-017029] 10 p1561 N85-19844
Electron bounce resonance heating in a bumpy cylinder
[DE85-001732] 10 p1561 N85-19845
Observations of bulk electron heating due to return current in a tokamak discharge started up by lower hybrid waves
[IPPJ-706] 12 p1937 N85-22172
Ruby wavefront-conjugation laser for obtaining high temperature plasma 13 p2044 N85-22795
Lower hybrid heating and current drive, and ion cyclotron heating experiments on the Alcator C and the Versator II Tokamaks
[DE85-004918] 13 p2161 N85-23412
Design, theoretical innovations in Tokamaks systems
14 p2289 N85-24190
Modeling longitudinal motions of thermal O+ and H+ ions in magnetic field tube convective through daytime polar cusp 15 p2481 N85-25314
Annual Review, April 1983 - March 1984
[ISSN-0547-1567] 15 p2654 N85-26369
High beta pinch plasma (STP-L)
15 p2655 N85-26381
Theoretical studies of Elmo Bumpy Torus
[DE85-007202] 15 p2658 N85-26402
Determining effective rate of plasma heating in outer equatorial ionosphere using data from ISIS-1 and ISIS-2 satellites 16 p2721 N85-26797
Velocity space diffusion of high energy ions induced by a lower hybrid wave in a nonuniform magnetic field
[IPPJ-714] 16 p2866 N85-27681
Tokamak systems code
[DE85-008147] 16 p2869 N85-27696
The effects of alpha particle production on the stability of an Elmo Bumpy Torus (EBT) reactor
19 p3369 N85-30695
Hard X-ray measurements of the hot electron rings in Nagoya BUMPY TORUS (NBT-1M)
[IPPJ-720] 19 p3370 N85-30699
Alternating current OHMIC heating in a toroidal stellerator 20 p3534 N85-31986
Self-consistent models for the X-ray emission from supernova remnants 20 p3548 N85-32082
Confinement and heating of high beta plasma with emphasis on compact toroids. Compact toroid research
[DE85-011463] 22 p3846 N85-33821
Computational study on excitation, propagation and 3 omega -heating due to the ion Bernstein wave
[IPPJ-733] 23 p3975 N85-34641
On the heat flux derived by the moment method in Lorentzian plasma between hot and cold walls
23 p3980 N85-34682
Integral representation for nonlinear heat transport
23 p3981 N85-34683
Scale separation closure and Alfven wave turbulence
[DE85-013124] 24 p4095 N85-35385
Confinement and heating of high beta plasmas with emphasis on compact toroids
[DE85-011459] 24 p4155 N85-35761
Proposed FRX-D experiment
[DE85-012766] 24 p4158 N85-35778

PLASMA INSTABILITY
U MAGNETOHYDRODYNAMIC STABILITY

PLASMA INTERACTION EXPERIMENT
SCATHA (spacecraft charging at high altitudes) plasma interaction experiment: SC-3 high energy particle spectrometer; SC-8 energetic ion composition experiment
[AD-A149728] 12 p1793 N85-21252
The PIX-2 experiment: An overview
13 p1993 N85-22494
Plasma interaction experiment 2 (PIX 2): Laboratory and flight results 13 p1993 N85-22495
Ram-wake effects on plasma current collection of the PIX 2 Langmuir probe 13 p1993 N85-22496

PLASMA INTERACTIONS
NT LASER PLASMA INTERACTIONS
NT PLASMA-ELECTROMAGNETIC INTERACTION
NT PLASMA-PARTICLE INTERACTIONS
Plasma surface interactions in magnetic fusion systems
[DE84-015255] 01 p0123 N85-10842
The effect of plasma on solar cell array arc characteristics
[NASA-TM-86887] 02 p0169 N85-11133
The effect of heat treatment on wear resistance of gas-plasma eutectic coatings
[BLL-M-35756-(5828.4)] 03 p0329 N85-12122
Study of plasma convection and wall interactions in magnetic confinement systems
[DE84-013959] 03 p0421 N85-12692
Brillouin scattering in underdense UV laser-produced plasmas
[DE84-015184] 04 p0567 N85-13614
Effects of the solar and extraterrestrial environments on space power systems 05 p0610 N85-13896
Proceedings of Workshop on Synergistic Effects in Surface Phenomena Related to Plasma-Wall Interactions
[IPPJ-AM-35] 06 p0864 N85-15488
Synergistic effects in fusion machines, session summary 06 p0864 N85-15489
Plasma surface interaction processes and possible synergisms 06 p0864 N85-15490
Synergisms in hydrogen recycling, session summary
06 p0864 N85-15491
Steady state hydrogen transport in solids
06 p0864 N85-15492
Synergisms in surface erosion, session summary
06 p0864 N85-15493
Synergism in materials erosion due to multispecies impact 06 p0864 N85-15494
Synergistic effects related to surface composition, session summary 06 p0865 N85-15495
Effects of monolayer coverages on substrate sputtering yields 06 p0865 N85-15496
Synergestic sputtering properties of binary alloys
06 p0865 N85-15497
Longer-scalelength plasma perturbations by an intense laser beam
[AD-A147005] 07 p1045 N85-16638
The environment of active galactic nuclei
07 p1057 N85-16712
Hydrogen trapping, diffusion, and recombination in austenitic stainless steels
[DE85-001871] 09 p1294 N85-18129
Developments and applications of laser fluorescence spectroscopy for studies of particle behaviours in fusion plasmas 09 p1389 N85-18735
Studies on impurity control and hydrogen pumping with chromium gettering in ISX-B
[DE85-001896] 09 p1394 N85-18771
Hydrodynamic response of a radiating Al plasma excited by a proton beam
[AD-A148904] 10 p1556 N85-19824
Plans for Interbol satellite experiment
13 p1977 N85-22407
Spacecraft Environmental Interactions Technology, 1983
[NASA-CP-2359] 13 p1989 N85-22470
Measured electron contribution to Shuttle plasma environment: Abbreviated update
13 p1990 N85-22476
Self-consistent simulation of plasma interactions with secondary-emitting insulators 13 p1993 N85-22492
Surface interactions and high-voltage current collection 13 p1993 N85-22493
The PIX-2 experiment: An overview
13 p1993 N85-22494
Plasma interaction experiment 2 (PIX 2): Laboratory and flight results 13 p1993 N85-22495
Discharges on a negatively biased solar cell array in a charged-particle environment 13 p1994 N85-22499
Spacecraft environmental interactions: A joint Air Force and NASA research and technology program
13 p1997 N85-22517
Space test program of high-voltage solar array-space plasma interactions 13 p1997 N85-22519
The Giotto spacecraft impact-induced plasma environment
[ESA-SP-224] 14 p2243 N85-23905
Measurements of integral yields of charged secondary particles using neutral beams simulating a cometary fly-by — Giotto mission 14 p2244 N85-23908
Simulations of satellite-plasma interaction, including electron space charges — Giotto mission
14 p2245 N85-23916
Anticipated impact plasma problems for the COPERNIC-RPA experiment in the cometary environment — Giotto mission 14 p2245 N85-23917
Spacecraft environment during the Giotto-Halley encounter: A summary 14 p2246 N85-23921
Preparatory experiments. 1: JIPP T-IIU
15 p2654 N85-26374
Discrete foundation for physics and experience
[DE85-008172] 16 p2872 N85-27720
Examination of a method for predicting the properties of railgun plasmas
[AR-004-322] 17 p3039 N85-28799
Microwave experimental studies of laser fusion
[DE85-008327] 17 p3041 N85-28814
Nonlinear plasma reactions on the antenna impedance of high transmission power satellites
[BMFT-FB-W-84-053] 18 p3192 N85-29799
Shocks in the solar wind between 1 and 8.5 AU: Voyager 1 observations
[NASA-CR-175911] 18 p3209 N85-29905
Cosmic ray modulation and turbulent interaction regions near 11 AU
[NASA-TM-86193] 18 p3209 N85-29906
Ion beam-plasma interactions
[DE85-010202] 19 p3371 N85-30913
On the role of the magnetic field strength in critical ionization velocity interaction
[TRITA-EPP-85-01] 20 p3536 N85-32003
Vehicle Charging And Potential (VCAP)
23 p3902 N85-34173
Latitude variation of recurrent fluxes in the outer solar system
[SH-4.1-13] 23 p4006 N85-34896
Beam potential measurement of an intense H(-) beam by use of the emissive probe technique
[DE85-012671] 24 p4155 N85-35782

PLASMA JETS
The effect of plasma on solar cell array arc characteristics
[NASA-TM-86887] 02 p0169 N85-11133
Investigation of heat exchange on models in subsonic jets of induction plasmatron 02 p0269 N85-11758
Dynamical models for radio jets
03 p0449 N85-12854
Laboratory electron beam simulation of cosmic radio jets
[DE84-016179] 04 p0590 N85-13764
The discharge mechanism of the high-temperature arc
[NASA-TM-77794] 07 p0922 N85-15837
Investigation of granules of molybdenum-base alloys obtained with pulsed discharges
[BLL-M-36012-(5828.4)] 07 p0926 N85-15871
Morphology and optical polarization of the 3C 273 jet — radio jet 08 p1236 N85-17803
On the hydrodynamical equations of astrophysical jets — active galactic nuclei 08 p1241 N85-17831
Four phase model for turbulent instabilities calculation in plasma jets
[IPF-84-2] 09 p1394 N85-18776
Cobalt-free permanent magnet alloys
[AD-A149272] 10 p1441 N85-19079
Electrodynamic interactions 11 p1643 N85-20340
Characteristics of multiarc plasma devices
12 p1841 N85-21554
Plasma performance of TFCX and jet with sawtoothing
[DE85-003335] 12 p1936 N85-22168
Determination of physical parameters of jets in radio galaxies 12 p1958 N85-22304
Hydrodynamics of astrophysical jets — active galactic nuclei 12 p1958 N85-22307
Viscous jets — extragalactic jets
12 p1958 N85-22308
Jets in galaxies 12 p1958 N85-22309
Development of theory of high-current high-pressure pulsed arc 15 p2645 N85-26314
Thermodynamic analysis of the plasma nitriding of ferrovanadium
[BLL-BISI-TRANS-22237-(9022.06)]
17 p2924 N85-28032
Implications for supersymmetry of the CERN monojets
[DE85-008178] 17 p3030 N85-28741
Examination of a method for predicting the properties of railgun plasmas
[AR-004-322] 17 p3039 N85-28799
Experimental research on electrical propulsion. Note 2: Experimental research on a plasma jet with vortex type stabilization for propulsion
[NASA-TM-77874] 18 p3067 N85-28988
Cavitation erosion of plasma sprayed alloys
[DE85-009542] 18 p3077 N85-29036
Ion-acoustic double layer in a magnetic picket fence configuration
[INPE-3552-PRE/764] 19 p3369 N85-30898
Plasma arc welding, equipment, installation and process control
[DE85-008481] 19 p3373 N85-30921
Limits on the Doppler factor in relativistic jets by means of gamma-ray observations
[OG-2.7-12] 22 p3872 N85-33985
Jets in air-jet family
[HE-3.2-1] 24 p4179 N85-35912
Search for anomalous C-jets in Chacaltaya emulsion chamber experiment
[HE-3.2-5] 24 p4179 N85-35913

PLASMA LAYERS
NT PLASMA SHEATHS
Plasma variables and tribological properties of coatings in low pressure (0.1 - 10.0 torr) plasma systems
[NASA-TM-83798] 02 p0189 N85-11281
Cold streams of ionospheric oxygen in the plasma sheet during the CDAW-6 event of March 22, 1979
[NASA-CR-174064] 03 p0393 N85-12513
On the cause of X-line formation in the near-Earth plasma sheet: Results of adiabatic convection of Plasma-Sheet-Plasma
[AD-A145835] 03 p0396 N85-12525

Electric field in plasma layer of magnetosphere during preliminary substorm phase 06 p0824 N85-15231
Development and application of low energy X-ray and electron physics
[AD-A149983] 12 p1926 N85-22099
Modeling plasma mantle of Earth's magnetosphere
16 p2720 N85-26790
The transport of neutral H, D, T and He and O in the boundary layers of a Tokamak plasma
[REPT-84-153] 17 p3041 N85-26817
Double layer formation due to contact of different temperature plasmas
[IPPJ-722] 19 p3370 N85-30900
Global effects of double layers — plasma layers
[TRITA-EPP-84-12] 20 p3536 N85-32002

PLASMA LOSS
Excitation of impurities by heavy particles and radiative losses of thermonuclear plasma
11 p1719 N85-20816
Numerical model for swirl cooling in high-heat-flux particle beam targets and the design of a swirl-flow-based plasma limiter
[DE85-003824] 11 p1732 N85-20894

PLASMA OSCILLATIONS
Hamiltonian and Lagrangian theory of gyrokinetic equations 02 p0283 N85-11845
Application of the energy problem to the problem of plasma flow stability
[DE84-013359] 05 p0730 N85-14691
Mechanism of damping of plasma oscillations in initial stage of injection of electron beams from spacecraft into ionosphere in active experiments
06 p0823 N85-15225
Waves and instabilities in collisionless shocks
[AD-A148689] 06 p0881 N85-15597
Longer-scalelength plasma perturbations by an intense laser beam
[AD-A147005] 07 p1045 N85-16638
Spacecraft-environment interaction: The environmental plasma aspect 13 p1990 N85-22479
The downshift of electron plasma oscillations in the electron foreshock region
[NASA-CR-175633] 14 p2423 N85-24945
Effects of finite current channel width on the current convective instability
[AD-A151414] 15 p2656 N85-26389
Stefan-Maxwell relations for plasma diffusion currents in magnetic field 17 p2942 N85-28160
Strong coupling effects on bound states in plasmas
[AD-A154353] 19 p3370 N85-30905
Low frequency instabilities driven by an ion temperature anisotropy
[AD-A154902] 21 p3707 N85-33016
Instrument to synchronize Thomson scattering diagnostic measurements with MHD activity in a Tokamak
[DE85-012032] 23 p3984 N85-34708
High energy plasma accelerators
[DE85-013121] 24 p4155 N85-35760

PLASMA PERTURBATION
U PLASMA OSCILLATIONS

PLASMA PHYSICS
Plasma drift equilibrium (gyration) in toroidal systems with complex magnetic-field geometry
[DE84-015627] 01 p0122 N85-10839
Fast waves near the lower hybrid frequency
[DE84-015217] 01 p0123 N85-10841
Plasma deposited diamondlike carbon on GaAs and InP
[NASA-TM-86670] 01 p0123 N85-10844
USSR report: Physics and mathematics
[JPRS-UPM-84-006] 02 p0256 N85-11676
Statistical Plasma Physics. Proceedings of the Workshop of the US-Japan Joint Institute for Fusion Theory Program
[IPPJ-689] 02 p0282 N85-11832
Behavior orbits of two coupled oscillators
02 p0282 N85-11833
Stochastic property of K-dV solitons perturbed by random forces — Korteweg-Devries equation
02 p0283 N85-11843
Chaotic behavior induced by solitons in perturbed integrable systems 02 p0283 N85-11844
Hamiltonian and Lagrangian theory of gyrokinetic equations 02 p0283 N85-11845
A simple transport model 02 p0284 N85-11853
Design, construction, and operational results of an 800-A, 10-kV hot deck amplifier
[DE84-014044] 04 p0496 N85-13162
Activities report in Earth and planetary environments physics
[CRPE-NT-134] 05 p0734 N85-14720
Proceedings on US-Japan Workshop on Tokamak Diagnostics by X-ray, VUV and Optical Radiations
[IPPJ-703] 09 p1386 N85-18719
Sources, densities, and transport of impurities in neutral-beam injected Tokamaks
09 p1388 N85-18731
Computational plasma physics and supercomputers
[DE85-001739] 09 p1393 N85-18766
Science Applications, part 1 11 p1643 N85-20346
Summary presentation of the Electrodynamics Interactions Panel 11 p1644 N85-20356
Fluctuations and transport in fusion plasmas
[DE85-003612] 11 p1732 N85-20893
Activities report of the Institute of Plasma Research
11 p1733 N85-20903
Simulation of thermal and electromagnetic processes in induction plasmatrons 12 p1841 N85-21552
Pressure-gradient-driven Tokamak resistive MHD instability in the banana-plateau collisionality regime
[DE85-004568] 12 p1937 N85-22171
University of Cambridge Institute of Astronomy report of activities 13 p2170 N85-23464
Evolution of strong inhomogeneities in ionospheric plasma, part 1 14 p2339 N85-24463
Slowing down of charged particles by the bound electrons in a plasma — ion beams, nuclear fusion
[LP-209] 14 p2419 N85-24929
Glossary of fusion energy
[DE84-017180] 14 p2425 N85-24958
USSR report: Physics and mathematics
[JPRS-UPM-85-003] 15 p2642 N85-26300
Annual Review, April 1983 - March 1984
[ISSN-0547-1567] 15 p2654 N85-26369
Scientific activities. A: Reacting plasma physics. 1: Introduction and overview 15 p2654 N85-26370
Preparatory experiments. 1: JIPP T-IIU
15 p2654 N85-26374
Basic studies. 1: Basic experiments in plasma physics 15 p2655 N85-26378
Plasma theory and computations
15 p2655 N85-26384
Propagation of wave packet in a dissipative dielectric medium
[IPPJ-710] 15 p2655 N85-26385
Optimizing computational efficiency and user convenience in plasma simulation codes
[DE85-007661] 16 p2866 N85-27682
Computational plasma physics and supercomputers, revision 1
[DE85-007228] 16 p2867 N85-27687
A four-field model for Tokamak plasma dynamics
[DE85-007111] 16 p2868 N85-27694
Plasma processing of materials
[AD-A152398] 17 p3039 N85-28800
Experimental plasma research: Plasma summaries
[DE85-008116] 17 p3039 N85-28805
Millimeter wave generation by relativistic electron beams
[AD-A153980] 18 p3179 N85-29708
ICRF antenna coupling and wave propagation in a tokamak plasma 19 p3369 N85-30893
The effects of weak turubience on parametric processes in an unmagnetized plasma 19 p3369 N85-30896
Perspectives of nonlinear dynamics
[IPPJ-723] 19 p3370 N85-30902
Effect of inner subshell ionization on emission lines OIV ions
[IPPJ-719] 19 p3370 N85-30903
Schottky theory of three component plasmas
[AD-A154461] 19 p3371 N85-30907
Slow tearing modes: Transitions to instability
20 p3534 N85-31989
Publications from the Department of Plasma Physics and the Unit of Accelerator Technology, index and abstracts, 1984
[TRITA-EPP-84-13] 20 p3534 N85-31991
USSR report: Physics and mathematics
[JPRS-UPM-85-004] 21 p3680 N85-32860
Modeling the exhaust of the pulsed plasma thruster
[AD-A155344] 21 p3707 N85-33018
Data Base Workshop: Availability-Reliability Modeling
[DE85-011570] 22 p3829 N85-33713
Electron and ion cyclotron heating calculations in the tandem-mirror
[DE85-011858] 22 p3842 N85-33797
Magnetic Fusion Program plan
[DE85-009861] 22 p3846 N85-33823
Waves in Space Plasmas (WISP)
23 p3901 N85-34164
Theoretical and Experimental Beam Plasma Physics (TEBPP) 23 p3901 N85-34166

PLASMA PINCH
NT THETA PINCH
NT ZETA PINCH
K-shell yield scaling law for conventional PRS loads
[AD-A145155] 01 p0121 N85-10831
Proceedings of the US-Japan Theory Workshop on 3-D MHD Studies
[DE84-012019] 04 p0568 N85-13620
Compact torroidal development: Activity plan for field reversed configurations
[DE84-017145] 05 p0730 N85-14695
Intense excitation source of blue-green laser
[AD-A147450] 07 p0971 N85-16168
High-power radiating plasma
[NASA-TM-77784] 07 p1045 N85-16637
Diffusion driven plasma current with turbulent dynamo
[IPPJ-700] 09 p1386 N85-18716
High beta pinch plasma (STP-3(M))
15 p2655 N85-26380
High beta pinch plasma (STP-L)
15 p2655 N85-26381
Poloidal rotation of magnetic fluctuations in reversed field pinch plasma
[IPPJ-715] 16 p2866 N85-27677

PLASMA POTENTIALS
Anomalously high potentials observed on ISEE
13 p1994 N85-22503
Screening phase transitions in two-dimensional Coulomb gas
[NOTA-INTERNA-830] 18 p3192 N85-29798
Space-time characteristics of field in longitudinal pulse-period discharge typical in pumping of self-terminating lasers 21 p3687 N85-32909
Model of azimuthal non-uniformities induced by RF heating in RFC-XXM 23 p3977 N85-34658

PLASMA POWER SOURCES
NT PLASMA ENGINES

PLASMA PROBES
NT ELECTROSTATIC PROBES
Novel probe for determining the size and position of a relativistic electron beam
[DE85-001044] 11 p1723 N85-20836
Vehicle Charging And Potential (VCAP)
23 p3902 N85-34173

PLASMA PROPULSION
Ring-cusp ion thruster with shell anode
[NASA-CASE-LEW-13881-1] 12 p1794 N85-21256

PLASMA PUMPING
Oscillating field current drive for reversed field pinch discharges
[DE84-015090] 04 p0567 N85-13610
Investigation of silicon surface passivation by silicon nitride deposition 06 p0829 N85-15266
High-power radiating plasma
[NASA-TM-77784] 07 p1045 N85-16637
Impurity and particle control systems for tokamak reactor experiments
[DE85-006124] 19 p3366 N85-30873
Radiation-cooled helicity-injecting reversed field pinch formed with relativistic electrons
[IPPJ-721] 19 p3370 N85-30901
New concept for pumping the edge plasma
[DE85-010180] 19 p3371 N85-30909
Space-time characteristics of field in longitudinal pulse-period discharge typical in pumping of self-terminating lasers 21 p3687 N85-32909
Transport issues in Phaedrus-type plasmas
23 p3976 N85-34653
Fokker-Planck calculation of hot electron formation in the thermal barrier region of tandem mirror Gamma-10
[IPPJ-726] 23 p3979 N85-34669

PLASMA RADIATION
Optical properties of laser erosion flares in plasma
02 p0270 N85-11764
A new maser effect in plasma turbulence
02 p0284 N85-11852
Imploding plasma radiation sources: Basic concepts
[AD-A145542] 02 p0284 N85-11856
High-power radiating plasma
[NASA-TM-77784] 07 p1045 N85-16637
Hydrodynamic response of a radiating Al plasma excited by a proton beam
[AD-A148904] 10 p1558 N85-19824
Influence of shock wave front on nature of luminescence of recombining laser plasma 11 p1719 N85-20818
Arguments for fundamental emission by the parametric process L yields T + S in interplanetary type III bursts — langmuir, electromagnetic, ion acoustic waves (L, T, S) 12 p1958 N85-22311
An Impurity Control Test Facility (ICTF) for the study of fusion reactor/plasma edge materials
[DE85-007946] 17 p3040 N85-28810
Plasma radiation sources. Quasi-adiabatic theory and numerical modeling in the electro-diffusive approximation
[AD-A154375] 19 p3370 N85-30906
Plasmodynamic methods for generating powerful light puses 21 p3693 N85-32943
Characteristics of optogalvanic effect in media with inverse populations 21 p3693 N85-32944
Investigation of space-time structure of glow of laser plasma colliding with flat screen
21 p3693 N85-32947

Beam potential measurement of an intense H(-) beam by use of the emissive probe technique
[DE85-012671] 24 p4155 N85-35762

PLASMA RENIN ACTIVITY
U IMMUNOASSAY

PLASMA RESONANCE
Exitation of low-frequency resonance waves by moving conductor in space plasma 13 p2067 N85-22912
Scattering of electromagnetic waves by charged particles 13 p2067 N85-22913
The application of laser resonance saturation to the development of efficient short wavelength lasers
[AD-A153951] 18 p3113 N85-29270
The determination of optical constants of thin metal films by surface plasma techniques 19 p3373 N85-30925
Influence of ECR-heating on MHD activity of plasma in tokamak-10 installation 21 p3694 N85-32949
Cyclotron resonance in a nonneutral plasma
[AD-A155248] 21 p3707 N85-33017
Nonlocal and nonadiabatic expression for the ponderomotive force near cyclotron resonance
[IPPJ-736] 23 p3974 N85-34636
Computational study on excitation, propagation and 3 omega -heating due to the ion Bernstein wave
[IPPJ-733] 23 p3975 N85-34641
Bounce resonance heating and radial transport of electrons 23 p3977 N85-34655
The heavy ion composition in 3HE-rich solar flares
[SH-2.2-7] 23 p4000 N85-34802

PLASMA RINGS
U TOROIDAL PLASMAS

PLASMA SHEATHS
Sun-aligned polar cap auroral arcs
[AD-A148052] 06 p1185 N85-17472
Reconsideration of sheath related to negative ion extraction
[IPPJ-706] 12 p1935 N85-22159
Direct measurements of severe spacecraft charging in auroral ionosphere 13 p1991 N85-22480
Polar plasmas as observed by Dynamics Explorers 1 and 2 13 p1991 N85-22483
Sheath ionization model of beam emissions from large spacecraft 13 p1992 N85-22489
The Giotto spacecraft impact-induced plasma environment
[ESA-SP-224] 14 p2243 N85-23905
Giotto plasmasheath and wake charging near Halley's Comet: Revised parameters 14 p2245 N85-23915
Anticipated impact plasma problems for the COPERNIC-RPA experiment in the cometary environment --- Giotto mission 14 p2245 N85-23917
An impact plasma monitor for cometary missions --- Giotto, VEGA 14 p2245 N85-23918
Plasma environment effects on the Giotto Ion Mass Spectrometer 14 p2245 N85-23919
Spacecraft environment during the Giotto-Halley encounter: A summary 14 p2246 N85-23921
Plasma and magnetospheric research
[NASA-CR-175675] 14 p2354 N85-24543
Research on thermionic plasmas
[AD-A150663] 14 p2423 N85-24944
Ionospheric effects on antenna impedance
[BMFT-FB-W-84-052] 17 p2950 N85-28217
Nonlinear plasma reactions on the antenna impedance of high transmission power satellites
[BMFT-FB-W-84-053] 18 p3192 N85-29799
Ion-acoustic double layer in a magnetic picket fence configuration
[INPE-3552-PRE/764] 19 p3369 N85-30898
Trajectories of charged particles traversing a plasma sheath in an oblique magnetic field
[DE85-011070] 19 p3371 N85-30911
Wave/particle interactions in the plasma sheet
[NASA-CR-171537] 20 p3547 N85-32072

PLASMA SOUND WAVES
U MAGNETOHYDRODYNAMIC WAVES
U PLASMA WAVES

PLASMA SPECTRA
High-power radiating plasma
[NASA-TM-77784] 07 p1045 N85-16637
Spectroscopic studies of a railgun muzzle flash
[MRL-R-952] 16 p2726 N85-26837
Projections of plasma cloud structures and their spectra
[AD-A153606] 18 p3189 N85-29776

PLASMA SPRAYING
Energy efficient engine high pressure turbine ceramic shroud support technology report
[NASA-CR-168036] 02 p0147 N85-10996
Mechanism of brittle heat fracture of inhomogenous solids by high temperature gas jets
02 p0265 N85-11731
Air force plasma spray at SA-ALC (San Antonio Air Logistics Center)
[AD-P004004] 03 p0308 N85-11984
High-temperature erosion of plasma-sprayed, yttria-stabilized zirconia in a simulated turbine environment
[NASA-TP-2406] 04 p0478 N85-13045
Study of phase composition of Al-B plasma coatings
11 p1598 N85-20050
Film and interstitial formation of metals in plasma-sprayed ceramics
[NASA-TM-86993] 13 p2038 N85-22756
Vacuum plasma coatings for turbine blades
16 p2734 N85-26869
Plasma spray screen repair method
[AD-D011713] 19 p3261 N85-30346
Thermal barrier coating system
[NASA-CASE-LEW-14057-1] 24 p4072 N85-35233

PLASMA STABILITY
U MAGNETOHYDRODYNAMIC STABILITY

PLASMA TEMPERATURE
Overheated open coronal regions
08 p1234 N85-17772
Modeling thermal plasma material processing experiments
[DE85-001551] 10 p1560 N85-19838
Heat flux in Lorentzian plasma
[IPPJ-704] 12 p1935 N85-22158
Radio frequency containment
15 p2654 N85-26375
Study of a constricted electric arc cooled by transpiration
[NASA-TM-77846] 17 p3038 N85-28796
A numerical solution technique for multitemperature plasma hydrodynamics
[AD-A152701] 17 p3039 N85-28801
Low plasma edge temperatures for the self-pumped limiter
[DE85-010155] 18 p3189 N85-29782
Theoretical and Experimental Beam Plasma Physics (TEBPP) 23 p3901 N85-34166

PLASMA THEORY
U PLASMA PHYSICS

PLASMA TURBULENCE
Stable distribution and Levy process in fractal turbulence 02 p0283 N85-11846
Strong Langmuir turbulence 02 p0284 N85-11851
A new maser effect in plasma turbulence
02 p0284 N85-11852
Relaxation of plasma rotation in a Tokamak in the presence of extraneous forces and corrugation of the magnetic field
[DE84-015628] 02 p0284 N85-11854
The flow of plasma in the solar terrestrial environment
[NASA-CR-174301] 06 p1224 N85-17707
Diffusion driven plasma current with turbulent dynamo
[IPPJ-700] 09 p1386 N85-18716
Four phase model for turbulent instabilities cnlculation in plasma jets
[IPF-84-2] 09 p1394 N85-18776
Space-time statistics of the turbulence in a Tokamak edge plasma
[DE85-002667] 10 p1559 N85-19834
Cosmic ray generation by plasma turbulence: Development of a new paradigm in physics
12 p1955 N85-22286
Arguments for fundamental emission by the parametric process L yields T + S in interplanetary type III bursts — langmuir, electromagnetic, ion acoustic waves (L, T, S) 12 p1958 N85-22311
Heating of coronal loops by tearing turbulence
14 p2448 N85-25114
Coronal heating by turbulent phase mixed MHD waves — solar corona 14 p2453 N85-25148
Turbulence and wave particle interactions in solar-terrestrial plasmas
[NASA-CR-175970] 18 p3209 N85-29906
Effects of a radial electric field on tokamak edge turbulence
[DE85-010401] 19 p3371 N85-30910
Runaway electrons and plasma turbulence in current ramping by lower hybrid waves in tokamak plasmas
[DE85-011390] 20 p3535 N85-31997
Caviton collapse of SRS by SBS
[DE85-009605] 20 p3535 N85-31999
Interplanetary plasma turbulence and the Doppler detection of a gravitational background radiation
[IFSI-85-1] 20 p3546 N85-32066
Investigation of ion-acoustic plasma turbulence in field of powerful electromagnetic wave by CO2-laser radiation scattering 21 p3691 N85-32935
The propagation of solar flare particles in a turbulent coronal loop
[SH-1.1-3] 23 p3989 N85-34730

PLASMA WAVES
NT ELECTROSTATIC WAVES
Bremsstrahlung radiation from longitudinal plasma waves caused by subthermal electrons in plasma
02 p0264 N85-11730
Strong Langmuir turbulence 02 p0284 N85-11851
A new maser effect in plasma turbulence
02 p0284 N85-11852
Reduction and analysis of data from the plasma wave instruments on the IMP-6 and IMP-8 spacecraft
[NASA-CR-175127] 04 p0460 N85-12918
Wave absorption and transport studies on Electron Cyclotron Resonance (ECR) heated stellarator plasma in W 7-A
[IPF-84-9] 09 p1395 N85-18782
Role of cavitons in laser-plasma interactions
[DE85-001842] 11 p1731 N85-20886
Dynamics of space charge waves in the laser beat wave accelerator
[AD-A149688] 12 p1936 N85-22183
On the spectrum of longitudinal waves in the hot degenerate plasma 12 p1955 N85-22280
Nonlinear waves in the magnetosphere of pulsars
12 p1955 N85-22281
Achievements of the International Magnetospheric Study (IMS) — conference
[ESA-SP-217] 14 p2354 N85-24544
Plasma waves at and near the neutral sheet
14 p2358 N85-24572
Pc 1-2 pulsations and related phenomena: A review — geomagnetic pulsations 14 p2364 N85-24611
Spatial characteristics of ULF pulsations and their modification by the ionosphere: IMS results
14 p2364 N85-24612
An evaluation of the contributions of the IMS to experimental and theoretical studies of ULF plasma
14 p2365 N85-24614
Observations of the MF-HF plasma wave emissions in active auroras by the sounding rocket experiments at Syowa station 14 p2366 N85-24620
VLF wave-particle interaction experiments by EXOS-B/Siple station transmissions
14 p2366 N85-24622
Energetic electron anisotropy and ELF waves onboard GEOS. How does quasi-linear diffusion work
14 p2366 N85-24623
The structure, stability, wave transmission and energy transfer at the Earth's magnetopause
14 p2372 N85-24661
Advances in magnetospheric plasma-wave research during the IMS 14 p2372 N85-24662
Active Magnetospheric Particle Tracing Explorers (AMPTE)
[AD-A151072] 14 p2374 N85-24674
Ionosphere effects may replace some communications satellites 15 p2484 N85-25337
Propagation of wave packet in a dissipative dielectric medium
[IPPJ-710] 15 p2655 N85-26385
Effects of finite current channel width on the current convective instability
[AD-A151414] 15 p2656 N85-26389
Two-dimensional beat wave acceleration simulation
[DE85-005861] 16 p2791 N85-27214
Plasma waves in the solar wind: Ten years of Helios observations 16 p2885 N85-27801
Plasma wake field accelerator
[DE85-010538] 18 p3191 N85-29791
Preliminary results on open accelerating structures
[DE85-010231] 18 p3191 N85-29793
More on shock-wave studies with Prognoz-10 satellite
19 p3296 N85-30432
Prognoz-10 intercosmos' station launched to study shock waves 19 p3296 N85-30434
Caviton collapse of SRS by SBS
[DE85-009605] 20 p3535 N85-31999
Analysis of spacecraft data
[NASA-CR-171587] 21 p3669 N85-32789

PLASMA-ELECTROMAGNETIC INTERACTION
NT LASER PLASMA INTERACTIONS
Theory of penderomotive forces
02 p0283 N85-11847
Plasma drift towards a plane equipotential surface
[TRITA-EPP-84-01] 02 p0285 N85-11860
An experimental and theoretical investigation of optogalvanic effects
[AD-A148089] 08 p1157 N85-17299
Effect of resonant microwave power on a PIG ion source
[DE85-001396] 09 p1379 N85-18673
Plasma states near surface of metal irradiated by CO2 laser 11 p1719 N85-20815
Explosive instability of strong electromagnetic wave in plasma 11 p1719 N85-20817
Monte Carlo studies of tandem mirror plasmas interacting with waves in the Ion Cyclotron Range of Frequencies (ICRF)
[DE85-002988] 11 p1731 N85-20883
Hydromagnetic precursors of interplanetary plasma burst 13 p1978 N85-22414

Report on final recommendations for IMPS engineering-science payload
[NASA-CR-175659] 13 p1988 N85-22464
Spacecraft-environment interaction: The environmental plasma aspect 13 p1990 N85-22479
Scattering of electromagnetic waves by charged particles 13 p2067 N85-22913
Diffraction of plane TM-wave on continuously irregular elliptical plasma 13 p2067 N85-22914
Basic experiments in plasma physics (TPL)
15 p2655 N85-26379
Direct electron and ion fluid computation of high electrostatic fields in dense inhomogeneous plasma with subsequent nonlinear optical and dynamical laser interaction 15 p2656 N85-26388
The formation of spokes in Saturn's rings
15 p2676 N85-26524
Millimeter wave generation by relativistic electron beams
[AD-A153960] 18 p3179 N85-29706

PLASMA-PARTICLE INTERACTIONS
Strong Langmuir turbulence 02 p0284 N85-11851
Spacecraft-environment interaction: The environmental plasma aspect 13 p1990 N85-22479
On-off characteristics of auroral pulsations
14 p2363 N85-24604
VLF wave-particle interaction experiments by EXOS-B/Siple station transmissions
14 p2366 N85-24622
Slowing down of charged particles by the bound electrons in a plasma — ion beams, nuclear fusion
[LP-209] 14 p2419 N85-24929
Modified betatron accelerator studies
[AD-A151420] 15 p2648 N85-26332
Selfsimilar time dependent shock structures
[OG-8.1-4] 23 p4017 N85-34894
A cosmic ray driven instability
[OG-8.1-5] 23 p4018 N85-34895

PLASMADYNAMIC LASERS
Metal vapor lasers and their applications
[ISL-CO-216/84] 22 p3791 N85-33488

PLASMAGUIDES
Multihole couplers for overmoded waveguide systems
[IPF-83-8] 09 p1394 N85-18773
Short mode selective directional couplers
[IPF-83-9] 09 p1394 N85-18774
Improved directional couplers for overmoded waveguide systems
[IPF-84-1] 09 p1394 N85-18775
Pc 1 pulsation source regions and their relationship to the plasma pause 14 p2368 N85-24638

PLASMAPAUSE
Precipitation of protons with E sub p approximately 1 MeV near plasmopause 02 p0161 N85-11093
Magnetohydrodynamic and gasdynamic theories for planetary bow waves
[NASA-CR-174132] 03 p0448 N85-12850
Observation of natural noise near upper hybrid resonance in terrestrial magnetosphere by Prognoz-5 satellite 06 p0822 N85-15221
Correlation of ring current and ionospheric gap in morning and evening hours 14 p2339 N85-24466
Whistler mode waves near the plasmapause: Results from the IMS VLF experiment at Halley, Antarctica
14 p2367 N85-24628
Pc 1 pulsation source regions and their relationship to the plasma pause 14 p2368 N85-24638
Plasma and magnetospheric research
[NASA-CR-171447] 15 p2591 N85-25976
Thermal ion heating in the vicinity of the plasmapause
[NASA-CR-176030] 20 p3535 N85-31993

PLASMAS (PHYSICS)
NT ARGON PLASMA
NT BETA PARTICLES
NT BOUNDARY LAYER PLASMAS
NT COLD PLASMAS
NT COLLISIONAL PLASMAS
NT COLLISIONLESS PLASMAS
NT COSMIC PLASMA
NT CYLINDRICAL PLASMAS
NT DENSE PLASMAS
NT DEUTERIUM PLASMA
NT ELECTRON PLASMA
NT ELLIPTICAL PLASMAS
NT HELIUM PLASMA
NT HIGH TEMPERATURE PLASMAS
NT HYDROGEN PLASMA
NT LASER PLASMAS
NT METALLIC PLASMAS
NT NITROGEN PLASMA
NT NONEQUILIBRIUM PLASMAS
NT NONUNIFORM PLASMAS
NT OXYGEN PLASMA
NT PLASMA FOCUS
NT RELATIVISTIC PLASMAS
NT ROTATING PLASMAS
NT SEMICONDUCTOR PLASMAS
NT SOLAR WIND
NT SPACE PLASMAS
NT SPHERICAL PLASMAS
NT STELLAR WINDS
NT STRONGLY COUPLED PLASMAS
NT THERMAL PLASMAS
NT TOROIDAL PLASMAS
MHD instabilities in simple plasma configuration
[AD-A144936] 01 p0121 N85-10829
Polarized electron cyclotron emission in the Tokapole 2 Tokamak
[DE84-014953] 01 p0122 N85-10838
Plasma variables and tribological properties of coatings in low pressure (0.1 - 10.0 torr) plasma systems
[NASA-TM-83798] 02 p0189 N85-11261
Numerical investigation of characteristics of current flow for different methods of obtaining discharge in high speed lasers. Mechanism underlying current flow in positive glow discharge column 02 p0264 N85-11728
Scattering of electromagnetic waves by plasma half-space after initiation of motion
02 p0264 N85-11729
Neutral beam interactions with materials
[AD-A145636] 02 p0285 N85-11857
In-line beam current monitor
[DE84-014054] 04 p0560 N85-13567
Theory of resistive ballooning modes in Tokamaks
[DE84-015626] 04 p0566 N85-13606
Internal helical mode m = 1 of a Tokamak in the plateau and banana regimes
[DE84-015623] 04 p0566 N85-13607
Rotation of a tenuous plasma with a high toroidal velocity in a Tokamak
[DE84-012990] 04 p0567 N85-13615
High-Beta plasma theory
[DE84-016471] 04 p0568 N85-13619
Magnetic helicity in the solar corona
05 p0745 N85-14780
Estimate of nuclear-pumped X-ray laser mechanism
06 p0748 N85-14795
The origin of plasma rotation in the early phase of an FRC produced by a reversed field theta pinch
[IPPJ-698] 06 p0863 N85-15482
A nonlocal expression for the ponderomotive potential
[IPPJ-699] 06 p0864 N85-15487
Plasma-surface interactions in large tandem mirror devices, MFTF-B
[DE85-001753] 06 p0865 N85-15499
Slow surface magnetoplasma waves in oblique magnetic field 07 p0952 N85-16034
Research relative to plasma transport across the magnetopause
[NASA-CR-174300] 07 p1045 N85-16636
The flow of plasma in the solar terrestrial environment
[NASA-CR-174301] 08 p1224 N85-17707
A research proposal for the theoretical study of the thermodynamic and transport properties of dense plasmas
[AD-A148040] 08 p1224 N85-17708
Diffusion driven plasma current with turbulent dynamo
[IPPJ-700] 09 p1386 N85-18716
MHD equilibrium and stability for stellarator/torsatron configurations
[DE85-001139] 09 p1391 N85-18750
Very high energy probes of the quark-gluon plasma
[DE84-016892] 09 p1392 N85-18763
Brief outline of analytic stability studies of magnetically insulated systems — bibliobliographies
[DE85-000212] 09 p1393 N85-18765
Optically induced intervalence-band transitions in germanium by the absorption of 1.06 micrometers picosecond pulses
[DE85-000946] 09 p1399 N85-18803
1984 AFOSR Research Meeting on Diagnostics of Reacting Flow held at New Haven, Connecticut on 21-22 March 1984
[AD-A149023] 10 p1484 N85-19367
Magnetic fusion energy plasma interactive and high heat flux components. Volume 3: Strategy for international collaborations in the areas of plasma materials interactions and high heat flux materials and components development
[DE85-001145] 10 p1559 N85-19829
Small, octopole-stabilized tandem mirror reactor
[DE85-002144] 10 p1559 N85-19832
Space-time statistics of the turbulence in a Tokamak edge plasma
[DE85-002667] 10 p1559 N85-19834
Finite-(beta) optimization of tandem mirrors
[DE85-002658] 10 p1560 N85-19835
Entrop production determination of the ambipolar solution nearest equilibrium
[DE85-003049] 10 p1560 N85-19836
Nonlinear saturation of stimulated Raman scattering in homogeneous plasma
[DE85-003120] 10 p1560 N85-19837
Role of multiple helicity nonlinear interaction of tearing modes in dynamo and anomalous thermal transport in the Reversed Pitch Field
[DE85-002176] 10 p1560 N85-19839
The 1984 review of the Applied Plasma Physics Program
[DE85-002136] 10 p1560 N85-19840
FRC translation dynamics and plasma confinement properties in FRX-C/T
[DE85-002386] 10 p1560 N85-19842
Resistive evolution of general plasma configuration
[DE85-002340] 10 p1561 N85-19843
Thermal barrier confinement experiments in TMX-U tandem mirror, revision 1
[DE84-017029] 10 p1561 N85-19844
A modeling analysis program for the JPL Table Mountain Io sodium cloud data
[NASA-CR-175493] 11 p1681 N85-20589
TMX-U neutral pressure measurement diagnostic systems
[DE85-000746] 11 p1730 N85-20881
Mirror fusion progress
[DE85-001187] 11 p1731 N85-20888
Covariant lie-transformed plasma action principle
[DE85-000285] 11 p1732 N85-20891
Design, construction and initial evaluation of an absolute, time-integrating/time-resolving spectrometer for the diagnostics of pulsed, high temperature plasma X-ray sources in the 100-10,000 eV region
[DE85-003526] 11 p1732 N85-20896
Edge diagnostics for tandem mirror machines
[DE85-001209] 11 p1733 N85-20902
Hollow cathode apparatus
[NASA-CASE-NPO-15560-1] 12 p1832 N85-21491
Investigation of plasma processes in electronic transition lasers
[AD-A149682] 12 p1834 N85-21506
The 60 GHz gyrotron development program
[DE85-000599] 12 p1836 N85-21522
Analysis and computations of microwave-atmospheric interactions
[AD-A149666] 12 p1869 N85-21854
Plasma mass and effective inductance in a small rainbow
[MRL-R-947] 12 p1936 N85-22162
Negative lithium emission from a tungsten surface in a plasma
[DE85-003456] 12 p1936 N85-22167
Spectroscopic study of sources and control of impurities in TMX-U: Revision 1
[DE85-004423] 12 p1937 N85-22170
Use of markets to elucidate reacting sputtering processes
[DE85-005723] 13 p2018 N85-22655
System for forming and focusing high current beam of deuterium ions 13 p2045 N85-22798
Calculation of amplitude-phase characteristics of signal scattered obliquely on meteor trail
13 p2073 N85-22948
Domain of applicability of asymptotic description of radio pulse fields near critical frequency
13 p2073 N85-22949
Meteoroidal impacts, plasma, fine structure of ringlets and spokes on Saturn's ring B 13 p2174 N85-23490
Interaction of the magnetospheric ions with the surfaces of the icy satellites of Saturn 13 p2174 N85-23491
Plasma production by meteoroid impact
13 p2174 N85-23492
Solar and stellar coronal plasmas
[NASA-CR-175623] 13 p2205 N85-23676
Numberical simulation of the effects of radially injected barium plasma in the ionosphere
[NASA-CR-175636] 14 p2354 N85-24542
Research on thermionic plasmas
[AD-A150663] 14 p2423 N85-24944
Current distribution in a plasma erosion opening switch
[AD-A150987] 14 p2424 N85-24949
ANTENA user guide
[DE85-004961] 14 p2424 N85-24953
Ionization equilibrium and equation of state in the solar interior 14 p2445 N85-25088
Plasma and magnetospheric research
[NASA-CR-171447] 15 p2591 N85-25976
Mean free paths, viscosity, and the limitations of perfect fluid hydrodynamics in the description of the quark-gluon plasma
[DE85-005501] 15 p2649 N85-26339
Finite orbit analysis for long wavelength modes in a plasma with a hot component
[DE85-006896] 15 p2658 N85-26404

Optimal control theory applied to fusion plasma thermal stabilization
[DE85-007599] 15 p2658 N85-26405

Eleven lectures on the physics of the quark-gluon plasma
[DE85-004321] 15 p2662 N85-26431

Space station as quark matter factory
[DE85-004606] 15 p2685 N85-26585

Digital image analysis of four-frame holographic plasma and neutral gas interferograms
[DE85-006397] 16 p2768 N85-27200

Equatorial F-region irregularity latitudinal extension and dynamo electric field
[INPE-3494-PRE/731] 16 p2826 N85-27433

Fundamentals of plasma simulation
[DE85-007699] 16 p2867 N85-27683

High efficiency ionizer using a hollow cathode discharge plasma
[DE85-006690] 16 p2868 N85-27693

The decomposition of gas phase formaldehyde by plasma discharge
[AD-A153202] 17 p2921 N85-28007

Geophysical plasmas and atmospheric modeling
[AD-A152805] 17 p2993 N85-28497

Time-integrated yield for the Joint European Torus (JET), April - September 1984
[AERE-M-3449] 17 p3038 N85-28797

Plasma processing of materials
[AD-A152398] 17 p3039 N85-28800

A numerical solution technique for multitemperature plasma hydrodynamics
[AD-A152701] 17 p3039 N85-28801

Multiple time-scale methods in particle simulations of plasmas
[DE85-007519] 17 p3040 N85-28808

Nonlinear plasma reactions on the antenna impedance of high transmission power satellites
[BMFT-FB-W-84-053] 18 p3192 N85-29799

Experiments in plasma initiation and laser absorption in flowing gases
[AD-A154303] 19 p3276 N85-30313

Plasma spray screen repair method
[AD-D011713] 19 p3281 N85-30346

Institute works on modeling thermonuclear plasma processes 19 p3296 N85-30435

Angle averaged Compton cross sections for degenerate electron gases
[AD-A154464] 19 p3371 N85-30908

New concept for pumping the edge plasma
[DE85-010180] 19 p3371 N85-30909

Publications from the Department of Plasma Physics and the Unit of Accelerator Technology, index and abstracts, 1984
[TRITA-EPP-84-13] 20 p3534 N85-31991

Nuclear responses in INTOR plasma stabilization elements
[DE85-010489] 20 p3535 N85-31995

Plasma erosion opening switch
[DE85-011384] 20 p3535 N85-31996

The space shuttle glow
[AD-A154937] 21 p3559 N85-32139

The plasma erosion opening switch
[AD-A154942] 21 p3580 N85-32259

Plasma mass and effective inductance in a small railgun
[AD-A154844] 21 p3589 N85-32304

Microwave-enhanced thin-film deposition
21 p3611 N85-32431

In-cavity laser IR spectrum analyzer for investigating non-steady-state processes 21 p3685 N85-32894

Infrared laser holography used in fusion plasma studies 21 p3687 N85-32905

Operational window for a plasma erosion opening switch used for voltage multiplication on pulsed power generators
[AD-A155482] 21 p3707 N85-33020

Research in particles and fields
[NASA-CR-176069] 21 p3724 N85-33103

Electron and ion cyclotron heating calculations in the tandem-mirror
[DE85-011856] 22 p3842 N85-33797

Confinement and heating of high beta plasma with emphasis on compact toroids. Compact toroid research
[DE85-011463] 22 p3846 N85-33821

Waves in Space Plasmas (WISP)
23 p3901 N85-34164

Theoretical and Experimental Beam Plasma Physics (TEBPP) 23 p3901 N85-34166

Electrodynamic tether 23 p3902 N85-34168

Magnetospheric multiprobes: MMP/CHEMSAT
23 p3902 N85-34171

Electronic imaging system and technique
[DE85-005740] 23 p3935 N85-34393

Some physical differences between sheet plasma and multicusp plasma as volume produced H- or D- ion sources
[IPPJ-726] 23 p3974 N85-34637

Effect of ECH and ICH on ambipolar potential in NBT-1M 23 p3978 N85-34661

Transports studies of ECH and ICRH-heated bumpy torus plasma in NBT-1M 23 p3978 N85-34662

Stability of ion distribution in strong ion shock structure 23 p3980 N85-34681

On the heat flux derived by the moment method in Lorentzian plasma between hot and cold walls
23 p3980 N85-34682

The role of cosmic rays and Alfven waves in the structure of the galactic halo
[OG-7.2-18] 23 p4016 N85-34885

Stochastic particle acceleration in flaring stars
[OG-8.3-9] 23 p4022 N85-34927

Very high energy probes of the quark-gluon plasma
24 p4147 N85-35706

Kinetic loss experiments on Mite
[DE85-012826] 24 p4158 N85-35780

The phi-meson and Chiral-mass-meson production in heavy-ion collisions as potential probes of quark-gluon-plasma and Chiral symmetry transitions
24 p4175 N85-35884

Heavy flavours production in quark-gluon plasma formed in high energy nuclear reactions
24 p4175 N85-35886

The maximum depth of shower with E sub 0 larger than 10(17) eV on average characteristics of EAS different components 24 p4188 N85-35961

PLASMASPHERE

Magnetospheric plasma studies using data from the dynamics high and low altitude plasma instruments
[AD-A145751] 03 p0392 N85-12505

On the cause of X-line formation in the near-Earth plasma sheet: Results of adiabatic convection of Plasma-Sheet-Plasma
[AD-A145835] 03 p0396 N85-12525

Plasma and magnetospheric research
[NASA-CR-175675] 14 p2354 N85-24543

Electric fields in the plasma sheet and plasma sheet boundary layer 14 p2357 N85-24562

VLF emissions observed by ISIS Satellites during the IMS 14 p2366 N85-24621

Plasma and magnetospheric research
[NASA-CR-171447] 15 p2591 N85-25976

Images of the Earth's aurora and geocorona from the Dynamics Explorer Mission
[NASA-CR-175983] 18 p3136 N85-29423

PLASMATRONS

Investigation of heat exchange on models in subsonic jets of induction plasmatron 02 p0269 N85-11756

Simulation of thermal and electromagnetic processes in induction plasmatrons 12 p1841 N85-21552

Reducing electric power losses in discharge chamber of induction plasmatron 12 p1841 N85-21553

PLASMOIDS

U PLASMAS (PHYSICS)

PLASMONS

Brillouin scattering in underdense UV laser-produced plasmas
[DE84-015184] 04 p0567 N85-13614

Confinement of low-energy electrons near metallic surfaces for plasmon generation
[DE85-001119] 09 p1381 N85-18688

Inelastic tunnel diodes
[NASA-CASE-LEW-13833-1] 12 p1832 N85-2[illegible]492

Solar energy converter using surface plasma waves
[NASA-CASE-LEW-13827-1] 12 p1876 N85-21768

The Valence- and conduction-band structure of the sapphire (1102) surface
[AD-A150001] 12 p1940 N85-22184

Research in the optical sciences
[AD-A150196] 13 p2159 N85-23401

Charge transfer, polarization and relaxation effects in the Auger lineshapes of Si
[AD-A150938] 14 p2252 N85-23954

PLASTIC COATINGS

Process for preparing highly optically transparent-colorless armomatic polyimide film
[NASA-CASE-LAR-13351-1] 12 p1811 N85-21360

X-ray photoelectron spectroscopy study of the compatibility of the explosive PETN with candidate plastic bonding materials
[DE85-010804] 19 p3251 N85-30161

New corrosion protection concept for very high voltage line towers
[BLL-OA-TRANS-2691-(6196.300)]
20 p3429 N85-31270

PLASTIC DEFORMATION

Evaluation of the role of diffusion creep in superplastic deformation 01 p0021 N85-10127

Fundamental studies of structure property relationship in transformation toughened ceramics
[DE84-015344] 01 p0033 N85-10204

Shear deformation plate continua of large double-layered space structures
01 p0059 N85-10391

Swaged Mo-5 percent W alloy and recrystallized commercially pure molybdenum
02 p0180 N85-11206

Plastic deformation and microstructural transformations of metals under shock waves 02 p0272 N85-11775

Features of plastic deformation and fracture of EP 741 nickel alloy under thermal strain
03 p0349 N85-12250

An experimental evaluation of the J integral in 50% sidegrooved compact geometry specimens
[AERE-R-11202] 03 p0374 N85-12366

Fast ions as probes in solid state research
03 p0430 N85-12740

Accuracy of preparation of three-dimensional reference grid
[BLL-M-35921-(5828.4)] 05 p0616 N85-13909

Iterative method for determining the distortion of elastic-plastic frames
[ISSN-0208-5658] 05 p0647 N85-14156

Compression of a band made of elastic, ideally Coulomb plastic material
[ISSN-0208-5658] 05 p0648 N85-14157

Use of coordinate functions to calculate deformation fields
[BLL-M-36010-(5828.4)] 07 p1028 N85-16524

The fundamentnls of dislocation transport of hydrogen in bcc iron
[AD-A148143] 08 p1129 N85-17117

A study of constitutive relations for polycrystalline aluminum during finite dynamic plastic deformation
08 p1172 N85-17388

Determination of the elastic constants of inhomogeneous materials with X-ray diffraction
[AD-A148469] 08 p1173 N85-17393

Creep deformation of compacted decomposed granite soils 09 p1303 N85-18187

Study of influence of cold plastic deformation on aging of VT30 alloy 10 p1448 N85-19124

Diffusion welding with forced deformation of heat-resistant nickel-based dispersion hardened alloy
10 p1449 N85-19130

Role of hydrogen in processes of deformation and fracture of metals 10 p1449 N85-19132

Influence of plastic deformation on structural stability of nichrome-tungsten composite materials
11 p1599 N85-20060

Effect of temperature and deformation rate on hardness of copper 11 p1605 N85-20090

Stress corrosion cracking behavior of tungsten heavy alloys
[AD-A149843] 12 p1806 N85-21329

An orthogonal grid technique for studying internal deformation and energy absorption in target penetration
[AD-A149969] 12 p1860 N85-21665

Critical events in inelastic deformation of glassy polymers in adsorptive medium
13 p2014 N85-22634

Development and study of two-matrix glass fiber composite with increased transverse deformation
13 p2027 N85-22700

Fatigue life, crack initiation, and propagation of 304 stainless steel with non-proportional axial-torsional strain-paths 13 p2101 N85-23094

Studies of deformation in niobium by X-ray topographic methods
[AD-A150726] 14 p2427 N85-24965

Thermal stability of titanium alloys after cold plastic deformation 15 p2515 N85-25515

Plastic deformation of crystalline polymers
[AD-A152090] 16 p2755 N85-26999

Multinomial form of the solution of problems of the statistics of elastic rectangular disks
[REPT-17/1984] 16 p2797 N85-27244

Determination of failure characteristics of materials and structures
[AD-A152073] 16 p2800 N85-27286

Thermomechanical softening treatment for bearing and tool steels
[BLL-BISI-TRANS-22432-(9022.06)]
17 p2925 N85-28035

Influence of eutectic silicate inclusions on micro-processes during deformation and fracture of 12G5 steel
[BLL-BISI-TRANS-22296-(9022.06)]
17 p2929 N85-28073

New method for determining stampability of sheet materials
[BLL-BISI-22486-(9022.06)] 17 p2972 N85-28360

State of stress and penetration of plastic deformation in forming
[BLL-BISI-22199-(9022.06)] 17 p2977 N85-28396
Effects of the structural state in thermo-bimetals on their resistance to microscopic plastic deformation
[BLL-BISI-TRANS-22403-(9022.06)] 17 p2979 N85-28412
Critical conditions for failure in materials subjected to high rates of loading
[AD-A153135] 17 p2980 N85-28420
Studies on surface processes during friction and wear
[AD-A153509] 18 p3117 N85-29296
State variable theories based on Hart's formulation
[DE85-009474] 19 p3239 N85-30082
Mechanical modification of friction surfaces of aluminum alloys by friction transfer 19 p3241 N85-30097
The initiation and growth of adiabatic shear bands
[AD-A154459] 19 p3287 N85-30382
Microstructural analysis of Pacific Ocean and Indian Ocean ultrabasites 19 p3291 N85-30405
On elastic-plastic fracture criterion
20 p3465 N85-31528
Fundamental investigations of failure during superplastic forming process
[AD-A154647] 21 p3568 N85-32194
Dynamic fracture of concrete and other heterogeneous materials
[AD-A154513] 21 p3596 N85-32343
The measurement of strain fields by X-ray topographic contour mapping
[AD-A154870] 21 p3599 N85-32348
Presentation of numerical simulation work in terminal ballistics using a few examples. Applications of the calculation model Program for Elastoplastic Simulation of Impacts (PEPSI) of the Franco-German Research Institute Saint Louis (ISL)
[ISL-CO-209/84] 22 p3834 N85-33741
Prediction of plasticity characteristics for three-dimensional fracture specimens comparison with experiment
[AD-A156425] 24 p4102 N85-35430
PLASTIC FILMS
U POLYMERIC FILMS
PLASTIC FLOW
NT TRESCA FLOW
Multiaxial yield behavior of 1100 aluminum following various magnitudes of prestrain
[DE84-013904] 05 p0617 N85-13949
The perfecting of the method of experimental-analytic solution of the problem of stationary plastic flow
[BLL-M-35938-(5828.4)] 05 p0634 N85-14065
The role of microstructure in the modelling of plastic flow in P/M superalloys at forging temperatures and strain rate 06 p0796 N85-15090
Flow and plasticity via nonequilibrium molecular dynamics
[DE85-001011] 10 p1555 N85-19804
Dependence of superplastic flow on state of grain boundaries 13 p2025 N85-22689
Influence of short-range order on deformation mechanisms in solid solutions
[DE85-006374] 14 p2258 N85-23969
On the accurate representation of large strain non-proportional plastic flow in ductile materials
[DE85-007106] 16 p2801 N85-27273
Conformational and mechanical properties at high strain rates
[AD-A153401] 17 p2959 N85-28272
PLASTIC MATERIALS
U PLASTICS
PLASTIC MEMORY
Effect of form memory in alloys based on Cu-Al systems 11 p1604 N85-20088
Production of shaped parts of NITINOL alloys by solid-state sintering
[AD-A152089] 16 p2749 N85-26966
PLASTIC PROPELLANTS
Effects of surface interactions and mechanical properties of PBXs (plastic bonded explosives) on explosive sensitivity
[AD-A146368] 06 p0773 N85-14944
PLASTIC PROPERTIES
NT ELASTOPLASTICITY
NT PHOTOPLASTICITY
NT SUPERPLASTICITY
NT THERMOPLASTICITY
NT VISCOPLASTICITY
NT YIELD POINT
Sensitivity analysis of limit state functions for probability-based plastic design
01 p0059 N85-10388
High temperature low-cycle fatigue mechanisms in single crystals of nickel-based superalloy Mar-M 200
[NASA-CR-174739] 03 p0331 N85-12130
Dependence of microplasticity of beryllium on grain size and heat treatment 03 p0353 N85-12273
Eta values for compact geometry specimens to calculate the J integral
[AERE-R-11126] 03 p0374 N85-12385
Numerical methods in metalforming
06 p0797 N85-15092
Finite element simulation of forging processes
06 p0797 N85-15093
Ultrahigh carbon steel
[AD-A147762] 08 p1128 N85-17113
Modeling of large-scale accretionary wedge and thin-skinned trust-and-fold belt mechanics
08 p1181 N85-17442
Nonlinear finite element analysis of elastic and elastic-plastic buckling of cylinders under complex combined loads 09 p1332 N85-18373
Influence of gaseous hydrogen on strength and ductility of nickel heat-resistant alloys 10 p1447 N85-19119
Flow and plasticity via nonequilibrium molecular dynamics
[DE85-001011] 10 p1555 N85-19804
Structure-phase state and properties of high-durability VAL8 alloy 11 p1597 N85-20046
Electron-plastic effect in metals
11 p1605 N85-20089
A remote source system for measuring relative positron annihilation line widths in individual slab cylindrical samples
[AERE-R-10549] 12 p1938 N85-22173
Some problems of optimum journal design for disk-drum rotors under antisymmetric loading
14 p2286 N85-24167
Effect of annealing procedures on structure and properties of VT6 alloy with initial large-grained structure
15 p2498 N85-25410
Effect of zirconium on forming ultrafine-grained structure in Al-Mg-Zr alloy 15 p2513 N85-25504
Dependence of plasticity of VT1-00 titanium alloy on microstructure 15 p2515 N85-25516
Predicting fully plastic mode 2 crack growth from an asymmetric defect
[AD-A152227] 16 p2801 N85-27269
Numerical resolution calculation for elastic-plastic impact problems
[AD-A152292] 16 p2801 N85-27270
On the accurate representation of large strain non-proportional plastic flow in ductile materials
[DE85-007106] 16 p2801 N85-27273
Properties of corrosion resistant stabilized ferritic steels
[BLL-BISI-TRANS-22519-(9022.06)]
17 p2925 N85-28039
The effect of microalloying with calcium and magnesium on the plasticity of Poldi AKN 20 Ni-based alloy
[BLL-BISI-TRANS-2174-(9022.06)]
17 p2929 N85-28075
The Shock and Vibration Digest, volume 17, no. 2
[AD-A153129] 17 p2977 N85-28400
Recent progress in the dynamic plastic behaviour of structures, part 4 17 p2978 N85-28402
Cyclic torsion of a circular cylinder and its residual stress distribution
[AD-A153347] 17 p2980 N85-28424
High tensile strength, punchable, hot rolled strips with good plasticity
[BMFT-FB-T-84-256] 18 p3076 N85-29040
Fatigue behavior of unidirectional FP-Al composites with circular holes
[AD-A153466] 18 p3121 N85-29322
Study of the influence of metallurgical factors on fatigue and fracture of aerospace structural materials
[AD-A153913] 18 p3122 N85-29328
Construction of constraint equation for stresses and strains
[BLL-M-36239-(5828.4)] 20 p3465 N85-31524
A numerical algorithm for endochronic plasticity and comparison with experiment 20 p3467 N85-31539
PLASTIC YIELDING
U PLASTIC DEFORMATION
PLASTICITY
U PLASTIC PROPERTIES
PLASTICIZERS
1-Fluoro-1,1,5-Trinitro-3-Oxa-5-Azahexane and method of preparation
[AD-D011421] 08 p1136 N85-17158
Plasticizer system for propellant compositions
[AD-D011502] 12 p1816 N85-21390
Plasticizer system for propellant compositions
[AD-D011506] 12 p1816 N85-21391
Azido nitramino ether containing solid propellants
[AD-D011511] 12 p1816 N85-21392
Plasticizer system for propellant compositions
[AD-D011514] 12 p1817 N85-21393
Plasticizer system for propellant compositions
[AD-D011516] 12 p1817 N85-21394
Plasticizer system for propellant compositions
[AD-D011517] 12 p1817 N85-21395
Propellant plasticizer
[AD-D011501] 20 p3434 N85-31306
Synthesis of energetic materials
[AD-A154887] 21 p3571 N85-32210
Polymer-water interaction studies
21 p3609 N85-32411
A new drawing technique for nylon 6 by reversible plasticization with iodine
[AD-A156272] 24 p4162 N85-35803
PLASTICS
NT ACRYLIC RESINS
NT CARBON FIBER REINFORCED PLASTICS
NT EPOXY RESINS
NT KEVLAR (TRADEMARK)
NT NYLON (TRADEMARK)
NT PHENOLIC RESINS
NT POLYAMIDE RESINS
NT POLYBUTADIENE
NT POLYESTER RESINS
NT POLYETHER RESINS
NT POLYETHYLENE TEREPHTHALATE
NT POLYETHYLENES
NT POLYISOBUTYLENE
NT POLYMETHYL METHACRYLATE
NT POLYPROPYLENE
NT POLYSTYRENE
NT POLYTETRAFLUOROETHYLENE
NT POLYVINYL ALCOHOL
NT POLYVINYL CHLORIDE
NT POLYVINYL FLUORIDE
NT REINFORCED PLASTICS
NT SYNTHETIC RESINS
NT TEFLON (TRADEMARK)
NT THERMOPLASTIC FILMS
NT THERMOPLASTIC RESINS
NT THERMOSETTING RESINS
NT VINYL COPOLYMERS
Comparison study of analytical methods for the determination of fluoride, chloride, and bromide in plastics
[DE84-015006] 04 p0470 N85-12989
Detection of cracks in a plastics pipe joint by reflection holography
[NPL-DMA(A)-87/MOM-70] 04 p0502 N85-13202
Method for forming electromagnetic-wave-screening composite 07 p0936 N85-15930
Polymer blends as high explosive binders
[DE85-001210] 11 p1611 N85-20131
Hydrolysis of plastic wastes with the aim of recovering and reprocessing the starting components (recycling)
[BMFT-FB-T-84-250] 12 p1885 N85-21829
Mechanism of strengthening plastics with rubbers
13 p2014 N85-22636
Chain dynamics and structure property relation in high impact strength polycarbonate plastic
[AD-A152011] 15 p2519 N85-25531
Status of French research in plastic batteries
15 p2530 N85-25603
Natural and accelerated aging of plastics
17 p2936 N85-28123
Qualitative and quantitative determination of aging by mechanical tests — plastics 17 p2977 N85-28393
Conservation and substitution technology for critical metals in bearings and related components for industrial equipment and opportunities for improved bearing performance
[PB85-176246] 18 p3082 N85-29069
Silvered polymer reflectors
[DE85-008782] 18 p3130 N85-29384
Plastic heliostat enclosure analysis
[DE85-009112] 18 p3130 N85-29387
X-ray photoelectron spectroscopy study of the compatibility of the explosive PETN with candidate plastic bonding materials
[DE85-010604] 19 p3251 N85-30161
Standard procedures to be used in specifying basic properties of plastics and polymers
[NPL-DMA(A)-99] 20 -3433 N85-31295
PLASTISOLS
NT SMOKE
PLATE (METAL)
U METAL PLATES
PLATE THEORY
On a general nonlinear theory of plates and shells: Formulation and applications 08 p1172 N85-17367
Numerical results of acoustic radiation, transmission and reflection of steel plate in water
[AMTE(N)-TM-84037] 13 p2155 N85-23378
PLATEAUS
NT PIEDMONTS
Oceanic plateaus, anomalous subduction, and the accretion of buoyant features at convergent margins
06 p0686 N85-14422
Basaltic pressure ridges: Formation and relationship to flow emplacement 13 p2186 N85-23567

Volcanism of the Colorado Plateau (basin and range transition): Implications for crustal processes
13 p2187 N85-23569

PLATELETS
The effect of +Gx acceleration on platelet activation as determined by plasma platelet factor 4 levels
[AD-A155881] 24 p4131 N85-35608

PLATES
An inverse source problem for elastic waves
03 p0371 N85-12368
Investigation of electromagnetic launcher behavior for impact fusion
[DE84-017401] 04 p0563 N85-13585
Modeling localized stress fields in composite laminates
[AD-A148630] 08 p1120 N85-17056
Large deformations of a nonlinear elastic solid and the diffusion of an ideal fluid treated as interacting continua
09 p1330 N85-18356
Coriolis effects on the vibrations of rotating beams, plates and shells 09 p1331 N85-18366

PLATES (STRUCTURAL MEMBERS)
NT ANISOTROPIC PLATES
NT CANTILEVER PLATES
NT CIRCULAR PLATES
NT ELASTIC PLATES
NT METAL PLATES
NT ORTHOTROPIC PLATES
NT PERFORATED PLATES
NT POROUS PLATES
NT RECTANGULAR PLATES
NT REINFORCED PLATES
Shear deformation plate continua of large double-layered space structures
01 p0059 N85-10391
Calculation of the optimum conditions for the forging of plates
[BLL-M-35757-(5828.4)] 02 p0189 N85-11260
Modeling the stress field in laminated composite plates near discontinuities
[PB84-219237] 03 p0327 N85-12103
The effects of microstructure on the temper embrittlement susceptibility of a Cr-2-1/4 1Mo forging
[AERE-R-11110] 03 p0334 N85-12151
Experimental study on transonic flutter characteristics of sweptback wing with core composite plates having different fiber orientations
[NAL-TR-827] 06 p0756 N85-14842
Evaluation of laterally loaded laminated glass units by theory and experiment
[PB85-111532/GAR] 09 p1300 N85-18166
Experimental verification of eddy-current flaw theory
[DE85-001288] 09 p1329 N85-18350
The problem of protecting the structure of a packet composite of optimal thinwall elements
10 p1444 N85-19101
Simple higher-order theory for laminated composite plates
[NASA-CR-174421] 10 p1496 N85-19445
Bending two-layer metal-polymer plates
11 p1604 N85-20085
Stress waves in an isotropic elastic plate excited by a circular transducer
[NASA-CR-3877] 11 p1650 N85-20390
Geometrically nonlinear analysis of laminated elastic structures
[NASA-CR-175809] 12 p1868 N85-21720
Machine analysis of resonance characteristics of plate-type radio electronic equipment constructions
13 p2085 N85-23018
Acoustic radiation from bilaminar plates
14 p2415 N85-24903
Symmetric composite laminate stress analysis
15 p2575 N85-25878
An elastic analysis of a plated bone to determine fracture gap motion 15 p2575 N85-25882
Design of shear deformable antisymmetric angle-ply laminates to maximize the fundamental frenquency and frequency separation
[CSIR-TWISK-333] 15 p2577 N85-25892
Model for computing late detonations initiated in propellants by impact (XDT reactions)
[DE85-007377] 16 p2756 N85-27019
Dynamic response of shells and plates subjected to variable magnitude traveling loads
16 p2798 N85-27250
The nonlinear analysis of thick composite plates using a cubic spline function 16 p2798 N85-27252
Stress analysis of the space telescope focal plane structure joint
[NASA-CR-175797] 16 p2803 N85-27284
Solution to eigenvalue problems of antisymmetric cross-ply and antisymmetric angle-ply laminated plates using affine transformations
[AD-A153040] 17 p2917 N85-27980
Acoustic oscillations of rods and plates
17 p2944 N85-28170
Numerical analysis of end effects in symmetric laminated plates
[NAL-TR-850] 18 p3068 N85-28977
Ultrasonic testing of plates containing edge cracks
[NASA-CR-3904] 18 p3119 N85-29307
A control concept for large flexible spacecraft using order reduction techniques 20 p3415 N85-31193
Durability of reinforced hard-alloy draw plates
[BLL-M-36278-(5828.4)] 20 p3465 N85-31526

PLATES (TECTONICS)
On gravity from SST, geoid from Seasat, and plate age and fracture zones in the Pacific
[E85-10020] 02 p0217 N85-11433
Seismic studies in southern Alaska
04 p0515 N85-13286
A computational study of two possible intraplate earthquake triggering mechanisms
05 p0674 N85-14329
Oceanic plateaus, anomalous subduction, and the accretion of buoyant features at convergent margins
05 p0688 N85-14422
Summaries of physical research in the geosciences
[DE85-001882] 06 p0818 N85-15194
Some trends in the modern Earth sciences — plate tectonics and Earth's crust 06 p0820 N85-15207
Anomalous magnetic field in northwestern Pacific Ocean and Pacific Ocean plate kinematics
06 p0820 N85-15210
Delineation of major geologic structures in Turkey using SIR-B data 08 p1149 N85-17249
Basic structural features and probable mechanism of formation of the Kuril Island system
10 p1501 N85-19472
Tectonic position and formation of young alkaline provinces of continents and oceans
10 p1502 N85-19480
Tectonic lineaments in the cenozoic volcanics of southern Guatemala: Evidence for a broad continental plate boundary zone
[NASA-CR-175456] 10 p1505 N85-19499
Science Applications, part 2 11 p1643 N85-20347
Absolute movement of Pacific Ocean plate during last 120 million years 13 p2107 N85-23126
Crustal dynamics studies in China
[NASA-CR-175617] 13 p2132 N85-23265
A tectonic model of an incipient spreading center and its margins: The Northern Red Sea and the Dead Sea rift 13 p2140 N85-23286
Absolute movement of Pacific Ocean plate based on paleoclimatic and paleomagnetic data and trajectory of hot spots during last 120 million years
14 p2334 N85-24435
Lateral inhomogeneity of mantle surface in western Eurasia 14 p2344 N85-24497
Density characteristics of asthenosphere in Atlantic Ocean 19 p3294 N85-30423
Geometry, velocity structure and penetration depths of descending slabs in the western Pacific
19 p3319 N85-30574
Geodynamics Branch research program
[NASA-TM-86223] 20 p3489 N85-31688
Contemporary plate motions from LAGEOS
20 p3489 N85-31689
Intraplate crustal deformation due to continental collisions 20 p3490 N85-31693
New stations supporting crustal dynamics project VLBI measurements 20 p3491 N85-31701
Global geomorphology 21 p3601 N85-32359
Techniques, problems and uses of mega-geomorphological mapping
21 p3604 N85-32378
Planetary perspective. Report of Working Group Number 4 21 p3605 N85-32385
The Aravalli sequence of Rajasthan, India: A Precambrian continental margin?
21 p3720 N85-33084
Subduction zone tectonic studies to develop concepts for the occurrence of sediment subduction
[DE85-011794] 22 p3815 N85-33632
Scaling differences between large interplate and intraplate earthquakes
[NASA-CR-176149] 23 p3948 N85-34467
Thermal evolution of coastal California with implications for hydrocarbon maturation 24 p4115 N85-35509
A dynamic model of Venus's gravity field
[NASA-CR-176173] 24 p4169 N85-35845

PLATFORMS
Orbiter processing facility: Access platforms Kennedy Space Center, Florida, from challenge to achievement
08 p1102 N85-16968
Analysis of interaction of dynamically adjustable gyroscopes on elastic platform by finite-element method
13 p2048 N85-22822

PLATING
NT ELECTROPLATING
NT ION PLATING
Mechanical locking between multi-layer printed wiring board conductors and through-hole plating
[AD-D011477] 10 p1481 N85-19352
Study of high performance alloy electroforming
[NASA-CR-175494] 11 p1596 N85-20040
Trace metal determinations in nickel-plating baths by polarographic methods
[DE85-007064] 15 p2511 N85-25488
Plating density standards
[DE85-010014] 21 p3591 N85-32318
Towards the development of technological processes for the preparation of cadmium plated steel articles
[BLL-M-36315-(5828.4)] 23 p3913 N85-34248

PLATINUM
Methods for producing platinum-group metal coatings from molten alkali cyanides
[PB84-225994] 01 p0029 N85-10181
Platinum thin film resistors as accurate and stable temperature sensors
[NASA-TM-77728] 01 p0049 N85-10322
Platinum group nuggets in deep sea sediments
06 p0683 N85-15611
Dispersed metal-toughened ceramics and ceramic brazing
[NASA-CR-174284] 07 p0933 N85-15916
Subtractively normalized interfacial Fourier transform infrared spectroscopy of difluorobenzene adsorbed at polycrystalline platinum electrodes
[AD-A148860] 08 p1123 N85-17080
Metal atom diffusion in amorphous silica and at the silica surface
[DE84-017351] 09 p1380 N85-18674
Response time correlations for platinum resistance thermometers in flowing fluids
[NASA-CR-172523] 12 p1850 N85-21606
Advanced thin film thermocouples
[NASA-CR-175541] 12 p1850 N85-21607
Power control of induction equipment for founding optical glass in array of platinum crucibles
14 p2267 N85-24044
C2H(n) fragments on metal surfaces
[AD-A151474] 15 p2505 N85-25449
Methanol adsorption on Pt(111)
[DE85-006802] 17 p2923 N85-28017
New catalysts and new electrolytes for acid fuel cells
[DE85-009940] 19 p3307 N85-30498
Opticals constant at X-ray wavelengths
[DE85-009743] 19 p3355 N85-30795
Defect production and recovery in FCC metals irradiated at 4.2 K
[DE85-010477] 20 p3538 N85-32014
Lead, platinum, and other heavy elements in the primary cosmic radiation: HEAO-3 results sec wg032961 cb553097 20 p3543 N85-32049
Characterization of catalysts with metal-support effects and of the species adsorbed on their surfaces
[DE85-012254] 24 p4096 N85-35394
Applications of the mineral resources data system and the international strategic minerals inventory in mineral-resource assessments by region and commodity
24 p4105 N85-35451

PLATINUM ALLOYS
Compatibility experiments of facilities, materials, and propellants for electrothermal thrusters
[NASA-TM-86956] 12 p1795 N85-21260
CO adsorption on (111) and (100) surfaces of the Pt sub 3 Ti alloy. Evidence for parallel binding and strong activation of CO
[NASA-CR-176077] 21 p3565 N85-32176

PLATINUM COMPOUNDS
Interactions between corrosion and creep of uncoated and coated superalloys in sulfate melts
04 p0477 N85-13038

PLAYBACKS
Playback amplifier with high interference immunity
13 p2077 N85-2297
Operation of autotracking system in various vide playback modes 16 p2764 N85-2705

PLETHYSMOGRAPHY
Vascular mechanisms of adaptation to antiorthosta position 22 p3822 N85-3367

PLEXIGLASS (TRADEMARK)
U POLYMETHYL METHACRYLATE

PLIES
U LAYERS

PLOTTERS
SPLOT: A plot program for finite element data, functi versus distance
[DE85-007129] 15 p2638 N85-262
Isotropic plotter
[PB85-175651] 18 p3150 N85-295

Defense Mapping Agency (DMA) raster-to-Vector analysis
[AD-A154153] 19 p3336 N85-30668
Defense Mapping Agency (DMA) raster-to-Vector benchmark testing
[AD-A154152] 19 p3338 N85-30683
Applied computer graphics in a geographic information system: Problems and successes
23 p3962 N85-34563

PLOTTING
Severe weather statistics STADTS decoder (SXW) and plotter (SWY)
[PB84-213693] 01 p0086 N85-10576
Plotting TDL coastal wind forecasts
[PB84-220789] 03 p0397 N85-12533
Computer-generated latitude and longitude templates for rapid determination of geographic positions in Alaska
04 p0516 N85-13268
A program to produce standard shewhart control charts for the statistics X-bar and R or S, P, NP, C, or U
[AD-A146971] 07 p1024 N85-16501
PLOT3D: An interactive graphics code for 3-dimensional plots
[AD-A147887] 07 p1026 N85-16514
Two-dimensional modeling for lineal and areal probabilities of weather conditions
[AD-A147970] 08 p1188 N85-17486
A FORTRAN plotting package for graphic VDUs
[AD-A148489] 08 p1204 N85-17577
User's manual: Menu-driven data graphing program for the Tektronix 7912AD and 7612D transient digitizer system
[DE85-002151] 09 p1370 N85-18610
Hurricane plotting program
[PB85-121432] 10 p1521 N85-19592
Plotfile appender
[PB85-109502] 11 p1688 N85-20616
Implementation of the computer program-system MOSS (Map Overlay and Statistical System) on a VAX-11 series computer under VMS
[AD-A149612] 12 p1914 N85-22019
Easyplot: An interactive, user-friendly graphics program
[AD-A150779] 14 p2404 N85-24824
NPLOT: An interactive plotting program for NASTRAN finite element models 15 p2573 N85-25869
Two interactive graphics postprocessors for NASTRAN 15 p2574 N85-25871
An unusual application of NASTRAN contour plotting capability 15 p2574 N85-25872
The interactive plotting program: GRAPH
[AD-A151371] 15 p2623 N85-26165
A heuristic solution to the spacing problem: Maximizing the minimum Euclidean distance among N points in a convex region
[AD-A152116] 16 p2855 N85-27603
Looking at more than three dimensions
[DE85-007754] 17 p3009 N85-28600
Computer program for plotting and fairing wind-tunnel data
[NASA-TM-85648] 20 p3387 N85-31009
A device-independent 2D plotting package written in FORTRAN
[RSRE-MEMO-3776] 23 p3956 N85-34514

PLOTTING INSTRUMENTS
U PLOTTERS

PLOWED FIELDS
U FARMLANDS

PLOWING
Prediction accuracy of the torques for rotary tillage by an analog tool
[AD-P004288] 09 p1408 N85-18865

PLUG NOZZLES
Jet noise suppression by porous plug nozzles
[NASA-CR-3613] 02 p0275 N85-11790
Experimental investigation of shock-cell noise reduction for dual-stream nozzles in simulated flight
[NASA-CR-3846] 04 p0557 N85-13549
Experimental investigation of shock-cell noise reduction for single stream nozzles in simulated flight
[NASA-CR-3845] 04 p0557 N85-13550
Thrust vectoring apparatus for maneuvering missile in flight
[AD-D011693] 19 p3226 N85-30004

PLUGS
Superconducting gyroscope research
[NASA-CR-171406] 15 p2560 N85-25795
Vapor-liquid phase separator studies
[NASA-CR-166545] 21 p3583 N85-32272

PLUMAGE
Microscopic identification of feathers in order to improve birdstrike statistics
[AD-P004187] 11 p1579 N85-19950

PLUMBANE
U LEAD COMPOUNDS
U METAL HYDRIDES

PLUMES
NT ROCKET EXHAUST
Collisional excitation cross sections
[AD-A145196] 01 p0117 N85-10800
Observed rate of tropospheric diffusion
[DE84-016047] 02 p0224 N85-11470
Modeling of propulsive jet plumes--extension of modeling capabilities by utilizing wall curvature effects
[AD-A146262] 03 p0362 N85-12324
Development of computational fluid dynamics at NASA Ames Research Center
[NASA-TM-86021] 04 p0452 N85-12886
Review of the attributes and performance of six urban diffusion models
[PB84-236850] 04 p0484 N85-13087
HS and E environmental sciences
[DE84-016183] 05 p0672 N85-14314
Measurements on the diffusion of hydrogen chloride in the waste gas plume of incineration ships in the North Sea. Part 1: Methodology, instrumentation and presentation of data
[GKSS-84-E-23-PT-1] 05 p0672 N85-14319
The properties of a round turbulent buoyant jet
[NAL-TR-826] 06 p0806 N85-15136
Shuttle system ascent aerodynamic and plume heating 08 p1103 N85-16975
Carbon vaporization/condensation effects
[NASA-TM-87430] 10 p1436 N85-19048
Meteorological support for the 1983 Deep Creek, Maryland experiment
[DE85-002616] 11 p1678 N85-20575
Preliminary analysis of tone-excited two-stream jet velocity decay
[NASA-TM-86951] 12 p1770 N85-21114
The influence on IR emission of engine parameters for an afterburn case. A sensitivity study on NATO infrared air target model (NIRATAM) version: 0.0
[AD-B089311L] 12 p1779 N85-21171
Hazardous air pollutants: Wet removal rates and mechanisms
[PB85-138626] 12 p1887 N85-21842
Time and space variability of turbulent concentration fluctuations
[AD-A149963] 12 p1896 N85-21898
Stagnation zone impaction on a simple terrain feature in stable flow 13 p2130 N85-23255
Deep water formation 15 p2601 N85-26030
A method for simulating 3-D aircraft flow fields with jet plume effects
[NASA-CR-175802] 16 p2699 N85-26664
The Terrain-Responsive Atmospheric Code (TRAC) for plume growth and dispersion in complex terrain
[DE85-010541] 19 p3309 N85-30513
Mechanisms of exhaust pollutants and plume formation in continuous combustion
[AD-A154169] 20 p3435 N85-31310
Manual for the computer program for the Gaussian plume model with percentile calculations
[KNMI-TR-60] 20 p3517 N85-31867
Laser beam interactions with vapor plumes during Nd:YAG laser welding on aluminum
[DE85-009793] 21 p3593 N85-32328
Assessment of the performance of an in-field Gaussian plume/puff model for overwater use
[AD-A155435] 21 p3614 N85-32460
VALMET: A valley air pollution model
[DE85-010820] 21 p3614 N85-32463
Modeling the exhaust of the pulsed plasma thruster
[AD-A155344] 21 p3707 N85-33018
Turbulence modelling for the prediction of turbulent jets: Wakes and plumes
[CFD/84/5] 22 p3784 N85-33447
Airborne cloud tracking measurements during the Three Mile Island nuclear station accident, Middletown, Pennsylvania. Date of survey: March - June 1979
[DE85-012060] 22 p3816 N85-33638
A dynamic model of Venus's gravity field
[NASA-CR-176173] 24 p4169 N85-35845

PLUNGERS
Design of inductive shift transducers
22 p3771 N85-33368

PLUTO (PLANET)
Research in planetary studies and operation of Mauna Kea Observatory
[NASA-CR-175616] 13 p2169 N85-23460
On the origin of Triton and Pluto
13 p2175 N85-23497
Photometric study of Pluto near perihelion. Part 2: Refinement of rotation period: Color indices
15 p2483 N85-25325
Magnetospheres of the outer planets
[AD-A154354] 19 p3384 N85-30996
Lightcurve CCD spectrophotometry of Pluto
20 p3545 N85-32057
Insolation changes on Pluto caused by orbital element variations
[AERONOMICA-ACTA-A-290-1984]
20 p3546 N85-32070

PLUTONIUM
NT PLUTONIUM ISOTOPES
NT PLUTONIUM 238
NT PLUTONIUM 239
General-purpose heat source development: Safety test program. Postimpact evaluation, design iteration test 5
[LA-10232-SR] 12 p1931 N85-22129
General-purpose heat source development: Safety test program. Postimpact evaluation, design iteration test 1
[LA-9680-SR] 12 p1931 N85-22131
Distribution of radium and plutonium in human bone
[DE85-005025] 13 p2142 N85-23298
Expected behavior of plutonium in the IFR fuel cycle
[DE85-006225] 18 p3161 N85-29725
Plutonium metal preparation and purification at Los Alamos, 1984
[DE85-010732] 19 p3239 N85-30085
Influence of chemical form, feeding regimen, and animal species on the gastrointestinal absorption of plutonium
[DE85-010291] 21 p3662 N85-32751
Measurement control for plutonium isotopic measurements using gamma-ray spectrometry
[DE85-013394] 24 p4097 N85-35397

PLUTONIUM COMPOUNDS
NT PLUTONIUM OXIDES

PLUTONIUM ISOTOPES
NT PLUTONIUM 238
NT PLUTONIUM 239
The I-Pu-Xe age of the Moon
04 p0584 N85-13729
Power flattening techniques for radioisotopic thermoelectric generators
[AD-A146365] 06 p0833 N85-15290
General-purpose heat source development: Safety test program. Postimpact evaluation, design iteration test
[LA-10034-SR] 23 p3969 N85-34606

PLUTONIUM OXIDES
Space nuclear safety program
[DE84-015074] 04 p0463 N85-12939
Space nuclear safety program
[DE84-015064] 04 p0463 N85-12940
Long-term exposure of pressed plutonium oxide heat sources to aquatic environments
[DE85-007385] 15 p2495 N85-25392
General-purpose heat source development: Safety test program. Postimpact evaluation, design iteration test
[LA-10034-SR] 23 p3969 N85-34606

PLUTONIUM 238
Environmental surveillance at Los Alamos during 1984
[DE85-011886] 22 p3811 N85-33605
Long-term exposure of (238) PuO2 to a terrestrial environment, volume 3
[DE85-011896] 22 p3840 N85-33781
Neutron flux, spectrum and dose equivalent measurements for a 4500-W(th) 238 PuO2 general purpose heat source
[DE85-011361] 22 p3841 N85-33786

PLUTONIUM 239
Historical review of californium-252 discovery and development
[DE85-010223] 19 p3362 N85-30844
The 1984 environmental monitoring program report for Idaho National Engineering Laboratory site
[DE85-011209] 22 p3812 N85-33611

PLUVIOGRAPHS
U RAIN GAGES
U RECORDING INSTRUMENTS

PLY ORIENTATION
Design sensitivity analysis of an antisymmetric angle-ply laminate
[CSIR-TWISK-318] 01 p0021 N85-10128
Design of shear deformable antisymmetric angle-ply laminates to maximize the fundamental frenquency and frequency separation
[CSIR-TWISK-333] 15 p2577 N85-25892

PLYWOOD
Self-heating to ignition measurements and computation of critical size for solar energy collector materials
[PB85-183374] 20 p3485 N85-31663

PNEUMATIC CONTROL
Development of an electro-pneumatic anti-G valve for high performance fighter aircraft
[AD-A148468] 08 p1201 N85-17561

PNEUMATIC EQUIPMENT
NT GAS VALVES
Noise reduction of the exhaust from pneumatic tools
[BMFT-FB-HA-83-021] 02 p0276 N85-11799
Pneumatic turbulators: A device for drag reduction at Reynolds numbers below 5 million
08 p1071 N85-16791
Tire inflation/deflation system
[AD-D011459] 10 p1493 N85-19426

Pneumatic clamping device
[AD-D011544] 12 p1858 N85-21656
Pneumohydraulic drive 14 p2268 N85-24050
Dynamic response of fluid transmission lines
[AD-A151926] 16 p2782 N85-27171
Thermo-electric valve
[AD-D011682] 19 p3252 N85-30165
PNEUMATIC RESET
U PNEUMATIC CONTROL
PNEUMATICS
Acoustic cross-correlation flowmeter for solid-gas flow
[DE85-005988] 23 p3935 N85-34391
POCKELS EFFECT
U BIREFRINGENCE
PODS (EXTERNAL STORES)
Equipment for preflight test of an Electronic Countermeasures (ECM) avionic system
07 p0939 N85-15949
POGO EFFECTS
STS-1 Pogo analysis
[NASA-TM-87433] 11 p1591 N85-20007
POIKILOTHERMIA
NT AMPHIBIA
NT FROGS
NT TURTLES
POINCARE PROBLEM
Stability of periodic satellite motions relative to center of mass in circular orbit 16 p2718 N85-26780
POINCARE SPHERES
Behavior orbits of two coupled oscillators
02 p0282 N85-11833
POINT DEFECTS
NT VACANCIES (CRYSTAL DEFECTS)
Radiation effects on structural materials
[DE84-014771] 01 p0029 N85-10178
Complex formation and temperature stability of electrophysical properties of GaAs seminsulating single crystals 02 p0258 N85-11689
Diffusion mechanisms and point defects in transition-metal oxides
[DE84-016238] 04 p0571 N85-13639
Analysis of diffusion in an ion-implanted alloy using a phenomenological model
[AERE-R-11527] 11 p1609 N85-20120
Oxidation of nickel-aluminum and iron-aluminum alloys
[DE85-006930] 15 p2512 N85-25497
Current understanding of point defects and diffusion processes in silicon 20 p3481 N85-31632
Thin-film reliability and engineering overview
21 p3612 N85-32450
The development and evaluation of point defect models for the growth of passive films on single crystal, polycrystalline, and amorphous metal surfaces
[AD-A154685] 21 p3709 N85-33023
Defect interactions at high concentrations in solid oxide electrolytes
[DE85-011824] 22 p3807 N85-33580
Formation of amorphous silicon by light ion damage
[DE85-012605] 23 p3972 N85-34623
POINT MATCHING METHOD (MATHEMATICS)
U BOUNDARY VALUE PROBLEMS
POINT SOURCES
Algorithm for astronomical, point source, signal to noise ratio calculations
[NASA-TP-2397] 03 p0445 N85-12834
Concentrator optical characterization using computer mathematical modelling and point source testing
[NASA-CR-174109] 04 p0528 N85-13375
Selection of parameters for image decomposition by television system for recognition of group of point sources 06 p0785 N85-15018
Study of low-frequency sound with point source in stream with shear 06 p0825 N85-15239
Analysis of processing 09 p1412 N85-18905
Sky coverage, confusion, completeness and reliability
09 p1412 N85-18906
Consolidation around a point heat source
[PB85-116549] 11 p1682 N85-20601
Electrical line source and point source interactions with anomalies in the ground
[DE85-009777] 18 p3095 N85-29161
Source characterization of point-like and distributed sources of acoustic emission 20 p3523 N85-31910
Mean intensity of wave reflected by wavefront reversing mirror in turbulent medium 22 p3782 N85-33432
Ninteenth International Cosmic Ray Conference. OG sessions, volume 1
[NASA-CP-2376-VOL-1] 22 p3860 N85-33902
A search for gamma-ray point sources with the Carpet shower array
[OG-2.1-12] 22 p3864 N85-33928
Detection of gamma-ray lines from the direction of the Crab Nebula 22 p3866 N85-33943
All sky Northern Hemisphere 10(15) EV gamma-ray survey
[OG-2.6-3] 22 p3870 N85-33968
Search for ultra high energy gamma-rays from various sources
[OG-2.6-7] 22 p3870 N85-33969
Diffusion-convection function of cosmic rays
[SH-3.2-10] 23 p4004 N85-34825
The cosmic ray composition as viewed from the chemical abundances of the solar system
[OG-7.1-8] 23 p4013 N85-34869
Electron capture decay of cosmic rays: A model of the inhomogeneous interstellar medium
[OG-7.1-10] 23 p4014 N85-34871
The model-independence of cosmic ray source determinations
[OG-7.2-1] 23 p4014 N85-34873
The effects of newly measured cross sections in hydrogen on the production of secondary nuclei during the propagation of cosmic rays through interstellar H
[OG-7.2-2] 23 p4014 N85-34874
A Cerenkov imaging telescope for high energy gamma rays
[OG-9.3-13] 23 p4028 N85-34968
A new ultra high energy gamma ray telescope at Ohya mine
[OG-9.4-3] 23 p4029 N85-34970
The Buckland Park air shower array
[OG-9.4-4] 23 p4029 N85-34971
An EAS experiment at mountain altitude for the detection of gamma-ray sources
[OG-9.4-5] 23 p4029 N85-34972
A new array for the study of ultra high energy gamma-ray sources
[OG-9.4-7] 23 p4029 N85-34974
Cerenkov light images of EAS produced by primary gamma
[OG-9.5-3] 23 p4030 N85-34979
A method to imprcve observations of gamma-ray sources near 10 (15) eV
[OG-9.5-5] 23 p4030 N85-34982
Note on the detection of high energy primary cosmic gamma rays by air shower observation
[OG-9.5-9] 23 p4031 N85-34986
Expected rates with mini-arrays for air showers
[HE-4.7-8] 24 p4199 N85-36059
A large area cosmic muon detector located at Ohya stone mine
[HE-5.1-7] 24 p4201 N85-36072
A study of atmospheric neutrinos with the IMB detector
[HE-5.3-7] 24 p4205 N85-36101
POINT SPREAD FUNCTIONS
Light scattered from polished optical surfaces: Wings of the point spread function 08 p1252 N85-17911
Improved continuum definition in high-background IUE images 11 p1761 N85-21078
Spatial resolution estimation of LANDSAT-4 Thematic Mapper data 12 p1872 N85-21741
POINTING CONTROL SYSTEMS
The design, fabrication and delivery of a spacelab neutral buoyancy Instrument Pointing System (IPS) mockup — underwater training simulator
[NASA-CR-171233] 04 p0462 N85-12934
Heavy duty precision pan and tilt head
[AD-A146669] 04 p0509 N85-13246
Attempts to contruct two-dimensional image of Sun from observations made with RATAN-600 radiotelescope by relay race method 06 p0783 N85-15005
Pointing and control system design study for the space infrared telescope facility (SIRTF)
[NASA-CR-166612] 07 p0915 N85-15795
Precise control of flexible manipulators
[NASA-CR-174210] 07 p0973 N85-16178
The UKIRT centre section structural investigation — United Kingdom Infrared Telescope (UKIRT)
[UKIRT-22] 09 p1414 N85-18920
Summary presentation of the Constellations Panel
11 p1644 N85-20359
Modal control of structural systems
[AD-A149734] 12 p1790 N85-21235
Impact of magnetic isolation on pointing system performance in the presence of structural flexibility
[NASA-CR-172481] 16 p2732 N85-26861
Modeling and analysis of pinhole occulter experiment: Initial study phase
[NASA-CR-175976] 19 p3272 N85-30287
Antenna pointing of large flexible telecommunications spacecraft 20 p3409 N85-31156
Design and evaluation of control systems for large communications satellites 20 p3409 N85-31157
Wideband disturbance accomodation in precision flexible space structures 20 p3415 N85-31194
Hubble space telescope: Pointing error effects on nonlinear ball joints
[NASA-TM-86511] 20 p3545 N85-32056
POINTS
Point processes associated with extreme value theory
[AD-A151211] 15 p2640 N85-26280
Inference and state estimation for stochastic point processes
[AD-A151216] 15 p2640 N85-26281
On the exceedance point process for a stationary sequence
[AD-A152827] 17 p3018 N85-28665
POINTS (MATHEMATICS)
NT FIXED POINTS (MATHEMATICS)
NT INFLECTION POINTS
NT POINT SPREAD FUNCTIONS
Spacefilling curves and the planer travelling salesman problem
[AD-A149337] 10 p1551 N85-19786
A description of the Langley wireframe geometry standard (LaWGS) format
[NASA-TM-85767] 13 p1971 N85-22300
A comparison of methods of least squares adjustment of traverses
[AD-A153612] 18 p3170 N85-29645
Method of and apparatus for generating an interstitial point in a data stream having an even number of data points
[NASA-CASE-MFS-25319-1] 22 p3827 N85-33701
POISEUILLE FLOW
U LAMINAR FLOW
POISONING (REACTION INHIBITION)
Effects of H2S on molten carbonate fuel cells
[DE84-015166] 02 p0195 N85-11307
POISONING (TOXICOLOGY)
U TOXIC DISEASES
POISONS
NT DDT
NT PESTICIDES
NT URETHANES
Bibliography of venomous and poisonous marine animals and their toxins
[AD-A148409] 08 p1192 N85-17514
Toxic hazards tests for vehicles and other equipment
[AD-A149164] 20 p3506 N85-31767
Emergency modeling of hazardous air pollutants
[AD-A155441] 21 p3614 N85-32461
POISSON DENSITY FUNCTIONS
Reversals of the Earth's magnetic field
04 p0521 N85-13332
A note on two papers in dependent central limit theory
[CWI-MS-R8410] 05 p0722 N85-14609
Distribution of atmospheric radio interference
06 p0792 N85-15083
Limiting distributions of functionals of Markov chains
[AD-A147832] 07 p1036 N85-16577
Digital elevation model computation using fast Poisson solutions 08 p1175 N85-17412
Inequalities for the M/G/Infinity queue and related shot noise processes
[AD-A149015] 10 p1545 N85-19737
A note on equivalent random theory
[CWI-OS-R8410] 14 p2412 N85-24872
Point processes associated with extreme value theory
[AD-A151211] 15 p2640 N85-26280
Inference and state estimation for stochastic point processes
[AD-A151216] 15 p2640 N85-26281
Poisson and multinomial shadowing processes
[AD-A151600] 15 p2640 N85-26286
On the exceedance point process for a stationary sequence
[AD-A152827] 17 p3018 N85-28665
Upward continuation of surface gravity anomalies
[AD-A154973] 21 p3631 N85-32560
On the statistical significance of excess events: Remarks of caution and the need for a standard method of calculation
[OG-9.5-10] 23 p4031 N85-34987
POISSON EQUATION
Optimum replacement of a system subject to shocks
[AD-A145811] 03 p0372 N85-12374
Unrestricted convergence for generalized Poisson integrals
[CTH-MATH-1984-13] 04 p0556 N85-13540
On the connection between multigrid and cyclic reduction
[NASA-TM-86020] 09 p1373 N85-18629
Twisting of segmental shafts
14 p2279 N85-24118
Macro for fitting nonlinear models to Poisson distributed data
[DE84-008569] 14 p2412 N85-24871
Investigation of the numerical method of moments for digital computer determination of differential equations
[AD-A151896] 15 p2638 N85-26258
Polycrystalline semiconductor heterojunction modeling (CdS/CuInSe(sub)2)
[DE85-002913] 16 p2671 N85-27713
Covariant Poisson brackets for classical fields
[DE85-010065] 18 p3171 N85-29654

Poisson formula for radon transformation and numerical image reconstruction algorithm
21 p3697 N85-32973

Admissible convergence of Poisson integrals in symmetric spaces
[CTH-MATH-1985-04] 22 p3836 N85-33750

POISSON PROCESS
U POISSON DENSITY FUNCTIONS
U STOCHASTIC PROCESSES

POISSON RATIO
The effect of pressure on the mechanical properties of polymers. Part 2: Measurement of the time-dependent Poisson's ratio
[DE85-002139] 06 p0772 N85-14938
Development and study of two-matrix glass fiber composite with increased transverse deformation
13 p2027 N85-22700
Research program on the effect of pressure on the mechanical properties of polymers, part 2
[DE85-000995] 13 p2037 N85-22761
Limiting values of stress state index after rupture of metals
[BLL-BISI-TRANS-22293-(9022.06)]
17 p2978 N85-28407

POLAND
Fungi of Mt. Babia Gora. 2: Indicative value of macromycetes in forest associations. A: Initial considerations
[NASA-TM-77485] 01 p0094 N85-10632
Fungi of Mount Babia Gora. 3: The indicating value of macromycetes in the forest associations
[NASA-TM-77486] 01 p0094 N85-10633
Development, production, application of robots assessed 03 p0343 N85-12211
Fiber optics development, prospects assessed
03 p0343 N85-12214
Polar research in Earth sciences described
08 p1142 N85-17204
Finnair, LOT, SAS reps in USSR on present operations, plans 09 p1278 N85-18035
National Machine Tools Conference slated for 1985: Conference agenda, papers 10 p1460 N85-19202
Automation of the process of speech signal segmentation in an analogic-numeric system
[REPT-5/1984] 16 p2768 N85-27082
Meteorological measurements with motor gliders in Poland 24 p4122 N85-35555

POLAR AURORAS
U AURORAS

POLAR CAPS
Seasonal variations in Triton's atmospheric mass and composition 02 p0301 N85-11948
Magnetospheric plasma studies using data from the dynamics high and low altitude plasma instruments
[AD-A145751] 03 p0392 N85-12505
Atlas of polar cap energetic particle observations. Volume 1: TIROS-N, 1 January 1979 - 28 February 1981
[PB84-233402] 04 p0535 N85-13419
Polar rain: Solar coronal electrons in the Earth's magnetosphere
[NASA-TM-86150] 07 p1060 N85-16726
Sun-aligned polar cap auroral arcs
[AD-A148052] 08 p1185 N85-17472
An atlas of polar cap energetic particle observations. Volume 2: NOAA-6, 8 July 1979 to 10 May 1983
[PB85-109072] 12 p1891 N85-21868
Polar cap formation on Ganymede
13 p2174 N85-23486
Properties of filamentary sublimation residues from dispersions of clay in ice 13 p2197 N85-23629
Afternoon radar aurora and polar cap convection pattern 14 p2361 N85-24592
The polar caps and the climatic evolution of Mars
22 p3854 N85-33866
Comparisons of the North Polar Cap of Mars and the Earth's Northern Hemisphere snow cover
[NASA-TM-86191] 23 p3989 N85-34728
On magnetic pair production above fast pulsar polar caps
[OG-8.2-13] 23 p4020 N85-34909

POLAR CUSPS
Birkeland currents correlated with dc-electric fields observed during the CENTAUR BBX rocket experiments
[DRI-6-84] 06 p0834 N85-15311

POLAR GASES
Equation of state study for polar fluids
[PB85-204345] 24 p4076 N85-35262

POLAR METEOROLOGY
On development mechanisms for polar lows
20 p3495 N85-31727

POLAR ORBITS
Tracking requirements for precise ERS-1 orbit determination 03 p0380 N85-12431
Ice sheets as invariant surfaces for radar altimeter calibration and orbit determination
03 p0383 N85-12449
S3-3 ONR-118 data analysis
[AD-A149725] 12 p1889 N85-21855
Direct measurements of severe spacecraft charging in auroral ionosphere 13 p1991 N85-22480
Charging of DMSP/F6 spacecraft in aurora on 10 January 1983 13 p1991 N85-22481
Average and worst-case specifications of precipitating auroral electron environment 13 p1991 N85-22482
Auroral-polar cap environment and its impact on spacecraft plasma interactions 13 p1991 N85-22484
Three-dimensional calculation of shuttle charging in polar orbit 13 p1992 N85-22486
Polar orbit electrostatic charging of objects in shuttle wake 13 p1992 N85-22487
Utilization of the polar platform of NASA's Space Station Program for operational Earth observations
[PB85-152502] 14 p2240 N85-23895
Universal time effects in polar ionosphere
14 p2338 N85-24461
Resonant rotations of satellite in polar orbit in magnetic and gravitational fields 15 p2479 N85-25302
Availability of the ARGOS system based on the orbital characteristics of the TIROS-N satellites --- oceanographic/meteorological data
16 p2813 N85-27352
The space station polar platform: NOAA systems considerations and requirements
[NOAA-TR-NESDIS-22] 22 p3740 N85-33182
Space Station Polar Platform: Integrating research and operational missions
[PB85-195279] 24 p4069 N85-35218

POLAR REGIONS
NT ANTARCTIC REGIONS
NT ARCTIC REGIONS
NT ROSS ICE SHELF
Convection of plasma in polar ionosphere, comparison of measurements from Cosmos-184 with model dependent on interplanetary magnetic field vector
02 p0160 N85-11086
Electric conductivities, currents and energy dissipation in the polar ionosphere 02 p0227 N85-11483
Occurrences of the polar slant E condition (SEC) at Narssarssuaq, Godhavn, Thule 1982
03 p0393 N85-12514
Mars polar volatiles: Topographic and geologic setting
[NASA-CR-174089] 04 p0581 N85-13708
Polar regions and climatic change
[PB84-237023] 05 p0688 N85-14421
Distribution of the K-corona over the polar regions of the solar disk: 1965-1983
[PB84-230077] 06 p0835 N85-15317
Region 1 birkeland currents from a global MHD simulation of the magnetosphere
[AD-A147435] 07 p0997 N85-16335
Diurnal freeze-thaw frequencies in selected regions of the high latitudes
[AD-A147276] 07 p1007 N85-16400
Polar research in Earth sciences described
08 p1142 N85-17204
Polar regions and climatic change: Appendix
[PB85-122679] 10 p1521 N85-19590
PMP-1 report: The fourth winter of PMP-1, 1981 - 1982: A winter with several interesting features
11 p1657 N85-20441
Passive microwave remote sensing for sea ice research
[NASA-CR-175570] 12 p1874 N85-21758
An atlas of polar cap energetic particle observations. Volume 2: NOAA-6, 8 July 1979 to 10 May 1983
[PB85-109072] 12 p1891 N85-21868
Carbonate chemistry of the Weddell Sea
[DOE/EV-110611/4] 12 p1898 N85-21916
Polar plasmas as observed by Dynamics Explorers 1 and 2 13 p1991 N85-22483
Mars: Stratigraphy of western highlands and polar regions 13 p2201 N85-23653
New directions in ARGOS instrumentation at Polar Research Lab (PRL) 14 p2323 N85-24350
Polar motions measurement study
[AD-A150690] 14 p2372 N85-24664
Space-time features of solar cosmic ray penetration into high latitude regions of Earth's magnetosphere based on Intercosmos-19 satellite data 15 p2481 N85-25310
SAM 2 measurements of the polar stratospheric aerosol, volume 5
[NASA-RP-1140] 15 p2590 N85-25970
A study of the generation mechanisms of high latitude and equatorial F-region irregularities using DE-2 data
[NASA-CR-175745] 16 p2825 N85-27423
Electron and ion distributions at high latitudes as measured by the Air Force polar orbiting satellites
[AD-A153242] 17 p2993 N85-28500
Preliminary documentation for the polar code
[AD-A154125] 19 p3336 N85-30667
Future prospects for a combined INMARSAT polar communication and search and rescue satellite system
20 p3406 N85-31137
Effects of Birkeland current limitation on high latitude convection patterns
[TRITA-EPP-84-10] 20 p3494 N85-31725
Airborne measurements of the vertical distribution of Arctic haze 21 p3647 N85-32657
Interplanetary magnetic field control of high-latitude electric fields and currents determined from Greenland magnetometer data
[DMI-GEOPHYS-PAPERS-R-69]
22 p3650 N85-33845
Comparisons of the North Polar Cap of Mars and the Earth's Northern Hemisphere snow cover
[NASA-TM-86191] 23 p3989 N85-34728
The influence of the Earth's magnetosphere on the high-energy solar protons
[SH-6.1-22] 23 p4046 N85-35093
The NORDA/FNOC (Naval Ocean Research and Development Activity's/Fleet Numerical Oceanography Center) Polar Ice Prediction System (PIPS)-Arctic: A technical description
[AD-A156332] 24 p4126 N85-35577

POLAR SUBSTORMS
Distribution of electric field near westward propagating bend in aurora 06 p0823 N85-15222

POLAR WANDERING (GEOLOGY)
Effects of the oceans on polar motion: Continued investigations
[E85-10037] 03 p0379 N85-12416
Earth rotation and polar wandering
14 p2399 N85-24785
Southern oscillation/El Nino excitation of the Earth's Chandler wobble 20 p3490 N85-31695
The Earth's wobble and associated ocean motions
20 p3490 N85-31696

POLARIMETERS
Imaging polarimeter-interferometer arrays for Tokamak measurements
[DE84-015916] 05 p0730 N85-14693
Far-infrared interferometry/polarimetry on the ISX-B Tokamak
[DE84-015401] 10 p1558 N85-19827
FIR interferometer/polarimeter system on ISX-B Tokamak
[DE85-001129] 11 p1731 N85-20887
Effects of focusing on HRS local-plane polarimeter measurements
[DE85-004627] 13 p2160 N85-23406
Ultraviolet Spectrometer and Polarimeter (UVSP) software development and hardware tests for the solar maximum mission
[NASA-CR-175279] 14 p2305 N85-24271
X-ray polarimetry: The measurement of the polarization of solar flare X-rays and the design of a Compton polarimeter 14 p2441 N85-25059
Polarimetric image recorder
[AD-D011605] 16 p2787 N85-27192
Measurements of vector fields with diode array
18 p3204 N85-29880
Analysis of the new polarimeter for the Marshall Space Flight Center vector magnetograph
18 p3205 N85-29881
The solar vector magnetograph of the Okayama Astrophysical Observatory 18 p3205 N85-29882
Vector magnetic field observations with the Haleakala polarimeter 18 p3205 N85-29883
Program for observations of Halley's comet
22 p3732 N85-33138

POLARIMETRY
Observations of plasma bubbles and their zonal drift using polarimeters
[INPE-3219-PRE/572] 05 p0729 N85-14686
Optical polarization as a probe of the local interstellar medium 06 p0875 N85-15560
First results of submillimeter polarimetry
08 p1246 N85-17861
Instrumentation for submillimeter polarimetry
08 p1250 N85-17889
Ultraviolet and optical spectroscopy and polarimetry of the helium weak star HD 21699: Evidence for a magnetically controlled stellar wind
11 p1759 N85-21065
Modern problems in polarimetry of solid surfaces of cosmic bodies 13 p1977 N85-22409
The Saturn ring particles from optical reflectance polarimetry 15 p2671 N85-26484
The San Fernando Observatory video Stokes polarimeter 18 p3205 N85-29885
The new solar magnetograph for the Canary Islands Observatory THEMIS 18 p3205 N85-29886
Diagnostics of vector magnetic fields
18 p3206 N85-29889

The nature and geometry of infrared reflection nebulae 24 p4167 N85-35835

POLARIS MISSILES
Polaris guidance system
[AD-D011324] 07 p0900 N85-15704

POLARITONS
NT PLASMONS
Splitting of surface polariton spectrum by holographic grating 02 p0272 N85-11771

POLARITY
Response of the F2 layer to the polarity of the interplanetary magnetic field
[REPT-561] 03 p0377 N85-12404
Relations between the particle precipitation events in mid-latitudes, the ring current intensity and the polarity of the interplanetary magnetic field
04 p0519 N85-13316
Characteristics of EMI generated by negative metal-positive dielectric voltage stresses due to spacecraft charging 13 p1995 N85-22505
A multipole model of the observed cerebral cortex magnetic field
[AD-A152237] 16 p2842 N85-27526
Luminescence probe studies of ionomers. I: Steady-state measurements from nafion membrane
[AD-A152475] 17 p3029 N85-28730
Effects of a wavy neutral sheet on cosmic ray anisotropies
[SH-4.2-11] 23 p4006 N85-34849
Latitudinal gradients of cosmic rays and the polarity reversal of the heliospheric magnetic field: A preliminary evaluation
[SH-4.2-16] 23 p4008 N85-34853
Isotropic intensity waves and features of their occurrence
[SH-4.3-8] 23 p4032 N85-34993
Cosmic ray sidereal diurnal variation of galactic origin observed by neutron monitors
[SH-4.4-2] 23 p4033 N85-35000
The sidereal semi-diurnal variation observed at high zenith angles at Mawson, 1968-1984, and the polarity of the solar main field
[SH-4.4-6] 23 p4033 N85-35004

POLARIZATION
Dust properties determined from backscattering in the interplanetary and interstellar medium
03 p0446 N85-12638

POLARIZATION (CHARGE SEPARATION)
NT DIELECTRIC POLARIZATION
NT ELECTROLYTIC POLARIZATION
Giacobini-Zinner comet: Polarimetric and physical observations
[NASA-TM-77771] 01 p0130 N85-10694
Simulation of the electrochemical machining process
[DE85-003797] 11 p1616 N85-20159
Stress corrosion cracking behavior of tungsten heavy alloys
[AD-A148843] 12 p1806 N85-21329
Theoretical and experimental comparisons of nearfield electrogalvanic fields due to nonlinear polarization layers
[AD-A152085] 16 p2779 N85-27149
The Hanle effect applied to magnetic field measurements 18 p3204 N85-29878
Applications and investigations of second harmonic generation 19 p3367 N85-30876
Equation of state study for polar fluids
[PB85-204345] 24 p4076 N85-35262

POLARIZATION (SPIN ALIGNMENT)
Performing (p vector,]ic]n), (d vector, n) and (n vector, n) measurements with a rotating magnet beam swinger
[DE84-017003] 04 p0562 N85-13582
Electron spin polarization effects in low energy electron diffraction, ion neutralization and metastable atom deexcitation at solid surfaces
[DE84-016550] 04 p0572 N85-13649
Magnetic alignment theory and the interpretation of polarization 06 p0860 N85-15590
Review of polarized proton beam techniques and a report on the workshop on polarized beams
[DE85-004390] 12 p1930 N85-22127
Effects of focusing on HRS focal-plane polarimeter measurements
[DE85-004627] 13 p2160 N85-23406
Theoretical and experimental studies of stabilized metastable helium
[AD-A150706] 14 p2417 N85-24913
Proceedings of the Workshop on Polarized Targets in Storage Rings
[DE85-002704] 16 p2862 N85-27653
Spin-polarized quantum systems
[DE85-006914] 16 p2864 N85-27667
Polarized internal target apparatus
[DE85-011611] 19 p3354 N85-30793
Polarization of fast particle beams by collisional pumping
[DE85-011621] 22 p3838 N85-33764

POLARIZATION (WAVES)
NT CIRCULAR POLARIZATION
NT CROSS POLARIZATION
NT LINEAR POLARIZATION
Polarization of ultrasound transmitted through boundary of magnetically inactive and equatorially magnetized media 02 p0257 N85-11682
Diffraction of plane polarized waves by noncircular cylindrical cavity 02 p0269 N85-11754
Nonlinear electromagnetic waves in ferromagnetic conducting media 03 p0346 N85-12232
Computer molecular dynamics of 2-D water (ice) structures under shock
[AD-A145818] 03 p0372 N85-12375
X-ray polarization in highly oriented pyrolytic graphite
[DE84-015573] 05 p0613 N85-13917
Detailed performance calculations: Goddard Group, appendix D 05 p0676 N85-14341
Polarization in chemically doped hydrogen-rich glasses
[DE84-017486] 06 p0771 N85-14936
Characteristics of polarization grids made of parallel metal strips during hemispherical scanning
06 p0792 N85-15062
Optical polarization as a probe of the local interstellar medium 06 p0875 N85-15560
Intrinsic polarization basis of radar target observed by system employing diversity reception
07 p0949 N85-16015
Reduction of signal modulation caused by polarization in visible optical scanning systems
[AD-D011389] 07 p1042 N85-16620
Nonlinear optical studies of rydberg atoms using degenerate four-wave mixing
[AD-A146827] 07 p1043 N85-16623
Instrumentation for submillimeter polarimetry
08 p1250 N85-17869
Analysis of Jovian decametric data: Study of radio emission mechanisms
[NASA-CR-174206] 08 p1258 N85-17917
Polarization angles of linearly polarized antennas and radio waves in satellite communications
[PB85-131613] 11 p1626 N85-20240
Generalized radome BSE (radome boresight error) characterization using superposition techniques
[AD-P004354] 12 p1825 N85-21448
Modern problems in polarimetry of solid surfaces of cosmic bodies 13 p1977 N85-22409
Interference flux during reflection of heterogeneous waves 13 p2078 N85-22977
Specifics of polarization structure of repeated scattering background in optical laser sounding signals
14 p2342 N85-24485
Holoswitch, phase 1
[AD-A152212] 16 p2787 N85-27198
Results of simultaneous measurements of absorption and polarization of radio waves reflected from ionosphere 16 p2807 N85-27313
Incident beam polarization for laser Doppler velocimetry employing a sapphire cylindrical window
[NASA-TM-87064] 17 p3037 N85-28786
Magnetism at interfaces and surfaces, as probed by neutron scattering
[DE85-007987] 18 p3176 N85-29690
The San Fernando Observatory video Stokes polarimeter 18 p3205 N85-29885
The new solar magnetograph for the Canary Islands Observatory THEMIS 18 p3205 N85-29886
The vector magnetograph of the Sayan Solar Observatory 18 p3206 N85-29887
Sensitive detection of tunable diode laser absorption by polarization rotation
[DE85-009621] 19 p3277 N85-30322
Lidar system using polarization discrimination techniques for molecular air pollution monitoring
19 p3308 N85-30504
Description and operation of CHISQMO, INVRTS, VOIGEN, VOIGTV, SMEAR, RUFF, AND POSCAR in the Stokes Analysis Program
[PB85-180628] 19 p3384 N85-30991
The Faraday effect in ruby and corundum in strong magnetic fields 21 p3697 N85-32967
Preparation and use of very pure o-D2
[DE85-009415] 22 p3843 N85-33800
Transient analysis of electromagnetic reflection from dispersive materials
[PB85-200186] 24 p4154 N85-35753

POLARIZATION CHARACTERISTICS
Checking optical-polarization measurements at interfaces 02 p0271 N85-11770
Measurements of polarization characteristics of radiation field of on-board aircraft antennas
03 p0346 N85-12230
Modeling rain polarization effects to millimeter wave frequencies
[PB84-231042] 03 p0357 N85-12296

Collisional pumping for the production of intense spin-polarized, neutral beams: Target considerations
[DE85-003459] 11 p1723 N85-20841
Modern problems in polarimetry of solid surfaces of cosmic bodies 13 p1977 N85-22409
The Fe XIII 10747 A and Fe XIV 5303 A coronal emission lines polarization 14 p2448 N85-25111
Spin physics at BNL
[DE85-009768] 20 p3520 N85-31885
Influence of mirror anisotropy and Brewster window orientation on radiation characteristics of ring lasers
21 p3664 N85-3[illegible]
Analysis of Jovian decametric data: Study of radio emission mechanisms
[NASA-CR-176057] 22 p3851 N85-33846

POLARIZATION CHARTS
U GRAPHS (CHARTS)
U POLARIZATION (WAVES)

POLARIZED ELECTROMAGNETIC RADIATION
NT POLARIZED LIGHT
NT SYNCHROTRON RADIATION
Specific absorption rate in a sitting rhesus model at 225, 1290, and 5950 MHz for E, H, and K polarizations
[AD-A145435] 02 p0234 N85-11524
Detection of submillimeter polarization in the Orion Nebula
[NASA-TM-86013] 04 p0579 N85-13700
Relation between polarization of artificial low frequency radiation and parameters of auroral ionosphere
06 p0785 N85-15018
Explosive instability of strong electromagnetic wave in plasma 11 p1719 N85-20817
Modern problems in polarimetry of solid surfaces of cosmic bodies 13 p1977 N85-22409
Small aperture analysis of the dual TEM (transverse electromagnetic) cell and an investigation of test object scattering in a single TEM cell
[PB85-159952] 14 p2306 N85-24277

POLARIZED LIGHT
The Saturn ring particles from optical reflectance polarimetry 15 p2671 N85-26484
Holoswitch, phase 1
[AD-A152212] 16 p2787 N85-27198
Bandpass filter formed by serial gratings operating in a wood's anomaly region
[AD-D011660] 18 p3093 N85-29148
Polarized internal target apparatus
[DE85-011611] 19 p3354 N85-30793

POLARIZED RADIATION
NT POLARIZED ELECTROMAGNETIC RADIATION
NT POLARIZED LIGHT
NT SYNCHROTRON RADIATION
Considerations for upgrading modifications to the Marshall Space Flight Center's X-ray calibration facility
12 p1946 N85-22226
The ultraviolet excess of quasars 3: The highly polarized quasars PKS 0736+017 and PKS 1510-089
[NASA-CR-175576] 12 p1953 N85-22298
Generation and transfer of polarized radiation in the solar atmosphere: Physical mechanisms and magnetic-field diagnostics 18 p3206 N85-29880
Dynamic models of flux tubes in the interpretation of polarization measurements 18 p3206 N85-29881
Contribution functions for Zeeman-split lines, and line formation in photospheric facules
18 p3207 N85-29882
Effect of polarized radiative transfer on the Hanle magnetic field determination in prominences: Analysis of hydrogen H alpha line observations at Pic-du-Midi
18 p3207 N85-29884
The inference of vector magnetic fields from polarization measurements with limited spectral resolution
18 p3207 N85-29888
Dual sense, circularly polarized helical antenna
[AD-D011680] 19 p3254 N85-30175
Commissioning the polarized beam in the AGS
[DE85-010958] 22 p3641 N85-33789

POLARIZERS
Characteristics of polarization grids made of parallel metal strips during hemispherical scanning
06 p0792 N85-15062
Polarization diversity addition to the 10 centimeter Doppler weather radar
[AD-A156062] 24 p4057 N85-35334

POLAROGRAPHS
U POLAROGRAPHY

POLAROGRAPHY
Homogeneous reaction involving components o different redox couples. 2: Polarographic studies of th interactions of alkali metal cations with anthracene an fluoroanthene dianions in N,N-dimethylformamide a acetonitrile
[AD-A148667] 08 p1124 N85-170
Trace metal determinations in nickel-plating baths b polarographic methods
[DE85-007064] 15 p2511 N85-254

Electrochemical reduction of titanium in dimethyl sulphoxide
[BLL-OA-TRANS-3225-(6196.300)] 20 p3429 N85-31267

POLARONS
Free energy and effective mass of the polaron at finite temperatures
[TUM-H6401] 03 p0417 N85-12567
Peltier heat of a small polaron in a magnetic semiconductor
[DE85-000470] 14 p2430 N85-24963

POLICE
Civil law enforcement missions 06 p0751 N85-14812

POLICIES
NT ENERGY POLICY
NT PATENT POLICY
Polychlorinated biphenyls (PCBs) in transit system electrical equipment
[PB84-222207] 01 p0045 N85-10291
Acid rain and transported air pollutants: Implications for public policy
[PB84-222967] 01 p0071 N85-10469
Second Symposium on Space Industrialization — space commercialization
[NASA-CP-2313] 02 p0149 N85-11011
Legal considerations and cooperative opportunities for space commercial activities 02 p0150 N85-11013
Emergency Mathematics and Science Education Act
[GPO-29-561] 03 p0435 N85-12770
Federal Telecommunications Privacy Act of 1984
[H-REPT-98-815] 03 p0441 N85-12807
Aircraft navigation and landing technology: Status of implementation
[GPO-38-615] 04 p0454 N85-12883
The Expendable Launch Vehicle Commercialization Act
[GPO-30-838] 04 p0460 N85-12919
Review of Space Shuttle requirements, operations, and future plans
[GPO-39-101] 04 p0461 N85-12927
Assessing erosion on US cropland: Land management and physical features
[PB84-219252] 04 p0526 N85-13366
Publications of the Executive Office of the President: January 20, 1981 - June 30, 1984
[PB84-230671] 06 p0871 N85-15533
Issues and findings 07 p0914 N85-15782
An evaluation of the effect of establishing a minimum Economic Order Quantity (EOQ) on the Air Force EOQ item management system
[AD-A147121] 07 p1051 N85-16673
Evaluation of the effectiveness of the weighted guidelines to induce contractor's investment in cost reducing facilities equipment
[AD-A147566] 07 p1053 N85-16681
Technical order managers handbook: Utilization assessment
[AD-A147579] 07 p1055 N85-16694
National airspace review enhancement plan, revision 3
[AD-A150743] 08 p1082 N85-16852
An analysis of production competition and award methodology
[AD-A147775] 08 p1228 N85-17733
International cooperation and competition in civilian space activities
[OTA-ISC-240] 08 p1231 N85-17750
Deep seabed stable reference areas
[PB84-241470] 09 p1360 N85-18555
Commission operation. National Low-Level Radioactive Waste Management Program
[DOE/LLW-33T] 09 p1383 N85-18699
Worldwide report: Telecommunications policy, research and development
[JPRS-TTP-85-002] 10 p1475 N85-19309
Worldwide report: Telecommunications policy, research and development
[JPRS-TTP-85-006] 10 p1476 N85-19314
Communications satellite needs examined 10 p1476 N85-19317
Strategic management for organizational effectiveness. The effect of human resource planning on retention and related issues, volume 3
[AD-A149400] 10 p1566 N85-19876
Strategic management for organizational effectiveness. The effect of human resource planning on retention and related issues: Methodological appendix
[AD-A149401] 10 p1566 N85-19877
FAA policy regarding solid waste disposal facilities
[AD-P004196] 11 p1581 N85-19963
Synthetic fuels policy
[GPO-34-227] 11 p1613 N85-20143
French research minister on policy, technology transfer 11 p1618 N85-20182
Debris in the geostationary orbit ring, the endless shooting gallery: The necessity for a disposal policy 12 p1786 N85-21214
Orbital debris policy issues: Battelle involvement and some personal observations 12 p1787 N85-21218
Considerations for policy on man-made debris propagation control 12 p1787 N85-21219
Spacecraft hazard and shielding requirements 12 p1788 N85-21224
Systems research on China in year 2000 12 p1820 N85-21418
Oversight review of the five-year outlook report on science and technology
[GPO-41-058] 12 p1949 N85-22243
1984 science and technology posture hearing with the director of the Office of Science and Technology Policy
[GPO-41-080] 12 p1949 N85-22244
USSR report: Space
[JPRS-USP-85-001] 13 p1977 N85-22403
INMARSAT marine satellite organization 13 p1985 N85-22456
USSR report: Science and technology policy
[JPRS-UST-85-002] 13 p2167 N85-23442
Militarization of space activity in United States 15 p2488 N85-25360
West Europe report: Science and technology
[JPRS-WST-84-014] 15 p2536 N85-25647
USSR report: Space
[JPRS-USP-85-004] 16 p2717 N85-26772
West Europe report: Science and technology
[JPRS-WST-84-024] 17 p2945 N85-28183
Social and political problems in Soviet basic research
[AD-P004565] 17 p3048 N85-28860
New ESA director on Ariane, space station, future trends 18 p3086 N85-29096
Inventory policy for high backorder items
[AD-A153696] 18 p3196 N85-29840
Computer center policy
[AD-A154416] 19 p3338 N85-30681
Methodology for assessing benefits and costs of government information collection
[DE85-010594] 19 p3361 N85-30975
FAA regulation of 9-seat and under passenger aircraft
[GPO-42-703] 20 p3391 N85-31032
West Europe report: Science and technology
[JPRS-WST-85-020] 20 p3438 N85-31333
Navy information systems: Planning, policy, organization, and management
[PB85-176113] 20 p3541 N85-32038
Opportunities for policy historians: The evolution of the US civilian space program 23 p4057 N85-35147
A guide for new environmental coordinators
[AD-A156327] 24 p4113 N85-35498

POLISHED METALS
U METAL POLISHING

POLISHING
NT ELECTROPOLISHING
NT METAL POLISHING
Development of a measuring procedure for the automatic evaluation of the flatness of reflective surfaces
[BMFT-FB-T-84-168] 03 p0421 N85-12688
Fabrication of monocrystalline GaAs solar cells utilizing NaCl sacrificial substrates
[DE84-013016] 11 p1673 N85-20544

POLITICS
International cooperation and competition in space
[GPO-38-001] 02 p0295 N85-11911
Statement of Otho E. Eskin, Director, Office of Advanced Technology, Department of State 02 p0296 N85-11914
Area handbook series. Honduras: A country study
[AD-A146510] 06 p0827 N85-15253
Outer space law: A problem of astronautics
[NASA-TM-77760] 07 p1055 N85-16697
Social and political problems in Soviet basic research
[AD-P004565] 17 p3048 N85-28860
Technology and Soviet political choices
[AD-P004566] 17 p3048 N85-28861
U.S.-China conference on science policy
[PB85-176345] 19 p3380 N85-30971
Satellites and politics: Weather, communications, and earth resources 23 p4057 N85-35144

POLLEN
Geographic and stratigraphic distribution of Miocene palynomorphs in north Idaho 03 p0390 N85-12498
Global paleoclimatic data base for 6000 years BP
[DE85-006628] 15 p2600 N85-26024

POLLUTANTS
U CONTAMINANTS

POLLUTION
NT AIR POLLUTION
NT ENVIRONMENT POLLUTION
NT GLOBAL AIR POLLUTION
NT INDOOR AIR POLLUTION
NT NOISE POLLUTION
NT OIL POLLUTION
NT WATER POLLUTION
Practical application of earth resistivity methods in phase 2 of the installation restoration program
[AD-P004148] 09 p1348 N85-18484
Acid rain: Towards automated monitoring 16 p2829 N85-27444
The seasonal cycle of atmospheric CO in the Southern Hemisphere 16 p2830 N85-27447
Protective systems and maintenance policies for marine environments 22 p3750 N85-33245
Solar energy meteorological research and training program: Region 4
[DE85-011783] 22 p3816 N85-33640

POLLUTION CONTROL
Operating experiences of reverse osmosis plants treating Rand Water Board (RWB) water: Pitfalls and problems 01 p0023 N85-10142
Demonstrating air quality improvements: A review of alternatives
[DE84-014274] 01 p0070 N85-10462
Acid rain and transported air pollutants: Implications for public policy
[PB84-222967] 01 p0071 N85-10469
Fabric filter system study
[PB84-229749] 03 p0342 N85-12206
Electrostatic augmentation of fabric filtration: Reverse-air pilot unit experience
[PB84-230002] 03 p0343 N85-12207
Effect of sealants of the sound absorption coefficients of acoustical friable insulating materials
[AD-A148541] 08 p1218 N85-17674
Proceedings of the Environmental Systems Symposium (13th) held at Bethesda, Md., 20-22 March 1984
[AD-A148194] 09 p1346 N85-18471
The application of emissions trading to DoD installations
[AD-P004136] 09 p1346 N85-18472
Compatible goals: Defense and environmental protection
[AD-P004137] 09 p1347 N85-18473
Environmental and energy audits of Air Force government owned-contractor operated installations
[AD-P004138] 09 p1347 N85-18474
Assessment of environmental costs at ordnance activities
[AD-P004140] 09 p1347 N85-18476
Protocol for aquifer cleanup decision making at military installations
[AD-P004151] 09 p1349 N85-18487
Versator divertor experiment: Preliminary designs
[DE84-017159] 09 p1393 N85-18769
Experimental investigation of a pulse combustor: Flow visualization by Schlieren photography
[DE85-002862] 11 p1636 N85-20304
Considerations for policy on man-made debris propagation control 12 p1787 N85-21219
Role of biological assessment in effluent control
[PB85-116101] 12 p1885 N85-21830
Papers from the Symposium on Emissions: The Value of Incentives and Guidelines for Control
[S-336] 15 p2590 N85-25967
Analytical methods for determination of POHC (Principal Organic Hazardous Constituents) in combustion products
[PB85-161578] 16 p2747 N85-26955
Environmental management needs
[DE85-007859] 18 p3133 N85-29405
Space station trace contaminant control 18 p3157 N85-29550
Control of acid deposition precursors through dry scrubbing
[DE85-010261] 19 p3235 N85-30056
Reduction of pollutant formation in combustion processes
[DE85-010181] 19 p3309 N85-30512
Technical guide for estimating fugitive dust impacts from coal handling operations, volume 2
[DE85-010939] 19 p3309 N85-30514
Technical guide for estimating fugitive dust impacts from coal handling operations. Volume 1: Project summary
[DE85-010948] 19 p3309 N85-30515
Third US/USSR Symposium on Particulate Control
[PB85-190890] 19 p3310 N85-30522
Sources of copper air emissions
[PB85-191136] 19 p3310 N85-30523
State-of-the-art of aquifer restoration. Volume 1: Sections 1 through 8
[PB85-181071] 20 p3478 N85-31612
State-of-the-art of aquifer restoration. Volume 2: Appendices A through G
[PB85-181089] 20 p3478 N85-31613
Historic emissions of sulfur and nitrogen oxides in the U.S. from 1900 to 1980. Volume 1: Results
[PB85-191195] 20 p3487 N85-31674

Historic emissions of sulfur and nitrogen oxides in the U.S. from 1900 to 1980. Volume 2: Data
[PB85-191203] 20 p3487 N85-31675

EPA (Environmental Protection Agency) research program guide, FY-1985, October 1, 1984 - September 30, 1985
[PB85-181881] 20 p3487 N85-31676

Environmental monitoring at Lawrence Livermore National Laboratory: 1984 report
[DE85-011593] 22 p3811 N85-33606

Technology of off-gas treatment for liquid-fed ceramic melters
[DE85-012467] 22 p3812 N85-33610

A guide for new environmental coordinators
[AD-A156327] 24 p4113 N85-35498

Review of US NOx abatement technology
[PB85-193522] 24 p4114 N85-35501

POLLUTION MONITORING

Mobile source exposure estimation
[PB84-224516] 01 p0095 N85-10643

Water resources by orbital remote sensing: Examples of applications
[E85-10015] 02 p0217 N85-11428

Analysis of Santa Barbara oxidant study
[PB84-229277] 03 p0388 N85-12486

Development and evaluation of cloud water collectors
[PB84-232529] 04 p0540 N85-13437

Portable instrument for the detection and identification of air pollutants
[DE84-014767] 05 p0672 N85-14316

Gas chromatographic determination of content of harmful substances in air of industrial locations
06 p0761 N85-14866

Measurement and analysis of ambient carbon monoxide concentrations for project-level air quality impact studies
[PB85-104602/GAR] 09 p1350 N85-18492

Laser air pollution monitoring system planned for Moscow 10 p1500 N85-19465

Comparative evaluation of GC/MS (Gas Chromatography/Mass Spectrometry) data analysis processing
[PB85-125664] 11 p1596 N85-20037

Research in environmental biology reviewed
11 p1622 N85-20211

Solid sorbent air sampler
[NASA-CASE-MSC-20653-1] 11 p1636 N85-20301

Development of a low cost electrochemical CO monitor based on stripping voltammetry
[PB85-113470] 11 p1637 N85-20312

User's guide for the Photochemical Box Model (PBM)
[PB85-137164] 11 p1682 N85-20602

Role of biological assessment in effluent control
[PB85-116101] 12 p1885 N85-21830

Evaluation of complex terrain air quality simulation models
[PB85-119485] 12 p1886 N85-21835

Atlantic Coast Unique Regional Atmospheric Tracer Experiment (ACURATE)
[PB85-128460] 12 p1886 N85-21839

Arabian gulf circulation — pollution monitoring
14 p2331 N85-24412

Utilization of remote sensing data in the evaluation of air pollution characteristics in the south coast/Southeast Desert Air Basin
[PB85-162063] 16 p2822 N85-27407

Symposium on Atmospheric Sciences in South Africa
[CSIR-S-331] 16 p2829 N85-27442

Elemental analysis of aerosols in Transvaal urban and power-producing areas using time and size-resolved samples 16 p2829 N85-27443

Acid rain: Towards automated monitoring
16 p2829 N85-27444

A wind-bivane/microprocessor system for on-line prediction and display of pollutant distributions
16 p2830 N85-27449

A study of gas solid reactions using coated piezoelectric detectors
[AD-A153047] 17 p2920 N85-28001

Elemental tracers of source regions of contaminants in precipitation
[DE85-007386] 18 p3133 N85-29407

Application of climatological analysis to minimize air pollution impacts in California
[PB85-172963] 18 p3149 N85-29502

Atmosphere monitoring requirements
18 p3158 N85-29553

Contamination control for increased crew productivity
18 p3158 N85-29555

Sources of copper air emissions
[PB85-191138] 19 p3310 N85-30523

Analysis of aldehydes and ketones in the gas phase
[PB85-181865] 20 p3426 N85-31261

VALMET: A valley air pollution model
[DE85-010820] 21 p3614 N85-32463

Laser Elektronika-01 for air pollution control lidar
21 p3684 N85-32887

Chemoreception and detection of micropollutants by means of a telemetric bionic detector
[DRIC-T-7460] 22 p3810 N85-33600

Environmental monitoring at Lawrence Livermore National Laboratory: 1984 report
[DE85-011593] 22 p3811 N85-33606

Modeling of auto exhaust smog chamber data for EKMA development
[PB85-186492] 22 p3813 N85-33619

Airborne cloud tracking measurements during the Three Mile Island nuclear station accident, Middletown, Pennsylvania. Date of survey: March - June 1979
[DE85-012060] 22 p3816 N85-33638

POLLUTION TRANSPORT

Space Shuttle Environmental Effects: The First 5 Flights
[NASA-CR-171812] 01 p0069 N85-10457

Solution of contaminant transport equations using an orthogonal-upstream finite element scheme
[DE84-014266] 01 p0070 N85-10463

The use of fixed-bed adsorber models to predict the fluxes of toxic substances in groundwaters and soil environments
[PB84-202563] 01 p0071 N85-10468

Acid rain and transported air pollutants: Implications for public policy
[PB84-222967] 01 p0071 N85-10469

Arctic haze: Meteorological aspects of long-range transport 02 p0230 N85-11499

Review of the attributes and performance of six urban diffusion models
[PB84-236850] 04 p0484 N85-13087

Transformation processes and wet deposition on the urban scale
[DE84-015294] 04 p0539 N85-13432

Spatial and temporal interpolation of NEROS radiosonde winds
[PB84-232545] 04 p0540 N85-13438

Calms processor (CALMPRO) user's guide
[PB84-229467] 04 p0540 N85-13439

Mean maximum mixing heights for northern Asia for the winter of 1978
[DE84-015980] 05 p0672 N85-14315

Cross-Appalachian Tracer Experiment (CAPTEX '83)
[PB84-238641] 06 p0834 N85-15307

NOx emissions near a heat pump with gas motor
[BLL-WH-782-(9091.9F)] 07 p0995 N85-16319

Climate and water quality 07 p1002 N85-16368

Installation restoration program. Phase 2: Stage 1 problem confirmation study, Duluth International Airport Duluth, Minnesota
[AD-A148318] 08 p1089 N85-16885

Determination of the laws governing the changes in the standard deviations of the distribution of pollution based on observations of the atmospheric turbulence spectrum and the possibility of simulating it in the laboratory
[BLL-TR-T6373/BG/MRS14883/84]
08 p1179 N85-17431

Penetration of the atmosphere by flammable mixtures as a result of spillage of LNG on the ground
08 p1179 N85-17432

Modeling of turbulent dispersion of neutral and buoyant contaminants released from two dimensional sources — air pollution
[VKI-TN-150] 08 p1180 N85-17436

Preliminary post-emplacement safety analysis of the subseabed disposal of high-level nuclear waste
[DE84-011162] 08 p1221 N85-17692

Meteorological factors responsible for high CO (carbon monoxide) levels in Alaskan cities
[PB85-115137/GAR] 09 p1350 N85-18493

TRAN-STAT: Statistics for environmental studies
[DE85-000829] 10 p1513 N85-19547

Study of pollutant dispersion in an urban street canyon
[DE85-002646] 11 p1677 N85-20571

Comparison of MESOI atmospheric dispersion estimates with data and estimates from other models
[DE85-002372] 11 p1678 N85-20572

Models and parameters for environmental radiological assessments
[DE81-027154] 11 p1678 N85-20573

Meteorological support for the 1983 Deep Creek, Maryland experiment
[DE85-002616] 11 p1678 N85-20575

Turbulence parameters impacting dispersion in an urban convection boundary layer
[PB85-116036] 11 p1682 N85-20586

Atmospheric dispersion of hypergolic liquid rocket fuels, volume 1
[AD-A149597] 12 p1817 N85-21399

ELECT groundwater transport research code
[DE85-003284] 12 p1884 N85-21824

Air quality criteria for ozone and other photochemical oxidants. External review draft, volume 2
[PB85-126043] 12 p1886 N85-21836

Hazardous air pollutants: Wet removal rates and mechanisms
[PB85-136626] 12 p1887 N85-21842

Continued research in mesoscale air pollution simulation modeling. Volume 6. Further studies in the modeling of microscale phenomena
[PB85-137370] 12 p1887 N85-21844

Observational study of transport in the free troposphere
[PB85-144145] 12 p1887 N85-21845

Sector analysis of relevant meteorological parameters for long range transport of air pollutants
[NR-27] 12 p1893 N85-21882

Drifting ice as mechanical factor in purifying and polluting hydrosphere 13 p2106 N85-23132

Arabian gulf circulation — pollution monitoring
14 p2331 N85-24412

PLUVIUS: A generalized 1-dimensional model of reactive pollutant behavior, including dry deposition, precipitation formation, and wet removal, 2nd edition
[DE85-005542] 14 p2353 N85-24538

Adjustment of the national dispersion model for air pollution from elevated sources
[KNMI-TR-57] 14 p2353 N85-24540

Operational methods for calculating atmospheric dispersion
[BLL-CE-TRANS-8040-(9022.09)]
15 p2588 N85-25955

Field validation of 6-particle puff model
[DE85-004073] 15 p2589 N85-25962

Analytical methods for determination of POHC (Principal Organic Hazardous Constituents) in combustion products
[PB85-161576] 16 p2747 N85-26955

Limiting profiles in contaminant transport through porous media — ground water pollution
[REPT-84-31] 17 p2960 N85-28282

Quality assurance for RESOLVE (Research on Operations-Limiting Visual Extinction). A visibility study in the California desert
[AD-A152383] 17 p2992 N85-28494

Vertical redistribution of a pollutant tracer due to cumulus convection
[PB85-172971] 18 p3134 N85-29415

Diffusion of trace gases in the ground level boundary layer 18 p3148 N85-29489

Global model of transport of pollutants in atmosphere
19 p3297 N85-30439

MELSAR: A mesoscale air quality model for complex terrain. Volume 2: Appendices
[DE85-010991] 19 p3310 N85-30519

Effect of vertical shear on regional-scale trajectories in near-frontal conditions
[DE85-007554] 19 p3317 N85-30561

Preliminary investigation of dispersion of pollutants in model building wake flows using bipolar space charge
[IC-AERO-84-04] 20 p3487 N85-31671

Modeling of chemical transformations of SO(x) and NO(x) in the polluted atmosphere: An overview of approaches and current status
[PB85-173169] 20 p3487 N85-31677

Errors and parameterizations of sub-grid scale processes in regional-scale atmospheric models
20 p3488 N85-31682

VALMET: A valley air pollution model
[DE85-010820] 21 p3614 N85-32463

Application of Particle Induced X-ray Emission analysis (PIXE) to aerosol long range transport studies
21 p3648 N85-32665

Sahara Desert dust transport to the south
21 p3648 N85-32666

Measurements of giant salt nuclei from inland in east China 21 p3648 N85-32668

on the transport of large condensation nuclei in the atmosphere at various altitudes over the territory of the USSR 21 p3653 N85-32698

MELSAR: A mesoscale air quality model for complex terrain. Volume 1: Overview, technical description and user's guide
[DE85-010943] 22 p3811 N85-33608

Airborne cloud tracking measurements during the Three Mile Island nuclear station accident, Middletown, Pennsylvania. Date of survey: March - June 1979
[DE85-012060] 22 p3816 N85-33638

Studies in thermo-hydro-chemical transport in porous and fractured media
[DE85-012555] 23 p3949 N85-34473

User's guide to the MATHEW/ADPIC models
[DE85-012952] 23 p3966 N85-3458

MATADOR (Methods for the Analysis of Transport And Deposition Of Radionuclides) code description and user's manual
[TI85-901402] 23 p3966 N85-3455

POLOIDAL FLUX

Versator divertor experiment: Preliminary designs
[DE84-017159] 09 p1393 N85-1876

The continuous spectrum of an axisymmetric, self-gravitating equilibrium in the presence of a poloidal magnetic field
12 p1959 N85-22315
The continuous spectrum of an axisymmetric equilibrium with a mixed poloidal and toroidal magnetic field with gravity included
14 p2450 N85-25128
Comparison study of toroidal-field divertors for a compact reversed-field pinch reactor
[DE85-009591] 18 p3189 N85-29781
Poloidal variations in toroidal fusion reactor wall power loadings
[DE85-009505] 19 p3362 N85-30648
Observation of helical sawtooth oscillations in a tokamak
[DE85-012062] 23 p3983 N85-34703

POLYACETYLENE
Control of electronic, magnetic and optical properties of doped polyacetylene conductors
[AD-A150117] 12 p1814 N85-21375
Polymeric electrolytes for ambient temperature lithium batteries
[DE85-001032] 12 p1835 N85-21518
Electron-donor dopant, method of improving conductivity of polymers by doping therewith, and a polymer so treated
[DE85-011640] 22 p3752 N85-33257
Electrically conductive doped block copolymer of polyacetylene and polyisoprene
[DE85-006500] 24 p4082 N85-35301

POLYACRYLATES
U ACRYLIC RESINS

POLYAMIDE RESINS
NT KEVLAR (TRADEMARK)
NT NYLON (TRADEMARK)
Thermoset-thermoplastic aromatic polyamide containing N-propargyl groups
[NASA-CASE-LAR-12723-1] 11 p1610 N85-20123
Process for preparing highly optically transparent-colorless armomatic polyimide film
[NASA-CASE-LAR-13351-1] 12 p1811 N85-21360
Fire and heat resistant laminating resins based on maleimido and citraconimido substituted 1-(diorgano oxyphosphonyl)methyl-2,4- and 2,6-diaminobenzenes
[NASA-CASE-ARC-11533-1] 12 p1812 N85-21364
Determination of the viscosity number of thermoplastics in dilute solution; polyamides (PA)
[NASA-TM-77673] 24 p4081 N85-35296

POLYATOMIC GASES
NT DIATOMIC GASES

POLYATOMIC MOLECULES
NT DIATOMIC MOLECULES
Collisional energy exchange in polyatomic molecules
[AD-A147710] 08 p1219 N85-17679
Identification and properties of molecular systems of potential use in solar-pumped lasers
[NASA-CR-175804] 16 p2769 N85-27207
Crossed molecular beam studies of the reactions of oxygen and fluorine atoms
[AD-A153302] 17 p2921 N85-28006

POLYBUTADIENE
Diblock copolymers of polystyrene/1,2 polybutadiene and polystyrene/polybutene-1: Molecular structure, morphology and mechanical properties
[AD-A144980] 01 p0033 N85-10201
Synthesis and characterization of a 1,4 Polybutadiene/Isotactic polypropylene block copolymer
[AD-A148199] 06 p1133 N85-17142
Deuterium isotope effect on the compatibility between polystyrene and polybutadiene
[AD-A148551] 06 p1134 N85-17145
LL-100: A new polybutadiene (resin system for radome applications)
[AD-P004368] 12 p1826 N85-21462
Effects of triazine components on physicochemical properties of polybutadiene: urethane block copolymers
13 p2014 N85-22635

POLYCARBONATES
Properties of miscible polymer blends
[AD-A147090] 07 p0931 N85-15903
Development of a heterogeneous laminating resin system
[NASA-CR-172459] 09 p1288 N85-18089
Chain dynamics and structure property relation in high impact strength polycarbonate plastic
[AD-A152011] 15 p2519 N85-25531
Laminated thermoplastic radome
[AD-D011664] 18 p3079 N85-29045

POLYCHLORINATED BIPHENYLS
Polychlorinated biphenyls (PCBs) in transit system electrical equipment
[PB84-222207] 01 p0045 N85-10291
Soil extraction kit
[AD-D011736] 22 p3742 N85-33190

POLYCRYSTALS
Life prediction and constitutive models for anisotropic materials
02 p0144 N85-10976
Surface chemistry of palladium
[DE84-014572] 02 p0173 N85-11163
The current status of diamond and cubic boron nitride composites
02 p0178 N85-11194
DOE/SERI polycrystalline thin-film photovoltaic research
[DE84-004516] 02 p0223 N85-11464
High temperature deformation of hot-pressed polycrystalline orthoenstatite
[NASA-CR-174026] 02 p0285 N85-11861
Development of a polysilicon process based on chemical vapor deposition of dichlorosilane in an advanced Siemen's reactor
[NASA-CR-174148] 04 p0483 N85-13083
Elastic wave propagation through polycrystals
[DE84-016772] 04 p0556 N85-13554
Process research of polycrystalline silicon material (PROPSM)
[NASA-CR-174130] 05 p0619 N85-13962
Electron channeling and EBIC studies of polycrystalline silicon sheets
[DE84-004515] 05 p0670 N85-14309
Analysis of spin echo signals in multi-pulse experiment
06 p0792 N85-15065
Process Research On Polycrystalline Silicon Material (PROPSM)
06 p0830 N85-15276
Subtractively normalized interfacial Fourier transform infrared spectroscopy of difluorobenzene adsorbed at polycrystalline platinum electrodes
[AD-A148660] 08 p1123 N85-17080
The fundamentals of dislocation transport of hydrogen in bcc iron
[AD-A148143] 08 p1129 N85-17117
The effect of tantalum on the structure/properties of two polycrystalline nickel-base superalloys: B-1900 + Hf MAR-M247
[NASA-CR-174847] 09 p1294 N85-18127
Process Research on Polycrystalline Silicon Material (PROPSM)
[NASA-CR-175461] 10 p1509 N85-19523
Quaternary narrow-band semiconductors (HgTe)x (InSb)1-x for far-infrared detectors
[AD-A149350] 10 p1562 N85-19852
Effect of macrostructure on durability of polycrystalline graphite
11 p1605 N85-20091
Development of a polysilicon process based on chemical vapor deposition of dichlorosilane in an advanced Siemen's reactor
[NASA-CR-174445] 11 p1672 N85-20532
Summary of recent research on mechanical behavior of polycrystalline solids
[DE85-004601] 12 p1942 N85-22199
Texture independent determination of residual stress in polycrystalline aggregates using Rayleigh waves
[AERE-R-11483] 12 p1943 N85-22203
High sheet resistance, arsenic implanted polycrystalline silicon for integrated circuit resistors
[DE85-004355] 13 p2065 N85-22902
The cyclic stress-strain behavior of nickel-base superalloy poly- and single crystals
14 p2254 N85-23969
Solar cells based on polycrystalline silicon with isothermal potential barriers along grain boundaries
14 p2275 N85-24091
Angular dependence of the Rayleigh-surface wave velocity in polycrystalline metals with small anisotropy
[AERE-R-11595] 15 p2509 N85-25476
Design of ductile polycrystaline Ni3Al alloys
[DE85-005572] 15 p2511 N85-25491
Summary of recent investigations of the mechanical properties of polycrystalline solids
[DE85-006776] 15 p2511 N85-25492
An analysis of the economics of turning titanium alloys with polycrystalline diamond tools
15 p2567 N85-25841
Process Research on Polycrystalline Silicon Material (PROPSM)
[NASA-CR-175761] 15 p2587 N85-25951
Thin-film polycrystalline silicon research
[DE85-002908] 15 p2663 N85-26434
Secondary ion mass spectrometry studies of solids and surfaces
[AD-A151744] 16 p2745 N85-26939
Mechanical properties of polycrystalline alpa titanium
[BLL-BISI-TRANS-21923-(9022.06)] 17 p2924 N85-28029
Semicrystalline casting process development and verification
[DE85-007695] 18 p3081 N85-29058
Electrohydrodynamic process for the production of large area polycrystalline silicon sheet
[DE85-008781] 19 p3261 N85-30225
Photoelectronic properties of zinc phosphide crystals and heterojunctions
[DE85-008777] 19 p3307 N85-30501
Neutron scattering study of the heavy fermion system UBe-13
[DE85-010955] 19 p3356 N85-30904
Compositional analysis of silicon
20 p3480 N85-31626
Surface passivation and junction formation using low energy hydrogen implants 20 p3480 N85-31628
The effect of diffusive hydrogen segregation on fracture of polycrystalline nickel
[AD-A155238] 21 p3567 N85-32186
Electrical and mechanical properties of intercalated graphite fibers
[AD-A155560] 21 p3570 N85-32205
Thermoelectric properties of beta-boron and some boron compounds
[DE85-011978] 21 p3582 N85-32270
Basic ice nucleation mechanisms on mono and microcrystals and ice forming nuclei. Theoretical analysis and experimental results achieved in the laboratory over the past ten years: Review paper
21 p3642 N85-32629
Mirror reflection of charged particles from + amorphous and polycrystalline surfaces 21 p3690 N85-32927
The development and evaluation of point defect models for the growth of passive films on single crystal, polycrystalline, and amorphous metal surfaces
[AD-A154685] 21 p3709 N85-33023
Method for preparing Pb-(beta)-aluminum ceramic
[DE85-011665] 22 p3752 N85-33256
Aluminum work function: Effect of oxidation, mechanical scraping and ion bombardment
[NASA-TM-87079] 23 p3915 N85-34265
Low noise polycrystalline semiconductor resistors by hydrogen passivation
[AD-D011721] 23 p3927 N85-34338
Noise in sodium beta alumina crystals
[AD-A156025] 24 p4161 N85-35796

POLYESTER RESINS
System for rapid repair of damaged airfield runways
[AD-D011325] 07 p0909 N85-15754
Properties of miscible polymer blends
[AD-A147090] 07 p0931 N85-15903
The synthesis and characterization of Poly(Oxy(2-Methyl-1,3-Phenylene) Methyl-1,3 -Phenylene) Oxyterephthaloyl)Oxy
[AD-A148269] 06 p1133 N85-17143
Interactions between F-111 fuselage fuel tank sealants. Part 2: Variation in performance properties of polysulfides after contact with polyester degradation products
[AD-A149777] 12 p1812 N85-21368
Scale-up of vanadium trineodecanoate
[AD-A149935] 12 p1813 N85-21370
Fluorinated polyesters
[AD-D011611] 16 p2753 N85-26988

POLYESTERS
Synthesis and characterization of unique liquid crystalline block copolyesters. A proposal for a polymer research center at the Atlanta University
[AD-A147280] 07 p0932 N85-15907
Stabilized unsaturated polyesters
[NASA-CASE-NPO-16103-1] 18 p3078 N85-29043
Polyesters: A review of the literature on products of combustion and toxicity
[NBSIR-85-3139] 20 p3433 N85-31296
Polymerizable ultraviolet stabilizers
21 p3606 N85-32406
Impact fracture mechanism of polymer plates containing a heavy inner material 23 p3908 N85-34215

POLYETHER RESINS
NT POLYMETHYL METHACRYLATE
Optimization of the injection process for thermostatic polyether-ether-ketone (Peek) thermoplastics reinforced with short carbon fibers
[SNIAS-842-422-102] 04 p0480 N85-13062
Structure-property relationships in thermoplastic elastomers. Part 1: Segmented polyether-polyurethanes
[AD-A148043] 06 p1133 N85-17138
Characterization of novel binders based on energetic thermoplastic elastomers
[AD-A148993] 10 p1451 N85-19139
Crystallinity determination by curvefit procedure for a semi-crystalline polymer
[NASA-TM-86412] 15 p2517 N85-25520
Phenoxy resins containing pendent ethynyl groups and cured resins obtained therefrom
[NASA-CASE-LAR-13262-1] 18 p3068 N85-28973
Mechanical properties of aligned short carbon fiber reinforced PES and PI laminates
[ESA-TT-898] 20 p3422 N85-31240

POLYETHYLENE TEREPHTHALATE
Description and characterization of deuterated polymers for the analysis with neutron scattering
03 p0431 N85-12746

Prediction of the long term stability of polyester-based recording media
[PB85-160133] 14 p2262 N85-24019

POLYETHYLENES
NT POLYETHYLENE TEREPHTHALATE
Nuclear Magnetic Resonance of Polymeric Materials
[AD-A145078] 01 p0032 N85-10192
13C and 1H NMR (Nuclear Magnetic Resonance) studies of solid polyolefines
[AD-P003909] 01 p0032 N85-10195
Equibiaxial extension of two polymer melts: Polystyrene and low density polyethylene
[AD-A144893] 01 p0032 N85-10200
Small angle neutron scattering (SANS) on polymer-oligomer mixtures and on deformed polyethylene melts 03 p0432 N85-12750
Apparatus for measuring dielectric characteristics of polymer materials in millimetric range of wavelengths at 4.2-300 K temperatures 06 p0788 N85-15032
Characterization of porosity in porous polymer implant materials
[PB85-119960] 10 p1454 N85-19161
Structural basis for the mechanical properties of polyethlenes
[PB85-149771] 11 p1613 N85-20142
Characterization and optimization of polyethylene resins and gas pipe
[PB85-118511] 12 p1815 N85-21382
Characterization of poly(ethylene oxide) drawn by solid state extrusion
[AD-A150967] 14 p2260 N85-24006
Uniaxial orientation of linear low density polyethylene
[AD-A151037] 14 p2261 N85-24009
Plastic deformation of crystalline polymers
[AD-A152090] 16 p2755 N85-26999
Properties of polyethylene gas piping materials
[PB85-187045] 18 p3082 N85-29068
Polyethylene imine-metal salt solid electrolyte
[AD-D011678] 19 p3305 N85-30485
Orientation and strength of semi-crystalline polymers
20 p3432 N85-31294
Interaction of solutes with stretched polymers
[AD-A154662] 21 p3569 N85-32196
Electron-donor dopant, method of improving conductivity of polymers by doping therewith, and a polymer so treated
[DE85-011640] 22 p3752 N85-33257
Polyethylene solidification of low-level wastes
[DE85-012568] 22 p3843 N85-33799
Method for making a low density polyethylene waste form for safe disposal of low level radioactive material
[DE85-006401] 23 p3920 N85-34292
Sensitivity of single and multiple cosmic ray neutrons to the surrounding medium in a lead-free monitor
[SH-9.1-10] 23 p4051 N85-35125
Structure and properties of polyethylene films used in heavy lift balloons
[NASA-CR-176227] 24 p4083 N85-35306

POLYGONS
NT RECTANGLES
Classical free-streamline flow over a polygonal obstacle
[NASA-CR-172448] 01 p0046 N85-10301
Origin of Martian polygonal terrain: Preliminary results
13 p2191 N85-23591
Chemical applications of topology and group theory. 17: An information theoretical approach to polyhedral symmetry
[AD-A152821] 17 p2919 N85-27995
Fourier coding and reconstruction of complicated contours
[REPT-84-39] 17 p3022 N85-28691
Shadow volumes for non-planar polygons
23 p3965 N85-34580
Reachable grasps on a polygon: The convex rope algorithm
[AD-A155913] 24 p4138 N85-35647

POLYHEDRONS
NT PARALLELEPIPEDS
NT PYRAMIDS

POLYIMIDE RESINS
Thermal deformation measurements of heat-resistant structural materials for aircraft by electro optical displacement transducer
[NAL-TR-810] 03 p0325 N85-12092
Polyimide resin characteristics, test
[DGT-24.322] 04 p0479 N85-13049
Flame resistant fibrous materials development
[NASA-CR-167817] 07 p0920 N85-15827
Phosphorus-containing imide resins
[NASA-CASE-ARC-11368-2] 12 p1809 N85-21347
Chemical approach for controlling nadimide cure temperature and rate with maleimide
[NASA-CASE-LEW-13770-3] 12 p1809 N85-21350
Chemical approach for controlling nadimide cure temperature and rate with maleimide
[NASA-CASE-LEW-13770-4] 12 p1810 N85-21351
Chemical approach for controlling nadimide cure temperature and rate
[NASA-CASE-LEW-13770-5] 12 p1810 N85-21352
Development and study of two-matrix glass fiber composite with increased transverse deformation
13 p2027 N85-22700
Adsorption behaviour of nitrogen compounds on to porous polymer beads and applications to atmospheric sampling
[BLL-DRIC-TRANS-7399-(3623.66)]
13 p2036 N85-22753
The effects of water and hydrogen on materials used in integrated circuit packages
[AD-A151893] 15 p2518 N85-25529
Chemical control of nadimide cure temperature and rate
[NASA-CASE-LEW-13770-2] 18 p3069 N85-28982
Chemical approach for controlling nadimide cure temperature and rate
[NASA-CASE-LEW-13770-6] 19 p3232 N85-30039
Adhesive evaluation of LARC-TPI and a water-soluble version of LARC-TPI
[NASA-TM-86428] 19 p3248 N85-30136
Graphite/PMR polyimide composites with improved toughness
[NASA-TM-87081] 21 p3561 N85-32148
Permeation of mixed penetrants through glassy polymer membranes
[AD-A155605] 21 p3570 N85-32207
Rigid zeolite containing polyurethane foams
[DE85-006406] 23 p3919 N85-34286

POLYIMIDES
NT KAPTON (TRADEMARK)
Thermoplastic/melt-processable polyimides
04 p0466 N85-12961
Effect of substituted phenylnadimides on processing and properties of PMR polyimide composites
[NASA-TM-86902] 06 p0770 N85-14929
Evaluation of colorless polyimide film for thermal control coating applications
[NASA-TM-86341] 07 p0930 N85-15894
The wear of small polyacetal and polymide gears in vacuum — spacecraft gears
[ESA-ESTL-058] 08 p1169 N85-17374
Tribological properties of graphite-fiber-reinforced, partially fluorinated polyimide composites
[NASA-TM-86926] 09 p1298 N85-18153
Characterization of a thermoplastic polyimidesulfone
[NASA-TM-86358] 10 p1450 N85-19135
Process for preparing solvent resistant, thermoplastic aromatic poly(imidesulfone)
[NASA-CASE-LAR-12858-2] 11 p1610 N85-20124
Process for preparing essentially colorless polyimide film containing phenoxy-linked diamines
[NASA-CASE-LAR-13353-1] 11 p1611 N85-20128
Oxidation protection coatings for polymers
[NASA-CASE-LEW-14072-1] 11 p1611 N85-20129
Elastomer toughened polyimide adhesives — bonding metal and composite material structures for aircraft and spacecraft
[NASA-CASE-LAR-12775-2] 12 p1809 N85-21349
Fire resistant polymers based on 1-(diorgano oxyphosphonyl)methyl-2,4- and 2,6-diamino benzenes
[NASA-CASE-ARC-11512-2] 12 p1811 N85-21362
Study of character of adhesive interaction and breaking of polyimid-aluminum foil junction during process of hardening 13 p2014 N85-22637
Spectroscopic analysis of radiation-generated changes in tensile properties of a polyetherimide film
[NASA-TP-2429] 15 p2502 N85-25435
Ion beam sputter-deposited thin film coatings for protection of spacecraft polymers in low Earth orbit
[NASA-TM-87051] 19 p3248 N85-30137
Mechanical properties of aligned short carbon fiber reinforced PES and PI laminates
[ESA-TT-898] 20 p3422 N85-31240
Synthesis and characterization of copolyimides with varying flexibilizing groups
[NASA-TM-86416] 20 p3433 N85-31296
STPI/LARC: A 200 deg C polyimide adhesive
[NASA-TM-86447] 20 p3433 N85-31297
Graphite/PMR polyimide composites with improved toughness
[NASA-TM-87081] 21 p3561 N85-32148
Fire-resistant phosphorus containing polyimides and copolyimides
[NASA-CASE-ARC-11522-2] 23 p3918 N85-34280

POLYISOBUTYLENE
The role of molecular diffusion in the adhesion of elastomers
[AD-A145576] 02 p0186 N85-11245

POLYISOPRENES
Plastic deformation of crystalline polymers
[AD-A152090] 16 p2755 N85-26999
Orientation and strength of semi-crystalline polymers
20 p3432 N85-31294

POLYMER CHEMISTRY
Method of obtaining polybenzimidazopyrrolones
[AD-A145140] 01 p0018 N85-10108
Method of obtaining heterocyclic polymers
[AD-A145127] 01 p0033 N85-10202
A new heat-resistant polymer from dimer diamine bismaleimide. Part 1: Preparation and free radical cure of dimer diamine bismaleimide
[AD-A145664] 02 p0186 N85-11247
The concept of solid solvent as processing aid
[AD-A146556] 06 p0771 N85-14934
Polyphosphazene solid electrolytes
[AD-A147008] 07 p0931 N85-15902
Rubber-modified epoxies. 1: Cure, transitions, and morphology
[AD-A147377] 07 p0932 N85-15908
Polymer electrolytes: An investigation of some poly (N-propylaziridine)/lithium salt compositions
[RAE-TR-84036] 08 p1131 N85-17130
Elastomers and other organic composites
[AD-A147624] 08 p1131 N85-17131
Stable polymeric carbon radicals. Part 2: Attempts at the preparation of polyradicals of the triphenylmethyl type linked by P-phenylene units
[NASA-TM-77799] 10 p1450 N85-19134
Polymer electrolytes: An investigation of some poly (N-propylaziridine)/lithium salt compositions
[AD-A149444] 10 p1452 N85-19146
Polymers and macromolecules
[DE85-003176] 10 p1454 N85-19160
USSR report: Chemistry
[JPRS-UCH-85-001] 13 p2013 N85-22629
Effect of alternative aging and accident simulations on polymer properties
[DE85-002642] 13 p2037 N85-22762
Abstracts of the 36th Southeastern Regional Meeting of the American Chemical Society
[AD-A151506] 15 p2496 N85-25394
Separating polymer solutions using high pressure LCST Lower Critical Solution Temperature) phenomena
[AD-A151538] 15 p2518 N85-25526
Polyaromatic ether-sulfone-keytones with fluoro-substituted-p-cyclophane units as cross-linking sites
[AD-D011649] 17 p2933 N85-28105
New polymers for composites: A summary of research on polystyrylpyridines
[NASA-CR-175886] 17 p2933 N85-28106
The synthesis and structure of polyphosphazenes
[AD-A153134] 17 p2934 N85-28112
Model for the growth of fractal silica polymers
[DE85-007884] 17 p2935 N85-28115
Chemical approach for controlling nadimide cure temperature and rate
[NASA-CASE-LEW-13770-6] 19 p3232 N85-30039
Mechanical modification of friction surfaces of aluminum alloys by friction transfer 19 p3241 N85-30097
Method for production of ceramic oxide and carbide bodies by polymer inclusion and decomposition
[DE85-011668] 19 p3250 N85-30152
Electrophoretic mobility of cells in a vertical Ficoll gradiant 20 p3499 N85-31753
Bubble dynamics in polymer solutions undergoing shear
[AD-A154575] 21 p3568 N85-32193
Importance and significance of transition temperatures
[AD-A154871] 21 p3569 N85-32198

POLYMER MATRIX COMPOSITES
Development of new and improved polymer matrix resin systems, phase 1
[NASA-CR-166595] 01 p0017 N85-10104
Friction and wear of polymers and polymer composite materials 01 p0054 N85-10361
Tough Composite Materials
[NASA-CP-2334] 04 p0463 N85-12941
Characterization of interlaminar crack growth in composites with the double cantilever beam specimen
04 p0463 N85-12942
Composite materials characterization and development at AFWAL 04 p0464 N85-12944
Investigation of toughened neat resins and their relations to advanced composite mechanical properties
04 p0464 N85-12949
Effect of polymer matrix on properties of fibers obtained by caking polymer dispersions 06 p0762 N85-14875
Investigation of the relations between resin and advanced composite mechanical properties. Volume 2: Appendices
[NASA-CR-172303-VOL-2] 06 p0763 N85-14880

Unidirectional fibers and polyurethane elastomer matrix based composites synthesis and properties
[NASA-TM-77501] 07 p0920 N85-15826
Characterization and selection of polymer materials for binary munitions storage. Part 2: Characterization of LLDPE resins
[AD-A148324] 08 p1133 N85-17144
New method for studying surface crack growth in laminated polymer composite materials
11 p1598 N85-20051
Electrical conduction in polymer dielectrics
13 p1996 N85-22514
Interlaminar fracture toughness in resin matrix composites
[AD-A150565] 13 p2015 N85-22640
Outlook for polymer composite materials
15 p2497 N85-25403
Research, development of composite materials described 15 p2497 N85-25404
Effect of counterface material type and its topography on the tribological properties of polyimide composites
[NASA-TM-87036] 16 p2754 N85-26993
Accuracy of the calculated stress field around a craze
[DE85-005520] 16 p2801 N85-27272
Experiments and micromechanical models for creep-rupture in polymer matrix composites
[DE85-008533] 17 p2935 N85-28118
Structure-property relationships in polymeric matrix materials
[AD-A153929] 18 p3080 N85-29050
Transversely reinforced piezoelectric composites
[AD-D011676] 19 p3260 N85-30214
Implementation of polymer impregnation as a bridge deck sealant
[PB85-185718] 22 p3753 N85-33265
Conductor-polymer composite electrode materials
[DE85-005766] 23 p3920 N85-34293

POLYMER PHYSICS
Equibiaxial extension of two polymer melts: Polystyrene and low density polyethylene
[AD-A144893] 01 p0032 N85-10200
Transport properties of multiphase systems
[DE84-015560] 02 p0173 N85-11159
Electrically conducting complexes of poly(3,6-n-methylcarbazolyl methylene)
[AD-A147884] 07 p0933 N85-15914
Critical events in inelastic deformation of glassy polymers in adsorptive medium
13 p2014 N85-22634
Effects of triazine components on physicochemical properties of polybutadiene: urethane block copolymers
13 p2014 N85-22635
Theory of relaxation processes in decomposing polymer materials during high-intensity convective heating
13 p2028 N85-22710
High performance mixed bisimide resins and composites based thereon
[NASA-CASE-ARC-11538-1-SB]
19 p3231 N85-30033
Importance and significance of transition temperatures
[AD-A154871] 21 p3569 N85-32199

POLYMERIC FILMS
NT KAPTON (TRADEMARK)
Optical constant determination of thin polymer films in the infrared
[AD-A145669] 02 p0287 N85-11877
Photophysical studies of triplet exciton processes in pure polymer films
[DE84-016258] 05 p0620 N85-13965
Synthesis of film-forming electron-accepting polymers
[AD-A146430] 06 p0771 N85-14931
The replacement of precious metal thick film inks using conductive polymer technology. Phase 1: Feasibility study
[AD-A147814] 07 p0933 N85-15913
Estimation of the rate of electron transfers between 2 contacting polymer surfaces
[AD-A148416] 08 p1122 N85-17072
Potential dependence of electrical conductivity and chemical charge storage of poly(pyrrole) films on electrodes
[AD-A148513] 08 p1122 N85-17075
Electrochemistry of polymer films. Applications to chemical analysis and energy conversion
[AD-A147737] 08 p1132 N85-17136
The kinetics of electron transfer reactions in and at films of electroactive polymers
[AD-A148597] 08 p1134 N85-17149
Mechanisms of gas permeation through polymer membranes
[DE84-017423] 09 p1293 N85-18117
Evaluation and prediction of long-term environmental effects of nonmetallic materials
[NASA-CR-171353] 10 p1450 N85-19137
Water absorption and conductivity in poly(ethylene oxide)-lithium tetrafluoroborate films
[AD-A147969] 10 p1450 N85-19136
Process for preparing essentially colorless polyimide film containing phenoxy-linked diamines
[NASA-CASE-LAR-13353-1] 11 p1611 N85-20128
Effect of interfacial characteristics of metal clad polymeric substrates on electrical high frequency interconnection performance
[NASA-TM-86948] 11 p1624 N85-20223
Mass analysis of neutral particles and ions released during electrical breakdowns on spacecraft surfaces
[NASA-CR-175585] 12 p1793 N85-21250
Process for preparing highly optically transparent-colorless armomatic polyimide film
[NASA-CASE-LAR-13351-1] 12 p1811 N85-21380
Effect of ultraviolet radiation on transparent polymer films as determined using in situ FTIR-RA spectroscopy. Volume 1: Photodegradation of transparent polymer films
[DE84-013039] 12 p1814 N85-21377
Polymeric electrolytes for ambient temperature lithium batteries
[DE85-001032] 12 p1835 N85-21518
Optimal design efforts in Shanghai described
13 p1972 N85-22386
Mass spectra of neutral particles released during electrical breakdown of thin polymer films
13 p1996 N85-22511
Study of character of adhesive interaction and breaking of polyimid-aluminum foil junction during process of hardening 13 p2014 N85-22637
Electrostatic forming and testing of polymer films on a 16-foot diameter test fixture
[NASA-TM-86328] 13 p2063 N85-22885
Uniaxial orientation of linear low density polyethylene
[AD-A151037] 14 p2261 N85-24009
Piezoelectric and electrostatic polymeric transducers for acoustic emission detection
[AD-A150683] 14 p2306 N85-24272
Monte Carlo lattice models for adsorbed polymer conformation
[NASA-TP-2453] 14 p2426 N85-24961
Investigation of the MBE growth of InSb and novel quantum well structures
[AD-A151014] 14 p2427 N85-24969
Finger materials for air cushion vehicles. Volume 1: Flexible coatings for finger materials
[AD-A151436] 15 p2522 N85-25545
Electrochemistry of polymer films not immersed in solution: Electron transfer on an ion budget
[AD-A152989] 17 p2920 N85-27998
Photophysical studies of triplet exciton processes in pure polymer films
[DE85-006571] 18 p3080 N85-29056
Silvered polymer reflectors
[DE85-006782] 18 p3130 N85-29384
Mass spectrometer based gas permeation apparatus
[DE85-011176] 19 p3273 N85-30299
Inhibited anticorrosion protection of automotive steel strip in the NLMK
[BLL-M-36250-(5826.4)] 20 p3430 N85-31274
Radiation-hardened polymeric films
[DE85-011636] 22 p3752 N85-33259
Development and demonstration of a spiral-wound thin-film composite membrane system for the economical production of oxygen-enriched air, phase 4
[DE85-012380] 23 p3920 N85-34288
Structure and properties of polyethylene films used in heavy lift balloons
[NASA-CR-176227] 24 p4083 N85-35306

POLYMERIZATION
NT COPOLYMERIZATION
NT VINYL COPOLYMERS
Method of obtaining polychalcones
[AD-A145051] 01 p0018 N85-10107
Preparation of large-particle-size monodisperse latexes in space: The STS-3, STS-4, and STS-7 mission results
02 p0151 N85-11021
The concept of doping of conducting polymers. The role of reduction potentials
[AD-A145480] 02 p0186 N85-11243
Microstructure development in polymers
[AD-A145960] 03 p0337 N85-12170
Aliphatic-aromatic heterocyclics as potential thermoplastics for composite matrices
04 p0466 N85-12962
Constituent properties and interrelationships
04 p0467 N85-12964
Influence of relaxation on the mechanical characteristics of a carbon-epoxy composite. Report no. 45.427/1
04 p0468 N85-12980
USSR report: Chemistry
[JPRS-UCH-84-012] 06 p0761 N85-14865
Polymerization and halogen scrambling behavior of phenyl-substituted cyclotriphosphazenes
[AD-A146366] 06 p0771 N85-14930
Boron-nitrogen polymers. 1: Mechanistic studies of borazine pyrolyses
[AD-A146470] 06 p0771 N85-14933
The concept of solid solvent as processing aid
[AD-A146556] 06 p0771 N85-14934
Preparation of polymers of functionalized acetylenes
[AD-D011296] 06 p0771 N85-14935
Optimization of the die entrance shape for polymeric extrusion
[DE85-001588] 06 p0772 N85-14937
Instruments for characterization of carbon black and polymers
[AD-A146475] 06 p0810 N85-15146
Pseudo-p-1,2,2,9,9,10,10-octofluoro (2,2)-p-cyclophane bis-acid chloride
[AD-D011393] 07 p0919 N85-15818
Gradient polymers
[AD-A146836] 07 p0931 N85-15900
Synthesis and characterization of unique liquid crystalline block copolyesters. A proposal for a polymer research center at the Atlanta University
[AD-A147280] 07 p0932 N85-15907
New synthesis of phosphazene polymers
[AD-A147567] 07 p0933 N85-15910
Elastomers and other organic composites
[AD-A147624] 08 p1131 N85-17131
Study of reaction kinetics and development of elastic properties in network polymerization systems by the impulse technique
[AD-A148187] 08 p1133 N85-17141
Applicability of linear elastic fracture mechanics to fatigue in polymers and short-fiber composites
09 p1298 N85-18152
Mechanism and process of flocculation by polymeric flocculant 09 p1303 N85-18185
Electromagnetic processing of materials
[AD-A148604] 09 p1311 N85-18241
Stable polymeric carbon radicals. Part 2: Attempts at the preparation of polyradicals of the triphenylmethyl type linked by P-phenylene units
[NASA-TM-77799] 10 p1450 N85-19134
Method for making heterocyclic block copolymers
[AD-D011446] 10 p1451 N85-19143
Characterization of acetylene-terminated resin cure states
[AD-A149463] 10 p1452 N85-19148
(Vinyloxy)chlorocyclotriphosphazenes
[AD-D011471] 10 p1453 N85-19152
SANS studies of polymers
[DE85-002471] 11 p1612 N85-20134
Characterization of the network structure of a hardened epoxy resin (TGMDA/DDS system)
[ONERA-RT-3/3346-M] 11 p1613 N85-20140
Status of specific FRG high tech research funded by BMFT 11 p1618 N85-20181
A brief review of the technology of microemulsions and other micellar systems
[AD-A149759] 12 p1800 N85-21289
Phthalocyanine polymers
[NASA-CASE-ARC-11413-1] 12 p1809 N85-21348
Fire resistant polymers based on 1-(diorgano oxyphosphonyl)methyl-2,4- and 2,6-diamino benzenes
[NASA-CASE-ARC-11512-2] 12 p1811 N85-21362
Fire and heat resistant laminating resins based on maleimido and citraconimido substituted 1-(diorgano oxyphosphonyl)methyl-2,4- and 2,6-diaminobenzenes
[NASA-CASE-ARC-11533-1] 12 p1812 N85-21364
Rheology of dissemination
[AD-A150006] 12 p1813 N85-21373
Plasticizer system for propellant compositions
[AD-D011516] 12 p1817 N85-21394
Amine salts as bonding agents
[AD-D011543] 12 p1817 N85-21396
LL-100: A new polybutadiene (resin system for radome applications)
[AD-P004366] 12 p1826 N85-21462
Synthesis and characterization of poly(vinylidene fluoride)
[AD-A150291] 13 p2037 N85-22759
Chiral polymers
[AD-A150366] 13 p2037 N85-22760
The mechanisms of phenylacetylene polymerization by molybdenum and titanium initiators
[AD-A150993] 14 p2260 N85-24007
Compressive strength of epoxy resin chocks subjected to elevated temperatures
[AD-A152018] 15 p2519 N85-25532
Electrical research on solar cells and photovoltaic materials
[NASA-CR-175899] 15 p2585 N85-25935
Oil resistant silicone elastomers
[AD-131523] 16 p2753 N85-26987

Formulation/cure technology for ultrahigh molecular weight silphenylene-siloxane polymers
[NASA-TP-2476] 16 p2753 N85-26990

Synthesis of phenols from metal-carbynes and diynes
[AD-A151913] 16 p2754 N85-26997

Theoretical studies of solar-pumped lasers
[NASA-CR-175801] 16 p2789 N85-27206

NBS (National Bureau of Standards) research reports
[PB85-127421] 16 p2879 N85-27764

Polyaromatic ether-sulfone-keytones with fluoro-substituted-p-cyclophane units as cross-linking sites
[AD-D011649] 17 p2933 N85-28105

Preparation of polystryene latex particles in a rotating reactor
[NASA-CR-171475] 17 p2933 N85-28108

Model for the growth of fractal silica polymers
[DE85-007884] 17 p2935 N85-28115

Light scattering and spectroscopic studies of polymerization processes
[AD-A153407] 18 p3069 N85-28984

Stabilized unsaturated polyesters
[NASA-CASE-NPO-16103-1] 18 p3078 N85-29043

Processable and stable conductive polymers
[AD-D011684] 19 p3249 N85-30143

Magnetically-localizable, polymerized lipid vesicles and method of disrupting same
[AD-D011686] 19 p3249 N85-30144

Molecular toxicology of chromatin: The role of Poly(ADP-Ribose) in gene control
[AD-A154415] 19 p3327 N85-30611

Development of a lithium secondary battery separator
20 p3444 N85-31378

Graphite/PMR polyimide composites with improved toughness
[NASA-TM-87081] 21 p3561 N85-32148

Introduction of structural variations into oxide polymers and their effect on sintering and crystallization
[AD-A155597] 21 p3570 N85-32206

Three-dimensional photochemical machining with lasers
[AD-A154711] 21 p3591 N85-32320

Polymerizable ultraviolet stabilizers
21 p3608 N85-32406

POLYMERS

Method of obtaining polychalcones
[AD-A145051] 01 p0018 N85-10107

Nuclear Magnetic Resonance of Polymeric Materials
[AD-A145078] 01 p0032 N85-10192

Dynamics of polymers in solution and melts
[AD-P003907] 01 p0032 N85-10193

NMR (Nuclear Magnetic Resonance) and macromolecular migration in a melt or in concentrated solutions
[AD-P003906] 01 p0032 N85-10194

13C and 1H NMR (Nuclear Magnetic Resonance) studies of solid polyolefines
[AD-P003909] 01 p0032 N85-10195

A determination of the photochemical quantum yields from 2 excited triplet states of biacetyl using holography
[AD-A145081] 01 p0050 N85-10326

An investigation of the suitability of using a Sieglaff-McKelvey high shear rate melt rheometer for the measurement of low viscosity polymer solutions
[AD-A146275] 03 p0338 N85-12174

Optimizing conductive polymer compounds
[BMFT-FB-T-84-145] 03 p0338 N85-12177

Insulating polymer concrete
[DE84-017239] 04 p0480 N85-13057

Determination of halogens and sulfur in organic compounds and polymers by combustion-ion chromatography
[DE84-016186] 05 p0614 N85-13921

USSR report: Chemistry
[JPRS-UCH-84-012] 06 p0761 N85-14865

Low temperature synthesis of polycaproamide copolymers grafted with polydimethylaminoethylmethacrylate
06 p0761 N85-14868

Synthesis of reinforced composite threads based on polymer mixtures 06 p0761 N85-14869

Polymer-carbon black interaction in electrically conducting fiber-forming composites
06 p0762 N85-14875

Effect of polymer matrix on properties of fibers obtained by caking polymer dispersions 06 p0762 N85-14876

Encapsulation materials and processing
06 p0830 N85-15269

Polymer-metal interface bond stability
06 p0830 N85-15272

Pseudo-p-1,2,2,9,9,10,10-octofluoro (2,2)-p-cyclophane bis-acid chloride
[AD-D011393] 07 p0919 N85-15818

Moisture absorbing anti-arcing coating and method for applying same
[AD-D011310] 07 p0932 N85-15904

New synthesis of phosphazene polymers
[AD-A147567] 07 p0933 N85-15910

Electrically conducting complexes of poly(3,6-n-methylcarbazolyl methylene)
[AD-A147884] 07 p0933 N85-15914

Mechanisms of gas permeation through polymer membranes
[DE84-017423] 09 p1293 N85-18117

Tribological properties of graphite-fiber-reinforced, partially fluorinated polyimide composites
[NASA-TM-86926] 09 p1296 N85-18153

Effective antireflection coatings of transparent polymeric materials by gas-phase surface fluorination
[DE84-013027] 09 p1385 N85-18711

On shrinkage and molecular extension
[AD-A149100] 10 p1451 N85-19144

Microstructural analysis of ion containing polymers
[DE85-001594] 10 p1453 N85-19157

Overview of major Swedish institutions in polymer research 11 p1592 N85-20014

Low temperature deposition of nickel films
[AD-D011568] 12 p1805 N85-21319

Control of electronic, magnetic and optical properties of doped polyacetylene conductors
[AD-A150117] 12 p1814 N85-21375

Polymer intermediates from limonene (follow-up project)
[BMFT-FB-T-84-243] 12 p1814 N85-21380

Research program on the effect of pressure on the mechanical properties of polymers, part 2
[DE85-000995] 13 p2037 N85-22761

HREELS and Auger studies of conducting polymers
[DE85-004541] 13 p2038 N85-22764

The replacement of precious metal thick film inks using conductive polymer technology
[AD-A152002] 16 p2749 N85-26965

Process for clarification of water
[DE85-007864] 17 p2923 N85-28023

Application of scattering methods to the studies of the structure of polymer blends
[IFPR-13/1984] 17 p2933 N85-28104

Development of concrete polymer materials
[DE85-005957] 17 p2934 N85-28114

Experiments and micromechanical models for creep-rupture in polymer matrix composites
[DE85-009533] 17 p2935 N85-28118

Polymer Research at Synchrotron Radiation Sources: Symposium Proceedings
[DE85-008466] 18 p3081 N85-29062

Synthesis and characterization of novel polymers from non-petroleum sources for use in enhanced oil recovery
[DE85-010922] 19 p3250 N85-30151

Polyethylene imine-metal salt solid electrolyte
[AD-D011678] 19 p3305 N85-30485

Orientation and strength of semi-crystalline polymers
20 p3432 N85-31294

Standard procedures to be used in specifying basic properties of plastics and polymers
[NPL-DMA(A)-99] 20 p3433 N85-31295

Synthesis and characterization of copolyimides with varying flexibilizing groups
[NASA-TM-86416] 20 p3433 N85-31296

EVA-glass interface bond stability
21 p3606 N85-32408

Process for improving moisture resistance of epoxy resins by addition of chromium ions
[NASA-CASE-LAR-13226-1] 23 p3919 N85-34282

Degradation mechanisms and accelerated aging test design
[TI85-003251] 23 p3940 N85-34420

Development of an NBS (National Bureau of Standards) polymer gage for dynamic soil stress measurement
[PB85-208494] 24 p4118 N85-35526

POLYMETHYL METHACRYLATE

Mechanochemical reactions of polymethyl methacrylate and polystyrene at high pressure
[DRIC-T-7307] 03 p0337 N85-12165

Gradient polymers
[AD-A146836] 07 p0931 N85-15900

Theory of relaxation processes in decomposing polymer materials during high-intensity convective heating
13 p2028 N85-22710

Light scattering and spectroscopic studies of polymerization processes
[AD-A153407] 18 p3069 N85-28984

A model for the combustion of polymethyl methacrylate in air in a laminar diffusion flame
[VTH-LR-439] 18 p3165 N85-29606

POLYMORPHISM

Synthesis and characterization of poly(vinylidene fluoride)
[AD-A150291] 13 p2037 N85-22759

POLYNOMIALS

NT BINOMIALS
NT HERMITIAN POLYNOMIAL

Simultaneous rational approximation of a function and its derivatives in the complex plane
[CSIR-TWISK-311] 01 p0109 N85-10730

Polynomial and power series FGS-rings have trivial coefficient rings
[TWISK-326] 01 p0109 N85-10737

A weighted polynomial inequality
[CSIR-TWISK-332] 01 p0110 N85-10741

Partitions of unity and approximation
[AD-A144717] 01 p0110 N85-10748

A trivariate Clough-Tocher scheme for tetrahedral data
[AD-A144740] 01 p0111 N85-10751

Methods for numerical differentiation
[AD-A145058] 01 p0112 N85-10758

Time invariant memoryless nonlinear systems identification method
[FUB-9-1983] 01 p0114 N85-10773

Estimates of Freud-Christoffel functions for some weights with the whole real line as support
[CSIR-TWISK-323] 01 p0114 N85-10775

PASCAL-MP algebraic and numerical manipulator for polynomials
[INPE-3229-TDL/176] 02 p0240 N85-11562

Control and identification of time varying systems
[AD-A145636] 02 p0252 N85-11649

Orthogonal polynomials and rigged Hilbert space
[TUM-M8313] 03 p0414 N85-12647

On the weak limits of elementary symmetric polynomials
[CWI-MS-R8407] 05 p0719 N85-14620

Orthogonal polynomials and a Dirichlet problem related to the Hilbert transform
[CWI-PM-R8406] 05 p0723 N85-14647

Performance of the h, p and h-p versions of the finite element method
[AD-A146940] 07 p1029 N85-16535

Probabilistic analysis of algorithms for NP-Complete problems
[AD-A148207] 08 p1215 N85-17653

On the quadratic mean radius of a polynomial in C2
[AD-A149189] 10 p1546 N85-19751

On the spans of polynomials and the spans of a Laguerre-Polya-Schur sequence of polynomials
[AD-A149384] 10 p1547 N85-19754

Some qualitative properties of bivariate Euler-Frobenius polynomials
[AD-A149408] 10 p1547 N85-19755

A note on the use of polynomial transformations in evaluating singular integrals
[MATHEMATICS-RESEARCH-165]
12 p1920 N85-22053

Approximate perturbing part of geopotential by polynomials of stipulated form 13 p1984 N85-22448

Polynomial parameterization in inverse gravimetric problem 13 p2115 N85-23174

Squares of Gegenbauer polynomials and Milin type inequalities
[CWI-PM-R8412] 14 p2410 N85-24862

A fast ray tracing routine for laterally inhomogeneous media
[AD-A150984] 14 p2421 N85-24938

Entire functions with spiral limits
15 p2634 N85-26241

Multinomial form of the solution of problems of the statistics of elastic rectangular disks
[REPT-17/1984] 16 p2797 N85-27244

Quadratic spaces over discrete Hodge algebras
16 p2853 N85-27593

Polynomial approaches for the characteristic velocity and flame temperature as a function of mixing compounding and pressure for the systems PMMA/O2, PMMA/air, PE/O2, PE/air, PS/O2 and PS/air
[VTH-LR-421] 17 p2924 N85-28024

Comparison of two algebraic methods for curve/curve intersection 17 p3007 N85-28591

Polynomial iteration for nonsymmetric indefinite linear systems
[AD-A153094] 17 p3019 N85-28671

A class of polynomials related to those of Laguerre
[CWI-AM-R8411] 17 p3022 N85-28693

Determinal representations of polynomials satisfying linear Ordinary Differential Equations (ODEs) or linear recurrence relations
[PREPRINT-417] 18 p3172 N85-29680

Evaluation of densities and distributions via hermite and generalized laguerre series employing high-order expansion coefficients determined recursively via moments or cumulants
[AD-A153950] 18 p3175 N85-29682

An algorithm for the generation of primitive polynomials
[FUB-17-1984] 22 p3631 N85-33730

POLYNUCLEAR ORGANIC COMPOUNDS

Analysis and characterization of organic carbon compounds in atmospheric particulate matter
[PB84-232636] 06 p0766 N85-14903

Prediction of retention indices of polynuclear aromatic hydrocarbons. Part 1: HPLC on nitrogen containing normal phase packing materials [DE85-001302] 10 p1436 N85-19051

Desorption efficiences of vapor phase polynuclear aromatic compounds on solid adsorbents [DE85-001303] 10 p1436 N85-19052

Prediction of retention indices of polynuclear aromatic hydrocarbons. Part 2: Capillary gas chromatography [DE85-001301] 10 p1437 N85-19053

Diesel engine emissions of particulates and associated organic matter [PB85-154425] 15 p2590 N85-25964

Identification and quantification of nitropolynuclear aromatic hydrocarbons in ambient and indoor air particulate samples [PB85-176790] 19 p3311 N85-30525

The interaction of polynuclear aromatic hydrocarbons PAH's with water vapor and their role as condensation nuclei in the formation of haze and fog 21 p3652 N85-32695

POLYPEPTIDES

Endocrine responses to hypotensive gravitational stress: Catecholamines, pancreatic polypeptide, and vasopressin 05 p0693 N85-14460

Primary light harvesting system: The relationship of phycobilisomes to photosystem 1 and 2 [DE85-003075] 11 p1689 N85-20622

POLYPHENYL ETHER

Contact angle and surface tension measurements of a five-ring polyphenyl ether [NASA-TM-86927] 07 p0930 N85-15897

Formation of high molecular weight products from benzene during boundary lubrication [NASA-TM-86966] 13 p2017 N85-22644

POLYPHENYLS

NT TRIPHENYLS

Stable polymeric carbon radicals. Part 2: Attempts at the preparation of polyradicals of the triphenylmethyl type linked by P-phenylene units [NASA-TM-77799] 10 p1450 N85-19134

The mechanisms of phenylacetylene polymerization by molybdenum and titanium initiators [AD-A150993] 14 p2260 N85-24007

POLYPROPYLENE

Nuclear Magnetic Resonance of Polymeric Materials [AD-A145078] 01 p0032 N85-10192

13C and 1H NMR (Nuclear Magnetic Resonance) studies of solid polyolefines [AD-P003909] 01 p0032 N85-10195

Synthesis and characterization of a 1,4 Polybutadiene/Isotactic polypropylene block copolymer [AD-A148199] 06 p1133 N85-17142

Determination of threshold and maximum operating electric stresses for selected high voltage insulation. Task 3: Investigation of high voltage capacitor insulation [DE84-017051] 09 p1316 N85-18274

Rep rated long life capacitor development: Phase 1 and 2 [DE85-000719] 11 p1629 N85-20256

Separating polymer solutions using high pressure LCST Lower Critical Solution Temperature) phenomena [AD-A151538] 15 p2518 N85-25528

Polymer blends for use in photoelectrochemical cells for conversion of solar energy to electricity [DE85-011602] 22 p3752 N85-33258

Strength properties of glassfiber reinforced thermoplastics 23 p3908 N85-34212

POLYQUINOXALINES

Fracture surface analysis in composite and titanium bonding: Part 1: Titanium bonding [NASA-CR-175750] 15 p2502 N85-25434

POLYSACCHARIDES

NT CELLULOSE

NT GLYCOGENS

NT STARCHES

POLYSTATION DOPPLER TRACKING SYSTEM

Fundamental limits to synchronization and tracking [AD-A149623] 12 p1833 N85-21504

POLYSTYRENE

Nuclear Magnetic Resonance of Polymeric Materials [AD-A145078] 01 p0032 N85-10192

Deuteron NMR (Nuclear Magnetic Resonance) in relation to the glass transition in polymers [AD-P003910] 01 p0032 N85-10196

Equibiaxial extension of two polymer melts: Polystyrene and low density polyethylene [AD-A144893] 01 p0032 N85-10200

Diblock copolymers of polystyrene/1,2 polybutadiene and polystyrene/polybutene-1: Molecular structure, morphology and mechanical properties [AD-A144980] 01 p0033 N85-10201

Mechanochemical reactions of polymethyl methacrylate and polystyrene at high pressure [DRIC-T-7307] 03 p0337 N85-12165

Photophysical studies of triplet exciton processes in pure polymer films [DE84-016258] 05 p0620 N85-13965

The effect of pressure on the mechanical properties of polymers. Part 2: Measurement of the time-dependent Poisson's ratio [DE85-002139] 06 p0772 N85-14938

Deuterium isotope effect on the compatibility between polystyrene and polybutadiene [AD-A148551] 08 p1134 N85-17145

Monodisperse Latex Reactor (MLR): A materials processing space shuttle mid-deck payload [NASA-TM-86487] 12 p1782 N85-21187

Development of a polystyrene insulation system [DE85-006950] 16 p2784 N85-27160

Preparation of polystryene latex particles in a rotating reactor [NASA-CR-171475] 17 p2933 N85-28108

Ac field-induced order in dense colloidal systems [DE85-009107] 17 p2935 N85-28119

Polymer solution-supercritical fluid behavior [AD-A154514] 21 p3568 N85-32192

POLYSULFIDES

Interactions between F-111 fuselage fuel tank sealants. Part 2: Variation in performance properties of polysulfides after contact with polyester degradation products [AD-A149777] 12 p1812 N85-21368

POLYTETRAFLUOROETHYLENE

Bending two-layer metal-polymer plates 11 p1604 N85-20085

Diffusely reflecting paints including polytetrafluoroethylene and method of manufacture [NASA-CASE-GSC-12883-1] 18 p3079 N85-29044

Detection threshold energy of high energy cascade showers using thermoluminescence PTFE-sheet and hot-gas reader [HE-7.1-5] 24 p4213 N85-36159

POLYTOPES

Some facets of the tri-index assignment polytope [AD-A149195] 10 p1547 N85-19753

POLYURETHANE FOAM

Electrically conductive rigid polyurethane foam [DE84-014490] 01 p0033 N85-10203

Polyimide-glass multilayer printed wiring boards [DE84-015092] 05 p0631 N85-14048

Thermal and mechanical properties of polyurethane foams and a survey of insulating concretes at cryogenic temperatures [PB85-100949/GAR] 07 p0934 N85-15918

Field test results of experimental EPDM (Ethylene Propylene Diene Monomer) and PUF (Polyurethane Foam) roofing [AD-A147697] 08 p1132 N85-17133

Pathophysiological study of poisoning due to thermal degradation of materials — aircraft cabins [CERMA-84-15] 11 p1692 N85-20640

X-ray gauge measures areal density variations as small as 0.1% [DE85-003774] 12 p1854 N85-21629

Damage caused to polyurethane foams by aging, simulated sunlight exposure, heat and fire [AD-A152040] 16 p2754 N85-26998

Buildup of electric charge in foil dielectrics during gamma irradiation 22 p3770 N85-33363

Rigid zeolite containing polyurethane foams [DE85-006406] 23 p3919 N85-34286

POLYURETHANE RESINS

Aircraft surface coatings [NASA-CR-3661] 02 p0137 N85-10935

Description and characterization of deuterated polymers for the analysis with neutron scattering 03 p0431 N85-12748

Protective coverings for fiber reinforced epoxy composites [PB84-231059] 04 p0480 N85-13063

Unidirectional fibers and polyurethane elastomer matrix based composites synthesis and properties [NASA-TM-77501] 07 p0920 N85-15626

Structure-property relationships in thermoplastic elastomers. Part 1: Segmented polyether-polyurethanes [AD-A148043] 08 p1133 N85-17138

Poly(dimethylsiloxane)-polyurethane elastomers: Synthesis and properties of segmented copolymers and related zwitterionomers [AD-A148571] 08 p1134 N85-17147

Fluorinated polyurethanes [AD-D011526] 12 p1810 N85-21353

Phase separation in polyurethanes: A deuterium NMR study [AD-A151515] 15 p2505 N85-25451

Finger materials for air cushion vehicles. Volume 1: Flexible coatings for finger materials [AD-A151438] 15 p2522 N85-25545

Structure-property relationships in thermoplastic elastomers. Part 3: Segmented polyacetal-polyurethanes [AD-A154897] 21 p3569 N85-32200

POLYVINYL ALCOHOL

Gel drawn fibers of poly(vinyl alcohol) [AD-A149062] 10 p1435 N85-19040

POLYVINYL CHLORIDE

New corrosion protection concept for very high voltage line towers [BLL-OA-TRANS-2691-(6196.300)] 20 p3429 N85-31270

Organic air pollutants during manufacturing and handling of PVC floor tiles [FOA-E-40018] 20 p3487 N85-31669

POLYVINYL FLUORIDE

Preliminary study for an IR-vidicon for the 8 to 14 micron range, phase 1 [BMFT-FB-W-84-025] 05 p0633 N85-14057

Effect of ultraviolet radiation on transparent polymer films as determined using in situ FTIR-RA spectroscopy. Volume 2: Photophysics of poly(vinylidene fluoride) films [DE84-013040] 09 p1299 N85-18159

Piezoelectric plastics — polyvinyl fluoride [ISL-CO-202/83] 14 p2262 N85-24017

Piezoelectric and pyroelectric polymers 16 p2756 N85-27008

Ferroelectric homopolymer PVF2 and P (VDF-TrFe) copolymers 24 p4089 N85-35347

PONDEROMOTIVE FORCES

A covariant derivation of the ponderomotive force [AD-A145054] 01 p0121 N85-10630

Theory of penderomotive forces 02 p0283 N85-11847

A nonlocal expression for the ponderomotive potential [IPPJ-699] 06 p0864 N85-15467

Direct electron and ion fluid computation of high electrostatic fields in dense inhomogeneous plasma with subsequent nonlinear optical and dynamical laser interaction 15 p2656 N85-26388

Nonlocal and nonadiabatic expression for the ponderomotive force near cyclotron resonance [IPPJ-736] 23 p3974 N85-34636

Transport issues in Phaedrus-type plasmas 23 p3976 N85-34653

PONDS

Potential for acidification of six remote ponds in the White Mountains of New Hampshire [PB84-207349] 02 p0225 N85-11475

Solar pond research at the Los Alamos National Laboratory [DE85-008631] 18 p3128 N85-29366

Salt-gradient solar ponds [DE85-008626] 18 p3129 N85-29380

Stable density stratification solar pond [NASA-CASE-NPO-15419-2] 19 p3303 N85-30474

Production of liquid fuels and chemicals by microalgae [DE85-008780] 22 p3819 N85-33658

Solar pond technology for Navy applications [AD-A155877] 24 p4112 N85-35488

PONTRYAGIN PRINCIPLE

On the Pontryagin principle for stochastic optimal control [TWISK-328] 01 p0112 N85-10762

POPULATION INVERSION

Imploding plasma X-ray laser research [DE85-000057] 09 p1326 N85-18331

Optimization of silicon-nitride-inversion layer solar cells 12 p1878 N85-21784

Population inversion in laser-initiated vacuum arcs [AD-A151958] 16 p2790 N85-27210

Coherently pumped two-frequency laser-type devices [AD-A154085] 19 p3275 N85-30311

Simplified analytical model for calculation of population inversion in channels of CW gasdynamic lasers operating at various transitions among levels pertaining to ccupled upsilon 1 and upsilon 2 modes of CO2 [STN-2] 20 p3461 N85-31498

Expansion ratio influence on population inversion in CO2/Ar CW gasdynamic lasers operating at various transitions within coupled upsilon 1 and upsilon 2 modes of CO2 [STN-4] 22 p3790 N85-33465

POPULATION THEORY

Maximum likelihood estimation of the survival functions of N stochastically ordered random variables [AD-A145429] 02 p0254 N85-11662

The growth and composition of supercritical branching populations on general type spaces [CTH-MATH-1984-16] 05 p0721 N85-14631

On the power functions of test statistics in order restricted inference [AD-A147126] 07 p1035 N85-16566

Empirical Bayes rules for selecting good binomial populations [AD-A147614] 08 p1214 N85-17646

Improved estimation procedures for item response functions
[AD-A147677] 06 p1215 N85-17648
Minimax multiple t-tests for comparing k normal populations with a control
[AD-A148306] 06 p1215 N85-17656
Study of mathematical models of mutation and selection in multi-locus systems
[DE85-000873] 09 p1376 N85-18848
On asymptotic joint distribution of the eigenvalues of the noncentral manova matrix for nonnormal populations
[AD-A151886] 15 p2642 N85-26294
The dynamical behavior of the age-size-distribution of a cell population
[CWI-AM-R8414] 17 p2996 N85-28538
A formal analysis of the evolution of cooperation
[AD-A152539] 17 p3018 N85-28662
Confidence intervals based on interpolated order statistics
[AD-A152607] 17 p3025 N85-28701
Spatial correlations in the decay from an unstable state in the Malthus Verhulst model — laser cavities
[NOTA-INTERNA-832] 18 p3114 N85-29260
Numerical simulation of the transient by the unstable state in a Lotka-Volterra model
[NOTA-INTERNA-833] 18 p3175 N85-29684

POPULATIONS
Response of algal populations to changes in stream water quality
[PB84-202464] 01 p0070 N85-10485
Results of the carbon monoxide study in Washington, D.C. and Denver, Colorado, in the winter of 1982-83
[PB84-230069] 06 p0634 N85-15309
NAAQS (National Ambient Air Quality Standards) Exposure Model (NEM) applied to carbon monoxide
[PB84-242551] 06 p0634 N85-15310
Hurricane experience levels of coastal county populations: Texas to Maine
[PB85-111383] 10 p1520 N85-19581
The use of image registration technique in Brasilia's urban growth monitoring
[INPE-3302-PRE/614] 10 p1569 N85-19896
Blackbirds and starlings: Population ecology and habits related to airport environments
[AD-P004190] 11 p1580 N85-19953
Feoktistov discusses need for space colonization
13 p1985 N85-22454
Study and estimation of planet-crossing asteroid populations: Discoveries and analysis
13 p2175 N85-23498

PORES
U POROSITY

POROSITY
NT MICROPOROSITY
Suppressing porosity in weld joints of 1420 aluminum alloy 01 p0020 N85-10123
Definition of global dispersion coefficients — aquifers
[PSE-83/4-B] 01 p0064 N85-10426
Study of the pore structure of ceramics prepared by the slip casting method
[NASA-TM-77495] 04 p0478 N85-13048
The variable polarity plasma arc welding process: Its application to the Space Shuttle external tank
[NASA-TM-86482] 05 p0641 N85-14115
Effect of polymer matrix on properties of fibers obtained by caking polymer dispersions 06 p0762 N85-14876
The influence of strain rate and porosity on the deformation and fracture of titanium and nickel
[AD-A148670] 08 p1130 N85-17123
The influence of porosity on the deformation and fracture of alloys
[AD-A148766] 08 p1130 N85-17124
Regularity of the free boundary for the porous medium equation
[AD-A147299] 08 p1210 N85-17611
Mechanisms of elevated temperature rupture in single phase ceramics
[DE85-000697] 09 p1299 N85-18156
Kinetics of saturation of porous titanium with low melting point metals 10 p1446 N85-19114
Behavior and specifics of fracture of porous fiber materials in extension 10 p1447 N85-19116
Collapse and removal of discontinuities in joint zone during diffusion welding 11 p1602 N85-20077
Effect of host-rock dissolution and precipitation on permeability in a nuclear waste repository in tuff
[DE85-000675] 11 p1727 N85-20660
Slip casting and nitridation of silicon powder
[NASA-TM-77809] 12 p1816 N85-21406
Problem of pore formation mechanism in welded joints of aluminum alloys in the system aluminum-magnesium-lithium 13 p2032 N85-22732
NDE methods for green ceramics
[DE85-004019] 13 p2038 N85-22766
Variational bounds on Darcy's constant
[DE85-006838] 15 p2580 N85-25916
Ultrasonic characterization of porosity: Theory
[DE85-005922] 15 p2646 N85-26325
Investigation to optimize the passive shock wave/boundary layer control for supercritical airfoil drag reduction
[NASA-CR-175786] 16 p2699 N85-26665
Continued development and testing of tungsten controlled porosity dispenser cathodes
[AD-A152595] 17 p2931 N85-28090
Detection of pores in hot continuously cast rounds
[BMFT-FB-T-85-007] 18 p3072 N85-29000
Variational bounds on Darcy's constant
[DE85-008959] 18 p3101 N85-29195
Interim rock mass properties and conditions for analyses of a repository in crystalline rock
[DE85-010700] 18 p3125 N85-29352
Analysis of the elastic and strength properties of Yucca Mountain tuff, Nevada
[DE85-008975] 19 p3300 N85-30460
A multiphase continuum model to describe dynamic loading effects in nonlinear porous media
[DE85-010102] 19 p3301 N85-30463
Measurement and analysis of two-phase flow through low permeability media, task 3
[PB85-188373] 20 p3435 N85-31313
Gas sensing with surface acoustic wave devices
[DE85-009125] 20 p3524 N85-31921
MPS solidification model. Analysis and calculation of macrosegregation in a casting ingot
[NASA-CR-171589] 21 p3566 N85-32178
KRAK: A computer program for two-phase two-component porous flow and fracture
[LA-9703] 22 p3782 N85-33434
Deep-burial diagenesis in carbonates
[DE85-011224] 22 p3802 N85-33554
WIPP horizon in situ permeability measurements
[DE85-012687] 22 p3802 N85-33557
The character of observed porosity and its possible effects on rolling contact fatigue life of M-50 steel
[AD-A155930] 24 p4079 N85-35279
Development and evaluation of sulfonated polysulfone membranes for the zinc-ferricyanide battery
[DE85-009104] 24 p4090 N85-35357
Simplified procedures for the evaluation of settlements in sands due to earthquake shaking
[PB85-197867] 24 p4118 N85-35527

POROUS BOUNDARY LAYER CONTROL
Progress in wind tunnel wall interference assessment/correction procedures at the NAE
03 p0314 N85-12025
Development of thermoconvective instabilities in porous media. Influence of boundary conditions
20 p3456 N85-31461

POROUS MATERIALS
Method of making a porous carbon cathode: A porous carbon cathode so made, and electrochemical cell including the porous carbon cathode
[AD-D011243] 02 p0195 N85-11301
Surface diffusion of high temperature vapors in porous alumina
[DE84-015968] 04 p0479 N85-13053
Numerical modelling of the drying of porous materials
[DE84-013056] 04 p0499 N85-13181
Theory of kinetics of impregnation of porous bodies
[BLL-M-35917-(5828.4)] 05 p0616 N85-13942
Characteristic impedance of a porous center during transmission of quasi-static sinusoidal vibrations
[ISSN-0208-5658] 05 p0647 N85-14155
Fatigue strength of different sintered steels and design criteria for porous material (PM) parts
[LBF-FB-170/84] 07 p0928 N85-15886
The influence of porosity on the deformation and fracture of alloys
[AD-A148766] 08 p1130 N85-17124
Response of saturated porous nonlinear materials to dynamic loadings
[AD-A148528] 08 p1173 N85-17394
Investigation of condensing, three-phase, two-component, flow through porous media
09 p1317 N85-18283
Natural convection experiments about a finite-length cylindrical heat source in a liquid-saturated porous medium
[DE84-012657] 09 p1320 N85-18298
Characterization of porosity in porous polymer implant materials
[PB85-119980] 10 p1454 N85-19161
Transition to detonation from rapid-compression (ramp-waves) generated in a burning porous bed
[AD-P004345] 10 p1455 N85-19169
Thermophysical properties of porous fiber materials
11 p1601 N85-20068
Adsorption behaviour of nitrogen compounds on porous polymer beads and applications to atmosphe sampling
[BLL-DRIC-TRANS-7399-(3823.66)]
13 p2036 N85-227
Molten carbonate fuel cell performance model upda draft
[DE85-005423] 13 p2129 N85-22
Impact crater scaling laws 13 p2181 N85-22
Model for high rate gas flows in deformable and reacti porous beds
[DE85-006140] 14 p2253 N85-2
Flow through very porous inclined screens
[NASA-TM-86979] 15 p2555 N85-2576
Variational bounds on Darcy's constant
[DE85-006838] 15 p2580 N85-2591
Ductility equation for porous metals and it linearization
[BLL-M-36118-(5828.4)] 16 p2748 N85-26
Two-d heat transfer through porous media with hea generation
[AD-A151965] 16 p2783 N85-2717
Interaction of finite-amplitude sound with air-filled porou materials
[NASA-CR-174885] 16 p2860 N85-276
Numerical study of porous airfoils in transonic flo
[NASA-TM-86713] 17 p2892 N85-278
Limiting profiles in contaminant transport through porou media — ground water pollution
[REPT-84-31] 17 p2960 N85-282
High temperature composite thermal storage system
[DE85-005073] 17 p2986 N85-2845
Variational bounds on Darcy's constant
[DE85-008959] 18 p3101 N85-2919
Diffusion of gases in porous solids: Simulation and measurements
[DE85-008870] 18 p3101 N85-2919
Dynamics of thin-film breakup in a constricted pore
[DE85-008442] 18 p3101 N85-2919
Distribution of density in closed-impression die forgin of axisymmetrical products from metal powders
19 p3245 N85-3011
Technical and historical overview of the study at Lawrence of porous antireflection coatings
[DE85-010925] 20 p3434 N85-3130
Natural convection experiments in a stratified liquid-saturated porous medium
[DE85-009003] 20 p3455 N85-3145
Development of thermoconvective instabilities in porous media. Influence of boundary conditions
20 p3456 N85-3146
Thermomigration in porous media. Study of the development of a drying zone 20 p3456 N85-3148
Vapor-liquid phase separator studies
[NASA-CR-166545] 21 p3583 N85-3227
Combustion-deflagration-detonation transition
[ISL-CO-221/84] 22 p3747 N85-3322
Detailed validation of a liquid and heat flow code against field performance
[DE85-009901] 23 p3932 N85-3436
Studies in thermo-hydro-chemical transport in porous and fractured media
[DE85-012555] 23 p3949 N85-3447
Method of preparing thin porous sheets of ceramic material
[DE85-006399] 24 p4082 N85-3530

POROUS PLATES
Behavior of the porous bed in a combustion-deflagration-detonation transition
[ISL-CO-220/84] 22 p3747 N85-3322

POROUS WALLS
Numerical simulation of natural convection in porous media — heat transfer
[CFD/84/10] 02 p0199 N85-1133
Jet noise suppression by porous plug nozzles
[NASA-CR-3613] 02 p0275 N85-1179
Investigations of reactive and non reactive acoustic boundary layers in porous walled ducts
13 p2000 N85-2253

PORPHYRINS
NT CHLOROPHYLLS
Three-dimensional photochemical machining with lasers
[AD-A145792] 03 p0365 N85-1234
Photoelectrochemistry with chemically modified electrodes
[DE84-016798] 04 p0471 N85-1299
Chemically modified electrodes and related solution chemistry
[DE84-017110] 05 p0614 N85-139
Investigation and optimization of fuel production using dye-based transition metal complexes as charge-transf intermediates
[PB85-161941] 14 p2264 N85-24

PORTABLE EQUIPMENT

Portable slotting device
[AD-D011213] 01 p0033 N85-10206

Evaluation of survival straws (pocket purifier)
[AD-A146240] 03 p0328 N85-12114

Portable real-time clock
[AD-A146218] 03 p0364 N85-12336

Improved robotic equipment for radiological emergencies
[DE84-017637] 04 p0509 N85-13249

Noise in small portable motocompressors. Experiments on limited-cost acoustic treatments to obtain progressive improvements
[CETIM-11-H-445] 04 p0558 N85-13557

Portable instrument for the detection and identification of air pollutants
[DE84-014767] 05 p0672 N85-14316

Testing of a field portable GPS (Global Positioning System) geodetic receiver
[AD-A148336] 06 p1082 N85-16859

Mobile accelerator neutron radiography system
[AD-A148808] 09 p1323 N85-18311

Location of volatile buried wastes by field portable instrumentation
[AD-P004147] 09 p1348 N85-18483

Fast data and voice transmission for mobile services with high immunity against multipath and co-channel interference 10 p1475 N85-19306

The use of small mobile radars to detect, monitor, and quantify bird movements
[AD-P004188] 11 p1580 N85-19951

Portable pallet weighing apparatus
[NASA-CASE-GSC-12789-1] 11 p1635 N85-20294

Development of a portable zenith chamber and its use on the 47th parallel
[SER-C-287] 11 p1741 N85-20946

Portable remote laser sensor for methane leak detection
[NASA-CASE-NPO-15790-1] 12 p1855 N85-21631

Portable electrochemical cell interrogator
[DE85-005186] 13 p2065 N85-22901

Technical manual: Description and operation Slaved Tracking System
[DE85-004807] 13 p2094 N85-23070

A concept for a mobile remote manipulator system
14 p2236 N85-23859

Fabrication of turbine parts with transportable tools
14 p2267 N85-24046

Deployable Core Automated Maintenance System (DCAMS)
[AD-A153695] 18 p3198 N85-29839

Expedient runway surfacing with post tensioning system for expeditionary airfields
[AD-D011677] 19 p3222 N85-29976

Field testing of a lightweight relocatable structure in a temperate environment
[AD-A155171] 21 p3599 N85-32350

PORTS (OPENINGS)

Wave guide branchings (n-port) types of representation of linear, time-independent and sourceless n-ports
[NASA-TM-77770] 01 p0037 N85-10233

Integral boost, heat protection, port covers and transition 07 p0918 N85-15813

Comparing different theoretical designs of six-port reflectometer junctions
[AD-A149419] 13 p2054 N85-22861

A preliminary human factors planning and design outline of parameters related to space station windows and CCTV monitoring 18 p3158 N85-29559

POSITION (LOCATION)
NT SOLAR POSITION

Drift characteristics of northeastern Bering Sea ice during 1982
[PB84-213982] 01 p0089 N85-10604

A trivariate Clough-Tocher scheme for tetrahedral data
[AD-A144740] 01 p0111 N85-10751

Problem of determining highly accurate coordinates of artificial satellites by photographic methods
02 p0162 N85-11096

The 7-Amino-4,6-Dinitrobenzofuroxan, an insensitive high explosive
[AD-A145865] 02 p0188 N85-11257

Estimation of target positioning using planar arrays
[RSRE-MEMO-3675] 02 p0189 N85-11266

Fungi of Mt. Babia Gora. 1: Mycoflora of forests
[NASA-TM-77484] 02 p0234 N85-11522

Interactions in localization
[NOTA-INTERNA-815] 02 p0279 N85-11818

Electrons in a disordered medium
[NOTA-INTERNA-816] 02 p0279 N85-11819

Realistic localizer courses for aircraft instrument landing simulators
[NASA-CR-172333] 04 p0455 N85-12885

Documentation for the machine-readable version of the Perth 75: A Catalogue of Positions of 2589 FK4 and FK4S Stars (Nikoloff and Hog 1982)
[NASA-TM-87376] 04 p0549 N85-13492

Documentation for the machine-readable version of the AGK3 Star Catalogue of Positions and Proper Motions North of -2 deg .5 declination (Dieckvoss and Collaborators 1975)
[NASA-TM-87378] 04 p0549 N85-13493

Terrestrial locating — of buoys from space
05 p0599 N85-13816

Documentation of earthquake algorithms
[PB84-235324] 05 p0677 N85-14351

High accuracy Doppler navigation employing optimum integrated position fix information
06 p1073 N85-16803

Data analysis techniques for vehicle attitudinal, positional and experimental measurements
[AD-A147752] 08 p1188 N85-17484

Spatiotemporal characteristics of visual localization
[AD-A148013] 08 p1200 N85-17555

The combinatorics of local constraints in model-based recognition and localization
[AD-A148338] 08 p1230 N85-17746

Three position estimation procedures
[AD-A148748] 09 p1278 N85-18042

Localization of destruction process
10 p1500 N85-19470

Fine figuring actuator
[AD-D011476] 10 p1557 N85-19819

Adjustable indicating device for load position
[NASA-CASE-MFS-28008-1] 11 p1635 N85-20300

Geodetic accuracy of LANDSAT 4 Multispectral Scanner and Thematic Mapper data — Washington, DC, California, Alabama, South Dakota, and Illinois
11 p1667 N85-20504

Performance of time-position discriminator of composite signal 13 p2072 N85-22941

Use of three omega radionavigation system position lines for solving problems in marine geodesy
13 p2107 N85-23131

Data Collection and Platform Location by Satellite: ARGOS Users' Conference 14 p2237 N85-23869

System performance, data distribution and technical files — ARGOS project 14 p2237 N85-23871

The ARGOS system status report
14 p2239 N85-23884

Three-dimensional sensing and interpretation
[AD-A150890] 14 p2311 N85-24304

Proceedings of the ARGOS Users Conference on Data Collection and Location by Satellite
14 p2322 N85-24348

Data Collection and Platform Location by Satellite: ARGOS Users' Conference 14 p2325 N85-24366

The ARGOS system main characteristics — satellite based localization 14 p2325 N85-24367

The ARGOS system after 3 years operation
14 p2325 N85-24368

The SARSAT program 14 p2327 N85-24385

Data Collection and Platform Location by Satellite: ARGOS users' Conference 14 p2328 N85-24391

Data Collection and Platform Location by Satellite: ARGOS Users' Conference 14 p2330 N85-24409

Location and synchronization — space-time coordinates 14 p2397 N85-24768

The ARGOS program — satellite based localization
14 p2397 N85-24775

The SARSAT/COSPAS system for assisting satellite based search and rescue 14 p2398 N85-24776

The TRANSIT and Global Positioning System (GPS) systems. Precision navigation and localization
14 p2398 N85-24777

Kitt Peak measurements of P/Halley positions
14 p2436 N85-25023

Measuring: The quantifying art
14 p2437 N85-25035

The orbital motion of Comet Halley
14 p2437 N85-25040

Documentation for the machine readable version of the Yale Catalogue of the Positions and Proper Motions of Stars between Declinations -60 deg and -70 deg (Fallon 1983)
[NASA-TM-87443] 14 p2439 N85-25051

Microcomputer application of aerospace asset surface search planning
[AD-A151833] 15 p2467 N85-25227

A FORTRAN program for deep space sensor analysis
[AD-A151700] 15 p2489 N85-25366

Low-resolution target classification from a staring infrared sensor
[AD-A151690] 15 p2652 N85-26358

Data Collection and Platform Location by Satellite: ARGOS Users' Conference 16 p2811 N85-27333

Location and data collection satellite system ARGOS. User's guide — satellite based localization
16 p2816 N85-27371

Real-time position determinations using the GPS TI4100/GEOSTAR receiver
[AD-A152551] 17 p2894 N85-27845

A comparison of methods of least squares adjustment of traverses
[AD-A153612] 18 p3170 N85-29645

A robust estimator of location using an adaptive spline model
[AD-A153662] 18 p3174 N85-29676

Ephemeral regions versus pseudo ephemeral regions
18 p3206 N85-29901

Use of Omega radio navigation system in geophysical work in Antarctica 19 p3298 N85-30448

The location of stress in clothing
[AD-A154423] 19 p3331 N85-30833

Touch-off: A method to determine the position of an object by means of a sensor-driven robot
[DE85-011178] 19 p3339 N85-30691

COSPAS/SARSAT: An overview
20 p3400 N85-31092

The COSPAS-SARSAT system
20 p3401 N85-31101

Comparing SLR and VLBI geodetic parameters
20 p3491 N85-31703

New optical satellite data 20 p3492 N85-31705

The potential of the NAVSTAR global positioning system for the Corps of Engineers, civil works
[AD-A154913] 21 p3554 N85-32109

Parameter estimation in communication system tracking satellite observations
[AD-A155137] 21 p3636 N85-32582

Estimating angular position of optical radiation source when received by array of photodetectors
22 p3778 N85-33413

Evaluation of coordinate measuring machines
[DE85-011712] 22 p3788 N85-33467

Dual optical mechanical position tracker
[AD-D011739] 22 p3844 N85-33811

What determines the location of satellites and planets? 22 p3853 N85-33858

Initial placement of STO instruments
23 p3902 N85-34174

Visual position determination for autonomous vehicle navigation
[AD-A156007] 24 p4063 N85-35181

Development of position sensors for microcomputer-oriented sensor systems
[BMFT-FB-T-85-021] 24 p4091 N85-35361

Materials and process development for microcomputer-compatible pressure, temperature, and position sensors
[BMFT-FB-T-85-024] 24 p4097 N85-35399

Evaluation of nuclear detonation location capability under high attack scenario
[AD-A155761] 24 p4149 N85-35729

POSITION ERRORS
NT BORESIGHT ERROR

Predictions of cockpit simulator experimental outcome using system models 05 p0702 N85-14504

A discussion of coning errors exhibited by inertial navigation systems
[RAE-TM-RAD-NAV-243] 06 p1082 N85-16854

Ordinary and proper location M-estimates for ARMA models, revised
[AD-A149705] 12 p1920 N85-22061

Positioning errors of commutating lenses and their influence on characteristics of high speed movie cameras 14 p2273 N85-24085

Angular error of position of RATAN-600 screens during radial displacement 15 p2476 N85-25286

Studies into location accuracy — ARGOS system
16 p2811 N85-27334

Positioning accuracy of the ARGOS system in operational use 16 p2811 N85-27335

An evaluation of the performance of a new storm tracking methodology
[AD-A152234] 16 p2835 N85-27484

Simulations of strapdown-system errors and error compensation methods — transport aircraft navigation
[DFVLR-MITT-84-22] 20 p3392 N85-31040

Search and rescue satellite (SARSAT) error analysis of the 406 MHz system 20 p3403 N85-31118

POSITION INDICATORS
NT ASTROLABES
NT PLAN POSITION INDICATORS
NT RADIO DIRECTION FINDERS
NT SPACECRAFT POSITION INDICATORS

Improved legislated emergency locating transmitters and emergency position indicating radio beacons
[NASA-CASE-GSC-12892-1] 11 p1624 N85-20226

Short-range radiotechnical point sensor
13 p2061 N85-22996

Enhacements to the TTS-502 time transfer system
17 p2963 N85-28296

High temperature position sensors based on monolithic GaAs Hall IC
[BMFT-FB-T-84-266] 17 p2969 N85-28337
A study of the application of differential techniques to the global positioning system for a helicopter precision approach
[NASA-CR-177326] 20 p3391 N85-31035
A device to detect Top Dead Center (TDC) position in motored engines
[REPT-84-RR-347] 20 p3458 N85-31475

POSITION SENSING
A position sensitive phoswich hard X-ray detector system
[OG-9.3-12] 23 p4028 N85-34967

POSITIONING
Linac quadrupole connections
[DE84-014694] 01 p0118 N85-10810
The facilities of the Calculation Center and Real Time Room for satellite positioning 05 p0599 N85-13819
Laser-guided measuring system for precisioning device 06 p0816 N85-15179
Recent development in astronomic position determinations
[AD-A148335] 08 p1082 N85-16858
Navigation for an intelligent mobile robot
[AD-A150051] 12 p1775 N85-21144
Orbital positioning and stationkeeping of geostationary satellites 14 p2397 N85-24772
Criteria for the classification of hydrographic positioning data
[AD-A152283] 16 p2705 N85-26697
Positioning of a robotic manipulator through the use of visual feedback
[AD-A151933] 16 p2851 N85-27577
Global positioning system carrier phase: Description and use
[PB85-174126] 19 p3216 N85-29946
Spillover minimization: An approach for actuators and sensors placement in distributed parameter study
[INPE-3525-PRE/746] 19 p3272 N85-30289
Optimal sensor locations for structural identification
20 p3417 N85-31209
The Galeleo spacecraft magnetometer boom
22 p3796 N85-33513
Time domain reflectometry for SLC BPM system
[DE85-012389] 24 p4155 N85-35756

POSITIONING DEVICES (MACHINERY)
NT BOOMS (EQUIPMENT)
NT CAMS
NT JIGS
Experimental study with parameter variations on a hydraulic positioning servo with computer implemented observer
[FOA-C-20545-E3] 02 p0256 N85-11673
Vehicle anchoring system
[AD-D011292] 06 p0815 N85-15173
Multi-directional straddle-lift carrier
[AD-D011315] 07 p0973 N85-16183
The space shuttle orbiter remote manipulator positioning mechanism 08 p1102 N85-16963
Design procedure for the new 70-meter antenna subreflector positioner 10 p1463 N85-19232
Automated parts storage and retrieval system positioning device and method
[AD-D011494] 11 p1647 N85-20379

POSITIVE IONS
Mean delta-ray energies in ion molecule collisions
[DE85-005524] 13 p2157 N85-23395
Quantitation of Na+, K+-ATPase enzyme activity in tissues of the mammalian vestibular system
15 p2613 N85-26102

POSITRON ANNIHILATION
Application of positron annihilation in materials science
[DE84-014733] 02 p0288 N85-11883
The Fermi surface and momentum space densities of ferromagnetic Gd using the Positron technique
09 p1396 N85-18788
A remote source system for measuring relative positron annihilation line widths in individual slab cylindrical samples
[AERE-R-10549] 12 p1938 N85-22173
Trapping model analysis of annihilation line narrowing in some plastically deformed metals and alloys
[AERE-R-10593] 14 p2258 N85-23995
Characterization of atomic defects and their aggregates using positron annihilation spectroscopy
[DE85-006206] 14 p2418 N85-24918
Positron annihilation studies of vacancy formation in tungsten, chromium, and niobium
[DE85-006837] 16 p2871 N85-27710
An investigation of molecular structure of copolymers using positron annihilation spectroscopy
[NASA-TM-86431] 17 p2916 N85-27977
Measurements of heavy quark and lepton lifetimes
[DE85-008321] 18 p3181 N85-29724
Theory of positron annihilation in vacancies in concentrated disordered alloys
[DE85-010267] 18 p3183 N85-29734
Study of the equilibrium vacancy ensemble in aluminum using 1D- and 2D-angular correlation of annihilation radiation
[DE85-008967] 18 p3194 N85-29813
Electron-proton collider option for the superconducting super collider
[DE85-010146] 18 p3196 N85-29822
Resolvability of defect ensembles with positron annihilation studies
[DE85-010041] 18 p3196 N85-29823
Determination of the vacancy formation enthalpy in chromium by positron annihilation
[DE85-010286] 19 p3239 N85-30084
PAS determination of the vacancy formation enthalpy in tungsten
[DE85-010283] 19 p3240 N85-30086
Low-temperature positron lifetime and Doppler-broadening measurements for single-crystal nickel oxide containing cation vacancies
[DE85-010238] 19 p3376 N85-30944
Reduction of the trapping of positrons in dislocated single crystals of iron when charged with hydrogen
[DE85-010235] 19 p3377 N85-30950
A positron annihilation Doppler broadening study of niobium
[DE85-010287] 20 p3527 N85-31936
Positron measurements in 2H-TaSe2 crystals
[DE85-010507] 20 p3529 N85-31949
Materials characterization with intense positron beams
[DE85-011850] 22 p3839 N85-33769
Search for positron annihilation line and continuum radiation from the Galactic Center
[OG-2.5-5] 22 p3869 N85-33962
Some evidence for large gravitational redshift in Seyfert galaxy NGC 4151
[OG-2.7-11] 22 p3872 N85-33984
On some problems of gamma-astronomy
[OG-2.7-15] 22 p3873 N85-33988
A coded aperture imaging system optimized for hard X-ray and gamma ray astronomy
[OG-9.2-3] 23 p4024 N85-34942
Forty-five years of e(+)e(-) annihilation physics: 1956 to 2001
[DE85-013052] 24 p4149 N85-35723

POSITRONIUM
Experimental method for measuring positronium reflection from surfaces
[DE85-010949] 20 p3531 N85-31967

POSITRONS
Positron ring system using Anger-type detectors
[DE84-016788] 04 p0503 N85-13212
Positron flux concentrator: An update
[DE84-016260] 04 p0561 N85-13576
Notes on the RF system for the SLC positron source
[DE85-002628] 11 p1722 N85-20830
Low-energy, high-intensity positron beam experiments with a linac
[DE85-001048] 11 p1723 N85-20835
Electron-positron pair equilibrium in strongly magnetized plasmas 12 p1957 N85-22296
Electron-positron pairs in a mildly relativistic plasma in active galactic nuclei 12 p1957 N85-22297
Theory of positron annihilation in vacancies in concentrated disordered alloys
[DE85-010267] 18 p3183 N85-29734
Additional muon calculations for the SLC positron source
[DE85-011212] 19 p3363 N85-30855
Reduction of the trapping of positrons in dislocated single crystals of iron when charged with hydrogen
[DE85-010235] 19 p3377 N85-30950
Materials characterization with intense positron beams
[DE85-011850] 22 p3839 N85-33769
Advanced instrumentation for Positron Emission Tomography
[DE85-011147] 22 p3840 N85-33779
Observation of cosmic ray positrons from 5 to 25 GeV
[OG-6.2-5] 22 p3889 N85-34104
An observation of cosmic ray positrons from 10-20 GeV
[OG-6.2-6] 22 p3889 N85-34105
Reestimation of the production spectra of cosmic ray secondary positrons and electrons in the ISM
[OG-6.2-8] 22 p3889 N85-34107
Electrons and positrons from expanding supernova envelopes in dense clouds
[OG-6.2-9] 22 p3889 N85-34108
Possible detection of flare-generated positrons by Helios 1 on 3 Jun 1982
[SH-1.4-10] 23 p3996 N85-34770
Pulsed-neutron-source models for the astrophysical s-process
[DE85-012927] 24 p4151 N85-35740
Vacuum system for the Argonne 6 GeV synchrotron ligh source
[DE85-012286] 24 p4157 N85-3577
Missing energies at pair creation
[HE-4.4-8] 24 p4190 N85-36

POST BOOST PROPULSION SYSTEM
Combined cycle ramjet engine
[AD-D011247] 06 p0760 N85-14

POSTMISSION ANALYSIS (SPACECRAFT)
Results of Space Shuttle Flight 41-C
[GPO-36-092] 04 p0461 N85-129
Statement of Captain Robert L. Crippen, USN, Commander of Space Shuttle Flight 41-C; Francis R. Scobee, pilot; Doctor George D. Nelson, Mission Specialist; Terry J. Hart, Mission Specialist; and Doctor James D. Van Hoften, Mission Specialist; accompanied by Frank Cepollina, Solar Maximum Repair Mission Project Manager, Goddard Space Flight Center
04 p0461 N85-1292
National Space Transportation Systems Program mission report
[NASA-TM-87456] 14 p2241 N85-23

POSTURE
Establishment of posture and working movements of pilot in air crash enquiries 07 p1010 N85-18417
Human body dimensions: Body outlines and envelope curves at different normal positions and movements
[HSE-TRANS-10866] 19 p3332 N85-30640
Postural adjustments associated with arm movements in weightlessness 20 p3509 N85-31813

POTABLE LIQUIDS
NT POTABLE WATER

POTABLE WATER
Reverse osmosis treatment to control inorganic and volatile organic contamination
[PB84-223528] 01 p0071 N85-10479
Ultrafiltration as pretreatment for the preparation of drinking water by reverse osmosis onboard ships
[PML-1984-32] 01 p0098 N85-10654
Corrosion of brass in potable water service
[CETIM-100390] 04 p0477 N85-13037
Tap noise-pressure fluctuations. Study of the acoustic behavior of hydraulic equipment in buildings as a function of the temperature
[CETIM-11-H-337] 04 p0502 N85-13201
Toxicology of natural and man-made toxicants in drinking water
[AD-P004035] 06 p0845 N85-15365
Closed-loop concepts for the Army: Water conservation, recycle, and reuse
[AD-A148839] 09 p1365 N85-18581
Literature review for development of the master analytical scheme for organic compounds in water
[PB85-152874] 15 p2507 N85-25488
Radiation-induced degradation of trichloroethylene and tetrachloroethylene in drinking water
[OEFZS-4298] 18 p3134 N85-29409
The degradation of pollutants in water and waste water by means of electron or gamma irradiation
[OEFZS-4317] 22 p3812 N85-33815
Experimental validation of allowable concentrations of sodium and potassium in recycled drinking water
22 p3823 N85-33885

POTASSIUM
NT LIQUID POTASSIUM
NT POTASSIUM 40
Measurement of magnetic sublevel differential scattering cross sections for potassium and mercury
[MPIS-10/1983] 01 p0119 N85-10815
Investigation on K (4 2P3/2) Hg interaction at collision energies from 0.5 to 5.7 eV
[MPIS-15/1983] 04 p0563 N85-1358
Titanium-potassium heat pipe corrosion studies
[DE84-015526] 05 p0637 N85-1409
Scattering experiments on interactions of excited atoms Differential cross sections of the system Na (3P)+K(4S
[MPIS-8/1984] 05 p0728 N85-1457
Calorimetric investigation into the possibility of a charge density wave ground state in alkali metals
[DE85-002006] 09 p1397 N85-1679
U, Th, K content, heat production and thermal conductivity of Sao Paulo, Brazil continental she sediments: A reconnaissance work
[INPE-3401-PRE/670] 10 p1515 N85-1995
Experimental investigations of thermal radiation fro potassium atoms in magnetohydrodynamic system Preliminary report
[DE85-003715] 12 p1936 N85-2218
Structural, morphological and optical characteristics o KGd(WO4)2 crystals 14 p2280 N85-2412
Performance characteristics of gravity-assiste potassium heat pipes
[DE85-010717] 19 p3287 N85-303
Circadian dynamics of potassium excretion in urine related to working on one and two shifts
19 p3325 N85-305

Passive Q-modulation of optical cavities by KCl crystals containing OH(-) -ions 21 p3668 N85-32915
Measurements of Fe and Ar fragmentation cross sections
[PAPER-OG-7.2-20] 21 p3714 N85-33047
Precision measurements of solar energetic particle elemental composition
[PAPER-SH-2.1-4] 21 p3715 N85-33052
Thermodynamics of the corrosion of chromium in molten carbonates
[DE86-011407] 24 p4079 N85-35282

POTASSIUM ALLOYS
Thermodynamic properties of liquid Li-Ph, Na-Pb and K-Pb]b alloys: Similarities and Differences
[DE85-004074] 18 p3197 N85-29630

POTASSIUM CHLORIDES
Investigation of the dissolution of CaCrO4 in molten LiCl-KCl eutectic
[DE84-016394] 04 p0489 N85-12965
Passive Q-modulation of optical cavities by KCl crystals containing OH(-) -ions 21 p3668 N85-32915

POTASSIUM COMPOUNDS
NT POTASSIUM CHLORIDES
NT POTASSIUM HYDROXIDES
NT POTASSIUM OXIDES
NT POTASSIUM PERCHLORATES
NT POTASSIUM PHOSPHATES
Phase behavior and QLS (Quasielastic Light Scattering) in potassium linoleate/n-alkanol microemulsions
[AD-A155028] 21 p3563 N85-32163
Luminescence and absorption of indium-activated potassium-borate glasses subjected to high-power excitation 21 p3661 N85-32868
Ames Laboratory measurements of alkali levels in the Curtiss-Wright PFBC gas stream
[DE85-011357] 22 p3745 N85-33214
Throughfall rate and chemistry studies: Whiteface Mountain
[DE85-012407] 23 p3947 N85-34464

POTASSIUM HYDROXIDES
Effects of additives and KOH electrolyte concentration on dissolution of iron electrodes
[DE84-014840] 02 p0173 N85-11162
Experimental evaluation of the thermodynamic properties of concentrated aqueous potassium hydroxide solutions
[DE85-010626] 23 p3912 N85-34238

POTASSIUM ISOTOPES
NT POTASSIUM 40

POTASSIUM OXIDES
Improved oxygen sources for breathing apparatus
[NASA-TM-86671] 24 p4134 N85-35623

POTASSIUM PERCHLORATES
Thermal conductivity of iron/potassium perchlorate heat powder
[DE84-017071] 04 p0476 N85-13035
Solid phase reactions among manganese, potassium perchlorate and barium chromate
[HSE-TRANS-11166] 19 p3237 N85-30071
Burn front velocity as a function of pellet density in iron-potassium perchlorate heat powders
[DE85-011448] 21 p3572 N85-32214
Friction, impact, and electrostatic discharge sensitivities of energetic materials
[DE85-013321] 24 p4083 N85-35309

POTASSIUM PHOSPHATES
Chemical engineering principles of constant temperature-constant supersaturation growth of potassium dihydrogen phosphate (KDP) crystals
[DE84-017061] 04 p0571 N85-13845
Rapid growth of potassium dihydrogen phosphate crystals
[DE85-007261] 17 p3045 N85-28639
Refractive indices and thermo-optic coefficients of nonlinear crystals isomorphic to KH2PO4
[DE85-012988] 22 p3847 N85-33831

POTASSIUM 40
Investigation of the daytime lunar atmosphere
[NASA-CR-175636] 14 p2440 N85-25057

POTATOES
Multi crop area estimation in Idaho using EDITOR
[E85-10054] 06 p0827 N85-15251
Alcohol: An alternate energy resource for community use
[DE85-007731] 18 p3084 N85-29075
Use of gamma radiation as a form of preservation of sweet potatoes
[DE85-011998] 22 p3841 N85-33787

POTENTIAL ENERGY
NT BIOELECTRIC POTENTIAL
NT COULOMB POTENTIAL
NT ELECTRIC POTENTIAL
NT GEOPOTENTIAL HEIGHT
NT IONIZATION POTENTIALS
NT LOW VOLTAGE
NT NUCLEAR POTENTIAL
NT OPEN CIRCUIT VOLTAGE
NT PHOTOVOLTAGES
NT PLASMA POTENTIALS
NT QUANTUM WELLS
Theoretical studies in molecular fragmentation: Processes, energetics and diagnostics
[AD-A146310] 03 p0418 N85-12673
Theoretical studies of highly ionized species
[DE84-016797] 04 p0561 N85-13574
The use of available potential energy to evaluate two GLAS FGGE data sets 05 p0682 N85-14387
Generation of available potential energy and other diagnostic studies during FGGE 05 p0683 N85-14388
Analysis of diabatic heating during FGGE 05 p0683 N85-14393
Potential at atomic bounderies in the TF (or TFD) model and equations of states 12 p1820 N85-21419
Translational and extensional energy release rates (the J- and M-integrals) for a crack layer in thermoelasticity
[NASA-CR-174872] 12 p1863 N85-21685
Theoretical studies of kinetic mechanisms of negative ion formation in plasmas
[AD-A150820] 14 p2423 N85-24946
Electronically excited alkaline earth oxides: Chemical production and collisional energy transfer processes
[AD-A153172] 17 p3044 N85-28833
Variational transition state theory
[DE85-010685] 19 p3235 N85-30059
Calculation of Franck-Condon factors for diatomic molecules
[AD-A154463] 19 p3353 N85-30784
Determination of the intramolecular potential flow from a neutron diffraction experiment
[B8563199] 20 p3532 N85-31978
Generation of available potential energy and the energy cycle during the global weather experiment
[NASA-CR-175301] 21 p3634 N85-32572
Horizontal and vertical structure of velocity, potential vorticity and energy in the gulf stream
[AD-A154753] 21 p3655 N85-32702

POTENTIAL FLOW
NT EQUIPOTENTIALS
PAN AIR: A computer program for predicting subsonic or supersonic linear potential flows about arbitrary configurations using a higher order panel method. Volume 3: Case manual (version 1.0)
[NASA-CR-3253] 02 p0135 N85-10922
Comparison of uniform perturbation solutions and numerical solutions for some potential flows past slender bodies
[NASA-CR-172485] 06 p0749 N85-14799
Supersonic nonlinear potential analysis
[NASA-CR-172456] 07 p0897 N85-15685
Inviscid compressible flow past a multi-element aerofoil 08 p1069 N85-16776
Spectral modeling of a potential vorticity equation for a barotropic flow on a beta-plane
[CWI-AM-R8406] 08 p1186 N85-17478
Potential applications of forced unsteady flows
[AD-P004155] 09 p1264 N85-17940
Numerical approach for the aerodynamic analysis if airfoils with laminar separation
[NASA-CR-172496] 09 p1273 N85-18001
A frozen vorticity approach to the axisymmetric strong interaction problem
[AD-A149101] 10 p1484 N85-19369
Numerical integration of the unsteady full-potential equation with applications to transonic flow about a two-dimensional airfoil
[NLR-MP-84022-U] 12 p1773 N85-21130
Robust calculation of three-dimensional transonic potential flow based on the nonlinear gas multigrid method and a mixed incomplete lower upper decomposition/strongly implicit procedure (ILU/SIP) algorithm
[NLR-MP-84003-U] 12 p1846 N85-21593
Comparison of measured and computed boundary layers at the tail-end of an axisymmetric body in an air-jet
[AMTE(N)-TM-83053] 14 p2209 N85-23700
Wind tunnel wall interference
[AD-A151212] 15 p2474 N85-25273
An experimental study of hairpin-type vortices as a potential flow structure of turbulent boundary layers 15 p2553 N85-25751
Investigation of potential and viscous flow effects contributing to dynamic stall
[AD-A151696] 15 p2557 N85-25773
A counterpart of Faxen's formula in potential flow
[REPT-84-09] 17 p2960 N85-28279
A study of aerodynamic control in stalled flight long laminar separation bubble analysis
[AD-A153850] 18 p3059 N85-28930
A first-order time-domain Green's function approach to supersonic unsteady flow
[NASA-CR-172208] 19 p3214 N85-29930
Floating shock-fitting in transonic potential flow calculations 20 p3387 N85-31007
Fuselage upwash effects on RSRA rotor systems
[NASA-CR-177349] 20 p3388 N85-31015
Numerical simulation of potential flow in transonic steady regimes 20 p3389 N85-31016
Vortex sheet modeling with higher order curved panels 20 p3451 N85-31428
The calculation of fully three dimensional flow through any type of turbomachine blade row 21 p3587 N85-32294
On the limiting configuration of interfacial gravity waves
[AD-A154821] 21 p3631 N85-32557
Calculation of compressible flow about three-dimensional inlets with auxiliary inlets, slats and vanes by means of a panel method
[NASA-CR-174975] 24 p4060 N85-35162

POTENTIAL GRADIENTS
Ohmic potential drop and gas bubble radius distribution in alkaline water electrolysis 17 p2924 N85-28025
Double layer formation due to contact of different temperature plasmas
[IPPJ-722] 19 p3370 N85-30900
A supersonic potential gradient method for the calculation of unsteady aerodynamic pressures on harmonically oscillating wings
[DFVLR-FB-85-11] 20 p3390 N85-31026
Influence of edge effects on performance of electrooptical lens 22 p3770 N85-33366
Possibility of potential generation by lower hybrid wave 23 p3977 N85-34654
Fokker-Planck calculation of hot electron formation in the thermal barrier region of tandem mirror Gamma-10
[IPPJ-726] 23 p3979 N85-34669

POTENTIAL THEORY
Self potentials of an electron ring in a torus for large ring displacement from the minor axis
[AD-A146086] 03 p0421 N85-12691
Boundary element methods in potential theory: Four lectures
[NPL-DITC-46/84] 05 p0718 N85-14604
Applications of the simple-layer logarithmic potential 05 p0718 N85-14606
Applications of Green's boundary formula 05 p0718 N85-14607
Three-dimensional and axisymmetric problems 05 p0718 N85-14608
A comparative study of the nonuniqueness problem of the potential equation
[NASA-TP-2385] 07 p0898 N85-15694
A fast algorithm of the finite difference method for computation of the transonic flow past an arbitrary airfoil with the conservative full-potential equation 11 p1619 N85-20191
Field theory analysis using the finite element method to determine the deliberation curves of three dimensional fracture mechanics specimens with a semicircular surface crack applying the electrical direct current potential method for crack depth measurement
[GKSS-84-E-53] 17 p2982 N85-28434
Nonlinear potential analysis techniques for supersonic-hypersonic configuration design
[NASA-CR-166078] 19 p3212 N85-29917
Computer simulation of elastic waves by a new mass-point system with potentials
[DRIC-T-7274] 20 p3469 N85-31553

POTENTIOMETERS (INSTRUMENTS)
A simple, low cost potentiostat for corrosion studies
[NPL-DMA(A)-47] 04 p0502 N85-13203
Ground-water level data and preliminary potentiometric-surface maps, Yucca Mountain and vicinity, Nye County, Nevada
[DE85-001771] 09 p1343 N85-18448
Development and testing of a spacecraft surface potential monitor 13 p2007 N85-22582
Using a single-board computer to maintain constant voltage, current sources 15 p2551 N85-25749

POTENTIOMETERS (RESISTORS)
The measurement of high value resistances at the NPL — electrical resistance
[NPL-DES-81] 22 p3758 N85-33291

POTTING COMPOUNDS
Electrical research on solar cells and photovoltaic materials
[NASA-CR-175699] 15 p2585 N85-25935
Electrical research on solar cells and photovoltaic materials
[NASA-CR-175897] 17 p2986 N85-28452

POWDER (PARTICLES)
NT FINES
NT METAL POWDER
NT POWDERED ALUMINUM

Powder containing 2H-type silicon carbide produced by reacting silicon dioxide and carbon powder in nitrogen atmosphere in the presence of aluminum
[NASA-TM-77597] 01 p0027 N85-10167
Processing ceramics
[NASA-TM-77603] 01 p0031 N85-10188
Milling of Si3N4 with Si3N4 hardware
[NASA-TM-86864] 01 p0031 N85-10191
Structure of silane coupling agents adsorbed on silicon powder
[AD-A145803] 03 p0327 N85-12105
Sintering behavior of ultrafine silicon carbide powders obtained by vapor phase reaction
[NASA-TM-77422] 03 p0336 N85-12161
Ceramic microstructure development
[AD-A145753] 03 p0337 N85-12166
Preparation of sinter-active silicon carbide powders
[BMFT-FB-T-84-189] 04 p0469 N85-12982
Structural changes during milling of aluminum oxide powders
[NASA-TM-77488] 04 p0472 N85-13008
Thermal conductivity of iron/potassium perchlorate heat powder
[DE84-017071] 04 p0476 N85-13035
Infrared thermography of burn front propagation in heat powders
[DE85-003307] 10 p1438 N85-19060
Factors influencing the ball milling of Si3N4 in water
[NASA-TM-86932] 10 p1450 N85-19136
Effect of powder characteristics on microstructure and properties in alkoxide prepared PZT ceramics
[AD-A149082] 10 p1451 N85-19141
Dynamic compaction of powders
[DE85-001062] 11 p1612 N85-20137
Influence of external electric field on structural-mechanical properties of powdered materials
13 p2013 N85-22630
Recent trends in particle size analysis techniques
[NASA-TM-77735] 13 p2017 N85-22645
A comprehensive review of black powder
[AD-A150455] 13 p2039 N85-22769
Comparative sinterability of combustion synthesized and commercial titanium carbides
[DE85-006255] 15 p2512 N85-25498
Interfacial and colloidal aspects of aqueous suspension containing oxidic powders
[DE85-005972] 15 p2519 N85-25534
Sintering phenomena of non-oxide silicon compounds
[DE85-006676] 15 p2520 N85-25535
Test and modeling for sintering theory
[DE85-007761] 16 p2755 N85-27004
High resolution powder diffraction
[DE85-008287] 17 p2922 N85-28015
Attenuated total reflection method for obtaining optical constants of powders
[AD-A154094] 19 p3367 N85-30881
Multilayer capacitor dielectrics produced from metallo-organic precursors
[AD-A154592] 21 p3580 N85-32254
Combustion-deflagration-detonation transition in a confined spherical powder
[ISL-R-108/84] 22 p3747 N85-33223
Quantitative determination of mineral composition by powder X-ray diffraction
[DE85-011654] 22 p3760 N85-33301
Method for removing oxide contamination from silicon carbide powders
[DE85-011648] 23 p3919 N85-34287
Dynamic compaction of a monosized spherical tungsten powder
[DE85-014808] 24 p4060 N85-35289
Computational methods for the explosive and impact compaction of powders
[AD-A156219] 24 p4139 N85-35653

POWDER METALLURGY
USSR report: Materials science and metallurgy, no. 93
[JPRS-84810] 01 p0018 N85-10110
Development of powder metallurgy in various sections of USSR 01 p0019 N85-10116
Fabrication and characterization of Si3N4 ceramics without additives by high pressure hot pressing
[NASA-TM-77724] 01 p0031 N85-10189
Microstructural design and control of sintered hard materials 02 p0176 N85-11180
Development of powder metallurgy 2XXX series Al alloys for high temperature aircraft structural applications
[NASA-CR-172408] 02 p0182 N85-11220
Hot isostatically pressed manufacture of high strength MERL 76 disk and seal shapes
[NASA-CR-165550] 02 p0183 N85-11225
Observation of oxide skin in powder metallurgy aluminum alloys
[AD-A145919] 03 p0331 N85-12135
USSR report: Materials science and metallurgy
[JPRS-UMS-84-007] 03 p0348 N85-12244
Breakdown of porous metals by laser radiation
03 p0349 N85-12249
Comparison between the properties of conventional wrought and powder metallurgical alloys for turbine disc applications 07 p0906 N85-15739
Influence of temperatures of reactants on nature of product of solid-phase reactions
[BLL-M-36019-(5828.4)] 07 p0921 N85-15832
Influence of pressure on compaction during compression of powders of iron and 40Kh and 10R6MS steels
[BLL-M-35995-(5828.4)] 07 p0926 N85-15866
Investigation of granules of molybdenum-base alloys obtained with pulsed discharges
[BLL-M-36012-(5828.4)] 07 p0926 N85-15871
Solid-phase sintering of tantalum carbide
[BLL-M-36013-(5828.4)] 07 p0926 N85-15872
Fatigue strength of different sintered steels and design criteria for porous material (PM) parts
[LBF-FB-170/84] 07 p0928 N85-15886
Rapid solidification processing and powder metallurgy of Al alloys
[AD-A148427] 08 p1130 N85-17120
Application of diffusion welding of nickel based metals and application of electron beam welding of hot isostatically pressed nickel based powdered metals
08 p1169 N85-17375
Deformation and fracture of P/M (Powder/Metallurgy) titanium alloys
[AD-A148672] 09 p1294 N85-18128
Sub-eutectic densification and second phase formation in Al2O3 - CaO
[DE85-002065] 09 p1398 N85-18796
Research on rapidly solidified alloys
[AD-A149380] 10 p1441 N85-19080
Characterization of Nb-8 wt % Al wires by analytical electron microscopy
[DE85-002726] 10 p1442 N85-19086
Alloys based on NiAl for high temperature applications
[NASA-TM-86976] 12 p1805 N85-21322
Stress corrosion cracking behavior of tungsten heavy alloys
[AD-A149843] 12 p1806 N85-21329
USSR report: Materials science and metallurgy
[JPRS-UMS-85-002] 13 p2025 N85-22688
Effect of phase state of TiC-NiTi powder composite materials on nature of failure and mechanical properties
13 p2027 N85-22702
Apparatus for producing amorphous and microcrystalline metal powders 13 p2030 N85-22720
Fabrication of ceramic substrate-reinforced and free forms
[NASA-TM-86994] 14 p2247 N85-23926
Pressure-density behavior for AlN, Al2O3, SiO2, TiB2, and TiC powders up to 3.5 GPa
[DE85-006146] 14 p2261 N85-24012
Powder metallurgy production problems
15 p2497 N85-25406
Mechanisms of corrosion fatigue in high strength I/M (Ingot Metallurgy) and P/M (Powder Metallurgy) aluminum alloys
[AD-A151177] 15 p2509 N85-25478
Metallurgical characterization of aluminum powder consolidation
[AD-A151990] 15 p2510 N85-25484
Interfacial and colloidal aspects of aqueous suspension containing oxidic powders
[DE85-005972] 15 p2519 N85-25534
Powder metallurgy bearings for advanced rocket engines 16 p2736 N85-26881
Microstructures and properties of rapidly solidified alloys
[NASA-CR-172377] 16 p2748 N85-26961
East Europe report: Science and technology
[JPRS-ESA-85-019] 16 p2767 N85-27077
Research on products obtained by powder metallurgy
16 p2768 N85-27081
Powder-metallurgy alloys and steels
[BLL-BISI-TRANS-22239-(9022.06)]
17 p2926 N85-28050
Sintering and properties of metal-ceramic alloys of the Kovar type
[BLL-BISI-TRANS-21822-(9022.06)]
17 p2927 N85-28060
Production and compaction of amorphous metal powders
[BLL-BISI-TRANS-22387-(9022.06)]
17 p2929 N85-28080
Dispersion-strengthened powder-metallurgical chromium steels
[BLL-BISI-TRANS-22323-(9022.06)]
17 p2929 N85-28081
Preparation of sinteractive silicon nitride powders
[BMFT-FB-T-84-303] 18 p3082 N85-29066
French, UK, Swedish research in powder metallurgy, HIP 18 p3088 N85-29109
Powder metallurgy forged gear development
[NASA-TM-87483] 18 p3117 N85-29256
USSR report: Materials Science and Metallurgy
[JPRS-UMS-85-005] 19 p3241 N85-30686
Hot isostatically pressed Sm(2)(TM)17 magnets
[AD-A155479] 21 p3582 N85-32257
Experimental attempt to achieve microstructure variations through temperature/time permutations for a nonwrought powder metallurgy uranium-6 niobium alloy
[DE85-013166] 23 p3916 N85-34272
The read-out system of spatial distribution of thermoluminescence in meteorites
[SH-9.1-16] 23 p4052 N85-35131
Method for measuring surface activity of silicon nitride powder
[NASA-TM-77906] 24 p4073 N85-35242
Oxidation resistant slurry coating for carbon-based materials
[NASA-CASE-LEW-13923-1] 24 p4077 N85-35267

POWDERED ALUMINUM
Observation of oxide skin in powder metallurgy aluminum alloys
[AD-A145919] 03 p0331 N85-12135
Non-steady combustion of composite solid propellants
[AD-A150827] 14 p2250 N85-22947
A fundamental study of liquid phase particle breakup. Revision
[AD-A150791] 14 p2301 N85-24249
Means for reducing hydrogen concentration upon surfacing of antifriction aluminum alloys with powder electrode 19 p3247 N85-30132

POWDERED METALS
U METAL POWDER

POWER
Circuit engineering and technological optimization of very high speed LSI logic elements and transistor structures 03 p0347 N85-12237

POWER AMPLIFIERS
Development of the Antares electron gun
[DE84-014043] 01 p0053 N85-10352
Spectrally matched modulation of radiation of injection laser in traveling-wave amplifier below 2 GHz
02 p0262 N85-11712
Metal oxide semiconductors power transistors
[CNES-84/OPE/FT/190] 04 p0496 N85-13168
Perceptibility of nonlinear distortions in power amplifier
06 p0789 N85-15041
Dual-gate MESFET variable gain constant output power amplifier
[AD-D011334] 07 p0945 N85-15982
Semiconductors at Leipzig Spring Fair
09 p1377 N85-18680
Combined microwave parallel amplifier-RF attenuator/modulator
[AD-D011535] 12 p1833 N85-21499
Proposal for continuation of research on megawatt gyrotrons for the period January 1, 1985 through December 31, 1986
[DE85-009962] 18 p3110 N85-29280
Methods of reliability design of semiconductor power devices 22 p3770 N85-33365
Research on gyrotrons
[AD-A154032] 23 p3934 N85-34380

POWER CONDITIONING
Multipurpose 5-MeV linear induction accelerator
[DE84-014523] 02 p0278 N85-11808
Space know-how, twenty years' space experience
04 p0461 N85-12925
Microcomputer control of a residential photovoltaic power conditioning system
[DE84-013867] 04 p0547 N85-13480
An Assessment of Integrated Flywheel System Technology
[NASA-CP-2346] 05 p0604 N85-13850
Microcomputer control of a residential photovoltaic power conditioning system
[DE84-014774] 07 p1022 N85-16485
Compilation of Sandia papers contributed to the 17th IEEE Photovoltaic Specialists Conference
[DE84-017456] 09 p1315 N85-18267
Variable speed generator technology options for wind turbine generators
[RR-84-4] 10 p1478 N85-19331
Inelastic tunnel diodes
[NASA-CASE-LEW-13833-1] 12 p1832 N85-21492
Autonomous uninterruptable power supply apparatus
[AD-D011571] 14 p2298 N85-24232
Advanced energy storage systems
[AD-A152244] 16 p2741 N85-26815
The plasma erosion opening switch
[AD-A154942] 21 p3580 N85-32259
Design and construction of an advanced power conditioning subsystem for small photovoltaic applications
[DE85-013940] 24 p4113 N85-35485

POWER DENSITY (ELECTROMAGNETIC)
U RADIANT FLUX DENSITY
POWER EFFICIENCY
Cylinder power fault diagnosis in military diesel engines
[TT-8405] 01 p0053 N85-10354
Measurements of satellite refrigeration compressor power consumption and efficiency
[DE84-016724] 05 p0632 N85-14056
High-power gate turn-off thyristors
06 p0793 N85-15071
New methods of fast switching of high power by means of semiconductor devices 06 p0794 N85-15075
Use of braking stages for control of turbine speed
09 p1306 N85-18215
Study of low energy density photovoltaic applications under varying rate structures
[DE85-000185] 10 p1511 N85-19538
Thermionic converter for space reactor described
11 p1621 N85-20208
The relevance of averaging period to wind power measurements and efficiency of Wind Energy Conversion Systems (WECS)
[GKSS-84-E-35] 11 p1676 N85-20562
Estimation of gas turbine engine boost provided by injecting water behind compressor
13 p2051 N85-22838
The ferrite permanent magnet AC motor: A technical and economical assessment
[DE85-002480] 13 p2066 N85-22903
Effect of diaphragm leakage on turbine stage characteristics 14 p2286 N85-24168
The effects of cooling on delay-time limits in IC's
14 p2297 N85-24224
The measurement of laser beam parameters
14 p2308 N85-24283
Aspects of CSSR CMOS integrated circuits discussed
15 p2533 N85-25627
Advanced energy storage systems
[AD-A152244] 16 p2741 N85-26915
Effect of precipitation on wind turbine performance
[NASA-TM-86986] 16 p2818 N85-27385
Commercialization of the power factor controller
[NASA-CR-171500] 17 p2951 N85-28221
On power effecient operation of the 2m x 2m transonic wind tunnel at the National Aerospace Laboratory
[NAL-TR-847] 18 p3064 N85-28953
Intense excitation source for high power laser
[AD-A153424] 18 p3112 N85-29267
Wind tunnel results of advanced high speed propellers in the takeoff, climb and landing operating regimes
[NASA-TM-87054] 19 p3213 N85-29925
Increased voltage photovoltaic cell
[NASA-CASE-NPO-16155-1] 19 p3303 N85-30475
Free-piston Stirling engine/linear alternator 1000-hour endurance test
[NASA-CR-174771] 19 p3304 N85-30481
A new large-scale, high-resolution multicolor software display concept
[AD-A155404] 22 p3827 N85-33703
Determination of DTL configurations
[DE85-010714] 22 p3830 N85-33719
Technology of magnetically driven accelerators
[DE85-011857] 23 p3983 N85-34700
Wingtip vortex propeller
[NASA-CASE-LAR-13019-1] 24 p4065 N85-35194
POWER FACTOR CONTROLLERS
Solar powered actuator with continuously variable auxiliary power control
[NASA-CASE-MFS-25637-1] 12 p1876 N85-21769
Power control for ac motor
[NASA-CASE-MFS-25861-1] 13 p2062 N85-22877
Commercialization of the power factor controller
[NASA-CR-171500] 17 p2951 N85-28221
POWER GENERATORS
U ELECTRIC GENERATORS
POWER LIMITERS
Monolithic planar doped barrier limiter
[AD-D011578] 15 p2548 N85-25723
POWER LINES
EMP injection on conduit entries, type Brattberg — electromagnetic pulse (EMP) injection
[FOA-E-30001-A3] 02 p0193 N85-11290
Pulsed-power system diagnostics: Electromagnetic data interpretation along pulse lines
[AD-A146607] 06 p0810 N85-15148
The ac power line protection for an IEEE 587 Class B environment 07 p1000 N85-16347
Adaptation of an air-dielectric RF cable for use as an oil-filled high voltage pulse transmission line
[DE84-017414] 11 p1630 N85-20265
Electromagnetic pulse (EMP) injection on cable entries, type ERA; EMP memo no. 10
[FOA-E-30003-A3] 12 p1830 N85-21484
Study of electric field and ion effects on HVDC lines
[DE85-002975] 12 p1833 N85-21503
Numerical/Electromagnetics Code (NEC)
[DE85-004999] 13 p2056 N85-22874
Operational test results of a prototype superconducting power transmission system and their extrapolation to the performance of a large system
[DE85-006731] 16 p2779 N85-27153
Unalloyed and alloyed line wires of improved properties
[BLL-BISI-TRANS-21930-(9022.06)]
16 p3073 N85-29008
Effects of Formvar coating and copper-nickel outer sheath on the ac losses of multi-strand subsize cables
[DE85-010413] 18 p3096 N85-29166
Protection products for the conductors of high voltage overhead lines
[BLL-OA-TRANS-3219-(6196.300)]
20 p3429 N85-31269
New corrosion protection concept for very high voltage line towers
[BLL-OA-TRANS-2691-(6196.300)]
20 p3429 N85-31270
Injector losses on Mite
[DE85-012356] 24 p4090 N85-35355
RFQ modeling computer program
[DE85-012665] 24 p4140 N85-35661
POWER PLANTS
Combustion chamber floatwall panel attachment arrangement
[AD-D011358] 07 p1047 N85-16647
Leak detectors for organic Rankine cycle power plants: On-line and manual methods
[DE85-002792] 12 p1852 N85-21617
A model for the economic assessment of solar power plants
[DE85-009355] 19 p3381 N85-30977
POWER PROCESSING SYSTEMS
U POWER CONDITIONING
POWER REACTORS
In-situ stress relief of expanded alloy 600 steam generator tubing
[DE84-014560] 04 p0513 N85-13273
A new rheological model for concrete structural analysis
[DE84-014743] 11 p1653 N85-20413
Development of the Cascade inertial-confinement-fusion reactor
[DE85-010933] 19 p3357 N85-30812
Transient three-phase three-component systems. Part 1: Formulation of the system of differential equations
[DE85-013267] 24 p4095 N85-35384
DEPTH-CHARGE static and time-dependent perturbation/sensitivity system for nuclear reactor core analysis, revision 1
[DE85-013103] 24 p4139 N85-35659
Applicability of 100kWe-class of space reactor power systems to NASA manned space station missions
[NASA-CR-174696] 24 p4149 N85-35728
POWER SERIES
NT TAYLOR SERIES
Polynomial and power series FGS-rings have trivial coefficient rings
[TWISK-326] 01 p0109 N85-10737
A simple and efficient algorithm to compute tail probabilities from transforms
[AD-A150928] 14 p2409 N85-24849
Use of REDUCE 2 for symbolic programming
[INPE-3355-PRE/633] 16 p2846 N85-27544
POWER SPECTRA
The average power density spectra of additive scrambler signals and their versions in AMI code
[FUB-27-1983] 01 p0040 N85-10258
Shape of power spectrum of intermittent chaos
02 p0283 N85-11841
Phase transition which exhibits 1/omega-spectrum: A rigorous result 02 p0283 N85-11842
Using measured variance of skywave radar sea-echo power spectra to estimate ionospheric Doppler broadening of mean spectra
[PB84-214071] 03 p0399 N85-12544
Noise analysis of the Coarse Optical Power Spectrum Estimator (COPSE) data acquisition system
[AD-A145918] 03 p0419 N85-12677
On syntheses of the X-ray background with power-law sources
[NASA-TM-82173] 03 p0448 N85-12840
Flight test technique for evaluation of gust load alleviation analysis methodology
[NASA-TM-86344] 06 p0754 N85-14833
Power spectrum analysis of astronomical photographs digitised with small apertures 07 p0965 N85-16127
Power spectral ensity of markov texture fields
07 p0986 N85-16262
Electrostatic wave observation during a space simulation Beam-Plasma-Discharge (BPD)
[NASA-CR-174286] 07 p1045 N85-16639
A nonlinear technique for high-resolution data processing
[AD-D011415] 08 p1203 N85-17570
NOAA OTEC CWP (National Oceanic and Atmospheric Administration Ocean Thermal Energy Conversion Cold Water Pipe) at-sea test. Volume 3, part 1: Tabulation of the power spectra for selected channels
[PB84-238955] 09 p1346 N85-18467
MTF analysis of LANDSAT-4 Thematic Mapper
12 p1871 N85-21737
The use of the spectral matrix in analyzing the propagation characteristics of electromagnetic emissions — magnetosphere 14 p2371 N85-24658
Evaluation of a magneto-optical filter and a Fabry-Perot interferometer for the measurement of solar velocity fields from space 14 p2442 N85-25067
Detection of solar gravity mode oscillations
14 p2442 N85-25070
Solar gravity modes from ACRIM-SWM irradiance data
14 p2443 N85-25071
Implications of observed frequencies of solar P modes
14 p2443 N85-25073
The effects of a nearly 100% duty cycle in observations of solar oscillations 14 p2443 N85-25078
Spectral information from gapped data. A comparison of technique 14 p2444 N85-25080
The stability of the low-degree 5-minute solar oscillations 14 p2444 N85-25084
An excitation mechanism fo: solar 5-minute oscillation of intermediate and high degree
14 p2444 N85-25085
Rational pulse-shaping filters for almost MSK-like modulation
[AD-A153065] 17 p2949 N85-28208
Projections of plasma cloud structures and their spectra
[AD-A153608] 18 p3189 N85-29776
Estimate of signal-to-interference energy ratio in discrete-data transmission 22 p3776 N85-33398
Cosmic ray biannual variation
[SH-4.4-15] 23 p4034 N85-35011
Cosmic ray power spectral variations. 3: Solar rotation periodicities
[SH-4.4-16] 23 p4034 N85-35012
A relation between the short time variations of cosmic rays and geomagnetic field change
[SH-5.1-14] 23 p4043 N85-35067
Pressure cross spectra in turbulent boundary layers in water
[AD-A156153] 24 p4094 N85-35378
Noise in sodium beta alumina crystals
[AD-A156025] 24 p4161 N85-35798
POWER SUPPLIES
DC switching regulated power supply for driving an inductive load
[DE84-014238] 01 p0044 N85-10285
Design, construction, and operational results of an 800-A, 10-kV hot deck amplifier
[DE84-014044] 04 p0496 N85-13162
Distributed energy store railguns experiment and analysis 09 p1313 N85-18256
All solid state high voltage power supply for neutral beam sources
[DE85-002531] 11 p1629 N85-20257
Photovoltaic industry progress through 1984
[DE85-013029] 22 p3809 N85-33596
POWER SUPPLY CIRCUITS
Isolated load switching with surge suppression
[AD-D011218] 01 p0042 N85-10274
Control aspects of the Schuchuli Village stand-alone photovoltaic power system
[NASA-TM-83790] 04 p0495 N85-13157
Developments in space power components for power management and distribution 05 p0608 N85-13877
Fuse status indicator system
[AD-D011294] 06 p0804 N85-15121
High-voltage, high-power, solid-state remote power controllers for aerospace applications
[NASA-TP-2437] 12 p1795 N85-21263
Erosion of electrodes due to switching of capacitor-bank discharge circuits
[AD-A151207] 15 p2547 N85-25718
China report: Science and technology
[JPRS-CST-85-011] 15 p2551 N85-25746
Improved Gonda's circuit described
15 p2551 N85-25748
Using a single-board computer to maintain constant voltage, current sources 15 p2551 N85-25749
POWER TRANSMISSION
Vibrational power transmission of an idealised gearbox
[ISVR-TR-124] 02 p0204 N85-11346
Operational characteristics of a 1000 MVA superconducting power transmission system
[DE85-000232] 09 p1314 N85-18263

Superconducting magnetic energy storage for asynchronous electrical systems
[DE85-005966] 22 p3847 N85-33832

POWER TRANSMISSION (LASERS)
Technology for satellite power conversion
[NASA-CR-174335] 09 p1343 N85-18451

POWERED LIFT AIRCRAFT
Future of V/STOL aircraft systems: A survey of opinions
[NASA-TM-86689] 18 p3061 N85-28937

POYNTING THEOREM
Theoretical approach to evolution of solar magnetic field 18 p3204 N85-29874

PPI (POSITION INDICATORS)
U PLAN POSITION INDICATORS

PPM (MODULATION)
U PULSE POSITION MODULATION

PRACTICES
U PROCEDURES

PRAESEPE STAR CLUSTERS
The behaviour of brighter binaries and yellow giants in open clusters 05 p0737 N85-14738

PRAIRIES
U GRASSLANDS

PRANDTL NUMBER
Influence of Prandtl number on natural convection heat transfer correlations
[DE84-013006] 05 p0637 N85-14089
High Marangoni number convection in a square cavity
[NASA-CR-174283] 07 p0959 N85-16078
Internal forced convection to low Prandtl number gas mixtures
[AD-A148932] 10 p1484 N85-19386
Contribution to the theory of stationary separation areas
[NASA-TM-77825] 14 p2300 N85-24244

PRANDTL-MEYER EXPANSION
The highly underexpanded exhaust plume from nozzles with boundary layers
[DFVLR-FB-85-10] 20 p3421 N85-31230

PRASEODYMIUM
Supercell band structure calculations of the two peak photo-and inverse photoemission spectra in Ce and Pr compounds
[DE84-017485] 06 p0867 N85-15513
Very low temperature studies of hyperfine effects in metals
[DE85-013367] 22 p3749 N85-33236

PRE-MAIN SEQUENCE STARS
Molecular hydrogen emission associated with high velocity flows. A tracer for low velocity shocks
03 p0443 N85-12819
X-ray activity in pre-main sequence stars
08 p1233 N85-17764
Active phenomena in the pre-main sequence star AB AUR 08 p1233 N85-17765
A search for young stellar chromospheres in NGC 2264 11 p1748 N85-20993

PREAMPLIFIERS
New preamplifier for particle detectors
[DE85-004115] 12 p1836 N85-21524
Tubes and transistors in audio amplifiers
12 p1837 N85-21532
Recommendation on use of series K157UL1 microcircuits 13 p2071 N85-22936
Fast scintillation counter preamplifier for the observation of Linsley effect
[HE-4.7-9] 24 p4199 N85-36060
A mini-array for large air showers
[HE-4.7-10] 24 p4199 N85-36061

PREBURNERS
Analysis of physical-chemical processes governing SSME internal fluid flows
[NASA-CR-174245] 06 p0760 N85-14862
An investigation of space shuttle main engine shutdown chugging instability 12 p1946 N85-22221
Fiber optic Raman thermometer for Space Shuttle main engine preburner profiling 16 p2739 N85-26904
SSME fuel preburner two-dimensional analysis
17 p2911 N85-27943

PRECAMBRIAN PERIOD
Archean sedimentation and tectonics in southern Africa
[NASA-CR-174156] 04 p0533 N85-13408
Constraints on lunar origin: Evidence preserved in Precambrian stromatolites 04 p0564 N85-13731
Synthesis of proterozoic data as a prerequisite for tectonic and thermal modeling
[NASA-CR-174252] 07 p0995 N85-16323
SIR-B analysis of the Precambrian shield of Sudan and Egypt: Penetration studies and subsurface mapping
08 p1145 N85-17219
Structural investigation of the Canadian Shield by orbital radar and LANDSAT 08 p1147 N85-17236
Late precambrian to ordovician metamorphism and orogenesis in the Blue Ridge and western Piedmont, Virginia Appalachians 09 p1352 N85-18503
Precambrian evolution and the rock record
21 p3656 N85-32711
Use of space photographs for analysis of structural and dynamic conditions of formation of ancient phlogopite and apatite deposits 22 p3735 N85-33153

PRECAUTIONS
U ACCIDENT PREVENTION

PRECESSION
NT QUENCHING (ATOMIC PHYSICS)
Earth rotation and polar wandering
14 p2399 N85-24785

PRECIOUS METALS
U NOBLE METALS

PRECIPITATION
Monthly and seasonal weather outlook for October 1984, volume 38, number 19, 29 September 1984
[PB85-113536] 11 p1687 N85-20610
Monthly and seasonal weather outlook for January 1985, volume 39, number 1
[PB85-148790] 12 p1898 N85-21915

PRECIPITATION (CHEMISTRY)
The X-ray Absorption Coefficient Fine Structure (EXAFS) study on precipitates in AlCu
[DESY-SR-84-15] 01 p0025 N85-10153
Rapid solidification processing and the control of structure/property relationships
02 p0176 N85-11178
A study of precipitation and boron distribution in 20 Cr 25Ni base stainless steels
[AERE-M-3353] 03 p0334 N85-12154
Investigation of the isothermal precipitation behavior of nickel-base alloys using electrochemical phase extraction
[JUEL-1903] 05 p0619 N85-13958
Microstructure, texture and formability of thin aluminium sheets 06 p0796 N85-15068
Clusters of defects in semiconductors
[AD-A147426] 07 p1048 N85-16655
Effect of powder characteristics on microstructure and properties in alkoxide prepared PZT ceramics
[AD-A149062] 10 p1451 N85-19141
Geothermal injection treatment: Process chemistry, field experiences, and design options
[DE85-002873] 11 p1675 N85-20554
Microstructural study on the processing and properties of high-field A15 superconducting materials
[DE85-004652] 13 p2164 N85-23423
MAP3S precipitation chemistry network
[DE85-005324] 14 p2353 N85-24539
An investigation of the structure and high temperature mechanical properties of oxide dispersion strengthened alloys
[AD-A151107] 15 p2509 N85-25477
A comparative evaluation of the effects of acid precipitation, natural acid production and harvesting of cation removal from forests
[DE85-005254] 15 p2589 N85-25961
Thermal annealing of Fe implanted Al2O3 in oxidizing and reducing environment: Revised version
[DE85-007546] 16 p2752 N85-26983
The precipitation mechanism in a metallic solid solution crystal: Case of the aluminum-copper and aluminum-silver systems
[DE85-009981] 18 p3077 N85-29032
North American acid deposition data base system (ADS) and its use in spatial analysis
[PB85-173235] 18 p3201 N85-29856
Electrochemical reduction of titanium in dimethyl sulphoxide
[BLL-OA-TRANS-3225-(6196.300)]
20 p3429 N85-31267
A study of the effect of a mismatch in gamma and gamma prime phase lattice spacings on the high temperature strength characteristics of dispersion-hardened nickel alloys
[BLL-CE-TRANS-8048-(9022.09)]
20 p3430 N85-31279
Effect of precipitation variables on the specific surface and explosion characteristics of pentaerythritol tetranitrate
[DE85-009620] 23 p3922 N85-34302

PRECIPITATION (METEOROLOGY)
NT ACID RAIN
NT RAIN
NT SNOW
NT SNOW COVER
Geostationary satellite cloud and precipitation analysis using an interactive computer system
01 p0076 N85-10506
Test results from RAINSAT 01 p0076 N85-10508
A tropical cyclone precipitation estimation technique using geostationary satellite data
[PB84-226703] 01 p0086 N85-10579
The identification of rain-bearing synoptic systems through principal component analysis
02 p0212 N85-11394
The application of principal component analysis in a study of rainfall 02 p0212 N85-11396
Spatial relationships in stream flow residuals
02 p0212 N85-11397
Forecast of the northeastern drought by the method of periodicities: Use and abuses
[INPE-3109-PRE/508] 02 p0230 N85-11502
Heat sources in the tropics and large scale flow anomalies associated with precipitation anomalies in northeast Brazil
[INPE-3211-TDL/175] 04 p0538 N85-13421
Weather research program report; FY 1983
[PB84-236694] 04 p0541 N85-13440
Studies of atmospheric water in storms with the Nimbus 7 scanning multichannel microwave radiometer
05 p0682 N85-14382
Trends in skill and accuracy of National Weather Service pop forecasts
[PB84-229053] 06 p0840 N85-15336
Precipitation characteristics of a dual mesoscale convective complex
[PB84-226711] 06 p0840 N85-15337
Revised Uniform Summary of Surface Weather Observations (RUSSWO). Alconbury RAF United Kingdom, parts A-F
[AD-A146913] 07 p1004 N85-16384
Revised Uniform Summary of Surface Weather Observations (RUSSWO). McChord AFB, Washington, parts A-F
[AD-A146914] 07 p1005 N85-16385
Revised Uniform Summary of Surface Weather Observations (RUSSWO). Mildenhall RAF, United Kingdom, parts A-F
[AD-A146915] 07 p1005 N85-16386
Revised Uniform Summary of Surface Weather Observations (RUSSWO). Dobbins AFB, Georgia, parts A-F
[AD-A146916] 07 p1005 N85-16387
Revised Uniform Summary of Surface Weather Observations (RUSSWO). Shemya AFB, Alaska, parts A-F
[AD-A146917] 07 p1005 N85-16388
Revised Uniform Summary of Surface Weather Observations (RUSSWO). Pope AFB, Fayetteville, North Carolina, parts A-F
[AD-A146918] 07 p1005 N85-16389
Revised Uniform Summary of Surface Weather Observations (RUSSWO). Sondestrom AB, Greenland, parts A-F
[AD-A146919] 07 p1005 N85-16390
Revised Uniform Summary of Surface Weather Observations (RUSSWO). England AFB, Alexandria, Lousiana, parts A-F
[AD-A146920] 07 p1006 N85-16391
Revised Uniform Summary of Surface Weather Observations (RUSSWO). Parts A-F: Homestead AFB, Florida
[AD-A147203] 07 p1007 N85-16396
Limited surface observations climatic summary (LISOCS). Camp Casey, Tong Du Chon, Korea
[AD-A147204] 07 p1007 N85-16397
Limited surface observatins climatic summary (LISOCS). Ansback AHP, Germany
[AD-A147205] 07 p1007 N85-16398
Revised Uniform Summary of Surface Weather Observations (RUSSWO). O'Hare International Airport, Chicago, parts A-F
[AD-A147206] 07 p1007 N85-16399
Methodology for the collection and analysis of trace metals in atmospheric precipitation
[CM-67] 09 p1350 N85-18491
Revised Uniform Summary of Surface Weather Observations (RUSSWO). Parts A-F Zweibrucken AB, Germany
[AD-A147165] 09 p1357 N85-18536
Mesoscale storm and dry period parameters from hourly precipitation data: Program documentation
[DE85-001366] 09 p1357 N85-18538
Sequential precipitation chemistry sampling program at Brookhaven National Laboratory with an analytical summary of 1976-1982 data
[DE85-002788] 10 p1513 N85-19545
Large scale circulation anomalies and prediction of northeast Brazil droughts
[INPE-3405-PRE/674] 10 p1518 N85-19571
Interannual variations of the winter circulation in the Northern Hemisphere and in the southern oscillation (meridian) and their possible connections with the climate of Northeast Brazil
[INPE-3333-TDL/182] 10 p1519 N85-19573
Frozen precipitation and concurrent weather: A case study for Munchen-Riem, West Germany
[AD-A149227] 10 p1519 N85-19577

Precipitation gage network operations for wintertime research in the Central Sierra Nevada [PB85-115020] 10 p1520 N85-19582

Computer-assisted data processing and analysis system for ground-based meteorological data collection, report on the Sierra Cooperative Pilot Project [PB85-115350] 10 p1520 N85-19587

Monthly and Seasonal Weather Outlook for November, 1984, Volume 38, Number 27, October 30, 1984 [PB85-116800] 10 p1521 N85-19588

Monthly and seasonal weather outlook for mid-October to mid-November 1984, volume 38, number 20, 13 October 1984 [PB85-113546] 11 p1687 N85-20611

Prospective investigations with DFVLR radar of possible relevance in the assessment of radio interference due to scattering from precipitations — meteorological radar [DFVLR-FB-84-42] 12 p1830 N85-21485

Combined effects of atmospheric deposition, internal acid production, and harvesting on nutrient gains and losses from forest ecosystems [DE85-002325] 12 p1884 N85-21821

OSCAR experiment high-density network data report [DE85-004907] 12 p1884 N85-21826

Hazardous air pollutants: Wet removal rates and mechanisms [PB85-138626] 12 p1887 N85-21842

On the wind error of the Finnish raingauge [REPT-37] 12 p1893 N85-21883

Moisture variation in northern hemisphere temperate latitudes 13 p2105 N85-23119

Relationship of Indian monsoon intensity to time of onset 13 p2106 N85-23120

Summary of Meteorological Observations, Surface (SMOS), Bermuda [AD-A150537] 13 p2138 N85-23278

Summary of Meteorological Observations, Surface (SMOS), Beaufort, South Carolina [AD-A150538] 13 p2138 N85-23279

Summary of Meteorological Observations Surface (SMOS), Sigonella, Sicily/Navy [AD-A150539] 13 p2138 N85-23280

Summary of Meteorological Observations, Surface (SMOS), Alameda, California [AD-A150609] 13 p2138 N85-23281

MAP3S precipitation chemistry network [DE85-005324] 14 p2353 N85-24539

Experimental investigation of annular air curtain domes [UTIAS-288] 15 p2521 N85-25543

An analysis of issues concerning acid rain, report to the Congress of the United States [TI85-901070] 15 p2589 N85-25959

Shuttle imaging radar-B (SIR-B) data analysis for identifying rainfall event occurrence and intensity [NASA-CR-175712] 15 p2594 N85-25986

Severe storm detection with passive 37 GHz observations 15 p2596 N85-25997

High-frequency microwave observations of convective precipitation 15 p2596 N85-26000

Model sensitivity studies of major east coast storms 15 p2598 N85-26016

Characteristics of precipitation regimes during first global atmospheric research project global experiments [AD-A151572] 15 p2599 N85-26021

Annual cycle. Part 2: The annual variation of precipitation over the United States and Canada [PB85-147684] 15 p2600 N85-26027

Cloud-seeding for regulating precipitation in Moscow area 16 p2807 N85-27308

Regularities in recent changes in surface air temperature and atmospheric precipitation fields 16 p2807 N85-27311

Effect of precipitation on wind turbine performance [NASA-TM-86986] 16 p2818 N85-27385

Precipitable water in the atmosphere, determined from surface dewpoint values 16 p2831 N85-27457

Summary of Meteorological Observations, Surface (SMOS), Dallas, Texas [AD-A150599] 16 p2835 N85-27480

A climatic data bank for Northern Hemisphere land areas, 1851-1980 [DE85-007863] 16 p2835 N85-27486

SCPP (Sierra Cooperative Pilot Project) data collection and analysis. Volume 1: Executive summary [PB85-156065] 16 p2837 N85-27494

Monthly and seasonal weather outlook for mid-January to mid-February 1985, volume 39, number 2, January 15, 1985 [PB85-164572] 16 p2837 N85-27500

Monthly and seasonal weather outlook for February 1985, volume 39, number 3, January 30, 1985 [PB85-159424] 16 p2838 N85-27502

Precipitation and snow cover data, 1977 [ISBN-951-697-215-2] 17 p2995 N85-28514

Environmental Research Division report: Atmospheric physics [DE85-009659] 18 p3133 N85-29404

Elemental tracers of source regions of contaminants in precipitation [DE85-007366] 18 p3133 N85-29407

Cloud physics 18 p3147 N85-29485

Areal coverage of storm precipitation [NASA-CR-176013] 19 p3315 N85-30550

Precipitation estimation using collocated GOES satellite and surface data [AD-A154248] 19 p3317 N85-30559

Monthly and seasonal weather outlook for mid-March to mid-April 1985, March 14, 1985, volume 39, no. 6 [PB85-174751] 19 p3317 N85-30565

Measurements of giant salt nuclei from inland in east China 21 p3648 N85-32668

Monthly and seasonal weather outlook for April 1985, March 30, 1985, volume 39, no. 7 [PB85-183604] 22 p3617 N85-33646

Throughfall rate and chemistry studies: Whiteface Mountain [DE85-012407] 23 p3947 N85-34464

PRECIPITATION HARDENING

Strain hardening and strain aging in Fe-Al-Mn alloys 02 p0178 N85-11198

The effect of potential on the corrosion fatigue behavior of a precipitation hardened aluminum alloy [AD-A146537] 06 p0768 N85-14916

Anomalies of aluminum structure and properties 13 p2026 N85-22693

Age hardening and atomic structure of an aluminum-6 at. % silver alloy [DE85-009977] 18 p3077 N85-29031

Influence of gamma-phase on magnetic properties and structure of KhK15YuB alloy during strain-aging [BLL-M-36281-(5828.4)] 20 p3431 N85-31260

Thermomechanical deformation in the presence of metallurgical changes 20 p3466 N85-31533

The dynamic strain ageing of A533B class 1 nuclear pressure vessel steel [AERE-R-11485] 24 p4078 N85-35274

PRECIPITATION PARTICLE MEASUREMENT

Experimental study of anisotropy of scattering of radar signals by clouds and precipitation 14 p2340 N85-24473

Modeling of radiothermal radiation of rain by Monte-Carlo method 14 p2341 N85-24476

Experimental and theoretical investigations of open resonators — precipitation measurement [DFVLR-FB-85-12] 20 p3449 N85-31414

PRECIPITATORS

NT ELECTROSTATIC PRECIPITATORS

Acoustic agglomeration methods and apparatus [NASA-CASE-NPO-15466-1] 12 p1927 N85-22104

PRECISION

Publications of Center for Manufacturing Engineering (of the National Bureau of Standards), 1978-1983 [PB84-224526] 01 p0036 N85-10228

East Europe report: Science and technology [JPRS-ESA-84-045] 06 p0815 N85-15175

Power of deterministic thinking in machine tool accuracy [DE85-001751] 07 p0974 N85-16188

Proceedings of the Workshop on Improvements to Photometry [NASA-CP-2350] 08 p1250 N85-17892

History of photometric precision 08 p1250 N85-17893

Photometric precision needed for planetary detection 08 p1250 N85-17894

Reduction to outside the atmosphere and statistical tests used in Geneva photometry 08 p1251 N85-17902

Operational experience with ion concentration sensors in orientation systems 13 p1980 N85-22422

Method for determining the number of correlative measurements required to validate the SBUV/2 ozone retrievals 13 p2105 N85-23114

Precision linear ramp function generator [DE85-011647] 22 p3760 N85-33304

Analyzer, flight line [AD-A155777] 24 p4067 N85-35207

PREDICTION ANALYSIS TECHNIQUES

Aerodynamics of airfoils subject to 3-dimensional periodic gusts [AD-A145149] 01 p0003 N85-10018

The use of fixed-bed adsorber models to predict the fluxes of toxic substances in groundwaters and soil environments [PB84-202563] 01 p0071 N85-10468

Prediction of deflections of the vertical by gravimetric methods [PB84-213727] 01 p0072 N85-10478

On probability forecasts for temperature 01 p0084 N85-10565

Automated aircraft icing forecast technique [AD-A144853] 01 p0085 N85-10571

A tropical cyclone precipitation estimation technique using geostationary satellite data [PB84-226703] 01 p0086 N85-10579

The prediction of observer responses from photometric data on smoke screens; an analysis of the Oldebroek 2 trials, May 1981 [IZF-1984-21] 01 p0095 N85-10642

Credibility approximations for Bayesian prediction of second moments [AD-A144[illegible]] 01 p0113 N85-10768

KrCl lasers for fusion [DE84-012210] 01 p0122 N85-10835

Structure and evolution of the large scale solar and heliospheric magnetic fields [NASA-CR-175268] 01 p0130 N85-10897

VORCOR: A computer program for calculating characteristics of wings with edge vortex separation by using a vortex-filament and-core model [NASA-CR-165902] 02 p0135 N85-10921

Nonlinear structural and life analyses of a turbine blade 02 p0141 N85-10954

Nonlinear structural and life analyses of a combustor liner 02 p0141 N85-10955

Gas side heat transfer: 2-D flow 02 p0142 N85-10965

Gas flow environment and heat transfer nonrotating 3D program 02 p0142 N85-10966

Life prediction and constitutive behavior: Overview 02 p0143 N85-10973

Validation of structural analysis methods using the in-house liner cyclic rigs 02 p0146 N85-10987

Three dimensional separation and vortex formation 02 p0196 N85-11308

A constitutive modeling technique based on a generalized rheological model to predict the response of materials 02 p0207 N85-11368

Reliability considerations for the total strain range version of strainrange partitioning [NASA-CR-174757] 02 p0209 N85-11380

Statistical interpretation of NWP model output: An overview of techniques used and results achieved [REPT-551.509.313] 02 p0231 N85-11503

An algorithm for least squares projections onto the intersection of shifted, convex cones [AD-A145428] 02 p0251 N85-11640

An asymptotic theory for logistic regression when some predictors are measured with error [AD-A145673] 02 p0254 N85-11666

Energetic electrons in impulsive solar flares 02 p0303 N85-11962

Estimation of helicopter performance using a program based on blade element analysis [AD-A146341] 03 p0318 N85-12055

Development of a pavement maintenance management system. Volume 9: Development of airfield pavement performance prediction models [AD-A146150] 03 p0321 N85-12069

Fatigue-impact studies in laminated composites [AD-A142841] 03 p0326 N85-12097

Modeling of propulsive jet plumes--extension of modeling capabilities by utilizing wall curvature effects [AD-A146262] 03 p0362 N85-12324

Laser velocimeter measurements and analysis in turbulent flows with combustion. Part 3: A correction lens for laser Doppler measurements in a cylindrical tube [AD-A146206] 03 p0366 N85-12348

Ballpark reliability estimation techniques [AD-A145971] 03 p0369 N85-12357

Computer molecular dynamics of 2-D water (ice) structures under shock [AD-A145818] 03 p0372 N85-12375

Recent examples of mesoscale numerical forecasts of severe weather events along the east coast [NASA-TM-86172] 03 p0395 N85-12523

Development of a microcomputer coupled atmospheric and oceanic boundary layer prediction model [AD-A146334] 03 p0397 N85-12530

Prediction of wave height of wind-generated seas in finite water depth [AD-A145996] 03 p0398 N85-12539

Filtering and prediction performance for a class of systems with uncertain parameters [AD-A146145] 03 p0411 N85-12630

Simple prediction of convergence zone propagation in waters around australia [AD-A145986] 03 p0416 N85-12659

Vertical coherence along a macroray path in an inhomogeneous anisotropic ocean [AD-A145992] 03 p0416 N85-12660

Prediction of long term strength of glass reinforced plastics in wet environments [NPL-DMA(A)-80] 04 p0477 N85-13041

Non-linear data fitting for the analysis of creep rupture data on GRP materials in aggressive environments --- glass reinforced plastics (GRP) [NPL-DMA(A)-79] 04 p0512 N85-13261
Weather research program report; FY 1983 [PB84-236694] 04 p0541 N85-13440
Computer programs to predict induced effects of jets exhausting into a crossflow [NASA-CR-166591] 05 p0592 N85-13776
Prediction of force coefficients for labyrinth seals 05 p0644 N85-14130
Critical evaluation of methods to calculate fatigue life 05 p0649 N85-14165
Sequence of effects in the crack initiation and crack propagation phase 05 p0649 N85-14168
Very short range statistical forecasting of automated weather observations [DOT/FAA/PM-84/31] 05 p0679 N85-14359
Some new mathematical methods for variational objective analysis 05 p0681 N85-14375
Extended range forecasting 05 p0681 N85-14376
The period of orbit as a test of the general theory of relativity 06 p0742 N85-14772
Method for predicting the creep rupture life of nickel-base precipitation-hardened superalloys from their chemical composition [BLL-PNR-90241-(8019.3153)] 06 p0768 N85-14910
A comparison of evaporation duct models for IREPS (Integrated Refractive Effects Prediction System) [AD-A146471] 06 p0799 N85-15103
Analyses to develop models to project failure rates and repair costs of electronic modules and subassemblies [AD-A146509] 06 p0816 N85-15180
Modelling of deformation and fracture in high-temperature structural materials [DE84-016906] 06 p0818 N85-15191
Predicting electrochemical breakdown in terrestrial photovoltaic modules 06 p0830 N85-15273
Probable maximum flood estimation - Eastern United States [AD-A146536] 06 p0839 N85-15324
Environmental research laboratories (of the National Oceanic and Atmospheric Administration) programs and plans: FY 1983 programs and FY 1984 plans [PB84-226729] 06 p0840 N85-15336
Prediction of percent body fat for U.S. Navy women from body circumferences and height [AD-A146456] 06 p0845 N85-15370
Parametric estimates of propulsion system maintenance manhours [AD-A147120] 07 p0894 N85-15662
Experiences with the material bevaviour and high temperature low cycle fatigue life prediction of the IN 738 blading alloy 07 p0906 N85-15746
View of future requirements for engine cyclic durability by analysis and testing 07 p0906 N85-15751
Exploring the use of structural models to improve remote sensing agricultural estimates 07 p0965 N85-16259
Evidence accumulation for spatial reasoning 07 p0965 N85-16261
An evaluation of an advection fog prediction model [AD-A147436] 07 p1008 N85-16403
Experiments in forecasting atmospheric marine horizontal visibility using model output statistics with conditional probabilities of discretized parameters [AD-A147574] 07 p1008 N85-16404
Robust prediction and interpolation for vector stationary processes, part 3 [AD-A147960] 07 p1036 N85-16579
Prediction of cruciform all-movable control characteristics at transonic speeds [AD-A147291] 08 p1078 N85-16832
Prediction of dynamic stall characteristics using advanced non-linear panel methods [AD-A148453] 08 p1078 N85-16836
The development and application of aerodynamic uncertainties: And flight test verification for the space shuttle orbiter 08 p1093 N85-16910
Model for prediction of the elastic response of composite materials over wide ranges of concentration [AD-A148186] 08 p1119 N85-17061
Analysis of deflagration to detonation transition in high-energy solid propellants [AD-A148302] 08 p1135 N85-17156
The role of nuclei size in transient cavitation threshold measurements [AD-A148334] 08 p1162 N85-17332
Age life prediction of nylon 66 parachute materials. Part 1: Mechanical properties [AD-A147698] 08 p1170 N85-17378
Atmospheric photochemical modeling of turbine engine fuels. Phase 1: Experimental studies. Volume 2: Environmental chamber data tabulations [AD-A147786] 08 p1185 N85-17470
Estimations of diabatic heating for an explosively-developing maritime cyclone [AD-A147676] 08 p1188 N85-17483
A scheme for short-term prediction of hydrometeors using advection and physical forcing [AD-A148011] 08 p1188 N85-17487
An application of discriminant analysis to the selection of software cost estimating models [AD-A147632] 08 p1204 N85-17580
Probable cause: A decision making framework [AD-A147642] 08 p1210 N85-17614
A variable span smoother [AD-A148241] 08 p1215 N85-17656
On estimating the cost growth of weapon systems [AD-A147297] 08 p1230 N85-17749
Synthesized airfoil data method for prediction of dynamic stall and unsteady airloads [NASA-CR-3672] 09 p1274 N85-18005
Theory of wing rock 09 p1282 N85-18064
Fracture mechanics analysis and prediction of delamination growth in composite structures [FFA-TN-1984-45] 09 p1289 N85-18092
Statistical aspects of shear fracture propagation [ERS-E.368] 09 p1341 N85-18434
Contribution of the study of light aircraft propeller noise [ESA-TT-865] 09 p1378 N85-18667
A comparison between a conventional method and an improved method for predicting tracked vehicle performance [AD-P004276] 09 p1406 N85-18852
A simple prediction model for soil compaction under various wheel loads and geometries as an aid to vehicle design [AD-P004298] 09 p1409 N85-18875
Mechanics of composite materials [DE85-003611] 10 p1432 N85-19031
A comparison between predicted and measured propagation loss in the VHF/UHF range in rugged terrain 10 p1471 N85-19285
Fluidelastic instability in shell and tube heat exchangers: A framework for a prediction method [DE84-006518] 10 p1496 N85-19444
Earthquake-modeling experiment using unique press 10 p1500 N85-19469
Large scale circulation anomalies and prediction of northeast Brazil droughts [INPE-3405-PRE/674] 10 p1518 N85-19571
Assessment of muscle strength and prediction of lifting capacity in US Army personnel [AD-A148846] 10 p1527 N85-19633
Predicting the performance of distributed knowledge-based systems: A modeling approach [AD-A149021] 10 p1545 N85-19738
Physical aspects of the prediction of solar flares [NASA-CR-175487] 10 p1572 N85-19915
Predicting stability of full-scale composite constructions of the basis of stiffness 11 p1599 N85-20054
Improvement of VHF(MB) model [AD-A150087] 12 p1829 N85-21480
Numerical studies of fluid spin-up from rest in a partially-filled cylinder [AD-A150079] 12 p1847 N85-21586
NASA: Model development for human factors interfacing [NASA-CR-175584] 12 p1910 N85-21985
Predicting a future response using rank predictive probabilities [MATHEMATICS-RESEARCH-166] 12 p1923 N85-22077
Method for the prediction of the installation aerodynamics of a propfan at subsonic speeds [NASA-CR-3887] 13 p1969 N85-22369
Reliability predictions for military avionics. Royal Signals and Radar Establishment reliability prediction method no. 250 [BR69221] 13 p1973 N85-22388
Snowmelt runoff model in Japan 13 p2124 N85-23227
Thermal and thermoelastic effects in rolling/sliding contacts [AD-A150435] 13 p2165 N85-23429
Advanced life analysis methods. Volume 4: Tabulated test data for attachment lugs [AD-A151016] 14 p2219 N85-23760
Shuttle payload bay dynamic environments: Summary and conclusion report for STS flights 1-5 and 9 [NASA-CR-175656] 14 p2241 N85-23896
Ordered carbon metal alloys for extraterrestrial power systems [AD-A150881] 14 p2255 N85-23977
Basic EMC (Electromagnetic Compatibility) technology advancement for C3 systems: Model revision for IEMCAP (Intrasystem Electromagnetic Compatibility Analysis Program) [AD-A150795] 14 p2292 N85-24206
Effect of flight sequences in complex load histories on crack front marking 14 p2316 N85-24326
Generation of marker lines by means of marker loads 14 p2318 N85-24327
Results of studies of wave field internal structure in prediction of geological cross section 14 p2346 N85-24504
Characteristics and behavior of atmospheric aerosols; application to prediction of infrared extinction [AD-A150691] 14 p2372 N85-24606
Sensitivity analysis of a coupled atmospheric-oceanic boundary layer model [AD-A150760] 14 p2382 N85-24690
Prediction of vortex-induced loads on wind-tunnel turning vanes [NASA-TM-86678] 15 p2462 N85-25204
Crack growth direction in unidirectional off-axis graphite epoxy [NASA-CR-175752] 15 p2502 N85-25430
Optimizing hot workability and controlling microstructures in difficult to process high strength and high temperature materials [AD-D011586] 15 p2510 N85-25482
Deepwater wind wave growth with fetch and duration [AD-A151604] 15 p2604 N85-26051
On failure modeling, revised [AD-A151411] 15 p2637 N85-26263
Confined turbulent swirling recirculating flow predictions [NASA-CR-174917] 16 p2709 N85-26718
Thrust chamber life prediction 16 p2733 N85-26865
Elevated temperature biaxial fatigue [NASA-CR-175795] 16 p2800 N85-27283
The practical and theoretical significance of small cracks: An evaluation [VTH-LR-432] 16 p2803 N85-27288
An appraisal of the duration of the recent drought in northeast Brazil and a forecast for 1985 [INPE-3477-PRE/720] 16 p2834 N85-27476
Predictions and measurements of isothermal flowfields in axisymmetric combustor geometries [NASA-CR-174916] 17 p2898 N85-27867
SRB filament wound case material property study [NASA-CR-171469] 17 p2910 N85-27940
Reexamination of cumulative fatigue damage laws 17 p2914 N85-27962
VLSI (Very large scale integrated circuits) device reliability models [AD-A153268] 17 p2954 N85-28245
Spectral decomposition and verification of NOGAPS 500MB medium-range forecasts [AD-A152550] 17 p2996 N85-28520
Electronically excited alkaline earth oxides: Chemical production and collisional energy transfer processes [AD-A153172] 17 p3044 N85-28833
Improved statistical analysis method for prediction of maximum inlet distortion [AD-A153767] 18 p3063 N85-28947
Time-averaged and time-dependent computations of isothermal flowfields in a centerbody combustor [AD-A153682] 18 p3100 N85-29189
Turbulent wake of a submerged flat plate [AD-A153776] 18 p3100 N85-29190
Numerical techniques for steady two-dimensional transcritical stratified flow problems, with an application to the intermediate field dynamics of ocean thermal energy conversion plants [DE85-008347] 18 p3151 N85-29509
Wake effects of the aerodynamic performance of horizontal axis wind turbines 19 p3211 N85-29915
Nonlinear potential analysis techniques for supersonic-hypersonic configuration design [NASA-CR-1[illegible]6078] 19 p3212 N85-29917
Fault detection and accommodation testing on an F100 engine in an F-15 airplane [NASA-TM-86735] 19 p3219 N85-29982
Experimental and theoretical study of fatigue crack initiation in metals 19 p3283 N85-30357
Strain-path modeling for geo-materials [AD-A154378] 19 p3286 N85-30380
Mathematical model of global processes in the biosphere 19 p3295 N85-30431
Flood-runoff forecasting with HEC1F [AD-A154286] 19 p3300 N85-30456
Analytical model for predicting emergency shutdown of a two-bladed horizontal axis wind turbine [NASA-TM-83472] 19 p3303 N85-30476
Workshop on objective analysis: Analysis strategies for field-dependent estimation [PB85-179901] 19 p3318 N85-30569
Measurements of folded path optical scintillation using a corner cube, a cat's eye and a flat mirror reflector [AD-A154044] 19 p3367 N85-30879

Radiometry: A useful prediction tool — atmospheric attenuation
[ESA-SP-1071] 20 p3399 N85-31084

Short term determination of the creep properties of high temperature materials
[CRIF-MT-160] 20 p3432 N85-31288

Prediction of lifetime for ceramic materials in the elastic and viscoelastic region by fracture mechanical methods
[ESA-TT-825] 20 p3434 N85-31305

Vortex sheet modeling with higher order curved panels
20 p3451 N85-31428

Heat transfer and fluid mechanics measurements in transitional boundary layer flows
20 p3453 N85-31439

A review and analysis of boundary layer transition data for turbine application 20 p3453 N85-31440

A comparison of millimeter wave, direct detect and heterodyne laser intersatellite links
[AD-A151964] 20 p3461 N85-31496

A comparison of two contemporary creep-fatigue life prediction methods 20 p3467 N85-31538

Two simplified procedures for predicting cyclic material response from a strain history 20 p3467 N85-31543

Creep crack growth predictions in INCO 718 using a continuum damage model 20 p3469 N85-31551

In-service supervision of a pressurized concrete pressure vessel
[OEFZS-4306] 20 p3470 N85-31564

The three-dimensional J-integral. An investigation into its use for post-yield fracture safety assessment
[WTHD-167] 20 p3472 N85-31576

An overview of nonlinear systems identification
[RR-271] 20 p3520 N85-31894

Wall flames and implications for upward flame spread
[FAA-CT-85-2] 21 p3553 N85-32103

Injection of drag reducing additives into turbulent water flows: Two-component velocity measurements and mixing length model predictions
[AD-A154604] 21 p3583 N85-32274

Assessment of the performance of an in-field Gaussian plume/puff model for overwater use
[AD-A155435] 21 p3614 N85-32460

Accuracy and operational use of medium and extended range numerical atmospheric forecasts: A review
[AD-A155027] 21 p3635 N85-32579

Forecasting of tropical cyclone motion using an EOF (Empirical Orthogonal Function) representation of wind forcing
[AD-A155034] 21 p3636 N85-32580

An evaluation of discretized conditional probability and linear regression threshold techniques in model output statistics forecasting of cloud amount and ceiling over the North Atlantic Ocean
[AD-A155100] 21 p3636 N85-32581

Medium range atmospheric forecast system: Evaluation report
[AD-A155240] 21 p3637 N85-32589

Forecasting atmospheric visibility over the summer north Atlantic using the principal discriminant method
[AD-A155537] 21 p3637 N85-32593

A numerical and analytical investigation of lee cyclogenesis
[AD-A155607] 21 p3638 N85-32594

Simulation of the coupled atmospheric and oceanic boundary layer model during MILDEX
[AD-A155166] 21 p3655 N85-32705

On the problem of linear programming with approximate data 21 p3698 N85-32978

A model for predicting propagation-related DSCS (Defense Communications Engineering Center) margin requirements
[AD-A155355] 22 p3756 N85-33281

Predicting electrical performance parameters of underwater cables 22 p3775 N85-33391

Finite element methods for viscoelastic flow
[AD-A154877] 22 p3783 N85-33437

The use of TOMS data in evaluating and improving the total ozone from TOVS measurements
[NOAA-TR-NESDIS-23] 22 p3814 N85-33626

Global environmental transport models for tritium
[DE85-011437] 22 p3816 N85-33639

Comments on the prediction of dynamic stall
[GU-AERO-8501] 23 p3894 N85-34125

Prediction of the flow-field interference induced by the long-range laser velocimeter in the Ames 40- by 80-foot and the 80- by 120-foot wind tunnels
[NASA-TM-86763] 23 p3898 N85-34146

Nonsimultaneous coupled laser velocimeter measurement technique: Error prediction for spatially noncoincident measurements
[NASA-TM-86718] 23 p3934 N85-34379

Lubrication and cooling for high speed gears
[NASA-TM-87096] 23 p3938 N85-34407

Forecasting future industrial SO2 and NC/sub x/ emissions, revised 23 p3947 N85-34461

Cerenkov radiation from periodic electron bunches for finite emission length in air
[AD-A156156] 24 p4090 N85-35352

Development and application of a unified viscoelastic constitutive model for the prediction of material response under thermomechanical loading
24 p4101 N85-35420

Development of a mathematical model for predicting the percentage fatigue life increase resulting from shot peened components
[AD-A155774] 24 p4101 N85-35425

Evaluation of the crack plane equilibrium model for predicting plastic fractures
[DE85-005558] 24 p4102 N85-35431

Meteorological data from the OPTOMA (Ocean Prediction Through Observations, Modeling and Analysis) program OPTOMA 2, leg D2. 30 Jun. - 10 Jul. 1984
[AD-A156134] 24 p4123 N85-35560

The NORDA/FNOC (Naval Ocean Research and Development Activity's/Fleet Numerical Oceanography Center) Polar Ice Prediction System (PIPS)-Arctic: A technical description
[AD-A156332] 24 p4126 N85-35577

Models for assessing workload of aircrews on long distance flights 24 p4129 N85-35599

SASSYS-1 computer code verification with EBR-2 test data
[DE85-012119] 24 p4139 N85-35657

A comparison of multipath arrival structures observed in the presence of a surface duct with predictions obtained using classical ray techniques and the parabolic equation method
[AD-A156024] 24 p4145 N85-35696

PREDICTIONS
NT FLOOD PREDICTIONS
NT IMPACT PREDICTION
NT LINEAR PREDICTION
NT NOISE PREDICTION
NT NOISE PREDICTION (AIRCRAFT)
NT PERFORMANCE PREDICTION

Predictor model for seasonal variations in skid resistance, volume 1
[PB84-226612] 01 p0036 N85-10229

Predicability of mesoscale phenomena
01 p0079 N85-10528

Estimating sunspot number
[NASA-TM-86471] 01 p0130 N85-10896

Effects of surface chemistry on hot corrosion life: Overview 02 p0145 N85-10960

Evaluation of an aerosol prediction model for coastal regions using marine aerosol generation and transport data
[AD-A145443] 02 p0231 N85-11510

Unified approach to sensitivity and uncertainty analysis
[DE84-014049] 02 p0255 N85-11689

On-line fatigue life prediction under stochastic loading by the time series modeling 03 p0370 N85-12362

Seismology today 04 p0523 N85-13346

Geothermal resource assessment for North Dakota
[DE84-016128] 04 p0526 N85-13367

Weather research program report; FY 1983
[PB84-236694] 04 p0541 N85-13440

Tide tables 1985, high and low water predictions, central and western Pacific Ocean and Indian Ocean
[PB84-238393] 04 p0542 N85-13451

Long-range predictive control using weighting-sequence models
[OUEL-1542/84] 04 p0553 N85-13521

Investigation of the relations between neat resin and advanced composite mechanical properties. Volume 1: Results
[NASA-CR-172303] 05 p0612 N85-13911

Evaluation of the crack initiation life behavior of fatigue loaded automotive components made from high strength aluminium alloys
[ESA-TT-733] 05 p0651 N85-14181

Predictions of cockpit simulator experimental outcome using system models 05 p0702 N85-14504

Practical application of IREPS (Integrated Refractive Effects Prediction System)
[AD-A146528] 06 p0838 N85-15323

Two-dimensional lake wave prediction system
[PB84-231034] 06 p0841 N85-15342

General model of earthquakes and the place of warnings in it 07 p0981 N85-16232

The problem of climate and climate variation
07 p1001 N85-16353

Meteorological aspects of the 1982-83 El Nino/southern oscillation episode 07 p1001 N85-16356

The ocean and the dynamics of the tropical atmosphere; its possible predicability 07 p1002 N85-16366

Prediction of cruciform all-movable control characteristics at transonic speeds
[AD-A147291] 08 p1078 N85-16832

Air traffic management concepts for the UK in the 1990's: A review of recent RSRE work
[AD-A147850] 08 p1082 N85-16853

Generalized predictor-corrector methods of high order for the time integration of parabolic differential equations
[CWI-NM-R8402] 08 p1214 N85-17644

A note on the prediction error for small time lags into the future
[AD-A148221] 08 p1215 N85-17654

Design of mismatched Smith predictors using plant step data
[RR-263] 08 p1217 N85-17664

Flame propagation and stabilization studies using Rayleigh scattering and laser Doppler velocimetry
[AD-A148802] 09 p1290 N85-18102

A free shear layer prediction of the turbulent wake of a flat plate towed below a free surface
[AD-A148699] 09 p1319 N85-18293

Prediction of in-sand tire and wheeled vehicle drawbar performance
[AD-P004265] 09 p1404 N85-1884

Prediction accuracy of the torques for rotary tillage by an analog tool
[AD-P004288] 09 p1408 N85-18865

Nonlocal and nonlinear effects on solar oscillations
09 p1416 N85-18934

Low energy antiproton interaction studies at Brookhaven
[DE85-001228] 11 p1720 N85-20820

Modeling 12 p1767 N85-21221

Minister B. V. Balmont on status of automation drive
14 p2284 N85-24151

Study of earthquake preparation processes from distribution of weak tremor epicenters
14 p2345 N85-24501

COSPAS-SARSAT satellite orbit predictor, volume 5
[NASA-TM-85015-VOL-5] 14 p2439 N85-25052

Shuttle fleet operations: A simulation analysis
[AD-A151383] 15 p2491 N85-25370

Significant parameters for predicting flame spread
[PB85-178002] 16 p2760 N85-27034

Use of forest modeling to project acid rain effects
[DE85-005251] 16 p2821 N85-27400

A study of the effect of gently varying terrain on atmospheric flow near the surface
16 p2823 N85-27411

Basic EMC technology advancement for C3 systems. Volume 4F: Prediction of crosstalk in flatpack coaxial cables
[AD-A153111] 17 p2954 N85-28242

Improving the effectiveness of integral property calculation in a CSG solid modeling system by exploiting predictability 17 p3006 N85-28586

Ozone and temperature trends due to the injection of trace species in the atmosphere
[AERONOMICA-ACTA-A-288-1984]
18 p3132 N85-29399

The impact of scatterometer data on limited-area model predictions of the QE 2 storm 18 p3139 N85-29436

SANDRAG: A computer code for predicting drag of bodies of revolution at zero angle of attack in incompressible flow
[DE85-011170] 19 p3338 N85-30684

Ozone in the 21st century: Increase or decrease
[AERONOMICA-ACTA-A-291-1984]
20 p3489 N85-31687

Understanding and laboratory prediction of the atmospheric corrosion behavior of steels and of non-ferrous metals and alloys
[AD-A154642] 21 p3586 N85-32179

Resource management for the tagged token dataflow architecture
[AD-A154773] 21 p3667 N85-32779

Oxidation states of iron in the terrestrial planets: Evidence and implications for accretion models
22 p3852 N85-33854

Comparison of experimental data on detonation velocity and Chapman-Jouget pressure vs initial HE density with predictions from Ree's model equation of state
[DE85-007266] 23 p3922 N85-34304

Evaluation of source strength and dispersion model predications with data from large nitrogen tetroxide field experiments
[DE85-011855] 23 p3947 N85-34465

System expectations for Pioneer 1 foil implosion experiments
[DE85-014129] 24 p4091 N85-35359

Calculation of trajectories of detached wind turbine blades and prediction of site risk levels associated with failures of HAWT's 24 p4110 N85-35475

PREDICTORS
U PREDICTIONS

PREFLIGHT ANALYSIS

Oral presentation of first year final report, appendix A
05 p0602 N85-13840

PREFLIGHT OPERATIONS
NT COUNTDOWN
PREFORMS
Equipment for performing surfaces of optical parts
14 p2266 N85-24043
Negative flexural behavior of precase composite slabs with steel joint 23 p3904 N85-34183
PREHEATERS
U HEATING EQUIPMENT
PREHEATING
U HEATING
PREIMPREGNATION
Quality assurance of composite materials, test report no. 45-649/F 04 p0489 N85-12961
Parametric study of the P9 HT glass fiber finish (Fatigue resistance). Lot no. 1: Report on the microfatigue tests
[CS-794] 05 p0620 N85-13968
PRELAUNCH PROBLEMS
Results of tests of K5NA and a revised formulation of EPDM/cork patch material in MSFC Hot Gas Facility
[NASA-CR-170890] 24 p4073 N85-35238
PRELAUNCH TESTS
NT STATIC FIRING
PRELOADING
U PRESTRESSING
PREMIXED FLAMES
Further developments of a nongradient theory of premixed turbulent flames
[NAL-TR-802T] 01 p0023 N85-10143
Gravitational effects on premixed particle cloud flames
02 p0171 N85-11144
Analysis of pressure gradient-velocity correlation in turbulent, premixed flames 09 p1272 N85-17994
Turbulent premixed flame study
[DE85-003220] 09 p1292 N85-18112
Asymptotic methods especially in combustion
[AD-A151505] 15 p2505 N85-25450
The overall reaction concept in premixed, laminar, steady-state flames. 2: Initial temperatures and pressures
[AD-A152132] 16 p2746 N85-26944
On the analytic calculation of premixed flames
[VTH-LR-417] 16 p2747 N85-26954
Flame acceleration mechanisms under conditions of partial confinement
[PB85-184083] 18 p3073 N85-29004
Vortex simulation of v-shaped flame
20 p3425 N85-31259
Comments on two matters related to turbulent combustion 22 p3743 N85-33204
Simultaneous measurement of velocity and density in a turbulent nonpremixed flame 22 p3744 N85-33209
Modeling of turbulent recirculating combusting flows
22 p3745 N85-33212

PREPARATION
NT PRESTRESSING
NT PRETREATMENT
Preparation of silicon carbide fibers
[DE84-014861] 01 p0022 N85-10137
1-Fluoro-1,1,5-Trinitro-3-Oxa-5-Azahexane and method of preparation
[AD-D011421] 08 p1136 N85-17158
Preparation methods: Past and potential methods of food preparation for space 14 p2393 N85-24738
A robotic system for preparing reagent and dilution vials
[DE85-008262] 16 p2793 N85-27231
Preparation of sinteractive silicon nitride powders
[BMFT-FB-T-84-303] 18 p3082 N85-29066
Plutonium metal preparation and purification at Los Alamos, 1984
[DE85-010732] 19 p3239 N85-30085
Improved process for the preparation of fiber-reinforced ceramic composites by chemical vapor deposition
[DE85-011584] 22 p3752 N85-33255
PREPOLYMERS
NT DIMERS
NT TRIMERS
Properties of ultra-violet cured poly(dimethylsiloxane)-urea acrylates
[AD-A148570] 08 p1134 N85-17146
PREPREGS
Development of new and improved polymer matrix resin systems, phase 1
[NASA-CR-166595] 01 p0017 N85-10104
Aliphatic-aromatic heterocyclics as potential thermoplastics for composite matrices
04 p0466 N85-12962
Evaluation of failure criterion for graphite/epoxy fabric laminates
[NASA-CR-172547] 10 p1431 N85-19025
Investigation of the effects of NaOH dopant level on the physical and mechanical properties of carbon/phenolic composite material 12 p1945 N85-22213
Development of an impact- and solvent-resistant thermoplastic composite matrix, phase 3
[NASA-CR-172568] 20 p3422 N85-31239
PREPROCESSING
Noise removal in multichannel images
[NASA-CR-174116] 04 p0554 N85-13526
Adaptive preprocessing system
[AD-D011327] 07 p0937 N85-15935
Scientific experiments. Preprocessing of scientific data — spaceborne experiments
14 p2398 N85-24779
A study of aerodynamic control in stalled flight leading-edge vortex formation analysis
[AD-A153758] 18 p3059 N85-26928
PRESELECTORS
U PREAMPLIFIERS
PRESERVING
Alternative food preservation techniques, new technology in food preparation and appropriateness of food supply for the permanently manned space station
14 p2393 N85-24739
Characterization-curing-property studies of HBRF 55A resin formulations
[NASA-CR-175836] 16 p2753 N85-26989
Use of gamma radiation as a form of preservation of sweet potatoes
[DE85-011998] 22 p3841 N85-33787
PRESIDENTIAL REPORTS
Publications of the Executive Office of the President: January 20, 1981 - June 30, 1984
[PB84-230671] 06 p0671 N85-15533
National Acid Precipitation Assessment Program. Report to the President and Congress (1983)
[PB85-116713] 11 p1679 N85-20581
President's private sector survey on cost control, report on research and development
[PB84-173269] 12 p1951 N85-22253
National aeronautical R and D goals: Technology for America's future 19 p3379 N85-30964
PRESINTERING
U SINTERING
PRESSES
Earthquake-modeling experiment using unique press
10 p1500 N85-19469
Automatic multi-layer welding of thick cylindrical structures under flux 13 p2035 N85-22746
Experience with introduction of Finish perforation of precision parts for optical instruments
16 p2761 N85-27038

PRESSING (FORMING)
NT STAMPING
Prediction of forming limit diagrams for deep drawing
08 p0796 N85-15089
Making high explosive bodies for shaped charges by casting or pressing. Shaped charge research at Research Institute of National Defence (FOA) in 1972 - 1983, part 1
[FOA-C-20554-D4-PT-1] 07 p0935 N85-15923
Summaries of press automation conference presented
08 p1139 N85-17173
Consolidation of thermites by pressing and sintering
[DE84-016943] 09 p1297 N85-18146
Robotized blanks loader for new forge press
10 p1461 N85-19216
Experience in use of optical theodolite for machine construction 14 p2267 N85-24049
Clutchless mechanism for engagement of forging press 14 p2268 N85-24051
USSR report: Machine tools and metalworking equipment
[JPRS-UMM-85-004] 14 p2284 N85-24152
Automated, robotized forge-press systems viewed
14 p2284 N85-24153
Robots for application in forge-press operation
14 p2284 N85-24154
Method of selecting robotized system design for pressing process 16 p2761 N85-27040
Industrial robots and automatic manipulators for forging and pressing operations at Second International Exhibition 16 p2762 N85-27044
Mechanizing of handling operations in drop forging with hammers and presses (conducted ergonomical examinations)
[BMFT-FB-HA-84-051] 17 p3002 N85-28561
Specifics of fine structure of pressed aluminum alloys manufactured by plasma atomization
19 p3242 N85-30102

PRESSURE
NT ATMOSPHERIC PRESSURE
NT BASE PRESSURE
NT BLOOD PRESSURE
NT CRITICAL PRESSURE
NT DENSIFICATION
NT DYNAMIC PRESSURE
NT FLUID PRESSURE
NT GAS PRESSURE
NT HIGH ALTITUDE PRESSURE
NT HIGH PRESSURE
NT HIGH VACUUM
NT HYDROSTATIC PRESSURE
NT HYPOXEMIA
NT ILLUMINANCE
NT IMPACT LOADS
NT INLET PRESSURE
NT INTERNAL PRESSURE
NT INTRAOCULAR PRESSURE
NT ISOSTATIC PRESSURE
NT LOW PRESSURE
NT LUMINANCE
NT LUMINOUS INTENSITY
NT OVERPRESSURE
NT OXYGEN TENSION
NT PARTIAL PRESSURE
NT RADIATION PRESSURE
NT SOUND PRESSURE
NT STAGNATION PRESSURE
NT STATIC PRESSURE
NT SUPERCRITICAL PRESSURES
NT TRANSIENT PRESSURES
NT TRANSITION PRESSURE
NT ULTRAHIGH VACUUM
NT VACUUM
NT VAPOR PRESSURE
NT WALL PRESSURE
NT WATER PRESSURE
NT WIND PRESSURE
Thermodynamic properties of isobutane-isopentane mixtures from -40 to +600(0)F and up to 1000 psia
[DE84-015137] 01 p0124 N85-10850
An alternative to reduction of surface pressure to sea level
[NASA-CR-174174] 04 p0538 N85-13422
Homogeneous condensation of gaseous mixtures of Si, Fe, O, N, and C in relative cosmic abundance and implications for astronomical condensation
06 p0887 N85-15632
Analysis of the surface load and radiated sound of a vibrating airfoil with application to the experiment of Brooks
[NASA-CR-3864] 07 p1038 N85-16590
Pressure tests in soil below tires of agricultural vehicles
[AD-P004294] 09 p1408 N85-16871
Flotation tires and subsurface compaction
[AD-P004299] 09 p1409 N85-16876
Airspeed sensing pressure valve system
[AD-D011472] 10 p1425 N85-16867
Electron storage ring beam lifetime dependence on pressure and pumping speed
[DE85-003208] 11 p1724 N85-20845
The sensitivity of solar eigenfrequencies to the treatment of the equation of state 14 p2445 N85-25089
Pressure-dependence of TiS(2) and TiSe(2) bandstructures
[AD-A151200] 15 p2659 N85-26410
Sources of improvement in quality of contact butt welding of wire
[BLL-M-36085-(5828.4)] 16 p2793 N85-27225
A study of aerodynamic control in stalled flight leading-edge vortex formation analysis
[AD-A153758] 18 p3059 N85-26928
Oscillating pressure device for dynamic calibration of pressure transducers
[NASA-CASE-LAR-13094-1] 18 p3104 N85-29217
An experimental study of the pressure in a fast bottom beneath the apex of an overlying fluid wedge
[AD-A153618] 18 p3177 N85-29686
An investigation of hydraulic transients in combination free surface and pressurized flows
19 p3264 N85-30239
Computation of three-dimensional, inviscid, rotational flows 21 p3587 N85-32296
X-ray spectroscopy of solids under pressure
[DE85-011486] 22 p3745 N85-33213
Finite element methods for viscoelastic flow
[AD-A154877] 22 p3783 N85-33437
Linear boundary detection using pressure buildup tests
[DE85-009926] 22 p3784 N85-33444
Adiabatic thermal models for planetary bodies
22 p3857 N85-33881

PRESSURE BREATHING
Hyperbaric physiology (status and prospects)
08 p1194 N85-17521
Manned testing of two closed-circuit oxygen underwater breathing apparatus: US Navy Emerson Rig and Fenzy PO.68
[AD-A148300] 08 p1200 N85-17530
PRESSURE CABINS
U PRESSURIZED CABINS
PRESSURE CHAMBERS
NT HYPERBARIC CHAMBERS
NT VACUUM CHAMBERS

Fokker wants to start new Netherlands space program
03 p0310 N85-11999

Small animal hypobaric chamber
[AD-A146196] 03 p0364 N85-12335

Pressure chamber simulation of 450-meter dive
20 p3505 N85-31788

Diving simulation experiment with pressure chambers
20 p3506 N85-31793

RESSURE DEPENDENCE

A hydrogen partitioning model for hydrogen assisted crack growth
[AD-A147365] 07 p0978 N85-16214

Electrical resistance measurements of metals to 40 GPa in the diamond cell
[DE85-001009] 11 p1629 N85-20262

Dynamic shock studies of PZT 95/5 ferroelectric ceramic
[DE85-006137] 14 p2261 N85-24015

X-ray spectroscopy of solids under pressure
[DE85-006939] 15 p2507 N85-25465

Electronic properties of new organic conductors
[DE85-005590] 15 p2549 N85-25736

Dynamics of vapor explosions
[DE85-008845] 18 p3101 N85-29194

RESSURE DISTRIBUTION

Integral equation of lifting surfaces in Laplace domain and analytic continuation of its pressure kernel
[NAL-TR-795T] 01 p0002 N85-10009

A study of aerodynamic characteristics of wing-body combinations. Part 2: Low-wing airplane
[NAL-TR-796] 01 p0002 N85-10010

Pressure distributions measured on research wing M100 mounted on an axisymmetric body
01 p0004 N85-10023

Pressure distributions measured on research wing M86 mounted on an axisymmetric body
01 p0004 N85-10024

Pressure distribution on a swept wing aircraft in flight
01 p0004 N85-10025

Effect of combined pressure and temperature distortion orientation on high-bypass-ratio turbofan engine stability
[NASA-TM-83771] 01 p0011 N85-10067

Visualization of the diverging two-phase flow pattern in a horizontal T-junction with vertical branch
[GKSS-84-E-25] 01 p0048 N85-10316

Transonic flow analysis for rotors. Part 1: Three-dimensional quasi-steady, full-potential calculation
[NASA-TP-2375-PT-1] 02 p0134 N85-10914

Effect of upstream sidewall boundary layer removal on an airfoil test — conducted in Langley 0.3-m transonic cryogenic tunnel 03 p0313 N85-12019

Performance of two transonic airfoil wind tunnels utilizing limited ventilation 03 p0313 N85-12020

Tunnel constraint for a jet in crossflow
03 p0314 N85-12027

Structure and properties of titanium alloys after isothermal deformation at low speeds
03 p0351 N85-12260

Internal heat transfer and pressure drop measurements in a variously baffled shell and tube heat exchanger
03 p0360 N85-12310

Summary of 1984 Atlantic seasonal tropical cyclone activity and verification of author's forecast
03 p0395 N85-12520

Investigations of boundary layers in the Emmen Federal Aircraft works transonic tunnel, Switzerland
[FW-FO-1641] 04 p0453 N85-12877

Flight and wind-tunnel comparisons of the inlet-airframe interaction of the F-15 airplane
[NASA-TP-2374] 04 p0455 N85-12884

Model equations describing unsteady fluid motion
[ESA-TT-850] 04 p0501 N85-13194

Experiments on the structure of turbulent reattaching flow 05 p0635 N85-14074

Static internal performance of single-expansion-ramp nozzles with various combinations of internal geometric parameters
[NASA-TM-86270] 06 p0749 N85-14797

A theoretical design method for 3-dimensional transonic wings
[NAL-TR-830] 06 p0754 N85-14834

Analysis of the flow field about a T-45 using PANAIR
[AD-A146811] 07 p0899 N85-15699

Some important problems in unsteady boundary layers including separation. 2: Unsteady boundary layers close to the stagnation region of slender bodies
[AD-A146964] 07 p0958 N85-16069

Analysis of the surface load and radiated sound of a vibrating airfoil with application to the experiment of Brooks
[NASA-CR-3864] 07 p1036 N85-16590

The NYU inverse swept wing code
[NASA-CR-3662] 08 p1077 N85-16830

A comparison of measured and predicted unsteady pressure on a fan blade in unstalled supersonic flutter
[PNR-90223] 08 p1079 N85-16839

An improved source model for aircraft interior noise studies
[NASA-CR-172517] 08 p1217 N85-17668

Acceleration of an electron ring in a modified betatron with transverse pressure
[AD-A148626] 08 p1221 N85-17688

Can the singularity be removed in time-dependent flows?
[AD-P004165] 09 p1265 N85-17950

Convective heat transfer coefficients for pipe flow with curvature induced secondary motion
09 p1318 N85-18265

Analysis of ground pressure distribution beneath tracked model with respect to external loading
[AD-P004275] 09 p1406 N85-18851

Detailed pressure distribution measurements obtained on several configurations of an aspect-ratio-7 variable twist wing
[NASA-TM-86308] 10 p1419 N85-18950

Transonic pressure distribution computations of a flexible wing 11 p1622 N85-20213

Measured unsteady transonic aerodynamic characteristics of an elastic supercritical wing with an oscillating control surface
[NASA-TM-86376] 12 p1771 N85-21116

An experimental investigation of flap turbulent heat transfer and pressure characteristics in hypersonic flow
12 p1821 N85-21426

Re-design of ARL/HLF (Heated Laminar Flow) body nose region
[AD-A150063] 12 p1846 N85-21585

Recent transonic unsteady pressure measurements at the NASA Langley Research Center
[NASA-TM-86408] 14 p2210 N85-23710

The influence of transition strips on the pressure distribution on transonic profiles
14 p2212 N85-23718

Problems of elastic hydrodynamic lubrication of helicopter transmission gears 14 p2222 N85-23784

Technology for pressure-instrumented thin airfoil models, phase 1
[NASA-CR-3891] 14 p2227 N85-23804

Some problems in improving reliability and accuracy of regulators with hydraulic amplifiers in main channel of power turbine 14 p2271 N85-24071

Interactions of unstable shear layers with leading edges and associated pressure fields 14 p2299 N85-24236

The photospheric temperature structure of magnetic flux tubes 14 p2447 N85-25102

Transonic pressure distributions on a two-dimensional 0012 and supercritical MBB-A3 profile oscillating in heave and pitch 15 p2457 N85-25173

Mathematical modeling of the AEDC (Arnold Engineering Development Center) propulsion wind tunnel (16T)
[AD-A151293] 15 p2475 N85-25275

Investigation to optimize the passive shock wave/boundary layer control for supercritical airfoil drag reduction
[NASA-CR-175788] 16 p2699 N85-26665

Flow rate and pressure profiles for 1 to 4 axially alined orifice inlets
[NASA-TP-2460] 16 p2782 N85-27165

Aerodynamic research in preparation for a new Dutch transport aircraft with supercritical wings
[B8580077] 17 p2893 N85-27836

Proceedings of the 9th US Air Force and the Federal Republic of Germany Data Exchange Agreement Meeting. Viscous and Interacting Flow Field Effects
[AD-A153020] 17 p2958 N85-28266

Characteristics of a confined jet thrust vector control nozzle
[AD-A153087] 17 p2958 N85-28268

Transport characteristics of slurries in pipelines: Flow regimes and pressure drop
[DE85-009453] 18 p3101 N85-29198

Pressure distribution data from tests of 2.29 M (7.5 feet) span EET high-lift transport aircraft model in the Ames 12-foot pressure tunnel
[NASA-TM-84517] 19 p3211 N85-29912

Transient combustion dynamics
[AD-A154430] 19 p3235 N85-30052

An experimental investigation of propfan installations on an upswept supercritical wing at transonic Mach numbers
[NASA-CR-172605] 20 p3388 N85-31013

Calculation of flow around the SF 310 airplane using a full potential equation method
[FFA-TN-1984-63] 20 p3389 N85-31022

Data set 8: ZKP wing, oscillating aileron
20 p3390 N85-31029

Trailing edge flow and aerodynamic sound. Part 1: Tonal pressure and velocity fluctuations. Part 2: Random pressure and velocity fluctuations
[AD-A154947] 21 p3552 N85-32097

Generation by conformal mappings of aerofoil sections and of certain other simple shapes suitable for both aerodynamic and stress-concentration problems
[AD-A154901] 22 p3728 N85-33112

Experimental study of collapse of thick-walled tube under external pressure and axial force
23 p3904 N85-34186

Pressure cross spectra in turbulent boundary layers in water
[AD-A156153] 24 p4094 N85-35378

PRESSURE DRAG
NT INTERFERENCE DRAG
NT WAVE DRAG

PRESSURE DROP

Heat transfer and pressure drop in blade cooling channels with turbulence promoters
[NASA-CR-3837] 03 p0361 N85-12315

Special topics reports for the reference tandem mirror fusion breeder: Liquid metal MHD pressure drop effects in the packet bed blanket, volume 1
[DE85-002142] 06 p0865 N85-15500

Determination of total pressure losses in stepped annular diffusors with curvilinear outer walls and uniform velocity field at inlet 09 p1306 N85-18203

PRESSURE EFFECTS

A thermodynamic surface for the critical region of ethylene
[PB84-217850] 01 p0025 N85-10159

Interpolation formulas for viscosity of six gases: Air, nitrogen, carbon dioxide, helium, argon and oxygen
[PB84-217801] 01 p0026 N85-10161

Calculation of the optimum conditions for the forging of plates
[BLL-M-35757-(5828.4)] 02 p0189 N85-11260

Nonlinear deformation and static linear buckling of structures under pressure
[CETIM-11-E-350] 04 p0514 N85-13281

The effect of temperature and pressure on the composition density of alkaline metals
[BLL-M-35940-(5828.4)] 05 p0616 N85-13934

Vityaz specialists study human adaptability to ocean depths 07 p0980 N85-16225

Investigation of the pressure-and velocity-coupled responses of solid propellants using impedance tube method 09 p1300 N85-18168

Studies on seismic earth pressure of cohesive backfill
09 p1303 N85-18186

Ignition phenomena of bulk aluminum alloy as a function of oxygen pressure 13 p1999 N85-22531

Pressure-density behavior for AlN, Al2O3, SiO2, TiB2, and TiC powders up to 3.5 GPa
[DE85-006146] 14 p2261 N85-24012

Stability of turbine runners in sliding bearings under external circulation forces 14 p2272 N85-24074

A numerical study of nonspherical black hole accretion 16 p2881 N85-27780

Thermal expansion effects in electrical transport in amorphous metals
[AD-A152477] 17 p2930 N85-28069

Stability of cylindrical shells with variable thickness under external pressure 17 p2943 N85-28164

A second-order pressure-correction method for viscous incompressible flow
[REPT-84-15] 17 p2960 N85-28280

Dynamics of vapor explosions
[DE85-008845] 18 p3101 N85-29194

Fast approach for calculating film thicknesses and pressures in elastohydrodynamically lubricated contacts at high loads
[NASA-TM-87032] 19 p3264 N85-30242

Interaction of slow electrons with high-pressure gases (quasi-liquids): Synthesis of our knowledge on slow electron-molecule interactions
[DE85-010061] 19 p3355 N85-30800

Pressure-shear loading of PBX-9404
[DE85-009982] 23 p3921 N85-34296

PRESSURE FIELDS
U PRESSURE DISTRIBUTION

PRESSURE GAGES
NT BAROMETERS
NT IONIZATION GAGES
NT MANOMETERS
NT PIEZOELECTRIC GAGES

Development of a polymer pressure gage with temperature compensation 03 p0365 N85-12340

Dynamic polymer pressure transducer with temperature compensation
[AD-D011373] 07 p0967 N85-16142

Performance assessment of Class 1E pressure transmitters subjected to environmental stresses
[DE85-001623] 12 p1854 N85-21626

Detonation velocity measurements of the explosives Datasheet C and Amatol
[AD-A152298] 16 p2757 N85-27015

A strain gauge manual
[AD-A151802] 16 p2787 N85-27197

PRESSURE GRADIENTS
Approximate solution of a laminar flow over a flat plate with suction and pressure gradient
[AD-A145482] 02 p0196 N85-11321
Numerical calculation of steady turbulent flows in adverse pressure gradients
[CFD/83/9] 04 p0501 N85-13195
Operational numerical forecasts: Survey and verification over the period 1978-1983
[KNMI-TR-49] 04 p0540 N85-13435
Drag reduction due to boundary-layer control by combined blowing and suction 08 p1070 N85-16785
On the relaxation of a turbulent boundary layer after an encounter with a forward facing step
08 p1071 N85-16789
Analysis of pressure gradient-velocity correlation in turbulent, premixed flames 09 p1272 N85-17994
Calculating secondary nonviscous gas flows in spatial cascades of turbines 09 p1305 N85-18202
Shock propagation in the exhaust gas handling system of the proposed large altitude rocket cell: Methods and preliminary analysis
[DE85-003055] 11 p1591 N85-20010
Nested subcritical flows within supercritical systems
[NASA-TM-86980] 12 p1845 N85-21574
Re-design of ARL/HLF (Heated Laminar Flow) body nose region
[AD-A150063] 12 p1848 N85-21585
Fine structure of vertical distribution of light attenuation index of sea water 13 p2109 N85-23140
Some problems in improving reliability and accuracy of regulators with hydraulic amplifiers in main channel of power turbine 14 p2271 N85-24071
Wind tunnel wall interference
[AD-A151212] 15 p2474 N85-25273
Two-phase fluid thermal transport for spacecraft
[AD-A151316] 15 p2493 N85-25376
A four-field model for Tokamak plasma dynamics
[DE85-007111] 16 p2868 N85-27694
The effects of microbubbles on turbulent boundary layer skin friction 20 p3451 N85-31425
Pressure correlations in turbulent reacting flows
22 p3744 N85-33205
Second order modelling in non-constant density flows
22 p3744 N85-33206
A design procedure to modify the trailing edge upper surface pressure gradient of a given aerofoil
[GU-AERO-8408] 23 p3894 N85-34120
Refrigerated dynamic seal to 6.9 MPa (1000 psi)
[NASA-TM-87108] 23 p3930 N85-34356
A three-dimensional turbulent boundary layer undergoing transverse strain and streamwise pressure gradient
[NASA-TM-86768] 23 p3930 N85-34358
Adverse pressure gradient and separating turbulent boundary-layer flows: The effect of disequilibrium in initial conditions 24 p4059 N85-35155
Computer code calculations of the TMI-2 accident: Initial and boundary conditions
[DE85-012613] 24 p4140 N85-35666

PRESSURE HEADS
Low-head hydroelectric power demonstration project: City of Gonzales, Texas
[DE85-010403] 22 p3809 N85-33595

PRESSURE ICE
Kinetic friction coefficient of ice
[AD-A155035] 21 p3660 N85-32859

PRESSURE MEASUREMENT
Inlet and airframe compatibility for a V/STOL fighter/attack aircraft with top-mounted inlets
[NASA-TM-84252] 01 p0003 N85-10015
Pressure distributions measured on research wing M100 mounted on an axisymmetric body
01 p0004 N85-10023
Pressure distributions measured on research wing M86 mounted on an axisymmetric body
01 p0004 N85-10024
Measurement and analysis of spark ignition engine pressure data to determine heat release profiles
[AD-A144770] 01 p0055 N85-10363
Turbine test report, addendum
[DE84-015130] 02 p0205 N85-11353
Spectroradiometric calibration of the Thematic Mapper and Multispectral Scanner system
[E85-10026] 02 p0218 N85-11439
Wind tunnel wall interference correction for aircraft models 03 p0314 N85-12029
Adaptation of a four-wall interference assessment/correction procedure for airfoil tests in the 0.3-m TCT 03 p0315 N85-12035
Internal heat transfer and pressure drop measurements in a variously baffled shell and tube heat exchanger
03 p0360 N85-12310
Microshell (trademark)-tipped optical fibers as sensors of high-pressure pulses in adverse environments
[DE84-015520] 03 p0365 N85-12338
Development of a polymer pressure gage with temperature compensation 03 p0365 N85-12340
Semiconductor-type transducer with universal strain gauge for measurement of low pressures
04 p0489 N85-13116
Development of components for micro-C oriented sensor systems
[BMFT-FB-T-84-126] 04 p0504 N85-13215
Unsteady pressure measurements on a biconvex airfoil in a transonic oscillating cascade
[NASA-TM-86914] 07 p0898 N85-15689
Steady- and unsteady-pressure measurements on a supercritical-wing model with oscillating control surfaces at subsonic and transonic speeds
[NASA-TM-84543] 08 p1077 N85-16831
Comparison of techniques to measure the low wavenumber wall pressure spectrum of a turbulent boundary layer
[AD-A148074] 08 p1162 N85-17331
Flow quality of NAL 2-dimensional transonic wind tunnel. Part 2: Extensive and systematic pressure fluctuations study in the settling chamber, test section and second throat of the NAL 2-D transonic wind tunnel
[NAL-TR-836-PT2] 09 p1283 N85-18066
Detailed pressure distribution measurements obtained on several configurations of an aspect-ratio-7 variable twist wing
[NASA-TM-86308] 10 p1419 N85-18950
Unsteady transonic pressure measurements on a semispan wind-tunnel model of a transport-type supercritical wing (Lann model). Part 2: Pressure distributions (plotted) and plots of the vibration modes
[AD-A130488] 10 p1421 N85-18965
Dynamic pressure test unit-ratio method
[AD-D011466] 10 p1488 N85-19392
Precision volume measuring system
[DE85-002589] 11 p1636 N85-20305
Unsteady transonic pressure measurements on a semi-span wind-tunnel model of a transport-type supercritical wing (Lann model). Part 2: Pressure distributions (plotted) and plots of the vibration modes
[AD-A130488] 12 p1846 N85-21579
The seven-hole pressure probe
[AD-A149799] 12 p1852 N85-21615
Method of and apparatus for measuring temperature and pressure — atmospheric sounding
[NASA-CASE-GSC-12558-1] 12 p1856 N85-21639
Seismic observation of infrasonic signals
[AD-A149574] 12 p1869 N85-21853
MFTF sensor verification computer program
[DE85-004452] 12 p1916 N85-22029
Liquid moment on a filled coning cylinder during spin-up: Ad hoc model
[AD-A150280] 13 p2092 N85-23060
Recent transonic unsteady pressure measurements at the NASA Langley Research Center
[NASA-TM-86408] 14 p2210 N85-23710
Transition detection using surface pressure holes
14 p2212 N85-23722
Surface pressure produced by Space Transportation System flight 41B
[AD-A150793] 14 p2242 N85-23901
Analysis of unsteady pressure measurements on a supercritical airfoil with a harmonically oscillating trailing edge flap at subsonic and transonic speeds
[DFVLR-FB-84-49] 17 p2893 N85-27837
Pressure measurement: Short course
[DE85-008644] 18 p3102 N85-29205
Measurement of turbofan-turbojet thrust from tailpipe static pressure
[AD-A154036] 19 p3220 N85-29967

PRESSURE OSCILLATIONS
An experimental investigation of combustion pressure oscillations in solid fuel ramjets
[AD-A144870] 01 p0024 N85-10147
Similarity criteria of spectra of pressure pulsations of turbulent boundary layer near wall
02 p0256 N85-11679
Pressure oscillations in liquid-fueled ramjet engines
05 p0596 N85-13797
Steady- and unsteady-pressure measurements on a supercritical-wing model with oscillating control surfaces at subsonic and transonic speeds
[NASA-TM-84543] 08 p1077 N85-16831
Effect of jet exit vanes on flow pulsations in an open-jet wind tunnel
[NASA-TM-86299] 09 p1273 N85-17999
Turbulent bouyant flow and pressure variations around a circular cylinder in a cross uniform flow near the ground 09 p1318 N85-18287
Measured unsteady transonic aerodynamic characteristics of an elastic supercritical wing with an oscillating control surface
[NASA-TM-86376] 12 p1771 N85-21116
An investigation of space shuttle main engine shutdown chugging instability 12 p1946 N85-22221
Nonlinear interactions between vortices and acoustic waves in a rocket combustion chamber
13 p1999 N85-22530
Comparisons of solid propellant with instability predictions and motor firing experience
13 p2001 N85-22541
Transonic pressure distributions on a two-dimensional 0012 and supercritical MBB-A3 profile oscillating in heave and pitch 15 p2457 N85-25173
Parametric study of autooscillation upon flow of supersonic jet into cylindrical cavity
16 p2765 N85-27060
Atmospherically forced, coastally trapped, long period gravity waves off the south coast of southern Africa
16 p2832 N85-27481

PRESSURE PROBES
U PRESSURE SENSORS

PRESSURE PULSES
Microshell (trademark)-tipped optical fibers as sensors of high-pressure pulses in adverse environments
[DE84-015520] 03 p0365 N85-12338
Long range effect of turbulent pressure pulsations in plane-parallel flows at different velocities with various flame fronts 09 p1308 N85-18220
Flow dynamic environment data base development for the SSME 16 p2736 N85-26985
Pulsed hydrojet propulsion
[DE85-010771] 22 p3784 N85-33448

PRESSURE RATIO
Design and off-design performance prediction of high pressure ratio centrifugal compressors
05 p0638 N85-14082
Mixing characteristics of an underexpanded multiple jet ejector
[AD-A149557] 10 p1485 N85-19375
Calibration of sonic valves for the laminar flow control, leading-edge flight test
[NASA-TP-2423] 14 p2210 N85-23707
Optimum geometry of interblade passages in impellers of thermomolecular vacuum pump
16 p2764 N85-27058
High pressure compressor component performance report
[NASA-CR-168245] 23 p3897 N85-34138

PRESSURE RECOVERY
Pressure recovery in a cylindrical heat pipe at high radial Reynolds numbers and at high Mach numbers
[DE85-010718] 19 p3269 N85-30274

PRESSURE REDUCTION
Internal heat transfer and pressure drop measurements in a variously baffled shell and tube heat exchanger
03 p0360 N85-12310
Pressure loss due to the tip clearance of impeller blades in centrifugal and axial blowers
05 p0636 N85-14083
Preliminary investigation of labyrinth packing pressure drops at onset of swirl-induced rotor instability
05 p0644 N85-14132
Safe decompression schedules for caisson workers
[PB85-103612/GAR] 07 p1017 N85-16460
Low loss injector for liquid propellant rocket engines
[NASA-CASE-MFG-25969-1] 11 p1591 N85-20008
Statistical comparison of pooled nitrogen washout data of various altitude decompression response groups
[NASA-TM-58265] 15 p2639 N85-26278
A feasibility study for using low boiling point fluids to change aircraft tire deflection
[AD-A152096] 16 p2706 N85-26701
A comprehensive strategy for saturation decompression with nitrogen-oxygen
[AD-A151800] 16 p2841 N85-27520
Method for growth of crystals by pressure reduction of supercritical or subcritical solution
[NASA-CASE-NPO-15772-1] 18 p3192 N85-29600
Diving simulation experiment with pressure chambers
20 p3506 N85-31790

PRESSURE REGULATORS
Simulation in the design of gas pressure control equipment
[ERS-E.352] 09 p1324 N85-18322

PRESSURE RIDGES
U PRESSURE ICE

PRESSURE SENSORS
Development of a floating element wall shear transducer
[AD-A144794] 01 p0049 N85-10324
Microshell (trademark)-tipped optical fibers as sensors of high-pressure pulses in adverse environments
[DE84-015520] 03 p0365 N85-12338
Development of a polymer pressure gage with temperature compensation 03 p0365 N85-12340
Semiconductor-type transducer with universal strain gauge for measurement of low pressures
04 p0489 N85-13116

Development of components for micro-C oriented
nsor systems
MFT-FB-T-84-126] 04 p0504 N85-13215
Aero-optics experimental techniques
D-A146755] 07 p0957 N85-16067
Dynamic polymer pressure transducer with temperature
mpensation
D-D011373] 07 p0967 N85-16142
Ultrasound instrumentation for the 7 inch Mach seven
nnel
ASA-CR-174277] 07 p1038 N85-16586
Development of a pressure transducer for usage in
gh-temperature and vibration environments. Phase 1:
easibility investigation
AD-A148695] 08 p1165 N85-17349
Pressure measurements in a hydrogen combustion
nvironment: An evaluation of 3 pressure transducers
TI85-003645] 09 p1323 N85-18312
A probe for direct measurement of flow direction
ESA-TT-853] 11 p1637 N85-20310
Heat pipe cooled probe
NASA-CASE-LAR-12586-1] 12 p1844 N85-21588
The seven-hole pressure probe
[AD-A148799] 12 p1852 N85-21615
Performance assessment of Class 1E pressure
ransmitters subjected to environmental stresses
[DE85-001623] 12 p1854 N85-21626
An advanced solid state pressure transducer for high
eliability SSME application 16 p2739 N85-26905
Oscillating pressure device for dynamic calibration of
pressure transducers
[NASA-CASE-LAR-13094-1] 18 p3104 N85-29217
Fluidic angular velocity sensor
[NASA-CASE-NPO-16479-1-CU]
18 p3104 N85-29219
Research pressure instrumentation for NASA space
shuttle main engine
[NASA-CR-176014] 19 p3227 N85-30006
Materials and process development for
microcomputer-compatible pressure, temperature, and
position sensors
[BMFT-FB-T-85-024] 24 p4097 N85-35399
RESSURE SUITS
NT SPACE SUITS
The Reports of Aeromedical Laboratory, volume 25, no.
1/2
[ISSN-0023-2858] 01 p0090 N85-10605
Assessment of the inflating characteristics of the
modified anti-G suit 01 p0090 N85-10609
Acceptance-testing procedures for air-line supplied-air
suits
[DE84-016980] 05 p0712 N85-14569
Development of an electro-pneumatic anti-G valve for
high performance fighter aircraft
[AD-A148468] 08 p1201 N85-17561
Servo operated anti-G suit pressurization system
[AD-D011468] 10 p1531 N85-19651
Analysis of the transient response of temporal artery
blood flow data relative to various anti-G suit pressure
schedules 10 p1533 N85-19660
Simulation of high +Gz onset in the dynamic
environment simulator
[AD-A155963] 24 p4131 N85-35610
PRESSURE TRANSDUCERS
U PRESSURE SENSORS
PRESSURE VESSEL DESIGN
Advanced nickel-hydrogen cell configuration study
[NASA-CR-174775] 01 p0067 N85-10444
Reactor pressure vessel steels ASME SA533B and
SA508 C 1.2
[VTT-340] 22 p3794 N85-33507
PRESSURE VESSELS
NT PREBURNERS
Ultralightweight oxygen container
[PB84-220730] 01 p0036 N85-10226
Detection of hydrogen assisted crack growth by
measurement of modulus changes and acoustic
emission
[DE84-015752] 02 p0184 N85-11236
Stress corrosion of pressure vessel steel A533-B in high
temperature water
[BLL-RISLEY-TR-4600-(9091.9F)]
03 p0330 N85-12125
Field installed brazed thermocouple feedthroughs for
high vacuum experiments
[DE84-013556] 04 p0503 N85-13207
Response of ferritic steels to nonsteady loading at
elevated temperatures
[DE84-014280] 04 p0513 N85-13272
Impact of NDE unreliability on pressure vessel fracture
predictions
[DE84-015586] 05 p0647 N85-14151
Static and dynamic fracture toughness characterization
of SA508 forging and SA533B welded plate — pressure
vessel steels
[CISE-2256] 08 p1131 N85-17127
Effect of temperature on the stress-relaxation response
of a pressure vessel steel
[TI85-003588] 09 p1339 N85-18424
Assessment of the need for an advanced high-strength
chromium-molybdenum steel for construction of
third-generation gasifier pressure vessels
[DE85-002865] 11 p1606 N85-20097
Optimization of pressure vessels with standard
intercepting spheres
[INPE-3276-PRE/600] 11 p1651 N85-20397
Effect of input distributions on the probabilistic fracture
mechanics analysis of reactor pressure vessels
[DE85-000632] 11 p1652 N85-20403
Mechanical properties and brittle fracture resistance of
welded multilayer elements for high pressure vessels
13 p2033 N85-22736
Welding technology: Japan — Conference
[ISBN-0-85300177-4] 15 p2565 N85-25823
Nondestructive equipment study
[NASA-CR-171865] 15 p2571 N85-25853
Sizing capability of automated ultrasonic time-of-flight
diffraction in thick section steel and aspects of reliable
inspection in practice
[AERE-R-11546] 15 p2571 N85-25855
Fatigue strength of Inconel 625 plate and weldments
used in the DIII-D configuration vacuum vessel
[DE85-006276] 17 p2981 N85-28427
Initial performance of advanced designs for IPV
nickel-hydrogen cells
[NASA-TM-87029] 17 p2984 N85-28444
Feasibility of electrolytic hydrogen production in the
Pacific Northwest
[DE85-008856] 18 p3064 N85-29080
Ten year environmental test of glass fiber/epoxy
pressure vessels
[NASA-TM-87058] 19 p3231 N85-30034
Literature survey of discontinuous-fiber-reinforced
composites with emphasis on pressure vessels
[DE85-010386] 19 p3232 N85-30038
Initial performance of advanced designs for IPV
nickel-hydrogen cells 20 p3448 N85-31404
In-service supervision of a pressurized concrete
pressure vessel
[OEFZS-4306] 20 p3470 N85-31564
Solid-state track recorder neutron dosimetry in the
Three-Mile Island Unit-2 reactor cavity
[DE85-011360] 20 p3531 N85-31966
Slideline verification for multilayer pressure vessels and
piping analysis including strain hardening
[DE85-005816] 22 p3801 N85-33549
Prestressed concrete vessel according to the hot liner
concept: A critical evaluation of experimental results with
a prototype vessel
[OEFZS-4313] 22 p3801 N85-33550
Effect of stainless steel weld overlay cladding on the
structural integrity of flawed steel plates in bending, series
1
[TI85-010349] 23 p3939 N85-34418
The dynamic strain ageing of A533B class 1 nuclear
pressure vessel steel
[AERE-R-11485] 24 p4078 N85-35274
PRESSURE WAVES
U ELASTIC WAVES
PRESSURE WELDING
NT DIFFUSION WELDING
NT EXPLOSIVE WELDING
NT ULTRASONIC WELDING
Pressure welding of corrosion-resistant steel with AMg6
aluminum 15 p2501 N85-25426
Thermocompression welding of parts made from AMts
and VT1 alloys 15 p2501 N85-25430
Welding techniques in pressure part technology
15 p2566 N85-25835
Solid state bonding of molybdenum and TZM
[BLL-T6439/BG/LRS/LRST751/85]
16 p2792 N85-27220
Low pressure arc butt welding of dissimilar metals
19 p3246 N85-30128
Welding of steel-aluminum cooling panels for the holds
of refrigerator vessels 19 p3246 N85-30129
Solid-state resistance welding cylinders and spheres
[DE85-010064] 20 p3469 N85-31555
PRESSURIZED CABINS
Aircraft cabin pressurization control system tester
[AD-D011225] 01 p0013 N85-10081
Distinctions in formation of microflora on construction
materials used in habitable pressurized compartments
22 p3823 N85-33683
Effect of dibazol on parameters of nonspecific resistance
of subjects in pressurized cabins
23 p3954 N85-34504
PRESSURIZED WATER REACTORS
Thermal fluid-structure interaction: A few scaling
considerations — nuclear reactors
[GKSS-84-E-18] 01 p0048 N85-10314
The detection and assessment of defects in automatic
ultrasonic inspection
[BLL-RISLEY-TR-4597-(9091.9F)]
05 p0647 N85-14150
Application of new welding technology in the fabrication
of nuclear power plant 15 p2566 N85-25829
Information presentation in power plant control rooms
[VTT-320] 16 p2864 N85-27668
Calculations on the feasibility of ultrasonic inspection
of steam generator tubing in pressurized water reactors
[AERE-R-10960] 23 p3940 N85-34419
PRESSURIZING
Behavior of pressurized tubes of candidate alloys in a
simulated low-Btu environment
[DE85-003403] 09 p1296 N85-18141
PRESTON TUBES
U PITOT TUBES
U SPEED INDICATORS
PRESTRAINING
U PRESTRESSING
PRESTRESSING
Measurement of the preloading of bolted joints by the
ultrasonic method
[CETIM-1-5H-38-6] 04 p0558 N85-13556
Multiaxial yield behavior of 1100 aluminum following
various magnitudes of prestrain
[DE84-013904] 05 p0617 N85-13949
Durability and behavior of prestressed concrete beams.
Posttensioned concrete beam investigation, supplemental
laboratory tests of beams exposed from 1961 to 1982
[AD-A148821] 09 p1304 N85-18191
Vibration and buckling of rotating, pretwisted, preconed
beams including Cooriolis effects
[NASA-TM-87004] 15 p2577 N85-25893
In-service supervision of a pressurized concrete
pressure vessel
[OEFZS-4306] 20 p3470 N85-31564
Monotonous stress-strain properties of structural steel
subjected to nonstationary repetitive pre-loading
23 p3904 N85-34185
Corrosion fatigue strength and crack growth in
prestrained 0.16% C carbon steel
23 p3905 N85-34192
PRETESTS
U TESTS
PRETREATMENT
NT PRESTRESSING
Influence of pretreatment, environment and strain rate
on stress corrosion cracking of the aluminum alloy
7075-T6
[VTH-LR-433] 16 p2752 N85-26985
PRETWISTING
U PRESTRESSING
U TWISTING
PREVENTION
NT ACCIDENT PREVENTION
NT CORROSION PREVENTION
NT FIRE PREVENTION
NT ICE PREVENTION
Jet lag prevention: Physiological mechanisms and
pharmacological therapy
[AD-A145444] 02 p0235 N85-11529
Tight Ribbon Arm Protection (TRAP) for aircrewman
ejection
[AD-A150464] 13 p2143 N85-23303
PRIMARY BATTERIES
NT ALKALINE BATTERIES
NT NICKEL ZINC BATTERIES
NT SODIUM SULFUR BATTERIES
NT THERMAL BATTERIES
Electrochemistry and storage
05 p0608 N85-13869
Electrochemistry and storage panel report
05 p0611 N85-13903
Safety characteristics of non-lithium battery systems
[AD-A155733] 22 p3606 N85-33574
PRIMARY COSMIC RAYS
NT SOLAR COSMIC RAYS
Anomalon search — heavy cosmic ray interactions
[NOTA-INTERNA-825] 02 p0305 N85-11970
Radiobiological studies on egg systems exposed to
heavy nuclei of cosmic galactic radiation — insects
05 p0690 N85-14440
Preliminary results of advanced Biostack experiments
with plant seeds and spores — cosmic ray effects
05 p0691 N85-14441
The radiobiological advanced Biostack experiment on
Spacelab 1 05 p0691 N85-14442
Isotopic composition of primary cosmic rays H-Fe for
ISEE-C
[NASA-CR-175266] 05 p0746 N85-14783
UCB cosmic ray experiment 09 p1417 N85-18941
The inner granulometric density of the tracks in nuclear
emulsions and its application to determine the chemical
spectrum of primary cosmic ray nuclidi
[OG-4.3-9] 22 p3879 N85-34034

Observations of ultraheavy cosmic ray particles at 10 GV cutoff rigidity
[OG-4.4-2] 22 p3879 N85-34035
Primary cosmic ray spectrum in the 10 to the 12th power - 10 to the 16th power eV energy range from the NUSEX experiment
[OG-5.1-5] 22 p3881 N85-34047
Study of composition of cosmic rays with energy .7 E 3 Ee
[OG-5.1-7] 22 p3881 N85-34049
On the possibility of the determining the average mass composition near 10 to the 14th power eV through the solar magnetic field
[OG-5.1-9] 22 p3882 N85-34051
A new method to determine the chemical composition of the cosmic rays beyond 10 to the 15th power eV
[OG-5.1-11] 22 p3882 N85-34052
Cosmic ray composition between 10 to the 15th power - 10 to the 17th power eV obtained by air shower experiments
[OG-5.1-12] 22 p3882 N85-34053
Fluctuations of development maximum depth and nuclear composition of primary cosmic radiation
[OG-5.1-13] 22 p3882 N85-34054
EAS spectrum in the primary energy region above 10 to the 15th power eV by the Akeno and Yakutsk array data
[OG-5.1-16] 22 p3882 N85-34057
Implication of EAS data for the study of primary cosmic rays above 10 to the 5th power GeV
[OG-5.2-7] 22 p3883 N85-34064
High-energy multiple muons and heavy primary cosmic-rays
[OG-5.2-9] 22 p3883 N85-34065
Composition of primary cosmic rays near the knee
[OG-5.2-10] 22 p3884 N85-34066
EAS Cerenkov measurements of the composition of the cosmic ray flux around 10 to the 16th power eV
[OG-5.2-11] 22 p3884 N85-34067
Electron and muon parameters of EAS and the composition of primary cosmic rays in 10(15) to approximately 10(16) eV
[OG-5.2-12] 22 p3884 N85-34068
Variations in the propagation of UH-nuclei
[OG-7.1-1] 23 p4012 N85-34863
Secondary to primary ratio and the continuous acceleration
[OG-8.3-4] 23 p4022 N85-34923
The response of ionization chambers to relativistic heavy nuclei
[OG-9.1-13] 23 p4024 N85-34938
Empirical model for the Earth's cosmic ray shadow at 400 KM: Prohibited cosmic ray access
[SH-6.1-14] 23 p4046 N85-35087
Cosmogenic-nuclide production by primary cosmic-ray protons
[SH-7.1-6] 23 p4047 N85-35096
The neutron moderated detector and groundbased cosmic ray modulation studies
[SH-9.1-13] 23 p4052 N85-35128
Measurement of low energy cosmic rays aboard Spacelab-1
[SH-10.1-6] 23 p4053 N85-35137
Heavy cosmic ray measurement aboard Spacelab-1
[SH-10.1-7] 23 p4053 N85-35138
Energy spectra of proton and nuclei of primary cosmic rays in energy region 10 TeV/particle
[HE-3.1-10] 24 p4178 N85-35908
Size distributions of air showers accompanied with high energy gamma ray bundles observed at Mt. Chacaltaya
[HE-3.3-9] 24 p4181 N85-35927
Multidimensional analysis of data obtained in experiments with X-ray emulsion chambers and extensive air showers
[HE-3.6-2] 24 p4184 N85-35951
LPM effect and primary energy estimations
[HE-3.6-4] 24 p4185 N85-35953
The lateral distributions of charged particles of energy greater than 0.3 E sub crit in electron-photon cascades in lead and air
[HE-3.6-10] 24 p4185 N85-35957
Result of Monte-Carlo simulation of electron-photon cascades in lead and layers of lead-scintillator
[HE-3.6-11] 24 p4185 N85-35958
Intensities of high-energy cosmic rays at Mount Kanbala
[HE-3.7-5] 24 p4186 N85-35964
Ultra high energy events in ECHOS series and primary energy spectrum
[HE-3.7-9] 24 p4186 N85-35966
Study of the energy spectrum of primary cosmic rays: EAS size fluctuations at a fixed primary energy
[HE-4.4-14] 24 p4194 N85-36020
Thickness of the particle swarm in cosmic ray air showers
[HE-4.7-14] 24 p4200 N85-36064
Relevance of multiple muons detected underground to the mass composition of primary cosmic rays
[HE-5.1-4] 24 p4201 N85-36069
Multimuons events and primary composition
[HE-5.1-5] 24 p4201 N85-36070
Muon groups and primary composition at 10 to the 13th power to 10 to the 15th power eV
[HE-5.1-12] 24 p4201 N85-36074
Primary chemical composition from simultaneous recording of muons induced cascades and accompanying muon group underground
[HE-5.1-13] 24 p4201 N85-36075
Multiple muons in MACRO
[HE-5.2-1] 24 p4202 N85-36079
Search for tachyons associated with extensive air showers in the ground level cosmic radiation
[HE-6.2-13] 24 p4212 N85-36149
Observation of genetic relation among new phenomena Geminion, Chiron and mini-Centauro
[HE-6.2-16] 24 p4212 N85-36152
Muon and neutrino fluxes
[HE-6.2-18] 24 p4213 N85-36154

PRIMATES
NT BABOONS
NT HUMAN BEINGS
NT MONKEYS
Primate experiments on SLS-1
15 p2687 N85-26592
A brief description of the two primate experiments to be carried out on SL-4 15 p2687 N85-26597
Morphological study of primate hypothalamus and hypophysis after experiment with antiorthostatic hypokinesia 19 p3325 N85-30603
Changes in nephron and juxtaglomerular system of primate kidneys under the effect of antiorthostatic hypokinesia 19 p3326 N85-30605

PRIMERS
Development of acceptance criteria for batches of silane primer for external tank thermal protection system bonding applications
[NASA-CR-171436] 15 p2518 N85-25523
Development of acceptance criteria for batches of silane primer for external tank thermal protection system bonding applications
[NASA-CR-175850] 16 p2754 N85-26995

PRIMERS (COATINGS)
Development of acceptance criteria for batches of silane primer for external tank thermal protection system bonding applications
[NASA-CR-171266] 04 p0478 N85-13043
Polarization in chemically doped hydrogen-rich glasses
[DE84-017486] 06 p0771 N85-14936
Evaluation of properties of varnishes, exterior stains and exterior primers
[PB84-243948] 06 p0772 N85-14940
An electrochemical study of the corrosion behavior of primer coated 2219-T87 aluminum
[NASA-TP-2459] 13 p2021 N85-22662
Development of acceptance criteria for batches of silane primer for external tank thermal protection system bonding applications
[NASA-CR-171428] 14 p2259 N85-23998
Adhesive evaluation of LARC-TPI and a water-soluble version of LARC-TPI
[NASA-TM-86428] 19 p3248 N85-30136
Results of tests of weathered K5NA closeout material in the MSFC Hot Gas Facility
[NASA-CR-170893] 24 p4073 N85-35239

PRIMITIVE EARTH ATMOSPHERE
Greenhouse effect in Earth's primordial atmosphere
16 p2807 N85-27310
The composition of the primitive atmosphere and the synthesis of organic compounds on the early Earth
21 p3717 N85-33065
The problem of the Earth's CO2 content and the iron core 21 p3718 N85-33069

PRIMITIVE EQUATIONS
Numerical studies of frontal dynamics
15 p2598 N85-26014
A split explicit model for short-term numerical weather prediction 16 p2831 N85-27460
A factored implicit scheme for numerical weather prediction with small factorization error
18 p3141 N85-29447
A comparison of the bounded derivative and the normal mode initialization methods using real data
18 p3144 N85-29463
An algorithm for the generation of primitive polynomials
[FUB-17-1984] 22 p3831 N85-33730

PRINCIPAL COMPONENTS ANALYSIS
Homogeneous macroclimatic zones of the lake states
[PB84-215821] 04 p0540 N85-13436
The use of principal components analysis technique Nimbus-7 coastal zone color scanner data to define mesoscale ocean features through a warm humid atmosphere
[AD-A148567] 08 p1176 N85-17416
Martian fretted terrain morphometry interpreted using principal components analysis 13 p2192 N85-22587
Determining mineral types and abundances from reflectance measurements 13 p2196 N85-22622

PRINTED CIRCUITS
NT LARGE SCALE INTEGRATION
Extractor for spring-lock pin connectors
[AD-D011235] 01 p0043 N85-10260
A generalized solution to a class of printed circuit antennas
[AD-A145626] 02 p0191 N85-11278
Depot level problems in the testing of printed circuit boards
[AD-P003932] 02 p0247 N85-11612
Swiss firm improves method for soldering printed circuits 03 p0341 N85-12150
Computerized circuit designs: Realization of masks to manufacture microwave circuits
[CNES-NT-107] 04 p0496 N85-13186
Polyimide-glass multilayer printed wiring boards
[DE84-015092] 05 p0631 N85-14048
Characteristics of circular-polarized printed radiators in planar phased antenna array 06 p0790 N85-15049
Diagnostic apparatus for radar pulse repetition frequency control circuit card
[AD-D011364] 07 p0937 N85-15208
MMIC devices for active phased array antennas
[NASA-CR-174281] 07 p0938 N85-15843
Evaluation of test equipment for the detection of contamination on electronic circuits — spacecraft electronics
[ESA-STM-234] 08 p1159 N85-17316
Mechanical locking between multi-layer printed wiring board conductors and through-hole plating
[AD-D011477] 10 p1481 N85-19052
CAD/CAM systems for printed circuit design, manufacture 11 p1619 N85-20188
Printed circuit balun with a dipole antenna
[AD-D011534] 12 p1833 N85-21498
Gain enhancement methods for printed circuit antennas
[AD-A150090] 12 p1835 N85-21517
The state of the art in printed wiring board inspection
[AD-A149871] 12 p1862 N85-21679
A generalized solution to a class of printed circuit antennas 13 p2062 N85-22882
Applications, specifications of Robotron CAD-CAM work stations 15 p2537 N85-25881
New designs from electronics R and D center
15 p2538 N85-25666
Design and swept-frequency measurement of printed circuit board log-periodic dipole arrays
[R-NIAS-23] 15 p2539 N85-25671
Ink jet printing of silver metallization for photovoltaics
[NASA-CR-175798] 15 p2586 N85-25943
Printed wiring board circuit isolator tool
[AD-D011638] 17 p2968 N85-28333
Drag soldering process control
[DE85-010853] 20 p3433 N85-31301
Digital integrated circuits 21 p3669 N85-32787
A comparison and analysis of Vintr's global routing algorithm with the Lee routing algorithm in two-layer printed circuit boards
[AD-A155600] 21 p3673 N85-32816
Heat sinking for printed circuitry
[DE85-011585] 22 p3783 N85-33440
Hermetic chip carrier compliant soldering pads
[AD-D011722] 23 p3938 N85-34410

PRINTERS
NT PRINTERS (DATA PROCESSING)
Program DISAS: A computer program to obtain hard-copy plots of an image displayed on a vector graphics device in a local-area-network
[AD-A153643] 18 p3162 N85-29886
Flexible satellite communications systems simulator phase 3
[AD-A155647] 21 p3577 N85-32247

PRINTERS (DATA PROCESSING)
East Europe report: Science and technology
[JPRS-ESA-84-030] 01 p0101 N85-10870
Two programs for the HP9836C computer to acquire frequency or voltage data from a source
[AD-A146632] 06 p0854 N85-15430
Computer equipment at 1984 Leipzig Spring Fair
09 p1378 N85-18862
Microprocessor AirborneData Acquisition and Replay (MADAR) system
[AD-A151728] 20 p3514 N85-31840
Dual optical mechanical position tracker
[AD-D011739] 22 p3844 N85-33811

PRINTING
NT LITHOGRAPHY
NT PHOTOLITHOGRAPHY

Optical recording of information on paper by CO2 and YAG-lasers
02 p0261 N85-11710

The electronic typesetting program programmer's manual
[AD-A147500] 07 p1025 N85-16508

Screen printed interdigitated back contact solar cell
[NASA-CASE-LEW-13414-1] 11 p1671 N85-20530

Applications of lasers in manufacturing
14 p2308 N85-24279

Ink jet printing of silver metallization for photovoltaics
[NASA-CR-175798] 15 p2586 N85-25943

A microcomputer-based program for printing check plots of integrated circuits specified in Caltech intermediate form
[AD-A151715] 15 p2829 N85-26205

T sub EX font tables
[DE85-011394] 19 p3339 N85-30687

Ink jet printing of silver metallization for photovoltaics
[NASA-CR-176019] 19 p3343 N85-30720

Ink jet printing of silver metallization for photovoltaics
[NASA-CR-176054] 22 p3805 N85-33569

Development of metallization process: FSA project, cells and module formation research area
[NASA-CR-176136] 23 p3945 N85-34447

PRISMATIC BARS

Study on a prismatic dye vat — laser systems
[CERT-2/6124-04-RO] 16 p2791 N85-27217

PRISMS
NT PRISMATIC BARS

Extending magnitude standards to faint stars with a sub-beam prism
07 p0965 N85-16124

Sub-beam prism used at the Bosscha Schmidt telescope
07 p0965 N85-16125

Stellar photographic photometry using a double wedge technique with a focal reducer system
07 p0966 N85-16133

Spectrophotometry of cool stars from objective prism spectra
07 p0966 N85-16134

Interpreting geothermal anomalies by special points method
07 p0982 N85-16238

High resolution diffraction grating
[AD-D011541] 12 p1933 N85-22141

Reflex attachment for line alignment in spectral diffraction devices
13 p2044 N85-22794

Three-mirror open resonator for millimeter wave band
13 p2077 N85-22972

Determination of parameters of elastically strained mirror facets of rapidly rotating prisms
14 p2282 N85-24137

Operation of Prisma flexible manufacturing system
15 p2524 N85-25564

Method and apparatus for generating a structured light beam array
[AD-D011590] 15 p2652 N85-26357

PRIVACY

Federal Telecommunications Privacy Act of 1984
[H-REPT-98-815] 03 p0441 N85-12807

PRIVATE AIRCRAFT
U GENERAL AVIATION AIRCRAFT

PROBABILITY
U PROBABILITY THEORY

PROBABILITY DENSITY FUNCTIONS
NT NORMAL DENSITY FUNCTIONS
NT PEARSON DISTRIBUTIONS
NT RAYLEIGH DISTRIBUTION
NT WEIBULL DENSITY FUNCTIONS

Total positivity. A review
[AD-A145205] 01 p0114 N85-10771

Efficient methods for mechanical and structural reliability analysis and design
02 p0205 N85-11355

Nonparametric maximum penalized likelihood estimation of a density from arbitrarily right-censored observations
[AD-A145569] 02 p0251 N85-11644

Algebraic functions of H-functions with specific dependency structure
[AD-A145598] 02 p0252 N85-11647

Likelihood estimation for generalized mixed exponential distributions
[AD-A145675] 02 p0252 N85-11651

Prediction of wave height of wind-generated seas in finite water depth
[AD-A145896] 03 p0398 N85-12539

Probability distribution density of normalized radar range
04 p0485 N85-13098

Multivariate spline methods in surface fitting
07 p0965 N85-16257

Some scientific subroutines in LISP
[AD-A147889] 07 p1026 N85-16515

A coaxial probe for measuring the current density profile of intense electron beams
[AD-D011407] 08 p1164 N85-17347

Flame propagation and stabilization studies using Rayleigh scattering and laser Doppler velocimetry
[AD-A148802] 09 p1290 N85-18102

Turbulent premixed flame study
[DE85-003220] 09 p1292 N85-18112

On the probability density of signal-to-noise ratio in an improved adaptive detector, part 1
[AD-A148856] 10 p1550 N85-19772

A stochastic-mechanical approach to acoustic pulse propagation in the deep ocean sound channel
[AD-A149598] 12 p1928 N85-22110

On filter binary processes
[AD-A150328] 13 p2063 N85-22890

Invariance of probability characteristics of detector to shape of optical pulse signals 13 p2090 N85-23048

Construction of efficient algorithms for the estimation of multivariate probability densities
[AD-A151509] 15 p2640 N85-26285

A non-parametric probability density estimator and some applications
[AD-A151853] 15 p2641 N85-26287

Measurement of damping of graphite expoxy materials
[NASA-CR-175793] 16 p2743 N85-26925

A data based algorithm for choosing the window width when estimating the integral of f2(x)
[AD-A152093] 16 p2847 N85-27553

An inequality and its application to the truncated distributions
17 p3020 N85-28673

Robust tests of mean vector in symmetrical multivariate distributions
[AD-A153116] 17 p3020 N85-28674

Conditional modelling in turbulent shear flows
20 p3424 N85-31250

The microstructure approach to conserved scalar pdf models
20 p3424 N85-31251

Assessment of superlayer contribution to the conserved scalar PDF in a hydrogen turbulent jet diffusion flame
20 p3425 N85-31255

Efficiency of discrimination in some invariant signal transformations
22 p3776 N85-33399

A new approach to evaluate gamma-ray measurements
[OG-9.5-11] 23 p4031 N85-34988

Relaxation phenomena and stability of probability densities
[AD-A155923] 24 p4143 N85-35682

PROBABILITY DISTRIBUTION FUNCTIONS

On probability forecasts for temperature
01 p0084 N85-10565

Probability distribution of leadtime demand
[AD-A144952] 01 p0113 N85-10766

An iterative procedure for obtaining I-projections onto the intersection of convex sets
[AD-A145402] 02 p0251 N85-11639

Weighted distributions arising out of methods of ascertainment
[AD-A145615] 02 p0252 N85-11648

The estimation of persistance statistics from cumulative probabilities of wave height
[NMI-R183] 03 p0397 N85-12534

Probability distribution density of normalized radar range
04 p0485 N85-13098

The undetected error probability for shortened hamming codes
[NASA-CR-174175] 04 p0555 N85-13535

Interval mathematics reports
[REPT-84/1] 04 p0556 N85-13536

Risk analysis without Monte Carlo methods
04 p0556 N85-13537

Stochastic cell model for hadronic multiparticle distributions
[DE84-016480] 04 p0562 N85-13578

Spline methods for approximating quantile functions and generating random samples
[NASA-TP-2389] 07 p1035 N85-16565

Pari-mutuel as a system of aggregation of information
[AD-A147210] 07 p1035 N85-16570

An analysis of robust and efficient priors associated with a finite Bayesian model for compliance testing
[AD-A148497] 08 p1213 N85-17635

Recent results on characterization of probability distributions: A unified approach through extensions of Deny's theorem
[AD-A147631] 08 p1214 N85-17647

Calculation of cumulative distributions and detection probabilities in communications and optics
[AD-A147781] 08 p1215 N85-17650

Analysis of characteristics of digital discriminators for phase-shift keyed signals 13 p2070 N85-22930

Informative geometry of probability spaces
[AD-A150510] 13 p2153 N85-23371

Approximating posterior distributions of system reliability derived from component test data
[AD-A152057] 15 p2572 N85-25857

On the probability density of signal-to-noise ratio in an improved detector
[AD-A152529] 17 p2952 N85-28232

A collection of probability distributions
[AD-A153128] 17 p3025 N85-28704

A numerical investigation of the overlap distribution among pure states in the spin glass phase
[PREPRINT-414] 18 p3172 N85-29659

Tables for distributions of quadratic forms
[AD-A154064] 19 p3347 N85-30745

Methodology for evaluating P sub nu distributions: Results to date
[DE85-007286] 20 p3530 N85-31956

Characterizations of generalized hyperexponential distributions
[AD-A155855] 24 p4142 N85-35680

PROBABILITY THEORY

Sensitivity analysis of limit state functions for probability-based plastic design
01 p0059 N85-10388

Estimation of the threshold in fatigue crack initiation models: A Bayesian approach
[AD-A144847] 01 p0062 N85-10410

Setting hurricane conditions of readiness with high confidence
[AD-A144785] 01 p0085 N85-10570

Some weak and strong laws of large numbers for d(0,1) - valued random variables
[AD-A144845] 01 p0111 N85-10754

Construction of approximate confidence intervals for probability-of-kill via the bootstrap
[AD-A144761] 01 p0113 N85-10764

Joint probability of selected cloud and visibility thresholds around Koblenz, Germany
[AD-A145294] 02 p0231 N85-11506

A fast, compact assignment algorithm
[NRIMS-TWISK-331] 02 p0250 N85-11632

An introduction to multilinear formula score theory
[AD-A145696] 02 p0254 N85-11667

Locally optimal subset selection rules based on ranks under joint type 2 censoring
[AD-A146179] 03 p0412 N85-12632

On choosing between two probabilistic choice sub-models in a dynamic multitask environment
05 p0711 N85-14563

On the Edgeworth expansion for the sum of a function of uniform spacings
[CWI-MS-R8404] 05 p0719 N85-14619

Asymptotic distributions of estimators for posterior probabilities in a classification model with both continuous and discrete variables
[CWI-MS-R8409] 05 p0722 N85-14637

Invariant measures and the equicontinuous structure relation 1
[CWI-PM-R8403] 05 p0723 N85-14645

Invariant measures and the equicontinuous structure relation 2: The relative case
[CWI-PM-R8404] 05 p0723 N85-14646

How many Earth-approaching asteroids are there?
[NASA-CR-174209] 06 p0890 N85-15650

Analysis of subpixel registration
07 p0966 N85-16267

Experiments in forecasting atmospheric marine horizontal visibility using model output statistics with conditional probabilities of discretized parameters
[AD-A147574] 07 p1008 N85-16404

The symmetry group and exponents of operator stable probability measures
[AD-A147187] 07 p1035 N85-16568

Ambiguity and uncertainty in probabilistic inference
[AD-A147378] 07 p1035 N85-16572

Belief structures
[AD-A147526] 07 p1036 N85-16575

The effect of assumptions about cost element probability distributions on operating and support cost risk analysis
[AD-A147553] 07 p1036 N85-16576

Development of a mixed scanning interactive system for decision support
[AD-A146895] 07 p1051 N85-16670

A technique for rapid determination of probability of detection in pulse Doppler radars
[AD-D011426] 08 p1154 N85-17288

Two-dimensional modeling for lineal and areal probabilities of weather conditions
[AD-A147970] 08 p1188 N85-17486

Large deviations for processes with independent increments
[AD-A147293] 08 p1210 N85-17610

Probable cause: A decision making framework
[AD-A147642] 08 p1210 N85-17614

On the probability generating functional for point processes
[AD-A147692] 08 p1210 N85-17615

A theorem on the optimal allocation of effort
[AD-A148026] 08 p1211 N85-17623

Empirical Bayes rules for selecting good binomial populations
[AD-A147614] 08 p1214 N85-17646
Recent results on characterization of probability distributions: A unified approach through extensions of Deny's theorem
[AD-A147631] 08 p1214 N85-17647
Calculation of cumulative distributions and detection probabilities in communications and optics
[AD-A147781] 08 p1215 N85-17650
Probabilistic analysis of algorithms for NP-Complete problems
[AD-A148207] 08 p1215 N85-17653
Prematurely terminated sequential tests for MIL-STD 781C
[AD-A148417] 08 p1216 N85-17657
Exact simultaneous confidence intervals for pairwise comparisons of three normal means
[AD-A148751] 09 p1375 N85-18645
Bounding the stochastic performance of continuum structure functions 2
[AD-A149458] 10 p1548 N85-19762
Characteristic functional of a probability measure absolutely continuous with respect to a Gaussian radon measure
[AD-A149482] 10 p1548 N85-19763
On large matchings and cycles in sparse random graphs
[AD-A149194] 10 p1550 N85-19778
Estimation of variance of the regression estimator
[AD-A149407] 10 p1551 N85-19780
Identification of dynamic systems, theory and formulation
[NASA-RP-1138] 10 p1551 N85-19784
The study of certain aspects of probability with applications in communications theory
[AD-A149620] 12 p1829 N85-21476
Predicting a future response using rank predictive probabilities
[MATHEMATICS-RESEARCH-166]
12 p1923 N85-22077
Proportional odds models for survival data and estimates using ranks
[MATHEMATICS-RESEARCH-172]
12 p1923 N85-22080
A replication and extension of the inducement of the availability heuristic
[AD-A149755] 12 p1923 N85-22083
Systems vulnerability and lethality in the development phase
[AD-A149737] 12 p1924 N85-22089
Stable measures and processes in statistical physics
[AD-A149592] 12 p1926 N85-22098
Reliability of structural brittle materials
12 p1946 N85-22222
A statistical approach to vendor selection
[AD-A149781] 12 p1950 N85-22249
Rejection of anomalous observations when determining spacecraft trajectories 13 p1979 N85-22421
A Monte Carlo sampling plan for estimating network reliability
[AD-A150511] 13 p2065 N85-22896
Error probability during optimal noncoherent reception of binary signals in multibeam channel
13 p2069 N85-22922
Probability of detection of pulsed signals employing zero-gating interference suppression
13 p2085 N85-23021
Noise tolerance of diversity reception in frequency-adaptive digital transmission systems
13 p2086 N85-23024
SIGPI: A user's manual for the fast computation of the probabilistic performance of a complex system
[DE85-005447] 13 p2148 N85-23336
Why do noninvertible estimated moving averages occur?
[AD-A150366] 13 p2153 N85-23366
Tracer diffusion in an ordered alloy: Application of the path probability and Monte Carlo methods
[DE85-002768] 14 p2257 N85-23966
Monthly and Seasonal Weather Outlook for mid-December 1984 mid-January 1985, volume 38, number 24, 14 December 1984
14 p2379 N85-24667
A simple and efficient algorithm to compute tail probabilities from transforms
[AD-A150926] 14 p2409 N85-24849
Properties of systems which lead to efficient computation of reliability
[AD-A151033] 14 p2409 N85-24853
Algorithms and approximations for queueing systems
[CWI-TRACT-8] 14 p2410 N85-24859
Probalistic analysis of combinatorial algorithms: An annotated bibliography
[CWI-OS-R8411] 14 p2411 N85-24864
Boundary crossing probabilities and statistical applications
[AD-A151027] 14 p2411 N85-24869
Inference and state estimation for stochastic point processes
[AD-A151216] 15 p2640 N85-26281
A non-parametric probability density estimator and some applications
[AD-A151853] 15 p2641 N85-26287
Lectures on probability and statistics
[DE85-007079] 15 p2641 N85-26291
The evolutive state: A new definition of system state to include sequencing of events
16 p2696 N85-26643
A mathematical model for calculating detection probability of a diffusion target
[AD-A152026] 16 p2854 N85-27601
An evaluation of discretized conditional probability and linear regression threshold techniques in model output statistics forecasting of visibility over the north Atlantic Ocean
[AD-A151955] 16 p2857 N85-27619
Probabilistic algorithms in group theory
[AD-A152253] 16 p2859 N85-27630
Refinements in the computation of collision probabilities
[DE85-006118] 16 p2864 N85-27663
Probabilistic structural analysis theory development
17 p2912 N85-27955
Probabilistic finite element development
17 p2913 N85-27956
Probabilistic structural analysis of SSME turbopump blades: Probabilistic geometry effects
17 p2913 N85-27958
Alternative theories of inference in expert systems for image analysis
[AD-A153649] 18 p3170 N85-29646
Accepting error to make less error
[AD-A153949] 18 p3171 N85-29651
Nonparametric renewal function estimation
[AD-A153474] 18 p3173 N85-29672
Nonparametric estimation of the probability of ruin
[AD-A153523] 18 p3174 N85-29674
Probabilistic analysis of combinational circuits with random delays 19 p3257 N85-30192
A comparison of four Monte Carlo methods for estimating the probability OF S=T connectedness
[AD-A154264] 19 p3348 N85-30749
Exponential order statistic models of software reliability growth
[NASA-CR-3909] 20 p3515 N85-31852
Monte Carlo: In the beginning and some great expectations
[DE85-010789] 20 p3518 N85-31872
Reliability of void detection in structural ceramics using scanning laser acoustic microscopy
[NASA-TM-87035] 21 p3597 N85-32337
Decomposing the joint distribution of several linear combinations of uniform spacings
[AD-A155056] 21 p3677 N85-32845
Analysis of unreplicated factorials allowing for possibly faulty observations
[AD-A154813] 21 p3678 N85-32848
Antistarshapedness, dispersiveness and mixtures
[AD-A155583] 21 p3678 N85-32849
Probabilistic analysis of automatic control systems for detection systems 22 p3765 N85-33335
SMACS: A system of computer programs for probabilistic seismic analysis of structures and subsystems. Volume 1: User's manual
[DE85-011853] 22 p3830 N85-33724
A formulation and analysis of combat games
[NASA-TP-2487] 22 p3835 N85-33745
The application of models to the assessment of fire hazard from consumer products
[NBSIR-85-3219] 23 p3925 N85-34325
Estimating risks of lead-induced hemoglobin decrements under conditions of uncertainty: Methodology, pilot judgments and illustrative calculations
[DE85-012293] 23 p3952 N85-34493
On the statistical significance of excess events: Remarks of caution and the need for a standard method of calculation
[OG-9.5-10] 23 p4031 N85-34987
Large deviations for the maxima of some random fields
[AD-A155909] 24 p4143 N85-35681
Relaxation phenomena and stability of probability densities
[AD-A155923] 24 p4143 N85-35682

PROBES
Precision tunable resonant microwave cavity
[NASA-CASE-LEW-13935-1] 11 p1628 N85-20248
Heat pipe cooled probe
[NASA-CASE-LAR-12568-1] 12 p1844 N85-21566

PROBLEM SOLVING
NT ASYMPTOTIC METHODS
NT ITERATIVE SOLUTION
NT THEOREM PROVING
Results of the technical exchange agreement between NASA and DuPont on the containerless drop tube solidification of NiAl3
[NASA-TM-86473] 01 p0014 N85-10097
RADC/NBS (Rome Air Development Center/National Bureau of Standards) Workshop. Moisture Measurement and Control for Semiconductor Devices, 3
[PB84-219559] 01 p0051 N85-10337
Research in Structures and Dynamics, 1984
[NASA-CP-2335] 01 p0057 N85-10377
Application of concurrent processing to structural dynamic response computations
01 p0057 N85-10380
Recursive calculation of curved finite element stiffness matrices
[CSIR-TWISK-303] 01 p0108 N85-10725
The convergence of Garlerkin approximation schemes for second-order hyperbolic equations with dissipation
[CSIR-TWISK-325] 01 p0109 N85-10736
Solution of the Boltzmann transport equations for a permeable base transistor
[AD-A144969] 01 p0112 N85-10757
Lattice dilation in metal-hydrogen systems
[BLL-M-35758-(5825.4)] 02 p0178 N85-11178
Parallel, iterative solution of sparse linear systems: Models and architectures
[NASA-CR-172457] 02 p0243 N85-11586
A representation for the functioning of devices that supports compilation of expert problem solving structures: An extended summary
[AD-P003921] 02 p0245 N85-11601
Knowledge based tools for electronic equipment maintenance
[AD-P003940] 02 p0248 N85-11620
Numerical methods for solving systems of linear equations
[INPE-3240-RPE/463] 02 p0250 N85-11633
The numerical solution of the Helmholtz equation for wave propagation problems in underwater acoustics
[NASA-CR-172454] 02 p0250 N85-11634
An algorithm for least squares projections onto the intersection of shifted, convex cones
[AD-A145428] 02 p0251 N85-11640
On some common interests among reliability, inventory and queuing
[AD-A145595] 02 p0251 N85-11646
Cognitive coordinate systems: Accounts of mental rotation and individual differences in spatial ability
[AD-A146149] 03 p0401 N85-12557
A sequential quadratic programming algorithm for solving large, sparse nonlinear programs
[AD-A145854] 03 p0407 N85-12597
Convergence of SIP (Strongly Implicit Procedure)
[AD-A145810] 03 p0410 N85-12621
Moving finite elements in 2-D
[AD-A146266] 03 p0412 N85-12637
Psychological issues in the design of expert systems
[AD-A146061] 03 p0438 N85-12702
Economic analysis handbook
[AD-A146263] 03 p0441 N85-12805
Conservation laws and the numerical solution of ODEs
[DE84-016206] 04 p0555 N85-13531
New integration techniques for chemical kinetic rate equations. 2: Accuracy comparison
[NASA-TM-86893] 05 p0596 N85-13798
On looking into the black box: Prospects and limits in the search for mental models 05 p0709 N85-14546
Use of artificial intelligence and simple mathematics to analyze a physiological model 05 p0717 N85-14587
Conservative and nonconservative schemes for the solution of the nonlinear Schroedinger equation
[CWI-NM-R8405] 05 p0720 N85-146
Situational interactive micro/graphic simulator system for improving maintenance performance
[AD-A146677] 06 p0757 N85-148
Method of aperture synthesis: Fundamental relations and data processing in aperture synthesis systems (review) 06 p0761 N85-149
Phase problem in aperture synthesis systems
06 p0782 N85-150
Limits of applicability of long wave theory in studies o oscillations of n-layer fluid 06 p0824 N85-152
A method for solving the inverse problem of transo cascade flow
[AD-A146739] 07 p0899 N85-15
Effects of individual mnemonic characteristics o problem solving 07 p1010 N85-164
Mental models and cooperative problem solving wi expert systems
[AD-A147843] 07 p1021 N85-164

Research in applied mathematics, numerical analysis, and computer science
[NASA-CR-172505] 07 p1021 N85-16480
Implementation of a constraint machine for prism - A parallel problem solver
[AD-A147844] 07 p1026 N85-16512
Lattice statistics
[AD-A146862] 07 p1029 N85-16530
Solution of finite element problems by preconditioned conjugate gradient and Lanczos methods
[AD-A146921] 07 p1029 N85-16532
Viscosity solutions of Hamilton-Jacobi equations at the boundary
[AD-A147444] 07 p1032 N85-16553
Splitting methods for the numerical solution of the incompressible Navier-Stokes equations
[AD-A147463] 07 p1032 N85-16554
Sequential and parallel matrix computations
[AD-A147871] 07 p1034 N85-16562
Development of a mixed scanning interactive system for decision support
[AD-A146895] 07 p1051 N85-16670
On the complexity of distributed decision problems
[AD-A147174] 07 p1052 N85-16674
Distributed knowledge base systems for diagnosis and information retrieval
[AD-A146890] 07 p1054 N85-16690
Vectorizable multigrid algorithms for transonic flow calculations
[NASA-CR-174326] 08 p1077 N85-16827
Hazard assessment of a hypothetical large rocket motor 08 p1117 N85-17042
Flexible manufacturing system concept features cache memory 08 p1140 N85-17186
COPES/ADS (Control Program for Engineering Synthesis) (Automated Design Synthesis) using the ADS optimization program
[AD-A148576] 08 p1206 N85-17588
A local refinement finite element method for time dependent partial differential equations
[AD-A147943] 08 p1211 N85-17620
Distributed asynchronous relaxation methods for convex network flow problems
[AD-A148027] 08 p1211 N85-17622
Probabilistic analysis of algorithms for NP-Complete problems
[AD-A148207] 08 p1215 N85-17653
Analysis of a potential hot-wire ignition problem
[DE84-017254] 09 p1301 N85-18174
Device modeling for advanced integrated circuits
09 p1314 N85-18258
An implicit, conservative, zonal-boundary scheme for Euler equation calculations
[NASA-CR-3865] 09 p1318 N85-18290
On the local behaviour of solutions of degenerate parabolic equations with measurable coefficients
[AD-A147412] 09 p1373 N85-18631
Solution of the h-equation for a single point source excitation of magnitude K
[DE84-017574] 09 p1374 N85-18638
Towards the construction of periodic solutions of pseudodifferential equations with the aid of algebraic operators 10 p1535 N85-19674
Distributing a distributed problem solving network simulator
[AD-A149065] 10 p1537 N85-19693
A program design for an adaptive, non-linear finite element solver
[AD-A148880] 10 p1539 N85-19705
Meta-level control through fault detection and diagnosis
[AD-A149064] 10 p1540 N85-19709
Qualitative process theory
[AD-A148987] 10 p1543 N85-19729
Efficient algorithm for fuzzy linear programming with multiple objectives
[AD-A149012] 10 p1544 N85-19736
A conformal mapping suitable for problems involving interaction between given geometries and known far fields
[AD-A149050] 10 p1545 N85-19744
Neumann type boundary conditions for Hamilton-Jacobi equations
[AD-A149069] 10 p1546 N85-19746
Hamilton-Jacobi equations in infinite dimensions. Part 1. Uniqueness of viscosity solutions
[AD-A149094] 10 p1546 N85-19749
Order picking in an aisle
[AD-A149553] 10 p1548 N85-19766
Construction of solutions for two-dimensional Riemann problems
[DE85-003136] 10 p1549 N85-19770
Contribution to the study of a numerical implicit method for solving the Euler equations
[ESA-TT-872] 10 p1549 N85-19771
Robust Kalman filtering and its applications
[AD-A149044] 10 p1550 N85-19775
Heuristics based on spacefilling curves for combinatorial problems in the plane
[AD-A149320] 10 p1552 N85-19788
Coordination in a distributed problem solving network
[AD-A148925] 10 p1565 N85-19872
A study of degenerate and nondegenerate critical points in three-dimensional flow fields
[DFVLR-FB-84-36] 11 p1633 N85-20288
East Europe report: Scientific affairs
[JPRS-ESA-84-006] 11 p1700 N85-20684
Polylith and environments for mathematical computation
[DE85-002967] 11 p1702 N85-20704
Solving partial differential equations on multiprocessors
[DE85-000745] 11 p1706 N85-20734
Solution of structured non-stiff ODEs
[DE85-004137] 11 p1707 N85-20741
An exact solution to the 2 point OC (Operating-Characteristic) curve determination
[AD-A148120] 11 p1708 N85-20746
The application of expert systems to corrosion problems
[AERE-M-3445] 12 p1804 N85-21316
On the accuracy of least squares methods in the presence of corner singularities
[NASA-CR-172552] 12 p1919 N85-22050
Numerical methods for tracking interfaces
[LA-9817-MS] 12 p1919 N85-22052
Satellite-to-satellite orbit determination using minimum, discrete range and range-rate data only
13 p1985 N85-22458
Sparse matrix computations
[DE85-004780] 13 p2152 N85-23362
Personal decision making: The influence of perceived locus of control and degree of rationality on information seeking strategies 13 p2167 N85-23446
Programmer/analyst workstation evaluation report
[NASA-CR-175289] 14 p2394 N85-24749
Implementation of a C1 triangular element based on the p-version of the finite element method
[AD-A150904] 14 p2404 N85-24825
The complexity of reliability computations in planar and acyclic graphs
[AD-A150759] 14 p2408 N85-24845
Maintaining soluation invariants in the numerical solution of ODEs
[DE85-005918] 14 p2410 N85-24857
Solving set covering problems using heuristics with branch and bound
[AD-A151905] 15 p2638 N85-26269
Finite-difference computations of rotor loads
[NASA-TM-86682] 16 p2700 N85-26669
Method for evaluating perturbation in algorithms for solving navigational problems 16 p2718 N85-26783
LU methods for the compressible Navier-Stokes equations 16 p2781 N85-27160
Explicit construction of contractivity matrices
[TRITA-NA-8309] 16 p2852 N85-27586
Augmented weighted diamond force of the linear nodal scheme for Cartesian coordinate systems
[DE85-005631] 17 p3020 N85-28679
A program for solving first kind Fredholm integral equations by means of regularization
[CWI-NM-R8416] 17 p3022 N85-28697
A variable-complexity norm maximization problem
[AD-A153514] 18 p3169 N85-29634
Extrapolation methods for multi-dimensional quadrature of singular and regular integrand functions
[DE85-009665] 18 p3172 N85-29655
Method for computing evolution of random hydropdynamic fields on basis of adjoint equations
19 p3292 N85-30412
Expanding expertise by use of an expert system
[DE85-010759] 19 p3344 N85-30723
On spectral multigrid methods for the time-dependent Navier-Stokes equations
[NASA-CR-172613] 19 p3344 N85-30725
On MGR (Upsilon) multigrid methods
[AD-A153887] 19 p3345 N85-30733
Numerical algorithms for solving linear algebra problems
[DE85-010310] 19 p3346 N85-30738
Floating shock-fitting in transonic potential flow calculations 20 p3387 N85-31007
Direct simulation techniques for the Boltzmann equation
[DFVLR-FB-85-13] 20 p3457 N85-31470
Compressible Lagrangian hydrodynamics without Lagrangian cells
[DE85-009597] 20 p3520 N85-31891
The formal specification of an abstract machine: Design and implementation
[AD-A155167] 21 p3672 N85-32808
A comprehensive study of the AFIT (Air Force Institute of Technology) software development environment
[AD-A155450] 21 p3672 N85-32812
A new fault-tolerant algorithm for clock synchronization
[AD-A154771] 21 p3676 N85-32836
A simulation study of Sylvester's problem in three dimensions
[AD-A155266] 21 p3679 N85-32854
Solution of problem of equilibrium confinement of plasma by magnetic field in an infinite circular cylinder
21 p3692 N85-32936
Solvability of some inverse problems in laser radiation focusing 21 p3696 N85-32963
On the problem of linear programming with approximate data 21 p3698 N85-32978
Flat is not necessarily good
[DE85-012819] 22 p3830 N85-33723
Implementing linear multistep formulas for solving DAES
[DE85-012400] 22 p3834 N85-33740
DISPL1: A software package for one and two spatially dimensioned kinetics-diffusion problems
[ANL-84-56] 23 p3956 N85-34516
A model for graphics interface tool development
23 p3960 N85-34545
Analytic solutions of inverse heat conduction problems
24 p4092 N85-35367
Algorithmic approaches in sets of good answers in inverse problems
[PM/84/18] 24 p4142 N85-35677

PROCEDURES
NT CREW PROCEDURES (INFLIGHT)
NT FINITE ELEMENT METHOD
NT FINITE VOLUME METHOD
NT OPTICAL CORRECTION PROCEDURE
NT PANEL METHOD (FLUID DYNAMICS)
The removal, mechanical handling and installation procedures for declination tachometer and Itek encoder — United Kingdom Infrared Telescope
[UKIRT-17] 09 p1414 N85-18915
The mechanical procedures for the 8 channel bolometer — United Kingdom Infrared Telescope
[UKIRT-18] 09 p1414 N85-18916
In situ washing procedures for the UKIRT 3.8 meter primary mirror — United Kingdom Infrared Telescope (UKIRT)
[UKIRT-20] 09 p1414 N85-18918
Development and evaluation of a procedure for the rapid analysis of fresh concrete
[AD-A149741] 12 p1868 N85-21703
A note on validity generalization procedures
[AD-A150065] 12 p1924 N85-22085
The acquisition of procedures from text. A production-system analysis of transfer of training
[AD-A151029] 14 p2382 N85-24732
Guide for the execution of reliability tests in the laboratory — aeronautical equipment
16 p2796 N85-27237
Method for preparing Pb-(beta)-aluminum ceramic
[DE85-011665] 22 p3752 N85-33256
Method for controlling the viscosity of siloxane oils
[DE85-011586] 23 p3909 N85-34221
Method for preparing hydride configurations and reactive metal surface
[DE85-006443] 23 p3917 N85-34274
Procedure for editing the fluxgate magnetometer data of the AFGL (Air Force Geophysics Laboratory) magnetometer network
[AD-A156331] 24 p4117 N85-35523

PROCEEDINGS
U CONFERENCES

PROCESS CONTROL (INDUSTRY)
Preparation of silicon carbide fibers
[DE84-014661] 01 p0022 N85-10137
Automated apparatus for producing gradient gels
[DE84-014507] 01 p0107 N85-10716
Computer aided process planning of machined metal parts
[AD-A145628] 02 p0189 N85-11263
Application of solidification theory to rapid solidification processing
[AD-A145953] 03 p0331 N85-12136
Critical dynamics for continuous rapid solidification processing
[AD-A146071] 03 p0332 N85-12137
DNC, CNC network for robotized machining cells
04 p0491 N85-13130
Self-tuning control of offset: A unified approach
[OUEL-1539/84] 04 p0553 N85-13520
Long-range predictive control using weighting-sequence models
[OUEL-1542/84] 04 p0553 N85-13521
Investigations regarding process analysis of liquids in the 1 to 2 micrometer spectral range
[BMFT-FB-T-84-169] 05 p0614 N85-13926

Controlled directionally solidified precision casting for superalloys and steels
[BMFT-FB-T-84-196] 05 p0619 N85-13960
Self-tuning controller design and implementation
[OUEL-1535/84] 05 p0621 N85-13975
Control of microstructure during hot working of Ti-6242 06 p0797 N85-15091
Finite element simulation of forging processes
06 p0797 N85-15093
Modelling temperature changes during hot working operations 06 p0798 N85-15095
Modelling microstructural changes during hot rolling of steels 06 p0798 N85-15096
Process research of non-Cz silicon material
06 p0830 N85-15275
Advanced dendritic web growth development
06 p0831 N85-15286
Aerosol reactor for silicon processing
06 p0832 N85-15292
Control technology for integrated circuit fabrication at Micro-Circuit Engineering, Incorporated, West Palm Beach, Florida
[PB85-100717/GAR] 07 p0949 N85-16013
An analysis of the effect of process controls on productivity and weapon system costs in DoD procurement
[AD-A147496] 07 p1052 N85-16678
Approximate models in multivariable process control: An inverse Nyquist array and robust tuning regulator interpretation
[RR-261] 08 p1216 N85-17663
Control of the manufacturing process and material flow in flexible manufacturing systems
[PNR-90234] 09 p1371 N85-18615
French firm has most advanced continuous-casting machine 11 p1592 N85-20017
Chemical approach for controlling nadimide cure temperature and rate with maleimide
[NASA-CASE-LEW-13770-3] 12 p1809 N85-21350
Chemical approach for controlling nadimide cure temperature and rate with maleimide
[NASA-CASE-LEW-13770-4] 12 p1810 N85-21351
Materials refining for solar cell silicon
12 p1877 N85-21775
Manufacturing perspective in the design of bevel gearing 14 p2221 N85-23777
Electrical features of new DNC, CNC system viewed — direct numerical control 15 p2524 N85-25562
Operation of Prisma flexible manufacturing system
15 p2524 N85-25564
East Europe report: Science and technology
[JPRS-ESA-85-018] 15 p2537 N85-25658
Process control systems for largely automated manufacturing 15 p2537 N85-25659
Summaries of FY 1984 engineering research
[DE85-006273] 15 p2664 N85-26442
Multivariable statistical modelling and its application
16 p2857 N85-27617
Integration of advanced preparation with coal liquefaction
[DE85-010432] 19 p3226 N85-30012
Identification of a mathematical model 1: Goodness of fit criterion
[HSE-TRANS-11109] 19 p3341 N85-30703
Plasma arc welding, equipment, installation and process control
[DE85-008481] 19 p3373 N85-30921
Contribution to the modelling of the gas carburizing process for steels
[BLL-OA-TRANS-3205-(6196.300)]
20 p3428 N85-31263
FAUST: Introduction and overview — self tuning control
[OUEL-1568/85] 20 p3519 N85-31882
Electrically conductive doped block copolymer of polyacetylene and polyisoprene
[DE85-006500] 24 p4082 N85-35301

PROCESS HEAT
Development and test of a high COP Rankine heat pump for generation of process steam. Phase 2: Fabrication and test
[DE85-002600] 11 p1632 N85-20275
Solar process heat: Technology program
[BMFT-FB-T-84-234] 12 p1882 N85-21812
Fuel cell applications literature review
[DE85-011891] 22 p3809 N85-33592
Solar central receiver preliminary design studies: Summary and review of contract results
[DE85-011385] 22 p3809 N85-33593
Solar thermal technologies program summary
[DE85-012253] 23 p3945 N85-34449

PROCESSES
Studies of collisional and nonlinear radiative process for development of coherent UV and XUV sources
[AD-A152001] 16 p2865 N85-27670

PROCESSING
Edge detection in SAR imagery using gradient operators — synthetic aperture radar (SAR)
[AD-A149411] 13 p2064 N85-22862
Low gravity exothermic heating/cooling apparatus
[NASA-CASE-MSC-25707-1] 16 p3104 N85-29214

PROCESSORS (COMPUTERS)
U CENTRAL PROCESSING UNITS

PROCUREMENT
NT GOVERNMENT PROCUREMENT
Electronic components for space applications
[CNES-NT-109] 04 p0496 N85-13169
An analysis of the effect of process controls on productivity and weapon system costs in DoD procurement
[AD-A147496] 07 p1052 N85-16678
Technical order managers handbook: Utilization assessment
[AD-A147579] 07 p1055 N85-16694
On estimating the cost growth of weapon systems
[AD-A147297] 08 p1230 N85-17749
Microcomputers in transit: A hardware handbook
[PB85-113660] 10 p1536 N85-19700
A statistical approach to vendor selection
[AD-A149781] 12 p1950 N85-22249
Visualization of computation results. Definition of a graphics satellite computer
[ONERA-RT-2/3587-CY] 20 p3514 N85-31845
National Aeronautics and Space Administration research and development 20 p3542 N85-32042
Lopez Energy Alternatives Project
[DE85-010589] 22 p3849 N85-33837

PROCUREMENT MANAGEMENT
Five-year plan for meeting the automatic data processing and telecommunications needs of the Federal Government. Volume 2: Major information technology systems acquisition plans of Federal executive agencies, 1984-1989
[PB84-214518] 03 p0436 N85-12778
Navy program manager's guide, 1985 edition
[AD-A151925] 16 p2876 N85-27744
Documentation for the West German Federal Cabinet's space policy decision 17 p3051 N85-28886
Progress report on implementing the recommendations of the White House Science Council's Federal Laboratory Review Panel, volume 1
[PB85-185072] 24 p4164 N85-35819

PRODUCT DEVELOPMENT
NT WEAPONS DEVELOPMENT
Abrasive products study
[PB84-223635] 01 p0033 N85-10205
Manufacturing Methods and Technology (MM/T) specifications for miniature cathode ray tube
[AD-A145597] 02 p0194 N85-11296
Development and utilization of advanced methods of neutron scattering 03 p0424 N85-12710
Construction, putting into operation, and utilization of a triple axis neutron spectrometer
03 p0425 N85-12715
Software configuration management across project boundaries and in distributed development environments
[RSRE-MEMO-3704] 04 p0549 N85-13494
Value analysis — industrial competition
[CNES-NT-110] 04 p0577 N85-13684
Special Developments and Methods in High Frequency Measuring Techniques — conferences
[PTB-E-24] 05 p0629 N85-14030
Present status and development tendencies in the field of high frequency measuring techniques
05 p0629 N85-14031
Development program: Nuclear magnetic resonance gyroscope (NMR-gyro). Phase 1: Development of an experimental model
[BMFT-FB-W-84-041] 05 p0639 N85-14101
Photovoltaic power supply units
05 p0662 N85-14252
Development and construction of a prototype photovoltaic energy supply unit
05 p0662 N85-14254
Siemens solar module: Status of the technique, development tendencies 05 p0662 N85-14255
Development and utilization of CdS/Cu2S
05 p0662 N85-14256
Existing measuring systems for wind energy units
05 p0669 N85-14302
Metallo-Organic Decomposition (MOD) silver metallization for photovoltaics 06 p0830 N85-15278
What do we want: Increased speed, resolution, contrast or DOE? — astronomical photography
07 p0964 N85-16115
Possibilities and impossibilities of microcomputer systems
[AD-1984-904] 07 p1026 N85-16522
USSR report: Machine tools and metalworking equipment
[JPRS-UMM-84-021] 08 p1138 N85-17168
Preliminary concepts of candidate elements for a potential European participation in a manned space station
[MBB-UR-E-749-84-O] 11 p1587 N85-[illegible]
The servicing vehicle of Columbus
[MBB-UR-E-750-84-O] 11 p1588 N85-[illegible]
Design and analysis of airborne scanning optical systems 11 p1623 N85-[illegible]
Development of the sonic pump levitator
[NASA-CR-171382] 12 p1782 N85-[illegible]
Process development for commercial production of natural rubber from Guayule
[PB85-124956] 12 p1815 N85-[illegible]
Development of miniature laser Doppler anemometers
[KU-SFB-210/ET/3] 12 p1857 N85-[illegible]
Development and prototype construction of photovoltaic energy supply units 12 p1878 N85-[illegible]
Development of an amorphous silicon panel
12 p1879 N85-[illegible]
Development of high-efficiency economic systems for photovoltaics 12 p1880 N85-21795
Development of a CdSe thin film solar cell
12 p1880 N85-21796
Development of new solar cells
12 p1880 N85-21797
Improved Y-11 general-purpose transport designated Y-12 13 p1972 N85-[illegible]
Giotto solar array: Design, manufacture and test
13 p2008 N85-[illegible]
The Olympus solar array development and test program 13 p2009 N85-[illegible]
Possibility of producing monolithic composite materials based on niobium carbide 13 p2029 N85-22707
The helicopter transmission design process
14 p2221 N85-23772
Manufacturing considerations related to aircraft gearboxes 14 p2222 N85-23778
Development of nitrile rubbers and foams having a high static modulus and low creep
[BR91485] 14 p2259 N85-24001
A 320 to have combined automatic pilot, flight control system 14 p2289 N85-[illegible]
Research on CAD/CAM support for microprocessor development surveyed 14 p2290 N85-[illegible]
An error generator to support the trials of the ZODIAC prototype system — raster links
[PHL-1984-71] 14 p2293 N85-[illegible]
New directions in ARGOS instrumentation at Polar Research Lab (PRL) 14 p2323 N85-[illegible]
Development of a low cost drifting buoy
14 p2330 N85-24408
A report on the DRIFTERS program — buoys
14 p2331 N85-24413
Flying objects
[CH-634516-A5] 15 p2469 N85-25242
Airfoil wing with flap
[CH-634787-A5] 15 p2469 N85-25243
Helicopter rotor
[CH-637890-A5] 15 p2470 N85-25245
Aircraft
[CH-642598-A5] 15 p2470 N85-25246
System for radio remote control of dropping bombs
[CH-639335-A5] 15 p2491 N85-25371
Satellite structure
[CH-642922-A5] 15 p2492 N85-25373
France develops own aluminum-based composite ceramic 15 p2534 N85-[illegible]
Development of an integrated control unit for the PDV bus concept
[BMFT-FB-T-84-300] 15 p2551 N85-[illegible]
The development of onboard laser velocimeter at the Saint Louis Institute (France) from 1976 to 1982
[ISL-NB-402/83] 16 p2791 N85-27218
Development of a Lagrangian drifting buoy
16 p2811 N85-[illegible]
Development of a fuselage forward section in Carbon Fiber Reinforced Plastic (CFRP) type of construction
[MBB/LFA34/CFK/PUB/008] 17 p2895 N85-[illegible]
Development of a microprocessor controlled communication system for ships
[BMFT-FB-T-84-275] 17 p2950 N85-[illegible]
Ceramic turbochargers: A case study of a near-term application of high-strength ceramics
[DE85-008495] 17 p2975 N85-[illegible]
Ultrasonic flaw detector with microcomputer interpretation
[BMFT-FB-T-84-272] 17 p2977 N85-[illegible]
Special topics in infrared interferometry — Michelson interferometer development
[NASA-TM-87472] 17 p3036 N85-[illegible]
Further development of high voltage SIPMOS FETs to fulfill market needs
[BMFT-FB-T-84-255] 17 p3045 N85-[illegible]
Detection of pores in hot continuously cast rounds
[BMFT-FB-T-85-007] 18 p3072 N85-[illegible]

Component problems plague French robotics industry
18 p3086 N85-29088

Development of corrosion resistant heat exchangers for e gas desulfurization
MFT-FB-T-84-281] 18 p3103 N85-29211

Aluminum pressure die casting process for the oduction of low porosity castings and new casting oys
MFT-FB-T-84-296] 18 p3123 N85-29335

Conceptual design of a fixed-pitch wind turbine generator stem rated at 400 kilowatts
ASA-CR-174877] 18 p3127 N85-29363

Fuel cells: A bibliography
DE85-004565] 18 p3128 N85-29371

Plastic heliostat enclosure analysis
DE85-009112] 18 p3130 N85-29387

Lithium-alloy/iron sulfide battery design studies
DE85-007891] 18 p3131 N85-29389

Development of a stationary carbon monoxide detector
BMFT-FB-T-84-253] 18 p3134 N85-29413

Development of a coal-water slurry-fueled diesel engine for industrial cogeneration. Task 1.0 topical report: Thermodynamic analysis
[DE85-010455] 19 p3238 N85-30062

Advanced evacuated tube collectors
[DE85-010271] 19 p3274 N85-30302

Studies toward a manned space station: Participation of European industry in NASA space station (MSS)
[SNIAS-S/DT-Y-25-212] 20 p3418 N85-31217

The ESA field emission electric propulsion program
[ESA-STR-213] 20 p3420 N85-31229

The Silica Aerogel Detector (SAD) story — Cherenkov detector
[USP-84-14] 20 p3459 N85-31485

Design, manufacture and testing of a medium accuracy star tracker
[REPT-TR/84-048] 20 p3459 N85-31488

Development of an active laser gyro for inertial rotation sensing in attitude/heading reference and inertial navigation systems, phase 1
[BMFT-FB-W-85-001] 20 p3460 N85-31489

The development of complex systems
20 p3539 N85-32021

Spin-offs from technical scientific infrastructures, no. 1
20 p3540 N85-32034

Spin-offs from technical commercial infrastructures, no. 2
20 p3540 N85-32035

Spin-offs from technical scientific research organizations, no. 5
20 p3540 N85-32036

On the relationship between electronics and chemistry
[DRIC-T-7480] 22 p3743 N85-33200

Automatic rotary valve actuator
[DE85-012797] 22 p3794 N85-33505

Development of an energy-absorbing passenger seat for a transport aircraft
22 p3796 N85-33515

Drag-compensated, precision-powered hinge system
22 p3796 N85-33517

Design and development of a linear thermal actuator
22 p3796 N85-33518

The design and development of a constant-speed solar array drive
22 p3796 N85-33519

The design and development of a spacecraft appendage tie down mechanism
22 p3797 N85-33522

Block 5 documentation and solar modules
[NASA-CR-176134] 22 p3805 N85-33564

Photovoltaics technical information guide
[DE85-002924] 22 p3808 N85-33585

User commands for product design and system management
[DE85-011706] 22 p3830 N85-33721

The development and evaluation of the creep and corrosion resistant alloy IN6201
[PNR-90253] 23 p3917 N85-34278

A rational approach to cam design
23 p3923 N85-34311

Cost effective single crystals: The Rolls Royce approach — gas turbine components
[PNR-90262] 23 p3985 N85-34717

New technologies at the forefront of industrial developments
24 p4061 N85-35168

Development of position sensors for microcomputer-oriented sensor systems
[BMFT-FB-T-85-021] 24 p4091 N85-35361

Development of contactless sensors for industrial and automotive applications
[BMFT-FB-T-85-031] 24 p4097 N85-35400

Monolithic photovoltaic series array for an energy coupler
[BMFT-FB-T-85-023] 24 p4113 N85-35486

Development and operation of a measuring data acquisition system for use in light airplanes
24 p4123 N85-35556

PRODUCTION

Study of catalysts and mechanisms in synthesis reactions
[DE84-015025] 04 p0470 N85-12990

Fiat, Peugeot introduce integrated robotized engine: CAD used
07 p0936 N85-15933

Technology planning for flexible manufacturing systems
08 p1139 N85-17170

An analysis of production competition and award methodology
[AD-A147775] 08 p1228 N85-17733

Impacts of robotic and flexible manufacturing technologies on manufacturing costs and employment
[AD-A150060] 12 p1860 N85-21666

Feasibility of electrolytic hydrogen production in the Pacific Northwest
[DE85-009856] 18 p3084 N85-29080

Preparation and use of very pure o-D2
[DE85-009415] 22 p3843 N85-33800

PRODUCTION COSTS

NT AIRCRAFT PRODUCTION COSTS

A buyer's guide to space infrastructure
07 p0914 N85-15784

Production rate variations cost models
[AD-A147708] 08 p1228 N85-17732

Amorphous silicon solar cells with a view to cheap production processes
12 p1879 N85-21789

A low cost approach with larger diameter silicon wafer — solar cells
13 p2006 N85-22572

Cost and schedule implications of multinational coproduction
[AD-A154358] 19 p3380 N85-30969

PRODUCTION ENGINEERING

NT PRODUCTION PLANNING

Development of powder metallurgy in various sections of USSR
01 p0019 N85-10116

USSR report: Machine tools and metalworking equipment
[JPRS-UMM-84-019] 01 p0035 N85-10214

Growth, future of Soviet robotics sector analyzed
01 p0035 N85-10217

A review of world wide development in stainless steels
02 p0177 N85-11190

Sensor technology for second, third generation industrial robots. Optical sensor applications
03 p0342 N85-12198

Activities report of the Department of Engineering
03 p0342 N85-12202

Automation of production of semiconductor power devices
03 p0346 N85-12229

Development of rapidly quenched alloys with special physical properties and of processes for their continuous production
[BMFT-FB-T-84-179] 04 p0477 N85-13039

East Europe report: Science and technology
[JPRS-ESA-84-041] 04 p0484 N85-13090

Developments in Soviet robot technology viewed
04 p0491 N85-13127

Manufacturing Sciences and Robotics Research and Development Act of 1984
[H-REPT-98-1078] 04 p0578 N85-13688

Full-scale testing, production and cost analysis data for the advanced composite stabilizer for Boeing 737 aircraft. Volume 1: Technical summary
[NASA-CR-3649] 05 p0612 N85-13912

Full-scale testing, production and cost analysis data for the advanced composite stabilizer for Boeing 737 aircraft, volume 2
[NASA-CR-166012] 05 p0613 N85-13915

USSR report: Engineering and equipment
[JPRS-UEQ-84-007] 06 p0775 N85-14954

Situational planning of production processes in a flexible automated production system
06 p0776 N85-14959

Control technology for integrated circuit fabrication at Micro-Circuit Engineering, Incorporated, West Palm Beach, Florida
[PB85-100717/GAR] 07 p0949 N85-16013

Manufacturing methods and technology project summary reports
[AD-A148209] 08 p1138 N85-17163

Control systems for robotic production lines
08 p1138 N85-17169

Coordinated research in robotics and integrated manufacturing
[AD-A148204] 08 p1168 N85-17365

Cognitive asymmetry and occupation. Computer programmers, students, and bank personnel, part 1 and part 2
[AD-A147125] 08 p1197 N85-17540

COPES/ADS (Control Program for Engineering Synthesis) (Automated Design Synthesis) using the ADS optimization program
[AD-A148576] 08 p1206 N85-17588

Production of concentrated nitric acid
[DE84-017191] 09 p1293 N85-18121

Scania, ASEA of Sweden use robots for all production phases
09 p1310 N85-18229

Status of the Li-Al/FeS battery manufacturing technology. An evaluation for the US Army, Belvoir R and D Center
[DE85-000776] 09 p1315 N85-18264

Role of engineering psychology
09 p1361 N85-18561

Control of the manufacturing process and material flow in flexible manufacturing systems
[PNR-90234] 09 p1371 N85-18615

Production method of nickel electrode
[NASA-TM-76946] 10 p1439 N85-19069

Method of producing nickel electrode
[NASA-TM-76944] 10 p1440 N85-19077

New PCB production for robotics application
11 p1617 N85-20169

Increased use of CNC in machine tool construction
11 p1617 N85-20170

Exploratory assessment of second generation robotics and sensor-based systems
[PB85-132793] 11 p1648 N85-20388

Process development for commercial production of natural rubber from Guayule
[PB85-124956] 12 p1815 N85-21368

Silicon band spraying technique for solar cells
12 p1877 N85-21778

Amorphous silicon solar cells with a view to cheap production processes
12 p1879 N85-21789

Production and characterization of amorphous silicon (a-Si:H) as base material for solar cells
12 p1879 N85-21791

Testing and optimization of the production technology of large-surface Cu2S/CdS solar generators
12 p1880 N85-21793

A 2 x 6 Back Surface Reflection (BSR) silicon solar cell
13 p2005 N85-22570

Development of very thin large area GaAs solar cells for space application
13 p2006 N85-22579

Economic mechanism of integration of science, production
13 p2167 N85-23443

Applications of lasers in manufacturing
14 p2308 N85-24279

Lasers in automobile production
14 p2309 N85-24286

Mini-Seminar on Non-Destructive Testing
[CSIR-TSD-0009/83] 14 p2316 N85-24308

Mini-Seminar on CAD/CAM
[CSIR-TSD-0007/83] 14 p2402 N85-24809

Resources for robotics research in Europe, by country
15 p2489 N85-25364

Production cells with IR 2SO robot examined
15 p2524 N85-25561

Flexible machining systems described
15 p2524 N85-25563

Operation of Prisma flexible manufacturing system
15 p2524 N85-25564

East Europe report: Science and technology
[JPRS-ESA-85-018] 15 p2537 N85-25658

Production technology of an electrolyte for Na/S batteries
[BMFT-FB-T-84-277] 15 p2550 N85-25742

Compositional control of plate steels
15 p2565 N85-25826

Welding technology and organisation in steel construction
15 p2566 N85-25828

Manufacturing and producibility technology
16 p2733 N85-26866

USSR report: Engineering and equipment
[JPRS-UEQ-84-006] 16 p2760 N85-27035

Calculating reliability and productivity of cold stamping robot complex as queuing system
16 p2761 N85-27039

Uses of laser technology described
16 p2768 N85-27080

Manufacturing methods and technology CAD/CAM (Computer-Aided Design/Computer-Aided Manufacturing) related efforts (FY 1980 - 1986)
[AD-A151817] 16 p2846 N85-27547

Integral profile method for production of carbon fiber sheets
[MBB/LFA34/CFK/PUB/006] 17 p2916 N85-27975

Uses of, experiences in production of custom designed IC's
17 p2945 N85-28180

Modern equipment for manufacture of IC's in Hungary
17 p2945 N85-28181

Manufacturing information system
[AD-A152715] 17 p3011 N85-28616

USSR report: Science and technology policy
[JPRS-UST-85-008] 17 p3049 N85-28872

Automated maintenance system test program increment VI production scheduling
[AD-A153694] 18 p3198 N85-29638

The evolution of the U.S. helicopter industry
[AD-A154280] 19 p3211 N85-29913

Producibility Engineering and Planning (PEP): Program management guidelines
[AD-A153730] 19 p3379 N85-30966
Cost and schedule implications of multinational coproduction
[AD-A154358] 19 p3380 N85-30969
Automated fabrication of composite structures for helicopters
[SNIAS-851-210-104] 20 p3393 N85-31049
Production process for steel with decarburized surface adapted for single coating enamelling
[BMFT-FB-T-85-022] 20 p3432 N85-31292
CEMA venture to develop FMS, robot technology
20 p3438 N85-31330
Hidden costs of robotized production systems revealed 20 p3438 N85-31332
Utilization of microwave measuring systems for the automation of composite materials manufacturing
[SNIAS-851-430-102] 22 p3742 N85-33197
Centralized surveillance of flexible workshops for the manufacturing of composite materials
[SNIAS-851-430-103] 23 p3910 N85-34227

PRODUCTION MANAGEMENT
Abrasive products study
[PB84-223635] 01 p0033 N85-10205
Automated plant, production management system
08 p1139 N85-17171
Development of AK18 alloy production technology based on electrothermic silumin
11 p1598 N85-20048
Robot production lines in operation
11 p1617 N85-20166
USSR report: Science and technology policy
[JPRS-UST-85-002] 13 p2167 N85-23442
Welding technology: Japan — Conference
[ISBN-0-85300177-4] 15 p2565 N85-25823
Some aspects of nuclear plant fabrication in Japan and the UK relating to automatic and robotic arc welding
15 p2566 N85-25834
Design-To-Cost (DTC) methodology to achieve affordable avionics 16 p2696 N85-26645
Standard series of direct-current motors for regulated electric drives 22 p3772 N85-33375

PRODUCTION METHODS
U PRODUCTION ENGINEERING

PRODUCTION PLANNING
Computer aided process planning of machined metal parts
[AD-A145626] 02 p0189 N85-11263
Automation of assembly of electrical products
03 p0346 N85-12226
Increase in the economy of design and process planning by integrated and graphic data processing, phase 2 — aircraft design
[BMFT-FB-W-84-028] 05 p0716 N85-14589
Situational planning of production processes in a flexible automated production system 06 p0776 N85-14959
Manufacturing methods and technology project summary reports
[AD-A148209] 08 p1138 N85-17163
The planning of flexible manufacturing systems
[PNR-90230] 09 p1371 N85-18613
USSR report: Science and technology policy
[JPRS-UST-85-002] 13 p2167 N85-23442
Riga institute seeking faster introduction of new technology 14 p2206 N85-23698
Electrical features of new DNC, CNC system viewed — direct numerical control 15 p2524 N85-25562
Industrial laser use expanding in the USSR
15 p2644 N85-26310
CEMA venture to develop FMS, robot technology
20 p3438 N85-31330
Robots, Manipulators 21 p3666 N85-32786

PRODUCTIVITY
The Marine Resources Experiment Program (MAREX)
[NASA-TM-87368] 01 p0086 N85-10580
Future robotics program at San Antonio ALC (Air Logistics Center)
[AD-P004011] 03 p0309 N85-11991
Improving operational reliability and productivity of robotized technological complexes
03 p0346 N85-12227
Technologies for space station autonomy
[NASA-CR-174112] 04 p0458 N85-12906
Advances of implementing NC machine tools discussed 04 p0491 N85-13131
Recent studies of the ocean nitrogen cycle
05 p0653 N85-14193
The climate in food production in Latin America
07 p1001 N85-16359
Contractor productivity measurement
[AD-A146756] 07 p1050 N85-16666
Feasibility of measuring technical productivity improvements in Air Force Logistics Command depot-level maintenance using the Data Envelopment Analysis (DEA) and Constrained Facet Analysis (CFA) models
[AD-A147329] 07 p1052 N85-16676
An appraisal of the USAF Technology Modernization Program
[AD-A147344] 07 p1052 N85-16677
Evaluation of the effectiveness of the weighted guidelines to induce contractor's investment in cost reducing facilities equipment
[AD-A147586] 07 p1053 N85-16681
Flexible manufacturing system for the production of aircraft parts
[BLL-PNR-90237-(8019.3153)]
08 p1137 N85-17159
USSR report: Machine tools and metalworking equipment
[JPRS-UMM-84-021] 08 p1138 N85-17168
Robotics research, integration overview presented. Application objectives cited 08 p1142 N85-17201
North American vegetation patterns observed with the NOAA-7 advanced very high resolution radiometer — North America
[E85-10062] 08 p1174 N85-17400
Advances in cutting tool technology surveyed
13 p2051 N85-22840
Scientific, technical progress as factor of intensification of economy 13 p2167 N85-23444
East Europe report: Science and technology
[JPRS-ESA-85-018] 15 p2537 N85-25658
Calculating reliability and productivity of cold stamping robot complex as queuing system
16 p2761 N85-27039
New stage in robotics development
16 p2762 N85-27045
Design of computer-related workstations in relation to job functions and productivity
[AD-A151936] 16 p2844 N85-27534
Management considerations for an information center
[AD-A151774] 16 p2875 N85-27742
World iron ore reserves
[BLL-BISI-TRANS-22260-(9022.06)]
17 p2963 N85-28435
Photosynthetic acclimation of Acer saccharum
[DE85-008247] 17 p2998 N85-28536
Proceedings of the Seminar on Space Station Human Productivity
[NASA-TM-86673] 18 p3156 N85-29539
Human productivity program definition
18 p3158 N85-29556
Mockups and human productivity studies
18 p3159 N85-29570
Rockwell experience applications to Ames space station mockup habitability/productivity studies
18 p3159 N85-29572
Capital investment motivational techniques used by prime contractors on subcontractors
[AD-A153660] 18 p3198 N85-29837
Encapsulation processing and manufacturing yield analysis 21 p3611 N85-32434
Human activity and production rate of secondary nuclei 21 p3645 N85-32645
Production of liquid fuels and chemicals by microalgae
[DE85-008760] 22 p3819 N85-33658
Resource evaluation and site selection for microalgae production systems
[DE85-008807] 23 p3951 N85-34485
Electronic information management and productivity
[DE85-013362] 24 p4164 N85-35818

PRODUCTS
NT ASPHALT
NT GREASES
NT PETROLEUM PRODUCTS
NT REACTION PRODUCTS

PROFICIENCY
U ABILITIES

PROFILE METHOD (FORECASTING)
Simulation experiments on the relative accuracy of inferred atmospheric states from idealized wind and temperature profiling systems 05 p0682 N85-14366

PROFILES
Designing the profile of turbine blades using an iteration technique 09 p1305 N85-18201
Influence of normalized frequency on time-dependent aerodynamic characteristics of vane blading profiles
09 p1306 N85-18204
Study of geological media based on scattered earthquake waves 13 p2114 N85-23168

PROFILOMETERS
Flight demonstration of new NRL real-time data acquisition system and laser video waveform sampler
[AD-A145126] 01 p0053 N85-10350
Evaluation of laser profile and deflection measuring system
[FAA-PM-84-24] 02 p0201 N85-11341
Characterization of lubricated bearing surfaces operated under high loads
[NASA-TM-86964] 12 p1811 N85-21357

PROGNOZ SATELLITES
Observation of natural noise near upper hybrid resonance in terrestrial magnetosphere by Prognoz-5 satellite 06 p0822 N85-15221
The measurements of Prognoz-4, -5, -6, -7 during IMS
14 p2355 N85-24548
Magnetic field in the Earth's outer magnetosphere: Prognoz-6, -7 data 14 p2356 N85-24536
X-ray experiment on Prognoz-9 artificial Earth satellite
15 p2478 N85-25295
More on shock-wave studies with Prognoz-10 satellite
19 p3296 N85-30432
Functions of Prognoz-10: Intercosmos' station explained 19 p3296 N85-30433
Prognoz-10 intercosmos' station launched to study shock waves 19 p3296 N85-30434

PROGRAM MANAGEMENT
U PROJECT MANAGEMENT

PROGRAM VERIFICATION (COMPUTERS)
On the formal description and derivation of tempora proof rules for program properties
[TUM-I8405] 01 p0101 N85-10675
Program flow analyzer, volume 2
[AD-A145521] 02 p0242 N85-11576
Program flow analyzer, volume 3
[AD-A145522] 02 p0242 N85-11577
Northern Telecom, Incorporated, NTI-585/565, ACOBOL/3 Release 4.1 Version H(01)
[PB84-226022] 03 p0404 N85-12574
Northern Telecom, Incorporated NTI-585/565, ACOBOL/3 Release 4.1 Version H(01) (COBOL technical report)
[PB84-226030] 03 p0404 N85-12575
Convergent Technologies, NGEN CP001, CT COBOL version 9.0
[PB84-227784] 03 p0404 N85-12576
Convergent Technologies, mega frame CTIX BASIC interpreter version 1.03
[PB84-227776] 03 p0404 N85-12579
Convergent Technologies, mega frame, CTIX FORTRAN 77 version 2.1
[PB84-227768] 03 p0404 N85-12580
Gould Incorporated, GOULD Concept 32/87, COBOL release 1.4
[PB84-227669] 04 p0548 N85-13484
Digital Equipment Corp., VAX/750, VAX COBOL versio 3.0
[PB84-227651] 04 p0548 N85-1348
Digital Equipment Corp., MICRO/PDP-11, COBOL-8 version 2.2
[PB84-227644] 04 p0548 N85-1348
Prime Computer, Inc., PRIME 750, FORTRAN-7 revision 19.4
[PB84-227628] 04 p0548 N85-134
C3, Incorporated, C50 System, C3 COBOL/75 versio 2.00
[PB84-226006] 04 p0548 N85-134
Burroughs Corporation B26-CPU, B20 COBOL, Relea 4.0
[PB84-216241] 04 p0551 N85-135
Burroughs Corporation B26-CPU, B20 COBOL Versi 4.0 (COBOL technical report)
[PB84-216258] 04 p0551 N85-135
Convergent technologies NGEN CP001, CT COB Version 9.0
[PB84-216266] 04 p0551 N85-135
Convergent Technologies, Incorporated, NGEN CP0 CT COBOL Version 9.0 (COBOL technical report)
[PB84-216274] 04 p0551 N85-13
Computer Sciences Corporation UNIVAC 1100/ CSTS COBOL Release COB250
[PB84-216282] 04 p0551 N85-13
Control Data Corporation CYBER 205 model FORTRAN 200 (G201-25)
[PB84-216290] 04 p0551 N85-13
C3, Incorporated NGEN CP001, COBOL Version
[PB84-216308] 04 p0552 N85-13
United Information Services, Inc., CRAY 1-S/2 FORTRAN CFT 1.10
[PB84-227685] 04 p0552 N85-13
Datapoint Corporation Datapoint 6600, 8600, COBOL Version 3.6
[PB84-242973] 04 p0552 N85-1
Northern Telecom, Inc., IBM 3033 (compile NTI-585/565 (execution), XCOBOL, release 4.1, v H(01) (COBOL technical report)
[PB84-226048] 05 p0714 N85-1
Experimental techniques of formal specifications f design of tested and reliable computer programs
[ENST-84E007] 05 p0716 N85-
Implementation assessment of a network service test responder exerciser specification
[NPL-DITC-44/84] 05 p0716 N85-

Data general Corporation, Eclipse C150, interactive COBOL Revision 1.30 (COBOL technical report)
[PB84-227834] 06 p0849 N85-15391
Data General Corporation, Eclipse C150, interactive COBOL Revision 1.30
[PB84-227891] 06 p0849 N85-15392
IBM Corporation, IBM Series/1 4955, IBM Series/1 host COBOL Release 1.1 EDX (COBOL technical report)
[PB84-227909] 06 p0849 N85-15393
IBM Corporation, IBM Series/1 4955, IBM Series/1 host COBOL Release 1.1 EDX
[PB84-227818] 06 p0849 N85-15394
IBM Corporation, IBM Series/1 4955, IBM Series/1 host COBOL Release 1.1 RPS
[PB84-227917] 06 p0850 N85-15395
IBM Corporation, IBM Series/1 4955, IBM Series/1 host COBOL Release 1.1 RPS (COBOL technical report)
[PB84-227925] 06 p0850 N85-15396
Gould Incorporated, Gould PS-3000, Gould PS-3000 COBOL V2.0
[PB84-229160] 06 p0850 N85-15403
Gould Incorporated, Gould PS-3000, Gould PS-3000 BASIC Interpreter Version 1.00
[PB84-229186] 06 p0851 N85-15404
Digital Equipment Corporation, PDP-11/23-PLUS PDP-11 FORTRAN-77 V5.0
[PB84-227610] 06 p0851 N85-15405
Plexus Computers, Inc., Plexus P/60, Plexus FORTRAN 77 Version 1.1
[PB84-227859] 06 p0851 N85-15407
Control Data Corporation, CYBER 835, COBOL Release 5.3 Level 614
[PB84-227842] 06 p0851 N85-15408
C3, Incorporated NGEN CP001, C3 COBOL Version 9.0 (COBOL Technical Report)
[PB84-216316] 06 p0855 N85-15435
Burroughs Corporation B26-CPU, Burroughs B20 BASIC Rel. 4.0
[PB84-216324] 06 p0855 N85-15436
Convergent Technologies NGEN CP001, CT BASIC Version 9.0
[PB84-216332] 06 p0855 N85-15437
Microsoft Corporation, Sun Microsystems, Microsoft COBOL Version 2.0
[PB84-243401] 06 p0856 N85-15443
Microsoft Corporation, IBM PC XT, Microsoft COBOL, Version 2.0
[PB84-243419] 06 p0856 N85-15444
On the generation of random variables for radar simulation purposes 07 p0938 N85-15947
Finite difference calculations of buoyant convection in an enclosure. Part 2: Verification of the nonlinear algorithm
[PB85-104065/GAR] 07 p0961 N85-16089
Ada compiler validation summary report: New York University (NYU Ada/Ed) compiler, version 1.4 for VAX 11/780, using VMS 3.5
[AD-A146924] 07 p1022 N85-16483
Ada compiler validation summary report: TeleSoft (TeleSoft Ada) compiler, version 2.0a for Sun 120 Motorola M68010, using 4.2 BSD UNIX-Sun Version 1.1
[AD-A146925] 07 p1022 N85-16484
Formal verification of mathematical software
[NASA-CR-172407] 07 p1023 N85-16489
NYU Ada/Ed user's guide: Version 1.4 for VAX/VMS systems
[AD-A146759] 07 p1024 N85-16495
Software test handbook
[AD-A146844] 07 p1024 N85-16498
Functional semantics of modules
[AD-A146923] 07 p1024 N85-16500
Debug testing and confidence testing
[AD-A147104] 07 p1025 N85-16504
Ada compiler validation summary report: TeleSoft (TeleSoft Ada) compiler, version 2.0a2 for Callan Unistar 300, using System V, version 4.1a
[AD-A147115] 07 p1025 N85-16505
The production of maintainable, trustworthy, and portable software 08 p1064 N85-16744
Software testing in an Ada programming environment 08 p1065 N85-16748
Investigating version dependence in fault-tolerant software 08 p1065 N85-16749
Software test handbook: Software test guidebook, volume 2
[AD-A147289] 08 p1204 N85-17578
DDL system: Design systhesis of digital systems
[NASA-CR-170759] 09 p1366 N85-18584
JOVIAL J73 automated verification system: Implementation phase
[AD-A148732] 09 p1368 N85-18597
High level languages in protocol specification and verification
[FUB-51-1983] 09 p1370 N85-18611
Gateway testing techniques — computer system interconnection
[NPL-DITC-49/84] 09 p1372 N85-18621
Digital Equipment Corporation VAX Ada Compiler Version T0.6-2 VAX-11/785, 11/750, 11/730, using VMS, Version 4.0 and MicroVAX 1, using MicroVMS Version 1.0
[AD-A149375] 10 p1538 N85-19696
Methodology investigation software testing of multiprocessor systems
[AD-A149446] 10 p1541 N85-19714
Four Phase Systems, Incorporated, Four Phase Series 5000, COBOL 1974 version BE08.8
[PB85-108017] 10 p1541 N85-19717
Four Phase Systems, Incorporated, Mini-Frame Series 6300, COBOL Series 6000
[PB85-108025] 10 p1541 N85-19718
Micro focus DEC Rainbow 100 + compact level 2 COBOL; V2.5
[PB85-108975] 10 p1542 N85-19719
Micro focus DEC Rainbow 100 + high performance level 2 COBOL; V2.5
[PB85-108983] 10 p1542 N85-19720
DTSS, Incorporated, DPS 8/44, DTSS COBOL Release 12
[PB85-108058] 10 p1542 N85-19721
Checking microcode algebraically
[AD-A149441] 10 p1547 N85-19759
Dynamic investigations of a spherical tank structure filled with liquid using ANSYS three-dimensional fluid elements
[MBB-UR-E-737-83-O] 11 p1654 N85-20418
Ada compiler validation summary report, Dansk Datamatik Center, VAX 11 compiler version 1.1
[AD-A149340] 11 p1699 N85-20681
Micro Focus, Intel Microprocessor Development System MDS221 CIS COBOL; V4.5
[PB85-110823] 11 p1699 N85-20682
A quality control experiment in a real time multiprocessor operating system: The Mara 860 — software testing 11 p1702 N85-20707
Validation Summary Report (VSR), Ryan-McFarland Corporation, AT and T 385, RM/COBOL Version 2.0
[PB85-102093] 11 p1703 N85-20709
Burroughs Corporation, Burroughs B3955 COBOL9 Version 6.8
[PB85-103110] 11 p1703 N85-20710
Burroughs Corporation, Burroughs B3955 FORT77 Version 6.8
[PB85-110328] 11 p1703 N85-20711
Micro Focus Plessy Micro Systems 68/50 Compact Level 2 COBOL; V2.5
[PB85-108934] 11 p1703 N85-20712
Micro Focus Plessy Micro Systems 68/50 High Performance Level 2 Cobol; V2.5
[PB85-108942] 11 p1703 N85-20713
Micro Focus IBM personal computer XT Compact Level 2 COBOL; V2.5
[PB85-108918] 11 p1703 N85-20716
Micro Focus IBM personal computer XT High Performance Level 2 COBOL; V2.5
[PB85-108926] 11 p1704 N85-20717
Micro focus Fortune 32:16 compact level 2 COBOL; V2.5
[PB85-108884] 11 p1704 N85-20718
Micro focus Fortune 32:16 high performance level 2 COBOL; V2.5
[PB85-108892] 11 p1704 N85-20719
Micro Focus IBM personal computer XT CIS COBOL; V4.5
[PB85-108868] 11 p1704 N85-20720
ICL, ICL 2988 COBOL C2COB. 1321
[PB85-108876] 11 p1704 N85-20721
MICRO FOCUS Intel Microprocessor Development System MDS221 Compact Level 2 COBOL; V2.5
[PB85-108900] 11 p1704 N85-20722
Micro focus IBM personal computer XT, high performance level, 2 COBOL, IBM PC tailored; V2.6
[PB85-110815] 11 p1705 N85-20725
A Gypsy-to-Ada program compiler
[TR-39] 12 p1913 N85-22005
Towards the generation of efficient code from verified programs
[TR-40] 12 p1914 N85-22017
Ryan-McFarland Corporation, IBM PC model XT, RM/FORTRAN, version 2.0.0
[PB85-107993] 12 p1917 N85-22037
Ryan-McFarland Corporation, sun microsystem with sky fast floating point processor, RM/FORTRAN version 1.5.0
[PB85-108009] 12 p1917 N85-22038
Requirements for a database management system
[DE85-004661] 12 p1951 N85-22259
Logic analyzer survey and reviews
[BAE-881/ELO/1645] 15 p2621 N85-26151
Using a logic analyser and trigger unit to de-bug a program
[BAE-881/ELO/1487] 15 p2626 N85-26180
The systematic integration of very large scale integrated circuit computer-aided design tools into a toolkit optimized for academic applications
[AD-A151813] 16 p2845 N85-27536
NASA guidelines for assuring the adequacy and appropriateness of security safeguards in sensitive applications
[NASA-CR-175489] 17 p3007 N85-28593
Software environment for conducting interactive statistical analysis
[AD-A153378] 17 p3012 N85-28626
Debugging distributed computations in a nested atomic action system
[AD-A153617] 18 p3162 N85-29585
Ada (trademark) compiler validation summary report: ALSYS ALSYCOMP-0001
[AD-A153750] 18 p3163 N85-29592
Specification of software quality attributes. Volume 2: Software quality specification guidebook
[AD-A153989] 18 p3163 N85-29594
Specification of software quality attributes. Volume 3: Software quality evaluation guidebook
[AD-A153990] 18 p3163 N85-29595
Statistical estimation of software reliability
[AD-A154097] 19 p3335 N85-30665
Discrete-element acoustic analysis of submerged structures using doubly asymptotic approximations
[AD-A154959] 21 p3700 N85-32987
A prototype PASCAL program validation system
[NPL-DITC-57/85] 23 p3956 N85-34513
Specifying and verifying concurrent programs
[AD-A156190] 24 p4138 N85-35652

PROGRAMMED INSTRUCTION
NT COMPUTER ASSISTED INSTRUCTION
Self-paced instruction. Factors critical to implementation in Air Force technical training: A preliminary inquiry
[AD-A145098] 01 p0097 N85-10647
Factors critical to the implementation of self-paced instruction: A background review
[AD-A145143] 01 p0097 N85-10648

PROGRAMMERS
Programming effort estimation
[AD-A145839] 03 p0406 N85-12595
Approaches to structuring the software development process
[AD-A147694] 08 p1205 N85-17582
Concept paper for the development of a DOD Ada (trademark) software engineering education and training plan
[AD-A148774] 08 p1206 N85-17592
Programmer/analyst workstation evaluation report
[NASA CR-175289] 14 p2394 N85-24749
A learning strategy approach for teaching novice computer programmers
[AD-A151523] 15 p2628 N85-26200
CLEANROOM software development: An empirical evaluation
[AD-A152924] 17 p3011 N85-28619
Data processing professionals and DP application users' perceptions and expectations of operational roles of persons working in a DP/application user interface group 24 p4165 N85-35821

PROGRAMMING (SCHEDULING)
Computer assisted flight schedule optimization
[AD-A151689] 16 p2858 N85-27623

PROGRAMMING LANGUAGES
NT ADA (PROGRAMMING LANGUAGE)
NT ASSEMBLY LANGUAGE
NT BASIC (PROGRAMMING LANGUAGE)
NT COBOL
NT FORTRAN
NT HIGH LEVEL LANGUAGES
NT LISP (PROGRAMMING LANGUAGE)
NT NATURAL LANGUAGE (COMPUTERS)
NT PASCAL (PROGRAMMING LANGUAGE)
NT PL/1
TEQUEL: The query language of SADDLE 01 p0058 N85-10382
Psychological testing on the computer
[R/PERS-618] 01 p0097 N85-10645
Activities of the MIT Laboratory for Computer Science
[AD-A145134] 01 p0100 N85-10661
PROGEN: An incremental programming environment
[NRIMS-TWISK-315] 02 p0241 N85-11568
Research on distributed languages and algorithms
[AD-A145661] 02 p0242 N85-11580
Application of the CSRL language to the design of expert diagnosis systems: The Auto-Mech experience
[AD-P003922] 02 p0245 N85-11602
Air Force Materials Laboratory plans/projects
[AD-P004010] 03 p0308 N85-11990

PROGRAMS

Convergent Technologies, mega frame, CTIX COBOL version 2.0
[PB84-227750] 03 p0404 N85-12581
DATAPLOT: Implementation tapes guide
[PB84-214063] 03 p0408 N85-12610
Technologies for space station autonomy
[NASA-CR-174112] 04 p0458 N85-12906
Control of walking: Local control and real time systems 05 p0715 N85-14583
Towards a specification of the B programming environment
[CWI-CS-R8406] 05 p0716 N85-14593
Design and analysis of an SQL (Structured Query Language) interface for a multi-backend database system
[AD-A146534] 06 p0656 N85-15447
Control system design language implementation of a gas turbine starting controller
[AD-A147896] 07 p0905 N85-15732
What a parallel programming language has to let you say
[AD-A147854] 07 p1026 N85-16513
Some scientific subroutines in LISP
[AD-A147889] 07 p1026 N85-16515
The production of maintainable, trustworthy, and portable software 08 p1064 N85-16744
Implementation of an Intel 8086 microprocessor-based realization library for the control system design language
[AD-A148506] 08 p1202 N85-17569
DDL system: Design systhesis of digital systems
[NASA-CR-170759] 09 p1366 N85-18584
FLAD user's manual: FLAD file contents
[AD-A148700] 09 p1368 N85-18594
Proposal for a small scheme implementation
[AD-A148707] 09 p1368 N85-18595
Partial evaluation as a means of language extensibility
[AD-A148730] 09 p1368 N85-18596
Multitasking kernel for the C and FORTRAN programming languages
[DE85-001799] 09 p1370 N85-18609
French firm develops 2D, 3D computer vision system
10 p1461 N85-19208
Research into self-timed VLSI circuits
[AD-A149140] 10 p1479 N85-19339
Ada (trademark) Joint Program Office objectives and progress through 1983
[AD-A149436] 10 p1541 N85-19713
SOLIDGEN: A solid finite element data generator. User's manual
[AD-A149490] 10 p1541 N85-19715
Software standards issues — space station software development 11 p1701 N85-20692
A survey of the project CIP: Computer aided, intuition-guided programming. Wide spectrum language and program transformations
[TUM-I8406] 12 p1912 N85-22000
The four forms of omega
[AD-A149694] 12 p1915 N85-22020
Principles of software engineering environment design
[AD-A150352] 13 p2147 N85-23324
LEXICON: A structured modeling system for optimization
[AD-A150536] 13 p2147 N85-23329
ROSS: An object-oriented language for constructing simulations
[AD-A150556] 13 p2147 N85-23330
Orphan detection in the Argus system
[AD-A150562] 13 p2148 N85-23331
Multidimensional digital signal processing
[AD-A150833] 14 p2292 N85-24209
GRAFIT language for simulating two-dimensional geometric entities and sketches
14 p2401 N85-24801
Automation of development of software for switching units that are implemented in the form of multiprocessor systems on a microcomputer base
14 p2401 N85-24802
An algebraic specification language and a syntax directed editor
[AD-A150664] 14 p2403 N85-24815
The enhancement of concurrent processing through functional programming languages
[AD-A150771] 14 p2404 N85-24822
CHIL: A comprehensive histogramming language
[DE85-005356] 14 p2405 N85-24830
The design and implementation of a syntax directed editor for a space constrained microcomputer
[AD-A151313] 15 p2623 N85-26163
Programming the digital computer ODRA-1204 in MOST-2 language
[NASA-TM-87482] 15 p2627 N85-26191
The development of a programming support system for rapid prototyping. Tasks 2 and 3
[AD-A151549] 15 p2629 N85-26202
Praxis language environment: Distribution package description, revision 1
[DE85-006699] 15 p2630 N85-26212
IPAD: Integrated Programs for Aerospace-vehicle Design
[NASA-CR-3690] 15 p2632 N85-26221
Graphic simulation of a machine-repairman model
[AD-A151761] 16 p2694 N85-26633
The systematic integration of very large scale integrated circuit computer-aided design tools into a toolkit optimized for academic applications
[AD-A151813] 16 p2845 N85-27538
Reliability models for dataflow computer systems
[NASA-CR-175813] 16 p2846 N85-27543
Parallel computation of multiple-scale problems
[DE85-007230] 16 p2849 N85-27563
Continued development and implementation of the Universal Network Interface Device (UNID) 2 in the Digital Engineering Laboratory Network (DELNET), volume 2
[AD-A151947] 16 p2850 N85-27570
Internation information networks for material properties: Revision 1
[DE85-007412] 16 p2850 N85-27572
AFIT GKS: A GKS implementation in the Ada programming language
[AD-A152954] 17 p3012 N85-28620
Ada validation summary report. ALS AdaVAX version 1.1 VAX-11/780 using VAX/VMS release 3.6
[AD-A153684] 18 p3162 N85-29588
Parallel computation of multiple-scale problems, revision 1
[DE85-009447] 18 p3164 N85-29598
Development and analysis of a global compaction technique of microprograms 19 p3334 N85-30654
The BLAZE language: A parallel language for scientific programming
[NASA-CR-172615] 19 p3334 N85-30656
The design, implementation and application of a table-driven syntax-directed editor
[AD-A154234] 19 p3336 N85-30670
Ada compiler validation summary report: University of Karlsruhe-GMD/German MOD VAX 11 compiler, version v1.0
[AD-A154370] 19 p3337 N85-30678
HANDTC: A FORTRAN program to calculate inner-zone terrain corrections
[DE85-011196] 19 p3340 N85-30699
Proceedings of the Argonne Workshop on Programming the Next Generation of Supercomputers
[DE85-008348] 19 p3343 N85-30718
Data communications-Oriented Production System Language (CPSL)
[DE85-011457] 20 p3440 N85-31352
The design and implementation of an object-oriented, production-rule interpreter
[AD-A154769] 21 p3671 N85-32803
Praxis release notes, version 7.3
[DE85-011862] 21 p3673 N85-32820
Evaluation and implementation of a functional microprogram generator
[AD-A155164] 21 p3674 N85-32823
Logical and physical modeling and design of scientific and statistical databases for energy research
[DE85-006061] 22 p3833 N85-33737
Graphics interaction in databases
23 p3958 N85-34534
Architecture of languages for large CAD systems development 23 p3962 N85-34557
Software maintenance relating to the input translator and z-80 realization volume of the computer systems design environment
[AD-A155849] 24 p4138 N85-35646
Benchmark evaluation of PC simscript
[AD-A156133] 24 p4138 N85-35651
Polylith: The early goals
[DE85-012534] 24 p4139 N85-35658
Artificial intelligence in Ada (trademark): Pattern-directed processing
[AD-A156230] 24 p4141 N85-35671

PROGRAMS
NT ACEE PROGRAM
NT AGRISTARS PROJECT
NT APOLLO APPLICATIONS PROGRAM
NT APOLLO PROJECT
NT BRAZILIAN SPACE PROGRAM
NT CANADIAN SPACE PROGRAM
NT DEFENSE PROGRAM
NT EARTH RESOURCES PROGRAM
NT EUROPEAN SPACE PROGRAMS
NT FRENCH SPACE PROGRAMS
NT GALILEO PROJECT
NT GLOBAL ATMOSPHERIC RESEARCH PROGRAM
NT HELIOS PROJECT
NT INDIAN SPACE PROGRAM
NT INTERNATIONAL GEOSPHERE-BIOSPHERE PROGRAM
NT JAPANESE SPACE PROGRAM
NT MACHINE-INDEPENDENT PROGRAMS
NT NASA PROGRAMS
NT PROJECT SETI
NT PROJECTS
NT SCOUT PROJECT
NT SKYLAB PROGRAM
NT SPACE PROGRAMS
NT SUPERSONIC CRUISE AIRCRAFT RESEARCH
NT SWEDISH SPACE PROGRAM
NT TIROS PROJECT
NT U.S.S.R. SPACE PROGRAM
NT UNIVERSITY PROGRAM
NT VOYAGER PROJECT
Electrochemical Energy Storage Branch
[DE85-007592] 18 p3131 N85-29381
Index of laser program publications and related reports, calendar year 1984
[DE85-011863] 23 p3936 N85-34398

PROGRESS
Scientific, technical progress as factor of intensification of economy 13 p2167 N85-23444
High-efficiency silicon solar cell research
21 p3609 N85-32417
Confinement experiments on ISX-B
[DE85-012346] 23 p3984 N85-34709

PROJECT MANAGEMENT
ACEE program rationale and implementation
[NASA-TM-84549] 02 p0133 N85-10908
Life prediction and constitutive behavior: Overview
02 p0143 N85-10973
Developing commercial users of space
02 p0154 N85-11044
Commercializing the transfer orbit stage
02 p0155 N85-11049
Research and technology
[NASA-TM-86321] 02 p0305 N85-11973
Methodology for the implementation of a domestic satellite communications network
04 p0493 N85-13148
Project resources planning and control
[NASA-TM-86339] 04 p0575 N85-13866
NASA's SESAC report on research and analysis in space and Earth sciences 04 p0579 N85-13897
The METEOSAT exploitation project, operational use of a remote sensing system 05 p0658 N85-14223
Knowledge-based communication and management support in a system development environment
05 p0717 N85-14596
The management of research institutions: A look at government laboratories
[NASA-SP-481] 07 p1050 N85-16665
National airspace review enhancement plan, revision 3
[AD-A150743] 08 p1082 N85-16852
Space station task force perspective
08 p1106 N85-16892
Air Force space technology center space technology: Emphasis 84 09 p1333 N85-18381
The R and D project selection problem with fuzzy coefficients
[INPE-3329-PRE/626] 10 p1565 N85-19871
Space Station Software Issues
[NASA-CP-2361] 11 p1700 N85-20689
Software development environment issues --- space station software development 11 p1700 N85-20691
Air Force satellite position management
12 p1787 N85-21217
Computer integration of engineering design and production: A national opportunity
[NASA-CR-175483] 12 p1820 N85-21414
Space Station technology planning
13 p1989 N85-22471
Solid fuel combustion chamber
[VTH-LR-415] 16 p2741 N85-2801
Organizing geological work tasks for 1985 outlined
16 p2806 N85-27303
The Helios missions 16 p2884 N85-2779
Managerial benefits of Helios for the Europea industry 16 p2887 N85-2780
Helios project support 16 p2887 N85-2781
Summer High School Apprenticeship Research Progra (SHARP) of the National Aeronautics and Spa Administration
[NASA-CR-175791] 17 p3046 N85-288
Technical services at NLR
[B8561898] 17 p3049 N85-2887
Space station study
[BL-6167] 18 p3066 N85-289
Program planning using the GMAP procedure SAS/GRAPH software
[DE85-008356] 18 p3199 N85-296
Thermal Energy Storage Program annual operating pl FY 1985
[DE85-006745] 19 p3307 N85-304

The development of an institutional structure for the Future Global Satellite System for Search and Rescue
20 p3406 N85-31138
Commission for Marine Meteorology
[WMO-640] 20 p3496 N85-31735
The development of complex systems
20 p3539 N85-32021
The 2nd World Meteorological Association Regional Association (Asia), 8th session
[WMO-642] 22 p3817 N85-33643
Project management using graphics
23 p3962 N85-34560
Analyzing performance of small projects using URS and PMAS, information pamphlet
[DE85-011964] 23 p3986 N85-34718
Management of large-scale technology
23 p4057 N85-35145

PROJECT PLANNING
Ada (trademark) training curriculum. Software engineering for managers m101 teacher's exercise guide
[AD-A145094] 01 p0104 N85-10695
AGARD bulletin technical programme, 1985
[AGARD-BUL-84-2] 02 p0305 N85-11971
Project resources planning and control
[NASA-TM-86339] 04 p0575 N85-13666
INFORM system 2-year plan, FY 1984-1985
[DE84-016044] 04 p0576 N85-13674
International Geosphere/Biosphere Program: 1984
[GPO-39-222] 04 p0578 N85-13691
Preliminary concepts of candidate elements for a potential European participation in a manned space station
[MBB-UR-E-749-84-O] 11 p1587 N85-19996
Systems research on China in year 2000
12 p1820 N85-21418
Global tropospheric chemistry: A plan for action
[NASA-CR-175545] 12 p1891 N85-21865
Space Station technology planning
13 p1989 N85-22471
Space station systems technology study (add-on task). Volume 3: Technology advancement program plan
[NASA-CR-171417] 15 p2475 N85-25280
The 1985 long-range program plan
[NASA-TM-87464] 15 p2664 N85-26440
National Airspace System Plan: Facilities, equipment and associated development 16 p2704 N85-26692
Space Station Engineering and Technology Development
[NASA-CR-175806] 16 p2731 N85-26851
Organizing geological work tasks for 1985 outlined
16 p2806 N85-27303
The significance of Helios for Europe
16 p2888 N85-27808
In orbit infrastructure. Volume 1: Executive summary – European space programs
[RX011-002/84-VOL-1] 17 p2906 N85-27928
Documentation for the West German Federal Cabinet's space policy decision 17 p3051 N85-28886
In orbit infrastructure — european space programs
[SNIAS-S/DT-24-996] 18 p3064 N85-28956
Study of a medium term flexible fixed satellite service mission
[DM51/CC-IM-0185.83] 18 p3091 N85-29136
Program planning using the GMAP procedure in SAS/GRAPH software
[DE85-006356] 18 p3199 N85-29842
Electric and hybrid vehicle program: FY 1985 program plan
[DE85-006933] 18 p3201 N85-29858
Thermal Energy Storage Program annual operating plan FY 1985
[DE85-006745] 19 p3307 N85-30499
Management of large-scale technology
23 p4057 N85-35145

PROJECT SETI
DSN 34-meter antenna optics analysis for wideband SETI investigations 10 p1465 N85-19244
The search for extraterrestrial intelligence
15 p2689 N85-26609

PROJECTILE CRATERING
Ion emission from solid surfaces: Comparison of dust impact with other excitations — Giotto mission
14 p2244 N85-23912

PROJECTILE PENETRATION
U TERMINAL BALLISTICS

PROJECTILES
NT HYPERVELOCITY PROJECTILES
NT SABOT PROJECTILES
Optical pin apparatus for measuring the arrival time and velocity of shock waves and particles
[DE84-014501] 01 p0120 N85-10624
Moment induced by liquid payload during spin-up without a critical layer
[AD-A145716] 02 p0199 N85-11327
Liquid payload moment equations
[AD-A145977] 03 p0362 N85-12319
The aerodynamics of some guided projectiles
[NASA-TM-86334] 06 p0747 N85-14788
A metallographic investigation of rotating bands for 7.5 cm artillery projectiles
[FOA-C-20551-D2] 07 p0929 N85-15888
Hypothetical zero yaw drag trajectory of spinning projectiles between M = 5 and M = 10
[AD-A148899] 10 p1421 N85-18963
Electromagnetic braking of a metallic projectile in flight
[AD-A149424] 10 p1480 N85-19345
Experimental simulation of the flow inside a gun barrel
[ISL-CO-208/83] 14 p2302 N85-24252
Experimental simulation of the flows in front of and behind a projectile with and without gas slippage
[ISL-CO-232/83] 14 p2302 N85-24258
A method of calculating the aim point for an unguided projectile fired at a moving target
[BAE-BT-12717] 15 p2489 N85-25365
Dispersion sensitivity of the eight inch advanced ramjet munitions technology projectile due to wind and minor thrust errors
[AD-A152145] 16 p2727 N85-26835
Model for computing late detonations initiated in propellants by impact (XDT reactions)
[DE85-007377] 16 p2758 N85-27019
Influence of behavior laws in the explosive deformation of metal plates
[ISL-R-122/83] 16 p2760 N85-27032
A method for the evaluation of the residual energy of a metallic fragment after perforation of a thin target
[ISL-R-113/83] 16 p2794 N85-27233
Using synchro-ballistic cameras to determine the velocity and spin rate of high-velocity projectiles
[DE85-010829] 19 p3367 N85-30884
Design and fabrication of projectiles for round bore railguns
[DE85-011871] 20 p3398 N85-31078
Preliminary considerations for the gasdynamic precompression of solid molecular hydrogen
[DE85-013256] 22 p3784 N85-33445
A 1984 environmental summary: Sandia National Laboratories Tonopah Test Range, Tonopah, Nevada
[DE85-011145] 22 p3812 N85-33612
OMEGA: Optoelectronic measurement of the incidence angle of a projectile
[ISL-CO-223/84] 23 p3974 N85-34634

PROJECTIVE GEOMETRY
NT MERCATOR PROJECTION
Choice of cartographic projection for space system data bank used in studying natural resources
02 p0165 N85-11119
The Gauss-Krueger projection of the Earth ellipsoid with direct calculation of elliptic integrals through Landen transformations
[SER-C-296] 11 p1666 N85-20495
Surfaces with canonical hyperplane sections
[CWI-TRACT-1] 14 p2410 N85-24858
Analysis of spectral operators in one-dimensional domains
[NASA-CR-172573] 15 p2633 N85-26228

PROJECTORS
Air combat visual simulation using a head slaved projector
[AD-P004327] 09 p1270 N85-17981

PROJECTS
NT AGRISTARS PROJECT
NT APOLLO PROJECT
NT GALILEO PROJECT
NT HELIOS PROJECT
NT PROJECT SETI
NT SCOUT PROJECT
NT TIROS PROJECT
NT VOYAGER PROJECT
Project manager's handbook for special projects
[AD-A147913] 07 p1053 N85-16683

PROMINENCES
NT SOLAR PROMINENCES

PROMOTION
NASA photography index
[NASA-TM-87457] 15 p2665 N85-26445

PRONE POSITION
Effect of body position and immobilization on intensity of spatial illusions in weightlessness
22 p3821 N85-33672

PROOFS
U PROVING

PROP-FAN TECHNOLOGY
Large-scale Advanced Propfan (LAP) performance, acoustic and weight estimation, January, 1984
[NASA-CR-174782] 13 p1969 N85-22366
Large-scale Advanced Propfan (LAP) program
[NASA-TM-87067] 19 p3220 N85-29964

PROPAGATION
Study of delamination cracking under static and cyclic loads of carbon-epoxy composite materials
[REPT-42-727/F] 03 p0327 N85-12102
Cosmic ray propagation in the local superbubble
[NASA-TM-85030] 03 p0449 N85-12855
ATA gas propagation: 1 foot tank experiment
[DE84-016395] 04 p0561 N85-13575
Experiments on ETA comparing wire-conditioned and non-wire-conditioned beam propagation
[DE85-004451] 11 p1725 N85-20648
Exponential anisotropy of solar cosmic rays
[SH-3.2-1] 23 p4002 N85-34817
Energetic solar particle events
[SH-3.2-2] 23 p4003 N85-34818
Channeled propagation of solar particles
[SH-3.2-3] 23 p4003 N85-34819
The local characteristic function of interplanetary particle propagation
[SH-3.2-8] 23 p4003 N85-34823

PROPAGATION (EXTENSION)
NT CRACK PROPAGATION
NT FLAME PROPAGATION

PROPAGATION MODES
Turbofan noise generation. Volume 2: Computer programs
[NASA-CR-167952] 02 p0275 N85-11791
Love and Rayleigh waves in irregular ground
04 p0523 N85-13348
Experimental determination of propagation rate of ELF signals employed by Omega radio navigation system for phase measurements 06 p0793 N85-15066
Transformation of mode composition of circular optical waveguide 07 p0950 N85-16023
Basic experiments in plasma physics (TPL)
15 p2655 N85-26379
Optical multiplexing on monomode fibers
[ENST-83E016] 20 p3533 N85-31982
Adjustment of radiation wavelength of multimode InP-GaInAsP injection heterolasers
21 p3688 N85-32913
The use of optical fibers in pulsed laser holography
[ISL-CO-226/84] 23 p3936 N85-34395
Advanced detectors and signal processing
[NASA-CR-176193] 24 p4088 N85-35343

PROPAGATION VELOCITY
Nondestructive evaluation of residual stress in low-carbon steel, introduction 04 p0512 N85-13265
Experimental determination of propagation rate of ELF signals employed by Omega radio navigation system for phase measurements 06 p0793 N85-15066
Velocity stack and slant stack inversion methods
09 p1351 N85-18497
Double reference pulsed phase locked loop (DRP-2L-2)
[NASA-CASE-LAR-13310-1] 12 p1824 N85-21441
Possibility of retrieving dynamics of reflected wave method records beneath low-velocity zone
14 p2346 N85-24503
Angular dependence of the Rayleigh-surface wave velocity in polycrystalline metals with small anisotropy
[AERE-R-11595] 15 p2509 N85-25476
Polynomial approaches for the characteristic velocity and flame temperature as a function of mixing compounding and pressure for the systems PMMA/O2, PMMA/air, PE/O2, PE/air, PS/O2 and PS/air
[VTH-LR-421] 17 p2924 N85-28024
Proceedings of the 1980 Workshop of the International Association of Seismology and Physics of the Earth's Interior on the Seismic Modeling of Laterally Varying Structures: Contributions based on data from the 1978 Saudi Arabian refraction profile
[GS-CIRC-937] 17 p2989 N85-28476
Preliminary interpretation of Saudi Arabian seismic refraction data 17 p2989 N85-28477
A preliminary examination of the 1978 refraction profiles in Saudi Arabia 17 p2990 N85-28482
The rifted margin of Saudi Arabia
17 p2990 N85-28483
On the propagation speed in relativistic quantum mechanics
[CWI-AM-R8410] 17 p3046 N85-28848
Lower bounds of propagation velocity of steady ionizing waves in field of strong electromagnetic wave
21 p3692 N85-32940
Amplification of electromagnetic wave by electron stream with negative velocity differences
21 p3692 N85-32941
The recovery of the cosmic ray flux from maximum solar modulation at IMP-8 (1 AU) and at Pioneer (R 30 AU
[SH-4.7-7] 23 p4041 N85-35052

PROPAGATORS
U PROPAGATION

PROPANE
Catalytic conversion of C3-C4 paraffins to gasoline
[DE85-004181] 10 p1458 N85-19187

Laser schlieren, shock tube studies of high temperature hydrocarbon pyrolysis rates
[DE85-003314] 11 p1636 N85-20303
Optical waveguide sensor for methane gas
[AD-D011691] 19 p3273 N85-30294
Investigation of the flame speeds of propane/methanol gas mixtures
[DE85-012817] 23 p3912 N85-34239

PROPARGYL GROUPS
Thermoset-thermoplastic aromatic polyamide containing N-propargyl groups
[NASA-CASE-LAR-12723-1] 11 p1610 N85-20123

PROPELLANT ADDITIVES
NT PROPELLANT BINDERS
NT SOLID ROCKET BINDERS
Transition to detonation from rapid-compression (ramp-waves) generated in a burning porous bed
[AD-P004345] 10 p1455 N85-19169
Workshop report: Catalysis of Burn Rate of Energetic Binder propellants 13 p2001 N85-22545
Mechanism of burning rate enhancement by ferric oxide 13 p2002 N85-22546
Propellant plasticizer
[AD-D011501] 20 p3434 N85-31306

PROPELLANT BINDERS
NT SOLID ROCKET BINDERS
Measurement of shock and induced reaction in rocket propellants by nanosecond infrared radiometry and photography
[DE84-013209] 04 p0482 N85-13070
Combustion properties of fuel-rich magnesium propellants with HTPB as binder
[FOA-C-20555-D1] 07 p0935 N85-15924
Workshop report: Catalysis of Burn Rate of Energetic Binder propellants 13 p2001 N85-22545
Effects of HMX addition on the combustion of energetic binders 13 p2004 N85-22560

PROPELLANT CHEMISTRY
The crystal and molecular structure of a new propellant compound: Triaminoguanidium Azide Nitrate (TAZN)
13 p2002 N85-22551

PROPELLANT COMBUSTION
NT SOLID PROPELLANT COMBUSTION
NT SOLID PROPELLANT IGNITION
HMX combustion modification
[AD-A145071] 01 p0024 N85-10149
Combustion properties of fuel-rich magnesium propellants with HTPB as binder
[FOA-C-20555-D1] 07 p0935 N85-15924
Transient combustion: An important consideration in deflagration-to-detonation transition
08 p1116 N85-17037
Twenty-first JANNAF Combustion Meeting, volume 1
[AD-A150981] 13 p1996 N85-22526
Status of boron combustion research
13 p1998 N85-22528
Development of a three-phrase combustion code for modeling liquid rocket engines 13 p2003 N85-22554
Atomization data requirements for rocket combustor modeling 13 p2003 N85-22555
Effects of HMX addition on the combustion of energetic binders 13 p2004 N85-22560
Study on the combustion of nitramine propulsion powder up to 1500 MPa and comparison of the performance with that of classical propulsion powders
[ISL-CO-203/83] 14 p2264 N85-24025

PROPELLANT EVAPORATION
An experimental study of spray thruster
[REPT-613] 12 p1845 N85-21578

PROPELLANT EXPLOSIONS
Hazard Studies for Solid Propellant Rocket Motors
[AGARD-CP-367] 08 p1114 N85-17025
Response of propellants to high dynamic stresses: The uses of gun launch techniques
08 p1116 N85-17035
Modelling the thermal explosion phenomenon in solid propellants: The case of fixed and variable temperatures 08 p1117 N85-17044

PROPELLANT GRAINS
Portable slotting device
[AD-D011213] 01 p0033 N85-10206
A model for grain misalignment in cylindrical port motors
[AD-A144856] 01 p0034 N85-10210
Closed vessel combustion of stick propellant
[AD-A147802] 08 p1135 N85-17154
A thermal-mechanical model of deflagration-to-detonation in granular energetic materials
[AD-P004346] 10 p1455 N85-19170
Curvilinear solid propellant grain
[AD-D011457] 10 p1458 N85-19183
Experimental high pressure equation of state of a very fast burning gun propellant
[DE85-001749] 10 p1458 N85-19184
Status of boron combustion research
13 p1998 N85-22528
Analysis of combustion oscillations in heterogeneous systems
[AD-A151999] 16 p2745 N85-26942
Fiber reinforcement of gun propellant
[AD-A152296] 16 p2757 N85-27014

PROPELLANT PROPERTIES
NT PROPELLANT SENSITIVITY
NT PROPELLANT STORABILITY

PROPELLANT SENSITIVITY
Sensitivity tests for solid propellants in Germany
08 p1115 N85-17028
Sensitiveness and explosiveness assessment at Perme Waltham Abbey 08 p1115 N85-17029
Study of the transition from deflagration to detonation of previously fragmented propellants
08 p1115 N85-17032
Effect of variable solid phase thermal properties on propellant combustion 13 p2002 N85-22547

PROPELLANT SPRAYS
An experimental study of spray thruster
[REPT-613] 12 p1845 N85-21578

PROPELLANT STORABILITY
Propellant plasticizer
[AD-D011501] 20 p3434 N85-31306

PROPELLANT STORAGE
Space station task force perspective
08 p1106 N85-16992
Earth-to-orbit propellant transportation overview
08 p1108 N85-17002
Active cooling requirements for propellant storage
08 p1108 N85-17004

PROPELLANT TANKS
An experimental study of jet impingement on a circular cylinder
[AD-A145583] 02 p0198 N85-11326
Ion thruster system (8-cm) cyclic endurance test
[NASA-CR-174745] 04 p0463 N85-12937
Propellant tank resupply system
[AD-D011288] 05 p0603 N85-13848
Fluid slosh dynamics of surface tension tanks in three axis stabilized spacecraft
[MBB-UR-E-739-84-O] 11 p1634 N85-20291
Dynamic investigations of a spherical tank structure filled with liquid using ANSYS three-dimensional fluid elements
[MBB-UR-E-737-83-O] 11 p1654 N85-20418

PROPELLANT TESTS
Review of USAF treatment of solid propellant rocket motor hazards 08 p1114 N85-17027
NATO AC/310 activities report on NATO STANAG 4170 and Allied Ordnance Publication 7 (Manual of Tests for Qualification of Explosive Materials for Military Use)
[AD-P004341] 10 p1454 N85-19165
Compatibility experiments of facilities, materials, and propellants for electrothermal thrusters
[NASA-TM-86956] 12 p1795 N85-21260
Characterization standards for solid propellant rocket motors
[AD-A150250] 13 p2013 N85-22627
Dissected motors-propellants motor number STM-012. Phase 15: Surveillance report, stage 1
[AD-A156068] 24 p4071 N85-35226

PROPELLANT TRANSFER
External tank GH2 vent arm 08 p1102 N85-16969
Propellant transfer: Attached depot
08 p1108 N85-17005
Propellant transfer: Tethered depot
08 p1108 N85-17006
OTV fluid mangement systems
08 p1108 N85-17007
Space Transportation System (STS) propellant scavenging system study. Volume 1: Technical report
[NASA-CR-171848-VOL-1] 11 p1589 N85-20000
Space Transportation System (STS) propellant scavenging system study. Volume 2: Supporting research and technology report
[NASA-CR-171849-VOL-2] 11 p1589 N85-20001
Space Transportatioin System (STS) propellant scavenging system study. Volume 3: Cost and work breakdown structure-dictionary
[NASA-CR-171850-VOL-3] 11 p1590 N85-20002
An investigation of space shuttle main engine shutdown chugging instability 12 p1946 N85-22221

PROPELLANTS
NT CASE BONDED PROPELLANTS
NT COMPOSITE PROPELLANTS
NT CRYOGENIC ROCKET PROPELLANTS
NT DOUBLE BASE PROPELLANTS
NT DOUBLE BASE ROCKET PROPELLANTS
NT GASEOUS ROCKET PROPELLANTS
NT GUN PROPELLANTS
NT HIGH ENERGY PROPELLANTS
NT HTPB PROPELLANTS
NT HYPERGOLIC ROCKET PROPELLANTS
NT LIQUID ROCKET PROPELLANTS
NT MONOPROPELLANTS
NT NITRAMINE PROPELLANTS
NT PLASTIC PROPELLANTS
NT RDX
NT ROCKET PROPELLANTS
NT SLURRY PROPELLANTS
NT SOLID PROPELLANTS
NT SOLID ROCKET PROPELLANTS
NT STORABLE PROPELLANTS
NT TATB
An optical and mass spectrometric study of the aluminum-oxygen flame
[AD-A147434] 07 p0923 N85-15849
Closed vessel combustion of stick propellant
[AD-A147802] 08 p1135 N85-17154
A thermal-mechanical model of deflagration-to-detonation in granular energetic materials
[AD-P004346] 10 p1455 N85-19170
Measurements of distributed combustion
13 p2001 N85-22542
Design of a Mobile Combustion Diagnostic Fixture (MCDF)
[AD-A151814] 16 p2746 N85-26941
Closed-bomb combustion of Hivelite-based, Very High Burn Rate (VHBR) propellant
[AD-A155740] 21 p3571 N85-32212

PROPELLER BLADES
Profile design for wings and propellers
[NASA-TM-77785] 10 p1419 N85-18953
Noise constraints effecting optimal propeller designs
[NASA-TM-86967] 11 p1575 N85-19923
Determination of aerodynamic and propulsion parameters of general aviation aircraft using steady state flight test data 13 p1971 N85-22377
Interaction of a turbulent vortex with a lifting surface
15 p2464 N85-25214
Low-speed wind-tunnel tests of an advanced eight-bladed propeller
[NASA-TM-86364] 19 p3214 N85-29928
Large-scale Advanced Propfan (LAP) program
[NASA-TM-87067] 19 p3220 N85-29984
Effects of propeller rotation direction on airplane interior noise levels
[NASA-TP-2444] 19 p3350 N85-30767
Impulsive noise due to transonic blade-vortex interactions 20 p3523 N85-31913
Two-plane balance and slip-ring design
22 p3799 N85-33536
Optimally designed propellers constrained by noise
24 p4065 N85-35196

PROPELLER DRIVE
NT HELICOPTER PROPELLER DRIVE

PROPELLER EFFICIENCY
Welcome to the Saclay Propeller Testing Center
[NASA-TM-77648] 14 p2225 N85-2379
Large-scale Advanced Propfan (LAP) program
[NASA-TM-87067] 19 p3220 N85-2998
Optimally designed propellers constrained by noise
24 p4065 N85-3519

PROPELLER FANS
Large-scale Advanced Propfan (LAP) performanc acoustic and weight estimation, January, 1984
[NASA-CR-174782] 13 p1969 N85-223
Wind tunnel results of advanced high speed propell in the takeoff, climb and landing operating regimes
[NASA-TM-87054] 19 p3213 N85-299

PROPELLER SLIPSTREAMS
Studies on the interference of wings and propel slipstreams
[NASA-CR-175753] 15 p2463 N85-252

PROPELLERS
NT PROPELLER FANS
NT VARIABLE PITCH PROPELLERS
Analysis of noise measured from a propeller in a w
[NASA-TP-2358] 02 p0274 N85-117
Screw expander for light duty diesel engines
04 p0508 N85-13
Evaluation of the Langley 4- by 7-meter tunnel propeller noise measurements
[NASA-TM-85721] 04 p0556 N85-13
Contribution of the study of light aircraft prope noise
[ESA-TT-865] 09 p1376 N85-18
Propeller propulsion system integration: Stat technology survey
[NASA-CR-3882] 12 p1771 N85-21
Towards a renewal of the propeller in aeronautics
[NASA-TM-77803] 12 p1779 N85-21
Further comparison of wind tunnel and airplane aco data for advanced design high speed propeller mo
[NASA-TM-86935] 12 p1927 N85-2
Method for the prediction of the install aerodynamics of a propfan at subsonic speeds
[NASA-CR-3887] 13 p1969 N85-2
Wind tunnel acoustic study of a propeller installed b an airplane empennage: Data report
[NASA-CR-177335] 13 p2154 N85-2

Wind tunnel results of advanced high speed propellers in the takeoff, climb and landing operating regimes
[NASA-TM-87054] 19 p3213 N85-29925
An experimental investigation of propfan installations on an upswept supercritical wing at transonic Mach numbers
[NASA-CR-172605] 20 p3388 N85-31013
Wingtip vortex propeller
[NASA-CASE-LAR-13019-1] 24 p4065 N85-35194

PROPHYLAXIS
A double blind comparative trial of powdered ginger root, hyoscine hydrobromide, and cinnarizine in the prophylaxis of motion sickness induced by cross coupled stimulation
11 p1695 N85-20657

PROPORTIONAL COUNTERS
In-beam tests of an air-core superconducting-solenoid particle spectrometer
[DE85-004029] 12 p1653 N85-21625
Wide-ranging radiation dose monitor
[DE85-011596] 22 p3787 N85-33463
Search for magnetic monopoles using proportional counters filled with helium gas
[HE-6.1-1] 24 p4209 N85-36127
Magnetic monopole search by 130 m(2)sr He gas proportional counter
[HE-6.1-2] 24 p4209 N85-36128
Limits on monopole fluxes from KFG experiment
[HE-6.1-6] 24 p4209 N85-36132
Results from the UCSD magnetic monopole search
[HE-6.1-12] 24 p4210 N85-36137
Results on nucleon life-time from the Kolar gold field experiment
[HE-6.2-3] 24 p4211 N85-36139
Data acquisition system for phase-2 KGF proton decay experiment
[HE-6.2-4] 24 p4211 N85-36140

PROPORTIONAL LIMIT
The effects of pin elasticity, clearance, and friction on the stresses in a pin-loaded orthotropic plate
[NASA-CR-175816] 16 p2743 N85-26927
Prediction of lifetime for ceramic materials in the elastic and viscoelastic region by fracture mechanical methods
[ESA-TT-825] 20 p3434 N85-31305

PROPRIOCEPTION
Estimating number, time and length; a baseline study
05 p0695 N85-14473

PROPRIOCEPTORS
Gravity perception and cardiac function in the spider
15 p2606 N85-26058

PROPULSION
NT ASCENT PROPULSION SYSTEMS
NT AUXILIARY PROPULSION
NT CHEMICAL PROPULSION
NT DESCENT PROPULSION SYSTEMS
NT ELECTRIC PROPULSION
NT ELECTROMAGNETIC PROPULSION
NT ELECTROSTATIC PROPULSION
NT HYBRID PROPULSION
NT ION PROPULSION
NT JET PROPULSION
NT LOW THRUST PROPULSION
NT MARINE PROPULSION
NT MASS DRIVERS (PAYLOAD DELIVERY)
NT NUCLEAR ELECTRIC PROPULSION
NT PLASMA PROPULSION
NT SOLAR PROPULSION
NT SPACECRAFT PROPULSION
Energy efficient engine. Volume 1: Component development and integration program
[NASA-CR-173084] 02 p0146 N85-10992
Report of the Department of Aerospace Engineering
03 p0307 N85-11977
Thrust characterization of very high burning rate propellants
[AD-A145891] 03 p0340 N85-12186
Research and technology, 1984: Marshall Space Flight Center
[NASA-TM-86476] 04 p0590 N85-13765
Embedment system for ultrahigh-burning rate propellants of solid propulsion subsystems
[AD-D011257] 06 p0773 N85-14942
Air Force space technology center space technology: Emphasis 84 09 p1333 N85-18381
Characterization standards for solid propellant rocket motors
[AD-A150250] 13 p2013 N85-22627
Future directions in aeropropulsion technology
[NASA-TM-87010] 14 p2207 N85-23665
AFRPL (Air Force Rocket Propulsion Laboratory) technical objective document FY 85
[AD-A151368] 15 p2495 N85-25389
Heat transfer in aeropropulsion systems
[NASA-TM-87066] 20 p3453 N85-31444
R and D programmes at the National Aeronautical Laboratory
[AR-22] 20 p3539 N85-32022
Clarke Stations and mercurian mass-drivers: Energy for large-scale transportation systems
[DE85-009607] 21 p3560 N85-32145
Three-Dimensional Techniques Applied to Internal Flows in Propulsion Systems
[AGARD-LS-140] 21 p3586 N85-32293
Status of advanced orbital transfer propulsion
[NASA-TM-87069] 24 p4071 N85-35225

PROPULSION SYSTEM CONFIGURATIONS
NT ASCENT PROPULSION SYSTEMS
NT DESCENT PROPULSION SYSTEMS
Investigation of a pulsed electrothermal thruster system
[NASA-CR-174768] 02 p0169 N85-11132
Continuing issues (FY 1983) concerning military use of the space transportation system
[AD-A146091] 03 p0323 N85-12080
The preliminary checkout, evaluation and calibration of a 3-component force measurement system for calibrating propulsion simulators for wind tunnel models
[NASA-CR-174113] 04 p0458 N85-12903
STOL simulation requirements for development of integrated flight/propulsion control systems
05 p0701 N85-14499
Parametric estimates of propulsion system maintenance manhours
[AD-A147120] 07 p0894 N85-15662
Installed nacelle drag-improvement tests of an M = 0.8 turboprop transport configuration
[NASA-TM-84302] 07 p0902 N85-15716
Ramjets with supersonic combustion
07 p0918 N85-15817
Propulsion and power systems perspective
08 p1098 N85-16938
Orbital Maneuvering system design evolution
08 p1098 N85-16943
OTV Propulsion Issues
[NASA-CP-2347] 08 p1106 N85-16989
Analysis and optimization of small Space Shuttle propulsion platforms
[DFVLR-FB-84-28] 10 p1431 N85-19023
The 1984 JANNAF Propulsion Systems Hazards Subcommittee Meeting, volume 1
[AD-A148665] 10 p1454 N85-19162
Propeller propulsion system integration: State of technology survey
[NASA-CR-3882] 12 p1771 N85-21119
Towards a renewal of the propeller in aeronautics
[NASA-TM-77803] 12 p1779 N85-21169
Fiscal year 1986 technical objective document
[AD-A151039] 14 p2432 N85-25000
Mathematical modeling of the AEDC (Arnold Engineering Development Center) propulsion wind tunnel (16T)
[AD-A151293] 15 p2475 N85-25275
Manrating orbital transfer vehicle propulsion
[NASA-TM-87019] 15 p2494 N85-25385
Future fundamental combustion research for aeropropulsion systems
[NASA-TM-87049] 17 p2898 N85-27870
The STOL and maneuver technology program integrated control system development 17 p2905 N85-27910
The Department of Defense statement on the Science and Technology Program by Colonel Donald I. Carter, USAF Acting Deputy Under Secretary of Defense for Research and Advanced Technology before the Subcommittee on Research and Development of the Committee on Armed Services of the United States House of Representatives, 99th Congress, first session
[AD-A152467] 17 p3046 N85-28850
Advanced beamed-energy and field propulsion concepts
[NASA-CR-176108] 22 p3741 N85-33186
Presentation of the acoustic and aerodynamic results of the Aladin 2 concept qualification testing
[NASA-TM-77883] 24 p4060 N85-35161

PROPULSION SYSTEM PERFORMANCE
Energy efficient engine component development and integration program
[NASA-CR-169496] 02 p0146 N85-10989
Investigation of a pulsed electrothermal thruster system
[NASA-CR-174768] 02 p0169 N85-11132
Nonlinear system identification methodology development based on F-4S flight test data analysis
[AD-A146289] 03 p0318 N85-12053
Continuing issues (FY 1983) concerning military use of the space transportation system
[AD-A146091] 03 p0323 N85-12080
LOX/LH2 propulsion system for launch vehicle upper stage, test results
[NASA-TM-77727] 03 p0324 N85-12089
Study on control of ion engine system
[EL-847] 07 p0916 N85-15800
An update of the Canada/USA augmentor-wing project 08 p1070 N85-16781
Space Shuttle Technical Conference, part 2
[NASA-CP-2342-PT-2] 08 p1098 N85-16937
NASA OAST perspective 08 p1106 N85-16990
Aerojet advanced engine concept
08 p1107 N85-16999
Advanced OTV engines and issues
08 p1108 N85-17000
The Altitude Wind Tunnel (AWT): A unique facility for propulsion system and adverse weather testing
[NASA-TM-86921] 09 p1283 N85-18067
Analysis and optimization of small Space Shuttle propulsion platforms
[DFVLR-FB-84-28] 10 p1431 N85-19023
Propeller propulsion system integration: State of technology survey
[NASA-CR-3882] 12 p1771 N85-21119
Optimization of guidance and control using function minimization and NAVSTAR/GPS
[AD-A149956] 12 p1775 N85-21141
Determination of aerodynamic and propulsion parameters of general aviation aircraft using steady state flight test data 13 p1971 N85-22377
Missions and vehicle concepts for modern, propelled, lighter-than-air vehicles
[NASA-TM-87461] 15 p2457 N85-25170
Performance and surge limits of a TF30-P-3 turbofan engine/axisymmetric mixed-compression inlet propulsion system at Mach 2.5
[NASA-TP-2461] 15 p2472 N85-25261
Mathematical modeling of the AEDC (Arnold Engineering Development Center) propulsion wind tunnel (16T)
[AD-A151293] 15 p2475 N85-25275
Error reduction program — combustor performance evaluation codes
[NASA-CR-174776] 16 p2852 N85-27584
Test devices for aeronautical research and technology
[NASA-TM-77651] 17 p2905 N85-27914
An evaluation of oxygen-hydrogen propulsion systems for the Space Station
[NASA-TM-87059] 18 p3067 N85-28971
Energy efficient engine integrated core/low spool test hardware design report
[NASA-CR-168137] 19 p3218 N85-29956
Performance improvements of a highly integrated digital electronic control system for an F-15 airplane
[NASA-TM-86748] 21 p3556 N85-32120

PROPULSIVE EFFICIENCY
NT PROPELLER EFFICIENCY
The preliminary checkout, evaluation and calibration of a 3-component force measurement system for calibrating propulsion simulators for wind tunnel models
[NASA-CR-174113] 04 p0458 N85-12903
Propulsive efficiency of vibrating wing in supersonic flow 05 p0724 N85-14656
Design study of technology requirements for high performance single-propeller-driven business airplanes
[NASA-CR-3863] 07 p0898 N85-15692
Missions and vehicle concepts for modern, propelled, lighter-than-air vehicles
[NASA-TM-87461] 15 p2457 N85-25170
Manrating orbital transfer vehicle propulsion
[NASA-TM-87019] 15 p2494 N85-25385
Propulsion efficiency of vibrating bodies in subsonic gas stream 17 p2942 N85-28159

PROPYL COMPOUNDS
Thermolysis of 4-methyl-4-(1-propenyl)malonyl peroxide: Mechanistic limits to chemiluminescence efficiency
[AD-A151567] 15 p2505 N85-25452

PROPYLENE
Field test results of experimental EPDM (Ethylene Propylene Diene Monomer) and PUF (Polyurethane Foam) roofing
[AD-A147697] 08 p1132 N85-17133
Stabilized unsaturated polyesters
[NASA-CASE-NPO-16103-1] 18 p3078 N85-29043

PROSPECTING
U EXPLORATION

PROSTAGLANDINS
The effect of naproxen on acute mountain sickness and vascular responses to hypoxia
[AD-A145144] 01 p0095 N85-10636

PROSTHETIC DEVICES
A comparative study of alternative controls and displays for by the severely physically handicapped
05 p0709 N85-14549
Metallic aid and technique in fitting voice prosthesis
[AD-D011356] 07 p1014 N85-16442

PROTEASE
Acid phosphatase and protease activities in immobilized rat skeletal muscles
[NASA-CR-174340] 08 p1192 N85-17509

PROTECTION
NT ACCELERATION PROTECTION
NT CIRCUIT PROTECTION
NT CORROSION PREVENTION

NT ENVIRONMENT PROTECTION
NT METEOROID PROTECTION
NT RADIATION PROTECTION
NT RADIATION SHIELDING
NT THERMAL PROTECTION

Impact tests of adjusters for the HBU-12 lap belt
[AD-A146021] 08 p1080 N85-16843

Power quality and protection of electric distribution systems with small, dispersed generation devices
[DE85-000990] 09 p1344 N85-18453

Improved ceramic anodes for corrosion protection
[AD-A149492] 10 p1452 N85-19149

Hurricane storm surge research
[GPO-40-048] 12 p1893 N85-21880

EOS (electrical overstress) protection for VLSI (Very Large Scale Integration) devices
[AD-A150333] 13 p2064 N85-22801

Fire pit tests of blue flight coverall program
[AD-A151884] 15 p2620 N85-26149

Fast shutter apparatus
[DE85-008501] 23 p3926 N85-34343

PROTECTIVE CLOTHING
NT HELMETS
NT PRESSURE SUITS
NT SPACE SUITS

The experimental mod 3 firefighters' aluminized crash-rescue, fire-proximity hood
[AD-A144993] 01 p0098 N85-10655

Resistance of Navy shipboard outerwear garments and fire-resistant fabrics to extreme heat
[AD-A145414] 02 p0238 N85-11546

Anthropometric cockpit compatibility assessment of US Army aircraft for large and small personnel wearing A cold weather, armored vest, chemical defense protective clothing configuration
[AD-A145472] 02 p0238 N85-11547

Acceptance-testing procedures for air-line supplied-air suits
[DE84-016960] 05 p0712 N85-14569

Windblast leg protector assembly
[AD-D011376] 07 p0899 N85-15700

Flame-resistant materials for use in pyrotechnic safety clothing
[AD-A146857] 07 p0931 N85-15901

The effect of modified spectacles on the field of view of the helmet display unit of the integrated helmet and display sighting system
[AD-A148693] 09 p1281 N85-18055

A systems analysis of alternative concepts for aircrew cold weather clothing
[AD-A148805] 09 p1365 N85-18580

Heat stress and personal protective equipment
[DE85-003552] 10 p1532 N85-19652

The application of anthropometric survey data to aircrew clothing sizing
[AD-A150545] 13 p2143 N85-23304

Fire pit tests of blue flight coverall program
[AD-A151884] 15 p2620 N85-26149

Investigation of the requirement for auxiliary heating of Canadian forces personnel
[AD-A151950] 16 p2841 N85-27522

The design of working systems on ergonomic principles. The importance of clothes and protective equipment in the design of the workplace
[HSE-TRANS-10865] 19 p3332 N85-30639

PROTECTIVE COATINGS
NT ANODIC COATINGS
NT CERAMIC COATINGS
NT PRIMERS (COATINGS)
NT REFRACTORY COATINGS

Single-drop impact damage prediction for low density, coated ceramic materials — rain erosion
01 p0061 N85-10402

Surface protection overview 02 p0144 N85-10978

Energy efficient engine high pressure turbine ceramic shroud support technology report
[NASA-CR-168036] 02 p0147 N85-10996

Development and performance of CVD-coatings on cutting tools 02 p0178 N85-11193

The development of CVD oxide coatings for the protection of metal surfaces — chemical vapor deposition (CVD) 03 p0332 N85-12142

New coatings for high temperature materials protection
[AERE-R-11367] 03 p0339 N85-12180

Protective coverings for fiber reinforced epoxy composites
[PB84-231059] 04 p0480 N85-13063

A review of metallic surface treatments for corrosion mitigation
[AD-A146701] 06 p0769 N85-14918

Arc-evaporated carbon films: Optical properties and electron mean free paths
[DE85-001246] 06 p0867 N85-15510

Mechanical aspects of high temperature coatings
07 p0906 N85-15749

Qualitative and quantitative compositional analysis of shale derived by gas chromatography and combined gas Chromatography/Mass spectrometry. Executive summary
[AD-A148369] 07 p0924 N85-15851

Process for preparation of crosslinked poly(tri-n-butyltin) methacrylate with simultaneous particle size reduction
[AD-D011313] 07 p0932 N85-15905

Effect of iron on the performance of IN 625 weld deposits
[BR91456] 08 p1169 N85-17376

Experimental and analytical study of ceramic-coated turbine-tip shroud seals for small turbine engines
[NASA-TM-86881] 09 p1281 N85-18057

Cavitation erosion resistant coatings for pumps
[PB85-120210/GAR] 09 p1300 N85-18167

Antifriction nickel-phosphorous coatings on aluminum alloy products 09 p1309 N85-18221

Low power microprocessor based measurements system for determining the integrity of coatings on buried pipelines
[ERS-E.380] 09 p1324 N85-18323

Effects of MAR-M247 substrate (modified) composition on coating oxidation coating/substrate interdiffusion — protective coatings for hot section components of gas turbine engines
[NASA-CR-174851] 10 p1440 N85-19073

Process for preparing essentially colorless polyimide film containing phenoxy-linked diamines
[NASA-CASE-LAR-13353-1] 11 p1611 N85-20128

Oxidation protection coatings for polymers
[NASA-CASE-LEW-14072-1] 11 p1611 N85-20129

A study of intumescent reaction mechanisms
[AD-A149605] 12 p1812 N85-21365

Formation of alumina layers on iron-base alloys
[BLL-T6418/BG/LRS/LRST737/84]
13 p2020 N85-22657

Properties of welded joints in argon arc welding of titanium alloy using a protective coating
13 p2032 N85-22733

Use of optical techniques in studies of wear rates of anodized aluminum and polymer coatings on aluminum
14 p2259 N85-23997

Development of acceptance criteria for batches of silane primer for external tank thermal protection system bonding applications
[NASA-CR-171428] 14 p2259 N85-23998

Dimensions of smooth mating parts with protective coatings 14 p2280 N85-24124

Self-substaining low-Z coatings for impurity control. Part 1: General considerations
[DE85-000427] 14 p2425 N85-24956

Development of coating for protection of backside of seam in welding of titanium alloys
15 p2500 N85-25421

Mechanical properties of TiN deposits obtained by PVD and TiN, TiC, TiC + TiN obtained by CVD
[BLL-RISLEY-TR-5097-(9091.9F)]
15 p2506 N85-25471

Detonation flame spraying extends life of automotive parts 15 p2513 N85-25507

Modified aluminosilicide coating for heat-resistant nickel alloys 15 p2514 N85-25509

Titanium diffusion method prevents metal corrosion
15 p2514 N85-25510

Inhibiting titanium corrosion in hot nitrogen nitrate solutions using sulfate ions 15 p2514 N85-25511

Protective coatings for aircraft structures: A review
[VTH-LR-413] 16 p2706 N85-26704

Effects of surface chemistry on hot corrosion life
[NASA-CR-174915] 16 p2706 N85-26711

Material technology 16 p2734 N85-26870

Characteristics of polyacrylic acid-complexed zinc phosphate conversion films deposited on metal surfaces
[DE85-004057] 16 p2750 N85-26974

Testing of materials and coatings for jet engine components under simulated operational conditions
[B8580073] 17 p2899 N85-27873

Properties of chromate coatings formed on electrolytic zinc substrates
[BLL-BISI-TRANS-22349-(9022.06)]
17 p2926 N85-28052

New process for production of bimetal with corrosion-resistant cladding layer
[BLL-BISI-TRANS-22371-(9022.06)]
17 p2927 N85-28056

Erosion of corrosion-resistant surface treatments on alloy steels
[DE85-008446] 17 p2932 N85-28100

New air-curing lacquer systems with high solids content
[BMFT-FB-T-85-005] 17 p2936 N85-28124

Technology development for thin-film-trace humidity sensors
[BMFT-FB-T-84-268] 17 p2969 N85-28338

Proper quality of anticorrosion work no matter how bad the atmospheric conditions
[BLL-BISI-TRANS-22080-(9022.06)]
17 p2975 N85-28380

Corrosion resistant coating
[NASA-CASE-NPO-15929-1] 18 p3073 N85-29005

Long-Term Materials Test Program
[DE85-003248] 18 p3077 N85-29034

Ceramic coatings for heat engine materials: Status and future needs
[DE85-006759] 18 p3080 N85-29033

Ceramic coatings for heat engine materials
[DE85-005236] 18 p3080 N85-29054

Spray applicator for spraying coatings and other fluids in space
[NASA-CASE-MSC-18652-1] 18 p3115 N85-29293

Physical-mechanical characteristics and wear resistance of coatings applied by microarc oxidation
19 p3242 N85-30104

Effect of prolonged high temperature on durability of coated high-temperature nickel alloys
19 p3243 N85-30105

Atomized magnetism-aluminum protective coatings
19 p3244 N85-30116

Ion beam sputter-deposited thin film coatings for protection of spacecraft polymers in low Earth orbit
[NASA-TM-87051] 19 p3248 N85-30137

Mechanical protection of DLC films on fused silica slides
[NASA-TM-87056] 19 p3248 N85-30138

Realization by vapor deposition of turbine blades covered with a silicon nitride layer
20 p3395 N85-31081

Protection products for the conductors of high voltage overhead lines
[BLL-OA-TRANS-3219-(6196.300)]
20 p3429 N85-31269

New corrosion protection concept for very high voltage line towers
[BLL-OA-TRANS-2691-(6196.300)]
20 p3429 N85-31270

Inhibited anticorrosion protection of automotive steel strip in the NLMK
[BLL-M-36250-(5828.4)] 20 p3430 N85-31274

Metallographic preparation of materials with various coatings
[BLL-DRIC-TRANS-7522-(3623.66)]
20 p3433 N85-31298

Silicon nitride protective coatings for silvered glass mirrors
[DE85-011637] 20 p3433 N85-31300

A study of adherent oxide scales
[AD-A155554] 21 p3567 N85-32186

Development of wide band recording materials
[AD-A154961] 21 p3589 N85-32309

Encapsulation materials research
21 p3606 N85-32407

Rationale in the selection of corrosion protective coating systems 22 p3750 N85-33242

Protective systems and maintenance policies for marine environments 22 p3750 N85-33245

Towards the development of technological processes for the preparation of cadmium plated steel articles
[BLL-M-36315-(5828.4)] 23 p3913 N85-34248

Diamondlike carbon protective coatings for IR materials
[NASA-TM-87083] 23 p3973 N85-34631

Wear-resistant coatings for tools intended for cold working
[BLL-RISLEY-TR-5040-(9091.9F)]
24 p4061 N85-35293

Space shuttle SRB TPS protective paint test and evaluation in NASA Hot Gas Facility and AEDC Tunnel C
[NASA-CR-170884] 24 p4061 N85-35294

PROTECTORS

Windblast leg protector assembly
[AD-D011376] 07 p0899 N85-15700

Flow through very porous screens
[NASA-TP-2436] 11 p1631 N85-20270

Windblast arm protector assembly
[AD-D011512] 12 p1909 N85-21884

Optoelectronic safety system for robotized technological complex 13 p2046 N85-22805

Results of tests of MTA-2 TPS on the SRB hold-down bolt blast container
[NASA-CR-170891] 24 p4070 N85-35224

PROTEIN METABOLISM
NT LIPID METABOLISM

Skeletal muscle metabolism in hypokinetic rats
[NASA-CR-174059] 02 p0233 N85-11520

Blood amino acids of cosmonauts before and after 211-day spaceflight 12 p1900 N85-21903

Calcium and calmodulin localization in gravitropically-responding plant organs
15 p2606 N85-26061

Role of glucocorticoids in the response to unloading of muscle protein and amino acid metabolism
15 p2609 N85-26077

PROTEIN SYNTHESIS

Skeletal muscle metabolism in hypokinetic rats
[NASA-CR-174059] 02 p0233 N85-11520

Nitrogen control of photosynthetic protein synthesis
[DE85-003513] 11 p1690 N85-20623

PROTEINS

NT ADENOSINE DIPHOSPHATE
NT ADENOSINE TRIPHOSPHATE
NT ADENOSINES
NT ASPARTATES
NT FIBRIN
NT GLOBULINS
NT GLUTATHIONE
NT LIPOPROTEINS
NT OXIDASE
NT OXYHEMOGLOBIN
NT PEPTIDES
NT POLYPEPTIDES

Nuclear Magnetic Resonance of Polymeric Materials
[AD-A145078] 01 p0032 N85-10192

NMR (Nuclear Magnetic Resonance) of solid biopolymers
[AD-P003912] 01 p0032 N85-10196

Static and quasielastic neutron scattering for the investigation of structure, dynamics and transport properties of lipid layers and lipid/protein compounds
03 p0432 N85-12753

Biochemistry and pathogenic hypotheses of organophosphorus-induced delayed neurotoxicity
[AD-P004026] 06 p0844 N85-15360

Plasmodium of myxomycete as research object in gravitational biology 15 p2483 N85-25327

Isolation of hybridomas for golgi-associated proteins and a plant calmodulin 15 p2613 N85-26103

Progress, goals in biotechnology summarized
17 p2945 N85-28192

Towards a statistical analysis of genetic sequences data with particular reference to protein sequences
[AD-A153005] 18 p3152 N85-29515

A computerized system for spot detection and analysis of two-dimensional electrophoresis images
23 p3958 N85-34531

Muscle protein and glycogen responses to recovery from hypogravity and unloading by tail-cast suspension
[NASA-CR-176181] 24 p4128 N85-35591

PROTOCOL (COMPUTERS)

Proceedings of the 5th LAN-Transport Workshop
[PB84-232867] 01 p0107 N85-10715

Specification of a transport protocol for computer communications. Volume 1: Overview and Services. Volume 2: Class 2 protocol. Volume 3: Class 4 protocol
[PB84-222850] 06 p0848 N85-15380

Specification of a transport protocol for computer communications. Volume 4: Service specifications. Volume 5: Guidance for the implementor. Volume 6: Guidance for implementation selection
[PB84-222868] 06 p0848 N85-15385

Specification of a transport protocol for computer communications. Volume 7: Testing OSL protocols, a compendium of papers. Volume 8: User's guide to the testing system for implementations of the ICST transport protocol. Volume 9: A test suite for implementations of the ICST transport protocol. Volume 10: Specification of a remote scenario interpreter for implementations of the ICST transport protocol
[PB84-222876] 06 p0848 N85-15386

Stuttgart Interconnection Network Project from PIX to NICS
[NASA-TM-77602] 06 p0870 N85-15528

Some experiences of testing protocol implementations — open systems interconnection
[NPL-DITC-46/84] 08 p1204 N85-17574

Interim protocol for the automated analysis of semivolatile organic compounds by Gas Chromatography/Fourier Transfer Infrared (GC/FT-IR) spectrometry
[PB85-115186] 11 p1595 N85-20035

Multicomputer communication system
[NASA-CASE-NPO-15433-1] 12 p1822 N85-21428

Evaluation of Ada (trademark) as a communications programming language. Volume 2: Communications protocols application
[AD-A152315] 16 p2848 N85-27560

Evaluation of Ada (trademark) as a communications programming language. Volume 3: Trusted software application
[AD-A152316] 16 p2848 N85-27561

A study of topologies and protocols for fiber optic local area network
[NASA-CR-175771] 16 p2864 N85-27669

A secure high-speed transaction protocol
[CWI-CS-R8417] 17 p3009 N85-28605

Performance measurement of OSI (Open System Interconnection) class 4 transport implementations
[PB85-177657] 18 p3161 N85-29582

Implementation assessment of the OSI network service. The test definition language
[NPL-DITC-52/84] 20 p3514 N85-31849

Satellite links in the ISO architecture: Models and performance evaluation
[ENST-84E017] 22 p3756 N85-33284

Petcom: A software instrument for the analysis of Petri networks, oriented towards communication protocols
[FUB-50-1983] 22 p3758 N85-33286

PROTON BEAMS

Accelerator technology program
[DE84-015052] 01 p0118 N85-10806

LAMPF transmition-region mechanical fabrication
[DE84-017078] 04 p0562 N85-13577

Tune shifts for coasting beams crossing at small angles
[DE84-017174] 04 p0562 N85-13579

Performing (p vector,]ic]n), (d vector, n) and (n vector, n) measurements with a rotating magnet beam swinger
[DE84-017003] 04 p0562 N85-13582

Accelerator Technology Program
[DE84-017083] 04 p0563 N85-13586

A proton laser accelerator by means of the inverse free electron laser mechanism
[DE85-000231] 06 p0813 N85-15163

Measurement of proton autoneutralization potential
[DE85-001752] 06 p0865 N85-15501

Study in spurious sensitivity of electronics in space
[AD-A148386] 08 p1158 N85-17305

Hydrodynamic response of a radiating Al plasma excited by a proton beam
[AD-A148904] 10 p1558 N85-19824

Review of polarized proton beam techniques and a report on the workshop on polarized beams
[DE85-004390] 12 p1930 N85-22127

Distortion functions
[DE85-007511] 16 p2862 N85-27655

Slow extraction of LAMPF 2
[DE85-010744] 19 p3356 N85-30805

Transverse emittance of a 2.0-MeV RFQ beam with high brightness
[DE85-012718] 22 p3837 N85-33758

Nuclear physics in the 10 to 300 MeV energy range using a pulsed white neutron source
[DE85-003713] 22 p3839 N85-33775

Acceleration of polarized H(-) in the BNL 200 MeV linac
[DE85-011836] 22 p3840 N85-33777

Commissioning the polarized beam in the AGS
[DE85-010958] 22 p3841 N85-33788

On gamma and neutrino radiation from Cyg X-3
[OG-2.1-7] 22 p3863 N85-33924

Injection of energetic particles following the gamma-ray flares on June 7, 1980, as observed on Helios 1
[SH-1.3-9] 23 p3993 N85-34756

Major facility overhauls at LAMPF
[DE85-012724] 24 p4156 N85-35765

Los Alamos high-current proton storage ring
[DE85-012664] 24 p4158 N85-35779

Hadrons registration in emulsion chamber with carbon block
[HE-3.7-3] 24 p4186 N85-35962

Intensities of high-energy cosmic rays at Mount Kanbala
[HE-3.7-5] 24 p4186 N85-35964

Muon and neutrino fluxes
[HE-6.2-18] 24 p4213 N85-36154

Acoustic detection of air shower cores
[HE-7.1-4] 24 p4213 N85-36158

PROTON BELTS

Boundary of modulation diffusion and stochastic instability of high energy protons in inner radiation belt
15 p2482 N85-25316

PROTON DENSITY (CONCENTRATION)

NT MAGNETOSPHERIC PROTON DENSITY

On the P1 data from GMS-SEM
12 p1894 N85-21890

Properties of the reflected beams from the Earth's bow shock: A simple model
[IFSI-84-14] 20 p3549 N85-32088

Fluctuations of development maximum depth and nuclear composition of primary cosmic radiation
[OG-5.1-13] 22 p3862 N85-34054

PROTON ENERGY

A compact time-of-flight energy analyzer of high resolution — for Tokamaks
[REPT-84-154] 09 p1324 N85-18318

An operational test of a time-of-flight analyzer at the ASDEX Tokamak
[REPT-84-155] 09 p1324 N85-18319

Protons with energies above 30 KeV in Earth's radiation belt at low altitudes during magnetically quiet time close to geomagnetic equator 13 p1980 N85-22423

Properties of the reflected beams from the Earth's bow shock: A simple model
[IFSI-84-14] 20 p3549 N85-32088

Solar modulation and interplanetary gradients of the galactic electron flux, 1977 - 1984
[PAPER-SH-4.7-4] 21 p3716 N85-33059

PROTON FLUX DENSITY

An atlas of polar cap energetic particle observations. Volume 2: NOAA-6, 8 July 1979 to 10 May 1983
[PB85-109072] 12 p1891 N85-21868

Boundary of modulation diffusion and stochastic instability of high energy protons in inner radiation belt
15 p2482 N85-25316

Search for proton decay
[DE85-008283] 19 p3353 N85-30786

Study of proton and neutron activation of metal samples in low Earth orbit
[NASA-CR-171596] 21 p3558 N85-32130

Latitude variation of recurrent fluxes in the outer solar system
[SH-4.1-13] 21 p3715 N85-33054

Further observations of protons resulting from the decay of neutrons ejected by solar flares
[SH-1.4-2] 23 p3994 N85-34763

Latitude variation of recurrent fluxes in the outer solar system
[SH-4.1-13] 23 p4006 N85-34836

PROTON IRRADIATION

Investigation of the degradation of GaAs photovoltaic cells by proton and electron irradiation
13 p2006 N85-22587

Isotropic proton irradiation of GaAs solar cells
13 p2012 N85-22622

NMR imaging and spectroscopy of the mammalian central nervous system after heavy ion radiation
[DE85-004509] 14 p2386 N85-24696

Study of proton and neutron activation of metal samples in low Earth orbit
[NASA-CR-171596] 21 p3558 N85-32130

PROTON PRECIPITATION

Precipitation of protons with E sub p approximately 1 MeV near plasmopause 02 p0161 N85-11093

Electron and proton precipitation in magnetic substorms — auroral substorms
14 p2360 N85-24585

PROTON RESONANCE

Slow extraction of LAMPF 2
[DE85-010744] 19 p3356 N85-30805

PROTON SCATTERING

Stochastic cell model for hadronic multiparticle distributions
[DE84-016480] 04 p0562 N85-13578

Perturbative treatment of quasi-resonant proton neutralization at alkali-halide surfaces
[AD-A154143] 19 p3356 N85-30806

The propagation of solar flare particles in a turbulent coronal loop
[SH-1.1-3] 23 p3989 N85-34730

The neutron moderated detector and groundbased cosmic ray modulation studies
[SH-9.1-13] 23 p4052 N85-35128

Observation of nuclei with energies 8-30 MeV per nucleon in the Earth's magnetosphere at the altitudes 350 KM
[SH-10.1-5] 23 p4053 N85-35136

Some nuclear data needs in astrophysics
[DE85-012916] 24 p4168 N85-35842

PROTON TELESCOPES

U PARTICLE TELESCOPES

PROTON-PROTON REACTIONS

Spin physics at BNL
[DE85-009768] 20 p3529 N85-31955

Exotic events of p bar p-collider: Excited quark or excited color boson? 21 p3691 N85-32930

Secondary antiproton production in relativistic plasmas
[OG-6.1-4] 22 p3868 N85-34095

Small air showers and collider physics
[HE-4.1-9] 24 p4187 N85-35975

A standard source for high energy neutrino astronomy
[HE-5.3-15] 24 p4206 N85-36109

Relationship of sea level muon charge ratio to primary composition including nuclear target effects
[HE-5.4-10] 24 p4208 N85-36121

PROTONS

NT SOLAR PROTONS

Study of proton and neutron activation of metal samples in low Earth orbit
[NASA-CR-171183] 01 p0026 N85-10164

NMR (Nuclear Magnetic Resonance) of solid biopolymers
[AD-P003912] 01 p0032 N85-10196

Proton pumping in purple membrane, appendix 1
[DE84-014801] 01 p0118 N85-10811

Energy deposition in microvolumes of silicon from high energy proton reactions
[AD-A144713] 01 p0123 N85-10845

The search for proton decay: Introduction
[DE84-014349] 01 p0131 N85-10904

Bremsstrahlung from nuclear scattering at low energy near a resonance
[DE84-014852] 04 p0561 N85-13572

A proton laser accelerator by means of the inverse free electron laser mechanism
[DE85-000231] 06 p0813 N85-15163

Bunch coalescing in the main ring to form intense proton and antiproton bunches without RF counterphasing
[DE85-001364] 09 p1382 N85-18692

Stopping powers of solids for low-energy protons
[DE85-001123] 09 p1382 N85-18693

Solar radio bursts, proton events and geomagnetic activity
[AD-A149016] 10 p1571 N85-19906

Proton NMR and susceptibility measurements in TiCoH/sub x
[DE85-003309] 12 p1807 N85-21336

Effects of focusing on HRS focal-plane polarimeter measurements
[DE85-004627] 13 p2160 N85-23406

The keV electrons and 80 keV protons in the vicinity of the high latitude magnetosphere and at the bow shock 14 p2355 N85-24554

NMR imaging and spectroscopy of the mammalian central nervous system after heavy ion radiation
[DE85-004509] 14 p2386 N85-24696

Radio frequency quadrupole and alternating phase focusing methods used in proton linear accelerator technology in the USSR
[AD-A150830] 14 p2418 N85-24916

Radiation effects induced in pin photodiodes by 40- and 85-MeV protons
[NASA-CR-175678] 14 p2426 N85-24960

Spectral characteristics of protons at low and high altitudes during geomagnetic storm of 29 July 1977
16 p2719 N85-26786

Measurements of fluxes of high-energy protons and electrons by 2 oppositely oriented spectrometers aboard Cosmos-368 artificial Earth satellite
16 p2722 N85-26800

East Europe report: Science and technology
[JPRS-ESA-85-017] 17 p2945 N85-28177

Proton induced X-ray emission method, its application in analytics 17 p2945 N85-28178

Experiments with light ions at CERN super proton synchrotron
[DE85-007625] 17 p3031 N85-28744

Cluster production and entropy
[DE85-007626] 17 p3032 N85-28752

One- and two-electron transfer processes in ion-surface scattering
[AD-A154206] 19 p3353 N85-30782

Search for proton decay
[DE85-008283] 19 p3353 N85-30786

Perturbative treatment of quasi-resonant proton neutralization at alkali-halide surfaces
[AD-A154143] 19 p3356 N85-30806

Proton ring trapping in a magnetic mirror
20 p3534 N85-31990

Sulfate-reducing bacteria: Microbiology and physiology 21 p3659 N85-32732

Solar modulation and interplanetary gradients of the galactic electron flux, 1977 - 1984
[PAPER-SH-4.7-4] 21 p3716 N85-33059

K(-) hydrogen bound and continuum states in momentum space
[DE85-010429] 22 p3841 N85-33789

Absolute rigidity spectrum of protons and helium nuclei above 10 GV/c
[OG-4.1-1] 22 p3875 N85-34007

Results of a search for deuterium at 25-50 GC/c using a magnetic spectrometer
[OG-4.2-4] 22 p3878 N85-34024

Parametrized energy spectrum of cosmic-ray protons with kinetic energies down to 1 GeV
[OG-4.2-11] 22 p3878 N85-34025

Primary cosmic ray spectrum in the 10 to the 12th power - 10 to the 16th power eV energy range from the NUSEX experiment
[OG-5.1-5] 22 p3881 N85-34047

Composition of primary cosmic rays at energies 10(15) to approximately 10(16) eV
[OG-5.2-4] 22 p3883 N85-34061

Electron and muon parameters of EAS and the composition of primary cosmic rays in 10(15) to approximately 10(16) eV
[OG-5.2-12] 22 p3884 N85-34066

Anisotropy of cosmic rays above 10(14) eV
[OG-5.4-11] 22 p3887 N85-34088

A model for the proton spectrum and cosmic ray anisotropy
[OG-5.4-12] 22 p3887 N85-34089

Interpretation of cosmic-ray anisotropy below 10(14) eV
[OG-5.4-13] 22 p3887 N85-34090

Two classes of solar energetic particle events associated with impulsive and long duration soft X-ray flares
[SH-1.2-12] 23 p3992 N85-34747

Solar flare gamma-ray line spectroscopy
[SH-2.1-14] 23 p3999 N85-34795

The central engine of quasars and AGNs: A relativistic proton radiative shock
[OG-8.1-7] 23 p4018 N85-34897

Pulsars as cosmic ray particle accelerators: Proton orbits
[OG-8.2-21] 23 p4021 N85-34917

Pulsars as cosmic ray accelerators: Energy development of protons
[OG-8.2-22] 23 p4021 N85-34918

Detection of 10 (1) GeV cosmic neutrinos with a space station
[OG-9.4-10] 23 p4030 N85-34977

Solar modulation and interplanetary gradients of the galactic electrons flux, 1977 - 1984
[SH-4.7-4] 23 p4040 N85-35049

Proton albedo spectrum observation in low latitude region at Hyderabad, India
[SH-6.1-8] 23 p4045 N85-35082

Calculation of heavy-ion tracks in liquid water
[DE85-012101] 24 p4149 N85-35725

Studies of relativistic heavy ion collisions
[DE85-014686] 24 p4152 N85-35745

Proton-air and proton-proton cross sections from air shower data
[HE-1.1-1] 24 p4170 N85-35849

Proton-air inelastic cross section at S(1/2) = 30 TeV
[HE-1.1-2] 24 p4170 N85-35850

Determination of the cross section of the proton, pion and neutron inelastic interaction with lead and carbon nuclei at 0.5 - 5.0 TeV energies (PION experiment)
[HE-1.1-5] 24 p4170 N85-35853

P(P bar)P elastic scattering and cosmic ray data
[HE-1.1-6] 24 p4170 N85-35854

The method for the study of the inelastic cross-section for high energy protons by means of shower arrays with the large calorimetric area
[HE-1.1-11] 24 p4171 N85-35858

A test of the Feynman scaling in the fragmentation region
[HE-1.2-9] 24 p4172 N85-35867

Nucleon-nucleus interactions from JACEE
24 p4173 N85-35869

Determination of primary energy in nucleus-nucleus collisions and the high P(sub)T tail of alpha-particles
24 p4173 N85-35875

Ringlike inelastic events in cosmic rays and accelerators 24 p4175 N85-35887

On the halo events observed by Mount Fuji and Mount Kanbala Emulsion Chamber Experiments
[HE-3.4-9] 24 p4182 N85-35937

Particle interactions at energies over 1000 TeV inferred from gamma-families observed at Mount Fuji
[HE-3.5-1] 24 p4183 N85-35940

Giant mini-clusters as possible origin of halo phenomena observed in super-families
[HE-3.5-4] 24 p4183 N85-35943

The electromagnetic component of albedo from superhigh energy cascades in dense media
[HE-3.5-11] 24 p4184 N85-35948

Peculiarities of gamma-quanta distribution at 20 TeV energy
[HE-3.7-10] 24 p4186 N85-35967

Electrons, muons and hadrons in extensive air showers and how do they depend on nuclear interaction model, part 2 24 p4187 N85-35969

Analysis of the hadron component in E.A.S.
24 p4187 N85-35971

Small air showers and collider physics
[HE-4.1-9] 24 p4187 N85-35975

Dependence of the average spatial and energy characteristics of the hadron-lepton cascade on the strong interaction parameters at superhigh energies
24 p4188 N85-35977

Preliminary results on underground muon bundles observed in the Frejus proton-decay detector
[HE-5.1-1] 24 p4200 N85-36067

Neutrino astronomy and the atmospheric background
[HE-5.3-17] 24 p4207 N85-36111

Multiple muons of conventional and exotic origin in DUMAND
[HE-5.4-4] 24 p4207 N85-36117

An experiment to detect gut monopoles
[HE-6.1-7] 24 p4210 N85-36133

Data acquisition system for phase-2 KGF proton decay experiment
[HE-6.2-4] 24 p4211 N85-36140

PROTOPLANETS

Tidal disruption and the origin of the Moon
04 p0586 N85-13739

A numerical investigation of planetesimal collision trajectories with a Moon accumulating in Earth orbit
04 p0586 N85-13740

Origin of the Moon 04 p0587 N85-13746

Geochemical evidence for the formation of the Moon by impact induced fission of the proto-Earth
04 p0587 N85-13747

Lunar origin: role of giant impacts
04 p0587 N85-13749

Models of angular momentum input to a circumterrestrial swarm from encounters with heliocentric planetesimals
04 p0587 N85-13750

Capture of planetesimals into a circumterrestrial swarm 04 p0588 N85-13751

The lunar angular momentum problem
04 p0588 N85-13752

A circumterrestrial compositional filter
04 p0588 N85-13753

Mechanical models of close approaches and collisions of large protoplanets 04 p0588 N85-13756

Lunar origin: Role of giant impacts
13 p2179 N85-23519

A circum-terrestrial compositional filter
13 p2179 N85-23520

Models of angular momentum input to a circum-terrestrial swarm from encounters with heliocentric planetesimals 13 p2179 N85-23521

Capture of planetesimals into a circumterrestrial swarm 13 p2179 N85-23522

Orbital resonances and planetary accretion in the solar nebula 13 p2179 N85-23523

Accumulation of the terrestrial planets
13 p2179 N85-23524

Evolution of grains in a turbulent solar nebula
13 p2179 N85-23525

The Formation of preplanetary disks from the collapse of rotating molecular cloud cores
13 p2180 N85-23526

The formation of the terrestrial planets from lunar sized planetesimals 15 p2678 N85-26533

Statistical theory of planet growth
15 p2678 N85-26534

Asteroid compositional rings: Clues to the compositions of primordial planetesimals in the middle solar system
15 p2678 N85-26537

Implications for the Earth of the early dynamical environment 21 p3719 N85-33079

Late-stage planetesimals: How big?
22 p3852 N85-33987

An impact-induced terrestrial atmosphere and iron-water reactions during accretion of the Earth
22 p3854 N85-33994

Study of the parameters affecting the collapse of a rotating protostellar cloud 24 p4166 N85-35837

PROTOPLASTS

Plant cell cultures in biological space experiments
05 p0690 N85-14434

Daylily as a system to study effects of space flight on plant development 15 p2607 N85-26088

PROTOSTARS

NT T TAURI STARS

Star Formation Workshop
[ROE-OR-13] 03 p0441 N85-12809

Compact infrared sources: Protostars before IRAS
03 p0442 N85-12812

Open cluster formation --- stellar evolution
03 p0442 N85-12815

Numerical models of the spectral appearance of protostellar envelopes 03 p0442 N85-12816

Spherical accretion onto a protostellar core
03 p0442 N85-12817

Future theoretical needs in studies of star formation
03 p0444 N85-12829

Dynamic thermal episodes in the protosolar nebula: Development of models from observations on CAI's
06 p0867 N85-15830

The relevance of QUASAT to the star formation problem 07 p1058 N85-16718

PROTOTYPES

SAGA: A project to automate the management of software production systems
[NASA-CR-174017] 01 p0103 N85-10865

Performance of a large area flash chamber prototype
[NOTA-INTERNA-807] 02 p0201 N85-11336

Use of prototyping for man-machine interface requirements definition on the AWDS (Automated Weather Distribution System) program
[AD-A146033] 03 p0396 N85-12535

Preliminary evaluation of RCA C83036E prototype photomultiplier
[DE84-016894] 04 p0496 N85-13165

Prototype concept design for US Army type 3A Air Traffic Control Tower (ATCT)
[AD-A148640] 09 p1284 N85-18070

A preliminary assessment of environmental noise from large Wind Energy Conversion Systems (WECS) based on experiences from Swedish prototypes
[FFA-TN-1984-48] 09 p1379 N85-18688

Improved Y-11 general-purpose transport designated Y-12 13 p1972 N85-22385

High reliability mechanical-hydraulic converter
14 p2268 N85-24055

Automated, robotized forge-press systems viewed
14 p2284 N85-24153

Solid state compressor
[AD-A150790] 14 p2311 N85-24302

The development of a programming support system for rapid prototyping. Tasks 2 and 3
[AD-A151549] 15 p2629 N85-26202

The design and implementation of an object-oriented, production-rule interpreter
[AD-A154769] 21 p3671 N85-32803

Prototyping with data dictionaries for requirements analysis
[AD-A156303] 24 p4139 N85-35654

PROTOZOA

Late Quaternary deep-water paleoceanography of the eastern equatorial Indian Ocean: Evidence from Bethnic foraminifers, carbonate dissolution, and stable isotopes
08 p1182 N85-17446

PROVING

NT THEOREM PROVING

Crewstation design and validation
06 p0752 N85-14822

Verification of a model of the Eastern Scheldt
[RAND/R-3108-NETH] 09 p1354 N85-18518

Perspective on demonstrations of compliance for high-level waste disposal
[DE85-000989] 09 p1383 N85-18696

Prime Computer, Incorporated, PRIME 750, BASICV revision 19.4
[PB85-108074] 11 p1699 N85-20683

Micro focus Cifer 2887 high performance level 2 COBOL; V2.5
[PB85-108959] 11 p1703 N85-20714

Micro focus Cifer 2887 compact level 2 COBOL; V2.5
[PB85-108967] 11 p1703 N85-20715

A note on validity generalization procedures
[AD-A150065] 12 p1924 N85-22085

Validation summary report, Burroughs Corporation, 820 FORTRAN release 4.0
[PB84-227792] 13 p2145 N85-23316

Get Away Special (GAS) thermal design summary
[X-732-85-8] 15 p2475 N85-25278

Peer Review of a Formal Verification/Design Proof Methodology
[NASA-CP-2377] 17 p3010 N85-28609

Ada validation summary report. ALS AdaVAX version 1.1 VAX-11/780 using VAX/VMS release 3.6
[AD-A153684] 18 p3162 N85-29588

Ada (trademark) compiler validation summary report. Honeywell information systems GCOS8 Ada version 1.1
[AD-A153746] 18 p3162 N85-29590

Ada compiler validation summary report, University of Karlsruhe-GMD/German MOD Siemens - BS 2000 version 7.30
[AD-A153747] 18 p3163 N85-29591

Ada (trademark) compiler validation summary report: ALSYS ALSYCOMP-0001
[AD-A153750] 18 p3163 N85-29592

A variable-complexity norm maximization problem
[AD-A153614] 18 p3169 N85-29634

Instrument Systems Analysis and Verification Facility (ISAVF) users guide
[NASA-TM-86226] 19 p3223 N85-29982

PROVISIONING

Food acquisition: Food ingredients, raw materials and supply 14 p2393 N85-24737

PROXIMITY

Focal plane array optical proximity sensor
[NASA-CASE-NPO-15155-1] 12 p1932 N85-22139

Design of an optical proximity sensor using multiple cones of light for measuring surface shape — application to a robot manipulator
[AD-A150050] 12 p1934 N85-22152

PROXIMITY EFFECT (ELECTRICITY)

Outlook for realization of proximity effect and Josephson direct current in helium-2 13 p2074 N85-22956

PSEUDOMONAS

Structural-functional changes in bacterial cells under spaceflight conditions 16 p2724 N85-26812

Genetics in methylotrophic bacteria
[DE85-011480] 19 p3327 N85-30615

PSEUDOPOTENTIALS

Pseudopotentials and total energy calculations: Applications to crystal stability, vibrational properties, phase transformations, and surface structures
[DE85-007657] 18 p3194 N85-29810

PSEUDORANDOM SEQUENCES

Precise bearing support ditherer
[AD-D011470] 10 p1493 N85-19428

Efficient parallel pseudo-random number generation
[AD-A152235] 16 p2655 N85-27608

An algorithm for the generation of primitive polynomials
[FUB-17-1984] 22 p3831 N85-33730

PSYCHOACOUSTICS

Aircraft noise effects: An interdisciplinary study of the effect of aircraft noise on man. Part 2: Appendix
[NASA-TM-75818] 10 p1527 N85-19630

Several specific and nonspecific responses of the human and animal body to ship noise
[NASA-TM-77483] 15 p2615 N85-26116

PSYCHOLINGUISTICS

Speech analysis system for assessing pilots' working fitness 22 p3819 N85-33661

PSYCHOLOGICAL EFFECTS

NT ILLUSIONS

NT JET LAG

Psychological states (mood, affect or emotion) experienced by JASDF pilots through flying duties. 3: Flying conditions causing pilots psychological disturbances 01 p0090 N85-10606

The relationship between emotional tension scale and psychological uneasiness of JASDF pilots in flying situations 01 p0090 N85-10608

Influence of activation of ASFS-2 on human emotional status 08 p1194 N85-17522

Aircraft noise effects: An interdisciplinary study of the effects of aircraft noise on man. Part 1: Basic report
[NASA-TM-75819] 10 p1526 N85-19629

Aircraft noise effects: An interdisciplinary study of the effect of aircraft noise on man. Part 2: Appendix
[NASA-TM-75818] 10 p1527 N85-19630

Aircraft noise effects: An inter-disciplinary study of the effect of aircraft noise on man. Part 3: Supplementary analyses of the social-scientific portion of the study on aircraft noise conducted by the DFG
[NASA-TM-75802] 10 p1527 N85-19631

Observations of physiological and psychological effects of terrain following flight based on in-flight test experience 10 p1532 N85-19657

Psychological aspects of phenomenon of spatial synchronization of EEG potential
11 p1691 N85-20632

Effect of prolonged hunger during experimental hikes
11 p1692 N85-20637

Simulator sickness: Reaction to a transformed perceptual world. 6: Preliminary site surveys
11 p1694 N85-20653

Some individual differences in human response to infrasound
[UTIAS-282] 12 p1905 N85-21960

Sleep deprivation and exercise tolerance
[AD-A150626] 13 p2142 N85-23297

Mechanizing of handling operations in drop forging with hammers and presses (conducted ergonomical examinations)
[BMFT-FB-HA-84-051] 17 p3002 N85-28561

Investigation of biochemical and psychological parameters of air traffic controllers in prestart state before beginning to work 19 p3325 N85-30599

Problems of aviation and space medicine and psychology discussed at 14th Gagarin lectures
23 p3954 N85-34509

PSYCHOLOGICAL FACTORS

The effects of feedback and predictability of human judgment
[AD-A145744] 02 p0237 N85-11542

Psychological issues in online adaptive task allocation
06 p0704 N85-14516

Job and family stress as predictors of pilot health, job satisfaction and performance
[AD-A142176] 07 p1018 N85-16464

A study of the relationship between user attitudes and the success of the MAJCOM and AFRCE work information management system
[AD-A146956] 07 p1051 N85-16671

An investigation of the relationship between stressful life events and psychological, behavioral and physiological outcomes
[AD-A147754] 08 p1197 N85-17541

Probable cause: A decision making framework
[AD-A147642] 08 p1210 N85-17614

A theory of preference reversals
[AD-A147952] 08 p1216 N85-17661

Captain development training at US Air
09 p1275 N85-18012

Management training for cockpit crews at Piedmont flight 09 p1276 N85-18013

Determination of functional mobility of human nervous system with the PNN-3 instrument
10 p1525 N85-19618

Research opportunities in human behavior and performance
[NASA-CR-175473] 10 p1529 N85-19640

Task influences in the analytic-intuitive approach to decision making
[AD-A149870] 12 p1950 N85-22250

Psychological and physiological basis of stereophonic effect 15 p2526 N85-25574

Psychological issues relevant to astronaut selection for long-duration space flight: A review of the literature
[AD-A154051] 19 p3330 N85-30627

Living aloft: Human requirements for extended spaceflight
[NASA-SP-483] 21 p3666 N85-32772

PSYCHOLOGICAL INDEXES

U PSYCHOLOGICAL TESTS

PSYCHOLOGICAL TESTS

Psychological testing on the computer
[R/PERS-618] 01 p0097 N85-10645

Conjunctive and disjunctive item response functions
[AD-A147815] 07 p1033 N85-16561

Cognitive asymmetry and occupation. Computer programmers, students, and bank personnel, part 1 and part 2
[AD-A147125] 08 p1197 N85-17540

Improved estimation procedures for item response functions
[AD-A147677] 08 p1215 N85-17648

Restructuring of the process of visual recognition as perception conditions alter 10 p1526 N85-19624

The effect of set size on color recognition
[AD-A150958] 14 p2391 N85-24726

Construction of a job-oriented test for the selection of air traffic controllers
[DFVLR-FB-84-51] 17 p3002 N85-28558

Equipercentile test equating: The effects of presmoothing and postsmoothing on the magnitude of sample-dependent errors
[AD-A154110] 19 p3347 N85-30746

PSYCHOLOGY

NT COGNITIVE PSYCHOLOGY

NT PSYCHOACOUSTICS

NT PSYCHOPHYSICS

Toward a computational neuropsychology of high-level vision
[AD-A145711] 02 p0236 N85-11540

European Scientific Notes, Number 38-9
[AD-A145683] 02 p0306 N85-11975

Evaluation of the National Library of Medicine's programs in the medical behavior sciences. Coverage of the Medical Behavioral Sciences (MBS) literature in monographic databases, study 5
[PB84-230531] 03 p0439 N85-12797

Evaluation of the National Library of Medicine's programs in the medical behavior sciences. Online searchers' reactions to database and vendor capabilities in the Medical Behavioral Sciences (MBS), study 4
[PB84-230523] 03 p0439 N85-12798

Evaluation of the National Library of Medicine's programs in the medical behavior sciences. Quality of indexing: The development and testing of a methodology comparing databases covering the Medical Behavioral Sciences (MBS) literature, study 3
[PB84-230515] 03 p0439 N85-12799

Evaluation of the National Library of Medicine's programs in the medical behavior sciences. Test retrievals in five major databases covering the Medical Behavioral Sciences (MBS) literature, study 2
[PB84-230507] 03 p0440 N85-12800

Evaluation of the National Library of Medicine's programs in the medical behavior sciences. Coverage, overlaps and gaps in bibliographic databases dealing with the Medical Behavioral Sciences (MBS) literature, study 1
[PB84-230499] 03 p0440 N85-12801

Evaluation of the National Library of Medicine's program in the medical behavior sciences. An analysis of the National Library of Medicine's (NLM) handling of Medical Behavioral Sciences (MBS) literatures: Some research tests of methods for evaluating bibliographic databases, executive summary
[PB84-230481] 03 p0440 N85-12802

USSR report: Life sciences. Biomedical and behavioral sciences
[JPRS-UBB-84-015] 07 p1010 N85-16416

Ambiguity and uncertainty in probabilistic inference
[AD-A147378] 07 p1035 N85-16572

ONR (Office of Naval Research) Far East Scientific Bulletin, volume 9, number 3, July to September 1984
[AD-A147282] 08 p1262 N85-17930

Psychobiology and food perception
14 p2394 N85-24745
Review of the psychological issues relating to the effectiveness of structured programming
[AD-A154593] 21 p3665 N85-32766
The priming effect in task design research
[AD-A154569] 21 p3679 N85-32852
PSYCHOMETRICS
An investigation of the effect of correlated abilities on observed test characteristics
[AD-A144669] 01 p0113 N85-10765
Revised Uniform Summary of Surface Weather Observations (RUSSWO). Spangdahlem AB, Germany, parts A-F
[AD-A147166] 07 p1006 N85-16392
Improvement of workload estimation techniques in piloting tasks
[NASA-CR-174374] 10 p1531 N85-19648
Human cognition and intelligence: Towards an integrated theoretical perspective
[CSIR-SR-PERS-350] 13 p2143 N85-23300
Psychometric evaluation of head injury among fliers referred to the AF School of Aerospace Medicine
[AD-A151479] 15 p2617 N85-26129
Conceptualizing in assembly tasks
[AD-A155564] 21 p3665 N85-32770
PSYCHOMOTOR PERFORMANCE
Measuring workload differences between short-term memory and long-term memory scenarios in a simulated flight environment 05 p0703 N85-14513
Fitts' law? A test of the relationship between information load and movement precision 05 p0705 N85-14523
A production system model of capturing reactive moving targets 05 p0706 N85-14524
The representation of action plans in long term memory 05 p0709 N85-14545
Speech-action interrelationships in operational work
07 p1010 N85-16418
Random pattern tracking acceleration tolerance tester
[AD-D011404] 07 p1017 N85-16459
Determination of functional mobility of human nervous system with the PNN-3 instrument
10 p1525 N85-19618
Restructuring of the process of visual recognition as perception conditions alter 10 p1526 N85-19624
Multiple resources and brain laterality
[AD-A148912] 10 p1530 N85-19643
Performance Evaluation Tests for Environmental Research (PETER) evaluation of 112 measures
[AD-A152317] 17 p2999 N85-28543
Biofeedback and performance: An update
[AD-A153228] 17 p3001 N85-28553
The effects of prolonged feeding meal, ready-to-eat (MRE) operational rations
[AD-A154763] 21 p3666 N85-32773
Performance of rolling ball and isometric joystick on a 2-D target alignment task
[RSRE-MEMO-3695] 22 p3826 N85-33699
PSYCHOPHYSICS
NT PSYCHOACOUSTICS
Electrophysiological correlates of Vernier acuity in human visual cortex
[AD-A146533] 06 p0846 N85-15371
Vision algorithms and psychophysics
[AD-A151888] 15 p2620 N85-26142
PSYCHOPHYSIOLOGY
NT WORKLOADS (PSYCHOPHYSIOLOGY)
Effects of individual mnemonic characteristics on problem solving 07 p1010 N85-16419
Functional inter-hemisphere asymmetry in recognition of visual stimuli of various classes
08 p1193 N85-17517
Encephalographic correlates of autogenous change in human functional state 08 p1193 N85-17518
Influence of activation of ASFS-2 on human emotional status 08 p1194 N85-17522
Simulator sickness: Sensorimotor disturbances induced in flight simulators
[AD-P004334] 09 p1271 N85-17988
Success in learning occupation of chemical production technician as function of certain personality traits and development of psychophysiological functions
09 p1362 N85-18568
USSR report: Life sciences. Biomedical and behavioral sciences
[JPRS-UBB-85-011] 10 p1525 N85-19616
Electrosleep therapy advanced at medical institute
10 p1526 N85-19623
Methods of monitoring mental work efficiency, emotional activity 10 p1526 N85-19627
Role of mental work in human tolerance in total-body vibration 12 p1901 N85-21940
Psychophysiological studies. 1: Performance and physiological response in learning, short-term memory and discrimination tasks
[AD-A151018] 14 p2392 N85-24731
Psychophysiological nature of aircraft feel
19 p3323 N85-30587
USSR report: Space Biology and Aerospace Medicine, volume 19, no. 2, March - April 1985
[JPRS-USB-85-004] 22 p3820 N85-33667
Psychophysiological distinctions of organization and regulation of daily cyclograms of crew activities during long-term spacecraft 22 p3821 N85-33669
Operator's functional comfort zone when controlling moving object 22 p3821 N85-33670
PTM (MODULATION)
U PULSE TIME MODULATION
PUBLIC HEALTH
Health and environmental effects document for photovoltaic energy systems, 1983
[DE84-017179] 04 p0532 N85-13399
USSR report: Life sciences. Biomedical and behavioral sciences
[JPRS-UBB-84-015] 07 p1010 N85-16416
Mercury health effects update: Health issue assessment
[PB85-123925] 10 p1528 N85-19639
Hygienic standardization of electromagnetic fields of radar systems 14 p2387 N85-24703
Biological and human health effects of extremely low frequency electromagnetic fields. Post-1977 literature review
[AD-A152731] 17 p2999 N85-28539
Geothermal hydrogen and health in Rotorua, New Zealand
[DE85-901283] 19 p3301 N85-30467
Hydrodynamics and sanitation
[CT-579] 20 p3487 N85-31672
PUBLIC LAW
NT LEGAL LIABILITY
NT LIABILITIES
Civil law enforcement missions
06 p0751 N85-14812
The need for a dedicated public service helicopter design 06 p0753 N85-14828
PUBLIC RELATIONS
Community relations activities at Department of Defense sites
[AD-P004150] 09 p1349 N85-18486
NASA photography index
[NASA-TM-87457] 15 p2665 N85-26445
Origin, processing, and dissemination of scientific news, with examples from 20 research institutes
[JUEL-1940] 17 p3060 N85-28882
PUBLICATIONS
U DOCUMENTS
PUERTO RICO
Meteor wind results from Atlanta, USA, and Ramey, Puerto Rico 11 p1662 N85-20474
PULLEYS
Feasibility demonstration of a novel, flat-belt, continuously variable transmission or automotive and electric-hybrid vehicle application
[NASA-CR-174430] 10 p1569 N85-19894
PULMONARY CIRCULATION
Oxygen delivery during exercise: Limitations to maximum flow 05 p0688 N85-14424
Pulmonary blood flow and oxygenation of arterial blood in a healthy subject upon 7 days hypokinesia
07 p1014 N85-16439
Human lung fluid content during 7-day head-down tilt
12 p1902 N85-21941
Spirolit-2 instrument used to test pulmonary ventilation
12 p1903 N85-21950
Effect of 120-day antiorthostatic bedrest on gas exchange and pulmonary circulation in man
19 p3323 N85-30589
PULMONARY FUNCTIONS
Interaction between lung mechanics and gas exchange by low volume high frequency pulmonary ventilation in patients with respiratory failure
[AD-A146604] 06 p0846 N85-15372
Human lung fluid content during 7-day head-down tilt
12 p1902 N85-21941
PULMONARY LESIONS
Deposition in the human lung during respiration of small particles suspended in the air
[BLL-RISLEY-TR-5021-(9091.9F)]
03 p0400 N85-12549
PULSARS
Observations of the pulsating hydrogen: Deficient star BD+13 deg 3224, during 1980 - 1981
01 p0128 N85-10882
A search for low luminosity pulsars and its implications for the pulsar luminosity functions
02 p0296 N85-11919
Measurement of pulsar parallax by Very Long Baseline Interferometry 03 p0444 N85-12830
The parallax of pulsar 0950+08 and the local free electron density 06 p0879 N85-15584
The X-ray structure of the Crab Nebula
11 p1741 N85-20948
Search for millisecond rotational periods in some low-mass X-ray binaries observed by EXOSAT
11 p1741 N85-20949
The X-ray structure of the Crab Nebula
11 p1742 N85-20954
Recent results on the Crab Pulsar X-ray light curve
11 p1742 N85-20955
EXOSAT observations of the 35d intensity variations of Her X-1 — X ray binary source
11 p1742 N85-20956
Pulse phase spectroscopy of Her X-1 with EXOSAT — X ray binary source 11 p1743 N85-20957
Simultaneous EXOSAT and optical observations of the pulsing X-ray binary H2252-035 / AO Psc
11 p1743 N85-20959
The axisymmetric pulsar magnetosphere
12 p1955 N85-22279
Nonlinear waves in the magnetosphere of pulsars
12 p1955 N85-22281
About static and dynamic solutions of the aligned rotator model — pulsar magnetospheres
12 p1958 N85-22308
An analytic model for hydromagnetospheres — stellar winds; pulsars; cosmic jets 12 p1959 N85-22313
The luminosity distribution of pulsars
12 p1959 N85-22317
Discriminant analysis of pulsar groups in the diagram P versus P 12 p1960 N85-22319
Pulsars and interstellar medium
12 p1960 N85-22320
Optical pulsar in the Large Magellanic Cloud remnant 0540-69.3
[DE85-006707] 16 p2883 N85-27788
The radiation of the Vela pulsar
20 p3548 N85-32080
A model of pulsed radiation from the Crab pulsar
20 p3548 N85-32081
Comments on RS-17 X-ray telescope
22 p3731 N85-33132
On gamma and neutrino radiation from Cyg X-3
[OG-2.1-7] 22 p3863 N85-33891
500 TeV gamma rays from Hercules X-1
[OG-2.2-7] 22 p3865 N85-33903
A model for the UHE gamma-rays from Hercules X-1
[OG-2.2-8] 22 p3865 N85-33904
High-resolution spectroscopic observation of Vela X-1 in the hard X-ray energy range
[OG-2.2-10] 22 p3865 N85-33906
Experimental results on gamma-ray sources at E sub 0 = 10(13) - 10(14) eV
[OG-2.2-12] 22 p3865 N85-33907
Very high energy gamma rays from the Crab Nebula
[OG-2.3-3] 22 p3866 N85-33940
Microburst of TeV gamma rays from the Crab pulsar
[OG-2.3-4] 22 p3866 N85-33941
Secondary periodicities of microbursts of TeV gamma rays from the Crab pulsar
[OG-2.3-5] 22 p3866 N85-33942
Detection of gamma-ray lines from the direction of the Crab Nebula 22 p3866 N85-33943
Observation of hard X-rays from the Crab pulsar and A0535+26
[OG-2.3-7] 22 p3866 N85-33944
Gamma rays of 0.3 to 30 MeV from PSR 0531+21
[OG-2.3-8] 22 p3866 N85-33945
The 1000 GeV gamma ray emission from radio pulsars 22 p3867 N85-33946
Pulsed emission of TeV gamma rays from Vela pulsar
22 p3867 N85-33947
The 1000 GeV gamma rays from ms pulsars
[OG-2.3-12] 22 p3867 N85-33948
A search in the COS-B data base for correlated time variability in regions containing objects of interest
[OG-2.5-9] 22 p3869 N85-33964
The 4U 0115+63: Another energetic gamma ray binary pulsar
[OG-2.6-11] 22 p3870 N85-33973
On some problems of gamma-astronomy
[OG-2.7-15] 22 p3873 N85-33986
Cosmic rays in the 10(16) to 10(19) eV range from pulsars
[OG-5.4-3] 22 p3886 N85-34080
Scaling from Jupiter to pulsars and the acceleration of cosmic ray particles by pulsars, 3
[OG-8.2-3] 23 p4019 N85-34904
On magnetic pair production above fast pulsar polar caps
[OG-8.2-13] 23 p4020 N85-34909
Pulsars as cosmic ray particle accelerators: Proton orbits
[OG-8.2-21] 23 p4021 N85-34917
Pulsars as cosmic ray accelerators: Energy development of protons
[OG-8.2-22] 23 p4021 N85-34918

Pulsars as cosmic ray particle accelerators: Dynamics of electrons [OG-8.2-23] 23 p4021 N85-34919

High energy radiation from neutron stars [DE85-014353] 24 p4169 N85-35843

ULSATING FLOW

U UNSTEADY FLOW

ULSE AMPLITUDE

Beam pulse length determination by spectral analysis [CSIR-NAC-83-05] 01 p0116 N85-10793

Slowly rotating pulsed radiation source 02 p0256 N85-11678

Gain instabilities in photomultipliers: How accurate are photon counting measurements? 08 p1251 N85-17903

Reception of signal with unknown amplitude and duration submerged in white noise 13 p2084 N85-23016

The latitudinal variation of geomagnetic pulsation amplitude and phase 14 p2370 N85-24646

An amplitude correlation and differencing method for the monitoring of flaws in repeat ultrasonic inspections [AERE-R-11416] 15 p2571 N85-25854

Acoustooptic pulse-echo transducer system [NASA-CR-175919] 17 p2951 N85-28224

Inherent angular tracking error in an amplitude comparison monopulse radar [AD-A154212] 19 p3255 N85-30185

A modified Fresnel scattering model for the parameterization of Fresnel returns, part 2.3A 21 p3618 N85-32483

Behaviors of stress waves in a conical bar 23 p3904 N85-34182

Cosmic ray north-south anisotropy 1961 - 1983 [SH-4.2-6] 23 p4007 N85-34844

Study of the shower maximum depth by the method of detection of the EAS Cerenkov light pulse shape [HE-4.4-15] 24 p4194 N85-36021

Analysis of Cerenkov pulses recorded simultaneously at two sites [HE-4.4-16] 24 p4194 N85-36022

Microprocessor-based single particle calibration of scintillation counter [HE-4.6-13] 24 p4198 N85-36049

Samarkand complex setup for investigation of cosmic ray variation in the energy range of 7 10 (9) - 10 (15) eV [HE-4.6-14] 24 p4198 N85-36050

The structure of the shower disk observed at Mt. Norikura [HE-4.7-1] 24 p4198 N85-36052

PULSE AMPLITUDE MODULATION

Investigation of characteristics of phased antenna array considering interaction between radiators and properties of power divider 06 p0790 N85-15051

PULSE CHARGING

Model that predicts pulse charged gas switching breakdown phenomena [DE85-013119] 22 p3761 N85-33313

PULSE CODE MODULATION

Switched Capacitor (SC) filter and design centering of integrated circuits, part 1 [BMFT-FB-T-84-190-PT-1] 05 p0633 N85-14062

Pulse code modulation telemetry: Properties of various binary modulation types [AD-A147214] 07 p0913 N85-15780

One-dimensional processing for adaptive image restoration [AD-A149314] 10 p1557 N85-19815

A method and apparatus for operating on companded PCM voice data [NASA-CASE-KSC-11285-1] 18 p3069 N85-29120

PULSE COMMUNICATION

A microcomputer aided measurement equipment for monitoring performance in digital radio relay systems [FUB-4-1984] 01 p0101 N85-10668

Timing performance of phase-locked loops in optical pulse position modulation communication systems [AD-A145403] 02 p0190 N85-11271

Designer on Aeroflot automated COMMO system development 08 p1067 N85-16765

Shuttle S-band communications technical concepts 08 p1099 N85-16948

Propagation Influences on Digital Transmission Systems: Problems and Solutions [AGARD-CP-363] 10 p1469 N85-19269

Limits of the propagation medium with respect to digital signal transmission 10 p1469 N85-19270

Digital data communications over microwave radio channels 10 p1469 N85-19272

EHF air-to-air communications 10 p1469 N85-19273

Equatorial transionospheric propagation conditions affecting digital communications 10 p1470 N85-19275

Measurements of propagation at 900 MHz in an urban zone for establishing a digital radiomobile system 10 p1472 N85-19286

Theoretical study of a dynamic simulator of selective fading for digital, wireless beam microwave links 10 p1473 N85-19294

Integrated support of tactical operations by satellite communications 11 p1709 N85-20754

The study of certain aspects of probability with applications in communications theory [AD-A149820] 12 p1829 N85-21476

Digital channel efficiency model [AD-A150084] 12 p1829 N85-21479

Use of electronic coding-frequency meters to measure parameters of pulsed radio signals 13 p2076 N85-22964

Secure digital speech communication [AD-D011572] 14 p2293 N85-24215

The performance of a new adaptive filter for digital communications [AD-A151890] 15 p2543 N85-25702

Rational pulse-shaping filters for almost MSK-like modulation [AD-A153065] 17 p2949 N85-28208

Measured noise performance of a new method of frequency hopping [AD-A152679] 17 p2953 N85-28234

A method and apparatus for operating on companded PCM voice data [NASA-CASE-KSC-11285-1] 18 p3069 N85-29120

Design of a jamming simulator for a binary communication system [AD-A154617] 21 p3573 N85-32221

Optimum predistortion of digital signals for transmission over parallel channels 22 p3776 N85-33397

New directional couplers for multimode circular waveguides applied to intense pulsed microwave systems [DE85-011753] 23 p3926 N85-34330

Joint services electronics program [AD-A154748] 23 p3927 N85-34336

Necessary bandwidth and spectral properties of digital modulation [PB85-185387] 24 p4088 N85-35340

PULSE COMPRESSION

Binary pulse compression techniques for MST radars 08 p1184 N85-17464

Rational pulse-shaping filters for almost MSK-like modulation [AD-A153065] 17 p2949 N85-28208

An approach to digital level compression using the zero-crossing points of programme signals [NHK-LABS-NOTE-308] 18 p3090 N85-29123

Huffman-coded pulse compression waveforms [AD-A155322] 21 p3576 N85-32243

Repetitive pulse accelerator technology for light ion inertial confinement fusion [DE85-012030] 23 p3982 N85-34693

PULSE DOPPLER RADAR

NT EARTH RESOURCES SHUTTLE IMAGING RADAR

NT MONOPULSE RADAR

Adaptive mutual interference suppression method [AD-D011268] 05 p0628 N85-14024

Test signal generator for coherent air-to-ground radars [AD-D011278] 05 p0628 N85-14025

Gain restoration after Doppler filtering [AD-D011425] 08 p1154 N85-17287

A technique for rapid determination of probability of detection in pulse Doppler radars [AD-D011426] 08 p1154 N85-17288

Development of the F-20 nose radome [AD-P004374] 12 p1827 N85-21468

PULSE DURATION

Notes on NAC report NAC-83-05: Beam Pulse Length Determination by Spectral Analysis [CSIR-NAC-83-06] 01 p0119 N85-10816

Estimating algorithmic error of digital recursive filters 12 p1839 N85-21543

Square-pulse generator 13 p2075 N85-22959

Use of electronic coding-frequency meters to measure parameters of pulsed radio signals 13 p2076 N85-22964

Flash radiography 14 p2317 N85-24316

Instrument for measuring dispersional distortions in optical fibers and cables 15 p2530 N85-25595

A sampling phasemeter design for pulsed continuous wave signals [AD-A155237] 21 p3581 N85-32264

A modified Fresnel scattering model for the parameterization of Fresnel returns, part 2.3A 21 p3618 N85-32483

Establishment of steady-state power level in pulse-periodic excimer laser 21 p3685 N85-32896

Voyager 0.2-lbf thruster valve assembly short pulse test report [NASA-CR-176121] 22 p3741 N85-33185

Method of designing digital band-pass filters with pulse response of finite duration 22 p3775 N85-33395

The 1000 GeV gamma ray emission from radio pulsars 22 p3867 N85-33946

The longitudinal thickness of air-shower fronts [OG-9.5-1] 23 p4030 N85-34978

Sub-luminal pulses from cosmic ray air showers [HE-4.7-13] 24 p4200 N85-36063

PULSE DURATION MODULATION

Formation of radio signals with low out-of-band radiation 07 p0950 N85-16018

Miniature high performance pulsed modulator apparatus [AD-D011427] 08 p1158 N85-17310

PULSE FREQUENCY MODULATION

Method and means for providing frequency agile operation of MTI (Moving Target Indicator) radar [AD-D011561] 12 p1823 N85-21436

Applicability of log-normal model to probabilitistic description of quasi-pulse interference 13 p2084 N85-23014

PULSE GENERATORS

Resistance and inductance calculations for helical flux compression generators [DE84-015068] 02 p0195 N85-11306

Optimization of ultrashort pulse generation mode of YAG laser 02 p0262 N85-11713

Power MOS fast switching techniques [DE84-015046] 05 p0732 N85-14707

High-speed power devices with field control 06 p0794 N85-15073

Repetitive pulse generation with inductive energy storage: A new technology for defense [DE84-017090] 06 p0805 N85-15122

Technical data on new engineering products 10 p1460 N85-19201

Investigation of the output parameters of the pulsed neutron generator NGI-5 [DE85-001823] 11 p1725 N85-20849

Power circuit utilizing self-excited Hall effect switch means [AD-D011505] 12 p1832 N85-21496

Square-pulse generator 13 p2075 N85-22959

Accuracy of approximation of Bayes estimates in presence of noninformative parameters 13 p2084 N85-23015

Optically triggered transferred-electron device microwave burst and single pulse generators [AD-D011614] 16 p2778 N85-27141

Generalization of the Child-Langmuir relation for 1-dimensional time-dependent diodes [DE85-007386] 16 p2779 N85-27152

Sub-optimal control of nonlinear flexible space structures 20 p3414 N85-31190

Coordinated research program in pulsed power physics [AD-A154629] 21 p3679 N85-32858

Operational window for a plasma erosion opening switch used for voltage multiplication on pulsed power generators [AD-A155482] 21 p3707 N85-33020

Capacitance measuring device [DE85-011643] 22 p3787 N85-33460

Series-counterpulse repetitive-pulse inductive storage circuit [DE85-006436] 23 p3928 N85-34342

Photoconductive pulse power switches: A review [DE85-014125] 24 p4091 N85-35360

Quality assurance considerations for the implementation of a pulsed power R and D project [DE85-012357] 24 p4148 N85-35720

Beam intensity increases at the intense pulsed neutron source accelerator [DE85-012377] 24 p4155 N85-35764

Power flow evaluations for HERMES 3 [DE85-013116] 24 p4156 N85-35769

PULSE HEATING

Optical monitoring of photo-acoustic pulse propagation in silicon wafers [AD-A151333] 15 p2651 N85-26352

PULSE HEIGHT

U PULSE AMPLITUDE

PULSE MODULATION

NT PULSE AMPLITUDE MODULATION

NT PULSE CODE MODULATION

NT PULSE DURATION MODULATION

NT PULSE FREQUENCY MODULATION

NT PULSE POSITION MODULATION

NT PULSE TIME MODULATION

Spectrally matched modulation of radiation of injection laser in traveling-wave amplifier below 2 GHz 02 p0262 N85-11712

Study of lower ionosphere by pulse cross-modulation method 10 p1500 N85-19467

Autostochastic behavior of solid state ring laser with low frequency periodic loss modulation 11 p1717 N85-20805

Synthesis of digital nonrecursive band-elimination filters for moving-target selectors 12 p1840 N85-21545
Pulsewidth modulated speed control of brushless dc motors
[AD-A151966] 16 p2778 N85-27148
Effect of powerful pulsed low-energy ion streams on GaAs 21 p3682 N85-32877
Self Q-modulation and generation of short pulses in distributed-feedback lasers 21 p3687 N85-32907
Cosmic ray modulatin and merged interaction regions
[SH-4.1-11] 23 p4005 N85-34834
Propagation of the phase of solar modulation
[SH-4.1-12] 23 p4005 N85-34835
The 1973-1984 solar modulation of cosmic ray nuclei
[SH-4.1-16] 23 p4006 N85-34838
Cosmic ray modulation in a random anisotropic magnetic field
[SH-4.1-20] 23 p4006 N85-34839
Evidence for regions of negligible cosmic-ray modulation in the inner heliosphere (10 AU)
[SH-4.1-21] 23 p4006 N85-34840
Drift and observations in cosmic-ray modulation, 1
[SH-4.2-4] 23 p4007 N85-34842
Drift and observations in cosmic-ray modulation, 2
[SH-4.2-5] 23 p4007 N85-34843
Variations of the cosmic ray general component in Antarctica
[SH-4.4-17] 23 p4035 N85-35013

PULSE POSITION MODULATION
Timing performance of phase-locked loops in optical pulse position modulation communication systems
[AD-A145403] 02 p0190 N85-11271
Formation of radio signals with low out-of-band radiation 07 p0950 N85-16018
Detection and symbol synchronization for multiple-bit per photon optical communications
10 p1463 N85-19228
Phase locked loop synchronization for direct detection optical PPM communication systems
[NASA-CR-176026] 19 p3254 N85-30178

PULSE RADAR
NT EARTH RESOURCES SHUTTLE IMAGING RADAR
NT MONOPULSE RADAR
NT PULSE DOPPLER RADAR
Measurement of snow cover thickness by radar sounding 03 p0344 N85-12216
Reference oscillator stability effect on clutter cancellation in a radar system 07 p0938 N85-15946
Binary pulse compression techniques for MST radars
08 p1184 N85-17464
Partial reflection spaced antenna wind measurements
08 p1185 N85-17467
Multiple channel adaptive filtering using a fast orthogonalization network: An application to efficient pulsed Doppler radar processing
[AD-A147929] 08 p1211 N85-17619
Pulse heterodyne equipment for measurements of range and velocity of moving targets-pulse radar
[ESA-TT-845] 09 p1312 N85-18246
Low sidelobe phased array antenna system
[AD-D011558] 12 p1823 N85-21435
Method and means for providing frequency agile operation of MTI (Moving Target Indicator) radar
[AD-D011561] 12 p1823 N85-21436
Summator of radio pulse signals
12 p1839 N85-21539
Interference suppressor for radar MTI
[AD-D011606] 16 p2769 N85-27086
Poseidon altimeter: Study of the hyperfrequency section and specifications of the prototype components
[CNES-84/DRT/TIT/HY/T/145]
20 p3419 N85-31219
Solid state altimeter model: Simulation description; analysis of first results (narrow band filters, weighting) — satellite-borne instruments
[CNES-DRT/TIT/RL-160-T] 20 p3419 N85-31220
Millimetre wave pulse technology — satellite mapping
[ESA-CR(P)-2004] 20 p3478 N85-31611
Huffman-coded pulse compression waveforms
[AD-A155322] 21 p3576 N85-32243
Observations of frontal zone structures with a VHF Doppler radar and radiosondes, part 1.2A
21 p3616 N85-32469
Characteristics of digital range finder with stroboscopic discretization 22 p3762 N85-33319
Detection of signals from coherent pulsed radars with random variation in parameters of sounding signals from pulse to pulse against background of worst-case Gaussian noise 22 p3763 N85-33324
Signal space models for antenna arrays
[AD-A156063] 24 p4067 N85-35335

PULSE RATE
NT PULSE REPETITION RATE
Contribution to the study and realization of the CARTHAGE multiservice local network
[ENST-84E006] 05 p0716 N85-14595
Semiconductor submicrosecond power commutator switches 06 p0795 N85-15061
A study of mode-locked argon ion-dye laser systems
16 p2789 N85-27205

PULSE RECORDERS
U COUNTERS

PULSE REPETITION RATE
Multipurpose 5-MeV linear induction accelerator
[DE84-014523] 02 p0278 N85-11808
Adaptive mutual interference suppression method
[AD-D011268] 05 p0628 N85-14024
Pulse transformer package for impedance matching a laser diode to a transmission line
[AD-D011499] 12 p1855 N85-21632
Repetitive energy transfers from an inductive energy store 13 p2062 N85-22881
Square-pulse generator 13 p2075 N85-22959

PULSE TIME MODULATION
NT PULSE DURATION MODULATION
NT PULSE POSITION MODULATION
Mg 2 emission of Pop. 2 long-period Cepheids
11 p1754 N85-21032

PULSE WIDTH
U PULSE DURATION

PULSE WIDTH MODULATION
U PULSE DURATION MODULATION

PULSED JET ENGINES
Investigation of a pulsed electrothermal thruster system
[NASA-CR-174768] 02 p0169 N85-11132

PULSED LASERS
NT Q SWITCHED LASERS
NT ULTRASHORT PULSED LASERS
NT ULTRAVIOLET LASERS
High repetition rate nitrogen ion laser
02 p0201 N85-11340
Diagnostics of ionization in air produced by infrared radiation from A pulse CO2 laser
[AD-A145376] 02 p0201 N85-11342
Time variability of directionality properties of pulsed EB-EDL (Electron Beam-Electric Discharge Laser) N2-CO2 lasers
[AD-A145546] 02 p0202 N85-11344
Studies of laser melting and rapid solidification using amorphous silicon
[DE84-014737] 02 p0202 N85-11345
Using two-beam interference method for measuring wavelength of tunable pulse lasers
02 p0272 N85-11772
Pulsed neodymium glass laser system for investigating nonlinear optical phenomena in gases
03 p0348 N85-12241
Laser balancing system for high material removal rates
[NASA-CR-174731] 03 p0365 N85-12341
Simulation of the interaction of single-pulsed optical lasers with targets in a vacuum
[DE84-016476] 05 p0640 N85-14107
Pulsed electric discharge laser technology. Electron beam window foil material
[AD-A146420] 06 p0813 N85-15162
Time-resolved studies of ultrarapid solidification of highly undercooled molten silicon formed by pulsed laser irradiation
[DE84-016664] 06 p0813 N85-15164
Self-generated magnetic fields and thermal flux inhibition
[AD-A147405] 07 p0971 N85-16166
Intense excitation source of blue-green laser
[AD-A147450] 07 p0971 N85-16168
Pulsed electric discharge laser technology. Electron beam window foil material
[AD-A147488] 07 p0972 N85-16171
Simulation of repetitively-pulsed laser irradiation of graphite-epoxy composite
[AD-A148698] 09 p1325 N85-18329
Electron-hole plasma formation in semiconductors due to the absorption of pulsed CO2 laser light
[DE85-001559] 09 p1392 N85-18757
Determination of vapor phase content when metals are struck by laser radiation pulses of various densities
10 p1445 N85-19106
Temperature variation of laser mirror stability criteria
10 p1445 N85-19108
Excitation modes and parameters of stress waves in metal exposed to single laser pulses
10 p1446 N85-19109
Picosecond laser pulse interactions with metallic and semiconductor surfaces
[AD-A149112] 10 p1490 N85-19405
Pulsed excimer laser processing for cost-effective solar cells
[NASA-CR-174429] 10 p1509 N85-19517
A method for determining in situ the absorption coefficient of particulate media using pulsed laser technique
[AD-D011548] 12 p1799 N85-21281
Mathematical modeling of two-frequency laser sounding of scattering media 13 p2089 N85-22046
Time-resolved ellipsometry and reflectivity measurements of the optical properties of silicon during pulsed excimer laser irradiation
[DE85-005091] 13 p2096 N85-22079
Activation of Si-N modes in silicon by pulsed laser annealing
[DE85-003988] 13 p2097 N85-22082
Time resolved X-ray studies during pulsed laser irradiation of Ge
[DE85-005263] 13 p2097 N85-22083
Time-resolved reflectivity measurement of extrinsic silicon during pulsed laser irradiation
[AD-A150350] 13 p2159 N85-23422
Laser Welding, Cutting and Surface Treatment
14 p2306 N85-24271
The measurement of laser beam parameters
14 p2306 N85-24275
Laser welding in the manufacture of heart pacemakers
14 p2306 N85-24288
Excimer laser annealing to fabricate low cost solar cells
[NASA-CR-175702] 14 p2351 N85-24520
Elementary processes of electronically excited particles. Part 5: Deactivation of CHF (A1a' (O, V'2, O) after excitation by a pulsed dye laser
[MPIS-13/1984] 14 p2420 N85-24930
An experimental technique for the study of velocity profiles in a laminar jet using a pulsed nitrogen laser
[AD-A151496] 15 p2556 N85-25771
Laser induced damage of zinc sulphide
[BAE-BT-13363] 15 p2562 N85-25803
Electric discharge excitation and energy source integration
[AD-A151502] 15 p2562 N85-25809
Characteristics of laser emission discharge created by pulsed CO2-laser 15 p2643 N85-26305
Theoretical investigation of lasing in 4.3 micron region in CO2 laser 15 p2643 N85-26306
Optical monitoring of photo-acoustic pulse propagation in silicon wafers
[AD-A151333] 15 p2651 N85-26352
Raman studies of surface temperature in laser-heated semiconductors
[AD-A151377] 15 p2659 N85-26412
Optogalvanic measurement of even parity Rydberg levels in krypton gas
[AD-A152113] 16 p2745 N85-26943
A study of mode-locked argon ion-dye laser systems
16 p2789 N85-27205
Surface modification of solids
[DE85-007543] 16 p2871 N85-27715
Quantum statistical theory of vibrational dynamics in a laser-driven admolecule-surface system
[AD-A152022] 16 p2872 N85-27719
X-ray crystallography of steel U8 after pulsed laser hardening
[BLL-BISI-22444-(9022.06)] 17 p2925 N85-28038
Obtaining amorphous coatings of FeW and Fe-Cr-P-B alloys using laser sputtering
[BLL-BISI-22493-(9022.06)] 17 p2927 N85-28057
Laser machining and some applications
[NHK-LABS-NOTE-307] 18 p3112 N85-29258
Quantum model of dephasing-enhanced laser desorption: Master equation approach
[AD-A153769] 18 p3112 N85-29259
The application of laser resonance saturation to the development of efficient short wavelength lasers
[AD-A153951] 18 p3113 N85-29270
A simple power meter for high energy pulsed lasers
[AD-D011661] 18 p3113 N85-29271
Definition of requirements for injection locking of pulsed UV lasers
[DE85-010126] 18 p3113 N85-29275
Dye laser traveling wave amplifier
[NASA-CR-175969] 19 p3275 N85-30308
Enhanced thermal coupling by a repetitively pulsed laser
[AD-A154435] 19 p3276 N85-30317
Spectral evolution of the pulse of a dual frequency dye laser
[CNES-83/168/T/CT/DRT/TIT/10]
20 p3461 N85-31487
Detection of excited states by laser-induced fluorescence
[AD-A155558] 21 p3592 N85-32326
Pulsed excimer laser processing for cost-effective solar cells 21 p3611 N85-32432
Excimer-laser generator of powerful UV picosecond pulses synchronized with picosecond pulses in visible and IR bands 21 p3686 N85-32903

Powerful XeCl excimer electric discharge laser with good temporal stability and fast response time
21 p3698 N85-32911

The moving thermoacoustic array: A theoretical feasibility study
[AD-A154510] 21 p3699 N85-32980

Sliding discharge in CO2 and excimer lasers
22 p3773 N85-33379

Pulsed lasers for filming color holographic film images
22 p3781 N85-33426

Metal vapor lasers and their applications
[ISL-CO-218/84] 22 p3791 N85-33488

The use of optical fibers in pulsed laser holography
[ISL-CO-226/84] 23 p3936 N85-34395

Theoretical and experimental analyses of the performance of two-color laser ranging systems
[NASA-CR-176159] 23 p3936 N85-34397

Ranging system which compares an object reflected component of a light beam to a reference component of the light beam
[NASA-CASE-NPO-15865-1] 23 p3973 N85-34629

Survey of mixing in metal/insulator systems
[DE85-011938] 23 p3965 N85-34714

ATA upgrade to 150 MeV
[DE85-013174] 24 p4098 N85-35404

PULSED RADIATION

NT ELECTROMAGNETIC PULSES

NT SYSTEM GENERATED ELECTROMAGNETIC PULSES

Slowly rotating pulsed radiation source
02 p0256 N85-11678

Transient optical nutation in CO2 laser
02 p0261 N85-11709

Efficiency of photoelectric conversion of short radiation pulses
03 p0348 N85-12240

Diffraction by the time-of-flight technique at pulsed neutron sources
[DE84-015839] 03 p0418 N85-12674

Developments of optical fast-gated imaging systems
[DE84-016170] 04 p0502 N85-13204

Pulsed irradiation of optimized, MBE grown, AlGaAs/GaAs radiation hardened photodiodes
[DE84-014984] 04 p0569 N85-13631

Pulsed photothermal radiometry for remote sensing of spectroscopic and physical properties of thin film
[AD-A149080] 10 p1435 N85-19041

Behavior degradation due to 1100-RAD pulsed radiation exposure (5.8:1 neutron/gamma ratio)
[AD-A149284] 11 p1689 N85-20621

Invariance of probability characteristics of detector to shape of optical pulse signals
13 p2090 N85-23048

Flash radiography
14 p2317 N85-24316

Calorimeter for measuring high-energy optical pulses
[PB85-160695] 15 p2561 N85-25799

Variations in intensity of secondary cosmic radiation observed on 10-11 August 1981
16 p2721 N85-26796

Technique for measuring surface diffusion by laser-beam-localized surface photochemistry
[DE85-007885] 18 p3113 N85-29273

A model of pulsed radiation from the Crab pulsar
20 p3548 N85-32081

Generation of single nanosecond high-contrast radiation pulse (lambda = 10.6 micrometers)
21 p3684 N85-32886

Laser radiation propagation in inertialess nonlinear medium
21 p3686 N85-32898

Optimal complex nonlinear processing of continuous and pulsed signals
22 p3763 N85-33323

Scientific Opportunities with Advanced Facilities for Neutron Scattering
[DE85-012113] 22 p3839 N85-33770

Observation of hard X-rays from the Crab pulsar and A0535 + 26
[OG-2.3-7] 22 p3866 N85-33944

Gamma rays of 0.3 to 30 MeV from PSR 0531 + 21
[OG-2.3-8] 22 p3866 N85-33945

The 1000 GeV gamma ray emission from radio pulsars
22 p3867 N85-33946

Pulsed emission of TeV gamma rays from Vela pulsar
22 p3867 N85-33947

Instrumentation for sensing moisture content of material using a transient thermal pulse
[NASA-CASE-NPO-15493-2] 23 p3933 N85-34373

Cosmic ray modulatin and merged interaction regions
[SH-4.1-11] 23 p4005 N85-34834

Study of the shower maximum depth by the method of detection of the EAS Cerenkov light pulse shape
[HE-4.4-15] 24 p4194 N85-36021

Analysis of Cerenkov pulses recorded simultaneously at two sites
[HE-4.4-16] 24 p4194 N85-36022

The experimental cascade curves of EAS at E sub 0 10(17) eV obtained by the method of detection of Cherenkov pulse shape
[HE-4.4-18] 24 p4194 N85-36024

PULSES

NT ELECTRIC PULSES

NT ELECTROMAGNETIC PULSES

NT GEOMAGNETIC PULSATIONS

NT PICOSECOND PULSES

NT PRESSURE PULSES

NT SYSTEM GENERATED ELECTROMAGNETIC PULSES

Regenerators of binary pulses for optical communication systems
04 p0465 N85-13099

Westinghouse programs in pulsed homopolar power supplies
05 p0606 N85-13662

Analysis of spin echo signals in multi-pulse experiment
06 p0792 N85-15065

Degenerate four-wave mixing lineshapes in sodium vapor under pulsed excitation
[AD-A148211] 08 p1222 N85-17686

Battery response to pulse loads: A mathematical model
[DE85-001149] 09 p1316 N85-18277

Study of the pulsations of the ZZ Ceti stars
09 p1414 N85-18923

A 10/sup 11/W high current pulse electron beam accelerator described
11 p1620 N85-20200

A stochastic-mechanical approach to acoustic pulse propagation in the deep ocean sound channel
[AD-A149598] 12 p1928 N85-22110

Surface forward scattering and reflection
[AD-A150115] 12 p1928 N85-22112

Strong iron accelerating by collisionless magnetosonic shock wave propagating perpendicular to a magnetic field
[IPPJ-709] 12 p1935 N85-22161

Domain of applicability of asymptotic description of radio pulse fields near critical frequency
13 p2073 N85-22949

Optimization of number of pulses in detection of fluctuating optical signals
13 p2081 N85-22993

Probability of detection of pulsed signals employing zero-gating interference suppression
13 p2085 N85-23021

Railgun conductor heating from multiple current pulses
[DE85-005333] 14 p2265 N85-24031

Pseudo bipolar nickel-cadmium batteries used as filter elements to pulsed current loads
[AD-A151192] 15 p2547 N85-25717

Studies in electron phenomena in MOS structures: The pulsed C-V method
15 p2659 N85-26407

Investigation of electron attachment and dissociation rates in C2F6/CH4 electric gas discharges
[AD-A151796] 16 p2862 N85-27649

Investigation on the application of the pulsed eddy current method of non-destructive testing using controlled signals (CS-technique)
[BLL-BISI-TRANS-22249-(9022.06)]
18 p3119 N85-29303

Design and testing of a pulsed current transformer
[AD-A154228] 19 p3259 N85-30208

Arctic acoustic tomography MIZEX 84
[AD-A154426] 19 p3320 N85-30580

Ultrasonic flowmetering with reflected pulses
[PB85-179885] 20 p3460 N85-31492

Amplitude stabilization of pulse signals
22 p3762 N85-33320

Comparative characteristics of optical multiposition pulse signals with intersymbol distortion
22 p3764 N85-33329

On gamma and neutrino radiation from Cyg X-3
[OG-2.1-7] 22 p3863 N85-33924

Multiple-stage integrating accelerometer
[DE85-006505] 23 p3935 N85-34388

Electronic imaging system and technique
[DE85-005740] 23 p3935 N85-34393

EML pulse ionization chamber systems for (222)Rn measurements
[DE85-012320] 23 p3970 N85-34610

PULTRUSION

Pultrusion process for fabrication of tethers (preliminary concepts)
11 p1646 N85-20371

PULVERIZING

U GRINDING (COMMINUTION)

PUMP IMPELLERS

Investigation of the HPFTP first stage impeller crack
[NASA-CR-171281] 07 p0977 N85-16208

Two-phase flow in centrifugal pumps
[BLL-CE-TRANS-8065-(9022.09)]
15 p2605 N85-26053

Optimum geometry of interblade passages in impellers of thermomolecular vacuum pump
16 p2764 N85-27058

PUMPS

NT CENTRIFUGAL PUMPS

NT FUEL PUMPS

NT ION PUMPS

NT JET PUMPS

NT MOLECULAR PUMPS

NT TURBINE PUMPS

NT VACUUM PUMPS

NT WINDPOWERED PUMPS

Photovoltaic pump systems
05 p0684 N85-14269

A study of wear characteristics due to pressure for hydraulic fixed displacement vane pumps
[AD-A146023] 06 p0814 N85-15169

Cavitation erosion resistant coatings for pumps
[PB85-120210/GAR] 09 p1300 N85-18167

Operational performance of the photovoltaic-powered grain mill and water pump at Tangaye, Burkina Faso (formerly Upper Volta)
[NASA-TM-86970] 13 p2128 N85-23243

Flat magnetohydrodynamic induction pump
17 p2939 N85-28145

Dependence of characteristics of centrifugal magnetohydrodynamic conduction pump on electrical conductance of end walls. Part 1: Experiment
17 p2939 N85-28146

Reciprocating magnetic refrigerator employing tandem porous matrices within a reciprocating displacer
[NASA-CASE-NPO-16257-1] 18 p3085 N85-29082

Fluidic angular velocity sensor
[NASA-CASE-NPO-16479-1-CU]
18 p3104 N85-29219

Remotely operable peristaltic pump
[NASA-CASE-MFS-28059-1] 18 p3116 N85-29288

Physiochemically controlled scour jet array system
[AD-D011688] 19 p3308 N85-30505

An analysis of the effects of active solar energy system control sensor degradation on system performance
[DE84-013023] 22 p3804 N85-33562

Combined cold compressor/ejector helium refrigerator
[DE85-006408] 23 p3925 N85-34326

Experimental lithium system
[DE85-013252] 24 p4094 N85-35382

PUNCHES

Experience with introduction of Finish perforation of precision parts for optical instruments
16 p2761 N85-27038

PURGING

Evacuate and backfill apparatus and method
[DE85-008018] 23 p3938 N85-34411

PURIFICATION

NT AIR PURIFICATION

Opportunities for space bioprocessing
02 p0150 N85-11018

Purification of biomaterials by phase partitioning
02 p0154 N85-11043

Evaluation of survival straws (pocket purifier)
[AD-A146240] 03 p0328 N85-12114

Development of a preprototype times wastewater recovery subsystem
[NASA-CR-171815] 03 p0388 N85-12480

Addendum: Development of a preprototype times wastewater recovery subsystem
[NASA-CR-171816] 03 p0388 N85-12481

Development of a preprototype times wastewater recovery subsystem: Appendices
[NASA-CR-171817] 03 p0388 N85-12482

Process for clarification of water
[DE85-007864] 17 p2923 N85-28023

Feasibility of melt casting strontium fluoride to produce high-density heat sources
[DE85-009429] 18 p3130 N85-29381

Plutonium metal preparation and purification at Los Alamos, 1984
[DE85-010732] 19 p3239 N85-30085

Flow cytometry of human embryonic kidney cells: A light scattering approach
20 p3503 N85-31778

New and revised methods of purifying mercuric iodide
[DE85-011684] 22 p3749 N85-33237

Method for removing oxide contamination from silicon carbide powders
[DE85-011648] 23 p3919 N85-34287

PURIFIERS

U PURIFICATION

PURITY

Chemistry Institute's advances in making extra-pure aluminum
10 p1443 N85-19093

Carbothermic production of silicon solar cells using high-purity starting materials
12 p1877 N85-21777

Low defect, high purity crystalline layers grown by selective deposition
[NASA-CASE-NPO-15813-1] 19 p3373 N85-30922

JPL in-house fluidized-bed reactor research
21 p3609 N85-32414

High-purity silicon crystal growth
21 p3612 N85-32444

Monosilane and disilane, 1984 report
[DE85-008776] 22 p3752 N85-33262

Method for preparing high purity vanadium
[DE85-008412] 23 p3913 N85-34242

An X-ray diffraction study of titanium oxidation
NASA-CR-176263] 23 p3915 N85-34264

PURPOSES
Broadening the debate 07 p0914 N85-15785
PURSUIT TRACKING
Effects of repetitive, small-spot, incoherent light flashes on pursuit tracking performance
[AD-A144848] 01 p0095 N85-10637
Space interception guidance with uncertain factors
13 p2042 N85-22781
Simple-motion pursuit-evasion differential games in the plane
[CSIR-TWISK-336] 14 p2412 N85-24874
Stochastic pursuit-evasion differential games in the plane
[CSIR-TWISK-343] 14 p2412 N85-24875
Pursuit tracking performance and flash disruption: The effects of training the non-dominant eye on target reacquisition
[AD-A153404] 17 p2999 N85-28541
PUSHBROOM SENSOR MODES
Imaging Science Panel. Multispectral Imaging Science Working Group joint meeting with Information Science Panel: Introduction 02 p0213 N85-11406
Application of pushbroom altimetry from space using large space antennas 14 p2230 N85-23817
INPE's line imaging camera: Preliminary results
[INPE-3476-PRE/719] 16 p2787 N85-27194
Investigations of the accuracy of the Digital Photogrammetry System (DPS), a rigorous three-dimensional compilation process for pushbroom imagery
[MBB-UA-753/83-O] 16 p2674 N85-27734
PWM (MODULATION)
U PULSE DURATION MODULATION
PYCNOMETERS
Pycnometer shaker
[PB85-174985] 20 p3460 N85-31491
PYLONS
Nacelle/pylon/wing integration on a transport model with a natural laminar flow nacelle
[NASA-TP-2439] 19 p3213 N85-29924
PYRAMIDS
Halfspace representations of extrusions, solids of revolution and pyramids
[DE84-015005] 01 p0104 N85-10700
Beamwidth control in pyramidal horns
[R-NIAS-27] 13 p2053 N85-22853
PYRANOMETERS
United States participation in International Energy Agency Task IX, Subtask (C): Pyranometry. 1984 participation
[DE85-009615] 18 p3110 N85-29256
PYRAZINES
NT AZINES
NT METHYLENE BLUE
PYRENEES MOUNTAINS (EUROPE)
Deep structure beneath the Pyrenees
04 p0524 N85-13351
Deep structure and seismicity in the Catalonia-Pyrenees region 04 p0524 N85-13352
Measurement of water equivalent of mountain snow cover — ARGOS system 14 p2327 N85-24386
PYRENES
Study of the kinetics of hydrogenation using aged catalysts
[DE85-010427] 19 p3230 N85-30025
PYREX (TRADEMARK)
U BOROSILICATE GLASS
PYRIDINES
Development of new and improved polymer matrix resin systems, phase 1
[NASA-CR-168595] 01 p0017 N85-10104
Chemically modified electrodes and related solution chemistry
[DE84-017110] 05 p0614 N85-13924
Electrochemistry and electrochemical methodology in molten salts
[AD-A149613] 12 p1799 N85-21284
The effect of Xe underlayers on the surface enhanced Raman scattering of pyridine on cold silver
[AD-A150109] 12 p1801 N85-21294
Evaluation of the PSP resin as a precursor of carbon
[ONERA-RT-11/1784-M] 16 p2744 N85-26932
New polymers for composites: A summary of research on polystyrylpyridines
[NASA-CR-175886] 17 p2933 N85-28106
PYRIMIDINES
NT MITOCHONDRIA
PYRITES
Improved solid-state laser sources, volume 2
[DE85-000759] 09 p1325 N85-18330
PYROELECTRICITY
Development of a polymer pressure gage with temperature compensation 03 p0365 N85-12340
Recording of acoustic wave in gaseous medium with thin-film pyroelectric transducers
15 p2525 N85-25571
Applications of piezoelectric and pyroelectric thin films: Opportunities for Langmuir-Blodgett technology
[AD-A149239] 15 p2659 N85-26406
Piezoelectric and pyroelectric polymers
16 p2756 N85-27008
PYROGRAPHALLOY
U COMPOSITE MATERIALS
U PYROLYTIC GRAPHITE
U REFRACTORY MATERIALS
PYROHELIOMETERS
Active Cavity Radiometer (ACR)
23 p3901 N85-34163
PYROLYSIS
HMX combustion modification
[AD-A145071] 01 p0024 N85-10149
The pyrolysis toxic gas analysis of aircraft interior materials
[AD-A146285] 03 p0328 N85-12115
Boron-nitrogen polymers. 1: Mechanistic studies of borazine pyrolyses
[AD-A146470] 06 p0771 N85-14933
Laser-assisted solar cell metallization processing
[NASA-CR-174213] 06 p0813 N85-15160
JPL in-house fluidized-bed reactor research
06 p0832 N85-15291
Aerosol reactor for silicon processing
06 p0832 N85-15292
Mechanism of soot formation
[AD-A146817] 07 p0922 N85-15841
Silazane precursors to silicon nitride
[AD-A146791] 07 p0931 N85-15899
Disclinations in carbon-carbon composites
[AD-A148290] 08 p1119 N85-17052
Laser schlieren, shock tube studies of high temperature hydrocarbon pyrolysis rates
[DE85-003314] 11 p1636 N85-20303
Synthesis, static and reactive characterization of supported organometallics
[DE85-004285] 12 p1806 N85-21340
Low cost, sprayed CuInSe2 solar cell research
[DE85-003467] 12 p1861 N85-21799
Methods/materials matrix of ultimate disposal techniques for spilled hazardous materials
[PB85-116853] 12 p1885 N85-21833
Shock tube study of the fuel structure effects on the chemical kinetic mechanisms responsible for soot formation, part 2
[NASA-CR-174880] 15 p2504 N85-25444
Thermolysis of 4-methyl-4-(1-propenyl)malonyl peroxide: Mechanistic limits to chemiluminescence efficiency
[AD-A151567] 15 p2505 N85-25452
Studies of the combustion of model fuels with low hydrogen content (pyrolysis of polycyclic aromatics-detection of soot precursors)
[DE85-005422] 15 p2521 N85-25541
Evaluation of the PSP resin as a precursor of carbon
[ONERA-RT-11/1784-M] 16 p2744 N85-26932
Preparation of silicon carbide-silicon nitride fibers by the pyrolysis of polycarbosilazane precursors
[NASA-TM-86505] 17 p2933 N85-28107
Sol-gel processing of lead zirconate titanate films
[ATR-85(8343)-2] 18 p3073 N85-29010
Structure-property relationships in polymeric matrix materials
[AD-A153929] 18 p3080 N85-29050
Combustion characterization of coals for industrial applications
[DE85-010673] 19 p3228 N85-30014
Supercritical solvent extraction of lignite to form carbonaceous chars
[DE85-010159] 19 p3229 N85-30019
Spray pyrolysis as a synthetic tool
[AD-A153891] 19 p3234 N85-30047
Comparison of isothermal kerogen decomposition results using reactors with different heat-up rates
[DE85-008563] 19 p3237 N85-30068
Processable and stable conductive polymers
[AD-D011684] 19 p3249 N85-30143
Flash pyrolysis of biomass with reactive and non-reactive gases
[DE85-010962] 19 p3306 N85-30496
Fuel-rich catalytic combustion: A soot-free technique for in situ hydrogen-like enrichment
[NASA-TP-2498] 20 p3423 N85-31244
Polyesters: A review of the literature on products of combustion and toxicity
[NBSIR-85-3139] 20 p3433 N85-31298
A fluidized-bed reactor for silane pyrolysis
21 p3609 N85-32413
Modeling of the silane FBR system
21 p3609 N85-32415
Silicon production in an aerosol reactor
21 p3609 N85-32416
Thermal reactions of aromatics with CaO
[DE85-010888] 22 p3742 N85-33193
Oxygen analyzer
[DE85-008002] 23 p3935 N85-34332
PYROLYTIC GRAPHITE
X-ray polarization in highly oriented pyrolytic graphite
[DE84-015573] 05 p0613 N85-13917
PYROLYTIC MATERIALS
NT PYROLYTIC GRAPHITE
Non-oxide ceramics: A new class of engineering materials 02 p0179 N85-11199
PYROMETALLURGY
Temperature, velocity, and species mapping in an induction plasma
[DE85-004005] 15 p2512 N85-25499
PYROMETERS
NT THERMOCOUPLE PYROMETERS
Dynamic gas temperature measurement system
02 p0141 N85-10958
Seven-wavelength pyrometer for determining surface temperature of ablation materials
[NASA-TM-77832] 14 p2305 N85-24288
Investigation of non-intrusive radiometers for entrained gasifier temperature measurement, revision 3
[DE85-011795] 23 p3934 N85-34325
PYROMETRY
U TEMPERATURE MEASUREMENT
PYROPHORIC MATERIALS
Pyrophoric alkylaluminum compounds in decoy flare
[FOA-C-20562-E4] 18 p3078 N85-29039
Review of zirconium-zircaloy pyrophoricity
[DE85-011169] 23 p3916 N85-34279
PYROTECHNICS
Effect of oxide coated thickness on thermal ignition of titanium-based pyrotechnics
[DE84-013061] 04 p0481 N85-13066
Laser for determining the ignition conditions of a pyrotechnic mixture
[FOA-C-20542-D1] 04 p0506 N85-13230
Flame-resistant materials for use in pyrotechnic safety clothing
[AD-A146857] 07 p0931 N85-15901
Modelling the thermal explosion phenomenon in solid propellants: The case of fixed and variable temperatures 08 p1117 N85-17044
CVD boron on calcium chromate powder
[DE85-000214] 09 p1299 N85-18158
Study of bridgewire size and pyrotechnic density relationships on all-fire levels
[DE84-016946] 09 p1302 N85-18177
NATO AC/310 activities report on NATO STANAG 4170 and Allied Ordnance Publication 7 (Manual of Tests for Qualification of Explosive Materials for Military Use)
[AD-P004341] 10 p1454 N85-19165
Measurement of the expension velocity of an aerosol cloud during pyrotechnical dispersion
[ISL-R-125/83] 14 p2303 N85-24282
Surveillance program for the dissection and analysis of explosive and pyrotechnic components
[DE85-006105] 16 p2757 N85-27016
Short Wavelength Chemical Laser (SWCL) Workshop
[AD-A151959] 16 p2790 N85-27211
Evaluation of pyrotechnic fire suppression system for six pyrotechnic compositions
[AD-A152995] 17 p2937 N85-28130
Fully redundant mechanical release actuator
[NASA-CASE-LAR-13196-1] 18 p3116 N85-28287
Ariane launcher system. Pyrotechnics subsystem: Definition of chains and pyrotechnic components
[CNES-84/CT/DRT/SST/SE/242(1)]
20 p3398 N85-31081
PYROXENES
NT ENSTATITE
Minor elements in relict olivine grains of deep-sea spheres: Match with Mg-rich olivines from C2 meteorites 06 p0883 N85-15810
PYROXYLIN
U CELLULOSE NITRATE
PYRRHOTITE
NT TROILITE
PYRROLES
NT CARBAZOLES
NT TRYPTOPHAN
Chemical derivatization of an array of three gold microelectrodes with polypyrrole: Fabrication of a molecule-based transistor
[AD-A146221] 03 p0359 N85-12304
Potential dependence of electrical conductivity and chemical charge storage of poly(pyrrole) films on electrodes
[AD-A148513] 08 p1122 N85-17075
Polymer blends for use in photoelectrochemical cells for conversion of solar energy to electricity
[DE85-011602] 22 p3752 N85-33258
P3V AIRCRAFT
U P-3 AIRCRAFT
P78-2 SATELLITE
U SCATHA SATELLITE

Q

Q DEVICES
Confinement and heating of high beta plasmas with emphasis on compact toroids
[DE85-011459] 24 p4155 N85-35761
Q FACTORS
Comparative descriptions of software quality measures
[GMD-STUDIES-81] 01 p0102 N85-10676
Influence of scattering on Q in the lithosphere
[AD-A149318] 10 p1515 N85-19563
Piezoelectric filter with low-Q inductances
13 p2070 N85-22932
Q SWITCHED LASERS
Efficiency of photoelectric conversion of short radiation pulses 03 p0348 N85-12240
Determination of the drag of free flying particles in supersonic flow with a pulsed laser
12 p1773 N85-21129
Investigation of plasma processes in electronic transition lasers
[AD-A149662] 12 p1834 N85-21506
Low jitter trigger for an excimer laser
[DE85-005732] 13 p2097 N85-23060
Developement of a theoretical model to describe the interaction between electric discharge and supersonic flow of a pulsed CO laser
[DFVLR-FB-84-45] 14 p2310 N85-24301
Q VALUES
Study of proton and neutron activation of metal samples in low Earth orbit
[NASA-CR-171596] 21 p3558 N85-32130
QCD
U QUANTUM CHROMODYNAMICS
QSO (RADIO SOURCES)
U QUASARS
QUADRATIC EQUATIONS
Quadratic spaces over discrete Hodge algebras
16 p2853 N85-27593
An overview of latest model reduction and control methods of large flexible space structures
20 p3414 N85-31191
Frequency domain control design of large space structures: A practical approach
20 p3415 N85-31192
A new problem in mathematical physics associated with the problem of coherent phase transformation
21 p3696 N85-32976
QUADRATIC PROGRAMMING
A research program in active control/aeroelasticity in the JIAFS at NASA Langley Research Center
[NASA-CR-174052] 02 p0148 N85-11001
A sequential quadratic programming algorithm for solving large, sparse nonlinear programs
[AD-A145854] 03 p0407 N85-12597
A dual quadratic programming algorithm
[AD-A147237] 07 p1031 N85-16547
Automatic control design procedures for restructurable aircraft control
[NASA-CR-172489] 12 p1780 N85-21173
User's guide for NPSOL (Version 2.1): A FORTRAN package for quadratic programming
[AD-A150078] 12 p1916 N85-22028
A decomposition procedure for convex quadratic programs
[AD-A151732] 16 p2854 N85-27595
A quadratic programming algorithm
[AD-A153476] 18 p3168 N85-29631
Model building and practical aspects of nonlinear programming
[AD-A155720] 22 p3829 N85-33711
QUADRATURE APPROXIMATION
U QUADRATURES
QUADRATURES
Oscillatory integrals by Hermite interpolatory rules
[CSIR-TWISK-301] 01 p0106 N85-10725
A lumped mass finite element method with quadrature for a nonlinear parabolic problem
[CTH-MATH-1984-22] 05 p0719 N85-14615
Calculation of cumulative distributions and detection probabilities in communications and optics
[AD-A147781] 08 p1215 N85-17650
A note on the use of polynomial transformations in evaluating singular integrals
[MATHEMATICS-RESEARCH-165]
12 p1920 N85-22053
The implementation of the Tanh transformations in the evaluation of singular integrals
[MATHEMATICS-RESEARCH-171]
12 p1920 N85-22054
Extrapolation methods for multi-dimensional quadrature of singular and regular integrand functions
[DE85-009665] 18 p3172 N85-29655
QUADRUPOLE LENSES
U MAGNETIC LENSES
QUADRUPOLE NETWORKS
RFQ modeling computer program
[DE85-012665] 24 p4140 N85-35661
QUADRUPOLES
Theory of nuclear magnetic relaxation
[AD-P003911] 01 p0032 N85-10197
Linac quadrupole connections
[DE84-014694] 01 p0118 N85-10810
Calculated parameters for the initial part of an accelerator with high-frequency quadrupole focusing
[RAE-TRANS-2122] 07 p1040 N85-16600
Crossing point conditions, quadrupole gradients and drift space lengths
[DE85-003223] 11 p1721 N85-20825
Ion quadrupole effects in spectral line broadening
[DE85-001504] 11 p1730 N85-20879
A computer controlled mass spectrometer system for investigating the decomposition of non-metallic materials under atmospheric conditions 12 p1948 N85-22237
Radio frequency quadrupole and alternating phase focusing methods used in proton linear accelerator technology in the USSR
[AD-A150830] 14 p2418 N85-24916
Moments in particle-in-cell simulations
[DE85-010792] 19 p3358 N85-30803
Mechanical considerations in cw linacs
[DE85-010728] 19 p3363 N85-30850
Proposed use of the radio-frequency quadrupole structure to funnel high-current ion beams
[DE85-010746] 19 p3364 N85-30857
Fabrication and test of modified quadrupole mass spectrometer
[AD-A155186] 21 p3590 N85-32312
Electron trajectories in a combined wiggler and alternating gradient quadrupole field
[DE85-010727] 22 p3842 N85-33794
QUALIFICATIONS
Certification of advanced systems
06 p0753 N85-14829
NATO AC/310 activities report on NATO STANAG 4170 and Allied Ordnance Publication 7 (Manual of Tests for Qualification of Explosive Materials for Military Use)
[AD-P004341] 10 p1454 N85-19165
IHE material qualification tests description and criteria
[DE85-004649] 13 p2040 N85-22770
Qualification of the T2 wind tunnel in cryogenic operation. B: Flow fluctuations, particle detection and qualification
[NASA-TM-77782] 14 p2227 N85-23806
Qualification needs for advanced integrated aircraft
[NASA-TM-86731] 22 p3729 N85-33119
QUALITATIVE ANALYSIS
Qualitative process theory
[AD-A148967] 10 p1543 N85-19729
Qualitative analysis of sign-bit processing
[AD-A154776] 21 p3671 N85-32804
Direct determination of metals in organic matrices by Inductively Coupled Plasma-Atomic Emission Spectrometry (ICP-AES)
[DE85-012015] 23 p3911 N85-34233
QUALITY
NT AIR QUALITY
NT ENVIRONMENTAL QUALITY
NT RIDING QUALITY
NT WATER QUALITY
Quality assurance for environmental analytical chemistry, 1983
[DE84-016045] 09 p1349 N85-18489
Characteristics of quality data
[DE85-001203] 10 p1566 N85-19889
Studies in quality improvement 2. An analysis for unreplicated fractional factorials
[AD-A153539] 18 p3169 N85-29640
The interpretation of flying qualities requirements for flight control system design
[NASA-CR-177942] 22 p3730 N85-33125
Acoustic scaling: The development of improved instrumentation
[BBC-RD-1985/7] 24 p4145 N85-35694
QUALITY CONTROL
Measurement assurance programs. Part 1: General introduction
[PB84-217868] 01 p0051 N85-10339
ICAM (Integrated Computer Aided Manufacturing) conceptual design for computer-integrated manufacturing. Volume 4, part 6: Task d. Quality assurance/quality control/technical requirement/tasks, quality assurance modeling and analysis, quality assurance program management standard recommendations (ISP)
[AD-A144891] 01 p0056 N85-10372
Comparative descriptions of software quality measures
[GMD-STUDIES-81] 01 p0102 N85-10676
Avionics integrity program (Avip). Volume 3: Program cost assessment - environmental stress screening and diagnostic techniques
[AD-A145644] 02 p0139 N85-10942
Avionics integrity program (Avip). Volume 1: Proc:rement phase issues: Design, manufacturing, and integration
[AD-A145651] 02 p0139 N85-10943
Advanced manufacturing development of a composite empennage component for L-1011 aircraft
[NASA-CR-165885] 02 p0170 N85-11141
A method for evaluating the contamination of steel in relation to the solidification curve
[BLL-M-35735-(5828.4)] 02 p0175 N85-11171
Investigation of the application of the marginal tension technique to test electronic devices, phase 3
[ESD-11-301] 02 p0208 N85-11360
Editorial urges improved aviation repair work quality
03 p0310 N85-12004
Development of a rapid test method for asphalt concrete content determination in hot-mix paving mixtures
[PB84-218892] 03 p0342 N85-12204
Prediction of weld defects using welding condition data
[VTT-RR-264] 03 p0370 N85-12359
Automating software design metrics
[AD-A145869] 03 p0407 N85-12598
Designing optimal AOQL sampling plans a computerized approach
[AD-A146288] 03 p0413 N85-12639
Test report no. 17.208: Statistics of the basic characteristics of carbon-epoxy composites
[DGT-23.426/A] 04 p0468 N85-12979
Quality assurance of composite materials, test report no. 45-849/F 04 p0469 N85-12981
Quality organization — quality control
[CNES-NT-106] 04 p0511 N85-13257
The ESA product assurance specification system: Explanatory note 04 p0511 N85-13259
Toward a non-bureaucratic approach to quality assurance in data processing
[DE84-007484] 04 p0550 N85-13497
Vandenberg space shuttle launch complex
[S-HRG-98-1075] 05 p0601 N85-13833
Statement of Edward C. Aldridge, Jr., Under Secretary of the Air Force, Department of the Air Force, accompanied by Lieutenant General Robert W. Bazley, Inspector General and Brigadier General Donald J. Kutyna, Director of Space Systems and Command, Control and Communications, Deputy Chief of Staff, Research, Development and Acquisition 05 p0601 N85-13834
Statement of Honorable James M. Beggs, Administrator, National Aeronautics and Space Administration
05 p0601 N85-13835
Quality assurance in the Antares Laser Fusion Construction Project
[DE84-015493] 05 p0640 N85-14104
Laboratory investigations 05 p0666 N85-14281
The effects of task structure on time-sharing efficiency and resource allocation optimality
05 p0711 N85-14562
Acceptance-testing procedures for air-line supplied-air suits
[DE84-016980] 05 p0712 N85-14569
Fabrication and quality assurance processes for superhybrid composite fan blades
[NASA-TM-83354] 06 p0763 N85-14882
Quality control of integrated circuits by parametric identification methods 06 p0796 N85-15065
Laser-guided measuring system for precisioning device 06 p0816 N85-15179
The effects of software quality control and baseline management on the acquisition of computer programs
[AD-A147051] 07 p1024 N85-16502
A survey and evaluation of software quality assurance
[AD-A147552] 07 p1026 N85-16510
An analysis of the effect of process controls on productivity and weapon system costs in DoD procurement
[AD-A147496] 07 p1052 N85-16678
A study of Air Force Quality Circle program effectiveness as viewed through facilitator's perceptions
[AD-A147633] 08 p1170 N85-17377
Improvements under way at Gorkiy airport
09 p1278 N85-18040
Quality control in soil compaction by behaviours of exciter
[AD-P004295] 09 p1408 N85-18872
Thematic Mapper: Design through flight evaluation
[E85-10078] 10 p1504 N85-19492
Robotics at Savannah River site: Activity report
[DE85-003657] 11 p1648 N85-20383
A quality control experiment in a real time multiprocessor operating system: The Mara 860 — software testing
11 p1702 N85-20707
An exact solution to the 2 point OC (Operating-Characteristic) curve determination
[AD-A148120] 11 p1708 N85-20746
Quality of scientific and engineering data
[DE85-000294] 11 p1739 N85-20936

Transportation
[JPRS-UTR-85-004] 12 p1769 N85-21105
Aviation repair plant directors on quality control measures 12 p1769 N85-21106
Development and evaluation of a procedure for the rapid analysis of fresh concrete
[AD-A149741] 12 p1868 N85-21703
A statistical approach to vendor selection
[AD-A149781] 12 p1950 N85-22249
Characterization standards for solid propellant rocket motors
[AD-A150250] 13 p2013 N85-22627
Measurement of internal thermal resistance for quality control of semiconductor devices
13 p2074 N85-22953
Ultrasonic non-destructive testing technique
14 p2316 N85-24313
Practical surface methods 14 p2316 N85-24314
Administration chief on air traffic control improvements
15 p2460 N85-25193
Quality control of radioelectronic apparatus components on basis of external characteristics in frequency domain
15 p2529 N85-25590
Detection and location of partial discharges in transformer windings using electrical methods
15 p2551 N85-25750
Welding technology and organisation in steel construction 15 p2566 N85-25828
Nondestructive tests of ceramic components for aircraft turbines 16 p2709 N85-26718
Cost prediction model for various payloads and instruments for the Space Shuttle Orbiter
[NASA-CR-175781] 16 p2729 N85-26842
A framework for software development
[AD-A152067] 16 p2847 N85-27551
Lidar ER2 (ozone). Crystal characterization for harmonic conversion — laser systems
[CERT-2/6129-00] 16 p2872 N85-27717
Examination of steels by chemical analysis for quality assurance
[BLL-BISI-TRANS-22068-(9022.06)]
17 p2929 N85-28074
Proper quality of anticorrosion work no matter how bad the atmospheric conditions
[BLL-BISI-TRANS-22080-(9022.06)]
17 p2975 N85-28383
Statistical models used in analyzing the quality of welded tubes
[BLL-BISI-TRANS-22232-(9022.06)]
17 p2976 N85-28384
Principal quality assurance measures in the manufacture of HF-welded high-pressure linepipe
[BLL-BISI-TRANS-21690-(9022.06)]
17 p2976 N85-28389
Integrating quality assurance and research and development
[DE85-007974] 17 p2976 N85-28392
Initial imperfection surveys on conical shells at Hoechst AG
[VTH-LR-407] 17 p2981 N85-28429
Quality assurance for RESOLVE (Research on Operations-Limiting Visual Extinction). A visibility study in the California desert
[AD-A152383] 17 p2992 N85-28494
Effects of inspection errors on curtailed Dorfman-type procedures
[AD-A152376] 17 p3024 N85-28699
Statistical effects of imperfect inspection sampling. Part 2: Double sampling, link sampling and grading
[AD-A152377] 17 p3024 N85-28700
Impurity control and vacuum pumping system design and analysis for next-generation Tokamaks
[DE85-009291] 17 p3041 N85-28815
Principles of quality assurance of chemical measurements
[PB85-177947] 18 p3072 N85-28997
Practical real-time quality control of antimisting kerosene
[DE/FAA/CT-85/1] 18 p3083 N85-29072
Specification of software quality attributes, volume 1
[AD-A153988] 18 p3163 N85-29593
Specification of software quality attributes. Volume 2: Software quality specification guidebook
[AD-A153989] 18 p3163 N85-29594
Specification of software quality attributes. Volume 3: Software quality evaluation guidebook
[AD-A153990] 18 p3163 N85-29595
Studies in quality improvement 2. An analysis for unreplicated fractional factorials
[AD-A153539] 18 p3169 N85-29640
Generic data entry quality assurance tool
[DE85-008359] 18 p3200 N85-29852
Improvements in safety testing of lithium cells
20 p3444 N85-31379
Design evaluation of high reliability lithium batteries
20 p3444 N85-31380
Philosophy of nondestructive control in aeronautics quality control. Knowledge of and improvements to nondestructive test safety
[SNIAS-851-551-101] 20 p3465 N85-31522
NASA/GSFC TOPEX gravity model operations group
20 p3492 N85-31709
Quality analysis 21 p3668 N85-32785
An automated quality assurance surveillance plan for ADP (Automated Data Processing) operations under the Navy's commercial activities program
[AD-A154767] 21 p3671 N85-32802
Current requirements for the design and maintenance against corrosion of UK military aircraft
22 p3750 N85-33244
EML pulse ionization chamber systems for (222)Rn measurements
[DE85-012320] 23 p3970 N85-34610
Quality assurance considerations for the implementation of a pulsed power R and D project
[DE85-012357] 24 p4148 N85-35720
Aeronautical Systems Division Manufacturing/Quality assurance orientation
[AD-A156128] 24 p4164 N85-35817

QUALITY FACTORS
U Q FACTORS

QUANTILES
Spline methods for approximating quantile functions and generating random samples
[NASA-TP-2389] 07 p1035 N85-16565
A kernel type estimator of a quantile function from right-censored data
[AD-A148753] 09 p1374 N85-18635
Scrawl plots, and letter and bletter strips
[DE85-001409] 11 p1707 N85-20739
Comments on estimating quantiles for Gaussian functionals by simulation
[AD-A154302] 19 p3348 N85-30750
On the confidence limits for Weibull reliability and quantiles: The case of maximum likelihood estimation from small size censored samples
[REPT-84-RR-345] 20 p3521 N85-31896

QUANTITATIVE ANALYSIS
Determination of halogens and sulfur in organic compounds and polymers by combustion-ion chromatography
[DE84-016186] 05 p0614 N85-13921
A study of the chemical interaction of gases with activated carbon
[AD-A147342] 07 p0923 N85-15846
Impact of aircraft emissions on air quality in the vicinity of airports. Volume 4. Nitrogen dioxide and hydrocarbons
[AD-A148253] 08 p1180 N85-17436
Background detection and correction in multicomponent analysis
[AD-A148251] 08 p1212 N85-17628
Multicomponent calibration and quantitation methods
[AD-A148252] 08 p1212 N85-17629
Quantitative determination of compound classes in jet turbine fuels by high performance liquid Chromatography/Differential refractive index detection: Part 2
[AD-A149298] 11 p1613 N85-20144
Interlaminar fracture toughness in resin matrix composites
[AD-A150565] 13 p2015 N85-22640
Trace metal determinations in nickel-plating baths by polarographic methods
[DE85-007064] 15 p2511 N85-25488
Procedure for certifying quantity of volatile organic compounds emitted by paint, ink and other coatings
[PB85-159044] 15 p2520 N85-25537
Quantitative analysis of defects in silicon-characterization of UCP, HAMCO, and microcrystalline material
[NASA-CR-175968] 18 p3079 N85-29046
Rapid rate-kinetic turbidometric assay for quantitation of antiviral complement-fixing antibodies
[AD-A153644] 18 p3152 N85-29516
Application of the reference intensity method to coal analysis
[DE85-009528] 19 p3228 N85-30015
Quantitative passive technique for assay of near-surface tritium in materials
[DE85-010661] 19 p3360 N85-30833
Rapid estimation of concentration of aromatic classes in middistillate fuels by high-performance liquid chromatography
[NASA-TP-2495] 20 p3434 N85-31307
Quantitative analysis in megageomorphology
21 p3603 N85-32376
Quantitative analysis of geomorphic processes using satellite image data at different scales
21 p3604 N85-32380
Quantitative geomorphologic studies from spaceborne platforms 21 p3604 N85-32381
Quantitative determination of mineral composition by powder X-ray diffraction
[DE85-011654] 22 p3760 N85-33301
Quantitative analysis of flare accelerated electrons through their hard X-ray and microwave radiation
[SH-1.2-7] 23 p3891 N85-34742

QUANTITY
U AMOUNT

QUANTIZATION
U MEASUREMENT

QUANTIZER
U COUNTERS

QUANTUM CHEMISTRY
Application of quantum chemistry of atmospheric chemistry
[AD-A147035] 07 p0922 N85-15843
Applications of molecular dynamics to the study of shock-induced chemistry
[AD-A148017] 08 p1121 N85-17086
Quantum Monte Carlo for molecules
[AD-A148159] 08 p1227 N85-17727
Atomic, Molecular and Solid-State Theory, and Computational Quantum Chemistry, part 1
[DE85-009401] 20 p3526 N85-31929

QUANTUM CHROMODYNAMICS
NT INSTANTONS
Research program in theoretical high-energy physics
[DE84-013717] 01 p0119 N85-10817
Gauge Theory on a Lattice, 1984: Proceedings
[DE84-014856] 02 p0291 N85-11892
Particle physics
[DE84-013834] 05 p0727 N85-14673
Very high energy probes of the quark-gluon plasma
[DE84-016992] 09 p1392 N85-16763
Cosmic axions
[DE85-001330] 09 p1418 N85-18044
Stochastic methods for the description of multiparticle production
[DE84-009981] 10 p1556 N85-19810
Experimental and theoretical high energy physics
[DE85-000644] 11 p1726 N85-20858
Axions in astrophysics and cosmology
[DE85-002720] 11 p1763 N85-21094
Jet topologies in hadron-hadron collisions
[DE85-001328] 12 p1929 N85-22119
Research in theoretical nuclear physics
[DE85-004349] 12 p1932 N85-22137
Resonances in photon-photon scattering
[DE85-004607] 14 p2419 N85-24928
Lattice Monte Carlo calculations of finite temperature QCD
[DE85-004035] 14 p2431 N85-24992
Space station as quark matter factory
[DE85-004606] 15 p2685 N85-26585
Discrete foundation for physics and experience
[DE85-008172] 16 p2872 N85-27720
Configuration space Faddeev calculations
[DE85-005813] 16 p2872 N85-27721
Photon structure function: Theory
[DE85-008064] 17 p3031 N85-28745
Measuring structure functions at SSC energies
[DE85-007515] 17 p3031 N85-28746
Experimental studies of diffractive phenomena
[DE85-006812] 17 p3031 N85-28749
Elementary particle theory
[DE85-006803] 17 p3034 N85-28771
Heavy quark production processes in QCD
[DE85-007240] 17 p3036 N85-28779
Some comments on SSC physics
[DE85-008444] 18 p3179 N85-29712
A comprehensive study of psi meson production
[DE85-008094] 18 p3180 N85-29718
Soliton matter as a model of dense nuclear matter
[DE85-009937] 19 p3359 N85-30825
Monte Carlo sampling strategies for lattice gauge calculations
[DE85-010756] 19 p3377 N85-30948
Toward the question of multi-quark configurations in nuclei 21 p3691 N85-32929
Spatial parity violation in elastic neutron-nuclei interaction channel 21 p3691 N85-32932
Quark structure of nuclei
[DE85-010781] 22 p3842 N85-33795
Duality of two-point functions for confined non-relativistic quark-antiquark systems
[DE85-012334] 23 p3971 N85-34618
Very high energy probes of the quark-gluon plasma
24 p4147 N85-35708
High energy physics at Tufts University
[DOE/ER-40085/7] 24 p4152 N85-35744
QCD-motivated description of very high energy particle interactions
[HE-1.2-2] 24 p4171 N85-35881

A cosmic ray super high energy multicore family event. 2: Structure and fragmentation characteristics of the jets
[HE-3.4-2] 24 p4181 N85-35931
QCD analysis of neutrino charged current structure function F2 in deep inelastic scattering
[HE-5.3-23] 24 p4207 N85-36114

QUANTUM COUNTERS
Noise tolerance of digital demodulator for complex signal system employing binary quantization
13 p2070 N85-22829
Lateral distribution on charged particles in EAS
[HE-4.3-15] 24 p4192 N85-36009

QUANTUM EFFICIENCY
Preliminary evaluation of RCA C83036E prototype photomultiplier
[DE84-016894] 04 p0496 N85-13165
Mercuric iodide photodetectors for scintillation spectroscopy
[DE85-001437] 10 p1437 N85-19056
Advanced high-efficiency concentrator cell
[DE85-000525] 14 p2351 N85-24533
A quantitative image evaluation study of a concurrent photon amplification treated emulsion
[AD-A151831] 15 p2560 N85-25798
Photon-counting image sensors for the ultraviolet
[NASA-CR-176062] 20 p3458 N85-31478

QUANTUM ELECTRODYNAMICS
Linear conformal gravitation 02 p0265 N85-11735
ASP: A new PEP experiment to measure single photons
[DE84-015732] 04 p0560 N85-13563
Implications of the chiral anomaly for quantum Hall effect devices
[NUB-2662] 05 p0629 N85-14029
Topics in high resolution spectroscopy of stored ions
[DE85-002093] 06 p0861 N85-15470
A superconducting quantum current standard
[NPL-QU-67] 08 p1224 N85-17710
Quantum noise effects in single-mode injection lasers
[FUB-11-1984] 09 p1327 N85-18336
Elementary particle theory
[DE85-006603] 17 p3034 N85-28771
The standard model and beyond
[DE85-010239] 19 p3362 N85-30847
Evaluation of parameters for particles acceleration by the zero-point field of quantum electrodynamics
[OG-8.2-16] 23 p4020 N85-34912

QUANTUM ELECTRONICS
Research activities of the Illinois University Coordinated Science Laboratory
[AD-A145569] 03 p0449 N85-12856
Electronics research at the University of Texas at Austin
[AD-A146900] 07 p0947 N85-15998
Solid state research
[NASA-CR-174285] 07 p1048 N85-16656
Quantum noise and excess noise in optical homodyne and heterodyne receivers
[AD-A148296] 08 p1157 N85-17303
Solid state research
[AD-A147640] 08 p1225 N85-17714
Annual report on electronics research at the University of Texas at Austin
[AD-A150836] 14 p2415 N85-24901
Joint services electronics program
[AD-A154348] 19 p3375 N85-30939
Solid state research
[AD-A154783] 21 p3709 N85-33025
Conferences of quantum-radiooptics section
22 p3773 N85-33380
Joint services electronics program
[AD-A154748] 23 p3927 N85-34336

QUANTUM MECHANICS
NT QUANTUM ELECTRODYNAMICS
Quantum characteristics of kinetic fracturing of solids
02 p0265 N85-11732
The identification of the scientific community's choice criteria in the history of scientific research: The case of quantum mechanics
[NOTA-INTERNA-797] 02 p0291 N85-11893
Theory of non-linear index of refraction of compound semiconductors
[DE84-013860] 04 p0569 N85-13626
Refractive index of ternary and quaternary compound semiconductors below the fundamental absorption edge: Linear and nonlinear effects
[DE84-012325] 05 p0640 N85-14105
Semiconductor superlattice photodetectors
[NASA-CR-174347] 09 p1397 N85-18791
Reduction of the wavepacket: How long does it take?
[DE84-016778] 09 p1400 N85-18815
Asymmetrical harmonic oscillator and fine-structure constant
[FUB-9-1984] 09 p1401 N85-18818
Accidental degeneracies, hidden supersymmetries, and spectrum-generating superalgebras
[DE85-003547] 11 p1736 N85-20930
Macroscopic quantum tunnelling in a current biased Josephson junction
[DE85-004603] 13 p2164 N85-23424
Parton dynamics in hadronic processes
[DE85-006072] 14 p2418 N85-24922
Soliton energetics in extended Peierls-Hubbard models: A quantum Monte Carlo study
[DE85-005409] 14 p2429 N85-24981
Identification and properties of molecular systems of potential use in solar-pumped lasers
[NASA-CR-175804] 16 p2789 N85-27207
Shallow impurity cluster states in n-type semiconductors
[INPE-3495-PRE/732] 16 p2869 N85-27699
Discrete foundation for physics and experience
[DE85-008172] 16 p2872 N85-27720
Configuration space Faddeev calculations
[DE85-005813] 16 p2872 N85-27721
Mutli-particle quantum mechanics obeying fractional statistics
[DE85-007830] 16 p2873 N85-27723
Memory function for cyclotron resonance of two-dimensional electron systems
[AD-A152632] 17 p3029 N85-28731
Nonrelativistic theory of heavy-ion collisions
[DE85-007538] 17 p3031 N85-28747
The strategy for time dependent quantum mechanical calculations using a Gaussian wave packet representation of the wave function
[AD-A152709] 17 p3046 N85-28845
On the propagation speed in relativistic quantum mechanics
[CWI-AM-R8410] 17 p3046 N85-28848
Adiatatic approach in the theory of polyatomic photodissociation: Application to C2N2
[DE85-008515] 18 p3071 N85-28996
Constructing a bit string universe
[DE85-006317] 18 p3197 N85-29829
Quantum effects in linear collider scaling laws
[DE85-009846] 19 p3363 N85-30851
Measurement problem in PROGRAM UNIVERSE
[DE85-008179] 19 p3378 N85-30959
Physical concepts in the development of constitutive equations 20 p3467 N85-31537
Atomic, Molecular and Solid-State Theory, and Computational Quantum Chemistry, part 1
[DE85-009401] 20 p3526 N85-31929
Lattice theory for nonspecialists, lecture notes
[NIKHEF-H/84-11] 20 p3539 N85-32019
Earth Albedo and the orbit of LAGEOS
[NASA-TM-86210] 21 p3558 N85-32131
Theoretical studies of structure and stability of hydrates of atmospheric sulfur species 21 p3650 N85-32684

QUANTUM NUMBERS
Proposal for the systematic naming of mesons and baryons
[DE85-008453] 17 p3035 N85-28773
Constructing a bit string universe
[DE85-006317] 18 p3197 N85-29829
Measurement problem in PROGRAM UNIVERSE
[DE85-008179] 19 p3378 N85-30959

QUANTUM STATISTICS
A measurement of the intensity of the cosmic background radiation at 3.9 cm
13 p2206 N85-23681
Boson degrees of freedom in Fermion many-body systems
[DE85-006997] 16 p2863 N85-27660
Spin-polarized quantum systems
[DE85-006914] 16 p2864 N85-27667

QUANTUM THEORY
Interactions in localization
[NOTA-INTERNA-815] 02 p0279 N85-11818
Toward unification of elementary particle physics and cosmology in 10-dimensions
[DE84-013950] 05 p0727 N85-14674
Stability questions for gravity in 4 and higher dimensions 05 p0734 N85-14716
Theory and applications of two-photon quantum optics
[AD-A147382] 07 p1044 N85-16631
Two-photon coherent state light - its generation and potential applications
[AD-A148245] 08 p1166 N85-17356
Hydrodynamic flow structures in quantum field theory
[DE84-015513] 09 p1401 N85-18817
Quasiparticle aggregation in the Fractional Quantum Hall Effect
[DE85-001574] 10 p1565 N85-19868
Ultraviolet divergences and supersymmetric theories
[DE85-001649] 11 p1729 N85-20875
Stable measures and processes in statistical physics
[AD-A149592] 12 p1926 N85-22098
Study of 1/f noise in solids
[AD-A151069] 14 p2428 N85-24972
Eigenvalue approximation methods for quantum lattice Hamiltonians 16 p2858 N85-27627
Quantum statistical theory of vibrational dynamics in a laser-driven admolecule-surface system
[AD-A152022] 16 p2872 N85-27719
The enhancement of molecular fluorescence and photochemistry by small metal particles
[AD-A152740] 17 p2919 N85-27994
Quantum model of dephasing-enhanced laser desorption: Master equation approach
[AD-A153769] 18 p3112 N85-29269
Research in the theory of condensed matter and elementary particles
[DE85-010447] 20 p3531 N85-31968
Bergson and the unification of the sciences
[DE85-009961] 20 p3538 N85-32018
Activities report of the Department of Astrophysics
20 p3546 N85-32064

QUANTUM WELLS
Strained-layer superlattices and strain-induced light holes
[DE85-003675] 14 p2431 N85-24990
Optical properties of heterostructures and superlattices
[AD-A156243] 24 p4162 N85-35802

QUARKS
Quark models of hadronic interactions
[DE84-013787] 04 p0561 N85-13570
Measurements of the A-dependence of deep-inelastic electron scattering from nuclei
[DE84-013865] 05 p0728 N85-14678
Very high energy probes of the quark-gluon plasma
[DE84-016992] 09 p1392 N85-18763
Thin end of the wedge
[DE84-016439] 09 p1401 N85-18816
Research in theoretical nuclear physics
[DE85-004349] 12 p1932 N85-22137
Standard model and beyond
[DE85-004269] 14 p2416 N85-24919
Eleven lectures on the physics of the quark-gluon plasma
[DE85-004321] 15 p2662 N85-26431
Overview of the physics issues at the SSC
[DE85-007074] 16 p2859 N85-27634
Heavy quark production processes in QCD
[DE85-007240] 17 p3036 N85-28779
Experimental methods of heavy quark detection
[DE85-006316] 17 p3036 N85-28781
Measurements of heavy quark and lepton lifetimes
[DE85-008321] 18 p3181 N85-29724
Soliton matter as a model of dense nuclear matter
[DE85-009937] 19 p3359 N85-30825
Deep-inelastic lepton scattering by nuclei: The pion-exchange model
[DE85-010498] 19 p3359 N85-30828
The standard model and beyond
[DE85-010239] 19 p3362 N85-30847
Systematics of quark mass matrices in the Standard Electroweak Model
[USIP-85-05] 20 p3532 N85-31972
Toward the question of multi-quark configurations in nuclei 21 p3691 N85-32929
Exotic events of p bar p-collider: Excited quark or excited color boson? 21 p3691 N85-32930
Heavy quarks and CP: Moriond 1985
[DE85-010563] 22 p3841 N85-33790
Quark structure of nuclei
[DE85-010781] 22 p3842 N85-33795
Detectors for relativistic nuclear collisions (report from the Fixed-Target Hadron Group)
24 p4146 N85-35701
Very high energy probes of the quark-gluon plasma
24 p4147 N85-35706
Propagation of cosmic rays through the atmosphere in the quark-gluon strings model 24 p4173 N85-35873
The phi-meson and Chiral-mass-meson production in heavy-ion collisions as potential probes of quark-gluon-plasma and Chiral symmetry transitions
24 p4175 N85-35884
Heavy flavours production in quark-gluon plasma formed in high energy nuclear reactions
24 p4175 N85-35886
A cosmic ray super high energy multicore family event. 2: Structure and fragmentation characteristics of the jets
[HE-3.4-2] 24 p4181 N85-35931
On mini-cluster observed by Chacaltaya emulsion chamber experiment
[HE-3.6-12] 24 p4185 N85-35959
The maximum depth of shower with E sub 0 larger than 10(17) eV on average characteristics of EAS different components 24 p4188 N85-35981

Calculation of intensity of high energy muon groups observed deep underground
[HE-5.4-13] 24 p4208 N85-36123
High energy cosmic ray signature of quark nuggets
[HE-6.2-11] 24 p4212 N85-36147
Progress report on a new search for free e/3 quarks in the cores of 10(15) - 10(16) eV air showers
[HE-6.2-15] 24 p4212 N85-36151
Tien-Shan effect and charmed particles
[HE-6.2-17] 24 p4212 N85-36153

QUARRIES
U MINES (EXCAVATIONS)

QUARTZ
New ages of radiolarian chert from the Rampart district, east-central Alaska 04 p0516 N85-13293
Metamorphic petrology of the Table Mountain area, Circle quadrangle, Alaska 04 p0516 N85-13295
Low noise multiple crystal-controlled oscillator
[AD-D011401] 07 p0948 N85-16010
Oscillator development
[AD-A149899] 12 p1834 N85-21509
Normal coordinate monolithic crystal filter
[AD-D011496] 12 p1941 N85-22188
Stress compensation crystal device
[AD-D011497] 12 p1941 N85-22189
Method of fabricating acceleration resistant crystal resonators and acceleration resistant crystal resonators so formed
[AD-D011630] 16 p2778 N85-27145
Acceleration sensitivity reduction method
[AD-D011631] 16 p2778 N85-27146
Research and development of subsurface acoustic wave devices for sensor applications
[AD-A152197] 16 p2661 N85-27642
A new precision time and frequency source for stationary PTTI applications 17 p2963 N85-28297
New features of different frequency generating systems due to the use of electrodeless rigidly mounted VBA quartz crystal resonator 18 p3106 N85-29231
Limiting processes laser CVD
[DE85-008848] 18 p3114 N85-29279
Physical and chemical changes to rock near electrically heated boreholes at Spent Fuel Test-Climax
[DE85-010834] 19 p3302 N85-30472
Dating Archean zircon by ion microprobe: New light on an old problem 21 p3722 N85-33094
Thermal reactions of aromatics with CaO
[DE85-010688] 22 p3742 N85-33193

QUARTZ CRYSTALS
Method of heating quartz resonators
[AD-D011454] 10 p1461 N85-19347
Quartz filter transceiver 12 p1836 N85-21538
Cylindrical crystal resonator
[AD-D011575] 14 p2426 N85-24974
Cut angles for quartz crystal resonators
[AD-D011652] 17 p2951 N85-28220
Acceleration insensitive oscillator
[AD-D011621] 17 p2953 N85-28236
Crystal resonator/oscillator test facility and test results
17 p2967 N85-28322
Power generation efficiency of piezoelectric crystals
20 p3537 N85-32006
JPL in-house fluidized-bed reactor research
21 p3609 N85-32414
Data analysis for lidar and quartz crystal microbalance systems
[NASA-CR-172601] 21 p3615 N85-32464

QUASARS
Measurement of pulsar parallax by Very Long Baseline Interferometry 03 p0444 N85-12830
Far-infrared photometry of compact extragalactic sources: OJ 187 and BL Lac
[NASA-TM-86022] 04 p0580 N85-13701
The 3a-F emulsion and the quasar redshift cut-off
07 p0964 N85-16112
X-ray and UV Emission from Active Galactic Nuclei — conference
[MPE-184] 08 p1236 N85-17790
Low excitation absorptions in the spectrum of the quasar PKS 1327-206 due to the galaxy MCG 03-34-085
08 p1237 N85-17801
X-ray surveys of quasars with the Einstein observatory
08 p1238 N85-17807
One to eight month X-ray light curves for active extragalactic objects 08 p1239 N85-17817
The high energy X-ray spectrum of 3C 273 — quasar
08 p1240 N85-17818
The X-ray properties of high-redshift, optically selected QSOs 08 p1240 N85-17821
On the broadband energy spectra of quasars and BL Lac objects 08 p1240 N85-17825
A universal spectrum for AGNs and QSOs — Active Galactic Nuclei (AGN) 08 p1241 N85-17826
Shock acceleration in active galactic nuclei and quasars 08 p1241 N85-17828
Collimated winds from active galactic nuclei
08 p1241 N85-17832
Active galactic nuclei and their cosmological evolution
08 p1243 N85-17842
An objective prism quasar survey with the Schmidt telescope on Calar Alto (Spain)
08 p1243 N85-17845
Broad emission features in active galactic nuclei
11 p1746 N85-20979
The UV spectra of intermediate redshift quasars
11 p1746 N85-20980
Multifrequency observations of BL LAC objects and violently variable quasars 11 p1746 N85-20981
Consequences of hot gas in the broad line region of active galactic nuclei
[NASA-TM-86176] 11 p1763 N85-21090
The ultraviolet excess of quasars 3: The highly polarized quasars PKS 0736+017 and PKS 1510-089
[NASA-CR-175576] 12 p1953 N85-22268
University of Cambridge Institute of Astronomy report of activities 13 p2170 N85-23464
A new luminosity component in 3C48
[NASA-CR-175840] 17 p3052 N85-28694
Evolution of the luminosity function of extragalactic objects
[NASA-CR-175977] 18 p3201 N85-29860
Milliarcsecond morphology of the twin quasar 0957 + 56A,B: The view through a gravitational lens
20 p3544 N85-32054
The ultraviolet spectra of intermediate redshift quasars
20 p3544 N85-32056
Activities report of the Institute of Astronomy
20 p3545 N85-32059
Cosmic gamma rays from quasars
[OG-2.7-10] 22 p3872 N85-33983
Limits on the Doppler factor in relativistic jets by means of gamma-ray observations
[OG-2.7-12] 22 p3872 N85-33985
The central engine of quasars and AGNs: A relativistic proton radiative shock
[OG-8.1-7] 23 p4018 N85-34897

QUASAT
QUASAT: A VLBI observatory in space — conferences
[ESA-SP-213] 07 p1056 N85-16700
The galaxy scene and QUASAT — VLBI satellite
07 p1056 N85-16703
The QUASAT mission: An overview
07 p1056 N85-16704
QUASAT: Technical aspects of the proposed mission — VLBI satellite 07 p1057 N85-16706
A study on the imaging potential of QUASAT — spaceborne VLBI 07 p1057 N85-16707
Correlator and data processing requirements for QUASAT 07 p1057 N85-16709
QUASAT, gravitational lenses, and studies of the interstellar, intracluster and intergalactic medium
07 p1058 N85-16715
The relevance of QUASAT to the star formation problem 07 p1058 N85-16718
Water masers and distance measurements: The impact of QUASAT 07 p1059 N85-16721
A short note on the high precision navigation of QUASAT 07 p1059 N85-16722
QUASAT: An orbiting very long baseline interferometer program using large space antenna systems
14 p2230 N85-23822
Antenna Technology for QUASAT application — radio antenna for very long base interferometry missions
14 p2231 N85-23828

QUASI-PARTICLES
U ELEMENTARY EXCITATIONS

QUASI-STELLAR RADIO SOURCES
U QUASARS

QUASILINEARITY
U NONLINEARITY

QUATERNARY ALLOYS
Zero-flux planes and flux reversals in multicomponent diffusion
[DE84-015212] 05 p0618 N85-13950

QUATERNIONS
Application of quaternions to problems of solid body dynamics in the atmosphere 15 p2481 N85-25313
Use of quaternions in flight mechanics
[AD-A152616] 17 p2899 N85-27875

QUENCHING (ATOMIC PHYSICS)
Electronically excited atomic and molecular oxygen
[AD-A147732] 08 p1121 N85-17064
X-ray emission in heavy ion collisions
[DE85-006350] 14 p2419 N85-24927
Elementary processes of electronically excited particles. Part 5: Deactivation of CHF (A1a' (O, V'2, O) after excitation by a pulsed dye laser
[MPIS-13/1984] 14 p2420 N85-24930
Lifetime and quenching measurements of C2H emission produced by vacuum ultraviolet photolysis of C2H2
[DE85-010769] 19 p3278 N85-30330

QUENCHING (COOLING)
Strain hardening and strain aging in Fe-Al-Mn alloys
02 p0178 N85-11186
Laminar flame propagation/quench for a parallel-wall duct
[DE84-009773] 04 p0470 N85-12963
Formation of superconductive Al(GeSi) alloys by low temperature laser quenching methods
[DE84-016867] 04 p0474 N85-13021
Study of residual stresses introduced into TA6ZrD (685) cylinders by quenching
[BLL-PNR-90240-(8019.3153)]
07 p0925 N85-15859
Study of residual stresses introduced into TA6ZrD (685) cylinders by quenching — compressor disk alloy
[PNR-90240] 09 p1341 N85-18435
Initial aging phenomena in copper-chromium alloys
[NASA-TM-77790] 10 p1439 N85-19070
Phase transformations in vanadium alloys of titanium during quenching and tempering
11 p1602 N85-20073
Quenching effects on iron site partitioning in the Apollo 17 orange glass composition 13 p2184 N85-23553
Experimental methods for quenching structures in lunar-analog silicate melts: Variations as a function of quench media and composition
13 p2184 N85-23554
Thermomechanical softening treatment for bearing and tool steels
[BLL-BISI-TRANS-22432-(9022.06)]
17 p2925 N85-28035
The state of martensite after quenching in a magnetic field
[BLL-BISI-TRANS-22297-(9022.06)]
17 p2926 N85-28051
Computer studies of the quench behavior of an SSC model-dipole
[DE85-010633] 19 p3360 N85-30629
Structural transformation of a 9% Cr - 2%Mo steel (type Z10CDNbV 09-02) for use in steam generators for fast neutron reactors
[BLL-CE-TRANS-7943-(9022.09)]
20 p3430 N85-31271
Application of the unloading compliance methods in fracture toughness measurements of a quenched and tempered steel
[BLL-CE-TRANS-7953-(9022.09)]
20 p3465 N85-31523

QUERY LANGUAGES
A methodology for supporting views in relational databases 03 p0437 N85-12763
Interpretation of natural language database queries using optimization methods 05 p0735 N85-14720
Tree Query Language Flat (TQLF) specifications
[PB84-217116] 06 p0855 N85-15438
Relational Query Language Flat (RQLF) specifications
[PB84-217405] 06 p0855 N85-15439
Network Query Language Flat (NQLF) specifications
[PB84-217538] 06 p0855 N85-15440
Design and analysis of an SQL (Structured Query Language) interface for a multi-backend database system
[AD-A146534] 06 p0856 N85-15447
Design of a pictorial program reference language
[AD-A149323] 10 p1540 N85-19711

QUEUEING THEORY
Development of a production order release methodology
[AD-A145213] 01 p0124 N85-10652
On some common interests among reliability, inventory and queuing
[AD-A145595] 02 p0251 N85-11648
Optimal control of waiting time in a M/G/1 queue
[INPE-2767-PRE/340] 02 p0255 N85-11671
Applications of functional analytic and Martingale methods
[AD-A145555] 02 p0255 N85-11672
On a program for solution of BCMP queueing network model
[NAL-TR-813] 03 p0405 N85-12586
The application of queueing theory to communications networks: A review
[AD-A146680] 04 p0492 N85-13140
One queue or two pushdown stores take square time on a one-head tape unit
[CWI-CS-R8406] 05 p0717 N85-14601
Relaxation times for queueing systems
[CWI-OS-R8407] 05 p0719 N85-14616
DYNA-SIM: A nonstationary queuing simulation with application to the automated test equipment problem
[AD-A146384] 06 p0857 N85-15455
Omni transforms: Applications to renewal theory
[AD-A146939] 07 p1029 N85-18534

A single server queue with mixed types of interruptions
[AD-A148536] 08 p1213 N85-17637
Inequalities for the M/G/Infinity queue and related shot noise processes
[AD-A149015] 10 p1545 N85-19737
The omni-transform in single-channel queues
[AD-A151019] 14 p2409 N85-24852
Algorithms and approximations for queueing systems
[CWI-TRACT-8] 14 p2410 N85-24859
Weak convergence of a sequence of queueing and storage processes to a singular diffusion
[AD-A150655] 14 p2411 N85-24866
A note on equivalent random theory
[CWI-OS-R8410] 14 p2412 N85-24872
Constructing unifying frameworks for the study of distributed system and algorithms
[AD-A151287] 15 p2637 N85-26261
Calculating reliability and productivity of cold stamping robot complex as queuing system
16 p2761 N85-27039
Replication methods for abstract data types
[AD-A153648] 18 p3162 N85-29587
Computer Performance Modeling Tool (CPMT)
[AD-A154436] 19 p3338 N85-30682
The architectural requirements and integration analysis of a database server for office automation
[AD-A155517] 21 p3674 N85-32625

QUINOLINE
Catalytic hydrotreatment studies with model compounds
[DE85-010167] 19 p3236 N85-30064

R

RABBITS
Influence of limboreticular complex on some reactions of rabbits 19 p3326 N85-30607

RACES
The 1981 transatlantic boat race contribution for marine meteorological measurements 14 p2324 N85-24361
NASA initiatives with historically black colleges and universities
[NASA-EP-210] 19 p3379 N85-30960

RACKS (FRAMES)
Preventing explosive propagation in racks or containers of tactical missiles
[AD-P004342] 10 p1455 N85-19168
Low-profile fastener
[AD-D011687] 19 p3280 N85-30343

RACON BEACONS
U RADAR BEACONS

RADAR
NT COHERENT RADAR
NT CONTINUOUS WAVE RADAR
NT DOPPLER RADAR
NT EARTH RESOURCES SHUTTLE IMAGING RADAR
NT IMAGING RADAR
NT INCOHERENT SCATTER RADAR
NT LANDING RADAR
NT METEOROLOGICAL RADAR
NT MONOPULSE RADAR
NT MOVING TARGET INDICATORS
NT MULTISPECTRAL RADAR
NT MULTISTATIC RADAR
NT OPTICAL RADAR
NT OVER-THE-HORIZON RADAR
NT PULSE DOPPLER RADAR
NT PULSE RADAR
NT RADAR MEASUREMENT
NT RANGE AND RANGE RATE TRACKING
NT SATELLITE-BORNE RADAR
NT SEARCH RADAR
NT SECONDARY RADAR
NT SIDE-LOOKING RADAR
NT SPACE BASED RADAR
NT SURVEILLANCE RADAR
NT SYNTHETIC APERTURE RADAR
NT TRACKING RADAR
Clutter generator for use in radar evaluation
[AD-D011234] 01 p0039 N85-10245
Programmable digital band integrators for the radar high-speed data acquisition system
05 p0624 N85-13994
SAR maritime missions 06 p0751 N85-14813
Radar frequency selection strategies
[AD-A147493] 07 p0941 N85-15867
LPI-radar for helicopter obstacle warning
08 p1074 N85-16810
In situ orbital debris experiment concepts
12 p1784 N85-21198
The ambiguity function and the Wigner distribution
[AD-A150095] 12 p1829 N85-21482
Remote sensing of directional wave spectra using the surface contour radar
[NASA-TM-84440] 14 p2347 N85-24510
Hygienic standardization of electromagnetic fields of radar systems 14 p2387 N85-24703
Hardware test program for evaluation of baseline range-range rate sensor concept
[NASA-CR-175794] 16 p2787 N85-27193
An analysis of the economic impact of the AN/APS-134 FLAR (Forward Looking Airborne Radar) retrofit on Coast Guard HC-130 aircraft
[AD-A152619] 17 p2949 N85-28204
Survivable ground base sensor
[AD-D011647] 17 p2950 N85-28213
The HURRA high resolution experimental radar system sampling unit
[FOA-C-30376-E1] 18 p3091 N85-29133
Optical techniques for signal distribution and control in advanced radar and communication systems
18 p3188 N85-29773
Orthogonalizer for inphase and quadrature digital data
[AD-D011679] 19 p3254 N85-30174
A single chip VLSI architecture for radar signal processing 19 p3257 N85-30195
The use of the glistening surface concept in rough surface scattering
[AD-A154922] 21 p3575 N85-32234
Power density and threshold control strategies for radar track initiation
[AD-A155357] 22 p3756 N85-33282
A planar version of a 4.0 gigahertz reactively steered adaptive array
[AD-A156029] 24 p4067 N85-35330

RADAR ALTIMETERS
U RADIO ALTIMETERS

RADAR ANTENNAS
Turnaround control for mechanically scanned radar antennas
[AD-D011236] 01 p0039 N85-10246
Structural aspects of SAR antenna for Japanese Earth Resources Satellite 1 05 p0626 N85-14007
Technology for the ERS-1 SAR antenna
05 p0626 N85-14008
CASA technological effort in the field of antennas — satellite radar antennas 05 p0626 N85-14010
Place of aperture synthesis in general theory of antennas (review) 06 p0781 N85-14993
Resolution and accuracy of radar measurements
06 p0789 N85-15044
Broadband pillbox antennas
[AD-A146569] 06 p0799 N85-15104
Fast switching driver for inductive load, such as a phase shifter
[AD-D011388] 08 p1143 N85-17207
Conformal phased array antenna pattern corrector
[AD-D011489] 10 p1468 N85-19266
Low sidelobe phased array antenna system
[AD-D011558] 12 p1823 N85-21435
Development of the F-20 nose radome
[AD-P004374] 12 p1827 N85-21468
Adaptive control of airborne radar antennas
13 p2080 N85-22989
Performance analysis of the N baseband assembly (Bba) Real-Time Combiner (RTC)
[NASA-CR-175877] 17 p2947 N85-28193
Inherent angular tracking error in an amplitude comparison monopulse radar
[AD-A154212] 19 p3255 N85-30185
Accuracy of velocity and power determination by the Doppler method 21 p3620 N85-32493
Improvement of vertical velocity measurements, part 3.4B 21 p3620 N85-32494
Mesospheric measurements of irregularity patches using a 3-antenna interferometer, part 3.6B
21 p3621 N85-32498
Summary of progress at the Poker Flat Observatory in Alaska 21 p3628 N85-32539
A note on the proposed UK VHF radar
21 p3629 N85-32545
Signal space models for antenna arrays
[AD-A156063] 24 p4087 N85-35335

RADAR APPROACH CONTROL
Planned office and facility consolidations: To improve system effectiveness and efficiency, FY 1985-87
[AD-A150441] 13 p1970 N85-22376
Investigation of imaging and flight guidance concepts for rotorcraft zero visibility approach and landing
[NASA-CR-166571] 17 p2894 N85-27843

RADAR ASTRONOMY
A review of radar observations of Saturn's rings
15 p2670 N85-26474
Saturn's rings resolved by the VLA — Very Larg Array (VLA) 15 p2670 N85-26476
Mars: Seasonally variable radar reflectivity
15 p2683 N85-26570

RADAR ATTENUATION
Using measured variance of skywave radar sea-echo power spectra to estimate ionospheric Doppler broadening of mean spectra
[PB84-214071] 03 p0399 N85-12544

RADAR BEACONS
Development and flight test of a helicopter compact, portable, precision landing system concept
08 p1076 N85-16821
Development and flight test of a helicopter, X-band, portable precision landing system concept
[NASA-TM-86710] 16 p2710 N85-26721

RADAR BEAMS
Radar echo enhancement using surface reflections
[AD-A148970] 07 p0930 N85-15855
Use of alternative solvents for low-temperature LPE growth of CdTe films
[AD-A149418] 10 p1562 N85-19853

RADAR CROSS SECTIONS
Simultaneous ocean cross-section and rainfall measurements from space with a nadir-pointing radar
[NASA-TM-86167] 07 p0967 N85-16273
Numerical methods for analyzing electromagnetic scattering
[NASA-CR-175507] 12 p1823 N85-21436
Research efforts in support of resonance extraction studies. Volume 1: Improvement and validation of TWFD (Thin-Wire Frequency-Domain): A thin-wire frequency-domain scattering code
[AD-A150296] 13 p2054 N85-22864
High frequency estimation of 2-dimensional cavity scattering
[AD-A151697] 15 p2542 N85-25696
Scattering center analysis for radar cross section modification 16 p2769 N85-27085
An empirical self-protection chaff model
[AD-A151928] 16 p2773 N85-27115
Radiation and scattering of spiral antennas
[AD-A151929] 16 p2773 N85-27116
Radar target identification through electromagnetic scattering studies
[AD-A154596] 21 p3573 N85-32220
The use of the glistening surface concept in rough surface scattering
[AD-A154922] 21 p3575 N85-32234
Head-on scattering of a tubular cylinder of finite length for radar target identification purposes
[AD-A155808] 21 p3577 N85-32246
Normal modes in an overmoded circular waveguide coated with lossy material
[NASA-CR-176186] 24 p4085 N85-35320

RADAR DATA
Preliminary assessment of very short term forecasting of rain from single radar data 01 p0078 N85-10523
Adaptive preprocessing system
[AD-D011327] 07 p0937 N85-15935
On the generation of random variables for radar simulation purposes 07 p0938 N85-15947
An adaptive Fast Fourier Transform weighting technique to increase small target sensitivity
[AD-D011424] 08 p1154 N85-17286
Programmable realtime interface between a block floating point processor and memory
[AD-D011431] 08 p1203 N85-17571
Rain volume estimation over areas using satellite and radar data
[NASA-CR-174434] 10 p1518 N85-19568
Digital coherent detector
[AD-D011560] 12 p1833 N85-21501
Visualization of radar altimetry data for Venus
13 p1982 N85-22437
Forth system for coherent-scatter radar data acquisition and processing
[NASA-CR-176055] 20 p3494 N85-31720
Hardware schemes for fast Fourier transform, part 7.4A 21 p3626 N85-32526
Criteria and algorithms for spectrum parameterization of MST radar signals 21 p3626 N85-32527

RADAR DETECTION
Optimization of moving-target selection radar devices for nonGaussian signals for stationary targets
06 p0789 N85-15043
Radar frequency selection strategies
[AD-A147493] 07 p0941 N85-15867
Intrinsic polarization basis of radar target observed by system employing diversity reception
07 p0949 N85-16015
NORAD's PARCS small satellite tests (1976 and 1978) 12 p1783 N85-21191
Use of ground radar to detect reentering debris
12 p1784 N85-21200
Survivable ground base sensor
[AD-D011647] 17 p2950 N85-2821

Convective storm downdraft outflows detected by NASA/MSFC's Airborne 10.6 micron pulsed Doppler Lidar System
[NASA-CR-3898] 17 p2995 N85-28511

Detection of signals from coherent pulsed radars with random variation in parameters of sounding signals from pulse to pulse against background of worst-case Gaussian noise 22 p3763 N85-33324

RADAR DIRECTION FINDERS
U RADIO DIRECTION FINDERS

RADAR DISPLAYS
U RADARSCOPES

RADAR ECHOES
NT CLUTTER
NT LUNAR RADAR ECHOES
NT VENUS RADAR ECHOES

A scheme for the delineation and extrapolation of thunderstorms from GOES satellite data
01 p0076 N85-10507

Simulation of information extraction from radar altimeter return echoes — ERS-1 (ESA satellite)
03 p0383 N85-12452

Using measured variance of skywave radar sea-echo power spectra to estimate ionospheric Doppler broadening of mean spectra
[PB84-214071] 03 p0399 N85-12544

Radar echo enhancement using surface reflections
[AD-A146970] 07 p0939 N85-15955

Design of an analog spectrum analyzer for probing experiments
[AD-A147384] 07 p0941 N85-15963

Test plan for the forest-echo experiment
[DE84-017175] 09 p1343 N85-18447

Digital coherent detector
[AD-D011580] 12 p1833 N85-21501

Preliminary results of associating cloud-to-ground lightning with surface convergence and radar reflectivity at Kennedy Space Center in 1983
[NASA-CR-175543] 12 p1897 N85-21910

Mars radar catalog 13 p2198 N85-23636

Experimental study of anisotropy of scattering of radar signals by clouds and precipitation
14 p2340 N85-24473

High frequency estimation of 2-dimensional cavity scattering
[AD-A151697] 15 p2542 N85-25696

The use of radar in determining precipitation processes in the BEWMEX area 16 p2831 N85-27455

Statistical comparison of radar echoes of convective precipitation between the northern Alps and its foreland
[DFVLR-FB-85-07] 17 p2950 N85-28215

Morphology of the scattering targets: Fresnel and turbulent mechanisms, part 2.1A
21 p3618 N85-32481

Signal statistics of the radar echoes: Angle-of-arrival statistics, part 2.2A 21 p3618 N85-32482

A modified Fresnel scattering model for the parameterization of Fresnel returns, part 2.3A
21 p3618 N85-32483

Observations of mesospheric turbulence by rocket probe and VHF radar, part 2.4A 21 p3619 N85-32484

Interpretation of radar returns from the mesosphere, part 2.3A 21 p3619 N85-32485

Radar echoes at 2.66 and 40.92 MHz from the mesosphere, part 2.6A 21 p3619 N85-32486

Anisotropy of the permittivity field inferred from aspect-sensitive radar echoes 21 p3620 N85-32492

Interferometer applications of VHF radars, part 3.6A
21 p3621 N85-32497

Most desirable terrain, e.g., flat vs valley location, part 5.1B 21 p3624 N85-32513

Interpolation problems in meteor radar analysis, part 7.6A 21 p3626 N85-32528

The effects of subrefractive layers and elevated ducts on airborne radar and ESM (Electronic Surveillance Measures)
[AD-A155524] 21 p3637 N85-32592

RADAR EQUIPMENT
NT PLAN POSITION INDICATORS
NT RADAR ANTENNAS
NT RADAR BEACONS
NT RADAR FILTERS
NT RADAR RECEIVERS
NT RADAR REFLECTORS
NT RADAR TRANSMITTERS
NT RADARSCOPES
NT RETROREFLECTORS

Radar, target and ranging
[AD-A145407] 02 p0190 N85-11272

Training capabilities test of Electronics Equipment Maintenance Trainer (EEMT): Findings and conclusions
[AD-A146075] 03 p0359 N85-12302

Diagnostic apparatus for radar pulse repetition frequency control circuit card
[AD-D011384] 07 p0937 N85-15938

Tracking servo compensator with rate aiding
[AD-D011372] 07 p0942 N85-15971

Propagation and scattering considerations for the 0.2-3.0 GHz frequency range for a space-based radar
[AD-A148504] 08 p1153 N85-17282

Measurement procedures for the radar spectrum engineering criteria
[PB85-119022/GAR] 09 p1313 N85-18254

The ambiguity function of random binary-phase-coded waveforms
[AD-A148906] 10 p1466 N85-19249

NORAD's PARCS small satellite tests (1976 and 1976) 12 p1783 N85-21191

Trajectory measurements for take-off and landing tests and other short-range applications, volume 16
[AGARD-AG-160-VOL-16] 15 p2561 N85-25801

High-power solid-state rf source for accelerator cavities
[DE85-012672] 22 p3761 N85-33309

Radar wind profilers in the Colorado network
[PB85-185486] 22 p3817 N85-33647

RADAR FILTERS

Gain restoration after Doppler filtering
[AD-D011425] 08 p1154 N85-17287

RADAR GEOLOGY

Volcanism and rift formation in Beta Regio, Venus: New radar results 13 p2176 N8F 23507

Classification of circular features on Venus
13 p2177 N85-23511

Shuttle imaging radar-A (SIR-A) data analysis — geology of the Ozark Plateau of southern Missouri, land use in western Illinois, and vegetation types at Koonamore Station, Australia
[NASA-CR-175765] 16 p2809 N85-27324

Planning for VRM: Radar and sonar studies of volcanic terrains on Earth, Venus and Mars
22 p3857 N85-33884

RADAR IMAGERY

A system for meteorological satellite, radar, conventional data and model analysis 01 p0082 N85-10551

Systematic data interpretation of remote sensing in the reception of hydrocarbons, volume 1
[E85-10006] 02 p0215 N85-11421

Production of optically correlated SEASAT-A (SEA satellite) SAR (Synthetic Aperture Radar) imagery at DREO (Defence Research Establishment Ottawa)
[AD-A145970] 03 p0355 N85-12281

Aspects and applications of SAR (Synthetic Aperture Radar) imagery for mensuration
[AD-A146301] 03 p0356 N85-12290

Multispectral (X and C band) crop classification with synthetic aperture radar (SAR-580) optical data
05 p0657 N85-14217

The SPOT data bank system
05 p0659 N85-14236

The SIR-B science investigations plan
[NASA-CR-174282] 08 p1143 N85-17208

The SIR-B science investigations plan: Introduction
08 p1143 N85-17209

Southern ocean sea-ice morphology and kinematics
08 p1144 N85-17217

SIR-B analysis of the Precambrian shield of Sudan and Egypt: Penetration studies and subsurface mapping
08 p1145 N85-17219

Quantitative use of multiincidence-angle SAR for geologic mapping 08 p1145 N85-17220

Geologic mapping of Indonesian rain forest with analysis of multiple SIR-B incidence angles
08 p1145 N85-17221

Evaluation of SIR-B data for identifying rainfall event occurrence and intensity 08 p1145 N85-17223

Microwave and optical remote sensing of forest vegetation 08 p1146 N85-17226

Evaluation of SIR-B imagery for geologic and geomorphic mapping, hydrology, and oceanography in Australia 08 p1146 N85-17229

The use of digital spaceborne SAR data for the delineation of surface features indicative of malaria vector breeding habitats 08 p1146 N85-17230

Interlobate comparison of glacial-depositional style as evidenced by small-relief glacial landscape features in Illinois, Indiana, and Ohio, utilizing SIR-B
08 p1146 N85-17231

SAR internal wave signature experiment
08 p1149 N85-17253

Information extraction and transmission techniques for spaceborne synthetic aperture radar images
[NASA-CR-174341] 08 p1150 N85-17256

SEASAT 3 and 4
[AD-A146343] 08 p1152 N85-17274

Second order Bragg scattering in a SAR
[AD-A146395] 08 p1152 N85-17275

Extraction of structural information from radar signals
[FOA-C-30370-E1] 08 p1155 N85-17292

The use of synthetic aperture radar imagery to detect hazards to navigation
[AD-A149324] 10 p1422 N85-1

Analysis of data acquired by synthetic aperture radar and LANDSAT Multispectral Scanner over Kershaw County, South Carolina, during the summer season
[E85-10071] 10 p1503 N85-1

Earth resources research using the Shuttle Imaging Radar system 11 p1713 N85-2

Research in image understanding as applied to 3-D tomographic imaging with near optical resolution
[AD-A150096] 12 p1829 N85-2

The imaging of internal waves by the SEASAT-A synthetic aperture radar
[AD-A149808] 12 p1875 N85-2

The imaging of internal waves by the SEASAT-A synthetic aperture radar
[ARE(PORTLAND)TN-720/84]
13 p2054 N85-2

Edge detection in SAR imagery using gradient operators — synthetic aperture radar (SAR)
[AD-A149411] 13 p2054 N85-2

Surfaces of asteroids and cometary nuclei
13 p2176 N85-2

Volcanism and rift formation in Beta Regio, Venus: New radar results 13 p2176 N85-2

Venus surface composition from radio/radar measurements 13 p2177 N85-2

Classification of circular features on Venus
13 p2177 N85-2

Correction and geological analysis of lunar 3.8 cm radar data 13 p2196 N85-2

Landform identification on radar images
13 p2196 N85-2

Mars radar catalog 13 p2196 N85-2

Radar and the detection of liquid water on Mars
13 p2190 N85-2

Intra-eruption geologic map from an x-band radar image during the May 18, 1980 eruption of Mount St. Helens, Washington 13 p2199 N85-2

Radar observations of fissure-fed basaltic lava flows, Craters of the Moon, Idaho 13 p2199 N85-2

Late Tertiary and Quaternary river systems of the eastern Sahara as mapped on shuttle radar and LANDSAT images 13 p2199 N85-2

Remote sensing of directional wave spectra using the surface contour radar
[NASA-TM-84440] 14 p2347 N85-2

Synthetic aperture radar data processing
14 p2398 N85-2

Increasing the accuracy of processing radar pictures by excluding systematic point coordinate error component
15 p2488 N85-2

Analysis of the Gran Desierto, Pinacate Region, Sonora, Mexico, via shuttle imaging radar
[NASA-CR-175711] 15 p2582 N85-2

Contamination of the fetch-limited directional wave spectrum by waves emanating from an embayment
[NASA-TM-84441] 15 p2604 N85-2

Radar return from vegetation covered terrains
[INPE-3470-PRE/713] 16 p2770 N85-2

Synthetic aperture side-looking radar image adjustment 16 p2806 N85-2

Investigation of imaging and flight guidance concepts for rotorcraft zero visibility approach and landing
[NASA-CR-166571] 17 p2894 N85-2

Evaluation of Defense Mapping Agency level 1 second edition digital data for training simulator applications
[AD-A152444] 17 p2983 N85-2

Application of artificial intelligence (AI) to radar image understanding
[AD-A152519] 17 p3017 N85-2

Further study of digital matching of dissimilar images
[AD-A153112] 17 p3019 N85-2

The multiple processor machine for image processing, volume 5
[ESA-CR(P)-1976-VOL-5] 18 p3164 N85-2

Geological analyses of the surface of Venus and Mars from lander spacecraft images and orbital radar observations 19 p3384 N85-3

Using ship wake patterns to evaluate SAR (Synthetic Aperture Radar) ocean wave imaging mechanisms. Joint US-Canadian Ocean Wave Investigation Project
[AD-A154633] 21 p3573 N85-3

Use of spaceborne imaging radar in regional geomorphic studies 21 p3603 N85-3

The Boot Lake MF imaging radar
21 p3626 N85-3

Basic properties and interpretation of synthesized radar images of sea waves with long synthetization time
22 p3773 N85-3

An experimental study of dielectric rod antennas for millimeter-wave imaging applications
[AD-A155832] 24 p4086 N85-3

Surface cyclogenesis as indicated by satellite imagery
[PB85-191815] 24 p4124 N85-3

Optical synthetic aperture techniques
AD-A156151] 24 p4154 N85-35752

DAR MAPS
NT RADAR IMAGERY
Progress in planetary radarclinometry
13 p2198 N85-23630
Mercury radar altimetry: A preliminary analysis
13 p2198 N85-23631
Millimetre wave pulse technology — satellite mapping
ESA-CR(P)-2004] 20 p3478 N85-31611
Geology and geomorphology of the Roraima group, utheastern Venezuela 24 p4115 N85-35511

ADAR MEASUREMENT
Thermosonde and UHF radar measurements of C2 sub e at Westford, Massachusetts - July 1981
[AD-A145398] 02 p0190 N85-11270
Measurement of snow cover thickness by radar sounding 03 p0344 N85-12216
Rain volume estimation over areas using satellite and radar data 06 p0686 N85-14406
Resolution and accuracy of radar measurements
06 p0789 N85-15044
Statistical analysis of visual wave observations and gage/radar measurements
[AD-A146358] 06 p0796 N85-15100
Lidar measurements of structural characteristics of atmospheric turbulence 06 p0824 N85-15229
Development of radar to measure sea ice merits prize nomination 06 p0826 N85-15244
Intermediate results of radar backscatter measurements from summer sea ice
[AD-A147212] 07 p0940 N85-15960
Design of an analog spectrum analyzer for probing experiments
[AD-A147384] 07 p0941 N85-15963
Simultaneous ocean cross-section and rainfall measurements from space with a nadir-pointing radar
[NASA-TM-86167] 07 p0987 N85-16273
MWR, Meteor Wind Radars 08 p1184 N85-17462
The MST radar technique 08 p1185 N85-17466
Partial reflection spaced antenna wind measurements
08 p1185 N85-17467
Airborne lidar measurements of El Chichon stratospheric aerosols, October 1982 to November 1982
[NASA-RP-1136] 10 p1514 N85-19550
Radar calibration using direct measurement equipment and oblique photometry
[AD-D011530] 12 p1822 N85-21433
Experimental test of the three subaperture method for estimating target elevation angle
[AD-A149687] 12 p1851 N85-21614
Progress in planetary radarclinometry
13 p2198 N85-23630
Mercury radar altimetry: A preliminary analysis
13 p2198 N85-23631
Mapping and geological analysis of Mercury and Venus radar ranging data 13 p2198 N85-23633
Landform identification on radar images
13 p2198 N85-23635
Intermediate results of the NORDSEE experiment
[AD-A151363] 15 p2542 N85-25693
Radar turbulence estimates. Effects of wind shear and reflectivity factor gradients
[AD-A151676] 15 p2509 N85-26023
Radar measurement of thickness of drifting ocean ice employing cepstral signal processing
15 p2644 N85-26313
Progress in radar meteorology
18 p3148 N85-29486
Use of radar with frequency modulation for studying atmospheric boundary layer 19 p3296 N85-30437
Geological analyses of the surface of Venus and Mars from lander spacecraft images and orbital radar observations 19 p3384 N85-30993
Comparison of wind and turbulence measurements from Doppler lidar and instrumented aircraft
[NASA-CR-171535] 20 p3495 N85-31729
Middle Atmosphere Program. Handbook for MAP. Volume 14: URSI/SCOSTEP Workshop on Technical Aspects of MST Radar
[NASA-CR-176085] 21 p3615 N85-32466
Gravity waves from the stratosphere to the mesosphere, part 1.3B 21 p3616 N85-32471
General circulation of the middle atmosphere, part 1.4B 21 p3617 N85-32474
Performance of the Colorado wind-profiling network, part 1.5A 21 p3617 N85-32475
Vertical transport in the atmosphere: Measurement capabilities and requirements of VHF radars, part 1.6A
21 p3617 N85-32476
Comparison of tropopause altitude determination by the Platteville Radar, Sunset Radar and the NWS Rawinsonde 21 p3617 N85-32477
Synoptic-scale dynamics with vertical velocity, part 1.8A 21 p3617 N85-32478
Practical use of a tropopause height determination algorithm on an MST radar data set, part 1.8B
21 p3618 N85-32479
Usefulness of multifrequency MST radar measurements, part 2.6B 21 p3619 N85-32487
Use of the VAD technique and measurements of momentum flux in the stratosphere at Aercibo, part 4.3A
21 p3622 N85-32505

RADAR NAVIGATION
Guidance and navigation programs and plans
06 p0751 N85-14809
National airspace review: Airport radar service area operational confirmation report
[DOT/FAA/AT-84/2] 07 p0901 N85-15707
Interplanetary navigation 14 p2396 N85-24781
Autofocus motion compensation for synthetic aperture radar and its compatibility with strapdown inertial navigation sensors on highly maneuverable aircraft
[AD-A151640] 16 p2704 N85-26693

RADAR NETWORKS
A multipurpose weather radar network
01 p0077 N85-10510
Operational precipitation observation system using digitized radar and rain gages 01 p0082 N85-10549
The French weather radar network: A status report
01 p0082 N85-10550
Project COST 72 (The European weather radar project) today 01 p0084 N85-10561
SIR-B coverage 08 p1143 N85-17211
Design and realization of a multiradar tracking system for air traffic control
[ENST-84E010] 09 p1279 N85-18044
The global meteor observation system (GLOBMET)
11 p1656 N85-20432
Middle Atmosphere Program. Handbook for MAP. Volume 14: URSI/SCOSTEP Workshop on Technical Aspects of MST Radar
[NASA-CR-176085] 21 p3615 N85-32466
Meteorological and aeronomical requirements for MST radar networks (keynote paper), part 1
21 p3615 N85-32467
Performance of the Colorado wind-profiling network, part 1.5A 21 p3617 N85-32475
Comparison of tropopause altitude determination by the Platteville Radar, Sunset Radar and the NWS Rawinsonde 21 p3617 N85-32477

RADAR OBSERVATION
U RADAR TRACKING

RADAR PHOTOGRAPHY
Metric evaluation of SAR-580 optical images for cartographic purposes 05 p0659 N85-14231
Geological analyses of the surface of Venus and Mars from lander spacecraft images and orbital radar observations 19 p3384 N85-30993

RADAR RANGE
Radar, target and ranging
[AD-A145407] 02 p0190 N85-11272
Probability distribution density of normalized radar range 04 p0485 N85-13096
SIR-B coverage 08 p1143 N85-17211
Pulse heterodyne equipment for measurements of range and velocity of moving targets-pulse radar
[ESA-TT-845] 09 p1312 N85-18246

RADAR RECEIVERS
Fast envelope detector with bias compensation
[AD-D011226] 01 p0038 N85-10243
Test and evaluation of a coherent 35 gigahertz radar repeater
[AD-A145714] 02 p0191 N85-11280
NAVSTAR GPS (Global Positioning System) marine receiver performance analysis
[AD-A146414] 06 p0753 N85-14831
Bistatic coherent radar receiving system
[AD-D011447] 10 p1466 N85-19252
Multiple loop sidelobe canceller
[AD-D011533] 12 p1823 N85-21434
Digital coherent detector
[AD-D011560] 12 p1833 N85-21501
Summator of radio pulse signals
12 p1839 N85-21539
Methods of digital correction for channels of multichannel radar receivers 13 p2082 N85-23005
Cryogenically-cooled, low-noise microwave receivers: Present status and future needs
14 p2298 N85-24226
The HURRA, a high resolution experimental radar system broadband receiver
[FOA-C-30375-E1] 16 p3091 N85-29132
A multi-channel radar receiver
[AD-A156058] 24 p4087 N85-35333

RADAR RECEPTION
Intrinsic polarization basis of radar target observed by system employing diversity reception
07 p0949 N85-16015
Survivable ground base sensor
[AD-D011647] 17 p2950 N85-28213
Criteria for site selection and frequency allocation (keynote paper), part 5 21 p3623 N85-32511
Sidelobe reduction of Barker codes, part 7.1C
21 p3625 N85-32522

RADAR REFLECTIONS
U RADAR ECHOES

RADAR REFLECTORS
A scheme for the delineation and extrapolation of thunderstorms from GOES satellite data
01 p0076 N85-10507
CASA activities in antenna technology — satellite antennas 05 p0627 N85-14015
Data appendix: F-number = 1.0 EMR with a flexible back electrode
[NASA-CR-172477] 07 p0946 N85-15994

RADAR RESOLUTION
Resolution and accuracy of radar measurements
06 p0789 N85-15044
Limitation of VLBI angular resolution
07 p1057 N85-16710
Landform identification on radar images
13 p2198 N85-23635

RADAR SCANNING
Turnaround control for mechanically scanned radar antennas
[AD-D011238] 01 p0039 N85-10246
Mathematical model of discriminator for signals with fluctuations and thermal noise 13 p2072 N85-22943
The development and application of volume scan and cell tracking capabilities for the analysis of convective cloud systems 16 p2830 N85-27451

RADAR SCATTERING
The use of dual polarisation radar for observing and predicting convective activity 01 p0077 N85-10512
Anglo-German millimeter wave backscatter measurements on snow, environmental data report
[REPT-7-84] 04 p0492 N85-13136
Scattering models in the microwave regime
[NASA-CR-174001] 04 p0525 N85-13361
A comparison between active and passive sensing of soil moisture from vegetated terrains
04 p0526 N85-13364
Simultaneous ocean cross-section and rainfall measurements from space with a nadir-pointing radar
[NASA-TM-86167] 07 p0987 N85-16273
Evaluation of the L-band scattering characteristics of volcanic terrain in aid of lithologic identification, assessment of SIR-B calibration, and development of planetary geomorphic analogs 08 p1146 N85-17232
Extraction of structural information from radar signals
[FOA-C-30370-E1] 08 p1155 N85-17292
Incoherent scatter radar studies of the mesosphere
08 p1184 N85-17463
The MST radar technique 08 p1185 N85-17466
Oceanographic and meteorological research based on the data products of SEASAT
[E85-10091] 12 p1874 N85-21753
Intermediate results of the NORDSEE experiment
[AD-A151363] 15 p2542 N85-25693
Radiation and scattering of spiral antennas
[AD-A151929] 16 p2773 N85-27116
Modeling the backscattering and transmission properties of vegetation canopies
[E85-10099] 16 p2809 N85-27320
An analysis of physical optics models for rough surface scattering
[AD-A154960] 21 p3575 N85-32235
A modified Fresnel scattering model for the parameterization of Fresnel returns, part 2.3A
21 p3618 N85-32483
Observations of mesospheric turbulence by rocket probe and VHF radar, part 2.4A 21 p3619 N85-32484
Interpretation of radar returns from the mesosphere, part 2.3A 21 p3619 N85-32485
Radar echoes at 2.66 and 40.92 MHz from the mesosphere, part 2.6A 21 p3619 N85-32486

RADAR SIGNATURES
Autoregressive modeling and the classification of land clutter — radar signatures
[ENST-C-84003] 03 p0356 N85-12292
Quantitative use of multiincidence-angle SAR for geologic mapping 08 p1145 N85-17220
Geologic mapping of Indonesian rain forest with analysis of multiple SIR-B incidence angles
08 p1145 N85-17221
An electronically controlled array for simulation of passive target/background signatures at millimeter wavelengths
[AD-D011456] 10 p1468 N85-19263
Hardware test program for evaluation of baseline range/range rate sensor concept
[NASA-CR-175910] 17 p2947 N85-28194
The use of the glistening surface concept in rough surface scattering
[AD-A154922] 21 p3575 N85-32234

Automated cell detection as a mesocyclone precursor tool
[AD-A154952] 21 p3636 N85-32577
Hardware test program for evaluation of baseline range-range rate sensor concept
[NASA-CR-176143] 23 p3893 N85-34377

RADAR TARGETS
Joint services electronics program
[AD-A145085] 01 p0042 N85-10276
Estimation of target positioning using planar arrays
[RSRE-MEMO-3675] 02 p0189 N85-11266
Intrinsic polarization basis of radar target observed by system employing diversity reception
07 p0949 N85-16015
Shuttle ku-band communications/radar technical concepts 08 p1090 N85-16940
An adaptive Fast Fourier Transform weighting technique to increase small target sensitivity
[AD-D011424] 08 p1154 N85-17286
Loop radiating elements
[AD-D011409] 08 p1158 N85-17308
Multi-bistatic radar for short range surveillance
[BAE-BT-10603] 15 p2539 N85-25673
Hardware test program for evaluation of baseline range/range rate sensor concept
[NASA-CR-175910] 17 p2947 N85-28194
Digital methods of the optimum processing of radar signals
[AD-A152469] 17 p2948 N85-28202
Inherent angular tracking error in an amplitude comparison monopulse radar
[AD-A154212] 19 p3255 N85-30185
Radar target identification through electromagnetic scattering studies
[AD-A154596] 21 p3573 N85-32220
Head-on scattering of a tubular cylinder of finite length for radar target identification purposes
[AD-A155606] 21 p3577 N85-32246
Broadside scattering of a tubular cylinder for evaluation of target identification
[AD-A155739] 21 p3577 N85-32248
Morphology of the scattering targets: Fresnel and turbulent mechanisms, part 2.1A
21 p3618 N85-32481
USSR report: Electronics and electrical engineering
[JPRS-UEE-84-015] 22 p3762 N85-33314
Method of static measurements of absolute scattering matrix of radar targets 22 p3762 N85-33316
Selectivity of weight compensator of passive interference to unknown velocities of detectable targets
22 p3762 N85-33317
Potential coordinate estimate accuracy estimation accuracy by multiposition radar systems
22 p3763 N85-33322

RADAR TRACKING
Estimation of target positioning using planar arrays
[RSRE-MEMO-3675] 02 p0189 N85-11266
Modelling of altimeter tracking over topographical surfaces — satellite antennas 03 p0363 N85-12450
A feasibility study on the use of wind profilers to support Space Shuttle launches
[NASA-CR-3861] 04 p0536 N85-13423
Tracking servo compensator with rate aiding
[AD-D011372] 07 p0942 N85-15971
Shuttle ku-band communications/radar technical concepts 08 p1090 N85-16940
Hybrid state estimation approach to multiobject tracking for airborne surveillance radars
[AD-A148459] 08 p1153 N85-17279
Methodology improvement program for the second generation miss distance radar (MIDI 2)
[AD-A148467] 08 p1153 N85-17281
Design and realization of a multiradar tracking system for air traffic control
[ENST-84E010] 09 p1279 N85-18044
Investigations relating to the simultaneous use of Combined Optical Adaptive Techniques (COAT) and angle-tracking
[ESA-TT-844] 09 p1365 N85-18712
Multi target tracking by dynamic scene analysis
[AD-A148922] 10 p1486 N85-19250
MTI system simulation and clutter output statistics
[AD-A149193] 10 p1487 N85-19255
Fundamental limits to synchronization and tracking
[AD-A149623] 12 p1833 N85-21504
Synthesis of optimum algorithms for secondary processing 13 p2080 N85-22992
High time-resolution studies of the auroral ionosphere
[AD-A150945] 14 p2409 N85-24850
Estimation of maneuvering targets
15 p2606 N85-26253
An empirical self-protection chaff model
[AD-A151928] 16 p2773 N85-27115
Ziv-Zakai bound applied to an amplitude-comparison monopulse radar
[AD-A151937] 16 p2773 N85-27118
A short range, high accuracy radar ranging system
[AD-A152195] 16 p2774 N85-27122
A constant altitude flight survey method for mapping atmospheric ambient pressures and systematic radar errors
[NASA-TM-86733] 19 p3217 N85-29961
Docking simulation analysis of range data requirements for the orbital maneuvering vehicle
[NASA-TM-86510] 20 p3407 N85-31143

RADAR TRANSMISSION
Pulse transmission through frozen silt
[AD-A147108] 07 p0940 N85-15958
Factorized algorithms for combined spatial and temporal processing of radar signals 13 p2081 N85-22997
A review of tropospheric refraction effects on Earth-to-satellite systems 18 p3107 N85-29235
Criteria and algorithms for spectrum parameterization of MST radar signals 21 p3626 N85-32527
Feasibility study of radar-transmitting materials
[AD-A155839] 24 p4087 N85-35329

RADAR TRANSMITTERS
Architecture for a demonstration radar-communication link
[AD-A147635] 08 p1150 N85-17260
Digital controller for the Wave Propagation Laboratory's VHF and UHF wind-profiling radars
[PB85-112142] 11 p1626 N85-20238
The Chinese remainder theorem and multi-PRF radars
[AD-A141375] 13 p2054 N85-22858
Summary of session on optimum transmitter and antenna configuration for MST radar, part 6
21 p3624 N85-32514
Increase of antenna area instead of transmitter power, part 6.3A 21 p3624 N85-32517

RADARSCOPES
NT PLAN POSITION INDICATORS
Visual attention to radar displays
05 p0704 N85-14514

RADIAL DISTRIBUTION
Transport experiments in the Texas experimental Tokamak 09 p1389 N85-18741
Numberical simulation of the effects of radially injected barium plasma in the ionosphere
[NASA-CR-175636] 14 p2354 N85-24542
On the radial structure of planetary rings
15 p2675 N85-26512
Inherent magnetic field error measurements in ELMO Bumpy Torus
[DE85-005855] 16 p2867 N85-27685
Testing and optimizing MST coaxial collinear arrays, part 6.4A 21 p3625 N85-32518
The galactic gamma-ray distribution and the radial cosmic ray gradient
[OG-3.1-4] 22 p3873 N85-33992
Radial distribution of cosmic ray intensity in the galaxy from gamma-ray data
[OG-3.1-5] 22 p3873 N85-33993
Constraints on the galactic distribution of cosmic rays from the COS-B gamma-ray data
[OG-3.1-6] 22 p3873 N85-33994
Breakdown of intrinsic ambipolarity for the radial diffusion due to a rotating RF field 23 p3977 N85-34660
Transports studies of ECH and ICRH-heated bumpy torus plasma in NBT-1M 23 p3978 N85-34662
Analytic and numerical calculations of the ambipolar electric field in a stellarator 23 p3978 N85-34665
Radial and latitudinal gradients of anomalous oxygen during 1977 - 1985
[SH-4.6-4] 23 p4039 N85-35042
The cosmic ray interplanetary radial gradient from 1972 - 1985
[SH-4.7-1] 23 p4040 N85-35046
A note on some statistical properties of rise time parameters used in muon arrival time measurements
[HE-4.7-12] 24 p4199 N85-36062

RADIAL DRAINAGE PATTERNS
U DRAINAGE PATTERNS

RADIAL FLOW
Turbine test report, addendum
[DE84-015130] 02 p0205 N85-11353
Stability of circular cylindrical shell with piecewise constant thickness subjected to radial pressure
06 p0779 N85-14982
The modelling of latitudinal gradients in the solar wind in the outer solar system 12 p1947 N85-22231
Coupling between velocity oscillations and solid propellant combustion
[AD-A151081] 14 p2247 N85-23927

RADIAL VELOCITY
South African Astronomical Observatory Circulars, no. 7
[SAAOC-7] 01 p0127 N85-10875
Simultaneous photometry and radial velocities of dwarf cepheids and Delta Scuti stars
01 p0128 N85-10878
A wide latitude CO survey of molecular clouds in the northern Milky Way 06 p0877 N85-1
High precision measurement of stellar radial velocity variations 08 p1250 N85-17
Atmospheric limitations in stellar seismology: Should one measure radial velocity or brightness fluctuations?
08 p1251 N85-17
A spectroscopic study of LMC X-4
[NASA-CR-174414] 10 p1571 N85-1
1983 observations of the eclipsing nucleus of the bipolar planetary nebula NGC 2346 11 p1747 N85-2
Multi-year and possibly periodic variations in the UV spectrum of 58 Pegasi 11 p1756 N85-21
Three short-period binaries seen at high-dispersion UX ARI, IOTA TRI and HA5110 11 p1756 N85-21
Precise measurements of radial velocities of emission lines in the far-ultraviolet spectra of late-type stars
11 p1758 N85-21
Experimental determination of optimum ratio of runner blade height at exit to runner blade height at entrance of radial inward-flow microturbines
13 p2049 N85-22
The effects of image motion on the I-nu diagram
14 p2443 N85-25
The ultraviolet spectra of intermediate redshift quasars
20 p3544 N85-32
The distribution and dynamics of planetary nebulae in M32 and the Andromeda Galaxy
20 p3546 N85-32
Use of the VAD technique and measurements of momentum flux in the stratosphere at Arecibo, part 4.3A
21 p3622 N85-32
Coding schemes for improving MST radar performance, part 7.1A 21 p3625 N85-32

RADIANCE
ISCCP Cloud Algorithm Intercomparison Workshop
01 p0073 N85-10
Spectroradiometric calibration of the Thematic Mapper and Multispectral Scanner system
[E85-10026] 02 p0216 N85-11
Report of the Third Session of the International Working Group on Data Management for the International Satellite Cloud Climatology Project (ISCCP)
[WCP-82] 02 p0231 N85-11
Theoretical elements of photometry
[BLL-RISLEY-TR-5022-(9091.9F)]
02 p0279 N85-11
Effects of atmospheric water vapor and clouds on NOAA (National Oceanic and Atmospheric Administration) AVHRR (Advanced Very High Resolution Radiometer) satellite data
[AD-A145425] 02 p0290 N85-11
LANDSAT instruments characterization
[E85-10032] 04 p0524 N85-13
Flux reconstruction and calibration
09 p1412 N85-18
PMP-1: A coordinated study of the behavior of the middle atmosphere in winter 11 p1654 N85-20
PMP-1 report: The fourth winter of PMP-1, 1981 - 1982: A winter with several interesting features
11 p1657 N85-20
Prelaunch absolute radiometric calibration of the reflective bands on the LANDSAT-4 protoflight Thematic Mapper 11 p1669 N85-20
Relative radiometric calibration of LANDSAT TM reflective bands 12 p1869 N85-21725
Evaluation of the radiometric integrity of LANDSAT 4 Thematic Mapper band 6 data 12 p1869 N85-21726
Thermal band characterization of the LANDSAT-4 Thematic Mapper 12 p1869 N85-21727
MTF analysis of LANDSAT-4 Thematic Mapper
12 p1871 N85-21737
GMS operational calibration procedure and status
12 p1885 N85-21
Analysis of selective chopper radiometer data
[NASA-CR-175157] 12 p1885 N85-21
Remote sensing of coastal wetlands biomass using Thematic Mapper wavebands — Lewes, Delaware
13 p2119 N85-2
The relationship between marine aerosol particles and satellite-detected radiance 13 p2131 N85-2
Sea surface temperatures from VAS MSI data
[NASA-CR-175706] 14 p2382 N85-2
Radiative forcing of the southwest summer monsoon (a satellite perspective) 15 p2593 N85-2
Diagnosis of vertical motions from VAS retrievals during a convective outbreak
[NASA-CR-171569] 19 p3316 N85-3
A transportable, machine oriented library of european sky and terrain radiance distributions with contemporary radiometric and meteorological profiles
[AD-A155254] 21 p3637 N85-3
Diurnal variations of cosmic ray geomagnetic cut-off threshold rigidities
[SH-6.1-21] 23 p4046 N85-3

RADIANT COOLING
Selective radiative cooling with MgO and/or LiF layers [DE85-011886] 19 p3262 N85-30228
RADIANT ENERGY
U RADIATION
RADIANT FLUX DENSITY
NT ELECTRON FLUX DENSITY
NT ILLUMINANCE
NT IRRADIANCE
NT LUMINANCE
NT LUMINOUS INTENSITY
NT NEUTRON FLUX DENSITY
NT PARTICLE FLUX DENSITY
NT PROTON FLUX DENSITY
NT RADIANCE
NT SOLAR CONSTANT
NT SOLAR FLUX DENSITY
Self-modulation of injection laser emission intensity due to external optical feedback 02 p0261 N85-11706
Einstein solid state spectrometer observation of the peculiar red dwarf Wolf 630 AB [NASA-TM-83947] 03 p0447 N85-12643
Software used with the flux mapper at the solar parabolic dish test site [NASA-CR-174108] 04 p0526 N85-13376
Device for measuring average power of laser radiation 06 p0786 N85-15026
Birkeland currents correlated with dc-electric fields observed during the CENTAUR BBX rocket experiments [DR-6-84] 06 p0834 N85-15311
NGC 2024: Multi-wavelength infrared and radio observations 08 p1246 N85-17865
New lighting technologies, their status and impacts on power densities [DE85-000712] 09 p1315 N85-18266
Temperature variation of laser mirror stability criteria 10 p1445 N85-19108
Thermionic converter for space reactor described 11 p1621 N85-20206
EXOSAT observations of the galactic bulge X-ray source GX17+2 — X ray binary star 11 p1742 N85-20951
Performance estimate of a reflecting light pipe for infrared detectors [AD-A141289] 13 p2158 N85-23398
Radiative forcing of the southwest summer monsoon (a satellite perspective) 15 p2593 N85-25981
Amplification of scattered induced radiation flux in high-gain laser rods 15 p2644 N85-26309
Screening ceramic materials for intense radiant heat applications [DE85-008880] 16 p2756 N85-27006
Microwave responses of the western North Atlantic [NASA-CR-175888] 17 p2946 N85-28191
Symposium on Luminescent Radiation Receivers and Converters 19 p3295 N85-30430
Plasma arc welding, equipment, installation and process control [DE85-008481] 19 p3373 N85-30921
Existence of smooth solutions in problems of electromagnetic radiation focusing 21 p3697 N85-32972
Gamma-ray line intensities for depleted uranium [DE85-012874] 22 p3843 N85-33804
Search for excess showers from Crab Nebula [OG-2.3-2] 22 p3866 N85-33939
The 1000 GeV gamma ray emission from radio pulsars 22 p3867 N85-33946
Cosmic gamma rays from quasars [OG-2.7-10] 22 p3872 N85-33983
Energy spectrum of extragalactic gamma-ray sources [OG-2.7-13] 22 p3872 N85-33986
Local interstellar medium and gamma-ray astronomy [OG-3.1-1] 22 p3873 N85-33989
The galactic gamma-ray distribution and the radial cosmic ray gradient [OG-3.1-4] 22 p3873 N85-33992
Radial distribution of cosmic ray intensity in the galaxy from gamma-ray data [OG-3.1-5] 22 p3873 N85-33993
Constraints on the galactic distribution of cosmic rays from the COS-B gamma-ray data [OG-3.1-6] 22 p3873 N85-33994
Local electron spectrum above 100 MeV derived from gamma-ray emissivity spectra [OG-3.1-7] 22 p3874 N85-33995
Relevance of cosmic gamma rays to the mass of gas in the galaxy [OG-3.1-8] 22 p3874 N85-33996
COS-B gamma-ray sources and interstellar gas [OG-3.1-9] 22 p3874 N85-33997
Excess gamma rays from the Loop I supernova remnant [OG-3.1-10] 22 p3874 N85-33998
Long term variability of the cosmic ray intensity [OG-3.1-11] 22 p3874 N85-33999
Spectrum of the gamma-ray diffuse component observed from HEAO-1 [OG-3.1-12] 22 p3874 N85-34000
Galactic antiprotons of 0.2-2 GeV energy [OG-6.1-11] 22 p3888 N85-34101
the role of shock waves in modulation of galactic cosmic rays [SH-4.1-7] 23 p4005 N85-34831
Cumulative effect of Forbush decreases in the heliospheric modulation during the present solar cycle [SH-4.1-10] 23 p4005 N85-34833
Cosmic ray modulatin and merged interaction regions [SH-4.1-11] 23 p4005 N85-34834
Propagation of the phase of solar modulation [SH-4.1-12] 23 p4005 N85-34835
Longitudinal distribution of cosmic rays in the heliosphere [SH-4.1-14] 23 p4006 N85-34837
The 1973-1984 solar modulation of cosmic ray nuclei [SH-4.1-16] 23 p4006 N85-34838
Evidence for regions of negligible cosmic-ray modulation in the inner heliosphere (10 AU) [SH-4.1-21] 23 p4006 N85-34840
Notes on drift theory [SH-4.2-3] 23 p4006 N85-34841
Drift and observations in cosmic-ray modulation, 2 [SH-4.2-5] 23 p4007 N85-34843
Propagation and nucleosynthesis of ultraheavy cosmic rays [OG-7.1-5] 23 p4013 N85-34867
High resolution Cherenkov detectors for cosmic ray isotope experiment [OG-9.1-4] 23 p4023 N85-34930
The final COS-B database now publicly available [OG-9.3-8] 23 p4028 N85-34963
The final COS-B database: In-flight calibration of instrumental parameters [OG-9.3-9] 23 p4028 N85-34964
An observatory to study 10 (10) to 10 (17) by EV gamma rays [OG-9.4-6] 23 p4029 N85-34973
Mini and super mini arrays for the study of highest energy cosmic rays [OG-9.4-9] 23 p4029 N85-34976
Cosmic ray biannual variation [SH-4.4-15] 23 p4034 N85-35011
Cosmic ray power spectral variations. 3: Solar rotation periodicities [SH-4.4-16] 23 p4034 N85-35012
The difference in the energy spectra of galactic cosmic rays at the minima of the 19th and 20th solar activity cycles [SH-4.4-18] 23 p4035 N85-35014
Cosmic ray variations with the period close to 27 days and their connection with solar activity longitudinal distribution [SH-4.4-19] 23 p4035 N85-35015
Azimuthal and meridional asymmetries of the solar wind and quasiperiodic variations of intensity of Galactic Cosmic Rays (GCR) [SH-4.4-20] 23 p4035 N85-35016
Dynamics of two-year cosmic ray variations inferred from the data of spacecraft and stratospheric measurements and from the neutron monitor data in 1959-1981 [SH-4.4-21] 23 p4035 N85-35017
Long-term modulation of galactic cosmic rays in high-energy region [SH-4.4-22] 23 p4035 N85-35018
Diurnal effect in cosmic rays at middle latitudes according to stratospheric measurements [SH-4.5-8] 23 p4036 N85-35026
Diurnal variation of galactic cosmic ray intensity on quiet days [SH-4.5-11] 23 p4037 N85-35029
Diurnal variations from muon data at Takeyama underground station [SH-4.5-13] 23 p4037 N85-35030
Long term changes in cosmic ray diurnal variations observed by ion chambers in Hong Kong and Japan [SH-4.5-14] 23 p4037 N85-35031
Cosmic ray density gradient and its dependence on the north-south asymmetry in solar activity [SH-4.5-17] 23 p4038 N85-35034
Diagnostic of electromagnetic conditions in space using cosmic rays [SH-4.5-19] 23 p4038 N85-35036
Solar cycle variations of the anomalous cosmic ray component [SH-4.6-2] 23 p4039 N85-35040
Temporal variations of the anomalous oxygen component, 1977 - 1984 [SH-4.6-3] 23 p4039 N85-35041
Radial and latitudinal gradients of anomalous oxygen during 1977 - 1985 [SH-4.6-4] 23 p4039 N85-35042
The cosmic ray interplanetary radial gradient from 1972 - 1985 [SH-4.7-1] 23 p4040 N85-35046
When did the average cosmic ray flux increase? [SH-7.1-4] 23 p4047 N85-35097
The structure of Herbig-Haro object 43 and Orion dark cloud extinction [NASA-TM-87503] 24 p4166 N85-35831
Measurement of interaction cross section of cosmic ray Fe nuclei (E4 GeV/N) with Al target [HE-1.1-7] 24 p4170 N85-35855
RADIANT HEATING
New concepts for measuring flame spread properties [NBSIR-84-2943] 03 p0327 N85-12104
Ceramic/ceramic seals by microwave heating [DE84-007486] 04 p0479 N85-13050
Summary of the origin of nonradiative heating/momentum in hot stars 08 p1236 N85-17789
Spontaneous ignition of organic solids by radiant heating 09 p1289 N85-18096
The thermal calculation of opaque heat screens [BLL-M-36273-(5828.4)] 20 p3450 N85-31421
The Konstantinov effect and absorption of sound in inhomogeneous media 21 p3660 N85-32861
Characterization of the optical and thermal properties of matter by photothermal techniques [DE85-012907] 24 p4076 N85-35260
Development of advanced high-temperature heat flux sensors. Phase 2: Verification testing [NASA-CR-174973] 24 p4096 N85-35391
RADIANT INTENSITY
U RADIANT FLUX DENSITY
RADIATION
Photothermal degradation of encapsulants 06 p0830 N85-15270
Most desirable terrain, e.g., flat vs valley location, part 5.1B 21 p3624 N85-32513
Longitudinal distribution of cosmic rays in the heliosphere [SH-4.1-14] 23 p4006 N85-34837
The identification of gamma ray induced EAS [HE-4.5-1] 24 p4195 N85-36026
RADIATION ABSORPTION
NT ATMOSPHERIC ATTENUATION
NT ELECTROMAGNETIC ABSORPTION
NT GAMMA RAY ABSORPTION
NT INFRARED ABSORPTION
NT MOLECULAR ABSORPTION
NT MULTIPHOTON ABSORPTION
NT PHOTOABSORPTION
NT ULTRAVIOLET ABSORPTION
NT X RAY ABSORPTION
Specific absorption rate in a sitting rhesus model at 225, 1290, and 5950 MHz for E, H, and K polarizations [AD-A145435] 02 p0234 N85-11524
Aharonov-Bohm effect in absorption of electromagnetic wave 06 p0786 N85-15022
Acoustoelectric interaction in double-layer semiconductors 06 p0786 N85-15023
Spectral estimators of absorbed photosynthetically active radiation in corn canopies [E85-10041] 07 p0963 N85-16242
Calculation of Si(Li) X-ray detector efficiencies [DE85-002732] 10 p1489 N85-19400
Techniques for measuring intercepted and absorbed PAR in corn canopies [E85-10061] 10 p1505 N85-19495
Latitudinal dependence of the energy input into the mesosphere by high energy electrons 11 p1664 N85-20489
Numerical investigation of propagation of radiation pulse at xxx 11 p1718 N85-20809
Surface physics and crystallography [DE85-003128] 11 p1735 N85-20810
A method for determining in situ the absorption coefficient of particulate media using pulsed laser technique [AD-D011548] 12 p1799 N85-21281
Control of electronic, magnetic and optical properties of doped polyacetylene conductors [AD-A150117] 12 p1814 N85-21375
Correctness of reflection characteristics of radio absorbent materials 13 p2081 N85-22995
A plasma initiation-flow chamber to study CW laser beamed energy absorption in light gases [AD-A151225] 15 p2562 N85-25806
Nuclear radiation induced absorption in optical materials [DE85-007128] 15 p2649 N85-26336
Gyrotron traveling-wave device including quarter wavelength anti-reflective dielectric layer to enhance microwave absorption [AD-D011690] 19 p3271 N85-30285

Influence of surface films of petroleum products on conditions for absorption of solar radiation by upper water layer 19 p3289 N85-30396
Detection of excited states by laser-induced fluorescence
[AD-A155558] 21 p3592 N85-32326
Absorption and scattering properties of aerosols of aggregated particles in the infrared spectral region
[AD-A155475] 21 p3637 N85-32591
Luminescence and absorption of indium-activated potassium-borate glasses subjected to high-power excitation 21 p3661 N85-32868
Absorption of laser radiation in substance with absorption coefficient depending linearly upon temperature 21 p3694 N85-32953
A practical guide to ionization chamber dosimetry at the AFRRI reactor
[AD-A155185] 21 p3703 N85-33003
An approach of reducing the background induced by neutrons
[OG-9.3-5] 23 p4027 N85-34960
Linear absorption and scattering of laser beams
[AD-A156167] 24 p4098 N85-35401
Some nuclear data needs in astrophysics
[DE85-012916] 24 p4168 N85-35842

RADIATION BELTS
NT INNER RADIATION BELT
NT OUTER RADIATION BELT
NT PROTON BELTS
Equatorial energetic distributions of ions of terrestrial radiation belt as function of solar corona temperature response 02 p0160 N85-11067
Earth's radiation belts
[AD-A147927] 07 p0998 N85-16339
Effects of the solar-terrestrial environment on satellite operations
[DE85-002413] 11 p1590 N85-20003
Longitude and pitch-angle distributions of streams of high-energy electrons under Earth's radiation belts
13 p1978 N85-22415
Protons with energies above 30 KeV in Earth's radiation belt at low altitudes during magnetically quiet time close to geomagnetic equator 13 p1980 N85-22423
SAMBO-GEOS: Substorm trapped particle particle boundary movements, particle precipitation and acceleration 14 p2361 N85-24569
Experimental check of ion transport mechanism in Earth's radiation belt with exposure to nonsteady-state electric fields 15 p2480 N85-25308
Substorms in energetic radiation belt particles according to data from Meteor artificial Earth satellite
16 p2719 N85-26768
Cosmic-ray transport in the galactic magnetosphere
[OG-7.2-17] 23 p4016 N85-34894

RADIATION CHEMISTRY
NT PHOTODECOMPOSITION
NT PHOTODISSOCIATION
NT PHOTOLYSIS
Magnetic resonance studies of transient radicals and radical ions
[DE84-011699] 03 p0328 N85-12116
USSR report: Chemistry
[JPRS-UCH-84-012] 06 p0761 N85-14865
Local phase transformation in alloys during charged-particle irradiation
[DE85-005012] 14 p2256 N85-23990
Measurements of radiation-induced segregation and diffusion in ion irradiated alloy using implanted manganese
[AERE-R-11528] 14 p2258 N85-23994

RADIATION COUNTERS
NT CERENKOV COUNTERS
NT NEUTRON COUNTERS
NT NEUTRON SPECTROMETERS
NT PARTICLE TELESCOPES
NT PROPORTIONAL COUNTERS
NT QUANTUM COUNTERS
NT SCINTILLATION COUNTERS
NT SPARK CHAMBERS
A system for monitoring radon and its decay products in the atmosphere
[INPE-3085-PRE/494] 03 p0391 N85-12502
Isotopic composition of primary cosmic rays H-Fe for ISEE-C
[NASA-CR-175266] 05 p0746 N85-14783
Comparison measurements on optical particle counters
[BLL-DOUNREAY-TR-934-(9091.9F)]
07 p0961 N85-16092
New preamplifier for particle detectors
[DE85-004115] 12 p1836 N85-21524
On the P1 data from GMS-SEM
12 p1894 N85-21890
Photon detection with cooled avalanche photodiodes: Theory and preliminary experimental results
16 p2770 N85-27096
Evaluation of a high pressure proportional counter for the detection of radioactive noble gases
[AD-A154436] 19 p3272 N85-30292
Photon-counting image sensors for the ultraviolet
[NASA-CR-176062] 20 p3458 N85-31476
Journal of Research of the National Bureau of Standards, volume 90, number 1, January - February 1985
[PB85-179089] 20 p3522 N85-31908
Plastic scintillator detectors for the study of transfer and breakup reactions at intermediate energies
[DE85-009945] 20 p3528 N85-31945
An absolute calibration of the solid state detectors in the narrow band neutrino beam at CERN
[NIKHEF-H/84-10] 20 p3536 N85-32017
Solar Ultraviolet Spectral Irradiance Monitor (SUSIM)
23 p3901 N85-34160
The response of ionization chambers to relativistic heavy nuclei
[OG-9.1-13] 23 p4024 N85-34939
Comparisons of monthly mean cosmic ray counting rates observes from worldwide network of neutron monitors
[SH-9.1-7] 23 p4051 N85-35122
Working group on penetrating probes at fixed target facilities 24 p4146 N85-35703
Microprocessor-based single particle calibration of scintillation counter
[HE-4.6-13] 24 p4198 N85-36049
The thickness of the shower disc as observed in showers produced by primaries above 10 (19)eV
[HE-4.7-6] 24 p4199 N85-36057
Search for anomalons using plastic nuclear track detectors
[HE-6.2-12] 24 p4212 N85-36148

RADIATION DAMAGE
NT LASER DAMAGE
Microwave susceptibility experiments
[DE84-016188] 02 p0192 N85-11281
Review: Role of refractory metal alloys in fusion reactor applications
[AERE-R-11317] 03 p0422 N85-12695
Investigation of internal fields and motions, radiation damages and recovery processes using beta and gamma active probe nuclei 03 p0427 N85-12726
Spectroscopic investigations on neutron induced impurity atoms and radiation defects
03 p0430 N85-12742
A study of defects in neutron transmutation doped silicon: Gallium by hall effect analysis
[AD-A146047] 03 p0433 N85-12758
Preliminary results of advanced Biostack experiments with plant seeds and spores — cosmic ray effects
05 p0691 N85-14441
Chemical protection against ionizing radiation
[AD-A147822] 07 p1016 N85-16457
Electron-irradiated effects in metals
[DE84-016989] 09 p1297 N85-18147
Facilities for studing radiation damage in nonmetals during irradiation
[DE85-000590] 10 p1554 N85-19601
Lithium counterdoped silicon solar cell
[NASA-CASE-LEW-14177-1] 11 p1672 N85-20535
Technological process effect on the carrier lifetime degradation of silicon solar cell base layer irradiated by 1 MeV electrons (boron doping case)
13 p2007 N85-22585
The effects of lithium counterdoping on radiation damage and annealing in n(+)p silicon solar cells
13 p2007 N85-22586
Investigation of the degradation of GaAs photovoltaic cells by proton and electron irradiation
13 p2008 N85-22587
In-orbit laser regeneration of the radiation damaged solar arrays 13 p2008 N85-22588
Analysis of optimum front cover thickness for lightweight solar arrays 13 p2010 N85-22606
Annealing of radiation damage in boron and gallium doped silicon solar cells 13 p2012 N85-22624
Some observations of heated gallium arsenide heteroface solar cells
[NASA-TM-86388] 14 p2246 N85-23925
Laser annealing of ion implanted HgCdTe
[AD-A150875] 14 p2427 N85-24966
ELF (Extremely Low Frequency) communications system ecological monitoring program: Measurements of ELF electromagnetic fields for site selection and characterization, 1983
[AD-A153120] 17 p2949 N85-28209
Radiation damage and repair in cells and cell components. Part 2: Physical radiations and biological significance
[DE85-008934] 18 p3152 N85-29518
Radiation damage and repair in cells and cell component, part 1
[DE85-008667] 18 p3152 N85-29519
Thin layered interference mirrors to reduce radiation damage
[DE85-009783] 18 p3185 N85-[illegible]
Summary of recent studies on AlGaAs/GaAs radiation hardened photodiodes
[DE85-009501] 18 p3194 N85-[illegible]
Electron spin resonance study of interface states induced by electron injection in metal-oxide-semiconductor devices
[DE85-009502] 18 p3195 N85-[illegible]
Collected epidemiological studies of the late effects of internal radium in man, and mechanistic investigations of those effects, part 2
[DE85-011174] 19 p3331 N85-[illegible]
Reduction of radiation damage in solar cells — spacecraft power supplies
[ESA-CR(P)-2005] 20 p3485 N85-[illegible]
Nuclear responses in INTOR plasma stabilization elements
[DE85-010489] 20 p3535 N85-[illegible]
Effects of laser radiation on surfaces and coatings
[DE85-010475] 22 p3790 N85-[illegible]
Ultraviolet radiation-damage absorption peak in solid deuterium-tritium, revision 1
[DE85-012969] 22 p3844 N85-[illegible]
Effects of space radiation on advanced semiconductor devices. Part 3: Further cosmic ray simulation studies of single event upsets and latch-up in CMOS memories
[AERE-G-3368-PT-3] 22 p3848 N85-[illegible]
The 1983 international intercomparison of nuclear accident dosimetry systems at Oak Ridge National Laboratory
[DE85-011303] 23 p3934 N85-[illegible]

RADIATION DETECTORS
NT DOSIMETERS
NT SILICON RADIATION DETECTORS
NT THRESHOLD DETECTORS (DOSIMETERS)
Thick film radiation detector
[AD-D011211] 01 p0046 N85-[illegible]
Report on solar neutrino experiments
[DE84-014567] 01 p0131 N85-[illegible]
Sensitivity improvement of a two-mode gravitational radiation detector through the use of a transducer not perfectly tuned to the antenna
[NOTA-INTERNA-812] 02 p0192 N85-[illegible]
High-bandwidth multichannel fiber optic system for measuring gamma rays
[DE84-014526] 04 p0584 N85-[illegible]
100 MHz fiber optic single transient gamma ray detection system
[DE84-016818] 05 p0729 N85-[illegible]
Sensor-atmosphere-target simulation. Computer program SENSAT
[DFVLR-FB-84-32] 08 p1176 N85-17410
P-I-N CdTe gamma-ray detectors by Liquid Phase Epitaxy (LPE)
[DE84-012276] 09 p1323 N85-[illegible]
Linear, position-sensitive X-ray detector used for real-time calculations of small-angle scattering parameters with submillisecond resolution
[DE85-002530] 10 p1489 N85-[illegible]
New preamplifier for particle detectors
[DE85-004115] 12 p1836 N85-21524
Dielectric detector device for registering heavy cosmic radiation particles 13 p2045 N85-[illegible]
Magnetic monopoles
[DE85-008178] 17 p3027 N85-[illegible]
Experiments and detectors for high energy heavy ion colliders
[DE85-007927] 17 p3031 N85-[illegible]
Polymer Research at Synchrotron Radiation Sources: Symposium Proceedings
[DE85-008486] 18 p3081 N85-[illegible]
The possibility of observing solar neutron events in the lower atmosphere
[NOTA-INTERNA-837] 18 p3200 N85-[illegible]
Improved fluid flow meter for measuring the rate of fluid flow in a conduit
[NASA-CASE-MFS-26030-1] 19 p3271 N85-[illegible]
Double photon excitation of high-Rydberg atoms as a long-lived submillimeter detector
[NASA-CASE-NPO-16372-1] 19 p3352 N85-[illegible]
The SLC program
[DE85-011433] 19 p3357 N85-[illegible]
Bismuth germanate scintillators: Applications in nuclear safeguards and health physics
[DE85-010730] 19 p3365 N85-[illegible]
Annual environmental monitoring report, January-December 1984
[DE85-011689] 20 p3486 N85-[illegible]
On the design of a global detection system for airborne radioactivity
[CM-66] 20 p3487 N85-31670
Detection of solar neutrons by ground based neutron monitors
[IFSI-84-11] 20 p3547 N85-[illegible]

Detector problems at the SSC
[DE85-010217] 21 p3703 N85-33007
Research in extreme ultraviolet and far ultraviolet astronomy
[NASA-CR-176068] 21 p3716 N85-33060
Batteryless magneto-driven portable radiac
[DE85-011622] 22 p3760 N85-33300
Beta response of selected instruments
[DE85-013270] 22 p3786 N85-33469
Advanced instrumentation for Positron Emission Tomography
[DE85-011147] 22 p3840 N85-33779
Detection of gamma-ray lines from the direction of the Crab Nebula 22 p3866 N85-33943
Relative abundances of elements (20 or = Z or = 26) at energies up to 70 GeV/amu using relativistic rise in ion chambers
[OG-4.1-7] 22 p3876 N85-34013
CYLTRAN calculations of electron effects on XD detectors
[LA-10384-MS] 23 p3969 N85-34601
Improved method for the stabilization of NaI-photomultiplier gamma detectors against thermal and other drift
[DE85-011830] 23 p3970 N85-34613
Cross sections for the production of fragments with Z greater than or equal to 6 by fragmentation of Z greater than or equal to 9 and less than or equal to 26 nuclei
[OG-7.2-22] 23 p4016 N85-34889
The development of a high energy cosmic ray detector for Spacelab-2
[OG-9.1-8] 23 p4023 N85-34934
Cherenkov-dE/dx-range measurements on cosmic ray iron group nuclei
[OG-9.1-12] 23 p4024 N85-34937
The response of ionization chambers to relativistic heavy nuclei
[OG-9.1-13] 23 p4024 N85-34939
A balloon-borne imaging gamma-ray telescope
[OG-9.2-2] 23 p4024 N85-34941
The Figaro experiment for the observation of time marked sources in the low energy gamma-ray range
[OG-9.2-11] 23 p4026 N85-34950
A position sensitive phoswich hard X-ray detector system
[OG-9.3-12] 23 p4028 N85-34967
The Buckland Park air shower array
[OG-9.4-4] 23 p4029 N85-34971
An EAS experiment at mountain altitude for the detection of gamma-ray sources
[OG-9.4-5] 23 p4029 N85-34972
Detection of 10 (1) GeV cosmic neutrinos with a space station
[OG-9.4-10] 23 p4030 N85-34977
Shower disc sampling and the angular resolution of gamma-ray shower detectors
[OG-9.5-2] 23 p4030 N85-34980
Angular resolution of air-shower array-telescopes
[OG-9.5-6] 23 p4030 N85-34983
Astrophysical applications of high angular resolution array-telescopes
[OG-9.5-7] 23 p4031 N85-34984
Results of ultra-low level 71ge counting for application in the Gallex-solar neutrino experiment at the Gran Sasso Underground Physics Laboratory
[SH-8.1-2] 23 p4049 N85-35108
Detector calibration of the Indian cosmic ray experiment (IONS) in Space-Shuttle Spacelab-13
[SH-8.1-2] 23 p4050 N85-35117
High resolution beam profile monitors in the SLC
[DE85-013375] 24 p4157 N85-35774
The structure of EAS at E 0.1 EeV
[HE-4.4-2] 24 p4193 N85-36012
Expected rates with mini-arrays for air showers
[HE-4.7-8] 24 p4199 N85-36059
A note on some statistical properties of rise time parameters used in muon arrival time measurements
[HE-4.7-12] 24 p4199 N85-36062
Multimuons events and primary composition
[HE-5.1-5] 24 p4201 N85-36070

RADIATION DISTRIBUTION
NT ANTENNA RADIATION PATTERNS
NT DIFFRACTION PATTERNS
NT RAINBOWS
NT SIDELOBES
Direction dependent radiation behavior in the classification of multispectral aircraft remote sensing data
[SER-C-290] 01 p0063 N85-10419
Measurements of polarization characteristics of radiation field of on-board aircraft antennas
03 p0346 N85-12230
Simple formula to estimate carbon dioxide gas effect in radiation balance of underlying surface
06 p0823 N85-15226
Theoretical studies relating to the interaction of radiation with matter: Atomic collision processes occurring in the presence of radiation fields
[AD-A148854] 07 p1040 N85-16602
Effect of scattering on instabilities in line-driven stellar winds 08 p1235 N85-17784
Radiative amplification of acoustic waves in hot stars
08 p1235 N85-17786
Evaluation of parameters of a signal (selected pages)
[AD-A148831] 09 p1312 N85-18243
Atmospheric diffusion in hilly region on middle reaches of the Cheng Jiang 11 p1620 N85-20196
MSG-7: Atmospheric penetration of solar radiation in the range of Schumann-Runge bands
11 p1657 N85-20443
Radiation safety of crew and passengers of air transportation in civil aviation. Provisional standards
[NASA-TM-77610] 11 p1692 N85-20636
USSR report: Physics and mathematics
[JPRS-UPM-85-001] 11 p1715 N85-20786
Problem of frequency space variation of sonic field in stratified media 11 p1715 N85-20787
Generation of sound by a vortex point in a steady flow of slightly compressible fluid 11 p1715 N85-20789
Stellar ultraviolet flux distributions in the 912-1200 A wavelength range 11 p1762 N85-21061
Numerical methods for analyzing electromagnetic scattering
[NASA-CR-175507] 12 p1823 N85-21438
The physical interactions of radiofrequency radiation fields and biological systems 16 p2775 N85-27129
Fiber optics in high dose radiation fields
[DE85-008649] 18 p3185 N85-29755
Cavityless optical bistability in systems of two-level atoms 18 p3186 N85-29764
Measurement of RF fields associated with ISM equipment as it relates to aeronautical services
[FAA-ES-84-2] 19 p3254 N85-30180
Measurement of radiated emissions from industrial heating device equipment as it relates to aeronautical services
[FAA-ES-85-2] 19 p3255 N85-30181
Research in particles and fields
[NASA-CR-176069] 21 p3724 N85-33103
Supernova explosion in dense clouds in the galaxy and the COS-B gamma-ray sources
[OG-2.5-3] 22 p3869 N85-33960
Galactic distribution of interstellar Al-26
[OG-3.2-3] 22 p3874 N85-34002
Longitudinal distribution of cosmic rays in the heliosphere
[SH-4.1-14] 23 p4006 N85-34837
Notes on drift theory
[SH-4.2-3] 23 p4006 N85-34841
The model-independence of cosmic ray source determinations
[OG-7.2-1] 23 p4014 N85-34873
A kinetic model for predicting oxidative degradation rates in combined radiation-thermal environments
[TI85-002629] 24 p4100 N85-35414
Multiplicity distributions in interaction models used for cascade simulations
[HE-1.2-5] 24 p4172 N85-35863
Angular distribution and multiplicity of backward hadrons in hFe interactions at 0.5-5.0 TeV energies (PION Experiment)
[HE-1.2-8] 24 p4172 N85-35866
Measurement of the local density spectrum
24 p4189 N85-35984

RADIATION DOSAGE
Radiofrequency and microwave radiation
[AD-A145492] 02 p0191 N85-11274
Thermoregulatory consequences of long-term microwave exposure at controlled ambient temperatures
[PB84-236603] 05 p0697 N85-14484
Characterizing X-ray machines
[AD-A146532] 06 p0862 N85-15481
A total dose characterization of five commercial analog multiplexers
[AD-A146886] 07 p0946 N85-15997
Computer subroutines for estimation of human exposure to radiation in low Earth orbit
[NASA-TM-86324] 08 p1199 N85-17550
Approaches to radiation guidelines for space travel
[DE85-001248] 09 p1363 N85-18576
Robotics at Savannah River site: Activity report
[DE85-003657] 11 p1648 N85-20383
Models and parameters for environmental radiological assessments
[DE81-027154] 11 p1676 N85-20573
Behavior degradation due to 1100-RAD pulsed radiation exposure (5.8:1 neutron/gamma ratio)
[AD-A149294] 11 p1689 N85-20621
Radiation exposure and performance of multiple burn LEO-GEO orbit transfer trajectories
[NASA-TM-86848] 12 p1788 N85-21228
Biological effects on radiofrequency radiation
[PB85-120848] 12 p1900 N85-21930
Distribution of radium and plutonium in human bone
[DE85-005025] 13 p2142 N85-23298
Space radiation studies for the reporting period, June 1983 - July 1984
[NASA-CR-171411] 15 p2685 N85-26583
Thermal consequences of localized SAR from RFR exposures 16 p2775 N85-27130
The medical results of human exposures to radio frequency radiation 16 p2776 N85-27133
Radio Frequency Radiation (RFR) measurements in operational settings 16 p2777 N85-27136
Energy and Technology Review
[DE85-004358] 17 p3049 N85-28668
Dosimeasurements with thermoluminescence dosimeters at a Febetron 701, 600 kV in room 022 of the Interuniversity Reactor Institute (IRI)
[IRI-190-84-02] 18 p3111 N85-29262
Radiation damage and repair in cells and cell components. Part 2: Physical radiations and biological significance
[DE85-008934] 18 p3152 N85-29518
Comparison of calculations and measurements of the off-axis radiation dose (SI) in liquid nitrogen as a function of radiation length
[AD-A153676] 18 p3176 N85-29704
Measurement of radiated emissions from industrial heating device equipment as it relates to aeronautical services
[FAA-ES-85-2] 19 p3255 N85-30181
Environmental monitoring at Argonne National Laboratory
[DE85-010613] 19 p3309 N85-30516
Effects of long-term low-level radiofrequency radiation exposure on rats. Volume 8: Evaluation of longevity, cause of death, and histopathological findings
[AD-A154283] 19 p3327 N85-30610
Research on the experimental verification of dosimetry calculations
[DE85-011282] 19 p3331 N85-30637
Additional muon calculations for the SLC positron source
[DE85-011212] 19 p3363 N85-30855
The DNA metabolism and poly-(ADP-ribose) synthesis in lymphocytes of persons exposed to low doses of ionizing radiation
[OEFZS-4307] 20 p3507 N85-31600
Dosimetry and limit values for internal contamination with radionuclides: From (International Commission on Radioactive Protection) ICRP-2 to ICRP-30
[IRI-190-84-03] 20 p3507 N85-31604
Sulfur activation at the Little Boy-Comet Critical Assembly: A replica of the Hiroshima bomb
[DE85-010261] 20 p3527 N85-31936
A practical guide to ionization chamber dosimetry at the AFRRI reactor
[AD-A155185] 21 p3703 N85-33003
Empirical correlation of residual gamma radiation resulting from operation of the Health Physics Research Reactor
[DE85-012075] 21 p3704 N85-33006
Wide-ranging radiation dose monitor
[DE85-011596] 22 p3787 N85-33463
Current internal-dosimetry practices at US Department of Energy facilities
[DE85-011718] 22 p3787 N85-33466
Error evaluation in measurements with thermoluminescent dosimeters
[ISS-T-84/6] 22 p3788 N85-33471
The 1984 effluent and environmental monitoring report for the Bettis Atomic Power Laboratory
[DE85-011533] 22 p3810 N85-33602
Control technology for radioactive emissions to the atmosphere at US Department of Energy facilities: The Los Alamos Meson Physics Facility
[DE85-011402] 22 p3811 N85-33609
Airborne cloud tracking measurements during the Three Mile Island nuclear station accident, Middletown, Pennsylvania. Date of survey: March - June 1979
[DE85-012060] 22 p3816 N85-33636
Global environmental transport models for tritium
[DE85-011437] 22 p3816 N85-33639
Investigation of some aspects of amino acid metabolism in man during brief exposure to antiorthostatic hypokinesia combined with ultraviolet radiation
22 p3822 N85-33678
Long-term exposure of (238) PuO2 to a terrestrial environment, volume 3
[DE85-011896] 22 p3840 N85-33781
Microdosimetric spectra measurements of JANUS neutrons
[DE85-012108] 22 p3843 N85-33801

Marine Sample Exploitation Project: Estimates regarding the sensitivity and technology for the detection of nuclear explosion debris in the marine environment
[DE85-013176] 23 p3947 N85-34462
Circuit approaches to increasing SRAM performance in total dose environments
[DE85-009441] 23 p3966 N85-34588
A kinetic model for predicting oxidative degradation rates in combined radiation-thermal environments
[TI85-002629] 24 p4100 N85-35414
Wholebody radiation counting system
[AD-A155842] 24 p4131 N85-35607
Tritium hazard via the ingestion pathway
[DE85-012897] 24 p4133 N85-35618
Calibration of a high-level photon irradiation
[DE85-013044] 24 p4151 N85-35738
Recent advances in remote handling at LAMPF
[DE85-012725] 24 p4157 N85-35775
Total integrated dose testing of solid-state scientific CD4011, CD4013, and CD4060 devices by irradiation with CO-60 gamma rays
[NASA-CR-176196] 24 p4161 N85-35795

RADIATION EFFECTS
NT LASER DAMAGE
NT RADIATION DAMAGE
NT RADIATION INJURIES
NT RADIOLYSIS

Radiation effects on structural materials
[DE84-014771] 01 p0029 N85-10178
Energy deposition in microvolumes of silicon from high energy proton reactions
[AD-A144713] 01 p0123 N85-10845
Cosmic ray effects on microelectronics. Part 3: Propagation of cosmic rays in the atmosphere
[AD-A145026] 01 p0131 N85-10902
Diagnostics of ionization in air produced by infrared radiation from A pulse CO2 laser
[AD-A145376] 02 p0201 N85-11342
The effect of temperature on the radiation induced losses of large diameter GPS (Germanium phosphosilicate) and GBS core optical fibers
[AD-A145409] 02 p0280 N85-11823
Internal friction, microstructure and radiation effects
[DE84-013906] 02 p0288 N85-11880
Breakdown of porous metals by laser radiation
03 p0349 N85-12249
Determination of bound water in biological tissue and energy dissipated in bound water by low level microwaves
[AD-A143101] 03 p0399 N85-12547
Evaluation of ferritic alloy Fe-2 1/4Cr-1Mo after neutron irradiation: Irradiation creep and swelling
[DE84-014647] 04 p0474 N85-13022
Radiation effects in amorphous metallic alloys
[DE84-014302] 04 p0475 N85-13025
Measuring transient radiation effects in optical fibers
[DE84-015044] 04 p0565 N85-13598
Gamma-induced leakage in junction field-effect transistors
[DE84-014990] 04 p0570 N85-13634
Effects of the solar and extraterrestrial environments on space power systems 05 p0610 N85-13896
Environmental interactions working group report
05 p0611 N85-13908
Effects of irradiation fluence and creep on fracture toughness of 347/348 stainless steel
[DE84-016091] 05 p0618 N85-13953
Plant responses to solar UV-B radiation
05 p0680 N85-14436
Spacelab 1 experiment: Microorganisms in space hard environment 05 p0691 N85-14443
Transient attenuation in optical fibers
[DE84-016487] 05 p0729 N85-14687
Synergisms in surface erosion, session summary
06 p0864 N85-15493
Synergism in materials erosion due to multispecies impact 06 p0864 N85-15494
Irradiation creep induced anisotropy in a/2110 dislocation populations
[DE84-016823] 06 p0888 N85-15520
A total dose characterization of five commercial analog multiplexers
[AD-A146886] 07 p0946 N85-15997
USSR report: Life sciences. Biomedical and behavioral sciences
[JPRS-UBB-84-015] 07 p1010 N85-16416
USSR report: Life sciences. Biomedical and behavioral sciences
[JPRS-UBB-84-027] 07 p1012 N85-16426
Effect of microwave radiation on local blood circulation and oxygenation of brain tissue
07 p1012 N85-16431
Chemical protection against ionizing radiation
[AD-A147822] 07 p1016 N85-16457

Effects of high energy radiation on the mechanical properties of epoxy-graphite fiber reinforced composites
[NASA-CR-174314] 08 p1118 N85-17047
Something in the air at Windscale — radioactive contaminants from the Sellafield nuclear Complex for reprocessing and storing irradiated fuel
[BLL-RISLEY-TR-4999-(9091.9F)]
08 p1179 N85-17429
Effect of ultraviolet radiation on transparent polymer films as determined using in situ FTIR-RA spectroscopy. Volume 2: Photophysics of poly(vinylidene fluoride) films
[DE84-013040] 09 p1299 N85-18150
Transient response of a small-signal microwave GaAs FET to X-rays
[DE85-000066] 09 p1315 N85-18265
Effect of neutron irradiation on the high temperature operation of injection laser diodes
[DE85-000068] 09 p1326 N85-18333
Effect of modulated ultrahigh frequency field on behavior and hormone level in female rats under emotional stress
09 p1361 N85-18562
Methodical approaches to determination of sanitation protective zone dimensions around TV centers and TV retransmitters 09 p1361 N85-18563
Functional and structural changes in human erythrocyte surface after irradiation by UV waves of various wavelengths. Report 1: Expression of ABO and Rhesus system antigen 09 p1361 N85-18564
Radiation response of optical fibers in a nuclear reactor
[DE84-017221] 09 p1385 N85-18710
Radiation effects in Strained-Layer Superlattice (SLS) structures
[DE85-001713] 09 p1398 N85-18799
Comparison of ionizing radiation and hot electron effects in MOS structures
[DE84-016766] 09 p1400 N85-18800
Isolated systems in general relativity
09 p1400 N85-18813
Lithography radiation effects study
[AD-A148552] 10 p1488 N85-19260
Genetic effects of microwave exposure on mammalian cells in vitro. Volume 2, Appendix A: Cytogenetics and growth kinetics data, 850 MHz
[AD-A148866] 10 p1522 N85-19599
Genetic effects of microwave exposure on mammalian cells in vitro. Volume 2, Appendix B: Cytogenetics and growth kinetics data, 1.2 GHz
[AD-A148867] 10 p1522 N85-19600
Genetic effects of microwave exposure on mammalian cells in vitro, volume 2
[AD-A148347] 10 p1523 N85-19603
Effects of the solar-terrestrial environment on satellite operations
[DE85-002413] 11 p1590 N85-20003
Metals and Ceramics Division Materials Science Program
[DE85-003795] 11 p1592 N85-20012
Conductivity changes in neutron-irradiated commercial copper alloys at approximately 450(O)C
[DE85-003007] 11 p1606 N85-20100
Design and use of nonstandard tensile specimens for irradiated materials testing
[DE85-001071] 11 p1652 N85-20408
Behavior degradation due to 1100-RAD pulsed radiation exposure (5.8:1 neutron/gamma ratio)
[AD-A149284] 11 p1669 N85-20621
Radiation safety of crew and passengers of air transportation in civil aviation. Provisional standards
[NASA-TM-77610] 11 p1692 N85-20638
Effects of neutron irradiation on the fracture properties of HT-9 weld
[DE85-001068] 12 p1807 N85-21339
Effect of ultraviolet radiation on transparent polymer films as determined using in situ FTIR-RA spectroscopy. Volume 1: Photodegradation of transparent polymer films
[DE84-013039] 12 p1814 N85-21377
Performance assessment of Class 1E pressure transmitters subjected to environmental stresses
[DE85-001623] 12 p1854 N85-21626
Research and technology activities at Ames Research Center's Biomedical Research Division
[NASA-TM-86692] 12 p1899 N85-21925
Biological effects on radiofrequency radiation
[PB85-120848] 12 p1900 N85-21930
Irradiation effects on fuels for space reactors
[DE84-016460] 12 p1931 N85-22134
Solar array dynamical simulation for illumination and temperature variation 13 p2011 N85-22611
Breakdown of thin plates by radiation
13 p2026 N85-22709
Effect of alternative aging and accident simulations on polymer properties
[DE85-002642] 13 p2037 N85-22762

Radiation-dominated snowmelt on Mars
13 p2191 N85-2
NASA space materials research
14 p2232 N85-2
Effect of elevated-temperature neutron irradiation o fracture toughness of ceramics
[DE85-000652] 14 p2261 N85-240
Radiological safety aspects of industrial radiography
14 p2316 N85-2431
NMR imaging and spectroscopy of the mammalian central nervous system after heavy ion radiation
[DE85-004509] 14 p2365 N85-2
Photoreactivation and other ultraviolet/visible ligh effects on DNA in human skin
[DE85-005135] 14 p2380 N85-247
Use of irradiated foods 14 p2393 N85-247
Influences of thermal spikes in ion beam mixing
[DE85-006130] 14 p2419 N85-24
Radiation effects induced in pin photodiodes by 40- an 85-MeV protons
[NASA-CR-175678] 14 p2426 N85-24
Spectroscopic analysis of radiation-generated change in tensile properties of a polyetherimide film
[NASA-TP-2429] 15 p2502 N85-254
Effects of ion bombardment on the morphology of la films
[DE85-007232] 15 p2511 N85-254
Effects of long-term low-level radiofrequency radiatio exposure on rats. Volume 7: Metabolism, growth an development
[AD-A150829] 15 p2615 N85-2611
Nuclear radiation induced absorption in optica materials
[DE85-007126] 15 p2649 N85-26
Radiation effects on structural materials
[DE85-007032] 15 p2649 N85-26
Physics effects of accidental submersion of space pow reactors in water
[DE85-005020] 15 p2650 N85-26
Assessment of present and future large-sca semiconductor detector systems
[DE85-006606] 15 p2662 N85-264
USSR report: Space
[JPRS-USP-85-004] 16 p2717 N85-2677
Satellite research on solar flares
16 p2717 N85-267
Swelling behavior of titanium-modified AISI 316 alloys
[DE85-007470] 16 p2752 N85-26
The Impact of Proposed Radio Frequency Radiation Standards on Military Operations
[AGARD-LS-138] 16 p2775 N85-2712
The physical interactions of radiofrequency radiatio fields and biological systems 16 p2775 N85-2712
The biological effects of radiofrequency radiation
16 p2775 N85-2713
The medical results of human exposures to radi frequency radiation 16 p2776 N85-2713
In situ HVEM studies of electron beam-driv composition changes in thin film alloys: Displacement-ra gradient effects
[DE85-007992] 17 p2931 N85-28
Biological and human health effects of extremely lo frequency electromagnetic fields. Post-1977 literatur review
[AD-A152731] 17 p2969 N85-28
Fiber optics in high dose radiation fields
[DE85-008649] 18 p3185 N85-297
Effects of gamma-ray irradiation on dislocations i sodium nitrate single crystals
[DE85-008291] 18 p3195 N85-29
Activities report in energy technology
[OEFZS-4302] 18 p3199 N85-29
Alloy development for irradiation performance
[DE85-010454] 19 p3240 N85-30
Method of reducing impurity and antisite defects i semiconductor crystal materials, and device and apparatu respectively produced from and utilizing same
[AD-D011696] 19 p3260 N85-30
Effects of long-term low-level radiofrequency radiatio exposure on rats. Volume 8: Evaluation of longevity, caus of death, and histopathological findings
[AD-A154283] 19 p3327 N85-30
Repair of DNA treated with lambda-irradiation an chemical carcinogens
[DE85-010266] 19 p3327 N85-30
Radiation interactions for tomography
[DE85-006961] 19 p3355 N85-307
Interaction of slow electrons with high-pressure gas (quasi-liquids): Synthesis of our knowledge on sl electron-molecule interactions
[DE85-010061] 19 p3355 N85-30
NBS (National Bureau of Standards) reactor: Summa of activities Jul. 1983 through Jun. 1984
[PB85-184836] 20 p3522 N85-31

Sulfur activation at the Little Boy-Comet Critical ssembly: A replica of the Hiroshima bomb
DE85-010201] 20 p3527 N85-31938
Polymer-water interaction studies
21 p3609 N85-32411
Nuclear thermal transmittance in the atmosphere using LOWTRAN-6 computer code
[AD-A154669] 21 p3630 N85-32553
USSR report: Life sciences. Biomedical and behavioral sciences
[JPRS-UBB-85-020] 21 p3663 N85-32752
USAFSAM review and analysis of radiofrequency radiation bioeffects literature
[AD-A155113] 21 p3664 N85-32760
Empirical correlation of residual gamma radiation resulting from operation of the Health Physics Research Reactor
[DE85-012075] 21 p3704 N85-33008
Tritium-helium effects in metals
[DE85-011507] 22 p3749 N85-33235
Effects of laser radiation on surfaces and coatings
[DE85-010475] 22 p3790 N85-33484
Hit-size effectiveness theory applied to high doses of low LET radiation for pink mutations in Tradescantia
[DE85-011835] 22 p3819 N85-33657
USSR report: Life sciences. Biomedical and behavioral sciences
[JPRS-UBB-85-018] 22 p3819 N85-33660
Investigation of some aspects of amino acid metabolism in man during brief exposure to antiorthostatic hypokinesia combined with ultraviolet radiation
22 p3822 N85-33678
Use of gamma radiation as a form of preservation of sweet potatoes
[DE85-011998] 22 p3841 N85-33787
Analysis of transient radiation upset in a 16K SRAM
[DE85-009442] 23 p3965 N85-34586
System expectations for Pioneer 1 foil implosion experiments
[DE85-014129] 24 p4091 N85-35359
A kinetic model for predicting oxidative degradation rates in combined radiation-thermal environments
[TI85-002629] 24 p4100 N85-35414
Biophysical research in space — radiation effects
24 p4130 N85-35603
Total integrated dose testing of solid-state scientific CD4011, CD4013, and CD4060 devices by irradiation with CO-60 gamma rays
[NASA-CR-176196] 24 p4161 N85-35795
Electron irradiation of N type cadmium telluride
[AD-A156117] 24 p4161 N85-35801

RADIATION EMISSION
U RADIATION

RADIATION EXPOSURE
U RADIATION DOSAGE

RADIATION FIELDS
U RADIATION DISTRIBUTION

RADIATION HARDENING
Pulsed irradiation of optimized, MBE grown, AlGaAs/GaAs radiation hardened photodiodes
[DE84-014964] 04 p0569 N85-13631
Radiation hardened ion-implanted GaAs field effect transistor and method for making the same specification
[AD-D011264] 05 p0731 N85-14897
Analytic models for radiation induced loss in optical fibers 2. A physical model
[AD-A147442] 07 p1044 N85-16832
The planned expansion of microelectronics capability at Sandia National Laboratory
[TI85-004326] 09 p1314 N85-18260
Corrosion behavior of Al4 aluminum alloy hardened by CO2 laser radiation 15 p2514 N85-25512
Radiation hardening for VLSI applications
[DE85-005493] 16 p2780 N85-27155
Summary of recent studies on AlGaAs/GaAs radiation hardened photodiodes
[DE85-008501] 18 p3194 N85-29812
A comparison of the radiation hardness of various VLSI technologies for defense applications
[DE85-008973] 19 p3263 N85-30236
Electron lithography STAR design guidelines. Part 2: The design of a STAR for space applications
[NASA-CR-170786] 20 p3513 N85-31841
Radiation-hardened polymeric films
[DE85-011636] 22 p3752 N85-33259
Circuit approaches to increasing SRAM performance in total dose environments
[DE85-009441] 23 p3966 N85-34588

RADIATION HAZARDS
Radiofrequency and microwave radiation
[AD-A145492] 02 p0191 N85-11274
Improved robotic equipment for radiological emergencies
[DE84-017697] 04 p0509 N85-13249
Space Nuclear Safety Program
[DE84-016973] 06 p0726 N85-14679
Assessment of radiation dosages obtained by intake of radioactive fallout contaminated food
[VTT-292] 07 p1017 N85-16460
Thermal radiation hazards from Liquified Petroleum Gas (LPG) fireballs
[VTT-304] 09 p1293 N85-18122
Approaches to radiation guidelines for space travel
[DE85-001249] 09 p1363 N85-18576
China report: Science and technology
[JPRS-CST-84-039] 11 p1621 N85-20206
Radiation safety of crew and passengers of air transportation in civil aviation. Provisional standards
[NASA-TM-77610] 11 p1692 N85-20636
The medical results of human exposures to radio frequency radiation
[AD-A149718] 12 p1905 N85-21962
The Impact of Proposed Radio Frequency Radiation Standards on Military Operations
[AGARD-LS-138] 16 p2775 N85-27126
The biological effects of radiofrequency radiation
16 p2775 N85-27131
The cumulative effects of long term exposure to low levels of radiofrequency radiation (RFR)
16 p2776 N85-27132
Review of epidemiological studies of human exposures to radiofrequency radiation 16 p2776 N85-27134
Hazards of VLF electromagnetic fields
16 p2776 N85-27136
Development and application of new radiofrequency radiation safety standards 16 p2777 N85-27137
The 10 MWe solar thermal central receiver pilot plant: Beam safety tests and analyses
[SAND-83-8035] 16 p2818 N85-27379
Use of environmental health-risk analysis for managing toxic substances
[DE85-008964] 18 p3160 N85-29574
Collected epidemiological studies of the late effects of internal radium in man, and mechanistic investigations of those effects, part 2
[DE85-011174] 19 p3331 N85-30636
MELCOR Accident Consequence Code System (MACCS)
[DE85-009712] 19 p3339 N85-30689
Bulk and thermal properties of the functional Tuffaceous Beds in holes USW G-1, UE-25 no. 1, and USW G-2, Yucca Mountain, Nevada
[DE85-011181] 19 p3365 N85-30866
The DNA metabolism and poly-(ADP-ribose) synthesis in lymphocytes of persons exposed to low doses of ionizing radiation
[OEFZS-4307] 20 p3507 N85-31800
ARAC status report, 1985
[DE85-012835] 22 p3810 N85-33603
Practical consequences of the assessment of different energy health risks
[DE85-004536] 22 p3825 N85-33696
Corrosion resistant storage container for radioactive material
[DE85-011666] 22 p3838 N85-33765
MATADOR (Methods for the Analysis of Transport And Deposition Of Radionuclides) code description and user's manual
[TI85-901402] 23 p3966 N85-34592
Biophysical research in space — radiation effects
24 p4130 N85-35603
Computer code calculations of the TMI-2 accident: Initial and boundary conditions
[DE85-012613] 24 p4140 N85-35666

RADIATION HEATING
U RADIANT HEATING

RADIATION INJURIES
Radiofrequency and microwave radiation
[AD-A145492] 02 p0191 N85-11274
Thermoregulatory consequences of long-term microwave exposure at controlled ambient temperatures
[PB84-238600] 06 p0897 N85-14464
The medical results of human exposures to radio frequency radiation
[AD-A149718] 12 p1905 N85-21962
Mouse oocyte killing by neutrons: Target considerations
[DE85-011362] 19 p3326 N85-30624
The 1983 international intercomparison of nuclear accident dosimetry systems at Oak Ridge National Laboratory
[DE85-011303] 23 p3834 N85-34382

RADIATION INTENSITY
U RADIANT FLUX DENSITY

RADIATION LAWS
NT KIRCHHOFF LAW OF RADIATION
NT STOKES LAW OF RADIATION

RADIATION MEASUREMENT
Radiation measuring system using transistor flux sensors
[AD-D011239] 01 p0050 N85-10326
Combustion system for radiation investigations
02 p0145 N85-10986
Energy-active zones in north Atlantic as manifestation of interannual variability of radiation balance
02 p0164 N85-11106
Analysis of radiocobalt in environmental samples
[DRIC-T-7334] 03 p0387 N85-12477
Isotopes in day to day life
[IAEA/PI/A.6E-84-00924] 03 p0417 N85-12688
High-bandwidth multichannel fiber optic system for measuring gamma rays
[DE84-014526] 04 p0564 N85-13596
Device for measuring average power of laser radiation
06 p0786 N85-15026
Microprocessors in geophysical instruments discussed
08 p1142 N85-17199
Radio Frequency Radiation (RFR) measurements in operational settings
[AD-A149717] 12 p1828 N85-21471
Operational experience with ion concentration sensors in orientation systems 13 p1980 N85-22422
Two-dimensional signal processing and storage and theory and applications of electromagnetic measurements
[AD-A150580] 13 p2065 N85-22899
Comprehensive, integrated, remote sensing at DOE sites
[DE85-004867] 13 p2126 N85-23240
Determining atmosphere moisture content from differences in two-frequency microwave radiation measurements 14 p2341 N85-24474
Space radiation monitor observations from Salyut-4 orbital station 15 p2482 N85-25317
The gamma thermometer: A new type of fixed internal instrumentation developed by EDF
[BLL-CE-TRANS-8080-(9022.09)]
15 p2560 N85-25791
Solar wind and cosmic rain 15 p2644 N85-26312
Space radiation studies for the reporting period, June 1983 - July 1984
[NASA-CR-171411] 15 p2685 N85-26583
Space radiation studies --- Spacelab 2 Payload
[NASA-CR-171410] 15 p2685 N85-26584
Measurement and interpretation of electron angle at MABE beam stop
[DE85-008583] 17 p3032 N85-28755
Dosimeasurements with thermoluminescence dosimeters at a Febetron 701, 600 kV in room 022 of the Interuniversity Reactor Institute (IRI)
[IRI-190-84-02] 18 p3111 N85-29262
Safety report, 1982 18 p3184 N85-29746
Design consideration for the X-ray Cerenkov experiment
[AD-A153636] 18 p3189 N85-29777
Measurement of RF fields associated with ISM equipment as it relates to aeronautical services
[FAA-ES-84-2] 19 p3254 N85-30180
Measurement of radiated emissions from industrial heating device equipment as it relates to aeronautical services
[FAA-ES-85-2] 19 p3255 N85-30181
Annual environmental monitoring report, January-December 1984
[DE85-011669] 20 p3488 N85-31665
Results from Astron orbiting telescope
22 p3732 N85-33134
Wide-ranging radiation dose monitor
[DE85-011596] 22 p3787 N85-33463
Environmental surveillance at Los Alamos during 1984
[DE85-011680] 22 p3811 N85-33605
The 1984 environmental monitoring report, Sandia National Laboratories, Albuquerque, New Mexico
[DE85-011175] 22 p3811 N85-33607
The 1984 environmental monitoring program report for Idaho National Engineering Laboratory site
[DE85-011209] 22 p3812 N85-33611
Airborne cloud tracking measurements during the Three Mile Island nuclear station accident, Middletown, Pennsylvania. Date of survey: March - June 1979
[DE85-012060] 22 p3816 N85-33636
Neutron flux, spectrum and dose equivalent measurements for a 4500-W(th) 238 PuO2 general purpose heat source
[DE85-011361] 22 p3841 N85-33786
The 1983 international intercomparison of nuclear accident dosimetry systems at Oak Ridge National Laboratory
[DE85-011303] 23 p3834 N85-34382
EML pulse ionization chamber systems for (222)Rn measurements
[DE85-012320] 23 p3970 N85-34610
Measurement and interpretation of electron angle at MABE beam stop
[DE85-011918] 23 p3983 N85-34698

Solar Coronal and photospheric abundances from solar energetic particle measurements
[SH-2.1-5] 23 p3998 N85-34786

Radiation measurements on magnesium flames
[BLL-CE-TRANS-8110-(9022.09)] 24 p4075 N85-35254

Study of hadron bundles observed in Chacaltaya two-story emulsion chamber
[HE-3.3-4] 24 p4160 N85-35922

RADIATION MEASURING INSTRUMENTS
NT ACTINOMETERS
NT BOLOMETERS
NT CERENKOV COUNTERS
NT DOSIMETERS
NT ELECTROPHOTOMETERS
NT ELECTROSTATIC PROBES
NT FABRY-PEROT SPECTROMETERS
NT FLIR DETECTORS
NT HODOSCOPES
NT INFRARED DETECTORS
NT INFRARED INSTRUMENTS
NT INFRARED RADIOMETERS
NT INFRARED SCANNERS
NT INFRARED SPECTROMETERS
NT INFRARED SPECTROPHOTOMETERS
NT MICROWAVE RADIOMETERS
NT NEUTRON COUNTERS
NT NEUTRON SPECTROMETERS
NT PARTICLE TELESCOPES
NT PASSIVE L-BAND RADIOMETERS
NT PHOTOMETERS
NT PROPORTIONAL COUNTERS
NT PYRANOMETERS
NT QUANTUM COUNTERS
NT RADIATION COUNTERS
NT RADIATION DETECTORS
NT RADIOMETERS
NT RIOMETERS
NT SCINTILLATION COUNTERS
NT SILICON RADIATION DETECTORS
NT SOLAR SPECTROMETERS
NT SPARK CHAMBERS
NT SPECTROHELIOGRAPHS
NT SPECTROPHOTOMETERS
NT SPECTRORADIOMETERS
NT THRESHOLD DETECTORS (DOSIMETERS)
NT ULTRAVIOLET SPECTROMETERS
NT ULTRAVIOLET SPECTROPHOTOMETERS

Software used with the flux mapper at the solar parabolic dish test site
[NASA-CR-174108] 04 p0528 N85-13376

Device for measuring average power of laser radiation
06 p0786 N85-15026

Operational problems with radiation survey meters: The university and accelerator
[DE84-015703] 06 p0811 N85-15151

Year-to-year variability of components of Earth's radiation budget according to satellite measurement data
16 p2725 N85-26821

Results from radiation monitoring equipment experiment on STS-8
[AD-A153241] 17 p3055 N85-28911

Results from radiation monitoring equipment experiments on STS-41C, 41D, 41G and 51A
[AD-A154676] 21 p3560 N85-32142

Wide-ranging radiation dose monitor
[DE85-011596] 22 p3787 N85-33463

Beta response of selected instruments
[DE85-013278] 22 p3788 N85-33469

EAS Cerenkov measurements of the composition of the cosmic ray flux around 10 to the 16th power eV
[OG-5.2-11] 22 p3884 N85-34067

Search for solar neutrons using NM-64 equipment
[SH-1.4-5] 23 p3995 N85-34765

Wholebody radiation counting system
[AD-A155842] 24 p4131 N85-35607

Monopole, astrophysics and cosmic ray observatory at Gran Sasso
[HE-6.1-4] 24 p4209 N85-36130

Monopole search below the Parker limit with the MACRO detector at Gran Sasso
[HE-6.1-5] 24 p4209 N85-36131

Upper limit on magnetic monopole flux from Baksan experiment
[HE-6.1-11] 24 p4210 N85-36136

RADIATION MEDICINE
U NUCLEAR MEDICINE

RADIATION METERS
U RADIATION MEASURING INSTRUMENTS

RADIATION NOISE
U ELECTROMAGNETIC NOISE

RADIATION PRESSURE
NT ILLUMINANCE
NT LUMINANCE
NT LUMINOUS INTENSITY
NT SOUND PRESSURE

Orbit perturbation — satellites
05 p0586 N85-13810

X-ray bursts: Observation versus theory
[NASA-CR-174415] 10 p1573 N85-19916

Dynamics of neutral small particles — in the solar system
15 p2676 N85-26521

Numerical integration through force discontinuities: Solar radiation pressure
16 p2805 N85-27296

Effect of solar eclipses on the LAGEOS semimajor axis
20 p3491 N85-31699

Effect of diffusely-reflected sunlight on the orbit of LAGEOS
20 p3491 N85-31700

RADIATION PROTECTION
NT RADIATION SHIELDING

Method for forming electromagnetic-wave-screening composite
07 p0936 N85-15930

Radiation safety of crew and passengers of air transportation in civil aviation. Provisional standards
[NASA-TM-77610] 11 p1692 N85-20638

Charge-to-mass dispersion methods for abrasion-ablation fragmentation models
[NASA-TM-86340] 11 p1726 N85-20857

Radio Frequency Radiation (RFR) measurements in operational settings
[AD-A149717] 12 p1828 N85-21471

China report: Science and technology
[JPRS-CST-85-013] 15 p2536 N85-25652

Report of the 11th Regional IRPA Congress on Recent Developments and New Trends in Radiation Protection
[IRI-190-83-13] 18 p3160 N85-29575

Working safely with ionizing radiation sources at the Interuniversity Reactor Institute (IRI) (meant for the introduction of new collaborators)
[IRI-190-84-01] 18 p3160 N85-29576

Safety system with microcomputer
[OEFZS-4294] 18 p3166 N85-29618

Radioprotective efficacy of ATP and adenosine with exposure to high energy protons
19 p3325 N85-30602

Study of a novel shielding principle for protection against intense gamma-ray beams
[AD-A154374] 19 p3357 N85-30808

East Europe report: Science and technology
[JPRS-ESA-85-023] 21 p3572 N85-32217

ARAC status report, 1985
[DE85-012835] 22 p3810 N85-33603

Design considerations for personnel access penetrations for the superconducting super collider
[DE85-013027] 24 p4162 N85-35807

RADIATION RESISTANCE
U RADIATION TOLERANCE

RADIATION SHIELDING

Computer subroutines for estimation of human exposure to radiation in low Earth orbit
[NASA-TM-86324] 08 p1199 N85-17550

Study of a novel shielding principle for protection against intense gamma-ray beams
[AD-A154374] 19 p3357 N85-30808

Additional muon calculations for the SLC positron source
[DE85-011212] 19 p3363 N85-30855

Solid-state track recorder neutron dosimetry in the Three-Mile Island Unit-2 reactor cavity
[DE85-011380] 20 p3531 N85-31966

Simulating the effects of plasma disruption with a 1 MA current pulse in a coaxial test fixture
[DE85-010491] 20 p3535 N85-31996

Key issues of fusion nuclear technology development (FINESSE)
[DE85-012599] 22 p3845 N85-33817

Container for radioactive materials
[DE85-005757] 23 p3972 N85-34626

A comparison of calculated and measured background noise rates in hard X-ray telescopes at balloon altitude
[OG-9.3-7] 23 p4028 N85-34962

Applicability of 100kWe-class of space reactor power systems to NASA manned space station missions
[NASA-CR-174896] 24 p4149 N85-35726

RADIATION SOURCES
NT MONOCHROMATORS
NT NEUTRON SOURCES
NT POINT SOURCES

Imploding plasma radiation sources: Basic concepts
[AD-A145542] 02 p0284 N85-11656

Developments of optical fast-gated imaging systems
[DE84-016170] 04 p0502 N85-13204

Method of aperture synthesis: Fundamental relations and data processing in aperture synthesis systems (review)
06 p0781 N85-14994

Developments and applications of laser fluorescence spectroscopy for studies of particle behaviours in fusion plasmas
09 p1369 N85-18735

Design and analysis of airborne scanning optical systems
11 p1623 N85-20218

Major facilities for materials research and relat
disciplines
[PB85-108850] 11 p1739 N85-20

Intense, broadband, pulsed I-R source at the Nationa
Synchrotron Light Source
[DE84-010542] 12 p1935 N85-2215

Possibility of mapping active tectonic structures fro
mercury gas aureoles over sea surface
13 p2113 N85-2318

Supersonic flow around weak radiation sources
17 p2942 N85-2812

Polymer Research at Synchrotron Radiation Source
Symposium Proceedings
[DE85-008488] 18 p3081 N85-2902

Plasma radiation sources. Quasi-adiabatic theory and
numerical modeling in the electro-diffusive approximatio
[AD-A154375] 19 p3370 N85-3086

Radiative-collision generation of sound in gase
subjected to single-pulse optical excitation
21 p3689 N85-3292

Correlation of intensities of different scattering
channels 21 p3694 N85-3292

Magnetically insulated diode for generating pulsed
neutron and gamma ray emissions
[DE85-011656] 22 p3760 N85-3330

Unthermalized plasma in bursts sources
[OG-1.1-5] 22 p3861 N85-3390

Optical monitoring of gamma-ray source fields
[OG-1.1-7] 22 p3861 N85-3390

Search for optical bursts from the gamma ray burst
source GBS 0526-66
[OG-1.1-8] 22 p3861 N85-3390

Search for infrared counterparts of gamma-ray
bursters
[OG-1.1-9] 22 p3861 N85-33910

A second catalog of gamma ray bursts: 1978 - 198
localizations from the interplanetary network
[OG-1.2-1] 22 p3861 N85-33912

Gamma ray burst size-frequency distributions: Spectral
selection effects
[OG-1.2-3] 22 p3862 N85-33913

An internally consistent gamma ray burst time history
phenomenology
[OG-1.2-6] 22 p3862 N85-33916

Relationships between log N-log S and celestial
distribution of gamma-ray bursts
[OG-1.2-10] 22 p3862 N85-33918

Search for gamma rays of energy 10(15) eV from Cygnus
X-3
[OG-2.1-1] 22 p3862 N85-33919

Observation of an excess of cosmic ray muons of
energies 2 TeV from the direction of Cygnus X-3
[OG-2.1-3] 22 p3863 N85-33920

Muon content of gamma ray induced EAS from Cygnus
X-3
[OG-2.1-4] 22 p3863 N85-33921

Gamma rays of energy or = 10(15) eV from Cyg X-3
[OG-2.1-5] 22 p3863 N85-33922

Experimental results on gamma-ray sources at E su
0 = 10(13) - 10(14) eV
[OG-2.2-12] 22 p3865 N85-3393

Observation of hard X-rays from the Crab pulsar an
A0535+26
[OG-2.3-7] 22 p3866 N85-3394

Periodic gamma-ray emissions from Geminga at or
10(12) eV
[OG-2.4-2] 22 p3867 N85-339

Search for periodicities near 59 s in the COS-
gamma-ray data of 2CG195+04 (Geminga)
[OG-2.4-3] 22 p3867 N85-339

On the 1983 observations of the gamma-ray sour
2CG195+4
[OG-2.4-5] 22 p3868 N85-339

Observations on TeV gamma rays from Geminga a
PSR 0950+08
[OG-2.4-6] 22 p3868 N85-339

Spectral evolution of gamma-rays from adiabatic
expanding sources in dense clouds
[OG-2.5-2] 22 p3869 N85-339

Supernova explosion in dense clouds in the galaxy
the COS-B gamma-ray sources
[OG-2.5-3] 22 p3869 N85-33

Galactic gamma-ray sources, SNOBs, and giant
regions
[OG-2.5-4] 22 p3869 N85-33

Observations of potential ultra high energy gamma
sources above 10(15) eV
[OG-2.6-9] 22 p3870 N85-3

COS-B gamma-ray sources and interstellar gas
22 p3874 N85-3
[OG-3.1-9]

Implications of new measurements of O-16 +
C-12,13, N-14,15 for the abundances of C, N isoto
the cosmic ray source
[OG-4.3-2] 22 p3878 N85-3

Type 3 solar radio bursts and 3HE-rich events
23 p4000 N85-3
[SH-2.2-3]

Germanium and lead: Significant differences between meteoritic and photospheric abundances?
[OG-7.1-2] 23 p4012 N85-34864

Implications of source abundances of ultraheavy cosmic rays
[OG-7.1-4] 23 p4013 N85-34866

Propagation and nucleosynthesis of ultraheavy cosmic rays
[OG-7.1-5] 23 p4013 N85-34867

A model for the origin of high-energy cosmic rays
[OG-8.1-8] 23 p4018 N85-34898

Approximate supernova remnant dynamics with cosmic ray production
[OG-8.1-12] 23 p4019 N85-34901

Scaling from Jupiter to pulsars and the acceleration of cosmic ray particles by pulsars, 3
[OG-8.2-3] 23 p4019 N85-34904

Cooling high intensity atomic hydrogen beams to liquid helium temperatures
[DE85-012515] 24 p4148 N85-35718

Calibration of a high-level photon irradiation
[DE85-013044] 24 p4151 N85-35738

RADIATION SPECTRA

NT ABSORPTION SPECTRA
NT BALMER SERIES
NT D LINES
NT ELECTROMAGNETIC SPECTRA
NT ELECTRONIC SPECTRA
NT EMISSION SPECTRA
NT FRAUNHOFER LINES
NT GAMMA RAY SPECTRA
NT H ALPHA LINE
NT H LINES
NT INFRARED SPECTRA
NT K LINES
NT LINE SPECTRA
NT LYMAN SPECTRA
NT MICROWAVE SPECTRA
NT RADIO SPECTRA
NT RAMAN SPECTRA
NT RYDBERG SERIES
NT SOLAR SPECTRA
NT STELLAR SPECTRA
NT UBV SPECTRA
NT ULTRAVIOLET SPECTRA
NT VIBRATIONAL SPECTRA
NT VISIBLE SPECTRUM
NT X RAY SPECTRA

New measurements of the spectrum of the cosmic microwave background
[DE84-016055] 05 p0746 N85-14785

Investigation of dynamics of radiation spectrum of injection lasers by infrared impulse Fourier spectroscopy
13 p2090 N85-23047

The 10 MWe solar thermal central receiver pilot plant: Beam safety tests and analyses
[SAND-83-8035] 16 p2818 N85-27379

Summary of the discussion of the theory of radiative processes
[DE85-007612] 19 p3371 N85-30914

Correlation of intensities of different scattering channels 21 p3694 N85-32952

Solid state radiative heat pump
[DE85-011605] 22 p3760 N85-33303

Implicit Monte Carlo methods and non-equilibrium Marshak wave radiative transport
[DE85-010711] 22 p3835 N85-33743

Detection of gamma-ray lines from the direction of the Crab Nebula 22 p3866 N85-33943

HEAO 3 upper limits to the expected 1634 KeV line from SS 433
[OG-2.4-9] 22 p3868 N85-33954

High-resolution spectrum of Cygnus X-1
[OG-2.4-12] 22 p3868 N85-33956

Spectrum of the gamma-ray diffuse component observed from HEAO-1
[OG-3.1-12] 22 p3874 N85-34000

Reestimation of the production spectra of cosmic ray secondary positrons and electrons in the ISM
[OG-6.2-8] 22 p3889 N85-34107

Nucleosynthesis in the terrestrial and solar atmospheres
[SH-2.2-2] 23 p4000 N85-34797

Penetration of solar protons into the Earth's magnetosphere on November 22, 1977
[SH-6.1-15] 23 p4046 N85-35088

Standard value for the radiation length in air
[HE-4.4-4] 24 p4193 N85-36013

Lateral-angular and temporal characteristics of EAS optical radiation
[HE-4.4-19] 24 p4194 N85-36025

RADIATION THERAPY

Biology and Medicine Division
[DE85-010636] 19 p3327 N85-30613

RADIATION TOLERANCE

Visible wavelength interferometer for high speed electron density diagnostics
[AD-A145686] 02 p0277 N85-11803

The relationship between radiation sensitivity and redox equilibria --- glass processing variables
[AD-A147216] 07 p0932 N85-15906

Lithium counterdoped silicon solar cell
[NASA-CASE-LEW-14177-1] 11 p1672 N85-20535

Hygienic standardization of electromagnetic fields of radar systems 14 p2367 N85-24703

Mouse oocyte killing by neutrons: Target considerations
[DE85-011362] 19 p3328 N85-30624

Additional muon calculations for the SLC positron source
[DE85-011212] 19 p3363 N85-30855

RADIATION TRANSPORT

SANDYL radiation transport code at the Naval Research Laboratory
[AD-A144890] 01 p0117 N85-10799

Radiation transport in the Earth atmosphere
04 p0522 N85-13341

Generation of radiation transport geometry from computer-generated design data --- monte carlo solution of the neutron transport equation
[DE84-017380] 09 p1370 N85-18606

Imaging through a multiple scattering medium
[DE85-002051] 10 p1557 N85-19821

Introduction to combinatorial geometry
[DE85-003266] 13 p2152 N85-23364

Intercomparison of Radiation Codes in Climate Models (ICRCCM)
[DE85-007251] 16 p2835 N85-27487

Nonlinear DSA difference schemes for radiative transfer applications
[DE85-005729] 16 p2856 N85-27611

Generation and transfer of polarized radiation in the solar atmosphere: Physical mechanisms and magnetic-field diagnostics 18 p3206 N85-29890

Additional muon calculations for the SLC positron source
[DE85-011212] 19 p3363 N85-30855

A new slab geometry radiation transport differencing scheme
[DE85-006681] 19 p3366 N85-30874

Radiation transport
[DE85-010333] 21 p3703 N85-33005

Global environmental transport models for tritium
[DE85-011437] 22 p3816 N85-33639

Monte Carlo and discrete ordinates calculations of 14-MeV neturons streaming through a stainless-steel duct (L/D = 4.6): Comparison with experiment
[DE85-011423] 22 p3840 N85-33776

Long-term exposure of (238) PuO2 to a terrestrial environment, volume 3
[DE85-011696] 22 p3840 N85-33781

Halo of NGC 4631 and models of cosmic-ray transport
[OG-6.2-3] 22 p3889 N85-34103

Coupled electron-photon transport calculations using the method of discrete ordinates
[DE85-009444] 23 p3967 N85-34597

Monte Carlo techniques for analyzing deep penetration problems
[DE85-011426] 23 p3966 N85-34596

Numerical descriptions of cosmic-ray transport
[SH-4.1-3] 23 p4004 N85-34829

Numerical and analytic descriptions of cosmic-ray transport
[SH-4.1-4] 23 p4005 N85-34830

Numerical studies of high current beam compression in heavy ion fusion
[DE85-011874] 24 p4158 N85-35783

RADIATIVE HEAT TRANSFER

Predicted heat transfer loss in the expansion cylinder of a 2 cylinder reciprocating engine
[AD-A144831] 01 p0055 N85-10366

Finite element analysis of thermoelasticity problems
02 p0208 N85-11369

Resistance of Navy shipboard outerwear garments and fire-resistant fabrics to extreme heat
[AD-A145414] 02 p0238 N85-11546

The radiative hydrodynamics of flare loops heated by impulsive bursts of energetic electrons
05 p0745 N85-14781

Methods for heat transfer and temperature field analysis of the insulated diesel
[NASA-CR-174783] 07 p1056 N85-16699

Simultaneous determination of radiation and convection heat transfer 08 p1194 N85-17523

Three-dimensional analysis of heat transfer and gas flow in a radiant furnace
[DE84-011732] 11 p1633 N85-20284

Radiation heat transfer within an open-cycle MHD generator channel --- mathematical models
[NLR-TR-83068-U] 14 p2304 N85-24267

Performance analysis of radiation cooled dc transmission lines for high power space systems
[NASA-TM-87040] 17 p2951 N85-28222

Performance analysis of mixed passive solar heating systems
[DE85-009624] 21 p3613 N85-32455

An analytical and numerical model of radiation heat transfer in direct injection-type diesel combustion
24 p4092 N85-35368

RADIATIVE LIFETIME

Studies of the chemistry of vibrationally and electronically excited species in planetary upper atmospheres
[NASA-CR-174134] 03 p0449 N85-12851

Absolute transition probabilities of lines in the spectra of astrophysical atoms, molecules, and ions
[NASA-CR-174141] 04 p0580 N85-13705

Lifetime and quenching measurements of C2H emission produced by vacuum ultraviolet photolysis of C2H2
[DE85-010769] 19 p3278 N85-30330

Search for proton decay
[DE85-006283] 19 p3353 N85-30786

RADIATIVE RECOMBINATION

Recombination and ionization in a nitrogen plasma
[AD-A155426] 22 p3645 N85-33613

RADIATIVE TRANSFER

NT RADIATIVE HEAT TRANSFER

Spectroradiometric calibration of the Thematic Mapper and Multispectral Scanner system
[E85-10026] 02 p0218 N85-11439

Effects of atmospheric water vapor and clouds on NOAA (National Oceanic and Atmospheric Administration) AVHRR (Advanced Very High Resolution Radiometer) satellite data
[AD-A145425] 02 p0280 N85-11824

Scattering models in the microwave regime
[NASA-CR-174001] 04 p0525 N85-13361

Scattering from randomly oriented scatterers of arbitrary shape in the low-frequency limit with application to vegetation 04 p0525 N85-13362

Non-LTE considerations in spectral diagnostics of thermal transport and implosion experiments
[DE84-015167] 05 p0730 N85-14669

Studies of radiative transfer in planetary atmospheres
[NASA-CR-174194] 05 p0745 N85-14778

Infrared emission and atomic transitions
[AD-A147640] 07 p1041 N85-16607

Radiation parameterization programs for use in general circulation models
[AD-A148015] 08 p1186 N85-17486

Evidence for non-radiative activity in hot stars
08 p1231 N85-17756

Summary of the origin of nonradiative heating/momentum in hot stars
08 p1236 N85-17789

Hydrodynamic response of a radiating Al plasma excited by a proton beam
[AD-A149904] 10 p1558 N85-19824

MAP in India 11 p1655 N85-20424

Aerosol multiple-scanning code, ASCAT
[LA-10046-MS] 12 p1823 N85-21440

Evaluation of the radiometric integrity of LANDSAT 4 Thematic Mapper band 6 data 12 p1869 N85-21726

Spectroradiometric calibration of the Thematic Mapper and Multispectral Scanner system
[E85-10094] 12 p1874 N85-21756

Atlas of relectance patterns for uniform earth and cloud surfaces (NIMBUS-7ERB-61 days)
[PB85-116382] 12 p1891 N85-21870

Mean free path lenght of photons with broken cloud cover 14 p2338 N85-24455

A numerical simulation of the formation of solar prominences 14 p2448 N85-25112

Technical development to improve satellite sounding over radiatively complex terrain
[NASA-CR-175746] 15 p2583 N85-25929

Radiative forcing of the southwest summer monsoon (a satellite perspective) 15 p2593 N85-25981

An Earth longwave radiation climate model
[NASA-CR-175749] 15 p2594 N85-25984

Microwave model prediction and verifications for vegetated terrain
[E85-10102] 16 p2809 N85-27322

Nonlinear DSA difference schemes for radiative transfer applications
[DE85-005729] 16 p2856 N85-27611

Solar radiance models for determination of ERBE scanner filter factor
[NASA-CR-172595] 17 p2995 N85-28513

Effect of polarized radiative transfer on the Hanle magnetic field determination in prominences: Analysis of hydrogen H alpha line observations at Pic-du-Midi
18 p3207 N85-29894

A new slab geometry radiation transport differencing scheme
[DE85-006681] 19 p3366 N85-30874

The suppression of convective wavebreaking by radiative transfer processes, part 1.3C
21 p3616 N85-32472

RADICALS
NT FREE RADICALS
NT HYDROXYL RADICALS
NT VINYL RADICAL
Magnetic resonance studies of transient radicals and radical ions
[DE84-011699] 03 p0328 N85-12116
Study of catalysts and mechanisms in synthesis reactions
[DE84-015025] 04 p0470 N85-12990
Study of combustion and flame processes initiated by laser-induced multiple-photon absorption
[DE84-017095] 04 p0471 N85-12996
Combustion kinetics of metal oxide and halide radicals
[AD-A148521] 08 p1122 N85-17076
Improved lithium-intercalation cathode material
[AD-A149319] 10 p1435 N85-19043
Stable polymeric carbon radicals. Part 2: Attempts at the preparation of polyradicals of the triphenylmethyl type linked by P-phenylene units
[NASA-TM-77799] 10 p1450 N85-19134
Toxicity, mutagenesis and aging due to endogenous oxygen radicals
[AD-A150121] 12 p1900 N85-21928
Ideal gas thermodynamic properties for the phenyl, phenoxy, and o-biphenyl radicals
[NASA-TM-83800] 12 p1943 N85-22204
Combustion kinetics of metal oxide and halide radicals
[AD-A150924] 14 p2251 N85-23952
Modeling the role of radicals in the ignition of and flame propagation in hydrogen-air and methane-air mixtures
16 p2744 N85-26935
A measurement of the vibrational band strength for the upsilon sub 3 band of the HO2 radical
[NASA-CR-175858] 16 p2744 N85-26936
Cometary atmospheres: Modeling the spatial distribution of observed neutral radicals
[NASA-CR-175852] 16 p2882 N85-27781
The electronic spectra of phthalocyanine radical anions and cations
[AD-A152328] 17 p2918 N85-27986
Measurement of Franck-Condon factors for the v'=0 progression in the B-X system of PO
[AD-A152734] 17 p2919 N85-27993
Cometary atmospheres: Modeling the spatial distribution of observed neutral radicals
[NASA-CR-175862] 17 p3054 N85-28904
Spray pyrolysis as a synthetic tool
[AD-A153891] 19 p3234 N85-30047
Nested dissection on a mesh-connected processor array
[AD-A154066] 19 p3342 N85-30711
Chromophores with auxochrome-like function
[NASA-TM-77849] 20 p3421 N85-31233
Measurements of the fragmentation of (40)Ar, (28)Si and (12)C in CH2C and H targets between 300 and 1500 MeV/nuc at the Bevalac
[OG-7.2-19] 23 p4016 N85-34886

RADII
NT LARMOR RADIUS
Experimental determination of the critical cavity radius in Fe-10% Cr for ion irradiation
[DE84-016570] 04 p0571 N85-13646
Lessons from the globular cluster NGC 5466
05 p0739 N85-14749
Galactic orbits of globular clusters
05 p0739 N85-14750
On the quadratic mean radius of a polynomial in Cz
[AD-A149189] 10 p1546 N85-19751
Ohmic potential drop and gas bubble radius distribution in alkaline water electrolysis 17 p2924 N85-28025
Single-dish high sensitivity determination of solar limb emission at 22 and 44 GHz
[INPE-3545-PRE/758] 19 p3385 N85-30999
Automatic sphericity interferometer for testing lens radii
[AD-A155736] 22 p3786 N85-33457

RADIO ALTIMETERS
ERS-1 radar altimeter data products — conferences
[ESA-SP-221] 03 p0379 N85-12419
The ERS-1 radar altimeter: An overview
03 p0379 N85-12421
The ERS-1 radar altimeter instrument
03 p0379 N85-12422
Wind speed determination from radar altimeters
03 p0380 N85-12424
Ocean wave parameters extraction using satellite short-pulse radar altimeters 03 p0380 N85-12425
The use of altimeter data for sea state forecasting
03 p0380 N85-12426
The impact of satellite altimeter data on wave research 03 p0380 N85-12427
Cryospheric data products available through satellite altimetry 03 p0380 N85-12428
Special difficulties of retrieving surface elevation over continental ice — satellite radar altimetry
03 p0380 N85-12429
Requirements and special problems of land altimetry — satellite altimetry 03 p0380 N85-12430
Determination of geoid undulations and ocean heights from ERS-1 radar altimetry data
03 p0381 N85-12432
Factors affecting the archiving, processing and dissemination of ERS-1 altimeter data
03 p0381 N85-12435
ERS-1 altimeter ground segment relations to other sensors and programs 03 p0381 N85-12436
Impact of ERS-1 observations on wave forecasting in the North Sea 03 p0381 N85-12437
Extraction of wave period from altimeter data
03 p0382 N85-12439
Sea ice characteristics derived from airborne altimetry
03 p0382 N85-12440
Radar altimetry over sea ice 03 p0382 N85-12441
Eddy detection in the Norwegian, Greenland, and Barents Seas with a radar altimeter
03 p0382 N85-12442
SEASAT altimeter data over the Mediterranean: Implications for ERS-1 03 p0382 N85-12443
Satellite altimetry for sea-surfacing topography determination and geoid improvement
03 p0382 N85-12444
The Precise Range and Range Rate Equipment (PRARE) and its possible support to the radar altimeter measurement for ERS-1 03 p0382 N85-12445
Determination of the altimetric geoid and gravity anomalies in the North Sea: Implications for a solution of the general circulation problem using ERS-1 data
03 p0382 N85-12446
Satellite altimetric measurements of lake levels
03 p0383 N85-12447
Ice sheets as invariant surfaces for radar altimeter calibration and orbit determination
03 p0383 N85-12449
Modelling of altimeter tracking over topographical surfaces — satellite antennas 03 p0383 N85-12450
ERS-1 radar altimeter system performance evaluation and calibration 03 p0383 N85-12451
Simulation of information extraction from radar altimeter return echoes — ERS-1 (ESA satellite)
03 p0383 N85-12452
The altimeter as a support to the scatterometer in the representation of winds and derived wave fields in coastal waters and enclosed seas: A research at its onset
03 p0383 N85-12453
The POSEIDON altimeter description
03 p0383 N85-12454
Standardization of data formats for radar altimeter data 03 p0384 N85-12455
Calibration and validation areas — satellite altimeters
03 p0384 N85-12456
Lessons from the SEASAT and GEOS-3 altimeters data projects 03 p0384 N85-12457
Components of the time variation of sea surface height from SEASAT altimeter data 05 p0658 N85-14227
A brief investigation into the validity of SEASAT radar altimeter data acquired over land
[AD-A146560] 06 p0827 N85-15254
Visualization of radar altimetry data for Venus
13 p1962 N85-22437
Application of pushbroom altimetry from space using large space antennas 14 p2230 N85-23817
Altitude of auroral scattering observed along auroral electrojets 14 p2339 N85-24465
On geoid heights and flexure of the lithosphere at seamounts
[AD-A151220] 15 p2604 N85-26050
Poseidon altimeter: Study of the hyperfrequency section and specifications of the prototype components
[CNES-84/DRT/TIT/HY/T/145]
20 p3419 N85-31219
Solid state altimeter model: Simulation description; analysis of first results (narrow band filters, weighting) — satellite-borne instruments
[CNES-DRT/TIT/RL-160-T] 20 p3419 N85-31220

RADIO ANTENNAS
NT MICROWAVE ANTENNAS
NT SPACETENNAS
An error analysis for the use of presently available lunar radio flux data in broadbeam antenna-system measurements
[PB84-218361] 01 p0016 N85-10097
HF broadband whip antenna evaluation
[AD-A149527] 10 p1467 N85-19258
Propagation influences on the performance of a reduced bandwidth quadrature phase shift keyed digital radio system 10 p1470 N85-19274
An electronically-steerable active receiving array fo h.f.
[BBC-RD-1985/2] 12 p1822 N85-2140
Antenna Technology for QUASAT application — radio antenna for very long base interferometry missions
14 p2231 N85-23
A description of the 64-meter antenna elevation driv gears and their strange wear 16 p2771 N85-27107
Repair of the DSS-14 pedestal concrete
16 p2772 N85-27108
On the possibilities of large-scale radio and fiber optics detectors in cosmic rays
[HE-4.6-2] 24 p4196 N85-36

RADIO ASTRONOMY
Activities report of the Radio Laboratory
[REPT-S-153] 02 p0192 N85-112
The mapping of the Sun at 8 mm wavelength and tracking of the active regions in the period 23 May - 5 June 1983
[REPT-S-149] 02 p0297 N85-1192
Documentation for the machine-readable version of A Catalogue of Extragalactic Radio Source Identifications (Veron-Cetty and Veron 1983)
[NASA-TM-87373] 03 p0405 N85-125
Measurement of pulsar parallax by Very Long Baseline Interferometry 03 p0444 N85-128
Aperture synthesis for radioastronomy
06 p0781 N85-149
Modern radioastronomical aperture synthesis systems (review) 06 p0782 N85-149
Approximating true radioluminance distribution from observations on aperture synthesis systems
06 p0783 N85-1500
Synthesis of radio image on RATAN-600 radiotelescope 06 p0783 N85-1500
QUASAT: A VLBI observatory in space — conferences
[ESA-SP-213] 07 p1056 N85-1670
Some prospects of space VLBI
07 p1056 N85-1670
QUASAT: Technical aspects of the proposed missio — VLBI satellite 07 p1057 N85-1670
The compact radio emission regions in active galacti nuclei — QUASAT VLBI mission
07 p1058 N85-1671
Very Long Base Interferometry (VLBI) in space and X-ra observations of compact sources in active galact nuclei 07 p1058 N85-1671
Opportunities for high angular and temporal resolutio of galactic objects at radio frequencies — QUASAT
07 p1059 N85-167
A 150 micron heterodyne spectrometer for airbor astronomy 08 p1249 N85-178
Tunable heterodyne receiver from 100 micron to 1,0 micron for airborne observations
08 p1249 N85-178
A new generation of sub mm telescopes, made of carb fiber reinforced plastic 08 p1250 N85-178
Spectroscopic observations of selected st systems
[NASA-CR-174288] 08 p1255 N85-178
FRG radiotelescope made of carbon fiber-reinforc plastic 09 p1309 N85-182
Observations of comets: Radio and otherwise conference
[TB-64] 11 p1762 N85-21
USSR report: Space
[JPRS-USP-85-001] 13 p1977 N85-22
All-Union conference of radio astronomers
13 p1977 N85-22
Studies of galactic HI in 21-centimeter absorption
13 p2170 N85-23
Venus surface composition from radio/r measurements 13 p2177 N85-23
Saturn's rings resolved by the VLA — Very Larg A (VLA) 15 p2670 N85-2
Voyager planetary radio astronomy: Grain and pa impacts shot noise in Saturn's ring plane
15 p2673 N85-2
Radio observations of comet P/Crommelin
[INPE-3480-PRE/723] 16 p2861 N85-2
Calibration methods in millimeter-wave radioastro
[INPE-3481-PRE/724] 16 p2861 N85-2
The Helios radio astronomy experiment
16 p2866 N85-2
Activity and magnetic fields on stars from observations
[NASA-CR-175966] 18 p3202 N85-2
Single-dish high sensitivity determination of sola emission at 22 and 44 GHz
[INPE-3545-PRE/758] 19 p3385 N85-3
Laboratory evaluation and application of micro absorption properties under simulated conditio planetary atmospheres
[NASA-CR-176078] 22 p3851 N85-

RADIO ATTENUATION
NT MANDELSTAM REPRESENTATION

Propagation measurements for land-mobile satellite systems at 1541 MHz
[CRC-TN-723] 09 p1310 N85-18232
UHF communications through forested propagation channels 10 p1470 N85-19280
Results of simultaneous measurements of absorption and polarization of radio waves reflected from ionosphere 16 p2807 N85-27313

RADIO AURORAS
Relation between polarization of artificial low frequency radiation and parameters of auroral ionosphere
06 p0785 N85-15016

RADIO BEACONS
Improved legislated emergency locating transmitters and emergency position indicating radio beacons
[NASA-CASE-GSC-12892-1] 11 p1624 N85-20226
Development of ARGOS platforms for tracking of basking sharks. Cetorhinus maximus
14 p2326 N85-24378
The sinking of the Les Mutuelles du Mans trimaran
14 p2327 N85-24384
Trajectory measurements for take-off and landing tests and other short-range applications, volume 16
[AGARD-AG-160-VOL-16] 15 p2561 N85-25801
The COSPAS-SARSAT system
20 p3401 N85-31101
The 121.5 MHz ELT: Past, present and future — Emergency Locator Transmitter (ELT)
20 p3401 N85-31105
The 406 MHz ELT/EPIRBs — Emergency Locator Transmitters/Emergency Position Indicating Radio Beacons (ELT/EPIRB) 20 p3402 N85-31106
Soviet Emergency Locator Transmitter/Emergency Position Indicating Radio Beacon (ELT/EPIRBs) at 121.5 and 406 MHz 20 p3402 N85-31107
The CCIR satellite EPIRB coordinated trials programme — Emergency Position Indicating Radio Beacon (EPIRB); International Radio Consultative Committee (CCIR) 20 p3402 N85-31111
The International Radio Consultative Committee (CCIR) recommended satellite Emergency Position Indicating Radio Beacon (EPIRB) system operating through geostationary satellites at 1.6 GHz
20 p3402 N85-31112
A 406 MHz ELT processor for geostationary satellites — Emergency Locator Transmitter (ELT)
20 p3403 N85-31114
Navigation data for Emergency Position Indicating Radio Beacons (EPIRBs) 20 p3403 N85-31115
Free-float Emergency Position Indicating Radio Beacons (EPIRBs) and release mechanism on board Norwegian ships. Main specifications and user experience
20 p3404 N85-31120
Experiments of a LORAN-C aided recovery system and a proposal of its application to rescue system
20 p3404 N85-31121
A special antenna for SARSAT EPIRBs providing circular polarization and hemispheric coverage for reliable transmission to satellites — Emergency Position Indicating Radio Beacon (EPIRB) 20 p3404 N85-31122
SARSAT 406 MHz system technical evaluation
20 p3404 N85-31124

RADIO BROADCASTING
U BROADCASTING

RADIO BURSTS
NT SOLAR RADIO BURSTS
NT TYPE 3 BURSTS
NT TYPE 4 BURSTS
Electron-cyclotron maser emission during solar and stellar flares
[NASA-CR-175883] 17 p3054 N85-28907

RADIO COMMUNICATION
NT CODE DIVISION MULTIPLE ACCESS
NT RADIO RELAY SYSTEMS
NT RADIO TELEMETRY
NT TELEPHONY
NT TIME DIVISION MULTIPLE ACCESS
Resistance to HF jamming interference in mobile radio networks by an adaptive, distributed reconfiguration technique
[AD-A145117] 01 p0038 N85-10238
Gaussian Wide Sense Stationary Uncorrelated Scattering (GWSSUS) channel simulation program to be used for mobile radio systems
[FUB-40-1983] 01 p0041 N85-10265
Planning guide for the review of telecommunications systems for frequency availability and electromagnetic compatibility
[PB84-210238] 01 p0041 N85-10268
Digital radio link: Comparison of the resistance of two different 4-phase modulation forms to multipath propagation
[FOA-C-30362-E] 02 p0193 N85-11291
Ministry wants better commo facilities for agroaviation
03 p0310 N85-12003
Operational requirements versus technological capabilities 08 p1072 N85-16798
Real-time estimation of amplitude and group delay distortion in a PSK line-of-sight communications channel
09 p1311 N85-18237
Calculation of the area covered by mobile radio systems using geographic data stored in a computer
[FUB-43-1983] 09 p1312 N85-18247
Adaptive signal processing for radio communications
10 p1473 N85-19295
Spectrum resource assessment of the Aeronautical Mobile Service between 400 MHz and 17.7 GHz
[PB85-125995] 11 p1626 N85-20241
Radioelectronics and space exploration
12 p1838 N85-21533
Satellite communications and amateur radio
12 p1838 N85-21534
INMARSAT marine satellite organization
13 p1985 N85-22456
Firefighters' communication transceiver test plan
[NASA-CR-171419] 13 p2053 N85-22854
A comparison of metropolitan and non-metropolitan employment characteristics: Indications of the size of non-metropolitan mobile communication services user classes
[NASA-CR-175648] 13 p2053 N85-22855
Use of Bigaussian approximation to describe fading in scattering communications channel
13 p2084 N85-23017
Tropospheric scatter communication system having angle diversity
[AD-D011448] 14 p2291 N85-24200
Trade-off between land vehicle antenna cost and gain for satellite mobile communications
[NASA-CR-175732] 15 p2540 N85-25681
Survey of narrow band vocoder technology
[AD-A151919] 16 p2773 N85-27114
Mobile television radio link
[AD-A152361] 17 p2946 N85-28201
Tone calibrated digital radio communication system
[NASA-CASE-NPO-16414-1-CU]
18 p3089 N85-29121
The determination of daily usage or occupancy in the land-mobile band 138-174 MHz at Montreal
[CRC-1383] 19 p3253 N85-30167
Performance interface document for the S-band diplexer for space users of NASA networks
[NASA-TM-86224] 23 p3900 N85-34155

RADIO DIRECTION FINDERS
Direction finder set, radio
[AD-A149958] 12 p1775 N85-21142
Experimental test of the three subaperture method for estimating target elevation angle
[AD-A149687] 12 p1851 N85-21614
Natural electromagnetic radiation in seismically active regions 13 p2111 N85-23152
Comprehensive radio direction finder with electronically stabilized radiation pattern 22 p3762 N85-33316

RADIO ECHOES
Analysis of spin echo signals in multi-pulse experiment
06 p0792 N85-15065
Measurements of partial reflections at 3.18 MHz using the CW radar technique 11 p1659 N85-20457

RADIO ELECTRONICS
USSR report: Electronics and electrical engineering
[JPRS-UEE-85-002] 13 p2066 N85-22907
Quality control of radioelectronic apparatus components on basis of external characteristics in frequency domain
15 p2529 N85-25590
Center for Electronics and Electrical Engineering technical progress bulletin covering center programs, July-September with 1985 CEEE events calendar
[PB85-191393] 24 p4091 N85-35363

RADIO EMISSION
NT CN EMISSION
NT HYDROXYL EMISSION
NT RADIO BURSTS
NT SOLAR RADIO BURSTS
NT SOLAR RADIO EMISSION
NT TYPE 3 BURSTS
NT TYPE 4 BURSTS
FCC (Federal Communication Commission) methods of measurement of radio noise emissions from computing devices
[PB84-243591] 06 p0849 N85-15387
The compact radio emission regions in active galactic nuclei — QUASAT VLBI mission
07 p1058 N85-16713
Observations of nonthermal radio emission from early-type stars 08 p1232 N85-17758
Nonthermal radio emission and the HR diagram
08 p1232 N85-17763
Synchrotron emission from chaotic stellar winds
08 p1234 N85-17774
Radio emission from RS CVn binary systems
09 p1417 N85-18939
Analysis of Jovian low frequency radio emissions
[NASA-CR-174449] 10 p1571 N85-19906
Determining vector of radiointerferometer base from observations of natural radio emission with narrow spectrum 13 p2112 N85-23158
Direct evidence for solar wind control of Jupiter's hectometer-wavelength radio emission
[NASA-TM-86073] 16 p2883 N85-27790
Sea surface radio emission at wavelengths 0.86 and 1.3 cm near Brewster angle 19 p3293 N85-30418
The radiation of the Vela pulsar
20 p3548 N85-32080
Analysis of Jovian decametric data: Study of radio emission mechanisms
[NASA-CR-176057] 22 p3851 N85-33846
Observations of potential ultra high energy gamma-ray sources above 10(15) eV
[OG-2.6-9] 22 p3870 N85-33971
The 4U 0115+63: Another energetic gamma ray binary pulsar
[OG-2.6-11] 22 p3870 N85-33973
Evidence for a dynamical halo around the edge-on galaxy NGC 4631
[OG-8.2-1] 22 p3889 N85-34102
The final COS-B database now publicly available
[OG-9.3-8] 23 p4028 N85-34963
Sporadic radio emission connected with a definite manifestation of solar activity in the near Earth space
[SH-10.1-8] 23 p4053 N85-35139
Near Earth space sporadic radio emission busts occurring during sunrise
[SH-10.1-9] 23 p4054 N85-35140
On the possibilities of large-scale radio and fiber optics detectors in cosmic rays
[HE-4.6-2] 24 p4196 N85-36039
On the production mechanism of radio-pulses from large extensive air showers
[HE-4.6-4] 24 p4196 N85-36041

RADIO EQUIPMENT
NT IONOSONDES
NT RADIO ANTENNAS
NT RADIO BEACONS
NT RADIO FILTERS
NT RADIO RECEIVERS
NT RADIO TELESCOPES
NT RADIO TRANSMITTERS
NT RADIOSONDES
NT RADIOTELEPHONES
NT RAWINSONDES
NT RECEPTION DIVERSITY
NT SPACECRAFT ANTENNAS
NT SUPERHETERODYNE RECEIVERS
NT TRANSMITTER RECEIVERS
NT TRANSPONDERS
NT VERY HIGH FREQUENCY RADIO EQUIPMENT
Shipboard and satellite-aided communications equipment in exhibition 06 p0819 N85-15203
Telecommunications equipment at 1984 Leipzig Spring Fair 08 p1140 N85-17179
Signal Hill solar-powered repeater report and recommendations
[DE85-000487] 09 p1316 N85-18273
Technical data on new engineering products
10 p1460 N85-19201
Application of the HARDMAN methodology to the single channel ground-airborne radio system (SINCGARS)
[NASA-CR-175486] 10 p1467 N85-19259
LOS microwave channel simulation: A survey of models, realizations and new concepts 10 p1472 N85-19291
Satellite communications and amateur radio
12 p1838 N85-21534
Algorithm for statistical simulation of electromagnetic compatibility characteristics of high-frequency transmission channels in radioelectronic facilities
12 p1842 N85-21580
Machine analysis of resonance characteristics of plate-type radio electronic equipment constructions
13 p2085 N85-23018
Results of comparison of long-wave radiation fluxes measured by Soviet and Japanese actinometric radiosounds 14 p2333 N85-24427
Application of space methods in geodesy
16 p2724 N85-26817
An analysis of the materiel fielding plan for the SINCGARS (Single Channel Ground and Airborne Radio System) radio
[AD-A155101] 21 p3578 N85-32236

RADIO FILTERS
Quartz filter transceiver 12 p1836 N85-21536
Theory of optimum M-filtration of signals against background of correlated interference
13 p2069 N85-22927
Combined processing method and matched filter for discrete composite frequency phase-shift keyed signal
13 p2070 N85-22931

Programmable filter with fanned interdigital surface acoustic wave transducer 13 p2083 N85-23008

RADIO FREQUENCIES
NT C BAND
NT EXTREMELY HIGH FREQUENCIES
NT EXTREMELY LOW RADIO FREQUENCIES
NT HIGH FREQUENCIES
NT LOW FREQUENCIES
NT MICROWAVE FREQUENCIES
NT SUPERHIGH FREQUENCIES
NT ULTRAHIGH FREQUENCIES
NT VERY HIGH FREQUENCIES
NT VERY LOW FREQUENCIES

Resistance to HF jamming interference in mobile radio networks by an adaptive, distributed reconfiguration technique
[AD-A145117] 01 p0036 N85-10238

Clutter generator for use in radar evaluation
[AD-D011234] 01 p0039 N85-10245

Transverse field interaction multibeam amplifier
[AD-D011241] 01 p0043 N85-10262

Radiofrequency and microwave radiation
[AD-A145492] 02 p0191 N85-11274

Use of a first-harmonic RF system in the NSLS booster
[DE84-016432] 02 p0277 N85-11806

The dc SQUID as a tuned radiofrequency amplifier
[DE85-000701] 06 p0805 N85-15123

A nonlocal expression for the ponderomotive potential
[IPPJ-699] 06 p0864 N85-15487

Polarization of radio molecular lines and mapping of magnetic field direction 06 p0878 N85-15561

Transmission line biased coherent array of Josephson oscillators
[AD-D01'323] 07 p0944 N85-15979

RF laser array driver apparatus
[AD-D011375] 07 p0969 N85-16155

Optical RF downconverter
[AD-D011336] 07 p1042 N85-16616

Opportunities for high angular and temporal resolutions of galactic objects at radio frequencies --- QUASAT
07 p1059 N85-16723

Dual mode radio frequency-infrared frequency system
[AD-D011402] 08 p1081 N85-16850

RF fiber optic link
[AD-A148679] 08 p1156 N85-17290

Slow wave antenna coupling to ion Bernstein waves for plasma heating in ICRF
[AD-B089094L] 09 p1386 N85-18717

LOS microwave channel simulation: A survey of models, realizations and new concepts 10 p1472 N85-19291

A review of transmission and channel evaluation techniques for digital communication systems
10 p1474 N85-19301

Narrowband spread spectrum systems
10 p1475 N85-19307

Genetic effects of microwave exposure on mammalian cells in vitro. Volume 2, Appendix A: Cytogenetics and growth kinetics data, 850 MHz
[AD-A148866] 10 p1522 N85-19599

Genetic effects of microwave exposure on mammalian cells in vitro, volume 2
[AD-A149047] 10 p1523 N85-19603

Precision tunable resonant microwave cavity
[NASA-CASE-LEW-13935-1] 11 p1628 N85-20246

Automated TEM (Transverse electromagnetic) cell calibration system
[PB85-134377] 11 p1638 N85-20319

Look at energy compression as an assist for high power RF production
[DE85-001568] 11 p1725 N85-20851

Biological effects on radiofrequency radiation
[PB85-120848] 12 p1900 N85-21920

Horizontal deflection TS-257
13 p2069 N85-22926

Combined processing method and matched filter for discrete composite frequency phase-shift keyed signal
13 p2070 N85-22931

Space-based antenna measurement system concepts for space station operation 14 p2236 N85-23860

Radio frequency quadrupole and alternating phase focusing methods used in proton linear accelerator technology in the USSR
[AD-A150630] 14 p2418 N85-24916

High field RF superconductivity: To pulse or not to pulse
[DE85-004381] 14 p2429 N85-24977

Quality control of radioelectronic apparatus components on basis of external characteristics in frequency domain
15 p2529 N85-25590

Land mobile satellite transmission measurements at 869 MHz: Selected results from the dedicated stratospheric balloon experiment of November 12 and 13, 1984
[NASA-CR-175734] 15 p2541 N85-25685

Annual Review, April 1983 - March 1984
[ISSN-0547-1567] 15 p2654 N85-26369

Radio frequency containment
15 p2654 N85-26375

Switching mixer
[AD-D011602] 16 p2777 N85-27139

Tone calibrated digital radio communication system
[NASA-CASE-NPO-16414-1-CU]
18 p3089 N85-29121

Performance of an RF beam monitor on the NBS-Los Alamos racetrack microtron
[DE85-010725] 19 p3262 N85-30232

Los Alamos Free-Electron Laser (FEL) RF system
[DE85-010719] 19 p3278 N85-30329

Mechanical considerations in cw linacs
[DE85-010728] 19 p3363 N85-30850

Proposed use of the radio-frequency quadrupole structure to funnel high-current ion beams
[DE85-010746] 19 p3364 N85-30857

Automated testing of developmental satellite communications systems and subsystems
[NASA-TM-87070] 20 p3440 N85-31348

Report of near field group
[DE85-010536] 20 p3527 N85-31940

VLF (Very low frequency) workshop held at San Diego California, 24-25 January 1985
[AD-A154652] 21 p3573 N85-32224

Microwave SAW (Surface Acoustic Wave) monochromator
[AD-D011718] 21 p3590 N85-32311

Radio-frequency radiation of storm clouds
21 p3692 N85-32939

Analysis of solution of Bloch's equations in time domain 22 p3771 N85-33371

Rf program for LAMPF 2
[DE85-012693] 22 p3837 N85-33760

Iris tilting and RF steering in the SLAC Linac
[DE85-011704] 22 p3841 N85-33783

Role of ECRH in potential formation for tandem mirrors
[DE85-011859] 22 p3848 N85-33834

Radio observations of four anticenter 2CG gamma-ray sources
[OG-2.5-10] 22 p3869 N85-33965

Breakdown of intrinsic ambipolarity for the radial diffusion due to a rotating RF field 23 p3977 N85-34860

Synthesis of ultrafine ceramic and metallic powders in a thermal argon rf plasma
[DE85-009634] 23 p3983 N85-34896

Sporadic radio emission connected with a definite manifestation of solar activity in the near Earth space
[SH-10.1-8] 23 p4053 N85-35139

Near Earth space sporadic radio emission busts occurring during sunrise
[SH-10.1-9] 23 p4054 N85-35140

Analyzer, flight line
[AD-A155777] 24 p4067 N85-35207

RF stabilization of interchange-ballooning modes
[DE85-012080] 24 p4090 N85-35353

Robinson instability and beam loading
[DE85-013301] 24 p4151 N85-35737

A new study on the emission of EM waves from large EAS
[HE-4.6-5] 24 p4197 N85-36042

Radio wave emitted by an extensive air showers in 10KHz to 1MHz region
[HE-4.6-15] 24 p4198 N85-36051

RADIO FREQUENCY DISCHARGE

Investigation of RF excited CW CO2 waveguide lasers
[NASA-CR-174106] 04 p0505 N85-13221

Microwave discharge in a supersonic flow for the excitation of a gas dynamic CO laser
[ESA-TT-833] 09 p1326 N85-18337

The effects of surface waves on RF discharge pumped lasers
[AD-A149689] 12 p1856 N85-21643

Statistical study of Saturnian electrostatic discharges observed by the Voyager Planetary Radio Astronomy experiment 15 p2673 N85-26500

An Earth-based attempt to detect Saturn Electrostatic Discharge (SED) at 21 centimeters
15 p2674 N85-26501

Fokker-Planck calculation of hot electron formation in the thermal barrier region of tandem mirror Gamma-10
[IPPJ-726] 23 p3979 N85-34869

RADIO FREQUENCY HEATING

High frequency plasma generator for ion thrusters
[NASA-CR-174772] 08 p1114 N85-17023

Analytical and numerical modeling of gyrotrons
[AD-A148100] 08 p1157 N85-17300

Proceedings on US-Japan Workshop on Tokamak Diagnostics by X-ray, VUV and Optical Radiations
[IPPJ-703] 09 p1386 N85-18719

X-rays spectroscopy on the PLT and TFTR Tokamaks
09 p1386 N85-18720

Electronics Engineering Department: EE technical review
[DE85-004360] 11 p1629 N85-20259

Computer simulation of equipment and processes involved in high-frequency heating of dielectrics
12 p1841 N85-21556

Observations of bulk electron heating due to return current in a tokamak discharge started up by lower hybrid waves
[IPPJ-708] 12 p1937 N85-22172

The design of megawatt gyrotrons
[DE85-007692] 17 p3032 N85-28754

Electron-cyclotron maser emission during solar and stellar flares
[NASA-CR-175883] 17 p3054 N85-28907

Measurement of radiated emissions from industrial heating device equipment as it relates to aeronautical services
[FAA-ES-85-2] 19 p3255 N85-30181

Activities of the RF Section 23 p3975 N85-34846

RF induced radial diffusion in tandem mirrors
23 p3976 N85-34849

Model of azimuthal non-uniformities induced by RF heating in RFC-XXM 23 p3977 N85-34858

RADIO FREQUENCY INTERFERENCE
NT ATMOSPHERICS
NT DAWN CHORUS
NT ELECTROMAGNETIC NOISE
NT HISS
NT IONOSPHERIC NOISE
NT SHOT NOISE
NT THERMAL NOISE
NT WHISTLERS
NT WHITE NOISE

Interference experiment with the Sirio-OTS satellites
[FUB-17-1983] 01 p0040 N85-10254

Revision of signal and interference space-time processing algorithms for implementation by microprocessors 04 p0487 N85-13105

Distribution of atmospheric radio interference
06 p0792 N85-15083

Asymptotically optimal ranking algorithms for quasi-determinate signal detection
06 p0792 N85-15084

Synoptic observations of the radio noise background in the frequency range 150-180 kHz to provide design data for the low frequency communications designer
[AD-A147438] 07 p0941 N85-15965

Measurement of signal separation between radio service and air navigation service
[IRT-TB-B-40/82] 08 p1083 N85-16860

Interference immunity of fiber-optic communication lines with spectral multiplexing of channels
13 p2069 N85-22924

Probability of detection of pulsed signals employing zero-gating interference suppression
13 p2085 N85-23021

Analysis of interference caused by interfering radio signals in communications systems with frequency separation of telephone channels and frequency modulation 13 p2086 N85-23025

Approximate rules for signal detection against background of Gaussian correlated interference
13 p2086 N85-23027

Noise immunity of information transmission system with pseudorandom frequency switching under worst-case interference conditions 13 p2086 N85-23029

FH/MFSK performance in multitone jamming
[NASA-CR-175667] 14 p2290 N85-24187

The distortion of AM broadcast antenna patterns as caused by nearby towers and highrise buildings
[CRC-1379] 15 p2538 N85-25988

Interference suppressor for radar MTI
[AD-D011606] 16 p2769 N85-27088

Predicting the effects of non-Gaussian interference in HF (High-Frequency) broadcasting. Part 1: A methodology for an analytic approach
[PB85-171544] 18 p3092 N85-29140

Measurement of RF fields associated with ISM equipment as it relates to aeronautical services
[FAA-ES-84-2] 19 p3254 N85-30180

Adaptive signal detection and other topics in real time signal processing
[AD-A154139] 19 p3255 N85-30184

Phase synchronizing large antenna arrays using the spatial correlation properties of radar clutter
20 p3439 N85-31344

Most desirable terrain, e.g., flat vs valley location, part 5.1B 21 p3624 N85-32513

Design of a freestanding noise measurement and recording system to predict the intensity and location of electromagnetic radiation from earthquakes
[AD-A155070] 21 p3632 N85-3256

Radio-frequency radiation of storm clouds
21 p3692 N85-32939

Adaptive antenna arrays for satellite communications: Design and testing
[NASA-CR-176162] 23 p3926 N85-3432

Television interference at the Maglarp (Sweden) wind turbine 24 p4111 N85-35480
Television interference measurement at Kalkugnen (Sweden) test windmill 24 p4111 N85-35481

RADIO FREQUENCY ION THRUSTOR ENGINES
U RIT ENGINES

RADIO FREQUENCY NOISE
U ELECTROMAGNETIC NOISE

RADIO FREQUENCY RADIATION
U RADIO WAVES

RADIO GALAXIES
Observations of 15 radio galaxies from Bologna survey using RATAN-600 radio telescope 02 p0162 N85-11097
The IRAS galaxy 0421+040P06: An active spiral (?) galaxy with extended radio lobes [NASA-CR-174208] 06 p0871 N85-15536
The environment of active galactic nuclei 07 p1057 N85-16712
The compact radio emission regions in active galactic nuclei — QUASAT VLBI mission 07 p1058 N85-16713
X-ray emission from Centaurus A — Vela 5B; radio galaxy 08 p1239 N85-17813
Collimated winds from active galactic nuclei 08 p1241 N85-17832
X-ray emission from Centaurus A [DE85-002030] 09 p1417 N85-18943
Determination of physical parameters of jets in radio galaxies 12 p1958 N85-22304
Magnetohydrodynamic (MHD) turbulence in radio galaxies 12 p1958 N85-22305
Morphology and energetics of narrow angle tail radio sources 14 p2455 N85-25164

RADIO INTERFERENCE
U RADIO FREQUENCY INTERFERENCE

RADIO INTERFEROMETERS
Apparatus of short baseline centrimetric wave radiointerferometer with cable communication lines for astrophysical research 06 p0782 N85-15001
Characteristics of lateral-scan interferometer 06 p0783 N85-15006
Primary data processing in very long baseline radiointerferometer 06 p0783 N85-15008
The wide-range space radio interferometer 07 p1058 N85-16717
Determining vector of radiointerferometer base from observations of natural radio emission with narrow spectrum 13 p2112 N85-23158
Accurate baseline determination by radio interferometry on NAVSTAR GPS satellite transmissions [AD-A150681] 14 p2291 N85-24202
Interferometer applications of VHF radars, part 3.6A 21 p3621 N85-32497

RADIO METEOROLOGY
Atmospheric channel performance measurements at 10 to 100 GHz [PB84-211325] 01 p0042 N85-10271
Neutral atmosphere properties determining D-region electron densities 11 p1658 N85-20451
Prospective investigations with DFVLR radar of possible relevance in the assessment of radio interference due to scattering from precipitations — meteorological radar [DFVLR-FB-84-42] 12 p1830 N85-21485
Additional possibilities of radiometeor azimuthal method for measuring wind velocity in lower thermosphere 19 p3296 N85-30438
Meteorological and aeronomical requirements for MST radar networks (keynote paper), part 1 21 p3615 N85-32467
Tropospheric-stratospheric exchange, part 1.1A 21 p3615 N85-32468
Observations of frontal zone structures with a VHF Doppler radar and radiosondes, part 1.2A 21 p3616 N85-32469
Gravity waves from the stratosphere to the mesosphere, part 1.3B 21 p3616 N85-32471
General circulation of the middle atmosphere, part 1.4B 21 p3617 N85-32474
Performance of the Colorado wind-profiling network, part 1.5A 21 p3617 N85-32475
Vertical transport in the atmosphere: Measurement capabilities and requirements of VHF radars, part 1.6A 21 p3617 N85-32476
Comparison of tropopause altitude determination by the Platteville Radar, Sunset Radar and the NWS Rawinsonde 21 p3617 N85-32477
Synoptic-scale dynamics with vertical velocity, part 1.8A 21 p3617 N85-32478
Sample interchange of MST radar data from the Urbana radar 21 p3627 N85-32531
MST radar data management 21 p3627 N85-32532
Data base for the Colorado profiling network 21 p3627 N85-32533
Further developments of EISCAT as an MST radar 21 p3627 N85-32534
Status of the Jicamarca radar 21 p3627 N85-32535
Recent results at the Sunset radar 21 p3627 N85-32536
The Boot Lake MF imaging radar 21 p3628 N85-32537
MENTOR: Adding an outlying receiver to an ST radar for meteor-wind measurement 21 p3628 N85-32538
Summary of progress at the Poker Flat Observatory in Alaska 21 p3628 N85-32539
Urbana radar systems: Possibilities and limitations 21 p3628 N85-32540
The Sondrestrom radar: Progress and proposed upgrades for ST work 21 p3628 N85-32541
Progress and plans for the Colorado Wind Profiler Network 21 p3628 N85-32542
The MU radar now partly in operation 21 p3628 N85-32543
Network ST radar and related measurements at Pennsylvania State University 21 p3629 N85-32544
A note on the proposed UK VHF radar 21 p3629 N85-32545
The Adelaide VHF radar: Capabilities and future plans 21 p3629 N85-32546
The Proust radar 21 p3629 N85-32547
Millstone Hill radar: Capabilities for S/T observations 21 p3629 N85-32548
The Ponape ST radar 21 p3629 N85-32549
Measurements of vertical velocity over flat terrain by ST radar and other related uses of the radar data set 21 p3630 N85-32550

RADIO METEORS
Additional possibilities of radiometeor azimuthal method for measuring wind velocity in lower thermosphere 19 p3296 N85-30438

RADIO NAVIGATION
NT LORAN
NT LORAN C
NT TACAN
NT VHF OMNIRANGE NAVIGATION
Experimental determination of propagation rate of ELF signals employed by Omega radio navigation system for phase measurements 06 p0793 N85-15066
Measurement of signal separation between radio service and air navigation service [IRT-TB-B-40/82] 08 p1083 N85-16860
INMARSAT marine satellite organization 13 p1965 N85-22456
Navigation: Accounting for copy 16 p2695 N85-26641
Allowance for differences in ellipsoids and geodetic control coordinate systems in determining ship's position using radio navigation systems 19 p3292 N85-30413
Use of Omega radio navigation system in geophysical work in Antarctica 19 p3298 N85-30448
Evaluation of radio navigation systems and their configuration with respect to minimum cost [ESA-TT-847] 20 p3392 N85-31043

RADIO OBSERVATION
Activity and magnetic fields on stars from radio observations [NASA-CR-175966] 18 p3202 N85-29861

RADIO OCCULTATION
Two-level model for formation of night ionosphere of Venus from radio occulation experiments 02 p0162 N85-11100
Radio scintillations observed during atmospheric occultations of Voyager: Internal gravity waves at Titan and magnetic field orientations at Jupiter and Saturn [NASA-CR-175554] 12 p1961 N85-22327
Occultations of stars and radio sources by comets: Predictions and observing prospects 14 p2437 N85-25034
Laboratory evaluation and application of microwave absorption properties under simulated conditions for planetary atmospheres [NASA-CR-176078] 22 p3851 N85-33847

RADIO PHYSICS
Decimetric-wave aperture synthesis system at Scientific Research Institute of Radiophysics 06 p0782 N85-15000
Study of lower ionosphere by pulse cross-modulation method 10 p1500 N85-19467
Millimeter-wave range masers: A review 13 p2089 N85-23042

RADIO PROBING
Experimental results of study of artificial perturbation region in upper and lower ionosphere disturbance by the method of vertical probing 06 p0784 N85-15011
Relation between polarization of artificial low frequency radiation and parameters of auroral ionosphere 06 p0785 N85-15016
Distortions of radio pulse during reflection from maximum region of ionospheric layer 06 p0792 N85-15061
Partial reflection D-region electron densities 08 p1184 N85-17461
Method and apparatus for calibrating the ionosphere and application to surveillance of geophysical events [NASA-CASE-NPO-15430-1] 12 p1887 N85-21846

RADIO PROPAGATION
U RADIO TRANSMISSION

RADIO RANGES
U RADIO BEACONS

RADIO RECEIVERS
NT SUPERHETERODYNE RECEIVERS
NT TRANSMITTER RECEIVERS
Digital radio receivers and problems of analog-to-digital conversion of narrow-band signals 04 p0486 N85-13101
Testing of a field portable GPS (Global Positioning System) geodetic receiver [AD-A148336] 08 p1082 N85-16859
Synthesis of optimum receiver and processor for signal packet of radio pulses 12 p1839 N85-21541
Receiver optimization for detection in doubly spread communication channels [AD-A151226] 15 p2541 N85-25689
The R-809 radio set [AD-A152370] 17 p2948 N85-28200
UHF IRIG G distribution system 17 p2965 N85-28308
Adaptive signal detection and other topics in real time signal processing [AD-A154139] 19 p3255 N85-30184
The NAVSTAR Global Positioning System (GPS) receiver development program, phase 1 [BMFT-FB-W-85-002] 20 p3399 N85-31085
Study of a low rate spread spectrum receiver [ENST-83E015] 20 p3441 N85-31354
New VLBI technology developments 20 p3491 N85-31702
Optimality criterion for high-frequency channel in receivers of discrete radio signals 22 p3776 N85-33401
Synthesis of system with nonideal components for optimal processing of radio signal 22 p3777 N85-33405
Developmental trends in radio receiver design 22 p3777 N85-33407
Waves in Space Plasmas (WISP) 23 p3901 N85-34164

RADIO RECEPTION
Energy correlation between natural extra-low-frequency noises at various frequencies 06 p0784 N85-15010
Evaluation of parameters of a signal (selected pages) [AD-A148831] 09 p1312 N85-18243
Ionosphere effects may replace some communications satellites 15 p2484 N85-25337
The distortion of AM broadcast antenna patterns as caused by nearby towers and highrise buildings [CRC-1379] 15 p2538 N85-25668
Receiver optimization for detection in doubly spread communication channels [AD-A151226] 15 p2541 N85-25689
Adaptive signal detection and other topics in real time signal processing [AD-A154139] 19 p3255 N85-30184

RADIO REFLECTION
U RADIO ECHOES

RADIO RELAY SYSTEMS
NT CODE DIVISION MULTIPLE ACCESS
NT TIME DIVISION MULTIPLE ACCESS
A microcomputer aided measurement equipment for monitoring performance in digital radio relay systems [FUB-4-1984] 01 p0101 N85-10668
Equipment for multiplexing multichannel radio-relay lines of communication [AD-A148402] 08 p1153 N85-17276
The impact of propagation effects on the design of high capacity digital microwave links in the 18 GHz frequency band 10 p1470 N85-19278
Wideband line-of-sight channel measurements and simulation: Application to digital radio links 10 p1471 N85-19283
Optimum path selection in automated radio relay link design 13 p2073 N85-22947
Automation of servicibility of radio-relay station equipment 15 p2527 N85-25582
System of light protection of antenna-mast structures of radio-relay lines 15 p2527 N85-25583

RADIO SCATTERING
Partial reflection D-region electron densities 08 p1184 N85-17461
D1 LF wind measurements in the 90 to 100 km height range 08 p1185 N85-17468
UHF communications through forested propagation channels 10 p1470 N85-19280

Correctness of reflection characteristics of radio absorbent materials 13 p2081 N85-22995

Ionosphere effects may replace some communications satellites 15 p2484 N85-25337

Radio wave scattering and intermittency of turbulence in the atmosphere 19 p3288 N85-30392

Radio wave scattering and turbulence intermittence in atmosphere 19 p3296 N85-30446

Theoretical investigation of single-frequency 8-element localizer signal scattering for critical area determination [FAA-PM-85-4] 20 p3391 N85-31037

RADIO SIGNAL ATTENUATION
U RADIO ATTENUATION

RADIO SIGNAL PROPAGATION
U RADIO TRANSMISSION

RADIO SIGNALS

Peculiarities of microprocessor implementation of algorithms for processing radio signals and noise in large antenna arrays 06 p0792 N85-15059

Formation of radio signals with low out-of-band radiation 07 p0950 N85-16018

Structure of frequency modulated and phase-shift keyed signals reflected from ionosphere at near-critical frequencies 07 p0952 N85-16035

Arctic marine acoustics [AD-A147492] 07 p1039 N85-16594

Digital coherent detector [AD-D011560] 12 p1833 N85-21501

Summator of radio pulse signals 12 p1839 N85-21539

The use of a high-speed 12-bit A/D converter for digital sampling of communication signal carriers [AD-A150578] 13 p2056 N85-22872

Space-time response characteristics of acoustooptic filter for compression of linearly frequency-modulated signal 13 p2071 N85-22937

Domain of applicability of asymptotic description of radio pulse fields near critical frequency 13 p2073 N85-22949

Reception noise immunity of multiposition signals 13 p2085 N85-23023

Analysis of interference caused by interfering radio signals in communications systems with frequency separation of telephone channels and frequency modulation 13 p2086 N85-23025

Investigation of influence of communications link and synchronization error on noise tolerence of group transmission of binary information based on orthogonal Walsh function 13 p2086 N85-23026

Approximate rules for signal detection against background of Gaussian correlated interference 13 p2086 N85-23027

Use of importance sampling to investigate signal detection systems by simulated method 13 p2086 N85-23028

Synthesis of system with nonideal components for optimal processing of radio signal 22 p3777 N85-33405

Radio signals from very large showers [HE-4.6-3] 24 p4196 N85-36040

RADIO SOURCES (ASTRONOMY)
NT CASSIOPEIA A
NT EXTRAGALACTIC RADIO SOURCES
NT PULSARS
NT QUASARS
NT RADIO GALAXIES
NT RADIO STARS

The catalogue of the discrete sources in the declination range from -13 deg to -2 deg [NASA-TM-77594] 01 p0129 N85-10887

Submilliarcsecond VLBI using compact close pairs of radio sources: Error analysis 05 p0622 N85-13981

Cross-shaped aperture synthesis system 06 p0782 N85-14999

Apparatus of short baseline centimetric wave radiointerferometer with cable communication lines for astrophysical research 06 p0782 N85-15001

Software for Crimea-Pushchino radiointerferometer 06 p0783 N85-15007

The IRAS galaxy 0421 + 040P06: An active spiral (?) galaxy with extended radio lobes [NASA-CR-174208] 06 p0871 N85-15536

Cosmology 07 p1056 N85-16701

The QUASAT mission: An overview 07 p1056 N85-16704

QUASAT: Technical aspects of the proposed mission — VLBI satellite 07 p1057 N85-16706

A study on the imaging potential of QUASAT — spaceborne VLBI 07 p1057 N85-16707

Ultraviolet and X-ray observations of active galactic nuclei: Constraints on models of the broad emission line region 11 p1744 N85-20966

A new radio emission at 3 kHz in the outer heliosphere 12 p1959 N85-22312

Absolute measurements of radiation intensity from Cassiopeia-A, Cygnus-A and crab nebula in 60-100 cm band 13 p2078 N85-22978

Comments on RS-17 X-ray telescope 22 p3731 N85-33132

Radio observations of four anticenter 2CG gamma-ray sources [OG-2.5-10] 22 p3869 N85-33965

A search for sources of ultra high energy gamma rays at air shower energies with Ooty EAS array [OG-2.6-8] 22 p3870 N85-33970

Search for the gamma-ray fluxes with energies above 10915) eV from various objects [OG-2.6-14] 22 p3871 N85-33975

CEN A observation at MeV-energies [OG-2.7-7] 22 p3871 N85-33980

The extent of the local hi halo [NASA-CR-176115] 23 p3987 N85-34724

Burst and Transient Source Experiment (BATSE) for the Gamma Ray Observatory (GRO) [OG-9.2-14] 23 p4026 N85-34953

Capabilities of the GRO/BATSE for monitoring of discrete sources [OG-9.2-16] 23 p4026 N85-34955

RADIO SPECTRA
NT MICROWAVE SPECTRA

Energy parameters of optical radiation space research systems 06 p0791 N85-15058

Radio Seyferts and the forbidden line region 08 p1236 N85-17793

The relationship between radio structures and stellar dynamics of nearby elliptical galaxies 08 p1236 N85-17794

VLBI observations of compact double radio sources 09 p1417 N85-18940

National Telecommunications and Information Administration authorization [GPO-38-660] 16 p2679 N85-27766

Microwave SAW (Surface Acoustic Wave) monochromator [AD-D011718] 21 p3590 N85-32311

Controllable companding in low-frequency FM radio communication systems 22 p3776 N85-33402

RADIO STARS
NT PULSARS

The 1000 GeV gamma rays from ms pulsars [OG-2.3-12] 22 p3867 N85-33948

RADIO TELEMETRY

Radio telemetry formula applications. A practical users guide [AD-A146247] 03 p0356 N85-12288

Meteorological Sounding System (MSS) standard operating procedures [AD-A149513] 10 p1519 N85-19578

Tracking pelagic dolphins by satellite 14 p2324 N85-24364

Polar bear telemetry results from the Nimbus-6 system 14 p2325 N85-24365

The ARGOS communications performance trials 14 p2326 N85-24376

Telemetered meteorological and engineering data from a deep sea moored body in the Long Term Upper Ocean Study (LOTUS) 14 p2329 N85-24402

The Data Acquisition Control and Telemetry (DACT) system — meteorological buoys 14 p2332 N85-24419

System for radio remote control of dropping bombs [CH-639335-A5] 15 p2491 N85-25371

RADIO TELESCOPES

Test measurements of the 100 m telescope at lambda = 7 mm [TR-18] 01 p0129 N85-10890

The Belikt experiment 02 p0159 N85-11079

Observations of 15 radio galaxies from Bologna survey using RATAN-600 radio telescope 02 p0162 N85-11097

The UK and Netherlands millimetre-wave telescope — Netherlands (NL) 05 p0625 N85-14003

Aperture synthesis (review) 06 p0781 N85-14995

Cross-shaped aperture synthesis system 06 p0782 N85-14999

Synthesis of radio image on RATAN-600 radiotelescope 06 p0783 N85-15004

Attempts to contruct two-dimensional image of Sun from observations made with RATAN-600 radiotelescope by relay race method 06 p0783 N85-15005

Research in geodesy based upon radio interferometric observations of extragalactic radio sources [AD-A147581] 07 p0988 N85-16280

FRG radiotelescope made of carbon fiber-reinforced plastic 09 p1309 N85-18226

Error in compensating phase fluctuations of wave field by means of adaptive reflectors with continuous or compound surface 13 p2080 N85-22988

QUASAT: An orbiting very long baseline interferometry program using large space antenna systems 14 p2230 N85-22822

Angular error of position of RATAN-600 screens during radial displacement 15 p2476 N85-25288

An Earth-based attempt to detect Saturn Electrostatic Discharge (SED) at 21 centimeters 15 p2674 N85-26801

Radio telescope with 256 antennas built in Siberia 22 p3732 N85-33126

RADIO TRACKING
NT WILDLIFE RADIOLOCATION

Data Collection and Platform Location by Satellite: ARGOS Users' Conference 14 p2325 N85-24368

The ARGOS contribution to the First GARP Global Experiment (FGGE) study of drifting buoys 14 p2325 N85-24371

The ARGOS system aboard research vehicles: 1981 experiment aboard the Le Suroit oceanographic vessel and the outlook [CNEXO/DFT/OPNAV/82-05] 14 p2327 N85-24382

Miscellaneous ARGOS maritime applications — yacht races 14 p2327 N85-24383

Synthesis of adaptive filters for tracking radio systems 22 p3763 N85-33325

RADIO TRANSMISSION
NT IONOSPHERIC PROPAGATION
NT MANDELSTAM REPRESENTATION
NT MICROWAVE ATTENUATION
NT MICROWAVE TRANSMISSION
NT MULTIPATH TRANSMISSION
NT SHORT WAVE RADIO TRANSMISSION
NT SINGLE SIDEBAND TRANSMISSION
NT SPREAD SPECTRUM TRANSMISSION
NT TRANSEQUATORIAL PROPAGATION

Digital radio link: Wave propagation measurements using narrow band technique [FOA-C-30364-E2] 04 p0494 N85-13152

Simulation of a transmission circuit composed of slightly nonlinear elements. Computation of the intermodulation on signals composed of N carriers [CNES-NT-105] 04 p0496 N85-13167

USSR report: Electronics and electrical engineering [JPRS-UEE-84-018] 07 p0949 N85-16014

Artificial ionospheric disturbances caused by powerful radio waves [AD-A148077] 08 p1186 N85-17473

UHF radiowave propagation through forests [AD-A149518] 10 p1467 N85-19256

Propagation Influences on Digital Transmission Systems: Problems and Solutions [AGARD-CP-363] 10 p1469 N85-19269

Limits of the propagation medium with respect to digital signal transmission 10 p1469 N85-19270

Propagation of wide bandwidth signals in a tropospheric ducting system 10 p1469 N85-19271

Propagation effects on the Doppler frequency shift of satellite transmissions 10 p1470 N85-19276

UHF communications through forested propagation channels 10 p1470 N85-19280

A comparison between predicted and measured propagation loss in the VHF/UHF range in rugged terrain 10 p1471 N85-19285

Measurements of propagation at 900 MHz in an urban zone for establishing a digital radiomobile system 10 p1472 N85-19288

A review of transmission and channel evaluation techniques for digital communication systems 10 p1474 N85-19301

A microprocessor controlled parallel model with FDPSK 10 p1475 N85-19304

Synopsis of mid-latitude radio wave absorption in Europe 11 p1659 N85-20454

L.F. RADIO-DATA: Specification of BBC phase-modulated transmissions on long-wave [BBC-RD-1984/19] 12 p1822 N85-21431

Disturbances in structure of lower ionosphere at terminators based on results of winde-band LW sounding 14 p2339 N85-24467

Land mobile satellite transmission measurements at 869 MHz: Selected results from the dedicated stratospheric balloon experiment of November 12 and 13, 1984 [NASA-CR-175734] 15 p2541 N85-25685

Meteorological conditions affecting electromagnetic propagation on the Arabian Peninsula [AD-A152019] 15 p2544 N85-25706

Active and passive remote sensing of ice [AD-A151741] 16 p2815 N85-27389

A transport theory of millimeter wave propagation in woods and forests [AD-A151883] 17 p2947 N85-28186

Effects of hydrometeors on electromagnetic wave propagation [AD-A155379] 22 p3759 N85-33297

Variation in radiowave propagation conditions in corona during solar activity cycle 22 p3763 N85-33327

O TRANSMITTERS
IONOSONDES
RADIO BEACONS
RADIOSONDES
RADIOTELEPHONES
RAWINSONDES
TRANSMITTER RECEIVERS
Development and testing of a 20-kW X-band transmitter n high phase stability 05 p0623 N85-13985
Estimation of requirements for acceptable noise iation level of communication transmitters 07 p0949 N85-16017
A reflectometer unit for a 500 kW HF balanced screened ader [BC-RD-1984/13] 10 p1477 N85-19322
Adaptive regulation of transmitter radiation power in do lines during delays of control signals 12 p1841 N85-21551
Equipment for the ARGOS system from Eidsvoll ectronics A.S. 14 p2239 N85-23885
The development of Platform Transmitter Terminal (PTT) d its application for drifting buoys 14 p2323 N85-24353
A new versatile ARGOS PTT for oceanographic plications -- Platform Transmit Terminal (PTT) 14 p2331 N85-24417
Foreshortened short-wave scattering on artificial nospheric inhomogeneities 14 p2340 N85-24488
Studies into location accuracy -- ARGOS system 16 p2811 N85-27334
The R-809 radio set [AD-A152370] 17 p2946 N85-28200
UHF IRIG G distribution system 17 p2965 N85-28308
Tone calibrated digital radio communication system [NASA-CASE-NPO-16414-1-CU] 18 p3089 N85-29121
Waves in Space Plasmas (WISP) 23 p3901 N85-34164
ADIO WAVE REFRACTION
Theory of radio wave propagation over the ocean 02 p0259 N85-11898
Field coherence function in layerwise nonhomogeneous troposphere 06 p0784 N85-15012
QUASAT, gravitational lenses, and studies of the interstellar, intracluster and intergalactic medium 07 p1058 N85-16715
Propagation effects on the Doppler frequency shift of satellite transmissions 10 p1470 N85-19276
Possibility of determining atmospheric weather parameters by radio and radiooptical measurements of refraction of cosmic sources 13 p2110 N85-23146
Saudi Arabian refraction profile: Crustal structure of the Red Sea-Arabian Shield transition 17 p2990 N85-28484
Beam diffusion in linear ionospheric layer 21 p3695 N85-32958
ADIO WAVES
NT CENTIMETER WAVES
NT CN EMISSION
NT DECAMETRIC WAVES
NT DECIMETER WAVES
NT EXTRATERRESTRIAL RADIO WAVES
NT GALACTIC RADIO WAVES
NT HYDROXYL EMISSION
NT IONOSPHERIC NOISE
NT LONG WAVE RADIATION
NT MICROWAVE EMISSION
NT MICROWAVES
NT MILLIMETER WAVES
NT RADIO BURSTS
NT RADIO EMISSION
NT SHORT WAVE RADIATION
NT SKY WAVES
NT SOLAR RADIO BURSTS
NT SOLAR RADIO EMISSION
NT SUBMILLIMETER WAVES
NT TYPE 3 BURSTS
NT TYPE 4 BURSTS
NT WHISTLERS
Planning guide for the review of telecommunications systems for frequency availability and electromagnetic compatibility [PB84-210238] 01 p0041 N85-10268
Formation of radio images by scanning around circle 02 p0264 N85-11727
Scattering of radio waves on magnitized meteor trail 03 p0344 N85-12221
The investigation of short wave signal structure in the vicinity of the caustic by means of a high-directed antenna [PR-194] 03 p0354 N85-12277
Artificial defocusing lens in ionosphere 05 p0724 N85-14854
Influence of Faraday effect in ionosphere on nonmutuality of meteor radio channel 07 p0952 N85-16037
Artificial ionospheric disturbances caused by powerful radio waves [AD-A148077] 08 p1186 N85-17473
Polarization angles of linearly polarized antennas and radio waves in satellite communications [PB85-131613] 11 p1626 N85-20240
Winter anomaly 1982/83 in comparison with earlier winters (1960-82) 11 p1660 N85-20461
Solar terrestrial influences on the D region as shown by the level of atmospheric radio noise 11 p1664 N85-20488
Radio Frequency Radiation (RFR) measurements in operational settings [AD-A149717] 12 p1828 N85-21471
The medical results of human exposures to radio frequency radiation [AD-A149718] 12 p1905 N85-21962
Calculation of amplitude-phase characteristics of signal scattered obliquely on meteor trail 13 p2073 N85-22948
Noninductive current drive in Tokamaks [DE85-005427] 14 p2424 N85-24951
Ionosphere effects may replace some communications satellites 15 p2484 N85-25337
The Impact of Proposed Radio Frequency Radiation Standards on Military Operations [AGARD-LS-138] 16 p2775 N85-27128
The physical interactions of radiofrequency radiation fields and biological systems 16 p2775 N85-27129
The biological effects of radiofrequency radiation 16 p2775 N85-27131
The cumulative effects of long term exposure to low levels of radiofrequency radiation (RFR) 16 p2776 N85-27132
Review of epidemiological studies of human exposures to radiofrequency radiation 16 p2776 N85-27134
Hazards of VLF electromagnetic fields 16 p2776 N85-27136
Radio Frequency Radiation (RFR) measurements in operational settings 16 p2777 N85-27138
Scintillation using NNSS satellites [AD-A152804] 17 p2949 N85-28207
A review of ionospheric effects on Earth-space propagation 18 p3106 N85-29233
Ionospheric limitations to time transfer by satellite 18 p3107 N85-29234
A review of tropospheric refraction effects on Earth-to-satellite systems 18 p3107 N85-29235
Meteorological and aeronomical requirements for MST radar networks (keynote paper), part 1 21 p3615 N85-32467
Morphology of the scattering targets: Fresnel and turbulent mechanisms, part 2.1A 21 p3618 N85-32481
Relationship of spaced antenna and Doppler techniques for velocity measurements (keynote paper), part 3 21 p3619 N85-32488
Radio telescope with 256 antennas built in Siberia 22 p3732 N85-33136
Onion-shell model for cosmic ray electrons and radio synchrotron emission in supernova remnants [OG-8.1-10] 23 p4018 N85-34900
RADICACTIVE AGE DETERMINATION
Automation of radiometric measurements in nuclear oceanology 14 p2337 N85-24452
Paleoenvironmental investigations at seed cave (Windust cave H-45FR46), Franklin County, Washington [AD-A154777] 21 p3635 N85-32576
Dating Archean zircon by ion microprobe: New light on an old problem 21 p3722 N85-33094
RADIOACTIVE CONTAMINANTS
Something in the air at Windscale --- radioactive contaminants from the Sellafield nuclear Complex for reprocessing and storing irradiated fuel [BLL-RISLEY-TR-4998-(9091.9F)] 08 p1179 N85-17429
Stabilization of contaminated soils by in situ vitrification [AD-P004144] 09 p1348 N85-18480
EPA (Environmental Protection Agency) research program guide, FY-1985, October 1, 1984 - September 30, 1985 [PB85-181881] 20 p3487 N85-31676
ARAC status report, 1985 [DE85-012835] 22 p3810 N85-33603
Control technology for radioactive emissions to the atmosphere at US Department of Energy facilities: The Los Alamos Meson Physics Facility [DE85-011402] 22 p3811 N85-33609
Estimation of Sr90 and Cs137 activity introduced and accumulation in the Po basin until 1983 [CISE-2515] 22 p3813 N85-33617
MATADOR (Methods for the Analysis of Transport And Deposition Of Radionuclides) code description and user's manual [TI86-901402] 23 p3966 N85-34592
RADIOACTIVE DATING
U RADIOACTIVE AGE DETERMINATION
RADIOACTIVE DECAY
NT ALPHA DECAY
NT NEUTRON EMISSION
Recent heavy particle decay in a matter dominated universe [NASA-CR-175501] 11 p1764 N85-21095
Study of 1/f noise in solids [AD-A151069] 14 p2428 N85-24972
Neutrino measurements on the Moon [DE85-007700] 16 p2884 N85-27791
Theoretical basis for the determination of the concentration of radon decay products in air from the activity of a particulate air sample [IRI-190-83-07] 17 p3035 N85-28774
Model computations of radon, and radon decay product, concentrations in an open system; the Hewlett-Packard 41C program RNSS, version 02 [IRI-190-83-12] 17 p3035 N85-28775
Theoretical studies of high energy phenomenon: Analysis of models of CP and T violation [DE85-007455] 17 p3036 N85-28782
Selected topics from J/psi decays [DE85-010537] 18 p3183 N85-29736
Early study of muons and muon decay [NOTA-INTERNA-835] 18 p3184 N85-29742
Topics in intermediate vector boson physics [NOTA-INTERNA-841] 18 p3184 N85-29743
AGS broad band neutrino beam [DE85-010954] 19 p3366 N85-30875
Summary of the discussion of the theory of radiative processes [DE85-007812] 19 p3371 N85-30914
Current experiments in elementary particle physics, revision 1-85 [DE85-011513] 20 p3529 N85-31950
Effects of CP violation in SU(2) sub L x SU(2) sub R x U(1) electroweak models [DE85-010801] 20 p3531 N85-31965
Phenomenology of the standard and nonstandard Higgs particles [USIP-85-03] 20 p3532 N85-31971
Tritium-helium effects in metals [DE85-011507] 22 p3749 N85-33235
Electron capture decay of cosmic rays: A model of the inhomogeneous interstellar medium [OG-7.1-10] 23 p4014 N85-34871
Preliminary results on underground muon bundles observed in the Frejus proton-decay detector [HE-5.1-1] 24 p4200 N85-36067
Muon and neutrino results from KGF experiment at a depth of 7000 hg/square cm [HE-5.1-2] 24 p4200 N85-36068
Relevance of multiple muons detected underground to the mass composition of primary cosmic rays [HE-5.1-4] 24 p4201 N85-36069
On muon energy spectrum in muon groups underground [HE-5.1-14] 24 p4201 N85-36076
RADIOACTIVE ELEMENTS
U RADIOACTIVE ISOTOPES
RADIOACTIVE ISOTOPES
NT AMERICIUM
NT AMERICIUM ISOTOPES
NT AMERICIUM 241
NT BERYLLIUM 7
NT BERYLLIUM 9
NT BERYLLIUM 10
NT CALIFORNIUM ISOTOPES
NT CARBON 14
NT CERIUM 144
NT CESIUM 134
NT CESIUM 137
NT COBALT 60
NT CURIUM
NT CURIUM 244
NT IRON 59
NT KRYPTON 85
NT PLUTONIUM
NT PLUTONIUM ISOTOPES
NT PLUTONIUM 238
NT PLUTONIUM 239
NT POTASSIUM 40
NT STRONTIUM 90
NT TRANSURANIUM ELEMENTS
NT TRITIUM

Radiotracer studies of the dispersion of solid pollutants in marine and estuarial environment: Measurement of diffusion coefficients and the phenomenon of dispersion by currents
[BLL-DRIC-TRANS-7104-(3623.66)] 02 p0224 N85-11466

Analysis of radiocobalt in environmental samples
[DRIC-T-7394] 03 p0367 N85-12477

Isotopes in day to day life
[IAEA/PI/A.6E-84-00924] 03 p0417 N85-12686

Hydrologic characteristics of the Mediterranean and Black Sea 07 p0961 N85-16226

Comparing computing formulas for estimating concentration ratios
[DE84-008644] 09 p1349 N85-18490

TRAN-STAT: Statistics for environmental studies
[DE85-000829] 10 p1513 N85-19547

Multiple element neutron-activation analysis of atmospheric aerosols with X-ray and gamma-spectrometric recording of radionuclides formed
13 p2013 N85-22631

Program RNTHR/2: An HP-41 C program for the calculation of RaA, RaB, and RaC concentrations in air based on three measurements of an air-dust sample
[IRI-190-83-10] 18 p3134 N85-29412

Collodial particle transport with simultaneous birth, growth and capture
[DE85-010366] 19 p3235 N85-30055

Evaluation of a high pressure proportional counter for the detection of radioactive noble gases
[AD-A154436] 19 p3272 N85-30292

Environmental monitoring at Argonne National Laboratory
[DE85-010613] 19 p3309 N85-30516

Radioluminescent lighting for Alaskan runway lighting and marking
[DE85-010405] 19 p3366 N85-30687

Dosimetry and limit values for internal contamination with radionuclides: From (International Commission on Radioactive Protection) ICRP-2 to ICRP-30
[IRI-190-84-03] 20 p3507 N85-31804

Source-term considerations for a potential radioactive-waste repository located in unsaturated tuff
[DE85-010090] 20 p3529 N85-31953

Current internal-dosimetry practices at US Department of Energy facilities
[DE85-011718] 22 p3787 N85-33466

Environmental surveillance at Los Alamos during 1984
[DE85-011686] 22 p3811 N85-33605

The 1984 environmental monitoring program report for Idaho National Engineering Laboratory site
[DE85-011209] 22 p3812 N85-33611

Measurement of radionuclides in waste packages
[DE85-011674] 22 p3838 N85-33786

MATADOR (Methods for the Analysis of Transport And Deposition Of Radionuclides) code description and user's manual
[TI85-901402] 23 p3966 N85-34592

Development of the osmium-191 yields iridium-191m radionuclide generator
[DE85-011165] 23 p3970 N85-34611

Current status of the Os-191 yields Ir-191m generator
[DE85-006306] 23 p3971 N85-34614

Elemental technetium as a cosmic-ray clock
[OG-7.1-9] 23 p4013 N85-34870

Bevalac calibration of the SOFIE range and hodoscope detectors
[OG-9.1-7] 23 p4023 N85-34933

High precise measurements of cosmogenic radiocarbon abundence by complex of scintillation equipments
[SH-7.1-14] 23 p4048 N85-35105

Wholebody radiation counting system
[AD-A155842] 24 p4131 N85-35607

Tritium hazard via the ingestion pathway
[DE85-012697] 24 p4133 N85-35618

RADIOACTIVE MATERIALS

Development of an automated miniature Charpy test method
[DE85-003011] 11 p1652 N85-20405

Examination of the feasibility for demonstration and use of radioluminescent lights for Alaskan remote runway lighting
[DE85-002503] 12 p1782 N85-21185

High altitude sampling program: Radioactivity in the stratosphere
[DE85-005924] 14 p2374 N85-24676

Scanning electron microscope facility for examination of radioactive materials
[DE85-008127] 17 p2969 N85-28335

Corrosion performance of metals and alloys in a tuff geochemical environment
[DE85-009449] 18 p3077 N85-29033

Concretization of high level radioactive source in marine sediment
[AD-D011703] 19 p3249 N85-30146

Petrologic and geochemical characterization of the Topopah Spring Member of the Paintbrush Tuff: Outcrop samples used in waste package experiments
[DE85-010449] 19 p3302 N85-30470

Container for radioactive materials
[DE85-005757] 23 p3972 N85-34626

Radiation safety problems in handling highly active tritium targets
[DE85-014266] 24 p4151 N85-35742

RADIOACTIVE NUCLIDES

U RADIOACTIVE ISOTOPES

RADIOACTIVE WASTES

Americium thermodynamic data for the EQ3/6 database
[DE84-017065] 04 p0573 N85-13656

HS and E environmental sciences
[DE84-016183] 05 p0672 N85-14314

Crystalline rocks of the northeastern United States
[DE84-013674] 05 p0677 N85-14347

Integrated data base program: A status report
[DE84-013604] 05 p0735 N85-14727

Conceptual design report for a remotely operated cask handling system, revision 1
[DE85-000348] 08 p1169 N85-17371

Preliminary post-emplacement safety analysis of the subseabed disposal of high-level nuclear waste
[DE84-011162] 08 p1221 N85-17692

Ground-water level data and preliminary potentiometric-surface maps, Yucca Mountain and vicinity, Nye County, Nevada
[DE85-001771] 09 p1343 N85-18448

Field implementation of geophysical diffraction tomography
[DE84-017594] 09 p1343 N85-18449

Stabilization of contaminated soils by in situ vitrification
[AD-P004144] 09 p1348 N85-18480

Consideration of future climatic changes in three geologic settings
[DE85-001704] 09 p1357 N85-18537

Measurements of sediment temperatures, conductivity and heat flow in the North Atlantic and their relevance to radioactive waste disposal
[IOS-172] 09 p1359 N85-18551

An assessment of biological processes close to the sea bed in a slope region and its significance to the assessment of sea-bed disposal of radioactive waste
[IOS-185] 09 p1360 N85-18554

Rockwell Hanford operations defense waste and byproducts management
[DE85-000553] 09 p1382 N85-18694

Nevada nuclear waste storage investigations preliminary repository concepts report
[DE85-002132] 09 p1383 N85-18696

Planning for greater-confinement disposal
[DE85-002143] 09 p1383 N85-18697

Perspective on demonstrations of compliance for high-level waste disposal
[DE85-000989] 09 p1383 N85-18698

Commission operation. National Low-Level Radioactive Waste Management Program
[DOE/LLW-33T] 09 p1383 N85-18699

Intrusion of radioactive industrially polluted water from North Sea into central Baltic Sea
10 p1498 N85-19454

China report: Science and technology
[JPRS-CST-84-025] 11 p1620 N85-20197

Index to published geologic maps in the region around the potential Yucca Mountain nuclear waste repository site, southern Nye County, Nevada
[DE85-000260] 11 p1669 N85-20518

Models and parameters for environmental radiological assessments
[DE81-027154] 11 p1678 N85-20573

Consolidation around a point heat source
[PB85-116549] 11 p1682 N85-20601

Man/machine interface for a nuclear cask remote handling control station: System design requirements
[DE85-000256] 11 p1697 N85-20667

WESF (173)Cs gamma ray sources
[DE85-000676] 11 p1727 N85-20859

Effect of host-rock dissolution and precipitation on permeability in a nuclear waste repository in tuff
[DE85-000675] 11 p1727 N85-20860

Radioactive waste isolation in salt: Peer review of the D'Appolonia report on schematic designs for penetration seals for a repository in the Permian Basin, Texas
[DE85-000693] 11 p1727 N85-20861

Field lysimeter facility for evaluating the performance of commercial solidified low-level waste
[DE85-003686] 11 p1727 N85-20863

High-level waste processing and disposal
[DE85-003564] 11 p1728 N85-20865

Shallow land burial technology: Humid
[DE85-004432] 12 p1932 N85-22136

Research and development related to the Nevada nuclear waste storage investigations
[DE85-002303] 12 p1932 N85-22139

Application of far-field models to the disposal of nuclear waste in geologic formations
[DE85-005489] 14 p2420 N85-24922

Physical-chemical model for the mechanism of glass corrosion with particular consideration of simulated radioactive waste glasses
[DE85-007713] 17 p2935 N85-28121

Corrosion performance of metals and alloys in a tuff geochemical environment
[DE85-009449] 18 p3077 N85-29033

Shales and other argillaceous strata in the United States
[DE85-010453] 18 p3125 N85-29053

Region-to-area screening methodology for the Crystalline Repository Project
[DE85-009802] 18 p3125 N85-29054

Implications about in situ stress at Yucca Mountain
[DE85-008068] 18 p3126 N85-29058

Radionuclide mobility in the shallow portion of an active high-temperature geothermal system
[DE85-010293] 18 p3182 N85-29729

Hydrolysis, formation and ionization constants at 25(0)C, and at high temperature-high ionic strength
[DE85-010645] 19 p3236 N85-30081

Mixtures experiment where the amount of the mixture is a factor under study
[DE85-010974] 19 p3250 N85-30153

High level radioactive waste vitrification process equipment component testing
[DE85-011143] 19 p3273 N85-30288

Development of HWVP melter/turntable components for canyon-remote maintenance and replacement
[DE85-010308] 19 p3273 N85-30289

Three-dimensional finite element impact analysis of a nuclear waste truck cask
[DE85-010653] 19 p3288 N85-30399

Reference data source documentation for performance assessment studies, Basalt Waste Isolation Project, Hanford Site, Washington
[DE85-010543] 19 p3301 N85-30468

Preliminary evaluation of alterant geophysical tomography in welded tuff
[DE85-010626] 19 p3302 N85-30469

Radioactive liquid wastes discharged to ground in the 200 areas during 1984
[DE85-010819] 19 p3310 N85-30517

TMI-2 technical information and examination program
[DE85-010614] 19 p3359 N85-30827

Qualitative comparison of fusion reactor materials for waste handling and disposal
[DE85-010473] 19 p3360 N85-30830

Radioactivity in gaseous waste discharged from the separations facilities during 1984
[DE85-011373] 19 p3360 N85-30831

Source Term Experiments Project (STEP): Aerosol characterization system
[DE85-010248] 19 p3361 N85-30839

Occurrence of uranium in ground water in the vicinity of the US Department of Energy Feed Materials Production Center, Fernald, Ohio
[DE85-010340] 19 p3364 N85-30862

Bulk and thermal properties of the functional Tuffaceous Beds in holes USW G-1, UE-25 no. 1, and USW G-2, Yucca Mountain, Nevada
[DE85-011181] 19 p3365 N85-30866

Dispersal From Deep Ocean Sources: Physical and Related Scientific Processes
[DE85-010420] 20 p3497 N85-31740

Development of processes for the inclusion of radioactive waste in glass-metal compounds and ceramic materials
[BLL-CE-TRANS-8014-(9022.09)] 20 p3526 N85-31931

Geologic and hydrologic characterization and evaluation of the basin and range province relative to the disposal of high-level radioactive waste. Part 1: Introduction and guidelines
[GS-CIRC-904-A] 20 p3526 N85-31932

Geologic and hydrologic characterization and evaluation of the basin and range province relative to the disposal of high-level radioactive waste. Part 2: Geologic and hydrologic characterization
[GS-CIRC-904-B] 20 p3526 N85-31933

Geologic and hydrologic characterization and evaluation of the basin and range province relative to the disposal of high-level radioactive waste. Part 3: Geologic and hydrologic evaluation
[GS-CIRC-904-A] 20 p3526 N85-31934

Source-term considerations for a potential radioactive-waste repository located in unsaturated tuff
[DE85-010090] 20 p3529 N85-31953

East Europe report: Science and technology
[JPRS-ESA-85-021] 21 p3566 N85-32190

Centrifugal castings of stainless steel spiked with radioactive tracers
[DE85-012003] 22 p3748 N85-33234
ARAC status report, 1985
[DE85-012835] 22 p3810 N85-33603
Technology of off-gas treatment for liquid-fed ceramic melters
[DE85-012467] 22 p3812 N85-33610
Corrosion resistant storage container for radioactive material
[DE85-011666] 22 p3836 N85-33765
Measurement of radionuclides in waste packages
[DE85-011674] 22 p3838 N85-33766
Design analysis for a repository in crystalline rock
[DE85-011802] 22 p3839 N85-33771
Office of Civilian Radioactive Waste Management
[DE85-012585] 22 p3839 N85-33774
Polyethylene solidification of low-level wastes
[DE85-012568] 22 p3843 N85-33799
Method for extracting lanthanides and actinides from acid solutions by modification of Purex solvent
[DE85-005763] 23 p3909 N85-34220
Research at the Institute of Oceanographic Sciences related to the possible disposal of radioactive waste on or beneath the seafloor
[IOS-204] 23 p3973 N85-34628
Simulated effects of increased recharge on the ground-water flow system of Yucca Mountain and vicinity, Nevada-California
[DE85-012865] 24 p4108 N85-35469

RADIOACTIVITY
A dispersion model for airborne particulates inside a building
[DE84-014981] 02 p0225 N85-11473
Evaluation of arctic test of improved tritium radioluminescent lighting
[AD-A148215] 08 p1089 N85-16884
Atmospheric science and power production
[DE84-005177] 09 p1354 N85-18521
Light your runways and taxiways without electricity
[DE85-000269] 11 p1586 N85-19991
Radiative ion beams: Hot stellar reactions in the laboratory
[DE85-001570] 11 p1722 N85-20633
High altitude sampling program: Radioactivity in the stratosphere
[DE85-005924] 14 p2374 N85-24676
A remote-operated manipulator vehicle
[HSE-TRANS-11133] 19 p3261 N85-30349
Nuclear data needs for fusion energy development
[DE85-010445] 20 p3536 N85-32000
The 1984 effluent and environmental monitoring report for the Bettis Atomic Power Laboratory
[DE85-011533] 22 p3810 N85-33602
The 1984 environmental monitoring report, Sandia National Laboratories, Albuquerque, New Mexico
[DE85-011175] 22 p3811 N85-33607

RADIOBIOLOGY
Radiobiological studies on egg systems exposed to heavy nuclei of cosmic galactic radiation — insects
05 p0690 N85-14440
Preliminary results of advanced Biostack experiments with plant seeds and spores — cosmic ray effects
05 p0691 N85-14441
The radiobiological advanced Biostack experiment on Spacelab 1 05 p0691 N85-14442
USSR report: Life sciences. Biomedical and behavioral sciences
[JPRS-UBB-84-015] 07 p1010 N85-16416
European scientific notes. Volume 38, number 11
[AD-A148228] 08 p1230 N85-17745
Radiation physics, biophysics, and radiation biology
[DE84-014885] 09 p1360 N85-18557
Effect of modulated ultrahigh frequency field on behavior and hormone level in female rats under emotional stress
09 p1361 N85-18562
Radiation damage and repair in cells and cell components. Part 2: Physical radiations and biological significance
[DE85-008934] 18 p3152 N85-29518
Biology and Medicine Division
[DE85-010638] 19 p3327 N85-30613
Collected epidemiological studies of the late effects of internal radium in man, and mechanistic investigations of those effects, part 2
[DE85-011174] 19 p3331 N85-30636
Biostack experiments on STS-flights and the impact for man in space 20 p3510 N85-31821
A practical guide to ionization chamber dosimetry at the AFRRI reactor
[AD-A155185] 21 p3703 N85-33003
Biophysical research in space — radiation effects
24 p4130 N85-35603

RADIOCHEMICAL SE. ARATION
Effects of primary recoil energy on the production rate of mobile defects during elevated temperature irradiation
[DE85-006218] 15 p2511 N85-25489

RADIOCHEMISTRY
NT RADIOCHEMICAL SEPARATION
Assessment of Techniques for Measuring Tropospheric H sub x O sub y
[NASA-CP-2332] 05 p0675 N85-14336
Hydrologic characteristics of the Mediterranean and Black Sea 07 p0961 N85-16228
Robotics in the radiochemical laboratory
[DE85-002624] 10 p1494 N85-19433
Activities in nuclear physics and high energy physics
11 p1728 N85-20866
Proposed solar neutrino experiment using (81)Br(nu,e(-e)) (81)Kr
[DE85-004802] 15 p2684 N85-26579
Proceedings of the Fifth International Conference on Nuclear Methods in Environmental and Energy Research
[DE84-017348] 19 p3310 N85-30521

RADIOGENIC MATERIALS
Late Paleozoic and early Mesozoic radiolarians in the Circle quadrangle, east-central Alaska
04 p0517 N85-13297
The relation between the age of the subconducting slab and the recycling of sediments into the mantle
21 p3717 N85-33063

RADIOGRAPHY
NT AUTORADIOGRAPHY
NT COMPUTER AIDED TOMOGRAPHY
NT NEUTRON RADIOGRAPHY
NT TOMOGRAPHY
Technical activities 1983, Office of Nondestructive Evaluation
[PB84-217074] 03 p0370 N85-12360
Flash radiography as a quantitative tool
[DE84-016485] 04 p0503 N85-13211
Development of a dynamic radiographic capability using high-speed video
[DE84-016477] 04 p0511 N85-13256
High-speed videography for optical and X-ray imaging
[DE84-012661] 04 p0564 N85-13595
Flywheel-powered X-ray generator
05 p0605 N85-13861
Collimation techniques for dense object flash radiography
[DE84-016461] 05 p0647 N85-14152
Characterizing X-ray machines
[AD-A146532] 06 p0862 N85-15481
X-radiography of slices of the Allende Meteorite
06 p0885 N85-15622
Metallic aid and technique in fitting voice prosthesis
[AD-D011356] 07 p1014 N85-16442
Improved radiographic viewing system
[AD-A147587] 07 p1016 N85-16456
Ultrasonic measurements, X-ray photographs and image processing
[BLL-RISLEY-TR-4596-(9091.9F)]
07 p1037 N85-16583
Proceedings of the 14th Army Science Conference. Volume 1: Principal Authors A through H
[AD-A149200] 10 p1573 N85-19920
China report: Science and technology
[JPRS-CST-84-025] 11 p1620 N85-20197
Radiographic inspection of butt welds described
11 p1620 N85-20198
Radiographic detectability limits for seeded voids in sintered silicon carbide and silicon nitride
[NASA-TM-86945] 12 p1861 N85-21674
A new NDE (Non-Destructive Evaluation) capability for thin-shelled structures
[AD-A149625] 12 p1862 N85-21678
In-situ burning rate determination using flash radiography 13 p2002 N85-22550
Mini-Seminar on Non-Destructive Testing
[CSIR-TSD-0009/83] 14 p2316 N85-24308
Basic principles of industrial radiography
14 p2316 N85-24310
Standing of industrial radiography in South Africa
14 p2316 N85-24311
Radiological safety aspects of industrial radiography
14 p2316 N85-24312
Flash radiography 14 p2317 N85-24316
New developments in industrial radiography
14 p2317 N85-24317
Axial topography from digitized real time radiography
[DE85-006767] 18 p3091 N85-29130
Visual simulation of radiographs
[DE85-010213] 18 p3110 N85-29255
Image processing: Mathematics, engineering or art
[DE85-007666] 18 p3154 N85-29527
Poisson formula for radon transformation and numerical image reconstruction algorithm
21 p3697 N85-32973

RADIOISOTOPE BATTERIES
Space nuclear safety program
[DE84-015074] 04 p0463 N85-12939
Space nuclear safety program
[DE84-015064] 04 p0463 N85-12940
General-purpose heat source development: Safety test program. Postimpact evaluation, design iteration test 2
[DE84-015978] 04 p0584 N85-13592
Technical support services for space and terrestrial systems programs
[DE84-009031] 05 p0597 N85-13806
Radioisotope space power programs
05 p0609 N85-13897
Development of advanced thermoelectric materials
[NASA-CR-175664] 14 p2351 N85-24532
LPCVD tungsten deposition on Si-Ge alloy
[DE85-005566] 16 p2750 N85-26970

RADIOLOGY
FLACS: A new sensitometer for measurement of extreme low intensity reciprocity in a controlled environment — X-ray films 07 p0963 N85-16104
Radiation physics, biophysics, and radiation biology
[DE84-014885] 09 p1360 N85-18557
China report: Science and technology
[JPRS-CST-85-013] 15 p2536 N85-25652

RADIOLYSIS
Magnetic resonance studies of transient radicals and radical ions
[DE84-011699] 03 p0328 N85-12116
Production of stable embryo particles in dense ion tracks of alpha particle emissions in the atmosphere
21 p3644 N85-32638

RADIOMETERS
NT INFRARED DETECTORS
NT INFRARED RADIOMETERS
NT INFRARED SCANNERS
NT MICROWAVE RADIOMETERS
NT PASSIVE L-BAND RADIOMETERS
NT SPECTRORADIOMETERS
A sphere-scanning radiometer for rapid directional measurements of sky and ground radiance: The PARABOLA field instrument
[NASA-TM-86171] 03 p0363 N85-12329
Self-study manual on optical radiation measurements. Part 1: Concepts. Chapter 11: Linearity considerations and calibrations
[PB84-218346] 03 p0421 N85-12690
Fidelity of satellite soundings
05 p0682 N85-14383
NBS (National Bureau of Standards) switching radiometers
[PB84-235894] 07 p0968 N85-16147
The radiation temperature of a cloud of particles
[FOA-C-30367-E4] 08 p1190 N85-17497
Photodiodes for astronomical stellar radiometry
08 p1252 N85-17908
Measurement of shock induced reaction in rocket propellants by nanosecond infrared radiometry and photography
[AD-P004349] 10 p1456 N85-19173
Liquid fuel spray processes in high-pressure gas flow
[NASA-TM-86944] 12 p1844 N85-21570
Microprocessor-controlled rotating shadowband radiometer
[DE85-003633] 12 p1854 N85-21630
Monolithic short wave infrared (SWIR) detector array
[NASA-CR-175284] 12 p1874 N85-21759
Analysis of selective chopper radiometer data
[NASA-CR-175157] 12 p1895 N85-21894
Application of field X-ray: Radiometric analysis in exploratory geology and means for its improvement
13 p2115 N85-23176
Automation of radiometric measurements in nuclear oceanology 14 p2337 N85-24452
Solar gravity modes from ACRIM-SWM irradiance data
14 p2443 N85-25071
Lidar and radiometer observations of thunderstorm tops 15 p2595 N85-25994
High-frequency microwave observations of convective precipitation 15 p2596 N85-26000
Galileo 15 p2688 N85-26601
Comparative study of the digital analysis of areas of the Earth's surface prepared for planting using different classification algorithms
[INPE-3359-PRE/637] 16 p2846 N85-27545
Radiometer integrated into a communication terminal
[AD-A151746] 17 p2947 N85-28195
Water vapor radiometry research and development phase
[NASA-CR-175887] 17 p2995 N85-28512
Offset reflector with horn feed array, used as an experimental sensor for radiometric measurements
[ESA-TT-830] 20 p3443 N85-31369
View-limiting shrouds for insolation radiometers
[NASA-CR-176041] 20 p3458 N85-31476
Ocean circulation studies 20 p3492 N85-31712

Calibration and use of clutter data for simulation
[AD-A154793] 21 p3574 N85-32229
Enhancing precision of remote temperature sensing data from satellites under cloudy atmospheric conditions
22 p3734 N85-33148
Determination of altitude of cloud cover top from Meteor satellite data 22 p0734 N85-33150
Active Cavity Radiometer (ACR)
23 p3901 N85-34163
Investigation of non-intrusive radiometers for entrained gasifier temperature measurement, revision 3
[DE85-011795] 23 p3934 N85-34385
Analyzer, flight line
[AD-A155777] 24 p4067 N85-35207
Development of advanced high-temperature heat flux sensors. Phase 2: Verification testing
[NASA-CR-174973] 24 p4096 N85-35391
Aeromagnetic and radiometric signatures of a possible porphyry system in the western Tusher Mountains, Utah
24 p4103 N85-35437

RADIOMETRIC CORRECTION
Characterizing the scientific potential of satellite sensors
[E85-10031] 05 p0654 N85-14200
Characterizing the scientific potential of satellite sensors — San Francisco, California
[E85-10044] 07 p0983 N85-16244
Characterizing the scientific potential of satellite sensors — San Francisco, California
[E85-10053] 07 p0984 N85-16249
Study of spectral/radiometric characteristics of the Thematic Mapper for land use applications
[E85-10057] 07 p0987 N85-16266
Study of spectral/radiometric characteristics of the Thematic Mapper for land use applications
[E85-10075] 10 p1504 N85-19489
Radiometric accuracy assessment of LANDSAT 4 Multispectral Scanner data 11 p1666 N85-20496
Radiometric calibration and geocoded precision processing of LANDSAT-4 Multispectral Scanner products by the Canada Centre for Remote Sensing
11 p1667 N85-20501
Radiometric calibration and processing procedure for reflective bands on LANDSAT-4 protoflight Thematic Mapper 11 p1668 N85-20510
A preliminary assessment of LANDSAT-4 Thematic Mapper data — Windsor, Ontario and Medicine Hat areas, Canada 12 p1869 N85-21728
Preliminary evaluation of the radiometric calibration of LANDSAT-4 Thematic Mapper data by the Canada Centre for Remote Sensing 12 p1870 N85-21729
In-progress absolute radiometric inflight calibration of the LANDSAT-4 sensors — New Mexico
12 p1870 N85-21733
LANDSAT-4 Thematic Mapper calibration and atmospheric correction 12 p1870 N85-21734
Scan angle and detector effects in Thematic Mapper radiometry — Iowa and Arkansas
12 p1871 N85-21735
Analysis and evaluation of the LANDSAT-4 MSS and TM sensors and ground data processing systems: Early results 13 p2117 N85-23189
LANDSAT-4/5 image data quality analysis
[E85-10105] 24 p4107 N85-35463

RADIOMETRIC RECTIFICATION
U RADIOMETRIC CORRECTION

RADIOMETRIC RESOLUTION
Study on spectral/radiometric characteristics of the Thematic Mapper for land use applications
[E85-10021] 02 p0218 N85-11434
LANDSAT instruments characterization
[E85-10032] 04 p0524 N85-13356
LANDSAT instruments characterization
[E85-10028] 05 p0654 N85-14197
LANDSAT instruments characterization
[E85-10030] 05 p0654 N85-14199
Radiation data and standards for Tokamak diagnostics
09 p1390 N85-18742
Study of spectral/radiometric characteristics of the Thematic Mapper for land use applications
[E85-10075] 10 p1504 N85-19489
Summary of MSS characterization investigations
11 p1666 N85-20497
Radiometric accuracy assessment of LANDSAT 4 Multispectral Scanner data 11 p1666 N85-20496
Investigation of radiometric properties of LANDSAT-4 MSS — California, North Carolina, South Carolina, and New England 11 p1666 N85-20500
Impact of LANDSAT MSS sensor differences on change detection analysis — New Mexico, San Francisco, CA, New Hampshire, and Connecticut
11 p1667 N85-20506
Prelaunch absolute radiometric calibration of the reflective bands on the LANDSAT-4 protoflight Thematic Mapper 11 p1669 N85-20515
Characterization of radiometric calibration of LANDSAT-4 reflective bands 11 p1669 N85-20516
LANDSAT-4 Science Characterization Early Results. Volume 3, part 2: Thematic Mapper (TM)
[E85-10089] 12 p1869 N85-21724
Relative radiometric calibration of LANDSAT TM reflective bands 12 p1869 N85-21725
Evaluation of the radiometric integrity of LANDSAT 4 Thematic Mapper band 6 data 12 p1869 N85-21726
Thermal band characterization of the LANDSAT-4 Thematic Mapper 12 p1869 N85-21727
A preliminary analysis of LANDSAT-4 Thematic Mapper radiometric performance 12 p1870 N85-21730
Evaluation of the radiometric quality of the TM data using clustering, linear transformations and multispectral distance measures — Illinois 12 p1870 N85-21731
Intraband radiometric performance of the LANDSAT 4 Thematic Mapper — Washington, DC, Arkansas, Massachusetts, Virginia, and Arizona
12 p1871 N85-21738
A preliminary evaluation of LANDSAT-4 Thematic Mapper data for their geometric and radiometric accuracies 12 p1871 N85-21739
The use of linear feature detection to investigate Thematic Mapper data performance and processing
12 p1872 N85-21740
Assessment of Thematic Mapper band-to-band registration by the block correlation method
12 p1872 N85-21743
LANDSAT 4 band 6 data evaluation
[E85-10093] 12 p1874 N85-21755
Spectroradiometric calibration of the Thematic Mapper and Multispectral Scanner system
[E85-10094] 12 p1874 N85-21756
VISSR infrared calibration by means of calculated radiances 12 p1894 N85-21889
Impact of Thematic Mapper sensor characteristics on classification accuracy — suburban Washington, D.C., Maryland, and the Chesapeake Bay
13 p2117 N85-23188
Assessing LANDSAT TM and MSS data for detecting submerged plant communities 13 p2120 N85-23203
The use of Thematic Mapper data for land cover discrimination: Preliminary results from the UK SATMaP programme 13 p2121 N85-23207
The 13 November 1984 occultation of BD +08 deg 0471 by (1) Ceres
[NASA-CR-176106] 23 p3987 N85-34725
Study of spectral/radiometric characteristics of the Thematic Mapper for land use applications
[E85-10106] 24 p4107 N85-35464

RADIONUCLIDES
U RADIOACTIVE ISOTOPES

RADIOPROTECTIVE AGENTS
U ANTIRADIATION DRUGS

RADIOSENSITIVITY
U RADIATION TOLERANCE

RADIOSONDES
NT IONOSONDES
NT RAWINSONDES
Three-dimensional mesoscale analysis of serial soundings 01 p0074 N85-10493
Thermosonde and UHF radar measurements of C2 sub n at Westford, Massachusetts - July 1981
[AD-A145398] 02 p0190 N85-11270
Measurements on the diffusion of hydrogen chloride in the waste gas plume of incineration ships in the North Sea. Part 1: Methodology, instrumentation and presentation of data
[GKSS-84-E-23-PT-1] 05 p0672 N85-14319
C2 sub n (optical) studies in the free atmosphere based on rawinsonde data
[AD-A147307] 07 p0997 N85-16332
Comparative investigation of three commercial radiosonde systems
[KNMI-TR-53] 07 p1008 N85-16409
Wind-weighting for sounding rockets with a telemetry system
[NASA-TP-2438] 12 p1792 N85-21246
Nowcasting applications of VAS
15 p2597 N85-26003
Role of jet streaks and boundary layer processes in organizing a pre-convective environment
15 p2597 N85-26008
Lightweight aerological radiosonde MARZ
16 p2807 N85-27309
Ship-to-ship propagation: Maritime data analyses
[AD-A155484] 21 p3592 N85-32325
Observations of frontal zone structures with a VHF Doppler radar and radiosondes, part 1.2A
21 p3616 N85-32469
A modified Fresnel scattering model for the parameterization of Fresnel returns, part 2.3A
21 p3618 N85-32483
Gravity-wave spectra in the atmosphere observed by MST radar, part 4.2B 21 p3622 N85-32502
Meteorological data from the OPTOMA (Ocean Prediction Through Observations, Modeling and Analysis) program OPTOMA 2, leg D2. 30 Jun. - 10 Jul. 1984
[AD-A156134] 24 p4123 N85-3

RADIOTELEPHONES
Estimation of requirements for acceptable safe radiation level of communication transmitters
07 p0949 N85-16917
Controllable companding in low-frequency FM radio communication systems 22 p3776 N85-3

RADIOTHERAPY
U RADIATION THERAPY

RADIUM
Distribution of radium and plutonium in human bone
[DE85-006025] 13 p2142 N85-2

RADIUS
U RADII

RADOME MATERIALS
Proceedings of the 17th Symposium on Electromagnetic Windows, part 1
[AD-A149165] 10 p1466 N85-1
Proceedings of the Symposium on Electromagnetic Windows (17th) held at Georgia Inst. of Technology, Engineering Experiment Station, Atlanta, Georgia on 25-27 July 1984. Part 2
[AD-A149125] 12 p1824 N85-21444
Design and calibration of a 35GHz dielectrometer
[AD-P004363] 12 p1826 N85-21457
Pressureless sintered silicon nitride as a promising candidate for radome materials
[AD-P004367] 12 p1826 N85-21461
LL-100: A new polybutadiene (resin system for radome applications)
[AD-P004368] 12 p1826 N85-21462
Broadband thermoplastic radomes
[AD-P004369] 12 p1827 N85-21463
Development of a high temperature single impact rain erosion test capability
[AD-P004371] 12 p1827 N85-21465
Laminated thermoplastic radome
[AD-D011664] 18 p3079 N85-28046

RADOMES
Tolerance synthesis of multilayer radome walls
07 p0953 N85-16041
Electromagnetic analysis of radomes by the moment method
[AD-P004351] 12 p1824 N85-21445
A computer analysis of the RF performance of a ground-mounted, air-supported radome
[AD-P004352] 12 p1824 N85-21446
Comparison of spherical wave ray tracing and exact boundary value solutions for spherical radomes
[AD-P004353] 12 p1824 N85-21447
Generalized radome BSE (radome boresight error) characterization using superposition techniques
[AD-P004354] 12 p1825 N85-21448
A subaperture approach to the calculation of flashlobes introduced by airborne radomes
[AD-P004355] 12 p1825 N85-21449
Near-field effects on radome boresight errors
[AD-P004356] 12 p1825 N85-21450
Dual band radome wall design
[AD-P004357] 12 p1825 N85-21451
Study of laminated dielectric behavior at microwave and millimeter-wave frequencies
[AD-P004358] 12 p1825 N85-21452
Image lobe analysis for large radomes
[AD-P004359] 12 p1825 N85-21453
Supersonic Tactical Missile (STM) radome development
[AD-P004360] 12 p1825 N85-21454
A millimeter wave apparatus for free-space measurement of dielectric constants at high temperature
[AD-P004361] 12 p1826 N85-21455
Automated radome testing
[AD-P004362] 12 p1826 N85-21456
Hot radome boresight error measurements
[AD-P004364] 12 p1826 N85-21458
A broadband kevlar radome for shipboard
[AD-P004365] 12 p1826 N85-21459
Fiber reinforced fused silica for hypersonic radome applications
[AD-P004366] 12 p1826 N85-21460
LL-100: A new polybutadiene (resin system for radome applications)
[AD-P004368] 12 p1826 N85-21462
Broadband thermoplastic radomes
[AD-P004369] 12 p1827 N85-21463
Infrared material optical damage by rain
[AD-P004372] 12 p1827 N85-21466
A radome for air traffic control SSR radar systems
[AD-P004373] 12 p1827 N85-21467
Development of the F-20 nose radome
[AD-P004374] 12 p1827 N85-21468

Nose and inlet duct radomes for the firebolt aerial target
[AD-P004376] 12 p1827 N85-21469
Laminated thermoplastic radome
[AD-D011664] 18 p3079 N85-29045

RADON
NT RADON ISOTOPES
A system for monitoring radon and its decay products in the atmosphere
[INPE-3086-PRE/494] 03 p0391 N85-12502
Characteristic functional of a probability measure absolutely continuous with respect to a Gaussian radon measure
[AD-A149462] 10 p1546 N85-19763
Radon concentration inversion in the troposphere: Still unexplained
[INPE-3380-PRE/638] 16 p2626 N85-27431
Atmospheric radon measurements in the Antarctic Peninsula: A preliminary report
[INPE-3386-PRE/667] 16 p2627 N85-27436
Program RNTHR/2: An HP-41 C program for the calculation of RaA, RaB, and RaC concentrations in air based on three measurements of an air-dust sample
[IRI-190-83-10] 18 p3134 N85-29412
Production of stable embryo particles in dense ion tracks of alpha particle emissions in the atmosphere
21 p3644 N85-32636
Study of the formation of particles from natural hydrocarbons released by vegetation
21 p3644 N85-32640
Aircraft investigations of the distribution of aerosols in the lower troposphere 21 p3647 N85-32659
Poisson formula for radon transformation and numerical image reconstruction algorithm
21 p3697 N85-32973
EML pulse ionization chamber systems for (222)Rn measurements
[DE85-012320] 23 p3970 N85-34610
Groundwater radon studies for earthquake precursors in southern California
[PB85-196871] 24 p4118 N85-35529

RADON ISOTOPES
Theoretical basis for the determination of the concentration of radon decay products in air from the activity of a particulate air sample
[IRI-190-83-07] 17 p3035 N85-28774
Model computations of radon and radon decay product, concentrations in an open system; the Hewlett-Packard 41C program RNSS, version 02
[IRI-190-83-12] 17 p3035 N85-28775
Temporal variations of Rn222 concentrations in Black Sea coastal zone 19 p3293 N85-30417
Some considerations about the natural atmospheric radioactive aerosol 21 p3647 N85-32662

RAFTS
NT LIFE RAFTS

RAIL TRANSPORTATION
Railroad safety program, volume 1
[NASA-CR-174333] 09 p1403 N85-18830
High-speed intercity rail passenger service
[GPO-35-896] 10 p1570 N85-19897
USSR report: Transportation
[JPRS-UTR-85-005] 14 p2207 N85-23688
USSR report: Transportation
[JPRS-UTR-84-008] 14 p2208 N85-23694
USSR report: Transportation
[JPRS-UTR-85-008] 15 p2460 N85-25189
USSR report: Transportation
[JPRS-UTR-84-017] 15 p2461 N85-25196
USSR report: Transportation
[JPRS-UTR-84-014] 15 p2467 N85-25229
Industry review: Locomotive dynamic characterization test-analysis
[NASA-CR-171467] 19 p3382 N85-30981
Fuel cell applications literature review
[DE85-011891] 22 p3809 N85-33592

RAILGUN ACCELERATORS
Resistance and inductance calculations for helical flux compression generators
[DE84-015068] 02 p0195 N85-11306
Preliminary analysis of space mission applications for electromagnetic launchers
[NASA-CR-174067] 03 p0321 N85-12071
Magnetic and photoconductive repetitive rail-gun opening switches
[DE84-017080] 04 p0496 N85-13163
Investigation of electromagnetic launcher behavior for impact fusion
[DE84-017401] 04 p0563 N85-13585
Distributed energy store railguns experiment and analysis 09 p1313 N85-18256
Materials physics
[DE84-017103] 09 p1377 N85-18658
Rail accelerator technology and applications
[NASA-TM-86947] 12 p1794 N85-21258
Arc-driven rail gun research
[NASA-CR-174816] 12 p1859 N85-21862
Plasma mass and effective inductance in a small rainbow
[MRL-R-947] 12 p1936 N85-22162
H-division materials physics progress
[DE85-004880] 13 p2165 N85-23430
Railgun conductor heating from multiple current pulses
[DE85-005333] 14 p2265 N85-24031
Spectroscopic studies of a railgun muzzle flash
[MRL-R-952] 16 p2728 N85-26837
Metal armatures for railguns
[AD-A152129] 16 p2728 N85-26838
Examination of a method for predicting the properties of railgun plasmas
[AR-004-322] 17 p3039 N85-28799
Numerical studies of ablation and ionization of railgun materials
[DE85-010741] 19 p3223 N85-29983
Design and fabrication of projectiles for round bore railguns
[DE85-011671] 20 p3398 N85-31078
Plasma mass and effective inductance in a small railgun
[AD-A154644] 21 p3589 N85-32304
A method of accurizing rail guns
[LA-10028-MS] 22 p3737 N85-33166
Use of the computer programs PARA 80 to study results from firing the railgun ERGS-1M
[MRL-R-900] 22 p3738 N85-33167
Generation of round bores in composite structure railguns
[DE85-011672] 22 p3793 N85-33501

RAILROADS
U RAIL TRANSPORTATION

RAIN
NT ACID RAIN
Layered sloping mesoscale structures and rainbands in atmospheric frontal regions and their relation to symmetric instability 01 p0075 N85-10497
Test results from RAINSAT 01 p0076 N85-10506
The use of dual polarisation radar for observing and predicting convective activity 01 p0077 N85-10512
Preliminary assessment of very short term forecasting of rain from single radar data 01 p0078 N85-10523
Operational precipitation observation system using digitized radar and rain gages 01 p0082 N85-10549
FRONTIERS: Progress with a system for nowcasting rain --- Forecasting Rain Optimized using New Techniques of Interactively Enhanced Radar and Satellite (FRONTIERS) 01 p0082 N85-10552
Northern Hemisphere atlas of 1-minute rainfall rates
[AD-A145411] 02 p0231 N85-11506
Southern Hemisphere atlas of 1-minute rainfall rates
[AD-A145421] 02 p0231 N85-11509
Modeling rain polarization effects to millimeter wave frequencies
[PB84-231042] 03 p0357 N85-12296
An interactive technique for satellite-improved rainfall monitoring 05 p0658 N85-14224
Diagnostics of rainfall anomalies in the nordeste during the global weather experiment 05 p0685 N85-14405
Rain volume estimation over areas using satellite and radar data 05 p0686 N85-14406
Probable maximum flood estimation - Eastern United States
[AD-A146536] 06 p0839 N85-15324
The influence of sample collection and methods of analysis on chemical concentrations measured in rainwater
[KNMI-TR-55] 07 p0924 N85-15853
Simultaneous ocean cross-section and rainfall measurements from space with a nadir-pointing radar
[NASA-TM-86167] 07 p0987 N85-16273
Antisoiling technology: Theories of surface soiling and performance of antisoiling surface coatings
[NASA-CR-174274] 07 p0991 N85-16296
Resolution enhancement of multichannel microwave imagery from the Nimbus-7 SMMR for maritime rainfall analysis
[NASA-CR-174367] 10 p1462 N85-19221
Nationwide urban runoff program. Relationship of urban runoff to land use and groundwater resources
[PB85-114692] 10 p1506 N85-19505
Cyclone diagnostics --- rainfall estimation, backscatter, and lidar
[NASA-CR-171337] 10 p1518 N85-19567
Rain volume estimation over areas using satellite and radar data
[NASA-CR-174434] 10 p1518 N85-19568
Modeling interception of rainfall by forests and the role of interception in the water balance
[DE85-002822] 12 p1884 N85-21825
OSCAR experiment high-density network data report
[DE85-004907] 12 p1884 N85-21826
Modeling of radiothermal radiation of rain by Monte-Carlo method 14 p2341 N85-24476
Rain rate determinations from electronic weight measurements: Instrument description and data reduction techniques
[AD-A150765] 14 p2378 N85-24691
Observation of precipitating clouds by a vertically pointing radar at Morino in the Iburi District, Hokkaido, Japan 15 p2582 N85-25922
Hurricane structure and dynamics from stereoscopic and infrared satellite observations and radar data
15 p2594 N85-25988
Estimation of convective rainfall from visible and infrared satellite data 15 p2596 N85-25999
Computers in the determination of rainfall depth-duration-frequencies in Natal
15 p2627 N85-26186
EHF attenuation derived from emission temperatures in light rain
[AD-A151166] 16 p2772 N85-27110
On the 1983 drought in northeast Brazil
[INPE-3412-PRE/676] 16 p2834 N85-27476
An appraisal of the duration of the recent drought in northeast Brazil and a forecast for 1985
[INPE-3477-PRE/720] 16 p2834 N85-27478
Statistical comparison of radar echoes of convective precipitation between the northern Alps and its foreland
[DFVLR-FB-85-07] 17 p2950 N85-28215
Laminated thermoplastic radome
[AD-D011664] 18 p3079 N85-29045
Some further aspects of the influence of raindrop-size distributions on millimeter-wave propagation
[PB85-168334] 18 p3092 N85-29138
Surface hydrologic characteristics of proposed repository locations in the Palo Duro Basin of the Texas Panhandle
[DE85-010530] 18 p3126 N85-29355
Influence of land-surface roughness on atmospheric circulation and rainfall: A sensitivity study with a GCM
18 p3146 N85-29479
Synthetic rainfall and its use in hydrologic modeling
19 p3314 N85-30542
On the dynamical climatology of the Amazon Basin and associated rain producing mechanisms
[INPE-3531-RPE/477] 19 p3315 N85-30552
Rain volume estimation over areas using satellite and radar data
[NASA-CR-176050] 21 p3634 N85-32570
The distribution of giant salt nuclei inside and outside cloud over the basin of Xin and Jiang
21 p3650 N85-32681
Tunisian climate seen through a Markov process
[CT-585] 23 p3950 N85-34482
Elemental tracers of source regions of contaminants in precipitation
[DE85-012858] 24 p4113 N85-35499
The kinematic structure of cold frontal rainbands
24 p4119 N85-35531

RAIN EROSION
Single-drop impact damage prediction for low density, coated ceramic materials --- rain erosion
01 p0061 N85-10402
Proceedings of the 17th Symposium on Electromagnetic Windows, part 1
[AD-A149185] 10 p1466 N85-19253
Development of a high temperature single impact rain erosion test capability
[AD-P004371] 12 p1827 N85-21465
Infrared material optical damage by rain
[AD-P004372] 12 p1827 N85-21466

RAIN FORESTS
Eddy correlation measurements of energy partition for Amazonian forest
[INPE-3195-PRE/559] 06 p0827 N85-15252
Relationship between forest clearing and biophysical factors in tropical environments: Implications for the design of a forest change monitoring approach --- Costa Rica
[E85-10051] 07 p0963 N85-16247
Geologic mapping of Indonesian rain forest with analysis of multiple SIR-B incidence angles
08 p1145 N85-17221
Information for space radar designers: Required dynamic range vs resolution and antenna calibration using the Amazon rain forest 08 p1147 N85-17239
The micrometeorology of an Amazonian rainforest
[INPE-3515-PRE/740] 19 p3315 N85-30551
Formation of particles in the air of the humid tropical forests 21 p3644 N85-32639

RAIN GAGES
Operational precipitation observation system using digitized radar and rain gages 01 p0082 N85-10549
The pluviometric recording stations in the 11 GHz radio link at Inviolatella Monte S. Pancrazio --- Italy
[FUB-6-1983] 01 p0086 N85-10575
Rain rate meter
[AD-D011381] 07 p0999 N85-16342

Precipitation gage network operations for wintertime research in the Central Sierra Nevada
[PB85-115029] 10 p1520 N85-19582
On the wind error of the Finnish raingauge
[REPT-37] 12 p1893 N85-21883

RAINBOWS
Classical rainbow scattering of alkali ions on metal surfaces. Application to the investigation of unknown surface structures
[MPIS-10/1984] 11 p1726 N85-20854

RAINMAKING
SCPP (Sierra Cooperative Pilot Project) Forecasting Support 16 p2837 N85-27493

RAINSTORMS
NT THUNDERSTORMS
Generation of deep convective clouds along mesoscale storm outflow boundaries 01 p0074 N85-10490
Rain bands and symmetric instability
01 p0075 N85-10496
NESDIS operational precipitation estimation techniques 01 p0076 N85-10505
Experiment on nowcasting of heavy rainfall and severe storms in central China in 1979-1981
01 p0081 N85-10545
Convection modeling and application to severe storms
15 p2595 N85-25991

RAMAN EFFECT
U RAMAN SPECTRA

RAMAN LASERS
Manual for Raman cells
[NASA-TM-77756] 01 p0052 N85-10342
Laser Raman techniques for studying flows and flames 11 p1576 N85-19929
Raman studies of laser damaged single and multi-layer optical coatings
[DE85-009431] 17 p2971 N85-28351

RAMAN SCATTERING
U RAMAN SPECTRA

RAMAN SPECTRA
Method and apparatus for determining pressure-induced frequency-shifts in shock-compressed materials
[DE84-014313] 01 p0024 N85-10151
Raman scattering from metastable GaSb(1-x) Ge(2x) alloys
[AD-A145897] 03 p0327 N85-12108
Folded acoustic and quantized optic phonons in semiconductor superlattices
[AD-A145935] 03 p0433 N85-12756
Structural properties of amorphous metals by Raman scattering
[DE84-016947] 04 p0475 N85-13027
Raman study of neutron irradiated GaAs
[DE84-016056] 05 p0731 N85-14702
In situ analysis of corrosive and passive surfaces by laser-excited Raman spectroscopy — lead, galvanized iron, and asbestos-cement pipes
[PB84-229756] 06 p0767 N85-14904
Electronics research at the University of Texas at Austin
[AD-A146900] 07 p0947 N85-15998
Rayleigh and Raman scattering for density in a swirling flow combustor 08 p1120 N85-17060
Raman sidescattering in laser-produced plasmas
[AD-A148905] 10 p1556 N85-19813
Nonlinear saturation of stimulated Raman scattering in collisional homogeneous plasma
[DE85-002814] 10 p1559 N85-19831
Nonlinear saturation of stimulated Raman scattering in homogeneous plasma
[DE85-003120] 10 p1560 N85-19837
Laser Raman techniques for studying flows and flames 11 p1576 N85-19929
Photon scattering and interaction analysis of interfacial corrosion and catalysis
[DE85-002534] 11 p1606 N85-20114
Application of Raman, TEM and other ion based techniques to oxidation problems
[AERE-R-11447] 11 p1610 N85-20121
Time resolved Raman studies of laser induced damage in TiO2 optical coatings
[DE85-003166] 11 p1640 N85-20332
The effect of Xe underlayers on the surface enhanced Raman scattering of pyridine on cold silver
[AD-A150109] 12 p1801 N85-21294
In situ monitoring of electrochemical reactions by surface enhanced Raman scattering
[PB85-149789] 12 p1803 N85-21312
Mathematical modeling of two-frequency laser sounding of scattering media 13 p2089 N85-23045
Resonant coherent anti-Stokes Raman scattering
[ESA-TT-876] 15 p2507 N85-25466
Raman scattering of light in epitaxial films of solid phosphide-gallium arsenide solutions
15 p2643 N85-26301
Raman studies of surface temperature in laser-heated semiconductors
[AD-A151377] 15 p2659 N85-26412
Fiber optic Raman thermometer for Space Shuttle main engine preburner profiling 16 p2739 N85-26904
Single-pulse Raman and photoacoustic spectroscopy studies of Triaminotrinitrobenzene (TATB) and related compounds
[DE85-010072] 18 p3084 N85-29078
An introductory view of Raman-Nath type equations
[PREPRINT-422] 18 p3172 N85-29664
High temperature Raman studies of phase transitions in thin film dielectrics
[DE85-010973] 19 p3263 N85-30234
Application of the Diffusion Raman Anti-Stokes Coherent (DRASC) method to a SNECMA combustion chamber
[YKC-3066/84] 20 p3425 N85-31260
Caviton collapse of SRS by SBS
[DE85-009605] 20 p3535 N85-31999
Temperature measurements on small droplets
21 p3653 N85-32699
Influence on bi-phonon states on Raman scattering of light in molecular crystals 21 p3680 N85-32865
Generation and amplification of radiation during stimulated Raman scattering in crystals
21 p3681 N85-32869
Participation of singlet oxygen in photodestruction of air-saturated solutions of coumarin dyes
21 p3685 N85-32891
Raman scattering studies in solids
[AD-A155528] 21 p3710 N85-33032
Measurement of velocity and concentration in free jets
[ISL-CO-215/84] 22 p3785 N85-33451
Time-resolved spectroscopic studies of detonating heterogeneous explosives
[DE85-009760] 23 p3921 N85-34297
Electronic structure and lattice dynamics of dimensionally constrained and disordered solids
[AD-A155927] 24 p4161 N85-35797

RAMAN SPECTROSCOPY
Investigation of the CARS spectrum of carbon monoxide at high pressure and temperature
[AD-A144816] 01 p0024 N85-10146
Kinetics of simple inner- and outer-sphere electrochemical reactions at rotating silver electrodes as examined using surface-enhanced Raman spectroscopy
[AD-A145606] 02 p0172 N85-11154
Raman and fluorescence spectroscopy in a methane-nitrous oxide laminar flame
[AD-A146092] 03 p0328 N85-12111
A study of structural phase transitions using light scattering techniques
[AD-A147261] 07 p1048 N85-16654
Cars temperature measurements in sooting, laminar diffusion flames
[AD-A148801] 09 p1319 N85-18294
New phases and chemical reactions in solid CO under pressure
[DE85-002033] 09 p1377 N85-18655
Laser Raman techniques for studying flows and flames 11 p1576 N85-19929
Velocity and volumetric measurement in free jets
11 p1576 N85-19931
Fundamental study of catalysts using laser Raman, infrared, auger electron spectroscopy and low energy electron diffraction
[DE85-001813] 11 p1595 N85-20033
Observation of standing spinwaves in thin Fe-films by means of Raman spectroscopy
[DE85-003036] 11 p1735 N85-20913
The effect of Xe underlayers on the surface enhanced Raman scattering of pyridine on cold silver
[AD-A150109] 12 p1801 N85-21294
Laser diagnostic analyses of sooting flames
[AD-A150478] 13 p2017 N85-22649
Raman structural studies of the nickel electrode
[NASA-CR-175619] 13 p2162 N85-23414
Picosecond lidar techniques in laboratory and field diagnostics
[AD-A150755] 14 p2309 N85-24294
Linewidth and bandwidth measurements of the q-branch of h2 using CW coherent anti-Stokes Raman spectroscopy
[AD-A151868] 15 p2506 N85-25456
Resonant coherent anti-Stokes Raman scattering
[ESA-TT-876] 15 p2507 N85-25466
Raman studies of laser damaged single and multi-layer optical coatings
[DE85-009431] 17 p2971 N85-28351
Studies of optical-beam phase-conjugation by nonlinear refraction
[AD-A152866] 17 p3037 N85-28788
Recent advances in optical measurement methods in physics and chemistry
[DE85-008695] 17 p3037 N85-28792
Properties of defects in Hg(1-x)Cd(x)Te
[AD-A153243] 17 p3044 N85-28835
Resonant CARS detection of OH radicals
[AD-A153842] 18 p3071 N85-28965
Single-pulse Raman and photoacoustic spectroscopy studies of Triaminotrinitrobenzene (TATB) and related compounds
[DE85-010072] 18 p3084 N85-29078
A basic study to assess the potential usefulness of resonance Raman spectroscopy as a means of rapidly detecting and identifying bacteria and other microorganisms
[AD-A153549] 18 p3152 N85-29513
The development of new techniques in laser spectroscopy 19 p3233 N85-30041
Participation of singlet oxygen in photodestruction of air-saturated solutions of coumarin dyes
21 p3685 N85-32891
The possibilities of remote analysis of atmospheric gases based on Raman scattering spectroscopy
21 p3685 N85-32892
Ionization detection of stimulated Raman spectra
[DE85-010672] 22 p3746 N85-33218

RAMJET ENGINES
NT SUPERSONIC COMBUSTION RAMJET ENGINES
An experimental investigation of combustion pressure oscillations in solid fuel ramjets
[AD-A144870] 01 p0024 N85-10147
Pressure oscillations in liquid-fueled ramjet engines
05 p0596 N85-13797
Combined cycle ramjet engine
[AD-D011247] 06 p0780 N85-14869
Ramjet and Ramrocket Propulsion Systems for Missiles
[AGARD-LS-136] 07 p0917 N85-15809
Ramjet and Ramrocket Propulsion Systems for Missiles: Introduction and overview 07 p0917 N85-15810
Ramjet air induction system design for tactical missile application 07 p0918 N85-15811
Some aspects of engine and airframe integration for Ramjet and Ramrocket powered missiles
07 p0918 N85-15812
Integral boost, heat protection, port covers and transition 07 p0918 N85-15813
Liquid-fueled Ramjet engines
07 p0918 N85-15814
Special problems of Ramjet with solid fuel
07 p0918 N85-15815
Combustion dynamics in rockets
[AD-A148478] 08 p1114 N85-17024
Analysis of sudden expansion flow in a two-dimensional duct with and without side-wall injection using the k-epsilon turbulence model 09 p1317 N85-18282
Window on science visit to the USA, 21 March - 22 April, 1984 — ramjets and solid propellant rocketry
[VTH-LR-426] 11 p1592 N85-20011
Study of HTPB-based SOFRAM fuels
[FOA-C-20563-D3] 11 p1614 N85-20150
Twenty-first JANNAF Combustion Meeting, volume 1
[AD-A150981] 13 p1998 N85-22526
Nonlinear interactions between vortices and acoustic waves in a rocket combustion chamber
13 p1999 N85-22533
Selection of air intake parameters for supersonic-flow operation 13 p2051 N85-22837
Mixing, chemical reaction and flow field development in ducted rockets
[DE85-004083] 14 p2247 N85-23928
Fiscal year 1986 technical objective document
[AD-A151039] 14 p2432 N85-25000
Gasdynamic evaluation of choking cascade turns
[AD-A151854] 15 p2557 N85-25776
Dispersion sensitivity of the eight inch advanced ramjet munitions technology projectile due to wind and minor thrust errors
[AD-A152145] 16 p2727 N85-26835
Solid fuel combustion chamber research in the Netherlands
[VTH-LR-444] 16 p2742 N85-26920
An experimental investigation of fuel regression rate control in solid fuel ramjets
[AD-A154251] 19 p3227 N85-30008
A model of hypersonic two-dimensional oblique detonation wave ramjet
[UTIAS-TN-257] 23 p3897 N85-34138

RAMJET MISSILES
Fuel-rich solid propellant boron combustion
[AD-A148522] 08 p1136 N85-17157

RAMP FUNCTIONS
Precision linear ramp function generator
[DE85-011647] 22 p3760 N85-33304
The collected data for ramp function tests on a NACA 23012 aerofoil. Volume 1: Description and pressure data
[GU-AERO-8413-VOL-1] 23 p3894 N85-34123

RANDOM ACCESS
Applications of functional analytic and Martingale methods
[AD-A146555] 02 p0255 N85-11672
RANDOM ACCESS MEMORY
Parallel update of minimum spanning trees in logarithmic time
[AD-A150497] 13 p2151 N85-23357
Parallel time 0(log N) acceptance of deterministic CFLs
[AD-A152255] 16 p2845 N85-27539
The design of an adaptive predictive coder using a single-chip digital signal processor
[AD-A152461] 17 p2952 N85-28231
Random access memory technologies
[AD-A153069] 17 p3008 N85-28597
Microcomputer controlled image processor
[AD-D011734] 22 p3833 N85-33735
Effects of space radiation on advanced semiconductor devices. Part 3: Further cosmic ray simulation studies of single event upsets and latch-up in CMOS memories
[AERE-G-3368-PT-3] 22 p3848 N85-33833
RANDOM DISTRIBUTIONS
U STATISTICAL DISTRIBUTIONS
RANDOM ERRORS
Spectral noise density and random errors of pulse frequency characteristic meters
03 p0346 N85-12231
Accepting error to make less error
[AD-A153949] 18 p3171 N85-29651
RANDOM LOADS
NT GUST LOADS
Fractographic observation and estimation of crack growth curve of aluminum alloy under ramdom flight simulation loading
[NAL-TR-824] 06 p0768 N85-14913
Stability of viscoelastic constructions subjected to steady random compressing loads 11 p1720 N85-20819
First passage times for combinations of random loads
[AD-A153275] 17 p2980 N85-28423
Safety and reliability of steel structural materials under random service impact loads 23 p3906 N85-34197
RANDOM NOISE
NT RANDOM SIGNALS
Noise analysis of the Coarse Optical Power Spectrum Estimator (COPSE) data acquisition system
[AD-A145918] 03 p0419 N85-12677
On estimating the phase of periodic waveform in additive Gaussian noise, part 2 05 p0622 N85-13962
Treatment and expression of measurement uncertainties 05 p0630 N85-14042
Variability of short-term eddy-correlation estimates of mass exchange
[DE84-007271] 05 p0677 N85-14349
Place of aperture synthesis in general theory of antennas (review) 06 p0781 N85-14993
The coding capacity of mismatched Gaussian channels
[AD-A149453] 10 p1551 N85-19782
Interference immunity of binary systems with second-order phase-difference modulation in various reception modes 13 p2072 N85-22944
Synthesis of quasi-optimum two-level signal discriminator with level changing at unknown point
13 p2083 N85-23010
Use of Bigaussian approximation to describe fading in scattering communications channel
13 p2084 N85-23017
Bayesian estimation of one dimensional discrete markov random fields
[AD-A151503] 15 p2640 N85-26284
Measurement of damping of graphite expoxy materials
[NASA-CR-175793] 16 p2743 N85-26925
Robust detection of fading narrow-band signals in non-Gaussian noise
[AD-A152262] 16 p2774 N85-27124
On the probability density of signal-to-noise ratio in an improved detector
[AD-A152529] 17 p2952 N85-28232
Global positioning system carrier phase: Description and use
[PB85-174126] 19 p3216 N85-29946
Modulation using four phase levels. Theoretical study of the degradation caused by a spurious phase modulation
[CNES-83/219/CT/DRT/TIT/TR]
20 p3441 N85-31360
Deterministic and random phase noise of oscillators --- synthetic aperture radar
[ESA-TT-848] 20 p3449 N85-31415
Detection of signals from coherent pulsed radars with random variation in parameters of sounding signals from pulse to pulse against background of worst-case Gaussian noise 22 p3763 N85-33324
A new description of combined trellis coding with asymmetric modulation
[NASA-CR-176197] 24 p4086 N85-35323
RANDOM NUMBERS
On the generation of random variables for radar simulation purposes 07 p0938 N85-15947
Regenerative structure of Markov chains simulated via common random numbers
[AD-A149092] 10 p1550 N85-19777
Efficient parallel pseudo-random number generation
[AD-A152235] 16 p2855 N85-27608
Probabilistic algorithms in group theory
[AD-A152253] 16 p2859 N85-27630
Monte Carlo learning-biasing experiment with intelligent random numbers
[DE85-010713] 22 p3834 N85-33742
A quickly tested Pascal random number generator for microcomputers
[AD-A156058] 24 p4136 N85-35633
RANDOM PROCESSES
NT RANDOM WALK
Dynamics of symmetry breaking: Phase coherence in finite and random systems
[NOTA-INTERNA-813] 02 p0253 N85-11658
Random processes and magnetohydrodynamic turbulence 02 p0271 N85-11767
The growth and composition of supercritical branching populations on general type spaces
[CTH-MATH-1984-18] 05 p0721 N85-14631
Distribution of atmospheric radio interference
06 p0792 N85-15063
A note on the prediction error for small time lags into the future
[AD-A148221] 08 p1215 N85-17654
Asymptotic analysis of Markovian access control computer communication networks
09 p1372 N85-18619
Regenerative structure of Markov chains simulated via common random numbers
[AD-A149092] 10 p1550 N85-19777
Models of discontinous random fields
13 p2079 N85-22983
On failure modeling, revised
[AD-A151411] 15 p2637 N85-26263
Anderson localization for large disorder or low energy
[PREPRINT-426] 18 p3176 N85-29692
Statistical methods for efficient design of community surveys of response to noise: Random coefficients regression models
[NASA-CR-177933] 21 p3698 N85-32979
RANDOM SAMPLING
Spline methods for approximating quantile functions and generating random samples
[NASA-TP-2389] 07 p1035 N85-16565
Small-sample properties of kernel density estimators from randomly right-censored data
[AD-A148752] 09 p1374 N85-18634
Nonparametric estimation of the probability of ruin
[AD-A153523] 18 p3174 N85-29674
A new approach to evaluate gamma-ray measurements
[OG-9.5-11] 23 p4031 N85-34988
RANDOM SIGNALS
Accuracy of random signal spectral parameter estimation against interference background in acoustooptical spectrum analyzers
13 p2090 N85-23052
Adaptive detection of noise signal according to Neumann-Pearson criterion 15 p2527 N85-25580
Optimal complex nonlinear processing of continuous and pulsed signals 22 p3763 N85-33323
RANDOM VARIABLES
Some weak and strong laws of large numbers for d(0,1) - valued random variables
[AD-A144845] 01 p0111 N85-10754
What is principal components analysis?
02 p0211 N85-11389
The information in the minor principal components
02 p0211 N85-11391
Algebraic functions of H-functions with specific dependency structure
[AD-A145598] 02 p0252 N85-11647
Maximum likelihood estimation of the survival functions of N stochastically ordered random variables
[AD-A145429] 02 p0254 N85-11662
Distributions of extreme values of sequences of autocorrelated random variables
[PB84-240746] 06 p0858 N85-15456
Rivista Tecnica Selenia, volume 9, number 1
07 p0938 N85-15945
On the generation of random variables for radar simulation purposes 07 p0938 N85-15947
On a random difference equation for matrices and a characterization of the gamma distribution
[AD-A146858] 07 p1029 N85-16529
Conditionally heteroscedastic autoregressions
[AD-A147166] 07 p1035 N85-16567
Generalized additive models
[AD-A147454] 07 p1036 N85-16573
Belief structures
[AD-A147526] 07 p1036 N85-16575
Recent results on characterization of probability distributions: A unified approach through extensions of Deny's theorem
[AD-A147631] 08 p1214 N85-17647
Calculation of cumulative distributions and detection probabilities in communications and optics
[AD-A147761] 08 p1215 N85-17650
Modelling and residual analysis of nonlinear auto-regressive time series in exponential variables
[AD-A149047] 10 p1550 N85-19776
The asymptotic behavior of the likelihood ratio statistic for testing a shift in mean in a sequence of independent normal variates
[AD-A149329] 10 p1550 N85-19779
Maximum matchings in a class of random graphs
[AD-A149663] 12 p1920 N85-22060
Statistics for the maximum of several positive random variables with application to networking
[AD-A150005] 12 p1922 N85-22069
Convergence rates in the strong law for bounded mixing sequences
[CWI-MS-R8412] 12 p1922 N85-22076
Skewed stable variables and processes
[AD-A150549] 13 p2153 N85-23372
A bilaterally deterministic rho-mixing stationary random sequence
[AD-A152856] 17 p3019 N85-28666
Central limit theorems in the area of large deviations for some dependent random variables
[AD-A153125] 17 p3043 N85-28831
A random layer model for reflection from ocean bottom sediments
[AD-A155019] 21 p3700 N85-32988
RANDOM VIBRATION
Non-Gaussian approach for parametric random vibration of non-linear structures 01 p0060 N85-10395
Stochastic motor blade dynamics
[AD-A146312] 03 p0318 N85-12054
Random vibrations of aircraft engine blades
06 p0777 N85-14967
The Shock and Vibration Digest, volume 16, no. 9
[AD-A146779] 07 p0976 N85-16200
Techniques for nonlinear random vibration problems
07 p0977 N85-16201
Investigation of dynamic noise affecting geodynamics information in a tethered subsatellite
[NASA-CR-174292] 08 p1174 N85-17405
Stresses in situ generating by bulldozers
[AD-P004270] 09 p1405 N85-18846
Centrifuge tests to provide closure bounds for switches subjected to random vibration
[DE85-002003] 10 p1482 N85-19357
Random vibration of nonlinear, parametrically excited systems 19 p3282 N85-30351
RANDOM WALK
Monte Carlo lattice models for adsorbed polymer conformation
[NASA-TP-2453] 14 p2426 N85-24961
Laser gyroscope random walk determination using a fast filtering technique 16 p2696 N85-26647
A trivariate version of Levy's equivalence
[AD-A153157] 17 p3025 N85-28705
The role of long term lamp fluctuations in the random walk of frequency behavior of the rubidium frequency standard: A case study
[AD-A155338] 21 p3590 N85-32314
Implicit Monte Carlo methods and non-equilibrium Marshak wave radiative transport
[DE85-010711] 22 p3835 N85-33743
Monte Carlo techniques for analyzing deep penetration problems
[DE85-011426] 23 p3968 N85-34598
RANGE
Directory of range data conversion and processing systems
[AD-A148996] 10 p1427 N85-19001
RANGE (EXTREMES)
NT FREQUENCY RANGES
NT PROPORTIONAL LIMIT
NT ROCHE LIMIT
Assessment of satellite power flux-density limits in the 2025-2300 MHz frequency range, part 2
[PB85-101244] 11 p1625 N85-20236
An empirical comparison of the accuracy of univariate and multivariate corrections for range restriction
[AD-A153071] 17 p3019 N85-28670
EOQ (Economic Order Quantity) range model
[AD-A153709] 19 p3379 N85-30965

Evaluation: Close-range photogrammetry for slope inventory and monitoring
[PB85-192755] 24 p4108 N85-35470
RANGE AND RANGE RATE TRACKING
Tracking requirements for precise ERS-1 orbit determination 03 p0380 N85-12431
The Precise Range and Range Rate Equipment (PRARE) and its possible support to the radar altimeter measurement for ERS-1 03 p0382 N85-12445
Measurements in satellite orbit tracing
05 p0596 N85-13812
Satellite-to-satellite orbit determination using minimum, discrete range and range-rate data only
13 p1965 N85-22458
Hardware test program for evaluation of baseline range-range rate sensor concept
[NASA-CR-175794] 16 p2787 N85-27193
Optimal relative data weights
16 p2605 N85-27296
RANGE CONTROL
U TRAJECTORY CONTROL
RANGE FINDERS
NT LASER RANGE FINDERS
NT OPTICAL RANGE FINDERS
USSR report: Electronics and electrical engineering
[JPRS-UEE-84-015] 22 p3762 N85-33314
Characteristics of digital range finder with stroboscopic discretization 22 p3762 N85-33319
Ranging system which compares an object reflected component of a light beam to a reference component of the light beam
[NASA-CASE-NPO-15865-1] 23 p3973 N85-34629
RANGE INDICATORS
U RANGE FINDERS
RANGE MEASUREMENT
U RANGEFINDING
RANGEFINDING
NT SOUND RANGING
Pulse heterodyne equipment for measurements of range and velocity of moving targets-pulse radar
[ESA-TT-845] 09 p1312 N85-18246
Three-dimensional sensing and interpretation
[AD-A150690] 14 p2311 N85-24304
A multi-element ultrasonic ranging array
[AD-A150698] 14 p2416 N85-24906
A short range, high accuracy radar ranging system
[AD-A152195] 16 p2774 N85-27122
Balanced system for ranging and synchronization between satellite pairs
[AD-D011697] 19 p3224 N85-29992
Hardware test program for evaluation of basline range-range rate sensor concept
[NASA-CR-176143] 23 p3933 N85-34377
RANGELANDS
The application of remote sensing to resource management and environmental quality programs in Kansas
[E85-10023] 02 p0218 N85-11436
An integrated remote sensing approach for identifying ecological range sites --- parker mountain
[E85-10050] 07 p0983 N85-16246
RANGES (FACILITIES)
NT TEST RANGES
Global coordinate system
[AD-A153678] 19 p3299 N85-30454
RANGING
U RANGEFINDING
RANK TESTS
Inference for censored matched pairs using signed ranks
[MATHEMATICS-RESEARCH-162]
12 p1923 N85-22078
Simplifications and approximations for linear rank statistics with censored data
[MATHEMATICS-RESEARCH-161]
12 p1923 N85-22079
RANKINE CYCLE
Modeling of a second-generation solar-driven Rankine air conditioner
[DE84-015132] 01 p0036 N85-10223
Overview of waste heat utilization systems
[NASA-TM-86901] 04 p0578 N85-13692
Dynamic power systems for power generation
05 p0609 N85-13892
Dynamic conversion working group summary
05 p0611 N85-13904
Phase 1-A development kinematic Sterling/Rankine commercial gas-fired heat pump research program
[PB85-100931/GAR] 07 p0936 N85-15926
Development and demonstration of a Stirling/Rankine heat activated heat pump. Phase 3B: Engine technology development testing
[DE85-004388] 10 p1486 N85-19383
Development and test of a high COP Rankine heat pump for generation of process steam. Phase 2: Fabrication and test
[DE85-002600] 11 p1632 N85-20275
Leak detectors for organic Rankine cycle power plants: On-line and manual methods
[DE85-002792] 12 p1852 N85-21617
Direct-contact condensers for solar pond power production
[DE84-004610] 12 p1876 N85-21771
Some solar dish/heat engine design considerations
[DE85-003479] 12 p1881 N85-21802
Development of an Organic Rankine-Cycle power module for a small community solar thermal power experiment
[NASA-CR-175660] 14 p2350 N85-24523
Test results of an organic Rankine-cycle power module for a small community solar thermal power experiment
[NASA-CR-175696] 14 p2350 N85-24524
Analysis of alkali liquid metal Rankine space power systems
[DE85-005089] 16 p2741 N85-26917
Technology for industrial waste heat recovery by organic Rankine cycle systems
[DE85-006719] 18 p3102 N85-29206
Comparative evaluation of three alternative power cycles for waste heat recovery from the exhaust of adiabatic diesel engines
[NASA-TM-86953] 20 p3542 N85-32043
RANKINE-HUGONIOT RELATION
Local stability analysis for a planar shock wave
[NASA-TP-2387] 04 p0452 N85-12864
Fast and optimal solution to the Rankine-Hugoniot problem
[NASA-TM-86214] 19 p3344 N85-30724
RANKING
Asymptotically optimal ranking algorithms for quasi-determinate signal detection
06 p0792 N85-15064
A computer package for ranking, selection and multiple comparisons with the best
[AD-A147617] 08 p1204 N85-17579
Analysis of a visual performance experiment
[DE85-000710] 10 p1530 N85-19645
Predicting a future response using rank predictive probabilities
[MATHEMATICS-RESEARCH-166]
12 p1923 N85-22077
Proportional odds models for survival data and estimates using ranks
[MATHEMATICS-RESEARCH-172]
12 p1923 N85-22080
Use of ranks to fit a linear model to cross-sectional data with an application to biological rhythms
[MATHEMATICS-RESEARCH-169]
12 p1923 N85-22081
Spaceborne power systems preference analyses. Volume 1: Summary
[NASA-CR-175644] 14 p2349 N85-24517
Spaceborne power systems preference analyses. Volume 2: Decision analysis
[NASA-CR-175645] 14 p2349 N85-24518
Streamlined Test Reporting And Planning (STRAP): Computerized human factors questionnaire
[AD-A150811] 14 p2395 N85-24751
A short bibliography of recent developments in selection and ranking procedures
[AD-A155646] 21 p3679 N85-32856
RAPCON (CONTROL)
U RADAR APPROACH CONTROL
RAPID BALLISTICS IDENTIFICATION
Short-time spectroscopic measurement of the temperature of solids
[ISL-CO-202/84] 20 p3450 N85-31486
Flash X-ray diffraction
[ISL-CO-227/84] 23 p3936 N85-34396
RAPID EYE MOVEMENT STATE
Sleep and wake physiology in weightlessness
20 p3510 N85-31819
RAPID QUENCHING (METALLURGY)
Rapid solidification of steels: Model and commercial alloys 02 p0176 N85-11184
Development of rapidly quenched alloys with special physical properties and of processes for their continuous production
[BMFT-FB-T-84-179] 04 p0477 N85-13039
Rapid solidification processing and powder metallurgy of Al alloys
[AD-A146427] 08 p1130 N85-17120
Rapidly solidified NiAl and FeAl
[NASA-TM-86941] 11 p1597 N85-20042
Rapid solidification processing of magnesium alloys
[AD-A150270] 13 p2022 N85-22668
Time-resolved studies of rapid solidification in highly undercooled molten silicon
[DE85-004657] 13 p2036 N85-22765
Metallurgical characterization of aluminum powder consolidation
[AD-A151990] 15 p2510 N85-25484
Investigation of the pitting potential of rapidly solidified aluminum-lithium alloys
[VTH-LR-434] 16 p2752 N85-25986
RARE EARTH ALLOYS
NT NEODYMIUM ALLOYS
Critical evaluation of binary rare Earth diagrams
[DE84-014860] 04 p0470 N85-12891
Critical evaluation of binary rare earth phase diagrams
[DE84-015057] 05 p0614 N85-13922
RARE EARTH COMPOUNDS
NT CERIUM COMPOUNDS
NT CERIUM OXIDES
NT ERBIUM COMPOUNDS
NT EUROPIUM COMPOUNDS
NT LUTETIUM COMPOUNDS
NT NEODYMIUM COMPOUNDS
NT SAMARIUM COMPOUNDS
Magnetism of the rare earth compounds --- intermetallic compounds 03 p0424 N85-12707
Growth and magnetic investigations of single crystals of intermetallic compounds of rare earths and uranium --- magnetic properties 03 p0425 N85-12712
Microstructure and mechanical properties of rare-earths-microalloyed high-speed tool steel
[BLL-BISI-TRANS-22043-(9022.06)]
17 p2928 N85-28084
Thin film phase transition materials development program
[AD-A154260] 19 p3259 N85-30209
Contact properties of rare-earth silicides and germanides on Si and Ge 19 p3374 N85-30931
Changes in lattice cell parameter of film intermetallic compounds RT2
[BLL-M-35874-(5828.4)] 23 p3915 N85-34261
RARE EARTH ELEMENTS
NT CERIUM
NT CERIUM 144
NT ERBIUM
NT GADOLINIUM
NT HOLMIUM
NT LANTHANUM
NT LUTETIUM
NT NEODYMIUM
NT NEODYMIUM ISOTOPES
NT PRASEODYMIUM
NT SAMARIUM
NT SCANDIUM
NT SCANDIUM ISOTOPES
NT YTTERBIUM
NT YTTRIUM
The marine geochemistry of the rare earth elements
[AD-A145132] 01 p0088 N85-10588
The influence of rare Earth elements on the temper embrittlement behaviour and mechanical properties of a low alloy steel 02 p0180 N85-11210
The chemistry of rare earth elements in the solar nebula 06 p0889 N85-15643
ESR (Electroslag Refining) technology in Australia: Laboratory research and industrial development
[AD-A147776] 08 p1129 N85-17114
Microscopic analysis of angular momentum projected HFB-states in terms of interacting bosons
[DE85-007629] 16 p2863 N85-27661
The influence of melting practice and of microalloying, with rare earth metals and with boron, on the quality of low-carbon steel
[BLL-BISI-22467-(9022.06)] 17 p2925 N85-28036
The corrosion resistance of chromium-nickel steel containing rare-earth metals
[BLL-BISI-TRANS-22477-(9022.06)]
17 p2925 N85-28041
Inoculation of non-metallic inclusions in steel 17GS
[BLL-BISI-TRANS-22431-(9022.06)]
17 p2925 N85-28042
Systematic view of transition intensities in the spectra of actinides and lanthanides in condensed phases
[DE85-010272] 19 p3354 N85-30789
Influence of gamma-phase on magnetic properties and structure of KhK15YuB alloy during strain-aging
[BLL-M-36281-(5828.4)] 20 p3431 N85-31280
Method for extracting lanthanides and actinides from acid solutions by modification of Purex solvent
[DE85-005763] 23 p3909 N85-34220
RARE GAS-HALIDE LASERS
NT KRYPTON FLUORIDE LASERS
NT XENON CHLORIDE LASERS
NT XENON FLUORIDE LASERS
KrCl lasers for fusion
[DE84-012210] 01 p0122 N85-10835
Investigation of plasma processes in electronic transition lasers
[AD-A155586] 21 p3583 N85-32327

RARE GASES
NT ARGON
NT ARGON ISOTOPES
NT HELIUM
NT HELIUM ATOMS
NT HELIUM ISOTOPES
NT KRYPTON
NT LIQUID HELIUM
NT LIQUID HELIUM 2
NT NEON
NT NEON ISOTOPES
NT RADON
NT RADON ISOTOPES
NT XENON
NT XENON ISOTOPES
NT XENON 129
The Boltzmann equation: Global existence for a rare gas in an infinite vacuum
[PREPRINT-78] 01 p0124 N85-10851
EXAFS and Moessbauer study of small metal clusters isolated in rare-gas solids
[DE84-015976] 04 p0470 N85-12994
The low-energy secondary cosmic ray flux: Detectors in iron meteorites 06 p0887 N85-15635
Where is the Earth's missing xenon?
06 p0888 N85-15641
Monte Carlo simulation of electron thermalization in rare gases
[NAL-TR-834T] 09 p1375 N85-18643
The behaviour of detonation waves in single phase heterogeneous systems
[AD-A149825] 12 p1846 N85-21581
Experimental study of steam condensation on water in countercurrent flow in presence of inert gases
[DE84-013028] 12 p1881 N85-21800
Effect of moisture in inert gases on density of seam metal and on mechanical characteristics of welded joints of aluminum and aluminum alloys
13 p2034 N85-22744
Evaluation of a high pressure proportional counter for the detection of radioactive noble gases
[AD-A154436] 19 p3272 N85-30292
Energy transfer and excimer formation in rare gas solids 19 p3374 N85-30930
Noble gases and the early history of the Earth: Inappropriate paradigms and assumptions inhibit research and communication 21 p3719 N85-33075
A review of noble gas geochemistry in relation to early Earth history 21 p3720 N85-33081
Terrestrial Planets: Comparative Planetology
[NASA-CR-176093] 22 p3851 N85-33849
Noble gases in meteorites and terrestrial planets
22 p3851 N85-33850
Relationships between chondritic meteorites and planets 22 p3851 N85-33851
Noble gas patterns in the atmospheres of Mars and Earth: A comparison via the SNC meteorites
22 p3852 N85-33853
Impact processes and their implications for planetary formation and early evolution 22 p3853 N85-33860
Heaterless ignition of inert gas ion thruster hollow cathodes
[NASA-TM-87096] 23 p3903 N85-34177
Gas shielding apparatus
[DE85-005992] 23 p3939 N85-34416
The 3HE in solar non-relativistic electron events
[SH-2.2-5] 23 p4000 N85-34800
Fluidized bed desulfurization
[NASA-CASE-NPO-15924-1] 24 p4075 N85-35253
Groundwater radon studies for earthquake precursors in southern California
[PB85-196871] 24 p4118 N85-35529

RAREFACTION
Construction of solutions for two-dimensional Riemann problems
[DE85-003136] 10 p1549 N85-19770

RAREFACTION WAVES
U ELASTIC WAVES

RAREFIED GAS DYNAMICS
Research activities of the Illinois University Coordinated Science Laboratory
[AD-A145569] 03 p0449 N85-12856
Study of stresses on surface of flat barrier immersed in under expanded jet of rarefied gas
16 p2765 N85-27061
The highly underexpanded exhaust plume from nozzles with boundary layers
[DFVLR-FB-85-10] 20 p3421 N85-31230
Unsteady transonic heat transfer in a transient facility
[NASA-CR-176145] 23 p3930 N85-34354

RAREFIED GASES
NT COSMIC GASES
NT INTERSTELLAR GAS
NT NEUTRAL GASES
Aerodynamic and thermal characteristics of stellate bodies in hypersonic flow of rarefied gas at angle of attack 06 p0778 N85-14974
Experimental investigation of heat transfer to bluff cylinders and cones in hypersonic rarefied gas flow
11 p1620 N85-20195
Nonequilibrium air radiation (Nequair) program: User's manual
[NASA-TM-86707] 19 p3353 N85-30780

RASERS
U MASERS

RATE METERS
U MEASURING INSTRUMENTS

RATES (PER TIME)
NT ACCELERATION (PHYSICS)
NT ACOUSTIC VELOCITY
NT AIRSPEED
NT ANGULAR ACCELERATION
NT ANGULAR VELOCITY
NT ARRHYTHMIA
NT BIT ERROR RATE
NT BURNING RATE
NT COLLISION PARAMETERS
NT COLLISION RATES
NT CRITICAL VELOCITY
NT CURRENT DENSITY
NT DECAY RATES
NT DECELERATION
NT DRIFT RATE
NT ELECTRON ACCELERATION
NT ELECTRON FLUX DENSITY
NT EVAPORATION RATE
NT EXHAUST VELOCITY
NT FLOW VELOCITY
NT FLUX (RATE)
NT FLUX DENSITY
NT GROUND SPEED
NT GROUP VELOCITY
NT HEART RATE
NT HEAT FLUX
NT HIGH ACCELERATION
NT HIGH GRAVITY ENVIRONMENTS
NT HIGH SPEED
NT HYPERSONIC SPEED
NT ILLUMINANCE
NT IMPACT ACCELERATION
NT ION PRODUCTION RATES
NT IRRADIANCE
NT LIGHT SPEED
NT LOADING RATE
NT LOW SPEED
NT LUMINANCE
NT LUMINOUS INTENSITY
NT MAGNETIC FLUX
NT MASS FLOW RATE
NT NEUTRON FLUX DENSITY
NT ORBITAL VELOCITY
NT PARTICLE ACCELERATION
NT PARTICLE FLUX DENSITY
NT PHASE VELOCITY
NT PHOTON DENSITY
NT PHYSIOLOGICAL ACCELERATION
NT PLASMA ACCELERATION
NT PROPAGATION VELOCITY
NT PROTON FLUX DENSITY
NT PULSE RATE
NT PULSE REPETITION RATE
NT RADIAL VELOCITY
NT RADIANCE
NT RADIANT FLUX DENSITY
NT RECOMBINATION COEFFICIENT
NT RELATIVISTIC VELOCITY
NT RESPIRATORY RATE
NT ROTOR SPEED
NT SIGNAL FADING RATE
NT SOLAR CONSTANT
NT SOLAR FLUX
NT SOLAR FLUX DENSITY
NT SOLAR VELOCITY
NT SOLAR WIND VELOCITY
NT SOUND INTENSITY
NT SPIN REDUCTION
NT STRAIN RATE
NT SUBSONIC SPEED
NT SUPERSONIC SPEEDS
NT TIP SPEED
NT TRANSONIC SPEED
NT TRANSVERSE ACCELERATION
NT WIND VELOCITY
Electron energy loss rates in N-2, O-2 and air
[AD-A145156] 01 p0072 N85-10476
Robust rate control system designs for a submersible
[AD-A144792] 01 p0111 N85-10753
Some of the features of movement of gas through a layer of free-flowing substances
[BLL-M-35732-(5828.4)] 02 p0196 N85-11312
Northern Hemisphere atlas of 1-minute rainfall rates
[AD-A145411] 02 p0231 N85-11508
Southern Hemisphere atlas of 1-minute rainfall rates
[AD-A145421] 02 p0231 N85-11509
Specific absorption rate in a sitting rhesus model at 225, 1290, and 5950 MHz for E, H, and K polarizations
[AD-A145435] 02 p0234 N85-11524
Ballpark reliability estimation techniques
[AD-A145971] 03 p0360 N85-12357
Analyses to develop models to project failure rates and repair costs of electronic modules and subassemblies
[AD-A146509] 06 p0816 N85-15180
Rain rate meter
[AD-D011361] 07 p0999 N85-16342
Snow characterization measurements from SNOW-TWO/Smoke Week 6
[AD-A147423] 07 p1008 N85-16402
An evaluation of flashtube signal characteristics
[AD-A149569] 10 p1423 N85-18974
Influence of extension rate on strength and deformation characteristics of titanium alloys over a broad temperature range 10 p1448 N85-19121
Development of a polysilicon process based on chemical vapor deposition of dichlorosilane in an advanced Siemen's reactor
[NASA-CR-174445] 11 p1672 N85-20532
Application of dimensional analysis to the problem of solar wind-magnetosphere energy coupling
[DE85-002414] 11 p1674 N85-20551
Influence of uncompensated solution resistance upon the evaluation of rate constants for rapid electrochemical reactions
[AD-A150657] 14 p2250 N85-23942
Use of optical techniques in studies of wear rates of anodized aluminum and polymer coatings on aluminum
14 p2259 N85-23997
Computer controlled acquistion of corrosion rate data from multiple sensors
[PB85-157378] 15 p2524 N85-25559
Removal of longitudinal internal flash from electrically welded tubes
[BLL-BISI-TRANS-22380-(9022.06)]
17 p2938 N85-28136
Inequalities for distributions with increasing failure rate
[AD-A152812] 17 p2976 N85-28390
Low-rate discharge of various electrochemical batteries for use with oceanographic instruments
[AD-A153965] 18 p3095 N85-29159
Method of characterizing critical timing paths and analyzing timing related failure modes in very large scale integrated circuits
[AD-D011731] 22 p3759 N85-33296
Limits to the burster repetition rate as deduced from the 2nd catalog of the interplanetary network
[OG-1.2-5] 22 p3862 N85-33915
Cyg X-3: Not seen in high-energy gamma rays by COS-B
[OG-2.2-2] 22 p3864 N85-33929
Constraints on cosmic-ray observation of Cygnus X-3
[OG-2.2-3] 22 p3864 N85-33930
Hercules X-1: Pulsed gamma-rays detected above 150 GeV
[OG-2.2-9] 22 p3866 N85-33935
Time-resolved spectroscopic studies of detonating heterogeneous explosives
[DE85-009760] 23 p3921 N85-34297
Dual-chamber plasma deposition of A-Si:H solar cells at high rates using disilane
[DE85-011828] 23 p3946 N85-34451
Analysis of transient radiation upset in a 16K SRAM
[DE85-009442] 23 p3965 N85-34586
Ranging system which compares an object reflected component of a light beam to a reference component of the light beam
[NASA-CASE-NPO-15865-1] 23 p3973 N85-34629
Injection of energetic particles following the gamma-ray flares on June 7, 1980, as observed on Helios 1
[SH-1.3-9] 23 p3993 N85-34756
Angular resolution of air-shower array telescopes
[OG-9.5-6] 23 p4030 N85-34983
The angular resolution of air shower gamma ray telescopes
[OG-9.5-14] 23 p4031 N85-34990
Recording system for the solar neutron monitoring at Mt. Norikura
[SH-9.1-8] 23 p4051 N85-35123
Burst size distributions in the digitized data of the ion chambers t Mt. Norikura and sea level stations
[SH-9.1-9] 23 p4051 N85-35124
Sensitivity of single and multiple cosmic ray neutrons to the surrounding medium in a lead-free monitor
[SH-9.1-10] 23 p4051 N85-35125
The neutron moderated detector and groundbased cosmic ray modulation studies
[SH-9.1-13] 23 p4052 N85-35126

A suggested standardized format for cosmic ray ground-level event data
[SH-9.1-15] 23 p4052 N85-35130

The application of bispectral analyses to aeroelastic phenomena 24 p4060 N85-35157

The structure of the shower disk observed at Mt. Norikura
[HE-4.7-1] 24 p4198 N85-36052

Methods for roof-top mini-arrays
[HE-4.7-7] 24 p4199 N85-36058

Fast scintillation counter preamplifier for the observation of Linsley effect
[HE-4.7-9] 24 p4199 N85-36060

RATINGS

The effect of beta adrenergic blockade on ratings of perceived exertion
[AD-A148053] 08 p1195 N85-17530

Streamlined Test Reporting And Planning (STRAP): Computerized human factors questionnaire
[AD-A150811] 14 p2395 N85-24751

RATIONS

NT SPACE RATIONS

Nutritional criteria for military rations and effects of prolonged feeding on acceptability
14 p2394 N85-24742

The effects of prolonged feeding meal, ready-to-eat (MRE) operational rations
[AD-A154763] 21 p3666 N85-32773

RATIOS

NT ASPECT RATIO
NT COMPRESSION RATIO
NT DIMENSIONLESS NUMBERS
NT FUEL-AIR RATIO
NT GRASHOF NUMBER
NT HIGH ASPECT RATIO
NT HIGH REYNOLDS NUMBER
NT INDEXES (RATIOS)
NT LIFT DRAG RATIO
NT LOW ASPECT RATIO
NT LOW REYNOLDS NUMBER
NT MACH NUMBER
NT MASS RATIOS
NT MASS TO LIGHT RATIOS
NT MODULAR RATIOS
NT NUSSELT NUMBER
NT POISSON RATIO
NT PRANDTL NUMBER
NT PRESSURE RATIO
NT RAYLEIGH NUMBER
NT REYNOLDS NUMBER
NT RICHARDSON NUMBER
NT SCALE (RATIO)
NT SIGNAL TO NOISE RATIOS
NT SIMILARITY NUMBERS
NT STRESS RATIO
NT STROUHAL NUMBER
NT VOID RATIO

The effect of occupational exposure and the body weight to height ratio on exhaled methylene chloride breath concentration in females at one, eighteen and sixty-six hours post exposure 14 p2388 N85-24708

Fuzzy hierarchical analysis
[DE85-006149] 17 p3021 N85-28685

Explanation of the secondary to primary ratio within the continuous Fermi accelerator model
[OG-8.3-2] 23 p4021 N85-34921

Propagation of injected cosmic rays under distributed reacceleration
[OG-8.3-3] 23 p4021 N85-34922

RATS

Hemopoiesis in rats submitted to weightlessness
01 p0091 N85-10613

General resistance of organism of rats under hypokinesia 05 p0694 N85-14462

An atropinized heat-stressed rat model: Dose response effects and pharmacokinetics
[AD-A146651] 07 p1011 N85-16423

Acute oral toxicity (LD50) of 4-nitrophenyl monochloromethyl (Phenyl) phosphinate (TA009) in male rats
[AD-A148337] 08 p1192 N85-17513

Results of sanitary-microbiological studies aboard Cosmos-1129 biosatellites 12 p1903 N85-21952

Rat tissue opioid peptide content during long-term hypokinesia 12 p1904 N85-21954

Effect of long-term repeated exposure to high-intensity stationary magnetic field on adrenomedullary activity
12 p1904 N85-21955

Chemical characterization and toxicologic evaluation of airborne mixtures. Inhalation toxicology of diesel fuel obscurant aerosol in Sprague-Dawley rats. Phase 3. Subchronic exposures
[AD-A150100] 12 p1905 N85-21966

Brain mechanisms underlying individual differences in reaction to stress: An animal model
[AD-A150195] 13 p2143 N85-23301

Structural development and gravity
15 p2608 N85-26071

The salutary effect of dietary calcium on bone mass in a rat model of simulated weightlessness
15 p2608 N85-26073

Role of glucocorticoids in the response to unloading of muscle protein and amino acid metabolism
15 p2609 N85-26077

Constant fiber number during skeletal muscle atrophy and modified arachidonate metabolism during hypertrophy 15 p2609 N85-26078

Blood pressure responses and mineral ocorticoid levels in the suspended rat model for weightlessness
15 p2609 N85-26079

Differential effect of denervation on free radical scavenging enzymes in slow and fast muscle of rat
[NASA-CR-175719] 15 p2614 N85-26110

Effects of long-term low-level radiofrequency radiation exposure on rats. Volume 7: Metabolism, growth and development
[AD-A150829] 15 p2615 N85-26112

Preliminary assessment of climatic change during late Wisconsin time, southwest Great Basin and vicinity, Arizona, California and Nevada
[DE85-008343] 16 p2836 N85-27486

Does a 50-cycle alternating field have central nervous effects?
[BLL-CE-TRANS-8083-(9022.09)]
16 p2839 N85-27507

Experiments in microwave exposure in the rat: Body temperature, serum chemistry and the use of chemical restraint
[PB85-156834] 16 p2840 N85-27512

Rat bone tissue after flight aboard Cosmos-1129 biosatellite 19 p3324 N85-30593

Effect of periodic accelerations on physiochemical properties and Ca2+ reactivity of actomyosin in white rat myocardium and skeletal muscles
19 p3324 N85-30594

Rat blood serum and liver carbohydrates and lipids in recovery period after 15-day hypokinesia
19 p3326 N85-30605

Effects of long-term low-level radiofrequency radiation exposure on rats. Volume 8: Evaluation of longevity, cause of death, and histopathological findings
[AD-A154283] 19 p3327 N85-30610

Changes in the impedance and bioelectrical activity of the cerebral cortex of rats under the action of anaesthetic drugs
[HSE-TRANS-10371] 19 p3327 N85-30617

Effects of coating rectangular microscopic electrophoresis chamber with methylcellulose
20 p3496 N85-31748

Changes in pentose and glucuronate pathway dehydrogenases in rat brains following single or multiple hypothermic episodes 20 p3505 N85-31790

General description of experiment dealing with rat ontogenesis aboard Cosmos-1514 biosatellite
22 p3822 N85-33679

Rat plasma hormone levels following flight aboard Cosmos-1129 biosatellite 22 p3823 N85-33681

The 1984 biotic studies of Yucca Mountain, Nevada test site, Nye County, Nevada
[DE85-011715] 23 p3951 N85-34487

Rat skeletal muscles with simulation of physiological effects of weightlessness (morphological study)
23 p3953 N85-34502

Lipogenesis in rat liver after flight aboard Cosmos-1129 biosatellite 23 p3954 N85-34506

Response of amino acids in hindlimb muscles to recovery from hypogravity and unloading by tail-cast suspension
[NASA-CR-176183] 24 p4128 N85-35589

Response of rat hindlimb muscles to 12 hours recovery from tail-cast suspension
[NASA-CR-176182] 24 p4128 N85-35590

RAWINSONDES

An evaluation and comparison of vertical profile data from the VISSR Atmospheric Sounder (VAS)
[NASA-TP-2425] 07 p1000 N85-16351

The effect of the arbitrary level assignment of satellite cloud motion wind vectors on wind analyses in the pre-thunderstorm environment
[NASA-TM-86186] 10 p1517 N85-19565

Upper-air data collection during CAPTEX
[DE85-006300] 16 p2827 N85-27438

Trends in the Southern Hemisphere
18 p3144 N85-29466

Processing methods of rawinsonde measurements at the descent by parachute
[KNMI-WR-84-7] 18 p3149 N85-29496

Comparison of tropopause altitude determination by the Platteville Radar, Sunset Radar and the NWS Rawinsonde 21 p3617 N85-32477

A modified Fresnel scattering model for the parameterization of Fresnel returns, part 2.3A
21 p3618 N85-32483

RAY ACOUSTICS

U GEOMETRICAL ACOUSTICS

RAY OPTICS

U GEOMETRICAL OPTICS

RAY TRACING

Nonlinear propagation in a depth-dependent ocean
[AD-A145079] 01 p0116 N85-10781

Concentrator optical characterization using computer mathematical modelling and point source testing
[NASA-CR-174109] 04 p0528 N85-13375

Ocean acoustics
[AD-A147062] 07 p1036 N85-16591

Simulation of bent crystal spectrometers
[DE85-002042] 09 p1385 N85-18709

Three dimensional ray tracing of the Jovian magnetosphere in the low frequency range
[NASA-CR-175462] 10 p1571 N85-19909

Electromagnetic analysis of radomes by the moment method
[AD-P004351] 12 p1824 N85-21445

Comparison of spherical wave ray tracing and exact boundary value solutions for spherical radomes
[AD-P004353] 12 p1824 N85-21447

A subaperture approach to the calculation of flashlobes introduced by airborne radomes
[AD-P004355] 12 p1825 N85-21449

Image lobe analysis for large radomes
[AD-P004359] 12 p1825 N85-21453

Surface forward scattering and reflection
[AD-A150115] 12 p1928 N85-22112

A fast ray tracing routine for laterally inhomogeneous media
[AD-A150984] 14 p2421 N85-24838

High frequency estimation of 2-dimensional cavity scattering
[AD-A151697] 15 p2542 N85-25696

LIGHT: A ray tracing code to simulate light collection in scintillation spectrometers and light pipes
[DE85-007213] 16 p2865 N85-27673

Saudi Arabian refraction profile: Crustal structure of the Red Sea-Arabian Shield transition
17 p2990 N85-28484

Saudi Arabian refraction profile: A preliminary interpretation for the Red Sea-Arabian Shield transition
17 p2991 N85-28485

A preliminary analysis of the Saudi Arabian deep seismic sounding data 17 p2991 N85-28489

The addition of advanced scene rendering techniques to a general purpose graphics package
[AD-A153323] 17 p3012 N85-28625

Ray tracing general sweep defined objects
[REPT-84-36] 17 p3014 N85-28636

Circular-beam ray tracing on a microcomputer
[DE85-010754] 19 p3338 N85-30885

View-limiting shrouds for insolation radiometers
[NASA-CR-176041] 20 p3458 N85-31476

A theoretical and empirical analysis of coherent ray-tracing 23 p3957 N85-34524

A simple but systematic CSG system
23 p3963 N85-34569

A ray trace program for line-of-sight microwave communication links
[AD-A156168] 24 p4087 N85-35336

RAYLEIGH DISTRIBUTION

Spline-based Rayleigh-Ritz methods for the approximation of the natural modes of vibration for flexible beams with tip bodies
[NASA-CR-172566] 13 p2102 N85-23100

An application of the Rayleigh distribution to contract cost data
[AD-A151551] 15 p2664 N85-26441

Bivariate Rayleigh distribution: Formulas and curves, for correlation computing using the distribution function
[FOA-C-30380-E2] 20 p3521 N85-31901

1000 GeV gamma rays from Cygnus X-3: An update
[OG-2.1-8] 22 p3863 N85-33925

A new approach to evaluate gamma-ray measurements
[OG-9.5-11] 23 p4031 N85-34888

A new statistic for the analysis of circular data in gamma-ray astronomy
[OG-9.5-13] 23 p4031 N85-34889

RAYLEIGH NUMBER

Natural convection in square partitioned enclosures
[AD-A153707] 18 p3197 N85-29828

RAYLEIGH SCATTERING

Extinction by dielectric particles at optical and infrared wavelengths
[AD-A146305] 03 p0413 N85-12840

Ionospheric turbulence: Interchange instabilities and chaotic fluid behavior
[AD-A147810] 07 p0996 N85-16337

Rayleigh and Raman scattering for density in a swirling flow combustor 08 p1120 N85-17060
Flame propagation and stabilization studies using Rayleigh scattering and laser Doppler velocimetry
[AD-A148602] 09 p1290 N85-18102
Fourier densitometry: A new optical method for measuring density fluctuations by Rayleigh scattering — turbulent jets 11 p1576 N85-19932
LANDSAT-4 Thematic Mapper calibration and atmospheric correction 12 p1870 N85-21734
A measurement of the intensity of the cosmic background radiation at 3.9 cm
13 p2206 N85-23681
Experimental determination of the mixing frequency parameter for coalescence/dispersion modeling of turbulent combustion
[DE85-011468] 19 p3270 N85-30280
Rayleigh scattering for density measurements in premixed flames: One point, time series data
20 p3424 N85-31253

RAYLEIGH WAVES
Rayleigh-Taylor instability in compressible media
[AD-A145491] 02 p0198 N85-11322
Measurement of areal mass variation in Rayleigh-Taylor unstable targets
[AD-A145541] 02 p0198 N85-11325
Research in quantitative NDE techniques
[AD-A145990] 03 p0369 N85-12358
Love and Rayleigh waves in irregular ground
04 p0523 N85-13348
Deep structure beneath the Pyrenees
04 p0524 N85-13351
Lightweight, broadband Rayleigh wave transducer
[AD-D011345] 07 p1037 N85-16584
Influence of Bragg reflecting lattice groove depth modulation on Rayleigh wave reflection coefficient
10 p1499 N85-19458
Texture independent determination of residual stress in polycrystalline aggregates using Rayleigh waves
[AERE-R-11483] 12 p1943 N85-22203
Angular dependence of the Rayleigh-surface wave velocity in polycrystalline metals with small anisotropy
[AERE-R-11595] 15 p2509 N85-25476
On Rayleigh waves and Rayleigh wave extension of surface micro-cracks 15 p2572 N85-25860
Inversion of Rayleigh wave group velocities from high-explosive tests
[AD-A152172] 16 p2783 N85-27175
Elastic wave gyrometer
[REPT-26/4924/HF] 20 p3459 N85-31484
Development of ultrasonic modeling techniques for the study of crustal inhomogeneities
[AD-A155206] 21 p3632 N85-32565

RAYS
Solar neutrino: Flux, cosmic rays and the 11 year solar cycle
[SH-8.1-7] 23 p4049 N85-35112

RC CIRCUITS
The design of high order active RC-filters
[DRIC-T-7147] 07 p0945 N85-15987
Development of thin film hybrid IC active filter for video band use
[NHK-LABS-NOTE-312] 18 p3094 N85-29153

RC NETWORKS
U RC CIRCUITS

RDX
The influence of inert particulate material on the properties of RDX/polyethylene wax compositions
[MRL-R-929] 03 p0336 N85-12159
Critical analysis of nitramine decomposition data. Preliminary comments on autoacceleration and autoinhibition in HMX and RDX decomposition
[AD-A146570] 06 p0774 N85-14946
Microstructural origins of hot spots in RDX explosive and a reference inert material
[AD-A146685] 06 p0774 N85-14947
Molecular dynamics in nitramines and modified nitramines
[AD-A148515] 08 p1220 N85-17686
The chemistry of RDX and HMX cluster ions
13 p2004 N85-22561
Combustion-deflagration-detonation transition in a confined spherical powder
[ISL-R-108/84] 22 p3747 N85-33223

REACTION BONDING
Quantum characteristics of kinetic fracturing of solids
02 p0265 N85-11732
Kinetics of reaction of metals and non-metals during diffusion welding 11 p1602 N85-20076
Radiographic detectability limits for seeded voids in sintered silicon carbide and silicon nitride
[NASA-TM-86945] 12 p1861 N85-21674
Sintered silicon carbide molded body and method for its production
[NASA-TM-77646] 14 p2259 N85-23999
Research and developmental study on MIS thin film solar cells of amorphous hydrogenated silicon, part 2
[BMFT-FB-T-84-290] 17 p2968 N85-28467

REACTION JETS
U JET FLOW
U JET THRUST

REACTION KINETICS
Comparison of numerical techniques for integration of stiff ordinary differential equations arising in combustion chemistry
[NASA-TP-2372] 01 p0011 N85-10065
CREKID: A computer code for transient, gas-phase combustion of kinetics
[NASA-TM-83806] 01 p0011 N85-10068
DYNKIN: A computer program for the description of detailed gas reactions in interaction with gas dynamics
[AD-B085364] 01 p0046 N85-10298
Second All-Union Seminar on Hydromechanics and Heat and Mass Exchange in Weightlessness, summaries of reports
[NASA-TM-77590] 01 p0047 N85-10305
Laser spectroscopy and gas-phase chemistry in CVD
[DE84-014959] 02 p0173 N85-11158
The oxidation of transition-metal ions by molecular oxygen
[BLL-M-29593-(5828.4)] 02 p0175 N85-11172
Impact cratering: The process and its effects on planetary evolution — and silicate-carbonate reactions on Venus
[NASA-CR-174016] 02 p0228 N85-11488
Study of singlet oxygen-pentavalent phosphorus reactions
[AD-A145896] 03 p0327 N85-12107
Mechanochemical reactions of polymethyl methacrylate and polystyrene at high pressure
[DRIC-T-7307] 03 p0337 N85-12165
Kinetics of fatigue factor of AT3 titanium alloys in air, distilled water and 3.5% aqueous NaCl solution
03 p0350 N85-12255
Organic aerosol formation: OH(hydroxyl radical) versus ozone oxidation pathways
[PB84-219880] 03 p0388 N85-12484
Reaction mechanisms in the formation of intercalation complexes, and properties of intercalated molecules
03 p0431 N85-12745
Low energy ion-molecule reaction dynamics and chemiionization kinetics
[DE84-015881] 04 p0559 N85-13562
New integration techniques for chemical kinetic rate equations. 2: Accuracy comparison
[NASA-TM-86893] 05 p0596 N85-13798
Space charge, interfacial kinetics, and electrical response of condensed matter
[AD-A146364] 06 p0765 N85-14893
Chemical kinetics and Earth's atmosphere
06 p0822 N85-15218
Integrating chemical kinetic rate equations by selective use of stiff and nonstiff methods
[NASA-TM-86923] 07 p0904 N85-15726
Reactions of butadiyne. 1: The reaction with hydrogen atoms
[NASA-TM-77805] 07 p0921 N85-15834
Interaction between chromium oxide and carbon
[BLL-M-36002-(5828.4)] 07 p0926 N85-15867
Solid-phase sintering of tantalum carbide
[BLL-M-36013-(5828.4)] 07 p0926 N85-15872
Kinetics of interaction between carbon and iron oxides of metallized materials in solid phase
[BLL-M-36023-(5828.4)] 07 p0926 N85-15873
Photochemistry and kinetics of the O*2-HI system
[AD-A147433] 07 p0971 N85-16167
Catalytic ignition and combustion of lean mixtures
[AD-A148101] 08 p1121 N85-17067
Combustion in high speed air flows
[AD-A148371] 08 p1122 N85-17070
Combustion kinetics of metal oxide and halide radicals
[AD-A148521] 08 p1122 N85-17076
The construction and behaviour of ultramicroelectrodes: Investigations of novel electrochemical systems
[AD-A148658] 08 p1123 N85-17079
Electrochemical features of the ferric sulfate leaching of CuFeS2/C aggregates
[AD-A148661] 08 p1123 N85-17081
Study of reaction kinetics and development of elastic properties in network polymerization systems by the impulse technique
[AD-A148187] 08 p1133 N85-17141
The kinetics of electron transfer reactions in and at films of electroactive polymers
[AD-A148597] 08 p1134 N85-17149
High pressure physics research focusing on composite materials 08 p1140 N85-17185
Study in molecular lasers
[AD-A148246] 08 p1166 N85-17357
Proceedings of the AFOSR/AFRPL Rocket Propulsion Research Meeting: Abstracts and Agenda
[AD-A148818] 09 p1288 N85-18085
Metal-support interactions: Their effects upon adsorption, electronics, and activity/selectivity properties of cobalt in hydrogenation
[DE85-003316] 09 p1292 N85-18113
Theoretical studies of the ignition and combustion of silane-hydrogen-air mixtures
[NASA-CR-3876] 10 p1433 N85-19032
An infrared study of the hydrogenation of carbon dioxide on supported rhodium catalysts
[AD-A149477] 10 p1436 N85-19049
Mechanisms and reaction dynamics related to methane combustion
[PB85-129690] 10 p1438 N85-19065
Kinetics of saturation of porous titanium with low melting point metals 10 p1446 N85-19114
Kinetics of oxidation of titanium alloy upon heating to 1000 deg C 10 p1448 N85-19122
Thermodynamics of the reactive flow model
[DE85-004405] 10 p1565 N85-19870
Dynamical studies of molecular systems
[DE85-003053] 11 p1594 N85-20028
A study of interdiffusion in beta + gamma/gamma + gamma prime Ni-Cr-Al
[NASA-CR-174852] 11 p1597 N85-20041
USSR report: Materials science and metallurgy
[JPRS-UMS-84-005] 11 p1597 N85-20044
Direct measurement of the temperature dependence of the velocity of the reaction of deuterium atoms with vibration-excited hydrogen molecules
[MPIS-12/1984] 11 p1726 N85-20856
A comparison of the efficiency of numerical methods for integrating chemical kinetic rate equations
[NASA-TM-83590] 12 p1778 N85-21162
Study of the kinetics of hydrogenation using aged catalysts
[DE85-004373] 12 p1802 N85-21302
Kinetics of nitric oxide formation in laminar and turbulent methane combustion
[PB85-149698] 12 p1804 N85-21313
A study of intumescent reaction mechanisms
[AD-A149605] 12 p1812 N85-21365
Optically pumped iodine monofluoride laser
[AD-D011555] 12 p1855 N85-21637
Chemical kinetics and photochemical data for use in stratospheric modeling. Evaluation number 6
[NASA-CR-175564] 12 p1888 N85-21849
State-selected ion-molecule reaction dynamics
[AD-A150068] 12 p1928 N85-22115
Theoretical nuclear physics
[DE85-003466] 12 p1932 N85-22135
Ignition of mixtures of SiH sub 4, CH sub 4, O sub 2, and Ar or N sub 2 behind reflected shock waves
[NASA-TP-2415] 13 p1974 N85-22395
Gasification of boron oxide drops and boron slurry agglomerates in combustion gases
13 p1999 N85-22529
Combustion kinetics of metal atoms and metallic radicals over wide temperature ranges 13 p1999 N85-22530
Combustion of zirconium carbide
13 p1999 N85-22532
Chemical kinetics of gas phase decomposition products of nitramine propellants 13 p2003 N85-22558
Kinetics of mechanism of the thermal decomposition of dimethylnitramine and dimethylnitrosamine
13 p2004 N85-22559
The chemistry of RDX and HMX cluster ions
13 p2004 N85-22561
Comprehensive mechanisms for combustion chemistry: An experimental and numerical study with emphasis on applied sensitivity analysis
[DE85-000173] 13 p2018 N85-22656
Estimating degree of development of physical-chemical interaction among components in Al B fiber composite material 13 p2027 N85-22705
Segregation of silicon in silumin-carbon fiber composites 13 p2028 N85-22706
Specifics of kinetics of polymorphous conversion upon heating of low carbon steels 13 p2030 N85-22721
Thermodynamic and kinetic studies of pulsed laser annealing from transient conductivity measurements
[DE85-003677] 13 p2096 N85-23078
Influence of uncompensated solution resistance upon the evaluation of rate constants for rapid electrochemical reactions
[AD-A150657] 14 p2250 N85-23942
Fundamental study of three dimensional two phase flow in combustion systems
[AD-A150739] 14 p2250 N85-23945
Evaluation of unimolecular rate constants for some outer-sphere electrochemical reactions
[AD-A150758] 14 p2250 N85-23946
Combustion kinetics of metal oxide and halide radicals
[AD-A150924] 14 p2251 N85-23952

best copy available

International Conference on Coordination Chemistry (23rd) held at Boulder, Colorado on 29 July - 3 August, 1984
[AD-A150960] 14 p2252 N85-23956
Block-implicit multigrid solution of Navier-Stokes equations in primitive variables
[DE85-004071] 14 p2301 N85-24250
Electricity production from coal through molten-carbonate fuel cells
[TI85-005072] 14 p2351 N85-24534
Extraction of ions from solutions at atmospheric pressure, mass spectrometric analysis of bioorganic substances 14 p2387 N85-24706
Theoretical studies of kinetic mechanisms of negative ion formation in plasmas
[AD-A150620] 14 p2423 N85-24948
Thermodynamic calculations and the chemical vapour deposition of hard materials 14 p2431 N85-24991
Detonations of solid explosives
[AD-A152012] 15 p2521 N85-25540
Kinetic studies following state selective laser excitations
[DE85-007173] 15 p2564 N85-25816
Dynamics of recrystallization and redistribution of impurities in semiconductors subjected to millisecond laser pulses 15 p2643 N85-26302
The overall reaction concept in premixed, laminar, steady-state flames. 2: Initial temperatures and pressures
[AD-A152132] 16 p2746 N85-26944
Transitional metal activation and functionalization of C-H bonds
[DE85-006816] 16 p2746 N85-26949
Evaluation of chemical reaction mechanisms for photochemical smog. Part 2: Quantitative evaluation of the mechanisms, revised
[PB85-166080] 16 p2822 N85-27408
The spectroscopy and reaction kinetics of coordinated unsaturated metal carbonyls
[AD-A153079] 17 p2920 N85-28003
Elementary reactions of importance in oxidation, combustion ignition and flame inhibitions
[AD-A153139] 17 p2921 N85-28004
Kinetics of hydrolysis and products of hydrolysis and photolysis of tetryl
[AD-A153144] 17 p2921 N85-28005
Study of self-propagating condensed phase reactions TiB(2) synthesis
[AD-A153198] 17 p2921 N85-28006
Kinetics of the formation of a complex alloyed boride coating on iron and its properties
[BLL-BISI-TRANS-22303-(9022.06)]
17 p2930 N85-28084
Rotational relaxation studies of hydrogen fluoride
[AD-A152711] 17 p3029 N85-28734
Rapid growth of potassium dihydrogen phosphate crystals
[DE85-007261] 17 p3045 N85-28839
Light scattering and spectroscopic studies of polymerization processes
[AD-A153407] 18 p3069 N85-28984
Chemical transformation modules for Eulerian acid deposition models. Volume 1: The gas-phase chemistry
[PB85-173714] 18 p3072 N85-29001
Spatial correlations in the decay from an unstable state in the Malthus Verhulst model — laser cavities
[NOTA-INTERNA-832] 18 p3114 N85-29280
Kinetics and intensity of photochemical processes in the atmosphere
[BPT-10/84] 18 p3134 N85-29411
Study of the chemical mechanism in lubrication
[DE85-010768] 19 p3228 N85-30013
Determination of the association constant for pertechnetic acid
[DE85-010224] 19 p3235 N85-30057
Variational transition state theory
[DE85-010685] 19 p3235 N85-30059
Burn rates of explosives at high pressures
[DE85-010806] 19 p3251 N85-30159
On the low temperature chemistry preceding end gas autoignition
[DE85-010471] 19 p3252 N85-30162
Flow field effects on nucleation in a reacting mixing layer
[ARL/AERO-R-165] 19 p3263 N85-30237
Experimental determination of the mixing frequency parameter for coalescence/dispersion modeling of turbulent combustion
[DE85-011468] 19 p3270 N85-30280
Production of gallium atoms by excimer laser photolysis of trimethyl gallium
[DE85-010742] 19 p3278 N85-30331
Instrumentation for particle-beams research using excited merging beams
[AD-A154155] 19 p3356 N85-30807
Carbon reduction of mixtures of MnO(2) and Fe(2)O(3)
[BLL-M-36260-(5828.4)] 20 p3422 N85-31241
Computer-controlled carburizing
[BLL-OA-TRANS-3204-(6196.300)]
20 p3429 N85-31268
Mechanistic and kinetic studies of the elementary processes in catalytic combustion of methane
[PB85-168306] 20 p3435 N85-31314
Theoretical modelling of the electro-chemistry in a corrosion fatigue crack. Part 2: Mathematical aspects of associated unsteady reaction equations
[NPL-DMA(A)-100-PT-2] 20 p3465 N85-31529
Self-heating to ignition measurements and computation of critical size for solar energy collector materials
[PB85-183374] 20 p3485 N85-31663
Modeling of chemical transformations of SO(x) and NO(x) in the polluted atmosphere: An overview of approaches and current status
[PB85-173169] 20 p3487 N85-31677
Fusion reactions at low energy
[DE85-010561] 20 p3528 N85-31944
Design of micelles as dephosphorylating agents
[AD-A155589] 21 p3564 N85-32166
Imbedded thermocouples as a solid propellant combustion probe
[AD-A155630] 21 p3564 N85-32167
Introduction of structural variations into oxide polymers and their effect on sintering and crystallization
[AD-A155597] 21 p3570 N85-32206
Multilayer capacitor dielectrics produced from metallo-organic precursors
[AD-A154592] 21 p3580 N85-32254
Experimental studies of the kinetics of deposition nucleation on an ice nucleant used in weather modification 21 p3638 N85-32598
The measured rate of condensation nucleation to droplets using the techniques of chemical kinetics
21 p3652 N85-32694
Resonant energy transfer during strong excitation
21 p3689 N85-32922
Jet flows: Modelling and experiments
22 p3744 N85-33208
Nonequilibrium chemistry in an isothermal turbulent flow 22 p3745 N85-33211
Static high pressure study of nitric oxide chemistry: Proposed mechanism for nitric oxide detonation
[DE85-010795] 22 p3746 N85-33220
Theoretical aspects of corrosion and practical implications for aircraft and related systems
22 p3749 N85-33240
Development of a chemical kinetic mechanism for the US EPA (Environmental Protection Agency) regional oxidant model
[PB85-185858] 22 p3813 N85-33618
Modeling of auto exhaust smog chamber data for EKMA development
[PB85-186492] 22 p3813 N85-33619
KIVA computer program for multidimensional chemically reactive fluid flows with fuel sprays
[DE85-012730] 22 p3830 N85-33722
An impact-induced terrestrial atmosphere and iron-water reactions during accretion of the Earth
22 p3854 N85-33864
Separation of gas mixtures by supported complexes
[DE85-011996] 23 p3912 N85-34236
Effects of hot deformation on the kinetics of the pearlite transformation in eutectoid steel
[BLL-M-35844-(5828.4)] 23 p3913 N85-34250
Metal alkoxides: Models for metal oxides. Alkoxide ligands in early transition metal organometallic chemistry
[DE85-011366] 23 p3916 N85-34269
Thermally induced chemical migration: A natural analog approach
[DE85-012306] 23 p3949 N85-34474
Application of evaluated fission-product delayed-neutron precursor data in reactor kinetics calculations
[DE85-012728] 23 p3972 N85-34624
Survey of mixing in metal/insulator systems
[DE85-011936] 23 p3985 N85-34714
FTIR studies of hydrocarbon synthesis on Pd/ZSM5 catalysts
[DE85-012430] 24 p4071 N85-35230
Basic research on pulse-combustion phenomena
[PB85-200228] 24 p4077 N85-35265
A study of the chemistry of alkali metals in the upper atmosphere
[AD-A156349] 24 p4117 N85-35524

REACTION PRODUCTS
Study of singlet oxygen-pentavalent phosphorus reactions
[AD-A145696] 03 p0327 N85-12107
Determination of Toluene's degradation products under simulated atmospheric conditions
05 p0674 N85-14331
Identification and properties of molecular systems of potential use in solar-pumped lasers
[NASA-CR-175804] 16 p2789 N85-27207
Current regulatory and licensing status for byproduct sources, facilities and applications
[DE85-010967] 22 p3842 N85-33796

REACTION RATE
U REACTION KINETICS

REACTION TIME
Pattern reversal visual evoked potentials and reaction time
[CSIR-SR-PERS-354] 01 p0087 N85-10644
Workload demand and CNS depressant stressor effects on spatial orientation information processing
[AD-A145211] 01 p0098 N85-10651
Fitts' law? A test of the relationship between information load and movement precision 05 p0705 N85-14523
A production system model of capturing reactive moving targets 05 p0705 N85-14524
A control model: Interpretation of Fitts' law
05 p0706 N85-14526
The effects of task structure on time-sharing efficiency and resource allocation optimality
05 p0711 N85-14562
Choice reaction time and color: An annotated bibliography
[AD-A149722] 12 p1906 N85-21979
Fast times at high temperatures
[DE85-003306] 12 p1943 N85-22205
The effect of set size on color recognition
[AD-A150958] 14 p2391 N85-24725
Eye movement in response to single and multiple targets
[AD-A151115] 15 p2617 N85-25125
Shape with and without redundant colour as coding mechanism for simulated radar displays in a time-extended simple vigilance task
[AD-A151683] 16 p2844 N85-27533
The effect of set size on time to recall color coded information
[AD-A155013] 21 p3665 N85-32767
Transformation of spectrum of phase-code keyed signal for scanning in time 22 p3765 N85-33338

REACTION WHEELS
Magnetically suspended reaction wheel assembly
05 p0607 N85-13870
Magnetic suspension options for spacecraft inertia-wheel applications 05 p0607 N85-13871
Reaction wheels for kinetic energy storage
05 p0607 N85-13874
Emitted vibration measurement device and method
[NASA-CASE-MFS-25981-1] 11 p1635 N85-20299

REACTIVITY
Alloying effects of reactive elements in ferritic stainless steels 02 p0178 N85-11196
Reactivity of ion implanted silicon carbide
[DE85-001543] 09 p1399 N85-18802
Ligand structural influences upon electrochemical reactivity: Organic substituent effects upon Carboxylatopentaamminecobalt(3) reductions at mercury and gold electrodes
[AD-A150685] 14 p2250 N85-23944
Mechanism of the catalytic gasification and reactivity of graphite
[DE85-009932] 19 p3229 N85-30020
Microscopic control of semiconductor surface oxidation
[AD-A154799] 21 p3709 N85-33029
Experimental studies of chemical reactivity during shock initiation of hexanitrostilbene
[DE85-011726] 22 p3754 N85-33270
Method for preparing hydride configurations and reactive metal surface
[DE85-006443] 23 p3917 N85-34274

REACTOR CHEMISTRY
U RADIOCHEMISTRY

REACTOR CORES
Multigrid iteration solution procedure for solving three-dimensional sets of coupled equations
[DE84-016515] 04 p0555 N85-13592
Expected behavior of plutonium in the IFR fuel cycle
[DE85-006225] 18 p3181 N85-29725
TFCX shielding optimization
[DE85-010503] 19 p3350 N85-30828
Superconducting toroidal field coil current densities for the TFCX
[DE85-010285] 20 p3530 N85-31959
MATADOR (Methods for the Analysis of Transport And Deposition Of Radionuclides) code description and user's manual
[TI85-901402] 23 p3966 N85-34592
Liquid uranium alloy-helium fission reactor
[DE85-006511] 23 p3970 N85-34607

DEPTH-CHARGE static and time-dependent rturbation/sensitivity system for nuclear reactor core alysis, revision 1
DE85-013103] 24 p4139 N85-35659
Neutronic calculations for a new high flux reactor
DE85-011651] 24 p4150 N85-35734
Thermal hydraulic features of the TMI accident
[DE85-014669] 24 p4152 N85-35747
ACTOR DESIGN
Instrumentation and controls evaluation for space nuclear power systems
[DE85-000963] 09 p1383 N85-18695
Magnetic divertor design for the compact reversed-field pinch reactor
[DE85-002031] 09 p1391 N85-18753
Optimization of pressure vessels with standard intercepting spheres
[INPE-3276-PRE/600] 11 p1651 N85-20397
Space nuclear-power reactor design based on combined neutronic and thermal-fluid analyses
[DE85-002433] 11 p1727 N85-20664
Tritium catalyzed deuterium Tokamaks
[DE85-004825] 12 p1936 N85-22166
Self-sustaining low-Z coatings for impurity control. Part 1: General considerations
[DE85-000427] 14 p2425 N85-24956
New directions in Tokamak reactors
[DE85-002548] 15 p2657 N85-26396
Methods of first wall structural analysis with applications to the long pulse commercial Tokamak reactor design
[DE85-004915] 15 p2657 N85-26397
Swelling behavior of titanium-modified AISI 316 alloys
[DE85-007470] 16 p2752 N85-26962
Ballooning beta limits of dee and bean shaped Tokamaks
[IPPJ-713] 16 p2866 N85-27676
TOKASTAR: A Tokamak stellarator hybrid with possible bean-shaped operation
[IPPJ-718] 16 p2866 N85-27680
Fusion-power-core design of a Compact Reversed-Field Pinch Reactor (CRFPR)
[DE85-007710] 16 p2868 N85-27692
Tokamak fusion core experiment maintenance study
[DE85-008040] 17 p3040 N85-28813
Preliminary proposal for a beryllium technology program for fusion applications
[DE85-009815] 18 p3183 N85-29737
Recent progress in stellarator reactor conceptual design
[DE85-008692] 18 p3189 N85-29760
Feasibility study of a fission-suppressed Tokamak fusion breeder
[DE85-008099] 18 p3190 N85-29786
Test cell modeling and optimization for FPD-2
[DE85-010636] 19 p3358 N85-30821
Advances in ICF power reactor design
[DE85-010930] 19 p3361 N85-30841
Poloidal variations in toroidal fusion reactor wall power loadings
[DE85-009505] 19 p3362 N85-30848
Tritium system design for the mirror reactors FPD-1, FPD-2 and FPD-3
[DE85-010490] 19 p3363 N85-30852
New concept for pumping the edge plasma
[DE85-010180] 19 p3371 N85-30909
Steady-state spheromak reactor studies
[DE85-009565] 19 p3372 N85-30916
Flow characteristics of the Cascade granular blanket
[DE85-010832] 20 p3420 N85-31227
Modeling and optimization of a test-cell upgrade for MFTF-B operating in the high neutron wall loading mode
[DE85-009997] 20 p3528 N85-31946
Simulating the effects of plasma disruption with a 1 MA current pulse in a coaxial test fixture
[DE85-010491] 20 p3535 N85-31996
Oxidation of formaldehyde solutions used for the preservation of reverse osmosis membranes
[PB85-186586] 22 p3742 N85-33194
Fusion Power Demonstration (FPD) maintenance and disassembly considerations
[DE85-011413] 22 p3846 N85-33820
Blanket optimization studies for Cascade
[DE85-010002] 22 p3846 N85-33824
REACTOR FUELS
U NUCLEAR FUELS
REACTOR MATERIALS
Heat exchanger
[DE84-014299] 01 p0047 N85-10309
Improved multiaxial creep-rupture strength criterion
[DE84-014273] 01 p0062 N85-10413
Method and apparatus for determining the content and distribution of a thermal neutron absorbing material in an object
[DE84-014319] 01 p0117 N85-10801
Materials studies for magnetic fusion energy applications at low temperatures, 7
[DE84-013487] 01 p0122 N85-10837
Stress corrosion of pressure vessel steel A533-B in high temperature water
[BLL-RISLEY-TR-4600-(9091.9F)] 03 p0330 N85-12125
Review: Role of refractory metal alloys in fusion reactor applications
[AERE-R-11317] 03 p0422 N85-12695
A physical interpretation of the structure and electron-optical data for spinel (MgAl2O4)
[AERE-R-11278] 03 p0434 N85-12767
Blanket materials for fusion reactors: Comparisons of thermochemical performance
[DE84-016240] 04 p0568 N85-13622
Proceedings of Workshop on Synergistic Effects in Surface Phenomena Related to Plasma-Wall Interactions
[IPPJ-AM-35] 06 p0864 N85-15488
Effects of monolayer coverages on substrate sputtering yields 06 p0865 N85-15496
Synergestic sputtering properties of binary alloys
06 p0865 N85-15497
Elevated temperature creep behavior of Inconel alloy 625
[DE84-015836] 09 p1297 N85-18144
Synergistic sputtering properties of binary alloys
[DE84-017493] 09 p1297 N85-18148
Magnetic fusion energy plasma interactive and high heat flux components. Volume 2: Technical assessment of the critical issues and problem areas in high heat flux materials and component development
[DE85-001155] 09 p1393 N85-18764
Magnetic fusion energy plasma interactive and high heat flux components. Volume 3: Strategy for international collaborations in the areas of plasma materials interactions and high heat flux materials and components development
[DE85-001145] 10 p1559 N85-19829
Leakage-flow-induced vibration of a tube-in-tube slip joint
[DE84-007301] 11 p1652 N85-20406
Ordered carbon metal alloys for extraterrestrial power systems
[AD-A150681] 14 p2255 N85-23977
Application of new welding technology in the fabrication of nuclear power plant 15 p2566 N85-25829
New directions in Tokamak reactors
[DE85-002548] 15 p2657 N85-26396
Differential between crack and pseudo-crack indications by means of objective magnetic flux leakage testing
[BLL-BISI-TRANS-22033-(9022.06)] 17 p2976 N85-28386
Sodium concrete reaction: Structural considerations
[DE85-009031] 18 p3081 N85-29063
Behavior of reinforced concrete at elevated temperatures
[DE85-009032] 18 p3123 N85-29332
Expected behavior of plutonium in the IFR fuel cycle
[DE85-006225] 18 p3181 N85-29725
Preliminary proposal for a beryllium technology program for fusion applications
[DE85-009815] 18 p3183 N85-29737
Load-carrying capabilities of refractory alloys for space reactor power applications
[DE85-010586] 19 p3240 N85-30087
Alloy development for irradiation performance
[DE85-010454] 19 p3240 N85-30091
Qualitative comparison of fusion reactor materials for waste handling and disposal
[DE85-010473] 19 p3360 N85-30830
Source Term Experiments Project (STEP): Aerosol characterization system
[DE85-010248] 19 p3361 N85-30839
Current state of development and expected performance of copper-lithium alloys as an impurity control system in fusion applications
[DE85-009673] 19 p3372 N85-30917
Nuclear data needs for fusion energy development
[DE85-010445] 20 p3536 N85-32000
Tritium-helium effects in metals
[DE85-011507] 22 p3749 N85-33235
Reactor pressure vessel steels ASME SA533B and SA508 C 1.2
[VTT-340] 22 p3794 N85-33507
Monte Carlo and discrete ordinates calculations of 14-MeV neturons streaming through a stainless-steel duct (L/D = 4.6): Comparison with experiment
[DE85-011423] 22 p3840 N85-33776
Stress corrosion cracking susceptibility of types 316NG and 316 stainless steel in an impurity environment
[TI85-006684] 23 p3917 N85-34277
Effect of stainless steel weld overlay cladding on the structural integrity of flawed steel plates in bending, series 1
[TI85-010349] 23 p3939 N85-34418
The dynamic strain ageing of A533B class 1 nuclear pressure vessel steel
[AERE-R-11485] 24 p4078 N85-35274
Analysis of reactor material experiments investigating oxide fuel crust stability and heat transfer in jet impingement flow
[DE85-012097] 24 p4151 N85-35739
REACTOR PHYSICS
The reactor dynamic code RETRANS: Structure and users guide
[OEFZS-4287] 07 p1041 N85-16614
Refinements in the computation of collision probabilities
[DE85-006116] 16 p2864 N85-27663
Radiation transport
[DE85-010333] 21 p3703 N85-33005
REACTOR SAFETY
A pilot study of future research on seismic hazards in Sweden
[FOA-C-20544-T1] 02 p0229 N85-11496
Space nuclear safety program
[DE84-015983] 04 p0564 N85-13591
Acoustic transducers for fast reactor instrumentation
[BLL-RISLEY-TR-4979-(9091.9F)] 07 p0961 N85-16091
Austrian contributions to fuel rod failure models shown at the International Standard Problem (ISP)-14
[OEFZS-4276] 07 p1041 N85-16613
Instrumentation and controls evaluation for space nuclear power systems
[DE85-000963] 09 p1383 N85-18695
Safety program considerations for space nuclear reactor systems
[DE85-003295] 10 p1558 N85-19806
Thermal stress-dependent dilation of concrete
[DE84-014686] 11 p1653 N85-20412
Parallel processing experiences on the Denelcor HEP computer
[DE85-000653] 11 p1702 N85-20703
Hydrogen flame acceleration and transition to detonation
[DE85-000611] 12 p1802 N85-21299
Proceedings of the 1984 DOE Nuclear Reactor and Facility Safety Conference, volume 1
[DE84-012130] 12 p1931 N85-22132
Proceedings of the DOE Nuclear Reactor and Facility Safety Conference, volume 2
[DE84-012694] 12 p1931 N85-22133
Steel containment buckling
[DE85-003744] 13 p2103 N85-23111
Physics effects of accidental submersion of space power reactors in water
[DE85-005020] 15 p2650 N85-26344
Sodium concrete reaction: Structural considerations
[DE85-009031] 18 p3081 N85-29063
Behavior of reinforced concrete at elevated temperatures
[DE85-009032] 18 p3123 N85-29332
Safety report, 1982 18 p3184 N85-29746
Flow visualization study of inverted annular flow of post dryout heat transfer region
[DE85-010482] 19 p3269 N85-30275
Liquid metal reactor programs: Safeguards and program assurance
[DE85-010621] 19 p3331 N85-30635
Graphic display development program, volume 1
[DE85-011076] 19 p3333 N85-30649
MELCOR Accident Consequence Code System (MACCS)
[DE85-008712] 19 p3339 N85-30689
Simulation and operation of the EBR-2 automatic control rod drive system
[DE85-010262] 19 p3360 N85-30832
Source Term Experiments Project (STEP): Aerosol characterization system
[DE85-010248] 19 p3361 N85-30839
Advances in ICF power reactor design
[DE85-010930] 19 p3361 N85-30841
A review of the SIMMER-2 analyses of liquid-metal-cooled fast breeder reactor core-disruptive accident fuel escape
[DE85-010803] 19 p3366 N85-30876
In-service supervision of a pressurized concrete pressure vessel
[OEFZS-4308] 20 p3470 N85-31564
Two-phase flow visualization in a transparent, atmospheric pressure, boiling water loop
[DE84-016057] 21 p3586 N85-32298
Tritium technology review
[DE85-010504] 21 p3703 N85-33006
MATADOR (Methods for the Analysis of Transport And Deposition Of Radionuclides) code description and user's manual
[TI85-901402] 23 p3966 N85-34592

Transient three-phase three-component systems. Part 1: Formulation of the system of differential equations
[DE85-013267] 24 p4095 N85-35384

REACTOR STARTUP TESTS
Instrumentation and controls evaluation for space nuclear power systems
[DE85-000963] 09 p1383 N85-18695
One-dimensional hybrid code for FRM dynamics
[DE85-010687] 19 p3361 N85-30840

REACTOR TECHNOLOGY
Means of varying conditions in the expanded boundary divertor without affecting energy confinement
[DE84-013840] 01 p0122 N85-10836
Hydrogen absorption on (110) tungsten planes at 30 K: An atom-probe field-ion microscope study
[DE84-015859] 04 p0560 N85-13565
Thermal contact conductance measurements on Doublet 3 armor tile traphile
[DE84-013554] 05 p0613 N85-13916
East Europe report: Science and technology
[JPRS-ESA-84-043] 08 p1142 N85-17198
USSR report: Engineering and equipment
[JPRS-UEQ-85-003] 13 p2042 N85-22782
Winding insulation in electromagnetic systems for Tokamak reactor plants 13 p2087 N85-23035
Glossary of fusion energy
[DE84-017180] 14 p2425 N85-24958
Comparison study of toroidal-field divertors for a compact reversed-field pinch reactor
[DE85-009591] 18 p3189 N85-29781
Liquid metal reactor programs: Safeguards and program assurance
[DE85-010621] 19 p3331 N85-30635
Touch-off: A method to determine the position of an object by means of a sensor-driven robot
[DE85-011178] 19 p3339 N85-30691
US blanket technology programs
[DE85-010505] 19 p3358 N85-30817
One-dimensional hybrid code for FRM dynamics
[DE85-010687] 19 p3361 N85-30840

REACTORS
Thermodynamical characteristics of heat storage reactors using metal hydrides
[NAL-TR-822] 06 p0869 N85-15524

READ-ONLY MEMORY DEVICES
Fast envelope detector with bias compensation
[AD-D011226] 01 p0038 N85-10243
Programmable digital temperature controller apparatus
[AD-D011221] 01 p0049 N85-10319
Fault tolerant computing research
[AD-A145640] 02 p0244 N85-11590
Logic elements for systems with variable structure
07 p0955 N85-16054
A method and apparatus for operating on compended PCM voice data
[NASA-CASE-KSC-11285-1] 18 p3089 N85-29120
Microcomputer controlled image processor
[AD-D011734] 22 p3833 N85-33735
Maintenance port system
[AD-D011724] 23 p3967 N85-34594

READERS
Comparative review of single-line and multiline optical character readers used in mail processing
[PB84-234624] 04 p0548 N85-13489
Optical mark reader
[AD-D011462] 10 p1557 N85-19818
Direct reading fast microwave interferometer for EBT
[DE85-000183] 11 p1636 N85-20306

READING
Comprehension of instructions for operating devices
[AD-A145263] 01 p0098 N85-10653
Investigation into the use of the TV magnifier in the Netherlands
[HSE-TRANS-11142] 20 p3533 N85-31986

READING MACHINES
U READERS

READJUSTMENT
U ADJUSTING

READOUT
A concept for a hadron calorimeter with photodiode readout
[MPI-PAE/EXP-E1-130] 01 p0050 N85-10332
Improvements in photodiode readout for small Cal (T1) crystals
[MPI-PAE/EXP-E1-131] 01 p0051 N85-10333
Fine grained hodoscopes based on scintillating optical fibers
[DE84-014849] 01 p0120 N85-10825
Characterization of electronic streak tubes including one with internal CCD readout
[DE84-016823] 05 p0639 N85-14098
CCDs: Their cause and cure
08 p1252 N85-17905
The ARGOS VHF direct readout mini-station and CML-80-MP data collection Platform Transmitter Terminals (PTTs) 14 p2238 N85-23873
ARGOS VHF direct readout mini-station
14 p2239 N85-23886
System for automatic recording of vibration parameters 14 p2282 N85-24135
Direct readout and dissemination of results using ARGOS keypad terminals 14 p2328 N85-24390
Digital tachometer 22 p3779 N85-33416
The read-out system of spatial distribution of thermoluminescence in meteorites
[SH-9.1-16] 23 p4052 N85-35131
Spatial distribution read-out system for thermoluminescence sheets
[HE-7.1-7] 24 p4213 N85-36161

REAGENTS
A robotic system for preparing reagent and dilution vials
[DE85-006262] 16 p2793 N85-27231
Basic research in novel inorganic reagents and fluorocarbon chemistry
[AD-A155340] 21 p3564 N85-32165

REAL NUMBERS
NT INTEGERS
Computable real analysis
[AD-A149079] 10 p1546 N85-19747

REAL TIME OPERATION
Real time sensing and control of out-of-plane distortion due to line heating by laser
[AD-A144773] 01 p0027 N85-10169
Clutter generator for use in radar evaluation
[AD-D011234] 01 p0039 N85-10245
The French weather radar network: A status report
01 p0082 N85-10550
Hardware for a real-time multiprocessor simulator
[NASA-TM-83605] 01 p0099 N85-10659
Ada (trademark) training curriculum. Real-time concepts I303 teacher's guide
[AD-A145093] 01 p0104 N85-10694
Chemoviscosity modeling for thermosetting resins - I
[NASA-CR-172443] 03 p0326 N85-12096
Wideband integrated voice/data technology
[AD-A146054] 03 p0355 N85-12283
Recent examples of mesoscale numerical forecasts of severe weather events along the east coast
[NASA-TM-86172] 03 p0395 N85-12523
Experimenting with the Rolm Ada language workshop for specifying and designing 03 p0408 N85-12607
A unified method for evaluating real-time computer controllers: A case study — aircraft control
[NASA-CR-174168] 04 p0547 N85-13478
Real-time planning by an intelligent robot
[DE84-016669] 04 p0553 N85-13519
The facilities of the Calculation Center and Real Time Room for satellite positioning 05 p0599 N85-13819
Information flow in event-driven large-scale systems
[DE84-014167] 05 p0735 N85-14728
The Western Aeronautical Test Range of NASA Ames Research Center
[NASA-TM-85924] 07 p0909 N85-15756
Some characteristics of automotive gasolines and their performance in a light aircraft engine
[FAA-CT-84-12] 07 p0934 N85-15919
Real-time analysis of space characteristics of microwave electromagnetic pulse fields by means of controllable layer structures 07 p0955 N85-16052
ILIR task of digital recoil travel measurement system
[AD-A147102] 07 p0967 N85-16140
Decentralized control of scheduling in distributed systems
[AD-A147446] 07 p1022 N85-16487
JPL Robotics Laboratory computer vision software library
[NASA-CR-174272] 07 p1023 N85-16491
Ada training curriculum. Real-time systems in Ada I401 teacher's guide, volume 1
[AD-A146782] 07 p1024 N85-16496
Ada training curriculum. Real-time systems in Ada I401 teacher's guide, volume 2
[AD-A146783] 07 p1024 N85-16497
The effect on software design of testing by symbolic execution 08 p1065 N85-16750
Reliable software design for avionics and space applications 08 p1065 N85-16751
Real-time estimation of amplitude and group delay distortion in a PSK line-of-sight communications channel
[AD-A147735] 08 p1151 N85-17266
A commentray on the utilization of real-time channel evaluation systems in HF spectrum management
[AD-A148616] 08 p1154 N85-17289
Programmable realtime interface between a block floating point processor and memory
[AD-D011431] 08 p1203 N85-17571
Operating system for a real-time multiprocessor propulsion system simulator. User's manual
[NASA-TP-2426] 08 p1207 N85-17596
Nonlinear real-time optical signal processing
[AD-A148293] 08 p1222 N85-17699
Improved real-time ultra-high resolution image projection display using laser-addressed liquid crystal light valve
[AD-D011414] 08 p1223 N85-17706
Decentralized control of scheduling in distributed systems
[AD-A147688] 08 p1226 N85-17731
Real-time estimation of amplitude and group delay distortion in a PSK line-of-sight communications channel
09 p1311 N85-18237
Development and operation of a real-time data acquisition system for the NASA-LaRC differential absorption lidar
[NASA-CR-174384] 09 p1366 N85-18583
Directory of range data conversion and processing systems
[AD-A148996] 10 p1427 N85-19001
An H.F. simulator for use with real time channel evaluation systems 10 p1473 N85-19290
Distributed data processing design methodology
[AD-A148888] 10 p1537 N85-19892
Distributing a distributed problem solving network simulator
[AD-A149065] 10 p1537 N85-19893
The feasibility of a multiprocessor architecture for real-time contour surface display generation
[AD-A149427] 10 p1538 N85-19897
RELTIM: A library of routines used in real time machine control applications
[PB85-116507] 10 p1542 N85-19725
Effect of water vapor and water droplets on the RAM-1 (Real-Time Aerosol Monitor): Preliminary results
[PB85-109429] 11 p1637 N85-20313
Real time algorithms for robotic control of teleoperators
[DE85-001137] 11 p1647 N85-20360
A quality control experiment in a real time multiprocessor operating system: The Mara 860 — software testing
11 p1702 N85-20707
Interface specifications for SCR (Software Cost Reduction) (A-7E) extended computer module, revised
[AD-A149948] 12 p1915 N85-22024
System for automatic recording of vibration parameters 14 p2282 N85-24135
The ARGOS communications performance trials
14 p2326 N85-24378
Structurization of programs for real-time microprocessor arrays 15 p2529 N85-25592
Real-time enhancement of a climatology or forecast of ocean thermal structure using observed ocean temperatures
[AD-A151118] 15 p2604 N85-26049
An extension of a microcomputer based system for analysis of line drawing quantization schemes
[AD-A152008] 15 p2624 N85-26171
Principles of organizing a real-time control system
15 p2625 N85-26177
High-capacity real-time computer system for processing hydrophysical data 15 p2625 N85-26178
Efficient implementation of real-time programs under the VAX/VMS operating system
[NASA-TM-86354] 15 p2627 N85-26193
Graphic simulation of a machine-repairmen model
[AD-A151761] 16 p2694 N85-26633
Maintaining consistency and accommodating network repair in a self-regenerative distributed database management system (a discussion of the means and cost) 16 p2696 N85-26656
Design and specification of a local area network architecture for use in real-time flight simulation
[AD-A152242] 16 p2716 N85-26762
Implementation of a real-time, interactive, continuous speech recognition system
[AD-A151936] 16 p2773 N85-27117
Data processing on the rotor test stand at DFVLR in Brunswick: Microprogrammable interfaces and array processor as key components in a PDP 11 real time data acquisition and processing system
[DFVLR-MITT-85-03] 17 p2906 N85-27921
Performance analysis of the DSN baseband assembly (Bba) Real-Time Combiner (RTC)
[NASA-CR-175877] 17 p2947 N85-28193
The design of an adaptive predictive coder using a single-chip digital signal processor
[AD-A152461] 17 p2952 N85-28231
Real-Time Multiprocessor Programming Language (RTMPL) user's manual
[NASA-TP-2422] 17 p3010 N85-28810
Optimal design and use of retry in fault tolerant real-time computer systems
[NASA-CR-175920] 17 p3015 N85-28843
Synchronization and fault-masking in redundant real-time systems
[NASA-TM-87478] 17 p3015 N85-28844
A real-time executive for multiple-computer clusters
[AD-A152961] 17 p3015 N85-28846

ial topography from digitized real time radiography
E85-006767] 18 p3091 N85-29130
ERMES-1: A mobile robot for navigation and
nipulation experiments
E85-008052] 18 p3118 N85-29301
The use of VLSI technology for the real-time generation
graphics displays: A proposal
D-A153766] 18 p3160 N85-29578
EDS operator and control software
E85-010470] 19 p3340 N85-30696
Implementation of a serial communication process for
fault tolerant, real time, multitransputer operating
stem
D-A154237] 19 p3343 N85-30714
A distributed real-time operating system
IKHEF-H/84-8] 20 p3518 N85-31876
Work in Amsterdam on local intelligence — artificial
telligence
IKHEF-H/84-9] 20 p3518 N85-31877
Interactive on-line conferences
[AD-A154723] 21 p3574 N85-32227
Hardware schemes for fast Fourier transform, part
7.4A 21 p3626 N85-32526
Real-time contour surface display generation
[AD-A155232] 21 p3668 N85-32780
Software for interactive on-line conferences
[AD-A154742] 21 p3670 N85-32801
A real time index of geomagnetic background noise for
the MAD (Magnetic Anomaly Detection) frequency band
[AD-A155717] 22 p3814 N85-33627
Modeling and measurement of fault-tolerant
multiprocessors
[NASA-CR-3920] 22 p3833 N85-33732
Linear filters as a method of real-time prediction of
geomagnetic activity
[DE85-010760] 22 p3860 N85-33899
Animengine: An engineering animation system
23 p3959 N85-34535
Real-time multiparameter pulse processing with decision
tables
[DE85-011683] 23 p3966 N85-34589
Space Missions for Automation and Robotics
Technologies (SMART) Program
[NASA-TM-86820] 24 p4066 N85-35210
Holoswitch
[AD-A155841] 24 p4096 N85-35392
Optimize computer throughput using array processors
[AD-A155843] 24 p4135 N85-35628
AL VARIABLES
NT ABEL FUNCTION
NT ASYMPTOTES
NT ASYMPTOTIC SERIES
NT BESSEL FUNCTIONS
NT BETHE-SALPETER EQUATION
NT BIHARMONIC EQUATIONS
NT BLASIUS EQUATION
NT BOREL SETS
NT BURGER EQUATION
NT CALCULUS OF VARIATIONS
NT CHANDRASEKHAR EQUATION
NT COLLINEARITY
NT COMPOSITE FUNCTIONS
NT COPLANARITY
NT DELTA FUNCTION
NT DIFFERENTIAL EQUATIONS
NT EINSTEIN EQUATIONS
NT ELLIPTIC DIFFERENTIAL EQUATIONS
NT EULER-CAUCHY EQUATIONS
NT EXISTENCE THEOREMS
NT EXTREMUM VALUES
NT FALKNER-SKAN EQUATION
NT FOKKER-PLANCK EQUATION
NT FOURIER SERIES
NT GAUSS EQUATION
NT GREEN'S FUNCTIONS
NT HELMHOLTZ VORTICITY EQUATION
NT HYPERBOLIC DIFFERENTIAL EQUATIONS
NT HYPERBOLIC FUNCTIONS
NT INTEGRAL CALCULUS
NT J INTEGRAL
NT JACOBI MATRIX METHOD
NT KERNEL FUNCTIONS
NT LAME WAVE EQUATIONS
NT LIAPUNOV FUNCTIONS
NT LIMITS (MATHEMATICS)
NT LINEAR EQUATIONS
NT LINEAR EVOLUTION EQUATIONS
NT LIOUVILLE EQUATIONS
NT LIPSCHITZ CONDITION
NT MAXIMA
NT MEASURE AND INTEGRATION
NT MONGE-AMPERE EQUATION
NT NEUMANN PROBLEM
NT NONLINEAR EQUATIONS
NT NONLINEAR EVOLUTION EQUATIONS
NT NUMERICAL DIFFERENTIATION
NT NUMERICAL INTEGRATION
NT PADE APPROXIMATION
NT PARABOLIC DIFFERENTIAL EQUATIONS
NT PARTIAL DIFFERENTIAL EQUATIONS
NT PERIODIC FUNCTIONS
NT POISSON EQUATION
NT POWER SERIES
NT QUADRATIC EQUATIONS
NT RUNGE-KUTTA METHOD
NT SERIES (MATHEMATICS)
NT STURM-LIOUVILLE THEORY
NT TANGENTS
NT TAYLOR SERIES
NT VECTOR ANALYSIS
NT VLASOV EQUATIONS
NT VORTICITY
NT WEIGHTING FUNCTIONS
Schubert varieties are arithmetically Cohen-Macaulay
16 p2853 N85-27592
SIGMA - A stochastic-integration global minimization algorithm
[AD-A154878] 21 p3671 N85-32806
REARWARD FACING STEPS
U BACKWARD FACING STEPS
REATTACHED FLOW
Experiments on the structure of turbulent reattaching
flow 05 p0635 N85-14074
Heat transfer and fluid mechanics measurements in the
turbulent reattaching flow behind a backward-facing step
15 p2553 N85-25753
An experimental study of compressible turbulent
reattaching free shear layers 16 p2781 N85-27161
REATTACHMENT
U ATTACHMENT
REB
U RELATIVISTIC ELECTRON BEAMS
REBREATHING
Cardiac output measured by mass spectroscopy
05 p0692 N85-14449
Cardiac output measurement with soluble gases
05 p0692 N85-14450
RECEIVERS
NT LINEAR RECEIVERS
NT LOGARITHMIC RECEIVERS
NT RADAR RECEIVERS
NT RADIO RECEIVERS
NT RADIOTELEPHONES
NT SUPERHETERODYNE RECEIVERS
NT TELEVISION RECEIVERS
The development of an optoelectronic assembly applied
to computer systems
[AD-A145028] 01 p0120 N85-10621
Experimental and theoretical study of a solar
thermochemical receiver module
[NASA-CR-174107] 04 p0528 N85-13374
Natural interference phenomena affecting spaceborne
receivers
[NASA-CR-174256] 07 p0916 N85-15796
Hardwire missile receiver coupler
[AD-D011350] 07 p0937 N85-15936
Spaceborne receivers: Basic principles
[NASA-CR-174269] 07 p0946 N85-15990
Lightweight, broadband Rayleigh wave transducer
[AD-D011345] 07 p1037 N85-16584
Using the control system design environment in the
design of a data link receiver unit for the Coast Guard
HH-65A helicopter
[AD-A148624] 08 p1068 N85-16860
TDRSS S-shuttle unique receiver equipment
08 p1100 N85-16951
A variable length and sensor spacing thermistor array
[AD-D011416] 08 p1113 N85-17017
The susceptibility of aeronautical navigational aids to
interference from adjacent-band broadcast transmissions
[BBC-RD-1984/12] 09 p1311 N85-18234
Coherent receiver phase and amplitude alignment
circuit
[AD-D011487] 10 p1468 N85-19265
SSPS-CRS advanced sodium receiver: Construction
experience report
[DE85-000625] 10 p1511 N85-19533
Direction finder set, radio
[AD-A149958] 12 p1775 N85-21142
Solid particle receiver experiments: Velocity
measurements
[DE85-000257] 12 p1853 N85-21623
Method of measuring sea surface water temperature
with a satellite including wideband passive
synthetic-aperture multichannel receiver
[NASA-CASE-NPO-15651-1] 12 p1869 N85-21723
Programmable filter with fanned interdigital surface
acoustic wave transducer 13 p2083 N85-23006
Invariance of probability characteristics of detector to
shape of optical pulse signals 13 p2090 N85-23048
Microwave blackbodies for spaceborne receivers
[NASA-CR-175647] 13 p2094 N85-23068
Optoacoustic receiver with semiconductor-type radiator
and photodetector 14 p2274 N85-24086
Photon detection with cooled avalanche photodiodes:
Theory and preliminary experimental results
16 p2770 N85-27096
Real-time position determinations using the GPS
TI4100/GEOSTAR receiver
[AD-A152551] 17 p2894 N85-27845
Thermal performance and design of a solid particle cavity
receiver
[DE85-010830] 19 p3274 N85-30300
Symposium on Luminescent Radiation Receivers and
Converters 19 p3295 N85-30430
Arctic acoustic tomography MIZEX 84
[AD-A154426] 19 p3320 N85-30580
Sensitivity of compressive receivers
[FOA-C-30365-E4] 22 p3756 N85-33288
Comparative characteristics of optical multiposition
pulse signals with intersymbol distortion
22 p3764 N85-33329
Binary signal detection in acoustooptic receivers
22 p3782 N85-33430
RECEIVING SYSTEMS
U RECEIVERS
RECEPTACLES (CONTAINERS)
U CONTAINERS
RECEPTION DIVERSITY
Analysis of space diversity techniques for EHF
(Extremely High Frequency) satellite downlinks
[AD-A151900] 15 p2544 N85-25705
Polarization diversity addition to the 10 centimeter
Doppler weather radar
[AD-A156062] 24 p4067 N85-35334
RECEPTORS (PHYSIOLOGY)
NT CHEMORECEPTORS
NT GRAVIRECEPTORS
NT MECHANORECEPTORS
NT PHOTORECEPTORS
NT PROPRIOCEPTORS
Dynamics of morphological changes in articulation
nervous system under hypokinetic conditions as a model
of a spaceflight factor 01 p0092 N85-10621
RECESSION
Results of variable enthalpy tests of CPR-488 TIP panels
in MSFC Hot Gas Facility
[NASA-CR-170889] 24 p4072 N85-35237
RECHARGING
Sixth DOE Electrochemical Contractor's Review.
Extended abstracts
[DE84-013679] 16 p2779 N85-27151
Geosynchronous performance of a lithium-titanium
disulfide battery 20 p3444 N85-31377
Deep reconditioning of batteries during DSCS 3 flight
operations 20 p3446 N85-31397
RECIPROCATING ENGINES
U PISTON ENGINES
RECIPROCATION
Reciprocating magnetic refrigerator employing tandem
porous matrices within a reciprocating displacer
[NASA-CASE-NPO-16257-1] 18 p3065 N85-29082
RECIPROCITY THEOREM
FLACS: A new sensitometer for measurement of
extreme low intensity reciprocity in a controlled
environment — X-ray films 07 p0963 N85-16104
RECIRCULATION
U CIRCULATION
RECIRCULATIVE FLUID FLOW
Characteristics of a turbulent plane offset jet
02 p0196 N85-11310
Momentum and heat transfers in a complex, but
well-defined turbulent fluid flow
[DE85-002857] 10 p1486 N85-19361
An experimental investigation of confined, multiple,
turbulent jet mixing with recirculation — flow distribution
in combustors with injection plates
15 p2555 N85-25764
Confined turbulent swirling recirculating flow
predictions
[NASA-CR-174917] 16 p2709 N85-26716
An experimental investigation of confined, multiple,
turbulent jet mixing with recirculation
20 p3451 N85-31426
A multilevel-multigrid method for recirculating flows
21 p3583 N85-32271
Modeling of turbulent recirculating combusting flows
22 p3745 N85-33212
RECLAMATION
NT GAS RECOVERY
NT MATERIALS RECOVERY
NT NUCLEAR FUEL REPROCESSING
NT WATER RECLAMATION
Proceedings of the Environmental Systems Symposium
(13th) held at Bethesda, Md., 20-22 March 1984
[AD-A148194] 09 p1346 N85-18471

Remedial action of hazardous waste US Army Corps of Engineers, Anniston, Alabama
[AD-P004141] 09 p1347 N85-18477

Practical application of earth resistivity methods in phase 2 of the installation restoration program
[AD-P004148] 09 p1348 N85-18484

Community relations activities at Department of Defense sites
[AD-P004150] 09 p1349 N85-18486

Protocol for aquifer cleanup decision making at military installations
[AD-P004151] 09 p1349 N85-18487

Technology for industrial waste heat recovery by organic Rankine cycle systems
[DE85-006719] 18 p3102 N85-29206

Orphans of the Valley: Abandoned surface mines in the Tennessee Valley. Volume 2: Maps
[DE85-901249] 19 p3301 N85-30465

RECOGNITION
NT CHARACTER RECOGNITION
NT PATTERN RECOGNITION
NT SPEECH RECOGNITION
NT TARGET RECOGNITION
NT TIMBER IDENTIFICATION

Eyelid motion sequences predictive of decision errors
[AD-A145702] 02 p0235 N85-11531

Modeling holographic recognition system by using number-theory convolution transformation
02 p0272 N85-11774

The effect of set size on color recognition
[AD-A150958] 14 p2391 N85-24726

RECOIL IONS

Dynamics and mechanisms of catalytic processes and hot chemistry
[DE85-002899] 09 p1292 N85-18114

RECOMBINATION COEFFICIENT

Ionic reactions of atmospheric importance
[AD-A147354] 07 p0997 N85-16333

Photoconductive pulse power switches: A review
[DE85-014125] 24 p4091 N85-35360

RECOMBINATION REACTIONS
NT ATOMIC RECOMBINATION
NT ELECTRON RECOMBINATION
NT ELECTRON-ION RECOMBINATION
NT HYDROGEN RECOMBINATIONS
NT ION RECOMBINATION
NT OXYGEN RECOMBINATION
NT RADIATIVE RECOMBINATION

Novel transport and recombination processes in semiconductors
[AD-A145969] 03 p0433 N85-12757

Estimate of nuclear-pumped X-ray laser mechanism
06 p0748 N85-14795

Barriers to achieving high efficiency
06 p0829 N85-15264

Study in molecular lasers
[AD-A148246] 08 p1166 N85-17357

Effect of inner subshell ionization for emission lines of OIV ion 09 p1388 N85-18729

Radiation effects in Straind-Layer Superlattice (SLS) structures
[DE85-001713] 09 p1398 N85-18799

Surface and allied studies in silicon solar cells
[NASA-CR-175468] 10 p1508 N85-19516

Development of high efficiency solar cells on silicon web
[NASA-CR-174435] 10 p1509 N85-19521

Electron production, electron attachment, and charge recombination process in high pressure gas discharges
[AD-A149535] 10 p1554 N85-19799

Surface and allied studies in silicon solar cells
[NASA-CR-174447] 11 p1671 N85-20531

Heavy doping effects in high efficiency silicon solar cells
[NASA-CR-175779] 16 p2818 N85-27383

Role and fate of ozone in the atmosphere
16 p2824 N85-27421

Experimental approaches to the measurement of dielectronic recombination
[DE85-006927] 17 p3030 N85-28743

Carrier loss in dispersive transport in amorphous semiconductors
[DE85-009122] 18 p3194 N85-29811

Recombination phenomena in high efficiency silicon solar cells 20 p3479 N85-31618

High efficiency solar cell processing
20 p3482 N85-31640

Measuring bulk recombination rates and boundary recombination velocities 21 p3609 N85-32419

Silicon surface passivation by silicon nitride deposition
21 p3610 N85-32423

Inter-zone auger recombination in GaSb laser structures 21 p3662 N85-32875

RECOMMENDATIONS

Fire protection review revisit no. 2, Argonne National Laboratory, Argonne, Illinois
[DE85-013245] 22 p3755 N85-33276

Current internal-dosimetry practices at US Department of Energy facilities
[DE85-011718] 22 p3787 N85-33486

Recommendations for content revision and alternate delivery modes for the Human Engineering Guide to Equipment Design (HEGED)
[AD-A155781] 24 p4134 N85-35624

RECOMPRESSION
U COMPRESSING

RECONNAISSANCE
NT AERIAL RECONNAISSANCE
NT PHOTORECONNAISSANCE
NT SPECTRAL RECONNAISSANCE

Satellite reconnaissance
[AD-B085034] 01 p0015 N85-10094

Marine helicopter missions 06 p0751 N85-14811

Modern signal processing and reconnaissance — conferences
[FOA-C-30374-E1] 07 p0942 N85-15975

Geothermal assessment of part of the east shore area, Davis and Weber Counties, Utah
[DE84-016817] 09 p1342 N85-18446

RECONNAISSANCE AIRCRAFT
NT MIRAGE AIRCRAFT
NT MIRAGE 3 AIRCRAFT
NT U-2 AIRCRAFT

Airworthiness and flight characteristics test of the RC-12D Guardrail V
[AD-A148046] 08 p1084 N85-16864

Electronic reconnaissance aircraft of the Soviet Union Navy
[AD-A154706] 21 p3551 N85-32091

RECONNAISSANCE SPACECRAFT

A method for determining mesoscale dynamic topography
[AD-D011412] 08 p1191 N85-17506

Target observability for satellite-based sensors
[AD-A156139] 24 p4069 N85-35217

RECONSTRUCTION
NT WAVE FRONT RECONSTRUCTION

Tomographic reconstruction of axially symmetric objects from a single radiograph
[DE84-016783] 04 p0565 N85-13599

Surface reconstruction preserving discontinuities
[AD-A146741] 07 p1026 N85-16526

Flux reconstruction and calibration
09 p1412 N85-18904

Reconstruction of past atmospheric CO/sub 2/ contents from the chemistry of the contemporary ocean: An evaluation
[DE85-006426] 18 p3133 N85-29401

RECORDERS

A limbus-sensing eye movement recorder
[AD-A144772] 01 p0049 N85-10323

RECORDING
NT DATA RECORDING
NT DATA SMOOTHING
NT MAGNETIC RECORDING
NT PHOTOGRAPHIC RECORDING

Low altitude high speed flight simulation using video disc technology
[AD-P004312] 09 p1268 N85-17986

Device for controlling operation of lithicon cathode-ray memory tube 12 p1839 N85-21542

Three-dimensional ballistocardiography in microgravity
20 p3510 N85-31818

Development of wide band recording materials
[AD-A154961] 21 p3589 N85-32309

Design of a freestanding noise measurement and recording system to predict the intensity and location of electromagnetic radiation from earthquakes
[AD-A155070] 21 p3632 N85-32563

RECORDING INSTRUMENTS
NT BATHYTHERMOGRAPHS
NT FLIGHT LOAD RECORDERS
NT OSCILLOGRAPHS
NT PLOTTERS
NT SEISMOGRAPHS
NT WEATHER DATA RECORDERS

Single viewpoint self calibration: A contribution to field calibration of recording chambers
[SER-C-269] 01 p0049 N85-10320

Acoustic scaling: The development of improved instrumentation
[BBC-RD-1985/7] 24 p4145 N85-35694

RECORDS
NT VIDEO DISKS

Primer on the registration of technical information in industry 03 p0436 N85-12786

Chronology of KSC and KSC related events for 1983
[NASA-TM-87435] 12 p1963 N85-22339

Records Disposal: A guidebook for laboratory offic
[AD-A156064] 24 p4165 N85-3

RECOVERABLE LAUNCH VEHICLES

Winged first stages of space transport appliance
[TUM-RT-TB-84/3] 02 p0167 N85-111

RECOVERABLE SPACECRAFT
NT APOLLO SPACECRAFT
NT CHALLENGER (ORBITER)
NT COLUMBIA (ORBITER)
NT DISCOVERY (ORBITER)
NT ENTERPRISE (ORBITER)
NT REUSABLE SPACECRAFT
NT SPACE SHUTTLES

RECOVERY

Calibration loading of a strain-gauged diverse helicopter weapon recovery system
[AD-A151486] 15 p2471 N85-252

RECOVERY PARACHUTES

Structural and mechanical design challenges of space shuttle solid rocket boosters separation and recovery subsystems 08 p1095 N85-1691

B-52B/DTV (Drop Test Vehicle) flight test results: Drop test missions
[NASA-CR-171530] 19 p3215 N85-2993

RECOVERY VEHICLES

Calibration loading of a strain-gauged diverse helicopter weapon recovery system
[AD-A151486] 15 p2471 N85-252

RECREATION

Combinations of remote sensing data with a digital map data base — regional planning 05 p0660 N85-1424

RECRYSTALLIZATION

Fundamental studies of structure property relationship in transformation toughened ceramics
[DE84-015344] 01 p0033 N85-1020

Time resolved calorimetry of 30 nm Te-films during laser annealing
[AD-A145047] 01 p0052 N85-1034

Electrolytic lapping technique for vanadium
[DE84-014710] 02 p0183 N85-1122

Structural recrystallization in titanium
03 p0351 N85-1225

Material problems for high-temperature, high-power space energy-conversion systems
[AD-A145940] 03 p0365 N85-1246

Amorphous materials and recrystallization
[DE85-001873] 09 p1336 N85-1800

Si-on-insulator formation using a line-source electron beam
[DE85-003449] 11 p1737 N85-2082

Enhanced diffusion from interstitial trapping during solid-phase-epitaxial growth of silicon alloys
[DE85-001265] 12 p1941 N85-2218

Dynamics of recrystallization and redistribution of impurities in semiconductors subjected to millisecond laser pulses 15 p2643 N85-2630

Thin films properties of sputtered niobium silicide on SiO2, Si3N4 and on n+ poly-Si
[AD-A152378] 17 p2952 N85-2822

Influence of recrystallization and solution on the tenacity of the 7010 and 7475 alloys. Olygocyclic fatigue of the 7010 alloy
[ONERA-RT-19/5069-M] 20 p3432 N85-312

System for electro-optical ceramic recrystallization
21 p3662 N85-3287

Crystallization of Polyetheretherketone (PEEK) in carbon fiber composites
[AD-A156316] 24 p4075 N85-352

RECTANGLES

An experimental investigation of an underexpanded rectangular jet ejector
[AD-A149656] 12 p1779 N85-2117

Theoretical prediction of stationary positions in the rectangular chamber during asymmetric electroosmotic flow 20 p3499 N85-3175

Acoustical absorption coefficient in a diffuse field of a plane, rectangular material of finite dimensions placed on an infinite perfectly reflecting surface
[NRC/CNR-TT-2113] 23 p3966 N85-345

RECTANGULAR BEAMS

Quantification of Saint-Venant's principle for a general prismatic member 04 p0467 N85-1297

Improved beam theory for anisotropic materials
04 p0468 N85-1297

Basic studies of multiple free and confined jets
[AD-A149556] 10 p1485 N85-1937

RECTANGULAR COORDINATES
U CARTESIAN COORDINATES

RECTANGULAR DRAINAGE
U DRAINAGE PATTERNS

RECTANGULAR PANELS

Nonlinear dynamic analysis of sandwich panels
01 p0080 N85-102

Noise transmission loss of a rectangular plate in an infinite baffle
[NASA-TP-2398] 12 p1927 N85-221

CTANGULAR PLANFORMS
T RECTANGULAR PANELS
T RECTANGULAR PLATES
T RECTANGULAR WINGS
Aerodynamic improvements by discrete wing tip jets
AD-A148981] 10 p1421 N85-18964
Basic studies of multiple free and confined jets
AD-A148556] 10 p1485 N85-19374
An investigation of compressible flows over open cavities including shear layer thickness effects
[AD-A150066] 12 p1847 N85-21588
CTANGULAR PLATES
Bulletin of the Faculty of Engineering, Hokkaido University, no. 123
[ISSN-0385-602-X] 04 p0482 N85-13075
Analysis based on Reissner theory for rectangular plates with all edges built-in 04 p0483 N85-13081
A buckling analysis for rectangular orthotropic plates with centrally located cutouts
[NASA-TM-86263] 04 p0513 N85-13268
Biaxial buckling of specially orthotropic, symmetric composite rectangular plates
[AD-A152958] 17 p2979 N85-28417
ECTANGULAR WAVEGUIDES
Multielement bend discontinuities in oversize rectangular waveguides
[PR-200] 03 p0354 N85-12275
Design and construction of a mode converter from rectangular TE 10 to circular TE 11
[REPT-84-158] 05 p0633 N85-14064
Scattering of H10-mode wave by narrow conducting plate inside rectangular waveguide
06 p0788 N85-15036
Magnetostatic-wave propagation in a finite YIG-Loaded rectangular waveguide
[AD-A150332] 13 p2055 N85-22865
Calculation of the propagation constant in a rectangular waveguide containing an inhomogeneous longitudinally magnetized plasma
[DE85-012072] 21 p3577 N85-32250
ECTANGULAR WINGS
On the flow processes in sharply inclined and stalled airfoils in parallel movement and rotation
[NASA-TM-77509] 10 p1419 N85-18952
Transonic pressure distributions on a two-dimensional 0012 and supercritical MBB-A3 profile oscillating in heave and pitch 15 p2457 N85-25173
Gust load alleviation of a cantilevered rectangular elastic wing. Wind tunnel experiment and analysis
[NAK-TR-88] 18 p3063 N85-28950
RECTENNAS
Technology for satellite power conversion
[NASA-CR-174335] 09 p1343 N85-18451
RECTIFICATION
NT GEOMETRIC RECTIFICATION (IMAGERY)
RECTIFIER ANTENNAS
U RECTENNAS
RECTIFIERS
NT AVALANCHE DIODES
NT GERMANIUM DIODES
NT SILICON CONTROLLED RECTIFIERS
NT THYRATRONS
NT THYRISTORS
Planar doped barrier semiconductor device
[AD-D011591] 20 p3537 N85-32010
T/R switch design for short-range measurements, part 8.1A 21 p3624 N85-32515
RECTUM
Weight loss, rectal temperature and heart rates following the 1984 Boston Marathon
[AD-A155984] 24 p4132 N85-35612
RECUPERATORS
U REGENERATORS
RECURSION FORMULAS
U RECURSIVE FUNCTIONS
RECURSIVE FUNCTIONS
Recursive algorithms for adaptive arrays based on estimates
[REPT-5-84] 01 p0107 N85-10718
Nonlinear regression with emphasis on spline methods
[AD-A146192] 03 p0412 N85-12633
A study of the recursion yn+1=yn+tau yn sup m
[CWI-NM-R8403] 05 p0723 N85-14848
Derivation of recursive digital filters by the step-invariant and the ramp-invariant transformations
[AD-A148500] 06 p0857 N85-15452
A note on using the integrated form of ARIMA forecasts
[AD-A146965] 07 p1030 N85-16536
Recursive moment formulas for regenerative simulation
[AD-A150112] 12 p1922 N85-22070
A general simulation program for robot manipulator arm dynamics
[AD-A152121] 16 p2793 N85-27230
Applied Kalman filtering: An overview
17 p2965 N85-28313
Kalman filter modeling 18 p3107 N85-29237
Determinal representations of polynomials satisfying linear Ordinary Differential Equations (ODEs) or linear recurrence relations
[PREPRINT-417] 18 p3172 N85-29660
An introductory view of Raman-Nath type equations
[PREPRINT-422] 18 p3172 N85-29664
The Hamiltonian structure of a complex version of the Burgers hierarchy
[PREPRINT-423] 18 p3173 N85-29665
Exact invariants in resonance form for time-dependent potentials
[DE85-010733] 19 p3346 N85-30739
Fast moving average recursive least mean square fit
[DE85-010036] 19 p3348 N85-30752
Recursive nonlinear filtering through complete linearization
[AD-A155029] 21 p3677 N85-32844
Reliability prediction of the series system with spares subject to Weibull failure 24 p4100 N85-35413
Recursive partitioning estimation
24 p4141 N85-35670
RECYCLING
COST 50 - materials for gas turbines, part 1 and 2 3UK9
[NPL-DMA(A)-74] 05 p0617 N85-13943
The microstructural characteristics of revert superalloys — for turbine blades
05 p0617 N85-13945
Adaptation of remelting procedures for the use of recycled metal in nickel-base superalloy castings
[PNR-90232] 09 p1297 N85-18149
Treatment of wastewater (red water) resulting from TNT (trinitrotoluene) purification
[AD-P004146] 09 p1348 N85-18482
Control of surface composition and hydrogen recycling by plasma conditioning
[DE85-001859] 11 p1731 N85-20889
Exploration of new methods to produce efficient sources of coherent near millimeter wave radiation
[AD-A150094] 12 p1829 N85-21481
Hydrolysis of plastic wastes with the aim of recovering and reprocessing the starting components (recycling)
[BMFT-FB-T-84-250] 12 p1865 N85-21826
The controlled ecological life support system
15 p2688 N85-26603
Recycling agent selection and tentative specification
[AD-A153529] 18 p3070 N85-28988
Current concepts and future directions of CELSS
18 p3155 N85-29532
Survey of CELSS concepts and preliminary research in Japan 18 p3155 N85-29533
Development of processes for the inclusion of radioactive waste in glass-metal compounds and ceramic materials
[BLL-CE-TRANS-8014-(9022.09)]
20 p3526 N85-31931
Neutral pumping rates for a next step tokamak ignition device
[DE85-012780] 24 p4157 N85-35776
RED BLOOD CELLS
U ERYTHROCYTES
RED DWARF STARS
Solar flares and laboratory experiments on magnetic reconnection in current sheaths
02 p0162 N85-11099
Einstein solid state spectrometer observation of the peculiar red dwarf Wolf 630 AB
[NASA-TM-83947] 03 p0447 N85-12843
Evidence for a solar companion star
[DE85-002069] 10 p1571 N85-19907
RED GIANT STARS
NT CARBON STARS
Balloon observations 01 p0014 N85-10086
Spectroscopic data for globular cluster giants. 1: Stars of the red giant tip 01 p0128 N85-10885
Combined ultraviolet studies of astronomical sources
[NASA-CR-174361] 09 p1413 N85-18910
Mass distribution and evolutionary scheme for central stars of planetary nebulae 11 p1751 N85-21012
Energy and Technology Review
[DE85-011767] 21 p3716 N85-33061
RED SEA
A tectonic model of an incipient spreading center and its margins: The Northern Red Sea and the Dead Sea rift 13 p2140 N85-23266
Saudi Arabian refraction profile: Crustal structure of the Red Sea-Arabian Shield transition
17 p2990 N85-28484
Saudi Arabian refraction profile: A preliminary interpretation for the Red Sea-Arabian Shield transition
17 p2991 N85-28485
A traveltime interpretation of the 1978 seismic refraction profile in the Kingdom of Saudi Arabia
17 p2991 N85-28486
Explanation of Russian models: Saudi Arabian seismic refraction profile 17 p2991 N85-28487
Interpretation of the data of USGS seismic refraction profile across the Arabian Shield in western Saudi Arabia 17 p2991 N85-28488
One-dimensional velocity-depth functions determined for the Arabian Shield and the southwestern Red Sea: A comparison of models 17 p2992 N85-28490
A comparison of crustal sections: Arabian Shield to the Red Sea 17 p2992 N85-28491
RED SHIFT
The 3a-F emulsion and the quasar redshift cut-off
07 p0964 N85-16112
The X-ray properties of high-redshift, optically selected QSOs 08 p1240 N85-17821
The UV spectra of intermediate redshift quasars
11 p1746 N85-20980
Evolution of the luminosity function of extragalactic objects
[NASA-CR-175977] 18 p3201 N85-29860
Formation of galaxies
[DE85-009537] 18 p3202 N85-29863
Color evolution in high redshift galaxies
20 p3544 N85-32055
The ultraviolet spectra of intermediate redshift quasars
20 p3544 N85-32056
Some evidence for large gravitational redshift in Seyfert galaxy NGC 4151
[OG-2.7-11] 22 p3872 N85-33984
Ultrahigh energy gamma rays: Carriers of cosmological information
[OG-2.7-14] 22 p3872 N85-33987
REDOX CELLS
Cycling performance of the iron-chromium redox energy storage system
[NASA-TM-87034] 16 p2819 N85-27387
Evaluation of developmental membranes for the mixed reactant iron-chromium redox system
[NASA-TM-87074] 23 p3944 N85-34443
Development of electrodes for the NASA iron/chromium
[NASA-CR-174724] 24 p4109 N85-35471
REDUCED GRAVITY
Second Symposium on Space Industrialization — space commercialization
[NASA-CP-2313] 02 p0149 N85-11011
Potential utilization of glass experiments in space
02 p0151 N85-11020
Preparation of large-particle-size monodisperse latexes in space: The STS-3, STS-4, and STS-7 mission results
02 p0151 N85-11021
Low-gravity solidification of cast iron and space technology applications 02 p0151 N85-11022
Producing gallium arsenide crystals in space
02 p0151 N85-11023
Microgravity containerless processing in long drop tubes 02 p0153 N85-11037
Purification of biomaterials by phase partitioning
02 p0154 N85-11043
Design and implementation of a low-gravity solidification experiment package for the F-104
02 p0156 N85-11053
Gravitational effects on premixed particle cloud flames
02 p0171 N85-11144
Transport phenomena in the boundary layer during solution solidification under microgravity. Ice growth from a water-salt solution
[BMFT-FB-W-84-031] 03 p0329 N85-12121
NBS (National Bureau of Standards): Materials measurements
[NASA-CR-174038] 03 p0332 N85-12143
Large-diameter astromast development
[NASA-CR-171201] 03 p0342 N85-12200
Intraocular fluid dynamics in microgravity
05 p0693 N85-14455
Bone structure and microgravity
05 p0694 N85-14463
Loss of bone substance in consequence of amputation as a model for the adaptation to microgravity
05 p0694 N85-14464
Caloric stimulation of the vestibular system in microgravity 05 p0695 N85-14469
Speculations on the formation of metallic meteorite phases 06 p0869 N85-15648
SPAR X technical report for experiment 76-22 directional solidification of magnetic composites
[NASA-CR-171271] 07 p0927 N85-15860
Commerce lab: Mission analysis and payload integration study
[NASA-CR-174381] 10 p1426 N85-18993
Investigation of surface tension phenomena using the KC-135 aircraft
[NASA-TM-82506] 10 p1426 N85-18995

Modular plant culture systems for life support functions
[NASA-CR-171853] 12 p1899 N85-21924

Investigation of foam flotation and phase partitioning techniques 12 p1945 N85-22216

Material research in microgravity
[NASA-TM-77626] 14 p2228 N85-23811

Thermoregulatory and vestibular systems in the rat
15 p2610 N85-26082

Microgravity: A new tool for basic and applied research in space
[EP-212] 16 p2716 N85-26767

Free-surface phenomena under low- and zero-gravity conditions
[NASA-CR-175885] 17 p2907 N85-27922

Fluid surface behavior in low gravity. Center discretionary fund no. 83-21
[NASA-TP-2486] 17 p2957 N85-28260

ESA presents plans for European manned space station 18 p3085 N85-29087

Spray applicator for spraying coatings and other fluids in space
[NASA-CASE-MSC-18852-1] 18 p3115 N85-29283

Crystallization of aluminum-based alloys in weightlessness 19 p3242 N85-30101

Concept development evaluation for John Deere/UA STS middeck experiment location
[NASA-CR-171541] 20 p3397 N85-31071

Microgravity silicon zoning investigation
[NASA-CR-171531] 20 p3397 N85-31073

On the measurement of material damping in a simulated space environment 20 p3411 N85-31169

Kidney cell electrophoresis
[NASA-CR-171869] 20 p3498 N85-31745

Kidney cell electrophoresis, continuing task
20 p3498 N85-31747

Effects of coating rectangular microscopic electrophoresis chamber with methylcellulose
20 p3498 N85-31748

Asymmetric electroosmotic flow and mobility measurements at nonstationary positions in the rectangular chamber 20 p3499 N85-31749

Evaluation of results of cell electrophoresis experiments on space shuttle STS-3 including pre-flight and post-flight laboratory experiments 20 p3502 N85-31772

Free zone electrophoresis simulation of static column electrophoresis in microgravity on shuttle flight STS-3
20 p3502 N85-31773

Microgravity electrophoresis: A study of the factors that affect free-fluid separation 20 p3502 N85-31774

Properties of electrophoretic fractions of human embryonic kidney cells separated on space shuttle flight STS-8 20 p3503 N85-31776

Evaluation of Results of Space Experiments in Physiology and Medicine and Informal Briefings by the F-16 Medical Working Group 20 p3506 N85-31806

Some results of the European vestibular experiments in the Spacelab-1 mission 20 p3508 N85-31809

Three-dimensional ballistocardiography in microgravity
20 p3510 N85-31818

Study of requirements for and method of multidimensional acoustic imaging — spaceborne experiments
[ESA-CR(P)-2020] 20 p3525 N85-31924

Research study for gel precursors as glass and ceramic starting materials for space processing applications research
[NASA-CR-176113] 22 p3751 N85-33250

NASA Developmental Biology Workshop: A summary
[NASA-TM-86756] 24 p4126 N85-35579

Effects of microgravity and hypergravity on invertebrate development 24 p4126 N85-35579

REDUCED ORDER FILTERS

Synthesis of digital nonrecursive band-elimination filters for moving-target selectors 12 p1840 N85-21545

REDUCTION

Life and reliability modeling of bevel gear reductions
[NASA-TM-87006] 16 p2780 N85-27227

REDUCTION (CHEMISTRY)

NT DEOXIDIZING
NT HYDROGENATION

Surface environmental effects in electrochemical kinetics: Outer-sphere chromium (3) reductions at mercury, gallium, lead, and thallium surfaces
[AD-A145807] 02 p0172 N85-11155

The concept of doping of conducting polymers. The role of reduction potentials
[AD-A145480] 02 p0186 N85-11243

Electrocatalysis of fuel cell reactions: Investigation of alternate electrolytes
[NASA-CR-174753] 02 p0222 N85-11455

Intramolecular electron transfer at metal surfaces. 4: Dependence of tunneling probability upon donor-acceptor separation distance
[AD-A145871] 02 p0287 N85-11876

Stability of several substituted ferrites in a reducing atmosphere
[AD-A146106] 03 p0328 N85-12112

Preparation of low-silicon vanadium metal
[DE84-014818] 04 p0476 N85-13031

Effect of water on hydrogen permeability — Stirling engines
[NASA-TM-86904] 06 p0761 N85-14864

Electrochemical behaviour of TiCl4 solutions in low melting point organic media
[BLL-OA-TRANS-3174-(6196.3)]
06 p0764 N85-14888

Electrolytic deposition of chromium from aqueous chromium solutions containing foreign anions
[BLL-MINTEK-TR-1170-(5810.5759)]
06 p0764 N85-14889

Interaction between chromium oxide and carbon
[BLL-M-36002-(5828.4)] 07 p0926 N85-15867

Kinetics of interaction between carbon and iron oxides of metallized materials in solid phase
[BLL-M-36023-(5828.4)] 07 p0926 N85-15873

Denitrification-efficiencies of alternate carbon sources
[AD-A148029] 08 p1119 N85-17050

Photoelectrochemical reduction of carbon dioxide
[PB85-129054] 11 p1596 N85-20036

Synthesis, static and reactive characterization of supported organometallics
[DE85-004295] 12 p1806 N85-21340

Polymeric electrolytes for ambient temperature lithium batteries
[DE85-001032] 12 p1835 N85-21518

Americium metal preparation on the multigram scale
[DE85-003735] 13 p2024 N85-22683

Temperature, velocity, and species mapping in an induction plasma
[DE85-004005] 15 p2512 N85-25499

Bifunctional oxygen electrodes
[DE85-006871] 17 p2955 N85-28248

Super hydrides
[AD-A153499] 18 p3070 N85-28986

Plutonium metal preparation and purification at Los Alamos, 1984
[DE85-010732] 19 p3239 N85-30085

Carbon reduction of mixtures of MnO(2) and Fe(2)O(3)
[BLL-M-36260-(5828.4)] 20 p3422 N85-31241

Electrochemical reduction of titanium in dimethyl sulphoxide
[BLL-OA-TRANS-3225-(6196.300)]
20 p3429 N85-31267

An analysis of the feasibility of producing silicon for solar cells by a dichlorosilane/fluidized-bed reactor process
[NASA-CR-176036] 20 p3478 N85-31614

Possible roles of manganese redox chemistry in the sulfur cycle 21 p3659 N85-32731

Phototrophic bacteria and their role in the biogeochemical sulfur cycle 21 p3660 N85-32735

Sulfur reduction in sediments of marine and evaporite environments 21 p3661 N85-32742

Cyanobacterial mats: Microanalysis of community metabolism 21 p3661 N85-32743

Microanalysis of dissolved iron and phosphate in pore waters of hypersaline sediment
21 p3661 N85-32744

Electron photoejection in carbanions
[DE85-011748] 23 p3912 N85-34237

Method for preparing high purity vanadium
[DE85-006412] 23 p3913 N85-34242

REDUCTION (MATHEMATICS)

U OPTIMIZATION

REDUNDANCY

Image signals encoding techniques oriented towards the reduction of perceptive redundance
[FUB-23-1983] 01 p0040 N85-10256

A human visual system investigation applicable to image contour coding
[FUB-36-1983] 01 p0096 N85-10640

Optimization of movements of manipulators with kinematic redundancy 04 p0488 N85-13112

Performance enhancements under dual-task conditions 05 p0707 N85-14537

Optimal query processing in distributed data base management systems with data redundancy
05 p0734 N85-14722

Analytical redundancy management mechanization and flight data analysis for the F-8 digital fly-by-wire aircraft flight control sensors
[NASA-CR-170396] 06 p0757 N85-14844

Evolution of shuttle avionics redundancy management/fault tolerance 08 p1090 N85-16890

Shuttle avionics software development trials: Tribulations and successes, the backup flight system
08 p1091 N85-16892

SSME digital control design characteristics
08 p1091 N85-16893

Voice data processing in packet switching modes
[FUB-44-1983] 09 p1312 N85-18248

Analytically redundant output feedback scheme for reduction of structural loads of a flexible transport aircraft
[TT-8303] 12 p1777 N85-21154

Low thrust bipropellant engine/redundant seat valve assembly
[AD-A150293] 13 p2013 N85-22

A theoretical basis for the analysis of redundant software subject to coincident errors
[NASA-TM-86369] 13 p2145 N85-23317

The kinematic control of redundant manipulators
15 p2566 N85-25

Some flight test results with redundant digital flight control systems 16 p2712 N85-26

A modular dissimilar redundant computer designed for high integrity control 16 p2714 N85-26781

A modular dissimilar redundant computer designed for high integrity control 17 p2904 N85-2790

Synchronization and fault-masking in redundant real-time systems
[NASA-TM-87478] 17 p3015 N85-2864

Replication methods for abstract data types
[AD-A153646] 18 p3162 N85-2953

Hexagonal uniformly redundant arrays for coded-aperture imaging
[OG-9.2-1] 21 p3714 N85-330

Intelligent redundant actuation system requirements and preliminary system design
[NASA-CR-177366] 23 p3896 N85-3413

Hexagonal uniformly redundant arrays for coded-aperture imaging
[OG-9.2-1] 23 p4024 N85-348

REDUNDANCY ENCODING

Redundancy of codes for detection and correction of unidirectional errors 12 p1642 N85-2155

Adaptation of bit error rate by coding — spacecraft transmissions
[ESA-CR(P)-1970] 15 p2545 N85-25711

REDUNDANT COMPONENTS

Synchronization and fault-masking in redundant real-time systems
[NASA-TM-87478] 17 p3015 N85-2864

Intelligent redundant actuation system requirements and preliminary system design
[NASA-CR-177366] 23 p3896 N85-3413

REDUNDANT STRUCTURES

U REDUNDANT COMPONENTS

REEFS

Diagenesis of niagaran (middle silurian) pinnacle reefs, northwest Michigan 09 p1352 N85-1850

Organogenic structures (submerged reefs) in Sitheran limestone of west Bengal basin
10 p1500 N85-194

REENTRY

NT HYPERSONIC REENTRY
NT SPACECRAFT REENTRY
NT UNCONTROLLED REENTRY (SPACECRAFT)

Terminal control of gliding in atmosphere
06 p0777 N85-14

Use of ground radar to detect reentering debris
12 p1784 N85-212

REENTRY BODIES

U REENTRY VEHICLES

REENTRY EFFECTS

Orbiter entry aerothermodynamics
08 p1104 N85-16

Correlation of predicted and measured sonic boom characteristics from the reentry of STS-1 orbiter
[NASA-TP-2475] 16 p3177 N85-28

REENTRY GLIDERS

U LIFTING REENTRY VEHICLES

REENTRY GUIDANCE

Terminal control of gliding in atmosphere
06 p0777 N85-14

Descent guidance and mission planning for space shuttle 08 p1092 N85-16

Space shuttle handling qualities
08 p1092 N85-16

REENTRY SHIELDING

Thermal design of the space shuttle external tank
08 p1103 N85-16

REENTRY TRAJECTORIES

Natural atmospheric reentry — satellite orbit decay
05 p0600 N85-13

REENTRY VEHICLES

NT APOLLO SPACECRAFT
NT CHALLENGER (ORBITER)
NT COLUMBIA (ORBITER)
NT DISCOVERY (ORBITER)
NT ENTERPRISE (ORBITER)
NT LIFTING REENTRY VEHICLES
NT REUSABLE SPACECRAFT

Numerical analysis of the 3-dimensional hypersonic flow around capsule-type bodies by alternate directional implicit method
[NAL-TR-799] 01 p0002 N85-1

Minimax optimal control in the reentry of a space glider 02 p0167 N85-11124

Navier-Stokes solution of 3-dimensional hypersonic afterbody flowfields over capsule-type vehicles
[NAL-TR-819] 03 p0311 N85-12010

Terminal control of gliding in atmosphere
06 p0777 N85-14866

Evaluation of inviscid/boundary layer and parabolized Navier-Stokes solutions for design of reentry vehicles
[DE84-014329] 10 p1428 N85-19006

One method of solving the problem of unsteady heat exchange of a body and its ablation
22 p3733 N85-33146

Thermal protection systems for reentry vehicles
[CNES-NT-113] 23 p3900 N85-34157

REFERENCE ATMOSPHERES

Model of atmospheric ozone for middle latitudes
02 p0161 N85-11091

Experience with proposed improvements of the International Reference Ionosphere (IRI)
[PB84-235670] 05 p0678 N85-14353

Processing methods of rawinsonde measurements at the descent by parachute
[KNMI-WR-84-7] 18 p3149 N85-29498

REFERENCE STARS

Desired characteristics of catalogs for cometary astrometry 14 p2436 N85-25030

Obtaining accurate comet positions despite some inaccurate catalog stars 14 p2437 N85-25032

One aspect of determination of direction of space survey base from photographs of planetary surface and star sky
15 p2487 N85-25352

REFERENCE SYSTEMS

Geology and geomorphology of the southern central Blue Ridge: An indexed bibliography
[PB84-225119] 01 p0072 N85-10480

Catalogue of earthquakes for the territory of Czechoslovakia for the period 1957 - 1980
[REPT-555] 03 p0376 N85-12396

Use and value of a geodetic reference system
[PB84-216167] 03 p0379 N85-12418

REFERENCES (STANDARDS)

U STANDARDS

REFILLING

Propellant tank resupply system
[AD-D011268] 05 p0603 N85-13848

REFINING

NT ELECTROSLAG REFINING

Preparation of low-silicon vanadium metal
[DE84-014816] 04 p0476 N85-13031

Distribution of oxygen between metal and basic slags
[BLL-M-35932-(5828.4)] 05 p0616 N85-13935

Grain refining and microstructural modification during solidification
[AD-A147705] 08 p1126 N85-17111

Improved silicon grinding method and apperatus
[NASA-CASE-NPO-16336-1-CU]
12 p1819 N85-21407

Materials refining for solar cell silicon
12 p1877 N85-21775

Lead shorage hastens need for improved storage batteries 15 p2461 N85-25195

Jet fuel property changes and their effect on producibility and cost in the U.S., Canada, and Europe
[NASA-CR-174840] 16 p2757 N85-27012

Experimental studies of glass refining
[NASA-CR-176130] 22 p3751 N85-33248

REFLECTANCE

NT SPECTRAL REFLECTANCE

Biophysical and spectral modeling for crop identification and assessment
[E85-10006] 02 p0215 N85-11419

A sphere-scanning radiometer for rapid directional measurements of sky and ground radiance: The PARABOLA field instrument
[NASA-TM-86171] 03 p0363 N85-12329

Anglo-German millimeter wave backscatter measurements on snow, environmental data report
[REPT-7-84] 04 p0492 N85-13136

Improvement of the accuracy of reflection factor measurements by a computer 05 p0629 N85-14033

Transformation of energy spread of laser pumping via phase conjugation 05 p0725 N85-14661

Nitriding of titanium and its alloys by N2, NH3 or mixtures of N2 + H2 in a dc arc plasma at low pressures (or = to torr)
[NASA-TM-83803] 06 p0814 N85-15166

Asteroid-meteorite connection: Regolith effects implied by lunar reflectance spectra 06 p0888 N85-15640

Reflection theorems for some anisotropic media
07 p0953 N85-16036

Determination of parameters of doped thin semiconductor layers from plasmatic minimum of reflection coefficient for infrared radiation
07 p0954 N85-16047

Changes in spectral properties of detached leaves
[E85-10042] 07 p0983 N85-16243

The extension of an invertible coniferous forest canopy reflectance model using SIR-B and LANDSAT data
08 p1149 N85-17246

Optical frequency domain reflectometry
08 p1222 N85-17695

Reflectivity measurements of laser gyro mirrors
[ESA-TT-851] 09 p1366 N85-18714

Laser rupture of composite materials
10 p1444 N85-19102

Influence of Bragg reflecting lattice groove depth modulation on Rayleigh wave reflection coefficient
10 p1499 N85-19458

Preliminary evaluation of the airborne imaging spectrometer for vegetation analysis
[NASA-CR-174440] 10 p1505 N85-19496

Nonlinear saturation of stimulated Raman scattering in homogeneous plasma
[DE85-003120] 10 p1560 N85-19837

Radiometric calibration and processing procedure for reflective bands on LANDSAT-4 protoflight Thematic Mapper 11 p1668 N85-20510

Wide-angle flat field telescope
[NASA-CASE-GSC-12825-1] 11 p1728 N85-20868

The Jovian Stratosphere in the ultraviolet
11 p1760 N85-21069

LSS 2018: A double-lined spectroscopic binary central star with an extremely large reflection effect
[NASA-CR-175503] 11 p1762 N85-21082

In-progress absolute radiometric inflight calibration of the LANDSAT-4 sensors — New Mexico
12 p1870 N85-21733

Investigations of vegetation and soils information contained in LANDSAT Thematic Mapper and Multispectral Scanner data
[E85-10082] 12 p1873 N85-21747

Atlas of relectance patterns for uniform earth and cloud surfaces (NIMBUS-7ERB-61 days)
[PB85-116362] 12 p1891 N85-21870

A study of low-level laser retinal damage
[AD-A150046] 12 p1905 N85-21965

Correctness of reflection characteristics of radio absorbent materials 13 p2061 N85-22995

Zero-crossings on lines of curvature
[AD-A150171] 13 p2150 N85-23345

Time-resolved reflectivity measurement of extrinsic silicon during pulsed laser irradiation
[AD-A150350] 13 p2159 N85-23403

Surface units on Venus derived from Pioneer-Venus altimetry, roughness, and reflectivity measurements
13 p2177 N85-23510

Unsupervised classification of global radar units on Venus 13 p2198 N85-23632

Scheme for measuring specular reflection coefficient at 10.6 microns wavelength with zigzag-path cell and integrating sphere 14 p2275 N85-24097

Quantitative roughness analysis of treated surfaces with higher-class finish by methods of X-ray reflectometry
14 p2282 N85-24136

Determining characteristics of optical radiation reflectors based on results of remote sensing
15 p2488 N85-25358

Measured performance of a broadband matching section for peripherally fed helical antennas
[R-NIAS-25] 15 p2539 N85-25670

Stimulated Brillouin scattering reflectivity in the presence of various aberrators
[AD-A151750] 15 p2563 N85-25812

Radar turbulence estimates. Effects of wind shear and reflectivity factor gradients
[AD-A151876] 15 p2599 N85-26023

Experimental and theoretical study of the infrared reflectance of thin oxide films on metals
[DE85-005799] 15 p2653 N85-26366

Mars: Seasonally variable radar reflectivity
15 p2683 N85-26570

Heliocentric sail problem with variable gravity field reduction 16 p2724 N85-26816

Effects of temperature on remotely sensed mafic mineral absorption features 16 p2809 N85-27323

Technique for measuring the effective source reflection coefficient of 2-resistor power splitters
[DE85-009964] 17 p2956 N85-28256

Light scattering by leaf layers with application to canopy reflectance modeling: The Scattering by Arbitrarily Inclined Leaves (SAIL) model
[NLR-MP-84011-U] 17 p3036 N85-28796

Diffusely reflecting paints including polytetrafluoroethylene and method of manufacture
[NASA-CASE-GSC-12863-1] 18 p3079 N85-29044

Novel analytical approaches to coal beneficiation
[DE85-010437] 19 p3229 N85-30021

Seperation of Drude and band-to-band spectra in polyvalent metals
[DE85-010247] 19 p3240 N85-30093

Spectral reflectances of natural targets for use in remote sensing studies
[NASA-RP-1139] 19 p3299 N85-30450

Preliminary investigations concerning a 90 GHz radiometer satellite experiment
[ESA-TT-860] 20 p3420 N85-31225

Usefulness of multifrequency MST radar measurements, part 2.6B 21 p3619 N85-32487

Thunderstorm phenomena and weather radar scanning strategies
[DOT/FAA/PM-85/14] 21 p3634 N85-32573

A random layer model for reflection from ocean bottom sediments
[AD-A155019] 21 p3700 N85-32988

Enhancing precision of remote temperature sensing data from satellites under cloudy atmospheric conditions
22 p3734 N85-33148

Fiber optic moisture sensor
[DE85-011651] 22 p3787 N85-33462

Empirical model for the Earth's cosmic ray shadow at 400 KM: Prohibited cosmic ray access
[SH-6.1-14] 23 p4046 N85-35087

REFLECTED RADIATION

U REFLECTED WAVES

REFLECTED RAYS

U REFLECTED WAVES

REFLECTED WAVES

Distortions of radio pulse during reflection from maximum region of ionospheric layer 06 p0792 N85-15061

Mathematical modeling of wave fields by superimposition of boundary waves in reflected earthquake waves method 10 p1501 N85-19476

Intensity fluctuations of focused laser beam during reflection in turbulent atmosphere
13 p2078 N85-22975

Reflected wave travel-time curves in stratified media with vertically heterogeneous layers and slightly sloping curved boundaries 13 p2114 N85-23167

Correcting depth line on nonlongitudinal seismic profile 13 p2117 N85-23184

Geological information content of reflected wave record form 14 p2345 N85-24502

Possibility of retrieving dynamics of reflected wave method records beneath low-velocity zone
14 p2346 N85-24503

Mean intensity of wave reflected by wavefront reversing mirror in turbulent medium 22 p3762 N85-33432

REFLECTING TELESCOPES

Observations of four Beta Cephei stars in NGC6231
01 p0126 N85-10677

Error in compensating phase fluctuations of wave field by means of adaptive reflectors with continuous or compound surface 13 p2080 N85-22989

Precision antenna reflector structures
14 p2232 N85-23834

The astrometry programme at Mt. John Observatory
14 p2436 N85-25026

Activities report of the Institute of Astronomy
20 p3545 N85-32059

REFLECTION

NT INFRARED REFLECTION
NT MACH REFLECTION
NT OPTICAL REFLECTION
NT RETROREFLECTION
NT SIGNAL REFLECTION
NT SPECULAR REFLECTION
NT WAVE REFLECTION

Bragg reflection of surface electroacoustic shear waves 04 p0485 N85-13096

Reflection of volume waves in multilayer structures
04 p0485 N85-13097

Coupling of multidirectional diffusions by reflection
[CTH-MATH-1984-20] 05 p0719 N85-14613

Radar echo enhancement using surface reflections
[AD-A146970] 07 p0939 N85-15955

Filter reflection image guide oscillator and solid state line scanning device
[AD-D011440] 10 p1479 N85-19336

Measurement of the configuration of a concave surface by the interference of reflected light
[NASA-TM-77796] 11 p1726 N85-20867

Influence of individual reflections on the precision of parameter estimates in least squares refinement
[DE85-000830] 11 p1735 N85-20909

Effect of ultraviolet radiation on transparent polymer films as determined using in situ FTIR-RA spectroscopy. Volume 1: Photodegradation of transparent polymer films
[DE84-013039] 12 p1814 N85-21377

Near-field effects on radome boresight errors
[AD-P004356] 12 p1825 N85-21450

Image lobe analysis for large radomes
[AD-P004359] 12 p1825 N85-21453

Wide angle phased array dome lens antenna with a reflection/transmission switch
[AD-D011562] 12 p1833 N85-21502

Analysis and computations of microwave-atmospheric interactions
[AD-A149666] 12 p1869 N85-21854
Calculation of ionospheric profiles by inverting VLF/LF reflection data. 2. Anisotropic propagation
[AD-A150105] 12 p1890 N85-21859
Multiple reflection theory for microwave measurement of solid propellant burning rates
13 p2002 N85-22549
Using color to separate reflection components
[AD-A150969] 14 p2405 N85-24826
Characterization of thin films and layered structures using X-ray absorption and reflection at grazing incidence
[DE85-006660] 15 p2682 N85-26429
Use of Goudrian model in studying laws of reflection in vegetation-soil system in optical range. 2: Influence of illumination conditions on spectral brightness coefficients 16 p2726 N85-26827
Energy reflection coefficient for H+ ions at energies between 10 and 80 keV
[DE85-007547] 16 p2863 N85-27662
LIGHT: A ray tracing code to simulate light collection in scintillation spectrometers and light pipes
[DE85-007213] 16 p2865 N85-27673
Selective radiative cooling with MgO and/or LiF layers
[DE85-011595] 19 p3262 N85-30228
Lidar techniques for search and rescue
[DE85-009588] 19 p3278 N85-30327
Attenuated total reflection method for obtaining optical constants of powders
[AD-A154064] 19 p3367 N85-30861
Effect of diffusely-reflected sunlight on the orbit of LAGEOS 20 p3491 N85-31700
Propagation and reflection of a finite amplitude ultrasonic beam including harmonic content: A numeric model
20 p3523 N85-31914
Experimental method for measuring positronium reflection from surfaces
[DE85-010849] 20 p3531 N85-31967
Improved Nominal Operating Cell Temperature (NOCT) test procedure 21 p3612 N85-32449
Mirror reflection of charged particles from +amorphous and polycrystalline surfaces 21 p3680 N85-32927
Dielectric mirror with ferromagnetic substrate
21 p3686 N85-32966
Calculating solar highlight and shadeless areas for scanning photographs from space and optimizing lighting conditions 22 p3736 N85-33160
Surface wave modes of a multilayered medium backed by a perfectly conducting ground plane: Computation of propagation constants
[DE85-011454] 22 p3829 N85-33715
Ranging system which compares an object reflected component of a light beam to a reference component of the light beam
[NASA-CASE-NPO-15865-1] 23 p3973 N85-34629
Radiation measurements on magnesium flames
[BLL-CE-TRANS-8110-(9022.09)]
24 p4075 N85-35254
Literature search for new physical methods for biological aerosol detection
[AD-A155863] 24 p4126 N85-35592

REFLECTION COEFFICIENT
U REFLECTANCE

REFLECTIVITY
U REFLECTANCE

REFLECTOMETERS
NT MICROWAVE REFLECTOMETERS
Influence of geometric conditions on the indicatrix of reflection of the perfect reflecting diffuser
[PTB-OPT-16] 03 p0420 N85-12686
Fundamentals and applications of the six port measuring technique — reflectometer 05 p0830 N85-14039
A reflectometer unit for a 500 kW HF balanced screened feeder
[BBC-RD-1984/13] 10 p1477 N85-19322
Optical reflectometer for multimode fiber lightpipes
13 p2075 N85-22961
Quantitative roughness analysis of treated surfaces with higher-class finish by methods of X-ray reflectometry
14 p2282 N85-24136

REFLECTOR SATELLITES
U PASSIVE SATELLITES

REFLECTORS
NT FRESNEL REFLECTORS
NT PARABOLIC REFLECTORS
NT PARABOLOID MIRRORS
NT RADAR REFLECTORS
NT RETROREFLECTORS
NT SOLAR COLLECTORS
NT SOLAR REFLECTORS
NT WIGGLER MAGNETS
Research on large, highly accurate, inflatable reflectors
[AD-A145080] 01 p0016 N85-10099
Effect of an underlayer of cadmium telluride on the reflection-reducing properties of zinc sulfide on mercury cadmium telluride
[AD-A146195] 03 p0414 N85-12649
Development of a measuring procedure for the automatic evaluation of the flatness of reflective surfaces
[BMFT-FB-T-84-168] 03 p0421 N85-12688
Dual band, low sidelobe, high efficiency mirror antenna
[AD-D011329] 07 p0944 N85-15980
Optimization of piezoceramic optical deflector
11 p1719 N85-20613
Intensity fluctuations of focused laser beam during reflection in turbulent atmosphere
13 p2078 N85-22975
Error in compensating phase fluctuations of wave field by means of adaptive reflectors with continuous or compound surface 13 p2080 N85-22988
Innovative research in the design and operation of large telescopes for space: Aspects of giant telescopes in space
[NASA-CR-175626] 13 p2170 N85-23462
Cable-catenary large antenna concept
14 p2231 N85-23829
Precision space structures 14 p2232 N85-23833
Application of modern Aperture Integration (AI) and Geometrical Theory of Diffraction (GTD) techniques for analysis of large reflector antennas
14 p2234 N85-23851
Feed system design considerations for large space antenna systems. Part 1: Multiple apertures with non-overlapping feeds 14 p2234 N85-23852
Diffraction analysis of mesh deployable reflector antennas 14 p2235 N85-23854
Utilization of space station by the large deployment reflector 14 p2235 N85-23857
Large Deployable Reflector (LDR) requirements for space station accommodations
14 p2236 N85-23858
Angular error of position of RATAN-600 screens during radial displacement 15 p2476 N85-25286
Null generation using discs on a reflector
[AD-A151897] 15 p2544 N85-25703
Defocusing losses in a log periodic-fed reflector
[AD-A151616] 15 p2547 N85-25722
The weighting function for scintillation on a folded path
[AD-A152659] 17 p2949 N85-28206
Echo-responses from crack-like two-dimensional reflectors in focused ultrasonic fields
17 p3027 N85-28724
Submillimeter local oscillators for spaceborne heterodyne applications
[NASA-RP-1147] 19 p3226 N85-30005
Measurements of folded path optical scintillation using a corner cube, a cat's eye and a flat mirror reflector
[AD-A154044] 19 p3367 N85-30879
Method of constructing folding umbrella-type antenna
22 p3774 N85-33386
Hoop/column antenna deployment mechanism overview 22 p3796 N85-33514
Optical receivers using rough reflectors
[NASA-CR-176200] 24 p4154 N85-35750

REFLEXES
NT VESTIBULAR NYSTAGMUS
Biological investigations of adaptive networks. Neuronal control of conditioned responding
[AD-A150959] 14 p2385 N85-24695
Test and evaluation of the 2.4-micron photorefractor ocular screening system
[NASA-TM-86492] 15 p2615 N85-26115

REFRACTED RADIATION
U REFRACTED WAVES

REFRACTED RAYS
U REFRACTED WAVES

REFRACTED WAVES
Structure of temperature field based on observations of refraction from high meteorological mast
06 p0819 N85-15199
Influence of refraction effects on informativeness of bistatic acoustical atmospheric sounding systems
06 p0825 N85-15237
Interpreting refracted waves method data on basis of automated determination of seismic drift
14 p2343 N85-24486
Saudi Arabian refraction profile: A preliminary interpretation for the Red Sea-Arabian Shield transition
17 p2991 N85-28485
A traveltime interpretation of the 1978 seismic refraction profile in the Kingdom of Saudi Arabia
17 p2991 N85-28486
Explanation of Russian models: Saudi Arabian seismic refraction profile 17 p2991 N85-28487
Interpretation of the data of USGS seismic refraction profile across the Arabian Shield in western Saudi Arabia 17 p2991 N85-[illegible]
A preliminary analysis of the Saudi Arabian deep seismic sounding data 17 p2991 N85-[illegible]
One-dimensional velocity-depth functions determined for the Arabian Shield and the southwestern Red Sea: A comparison of models 17 p2992 N85-[illegible]
A theoretical study of electron capture in ion-ion and ion-atom collisions
[DE85-011154] 19 p3362 N85-30942

REFRACTING TELESCOPES
Saturn rings: Divisions, gaps and ringlets from ground-based telescopes 15 p2672 N85-[illegible]
Stokes parameters modulator for birefringent filters
18 p3205 N85-[illegible]

REFRACTION
NT ATMOSPHERIC REFRACTION
NT BIREFRINGENCE
NT RADIO WAVE REFRACTION
Hole shots along refraction profile R4/78 recorded at the temporary seismic station near Stary Plzenec (west Bohemia)
[REPT-549] 03 p0375 N85-[illegible]
Design and testing of a refractive laser beam homogenizer
[AD-A148997] 07 p0970 N85-16182
Acoustic energy exchange in sheared mean flow – solid rocket motors 13 p1999 N85-22594
Reflected wave travel-time curves in stratified media with vertically heterogeneous layers and slightly sloping curved boundaries 13 p2114 N85-23167
Test and evaluation of the 2.4-micron photorefractor ocular screening system
[NASA-TM-86492] 15 p2615 N85-26115
Inversion of Rayleigh wave group velocities from high-explosive tests
[AD-A152172] 16 p2783 N85-27175
Astrometric method advances Astronomy, geodesy
16 p2806 N85-27306
High precision materials characterization in the near millimeter wave-length range
[AD-A153267] 17 p2988 N85-28331
Journal of Research of the National Bureau of Standards, volume 90, number 1, January - February 1985
[PB85-179063] 20 p3522 N85-31906
The effects of subrefractive layers and elevated ducts on airborne radar and ESM (Electronic Surveillance Measures)
[AD-A155524] 21 p3637 N85-32592
Refraction of narrow probing light beam in multilayer optical fiber 22 p3764 N85-33330
Crustal structure in southern California from array data
24 p4115 N85-35512

REFRACTIVE INDEX
U REFRACTIVITY

REFRACTIVITY
Compound class quantitation of JP-5 jet fuels by high performance liquid chromatography-differential refractive index detection
[AD-A145754] 03 p0340 N85-12185
Refractive index of ternary and quaternary compound semiconductors below the fundamental absorption edge: Linear and nonlinear effects
[DE84-012325] 05 p0640 N85-14105
C2 sub n (optical) studies in the free atmosphere based on rawinsonde data
[AD-A147307] 07 p0997 N85-16032
Thermosonde C2N measurements in Hawaii-August 1982
[AD-A146016] 08 p1189 N85-17489
Quantitative determination of compound classes in jet turbine fuels by high performance liquid Chromatography/Differential refractive index detection: Part 2
[AD-A149298] 11 p1613 N85-20144
Optical guiding in a free electron laser
[DE85-003141] 11 p1639 N85-20327
Photorefractor ocular screening system
[NASA-CASE-MFS-26011-1SB]
11 p1692 N85-20639
Imaging apparatus for transverse electrode electro-optic tunable filter
[AD-D011524] 12 p1832 N85-21487
Multifunctional elements for integrated optics
13 p2068 N85-22313
Dispersion characteristics of small-mode gradient optical fibers 13 p2082 N85-23004
Possibility of determining atmospheric weather parameters by radio and radiooptical measurements of refraction of cosmic sources 13 p2110 N85-23146
Nonuniform interference coatings with thickness-dependent refractive index
14 p2281 N85-24131
Scattering properties of a moving dielectric object
[AD-A151974] 15 p2544 N85-25706

Sound propagation through directional internal wave fields
[AD-A151168] 15 p2646 N85-26321
Design of a variable-focal-length optical system
[NASA-CR-175710] 15 p2651 N85-26349
Impurity studies
[DE85-006235] 15 p2661 N85-26423
The problem of atmospheric turbulence
[NASA-CR-175783] 16 p2832 N85-27464
LIGHT: A ray tracing code to simulate light collection in scintillation spectrometers and light pipes
[DE85-007213] 16 p2865 N85-27673
Proceedings of the 1980 Workshop of the International Association of Seismology and Physics of the Earth's Interior on the Seismic Modeling of Laterally Varying Structures: Contributions based on data from the 1978 Saudi Arabian refraction profile
[GS-CIRC-937] 17 p2989 N85-28476
A crustal section for the Arabian Shield and adjacent Red Sea margin derived from first-arrival data
17 p2990 N85-28480
A seismic refraction profile across the Arabian Shield
17 p2990 N85-28481
A preliminary examination of the 1978 refraction profiles in Saudi Arabia 17 p2990 N85-28482
An assessment of atmospheric refractivity in the northern marginal ice zone
[AD-A152346] 17 p2992 N85-28493
Optical waveguide characterization using grating couplers
[AD-A153063] 17 p3037 N85-28789
Optical modulators and bistable devices using molecular gases 18 p3186 N85-29761
An experimental nonlinear optical waveguide device
18 p3186 N85-29762
Design consideration for the X-ray Cerenkov experiment
[AD-A153636] 18 p3189 N85-29777
Radio wave scattering and intermittency of turbulence in the atmosphere 19 p3288 N85-30392
Radio wave scattering and turbulence intermittence in atmosphere 19 p3296 N85-30446
Haze over eastern North America. Part 1: Haze properties
[PB85-181857] 19 p3311 N85-30526
A comparison of electronic heterodyne moire deflectometry and electronic heterodyne holographic interferometry for flow measurements
[NASA-TM-87071] 21 p3588 N85-32302
Some recent developments in the interpretation of MST radar returns from clear air (keynote paper), part 2
21 p3618 N85-32480
Morphology of the scattering targets: Fresnel and turbulent mechanisms, part 2.1A
21 p3618 N85-32481
A modified Fresnel scattering model for the parameterization of Fresnel returns, part 2.3A
21 p3618 N85-32483
Observations of mesospheric turbulence by rocket probe and VHF radar, part 2.4A 21 p3619 N85-32484
Interpretation of radar returns from the mesosphere, part 2.3A 21 p3619 N85-32485
Usefulness of multifrequency MST radar measurements, part 2.6B 21 p3619 N85-32487
Variation of the submicron aerosol structure
21 p3647 N85-32661
Beam diffusion in linear ionospheric layer
21 p3695 N85-32958
Transmission of light by disperse medium of densely packed optically soft particles 21 p3697 N85-32969
Refraction of narrow probing light beam in multilayer optical fiber 22 p3764 N85-33330
Temperature sensitivity of fiber-optic transmission line
22 p3764 N85-33331
Refractive indices and thermo-optic coefficients of nonlinear crystals isomorphic to KH2PO4
[DE85-012968] 22 p3847 N85-33831
The use of a laser Doppler velocimeter in a standard flammability tube
[NASA-CR-174980] 24 p4096 N85-35389
REFRACTORY COATINGS
Corrosion study on zirconium refractory coatings. 1: Oxidation of zirconium nitride coatings by oxygen
[BLL-RISLEY-TR-5044-(9091.9F)]
07 p0925 N85-15857
Thermal barrier coating system
[NASA-CASE-LEW-13324-2] 12 p1796 N85-21266
REFRACTORY MATERIALS
NT CHROMIUM
NT CHROMIUM ISOTOPES
NT IRIDIUM
NT MOLYBDENUM
NT MOLYBDENUM ALLOYS
NT NIOBIUM
NT NIOBIUM ALLOYS
NT OSMIUM
NT OSMIUM ISOTOPES
NT REFRACTORY METAL ALLOYS
NT REFRACTORY METALS
NT RENE 95
NT RHENIUM
NT RHENIUM ALLOYS
NT TANTALUM
NT TANTALUM ALLOYS
NT TUNGSTEN
NT TUNGSTEN ALLOYS
USSR report: Materials science and metallurgy, no. 93
[JPRS-84810] 01 p0016 N85-10110
Silicon nitride powder
[NASA-TM-77731] 01 p0022 N85-10132
Milling of Si3N4 with Si3N4 hardware
[NASA-TM-86864] 01 p0031 N85-10191
Resistance of Navy shipboard outerwear garments and fire-resistant fabrics to extreme heat
[AD-A145414] 02 p0236 N85-11546
New coatings for high temperature materials protection
[AERE-R-11387] 03 p0339 N85-12160
Improved apparatus and techniques for high temperature and pressure deformation of crystalline materials
[DE84-016049] 04 p0569 N85-13629
Modelling of deformation and fracture in high-temperature structural materials
[DE84-016906] 06 p0818 N85-15191
A program to develop thermite reactions to produce refractory borides and carbides
[AD-A148972] 10 p1434 N85-19037
Nonlinear analysis for high-temperature multilayered fiber composite structures — turbine blades
[NASA-TM-83754] 12 p1797 N85-21273
Viscoplastic constitutive relationships with dependence on thermomechanical history
[NASA-CR-174836] 12 p1864 N85-21691
Experimental study of enthalpy of quasimonocrystal of graphite and carbon glass in temperature range of 2890-3818 deg K 13 p2036 N85-22751
Optimizing hot workability and controlling microstructures in difficult to process high strength and high temperature materials
[AD-D011586] 15 p2510 N85-25482
Refractory inclusions in the Ornans C30 chondrite
15 p2660 N85-26553
Method of fabricating material for the electrodes of gas discharge devices
[DE85-007452] 16 p2780 N85-27157
High temperature fracture mechanics of silicon nitride
[BMFT-FB-T-84-285] 17 p2961 N85-28433
Convoluted nozzle design for the RL10 derivative 2B engine
[NASA-CR-174953] 19 p3220 N85-29965
Thermo-mechanical and thermal behavior of high-temperature structural materials
[AD-A154154] 19 p3266 N85-30251
Thermodynamics of high temperature materials
[AD-A154269] 19 p3376 N85-30956
Short term determination of the creep properties of high temperature materials
[CRIF-MT-160] 20 p3432 N85-31266
Welding methods for high melting metals
22 p3794 N85-33506
Thermal protection systems for reentry vehicles
[CNES-NT-113] 23 p3900 N85-34157
REFRACTORY METAL ALLOYS
NT MOLYBDENUM ALLOYS
NT NIOBIUM ALLOYS
NT RHENIUM ALLOYS
NT TANTALUM ALLOYS
NT TUNGSTEN ALLOYS
Superpure materials research planned
03 p0353 N85-12270
Review: Role of refractory metal alloys in fusion reactor applications
[AERE-R-11317] 03 p0422 N85-12695
Effect of stress concentration fatigue resistance of refractory nickel alloys under asymmetrical multicycle loading, communication 1 11 p1604 N85-20086
Obtaining amorphous coatings of FeW and Fe-Cr-P-B alloys using laser sputtering
[BLL-BISI-22493-(9022.06)] 17 p2927 N85-28057
Load-carrying capabilities of refractory alloys for space reactor power applications
[DE85-010566] 19 p3240 N85-30087
REFRACTORY METALS
NT CHROMIUM
NT CHROMIUM ISOTOPES
NT IRIDIUM
NT MOLYBDENUM
NT NIOBIUM
NT OSMIUM
NT OSMIUM ISOTOPES
NT RHENIUM
NT TANTALUM
NT TUNGSTEN
Material problems for high-temperature, high-power space energy-conversion systems
[AD-A145940] 03 p0385 N85-12466
Electronic transport processes in refractory metal silicides
[AD-A146495] 06 p0861 N85-15468
Method for making alloy additions to base metals having higher melting points
[AD-D011403] 07 p0928 N85-15884
Studies of silicon-refractory metal interfaces: Photoemission study of interface formation and compound nucleation
[AD-A150075] 12 p1800 N85-21293
Update of thermal conductivity and electrical resistivity of electrolytic iron, tungsten and stainless steel
[PB85-115814] 12 p1803 N85-21311
An investigation of the irradiation swelling mechanisms in refractory metals at high temperatures
[AD-A154149] 19 p3238 N85-30079
Thermodynamics of high temperature materials
[AD-A154269] 19 p3376 N85-30956
REFRACTORY PERIOD
Relaxation lens in inhomogeneous binary mixture
21 p3695 N85-32957
REFRASIL (TRADEMARK)
U FIBERS
U SILICON DIOXIDE
REFRIGERANTS
Investigation of an ejector heat pump by analytical methods
[DE84-016675] 04 p0500 N85-13169
DOE/ORNL electric systems program overview
[DE85-003334] 10 p1459 N85-19197
Optimization of a ground coupled heat pump
[DE85-000273] 10 p1486 N85-19380
Determination of properties of zeolite/refrigerant combinations for solar refrigeration systems
[DE85-012009] 23 p3945 N85-34448
REFRIGERATING
Hybrid system for producing and storing ice
[DE84-017474] 09 p1304 N85-18195
Magnetic refrigeration and heat pumping design options
[DE85-003405] 13 p2092 N85-23064
Evaluation study of mechanical refrigeration systems for application to space missions — infrared astronomy
[SNIAS-1029ACA/LL/V] 22 p3755 N85-33277
Heat-mass flow enhancement system for a metal hydride assembly
[DE85-010696] 22 p3783 N85-33441
Refrigerated dynamic seal to 6.9 MPa (1000 psi)
[NASA-TM-87108] 23 p3930 N85-34356
REFRIGERATING MACHINERY
NT REFRIGERATORS
Magentically actuated compressor
[NASA-CASE-GSC-12799-1] 12 p1818 N85-21404
Testing and further development of a solar absorption cooling plant
[BMFT-FB-T-84-264] 15 p2588 N85-25954
REFRIGERATORS
Selection of regenerator geometry for magnetic refrigerator applications
[DE84-012637] 11 p1616 N85-20160
Gas-fired duplex free-piston Stirling refrigerator
12 p1819 N85-21413
Reciprocating magnetic refrigerator employing tandem porous matrices within a reciprocating displacer
[NASA-CASE-NPO-16257-1] 18 p3085 N85-29082
Ten degree Kelvin hydride refrigerator
[NASA-CASE-NPO-16393-1-CU]
18 p3085 N85-29084
Welding of steel-aluminum cooling panels for the holds of refrigerator vessels 19 p3246 N85-30129
Intrinsically irreversible acoustic heat engines
[DE85-007672] 19 p3270 N85-30276
Combined cold compressor/ejector helium refrigerator
[DE85-008408] 23 p3925 N85-34326
REFUELING
NT AIR TO AIR REFUELING
Orbit of Salyut-7 station boosted
02 p0157 N85-11067
Salyut-7 crew in orbit 150 days
02 p0157 N85-11068
Propellant tank resupply system
[AD-D011288] 05 p0603 N85-13848
Propellant transfer: Tethered depot
08 p1108 N85-17006
Safety recommendation(s), A-84-103
[REPT-3909B/101B] 14 p2216 N85-23745
Inspection evaluation and repair of the flawed feedwater nozzle of the 50 MWe Dodewaard GKN boiling water reactor
[ISBN-90-353-0017-3] 17 p2977 N85-28394

NASA space station automation: AI-based technology review. Executive summary
[NASA-CR-176096] 21 p3558 N85-32135

REGENERATION (ENGINEERING)

Recursive moment formulas for regenerative simulation
[AD-A150112] 12 p1922 N85-22070

In-orbit laser regeneration of the radiation damaged solar arrays 13 p2008 N85-22588

Regenerative stochastic Petri nets
[AD-A150343] 13 p2151 N85-23355

Regenerative simulation of non-Markovian stochastic systems
[AD-A150344] 13 p2153 N85-23367

Space shuttle revitalization system
18 p3157 N85-29548

Composite desiccant structure
[DE85-006400] 23 p3910 N85-34226

REGENERATION (PHYSIOLOGY)

Problems associated with the utilization of algae in bioregenerative life support systems
[NASA-CR-166615] 07 p1019 N85-16469

Feasibility of producing a range of food products from a limited range of undifferenitiated major food components
[NASA-CR-177329] 07 p1020 N85-16473

Current concepts and future directions of CELSS
18 p3155 N85-29532

Survey of CELSS concepts and preliminary research in Japan 18 p3155 N85-29533

Advanced regenerative environmental control and life support systems: Air and water regeneration
18 p3155 N85-29535

Atmosphere behavior in gas-closed mouse-algal systems: An experimental and modelling study
18 p3155 N85-29536

Dynamic considerations for control of closed life support systems 18 p3155 N85-29537

CELSS transportation analysis
18 p3158 N85-29538

Composition and dynamics of bacteriocenosis associated with algae in human life-support systems
22 p3823 N85-33684

Experimental validation of allowable concentrations of sodium and potassium in recycled drinking water
22 p3823 N85-33685

REGENERATIVE CYCLES
U REGENERATION (ENGINEERING)

REGENERATIVE FUEL CELLS

Regenerative fuel cell energy storage system for a low Earth orbit space station
[NASA-CR-174802] 04 p0527 N85-13371

Electrochemistry and storage panel report
05 p0611 N85-13903

Investigation of bromine complexed hydrogen/bromine regenerative fuel cells for portable electric power
[AD-A146401] 06 p0833 N85-15300

Engineering model system study for a regenerative fuel cell: Study report
[NASA-CR-174801] 07 p0991 N85-16292

Develop and test fuel cell powered on-site integrated total energy systems. Phase 3: Full-scale power plant development
[NASA-CR-168338] 19 p3304 N85-30483

Regenerative fuel cell systems for space station
20 p3443 N85-31372

System level electrochemical principles
20 p3443 N85-31375

REGENERATORS
NT THERMOSIPHONS

Preliminary mechanical redesign of an existing gas-turbine engine to incorporate a high-efficiency, low-pressure-ratio, highly regenerative cycle for marine applications
[AD-A144808] 01 p0011 N85-10070

Selecting the proper ceramic material for a regenerator experiencing large temperature gradients
[AD-A144796] 01 p0032 N85-10199

Regenerators of binary pulses for optical communication systems 04 p0485 N85-13099

Selection of regenerator geometry for magnetic refrigerator applications
[DE84-012637] 11 p1616 N85-20160

REGGE POLES

Is the inelastic charge-exchange contribution constant at the large X and superhigh energies? Qaut 01Kuchin, I. A. 24 p4173 N85-35871

REGIONAL PLANNING
NT URBAN PLANNING

Combinations of remote sensing data with a digital map data base — regional planning 05 p0660 N85-14240

Climate Conference for Latin America and the Caribbean
[WMO-632] 07 p1000 N85-16352

Climate applications: General
07 p1001 N85-16355

The challenge of food production: The importance of climate 07 p1001 N85-16361

The management of atmospheric resources in food production 07 p1002 N85-16362

Requirements for training in climate-related subjects
07 p1004 N85-16378

Applied climatology — regional planning
18 p3147 N85-29486

REGIONS
NT AMAZON REGION (SOUTH AMERICA)
NT ANTARCTIC REGIONS
NT ARCTIC REGIONS
NT AURORAL ZONES
NT BRILLOUIN ZONES
NT CENTRAL ATLANTIC REGION (US)
NT D REGION
NT E REGION
NT EQUATORIAL REGIONS
NT F REGION
NT FRESNEL REGION
NT HABITATS
NT INTERTROPICAL CONVERGENT ZONES
NT M REGION
NT NEW ENGLAND (US)
NT NULL ZONES
NT PACIFIC NORTHWEST (US)
NT POLAR REGIONS
NT REMOTE REGIONS
NT ROSS ICE SHELF
NT SOUTHERN CALIFORNIA
NT SUBARCTIC REGIONS
NT TEMPERATE REGIONS
NT TROPICAL REGIONS

Simple mesoscale models for operational use in regions of topographic and thermal forcing: Development and evaluation
[AD-A146667] 06 p0839 N85-15325

Modeling longitudinal motions of thermal O+ and H+ ions in magnetic field tube convective through daytime polar cusp 15 p2481 N85-25314

Annual cycle. Part 2: The annual variation of precipitation over the United States and Canada
[PB85-147684] 15 p2600 N85-26027

Discovery in earthquake forecasting and seismic zoning recorded 19 p3295 N85-30426

A new approach to linear quadtrees
23 p3961 N85-34550

An analysis and algorithm for filling propagation
23 p3961 N85-34551

REGISTERS (COMPUTERS)

Siemens introduces fast computer with pipeline architecture 11 p1618 N85-20178

Interprocess communication
[AD-A156337] 24 p4088 N85-35337

REGOLITH

Physical and mechanical properties of lunar soil as function of specifics of relief and processes in vicinity of operation of Lunokhod-2 02 p0161 N85-11090

Megaregolith thickness, heat flow, and the bulk composition of the Moon 04 p0583 N85-13723

Grainsize evolution and differential comminution in an experimental regolith 06 p0888 N85-15638

Asteroid-meteorite connection: Regolith effects implied by lunar reflectance spectra 06 p0888 N85-15640

Progress on Experimental impact studies
13 p2181 N85-23534

Multispectral analysis of the Kasei Vallis-Lanae Planum region of Mars 13 p2193 N85-23607

Investigation of the daytime lunar atmosphere
[NASA-CR-175636] 14 p2440 N85-25057

Earth's primordial differentiation, and its after-effects
21 p3722 N85-33092

Interpretation of photometric measurements of airless bodies 22 p3855 N85-33871

REGRESSION (STATISTICS)
U REGRESSION ANALYSIS

REGRESSION ANALYSIS
NT REGRESSION COEFFICIENTS

The effects of seven alloying elements on the microstructure and stress-rupture behavior of nickle-base superalloys
[NASA-TM-83791] 01 p0027 N85-10168

Statistical tropical cyclone forecasting techniques for the Southern Hemisphere
[AD-A144752] 01 p0085 N85-10569

A combined logistic regression and Zionts-Wallenius methodology for multiple criteria linear programming
[TWISK-314] 01 p0102 N85-10679

Location of several outliers in multiple regression data using elemental data
[CSIR-TWISK-300] 01 p0108 N85-10724

The information in the minor principal components
[CSIR-TWISK-320] 01 p0109 N85-10735

Statistical analysis of 11-year and 80-year solar cycles
02 p0161 N85-11095

Life distribution properties of devices subject to deterioration
[AD-A145554] 02 p0208 N85-1139

Description of a data matrix structure and model diagnosis by means of row and column Euclidean maps
02 p0211 N85-1130

Limit theory for the sample covariance and correlation functions of moving averages
[AD-A145488] 02 p0251 N85-1164

Auto-regressive moving average spectral estimation using modified and least squares modified Yule-Walker estimates
[AD-A145516] 02 p0254 N85-1168

An asymptotic theory for logistic regression when some predictors are measured with error
[AD-A145673] 02 p0254 N85-1169

Least squares estimation of conditionally heteroscedastic autoregressions
[AD-A145994] 03 p0411 N85-1260

An introduction to fuzzy regression analysis with a ballistic application
[AD-A146093] 03 p0411 N85-1260

Nonlinear regression with emphasis on spline methods
[AD-A146192] 03 p0412 N85-1260

Users manual for BRGLM: Interactive general linear model regression, version 3
[DE84-017386] 04 p0550 N85-13001

Least squares spline regression with block-diagonal variance matrices
[NPL-DITC-40/84] 04 p0554 N85-13023

Development of structured regression hypotheses/interactive descriptive geometry through five dimensions
[INT-324] 04 p0554 N85-13024

Parametric estimates of propulsion system maintenance manhours
[AD-A147120] 07 p0894 N85-1592

Exploring the use of structural models to improve remote sensing agricultural estimates 07 p0985 N85-1625

Calibration or inverse regression: Which is appropriate for crop surveys using LANDSAT data?
07 p0985 N85-1626

Experiments in forecasting atmospheric marine horizontal visibility using model output statistics with conditional probabilities of discretized parameters
[AD-A147574] 07 p1008 N85-16404

Some scientific subroutines in LISP
[AD-A147889] 07 p1026 N85-16515

Estimation for a semimartingale regression model using the method of sieves
[AD-A146609] 07 p1028 N85-16527

Conditional regression models for transient state survival analysis
[AD-A147872] 07 p1034 N85-16560

Generalized additive models
[AD-A147454] 07 p1036 N85-16573

Infinite order autoregressive representations of multivariate stationary stochastic processes
[AD-A147863] 07 p1036 N85-16580

Completely monotone regression estimates of software failure rates
[NASA-CR-174319] 08 p1204 N85-17575

The EM algorithm for censored data
[AD-A148136] 08 p1212 N85-17626

A power transformation exponential regression model for censored failure time data
[AD-A148377] 08 p1212 N85-17632

Multivariable Autoregressive Moving Average (ARMA) models: A time approach to antenna processing
[ENST-84E015] 09 p1313 N85-18252

Estimation of variance of the regression estimator
[AD-A149407] 10 p1551 N85-19780

The likelihood displacement: A unifying principle for influence measures
[AD-A149456] 10 p1551 N85-19783

Statistical analysis of autoregressive spectral estimates for noise corrupted autoregressive series
[AD-A149543] 11 p1706 N85-20747

A note on some simple influence diagnostics in accelerated life testing
[AD-A149593] 12 p1862 N85-21877

Analysis of selective chopper radiometer data
[NASA-CR-175157] 12 p1895 N85-21894

Ordinary and proper location M-estimates for ARMA models, revised
[AD-A149705] 12 p1920 N85-22061

Inference for censored matched pairs using signed ranks
[MATHEMATICS-RESEARCH-162]
12 p1923 N85-22078

Proportional odds models for survival data and estimates using ranks
[MATHEMATICS-RESEARCH-172]
12 p1923 N85-22080

Pulsars and interstellar medium
12 p1960 N85-22320

Expansion of functions describing planetary surface and gravity field 13 p1978 N85-22410
Approaches and algorithms for robust signal processing 13 p2062 N85-22878
Ozone Correlative Measurements Workshop
[NASA-CP-2362] 13 p2105 N85-23112
Measurement requirements for the detection of ozone sonde 13 p2105 N85-23115
Consistency of smoothing with running linear fits
[AD-A150232] 13 p2150 N85-23349
A model for large sparse contingency tables
[AD-A150320] 13 p2151 N85-23350
A note about the strong convergence of the nonparametric estimation of a regression function
[AD-A150325] 13 p2151 N85-23353
Determining optimum service conditions for concentrator mirrors by methods of mathematically planned experiment 14 p2274 N85-24090
Classification and multiple regression through projection pursuit
[AD-A150797] 14 p2411 N85-24867
Thermal traction contact performance evaluation under fully flooded and starved conditions
[NASA-CR-168173] 15 p2568 N85-25848
Statistical analysis techniques for small sample sizes
[NASA-CR-171872] 15 p2639 N85-26279
Statistical regularization methods in problem of navigational determination of space vehicle orbits
16 p2719 N85-26764
Multiple regression analysis of photographic image of soil properties 16 p2726 N85-26825
An interactive computer package for use with simulation models which performs multidimensional sensitivity analysis by employing the techniques of response surface methodology
[AD-A151956] 16 p2846 N85-27548
Some new estimation methods for weighted regression when there are possible outliers
[AD-A152104] 16 p2854 N85-27602
Locally-weighted-regression scatter-plot smoothing (LOWESS): A graphical exploratory data analysis technique
[AD-A152239] 16 p2855 N85-27609
An evaluation of discretized conditional probability and linear regression threshold techniques in model output statistics forecasting of visibility over the north Atlantic Ocean
[AD-A151955] 16 p2857 N85-27619
Local likelihood estimation
[DE85-007236] 16 p2857 N85-27620
Surveillance report. Stage 1: Dissected motors-propellants motor number 0012199, phase 15
[AD-A153206] 17 p2916 N85-27973
MM2 LRSLA testing stage 3 propellant
[AD-A152540] 17 p2937 N85-28128
The measurement of linear frequency drift in oscillators 17 p2968 N85-28316
Robust regression through robust covariances
[AD-A153301] 17 p3020 N85-28677
Fuzzy hierarchical analysis
[DE85-008149] 17 p3021 N85-28685
A multiple regression technique for detecting outliers
[REPT-84-33] 17 p3025 N85-28706
Fixed width interval estimation in linear regression
[AD-A153633] 18 p3174 N85-29675
An experimental investigation of fuel regression rate control in solid fuel ramjets
[AD-A154251] 19 p3227 N85-30008
Regression diagnostics in practice: Experiences from modelling jet engine costs
[AD-A154199] 19 p3347 N85-30748
Using regression analysis for determining air data sensor errors by means of an inertial navigation system
[ESA-TT-886] 20 p3392 N85-31041
A multiple linear regression analysis of hot corrosion attack on a series of nickel base turbine alloys
[NASA-TM-87020] 20 p3431 N85-31284
Regression metamodel summarization of model behavior
[FEW-120] 20 p3522 N85-31902
On the interpretation of variables — simulation and regression models
[FEW-136] 20 p3522 N85-31903
Statistical methods for efficient design of community surveys of response to noise: Random coefficients regression models
[NASA-CR-177933] 21 p3698 N85-32979
Kalman filter time series analysis of gamma-ray data from NaI(T1) detectors for the ND6620 computer
[AD-A154995] 21 p3705 N85-33014
Regression analysis of aircraft and ground measurement data on vegetation cover 22 p3735 N85-33156
Direct regression analysis of remote sensing data (using example of grass cover) 22 p3736 N85-33157

Development of NATOPS performance software for the SH-3D and SH-3H helicopters
[AD-A156140] 24 p4065 N85-35192

REGRESSION COEFFICIENTS
A two-dimensional smoothing spline and a regression problem
[AD-A149524] 12 p1921 N85-22067
Statistical methods for efficient design of community surveys of response to noise: Random coefficients regression models
[NASA-CR-177933] 21 p3698 N85-32979

REGULARITY
Regularity of the free boundary for the porous medium equation
[AD-A147299] 06 p1210 N85-17611

REGULATION
U CONTROL

REGULATIONS
Polychlorinated biphenyls (PCBs) in transit system electrical equipment
[PB84-222207] 01 p0045 N85-10291
Major institutional arrangements affecting ground water in New York state
[PB84-202506] 01 p0065 N85-10429
Airliner cabin air quality
[S-REPT-98-468] 03 p0402 N85-12560
Commercial Space Launch Act
[GPO-39-613] 04 p0578 N85-13690
The application of emissions trading to DoD installations
[AD-P004136] 09 p1346 N85-18472
Strategies for preparing and submitting a part B application for a DoD facility
[AD-P004139] 09 p1347 N85-18475
Perspective on demonstrations of compliance for high-level waste deiposal
[DE85-000989] 09 p1383 N85-18698
Airport bird hazards associated with solid waste disposal facilities
[AD-P004197] 11 p1581 N85-19964
The FAA grant-in-aid assurances: FAR part 139, and airport hazards
[AD-P004209] 11 p1583 N85-19976
Interim protocol for the automated analysis of semivolatile organic compounds by Gas Chromatography/Fourier Transfer Infrared (GC/FT-IR) spectrometry
[PB85-115186] 11 p1595 N85-20035
Ultralight aircraft technology and public safety
[GPO-38-948] 12 p1773 N85-21131
Do new aircraft need new technologies and certification rules? 14 p2224 N85-23795
Civil air code international flights section explained
15 p2460 N85-25194
Protecting the nation's groundwater from contamination, volume 1
[PB85-154201] 15 p2590 N85-25965
Protecting the nation's groundwater from contamination, volume 2
[PB85-154219] 15 p2590 N85-25966
White paper on new international satellite systems
[PB85-162501] 16 p2775 N85-27127
Gordon Research Conference on Composites
[AD-A152888] 17 p2917 N85-27979
FAA regulation of 9-seat and under passenger aircraft
[GPO-42-703] 20 p3391 N85-31032
Current regulatory and licensing status for byproduct sources, facilities and applications
[DE85-010967] 22 p3842 N85-33796

REGULATORS
NT AUTOMATIC FREQUENCY CONTROL
NT CURRENT REGULATORS
NT FLOW REGULATORS
NT FREQUENCY CONTROL
NT PRESSURE REGULATORS
NT SPEED REGULATORS
NT THERMOSTATS
NT VOLTAGE REGULATORS
Adaptive regulation of transmitter radiation power in radio lines during delays of control signals
12 p1841 N85-21551
Construction of high speed guaranteed regulators
14 p2270 N85-24063
Modal synthesis of multidimensional PI-regulators for objects with inertial sections 14 p2270 N85-24064
Some problems in improving reliability and accuracy of regulators with hydraulic amplifiers in main channel of power turbine 14 p2271 N85-24071
Some new results on the discrete-time Riccati Equation and their use in the design of optimal regulators and observer-estimators
[AD-A151934] 16 p2854 N85-27597

REHEATING
U HEATING

REIGNITION
U IGNITION

REINFORCED MATERIALS
U COMPOSITE MATERIALS

REINFORCED PLASTICS
NT GLASS FIBER REINFORCED PLASTICS
Impressions from a study tour in Finland concerning fiber reinforced plastics, June 1984
[FOA-C-20552-D2(E4,F9)] 07 p0921 N85-15831
Theoretical and experimental study of crack resistance and macrocrack growth rate in organic fiber reinforced plastic under pure shear condition
11 p1598 N85-20053
Outlook for polymer composite materials
15 p2497 N85-25403
New material, process spins off from Volvo LCP 2000 program 15 p2536 N85-25648

REINFORCED PLATES
Impact fracture mechanism of polymer plates containing a heavy inner material 23 p3908 N85-34215

REINFORCED SHELLS
Normal mode method of solving problem forced oscillations of rib-reinforced shell of revolution in liquid
02 p0273 N85-11781
Finite element procedures applicable to nonlinear analysis of reinforced concrete shell structures
[AD-A146796] 07 p0978 N85-16209
Testing of wound materials for strength with loading in the reinforcement plane 13 p2027 N85-22701
Strength computation of thin walled shell by discreet-continuous model 14 p2288 N85-24181
Natural vibrations of reinforced spherical shells
17 p2943 N85-28165
Method of solving problems of statics for multilayer shells of revolution 17 p2943 N85-28167

REINFORCEMENT (STRUCTURES)
Development of advanced constitutive model for reinforced concrete
[AD-A145050] 01 p0062 N85-10411
Improved reinforcement metal
03 p0353 N85-12271
Dynamic shear failure of shallow-buried flat-roofed reinforced concrete strucuires subjected to blast loading
[AD-A145974] 03 p0373 N85-12378
Refined modeling of reinforced concrete columns of seismic analysis
[PB84-234384] 04 p0484 N85-13069
Measuring the corrosion rate of reinforcing steel in concrete
[PB84-244532] 06 p0770 N85-14925
Response of earth-covered slabs in clay and sand backfills
[AD-A149296] 11 p1615 N85-20157
An approach for user controlled reinforced concrete design optimization 15 p2627 N85-26187
Effects of humidity cycles on the corrosion of galvanised reinforcements in carbonated and uncarbonated mortars
[BLL-CE-TRANS-8039-(9022.09)]
20 p3430 N85-31272
Membrane reinforcement in concrete shells: Design versus nonlinear behavior 24 p4084 N85-35312
User's guide: A computer program for strength analysis of non-hydraulic concrete structural elements. Report 2. Strength design of reinforced concrete column sections (PCAUC)
[AD-A156393] 24 p4102 N85-35429

REINFORCING FIBERS
NT BORON FIBERS
NT CARBON FIBERS
High performance fibers for structurally reliable metal and ceramic composites — advanced gas turbine engine materials
[NASA-TM-86878] 03 p0325 N85-12095
Impressions from a study tour in Finland concerning fiber reinforced plastics, June 1984
[FOA-C-20552-D2(E4,F9)] 07 p0921 N85-15831
Quantitative estimate of compatibility of fiber composite material components 10 p1444 N85-19099
Evaluation of features of reinforcing fibers by testing bundles 11 p1599 N85-20059
Preparation of silicon carbide-silicon nitride fibers by the pyrolysis of polycarbosilazane precursors
[NASA-TM-86505] 17 p2933 N85-28107
Lightweight piston
[NASA-CASE-LAR-13150-1] 18 p3068 N85-28975
Effect of matrix composition on steel fiber reinforced concrete properties 19 p3230 N85-30026
Features of the interaction between fibers and matrix in production of aluminum-boron composite material
19 p3244 N85-30117
Matrix fracture in fiber-reinforced ceramics
[AD-A154704] 21 p3569 N85-32197
Improved process for the preparation of fiber-reinforced ceramic composites by chemical vapor deposition
[DE85-011584] 22 p3752 N85-33255
Substitution of asbestos by aramid fibers and fiber blends in industrial textiles and composites with organic binders
[BMFT-FB-T-85-006] 23 p3920 N85-34294

REINFORCING MATERIALS
Related studies to cathodic protection of reinforced concrete structures
[PB84-218114] 03 p0333 N85-12145
Reinforcement of molybdenum disilicide with nematic crystals of aluminum oxide 03 p0353 N85-12269
Improved reinforcement metal
03 p0353 N85-12271
Ultrasonic analysis of spherical composite test specimens
[DE85-001591] 07 p0976 N85-16197
Mechanism of strengthening plastics with rubbers
13 p2014 N85-22636
Particulate and whisker toughened alumina composites
[DE85-005239] 16 p2743 N85-26930
Anticorrosion protection of reinforcing steel in prestressed gypsum and anhydrite concrete
[BLL-BISI-TRANS-22079-(9022.06)]
17 p2926 N85-28044
Behavior of reinforced concrete at elevated temperatures
[DE85-009032] 18 p3123 N85-29332
Durability of reinforced hard-alloy draw plates
[BLL-M-36278-(5828.4)] 20 p3485 N85-31526

REISSNER THEORY
Modeling the stress field in laminated composite plates near discontinuities
[PB84-219237] 03 p0327 N85-12103
Bulletin of the Faculty of Engineering, Hokkaido University, no. 123
[ISSN-0385-602-X] 04 p0432 N85-13075
Analysis based on Reissner theory for rectangular plates with all edges built-in 04 p0483 N85-13081
Interaction of part-through cracks in a flat plate
[NASA-CR-175588] 12 p1864 N85-21692

REJECTION
Choice of criteria for rejection of insulating components in high-voltage surge equipment
06 p0785 N85-15021

RELATIONSHIPS
Compressive strength-maturity relationships of mortar containing fly ash
[AD-A148705] 09 p1339 N85-18423

RELATIVISTIC EFFECTS
An alternative to relativistic beaming in AGN — Active Galactic Nuclei (AGN) 08 p1242 N85-17833
Viking radio science data analysis and synthesis
[NASA-CR-175631] 13 p2171 N85-23471
Activities report of the Department of Astrophysics
20 p3546 N85-32064
A derivation of relativistic effects in satellite tracking
[AD-A154620] 21 p3558 N85-32132

RELATIVISTIC ELECTRON BEAMS
NRL (Naval Research Laboratory) FEL (Free Electron Laser) program
[AD-A145057] 01 p0052 N85-10347
Cerenkov radiation in the neighborhood of the emission threshold, revised
[AD-A145458] 02 p0284 N85-11855
Time-resolved tomographic images of a relativistic electron beam
[DE84-015021] 04 p0565 N85-13597
Explosive emission cathode plasmas in intensive relativistic electron beam diodes
[AD-A147917] 07 p1046 N85-16642
SIMM1: A linearized particle code
[AD-A148627] 08 p1221 N85-17689
IREB (Intense Relativistic Electron Beam) converter to ac pulses
[AD-D011479] 10 p1554 N85-19800
Directivity of Bremsstrahlung radiation from relativistic beams and the Gamma-Rays from solar flares
[NASA-CR-174433] 10 p1572 N85-19913
Novel probe for determining the size and position of a relativistic electron beam
[DE85-001044] 11 p1723 N85-20836
Theoretical study of collective ion acceleration in the Luce diode
[AD-A150107] 12 p1929 N85-22116
Collective acceleration of ions using high current relativistic electron beams
[DE85-004889] 13 p2157 N85-23393
Explosive emission cathode plasmas in intense relativistic electron beam diodes
[AD-A150669] 14 p2417 N85-24912
Principle and design of a medium-enhanced free-electron laser 15 p2561 N85-25802
Beam trapping in high current cyclic accelerators with strong focusing fields
[AD-A151392] 15 p2648 N85-26331
Microwave emission from relativistic electron beams
[AD-A151472] 15 p2648 N85-26333
Bursts of relativistic electrons in magnetopause and in outer radiation belt 16 p2722 N85-26801
Comparison of calculations and measurements of the off-axis radiation dose (SI) in liquid nitrogen as a function of radiation length
[AD-A153676] 18 p3178 N85-29704
Millimeter wave generation by relativistic electron beams
[AD-A153980] 18 p3179 N85-29706
Gyrotron traveling-wave device including quarter wavelength anti-reflective dielectric layer to enhance microwave absorption
[AD-D011690] 19 p3271 N85-30285
Profile of a relativistic electron beam propagated through a linear wiggler and an axial guide field
[AD-A154403] 19 p3353 N85-30783
Quasioptical gyroklystron
[AD-D011686] 19 p3356 N85-30801
Further studies of X-ray structure of the Perseus cluster
[OG-2.5-12] 22 p3870 N85-33967
Injection of energetic particles following the gamma-ray flares on June 7, 1980, as observed on Helios 1
[SH-1.3-9] 23 p3993 N85-34756
Ultrarelativistic electrons and solar flare gamma-radiation
[SH-1.3-11] 23 p3993 N85-34757

RELATIVISTIC PARTICLES
NT RELATIVISTIC ELECTRON BEAMS
A covariant derivation of the ponderomotive force
[AD-A145054] 01 p0121 N85-10830
Physics of nonmagnetic relativistic thermal plasmas
09 p1386 N85-18715
Pulsations of cosmic ray intensities before increasing flux of relativistic particles from solar flares
15 p2477 N85-25292
Contributions to the 19th International Cosmic Ray Conference
[NASA-CR-176049] 20 p3543 N85-32044
Classical emission of relativistic charged particles during axial channeling 21 p3681 N85-32871
Relativistic electron in curved magnetic fields
[OG-6.2-11] 22 p3890 N85-34110
Simulation studies on stability of hot electron plasma
23 p3978 N85-34664
Multiple inner shell vacancies in laser-irradiated Au plasma 23 p3981 N85-34687
Neutron-induced 2.2 MeV background in gamma ray telescopes
[OG-9.3-6] 23 p4027 N85-34961
A bi-directional charged particle telescope to observe flux, energy spectrum and angular distribution of relativistic and non-relativistic particles
[SH-9.1-4] 23 p4050 N85-35119
Proceedings of the Workshop on Detectors for Relativistic Nuclear Collisions
[LBL-18225] 24 p4146 N85-35700
Report of working group on detectors for hadrons and event parameters at colliders 24 p4146 N85-35705
A simulation of ultra-relativistic nucleus-nucleus collisions 24 p4146 N85-35707
A holographic streamer chamber for relativistic nucleus-nucleus collision experiments
24 p4147 N85-35710
Fractional charge resolution in music
24 p4147 N85-35712
Hadron thermodynamics in relativistic nuclear collisions
[HE-1.1-8] 24 p4171 N85-35856
Structure of air shower disc near the core
[HE-4.7-2] 24 p4198 N85-36053
High energy cosmic ray signature of quark nuggets
[HE-6.2-11] 24 p4212 N85-36147
Search for anomalons using plastic nuclear track detectors
[HE-6.2-12] 24 p4212 N85-36148

RELATIVISTIC PLASMAS
The environment of active galactic nuclei
07 p1057 N85-16712
Physical processes in relativistic plasmas --- active galactic nuclei 08 p1240 N85-17824
Power law X- and gamma-ray emission from relativistic thermal plasmas 08 p1241 N85-17829
Centrifugally driven magnetohydrodynamic (MHD) winds and the nonthermal emission regions in Active Galactic Nuclei (AGN) 08 p1242 N85-17835
Physics of nonmagnetic relativistic thermal plasmas
09 p1386 N85-18715
On the spectrum of longitudinal waves in the hot degenerate plasma 12 p1955 N85-22280
Electron-positron pair equilibrium in strongly magnetized plasmas 12 p1957 N85-22296
Electron-positron pairs in a mildly relativistic plasma in active galactic nuclei 12 p1957 N85-22297
Spacecraft-environment interaction: The environmental plasma aspect 13 p1990 N85-22479
High energy beam experiment
15 p2654 N85-26376
Limits on the Doppler factor in relativistic jets by means of gamma-ray observations
[OG-2.7-12] 22 p3872 N85-33985
Secondary antiproton production in relativistic plasmas
[OG-6.1-4] 22 p3888 N85-33996
Multiple inner shell vacancies in laser-irradiated Au plasma 23 p3981 N85-34687
Monte Carlo calculations of relativistic solar proton propagation in interplanetary space
[SH-3.2-11] 23 p4004 N85-34825
Selfsimilar time dependent shock structures
[OG-8.1-4] 23 p4017 N85-34884
Detectors for relativistic nuclear collisions (report from the Fixed-Target Hadron Group)
24 p4146 N85-35701

RELATIVISTIC THEORY
NT MANDELSTAM REPRESENTATION
Topics in black-hole physics: Geometric constraints on noncollapsing, gravitating systems, and tidal distortions of a Schwarzschild black hole 05 p0742 N85-14768
The determination of the post-Newtonian parameters in gravitational theory using laser ranging to the Lageos satellite 09 p1414 N85-18804
Viking radio science data analysis and synthesis
[NASA-CR-175631] 13 p2171 N85-23471

RELATIVISTIC VELOCITY
Testing theories of superluminal motion — QUASAT
07 p1058 N85-16714
On the propagation speed in relativistic quantum mechanics
[CWI-AM-R8410] 17 p3046 N85-28848
Spectra of solar proton ground level events using neutron monitor and neutron moderated detector recordings
[SH-1.3-14] 23 p3994 N85-34759

RELATIVITY
Contributions to the error analysis in the relativity gyroscope experiment 05 p0636 N85-14695
The period of orbit as a test of the general theory of relativity 05 p0742 N85-14772
Isolated systems in general relativity
09 p1400 N85-18813
Drag-free satellite simulator
[REPT-615] 12 p1789 N85-21229
Suspension torques on a gimballed electrostatically supported gyroscope and requirements on the gyroscope and spacecraft for the relativity gyroscope experiment
12 p1851 N85-21908
Conserved quantities and radiative aspects of asymptotically anti-de Sitter space-times
12 p1956 N85-22303
Solutions of field equations in General Relativity with spinor connection 15 p2663 N85-26436
An improved servo-controlled inertial clock for laboratory tests of general relativity 19 p3378 N85-30665
The dimensional reduction transition
[DE85-003948] 19 p3383 N85-30690
Bergson and the unification of the sciences
[DE85-009961] 20 p3538 N85-32018

RELAXATION
NMR (Nuclear Magnetic Resonance) of solid biopolymers
[AD-P003912] 01 p0032 N85-10188

RELAXATION (MECHANICS)
NT SPIN-LATTICE RELAXATION
NT STRESS RELAXATION
Effect of the Basset term on particle relaxation behind normal shock waves
[AD-A145446] 02 p0198 N85-11320
Influence of translational and hyperfine relaxation on energy characteristics of oxygen-iodine laser
02 p0261 N85-11707
Relaxation of plasma rotation in a Tokamak in the presence of extraneous forces and corrugation of the magnetic field
[DE84-015628] 02 p0284 N85-11854
Internal friction, microstructure and radiation effects
[DE84-013905] 02 p0288 N85-11880
Parameters of structural relaxation and mechanical properties of amorphous alloys
03 p0349 N85-12248
Structure and properties of grain boundaries
[DE84-014368] 04 p0570 N85-13636
Transport and relaxation processes in supercritical fluids
[DE84-006591] 05 p0731 N85-14686
Structural relaxation and isoconfigurational flow of a metallic glass near equilibrium
[AD-A147888] 07 p0933 N85-15915
On the relaxation of a turbulent boundary layer after an encounter with a forward facing step
08 p1071 N85-16780
Electrical resistivity and structural changes upon relaxation and crystallization of (Mo/sub 0.6/Ru/sub 0.4)sub 100-x/B/sub x/ metallic glasses
[DE84-017281] 09 p1299 N85-18180

Reduction of the wavepacket: How long does it take?
[DE84-016778] 09 p1400 N85-18815

On relaxation of transonic flows around zero-lift airfoils and convergence of self-correcting wing tunnels
11 p1622 N85-20214

Mini-model testing of wind turbines using novel excitation
[DE85-000666] 11 p1654 N85-20417

Energy spectrum of processes of structural relaxation of amorphous alloy FeCo70Si15B10
13 p2035 N85-22750

Numerical simulation of inverters with I2L elements including effects of high doping level
13 p2088 N85-23039

Relaxation properties and fatigue fracture resistance of austenitic spring steel
[BLL-BISI-TRANS-22300-(9022.06)]
17 p2978 N85-28406

Recent advances in d-c relaxation techniques for the measurement of kinetics of fast electrode reactions
[DE85-005029] 22 p3745 N85-33216

RELAXATION (PHYSIOLOGY)

Catecholamine excretion and subjective ratings of tension during autogenic training and mental stress
[REPT-172] 05 p0697 N85-14483

Responses of skeletal muscle to unloading, a review
[NASA-CR-176177] 24 p4128 N85-35594

Relaxation techniques
[AD-A156248] 24 p4133 N85-35621

RELAXATION METHOD (MATHEMATICS)

Relaxation times for queueing systems
[CWI-OS-R8407] 05 p0719 N85-14618

Theoretical contributions to transonic flow analysis for transport aircraft
[BMFT-FB-W-84-036] 06 p1078 N85-16838

Distributed asynchronous relaxation methods for convex network flow problems
[AD-A148027] 08 p1211 N85-17622

Investigation of three-dimensional mesh generation with precise controls
[AD-A148759] 09 p1374 N85-18636

To the theory of approximation of experimental curves by smooth functions
[PREPRINT-438] 18 p3173 N85-29671

A parallelized point successive over-relaxation method on a multiple instruction multiple data stream computer
[AD-A154377] 19 p3337 N85-30679

Optimization of a numerical method to calculate elliptic flows
[ESA-TT-889] 20 p3457 N85-31472

Relaxation phenomena and stability of probability densities
[AD-A155923] 24 p4143 N85-35682

RELAXATION TIME

Kinetics of short-range ordering in metallic glasses: Analysis of the crossover effect
[DE84-015524] 02 p0187 N85-11251

Influence of translational and hyperfine relaxation on energy characteristics of oxygen-iodine laser
02 p0261 N85-11707

Numerical experiments and theoretical analysis of the flow of an elastic liquid of the Maxwell-Oldroyd type in the presence of geometrical singularities
[WTHD-164] 06 p1163 N85-17340

NMR imaging and spectroscopy of the mammalian central nervous system after heavy ion radiation
[DE85-004509] 14 p2386 N85-24696

Infrared nonlinear processes in semiconductors
[AD-A150966] 14 p2427 N85-24968

A statistical approach to relaxation in glassy materials
[AD-A151285] 15 p2518 N85-25524

Rotational relaxation studies of hydrogen fluoride
[AD-A152711] 17 p3029 N85-28734

RELEASING

Dynamic compression and volatile release of carbonates
[NASA-CR-174076] 03 p0391 N85-12504

Theoretical thermodynamics of mixtures at high pressures 13 p2183 N85-23550

Fully redundant mechanical release actuator
[NASA-CASE-LAR-13198-1] 18 p3116 N85-29287

Slide release mechanism — for space shuttle orbiter/external tank connection device
[NASA-CASE-MSC-20080-1] 19 p3279 N85-30334

Free-float Emergency Position Indicating Radio Beacons (EPIRBs) and release mechanism on board Norwegian ships. Main specifications and user experience
20 p3404 N85-31120

RELIABILITY

NT AIRCRAFT RELIABILITY
NT CIRCUIT RELIABILITY
NT COMPONENT RELIABILITY
NT STRUCTURAL RELIABILITY

Free-piston Stirling engine development
[PB84-237767] 01 p0056 N85-10369

Ada (trademark) training curriculum. Software engineering for managers m101 teacher's exercise guide
[AD-A145094] 01 p0104 N85-10695

An integral inequality with applications to order statistics
[AD-A145081] 01 p0113 N85-10770

Total positivity. A review
[AD-A145205] 01 p0114 N85-10771

Avionics integrity program (Avip). Volume 3: Program cost assessment - environmental stress screening and diagnostic techniques
[AD-A145644] 02 p0139 N85-10942

Simulation study of a new inverse-pinch high Coulomb transfer switch
[NASA-CR-172420] 02 p0194 N85-11294

Efficient methods for mechanical and structural reliability analysis and design 02 p0205 N85-11355

Computing the reliability of k out of n systems
[AD-A145505] 02 p0206 N85-11357

Proposal for a semiautomatic program testing system
[INPE-3262-TDL/178] 02 p0240 N85-11561

On some common interests among reliability, inventory and queuing
[AD-A145595] 02 p0251 N85-11646

Editorial urges improved aviation repair work quality
03 p0310 N85-12004

Improving operational reliability and productivity of robotized technological complexes
03 p0346 N85-12227

The 30 GHz solid state amplifier for low cost low data rate ground terminals
[NASA-CR-174795] 03 p0358 N85-12300

The Lindstrom-Madden method for series systems with repeated components
[AD-A146265] 03 p0412 N85-12636

Determination sample sizes for diversified reliability test programs
[DE84-015003] 04 p0511 N85-13255

Human reliability data bank: Feasibility study
[DE84-015215] 04 p0546 N85-13476

Test experience on an ultrareliable computer communication network
[NASA-TM-85915] 04 p0552 N85-13514

Potential of flywheels for spacecraft energy storage
05 p0609 N85-13890

Analyses to develop models to project failure rates and repair costs of electronic modules and subassemblies
[AD-A146509] 06 p0816 N85-15180

More than you want to know about maximum likelihood estimation
[NASA-TM-85905] 07 p0909 N85-15752

The theory of optimal confidence limits for systems reliability with counterexamples for results on optimal confidence limits for series systems
[AD-A147236] 07 p1031 N85-16546

EDP computer tapes described
08 p1142 N85-17203

On modeling the performance and reliability of multi-mode computer systems
[AD-A148444] 08 p1208 N85-17599

An analysis of robust and efficient priors associated with a finite Bayesian model for compliance testing
[AD-A148497] 08 p1213 N85-17635

NBS (National Bureau of Standards) solar collector durability-reliability test program
[PB85-113603/GAR] 09 p1346 N85-18469

SPADE: Series-parallel directed acyclic graph evaluator
[AD-A148458] 09 p1368 N85-18592

Beyond fault trees to fault graphs
[DE84-017022] 09 p1370 N85-18608

An ultra reliable computer communication network: The dispersed sensor processing mesh
09 p1372 N85-18620

Sky coverage, confusion, completeness and reliability
09 p1412 N85-18906

Integrated Technology Rotor/Flight Research Rotor (ITR/FRR) concept definition
[NASA-CR-166445] 10 p1423 N85-18979

Integrated Technology Rotor/Flight Research Rotor (ITR/FRR) concept definition study
[NASA-CR-166444] 10 p1424 N85-18981

Reliability of adhesive bonds under severe environments. Report of the Committee on Reliability of Adhesive Bonds in Severe Environments
[AD-A149010] 10 p1451 N85-19140

Reliability studies of ceramic capacitors
[AD-A149126] 10 p1479 N85-19338

Design of explosive logic elements
[DE84-009611] 11 p1614 N85-20146

Reliability of DNC system examined
11 p1617 N85-20171

New CNC systems described
11 p1617 N85-20172

A summary and assessment of historical reliability and maintainability data for solar hot water and space conditioning systems
[DE84-004521] 12 p1876 N85-21770

AFOS (Automation of Field Operations and Services)-ERA forecast verification, September 1984
[PB85-137578] 12 p1897 N85-21912

Reliability of structural brittle materials
12 p1946 N85-22222

Effects of assuming independent component failure times, if they are actually dependent, in a series system
[AD-A150582] 13 p2101 N85-23092

Parallel test method for LSI (Large Scale Integration) microprocessors
[AD-A150237] 13 p2144 N85-23310

Contribution of instrumentation and control software to system reliability
[DE85-004693] 13 p2149 N85-23340

Electric and hybrid vehicle demonstration project
[DE85-003939] 13 p2169 N85-23455

Special power train requirements for the next generation of rotary-wing aircraft 14 p2220 N85-23769

Fine filtration: An attractive route towards lower helicopter operating costs 14 p2221 N85-23774

Estimate of fatigue stability of gas-turbine engine compressor vanes in probabilistic aspect
14 p2287 N85-24169

Cold electronics: An overview
14 p2297 N85-24221

Some recent developments in systems reliability
[AD-A150661] 14 p2317 N85-24318

Supplement to evaluation of satellite derived estimates of solar radiation
[E85-10086] 14 p2346 N85-24506

Evaluation of satellite derived estimates of solar radiation
[E85-10087] 14 p2346 N85-24507

Properties of systems which lead to efficient computation of reliability
[AD-A151033] 14 p2409 N85-24853

Convolution of the IFRA (Increasing Failure Rate Average) scaled-mins class
[AD-A151070] 14 p2411 N85-24870

Shuttle fleet operations: A simulation analysis
[AD-A151383] 15 p2491 N85-25370

Sizing capability of automated ultrasonic time-of-flight diffraction in thick section steel and aspects of reliable inspection in practice
[AERE-R-11548] 15 p2571 N85-25855

Care 3 model overview and user's guide, first revision
[NASA-TM-86404] 15 p2627 N85-26192

On failure modeling, revised
[AD-A151411] 15 p2637 N85-26263

Statistical aspects of reliability, maintainability and availability
[AD-A151228] 15 p2640 N85-26282

The evolutive state: A new definition of system state to include sequencing of events
16 p2696 N85-26643

Avionics integrity issues presented during NAECON (National Aerospace and Electronics Convention) 1984
[AD-A151923] 16 p2707 N85-26707

Technical evaluation report on the Flight Mechanics Symposium on Active Control Systems: Review, Evaluation and Projections
[AGARD-AR-220] 16 p2711 N85-26730

Active control technology: Past, present, future
16 p2711 N85-26731

Initial quality of advanced joining concepts
[AD-A152241] 16 p2759 N85-27027

Research on products obtained by powder metallurgy
16 p2766 N85-27081

Life and reliability modeling of bevel gear reductions
[NASA-TM-87006] 16 p2793 N85-27227

Photovoltaic cell reliability research: Investigation of accelerated stress factors and failure-degradation mechanisms in terrestrial solar cells
[NASA-CR-175815] 16 p2819 N85-27388

VLSI (Very large scale integrated circuits) device reliability models
[AD-A153268] 17 p2954 N85-28245

Test and evaluation plan for the Centralized Storm Information System 17 p2994 N85-28506

Reliability report for communication networks
[AD-A153764] 18 p3090 N85-29127

Silicide conductors reliability research
[AD-A153768] 18 p3095 N85-29157

Small central receiver Brayton cycle study
[DE85-006882] 18 p3128 N85-29369

Guidance on planning and implementing computer system reliability
[PB85-177996] 18 p3161 N85-29581

Specification of software quality attributes. Volume 3: Software quality evaluation guidebook
[AD-A153990] 18 p3183 N85-29595

Ultrareliable, fault-tolerant control systems: A conceptual description
[NASA-TM-86017] 19 p3221 N85-29972
A Lotus 1-2-3 based system reliability program
[DE85-010633] 19 p3340 N85-30701
Results of analysis on the design variable cells
20 p3445 N85-31386
Exponential order statistic models of software reliability growth
[NASA-CR-3909] 20 p3515 N85-31852
Globally-asynchronous locally-synchronous systems
[AD-A154624] 21 p3573 N85-32222
The optimality of lower confidence limits for the reliability of series systems obtained by the method of key test results or other related techniques
[AD-A154880] 21 p3597 N85-32338
Reliability physics 21 p3606 N85-32402
Advanced module development overview
21 p3612 N85-32445
Thin-film reliability and engineering overview
21 p3612 N85-32450
Los Alamos optical materials reliability, maintainability, and exposure testing program
[DE85-011894] 21 p3613 N85-32456
Further developments of EISCAT as an MST radar
21 p3627 N85-32534
Survival function of hypo-exponential distributions
[AD-A155518] 21 p3672 N85-32814
Ice fog as an electro-optical obscurant
[AD-A155059] 21 p3705 N85-33015
Methods of reliability design of semiconductor power devices 22 p3770 N85-33365
Photovoltaics technical information guide
[DE85-002924] 22 p3806 N85-33585
CARE 3 MENU maintenance manual
[NASA-CR-172609] 22 p3828 N85-33708
Analytical ultrasonics for structural materials
[TI85-006132] 23 p3968 N85-34600
Development of an NBS (National Bureau of Standards) polymer gage for dynamic soil stress measurement
[PB85-208494] 24 p4118 N85-35526

RELIABILITY ANALYSIS
On discrete failure models
[AD-A145579] 02 p0206 N85-11359
Reliability considerations for the total strain range version of strainrange partitioning
[NASA-CR-174757] 02 p0209 N85-11380
Research in data management and system reliability
[AD-A145496] 03 p0436 N85-12773
Climate of the Northern Hemisphere, 1851 - 1900 compared to contemporary climate
[DE84-016368] 04 p0539 N85-13426
Analysis of the impact of error detection on computer performance
[NASA-CR-174167] 04 p0547 N85-13477
Impact of NDE unreliability on pressure vessel fracture predictions
[DE84-015586] 05 p0647 N85-14151
Predicting changes in reliability characteristics of gas turbine engines during operation
06 p0776 N85-14964
Reliability analysis of local area networks, intermediate report
[BLL-WH-610-(9091.9F)] 07 p1027 N85-16520
Completely monotone regression estimates of software failure rates
[NASA-CR-174310] 08 p1204 N85-17575
Improved models for increasing wind penetration, economics and operating reliability
[NASA-CR-175536] 11 p1674 N85-20545
Reliability analysis of automatic systems
[VTT-301] 12 p1863 N85-21682
An experiment in software reliability
[NASA-CR-172553] 14 p2403 N85-24813
Approximating posterior distributions of system reliability derived from component test data
[AD-A152057] 15 p2572 N85-25857
Cost prediction model for various payloads and instruments for the Space Shuttle Orbiter
[NASA-CR-175781] 16 p2729 N85-26842
Calculating reliability and productivity of cold stamping robot complex as queuing system
16 p2761 N85-27039
Determining availability characteristics of DSN data systems using discrepancy report data
16 p2772 N85-27109
Fatigue criterion to system design, life and reliability
[NASA-TM-87017] 16 p2793 N85-27226
Extreme evaluation of reliability indices for components of metallurgical equipment
[BLL-M-36070-(5828.4)] 16 p2796 N85-27234
An abstract specification language for Markov reliability models
[NASA-TM-86423] 16 p2857 N85-27616
Performance evaluation of fiber-optic converters
17 p2941 N85-28154
Engineering significance of fatigue thresholds and short fatigue cracks for structural design
[NLR-MP-84001-U] 17 p2981 N85-28430
There is no I/O like no I/O
[DE85-009115] 17 p3014 N85-28634
Statistical estimation of software reliability
[AD-A154097] 19 p3335 N85-30665
Weibull distribution based on maximum likelihood with interval inspection data
[NASA-TM-86515] 21 p3678 N85-32847
Reliability prediction of the series system with spares subject to Weibull failure 24 p4100 N85-35413

RELIABILITY CONTROL
U QUALITY CONTROL
U RELIABILITY ENGINEERING

RELIABILITY ENGINEERING
Component reliability and assembling technologies
[CNES-NT-106] 04 p0511 N85-13256
Design and test requirements for development of today's engines 07 p0906 N85-15737
Nondestructive inspection: Improved capabilities of technicians
[AD-A147388] 07 p0975 N85-16196
Ultrasonic transducers, performance variability, design, and manufacturing procedures
[AD-A148575] 08 p1158 N85-17306
A unified model for performance and reliability of Fault-Tolerant/Multi-Mode systems
[AD-A148789] 08 p1208 N85-17601
Material flow in the manufacturing system: Fault-diagnosis systems as support for the maintenance of highly automated manufacturing systems
[PNR-90238] 09 p1371 N85-18618
AIRLAB: A laboratory for flight-crucial-electronics system research 13 p1968 N85-22362
Introduction to methods of evaluating the operational reliability of complex systems: Application to satellite control ground support 14 p2397 N85-24771
Guide for the execution of reliability tests in the laboratory — aeronautical equipment
16 p2796 N85-27237
Characterization of solderless miniwrapping connections
[CNES-NT-112] 16 p2796 N85-27238
Lightweight piston
[NASA-CASE-LAR-13150-1] 18 p3088 N85-28975
Note for a research feasibility project: High reliability design in the aeronautical field
[REPT-84-RR-350] 20 p3387 N85-31005
Statistical pooling method of fatigue data for reliability design 23 p3906 N85-34196

RELIC RADIATION
Search for the radiative decay of a cosmic relic particle with IUE
[PREPRINT-410] 04 p0580 N85-13707

RELIEF MAPS
Combinations of remote sensing data with a digital map data base — regional planning 05 p0660 N85-14240
Expansion of functions describing planetary surface and gravity field 13 p1978 N85-22410
Visualization of radar altimetry data for Venus
13 p1982 N85-22437
Mars planimetric mapping 13 p2203 N85-23666
Voyager cartography 13 p2203 N85-23668

RELIEVING
NT STRESS RELIEVING
Theory of diaphragm light modulators with electrical input signal 13 p2082 N85-23002

RELOCATION
An inexpensive radar-responding relocation device for drifting oceanographic instruments
[AD-A152170] 16 p2836 N85-27505
Predictors of transfer adjustment: A longitudinal study
[AD-A152462] 17 p3000 N85-28548

REMAGNETIZATION
U MAGNETIZATION

REMELTING
U MELTING

REMOTE CONTROL
Controlling rotation of elastic manipulator link
04 p0488 N85-13113
The human role in space. Volume 3: Generalizations on human roles in space
[NASA-CR-171225] 04 p0546 N85-13475
Application of robotics in remote fuel fabrication operations
[DE84-011481] 05 p0646 N85-14144
Review of teleoperator research
05 p0703 N85-14511
Visual systems for remotely controlled vehicles
05 p0703 N85-14512
Closing the design loop on HIMAT (highly maneuverable aircraft technology)
[NASA-TM-85923] 06 p0754 N85-14836
National airspace system configuration management interface control document. Maintenance processor subsystem to remote monitoring subsystems and remote monitoring subsystem concentrators
[NAS-MD-790] 07 p0900 N85-15786
Determining grasp points using photometric stereo and the PRISM binocular stereo system
[AD-A147762] 08 p1222 N85-17697
The influence of modern control techniques on the gas industry
[ERS-E.395] 09 p1325 N85-18329
The optimal control and design of a flexible manipulator arm 09 p1327 N85-18340
Robotics in the radiochemical laboratory
[DE85-002824] 10 p1494 N85-19433
A remotely controlled orbiting retriever
12 p1786 N85-21212
A concept for a mobile remote manipulator system
14 p2236 N85-23869
System for radio remote control of dropping bombs
[CH-639335-A5] 15 p2491 N85-25271
Optimal open loop and nonlinear feedback control for remote orbital capture
[AD-A151967] 16 p2732 N85-26859
Scanning electron microscope facility for examination of radioactive materials
[DE85-008127] 17 p2969 N85-28335
Retinally stabilized differential resolution television display
[NASA-CASE-NPO-15432-1] 18 p3089 N85-29117
Digital control of diode laser for atmospheric spectroscopy
[NASA-CASE-NPO-16000-1] 18 p3112 N85-29264
Remotely operable peristaltic pump
[NASA-CASE-MFS-28059-1] 18 p3116 N85-29288
High level radioactive waste vitrification process equipment component testing
[DE85-011143] 19 p3273 N85-30296
Development of HWVP melter/turntable components for canyon-remote maintenance and replacement
[DE85-010308] 19 p3273 N85-30298
Remote medical diagnosis 21 p3663 N85-32753
Space robot simulator vehicle
[NASA-CR-176133] 22 p3739 N85-33176
Remote temperature-set-point controller
[DE85-011614] 22 p3787 N85-33459
Telepresence work system concepts
22 p3797 N85-33525
Dual arm master controller development
22 p3797 N85-33526

REMOTE HANDLING
Advancement of remote systems technology: Past perspectives and future plans
[DE84-016710] 04 p0509 N85-13250
Conceptual design report for a remotely operated cask handling system, revision 1
[DE85-000348] 08 p1169 N85-17371
Advancement of remote technology: Past perspectives and future plans
[DE85-000934] 09 p1327 N85-18342
Advanced remotely maintainable force-reflecting servomanipulator concept
[DE85-001902] 09 p1328 N85-18345
Man/machine interface for a nuclear cask remote handling control station: System design requirements
[DE85-000256] 11 p1697 N85-20667
Tokamak fusion core experiment maintenance study
[DE85-006040] 17 p3040 N85-28613
Precision manipulator heating and cooling apparatus for use in UHV systems with sample transfer capability
[NASA-CASE-LAR-13040-1] 18 p3116 N85-29286
HERMIES-1: A mobile robot for navigation and manipulation experiments
[DE85-008652] 18 p3118 N85-29301
High level radioactive waste vitrification process equipment component testing
[DE85-011143] 19 p3273 N85-30296
Development of HWVP melter/turntable components for canyon-remote maintenance and replacement
[DE85-010308] 19 p3273 N85-30298
Manipulators in teleoperation
[DE85-010583] 20 p3512 N85-31933
NASA space station automation: AI-based technology review. Executive summary
[NASA-CR-176096] 21 p3558 N85-32135
Latch assembly
[DE85-011660] 22 p3792 N85-33492
Portable cutting apparatus
[DE85-011635] 22 p3792 N85-33498
Future of robots in nuclear plants and processes
[DE85-011505] 22 p3793 N85-33500
Telepresence work system concepts
22 p3797 N85-33525
Dual arm master controller development
22 p3797 N85-33526

Recent advances in remote handling at LAMPF
[DE85-012725] 24 p4157 N85-35775
REMOTE MANIPULATOR SYSTEM
Six degrees of freedom control with each hand?
05 p0700 N85-14492
The space shuttle orbiter remote manipulator positioning mechanism 08 p1102 N85-16963
An overview of the space remote manipulator system
08 p1102 N85-16964
Simulation 09 p1277 N85-18024
A concept for a mobile remote manipulator system
14 p2236 N85-23859
Touch-off: A method to determine the position of an object by means of a sensor-driven robot
[DE85-011178] 19 p3339 N85-30691
Telepresence work system concepts
22 p3797 N85-33525
REMOTE REGIONS
NT ANTARCTIC REGIONS
NT ARCTIC REGIONS
Project manager's handbook for special projects
[AD-A147913] 07 p1053 N85-16663
REMOTE SENSING
Satellite reconnaissance
[AD-B085034] 01 p0015 N85-10094
Direction dependent radiation behavior in the classification of multispectral aircraft remote sensing data
[SER-C-290] 01 p0063 N85-10419
Remote sensing of atmospheric particulates: Technological innovation and physical limitations in applications to short-range weather prediction
[NSF ATM-82-09684] 01 p0077 N85-10511
A lightning detection system in Sweden
01 p0078 N85-10519
The Marine Resources Experiment Program (MAREX)
[NASA-TM-87368] 01 p0086 N85-10580
Second Symposium on Space Industrialization — space commercialization
[NASA-CP-2313] 02 p0149 N85-11011
Land remote sensing commercialization: A status report 02 p0151 N85-11024
The future of satellite remote sensing: A worldwide assessment and prediction 02 p0151 N85-11025
Industrial use of land observation satellite systems
02 p0151 N85-11026
Space America's commercial space program
02 p0152 N85-11027
LANDSAT data and interactive computer mapping
02 p0152 N85-11028
Agribusiness and space: No limits to growth
02 p0152 N85-11029
Space research benefits national economy
02 p0163 N85-11107
Some statistical characteristics of atmospheric optical thickness in visible spectral range
02 p0164 N85-11109
Predicting optical image displacement velocity in survey of Earth's surface 02 p0165 N85-11116
Technological approach to automation of specialized processing of survey data 02 p0165 N85-11118
Activities report of the Radio Laboratory
[REPT-8-153] 02 p0192 N85-11288
Reducing spectral dimension of remotely sensed data using principal components analysis and a Peano scanning 02 p0212 N85-11399
The feasibility of satellite remote sensing as a technique for evaluating coal mine surface features
02 p0213 N85-11401
Relationships between grass canopy characteristics and LANDSAT Thematic Mapper bands
02 p0213 N85-11402
Active remote sensing of ocean parameters, an engineering study 02 p0213 N85-11403
Multispectral Imaging Science Working Group for Hydrologic Science: Executive summary
02 p0214 N85-11414
Fundamental remote sensing science research program. Part 1: Status report of the mathematical pattern recognition and image analysis project
[E85-10004] 02 p0215 N85-11417
A preliminary study of the feasibility of detecting the floating macrophytes by means of digital processing of MSS/LANDSAT data
[E85-10005] 02 p0215 N85-11418
Hypothesis on the origin of lineaments in the LANDSAT and SLAR images of precambrian soil in the low Contas River Valley (southern Bahia)
[E85-10007] 02 p0215 N85-11420
Utilization of LANDSAT orbital imagery in the soil survey processes at Rio Grande do Norte state
[E85-10009] 02 p0216 N85-11422
Remote sensing as a mineral prospecting technique
[E85-10010] 02 p0216 N85-11423
Development and testing of a rural credit supervision system at the level of counties and rural properties utilizing remote sensing techniques
[E85-10018] 02 p0217 N85-11431
The application of remote sensing to resource management and environmental quality programs in Kansas
[E85-10023] 02 p0218 N85-11436
Shuttle Experimental Radar for Geological Exploration (SERGE) project: Field work relating to the Shuttle Experimental Radar A (SIR-A) in Brazil (phase 2)
[NASA-CR-174033] 02 p0219 N85-11444
Applications of remote sensing techniques to oceanography and sea ice
[FOA-B-60004-M7] 02 p0220 N85-11448
Atmospheres of Uranus and Neptune
02 p0296 N85-11929
East Europe report: Scientific affairs, no. 791
[JPRS-84624] 03 p0341 N85-12195
Satellite, airborne remote sensing development outlined 03 p0342 N85-12199
East Europe report: Science and technology
[JPRS-ESA-84-038] 03 p0343 N85-12210
Achievements in development of space meteorology
03 p0343 N85-12212
Remote sensing for landforms and soils in the arid southwest United States 03 p0378 N85-12410
ERS-1 radar altimeter data products — conferences
[ESA-SP-221] 03 p0379 N85-12419
The NASA/JPL pilot ocean data system
03 p0381 N85-12433
International banking of satellite and in-situ wave data by the Marine Information and Advisory Services (MIAS)
03 p0381 N85-12434
Satellite altimetric measurements of lake levels
03 p0383 N85-12447
Report of the Division of Atmospheric Physics, 1980-1983 03 p0391 N85-12501
Millimeter-wave propagation and remote sensing of the atmosphere
[AD-A146339] 03 p0393 N85-12512
Ice-soil mixtures: Visual and near-infrared remote sensing techniques
[NASA-CR-174087] 04 p0525 N85-13358
A comparison between active and passive sensing of soil moisture from vegetated terrains
04 p0526 N85-13364
A feasibility study on the use of wind profilers to support Space Shuttle launches
[NASA-CR-3861] 04 p0538 N85-13423
Some principles of plant resources evaluation using remotely sensed data 04 p0543 N85-13459
The 1984 ASEE-NASA summer faculty fellowship program (aeronautics and research)
[NASA-TM-87393] 04 p0575 N85-13664
Basic investigation concerning the applicability of multispectral radiation data from microwave radiometry measurements to geoscientific objectives of remote sensing
[ESA-TT-846] 05 p0628 N85-14027
Development of a capacitive sensor system for high temperature application
[BMFT-FB-HA-84-027] 05 p0646 N85-14147
Air-sea heat exchange, an element of the water cycle
05 p0653 N85-14195
Contributions to remote sensing : Applications of thermal infrared
[COMMUN-34/1984] 05 p0654 N85-14196
Land Remote-Sensing Commercialization Act
[S-REPT-98-458] 05 p0654 N85-14201
EARSeL/ESA Symposium on Integrative Approaches in Remote Sensing
[ESA-SP-214] 05 p0655 N85-14202
The Interactive Planetary Image Processing System (IPIPS): A major facility for research and teaching in remote sensing 05 p0655 N85-14203
Digital comparison and correlation techniques of remote sensing images with differing spatial resolutions
05 p0655 N85-14204
The integrated use of digital cartographic data and remotely sensed imagery 05 p0655 N85-14206
Methodological research in connection with the handling of LANDSAT satellite data for archaeology
05 p0655 N85-14207
Methods for correlating geological, geochemical and geophysical data with satellite imagery in central Ireland
05 p0655 N85-14208
International cooperation in remote sensing applications 05 p0656 N85-14209
A comparison of TIROS-N series satellite data and LANDSAT data over Scotland 05 p0656 N85-14210
The Finnish approach to microwave remote sensing of snow 05 p0656 N85-14212
The areal pattern of latent and sensible heat fluxes: The combination of soil physics and remotely sensed data 05 p0656 N85-14213
Forest cover monitoring by remote sensing in Great Britain 05 p0656 N85-14214
Remote sensing of plant stress and diseases
05 p0657 N85-14216
Study of the improvement in analyzing passive microwave remote sensing data by integrated use of ground data 05 p0658 N85-14226
Remote sensing data in support of conventional data
05 p0659 N85-14232
A geoinformation expert system for synergetic use of map and image data 05 p0659 N85-14233
A methodology for an integrated spatial data model and its application to image classification
05 p0659 N85-14234
The SPOT data bank system
05 p0659 N85-14236
Evaluation of SPOT simulation data of the S GEOS campaign of the EEC by data of the test sites Freiburg and Staubing (West Germany) 05 p0659 N85-14237
Perspectives of remote sensing at the end of the decade 05 p0659 N85-14238
Combining Heat Capacity Mapping Mission (HCMM) LANDSAT and thematic map information into a unique high precision merged multichannel system — climatology 05 p0660 N85-14239
Combinations of remote sensing data with a digital map data base — regional planning 05 p0660 N85-14240
Application of high frequency 2-D digital filtering to remote sensing image processing
05 p0660 N85-14242
A multiple approach in remote sensing for structural and lithological mapping by use Modular Optoelectronic Multispectral Scanner (MOMS)/LANDSAT/Heat Capacity Mapping Mission (HCMM) data
05 p0660 N85-14244
Inventory and monitoring of national park landscapes — remote sensing 05 p0660 N85-14245
The role of expert systems in remote sensing
05 p0661 N85-14246
Electronic satellite imaging system MOMS-ESA
[BMFT-FB-W-84-033] 05 p0661 N85-14248
A diagnostic approach to obtaining planetary boundary layer winds using satellite-derived thermal data
05 p0674 N85-14330
Global Scale Atmospheric Processes Research Program Review
[NASA-CP-2344] 05 p0679 N85-14360
An investigation of the marine boundary layer during cold air outbreak 05 p0680 N85-14368
Rain volume estimation over areas using satellite and radar data 05 p0686 N85-14406
Development of a van-portable remote-sensing laser system for selective detection of natural gas leaks
[PB85-101939/GAR] 06 p0811 N85-15156
Development of radar to measure sea ice merits prize nomination 06 p0826 N85-15244
A geographic information system for resource managers based on multi-level remote sensing data
[E85-10047] 06 p0827 N85-15249
Effective use of remote sensing products in litigation
[E85-10048] 06 p0827 N85-15250
Upper Atmosphere Research Satellite (UARS) trade analysis
[NASA-CR-175269] 07 p0912 N85-15774
Intermediate results of radar backscatter measurements from summer sea ice
[AD-A147212] 07 p0940 N85-15960
Power transfer from natural emitters to collection apertures at microwave wavelengths
[NASA-CR-174275] 07 p0945 N85-15989
Stereo Electro-optical Tracking System (SETS)
[NASA-CR-172471] 07 p0962 N85-16098
Enhancement of multispectral scanner images by digital filtering
[ESA-TT-624] 07 p0969 N85-16284
Remote sensing of atmospheric gases with CO2 lasers. Continuation and conclusion of spectroscopic investigations
[BMFT-FB-W-84-030] 07 p0969 N85-16285
Remote sensing of the high latitude ionosphere
[AD-A147881] 07 p1008 N85-16405
Use of SIR-B multiincidence-angle imagery to study iceberg detectability and offshore ocean feature extraction 08 p1145 N85-17225
Geological, structural, and geomorphological analyses from SIR-B 08 p1145 N85-17226
Microwave and optical remote sensing of forest vegetation 08 p1146 N85-17228
Evaluation of SIR-B imagery for geologic and geomorphic mapping, hydrology, and oceanography in Australia 08 p1146 N85-17229
The use of digital spaceborne SAR data for the delineation of surface features indicative of malaria vector breeding habitats 08 p1146 N85-17230

Interlobate comparison of glacial-depositional style as evidenced by small-relief glacial landscape features in Illinois, Indiana, and Ohio, utilizing SIR-B
08 p1146 N85-17231

Evaluation of the L-band scattering characteristics of volcanic terrain in aid of lithologic identification, assessment of SIR-B calibration, and development of planetary geomorphic analogs 08 p1146 N85-17232

The investigation of selected oceanographic applications of spaceborne synthetic-aperture radar
08 p1146 N85-17233

Investigation of SIR-B images for lithologic mapping
08 p1148 N85-17241

Remote sensing of soil moisture
08 p1149 N85-17252

Spaceborne microwave radiometers: Background and technology requirements
[LD-R-267] 08 p1165 N85-17350

Papers of the 15th International Society for Photogrammetry and Remote Sensing (ISPRS) Congress — conferences
[TRITA-FMI-9] 08 p1175 N85-17406

Advanced technology for hydrographic mapping
[FOA-C-30371-E1] 08 p1176 N85-17418

Development of an airborne measuring system for remote sensing of Earth surface and atmosphere, spectroscopic investigations
[BMFT-FB-W-84-029] 08 p1176 N85-17420

X rays from the aurora
[AD-A148626] 08 p1186 N85-17477

Low power microprocessor based measurements system for determining the integrity of coatings on buried pipelines
[ERS-E.360] 09 p1324 N85-18323

Development and operation of a real-time data acquisition system for the NASA-LaRC differential absorption lidar
[NASA-CR-174384] 09 p1366 N85-18583

Technical evaluation report on the 48th Symposium of the Avionics Panel on Space System Applications to Tactical Operations
[AGARD-AR-203] 10 p1425 N85-18988

Pulsed photothermal radiometry for remote sensing of spectroscopic and physical properties of thin film
[AD-A149080] 10 p1435 N85-19041

Resolution enhancement of multichannel microwave imagery from the Nimbus-7 SMMR for maritime rainfall analysis
[NASA-CR-174367] 10 p1462 N85-19221

CNES, INRA do joint remote-sensing research
10 p1477 N85-19321

Brazilian Remote Sensing Shuttle Experiment (BRESEX): Characteristics and future utilization on satellites
[INPE-3313-PRE/620] 10 p1487 N85-19385

The BRESEX multispectral camera: Preliminary characteristics
[INPE-3357-PRE/635] 10 p1487 N85-19386

Earth resources: A continuing bibliography with indexes
[NASA-SP-7041(44)] 10 p1503 N85-19484

Brazilian remote sensing receiving, recording and processing ground systems in the 1980's
[E85-10079] 10 p1504 N85-19493

Preliminary evaluation of the airborne imaging spectrometer for vegetation analysis
[NASA-CR-174440] 10 p1505 N85-19496

SIR-A imagery in geologic studies of the Sierra Madre Oriental, northeastern Mexico. Part 1 (Regional stratigraphy): The use of morphostratigraphic units in remote sensing mapping
[NASA-CR-175457] 10 p1505 N85-19497

Remote sensing activities in Latin America
[INPE-3297-PRE/612] 10 p1506 N85-19501

The sharing of remote sensing techniques in Brazilian geographic research
[INPE-3307-PRE/617] 10 p1506 N85-19502

Nautical charting with remotely sensed imagery, volume 1
[AD-A149361] 10 p1506 N85-19503

Nautical charting with remotely sensed imagery. Volume 2: Case studies
[AD-A149362] 10 p1506 N85-19504

The use of image registration technique in Brasilia's urban growth monitoring
[INPE-3302-PRE/614] 10 p1569 N85-19896

Remote sensing technology now playing practical roles 11 p1619 N85-20190

Airborne remote sensing CCD imaging system
11 p1623 N85-20220

Earth observations and the polar platform
[NOAA-TR-NESDIS-18] 11 p1669 N85-20517

Influence of the atmosphere on remotely sensed reflection from vegetation surfaces
[DE85-000658] 11 p1670 N85-20521

Space System Applications to Tactical Operations
[AGARD-CP-344] 11 p1709 N85-20751

Defense Meteorological Satellite Program (DMSP)
11 p1711 N85-20766

The spot operational remote sensing satellite system: Current status and perspectives
11 p1713 N85-20776

The ESA remote sensing satellite system (ERS-1)
11 p1713 N85-20777

Preserve the sense of Earth from space — achieves of remote sensing data
[PB85-124121] 11 p1740 N85-20942

In situ orbital debris experiment concepts
12 p1784 N85-21196

Passive microwave remote sensing for sea ice research
[NASA-CR-175570] 12 p1874 N85-21758

Workshop on Remote Sensing/Lineament Applications for Energy Extraction
[DE84-008291] 12 p1875 N85-21763

Method and apparatus for calibrating the ionosphere and application to surveillance of geophysical events
[NASA-CASE-NPO-15430-1] 12 p1887 N85-21846

USSR report: Space
[JPRS-USP-85-001] 13 p1977 N85-22403

Remote sensing used for study of forest resources
13 p1983 N85-22440

China report: Science and technology
[JPRS-CST-85-005] 13 p2052 N85-22843

Geological remote sensing develops rapidly, finds broad applications 13 p2052 N85-22848

Radiosodar system for remote synchronous measurements of wind speed, temperature and its fluctuations 13 p2110 N85-23145

Remote Sensing of Snow and Evapotranspiration
[NASA-CP-2363] 13 p2123 N85-23223

NASA's land remote sensing plans for the 1980's
13 p2124 N85-23224

General report of the researches of snowpack properties, snowmelt runoff and evapotranspiration in Japan 13 p2124 N85-23225

Snowmelt-runoff model utilizing remotely-sensed data
13 p2124 N85-23226

Microwave radiometer observations of snowpack properties and comparison of U.S. Japanese results — Hokkaido, Japan and Vermont and North Dakota test sites 13 p2125 N85-23230

Estimation of regional evapotranspiration using remotely sensed land surface temperature. Part 1: Measurement of evapotranspiration at the Environmental Research Center and determination of Priestley-Taylor parameter
13 p2125 N85-23233

Estimation of regional evapotranspiration using remotely sensed land surface temperature. Part 2: Application of equilibrium evaporation model to estimate evapotranspiration by remote sensing technique — Japan 13 p2125 N85-23234

Characteristic vector analysis of inflection ratio spectra: New technique for analysis of ocean color data
[NASA-TP-2428] 13 p2126 N85-23237

Feature extraction assessment study
[AD-A150189] 13 p2126 N85-23239

Comprehensive, integrated, remote sensing at DOE sites
[DE85-004867] 13 p2126 N85-23240

Accomplishments of Institute of Cartography summarized 13 p2166 N85-23435

Zeolites on Mars: Prospects for remote sensing
13 p2195 N85-23615

Analysis of SMIRR data for volcanic and sedimentary terrains of the trans-Pecos region, Texas
13 p2197 N85-23626

Orbiting multi-beam microwave radiometer for soil moisture remote sensing 14 p2230 N85-23818

Low-frequency microwave radiometer for N-ROSS
14 p2230 N85-23819

Large space antenna technology applied to radar-imaging, rain-rate measurements, and ocean wind sensing 14 p2230 N85-23820

Advanced 2-frequency ocean sensing radar using high resolution antenna beams 14 p2230 N85-23821

The use of the ARGOS system for the study of the drift of Antarctic icebergs 14 p2240 N85-23890

China report: Science and technology
[JPRS-CST-84-012] 14 p2283 N85-24140

Remote sensing: New tool for China's geologists
14 p2283 N85-24141

Geometric error analysis for shuttle imaging spectrometer experiment
[NASA-CR-175665] 14 p2305 N85-24269

Remote sensing of directional wave spectra using the surface contour radar
[NASA-TM-84440] 14 p2347 N85-24510

Evaluation of carrying capacity and landscape damage in northern Kenya by multistage remote sensing
[DFVLR-FB-84-47] 14 p2347 N85-24514

Determination of ionospheric electron density profiles from satellite UV (ultraviolet) emission measurements
[AD-A150734] 14 p2373 N85-24687

Scientific experiments. Preprocessing of scientific data — spaceborne experiments
14 p2398 N85-24779

USSR report: Space
[JPRS-USP-85-003] 15 p2476 N85-25284

Optimization of system for observing Northern Hemisphere atmospheric pressure field
15 p2485 N85-25336

Use of space information in petroleum- and gas-prospecting work (example of Southern Mongolia)
15 p2485 N85-25341

Evaluating identifiability in remote sensing problems
15 p2486 N85-25347

Determining characteristics of optical radiation reflectors based on results of remote sensing
15 p2488 N85-25368

Details on spot remote sensing satellite propulsion unit 15 p2535 N85-25640

Analysis of suspended sediment distributions in the surface waters of Delaware Bay using remote sensing of optical properties 15 p2582 N85-25925

Survey of remote sensing techniques for wave measurement
[NASA-TM-84429] 15 p2583 N85-25929

SAM 2 measurements of the polar stratospheric aerosol, volume 5
[NASA-RP-1140] 15 p2590 N85-25970

Shuttle imaging radar-B (SIR-B) data analysis for identifying rainfall event occurrence and intensity
[NASA-CR-175712] 15 p2594 N85-25996

Potential climatic effects on the Greenland ice sheet
15 p2603 N85-26044

Connection between time- and frequency-domain three-dimensional inverse problems for the Schroedinger equation
[DE85-005914] 15 p2639 N85-26274

Tenth Conference of Working Group of Socialist Countries on Remote Sensing of Earth under Intercosmos Program 16 p2725 N85-26820

One approach to remote sensing of total ozone content 16 p2725 N85-26822

Scheme for atmospheric thermal sensing from satellites with enhanced vertical resolution
16 p2726 N85-26823

Multiple regression analysis of photographic image of soil properties 16 p2726 N85-26825

Contribution to space program reviewed
16 p2727 N85-26834

Radar return from vegetation covered terrains
[INPE-3470-PRE/713] 16 p2770 N85-27080

The Bresex multispectral camera: Preliminary characteristics
[INPE-3424-PRE/687] 16 p2787 N85-27195

China's integrated circuit production
16 p2806 N85-27302

Study of the urban evolution of Brasilia with the use of LANDSAT data
[E85-10101] 16 p2809 N85-27321

Simultaneous Earth observations from 2 satellites
[NASA-TM-86204] 16 p2810 N85-27325

System of interpretation of remote sensing data when hydrocarbons are present, volume 2
[INPE-3087-TDL/162-VOL-2] 16 p2810 N85-27326

SELPER (Latin American Society of Remote Sensing Specialists)
[INPE-3315-PRE/622] 16 p2810 N85-27328

Function of remote sensing in Brazil
[INPE-3314-PRE/621] 16 p2810 N85-27329

The relevance of remote sensing to Brazil
[INPE-3421-PRE/686] 16 p2811 N85-27332

Utilization of remote sensing data in the evaluation of air pollution characteristics in the south coast/Southeast Desert Air Basin
[PB85-162063] 16 p2822 N85-27407

In-situ stratospheric ozone measurements: Recent results and their implications 16 p2824 N85-27418

SAM II measurements of the polar stratospheric aerosol. Volume 6: April to October 1981
[NASA-RP-1141] 16 p2825 N85-27422

Ground-based remote sensing of atmospheric pollution 16 p2832 N85-27462

Atmospheric frontal zone studies
[NASA-CR-175293] 16 p2833 N85-27469

Experience of the Institute of Space Research with the use of remote sensing in urban planning studies
[INPE-3159-PRE/533] 16 p2860 N85-27770

Remote sensing of the plasma with time delay measurements (coronal sounding)
16 p2866 N85-27804

Solar activity monitoring satellite (SAMSAT): Impact on space environment services
[PB85-165066] 16 p2888 N85-27818

Test devices for aeronautical research and technology [NASA-TM-77651] 17 p2905 N85-27914

Earth observation modeling based on layer scattering matrices [NLR-MP-84015-U] 17 p2984 N85-28440

Developments in remote sensing [illegible] 17 p2984 N85-28441

Convective storm downdraft outflows detected by NASA/MSFC's Airborne 10.6 micron pulsed Doppler Lidar System [NASA-CR-3898] 17 p2995 N85-28511

Light scattering by leaf layers with application to canopy reflectance modeling: The Scattering by Arbitrarily Inclined Leaves (SAIL) model [NLR-MP-84011-U] 17 p3038 N85-28796

Experimental philosophy leading to a small scale digital data base of the conterminous United States for designing experiments with remotely sensed data [NASA-TM-85009] 17 p3049 N85-28877

German contributions to the cartography of Antarctica by means of photogrammetry and remote sensing 18 p3124 N85-29342

Looking down looking forward: Earth observation, sciences and applications, a perspective [ESA-SP-1073] 18 p3149 N85-29497

Arctic mixed layer dynamics [AD-A153582] 18 p3150 N85-29505

ERS economic impace study [ESA-CR(P)-1979] 18 p3199 N85-29847

Technology assessment of high pulse energy CO(2) lasers for remote sensing from satellites [NASA-TM-86415] 19 p3275 N85-30309

Space methods for geological research 19 p3295 N85-30429

Spectral reflectances of natural targets for use in remote sensing studies [NASA-RP-1139] 19 p3299 N85-30450

Nimbus 7 Coastal Zone Color Scanner (CZCS). Level 2 data product users' guide [NASA-TM-86202] 19 p3299 N85-30452

Nimbus 7 Coastal Zone Color Scanner (CZCS). Level 1 data product users' guide [NASA-TM-86203] 19 p3299 N85-30453

Active and passive remote sensing of ice [AD-A154406] 19 p3300 N85-30459

Geologic interpretation of remote sensing data for the Martian volcano Ascraeus Mons 19 p3384 N85-30992

Microwave hydrology: A trilogy [NASA-CR-176042] 20 p3477 N85-31603

Influence of spatial variability of hydraulic characteristics of soils on surface parameters obtained from remote sensing data in infrared and microwaves [NASA-TM-77902] 20 p3477 N85-31604

Remote Sensing Technology: Symposium Proceedings [DE85-010212] 20 p3477 N85-31606

Millimetre wave pulse technology — satellite mapping [ESA-CR(P)-2004] 20 p3478 N85-31611

Tropical Ocean and Global Atmosphere (TOGA) heat exchange project: A summary report [NASA-CR-176038] 20 p3496 N85-31738

A new global geomorphology? 21 p3601 N85-32358

Geomorphological similarity and uniqueness 21 p3601 N85-32361

Regional landform thresholds 21 p3601 N85-32362

Mega-geomorphology and neotectonics 21 p3602 N85-32366

Andrean examples of mega-geomorphology themes 21 p3602 N85-32367

Space imagery and some geomorphological problems of the Guiana Shield, South America 21 p3602 N85-32368

Deep sea mega-geomorphology: Progress and problems 21 p3602 N85-32369

Use of the synoptic view: Examples from Earth and other planets 21 p3602 N85-32371

Geomorphic analyses from space imagery 21 p3603 N85-32374

Use of spaceborne imaging radar in regional geomorphic studies 21 p3603 N85-32377

Techniques, problems and uses of mega-geomorphological mapping 21 p3604 N85-32378

Global geomorphology: Report of Working Group Number 1 21 p3604 N85-32382

Process thresholds: Report of Working Group Number 3 21 p3604 N85-32384

Biogeochemical cycling and remote sensing 21 p3659 N85-32733

Remote medical diagnosis 21 p3663 N85-32753

Participation of singlet oxygen in photodestruction of air-saturated solutions of coumarin dyes 21 p3665 N85-32891

The possibilities of remote analysis of atmospheric gases based on Raman scattering spectroscopy 21 p3665 N85-32892

Cosmonauts participate in multilevel remote sensing experiment 22 p3731 N85-33130

Spacecraft-aided research discussed at geology Congress 22 p3734 N85-33147

Enhancing precision of remote temperature sensing data from satellites under cloudy atmospheric conditions 22 p3734 N85-33148

Impact of fluctuations in optical properties of atmosphere on the ratio of spectral brightness from remote sensing of agricultural land 22 p3734 N85-33149

Determination of altitude of cloud cover top from Meteor satellite data 22 p3734 N85-33150

Landscape interpretation capabilities using space photographs of regions of a multistage platform mantle structure 22 p3734 N85-33151

Interpretation of multiband photographs made during Telefoto-80 experiment for the purpose of discriminating agricultural crops 22 p3735 N85-33152

Using remote photographs in prospecting for hydrocarbons on the Kerch Peninsula 22 p3735 N85-33154

Cataloging the spectral brightness coefficients of the forested region of the European territory of the USSR 22 p3735 N85-33155

Regression analysis of aircraft and ground measurement data on vegetation cover 22 p3735 N85-33156

Direct regression analysis of remote sensing data (using example of grass cover) 22 p3736 N85-33157

Optical-fiber/microprocessor-based remote velocity sensor [DE85-010071] 22 p3788 N85-33470

Fracture detection and characterization for geothermal reservoir definition [DE85-008677] 22 p3815 N85-33630

Potential spin-offs of the carbon dioxide observational platform system (CO-OPS) for remote sensing opportunities [NASA-TP-2510] 23 p3899 N85-34149

The scientific and technical issues in integrating remotely sensed imagery with geocoded data bases 23 p3960 N85-34547

Selection of segment similarity measures for hierarchical picture segmentation 23 p3960 N85-34548

The International Cometary Explorer (ICE)wallsheet teacher's guide [NASA-TM-87498] 23 p3988 N85-34727

Microwave properties of a quiet sea [NASA-CR-176199] 24 p4085 N85-35322

Processing of LANDSAT imagery to map surface mineral alteration on the Alaska Peninsula, Alaska 24 p4106 N85-35455

The development of assessment techniques program 24 p4106 N85-35457

Remote sensing of hydrologic transport processes using spot simulation data [DE85-012412] 24 p4108 N85-35467

Kinematic analysis of Hurricane Frederick (1979) using satellite, aircraft and rawinsonde data [NASA-CR-176167] 24 p4119 N85-35533

Sea surface and remotely sensed temperatures off Cape Mendocino, California [NASA-TM-86712] 24 p4125 N85-35573

REMOTE SENSORS

Flight demonstration of new NRL real-time data acquisition system and laser video waveform sampler [AD-A145126] 01 p0053 N85-10350

Middle infrared spectral studies of geologic materials in their natural state using photothermal beam deflection spectroscopy [AD-A144894] 01 p0120 N85-10820

Earth Resources, A Continuing Bibliography with Indexes [NASA-SP-7041(43)] 03 p0378 N85-12411

Thematic Mapper. Volume 1: Calibration report flight model, LANDSAT 5 [E85-10059] 07 p0987 N85-16270

Thematic Mapper. Volume 2: Flight model prechipment review [E85-10060] 07 p0987 N85-16271

On-board processing for linescan sensors in miniature unmanned aircraft [RAE-TM-SPACE-327] 08 p1065 N85-16870

Development of the GASCOPACT (R) pipe and cable tracer [ERS-E.340] 09 p1324 N85-18320

GASCOPACT: A new approach to pipe and cable location [ERS-E.383] 09 p1325 N85-18324

Nautical charting with remotely sensed imagery, volume 1 [AD-A149361] 10 p1506 N85-19503

An evaluation of wind measurements by four Doppler sodars [PB85-115301] 10 p1520 N85-19586

Spectral characterization of the LANDAT-4 MSS sensors 11 p1666 N85-20499

LANDSAT-4 Science Characterization Early Results. Volume 2, part 1: Thematic Mapper (TM) [E85-10068] 11 p1668 N85-20508

An overview of LANDSAT-4 and the Thematic Mapper 11 p1668 N85-20509

Remote self-contained undersea monitor [AD-D011520] 12 p1849 N85-21599

Method of and apparatus for measuring temperature and pressure — atmospheric sounding [NASA-CASE-GSC-12558-1] 12 p1856 N85-21639

Spatial resolution estimation of LANDSAT-4 Thematic Mapper data 12 p1872 N85-21741

Digital processing of mesoscale analysis and space sensor data [NASA-CR-171429] 13 p2146 N85-23319

The remote detection of polynuclear aromatic hydrocarbons using laser-induced fluorescence [AD-A152294] 16 p2757 N85-27013

Active and passive remote sensing of ice [AD-A151741] 16 p2815 N85-27369

A transduction path method of solid state sensor analysis and investigation [AD-A152123] 16 p2870 N85-27707

Development of an EM-Based lifeform detector [AD-A153504] 18 p3151 N85-29512

Chemometric analysis of multisensor arrays [AD-A153805] 18 p3174 N85-29680

A laser slope gauge and a spar buoy wave gauge: Tools for the validation of microwave remote sensors [AD-A154038] 19 p3272 N85-30290

Touch-off: A method to determine the position of an object by means of a sensor-driven robot [DE85-011178] 19 p3339 N85-30891

System enhancements of Mesoscale Analysis and Space Sensor (MASS) computer system [NASA-CR-171463] 19 p3342 N85-30708

Spectroradiometric calibration of the Thematic Mapper and Multispectral Scanner system [E85-10104] 20 p3476 N85-31601

Characteristics and sources of E-region ionization in the continuous aurora [AD-A155018] 21 p3632 N85-32562

Target observability for satellite-based sensors [AD-A156139] 24 p4069 N85-35217

REMOTELY PILOTED VEHICLES

Characterization of atmospheric conditions along transmission paths from a remotely piloted vehicle [AD-A145527] 02 p0232 N85-11511

Visual systems for remotely controlled vehicles 05 p0703 N85-14512

Technology development for unmanned untethered submersible vehicle systems [AD-A148794] 09 p1304 N85-18190

Operational effectiveness of a Multiple Aquila Control System (MACS) [NASA-CR-174436] 10 p1427 N85-19000

Operation and maintenance requirements of the Army Remotely Piloted Vehicle (RPV) [NASA-CR-175714] 14 p2218 N85-23755

Remote control of an impact demonstration vehicle [NASA-TM-85925] 14 p2225 N85-23797

The PINGUIN B3: A remotely piloted vehicle for mine identification and disposal [MBB-UM-1/84-O] 16 p2874 N85-27735

British super-shuttle 18 p3067 N85-29104

A remote-operated manipulator vehicle [HSE-TRANS-11133] 19 p3281 N85-30349

A survey of the turbulence in the marine surface layer for the operation of low-Reynolds number aircraft [AD-A154133] 19 p3316 N85-30558

Flight test experience and controlled impact of a large, four-engine, remotely piloted airplane [NASA-TM-86738] 22 p3730 N85-33123

REMOVAL

Heliport snow and ice control methods and guidelines [DOT/FAA/PM-84/22] 01 p0012 N85-10073

Digital Terrain Elevation Data (DTED) anomaly removal through the use of an interactive Fourier frequency filtering process [AD-A145433] 02 p0219 N85-11445

Laser paint removal [AD-P004009] 03 p0306 N85-11989

Alternatives for runway rubber removal from porous friction surfaces [DOT/FAA/PM-84/28] 05 p0597 N85-13803

A method of making the gas-electric removal of highly dispersed particles more effective [BLL-M-36030-(5828.4)] 06 p0765 N85-14890

The mechanical procedures for the 8 channel bolometer — United Kingdom Infrared Telescope [UKIRT-18] 09 p1414 N85-18916

The removal, mechanical handling and installation procedures for the RA Ilek encoder
[UKIRT-21] 09 p1414 N85-18919
Removal of heavy metals by artificial wetlands
[PB85-116127] 10 p1513 N85-19548
Improved techniques for removal of sediments contaminated with hazardous materials
[PB85-116093] 11 p1679 N85-20580
Hydrogen embrittlement of cadmium-plated ultra-high strength steels in paint strippers
[ARL/MAT-R-117] 12 p1806 N85-21326
Hazardous air pollutants: Dry-deposition phenomena
[PB85-138279] 12 p1867 N85-21843
The behaviour of nitride inclusions in nickel-base alloys
[BLL-BISI-TRANS-22396-(9022.06)]
17 p2927 N85-28058
A comparative evaluation of the effects of acid precipitation, natural acid production and harvesting on cation removal from forests
[DE85-010621] 19 p3309 N85-30511
Method for removing chlorine compounds from hydrocarbon mixtures
[DE85-011608] 22 p3742 N85-33191

REMS
U RAPID EYE MOVEMENT STATE

RENAL FUNCTION
The behavior of renal-regulating hormones during hypogravic stress
[NASA-CR-171877] 15 p2616 N85-26123
Mathematical modeling of fluid-electrolyte alterations during weightlessness
[NASA-CR-171881] 15 p2617 N85-26125
Fluid-electrolyte metabolism and renal function in cosmonauts following 185-day spaceflight
23 p3952 N85-34495

RENDEZVOUS
NT ORBITAL RENDEZVOUS
NT SPACE RENDEZVOUS

RENDEZVOUS GUIDANCE
Automatic assembly of space stations
20 p3409 N85-31153

RENDEZVOUS SPACECRAFT
Rendezvous with Saturn's rings
15 p2679 N85-26543

RENE 95
Comparison between the properties of conventional wrought and powder metallurgical alloys for turbine disc applications 07 p0906 N85-15739

REORIENTATION
U RETRAINING

REPAIRING
U MAINTENANCE

REPEATERS
Test and evaluation of a coherent 35 gigahertz radar repeater
[AD-A145714] 02 p0191 N85-11260
Signal Hill solar-powered repeater report and recommendations
[DE85-000487] 09 p1316 N85-18273
Preliminary investigation of the performance of repeater technology for satellite sound broadcasting
[SSP/017/82] 18 p3092 N85-29137

REPETITION
A high-repetition rate, inductively stabilized, long-pulse excimer laser
[DE84-016827] 04 p0506 N85-13229
An evaluation of flashtube signal characteristics
[AD-A149569] 10 p1423 N85-18974
Limits to the burster repetition rate as deduced from the 2nd catalog of the interplanetary network
[OG-1.2-5] 22 p3662 N85-33915
Vector calculation of particle code
23 p3981 N85-34666

REPLACING
The effect of replacing molybdenum with vanadium on the corrosion resistant properties of stainless steels
02 p0178 N85-11197
Life distribution properties of devices subject to deterioration
[AD-A145554] 02 p0206 N85-11358
The replacement of precious metal thick film inks using conductive polymer technology. Phase 1: Feasibility study
[AD-A147614] 07 p0933 N85-15913
On maximizing the expected lifetime of replaceable systems
[AD-A150003] 12 p1862 N85-21680
The role of mock-ups in the development of Orbital Replaceable Units (ORU) 18 p3160 N85-29573
F-111 automatic test equipment replacement program
20 p3437 N85-31322
Negative flexural behavior of precase composite slabs with steel joint 23 p3904 N85-34183

REPLENISHMENT
Computer simulation of multiple stability regions in an internally cooled superconducting conductor and of helium replenishment in a bath-cooled conductor
[DE85-002112] 09 p1399 N85-18805
A replenishment phase study for the NAVSTAR global positioning system
[AD-A152030] 16 p2704 N85-26695
Renewable energy research and development outlook, volume 1
[DE85-011577] 20 p3540 N85-32033
Feasibility of applications of Competition Decision Assist Package (CDAP) to spare parts
[AD-A154716] 21 p3712 N85-33036

REPLICAS
Application of extraction replicas and analytical electron microscopy to precipitate phase studies
[DE85-001253] 06 p0769 N85-14919

REPORTS
NT CONGRESSIONAL REPORTS
NT PRESIDENTIAL REPORTS
Research and technology highlights of the Lewis Research Center
[NASA-TM-86899] 08 p1261 N85-17928
Research and technology, Lyndon B. Johnson Space Center
[NASA-TM-58263] 08 p1262 N85-17929
West Europe report: Science and technology
[JPRS-WST-85-003] 09 p1309 N85-18224
USSR report: Life sciences. Biomedical and behavioral sciences
[JPRS-UBB-85-011] 10 p1525 N85-19616
USSR report: Physics and mathematics
[JPRS-UPM-85-001] 11 p1715 N85-20786
Research in surface sciences, disordered materials, and solidification and growth
[PB85-132140] 11 p1737 N85-20927
Transportation
[JPRS-UTR-85-004] 12 p1769 N85-21105
Activities of the Jet Propulsion Laboratory, 1 January - 31 December 1983
[NASA-CR-175555] 13 p2167 N85-23447
Investigations carried out under the Director's Discretionary Fund
[NASA-CR-175676] 14 p2432 N85-24999
USSR report: Transportation
[JPRS-UTR-84-025] 17 p2894 N85-27841
Experimental plasma research: Plasma summaries
[DE85-008116] 17 p3039 N85-28805
Analytical Chemistry Division
[DE85-010585] 18 p3066 N85-28974
National Archives and Records Service (NARS) twenty year preservation plan
[PB85-177640] 18 p3200 N85-29854
High-efficiency silicon solar cell research
21 p3609 N85-32417
National Center for Atmospheric Research
[PB85-191237] 22 p3848 N85-33835
NBS (National Bureau of Standards) library serial holdings, 1985
[PB85-191948] 22 p3849 N85-33839
Confinement experiments on ISX-B
[DE85-012346] 23 p3984 N85-34709

REPRESENTATIONS
A representation for the functioning of devices that supports compilation of expert problem solving structures: An extended summary
[AD-P003921] 02 p0245 N85-11601

REPRODUCTION (BIOLOGY)
Pollutant body burdens and reproduction in Platichthys stellatus from San Francisco Bay
[DE85-010407] 19 p3308 N85-30509
Vertebrate development in space: Gravity is a drag (and has been for eons and eons) 24 p4126 N85-35580

REPRODUCTION (COPYING)
Photocopiers: Do they pose a health hazard?
[P83-1E] 02 p0234 N85-11527
An investigation into the fidelity of reproduction of UKST original objective prism plates on to film — United Kingdom Schmidt Telescope (UKST) 07 p0965 N85-16123

REPTILES
NT TURTLES

REPUBLIC AIRCRAFT
NT A-10 AIRCRAFT

REPUBLIC MILITARY AIRCRAFT
U MILITARY AIRCRAFT

REPUBLIC OF CHINA
U TAIWAN

REPUBLIC OF SOUTH AFRICA
The SANCOR estuaries programme, 1982-1986
[ISBN-0-7988-2662-2] 01 p0068 N85-10454
The SANCOR programme on coastal processes, April 1982 - March 1988
[REPT-68] 01 p0069 N85-10455
Estuaries of the Cape. Part 2: Synopses of available information on individual systems. Report 12: [illegible] (WES) (CSW 1), Elsies (CSW 2), Sir Lowry's Pass (CSW, Steenbras (CSW 9), and Buffels (OOS) (CSW 11)
[CSIR-RR-411-PT-2] 01 p0086 N85-105
Estuaries of the Cape. Part 2: Synopses of available information on individual systems. Report no. 14: [illegible] (CSW 4)
[CSIR-RR-413-PT-2] 01 p0086 N85-10
Estuaries of the Cape. Part 2: Synopses of available information on individual systems. Report no. 15: [illegible] (CSW 5)
[CSIR-RR-414-PT-2] 01 p0087 N85-10
Estuaries of the Cape. Part 2: Synopses of available information on individual systems. Report no. 16: [illegible] (CSW 6)
[CSIR-RR-415-PT-2] 01 p0087 N85-10

REPULSION
U FORCE

REQUIREMENTS
Information requirements analysis: An application
[AD-A144696] 01 p0125 N85-10
DOD related software technology requirements, practices, and prospects for the future
[AD-A145493] 02 p0242 N85-1157
Design of a scientific information collation and dissemination system, volumes 1 thru 3
[AD-A146002] 03 p0436 N85-127
Operational requirements - system concepts
06 p0752 N85-14
Man-machine interface requirements - advanced technology 06 p0753 N85-14
View of future requirements for engine cyclic durability by analysis and testing 07 p0906 N85-1575
Estimating wartime support resource requirements. Statistical and related policy issues
[AD-A147923] 07 p1053 N85-16
Overview od STS ground operations/orbiter turnaround STS-1 through STS-7 08 p1096 N85-16
Safety requirements for wiring systems and connectors for photovoltaic systems
[NASA-CR-174431] 10 p1477 N85-18
Distributed data processing design methodology
[AD-A148688] 10 p1537 N85-19
A proposed integration among organizational information requirements, media richness and structural design
[AD-A149317] 10 p1567 N85-19
Requirements formulation subtask 1.A of the Major Item System Mapping (MISM) project
[DE85-000978] 11 p1740 N85-20
GSFC specification electronic data processing magnetic recording tape
[NASA-TM-80599] 12 p1851 N85-21
1985 Resident research associateships: Postdoctoral and senior research awards
[NASA-TM-87458] 12 p1963 N85-22
Safety with industrial manufacturing lasers
14 p2306 N85-24
Procedures for use in compiling requirements specifications for computerized library systems
[CSTI-76] 15 p2665 N85-25
Design and implementation of the digital engineering laboratory distributed database management system
[AD-A151694] 15 p2665 N85-25
Technical overview structural dynamics
16 p2736 N85-26
USAF damage tolerant design handbook: Guidelines for the analysis and design of damage tolerant aircraft structures, revision B
[AD-A153161] 17 p2896 N85-27
Steel Tubes
[BLL-BISI-TRANS-22064-(9022.06)]
17 p2973 N85-28
Functional and performance requirements of the next NOAA-Kasas City computer system
17 p2994 N85-28
A systematic determination of skill and simulator requirements for airline transport pilot certification
[AD-A154135] 19 p3330 N85-30
Proceedings of the Workshop on Detectors for Relativistic Nuclear Collisions
[LBL-18225] 24 p4146 N85-357

RESCUE OPERATIONS
SAR maritime missions 06 p0751 N85-148
HH-60D night hawk helicopter
06 p0752 N85-14817
Avionics system design for requirements for the United States Coast Guard HH-65A Dolphin
06 p0753 N85-1482
Shipboard and satellite-aided communications equipment in exhibition 06 p0819 N85-15
Experimental satellite system for determining coordinates of maritime distress
09 p1308 N85-182

he sinking of the Les Mutuelles du Mans trimaran
14 p2327 N85-24384

he SARSAT program 14 p2327 N85-24385

he ARGOS contribution to the demonstration of the ctiveness of a satellite-based search and rescue stem
14 p2330 N85-24404

The SARSAT/COSPAS system for assisting satellite ed search and rescue 14 p2398 N85-24776

icrocomputer application of aerospace asset surface rch planning
D-A151893] 15 p2487 N85-25227

nternational conference on COSPAS-SARSAT system
15 p2484 N85-25336

Lidar techniques for search and rescue
DE85-006586] 19 p3278 N85-30327

Satellite aided search and rescue. Experimental results nd operational prospects — conference
SBN-2-85428-120-9] 20 p3400 N85-31088

The international organization of maritime search and escue 20 p3400 N85-31089

Search and rescue services for international civil viation 20 p3400 N85-31090

INMARSAT: An overview 20 p3400 N85-31091

COSPAS/SARSAT: An overview
20 p3400 N85-31092

Maritime search and rescue cooperation and planning
20 p3400 N85-31093

Search and rescue at sea in the USSR
20 p3400 N85-31094

The contribution of an operational SAR satellite system to the UK SAR organisation — search and rescue (SAR)
20 p3400 N85-31095

Search and rescue of aircraft in distress in France. Organization, means 20 p3401 N85-31096

Specific aspects of maritime search and rescue in French metropolitan and overseas territories: Expected benefits rom a detection and location of distress system by satellites 20 p3401 N85-31097

Search and rescue in Canada
20 p3401 N85-31098

The national Search and Rescue (SAR) needs and organization in Norway 20 p3401 N85-31099

Possible use of the COSPAS/SARSAT system within the Swedish mountain rescue organization
20 p3401 N85-31100

The COSPAS-SARSAT system
20 p3401 N85-31101

The COSPAS-SARSAT space segment: Present status and evolution 20 p3401 N85-31102

Rescue satellite COSPAS 20 p3401 N85-31103

The 121.5 MHz ELT: Past, present and future — Emergency Locator Transmitter (ELT)
20 p3401 N85-31105

The 406 MHz ELT/EPIRBs — Emergency Locator Transmitters/Emergency Position Indicating Radio Beacons (ELT/EPIRB) 20 p3402 N85-31106

Soviet Emergency Locator Transmitter/Emergency Position Indicating Radio Beacon (ELT/EPIRBs) at 121.5 and 406 MHz 20 p3402 N85-31107

Ground segment of COSPAS system
20 p3402 N85-31108

Existing and potential INMARSAT capabilities for the Future Global Maritime Distress and Safety System
20 p3402 N85-31110

The International Radio Consultative Committee (CCIR) recommended satellite Emergency Position Indicating Radio Beacon (EPIRB) system operating through geostationary satellites at 1.6 GHz
20 p3402 N85-31112

A 406 MHz geostationary satellite SARSAT experiment 20 p3403 N85-31113

Evolution of 406 MHz Search and Rescue (SAR) processor 20 p3403 N85-31116

Free-float Emergency Position Indicating Radio Beacons (EPIRBs) and release mechanism on board Norwegian ships. Main specifications and user experience
20 p3404 N85-31120

Experiments of a LORAN-C aided recovery system and a proposal of its application to rescue system
20 p3404 N85-31121

SARSAT 406 MHz system technical evaluation
20 p3404 N85-31124

The COSPAS system tests. Technical results
20 p3404 N85-31125

Use of 121.5/243.0 MHz COSPAS-SARSAT data by North American SAR agencies — search and rescue (SAR) 20 p3405 N85-31127

The COSPAS/SARSAT demonstration and evaluation. Results of the first year in the United States
20 p3405 N85-31128

COSPAS-SARSAT demonstration and evaluation results in Canada 20 p3405 N85-31129

COSPAS-SARSAT demonstration and evaluation phase: COSPAS tests in the USSR and their results
20 p3405 N85-31130

The SARSAT-COSPAS demonstration in France
20 p3405 N85-31131

UK experience with COSPAS-SARSAT and INMARSAT distress systems 20 p3406 N85-31132

The COSPAS-SARSAT system evaluation in Norway
20 p3406 N85-31133

INMARSAT distress and safety communication
20 p3406 N85-31134

Maritime mobile satellite techniques as an integral part of the Future Global Maritime Distress and Safety System (FGMDSS): The position of the Federal Republic of Germany 20 p3406 N85-31136

Future prospects for a combined INMARSAT polar communication and search and rescue satellite system
20 p3406 N85-31137

The development of an institutional structure for the Future Global Satellite System for Search and Rescue
20 p3406 N85-31138

Aircraft accident report: World Airways Inc., Flight 30H, McDonnell Douglas DC-10-30CF, N113WA, Boston-Logan International Airport, Boston, Massachusetts, January 23, 1982
[PB85-910406] 22 p3728 N85-33114

RESEARCH

NT DYNAMIC PROGRAMMING
NT LINEAR PROGRAMMING
NT LOW DENSITY RESEARCH
NT MARKET RESEARCH
NT MATHEMATICAL PROGRAMMING
NT NONLINEAR PROGRAMMING
NT NUCLEAR RESEARCH
NT QUADRATIC PROGRAMMING

South African Antarctic research report to SCAR, no. 24, 1982. 1: Record of activities: April 1981 - September 1982. 2: Planned activities: October 1982 - September 1983. 3: Recent publications: 1981/1982
[CSIR-SR-SCAR-24] 01 p0063 N85-10417

National Science Foundation, fiscal year 1983, volume 1
[PB84-212315] 01 p0124 N85-10853

Publications of the National Bureau of Standards, 1983 catalog
[PB84-218031] 01 p0126 N85-10869

Artificial intelligence applications to maintenance
[AD-P003914] 02 p0244 N85-11594

Navy programs on ion implantation for materials modification
[AD-P003952] 02 p0286 N85-11868

Characteristics of systems engineering in aviation science research
[AD-A145602] 02 p0292 N85-11899

Computer equipment for research in statistics
[AD-A145755] 03 p0406 N85-12591

Priorities for a national program of continental drilling for scientific purposes 04 p0534 N85-13418

The 1984 NASA/ASEE summer faculty fellowship program
[NASA-TM-87392] 04 p0574 N85-13662

Activities at the Lunar and Planetary Institute
[NASA-CR-174069] 04 p0579 N85-13694

Activities at the Lunar and Planetary Institute, introduction 04 p0579 N85-13695

Resident research associateships. Postdoctoral and senior research awards
[NASA-TM-87399] 05 p0734 N85-14717

Research into topics in transonic flow theory
[AD-A148526] 06 p1078 N85-16837

Beam propagation studies at NRL (Naval Research Laboratory) July 1983 to June 1984, volume 2
[AD-A148198] 08 p1152 N85-17270

Use of iterative linear and nonlinear algebraic methods for solving large stiff systems of ODEs
[AD-A148516] 08 p1213 N85-17836

Research in stochastic processes
[AD-A148622] 08 p1216 N85-17860

Resident research associateships. Postdoctoral and senior research awards: Opportunities for research at the Jet Propulsion Laboratory
[NASA-CR-174343] 09 p1418 N85-18945

Keyword thesaurus: A list of terms and codes to identify areas of interest for research and other types of sponsored programs (revised October 1984)
[PB85-136883] 10 p1568 N85-19690

China report: Science and technology
[JPRS-CST-84-026] 11 p1619 N85-20189

China report: Science and technology
[JPRS-CST-84-025] 11 p1620 N85-20197

Thermophysical properties of matter
11 p1620 N85-20199

China report: Science and technology
[JPRS-CST-85-008] 12 p1820 N85-21416

Report on the Second Annual Review Meeting of the National Acid Precipitation Assessment Program. Research to assist decisionmaking: Summary
[DE85-003003] 12 p1884 N85-21820

Bibliography of Lewis Research Center technical publications announced in 1983
[NASA-TM-83693] 12 p1951 N85-22255

University of Cambridge Institute of Astronomy report of activities 13 p2170 N85-23464

O. F. Mossotti and the physics of molecules
[NOTA-INTERNA-822] 14 p2420 N85-24931

Discovery refutation and verification refutation: The proposals of Von Neumann and Wiener in the development of 20th century physics
[NOTA-INTERNA-840] 14 p2431 N85-24993

The conservation and utilization of scientific research documents: Practical aspects and organization
[NOTA-INTERNA-834] 14 p2433 N85-25006

AFRPL (Air Force Rocket Propulsion Laboratory) technical objective document FY 85
[AD-A151368] 15 p2495 N85-25389

China report: Science and technology
[JPRS-CST-85-011] 15 p2551 N85-25746

Physics, Computer Science and Mathematics Div.
[DE85-006868] 15 p2642 N85-26298

Theoretical studies of Elmo Bumpy Torus
[DE85-007202] 15 p2658 N85-26402

Summaries of FY 1984 engineering research
[DE85-006273] 15 p2664 N85-26442

The search for extraterrestrial intelligence
15 p2689 N85-26609

Recent Naval Postgraduate School publications
[AD-A151723] 16 p2875 N85-27740

Magnetic monopoles
[DE85-008176] 17 p3027 N85-28719

Laboratory research: A question of when, not if
[AD-A153296] 17 p3046 N85-28867

Catalog of research projects at Lawrence Berkeley Laboratory, 1985
[DE85-008679] 17 p3049 N85-28869

Silicide conductors reliability research
[AD-A153768] 18 p3095 N85-29157

Photovoltaic Systems Development Project: An activity summary
[DE85-009994] 18 p3129 N85-29379

Proceedings of the 14th European Solid State Device Research Conference Including Solid State Device Technology, ESSDERC 84
[AD-A153409] 18 p3193 N85-29804

Space station automation study. Volume 1: Executive summary. Autonomous systems and assembly
[NASA-CR-171514] 19 p3226 N85-30002

High-efficiency silicon solar cell research
21 p3609 N85-32417

Activities report of the Aeronomy Department
[G-774-1984] 21 p3633 N85-32569

Air force technical objective document, Aerospace Medical Division, Fiscal Year 1986
[AD-A155195] 21 p3664 N85-32762

Air Force Office of Scientific Research (AFOSR). Technical report summaries: First quarter (CY)
[AD-A154757] 21 p3713 N85-33041

Investigation of DBMS (Data Base Management Systems) for use in a research environment
[AD-A154882] 21 p3713 N85-33042

The flow of scientific and technical information in the US Army Research Laboratories
[AD-A155050] 21 p3713 N85-33043

Energy efficient transport technology: Program summary and bibliography
[NASA-RP-1135] 22 p3729 N85-33116

National Center for Atmospheric Research
[PB85-191237] 22 p3848 N85-33835

RESEARCH AIRCRAFT

NT B-70 AIRCRAFT
NT ROTOR SYSTEMS RESEARCH AIRCRAFT
NT U-2 AIRCRAFT
NT X-15 AIRCRAFT

A preliminary flight evaluation of the peripheral vision display using the NT-33A aircraft
[AD-A145123] 01 p0010 N85-10060

YO-3A acoustics research aircraft systems manual
[NASA-TM-85968] 01 p0012 N85-10074

Role of research aircraft in technology development
[NASA-TM-85913] 02 p0137 N85-10932

First stage of equipping a Do 28 as a research aircraft for icing, and first research results
[ESA-TT-855] 11 p1584 N85-19982

ADAPS (Airborne Data Acquisition and Processing System) operation and maintenance manual
[AD-A149297] 11 p1585 N85-19983

Miniature electrooptical air flow sensor
[NASA-CASE-LAR-13065-1] 11 p1635 N85-20295

Civil avionics flight testing with the RAE(B) BAC1-11
13 p1967 N85-22354

Multivariable control law design for the X-29 aircraft
[AD-A151828] 15 p2472 N85-25259

X-29 digital flight control system design
17 p2901 N85-27889

The flight control system for the Experimental Aircraft Programme (EAP) demonstration aircraft
17 p2904 N85-27908
West Europe report: Science and technology
[JPRS-WST-85-020] 20 p3438 N85-31333
MBB demonstrates new research aircraft ATTAS
20 p3438 N85-31334

RESEARCH AND DEVELOPMENT
Aeronautics Technology Possibilities for 2000: Report of a workshop
[NASA-CR-174018] 01 p0001 N85-10001
East Europe report: Science and technology
[JPRS-ESA-84-029] 01 p0115 N85-10783
Lagging development of biotechnology described
01 p0115 N85-10787
Canada report to COSPAR 01 p0131 N85-10906
Space commercialization: Analysis of R and D investments with long time horizons
02 p0155 N85-11052
Development of space instrumentation of Intercosmos member countries 02 p0163 N85-11106
The need for improvements in weapon system maintenance: What can AI (Artificial Intelligence) contribute?
[AD-P003913] 02 p0244 N85-11593
Research and development requirements for ion implantation
[AD-P003951] 02 p0286 N85-11867
The status of synthetic fuels and cost-shared energy R and D facilities
[GPO-36-903] 03 p0339 N85-12182
Project resources planning and control
[NASA-TM-86339] 04 p0575 N85-13666
Research report 1979-1982. Part 2: Projects
[ISBN-3-7983-0960-4] 04 p0575 N85-13667
The characteristics of generation and the rate of distribution for science and technology information in our country (China)
[AD-A141037] 04 p0575 N85-13671
The Uniform Science and Technology Research and Development Utilization Act
[GPO-36-327] 04 p0577 N85-13685
Uniform Science and Technology Research and Development Utilization Act
[H-REPT-98-963-PT-1] 04 p0577 N85-13686
International comparative study of systems for the government advancement of research and development
[NASA-TM-77589] 04 p0578 N85-13689
The 15 photovoltaic pilot projects of the European Communities 05 p0663 N85-14263
The management of research institutions: A look at government laboratories
[NASA-SP-481] 07 p1050 N85-16665
Organizations and information processing: A field study of research and development units within the United States Air Force Systems Command
[AD-A147381] 07 p1054 N85-16691
Research and technology, 1984 report
[NASA-TM-83096] 07 p1061 N85-16730
Technology developments for laminar boundary layer control on subsonic transport aircraft
08 p1071 N85-16787
Blade technology program for large wind turbines, phase 1
[BMFT-FB-T-84-217] 08 p1179 N85-17426
Aeroacoustics at the DFVLR Brunswick Research Center: A survey on recent and current activities
[DFVLR-MITT-84-14] 08 p1219 N85-17677
Autonomy in the industrial R and D lab
[AD-A148075] 08 p1228 N85-17736
Outlook for expanding the Federal research in progress system
[AD-A148354] 08 p1229 N85-17737
Research and technology highlights of the Lewis Research Center
[NASA-TM-86899] 08 p1261 N85-17928
Research and technology, Lyndon B. Johnson Space Center
[NASA-TM-58263] 08 p1262 N85-17929
Innovation in British industry (notably the aircraft industry) and its value: Collected papers
[BAE-KRS-N-GEN-296] 09 p1263 N85-17933
Emerging role of the national laboratory in the development and transfer of materials technology
[DE85-001252] 09 p1288 N85-18086
Activities report in aerospace in West Germany
[ISSN-0070-3966] 09 p1418 N85-18947
Worldwide report: Telecommunications policy, research and development
[JPRS-TTP-85-002] 10 p1475 N85-19309
The R and D project selection problem with fuzzy coefficients
[INPE-3329-PRE/626] 10 p1565 N85-19871
Characteristics of quality data
[DE85-001203] 10 p1568 N85-19889
Calendar of selected aeronautical and space meetings
[AGARD-CAL-84/2] 10 p1573 N85-19917
Activities in French aerospace
11 p1587 N85-19995
French research minister on policy, technology transfer 11 p1618 N85-20182
China report: Science and technology
[JPRS-CST-84-039] 11 p1621 N85-20206
Research in environmental biology reviewed
11 p1622 N85-20211
Oversight review of the five-year outlook report on science and technology
[GPO-41-058] 12 p1949 N85-22243
An agenda for a study of government science policy
[GPO-40-860] 12 p1949 N85-22245
President's private sector survey on cost control, report on research and development
[PB84-173269] 12 p1951 N85-22253
1985 Resident research associateships: Postdoctoral and senior research awards
[NASA-TM-87458] 12 p1963 N85-22336
Research and technology: Fiscal year 1984 report
[NASA-TM-85231] 12 p1964 N85-22340
China report: Science and technology
[JPRS-CST-84-030] 13 p2041 N85-22777
Physicists' role in new technological development discussed 13 p2166 N85-23436
Activities in flight mechanics and flight control
[ISSN-0720-7808] 14 p2227 N85-23803
Applications of ultrasonic technology
14 p2283 N85-24144
Thirty-three years of research with shock tubes in the Franco-German Research Institute, Saint Louis (France)
[ISL-CO-226/83] 14 p2302 N85-24257
Summaries of FY 1984 research in high energy physics
[DE85-005641] 14 p2420 N85-24934
Accomplishments of science by the year 2000
14 p2432 N85-24996
Investigations carried out under the Director's Discretionary Fund
[NASA-CR-175676] 14 p2432 N85-24999
Research and technology
[NASA-TM-86662] 14 p2456 N85-25166
Air Force Office of Scientific Research (AFOSR): Technical report summaries. Fourth quarter (CY)
[AD-A150860] 14 p2456 N85-25167
Resources for robotics research in Europe, by country
15 p2489 N85-25364
Outlook for polymer composite materials
15 p2497 N85-25403
Research, devolopment of composite materials described 15 p2497 N85-25404
France officially proposes development of Ariane 5 to ESA 15 p2532 N85-25613
Academic science and engineering: R and D funds, fiscal year 1982 (detailed statistical tables)
[PB85-154763] 15 p2664 N85-26443
AGARD bulletin: Meetings, publications, membership
[AGARD-BUL-85-1] 15 p2686 N85-26589
Flight testing and development of the F/A-18A digital flight control system 16 p2713 N85-26743
East Europe report: Science and technology
[JPRS-ESA-84-032] 16 p2727 N85-26833
Research and development. Technical and scientific reports 1984 16 p2873 N85-27724
NBS (National Bureau of Standards) research reports
[PB85-127421] 16 p2879 N85-27764
Activities in aerospace 17 p2891 N85-27821
Test devices for aeronautical research and technology
[NASA-TM-77651] 17 p2905 N85-27914
Gordon Research Conference on Composites
[AD-A152868] 17 p2917 N85-27979
Integrating quality assurance and research and development
[DE85-007974] 17 p2976 N85-28392
Experimental plasma research: Plasma summaries
[DE85-008116] 17 p3039 N85-28805
The Department of Defense statement on the Science and Technology Program by Colonel Donald I. Carter, USAF Acting Deputy Under Secretary of Defense for Research and Advanced Technology before the Subcommittee on Research and Development of the Committee on Armed Services of the United States House of Representatives, 99th Congress, first session
[AD-A152467] 17 p3046 N85-28850
Multicriteria decision analysis as an aid to strategic planning of energy research and development
[REPT-84-02] 17 p3049 N85-28870
Bibliography of Lewis Research Center technical publications announced in 1984
[NASA-TM-87012] 17 p3049 N85-28876
Multi-ducted inlet combustor research and development
[AD-A153753] 18 p3063 N85-28946
Space station study
[BI-6167] 18 p3066 N85-28969
West Europe report: Science and technology
[JPRS-WST-84-022] 18 p3065 N85-29066
Results of Italian research in high power lasers
18 p3066 N85-29067
Rifa of Sweden conducts research in 3-5 materials
18 p3068 N85-29107
SERI photovoltaic advanced research and development project: FY 1984 accomplishments
[DE85-002939] 18 p3128 N85-29389
Electrochemical Energy Storage Branch
[DE85-007592] 18 p3131 N85-29391
Activities at the Lunar and Planetary Institute
[NASA-CR-175914] 18 p3201 N85-29859
Alloy development for irradiation performance
[DE85-010454] 19 p3240 N85-30091
Present and future directions of atomic physics research with multiply-charged ions at Brookhaven National Laboratory
[DE85-010960] 19 p3354 N85-30788
Strained-layer-superlattice optoelectronic devices
[DE85-009148] 19 p3377 N85-30953
The economics of private sector R and D decisionmaking in aeronautics
[NASA-CR-176007] 19 p3379 N85-30962
National Aeronautics and Space Administration
19 p3382 N85-30980
Note for a research feasibility project: High reliability design in the aeronautical field
[REPT-84-RR-350] 20 p3387 N85-31005
Space research at NLR 20 p3397 N85-31075
NASA Space controls research and technology program 20 p3406 N85-31149
Reciprocating Brayton cycle motor
[REPT-84-RR-336] 20 p3462 N85-31507
The Department of Defense report on the technology base and support of university research
[AD-A154309] 20 p3540 N85-32030
Renewable energy research and development outlook, volume 1
[DE85-011577] 20 p3540 N85-32033
Spin-offs from technical scientific infrastructures, no. 1
20 p3540 N85-32034
Spin-offs from technical scientific research organizations, no. 5 20 p3540 N85-32036
A comprehensive study of the AFIT (Air Force Institute of Technology) software development environment
[AD-A155450] 21 p3672 N85-32812
Management of Corrosion
[AGARD-LS-141] 22 p3749 N85-33238
Photovoltaics technical information guide
[DE85-002924] 22 p3806 N85-33585
Transfer of battery technology developed by the US Department of Energy
[DE85-009868] 22 p3808 N85-33588
Electron photoejection in carbanions
[DE85-011747] 23 p3911 N85-34230
Development of flight mechanics research in Brunswick 24 p4061 N85-35186
Piezoelectric transducers, state of research
24 p4089 N85-35345
Development and evaluation of sulfonated polysulfone membranes for the zinc-ferricyanide battery
[DE85-009104] 24 p4090 N85-35357
United States Army welding research and development topical and coordination meeting
[AD-A155834] 24 p4099 N85-35409
Quality assurance considerations for the implementation of a pulsed power R and D project
[DE85-012357] 24 p4148 N85-35720
The 1986 National Aeronautics and Space Administration authorization
[GPO-47-635] 24 p4166 N85-35829

RESEARCH FACILITIES
Mathmatics and Computer Science Division activities
[DE84-014842] 01 p0104 N85-10701
Ocean energy systems at the Johns Hopkins University Applied Physics Laboratory
[PB84-225705] 03 p0387 N85-12474
Investigation of special facilities for a spallation neutron source 03 p0427 N85-12724
Hydrogen technology evaluation center at Brookhaven National Laboratory
[DE84-014099] 04 p0470 N85-12988
Instrumentation at national facilities for synchrotron radiation topography
[DE84-016256] 04 p0564 N85-13650
Summary and analysis of hearing on improving the research infrastructure at US universities and colleges
[GPO-36-854] 04 p0574 N85-13680
Improving the research infrastructure at US universities and colleges
[GPO-35-290] 04 p0574 N85-13681
NASA-Ames vertical gun 04 p0579 N85-13696

pper Atmosphere Research Satellite (UARS) trade
alysis
ASA-CR-175269] 07 p0912 N85-15774
ectronics research at the University of Texas at
stin
D-A146900] 07 p0947 N85-15996
The management of research institutions: A look at
ernment laboratories
ASA-SP-481] 07 p1050 N85-16665
Hybrid data processing research facility
D-A148092] 08 p1202 N85-17567
Research and technology highlights of the Lewis
esearch Center
ASA-TM-86899] 08 p1261 N85-17928
Research and technology, Lyndon B. Johnson Space
enter
ASA-TM-58263] 08 p1262 N85-17929
The Prandtl Hergesell project of a national research
stablishment for aeronautics
ESA-TT-835] 09 p1272 N85-17993
The planned expansion of microelectronics capability
at Sandia National Laboratory
[TI85-004326] 09 p1314 N85-18260
Air Force space technology center space technology:
Emphasis 84 09 p1333 N85-18381
Decade of the Varilov Kupola
10 p1497 N85-19448
Rocky Flats Wind Energy Research Center FY 1983
report
[DE85-004500] 10 p1511 N85-19535
Personal desktop computing in a research and
development laboratory
[DE85-002765] 11 p1705 N85-20728
Research in surface sciences, disordered materials, and
solidification and growth
[PB85-132140] 11 p1737 N85-20927
Major facilities for materials research and related
disciplines
[PB85-108850] 11 p1739 N85-20934
Task and future of the Large Institutes of Technology
(LIT)
[B8474720] 11 p1741 N85-20945
Computing Division two-year operational plan, FY 1984
- 1985
[LA-9978-MS] 12 p1913 N85-22006
1985 Resident research associateships: Postdoctoral
and senior research awards
[NASA-TM-87456] 12 p1963 N85-22338
Activities of the Jet Propulsion Laboratory, 1 January -
31 December 1983
[NASA-CR-175555] 13 p2167 N85-23447
JESS facility modification and environmental/power
plans
[NASA-CR-175685] 14 p2227 N85-23807
Frenrh robotics research at Grenoble labs
15 p2523 N85-25555
Soviet institute director on GDR-USSR welding
technology 15 p2538 N85-25662
Geophysical Fluid Dynamics Laboratory activities, FY84,
plans, FY85
[PB85-147601] 15 p2558 N85-25783
Basic studies. 1: Basic experiments in plasma
physics 15 p2355 N85-26378
High beta pinch plasma (STP-3(M))
15 p2655 N85-26380
Ignition of metals in high pressure oxygen
16 p2735 N85-26874
A summary of the Naval Postgraduate School research
program
[AD-A151721] 16 p2875 N85-27738
Nucleon-nucleon program at TRIUMF
[DE85-900430] 17 p3032 N85-28756
Origin, processing, and dissemination of scientific news,
with examples from 20 research institutes
[JUEL-1940] 17 p3050 N85-28882
Selected university laboratory needs in support of
national security
[AD-A153611] 18 p3197 N85-29833
Metrology and Oceanology Institutes' underwater
acoustics R and D 19 p3289 N85-30394
The SLC program
[DE85-011433] 19 p3357 N85-30813
Additional muon calculations for the SLC positron
source
[DE85-011212] 19 p3363 N85-30855
High efficiency solar cell research for space
applications 20 p3480 N85-31624
Fixed-target physics at Fermilab
[DE85-010141] 20 p3528 N85-31942
R and D activities of the Computer Centre
20 p3540 N85-32029
The flow of scientific and technical information in the
US Army Research Laboratories
[AD-A155050] 21 p3713 N85-33043
Current internal-dosimetry practices at US Department
of Energy facilities
[DE85-011718] 22 p3787 N85-33466
Langley aeronautics and space test highlights, 1984
[NASA-TM-87585] 23 p4057 N85-35151
United States Army welding research and development
topical and coordination meeting
[AD-A155834] 24 p4099 N85-35409

RESEARCH MANAGEMENT
Exploratory investigation of the need for and feasibility
of a Lower Atmosphere Research Satellite (LARS)
program
[NASA-CR-171181] 01 p0015 N85-10091
Research study: Studies in atmospheric processes from
Space Platforms
[NASA-CR-171176] 01 p0072 N85-10473
Numerical algorithms and parallel tasking
[AD-A145090] 01 p0104 N85-10693
Fusion and its future in Illinois
[DE84-014686] 01 p0122 N85-10833
Publications of the National Bureau of Standards, 1983
catalog
[PB84-218031] 01 p0126 N85-10869
Conceptual design and evaluation of selected Space
Station concepts, volume 1
[NASA-TM-87383] 02 p0168 N85-11129
Proceedings of the Ion Implantation for Army Needs
Workshop
[AD-A145474] 02 p0286 N85-11863
Navy programs on ion implantation for materials
modification
[AD-P003952] 02 p0286 N85-11868
Characteristics of systems engineering in aviation
science research
[AD-A145602] 02 p0292 N85-11899
Research and technology
[NASA-TM-86321] 02 p0305 N85-11973
Air Force Materials Laboratory plans/projects
[AD-P004010] 03 p0308 N85-11990
Scientific communications and national security
[GPO-36-093] 04 p0492 N85-13138
International coordination in scientific research
04 p0519 N85-13311
Five year research plan, 1984-1988. Photovoltaics:
Electricity from sunlight
[DE84-013009] 04 p0528 N85-13377
R and D project selection with nonnumerical returns
[INPE-2760-PRE/335] 04 p0575 N85-13665
International comparative study of systems for the
government advancement of research and development
[NASA-TM-77589] 04 p0578 N85-13689
NASA's SESAC report on research and analysis in space
and Earth sciences 04 p0579 N85-13697
Activities of the Coastal Research Center
[PB84-231323] 05 p0672 N85-14320
A summary of the foundation research program
[AD-A146524] 06 p0891 N85-15656
Integrated technology wing study (oral presentation)
[NASA-CR-169497] 07 p0902 N85-15718
Evaluation of the musculoskeletal diseases program
[PB84-230648] 07 p1017 N85-16461
Organizations and information processing: A field study
of research and development units within the United States
Air Force Systems Command
[AD-A147361] 07 p1054 N85-16691
UK, FRG, France: R and D in sensors, related fields
08 p1142 N85-17197
On the validation of computer science theories
[AD-A148637] 08 p1203 N85-17572
Autonomy in the industrial R and D lab
[AD-A148075] 08 p1228 N85-17736
Outlook for expanding the Federal research in progress
system
[AD-A148354] 08 p1229 N85-17737
An overview of the research program at the visual
technology research simulator
[AD-P004321] 09 p1269 N85-17975
Emerging role of the national laboratory in the
development and transfer of materials technology
[DE85-001252] 09 p1288 N85-18066
Evaluation of the Fundamental Research on Explosives
(FRE) program
[DE85-001537] 09 p1301 N85-18172
European Scientific Notes, volume 38, number 12
[AD-A148713] 09 p1418 N85-18946
Biomechanical studies of impact acceleration research
[AD-A149077] 10 p1522 N85-19601
National solar-terrestrial research program, part 1.
Solar-terrestrial research for the 1980's, part 2
[AD-A149542] 11 p1681 N85-20591
Needs, opportunities, and options for large scale
systems research
[DE85-002684] 11 p1709 N85-20750
Task and future of the Large Institutes of Technology
(LIT)
[B8474720] 11 p1741 N85-20945
Systems research on China in year 2000
12 p1820 N85-21418
Global tropospheric chemistry: A plan for action
[NASA-CR-175545] 12 p1891 N85-21865
1985 Resident research associateships: Postdoctoral
and senior research awards
[NASA-TM-87456] 12 p1963 N85-22338
Research in the optical sciences
[AD-A150196] 13 p2159 N85-23401
Activities of the Jet Propulsion Laboratory, 1 January -
31 December 1983
[NASA-CR-175555] 13 p2167 N85-23447
Authorizing appropriations to the National Aeronautics
and Space Administration for fiscal year 1986
[H-REPT-99-32] 13 p2168 N85-23452
Investigations carried out under the Director's
Discretionary Fund
[NASA-CR-175676] 14 p2432 NF5-24999
Wind energy systems: Program summary for fiscal year,
1983
[DE85-002927] 17 p2965 N85-28451
Nucleon-nucleon program at TRIUMF
[DE85-900430] 17 p3032 N85-28756
Air Force technical objective document FY 86
[AD-A152730] 17 p3047 N85-28855
Science and Technology in the Soviet Union
[AD-A152828] 17 p3047 N85-28856
The outlook for Soviet advanced technologies
[AD-P004564] 17 p3048 N85-28859
Social and political problems in Soviet basic research
[AD-P004565] 17 p3048 N85-28860
Close encounters with S/T (science and technology)
in the Soviet Union
[AD-P004570] 17 p3048 N85-28864
R/D contracts in the Soviet Union
[AD-P004569] 17 p3048 N85-28865
Laboratory research: A question of when, not if
[AD-A153298] 17 p3048 N85-28867
Research on structural analysis at the DFVLR,
Brunswick 18 p3120 N85-29314
The evolution of the U.S. helicopter industry
[AD-A154290] 19 p3211 N85-29913
EPA (Environmental Protection Agency) research
program guide, FY-1985, October 1, 1984 - September
30, 1985
[PB85-181881] 20 p3487 N85-31676
Commission for Marine Meteorology
[WMO-640] 20 p3496 N85-31735
Human factors engineering contracts in Sweden: An
overview
[FOA-C-56043-H2] 20 p3513 N85-31836
The Department of Defense report on the technology
base and support of university research
[AD-A154309] 20 p3540 N85-32030
The Human Resource Management Information
Network (HRMIN): A cost comparison in accordance with
Office of Management and Budget (OMB) Circular no.
A-76, 5 April 1979
[AD-A154563] 21 p3713 N85-33039
Investigation of DBMS (Data Base Management
Systems) for use in a research environment
[AD-A154862] 21 p3713 N85-33042
Research report program of the US Army in Europe
24 p4061 N85-35167
DoD Value Engineering conference report. Value
Engineering (VE): A tool that benefits line management.
Part 3, Workshop A: VE in the program office
[AD-A156069] 24 p4163 N85-35812

RESEARCH PROJECTS
The application of remote sensing to resource
management and environmental quality programs in
Kansas
[E85-10023] 02 p0218 N85-11436
Determination sample sizes for diversified reliability test
programs
[DE84-015003] 04 p0511 N85-13255
High-Beta plasma theory
[DE84-016471] 04 p0568 N85-13619
Research report 1979-1982. Part 2: Projects
[ISBN-3-7983-0960-4] 04 p0575 N85-13667
International comparative study of systems for the
government advancement of research and development
[NASA-TM-77589] 04 p0578 N85-13689
Lightning research: A user's lament
07 p0999 N85-16346
An overview of the research program at the visual
technology research simulator
[AD-P004321] 09 p1269 N85-17975
Evaluation of the Fundamental Research on Explosives
(FRE) program
[DE85-001537] 09 p1301 N85-18172
European Scientific Notes. Volume 39, number 1
[AD-A149496] 10 p1568 N85-19686
Space Station Spartan study
[NASA-TM-86215] 16 p2731 N85-26852

Summary of research for the Inertial Confinement Fusion Program at Los Alamos National Laboratory
[DE85-010330] 19 p3361 N85-30836

RESEARCH VEHICLES

NT UNDERWATER RESEARCH LABORATORIES

Machine Mechanics Institute builds walking vehicle
04 p0543 N85-13455

The transpacific experimental sailing by YASEIGO 3
14 p2327 N85-24380

Test plan for acceptance, verification and performance testing of the Bedford Lucas Chloride Electric Van. Part 1: Acceptance and verification testing at EG and G Automotive Research. Part 2: INEL performance testing, revision 1
[DE85-005157] 17 p3051 N85-28888

Preliminary results of an ALVIN dive program on active hydrothermal vents at the southern Juan de Fuca Ridge
24 p4106 N85-35454

RESERVES

International strategic minerals inventory. Summary report: Manganese
[GS-CIRC-930-A] 02 p0219 N85-11442

Geology and resources of the Tar Sand Triangle, southeastern Utah
[DE84-012017] 05 p0677 N85-14346

World iron ore reserves
[BLL-BISI-TRANS-22260-(9022.06)]
17 p2983 N85-28435

AUTSKED: An addendum
[DE85-010410] 22 p3829 N85-33712

Preliminary SPR thermal model description and results for WH-11 and BM-4
[DE85-013171] 23 p3931 N85-34360

RESERVOIRS

Identification and parameter estimation of phosphate balance models in drinking water reservoirs
[PUBL-313] 08 p1181 N85-17439

Electrical resistivity technique to assess the integrity of geomembrane liners
[PB85-122414/GAR] 09 p1325 N85-18327

Results from geopressured-geothermal subsidence studies
[DE84-016279] 09 p1354 N85-18520

Laboratory investigation of formation damage of an artificial fracture at simulated geothermal conditions
[DE85-010301] 18 p3102 N85-29201

Modeling water resources systems for water quality
[AD-A154288] 19 p3300 N85-30457

Hydrodynamic solutions for the diffusion of components in confined media 20 p3456 N85-31464

Empirical methods for predicting eutrophication in impoundments. Report 3. Phase 2. Model refinements
[AD-A155483] 21 p3614 N85-32462

Carbon and sulfur cycling through geologic time
21 p3658 N85-32720

Fracture detection and characterization for geothermal reservoir definition
[DE85-008677] 22 p3815 N85-33630

Comprehensive fracture diagnostics experiement. Part 2: Comparison of seven fracture azimuth measurements
[DE85-011707] 23 p3948 N85-34470

Studies in thermo-hydro-chemical transport in porous and fractured media
[DE85-012555] 23 p3949 N85-34473

National program for inspection of non-federal dams. Woodward reservoir dam (VT 00209), Connecticut River Basin, Plymouth, Vermont. Phase 1 inspection report
[AD-A156256] 24 p4144 N85-35693

RESIDENTIAL ENERGY

Microcomputer control of a residential photovoltaic power conditioning system
[DE84-013867] 04 p0547 N85-13480

Correlations of solar irradiance and daylight illuminance for building energy analysis
[DE85-001736] 06 p0839 N85-15326

Microcomputer control of a residential photovoltaic power conditioning system
[DE84-014774] 07 p1022 N85-16488

An assessment of ground-coil heat-pump technology
[DE85-002567] 10 p1486 N85-19382

Solar collection
[DE85-000060] 10 p1512 N85-19540

Solar-gas systems impact analysis study
[PB85-129066] 11 p1616 N85-20163

Latent heat storage technology and application workshop. Summary report: Session 6
[DE85-001097] 12 p1882 N85-21806

A multifunction wall system for application with solar heating and ground cooling
[DE85-006792] 16 p2820 N85-27395

Solid desiccant dehumidification systems for residential applications
[PB85-198489] 22 p3755 N85-33279

Advanced heat pump research and development
[DE85-009540] 23 p3932 N85-34372

Design and construction of an advanced power conditioning subsystem for small photovoltaic applications
[DE85-013940] 24 p4113 N85-35495

RESIDUAL STRENGTH

The three-dimensional J-integral. An investigation into its use for post-yield fracture safety assessment
[WTHD-167] 20 p3472 N85-31578

RESIDUAL STRESS

Nondestructive evaluation of residual stress in low-carbon steel
[NASA-CR-174157] 04 p0512 N85-13264

Nondestructive evaluation of residual stress in low-carbon steel, introduction 04 p0512 N85-13265

Flexible matrix composite laminated disk/ring flywheel
05 p0606 N85-13866

The fourth LBF colloquium
[ISSN-0721-5320] 05 p0648 N85-14163

Fatigue life improvement due to mechanically induced compressive residual stresses 05 p0650 N85-14175

Influence of residual stresses resulting from manufacturing on the fatigue strength of welded joints
05 p0650 N85-14177

Influence of the shape and distribution of inclusions of the fatigue strength of bearing steels in rotary bending
[BLL-PNR-90243-(8019.3153)]
06 p0766 N85-14912

Stress studies in EFG 06 p0831 N85-15285

Silicon-sheet surface studies
06 p0831 N85-15287

Study of residual stresses introduced into TA6ZrD (685) cylinders by quenching
[BLL-PNR-90240-(8019.3153)]
07 p0925 N85-15859

Residual stresses at small diffusion welds
[DE84-014982] 07 p0974 N85-16169

Nondestructive measurement of bulk residual stresses
[AD-A147063] 07 p0978 N85-16211

In-situ stress determination in soil and rock using the acoustic emission method
[AD-A147459] 07 p0979 N85-16215

A finite element analysis of viscoelastic materials with varying time scales 09 p1330 N85-18355

Study of residual stresses introduced into TA6ZrD (685) cylinders by quenching — compressor disk alloy
[PNR-90240] 09 p1341 N85-18435

Calculating residual stresses in composite materials
10 p1443 N85-19095

Evaluation of residual stress in laminated metallic composites 11 p1598 N85-20052

Residual stress after laser processing
11 p1600 N85-20065

Evaluation of machining damage in brittle materials
[DE85-001794] 11 p1612 N85-20136

The measurement of residual stresses using ultrasonics
[AERE-R-11415] 12 p1868 N85-21722

Texture independent determination of residual stress in polycrystalline aggregates using Rayleigh waves
[AERE-R-11483] 12 p1943 N85-22203

Brittle fracture resistance of electron beam-welded joints in titanium Alpha alloys 15 p2500 N85-25419

On residual stresses and stress intensity factors in composite materials 15 p2572 N85-25859

Evaluation of the blind hole drilling method for the measurement of residual stress
[AD-A151459] 15 p2579 N85-25905

A study of the time dependence in fracture processes relating to service prediction of adhesive joints and advanced composites
[AD-A152064] 15 p2579 N85-25910

Advanced life analysis methods. Volume 6: User's manual for LUGRO computer program to predict crack growth in attachment lugs
[AD-A151235] 15 p2628 N85-26195

Mechanical properties of high performance carbon fibers 16 p2742 N85-26922

Study of oscillations of composite cylindrical shells using a dynamic stiffness technique 16 p2766 N85-27066

Stressed-strained state of tubular shells under uniformly distributed pressure 16 p2766 N85-27067

On residual stress in an elastic body
16 p2798 N85-27248

Principles of wave formation along web of H-beams
[BLL-M-36041-(5828.4)] 16 p2798 N85-27253

An X-ray study of residual stresses in narrow groove TIG weldments
[DE85-006485] 16 p2802 N85-27274

Local heat treatment of welded joints of pipes and rotary vessels 17 p2924 N85-28028

X-ray diffraction study of changes in stress-strain distributions during fatigue of a 2-phase alloy
[AD-A152367] 17 p2930 N85-28087

An X-ray diffraction study of the residual stress-strain distribution in shot-peened 2-phase brass
[AD-A152418] 17 p2930 N85-28088

Local heat treatment of welded joints of pipes and rotary vessels
[BLL-BISI-TRANS-22197-(9022.06)]
17 p2972 N85-28054

Cyclic torsion of a circular cylinder and its residual stress distribution
[AD-A153347] 17 p2980 N85-28424

Residual stress distributions in (plastically) surface deformed two-phase materials 19 p3283 N85-30358

Effect of nonuniform size on internal stresses in a rapid, simple shear flow of granular materials. Part 1: Two grain sizes
[AD-A154045] 19 p3285 N85-30372

Fundamental studies related to failure of adhesively bonded structures
[AD-A154072] 19 p3285 N85-30374

Measurement and analysis of critical crack tip processes during fatigue crack growth
[NASA-CR-172597] 21 p3598 N85-32342

Stress concentration in the elastoplastic state and residual stress after unloading
[AD-A155628] 21 p3600 N85-32356

Effects of residual stresses and distortion on the nickel 200 and stainless steel 304 weldments
[DE85-011868] 22 p3748 N85-33230

Stresses and deformations in cross-ply composite tubes subjected to a uniform temperature change: Elasticity and Approximate Solutions
[NASA-CR-176147] 22 p3800 N85-33545

X-ray residual stress analysis on the coarse grain of copper and its application to the brazed copper
23 p3907 N85-34202

Study on the correlation between grinding conditions and residual stresses in ground surface of steel by the X-ray method 23 p3907 N85-34203

Multiaxial stress analysis taking account of penetration depth of X-rays. A solution by means of polynomial approximation 23 p3907 N85-34204

Influence of cyclic thermal loading on internal stress in casted epoxy resin 23 p3908 N85-34211

Development of a mathematical model for predicting the percentage fatigue life increase resulting from shot peened components
[AD-A155774] 24 p4101 N85-35425

RESIDUES

Analysis of Nonvolatile Residue (NVR) from spacecraft systems
[NASA-TM-86184] 08 p1113 N85-17019

Transformation of polar ice sublimate residue into Martian circumpolar sand 13 p2189 N85-23580

RESILIENCE

Experimental AC (Asphalt Concrete) overlays of PCC pavement
[PB84-218171] 03 p0342 N85-12203

New deformable secondary aluminum alloys
13 p2026 N85-22694

RESIN MATRIX COMPOSITES

NT GRAPHITE-EPOXY COMPOSITES

Tough Composite Materials
[NASA-CP-2334] 04 p0463 N85-12941

Characterizing delamination resistance of toughened resin composites 04 p0464 N85-12943

Composite materials characterization and development at AFWAL 04 p0464 N85-12944

Effects of constituent properties on compression failure mechanisms 04 p0464 N85-12946

The effect of matrix and fiber properties on impact resistance 04 p0464 N85-12947

Fundamental studies of composite toughness
04 p0464 N85-12948

Development of a heterogeneous laminating resin
04 p0465 N85-12956

System for rapid repair of damaged airfield runways
[AD-D011325] 07 p0909 N85-15754

The use of microdielectrometry in monitoring the cure of resins and composites
[AD-A148619] 08 p1119 N85-17055

Fatigue-creep interaction in + or - 45 deg carbon-resin composites — aircraft construction materials
[ONERA-RT/40/7086/M] 11 p1594 N85-20027

Interlaminar fracture toughness in resin matrix composites
[AD-A150565] 13 p2015 N85-22540

NASA/aircraft industry standard specification for graphite fiber toughened thermoset resin composite material
[NASA-RP-1142] 16 p2742 N85-26923

Characterization-curing-property studies of HBRF 55A resin formulations
[NASA-CR-175836] 16 p2753 N85-26989

High performance mixed bisimide resins and composites based thereon
[NASA-CASE-ARC-11538-1-SB]
19 p3231 N85-30033

Transversely reinforced piezoelectric composites
[AD-D011676] 19 p3260 N85-30214

Development of an impact- and solvent-resistant hermoplastic composite matrix, phase 3
ASA-CR-172568] 20 p3422 N85-31239
Effect of strain rate on the initial failure of notched GRP aminates 23 p3908 N85-34214

SINS
NT ACRYLIC RESINS
NT ALKYD RESINS
NT EPOXY RESINS
NT ION EXCHANGE RESINS
NT KEVLAR (TRADEMARK)
NT NYLON (TRADEMARK)
NT PHENOLIC RESINS
NT POLYAMIDE RESINS
NT POLYESTER RESINS
NT POLYETHER RESINS
NT POLYIMIDE RESINS
NT POLYMETHYL METHACRYLATE
NT POLYURETHANE RESINS
NT SILICONE RESINS
NT SYNTHETIC RESINS
NT THERMOPLASTIC FILMS
NT THERMOPLASTIC RESINS
NT THERMOSETTING RESINS
NT VINYL COPOLYMERS
Development of new and improved polymer matrix resin systems, phase 1
[NASA-CR-166595] 01 p0017 N85-10104
Quasi-steady analysis of aircraft panel flammability
[AD-A145461] 02 p0138 N85-10936
Moisture absorbing anti-arcing coating and method for applying same
[AD-D011310] 07 p0932 N85-15904
Development of a heterogeneous laminating resin system
[NASA-CR-172459] 09 p1288 N85-18089
Synthesis and thermomechanical properties of new AT-Phenylene R systems
[AD-A148961] 12 p1813 N85-21372
Characterization and optimization of polyethylene resins and gas pipe
[PB85-118511] 12 p1815 N85-21382
High performance mixed bisimide resins and composites based thereon
[NASA-CASE-ARC-11538-1-SB] 19 p3231 N85-30033

RESISTANCE
Influence of tire on resistance and steering forces of tires
[AD-P004306] 09 p1410 N85-18883
Basic study on the turning resistance of track
[AD-P004307] 09 p1410 N85-18884
Theoretical and experimental study of crack resistance and macrocrack growth rate in organic fiber reinforced plastic under pure shear condition 11 p1596 N85-20053
Flow through very porous screens
[NASA-TP-2436] 11 p1631 N85-20270

RESISTANCE COEFFICIENTS
U RESISTANCE

RESISTANCE HEATING
Reducing electric power losses in discharge chamber of induction plasmatron 12 p1841 N85-21553
Instrumentation for sensing moisture content of material using a transient thermal pulse
[NASA-CASE-NPO-15493-2] 23 p3933 N85-34373
High Temperature Heating System (HTHS)
[PB85-188340] 24 p4084 N85-35316

RESISTANCE THERMOMETERS
Platinum thin film resistors as accurate and stable temperature sensors
[NASA-TM-77726] 01 p0049 N85-10322
High temperature static strain sensor development program 02 p0141 N85-10959
Effects of temperature on the response time of thermocouples and resistance thermometers
[DE84-016855] 06 p0811 N85-15154
Response time correlations for platinum resistance thermometers in flowing fluids
[NASA-CR-172523] 12 p1850 N85-21606
MFTF sensor verification computer program
[DE85-004452] 12 p1916 N85-22029

RESISTIVITY
U ELECTRICAL RESISTIVITY

RESISTOJET ENGINES
Compatibility experiments of facilities, materials, and propellants for electrothermal thrusters
[NASA-TM-86956] 12 p1795 N85-21260
Space station propulsion: The advanced development program at Lewis
[NASA-TM-86999] 15 p2494 N85-25386
An evaluation of oxygen-hydrogen propulsion systems for the Space Station
[NASA-TM-87059] 18 p3067 N85-28971

RESISTOJETS
U RESISTOJET ENGINES

RESISTORS
NT POTENTIOMETERS (RESISTORS)
NT THERMISTORS
Platinum thin film resistors as accurate and stable temperature sensors
[NASA-TM-77726] 01 p0049 N85-10322
High sheet resistance, arsenic implanted polycrystalline silicon for integrated circuit resistors
[DE85-004355] 13 p2065 N85-22902
Stability of highly nonlinear oxide-zinc resistors under continuous voltage of industrial frequency 13 p2087 N85-23030
Derated application of parts for (Electronic Systems Division) systems development. Revision
[AD-A153299] 17 p2955 N85-28246
Technique for measuring the effective source reflection coefficient of 2-resistor power splitters
[DE85-009964] 17 p2956 N85-28256
Morphology of GaAs/sub 1-x/P/sub x/ superlattices grown by MOCVD and chloride VPE
[DE85-002944] 17 p3045 N85-28842
Low noise polycrystalline semiconductor resistors by hydrogen passivation
[AD-D011721] 23 p3927 N85-34338

RESOLUTION
NT ANGULAR RESOLUTION
NT HIGH RESOLUTION
NT IMAGE RESOLUTION
NT RADAR RESOLUTION
NT RADIOMETRIC RESOLUTION
NT SPATIAL RESOLUTION
NT SPECTRAL RESOLUTION
NT TEMPORAL RESOLUTION
Characteristics of lateral-scan interferometer 06 p0783 N85-15006
An operator method for computing the asymptotics of a collision resolution interval
[AD-A146837] 07 p1028 N85-16528
SODERN Visualization System (SVS) for flight simulation
[AD-P004320] 09 p1269 N85-17974
Study of resolution of deep MT soundings by means of physical model 13 p2112 N85-23155
Rayleigh criteria resolution of optical correlations
[AD-A151711] 15 p2652 N85-26359
Improvements in the energy resolution and high-count-rate performance of bismuth germanate
[DE85-010763] 19 p3240 N85-30092
Resolution at its current limit: Applications of the Berkeley ARM
[DE85-009959] 19 p3274 N85-30301
Optical image of bounded objects 21 p3697 N85-32968
Single-point diamond crushing of Zerodur with in-situ polishing and metrology on a diamond turning machine
[DE85-012918] 24 p4083 N85-35305
LANDSAT-4/5 image data quality analysis
[E85-10105] 24 p4107 N85-35463

RESOLVERS
Angular measurement system
[NASA-CASE-MFS-25825-1] 11 p1635 N85-20298

RESOLVING POWER
U RESOLUTION

RESONANCE
NT BARYON RESONANCE
NT CYCLOTRON RESONANCE
NT ELECTRON PARAMAGNETIC RESONANCE
NT FERROMAGNETIC RESONANCE
NT MAGNETIC RESONANCE
NT MAGNETOSONIC RESONANCE
NT MICROWAVE RESONANCE
NT NUCLEAR MAGNETIC RESONANCE
NT OPTICAL RESONANCE
NT PLASMA RESONANCE
NT PROTON RESONANCE
NT RESONANT VIBRATION
NT SPIN RESONANCE
Semiclassical theory of resonances
[REPT-67] 01 p0114 N85-10777
Rapid nonresonant rotation of a spacecraft in nominally periodic orbits in limited 3 body problem 02 p0160 N85-11083
Vibrational power transmission of an idealised gearbox
[ISVR-TR-124] 02 p0204 N85-11346
Selective observation of elastic-body resonances via their ringing in transient acoustic scattering
[AD-A145868] 03 p0416 N85-12658
Resonance model of Pc3 in subtropical regions --- geomagnetism 04 p0520 N85-13323
Bremsstrahlung from nuclear scattering at low energy near a resonance
[DE84-014652] 04 p0561 N85-13572
Experimental on-stream elimination of resonant whirl in a large centrifugal compressor 05 p0642 N85-14121
Multiphoton ionization of benzene in solution
[DE85-000893] 06 p0766 N85-14899
Resonant scattering of acoustic waves by elastic spherical shell in fluid 06 p0778 N85-14972
Laser ablation studies using RIS
[DE85-001118] 09 p1326 N85-18336
Experimental investigations of driven Alfven wave resonances in a Tokamak plasma using carbon dioxide laser interferometry
[DE85-001049] 09 p1392 N85-18758
A picosecond population modulation study of near interband resonances in semiconductors 09 p1396 N85-18787
Resonant activation of a Josephson junction
[DE85-000702] 10 p1563 N85-19857
Precision tunable resonant microwave cavity
[NASA-CASE-LEW-13935-1] 11 p1626 N85-20248
Gain enhancement methods for printed circuit antennas
[AD-A150090] 12 p1835 N85-21517
Dipole active surface vibrational resonances on clean and hydrogen covered Ni(110)
[AD-A150546] 13 p2163 N85-23420
Stability of the Galilean satellites in deep orbital resonance 13 p2172 N85-23477
Studies of planetary rings 13 p2174 N85-23488
Orbital resonances and planetary accretion in the solar nebula 13 p2179 N85-23523
Theoretical aspects of the nucleon-nucleon workshop
[DE85-003740] 14 p2420 N85-24933
The resonant count diagram and solar g mode oscillations 14 p2445 N85-25086
Vapor sensing by means of a ZnO-on-Si surface acoustic wave resonator
[DE85-003250] 15 p2646 N85-26324
Pyrotechnic shock simulation using the controlled response of a resonating bar fixture
[DE85-006537] 16 p2784 N85-27181
Distortion functions
[DE85-007511] 16 p2862 N85-27655
Resonance ionization mass spectrometry of carbon
[DE85-009040] 17 p2923 N85-28018
Transverse electron resonance accelerator
[DE85-008289] 17 p3032 N85-28758
On the origin of streamwise vortices in a turbulent boundary layer
[AD-A153651] 18 p3100 N85-29186
The application of laser resonance saturation to the development of efficient short wavelength lasers
[AD-A153951] 18 p3113 N85-29270
Stochastic resonance in the Landau-Ginzburg equation
[PREPRINT-430] 18 p3175 N85-29685
Arrangement for damping the resonance in a laser diode
[NASA-CASE-NPO-15980-1] 19 p3274 N85-30305
Shifts and widths of hydrogenic ion lines
[DE85-011375] 19 p3277 N85-30323
An algorithm for the influence numbers in the expansion of the lumped gravitational potential coefficients in the presence of resonant inclination variation
[AD-A154229] 19 p3336 N85-30689
Exact invariants in resonance form for time-dependent potentials
[DE85-010733] 19 p3346 N85-30739
Spontaneous emission by two atoms with different resonance frequencies near a metal surface
[AD-A154115] 19 p3353 N85-30781
Resonant-transfer-and-excitation for highly charged ions (16 or = Z or = 23) in collisions with helium
[DE85-010550] 19 p3359 N85-30823
Fundamentals of radio optical theory of resonant and directional quasi-optical devices 22 p3780 N85-33420
Photoionization of alkali and alkaline earth atoms: Na and Mg
[DE85-011812] 22 p3837 N85-33755
Accelerator vibration issues
[DE85-010766] 22 p3842 N85-33791
Role of ECRH in potential formation for tandem mirrors
[DE85-011859] 22 p3848 N85-33834
Calculating the interatomic pair potential allowing for resonance interaction in titanium, nickel and vanadium
[BLL-M-35843-(5826.4)] 23 p3913 N85-34249
Capture in the 1.15-keV iron resonance
[DE85-011913] 23 p3970 N85-34612
Some aspects of internal gravity waves in a multi-layered moving stratified flow 24 p4092 N85-35369
Width of nonlinear difference resonances
[DE85-013026] 24 p4148 N85-35719
Exit channels of autoionization resonances in atoms
[DE85-012299] 24 p4149 N85-35726
Resonance localization in tokamaks excited with ICRF waves
[DE85-014559] 24 p4160 N85-35791

RESONANCE FLUORESCENCE
Development of novel lamps for study of enhanced production of resonance by low-density mercury discharges
[DE84-016689] 05 p0632 N85-14053
Degenerate four-wave mixing lineshapes in sodium vapor under pulsed excitation
[AD-A148211] 08 p1222 N85-17698
The enhancement of molecular fluorescence and photochemistry by small metal particles
[AD-A152740] 17 p2919 N85-27994
RESONANCE LINES
Narrow absorption components in Be star winds
08 p1232 N85-17780
An episodic red-wing structure of SiIV, lambda 1394A, in gamma Cas 11 p1750 N85-21009
Variability of ultraviolet emission lines in the carbon star TX Psc 11 p1753 N85-21027
Atmospheric properties of RU Lupi derived from high- and low-resolution IUE spectra
11 p1754 N85-21031
Betageuse at maximum luminosity
11 p1758 N85-21061
RESONANCE PROBES
NT CYCLOTRON RESONANCE DEVICES
Proposal for continuation of research on megawatt gyrotrons for the period January 1, 1985 through December 31, 1986
[DE85-009962] 18 p3110 N85-29260
The heavy ion composition in 3HE-rich solar flares
[SH-2.2-7] 23 p4000 N85-34802
RESONANCE RADIATION
U RESONANCE FLUORESCENCE
RESONANCE SCATTERING
Observation of pure resonance and threshold effects in electron impact experiments in high intensity laser fields
[AD-A150725] 14 p2309 N85-24293
Resonances in photon-photon scattering
[DE85-004807] 14 p2419 N85-24928
Influence on bi-phonon states on Raman scattering of light in molecular crystals 21 p3660 N85-32865
Circumstellar shells of late-type stars: A study at millimeter and infrared wavelengths
24 p4167 N85-35836
RESONANT CAVITIES
U CAVITY RESONATORS
RESONANT FREQUENCIES
Resonant frequencies and mode shapes for single and double cylindrical shells
[AD-A144778] 01 p0062 N85-10408
Hardware and software selection for experimental modal analysis 02 p0208 N85-11373
NATFREQ users manual: A FORTRAN 4 program for computing natural frequencies, mode shapes and drag coefficients for taut strumming cables with attached masses and spring-mass combinations
[AD-A146058] 03 p0407 N85-12600
Analysis of piezoelectric disks and cylinders using finite element method
[AD-A146323] 03 p0414 N85-12650
The use of an optical data acquisition system for bladed disk vibration analysis
[NASA-TM-86691] 06 p0817 N85-15184
Electromagnetic resonances of cylinders and aircraft model with resistive wires
[NASA-CR-174203] 06 p0838 N85-15319
Evaluation of resonant modes in isolated dielectric resonators using a surface integral equation formulation
[PB85-110831] 12 p1837 N85-21528
Compensation of acoustic wave devices
[AD-D011582] 15 p2646 N85-26322
Approximate solution of the problem of fluid oscillations in cavities of revolution 16 p2764 N85-27056
Acoustic oscillations of rods and plates
17 p2944 N85-28170
Methods to recover the narrow Dicke sub-Doppler feature in evacuated wall-coated cells without restrictions on cell size 18 p3105 N85-29225
Diode laser 87Rb optical pumping in an evacuated wall-coated cell 18 p3105 N85-29226
Coherently pumped two-frequency laser-type devices
[AD-A154085] 19 p3275 N85-30311
Self-tuning adaptive-controller using online frequency identification 20 p3417 N85-31205
Adaptive filtering for large space structures: A closed-form solution 20 p3417 N85-31206
Experimental and theoretical investigations of open resonators — precipitation measurement
[DFVLR-FB-85-12] 20 p3449 N85-31414
Substructure coupling in the frequency domain
[NASA-CR-176140] 22 p3800 N85-33543
Rotor blade test apparatus
[AD-D011725] 23 p3934 N85-34381
RESONANT VIBRATION
Experimental investigation of vibroimpact of two cantilever beams 09 p1336 N85-18399
Acoustic agglomeration methods and apparatus
[NASA-CASE-NPO-15466-1] 12 p1927 N85-22104
Turbine blade friction damping study
16 p2736 N85-26886
Solar array flight experiment
[NASA-TM-86506] 17 p2909 N85-27935
Acoustic resonances in cylinder bundles oscillating in a compressible fluid
[DE85-004066] 24 p4145 N85-35699
RESONATORS
NT CAVITY RESONATORS
NT HELMHOLTZ RESONATORS
NT MULTIMODE RESONATORS
NT OPTICAL RESONATORS
Acoustic resonator and method of making same
[DE84-014655] 01 p0116 N85-10792
Sensitivity improvement of a two-mode gravitational radiation detector through the use of a transducer not perfectly tuned to the antenna
[NOTA-INTERNA-812] 02 p0192 N85-11265
Biaxial-crystal laser with waveguide resonator
02 p0262 N85-11717
Forced oscillations theory for resonant extended interaction electron devices
[PR-206] 03 p0358 N85-12298
Analyses of energy extraction efficiency of unstable resonators
[AD-A146391] 06 p0813 N85-15161
Reverse wave suppression in unstable ring resonator
[AD-A146825] 07 p0939 N85-15952
Low noise multiple crystal-controlled oscillator
[AD-D011401] 07 p0948 N85-16010
Microwave resonator using lateral excitation
[AD-D011374] 07 p1039 N85-16596
Status of RF superconductivity at Argonne National Laboratory
[DE85-002145] 09 p1312 N85-18245
Method of heating quartz resonators
[AD-D011454] 10 p1481 N85-19347
KMSF X-ray laser experiments, task no. 2
[DE85-000291] 11 p1640 N85-20335
Oscillator development
[AD-A149699] 12 p1834 N85-21509
Evaluation of resonant modes in isolated dielectric resonators using a surface integral equation formulation
[PB85-110831] 12 p1837 N85-21528
Stress compensation crystal device
[AD-D011497] 12 p1941 N85-22189
Three-mirror open resonator for millimeter wave band
13 p2077 N85-22972
Effect of space-charge field on output characteristics of O-type oscillators with distributed interaction
13 p2089 N85-23043
Dielectric resonator
[AD-D011573] 14 p2299 N85-24233
Cylindrical crystal resonator
[AD-D011575] 14 p2428 N85-24974
Suppression of vibration effects on piezoelectric crystal resonators
[AD-D011625] 16 p2778 N85-27142
Acceleration-resistant crystal resonator
[AD-D011627] 16 p2778 N85-27144
Method of fabricating acceleration resistant crystal resonators and acceleration resistant crystal resonators so formed
[AD-D011630] 16 p2778 N85-27145
Acceleration sensitivity reduction method
[AD-D011631] 16 p2778 N85-27146
Cut angles for quartz crystal resonators
[AD-D011652] 17 p2951 N85-28220
High performances from a new design of crystal oscillator 17 p2966 N85-28318
Design of SC cut 10 MHZ H.Q. crystals with G. sensitivity better than 2.10(-10)/G 17 p2966 N85-28319
Crystal resonator/oscillator test facility and test results
17 p2967 N85-28322
The superconducting cavity stability ruby maser oscillator 17 p2967 N85-28324
New features of different frequency generating systems due to the use of electrodeless rigidly mounted VBA quartz crystal resonator 18 p3106 N85-29231
Passivation on high Q acoustic strain sensor for accelerometer
[AD-A153565] 18 p3177 N85-29695
Dielectric resonator stabilized microstrip oscillator
[AD-D011708] 19 p3261 N85-30219
Dielectric resonator oscillators with digital temperature compensation
[AD-D011715] 19 p3261 N85-30221
Miniature two-mode filters 22 p3775 N85-33394
Fundamentals of radio optical theory of resonant and directional quasi-optical devices
22 p3780 N85-33420
RESOURCE ALLOCATION
The effects of task structure on time-sharing efficiency and resource allocation optimality
05 p0711 N85-14582
Control and modeling of a CELSS (Controlled Ecological Life Support System)
[NASA-CR-177324] 07 p1020 N85-16472
The international environment UNISPACE '82 and the ITU: A relationship between orbit-spectrum resource allocation and orbital debris 12 p1767 N85-21215
Metal waste in machine tool industry examined
14 p2263 N85-24147
Glossary of landscape and vegetation ecology for Alaska
[PB85-153831] 16 p2816 N85-27372
Selected university laboratory needs in support of national security
[AD-A153511] 18 p3197 N85-29633
Routing algorithms and stochastic analysis for large communications networks
[AD-A154654] 21 p3573 N85-32225
Resource allocation in cerebral specialization of function: Behavioral and electrophysiological studies
[AD-A155092] 21 p3664 N85-32758
RESOURCES
NT AQUIFERS
NT COAL
NT CRUDE OIL
NT EARTH RESOURCES
NT EXTRATERRESTRIAL RESOURCES
NT FORESTS
NT FOSSIL FUELS
NT GEOTHERMAL RESOURCES
NT GEYSERS
NT GLACIERS
NT ICEBERGS
NT LAND ICE
NT LIGNITE
NT MARINE RESOURCES
NT OIL FIELDS
NT RAIN FORESTS
NT SPRINGS (WATER)
NT TAR SANDS
NT THERMAL RESOURCES
NT UNDERWATER RESOURCES
NT WATER RESOURCES
Arctic and offshore research
[DE85-001995] 22 p3818 N85-33653
Expert systems research in regional resource evaluation: Experiences in the application of microcomputer technologies 24 p4105 N85-35450
Applications of the mineral resources data system and the international strategic minerals inventory in mineral-resource assessments by region and commodity
24 p4105 N85-35451
RESOURCES MANAGEMENT
NT FOREST MANAGEMENT
NT LAND MANAGEMENT
Estuaries of the Cape. Part 2: Synposes of available information on individual systems. Report no. 19: Groot (WES) (CMS 23) and Sout (CMS 22)
[CSIR-RR-418] 01 p0087 N85-10569
Cartography 02 p0214 N85-11412
Multispectral Imaging Science Working Group for Hydrologic Science: Executive summary
02 p0214 N85-11414
ONR (Office of Naval Research) Far east Scientific Bulletin, Volume 9, Number 2, April - June 1984
[AD-A145681] 02 p0305 N85-11974
A methodology for comparing the variable costs of the continuous and periodic review models
[AD-A146351] 03 p0436 N85-12776
Assessing erosion on US cropland: Land management and physical features
[PB84-219252] 04 p0526 N85-13306
Project resources planning and control
[NASA-TM-86339] 04 p0575 N85-13666
Remote sensing data in support of conventional data
05 p0659 N85-14232
A geographic information system for resource managers based on multi-level remote sensing data
[E85-10047] 06 p0827 N85-15249
Climate Conference for Latin America and the Caribbean
[WMO-632] 07 p1000 N85-16352
The management of atmospheric resources in food production 07 p1002 N85-16362
Evaluation of the climatic resources of Cuba applied to agricultural work 07 p1004 N85-16380
Managing recoverable aircraft components in the PPB and related processes: Executive summary
[AD-A146806] 07 p1050 N85-16667

Feasibility of measuring technical productivity improvements in Air Force Logistics Command depot-level maintenance using the Data Envelopment Analysis (DEA) and Constrained Facet Analysis (CFA) models
[AD-A147329] 07 p1052 N85-16676
Estimating wartime support resource requirements. Statistical and related policy issues
[AD-A147923] 07 p1053 N85-16685
Cockpit resource management training
09 p1276 N85-18023
Compatible goals: Defense and environmental protection
[AD-P004137] 09 p1347 N85-18473
An integrated GIS/remote sensing data base in North Cache soil conservation district, Utah: A pilot project for the Utah Department of Agriculture's RIMS (Resource Inventory and Monitoring System)
[E85-10073] 10 p1504 N85-19487
The evolution from data processing to information resource management
[AD-A149429] 10 p1567 N85-19878
Remote sensing technology now playing practical roles 11 p1619 N85-20190
Proceedings of the 1st Glacier Bay Science Symposium
[PB85-115913] 11 p1662 N85-20599
Remote sensing research for agricultural applications — San Joaquin County, California and Snake River Plain and Twin Falls area, Idaho
[E85-10090] 12 p1873 N85-21752
Building a functional, integrated GIS/remote sensing resource analysis and planning system — Utah
[E85-10092] 12 p1874 N85-21754
Review of computer mapping and display techniques applicable to regional analysis
[DE85-003545] 12 p1875 N85-21764
A formal method for specifying computer resources in an implementation independent manner
[AD-A149955] 12 p1918 N85-22043
Technologies to sustain tropical forest resources
[TI85-901065] 13 p2126 N85-23241
Metal waste in machine tool industry examined
14 p2283 N85-24147
Geometric error analysis for shuttle imaging spectrometer experiment
[NASA-CR-175665] 14 p2305 N85-24289
Managing recoverable aircraft components in the PPB (Planning, Programming and Budgeting) and related processes. Technical volume
[AD-A152014] 15 p2457 N85-25169
Navy geothermal plan
[AD-A152478] 17 p2985 N85-28450
Assessment of computer resource management plan for division support weapon system
[AD-A154142] 19 p3342 N85-30712
Resource management for the tagged token dataflow architecture
[AD-A154773] 21 p3667 N85-32779
Solar energy meteorological research and training program: Region 4
[DE85-011783] 22 p3816 N85-33640
Some recent deposit modeling efforts
24 p4106 N85-35453
Mineral resources programs 24 p4106 N85-35456
Federal Mineral Land Information System
24 p4106 N85-35459
USGS coastal research, studies and maps: A source of information for coastal decision making
[USGS-CIRC-883] 24 p4106 N85-35485

RESPIRATION
NT HIGH ALTITUDE BREATHING
NT PRESSURE BREATHING
Carbon cycle: Terrestrial interactions
05 p0652 N85-14187
Control technology for fiber reinforced plastics industry at AMF Hatteras Yachts, New Bern Division, New Bern, North Carolina
[PB85-109015] 10 p1460 N85-19198
Mercury health effects update: Health issue assessment
[PB85-123925] 10 p1528 N85-19639
USSR report: Space Biology and Aerospace Medicine, volume 18, no. 6, November - December 1984
[JPRS-USB-85-002] 12 p1900 N85-21931
Main component method used to study variations of cardiovascular parameters 12 p1901 N85-21939
Chemical characterization and toxicologic evaluation of airborne mixtures. Inhalation toxicology of diesel fuel obscurant aerosol in Sprague-Dawley rats. Phase 3. Subchronic exposures
[AD-A150100] 12 p1905 N85-21966
Hazards in welding due to oxygen changes in the workplace atmosphere
[BLL-WI-TRANS-684-(9312.57)]
16 p2792 N85-27224
Development of an EM-Based lifeform detector
[AD-A153504] 18 p3151 N85-29512
Changes in the impedance and bioelectrical activity of the cerebral cortex of rats under the action of anaesthetic drugs
[HSE-TRANS-10371] 19 p3327 N85-30617
Typological characteristics of hemodynamic states of healthy subjects in orthostatic position
22 p3821 N85-33673
Effect of short-term antiorthostatic hypokinesia on dynamics of cardiorespiratory parameters during graded physical exercise 22 p3822 N85-33677
An analysis of aerobic capacity in a large United States population
[AD-A156200] 24 p4132 N85-35614

RESPIRATORS
Respiratory protection for children 3 - 6 years of age
[FOA-C-40197-C2] 02 p0238 N85-11550

RESPIRATORY DISEASES
NT ASTHMA
NT INFLUENZA
Interaction between lung mechanics and gas exchange by low volume high frequency pulmonary ventilation in patients with respiratory failure
[AD-A146604] 06 p0846 N85-15372

RESPIRATORY PHYSIOLOGY
Effect of maximum physical load on oxygen-transport properties of blood 01 p0093 N85-10627
Interaction between lung mechanics and gas exchange by low volume high frequency pulmonary ventilation in patients with respiratory failure
[AD-A146604] 06 p0846 N85-15372
Short-term human respiratory effects of nitrogen dioxide: Determination of quantitative dose-response profiles. Phase 2: Exposure of asthmatic volunteers to 4 PPM NO2
[PB85-104388/GAR] 07 p1017 N85-16462
Dynamics of external respiration and gas metabolism under combined effect of hypoxia and hypercapnia
08 p1193 N85-17519
Hyperbaric physiology (status and prospects)
08 p1194 N85-17521

RESPIRATORY RATE
Factors determining effectiveness of voluntary decrease in ventilation during muscular work using instrumented feedback 08 p1193 N85-17520
Scattering of electromagnetic waves by human body and its applications 09 p1363 N85-18572
External respiration, gas exchange and energy expenditures of man in weightlessness
12 p1900 N85-21932

RESPIRATORY SYSTEM
NT BRONCHI
NT DIAPHRAGM (ANATOMY)
NT LUNGS
Deposition in the human lung during respiration of small particles suspended in the air
[BLL-RISLEY-TR-5021-(9091.9F)]
03 p0400 N85-12549
Respiratory chain of alkalophilic bacteria
[DE84-012558] 09 p1360 N85-18556
Air quality criteria for ozone and other photochemical oxidants. External review draft, volume 4
[PB85-126068] 12 p1886 N85-21838
Human lung fluid content during 7-day head-down tilt
12 p1902 N85-21941
Spirolit-2 instrument used to test pulmonary ventilation
12 p1903 N85-21950
Principal patterns of functional changes of human respiratory system in adaptation to high pressure
14 p2387 N85-24704
Cardiorespiratory function and work performance during adaptation to industrial labor in midalpine conditions
22 p3820 N85-33665

RESPONDERS
U TRANSPONDERS

RESPONSE TIME (COMPUTERS)
On a program for solution of BCMP queueing network model
[NAL-TR-813] 03 p0405 N85-12585
Development of graphical time response using the OPTSYSX program
[AD-A152221] 16 p2848 N85-27557
Using percent-done program indicators to enhance user interfaces 23 p3960 N85-34546

RESPONSES
NT DYNAMIC RESPONSE
NT GALVANIC SKIN RESPONSE
NT HEMODYNAMIC RESPONSES
NT MODAL RESPONSE
NT PHYSIOLOGICAL RESPONSES
NT TRANSIENT RESPONSE
Conjunctive and disjunctive item response functions
[AD-A147815] 07 p1033 N85-16561
Models for mixture experiments when the response depends on the total amount
[DE85-000370] 09 p1374 N85-18637
The response of explosive systems to thermal stimuli: A state-of-the-art assessment
[DE85-000919] 11 p1614 N85-20146
Temperature responses of composite panels
[AD-A150053] 12 p1798 N85-21277
Use of the ORACLE DEMS in determining the response of complex scientific instrumentation
[DE85-001742] 12 p1853 N85-21621
Optimized response functions for 2-dimensional observations of solar oscillations
14 p2443 N85-25075
Airsickness control using biofeedback to self-regulate psychophysiological responses
[AD-A151167] 15 p2617 N85-26128
An interactive computer package for use with simulation models which performs multidimensional sensitivity analysis by employing the techniques of response surface methodology
[AD-A151956] 16 p2846 N85-27548
Controller requirements for uncoupled aircraft motion, volume 2
[AD-A153300] 17 p2900 N85-27879
Optical fiber magnetic field sensor with nanosecond response time
[DE85-008409] 18 p3110 N85-29259
Interaction of opiate and phencyclidine derivatives with the acetylcholine receptor
[AD-A155119] 21 p3664 N85-32761
The effect of set size on time to recall color coded information
[AD-A155013] 21 p3665 N85-32767
Models for multidimensional tests and hierarchically structured training materials
[AD-A155231] 21 p3665 N85-32768
Powerful XeCl excimer electric discharge laser with good temporal stability and fast response time
21 p3688 N85-32911
Relaxation phenomena and stability of probability densities
[AD-A155923] 24 p4143 N85-35682

REST
NT BED REST

RESTORATION
Restoration of multichannel microwave radiometric images
[NASA-CR-174115] 04 p0554 N85-13527
State-of-the-art of aquifer restoration. Volume 1: Sections 1 through 8
[PB85-181071] 20 p3478 N85-31612
State-of-the-art of aquifer restoration. Volume 2: Appendices A through G
[PB85-181089] 20 p3478 N85-31613

RESTRAINTS
U CONSTRAINTS

RESTRICTIONS
U CONSTRICTIONS

RESUSCITATION
Liposome-encapsulated hemoglobin for emergency resuscitation
[AD-A146794] 07 p1015 N85-16446

RETAINING
Studies on seismic earth pressure of cohesive backfill
09 p1303 N85-18186

RETARDANTS
NT FLAME RETARDANTS

RETARDERS (DEVICES)
Sensitivity of single and multiple cosmic ray neutrons to the surrounding medium in a lead-free monitor
[SH-9.1-10] 23 p4051 N85-35125

RETARDING
Suppression of vibration effects on piezoelectric crystal resonators
[AD-D011625] 16 p2778 N85-27142
Dual species ion implantation of ternary compounds based on In-Ga-As
[AD-D011617] 16 p2869 N85-27698

RETARDING ION MASS SPECTROMETERS
U MASS SPECTROMETERS

RETENTION (PSYCHOLOGY)
Problems of psychological support of automated organization control systems 09 p1362 N85-18570
Oral discussion, group-to-individual transfer and achievement in cooperative learning groups
[AD-A153209] 17 p3001 N85-28552

RETICLES
Derivation of model topography
18 p3141 N85-29449

RETINA
A study of low-level laser retinal damage
[AD-A150046] 12 p1905 N85-21965
Mammalian tissue sensitivity to long-term exposure to high-intensity stationary magnetic fields
22 p3823 N85-33686

RETINAL ADAPTATION
NT DARK ADAPTATION
NT LIGHT ADAPTATION
Predictive model of electron beam induced flashblindness
[AD-A155260] 21 p3664 N85-32763
RETINAL IMAGES
Retinal information mapping system
[AD-D011531] 12 p1849 N85-21601
Retinally stabilized differential resolution television display
[NASA-CASE-NPO-15432-1] 18 p3089 N85-29117
RETIREMENT FOR CAUSE
Exploratory development of advanced surface flaw detection methods
[AD-A148757] 09 p1281 N85-18060
RETRACTABLE EQUIPMENT
Electronic module insertion and retraction mechanism
[AD-D011309] 07 p0947 N85-16002
Blanket integrated cushioning of foldable and retractable solar arrays 13 p2011 N85-22612
Concept for controlled fold by fold deployment and retraction of flexible, foldable solar generators
13 p2011 N85-22613
Growth capabilities of European retractable solar arrays 13 p2012 N85-22625
Selection of effective arrangement of heavy undercarriage systems for use with concrete runways
14 p2285 N85-24158
Retractable Rigid Solar Generator (GSR)
[SNIAS-851-440-101] 20 p3484 N85-31654
RETRACTABLE LANDING GEAR
U LANDING GEAR
U RETRACTABLE EQUIPMENT
RETRAINING
Data processing professionals and DP application users' perceptions and expectations of operational roles of persons working in a DP/application user interface group 24 p4165 N85-35821
RETRIEVAL
NT DATA RETRIEVAL
NT INFORMATION RETRIEVAL
NT PAYLOAD RETRIEVAL (STS)
The ARGOS contribution to the successful dredging of a deep moored current meter 14 p2327 N85-24381
RETROFITTING
NT ACOUSTIC RETROFITTING
Natural gas the new locomotive fuel
[DE84-901824] 09 p1302 N85-18179
Computer-generated display system guidelines. Volume 1: Display design
[DE85-000679] 11 p1701 N85-20699
RETROREFLECTION
Transparent electrode for optical switch
[DE85-011618] 22 p3761 N85-33310
RETROREFLECTORS
Retroreflective armbands: Influences of wearing mode, aging and other factors on the visibility distance
[IZF-1984-28] 14 p2422 N85-24942
RETURN BEAM VIDICONS
NT THERMICONS
Preliminary study for an IR-vidicon for the 8 to 14 micron range, phase 1
[BMFT-FB-W-84-025] 05 p0633 N85-14057
REUSABLE HEAT SHIELDING
Results of tests of advanced flexible insulation vortex and flow environments in the North American Aerodynamics Laboratory lowspeed wind tunnel using 0.0405-scale Space Shuttle Orbiter model 16-0 (test OA-309)
[NASA-CR-167692] 01 p0015 N85-10096
Verification tests of durable TPS concepts
[NASA-TM-86313] 03 p0323 N85-12085
The challenging scales of the bird: Shuttle tile structural integrity 08 p1095 N85-16919
Study of outgassing and decomposition of space shuttle heat protection tiles, fillers and adhesive
[NASA-CR-175565] 12 p1791 N85-21242
Electron beam charging of Space Shuttle thermal protection system tiles 13 p1990 N85-22478
Thermal protection systems for reentry vehicles
[CNES-NT-113] 23 p3900 N85-34157
Experimental aerodynamic heating to simulated space shuttle tiles in laminar and turbulent boundary layers with variable flow angles at a nominal Mach number of 7
[NASA-TP-2307] 23 p3929 N85-34351
REUSABLE LAUNCH VEHICLES
Future launching systems, 3rd prospective phase
[SNIAS-S/DT/Y-25-063] 11 p1589 N85-19999
REUSABLE ROCKET ENGINES
Methane heat transfer investigation
[NASA-CR-171199] 03 p0362 N85-12316
The aerodynamic challenges of SRB recovery
08 p1093 N85-16908
Aerojet advanced engine concept
08 p1107 N85-16999
Studies on rocket engines for future European launchers
[SEP-TPRL/K-19572/84] 15 p2495 N85-25393
Structural Integrity and Durability of Reusable Space Propulsion Systems
[NASA-CP-2381] 17 p2910 N85-27941
REUSABLE SPACECRAFT
NT CHALLENGER (ORBITER)
NT COLUMBIA (ORBITER)
NT DISCOVERY (ORBITER)
NT ENTERPRISE (ORBITER)
NT SPACE SHUTTLES
Winged first stages of space transport appliances
[TUM-RT-TB-84/3] 02 p0167 N85-11125
Ground man-machine interfaces for orbiter checkout
08 p1091 N85-16897
Drives and benefits overview
08 p1107 N85-16998
Advanced research and technology programs for advanced high-pressure oxygen-hydrogen rocket propulsion
[NASA-TM-86969] 12 p1789 N85-21231
British super-shuttle 18 p3087 N85-29104
REUSE
Reusable software
[AD-A146575] 06 p0854 N85-15427
Reusable software: A concept for cost reduction
16 p2697 N85-26655
REVENUE
Financing considerations and Federal budget impacts
07 p0915 N85-15792
REVERBERATION
Total area of diffusion elements in a reverberation chamber and measured degree of sound absorption
[NRC/CNR-TT-2110] 03 p0415 N85-12653
Reverberation effects on directionality and response of stationary monopole and dipole sources in a wind tunnel
[NASA-TM-87063] 20 p3453 N85-31443
Toward the theory of acoustic scattering on uneven free surface 21 p3680 N85-32862
REVERSE FIELD PINCH
NT CYLINDRICAL PLASMAS
Physics of reversed-field pinch profile sustainment
[DE84-014024] 04 p0565 N85-13602
Theoretical studies of Field-Reversed Configurations (FRC) and experimental study of the FRC during translation
[DE84-016467] 04 p0566 N85-13603
Oscillating field current drive for reversed field pinch discharges
[DE84-015090] 04 p0567 N85-13610
Transport experiments in the Texas experimental Tokamak 09 p1389 N85-18741
Design and construction details of the FRX-C/T device: A compact toroid plasma translation experiment
[DE85-001527] 09 p1390 N85-18749
Magnetic divertor design for the compact reversed-field pinch reactor
[DE85-002031] 09 p1391 N85-18753
Role of multiple helicity nonlinear interaction of tearing modes in dynamo and anomalous thermal transport in the Reversed Pitch Field
[DE85-002176] 10 p1560 N85-19639
FRC translation dynamics and plasma confinement properties in FRX-C/T
[DE85-002386] 10 p1560 N85-19642
Magnetic fluctuations, field reversal maintenance, and anomalous thermal transport in the reversed field pinch
[DE85-003804] 11 p1732 N85-20892
High beta pinch plasma (STP-3(M))
15 p2655 N85-26380
High beta pinch plasma (STP-L)
15 p2655 N85-26381
Asymmetric flux generation and its relaxation in reversed field pinch
[IPPJ-712] 15 p2656 N85-26387
Internal field probing of translating FRCs
[DE85-003732] 15 p2657 N85-26394
Poloidal rotation of magnetic fluctuations in reversed field pinch plasma
[IPPJ-715] 16 p2866 N85-27677
Fusion-power-core design of a Compact Reversed-Field Pinch Reactor (CRFPR)
[DE85-007710] 16 p2868 N85-27692
Two-dimensional TBR calculations for conceptual compact reversed-field pinch reactor blanket
[DE85-007636] 17 p3040 N85-28812
Reversed field pinch dynamics and transport studies
[DE85-007553] 18 p3189 N85-29778
Comparison study of toroidal-field divertors for a compact reversed-field pinch reactor
[DE85-009591] 18 p3189 N85-29781
One-dimensional hybrid code for FRM dynamics
[DE85-010687] 19 p3361 N85-30840
Radiation-cooled helicity-injecting reversed field pinch formed with relativistic electrons
[IPPJ-721] 19 p3370 N85-30091
Proposed FRX-D experiment
[DE85-012766] 24 p4158 N85-35779
REVERSE OSMOSIS
Operating experiences of reverse osmosis plants treating Rand Water Board (RWB) water: Pitfalls and problems 01 p0023 N85-10142
Reverse osmosis treatment to control inorganic and volatile organic contamination
[PB84-223528] 01 p0071 N85-10470
Ultrafiltration as pretreatment for the preparation of drinking water by reverse osmosis onboard ships
[PML-1984-32] 01 p0098 N85-10654
Feasibility study for small group water desalination equipment
[AD-A155108] 21 p3563 N85-32164
Oxidation of formaldehyde solutions used for the preservation of reverse osmosis membranes
[PB85-185585] 22 p3742 N85-33194
REVERSE TIME
U REACTION TIME
REVERSED FLOW
Characteristics of a turbulent plane offset jet
02 p0196 N85-11310
Dilution jet configurations in a reverse flow combustor
[NASA-CR-174888] 13 p1974 N85-22392
Determination of boundary line between reverse jet and surrounding stream 13 p2043 N85-22799
Small gas turbine combustor study: Fuel injector performance in a transpiration-cooled liner
[NASA-TM-86989] 15 p2473 N85-25294
REVERSING
Mean intensity of wave reflected by wavefront reversing mirror in turbulent medium 22 p3782 N85-33432
Latitudinal gradients of cosmic rays and the polarity reversal of the heliospheric magnetic field: A preliminary evaluation
[SH-4.2-16] 23 p4008 N85-34653
A new drawing technique for nylon 6 by reversible plasticization with iodine
[AD-A156272] 24 p4162 N85-35800
REVIEWING
A review of some aspects of robust inference for time series
[AD-A149706] 12 p1923 N85-22962
REVISIONS
Preliminary mechanical redesign of an existing gas-turbine engine to incorporate a high-efficiency, low-pressure-ratio, highly regenerative cycle for marine applications
[AD-A144808] 01 p0011 N85-10070
United States Air force aircraft modification process: A system dynamics analysis
[AD-A146954] 07 p0893 N85-15660
Reanalysis of continuous dynamic systems with continuous modifications 09 p1337 N85-18411
Testing of scanner-assisted revision of the topographic map 1:25,000 (TK 25) 16 p2814 N85-27359
Automatic engraving of map frames in the revision of the TK 25, 1:25,000 topographical map
16 p2814 N85-27382
A concept for map updating using digital image processing methods 16 p2815 N85-27384
Structural dynamics modification of generalized beams using a local eigenvalue modification procedure
19 p3282 N85-30053
Modification of the grain size of sputtered copper with additions of oxygen, krypton, silver, or yttrium
[DE85-010975] 21 p3567 N85-32180
Progress and plans for the Colorado Wind Profiler Network 21 p3626 N85-32542
AUTSKED: An addendum
[DE85-010410] 22 p3829 N85-33712
REVOLUTION (MOTION)
U REVOLVING
REVOLVING
Variable loading of elastic-plastic shells of revolution
06 p0779 N85-14981
REYNOLDS EQUATION
A local dynamical interpretation method of numerical weather forecasting 01 p0080 N85-10536
Applications of Canuto's method to Rayleigh-Taylor-initiated turbulence
[DE85-010835] 18 p3102 N85-29202
Turbulent mixing and combustion
22 p3744 N85-33207
REYNOLDS LAW
U REYNOLDS EQUATION
REYNOLDS NUMBER
NT HIGH REYNOLDS NUMBER
NT LOW REYNOLDS NUMBER
A review and analysis of boundary layer transition data for turbine application
[NASA-TM-86880] 01 p0047 N85-10306

amina: flow heat exchangers. Viscosity induced
-uniform flow
D-A144777] 01 p0047 N85-10307
Development of the code NSFOIL for analyzing high
ynolds number transonic flow around an airfoil
AL-TR-816] 06 p0749 N85-14801
High Marangoni number convection in a square cavity
ASA-CR-174263] 07 p0959 N85-16076
Pneumatic turbulators: A device for drag reduction at
ynolds numbers below 5 million
08 p1071 N85-16791
A visual study of a delta wing in steady and unsteady
otion
D-P004156] 09 p1264 N85-17943
Skin friction measurements for 2 relatively thick airfoil
ections at high Reynolds number
AD-A150021] 12 p1772 N85-21125
Application of large eddy interaction model to channel
low
NASA-TM-86691] 12 p1844 N85-21572
Surface-slip equations for multicomponent
onequilibrium air flow
NASA-TM-85820] 12 p1845 N85-21573
Cryogenic wind tunnels: A selected annotated
bibliography
NASA-TM-86346] 13 p1976 N85-22401
The structure of separated flow regions occurring near
the leading edge of airfoils, including transition
NASA-CR-175670] 14 p2209 N85-23703
Flat magnetohydrodynamic induction pump
17 p2939 N85-28145
Instability at the interface between two shearing fluids
in a channel
[AD-A153532] 18 p3099 N85-29185
Experimental investigations of the unsteady turbulent
friction behavior with pressure impulses in a circular pipe
[MAWI-MITT-102] 18 p3103 N85-29210
High Reynolds number tests of a NASA SC(3)-0712(B)
airfoil in the Langley 0.3-meter transonic cryogenic
tunnel
[NASA-TM-86371] 19 p3213 N85-29926
Pressure distribution from high Reynolds number tests
of a NASA SC(3)-0712(B) airfoil in the Langley 0.3-meter
transonic cryogenic tunnel
[NASA-TM-86370] 19 p3213 N85-29927
Low-speed tests of a high-aspect-ratio,
supercritical-wing transport model equipped with a high-lift
flap system in the Langley 4- by 7-meter and Ames 12-foot
pressure tunnels
[NASA-TP-2097] 20 p3388 N85-31010
Transition in a disturbed environment
20 p3452 N85-31436
Heat transfer in aeropropulsion systems
[NASA-TM-87066] 20 p3453 N85-31444
Development of a new laser Doppler velocimeter for
the Ames High Reynolds Channel No. 2
[NASA-TM-86772] 20 p3458 N85-31477
A numerical study of Taylor-Vortex flow
[AD-A154787] 21 p3584 N85-32277
Numerical solutions of turbulent models for flow over
a flat plate with angle of attack
[DE85-010380] 21 p3585 N85-32286
The aerodynamic characteristics of a GU25-5(11)8
aerofoil for low Reynolds numbers
[GU-AERO-8410] 23 p3894 N85-34121

EYNOLDS STRESS
A study of Reynolds-stress closure model
[NASA-CR-174342] 08 p1161 N85-17324
Analysis of sudden expansion flow in a two-dimensional
duct with and without side-wall injection using the k-epsilon
turbulence model 09 p1317 N85-18282
On the influence of turbulent motions on non-radial
oscillations 14 p2444 N85-25083
Computational models of the viscous sublayer and
limiting behavior of turbulence near a wall
[AD-A151198] 15 p2556 N85-25767
Turbulent wake of a submerged flat plate
[AD-A153776] 18 p3100 N85-29190
A study of the second and third order closure models
of turbulence for prediction of separated shear flows
[NASA-CR-176127] 23 p3929 N85-34353

F-8 AIRCRAFT
U F-8 AIRCRAFT

F-4 AIRCRAFT
Peripheral vision horizon display testing in RF-4C
aircraft 01 p0009 N85-10054

H-2 HELICOPTER
U UH-1 HELICOPTER

HENIUM
Compatibility experiments of facilities, materials, and
propellants for electrothermal thrusters
[NASA-TM-86956] 12 p1795 N85-21260

HENIUM ALLOYS
Solution softening in molybdenum-rhenium alloys
[DE85-006706] 16 p2750 N85-26972

RHEOENCEPHALOGRAPHY
Effect of 120-day antiorthostatic bedrest on gas
exchange and pulmonary circulation in man
19 p3323 N85-30589

RHEOLOGY
The rheology of icy satellites
[NASA-CR-174024] 02 p0302 N85-11959
Elastomers and other organic composites
[AD-A147624] 08 p1131 N85-17131
The stress-strain-time graph of rheological soils and its
application
[AD-P004286] 09 p1407 N85-18863
A new rheological model for concrete structural
analysis
[DE84-014743] 11 p1653 N85-20413
Rheology of dissemination
[AD-A150006] 12 p1813 N85-21373
Thermal and thermoelastic effects in rolling/sliding
contacts
[AD-A150435] 13 p2165 N85-23429
Sulfur volcanoes on Io? 13 p2173 N85-23479
Geomorphic classification of lava flows on Io
13 p2173 N85-23480
Emplacement of long lava flows on Mauna Loa (Hawaii)
and Alba (Mars) 13 p2186 N85-23563
Field measurements of the 1983 Royal Gardens lava
flows, Kilauea Volcano, and 1984 Mauna Loa lava flows,
Hawaii 13 p2186 N85-23565
Surface structures of Hawaiian lavas
13 p2186 N85-23566
Submarine volcanic eruptions and potential analogs for
Venus 13 p2187 N85-23573
Creep of ice: Further studies
13 p2201 N85-23655
Theoretical and experimental studies of the mechanics
of viscoelastic liquids
[AD-A153505] 18 p3070 N85-28987
Characteristics of charge transfer in the dispersed phase
of electrorheological suspensions
[RAE-TRANS-2125] 19 p3233 N85-30040
Synthesis and characterization of copolyimides with
varying flexibilizing groups
[NASA-TM-86416] 20 p3433 N85-31296
Intraplate crustal deformation due to continental
collisions 20 p3490 N85-31693
Finite element methods for viscoelastic flow
[AD-A154877] 22 p3783 N85-33437
Vascular mechanisms of adaptation to antiorthostatic
position 22 p3822 N85-33675
Cerebral hemodynamics and ventricular function in -15
deg antiorthostatic position 22 p3822 N85-33676
A solid-state framework for terrestrial upper mantles
22 p3856 N85-33878

RHEOMETERS
An investigation of the suitability of using a
Siegiaff-McKelvey high shear rate melt rheometer for the
measurement of low viscosity polymer solutions
[AD-A146275] 03 p0338 N85-12174
Natural electrical activity of human sympathetic nerve
fibers, recorded from body surface
07 p1013 N85-16433

RHODIUM
Characterization of CO binding sites on Rh(111) and
Rh(331) surfaces by XPS and LEED (Low Energy Electron
Diffraction): Comparison to EELS (Electron Energy Loss
Spectroscopy) results
[AD-A149331] 10 p1435 N85-19044
An infrared study of isotopic exchange during
methanation over supported rhodium catalysts; an inverse
spillover effect
[AD-A149390] 10 p1435 N85-19046
An infrared study of the hydrogenation of carbon dioxide
on supported rhodium catalysts
[AD-A149477] 10 p1436 N85-19049
An infrared study of the oxidation of carbon monoxide
over supported rhodium catalysts
[AD-A149478] 10 p1436 N85-19050
Optical second harmonic generation for surface
studies
[DE85-000670] 11 p1640 N85-20333
An infrared study of the dissociation of carbon dioxide
over supported rhodium catalysts
[AD-A149813] 12 p1800 N85-21291
Advanced thin film thermocouples
[NASA-CR-175541] 12 p1850 N85-21607
Transition metal catalyzed transformations of
unsaturated molecules
[DE85-009531] 18 p3080 N85-29055

RHODIUM COMPOUNDS
Anomalous magnetism of CeRh3B2 under pressure
[DE85-003069] 13 p2164 N85-23425
Magnitude and range of the RKKy interaction in
SmRh4B4
[DE85-012284] 23 p3985 N85-34712

RHOMBIC ANTENNAS
Surface wave excitation study
[DE85-005301] 13 p2056 N85-22875

RHYTHM (BIOLOGY)
NT CIRCADIAN RHYTHMS
Mathematical Models of the Circadian Sleep-Wake
Cycle
[AD-A145712] 02 p0235 N85-11532
Timing in dry seeds 05 p0690 N85-14437
The physiology of ultradian rhythms and their role in
affecting disease resistance
[AD-A148842] 09 p1363 N85-18575
Effect of stationary magnetic field on bleeding time
12 p1904 N85-21956
Use of ranks to fit a linear model to cross-sectional data
with an application to biological rhythms
[MATHEMATICS-RESEARCH-169]
12 p1923 N85-22081

RIBBONS
Silicon-sheet surface studies
06 p0831 N85-15267
Ribbon growing method and apparatus
[NASA-CASE-NPO-16306-1-CU]
19 p3375 N85-30934

RIBONUCLEIC ACIDS
Phylogenic distribution of the large 5S rRNA from
Halococcus morrhuae
[NASA-CR-174019] 02 p0234 N85-11523
Development of a new class of chemical and biological
ultrasensors: Ribonuclease contamination and control
[NASA-CR-175466] 11 p1635 N85-20296
Insights into the phylogenetic positions of photosynthetic
bacteria obtained from 5S rRNA and 16S rRNA sequence
data 21 p3658 N85-32719

RIBOSE
Molecular toxicology of chromatin: The role of
Poly(ADP-Ribose) in gene control
[AD-A154415] 19 p3327 N85-30611
The DNA metabolism and poly-(ADP-ribose) synthesis
in lymphocytes of persons exposed to low doses of ionizing
radiation
[OEFZS-4307] 20 p3507 N85-31800
Insights into the phylogenetic positions of photosynthetic
bacteria obtained from 5S rRNA and 16S rRNA sequence
data 21 p3658 N85-32719

RIBS (SUPPORTS)
Heat transfer and pressure drop in blade cooling
channels with turbulence promoters
[NASA-CR-3837] 03 p0361 N85-12315
The residual strength of cracked specimens
representing a section of the mirage into wing main spar
[ARL/STRUC-R-408] 12 p1865 N85-21699
Research in the field of rib stiffened shell stability
16 p2766 N85-27068

RICCATI EQUATION
Numerical algorithms and software for matrix Riccati
equations
[AD-A150148] 13 p2150 N85-23344
Some new results on the discrete-time Riccati Equation
and their use in the design of optimal regulators and
observer-estimators
[AD-A151934] 16 p2854 N85-27597

RICE
Remote sensing of rice fields and sea pollution by
SIR-B 08 p1145 N85-17222

RICHARDSON NUMBER
On the classification and nonlinear solution of one type
of stratified shear flow
[AD-A148832] 09 p1319 N85-18295
Three-dimensional baroclinic instability of a Hadley cell
for small Richardson number
[NASA-TP-2450] 11 p1687 N85-20605
Modeling of shear flow in a stratified fluid
14 p2340 N85-24469

RICHARDSON-DUSHMAN EQUATION
U TEMPERATURE EFFECTS
U THERMIONIC EMISSION

RIDGES
New data on structure of Shirshov Ridge (Bering Sea)
10 p1496 N85-19456

RIDING QUALITY
Design of a digital ride quality augmentation system for
commuter aircraft
[NASA-CR-172419] 01 p0006 N85-10037
Design of a digital ride quality augmentation system for
commuter aircraft
[AD-A148233] 08 p1086 N85-16879
Ride comfort of off-road vehicles
[AD-P004279] 09 p1406 N85-18855
Further development in ride quality assessment
[AD-P004280] 09 p1406 N85-18856
Comparison of measured and simulated ride comfort
for an agricultural tractor and influence of travel speed
and tyre-inflation pressure on dynamic response
[AD-P004281] 09 p1407 N85-18857

Seakeeping and vibration tests of the Coast Guard 110 foot surface effect ship SEA BIRD class (WSES)
[AD-A154150] 19 p3252 N85-30166

RIEMANN INTEGRAL
U MEASURE AND INTEGRATION

RIEMANN MANIFOLD
Unrestricted convergence for generalized Poisson integrals
[CTH-MATH-1984-13] 04 p0556 N85-13540
A geometric approach to high resolution TVD schemes
[NASA-CR-172484] 06 p0857 N85-15449
Riemann foliations on simply connected varieties
11 p1699 N85-20677
Nonlinear sigma-models and integration methods
[DE85-004447] 12 p1922 N85-22071
On meromorphic functions continuous on the Stollow boundary 15 p2633 N85-26232
Conditions for the possibility of conformal sewing
[ST-AASF-IMD-58] 16 p2858 N85-27625
Admissible convergence of Poisson integrals in symmetric spaces
[CTH-MATH-1985-04] 22 p3636 N85-33750

RIEMANN PROBLEM
U CAUCHY PROBLEM

RIEMANN SPACE
U RIEMANN MANIFOLD

RIEMANN SPHERE
U RIEMANN MANIFOLD

RIFT VALLEYS
U VALLEYS

RIFTS
U GEOLOGICAL FAULTS

RIGGING
Behavior of the lean methane-air flame at zero-gravity
[NASA-CR-175586] 12 p1799 N85-21263
A novel type of stayed tower for wind turbines
[ISD-295] 15 p2587 N85-25952
Actuator rigging test set electromagnetic interference test (CE03)
[AD-A155819] 24 p4086 N85-35327

RIGID BODIES
U RIGID STRUCTURES

RIGID MOUNTING
New features of different frequency generating systems due to the use of electrodeless rigidly mounted VBA quartz crystal resonator 18 p3106 N85-29231

RIGID ROTOR HELICOPTERS
Application of Floquet theory to helicopter blade flapping stability
[AD-A154460] 19 p3218 N85-29952

RIGID ROTORS
The analysis on the dynamic performance of a single lug
[AD-P004289] 09 p1406 N85-18886

RIGID ROTORS (PLASMA PHYSICS)
NT PLASMA PHYSICS

RIGID STRUCTURES
NT RIGID ROTORS
NT RIGID WINGS
A rigid body mechanism in structural dynamics
02 p0206 N85-11361
Measurement of the inertial constants of a rigid or flexible structure of arbitrary share through a vibration test
[NASA-TM-77557] 02 p0209 N85-11381
Elimination of uncontrollable rigid body mode, appendix C 05 p0603 N85-13842
Composite repair of aircraft structures
08 p1120 N85-17059
Least favorable response of inelastic structures
09 p1336 N85-18398
Planar dynamics of a uniform beam with rigid bodies affixed to the ends
[NASA-CR-175566] 12 p1864 N85-21693
Computer aided engineering applied to the design and verification of the generic Advanced Rigid Array (ARA) — solar array 13 p2006 N85-22593
Development and qualification of the electrical part of the Advanced Rigid Array (ARA) — solar array
13 p2006 N85-22594
Rigid Solar Generator (GSR) solar arrays
13 p2009 N85-22596
Retractable Rigid Solar Generator (GSR)
13 p2009 N85-22597
Generic design and verification of an Advanced Rigid Array (ARA) — solar array 13 p2012 N85-22621
Sound emission by particle beam passing through hole in rigid shield 15 p2525 N85-25570
Experience with free bodies 15 p2576 N85-25887
An improved torsional method for determining the fracture toughness of stiff materials and of adhesive joints
[AD-A152091] 16 p2800 N85-27267
The stability and dynamics of elastic structures and fluid flows
[AD-A154188] 19 p3266 N85-30252
Space station dynamic modeling, disturbance accommodation, and adaptive control
20 p3409 N85-31154
Retractable Rigid Solar Generator (GSR)
[SNIAS-851-440-101] 20 p3484 N85-31654
Rigid Solar Generator (GSR) solar arrays
[SNIAS-851-440-102] 20 p3484 N85-31655
Joint design for improved fatigue life of diffusion-bonded box-stiffened panels
[NASA-TP-2480] 22 p3799 N85-33537
The dynamics of articulated rigid bodies for purposes of animation 23 p3965 N85-34579
Identification and control of structures in space
[NASA-CR-176175] 24 p4089 N85-35214

RIGID WINGS
Theoretical study of non-linear unsteady aerodynamics of a non-rigid lifting body
[AD-P004169] 09 p1266 N85-17954
The aerodynamic characteristics of a GU25-5(11)8 aerofoil for low Reynolds numbers
[GU-AERO-8410] 23 p3894 N85-34121

RIGIDITY
Rigid zeolite containing polyurethane foams
[DE85-006406] 23 p3919 N85-34286
Effects of solar magnetic field on cosmic rays
[SH-4.2-12] 23 p4008 N85-34850
The expected cosmic ray density and stream distributions at the heliolatitudinal asymmetry of solar wind
[SH-4.2-14] 23 p4008 N85-34852
The dependence of solar modulation on the sign of the cosmic ray particle charge
[SH-4.2-23] 23 p4009 N85-34860
Observation of nuclei with energies 8-30 MeV per nucleon in the Earth's magnetosphere at the altitudes 350 KM
[SH-10.1-5] 23 p4053 N85-35136

RILLS
U VALLEYS

RIMS
Chondrule rims and interchondrule matrix in UOC
06 p0882 N85-15604

RING CURRENTS
Relations between the particle precipitation events in mid-latitudes, the ring current intensity and the polarity of the interplanetary magnetic field
04 p0519 N85-13316
Earth's radiation belts
[AD-A147927] 07 p0998 N85-16339
Correlation of ring current and ionospheric gap in morning and evening hours 14 p2339 N85-24466
Ring current dynamics and plasma sheet sources — magnetic storms 14 p2359 N85-24577
The temporal evolution of a small auroral substorm as viewed from high altitudes with Dynamics Explorer 1
[NASA-CR-176064] 20 p3493 N85-31718

RING LASERS
Experimental properties of an inhomogeneously broadened He-Xe unstable ring laser
[AD-A144824] 01 p0052 N85-10344
Autostochastic behavior of solid state ring laser with low frequency periodic loss modulation
11 p1717 N85-20605
Status of and outlook for producing means of transmitting units of plane angle, angular velocity and acceleration with ring lasers 13 p2074 N85-22955
Measurements of laser gyro errors as a function of the beam path
[DFVLR-FB-85-02] 17 p2969 N85-28336
Fiber optic gyroscope with alternating output signal
[AD-D011689] 19 p3271 N85-30284
Influence of mirror anisotropy and Brewster window orientation on radiation characteristics of ring lasers
21 p3684 N85-32889
Possibility of measurement of small displacements by ring laser 21 p3687 N85-32904

RING STRUCTURES
Seismotectonic nature of some annular photoanomalies registered by remote methods 02 p0164 N85-11110
Large-scale bubble structure of the interstellar medium (ISM) and properties of the Local Spiral Arm (LSA)
06 p0879 N85-15586
Method for introducing fluorine into an aromatic ring
[AD-D011397] 08 p1120 N85-17061
Two-dimensional shock response of a mass on energy-absorbing shock mounts
09 p1334 N85-18389
The structure and dynamics of ringed galaxies
09 p1415 N85-18926
Solar system studies with the IUE: 1982 - 1984
11 p1744 N85-20964
Torso sizing ring construction for hard space suit
[NASA-CASE-ARC-11616-1] 12 p1910 N85-21987
Observations of high resistance on slip-rings employing Ag/MoS2/Cu brushes — solar array drives
[ESA-ESTL-70] 18 p3123 N85-29333
A rotating electrical transfer device
22 p3798 N85-33520
Two-plane balance and slip-ring design
22 p3799 N85-33538
SRB attach ring phenolic TPS fishtail seal evaluation tests
[NASA-CR-170887] 24 p4096 N85-35407

RINGS
Flexible matrix composite laminated disk/ring flywheel
05 p0606 N85-13868
Acceleration of an electron ring in a modified betatron with transverse pressure
[AD-A148626] 08 p1221 N85-17888

RINGS (MATHEMATICS)
Polynomial and power series FGS-rings have trivial coefficient rings
[TWISK-326] 01 p0109 N85-10737
On Bezout domains, elementary divisor rings, and pole assignability
[CSIR-TWISK-330] 01 p0110 N85-10740
On localization of injective modules
[CSIR-TWISK-342] 14 p2413 N85-24878
Quadratic spaces over discrete Hodge algebras
16 p2853 N85-27580
On the turning lozange of constant side whose vertices alternate between two fixed circles of a ring
[AD-A154803] 21 p3677 N85-32840

RIO GRANDE (NORTH AMERICA)
Rio Grande rift: Problems and perspectives
[DE84-015492] 04 p0534 N85-13417
Water resources data for Colorado, water year 1983. Volume 1: Missouri River Basin, Arkansas River Basin and Rio Grande Basin
[PB85-123859] 11 p1671 N85-20528
Evaluation of geothermal potential of Rio Grande rift and Basin and Range province, New Mexico
[DE85-901380] 19 p3301 N85-30466

RIOMETERS
Autumn and winter anomalies in ionospheric absorption as measured by riometers 11 p1660 N85-20460

RIPPLES
Ripple ring basins on Ganymede and Callisto
13 p2183 N85-23547
Water wave propagation over uneven bottoms
[AD-A151450] 15 p2556 N85-25769
Neoclassical diffusion including ellipticity in a heliotron-like configuration 23 p3976 N85-34667

RISK
Differences in health risks by aircraft model among US Navy pilots
[AD-A146147] 03 p0401 N85-12558
Interval mathematics reports
[REPT-84/1] 04 p0556 N85-13536
Risk analysis without Monte Carlo methods
04 p0556 N85-13537
Conditional regression models for transient state survival analysis
[AD-A147872] 07 p1034 N85-16563
Ambiguity and uncertainty in probabilistic inference
[AD-A147378] 07 p1035 N85-16572
A theory of preference reversals
[AD-A147952] 08 p1216 N85-17861
Application of the isoenergy principle and the A weighting to evaluate lesion risks due to noise in a military environment
[ISL-CO-231/83] 14 p2390 N85-24720
LFMR definition study
[AD-A153691] 18 p3090 N85-29126
The human role in space (THURIS)
18 p3158 N85-29557
Procedure for estimating orbital debris risks
[NASA-TP-2507] 22 p3736 N85-33169
Description of a test site for large-scale heavy gas dispersion and combustion experiments
[DE85-004987] 23 p3911 N85-34231
The application of models to the assessment of fire hazard from consumer products
[NBSIR-85-3219] 23 p3925 N85-34325
Fire service emergency management handbook
[AD-A155780] 24 p4064 N85-35313
Calculation of trajectories of detached wind turbine blades and prediction of site risk levels associated with failures of HAWT's 24 p4110 N85-35475
The physical and empirical basis for a specific clear-air turbulence risk index
[NASA-CR-178522] 24 p4120 N85-35549
Risk analysis and sensitivity: Antithesis or synthesis
[B8562444] 24 p4144 N85-35887

RIT ENGINES
Analysis of beam interaction of the electrical thruster RIT 10 (particle emission) with surfaces
[ESA-TT-826] 20 p3421 N85-31231

RITZ AVERAGING METHOD
Comparison of free component mode synthesis techniques using MSC/NASTRAN
[DE84-014451] 04 p0514 N85-12276

pline-based Rayleigh-Ritz methods for the roximation of the natural modes of vibration for flexible ms with tip bodies
SA-CR-172566] 13 p2102 N85-23100
A study of internal and distributed damping for vibrating omachiner blades
ASA-CR-175901] 17 p2898 N85-27868
R BASINS
T MISSOURI RIVER BASIN (US)
Systematic data interpretation of remote sensing in the ection of hydrocarbons, volume 1
85-10006] 02 p0215 N85-11421
Evaluation of criteria for selecting the spectral attributes digital LANDSAT MSS imagery for discriminating ological units in the lower Curaca River Valley, Bahia - Brazil
E85-10036] 03 p0379 N85-12415
Late quarterly glaciolacustrine and vegetational history of the Copper River Basin, south-central Alaska
03 p0391 N85-12499
Report of the field work performed in the Basins of the Quebra Osso and Tanque Petro Rivers in the Catas Altas quadrangle, Minas Gerais
[INPE-3268-NTE/225] 04 p0525 N85-13359
Deforestation, floodplain dynamics, and carbon biogeochemistry in the Amazon Basin
08 p1144 N85-17216
Comparison of land cover information from LANDSAT Multispectral Scanner (MSS) and airborne Thematic Mapper simulator (TMS) data for hydrologic applications — Clinton River Basin, Michigan
13 p2122 N85-23211
General report of the researches of snowpack properties, snowmelt runoff and evapotranspiration in Japan 13 p2124 N85-23225
Snowmelt-runoff model utilizing remotely-sensed data
13 p2124 N85-23226
Snowmelt runoff model in Japan
13 p2124 N85-23227
Application of Martinec-Rango model to river basin in Japan 13 p2124 N85-23228
Distribution of snow and maximum snow water equivalent obtained by LANDSAT data and degree day method 13 p2124 N85-23229
The geology of East Butte, a rhyolitic volcanic dome on the Eastern Snake River Plain, Idaho
13 p2187 N85-23570
Automatic hydrological data collection facility using ARGOS 14 p2324 N85-24363
The ARGOS system and hydrology: The use of Platform Terminal Transmitter (PTT) with built-in memory and direct reception by the Seine basin hydrology service
14 p2328 N85-24389
Study of Volga river delta using space photosurvey materials 15 p2485 N85-25340
Estimation of Sr90 and Cs137 activity introduced and accumulation in the Po basin until 1983
[CISE-2515] 22 p3813 N85-33617
RIVERS
NT COLORADO RIVER (NORTH AMERICA)
NT MISSISSIPPI RIVER (US)
NT RIO GRANDE (NORTH AMERICA)
The SANCOR estuaries programme, 1982-1986
[ISBN-0-7988-2662-2] 01 p0068 N85-10454
Estuaries of the Cape. Part 2: Synopses of available information on individual systems. Report 12: Buffels (WES) (CSW 1), Elsies (CSW 2), Sir Lowry's Pass (CSW8), Steenbras (CSW 9), and Buffels (OOS) (CSW 11)
[CSIR-RR-411-PT-2] 01 p0086 N85-10581
Estuaries of the Cape. Part 2: Synopses of available information on individual systems. Report no. 14: Sand (CSW 4)
[CSIR-RR-413-PT-2] 01 p0086 N85-10583
Estuaries of the Cape. Part 2: Synopses of available information on individual systems. Report no. 15: Zeekoe (CSW 5)
[CSIR-RR-414-PT-2] 01 p0087 N85-10584
Estuaries of the Cape. Part 2: Synopses of available information on individual systems. Report no. 18: Bot/Kleinmond system (CSW 13)
[CSIR-RR-417-PT-2] 01 p0087 N85-10587
Spatial relationships in stream flow residuals
02 p0212 N85-11397
Petrology of deep crustal xenoliths from the eastern Snake River Plain, Idaho 02 p0226 N85-11477
Geothermal assessment of the lower Bear River drainage and northern East Shore ground-water areas, Box Elder County, Utah
[DE84-017358] 04 p0526 N85-13368
Carbon cycle: Terrestrial interactions
05 p0652 N85-14187
Image-to-image correspondence: Linear structure matching 07 p0986 N85-16266
Forecasting water temperature decline and freeze-up in rivers
[AD-A147068] 07 p0987 N85-16274
Verification of a model of the Eastern Scheldt
[RAND/R-3108-NETH] 09 p1354 N85-18518
Freeze-up, breakup and date of maximum ice thickness for the Saint Lawrence River, 1971 - 1978
[PB85-119451] 10 p1507 N85-19509
Examples of environment services: Hydrological and pollution measurements in the Po River (Italy)
[CISE-2299] 11 p1679 N85-20578
A comparison of terrestrial saltation flux in the laboratory and the field 13 p2189 N85-23582
The ARGOS system and hydrology. Results obtained by ORSTROM and benefits of a degree of standardization 14 p2239 N85-23881
Applications of Kalman filtering and recursive least-squares in river flow modelling
15 p2636 N85-26254
Modeling water resources systems for water quality
[AD-A154288] 19 p3300 N85-30457
Sand dispersion from an ephemeral river delta on the wave-dominated central California coast
[AD-A154352] 19 p3300 N85-30458
Microwave hydrology: A trilogy
[NASA-CR-176042] 20 p3477 N85-31603
Depositional systems and coal occurrence in the Fort Union Formation (Paleocene), Powder River Basin, Wyoming and Montana 24 p4114 N85-35505
Bibliography on tidal hydraulics. Report 2. Supplement 9: Supplementary material compiled from June 1980 - June 1983. Tidal flows in rivers and harbors
[AD-A155990] 24 p4125 N85-35574
RIVETED JOINTS
Defect detection threshold in riveted joints, test report no.44-833/F — in aircraft 04 p0511 N85-13260
The influence of fastener flexibility on load transfer and fatigue life predictions for multirow bolted and riveted joints — aircraft structures
[LBF-FB-172/84] 07 p0979 N85-16219
The application of BRILES rivets for mechanical jointing of Aramid Reinforced Aluminum Laminate (ARALL)
[VTH-LR-387] 16 p2802 N85-27279
Mechanical jointing in Aramid fiber composites: An experimental study
[VTH-LR-371] 16 p2802 N85-27280
RIVETING
The application of BRILES rivets for mechanical jointing of Aramid Reinforced Aluminum Laminate (ARALL)
[VTH-LR-387] 16 p2802 N85-27279
Utilization of an automated riveting system in aircraft construction
[MBB-UT-11/84-O] 16 p2875 N85-27738
RIVETS
Future robotics program at San Antonio ALC (Air Logistics Center)
[AD-P004011] 03 p0309 N85-11991
The application of BRILES rivets for mechanical jointing of Aramid Reinforced Aluminum Laminate (ARALL)
[VTH-LR-387] 16 p2802 N85-27279
RL-10 ENGINES
Convoluted nozzle design for the RL10 derivative 2B engine
[NASA-CR-174953] 19 p3220 N85-29965
RNA
U RIBONUCLEIC ACIDS
ROADS
NT HIGHWAYS
Pavement friction measurements on nontangent sections of roadways, vol. 1
[PB84-219732] 01 p0036 N85-10227
A study of bituminous pavements to determine a correlation between pavement structure designs and tripping of asphalt cement
[PB84-217751] 01 p0037 N85-10231
Automatic land vehicle navigation using road map data
[DE84-017178] 09 p1278 N85-18043
Microwave methods for paving
[DE85-004194] 14 p2265 N85-24032
A greedy algorithm for the transhipment along a single road problem
[AD-A152343] 17 p3025 N85-28709
Review of rigid pavement design for vehicular parking areas
[AD-A154284] 19 p3222 N85-29975
Design and implementation of an interactive route editor 23 p3962 N85-34559
ROASTING
Sintered silicon nitride workpiece
[NASA-TM-77600] 01 p0021 N85-10129
ROBOTICS
Terrain navigation concepts for autonomous vehicles
[AD-A144994] 01 p0005 N85-10031
USSR report: Machine tools and metalworking equipment
[JPRS-UMM-84-019] 01 p0035 N85-10214
Growth, future of Soviet robotics sector analyzed
01 p0035 N85-10217
Publications of Center for Manufacturing Engineering (of the National Bureau of Standards), 1978-1983
[PB84-224526] 01 p0036 N85-10228
East Europe report: Science and technology
[JPRS-ESA-84-030] 01 p0101 N85-10670
Robotics investment decision model user's manual
[AD-A145467] 02 p0204 N85-11347
European Scientific Notes, Number 38-9
[AD-A145663] 02 p0306 N85-11975
Current successful robotics applications by the Automatix Company
[AD-P003998] 03 p0307 N85-11979
Air Force Materials Laboratory plans/projects
[AD-P004010] 03 p0308 N85-11990
Future robotics program at San Antonio ALC (Air Logistics Center)
[AD-P004011] 03 p0309 N85-11991
Robotics in nondestructive inspection at Sacramento Air Logistics Center
[AD-P004012] 03 p0309 N85-11992
Supply center processes
[AD-P004014] 03 p0309 N85-11993
Potential application of robotics and state-of-the art end effectors at Letterkenny Army Depot
[AD-P004015] 03 p0309 N85-11994
Field applications for robotic material handling
[AD-P004016] 03 p0309 N85-11995
West Europe report: Science and technology, no. 166
[JPRS-84845] 03 p0341 N85-12190
French firms develop artificial intelligence robot
03 p0341 N85-12192
East Europe report: Scientific affairs, no. 791
[JPRS-84624] 03 p0341 N85-12195
Sensor technology for second, third generation industrial robots. Optical sensor applications
03 p0342 N85-12196
Test-bed for programmable automation research. Phase 1
[AD-A145872] 03 p0409 N85-12614
USSR report: Machine tools and metalworking equipment
[JPRS-UMM-84-020] 04 p0491 N85-13126
Developments in Soviet robot technology viewed
04 p0491 N85-13127
DNC, CNC network for robotized machining cells
04 p0491 N85-13130
Development of robot technology in Shanghai surveyed 04 p0492 N85-13134
Machine Mechanics Institute builds walking vehicle
04 p0543 N85-13455
Evaluation of automated decisionmaking methodologies and development of an integrated robotic system simulation
[NASA-CR-172401] 04 p0552 N85-13516
Manufacturing Sciences and Robotics Research and Development Act of 1984
[H-REPT-98-1078] 04 p0578 N85-13888
Instantaneous kinematics and joint displacement analysis of fully-parallel robotic devices
05 p0641 N85-14113
Application of robotics in remote fuel fabrication operations
[DE84-011481] 05 p0646 N85-14144
Robotic technology: An assessment and forecast
[AD-A146672] 06 p0815 N85-15171
NC programming, machine tool information
06 p0816 N85-15178
Fiat, Peugeot introduce integrated robotized engine: CAD used 07 p0936 N85-15933
Improvement of electromechanical systems by utilization of microelectronic technology 07 p0955 N85-16053
Computer science research in Europe
[AD-A146905] 07 p1022 N85-16482
JPL Robotics Laboratory computer vision software library
[NASA-CR-174272] 07 p1023 N85-16491
USSR report: Machine tools and metalworking equipment
[JPRS-UMM-84-021] 08 p1138 N85-17168
Control systems for robotic production lines
08 p1138 N85-17169
USSR report: Machine tools and metalworking equipment
[JPRS-UMM-85-001] 08 p1139 N85-17172
Design features, applications of new robots
08 p1139 N85-17174
East Europe report: Science and technology
[JPRS-ESA-84-046] 08 p1139 N85-17176
Man-machine communication research for robotics reported 08 p1139 N85-17177
Robotics application in construction industry assessed
08 p1139 N85-17178
East Europe report: Science and technology
[JPRS-ESA-84-047] 08 p1140 N85-17183
Researchers on third generation robotics development
08 p1140 N85-17184

Flexible manufacturing system concept features cache memory 08 p1140 N85-17186

East Europe report: Science and technology [JPRS-ESA-84-043] 08 p1142 N85-17198

Chemical, material electronics studies established 08 p1142 N85-17200

Robotics research, integration overview presented. Application objectives cited 08 p1142 N85-17201

Coordinated research in robotics and integrated manufacturing [AD-A148204] 08 p1168 N85-17365

Conceptual design report for a remotely operated cask handling system, revision 1 [DE85-000348] 08 p1169 N85-17371

Cognitive asymmetry and occupation. Computer programmers, students, and bank personnel, part 1 and part 2 [AD-A147125] 08 p1197 N85-17540

Recognition of complex 3-dimensional objects using 3-dimensional moment invariants [AD-A148119] 08 p1212 N85-17625

Investigation on experimental techniques to detect, locate and quantify gear noise in helicopter transmissions [NASA-CR-3847] 08 p1217 N85-17667

Advancement of remote technology: Past perspectives and future plans [DE85-000934] 09 p1327 N85-18342

Optical data processing for missile guidance [AD-A149346] 10 p1422 N85-18972

Researchers, projects at French intelligent machine center 10 p1460 N85-19207

French firm develops 2D, 3D computer vision system 10 p1461 N85-19208

USSR report: Machine tools and metalworking equipment [JPRS-UMM-85-003] 10 p1461 N85-19211

Dean of Kiev State University on impact of robots 10 p1461 N85-19213

Robotized blanks loader for new forge press 10 p1461 N85-19216

Flexible applications robot used in Moscow training course 10 p1462 N85-19217

Control system of complex CNC machining cell 10 p1462 N85-19218

On motion planning with uncertainty: Revised [AD-A149521] 10 p1492 N85-19421

Contact insertion and wire lay robotic end effector apparatus [AD-D011451] 10 p1492 N85-19424

New developments in robotics: The Robots 8 Conference and Exposition [DE85-000263] 10 p1493 N85-19429

Robotics in the radiochemical laboratory [DE85-002824] 10 p1494 N85-19433

Optical implementation of the synthetic discriminant function [AD-A149562] 10 p1557 N85-19817

Novel concept in design of ASEA's new assembly robot 11 p1592 N85-20016

East Europe report: Science and technology [JPRS-ESA-85-009] 11 p1616 N85-20165

New PCB production for robotics application 11 p1617 N85-20169

Overview of leading-edge research at French CNRS lab 11 p1618 N85-20179

French panel makes specific proposals for robotics research. Current state of French robotics 11 p1618 N85-20180

Real time algorithms for robotic control of teleoperators [DE85-001137] 11 p1647 N85-20380

Robotics at Savannah River site: Activity report [DE85-003657] 11 p1648 N85-20383

Advanced industrial robot control systems [PB85-110773] 11 p1648 N85-20385

Advanced industrial robot control systems [PB85-110781] 11 p1648 N85-20386

Dynamic world modeling for an intelligent mobile robot using a rotating ultra-sonic ranging device [AD-A149979] 12 p1775 N85-21143

Impacts of robotic and flexible manufacturing technologies on manufacturing costs and employment [AD-A150060] 12 p1860 N85-21668

Mechanical properties for the grasp of a robotic hand [AD-A150062] 12 p1860 N85-21669

A formal method for specifying computer resources in an implementation independent manner [AD-A149955] 12 p1918 N85-22043

Design of an optical proximity sensor using multiple cones of light for measuring surface shape — application to a robot manipulator [AD-A150050] 12 p1934 N85-22152

Sensor control of robot arc welding 12 p1948 N85-22233

Advancing automation and robotics technology for the Space Station and for the US economy. Volume 1: Executive overview [NASA-TM-87566-VOL-1] 13 p1986 N85-22460

Advancing automation and robotics technology for the Space Station and for the US economy, volume 2 [NASA-TM-87566-VOL-2] 13 p1987 N85-22461

Reliability of robotized welding apparatus 13 p2034 N85-22741

Optoelectronic safety system for robotized technological complex 13 p2046 N85-22805

Optimum design of electrical motors for multilink manipulators and automated manufacturing systems 13 p2062 N85-22880

Motion planning with six degrees of freedom [AD-A150312] 13 p2165 N85-23432

Classification of holding jigs for objects of robotized assembly 14 p2266 N85-24039

USSR report: Machine tools and metalworking equipment [JPRS-UMM-85-004] 14 p2284 N85-24152

Automated, robotized forge-press systems viewed 14 p2284 N85-24153

Robots for application in forge-press operation 14 p2284 N85-24154

Modular design, versatility of robots viewed 14 p2284 N85-24155

Integrated control system for FMS components 14 p2285 N85-24156

Robotized system for treating gear wheels 14 p2285 N85-24162

Investigation of transport operations of ergatic robot 14 p2286 N85-24166

East Europe report: Science and technology [JPRS-ESA-85-015] 14 p2289 N85-24189

Plans, developments in robotics 14 p2289 N85-24191

3D (Three-Dimensional) sensor for adaptive suspension vehicle [AD-A150921] 14 p2311 N85-24305

Our future in the cosmos: Computers 14 p2432 N85-24997

West Europe report: Science and technology [JPRS-WST-85-014] 15 p2489 N85-25362

Resources for robotics research in Europe, by country 15 p2489 N85-25364

Study of experimental robotized system for arc welding based on Universal-15 manipulator 15 p2500 N85-25423

West Europe report: Science and technology [JPRS-WST-84-012] 15 p2523 N85-25552

French robotics research at Grenoble labs 15 p2523 N85-25555

French firm develops new kind of CTD camera for robots 15 p2523 N85-25556

China report: Science and technology [JPRS-CST-85-009] 15 p2530 N85-25596

Development of robots, robotics discussed 15 p2530 N85-25599

West Europe report: Science and technology [JPRS-WST-84-027] 15 p2532 N85-25612

A preliminary investigation into the intelligibility of Microspeech-2, a speech synthesiser [BAE-BT-12284] 15 p2539 N85-25675

Robotic arc welding 15 p2566 N85-25830

Automation and robotics in welding 15 p2566 N85-25831

Some aspects of nuclear plant fabrication in Japan and the UK relating to automatic and robotic arc welding 15 p2566 N85-25834

The kinematic control of redundant manipulators 15 p2566 N85-25836

Development of robots and application to industrial processes [NASA-CR-175754] 15 p2567 N85-25840

East Europe report: Science and technology [JPRS-ESA-84-032] 16 p2727 N85-26833

Optimal open loop and nonlinear feedback control for remote orbital capture [AD-A151967] 16 p2732 N85-26859

Method of selecting robotized system design for pressing process 16 p2761 N85-27040

Experience of sheet stamping robotic complexes 16 p2761 N85-27041

USSR report: Machine tools and metalworking equipment [JPRS-UMM-84-010] 16 p2767 N85-27071

New robotized, vertical broaching machine featured 16 p2767 N85-27074

Guidelines for optimization of robotized machining cells 16 p2767 N85-27076

A robotic system for preparing reagent and dilution vials [DE85-008262] 16 p2793 N85-27231

Automation and robotics for the National Space Program [NASA-CR-175881] 17 p2909 N85-27938

Engineering robot actions in a computer integrated manufacturing environment [CWI-CS-R8415] 17 p2938 N85-28138

USSR report: Machine tools and metalworking equipment [JPRS-UMM-84-014] 17 p2946 N85-28183

Applications of robots in machine tool industry reviewed 17 p2946 N85-28186

Robotic safety systems and methods: Savannah River site [DE85-008261] 17 p2974 N85-28375

West Europe report: Science and technology [JPRS-WST-84-022] 18 p3085 N85-29088

Component problems plague French robotics industry 18 p3085 N85-29089

Multinational program to develop intelligent robots 18 p3086 N85-29094

Analysis of remote operating systems for space-based servicing operations, volume 1 [NASA-CR-171885] 19 p3225 N85-29993

Analysis of remote operating systems for space-based servicing operations. Volume 2: Study results [NASA-CR-171886] 19 p3225 N85-29994

Space station automation study-satellite servicing. Volume 1: Executive summary [NASA-CR-171512] 19 p3226 N85-29999

Space station automation study-satellite servicing, volume 2 [NASA-CR-171513] 19 p3226 N85-30000

Some examples of the application of automatically guided vehicle systems [HSE-TRANS-11134] 19 p3281 N85-30349

Touch-off: A method to determine the position of an object by means of a sensor-driven robot [DE85-011176] 19 p3339 N85-30681

Acoustic imaging systems (for robotic object acquisition) [AD-A154043] 19 p3351 N85-30772

Space optics [CNES-84/105/T/CT/DRT/TIT/10] 20 p3533 N85-31985

NASA space station automation: AI-based technology review [NASA-CR-176094] 21 p3558 N85-32134

NASA space station automation: AI-based technology review. Executive summary [NASA-CR-176096] 21 p3558 N85-32135

East Europe report: Science and technology [JPRS-ESA-85-021] 21 p3568 N85-32190

East Europe report: Science and technology [JPRS-ESA-85-023] 21 p3572 N85-32217

Importance of automation, robotization in economy 21 p3572 N85-32219

Ultrasonic position reference systems for an autonomous sentry robot and a robot manipulator arm [AD-A155481] 21 p3596 N85-32338

Space station automation and robotics study. Operator-systems interface [NASA-CR-176095] 22 p3738 N85-33172

Testimony of Robert A. Frosch before the Subcommittee on HUD and Independent Agencies of the Senate Committee on Appropriations [NASA-TM-87496] 22 p3738 N85-33173

Statement of Aaron Cohen, Director, Research and Engineering, Johnson Space Center and Chairman, Space Station Advanced Technology Advisory Committee, National Aeronautics and Space Administration, before the Subcommittee on Science, Technology, and Space, Committee on Commerce, Science, and Transportation, United States Senate [NASA-TM-87497] 22 p3739 N85-33174

Space station automation study: Autonomous systems and assembly, volume 2 [NASA-CR-176092] 22 p3739 N85-33175

Study and realization of a command system adapted to space robotics [SNIAS-851-440-106] 22 p3740 N85-33183

Robotic order picking [AD-D011737] 22 p3792 N85-33483

Machine intelligence for robotics applications [DE85-011430] 22 p3793 N85-33500

A strategy planner for NASA robotics applications [NASA-CR-175319] 22 p3834 N85-33739

Space Missions for Automation and Robotics Technologies (SMART) Program [NASA-TM-86820] 24 p4068 N85-35210

Investment justification of robotic technology in aerospace manufacturing. User's manual [AD-A156193] 24 p4099 N85-35410

TRICCS: A proposed teleoperator/robot integrated command and control system for space applications [NASA-TM-87577] 24 p4136 N85-35837

OBOTS

Optical seam tracking of robotic arc welding
[VTT-272] 01 p0055 N85-10368

Methods, applications of image processing
01 p0115 N85-10785

DoD Robotics Application Workshop Proceedings
[AD-A145867] 03 p0307 N85-11978

Current successful robotics applications by the Automatix Company
[AD-P003998] 03 p0307 N85-11979

Air force, robotic painting
[AD-P004006] 03 p0308 N85-11986

East Europe report: Science and technology
[JPRS-ESA-84-038] 03 p0343 N85-12210

Development, production, application of robots assessed 03 p0343 N85-12211

Industrial robots and transmanipulations: Important link in setup of automated production lines
03 p0345 N85-12222

Modular electromechanical industrial robots
03 p0345 N85-12223

International exhibition: Industrial Robots, 1982
03 p0345 N85-12224

Robotization of electric welding processes
03 p0345 N85-12225

Robotization of technological processes in high-frequency heating and welding
03 p0345 N85-12226

Improving operational reliability and productivity of robotized technological complexes
03 p0346 N85-12227

Test-bed for programmable automation research. Phase 1
[AD-A145872] 03 p0409 N85-12614

East Europe report: Science and technology
[JPRS-ESA-84-041] 04 p0484 N85-13090

Use of robotics in heavy machinery, equipment construction industry 04 p0485 N85-13093

Robotics technology application assessed, statistics
04 p0485 N85-13094

Mathematical modeling of assembly processes involving use of sensitized robots 04 p0488 N85-13111

Optimization of movements of manipulators with kinematic redundancy 04 p0488 N85-13112

Soviet robot exhibition reviewed
04 p0491 N85-13128

Development, new application of Soviet robots
04 p0491 N85-13129

China report: Science and technology
[JPRS-CST-84-003] 04 p0491 N85-13132

Development of robot technology in Shanghai surveyed 04 p0492 N85-13134

Improved robotic equipment for radiological emergencies
[DE84-017637] 04 p0509 N85-13249

Design of a flexible machining system
[CETIM-1-3E-140] 04 p0510 N85-13252

Real-time planning by an intelligent robot
[DE84-016669] 04 p0553 N85-13519

The acquisition, processing, and use of tactile sensor data in robot control 05 p0641 N85-14114

Robotic technology: An assessment and forecast
[AD-A146672] 06 p0815 N85-15171

East Europe report: Science and technology
[JPRS-ESA-84-045] 06 p0815 N85-15175

New concepts for industrial robots outlined
06 p0815 N85-15176

Translational control of a graphically simulated robot arm by kinematic rate equations that overcome elbow joint singularity
[NASA-TP-2376] 06 p0856 N85-15446

NyKINM, a further development of KINM 22 — simulation of a robot attack on an aircraft
[FOA-C-20559-D8(E3)] 07 p0903 N85-15720

Precise control of flexible manipulators
[NASA-CR-174210] 07 p0973 N85-16178

Vision by man and machine: How the brain processes visual information may be suggested by studies in computer vision (and vice versa)
[AD-A147890] 07 p1017 N85-16458

New applications for robot loaders, unloaders
08 p1139 N85-17175

General assessment of GDR microelectronics industry, applications 08 p1142 N85-17202

The combinatorics of local constraints in model-based recognition and localization
[AD-A148338] 08 p1230 N85-17746

Dutch institutes do research in tactile visual robot sensors 09 p1310 N85-18228

Scania, ASEA of Sweden use robots for all production phases 09 p1310 N85-18229

The optimal control and design of a flexible manipulator arm 09 p1327 N85-18340

Parallel algorithms for robot dynamics
[DE84-016563] 09 p1369 N85-18605

Strategy planning by an intelligent machine
[DE84-016609] 09 p1372 N85-18624

Double pinch-push contact insertion end-effector
[AD-D011485] 10 p1459 N85-19196

Armenia markets new drive motors for machine tools
10 p1461 N85-19212

Production turret lathe retrofitted with robot
10 p1461 N85-19214

Specifications, applications of gantry robots viewed
10 p1461 N85-19215

Planning of minimum-time trajectories for robot arms
[AD-A148956] 10 p1492 N85-19418

Simplified grasping and manipulation with dextrous robot hands
[AD-A148962] 10 p1492 N85-19419

Fourth International Conference on Robot Vision and Sensory Controls
[AD-A149524] 10 p1492 N85-19422

Contact insertion and wire lay robotic end effector apparatus
[AD-D011451] 10 p1492 N85-19424

New developments in robotics: The Robots 8 Conference and Exposition
[DE85-000263] 10 p1493 N85-19429

Robotic safety
[DE85-002314] 10 p1493 N85-19431

Robotics in the radiochemical laboratory
[DE85-002824] 10 p1494 N85-19433

Monitoring the execution of plans in SIPE (System for Interactive Planning and Execution) monitoring
[AD-A149138] 10 p1544 N85-19731

Novel concept in design of ASEA's new assembly robot 11 p1592 N85-20016

East Europe report: Science and technology
[JPRS-ESA-85-009] 11 p1616 N85-20165

Robot production lines in operation
11 p1617 N85-20166

Increased use of CNC in machine tool construction
11 p1617 N85-20170

Robotics at Savannah River site: Activity report
[DE85-003657] 11 p1648 N85-20383

Exploratory assessment of second generation robotics and sensor-based systems
[PB85-132793] 11 p1648 N85-20388

Man/machine interface for a nuclear cask remote handling control station: System design requirements
[DE85-000256] 11 p1697 N85-20667

Navigation for an intelligent mobile robot
[AD-A150051] 12 p1775 N85-21144

A functional vehicle for autonomous mobile robot research
[AD-A150052] 12 p1860 N85-21666

Dynamic visual servo control of robots: An adaptive image-based approach
[AD-A150057] 12 p1860 N85-21667

Impacts of robotic and flexible manufacturing technologies on manufacturing costs and employment
[AD-A150060] 12 p1860 N85-21668

Mechanical properties for the grasp of a robotic hand
[AD-A150062] 12 p1860 N85-21669

Oversight review of the five-year outlook report on science and technology
[GPO-41-058] 12 p1949 N85-22243

Cyclic industrial robots with mechanical energy storing devices: Multipositional system with one or several degrees of freedom 13 p2045 N85-22803

Hydraulic brakes for industrial robots
13 p2046 N85-22806

Cyclic industrial robots with mechanical energy storing devices: Principles of drive design
13 p2046 N85-22807

Assembly robot control algorithms
13 p2046 N85-22808

Optimum design and automated dynamic analysis of flexible mechanisms
[AD-A150152] 13 p2099 N85-23088

USSR report: Machine tools and metalworking equipment
[JPRS-UMM-85-006] 14 p2283 N85-24146

New CNC turning centers described
14 p2284 N85-24148

Minister B. V. Balmont on status of automation drive
14 p2284 N85-24151

Auxiliary units for Robots 14 p2285 N85-24161

Robotized system for treating gear wheels
14 p2285 N85-24162

Investigation of transport operations of ergatic robot
14 p2286 N85-24166

Robotic deburring. Part 2: Evaluation of cutters and noncompliant tooling
[DE85-006182] 14 p2311 N85-24306

Production cells with IR 2SO robot examined
15 p2524 N85-25561

Development of robots, robotics discussed
15 p2530 N85-25599

Robot use in FRG increases but sensor technology lags 15 p2531 N85-25605

West Europe report: Science and technology
[JPRS-WST-84-009] 15 p2535 N85-25639

French consulting firm develops own robotics
15 p2535 N85-25642

Italy invents robot to compete with Asea, Hitachi
15 p2535 N85-25643

Italy's Fiat uses Sweden's Asea seeing robot
15 p2536 N85-25650

Applicability of modular versus universal robots discussed 15 p2538 N85-25664

Sonars with high noise and clutter rejection for use with adaptive robots
[AD-A151875] 15 p2543 N85-25701

Manipulation and simulation of general robots using the zero-position description 15 p2567 N85-25838

Artificial intelligence based control of a sensor-driven machine
[DE85-006972] 15 p2633 N85-26227

Structural design and kinematic configuration of two-armed robots 16 p2761 N85-27037

Calculating reliability and productivity of cold stamping robot complex as queuing system
16 p2761 N85-27039

Automatic manipulators for forging rollers
16 p2762 N85-27042

Updating model RPD-1.25 industrial robot
16 p2762 N85-27043

Industrial robots and automatic manipulators for forging and pressing operations at Second International Exhibition 16 p2762 N85-27044

New stage in robotics development
16 p2762 N85-27045

Control of motion of manipulator robots on basis of first-order kinematic algorithms
16 p2762 N85-27047

Robotic thermal battery pellet fabrication
[DE85-007755] 16 p2779 N85-27154

Creating a Mobile Autonomous Robot Research System (MARRS)
[AD-A151963] 16 p2793 N85-27229

A general simulation program for robot manipulator arm dynamics
[AD-A152121] 16 p2793 N85-27230

Kinematic rate control of simulated robot hand at or near wrist singularity
[NASA-TP-2440] 16 p2851 N85-27575

Positioning of a robotic manipulator through the use of visual feedback
[AD-A151933] 16 p2851 N85-27577

Robots, automatic devices inside VW's Wolfsburg plant 17 p2946 N85-28186

Future directions of robotics, automation in Italy
17 p2946 N85-28187

Component problems plague French robotics industry
18 p3085 N85-29088

Multinational program to develop intelligent robots
18 p3086 N85-29094

HERMIES-1: A mobile robot for navigation and manipulation experiments
[DE85-008652] 18 p3118 N85-29301

Short and long-term robot feedback
[PB85-180735] 19 p3281 N85-30347

A remote-operated manipulator vehicle
[HSE-TRANS-11133] 19 p3281 N85-30349

Acoustic imaging systems (for robotic object acquisition)
[AD-A154043] 19 p3351 N85-30772

CEMA venture to develop FMS, robot technology
20 p3438 N85-31330

CEMA cooperation in development of robotics, FMS viewed 20 p3438 N85-31331

Hidden costs of robotized production systems revealed 20 p3438 N85-31332

West Europe report: Science and technology
[JPRS-WST-85-020] 20 p3438 N85-31333

Robot, laser tridimensional cutting technology detailed
20 p3438 N85-31335

An analysis of multi-fingered hands
20 p3462 N85-31504

Philosophy of nondestructive control in aeronautics quality control. Knowledge of and improvements to nondestructive test safety
[SNIAS-851-551-101] 20 p3465 N85-31522

Discovery regarding visual neuron adaptation applicable to robot use 20 p3504 N85-31786

Manipulators in teleoperation
[DE85-010563] 20 p3512 N85-31833

Coordinate transformations and programming for small revolute coordinate robots
[RR-273] 20 p3519 N85-31881

Ultrasonic position reference systems for an autonomous sentry robot and a robot manipulator arm
[AD-A155481] 21 p3596 N85-32336

East Europe report: Science and technology. Selections on CSSR computer technology
[JPRS-ESA-84-017] 21 p3666 N85-32781
Robots, Manipulators 21 p3666 N85-32786
Space station automation and robotics study. Operator-systems interface
[NASA-CR-176095] 22 p3738 N85-33172
Space robot simulator vehicle
[NASA-CR-176133] 22 p3739 N85-33176
Study and realization of a command system adapted to space robotics
[SNIAS-851-440-106] 22 p3740 N85-33183
Latch assembly
[DE85-011660] 22 p3792 N85-33492
Future of robots in nuclear plants and processes
[DE85-011506] 22 p3793 N85-33500
Research on distributed artificial intelligence
[AD-A155356] 22 p3833 N85-33733
Multi-robot assembly of IC's 23 p3964 N85-34577
Robot environment expert system
[NASA-CR-3915] 23 p3967 N85-34593
The compliance of end effector force sensors for robot manipulator control 24 p4098 N85-35406
Testbed for sensory control of intelligent machines
[DE85-012355] 24 p4099 N85-35412

ROBUSTNESS (MATHEMATICS)
Location of several outliers in multiple regression data using elemental data
[CSIR-TWISK-300] 01 p0106 N85-10724
Robust rate control system designs for a submersible
[AD-A144792] 01 p0111 N85-10753
Influential observations in time series
[AD-A144719] 01 p0112 N85-10763
The numerical range: A tool for robust stability studies — multivariable feedback systems
[RR-255] 02 p0253 N85-11660
On the relationship between Lehtomaki's robustness test and an inverse Nyquist based test
[OUEL-1526/84] 03 p0409 N85-12616
An H-infinity-minimax approach to the design of robust control systems
[OUEL-1537/84] 05 p0717 N85-14600
Utilization of numerical optimization techniques in the design of robust multi-input, multi-output control systems
[AD-A148289] 08 p1212 N85-17630
An analysis of robust and efficient priors associated with a finite Bayesian model for compliance testing
[AD-A148497] 08 p1213 N85-17635
The performance of variable sampling plans when the normal distribution is truncated
[AD-A147717] 08 p1215 N85-17649
Approximate models in multivariable process control: An inverse Nyquist array and robust tuning regulator interpretation
[RR-261] 08 p1216 N85-17663
Methods of computer-aided analysis of non-Gaussian noise and application to robust adaptive detection, part 2
[AD-A148879] 10 p1539 N85-19704
Robust Kalman filtering and its applications
[AD-A149044] 10 p1550 N85-19775
Robustness of discrete-time dynamical systems: Application to the multivariable digital control of combat aircraft
[ONERA-NT-1984-2] 11 p1585 N85-19986
Automatic control design procedures for restructurable aircraft control
[NASA-CR-172489] 12 p1780 N85-21173
A review of some aspects of robust inference for time series
[AD-A149706] 12 p1923 N85-22062
Asymptotics for configural estimators
[AD-A150106] 12 p1924 N85-22067
Approaches and algorithms for robust signal processing 13 p2062 N85-22878
Bootstrapping the Kalman filter
[AD-A150509] 13 p2153 N85-23370
A research program in active control/aeroelasticity
[NASA-CR-175674] 14 p2218 N85-23752
Estimation of optimum scores for partition detectors using stochastic approximation techniques
14 p2411 N85-24865
Compensator development and examination of performance and robustness
[NASA-CR-175703] 15 p2540 N85-25676
Robust detection of fading narrow-band signals in non-Gaussian noise
[AD-A152262] 16 p2774 N85-27124
Robust regression through robust covariances
[AD-A153301] 17 p3020 N85-28677
On the stability of collocated controllers in the presence or uncertain nonlinearities and other perils
20 p3416 N85-31201
Robust adaptive control 20 p3417 N85-31207
Feedforward-feedback control logic for robust target-tracking 20 p3436 N85-31317
Extensions of the small-mu test for robust stability — control stability
[OUEL-1573/85-REV] 20 p3519 N85-31884
Decentralized stabilization by high gain feedback
[BU-115] 24 p4144 N85-35689

ROCHE LIMIT
The Moon's orbit history and inferences on its origin
04 p0585 N85-13735
Formation of the prelunar accretion disk
04 p0588 N85-13755
Mechanical models of close approaches and collisions of large protoplanets 04 p0588 N85-13756

ROCK INTRUSIONS
NT BATHOLITHS
Rio Grande rift: Problems and perspectives
[DE84-015492] 04 p0534 N85-13417
High-resolution microseismicity study of possible magmatic intrusion in the Long Valley Caldera
[DE85-001076] 11 p1681 N85-20593
Nd-isotopic evidence for the origin of the Sudbury complex by meteoritic impact 15 p2660 N85-26554
Three-dimensional gravity ideal body studies in rough terrain
[DE85-014097] 24 p4118 N85-35525

ROCK MECHANICS
Remote sensing as a mineral prospecting technique
[E85-10010] 02 p0216 N85-11423
Seismology in rockburst research
[REPT-551] 03 p0375 N85-12394
Summaries of physical research in the geosciences
[DE85-001882] 06 p0818 N85-15194
Some specifics of methods for mass detailed studies of rock heat conductivity 10 p1502 N85-19477
Rock mechanics: Issues and research needs in the disposal of wastes in hydraulic fractures
[DE85-001399] 10 p1556 N85-19809
Improved model for fluid-driven cracks in jointed rock
[DE85-008963] 18 p3125 N85-29349
Thermal-cycle testing of the G-tunnel heated block
[DE85-008408] 18 p3126 N85-29359
Measurement and calculation of the mechanical response of a highly fractured rock
[DE85-008421] 18 p3127 N85-29362
Comparison and evaluation of field and numerical results from the Site A heater test at Avery Island
[DE85-010625] 19 p3268 N85-30269
Geologic and hydrologic characterization and evaluation of the basin and range province relative to the disposal of high-level radioactive waste. Part 2: Geologic and hydrologic characterization
[GS-CIRC-904-B] 20 p3526 N85-31933
Geologic and hydrologic characterization and evaluation of the basin and range province relative to the disposal of high-level radioactive waste. Part 3: Geologic and hydrologic evaluation
[GS-CIRC-904-A] 20 p3526 N85-31934
Precambrian evolution and the rock record
21 p3656 N85-32711
Calibrator for displacement gages used in the rock mechanics laboratory
[DE85-013257] 24 p4096 N85-35393
Seismic stratigraphic analysis of the Mississippi Fan
24 p4115 N85-35507
Crustal structure in southern California from array data
24 p4115 N85-35512

ROCKET BOOSTERS
U BOOSTER ROCKET ENGINES

ROCKET CHAMBERS
U THRUST CHAMBERS

ROCKET ENGINE CASES
The effect of 2 strength reducing techniques on the ultimate tensile strength of AISI 4130 steel: Rocket motor case venting
[AD-A145526] 02 p0169 N85-11134
Integral boost, heat protection, port covers and transition 07 p0918 N85-15813
Solid rocket booster retrieval operations
08 p1096 N85-16928
A study on a medium-sized rocket with Burnout frame
[NAL-TR-821] 09 p1287 N85-18082
Integrated insulation wall assembly — for a solid rocket motor case
[AD-D011553] 12 p1794 N85-21257
Characterization standards for solid propellant rocket motors
[AD-A150250] 13 p2013 N85-22627
Verification of the SRB motor case pin retainer band tips
[NASA-CR-170882] 24 p4070 N85-35220

ROCKET ENGINE CONTROL
Shuttle avionics software trials, tribulations and success 08 p1090 N85-16891
Man-machine interface and control of the shuttle digital flight system 08 p1091 N85-16894
Space shuttle main engine hardware simulation
08 p1091 N85-16895

ROCKET ENGINE DESIGN
Ramjet air induction system design for tactical missile application 07 p0918 N85-15811
Design and analysis report for the RL10-2B breadboard low thrust engine
[NASA-CR-174857] 10 p1430 N85-19020
Studies on rocket engines for future European launchers
[SEP-TPRL/K-19572/84] 15 p2495 N85-25391

ROCKET ENGINES
NT ARC JET ENGINES
NT BOOSTER ROCKET ENGINES
NT DUCTED ROCKET ENGINES
NT ELECTROSTATIC ENGINES
NT ELECTROTHERMAL ENGINES
NT HYDRAZINE ENGINES
NT HYDROGEN OXYGEN ENGINES
NT ION ENGINES
NT LIQUID PROPELLANT ROCKET ENGINES
NT MERCURY ION ENGINES
NT MICROROCKET ENGINES
NT ORBIT MANEUVERING ENGINE (SPACE SHUTTLE)
NT RESISTOJET ENGINES
NT REUSABLE ROCKET ENGINES
NT RIT ENGINES
NT RL-10 ENGINES
NT SOLID PROPELLANT ROCKET ENGINES
NT SPACE SHUTTLE MAIN ENGINE
NT TURBOROCKET ENGINES
NT UPPER STAGE ROCKET ENGINES
Characterization of 8-cm engineering model thruster
[NASA-CR-174673] 02 p0169 N85-11131
Ramjet and Ramrocket Propulsion Systems for Missiles
[AGARD-LS-136] 07 p0917 N85-15809
Ramjet and Ramrocket Propulsion Systems for Missiles: Introduction and overview 07 p0917 N85-15810
Some aspects of engine and airframe integration for Ramjet and Ramrocket powered missiles
07 p0918 N85-15812
Drives and benefits overview
08 p1107 N85-16999
Advanced OTV engines and issues
08 p1108 N85-17000
Advanced OTV engine concepts
08 p1108 N85-17001
Proceedings of the AFOSR/AFRPL Rocket Propulsion Research Meeting: Abstracts and Agenda
[AD-A148818] 09 p1268 N85-18065
One rocket multiple satellite launch technology
[AD-A149226] 10 p1427 N85-19002
Design and analysis report for the RL10-2B breadboard low thrust engine
[NASA-CR-174857] 10 p1430 N85-19020
A diffuser heat transfer code
[AD-A149270] 10 p1430 N85-19022
Ring-cusp ion thruster with shell anode
[NASA-CASE-LEW-13881-1] 12 p1764 N85-21258
An experimental study of spray thruster
[REPT-613] 12 p1845 N85-21578
Twenty-first JANNAF Combustion Meeting, volume 1
[AD-A150981] 13 p1998 N85-22528
Minimizing plume contamination production in bipropellant thrusters 13 p2003 N85-22557
West Europe report: Science and technology
[JPRS-WST-84-027] 15 p2532 N85-25812
France officially proposes development of Ariane 5 to ESA 15 p2532 N85-25813
SEP of France to make Ariane HM-60 cryogenic engine 15 p2532 N85-25814
Ion sensor signal fluctuations during operation of spacecraft reaction engines 16 p2724 N85-26815
Liquid rocket combustor computer code development
16 p2740 N85-26910
Model for computing late detonations initiated in propellants by impact (XDT reactions)
[DE85-007377] 16 p2758 N85-27018
A theoretical study of two stage thrust augmenting ejectors
[ARL/AERO-R-166] 19 p3218 N85-29954
Solar rocket component study
[AD-A154166] 19 p3227 N85-30007
Modeling the exhaust of the pulsed plasma thruster
[AD-A155344] 21 p3707 N85-33016
Voyager 0.2-lbf thruster valve assembly short pulse test report
[NASA-CR-176121] 22 p3741 N85-33185
SRB attach ring phenolic TPS fishtail seal evaluation tests
[NASA-CR-170887] 24 p4098 N85-35407

ROCKET EXHAUST
Description and use of the single-color transmissometer plume diagnostic code A32CODE
[AD-A146181] 03 p0325 N85-12090

High altitude chemically reacting gas particle mixtures. olume 1: A theoretical analysis and development of the merical solution — rocket nozzle and orbital plume flow elds
[NASA-CR-171826] 07 p0916 N85-15801
High altitude chemically reacting gas particle mixtures. Volume 2: Program manual for RAMP2 — rocket nozzle and orbital plume flow fields
[NASA-CR-171827] 07 p0916 N85-15802
High altitude chemically reacting gas particle mixtures. Volume 3: Computer code user's and applications manual — rocket nozzle and orbital plume flow fields
[NASA-CR-171828] 07 p0917 N85-15803
Proceedings of the AFOSR/AFRPL Rocket Propulsion Research Meeting: Abstracts and Agenda
[AD-A148818] 09 p1288 N85-18085
Particle size, number, composition and velocity from solid rocket motors 12 p1765 N85-21201
Minimizing plume contamination production in bipropellant thrusters 13 p2003 N85-22557
Technical manual: Description and operation Slaved Tracking System
[DE85-004807] 13 p2094 N85-23070
Surface pressure produced by Space Transportation System flight 41B
[AD-A150793] 14 p2242 N85-23901
The highly underexpanded exhaust plume from nozzles with boundary layers
[DFVLR-FB-85-10] 20 p3421 N85-31230

ROCKET LAUNCHERS
Lightweight composite launcher pod
[AD-D011236] 01 p0015 N85-10092

ROCKET LAUNCHING
NT ORBITAL LAUNCHING
Rocket observations 01 p0014 N85-10084
Launch summary for 1978 - 1982 — sounding rockets, space probes, and satellites
[NASA-TM-87375] 04 p0461 N85-12924
Rocket body charge neutralization processes in ARAKS experiment (data from two launches)
13 p1960 N85-22426
Ariane space general director on satellite launcher market 18 p3087 N85-29103

ROCKET LININGS
Alternate nozzle ablative materials program
[NASA-CR-175658] 14 p2246 N85-23924

ROCKET MOTOR CASES
U ROCKET ENGINE CASES

ROCKET NOZZLES
A computer program for the performance analysis of scarfed nozzles
[AD-A147370] 07 p0905 N85-15730
Carbon/carbon rocket motor exit cone reinforcement
[AD-D011380] 07 p0916 N85-15799
High altitude chemically reacting gas particle mixtures. Volume 1: A theoretical analysis and development of the numerical solution — rocket nozzle and orbital plume flow fields
[NASA-CR-171826] 07 p0916 N85-15801
High altitude chemically reacting gas particle mixtures. Volume 2: Program manual for RAMP2 — rocket nozzle and orbital plume flow fields
[NASA-CR-171827] 07 p0916 N85-15802
High altitude chemically reacting gas particle mixtures. Volume 3: Computer code user's and applications manual — rocket nozzle and orbital plume flow fields
[NASA-CR-171828] 07 p0917 N85-15803
Thermophysical property testing using transient techniques
[AD-A147085] 07 p1049 N85-16664
Characterization standards for solid propellant rocket motors
[AD-A150250] 13 p2013 N85-22627
Alternate nozzle ablative materials program
[NASA-CR-175658] 14 p2246 N85-23924
An experimental study of clustered, two-dimensional rocket nozzles
[AD-A151889] 15 p2495 N85-25390
Effective specific impulse of secondary flow injected into a rocket nozzle
[NAL-TR-846T] 18 p3067 N85-28970
Thrust vectoring apparatus for maneuvering missile in flight
[AD-D011693] 19 p3226 N85-30004
Recession of graphitic nozzles in rocket motors
21 p3560 N85-32144

ROCKET PLANES
NT X-15 AIRCRAFT

ROCKET PROPELLANT TANKS
U PROPELLANT TANKS

ROCKET PROPELLANTS
NT CRYOGENIC ROCKET PROPELLANTS
NT DOUBLE BASE ROCKET PROPELLANTS
NT GASEOUS ROCKET PROPELLANTS
NT HYPERGOLIC ROCKET PROPELLANTS
NT LIQUID ROCKET PROPELLANTS
NT MONOPROPELLANTS
NT NITRAMINE PROPELLANTS
NT SLURRY PROPELLANTS
NT SOLID ROCKET PROPELLANTS
NT TATB
Measurement of shock and induced reaction in rocket propellants by nanosecond infrared radiometry and photography
[DE84-013209] 04 p0482 N85-13070
The 1984 JANNAF Propulsion Systems Hazards Subcommittee Meeting, volume 1
[AD-A148865] 10 p1454 N85-19162
Twenty-first JANNAF Combustion Meeting, volume 1
[AD-A150981] 13 p1998 N85-22526
Mixing, chemical reaction and flow field development in ducted rockets
[DE85-004083] 14 p2247 N85-23928
Model for computing late detonations initiated in propellants by impact (XDT reactions)
[DE85-007377] 16 p2758 N85-27019

ROCKET PROPELLED SLEDS
Nondestructive deceleration of a rocket sled — target penetration tests
[FOA-C-20549-D3] 07 p0912 N85-15771

ROCKET SONDES
U SOUNDING ROCKETS

ROCKET SOUNDING
Lyman alpha coronagraph research sounding rocket program
[NASA-CR-174376] 09 p1354 N85-18517
Rocket observations of the ionosphere during the eclipse of 26 February 1979
[NASA-CR-175513] 12 p1888 N85-21850
Experiment for measuring electric fields within the sounding rocket project Energy Budget
[BMFT-FB-W-84-048] 12 p1891 N85-21886
Characteristics of the electrodynamics of auroral arcs as inferred from rocket and ground-base observations during IMS 14 p2363 N85-24601
Observations of the MF-HF plasma wave emissions in active auroras by the sounding rocket experiments at Syowa station 14 p2366 N85-24620
Experimental research on ionospheric disturbance caused by cumulative barium vapor injection
16 p2719 N85-26787
Observations of airglow O2(1-Sigma) atmospheric band at 8645 A and the rotational temperature at 23 deg S
[INPE-3378-PRE/653] 16 p2826 N85-27435
Rocket measurements of mesospheric ionization irregularities
[NASA-CR-176056] 20 p3494 N85-31721

ROCKET TEST FACILITIES
Making sure: A brief outline and history of ESA's test and checkout services
[ESA-BR-22] 09 p1286 N85-18077

ROCKET THRUST
Experiments on residual thrust and prediction for upper-stage solid propellant rockets
[NAL-TR-800] 03 p0324 N85-12087
Orbital maneuvers with finite thrust. Volume 1: Mathematical formulation, numerical methods, catalog concept
[ESA-CR(P)-1910-VOL-1] 06 p0758 N85-14848
Orbit maneuvers with finite thrust. Volume 2: Reference manual, part 1
[ESA-CR(P)-1910-VOL-2-PT-1]
06 p0758 N85-14849
Orbit maneuvers with finite thrust. Volume 3: User's guide, part 2
[ESA-CR(P)-1910-VOL-3-PT-2]
06 p0758 N85-14850
Orbit maneuvers with finite thrust. Volume 3: Reference catalog, parts 1 and 2
[ESA-CR(P)-1910-VOL-3-PT-1/2]
06 p0758 N85-14851
Gyrodynamic fixture for measuring thrust force components
[AD-D011258] 06 p0760 N85-14860
Qualification of an electrothermal hydrazine thruster with a vacuum thrust of 0.5 to 2.0 N
[BMFT-FB-W-84-043] 07 p0917 N85-15808
Advanced OTV engines and issues
08 p1108 N85-17000
Ion sensor signal fluctuations during operation of spacecraft reaction engines 16 p2724 N85-26815
Heaterless ignition of inert gas ion thruster hollow cathodes
[NASA-TM-87086] 23 p3903 N85-34177

ROCKET VEHICLES
NT ARIANE LAUNCH VEHICLE
NT ATLAS CENTAUR LAUNCH VEHICLE
NT CENTAUR LAUNCH VEHICLE
NT MULTISTAGE ROCKET VEHICLES
NT SOUNDING ROCKETS
NT TITAN CENTAUR LAUNCH VEHICLE
NT VEGA LAUNCH VEHICLE

ROCKET-BORNE INSTRUMENTS
Launch summary for 1978 - 1982 — sounding rockets, space probes, and satellites
[NASA-TM-87375] 04 p0461 N85-12924
The multi-anode microchannel array detector system: Current status and future prospects
11 p1761 N85-21080
Stellar ultraviolet flux distributions in the 912-1200 A wavelength range 11 p1762 N85-21081
An improved rocket-borne electric field meter for the middle atmosphere
[NASA-CR-175510] 12 p1888 N85-21851
A rocket-borne X-ray observation of SN1006 with the imaging gas scintillation proportional counter
14 p2435 N85-25014

ROCKS
NT ANORTHOSITE
NT BALTIC SHIELD (EUROPE)
NT BASALT
NT BEDROCK
NT BRECCIA
NT COAL
NT ECLOGITE
NT GNEISS
NT GRANITE
NT IGNEOUS ROCKS
NT LIGNITE
NT LIMESTONE
NT LUNAR ROCKS
NT PERIDOTITE
NT REGOLITH
NT SANDSTONES
NT SCHIST
NT SEDIMENTARY ROCKS
NT SHALES
Compilation of elemental concentration data for NBS (National Bureau of Standards) biological, geological and environmental standard reference materials, 1982
[PB84-218338] 01 p0025 N85-10158
Middle infrared spectral studies of geologic materials in their natural state using photothermal beam deflection spectroscopy
[AD-A144894] 01 p0120 N85-10820
A paleomagnetic study of the Prince William terrane and Nixon Fork terrane, Alaska 02 p0226 N85-11478
Magnetic characteristics of some volcanic rocks of the west Carpathians
[REPT-557] 03 p0376 N85-12400
Electric properties of neovolcanic rocks of central and east Slovakia
[REPT-558] 03 p0376 N85-12401
Reconnaissance geology of the northern part of the Unalakleet quadrangle 04 p0516 N85-13291
Stratigraphy, petrology, and structure of the Pingston terrane, Mount Hayes C-5 and C-6 quadrangles, eastern Alaska Range, Alaska 04 p0517 N85-13301
Paleomagnetic latitude of paleocene volcanic rocks of the Cantwell Formation, central Alaska
04 p0517 N85-13302
Paleogene volcanic rocks of the Matanuska Valley area and the displacement history of the Castle Mountain fault 04 p0518 N85-13303
Progress in lead/uranium zircon studies of lower paleozoic rocks of the southern Alexander terrane
04 p0518 N85-13304
The northern coast plutonic-metamorphic complex, southeastern Alaska and northwestern British Columbia
04 p0518 N85-13305
Cretaceous plutonic rocks, Mitkof and Kupreanof Islands, Petersburg quadrangle, southeastern Alaska
04 p0518 N85-13306
Late oligocene gabbro near Ketchikan, southeastern Alaska 04 p0518 N85-13307
Petrology and petrogenesis of Batholitic rocks, San Jacinto Mountains, southern California
05 p0673 N85-14322
Sedimentation, structure and tectonics of the Umpqua group (paleocene to early eocene), southwestern Oregon 05 p0678 N85-14354
Geochemical data for rock samples from the Petersburg and parts of the Port Alexander and Sumdum quadrangles, southeastern Alaska (documentation)
[PB84-234434] 06 p0836 N85-15318
In-situ stress determination in soil and rock using the acoustic emission method
[AD-A147459] 07 p0979 N85-16215
Geology of the Batopilas mining district, Chihuahua, Mexico, volumes 1 and 2 09 p1351 N85-18496
Quaternary stratigraphy of the lower Iowa and Cedar River Valleys, southeast Iowa 09 p1352 N85-18504
Part 1. Stratigraphy, structure and petrology of the Peterborough 1.5-minute quadrangle, New Hampshire and part 2. Graphite textural and isotropic variations in plutonic rocks, south-central New Hampshire
09 p1353 N85-18511

Study of the physical properties of crystalline rocks in the southeast Voronezh anteclise
[NASA-TM-77823] 10 p1514 N85-19551
China report: Science and technology
[JPRS-CST-84-025] 11 p1620 N85-20197
Micro-deformation of quartz under dynamic action and its applications 11 p1620 N85-20201
Piezoelectric stress transducer used for measurements of explosions in hard rock 11 p1638 N85-20316
Effect of host-rock dissolution and precipitation on permeability in a nuclear waste repository in tuff
[DE85-000675] 11 p1727 N85-20860
Effects of fracture roughness on fluid flow through a single deformable fracture
[DE85-004593] 13 p2092 N85-23062
Geomagnetic field dynamics 13 p2116 N85-23182
Assessment of computer based geologic mapping of rock units in the LANDSAT-4 scene of northern Death Valley, California 13 p2119 N85-23195
Geological information content of reflected wave record form 14 p2345 N85-24502
Location of continental Permian volcanites of central Asia and its tectonic interpretation
14 p2346 N85-24505
The impact ejection of living organisms into space
15 p2682 N85-26566
In-situ rock melting applied to lunar base construction and for exploration drilling and coring on the moon
[DE85-006716] 16 p2717 N85-26770
Analysis of mesofissuring on space photographs: New technique for study of petroleum and gas deposits
16 p2726 N85-26828
In situ Tuff water migration/heater experiment
[DE85-010415] 18 p3101 N85-29200
Laboratory investigation of formation damage of an artificial fracture at simulated geothermal conditions
[DE85-010301] 18 p3102 N85-29201
Improved model for fluid-driven cracks in jointed rock
[DE85-008963] 18 p3125 N85-29349
Interim rock mass properties and conditions for analyses of a repository in crystalline rock
[DE85-010700] 18 p3125 N85-29352
Implications about in situ stress at Yucca Mountain
[DE85-008068] 18 p3126 N85-29356
Measurement and calculation of the mechanical response of a highly fractured rock
[DE85-008421] 18 p3127 N85-29362
Hot Dry Rock Geothermal Energy Developement Program
[DE85-010570] 19 p3268 N85-30264
Ultramicroscopic study of structure of phosphorites from Sea of Japan floor 19 p3290 N85-30400
Microstructural analysis of Pacific Ocean and Indian Ocean ultrabasites 19 p3291 N85-30405
Analysis of the elastic and strength properties of Yucca Mountain tuff, Nevada
[DE85-006975] 19 p3300 N85-30460
Preliminary evaluation of alterant geophysical tomography in welded tuff
[DE85-010626] 19 p3302 N85-30469
Structural and tectonic history of the Golconda allochton, southern Toiyabe Range, Nevada
19 p3312 N85-30529
Stratigraphic analysis of Pennsylvania rocks using hierarchy of transgressive-regressive units
19 p3312 N85-30531
Geometry, velocity structure and penetration depths of descending slabs in the western Pacific
19 p3319 N85-30574
Geothermal COMPAX drill hit development
[DE85-011353] 20 p3469 N85-31556
Source-term considerations for a potential radioactive-waste repository located in unsaturated tuff
[DE85-010090] 20 p3529 N85-31953
Hydrothermal alteration in the 3.5 b.y. old Onverwacht Group of South Africa 21 p3718 N85-33071
The 3.5 b.y. old Onverwacht Group: A remnant of ancient oceanic crust 21 p3718 N85-33073
The Aravalli sequence of Rajasthan, India: A Precambrian continental margin?
21 p3720 N85-33084
Deep-burial diagenesis in carbonates
[DE85-011224] 22 p3802 N85-33554
Discontinuous deformation analysis
[DE85-011208] 22 p3814 N85-33628
Subcritical fracture propagation in rocks: An examination using the methods of fracture mechanics and non-destructive testing 24 p4116 N85-35516
Underwater measurements of muon intensity
[HE-5.1-16] 24 p4202 N85-36078
Results of low energy background measurements with the Liquid Scintillation Detector (LSD) of the Mont Blanc Laboratory
[HE-5.3-5] 24 p4205 N85-36099
The research program of the Liquid Scintillation Detector (LSD) in the Mont Blanc Laboratory
[HE-5.3-6] 24 p4205 N85-36100

ROCKY MOUNTAINS (NORTH AMERICA)
On the nowcasting of mountain-generated thunderstorm systems 01 p0074 N85-10489
Measurements of the surface energy budget in the southern Gobi Desert of China, and in the Rocky Mountains of Colorado
[NASA-CR-175506] 12 p1888 N85-21847

RODENTS
NT GUINEA PIGS
NT MICE
NT RABBITS
NT RATS

RODS
NT CONTROL RODS
Physical-chemical properties of articulated rodlike polymers
[AD-A145549] 02 p0186 N85-11244
Post buckling behavior of a circular rod constrained within a circular cylinder 02 p0207 N85-11365
Nonlinear waves in a rod. Results for incompressible elastic materials
[AD-A147485] 07 p0979 N85-16216
Acoustic oscillations of rods and plates
17 p2944 N85-28170
Torsion-tension coupling in rods
18 p3120 N85-29315
Stress-intensity factors for circumferential surface cracks in pipes and rods under tension and bending loads
[NASA-TM-87594] 24 p4101 N85-35424

ROENTGEN SATELLITE
U ROSAT MISSION

ROGALLO WINGS
U FLEXIBLE WINGS
U FOLDING STRUCTURES

ROLL
Mean and random errors of visual roll rate perception from central and peripheral visual displays
05 p0704 N85-14519
Accuracy of system step response roll magnitude estimation from central and peripheral visual displays and simulator cockpit motion 05 p0705 N85-14522
Models for the effects of G-seat cuing on roll-axis tracking performance 05 p0707 N85-14532
Theory of wing rock 09 p1282 N85-18064
Forces on undriven, angled wheels
[AD-P004303] 09 p1409 N85-18880
Some effects of display format variables on the perception of aircraft spatial orientation
10 p1534 N85-19686
Perception of roll rate from an artificial horizon and peripheral displays
[VTH-LR-403] 17 p3002 N85-28557
In-flight evaluation of pure time delays in pitch and roll
[NASA-TM-86744] 21 p3556 N85-32123

ROLL CONTROL
U LATERAL CONTROL

ROLL FORMING
Microstructural design in low alloy steels
02 p0176 N85-11179
The influence of aluminum on the qualities of low and medium carbon steel
[BLL-M-35754-(5828.4)] 03 p0330 N85-12123
Defining effect of hardening on mean yield strength in deformation zone
[BLL-M-35934-(5828.4)] 05 p0647 N85-14154
Development of surface cracks in AMg6 alloy under low-cycle loading conditions 10 p1442 N85-19089
Hot rolling of ceramics by the use of self propagating synthesis
[AD-D011486] 10 p1453 N85-19154
Method for continuously casting
[AD-D011481] 10 p1459 N85-19195
Division boundary in Al-B composite material with boron in contact with solid and liquid aluminum
13 p2027 N85-22704
Ultrasonic SH wave velocity in textured aluminum plates
[AERE-R-11516] 15 p2509 N85-25475
Superplasticity in a thermo-mechanically processed Aluminum-10.2%Mg-0.52%Mn alloy
[AD-A152016] 15 p2510 N85-25485
Development of high strength ship hull steel for high heat input welding — controlled rolling and accelerated cooling 15 p2565 N85-25827
Automatic manipulators for forging rollers
16 p2762 N85-27042
Principles of wave formation along web of H-beams
[BLL-M-36041-(5828.4)] 16 p2796 N85-27253
High tensile strength, punchable, hot rolled strips with good plasticity
[BMFT-FB-T-84-256] 18 p3078 N85-29040
Rolling contact fatigue testing of thermomechanically processed M-50 steel
[AD-A153640] 18 p3122 N85-[illegible]
The character of observed porosity and its possible effects on rolling contact fatigue life of M-50 steel
[AD-A155930] 24 p4079 N85-[illegible]
Effect of prior warm rolling on the retained austenite content and hardening response of VIM-VAR (vacuum-induction melted-vacuum-arc remelted) AISI M-50 steel
[AD-A158145] 24 p4079 N85-[illegible]

ROLLER BEARINGS
Performance evaluation of automotive wheel bearing greases
[AD-A145948] 03 p0337 N85-12[illegible]
Effect of two inner-ring oil-flow distribution schemes on the operating characteristics of a 35 millimeter bore ball bearing to 2.5 million DN
[NASA-TP-2404] 04 p0507 N85-13[illegible]
Influence of shot-peening methods on surface quality and service life of bearings 06 p0776 N85-14[illegible]
Grease versus oil lubrication of wheel bearings in Army equipment
[AD-A147546] 07 p0973 N85-16[illegible]
Lubrication and performance of high-speed rolling-element bearings
[NASA-TM-86958] 12 p1859 N85-21[illegible]
Load capacity of cages of roller bearings for planet wheels 14 p2221 N85-23775
The characteristics of surface roughness important to gear and rolling bearing problems
14 p2222 N85-23782
Effect of speed and press fit on fatigue life of roller-bearing inner-race contact
[NASA-TP-2496] 20 p3463 N85-31511
The use of ultrasound to monitor incipient failure of rolling element bearings 23 p3924 N85-34317
Elastohydrodynamic lubrication calculations used as a tool to study scuffing
[NASA-TM-87097] 23 p3938 N85-34[illegible]
Design and lubrication of high-speed rolling-element bearings
[NASA-TM-87107] 23 p3938 N85-34[illegible]
Planetary-gear-support bearing test rig design
[NASA-CR-174927] 24 p4064 N85-35[illegible]

ROLLERS
Roller crosshead analysis 04 p0507 N85-13[illegible]
Stability of rigid motions and rollers in bicomponent flows of immiscible liquids
[AD-A147302] 07 p0960 N85-16[illegible]
No-slump Roller-Compacted Concrete (RCC) for use in mass concrete construction
[AD-A148564] 08 p1138 N85-17184
A rotating electrical transfer device
22 p3798 N85-33[illegible]

ROLLING CONTACT LOADS
Numerical analysis of some problems related to the mechanics of pneumatic tires: Finite deformation/rolling contact of a viscoelastic cylinder and finite deformation of cord-reinforced rubber composites
01 p0060 N85-10[illegible]
The characteristics of surface roughness important to gear and rolling bearing problems
14 p2222 N85-23782
Evaluation of the blind hole drilling method for the measurement of residual stress
[AD-A151459] 15 p2579 N85-25[illegible]
Temperature and surface damage under lubricated sliding-rolling contacts 19 p3280 N85-30[illegible]
Effect of speed and press fit on fatigue life of roller-bearing inner-race contact
[NASA-TP-2496] 20 p3463 N85-31511
Rolling, slip and traction measurements on low modulus materials
[NASA-CR-174909] 22 p3791 N85-33[illegible]
The properties of thin-section, four-point-contact ball bearings in space 22 p3797 N85-33521

ROLLING MOMENTS
The generation of rolling moments with the superconducting solenoid model
[NASA-CR-172520] 09 p1283 N85-18[illegible]
Operational and developmental experience with the F/A-18A digital flight control system
16 p2713 N85-26742
Experimental and theoretical determination of the wing-induced lateral wind on the tail surfaces in oscillating rolling motion. Part 1: Application of the Mobile Oscillating Derivatives (MOD) on an experimental part
[IFD-1/84-PT-1] 18 p3061 N85-[illegible]

ROLLUP SOLAR ARRAYS
U SOLAR ARRAYS

ROOFS
Field test results of experimental EPDM (Ethylene Propylene Diene Monomer) and PUF (Polyurethane Foam) roofing
[AD-A147697] 08 p1132 N85-17133

otovoltaic roofing tile systems
12 p1878 N85-21783

aluating wind flow around buildings on heliport
ement
A-PM-84-25] 12 p1893 N85-21881

TEMPERATURE

able and ultraviolet lasers based on excimer
ations in the homonuclear halogens
D011311] 07 p0971 N85-16163

emperature: Curvature relationships for unsymmetric
phite-epoxy laminates
E-85-08] 16 p2743 N85-26926

ffects of temperature on remotely sensed mafic mineral
orption features 16 p2800 N85-27323

A study of Ga(.47)In(.53)As and Al(.48)In(.52)As for very
h frequency device applications
D-A151995] 16 p2870 N85-27706

Strength and failure analysis of composite laminates with
es at room and elevated temperatures
D-A153283] 17 p2917 N85-27981

T CLEAN ROOMS

Penetration of short duration airblast into protective
uctures 09 p1336 N85-18404

Acoustic scaling: A re-evaluation of the acoustic model
Manchester Studio 7
BC-RD-1984/18] 12 p1822 N85-21432

T-MEAN-SQUARE ERRORS

An objective error measure for the comparison of
lculated and measured transient response histories
09 p1335 N85-18395

Clock characterization tutorial
17 p2965 N85-28311

Satellite measurements of atmospheric aerosols
D-A153607] 19 p3316 N85-30556

1000 GeV gamma rays from Cygnus X-3: An update
G-2.1-8] 22 p3863 N85-33925

Comparative analysis of operational forecasts versus
ctual weather conditions in airline flight planning, volume

ASA-CR-167864] 24 p4120 N85-35536

Study of the time-differentiated particle flux density at
rious distances from EAS axis
E-4.7-15] 24 p4200 N85-36065

OTS OF EQUATIONS

On edge detection
D-A148573] 08 p1223 N85-17703

Zero-crossings on lines of curvature
D-A150171] 13 p2150 N85-23345

Convergence of Newton's method for a single real
uation
ASA-TP-2489] 17 p3017 N85-28656

Finding the roots of the transcendental equations in
roblems in determining the thermal conductivity of
pheres with heterogeneous boundary conditions
LL-M-35878-(5828.4)] 23 p3929 N85-34347

AT MISSION

The ROSAT all-sky survey in X-rays
08 p1243 N85-17843

The ROSAT XUV wide field camera
08 p1243 N85-17844

On the unique capabilities of the Hubble space telescope
r studies of ROSAT deep-survey X-ray sources
08 p1243 N85-17846

X-ray satellite
ASA-TM-77882] 20 p3407 N85-31145

The design, development, testing, fabrication, calibration
nd integration of a High Resolution Imager (HRI) for the
ontgen Satellite (ROSAT)
ASA-CR-175302] 22 p3741 N85-33184

S ICE SHELF

Microbial ecology of extreme environments: Antarctic
easts and growth in substrate-limited habitats
ASA-CR-175810] 16 p2839 N85-27509

Aerosol formation by wave action over Ross Sea,
ntarctica 21 p3651 N85-32686

SBY REGIMES

Spectral modeling of a potential vorticity equation for
barotropic flow on a beta-plane
CWI-AM-R8408] 08 p1186 N85-17478

Combined effects of baroclinic and barotropic instability
a nonlinear low order model
DM-41] 09 p1358 N85-18544

Evolution of set of Rossby waves toward anisotropic
quilibrium state 13 p2109 N85-23141

Stability of Rossby waves within framework of
ree-component analysis 13 p2109 N85-23142

Study of the functions of similarity of the planetary
oundary layer. Part 1: Theory
NPE-3129-PRE/520-PT-1] 16 p2826 N85-27428

The effect of the Benthic Boundary Layer on the physics
f intense mesoscale eddies
AD-A153193] 17 p2958 N85-28270

Finite amplitude stability of a Rossby wave in a
hannel 19 p3314 N85-30543

ROSSBY WAVES
U PLANETARY WAVES

ROTARY DRIVES
U MECHANICAL DRIVES

ROTARY ENGINES

Evaluation of heat engine for hybrid vehicle application
[NASA-CR-174163] 04 p0508 N85-13245

Stratified charge rotary aircraft engine technology enablement program
[NASA-CR-174812] 12 p1778 N85-21163

Installation, maintenance and operating manual for the Lucas-type fuel injection system of the 3 B rotary engine
[NASA-TM-77872] 15 p2568 N85-25846

ROTARY GYROSCOPES

Fiber optic gyroscope with alternating output signal
[AD-D011689] 19 p3271 N85-30284

ROTARY STABILITY
NT GYROSCOPIC STABILITY

Structural response of a rotating bladed disk to rotor whirl
[NASA-CR-175605] 13 p1973 N85-22391

Rotational motion of a satellite
13 p1981 N85-22428

Damping seals for turbomachinery
16 p2738 N85-26894

Housing flexibility effects on rotor stability
16 p2738 N85-26896

Influence of materials creep on rotor dynamics
[DE85-008545] 17 p2981 N85-28426

Application of Floquet theory to helicopter blade flapping stability
[AD-A154460] 19 p3218 N85-29952

Recent developments in rotary-balance testing of fighter aircraft configurations at NASA Ames Research Center
[NASA-TM-86714] 21 p3551 N85-32090

ROTARY WING AIRCRAFT
NT BO-105 HELICOPTER
NT CH-47 HELICOPTER
NT HELICOPTERS
NT MILITARY HELICOPTERS
NT P-531 HELICOPTER
NT RIGID RCTOR HELICOPTERS
NT ROTOR SYSTEMS RESEARCH AIRCRAFT
NT TILT ROTOR AIRCRAFT
NT UH-1 HELICOPTER
NT UH-60A HELICOPTER

Rotary-wing aircraft noise measurements: Analysis of variations and proposed measurement standard
[AD-A146207] 03 p0416 N85-12662

Mission-oriented requirements for updating MIL-H-8501. Volume 1: STI proposed structure — military rotorcraft
[NASA-CR-177331-VOL-1] 08 p1088 N85-16877

Mission-oriented requirements for updating MIL-H-8501. Volume 2: STI background and rationale — military rotorcraft
[NASA-CR-177331-VOL-2] 08 p1088 N85-16878

A methodology for the determination of rotary wing aircraft vulnerabilities in air-to-air combat simulation
[AD-A148984] 10 p1424 N85-18984

Special power train requirements for the next generation of rotary-wing aircraft 14 p2220 N85-23769

Rotorcraft digital advanced avionics system (RODAAS) functional description
[NASA-CR-166611] 15 p2468 N85-25237

Rotorcraft research testing in the National Full-Scale Aerodynamics Complex at NASA Ames Research Center
[NASA-TM-86687] 17 p2896 N85-27854

Analysis of rotorcraft crash dynamics for development of improved crashworthiness design criteria
[FAA-CT-85-11] 20 p3391 N85-31031

Fixed gain and adaptive techniques for rotorcraft vibration control
[NASA-CR-177344] 22 p3728 N85-33111

ROTARY WINGS
NT BEARINGLESS ROTORS
NT LIFTING ROTORS
NT RIGID ROTORS
NT TILTING ROTORS
NT TIP DRIVEN ROTORS

Helicopter rotor blade design for minimum vibration
[NASA-CR-3825] 01 p0006 N85-10032

DFVLR rotorcraft: Construction and engineering
[NASA-TM-77740] 01 p0006 N85-10035

Data input, processing and presentation — helicopter rotor balance measurement
[NASA-TM-77739] 01 p0125 N85-10856

Transonic flow analysis for rotors. Part 1: Three-dimensional quasi-steady, full-potential calculation
[NASA-TP-2375-PT-1] 02 p0134 N85-10914

Lifting surface theory for a helicopter rotor in forward flight
[NASA-TM-86315] 02 p0134 N85-10916

Extended aeroelastic analysis for helicopter rotors with prescribed hub motion and blade appended pendulum vibration absorbers
[NASA-CR-172455] 03 p0315 N85-12036

Stochastic motor blade dynamics
[AD-A146312] 03 p0318 N85-12054

Estimation of helicopter performance using a program based on blade element analysis
[AD-A146341] 03 p0318 N85-12055

Detection, classification, and extraction of helicopter-radiated noise
[AD-A145993] 03 p0416 N85-12661

Initial feasibility ground test of a proposed photogrammetric system for measuring the shapes of ice accretions on helicopter rotor blades during forward flight
[NASA-TM-87391] 04 p0455 N85-12887

An experimental investigation of the parallel blade-vortex interaction
[NASA-TM-86005] 05 p0592 N85-13777

Study to eliminate ground resonance using active controls
[NASA-CR-166609] 07 p0902 N85-15715

Helicopter active control with rotor blades relaxation
08 p1075 N85-16819

Integrated technology rotor/flight research rotor concept definition study
[NASA-CR-166446] 10 p1424 N85-18980

Experimental study of main rotor tip geometry and tail rotor interactions in hover. Volume 1. Text and figures
[NASA-CR-177336-VOL-1] 13 p1965 N85-22344

Experimental study of main rotor tip geometry and tail rotor interactions in hover. Volume 2: Run log and tabulated data
[NASA-CR-177336-VOL-2] 13 p1965 N85-22345

Study for prediction of rotor/wake/fuselage interference, part 1
[NASA-CR-177340-VOL-1] 13 p1965 N85-22346

Study for prediction of rotor/wake/fuselage interference. Part 2: Program users guide
[NASA-CR-177340-VOL-2] 13 p1966 N85-22347

Simple theoretical models for composite rotor blades
[NASA-CR-175620] 13 p1971 N85-22382

Computations of two-dimensional airfoil-vortex interactions — helicopter rotor flowfields
[NASA-CR-3885] 14 p2210 N85-23709

Unsteady analysis of rotor blade tip flow
[NASA-CR-3868] 15 p2462 N85-25202

Interaction of a turbulent vortex with a lifting surface
15 p2464 N85-25214

Helicopter rotor
[CH-637690-A5] 15 p2470 N85-25245

Rotor blade flap-lag stability and response in forward flight in turbulent flows 16 p2705 N85-26698

Helicopter Aeromechanics
[AGARD-LS-139] 18 p3057 N85-28913

Rotorcraft noise 18 p3057 N85-28916

Recent developments in the dynamics of advanced rotor systems 18 p3057 N85-28917

Application of Floquet theory to helicopter blade flapping stability
[AD-A154460] 19 p3218 N85-29952

Design of helicopter rotor blades for optimum dynamic characteristics
[NASA-CR-176076] 20 p3393 N85-31044

Impulsive noise due to transonic blade-vortex interactions 20 p3523 N85-31913

Tip vortex computer code SRATIP. User's guide
[NASA-CR-172603] 21 p3551 N85-32093

A three-dimensional viscous flow analysis for the helicopter tip vortex generation problem
[NASA-CR-3906] 23 p3893 N85-34114

An evaluation of three helicopter rotor sections
[NASA-TM-86719] 23 p3893 N85-34115

The effects of parameter variation on helicopter performance
[AD-A156027] 24 p4064 N85-35189

ROTATING
U ROTATION

ROTATING BODIES
NT BEARINGLESS ROTORS
NT COMPRESSOR ROTORS
NT FLYWHEELS
NT HELICOPTER TAIL ROTORS
NT IMPELLERS
NT LIFTING ROTORS
NT LUNAR ROTATION
NT PUMP IMPELLERS
NT RIGID ROTORS
NT ROTARY WINGS
NT ROTATING CYLINDERS
NT ROTATING DISKS
NT ROTATING SPHERES
NT ROTORS
NT TAIL ROTORS

NT TILTING ROTORS
NT TIP DRIVEN ROTORS
NT TURBINE WHEELS

Slowly rotating pulsed radiation source
02 p0256 N85-11678

Advanced high-power transfer through rotary interfaces 05 p0507 N85-13675

Lateral fluid forces acting on a whirling centrifugal impeller in vaneless and vaned diffuser
05 p0643 N85-14123

Design of two-mirror scanner with axes of rotation not in plane of mirrors 06 p0777 N85-14969

Hypothetical zero yaw drag trajectory of spinning projectiles between M = 5 and M = 10
[AD-A148899] 10 p1421 N85-18963

Flight dynamics of axisymmetrical rotating bodies in air medium 13 p2043 N85-22791

Axisymmetrical oscillations of shell systems subjected to impulse loads 13 p2047 N85-22814

Optimum rotation of solid body with 1 axis of symmetry 16 p2718 N85-26781

Nonlinear equations for dynamics of pretwisted beams undergoing small strains and large rotations
[NASA-TP-2470] 16 p2709 N85-27258

Dynamic stability of a spinning tube conveying a flowing fluid
[DE85-007583] 18 p3102 N85-29207

Speckle interferometry applied to asteroids and other solar system objects
[NASA-CR-175976] 19 p3384 N85-30995

A rotating electrical transfer device
22 p3796 N85-33529

ROTATING CYLINDERS

A study of the critical layer in a rotating liquid payload
[AD-A146094] 03 p0362 N85-12321

The use of horizontal clinostats in studies of plant statocyte development 05 p0690 N85-14435

Turbulent flow around circular cylinder uniformly rotating in infinite incompressible fluid 14 p2277 N85-24109

Stability of steady rotation of a cylinder filled with a stratified viscous incompressible fluid
14 p2278 N85-24112

Flow around rotating and nonmoving circular cylinder near flat screen. Report 1: Aerodynamic forces in cylinder 16 p2785 N85-27059

The Mises yield condition for thin rotationally symmetric shells
[BLL-BISI-TRANS-22047-(9022.06)]
17 p2978 N85-28409

Non-backdriveable free wheeling coupling
[NASA-CASE-MSC-20475-1] 18 p3116 N85-29290

ROTATING DISKS

Analysis of turbomachine blades: A review
02 p0208 N85-11374

Corrosion of a zinc rotating disk in one molar hydrochloric acid
[DE84-015974] 04 p0474 N85-13015

Development of a mass transfer machine for gas/liquid operations in the absence of gravity
[BMFT-FB-W-84-027] 05 p0637 N85-14091

CFM 56-2. Oligocyclic fatigue of the turbofan disk: Dimensionning and tests for verification and improvements 07 p0908 N85-15750

Possibilities for a more accurate life prediction of components — gas turbine disks
07 p0976 N85-16198

Some problems of optimum journal design for disk-drum rotors under antisymmetric loading
14 p2286 N85-24167

Abrasive cutting-off wheel 15 p2568 N85-25843

A rational approach to cam design
23 p3923 N85-34311

ROTATING ENVIRONMENTS

Internal gravity waves in real atmosphere
06 p0825 N85-15236

Small scale structure and the Spinar model for active galactic nuclei 12 p1959 N85-22316

ROTATING FLUIDS

NT ROTATING LIQUIDS

Linear long-wave stability of cylindrical steady laminar flame in rotating medium 02 p0266 N85-11752

Fluid motion in a rotating and nutating container
[AD-A146175] 03 p0362 N85-12322

Corotating interaction regions in stellar winds: Particle acceleration and non-thermal radio emission in hot stars
08 p1234 N85-17773

Winds from rotating, magnetic, hot stars
08 p1234 N85-17775

Turbulent jet flow in a channel with a circulation region
09 p1308 N85-18218

Regions of propagation of short-wave perturbations in spherical layer of rotating fluid 13 p2107 N85-23130

Turbulent flow around circular cylinder uniformly rotating in infinite incompressible fluid 14 p2277 N85-24109

Solution of Onsager's equation for a rotating compressible fluid in a multiply-connected domain
[DE85-007048] 16 p2784 N85-27178

Boundary layer and parabolic flows
[DFVLR-FB-84-46] 17 p2960 N85-28285

ROTATING GENERATORS

NT AC GENERATORS
NT DYNAMOMETERS
NT HOMOPOLAR GENERATORS
NT TURBOGENERATORS

Assessing expired fatigue life in large turbine shafts
[DE84-016676] 09 p1340 N85-18427

A device for generating motive force through the expansion of a non-elastic dense fluid
[NASA-TM-77684] 20 p3454 N85-31446

A small-scale self-excited rotor electrostatic generator
[AD-A155264] 21 p3581 N85-32265

ROTATING LIQUIDS

A study of the critical layer in a rotating liquid payload
[AD-A146094] 03 p0362 N85-12321

Double and inverse Taylor-Hogg vortices in a stratified ocean 13 p2108 N85-23137

Very high speed lap with positive lift effect
[AD-D011710] 19 p3280 N85-30344

Very high speed lap with negative lift effect
[AD-D011711] 19 p3281 N85-30345

ROTATING MIRRORS

Dual band, low sidelobe, high efficiency mirror antenna
[AD-D011329] 07 p0944 N85-15980

Determination of parameters of elastically strained mirror facets of rapidly rotating prisms
14 p2282 N85-24137

ROTATING PLASMAS

Fluctuation spectrum for linear gyroviscous MHD
[IPP-6/237] 01 p0121 N85-10828

Pressure-gradient-driven Tokamak resistive MHD instability in the banana-plateau collisionality regime
[DE85-004588] 12 p1937 N85-22171

About static and dynamic solutions of the aligned rotator model — pulsar magnetospheres
12 p1958 N85-22306

ROTATING SHAFTS

NT SHAFTS (MACHINE ELEMENTS)
NT TURBOSHAFTS

Identification of dynamic coefficients of annular turbulent seals 05 p0644 N85-14133

Analysis of experimental shaft seal data for high-performance turbomachines, as for Space Shuttle main engines
[NASA-TM-86928] 12 p1844 N85-21569

Study of fatigue strength of shafts with segmented channels 14 p2282 N85-24138

An analytical investigation of dynamic coupling in nonlinear, geared rotor systems
16 p2792 N85-27218

Variable force, eddy-current or magnetic damper
[NASA-CASE-LEW-13717-1] 19 p3279 N85-30333

ROTATING SPHERES

Some important problems in unsteady boundary layers including separation. 2: Unsteady boundary layers close to the stagnation region of slender bodies
[AD-A146964] 07 p0958 N85-16069

Sedimentation of two arbitrarily oriented spheroids in a viscous fluid
[AD-A147303] 07 p0960 N85-16082

Finite element analysis of nonlinear oscillations and flutter of shells of revolution
[AD-A149071] 10 p1496 N85-19440

The effect of power law body forces on a thermally-driven flow between concentric rotating spheres
[NASA-TM-87596] 24 p4093 N85-35374

ROTATING STALLS

Subsynchronous vibrations in a high pressure centrifugal compressor: A case history 05 p0642 N85-14118

A theory of post-stall transients in multistage axial compression systems
[NASA-CR-3878] 12 p1771 N85-21117

ROTATING VEHICLES

U ROTATING BODIES

ROTATION

NT EARTH ROTATION
NT MOLECULAR ROTATION
NT MUON SPIN ROTATION
NT PLANETARY ROTATION
NT SATELLITE ROTATION
NT SOLAR ROTATION
NT STELLAR ROTATION

The NBS tri-directional test facility
[PB84-217482] 01 p0051 N85-10334

A short-term forecast model for thunderstorm rotation
01 p0081 N85-10542

Environmentally independent fiber optic rotation sensor
[AD-D011219] 01 p0119 N85-10818

Experimental observation of neoclassical currents
[DE84-015113] 01 p0122 N85-10834

Relaxation of plasma rotation in a Tokamak in the presence of extraneous forces and corrugation of the magnetic field
[DE84-015626] 02 p0294 N85-11884

Dynamics of the Uranian rings
02 p0302 N85-11888

Fluid motion in a rotating and nutating container
[AD-A146175] 03 p0362 N85-12322

Controlling rotation of elastic manipulator link
04 p0488 N85-13113

Rotation of a tenuous plasma with a high toroidal velocity in a Tokamak
[DE84-012990] 04 p0587 N85-13615

Experimental on-stream elimination of resonant whirl in a large centrifugal compressor 05 p0642 N85-14121

Hydraulic forces on a centrifugal impeller undergoing synchronous whirl 05 p0643 N85-14124

Two-dimensional unsteady analysis of fluid forces on a whirling centrifugal impeller in a volute
05 p0643 N85-14125

Controllable rotation of system of two solid bodies with elastic elements 06 p0780 N85-14988

A free electron laser with a rotating quadrupole wiggler
[AD-A149052] 10 p1489 N85-19404

Theory of oriented nucleation with asymmetric single elements. 2: Effects of rotational diffusion
[IFTR-32/1984] 12 p1939 N85-22176

Study of energy versus misorientation for grain boundaries in gold by crystallite rotation method. 1: 001 twist boundaries
[DE85-004596] 12 p1943 N85-22201

Absolute stability of unsteady movement of axisymmetrical rotating flight vehicle
13 p2044 N85-22780

The unsteady boundary layer on an elliptic cylinder following the impulsive onset of translational and rotational motion — dynamic stall 14 p2209 N85-23690

Linearization of digital derived rate algorithm for use in linear stability analysis
[NASA-TM-87000] 14 p2243 N85-23904

Precise mounting of instruments in universal suspension with skewed axes 14 p2273 N85-24080

Polar motions measurement study
[AD-A150690] 14 p2372 N85-24684

On the boundary behaviour of a rotation automorphic function with finite spherical Dirichlet integral
15 p2634 N85-26238

High beta pinch plasma (STP-L)
15 p2655 N85-26381

Damping seals for turbomachinery
16 p2738 N85-26894

Poloidal rotation of magnetic fluctuations in reversed field pinch plasma
[IPPJ-715] 16 p2866 N85-27677

Use of quaternions in flight mechanics
[AD-A152616] 17 p2899 N85-27875

Influence of materials creep on rotor dynamics
[DE85-006545] 17 p2981 N85-28425

Efficient parallel solution of linear systems with hyperbolic rotations
[AD-A152355] 17 p3018 N85-28661

Experimental and theoretical investigation of microwave and millimeter wave radiation from hollow, rotating electron beams
[AD-A153627] 18 p3179 N85-29706

Load-induced rotordynamic instabilities in turbomachinery 19 p3280 N85-30340

Analysis and modeling of variations in length of day
19 p3349 N85-30781

Development of the Cascade inertial-confinement fusion reactor
[DE85-010933] 19 p3357 N85-30812

Viscous flows in rotating pipes with internal cavities and related vortex breakdowns
[NASA-TM-86761] 20 p3454 N85-31447

Development of an active laser gyro for inertial rotation sensing in attitude/heading reference and inertial navigation systems, phase 1
[BMFT-FB-W-85-001] 20 p3460 N85-31489

A model of pulsed radiation from the Crab pulsar
20 p3548 N85-32081

Aerodynamic characteristics of the standard dynamics model in coning motion at Mach 0.6
[NASA-TM-86717] 21 p3552 N85-32094

Automatic rotary valve actuator
[DE85-012797] 22 p3794 N85-33505

Development of a microorifice uniform deposit cascade impactor
[DE85-006765] 22 p3812 N85-33614

Breakdown of intrinsic ambipolarity for the radial diffusion due to a rotating RF field 23 p3977 N85-34690

surement of low energy cosmic rays aboard
lab-1
23 p4053 N85-35137
0.1-6]
ry cosmic ray measurement aboard Spacelab-1
23 p4053 N85-35138
0.1-7]
imally designed propellers constrained by noise
24 p4065 N85-35196

IONAL FLOW
FLUID FLOW
ORTICES

S
aling violation in the fragmentation region of inclusive
on spektrum 24 p4173 N85-35874

R AERODYNAMICS
ome considerations on Aeroelastic instabilities caused
upling between propeller-type rotor and its supporting
ucture
AL-TR-804] 01 p0003 N85-10013
Data input, processing and presentation — helicopter
r balance measurement
ASA-TM-77739] 01 p0125 N85-10856
Lifting surface theory for a helicopter rotor in forward
ht
ASA-TM-86315] 02 p0134 N85-10916
Extended aeroelastic analysis for helicopter rotors with
scribed hub motion and blade appended penduluum
bration absorbers
ASA-CR-172455] 03 p0315 N85-12038
Rotordynamic Instability Problems in High-Performance
urbomachinery
ASA-CP-2338] 05 p0642 N85-14116
Analysis for leakage and rotordynamic coefficients of
rface roughened tapered annular gas seals
05 p0644 N85-14135
Effects of fluid inertia and turbulence on force
coefficients for squeeze film dampers
05 p0645 N85-14137
The UH-1H helicopter icing flight test program: An
overview
NASA-TM-86925] 07 p0900 N85-15702
Clearance flow-generated transverse forces at the rotors
of thermal turbomachines
NASA-TM-77292] 07 p0973 N85-16180
Synthesized airfoil data method for prediction of dynamic
stall and unsteady airloads
NASA-CR-3672] 09 p1274 N85-18005
Integrated technology rotor/flight research rotor hub
concept definition
[NASA-CR-166447] 09 p1280 N85-18051
Theory versus experiment for the rotordynamic
coefficients of annular gas seals. Part 2: Constant
clearance and convergent-tapered geometry
[NASA-CR-174413] 10 p1491 N85-19416
Theory versus experiment for the rotordynamic
coefficients of annular gas seals. Part 1: Test facility
and apparatus
[NASA-CR-174409] 10 p1491 N85-19417
A study for calculating rotor loads using free vortex
concept 11 p1620 N85-20194
Analytical and flight investigation of the influence of rotor
and other high-order dynamics on helicopter flight-control
system bandwidth
[NASA-TM-86696] 12 p1780 N85-21174
Computer analysis of wind turbine blade dynamic
loads
[DE85-000530] 12 p1867 N85-21714
Research Reports: 1984 NASA/ASEE Summer Faculty
Fellowship Program
[NASA-CR-171317] 12 p1944 N85-22210
Study for prediction of rotor/wake/fuselage interference,
part 1
[NASA-CR-177340-VOL-1] 13 p1965 N85-22346
Study for prediction of rotor/wake/fuselage interference.
Part 2: Program users guide
[NASA-CR-177340-VOL-2] 13 p1966 N85-22347
Flight dynamics of axisymmetrical rotating bodies in air
medium 13 p2043 N85-22791
Recent developments in the dynamics of advanced rotor
systems
[NASA-TM-86669] 14 p2317 N85-24320
Finite-difference computations of rotor loads
[NASA-TM-86682] 16 p2700 N85-26669
Vibration characteristics of the HPOTP (High Pressure
Oxygen Turbopump) of the SSME (Space Shuttle Main
Engine) 16 p2738 N85-26895
Housing flexibility effects on rotor stability
16 p2738 N85-26896
Operating characteristics of a 0.87 kW-hr flywheel
energy storage module
[NASA-TM-87038] 17 p2974 N85-28371
Helicopter Aeromechanics
[AGARD-LS-139] 18 p3057 N85-28913
A survey of recent development in helicopter
aerodynamics 18 p3057 N85-28915
Rotorcraft noise 18 p3057 N85-28916
Recent developments in the dynamics of advanced rotor
systems 18 p3057 N85-28917
Vibration control of rotor shaft
[NASA-TM-87053] 18 p3117 N85-29292

ROTOR BLADES
Turbofan noise generation. Volume 2: Computer
programs
[NASA-CR-167952] 02 p0275 N85-11791

ROTOR BLADES (TURBOMACHINERY)
Thermal fatigue of gas turbine engine blades made of
material based on silicon nitride and silicon carbide
01 p0019 N85-10115
Variable geometry Darrieus wind machine
[PB84-207261] 01 p0068 N85-10453
Coolant passage heat transfer with rotation
02 p0143 N85-10968
Structural analysis 02 p0143 N85-10969
Incompressible lifting-surface aerodynamics for a
rotor-stator combination
[NASA-TM-83767] 03 p0316 N85-12039
Evaluation of the unsteady effects for a class of wind
turbines 05 p0592 N85-13772
In-flight evalution of LCF life consumption of critical rotor
components subjected to high transient thermal stress
07 p0906 N85-15734
Helicopter model rotor-blade vortex interaction impulsive
noise: Scalability and parametric variations
[NASA-TM-86007] 08 p1077 N85-16826
Blade technology program for large wind turbines, phase
1
[BMFT-FB-T-84-217] 08 p1179 N85-17426
A feasibility study of free-tip rotor application as a passive
cyclic control device 09 p1279 N85-18046
Integrated technology rotor/flight research rotor hub
concept definition
[NASA-CR-166447] 09 p1280 N85-18051
Influence of normalized frequency on time-dependent
aerodynamic characteristics of vane blading profiles
09 p1306 N85-18204
Influence of secondary flow rate on dynamic stresses
in turbine rotor blades 09 p1306 N85-18205
One-piece HPTR blade squealer tip
[AD-D011452] 10 p1425 N85-18969
High pressure turbine rotor two-piece blade retainer
[AD-D011498] 12 p1858 N85-21653
Cooled turbine blade tip closure
[AD-D011525] 12 p1858 N85-21654
Structural response of a rotating bladed disk to rotor
whirl
[NASA-CR-175605] 13 p1973 N85-22391
Experimental determination of optimum ratio of runner
blade height at exit to runner blade height at entrance of
radial inward-flow microturbines
13 p2049 N85-22827
An experimental investigation of the chopping of
helicopter main rotor tip vortices by the tail rotor
[NASA-CR-177338] 13 p2154 N85-23376
Calculation of three-dimensional, viscous flow through
turbomachinery blade passages by parabolic marching
[NASA-TM-86984] 14 p2211 N85-23711
Vibration and buckling of rotating, pretwisted, preconed
beams including Cooriolis effects
[NASA-TM-87004] 15 p2577 N85-25893
Development of a rotor wake-vortex model, volume 1
[NASA-CR-174849] 16 p2699 N85-26668
Aerodynamic detuning analysis of an unstalled
supersonic turbofan cascade
[NASA-TM-87001] 16 p2700 N85-26670
Ice shapes and the resulting drag increase for a NACA
0012 airfoil
[NASA-TM-83556] 17 p2894 N85-27839
A survey of recent development in helicopter
aerodynamics 18 p3057 N85-28915
Rotor blade test apparatus
[AD-D011725] 23 p3934 N85-34381
Reflection plane tests of a wind turbine blade tip section
with ailerons
[NASA-TM-87018] 23 p3945 N85-34444

ROTOR DISKS
U TURBINE WHEELS

ROTOR HUBS
U HUBS
U ROTORS

ROTOR SPEED
Shutdown characteristics of the Mod-O wind turbine with
aileron controls
[NASA-TM-86918] 07 p0992 N85-16299
Experimental study of main rotor tip geometry and tail
rotor interactions in hover. Volume 1. Text and figures
[NASA-CR-177336-VOL-1] 13 p1965 N85-22344
Development of a rotor wake-vortex model, volume 1
[NASA-CR-174849] 16 p2699 N85-26668
Improved turbopump dynamics
[NASA-TM-86514] 20 p3462 N85-31509
A comparison of experimental and theoretical results
for rotordynamic coefficients of four annular gas seals
[NASA-CR-176086] 21 p3596 N85-32332

ROTOR SYSTEMS RESEARCH AIRCRAFT
Rotor systems research aircraft airplane configuration
flight-test results
[NASA-TM-85911] 01 p0006 N85-10034
Numerical analysis of the first static calibration of the
RSRA helicopter active-isolator rotor balance system
[NASA-TM-85975] 08 p1083 N85-16863
Fuselage upwash effects on RSRA rotor systems
[NASA-CR-177349] 20 p3368 N85-31015
Estimation of dynamic rotor loads for the rotor systems
research aircraft: Methodology development and
validation
[NASA-CR-177382] 20 p3393 N85-31045
Flight testing the fixed-wing configuration of the Rotor
Systems Research Aircraft (RSRA)
[NASA-TM-86762] 23 p3896 N85-34135

ROTORCRAFT
U ROTARY WING AIRCRAFT

ROTORCRAFT AIRCRAFT
Effects of side-stick controllers on rotorcraft handling
qualities for terrain flight
[NASA-TM-86688] 15 p2473 N85-25267

ROTORS
NT BEARINGLESS ROTORS
NT COMPRESSOR ROTORS
NT FLYWHEELS
NT HELICOPTER TAIL ROTORS
NT IMPELLERS
NT LIFTING ROTORS
NT PUMP IMPELLERS
NT RIGID ROTORS
NT ROTARY WINGS
NT TAIL ROTORS
NT TILTING ROTORS
NT TIP DRIVEN ROTORS
NT TURBINE WHEELS
Some considerations on Aeroelastic instabilities caused
by coupling between propeller-type rotor and its supporting
structure
[NAL-TR-804] 01 p0003 N85-10013
A mathematical simulation model of the CH-47B
helicopter, volume 1
[NASA-TM-84351-VOL-1] 01 p0006 N85-10033
Singular asymptotic expansions in nonlinear
rotordynamics
[NASA-CR-174012] 01 p0017 N85-10100
Rotordynamic analysis of the SSME turbopumps using
reduced models
[NASA-CR-171170] 01 p0054 N85-10355
Aileron controls for wind turbine applications
[NASA-TM-86867] 02 p0222 N85-11458
Laser balancing system for high material removal
rates
[NASA-CR-174731] 03 p0365 N85-12341
European development experience on energy storage
wheels for space 05 p0605 N85-13856
Summary results of the DOE flywheel development
effort 05 p0606 N85-13865
General Electric composite ring-disk flywheel: Recent
and potential developments 05 p0606 N85-13867
Flywheel containment and safety considerations
05 p0606 N85-13869
Control of rotordynamic instability in a typical gas
turbine's power system 05 p0642 N85-14120
Hydrodynamic impeller stiffness, damping, and inertia
in the rotordynamics of centrifugal flow pumps
05 p0643 N85-14125
Preliminary investigation of labyrinth packing pressure
drops at onset of swirl-induced rotor instability
05 p0644 N85-14132
Design of electromagnetic bearing for vibration control
of flexible transmission shaft 05 p0645 N85-14136
Squeeze-film dampers for turbomachinery stabilization
05 p0645 N85-14138
Damping capacity of a sealed squeeze film bearing
05 p0645 N85-14139
Dynamic stiffness characteristics of high eccentricity
ratio bearings and seals by perturbation testing
05 p0645 N85-14141
Measurement data acquisition and processing system
for wind rotor measurements in the wind channel of Bremen
University 05 p0668 N85-14296
Device for measuring relative axial expansion of turbine
rotor employing space-vector tracking method
06 p0776 N85-14962
Two-rotor alternators with superconductor field
winding 06 p0795 N85-15082
The use of an optical data acquisition system for bladed
disk vibration analysis
[NASA-TM-86891] 06 p0817 N85-15184
Superconducting rotor dynamics
[AD-A147176] 07 p0947 N85-16000

Development of a Navier-Stokes rotor and stator analysis
[AD-A146967] 07 p0958 N85-16070
Theoretical and experimental study of hydro-elastic instability on the line of shafting of a rotating machine
[BLL-DOUNREAY-TR-937-(9091.9F)]
07 p0972 N85-16174
Experimental investigation of the oscillation behaviour of a liquid-filled rotor with centrifugal motion
[BLL-DOUNREAY-TR-936-(9091.9F)]
08 p1160 N85-17317
Eigenvalues of rotating machinery
08 p1167 N85-17361
Prediction accuracy of the torques for rotary tillage by an analog tool
[AD-P004288] 09 p1406 N85-18665
Integrated Technology Rotor/Flight Research Rotor (ITR/FRR) concept definition
[NASA-CR-166443] 10 p1423 N85-18978
Integrated Technology Rotor/Flight Research Rotor (ITR/FRR) concept definition
[NASA-CR-166445] 10 p1423 N85-18979
Singular asymptotic expansions in nonlinear rotordynamics 12 p1945 N85-22218
Oscillations of gas turbine installation rotors under operating conditions 14 p2272 N85-24077
Stability of steady modes of motion by axis of rotating wheel in nonlinear bearings 14 p2279 N85-24117
Stability of permanent rotation modes of asymmetric heavy solid body 14 p2279 N85-24118
Thermal deformation of flexible rotors in friction bearings 14 p2280 N85-24123
Superconducting gyroscope research
[NASA-CR-171406] 15 p2560 N85-25795
Rotordynamics 16 p2737 N85-26888
Effects of bearing deadbands on bearing loads and rotor stability 16 p2737 N85-26889
Rotor response for transient unbalance changes in a nonlinear simulation 16 p2737 N85-26892
Damping seals for turbomachinery
16 p2738 N85-26894
Vibration characteristics of the HPOTP (High Pressure Oxygen Turbopump) of the SSME (Space Shuttle Main Engine) 16 p2738 N85-26895
Reusable rocket engine turbopump condition monitoring 16 p2740 N85-26907
An analytical investigation of dynamic coupling in nonlinear, geared rotor systems
16 p2792 N85-27218
Vibrations of rotors connected through couplings with backlash 17 p2940 N85-28147
Influence of materials creep on rotor dynamics
[DE85-008545] 17 p2981 N85-28426
Damping seal for turbomachinery
[NASA-CASE-MFS-25842-2] 19 p3260 N85-30341
Effect of ground and/or ceiling planes on thrust of rotors in hover
[NASA-TM-86754] 20 p3388 N85-31014
Estimation of dynamic rotor loads for the rotor systems research aircraft: Methodology development and validation
[NASA-CR-177362] 20 p3393 N85-31045
A theoretical model for the study of nonlinear dynamics of magnetic bearings 20 p3462 N85-31505
R and D activities of the Structural Sciences Division
20 p3539 N85-32026
A panel method study of vortex sheets with special emphasis on sheets of axisymmetric geometry
[NASA-CR-177365] 21 p3552 N85-32095
A phase-locked frequency multiplier for the signal averaging of the vibration of the Wessex helicopter input spiral bevel pinion
[AD-A154914] 21 p3555 N85-32113
Proposal for modifications to the Wessex helicopter main rotor gearbox vibration monitoring program
[AD-A155196] 21 p3555 N85-32117

ROUGHNESS
NT SEA ROUGHNESS
NT SURFACE ROUGHNESS
Comparison of predicted and measured friction for a tilt-pad thrust bearing with crown and roughness under hydrodynamic and mixed lubrication
[AD-A145752] 03 p0371 N85-12371
Hydraulic drag of rod with artificial microroughness in longitudinal flow 14 p2278 N85-24111
Predicting microfracture in ceramics via a microcontract model
[DE85-005654] 18 p3061 N85-29060
Mechanical properties of plasma arc cut steel
23 p3905 N85-34186

ROUND TRIP TRAJECTORIES
Mars exploration, Venus swingby and conjunction class mission modes, time period 2000 to 2045
[NASA-TM-86477] 02 p0303 N85-11961

ROUTES
Asynchronous distributed flow control algorithms
[AD-A146452] 08 p1206 N85-17600
Local search in routing problems with time windows
[CWI-OS-R8409] 12 p1922 N85-22075
Routing algorithms and stochastic analysis for large communications networks
[AD-A154654] 21 p3573 N85-32225

ROVING VEHICLES
NT LUNOKHOD LUNAR ROVING VEHICLES
An autonomous roving vehicle for the planet Mars: A summary of over 15 years of research
[RPI-TR-MP-83] 07 p0973 N85-16179
Mathematical model for rollout of planet roving vehicle from landing craft 15 p2484 N85-25334
Mars landing sites 22 p3859 N85-33893

RPV
U REMOTELY PILOTED VEHICLES

RUBBER
NT CHLOROPRENE RESINS
NT ELASTOMERS
NT LATEX
NT SILICONE RUBBER
NT SYNTHETIC RUBBERS
NT VULCANIZED ELASTOMERS
Diblock copolymers of polystyrene/1,2 polybutadiene and polystyrene/polybutene-1: Molecular structure, morphology and mechanical properties
[AD-A144980] 01 p0033 N85-10201
Guide to the selection of rubbers
[AMTE(N)-TM-84301] 03 p0336 N85-12164
Modified epoxy composites 04 p0466 N85-12957
Alternatives for runway rubber removal from porous friction surfaces
[DOT/FAA/PM-84/28] 05 p0597 N85-13803
Low frequency electrical properties of selected dielectrics
[DE84-016220] 05 p0632 N85-14052
Rubber-modified epoxies. 1: Cure, transitions, and morphology
[AD-A147377] 07 p0932 N85-15908
Rubber-modified epoxies. Part 2: Morphology, transitions, and mechanical properties
[AD-A147962] 08 p1132 N85-17137
Runway rubber removal specification development field evaluation procedures development
[FAA-PM-84-27] 12 p1781 N85-21179
Rubber modified epoxy adhesive
[AD-D011527] 12 p1810 N85-21354
Process development for commercial production of natural rubber from Guayule
[PB85-124956] 12 p1815 N85-21388
Finger materials for air cushion vehicles. Volume 2: Base fabrics for finger materials
[AD-A149701] 12 p1819 N85-21408
Mechanism of strengthening plastics with rubbers
13 p2014 N85-22636

RUBBER COATINGS
Design, manufacture, and testing of compliant coatings for reduction of turbulent drag
[AD-A145510] 02 p0198 N85-11323
Anticorrosion protection of reinforcing steel in prestressed gypsum and anhydrite concrete
[BLL-BISI-TRANS-22079-(9022.06)]
17 p2926 N85-28044
Description of an holographic interferometry nondestructive test installation: Application to bond tests
[SNIAS-851-430-101] 20 p3464 N85-31521

RUBIDIUM
NT RUBIDIUM ISOTOPES
Calorimetric investigation into the possibility of a charge density wave ground state in alkali metals
[DE85-002006] 09 p1397 N85-18795
Lifetime and reliability of rubidium discharge lamps for use in atomic frequency standards
[AD-A150787] 14 p2417 N85-24915
Physics element design aspects for a tactical rubidium frequency standard 17 p2967 N85-28321
On-orbit frequency stability analysis of the GPS NAVSTAR-1 quartz clock and the NAVSTARs-6 and -8 rubidium clocks 18 p3105 N85-29227
A miniature tactical Rb frequency standard
18 p3106 N85-29229
The Rubidium-Crystal Oscillator Hybrid Development Program 18 p3106 N85-29230
The system design of a rubidium maser frequency standard 18 p3106 N85-29232
The role of long term lamp fluctuations in the random walk of frequency behavior of the rubidium frequency standard: A case study
[AD-A155338] 21 p3590 N85-32314

RUBIDIUM ISOTOPES
Diode laser 87Rb optical pumping in an evacuated wall-coated cell 18 p3105 N85-29226

RUBY
The Faraday effect in ruby and corundum in strong magnetic fields 21 p3697 N85-3[illegible]

RUBY LASERS
Neutral beam interactions with materials
[AD-A145636] 02 p0265 N85-11857
Coherent amplification of ultrasonic pulses in activated crystals 05 p0724 N85-14[illegible]
High-speed, eight-frame electro-optic camera with multipulsed ruby laser illuminator
[DE85-001748] 09 p1323 N85-18914
Effect of transparent coatings on generation of laser-induced shock waves in metals
13 p2028 N85-22711
Ruby wavefront-conjugation laser for obtaining high temperature plasma 13 p2044 N85-22776
System for lower hybrid current startup
15 p2654 N85-26073
Visibility and vertical structure measurements in southern Germany
[AD-A154714] 21 p3635 N85-32574
Operation of solid state lasers exposed to electron beam 21 p3685 N85-32865
Instrument to synchronize Thomson scattering diagnostic measurements with MHD activity in a Tokamak
[DE85-012082] 23 p3984 N85-34706

RUDDERS
NT AERIAL RUDDERS
Flight-service program for advanced composite rudders on transport aircraft
[NASA-CR-174537] 19 p3217 N85-29960

RULES
NT INSTRUMENT FLIGHT RULES
NT VISUAL FLIGHT RULES
Safety with industrial manufacturing lasers
14 p2306 N85-24281

RUN TIME (COMPUTERS)
Relative performance of micro and mainframe computers
[AD-A149281] 10 p1538 N85-19886
Exploiting multiprocessors: Issues and options
[DE85-003144] 13 p2145 N85-22313
Trends in computational capabilities for fluid dynamics
15 p2457 N85-25172
Efficient implementation of real-time programs under the VAX/VMS operating system
[NASA-TM-86354] 15 p2627 N85-26190
The completion time of a job on multi-mode systems
[AD-A154113] 19 p3338 N85-30886
Experiments and improvements of the ordinary differential equation solvers DEPAC on the CRAY computer
[DE85-013260] 22 p3831 N85-33728

RUNGE-KUTTA METHOD
Computation of the nonequilibrium flow in a gasdynamic laser
[AD-A141022] 04 p0505 N85-13224
Art of programming programmable microcalculators. Part 12: Solution of differential equations
07 p0953 N85-16040
Fixed vs. variable order Runge-Kutta
[DE85-001320] 09 p1374 N85-18839
Solution of structured non-stiff ODEs
[DE85-004137] 11 p1707 N85-20741
Electromagnetic rail launcher as a circuit element
[AD-A150067] 12 p1835 N85-21518
The performance of a type-insensitive Runge-Kutta code on a personal computer
[TUM-I8410] 12 p1919 N85-22046
Runge-Kutta formula with cheap error estimate
[DE85-005674] 13 p2152 N85-22383
On the algebraic equations in implicit Runge-Kutta methods
[CWI-NM-R8413] 17 p3022 N85-2[illegible]
Compressible two-phase flow instabilities simulated with a hybrid Lagrange-Euler pseudospectral method
[DE85-009904] 23 p3931 N85-34381

RUNNING
The energy cost of women walking and running in shoes and boots
[AD-A151022] 14 p2389 N85-24719
Weight loss, rectal temperature and heart rates following the 1984 Boston Marathon
[AD-A155984] 24 p4132 N85-35612

RUNOFFS
U DRAINAGE

RUNWAY ALIGNMENT
Closely spaced independent parallel runway simulation
[DOT/FAA/CT-84/45] 04 p0457 N85-12862

RUNWAY CONDITIONS
Aircraft accident report: Flying Tigers, Inc., Flight [illegible], McDonell Douglas DC8-63, N797FT, Chambers Field, Naval Air Station, Norfolk, Virginia, October 25, 198[illegible]
[PB84-910408] 02 p0136 N85-10[illegible]

osely spaced independent parallel runway simulation
OT/FAA/CT-84/45] 04 p0457 N85-12902

o take off and to land safely, Hoechst 1678 for ice
l snow free runways 05 p0595 N85-13791

A model for forecasting runway surface temperature and
lication with subjective forecasts
R-8] 10 p1518 N85-19569

Aircraft accident report: World Airways Inc., Flight 30H,
cDonnell Douglas DC-10-30CF, N113WA, Boston-Logan
ernational Airport, Boston, Massachusetts, January 23,
82
B85-910406] 22 p3726 N85-33114

WAY LIGHTS

Flares and photoflash items
AD-A145442] 02 p0187 N85-11253

Evaluation of arctic test of improved tritium radioluminescent lighting
[DE84-014887] 05 p0597 N85-13805

Wind-powered electric generation runway lighting system demonstration project
[DE84-014962] 05 p0670 N85-14311

Light your runways and taxiways without electricity
[DE85-000269] 11 p1586 N85-19991

Examination of the feasibility for demonstration and use of radioluminescent lights for Alaskan remote runway lighting
[DE85-002503] 12 p1782 N85-21185

Radioluminescent lighting for rural Alaskan runway lighting and marking
[DE85-007022] 16 p2716 N85-26784

Acceptability testing of radioluminescent lights for VFR-night air taxi operations
[DE85-007303] 16 p2716 N85-26785

Radioluminescent lighting for Alaskan runway lighting and marking
[DE85-010405] 19 p3368 N85-30887

UNWAYS

Materials for emergency repair of runways
[AD-A146139] 03 p0320 N85-12068

Development of a pavement maintenance management system. Volume 9: Development of airfield pavement performance prediction models
[AD-A146150] 03 p0321 N85-12069

Alternatives for runway rubber removal from porous friction surfaces
[DOT/FAA/PM-84/28] 05 p0597 N85-13803

Prefabricated panels for rapidly runway repair and expedient airfield surfacing
[AD-D011277] 05 p0597 N85-13804

System for rapid repair of damaged airfield runways
[AD-D011325] 07 p0909 N85-15754

Development of a preliminary ALRS stabilized material pavement analysis system (SPAS)
[AD-A147116] 07 p0910 N85-15760

International projects, other work of Aeroproyekt Institute 08 p1068 N85-16767

Aeroproyekt develops improved runway surfacing
08 p1068 N85-16770

New runway enables IL-76 flights to Tenkeli in far north 12 p1769 N85-21106

Runway rubber removal specification development field evaluation procedures development
[FAA-PM-84-27] 12 p1781 N85-21179

Field validation of statistically-based acceptance plan for bituminous airport pavements. Volume 1: Correlation analysis of Marshall properties of laboratory-compacted specimens
[FAA-PM-84-12-VOL-1] 12 p1781 N85-21180

Field validation of statistically-based acceptance plan for bituminous airport pavements. Volume 2: Statistical analysis of Marshall properties of plant-produced bituminous materials
[FAA-PM-84-12-VOL-2] 12 p1781 N85-21181

Field validation of statistically-based acceptance plan for bituminous airport pavements. Volume 3: Statistical analysis of 3 methods for determining maximum specific gravity of bituminous concrete mixtures
[FAA-PM-84-12-VOL-3] 12 p1781 N85-21182

Field validation of statistically-based acceptance plan for bituminous airport pavements. Volume 4: Computer simulation of multiple acceptance criteria
[FAA-PM-84-12-VOL-4] 12 p1782 N85-21183

Field validation of statistically-based acceptance plan for bituminous airport pavements. Volume 5: Summary of validation studies
[FAA-PM-84-12-VOL-5] 12 p1782 N85-21184

Probabilistic computer model of optimal runway turnoffs
[NASA-CR-172549] 16 p2715 N85-26760

Study of acceptance criteria for joint densities in bituminous airport pavements
[FAA-PM-85-5] 16 p2715 N85-26761

OWEMA report: A project study concerning the possibilities and the desirability of a east-west runway for Maastricht Airport (Netherlands) as a Euro-regional air freight center
[B8476490] 18 p3064 N85-28955

Review of rigid pavement design for vehicular parking areas
[AD-A154284] 19 p3222 N85-29975

Expedient runway surfacing with post tensioning system for expeditionary airfields
[AD-D011677] 19 p3222 N85-29976

Guidelines for the evaluation of visual approach slope indicators
[ARL/SYS-R-32] 23 p3896 N85-34132

RUPTURING

Toughness in high speed steels and hard metals
02 p0176 N85-11181

Laser rupture of composite materials
10 p1444 N85-19102

Preliminary review of statistical treatment of S-glass/epoxy stress rupture data
[AD-A149810] 12 p1797 N85-21275

Limiting values of stress state index after rupture of metals
[BLL-BISI-TRANS-22293-(9022.06)]
17 p2978 N85-28407

A continuous damage model based on stepwise-stress creep rupture tests
[NASA-CR-174941] 21 p3597 N85-32341

RURAL AREAS

Examination of the feasibility for demonstration and use of radioluminescent lights for Alaskan remote runway lighting
[DE85-002503] 12 p1782 N85-21185

A comparison of metropolitan and non-metropolitan employment characteristics: Indications of the size of non-metropolitan mobile communication services user classes
[NASA-CR-175646] 13 p2053 N85-22855

Trace element concentrations in atmospheric aerosol over Hungary 21 p3646 N85-32652

Motor glider measurements during the Urban Atmosphere Energy Budget Experiment (EESA 1)
24 p4122 N85-35553

RURAL LAND USE

Development and testing of a rural credit supervision system at the level of counties and rural properties utilizing remote sensing techniques
[E85-10018] 02 p0217 N85-11431

A field control methodology of remotely sensed data for statistical purposes: An example of SPOT simulated data in eastern Belgium --- land use statistics
05 p0660 N85-14241

The challenge of food production: The importance of climate 07 p1001 N85-16361

RUSTING

Continuous measurement of zircaloy corrosion in air with an ultrasonic corrosion monitor
[DE85-003663] 12 p1807 N85-21337

Forming of coating protection system: Mechanism of paint-coating anti-corrosion protection of steel
[BLL-BISI-TRANS-22061-(9022.06)]
17 p2925 N85-26033

RUTHENIUM

Laser studies of chemical dynamics at the gas-solid interface
[DE84-017590] 11 p1736 N85-20920

Technology of off-gas treatment for liquid-fed ceramic melters
[DE85-012467] 22 p3812 N85-33610

RUTHENIUM ALLOYS

Electrical resistivity and structural changes upon relaxation and crystallization of (Mo/sub 0.6/Ru/sub 0.4)sub 100-x/B/sub x/ metallic glasses
[DE84-017281] 09 p1299 N85-18160

RUTHENIUM COMPOUNDS

Transition metal carbene complexes
[AD-A144879] 01 p0028 N85-10173

Chemically modified electrodes and related solution chemistry
[DE84-017110] 05 p0614 N85-13924

RUTILE

Mechanisms of impurity diffusion in rutile
[DE84-014741] 06 p0788 N85-14902

RYDBERG SERIES

Physico-chemical investigation of some areas of fundamental significance to biophysics
[DE84-016385] 04 p0471 N85-12999

Infrared emission and atomic transitions
[AD-A147840] 07 p1041 N85-16607

Nonlinear optical studies of rydberg atoms using degenerate four-wave mixing
[AD-A146827] 07 p1043 N85-16623

Collision-induced dipole moments
[AD-A147682] 08 p1121 N85-17063

Basic studies of atomic dynamics
[DE84-015661] 09 p1380 N85-18675

Alignment of high Ryberg states in hydrogen
[DE85-000582] 09 p1380 N85-18677

Photoelectron studies of autoionizing Rydberg states in HCl
[DE85-011813] 21 p3702 N85-33001

S

S BAND
U SUPERHIGH FREQUENCIES
U ULTRAHIGH FREQUENCIES

S GLASS

Passive Orbital Disconnect Strut (PODS 3) structural test program
[NASA-CR-177325] 08 p1113 N85-17020

Preliminary review of statistical treatment of S-glass/epoxy stress rupture data
[AD-A149810] 12 p1797 N85-21275

S MATRIX THEORY

Semiclassical theory of resonances
[REPT-67] 01 p0114 N85-10777

The S-matrix and acoustic signal structure in simple and compound waveguides
[PP-583] 03 p0415 N85-12652

Scattering matrix of antenna array with Joule losses in radiators 06 p0791 N85-15053

Theory of resonant light scattering from a rough surface 09 p1383 N85-18701

Shielded enclosures for experimental studies of shielding topology
[AD-A149292] 11 p1624 N85-20227

S-matrix theory of nuclear forces
[DE85-007633] 18 p3179 N85-29710

Method of static measurements of absolute scattering matrix of radar targets 22 p3762 N85-33316

Interrelations for the elements of the scattering matrix
22 p3855 N85-33872

Duality of two-point functions for confined non-relativistic quark-antiquark systems
[DE85-012334] 23 p3971 N85-34618

S STARS
NT CARBON STARS
NT GIANT STARS
NT RED GIANT STARS

S WAVES

Response and characteristics of structures subjected to S-H waves 01 p0060 N85-10396

Bragg reflection of surface electroacoustic shear waves 04 p0485 N85-13096

Propagation of acoustic shear waves through active periodic structure 04 p0490 N85-13125

Characterization of stressed metals using acoustic shear waves 05 p0648 N85-14159

Optical method of measuring velocity of shear waves
06 p0787 N85-15029

Modeling of real UT transducer field/flaw interactions
[DE85-000341] 09 p1329 N85-18351

Experimental high pressure equation of state of a very fast burning gun propellant
[DE85-001749] 10 p1456 N85-19184

Effects of magnetic shear on lower hybrid waves in the supraauroral region
[AD-A151960] 15 p2656 N85-26392

Radar echoes at 2.66 and 40.92 MHz from the mesosphere, part 2.6A 21 p3619 N85-32486

On the cosmic ray diffusion in a violent interstellar medium
[OG-7.2-14] 23 p4015 N85-34881

Scale separation closure and Alfven wave turbulence
[DE85-013124] 24 p4095 N85-35385

S-A-W DEVICES
U SURFACE ACOUSTIC WAVE DEVICES

S-N DIAGRAMS

Fatigue behavior of HY-130 steel weldments containing fabrication discontinuities
[AD-A153630] 18 p3122 N85-29326

Controlled indentation flaws for the construction of toughness and fatigue master maps
[PB85-179067] 20 p3473 N85-31582

SABOT PROJECTILES

Stress in axially symmetrical heavy metal projectiles during discharge --- numerical simulation
[ISL-CO-219/83] 14 p2321 N85-24345

Metal armatures for railguns
[AD-A152129] 16 p2726 N85-26836

SACCADIC EYE MOVEMENTS

Application of the system identification technique to goal-directed saccades
[AD-A150132] 12 p1908 N85-21967

SACCHARIDES
U CARBOHYDRATES

SACRAMENTO VALLEY (CA)
Investigation of several aspects of LANDSAT 4/5 data quality
[E85-10038] 04 p0525 N85-13357
SADDLE POINTS
NT SADDLE POINTS (GAME THEORY)
Existence, uniqueness and stability conditions for general finite element methods in linear elasticity
09 p1332 N85-16372
Analysis of the convergence of mixed finite element methods
[HTKK-MAT-A227] 16 p2656 N85-27613
SADDLE POINTS (GAME THEORY)
General saddlepoint approximations with applications to l-statistics
[AD-A150073] 12 p1924 N85-22086
SAFETY
NT AEROSPACE SAFETY
NT AIRCRAFT SAFETY
NT FLIGHT SAFETY
NT INDUSTRIAL SAFETY
NT REACTOR SAFETY
Manual for Raman cells
[NASA-TM-77756] 01 p0052 N85-10342
A dispersion model for airborne particulates inside a building
[DE84-014961] 02 p0225 N85-11473
Photocopiers: Do they pose a health hazard?
[P83-1E] 02 p0234 N85-11527
The IMX double direct process
[AD-A146250] 03 p0340 N85-12186
Activities report in technology
[ISBN-951-38-1996-1] 04 p0577 N85-13661
Flywheel containment and safety considerations
05 p0606 N85-13869
The detection and assessment of defects in automatic ultrasonic inspection
[BLL-RISLEY-TR-4597-(9091.9F)]
05 p0647 N85-14150
Computer science and technology: Overview of computer security certification and accreditation
[PB84-217819] 06 p0848 N85-15384
Flame-resistant materials for use in pyrotechnic safety clothing
[AD-A146857] 07 p0931 N85-15901
Safety evaluation of an electronic totalizer containing a Li/(CF)x cell
[AD-A147306] 07 p0993 N85-16305
Aims and requirements of NATO group AC/310
08 p1114 N85-17026
Sensitivity tests for solid propellants in Germany
08 p1115 N85-17028
Sensitiveness and explosiveness assessment at Perme Waltham Abbey 08 p1115 N85-17029
Penguin warhead safety tests
08 p1115 N85-17031
The vulnerability of cast double base rocket motors to thermomechanical attack 08 p1115 N85-17033
Tolerance endpoint for evaluating the effects of heat stress in dogs
[AD-A148104] 08 p1192 N85-17511
A study on a medium-sized rocket with Burnout frame
[NAL-TR-821] 09 p1287 N85-18082
Railroad safety program, volume 1
[NASA-CR-174333] 09 p1403 N85-18830
Preventing explosive propagation in racks or containers of tactical missiles
[AD-P004342] 10 p1455 N85-19166
Safety aspects of prepackaged liquid propellant stages for strategic missiles
[AD-P004350] 10 p1456 N85-19174
A review of hazard assessment procedures for liquid gun propellants
[AD-A149470] 10 p1457 N85-19182
Ultralight aircraft technology and public safety
[GPO-38-946] 12 p1773 N85-21131
General-purpose heat source development: Safety test program. Postimpact evaluation, design iteration test 4
[LA-10217-SR] 12 p1930 N85-22128
US Army human Engineering Laboratory Communications Survey: A Pilot Study (HELCOMS-PS)
[AD-A151434] 15 p2521 N85-25544
Pavement-marking materials: New York's experience
[PB85-153294] 15 p2523 N85-25556
Some aspects of how to design cost-effective flight control systems 16 p2695 N85-26639
The certification of airborne complex digital systems
16 p2714 N85-26754
A review of safety practices and safety training for the explosives field
[AD-A152295] 16 p2759 N85-27028
Space Station crew safety alternatives study. Volume 5: Space Station safety plan
[NASA-CR-3858] 17 p2906 N85-27930
Space Station crew safety alternatives study. Volume 4: Appendices
[NASA-CR-3857] 18 p3065 N85-28958
Space station crew safety: Human factors interaction model 18 p3156 N85-29540
Space station crew safety alternatives study, third quarter briefing 18 p3156 N85-29541
Experimental program to determine maximum temperatures for dry storage of spent fuel
[DE85-010307] 19 p3236 N85-30060
Working with flammable solvents, thinners, paints and adhesives
[HSE-TRANS-11066] 19 p3250 N85-30154
SAFEORD: Safety of explosive ordnance databank
[AD-A154058] 19 p3380 N85-30972
The CCIR satellite EPIRB coordinated trials programme -- Emergency Position Indicating Radio Beacon (EPIRB); International Radio Consultative Committee (CCIR) 20 p3402 N85-31111
The International Radio Consultative Committee (CCIR) recommended satellite Emergency Position Indicating Radio Beacon (EPIRB) system operating through geostationary satellites at 1.6 GHz
20 p3402 N85-31112
Improvements in safety testing of lithium cells
20 p3444 N85-31379
Safety of Li-SOCl2 cells 20 p3444 N85-31383
Basic cryogenics and materials. Phase 1
[NASA-CR-177932] 21 p3572 N85-32215
Safety characteristics of non-lithium battery systems
[AD-A155733] 22 p3806 N85-33574
Experimental lithium system
[DE85-013252] 24 p4094 N85-35382
SAFETY DEVICES
NT ARRESTING GEAR
NT EJECTION SEATS
NT HELMETS
NT SEAT BELTS
NT SPACE SUITS
Safing and arming mechanism
[AD-D011261] 05 p0621 N85-13969
Flow of nitrogen-pressurized Halon 1301 in fire extinguishing systems
[NASA-CR-174271] 07 p0900 N85-15701
Powered articulated headrest system
[AD-D011353] 07 p0901 N85-15710
S-3A ballast block final design and engineering tests
[AD-A147685] 08 p1080 N85-16842
SPH-4 US Army flight helmet performance, 1972 - 1983
[AD-A148674] 08 p1201 N85-17562
Optoelectronic safety system for robotized technological complex 13 p2046 N85-22805
Retroreflective armbands: Influences of wearing mode, aging and other factors on the visibility distance
[IZF-1984-28] 14 p2422 N85-24942
Parachute extraction device for ultralight gliders
[CH-643499-A5] 16 p2699 N85-26663
Torso restraint system
[AD-D011609] 16 p2702 N85-26684
Robotic safety systems and methods: Savannah River site
[DE85-008261] 17 p2974 N85-28375
Investigation, development, and certification of a burst disk for cryogenic fuel tanks
[GCP-3/MT-CM-21-2546] 18 p3067 N85-28972
Development of a stationary carbon monoxide detector
[BMFT-FB-T-84-253] 18 p3134 N85-29413
The design of working systems on ergonomic principles. The importance of clothes and protective equipment in the design of the workplace
[HSE-TRANS-10865] 19 p3332 N85-30639
Free-float Emergency Position Indicating Radio Beacons (EPIRBs) and release mechanism on board Norwegian ships. Main specifications and user experience
20 p3404 N85-31120
Fast shutter apparatus
[DE85-006501] 23 p3928 N85-34343
SAFETY FACTORS
Aircraft chocks
[AD-A145135] 01 p0012 N85-10077
System engineering and integration contract for implementation of the National Airspace System plan, volume 1, sections 1.0-4.0, 6.0
[AD-A145763] 03 p0317 N85-12046
Test methods for cable cars
[CETIM-1-5K-45-1] 04 p0515 N85-13282
Vandenberg space shuttle launch complex
[S-HRG-98-1075] 05 p0601 N85-13833
Statement of Edward C. Aldridge, Jr., Under Secretary of the Air Force, Department of the Air Force, accompanied by Lieutenant General Robert W. Bazley, Inspector General and Brigadier General Donald J. Kutyna, Director of Space Systems and Command, Control and Communications, Deputy Chief of Staff, Research, Development and Acquisition 05 p0601 N85-13834
Statement of Honorable James M. Beggs, Administrator, National Aeronautics and Space Administration
05 p0601 N85-13835
Space Nuclear Safety Program
[DE84-016973] 05 p0728 N85-14879
Electric and hybrid vehicle demonstration project
[DE84-014622] 06 p0871 N85-15535
Safety requirements for wiring systems and connectors for photovoltaic systems
[NASA-CR-174431] 10 p1477 N85-19324
Design of explosive logic elements
[DE84-009611] 11 p1614 N85-20146
Six-inch HYGE vertical impact facility
[AD-A150665] 14 p2228 N85-23809
Ultrasonic non-destructive testing technique
14 p2316 N85-24313
Evaluation of adequacy pf JP54 protection level for large electric machines 15 p2528 N85-25566
Development and application of new radiofrequency radiation safety standards 16 p2777 N85-27137
Space station crew safety alternatives study, volume 1
[NASA-CR-3854] 19 p3223 N85-29985
Organic air pollutants during manufacturing and handling of PVC floor tiles
[FOA-E-40018] 20 p3487 N85-31669
Space Station crew safety alternatives study. Volume 2: Threat development
[NASA-CR-3855] 21 p3558 N85-32133
Safety and reliability of steel structural materials under random service impact loads 23 p3906 N85-34197
General-purpose heat source development: Safety test program. Postimpact evaluation, design iteration test
[LA-10034-SR] 23 p3969 N85-34606
SAFETY MANAGEMENT
Safety requirements for wiring systems and connectors for photovoltaic systems
[NASA-CR-174211] 06 p0803 N85-15110
The aviation safety reporting system
09 p1276 N85-18021
The development of fire evaluation system for detention and correctional occupancies
[NBSIR-84-2976] 10 p1459 N85-19192
Safety program considerations for space nuclear reactor systems
[DE85-003295] 10 p1556 N85-19808
Airport bird hazards associated with solid waste disposal facilities
[AD-P004197] 11 p1581 N85-19964
Successful control of gulls and other birds at a sanitary landfill
[AD-P004198] 11 p1582 N85-19965
Effectiveness of an overhead wire barrier system in reducing gull use at the BFI Jedburg sanitary landfill, Berkeley and Dorchester counties, South Carolina
[AD-P004200] 11 p1582 N85-19967
Control technology for integrated circuit fabrication at Honeywell Optoelectronics Division, Richardson, Texas
[PB85-109023] 11 p1616 N85-20162
Radiation safety of crew and passengers of air transportation in civil aviation. Provisional standards
[NASA-TM-77610] 11 p1692 N85-20638
Aerospace Safety Advisory Panel
[NASA-TM-87428] 12 p1774 N85-21135
Geosynchronous satellite collision avoidance
12 p1784 N85-21197
General-purpose heat source development: Safety test program. Postimpact evaluation, design iteration test 5
[LA-10232-SR] 12 p1931 N85-22129
Radiological safety aspects of industrial radiography
14 p2316 N85-24312
Dosimeasurements with thermoluminescence dosimeters at a Febetron 701, 600 kV in room 022 of the Interuniversity Reactor Institute (IRI)
[IRI-190-84-02] 18 p3111 N85-29292
Ambient air contamination: Characterization and detection techniques 18 p3157 N85-29546
Report of the 11th Regional IRPA Congress on Recent Developments and New Trends in Radiation Protection
[IRI-190-83-13] 18 p3160 N85-29575
Working safely with ionizing radiation sources at the Interuniversity Reactor Institute (IRI) (meant for the introduction of new collaborators)
[IRI-190-84-01] 18 p3160 N85-29576
Safety system with microcomputer
[OEFZS-4294] 18 p3168 N85-29618
Safety report, 1982 18 p3184 N85-29746
Space station crew safety alternatives study, volume 1
[NASA-CR-3854] 19 p3223 N85-29985

Description of a test site for large-scale heavy gas persion and combustion experiments
DE85-004987] 23 p3911 N85-34231
E SATELLITE
Utilization of SAGE aerosol profiles in the analysis of auna Loa stratospheric lidar data
NASA-CR-174196] 05 p0675 N85-14332
Development of algorithms for using satellite eteorological data sets to study global transport of ratospheric aerosols and ozone
NASA-CR-172540] 15 p2591 N85-25974
HARA DESERT (AFRICA)
Late Tertiary and Quaternary river systems of the eastern Sahara as mapped on shuttle radar and LANDSAT images 13 p2199 N85-23641
Sahara Desert dust transport to the south 21 p3648 N85-32666
AILPLANES
U GLIDERS
AILS
NT SOLAR SAILS
The Satellite sail 11 p1647 N85-20376
La Recherche Aerospatiale Bimonthly Bulletin, Number 1984-4, 221/July-August
[ESA-TT-884] 16 p2695 N85-26637
Clarke Stations and mercurian mass-drivers: Energy for large-scale transportation systems
[DE85-009807] 21 p3560 N85-32145
AINT VENANT FLEXURE PROBLEM
U SAINT VENANT PRINCIPLE
AINT VENANT PRINCIPLE
Quantification of Saint-Venant's principle for a general prismatic member 04 p0467 N85-12972
ALINITY
The gulf stream deflection and meander energetics experiment. Current meter and bottom pressure gauge data report for the September, 1981 to April, 1982 mooring period
[AD-A144977] 01 p0088 N85-10595
Site-specific research conducted in support of the Salton Sea Solar Pond Project, FY 1982 report
[NASA-CR-174182] 05 p0666 N85-14280
Solar pond overview 05 p0667 N85-14287
Solar pond fluid dynamics and heat transfer 05 p0667 N85-14288
Summary of salt gradient solar pond research 05 p0667 N85-14292
Hydrographic data collected in 1982 and 1983 for EPOCS (Equatorial Pacific Ocean Climate Studies)
[PB85-110799] 12 p1876 N85-21765
Geographic variation in the relationships of temperature, salinity or sigma sub t versus plant nutrient concentrations in the world ocean — silicic acid, nitrate, and phosphate concentration
[NASA-CR-175621] 13 p2140 N85-23287
Frontal nature of Cromwell Current 14 p2336 N85-24445
Representation of temperature and salinity fields using statisticallyt orthogonal functions (in example of polymode data) 14 p2337 N85-24449
Nationwide Urban Runoff Project, Champaign, Illinois: The biological impact of urban runoff on the Saline Branch Drainage Ditch and Boneyard Creek
[PB85-150274] 14 p2348 N85-24515
An experimental study of brine upward migration in thin sea ice 15 p2582 N85-25923
Characteristics of snow cover on sea ice and formation of snow ice II 15 p2582 N85-25924
Characteristics of fast sea ice collected near Barrow, Alaska 15 p2582 N85-25925
North Atlantic Deep Water Formation
[NASA-CP-2367] 15 p2601 N85-26028
Review of North Atlantic source waters 15 p2601 N85-26029
Temporal and spatial scales of Labrador Sea water formation 15 p2601 N85-26031
Chemical signatures associated with the freshening of Northern Atlantic waters between 1972 and 1981 15 p2601 N85-26032
North Atlantic Deep Water and the world ocean 15 p2602 N85-26033
Ocean circulation and meteorology off the Georgia coast. Part 1: Real-time telemetry system for data collection
[PB85-155935] 15 p2605 N85-26052
The effects of sea water and concentrated salt solutions on the fatigue of nylon 6,6 fibers 17 p2979 N85-28416
Chemical, biological, and physical measurements from the subtropical western North Atlantic Ocean. Summer 1982, USNS Lynch, cruise 710-82
[AD-A153623] 18 p3201 N85-29857
Microbiology of solar salt ponds 21 p3658 N85-32724
The role of sulfur in osmoregulation and salinity tolerance in cyanobacteria, algae, and plants 21 p3660 N85-32736
Sulfur reduction in sediments of marine and evaporite environments 21 p3661 N85-32742
Microanalysis of dissolved iron and phosphate in pore waters of hypersaline sediment 21 p3361 N85-32744
Salinity driven oceanographic upwelling
[DE85-011664] 22 p3818 N85-33652
SALT BATHS
Development of low-melting fused salts 8: Formation of molybdenum film from molten ammonium formate bath
[BLL-OA-TRANS-3195-(8196.300)] 20 p3429 N85-31264
SALT BEDS
Landform evaluation through integrated remote sensing methods. A case study in parts of Haryana, India 05 p0657 N85-14221
Radioactive waste isolation in salt: Peer review of the Office of Nuclear Waste Isolation's report on the organic geochemistry of deep groundwaters from the Palo Duro Basin, Texas
[DE85-001439] 10 p1556 N85-19811
Radioactive waste isolation in salt: Peer review of the D'Appolonia report on schematic designs for penetration seals for a repository in the Permian Basin, Texas
[DE85-000693] 11 p1727 N85-20861
Comparison and evaluation of field and numerical results from the Site A heater test at Avery Island
[DE85-010625] 19 p3268 N85-30269
Microbiology of solar salt ponds 21 p3658 N85-32724
WIPP horizon in situ permeability measurements
[DE85-012687] 22 p3802 N85-33557
Preliminary SPR thermal model description and results for WH-11 and BM-4
[DE85-013171] 23 p3931 N85-34360
SALT FLATS
U FLATS (LANDFORMS)
SALT SPRAY TESTS
Influence of 3% NaCl solution on rate of accumulation of damage and residual strength of aluminum-boron composite 13 p2027 N85-22699
SALTON SEA (CA)
Site-specific research conducted in support of the Salton Sea Solar Pond Project, FY 1982 report
[NASA-CR-174182] 05 p0666 N85-14280
Laboratory investigations 05 p0666 N85-14281
Analytical models 05 p0666 N85-14282
Material selection consideration for solar ponds 05 p0666 N85-14284
Salton Sea solar pond power plant design study and regional applicability 05 p0667 N85-14290
SALTS
Airfoil deposition model 02 p0144 N85-10979
New data on presence of ores in salt dome structures of Dnieper-Donets Basin 07 p0981 N85-16234
Measurements of giant salt nuclei from inland in east China 21 p3648 N85-32666
The distribution of giant salt nuclei inside and outside cloud over the basin of Xin and Jiang 21 p3650 N85-32681
Experimental characterization and stability of salt- and nonsalt-containing grouts and mortars (BCT-1F- and BCT-1FF-related)
[DE85-012339] 22 p3753 N85-33263
SALYUT SPACE STATION
Vitamin metabolism in cosmonauts following short-term flights 01 p0091 N85-10615
USSR report: Space
[JPRS-USP-84-005] 02 p0156 N85-11060
Features of new solar panels on Salyut-7 02 p0157 N85-11062
Tass reports launch of Progress-22 02 p0157 N85-11063
Progress-22 docks with Salyut-7 02 p0157 N85-11064
Cosmonauts complete 4th month aboard Salyut-7 02 p0157 N85-11065
Geophysical experiments, photography aboard Salyut-7 02 p0157 N85-11066
Orbit of Salyut-7 station boosted 02 p0157 N85-11067
Salyut-7 crew in orbit 150 days 02 p0157 N85-11068
Commentary on cosmonauts geological mapping, photography 02 p0158 N85-11069
Tass reports launch of Soyuz T-12 02 p0158 N85-11070
Tass reports medical, materials studies aboard Salyut-7 02 p0158 N85-11071
Commentary on Salyut-7 electrophoresis, plugging mortar experiments 02 p0158 N85-11072
Tass reports experiments during visiting crew's third day 02 p0158 N85-11073
Commentary on derivation of biological materials, cosmonaut adaptation 02 p0158 N85-11074
Tass reports astrophysical, atmospheric studies on Salyut-7 02 p0158 N85-11075
EVA of cosmonauts Savitskaya and Dzhanibekov 02 p0158 N85-11076
Commentary on hand tool used in cosmonaut EVA 02 p0159 N85-11077
Further details in welding, spray-coating tool 02 p0159 N85-11078
Lyakhov and Aleksandrov on 150-day flight 13 p1977 N85-22405
Comments on Salyut-7 150-day flight 13 p1977 N85-22406
Remote sensing used for study of forest resources 13 p1983 N85-22440
USSR report: Space
[JPRS-USP-85-004] 16 p2717 N85-26772
Tass reports program for Salyut-7 fully completed 16 p2717 N85-26773
Cosmonaut Savitskaya says many women in cosmonaut training 16 p2717 N85-26774
Cosmonauts' postural reactions after long-term missions aboard Salyut-6 orbital station 19 p3323 N85-30585
Cosmonauts' cardiovascular system function during long-term orbital flights aboard Salyut-6 station 22 p3733 N85-33141
Vatra telvision complex for Salyut orbital space station 22 p3763 N85-33321
SAMARIUM
The growth of metastable peritectic compounds
[NASA-CR-171289] 07 p0920 N85-15824
SAMARIUM COMPOUNDS
Magnitude and range of the RKKy interaction in SmRh4B4
[DE85-012284] 23 p3965 N85-34712
SAMPLED DATA
U DATA SAMPLING
SAMPLED DATA SYSTEMS
U DATA SAMPLING
SAMPLERS
Precision digital sampler
[AD-D011285] 06 p0809 N85-15143
Sampling device
[AD-D011256] 06 p0814 N85-15166
New stage in robotics development 16 p2762 N85-27045
Acid rain: Towards automated monitoring 16 p2829 N85-27444
Microstore: The Stanford analog memory unit
[DE85-005534] 18 p3095 N85-29160
Liquid sampling system
[DE85-011673] 19 p3265 N85-30248
Soil extraction kit
[AD-D011736] 22 p3742 N85-33190
SAMPLES
Study of proton and neutron activation of metal samples in low Earth orbit
[NASA-CR-171183] 01 p0026 N85-10164
Statistical analysis techniques for small sample sizes
[NASA-CR-171872] 15 p2639 N85-26279
A gel-halo sample pellet: The best of both worlds? Stubby zones without a constricted sample gate 20 p3502 N85-31770
Efficiency tests of samplers for microbiological aerosols, a review
[FOA-C-40199-B1] 20 p3504 N85-31783
Optimization of sampling in statistical physics experiments 21 p3696 N85-32975
SAMPLING
NT AIR SAMPLING
NT CORE SAMPLING
NT DATA SAMPLING
NT PARTICULATE SAMPLING
NT RANDOM SAMPLING
Designing optimal AOQL sampling plans a computerized approach
[AD-A146266] 03 p0413 N85-12639
The growth and composition of supercritical branching populations on general type spaces
[CTH-MATH-1984-18] 05 p0721 N85-14631
The influence of sample collection and methods of analysis on chemical concentrations measured in rainwater
[KNMI-TR-55] 07 p0924 N85-15853
A complete characterization of triply balanced matrices with applications to survey sampling
[AD-A147083] 07 p1031 N85-16542
Bayesian estimation of undetected errors
[AD-A147196] 07 p1031 N85-16545
Developing double sampling plans for attributes to meet sample size criteria
[AD-A148144] 08 p1205 N85-17587

SAMPLING DEVICES

A numerical analysis of sampling plans based on prior distribution and costs
[AD-A147718] 08 p1210 N85-17616
The performance of variable sampling plans when the normal distribution is truncated
[AD-A147717] 08 p1215 N85-17649
Antisampling for estimation: An overview
[AD-A148545] 08 p1216 N85-17659
Applying an innovative approach to field investigations at a remedial action site
[AD-P004145] 09 p1348 N85-18481
Location of volatile buried wastes by field portable instrumentation
[AD-P004147] 09 p1348 N85-18483
Sampling errors. They may deprive the analytical results of any meaning
[BLL-MINTEK-TR-1169-(5810.5759)] 09 p1373 N85-18625
Simple approximate variances for b-letter values. A sampling enquiry: Supplement
[DE85-001410] 09 p1376 N85-18647
An optically coupled sampling system with 4 GHz bandwith
[AD-A148057] 09 p1384 N85-18702
Ground-based snow and ice crystal observation system used in Sierra Nevada winter orographic storms
[PB85-115343] 10 p1520 N85-19564
W.E. Johnson's Sufficientness postulate
[AD-A149014] 10 p1550 N85-19774
Estimation of variance of the regression estimator
[AD-A149407] 10 p1551 N85-19780
Asymptotic distributions of the sample mean, autocovariances and autocorrelations of long-memory time series
[AD-A149409] 10 p1551 N85-19781
A computer system for generating single and double sampling plans for attributes data
[AD-A149548] 11 p1701 N85-20698
Inference for censored matched pairs using signed ranks
[MATHEMATICS-RESEARCH-162] 12 p1923 N85-22078
Simplifications and approximations for linear rank statistics with censored data
[MATHEMATICS-RESEARCH-161] 12 p1923 N85-22079
The use of a high-speed 12-bit A/D converter for digital sampling of communication signal carriers
[AD-A150578] 13 p2056 N85-22872
A Monte Carlo sampling plan for estimating network reliability
[AD-A150511] 13 p2065 N85-22898
Use of importance sampling to investigate signal detection systems by simulated method
13 p2086 N85-23028
Tutorial discussion of electronic sampling systems for recording wide-bandwidth transient signals
[DE85-006577] 15 p2549 N85-25735
Multivariable statistical modelling and its application
16 p2857 N85-27617
Statistical effects of imperfect inspection sampling. Part 2: Double sampling, link sampling and grading
[AD-A152377] 17 p3024 N85-28700
Estimating random integrals from noisy observations: Sampling designs and their performance
[AD-A152926] 17 p3025 N85-28702
Moisture content and gas sampling device
[NASA-CASE-MSC-18866-1] 18 p3103 N85-29213
Effect of some estimators on a large sample approximation to the non-null distribution of the pearson chi-square statistic
[AD-A153515] 18 p3173 N85-29673
Liquid sampling system
[DE85-011673] 19 p3265 N85-30248
A comparison of four Monte Carlo methods for estimating the probability OF S=T connectedness
[AD-A154264] 19 p3348 N85-30749
A critique of Deming's discussion of acceptance sampling procedures
[AD-A154305] 19 p3348 N85-30751
Low-discrepancy point sets in transport codes
[DE85-010786] 19 p3348 N85-30755
Intermittency, conditional sampling and turbulent combustion 20 p3424 N85-31249
Organic air pollutants during manufacturing and handling of PVC floor tiles
[FOA-E-40018] 20 p3487 N85-31669
Optimization of sampling in statistical physics experiments 21 p3698 N85-32975
The 1984 environmental monitoring program report for Idaho National Engineering Laboratory site
[DE85-011209] 22 p3812 N85-33611
Marine Sample Exploitation Project: Estimates regarding the sensitivity and technology for the detection of nuclear explosion debris in the marine environment
[DE85-013176] 23 p3947 N85-34462
Ultrasonic inspection of carbon fiber reinforced plastic by means of sample-recognition methods
[NASA-TM-77896] 24 p4074 N85-35245

SAMPLING DEVICES
U SAMPLERS

SAN ANDREAS FAULT
Geodynamics Branch research program
[NASA-TM-86223] 20 p3489 N85-31688
First epoch measurements by Mark III VLBI of the San Andreas Fault experiment baseline
20 p3490 N85-31691
Geophysical interpretation of satellite laser ranging measurements 20 p3490 N85-31692
Carbon fiber strainmeter studies in southern California
[PB85-196889] 24 p4118 N85-35528

SAN ANDREAS FAULT EXPERIMENT
Geodynamics Branch research program
[NASA-TM-86223] 20 p3489 N85-31688
First epoch measurements by Mark III VLBI of the San Andreas Fault experiment baseline
20 p3490 N85-31691
Geophysical interpretation of satellite laser ranging measurements 20 p3490 N85-31692

SAN FRANCISCO (CA)
Characterizing the scientific potential of satellite sensors --- San Francisco, California
[E85-10044] 07 p0963 N85-16244
Characterizing the scientific potential of satellite sensors --- San Francisco, California
[E85-10053] 07 p0984 N85-16249
Impact of LANDSAT MSS sensor differences on change detection analysis --- New Mexico, San Francisco, CA, New Hampshire, and Connecticut
11 p1667 N85-20506

SAN FRANCISCO BAY (CA)
Field studies of run-up generated by wind waves on dissipative beaches
[AD-A148793] 09 p1359 N85-18548
Pollutant body burdens and reproduction in Platichthys stellatus from San Francisco Bay
[DE85-010407] 19 p3308 N85-30509

SAND DUNES
U DUNES

SANDS
NT TAR SANDS
Submarine sand ridges: Geology and development, New Jersey, USA 02 p0227 N85-11482
Application of SIR-B data for groundwater exploration in the Arabian shield and sand-drift monitoring in the AN Nafud and Al Jafurah fringe areas, Kingdom of Saudi Arabia 08 p1144 N85-17214
A wind-tunnel study of the saltation of heterogeneous (size, density) sands 08 p1182 N85-17449
Influence of grain size distribution on the undrained dynamic properties of saturated sand
[PB85-102382/GAR] 09 p1305 N85-18197
The rolling resistance and sinkage of towed dual wheel combination in sand
[AD-P004261] 09 p1404 N85-18837
Performance prediction of pneumatic tyres on sand
[AD-P004262] 09 p1404 N85-18838
Prediction of in-sand tire and wheeled vehicle drawbar performance
[AD-P004265] 09 p1404 N85-18841
Compaction of sand using ordinary off-road vehicles
[AD-P004297] 09 p1409 N85-18874
Transformation of polar ice sublimate residue into Martian circumpolar sand 13 p2189 N85-23580
A comparison of terrestrial saltation flux in the laboratory and the field 13 p2189 N85-23582
Potential bedforms on Venus: Wind tunnel simulations
13 p2189 N85-23583
Experimentally determined distribution of stress around a horizontally loaded model pile in dense sand
[CE-43] 16 p2796 N85-27230
Western gas sands
[DE85-001985] 18 p3126 N85-29360
Sand dispersion from an ephemeral river delta on the wave-dominated central California coast
[AD-A154352] 19 p3300 N85-30458
Propagation of sound in a layered laboratory model
[AD-A155141] 21 p3700 N85-32989
Steamflood pilots in the O'Connell Ranch field and the T-4 Ranch field
[DE85-901363] 24 p4108 N85-35468
Simplified procedures for the evaluation of settlements in sands due to earthquake shaking
[PB85-197887] 24 p4118 N85-35527

SANDSTONES
Paleoenvironmental interpretation of the upper cretaceous Point Lookout sandstone: Implications for shoreline progradation and basin tectonic history, San Juan basin, New Mexico 02 p0227 N85-11486
Sedimentary petrology and provenance of the upper Jackforth Sandstone (Morrowan) Quachita Mountains, Arkansas, USA 08 p1182 N85-17447
Lithologic and environmental atlas of Berea Sandstone (Mississippian) in the Appalachian Basin
[PB85-129039] 11 p1682 N85-20690
Subsurface petroleum geology of Santa Rosa sandstone (Triassic), northeast New Mexico
[TI85-901364] 19 p3313 N85-30338
Crosswell acoustic surveying in gas sands: Travel-time pattern recognition, seismic Q and channel waves
[DE85-010777] 19 p3352 N85-30770
Measurement and analysis of two-phase flow through low permeability media, task 3
[PB85-188373] 20 p3435 N85-31313
Steamflood pilots in the O'Connell Ranch field and the T-4 Ranch field
[DE85-901363] 24 p4108 N85-35468

SANDWICH CONSTRUCTION
U SANDWICH STRUCTURES

SANDWICH STRUCTURES
Development of new and improved polymer matrix resin systems, phase 1
[NASA-CR-166595] 01 p0017 N85-10104
Nonlinear dynamic analysis of sandwich panels
01 p0060 N85-10394
Simulation of vibration processes in damped structures with allowance for temperature-frequency characteristics of vibration absorbing materials
02 p0257 N85-11660
Numerical simulations of compliant material response to turbulent flow, revision 1
[AD-A145801] 03 p0372 N85-12373
Composite repair of aircraft structures
08 p1120 N85-17069
Mechanical locking between multi-layer printed wiring board conductors and through-hole plating
[AD-D011477] 10 p1481 N85-19352
OTEC (Ocean Thermal Energy Conversion) Cold Water Pipe At-Sea Test Program. Phase 2: Suspended pipe test
[PB85-119931] 10 p1512 N85-19542
Aircraft safety improvement 15 p2688 N85-26602
Stability of anisotropic cylindrical sandwich shells
16 p2766 N85-27065
Method of solving problems of statics for multilayer shells of revolution 17 p2943 N85-28167

SANITATION
Design concept definition study for an improved shuttle waste collection subsystem
[NASA-CR-171834] 08 p1198 N85-17546
Hydrodynamics and sanitation
[CT-579] 20 p3487 N85-31672

SAPPHIRE
Factors affecting SOS (Silicon-On-Sapphire) yield and reliability
[AD-A150004] 12 p1835 N85-21515
The Valence- and conduction-band structure of the sapphire (1102) surface
[AD-A150001] 12 p1940 N85-22184
Incident beam polarization for laser Doppler velocimetry employing a sapphire cylindrical window
[NASA-TM-87064] 17 p3037 N85-28785
Producing titanium-sapphire items by solid-phase bonding through aluminum gasket
19 p3246 N85-30127
Size and shape dependence of CO adsorption sites on sapphire supported Fe microcrystals
[NASA-CR-176171] 24 p4160 N85-35794

SARCOMA
U CANCER

SARSAT
Terrestrial locating --- of buoys from space
05 p0599 N85-13618
The Search And Rescue Satellite Aided Tracking (SARSAT) experiment. Presentation of CNES processing for the SARGOS project: Context and orbit processing
05 p0600 N85-13620
Experimental satellite system for determining coordinates of maritime distress
09 p1308 N85-18215
The SARSAT program 14 p2327 N85-24365
The SARSAT/COSPAS system for assisting satellite based search and rescue 14 p2398 N85-24778
COSPAS-SARSAT satellite orbit predictor, volume 5
[NASA-TM-85015-VOL-5] 14 p2439 N85-25082
International conference on COSPAS-SARSAT system
15 p2484 N85-25336
Satellite aided search and rescue. Experimental results and operational prospects --- conference
[ISBN-2-85428-120-9] 20 p3400 N85-31098
COSPAS/SARSAT: An overview
20 p3400 N85-31092
Possible use of the COSPAS/SARSAT system within the Swedish mountain rescue organization
20 p3401 N85-31100
The COSPAS-SARSAT system
20 p3401 N85-31101

The COSPAS-SARSAT space segment: Present status nd evolution 20 p3401 N85-31102
Canadian Astronautics Limited's SARSAT ground ations 20 p3401 N85-31104
The 406 MHz ELT/EPIRBs — Emergency Locator ransmitters/Emergency Position Indicating Radio eacons (ELT/EPIRB) 20 p3402 N85-31106
Soviet Emergency Locator Transmitter/Emergency osition Indicating Radio Beacon (ELT/EPIRBs) at 121.5 nd 406 MHz 20 p3402 N85-31107
Ground segment of COSPAS system 20 p3402 N85-31108
The COSPAS/SARSAT local user terminal in Tromso, Norway. Special considerations and experience with high atitude location (69 deg, 43 min N) 20 p3402 N85-31109
A 406 MHz geostationary satellite SARSAT experiment 20 p3403 N85-31113
Evolution of 406 MHz Search and Rescue (SAR) processor 20 p3403 N85-31116
A micro/PDP-11 system for 406 MHz COSPAS/SARSAT processing 20 p3403 N85-31117
Search and rescue satellite (SARSAT) error analysis of the 406 MHz system 20 p3403 N85-31118
A special antenna for SARSAT EPIRBs providing circular polarization and hemispheric coverage for reliable transmission to satellites — Emergency Position Indicating Radio Beacon (EPIRB) 20 p3404 N85-31122
Fault tolerant multiprocessor SARSAT-COSPAS 406 MHz local user terminal 20 p3404 N85-31123
SARSAT 406 MHz system technical evaluation 20 p3404 N85-31124
SARSAT 121.5/243 MHz technical evaluation 20 p3405 N85-31126
Use of 121.5/243.0 MHz COSPAS-SARSAT data by North American SAR agencieu — search and rescue (SAR) 20 p3405 N85-31127
The COSPAS/SARSAT demonstration and evaluation. Results of the first year in the United States 20 p3405 N85-31128
COSPAS-SARSAT demonstration and evaluation results in Canada 20 p3405 N85-31129
COSPAS-SARSAT demonstration and evaluation phase: COSPAS tests in the USSR and their results 20 p3405 N85-31130
The SARSAT-COSPAS demonstration in France 20 p3405 N85-31131
UK experience with COSPAS-SARSAT and INMARSAT distress systems 20 p3406 N85-31132
The COSPAS-SARSAT system evaluation in Norway 20 p3406 N85-31133
JANUS: An autonomous platform optimized for SARSAT type missions 20 p3406 N85-31135
United States-Soviet satellite accord: SARSAT/Cospas search-and-rescue program
[GPO-41-113] 20 p3541 N85-32040
LOCAT: A data retrieval program
[AD-A156004] 24 p4165 N85-35822

SAS-D
U IUE

SATAN (SENSOR)
U TERRAIN ANALYSIS

SATELLITE ANTENNAS
Workshop on Mechanical Technology for Antennas — conferences; satellite antennas
[ESA-SP-225] 05 p0625 N85-13999
Antenna mechanical technologies within ESA 05 p0625 N85-14000
High performance deployable antenna structures 05 p0625 N85-14001
Offset unfurlable antenna concepts 05 p0625 N85-14002
Distortional measurement of antennas under space simulation conditions by means of holography 05 p0625 N85-14005
Electrical consequences of mechanical antenna characteristics 05 p0625 N85-14006
Structural aspects of SAR antenna for Japanese Earth Resources Satellite 1 05 p0626 N85-14007
Technology for the ERS-1 SAR antenna 05 p0626 N85-14008
Mechanical/thermal design of a polarization sensitive reflector — communication satellites 05 p0626 N85-14009
CASA technological effort in the field of antennas — satellite radar antennas 05 p0626 N85-14010
BAe antenna hardware technology for current satellite projects 05 p0626 N85-14011
Technology and performances of structural thermal mechanical equipment used for antenna of TV.SAT-TDF 1 program 05 p0626 N85-14012
The dimensional stability of advanced composite antenna reflectors: Analytical and test evaluation — satellite antennas 05 p0626 N85-14014
CASA activities in antenna technology — satellite antennas 05 p0627 N85-14015
Structural design and thermal stability of TELE-X antenna tower 05 p0627 N85-14016
Analytical thermal formulations for antenna dishes — satellite antennas 05 p0627 N85-14017
In-orbit performance of INTELSAT V communications antennas deployment systems 05 p0627 N85-14018
Study of structure control dynamic interaction for radio frequency antenna control systems — satellite antennas 05 p0627 N85-14020
Hemispherical antenna pointing mechanism — satellite antennas 05 p0627 N85-14021
ARABSAT spacecraft: Rx and Tx antenna mechanisms 05 p0628 N85-14022
Configuration study for a 30 GHz monolithic receive array, volume 2
[NASA-CR-174897-VOL-2] 09 p1311 N85-16240
Operational fitness of box truss antennas in response to dynamic slewing
[NASA-CR-172470] 10 p1429 N85-19012
Polarization angles of linearly polarized antennas and radio waves in satellite communications
[PB85-131613] 11 p1626 N85-20240
The Ferranti Tactical SHF SATCOM station (MANSAT) 11 p1710 N85-20759
Large Space Antenna Systems Technology, 1984
[NASA-CP-2368-PT-1] 14 p2229 N85-23813
NASA mobile satellite program 14 p2229 N85-23814
Alternatives for satellite sound broadcast systems at HF and VHF ·14 p2229 N85-23815
Development concerns for satellite-based air traffic control surveillance systems 14 p2230 N85-23816
Application of pushbroom altimetry from space using large space antennas 14 p2230 N85-23817
Orbiting multi-beam microwave radiometer for soil moisture remote sensing 14 p2230 N85-23818
Space-based antenna measurement system concepts for space station operation 14 p2236 N85-23860
Satellite reception of reentry vehicle telemetry
[AD-A151851] 15 p2492 N85-25372
Thin Route Project 15 p2687 N85-26596
Communications 15 p2687 N85-26600
Earth station antenna sidelobe characteristics
[PB85-164986] 16 p2780 N85-27159
Ionospheric effects on antenna impedance
[BMFT-FB-W-84-052] 17 p2950 N85-28217
Nonlinear plasma reactions on the antenna impedance of high transmission power satellites
[BMFT-FB-W-84-053] 18 p3192 N85-29799
High reflective surfaces for millimeter RF waves, phase A — satellite antenna reflectors
[HRS-FR-01] 20 p3442 N85-31366

SATELLITE ATMOSPHERES
NT LUNAR ATMOSPHERE
Composition, structure and evolution of Uranian and Neptunian satellites 02 p0300 N85-11944
Satellite masses in the Uranus and Neptune systems
[PSI-CONTRIB-198] 02 p0301 N85-11947
Seasonal variations in Triton's atmospheric mass and composition 02 p0301 N85-11948
Do the satellites of Uranus control its magnetosphere? 02 p0301 N85-11952
Outer satellite atmospheres: Their nature and planetary interactions
[NASA-CR-174146] 04 p0589 N85-13759
Extended atmospheres of outer planet satellites and comets
[NASA-CR-174398] 09 p1416 N85-18933
A modeling analysis program for the JPL Table Mountain Io sodium cloud data
[NASA-CR-175493] 11 p1681 N85-20589
Radio scintillations observed during atmospheric occultations of Voyager: Internal gravity waves at Titan and magnetic field orientations at Jupiter and Saturn
[NASA-CR-175554] 12 p1961 N85-22327
Extended atmospheres of outer planet satellites and comets
[NASA-CR-175673] 14 p2440 N85-25058
A modeling analysis program for the JPL table mountain Io sodium cloud
[NASA-CR-175851] 16 p2833 N85-27468
Volatiles in the outer solar system. 1: Thermodynamics of clathrate hydrates. 2: Ethane ocean on Titan. 3: Evolution of primordial Titan atmosphere 19 p3382 N85-30964
Quasi non-intrusive sampling and analysis of gases associated with the boundary layer on the tethered satellite and similar supersonic and hypersonic research vehicles
[NASA-CR-176075] 20 p3407 N85-31140
Extended atmospheres of outer planet satellites and comets
[NASA-CR-176137] 22 p3851 N85-33848

SATELLITE ATTITUDE CONTROL
In-orbit experiments on IRAS for application to the ISO satellite
[FOK-TR-R-84-057] 03 p0322 N85-12078
Overview of Autonomous Payload Control Experiment 04 p0459 N85-12911
Satellite attitude determination 05 p0599 N85-13814
Stationkeeping strategies for geostationary satellites 05 p0600 N85-13825
Magnetically suspended flywheel system study 05 p0607 N85-13873
Reaction wheels for kinetic energy storage 05 p0607 N85-13874
Study of structure control dynamic interaction for radio frequency antenna control systems — satellite antennas 05 p0627 N85-14020
Qualification of a hydrazine gas generator system with electrothermal/catalytic gas generator
[BMFT-FB-W-84-040] 08 p1110 N85-17016
Satellite description 09 p1412 N85-18900
Application Number 3: Using tethers for attitude control 11 p1646 N85-20373
Application of model following control and estimation techniques to attitude control of maneuvering spacecraft. Part 2: Simulation software description
[NLR-TR-82116-U-PT-2] 12 p1793 N85-21254
Minimizing plume contamination production in bipropellant thrusters 13 p2003 N85-22557
Modeling needed for the design and definition of spacecraft attitude and orbit control systems 14 p2397 N85-24766
Spaceborne automatic data processing 14 p2397 N85-24769
Details on spot remote sensing satellite propulsion unit 15 p2535 N85-25640
Optimum parameters of aerogyroscopic satellite orientation system 16 p2718 N85-26782
Maximizing the semi-major axis for a freely coning solar sailcraft
[AD-A153175] 17 p2909 N85-27938
Application of model following control and estimation techniques to attitude control of maneuvering spacecraft. Part 1: Theory and simulation results
[NLR-TR-82116-U-PT-1] 18 p3065 N85-28957
The attitude control model tests for the Infrared Astronomical Satellite (IRAS)
[B8560071] 18 p3067 N85-28967
Research on an expert system for database operation of simulation-emulation math models. Volume 1, Phase 1: Results
[NASA-CR-176087] 21 p3669 N85-32792
Research on an expert system for database operation of simulation-emulation math models. Volume 2, Phase 1: Results
[NASA-CR-176088] 21 p3669 N85-32793

SATELLITE ATTITUDE DISTURBANCE
U ATTITUDE STABILITY
U SPACECRAFT STABILITY

SATELLITE CAPTURE
U SPACECRAFT RECOVERY

SATELLITE COMMUNICATION
U SPACECRAFT COMMUNICATION

SATELLITE CONFIGURATIONS
Shuttle tethered satellite system program overview 11 p1642 N85-20342
TSS Satellite overview 11 p1642 N85-20343
Satellite module design 11 p1642 N85-20344
Multimission advanced configurations study — telecommunication satellites
[MATRA-DM.51/CC/FL/0151.83] 12 p1790 N85-21237
A study of spacecraft technology and design concepts, volume 1
[NASA-CR-172579-VOL-1] 16 p2730 N85-26844
A study of spacecraft technology and design concepts. Volume 2: Appendices
[NASA-CR-172579-VOL-2] 16 p2730 N85-26845
Spacecraft configuration study for second generation mobile satellite system
[NASA-CR-175774] 16 p2730 N85-26849
Stuuy of a medium term flexible fixed satellite service mission
[DM51/CC-IM-0185.83] 18 p3091 N85-29136

SATELLITE CONTROL
NT SATELLITE ATTITUDE CONTROL
The application of microprocessors in the command and control of satellites by the MECB stations
[INPE-3282-RPE/466] 02 p0239 N85-11553
Telemetry (TM)/telecommand (TC) processor study
[ESA-CR(P)-1915] 03 p0323 N85-12061
Inertial storage for satellites 05 p0605 N85-13859
Air Force space technology center space technology: Emphasis 84 09 p1333 N85-18381
Effects of the solar-terrestrial environment on satellite operations
[DE85-002413] 11 p1590 N85-20003
Definition of ground test for Large Space Structure (LSS) control verification
[NASA-TM-86495] 12 p1792 N85-21249

Space Mathematics for the Preparation and Development of satellite Exploitation [ISBN-2-86428-115-2] 14 p2395 N85-24753
Introduction to methods of evaluating the operational reliability of complex systems: Application to satellite control ground support 14 p2397 N85-24771
Orbital positioning and stationkeeping of geostationary satellites 14 p2397 N85-24772
The steering of GPS time 17 p2984 N85-28301
Timing of spacecraft data: Time accuracy requirements and timing facilities of the European Space Agency (ESA) 17 p2984 N85-28307
A study of the ESA-NAVSAT control segment [ESA-CR(P)-2000] 20 p3396 N85-31079
Advanced (unfloated) gyros for satellite control [ESA-CR(P)-2010] 20 p3419 N85-31222

SATELLITE DEFENSE
U SPACECRAFT DEFENSE

SATELLITE DESIGN
The ESA remote sensing satellite system (ERS-1) 03 p0379 N85-12420
Conceptual ideas for a second generation METEOSAT system 06 p0858 N85-14226
QUASAT: Technical aspects of the proposed mission — VLBI satellite 07 p1057 N85-16706
UK Skynet 4 communications satellites 11 p1710 N85-20757
Drag-free satellite simulator [REPT-615] 12 p1789 N85-21229
Multimission advanced configurations study — telecommunication satellites [MATRA-DM.51/CC/FL/0151.83] 12 p1790 N85-21237
Satellite structure [CH-642922-A5] 15 p2492 N85-25373
Shuttle-tethered satellite system definition study. Volume 1: Executive study [NASA-CR-171474] 17 p2907 N85-27924
IRAS: Space technology from the Netherlands [B8561841] 17 p2908 N85-27929
JANUS: An autonomous platform optimized for SARSAT type missions 20 p3406 N85-31135
Evolution of spacecraft design methods as a function of environmental and geometrical constraints [ESA-CR(P)-2012] 20 p3418 N85-31216
Second-generation mobile satellite system. A conceptual design and trade-off study [NASA-CR-176195] 24 p4086 N85-35325

SATELLITE DOPPLER POSITIONING
Diagnosis and therapy of geodetic satellite networks of Doppler type — error analysis [SER-C-293] 01 p0015 N85-10090
Data Collection and Platform Location by Satellite: ARGOS Users' Conference 14 p2237 N85-23869
The ARGOS system status report after 2 years operation 14 p2237 N85-23870
Data Collection and Platform Location by Satellite: ARGOS Users' Conference 14 p2239 N85-23883
The ARGOS system status report 14 p2239 N85-23884
Some experience from ARGOS stations in the open sea 14 p2240 N85-23891
Proceedings of the ARGOS Users Conference on Data Collection and Location by Satellite 14 p2322 N85-24348
Improvements brought about to the system since 1978 and statements on future development 14 p2323 N85-24349
New directions in ARGOS instrumentation at Polar Research Lab (PRL) 14 p2323 N85-24350
The Edmonton data collection platform processing and locating facility 14 p2323 N85-24352
The development of Platform Transmitter Terminal (PTT) and its application for drifting buoys 14 p2323 N85-24353
US programs using the ARGOS data collection and platform location system 14 p2323 N85-24355
Data Collection and Platform Location by Satellite: ARGOS Users' Conference 14 p2325 N85-24366
The ARGOS system main characteristics — satellite based localization 14 p2325 N85-24367
The ARGOS system after 3 years operation 14 p2325 N85-24368
Location and data collection for long stratospheric balloon flights 14 p2326 N85-24377
The ARGOS contribution to the successful dredging of a deep moored current meter 14 p2327 N85-24381
The ARGOS system aboard research vehicles: 1981 experiment aboard the Le Suroit oceanographic vessel and the outlook [CNEXO/DFT/OPNAV/82-05] 14 p2327 N85-24382
The SARSAT program 14 p2327 N85-24385
Data Collection and Platform Location by Satellite: ARGOS users' Conference 14 p2328 N85-24391
US programs using the ARGOS data collection and platform location system 14 p2329 N85-24401
Data Collection and Platform Location by Satellite: ARGOS Users' Conference 14 p2330 N85-24409
US program using the ARGOS data collection and platform location system 14 p2330 N85-24410
Moored buoy stationkeeping and location system 14 p2331 N85-24416
The ARGOS program — satellite based localization 14 p2397 N85-24775
The SARSAT/COSPAS system for assisting satellite based search and rescue 14 p2398 N85-24776
The TRANSIT and Global Positioning System (GPS) systems. Precision navigation and localization 14 p2398 N85-24777
DORIS: Prediction in Doppler measurement — satellite onboard measurement [CNES-CT/DTI/MS/AE/170] 16 p2729 N85-26843
Data Collection and Platform Location by Satellite: ARGOS Users' Conference 16 p2811 N85-27333
Studies into location accuracy — ARGOS system 16 p2811 N85-27334
Positioning accuracy of the ARGOS system in operational use 16 p2811 N85-27335
Checking on the position of navigation marker buoys by the ARGOS system 16 p2813 N85-27354
Location and data collection satellite system ARGOS. User's guide — satellite based localization 16 p2816 N85-27371
Influence of coherent mesoscale structures on satellite-based Doppler lidar wind measurements [NASA-CR-175853] 16 p2833 N85-27467
COSPAS/SARSAT: An overview 20 p3400 N85-31092
The contribution of an operational SAR satellite system to the UK SAR organisation — search and rescue (SAR) 20 p3400 N85-31095
Specific aspects of maritime search and rescue in French metropolitan and overseas territories: Expected benefits from a detection and location of distress system by satellites 20 p3401 N85-31097
The COSPAS-SARSAT system 20 p3401 N85-31101
The COSPAS-SARSAT space segment: Present status and evolution 20 p3401 N85-31102
Canadian Astronautics Limited's SARSAT ground stations 20 p3401 N85-31104
A 406 MHz ELT processor for geostationary satellites — Emergency Locator Transmitter (ELT) 20 p3403 N85-31114
Fault tolerant multiprocessor SARSAT-COSPAS 406 MHz local user terminal 20 p3404 N85-31123
SARSAT 406 MHz system technical evaluation 20 p3404 N85-31124
The COSPAS system tests. Technical results 20 p3404 N85-31125
SARSAT 121.5/243 MHz technical evaluation 20 p3405 N85-31126
The COSPAS/SARSAT demonstration and evaluation. Results of the first year in the United States 20 p3405 N85-31128
COSPAS-SARSAT demonstration and evaluation results in Canada 20 p3405 N85-31129
The SARSAT-COSPAS demonstration in France 20 p3405 N85-31131
UK experience with COSPAS-SARSAT and INMARSAT distress systems 20 p3406 N85-31132
Interplanetary plasma turbulence and the Doppler detection of a gravitational background radiation [IFSI-85-1] 20 p3546 N85-32066

SATELLITE DRAG
Drag-free satellite simulator [REPT-615] 12 p1789 N85-21229
Optical best arc RMS test results 16 p2604 N85-27290
Consummative expressions for satellite drag perturbations in a spherically symmetrical atmosphere [AD-A154230] 19 p3222 N85-29981

SATELLITE GROUND SUPPORT
The current formal status of the ERS-1 ground segment 03 p0380 N85-12423
ERS-1 altimeter ground segment relations to other sensors and programs 03 p0381 N85-12436
The 2 GHz network and the network operations center — satellite tracking 05 p0599 N85-13817
The facilities of the Calculation Center and Real Time Room for satellite positioning 05 p0599 N85-13819
The satellite maneuvers determination department 05 p0599 N85-13820
The operational orbit tracking center 05 p0599 N85-13821
Development of the TT and C station equipment at INPE [INPE-3327-PRE/625] 10 p1427 N85-18999
Introduction to methods of evaluating the operational reliability of complex systems: Application to satellite control ground support 14 p2397 N85-24771
A study of the ESA-NAVSAT control segment [ESA-CR(P)-2000] 20 p3396 N85-31079

SATELLITE GROUND TRACKS
Altimetry, orbits and tides [E85-10066] 08 p1174 N85-17484
Scientific requirements for ozone measurements 13 p2105 N85-20113
Comparison of gravity field solution techniques 16 p2805 N85-27886

SATELLITE GUIDANCE
The facilities of the Calculation Center and Real Time Room for satellite positioning 05 p0599 N85-13819
Satellite positioning — in geosynchronous orbit 05 p0600 N85-13823

SATELLITE IMAGERY
ISCCP Cloud Algorithm Intercomparison Workshop 01 p0073 N85-10465
A system for meteorological satellite, radar, conventional data and model analysis 01 p0082 N85-10551
The future of satellite remote sensing: A worldwide assessment and prediction 02 p0151 N85-11005
LANDSAT data and interactive computer mapping 02 p0152 N85-11006
Seismotectonic nature of some annular photoanomalies registered by remote methods 02 p0164 N85-11110
Predicting fracturing zones in Caspian depression subsalt deposits on basis of space information and geological-geophysical data 02 p0164 N85-11111
Method for interpreting soil cover of flowed fields using spectral brightnesses measured from space photographs 02 p0164 N85-11112
Space observation of latitudinal changes in vegetation cover 02 p0164 N85-11113
Choice of cartographic projection for space system data bank used in studying natural resources 02 p0165 N85-11119
The application of principal components analysis to LANDSAT MSS data 02 p0212 N85-11396
The Multispectral Imaging Science Working Group. Volume 1: Executive summary [E85-10001] 02 p0213 N85-11404
The Multispectral Imaging Science Working Group. Volume 2: Working group reports [E85-10002] 02 p0213 N85-11405
Workshop on the Use of Future Multispectral Imaging Capabilities for Lithologic Mapping: Workshop summary 02 p0214 N85-11413
Utilization of LANDSAT orbital imagery in the soil survey processes at Rio Grande do Norte state [E85-10009] 02 p0216 N85-11422
Spectroradiometric calibration of the Thematic Mapper and Multispectral Scanner system [E85-10026] 02 p0218 N85-11439
Production of optically correlated SEASAT-A (SEA satellite) SAR (Synthetic Aperture Radar) imagery at DREO (Defence Research Establishment Ottawa) [AD-A145970] 03 p0355 N85-12281
Specification and preliminary design of the CARTA system for satellite cartography [E85-10035] 03 p0378 N85-12414
Evaluation of criteria for selecting the spectral attributes of digital LANDSAT MSS imagery for discriminating lithological units in the lower Curaca River Valley, Bahia — Brazil [E85-10036] 03 p0379 N85-12415
The United States Geological Survey in Alaska: Accomplishments during 1981 [USGS-CIRC-868] 04 p0515 N85-13283
Summary of LANDSAT quadrangle studies in Alaska 04 p0515 N85-13284
Investigations of severe/tornadic thunderstorm development and evolution based on satellite and AVE/SESAME/VAS data [NASA-CR-174154] 04 p0536 N85-13424
Noise removal in multichannel images [NASA-CR-174116] 04 p0554 N85-13605
Mars polar volatiles: Topographic and geologic setting [NASA-CR-174089] 04 p0581 N85-13709
Air-sea heat exchange, an element of the water cycle 05 p0653 N85-14185
LANDSAT instruments characterization [E85-10028] 05 p0654 N85-14197
LANDSAT instruments characterization [E85-10029] 05 p0654 N85-14198
Classification of vegetation communities in the Battle Mountain SE quadrangle, Nevada with MSS digital data [E85-10043] 06 p0826 N85-15246
Experiences with digital processing of images at INPE [E85-10045] 06 p0826 N85-15247
An integrated LANDSAT/ancillary data classification of desert rangeland [E85-10046] 06 p0826 N85-15248
A geographic information system for resource management based on multi-level remote sensing data [E85-10047] 06 p0827 N85-15249

Multi crop area estimation in Idaho using EDITOR
85-10064] 06 p0627 N85-15251
Characterizing the scientific potential of satellite ensors — San Francisco, California
E85-10044] 07 p0983 N85-16244
Characterizing the scientific potential of satellite ensors — San Francisco, California
E85-10063] 07 p0984 N85-16249
LANDSAT-4 Thematic Mapper Modulation Transfer Function (MFT) evaluation — California and New Mexico
[E85-10065] 07 p0984 N85-16250
Proceedings of the Second Annual Symposium on athematical Pattern Recognition and Image Analysis Program
[E85-10066] 07 p0984 N85-16251
Exploring the use of structural models to improve remote sensing agricultural estimates 07 p0985 N85-16259
Calibration or inverse regression: Which is appropriate for crop surveys using LANDSAT data?
07 p0985 N85-16260
Rectification of single and multiple frames of satellite scanner imagery using points and edges as control
07 p0986 N85-16263
The influence of the number of ground control points on the scene-to-map registration accuracy — Kansas, Louisiana, Mississipp, and Missouri
07 p0986 N85-16264
Southern ocean sea-ice morphology and kinematics
08 p1144 N85-17217
Optical wave propagation and imaging in the atmosphere 08 p1222 N85-17694
SIRTF: The next step 08 p1250 N85-17891
Resolution enhancement of multichannel microwave imagery from the Nimbus-7 SMMR for maritime rainfall analysis
[NASA-CR-174367] 10 p1462 N85-19221
Assessment of LANDSAT for rangeland mapping, Rush Valley, Utah
[E85-10072] 10 p1503 N85-19486
Anaysis of the quality of image data required by the LANDSAT-4 Thematic Mapper and Multispectral Scanner — agricultural and forest cover types in California
[E85-10074] 10 p1504 N85-19488
Thematic Mapper: Design through flight evaluation
[E85-10078] 10 p1504 N85-19492
The sharing of remote sensing techniques in Brazilian geographic research
[INPE-3307-PRE/617] 10 p1506 N85-19502
Satellite support to the Sierra Cooperative Pilot Project: 1979/80 and 1980/81
[PB85-115079] 10 p1520 N85-19583
LANDSAT-4 Science Characterization Early Results. Volume 1: Multispectral Scanner (MSS)
[E85-10067] 11 p1666 N85-20496
Summary of MSS characterization investigations
11 p1666 N85-20497
Radiometric accuracy assessment of LANDSAT 4 Multispectral Scanner data 11 p1666 N85-20498
Investigation of radiometric properties of LANDSAT-4 MSS — California, North Carolina, South Carolina, and New England 11 p1666 N85-20500
Radiometric calibration and geocoded precision processing of LANDSAT-4 Multispectral Scanner products by the Canada Centre for Remote Sensing
11 p1667 N85-20501
Geodetic accuracy of LANDSAT 4 Multispectral Scanner and Thematic Mapper data — Washington, DC, California, Alabama, South Dakota, and Illinois
11 p1667 N85-20504
Geometric accuarcy assessment of LANDSAT-4 Multispectral Scanner (MSS) data
11 p1667 N85-20505
LS-4 MSS geometric correction: Methods and results
11 p1668 N85-20507
LANDSAT-4 Science Characterization Early Results. Volume 2, part 1: Thematic Mapper (TM)
[E85-10068] 11 p1668 N85-20508
TM digital image products for applications
11 p1668 N85-20512
Canadian plans for Thematic Mapper data
11 p1668 N85-20513
Development of satellite data presentation for environmental forecasting 11 p1712 N85-20770
Practical applications of satellite-derived meteorological and oceanographic data in Naval operations
11 p1712 N85-20771
LANDSAT-4 Science Characterization Early Results. Volume 3, part 2: Thematic Mapper (TM)
[E85-10069] 12 p1869 N85-21724
A preliminary assessment of LANDSAT-4 Thematic Mapper data — Windsor, Ontario and Medicine Hat areas, Canada 12 p1869 N85-21728
Evaluation of the radiometric quality of the TM data using clustering, linear transformations and multispectral distance measures — Illinois 12 p1870 N85-21731
TM geometric performance: Line to Line Displacement Analysis (LLDA) — New Mexico
12 p1870 N85-21732
In-progress absolute radiometric inflight calibration of the LANDSAT-4 sensors — New Mexico
12 p1870 N85-21733
Scan angle and detector effects in Thematic Mapper radiometry — Iowa and Arkansas
12 p1871 N85-21735
Thematic Mapper spectral dimensionality and data structure 12 p1871 N85-21736
Intraband radiometric performance of the LANDSAT 4 Thematic Mapper — Washington, DC, Arkansas, Massachusetts, Virginia, and Arizona
12 p1871 N85-21738
Tests of low-frequency geometric distortions in LANDSAT 4 images 12 p1872 N85-21744
Investigation of TM band-to-band registration using the JSC registration processor 12 p1872 N85-21745
Meteorological Satellite Center Technical Note No. 10, 1984
[MSC-TN-10] 12 p1894 N85-21884
On the relative motion of typhoons: In the case of Typhoon 8305 and Typhoons 8306 and 8307
12 p1894 N85-21885
Accuracy of typhoon center determined by GMS imagery 12 p1894 N85-21887
The development of image processing of NOAA AVHRR data and its application to sea surface temperature
12 p1895 N85-21891
A supplement study on the subsynoptic cloud system off the south coast of Japan 12 p1895 N85-21892
Nation said to rank high with 15 satellites
13 p2041 N85-22778
LANDSAT-4 Science Characterization Early Results. Volume 4: Applications — agriculture, soils land use, geology, hydrology, wetlands, water quality, biomass identification, and snow mapping
[E85-10070] 13 p2117 N85-23186
Overview of TM applications research reports
13 p2117 N85-23187
Characterization of LANDSAT-4 TM and MSS image quality for the interpretation of California's agricultural resources — Central Valley 13 p2118 N85-23190
Preliminary evaluation of Thematic Mapper image data quality 13 p2118 N85-23194
A concept for the processing and display of Thematic Mapper data 13 p2119 N85-23196
Quick look analysis of TM data of the Washington, District of Columbia, area 13 p2119 N85-23197
A preliminary comparison of the information content of data from the LANDSAT 4 Thematic Mapper and Multispectral Scanner — Arkansas
13 p2119 N85-23199
Thematic Mapper data quality and performance assessment in renewable resources/agriculture/remote sensing 13 p2120 N85-23201
Preliminary evaluation of TM for soils information
13 p2121 N85-23206
Comparison of MSS and TM data for landcover classification in the Chesapeake Bay area: A preliminary report — Taylor's Island, Maryland
13 p2121 N85-23210
An investigation of several aspects of LANDSAT-5 data quality — Palmer County, Shelby, mt; White sands, NM; Great Salt Lake, UT; San Matted Bridge and Sacramento, California
[E85-10096] 13 p2122 N85-23214
Distribution of snow and maximum snow water equivalent obtained by LANDSAT data and degree day method 13 p2124 N85-23229
Analysis of NIMBUS-7 SMMR data — Hokkaido, Japan snow cover 13 p2125 N85-23232
The relationship between marine aerosol particles and satellite-detected radiance 13 p2131 N85-23263
Analysis of the inflow layer and air-sea interactions in Hurricane Frederic (1979)
[NASA-CR-175616] 13 p2137 N85-23271
Use of space photographic information to map plant cover 15 p2486 N85-25359
Identification of structure of soil-vegetation cover using aerial and space photographs 16 p2726 N85-26826
Contribution to space program reviewed
16 p2727 N85-26834
China's integrated circuit production
16 p2806 N85-27302
CNPq/INPE LANDSAT system: Report of activities from October 1, 1983 to September 30, 1984 — Brazil
[E85-10097] 16 p2808 N85-27318
Noise correction on LANDSAT images using a spline-like algorithm
[E85-10098] 16 p2808 N85-27319
The relevance of remote sensing to Brazil
[INPE-3421-PRE/666] 16 p2811 N85-27332
Experience of the Institute of Space Research with the use of remote sensing in urban planning studies
[INPE-3159-PRE/533] 16 p2880 N85-27770
Information relative to cartography and geodesy. Series 2: Translations, number 42, volume 1
[ISSN-0469-4244] 18 p3123 N85-29338
Two satellite image maps of Central Europe
18 p3123 N85-29339
Digital image mapping of Antarctica using NOAA-7 AVHRR imagery 18 p3124 N85-29340
Satellite measurements of atmospheric aerosols
[AD-A153607] 19 p3316 N85-30556
Microwave hydrology: A trilogy
[NASA-CR-176042] 20 p3477 N85-31603
Regional landform thresholds
21 p3601 N85-32362
Geomorphology, tectonics, and exploration
21 p3601 N85-32365
Quantitative analysis of geomorphic processes using satellite image data at different scales
21 p3604 N85-32380
Use of space photographs for analysis of structural and dynamic conditions of formation of ancient phlogopite and apatite deposits 22 p3735 N85-33153
Physico-geographical regionalization of Caspian lowland based on space survey materials
22 p3736 N85-33162
Repetition of dense cloud cover above Indian Ocean from generalized satellite data 22 p3737 N85-33165

SATELLITE INSTRUMENTS
NT MULTISPECTRAL LINEAR ARRAYS
Optical analysis of the star-tracker telescope for Gravity Probe
[NASA-TM-86474] 01 p0129 N85-10888
An overview of Multispectral Electro-Optical Stereo Scanner (MEOSS) mission 04 p0458 N85-12906
Research relative to the development of a cryogenic microwave cavity gradiometer for orbital use
[NASA-CR-174249] 07 p0962 N85-16095
Thematic Mapper. Volume 1: Calibration report flight model, LANDSAT 5
[E85-10059] 07 p0987 N85-16270
Thematic Mapper. Volume 2: Flight model preshipment review
[E85-10060] 07 p0987 N85-16271
Solar Corona Explorer: A mission for the physical diagnosis of the solar corona
[NASA-TM-87416] 10 p1572 N85-19912
Instrumentation for Application Number 1: Mass spectrometric analysis of the boundary layer associated with the tethered satellite 11 p1646 N85-20372
Development of Faraday cup onboard MS-T5 for solar wind measurements
[REPT-616] 12 p1794 N85-21256
Development and testing of a spacecraft surface potential monitor 13 p2007 N85-22582
Kovtunenko comments on Vega flight plan, instrumentation 15 p2482 N85-25318
French and West German equipment for Vega Project
16 p2722 N85-26805
Comparison of ERS-1 scatterometer Monte Carlo performance simulations using a weighted nonlinear least squares and a maximum likelihood estimation method
20 p3420 N85-31224
SAR swath widening techniques — satellite radar
[BL-6198] 20 p3441 N85-31358
Six mechanisms used on the SSM/1 radiometer
22 p3798 N85-33534

SATELLITE LAUNCHING
U SPACECRAFT LAUNCHING

SATELLITE LIFETIME
Satellite observations 01 p0013 N85-10083
Natural atmospheric reentry — satellite orbit decay
05 p0600 N85-13829
Natural reentry of satellites 14 p2397 N85-24774

SATELLITE MANEUVERS
U SPACECRAFT MANEUVERS

SATELLITE NAVIGATION SYSTEMS
Diagnosis and therapy of geodetic satellite networks of Doppler type — error analysis
[SER-C-293] 01 p0015 N85-10090
Satellite navigation
[S-HRG-98-856] 08 p1082 N85-16851
The Global Positioning System (GPS): Program status update 11 p1710 N85-20761
Program INNAVSAT: Global Positioning System (GPS): Test and demonstration program
[BMFT-FB-W-84-047] 12 p1776 N85-21145
Global positioning system: A modification to the baseline satellite constellation for improved geometric performance
[AD-A151692] 15 p2489 N85-25239
CPS navigation experiment using high precision GPS timing receivers 17 p2963 N85-28299
A review of tropospheric refraction effects on Earth-to-satellite systems 18 p3107 N85-29235

Using GPS and VLBI technology to maintain 14 digit synchronization 16 p3109 N85-29250

Allowance for differences in ellipsoids and geodetic control coordinate systems in determining ship's position using radio navigation systems 19 p3292 N85-30413

A study of the ESA-NAVSAT control segment
[ESA-CR(P)-2000] 20 p3398 N85-31079

The NAVSTAR Global Positioning System (GPS) receiver development program, phase 1
[BMFT-FB-W-85-002] 20 p3399 N85-31085

SATELLITE NETWORKS

Simple methods in very short-range forecasting based on data from a mesoscale network of automatic stations (ANETZ) and from satellite (Meteosat) and radar — Swiss Alps 01 p0082 N85-10548

SLIM TDMA ANIK B pilot project
[CRC-REPT-1366] 03 p0354 N85-12278

The NASA/JPL pilot ocean data system 03 p0361 N85-12433

Ongoing activities in the field of communication at DFVLR 04 p0459 N85-12913

APOLLO system requirements specification — electronic document delivery
[ESA-SP-1068] 04 p0494 N85-13150

The motion of the Earth by Doppler observing campaign (MEDOC) 05 p0601 N85-13831

Demand for satellite-provided domestic communications services up to the year 2000
[NASA-TM-86694] 06 p0798 N85-15099

Shipboard and satellite-aided communications equipment in exhibition 06 p0819 N85-15203

Satellite broadcasting: The performance of C-MAC in a hardware simulation of a DBS transmission chain
[BBC-RD-1984/9] 08 p1143 N85-17206

Experimental satellite system for determining coordinates of maritime distress 09 p1306 N85-18216

China's future domestic satellite communications systems 10 p1476 N85-19312

The Global Positioning System (GPS): Program status update 11 p1710 N85-20761

GPS system field testing 11 p1711 N85-20762

Coverage and buildup of the Navstar constellation 11 p1711 N85-20764

Tactical applications of GPS user equipment 11 p1711 N85-20765

Combat capable space systems for tactical support 11 p1713 N85-20775

Assessment of effectiveness of signal-code constructions in time division-multi-access satellite systems 13 p2066 N85-22906

Satellite bridges in communications networks 13 p2067 N85-22910

Onboard demand scheduling of a multibeam SS/TDMA satellite with integrated circuit and packet switching 14 p2229 N85-23812

The ARGOS system status report after 2 years operation 14 p2237 N85-23870

System performance, data distribution and technical files — ARGOS project 14 p2237 N85-23871

Applications of ARGOS data collection systems in Arctic regions 14 p2238 N85-23875

The ARGOS system and hydrology. Results obtained by ORSTROM and benefits of a degree of standardization 14 p2239 N85-23881

The ARGOS system status report 14 p2239 N85-23884

Operational experiences with the ARGOS system in oceanography and oil spill emergency planning. Future plans for the use of the ARGOS system as a component in offshore data collection system 14 p2239 N85-23887

The experience of the Swedish Meteorological and Hydrological Institute (SMHI) with the ARGOS system
[PM-U1/81] 14 p2240 N85-23892

Applications of ARGOS data collection system for automatic meteorological observatories in Arctic regions 14 p2240 N85-23893

Automatic weather stations in Antarctica 14 p2324 N85-24360

Automatic hydrological data collection facility using ARGOS 14 p2324 N85-24363

The ARGOS system after 3 years operation 14 p2325 N85-24368

The ARGOS contribution to the First GARP Global Experiment (FGGE) study of drifting buoys 14 p2325 N85-24371

The ARGOS communications performance trials 14 p2326 N85-24376

Miscellaneous ARGOS maritime applications — yacht races 14 p2327 N85-24383

The SARSAT program 14 p2327 N85-24385

Measurement of water equivalent of mountain snow cover — ARGOS system 14 p2327 N85-24386

Hydrology and climatic conditions in Greenland 14 p2327 N85-24387

The ARGOS system and hydrology: The use of Platform Terminal Transmitter (PTT) with built-in memory and direct reception by the Seine basin hydrology service 14 p2328 N85-24389

Direct readout and dissemination of results using ARGOS keypad terminals 14 p2328 N85-24390

Service ARGOS technical report and improvement 14 p2328 N85-24395

Antarctic automatic weather stations 14 p2329 N85-24397

Collecting meteorological reports with the ARGOS system 14 p2329 N85-24398

Telemetered meteorological and engineering data from a deep sea moored body in the Long Term Upper Ocean Study (LOTUS) 14 p2329 N85-24402

The ARGOS contribution to the demonstration of the effectiveness of a satellite-based search and rescue system 14 p2330 N85-24404

Drifting buoy development and future programs — Japanese ARGOS program 14 p2330 N85-24406

Data transmission using ARGOS keypad platform transmitter terminals (PTT) 14 p2330 N85-24407

Applications of ARGOS measurements in equatorial Pacific Ocean-atmosphere interaction studies 14 p2331 N85-24414

Overview of data processing at AES local user terminals — Canadian Atmospheric Environment Service (AES) 14 p2331 N85-24418

The SARSAT/COSPAS system for assisting satellite based search and rescue 14 p2398 N85-24776

Methods for cloud cover estimation 14 p2444 N85-25081

White paper on new international satellite systems
[PB85-162501] 16 p2775 N85-27127

Routine wave and meteorological measurements in offshore areas using ARGOS data surveillance 16 p2812 N85-27344

Present stage of utilization of the ARGOS system by the ORSTOM hydrological service for hydrometric data collection 16 p2813 N85-27348

The ARGOS system in Brazil — hydrology 16 p2813 N85-27349

A seismic ARGOS data collection platform 16 p2813 N85-27350

An operational buoy network collecting meteorological data 16 p2813 N85-27351

Operational experiences with the ARGOS system in Greenland 16 p2813 N85-27353

Personal mobile communications by satellite
[REPT-15-4572] 18 p3091 N85-29135

Study of a medium term flexible fixed satellite service mission
[DM51/CC-IM-0185.83] 18 p3091 N85-29136

Time transfer techniques: Historical overview, current practices and future capabilities 18 p3106 N85-29245

Satellite aided search and rescue. Experimental results and operational prospects — conference
[ISBN-2-85428-120-9] 20 p3400 N85-31088

INMARSAT: An overview 20 p3400 N85-31091

COSPAS/SARSAT: An overview 20 p3400 N85-31092

The contribution of an operational SAR satellite system to the UK SAR organisation — search and rescue (SAR) 20 p3400 N85-31095

The COSPAS-SARSAT system 20 p3401 N85-31101

The COSPAS-SARSAT space segment: Present status and evolution 20 p3401 N85-31102

The CCIR satellite EPIRB coordinated trials programme --- Emergency Position Indicating Radio Beacon (EPIRB); International Radio Consultative Committee (CCIR) 20 p3402 N85-31111

Navigation data for Emergency Position Indicating Radio Beacons (EPIRBs) 20 p3403 N85-31115

INMARSAT distress and safety communication 20 p3406 N85-31134

The development of an institutional structure for the Future Global Satellite System for Search and Rescue 20 p3406 N85-31138

Remote medical diagnosis 21 p3663 N85-32753

International prototype network in Dubna experimental satellite communications system 22 p3773 N85-33383

Pluribus satellite IMP (Interface Message Processors) development mobile access terminal network
[AD-A155754] 24 p4060 N85-35216

Second-generation mobile satellite system. A conceptual design and trade-off study
[NASA-CR-176195] 24 p4086 N85-35325

SATELLITE OBSERVATION

Exploratory investigation of the need for and feasibility of a Lower Atmosphere Research Satellite (LARS) program
[NASA-CR-171161] 01 p0016 N85-10031

Satellite reconnaissance
[AD-B065034] 01 p0015 N85-10[illegible]

The Marine Resources Experiment Program (MAREX)
[NASA-TM-87368] 01 p0086 N85-10[illegible]

Industrial use of land observation satellite systems 02 p0151 N85-110[illegible]

A proof-of-principle getaway special free-flying satellite demonstration 02 p0155 N85-110[illegible]

The feasibility of satellite remote sensing as a technique for evaluating coal mine surface features 02 p0213 N85-11401

A prospectus for Thematic Mapper research in the Earth sciences
[E85-10003] 02 p0215 N85-11416

A report on the training course at Fortaleza (Ceara)
[E85-10013] 02 p0216 N85-11426

Achievements in development of space meteorology 03 p0343 N85-12212

Earth Resources, A Continuing Bibliography with Indexes
[NASA-SP-7041(43)] 03 p0378 N85-12411

The structures and the role of an international agency for the control of satellites
[NASA-TM-76765] 03 p0441 N85-12[illegible]

Space observations of solar flares 04 p0519 N85-13313

Weather research program report; FY 1983
[PB84-236694] 04 p0541 N85-13446

A diagnostic approach to obtaining planetary boundary layer winds using satellite-derived thermal data 05 p0674 N85-14330

Spectral general circulation model development 05 p0679 N85-14[illegible]

Applications of sequential estimation to numerical weather prediction 05 p0681 N85-14374

Investigation of satellite measurements in the presence of clouds, forcing influences on clouds and feedback to the large scale following convection 05 p0682 N85-14381

The use of available potential energy to evaluate two GLAS FGGE data sets 05 p0682 N85-14387

Energy diagnostics and impact studies of FGGE global data sets and GLAS GCM simulations 05 p0683 N85-14390

Numerical prediction of the president's day cyclone 05 p0684 N85-14396

Rain volume estimation over areas using satellite and radar data 05 p0686 N85-14406

Mixed layers and satellite retrievals 05 p0686 N85-14411

Autoregressive spectral estimation for two dimensional time series 07 p0985 N85-16258

Remote sensing of the high latitude ionosphere
[AD-A147881] 07 p1008 N85-16405

Testing of a field portable GPS (Global Positioning System) geodetic receiver
[AD-A148336] 08 p1082 N85-16859

North American vegetation patterns observed with the NOAA-7 advanced very high resolution radiometer — North America
[E85-10062] 08 p1174 N85-17400

Solitons and SEASAT
[AD-A148398] 08 p1176 N85-17414

Satellite stratospheric aerosol measurement validation
[NASA-TM-86003] 08 p1187 N85-17479

Earth resources: A continuing bibliography with indexes
[NASA-SP-7041(44)] 10 p1503 N85-19484

Remote sensing activities in Latin America
[INPE-3297-PRE/612] 10 p1506 N85-19501

The effect of the arbitrary level assignment of satellite cloud motion wind vectors on wind analyses in the pre-thunderstorm environment
[NASA-TM-86186] 10 p1517 N85-19555

Rain volume estimation over areas using satellite and radar data
[NASA-CR-174434] 10 p1518 N85-19566

Cut-off lows and their influence on the weather in Switzerland
[REPT-45] 10 p1519 N85-19574

Preserve the sense of Earth from space — achieve of remote sensing data
[PB85-124121] 11 p1740 N85-20942

Evaluating accuracy in determining position of Earth's center of mass and elements of orientation of geodetic coordinate system 13 p1983 N85-22441

New method of reconstructing conditions of recent differentiation of oil and gas in the Amudarya Basin (based on results of interpretation of space photographs) 13 p1984 N85-22446

T anomaly field data of the crustal properties
a
0] 13 p2122 N85-23215
od for estimating soil moisture availability
R-175806] 13 p2126 N85-23238
gement concerns for satellite-based air traffic
urveillance systems 14 p2230 N85-23816
ment to evaluation of satellite derived estimates
adiation
86] 14 p2346 N85-24506
tion of satellite derived estimates of solar
987] 14 p2346 N85-24507
tional mesoscale satellite data assimilation and
ion
CR-175704] 14 p2378 N85-24680
fic experiments. Preprocessing of scientific
spaceborne experiments
14 p2396 N85-24779
ods for cloud cover estimation
14 p2444 N85-25061
ce radiation monitor observations from Salyut-4
tation 15 p2482 N85-25317
minary processing of laser ranging data from
OS artificial Earth satellite during short merit program
ation period 15 p2488 N85-25355
ORTRAN program for deep space sensor analysis
151700] 15 p2489 N85-25366
oscale Atmospheric Processes Research Program
e Review
A-TM-87465] 15 p2594 N85-25967
icane structure and dynamics from stereoscopic and
d satellite observations and radar data
15 p2594 N85-25968
itoring tropical cyclone growth using GOES
R/VAS and Nimbus-7 TOMS data
15 p2595 N85-25969
ration of satellite data in mesoscale modeling of
e weather 15 p2597 N85-26007
ee-dimensional/perspective display techniques for
orological data sets 15 p2599 N85-26018
ng-term observations of Cyg X-3 with Vela 5B
5-005556] 15 p2686 N85-26586
ar-to-year variability of components of Earth's
ation budget according to satellite measurement
16 p2725 N85-26821
avity model development software status
16 p2804 N85-27289
mospheric frontal zone studies
SA-CR-175293] 16 p2833 N85-27469
lar activity monitoring satellite (SAMSAT): Impact on
e environment services
95-165066] 16 p2868 N85-27818
search Review, 1983
SA-TM-86219] 18 p3139 N85-29433
ilization of satellite data and regional scale numerical
els in short range weather forecasting
SA-CR-175960] 19 p3314 N85-30545
agnosis of vertical motions from VAS retrievals during
nvective outbreak
SA-CR-171569] 19 p3316 N85-30554
ecipitation estimation using collocated GOES satellite
surface data
-A154248] 19 p3317 N85-30559
nproving the geological interpretation of magnetic and
ity satellite anomalies
5-10103] 20 p3473 N85-31585
eologic analysis of averaged magnetic satellite
malies 20 p3474 N85-31588
tatistical magnetic anomalies from satellite
asurements for geologic analysis
20 p3474 N85-31589
inning of satellite magnetic anomalies
20 p3474 N85-31590
Continental and oceanic magnetic anomalies:
hancement through GRM 20 p3476 N85-31598
Results of the MIZEX preliminary campaign: 29 June
19 July 1983 — Marginal Ice Zone Experiment (MIZEX),
ellite observation
NES-84/142/T/CT/DRT/TIT/RL]
20 p3478 N85-31609
Structure of the distant geotail: ISEE-3 observations
20 p3488 N85-31678
Geophysical interpretation of satellite laser ranging
asurements 20 p3490 N85-31692
New optical satellite data 20 p3492 N85-31705
NASA/GSFC TOPEX gravity model operations group
20 p3492 N85-31709
Ocean circulation studies 20 p3492 N85-31712
Ocean tidal parameters from LAGEOS
20 p3493 N85-31716
Tropical Ocean and Global Atmosphere (TOGA) heat
xchange project: A summary report
NASA-CR-176038] 20 p3496 N85-31738

Space optics
[CNES-84/105/T/CT/DRT/TIT/10]
20 p3533 N85-31985
Radio counterparts of galactic gamma-ray sources
20 p3549 N85-32085
Doppler satellite data characteristics
[AD-A154868] 21 p3575 N85-32231
Use of the synoptic view: Examples from Earth and other planets 21 p3602 N85-32371
Rain volume estimation over areas using satellite and radar data
[NASA-CR-176050] 21 p3634 N85-32570
Parameter estimation in communication system tracking satellite observations
[AD-A155137] 21 p3636 N85-32582
Large-scale sea surface temperature variability from satellite and shipboard measurements
[NASA-CR-176123] 22 p3818 N85-33651
Method and apparatus for Delta Kappa synthetic aperture radar measurement of ocean current
[NASA-CASE-NPO-15704-1] 23 p3925 N85-34327
Target observability for satellite-based sensors
[AD-A156139] 24 p4069 N85-35217
Remote sensing of hydrologic transport processes using spot simulation data
[DE85-012412] 24 p4108 N85-35467
Two-dimensional quasineutral description of particles and fields above discrete auroral arcs
[NASA-CR-176170] 24 p4116 N85-35517
Mean cloudiness over the global tropics from satellite observations
[AD-A156188] 24 p4123 N85-35561
SATELLITE ORBIT CALCULATION
U ORBIT CALCULATION
SATELLITE ORBITS
NT GEOSYNCHRONOUS ORBITS
NT PARKING ORBITS
NT POLAR ORBITS
NT STATIONARY ORBITS
Geopotential harmonics of order 15 and 30, from analysis of the orbit of satellite 1971-10B
[RAE-TR-84006] 02 p0165 N85-11121
Satellite motion: Lectures and exercises on space mechanics
[ISBN-2-85428-114-4] 05 p0598 N85-13607
Keplerian and perturbed motion — satellite motion
05 p0598 N85-13608
Orbit extrapolation — satellite orbits
05 p0598 N85-13611
Measurements in satellite orbit tracing
05 p0598 N85-13612
Satellite orbit determination 05 p0598 N85-13613
The satellite maneuvers determination department
05 p0599 N85-13620
The operational orbit tracking center
05 p0599 N85-13621
Heliosynchronism and phasing. Application to the SPOT orbit 05 p0600 N85-13826
Choice of orbit for scientific satellites: SIGMA, the submillimeter telescope — Ariane-borne gamma imagery satellite (SIGMA) 05 p0600 N85-13828
The Search And Rescue Satellite Aided Tracking (SARSAT) experiment. Presentation of CNES processing for the SARGOS project: Context and orbit processing
05 p0600 N85-13830
Spatial mechanics formulas and exercises
05 p0601 N85-13832
Individual geopotential coefficients of order 15 and 30, from resonant satellite orbits
[AD-A148687] 06 p0826 N85-15256
Thermal and cryogenic design study for space infrared telescope facility (SIRTF)
[NASA-CR-166613] 07 p0915 N85-15793
Individual geopotential coefficients of order 15 and 30, from resonant satellite orbits
[RAE-TR-84021] 08 p1105 N85-16985
Altimetry, orbits and tides
[E85-10066] 08 p1174 N85-17404
Theory of the orbital motion of an artificial Earth Satellite
[NAL-TR-807] 09 p1285 N85-18075
The determination of the post-Newtonian parameters in gravitational theory using laser ranging to the Lageos satellite 09 p1414 N85-18924
A modeling analysis program for the JPL table mountain Io sodium cloud data
[NASA-CR-175474] 10 p1572 N85-19910
Tactical military communications by satellite relay at high latitudes 11 p1709 N85-20756
Proposed preliminary design criteria model environment for the 1990's 12 p1784 N85-21194
Transmission and orbital constraints in space-related programs: Briefing summary 12 p1787 N85-21216
Air Force satellite position management
12 p1787 N85-21217

Engineering calculations for communications satellite systems planning
[NASA-CR-175552] 12 p1789 N85-21233
Nontraditional method for determining unperturbed orbits of unknown space objects using incomplete optical observational data 13 p1979 N85-22417
Satellite oscillations in elliptical orbit
13 p1981 N85-22429
Satellite-to-satellite orbit determination using minimum, discrete range and range-rate data only
13 p1985 N85-22458
Method for determining the number of correlative measurements required to validate the SBUV/2 ozone retrievals 13 p2105 N85-23114
Small solar system bodies 13 p2175 N85-23499
Motion of satellite with total dynamic symmetry around rotating aspherical Earth 14 p2287 N85-24174
Space Mathematics for the Preparation and Development of satellite Exploitation
[ISBN-2-85428-115-2] 14 p2395 N85-24753
Orbit perturbation. Extrapolation of perturbed orbits
14 p2396 N85-24763
Orbit reconstitution — satellite orbits
14 p2396 N85-24765
COSPAS-SARSAT satellite orbit predictor, volume 5
[NASA-TM-85015-VOL-5] 14 p2439 N85-25052
Global positioning system: A modification to the baseline satellite constellation for improved geometric performance
[AD-A151692] 15 p2469 N85-25239
Some numerical estimates of perturbation of orbital elements of artificial Earth satellite with total dynamic symmetry about rotating aspherical Earth
15 p2478 N85-25294
Use of atmospheric models in predicting artificial Earth satellite motion 15 p2478 N85-25296
Using velocity vector in determining Keplerian orbit of geodectic satellite 15 p2478 N85-25297
Minimax problem of estimating trajectory parameters in continuous formulation 15 p2479 N85-25301
Construction of conditionally periodic solutions of problem of reciprocating motion of axially symmetric satellite of triaxial planet 15 p2480 N85-25304
List of recent Soviet space launches
15 p2489 N85-25361
Statistical regularization methods in problem of navigational determination of space vehicle orbits
16 p2719 N85-26784
Satellite physical and orbital characteristics
16 p2804 N85-27287
Radial orbit error spectrum for Topex
16 p2805 N85-27292
Analytical generation of satellite orbits at the RAE (Royal Aircraft Establishment)
[AD-A152655] 17 p3053 N85-28901
An introduction to satellite orbits
[RAE-TM-SPACE-344] 20 p3397 N85-31076
Update on the evolution of the LAGEOS orbit
20 p3491 N85-31698
Error spectrum of Goddard satellite models for the gravity field 20 p3491 N85-31704
New optical satellite data 20 p3492 N85-31705
Optical best arc RMS test results
20 p3492 N85-31706
Spacecraft-aided research discussed at geology Congress 22 p3734 N85-33147
SATELLITE ORIENTATION
Attitude measurements and determination
14 p2397 N85-24767
Consummative expressions for satellite drag perturbations in a spherically symmetrical atmosphere
[AD-A154230] 19 p3222 N85-29981
Doppler satellite data characteristics
[AD-A154868] 21 p3575 N85-32231
SATELLITE PERTURBATION
Periodic oscillation of gyrostat-satellite about its center of mass in an elliptical orbit 02 p0159 N85-11080
Keplerian and perturbed motion — satellite motion
05 p0598 N85-13608
Orbit perturbation — satellites
05 p0598 N85-13610
Perturbations in geostationary orbit
05 p0600 N85-13824
Spatial mechanics formulas and exercises
05 p0601 N85-13832
Theory of the orbital motion of an artificial Earth Satellite
[NAL-TR-807] 09 p1285 N85-18075
Approximate perturbing part of geopotential by polynomials of stipulated form 13 p1984 N85-22448
Orbit perturbation. Extrapolation of perturbed orbits
14 p2396 N85-24763
Some numerical estimates of perturbation of orbital elements of artificial Earth satellite with total dynamic symmetry about rotating aspherical Earth
15 p2478 N85-25294

Application of perturbation theory to problem in orbital theory 15 p2537 N85-25656
Accuracy in predicting orbital motion of artificial Earth satellite 16 p2720 N85-26793
Satellite selection criteria 16 p2804 N85-27288
The study of the physics of cometary nuclei [NASA-CR-175817] 17 p3054 N85-28905
Consummative expressions for satellite drag perturbations in a spherically symmetrical atmosphere [AD-A154230] 19 p3222 N85-29981
Investigation of dynamic noise affecting geodynamics information in a tethered subsatellite [NASA-CR-176031] 20 p3476 N85-31602
Spaceborne gradiometer error analysis 20 p3492 N85-31707

SATELLITE RENDEZVOUS
U ORBITAL RENDEZVOUS

SATELLITE ROTATION
Rapid nonresonant rotation of a spacecraft in nominally periodic orbits in limited 3 body problem 02 p0160 N85-11083
Magnetic spin reduction system for free spinning objects [NASA-CASE-MFS-25966-1] 02 p0166 N85-11122
Development of Faraday cup onboard MS-T5 for solar wind measurements [REPT-616] 12 p1794 N85-21255
Non-contacting electromagnetic de-spin system for Earth orbiting satellites 12 p1946 N85-22225
Motion of symmetrical satellite with flexible viscoelastic rods about center of mass in circular orbit 13 p1979 N85-22420
Rotational motion of a satellite 13 p1981 N85-22428
Electric field effects on ion currents in satellite wakes 13 p1991 N85-22485
Patterns of fracture and tidal stresses due to nonsynchronous rotation: Implications for fracturing on Europa 13 p2173 N85-23483
Resonant rotations of satellite in polar orbit in magnetic and gravitational fields 15 p2479 N85-25302
The investigation of tethered satellite system dynamics [NASA-CR-171433] 15 p2492 N85-25375
Investigation of dynamic noise affecting geodynamics information in a tethered subsatellite [NASA-CR-176031] 20 p3476 N85-31602

SATELLITE SOUNDING
The past, present, and anticipated future contributions of geosynchronous satellites to short range prediction 01 p0076 N85-10503
Use of satellite soundings and imagery for nowcasting and very-short-range forecasting 01 p0076 N85-10504
Variation of fast charged particles in event of 22 November 1977 based on Cosmos-900 satellite data 02 p0161 N85-11092
International banking of satellite and in-situ wave data by the Marine Information and Advisory Services (MIAS) 03 p0381 N85-12434
Water vapor profile retrievals from the HIRS/MSU satellite sounder 05 p0661 N85-14378
Applications of TOMS ozone data and clustering techniques in satellite soundings 05 p0661 N85-14379
Fidelity of satellite soundings 05 p0662 N85-14383
Actual altitudes of radioacoustic sounding in decimeter wavelength band 06 p0826 N85-15243
Convective scale weather analysis and forecasting [NASA-CR-174185] 06 p0836 N85-15320
Environmental satellites 14 p2328 N85-24392
VLF wave-particle interaction experiments by EXOS-B/Siple station transmissions 14 p2366 N85-24622
Advances in magnetospheric plasma diagnosis by active experiments — IMS satellites 14 p2371 N85-24654
Technical development to improve satellite sounding over radiatively complex terrain [NASA-CR-175746] 15 p2583 N85-25829
Substorms in energetic radiation belt particles according to data from Meteor artificial Earth satellite 16 p2719 N85-26786
Determining effective rate of plasma heating in outer equatorial ionosphere using data from ISIS-1 and ISIS-2 satellites 16 p2721 N85-26797
The validation of sea surface temperatures determined from AVHRR data using in situ data recovered via system ARGOS 16 p2812 N85-27342
Assessment of VAS soundings in the analysis of a preconvective environment [NASA-TM-86205] 16 p2825 N85-27427
Remote sensing of the plasma with time delay measurements (coronal sounding) 16 p2886 N85-27804
Applications of fuzzy set theory to satellite soundings 18 p3141 N85-29445
Applications of some artificial intelligence methods to satellite soundings 18 p3141 N85-29446
Utilization of satellite data and regional scale numerical models in short range weather forecasting [NASA-CR-175980] 19 p3314 N85-30545
Observations of low energy magnetospheric plasma outside the plasmasphere [KGI-PREPRINT-075] 20 p3536 N85-32004

SATELLITE SURFACES
The rheology of icy satellites [NASA-CR-174024] 02 p0302 N85-11959
The violet absorber on Io: Disulfur monoxide derivatives 13 p2173 N85-23482
Polar cap formation on Ganymede 13 p2174 N85-23486
Interaction of the magnetospheric ions with the surfaces of the icy satellites of Saturn 13 p2174 N85-23491
Plasma production by meteoroid impact 13 p2174 N85-23492
Ripple ring basins on Ganymede and Callisto 13 p2183 N85-23547
Permafrost and subsurface ice in the solar system 13 p2191 N85-23594
Planetary analogs in Antarctica: Icy satellites 13 p2193 N85-23605
The geomorphology of Rhea 13 p2193 N85-23606
Io: Precise comparison of Voyager spectral curves with laboratory measurements 13 p2196 N85-23619
Photometric analysis of Jupiter-illuminated images of Io 13 p2196 N85-23620
Spectral units on Europa and Ganymede 13 p2196 N85-23621
Fault offsets and lateral crustal movement on Europa 13 p2201 N85-23656
Lineaments on Ganymede: New evidence for late tectonic activity 13 p2202 N85-23658
Global tectonics on Ganymede 13 p2202 N85-23659
Tectonics of the Galileo Regio on Ganymede 13 p2202 N85-23660
Importance of the tectonic motions on Ganymede 13 p2202 N85-23661
Tectonics of the Valhalla structure on Callisto 13 p2202 N85-23662
The Galilean Satellite Geological Mapping Program, 1984 13 p2203 N85-23664
Geology of the Ganymede quadrangle Jg7 13 p2203 N85-23665
Voyager cartography 13 p2203 N85-23668
Jupiter/Voyager data analysis [NASA-CR-175723] 15 p2679 N85-26545

SATELLITE TELEVISION
Technology and performances of structural thermal mechanical equipment used for antenna of TV.SAT-TDF 1 program 05 p0626 N85-14012
Activities of Istituto Elettrotecnico Nazionale Galileo Ferraris 18 p3199 N85-29845

SATELLITE TEMPERATURE
Space environment simulation to test satellite thermal control coatings, volume 1 [CERT-4128-VOL-1] 06 p1109 N85-17012
Space environment simulation to test satellite thermal control coatings. Volume 2: Annex 1 [ESA-CR(P)-1870-VOL-2] 06 p1109 N85-17013
Space environment simulation to test satellite thermal control coatings. Volume 2: Annexes 2, 3, 4 [ESA-CR(P)-1870-VOL-3] 06 p1109 N85-17014
On the improvement of satellite temperature retrievals by means of boundary layer models 18 p3140 N85-29443

SATELLITE TRACKING
Tracking requirements for precise ERS-1 orbit determination 03 p0380 N85-12431
Measurements in satellite orbit tracing 05 p0598 N85-13812
The 2 GHz network and the network operations center — satellite tracking 05 p0599 N85-13817
The operational orbit tracking center 05 p0599 N85-13821
Development of the TT and C station equipment at INPE [INPE-3327-PRE/625] 10 p1427 N85-18999
Orbital Debris [NASA-CP-2360] 12 p1783 N85-21188
NCRAD operational system 12 p1783 N85-21189
History of satellite break-ups in space 12 p1783 N85-21190
Geosynchronous satellite collision avoidance 12 p1784 N85-21197
China report: Science and technology [JPRS-CST-85-005] 13 p2052 N85-22843
Development, prospect of satellite dynamics discussed 13 p2052 N85-22847
Proceedings of the ARGOS Users Conference on Data Collection and Location by Satellite 14 p2322 N85-24348
One thousand days in the brine — platform transmitter terminals 14 p2324 N85-24359
Tracking pelagic dolphins by satellite 14 p2324 N85-24364
Polar bear telemetry results from the Nimbus-6 system 14 p2325 N85-24385
Data Collection and Platform Location by Satellite: ARGOS users' Conference 14 p2328 N85-24391
US programs using the ARGOS data collection and platform location system 14 p2329 N85-24401
Tracking whale migrations with the ARGOS satellite system 14 p2330 N85-24403
Data Collection and Platform Location by Satellite: ARGOS Users' Conference 14 p2330 N85-24409
US program using the ARGOS data collection and platform location system 14 p2330 N85-24410
Arabian gulf circulation — pollution monitoring 14 p2331 N85-24412
Drifting buoys on the Labrador shelf 14 p2331 N85-24415
Some methods of computing platform transmitter terminal location estimates — ARGOS system; whale tracking 14 p2332 N85-24420
The ARGOS system used for tracking gray whales 14 p2332 N85-24421
The MEDOC 2: Experimental Doppler measurement of Earth kinematics 14 p2399 N85-24798
Data Collection and Platform Location by Satellite: ARGOS Users' Conference 16 p2811 N85-27333
Long term drifting float for measuring mean oceanic circulation using ARGOS system 16 p2811 N85-27339
Results of an initial trial of a satellite telemetering buoy measuring near surface current 16 p2812 N85-27345
The ARGOS system used for tracking gray whales 16 p2812 N85-27347
A new precision time and frequency source for stationary PTTI applications 17 p2963 N85-28297
CPS navigation experiment using high precision GPS timing receivers 17 p2963 N85-28299
International time transfer and portable clock evaluation using GPS timing receivers: Preliminary results 17 p2964 N85-28303
Maintenance of time and frequency in the Jet Propulsion Laboratory's Deep Space Network using the Global Positioning System 18 p3109 N85-29249
Fault tolerant multiprocessor SARSAT-COSPAS 406 MHz local user terminal 20 p3404 N85-31123
Optical best arc RMS test results 20 p3492 N85-31706
United States-Soviet satellite accord: SARSAT/Cospas search-and-rescue program [GPO-41-113] 20 p3541 N85-32040
Interplanetary plasma turbulence and the Doppler detection of a gravitational background radiation [IFSI-85-1] 20 p3546 N85-32098
A derivation of relativistic effects in satellite tracking [AD-A154620] 21 p3558 N85-32132

SATELLITE TRANSMISSION
Ongoing activities in the field of communication at DFVLR 04 p0459 N85-12913
Television transmission in frequency modulation 04 p0493 N85-13146
A transmission analysis for the use of 2-4 PSK modulation in satellite broadcasting [ESA-STM-231] 04 p0494 N85-13151
Satellite broadcasting: The performance of C-MAC in a hardware simulation of a DBS transmission chain [BBC-RD-1984/9] 08 p1143 N85-17206
Study of factors affecting an HF/VHF direct broadcasting satellite service [PB85-120889/GAR] 09 p1313 N85-18256
Equatorial transionospheric propagation conditions affecting digital communications 10 p1470 N85-19275
Propagation effects on the Doppler frequency shift of satellite transmissions 10 p1470 N85-19276
A technical solution to fadings in tactical satellite digital transmissions 10 p1473 N85-19297
China's domestic satellite communications 10 p1476 N85-19313
Satellite-computer interface 10 p1476 N85-19319
Development of a 20 GHz modulator for the payload of a satellite for propagation and transmission experiments including the required converters of the test equipment [BMFT-FB-W-84-044] 11 p1590 N85-20004
The Ferranti Tactical SHF SATCOM station (MANSAT) 11 p1710 N85-20759
Tactical satellite terminals for land and airborne C3 applications 11 p1710 N85-20760
Coverage and buildup of the Navstar constellation 11 p1711 N85-20764

Tactical applications of GPS user equipment
11 p1711 N85-20765
Brussels Satellite Convention
EXEC-REPT-98-52] 12 p1790 N85-21234
Assessment of effectiveness of signal-code nstructions in time division-multi-access satellite stems
13 p2066 N85-22906
Satellite bridges in communications networks
13 p2067 N85-22910
Development of TV systems for spacecraft
15 p2484 N85-25332
Propagation considerations in land mobile satellite ansmission
NASA-CR-175733] 15 p2540 N85-25684
SESC (Space Environment Services Center) satellite oadcasting 10-year plan
[PB85-163541] 16 p2775 N85-27126
Station for in-orbit testing of satellites
[MBB-UR-708/84-O] 16 p2874 N85-27733
Time synchronization experiments with APPLE
17 p2967 N85-28323
Preliminary investigation of the performance of repeater technology for satellite sound broadcasting
[SSP/017/82] 18 p3092 N85-29137
Nonlinear plasma reactions on the antenna impedance of high transmission power satellites
[BMFT-FB-W-84-053] 18 p3192 N85-29799
Radiometry: A useful prediction tool — atmospheric attenuation
[ESA-SP-1071] 20 p3399 N85-31084
Modulation using four phase levels. Theoretical study of the degradation caused by a spurious phase modulation
[CNES-83/219/CT/DRT/TIT/TR]
20 p3441 N85-31360
Study of a limited band signal transmission chain
[CNES-CT/DRT/TIT/TR-83/221]
20 p3442 N85-31361
Adaptive antenna arrays for satellite communications: Design and testing
[NASA-CR-176162] 23 p3926 N85-34329

SATELLITE-BORNE INSTRUMENTS
Periodic oscillation of gyrostat-satellite about its center of mass in an elliptical orbit 02 p0159 N85-11080
The ESA remote sensing satellite system (ERS-1)
03 p0379 N85-12420
The ERS-1 radar altimeter: An overview
03 p0379 N85-12421
The ERS-1 radar altimeter instrument
03 p0379 N85-12422
Wind speed determination from radar altimeters
03 p0380 N85-12424
Ocean wave parameters extraction using satellite short-pulse radar altimeters 03 p0380 N85-12425
The use of altimeter data for sea state forecasting
03 p0380 N85-12426
The impact of satellite altimeter data on wave research 03 p0380 N85-12427
Cryospheric data products available through satellite altimetry 03 p0380 N85-12428
Special difficulties of retrieving surface elevation over continental ice — satellite radar altimetry
03 p0380 N85-12429
Requirements and special problems of land altimetry — satellite altimetry 03 p0380 N85-12430
ERS-1 altimeter ground segment relations to other sensors and programs 03 p0381 N85-12436
Satellite altimetry for sea-surfacing topography determination and geoid improvement
03 p0382 N85-12444
Satellite altimetric measurements of lake levels
03 p0383 N85-12447
Modelling of altimeter tracking over topographical surfaces — satellite antennas 03 p0383 N85-12450
ERS-1 radar altimeter system performance evaluation and calibration 03 p0383 N85-12451
The POSEIDON altimeter description
03 p0383 N85-12454
Standardization of data formats for radar altimeter data 03 p0384 N85-12455
Calibration and validation areas — satellite altimeters
03 p0384 N85-12456
Feasibility study of a satellite-borne 90 GHz radiometer 04 p0459 N85-12914
Launch summary for 1978 - 1982 — sounding rockets, space probes, and satellites
[NASA-TM-87375] 04 p0461 N85-12924
Conceptual ideas for a second generation METEOSAT system 05 p0658 N85-14228
Spaceborne microwave radiometers: Background and technology requirements
[LD-R-267] 08 p1165 N85-17350
Development of a 20 GHz modulator for the payload of a satellite for propagation and transmission experiments, including the required converters of the test equipment
[BMFT-FB-W-84-044] 11 p1590 N85-20004
MAP-related activities in the United States
11 p1655 N85-20427
UK Skynet 4 communications satellites
11 p1710 N85-20757
The multi-anode microchannel array detector system: Current status and future prospects
11 p1761 N85-21080
Method of measuring sea surface water temperature with a satellite including wideband passive synthetic-aperture multichannel receiver
[NASA-CASE-NPO-15651-1] 12 p1869 N85-21723
Spatial resolution estimation of LANDSAT-4 Thematic Mapper data 12 p1872 N85-21741
On the P1 data from GMS-SEM
12 p1894 N85-21690
Dielectric detector device for registering heavy cosmic radiation particles 13 p2045 N85-22799
Scientific requirements for ozone measurements
13 p2105 N85-23113
Results of the Langmuir-probe experiment on board Intercosmos-18 — ionosphere-magnetosphere interaction 14 p2362 N85-24596
Optic's institute's development of equipment for comet probe 15 p2484 N85-25333
Development of algorithms for using satellite meteorological data sets to study global transport of stratospheric aerosols and ozone
[NASA-CR-172540] 15 p2591 N85-25974
Satellite detection of severe thunderstorms
15 p2596 N85-25996
Severe storm detection with passive 37 GHz observations 15 p2596 N85-25997
Soil moisture and evapotranspiration estimates based on satellite data 15 p2596 N85-25998
Estimation of convective rainfall from visible and infrared satellite data 15 p2596 N85-25999
Mesoscale analysis and modeling group
15 p2596 N85-26001
Carbon foil secondary electron emission during ion passage through the 40 to 500 keV energy field
[MPE-190] 18 p3184 N85-29747
Some design considerations for a satellite-borne magnetograph 18 p3204 N85-29879
Poseidon altimeter: Study of the hyperfrequency section and specifications of the prototype components
[CNES-84/DRT/TIT/HY/T/145]
20 p3419 N85-31219
Solid state altimeter model: Simulation description; analysis of first results (narrow band filters, weighting) — satellite-borne instruments
[CNES-DRT/TIT/RL-160-T] 20 p3419 N85-31220
Preliminary investigations concerning a 90 GHz radiometer satellite experiment
[ESA-TT-860] 20 p3420 N85-31225
Spacecraft-aided research discussed at geology Congress 22 p3734 N85-33147
SONTRAC: A solar neutron track chamber detector
[SH-9.1-12] 23 p4052 N85-35127
Measurement of low energy cosmic rays aboard Spacelab-1
[SH-10.1-6] 23 p4053 N85-35137

SATELLITE-BORNE PHOTOGRAPHY
Use of satellite soundings and imagery for nowcasting and very-short-range forecasting
01 p0076 N85-10504
Method for interpreting soil cover of flowed fields using spectral brightnesses measured from space photographs
02 p0164 N85-11112
Economic evaluation of space survey materials use in land improvement engineering field work
02 p0165 N85-11115
Methods for determining atmospheric optical parameters using results of space survey of Earth's surface
02 p0165 N85-11117
Methods for correlating geological, geochemical and geophysical data with satellite imagery in central Ireland
05 p0655 N85-14206
Use of photographs of meteorologic satellites in synoptic analysis
[SESIT-5] 05 p0679 N85-14357
Evaluating accuracy in orientation of topographic photograph and satellite-centered direction from star photograph 13 p1983 N85-22442
New method of reconstructing conditions of recent differentiation of oil and gas in the Amudarya Basin (based on results of interpretation of space photographs)
13 p1984 N85-22446
One aspect of determination of direction of space survey base from photographs of planetary surface and star sky
15 p2487 N85-25352
Minimizing influence of Earth's curvature in projective rectification of space photographs into photoplans and photomaps 16 p2727 N85-26829
First results of oceanography utilization of infrared high resolution picture transmission images
[KNMI-TR-59] 18 p3151 N85-29511
Spacecraft-aided research discussed at geology Congress 22 p3734 N85-33147
Landscape interpretation capabilities using space photographs of regions of a multistage platform mantle structure 22 p3734 N85-33151
Surface cyclogenesis as indicated by satellite imagery
[PB85-191815] 24 p4124 N85-35586

SATELLITE-BORNE RADAR
Terrestrial locating — of buoys from space
05 p0599 N85-13816
Earth resources research using the Shuttle Imaging Radar system 11 p1713 N85-20779
Synthetic aperture radar data processing — satellite-borne radar
[CNES-196-T-CT/DRT/TIT/RL]
20 p3442 N85-31363
Digital signal processing for spaceborne synthetic aperture radar
[FOA-C-30361-E1] 20 p3442 N85-31364

SATELLITES
NT AERONAUTICAL SATELLITES
NT AEROS SATELLITE
NT ALOUETTE 2 SATELLITE
NT ANIK SATELLITES
NT ARABSAT
NT ARTIFICIAL SATELLITES
NT ASTRONOMICAL SATELLITES
NT ATS
NT BIOSATELLITES
NT CALLISTO
NT CHARON
NT COMMUNICATION SATELLITES
NT COMMUNICATIONS TECHNOLOGY SATELLITE
NT COS-B SATELLITE
NT COSMOS SATELLITES
NT COSMOS 936 SATELLITE
NT COSMOS 1129 SATELLITE
NT COSPAS
NT DEIMOS
NT DMSP SATELLITES
NT DYNAMICS EXPLORER 1 SATELLITE
NT ENCELADUS
NT EOSS
NT ERS-1 (ESA SATELLITE)
NT EUROPA
NT EUROPEAN COMMUNICATIONS SATELLITE
NT EXOSAT SATELLITE
NT EXPLORER SATELLITES
NT EXPLORER 10 SATELLITE
NT EXPLORER 43 SATELLITE
NT EXPLORER 46 SATELLITE
NT EXPLORER 50 SATELLITE
NT EXPLORER 51 SATELLITE
NT EXTREME ULTRAVIOLET EXPLORER SATELLITE
NT FAR UV SPECTROSCOPIC EXPLORER
NT GALILEAN SATELLITES
NT GANYMEDE
NT GEODETIC SATELLITES
NT GEOPHYSICAL SATELLITES
NT GEOS SATELLITES (ESA)
NT GEOS 1 SATELLITE
NT GEOS 2 SATELLITE
NT GEOS 3 SATELLITE
NT GOES SATELLITES
NT GOES 5
NT GRAVITY GRADIENT SATELLITES
NT HEAO 1
NT HEAO 2
NT HEAO 3
NT HELIOS SATELLITES
NT HELIOS 1
NT HELIOS 2
NT HEOS B SATELLITE
NT HUBBLE SPACE TELESCOPE
NT IMP
NT INFRARED ASTRONOMY SATELLITE
NT INTELSAT SATELLITES
NT INTERCOSMOS SATELLITES
NT INTERNATIONAL SUN EARTH EXPLORER 1
NT INTERNATIONAL SUN EARTH EXPLORER 2
NT INTERNATIONAL SUN EARTH EXPLORER 3
NT INTERNATIONAL SUN EARTH EXPLORERS
NT IO
NT ISIS SATELLITES
NT IUE
NT JUPITER SATELLITES
NT L-SAT
NT LAGEOS (SATELLITE)
NT LANDSAT SATELLITES
NT LANDSAT 1
NT LANDSAT 4
NT LANDSAT 5
NT LONG DURATION EXPOSURE FACILITY
NT LUNAR SATELLITES
NT MAGSAT SATELLITES
NT MARISAT SATELLITES

NT MARITIME SATELLITES
NT METEOROLOGICAL SATELLITES
NT METEOSAT SATELLITE
NT MIRANDA SATELLITE
NT MOON
NT MULTISPECTRAL RESOURCE SAMPLER
NT NATURAL SATELLITES
NT NAVIGATION SATELLITES
NT NAVSTAR SATELLITES
NT NIMBUS SATELLITES
NT NIMBUS 5 SATELLITE
NT NIMBUS 7 SATELLITE
NT NOAA SATELLITES
NT NOAA 6 SATELLITE
NT NOAA 7 SATELLITE
NT NOAA 8 SATELLITE
NT OAO 3
NT OGO
NT ORBITAL SPACE STATIONS
NT OTS (ESA)
NT PASSIVE SATELLITES
NT PROGNOZ SATELLITES
NT QUASAT
NT ROSAT MISSION
NT SAGE SATELLITE
NT SARSAT
NT SATURN SATELLITES
NT SCATHA SATELLITE
NT SCIENTIFIC SATELLITES
NT SEASAT SATELLITES
NT SEASAT 1
NT SIRIO SATELLITE
NT SIRS B SATELLITE
NT SKYNET SATELLITES
NT SOLAR MESOSPHERE EXPLORER
NT SOLAR POWER SATELLITES
NT SPACE INFRARED TELESCOPE FACILITY
NT SPARTAN SATELLITES
NT SPOT (FRENCH SATELLITE)
NT STORMSAT SATELLITE
NT SYMPHONIE SATELLITES
NT SYNCHRONOUS SATELLITES
NT TDR SATELLITES
NT TETHERED SATELLITES
NT TIROS N SERIES SATELLITES
NT TIROS SATELLITES
NT TITAN
NT TRANSIT SATELLITES
NT TRITON
NT UK SATELLITES
NT VELA SATELLITES
NT VENERA SATELLITES
NT VENERA 11 SATELLITE

On-orbit support of DARPA-301 payload
[AD-A146897] 07 p0911 N85-15767

The BRESEX multispectral camera: Preliminary characteristics
[INPE-3357-PRE/635] 10 p1487 N85-19386

Modeling 12 p1787 N85-21221

West Europe report: Science and technology
[JPRS-WST-85-013] 14 p2289 N85-24183

Ariane space general director on satellite launcher market 18 p3087 N85-29103

Images of the Earth's aurora and geocorona from the Dynamics Explorer Mission
[NASA-CR-175983] 18 p3136 N85-29423

Fuel cell applications literature review
[DE85-011691] 22 p3809 N85-33592

SATURATED HYDROCARBONS
U ALKANES

SATURATION

Response of saturated porous nonlinear materials to dynamic loadings
[AD-A148528] 08 p1173 N85-17394

A comprehensive strategy for saturation decompression with nitrogen-oxygen
[AD-A151800] 16 p2841 N85-27520

Saturation effect in multilevel lasing media
21 p3686 N85-32901

SATURATION (CHEMISTRY)

Influence of grain size distribution on the undrained dynamic properties of saturated sand
[PB85-102382/GAR] 09 p1305 N85-18197

Kinetics of saturation of porous titanium with low melting point metals 10 p1446 N85-19114

Mechanism of heterogeneous deposition ice nucleation near water-saturation 21 p3638 N85-32597

SATURN (PLANET)

Charged particle erosion of icy satellites: Coronal atmospheres and surface redistribution
03 p0448 N85-12845

Detection of the J-10 manifold of the pure rotational band of phosphine on Saturn 08 p1245 N85-17855

Investigations of planetary ring phenomena
13 p2174 N85-23487

Studies of planetary rings 13 p2174 N85-23488

Dynamical studies of Saturn's rings
13 p2174 N85-23489

Meteoroidal impacts, plasma, fine structure of ringlets and spokes on Saturn's ring B 13 p2174 N85-23490

Interaction of the magnetospheric ions with the surfaces of the icy satellites of Saturn 13 p2174 N85-23491

Plasma production by meteoroid impact
13 p2174 N85-23492

Origin and evolution of the Saturn system
13 p2175 N85-23493

Saturn electrostatic discharges
15 p2673 N85-26499

Statistical study of Saturnian electrostatic discharges observed by the Voyager Planetary Radio Astronomy experiment 15 p2673 N85-26500

An Earth-based attempt to detect Saturn Electrostatic Discharge (SED) at 21 centimeters
15 p2674 N85-26501

Electrons and cosmic ray produced protons in Saturn's inner magnetosphere
[NASA-TM-87469] 15 p2679 N85-26546

Extended atmospheres of outer planet satellites and comets
[NASA-CR-176137] 22 p3851 N85-33848

SATURN ATMOSPHERE

Exploration of the solar system by airborne astronomy
08 p1244 N85-17851

Near infrared modeling of the equatorial regions of Jupiter and Saturn 09 p1415 N85-18930

Dynamics of charged small particles — Jupiter, Saturn magnetospheres 15 p2676 N85-26522

Possible period of Jovian activity and possibility of seasons 16 p2723 N85-26810

SATURN RINGS

A review of radar observations of Saturn's rings
15 p2670 N85-26474

Microwave emission from Saturn's rings
15 p2670 N85-26475

Saturn's rings resolved by the VLA — Very Larg Array (VLA) 15 p2670 N85-26476

Apparent thickness of Saturn's rings from the observations of the ring plane crossing
15 p2671 N85-26477

Azimuthal variations in Saturn's A ring
15 p2671 N85-26478

A model containing blobs for the A ring of Saturn
15 p2671 N85-26479

Saturn's E-ring in the red spectral region
15 p2671 N85-26480

Saturn's E ring 15 p2671 N85-26481

Summary of optical groundbased E ring observations at the University of Arizona 15 p2671 N85-26482

Photometric study of the Saturn E ring
15 p2671 N85-26483

The Saturn ring particles from optical reflectance polarimetry 15 p2671 N85-26484

Saturn rings: Divisions, gaps and ringlets from ground-based telescopes 15 p2672 N85-26485

Physical properties of Saturn's rings
15 p2672 N85-26493

Structure and dynamics of Saturn's rings as seen by the Voyager stellar occultation 15 p2673 N85-26494

The C ring of Saturn: A high resolution view of some of its structure 15 p2673 N85-26495

The eccentric ringlet at 1.29 R sub S — Saturn radius (RS) 15 p2673 N85-26496

Voyager UVS observations of stellar occultations by the rings of Saturn — ultraviolet spectrometer (UVS)
15 p2673 N85-26497

Voyager planetary radio astronomy: Grain and particle impacts shot noise in Saturn's ring plane
15 p2673 N85-26498

Saturn electrostatic discharges
15 p2673 N85-26499

Solved und unsolved problems in planetary ring dynamics 15 p2674 N85-26502

Resonance identifications in Saturn's rings
15 p2674 N85-26504

A simple model of Saturn's rings revisited
15 p2674 N85-26506

Viscosity in Saturn's rings 15 p2674 N85-26507

Physical and geological nature of Saturn's larger ring particles 15 p2674 N85-26509

Effects of shepherd conjunctions on Saturn's F-ring
15 p2675 N85-26511

Orbital elements of Saturn's F ring and its shepherding satellites 15 p2675 N85-26515

Dense but collisionless orbiting rings — Saturn rings
15 p2675 N85-26517

Instabilities and the fine structure of Saturn's rings
15 p2676 N85-26520

The formation of spokes in Saturn's rings
15 p2676 N85-26524

On the role of mother-planet magnetic field in spiral structure explanation of formation of spokes — Saturn rings 15 p2676 N85-26525

On planetary rings as sources and sinks of magnetospheric plasmas 15 p2677 N85-26526

The E-ring of Saturn 15 p2677 N85-26527

Macrostructure and microphysics of Saturn's E-ring
15 p2677 N85-26528

Multivalued electrostatic potentials; chance or necessity for the charge of solid particles near Saturn?
15 p2677 N85-26529

A priority of space exploration: Observation of Saturn's rings from a Saturn orbiter 15 p2679 N85-26542

Rendezvous with Saturn's rings
15 p2679 N85-26543

SATURN SATELLITES
NT ENCELADUS
NT TITAN

Voyager cartography 13 p2203 N85-2366

The control networks of the satellites of Jupiter and Saturn 13 p2204 N85-23671

Orbital elements of Saturn's F ring and its shepherding satellites 15 p2675 N85-26515

Jupiter/Voyager data analysis
[NASA-CR-175723] 15 p2679 N85-26545

SAUDI ARABIA

Meteorological conditions affecting electromagnetic propagation on the Arabian Peninsula
[AD-A152019] 15 p2544 N85-2570

Saudi Arabian refraction profile: Crustal structure of the Red Sea-Arabian Shield transition
17 p2990 N85-28484

Saudi Arabian refraction profile: A preliminary interpretation for the Red Sea-Arabian Shield transition
17 p2991 N85-28485

A traveltime interpretation of the 1978 seismic refraction profile in the Kingdom of Saudi Arabia
17 p2991 N85-28486

Explanation of Russian models: Saudi Arabian seismic refraction profile 17 p2991 N85-28487

Interpretation of the data of USGS seismic refraction profile across the Arabian Shield in western Saudi Arabia 17 p2991 N85-28488

A preliminary analysis of the Saudi Arabian deep seismic sounding data 17 p2991 N85-28489

One-dimensional velocity-depth functions determined for the Arabian Shield and the southwestern Red Sea: A comparison of models 17 p2992 N85-28490

A comparison of crustal sections: Arabian Shield to the Red Sea 17 p2992 N85-28491

SAVANNAHS
U GRASSLANDS

SAWS

Ingot slicing machine and method
[NASA-CASE-NPO-15483-1] 12 p1857 N85-21650

SAWTOOTH WAVEFORMS

A simulation of weather in 3D space
[AD-A155221] 21 p3636 N85-3258

SCALAR MAGNETIC CHARGE
U MAGNETIC CHARGE DENSITY

SCALARS

Renormalization theory in four dimensional scalar fields
[NOTA-INTERNA-824] 02 p0292 N85-118

Second order modeling of scalar turbulent flows
03 p0360 N85-12311

Accuracy of the finite analytic method for scalar transport calculations
[DE85-001474] 09 p1320 N85-18

Nonlinear sigma-models and integration methods
[DE85-004447] 12 p1922 N85-22071

Did bosonic sneutrino stars ever exist
[PREPRINT-421] 18 p3202 N85-29

On the convergence of difference approximations to scalar conservation laws
[NASA-CR-172614] 19 p3344 N85-307

Intermittency, conditional sampling and turbulent combustion 20 p3424 N85-31249

Conditional modelling in turbulent shear flows
20 p3424 N85-31250

The microstructure approach to conserved scalar pdf models 20 p3424 N85-31251

Recent measurements in turbulent jet flames at Sandia Combustion Research Facility 20 p3424 N85-31254

Assessment of superlayer contribution to the conserved scalar PDF in a hydrogen turbulent jet diffusion flame
20 p3425 N85-31255

Experimental and theoretical investigations of open resonators — precipitation measurement
[DFVLR-FB-85-12] 20 p3449 N85-31414

Vortex dynamics simulation of conserved scalar dissipation 22 p3745 N85-33210

Scalar/Vector potential formulation for compressible viscous unsteady flows
[NASA-CR-3921] 23 p3893 N85-34113

Three-dimensional gravity ideal body studies in rough terrain
[DE85-014097] 24 p4118 N85-35

del robust response surface designs: Scaling 2-level
rials
A147484] 07 p1033 N85-16556
E (CORROSION)
udy of the reactive-element effect in oxidation of Fe-Cr
s using transverse section analytical electron
oscopy
84-016237] 04 p0571 N85-13641
levated temperature erosion corrosion of 9Cr1Mo
l
85-008445] 18 p3074 N85-29016
orrosion Research Center of the University of
nesota
85-008418] 18 p3075 N85-29022
orrosion-erosion rates/mechanisms of 9Cr1Mo steel
85-008506] 18 p3076 N85-29029
he effect of temperature on the corrosion-erosion of
r1Mo steel
E85-008507] 18 p3076 N85-29030
Optimisation of MCr Al coating compositions for marine
s turbines
R81159] 20 p3394 N85-31056
A study of adherent oxide scales
D-A155554] 21 p3567 N85-32188
The preparation of TEM specimens showing oxide scales
transverse cross-section
ERE-R-11579] 24 p4078 N85-35276
LE (RATIO)
Color and grey scale in sonar displays
05 p0710 N85-14552
Mars radar catalog 13 p2196 N85-23636
Design of a physical model of the cochlea. Displacement
nsor for small amplitudes in a highly viscous liquid
TN-6] 20 p3507 N85-31802
The problem of scale in planetary geomorphology
21 p3603 N85-32375
Quantitative analysis of geomorphic processes using
ellite image data at different scales
21 p3604 N85-32380
Scaling violation in the fragmentation region of inclusive
ckon spektrum 24 p4173 N85-35874
ALE EFFECT
Investigations into the effects of scale and
ompressibility on lift and drag in the RAE 5m pressurized
w-speed wind tunnel 08 p1068 N85-16773
Investigations into the effects of scale and
ompressibility on lift and drag in the RAE 5m pressurised
w-speed wind tunnel
RAE-TM-AERO-2006] 13 p1969 N85-22372
The Shock and Vibration Digest, volume 17, no. 2
AD-A153129] 17 p2977 N85-28400
Recent progress in the dynamic plastic behaviour of
tructures, part 4 17 p2978 N85-28402
Least-squares approximation to minimum chi-square
estimators of location and scale parameters and their effect
n the Pearson chi-square test
AD-A153534] 18 p3169 N85-29638
Hard X-ray measurements of the hot electron rings in
Nagoya BUMPY TORUS (NBT-1M)
IPPJ-720] 19 p3370 N85-30899
Scale separation closure and Alfven wave turbulence
DE85-013124] 24 p4095 N85-35385
ALE MODELS
Model study of the interaction of a blast wave with the
superstructure of ships. Part 5: Application of optical
measurement methods to the study of blast interaction
[PML-1984-12-PT-5] 01 p0057 N85-10375
Singular perturbations, coherency and aggregation of
dynamic systems
[DE84-014166] 01 p0114 N85-10772
Review of requirements and status of simulation and
scaling of transonic, viscous flows
[AD-A146357] 06 p0808 N85-15137
Discrete modifications to continuous dynamic structural
systems 09 p1337 N85-18410
Analysis of ground pressure distribution beneath tracked
model with respect to external loading
[AD-P004275] 09 p1406 N85-18851
Acoustic scaling: A re-evaluation of the acoustic model
of Manchester Studio 7
[BBC-RD-1984/16] 12 p1822 N85-21432
A new model for thin plates with rapidly varying thickness.
Part 3: Comparison of different scalings
[AD-A149748] 12 p1866 N85-21704
Impact studies of a 1/3-scale model of an air cushion
vehicle
[NASA-TM-86360] 14 p2218 N85-23757
An evaluation of proposed acoustic treatments for the
NASA LaRC 4 x 7 meter wind tunnel
[NASA-CR-172577] 15 p2646 N85-26319
Plasma heating 15 p2654 N85-26372
Wind-tunnel evaluation of a 21-percent-scale powered
model of a prototype advanced scout helicopter
[NASA-TP-2420] 18 p3058 N85-28923

Design of a physical model of the cochlea. Displacement sensor for small amplitudes in a highly viscous liquid
[STN-6] 20 p3507 N85-31802
Reverification of the Chesapeake Bay model
[AD-A155486] 21 p3655 N85-32706
SCALERS
Construction of solutions for two-dimensional Riemann problems
[DE85-003136] 10 p1549 N85-19770
SCALING
Universal binding energy relations in metallic adhesion
[NASA-TM-86889] 03 p0331 N85-12132
SCALING LAWS
Thermal fluid-structure interaction: A few scaling considerations — nuclear reactors
[GKSS-84-E-18] 01 p0048 N85-10314
K-shell yield scaling law for conventional PRS loads
[AD-A145155] 01 p0121 N85-10631
Factor analysis applied to a silane coupling agent on E-glass fiber system
[AD-A145687] 02 p0187 N85-11249
Similarity considerations in 1-component 2-phase flow
[DE84-016370] 04 p0499 N85-13184
Theoretical studies of Field-Reversed Configurations (FRC) and experimental study of the FRC during translation
[DE84-016467] 04 p0566 N85-13603
A nonlocal expression for the ponderomotive potential
[IPPJ-699] 06 p0864 N85-15487
Wavelength scaling of laser plasma coupling
[DE84-014637] 06 p0866 N85-15505
On existence and uniqueness of solutions of Hamilton-Jacobi equations
[AD-A147597] 07 p1033 N85-16560
Hazard assessment of a hypothetical large rocket motor 08 p1117 N85-17042
The scaling of coronal models from one star to another 08 p1233 N85-17771
FRC translation dynamics and plasma confinement properties in FRX-C/T
[DE85-002366] 10 p1560 N85-19842
Magnetic fluctuations, field reversal maintenance, and anomalous thermal transport in the reversed field pinch
[DE85-003604] 11 p1732 N85-20892
Impact crater scaling laws 13 p2181 N85-23532
Los Alamos Science, Number 11, Summer-Fall, 1984
[DE85-004634] 14 p2419 N85-24926
Experimental investigation of annular air curtain domes
[UTIAS-288] 15 p2521 N85-25543
Theoretical studies of Elmo Bumpy Torus
[DE85-007202] 15 p2658 N85-26402
Restrike particle beam experiments on a dense plasma focus. Opening switch research on a dense plasma focus
[AD-A152991] 17 p3039 N85-28802
Quantum effects in linear collider scaling laws
[DE85-009846] 19 p3363 N85-30851
Computer programs for smoothing and scaling airfoil coordinates
[NASA-TM-84666] 20 p3388 N85-31011
TNT equivalency of EAK explosive
[AD-A155737] 21 p3571 N85-32211
Soil extraction kit
[AD-D011736] 22 p3742 N85-33190
Magnetic field generation in the cores of terrestrial bodies 22 p3859 N85-33894
Scaling parameters of flashover
[NBS-GCR-85-497] 23 p3911 N85-34229
Scaling differences between large interplate and intraplate earthquakes
[NASA-CR-176149] 23 p3948 N85-34467
Confinement experiments on ISX-B
[DE85-012346] 23 p3984 N85-34709
Model robust response surface designs: Scaling two-level factorials
[AD-A156218] 24 p4143 N85-35686
Scaling violation in hadron-nucleus interaction
[HE-3.2-8] 24 p4179 N85-35916
Particle interactions at energies over 1000 TeV inferred from gamma-families observed at Mount Fuji
[HE-3.5-1] 24 p4183 N85-35940
Multidimensional analysis of data obtained in experiments with X-ray emulsion chambers and extensive air showers
[HE-3.6-2] 24 p4184 N85-35951
Hadrons registration in emulsion chamber with carbon block
[HE-3.7-3] 24 p4186 N85-35962
Intensities of high-energy cosmic rays at Mount Kanbala
[HE-3.7-5] 24 p4186 N85-35964
Simulation of EAS properties on the basis of high energy interaction model deduced from the accelerator data
24 p4187 N85-35973

SCANDINAVIA
Ground magnetic observations of high-latitude Pi2 pulsations: Scandinavian magnetometer array results
14 p2370 N85-24649
SCANDIUM
NT SCANDIUM ISOTOPES
Effect of ScAl3 phase dispersion on hardening of alloy Al-6.3 percent Mg-0.21 percent Sc
19 p3241 N85-30096
Possible causes of modification and strengthening of aluminum by scandium 19 p3241 N85-30099
The isotopic composition of cosmic ray calcium
[OG-4.3-5] 22 p3879 N85-34030
SCANDIUM ISOTOPES
Mechanisms of impurity diffusion in rutile
[DE84-014741] 06 p0766 N85-14902
SCANDIUM 46
U SCANDIUM ISOTOPES
SCANNERS
NT COASTAL ZONE COLOR SCANNER
NT HORIZON SCANNERS
NT INFRARED SCANNERS
NT MULTISPECTRAL BAND SCANNERS
NT OPTICAL SCANNERS
NT ULTRASONIC SCANNERS
A scanning alarm electronic processor
[AD-D011419] 08 p1158 N85-17309
Filter reflection image guide oscillator and solid state line scanning device
[AD-D011440] 10 p1479 N85-19336
Defense Mapping Agency (DMA) raster-to-Vector benchmark testing
[AD-A154152] 19 p3338 N85-30683
Six mechanisms used on the SSM/1 radiometer
22 p3798 N85-33534
Method and apparatus for measuring areas of photoelectric cells and photoelectric cell performance parameters
[DE85-011629] 22 p3810 N85-33599
Cylindrical lens-array antenna for wideband electronic scanning
[AD-A156085] 24 p4090 N85-35350
SCANNING
NT CONICAL SCANNING
NT FREQUENCY SCANNING
NT RADAR SCANNING
Characteristics of polarization grids made of parallel metal strips during hemispherical scanning
06 p0792 N85-15062
Filter reflection image guide oscillator and solid state line scanning device
[AD-D011440] 10 p1479 N85-19336
New high resolution scanning ion microprobe and focused ion beam applications
[AD-A149992] 12 p1852 N85-21616
NDE methods for green ceramics
[DE85-004019] 13 p2036 N85-22766
Factors affecting dwell times on digital displaying
[NASA-TM-86406] 14 p2390 N85-24722
A new NASTRAN capability for data reduction
15 p2574 N85-25874
Eye movement in response to single and multiple targets
[AD-A151115] 15 p2617 N85-26126
An error-dependent model of instrument-scanning behavior in commercial airline pilots
[NASA-CR-3908] 21 p3665 N85-32765
Intermolecular explosives
[DE85-009609] 23 p3921 N85-34296
LANDSAT-4/5 image data quality analysis
[E85-10105] 24 p4107 N85-35463
SCANNING DEVICES
U SCANNERS
SCANNING LASER ACOUSTIC MICROSCOPE (SLAM)
U ACOUSTIC MICROSCOPES
SCAR PROGRAM
U SUPERSONIC CRUISE AIRCRAFT RESEARCH
SCARFING
Detection of pores in hot continuously cast rounds
[BMFT-FB-T-85-007] 18 p3072 N85-29000
SCARPS
U ESCARPMENTS
SCARS (GEOLOGY)
U EROSION
SCATHA SATELLITE
SCATHA (spacecraft charging at high altitudes) plasma interaction experiment: SC-3 high energy particle spectrometer; SC-8 energetic ion composition experiment
[AD-A149728] 12 p1793 N85-21252
Aerospace spacecraft-charging guidelines document
13 p1994 N85-22501
Automatic charge control system for satellites
13 p1995 N85-22508
Results of the SCATHA ion composition experiment during the IMS 14 p2359 N85-24580

SCATTER PROPAGATION

Research on acoustical and optical scattering, optics of bubbles, diffraction catastrophes, laser generation of sound, and shock induced cavitation
[AD-A146703] 06 p0660 N85-15466

Limits of the propagation medium with respect to digital signal transmission 10 p1469 N85-19270

Tropospheric scatter communication system having angle diversity
[AD-D011448] 14 p2291 N85-24200

A transport theory of millimeter wave propagation in woods and forests
[AD-A151683] 17 p2947 N85-28196

Implications of cross section errors for cosmic ray propagation
[OG-7.2-3] 23 p4014 N85-34875

Alfven wave scattering and the secondary to primary ratio
[OG-7.2-9] 23 p4015 N85-34878

Interstellar turbulence, random density variations, and scintillation measurements
[OG-7.2-13] 23 p4015 N85-34880

Relativistic transport theory for cosmic-rays
[OG-8.3-8] 23 p4022 N85-34926

An experiment to measure the energy spectrum of cosmic ray antiprotons from 100 to 1000 MeV
[OG-9.1-3] 23 p4022 N85-34929

Linear absorption and scattering of laser beams
[AD-A156167] 24 p4096 N85-35401

SCATTERERS
U SCATTERING

SCATTERING
NT ACOUSTIC SCATTERING
NT ATMOSPHERIC SCATTERING
NT BACKSCATTERING
NT COHERENT SCATTERING
NT COMPTON EFFECT
NT ELASTIC SCATTERING
NT ELECTROMAGNETIC SCATTERING
NT ELECTRON SCATTERING
NT FORWARD SCATTERING
NT HALOS
NT INCOHERENT SCATTERING
NT INELASTIC SCATTERING
NT INVERSE SCATTERING
NT ION SCATTERING
NT LIGHT SCATTERING
NT MICROWAVE SCATTERING
NT MIE SCATTERING
NT NEUTRON SCATTERING
NT NUCLEAR SCATTERING
NT NUCLEON-NUCLEON SCATTERING
NT PROTON SCATTERING
NT RADAR SCATTERING
NT RAMAN SPECTRA
NT RAYLEIGH SCATTERING
NT RESONANCE SCATTERING
NT REVERBERATION
NT THOMSON SCATTERING
NT TROPOSPHERIC SCATTERING
NT WAVE SCATTERING
NT X RAY SCATTERING

Spline-Galerkin solution of integral equations for 3-body scattering above break-up
[TWISK-327] 01 p0109 N85-10738

A finite element projection method for the solution of particle transport problems with anisotropic scattering
[AD-A145382] 02 p0250 N85-11637

Total area of diffusion elements in a reverberation chamber and measured degree of sound absorption
[NRC/CNR-TT-2110] 03 p0415 N85-12653

Scattering from multi-scale surface — infrared lasers
[RSRE-MEMO-3656] 04 p0505 N85-13222

Laboratory studies of atomic collision processes of importance in planetary atmospheres
[NASA-CR-174142] 04 p0569 N85-13758

Transient currents of ideally conducting body of revolution with transient diffraction
06 p0785 N85-15019

Structural studies of amorphous Mo-Ge alloys using synchrotron radiation
[DE85-002061] 08 p1131 N85-17125

Effects of heterogeneities on the propagation, scattering and attenuation of seismic waves and the characterization of seismic source
[AD-A148284] 08 p1186 N85-17476

Optical wave propagation and imaging in the atmosphere 08 p1222 N85-17694

Effect of scattering on instabilities in line-driven stellar winds 08 p1235 N85-17784

DSN 34-meter antenna optics analysis for wideband SETI investigations 10 p1465 N85-19244

Influence of scattering on Q in the lithosphere
[AD-A149316] 10 p1515 N85-19563

Quantum mechanical and semiclassical approaches to molecular dynamics
[DE85-003458] 10 p1555 N85-19803

Imaging through a multiple scattering medium
[DE85-002051] 10 p1557 N85-19821

Dynamical studies of molecular systems
[DE85-003063] 11 p1594 N85-20028

Electron acceleration by laser fields in a gas
[DE85-000575] 11 p1639 N85-20323

Self-Optimized Sector (SOS) model of self-consistent energy loss and scattering for an electron beam propagating in air
[DE85-003161] 11 p1722 N85-20831

An iteration method for complex scattering problems
[AD-A150038] 12 p1934 N85-22151

High energy facilities advanced projects: Intrabeam scattering for a beam of gold ions
[DE85-000887] 12 p1941 N85-22192

Paramagnetic scattering from Ni
[DE85-004207] 12 p1942 N85-22198

Mathematical modeling of two-frequency laser sounding of scattering media 13 p2089 N85-23045

Improvement in magnetic field properties of vanadium-gallium superconductors by enhancement of spin-orbit scattering
[DE85-002893] 13 p2164 N85-23422

Receiver optimization for detection in doubly spread communication channels
[AD-A151226] 15 p2541 N85-25689

Space shuttle molecular and wake vacuum measurements
[NASA-TM-86509] 19 p3222 N85-29978

Microwave bandstop filter
[AD-D011716] 19 p3261 N85-30222

Measurement problem in PROGRAM UNIVERSE
[DE85-008179] 19 p3378 N85-30959

Guided-mode launching in a slab waveguide by way of diffraction at the edge of a conducting screen residing on one surface of the slab
[AD-A154886] 21 p3575 N85-32232

Interpretation of photometric measurements of airless bodies 22 p3855 N85-33871

Monte Carlo techniques for analyzing deep penetration problems
[DE85-011426] 23 p3968 N85-34598

Fokker-Planck calculation of hot electron formation in the thermal barrier region of tandem mirror Gamma-10
[IPPJ-726] 23 p3979 N85-34669

Stochastic particle acceleration in solar flares
[SH-1.1-4] 23 p3989 N85-34731

Exponential anisotropy of solar cosmic rays
[SH-3.2-1] 23 p4002 N85-34817

Energetic solar particle events
[SH-3.2-2] 23 p4003 N85-34818

Channeled propagation of solar particles
[SH-3.2-3] 23 p4003 N85-34819

The local characteristic function of interplanetary particle propagation
[SH-3.2-8] 23 p4003 N85-34823

Spatial distribution of cosmic rays in magnetic cycles of the Sun
[SH-4.2-20] 23 p4009 N85-34857

SONTRAC: A solar neutron track chamber detector
[SH-9.1-12] 23 p4052 N85-35127

The HEAO-2 Guest Investigator Program: Non-linear growth of instabilities in line-driven stellar winds
[NASA-CR-176168] 24 p4168 N85-35840

Scattering and stopping of hadrons in nuclear matter
24 p4174 N85-35862

The hump in the Cerenkov lateral distribution of gamma ray showers
[HE-4.5-9] 24 p4185 N85-36032

Search for tachyons associated with extensive air showers in the ground level cosmic radiation
[HE-6.2-13] 24 p4212 N85-36149

SCATTERING AMPLITUDE

Scattering of plane wave on cylindrical shell in low-frequency region 02 p0256 N85-11677

Nonlinear saturation of stimulated Raman scattering in homogeneous plasma
[DE85-003120] 10 p1560 N85-19837

Calculation of amplitude-phase characteristics of signal scattered obliquely on meteor trail
13 p2073 N85-22948

Measurement and analysis of critical crack tip processes during fatigue crack growth
[NASA-CR-172597] 21 p3598 N85-32342

SCATTERING COEFFICIENTS

Relation between atmospheric scattering and backscattering coefficient
[ESA-TT-837] 05 p0777 N85-14350

Evaluation of machining damage in brittle materials
[DE85-001794] 11 p1612 N85-20136

A method for determining in situ the absorption coefficient of particulate media using pulsed laser technique
[AD-D011548] 12 p1799 N85-21281

Test of lidar inversion algorithm sensitivity to atmospheric backscatter and extinction parameters, revision A
[AD-A152062] 16 p2865 N85-27671

Light scattering by leaf layers with application to canopy reflectance modeling: The Scattering by Arbitrarily Inclined Leaves (SAIL) model
[NLR-MP-84011-U] 17 p3038 N85-28796

Active and passive remote sensing of ice
[AD-A154406] 19 p3300 N85-30459

Variability of rural aerosols under stable weather conditions 21 p3647 N85-32863

SCATTERING CROSS SECTIONS

Study of structure of nuclei with neutrons and nuclear data measurements for MFE
[DE84-015128] 01 p0117 N85-10602

Measurement of magnetic sublevel differential scattering cross sections for potassium and mercury
[MPIS-10/1983] 01 p0119 N85-10615

Influence of strut cross-section on strut radiation of reflector antennas
[FI-455-TBR-39] 03 p0357 N85-12285

Acoustic scattering cross sections for truly composite wind-wave surfaces. Scattering without bubbles
[AD-A145672] 03 p0415 N85-12655

Fast neutron capture with a white neutron source
[DE84-016799] 04 p0562 N85-13580

Energy transfer in atom-molecule scattering experiments in the 1eV region with SF6-Ar, CF4-Ne and Xe-CO2 systems as examples
[REPT-11/1983] 04 p0563 N85-13588

Investigation on K (4 2P3/2) Hg interaction at collision energies from 0.5 to 5.7 eV
[MPIS-15/1983] 04 p0563 N85-13589

Rotational inelastic scattering of He-atoms at HF-, HCl-, CF4-, SF6-, C2H6- and C2F6-molecules
[MPIS-9/1984] 04 p0564 N85-13590

Measurement of scattering cross sections of liquid and solid hydrogen deuterium and deuterium hydride for thermal neutrons
[DE84-014814] 05 p0727 N85-14671

Scattering experiments on interactions of excited atoms: Differential cross sections of the system Na (3P)+K(4S)
[MPIS-8/1984] 05 p0728 N85-14677

Measurements of the A-dependence of deep-inelastic electron scattering from nuclei
[DE84-013865] C5 p0728 N85-14678

Pion inelastic scattering to the first three excited states of Lithium-6
[AD-A147560] 07 p1041 N85-16606

Theoretical cross sections for inner-shell vacancy production by high-energy electrons
[DE84-007346] 11 p1721 N85-20627

Theoretical study of near-threshold electron-molecule scattering
[DE85-004530] 12 p1930 N85-22126

Particle shape characterization
[AD-A151981] 15 p2544 N85-25707

Theory of electron-impact atomic ionization cross sections
[AD-A151763] 16 p2861 N85-27648

Electromagnetic transmission through a slot in a perfectly conducting plane
[AD-A153224] 17 p2949 N85-28210

Application of forward scattering renormalization to scattering in turbid media
[AD-A153232] 17 p2959 N85-28271

A study of excitations during collisionally-induced electron detachment of negative ions
[AD-A152879] 17 p3030 N85-28739

New experimental results in two photon physics
[NIKHEF-H/84-16] 17 p3035 N85-28776

Theory of high energy collision processes
[DE85-010183] 19 p3362 N85-30846

AGS broad band neutrino beam
[DE85-010954] 19 p3386 N85-30875

Study of proton and neutron activation of metal samples in low Earth orbit
[NASA-CR-171596] 21 p3556 N85-32130

The use of the glistening surface concept in rough surface scattering
[AD-A154922] 21 p3575 N85-32234

An analysis of physical optics models for rough surface scattering
[AD-A154960] 21 p3575 N85-32235

Head-on scattering of a tubular cylinder of finite length for radar target identification purposes
[AD-A155808] 21 p3577 N85-32246

Radar echoes at 2.66 and 40.92 MHz from the mesosphere, part 2.6A 21 p3619 N85-32468

mplicit Monte Carlo methods and non-equilibrium arshak wave radiative transport
DE86-010711] 22 p3835 N85-33743

mplications of cross section errors for cosmic ray propagation
[OG-7.2-3] 23 p4014 N85-34875

On the importance of interstellar helium for the propagation of heavy cosmic rays
[OG-7.2-11] 23 p4015 N85-34879

Proton-air and proton-proton cross sections from air shower data
[HE-1.1-1] 24 p4170 N85-35849

Proton-air inelastic cross section at S(1/2) = 30 TeV
[HE-1.1-2] 24 p4170 N85-35850

Hadron cross sections at ultra high energies and unitarity bounds on diffraction dissociation
[HE-1.1-3] 24 p4170 N85-35851

On total cross sections and slopes at superhigh energies
[HE-1.1-4] 24 p4170 N85-35852

Determination of the cross section of the proton, pion and neutron inelastic interaction with lead and carbon nuclei at 0.5 - 5.0 TeV energies (PION experiment)
[HE-1.1-5] 24 p4170 N85-35853

P(P bar)P elastic scattering and cosmic ray data
[HE-1.1-6] 24 p4170 N85-35854

Measurement of interaction cross section of cosmic ray Fe nuclei (E4 GeV/N) with Al target
[HE-1.1-7] 24 p4170 N85-35855

Hadron thermodynamics in relativistic nuclear collisions
[HE-1.1-8] 24 p4171 N85-35856

The method for the study of the inelastic cross-section for high energy protons by means of shower arrays with the large calorimetric area
[HE-1.1-11] 24 p4171 N85-35858

QCD-motivated description of very high energy particle interactions
[HE-1.2-2] 24 p4171 N85-35861

Is the inelastic charge-exchange contribution constant at the large X and superhigh energies? Qeut 01Kuchin, I. A. 24 p4173 N85-35871

General consequences of the violated Feynman scaling 24 p4173 N85-35872

Intensities of high-energy cosmic rays at Mount Kanbala
[HE-3.7-5] 24 p4186 N85-35964

SCATTERING FUNCTIONS

Scattering theory by Enss' method for operator valued matrices: Dirac operator in an electric field
[REPT-64] 01 p0045 N85-10290

Calculation of the scattering function of rotating molecules with emphasis on the tunnel spectra of absorbed molecules 03 p0427 N85-12725

Scattering of waves by axisymmetrical edge
13 p2080 N85-22967

Numerical solution of a first kind Fredholm integral equation arising in electron-atom scattering
[CWI-NM-R8414] 14 p2414 N85-24897

Multiple scattering of electromagnetic waves in discrete random media
[AD-A151766] 16 p2772 N85-27112

Characteristics of optical information-measurement channels with utilization of scattering effects
22 p3781 N85-33429

SCATTERING MATRIX
U S MATRIX THEORY

SCATTEROMETERS

The altimeter as a support to the scatterometer in the representation of winds and derived wave fields in coastal waters and enclosed seas: A research at its onset
03 p0383 N85-12453

Studies of coastal mesoscale winds using SIR-B
06 p1147 N85-17238

Information for space radar designers: Required dynamic range vs resolution and antenna calibration using the Amazon rain forest 06 p1147 N85-17239

Science opportunities using the NASA scatterometer on N-ROSS
[NASA-CR-175639] 13 p2123 N85-23222

The impact of scatterometer data on limited-area model predictions of the QE 2 storm 18 p3139 N85-29436

Utilization of the SEASAT scatterometer winds for ocean mixed layer modeling
[AD-A153748] 18 p3150 N85-29506

Comparison of ERS-1 scatterometer Monte Carlo performance simulations using a weighted nonlinear least squares and a maximum likelihood estimation method
20 p3420 N85-31224

Results of the MIZEX preliminary campaign: 29 June to 19 July 1983 — Marginal Ice Zone Experiment (MIZEX), satellite observation
[CNES-84/142/T/CT/DRT/TIT/RL]
20 p3478 N85-31609

AMI calibration study. Volume 1: SAR calibration. Volume 2: Ground Targets. Volume 3: Scatterometer calibration — Active Microwave Instrument (AMI) ERS-1
[C2248/4/4-VOL-1] 23 p3936 N85-34394

SCAVENGING

Earth-to-orbit propellant transportation overview
06 p1106 N85-17002

Space Transportation System (STS) propellant scavenging system study. Volume 1: Technical report
[NASA-CR-171848-VOL-1] 11 p1589 N85-20000

Space Transportation System (STS) propellant scavenging system study. Volume 2: Supporting research and technology report
[NASA-CR-171849-VOL-2] 11 p1589 N85-20001

Space Transportatioin System (STS) propellant scavenging system study. Volume 3: Cost and work breakdown structure-dictionary
[NASA-CR-171850-VOL-3] 11 p1590 N85-20002

SCENE ANALYSIS

Analysis of accretion and deletion at boundaries in dynamic scenes
[AD-A145944] 03 p0419 N85-12678

Texture classification using autoregressive filtering
07 p0984 N85-16254

Multi target tracking by dynamic scene analysis
[AD-A148922] 10 p1466 N85-19250

A method for reduction of ambiguity in segmentation of images
[INPE-3394-TDL/186] 11 p1697 N85-20664

Preliminary study of information extraction of LANDSAT TM data for a suburban/regional test site
13 p2121 N85-23208

Validation of the ERBE scanner scene identification methodology: Analysis with Nimbus-7 ERB data
[NASA-CR-172596] 16 p2832 N85-27466

Scene analysis using recursive frequency domain correlation with energy normalization
[AD-A151777] 16 p2854 N85-27596

An image compression survey and algorithm switching based on scene activity
[NASA-TP-2458] 22 p3727 N85-33106

SCF
U SELF CONSISTENT FIELDS

SCHEDULES
NT COUNTDOWN

List of recent Soviet space launches
02 p0165 N85-11120

AGARD bulletin technical programme, 1985
[AGARD-BUL-84-2] 02 p0305 N85-11971

Space telescope cost, schedule, and performance review, 1984
[GPO-39-065] 04 p0579 N85-13696

Overview od STS ground operations/orbiter turnaround STS-1 through STS-7 08 p1096 N85-16926

Calendar of selected aeronautical and space meetings
[AGARD-CAL-84/2] 10 p1573 N85-19917

Space Transportation System. Space shuttle payload flight assignments
[NASA-TM-87492] 19 p3224 N85-29989

Space Transportation System. Space shuttle payload flight assignments
[NASA-TM-87491] 19 p3224 N85-29990

SCHEDULING
NT PREDICTION ANALYSIS TECHNIQUES

Constraint-based scheduling in an intelligent logistics support system: An artificial intelligence approach
[AD-A145613] 02 p0293 N85-11900

Decentralized control of scheduling in distributed systems
[AD-A147446] 07 p1022 N85-16487

Transmission scheduling to reduce convex delay costs in packet networks
[AD-A148451] 08 p1153 N85-17278

Order picking in an aisle
[AD-A149553] 10 p1548 N85-19766

On maximizing the expected lifetime of replaceable systems
[AD-A150003] 12 p1862 N85-21680

State dependent priority rules for scheduling
[AD-A149972] 12 p1924 N85-22090

Onboard demand scheduling of a multibeam SS/TDMA satellite with integrated circuit and packet switching
14 p2229 N85-23812

Information technology applications in voluntary sector transport operations. SP1: Objectives and programme of work
[TT-8501] 15 p2667 N85-26457

Large scale electricity production scheduling via nonlinear optimization
[REPT-84-07] 17 p3017 N85-28655

Automated maintenence system test program increment VI production scheduling
[AD-A153694] 18 p3198 N85-29838

Cost and schedule implications of multinational coproduction
[AD-A154358] 19 p3380 N85-30969

Simulation studies of time-control procedures for the advanced air traffic control system
[NASA-TP-2493] 21 p3553 N85-32101

Aviation system delays
[S-HRG-98-1241] 21 p3553 N85-32102

Deficit irrigation feasibility study and demonstration project
[DE85-011531] 22 p3802 N85-33555

SCHEMATICS
U CIRCUIT DIAGRAMS

SCHIFF BASES
U IMINES

SCHIST

Metamorphic petrology of the Table Mountain area, Circle quadrangle, Alaska 04 p0516 N85-13295

SCHLIEREN PHOTOGRAPHY

Experimental investigation of a pulse combustor: Flow visualization by Schlieren photography
[DE85-002862] 11 p1636 N85-20304

SCHMIDT CAMERAS

Some aspects of photography with a small Schmidt camera — astronomical photography
07 p0964 N85-16116

The UK Schmidt telescope and the facilities in Edinburgh 07 p0965 N85-16121

Astronomers' problems with the calibration of Schmidt plates 07 p0965 N85-16126

Cometary astrometry with Schmidt cameras
14 p2435 N85-25020

Astometry at La Silla 14 p2436 N85-25025

SCHMIDT TELESCOPES

What do we want: Increased speed, resolution, contrast or DOE? — astronomical photography
07 p0964 N85-16115

The UK Schmidt telescope and the facilities in Edinburgh 07 p0965 N85-16121

An investigation into the fidelity of reproduction of UKST original objective prism plates on to film — United Kingdom Schmidt Telescope (UKST) 07 p0965 N85-16123

Sub-beam prism used at the Bosscha Schmidt telescope 07 p0965 N85-16125

The Malin effect in stellar photography
07 p0966 N85-16131

An objective prism quasar survey with the Schmidt telescope on Calar Alto (Spain)
08 p1243 N85-17845

SCHOOLS

Computer Literacy Act of 1983, part 2
[H-REPT-98-752-PT-2] 04 p0578 N85-13687

Recent Naval Postgraduate School publications
[AD-A151723] 16 p2875 N85-27740

SCHOTTKY BARRIER DIODES
U SCHOTTKY DIODES

SCHOTTKY DIODES

Coplanar Schottky variable phase shifter
[AD-A146304] 03 p0359 N85-12305

Effect of barrier height on friction behavior of the semiconductors silicon and gallium arsenide in contact with pure metals
[NASA-TP-2405] 04 p0478 N85-13044

Planning of hybrid integrated circuits for microwave-band oscillators 04 p0490 N85-13124

Imaging polarimeter-interferometer arrays for Tokamak measurements
[DE84-015916] 05 p0730 N85-14693

Amorphous metallic layers in Si metallization systems
06 p0830 N85-15277

Photoluminescent and electroluminescent properties of Cd sub 0.95 Mn sub 0.05 Se electrodes
[AD-A146775] 07 p0946 N85-15995

Buried junction enhanced Schottky barrier device
[AD-D011399] 07 p1044 N85-16635

Electronics component R and D, production capability reviewed 08 p1140 N85-17181

Low capacitance e-beam fabricated beam-lead Schottky barrier diodes
[AD-A150238] 13 p2063 N85-22866

Fabrication and I-V characterization of AlGaAs/GaAs MODFETs with P-type surface layers grown by molecular beam epitaxy
[AD-A151695] 15 p2660 N85-26415

Completely consumed carbide: A new process for dielectric isolation
[AD-A152379] 17 p2918 N85-27987

Research and developmental study on MIS thin film solar cells of amorphous hydrogenated silicon, part 2
[BMFT-FB-T-84-290] 17 p2966 N85-28467

Heterojunction Schottky gate MESFET with lower channel ridge barrier
[AD-D011673] 19 p3258 N85-30199

Schottky theory of three component plasmas
[AD-A154461] 19 p3371 N85-30907

Contact properties of rare-earth silicides and germanides on Si and Ge 19 p3374 N85-30931

Numerical simulation of nonisothermal transient processes in GaAs diode structures
22 p3767 N85-33350

SCHOTTKY EFFECT
U WORK FUNCTIONS

SCHROEDINGER EQUATION
Semiclassical theory of resonances
[REPT-67] 01 p0114 N85-10777
Reduction of nonlinear problems to Schroedinger or heat equations: Formation of Kepler orbits, singular solutions for hydrodynamical equations
[REPT-72] 01 p0129 N85-10892
Difference schemes for equations of Schrodinger type
[AD-A145812] 03 p0410 N85-12622
Conservative and nonconservative schemes for the solution of the nonlinear Schroedinger equation
[CWI-NM-R8405] 05 p0720 N85-14628
Multidimensional inverse scattering for first order systems
[AD-A148711] 06 p1214 N85-17642
Connection between time- and frequency-domain three-dimensional inverse problems for the Schroedinger equation
[DE85-005914] 15 p2639 N85-26274
Computer modeling of vibrational energy levels of potential laser candidates (diatomic molecules)
[AD-A151765] 16 p2790 N85-27209
Anderson localization for large disorder or low energy
[PREPRINT-426] 18 p3176 N85-29692
Attractors for the Kuramoto-Sivashinsky equations
[DE85-009831] 20 p3520 N85-31892
K(-) hydrogen bound and continuum states in momentum space
[DE85-010429] 22 p3841 N85-33789

SCHUMANN-RUNGE BANDS
MSG-7: Atmospheric penetration of solar radiation in the range of Schumann-Runge bands
11 p1657 N85-20443
Determination of band oscillator strengths of atmospheric molecules from high resolution vacuum ultraviolet cross section measurements
[NASA-CR-176150] 22 p3814 N85-33624

SCHWARTZ INEQUALITY
Some ideas for decomposing the domain of elliptic partial differential equations in the Schwarz process
[DE85-011844] 22 p3834 N85-33739

SCHWARZSCHILD METRIC
A derivation of relativistic effects in satellite tracking
[AD-A154620] 21 p3558 N85-32132

SCIATIC REGION
Differential effect of denervation on free radical scavenging enzymes in slow and fast muscle of rat
[NASA-CR-175719] 15 p2614 N85-26110
Changes in the cholinergic system of rat sciatic nerve and skeletal muscle following suspension induced disuse
[NASA-CR-175718] 15 p2615 N85-26111

SCIENCE
Emergency Mathematics and Science Education Act
[GPO-29-561] 03 p0435 N85-12770
European Scientific Notes, volume 38, number 12
[AD-A148713] 09 p1418 N85-18946
China report: Science and technology
[JPRS-CST-84-037] 10 p1424 N85-18982
West Europe report: Science and technology
[JPRS-WST-85-005] 11 p1592 N85-20013
The Impact of Science on Society
[NASA-SP-482] 14 p2431 N85-24994
The legacy of science 14 p2432 N85-24995
East European report: Science and technology
[JPRS-ESA-85-010] 15 p2524 N85-25560
Characteristics of recent science/engineering graduates, 1982: Detailed statistical tables
[PB85-149060] 15 p2663 N85-26437
Academic science and engineering: Graduate enrollment and support, fall 1982 (detailed statistical tables)
[PB85-154730] 15 p2664 N85-26438
Academic science and engineering: R and D funds, fiscal year 1982 (detailed statistical tables)
[PB85-154763] 15 p2664 N85-26443

SCIENTIFIC SATELLITES
NT ASTRONOMICAL SATELLITES
NT ATS
NT EXOSAT SATELLITE
NT MAGSAT SATELLITES
NT UK SATELLITES
Space Research in Japan. National report
01 p0013 N85-10082
Satellite observations 01 p0013 N85-10083
The galaxy scene and QUASAT — VLBI satellite
07 p1056 N85-16703
The QUASAT mission: An overview
07 p1056 N85-16704
Solar Corona Explorer: A mission for the physical diagnosis of the solar corona
[NASA-TM-87416] 10 p1572 N85-19912
Drag-free satellite simulator
[REPT-615] 12 p1789 N85-21229
S3-3 ONR-118 data analysis
[AD-A149725] 12 p1889 N85-21855
Assessment study of liquid content measurement methods applicable to space missions — Infrared Space Observatory
[TU-HH-TRI-ESA-84-2] 17 p2938 N85-28135

SCIENTISTS
Synthesis and characterization of advanced materials
[PB84-215326] 01 p0025 N85-10156
A bibliography of planetary geology and geophysics principal investigators and their associates, 1983 - 1984
[NASA-TM-87361] 01 p0127 N85-10874
The identification of the scientific community's choice criteria in the history of scientific research: The case of quantum mechanics
[NOTA-INTERNA-797] 02 p0291 N85-11893
Fiber optics development, prospects assessed
03 p0343 N85-12214
Scientific communications and national security
[GPO-36-093] 04 p0492 N85-13138
Fr. Angelo Secchi, a pioneer in the study of solar-terrestrial relationships 04 p0519 N85-13312
The 1984 NASA/ASEE summer faculty fellowship program
[NASA-TM-87392] 04 p0574 N85-13662
Training guide for scientific and engineering trainees 1984
[AD-A147963] 08 p1198 N85-17542
Fundamentals of computer programming for engineers
[AD-A147964] 08 p1205 N85-17583
Middle Atmosphere Program. Handbook for MAP, volume 6
[NASA-CR-175460] 11 p1656 N85-20436
China report: Science and technology
[JPRS-CST-85-003] 13 p2166 N85-23433
Physicists' role in new technological development discussed 13 p2166 N85-23436
Some historical and other notes about the Mertens conjecture and its recent disproof
[CWI-NM-R8415] 14 p2414 N85-24898
O. F. Mossotti and the physics of molecules
[NOTA-INTERNA-822] 14 p2420 N85-24931
Discovery refutation and verification refutation: The proposals of Von Neumann and Wiener in the development of 20th century physics
[NOTA-INTERNA-840] 14 p2431 N85-24993
Institute's contribution to Soviet welding technology noted 16 p2767 N85-27072
Span graphics display utilities handbook, first edition
[NASA-TM-86500] 16 p2849 N85-27567
Harold Hazen and the theory and design of servomechanism
[RR-270] 22 p3794 N85-33506

SCINTILLATION
Scattering from multi-scale surface — infrared lasers
[RSRE-MEMO-3656] 04 p0505 N85-13222
Ionospheric scintillation: A brief review
04 p0522 N85-13337
Observations of plasma bubbles and their zonal drift using polarimeters
[INPE-3219-PRE/572] 05 p0729 N85-14688
Unsteady pressure measurements on a biconvex airfoil in a transonic oscillating cascade
[NASA-TM-86914] 07 p0898 N85-15689
Optical wave propagation and imaging in the atmosphere 06 p1222 N85-17694
Description of amplitude scintillations on a 11 GHz slant path in terms of forward scattering from turbulent layers
[FI-455-TBR-76] 11 p1625 N85-20232
Remote sensing of irregularities in the equatorial ionosphere using the radio scintillation technique
16 p2806 N85-27317
Scintillation using NNSS satellites
[AD-A152804] 17 p2949 N85-28207
Measurements of folded path optical scintillation using a corner cube, a cat's eye and a flat mirror reflector
[AD-A154044] 19 p3367 N85-30679
Equitorial scintillations: Advances since ISEA-6
[AD-A154962] 21 p3631 N85-32559
EAS spectrum in the primary energy region above 10 to the 15th power eV by the Akeno and Yakutsk array data
[OG-5.1-16] 22 p3882 N85-34057
Methods and software for cosmic ray scintillation studies
[SH-9.1-17] 23 p4052 N85-35132
Air fluorescence detection of large air showers below the horizon
[HE-4.6-6] 24 p4197 N85-36043

SCINTILLATION COUNTERS
Improvements in photodiode readout for small CsI (T1) crystals
[MPI-PAE/EXP-E1-131] 01 p0051 N85-10333
Fine grained hodoscopes based on scintillating optical fibers
[DE84-014849] 01 p0120 N85-10825
Recent progress in BGO development for high resolution calorimetry
[MPI-PAE/EXP-E1-129] 01 p0124 N85-10848
Study for a large area underground detector made with organic scintillators for searching for magnetic monopoles
[NOTA-INTERNA-814] 02 p0201 N85-11339
Advances in room-temperature solid-state gamma-ray spectrometry
[DE84-015944] 04 p0489 N85-12987
Simulation of optical configurations and signal processing methods in Anger-type neutron-position scintillation detector
[DE84-012095] 04 p0503 N85-13210
Scintillator-fiber charged particle track-imaging detector
[NASA-CR-174160] 04 p0559 N85-13560
Mercuric iodide photodetectors for scintillation spectroscopy
[DE85-001437] 10 p1437 N85-19056
The effect of the choice or response matrix on unfolded bonner sphere spectra
[AD-A150462] 13 p2159 N85-23404
Assessment of present and future large-scale semiconductor detector systems
[DE85-006606] 15 p2662 N85-26430
LIGHT: A ray tracing code to simulate light collection in scintillation spectrometers and light pipes
[DE85-007213] 16 p2865 N85-27673
A possible digital circuit able to recognize magnetic monopoles crossing a thick scintillator counter
[NOTA-INTERNA-826] 18 p3097 N85-29173
Study for a large area acrylic scintillator detector — magnetic monopoles
[NOTA-INTERNA-827] 18 p3097 N85-29174
Measurement of the attenuation length of an acrylic scintillator — magnetic monopoles
[NOTA-INTERNA-828] 18 p3097 N85-29175
Experimental performance of a digital circuit able to recognize magnetic monopole events
[NOTA-INTERNA-838] 18 p3097 N85-29176
New concept for a wall detector for alpha particles
[DE85-009037] 18 p3183 N85-29740
Improvements in the energy resolution and high-count-rate performance of bismuth germanate
[DE85-010763] 19 p3240 N85-30092
Bismuth germanate scintillators: Applications in nuclear safeguards and health physics
[DE85-010730] 19 p3365 N85-30665
Plastic scintillator detectors for the study of transfer and breakup reactions at intermediate energies
[DE85-009945] 20 p3528 N85-31945
Search for neutrino oscillations at the Brookhaven AGS
[DE85-009766] 20 p3530 N85-31957
Intercomparison of the calculated absolute efficiency values between true coaxial and true closed-end coaxial Ge (Li) and NaI detectors
[REPT-5-1984] 20 p3532 N85-31976
Reduction of reabsorption effects in scintillators by employing solutes with large Stokes shifts
[DE85-011645] 22 p3838 N85-33767
Observation of hard X-rays from the Crab pulsar and A0535+26
[OG-2.3-7] 22 p3866 N85-33944
Specificity of (71)Ga(p,n) (71)Ge at 35 MeV for Gamow-Teller strength
[DE85-011837] 23 p3971 N85-34615
A balloon-borne imaging gamma-ray telescope
[OG-9.2-2] 23 p4024 N85-34941
Gamma-ray burst spectroscopy capabilities of the BATSE/GRO experiment
[OG-9.2-15] 23 p4026 N85-34954
A position sensitive phoswich hard X-ray detector system
[OG-9.3-12] 23 p4028 N85-34967
The Buckland Park air shower array
[OG-9.4-4] 23 p4029 N85-34971
A new array for the study of ultra high energy gamma-ray sources
[OG-9.4-7] 23 p4029 N85-34974
Akeno 20 km (2) air shower array (Akeno Branch)
[OG-9.4-8] 23 p4029 N85-34975
The longitudinal thickness of air-shower fronts
[OG-9.5-1] 23 p4030 N85-34976
Shower disc sampling and the angular resolution of gamma-ray shower detectors
[OG-9.5-2] 23 p4030 N85-34980

Angular resolution of air-shower array-telescopes
G-9.5-6] 23 p4030 N85-34983
Astrophysical applications of high angular resolution ray-telescopes
OG-9.5-7] 23 p4031 N85-34984
The angular resolution of air shower gamma ray elescopes
OG-9.5-14] 23 p4031 N85-34990
Study of cosmic ray scintillations from 5-minute data f the scintillations telescope Izmran and world-wide etwork stations
[SH-5.1-18] 23 p4043 N85-35071
High precise measurements of cosmogenic radiocarbon bundance by complex of scintillation equipments
[SH-7.1-14] 23 p4048 N85-35105
Plastic scintillators in coincidence for the study of multi-particle production of sea level cosmic rays in dense medium
[SH-9.1-11] 23 p4052 N85-35126
Wholebody radiation counting system
[AD-A155842] 24 p4131 N85-35607
A lead glass tubing drift calorimeter
24 p4147 N85-35711
The response of a scintillation counter below an emulsion chamber to heavy nucleus interactions in the chamber 24 p4175 N85-35889
Result of Monte-Carlo simulation of electron-photon cascades in lead and layers of lead-scintillator
[HE-3.6-11] 24 p4185 N85-35958
Application of photodiodes to the detection of electromagnetic bursts 24 p4189 N85-35988
Study of muons near shower cores at sea level using the E594 neutrino detector 24 p4191 N85-36000
Average features of the muon component of EAS or = 10(17) eV
[HE-4.3-10] 24 p4191 N85-36004
Transition effect of air shower particles in plastic scintillators
[HE-4.4-9] 24 p4193 N85-36017
A new study on the emission of EM waves from large EAS
[HE-4.6-5] 24 p4197 N85-36042
Fast scintillation counter system and performance
[HE-4.6-10] 24 p4197 N85-36047
Performance of a local electron density trigger to select extensive air showers at sea level
[HE-4.6-11] 24 p4198 N85-36048
Microprocessor-based single particle calibration of scintillation counter
[HE-4.6-13] 24 p4198 N85-36049
Samarkand complex setup for investigation of cosmic ray variation in the energy range of 7 10 (9) - 10 (15) eV
[HE-4.6-14] 24 p4198 N85-36050
The structure of the shower disk observed at Mt. Norikura
[HE-4.7-1] 24 p4198 N85-36052
Arrival time distributions of electrons in air showers with primary energies above 10 (18)eV observed at 900m above sea level
[HE-4.7-5] 24 p4199 N85-36056
Methods for roof-top mini-arrays
[HE-4.7-7] 24 p4199 N85-36058
Fast scintillation counter preamplifier for the observation of Linsley effect
[HE-4.7-9] 24 p4199 N85-36060
A mini-array for large air showers
[HE-4.7-10] 24 p4199 N85-36061
Sub-luminal pulses from cosmic ray air showers
[HE-4.7-13] 24 p4200 N85-36063
Thickness of the particle swarm in cosmic ray air showers
[HE-4.7-14] 24 p4200 N85-36064
Study of the time-differentiated particle flux density at various distances from EAS axis
[HE-4.7-15] 24 p4200 N85-36065
On method of muon spectrum measurements by the scintillation detectors of a large thickness T4t sub o
[HE-5.2-18] 24 p4204 N85-36094
Results of low energy background measurements with the Liquid Scintillation Detector (LSD) of the Mont Blanc Laboratory
[HE-5.3-5] 24 p4205 N85-36099
The research program of the Liquid Scintillation Detector (LSD) in the Mont Blanc Laboratory
[HE-5.3-6] 24 p4205 N85-36100
Search for stellar collapse with the MACRO detector at Gran Sasso
[HE-5.3-11] 24 p4206 N85-36105
The homestake surface-underground scintillations: Description
[HE-6.1-9] 24 p4210 N85-36135
A search for heavy long lived particles in high energy cosmic rays
[HE-6.2-7] 24 p4211 N85-36143
Delayed particles in EAS at Akeno
[HE-6.2-8] 24 p4211 N85-36144
Energetic delayed hadrons in large air showers observed at 5200m above sea level
[HE-6.2-9] 24 p4211 N85-36145
Search for long-lived massive particles in extensive air showers
[HE-6.2-10] 24 p4212 N85-36146
Search for tachyons associated with extensive air showers in the ground level cosmic radiation
[HE-6.2-13] 24 p4212 N85-36149
Progress report on a new search for free e/3 quarks in the cores of 10(15) - 10(16) eV air showers
[HE-6.2-15] 24 p4212 N85-36151
Exploring results of the possibility on detecting cosmic ray particles by acoustic way
[HE-7.1-3] 24 p4213 N85-36157

SCINTILLATORS
U SCINTILLATION COUNTERS

SCINTILLOMETERS
U SCINTILLATION COUNTERS

SCOOPS
Ramjets with supersonic combustion
07 p0918 . N85-15817

SCORING
An introduction to multilinear formula score theory
[AD-A145696] 02 p0254 N85-11667
Efficient scores, variance decompositions and Monte Carlo swindles
[AD-A146673] 06 p0858 N85-15458
A 2 x 6 Back Surface Reflection (BSR) silicon solar cell 13 p2005 N85-22570

SCOUT HELICOPTER
U P-531 HELICOPTER

SCOUT PROJECT
User's operating procedures. Volume 1: Scout project information programs
[NASA-CR-177948] 23 p3956 N85-34518
User's operating procedures. Volume 1: Scout project financial analysis program
[NASA-CR-177949] 23 p3956 N85-34519

SCPC TRANSMISSION
U SINGLE CHANNEL PER CARRIER TRANSMISSION

SCR (RECTIFIERS)
U SILICON CONTROLLED RECTIFIERS

SCRAMBLING (COMMUNICATION)
The average power density spectra of additive scrambler signals and their versions in AMI code
[FUB-27-1983] 01 p0040 N85-10258
Digital scrambling for shuttle communication links: Do drawbacks outweigh advantages?
08 p1101 N85-16956

SCRAMJET ENGINES
U SUPERSONIC COMBUSTION RAMJET ENGINES

SCRAMJETS
U SUPERSONIC COMBUSTION RAMJET ENGINES

SCRAP
Spectral characteristics of grinding sparks used for identification of scrap metals
[PB85-198570] 24 p4080 N85-35290
Deposition of nickel-cobalt alloys by controlled-potential electrolysis
[PB85-198562] 24 p4081 N85-35291

SCREEN EFFECT
Method for forming electromagnetic-wave-screening composite 07 p0936 N85-15930

SCREENS
Diffraction of electromagnetic wave by screen of arbitrary shape 02 p0273 N85-11778
Flow through very porous inclined screens
[NASA-TM-86979] 15 p2555 N85-25761
The thermal calculation of opaque heat screens
[BLL-M-36273-(5828.4)] 20 p3450 N85-31421
Development of metalization process: FSA project, cells and module formation research area
[NASA-CR-176136] 23 p3945 N85-34447

SCREW DISLOCATIONS
Fracture toughness of materials
[DE85-004306] 12 p1867 N85-21713
Determination of edge and screw dislocation density in single crystals of high-purity iron
[DE85-010237] 20 p3537 N85-32012

SCREWS
Alignment and assembly tool for very large diameter cylinders
[NASA-CASE-MFS-28001-1] 18 p3116 N85-29289
Failure analysis of fractured capscrews in centrifugal coolant compressor
[DE85-010029] 19 p3287 N85-30384

SCRIBING
U SCORING

SCRUBBERS
Operating and maintenance guidelines for the kinergetics (trade name) environmental control system. Carbon dioxide scrubber model DH-10 and heat exchanger model CCU-01
[AD-A148107] 08 p1200 N85-17557
Nebulization reflux concentrator
[NASA-CASE-LAR-13254-1] 11 p1615 N85-20154
Control of acid deposition precursors through dry scrubbing
[DE85-010281] 19 p3235 N85-30056
Evaluation of the Santee limestone for use in flue-gas desulfurization systems
[DE85-901277] 19 p3249 N85-30148
Technology of off-gas treatment for liquid-fed ceramic melters
[DE85-012467] 22 p3812 N85-33610
A study of the control of particulate emissions from turbine engine test cells 24 p4067 N85-35205

SCRUBBING
U WASHING

SCRUBS (BOTANY)
U BRUSH (BOTANY)

SDV
U SHUTTLE DERIVED VEHICLES

SEA BREEZE
Sea breeze-induced mesoscale systems and severe weather
[NASA-CR-174317] 08 p1187 N85-17480
Sea breeze-induced mesoscale systems and severe weather 15 p2596 N85-26012
Air flow of the western coastal boundary of South Africa and its influence on the ocean 16 p2631 N85-27459

SEA ICE
NT ICE FLOES
NT ICEBERGS
NT PRESSURE ICE
Sea ice data buoys in the Weddell Sea
[AD-A144953] 01 p0088 N85-10594
Investigation of ice dynamics in the marginal ice zone
[AD-A145110] 01 p0088 N85-10597
Drift characteristics of northeastern Bering Sea ice during 1982
[PB84-213982] 01 p0089 N85-10604
Active microwave measurements of sea ice under fall conditions: The RADARSAT/FIREX fall experiment — in the Canadian Arctic
[E85-10019] 02 p0217 N85-11432
Applications of remote sensing techniques to oceanography and sea ice
[FOA-B-60004-M7] 02 p0220 N85-11448
Handbook for sea ice analysis and forecasting
[AD-A145286] 02 p0233 N85-11516
MIZEX. A program for mesoscale air-ice-ocean interaction experiments in arctic marginal ice zones. III: Modeling the marginal ice zone
[AD-A145351] 02 p0233 N85-11517
Sea ice characteristics derived from airborne altimetry
03 p0382 N85-12440
Radar altimetry over sea ice 03 p0382 N85-12441
Physical oceanography report. Helicopter-based STD data from MIZEX 83 (Marginal ice zone experiment)
[AD-A145848] 03 p0398 N85-12538
Eastern-Western Arctic Sea ice analysis 1983
[AD-A146133] 03 p0398 N85-12541
A comparison between active and passive sensing of soil moisture from vegetated terrains
04 p0526 N85-13384
Dynamics of coupled ice-ocean system in the marginal ice zone: Study of the mesoscale processes and of constitutive equations for sea ice
[NASA-CR-174171] 04 p0542 N85-13448
Arctic ice island and sea ice movements and mechanical properties
[DE84-016323] 04 p0542 N85-13450
Development of radar to measure sea ice merits prize nomination 06 p0826 N85-15244
Intermediate results of radar backscatter measurements from summer sea ice
[AD-A147212] 07 p0940 N85-15960
Ice dynamics
[AD-A147376] 07 p0968 N85-16278
Investigation of the ice dynamics in the marginal ice zone
[AD-A146729] 07 p1009 N85-16411
Southern ocean sea-ice morphology and kinematics
08 p1144 N85-17217
MIZEX. A program for mesoscale Air-Ice-Ocean interaction experiments in arctic marginal ice zones. 4: Initial results and analysis from MIZEX 83
[AD-A148255] 08 p1173 N85-17399
Shore ice ride-up and pile-up features. Part 2. Alaska's Beaufort Sea coast, 1983 - 1984
[AD-A148428] 08 p1190 N85-17501
SAI (Science Applications, Inc.) Interim Scattering Model/Ice (SISM/ICE)
[AD-A148596] 08 p1213 N85-17638
Crystalline structure of urea ice sheets used in modeling experiments in the CRREL test basin
[AD-A148434] 08 p1226 N85-17722

Data report on variations in the composition of sea ice during MIZEX/East'83 with the Nimbus-7 SMMR
[NASA-TM-86170] 09 p1342 N85-18443

Atlas of the Beaufort Sea
[AD-A149545] 11 p1669 N85-20619

Report of the International Ice Patrol Services in the North Atlantic Ocean, season of 1982
[AD-A149595] 12 p1896 N85-21917

Drifting ice as mechanical factor in purifying and polluting hydrosphere 13 p2108 N85-23132

Digital processing of passive Ka-band microwave images for sea-ice classification
[AD-A150686] 14 p2347 N85-24511

Low Temperature Science. Series A: Physical Sciences
[ISSN-0439-3538] 15 p2581 N85-25917

An experimental study of brine upward migration in thin sea ice 15 p2582 N85-25923

Characteristics of snow cover on sea ice and formation of snow ice II 15 p2582 N85-25924

Characteristics of fast sea ice collected near Barrow, Alaska 15 p2582 N85-25925

Oceanographic variations in recent decades and their impact on the fertility of the Iceland Sea
15 p2602 N85-26034

Glacial-to-interglacial changes in NADW fluxes?
15 p2602 N85-26037

Numerical simulation of North Atlantic Sea ice variability, 1951 - 1980 15 p2603 N85-26040

Sea ice, climate and Fram Strait
15 p2603 N85-26042

Greenland ice sheet mass balance
15 p2603 N85-26043

Potential climatic effects on the Greenland ice sheet
15 p2603 N85-26044

Active and passive remote sensing of ice
[AD-A151741] 16 p2815 N85-27369

An assessment of atmospheric refractivity in the northern marginal ice zone
[AD-A152346] 17 p2992 N85-28493

Regional meteorology of the Bering Sea during MIZEX-West, February and March 1983
[PB85-173699] 18 p3150 N85-29503

Arctic mixed layer dynamics
[AD-A153582] 18 p3150 N85-29505

MIZEX, 1984, NASA CV-990 flight report
[NASA-TM-86216] 19 p3299 N85-30451

Arctic acoustic tomography MIZEX 84
[AD-A154426] 19 p3320 N85-30580

Numerical modeling of sea ice dynamics and ice thickness characteristics
[AD-A154600] 21 p3654 N85-32700

Arctic and offshore research
[DE85-001995] 22 p3818 N85-33653

The NORDA/FNOC (Naval Ocean Research and Development Activity's/Fleet Numerical Oceanography Center) Polar Ice Prediction System (PIPS)-Arctic: A technical description
[AD-A156332] 24 p4126 N85-35577

SEA LEVEL

Sea-level in the world ocean. Part 5: The North-East Pacific and Arctic Oceans, a catalogue of measurements
[CSIR-T/SEA-8303-5] 01 p0087 N85-10589

Sea-level in the world ocean. Part 6: The South Atlantic and South Pacific Oceans, a catalogue of measurements
[CSIR-T/SEA-8303-6] 01 p0087 N85-10590

Sea-level in the world ocean. Part 7: The Indian Ocean, a catalogue of measurements
[CSIR-T/SEA-8303-7] 01 p0087 N85-10591

Determination of geoid undulations and ocean heights from ERS-1 radar altimetry data
03 p0381 N85-12432

Parameterizing extreme still water levels and waves in design level studies
[IOS-183] 03 p0396 N85-12542

An alternative to reduction of surface pressure to sea level
[NASA-CR-174174] 04 p0538 N85-13422

The Midway Atoll coral cap: Meteoric diagenesis, amplitude of sea-level fluctuation and dolomitization
09 p1351 N85-18499

The wobble of the Earth and the low frequency dynamics of the ocean 09 p1358 N85-18546

Hemodynamics responses to upright tilt at sea level and high altitude
[AD-A148648] 10 p1527 N85-19634

Calculation of level surface in problems of large-scale ocean circulation 13 p2106 N85-23136

Global paleoclimatic data base for 6000 years BP
[DE85-008628] 15 p2600 N85-26024

The sea level response to weather along the coast of southern Africa 16 p2829 N85-27446

Trends in the Southern Hemisphere
18 p3144 N85-29466

Stratigraphic analysis of Pennsylvania rocks using hierarchy of transgressive-regressive units
19 p3312 N85-30531

The worldwide distribution of the seasonal cycle of mean sea level
[IOS-190] 20 p3497 N85-31743

Composition of primary cosmic rays near the bend from a study of hadrons in air showers at sea level
[OG-5.2-2] 22 p3883 N85-34059

The composition of cosmic rays near the Bend (10 to the 15th power eV) from a study of muons in air showers at sea level
[OG-5.2-3] 22 p3883 N85-34060

Plastic scintillators in coincidence for the study of multi-particle production of sea level cosmic rays in dense medium
[SH-9.1-11] 23 p4052 N85-35126

The neutron moderated detector and groundbased cosmic ray modulation studies
[SH-9.1-13] 23 p4052 N85-35128

Strong earthquakes, novae and cosmic ray environment
[SH-10.1-3] 23 p4053 N85-35135

Particle distributions in approximately 10(14) 10(16) eV air shower cores at sea level 24 p4189 N85-35990

Comparison of simulation results with sea-level experimental data on 10(14) - 10(16) air shower cores
24 p4190 N85-35993

Particle distributions in approximately 10(13) - 10(16) eV air shower cores at mountain altitude and comparison with Monte Carlo simulations
[HE-4.2-18] 24 p4190 N85-35994

Energy spectrum of cascades generated by muons in Baksan underground scintillation telescope
[HE-5.1-15] 24 p4202 N85-36077

Range fluctuations of high energy muons passing through matter
[HE-5.2-19] 24 p4204 N85-36095

SEA OF JAPAN

Ultramicroscopic study of structure of phosphorites from Sea of Japan floor 19 p3290 N85-30400

SEA ROUGHNESS

The spatial evolution of t he directional wave spectrum in the Southern Ocean: Its relation to extreme waves in Agulhas Current 08 p1144 N85-17213

Rip in White Sea 19 p3290 N85-30401

SEA STATES

The use of altimeter data for sea state forecasting
03 p0380 N85-12426

Evaluation of wave energy resources on the French Atlantic seaboard 14 p2325 N85-24369

SEA SURFACE TEMPERATURE

Heat sources in the tropics and large scale flow anomalies associated with precipitation anomalies in northeast Brazil
[INPE-3211-TDL/175] 04 p0538 N85-13421

Study of the improvement in analyzing passive microwave remote sensing data by integrated use of ground data 05 p0658 N85-14226

Energy active areas of ocean
06 p0820 N85-15204

Droughts and floods in South America due to the 1982-83 El Nino-southern oscillation episode
[INPE-3408-PRE/677] 09 p1357 N85-18535

Planetary scale circulation anomalies associated with droughts over northeast Brazil
[INPE-3351-PRE/630] 10 p1518 N85-19570

Method of measuring sea surface water temperature with a satellite including wideband passive synthetic-aperture multichannel receiver
[NASA-CASE-NPO-15651-1] 12 p1669 N85-21723

The development of image processing of NOAA AVHRR data and its application to sea surface temperature
12 p1895 N85-21891

Low-frequency microwave radiometer for N-ROSS
14 p2230 N85-23819

Proposed use of system ARGOS with data buoys for calibration of thermal infrared imagery of North British waters for sea surface temperature maps
14 p2240 N85-23869

Applications of ARGOS measurements in equatorial Pacific Ocean-atmosphere interaction studies
14 p2331 N85-24414

Sea surface temperatures from VAS MSI data
[NASA-CR-175706] 14 p2382 N85-24660

China's integrated circuit production
16 p2806 N85-27302

The validation of sea surface temperatures determined from AVHRR data using in situ data recovered via system ARGOS 16 p2812 N85-27342

Observations of surface water temperature in the Netherlands since 1860: Statistics
[KNMI-WR-84-3] 17 p2997 N85-28531

Observations of surface water temperature in the Netherlands since 1860: Tables for light vessels
[KNMI-WR-84-4] 17 p2998 N85-28532

Observations of surface water temperature in the Netherlands since 1860: Series from KNMI-RWS
[KNMI-WR-84-5] 17 p2998 N85-28533

Mechanistic experiments to determine the origin of Southern Hemisphere stationary waves
18 p3143 N85-29461

Atmospheric planetary wave response to external forcing
[NASA-CR-176000] 19 p3315 N85-30543

Tropical Ocean and Global Atmosphere (TOGA) heat exchange project: A summary report
[NASA-CR-176038] 20 p3496 N85-31738

Sea surface and remotely sensed temperatures off Cape Mendocino, California
[NASA-TM-86712] 24 p4125 N85-35573

SEA TRUTH

Study of the improvement in analyzing passive microwave remote sensing data by integrated use of ground data 05 p0658 N85-14226

An assessment of the potential role of multispectral imagery in bathymetric charting
[AD-A152460] 17 p2964 N85-28438

SEA WATER

Evaluation of hollow fiber ultrafiltration as a pretreatment for reverse osmosis desalinaton of seawater
[PB84-212406] 01 p0026 N85-10160

Bifouling and corrosion studies at the Seacoast Test Facility in Hawaii
[DE84-014643] 01 p0029 N85-10180

Sea water rope batteries
[AD-A144775] 01 p0042 N85-10275

The development of a diode laser Doppler velocimeter for boundary layer measurements under ice: A feasibility investigation
[AD-A145076] 01 p0053 N85-10346

Variations with time of the carbon dioxide partial pressure in central and south Atlantic surface waters
[AD-A145825] 03 p0398 N85-12597

A simple, low cost potentiostat for corrosion studies
[NPL-DMA(A)-47] 04 p0502 N85-13200

Hydrologic characteristics of the Mediterranean and Black Sea 07 p0981 N85-16226

Propagation of electromagnetic fields along the sea/sea-bed interface
[AD-A149523] 10 p1467 N85-19257

Possible role of ocean biota in global carbon balance — phytoplankton production 13 p2107 N85-23128

Mathematical-cartographic model for study of distribution of hydrochemical elements in sea water (using dissolved oxygen in the Pacific Ocean as an example)
13 p2109 N85-23136

Geographic variation in the relationships of temperature, salinity or sigma sub t versus plant nutrient concentrations in the world ocean — silicic acid, nitrate, and phosphate concentration
[NASA-CR-175621] 13 p2140 N85-23287

Luminescence in the ocean
[AD-B089136L] 13 p2140 N85-23288

Variability in constant-load-amplitude fatigue crack growth rates in marine environments
[AD-A150786] 14 p2255 N85-23975

Resistance of optical coatings to alkali solutions and sea water 14 p2261 N85-24129

Some approximations of geophysical hydrodynamics
14 p2336 N85-24448

Representation of temperature and salinity fields using statisticallyt orthogonal functions (in example of polymode data) 14 p2337 N85-24449

Real-time enhancement of a climatology or forecast of ocean thermal structure using observed ocean temperatures
[AD-A151118] 15 p2604 N85-26049

Fatigue of synthetic fibers for marine rope applications
[MIT-R84-2] 17 p2979 N85-28414

The effects of sea water and concentrated salt solutions on the fatigue of nylon 6,6 fibers
17 p2979 N85-28416

Resistance to corrosion fatigue in aluminum alloy 1561 in sea water 19 p3243 N85-30108

Concretization of high level radioactive source in marine sediment
[AD-D011703] 19 p3249 N85-30146

Geochemistry of manganese in ocean
19 p3291 N85-30408

Sea water photoluminescence
19 p3292 N85-30415

Environmental background measurement program
[AD-A153860] 19 p3319 N85-30577

Theoretical modelling of the electro-chemistry in a corrosion fatigue crack. Part 2: Mathematical aspects of associated unsteady reaction equations
[NPL-DMA(A)-100-PT-2] 20 p3465 N85-31520

A microprocessor-controlled, multichannel fluorimeter for analysis of sea water
[AD-A154986] 21 p3590 N85-32310

Granulometric study of the acidity and sulfate excess in marine aerosols 21 p3652 N85-32691
Determination of organobromide compounds in water by gas chromatography-negative ion chemical ionisation mass spectrometry
[DRIC-T-7411] 22 p3743 N85-33199
A manual of methods for the continuous flow determination of ammonia, nitrate-nitrite, phosphate and silicate in seawater
[IOS-177] 23 p3913 N85-34243
Microwave properties of a quiet sea
[NASA-CR-176199] 24 p4085 N85-35322
Underwater measurements of muon intensity
[HE-5.1-16] 24 p4202 N85-36078
Background light measurements at the DUMAND site
[HE-5.2-7] 24 p4203 N85-36084
Measurements of light background at large depth in the ocean
[HE-5.2-8] 24 p4203 N85-36085
Analytical calculation of muon intensities under deep sea-water
[HE-5.2-16] 24 p4204 N85-36092
Modular detector for deep underwater registration of muons and muon groups
[HE-5.4-15] 24 p4208 N85-36125

SEALANTS
U SEALERS

SEALERS
Sealing ceramic material in low melting point glass
[NASA-TM-77599] 01 p0031 N85-10190
Encapsulation materials and processing
06 p0830 N85-15269
Effect of sealants of the sound absorption coefficients of acoustical friable insulating materials
[AD-A148541] 08 p1218 N85-17674
Interactions between F-111 fuselage fuel tank sealants. Part 2: Variation in performance properties of polysulfides after contact with polyester degradation products
[AD-A149777] 12 p1812 N85-21368
Fuel cell separator plate with bellows-type sealing flanges
[DE85-005991] 23 p3947 N85-34459

SEALING
NT SELF SEALING
Low leakage turbine shaft seals for advanced combined cycle systems
[AD-A149372] 10 p1492 N85-19420
Radioactive waste isolation in salt: Peer review of the D'Appolonia report on schematic designs for penetration seals for a repository in the Permian Basin, Texas
[DE85-000693] 11 p1727 N85-20861
Preventing the formation of an anomalous structure in chemically sealed low carbon steel
[BLL-BISI-TRANS-22373-(9022.06)]
17 p2930 N85-28085
Sodium nitrate containing mixture for producing ceramic-glass-ceramic seal by microwave heating
[DE85-011610] 22 p3751 N85-33254
Experimental characterization and stability of salt- and nonsalt-containing grouts and mortars (BCT-1F- and BCT-1FF-related)
[DE85-012339] 22 p3753 N85-33263

SEALS (ANIMALS)
Motivation for satellite tracking of southern elephant seals Mirounga leonina at sea 16 p2812 N85-27346

SEALS (STOPPERS)
NT GASKETS
NT GLANDS (SEALS)
NT HERMETIC SEALS
NT LABYRINTH SEALS
NT O RING SEALS
NT PACKINGS (SEALS)
NT PLUGS
Collapsable seal member
[DE84-014300] 01 p0055 N85-10367
High-temperature erosion of plasma-sprayed, yttria-stabilized zirconia in a simulated turbine environment
[NASA-TP-2406] 04 p0478 N85-13045
Identification of dynamic coefficients of annular turbulent seals 05 p0644 N85-14133
Analysis and testing for rotordynamic coefficients of turbulent annular seals with different, directionally homogeneous surface-roughness treatment for rotor and stator elements 05 p0644 N85-14134
Analysis for leakage and rotordynamic coefficients of surface roughened tapered annular gas seals
05 p0644 N85-14135
Dynamic stiffness characteristics of high eccentricity ratio bearings and seals by perturbation testing
05 p0645 N85-14141
Analysis of physical-chemical processes governing SSME internal fluid flows
[NASA-CR-174245] 06 p0760 N85-14362
High temperature ultra-high vacuum infrared window seal
[AD-D011339] 07 p0929 N85-15890
Cryogenic glass-to-metal seal
[AD-D011370] 07 p0933 N85-15911
Space shuttle elevon seal panel mechanism
08 p1101 N85-16951
Computational fluid mechanics utilizing the variational principle of modeling damping seals
[NASA-CR-174332] 08 p1161 N85-17325
Sealing assembly
[AD-D011463] 10 p1452 N85-19151
Experimental study of ceramic coated tip seals for turbojet engines
[NASA-TM-86939] 10 p1483 N85-19363
Ribbon burner simulation of T-700 turbine shroud for ceramic lined seals research
[NASA-TM-86940] 10 p1483 N85-19364
Theory versus experiment for the rotordynamic coefficients of annular gas seals. Part 2: Constant clearance and convergent-tapered geometry
[NASA-CR-174413] 10 p1491 N85-19416
Theory versus experiment for the rotordynamic coefficients of annular gas seals. Part 1: Test facility and apparatus
[NASA-CR-174409] 10 p1491 N85-19417
Low leakage turbine shaft seals for advanced combined cycle systems
[AD-A149372] 10 p1492 N85-19420
Variable friction secondary seal for face seals
[NASA-CASE-LEW-14170-1] 11 p1647 N85-20377
Finger materials for air cushion vehicles. Volume 2: Base fabrics for finger materials
[AD-A149701] 12 p1819 N85-21406
Sliding seal materials for adiabatic engines
[NASA-CR-174893] 13 p2037 N85-22757
Experimental stiffness of tapered bore seals
[NASA-TM-86978] 15 p2568 N85-25847
Damping seal verification setup
16 p2738 N85-26893
Damping seals for turbomachinery
16 p2738 N85-26894
Spacer structure
[AD-D011641] 17 p2897 N85-27868
Damping seal for turbomachinery
[NASA-CASE-MFS-25842-2] 19 p3280 N85-30341
SSME seal test program: Test results for hole-pattern damper seals
[NASA-CR-171595] 20 p3395 N85-31059
A comparison of experimental and theoretical results for rotordynamic coefficients of four annular gas seals
[NASA-CR-176086] 21 p3596 N85-32332
Tape casting as an approach to an all-ceramic turbine shroud seal
[NASA-TM-87078] 21 p3596 N85-32333
Mechanical connection for a tubular assembly
[DE85-011590] 22 p3792 N85-33497
Refrigerated dynamic seal to 6.9 MPa (1000 psi)
[NASA-TM-87108] 23 p3930 N85-34356
Oxidizing seal for a turbine tip gas path
[NASA-CASE-LEW-14053-1] 23 p3937 N85-34402
Thermal stress analysis of a new turbine shroud seal concept
[NASA-TM-87082] 23 p3938 N85-34406
SRB attach ring phenolic TPS fishtail seal evaluation tests
[NASA-CR-170887] 24 p4098 N85-35407

SEAMOUNTS
On geoid heights and flexure of the lithosphere at seamounts
[AD-A151220] 15 p2604 N85-26050

SEAMS (JOINTS)
Optical seam tracking of robotic arc welding
[VTT-272] 01 p0055 N85-10368
Softening of metal near seam during welding of heat-resistant nickel alloys 13 p2035 N85-22747
Increasing seam formation stability in electron beam welding of very thick titanium alloys
15 p2500 N85-25420
Development of coating for protection of backside of seam in welding of titanium alloys
15 p2500 N85-25421
Study of acceptance criteria for joint densities in bituminous airport pavements
[FAA-PM-85-5] 16 p2715 N85-26761

SEAPLANES
The effect of changes in the angle of incidence in the event of a richochet at a float step
[RAE-TRANS-2120] 07 p0902 N85-15712

SEARCH AND RESCUE SATELLITE
U SARSAT

SEARCH FOR EXTRATERRESTRIAL INTELLIGENCE
U PROJECT SETI

SEARCH PROFILES
Guide to human factors information sources
[AD-A149102] 10 p1531 N85-19649
Local search in routing problems with time windows
[CWI-OS-R8409] 12 p1922 N85-22075
Evaluation of the vocabulary switching systems
[PB85-127157] 12 p1951 N85-22260
Document retrieval from a relational database management system: An investigation of multiple-line query formulation using SEQUEL
15 p2665 N85-26447
Retrieval performance in a full text journal article database 16 p2677 N85-27747
Individual differences in online search behavior: The effect of learning styles and cognitive abilities on process and outcome 20 p3541 N85-32037

SEARCH RADAR
NT OVER-THE-HORIZON RADAR
Terrestrial locating --- of buoys from space
05 p0599 N85-13816

SEARCHING
NT SEARCH PROFILES
Optimizing search with positive information feedback
[CSIR-TWISK-313] 01 p0125 N85-10855
Some attributes of online search intermediaries that relate to search outcome 05 p0734 N85-14721
Shipboard and satellite-aided communications equipment in exhibition 06 p0819 N85-15203
Experimental satellite system for determining coordinates of maritime distress
09 p1306 N85-18216
Online database search strategies and thesaural relationship models 09 p1402 N85-18622
The ARGOS contribution to the successful dredging of a deep moored current meter 14 p2327 N85-24381
The SARSAT program 14 p2327 N85-24385
The ARGOS contribution to the demonstration of the effectiveness of a satellite-based search and rescue system 14 p2330 N85-24404
The SARSAT/COSPAS system for assisting satellite based search and rescue 14 p2398 N85-24776
Microcomputer application of aerospace asset surface search planning
[AD-A151633] 15 p2467 N85-25227
Visual search strategy predictions: The use of aspect ratio as a cue
[BAE-BT-12565] 15 p2619 N85-26138
Forward library searching of previously-quantitated peaks, using a scan list created from a quantitation list by a novel FORTRAN program for the INCOS data system
[PB85-165835] 16 p2845 N85-27541
Satellite aided search and rescue. Experimental results and operational prospects --- conference
[ISBN-2-85428-120-9] 20 p3400 N85-31088
The international organization of maritime search and rescue 20 p3400 N85-31089
Search and rescue services for international civil aviation 20 p3400 N85-31090
COSPAS/SARSAT: An overview
20 p3400 N85-31092
Maritime search and rescue cooperation and planning
20 p3400 N85-31093
Search and rescue at sea in the USSR
20 p3400 N85-31094
The contribution of an operational SAR satellite system to the UK SAR organisation — search and rescue (SAR)
20 p3400 N85-31095
Search and rescue of aircraft in distress in France. Organization, means 20 p3401 N85-31096
Specific aspects of maritime search and rescue in French metropolitan and overseas territories: Expected benefits from a detection and location of distress system by satellites 20 p3401 N85-31097
Search and rescue in Canada
20 p3401 N85-31098
The national Search and Rescue (SAR) needs and organization in Norway 20 p3401 N85-31099
The COSPAS-SARSAT system
20 p3401 N85-31101
The COSPAS-SARSAT space segment: Present status and evolution 20 p3401 N85-31102
Rescue satellite COSPAS 20 p3401 N85-31103
The 121.5 MHz ELT: Past, present and future — Emergency Locator Transmitter (ELT)
20 p3401 N85-31105
The 406 MHz ELT/EPIRBs --- Emergency Locator Transmitters/Emergency Position Indicating Radio Beacons (ELT/EPIRB) 20 p3402 N85-31106
Soviet Emergency Locator Transmitter/Emergency Position Indicating Radio Beacon (ELT/EPIRBs) at 121.5 and 406 MHz 20 p3402 N85-31107
Ground segment of COSPAS system
20 p3402 N85-31108
Existing and potential INMARSAT capabilities for the Future Global Maritime Distress and Safety System
20 p3402 N85-31110

The International Radio Consultative Committee (CCIR) recommended satellite Emergency Position Indicating Radio Beacon (EPIRB) system operating through geostationary satellites at 1.6 GHz
20 p3402 N85-31112

A 406 MHz geostationary satellite SARSAT experiment 20 p3403 N85-31113

Evolution of 406 MHz Search and Rescue (SAR) processor 20 p3403 N85-31116

Free-float Emergency Position Indicating Radio Beacons (EPIRBs) and release mechanism on board Norwegian ships. Main specifications and user experience
20 p3404 N85-31120

Experiments of a LORAN-C aided recovery system and a proposal of its application to rescue system
20 p3404 N85-31121

SARSAT 406 MHz system technical evaluation
20 p3404 N85-31124

The COSPAS system tests. Technical results
20 p3404 N85-31125

Use of 121.5/243.0 MHz COSPAS-SARSAT data by North American SAR agencies — search and rescue (SAR) 20 p3405 N85-31127

The COSPAS/SARSAT demonstration and evaluation. Results of the first year in the United States
20 p3405 N85-31128

COSPAS-SARSAT demonstration and evaluation results in Canada 20 p3405 N85-31129

COSPAS-SARSAT demonstration and evaluation phase: COSPAS tests in the USSR and their results
20 p3405 N85-31130

The SARSAT-COSPAS demonstration in France
20 p3405 N85-31131

UK experience with COSPAS-SARSAT and INMARSAT distress systems 20 p3406 N85-31132

The COSPAS-SARSAT system evaluation in Norway
20 p3406 N85-31133

INMARSAT distress and safety communication
20 p3406 N85-31134

Maritime mobile satellite techniques as an integral part of the Future Global Maritime Distress and Safety System (FGMDSS): The position of the Federal Republic of Germany 20 p3406 N85-31136

Future prospects for a combined INMARSAT polar communication and search and rescue satellite system
20 p3406 N85-31137

The development of an institutional structure for the Future Global Satellite System for Search and Rescue
20 p3406 N85-31138

SEAS
NT ARABIAN SEA
NT BALTIC SEA
NT BARENTS SEA
NT BEAUFORT SEA (NORTH AMERICA)
NT BERING SEA
NT BLACK SEA
NT CARIBBEAN SEA
NT CASPIAN SEA
NT MEDITERRANEAN SEA
NT NORTH SEA
NT RED SEA
NT SALTON SEA (CA)
NT SEA OF JAPAN

Prediction of wave height of wind-generated seas in finite water depth
[AD-A145996] 03 p0398 N85-12539

Multivariate analyses of sedimentological data at two early Bronze age sites, Bab edh-Dhra and Numeira, southeast Dead Sea Graben, Jordan
05 p0674 N85-14326

Behavior of mode frequency characteristics in shallow sea with variation of P-wave veocity in bottom sediment layer and sonic velocity profile in water layer
10 p1498 N85-19457

Preliminary results of study of space-time variability of shallow sea on steady acoustical path
10 p1499 N85-19459

Studies of the development of cyclones over Southern China coastal areas and adjacent seas
[AD-A150108] 12 p1896 N85-21901

Preliminary results of the oceanographic cruise of USCGC NORTHWIND to the Greenland Sea
[AD-A149802] 12 p1898 N85-21919

Maritime search and rescue cooperation and planning
20 p3400 N85-31093

SEASAT altimetry for surface height of inland seas
20 p3493 N85-31714

Aerosol formation by wave action over Ross Sea, Antartica 21 p3651 N85-32686

Marine Sample Exploitation Project: Estimates regarding the sensitivity and technology for the detection of nuclear explosion debris in the marine environment
[DE85-013176] 23 p3947 N85-34462

SEASAT SATELLITES
NT SEASAT 1

Lithospheric structure in the Pacific geoid
[NASA-CR-174155] 04 p0526 N85-13365

Components of the time variation of sea surface height from SEASAT altimeter data 05 p0658 N85-14227

SAR internal wave signature experiment
06 p1149 N85-17253

SEASAT 3 and 4
[AD-A148343] 08 p1152 N85-17274

Solitons and SEASAT
[AD-A148396] 08 p1176 N85-17414

Along-track deflection of the vertical from SEASAT: GEBCO (General Bathymetric Chart of the Oceans) overlays
[PB85-129641] 12 p1876 N85-21767

Advanced 2-frequency ocean sensing radar using high resolution antenna beams 14 p2230 N85-23821

SEASAT report
[AD-A151283] 15 p2583 N85-25931

Utilization of the SEASAT scatterometer winds for ocean mixed layer modeling
[AD-A153748] 18 p3150 N85-29506

Global mean sea surface based upon a combination of the GEOS-3 and SEASAT altimeter data
20 p3492 N85-31710

SEASAT altimetry for surface height of inland seas
20 p3493 N85-31714

SEASAT 1

Production of optically correlated SEASAT-A (SEA satellite) SAR (Synthetic Aperture Radar) imagery at DREO (Defence Research Establishment Ottawa)
[AD-A145970] 03 p0355 N85-12281

Intercomparison of GEOS 3/SEASAT wave data and wave model data 03 p0381 N85-12438

SEASAT altimeter data over the Mediterranean: Implications for ERS-1 03 p0382 N85-12443

Lessons from the SEASAT and GEOS-3 altimeters data projects 03 p0384 N85-12457

A brief investigation into the validity of SEASAT radar altimeter data acquired over land
[AD-A146560] 06 p0827 N85-15254

The imaging of internal waves by the SEASAT-A synthetic aperture radar
[ARE(PORTLAND)TN-720/84]
13 p2054 N85-22860

SEASONAL VARIATIONS
U ANNUAL VARIATIONS

SEASONS
NT SUMMER
NT WINTER

Predictor model for seasonal variations in skid resistance, volume 1
[PB84-226612] 01 p0036 N85-10229

Seasonal variations in Triton's atmospheric mass and composition 02 p0301 N85-11948

Spring changeover of the middle atmosphere circulation compared with rocket wind data up to 80 km
11 p1661 N85-20466

Annual cycle. Part 1: The annual variation of surface temperatures over the United States and Canada
[PB85-147676] 15 p2600 N85-26026

The worldwide distribution of the seasonal cycle of mean sea level
[IOS-190] 20 p3497 N85-31743

SEAT BELTS

Impact tests of adjusters for the HBU-12 lap belt
[AD-A148021] 08 p1080 N85-16843

Impact tests of automatic lap belt configurations
[AD-A148034] 08 p1081 N85-16844

Improving inflight negative Gz restraint for aircrewmen
[AD-A151909] 16 p2703 N85-26688

SEATS
NT EJECTION SEATS

Low thrust bipropellant engine/redundant seat valve assembly
[AD-A150293] 13 p2013 N85-22626

Thermal response of aircraft cabin ceiling materials during a post-crash, external fuel-spill, fire scenario
[PB85-145647] 14 p2220 N85-23764

Seat experiments for the full-scale transport aircraft controlled impact demonstration
[AD-A155024] 21 p3553 N85-32106

Development of an energy-absorbing passenger seat for a transport aircraft 22 p3796 N85-33515

Design and testing of an energy-absorbing crewseat for the F/FB-111 aircraft, volume 1
[NASA-CR-3916] 23 p3896 N85-34133

Design and testing of an energy-absorbing crewseat for the F/FB-111 aircraft. Volume 3: Data from crew module testing
[NASA-CR-3918] 23 p3896 N85-34134

SECONDARY BATTERIES
U STORAGE BATTERIES

SECONDARY COSMIC RAYS

Variations in intensity of secondary cosmic radiation observed on 10-11 August 1961
16 p2721 N85-26796

Early study of muons and muon decay
[NOTA-INTERNA-836] 18 p3184 N85-28742

The isotopic composition of cosmic ray chlorine
[OG-4.3-3] 22 p3678 N85-34028

Propagation and secondary production of low energy antiprotons in the atmosphere
[OG-6.1-3] 22 p3687 N85-34094

Secondary antiproton production in relativistic plasmas
[OG-6.1-4] 22 p3688 N85-34095

Observed antiprotons and energy dependent confinement of cosmic rays: A conflict?
[OG-6.1-7] 22 p3688 N85-34096

Reestimation of the production spectra of cosmic ray secondary positrons and electrons in the ISM
[OG-6.2-6] 22 p3689 N85-34107

The effects of newly measured cross sections in hydrogen on the production of secondary nuclei during the propagation of cosmic rays through interstellar H
[OG-7.2-2] 23 p4014 N85-34874

Cosmic ray secondary nuclei and the structure of the galaxy
[OG-7.2-4] 23 p4014 N85-34876

Alfven wave scattering and the secondary to primary ratio
[OG-7.2-9] 23 p4015 N85-34879

Influence of the source distribution on the age distribution of galactic cosmic rays
[OG-8.3-1] 23 p4021 N85-34920

Explanation of the secondary to primary ratio within the continuous Fermi accelerator model
[OG-8.3-2] 23 p4021 N85-34921

Secondary to primary ratio and the continuous acceleration
[OG-8.3-4] 23 p4022 N85-34923

The multiplicity and the spectra of secondaries correlated with the leading particle energy
[HE-3.2-11] 24 p4179 N85-35819

Characteristics of anomalously high multiplicity cosmic ray interactions
[HE-3.3-1] 24 p4180 N85-35820

Peculiarities of gamma-quanta distribution at 20 TeV energy
[HE-3.7-10] 24 p4186 N85-35867

SECONDARY EMISSION

Textured carbon surfaces on copper
[NASA-CASE-LEW-14130-1] 11 p1615 N85-20156

Correlated 2 electron effects in collisions of multiply charged Au ions with He
[DE85-003064] 11 p1723 N85-20837

Coincidence studies of secondary electron emission in light ion-atom collisions
[DE85-002373] 11 p1725 N85-20852

Calculation of secondary-electron escape currents from inclined-spacecraft surfaces in a magnetic field
13 p1992 N85-22481

Self-consistent simulation of plasma interactions with secondary-emitting insulators 13 p1993 N85-22482

Electron yields from spacecraft materials
13 p1996 N85-22512

Measurement of charged secondary particle emission under ion and neutral impact --- Giotto mission
14 p2243 N85-22906

Measurements of integral yields of charged secondary particles using neutral beams simulating a cometary fly-by --- Giotto mission 14 p2244 N85-22908

Simulations of satellite-plasma interaction, including electron space charges --- Giotto mission
14 p2245 N85-22916

Electron stimulated desorption and the role of secondary electrons
[AD-A150974] 14 p2252 N85-22955

Convoy electron production by heavy ions in solids
[DE85-005256] 15 p2660 N85-26416

Multivalued electrostatic potentials; chance or necessity for the charge of solid particles near Saturn?
15 p2677 N85-26529

Wide-angle optics with strong magnetic fields for efficient generation of secondary-particle beams
[DE85-007727] 18 p3179 N85-28713

Carbon foil secondary electron emission during ion passage through the 40 to 500 keV energy field
[MPE-190] 18 p3184 N85-28747

Characteristics of slow particles emitted in the charged current interactions of neutrinos with emulsion nuclei
[HE-5.3-22] 24 p4207 N85-36113

Underground measurements on secondary cosmic rays
[HE-5.4-1] 24 p4207 N85-36116

Analysis of the electron component of EAS at observational level 700 g x cm(-2) with a scale breaking interaction model and gammaisation hypothesis
[HE-5.4-6] 24 p4208 N85-36119

SECONDARY FLOW

Turbulent boundary layers with secondary flow
[NASA-TM-77494] 04 p0496 N85-13176

Computation of flow and heat transfer in flow around a 180 deg bend
[AD-A148065] 08 p1162 N85-17330
Secondary flow in cascades
[AD-A148415] 08 p1162 N85-17339
Basic consideration of the lifting capability of stoppable rotors
[AD-A150650] 14 p2219 N85-23759
Effective specific impulse of secondary flow injected into a rocket nozzle
[NAL-TR-845T] 18 p3067 N85-28970
Experiments on the influence of active walls on the initial amplitudes and growths of instability waves
[AD-A154630] 21 p3583 N85-32275

SECONDARY RADAR
Synthesis of optimum algorithms for secondary processing 13 p2060 N85-22992
Developments in the area of air traffic control systems and the relation with meteorology
[NLR-MP-84029-U] 17 p2895 N85-27848

SECONDARY WAVES
U S WAVES

SECRETIONS
NT ADRENOCORTICOTROPIN (ACTH)
NT HORMONES
NT HYDROXYCORTICOSTEROID
NT INSULIN
NT PROSTAGLANDINS
NT SWEAT
Biligenic function of white rat liver
01 p0093 N85-10624

SECULAR PERTURBATION
U LONG TERM EFFECTS

SECULAR VARIATIONS
Geomagnetic secular variation: A jerk in 1970
04 p0521 N85-13329
Comparisons of secular variation in two-dipole and spherical harmonic models with observatory data in Eurasia, 1965-1975 04 p0521 N85-13330
Geomagnetic secular variation at Ebro Observatory during the past 70 years 04 p0521 N85-13331
Insolation changes on Pluto caused by orbital element variations
[AERONOMICA-ACTA-A-290-1984]
20 p3546 N85-32070
Cosmic ray secular variations in terrestrial records and aurorae
[SH-7.1-3] 23 p4047 N85-35096

SECURITY
NT COMPUTER INFORMATION SECURITY
Scientific communications and national security
[GPO-36-093] 04 p0492 N85-13136
Semiannual report to Congress on the effectiveness of the civil aviation security program
[AD-A146522] 10 p1421 N85-18967
Brussels Satellite Convention
[S-EXEC-REPT-98-52] 12 p1790 N85-21234
Literature survey of underground construction methods for application to hardened facilities
[AD-A155212] 21 p3599 N85-32351

SEDIMENT TRANSPORT
Dynamic response of electromagnetic current meters
[PB84-229731] 06 p0842 N85-15344
Analysis of suspended sediment distributions in the surface waters of Delaware Bay using remote sensing of optical properties 15 p2582 N85-25926
Modern sedimentation in the northern Barents Sea: Input, dispersal and deposition of suspended sediments from glacial meltwater
[AD-A152520] 17 p2997 N85-28530
Use of a two-dimensional flow model to quantify aquatic habitat
[AD-A154287] 19 p3266 N85-30253
Sand dispersion from an ephemeral river delta on the wave-dominated central California coast
[AD-A154352] 19 p3300 N85-30456
New estimating procedures for surface runoff, sediment yield, and contaminant transport in Los Alamos County, New Mexico
[DE85-011690] 21 p3606 N85-32393

SEDIMENTARY ROCKS
NT COAL
NT LIGNITE
NT LIMESTONE
NT PEAT
NT SANDSTONES
NT SHALES
Franciscan and related rocks of southern Humbolt County, northern California coast ranges: Analysis of structure, tectonics, sedimentary petrology, paleogeography, depositional histroy, and thermal maturity 03 p0390 N85-12495
Post-Sonoman conodont biofacies of the Triassic of northwestern Nevada 03 p0390 N85-12497
The Kanayut Conglomerate in the westernmost Brooks Range, Alaska 04 p0516 N85-13289
Reconnaissance geology of the northern part of the Unalakleet quadrangle 04 p0516 N85-13291
Newly recognized sedimentary environments in the Shelikof Formation, Alaska 04 p0516 N85-13292
New ages of radiolarian chert from the Rampart district, east-central Alaska 04 p0516 N85-13293
Concordant bands of augen gneiss within metasedimentary rocks in the Big Delta C-2 quadrangle, east-central Alaska 04 p0516 N85-13294
Lacustrine and eolian deposits of Wisconsin age at Riverside Bluff in the upper Tanana River valley, Alaska
04 p0517 N85-13299
Archean sedimentation and tectonics in southern Africa
[NASA-CR-174156] 04 p0533 N85-13408
The Georges Bank monitoring program 1983: Analysis of trace metals in bottom sediments
[CIRC-915] 05 p0688 N85-14423
Normal-fault and fold development in sedimentary rocks above a pre-existing basement normal fault
13 p2131 N85-23259
Evaluating structure-forming role of late Paleozoic and Mesozoic-Cenozoic tectonic movements in Baltic Sea region 14 p2337 N85-24450
Carbon isotope geochemistry and geobiology
21 p3657 N85-32716
Archean sedimentary systems and crustal evolution
21 p3720 N85-33082
Organic solvent alteration of hydraulic properties of sedimentary rocks of low permeability: A review
[DE85-012537] 22 p3815 N85-33635
Marine phosphorite deposits model for exploration, with emphasis on deposits in the US Atlantic coastal plain
24 p4104 N85-35439
Seismic stratigraphic analysis of the Mississippi Fan
24 p4115 N85-35507
Geology and geomorphology of the Roraima group, southeastern Venezuela 24 p4115 N85-35511

SEDIMENTS
NT SANDS
NT TAR SANDS
Chemistry of fuel deposits and sediments and their precursors
[NASA-CR-174778] 01 p0034 N85-10209
Erosion and sedimentation chronology of three watersheds in Maryland
[PB84-207356] 01 p0071 N85-10467
Late quaternary glacial cycles in the Bahamian deep basins and in the adjacent Atlantic Ocean
02 p0226 N85-11476
Paleohydrology and geomorphology of selected reaches of the upper Wabash Valley, Indiana
02 p0226 N85-11481
Paleoenvironmental interpretation of the upper cretaceous Point Lookout sandstone: Implications for shoreline progradation and basin tectonic history, San Juan basin, New Mexico 02 p0227 N85-11486
Stratigraphy, sedimentology and tectonic significance of the Upper Cretaceous Virginian Ridge formation, Method Basin, Washington: Implications for tectonic history of the North Cascades 03 p0390 N85-12494
Late quarterly glaciolacustrine and vegetational history of the Copper River Basin, south-central Alaska
03 p0391 N85-12499
Glacial-lake deposits in the Mount Harper area, Yukon-Tanana Upland 04 p0517 N85-13300
Constraints on lunar origin: Evidence preserved in Precambrian stromatolites 04 p0584 N85-13731
Multivariate analyses of sedimentological data at two early Bronze age sites, Bab edh-Dhra and Numeira, southeast Dead Sea Graben, Jordan
05 p0674 N85-14326
Sedimentation, structure and tectonics of the Umpqua group (paleocene to early eocene), southwestern Oregon 05 p0678 N85-14354
The Georges Bank monitoring program 1983: Analysis of trace metals in bottom sediments
[CIRC-915] 05 p0688 N85-14423
Storage stability of jet fuels
[AD-A146360] 06 p0773 N85-14943
Manganese in recent sediments of Ukrainian SSR Black Sea shelf 06 p0819 N85-15200
Unsinkability of ferromanganese nodules
06 p0819 N85-15202
Some methodological aspects of study of layer associations in continents and oceans
06 p0820 N85-15205
Platinum group nuggets in deep sea sediments
06 p0883 N85-15611
Pulse transmission through frozen silt
[AD-A147108] 07 p0940 N85-15958
Ocean acoustics
[AD-A147062] 07 p1036 N85-16591
Soil formation on tertiary landsurfaces of the New Jersey coastal plain 08 p1181 N85-17441
Preliminary post-emplacement safety analysis of the subseabed disposal of high-level nuclear waste
[DE84-011162] 08 p1221 N85-17692
The pleistocene geology of Vilas County, Wisconsin
09 p1353 N85-18509
Quaternary stratigraphy, geochronology and carbon isotope geology of alluvial deposits in the Texas panhandle 09 p1353 N85-18514
Measurements of sediment temperatures, conductivity and heat flow in the North Atlantic and their relevance to radioactive waste disposal
[IOS-172] 09 p1359 N85-18551
Evolution of sedimentation basins in Earth's history
10 p1497 N85-19451
Behavior of mode frequency characteristics in shallow sea with variation of P-wave veocity in bottom sediment layer and sonic velocity profile in water layer
10 p1498 N85-19457
Aluminum in biogenic cycle and forms of its occurence in ocean 10 p1499 N85-19463
SIR-A imagery in geologic studies of the Sierra Madre Oriental, northeastern Mexico. Part 1 (Regional stratigraphy): The use of morphostratigraphic units in remote sensing mapping
[NASA-CR-175457] 10 p1505 N85-19497
U, Th, K content, heat production and thermal conductivity of Sao Paulo, Brazil continental shelf sediments: A reconnaissance work
[INPE-3401-PRE/670] 10 p1515 N85-19558
Improved techniques for removal of sediments contaminated with hazardous materials
[PB85-116093] 11 p1679 N85-20580
Special features of computations of vertical distribution of concentration of suspended sediments under marine conditions 13 p2106 N85-23125
Determining adsorption of surface-active substances by sea bottom deposits 13 p2107 N85-23128
Review of problems in lithology
13 p2113 N85-23160
A first evaluation of LANDSAT TM data to monitor suspended sediments in lakes — Lake Chicot, Arkansas
13 p2120 N85-23204
Electromagnetic field of currents and its use to estimate total conductivity of sedimentary deposits in Western Black Sea 14 p2334 N85-24434
Absolute movement of Pacific Ocean plate based on paleoclimatic and paleomagnetic data and trajectory of hot spots during last 120 million years
14 p2334 N85-24435
Evaluating structure-forming role of late Paleozoic and Mesozoic-Cenozoic tectonic movements in Baltic Sea region 14 p2337 N85-24450
Modern sedimentation in the northern Barents Sea: Input, dispersal and deposition of suspended sediments from glacial meltwater
[AD-A152520] 17 p2997 N85-28530
Numerical benchmark study for the finite element computer code NEPTUNE
[DE85-008400] 17 p3013 N85-28630
Structure of Reykjanes Ridge rift zone and Icelandic thermal anomaly 19 p3289 N85-30395
Natural gas anomaly in bottom waters of South China Sea 19 p3290 N85-30399
Sand dispersion from an ephemeral river delta on the wave-dominated central California coast
[AD-A154352] 19 p3300 N85-30456
Physiochemically controlled scour jet array system
[AD-D011686] 19 p3308 N85-30505
Offshore oceanographic and environmental monitoring services for the Strategic Petroleum Reserve, volume 3
[DE85-009907] 20 p3497 N85-31741
Sulfur diagenesis in marine sediments
21 p3658 N85-32721
Sulfur cycling in freshwater sediments
21 p3658 N85-32726
Sulfur and carbon cycling in organic-rich marine sediments 21 p3659 N85-32729
Sulfur reduction in sediments of marine and evaporite environments 21 p3661 N85-32742
Microanalysis of dissolved iron and phosphate in pore waters of hypersaline sediment
21 p3661 N85-32744
A random layer model for reflection from ocean bottom sediments
[AD-A155019] 21 p3700 N85-32988
Archean sedimentary systems and crustal evolution
21 p3720 N85-33082
Subduction zone tectonic studies to develop concepts for the occurrence of sediment subduction
[DE85-011794] 22 p3815 N85-33632
Bedrock geology of the Brattleboro Quadrangle, Vermont-New Hampshire
[DE85-011027] 22 p3815 N85-33634
Origin of sedimentary humic acids, potential carriers of ore-forming elements 24 p4104 N85-35443

Depositional systems and coal occurrence in the Fort Union Formation (Paleocene), Powder River Basin, Wyoming and Montana 24 p4114 N85-35505
Bibliography on tidal hydraulics. Report 2. Supplement 9: Supplementary material compiled from June 1980 - June 1983. Tidal flows in rivers and harbors [AD-A155990] 24 p4125 N85-35574
SEEBECK COEFFICIENT
U SEEBECK EFFECT
SEEBECK EFFECT
Anomalous electronic transport in boron carbides [DE84-015620] 06 p0868 N85-15518
SEEDING (INOCULATION)
U INOCULATION
SEEDS
Timing in dry seeds 05 p0690 N85-14437
Attempts to localize and identify the gravity sensing device of plant seedlings 15 p2607 N85-26064
Effect of seeds of heavy charged particles of galactic cosmic radiation 23 p3954 N85-34505
SEEKERS
U HOMING DEVICES
SEGMENTS
Integrating non-semantic knowledge into image segmentation processes [AD-A149571] 12 p1851 N85-21612
Twisting of segmental shafts 14 p2279 N85-24119
Study of fatigue strength of shafts with segmented channels 14 p2282 N85-24138
Computations for segmented radial bearings 14 p2288 N85-24180
Selection of segment similarity measures for hierarchical picture segmentation 23 p3960 N85-34548
SEGREGATION
U SEPARATION
SEISMIC ENERGY
Horizontal-strain observations in the Shumagin Island and Yakataga seismic gaps, Alaska 04 p0515 N85-13237
Deployment of a regional array in Norway [AD-A147032] 07 p0997 N85-16330
Interrelationship of earthquake magnitude and lithospheric-asthenospheric thermodynamic parameters in seismically active zones 13 p2116 N85-23183
Relationship between seismic status of Earth and relative position of bodies in sun-earth-moon system 14 p2345 N85-24499
Study of earthquake preparation processes from distribution of weak tremor epicenters 14 p2345 N85-24501
Development of ultrasonic modeling techniques for the study of crustal inhomogeneities [AD-A155206] 21 p3632 N85-32565
SMACS: A system of computer programs for probabilistic seismic analysis of structures and subsystems. Volume 1: User's manual [DE85-011853] 22 p3830 N85-33724
SEISMIC WAVES
NT LOVE WAVES
NT MICROSEISMS
NT RAYLEIGH WAVES
Response and characteristics of structures subjected to S-H waves 01 p0060 N85-10386
Specific phenomena associated with the propagation of seismic waves in central Europe [REPT-548] 03 p0375 N85-12391
Hole shots along refraction profile R4/78 recorded at the temporary seismic station near Stary Plzenec (west Bohemia) [REPT-549] 03 p0375 N85-12392
In situ experiment on shear waves generation and determination of elastic properties of soils [REPT-550] 03 p0375 N85-12393
Finite-difference synthetic seismograms for SH waves [AD-A145834] 03 p0392 N85-12508
Coupling of airborne sound into the Earth [AD-A146231] 03 p0416 N85-12663
Characteristics of a recent Columbian earthquake, December 12, 1979 04 p0523 N85-13347
Possible effects of interaction of electric seismic fields with the ionosphere 06 p0823 N85-15228
Nonlinear wave propagation study [AD-A147011] 07 p0996 N85-16329
Short period guided waves over oceanic and continental paths [AD-A147053] 07 p0997 N85-16331
The Shock and Vibration Digest, volume 16, no. 11 [AD-A148466] 08 p1171 N85-17382
On seismic waves 08 p1171 N85-17383
Seismic performance of low-rise light-framed wood buildings 08 p1171 N85-17384
Effects of heterogeneities on the propagation, scattering and attenuation of seismic waves and the characterization of seismic source [AD-A148284] 08 p1186 N85-17476
Studies on seismic earth pressure of cohesive backfill 09 p1303 N85-18186
Earthquake-modeling experiment using unique press 10 p1500 N85-19469
Mathematical modeling of wave fields by superimposition of boundary waves in reflected earthquake waves method 10 p1501 N85-19476
Influence of scattering on Q in the lithosphere [AD-A149318] 10 p1515 N85-19583
An analysis of short-to-medium-range seismic attenuation tests using a multilayered viscoelastic seismic propagation model [AD-A149771] 12 p1889 N85-21856
Twenty-five sound propagation tests on the continental shelf between Long Island, New York and Cape Canaveral, Florida [AD-A149869] 12 p1928 N85-22111
Two-and-one-half dimensional in-plane wave propagation [AD-A150467] 13 p2055 N85-22867
Determining degree of partial melting of asthenosphere from seismic data 13 p2107 N85-23127
More precise curve of dependence between density and velocity of longitudinal waves in consolidated crust and top of mantle in oceanic structures 13 p2110 N85-23143
Nature of seismic images with amplitude and time fluctuations of recorded oscillations 13 p2112 N85-23156
Magmatism in continent-ocean transition zone (development of ideas of A. N. Zavaritskiy) 13 p2113 N85-23161
Boundary velocities of longitudinal seismic waves and lateral inhomogeneities of upper ocean mantle 13 p2113 N85-23165
Seismic waves and dispersion relations 13 p2116 N85-23181
Interrelationship of earthquake magnitude and lithospheric-asthenospheric thermodynamic parameters in seismically active zones 13 p2116 N85-23183
Correcting depth line on nonlongitudinal seismic profile 13 p2117 N85-23184
Attenuation of seismic waves at regional distances [AD-A150198] 13 p2132 N85-23267
Influence scattering and Q in the lithosphere [AD-A150939] 14 p2293 N85-24213
Seismic analysis of rotating mechanical systems [PB85-149599] 14 p2311 N85-24307
Interpreting refracted waves method data on basis of automated determination of seismic drift 14 p2343 N85-24486
Determining geometrical divergence using seismic observation data 14 p2343 N85-24489
New methods for interpreting seismic time fields in media with variable velocities 14 p2343 N85-24490
Possibility of retrieving dynamics of reflected wave method records beneath low-velocity zone 14 p2346 N85-24503
Results of studies of wave field internal structure in prediction of geological cross section 14 p2346 N85-24504
Regional seismic wave propagation [AD-A150801] 14 p2373 N85-24671
Asymptotic construction of a procedure for plane-wave synthesis and migration [AD-A150969] 14 p2374 N85-24672
Seafloor seismic measurements in the southern Bering [DE85-004908] 14 p2374 N85-24675
On coupling factors of explosion 15 p2551 N85-25747
Connection between time- and frequency-domain three-dimensional inverse problems for the Schroedinger equation [DE85-005914] 15 p2639 N85-26274
The Shock and Vibration Digest, volume 17, no. 2 [AD-A153129] 17 p2977 N85-28400
The effects of seismic waves 17 p2978 N85-28401
Proceedings of the 1980 Workshop of the International Association of Seismology and Physics of the Earth's Interior on the Seismic Modeling of Laterally Varying Structures: Contributions based on data from the 1978 Saudi Arabian refraction profile [GS-CIRC-937] 17 p2989 N85-28476
Two-dimensional inverse kinematic problem: Application to the Saudi Arabian refraction profile 17 p2990 N85-28478
Crustal structure of the Red Sea-Arabian Shield transition 17 p2990 N85-28479
A seismic refraction profile across the Arabian Shield 17 p2990 N85-28481
The rifted margin of Saudi Arabia 17 p2990 N85-28483
Surface waveseismic yields as measured by the Regional Seismic Test Network [DE85-010532] 18 p3137 N85-29425
Wave-theoretical approach to seismic modeling problems (WELMOD) [BMFT-FB-T-84-258] 18 p3137 N85-29429
Discovery in earthquake forecasting and seismic zoning recorded 19 p3295 N85-30426
Well-posedness of one-way wave equations and absorbing boundary conditions [NASA-CR-172619] 19 p3345 N85-30727
Crosswell acoustic surveying in gas sands: Travel-time pattern recognition, seismic Q and channel waves [DE85-010777] 19 p3352 N85-30778
Effects of contact area of an interface on acoustic wave transmission characteristics [DE85-009935] 20 p3524 N85-31920
Robust detection and classification of regional seismic signals using a two mode/two stage cascaded adaptive arma (CAARMA) model [AD-A154710] 21 p3630 N85-32554
The Norwegian seismic array (NORSAR) [AD-A154751] 21 p3631 N85-32555
Experimental and analytic characterization of nonlinear seismic attenuation [AD-A154760] 21 p3631 N85-32556
Design of a freestanding noise measurement and recording system to predict the intensity and location of electromagnetic radiation from earthquakes [AD-A155070] 21 p3632 N85-32563
Qualitative analysis of sign-bit processing [AD-A154776] 21 p3671 N85-32804
Attenuation properties of the Petatlan region, Mexico, and a local magnitude scale for microearthquakes in this area 24 p4116 N85-35513
Applications of the Kirchoff-Helmholtz integral to problems in body wave seismology 24 p4116 N85-35515
Workshop Proceedings: Interpretation of Seismic Wave Propagation in Laterally Heterogeneous Structures [BMR-258] 24 p4118 N85-35530
SEISMOGRAMS
Finite-difference synthetic seismograms for SH waves [AD-A145834] 03 p0392 N85-12508
SEISMOGRAPHS
Standardization of amplitude characteristics of galvanometric seismographs in the KAPG network [REPT-552] 03 p0375 N85-12395
SVKD and SVKM-3 seismographs with a low-sensitivity channel [REPT-553] 03 p0376 N85-12396
Short-period seismograph SVSN-6 [REPT-554] 03 p0376 N85-12397
Microseism level, time variations at Turkmen seismic stations studied 07 p0961 N85-16231
Deployment of a regional array in Norway [AD-A147032] 07 p0997 N85-16330
Seismic performance of low-rise light-framed wood buildings 08 p1171 N85-17384
Use of mobile surface station for synchronous seismic measurements in seismological research 13 p1984 N85-22447
A seismic ARGOS data collection platform 16 p2813 N85-27350
SEISMOLOGY
NT HELIOSEISMOLOGY
Microseismic monitoring of Chocolate Bayou, Texas: The Pleasant Bayou no. 2 geopressured/geothermal energy test well program [DE84-014825] 01 p0072 N85-10477
Seismotectonic nature of some annular photoanomalies registered by remote methods 02 p0184 N85-11110
A comparison of seismic properties of young and mature oceanic crust 02 p0226 N85-11479
Seismology 1983: Nuclear test ban verification, earthquake and Earth resource investigation [FOA-C-20537-T1] 02 p0229 N85-11485
A pilot study of future research on seismic hazards in Sweden [FOA-C-20544-T1] 02 p0229 N85-11486
Archiving and exchange of a computerized marine seismic database: The ROSE (Rivera Ocean Seismic Experiment) data archive system [AD-A145658] 02 p0294 N85-11908
Geophysical Works during 1981, volume 29, no. 547-566 03 p0375 N85-12390
In situ experiment on shear waves generation and determination of elastic properties of soils [REPT-550] 03 p0375 N85-12393
Seismology in rockburst research [REPT-551] 03 p0375 N85-12394
Coupling of airborne sound into the Earth [AD-A146231] 03 p0416 N85-12663
Seismic studies in southern Alaska 04 p0515 N85-13236

Scientific contributions in commemoration of Ebro Observatory's 75th anniversary — conference
[ISBN-84-00-05380-X] 04 p0518 N85-13306
Seismology today 04 p0523 N85-13346
A review of seismicity in peninsular Spain
04 p0523 N85-13349
Deep structure beneath the Pyrenees
04 p0524 N85-13351
Earthquake catalog for northern New Mexico
[DE84-016964] 04 p0534 N85-13416
Archiving and exchange of a computerized marine seismic databases: The ROSE data archive system
[DE84-901453] 04 p0576 N85-13677
Documentation of earthquake algorithms
[PB84-235324] 05 p0677 N85-14351
Evaluation of the RSTN (Regional Seismic Test Network) network and further improvement to automatic association
[AD-A146395] 06 p0835 N85-15312
Microseism level, time variations at Turkmen seismic stations studied 07 p0961 N85-16231
General model of earthquakes and the place of warnings in it 07 p0961 N85-16232
Research activities of the Norwegian seismic array (NORSAR)
[AD-A146778] 07 p0996 N85-16326
Deployment of a regional array in Norway
[AD-A147032] 07 p0997 N85-16330
Short period guided waves over oceanic and continental paths
[AD-A147053] 07 p0997 N85-16331
Seismicity of southern Sweden
[FOA-C-20543-T1] 07 p0998 N85-16340
Research of inverse methods to describe the structure of the earth and ocean bottom
[AD-A147082] 07 p1030 N85-16541
An efficient numerical solution technique for wave propagation in horizontally stratified ocean environments
[AD-A148637] 08 p1190 N85-17502
Detailed oceanic crustal modeling
[AD-A148589] 08 p1191 N85-17507
Atmospheric limitations in stellar seismology: Should one measure radial velocity or brightness fluctuations?
08 p1251 N85-17899
Technology reports of the Yamaguchi University, volume 3, no. 3
[ISSN-0386-3433] 09 p1302 N85-18182
Earth Sciences Division report, 1983
[DE85-001036] 09 p1341 N85-18436
Field implementation of geophysical diffraction tomography
[DE84-017594] 09 p1343 N85-18449
Velocity stack and slant stack inversion methods
09 p1351 N85-18497
Nonlinear seismology 10 p1503 N85-19482
Statistical study of anthropogenic seismic noise with IVK-7 computer system 10 p1503 N85-19483
High-resolution microseismicity study of possible magmatic intrusion in the Long Valley Caldera
[DE85-001076] 11 p1681 N85-20593
Resolution of 2-dimensional seismologic problems by a finite element approximation. Application to the Love wave propagation through the Atlantic border of the Iberic Peninsula 11 p1681 N85-20594
Resolution of 2-dimensional seismologic problems by a finite element approximation. Application to the Love wave propagation through the Atlantic border of the Iberic Peninsula. Appendix: Graphs of results — Lagrange coordinates 11 p1681 N85-20595
Seismic observation of infrasonic signals
[AD-A149574] 12 p1889 N85-21853
Use of mobile surface station for synchronous satellite measurements in seismological research
13 p1984 N85-22447
Geophysical laser interferometer with 12.5 meter base
13 p2089 N85-23046
Crustal and upper mantle density model of Owen fault zone 13 p2110 N85-23144
Observation of long-period oscillations of Earth
13 p2110 N85-23149
Natural electromagnetic radiation in seismically active regions 13 p2111 N85-23152
Determination of density of the crust and upper mantle from deep seismic sounding and gravimetry, 2
13 p2111 N85-23153
Geomagnetic precursors of intensive earthquakes in the 1-0.2 Hz frequency range of geomagnetic pulsations
13 p2116 N85-23178
Correcting depth line on nonlongitudinal seismic profile 13 p2117 N85-23184
Method for processing broad-profile data
13 p2117 N85-23185
Attenuation of seismic waves at regional distances
[AD-A150196] 13 p2132 N85-23267
Seismic analysis of rotating mechanical systems
[PB85-149599] 14 p2311 N85-24307
USSR report: Earth sciences
[JPRS-UES-85-004] 14 p2332 N85-24424
Evaluating structure-forming role of late Paleozoic and Mesozoic-Cenozoic tectonic movements in Baltic Sea region 14 p2337 N85-24450
Interpreting refracted waves method data on basis of automated determination of seismic drift
14 p2343 N85-24486
Electromagnetic fields migration method
14 p2343 N85-24487
New methods for interpreting seismic time fields in media with variable velocities 14 p2343 N85-24490
Asymptotic construction of a procedure for plane-wave synthesis and migration
[AD-A150969] 14 p2374 N85-24672
Seafloor seismic measurements in the southern Bering
[DE85-004908] 14 p2374 N85-24675
A fast ray tracing routine for laterally inhomogeneous media
[AD-A150984] 14 p2421 N85-24936
China report: Science and technology
[JPRS-CST-85-011] 15 p2551 N85-25746
On coupling factors of explosion
15 p2551 N85-25747
Frequency dependence of Q in the mantle underlying the shield areas of eurasia
[AD-A151367] 15 p2582 N85-25978
GEMINI: A computer program for two and three dimensional linear static and seismic structural analysis, CDC 7600 version
[DE85-007496] 15 p2631 N85-26218
A seismic ARGOS data collection platform
16 p2813 N85-27350
Response of a wind turbine blade to seismic and turbulent wind excitations 16 p2817 N85-27375
Symposium on Atmospheric Sciences in South Africa
[CSIR-S-331] 16 p2829 N85-27442
Born inversion with a stratified reference velocity
[AD-A149222] 16 p2853 N85-27594
The Shock and Vibration Digest, volume 17, no. 2
[AD-A153129] 17 p2977 N85-28400
The effects of seismic waves
17 p2978 N85-28401
Australian seismological report, 1980
[REPT-252] 17 p2989 N85-28473
Proceedings of the 1980 Workshop of the International Association of Seismology and Physics of the Earth's Interior on the Seismic Modeling of Laterally Varying Structures: Contributions based on data from the 1978 Saudi Arabian refraction profile
[GS-CIRC-937] 17 p2989 N85-28476
Preliminary interpretation of Saudi Arabian seismic refraction data 17 p2989 N85-28477
Two-dimensional inverse kinematic problem: Application to the Saudi Arabian refraction profile
17 p2990 N85-28478
Crustal structure of the Red Sea-Arabian Shield transition 17 p2990 N85-28479
A crustal section for the Arabian Shield and adjacent Red Sea margin derived from first-arrival data
17 p2990 N85-28480
A seismic refraction profile across the Arabian Shield
17 p2990 N85-28481
A preliminary examination of the 1978 refraction profiles in Saudi Arabia 17 p2990 N85-28482
The rifted margin of Saudi Arabia
17 p2990 N85-28483
Saudi Arabian refraction profile: Crustal structure of the Red Sea-Arabian Shield transition
17 p2990 N85-28484
Saudi Arabian refraction profile: A preliminary interpretation for the Red Sea-Arabian Shield transition
17 p2991 N85-28485
A traveltime interpretation of the 1978 seismic refraction profile in the Kingdom of Saudi Arabia
17 p2991 N85-28486
Explanation of Russian models: Saudi Arabian seismic refraction profile 17 p2991 N85-28487
Interpretation of the data of USGS seismic refraction profile across the Arabian Shield in western Saudi Arabia 17 p2991 N85-28488
A preliminary analysis of the Saudi Arabian deep seismic sounding data 17 p2991 N85-28489
One-dimensional velocity-depth functions determined for the Arabian Shield and the southwestern Red Sea: A comparison of models 17 p2992 N85-28490
Revised draft: Southeastern regional geologic characterization report
[DE85-008285] 18 p3125 N85-29351
Surface waveseismic yields as measured by the Regional Seismic Test Network
[DE85-010532] 18 p3137 N85-29425
Seismic analysis of liquid-filled tanks with an eccentric core barrel
[DE85-010249] 19 p3269 N85-30272
Analysis of seismic sloshing of reactor tanks considering submerged components and seismic isolation
[DE85-010499] 19 p3269 N85-30273
Tectonic structure features of some deep faults in Atlantic and Pacific Oceans (according to deep seismic sounding-reflected waves method data)
19 p3295 N85-30428
Deployment of a regional array in Norway
[AD-A154120] 19 p3313 N85-30536
Seismic discrimination
[AD-A154167] 20 p3494 N85-31722
The Norwegian seismic array (NORSAR)
[AD-A154751] 21 p3631 N85-32555
Tectonic stability and expected ground motion at Yucca Mountain
[DE85-012004] 22 p3814 N85-33629
SMACS: A system of computer programs for probabilistic seismic analysis of structures and subsystems. Volume 1: User's manual
[DE85-011853] 22 p3830 N85-33724
Geophysical-geological studies of possible extensions of the New Madrid fault zone
[TI85-901341] 23 p3949 N85-34475
Strong earthquakes, novae and cosmic ray environment
[SH-10.1-3] 23 p4053 N85-35135
Seismic stratigraphic analysis of the Mississippi Fan
24 p4115 N85-35507
Attenuation properties of the Petatlan region, Mexico, and a local magnitude scale for microearthquakes in this area 24 p4116 N85-35513
Applications of the Kirchoff-Helmholtz integral to problems in body wave seismology
24 p4116 N85-35515

SEISMOMETERS
U SEISMOGRAPHS

SELECTION
NT PERSONNEL SELECTION
NT PILOT SELECTION
NT SITE SELECTION
Guide to the selection of rubbers
[AMTE(N)-TM-84301] 03 p0336 N85-12164
R and D project selection with nonnumerical returns
[INPE-2760-PRE/335] 04 p0575 N85-13665
On choosing between two probabilistic choice sub-models in a dynamic multitask environment
05 p0711 N85-14563
A theoretical method for selecting space craft and space suit atmospheres
[AD-A148219] 08 p1200 N85-17559
A computer package for ranking, selection and multiple comparisons with the best
[AD-A147617] 08 p1204 N85-17579
The R and D project selection problem with fuzzy coefficients
[INPE-3329-PRE/626] 10 p1565 N85-19871
Selection criteria for a CAD/CM system
14 p2402 N85-24810
Selection criteria and computer aided design (CAD) systems
[NLR-MP-84037-U] 14 p2406 N85-24834
Method of selecting robotized system design for pressing process 16 p2761 N85-27040
Satellite selection criteria 16 p2804 N85-27288
A short bibliography of recent developments in selection and ranking procedures
[AD-A155648] 21 p3679 N85-32856
Robotic order picking
[AD-D011737] 22 p3792 N85-33493
Knowledge engineering application in image processing 23 p3965 N85-34583

SELECTIVE DISSEMINATION OF INFORMATION
Environmental geologic atlas of the North Carolina coastal zone: Dare, Hyde, Tyrrell and Washington Counties
[PB84-222975] 01 p0066 N85-10439
International strategic minerals inventory. Summary report: Manganese
[GS-CIRC-930-A] 02 p0219 N85-11442
Ocean services user needs assessment. Volume 1: Survey results, conclusions and recommendations
[NASA-CR-174104] 04 p0541 N85-13445
Nuclear criticality information system: Database examples
[DE84-014462] 04 p0576 N85-13678
Organization of scientific, technical information services 17 p3049 N85-28873
The U.S. Geological Survey in Alaska: Accomplishments during 1982
[US-GEOL-SURV-CIRC-939] 20 p3493 N85-31719
Source header list, supplement 3
[AD-A156100] 24 p4165 N85-35824
Source hierarchy list. Volume 2: I through Z
[AD-A156301] 24 p4165 N85-35826

SELECTIVE FADING
Digital radio link: Wave propagation measurements using narrow band technique
[FOA-C-30384-E2] 04 p0494 N85-13152
Digital data communications over microwave radio channels 10 p1469 N85-19272
Theoretical study of a dynamic simulator of selective fading for digital, wireless beam microwave links
10 p1473 N85-19294
SELECTIVE SURFACES
Selective coatings for solar-to-thermal energy converters 14 p2260 N85-24127
High-altitude testing of selective optical coatings for solar radiators and collectors 17 p2939 N85-28143
Selective coatings for solar heat converters
17 p2939 N85-28144
Thickness-insensitive selective surface paint
[DE85-010568] 19 p3250 N85-30150
SELECTIVITY
Color-selective coating for viewfinder in optical instruments 14 p2276 N85-24098
Correlation of zeolite ZSM-5 acid strength with catalytic activity and selectivity
[DE85-005415] 17 p2922 N85-28013
High-altitude testing of selective optical coatings for solar radiators and collectors 17 p2939 N85-28143
Selective coatings for solar heat converters
17 p2939 N85-28144
Waveguide dielectric millimeter band filter with enhanced selectivity 22 p3780 N85-33421
SELECTORS
High-frequency input device for superheterodyne radio receiver with wideband preselector
12 p1839 N85-21540
Gyrator frequency selectors with bandwidth independent of input signal level 13 p2063 N85-23009
SELENIDES
NT CADMIUM SELENIDES
NT COPPER SELENIDES
NT ZINC SELENIDES
Thio and seleno compounds of the transition metals with the d (o) configuration
[BLL-MINTEK-TR-1177-(5810.5759)]
07 p0925 N85-15863
Positron measurements in 2H-TaSe2 crystals
[DE85-010507] 20 p3529 N85-31949
SELENIUM
Environmental surveillance at Los Alamos during 1984
[DE85-011686] 22 p3811 N85-33605
SELENIUM ALLOYS
Philips tested new materials for optical data storage
15 p2532 N85-25620
SELENIUM COMPOUNDS
NT CADMIUM SELENIDES
NT COPPER SELENIDES
NT SELENIDES
NT ZINC SELENIDES
Effect of light pulses on film of chalcogenide vitreous semiconductors 02 p0258 N85-11667
SELENOGRAPHY
Analysis of systematic errors in systems of selenodetic coordinates 13 p1982 N85-22435
SELENOLOGY
NT LUNAR CORE
Activities at the Lunar and Planetary Institute
[NASA-CR-174069] 04 p0579 N85-13694
Activities at the Lunar and Planetary Institute, introduction 04 p0579 N85-13695
Volatile elements in and on lunar volcanic glasses: What do they tell us about lunar genesis?
04 p0584 N85-13726
The origin of the Moon 04 p0586 N85-13754
A unified lunar control network
13 p2203 N85-23669
Surface exploration geophysics applied to the Moon
[DE85-006714] 16 p2894 N85-27793
SELF ADAPTIVE CONTROL SYSTEMS
Self-tuning control of offset: A unified approach
[OUEL-1539/84] 04 p0553 N85-13520
Error correction coding for a self-adaptive modem: Theoretical and experimental results
10 p1474 N85-19303
Adaptive control of airborne radar antennas
13 p2080 N85-22969
Technical evaluation report on the Flight Mechanics Symposium on Active Control Systems: Review, Evaluation and Projections
[AGARD-AR-220] 16 p2711 N85-26730
High gain adaptive control of decentralized systems
[DE85-010040] 19 p3339 N85-30686
FAUST: Introduction and overview — self tuning control
[OUEL-1568/85] 20 p3519 N85-31882
Multivariable model-following self-tuning control with offset rejection
[OUEL-1572/85] 20 p3519 N85-31883
SELF ALIGNMENT
Simulation of gyrocompassing alignment and calibration of strapdown inertial navigation system in a swaying vehicle
[DFVLR-MITT-84-20] 17 p2895 N85-27850
Self-aligned GaAs FET with low 1/F noise
[AD-D011667] 19 p3260 N85-30215
Space station dynamic modeling, disturbance accommodation, and adaptive control
20 p3409 N85-31154
SELF CONSISTENT FIELDS
Field consistency and the finite element analysis of multifield structural problems 18 p3120 N85-29316
A method to estimate the self-consistency effects on electronic structure calculations
[INPE-3536-PRE/752] 19 p3375 N85-30936
SELF DEPLOYING SPACE STATIONS
U SELF ERECTING DEVICES
U SPACE STATIONS
SELF DIFFUSION (SOLID STATE)
Mossbauer spectroscopic investigations of the diffusion and correlation of lattice defects (complementary to neutron spectroscopic investigations)
03 p0429 N85-12736
Comparisons between computed and observed grain boundary structures and properties in metals
[DE85-002596] 10 p1442 N85-19085
SELF ERECTING DEVICES
Hoop/column antenna deployment mechanism overview 22 p3796 N85-33514
SELF EXCITATION
Internal hysteresis experienced on a high pressure syn gas compressor 05 p0642 N85-14122
Theoretical approach to labyrinth seal forces - cross-coupled stiffness of a straight-through labyrinth seal 05 p0643 N85-14127
Experimental investigation of lateral forces induced by flow through model labyrinth glands
05 p0643 N85-14128
Buildup of oscillations in two-mode gyrotron
06 p0788 N85-15037
Clearance flow-generated transverse forces at the rotors of thermal turbomachines
[NASA-TM-77292] 07 p0973 N85-16180
Leakage-flow-induced vibration of a tube-in-tube slip joint
[DE84-007301] 11 p1652 N85-20406
Turbine blade-tip clearance excitation forces
[NASA-CR-171534] 19 p3220 N85-29963
Random vibration of nonlinear, parametrically excited systems 19 p3282 N85-30351
SELF FOCUSING
Brillouin scattering in underdense UV laser-produced plasmas
[DE84-015164] 04 p0567 N85-13614
SELF INDUCED VIBRATION
NT SUBSONIC FLUTTER
NT SUPERSONIC FLUTTER
NT TRANSONIC FLUTTER
Stability of turbine runners in sliding bearings under external circulation forces 14 p2272 N85-24074
SELF LUBRICATING MATERIALS
Mechanical modification of friction surfaces of aluminum alloys by friction transfer 19 p3241 N85-30097
SELF LUBRICATION
Observations of high resistance on slip-rings employing Ag/MoS2/Cu brushes — solar array drives
[ESA-ESTL-70] 18 p3123 N85-29333
SELF ORGANIZING SYSTEMS
A self-organizing database system: A different approach to query optimization 05 p0735 N85-14725
SELF OSCILLATION
Parametric study of autooscillation upon flow of supersonic jet into cylindrical cavity
16 p2765 N85-27060
SELF PROPAGATION
Hot rolling of ceramics by the use of self propagating synthesis
[AD-D011486] 10 p1453 N85-19154
SELF REGULATING
U AUTOMATIC CONTROL
SELF SEALING
Experimental stiffness of tapered bore seals
[NASA-TM-86978] 15 p2568 N85-25847
Refrigerated dynamic seal to 6.9 MPa (1000 psi)
[NASA-TM-87108] 23 p3930 N85-34356
SELF SUBTRACTION HOLOGRAPHY
U HOLOGRAPHIC SUBTRACTION
SELSYNS (TRADEMARK)
U SERVOMOTORS
SEMANTICS
Model theory for infinitely deep languages
[ISSN-0355-0087] 01 p0101 N85-10874
On update semantics and relational views
[AD-A145622] 02 p0294 N85-11907
Research in knowledge representation for natural language understanding
[AD-A145807] 03 p0409 N85-12813
Knowledge representation and natural-language semantics
[AD-A146025] 03 p0409 N85-12815
Crew communication as a factor in aviation accidents
05 p0710 N85-14865
Functional semantics of modules
[AD-A146923] 07 p1024 N85-16600
Speech analysis by parametric methods: A survey
[ENST-84C004] 09 p1313 N85-18251
JOVIAL J73 automated verification system: Implementation phase
[AD-A148732] 09 p1369 N85-18687
Precedency control and other semantic integrity issues in a workbench database 13 p2123 N85-23230
The identification of semantics for the file/database problem domain and their use in a template-based software environment 14 p2401 N85-24803
Functional analysis of programs
[AD-A150742] 14 p2404 N85-24819
Semantic networks and neural nets
[AD-A150750] 14 p2407 N85-24840
Research in knowledge representation for natural language understanding
[AD-A152260] 16 p2851 N85-27579
Towards a uniform topological treatment of streams and functions on streams
[CWI-CS-R8422] 17 p3014 N85-28609
Survey of Ada (Trademark)-based PDLs (Program Design Language)
[AD-A154402] 19 p3338 N85-30680
Design and implementation of an intelligence database
[AD-A154095] 19 p3361 N85-30873
The formal specification of an abstract machine: Design and implementation
[AD-A155167] 21 p3672 N85-32508
Research on distributed artificial intelligence
[AD-A155356] 22 p3833 N85-33733
SEMICONDUCTING FILMS
Studies of hydrogenated amorphous silicon
[DE84-013036] 01 p0067 N85-10443
Effect of liquid phase composition on thickness of epitaxial Ga sub (1-x) Al sub x As films
02 p0257 N85-11683
Determining composition in surface region of semiconductor crystals by method of sudden changes in X-ray photoelectric effect 02 p0267 N85-11746
Some investigations of molecular beam epitaxial growth of 3-5 semiconductor films via Monte-Carlo computer simulations, carrier tunneling and spectroscopic ellipsometry
[AD-A149465] 10 p1563 N85-19854
Method for the preparation of epitaxial films of mercury cadmium telluride
[AD-D011532] 12 p1936 N85-22175
Process for the epitaxial deposition of III-V compounds utilizing a continuous in-situ hydrogen chloride etch
[AD-D011557] 12 p1939 N85-22177
Non-linear optical techniques for visible and UV lasers and thin film deposition
[AD-A150489] 13 p2096 N85-23077
Investigation of a Si and related semiconductors as materials for photovoltaic conversion
[DE85-002932] 18 p3096 N85-29180
Glow discharge deposition at high rates using disilane
[DE85-010236] 19 p3263 N85-30235
Microwave-enhanced thin-film deposition
21 p3611 N85-32431
SEMICONDUCTOR DEVICES
NT AVALANCHE DIODES
NT BIPOLAR TRANSISTORS
NT CHARGE COUPLED DEVICES
NT CHARGE INJECTION DEVICES
NT CHARGE TRANSFER DEVICES
NT CMOS
NT FIELD EFFECT TRANSISTORS
NT GALLIUM ARSENIDE LASERS
NT GERMANIUM DIODES
NT HETEROJUNCTION DEVICES
NT JFET
NT JUNCTION DIODES
NT JUNCTION TRANSISTORS
NT LIGHT EMITTING DIODES
NT METAL OXIDE SEMICONDUCTORS
NT MIM (SEMICONDUCTORS)
NT MIM DIODES
NT MIS (SEMICONDUCTORS)
NT PHOTODIODES
NT PHOTOTRANSISTORS
NT PHOTOVOLTAIC CELLS
NT SCHOTTKY DIODES
NT SEMICONDUCTOR LASERS
NT SILICON CONTROLLED RECTIFIERS

CON TRANSISTORS
RMISTORS
RISTORS
NSISTOR AMPLIFIERS
NSISTORS
RACTOR DIODES
RISTORS

r for Electronics and Electrical Engineering l Bulletin covering center programs with 1984 ents calendar
22785] 01 p0045 N85-10292

r for Electronics and Electrical Engineering l Bulletin covering center programs with 1984 ents calendar
23804] 01 p0045 N85-10293

r for Electronics and Electrical Engineering al Bulletin covering center programs
219716] 01 p0045 N85-10295

ation measuring system using transistor flux s
011239] 01 p0050 N85-10328

C/NBS (Rome Air Development Center/National of Standards) Workshop. Moisture Measurement ontrol for Semiconductor Devices, 3
-219550] 01 p0051 N85-10337

ersible change in parameters of GaAs-based ce-barrier metal-semiconductor diodes induced by gen absorption-desorption
02 p0258 N85-11690

thod of splitting for solution of problems in onductor physics 02 p0265 N85-11736

ceedings of the Ion Implantation for Army Needs shop
A145474] 02 p0286 N85-11863

omation of production of semiconductor power es 03 p0346 N85-12229

search activities of the Illinois University Coordinated ce Laboratory
A145589] 03 p0449 N85-12856

mprehensive silicon solar cell computer modeling
SA-CR-174151] 04 p0530 N85-13386

miconductor high-voltage power devices: State of nd outlook 06 p0794 N85-15074

w methods of fast switching of high power by means miconductor devices 06 p0794 N85-15075

egrated power devices with three-dimensional ection for automation systems
06 p0794 N85-15077

evelopment of technology of silicon single-crystal uction semiconductor power devices: State of art ook 06 p0795 N85-15078

urrent-voltage characteristics of semiconductor power ices operating at high current densities
06 p0795 N85-15079

heoretical investigation of device aspects of iconductor superlattices
-A146641] 06 p0867 N85-15509

obility and trapping time measurements in HgI2
E84-015954] 06 p0869 N85-15522

harge domain filters for enhanced monolithic signal cessing
D-A147428] 07 p0941 N85-15964

n asymptotic analysis of a transient p-n junction del
D-A147270] 07 p0947 N85-16004

he constant current strain gauge bridge
RL/STRUC-TM-385] 07 p0962 N85-16097

Superlattice ultrasonic wave generator
D-D011363] 07 p1038 N85-16585

Two carrier dual injector apparatus
D-D011357] 07 p1047 N85-16646

Characterization of III-V compound semiconductor vice materials
D-A148203] 08 p1226 N85-17719

Gallium arsenide/AlGaAs multilayer structures with ecial doping profiles for microwave and optoelectronic vices
MFT-FB-T-84-207] 08 p1227 N85-17725

East Europe report: Science and technology
PRS-ESA-85-005] 09 p1377 N85-18659

Semiconductors at Leipzig Spring Fair
09 p1377 N85-18660

Semiconductor superlattice photodetectors
NASA-CR-174347] 09 p1397 N85-18791

Asymptotic representation of solutions of the basic miconductor device equations
AD-A149040] 10 p1545 N85-19741

A new very high voltage semiconductor switch
NASA-TM-86957] 11 p1627 N85-20246

Method and apparatus for measuring minority carrier lifetime in a direct band-gap semiconductor
NASA-CASE-NPO-163371-1] 11 p1628 N85-20251

Measurement of the configuration of a concave surface y the interference of reflected light
NASA-TM-77796] 11 p1728 N85-20867

Low stress semiconductor-insulator interface for cryogenic device applications
[NASA-CASE-NPO-16394-1] 11 p1734 N85-20906

Inelastic tunnel diodes
[NASA-CASE-LEW-13833-1] 12 p1832 N85-21492

Method for the fabrication of dielectric isolated junction field effect transistor and PNP transistor
[AD-D011500] 12 p1832 N85-21494

Process for the epitaxial deposition of III-V compounds utilizing a continuous in-situ hydrogen chloride etch
[AD-D011557] 12 p1939 N85-22177

Investigation of device and electronic interactions in GaAs device processing
[AD-A149747] 12 p1940 N85-22182

Electrical performance of semiconductor devices at cryogenic temperatures 12 p1948 N85-22239

Drift fields and boundary conditions at grain boundaries in bipolar P/N junction silicon devices
13 p2062 N85-22879

Electrical overstress protection of submicron devices
[AD-A150334] 13 p2064 N85-22892

Measurement of internal thermal resistance for quality control of semiconductor devices
13 p2074 N85-22953

Requirements placed on information processing equipment
[BLL-CE-TRANS-7983-(9022.09)]
13 p2144 N85-23307

Solar cells based on polycrystalline silicon with isothermal potential barriers along grain boundaries
14 p2275 N85-24091

Proceedings of the Cold Electronics Workshop
[NASA-CR-175662] 14 p2297 N85-24220

Cold electronics: An overview
14 p2297 N85-24221

Acoustic emission of semiconductor devices
15 p2529 N85-25593

Developments in microelectronics: Past and future
15 p2530 N85-25597

Future prospects of China's microwave semiconductor technology 15 p2530 N85-25598

China report: Science and technology
[JPRS-CST-85-013] 15 p2536 N85-25652

Heavy doping effects in high efficiency silicon solar cells
[NASA-CR-175681] 15 p2586 N85-25940

Solution of coupled system of PDE by the transistorized multigrid method
[DE85-006377] 15 p2639 N85-26276

Charge isolation in a spatial light modulator
[AD-D011581] 15 p2652 N85-26356

Assessment of present and future large-scale semiconductor detector systems
[DE85-006606] 15 p2662 N85-26430

Space power plants 16 p2724 N85-26813

Cryostat and electronic development associated with multi-detector spectrometer systems
[DE85-007624] 16 p2788 N85-27203

Shallow impurity cluster states in n-type semiconductors
[INPE-3495-PRE/732] 16 p2869 N85-27699

Investigation of superlattice device structures
[NASA-CR-3903] 18 p3094 N85-29152

Optical fiber magnetic field sensor with nanosecond response time
[DE85-006409] 18 p3110 N85-29259

A stored data acquisition system: Update
[DE85-010534] 18 p3166 N85-29616

Optically nonlinear and bistable behaviour of direct gap semiconductors 18 p3186 N85-29759

The potential of semiconductors for optical integrated circuits 18 p3187 N85-29768

Electron spin resonance study of interface states induced by electron injection in metal-oxide-semiconductor devices
[DE85-009502] 18 p3195 N85-29817

Low defect, high purity crystalline layers grown by selective deposition
[NASA-CASE-NPO-15813-1] 19 p3373 N85-30922

Theoretical investigation of material characteristics of semiconductor superlattices
[AD-A154126] 19 p3375 N85-30938

Planar doped barrier semiconductor device
[AD-D011591] 20 p3537 N85-32010

Microwave semiconductor research: Materials, devices and circuits and gallium arsenide ballistic electron transistors
[AD-A154698] 21 p3709 N85-33024

A second order difference scheme for transient semiconductor device simulation
[AD-A154824] 21 p3709 N85-33027

A review of the physics and response models for burnout of semiconductor devices
[AD-A155031] 21 p3709 N85-33028

Modulation doped GaAs/Al(x)Ga(1-x)As layered structures with applications to field effect transistors
[AD-A155360] 22 p3759 N85-33296

Thermoelectric generator and method for the fabrication thereof
[DE85-011650] 22 p3760 N85-33302

Solid state radiative heat pump
[DE85-011605] 22 p3760 N85-33303

Electron beam enhanced surface modification for making highly resolved structures
[DE85-011609] 22 p3760 N85-33305

TEMO and TEB thermoelectronic devices
22 p3779 N85-33415

Transient two-dimensional simulation of SEU in a CMOS SRAM cell
[DE85-008419] 22 p3890 N85-34111

Joint services electronics program
[AD-A154748] 23 p3927 N85-34336

Applications of CdTe to nuclear medicine
[DE85-011877] 23 p3952 N85-34492

Analysis of transient radiation upset in a 16K SRAM
[DE85-009442] 23 p3965 N85-34586

Circuit approaches to increasing SRAM performance in total dose environments
[DE85-009441] 23 p3966 N85-34588

Error-correcting codes for computer memories
24 p4136 N85-35636

Electron irradiation of N type cadmium telluride
[AD-A156117] 24 p4161 N85-35801

Optical properties of heterostructures and superlattices
[AD-A156243] 24 p4162 N85-35802

SEMICONDUCTOR DIODES
NT AVALANCHE DIODES
NT GERMANIUM DIODES
NT GUNN DIODES
NT JUNCTION DIODES
NT LIGHT EMITTING DIODES
NT PHOTODIODES
NT SCHOTTKY DIODES
NT TUNNEL DIODES
NT VARACTOR DIODES

The behavior of Pb(1-x)Sn(x)Te semiconductor laser diodes in a magnetic field
[AD-A145431] 02 p0287 N85-11872

Heatsink requirements for coherent operation of high-power semiconductor laser arrays
[AD-A146184] 03 p0366 N85-12346

Lifetime of excess charge carriers in weakly doped epitaxial GaAs layers 04 p0487 N85-13108

Strained-layer superlattice emitter and detector structures using modulation-doped active regions
[DE85-000064] 06 p0867 N85-15511

AlAs/GaAs superlattice barrier unipolar diode structure
[DE85-001904] 11 p1736 N85-20921

Pulse transformer package for impedance matching a laser diode to a transmission line
[AD-D011499] 12 p1855 N85-21632

SEM (Scanning Electron Microscope) investigation of silicon diodes using the electron beam induced current method
[AD-A150356] 13 p2064 N85-22894

Monolithic planar doped barrier limiter
[AD-D011578] 15 p2548 N85-25723

Controlled-linewidth laser source
[AD-D011681] 19 p3274 N85-30306

SEMICONDUCTOR INSULATOR SEMICONDUCTORS
U SIS (SEMICONDUCTORS)

SEMICONDUCTOR JUNCTIONS
NT P-I-N JUNCTIONS
NT P-N JUNCTIONS
NT P-N-P JUNCTIONS
NT P-N-P-N JUNCTIONS
NT SILICON JUNCTIONS

Multijunction cells for concentrators: Technology prospects
[NASA-CR-174259] 07 p0981 N85-16295

Advanced high-efficiency concentrator cells
[DE84-013020] 09 p1344 N85-18459

Screen printed interdigitated back contact solar cell
[NASA-CASE-LEW-13414-1] 11 p1671 N85-20530

Drift fields and boundary conditions at grain boundaries in bipolar P/N junction silicon devices
13 p2062 N85-22879

Flat-plate solar array project process development area: Process research of non-CZ silicon material
[NASA-CR-175777] 16 p2818 N85-27382

A second order difference scheme for transient semiconductor device simulation
[AD-A154824] 21 p3709 N85-33027

Flat-plate solar array project process development area process research of non-CZ silicon material
[NASA-CR-176117] 23 p3945 N85-34445

Rapid annealing of temperature-compensated, precision voltage references following fast-neutron irradiation
[DE85-009821] 23 p3970 N85-34609
HgCdTe surface and defect study program
[AD-A158079] 24 p4161 N85-35799

SEMICONDUCTOR LASERS
NT GALLIUM ARSENIDE LASERS
Synchronously pumped mode-locked semiconductor platelet laser
[AD-D011214] 01 p0051 N85-10340
Tunable CW semiconductor platelet laser
[AD-D011215] 01 p0052 N85-10341
High frequency phase-noise in semiconductor lasers
[FUB-20-1983] 01 p0053 N85-10353
Biaxial-crystal laser with waveguide resonator
02 p0262 N85-11717
Theoretical analysis of physical processes of lasing medium degradation in semiconductor lasers
02 p0269 N85-11759
The behavior of Pb(1-x)Sn(x)Te semiconductor laser diodes in a magnetic field
[AD-A145431] 02 p0287 N85-11872
Diffusion barrier for long wavelength laser diodes
[AD-D011390] 07 p0970 N85-16157
Phased locked array laser systems
[AD-D011317] 07 p0971 N85-16164
Optical computer studies at UK's Heriot-Watt University 09 p1309 N85-18227
Effect of neutron irradiation on the high temperature operation of injection laser diodes
[DE85-000068] 09 p1326 N85-18333
Quantum noise effects in single-mode injection lasers
[FUB-11-1984] 09 p1327 N85-18338
Effect of impurities on absorption in semiconductors and lasing of semiconductor lasers 11 p1718 N85-20797
Pulse transformer package for impedance matching a laser diode to a transmission line
[AD-D011499] 12 p1855 N85-21632
Mode control and wavelength tuning in open ended Michelson interferometric semiconductor laser
13 p2095 N85-23073
Wavelength dependent, tunable, optical time delay system for electrical signals
[AD-D011584] 15 p2548 N85-25725
Possible uses of tunable diode lasers in infrared spectroscopy
[ESA-TT-889] 15 p2584 N85-25818
The construction and study of improved Al(x)Ga(1-x)As-GaAs heterostructure devices
[AD-A153264] 17 p2954 N85-28244
Injection laser structure design
[AD-A153210] 17 p2971 N85-28345
Diode laser 87Rb optical pumping in an evacuated wall-coated cell 18 p3105 N85-29226
1.5 micrometer GaInAsP high pulsed power diode lasers
[AD-A153568] 18 p3193 N85-29805
Controlled-linewidth laser source
[AD-D011881] 19 p3274 N85-30306
Sensitive detection of tunable diode laser absorption by polarization rotation
[DE85-009821] 19 p3277 N85-30322
Optical properties of heterostructures and superlattices
[AD-A156243] 24 p4162 N85-35802

SEMICONDUCTOR PLASMAS
Demonstration of feasibility of depositing semiconductor layers using microwave enhanced plasma techniques
[NASA-CR-174392] 13 p2163 N85-23421
Some dynamic electronic properties of semiconductor surfaces and interfaces 20 p3537 N85-32007

SEMICONDUCTORS (MATERIALS)
NT ACCEPTOR MATERIALS
NT AMORPHOUS SEMICONDUCTORS
NT CHARGE TRANSFER DEVICES
NT CMOS
NT DONOR MATERIALS
NT METAL OXIDE SEMICONDUCTORS
NT MIM (SEMICONDUCTORS)
NT MIS (SEMICONDUCTORS)
NT N-TYPE SEMICONDUCTORS
NT ORGANIC SEMICONDUCTORS
NT P-TYPE SEMICONDUCTORS
NT PHOTOCONDUCTORS
NT SUPERLATTICES
Center for Electronics and Electrical Engineering Technical Bulletin covering center programs with 1984 CEEE events calendar
[PB84-222785] 01 p0045 N85-10292
Preparation and properties of single crystals of hydrogen bis(phthalocyaninato) neodymium(3)
[AD-A144933] 01 p0123 N85-10846
Solidification and crystal growth of solid solution semiconducting alloys 02 p0155 N85-11046
Experiments with phase transitions at very high pressure
[NASA-CR-174029] 02 p0172 N85-11148
Complex formation and temperature stability of electrophysical properties of GaAs semiinsulating single crystals 02 p0258 N85-11689
Formation of lattice defects by nitrogen laser exposure in A2B6 semiconductors with wide forbidden band
02 p0258 N85-11692
USSR report: Physics and mathematics
[JPRS-UPM-84-004] 02 p0266 N85-11737
Nonlinear absorption of laser radiation in InP and in GaAs 02 p0266 N85-11740
Photocurrent oscillations in Bi12GeO20 metal-semiconductor-metal structures
02 p0266 N85-11741
Capacitive reactance of compensated semiconductors with deep centers under conditions of transmission of exclusion and double injection currents
02 p0266 N85-11742
Magnetoabsorption of weak light wave in presence of intense light wave in semiconductor with narrow forbidden band 02 p0267 N85-11743
Mechanisms of laser annealing of semiconductors
02 p0267 N85-11744
Instability in semiconductors exposed to ionizing radiation 02 p0267 N85-11747
Injection lasers based on AlGaAsSb/GaSb and InGaAsSb/GaSb heterostructures
02 p0270 N85-11761
Characteristics of ion implanters for fabrication of electronic devices
[AD-P003949] 02 p0286 N85-11865
Current controlled LPE (Liquid Phase Epitaxy) growth of semiconductors
[AD-A145536] 02 p0287 N85-11875
Nonlinear electromagnetic waves in ferromagnetic conducting media 03 p0346 N85-12232
Producing semiconductor materials by superfast cooling of melt 03 p0354 N85-12274
Center for Electronic and Electrical Engineering Technical Progress Bulletin, January - March 1985, no. 2
[PB84-231224] 03 p0360 N85-12306
Inelastic neutron scattering on crystals for the clarification of structure and semiconductor properties
03 p0425 N85-12714
Measurement of state and dynamic solid state properties in nonmetals using excited probe nuclei on the Erlanger 12 MeV tandem accelerator 03 p0428 N85-12730
Neutron irradiation of semiconductors --- lattice defects, electron irradiation 03 p0428 N85-12732
Studies of grown-in defects versus growth parameters in 3-4 compound semiconductors
[AD-A145864] 03 p0433 N85-12755
Research activities of the Illinois University Coordinated Science Laboratory
[AD-A145589] 03 p0449 N85-12856
Effect of barrier height on friction behavior of the semiconductors silicon and gallium arsenide in contact with pure metals
[NASA-TP-2405] 04 p0478 N85-13044
Nonthermal mechanism for laser annealing of semiconductors and formation of super structure
04 p0487 N85-13109
Investigation of effect of photocurrent amplification in meta-dielectric-semiconductor structures based on silicon 04 p0488 N85-13110
Physics and design of advanced infrared bolometers and photoconductors
[DE84-016883] 04 p0503 N85-13213
Silicon for solar cells
[DE84-004503] 04 p0529 N85-13381
Materials characterization using ion, electron, and photon probes
[DE84-004518] 04 p0560 N85-13568
Theory of non-linear index of refraction of compound semiconductors
[DE84-013660] 04 p0569 N85-13626
Single crystal semiconductor multilayers for electrically active optical interference filters
[DE84-015614] 04 p0571 N85-13640
Refractive index of ternary and quaternary compound semiconductors below the fundamental absorption edge: Linear and nonlinear effects
[DE84-012325] 05 p0640 N85-14105
USSR report: Physics and mathematics
[JPRS-UPM-84-007] 05 p0723 N85-14651
LPE (Liquid phase epitaxy) semiconductor material transfer method
[AD-D011250] 05 p0731 N85-14696
InAsSb strained-layer superlattices (SLSs) for long wavelength detector applications
[DE84-016111] 05 p0732 N85-14706
Acoustoelectric interaction in double-layer semiconductors 06 p0786 N85-15023
Computer investigation of effects of high injection in transistor large integrated circuit structures
06 p0793 N85-15069
Trends in development of bipolar power transistors
06 p0793 N85-15072
Investigation of structural and electrical properties of low-angle silicon sheet 06 p0831 N85-15288
Characterization of surface electronic properties of semi-insulating InP
[AD-A146553] 06 p0866 N85-15507
The growth and properties of semiconductor strained-layer superlattices
[DE84-012979] 06 p0868 N85-15515
Float zone experiments in space
[NASA-CR-171284] 07 p0911 N85-15788
Determination of moments of initial estimate during linear approximation of distribution of ejected impurity
07 p0954 N85-16045
Determination of parameters of doped thin semiconductor layers from plasmatic minimum of reflection coefficient for infrared radiation
07 p0954 N85-16047
Superlattice ultrasonic wave generator
[AD-D011363] 07 p1038 N85-16585
Ion microscopy of metals and semiconductors
[AD-A147118] 07 p1043 N85-16626
Ion implantation and laser processing of III-V compound semiconductors with applications to the fabrication of microwave devices
[AD-A146846] 07 p1047 N85-16651
Laser annealing of ion implanted semiconductors
[AD-A146979] 07 p1047 N85-16652
Method of preparing single crystalline cubic silicon carbide layers
[AD-D011305] 07 p1048 N85-16653
Clusters of defects in semiconductors
[AD-A147426] 07 p1048 N85-16655
Electron distribution function and mobility in 3-5 compounds for high and low fields
[AD-A147447] 07 p1048 N85-16658
X-ray and backscattering analysis of ion implantation phenomena in GaAs and related compounds
[AD-A147449] 07 p1048 N85-16659
Transport properties and distribution functions in 3-5 semiconductors
[AD-A147525] 07 p1049 N85-16660
Electronics component R and D, production capability reviewed 08 p1140 N85-17181
French research on gallium arsenide devices
08 p1141 N85-17196
General assessment of GDR microelectronics industry, applications 08 p1142 N85-17202
Life cycle cost model for very high speed integrated circuits
[AD-A147798] 08 p1157 N85-17296
Formation of a limiting composition in the preparation of ternary 3-5 semiconductors by the VPE (Vapor Phase Epitaxy) Hydride technique
[AD-A147639] 08 p1225 N85-17713
Electronic structure of semiconductor interfaces
[AD-A147663] 08 p1225 N85-17715
Characterization of III-V compound semiconductor device materials
[AD-A148203] 08 p1226 N85-17719
Ion implantation in 3-5 compound semiconductors
[AD-A148462] 08 p1226 N85-17720
Device modeling for advanced integrated circuits
09 p1314 N85-18258
Nondestructive characterization of semiconductor surfaces and interfaces 09 p1329 N85-18349
Electron-hole plasma formation in semiconductors due to the absorption of pulsed CO2 laser light
[DE85-001559] 09 p1392 N85-18757
A picosecond population modulation study of near interband resonances in semiconductors
09 p1396 N85-18767
Ion-implantation doping of strained-layer superlattices
[DE85-001903] 09 p1400 N85-18811
Siemens' CAD system designs VLSI circuits
10 p1461 N85-19209
Picosecond laser pulse interactions with metallic and semiconductor surfaces
[AD-A149112] 10 p1490 N85-19405
Silicon film solar cell process
[NASA-CR-174446] 10 p1506 N85-19514
Metal-nonmetal transitions in N-doped many-valley Si and Ge
[INPE-3358-PRE/636] 10 p1562 N85-19848
Quaternary narrow-band semiconductors (HgTe)x(InSb)1-x for far-infrared detectors
[AD-A149350] 10 p1562 N85-19852
Applications of the Heavy-Iron Rutherford Backscattering Spectrometry (HIRBS) to the analysis of contact structures on GaAs and Ge
[DE85-000671] 10 p1564 N85-19861

olar fuel synthesis based on colloidal and particulate iconductors
85-129104] 11 p1614 N85-20152
ethod for increasing linearity of load cell
11 p1623 N85-20221
Optically bistable devices using semiconductor aterials
D-A149551] 11 p1628 N85-20253
USSR report: Physics and mathematics
PRS-UPM-85-001] 11 p1715 N85-20786
Effect of impurities on absorption in semiconductors and ing of semiconductor lasers 11 p1716 N85-20797
Laser-plasma interactions for the deposition and etching semiconductor materials
DE85-000458] 11 p1731 N85-20885
Determination of the mobility profile in aAs-MESFETs
NASA-TM-77816] 11 p1734 N85-20905
Subnanosecond time-resolved emission study of Cu2O nd GaAs
DE85-002070] 11 p1735 N85-20912
Preliminary studies on the low-cost preparation of halcogenide semiconductors from solution depositions
[DE85-000536] 11 p1736 N85-20918
Impurity complexes in pure elemental semiconductors
11 p1736 N85-20919
Research in surface sciences, disordered materials, and solidification and growth
[PB85-132140] 11 p1737 N85-20927
GaAs and 3-5 compound solar cells status and prospects for use in space
[NASA-TM-86960] 12 p1795 N85-21261
Transmissive Dewar cooling chamber for optically pumped semiconductor ring lasers
[AD-D011550] 12 p1855 N85-21636
Process for the epitaxial deposition of III-V compounds utilizing a continuous in-situ hydrogen chloride etch
[AD-D011557] 12 p1939 N85-22177
Total immersion crystal growth
[NASA-CASE-NPO-15800-2] 12 p1939 N85-22178
Semiconductor materials for high frequency solid state sources
[AD-A150020] 12 p1940 N85-22186
Germanium resistance thermometer calibration at superfluid helium temperatures
12 p1947 N85-22226
Clustering and ordering in 3-5 alloys
[AD-A150604] 13 p2022 N85-22670
Noise characteristics of sulfur-doped silicon diodes
13 p2073 N85-22952
Numerical simulation of inverters with I2L elements including effects of high doping level
13 p2088 N85-23039
Electronic transport in hydrogenated amorphous silicon films
[DE85-002901] 13 p2164 N85-23426
Proceedings of the Cold Electronics Workshop
[NASA-CR-175662] 14 p2297 N85-24220
Cold electronics: An overview
14 p2297 N85-24221
Recent developments in semiconductor research
14 p2297 N85-24222
AlN insulator for 3-5 MIS applications
[AD-A150674] 14 p2426 N85-24962
Electrical and thermal transport property studies of high-temperature thermoelectric materials
[AD-A150900] 14 p2427 N85-24967
Infrared nonlinear processes in semiconductors
[AD-A150966] 14 p2427 N85-24968
Theory and calculations of the electronic structure of solids having directional bonding
[AD-A151062] 14 p2428 N85-24971
Strained-layer superlattices and strain-induced light holes
[DE85-003675] 14 p2431 N85-24990
Future directions in computers
15 p2626 N85-26183
USSR report: Physics and mathematics
[JPRS-UPM-85-003] 15 p2642 N85-26300
Pressure-dependence of TiS(2) and TiSe(2) bandstructures
[AD-A151200] 15 p2659 N85-26410
ONR (Office of Naval Research) Far East Scientific Bulletin, Volume 9, Number 4, October-December 1984
[AD-A151274] 15 p2665 N85-26448
The impact of VLSI on guidance and control system design 16 p2697 N85-26654
Periodic cluster simulation of a disordered impurity system
[INPE-3453-PRE/706] 16 p2858 N85-27628
On some physical impurity properties of doped-indirect gap semiconductors at low and intermediate concentrations
[INPE-3452-PRE/704] 16 p2869 N85-27701
Density of impurity states associated to inversion layers
[INPE-3406-PRE/675] 16 p2869 N85-27702
Optimum convection conditions for Czochralski growth of semiconductors
[INPE-3395-PRE/665] 16 p2870 N85-27703
Impurity bands associated with MOS inversion layers
[INPE-3463-PRE/726] 16 p2870 N85-27704
On the choice of coordinates for semiconductor simulation
[AD-A152214] 16 p2870 N85-27708
Heat pipe and method of making same
[AD-D011654] 17 p2959 N85-28273
Laser measurement techniques: Laser spectroscopy in semiconductors
[DE85-007667] 17 p2971 N85-28350
Optical waveguide characterization using grating couplers
[AD-A153063] 17 p3037 N85-28789
Morphology of GaAs/sub 1-x/P/sub x/ superlattices grown by MOCVD and chloride VPE
[DE85-002944] 17 p3045 N85-28842
Research on electrochemical photovoltaic cells
[DE85-008775] 18 p3131 N85-29392
The potential of semiconductors for optical integrated circuits 18 p3187 N85-29768
Process for the epitaxial deposition of 3-5 compounds utilizing a binary alloy as the metallic source
[AD-D011683] 18 p3193 N85-29801
Growth mechanism and properties of the thermal and anodic oxides of the 3-5 compound semiconductors
[AD-A153406] 18 p3193 N85-29803
Processable and stable conductive polymers
[AD-D011684] 19 p3249 N85-30143
Electron irradiation of light emitting diodes
[AD-A154441] 19 p3260 N85-30213
Method of reducing impurity and antisite defects in semiconductor crystal materials, and device and apparatus respectively produced from and utilizing same
[AD-D011696] 19 p3260 N85-30216
Method for producing high quality germanium-germanium nitride interfaces for germanium semiconductors and device produced thereby
[AD-D011702] 19 p3260 N85-30218
Method for determining the point of zero zeta potential of semiconductor
[NASA-CASE-LAR-12693-1] 19 p3373 N85-30923
Fluorescence quenching by metal semiconductor and insulator surfaces 19 p3374 N85-30929
Method for growing low defect, high purity crystalline layers
[NASA-CASE-NPO-15813-2] 19 p3374 N85-30933
Crystal growth of device quality GaAs in space
[NASA-CR-176024] 19 p3375 N85-30935
Theoretical investigation of material characteristics of semiconductor superlattices
[AD-A154126] 19 p3375 N85-30936
Chemistry and physics of silicon-based amorphous semiconductors
[DE85-001931] 19 p3377 N85-30949
Strained-layer-superlattice optoelectronic devices
[DE85-009148] 19 p3377 N85-30953
Predamage threshold electron emission from insulator and semiconductor surfaces
[DE85-006968] 19 p3377 N85-30954
Leading-edge microelectronics research at Sweden's Chalmers 20 p3438 N85-31337
Swedish program for sensor research, development
20 p3438 N85-31338
Center for Electronics and Electrical Engineering technical progress bulletin covering center programs, April-June 1984 with 1984 CEEE (Center for Electronics and Electrical Engineering) events calendar, issue 7
[PB85-187540] 20 p3450 N85-31419
Interface chemistry of Hg(1-x)Cd(x)Te
[AD-A154876] 21 p3563 N85-32161
Z-contrast imaging and electron channeling analysis of dopants in semiconductors
[DE85-011410] 21 p3582 N85-32269
On the dependence of the convergence of Gummel's algorithm on the regularity of the solution
[AD-A154626] 21 p3675 N85-32832
Influence on bi-phonon states on Raman scattering of light in molecular crystals 21 p3680 N85-32865
Influence of coherent light beams on free carriers in semiconductors 21 p3681 N85-32867
Quasi-steady-state melting mode during combined laser irradiation of semiconductor materials
21 p3682 N85-32874
Photo-acoustic effect in finite-dimensional semiconductors 21 p3682 N85-32876
Effect of powerful pulsed low-energy ion streams on GaAs 21 p3682 N85-32877
A second order difference scheme for transient semiconductor device simulation
[AD-A154824] 21 p3709 N85-33027
Raman scattering studies in solids
[AD-A155528] 21 p3710 N85-33032
Electronic phenomena near semiconductor grain boundaries
[DE85-011543] 21 p3711 N85-33035
Consortium program for the study of boron-rich borides
[DE85-011378] 22 p3752 N85-33260
In-situ observations of the development of heavy-ion damage in semiconductors
[DE85-010288] 22 p3761 N85-33307
Photovoltaics technical information guide
[DE85-002924] 22 p3808 N85-33585
Electronic structure and lattice dynamics of dimensionally constrained and disordered solids
[AD-A155927] 24 p4161 N85-35797
Investigations of the molecular beam epitaxial growth and characteristics of external excitation induced non-equilibrium phases of immiscible 3-5 compound semiconductors
[AD-A156325] 24 p4162 N85-35804

SEMIMETALS
U METALLOIDS

SENDERS
U TRANSMITTERS

SENSE ORGANS
NT CHEMORECEPTORS
NT COCHLEA
NT EAR
NT EYE (ANATOMY)
NT GRAVIRECEPTORS
NT LABYRINTH
NT MECHANORECEPTORS
NT OCULOMOTOR NERVES
NT OTOLITH ORGANS
NT PHOTORECEPTORS
NT PROPRIOCEPTORS
NT RETINA
NT VESTIBULES

SENSES
U SENSORY PERCEPTION

SENSIBILITY
U SENSITIVITY

SENSING
U DETECTION

SENSITIVITY
NT IMPACT RESISTANCE
NT LIGHT ADAPTATION
NT NOTCH SENSITIVITY
NT PHOTOSENSITIVITY
NT PHOTOTROPISM
NT PROPELLANT SENSITIVITY
NT RADIATION TOLERANCE
NT SENSITOMETRY
NT SPECTRAL SENSITIVITY
Design sensitivity analysis of an antisymmetric angle-ply laminate
[CSIR-TWISK-318] 01 p0021 N85-10128
Motion sensor evaluation using simulation
[DE84-014969] 01 p0050 N85-10331
Sensitivity analysis of limit state functions for probability-based plastic design
01 p0059 N85-10388
Sensitivity analysis in generalized rational approximation with restricted denominator
[CSIR-TWISK-319] 01 p0109 N85-10734
Definition of acceptable levels of mismatch for equivalent systems of augmented CTOL (Conventional Take-Off and Landing) aircraft
[AD-A145619] 02 p0149 N85-11007
Unified approach to sensitivity and uncertainty analysis
[DE84-014049] 02 p0255 N85-11669
New uses for sensitivity analysis: How different movement tasks effect limb model parameter sensitivity
05 p0706 N85-14529
Sensitivity analysis of discrete structural systems: A survey
[NASA-TM-86333] 06 p0817 N85-15186
Human reactions to transient electric currents, volume 12
[PB84-231463] 06 p0846 N85-15374
Optical fibers with reduced pressure sensitivity to high frequency acoustic field
[AD-D011306] 07 p1043 N85-16627
An adaptive Fast Fourier Transform weighting technique to increase small target sensitivity
[AD-D011424] 08 p1154 N85-17286
CP DDT detonators. Part 1: Design sensitivity study
[DE84-017255] 09 p1302 N85-18160
Treatment of general boundary conditions and point-wise state variable constraints in optimum design for static and dynamic response
09 p1330 N85-18358

Issues in sensitivity and statistical analysis of large-scale, computer-based models [PB85-116317/GAR] 09 p1378 N85-18880

Dual adaptive control based upon sensitivity functions [NASA-CR-169331] 10 p1543 N85-19727

Radiographic detectability limits for seeded voids in sintered silicon carbide and silicon nitride [NASA-TM-86945] 12 p1861 N85-21674

Structural sensitivity analysis: Methods, applications and needs [NASA-TM-85827] 12 p1865 N85-21695

Investigation of adaptive distinctions of mechanism of controlled glycemia in Macaca rhesus monkeys 12 p1902 N85-21946

A user's guide to sensitivity testing on computer models at Los Alamos National Laboratory [LA-10104-M] 12 p1914 N85-22018

Comprehensive mechanisms for combustion chemistry: An experimental and numerical study with emphasis on applied sensitivity analysis [DE85-000173] 13 p2018 N85-22656

Visual simulation requirements for aircraft aspect recognition at real world distances [AD-A151040] 14 p2226 N85-23810

Measurement of sensitivity of shadowgraphic instruments with spherical autocollimating mirror 14 p2274 N85-24067

Thresholds of optical breakdown in alkali-halide crystals under pulses from CO2-laser 14 p2282 N85-24124

Effect of axisymmetric vibration modes on sensitivity and directivity characteristics of piezoceramic sphere — hydrophones 15 p2526 N85-25569

Acceleration-resistant crystal resonator [AD-D011627] 16 p2778 N85-27144

Acceleration sensitivity reduction method [AD-D011681] 16 p2778 N85-27146

Earth station antenna sidelobe characteristics [PB85-164986] 16 p2780 N85-27159

An interactive computer package for use with simulation models which performs multidimensional sensitivity analysis by employing the techniques of response surface methodology [AD-A151956] 16 p2846 N85-27548

Design of SC cut 10 MHZ H.Q. crystals with G. sensitivity better than 2.10(-10)/G 17 p2886 N85-28319

Mass spectrometry technology at the Jet Propulsion Laboratory (JPL) 18 p3157 N85-29552

Surface acoustic wave devices as chemical vapor microsensors [AD-A153752] 18 p3177 N85-29696

Fiber optic gyroscope with alternating output signal [AD-D011689] 19 p3271 N85-30284

New concepts in free electron lasers 20 p3480 N85-31493

Test evaluation of the Honeywell GG1111 Single-Degree-of-Freedom (SDF) strapdown gyroscope [AD-A154768] 21 p3589 N85-32307

Visibility and vertical structure measurements in southern Germany [AD-A154714] 21 p3625 N85-32574

Rhodium-103 and Indium-115 inelastic scattering reactions for fission neutron dosimetry 21 p3703 N85-33004

Sensitivity and performance characterization of DINGU [DE85-010750] 22 p3754 N85-33269

Sensitivity of compressive receivers [FOA-C-30385-E4] 22 p3756 N85-33288

Determination of sensitivity functions for discrete dynamic systems from results of function modeling on digital computer 22 p3760 N85-33359

Design of inductive shift transducers 22 p3771 N85-33366

Selecting step sizes in sensitivity analysis by finite differences [NASA-TM-86382] 22 p3796 N85-33536

Experimental test for interpreting the increase in sensibility of doped CR-39 [DG-4-4-11] 22 p3880 N85-34042

A multi-touch three dimensional touch-sensitive tablet (executive summary) 23 p3961 N85-34563

The final COS-B database: In-flight calibration of instrumental parameters [DG-9349] 23 p4028 N85-34964

Friction, impact, and electrostatic discharge sensitivities of energetic materials [DE85-012221] 24 p4085 N85-35309

Assessment of metal heating technologies for ferrous forging: A pilot study of the form value of natural gas [PB85-204384] 24 p4094 N85-35314

Reliability prediction of the series system with spares subject to Weibull failure 24 p4100 N85-35413

Risk analysis and sensitivity: Antithesis or synthesis [B8562444] 24 p4144 N85-35687

Measurement of uranium enrichment for gaseous uranium at low pressure [DE85-012887] 24 p4160 N85-35733

SENSITIZING

Investigation and optimization of fuel production using dye-based transition metal complexes as charge-transfer intermediates [PB85-161941] 14 p2264 N85-24029

Stereotype traits can be processed automatically [AD-A150947] 14 p2391 N85-24725

SENSITOMETRY

Astronomical photography 1984 — conferences [ROE-OR-14] 07 p0962 N85-16102

Recalibration of the KPNO spot sensitometers — Kitt Peak National Observatory 07 p0963 N85-16103

FLACS: A new sensitometer for measurement of extreme low intensity reciprocity in a controlled environment — X-ray films 07 p0963 N85-16104

SENSIT.FOR: A program for sensitometric reduction 07 p0963 N85-16105

A spectrosensitometer with an absolute calibration 07 p0963 N85-16106

Effects of tasks on responses of human skin mechanoreceptors 11 p1691 N85-20635

SENSORIMOTOR PERFORMANCE

NT PSYCHOMOTOR PERFORMANCE

Medication interference with space research: An example from a mass-discrimination experiment on Spacelab 1 05 p0685 N85-14472

Estimating number, time and length; a baseline study 05 p0685 N85-14473

Effect of modulated ultrahigh frequency field on behavior and hormone level in female rats under emotional stress 09 p1361 N85-18582

Topography of human brain electric potentials and dominance 11 p1691 N85-20633

Psychological components in the development and prevention of air sickness 11 p1695 N85-20659

Role of mental work in human tolerance in total-body vibration 12 p1901 N85-21940

A portable battery for objective, non-obstrusive measures of human performances [NASA-CR-171868] 15 p2586 N85-25942

Measurement and modification of sensory system EEG (electroencephalographic) characteristics during visual-motor performance [AD-A151801] 15 p2618 N85-26133

M-BLASER: A device to study pursuit tracking in the rhesus monkey [AD-A152086] 17 p2998 N85-28534

Psychophysiological nature of aircraft feel 19 p3323 N85-30587

Effect of triphthasine and elenium on changes in evoked bioelectrical activity of the brain exposed to stationary magnetic field 19 p3325 N85-30601

SENSORS

Non-intrusive speed sensor — space shuttle main engine turbopumps [NASA-CR-171204] 03 p0364 N85-12331

Variability of short-term eddy-correlation estimates of mass exchange [DE84-007271] 05 p0677 N85-14349

Dutch institutes do research in tactile visual robot sensors 09 p1310 N85-18228

An ultra reliable computer communication network: The dispersed sensor processing mesh 09 p1372 N85-18620

Infrared horizon sensor modeling for attitude determination and control: Analysis and mission experience [NASA-TM-86181] 10 p1429 N85-19016

NORAD operational system 12 p1763 N85-21186

New atmospheric sensor analysis study [NASA-CR-171426] 13 p2094 N85-23069

Technical Digest: Symposium on Optical Fiber measurements, 1984 [PB85-114780] 13 p2160 N85-23407

A FORTRAN program for deep space sensor analysis [AD-A151790] 15 p2489 N85-25366

New sensor for industrial metrology developed 15 p2536 N85-25665

Low-resolution target classification from a staring infrared sensor [AD-A151690] 15 p2652 N85-26358

Hardware test program for evaluation of baseline range/range rate sensor concept [NASA-CR-175910] 17 p2947 N85-28194

Trace water sensor [NASA-CASE-NPO-15722-1] 18 p3103 N85-29212

Experiments in structural dynamics and control using a grid 20 p3410 N85-31165

The experimental computer control of a two-dimensional hyperbolic system 20 p3411 N85-31166

Optimal sensor locations for structural identification 20 p3417 N85-31209

Electrochemical methane sensor [DE85-011663] 22 p3787 N85-33464

Optical-fiber/microprocessor-based remote velocity sensor [DE85-010071] 22 p3788 N85-33470

Electronic temperature equalizer [PB85-181465] 22 p3789 N85-33475

Durability of oxygen sensors [PB85-183083] 22 p3789 N85-33477

Atmospheric nitrogen oxides: Their detection and chemistry [PB85-193910] 24 p4114 N85-35502

SENSORY DEPRIVATION

G-induced Loss of Consciousness (GLC) 20 p3610 N85-31623

SENSORY DISCRIMINATION

NT TACTILE DISCRIMINATION

NT VISUAL DISCRIMINATION

Reflection of laterization of sound stimuli in evoked potentials of human brain 04 p0544 N85-13460

SENSORY FEEDBACK

What is being done to control motion sickness? 15 p2687 N85-26596

SENSORY PERCEPTION

NT AUDITORY PERCEPTION

NT CONSCIOUSNESS

NT PROPRIOCEPTION

NT SPACE PERCEPTION

NT TACTILE DISCRIMINATION

NT TOUCH

NT VERTICAL PERCEPTION

NT VISUAL DISCRIMINATION

NT VISUAL PERCEPTION

Reflection of laterization of sound stimuli in evoked potentials of human brain 04 p0544 N85-13460

Susceptibility to kinetoses and the amplitude perceived from sensory illusions 11 p1694 N85-20651

Psychophysiological nature of aircraft feel 19 p3323 N85-30587

Reinterpretation of otolith input as a primary factor in space motion sickness 20 p3509 N85-31812

Dissociation of autonomic and sensory vestibular reactions 23 p3953 N85-34501

Testbed for sensory control of intelligent machines [DE85-012355] 24 p4099 N85-35412

A review of motion sickness with special reference to simulator sickness [AD-A155675] 24 p4131 N85-35611

Thirst and fluid intake following graded hypohydration levels in humans [AD-A156201] 24 p4132 N85-35615

SENSORY STIMULATION

USSR report: Life Sciences: Biomedical and behavioral sciences [JPRS-UBB-84-026] 04 p0543 N85-13457

Central regulation of sensory flow in human visual system 07 p1013 N85-1643

SENTENCES

NT WORDS (LANGUAGE)

SEO (INDIAN SPACECRAFT)

U INDIAN SPACECRAFT

SEPARATED FLOW

NT BOUNDARY LAYER SEPARATION

Oil flow patterns of separated flow on a hemispherical cylinder at incidence [DFVLR-FB-84-20] 01 p0048 N85-1001

The structure of the vorticity field in turbulent channel flow. Part 2: Study of ensemble-averaged fields [NASA-TM-86657] 03 p0361 N85-1231

Laminar and turbulent boundary layers in a plane of symmetry [AD-A146261] 03 p0362 N85-1232

Laser anemometer study of separated flow on wing profiles [ISL-CO-214/83] 04 p0459 N85-1287

Simulation of separated transonic airfoil flow by finite-difference viscous-inviscid interaction 05 p0591 N85-1379

Experiments on the structure of turbulent reattaching flow 05 p0635 N85-1407

Investigation of phase separation models in RELAP 4/MOD 6 [OEFZS-4286] 05 p0636 N85-1408

Flight test results on stall characteristics of a large jet transport [NAL-TR-817] 06 p0754 N85-1480

A collection of flow visualization techniques used in the Aerodynamic Research Branch [NASA-TM-85998] 06 p0800 N85-1513

A scanning laser velocimeter for turbulence research [NASA-CR-172493] 07 p0897 N85-1568

The structure of dilute combusting sprays [NASA-CR-174836] 07 p0905 N85-1573

Turbulent bubbles behind airfoils and wings at high angle of attack 08 p1069 N85-1677

Application of the vortex-lattice concept to flows with smooth-surface separation 08 p1100 N85-1702

roceedings of the workshop on unsteady separated w held at the United States Air Force Academy on August -11, 1983
D-A148249] 09 p1263 N85-17937

otential applications of forced unsteady flows
D-P004156] 09 p1264 N85-17940

A visual study of a delta wing in steady and unsteady ation
D-P004158] 09 p1264 N85-17943

Comparative visualization of accelerating flow around rious bodies, starting from rest
D-P004159] 09 p1264 N85-17944

Numerical solution of the Navier-Stokes equations for nsteady separated flows
AD-P004161] 09 p1265 N85-17946

Some structural features of unsteady separating urbulent shear flows
AD-P004164] 09 p1265 N85-17949

Unsteady separated flow: Forced and common vorticity bout oscillating airfoils
AD-P004167] 09 p1265 N85-17952

Unsteady separated flows: Generation and use by nsects
[AD-P004168] 09 p1266 N85-17953

Experiments on controlled, unsteady, separated turbulent boundary layers
[AD-P004172] 09 p1266 N85-17957

Flow separation induced by periodic aerodynamic interference
[AD-P004174] 09 p1266 N85-17959

On the flow processes in sharply inclined and stalled airfoils in parallel movement and rotation
[NASA-TM-77509] 10 p1419 N85-18952

Vacuum chamber pressure effects on thrust measurements of low Reynolds number nozzles
[NASA-TM-86955] 12 p1794 N85-21259

Theoretical and empirical studies of the basic structure of turbulent shear flows, including separated flows and effects of wall curvature
[AD-A149657] 12 p1846 N85-21580

Annular groove in compressor casing as device for control of air stream 13 p2050 N85-22632

Transonic merging separated flows
[AD-A150667] 14 p2213 N85-23724

Investigation of the turbulent separated flow behind a spoiler
[ISL-CO-240/83] 14 p2213 N85-23726

Calculation of an unsteady transonic flow with shock waves and separation in Laval nozzles
[MPIS-14/1984] 14 p2213 N85-23728

Stability of vortex structures during separation flow past array of wings 14 p2278 N85-24110

Contribution to the theory of stationary separation areas
[NASA-TM-77825] 14 p2300 N85-24244

Calculation of unsteady transonic separated flows by viscous-inviscid interaction 15 p2458 N85-25178

Heat transfer and fluid mechanics measurements in the turbulent reattaching flow behind a backward-facing step
15 p2553 N85-25753

An exploratory investigation of sharp fin-induced shock wave/turbulent boundary layer interactions at high shock strengths
[AD-A151571] 15 p2556 N85-25772

Problems and opportunities with three-dimensional boundary layers — aircraft, missile, and ship components 15 p2559 N85-25789

The role of computational fluid dynamics in aeronautical engineering 16 p2694 N85-26829

Numerical analysis of flow non-uniformity in the hot gas manifold of the Space Shuttle main engine
16 p2738 N85-26899

Structural stability and bifurcation in conical flow fields
[VTH-LR-424] 16 p2803 N85-27282

Method of calculating separation flow of subsonic gas stream around wings 17 p2942 N85-28161

Proceedings of the 9th US Air Force and the Federal Republic of Germany Data Exchange Agreement Meeting. Viscous and Interacting Flow Field Effects
[AD-A153020] 17 p2956 N85-28266

Characteristics of a confined jet thrust vector control nozzle
[AD-A153087] 17 p2956 N85-28268

A three-dimensional turbulent separated flow and related measurements
[NASA-CR-175913] 18 p3098 N85-29181

Additional flow field studies of the GA(W)-1 airfoil with 30-percent chord Fowler flap including slot-gap variations and cove shape modifications
[NASA-CR-3687] 19 p3212 N85-29919

High Re separated flow solutions using the Navier-Stokes and approximate equations
[AD-A152252] 20 p3454 N85-31451

Two-dimensional separation in an incompressible fluid — boundary layer separation
[ONERA-RTS-16/3232-RY-060-R]
20 p3456 N85-31459

Experimental investigations on airfoils with different geometries in the domain of high angles of attack-flow separation
[NASA-TM-77892] 22 p3728 N85-33110

Modelling of unsteady, incompressible separation on an aerofoil using an inviscid flow algorithm
[GU-AERO-8412] 23 p3894 N85-34122

A study of the second and third order closure models of turbulence for prediction of separated shear flows
[NASA-CR-176127] 23 p3929 N85-34353

Block-implicit calculations of three-dimensional laminar flow in strongly curved ducts
[DE85-003047] 23 p3931 N85-34363

SEPARATION

Ge abundances in the lunar mantle and implications for the origin of the Moon 04 p0582 N85-13721

Investigation of structure-permeability relationships of silicone polymer membranes
[PB85-148476] 11 p1596 N85-20038

Investigation of foam flotation and phase partitioning techniques 12 p1945 N85-22216

Grain boundary composition and intergranular fracture of steels. Volume 1: Detection of grain boundary segregation in steels
[DE85-006850] 15 p2662 N85-26428

Dual optical mechanical position tracker
[AD-D011739] 22 p3844 N85-33811

Separation of gas mixtures by supported complexes
[DE85-011996] 23 p3912 N85-34236

Separation of uranium from technetium in recovery of spent nuclear fuel
[DE85-006499] 23 p3972 N85-34627

SEPARATORS

NT AIR FILTERS
NT DRYING APPARATUS
NT DUST COLLECTORS
NT ELECTROSTATIC PRECIPITATORS
NT EVAPORATORS
NT FLUID FILTERS
NT PRECIPITATORS
NT SIEVES
NT STILLS

Purification of biomaterials by phase partitioning
02 p0154 N85-11043

Separation of metal species by supported liquid membranes
[DE84-014536] 04 p0470 N85-12992

Development of a mass transfer machine for gas/liquid operations in the absence of gravity
[BMFT-FB-W-84-027] 05 p0637 N85-14091

Phosphoric and electric utility fuel cell technology development
[NASA-CR-174215] 06 p0805 N85-15124

Design and development of a sealed 100-Ah nickel-hydrogen battery
[DE84-016935] 06 p0805 N85-15128

Electric utility acid fuel cell stack technology advancement
[NASA-CR-174804] 08 p1178 N85-17422

Diffusion separation of reacting gas mixtures
11 p1718 N85-20810

Improved silicon grinding method and apparatus
[NASA-CASE-NPO-16336-1-CU]
12 p1819 N85-21407

Supported liquid membrane battery separators
[DE85-001031] 12 p1836 N85-21519

Research on separators for alkaline zinc batteries
[DE85-003062] 12 p1836 N85-21523

Magnetic field in main gap of separator
12 p1843 N85-21563

Development of molten carbonate fuel cell power plant technology
[DE84-016839] 14 p2352 N85-24536

Alkaline battery containing a separator of a cross-linked copolymer of vinyl alcohol and unsaturated carboxylic acid
[NASA-CASE-LEW-13102-1] 18 p3093 N85-29144

Aluminum-air power cell: The M3-3 experiment
[DE85-008678] 18 p3096 N85-29168

Development of a lithium secondary battery separator
20 p3444 N85-31379

RCA's planned test program to compare the performance and life of NiCd cells containing Pellon 2536 in contrast with Pellon 2505 separator material
20 p3445 N85-31385

Free zone electrophoresis simulation of static column electrophoresis in microgravity on shuttle flight STS-3
20 p3502 N85-31773

Microgravity electrophoresis: A study of the factors that affect free-fluid separation 20 p3502 N85-31774

Properties of electrophoretic fractions of human embryonic kidney cells separated on space shuttle flight STS-8 20 p3503 N85-31776

Vapor-liquid phase separator studies
[NASA-CR-166545] 21 p3583 N85-32272

Drying of pulverized material with heated condensible vapor
[DE85-011656] 22 p3783 N85-33438

Development of a prototype energy meter
[PB85-196430] 22 p3789 N85-33476

Molten carbonate fuel cell separator
[DE85-011615] 22 p3806 N85-33577

Fuel cell separator plate with bellows-type sealing flanges
[DE85-005991] 23 p3947 N85-34458

Cationic exchange membrane for the zinc-ferricyanide battery
[DE85-013152] 24 p4112 N85-35489

SEQUENCING

Comprehension of instructions for operating devices
[AD-A145263] 01 p0098 N85-10653

Modular detonator device
[AD-D011232] 03 p0340 N85-12164

Sequence of effects in the crack initiation and crack propagation phase 05 p0649 N85-14168

Steps towards parsing of query sequences to a database
[AD-A148769] 08 p1206 N85-17590

Low-resolution target classification from a staring infrared sensor
[AD-A151690] 15 p2652 N85-26358

The evolutive state: A new definition of system state to include sequencing of events
16 p2696 N85-26843

Bandpass filter formed by serial gratings operating in a wood's anomaly region
[AD-D011660] 18 p3093 N85-29148

Towards a statistical analysis of genetic sequences data with particular reference to protein sequences
[AD-A153805] 18 p3152 N85-29515

Study of a low rate spread spectrum receiver
[ENST-83E015] 20 p3441 N85-31354

Construction of complementary code sequence sets, part 7.1D 21 p3625 N85-32523

SEQUENTIAL ANALYSIS

Model for non-linear crack growth prediction, taking load sequence (LOSEQ) effects into consideration
[BLL-RAE-TRANS-2114-(5207)]
02 p0208 N85-11371

Nonlinear processing of optical pulse signals
07 p0951 N85-16026

Local dependence and point processes of exceedances in stationary sequences
[AD-A147858] 07 p1036 N85-16676

Sequential data processing for photogrammetric acquisition of digital elevation models
08 p1176 N85-17413

Sequential minimization for sum of squares of unknown functions
[DE85-004162] 11 p1707 N85-20738

Automatic pickup of trajectory by method of sequential analysis taking into account deviation of radar markers from center of strobe 12 p1838 N85-21535

Boundary crossing probabilities and statistical applications
[AD-A151027] 14 p2411 N85-24869

A software simulation study of a sequential decoder using the Fano algorithm 16 p2771 N85-27100

Sequential regularization solution of the inverse heat conduction problem
[DE85-010657] 23 p3931 N85-34362

SEQUENTIAL COMPUTERS

Construction of complementary code sequence sets, part 7.1D 21 p3625 N85-32523

SEQUENTIAL CONTROL

Sequential syndrome decoding of convolutional codes
05 p0624 N85-13992

Asymptotically optimum multialternative sequential procedures for discernment of processes minimizing average length of observations
13 p2084 N85-23212

Principles of organizing a real-time control system
15 p2625 N85-26177

A comparison of methods of least squares adjustment of traverses
[AD-A153812] 18 p3170 N85-29840

SERIES (MATHEMATICS)

NT ASYMPTOTIC SERIES
NT FOURIER SERIES
NT PADE APPROXIMATION
NT POWER SERIES
NT TAYLOR SERIES

The Lindstrom-Madden method for series systems with repeated components
[AD-A149285] 20 p3412 N85-[illegible]

Local dependence and point processes of exceedances in stationary sequences
[AD-A147859] 07 p1036 N85-16578
On the spans of polynomials and the spans of a Laguerre-Polya-Schur sequence of polynomials
[AD-A149364] 10 p1547 N85-19754
Effects of assuming independent component failure times, if they are actually dependent, in a series system
[AD-A150582] 13 p2101 N85-23092
An integral representation of the generalized Euler-Mascheroni constants
[NASA-TP-2456] 13 p2144 N85-23305
Squares of Gegenbauer polynomials and Milin type inequalities
[CWI-PM-R8412] 14 p2410 N85-24882
Disproof of the Mertens conjecture
[CWI-NM-R8412] 14 p2414 N85-24896
On the exceedance point process for a stationary sequence
[AD-A152627] 17 p3018 N85-28665
The optimality of lower confidence limits for the reliability of series systems obtained by the method of key test results or other related techniques
[AD-A154880] 21 p3597 N85-32338
Method of estimating convergence of Haar coefficients in message compression problems
22 p3769 N85-33358

SERIES EXPANSION
Model diagnosis in two-way tables by means of row and column Euclidean maps
[CSIR-TWISK-307] 01 p0108 N85-10730
Upwind compact finite difference schemes
[CSIR-TWISK-334] 01 p0110 N85-10742
Scattering by a parabolic cylinder: A uniform asymptotic expansion
[AD-A145686] 02 p0252 N85-11652
On the Edgeworth expansion for the sum of a function of uniform spacings
[CWI-MS-R8404] 05 p0719 N85-14619
A propagator expansion method for solving linearized plasma kinetic equations with collisions
[AD-A147524] 07 p1045 N85-16640
First derivatives of flow quantities behind two-dimensional, nonuniform supersonic flow over a convex corner
[NASA-TM-86272] 08 p1077 N85-16828
A series expansion study of the Navier-Stokes equations
[DFVLR-FB-84-34] 09 p1321 N85-18306
A convergent series expansion for hyperbolic systems of conservation laws
[NASA-CR-172557] 12 p1910 N85-21990
Transient analysis of loaded thin-wire antennas and transmission lines 13 p2053 N85-22852
Asymptotic expansions of the distribution of test statistics associated with several two parameter exponential distributions
[AD-A151906] 15 p2641 N85-26289
Asymptotic expansion of Jacobi polynomials
[REPT-84-35] 17 p3021 N85-28689
Uniform asymptotic expansions of integrals
[CWI-AM-R8412] 17 p3022 N85-28694
Evaluation of densities and distributions via hermite and generalized laguerre series employing high-order expansion coefficients determined recursively via moments or cumulants
[AD-A153950] 18 p3175 N85-29682
Asymptotic expansions for finite element eigenvalues and finite element solution 19 p3345 N85-30730

SERPENTINE
The mineralogy of global magnetic anomalies
[E85-10061] 07 p0987 N85-16272

SERUMS
The role of vitamin D in the bone changes associated with simulated weightlessness 15 p2608 N85-26072
Experiments in microwave exposure in the rat: Body temperature, serum chemistry and the use of chemical restraint
[PB85-156834] 16 p2840 N85-27512
Rat blood serum and liver carbohydrates and lipids in recovery period after 15-day hypokinesia
19 p3326 N85-30606

SERVICE LIFE
Retardation analytical model to extend service life
[NASA-CR-171177] 01 p0057 N85-10376
Avionics integrity program (Avip). Volume 4: Force management. Economic life considerations
[AD-A145592] 02 p0138 N85-10941
Equivalent damage: A critical assessment
02 p0140 N85-10952
On discrete failure models
[AD-A145579] 02 p0206 N85-11359
Performance of improved lead acid batteries for electric vehicles
[DE84-015845] 04 p0495 N85-13160
A high-repetition rate, inductively stabilized, long-pulse excimer laser
[DE84-016827] 04 p0506 N85-13229
Perspectives on energy storage wheels for space station application 05 p0605 N85-13860
Influence of shot-peening methods on surface quality and service life of bearings 06 p0776 N85-14960
Predicting changes in reliability characteristics of gas turbine engines during operation
06 p0776 N85-14964
Longevity of thin-walled engine parts subjected to transient stresses under creep conditions
06 p0777 N85-14966
Performance on advanced lead-acid batteries for load-leveling applications
[DE84-015817] 06 p0805 N85-15125
Impact of temperature on cycle life of globe ISOA EV-3000 lead-acid batteries
[DE84-015840] 06 p0805 N85-15126
Predicting electrochemical breakdown in terrestrial photovoltaic modules 06 p0830 N85-15273
Structural flight load measurement demonstration of structural integrity 07 p0895 N85-15670
CF-5 vertical stabilizer flight load survey
07 p0895 N85-15673
US Army helicopter operational flight loads
07 p0895 N85-15675
Helicopter data acquisition in WHL
07 p0896 N85-15676
Prematurely terminated sequential tests for MIL-STD 781C
[AD-A148417] 08 p1216 N85-17657
Determination of blade service life under irregular loading conditions 09 p1309 N85-18222
A kernel type estimator of a quantile function from right-censored data
[AD-A148753] 09 p1374 N85-18635
Measurement techniques for evaluating solar reflector materials
[DE85-002194] 10 p1510 N85-19531
Seven-year thermal-vacuum real-life test of a solar array drive mechanism manufactured by Marconi Space and Defence Systems (Model No. 002)
[ESA-ESTL-62] 11 p1616 N85-20161
Rep rated long life capacitor development: Phase 1 and 2
[DE85-000719] 11 p1629 N85-20256
Tailored airfoils for vertical axis wind turbines
[DE85-004628] 12 p1772 N85-21126
Finger materials for air cushion vehicles. Volume 2: Base fabrics for finger materials
[AD-A149701] 12 p1819 N85-21408
Supported liquid membrane battery separators
[DE85-001031] 12 p1836 N85-21519
On maximizing the expected lifetime of replaceable systems
[AD-A150003] 12 p1862 N85-21680
Approach for service life extension of explosive devices for aircraft escape systems
[NASA-TM-86323] 13 p1971 N85-22381
Survival testing of silicon solar modules
13 p2009 N85-22602
Development of molten carbonate fuel cell power plant technology
[DE84-016839] 14 p2352 N85-24536
Long-life high performance fuel cell program
[NASA-CR-174874] 15 p2494 N85-25384
NASA welding assessment program
[NASA-CR-175683] 15 p2568 N85-25845
Thrust chamber life prediction
16 p2733 N85-26865
Fatigue criterion to system design, life and reliability
[NASA-TM-87017] 16 p2793 N85-27226
Bifunctional oxygen electrodes
[DE85-006871] 17 p2955 N85-28248
DOE/Sandia point-focus concentrator program, draft
[DE85-008209] 17 p3038 N85-28793
Additional experiments relative to the shelf life of Li(Si)/FeS2 thermal batteries
[DE85-008482] 18 p3095 N85-29162
Nickel-cadmium cell design variable program data analysis
[NASA-TM-86196] 19 p3258 N85-30203
Life cycle test results of a bipolar nickel hydrogen battery
[NASA-TM-87046] 19 p3304 N85-30480
Free-piston Stirling engine/linear alternator 1000-hour endurance test
[NASA-CR-174771] 19 p3304 N85-30481
Design evaluation of high reliability lithium batteries
20 p3444 N85-31380
RAY-O-VAC BR2325 lithium carbon monofluoride cell performance 20 p3444 N85-31382
AUSSAT battery life test program
20 p3446 N85-31395
Design principles for nickel-hydrogen cells and batteries
[NASA-TM-87037] 20 p3483 N85-31648
High temperature electronics technology: Life test report
[AD-A154681] 21 p3580 N85-32257
Los Alamos optical materials reliability, maintainability, and exposure testing program
[DE85-011894] 21 p3613 N85-32458
Performance improvements from surfacing in aero engine components
[PNR-90257] 23 p3897 N85-34142

SERVICES
NT MEDICAL SERVICES
NT METEOROLOGICAL SERVICES
Demand for satellite-provided domestic communications services up to the year 2000
[NASA-TM-86894] 06 p0798 N85-15099
A comparison of metropolitan and non-metropolitan employment characteristics: Indications of the size of non-metropolitan mobile communication services user classes
[NASA-CR-175648] 13 p2053 N85-22855
Food service management 14 p2393 N85-24736

SERVOCONTROL
Active dispersion control for a Doppler broadened laser
[AD-D011570] 14 p2310 N85-24297
Control of motion of manipulator robots on basis of first-order kinematic algorithms
16 p2762 N85-27047
An improved servo-controlled inertial clock for laboratory tests of general relativity 19 p3378 N85-30955

SERVOMECHANISMS
NT SERVOMOTORS
Experimental study with parameter variations on a hydraulic positioning servo with computer implemented observer
[FOA-C-20545-E3] 02 p0256 N85-11673
Tracking servo compensator with rate aiding
[AD-D011372] 07 p0942 N85-15971
Improvement of electromechanical systems by utilization of microelectronic technology 07 p0955 N85-16053
Mirror actuator control system
[AD-D011383] 07 p1042 N85-16619
Control and electronic subsystems for the advanced servomanipulator
[DE85-001900] 09 p1327 N85-18343
Dual arm master controller concept
[DE85-001901] 09 p1327 N85-18344
Advanced remotely maintainable force-reflecting servomanipulator concept
[DE85-001902] 09 p1328 N85-18345
Servo operated anti-G suit pressurization system
[AD-D011468] 10 p1531 N85-19651
Flutter taming: A new tool for the aeroelastic designer
[AD-A150834] 14 p2226 N85-23802
New equipment complex Kaskad 2 for automatic control 14 p2266 N85-24042
Italy's Fiat uses Sweden's Asea seeing robot
15 p2536 N85-25650
Control of motion of manipulator robots on basis of first-order kinematic algorithms
16 p2762 N85-27047
Proceedings of the Workshop on Identification and Control of Flexible Space Structures, volume 1
[NASA-CR-176051] 20 p3408 N85-31148
A study on the control of third generation spacecraft
20 p3415 N85-31196
Harold Hazen and the theory and design of servomechanism
[RR-270] 22 p3794 N85-33506
Application of traction drives as servo mechanisms
22 p3797 N85-33520
Dual arm master controller development
22 p3797 N85-33528

SERVOMOTORS
Design and test of a four channel motor for electromechanical flight control actuation
[NASA-CR-171838] 08 p1156 N85-17294
Analysis and design of hydraulic servo systems within the scope of the improvement of a fatigue testing installation of the Royal Dutch Army
[LEOK-TR-1984-09] 14 p2265 N85-24033
Novel drives for machine tools
14 p2268 N85-24053
Robot use in FRG increases but sensor technology lags 15 p2531 N85-25605
Basic development of one-chip control circuitry for commutatorless dc motors
[BMFT-FB-T-84-305] 18 p3098 N85-29178
Computer simulation of a cruise missile using brushless dc motor fin control
[AD-A155935] 24 p4089 N85-35349

SERVOS
U SERVOMOTORS

SERVOSTABILITY CONTROL
U SERVOCONTROL
SES
U SURFACE EFFECT SHIPS
SET THEORY
NT BOREL SETS
NT EQUIVALENCE
NT THRESHOLD LOGIC
Set-theoretic problems of null completion in relational databases
[AD-A145045] 01 p0125 N85-10861
An iterative procedure for obtaining i-projections onto the intersection of convex sets
[AD-A145402] 02 p0251 N85-11639
Constrained optimization using iterated partial Kuhn-Tucker vectors
[AD-A145476] 02 p0251 N85-11641
An investigation into fuzzy clustering and classification
[AD-A145571] 02 p0251 N85-11645
Advanced Ada (trademark)
[AD-A146257] 03 p0407 N85-12602
Locally optimal subset selection rules based on ranks under joint type 2 censoring
[AD-A146179] 03 p0412 N85-12632
Stable monotone variational inequalities
[AD-A147123] 07 p1031 N85-16544
Condenser capacities and removable sets in W1p1
10 p1536 N85-19682
Relative-entropy minimization with uncertain constraints--theory and application to spectrum analysis
[AD-A149192] 10 p1546 N85-19752
Some facets of the tri-index assignment polytope
[AD-A149195] 10 p1547 N85-19753
Connected simple systems and the Conley index of isolated invariant sets
[AD-A149383] 10 p1552 N85-19789
Some data manipulation requirements for the exploratory analysis of large data sets
[DE85-002541] 10 p1568 N85-19887
Maximum matchings in a class of random graphs
[AD-A149863] 12 p1920 N85-22060
Optimal designs for comparisons between two sets of treatments
[AD-A150621] 13 p2152 N85-23360
Topology and Order Structures, part 2
[MCT-169-PT-2] 14 p2413 N85-24879
When is a GO-space JO(2)? 14 p2414 N85-24889
Solving the minimal least squares problem subject to bounds on the variables
[TRITA-NA-8215] 16 p2852 N85-27580
Schubert varieties are arithmetically Cohen-Macaulay
16 p2853 N85-27592
A note on integral operators
[REPT-83-26] 17 p3021 N85-28688
Applications of fuzzy set theory to satellite soundings
18 p3141 N85-29445
Applications of some artificial intelligence methods to satellite soundings 18 p3141 N85-29446
Ada developments
[REPT-84-28] 18 p3164 N85-29604
Hybrid uncertainty theory
[DE85-008357] 18 p3167 N85-29622
A variable-complexity norm maximization problem
[AD-A153514] 18 p3169 N85-29634
On approximating a set-valued function locally
[AD-A153540] 18 p3170 N85-29641
Construction of complementary code sequence sets, part 7.1D 21 p3625 N85-32523
SETI
U PROJECT SETI
SETTING
Setting hurricane conditions of readiness with high confidence
[AD-A144785] 01 p0065 N85-10570
SEVERE STORMS OBSERVING SATELLITE
U STORMSAT SATELLITE
SEWAGE
NT SOLID WASTES
SEWERS
Hydrodynamics and sanitation
[CT-579] 20 p3487 N85-31672
SEWING
Re-designing a mechanism for higher speed: A case history from textile machinery 23 p3923 N85-34310
SEX FACTOR
Physiological differences between men and women in exercise-heat tolerance and heat acclimation
[AD-A152048] 15 p2618 N85-26135
SEYFERT GALAXIES
X-ray observations of the Seyfert 1 galaxies AKN120 and MCG8-11-11
[NASA-TM-86063] 03 p0446 N85-12839
The X-ray spectrum and time variability of narrow emission line galaxies
[NASA-TM-83859] 03 p0446 N85-12842
The IRAS galaxy 0421+040P06: An active spiral (?) galaxy with extended radio lobes
[NASA-CR-174208] 06 p0871 N85-15536
X-ray and UV Emission from Active Galactic Nuclei -- conference
[MPE-184] 08 p1236 N85-17790
Radio Seyferts and the forbidden line region
08 p1236 N85-17793
A new estimate of the local luminosity function of Seyfert 1 nuclei 08 p1237 N85-17796
Continuous transition from star burst galaxies to Seyfert galaxies 08 p1237 N85-17798
Spatially resolved optical spectroscopy of the radio jet of the X-ray galaxy NGC 2110 08 p1238 N85-17804
EXOSAT observations of active galactic nuclei
08 p1238 N85-17809
The X-ray spectra of NGC 4151 -- Seyfert galaxy
08 p1239 N85-17815
An inverse Compton model of the X-ray emission in Seyfert galaxies 08 p1241 N85-17827
Theoretical studies of emission line variability in type 1 Seyfert galaxies 08 p1242 N85-17839
Active galactic nuclei and their cosmological evolution
08 p1243 N85-17842
Ultraviolet and X-ray observations of active galactic nuclei: Constraints on models of the broad emission line region 11 p1744 N85-20966
Broad emission features in active galactic nuclei
11 p1746 N85-20979
Fluorescent excitation of Fe 2, Mn 2, Ti 2, N 1 lines by V 4, N 5, O 6: Emission lines in the spectra of symbiotic stars and Seyfert galaxies 11 p1746 N85-20984
A model for the variable continuum of the Seyfert 1 galaxy NGC 5548 11 p1747 N85-20985
X-ray emission from active galactic nuclei
[NASA-TM-86175] 11 p1763 N85-21088
IRAS observations of Seyfert galaxies
[NASA-CR-175557] 12 p1953 N85-22267
IRAS observations of active galaxies
[NASA-CR-175720] 15 p2668 N85-26463
The ultraviolet spectra of intermediate redshift quasars
20 p3544 N85-32056
Interactions of galaxies and their nuclear activity
20 p3545 N85-32060
Balloon observations of hard X-rays from NGC 4151 and an X-ray transient source
[OG-2.7-6] 22 p3871 N85-33979
Gamma-radiation with E gamma 5 MeV detected from Seyfert galaxy 3C120 and region with 1' = 190 deg and b' = 20 deg
[OG-2.8-8] 22 p3871 N85-33981
Some evidence for large gravitational redshift in Seyfert galaxy NGC 4151
[OG-2.7-11] 22 p3872 N85-33984
SFERICS
U ATMOSPHERICS
SGEMP
U SYSTEM GENERATED ELECTROMAGNETIC PULSES
SHADOWGRAPH PHOTOGRAPHY
NT SCHLIEREN PHOTOGRAPHY
Measurement of sensitivity of shadowgraphic instruments with spherical autocollimating mirror
14 p2274 N85-24087
Optical system for measuring shadowgraph data
[AD-D011642] 17 p3036 N85-28784
SHADOWGRAPHS
U SHADOWGRAPH PHOTOGRAPHY
SHADOWS
NT PENUMBRAS
Numerical simulation of static and dynamic shadow patterns using an atomistic description of crack initiation and propagation
[DE85-003226] 12 p1867 N85-21715
Poisson and multinomial shadowing processes
[AD-A151600] 15 p2640 N85-26286
On the possibility of the determining the average mass composition near 10 to the 14th power eV through the solar magnetic field
[OG-5.1-9] 22 p3882 N85-34051
Shadow volumes for non-planar polygons
23 p3955 N85-34580
Empirical model for the Earth's cosmic ray shadow at 400 KM: Prohibited cosmic ray access
[SH-6.1-14] 23 p4046 N85-35087
SHAFTS (MACHINE ELEMENTS)
NT TURBOSHAFTS
Stability of hollow shafts under torsion
06 p0780 N85-14986
Improvement of the corrosion resistance of turbine engine bearings
[AD-A147430] 07 p0905 N85-15731
Theoretical and experimental study of hydro-elastic instability on the line of shafting of a rotating machine
[BLL-DOUNREAY-TR-937-(9091.9F)]
07 p0972 N85-16174
Measurement and evaluation of the loading of shafts by torsional vibrations 07 p0980 N85-16222
Assessment of the operating characteristics of the SSME LOX turbopump pump-end bearing
[NASA-CR-171287] 08 p1167 N85-17362
Effect of coupled torsional-flexural vibration of a geared shaft system on the dynamic tooth load
09 p1338 N85-18415
Assessing expired fatigue life in large turbine shafts
[DE84-016876] 09 p1340 N85-18427
Low leakage turbine shaft seals for advanced combined cycle systems
[AD-A149372] 10 p1492 N85-19420
Angular measurement system
[NASA-CASE-MFS-25825-1] 11 p1635 N85-20298
Influence of axial shaft load on operation of magnetoelastic torque transducer
14 p2270 N85-24065
Twisting of segmental shafts
14 p2279 N85-24119
Some problems of optimum journal design for disk-drum rotors under antisymmetric loading
14 p2286 N85-24167
SHAFT: Interactive shaft design program
[DE85-007333] 15 p2568 N85-25850
Electric motors with elastically mounted rotors
16 p2763 N85-27048
Monitoring of turbo-machines by shaft vibration measurement
[BLL-CE-TRANS-7900-(9022.09)]
16 p2799 N85-27255
Quasi-steady vibrations of a rotating shaft grazing an obstacle: Spiral vibration
[BLL-CE-TRANS-7962-(9022.09)]
16 p2799 N85-27256
Calculation of friction at spherical bearing journals in turbomachines 17 p2940 N85-28150
Determination of wear intensity and resource of crankshafts and cylinder liners of ZIL-130 and ZMZ-53 engines
[BLL-BISI-TRANS-21393-(9022.06)]
17 p2972 N85-28355
Muthod for driving two-phase turbines with enhanced efficiency
[NASA-CASE-NPO-15037-2] 18 p3115 N85-29282
Non-backdriveable free wheeling coupling
[NASA-CASE-MSC-20475-1] 18 p3116 N85-29290
Vibration control of rotor shaft
[NASA-TM-87053] 18 p3117 N85-29292
SHAKERS
Pycnometer shaker
[PB85-174985] 20 p3460 N85-31491
Measurement of damping of graphite epoxy materials
[NASA-CR-176073] 21 p3596 N85-32334
SHAKING
NT DITHERS
Mechanical stress regulation of plant growth and development 15 p2610 N85-26087
SHALE OIL
Mechanisms of syncrude-synfuel degradation
[DE84-015206] 01 p0034 N85-10212
Lubricity of well-characterized jet and broad-cut fuels by ball-on-cylinder machine
[NASA-TM-83807] 03 p0339 N85-12183
Oil-shale exploration expansion urged
07 p0994 N85-16317
Data base of all known, published data on trace elements in oil shale and its products
[DE85-003399] 18 p3126 N85-29357
Aspects of high-resolution gas chromatography as applied to the analysis of hydrocarbon fuels and other complex organic mixtures. Volume 1
[AD-A156154] 24 p4076 N85-35257
SHALES
Workshop on Remote Sensing/Lineament Applications for Energy Extraction
[DE84-009291] 12 p1875 N85-21763
Shales and other argillaceous strata in the United States
[DE85-010453] 18 p3125 N85-29353
SHALLOW SHELLS
Buckling and postbuckling behavior of shallow shells
18 p3120 N85-29317
SHALLOW WATER
An analytical model of periodic waves in shallow water
[AD-A147501] 07 p0960 N85-16085
An analytical model of periodic waves in shallow water
[AD-A147502] 07 p0960 N85-16086
The investigation of selected oceanographic applications of spaceborne synthetic-aperture radar
08 p1146 N85-17233
Weakly-reflective boundary conditions for two-dimensional shallow water flow problems
[PUBL-322] 08 p1163 N85-17341

Evaluation of time integrators for the shallow water equations
[CWI-NM-R8406] 11 p1634 N85-20292
Modifications to a propagation model for the combinded refraction-diffraction of stokes waves; shallow water, large angle and breaking wave effects
[AD-A151428] 15 p2556 N85-25768
The theoretical response of a vertical line array to wind-generated noise in shallow water
[AD-A151730] 16 p2860 N85-27636
Rip in White Sea 19 p3290 N85-30401
Propagation of sound in a layered laboratory model
[AD-A155141] 21 p3700 N85-32969

SHANKS
U JOINTS (JUNCTIONS)

SHANNON INFORMATION THEORY
U INFORMATION THEORY

SHAPE CONTROL
Constellations 11 p1643 N85-20352
Control Of Flexible Structures (COFS) flight experiment background and description 14 p2236 N85-23664
The effect of sensor and actuator errors on static shape control for large space structures
[NASA-TM-86446] 19 p3225 N85-29998
Multivariable control of a soft coupled space station
20 p3408 N85-31151
Stiffness control of large space structures
20 p3414 N85-31189
Sub-optimal control of nonlinear flexible space structures 20 p3414 N85-31190

SHAPE MEMORY ALLOYS
NT NITINOL ALLOYS
Effect of form memory in alloys based on Cu-Al systems 11 p1604 N85-20066
The effect of prior parent phase cold work on martensite transformation in Cu-Zn-Al shape memory alloys
[AD-A155140] 21 p3566 N85-32183
Comparison of the response of shape memory alloy actuators using air-cooling and water-cooling
[AD-A155216] 21 p3567 N85-32185
Shape memory effect in uranium-niobium alloys below room temperature
[DE85-012964] 23 p3916 N85-34268

SHAPED CHARGES
Making high explosive bodies for shaped charges by casting or pressing. Shaped charge research at Research Institute of National Defence (FOA) in 1972 - 1983, part 1
[FOA-C-20554-D4-PT-1] 07 p0935 N85-15923
Generation of detonation waves of given spatial and temporal characteristics
[ISL-R-103/83] 16 p2758 N85-27021
SCAP: A Shaped Charge Analysis Program. User's manual for SCAP 1.0
[DE85-011182] 20 p3515 N85-31854

SHAPES
NT CONVEXITY
NT ELLIPTICITY
NT FLATNESS
NT LINE SHAPE
An error analysis for the use of presently available lunar radio flux data in broadbeam antenna-system measurements
[PB84-216361] 01 p0016 N85-10097
Resonant frequencies and mode shapes for single and double cylindrical shells
[AD-A144778] 01 p0062 N85-10408
Optimization of the die entrance shape for polymeric extrusion
[DE85-001588] 06 p0772 N85-14937
Effects of body shape on the aerodynamics of a body of revolution at Mach numbers from 1.6 to 4.6
[NASA-TM-86345] 07 p0893 N85-15657
Free-surface boundary layer and the origin of bow vortices
[AD-A147427] 07 p0980 N85-16083
Experimental investigation of a turbulent incompressible boundary layer on a curved wall
11 p1577 N85-19936
Semianalytic modeling of aerodynamic shapes
[NASA-TP-2413] 12 p1771 N85-21120
A stochastic-mechanical approach to acoustic pulse propagation in the deep ocean sound channel
[AD-A149598] 12 p1928 N85-22110
A description of the Langley wireframe geometry standard (LaWGS) format
[NASA-TM-85767] 13 p1971 N85-22380
Shape optimization for minimal stress concentration
13 p2101 N85-23093
Surfaces of asteroids and cometary nuclei
13 p2176 N85-23503
Some problems of optimum journal design for disk-drum rotors under antisymmetric loading
14 p2286 N85-24167
Effect of form and clearance of a piston launched in a tube on the boundary layer and the heat transfer
[ISL-CO-216/83] 14 p2302 N85-24255
Scattering properties of a moving dielectric object
[AD-A151974] 15 p2544 N85-25706
An IKBS approach to image understanding
[AD-A151992] 16 p2854 N85-27599
Fluid surface behavior in low gravity. Center discretionary fund no. 83-21
[NASA-TP-2486] 17 p2957 N85-28260
Shape preserving spline interpolation
17 p3003 N85-28564
The construction of curves and surfaces using numerical optimization techniques 17 p3003 N85-28565
Free-form design in solid modelling
17 p3004 N85-28569
Triangular Berstein-Bezier patches, a survey and new results 17 p3005 N85-28577
Urn models and beta-splines
17 p3005 N85-28580
A new technique for system-to-system transfer of surface data 17 p3007 N85-28589
Texture perception and shape from texture
[AD-A154276] 19 p3336 N85-30672
Spectrum of the gamma-ray diffuse component observed from HEAO-1
[OG-3.1-12] 22 p3874 N85-34000
Spectral shape variation of interstellar electrons at high energies
[OG-6.2-7] 22 p3889 N85-34106
Block-implicit calculations of three-dimensional laminar flow in strongly curved ducts
[DE85-003047] 23 p3931 N85-34363
A user-friendly computer-aided construction of boundaries 23 p3962 N85-34564
Non-rigid body motion 23 p3964 N85-34576

SHARKS
Development of ARGOS platforms for tracking of basking sharks. Cetorhinus maximus
14 p2326 N85-24376

SHATTERING
U FRAGMENTATION

SHEAR
Shear deformation plate continua of large double-layered space structures
01 p0059 N85-10391

SHEAR CREEP
The effects of radial yarns, 3-dimensionally reinforced carbon-carbon composite
[AD-A144751] 01 p0022 N85-10134

SHEAR DISTURBANCES
U S WAVES

SHEAR FATIGUE
U SHEAR STRESS

SHEAR FLOW
A perturbation solution for rigid dumbbell suspensions in steady shear flow
[AD-A144876] 01 p0111 N85-10755
Study of the structure of turbulent shear flows at supersonic speeds and high Reynolds number
[NASA-CR-174144] 04 p0452 N85-12865
Progress in the development of a two-fluid model of turbulence for near-wall flows, part 1
[CFD/84/7-PT-1] 04 p0501 N85-13196
Turbulent shear fields for dispersion of aqueous drops in organic liquids and application to gel-sphere processes
[DE84-016562] 06 p0809 N85-15141
Study of low-frequency sound with point source in stream with shear 06 p0825 N85-15239
Some structural features of unsteady separating turbulent shear flows
[AD-P004164] 09 p1265 N85-17949
Single integral constitutive equations for viscoelastic fluids
[AD-A149410] 10 p1547 N85-19756
A three-dimensional spectral algorithm for simulations of transition and turbulence
[NASA-CR-172561] 12 p1845 N85-21575
Theoretical and empirical studies of the basic structure of turbulent shear flows, including separated flows and effects of wall curvature
[AD-A149657] 12 p1846 N85-21580
Acoustic energy exchange in sheared mean flows -- solid rocket motors 13 p1999 N85-22534
Modeling of shear flow in a stratified fluid
14 p2340 N85-24469
Three-dimensional boundary layers and shear flows activities at ONERA/CERT 15 p2558 N85-25785
An experimental study of the noise generated by vaporous cavitation in turbulent shear flows produced by confined orifice plates 15 p2645 N85-26316
Studies of structure and modeling in turbulent shear flows
[AD-A151607] 16 p2782 N85-27170
Practical real-time quality control of antimisting kerosene
[DE/FAA/CT-85/1] 18 p3063 N85-29072
Transverse vorticity measurements using an array of four hot-wire probes
[FSFL-R-85-006] 18 p3099 N85-29184
Effect of nonuniform size on internal stresses in a rapid, simple shear flow of granular materials. Part 1: Two grain sizes
[AD-A154045] 19 p3285 N85-30072
Effect of nonuniform size on internal stresses in a rapid, simple shear flow of granular materials. Part 2: Multiple grain sizes
[AD-A154046] 19 p3285 N85-30073
Intermittency, conditional sampling and turbulent combustion 20 p3424 N85-31249
Conditional modelling in turbulent shear flows
20 p3424 N85-31250
Turbulent reacting flows 20 p3451 N85-31427
Wall effect on lateral migration of spherical particles in a linear shear flow 20 p3452 N85-31432
Moist barotropic instability in the tropics
20 p3489 N85-31683
On the solution for the sound field in a semi-infinite uniform duct with sheared mean flow
20 p3523 N85-31912
Techniques for the study of gravity waves and turbulence (keynote paper), part 4 21 p3621 N85-32489
Second order modelling in non-constant density flows
22 p3744 N85-33206
Turbulent mixing and combustion
22 p3744 N85-33207
Modeling of turbulent recirculating combusting flows
22 p3745 N85-33212
Turbulence modelling for the prediction of turbulent jets: Wakes and plumes
[CFD/84/5] 22 p3784 N85-33447
A study of the second and third order closure models of turbulence for prediction of separated shear flows
[NASA-CR-176127] 23 p3829 N85-34353

SHEAR LAYERS
The aerodynamics of bluff bodies in turbulent shear layers 05 p0593 N85-13780
Amiet shear layer correction with an additional temperature gradient considered: Nomograms for the correction of noise signatures from open jet wind tunnel tests
[DFVLR-MITT-84-11] 05 p0726 N85-14689
Aero-optics experimental techniques
[AD-A146755] 07 p0957 N85-16067
Modelling circulation control by blowing --- airfoils
08 p1069 N85-16778
A free shear layer prediction of the turbulent wake of a flat plate towed below a free surface
[AD-A148699] 09 p1319 N85-18293
On the interaction of a sound pulse with the shear layer of an axisymmetric jet. Part 3: Nonlinear effects
[NASA-CR-172512] 09 p1378 N85-18683
Effects of a periodic disturbance on structure and mixing in turbulent shear layers and wakes
[AD-A149278] 10 p1484 N85-19370
An investigation of compressible flows over open cavities including shear layer thickness effects
[AD-A150086] 12 p1847 N85-21588
Variations in resistivity of upper crustal layer
13 p2113 N85-23164
Interactions of unstable shear layers with leading edges and associated pressure fields 14 p2299 N85-24236
An experimental study of compressible turbulent reattaching free shear layers 16 p2781 N85-27161
Transverse vorticity measurements using an array of four hot-wire probes
[FSFL-R-85-006] 18 p3099 N85-29184
Transient combustion dynamics
[AD-A154430] 19 p3235 N85-30062
Effect of vertical shear on regional-scale trajectories in near-frontal conditions
[DE85-007554] 19 p3317 N85-30581
Turbulent solutions of equations of fluid motion
20 p3453 N85-31441
Amiet shear layer correction with an additional temperature gradient considered: Nomograms for the correction of noise signatures from open jet wind tunnel tests
[ESA-TT-897] 20 p3525 N85-31889
Comments on two matters related to turbulent combustion 22 p3743 N85-33204

SHEAR PROPERTIES
NT SHEAR STRENGTH
Butene oxidation by molybdenum crystalographic shear compounds
[DE84-013910] 05 p0614 N85-13923
Strain rate effects and temperature history effects for three different tempers of 4340 VAR steel
[AD-A146372] 06 p0768 N85-14915

Declinations in carbon-carbon composites [AD-A148290] 08 p1119 N85-17052

Natural unsteadiness of a separation bubble behind a backward-facing step [AD-P004176] 09 p1267 N85-17961

A free shear layer prediction of the turbulent wake of a flat plate towed below a free surface [AD-A148899] 09 p1319 N85-18293

Verification and application of the Iosipescu shear test method [NASA-CR-174346] 09 p1333 N85-18376

Determination of shear coefficient of a general beam cross section by finite element method 09 p1338 N85-18413

Antiplane cracks in solid propellants [AD-P004344] 10 p1455 N85-19168

Journal of Research of the National Bureau of Standards, volume 89, number 2, March - April 1984 [PB85-115426] 12 p1926 N85-22103

In-plane shear properties of graphite Fibre/Epoxy composites for aerospace applications: Evaluation of test methods by the decision analysis technique [AD-A151599] 15 p2503 N85-25440

Effects of magnetic shear on lower hybrid waves in the suprauroral region [AD-A151980] 15 p2656 N85-26392

Studies of structure and modeling in turbulent shear flows [AD-A151807] 16 p2782 N85-27170

Coherent structure reflective turbulent viscous flow modeling [AD-A153086] 17 p2958 N85-28267

Analytical shear buckling investigation of curved composite panels [AD-A153138] 17 p2960 N85-28421

Structural characteristics of high temperature composites [NASA-CR-175996] 19 p3232 N85-30037

On design of off-axis specimens [AD-A154328] 19 p3286 N85-30379

Shear-stress distribution and shear stiffness in the case represented by a non-homogeneous cross-section, of any shape, but composed of an orthotropic material, when subjected to a shear force [DRIC-T-7430] 20 p3469 N85-31554

Modeling granular explosive detonations with shear band concepts [DE85-011823] 22 p3754 N85-33271

Pressure-shear loading of PBX-9404 [DE85-009982] 23 p3921 N85-34298

SHEAR STRAIN

Deformation measurements of composite multi-span beam shear specimens by Moire interferometry [NASA-CR-3844] 02 p0169 N85-11135

Effective moduli of elasticity of unidirectional fibrous composite 02 p0265 N85-11733

Simple higher-order theory for laminated composite plates [NASA-CR-174421] 10 p1496 N85-19445

Elastic equilibrium of composite shells with finite shear rigidity 17 p2942 N85-28163

Shear-stress distribution and shear stiffness in the case represented by a non-homogeneous cross-section, of any shape, but composed of an orthotropic material, when subjected to a shear force [DRIC-T-7430] 20 p3469 N85-31554

SHEAR STRENGTH

Dynamic shear failure of shallow-buried flat-roofed reinforced concrete structures subjected to blast loading [AD-A145974] 03 p0373 N85-12376

The chemical nature of the fiber/resin interface in composite materials 04 p0465 N85-12953

Composite property dependence on the fiber, matrix, and the interphase 04 p0465 N85-12954

Exploratory study of shear strength of joints for precast segmental bridges [PB84-235449] 05 p0651 N85-14182

Mechanical property data 7050-t736511 alloy [AD-A147365] 07 p0928 N85-15882

Imide modified epoxy matrix resins [NASA-CR-174695] 07 p0930 N85-15892

Laboratory investigation on adhesives for Naval facilities construction [AD-A147453] 07 p0932 N85-15909

Graphite/PMR polyimide composites with improved toughness [NASA-TM-87081] 21 p3561 N85-32148

Pressure-shear loading of PBX-9404 [DE85-009982] 23 p3921 N85-34298

SHEAR STRESS

NT TORSIONAL STRESS

Development of a floating element wall shear transducer [AD-A144794] 01 p0040 N85-10324

Three programs for evaluating bending moments, deflections and shear forces in simply-supported uniform bridge decks under South African NA loading: NAB, NAD and NAS. NITRR manual P13 [ISBN-0-7988-2283-X] 01 p0102 N85-10681

Mechanochemical reactions of elastomers with metals [AD-A145657] 02 p0186 N85-11246

The structure of the vorticity field in turbulent channel flow. Part 2: Study of ensemble-averaged fields [NASA-TM-86857] 03 p0361 N85-12317

Composite materials characterization and development at AFWAL 04 p0464 N85-12944

Studies of the wall shear stress in a turbulent pulsating pipe flow [AD-A146772] 07 p0957 N85-16068

Effects of high energy radiation on the mechanical properties of epoxy-graphite fiber reinforced composites [NASA-CR-174314] 08 p1118 N85-17047

A study of Reynolds-stress closure model [NASA-CR-174342] 08 p1161 N85-17324

Development of a floating element wall shear transducer [AD-A148450] 08 p1164 N85-17346

Crack problems for bonded nonhomogeneous materials under antiplane shear loading [NASA-CR-172532] 10 p1495 N85-19438

Theoretical and experimental study of crack resistance and macrocrack growth rate in organic fiber reinforced plastic under pure shear condition 11 p1598 N85-20053

Influence of external electric field on structural-mechanical properties of powdered materials 13 p2013 N85-22630

Longitudinal splitting in unidirectional composites, analysis and experiments [NASA-CR-3881] 13 p2015 N85-22639

Study of stresses on surface of flat barrier immersed in under expanded jet of rarefied gas 16 p2765 N85-27061

Recent progress in the dynamic plastic behaviour of structures, part 4 17 p2978 N85-28402

Investigations of the material factors in the adiabatic shearing of steels [AD-A153084] 17 p2979 N85-28418

Surface shear stress characteristics in turbulent flows 19 p3211 N85-29914

Granular Flow Project [DE85-010015] 19 p3270 N85-30279

The initiation and growth of adiabatic shear bands [AD-A154459] 19 p3287 N85-30382

Shear-stress distribution and shear stiffness in the case represented by a non-homogeneous cross-section, of any shape, but composed of an orthotropic material, when subjected to a shear force [DRIC-T-7430] 20 p3469 N85-31554

A refinement of the transverse shear deformation theory for multilayered anisotropic plates [STN-5] 20 p3471 N85-31571

A cracked orthotropic sheet stiffened by a semi-infinite orthotropic sheet [NASA-TP-2455] 21 p3597 N85-32339

Pressure-shear loading of PBX-9404 [DE85-009982] 23 p3921 N85-34298

Stress analysis of axisymmetric sandwich shells of variable thickness 24 p4101 N85-35419

SHEAR WAVES

U S WAVES

SHEARING

The shearing contribution in transformation toughening of brittle materials [AD-A154656] 21 p3568 N85-32195

SHEARING STRESS

U SHEAR STRESS

SHEATHS

NT ION SHEATHS

NT PLASMA SHEATHS

Subcable test facility [DE85-002103] 09 p1315 N85-18269

SHEEP

The 1984 environmental monitoring program report for Idaho National Engineering Laboratory site [DE85-011209] 22 p3812 N85-33611

SHEET METAL

U METAL SHEETS

SHELL ANODES

Ring-cusp ion thruster with shell anode [NASA-CASE-LEW-13881-1] 12 p1794 N85-21256

SHELL STABILITY

Variable loading of elastic-plastic shells of revolution 06 p0779 N85-14981

Stability of circular cylindrical shell with piecewise constant thickness subjected to radial pressure 06 p0779 N85-14982

Analysis of shell type structures subjected to time dependent mechanical and thermal loading [NASA-CR-175747] 15 p2577 N85-25896

Dynamic creep buckling: Analysis of shell structures subjected to time-dependent mechanical and thermal loading 17 p2913 N85-27959

Elastic equilibrium of composite shells with finite shear rigidity 17 p2942 N85-28163

Stability of cylindrical shells with variable thickness under external pressure 17 p2943 N85-28164

Initial imperfection surveys on conical shells at Hoechst AG [VTH-LR-407] 17 p2981 N85-28429

Stress analysis of axisymmetric sandwich shells of variable thickness 24 p4101 N85-35419

SHELL THEORY

Numerical modeling of complex interaction of shell of revolution and its filler with allowance for friction 06 p0779 N85-14980

A review of imperfection sensitivity of stiffened shells [AD-A147311] 07 p0978 N85-16213

On a general nonlinear theory of plates and shells: Formulation and applications 08 p1172 N85-17387

The principle of virtual work and associated variational principles [ESA-TT-873] 09 p1340 N85-18428

Shell-model Lanczos-method studies of the Gamow-Teller strength function in astrophysics [DE85-004205] 11 p1763 N85-21093

Vacancy-rearrangement theory in the first Magnus approximation [DE85-004435] 12 p1930 N85-22123

The nonlinear analysis of thick composite plates using a cubic spline function [AD-A152115] 16 p2801 N85-27268

An analysis for axially compressed orthotropic shells with a multimode imperfection representation [VTH-LR-422] 16 p2803 N85-27281

Dynamic creep buckling: Analysis of shell structures subjected to time-dependent mechanical and thermal loading 17 p2913 N85-27959

Elastic equilibrium of composite shells with finite shear rigidity 17 p2942 N85-28163

Method of solving problems of statics for multilayer shells of revolution 17 p2943 N85-28167

SHELLS (STRUCTURAL FORMS)

NT ANISOTROPIC SHELLS

NT CIRCULAR SHELLS

NT CONICAL SHELLS

NT CORRUGATED SHELLS

NT CYLINDRICAL SHELLS

NT ELASTIC SHELLS

NT FLUID FILLED SHELLS

NT LIQUID FILLED SHELLS

NT METAL SHELLS

NT ORTHOTROPIC SHELLS

NT RADOMES

NT REINFORCED SHELLS

NT SHALLOW SHELLS

NT SPHERICAL CAPS

NT SPHERICAL SHELLS

NT THIN WALLED SHELLS

NT TOROIDAL SHELLS

Heat exchanger [DE84-014299] 01 p0047 N85-10309

Internal heat transfer and pressure drop measurements in a variously baffled shell and tube heat exchanger 03 p0360 N85-12310

Complex frequency analysis of damped thin-walled beams with open cross sections 03 p0371 N85-12366

Finite element procedures applicable to nonlinear analysis of reinforced concrete shell structures [AD-A146796] 07 p0978 N85-16209

A review of imperfection sensitivity of stiffened shells [AD-A147311] 07 p0978 N85-16213

Coriolis effects on the vibrations of rotating beams, plates and shells 09 p1331 N85-18366

Fluidelastic instability in shell and tube heat exchangers: A framework for a prediction method [DE84-006518] 10 p1496 N85-19444

A solution method for nonlinear dynamic analysis of shell structures [AD-A149646] 12 p1866 N85-21708

Nonlinear analysis of layered composite plates and shells [PB85-127181] 12 p1866 N85-21719

Geometrically nonlinear analysis of laminated elastic structures [NASA-CR-175609] 12 p1866 N85-21720

USSR report: Engineering and equipment [JPRS-UEQ-85-003] 13 p2042 N85-22782

Stability of three-layer glass-reinforced plastic shells of rotation 13 p2047 N85-22813

Axisymmetrical oscillations of shell systems subjected to impulse loads 13 p2047 N85-22814

Reaction of piezoceramic shell to concentrated forces 14 p2279 N85-24115

Stressed-strained state of tubular shells under uniformly distributed pressure 16 p2766 N85-27067
Research in the field of rib stiffened shell stability
16 p2766 N85-27068
Dynamic response of shells and plates subjected to variable magnitude traveling loads
16 p2796 N85-27250
The statistical analysis of initial imperfection measurements --- shell profiles
[VTH-LR-442] 16 p2857 N85-27622
Propagation of non-axisymmetric elastic waves through shell with filler under radial load at one end
17 p2943 N85-28169
The Mises yield condition for thin rotationally symmetric shells
[BLL-BISI-TRANS-22047-(9022.06)]
17 p2976 N85-28409
Computer-aided thermohydraulic design of TEMA type E shell and tube heat exchangers for use in low pressure, liquid-to-liquid, single phase applications
[AD-A153779] 18 p3100 N85-29191
An investigation into the comparisons of the underwater shock effects on a stiffened flat plate to the predictive nature of a computer model
[AD-A156612] 21 p3600 N85-32355
Membrane reinforcement in concrete shells: Design versus nonlinear behavior 24 p4084 N85-35312
Response of a BWR Mark 2 containment vessel head to loads beyond the design basis
[DE85-010524] 24 p4103 N85-35432

SHELTERS
NT LUNAR SHELTERS
A comparison of lightning and nuclear electromagnetic pulse response of tactical shelters
07 p1000 N85-16350
Field testing of a lightweight relocatable structure in a temperate environment
[AD-A155171] 21 p3599 N85-32350
SHELTER: Description of a program code --- indoor climate
[FOA-C-56002-H1] 22 p3755 N85-33278

SHIELDING
NT ELECTROMAGNETIC SHIELDING
NT ELECTROSTATIC SHIELDING
NT HEAT SHIELDING
NT MAGNETIC SHIELDING
NT RADIATION SHIELDING
NT REENTRY SHIELDING
NT REUSABLE HEAT SHIELDING
NT SPACECRAFT SHIELDING
EMP injection on conduit entries, type Brattberg --- electromagnetic pulse (EMP) injection
[FOA-E-30001-A3] 02 p0193 N85-11290
Experimental study of aerodynamic shielding of turbojet engine air intake against exhaust gases
09 p1307 N85-18210
Explosion-proof properties and hydraulic resistance of fire-barrier elements based on knitted metallic screens
11 p1601 N85-20067
Shielded enclosures for experimental studies of shielding topology
[AD-A149292] 11 p1624 N85-20227
TFCX shielding optimization
[DE85-010503] 19 p3359 N85-30626
MFTF-(alpha) + T shield design
[DE85-010496] 20 p3529 N85-31948
Rhodium-103 and Indium-115 inelastic scattering reactions for fission neutron dosimetry
21 p3703 N85-33004
Calculation of external magnetic field of a shielded transformer 22 p3771 N85-33373
Magnetic field and equivalent circuit of induction motors with shielded poles 22 p3772 N85-33378
Removable cleanable antireflection shield
[AD-D011735] 22 p3844 N85-33810
Gas shielding apparatus
[DE85-005992] 23 p3939 N85-34416
Coupled electron-photon transport calculations using the method of discrete ordinates
[DE85-009444] 23 p3967 N85-34597
Monte Carlo techniques for analyzing deep penetration problems
[DE85-011426] 23 p3966 N85-34596
Design considerations for personnel access penetrations for the superconducting super collider
[DE85-013027] 24 p4162 N85-35807

SHIELDS (GEOLOGY)
U BEDROCK

SHIFT REGISTERS
A two-cycle shift register with error detection
[AD-A150766] 14 p2400 N85-24791

SHIP HULLS
Design proposals for torsional buckling of stiffeners
[AD-A144783] 01 p0062 N85-10409
Numerical simulations of compliant material response to turbulent flow, revision 1
[AD-A145601] 03 p0372 N85-12373
Direct energy minimization approach to whipping analysis of pressure hulls 09 p1335 N85-18393
Remote self-contained undersea monitor
[AD-D011520] 12 p1840 N85-21599
Corrosion problems in the Canadian maritime forces
[AD-A151594] 15 p2509 N85-25481
Development of high strength ship hull steel for high heat input welding --- controlled rolling and accelerated cooling 15 p2565 N85-25827
Seakeeping and vibration tests of the Coast Guard 110 foot surface effect ship SEA BIRD class (WSES)
[AD-A154150] 19 p3252 N85-30166
Fatigue characterization of fabricated ship details for design
[SSC-318] 19 p3265 N85-30371
Design of transversely stiffenend FRP panels under compressive load --- fiber reinforced plastic (FRP) ships
[AMTE(S)-R-84104] 23 p3940 N85-34424

SHIP TO SHORE COMMUNICATION
Shipboard and satellite-aided communications equipment in exhibition 06 p0819 N85-15203
Development of a microprocessor controlled communication system for ships
[BMFT-FB-T-84-275] 17 p2950 N85-28216
Navigation data for Emergency Position Indicating Radio Beacons (EPIRBs) 20 p3403 N85-31115

SHIPS
NT AIRCRAFT CARRIERS
NT SUBMARINES
NT SURFACE EFFECT SHIPS
NT TANKER SHIPS
Model study of the interaction of a blast wave with the superstructure of ships. Part 5: Application of optical measurement methods to the study of blast interaction
[PML-1984-12-PT-5] 01 p0057 N85-10375
The climate of Denmark. Summaries of observations from light vessels. 3: Sea temperature
[ISBN-87-7478-215-0] 01 p0073 N85-10481
Experiences with a high-blockage model tested in the NASA Ames 12-foot pressure wind tunnel
03 p0315 N85-12032
Theoretical and experimental modal analysis of a rotor test rig --- shipboard equipment
[AMTE(N)-TM-83079] 03 p0371 N85-12370
Solar power supplies for ships
05 p0665 N85-14274
Simulation evaluation of two VTOL control/display systems in IMC approach and shipboard landing
[NASA-TM-85996] 06 p0756 N85-14841
Copper-nickel sheathing study, phase 2. Two-year service performance of test panels on the ARCO TEXAS
[PB84-242411] 06 p0775 N85-14952
Mariners weather log, volume 28, no. 3, July-August-September 1984
[PB85-107266] 06 p0840 N85-15334
Free-surface boundary layer and the origin of bow vortices
[AD-A147427] 07 p0960 N85-16083
Installation options for the NAVSTAR global positioning system in surface ships
[AD-A148190] 08 p1082 N85-16856
Using the control system design environment in the design of a data link receiver unit for the Coast Guard HH-65A helicopter
[AD-A148624] 08 p1086 N85-16880
Solid rocket booster retrieval operations
08 p1096 N85-16926
Improvements in linked-spar motion-compensated lifting system
[AD-D011413] 08 p1136 N85-17165
SEASAT 3 and 4
[AD-A148343] 08 p1152 N85-17274
Second order Bragg scattering in a SAR
[AD-A148395] 08 p1152 N85-17275
Speed governor for diesel engine
09 p1307 N85-18214
Use of braking stages for control of turbine speed
09 p1308 N85-18215
Reflections on trends in dynamics: The Navy's perspective 09 p1334 N85-18382
The Shock and Vibration Bulletin 54. Part 2: Ship shock, shock and blast and ground shock
[AD-A148132] 09 p1334 N85-18386
Two-dimensional shock response of a mass on energy-absorbing shock mounts
09 p1334 N85-18389
Shipboard shock response of the model structure DSM: Experimental results versus responses predicted by eight participants 09 p1335 N85-18392
High-strength composite materials for aircraft, body armor 11 p1589 N85-20057
International list of selected, supplementary and auxiliary ships --- WMO
[WMC-47-ED-84] 11 p1687 N85-20800
A broadband kevlar radome for shipboard
[AD-P004366] 12 p1826 N85-21409
INMARSAT marine satellite organization
13 p1965 N85-22456
Uses of composite materials
13 p2027 N85-22898
USSR report: Transportation
[JPRS-UTR-85-005] 14 p2207 N85-23966
USSR report: Engineering and equipment
[JPRS-UEQ-84-001] 14 p2265 N85-24084
Investigation of errors of acoustic goniometer information-measurement systems on rocking base
14 p2283 N85-24139
Pluribus Satellite IMP (Interface Message Provision) development mobile access terminal network
[AD-A151312] 15 p2542 N85-25662
Several specific and nonspecific responses of the human and animal body to ship noise
[NASA-TM-77483] 15 p2615 N85-26116
Special features of the one-sided automatic welding of structures of Al-Mg alloys 16 p2792 N85-27222
An inexpensive radar-responding relocation device for drifting oceanographic instruments
[AD-A152170] 16 p2836 N85-27505
The PINGUIN B3: A remotely piloted vehicle for mine identification and disposal
[MBB-UM-1/84-O] 16 p2874 N85-27736
USSR report: Engineering and equipment
[JPRS-UEQ-85-004] 17 p2939 N85-28142
Operation guiding light-scientific program and field plan. The pilot field experiment for NORDA project chemical dynamics in ocean frontal areas
[AD-A153765] 18 p3150 N85-29507
Fatigue characterization of fabricated ship details for design
[SSC-318] 19 p3265 N85-30371
Soviet Emergency Locator Transmitter/Emergency Position Indicating Radio Beacon (ELT/EPIRBs) at 121.5 and 406 MHz 20 p3402 N85-31107
Existing and potential INMARSAT capabilities for the Future Global Maritime Distress and Safety System
20 p3402 N85-31110
The CCIR satellite EPIRB coordinated trials programme --- Emergency Position Indicating Radio Beacon (EPIRB); International Radio Consultative Committee (CCIR) 20 p3402 N85-31111
The International Radio Consultative Committee (CCIR) recommended satellite Emergency Position Indicating Radio Beacon (EPIRB) system operating through geostationary satellites at 1.6 GHz
20 p3402 N85-31112
Free-float Emergency Position Indicating Radio Beacons (EPIRBs) and release mechanism on board Norwegian ships. Main specifications and user experience
20 p3404 N85-31120
Experiments of a LORAN-C aided recovery system and a proposal of its application to rescue system
20 p3404 N85-31121
LORAN-C harbor and harbor entrance survey: Charleston, South Carolina
[AD-A154875] 21 p3554 N85-32108
Fuel cell applications literature review
[DE85-011891] 22 p3809 N85-33592
A life-saving device for ships
[NASA-TM-77670] 23 p3895 N85-34120

SHIVERING
NT DITHERS

SHOCK (PHYSIOLOGY)
Fatal hemorrhagic shock and acetate solutions
[AD-A146754] 07 p1014 N85-16444
Hazards of VLF electromagnetic fields
16 p2776 N85-27135

SHOCK ABSORBERS
Simulation of vibration processes in damped structures with allowance for temperature-frequency characteristics of vibration absorbing materials
02 p0257 N85-11660
Multiple rate shock isolator damping valve
[AD-D011429] 08 p1168 N85-17380
Optimum design for nonlinear shock mounts for transient inputs 09 p1334 N85-18390
Missile launcher integral shock isolation and running gear system
[AD-D011490] 11 p1569 N85-19969
Development of an energy-absorbing passenger seat for a transport aircraft 22 p3796 N85-33515

SHOCK DIFFUSERS
U DIFFUSERS
U SHOCK WAVE ATTENUATION

SHOCK DISCONTINUITY
Characteristics of steady-state hypersonic flow about blunted bodies with discontinuities in generators
17 p2941 N85-28155

RONTS
al pin apparatus for measuring the arrival time and
of shock waves and particles
014501] 01 p0120 N85-10624
utral gas jet in a low velocity shock front at the
ry of the Draco Nebula 06 p0878 N85-15576
k acceleration in active galactic nuclei and
s 08 p1241 N85-17828
ence of shock wave front on nature of luminescence
mbining laser plasma 11 p1719 N85-20818
2-D simulations of the NRL (Naval Research
tory) laser experiment
154915] 21 p3592 N85-32321
rgetic ion acceleration at collisionless shocks
5-3] 23 p3996 N85-34772
reflecting boundary behind the Earth's orbit at
gation of fast particles from solar flares
2-13] 23 p4004 N85-34827
nucleosynthesis of deterium and helium-3
3.2-18] 23 p4020 N85-34914
clear reactions in shock wave front during supernova
s
8.2-19] 23 p4021 N85-34915
opagation of injected cosmic rays under distributed
celeration
8.3-3] 23 p4021 N85-34922
operties of 10 (18)-10 (19)eV EAS at far core
nce
4.7-3] 24 p4198 N85-36054
note on some statistical properties of rise time
meters used in muon arrival time measurements
4.7-12] 24 p4199 N85-36062
K HEATING
easurement of shock and induced reaction in rocket
ellants by nanosecond infrared radiometry and
ography
84-013209] 04 p0482 N85-13070
ysical conditions in low-luminosity active galactic
ei 05 p0742 N85-14771
uttle system ascent aerodynamic and plume
ing 08 p1103 N85-16975
entrifugally driven magnetohydrodynamic (MHD) winds
the nonthermal emission regions in Active Galactic
ei (AGN) 08 p1242 N85-17835
easurement of shock induced reaction in rocket
pellants by nanosecond infrared radiometry and
tography
-P004349] 10 p1456 N85-19173
udy of structural changes of dual-phase titanium alloy
ng shock wave loading 15 p2498 N85-25408
K LAYERS
erothermal tests of a 12.5 percent cone at Mach 6.7
various Reynolds numbers, angles of attack and nose
pes — conducted in Langley 8-foot high temperature
nel
ASA-TP-2345] 08 p1161 N85-17322
K LOADS
BLAST LOADS
ethod and apparatus for determining pressure-induced
quency-shifts in shock-compressed materials
E84-014313] 01 p0024 N85-10151
he Shock and Vibration Digest, volume 16, no. 8
D-A145653] 02 p0206 N85-11372
Constitutive features of solids at shock-wave loading
es
E84-015715] 03 p0362 N85-12325
Optimum replacement of a system subject to shocks
D-A145811] 03 p0372 N85-12374
Computer molecular dynamics of 2-D water (ice)
uctures under shock
D-A145818] 03 p0372 N85-12375
Shock-induced CO2 loss from CaCO3: Implications for
rly planetary atmospheres
ASA-CR-174197] 05 p0745 N85-14777
Shock response analysis by personal computer using
e extended IFT algorithm 09 p1335 N85-18397
Models for shock damage to marine structural
aterials 09 p1336 N85-18400
A study of the effect of mass loading on the shock
vironment 09 p1336 N85-18401
Assessment of seismic survivability
09 p1336 N85-18402
Ground shock effect on soil field inclusions
09 p1336 N85-18403
Shock propagation in the exhaust gas handling system
f the proposed large altitude rocket cell: Methods and
eliminary analysis
DE85-003055] 11 p1591 N85-20010
Evaluation of air and ground launched cruise missile
avigational element containers
AD-A149654] 12 p1774 N85-21138
Comparison of shock-induced displacements with
isplacements produced by a centrifuge acceleration
DE85-000467] 12 p1852 N85-21618
Sound velocity of carbon at high pressures
DE85-002016] 12 p1926 N85-22113

Molecular dynamics studies of energy transfer processes in crystal systems
[AD-A150161] 13 p2163 N85-23416
Dynamic shock studies of PZT 95/5 ferroelectric ceramic
[DE85-006137] 14 p2261 N85-24015
Preliminary considerations for the gasdynamic precompression of solid molecular hydrogen
[DE85-013256] 22 p3784 N85-33445
SHOCK RESISTANCE
NT IMPACT RESISTANCE
The Shock and Vibration Digest, volume 16, no. 11
[AD-A148466] 08 p1171 N85-17382
The Shock and Vibration Bulletin 54. Part 2: Ship shock, shock and blast and ground shock
[AD-A148132] 09 p1334 N85-18388
Shipboard shock response of the model structure DSM: Experimental results versus responses predicted by eight participants 09 p1335 N85-18392
Prediction of the resistance of structural materials to cavitation erosion
[BLL-DRIC-TRANS-7435-(3623.66)]
13 p2020 N85-22659
Dispersed-metal-toughened alumina
[NASA-CR-174687] 13 p2037 N85-22758
Design of SC cut 10 MHZ H.Q. crystals with G. sensitivity better than 2.10(-10)/G 17 p2966 N85-28319
SHOCK SIMULATORS
The Shock and Vibration Digest, volume 16, no. 11
[AD-A148466] 08 p1171 N85-17382
SHOCK SPECTRA
The Shock and Vibration Digest, volume 16, no. 11
[AD-A148466] 08 p1171 N85-17382
Alternative shock characterizations for consistent shock test specifications 09 p1335 N85-18396
Least favorable response of inelastic structures
09 p1336 N85-18398
Recovery of pyroshock data from distorted acceleration records
[NASA-TP-2494] 20 p3407 N85-31141
Short-time spectroscopic measurement of the temperature of solids
[ISL-CO-202/84] 20 p3459 N85-31486
SHOCK TESTS
Vibration, acoustic, and shock design and test criteria for components on the Solid Rocket Boosters (SRB), Lightweight External Tank (LWT), and Space Shuttle Main Engines (SSME)
[NASA-RP-1127] 01 p0061 N85-10405
Particle velocity experiments in anorthosite and gabbro
[NASA-CR-174158] 04 p0533 N85-13407
Shock testing of a nitrogen tank (Cryo diffusion type 220 VLR) on the middle weight shock stand
[NASA-TM-77747] 06 p0817 N85-15183
Sensitivity tests for solid propellants in Germany
08 p1115 N85-17026
Evaluation of air and ground launched cruise missile navigational element containers
[AD-A149654] 12 p1774 N85-21138
SHOCK TUBES
Particle entrainment in a compressible vortex
[ISL-CO-230/83] 04 p0500 N85-13192
A Van Leer shock capturing algorithm for the Euler equations
[AD-A148761] 08 p1163 N85-17335
Pseudo-stationary oblique-shock-wave reflections in a polyatomic gas, sulfur hexafluoride
[UTIAS-TN-253] 12 p1845 N85-21577
Turbulence measurements in shock induced flows
13 p2091 N85-23055
Collaborative shock tube studies of benzene pyrolysis
[DE85-006347] 14 p2253 N85-23962
Experimental simulation of the flow inside a gun barrel
[ISL-CO-208/83] 14 p2302 N85-24252
Thirty-three years of research with shock tubes in the Franco-German Research Institute, Saint Louis (France)
[ISL-CO-226/83] 14 p2302 N85-24257
Experimental simulation of the flows in front of and behind a projectile with and without gas slippage
[ISL-CO-232/83] 14 p2302 N85-24258
Compression waves in front of and behind a piston launched in a shock tube
[ISL-R-101/83] 14 p2303 N85-24260
Simulation of interior ballistics flows in a shock tube
[ISL-CO-222/83] 16 p2784 N85-27183
Investigation of heat transfer to a turbine blade cascade using a shock tube
[AD-A153090] 17 p2898 N85-27871
Characteristics of steady-state hypersonic flow about blunted bodies with discontinuities in generators
17 p2941 N85-28155
Impact starting of plane nozzles with wide divergence angle 17 p2941 N85-28156
Experimental observation of transition behavior on a flat plate 20 p3452 N85-31437

Environmental airblast around large shock tubes
[DE85-010654] 20 p3463 N85-31512
Shock tube measurements of growth constants in the branched-chain ethane-carbon monoxide-oxygen system
[NASA-TM-87068] 21 p3562 N85-32156
A variable node finite element method applied to the gas dynamics equations
[AD-A155211] 21 p3584 N85-32281
Velocity and transient measurements in a shock tube using a hot-wire anemometer
[AD-A154694] 21 p3589 N85-32305
Experimental simulation of in-bore flows using a high pressure shock tube
[ISL-CO-217/84] 22 p3765 N85-33452
SHOCK WAVE ATTENUATION
Supersonic flow with feeding of energy
[NASA-TM-77912] 24 p4061 N85-35163
Attenuation properties of the Petatlan region, Mexico, and a local magnitude scale for microearthquakes in this area 24 p4116 N85-35513
SHOCK WAVE CONTROL
Selection of air intake parameters for supersonic-flow operation 13 p2051 N85-22837
SHOCK WAVE GENERATORS
NT SHOCK TUBES
Flow-induced vibrations of a circular cylinder due to turbulent internal flows
[DE85-002766] 13 p2103 N85-23110
Shock compression of liquid helium to 56 GPa (560) kbar 13 p2184 N85-23551
Generation of detonation waves of given spatial and temporal characteristics
[ISL-R-103/83] 16 p2756 N85-27021
SHOCK WAVE INTERACTION
Experimental study of Mach reflection of weak shock waves 02 p0260 N85-11703
Geometric characteristics of turbulent boundary layer separation upon action with direct shock wave in conical flows 02 p0269 N85-11755
Shock/turbulent boundary layer interaction and its control 08 p1071 N85-16792
Oblique shock wave-turbulent boundary layer interaction on a porous wall with suction 08 p1072 N85-16794
Active and passive shock/boundary layer interaction control on supercritical airfoils 08 p1072 N85-16795
Transonic shock interaction with a tangentially-injected turbulent boundary layer 08 p1072 N85-16796
Velocity measurements in a 3D shock wave laminar boundary layer interaction. Part 1: Low speed 2D LDV measurements
[AD-A149533] 10 p1485 N85-19373
Influence of shock wave front on nature of luminescence of recombining laser plasma 11 p1719 N85-20818
The behaviour of detonation waves in single phase heterogeneous systems
[AD-A149825] 12 p1846 N85-21581
Study of geological media based on scattered earthquake waves 13 p2114 N85-23168
Application possibilities of laser Doppler anemometry in the investigation of the transonic interaction between shock wave and boundary layer
[ISL-R-131/83] 14 p2304 N85-24265
An exploratory investigation of sharp fin-induced shock wave/turbulent boundary layer interactions at high shock strengths
[AD-A151571] 15 p2556 N85-25772
Viscous effects on blast wave flowfields
[AD-A152013] 15 p2558 N85-25779
A curved test section for research on transonic shock wave-boundary layer interaction
[VTH-LR-414] 16 p2701 N85-26682
Numerical solution of transonic normal shock wave-boundary layer interaction using the Bohning-Zierop model — wind tunnel flow
[VTH-LR-416] 16 p2701 N85-26683
Theoretical investigation of three-dimensional shock wave turbulent boundary layer interactions. Part 3
[AD-A152251] 16 p2783 N85-27177
An experimental investigation of the interaction between a shock wave and a turbulent boundary layer on a convex wall
[VTH-LR-428] 16 p2785 N85-27187
Underwater shock-induced responses of stiffened flat plates: An investigation into the predictive capabilities of the USA-STAGS code
[AD-A154245] 19 p3286 N85-30377
The application of laser anemometry to the study of transonic shock boundary-layer interactions
[ISL-CO-204/84] 20 p3396 N85-31067
Shock waves in adjacent engine inlets
[ISL-R-104/84] 20 p3396 N85-31068
SHOCK WAVE LUMINESCENCE
A program of ground-based astronomy to complement einstein observations
[AD-A151111] 15 p2666 N85-26466

SHOCK WAVE PROFILES
Deceleration of a supersonic flow behind a curved shock wave with isentropic precompression
[NASA-TM-77920] 24 p4061 N85-35164
Ground motion measurements for the QUESO nuclear event
[DE85-014806] 24 p4151 N85-35743

SHOCK WAVE PROPAGATION
Self-similar expansion of dense matter due to heat transfer by nonlinear conduction
[MPQ-81] 01 p0046 N85-10297
Plastic deformation and microstructural transformations of metals under shock waves 02 p0272 N85-11775
An experimental investigation of the parallel blade-vortex interaction
[NASA-TM-86005] 05 p0592 N85-13777
Research on acoustical and optical scattering, optics of bubbles, diffraction catastrophes, laser generation of sound, and shock induced cavitation
[AD-A146703] 06 p0860 N85-15486
Strong iron accelerating by collisionless magnetosonic shock wave propagating perpendicular to a magnetic field
[IPPJ-709] 12 p1936 N85-22161
Interplanetary shock waves during April and May of 1981 13 p1962 N85-22434
Molecular spectroscopy from the Kuiper Airborne Observatory
[NASA-CR-175748] 16 p2662 N85-27783
Impact starting of plane nozzles with wide divergence angle 17 p2941 N85-28156
Supersonic flow around blunt wedge
17 p2942 N85-28158
Proceedings of the 1980 Workshop of the International Association of Seismology and Physics of the Earth's Interior on the Seismic Modeling of Laterally Varying Structures: Contributions based on data from the 1978 Saudi Arabian refraction profile
[GS-CIRC-937] 17 p2989 N85-28476
Preliminary interpretation of Saudi Arabian seismic refraction data 17 p2989 N85-28477
Two-dimensional inverse kinematic problem: Application to the Saudi Arabian refraction profile
17 p2990 N85-28478
Crustal structure of the Red Sea-Arabian Shield transition 17 p2990 N85-28479
A seismic refraction profile across the Arabian Shield
17 p2990 N85-28481
A preliminary examination of the 1978 refraction profiles in Saudi Arabia 17 p2990 N85-28482
The rifted margin of Saudi Arabia
17 p2990 N85-28483
Solar wind observations associated with a slow forward shock wave at 0.31 AU
[MPAE-W-79-84-46] 17 p3055 N85-28909
Wave-theoretical approach to seismic modeling problems (WELMOD)
[BMFT-FB-T-84-258] 18 p3137 N85-29429
Shock waves in adjacent engine inlets
[ISL-R-104/84] 20 p3396 N85-31066
Weak shock waves propagating in fluid-gas mixtures
[AD-A154759] 21 p3584 N85-32276
Resonant ion acceleration by oblique magnetosonic shock wave in a collisionless plasma
[IPPJ-735] 23 p3975 N85-34643
Workshop report on Simulation Techniques for Shock Wave Phenomena and Characteristics of Plasmas in Inertial Confinement Fusion
[IPPJ-725] 23 p3979 N85-34670
Simulation of instability of cylindrically converging shock waves 23 p3980 N85-34679
Stability of ion distribution in strong ion shock structure 23 p3980 N85-34681
First-order shock acceleration in solar flares
[SH-1.1-5] 23 p3989 N85-34732
On reflecting boundary behind the Earth's orbit at propagation of fast particles from solar flares
[SH-3.2-13] 23 p4004 N85-34827
The intensity recovery of Forbush-type decreases as a function of heliocentric distance and its relationship to the 11-year variation
[SH-4.1-9] 23 p4006 N85-34832
On the cosmic ray diffusion in a violent interstellar medium
[OG-7.2-14] 23 p4015 N85-34881
The central engine of quasars and AGNs: A relativistic proton radiative shock
[OG-8.1-7] 23 p~018 N85-34897
Propagation of cosmic rays and new evidence for distributed acceleration
[OG-8.3-5] 23 p4022 N85-34924
Ground motion measurements for the QUESO nuclear event
[DE85-014806] 24 p4151 N85-35743

SHOCK WAVES
NT DETONATION WAVES
NT NORMAL SHOCK WAVES
NT OBLIQUE SHOCK WAVES
NT SONIC BOOMS
Observations from varying the lift and drag inputs to a noise prediction method for supersonic helical tip speed propellers
[NASA-TM-83797] 01 p0115 N85-10786
Optical pin apparatus for measuring the arrival time and velocity of shock waves and particles
[DE84-014501] 01 p0120 N85-10624
Weak shocks and steady waves in a nonlinear elastic rod or granular material
[AD-A145715] 02 p0209 N85-11383
Experimental study of Mach reflection of weak shock waves 02 p0260 N85-11703
Using fiber-optics light guides in diagnosing intense shock waves 02 p0272 N85-11773
Problems in theory of diffusion under shock wave
02 p0272 N85-11776
Review of simulation of quasiparallel collisionless shocks
[DE84-015469] 02 p0304 N85-11967
Numerical studies of unsteady transonic flow over an oscillating airfoil
[NASA-TM-86011] 03 p0361 N85-12316
Constitutive features of solids at shock-wave loading rates
[DE84-015715] 03 p0362 N85-12325
Magnetohydrodynamic and gasdynamic theories for planetary bow waves
[NASA-CR-174132] 03 p0446 N85-12850
Local stability analysis for a planar shock wave
[NASA-TP-2367] 04 p0452 N85-12864
Seismic studies in southern Alaska
04 p0515 N85-13286
Experimental investigation of shock-cell noise reduction for dual-stream nozzles in simulated flight
[NASA-CR-3846] 04 p0557 N85-13549
Lunar origin from impact on the Earth
04 p0586 N85-13757
Pressure oscillations in liquid-fueled ramjet engines
05 p0596 N85-13797
Experimental investigation and analysis of oscillations of thin-walled spherical shell during pulse loading
05 p0725 N85-14662
Multiple steady states for characteristic initial value problems
[NASA-CR-172486] 06 p0749 N85-14800
A model of the soft X-ray background as a blast wave viewed from inside 06 p0679 N85-15586
Waves and instabilities in collisionless shocks
[AD-A146689] 06 p0881 N85-15507
A comparative study of the nonuniqueness problem of the potential equation
[NASA-TP-2385] 07 p0898 N85-15694
Numerical reconstruction of part of an actual blast-wave flow field to agree with available experimental data
[UTIAS-TN-251] 07 p0956 N85-16061
Bulk cavitation caused by a plane shock wave
[AD-A147031] 07 p0958 N85-16072
On the asymptotic analysis of travelling shocks and phase boundaries in elastic bars
[AD-A147239] 07 p0959 N85-16076
Nonlinear waves in a rod. Results for incompressible elastic materials
[AD-A147485] 07 p0979 N85-16216
Shock/turbulent boundary layer interaction and its control 08 p1071 N85-16792
Active and passive shock/boundary layer interaction control on supercritical airfoils 08 p1072 N85-16795
Transonic shock interaction with a tangentially-injected turbulent boundary layer 08 p1072 N85-16796
Shock waves in transonic flows at moderate Reynolds Number 08 p1076 N85-16823
The NYU inverse swept wing code
[NASA-CR-3862] 08 p1077 N85-16830
Analysis of Deflagration to Shock to Detonation Transition (DSDT) in porous energetic solid propellants
08 p1115 N85-17030
Numerical simulation of the shock detonation transition 08 p1116 N85-17039
Shock and impact response of solid rocket propellants: Experimental and theoretical 08 p1116 N85-17040
A numerical study of several supersonic flows
09 p1272 N85-17995
The Shock and Vibration Bulletin 54. Part 1: Welcome, keynote address, invited papers MIL-STD-810D, MIL-STD-810D panel session
[AD-A148131] 09 p1333 N85-18377
Keynote address 09 p1333 N85-18378
Analysis of Shock to Detonation Transition (SDT) of porous high energy propellant from ramp-wave compression loading
[AD-A149333] 10 p1457 N85-19180
A shock wave capability for the improved Two-Dimensional Kinetics (TDK) computer program
[NASA-CR-171302] 10 p1483 N85-1930
Velocity measurements in a 3D shock wave laminar boundary layer interaction. Part 1: Low speed 2D LDV measurements
[AD-A149533] 10 p1485 N85-1937
Construction of solutions for two-dimensional Riemann problems
[DE85-003136] 10 p1549 N85-1977
Research study of space plasma boundary processes
[NASA-CR-174351] 10 p1558 N85-1980
Micro-deformation of quartz under dynamic action and its applications 11 p1620 N85-20201
On detached shock wave of sphere moving with transonic velocities 11 p1622 N85-20215
Magnetic and structural properties of shock-synthesized zinc ferrite
[DE85-000469] 11 p1736 N85-20815
Wavecode constitutive models: Nonhomogeneous mixtures
[DE85-000836] 12 p1798 N85-21278
Pseudo-stationary oblique-shock-wave reflections in a polyatomic gas, sulfur hexafluoride
[UTIAS-TN-253] 12 p1845 N85-21577
Front tracking and two dimensional Riemann problems: A conference report
[DE85-002209] 12 p1847 N85-2158
Biological effects of blast and impact waves
[FOA-C-52006-H4-D7] 12 p1906 N85-2198
Adaptive meshes in the 2DL code
[LA-9938-MS] 12 p1914 N85-22011
Recovering pointwise values of discontinuous data within spectral accuracy
[NASA-CR-172535] 12 p1919 N85-2204
Self-similar modified shock structures — cosmic rays
12 p1956 N85-2229
Aerodynamic heating rate distributions induced by trailing edge controls on hypersonic aircraft configurations at Mach 8
[NASA-TM-87453] 13 p1969 N85-2237
Ignition of mixtures of SiH sub 4, CH sub 4, O sub 2, and Ar or N sub 2 behind reflected shock waves
[NASA-TP-2415] 13 p1974 N85-2238
Effect of transparent coatings on generation of laser-induced shock waves in metals
13 p2026 N85-22711
Space and time distribtuion of aftershocks
13 p2112 N85-23157
Study of geological media based on scattered earthquake waves 13 p2114 N85-2318
Physics of the inner heliosphere: Mechanisms, models and observational signatures
[NASA-CR-175632] 13 p2205 N85-2367
Wave motion of three-component medium under load moving on plane boundary 14 p2277 N85-24105
Compression waves in front of and behind a piston launched in a shock tube
[ISL-R-101/83] 14 p2303 N85-2428
Diagram of nonstationary rejoining of magnetic force lines 14 p2344 N85-2446
Electric field and plasma observations near the magnetopause and bow shock during a rapid compression 14 p2355 N85-2455
The keV electrons and 80 keV protons in the vicinity of the high latitude magnetosphere and at the bow shock 14 p2355 N85-2455
The downshift of electron plasma oscillations in the electron foreshock region
[NASA-CR-175633] 14 p2423 N85-2484
Numerical studies of unsteady transonic flow over oscillating airfoil 15 p2458 N85-25174
Magnetohydrodynamics of Earth's bow shock
15 p2481 N85-25011
Vapor explosions in superheated liquids and fundamental studies of the physics of detonation
[AD-A151362] 15 p2504 N85-25447
Measurement of material properties to Mbar pressure using time-resolved shock wave techniques
[DE85-007319] 15 p2558 N85-2578
An experimental investigation into the dynamic response of a stiffened flat plate loaded impulsively by an underwater shockwave
[AD-A151321] 15 p2578 N85-259
Investigation to optimize the passive shock wave/boundary layer control for supercritical airfoil drag reduction
[NASA-CR-175788] 16 p2699 N85-268
Evaluation of an algorithm for the solution of the time-dependent Euler equations
[AD-A151993] 16 p2854 N85-2790
Analyses of orderly structures in jets and the relationship with emitted noise
[ISL-R-117/83] 16 p2861 N85-2794

The soft X-ray background as a supernova blast wave from inside: Solar abundance models
ASA-CR-175767] 16 p2867 N85-27813

Characteristics of steady-state hypersonic flow about bodies with discontinuities in generators
17 p2941 N85-28155

Formation of a fine structure during shock wave
ding
LL-BISI-TRANS-22401-(9022.06)]
17 p2973 N85-28368

Australian seismological report, 1980
EPT-252] 17 p2980 N85-28473

The shock desensitization of PBX-9404 and composition
B-3
[DE85-009604] 18 p3084 N85-29077

Shock capturing
[NASA-CR-172582] 18 p3168 N85-29627

Shocks in the solar wind between 1 and 8.5 AU: Voyager 1 observations
[NASA-CR-175911] 18 p3209 N85-29905

A numerical solution of a nonisothermal wall using the two-dimensional Navier-Stokes equations
[AD-A154487] 19 p3266 N85-30257

Highly accurate shock flow calculations with moving grids and mesh refinements, revision 1
[DE85-010929] 19 p3267 N85-30260

Strain-path modeling for geo-materials
[AD-A154378] 19 p3286 N85-30380

More on shock-wave studies with Prognoz-10 satellite
19 p3296 N85-30432

Functions of Prognoz-10: Intercosmos' station explained 19 p3296 N85-30433

Prognoz-10 Intercosmos' station launched to study shock waves 19 p3296 N85-30434

A multiphase continuum model to describe dynamic loading effects in nonlinear porous media
[DE85-010102] 19 p3301 N85-30463

Fast and optimal solution to the Rankine-Hugoniot problem
[NASA-TM-86214] 19 p3344 N85-30724

Floating shock-fitting in transonic potential flow calculations 20 p3387 N85-31007

Interaction between an interplanetary shock and the Earth's magnetosphere on 27 August 1978: ISEE-1 electric field and ISEE-2 plasma observations
[IFSI-84-15] 20 p3548 N85-32078

Properties of the reflected beams from the Earth's bow shock: A simple model
[IFSI-84-14] 20 p3549 N85-32086

Development of a temperature-compensated hot-film anemometer system for boundary-layer transition detection on high-performance aircraft
[NASA-TM-86732] 22 p3730 N85-33121

Static high pressure study of nitric oxide chemistry: Proposed mechanism for nitric oxide detonation
[DE85-010795] 22 p3746 N85-33220

Experimental studies of chemical reactivity during shock initiation of hexanitrostilbene
[DE85-011726] 22 p3754 N85-33270

Modeling granular explosive detonations with shear band concepts
[DE85-011823] 22 p3754 N85-33271

Two-dimensional simulation of instability growth due to shocks
[DE85-011869] 22 p3784 N85-33442

Gradient scaling for nonuniform meshes
[DE85-009625] 22 p3784 N85-33443

Detonation in tungsten-loaded HMX
[DE85-009806] 23 p3922 N85-34299

Three-dimensional hydrodynamic hot-spot model
[DE85-009587] 23 p3922 N85-34301

Shock and release equation of state of calcite
[DE85-013151] 23 p3942 N85-34432

Cubic interpolated pseudo-particle method (CIP) for solving hyperbolic-type equation
23 p3979 N85-34673

Moving finite element method for ICF target implosion
23 p3980 N85-34675

Numerical calculations on shock loaded materials
23 p3980 N85-34676

Simulation of instability of cylindrically converging shock waves 23 p3980 N85-34679

Stochastic particle acceleration in solar flares
[SH-1.1-4] 23 p3989 N85-34731

Prompt acceleration of ions by oblique turbulent shocks in solar flares
[SH-1.1-6] 23 p3989 N85-34733

Shock and statistical acceleration of energetic particles in the interplanetary medium
[SH-1.5-1] 23 p3996 N85-34771

Energetic ion acceleration at collisionless shocks
[SH-1.5-3] 23 p3996 N85-34772

Pitch angle distributions of 35-1000 keV protons at quasi-perpendicular interplanetary shocks
[SH-1.5-6] 23 p3996 N85-34775

Spatial dependence of the local diffusion coefficient measured upstream of the November 12, 1978 interplanetary traveling shock
[SH-1.5-12] 23 p3996 N85-34776

Latitude dependence of co-rotating shock acceleration
[SH-1.5-14] 23 p3997 N85-34777

Cosmic ray acceleration by stellar wind. Simulation for heliosphere
[SH-1.5-17] 23 p3997 N85-34780

the role of shock waves in modulation of galactic cosmic rays
[SH-4.1-7] 23 p4005 N85-34831

Cosmic ray secondary nuclei and the structure of the galaxy
[OG-7.2-4] 23 p4014 N85-34876

On the cosmic ray diffusion in a violent interstellar medium
[OG-7.2-14] 23 p4015 N85-34881

The cosmic-ray shock structure problem for relativistic shocks
[OG-8.1-1] 23 p4017 N85-34891

Instabilities in decelerating supersonic flows with applications to cosmic ray shocks
[OG-8.1-2] 23 p4017 N85-34892

Time-dependent nonlinear cosmic ray shocks confirming abstract
[OG-8.1-3] 23 p4017 N85-34893

Selfsimilar time dependent shock structures
[OG-8.1-4] 23 p4017 N85-34894

A cosmic ray driven instability
[OG-8.1-5] 23 p4018 N85-34895

Relativistic cosmic ray spectra in the full non-linear theory of shock acceleration
[OG-8.1-6] 23 p4018 N85-34896

The central engine of quasars and AGNs: A relativistic proton radiative shock
[OG-8.1-7] 23 p4018 N85-34897

A model for the origin of high-energy cosmic rays
[OG-8.1-8] 23 p4018 N85-34898

Acceleration of cosmic rays in supernova-remnants
[OG-8.1-9] 23 p4018 N85-34899

Efficiency of regular acceleration of particles by a shock wave at different injection regimes
[OG-8.1-13] 23 p4019 N85-34902

A numerical study of diffusive shock acceleration of cosmic rays in supernova shocks
[OG-8.2-2] 23 p4019 N85-34903

Nuclear reactions in shock wave front during supernova events
[OG-8.2-19] 23 p4021 N85-34915

The theoretical and experimental investigation of cosmic ray Forbush-effects
[SH-5.1-20] 23 p4044 N85-35072

Finite analytic solutions of supersonic flows in two-dimensional non-symmetrical channels
24 p4059 N85-35154

Unsteady flow in a supersonic cascade with two in-passage shocks
[NASA-CR-3925] 24 p4060 N85-35158

Numerical studies of 2-dimensional flows
[NASA-CR-3930] 24 p4060 N85-35160

Computation of three-dimensional shock wave and boundary-layer interactions
[NASA-TM-86780] 24 p4093 N85-35372

SHOES

The energy cost of women walking and running in shoes and boots
[AD-A151022] 14 p2389 N85-24716

SHOOTING STAR AIRCRAFT

U T-33 AIRCRAFT

SHOPS

Development of a production order release methodology
[AD-A145213] 01 p0124 N85-10852

SHORELINES

Progress in developing tidal electric power plants reported 07 p0994 N85-16314

Shore ice ride-up and pile-up features. Part 2. Alaska's Beaufort Sea coast, 1983 - 1984
[AD-A148428] 08 p1190 N85-17501

Establishment of hydrographic shore control by Doppler satellite techniques
[AD-A150709] 14 p2347 N85-24512

Sand dispersion from an ephemeral river delta on the wave-dominated central California coast
[AD-A154352] 19 p3300 N85-30458

SHORT CIRCUIT CURRENTS

New high-efficiency silicon solar cells
[NASA-CR-175643] 13 p2128 N85-23244

Process Research on Polycrystalline Silicon Material (PROPSM)
[NASA-CR-175761] 15 p2587 N85-25951

Measurement of electrical parameters and current components in the bulk of silicon solar cells
20 p3481 N85-31635

SHORT CIRCUITS

Diagnosis of insulation defects in 1000+ V distribution networks with insulated neutral
07 p0954 N85-16044

Surface and allied studies in silicon solar cells
[NASA-CR-174447] 11 p1671 N85-20531

Nickel-cadmium battery cell reversal from resistive network effects
[AD-A149626] 12 p1834 N85-21505

Study of the degradation of short-circuit current and the open-circuit tension of spatial solar cells as a function of the fluency of 1MeV electrons
[INPE-3356-PRE/634] 16 p2667 N85-27614

Failure modes experienced on spacecraft NiCd batteries 20 p3445 N85-31386

Nickel-cadmium battery cell reversal from resistive network effects 20 p3446 N85-31392

Thin-film reliability and engineering overview
21 p3612 N85-32450

SHORT HAUL AIRCRAFT

NT A-310 AIRCRAFT
NT A-320 AIRCRAFT
NT CESSNA 402B AIRCRAFT
NT EUROPEAN AIRBUS

SHORT TAKEOFF AIRCRAFT

NT A-310 AIRCRAFT
NT A-320 AIRCRAFT
NT ALADIN 2 AIRCRAFT
NT EUROPEAN AIRBUS

STOL simulation requirements for development of integrated flight/propulsion control systems
05 p0701 N85-14499

Circulation control: A bibliography of DTNSRDC research and selected outside references: Update
[AD-A146966] 07 p0893 N85-15661

Low-speed wind tunnel tests of the NAL fan-jet STOL research aircraft model with ground simulation by tangential blowing
[NAL-TR-828] 10 p1423 N85-18976

The use of pressure sensing taps on the aircraft wing as sensor for flight control systems
16 p2696 N85-26660

The STOL and maneuver technology program integrated control system 16 p2715 N85-26757

Analysis of control system from a viewpoint of desired pole placement and desired degree of robustness
[AD-A152627] 17 p2899 N85-27876

The STOL and maneuver technology program integrated control system development 17 p2905 N85-27910

Discussion of the paper, Some Aspects of Propulsion for the Augmenter-Wing Concept, by D. C. Whittley
[NASA-TM-77884] 22 p3727 N85-33106

Presentation of the acoustic and aerodynamic results of the Aladin 2 concept qualification testing
[NASA-TM-77883] 24 p4060 N85-35161

SHORT WAVE RADIATION

NT CENTIMETER WAVES
NT DECIMETER WAVES
NT MICROWAVE EMISSION
NT MICROWAVES
NT MILLIMETER WAVES
NT SUBMILLIMETER WAVES

SWIR and visible atomic emission from laser-produced oxygen and nitrogen plasmas
[AD-A147528] 07 p1045 N85-16641

Two-stage free electron laser research
[AD-A148951] 10 p1489 N85-19402

Explanation of the normal winter anomaly from the seasonal variation of short wave absorption
11 p1660 N85-20463

Year-to-year variability of components of Earth's radiation budget according to satellite measurement data 16 p2725 N85-26821

Short Wavelength Chemical Laser (SWCL) Workshop
[AD-A151959] 16 p2790 N85-27211

Solar radiance models for determination of ERBE scanner filter factor
[NASA-CR-172595] 17 p2995 N85-28513

Global geoid and gravity anomaly predictions using the collocation and point mass techniques
[AD-A154517] 21 p3605 N85-32387

Developmental trends in radio receiver design
22 p3777 N85-33407

SHORT WAVE RADIO TRANSMISSION

Theory of radio wave propagation over the ocean
02 p0259 N85-11696

The investigation of short wave signal structure in the vicinity of the caustic by means of a high-directed antenna
[PR-194] 03 p0354 N85-12277

Experimental results of study of artificial perturbation region in upper and lower ionosphere disturbance by the method of vertical probing 06 p0784 N85-15011

A reflectometer unit for a 500 kW HF balanced screened feeder
[BBC-RD-1984/13] 10 p1477 N85-19322

Measurements and predictions of HF ground wave radio propagation over irregular, inhomogeneous terrain
[PB85-110666] 12 p1830 N85-21487
Influence of tropical F region in ionosphere on propagation of short radio waves
16 p2721 N85-26798

SHORTENING
U REDUCTION

SHOT NOISE
Inequalities for the M/G/Infinity queue and related shot noise processes
[AD-A149015] 10 p1545 N85-19737
Voyager planetary radio astronomy: Grain and particle impacts shot noise in Saturn's ring plane
15 p2673 N85-26496

SHOT PEENING
Influence of shot-peening methods on surface quality and service life of bearings 06 p0776 N85-14960
Residual stress distributions in (plastically) surface deformed two-phase materials 19 p3283 N85-30356
Development of a mathematical model for predicting the percentage fatigue life increase resulting from shot peened components
[AD-A156774] 24 p4101 N85-35425

SHOULDERS
Shoulder and hip joint for hard space suits and the like
[NASA-CASE-ARC-11543-1] 12 p1910 N85-21986
The position and mobility of the shoulder, spinal column and pelvis in seated subjects
[AD-A153751] 18 p3153 N85-29524

SHOWERS
Fast electromagnetic (EM) shower simulation
[NOTA-INTERNA-831] 18 p3175 N85-29663

SHRAPNEL
Holographic assembly for measuring velocity fields of supersonic ballistic splinters at a large distance
[ISL-CO-203/84] 20 p3459 N85-31487

SHRINKAGE
Method for calculating linear shrinkage and expansion of metals and alloys
[BLL-M-35747-(5828.4)] 02 p0175 N85-11173
On shrinkage and molecular extension
[AD-A149100] 10 p1451 N85-19144
Microshrink, tensile properties, and the detection of microshrink
[AD-A155875] 24 p4079 N85-35278

SHROUDED BODIES
U SHROUDS

SHROUDED TURBINES
Ribbon burner simulation of T-700 turbine shroud for ceramic lined seals research
[NASA-TM-86940] 10 p1483 N85-19364
Shroud segments for unshrouded blade turbines
[PNR-90260] 23 p3897 N85-34143
Thermal stress analysis of a new turbine shroud seal concept
[NASA-TM-87082] 23 p3938 N85-34406

SHROUDS
Energy efficient engine high pressure turbine ceramic shroud support technology report
[NASA-CR-168036] 02 p0147 N85-10996
An experimental investigation of two-dimensional thrust augmenting ejectors, part 2
[NASA-CR-174110] 04 p0456 N85-12895
Experimental and analytical study of ceramic-coated turbine-tip shroud seals for small turbine engines
[NASA-TM-86881] 09 p1281 N85-18057
View-limiting shrouds for insolation radiometers
[NASA-CR-176041] 20 p3458 N85-31476
Shroud segments for unshrouded blade turbines
[PNR-90260] 23 p3897 N85-34143

SHUNTS
U BYPASSES
U CIRCUITS

SHUTDOWNS
Shutdown characteristics of the Mod-O wind turbine with aileron controls
[NASA-TM-86916] 07 p0992 N85-16299
Analytical model for predicting emergency shutdown of a two-bladed horizontal axis wind turbine
[NASA-TM-83472] 19 p3303 N85-30476

SHUTTLE BOOSTERS
U SPACE SHUTTLE BOOSTERS

SHUTTLE DERIVED VEHICLES
Assessment of candidate-expendable launch vehicles for large payloads
[NASA-CR-175540] 14 p2237 N85-23867
East Europe report: Science and technology
[JPRS-ESA-84-016] 15 p2533 N85-25624
Flight tests of experimental shuttle craft described
15 p2533 N85-25625

SHUTTLE IMAGING RADAR
The SIR-B science investigations plan
[NASA-CR-174282] 08 p1143 N85-17208
The SIR-B science investigations plan: Introduction
08 p1143 N85-17209
Experiment description 08 p1143 N85-17210
SIR-B coverage 08 p1143 N85-17211
The interpretation of SIR-B imagery of surface waves and other oceanographic features using in-situ, meteorological satellite, and infrared satellite data
08 p1143 N85-17212
The spatial evolution of t he directional wave spectrum in the Southern Ocean: Its relation to extreme waves in Agulhas Current 08 p1144 N85-17213
Application of SIR-B data for groundwater exploration in the Arabian shield and sand-drift monitoring in the AN Nafud and Al Jafurah fringe areas, Kingdom of Saudi Arabia 08 p1144 N85-17214
Tectonic, volcanic, and climatic geomorphology study of the Sierras Pampeanas Andes, northwestern Argentina 08 p1144 N85-17215
Deforestation, floodplain dynamics, and carbon biogeochemistry in the Amazon Basin
08 p1144 N85-17216
Southern ocean sea-ice morphology and kinematics
08 p1144 N85-17217
New Zealand SIR-B science investigations
08 p1144 N85-17218
SIR-B analysis of the Precambrian shield of Sudan and Egypt: Penetration studies and subsurface mapping
08 p1145 N85-17219
Quantitative use of multiincidence-angle SAR for geologic mapping 08 p1145 N85-17220
Geologic mapping of Indonesian rain forest with analysis of multiple SIR-B incidence angles
08 p1145 N85-17221
Remote sensing of rice fields and sea pollution by SIR-B 08 p1145 N85-17222
Evaluation of SIR-B data for identifying rainfall event occurrence and intensity 08 p1145 N85-17223
SIR-B interferometric topography
08 p1145 N85-17224
Use of SIR-B multiincidence-angle imagery to study iceberg detectability and offshore ocean feature extraction 08 p1145 N85-17225
Geological, structural, and geomorphological analyses from SIR-B 08 p1145 N85-17226
Amplitude calibration experiment for SIR-B
08 p1146 N85-17227
Microwave and optical remote sensing of forest vegetation 08 p1146 N85-17228
Evaluation of SIR-B imagery for geologic and geomorphic mapping, hydrology, and oceanography in Australia 08 p1146 N85-17229
Interlobate comparison of glacial-depositional style as evidenced by small-relief glacial landscape features in Illinois, Indiana, and Ohio, utilizing SIR-B
08 p1146 N85-17231
Evaluation of the L-band scattering characteristics of volcanic terrain in aid of lithologic identification, assessment of SIR-B calibration, and development of planetary geomorphic analogs 08 p1146 N85-17232
The investigation of selected oceanographic applications of spaceborne synthetic-aperture radar
08 p1146 N85-17233
SIR-B cartography and stereo topographic mapping
08 p1147 N85-17234
Monitoring of the tidal dynamics of the Dutch Waddensee by SIR-B 08 p1147 N85-17235
Structural investigation of the Canadian Shield by orbital radar and LANDSAT 08 p1147 N85-17236
Structural investigation of the Grenville Province by radar and other imaging and nonimaging sensors
08 p1147 N85-17237
Information for space radar designers: Required dynamic range vs resolution and antenna calibration using the Amazon rain forest 08 p1147 N85-17239
Development and evaluation of techniques for using combined microwave and optical image data for vegetation studies 08 p1148 N85-17240
Investigation of SIR-B images for lithologic mapping
08 p1148 N85-17241
Australian Multiexperimental Assessment of SIR-B (AMAS) 08 p1148 N85-17243
Application and calibration of the subsurface mapping capability of SIR-B in desert regions
08 p1148 N85-17244
German Radar Observation Shuttle Experiment (ROSE) 08 p1148 N85-17245
The extension of an invertible coniferous forest canopy reflectance model using SIR-B and LANDSAT data
08 p1149 N85-17246
An investigation of ionospheric irregularity effects on SIR-B image processing and information extraction
08 p1149 N85-17247
Analysis of SIR-B radar illumination of geometry for depth of penetration and surface feature and vegetation detection, Nevada and California
08 p1149 N85-17248
Delineation of major geologic structures in Turkey using SIR-B data 08 p1149 N85-17249
Evaluation of the radar response to land surfaces and volumes: Examination of theoretical models, target statistics, and applications 08 p1149 N85-17250
Ground truth for SIR-B images obtained by SIR system 8 impulse radar 08 p1149 N85-17251
Remote sensing of soil moisture
08 p1149 N85-17252
SAR internal wave signature experiment
08 p1149 N85-17253
Data user's manual 08 p1150 N85-17254
SIR-A imagery in geologic studies of the Sierra Madre Oriental, northeastern Mexico. Part 1 (Regional stratigraphy): The use of morphostratigraphic units in remote sensing mapping
[NASA-CR-175457] 10 p1505 N85-19497
Earth resources research using the Shuttle Imaging Radar system 11 p1713 N85-20779
Analysis of the Gran Desierto, Pinacte Region, Sonora, Mexico, via shuttle imaging radar
[NASA-CR-175711] 15 p2582 N85-25927
Shuttle imaging radar-B (SIR-B) data analysis for identifying rainfall event occurrence and intensity
[NASA-CR-175712] 15 p2584 N85-25986
Shuttle imaging radar-A (SIR-A) data analysis — geology of the Ozark Plateau of southern Missouri, land use in western Illinois, and vegetation types at Koonamore Station, Australia
[NASA-CR-175785] 16 p2809 N85-27324
Design of a shuttle-borne SAR for the DFVLR's planning study
[ERYS-019/84] 20 p3419 N85-31218

SHUTTLE ORBITERS
U SPACE SHUTTLE ORBITERS

SIALON
Oxidation resistance of silicon ceramics
[NASA-TM-77429] 07 p0931 N85-15888

SIBERIA
Deep structure of terrestrial crust and upper mantle in southeastern Siberia and Far East according geological-geophysical data 06 p0821 N85-15212
Deep structure of Western Siberia
07 p0961 N85-16235
The dynamics of ionospheric D region over East Siberia 11 p1662 N85-20477
Snow cover in the Siberian forest-steppe
[NASA-TM-77914] 23 p3943 N85-34435

SICKNESSES
NT ALTITUDE SICKNESS
NT DECOMPRESSION SICKNESS
Morbidity and mortality associated with exposure to Otto Fuel II in the U.S. Navy 1966-1979
[AD-A148726] 09 p1363 N85-18574

SID (IONOSPHERIC DISTURBANCES)
U SUDDEN IONOSPHERIC DISTURBANCES

SIDE-LOOKING RADAR
NT RADAR IMAGERY
Intra-eruption geologic map from an x-band radar image during the May 18, 1980 eruption of Mount St. Helens, Washington 13 p2199 N85-23639
Synthetic aperture side-looking radar image adjustment 16 p2806 N85-27304
Developments in remote sensing
[B8580069] 17 p2984 N85-28441

SIDEBANDS
The spectral distribution of field components for a sinusoidal power modulated monofrequency optical carrier source
[FI-44-TBR-94] 04 p0565 N85-13601
Wideband phase keyers 12 p1839 N85-21544

SIDELOBE REDUCTION
Influence of strut cross-section on strut radiation of reflector antennas
[FI-455-TBR-39] 03 p0357 N85-12285
Configuration study for a 30 GHz monolithic receive array, volume 2
[NASA-CR-174697-VOL-2] 09 p1311 N85-18240
Criteria for site selection and frequency allocation (keynote paper), part 5 21 p3623 N85-32511
Sidelobe reduction of Barker codes, part 7.1C
21 p3625 N85-32522

SIDELOBES
Reflector antenna having sidelobe suppression elements
[AD-D011227] 01 p0039 N85-10244
The 20 GHz proof-of-concept test model results for a multiple scan beam dual reflector antenna
[NASA-CR-174268] 07 p0938 N85-15944
Array sidelobes, error tolerance, gain, and beamwidth
[AD-A147004] 07 p0940 N85-15956
Multiple loop sidelobe canceller
[AD-D011533] 12 p1823 N85-21434
Low sidelobe phased array antenna system
[AD-D011558] 12 p1823 N85-21435

Accuracy of velocity and power determination by the ppler method 21 p3620 N85-32493
Reducing grating lobes due to subarray amplitude pacing
AD-D011723] 23 p3927 N85-34339
DEREAL TIME
The sidereal anisotropy of cosmic rays around 3 x 10 15) eV observed at a middle north latitude
[OG-5.3-6] 22 p3884 N85-34072
Cosmic ray intensity variations at primary rigidities near 1000 GV
[OG-5.3-0] 22 p3885 N85-34075
Cosmic ray sidereal diurnal variation of galactic origin observed by neutron monitors
[SH-4.4-2] 23 p4033 N85-35000
Sidereal anisotropies in the median rigidity range 60-600GV in 1978-1983
[SH-4.4-3] 23 p4033 N85-35001
Sidereal variations deep underground in Tasmania
[SH-4.4-4] 23 p4033 N85-35002
The effect of the interplanetary magnetic field on sidereal variations observed at medium depth underground detectors
[SH-4.4-5] 23 p4033 N85-35003
The sidereal semi-diurnal variation observed at high zenith angles at Mawson, 1968-1984, and the polarity of the solar main field
[SH-4.4-6] 23 p4033 N85-35004
Corrected sidereal anisotropy for underground moons
[SH-4.4-7] 23 p4033 N85-35005
Sidereal anisotropy of cosmic rays
[SH-4.4-8] 23 p4034 N85-35006
DERITE METEORITES
U IRON METEORITES
IDERITES
Origin of mesosiderites as a natural consequence of planet formation 15 p2683 N85-26574
SIDES
Effect of upstream sidewall boundary layer removal on an airfoil test — conducted in Langley 0.3-m transonic cryogenic tunnel 03 p0313 N85-12019
SIDESLIP
Wind tunnel calibration of a hemispherical head angle of attack and angle of sideslip indicator
[FFA-TN-1984-11] 02 p0135 N85-10923
Supermaneuverability
[AD-P004153] 09 p1263 N85-17938
Aerodynamic characteristics of the standard dynamics model in coning motion at Mach 0.6
[NASA-TM-86717] 21 p3552 N85-32094
SIDEWINDER MISSILES
Air force, robotic painting
[AD-P004006] 03 p0308 N85-11986
SIERRA NEVADA MOUNTAINS (CA)
Precipitation gage network operations for wintertime research in the Central Sierra Nevada
[PB85-115020] 10 p1520 N85-19582
Ground-based snow and ice crystal observation system used in Sierra Nevada winter orographic storms
[PB85-115343] 10 p1520 N85-19584
SIEVES
Estimation for a semimartingale regression model using the method of sieves
[AD-A146809] 07 p1028 N85-16527
Rigid zeolite containing polyurethane foams
[DE85-006406] 23 p3919 N85-34286
Molecular and macromolecular sieving by asymmetric ultrafiltration membranes
[PB85-157766] 24 p4077 N85-35266
SIGHT
U VISUAL PERCEPTION
SIGNAL ANALYSIS
NT CEPSTRAL ANALYSIS
Autoregressive nonsteady methods for the analysis and synthesis of the human voice
[FUB-3-1984] 01 p0041 N85-10266
On maximum entropy signal analysis
[AD-A144374] 03 p0410 N85-12618
Automatic correction of static characteristics of measurement channel of digital oscillograph
06 p0795 N85-15083
Interactive Signal Analysis Software (ISAS). User's manual
[AD-A146699] 07 p1022 N85-16485
Use of the analytic signal in ultrasonic imaging
[DE84-016843] 07 p1039 N85-16596
Initialization of Thompson-Pisarenko's algorithm — sinusoidal signal parameter estimation
[FUB-46-1983] 09 p1375 N85-18641
Performance of time-position discriminator of composite signal 13 p2072 N85-22941
Synthesis of quasi-optimum two-level signal discriminator with level changing at unknown point
13 p2083 N85-23010
Accuracy of approximation of Bayes estimates in presence of noninformative parameters
13 p2084 N85-23015
Signal analysis techniques for incipient failure detection in turbomachinery 16 p2736 N85-26884
Algorithms for determining the relative complexity of dynamic signals
[BLL-M-36111-(5828.4)] 16 p2851 N85-27574
Synthesis of adaptive filters for tracking radio systems
22 p3763 N85-33325
SIGNAL ANALYZERS
Noise analysis of the Coarse Optical Power Spectrum Estimator (COPSE) data acquisition system
[AD-A145916] 03 p0419 N85-12677
China report: Science and technology
[JPRS-CST-84-001] 04 p0557 N85-13545
Present status, future prospects of domestic acoustical instruments 04 p0557 N85-13548
The adaptive spectrum analyser
05 p0622 N85-13978
Design of an analog spectrum analyzer for probing experiments
[AD-A147384] 07 p0941 N85-15963
The Statistical Loop Analyzer (SLA)
08 p1100 N85-16955
Development of a modified time delay spectrometry technique for underwater acoustic measurements in a multipath environment
[AD-A152111] 16 p2860 N85-27639
A portable pulse analyzer for nuclear geophysics using a Sinclair-TK microcomputer
[INPE-3278-PRE/601] 16 p2864 N85-27666
Measurement of permittivity and permeability of microwave materials
[AD-D011656] 18 p3176 N85-29688
Hierarchical beamforming with application to a large aperture array system 20 p3439 N85-31345
Transmitter spectrum analyzer
22 p3774 N85-33389
SIGNAL DETECTION
NT CORRELATION DETECTION
Detection and coding techniques of contours in image signals
[FUB-8-1983] 01 p0039 N85-10251
Rules for post-detector detection of weak signals in non-Gaussian noise of unknown power
03 p0344 N85-12218
Optoacoustic spectroscopy
[AD-A145995] 03 p0419 N85-12679
A model for the effectiveness of aircraft alerting and warning systems 05 p0702 N85-14506
Selection of parameters for image decomposition by television system for recognition of group of point sources 06 p0785 N85-15018
Asymptotically optimal ranking algorithms for quasi-determinate signal detection
06 p0792 N85-15064
Human engineer's guide to auditory displays. Volume 2: Elements of signal reception and resolution affecting auditory displays
[AD-A146513] 06 p0859 N85-15462
Potential effectiveness of spatial processing in detecting signals against background of interfering reflections
07 p0952 N85-16032
A technique for rapid determination of probability of detection in pulse Doppler radars
[AD-D011426] 08 p1154 N85-17288
Quantum noise and excess noise in optical homodyne and heterodyne receivers
[AD-A148298] 08 p1157 N85-17303
Experimental satellite system for determining coordinates of maritime distress
09 p1308 N85-18216
Methods of computer-aided analysis of non-Gaussian noise and application to robust adaptive detection, part 2
[AD-A148679] 10 p1539 N85-19704
Digital coherent detector
[AD-D011580] 12 p1833 N85-21501
Method and apparatus for detecting acoustic emissions from metal matrix wire
[AD-D011556] 12 p1927 N85-22107
Theory of optimum M-filtration of signals against background of correlated interference
13 p2069 N85-22927
Effect of variance of photoreceiver frequency characteristics on characteristics of measuring instruments 13 p2076 N85-22965
Asymptotically optimum multialternative sequential procedures for discernment of processes minimizing average length of observations
13 p2084 N85-23012
Extraction of signals from background interference with unknown parameters in quantized sample
13 p2084 N85-23013
Reception of signal with unknown amplitude and duration submerged in white noise 13 p2084 N85-23016
Synthesis of quasi-optimum algorithms for signal recognition against background of correlated noise employing discrete spectral transformations
13 p2085 N85-23020
Probability of detection of pulsed signals employing zero-gating interference suppression
13 p2085 N85-23021
Approximate rules for signal detection against background of Gaussian correlated interference
13 p2086 N85-23027
Use of importance sampling to investigate signal detection systems by simulated method
13 p2086 N85-23028
Transition detection using surface pressure holes
14 p2212 N85-23722
Investigations of the experimental detection of boundary layer transitions 14 p2213 N85-23723
Adaptive detection of noise signal according to Neumann-Pearson criterion 15 p2527 N85-25580
Statistical techniques for signal processing
[AD-A151231] 15 p2541 N85-25690
Nonparametric detection of narrowband signals
[AD-A151280] 15 p2542 N85-25691
Bit error rate of coherent M-ary PSK
16 p2770 N85-27098
Robust detection of fading narrow-band signals in non-Gaussian noise
[AD-A152262] 16 p2774 N85-27124
Phase-lock fiber optic interferometer
[AD-D011603] 16 p2786 N85-27191
Microwave responses of the western North Atlantic
[NASA-CR-175868] 17 p2946 N85-28191
Research on signal detection and block truncation cooling for image compression
[AD-A153444] 18 p3168 N85-29628
Adaptive signal detection and other topics in real time signal processing
[AD-A154139] 19 p3255 N85-30184
Fiber optic gyroscope with alternating output signal
[AD-D011689] 19 p3271 N85-30284
Robust detection and classification of regional seismic signals using a two mode/two stage cascaded adaptive arma (CAARMA) model
[AD-A154710] 21 p3630 N85-32554
Selectivity of weight compensator of passive interference to unknown velocities of detectable targets
22 p3762 N85-33317
Detection of signals from coherent pulsed radars with random variation in parameters of sounding signals from pulse to pulse against background of worst-case Gaussian noise 22 p3763 N85-33324
Efficiency of discrimination in some invariant signal transformations 22 p3776 N85-33399
Optimality criterion for high-frequency channel in receivers of discrete radio signals
22 p3776 N85-33401
Binary signal detection in acoustooptic receivers
22 p3782 N85-33430
Manual and computer-aided sequential diagnostic inference
[AD-A156229] 24 p4133 N85-35620
SIGNAL DETECTORS
Minimization of anomalous errors in measuring systems employing search and testing devices
03 p0344 N85-12219
A miniature urethane molded acoustic transducer
[AD-A146459] 06 p0804 N85-15114
Lightweight, broadband Rayleigh wave transducer
[AD-D011345] 07 p1037 N85-16584
Detection of angular modulated electromagnetic signals
[AD-D011563] 12 p1823 N85-21437
Digital detector of harmonic signals
12 p1840 N85-21549
Method and apparatus for detecting acoustic emissions from metal matrix wire
[AD-D011556] 12 p1927 N85-22107
Efficiency of multitarget signal detection by digital radar data processing devices 13 p2080 N85-22991
Short-range radiotechnical point sensor
13 p2081 N85-22996
Synthesis of quasi-optimum two-level signal discriminator with level changing at unknown point
13 p2083 N85-23010
Statistical techniques for signal processing
[AD-A151231] 15 p2541 N85-25690
Research and development of subsurface acoustic wave devices for sensor applications
[AD-A152197] 16 p2861 N85-27642
Calibration and use of clutter data for simulation
[AD-A154793] 21 p3574 N85-32229
Advanced detectors and signal processing
[NASA-CR-176193] 24 p4086 N85-35343

SIGNAL DISCRIMINATORS
U SIGNAL DETECTORS
SIGNAL DISTORTION
The average power density spectra of additive scrambler signals and their versions in AMI code [FUB-27-1983] 01 p0040 N85-10258
Electrical consequences of mechanical antenna characteristics 05 p0625 N85-14006
Distortions of radio pulse during reflection from maximum region of ionospheric layer 06 p0792 N85-15061
Real-time estimation of amplitude and group delay distortion in a PSK line-of-sight communications channel 09 p1311 N85-18237
Digital data communications over microwave radio channels 10 p1469 N85-19272
Some propagation experimental results on protection techniques for line-of-sight digital systems 10 p1472 N85-19286
Ionospheric distortions of digital signals with wideband modulation 13 p2072 N85-22945
Simple detonation meter 13 p2077 N85-22971
Nature of seismic images with amplitude and time fluctuations of recorded oscillations 13 p2112 N85-23156
The effects of seeing on noise 14 p2443 N85-25077
Specifics of laser sounding of atmosphere along horizontal and slightly slanting paths over water surface 19 p3297 N85-30441
Recovery of pyroshock data from distorted acceleration records [NASA-TP-2/04] 20 p3407 N85-31141
Solid state altimeter model: Simulation description; analysis of test results (narrow band filters, weighting) --- satellite-borne instruments [CNES-DRT/TIT/RL-160-T] 20 p3419 N85-31220
Compression of spread spectrum signals on an excessively dispersive channel [AD-A155184] 21 p3576 N85-32240
An image compression survey and algorithm switching based on scene activity [NASA-TP-2456] 22 p3727 N85-33106
Optimum predistortion of digital signals for transmission over parallel channels 22 p3776 N85-33397
Study of nonlinear distortion in microwave amplifiers using Schottky gate field effect transistors 22 p3780 N85-33423
SIGNAL ENCODING
Improvement of the narrowband linear predictive coder. Part 2: Synthesis improvements [AD-A145031] 01 p0038 N85-10237
Detection and coding techniques of contours in image signals [FUB-8-1983] 01 p0039 N85-10251
Image signals encoding techniques oriented towards the reduction of perceptive redundance [FUB-23-1983] 01 p0040 N85-10256
The average power density spectra of additive scrambler signals and their versions in AMI code [FUB-27-1983] 01 p0040 N85-10258
Voice phonetic coding and decoding processes [FUB-29-1983] 01 p0040 N85-10259
A human visual system investigation applicable to image contour coding [FUB-36-1983] 01 p0085 N85-10640
Improved digital baseband transmission by application of maximum likelihood decoding to an 8-level signal generated by convolution and block coding [FI-44-TBR-83] 07 p0942 N85-15973
A public key cryptographic algorithm based on a generalization of the knapsack problem [FUB-7-1984] 09 p1313 N85-18250
Tally cell circuit [AD-D011492] 11 p1629 N85-20254
Fundamental limits to synchronization and tracking [AD-A149623] 12 p1833 N85-21504
Secure digital speech communication [AD-D011572] 14 p2298 N85-24215
Synchronizing heavily encoded data in bad weather 16 p2770 N85-27099
Symbol stream combining in a convolutionally coded system 16 p2771 N85-27101
Combined trellis coding with asymmetric MPSK modulation: An MSAT-X report [NASA-CR-176039] 20 p3440 N85-31347
Study of a low rate spread spectrum receiver [ENST-83E015] 20 p3441 N85-31354
Coding schemes for improving MST radar performance, part 7.1A 21 p3625 N85-32520
SIGNAL FADEOUT
U SIGNAL FADING
SIGNAL FADING
NT SELECTIVE FADING
Propagation measurements for land-mobile satellite services in the 800 MHz band [CRC-TN-724] 09 p1310 N85-18231
A technical solution to fadings in tactical satellite digital transmissions 10 p1473 N85-19297
Fast data and voice transmission for mobile services with high immunity against multipath and co-channel interference 10 p1475 N85-19306
Effective millimeter wave transmission under severe multipath conditions 10 p1475 N85-19308
Optimal threshold and weight sorting of elevation angle readings under conditions of fadeouts of a directed signal 12 p1840 N85-21547
Robust detection of fading narrow-band signals in non-Gaussian noise [AD-A152262] 16 p2774 N85-27124
Radiometry: A useful prediction tool --- atmospheric attenuation [ESA-SP-1071] 20 p3399 N85-31094
SIGNAL FADING RATE
Moving random surfaces and correlation analysis [CRC-1384] 19 p3253 N85-30168
SIGNAL GENERATORS
NT FREQUENCY SYNTHESIZERS
NT FUNCTION GENERATORS
China report: Science and technology [JPRS-CST-84-001] 04 p0557 N85-13545
Present status, future prospects of domestic acoustical instruments 04 p0557 N85-13548
Test signal generator for coherent air-to-ground radars [AD-D011278] 05 p0628 N85-14025
Formation of radio signals with low out-of-band radiation 07 p0950 N85-16018
Application of K176-series microcircuits 13 p2077 N85-22973
Computing convolution of multifrequency signal employing truncated fast Fourier transform algorithms 13 p2085 N85-23019
Dielectric resonator [AD-D011573] 14 p2299 N85-24233
Rotor blade test apparatus [AD-D011725] 23 p3934 N85-34381
SIGNAL MEASUREMENT
Digital radio link: Wave propagation measurements using narrow band technique [FOA-C-30384-E2] 04 p0494 N85-13152
Noncontact photo-thermal probe-beam deflection measurement of thermal diffusivity in an confined hot gas [AD-A147481] 07 p0971 N85-16170
A sampling phasemeter design for pulsed continuous wave signals [AD-A155237] 21 p3581 N85-32264
Visibility and vertical structure measurements in southern Germany [AD-A154714] 21 p3635 N85-32574
SIGNAL MIXING
Error probability during optimal noncoherent reception of binary signals in multibeam channel 13 p2069 N85-22922
SIGNAL PROCESSING
Fast envelope detector with bias compensation [AD-D011226] 01 p0036 N85-10243
Center for Electronics and Electrical Engineering Technical Bulletin covering center programs with 1984 CEEE events calendar [PB84-222785] 01 p0045 N85-10292
Center for Electronics and Electrical Engineering Technical Bulletin covering center programs [PB84-219716] 01 p0045 N85-10295
Guided-wave optic devices for integrated optic information processing [AD-A145695] 02 p0280 N85-11827
Aspects and applications of SAR (Synthetic Aperture Radar) imagery for mensuration [AD-A146301] 03 p0356 N85-12290
Center for Electronic and Electrical Engineering Technical Progress Bulletin, January - March 1983, no. 2 [PB84-231224] 03 p0360 N85-12308
Electronic bandwidth compression module [AD-A145843] 03 p0366 N85-12343
Simulation of information extraction from radar altimeter return echoes --- ERS-1 (ESA satellite) 03 p0383 N85-12452
Signal processing algorithms [AD-A145748] 03 p0406 N85-12590
Extinction by dielectric particles at optical and infrared wavelengths [AD-A146305] 03 p0413 N85-12640
Research on materials and components for opto-electronic signal processing [AD-A145806] 03 p0433 N85-12754
Research activities of the Illinois University Coordinated Science Laboratory [AD-A145589] 03 p0449 N85-12856
USSR report: Electronics and electrical engineering [JPRS-UEE-84-010] 04 p0485 N85-13095
Bragg reflection of surface electroacoustic shear waves 04 p0485 N85-13096
Interference immunity of digital equipment for coherent processing of wideband signals 04 p0486 N85-13100
Digital radio receivers and problems of analog-to-digital conversion of narrow-band signals 04 p0486 N85-13101
Architecture of adaptive space-frequency-time signal processing system 04 p0486 N85-13103
Microprocessor implementation of algorithms of nonlinear filtration 04 p0486 N85-13104
Revision of signal and interference space-time processing algorithms for implementation by microprocessors 04 p0487 N85-13105
Efficiency of computer system digital processing of signals 04 p0487 N85-13106
Carrier acquisition and tracking by a COSTAS loop with automatic frequency control [ESA-TT-838] 04 p0483 N85-13149
On estimating the phase of periodic waveform in additive Gaussian noise, part 2 05 p0622 N85-1398
Parametric models for signal processing: Autoregressive (AR), Moving Average (MA) and mixed autoregressive with moving average (ARMA) [ENST-84D001] 05 p0628 N85-1403
Study and realization of a Doppler system with pulsed, directional, multiport (128) emission and sequential signal treatment --- ultrasonic echography, blood flow [ENST-84E008] 05 p0639 N85-14102
Detailed performance calculations: Portland State Group, appendix F 06 p0676 N85-1484
Fast algorithms and specialized architectures 06 p0714 N85-1487
Fly's eye sensor nonlinear signal processing [AD-D011290] 06 p0729 N85-1488
Place of aperture synthesis in general theory of antennas (review) 06 p0781 N85-1498
Primary data processing in very long baseline radiointerferometer 06 p0783 N85-1500
Device for frequency stabilization of microwave oscillators 06 p0788 N85-1503
USSR report: Electronics and electrical engineering [JPRS-UEE-84-011] 06 p0789 N85-1504
Synthesis of systems for coherent weighted signal processing against background of correlated interference 06 p0790 N85-1504
Teletrack: A special effect [BBC-RD-1984/10] 06 p0798 N85-1508
Wavelength coded image transmission and holographic optical elements [AD-A146490] 06 p0810 N85-15147
Actual altitudes of radioacoustic sounding in decimeter wavelength band 06 p0826 N85-1524
Development of radar to measure sea ice melt pond nomination 06 p0826 N85-1524
Evaluation of the RSTN (Regional Seismic Test Network) network and further improvement to automatic association [AD-A146395] 06 p0836 N85-15312
Adaptive MTI (Moving Target Indicator) system [AD-D011361] 07 p0937 N85-1596
Two-dimensional signal processing and storage and theory and applications of electromagnetic measurements. Supplemental appendix [AD-A146848] 07 p0939 N85-1596
Studies in statistical signal processing [AD-A147130] 07 p0940 N85-1596
Charge domain filters for enhanced monolithic signal processing [AD-A147428] 07 p0941 N85-1596
New technology high efficiency and high stability color motion video compression system [AD-A147523] 07 p0941 N85-1596
Parallel processor configuration for adaptive antenna arrays [AD-D011347] 07 p0942 N85-15970
Modern signal processing and reconnaissance -- conferences [FOA-C-30374-E1] 07 p0942 N85-15975
Electronics research at the University of Texas at Austin [AD-A146900] 07 p0947 N85-1599
USSR report: Electronics and electrical engineering [JPRS-UEE-84-018] 07 p0949 N85-1601
Digital signal demodulators with single-sideband 07 p0950 N85-1601
USSR report: Electronics and electrical engineering [JPRS-UEE-84-017] 07 p0951 N85-1602
Nonlinear processing of optical pulse signals 07 p0951 N85-1602
Analysis of effectiveness of partial optimization of spatial processing systems 07 p0952 N85-1603
Potential effectiveness of spatial processing in detecting signals against background of interfering reflections 07 p0952 N85-1603
Digital thermometer with linearizer on slide wire 07 p0954 N85-1604

provement of electromechanical systems by utilization
icroelectronic technology 07 p0955 N85-16053

hite-light optical information processing and
graphy
A146936] 07 p0967 N85-16138

teractive Signal Analysis Software (ISAS). User's
ual
-A146999] 07 p1022 N85-16485

lectro-optical target detection
-D011386] 07 p1042 N85-16617

olid state research
ASA-CR-174285] 07 p1048 N85-16656

NSWC-NADC interactive communication links for
/UYS-1 loadtape creation and retrieval
D-A149416] 08 p1153 N85-17277

An adaptive Fast Fourier Transform weighting technique
increase small target sensitivity
D-D011424] 08 p1154 N85-17286

A technique for rapid determination of probability of
tection in pulse Doppler radars
AD-D011425] 08 p1154 N85-17288

Extraction of structural information from radar signals
FOA-C-30370-E1] 08 p1155 N85-17292

A scanning alarm electronic processor
AD-D011419] 08 p1158 N85-17309

Data acquisition channel apparatus
AD-D011428] 08 p1159 N85-17311

Electromagnetic inspection of wire ropes using sensor
arrays
AD-A148317] 08 p1170 N85-17379

Lidar studies of temperature and density using Rayleigh
scattering 08 p1184 N85-17450

Programmable realtime interface between a block
floating point processor and memory
[AD-D011431] 08 p1203 N85-17571

Multidimensional digital signal processing
[AD-A148055] 08 p1205 N85-17586

Multiple channel adaptive filtering using a fast
orthogonalization network: An application to efficient
pulsed Doppler radar processing
[AD-A147929] 08 p1211 N85-17619

Robust linear filtering for multivariable stationary time
series, part 3
[AD-A148169] 08 p1212 N85-17627

Calculation of cumulative distributions and detection
probabilities in communications and optics
[AD-A147781] 08 p1215 N85-17650

Research in stochastic processes
[AD-A148622] 08 p1216 N85-17660

Nonlinear real-time optical signal processing
[AD-A148293] 08 p1222 N85-17699

Matrix-matrix multiplication using an electrooptical
systolic-engagement array processing architecture
[AD-D011410] 08 p1223 N85-17704

Subjective evaluation of the effect of noise and
interference on frequency modulated NTSC television
signals
[CRC-1367] 09 p1310 N85-18230

Multivariable Autoregressive Moving Average (ARMA)
models: A time approach to antenna processing
[ENST-84E015] 09 p1313 N85-18252

Signal Hill solar-powered repeater report and
recommendations
[DE85-000487] 09 p1316 N85-18273

Neurocognitive pattern analysis of an auditory and visual
numeric motor control task. Part 1: Development of
methods
[AD-A148809] 09 p1364 N85-18578

Survey of VLF-OMEGA transmissions received during
summer at Antarctic peninsula
[INPE-3389-PRE/666] 10 p1462 N85-19223

Performance of the DSA's subcarrier demodulation
digital loop 10 p1465 N85-19242

The ambiguity function of random binary-phase-coded
waveforms
[AD-A148906] 10 p1466 N85-19249

An object-oriented signal processing environment: The
knowledge-based signal processing package
[AD-A148963] 10 p1468 N85-19251

Adaptive signal processing for radio communications
10 p1473 N85-19295

Time and space domain filtering for improved HF
communication 10 p1473 N85-19298

Overview of RADC adaptive antenna developments for
communications 10 p1474 N85-19299

Asynchronous transmission with strong spectral
spread 10 p1474 N85-19300

Effective millimeter wave transmission under severe
multipath conditions 10 p1475 N85-19308

On the probability density of signal-to-noise ratio in an
improved adaptive detector, part 1
[AD-A148958] 10 p1550 N85-19772

Elimination of sensor artifacts from infrared data
[AD-A149048] 10 p1556 N85-19814

Optical implementation of the synthetic discriminant
function
[AD-A149562] 10 p1557 N85-19817

Signal processing and range spreading in the FM-CW
radar
[PB85-108256] 11 p1626 N85-20239

Processing circuit with asymmetry corrector and
convolutional encoder for digital data
[NASA-CASE-MSC-20167-1] 11 p1629 N85-20249

Optical eigenvector
[AD-A149550] 11 p1729 N85-20871

Direction finder set, radio
[AD-A149958] 12 p1775 N85-21142

Detection of angular modulated electromagnetic
signals
[AD-D011563] 12 p1823 N85-21437

Digital coherent detector
[AD-D011560] 12 p1833 N85-21501

Tubes and transistors in audio amplifiers
12 p1837 N85-21532

Summator of radio pulse signals
12 p1839 N85-21539

Synthesis of optimum receiver and processor for signal
packet of radio pulses 12 p1839 N85-21541

Multichannel digital processing of wideband signals
12 p1840 N85-21548

Optimal discrete filtration of intricate phase-keyed
signals 12 p1840 N85-21550

Retinal information mapping system
[AD-D011531] 12 p1849 N85-21601

Application of homomorphic signal processing to stress
wave factor analysis
[NAS 1.26:174871] 12 p1861 N85-21673

Seismic observation of infrasonic signals
[AD-A149574] 12 p1889 N85-21853

Electrical characterization of analog microprocessors
[AD-A149629] 12 p1911 N85-21995

Instrumentation award
[AD-A150081] 12 p1912 N85-21999

Topics in optical materials and device research, 3:
Volume 1
[AD-A149726] 12 p1933 N85-22145

Switchable zero order diffraction gratings as light
valves
[AD-A150129] 12 p1934 N85-22153

The future of lightwave technology
[PB85-109759] 12 p1935 N85-22155

Approaches and algorithms for robust signal
processing 13 p2062 N85-22878

Acousto-optically addressed Fourier transform matched
filters
[AD-A150298] 13 p2063 N85-22889

Two-dimensional signal processing and storage and
theory and applications of electromagnetic
measurements
[AD-A150590] 13 p2065 N85-22899

USSR report: Electronics and electrical engineering
[JPRS-UEE-85-002] 13 p2066 N85-22907

Assessment of effectiveness of signal-code
constructions in time division-multi-access satellite
systems 13 p2066 N85-22908

Processing of signals in experiments with scattering of
short radio pulses by conducting sphere
13 p2068 N85-22917

Dispersion of phase-shift keyed systems with fixed
number of blocks 13 p2070 N85-22928

Noise tolerance of digital demodulator for complex signal
system employing binary quantization
13 p2070 N85-22929

Combined processing method and matched filter for
discrete composite frequency phase-shift keyed signal
13 p2070 N85-22931

Space-time response characteristics of acoustooptic
filter for compression of linearly frequency-modulated
signal 13 p2071 N85-22937

Dynamics of adaptive signal corrector
13 p2071 N85-22940

Spectra of incidental interference resulting from
nonlinear conversion of signals from transmitter
13 p2073 N85-22950

Models of discontinous random fields
13 p2079 N85-22983

Synthesis of optimum single-channel discrete signals
and filters 13 p2080 N85-22990

Synthesis of optimum algorithms for secondary
processing 13 p2080 N85-22992

Factorized algorithms for combined spatial and temporal
processing of radar signals 13 p2081 N85-22997

Electrothermal transducer with short time constant
13 p2088 N85-23040

Acoustooptic demodulation of frequency-modulated
signals 13 p2090 N85-23050

Optical processing in radon space
[AD-A150269] 13 p2159 N85-23402

Condition monitoring of helicopter gearboxes using
automatic vibration analysis techniques
14 p2223 N85-23790

Six-inch HYGE vertical impact facility
[AD-A150665] 14 p2228 N85-23809

Multidimensional digital signal processing
[AD-A150833] 14 p2292 N85-24209

Advanced detectors and signal processing for bubble
memories
[NASA-CR-172534] 14 p2297 N85-24219

Design, fabrication and testing of a multibeam forming
network
[NASA-CR-175695] 14 p2298 N85-24228

Picosecond lidar techniques in laboratory and field
diagnostics
[AD-A150755] 14 p2309 N85-24294

Annual report on electronics research at the University
of Texas at Austin
[AD-A150636] 14 p2415 N85-24901

USSR report: Electronics and electrical engineering
[JPRS-UEE-85-005] 15 p2524 N85-25565

Space processing of acoustic signals in plane-parallel
waveguide — antenna arrays 15 p2525 N85-25572

Converters of sum/differnce of codes to frequency
15 p2526 N85-25576

Analysis of spectral characteristics of multilevel digital
computing synthesis 15 p2527 N85-25579

MHB4046 phase-lock circuit 15 p2533 N85-25629

Additional PLL designs 15 p2534 N85-25632

Receiver optimization for detection in doubly spread
communication channels
[AD-A151226] 15 p2541 N85-25689

Statistical techniques for signal processing
[AD-A151231] 15 p2541 N85-25690

Nonparametric detection of narrowband signals
[AD-A151260] 15 p2542 N85-25691

Processing speech for analysis using optical Fourier
techniques
[AD-A151698] 15 p2544 N85-25704

Conversion of algorithms to custom integrated circuit
devices
[AD-A151288] 15 p2547 N85-25720

Wavelength dependent, tunable, optical time delay
system for electrical signals
[AD-D011584] 15 p2548 N85-25725

Parallel programmable charge domain device
[AD-D011599] 15 p2549 N85-25733

Radar measurement of thickness of drifting ocean ice
employing cepstral signal processing
15 p2644 N85-26313

Ultrasonic characterization of porosity: Theory
[DE85-005922] 15 p2646 N85-26325

Mode dependent, optical time delay system for electrical
signals
[AD-D011596] 15 p2653 N85-26363

Three new fiber-optic components
[DE85-006269] 15 p2653 N85-26364

The impact of VLSI on guidance and control system
design 16 p2697 N85-26654

Synchronizing heavily encoded data in bad weather
16 p2770 N85-27099

Symbol stream combining in a convolutionally coded
system 16 p2771 N85-27101

High-speed digital baseband mixer
16 p2771 N85-27103

Signal processing for the analysis of transient
electromagnetic data
[DE85-007244] 16 p2774 N85-27125

The origin of brain potentials associated with selective
visual attention
[AD-A152291] 16 p2840 N85-27511

Algorithms for determining the relative complexity of
dynamic signals
[BLL-M-36111-(5826.4)] 16 p2851 N85-27574

Topics in time delay estimation
[AD-A152231] 16 p2855 N85-27607

Performance analysis of the DSN baseband assembly
(Bba) Real-Time Combiner (RTC)
[NASA-CR-175876] 17 p2946 N85-28190

Digital methods of the optimum processing of radar
signals
[AD-A152469] 17 p2948 N85-28202

Pipelined programmable charge domain device
[AD-D011598] 17 p2951 N85-28225

Research on superconductive signal-processing
devices
[AD-A152703] 17 p2953 N85-28235

A plan for the development of inertial reconstruction
of initial state clock (IRIS) 17 p2966 N85-28317

Studies of optical-beam phase-conjugation by nonlinear
refraction
[AD-A152865] 17 p3037 N85-28798

An approach to digital level compression using the
zero-crossing points of programme signals
[NHK-LABS-NOTE-308] 18 p3090 N85-29123

Theoretical investigations of the propagation and interactions of surface waves
[AD-A153548] 18 p3165 N85-29753

Digital Optical Circuit Technology
[AGARD-CP-362] 18 p3165 N85-29757

Prospects for parallel nonlinear optical signal processing using GaAs etalons and ZnS interference filters
18 p3167 N85-29765

Multiport optical detectors 18 p3167 N85-29769

Optical techniques for signal distribution and control in advanced radar and communication systems
18 p3168 N85-29773

A study of reflex optoelectronic switching matrices and their derivatives
[CRC-TN-720] 19 p3253 N85-30169

Orthogonalizer for inphase and quadrature digital data
[AD-D011679] 19 p3254 N85-30174

Control and regulation of generalized linear systems
19 p3257 N85-30193

A single chip VLSI architecture for radar signal processing 19 p3257 N85-30195

Linear time-invariant, space-variant filters and the WKB approximation with applications to underwater acoustic signal processing
[AD-A154250] 19 p3352 N85-30775

A 406 MHz ELT processor for geostationary satellites — Emergency Locator Transmitter (ELT)
20 p3403 N85-31114

Adaptive identification and control of structural dynamics systems using recursive lattice filters
[NASA-TP-2371] 20 p3407 N85-31142

Swedish program for sensor research, development
20 p3438 N85-31338

Scattering models in signal processing
20 p3439 N85-31339

Fast eigenvector methods for digital signal processing
20 p3439 N85-31341

Hierarchical beamforming with application to a large aperture array system 20 p3439 N85-31345

Combined trellis coding with asymmetric MPSK modulation: An MSAT-X report
[NASA-CR-176039] 20 p3440 N85-31347

Synthetic aperture radar data processing — satellite-borne radar
[CNES-196-T-CT/DRT/TIT/RL]
20 p3442 N85-31363

Digital signal processing for spaceborne synthetic aperture radar
[FOA-C-30381-E1] 20 p3442 N85-31364

Center for Electronics and Electrical Engineering technical progress bulletin covering center programs, April-June 1984 with 1984 CEEE (Center for Electronics and Electrical Engineering) events calendar, issue 7
[PB85-187540] 20 p3450 N85-31419

Forth system for coherent-scatter radar data acquisition and processing
[NASA-CR-176055] 20 p3494 N85-31720

An overview of nonlinear systems identification
[RR-271] 20 p3520 N85-31894

Spectral methods for the estimation of acoustic intensity, energy density, and surface velocity using a multimicrophone probe 20 p3524 N85-31916

Particle sizing from forward scattered light at two angles using a Variable-Focal-Length optical system
[AD-A154164] 20 p3533 N85-31980

Electronics Division research and development
[DE85-011887] 20 p3540 N85-32032

A phase-locked frequency multiplier for the signal averaging of the vibration of the Wessex helicopter input spiral bevel pinion
[AD-A154914] 21 p3555 N85-32113

Calibration and use of clutter data for simulation
[AD-A154793] 21 p3574 N85-32229

Compression of spread spectrum signals on an excessively dispersive channel
[AD-A155184] 21 p3576 N85-32240

A high-speed digital signal processor for atmospheric radar, part 7.3A 21 p3626 N85-32525

Qualitative analysis of sign-bit processing
[AD-A154776] 21 p3671 N85-32804

Bayesian vs MAP multiple model adaptive estimation for field of view expansion in tracking airborne targets
[AD-A155466] 21 p3679 N85-32855

Solid state research
[AD-A154783] 21 p3709 N85-33025

USSR report: Electronics and electrical engineering
[JPRS-UEE-84-015] 22 p3762 N85-33314

Signal processing in quasi-holographic system as an inverse problem 22 p3762 N85-33315

Method of static measurements of absolute scattering matrix of radar targets 22 p3762 N85-33316

Characteristics of digital range finder with stroboscopic discretization 22 p3762 N85-33319

Amplitude stabilization of pulse signals
22 p3762 N85-33320

Potential coordinate estimate accuracy estimation accuracy by multiposition radar systems
22 p3763 N85-33322

Optimal complex nonlinear processing of continuous and pulsed signals 22 p3763 N85-33323

Variation in radiowave propagation conditions in corona during solar activity cycle 22 p3763 N85-33327

Adaptive synthesis of antennas with separation of signals by direction of arrival 22 p3764 N85-33328

Probabilistic analysis of automatic control systems for detection systems 22 p3765 N85-33335

Transformation of spectrum of phase-code keyed signal for scanning in time 22 p3765 N85-33336

Synthesis of optimum receiver and processor for interfering radio pulse signals 22 p3769 N85-33361

Design of digital bandpass filters with finite memory
22 p3775 N85-33392

Method of designing digital band-pass filters with pulse response of finite duration 22 p3775 N85-33395

Generalization of discrete Fourier transform for interpolation in time domain 22 p3775 N85-33396

Generalization of discrete Fourier transformation for interpolation in time domain 22 p3776 N85-33400

Controllable companding in low-frequency FM radio communication systems 22 p3776 N85-33402

Synthesis of system with nonideal components for optimal processing of radio signal
22 p3777 N85-33405

General design principles of high speed frequency synthesizers based on phase synchronization systems
22 p3779 N85-33417

Methods for the optical processing of signals
[DRIC-T-7439] 22 p3844 N85-33809

The improved display of 625-line television pictures: Adaptive interpolation
[BBC-RD-1985/5] 23 p3925 N85-34328

A general purpose image processing package
23 p3961 N85-34549

Nonlinear digital phase-locked loops with application to Loran-C receivers 24 p4063 N85-35178

Advanced detectors and signal processing
[NASA-CR-176193] 24 p4066 N85-35343

Aspects of input signal design for order and parameter estimation in linear dynamical systems
[ER-83/05] 24 p4091 N85-35362

SIG: A general-purpose signal processing program. User's manual: Revision 1
[DE85-013035] 24 p4140 N85-35662

SIGNAL RECEPTION

NT SYMBOLS
NT TELEVISION RECEPTION

Reflector antenna having sidelobe suppression elements
[AD-D011227] 01 p0039 N85-10244

Detection, classification, and extraction of helicopter-radiated noise
[AD-A145993] 03 p0416 N85-12661

Analysis of threshold effects during estimation of arrival time of optical signals 07 p0951 N85-16030

Structure of frequency modulated and phase-shift keyed signals reflected from ionosphere at near-critical frequencies 07 p0952 N85-16035

DSN 34-meter antenna optics analysis for wideband SETI investigations 10 p1465 N85-19244

Base communications issues for the 1980s
[AD-A149764] 12 p1828 N85-21474

Optimal threshold and weight sorting of elevation angle readings under conditions of fadeouts of a directed signal 12 p1840 N85-21547

Error probability during optimal noncoherent reception of binary signals in multibeam channel
13 p2069 N85-22922

Regular synthesis of pairs of phase-keyed binary minimax signals 13 p2069 N85-22923

Interference immunity of binary systems with second-order phase-difference modulation in various reception modes 13 p2072 N85-22944

Reception of signal with unknown amplitude and duration submerged in white noise 13 p2084 N85-23016

Reception noise immunity of multiposition signals
13 p2085 N85-23023

Measurement results from a balloon experiment simulating land mobile satellite transmissions
[NASA-CR-175740] 15 p2540 N85-25683

Global positioning system carrier phase: Description and use
[PB85-174126] 19 p3216 N85-29946

Specifics of laser sounding of atmosphere along horizontal and slightly slanting paths over water surface
19 p3297 N85-30441

Study of the interferences of 2 GHz radio beams with a DORIS system — precise low orbit determination system (DORIS)
[CNES-CT/DRT/TIT/RL-84/140-T]
20 p3442 N85-31362

SIGNAL REFLECTION

Potential effectiveness of spatial processing in detecting signals against background of interfering reflections
07 p0952 N85-16032

Velocity inversion using a stratified reference
[AD-A150082] 12 p1889 N85-21658

Parameters of amplitude-modulated signal upon reflections 13 p2076 N85-22966

Axial focusing of signal from distant point radiator reflected twice in deep paraboloid
13 p2078 N85-22979

Digital RF delay line for ECM (electronic countermeasure) look-through
[AD-A152120] 16 p2774 N85-27120

Kirchhoff modeling via wave equation datuming
[AD-A152399] 17 p3026 N85-28727

Small-scale structure of ionospheric F-region
19 p3297 N85-30440

A random layer model for reflection from ocean bottom sediments
[AD-A155019] 21 p3700 N85-32996

Theoretical and experimental analyses of the performance of two-color laser ranging systems
[NASA-CR-176159] 23 p3936 N85-34387

SIGNAL TO NOISE RATIOS

A limbus-sensing eye movement recorder
[AD-A144772] 01 p0049 N85-10322

The development of a diode laser Doppler velocimeter for boundary layer measurements under ice: A feasibility investigation
[AD-A145076] 01 p0053 N85-10348

A Monte Carlo comparison of the recovery of winds near upwind and downwind from the SASS-1 model function by means of the sum of squares algorithm and a maximum likelihood estimator
[NASA-CR-3839] 01 p0064 N85-10421

Radio telemetry formula applications. A practical users guide
[AD-A146247] 03 p0356 N85-12286

Algorithm for astronomical, extended source, signal-to-noise radio calculations
[NASA-TP-2396] 03 p0445 N85-12833

Algorithm for astronomical, point source, signal to noise ratio calculations
[NASA-TP-2397] 03 p0445 N85-12834

Television transmission in frequency modulation
04 p0493 N85-13146

Thermal shock as a carbide grade development tool
[DE84-016939] 04 p0509 N85-13251

Synthesis of systems for coherent weighted signal processing against background of correlated interference 06 p0790 N85-15046

Efficiency in integral active antennas
06 p0792 N85-15080

A noise-suppressing digital frequency meter
06 p0796 N85-15084

Reference oscillator stability effect on clutter cancellation in a radar system 07 p0038 N85-15946

Improved digital baseband transmission by application of maximum likelihood decoding to an 8-level signal generated by convolution and block coding
[FI-44-TBR-93] 07 p0942 N85-15973

Some applications of signal-to-noise in photographic stellar photometry 07 p0966 N85-16132

Electro-optical target detection
[AD-D011366] 07 p1042 N85-16617

Measurement of signal separation between radio service and air navigation service
[IRT-TB-B-40/82] 08 p1083 N85-16860

Configuration study for a 30 GHz monolithic receive array, volume 2
[NASA-CR-174697-VOL-2] 09 p1311 N85-18240

Further results on rate 1/N convolutional code constructions with minimum required SNR criterion
10 p1464 N85-19235

Performance of the DSA's subcarrier demodulation digital loop 10 p1465 N85-19242

On the probability density of signal-to-noise ratio in an improved adaptive detector, part 1
[AD-A148856] 10 p1550 N85-19772

The noise of laser diodes with modulated injection current
[FI-465-TBR-23] 11 p1625 N85-20233

Detection of angular modulated electromagnetic signals
[AD-D011563] 12 p1823 N85-21437

Fundamental limits to synchronization and tracking
[AD-A149623] 12 p1833 N85-21504

Optimal threshold and weight sorting of elevation angle readings under conditions of fadeouts of a directed signal 12 p1840 N85-21547

Shuttle flight test of an advanced gamma-ray detection system
[AD-A150316] 13 p1966 N85-22469

Moving target detection 13 p2067 N85-22915

Theory of optimum M-filtration of signals against ackground of correlated interference
13 p2069 N85-22927
Performance of time-position discriminator of composite ignal 13 p2072 N85-22941
Effect of variance of photoreceiver frequency characteristics on characteristics of measuring instruments 13 p2076 N85-22965
Accuracy of approximation of Bayes estimates in presence of noninformative parameters
13 p2084 N85-23015
Reception of signal with unknown amplitude and duration submerged in white noise 13 p2084 N85-23016
Synthesis of quasi-optimum algorithms for signal recognition against background of correlated noise employing discrete spectral transformations
13 p2085 N85-23020
Noise tolerance of diversity reception in frequency-adaptive digital transmission systems
13 p2086 N85-23024
Algorithms for reconstruction of partially known, band limited Fourier transform pairs from noisy data
[AD-A150194] 13 p2150 N85-23347
An examination of signal-to-noise enhancement at the Edsall CDAA (Circular Disposed Antenna Array)
[AD-A150706] 14 p2291 N85-24204
Frequency selective signals-to-noise enhancer/limiter apparatus
[AD-D011583] 15 p2548 N85-25724
Performance of charge-injection-device infrared detector arrays at low and moderate backgrounds
[NASA-TM-86667] 15 p2560 N85-25793
On the probability density of signal-to-noise ratio in an improved detector
[AD-A152529] 17 p2952 N85-28232
Experimental performance of a frequency measurement circuit
[AD-A152951] 17 p2953 N85-28239
Improved high performance television receiver
[PB85-170751] 18 p3092 N85-29139
Modulation using four phase levels. Theoretical study of the degradation caused by a spurious phase modulation
[CNES-83/219/CT/DRT/TIT/TR]
20 p3441 N85-31380
Sidelobe reduction of Barker codes, part 7.1C
21 p3625 N85-32522
Qualitative analysis of sign-bit processing
[AD-A154776] 21 p3671 N85-32804
Sensitivity of compressive receivers
[FOA-C-30385-E4] 22 p3756 N85-33288
Adaptive corrector operating in frequency domain
22 p3765 N85-33337
Estimate of signal-to-interference energy ratio in discrete-data transmission 22 p3776 N85-33398
A new array for the study of ultra high energy gamma-ray sources
[OG-9.4-7] 23 p4029 N85-34974
Astrophysical applications of high angular resolution array-telescopes
[OG-9.5-7] 23 p4031 N85-34984
Search for acoustic signals from high energy cascades
[HE-7.1-1] 24 p4213 N85-36155
Acoustic detection of air shower cores
[HE-7.1-4] 24 p4213 N85-36158
SIGNAL TRANSMISSION
NT CODE DIVISION MULTIPLE ACCESS
NT DATA TRANSMISSION
NT FREQUENCY DIVISION MULTIPLE ACCESS
NT IONOSPHERIC PROPAGATION
NT MANDELSTAM REPRESENTATION
NT MICROWAVE ATTENUATION
NT MICROWAVE TRANSMISSION
NT MULTIPATH TRANSMISSION
NT MULTIPLE ACCESS
NT PCM TELEMETRY
NT RADAR TRANSMISSION
NT RADIO TELEMETRY
NT RADIO TRANSMISSION
NT SATELLITE TRANSMISSION
NT SHORT WAVE RADIO TRANSMISSION
NT SINGLE CHANNEL PER CARRIER TRANSMISSION
NT SINGLE SIDEBAND TRANSMISSION
NT TELEMETRY
NT TELEVISION TRANSMISSION
NT TRANSEQUATORIAL PROPAGATION
An optically isolated amplifier
[CSIR-SR-ELEK-257] 01 p0049 N85-10321
Development of a microcomputer coupled atmospheric and oceanic boundary layer prediction model
[AD-A146334] 03 p0397 N85-12530
Detailed performance calculations: Georgia Institute of Technology Group, appendix E
05 p0676 N85-14342
Hardwire missile receiver coupler
[AD-D011350] 07 p0937 N85-15936
Improved digital baseband transmission by application of maximum likelihood decoding to an 8-level signal generated by convolution and block coding
[FI-44-TBR-93] 07 p0942 N85-15973
NTT (Nippon Telegraph and Telephone Public Corporation) develops new optical fiber
10 p1476 N85-19311
Effect of interfacial characteristics of metal clad polymeric substrates on electrical high frequency interconnection performance
[NASA-TM-86948] 11 p1624 N85-20223
Signal propagation delay, wire length distribution and the efficiency of VLSI circuits
[CWI-CS-R8412] 11 p1630 N85-20266
Circuit topology, signal propagation delay and the efficiency of VLSI circuits
[CWI-CS-R8414] 11 p1630 N85-20267
The use of a high-speed 12-bit A/D converter for digital sampling of communication signal carriers
[AD-A150576] 13 p2056 N85-22872
Analysis and design of linear microwave transistor amplifiers 13 p2068 N85-23036
Frequency selection for dispersion signal in satellite communication lines 15 p2528 N85-25584
Signal flow model for sequential logic built from combinational logic elements and its implementation in Prolog
[DE85-005792] 15 p2549 N85-25734
Measurements of VHF/UHF radio propagation in a maritime temperate climate
[CRC-1380] 18 p3089 N85-29119
The determination of daily usage or occupancy in the land-mobile band 138-174 MHz at Montreal
[CRC-1383] 19 p3253 N85-30167
Combined trellis coding with asymmetric MPSK modulation: An MSAT-X report
[NASA-CR-176039] 20 p3440 N85-31347
Center for Electronics and Electrical Engineering technical progress bulletin covering center programs, April-June 1984 with 1984 CEEE (Center for Electronics and Electrical Engineering) events calendar, issue 7
[PB85-187540] 20 p3450 N85-31419
Testing and optimizing MST coaxial collinear arrays, part 6.4A 21 p3625 N85-32518
Criteria and algorithms for spectrum parameterization of MST radar signals 21 p3626 N85-32527
Transformation of spectrum of phase-code keyed signal for scanning in time 22 p3765 N85-33338
Digital matched filter 22 p3765 N85-33339
Optimum predistortion of digital signals for transmission over parallel channels 22 p3776 N85-33397
Photothyristor optrons and optron microcircuits, part 1
22 p3781 N85-33424
Characteristics of optical information-measurement channels with utilization of scattering effects
22 p3781 N85-33429
Signal space models for antenna arrays
[AD-A156063] 24 p4037 N85-35335
SIGNALS
Digital sound: Programme-modulated noise levels in sound signals subjected to a number of digital companding processes
[BBC-RD-1984/11] 09 p1310 N85-18233
Evaluation of parameters of a signal (selected pages)
[AD-A148831] 09 p1312 N85-18243
SIGNATURE ANALYSIS
Description of the Dutch-Danish (DUDA) scanner --- thermal signatures
[AD-B084893] 01 p0121 N85-10826
Basic principles, methodology, and applications of remote sensing in agriculture
[E85-10016] 02 p0217 N85-11429
The monitoring of machines
[CETIM-15-J-041] 04 p0510 N85-13253
Solar physics applications of computer graphics and image processing 18 p3208 N85-29903
Hardware test program for evaluation of basline range-range rate sensor concept
[NASA-CR-176143] 23 p3933 N85-34377
SIGNATURES
NT MAGNETIC SIGNATURES
NT RADAR SIGNATURES
NT SPECTRAL SIGNATURES
Joint services electronics program
[AD-A145085] 01 p0042 N85-10276
Digital signatures: An update
[NPL-DITC-51/84] 09 p1367 N85-18589
Real-time automated detection of mesocyclones and tornado vortex signatures
[AD-A154968] 21 p3635 N85-32578
SIGNS (SYMBOLS)
U SYMBOLS
SIGNS AND SYMPTOMS
The effects of prolonged feeding meal, ready-to-eat (MRE) operational rations
[AD-A154763] 21 p3666 N85-32773
Labyrinthine and extralabyrinthine mechanisms of development of motion sickness in weightlessness
22 p3821 N85-33666
A review of motion sickness with special reference to simulator sickness
[AD-A155975] 24 p4131 N85-35611
SIKORSKY AIRCRAFT
NT UH-60A HELICOPTER
SILANES
NT CHLOROSILANES
Chemical vapor deposition of amorphous silicon films produced by using higher order silanes
[DE84-004519] 01 p0123 N85-10847
The silane interphase of composites: Effects of process conditions on gamma-aminopropyltriethoxysilane
[AD-A145578] 02 p0171 N85-11143
Laser spectroscopy and gas-phase chemistry in CVD
[DE84-014959] 02 p0173 N85-11158
Factor analysis applied to a silane coupling agent on E-glass fiber system
[AD-A145687] 02 p0187 N85-11249
Structure of silane coupling agents adsorbed on silicon powder
[AD-A145803] 03 p0327 N85-12105
Development of acceptance criteria for batches of silane primer for external tank thermal protection system bonding applications
[NASA-CR-171266] 04 p0478 N85-13043
Development of a polysilicon process based on chemical vapor deposition of dichlorosilane in an advanced Siemen's reactor
[NASA-CR-174148] 04 p0483 N85-13083
Electrical properties of 10-50 nm TEOS (Tetraethoxysilane) LPCVD (Low Pressure Chemical Vapor Deposition) films
[AD-A146416] 06 p0803 N85-15111
Electrochemical production of silicon
06 p0832 N85-15290
Theoretical studies of the ignition and combustion of silane-hydrogen-air mixtures
[NASA-CR-3876] 10 p1433 N85-19032
Development of a polysilicon process based on chemical vapor deposition of dichlorosilane in an advanced Siemen's reactor
[NASA-CR-174445] 11 p1672 N85-20532
Process for producing tris s(n-methylamino) methylsilane
[NASA-CASE-MFS-25721-1] 12 p1799 N85-21280
Ignition of mixtures of SiH sub 4, CH sub 4, O sub 2, and Ar or N sub 2 behind reflected shock waves
[NASA-TP-2415] 13 p1974 N85-22395
Development of acceptance criteria for batches of silane primer for external tank thermal protection system bonding applications
[NASA-CR-171428] 14 p2250 N85-23998
Development of acceptance criteria for batches of silane primer for external tank thermal protection system bonding applications
[NASA-CR-171436] 15 p2518 N85-25523
Development of acceptance criteria for batches of silane primer for external tank thermal protection system bonding applications
[NASA-CR-175850] 16 p2754 N85-26095
Self-developing polysilane deep-UV resists: Photochemistry, photophysics and submicron lithography
[DE85-007606] 19 p3237 N85-30067
A fluidized-bed reactor for silane pyrolysis
21 p3609 N85-32413
Modeling of the silane FBR system
21 p3609 N85-32415
Silicon production in an aerosol reactor
21 p3609 N85-32416
Monosilane and disilane, 1984 report
[DE85-006776] 22 p3752 N85-33262
1985 Amorphous Silicon Review Meeting
[DE85-006794] 22 p3807 N85-33582
Dual-chamber plasma deposition of A-Si:H solar cells at high rates using disilane
[DE85-011828] 23 p3946 N85-34451
SILENCERS
Exhaust systems for passenger vehicles: Test procedure for resistance to internal corrosion of silencers
[BLL-BISI-TRANS-22360-(9022.06)]
17 p2973 N85-28361
SILICA
U SILICON DIOXIDE
SILICA GEL
Structure and chemistry of sol-gel derived transparent silica aerogel
[DE85-009802] 20 p3434 N85-31303

The Silica Aerogel Detector (SAD) story — Cherenkov detector
[USIP-84-14] 20 p3459 N85-31485

SILICA GLASS
Optical contacting for gravity probe star tracker
[NASA-TM-86475] 01 p0120 N85-10819
Emissivity enhancement of fused silica for space applications — solar cells 13 p2011 N85-22615
Downdraw extrusion of ULE(TM) glass
[AD-A153783] 18 p3079 N85-29048

SILICATES
NT ALUMINUM SILICATES
NT BERYL
NT ENSTATITE
NT FELDSPARS
NT GARNETS
NT PYROXENES
NT SODIUM SILICATES
NT YTTRIUM-ALUMINUM GARNET
NT YTTRIUM-IRON GARNET
NT ZEOLITES
Impact cratering: The process and its effects on planetary evolution — and silicate-carbonate reactions on Venus
[NASA-CR-174016] 02 p0228 N85-11486
The effect of temperature on the radiation induced losses of large diameter GPS (Germanium phosphosilicate) and GBS core optical fibers
[AD-A145409] 02 p0280 N85-11823
The problem of iron partition between Earth and Moon during simultaneous formation as a double planet system 04 p0587 N85-13744
Dynamic crystallization of silicate melts
[NASA-CR-174103] 05 p0743 N85-14774
Calculation of energy of atomization in silicate tetrahedron SiA(4-)
[BLL-M-36000-(5828.4)] 07 p1040 N85-16599
A circum-terrestrial compositional filter
13 p2179 N85-23520
Quenching effects on iron site partitioning in the Apollo 17 orange glass composition 13 p2184 N85-23553
Experimental methods for quenching structures in lunar-analog silicate melts: Variations as a function of quench media and composition
13 p2184 N85-23554
Mechanical properties of lunar materials under anhydrous, hard vacuum conditions: Applications of lunar glass structural components
[DE85-006682] 16 p2801 N85-27271
Influence of eutectic silicate inclusions on micro-processes during deformation and fracture of 12GS steel
[BLL-BISI-TRANS-22296-(9022.06)]
17 p2929 N85-28073
Model for the growth of fractal silica polymers
[DE85-007684] 17 p2935 N85-28115
Chemical constraints on the evolution of Archean continental crust 21 p3722 N85-33093
Dating Archean zircon by ion microprobe: New light on an old problem 21 p3722 N85-33094
Thermodynamic data for mineral technology
[PB85-184331] 22 p3803 N85-33560
Volatile loss following very large impacts
22 p3853 N85-33862

SILICIDES
NT DISILICIDES
Electronic transport processes in refractory metal silicides
[AD-A148495] 06 p0861 N85-15468
Preparation and electronic properties of MoS(2) and WS(2) single crystals grown in the presence of cobalt
[AD-A146506] 06 p0866 N85-15506
Improving operational properties of titanium alloys by diffusion siliciding 11 p1602 N85-20075
Thin films properties of sputtered niobium silicide on SiO2, Si3N4 and on n+ poly-Si
[AD-A152376] 17 p2952 N85-28228
Silicide conductors reliability research
[AD-A153766] 18 p3095 N85-29157
Contact properties of rare-earth silicides and germanides on Si and Ge 19 p3374 N85-30931
Flux-line lattice anisotropy in V3Si: Observation and interpretation
[DE85-011935] 23 p3985 N85-34713

SILICON
NT SILICON ISOTOPES
Center for Electronics and Electrical Engineering Technical Bulletin covering center programs
[PB84-218056] 01 p0045 N85-10296
Process Research of Polycrystalline Silicon Material (PROPSM)
[NASA-CR-173838] 01 p0067 N85-10446
Energy deposition in microvolumes of silicon from high energy proton reactions
[AD-A144713] 01 p0123 N85-10845
Studies of laser melting and rapid solidification using amorphous silicon
[DE84-014737] 02 p0202 N85-11345
Silicon sheet with molecular beam epitaxy for high efficiency solar cells
[NASA-CR-174022] 02 p0222 N85-11459
Hydrogen passivation of electrically active defects in crystalline silicon solar cells
[DE84-004590] 02 p0223 N85-11461
Large-area sheet task advanced dendritic web growth development
[NASA-CR-174021] 02 p0223 N85-11463
Research on crystalline silicon solar cells
[DE84-114591] 02 p0223 N85-11465
Optimized conditions for the formation of buried insulating layers in Si by high dose implantation of oxygen
[DE84-015369] 02 p0288 N85-11882
Structure of silane coupling agents adsorbed on silicon powder
[AD-A145803] 03 p0327 N85-12105
NBS (National Bureau of Standards): Materials measurements
[NASA-CR-174036] 03 p0332 N85-12143
Application of a silicon compiler to VLSI (Very Large Scale Integrated circuits) design of digital pipelined multipliers
[AD-A146326] 03 p0403 N85-12569
A study of defects in neutron transmutation doped silicon: Gallium by hall effect analysis
[AD-A146047] 03 p0433 N85-12758
Thermodynamics and phase equilibria in the vanadium-silicon system
[AD-A145870] 03 p0435 N85-12769
Preparation of low-silicon vanadium metal
[DE84-014818] 04 p0476 N85-13031
Effect of barrier height on friction behavior of the semiconductors silicon and gallium arsenide in contact with pure metals
[NASA-TP-2405] 04 p0478 N85-13044
Photoconductivity and emission from the impurity excited states in silicon
[DE84-015563] 04 p0479 N85-13052
Investigation of effect of photocurrent amplification in meta-dielectric-semiconductor structures based on silicon 04 p0486 N85-13110
NMOS test chip for a course in semiconductor parameter measurements
[PB84-216506] 04 p0497 N85-13174
Silicon for solar cells
[DE84-004503] 04 p0529 N85-13361
CO-2-silica geothermometer for low temperature geothermal resource assessment, with application to resources in the Safford Basin, Arizona
[DE84-013958] 04 p0534 N85-13411
On the origins of structural defects in BF2(+)-implanted and rapid thermally annealed silicon: Conditions for defect free regrowth
[DE84-016080] 04 p0572 N85-13650
Trends in space photovoltaic technology
05 p0609 N85-13868
Testing of production of silicon-titanium-magnesium alloying composition
[BLL-M-35904-(5828.4)] 05 p0616 N85-13937
Process research of polycrystalline silicon material (PROPSM)
[NASA-CR-174130] 05 p0619 N85-13962
Solar generators made of amorphous silicon
05 p0662 N85-14257
Material models and device structures for GaAs solar cells
[DE85-000501] 05 p0665 N85-14275
GaAs material properties and models
05 p0665 N85-14277
Electron channeling and EBIC studies of polycrystalline silicon sheets
[DE84-004516] 05 p0670 N85-14309
EPR linewidth studies of unpaired electrons at the Si-SiO2
[DE84-016727] 05 p0733 N85-14712
New methods of fast switching of high power by means of semiconductor devices 05 p0794 N85-15075
Development of technology of silicon single-crystal production semiconductor power devices: State of art outlook 05 p0795 N85-15076
Time-resolved studies of ultrarapid solidification of highly undercooled molten silicon formed by pulsed laser irradiation
[DE84-016664] 06 p0813 N85-15164
Development of high-efficiency solar cells on silicon web
[NASA-CR-174212] 06 p0826 N85-15259
Process research of non-Cz silicon material
06 p0830 N85-15275
Process Research On Polycrystalline Silicon Material (PROPSM) 06 p0830 N85-15276
Amorphous metallic layers in Si metallization systems
06 p0830 N85-15277
Silicon-sheet surface studies
06 p0831 N85-15287
Investigation of structural and electrical properties of low-angle silicon sheet 06 p0831 N85-15288
Semicrystalline casting process development and verification 06 p0832 N85-15289
Electrochemical production of silicon
06 p0832 N85-15290
Aerosol reactor for silicon processing
06 p0832 N85-15292
Proceedings of the 22nd Project Integration Meeting
[DE85-000334] 06 p0833 N85-15302
Advances and opportunities in the amorphous silicon research field
[DE84-004526] 06 p0833 N85-15304
Recent developments in photovoltaics
[DE84-004528] 06 p0833 N85-15305
Specialized silicon compilers for language recognition
[AD-A146526] 06 p0853 N85-15425
Charge trapping in low temperature MOS (Metal-Oxide-Silicon) oxides
[AD-A146450] 06 p0860 N85-15487
Evidence for pairing of implanted nitrogen in silicon
[DE84-015622] 06 p0868 N85-15517
Microbiological method for the desiliconization of high-silica bauxites
[BLL-MINTEK-TR-1166-(5810.5759)]
07 p0925 N85-15884
Silicon superlattices. 2: Si-Ge heterostructures and MOS systems
[NASA-CR-174287] 08 p1224 N85-17711
Advanced NMR characterization of zeolite catalysts
[DE85-000456] 09 p1291 N85-18104
Calculations of high-current characteristics of silicon diodes at microwave frequencies
[AD-A147406] 09 p1314 N85-18281
Theory of silicon superlattices: Band structure and mobility enhancement 09 p1396 N85-18789
Influence of the amorphous-crystalline interface morphology on dislocation nucleation in pre-amorphized silicon
[DE85-002068] 09 p1396 N85-18800
Ion beam processes in Si
[DE85-001254] 09 p1399 N85-1080
Single crystal silicon as a low-temperature structural material
[DE84-017469] 09 p1400 N85-18810
The Si/SiO2 intrinsic states and interface charges Chapter 1: Origin, properties, models, impact
[HMI-B-413] 09 p1400 N85-18812
Calculation of Si(Li) X-ray detector efficiencies
[DE85-002732] 10 p1489 N85-1940
Picosecond laser pulse interactions with metallic an semiconductor surfaces
[AD-A149112] 10 p1490 N85-194
Stress studies in EFG
[NASA-CR-174441] 10 p1508 N85-1951
Surface and allied studies in silicon solar cells
[NASA-CR-175466] 10 p1508 N85-1951
Investigation of welded interconnection of large ar wraparound contacted silicon solar cells
[NASA-CR-174436] 10 p1509 N85-1951
Stress-strain analysis of silicon ribbon
[NASA-CR-175459] 10 p1510 N85-195
US Amorphous Silicon Research Project
[DE85-000536] 10 p1511 N85-195
Metal-nonmetal transitions in N-doped many-valley and Ge
[INPE-3358-PRE/636] 10 p1582 N85-19
Microstrain analysis in bent single crystal silicon double crystal X-ray topography technique
[DE85-000422] 10 p1584 N85-19
Development of AK18 alloy production technol based on electrothermic silumin
11 p1598 N85-20
Effect of silicon and titanium properties on N85Co steel 11 p1601 N85-20
Optical second harmonic generation for sur studies
[DE85-000670] 11 p1640 N85-2
Development of a polysilicon process based on che vapor deposition of dichlorosilane in an adva Siemen's reactor
[NASA-CR-174445] 11 p1672 N85-2
Research on the basic understanding of high effic in silicon solar cells
[DE85-000507] 11 p1672 N85-
Electronic structure of silicon superlattices
[NASA-CR-175536] 11 p1736 N85-
An episodic red-wing structure of SiIV, lambda in gamma Cas 11 p1750 N85
Carbon, silicon, and oxygen in the white dwarf 40 11 p1752 N85

The abundances of the elements -carbon to silicon- in Nova Corona Austrina 1981 11 p1753 N85-21024

Preparation of crystal growth experiments in Spacelab: Si (FSLP), CdTe (D1), ZnS (D1)
[BMFT-FB-W-84-045] 12 p1788 N85-21227

Slip casting and nitridation of silicon powder
[NASA-TM-77809] 12 p1818 N85-21406

Improved silicon grinding method and apparatus
[NASA-CASE-NPO-16336-1-CU] 12 p1819 N85-21407

Factors affecting SOS (Silicon-On-Sapphire) yield and reliability
[AD-A150004] 12 p1835 N85-21515

Crystallization methods for solar cell silicon 12 p1877 N85-21774

Materials refining for solar cell silicon 12 p1877 N85-21775

Flat-plate silicon for solar cells 12 p1877 N85-21776

Silicon band spraying technique for solar cells 12 p1877 N85-21778

Development of silicon nitride materials for the casting of solar cell silicon 12 p1878 N85-21779

Development of new process technologies for solar cells with high efficiency starting from purified silicon 12 p1878 N85-21785

Investigation of the optical properties of solar elements 12 p1879 N85-21786

Pin solar cells made of amorphous silicon 12 p1879 N85-21787

Development of an amorphous silicon panel 12 p1879 N85-21788

Amorphous silicon solar cells with a view to cheap production processes 12 p1879 N85-21789

Plasmachemical evaporation and doping of amorphous silicon 12 p1879 N85-21790

Gallium arsenide arrays versus silicon arrays for space application 13 p2006 N85-22574

Availability of AlGaAs/GaAs solar cells in space 13 p2006 N85-22576

Technological process effect on the carrier lifetime degradation of silicon solar cell base layer irradiated by 1 MeV electrons (boron doping case) 13 p2007 N85-22585

The effects of lithium counterdoping on radiation damage and annealing in n(+)p silicon solar cells 13 p2007 N85-22586

Study of processes of modification of Al-Si alloys 13 p2026 N85-22695

Segregation of silicon in silumin-carbon fiber composites 13 p2028 N85-22706

Time-resolved studies of rapid solidification in highly undercooled molten silicon
[DE85-004857] 13 p2038 N85-22765

Drift fields and boundary conditions at grain boundaries in bipolar P/N junction silicon devices 13 p2062 N85-22879

SEM (Scanning Electron Microscope) investigation of silicon diodes using the electron beam induced current method
[AD-A150366] 13 p2064 N85-22894

High sheet resistance, arsenic implanted polycrystalline silicon for integrated circuit resistors
[DE85-004366] 13 p2065 N85-22902

Noise characteristics of sulfur-doped silicon diodes 13 p2073 N85-22952

Thermodynamic and kinetic studies of pulsed laser annealing from transient conductivity measurements
[DE85-003877] 13 p2096 N85-23078

Time-resolved ellipsometry and reflectivity measurements of the optical properties of silicon during pulsed excimer laser irradiation
[DE85-005081] 13 p2096 N85-23079

Time-resolved reflectivity measurement of extrinsic silicon during pulsed laser irradiation
[AD-A150350] 13 p2158 N85-23403

Transport properties of silica thermally grown on silicon
[AD-A150304] 13 p2163 N85-23418

Demonstration of feasibility of depositing semiconductor layers using microwave enhanced plasma techniques
[NASA-CR-174302] 13 p2163 N85-23421

Electronic transport in hydrogenated amorphous silicon films
[DE85-002901] 13 p2164 N85-23426

Influence of substrate heating and thermal annealing on the surface crystallinity in single Si crystals implanted with high doses of (16)O
[DE85-005284] 13 p2164 N85-23428

Charge transfer, polarization and relaxation effects in the Auger lineshapes of Si
[AD-A150938] 14 p2252 N85-23954

Dependence of parameters of silicon photovoltaic cells on temperature and light intensity 14 p2275 N85-24094

Characterization of terrestrial solar cells for space applications: Electrical characteristics of thin Westinghouse dendritic web cells as a function of solar intensity, temperature, and incidence angle
[NASA-CR-175642] 14 p2349 N85-24516

Silicon-sheet and thin-film cell and module technology potential: Issue study
[NASA-CR-175654] 14 p2349 N85-24520

Solid/melt interface studies of high-speed silicon sheet growth
[NASA-CR-175698] 14 p2350 N85-24525

Laser-assisted solar cell metallization processing
[NASA-CR-175668] 14 p2350 N85-24528

Excimer laser annealing to fabricate low cost solar cells
[NASA-CR-175702] 14 p2351 N85-24529

Stress and efficiency studies
[NASA-CR-175688] 14 p2351 N85-24531

High resolution Z-contrast imaging and lattice location analysis of dopants in ion-implanted silicon
[DE85-005261] 14 p2429 N85-24960

Dopant incorporation in silicon during nonequilibrium solidification: Comparison of 2 processes
[DE85-005568] 14 p2430 N85-24968

Ion beam mixing of marker layers in Al and Si
[DE85-006227] 15 p2511 N85-25490

Reduced-chromium stainless steel substitutes containing silicon and aluminum
[PB85-160786] 15 p2513 N85-25502

Heavy doping effects in high efficiency silicon solar cells
[NASA-CR-175687] 15 p2585 N85-25937

Investigation of silicon surface passivation by silicon nitride film deposition
[NASA-CR-175693] 15 p2585 N85-25938

Heavy doping effects in high efficiency silicon solar cells
[NASA-CR-175681] 15 p2586 N85-25940

Vapor sensing by means of a ZnO-on-Si surface acoustic wave resonator
[DE85-003250] 15 p2646 N85-26324

Raman studies of surface temperature in laser-heated semiconductors
[AD-A151377] 15 p2659 N85-26412

Chemical vapor deposition of amorphous semiconductor films
[DE85-002917] 15 p2661 N85-26421

Thin-film polycrystalline silicon research
[DE85-002908] 15 p2663 N85-26434

An advanced solid state pressure transducer for high reliability SSME application 16 p2739 N85-26905

Effect of nickel addition on the thermal, magnetic and magnetomechanical properties of Fe(80)B(15)Si(5)
[AD-A152261] 16 p2749 N85-26967

Flat-plate solar array project process development area: Process research of non-CZ silicon material
[NASA-CR-175777] 16 p2818 N85-27382

Heavy doping effects in high efficiency silicon solar cells
[NASA-CR-175779] 16 p2818 N85-27383

Electronic density of states for the double donor system Si:P, As
[INPE-3447-PRE/700] 16 p2869 N85-27700

Influence of manganese and heat treatment on structure and properties of Fe-0.1 percent-C-14 percent Cr-based steels
[BLL-BISI-TRANS-22299-(9022.06)] 17 p2926 N85-28071

Fracture mechanics analysis of cold drawn Si-Cr valve steel
[BLL-BISI-TRANS-22216-(9022.06)] 17 p2976 N85-28405

Comprehensive silicon solar cell computer modeling
[NASA-CR-175869] 17 p2987 N85-28461

Research and developmental study on MIS thin film solar cells of amorphous hydrogenated silicon, part 2
[BMFT-FB-T-84-290] 17 p2988 N85-28467

The effect of ion-bombardment-induced atomic mixing on depth-profiling of interfaces
[AD-A153199] 17 p3044 N85-28834

Quantitative analysis of defects in silicon-characterization of UCP, HAMCO, and microcrystalline matural
[NASA-CR-175968] 18 p3079 N85-29046

Semicrystalline casting process development and verification
[DE85-007695] 18 p3081 N85-29058

Silicide conductors reliability research
[AD-A153768] 18 p3095 N85-29157

Investigation of a Si and related semiconductors as materials for photovoltaic conversion
[DE85-002932] 18 p3096 N85-29163

Evaluation of VLSI technology — space applications
[CD.8501702] 18 p3098 N85-29177

Mechanically-stacked multijunction solar cells
[DE85-010389] 18 p3129 N85-29377

Electronic states in silicon and on its interfaces
[AD-A153664] 18 p3193 N85-29807

Oxygen-nitrogen interactions in ion-implanted silicon
[DE85-010091] 18 p3195 N85-29819

Research pressure instrumentation for NASA space shuttle main engine
[NASA-CR-176014] 19 p3227 N85-30006

Action of plasma and explosion products on silumins 19 p3242 N85-30100

Influence of type of processing of AK4 alloy on its surface state and strength of bonding of plasma coatings 19 p3242 N85-30103

Glow discharge deposition at high rates using disilane
[DE85-010236] 19 p3263 N85-30235

Increased voltage photovoltaic cell
[NASA-CASE-NPO-16155-1] 19 p3303 N85-30475

Current status of silicon materials research for photovoltaic applications
[DE85-006799] 19 p3304 N85-30482

Research on the basic understanding of high efficiency in silicon solar cells
[DE85-008774] 19 p3305 N85-30487

Ribbon growing method and apparatus
[NASA-CASE-NPO-16306-1-CU] 19 p3375 N85-30934

Chemistry and physics of silicon-based amorphous semiconductors
[DE85-001931] 19 p3377 N85-30949

Leading-edge microelectronics research at Sweden's Chalmers 20 p3438 N85-31337

An analysis of the feasibility of producing silicon for solar cells by a dichlorosilane/fluidized-bed reactor process
[NASA-CR-176036] 20 p3478 N85-31614

Historical perspective of barriers to achieving high-efficiency silicon solar cells 20 p3479 N85-31616

Aspects of silicon bulk lifetimes 20 p3479 N85-31617

Silicon solar cell efficiency improvement: Status and outlook 20 p3479 N85-31619

Some practical considerations for economical back contact formation on high efficiency solar cells 20 p3479 N85-31620

Silicon MINP solar cells 20 p3480 N85-31623

New adatom model for Si(11) 7X7 and Si(111)Ge 5X5 reconstructed surfaces 20 p3480 N85-31625

Compositional analysis of silicon 20 p3480 N85-31626

Surface passivation and junction formation using low energy hydrogen implants 20 p3480 N85-31628

Chemical structure of interfaces 20 p3480 N85-31629

Structural defects in crystalline silicon 20 p3481 N85-31630

Oxygen and carbon impurities and related defects in silicon 20 p3481 N85-31631

Current understanding of point defects and diffusion processes in silicon 20 p3481 N85-31632

Electrical and structural characterization of web dendrite crystals 20 p3481 N85-31633

EBIC characterization and hydrogen passivation in silicon sheet 20 p3481 N85-31634

Current status of one- and two-dimensional numerical models: Successes and limitations 20 p3482 N85-31636

Application of closed-form solutions to a mesh point field in silicon solar cells 20 p3482 N85-31637

Phenomena simulation for heavy doping and surface recombination velocity 20 p3482 N85-31638

High efficiency large area polysilicon solar cells 20 p3482 N85-31639

High efficiency solar cell processing 20 p3482 N85-31640

Process and design considerations for high-efficiency solar cells 20 p3482 N85-31641

Processing technology for high efficiency silicon solar cells 20 p3483 N85-31642

Recent improvements in materials for thin GaAs and multibandgap solar cells
[DE85-008600] 20 p3484 N85-31651

Gallium arsenide arrays versus silicon arrays for space application
[SNIAS-851-440-104] 20 p3485 N85-31657

Infrared absorption of oxygen complexes in electron-irradiated silicon
[FOA-C-30379-E1,E2,E3,E4] 20 p3538 N85-32015

High temperature electronics technology: Life test report
[AD-A154881] 21 p3580 N85-32257

Electrical properties of bulk grown nitrogen doped silicon
[AD-A155471] 21 p3581 N85-32266

Thermoelectric properties of beta-boron and some boron compounds
[DE85-011978] 21 p3582 N85-32270

High-frequency furnace
[DE85-011210] 21 p3566 N85-32291

Predicting photothermal field performance
21 p3608 N85-32404

Interfacial bonding stability 21 p3608 N85-32409

Silicon refinement by chemical vapor transport
21 p3609 N85-32412

JPL in-house fluidized-bed reactor research
21 p3609 N85-32414

Silicon production in an aerosol reactor
21 p3609 N85-32416

Physics of heavily doped silicon and solar-cell parameter measurement 21 p3609 N85-32418

Measuring bulk recombination rates and boundary recombination velocities 21 p3609 N85-32419

Studies of oxygen- and carbon-related defects in high-efficiency silicon solar cells
21 p3609 N85-32420

Comprehensive silicon solar-cell computer modeling
21 p3609 N85-32421

Sensitivity analysis of high-efficiency silicon solar-cell design parameters 21 p3610 N85-32422

Silicon surface passivation by silicon nitride deposition
21 p3610 N85-32423

Important loss mechanisms in high-efficiency solar cells 21 p3610 N85-32424

Development of high-efficiency solar cells on silicon web 21 p3610 N85-32425

Simultaneous junction formation
21 p3610 N85-32426

Amorphous metallic films in silicon metallization systems 21 p3610 N85-32427

Silicon dendritic web growth 21 p3611 N85-32435

Temperature-stress modeling
21 p3611 N85-32436

Silicon ribbon stress-strain activities
21 p3611 N85-32437

Analysis of stress-strain relationships in silicon ribbon
21 p3611 N85-32438

Stress and buckling analysis 21 p3611 N85-32439

Stress and efficiency studies in EFG
21 p3611 N85-32440

Silicon sheet surface studies
21 p3611 N85-32441

Analysis of inclined growth of silicon sheet
21 p3612 N85-32442

Edge-defined film-fed growth of thin silicon sheets
21 p3612 N85-32443

High-purity silicon crystal growth
21 p3612 N85-32444

Thin-film reliability and engineering overview
21 p3612 N85-32450

Defect formation in amorphous hydrated silicon subjected to laser radiation 21 p3682 N85-32873

Influence of background electrically neutral argon admixture on mechanical strength of silicon crystals
21 p3683 N85-32878

Microscopic control of semiconductor surface oxidation
[AD-A154799] 21 p3709 N85-33026

A theory of exciton photoluminescence for two types of neutral acceptors in silicon. A study of the systems Si:(B, IN), Si:(Al), (Si), Si:(Ga, In), Si:(B, Al), Si:(B, Ga), and Si:(Al, GA)
[AD-A155452] 21 p3710 N85-33031

Cryogenic laser calorimetry for impurity analysis
[NASA-CR-176102] 22 p3743 N85-33201

Solid-melt interface studies of high-speed silicon sheet growth
[NASA-CR-176112] 22 p3751 N85-33249

Stress and efficiency studies in EFG
[NASA-CR-176125] 22 p3751 N85-33251

In-situ observations of the development of heavy-ion damage in semiconductors
[DE85-010269] 22 p3761 N85-33307

Method and apparatus for casting conductive and semi-conductive materials
[DE85-011666] 22 p3792 N85-33494

Development of high-efficiency solar cells on silicon web
[NASA-CR-176101] 22 p3805 N85-33568

Ultrasonic seam welding on thin silicon solar cells
[NASA-CR-176116] 22 p3805 N85-33570

Use of low energy hydrogen ion implants in high efficiency crystalline silicon solar cells
[NASA-CR-176109] 22 p3806 N85-33571

Investigation of the microstructure and photovoltaic properties of semicrystalline silicon
22 p3806 N85-33573

1985 Amorphous Silicon Review Meeting
[DE85-008794] 22 p3807 N85-33582

Low-cost high-performance silicon concentrator cells
[DE85-008875] 22 p3807 N85-33584

Striation free doped silicon
[AD-A155730] 22 p3847 N85-33827

Apparatus and method for the horizontal, crucible-free growth of silicon sheet crystals
[DE85-011588] 22 p3847 N85-33829

A new analysis of cosmic ray isotopes at 3 GeV/n from HEA03-C2 data
[OG-4.3-6] 22 p3879 N85-34031

Enthalpies of formation of liquid Fe-Ce-Si and Fe-Ce-Al three-component alloys
[BLL-M-36296-(5828.4)] 23 p3913 N85-34247

Dual-chamber plasma deposition of A-Si:H solar cells at high rates using disilane
[DE85-011828] 23 p3946 N85-34451

Formation of amorphous silicon by light ion damage
[DE85-012605] 23 p3972 N85-34623

Silicon to iron abundances in solar cosmic rays and in the sun
[SH-2.1-6] 23 p3998 N85-34787

The mean ionic charge of silicon in 3HE-rich solar flares
[SH-2.2-8] 23 p4000 N85-34803

A silicon surface barrier telescope for solar particles identification
[SH-9.1-3] 23 p4050 N85-35118

Oxidation resistant slurry coating for carbon-based materials
[NASA-CASE-LEW-13923-1] 24 p4077 N85-35267

Dangling bonds and sub-gap optical absorption in silicon
[DE85-011752] 24 p4082 N85-35302

Advanced detectors and signal processing
[NASA-CR-176193] 24 p4086 N85-35343

Photoconductive pulse power switches: A review
[DE85-014125] 24 p4091 N85-35360

Cryogenic laser calorimetry for impurity analysis
[NASA-CR-176179] 24 p4097 N85-35395

Electronic structure and lattice dynamics of dimensionally constrained and disordered solids
[AD-A155927] 24 p4161 N85-35797

SILICON ALLOYS

Alloying specially low carbon silicon-bearing steel with nitrogen
[BLL-M-35707-(5828.4)] 02 p0175 N85-11170

Optical properties of composite materials
[AD-A146768] 07 p0920 N85-15828

Fluctuation phenomena studies in chemically sensitive field effect transistor. Part 1: Corrosion of aluminum
[AD-A148240] 08 p1129 N85-17118

Radiation-induced compositional redistribution and local phase transformation in irradiated alloys
[DE85-000060] 10 p1441 N85-19082

Structure-phase state and properties of high-durability VAL8 alloy 11 p1597 N85-20046

Enhanced diffusion from interstitial trapping during solid-phase-epitaxial growth of silicon alloys
[DE85-001285] 12 p1941 N85-22193

The structural and electronic properties of amorphous silicon based alloy materials
[DE85-002909] 15 p2660 N85-26419

Compensation of dangling bonds in A-Si, Ge:H alloys
[DE85-002905] 15 p2662 N85-26433

LPCVD tungsten deposition on Si-Ge alloy
[DE85-005588] 16 p2750 N85-26970

Experimental and theoretical study of fatigue crack initiation in metals 19 p3283 N85-30357

Development of improved thermoelectric materials for space nuclear power systems
[DE85-013079] 22 p3844 N85-33807

Studies of the crystallization process of aluminum-silicon alloys using a high temperature microscope
[NASA-TM-77869] 24 p4078 N85-35272

SILICON CARBIDES

Treating silicon carbide sinter by heating in nitrogen
[NASA-TM-77601] 01 p0021 N85-10130

Silicon nitride sintered body
[NASA-TM-77602] 01 p0021 N85-10131

Preparation of silicon carbide fibers
[DE84-014661] 01 p0022 N85-10137

Powder containing 2H-type silicon carbide produced by reacting silicon dioxide and carbon powder in nitrogen atmosphere in the presence of aluminum
[NASA-TM-77597] 01 p0027 N85-10167

Critical conditions for the growth of SiC, Si3N4, and SiO2
[DE84-014824] 01 p0030 N85-10185

Silicon carbide ceramic production
[NASA-TM-77598] 01 p0035 N85-10220

Injection molding of silicon carbide capable of being sintered without pressure
[NASA-TM-77736] 01 p0035 N85-10221

Sintering behavior of ultrafine silicon carbide powders obtained by vapor phase reaction
[NASA-TM-77422] 03 p0336 N85-12161

Bending strength studies on hot-pressed silicon carbide
[NASA-TM-77512] 03 p0371 N85-12369

Development and fabrication of refractory bodies for gas turbine engines
[BMFT-FB-T-84-180] 04 p0457 N85-129

Preparation of sinter-active silicon carbide powders
[BMFT-FB-T-84-189] 04 p0469 N85-129

Electrokinetic potential and stability of SiC suspensions in electrolyte solutions
[NASA-TM-77492] 04 p0469 N85-1298

Reactive sintering of SiC 04 p0473 N85-13010

High temperature corrosion of ceramics
[DE84-017084] 05 p0620 N85-1398

Creep of chemically vapor deposited SiC fibers
[NASA-TM-86897] 06 p0763 N85-1487

Fatigue behavior of continuous fiber silicon-carbide-aluminum composites
[NASA-TM-86332] 06 p0763 N85-14879

Fundamental tribological properties of ceramics
[NASA-TM-86915] 07 p0930 N85-158

Oxidation resistance of silicon ceramics
[NASA-TM-77429] 07 p0931 N85-158

Development and production of improved silicon carbide powder for pressureless sintering and hot pressing
[BMFT-FB-T-84-211] 07 p0934 N85-15917

Gas cooled fuel cell systems technology development
[NASA-CR-174732] 07 p0991 N85-16291

Method of preparing single crystalline cubic silicon carbide layers
[AD-D011305] 07 p1048 N85-168

Fabrication of SiC whiskers and composites
[DE85-002036] 09 p1269 N85-18091

Fabrication of ceramic-ceramic composites by chemical vapor deposition
[DE85-000961] 09 p1298 N85-18155

Reactivity of ion implanted silicon carbide
[DE85-001543] 09 p1309 N85-188

Amorphization of ceramics by ion beams
[DE85-000936] 10 p1453 N85-191

Fundamental studies of growth, doping and transformation in beta silicon carbide
[AD-A149339] 10 p1582 N85-19851

Tensile testing of SiC whiskers
[DE85-003712] 11 p1593 N85-20025

High temperature corrosion of ceramics
[DE85-002179] 11 p1612 N85-20139

West Europe report: Science and technology
[JPRS-WST-85-006] 11 p1618 N85-20183

SEP of France manufactures its first silicon carbide fibers 11 p1618 N85-20184

NDE for heat engine ceramics
[NASA-TM-86949] 11 p1649 N85-203

Slit-ring test for evaluating fracture in tubular cross sections
[DE85-003550] 11 p1654 N85-20416

Parametric evaluation of ball milling of SiC in water
[NASA-TM-86974] 12 p1811 N85-213

Radiographic detectability limits for seeded voids in sintered silicon carbide and silicon nitride
[NASA-TM-86945] 12 p1861 N85-21674

Silicon carbide-silicon nitride fibers: Preparation and characterization of polycarbosilazane precursors
12 p1945 N85-22214

Particulate toughened silicon carbide
[DE85-004797] 13 p2016 N85-229

The effect of notch acuity on the fracture toughness of silicon carbide/aluminum metal matrix composites
[AD-A150970] 14 p2248 N85-239

Localized corrosion currents from graphite/aluminum and welded SiC/Al metal matrix composites
[AD-A150988] 14 p2256 N85-239

Sintered silicon carbide molded body and method for its production
[NASA-TM-77646] 14 p2259 N85-239

Environmental effects on the tensile strength of chemically vapor deposited silicon carbide fibers
[NASA-TM-86961] 14 p2259 N85-24000

A novel polymeric organosilazane precursor to Si3N4/SiC ceramics
[AD-A150748] 14 p2260 N85-24003

Thermodynamic calculations and the chemical vapour deposition of hard materials 14 p2431 N85-24091

Effect of fatigue and thermal loads on silicon carbide fiber reinforced glass matrix composites
[DE85-006069] 15 p2503 N85-25441

Fabrication of fiber reinforced ceramic composites by chemical vapor infiltration
[DE85-007565] 15 p2520 N85-2553

Fundamental studies of growth, doping and transformation in beta silicon carbide
[AD-A152047] 15 p2660 N85-2641

Particulate and whisker toughened alumi composites
[DE85-005239] 16 p2743 N85-269

Reaction-bonded and fiber-reinforced SiC static an dynamic gas turbine components
[BMFT-FB-T-84-302] 17 p2899 N85-278

Completely consumed carbide: A new process for dielectric isolation
[AD-A152379] 17 p2918 N85-27987
Titanium metal-matrix composites
[AD-D011643] 17 p2930 N85-28086
Preparation of silicon carbide-silicon nitride fibers by the pyrolysis of polycarbosilazane precursors
[NASA-TM-86505] 17 p2933 N85-28107
Development of high temperature resistant noncorrodible silicon carbide components for gas turbine applications, follow-up report
[BMFT-FB-T-85-016] 17 p2936 N85-28125
Limiting processes laser CVD
[DE85-008646] 18 p3114 N85-29279
Burner rig corrosion of SiC at 1000 deg C
[NASA-TM-87061] 19 p3227 N85-30011
Mechanism of strength degradation for hot corrosion of alpha-SiC
[NASA-TM-87052] 19 p3248 N85-30135
Development of the Cascade inertial-confinement-fusion reactor
[DE85-010993] 19 p3357 N85-30812
Reliability of void detection in structural ceramics using scanning laser acoustic microscopy
[NASA-TM-87035] 21 p3597 N85-32337
Dispersion toughened ceramic composites and method for making same
[DE85-011601] 22 p3751 N85-33252
Woven heat exchanger
[DE85-011633] 22 p3783 N85-33439
Rotating bending fatigue strength of silicon carbide and alumina-fiber reinforced aluminum
23 p3907 N85-34208
Mechanical properties of SiC fiber-reinforced reaction-bonded Si3N4 composites
[NASA-TM-87085] 23 p3909 N85-34223
Method for removing oxide contamination from silicon carbide powders
[DE85-011648] 23 p3919 N85-34267
Oxidation resistant slurry coating for carbon-based materials
[NASA-CASE-LEW-13923-1] 24 p4077 N85-35267

SILICON COMPOUNDS
NT ALUMINUM SILICATES
NT BERYL
NT CHLOROSILANES
NT DISILICIDES
NT ENSTATITE
NT FELDSPARS
NT GARNETS
NT ORGANIC SILICON COMPOUNDS
NT PYROXENES
NT QUARTZ
NT SILANES
NT SILICATES
NT SILICIDES
NT SILICON CARBIDES
NT SILICON DIOXIDE
NT SILICON NITRIDES
NT SILICON OXIDES
NT SODIUM SILICATES
NT YTTRIUM-ALUMINUM GARNET
NT YTTRIUM-IRON GARNET
NT ZEOLITES
Two silicon phthalocyanines and a silicon naphthalocyanine: Synthesis, electrochemistry and electrogenerated chemiluminescence
[AD-A144760] 01 p0023 N85-10145
A silicon phthalocyanine and a silicon naphthalocyanine: Synthesis, electrochemistry, and electrogenerated chemiluminescence
[AD-A146441] 06 p0765 N85-14895
Electronic and redox properties of stacked-ring silicon phthalocyanines from molecular orbital theory
[AD-A147161] 07 p0922 N85-15844
Effects of primary recoil energy on the production rate of mobile defects during elevated temperature irradiation
[DE85-006218] 15 p2511 N85-25489
Chemical structure of interfaces
20 p3480 N85-31629
A fluidized-bed reactor for silane pyrolysis
21 p3609 N85-32413
Advanced module development overview
21 p3612 N85-32445
An enhanced photoresponse at dislocation subgrain boundaries revealed by X-ray topography of polysilicon solar cells 22 p3806 N85-33572
Calculation of mixed depth for some metal-Si systems
[DE85-011907] 23 p3971 N85-34616
Center for Electronics and Electrical Engineering technical progress bulletin covering center programs, July-September with 1985 CEEE events calendar
[PB85-191393] 24 p4091 N85-35363
Circumstellar shells of late-type stars: A study at millimeter and infrared wavelengths
24 p4167 N85-35836

SILICON CONTROLLED RECTIFIERS
Isolated load switching with surge suppression
[AD-D011218] 01 p0042 N85-10274
Random access memory technologies
[AD-A153089] 17 p3008 N85-28597

SILICON DIOXIDE
NT QUARTZ
The rheology of icy satellites
[NASA-CR-174024] 02 p0302 N85-11959
The development of CVD oxide coatings for the protection of metal surfaces --- chemical vapor deposition (CVD) 03 p0332 N85-12142
Transient attenuation in optical fibers
[DE84-016487] 05 p0729 N85-14887
Oxide charge characteristics of low temperature MOS (Metal-Oxide-Silicon) oxide films
[AD-A146447] 06 p0803 N85-15113
Metal atom diffusion in amorphous silica and at the silica surface
[DE84-017351] 09 p1380 N85-18674
The Si/SiO2 intrinsic states and interface charges. Chapter 1: Origin, properties, models, impact
[HMI-B-413] 09 p1400 N85-18812
Fiber reinforced fused silica for hypersonic radome applications
[AD-P004366] 12 p1826 N85-21460
Transport properties of silica thermally grown on silicon
[AD-A150304] 13 p2163 N85-23418
A silicic shield volcano in Bolivia
13 p2187 N85-23572
Dendritic growth from amorphous matrix
[DE85-007630] 16 p2871 N85-27712
Influence of eutectic silicate inclusions on micro-processes during deformation and fracture of 12GS steel
[BLL-BISI-TRANS-22296-(9022.06)]
17 p2929 N85-28073
Analysis of time dependent dielectric failures
[AD-A153200] 17 p2954 N85-28243
Silica problem in the design of geothermal power plants
[DE85-008245] 17 p2986 N85-28453
Mechanical protection of DLC films on fused silica slides
[NASA-TM-87056] 19 p3248 N85-30138
Nitridation of SiO2 for surface passivation
20 p3480 N85-31627
Process for improving the quality of epitaxial silicon films grown on insulating substrates
[AD-D011730] 22 p3847 N85-33828
Uranium, thorium isotopic analyses and uranium-series ages of calcite and opal and stable isotopic compositions of calcite from drill cores UE25a no. 1, USR G-2 and USW G-3/GU-3, Yucca Mountain, Nevada
[DE85-013039] 23 p3948 N85-34471
Characterization of catalysts with metal-support effects and of the species adsorbed on their surfaces
[DE85-012254] 24 p4096 N85-35394

SILICON FILMS
Studies of hydrogenated amorphous silicon
[DE84-013038] 01 p0067 N85-10443
Chemical vapor deposition of amorphous silicon films produced by using higher order silanes
[DE84-004519] 01 p0123 N85-10847
Effect of heat treatment on phase composition and crystal structure of thin WSi2 films on silicon substrates
03 p0350 N85-12253
Material models and device structures for GaAs solar cells, introduction 05 p0665 N85-14276
Evaluation of the ion implantation process for production of solar cells from silicon sheet materials
06 p0831 N85-15281
Ion cluster beam deposition research
06 p0831 N85-15283
Miniworkshop on effects of stress and strain in high-speed-growth silicon ribbons
06 p0831 N85-15284
Stress studies in EFG 06 p0831 N85-15285
Research on submicrometer structures
[AD-A146578] 06 p0867 N85-15508
Density of states and recombination in amorphous silicon (a-Si:H)
[BMFT-FB-T-84-216] 08 p1135 N85-17151
French research on gallium arsenide devices
08 p1141 N85-17196
Silicon film solar cell process
[NASA-CR-174446] 10 p1508 N85-19514
Infrared modulation of photoluminescence in glow discharge amorphous silicon
[DE85-016993] 11 p1737 N85-20922
Ingot slicing machine and method
[NASA-CASE-NPO-15483-1] 12 p1857 N85-21650
Technology of thin silicon foils for the fabrication of monolithic integrated sensors
[BMFT-FB-T-84-209] 12 p1943 N85-22202
Investigation of silicon surface passivation by silicon nitride film deposition
[NASA-CR-175693] 15 p2585 N85-25938
Diagnostics of a glow discharge used to produce hydrogenated amorphous silicon films
[DE85-002914] 15 p2661 N85-26420
In plane stress analysis
[NASA-CR-175775] 16 p2799 N85-27250
Photovoltaic cell reliability research: Investigation of accelerated stress factors and failure-degradation mechanisms in terrestrial solar cells
[NASA-CR-175815] 16 p2819 N85-27388
Investigation of superlattice device structures
[NASA-CR-3903] 18 p3094 N85-29152
Superconducting electronic film structures
[AD-A154196] 19 p3259 N85-30207
Electrohydrodynamic process for the production of large area polycrystalline silicon sheet
[DE85-006781] 19 p3261 N85-30225
High-efficiency cell concepts on low-cost silicon sheets 20 p3479 N85-31621
The development and evaluation of point defect models for the growth of passive films on single crystal, polycrystalline, and amorphous metal surfaces
[AD-A154685] 21 p3709 N85-33023
Process for improving the quality of epitaxial silicon films grown on insulating substrates
[AD-D011730] 22 p3847 N85-33828

SILICON ISOTOPES
Measurements of the fragmentation of (40)Ar, (28)Si and (12)C in CH2C and H targets between 300 and 1500 MeV/nuc at the Bevalac
[OG-7.2-19] 23 p4016 N85-34686

SILICON JUNCTIONS
Solar cells based on polycrystalline silicon with isothermal potential barriers along grain boundaries
14 p2275 N85-24091
The future of crystalline silicon technology in the US Department of Energy program
21 p3607 N85-32399
Advanced module development overview
21 p3612 N85-32445

SILICON NITRIDES
Sintered silicon nitride workpiece
[NASA-TM-77600] 01 p0021 N85-10129
Silicon nitride powder
[NASA-TM-77731] 01 p0022 N85-10132
Critical conditions for the growth of SiC, Si3N4, and SiO2
[DE84-014824] 01 p0030 N85-10185
Fabrication and characterization of Si3N4 ceramics without additives by high pressure hot pressing
[NASA-TM-77724] 01 p0031 N85-10189
Milling of Si3N4 with Si3N4 hardware
[NASA-TM-86864] 01 p0031 N85-10191
Silicon nitride joining
[AD-A145668] 02 p0187 N85-11248
Development and fabrication of refractory bodies for gas turbine engines
[BMFT-FB-T-84-180] 04 p0457 N85-12899
Study of the pore structure of ceramics prepared by the slip casting method
[NASA-TM-77495] 04 p0478 N85-13046
High temperature corrosion of ceramics
[DE84-017084] 05 p0620 N85-13967
Investigation of silicon surface passivation by silicon nitride deposition 06 p0829 N85-15266
Development and production of improved alpha-phase silicon nitride powders for hot pressing and sintering
[BMFT-FB-T-84-208] 07 p0921 N85-15830
Oxidation resistance of silicon ceramics
[NASA-TM-77429] 07 p0931 N85-15898
Silazane precursors to silicon nitride
[AD-A146791] 07 p0931 N85-15899
Fluctuation phenomena studies in chemically sensitive field effect transistors. Part 2: Corrosion of silicon oxynitride
[AD-A148227] 08 p1157 N85-17302
Tensile test of pressureless-sintered silicon nitride at elevated temperature
[NASA-TM-77777] 08 p1172 N85-17390
Factors influencing the ball milling of Si3N4 in water
[NASA-TM-86932] 10 p1450 N85-19136
Evaluation of machining damage in brittle materials
[DE85-001794] 11 p1612 N85-20136
High temperature corrosion of ceramics
[DE85-002179] 11 p1612 N85-20139
NDE for heat engine ceramics
[NASA-TM-86949] 11 p1649 N85-20389
Oxidation and hot corrosion of hot-pressed Si3N4 at 1000 deg C
[NASA-TM-86977] 12 p1811 N85-21358
Pressureless sintered silicon nitride as a promising candidate for radome materials
[AD-P004367] 12 p1826 N85-21461

Radiographic detectability limits for seeded voids in sintered silicon carbide and silicon nitride
[NASA-TM-86945] 12 p1861 N85-21674
Development of silicon nitride materials for the casting of solar cell silicon 12 p1878 N85-21779
Optimization of silicon-nitride-inversion layer solar cells
12 p1878 N85-21784
Silicon carbide-silicon nitride fibers: Preparation and characterization of polycarbosilazane precursors
12 p1945 N85-22214
Degassification of silicon nitride powders of various origins 13 p2030 N85-22718
Ammonia formation caused by the presence of water in the wet grinding of silicon nitride powder
[NASA-TM-77746] 14 p2249 N85-23937
A novel polymeric organosilazane precursor to Si3N4/SiC ceramics
[AD-A150748] 14 p2260 N85-24003
Sintering phenomena of non-oxide silicon compounds
[DE85-006676] 15 p2520 N85-25535
Fabrication of fiber reinforced ceramic composites by chemical vapor infiltration
[DE85-007565] 15 p2520 N85-25536
Fiat conducts R and D in ceramic parts for diesel engine 15 p2534 N85-25637
Sweden invents new ceramic for more durable cutting tools 15 p2536 N85-25645
Investigation of silicon surface passivation by silicon nitride film deposition
[NASA-CR-175693] 15 p2565 N85-25936
Preparation of silicon carbide-silicon nitride fibers by the pyrolysis of polycarbosilazane precursors
[NASA-TM-86505] 17 p2933 N85-28107
Development of high temperature resistant, noncorrosible, non-metallic ceramic materials, especially silicon nitride in gas turbine application
[BMFT-FB-T-85-015] 17 p2936 N85-28125
High temperature fracture mechanics of silicon nitride
[BMFT-FB-T-84-285] 17 p2981 N85-28433
Preparation of sinteractive silicon nitride powders
[BMFT-FB-T-84-303] 18 p3082 N85-29066
High-temperature oxidation of reaction-roasted silicon nitride with various additives 19 p3244 N85-30114
Method for producing high quality germanium-germanium nitride interfaces for germanium semiconductors and device produced thereby
[AD-D011702] 19 p3260 N85-30218
Vibrational properties of disordered solids: Far infrared studies
[DE85-010400] 19 p3377 N85-30951
Realization by vapor deposition of turbine blades covered with a silicon nitride layer
20 p3395 N85-31061
Silicon nitride protective coatings for silvered glass mirrors
[DE85-011637] 20 p3433 N85-31300
Reliability of void detection in structural ceramics using scanning laser acoustic microscopy
[NASA-TM-87035] 21 p3597 N85-32337
Silicon surface passivation by silicon nitride deposition
21 p3610 N85-32423
Mechanical properties of SiC fiber-reinforced reaction-bonded Si3N4 composites
[NASA-TM-87085] 23 p3909 N85-34223
Reliability of two sintered silicon nitride materials
[NASA-TM-87092] 23 p3919 N85-34284
Method for measuring surface activity of silicon nitride powder
[NASA-TM-77906] 24 p4073 N85-35242

SILICON OXIDES
NT QUARTZ
NT SILICON DIOXIDE
Critical conditions for the growth of SiC, Si3N4, and SiO2
[DE84-014824] 01 p0030 N85-10185
Phase transformations of AlPO4 with SiO2 structures
03 p0425 N85-12713
High temperature corrosion of ceramics
[DE84-017084] 05 p0620 N85-13967
The atomic structure of Si-SiO2 interfaces suggesting a ledge mechanism of silicon oxidation
[DE84-016057] 05 p0731 N85-14703
EPR linewidth studies of unpaired electrons at the Si-SiO2
[DE84-016727] 05 p0733 N85-14712
Density and thermal expansion measurements of several mixed oxide glasses in the solid and liquid regions
[DE85-006134] 14 p2261 N85-24014
Impurity bands associated with MOS inversion layers
[INPE-3483-PRE/726] 16 p2670 N85-27704

SILICON POLYMERS
NT METHYL POLYSILOXANE
NT SILICONE RESINS
NT SILICONES
NT SILOXANES
Thin polymer film collectors as a contribution to the solar industry
[DE84-015299] 04 p0529 N85-13383
French research on gallium arsenide devices
08 p1141 N85-17196
Investigation of structure-permeability relationships of silicone polymer membranes
[PB85-148476] 11 p1596 N85-20038
EOS (electrical overstress) protection for VLSI (Very Large Scale Integration) devices
[AD-A150333] 13 p2064 N85-22891
A novel polymeric organosilazane precursor to Si3N4/SiC ceramics
[AD-A150748] 14 p2260 N85-24003
Preparation of silicon carbide-silicon nitride fibers by the pyrolysis of polycarbosilazane precursors
[NASA-TM-86505] 17 p2933 N85-28107
EVA-glass interface bond stability
21 p3606 N85-32408
Interfacial bonding stability 21 p3606 N85-32409
Topics in electrochemical degradation of photovoltaic modules 21 p3606 N85-32410
Polymer-water interaction studies
21 p3609 N85-32411

SILICON RADIATION DETECTORS
The Silica Aerogel Detector (SAD) story — Cherenkov detector
[USIP-84-14] 20 p3459 N85-31485

SILICON SOLAR CELLS
U SOLAR CELLS

SILICON TRANSISTORS
The construction and study of improved Al(x)Ga(1-x)As-GaAs heterostructure devices
[AD-A153264] 17 p2954 N85-28244
KT3127A, KT3128A transistors
22 p3779 N85-33414

SILICONE RESINS
Thermal conductivity and interface resistance of particle-filled silicone resin
[DE84-011681] 04 p0479 N85-13056

SILICONE RUBBER
General studies on composite materials. Evaluation of auxiliary products of national origin
[SNIAS-2500/DCI-PR/84] 03 p0326 N85-12101
Simple EOS for the silicone rubber Sylgard 184
[DE85-001394] 12 p1814 N85-21376
Oil resistant silicone elastomers
[AD-131523] 16 p2753 N85-26987

SILICONES
NT METHYL POLYSILOXANE
NT SILOXANES
Development of a polysilicon process based on chemical vapor deposition of dichlorosilane in an advanced Siemen's reactor
[NASA-CR-174148] 04 p0483 N85-13083
Vacuum ultraviolet electronic properties of liquids
[DE85-000305] 10 p1563 N85-19858
Model for the growth of fractal silica polymers
[DE85-007884] 17 p2935 N85-28115

SILICONIZING
Studies of the crystallization process of aluminum-silicon alloys using a high temperature microscope
[NASA-TM-77869] 24 p4078 N85-35272

SILOS (MISSILE STORAGE)
U MISSILE SILOS

SILOXANES
Neutron scattering on polysiloxanes
03 p0432 N85-12751
Properties of ultra-violet cured poly(dimethylsiloxane)-urea acrylates
[AD-A148570] 08 p1134 N85-17146
Poly(dimethylsiloxane)-polyurethane elastomers: Synthesis and properties of segmented copolymers and related zwitterionomers
[AD-A148571] 08 p1134 N85-17147
High performance size exclusion chromatography (IX) bulk and component analysis of silanol groups in polydimethylsiloxanes: Process development endeavor
[DE85-006853] 15 p2506 N85-25458
Formulation/cure technology for ultrahigh molecular weight silphenylene-siloxane polymers
[NASA-TP-2476] 16 p2753 N85-26990
Thermally stable elastomers: Review of silarylene-siloxane polymers and polysilmethylenes
[AD-A152323] 17 p2934 N85-28111
Self-developing polysilane deep-UV resists: Photochemistry, photophysics and submicron lithography
[DE85-007606] 19 p3237 N85-30067
Method for controlling the viscosity of siloxane oils
[DE85-011586] 23 p3909 N85-34221

SILTS
U SEDIMENTS

SILVER
Relationships between electronic structure and stability of metallic glasses
[AD-A145141] 01 p0026 N85-10176
Kinetics of simple inner- and outer-sphere electrochemical reactions at rotating silver electrodes as examined using surface-enhanced Raman spectroscopy
[AD-A145606] 02 p0172 N85-11184
EXAFS and Moessbauer study of small metal clusters isolated in rare-gas solids
[DE84-015976] 04 p0470 N85-12984
Behaviour of lead-silver anodes in zinc electrodeposition from sulphuric acid baths
[BLL-MINTEK-TR-1180-(5810.5759)]
06 p0764 N85-14887
Effects of silver and group 2 fluorides addition to plasma sprayed chromium carbide high temperature solid lubricant for foil gas bearing to 650 deg C
[NASA-TM-86895] 06 p0770 N85-14928
Metallo-Organic Decomposition (MOD) silver metallization for photovoltaics 06 p0830 N85-15276
Ion cluster beam deposition research
06 p0831 N85-15280
Electronic structure, chemical bonding, and superconductivity of silver films on germanium
[AD-A147720] 08 p1128 N85-17112
Silver metallogeny in Earth's Pacific Ocean segment
10 p1496 N85-19485
The role of silver in self-lubricating coatings for use at extreme temperatures
[NASA-TM-86943] 11 p1611 N85-20127
The effect of Xe underlayers on the surface enhanced Raman scattering of pyridine on cold silver
[AD-A150109] 12 p1801 N85-21294
EXAFS of monolayers on silver electrodes: SSRL proposal number 717M
[AD-A150623] 13 p2018 N85-22652
Ink jet printing of silver metallization for photovoltaics
[NASA-CR-175798] 15 p2586 N85-25943
MOD silver metallization for photovoltaics
[NASA-CR-175773] 16 p2818 N85-27381
The loss of material from the cathode of metal arcs
[NASA-TM-77845] 17 p2918 N85-27985
Silvered polymer reflectors
[DE85-008782] 18 p3130 N85-29384
Modification of the grain size of sputtered copper with additions of oxygen, krypton, silver, or yttrium
[DE85-010975] 21 p3567 N85-32189
MOD silver metallization for photovoltaics
21 p3610 N85-32428
Ice nucleation of single water droplet by silver iodide: A laboratory observation 21 p3643 N85-32630
Monte Carlo studies of H2O layers adsorbed on a model basal face of AgI 21 p3643 N85-32633
Method of bonding silver to glass and mirrors produced according to this method
[DE85-011642] 22 p3792 N85-33465
Ink jet printing of silver metallization for photovoltaics
[NASA-CR-176054] 22 p3805 N85-33589
Environmental surveillance at Los Alamos during 1984
[DE85-011886] 22 p3811 N85-33805
Polarisation insensitive achromatic cube beamsplitter — binocular microscopes
[NPL-MOM-72] 23 p3973 N85-34630
Noise in silver beta alumina ceramics
[AD-A156135] 24 p4062 N85-35297
New silver resource map of the United States: Potential for increased domestic silver production
24 p4105 N85-35445

SILVER ALLOYS
Alloy supercooling on Salyut-7
11 p1604 N85-20083
Application of solidification theory to rapid solidification processing
[AD-A151251] 15 p2509 N85-25480
Study of the kinetics and thermodynamics of hydrogen in Pd-based alloys
[DE85-007341] 16 p2750 N85-26969
Age hardening and atomic structure of an aluminum-6 at. % silver alloy
[DE85-009977] 18 p3077 N85-29031
The precipitation mechanism in a metallic solid solution crystal: Case of the aluminum-copper and aluminum-silver systems
[DE85-009981] 18 p3077 N85-29032
Studies of the crystallization process of aluminum-silicon alloys using a high temperature microscope
[NASA-TM-77869] 24 p4078 N85-35272

SILVER CHLORIDES
Determination of low chloride values in Rocky Flats scrub alloy solutions and other complex matrices
[DE85-011506] 23 p3911 N85-34234

SILVER COMPOUNDS
NT SILVER CHLORIDES
NT SILVER HALIDES
NT SILVER IODIDES

SILVER HALIDES
NT SILVER CHLORIDES
NT SILVER IODIDES

nfrared presensitization photography
D-A146966] 07 p0967 N85-16139
nfrared presensitization photography
16 p2766 N85-27189
ER HYDROGEN BATTERIES
Analysis and testing of the thermal properties of space
ttery cells, phase B, draft
SA-CR(P)-1971] 15 p2550 N85-25741
ER IODIDES
Inactivation of silver iodide by atmospheric nucleation
hibitors 21 p3636 N85-32599
Ice nucleation by silver iodine particles with nearly critical
ions 21 p3638 N85-32600
Photoinduced active sites on ice nucleating aerosol of
ilver iodide 21 p3639 N85-32601
COR (IMAGE CORRELATOR)
U IMAGE CORRELATORS
ILARITIES
U ANALOGIES
ILARITY NUMBERS
Study of the functions of similarity of the planetary
boundary layer. Part 2: Results
[INPE-3130-PRE/521-VOL-2] 16 p2826 N85-27429
Application of field similitude theory to calculation of
stripline heating 22 p3780 N85-33419
Selection of segment similarity measures for hierarchical
picture segmentation 23 p3960 N85-34548
ILARITY THEOREM
Similarity criteria of spectra of pressure pulsations of
turbulent boundary layer near wall
02 p0256 N85-11679
Study of the functions of similarity of the planetary
boundary layer. Part 1: Theory
[INPE-3129-PRE/520-PT-1] 16 p2825 N85-27428
Parameterization of surface fluxes in the VVR Fourth
Order GCM 18 p3142 N85-29454
PLEX METHOD
New labeling procedures for the basis graph in
generalized networks
[AD-A146217] 03 p0407 N85-12601
The stable evaluation of multivariate b-splines
[AD-A147386] 07 p1032 N85-16551
An iterative scheme for linear complementarity
problems
[AD-A147464] 07 p1032 N85-16555
Minimal cost flow in processing networks: A primal
approach
[CWI-TRACT-4] 14 p2432 N85-25001
A greedy algorithm for the transhipment along a single
road problem
[AD-A152343] 17 p3025 N85-28709
On the step size in Karmarkar's algorithm
[AD-A154040] 19 p3335 N85-30661
A practical approach to Karmarkar's algorithm
[AD-A155714] 21 p3673 N85-32818
SIMULATED ALTITUDE
U ALTITUDE SIMULATION
SIMULATION
NT ALTITUDE SIMULATION
NT ANALOG SIMULATION
NT ATMOSPHERIC ENTRY SIMULATION
NT COMPUTER SYSTEMS SIMULATION
NT COMPUTERIZED SIMULATION
NT CONTROL SIMULATION
NT DIGITAL SIMULATION
NT ENVIRONMENT SIMULATION
NT EXHAUST FLOW SIMULATION
NT FLIGHT SIMULATION
NT LANDING SIMULATION
NT MOTION SIMULATION
NT SOLAR SIMULATION
NT SPACE ENVIRONMENT SIMULATION
NT SYSTEMS SIMULATION
NT THERMAL SIMULATION
NT WEIGHTLESSNESS SIMULATION
Simulation of contact surface erosion for impact
problems 01 p0060 N85-10398
Simulation uses of the exponential distribution
[AD-A144940] 01 p0112 N85-10756
Simulation of vibration processes in damped structures
with allowance for temperature-frequency characteristics
of vibration absorbing materials
02 p0257 N85-11680
The structure of the vorticity field in turbulent channel
flow. Part 2: Study of ensemble-averaged fields
[NASA-TM-86657] 03 p0361 N85-12317
Surge transient simulation in turbo-jet engine
05 p0596 N85-13796
Possibilities of increasing the simulation quality of
multiaxial test stands — vehicle testing
05 p0649 N85-14169
Massively parallel processor 05 p0680 N85-14366
NOAA/NASA joint simulation of AMTS and HIRS
05 p0682 N85-14384
ECMWF/NMC/GLAS joint simulation study
05 p0682 N85-14385
Simulation evaluation of two VTOL control/display
systems in IMC approach and shipboard landing
[NASA-TM-85996] 06 p0756 N85-14841
Review of requirements and status of simulation and
scaling of transonic, viscous flows
[AD-A146357] 06 p0808 N85-15137
Region 1 birkeland currents from a global MHD
simulation of the magnetosphere
[AD-A147435] 07 p0997 N85-16335
Matrix display simulation
[AD-D011371] 07 p1055 N85-16895
Automatic software for controlling cryogenic systems
08 p1097 N85-16932
Small-sample properties of kernel density estimators
from randomly right-censored data
[AD-A148752] 09 p1374 N85-18634
A tracked vehicle test plant for the simulation of dynamic
operation
[AD-P004305] 09 p1410 N85-18882
Simulation of the ion-beam-driven drift instability in a
magnetic trap, 1
[AD-A149451] 10 p1452 N85-19147
An electronically controlled array for simulation of
passive target/background signatures at millimeter
wavelengths
[AD-D011456] 10 p1488 N85-19263
LOS microwave channel simulation: A survey of models,
realizations and new concepts 10 p1472 N85-19291
Simulation of the ion-beam-driven drift instability in a
magnetic trap, 2
[AD-A149452] 10 p1554 N85-19798
Compensator development and examination of
performance and robustness
[NASA-CR-175470] 11 p1627 N85-20244
Radiative ion beams: Hot stellar reactions in the
laboratory
[DE85-001570] 11 p1722 N85-20833
Algorithm for statistical simulation of electromagnetic
compatibility characteristics of high-frequency
transmission channels in radioelectronic facilities
12 p1842 N85-21560
NOAA-AISC user's guide for implementing CERES
wheat model for large area yield estimation
[E85-10085] 12 p1873 N85-21750
Estimating solar radiation for plant simulation models
[E85-10089] 12 p1873 N85-21751
Recursive moment formulas for regenerative
simulation
[AD-A150112] 12 p1922 N85-22070
Air combat simulation: Methods, models, trends
13 p1967 N85-22359
Microwave blackbodies for spaceborne receivers
[NASA-CR-175647] 13 p2094 N85-23066
Markov method for simulating non-Gaussian wind speed
time series
[DE85-003450] 13 p2139 N85-23284
Calculating boundary layer on profile with laminar and
turbulent flow zone 14 p2288 N85-24177
Synthetic aperture radar simulation study
[AD-A151000] 14 p2293 N85-24214
Investigation of a failure detection/identification system
for a tactical aircraft navigation system
[AD-A151846] 15 p2469 N85-25240
Shuttle communications and tracking systems modeling
and TDRSS link simulations studies
[NASA-CR-171861] 15 p2491 N85-25369
Compensator development and examination of
performance and robustness
[NASA-CR-175703] 15 p2540 N85-25678
Numerical experiments of jet streak ageostrophic
circulations using pseudo-geostrophic initialization and
perspectives 15 p2590 N85-25969
Aerosol deposition along the respiratory tract at zero
gravity: A theoretical study
[DE85-006703] 15 p2619 N85-26136
Evaluating computer-communication networks with
simulation techniques
[AD-A151852] 15 p2632 N85-26222
Solution of coupled system of PDE by the transistorized
multigrid method
[DE85-006377] 15 p2639 N85-26276
Flight testing and development of the F/A-18A digital
flight control system 16 p2713 N85-26743
Development of a persistent chemical agent simulation
system
[NASA-CR-175780] 16 p2745 N85-26937
Development of a Persistent Chemical Agent Simulator
System (PCASS)
[NASA-CR-175776] 16 p2745 N85-26938
Pyrotechnic shock simulation using the controlled
response of a resonating bar fixture
[DE85-006537] 16 p2784 N85-27181
In plane stress analysis
[NASA-CR-175775] 16 p2799 N85-27259
The selection of the starting field: General versus
tailored model 16 p2805 N85-27294
Comparison of gravity field solution techniques
16 p2805 N85-27295
Kinetic theory and simulation of multi-species plasmas
in Tokamaks excited with ICRF microwaves
[DE85-006119] 16 p2868 N85-27691
The evolution of ACS for helicopters: Conceptual
simulation studies to preliminary design
17 p2902 N85-27890
Physical-chemical model for the mechanism of glass
corrosion with particular consideration of simulated
radioactive waste glasses
[DE85-007713] 17 p2935 N85-28121
Conformational and mechanical properties at high strain
rates
[AD-A153401] 17 p2959 N85-28272
Study of a simulated test for assessing the machinability
of steels
[BLL-BISI-TRANS-22344-(9022.06)]
17 p2972 N85-28357
Mathematical modeling and simulation of climate and
climatic change
[DE85-008974] 17 p2997 N85-28526
Robust regression through robust covariances
[AD-A153301] 17 p3020 N85-28677
An experimental investigation of the angular scattering
and backscattering behaviors of the simulated clouds of
the outer planets
[NASA-CR-175909] 17 p3052 N85-28896
Multi-ducted inlet combustor research and
development
[AD-A153753] 18 p3063 N85-28946
Diffusion of gases in porous solids: Simulation and
measurements
[DE85-008870] 18 p3101 N85-29196
Methods for simulating gas phase SO2 oxidation in
atmospheric models
[PB85-173110] 18 p3135 N85-29418
Forecast impact simulation studies
18 p3139 N85-29435
Preliminary results from numerical experiments on the
summer 1980 heat wave and drought
18 p3140 N85-29436
A numerical study of the Pacific polar low
[AD-A153777] 18 p3149 N85-29495
Simulation for human factors research. A central
question: Fidelity 18 p3159 N85-29588
Limit theorems for the method of replication
[AD-A153541] 18 p3170 N85-29642
Fault detection and accommodation testing on an F100
engine in an F-15 airplane
[NASA-TM-86735] 19 p3219 N85-29962
Decay of a coherent scalar disturbance in a turbulent
flow
[NASA-TM-86700] 19 p3264 N85-30244
Highly accurate shock flow calculations with moving
grids and mesh refinements, revision 1
[DE85-010929] 19 p3267 N85-30260
Numerical simulation of chemical and physical properties
of cumulus clouds
[DE85-009744] 19 p3317 N85-30564
One-dimensional model hindcasts of warm anomalies
in the North Pacific Ocean
[AD-A154126] 19 p3320 N85-30579
Evaluation of curve-smoothing techniques
[HSE-TRANS-11108] 19 p3349 N85-30759
Double layer formation due to contact of different
temperature plasmas
[IPPJ-722] 19 p3370 N85-30900
Monte Carlo simulations of fermion systems: The
determinant method
[DE85-010708] 19 p3376 N85-30947
Venus thermospheric circulation
[PB85-180420] 19 p3384 N85-30997
A study of the application of differential techniques to
the global positioning system for a helicopter precision
approach
[NASA-CR-177326] 20 p3391 N85-31035
Vortex simulation of v-shaped flame
20 p3425 N85-31259
Simulation and analysis of airborne antenna radiation
patterns 20 p3439 N85-31342
Coal slurry ignition in a diesel engine simulator
[DE85-010987] 20 p3463 N85-31513
Pressure chamber simulation of 450-meter dive
20 p3505 N85-31788
Diving simulation experiment with pressure chambers
20 p3506 N85-31793
A systems analysis of the erythropoietic responses to
weightlessness. Volume 1: Mathematical model
simulations of the erythropoietic responses to
weightlessness
[NASA-CR-171890] 20 p3506 N85-31794
Simulation model of acoustic emission due to
microscopic fracture in metals
[BLL-BISI-TRANS-22367-(9022.06)]
20 p3523 N85-31909

Impulsive noise due to transonic blade-vortex interactions 20 p3523 N85-31913

Simulating the effects of plasma disruption with a 1 MA current pulse in a coaxial test fixture
[DE85-010491] 20 p3535 N85-31986

Cavitation collapses of SRS by SBS
[DE85-009605] 20 p3535 N85-31989

Two-phase flow visualization in a transparent, atmospheric pressure, boiling water loop
[DE84-016857] 21 p3566 N85-32286

The 2-D simulations of the NRL (Naval Research Laboratory) laser experiment
[AD-A154915] 21 p3592 N85-32321

A simulation of weather in 3D space
[AD-A155221] 21 p3636 N85-32586

Numerical modeling of sea ice dynamics and ice thickness characteristics
[AD-A154600] 21 p3654 N85-32700

On the dependence of the convergence of Gummel's algorithm on the regularity of the solution
[AD-A154628] 21 p3675 N85-32832

The priming effect in task design research
[AD-A154589] 21 p3679 N85-32852

A simulation study of Sylvester's problem in three dimensions
[AD-A155268] 21 p3679 N85-32854

Intracardiac hemodynamics and human heart function in simulated weightlessness 22 p3733 N85-33140

Synthesis of optimum receiver and processor for interfering radio pulse signals 22 p3769 N85-33361

New formulation for linear accelerator design
[DE85-011171] 22 p3842 N85-33792

Laboratory evaluation and application of microwave absorption properties under simulated conditions for planetary atmospheres
[NASA-CR-176078] 22 p3851 N85-33847

Late-stage planetesimals: How big?
22 p3852 N85-33857

A simulation of high energy cosmic ray propagation 2
[OG-5.4-2] 22 p3885 N85-34079

Effect of interference on the performance of a minimum TCAS 2
[FAA-PM-84-33] 23 p3896 N85-34131

The 1983 international intercomparison of nuclear accident dosimetry systems at Oak Ridge National Laboratory
[DE85-011303] 23 p3934 N85-34382

Image synthesis: Optical identity or pictorial communication? 23 p3963 N85-34565

Simulation studies on stability of hot electron plasma
23 p3978 N85-34664

Numerical simulation in astrophysics: Smoothed particle methods 23 p3979 N85-34674

Simulation of instability of cylindrically converging shock waves 23 p3980 N85-34679

A position sensitive phoswich hard X-ray detector system
[OG-9.3-12] 23 p4028 N85-34967

Simulated effects of increased recharge on the ground-water flow system of Yucca Mountain and vicinity, Nevada-California
[DE85-012965] 24 p4108 N85-35469

Application of pulsed power in the simulation of severe natural lightning
[DE85-012866] 24 p4124 N85-35564

Simulation of high +Gz onset in the dynamic environment simulator
[AD-A155963] 24 p4131 N85-35610

Constrained stiffness matrix adjustment using mode data
[AD-A155968] 24 p4143 N85-35685

A simulation of ultra-relativistic nucleus-nucleus collisions 24 p4146 N85-35707

Detector requirements for intensity interferometry measurements 24 p4147 N85-35709

A lead glass tubing drift calorimeter
24 p4147 N85-35711

Pulsed-neutron-source models for the astrophysical s-process
[DE85-012927] 24 p4151 N85-35740

Numerical studies of high current beam compression in heavy ion fusion
[DE85-011874] 24 p4158 N85-35783

Multiplicity distributions in interaction models used for cascade simulations
[HE-1.2-5] 24 p4172 N85-35863

Some remarks about simulation of cosmic ray phenomena with use of nuclear interaction models based on the current SPS proton-antiproton data
[HE-1.2-6] 24 p4172 N85-35864

Relation between gamma-ray family and EAS core: Monte-Carlo simulation of EAS core
[HE-3.6-7] 24 p4185 N85-35955

The lateral distributions of charged particles of energy greater than 0.3 E sub crit in electron-photon cascades in lead and air
[HE-3.6-10] 24 p4185 N85-35957

Result of Monte-Carlo simulation of electron-photon cascades in lead and layers of lead-scintillator
[HE-3.6-11] 24 p4185 N85-35958

A study of gamma-families generated in nucleon-nucleus (NA) and pion-nucleus (pi A) interactions
[HE-3.7-2] 24 p4186 N85-35961

Hadrons registration in emulsion chamber with carbon block
[HE-3.7-3] 24 p4186 N85-35962

New analysis of nuclear interaction observed by Mt. Kanbara emulsion chamber experiment
[HE-3.7-4] 24 p4186 N85-35963

Intensities of high-energy cosmic rays at Mount Kanbala
[HE-3.7-5] 24 p4186 N85-35964

Structured events in Pamir carbon X-ray chambers
[HE-3.7-7] 24 p4186 N85-35965

Ultra high energy events in ECHOS series and primary energy spectrum
[HE-3.7-9] 24 p4186 N85-35966

Peculiarities of gamma-quanta distribution at 20 TeV energy
[HE-3.7-10] 24 p4186 N85-35967

Analysis of equi-intensity curves and NU distribution of EAS 24 p4187 N85-35970

Electrons, muons and hadrons in extensive air showers and how do they depend on nuclear interaction model, part 1 24 p4187 N85-35972

Simulation of EAS properties on the basis of high energy interaction model deduced from the accelerator data
24 p4187 N85-35973

New aspects in nucleon-nucleus collisions and EAS properties around 10(6) GeV 24 p4187 N85-35974

Small air showers and collider physics
[HE-4.1-9] 24 p4187 N85-35975

High energy hadrons in extensive air showers
24 p4187 N85-35976

Hadronic components of EAS by rigorous saddle point method in the energy range between 10(5) and 10(8) GeV 24 p4188 N85-35978

About increase of the large transvere momentum processes fraction in hA interactions at energies 5.10(14) - 10(16) eV according to the data on E.A.S. hadrons
24 p4188 N85-35979

Phenomenology of soft hadron interactions and the relevant EAS data 24 p4188 N85-35980

Theoretical study of EAS hadronic structure
24 p4189 N85-35991

Comparison of simulation results with sea-level experimental data on 10(14) - 10(16) air shower cores
24 p4190 N85-35993

Particle distributions in approximately 10(13) - 10(16) eV air shower cores at mountain altitude and comparison with Monte Carlo simulations
[HE-4.2-18] 24 p4190 N85-35994

The longitudinal development of muons in cosmic ray air showers at energies 10(15) - 10(17) eV
[HE-4.3-12] 24 p4192 N85-36006

Topological aspects of age parameter
[HE-4.3-13] 24 p4192 N85-36007

Monte Carlo simulation of EAS generated by 10(14) - 10(16) eV protons
[HE-4.3-14] 24 p4192 N85-36008

Hybrid TLC-pair meter for the Sphinx Project
[HE-5.2-10] 24 p4203 N85-36086

SIMULATOR TRAINING

U TRAINING SIMULATORS

SIMULATORS

NT COCKPIT SIMULATORS
NT CONTROL SIMULATION
NT ENVIRONMENT SIMULATORS
NT FLIGHT SIMULATORS
NT MOTION SIMULATORS
NT SHOCK SIMULATORS
NT SOLAR SIMULATORS
NT SPACE SIMULATORS
NT SPACECRAFT CABIN SIMULATORS
NT TARGET SIMULATORS
NT TRAINING SIMULATORS
NT VIBRATION SIMULATORS

Clutter generator for use in radar evaluation
[AD-D011234] 01 p0039 N85-10245

Effects of repetitive, small-spot, incoherent light flashes on pursuit tracking performance
[AD-A144848] 01 p0095 N85-10637

Hardware for a real-time multiprocessor simulator
[NASA-TM-83805] 01 p0099 N85-10659

Test signal generator for coherent air-to-ground radars
[AD-D011276] 05 p0628 N85-14025

POPCORN: A supervisory control simulation for workload and performance research
05 p0704 N85-14515

A simulator for studying helicopter weapons systems
08 p1075 N85-16816

Novel applications of the NASA/GSFC Viterbi decoder hardware simulator 08 p1101 N85-16867

Operating system for a real-time multiprocessor propulsion system simulator. User's manual
[NASA-TP-2426] 08 p1207 N85-17596

An electronically controlled array for simulation of passive target/background signatures at millimeter wavelengths
[AD-D011458] 10 p1468 N85-19203

An H.F. simulator for use with real time channel evaluation systems 10 p1473 N85-19280

Theoretical study of a dynamic simulator of selective fading for digital, wireless beam microwave links
10 p1473 N85-19284

Drag-free satellite simulator
[REPT-615] 12 p1789 N85-21220

Rotorcraft digital advanced avionics system (Rodaas)
15 p2686 N85-28008

The gust simulation apparatus of the 3m x 3m low speed wind tunnel of the DFVLR in Goettingen, West Germany
[DFVLR-FB-85-04] 17 p2906 N85-27920

SAPIENS Memo 8: Electromagnetic properties of the EMP simulator SAPIENS
[FOA-C-30382-A3] 20 p3442 N85-31385

PHOENICS 84: A multi-dimensional multi-phase general-purpose computer simulator for fluid flow, heat transfer and combustion: 36 lecture panels
[CFD/84/18] 20 p3457 N85-31486

Construction of University of Missouri, Rolla's full scale cloud simulation chamber and applied research
[AD-A154682] 21 p3557 N85-32128

Design of a jamming simulator for a binary communication system
[AD-A154617] 21 p3573 N85-32221

Flexible satellite communications systems simulator, phase 3
[AD-A155647] 21 p3577 N85-32247

Reference-cell calibration activities
21 p3613 N85-32453

Gust simulation for flight mechanical wind tunnel tests
24 p4062 N85-35172

A review of motion sickness with special reference to simulator sickness
[AD-A155975] 24 p4131 N85-35611

SIMULTANEOUS EQUATIONS

Method and apparatus for self-calibration and phasing of array antenna
[NASA-CASE-NPO-15920-1] 12 p1832 N85-21493

MATRIX: A program that shows how row and column orderings affect matrix fill-in
[DE85-007522] 15 p2630 N85-26213

SIMULTANEOUS IMAGE CORRELATOR

U IMAGE CORRELATORS

SINE WAVES

The ML (Maximum Likelihood) method for frequency estimation of real sinusoids in noise
[AD-A146053] 03 p0411 N85-12628

Effect of a thermal gradient applied to a sinusoidal surface profile
[DE84-015649] 03 p0434 N85-12765

Characteristic impedance of a porous center during transmission of quasi-static sinusoidal vibrations
[ISSN-0208-5658] 05 p0647 N85-14155

Initialization of Thompson-Pisarenko's algorithm -- sinusoidal signal parameter estimation
[FUB-46-1983] 09 p1375 N85-18541

Modulated sinusoidal currents in management of vibration sickness 10 p1524 N85-19612

Microwave SAW (Surface Acoustic Wave) monochromator
[AD-D011718] 21 p3590 N85-32311

SINGLE CHANNEL PER CARRIER TRANSMISSION

Analog voice processing for FM transmission in a telephone channel
[INPE-2798-PRE/359] 03 p0354 N85-12279

SINGLE CRYSTALS

Morphological changes of gamma prime precipitates in nickel-base superalloy single crystals
[NASA-TM-83698] 01 p0026 N85-10165

Process Research of Polycrystalline Silicon Material (PROPSM)
[NASA-CR-173838] 01 p0067 N85-10448

Preparation and properties of single crystals of hydrogen bis(phthalocyaninato) neodymium(3)
[AD-A144933] 01 p0123 N85-10846

Life prediction and constitutive models for anisotropic materials 02 p0144 N85-10976

Trivalent ion exchange in beta alumina
[AD-A145373] 02 p0172 N85-11151

Surface chemistry of palladium
[DE84-014572] 02 p0173 N85-11153

The transient oxidation of single crystal NiAl+Zr
[NASA-CR-174756] 02 p0182 N85-11221

The effect of tantalum and carbon on the structure/properties of a single crystal nickel-base superalloy
[NASA-CR-174779] 02 p0182 N85-11223
Preparation and properties of evaporated CdTe films compared with single crystal CdTe
[DE85-000502] 02 p0222 N85-11452
Complex formation and temperature stability of electrophysical properties of GaAs seminsulating single crystals 02 p0258 N85-11689
Focusing beam of 1-GeV protons with volumetric capture to the mode of channeling by bent single crystal
02 p0268 N85-11750
Splitting of surface polariton spectrum by holographic grating 02 p0272 N85-11771
Biaxial constitutive equation development for single crystals
[NASA-CR-174056] 02 p0286 N85-11862
Plastic strain localization in superalloy single crystals
[AD-A145705] 02 p0288 N85-11878
The effect of orientation on fatigue growth in a nickel-based single crystal superalloy
[PNR-90207] 03 p0332 N85-12141
Diffusion of Fe-55 in Fe-2O-3 single crystals
[AERE-R-11286] 03 p0333 N85-12147
Growth and magnetic investigations of single crystals of intermetallic compounds of rare earths and uranium — magnetic properties 03 p0425 N85-12712
Quasielastic neutron scattering on single crystals of solid ionic conductor 03 p0426 N85-12719
Construction of a neutron single crystal diffractometer
03 p0427 N85-12723
Spectroscopic investigations on neutron induced impurity atoms and radiation defects
03 p0430 N85-12742
Neutron scattering on macromolecular solid state materials, solutions and melts 03 p0431 N85-12747
Kohn anomaly in metastable fcc lanthanum at low temperatures
[DE84-015459] 04 p0569 N85-13628
Magnetic susceptibility, electrical resistivity, and specific heat of single crystal LaFe-4P-12
[DE84-009979] 04 p0570 N85-13633
Single crystal semiconductor multilayers for electrically active optical interference filters
[DE84-015814] 04 p0571 N85-13640
Development of high responsitivity Ge:Ga photoconductors
[DE84-016902] 04 p0571 N85-13643
Luminescent properties of graded cadmium sulfoselenide electrodes prepared from cadmium sulfide substrates
[AD-A146710] 06 p0766 N85-14898
Development of technology of silicon single-crystal production semiconductor power devices: State of art outlook 06 p0795 N85-15078
Analysis of optical and electrical performance of a TCP-coated solar cell 06 p0832 N85-15293
Preparation and electronic properties of MoS(2) and WS(2) single crystals grown in the presence of cobalt
[AD-A146508] 06 p0866 N85-15506
Low noise multiple crystal-controlled oscillator
[AD-D011401] 07 p0948 N85-16010
Crystal growth and characterization of BaMgF4
[AD-A146805] 07 p1047 N85-16650
The fundamentals of dislocation transport of hydrogen in bcc iron
[AD-A148143] 08 p1129 N85-17117
Process development for the production of technically high quality monocrystalline diamond grits
[BMFT-FB-T-84-204] 08 p1136 N85-17166
Automatic Monoellipsoidal Mirror Furnace Facility (AMMFF), volume 1 — spaceborne crystal growth
[AMF-RP.100-DS-015-VOL-1] 09 p1285 N85-18073
Improved solid-state laser sources, volume 2
[DE85-000759] 09 p1325 N85-18330
The growth of large diameter single crystals by vertical solidification of the melt
[AD-A148756] 09 p1397 N85-18792
Single crystal silicon as a low-temperature structural material
[DE84-017469] 09 p1400 N85-18810
Characterization of CO binding sites on Rh(111) and Rh(331) surfaces by XPS and LEED (Low Energy Electron Diffraction): Comparison to EELS (Electron Energy Loss Spectroscopy) results
[AD-A149331] 10 p1435 N85-19044
Low cycle fatigue of MAR-M 200 single crystals at 760 and 870 deg C
[NASA-TM-86933] 10 p1440 N85-19074
Magnetic excitation in CuMn spin glass alloy
[DE85-002564] 10 p1453 N85-19159
Method for synthesizing indium phosphide
[AD-D011475] 10 p1563 N85-19855
Microstrain analysis in bent single crystal silicon by double crystal X-ray topography technique
[DE85-000422] 10 p1584 N85-19863
Studies of the kinetics and mechanisms of ammonia synthesis and hydrodesulfurization on metal single crystal surfaces
[DE85-001650] 11 p1595 N85-20030
Phonon-impurity relaxation and acoustic wave absorption in yttrium-aluminum garnet crystals with impurities 11 p1715 N85-20790
Electron-oscillatory spectra of yttrium-erbium-aluminum garnet of crystals and their role in laser pumping
11 p1715 N85-20791
Low stress semiconductor-insulator interface for cryogenic device applications
[NASA-CASE-NPO-16394-1] 11 p1734 N85-20906
Diamondlike flakes
[NASA-CASE-LEW-13637-2] 12 p1796 N85-21267
Fracture toughness of materials
[DE85-004306] 12 p1867 N85-21713
Total immersion crystal growth
[NASA-CASE-NPO-15800-2] 12 p1939 N85-22178
Orientation and temperature dependence of some mechanical properties of the single-crystal nickel-base superalloy Rene N4. 3: Tension-compression anisotropy
[NASA-TM-86982] 13 p2021 N85-22660
Basis and pyramidal slipping in single crystals of alpha-alloy Ti-Al-Sn 13 p2032 N85-22730
Fracture mechanics evaluation of GaAs
[NASA-CR-175657] 13 p2102 N85-23101
Influence of substrate heating and thermal annealing on the surface crystallinity in single Si crystals implanted with high doses of (16)O
[DE85-005264] 13 p2164 N85-23428
The cyclic stress-strain behavior of nickel-base superalloy poly- and single crystals
14 p2254 N85-23969
Effect of elevated-temperature neutron irradiation on fracture toughness of ceramics
[DE85-000652] 14 p2261 N85-24010
A two-cycle shift register with error detection
[AD-A150768] 14 p2400 N85-24791
Ferroelectric tungsten bronze bulk crystals and epitaxial thin films for electro-optic device applications
[AD-A151044] 14 p2427 N85-24970
Surface acoustic wave structure and volume waves
15 p2525 N85-25568
Materials for advanced rocket engine turbopump turbine blades 16 p2734 N85-26872
High-pressure hydrogen testing of single crystal superalloys for advanced rocket engine turbopump turbine blades 16 p2735 N85-26875
Secondary ion mass spectrometry studies of solids and surfaces
[AD-A151744] 16 p2745 N85-26939
Effects of wear on structure-sensitive magnetic properties of ceramic ferrite in contact with magnetic tape
[NASA-TM-87007] 16 p2753 N85-26991
Acceleration-resistant crystal resonator
[AD-D011627] 16 p2778 N85-27144
Studies of strain rate effects in the deformation of solids by means of stress pulses and ultrasonic methods
[DE85-009463] 18 p3122 N85-29329
Study of the equilibrium vacancy ensemble in aluminum using 1D- and 2D-angular correlation of annihilation radiation
[DE85-008967] 18 p3194 N85-29813
Effects of gamma-ray irradiation on dislocations in sodium nitrate single crystals
[DE85-008291] 18 p3195 N85-29818
Laser Schlieren crystal monitor
[NASA-CASE-MFS-28060-1] 19 p3374 N85-30932
Crystal growth of device quality GaAs in space
[NASA-CR-176024] 19 p3375 N85-30935
Low-temperature positron lifetime and Doppler-broadening measurements for single-crystal nickel oxide containing cation vacancies
[DE85-010238] 19 p3376 N85-30944
Debye temperature and static displacements in LuH sub x single crystals from energy dispersive X-ray diffraction
[DE85-010961] 19 p3376 N85-30946
Reduction of the trapping of positrons in dislocated single crystals of iron when charged with hydrogen
[DE85-010235] 19 p3377 N85-30950
Microgravity silicon zoning investigation
[NASA-CR-171531] 20 p3397 N85-31073
Photoeffects of semiconductor electrolyte interfaces
[AD-A154163] 20 p3449 N85-31411
Constitutive modeling of superalloy single crystals and directionally solidified materials
20 p3466 N85-31535
Compositional analysis of silicon
20 p3480 N85-31626
Positron measurements in 2H-TaSe2 crystals
[DE85-010507] 20 p3529 N85-31949
Temperature field around a spherical, cylindrical, and needle-shaped crystal, growing in a pre-cooled melt
[NASA-TM-77889] 20 p3537 N85-32011
Determination of edge and screw dislocation density in single crystals of high-purity iron
[DE85-010237] 20 p3537 N85-32012
The measurement of strain fields by X-ray topographic contour mapping
[AD-A154870] 21 p3599 N85-32348
A fluidized-bed reactor for silane pyrolysis
21 p3609 N85-32413
Basic ice nucleation mechanisms on mono and microcrystals and ice forming nuclei. Theoretical analysis and experimental results achieved in the laboratory over the past ten years: Review paper
21 p3642 N85-32629
Spectral-luminescence characteristics and induced emission of Nd-3(+) ion in Gd(2-x)Nd(x)(WO4)3 crystals
21 p3688 N85-32912
The development and evaluation of point defect models for the growth of passive films on single crystal, polycrystalline, and amorphous metal surfaces
[AD-A154685] 21 p3709 N85-33023
Microstructure-mechanical property relationships in the transformation-toughened ceramics
[DE85-011946] 22 p3752 N85-33261
Infrared studies of the influence of alkali metals on the C-O bond in chemisorbed carbon monoxide
[DE85-005306] 23 p3911 N85-34232
Cost effective single crystals: The Rolls Royce approach — gas turbine components
[PNR-90262] 23 p3985 N85-34717
Wholebody radiation counting system
[AD-A155842] 24 p4131 N85-35607

SINGLE SIDEBAND MODULATION
U SINGLE SIDEBAND TRANSMISSION

SINGLE SIDEBAND TRANSMISSION
Digital signal demodulators with single-sideband
07 p0950 N85-16019
Use of the analytic signal in ultrasonic imaging
[DE84-016843] 07 p1039 N85-16596
Study of phase radiogeodetic systems with phase-locked loops 13 p2115 N85-23172

SINGULAR INTEGRAL EQUATIONS
Sinc method of solution of singular integral equations
[AD-A146155] 03 p0411 N85-12631
A note on the use of polynomial transformations in evaluating singular integrals
[MATHEMATICS-RESEARCH-165]
12 p1920 N85-22053
Calculating dominant (quasi-t) mode group velocity in shielded microstrip line 22 p3780 N85-33422

SINGULARITY (MATHEMATICS)
Implementation of the supersonic triplet singularity into the USTORE computer code
[CSIR-NIAST-83/47] 01 p0001 N85-10006
Stable and chaotic dynamical systems and their singularities in the complex time plan
[DE84-011780] 01 p0035 N85-10222
Classical free-streamline flow over a polygonal obstacle
[NASA-CR-172448] 01 p0046 N85-10301
Applications of integral equations with strong singularities in fracture mechanics
03 p0371 N85-12367
Removal of singularities in Tresca and Mohr-Coulomb yield functions
[OUEL-1528/84] 03 p0413 N85-12642
Singularity model for the analysis of wall interference in closed wind tunnels according to the wall pressure signature method (blockage and lift)
[FW-FO-1612] 04 p0453 N85-12874
Computation of the nonequilibrium flow in a gasdynamic laser
[AD-A141022] 04 p0505 N85-13224
Flow calculation on a thin wing, with specific attention to separation point at the trailing edge
[FTW-FO-1721] 05 p0594 N85-13787
Translational control of a graphically simulated robot arm by kinematic rate equations that overcome elbow joint singularity
[NASA-TP-2376] 06 p0856 N85-15446
Numerical experiments and theoretical analysis of the flow of an elastic liquid of the Maxwell-Oldroyd type in the presence of geometrical singularities
[WTHD-164] 08 p1163 N85-17340
Topological triviality of versal unfoldings of complete intersections 11 p1699 N85-20678
On the accuracy of least squares methods in the presence of corner singularities
[NASA-CR-172552] 12 p1919 N85-22050
Transient analysis of loaded thin-wire antennas and transmission lines 13 p2053 N85-22852

Structural stability and bifurcation in conical flow fields
[VTH-LR-424] 16 p2803 N85-27262

SINKS
NT HEAT SINKS
Three dimensional global modeling of atmospheric CO2 06 p0652 N85-14189
The nitrogen cycle: Atmosphere interactions
05 p0653 N85-14191
Evolution of set of Rossby waves toward anisotropic equilibrium state 13 p2109 N85-23141
Flow past a flat plat with a vortex/sink combination
[JIAA-TR-58] 15 p2464 N85-25215
On planetary rings as sources and sinks of magnetospheric plasmas 15 p2677 N85-26526
Tribological sinks: Money down the drain
[DE85-010019] 17 p2974 N85-28376

SINKS (GEOLOGY)
U STRUCTURAL BASINS

SINTERED ALUMINUM POWDER
Engineering property comparisons of PM and IM aluminum alloy forgings
[AD-B088146L] 08 p1173 N85-17398

SINTERING
Sintered silicon nitride workpiece
[NASA-TM-77600] 01 p0021 N85-10129
Treating silicon carbide sinter by heating in nitrogen
[NASA-TM-77601] 01 p0021 N85-10130
Silicon nitride sintered body
[NASA-TM-77602] 01 p0021 N85-10131
Silicon carbide ceramic production
[NASA-TM-77598] 01 p0035 N85-10220
Injection molding of silicon carbide capable of being sintered without pressure
[NASA-TM-77736] 01 p0035 N85-10221
Erosion of sintered WC-Co alloys
02 p0179 N85-11201
An investigation of the role of sintering in gas-solid interactions
[DE84-015481] 02 p0288 N85-11884
Ceramic powder for sintering materials
[NASA-TM-77434] 03 p0336 N85-12160
Sintering behavior of ultrafine silicon carbide powders obtained by vapor phase reaction
[NASA-TM-77422] 03 p0336 N85-12161
Ceramic microstructure development
[AD-A145753] 03 p0337 N85-12166
Preparation of sinter-active silicon carbide powders
[BMFT-FB-T-84-189] 04 p0469 N85-12982
Reactive sintering of SiC 04 p0473 N85-13010
Tests and modeling for sintering theory
[DE84-015110] 04 p0473 N85-13012
Fatigue behavior of sintered steels and measurement criteria for sintered prefabricated parts
05 p0650 N85-14174
Development and production of improved alpha-phase silicon nitride powders for hot pressing and sintering
[BMFT-FB-T-84-208] 07 p0921 N85-15830
Influence of size grading of sintering ore on the sintering process
[BLL-M-36004-(5828.4)] 07 p0924 N85-15854
Procedure for investigating high-temperature properties of iron-ore materials
[BLL-M-36020-(5828.4)] 07 p0926 N85-15868
The determination of vertical sintering speed of sinter charges
[BLL-M-36033-(5828.4)] 07 p0926 N85-15869
Solid-phase sintering of tantalum carbide
[BLL-M-36013-(5828.4)] 07 p0926 N85-15872
Fatigue strength of different sintered steels and design criteria for porous material (PM) parts
[LBF-FB-170/84] 07 p0928 N85-15886
Development and production of improved silicon carbide powder for pressureless sintering and hot pressing
[BMFT-FB-T-84-211] 07 p0934 N85-15917
Tensile test of pressureless-sintered silicon nitride at elevated temperature
[NASA-TM-77777] 08 p1172 N85-17390
Consolidation of thermites by pressing and sintering
[DE84-016943] 09 p1297 N85-18146
Sub-eutectic densification and second phase formation in Al2O3 - CaO
[DE85-002065] 09 p1396 N85-18796
Optimization of production of composite diamond-containing materials using titanium carbide-steel alloys 10 p1446 N85-19113
Kinetics of saturation of porous titanium with low melting point metals 10 p1446 N85-19114
Behavior and specifics of fracture of porous fiber materials in extension 10 p1447 N85-19118
Densification of submicron YSZ (Yttria-Stabilized Zirconia) powders with alumina and borate additives
[AD-A149520] 10 p1452 N85-19150
Positive electrodes of nickel-cadmium batteries
[NASA-TM-77808] 10 p1478 N85-19330
Structure and properties of copper-titanium-aluminum composites obtained by thermoreactive sintering
11 p1600 N85-20061
Laser processing of ceramics
[DE85-001184] 11 p1612 N85-20135
High-temperature, solid oxide electrolyte fuel cell power generation system
[DE85-002978] 11 p1675 N85-20552
Slip casting and nitridation of silicon powder
[NASA-TM-77809] 12 p1818 N85-21406
Pressureless sintered silicon nitride as a promising candidate for radome materials
[AD-P004367] 12 p1826 N85-21461
Development of a sintered shim
[DE85-006183] 13 p2025 N85-22685
Densification and deformation in the presence of a liquid phase
[DE85-005101] 13 p2038 N85-22763
Sintered silicon carbide molded body and method for its production
[NASA-TM-77646] 14 p2250 N85-23999
Influence of oxygen traces on the properties of tungsten heavy metals
[BLL-RARDE-TR-1177-(7291.7965)]
15 p2508 N85-25470
Comparative sinterability of combustion synthesized and commercial titanium carbides
[DE85-006255] 15 p2512 N85-25498
Sintering phenomena of non-oxide silicon compounds
[DE85-006676] 15 p2520 N85-25535
Fiat conducts R and D in ceramic parts for diesel engine 15 p2534 N85-25637
Production of shaped parts of NITINOL alloys by solid-state sintering
[AD-A152069] 16 p2749 N85-26966
Test and modeling for sintering theory
[DE85-007761] 16 p2755 N85-27004
Impact of optical inhomogeneity in sintered interface between glasses on laser emission characteristics
16 p2763 N85-27053
Reaction-bonded and fiber-reinforced SiC static and dynamic gas turbine components
[BMFT-FB-T-84-302] 17 p2899 N85-27874
Powder-metallurgy alloys and steels
[BLL-BISI-TRANS-22239-(9022.06)]
17 p2926 N85-28050
Sintering and properties of metal-ceramic alloys of the Kovar type
[BLL-BISI-TRANS-21822-(9022.06)]
17 p2927 N85-28060
Process for making electrodes for discharge tubes
[DE85-008898] 17 p2955 N85-28247
Electrodes for flash discharge lamps
[DE85-008897] 17 p2955 N85-28250
Effects of processing chemistry on electrical properties of high field ZnO varistors
[DE85-007666] 17 p2956 N85-28254
Sintering reactions, structure and properties of a cobalt free nonconventional hard material
[DE85-007704] 18 p3076 N85-29025
French, UK, Swedish research in powder metallurgy, HIP 18 p3088 N85-29109
Powder metallurgy forged gear development
[NASA-TM-87483] 18 p3117 N85-29295
Joining of sintered composite TiC-steel materials by welding
[BLL-M-36253-(5828.4)] 20 p3461 N85-31502
Introduction of structural variations into oxide polymers and their effect on sintering and crystallization
[AD-A155597] 21 p3570 N85-32206
Sintering studies project
[AD-A154750] 21 p3572 N85-32216
Hot isostatically pressed Sm(2)(TM)17 magnets
[AD-A155479] 21 p3582 N85-32267
Reliability of void detection in structural ceramics using scanning laser acoustic microscopy
[NASA-TM-87035] 21 p3597 N85-32337
Influence of particle arrangement on sintering
[AD-A155337] 21 p3599 N85-32352
Ultra-trace analysis of sinter tantalum with SIMS
[BLL-RARDE-TR-1220-(7291.7965)]
23 p3913 N85-34245
Reliability of two sintered silicon nitride materials
[NASA-TM-87092] 23 p3919 N85-34284

SINUSOIDS
U SINE WAVES

SIPHONS
A siphon flow model for Evershed motion --- sunspot regions 14 p2453 N85-25147

SIR-A
U SHUTTLE IMAGING RADAR

SIR-B
U SHUTTLE IMAGING RADAR

SIRIO SATELLITE
Interference experiment with the Sirio-OTS satellites
[FUB-17-1983] 01 p0040 N85-10254
Attenuation experimental data bank in the COST 205 project. Structure and management of the final support
[FUB-5-1983] 01 p0126 N85-10986

SIRS B SATELLITE
SIR-B cartography and stereo topographic mapping
08 p1147 N85-17234
Monitoring of the tidal dynamics of the Dutch Waddensea by SIR-B 08 p1147 N85-17235
Studies of coastal mesoscale winds using SIR-B
08 p1147 N85-17238

SIS (SEMICONDUCTORS)
AlAs/GaAs superlattice barrier unipolar diode structure
[DE85-001904] 11 p1736 N85-20821

SITE SELECTION
A pilot study of future research on seismic hazards in Sweden
[FOA-C-20544-T1] 02 p0229 N85-11496
Calibration and validation areas --- satellite altimeters
03 p0384 N85-12458
Carbon monoxide study, Anchorage, Alaska, November 22, 1982 to February 11, 1983
[PB84-236595] 05 p0673 N85-14321
Potential affiliate stations to work with the EVN -- European VLBI Network; QUASAT
07 p1057 N85-16708
Ground-water level data and preliminary potentiometric-surface maps, Yucca Mountain and vicinity, Nye County, Nevada
[DE85-001771] 09 p1343 N85-18446
Preliminary survey of wind generation in Washington: Site studies and selected wind speed data
[DE85-000058] 09 p1345 N85-18462
Assessment of wave power available at key United Kingdom sites
[IOS-186] 09 p1346 N85-18466
Planning for greater-confinement disposal
[DE85-002143] 09 p1383 N85-18697
Airport site selection and design
[AD-P004193] 11 p1581 N85-19959
Index to published geologic maps in the region around the potential Yucca Mountain nuclear waste repository site, southern Nye County, Nevada
[DE85-000260] 11 p1669 N85-20518
Shallow magma targets in the western US
[DE85-003274] 12 p1881 N85-21803
Optimum path selection in automated radio relay link design 13 p2073 N85-22947
Selection of promising sites for magma energy experiments
[DE85-006832] 16 p2820 N85-27393
Parabolic dish test site: History and operating experience
[NASA-CR-175892] 17 p2985 N85-28447
Conceptual hydrologic model of flow in the unsaturated zone, Yucca Mountain, Nevada
[DE85-008346] 18 p3125 N85-29350
Region-to-area screening methodology for the Crystalline Repository Project
[DE85-009892] 18 p3125 N85-29354
Reference data source documentation for performance assessment studies, Basalt Waste Isolation Project, Hanford Site, Washington
[DE85-010543] 19 p3301 N85-30468
Design of the National Trends Network for monitoring the chemistry of atmospheric precipitation
[GS-CIRC-964] 20 p3486 N85-31684
Detection of solar neutrons by ground based neutron monitors
[IFSI-84-11] 20 p3547 N85-32076
Criteria for site selection and frequency allocation (keynote paper), part 5 21 p3623 N85-32511
Frequency and site selection criteria for MST radars, part 5.1A 21 p3624 N85-32512
Fusion facility siting considerations
[DE85-012694] 22 p3843 N85-33805
Mars landing sites 22 p3859 N85-33893
Reports from the German Meteorological Service. No. 166: The optimal spectral density of climatological station networks
[ISBN-3-88148-214-8] 23 p3950 N85-34478
Resource evaluation and site selection for microalgae production systems
[DE85-008807] 23 p3951 N85-34485
The 1984 biotic studies of Yucca Mountain, Nevada test site, Nye County, Nevada
[DE85-011715] 23 p3951 N85-34487
Simulated effects of increased recharge on the ground-water flow system of Yucca Mountain and vicinity, Nevada-California
[DE85-012985] 24 p4106 N85-35480
Siting of large scale wind turbines in Denmark
24 p4111 N85-35483
Special questions of siting wind turbine arrays and networks --- West Germany 24 p4111 N85-35484

Environmental aspects of the Netherlands wind farm project 24 p4111 N85-35485
Visual impact of GROWIAN and resulting recommendations for siting of large wind energy converters 24 p4112 N85-35486

ITES
NT LANDING SITES
NT LAUNCHING PADS
NT LAUNCHING SITES
Community relations activities at Department of Defense sites [AD-P004150] 09 p1349 N85-18486
Adsorption site, adsorption energy and normal vibration frequency of H/Ni(100) via total energy calculations [AD-A150555] 13 p2156 N85-23388
Literature survey of underground construction methods for application to hardened facilities [AD-A155212] 21 p3590 N85-32351

SITTING POSITION
Effect of body position and immobilization on intensity of spatial illusions in weightlessness 22 p3621 N85-33672

SIZE (DIMENSIONS)
NT GRAIN SIZE
Size specific total particulate emission factors for mobile sources [PB84-226653] 01 p0071 N85-10471
The smallest sizes of diffuse interstellar clouds 06 p0878 N85-15578
Space nuclear-power reactor design based on combined neutronic and thermal-fluid analyses [DE85-002433] 11 p1727 N85-20884
Torso sizing ring construction for hard space suit [NASA-CASE-ARC-11616-1] 12 p1910 N85-21987
A Gimbal sizing analysis for an IPACS rotating assembly [NASA-CR-172524] 16 p2741 N85-26913
Grain structure identification by ultrasound frequency averaging and deconvolution [AD-A154332] 19 p3352 N85-30777
The effect of set size on time to recall color coded information [AD-A155013] 21 p3666 N85-32767
An exploratory study of the effect of screen size and resolution on the legibility of graphics in automated job performance aids [AD-A155989] 24 p4136 N85-35632

SIZE DETERMINATION
NT PRECIPITATION PARTICLE MEASUREMENT
The size of the lunar core 04 p0581 N85-13713
Programming and application of numerical controlled measuring machines (NCMES) [BMFT-FB-T-84-153] 05 p0717 N85-14599
Size dependence of chondrule textural types 06 p0882 N85-15606
Computer sizing of fighter aircraft [NASA-TM-86351] 08 p1067 N85-16759
Research study of droplet sizing technology leading to the development of an advanced droplet sizing system [NASA-CR-174839] 12 p1850 N85-21604
Recent trends in particle size analysis techniques [NASA-TM-77735] 13 p2017 N85-22645

SIZE DISTRIBUTION
NT PARTICLE SIZE DISTRIBUTION
Experimental study of the spray characteristics of a research airblast atomizer [NASA-TM-86911] 07 p0904 N85-15727
Measurement of drop-size distributions with the aid of a scattered light particle size counting analyser [BLL-TRANS-WH-620-(9091.9F)] 09 p1317 N85-18278
Application of scattered light particle size counting analysis to the determination of wide drop size distributions [BLL-TRANS-WH-619-(9091.9F)] 09 p1317 N85-18279
Asteroid collisional evolution studies 13 p2176 N85-23501
Evolution of stratospheric aerosol size distribution from ground-based radiometric measurements: A study of El Chichon aerosol [DE85-007555] 16 p2827 N85-27439
Elemental analysis of aerosols in Transvaal urban and power-producing areas using time and size-resolved samples 16 p2829 N85-27443
The dynamical behavior of the age-size-distribution of a cell population [CWI-AM-R8414] 17 p2996 N85-28538
Ice fog as an electro-optical obscurant [AD-A155059] 21 p3705 N85-33015
Burst size distributions in the digitized data of the ion chambers t Mt. Norikura and sea level stations [SH-9.1-9] 23 p4051 N85-35124
Atmospheric neutrinos observed in underground detectors [HE-5 3-6] 24 p4205 N85-36102

SIZE SEPARATION
Improved silicon grinding method and apparatus [NASA-CASE-NPO-16336-1-CU] 12 p1819 N85-21407
Acoustic particle separation [NASA-CASE-NPO-155559-1] 19 p3350 N85-30765
Size and DNA distributions of electrophoretically seperated cultured human kidney cells 20 p3500 N85-31759

SIZING (SEPARATION)
U SIZE SEPARATION

SIZING (SHAPING)
Application of finite element method to the sizing of mechanical parts — helicopter design [SNIAS-851-210-105] 20 p3463 N85-31515
Preliminary sizing and performance of aircraft [NASA-TM-86357] 21 p3554 N85-32111

SIZING (SURFACE TREATMENT)
The application of anthropometric survey data to aircrew clothing sizing [AD-A150545] 13 p2143 N85-23304

SKELETON
U MUSCULOSKELETAL SYSTEM

SKEWNESS
Transformation of heterogeneous surface waves by skewed streams 02 p0259 N85-11697
Compensation of skew passband of a SAW filter using predistortion 12 p1821 N85-21422
Skewed stable variables and processes [AD-A150549] 13 p2153 N85-23372

SKID LANDINGS
Aircraft accident report: World Airways Inc., Flight 30H, McDonnell Douglas DC-10-30CF, N113WA, Boston-Logan International Airport, Boston, Massachusetts, January 23, 1982 [PB85-910406] 22 p3728 N85-33114

SKIDDING
Predictor model for seasonal variations in skid resistance, volume 1 [PB84-226612] 01 p0036 N85-10229
Predictor model for seasonal variations in skid resistance. Volume 2: Comprehensive report [PB84-226620] 01 p0037 N85-10230
Skid resistance of bituminous surfaces in Ohio [PB84-234491] 04 p0484 N85-13086
Evaluation of Epoxo 300-C nonskid coating for use on bridge decks [PB85-108643] 12 p1819 N85-21412
Skid steering of wheeled and tracked vehicles: Analysis with Coulomb friction assumptions [AD-A149626] 12 p1860 N85-21664

SKILLS
U ABILITIES

SKIN (ANATOMY)
NT EPITHELIUM
In vivo dermal absorption method and system for laboratory animals [AD-D011231] 01 p0094 N85-10635
Natural electrical activity of human sympathetic nerve fibers, recorded from body surface 07 p1013 N85-16433
Technique for measuring body circumferences and skinfold thicknesses [AD-A148166] 08 p1195 N85-17532
Specifics of human thermal regulatory reactions upon exposure to coriolis acceleration 10 p1525 N85-19617
Evaluation of a field expedient technique for sweat sample collection [AD-A151916] 16 p2841 N85-27521
Carcinogenesis of nitrated toluenes and benzenes skin and lung tumor assays in mice [AD-A155723] 22 p3818 N85-33655

SKIN (STRUCTURAL MEMBER)
Zero adhesion system [AD-D011237] 01 p0015 N85-10093
Low power laminar aircraft structures 04 p0451 N85-12857
Aircraft skin penetrator and agent applicator. Volume 2: Test and evaluation [AD-A151609] 15 p2466 N85-25225
Development of a field repair technique for mini-sandwich Kevlar/epoxy aircraft skin [AD-A151369] 15 p2503 N85-25439
Friction and wear behavior of aluminum and composite I-beam stiffened airplane skins [NASA-TM-86418] 17 p2895 N85-27852
Laminated thermoplastic radome [AD-D011664] 18 p3079 N85-29045
Impact dynamics research on composite transport structures [NASA-TM-86391] 19 p3264 N85-30367
A normal incidence X-ray telescope sounding rocket payload [NASA-CR-176169] 24 p4153 N85-35749

SKIN FRICTION
NT AERODYNAMIC DRAG
NT FRICTION DRAG
NT VISCOUS DRAG
Turbulent boundary layers over rough surfaces hypersonic flow [AD-A145040] 01 p0003 N85-10016
Full scale experiments into the use of large eddy breakup devices for drag reduction on aircraft 08 p1071 N85-16790
A two-axis, self-nulling skin friction balance [NASA-CASE-LAR-13294-1] 12 p1851 N85-21610
Surface shear stress characteristics in turbulent flows 19 p3211 N85-29914
The effects of microbubbles on turbulent boundary layer skin friction 20 p3451 N85-31425
Numerical solutions of turbulent models for flow over a flat plate with angle of attack [DE85-010380] 21 p3585 N85-32286
A three-dimensional turbulent boundary layer undergoing transverse strain and streamwise pressure gradient [NASA-TM-86766] 23 p3930 N85-34358

SKIN TEMPERATURE (BIOLOGY)
Specifics of human thermal regulatory reactions upon exposure to coriolis acceleration 10 p1525 N85-19617
Circadian rhythm of human body temperature during spaceflights 12 p1901 N85-21934

SKIN TEMPERATURE (NON-BIOLOGICAL)
Turbine heat transfer 02 p0142 N85-10964

SKIRTS
Water impact laboratory and flight test results for the space shuttle solid rocket booster aft skirt 09 p1335 N85-18394
Finger materials for air cushion vehicles. Volume 2: Base fabrics for finger materials [AD-A149701] 12 p1819 N85-21408
Results of tests on a specimen of the SRB aft skirt heat shield curtain in the MSFC LRLF [NASA-CR-170883] 24 p4070 N85-35221
SRB TPS closeout materials characterization [NASA-CR-170885] 24 p4070 N85-35222
Study of NSI and related cable performance during tests performed in the NASA Hot Gas Facility [NASA-CR-170886] 24 p4101 N85-35423

SKIS
Determination of parameters of cupped aircraft landing ski 06 p0775 N85-14856

SKULL
SSMIR (Solid State Memory Instrumentation Recorder): A new approach to acquiring data during an aircraft seat/sled ejection sequence [AD-A154780] 21 p3589 N85-32308

SKY
NT NIGHT SKY
HEAO-1 diffuse soft X-ray sky maps 06 p0877 N85-15570
A FORTRAN program for deep space sensor analysis [AD-A151700] 15 p2489 N85-25366
Issue of sky conditions [DE85-010590] 19 p3317 N85-30562
Correlation analysis of 1 to 30 MeV celestial gamma rays 20 p3549 N85-32083
A transportable, machine oriented library of european sky and terrain radiance distributions with contemporary radiometric and meteorological profiles [AD-A155254] 21 p3637 N85-32590

SKY BRIGHTNESS
NBS (National Bureau of Standards) daylight availability database [PB84-245745] 07 p1054 N85-16688
The IRAS mission 09 p1412 N85-18901
Flux reconstruction and calibration 09 p1412 N85-18904
Analysis of processing 09 p1412 N85-18905
Investigating statistical characteristics of atmospheric background brightness and star background density in equatorial region of celestial sphere 15 p2478 N85-25298
Issue of sky conditions [DE85-010590] 19 p3317 N85-30562

SKY RADIATION
NT AIRGLOW
NT GEOCORONAL EMISSIONS
NT NIGHTGLOW
NT TWILIGHT GLOW
Thermal characterization of photovoltaic modules in natural environments 06 p0832 N85-15296
Improved Nominal Operating Cell Temperature (NOCT) test procedure 21 p3612 N85-32449

SKY WAVES
NT WHISTLERS
Skywave radar detectability of volcanic aersols [AD-A151448] 15 p2542 N85-25694

SKYLAB PROGRAM

The evolution of civilian in-space infrastructure, i.e., space station concepts in the United States
07 p0914 N85-15788

Material research in microgravity
[NASA-TM-77626] 14 p2228 N85-23811

Primate experiments on SLS-1
15 p2687 N85-26592

SKYLAB 3

Relative abundances of sub-iron to iron nuclei in low energy (50-250 MeV/N) cosmic rays as observed in the Skylab experiment
[OG-4.1-4] 22 p3676 N85-34010

SKYLAB 4

Hypervelocity impacts on Skylab 4/Apollo windows
12 p1785 N85-21202

Hypervelocity impact investigations and meteoroid shielding experience related to Apollo and Skylab
12 p1785 N85-21206

SKYNET SATELLITES

UK Skynet 4 communications satellites
11 p1710 N85-20757

SL 3
U SKYLAB 3

SL 4
U SKYLAB 4

SLABS

Microwave measurement of the complex dielectric tensor at anisotropic slab materials
[DE84-017050] 04 p0493 N85-13144

A remote source system for measuring relative positron annihilation line widths in individual slab cylindrical samples
[AERE-R-10549] 12 p1938 N85-22173

Guided-mode launching in a slab waveguide by way of diffraction at the edge of a conducting screen residing on one surface of the slab
[AD-A154886] 21 p3575 N85-32232

Multiple collision solutions for time-dependent neutron transport in slabs of finite thickness
[OEFZS-4312] 22 p3838 N85-33762

Negative flexural behavior of precase composite slabs with steel joint 23 p3904 N85-34183

SLAGS

The electrochemical deoxidation of molten oxide substances
[BLL-M-35962-(5828.4)] 05 p0614 N85-13920

Distribution of oxygen between metal and basic slags
[BLL-M-35932-(5828.4)] 05 p0616 N85-13935

Calculation of energy of atomization in silicate tetrahedron Si4(4-)
[BLL-M-36000-(5828.4)] 07 p1040 N85-16599

The development of titanium production in the USSR
[BLL-OA-TRANS-3226-(6196.3)]
23 p3913 N85-34244

SLANT
U SLOPES

SLANT PERCEPTION
U SPACE PERCEPTION

SLASHES
U CLEARINGS (OPENINGS)

SLEDS
NT ROCKET PROPELLED SLEDS

Design and testing of an energy-absorbing crewseat for the F/FB-111 aircraft. Volume 2: Data from seat testing
[NASA-CR-3917] 24 p4064 N85-35184

SLEEP

The effect of sleep loss on the human visual event-related potential
[AD-A145364] 02 p0234 N85-11528

Effect of physical work and sleep loss on recovery sleep
[AD-A146082] 03 p0401 N85-12554

Sleep physiology in weightlessness (experiment 1ES 030) — Spacelab 05 p0695 N85-14474

Computerized sleep staging by detecting eye and hand movement, delta EEG activity and EMG, using portable solid state technique — spaceborne experiments
05 p0695 N85-14475

Laboratory note: Effect on sleep latency of pre-sleep AEP (Auditory Evoked Potential) procedures
[AD-A147620] 08 p1194 N85-17527

Electrosleep therapy advanced at medical institute
10 p1526 N85-19623

Homeostasis in primates in the hyperdynamic environment — circadian timekeeping and effects of lower body positive pressure on sleep
15 p2610 N85-26085

Sleep and wake physiology in weightlessness
20 p3510 N85-31819

SLEEP DEPRIVATION

The effect of sleep loss on the human visual event-related potential
[AD-A145364] 02 p0234 N85-11528

Cognitive performance during successive sustained physical work episodes
[AD-A148061] 08 p1200 N85-17556

Effects of partial deprivation of slow-wave sleep on sleep-wakefulness cycles 10 p1524 N85-19613

Sleep deprivation and exercise tolerance
[AD-A150180] 13 p2142 N85-23295

Sleep deprivation and exercise tolerance
[AD-A150566] 13 p2142 N85-23296

Sleep deprivation and exercise tolerance
[AD-A150626] 13 p2142 N85-23297

Sleep deprivation and performance: Older age performance and limited sleep period use
[AD-A153102] 17 p2999 N85-28540

Human performance in continuous/sustained operations and the demands of extended work/rest schedules. An annotated bibliography
[AD-A155619] 21 p3686 N85-32771

SLEEVES

Manifold insulated with knitted impregnated sleeve
[AD-D011270] 06 p0814 N85-15167

Windblast arm protector assembly
[AD-D011512] 12 p1909 N85-21984

Direct transient analysis of a fuze assembly by axisymmetric solid elements 15 p2576 N85-25890

SLENDER BODIES
NT SLENDER CONES

Comparison of uniform perturbation solutions and numerical solutions for some potential flows past slender bodies
[NASA-CR-172485] 06 p0749 N85-14799

Transonic flow of elastic medium past slender solid body 06 p0776 N85-14976

Some important problems in unsteady boundary layers including separation. 2: Unsteady boundary layers close to the stagnation region of slender bodies
[AD-A146964] 07 p0958 N85-16069

Generation of a pair of symmetric eddies behind a slender axisymmetric body with pitch angle
[ISL-R-121/83] 11 p1577 N85-19934

An experimental and analytical study of the aerodynamic interference effects between two Sears-Haack bodies at Mach 2.7
[NASA-TM-85729] 16 p2700 N85-26673

SLENDER CONES

Experimental investigations of prismatic cylinders in flow with harmonic pulsations
[KU-SFB-210/E/4] 16 p2785 N85-27186

SLENDER WINGS

Transonic wing and far field test data on a high aspect ratio transport wing for three dimensional computational method evaluation 01 p0004 N85-10021

Flutter parametric studies of cantilevered twin-engine transport type wing with and without winglet. Volume 2: Transonic and density effect investigations
[NASA-CR-172410-VOL-2] 04 p0513 N85-13270

A calculation of slender delta wing with leading-edge separation by quasi-vortex-lattice method
12 p1821 N85-21423

Numerical simulation of transonic flutter of a high-aspect ratio transport wing 16 p2694 N85-26630

Aerodynamic performance of a wing in ground effect using the PANAIR program
[AD-A153303] 17 p2892 N85-27832

Low-speed tests of a high-aspect-ratio, supercritical-wing transport model equipped with a high-lift flap system in the Langley 4- by 7-meter and Ames 12-foot pressure tunnels
[NASA-TP-2097] 20 p3368 N85-31010

SLEWING

Operational fitness of box truss antennas in response to dynamic slewing
[NASA-CR-172470] 10 p1429 N85-19012

Time-optimal bang-bang slew of rigidized SCOLE configuration 20 p3410 N85-31164

SLICING

The read-out system of spatial distribution of thermoluminescence in meteorites
[SH-9.1-16] 23 p4052 N85-35131

SLICKS
U OIL SLICKS

SLIDES
U CHUTES

SLIDES (MICROSCOPY)

The Fibrin slide assay for detecting urokinase activity in human fetal kidney cells 20 p3502 N85-31768

SLIDING

Control of tractors on sloping ground
[AD-P004292] 09 p1408 N85-18869

Sealing assembly
[AD-D011463] 10 p1452 N85-19151

Interaction among inhomogeneities and inclusions
[AD-A153114] 17 p2979 N85-28419

The effect of stress and hot corrosion on nickel-base superalloys
[AD-A154722] 21 p3566 N85-32181

SLIDING FRICTION

An experimental investigation and numerical simulation of the thermomechanical phenomena in compressor rotor tip rubbing 03 p0367 N85-12352

Effect of barrier height on friction behavior of the semiconductors silicon and gallium arsenide in contact with pure metals
[NASA-TP-2405] 04 p0478 N85-13044

Effect of asperity interactions on scuffing
[AD-A146544] 06 p0814 N85-15170

Computational methods for nonlinear dynamics problems in solid and structural mechanics
[AD-A148352] 08 p1172 N85-17392

Analytical and experimental investigation of rubbing interaction in labyrinth seals for a liquid hydrogen fuel pump — space shuttle main engine
[NASA-CR-174657] 09 p1287 N85-18084

Sliding seal materials for adiabatic engines
[NASA-CR-174893] 13 p2037 N85-22757

Significant parameters of the behavior and of the surface damage of the lubricated Hertzian contact: An application to gears 14 p2222 N85-23783

Wear reduction by lubricants in confined contacts
14 p2223 N85-23786

Sliding interfaces with contact-impact in large scale Lagrangian computations
[DE85-006451] 15 p2639 N85-26277

Mechanical interactions of rough surfaces
[DE85-005653] 18 p3118 N85-29299

Granular Flow Project
[DE85-010015] 19 p3270 N85-30279

Kinetic friction coefficient of ice
[AD-A155035] 21 p3680 N85-32859

Rolling, slip and traction measurements on low modulus materials
[NASA-CR-174909] 22 p3791 N85-33491

Anti wear property of two phasic metal composite
23 p3906 N85-34199

SLIP BANDS
U EDGE DISLOCATIONS

SLIP CASTING

Study of the pore structure of ceramics prepared by the slip casting method
[NASA-TM-77495] 04 p0478 N85-13048

Nitinol devices, phase 2, integration of slip ring system and tracking mechanism with memory drive
[BMFT-FB-W-84-032] 05 p0619 N85-13959

Slip casting and nitridation of silicon powder
[NASA-TM-77809] 12 p1818 N85-21406

SLIPSTREAMS
NT PROPELLER SLIPSTREAMS

Turbulent jet flow in a channel with a circulation region
09 p1306 N85-18218

An experimental investigation of propfan installations on an upswept supercritical wing at transonic Mach numbers
[NASA-CR-172605] 20 p3386 N85-31013

SLITS

The effect of grazing flow on the impedance of the Helmholtz resonator 05 p0635 N85-14076

SLOPES
NT GLIDE PATHS

Terrain analysis procedural guide for surface configuration
[AD-A145637] 02 p0219 N85-11446

Occurrences of the polar slant E condition (SEC) at Narssarssuaq, Godhavn, Thule 1982
03 p0393 N85-12514

Relationship between forest clearing and biophysical factors in tropical environments: Implications for the design of a forest change monitoring approach — Costa Rica
[E85-10051] 07 p0963 N85-16247

Study of the motion of agricultural vehicles on steep grass-covered slopes
[AD-P004290] 09 p1408 N85-18867

Some stability and control problems with trailed farm tankers on slopes
[AD-P004291] 09 p1408 N85-18868

Control of tractors on sloping ground
[AD-P004292] 09 p1408 N85-18869

Analysis of slope stability, Wilmington to Lindenkohl Canyons, US mid-Atlantic margin
[DE84-012278] 12 p1899 N85-21921

Relationship between brightness spectrum of photographic image and spectrum of rises on a water surface with waves 13 p2115 N85-23171

A statistical treatment of the regional slope characteristics of Venus and Earth
13 p2178 N85-23517

Lithologic and structural control on slope morphology in the Valles Marineris 13 p2201 N85-23651

Guidelines for the evaluation of visual approach slope indicators
[ARL/SYS-R-32] 23 p3896 N85-3413

Evaluation: Close-range photogrammetry for slope inventory and monitoring
[PB85-192755] 24 p4108 N85-35470
Turbulent structure of stably stratified nocturnal slope flows
[AD-A155845] 24 p4123 N85-35559

SLOSHING
U LIQUID SLOSHING

SLOT ANTENNAS
Experimental measurements of the ion cyclotron antennas' coupling and RF characteristics
[DE85-011569] 23 p3982 N85-34694
Characteristic modes for slots in a ground plane TE case
[AD-A155757] 24 p4086 N85-35326

SLOTS
Portable slotting device
[AD-D011213] 01 p0033 N85-10206
Electromagnetic transmission through a slot in a perfectly conducting plane
[AD-A153224] 17 p2949 N85-28210
A multiplying slot array
[AD-A155570] 21 p3576 N85-32245
Induction motors with minimum waste of magnetic iron
22 p3772 N85-33377
Dual optical mechanical position tracker
[AD-D011739] 22 p3844 N85-33811

SLOTTED ANTENNAS
U SLOT ANTENNAS

SLOTTED WIND TUNNELS
Interference from slotted walls
03 p0314 N85-12028
An inerference assessment approach for a three-dimensional slotted tunnel with sparse wall pressure data
03 p0314 N85-12030
A local slot boundary condition for transonic flow calculations in slotted-wall test sections of wind tunnels
[FFA-TN-1984-34] 04 p0453 N85-12879
Investigation for the improvement of the transonic tunnel working section of the Emmen Federal Aircraft Works (Switzerland)
[FW-FO-1681] 04 p0458 N85-12904
Flow quality of NAL 2-dimensional transonic wind tunnel. Part 2: Extensive and systematic pressure fluctuations study in the settling chamber, test section and second throat of the NAL 2-D transonic wind tunnel
[NAL-TR-836-PT2] 09 p1283 N85-18066
Finite difference computation of the flow around airfoils in two-dimensional transonic slotted wall wind tunnel
11 p1623 N85-20216
Wind tunnel wall interference
[AD-A151212] 15 p2474 N85-25273

SLOW NEUTRONS
U THERMAL NEUTRONS

SLUDGE
Remedial action of hazardous waste US Army Corps of Engineers, Anniston, Alabama
[AD-P004141] 09 p1347 N85-18477

SLURRIES
Additives for heat engine coal slurry fuels
[DE84-016434] 05 p0621 N85-13971
Gasification of boron oxide drops and boron slurry agglomerates in combustion gases
13 p1999 N85-22529
Catalyst and reactor development for a liquid phase Fischer-Tropech process
[DE85-005894] 17 p2922 N85-28014
Transport characteristics of slurries in pipelines: Flow regimes and pressure drop
[DE85-009453] 18 p3101 N85-29196
Development of a coal-water slurry-fueled diesel engine for industrial cogeneration. Task 1.0 topical report: Thermodynamic analysis
[DE85-010455] 19 p3236 N85-30062
Very high speed lap with positive lift effect
[AD-D011710] 19 p3280 N85-30344
Very high speed lap with negative lift effect
[AD-D011711] 19 p3281 N85-30345
Effect of nonuniform size on internal stresses in a rapid, simple shear flow of granular materials. Part 1: Two grain sizes
[AD-A154045] 19 p3285 N85-30372
Coal slurry ignition in a diesel engine simulator
[DE85-010087] 20 p3463 N85-31513
Superheated fuel injection for combustion of liquid-solid slurries
[DE85-011624] 22 p3753 N85-33266
Drying of pulverized material with heated condensible vapor
[DE85-011656] 22 p3783 N85-33438
Method of preparing thin porous sheets of ceramic material
[DE85-006399] 24 p4082 N85-35300

SLURRY PROPELLANTS
Status of boron combustion research
[AD-A154762] 21 p3563 N85-32160

SMALL PERTURBATION FLOW
Robust calculation of three-dimensional transonic potential flow based on the nonlinear gas multigrid method and a mixed incomplete lower upper decomposition/strongly implicit procedure (ILU/SIP) algorithm
[NLR-MP-84003-U] 12 p1848 N85-21593
Extension of the small perturbations method in three-dimensional transonic, unsteady flow to the case of real wings
[ONERA-NT-17/3064-RY-070-R]
20 p3389 N85-31017

SMELTING
New ferrous metallurgy technology
01 p0019 N85-10114
Sweden develops new rapid solidification process
15 p2531 N85-25610
Assessment of metal heating technologies for ferrous forging: A pilot study of the form value of natural gas
[PB85-204394] 24 p4064 N85-35314

SMOG
Impact of alcohol fuels on urban air pollution: Methanol photochemistry study
[DE84-012950] 04 p0531 N85-13397
Evaluation of chemical reaction mechanisms for photochemical smog. Part 2: Quantitative evaluation of the mechanisms, revised
[PB85-166060] 16 p2822 N85-27408
Effect of traffic and meteorology on air pollution
16 p2830 N85-27452
Development of a chemical kinetic mechanism for the US EPA (Environmental Protection Agency) regional oxidant model
[PB85-185858] 22 p3813 N85-33618
Modeling of auto exhaust smog chamber data for EKMA development
[PB85-186492] 22 p3813 N85-33619
Atmospheric reaction products from hazardous air pollutant degradation
[PB85-185841] 22 p3813 N85-33620
Studies in photochemical smog chemistry. 1: Atmospheric chemistry of toulene. 2: Analysis of chemical reaction mechanisms for photochemical smog
24 p4113 N85-35497

SMOKE
The perceptual quality of smoke screens: An analysis of the Oldebroek 2 trials, May 1981
[IZF-1984-20] 01 p0095 N85-10641
The prediction of observer responses from photometric data on smoke screens; an analysis of the Oldebroek 2 trials, May 1981
[IZF-1984-21] 01 p0095 N85-10642
Analytical fuel property effects: Small combustors, phase 2
[NASA-CR-174848] 10 p1456 N85-19175
Continuous laminar smoke generator
[NASA-CASE-LAR-13014-1] 12 p1781 N85-21178
Ionic mechanisms of soot formation in flames
[AD-A150119] 12 p1801 N85-21297
Time and space variability of turbulent concentration fluctuations
[AD-A149963] 12 p1896 N85-21898
Effects of interactive transport and scavenging of smoke on the calculated temperature change resulting from large amounts of smoke
[DE85-006450] 14 p2378 N85-24684
Advanced smoke meter development survey and analysis
[NASA-CR-168287] 15 p2560 N85-25792
Evaluation of pyrotechnic fire suppression system for six pyrotechnic compositions
[AD-A152995] 17 p2937 N85-28130

SMOKE ABATEMENT
Laboratory simulation of smoke reduction from aircraft engine test cell exhaust using a fluidized bed filter
[AD-A148600] 08 p1089 N85-16886
Numerical simulations of the effect of floor and ceiling venting on fire and smoke spread in aircraft cabins
[PB85-178333] 19 p3216 N85-29939

SMOKE DETECTORS
Test results from a comparative evaluation of a condensation nuclei fire detector
[NASA-CR-3874] 12 p1862 N85-21675
Evaluation of pyrotechnic fire suppression system for six pyrotechnic compositions
[AD-A152995] 17 p2937 N85-28130

SMOKE TRAILS
Numerical simulations of the effect of floor and ceiling venting on fire and smoke spread in aircraft cabins
[PB85-178333] 19 p3216 N85-29939

SMOOTHING
NT DATA SMOOTHING
Improved carrier tracking by smoothing estimators
05 p0623 N85-13989
Recovering pointwise values of discontinuous data within spectral accuracy
[NASA-CR-172535] 12 p1919 N85-22049
Consistency of smoothing with running linear fits
[AD-A150232] 13 p2150 N85-23349
Kalman filtering and exponential smoothing in economics 15 p2635 N85-26246
Uniformly high-order accurate non-oscillatory schemes, 1
[NASA-CR-175766] 16 p2853 N85-27569
The essence of invexity
[CSIR-TWISK-321] 16 p2858 N85-27626
To the theory of approximation of experimental curves by smooth functions
[PREPRINT-438] 18 p3173 N85-29671
Computer programs for smoothing and scaling airfoil coordinates
[NASA-TM-84666] 20 p3388 N85-31011
A residuals approach to filtering, smoothing and identification for static distributed systems
20 p3418 N85-31213

SNAKING
U LATERAL OSCILLATION

SNAP
SNAP (Space Nuclear Auxiliary Power) reactor overview
[AD-A146831] 07 p1041 N85-16612

SNATCHING
U SPACECRAFT RECOVERY

SNOW
Heliport snow and ice control methods and guidelines
[DOT/FAA/PM-84/22] 01 p0012 N85-10073
Some mesoscale weather effects and the very short-range forecasting impact of variable snow cover
01 p0075 N85-10499
Fractals: From snow flakes to galactic clusters
[NOTA-INTERNA-796] 02 p0296 N85-11918
Anglo-German millimeter wave backscatter measurements on snow, environmental data report
[REPT-7-84] 04 p0492 N85-13136
The Finnish approach to microwave remote sensing of snow 05 p0656 N85-14212
Snow characterization measurements from SNOW-TWO/Smoke Week 6
[AD-A147423] 07 p1008 N85-16402
Climate at CRREL (Cold Regions Research and Engineering Laboratory) Hanover, New Hampshire
[AD-A148400] 08 p1189 N85-17495
Regional and seasonal variations in snow-cover density in the USSR
[AD-A148429] 08 p1189 N85-17496
Atlas of snow and ice resources
10 p1497 N85-19449
Ground-based snow and ice crystal observation system used in Sierra Nevada winter orographic storms
[PB85-115343] 10 p1520 N85-19584
Snow reflectance from Thematic Mapper
13 p2120 N85-23205
Remote Sensing of Snow and Evapotranspiration
[NASA-CP-2363] 13 p2123 N85-23223
General report of the researches of snowpack properties, snowmelt runoff and evapotranspiration in Japan 13 p2124 N85-23225
Snowmelt-runoff model utilizing remotely-sensed data
13 p2124 N85-23226
Snowmelt runoff model in Japan
13 p2124 N85-23227
Studies on physical properties of snow based on multi channel microwave radiometer
13 p2125 N85-23231
Radiation-dominated snowmelt on Mars
13 p2191 N85-23592
An equation of profile of snow drift density during snowfall 15 p2581 N85-25919
Measuring methods of atmospheric electric elements at the Earth's surface during snowfall and investigation of these relationships 15 p2581 N85-25920
Case studies of snow clouds by means of snow crystal sondes 15 p2581 N85-25921
A survey of major east coast snowstorms, 1960-1983. Part 2. Summary of surface and upperlevel characteristics
[NASA-TM-86195] 16 p2833 N85-27471
A survey of major east coast snowstorms, 1960-1983. Part 2: Case studies of eighteen storms
[NASA-TM-86196] 16 p2833 N85-27472
Snow Scale/Rate meter
[AD-D011648] 17 p2994 N85-28505
The capture of ice nucleating and non ice-nucleating aerosols by ice phase precipitation
21 p3641 N85-32620
Ice-forming efficiency of the soluble and insoluble portions of dust contained in snow
21 p3643 N85-32631

Scavenging of submicron aerosol particles by snow crystals: Theory and experiments
21 p3646 N85-32667

Elemental tracers of source regions of contaminants in precipitation
[DE85-012658] 24 p4113 N85-35499

SNOW COVER

Measurement of snow cover thickness by radar sounding 03 p0344 N85-12216

Scattering from snow backgrounds at 35, 98, and 140 GHz
[AD-A145798] 03 p0355 N85-12260

A comparison between active and passive sensing of soil moisture from vegetated terrains
04 p0526 N85-13364

Synoptical observations of snow depths at Dutch meteorological stations, 1956 - 1977
[KNMI-TR-51] 07 p1008 N85-16407

Microwave emissions from snow
[E85-10065] 08 p1174 N85-17403

Application of Martinec-Rango model to river basin in Japan 13 p2124 N85-23228

Distribution of snow and maximum snow water equivalent obtained by LANDSAT data and degree day method 13 p2124 N85-23229

Microwave radiometer observations of snowpack properties and comparison of U.S. Japanese results — Hokkaido, Japan and Vermont and North Dakota test sites 13 p2125 N85-23230

Analysis of NIMBUS-7 SMMR data — Hokkaido, Japan snow cover 13 p2125 N85-23232

Estimation of regional evapotranspiration using remotely sensed land surface temperature. Part 2: Application of equilibrium evaporation model to estimate evapotranspiration by remote sensing technique --- Japan 13 p2125 N85-23234

Measurement of water equivalent of mountain snow cover — ARGOS system 14 p2327 N85-24386

Low Temperature Science. Series A: Physical Sciences
[ISSN-0439-3538] 15 p2581 N85-25917

The temperature fluctuation in stable stratification above snow cover 15 p2581 N85-25918

Characteristics of snow cover on sea ice and formation of snow ice II 15 p2582 N85-25924

Atmospheric frontal zone studies
[NASA-CR-175293] 16 p2833 N85-27469

Precipitation and snow cover data, 1977
[ISBN-951-697-215-2] 17 p2995 N85-28514

Permafrost, seasonally frozen ground, snow cover and vegetation in the USSR
[AD-A153628] 18 p3124 N85-29346

Snow cover in the Siberian forest-steppe
[NASA-TM-77914] 23 p3943 N85-34435

Comparisons of the North Polar Cap of Mars and the Earth's Northern Hemisphere snow cover
[NASA-TM-86191] 23 p3989 N85-34726

SNOWPLOW EFFECT

U PLASMA DYNAMICS

SNOWSTORMS

East coast snowstorm survey
15 p2598 N85-26013

A survey of major east coast snowstorms, 1960-1983. Part 2. Summary of surface and upperlevel characteristics
[NASA-TM-86195] 16 p2833 N85-27471

A survey of major east coast snowstorms, 1960-1983. Part 2: Case studies of eighteen storms
[NASA-TM-86196] 16 p2833 N85-27472

Circulation analysis of two snowstorms during the SNOW-TWO program
[AD-A155225] 21 p3637 N85-32587

SOBOLEV SPACE

Loeb Sobolev spaces with applications to variational integrals and differential equations
[CTH-MATH-1984-19] 04 p0556 N85-13544

A non-hypoelliptic Dirichlet problem from stochastics
10 p1537 N85-19667

On the accuracy of least squares methods in the presence of corner singularities
[NASA-CR-172552] 12 p1919 N85-22050

Some properties of Loeb-Sobolev spaces
[CTH-MATH-1985-01] 22 p3835 N85-33748

SOCIAL FACTORS

Some aspects of matching nowcasting and Very-Short-Range Forecasting (VSRF) products with the need of a multilingual community of a mountainous country — Swiss Alps 01 p0084 N85-10566

The identification of the scientific community's choice criteria in the history of scientific research: The case of quantum mechanics
[NOTA-INTERNA-797] 02 p0291 N85-11893

Area handbook series. Honduras: A country study
[AD-A146510] 06 p0827 N85-15253

Socio-economic impact of climate — Mexico
07 p1003 N85-16372

Climate and fisheries: A Peruvian case study
07 p1003 N85-16373

Job and family stress as predictors of pilot health, job satisfaction and performance
[AD-A142176] 07 p1018 N85-16464

Aeronautical Engineering: A continuing bibliography with indexes, supplement 186
[NASA-SP-7037(186)] 13 p1965 N85-22342

Disturbance to the population due to flight operations at landing fields. Questionnaire on community reaction to non-commercial and sporting aviation
[NASA-TM-76531] 14 p2353 N85-24537

The effects of controversy and concurrence seeking on effective decision making
[AD-A153370] 17 p3002 N85-28555

Social and political problems in Soviet basic research
[AD-P004565] 17 p3048 N85-28860

Symbolic and interactional perspectives on leadership: An integrative framework
[AD-A155247] 21 p3665 N85-32769

SOCIOLOGY

NT SOCIAL FACTORS

National Science Foundation grants and awards for fiscal year 1983, volume 2
[PB84-212323] 01 p0125 N85-10654

An open-ended future: In defense of a new humanism
[NASA-TM-77613] 12 p1944 N85-22209

The Impact of Science on Society
[NASA-SP-482] 14 p2431 N85-24994

Accomplishments of science by the year 2000
14 p2432 N85-24996

Our future in the cosmos: Space
14 p2432 N85-24998

Science and Technology in the Soviet Union
[AD-A152626] 17 p3047 N85-28856

Space ventures and society long-term perspectives
[NASA-CR-176012] 19 p3379 N85-30963

SODAR

An operational forecasting system for stratus and fog with sodar 01 p0061 N85-10539

An evaluation of wind measurements by four Doppler sodars
[PB85-115301] 10 p1520 N85-19586

Radiosodar system for remote synchronous measurements of wind speed, temperature and its fluctuations 13 p2110 N85-23145

Verification of Doppler sodar measurements --- atmospheric boundary layer
[KNMI-WR-85-2] 22 p3817 N85-33645

SODIUM

NT LIQUID SODIUM
NT SODIUM ISOTOPES
NT SODIUM VAPOR

Trivalent ion exchange in beta alumina
[AD-A145373] 02 p0172 N85-11151

Scattering experiments on interactions of excited atoms: Differential cross sections of the system Na (3P) + K(4S)
[MPIS-8/1984] 05 p0728 N85-14677

A high-resolution study of local interstellar sodium
06 p0875 N85-15556

Forces on neutral atoms due to electromagnetic fields
[AD-A146984] 07 p1040 N85-16603

Collision-induced dipole moments
[AD-A147682] 08 p1121 N85-17063

SSPS-CRS advanced sodium receiver: Construction experience report
[DE85-000625] 10 p1511 N85-19533

First sodium nightglow results for Natal
[INPE-3397-PRE/666] 10 p1515 N85-19560

A modeling analysis program for the JPL table mountain Io sodium cloud data
[NASA-CR-175474] 10 p1572 N85-19910

Study of processes of modification of Al-Si alloys
13 p2026 N85-22695

Sodium and lithium corrosion in molybedenum heat pipes
[DE85-005561] 16 p2784 N85-27179

A modeling analysis program for the JPL table mountain Io sodium cloud
[NASA-CR-175851] 16 p2833 N85-27468

Sodium concrete reaction: Structural considerations
[DE85-009031] 18 p3081 N85-29063

Intrinsically irreversible acoustic heat engines
[DE85-007672] 19 p3270 N85-30276

Intercomparison of the calculated absolute efficiency values between true coaxial and true closed-end coaxial Ge (Li) and NaI detectors
[REPT-5-1984] 20 p3532 N85-31976

The diurnal variation of the neutral sodium species in the upper atmosphere: A model study
[AD-A154986] 21 p3631 N85-32561

Physical and chemical aerosol characteristics in extremely clean air masses at Cape Grim, Tasmania
21 p3646 N85-32655

Photoionization of alkali and alkaline earth atoms. Na and Mg
[DE85-011612] 22 p3837 N85-3

Effect of temperature and ionic impurities at very low concentrations on stress corrosion cracking of Type 304 stainless steel
[TI85-003048] 24 p4079 N85-3

Development and evaluation of sulfonated polysulfone membranes for the zinc-ferricyanide battery
[DE85-009104] 24 p4090 N85-3

A study of the chemistry of alkali metals in the upper atmosphere
[AD-A156349] 24 p4117 N85-3

Noise in sodium beta alumina crystals
[AD-A156025] 24 p4161 N85-3

A new drawing technique for nylon 6 by reversible plasticization with iodine
[AD-A156272] 24 p4162 N85-3

SODIUM ALLOYS

Thermodynamic properties of liquid Li-Pb, Na-Pb and K-Plc]b alloys: Similarities and Differences
[DE85-004074] 18 p3197 N85-2

SODIUM CHLORIDES

Effect of fluid and salt supplements to food allowance on endurance of head-to-pelvis accelerations following 7-day dry immersion and under ordinary motor activity conditions 01 p0092 N85-10616

Salt action on concrete
[AD-A147812] 07 p0933 N85-15912

Application of electrochemical engineering methods and theory to solving corrosion and adhesion problems with organic coatings
[AD-A147799] 08 p1129 N85-17115

Thermodynamic properties of aqueous NaCl from 273 to 823 K with estimates for higher temperatures
[DE85-000392] 09 p1292 N85-18116

Mechanisms of heat and mass transfer across a double-diffusive interface
[PB85-148468] 12 p1848 N85-21584

Resistance of hydrogenated alpha-titanium alloys to corrosion-fatigue fracture 15 p2499 N85-25413

The use of moments of momentum to account for crystal habits
[NASA-CR-3907] 20 p3421 N85-31222

Experimental investigation of radiative-acoustic effects in the water by the thermodynamical conditions of Dumand
[HE-7.1-2] 24 p4213 N85-36158

SODIUM COMPOUNDS

NT SODIUM CHLORIDES
NT SODIUM IODIDES
NT SODIUM NITRATES
NT SODIUM SILICATES
NT SODIUM SULFATES

Synthesis and properties of Hexachloromolybdates(5) and related species
[AD-A139599] 07 p0924 N85-15852

Ames Laboratory measurements of alkali levels in the Curtiss-Wright PFBC gas stream
[DE85-011357] 22 p3745 N85-33214

SODIUM IODIDES

Measurement of nuclear lines with a dual Ge(Li) telescope aboard a stratospheric balloon
[INPE-3380-TDL/185] 11 p1762 N85-21083

Improved method for the stabilization of NaI-photomultiplier gamma detectors against thermal and other drift
[DE85-011830] 23 p3970 N85-34613

SODIUM ISOTOPES

Cosmogenic Na-22 and Al-26 in Luna-24 lunar drill core soil samples 13 p1961 N85-22427

SODIUM NITRATES

Effects of gamma-ray irradiation on dislocations in sodium nitrate single crystals
[DE85-008291] 18 p3195 N85-29618

Sodium nitrate containing mixture for producing ceramic-glass-ceramic seal by microwave heating
[DE85-011610] 22 p3751 N85-33254

SODIUM SILICATES

EXAFS studies of sodium silicate glasses containing dissolved actinides
[DE84-015835] 04 p0479 N85-13051

SODIUM SULFATES

Interactions between corrosion and creep of uncoated and coated superalloys in sulfate melts
04 p0477 N85-13039

SODIUM SULFUR BATTERIES

Physico-chemical investigations on the electronic partial conductivity of molten electrolytes, especially of the eutectic mixture LiCl-KCl
[BMFT-FB-T-84-205] 05 p0633 N85-14863

BBC of Switzerland develops electric car
08 p1141 N85-17182

Prospects for advanced storage battery technologies
[DE84-015708] 09 p1345 N85-19484

Production technology of an electrolyte for Na/S batteries
[BMFT-FB-T-84-277] 15 p2550 N85-25742
Degradation phenomena in solid electrolytes
[DE85-007066] 15 p2587 N85-25949
Sixth DOE Electrochemical Contractor's Review. Extended abstracts
[DE84-013679] 16 p2779 N85-27151
Transfer of battery technology developed by the US Department of Energy
[DE85-009666] 22 p3808 N85-33588

SODIUM VAPOR
Degenerate four-wave mixing lineshapes in sodium vapor under pulsed excitation
[AD-A148211] 08 p1222 N85-17696
Astronomy and sodium lighting
[RAND/N-2069-RC] 09 p1413 N85-18914
A modeling analysis program for the JPL Table Mountain Io sodium cloud data
[NASA-CR-175493] 11 p1681 N85-20589
Instrumentation for particle-beams research using excited merging beams
[AD-A154155] 19 p3356 N85-30807

SOFT LANDING SPACECRAFT
NT APOLLO SPACECRAFT

SOFTENING
Response of ferritic steels to nonsteady loading at elevated temperatures
[DE84-014260] 04 p0513 N85-13272
Non equilibrium ionization in the local hot bubble
06 p0879 N85-15587
Softening of metal near seam during welding of heat-resistant nickel alloys 13 p2035 N85-22747
Solution softening in molybdenum-rhenium alloys
[DE85-006706] 16 p2750 N85-26972
Thermomechanical softening treatment for bearing and tool steels
[BLL-BISI-TRANS-22432-(9022.06)]
17 p2925 N85-28035

SOFTNESS
Strength and aging behaviour of soft soldered joints
[BLL-T6365/BG/WH600/84] 07 p0925 N85-15662

SOFTWARE (COMPUTERS)
U COMPUTER PROGRAMS
U COMPUTER SYSTEMS PROGRAMS

SOFTWARE ENGINEERING
NT ASSEMBLER ROUTINES
NT COMPUTER PROGRAMMING
NT LANGUAGE PROGRAMMING
NT LOGIC PROGRAMMING
NT MICROPROGRAMMING
NT MULTIPROGRAMMING
NT PARALLEL PROGRAMMING
NT SYMBOLIC PROGRAMMING
Potential use of dialogue with computers in biomedical research 01 p0091 N85-10614
Comparative descriptions of software quality measures
[GMD-STUDIES-81] 01 p0102 N85-10676
SAGA: A project to automate the management of software production systems
[NASA-CR-174017] 01 p0103 N85-10685
Ada (trademark) training curriculum. Software engineering for managers m101 teacher's exercise guide
[AD-A145094] 01 p0104 N85-10695
Mathmatics and Computer Science Division activities
[DE84-014842] 01 p0104 N85-10701
Establishing a Software Engineering Technology (SET)
[PB84-212141] 01 p0105 N85-10702
Microcomputers in Hungary 01 p0115 N85-10786
Software engineering environments for mission critical applications: STARS alternative programmatic approaches
[AD-A145265] 02 p0241 N85-11571
Program flow analyzer, volume 1
[AD-A145320] 02 p0241 N85-11572
Description of the software acquisition process (SWAP) model
[AD-A145413] 02 p0241 N85-11573
DOD related software technology requirements, practices, and prospects for the future
[AD-A145493] 02 p0242 N85-11575
Program flow analyzer, volume 3
[AD-A145522] 02 p0242 N85-11577
Concurrent processing and the decomposition of problems
[DE84-015265] 02 p0242 N85-11581
A representation for the functioning of devices that supports compilation of expert problem solving structures: An extended summary
[AD-P003921] 02 p0245 N85-11601
Artificial intelligence applications to automatic test equipment
[AD-P003936] 02 p0247 N85-11616
Programming effort estimation
[AD-A145839] 03 p0406 N85-12595
Automating software design metrics
[AD-A145869] 03 p0407 N85-12598
Configuration management for mission-critical software: The Los Alamos solution
[DE84-015515] 03 p0408 N85-12606
Information Center handbook
[PB84-211341] 03 p0439 N85-12795
Software configuration management across project boundaries and in distributed development environments
[RSRE-MEMO-3704] 04 p0549 N85-13494
Documentation for DIGLIB: Device independent graphics library
[DE84-017365] 04 p0550 N85-13500
Burroughs Corporation B26-CPU, B20 COBOL Version 4.0 (COBOL technical report)
[PB84-216256] 04 p0551 N85-13506
Convergent Technologies, Incorporated, NGEN CP001, CT COBOL Version 9.0 (COBOL technical report)
[PB84-216274] 04 p0551 N85-13508
Research in computer science
[NASA-CR-174066] 05 p0713 N85-14572
Technical Workshop: Advanced Helicopter Cockpit Design
[NASA-CP-2351] 06 p0750 N85-14806
Reusable software
[AD-A146575] 06 p0854 N85-15427
Trends in development of software for computer-aided analysis of large-scale integrated circuits
07 p0955 N85-16055
JPL Robotics Laboratory computer vision software library
[NASA-CR-174272] 07 p1023 N85-16491
Software test handbook
[AD-A146844] 07 p1024 N85-16498
Functional semantics of modules
[AD-A146923] 07 p1024 N85-16500
On the structure of information in software
[AD-A147580] 07 p1026 N85-16511
Ultrasound instrumentation for the 7 inch Mach seven tunnel
[NASA-CR-174277] 07 p1038 N85-16586
Built-in-test for first line testing
08 p1064 N85-16739
Functional built-in-test in a pipelined image processor
08 p1064 N85-16740
The production of maintainable, trustworthy, and portable software 08 p1064 N85-16744
Documentation and separate test program development is most important for test/maintenance
08 p1065 N85-16745
Effective life cycle software support: A study in discipline and versatility 08 p1065 N85-16746
Experience in using on-aircraft software for testing integrated systems 08 p1065 N85-16747
Software testing in an Ada programming environment
08 p1065 N85-16748
Cryogenic propellant management: Integration of design, performance and operational requirements
08 p1098 N85-16939
Fast arithmetic for microcomputers
08 p1140 N85-17180
Researchers on third generation robotics development
08 p1140 N85-17184
ES devices at fair 08 p1141 N85-17187
East Europe report: Science and technology
[JPRS-ESA-84-043] 08 p1142 N85-17196
Plasma and magnetospheric research
[NASA-CR-171293] 08 p1163 N85-17451
VICOM technical description
[REPT-611-0012-REV-A] 08 p1202 N85-17563
Software test handbook: Software test guidebook, volume 2
[AD-A147289] 08 p1204 N85-17578
Concept paper for the development of a DOD Ada (trademark) software engineering education and training plan
[AD-A148774] 08 p1206 N85-17592
Study of application of space telescope science operations software for SIRTF use
[NASA-CR-177337] 09 p1267 N85-18060
Development and operation of a real-time data acquisition system for the NASA-LaRC differential absorption lidar
[NASA-CR-174384] 09 p1366 N85-18583
Concepts and tools for the software life cycle
10 p1464 N85-19236
A program design for an adaptive, non-linear finite element solver
[AD-A148880] 10 p1539 N85-19705
Selected NBSNET software
[PB85-109148] 10 p1542 N85-19723
French work toward flexible software workshops
11 p1592 N85-20015
Space Station Software Issues
[NASA-CP-2361] 11 p1700 N85-20689
Software management issues — space station software development 11 p1700 N85-20690
Software development environment issues — space station software development 11 p1700 N85-20691
Software standards issues — space station software development 11 p1701 N85-20692
Information systems issues 11 p1701 N85-20693
Shuttle software production facility
11 p1701 N85-20694
Software technology within NASA
11 p1701 N85-20695
Communications software for Olympics Micromation Computer System
[PB85-109510] 11 p1704 N85-20723
AFOS (Automation of Field Operations and Service) surface observation decoding
[PB85-137586] 12 p1898 N85-21913
A survey of the project CIP: Computer aided, intuition-guided programming. Wide spectrum language and program transformations
[TUM-I8406] 12 p1912 N85-22000
Earth radiation budget experiment software development
[NASA-CR-172567] 12 p1912 N85-22002
DOS 21: PCDOS 2.0 support subroutine package for the IBM personal computer
[LA-10142-MS] 12 p1914 N85-22012
Microcomputers in transit: A software handbook
[PB85-136414] 12 p1918 N85-22042
A formal method for specifying computer resources in an implementation independent manner
[AD-A149955] 12 p1918 N85-22043
Validation summary report, Burroughs Corporation, 820 FORTRAN release 4.0
[PB84-227792] 13 p2145 N85-23316
Principles of software engineering environment design
[AD-A150352] 13 p2147 N85-23324
Measurement of SIFT operating system overhead
[NASA-TM-86322] 13 p2149 N85-23337
Investigation of doubly-fed machine in variable speed application
[DE85-004378] 14 p2299 N85-24234
Ultraviolet Spectrometer and Polarimeter (UVSP) software development and hardware tests for the solar maximum mission
[NASA-CR-175279] 14 p2305 N85-24271
The identification of semantics for the file/database problem domain and their use in a template-based software environment 14 p2401 N85-24803
An experiment in software reliability
[NASA-CR-172553] 14 p2403 N85-24813
An algebraic specification language and a syntax directed editor
[AD-A150664] 14 p2403 N85-24815
Computers and the consulting engineer
15 p2626 N85-26184
A learning strategy approach for teaching novice computer programmers
[AD-A151523] 15 p2628 N85-26200
Extension of the software development workbench to include microcomputer workstations
[AD-A151903] 15 p2630 N85-26207
Praxis language environment: Distribution package description, revision 1
[DE85-006699] 15 p2630 N85-26212
IPAD: Integrated Programs for Aerospace-vehicle Design
[NASA-CR-3890] 15 p2632 N85-26221
Mathematical software for hyperbolic equations and two point boundary value problems
[AD-A151982] 15 p2638 N85-26270
Space radiation studies — Spacelab 2 Payload
[NASA-CR-171410] 15 p2685 N85-26584
Active control technology: Past, present, future
16 p2711 N85-26731
East Europe report: Science and technology
[JPRS-ESA-84-032] 16 p2727 N85-26833
A robotic system for preparing reagent and dilution vials
[DE85-008262] 16 p2793 N85-27231
Fujian forges ahead in electronic production
16 p2806 N85-27301
Symbiosis between postgraduate training and research projects: A successful experience
[INPE-3216-PRE/569] 16 p2810 N85-27330
A framework for software development
[AD-A152067] 16 p2847 N85-27551
Diagnosis: Using automatic test equipment and an artificial intelligence expert system
[AD-A151918] 16 p2851 N85-27576
Software for reflectivity calculations of X-ray mirrors, revision 1
[DE85-006642] 16 p2867 N85-27688
COSMIC Software Catalog, 1985 edition
[NASA-CR-174070] 17 p3010 N85-28608

Peer Review of a Formal Verification/Design Proof Methodology
[NASA-CP-2377] 17 p3010 N85-28609
Automatic distribution of programs in MASCOT and Ada (trademark) environments: A feasibility study
[AD-A152665] 17 p3010 N85-28614
Implementation of a general finite element code on an IBM PC compatible microcomputer
[AD-A152661] 17 p3011 N85-28615
A test methodology for an automated and interactive software development environment
[AD-A152657] 17 p3011 N85-28618
CLEANROOM software development: An empirical evaluation
[AD-A152924] 17 p3011 N85-28619
CAMAC 488 module: 68000 based GPIB interface module
[DE85-009367] 17 p3014 N85-28635
Micro-CAE mechanical engineering software development at Lawrence Livermore National Laboratory and participating universities and technology transfer
[DE85-008880] 18 p3163 N85-29597
Annotated bibliography of recent papers on software engineering environments
[PB85-191385] 18 p3165 N85-29607
Statistical estimation of software reliability
[AD-A154097] 19 p3335 N85-30665
Implementation of a proposed system for automated microcode generation
[AD-A154235] 19 p3336 N85-30671
Guide on logical database design
[PB85-177970] 19 p3361 N85-30976
PIPE-1000: An implementation of piping on an HP-1000 minicomputer
[PB85-191955] 20 p3514 N85-31847
Evaluative report on the Institute for Computer Sciences and Technology, National Bureau of Standards, fiscal year 1984
[PB85-176097] 20 p3514 N85-31848
Implementation assessment of the OSI network service. The test definition language
[NPL-DITC-52/84] 20 p3514 N85-31849
Integrated software engineering system (SIGL)
[DT/GL/7254/Z462/G-C./MJ]
20 p3516 N85-31863
Study of the applicability of higher order languages for on-board satellite software production
[ESA-CR(P)-2024] 20 p3516 N85-31864
Determining functional requirements for NASA Goddard's command management system software design using expert systems 20 p3539 N85-32020
The effect of communication-language designs on software specifications
[AD-A155173] 21 p3672 N85-32809
A comprehensive study of the AFIT (Air Force Institute of Technology) software development environment
[AD-A155450] 21 p3672 N85-32812
Experiments and improvements of the ordinary differential equation solvers DEPAC on the CRAY computer
[DE85-013260] 22 p3831 N85-33726
Software for mechanism design
23 p3925 N85-34324
A prototype PASCAL program validation system
[NPL-DITC-57/85] 23 p3956 N85-34513
The parser generator as a general purpose tool
[NASA-CR-177955] 23 p3957 N85-34521
Calculation of the diffusion of light by aerosols: Description of the MIELOR software and results obtained
[REPT-80] 24 p4137 N85-35638
CRAYCDC
[NASA-CR-177374] 24 p4137 N85-35639
CDCCRAY
[NASA-CR-177375] 24 p4137 N85-35640
Study of fault tolerant software technology for dynamic systems
[NASA-CR-172618] 24 p4137 N85-35642
Attacking software crisis: A macro approach
[AD-A155846] 24 p4138 N85-35645
Prototyping with data dictionaries for requirements analysis
[AD-A156303] 24 p4139 N85-35654
Toolpack
[DE85-013135] 24 p4140 N85-35665

SOFTWARE TOOLS
Remote data processing system software in Hungary
01 p0101 N85-10673
FSTC (Federal Software Testing Center) software tool catalog
[PB84-212158] 01 p0105 N85-10703
Study on spectral/radiometric characteristics of the Thematic Mapper for land use applications
[E85-10021] 02 p0218 N85-11434
Proposal for a semiautomatic program testing system
[INPE-3262-TDL/178] 02 p0240 N85-11561
Program flow analyzer, volume 1
[AD-A145320] 02 p0241 N85-11572
Program flow analyzer, volume 2
[AD-A145521] 02 p0242 N85-11576
Program flow analyzer, volume 3
[AD-A145522] 02 p0242 N85-11577
Software for Crimea-Pushchino radiointerferometer
06 p0783 N85-15007
Some experiences of testing protocol implementations — open systems interconnection
[NPL-DITC-48/84] 08 p1204 N85-17574
Multidimensional digital signal processing
[AD-A146055] 08 p1205 N85-17585
Solutions to structural dynamics problems
09 p1334 N85-18384
Identification of emerging designer needs and high payoff CAE tools
[DE85-000755] 09 p1369 N85-18599
High level languages in protocol specification and verification
[FUB-51-1983] 09 p1370 N85-18611
Concepts and tools for the software life cycle
10 p1464 N85-19236
A low-cost, general purpose image processing system
[INPE-3292-PRE/607] 10 p1537 N85-19690
FORTRAN 66 analyser: User's manual
[PB85-111748] 10 p1542 N85-19724
Microcomputers and the electrical engineer
[AD-A150499] 13 p2147 N85-23325
The HORNE reasoning system, revision
[AD-A150963] 14 p2405 N85-24827
CaD systems for electronic component design reviewed 15 p2537 N85-25660
Symposium on Computers in Civil Engineering 1983
[CSIR-S-298] 15 p2626 N85-26182
Programme development: A state of the art
15 p2626 N85-26185
Extension of the software development workbench to include microcomputer workstations
[AD-A151903] 15 p2630 N85-26207
VAX-based graphics mail system
[DE85-007231] 15 p2630 N85-26214
Development of computer aided database design and maintenance tools
[AD-A151782] 16 p2845 N85-27537
Further development of an Interactive Control Engineering Computer Analysis Package (ICECAP) for discrete and continuous systems
[AD-A151783] 16 p2846 N85-27546
The interactive generation of specifications for an onboard software series (GISELE)
17 p2904 N85-27906
COSMIC Software Catalog, 1985 edition
[NASA-CR-174070] 17 p3010 N85-28608
ZOG-Vinson technology demonstration project. Volume 2: System description
[AD-A153871] 19 p3333 N85-30645
Production verification of the acoustic emission weld monitor
[AD-A154168] 20 p3464 N85-31519
Integrated software engineering system (SIGL)
[DT/GL/7254/Z462/G-C./MJ]
20 p3516 N85-31863
Integrated Support Software System (ISSS)
[AD-A155715] 22 p3829 N85-33710
The parser generator as a general purpose tool
[NASA-CR-177955] 23 p3957 N85-34521
Developing graphical tools with minimal GKS
23 p3964 N85-34573
Study of fault tolerant software technology for dynamic systems
[NASA-CR-172618] 24 p4137 N85-35642
Attacking software crisis: A macro approach
[AD-A155846] 24 p4138 N85-35645
Error message recording and reporting in the SLC control system
[DE85-013057] 24 p4140 N85-35664

SOIL EROSION
Erosion and sedimentation chronology of three watersheds in Maryland
[PB84-207356] 01 p0071 N85-10467
Assessing erosion on US cropland: Land management and physical features
[PB84-219252] 04 p0526 N85-13366
Mineral aerosols and source identification
21 p3646 N85-32654

SOIL MAPPING
Method for interpreting soil cover of flowed fields using spectral brightnesses measured from space photographs
02 p0164 N85-11112
Utilization of LANDSAT orbital imagery in the soil survey processes at Rio Grande do Norte state
[E85-10009] 02 p0216 N85-11422
Remote sensing for landforms and soils in the arid southwest United States 03 p0378 N85-12410
The use of Thematic Mapper data for land cover survey 05 p0657 N85-14220
Evaluation of SIR-B imagery for geologic and geomorphic mapping, hydrology, and oceanography in Australia 08 p1146 N85-17229
Preliminary evaluation of TM for soils information
13 p2121 N85-23206
Variability of coefficients of spectral brightness of soils
15 p2486 N85-25346
Identification of structure of soil-vegetation cover using aerial and space photographs 16 p2726 N85-26826
Airphoto interpretation of vegetation and landforms for soil mapping 17 p2983 N85-28436
Space imagery and some geomorphological problems of the Guiana Shield, South America
21 p3802 N85-32366

SOIL MECHANICS
Multispectral passive microwave correlations with an antecedent precipitation index using the Nimbus 7 SMMR
[AD-A145419] 02 p0200 N85-11334
In situ experiment on shear waves generation and determination of elastic properties of soils
[REPT-550] 03 p0375 N85-12393
Development of a preliminary ALRS stabilized material pavement analysis system (SPAS)
[AD-A147116] 07 p0910 N85-15760
Computer program for determining induced stresses and consolidation settlements (CSETT)
[AD-A146730] 07 p1023 N85-16493
Technology reports of the Yamaguchi University, volume 3, no. 3
[ISSN-0386-3433] 09 p1302 N85-18182
Studies on seismic earth pressure of cohesive backfill
09 p1303 N85-18186
Creep deformation of compacted decomposed granite soils 09 p1303 N85-18187
Influence of grain size distribution on the undrained dynamic properties of saturated sand
[PB85-102382/GAR] 09 p1305 N85-18197
Approximation of difference in water table positions by horizontal stratum in studies of their influence on gravity
10 p1502 N85-19478
Analysis of slope stability, Wilmington to Lindenkohl Canyons, US mid-Atlantic margin
[DE84-012278] 12 p1899 N85-21921
Engineering geology of selected areas, US army engineer division, lower Mississippi valley. The American bottom area, MO-IL. Volume 1
[AD-A154258] 19 p3299 N85-30455
Influence of spatial variability of hydraulic characteristics of soils on surface parameters obtained from remote sensing data in infrared and microwaves
[NASA-TM-77902] 20 p3477 N85-31604

SOIL MOISTURE
Multispectral passive microwave correlations with an antecedent precipitation index using the Nimbus 7 SMMR
[AD-A145419] 02 p0200 N85-11334
Surface soil moisture measurements of the White Sands, New Mexico
[NOAA-TM-NESDIS-7] 02 p0219 N85-11441
Scattering models in the microwave regime
[NASA-CR-174001] 04 p0525 N85-13361
A comparison between active and passive sensing of soil moisture from vegetated terrains
04 p0526 N85-13364
New Zealand SIR-B science investigations
08 p1144 N85-17218
Evaluation of the radar response to land surfaces and volumes: Examination of theoretical models, target statistics, and applications 08 p1149 N85-17250
Ground truth for SIR-B images obtained by SIR system 8 impulse radar 08 p1149 N85-17251
Remote sensing of soil moisture
08 p1149 N85-17252
The effects of soil moisture on bistatic clutter power
[AD-A147636] 08 p1150 N85-17261
The influence of soil moisture distribution on the severe-storm environment of the southern Great Plains: A numerical study of the SESAME 4 case
09 p1357 N85-18534
Investigations of vegetation and soils information contained in LANDSAT Thematic Mapper and Multispectral Scanner data
[E85-10082] 12 p1873 N85-21747
Estimation of regional evapotranspiration using remotely sensed land surface temperature. Part 1: Measurement of evapotranspiration at the Environmental Research Center and determination of Priestley-Taylor parameter
13 p2125 N85-23233
Microwave remote sensing of soil moisture
13 p2125 N85-23235

Testing an energy balance model for estimating actual evapotranspiration using remotely sensed data — Hannover, West Germany barley and wheat fields
13 p2125 N85-23236

A method for estimating soil moisture availability
[NASA-CR-175606] 13 p2126 N85-23238

Orbiting multi-beam microwave radiometer for soil moisture remote sensing 14 p2230 N85-23818

Development of the microwave antenna range of the national antenna test facility at Paardefontein
[R-NIAS-21] 15 p2539 N85-25669

Soil moisture and evapotranspiration estimates based on satellite data 15 p2596 N85-25998

Aerospace technology determines forest-fire danger
19 p3295 N85-30427

Thermomigration in porous media. Study of the development of a drying zone 20 p3456 N85-31462

Influence of spatial variability of hydraulic characteristics of soils on surface parameters obtained from remote sensing data in infrared and microwaves
[NASA-TM-77902] 20 p3477 N85-31604

SOIL SCIENCE

Utilization of LANDSAT orbital imagery in the soil survey processes at Rio Grande do Norte state
[E85-10009] 02 p0216 N85-11422

International strategic minerals inventory. Summary report: Manganese
[GS-CIRC-930-A] 02 p0219 N85-11442

Applying an innovative approach to field investigations at a remedial action site
[AD-P004145] 09 p1348 N85-18481

Growth of soil bacteria in presence of Martian soil analog, carbon dioxide and hydrogen peroxide
09 p1361 N85-18560

Glossary of the soil sciences
[PB85-133452] 12 p1952 N85-22263

Microbial ecology of extreme environments: Antarctic yeasts and growth in substrate-limited habitats
[NASA-CR-175810] 16 p2839 N85-27509

Mathematical model of the nitrogen cycle in a nonsaturated area of cultivated soil
20 p3478 N85-31610

Mineral aerosols and source identification
21 p3646 N85-32654

The 1984 environmental monitoring program report for Idaho National Engineering Laboratory site
[DE85-011209] 22 p3812 N85-33611

SOILS
NT ALLUVIUM
NT DIRT
NT LUNAR SOIL
NT PERMAFROST
NT SANDS
NT TAR SANDS

Response and characteristics of structures subjected to S-H waves 01 p0060 N85-10396

The use of fixed-bed adsorber models to predict the fluxes of toxic substances in groundwaters and soil environments
[PB84-202583] 01 p0071 N85-10468

Remote sensing for landforms and soils in the arid southwest United States 03 p0378 N85-12410

Ice-soil mixtures: Visual and near-infrared remote sensing techniques
[NASA-CR-174087] 04 p0525 N85-13358

Thermal properties of soils and soils testing
[DE84-015312] 04 p0525 N85-13360

Effects of acid rain on plant microbial associations in California
[PB84-242122] 04 p0532 N85-13404

The areal pattern of latent and sensible heat fluxes: The combination of soil physics and remotely sensed data 05 p0656 N85-14213

Development of a preliminary ALRS stabilized material pavement analysis system (SPAS)
[AD-A147116] 07 p0910 N85-15760

In-situ stress determination in soil and rock using the acoustic emission method
[AD-A147459] 07 p0979 N85-16215

An integrated remote sensing approach for identifying ecological range sites — parker mountain
[E85-10050] 07 p0983 N85-16246

Relationship between forest clearing and biophysical factors in tropical environments: Implications for the design of a forest change monitoring approach — Costa Rica
[E85-10051] 07 p0983 N85-16247

Fate and disposition of trichloroethylene in surface soils
[AD-A147918] 07 p0995 N85-16321

Computer program to compute soil thermal conductivity from transient temperature measurements
[PB85-100550] 07 p0998 N85-16341

Computer program for determining induced stresses and consolidation settlements (CSETT)
[AD-A146730] 07 p1023 N85-16493

Interactions of hydrazine and of hydrazine derivatives with soil constituents and with soils
[AD-A148475] 08 p1122 N85-17074

Response of saturated porous nonlinear materials to dynamic loadings
[AD-A148528] 08 p1173 N85-17394

Soil formation on tertiary landsurfaces of the New Jersey coastal plain 08 p1181 N85-17441

Chronologic and climatic control on soil development, northern Bighorn Basin, Wyoming and Montana
08 p1181 N85-17443

Ground shock effect on soil field inclusions
09 p1336 N85-18403

Incineration of explosives contaminated soils
[AD-P004142] 09 p1347 N85-18478

Stabilization of contaminated soils by in situ vitrification
[AD-P004144] 09 p1348 N85-18480

Applying an innovative approach to field investigations at a remedial action site
[AD-P004145] 09 p1348 N85-18481

Location of volatile buried wastes by field portable instrumentation
[AD-P004147] 09 p1348 N85-18483

Community relations activities at Department of Defense sites
[AD-P004150] 09 p1349 N85-18486

Protocol for aquifer cleanup decision making at military installations
[AD-P004151] 09 p1349 N85-18487

Results from geopressured-geothermal subsidence studies
[DE84-016279] 09 p1354 N85-18520

Modelling of off-road tyres and soil for improved traction
[AD-P004258] 09 p1404 N85-18834

Development of a soil-wheel interaction model
[AD-P004259] 09 p1404 N85-18835

Soil compliance influence on tyre performance
[AD-P004260] 09 p1404 N85-18836

Effects of slip on energy distribution between tyre and soil
[AD-P004263] 09 p1404 N85-18839

Traction forces of drive tyre on the compacted soil
[AD-P004264] 09 p1404 N85-18840

A rig for testing the soft soil performance of track systems
[AD-P004272] 09 p1405 N85-18848

The dependence of soil bearing capacity and drawbar pull on the spacing between track
[AD-P004273] 09 p1406 N85-18849

The dynamic interaction between track and soil
[AD-P004274] 09 p1406 N85-18850

Effect of hitch positions on the performance of track-grouser systems
[AD-P004277] 09 p1406 N85-18853

The research of driving wheel with movable lugs of the paddy field floating tractor
[AD-P004283] 09 p1407 N85-18860

Mobility of the small combine (track type) on soft ground-relationship between the position of the center of gravity and the mobility
[AD-P004285] 09 p1407 N85-18862

The stress-strain-time graph of rheological soils and its application
[AD-P004286] 09 p1407 N85-18863

Behaviour of soil under a lugged wheel
[AD-P004287] 09 p1407 N85-18864

Prediction accuracy of the torques for rotary tillage by an analog tool
[AD-P004288] 09 p1408 N85-18865

The analysis on the dynamic performance of a single lug
[AD-P004289] 09 p1408 N85-18866

Pressure tests in soil below tires of agricultural vehicles
[AD-P004294] 09 p1408 N85-18871

Quality control in soil compaction by behaviours of exciter
[AD-P004295] 09 p1408 N85-18872

Smoother terrain-machine
[AD-P004296] 09 p1409 N85-18873

A simple prediction model for soil compaction under various wheel loads and geometries as an aid to vehicle design
[AD-P004298] 09 p1409 N85-18875

Flotation tires and subsurface compaction
[AD-P004299] 09 p1409 N85-18876

Tractor power selection with compaction constraints
[AD-P004300] 09 p1409 N85-18877

Composition and method for cleaning embedded soil from surfaces having low gloss coatings
[AD-D011465] 10 p1459 N85-19194

An assessment of ground-coil heat-pump technology
[DE85-002567] 10 p1486 N85-19382

Consolidation around a point heat source
[PB85-116549] 11 p1682 N85-20601

Field lysimeter facility for evaluating the performance of commercial solidified low-level waste
[DE85-003666] 11 p1727 N85-20663

Thematic Mapper spectral dimensionality and data structure 12 p1871 N85-21736

Remote sensing research for agricultural applications — San Joaquin County, California and Snake River Plain and Twin Falls area, Idaho
[E85-10090] 12 p1873 N85-21752

Glossary of the soil sciences
[PB85-133452] 12 p1952 N85-22263

Characterization of LANDSAT-4 TM and MSS image quality for the interpretation of California's agricultural resources — Central Valley 13 p2118 N85-23190

Preliminary comparisons of the information content and utility of TM versus MSS data 13 p2120 N85-23202

Calculations of microwave brightness temperature of rough soil surfaces: Bare field
[NASA-TM-86200] 13 p2123 N85-23221

Areas with forest soils sensitive to acidic deposition under alternative damage hypotheses
[DE85-005257] 13 p2130 N85-23257

Chemical weathering of soils from the dry valleys of Antarctica: A terrestrial analog of Martian weathering processes 13 p2197 N85-23628

Determination of electromagnetic properties of mesh material using advanced radiometer techniques
14 p2235 N85-23855

Innovation in earthquake and natural hazards research: Determining soil liquefaction potential
[PB85-149573] 14 p2374 N85-24678

Impact of soil moisture in organizing a severe storm outbreak 15 p2597 N85-26009

Multiple regression analysis of photographic image of soil properties 16 p2726 N85-26825

Use of Goudrian model in studying laws of reflection in vegetation-soil system in optical range. 2: Influence of illumination conditions on spectral brightness coefficients 16 p2726 N85-26827

Interactive effects of acid rain and gaseous air pollutants on natural terrestrial vegetation
[DE85-005255] 16 p2821 N85-27401

Ultrasonic dispersion of soils for routine particle size analysis: Recommended procedures
[DE85-005530] 16 p2861 N85-27643

Effect of the agressive action of soil on metallic pipelines. New possibilities for the passive and active corrosion protection
[BLL-BISI-TRANS-21630-(9022.06)]
17 p2928 N85-28070

Constitutive modeling for blast-induced wave propagation
[AD-A153576] 18 p3099 N85-29187

Survival of microorganisms and bacterial predation in nature
[AD-A153574] 18 p3152 N85-29514

Soil temperature extrema recovery rates after precipitation cooling 20 p3491 N85-31697

Numerical modeling of subsurface communication
[DE85-012818] 21 p3577 N85-32249

Mineral aerosols and source identification
21 p3646 N85-32654

Biogeochemical cycling and remote sensing
21 p3659 N85-32733

Soil extraction kit
[AD-D011736] 22 p3742 N85-33190

WIPP horizon in situ permeability measurements
[DE85-012687] 22 p3802 N85-33557

Geologic, technical, and economic sensitivity analysis in support of the GRI (Gase Research Institute) tight gas reservoirs project area
[PB85-192276] 22 p3802 N85-33559

Environmental surveillance at Los Alamos during 1984
[DE85-011886] 22 p3811 N85-33605

Global environmental transport models for tritium
[DE85-011437] 22 p3816 N85-33639

Arctic and offshore research
[DE85-001995] 22 p3818 N85-33653

Development of solid thorium-232 reference materials
[DE85-011453] 22 p3841 N85-33785

Effects of acid rain on forest nutrient status
[DE85-012486] 23 p3947 N85-34463

Multi-solute subsurface transfer modeling for energy solid wastes: Highlights FY 1984
[DE85-012786] 23 p3966 N85-34591

Mineral deposit models: Theory and practice
24 p4105 N85-35448

Development of an NBS (National Bureau of Standards) polymer gage for dynamic soil stress measurement
[PB85-208494] 24 p4118 N85-35526

The measurement of nitrogen oxide (NO, NO2) exchange over plant/soil surfaces
[CSIRO-DAR-TP-8] 24 p4127 N85-35587

best copy available

SOL-GEL PROCESSES

Structural evolution during the gel to glass conversion
[DE84-014954] 06 p0772 N85-14939

Sol-gel-derived AR coatings for solar receivers
[DE85-000192] 11 p1673 N85-20541

SOLAR ACTIVITY

NT FACULAE
NT SOLAR FLARES
NT SOLAR PROMINENCES
NT SOLAR STORMS
NT SPICULES
NT STELLAR FLARES
NT SUNSPOTS

Research study: Studies in atmospheric processes from Space Platforms
[NASA-CR-171176] 01 p0072 N85-10473

The mapping of the Sun at 8 mm wavelength and tracking of the active regions in the period 23 May - 5 June 1983
[REPT-S-149] 02 p0297 N85-11924

Variability of Neptune 02 p0299 N85-11938

The soft X-ray diffuse background: Implications for the nature of the local interstellar medium
06 p0876 N85-15566

Solar-geophysical data number 478, June 1984. Part 1 (prompt reports): Data for May 1984, Apr. 1984, and late data
[PB84-243153] 06 p0890 N85-15653

Solar-geophysical data number 478, June 1984. Part 2 (comprehensive reports): Data for December 1983 and miscellanea
[PB84-243161] 06 p0890 N85-15654

User's guide for the Nimbus 7 ERB Solar Analysis Tape (ESAT)
[NASA-TM-86143] 10 p1572 N85-19914

Explanation of the normal winter anomaly from the seasonal variation of short wave absorption
11 p1660 N85-20463

Aeronomical aspects of mesospheric photodissociation: Processes resulting from the solar H Lyman alpha line
[AERONOMICA-ACTA-A-285-1984]
11 p1680 N85-20587

National solar-terrestrial research program, part 1. Solar-terrestrial research for the 1980's, part 2
[AD-A149542] 11 p1681 N85-20591

Solar-Geophysical Data. Part 1: (Prompt reports)
[PB85-112068] 11 p1766 N85-21100

Plasma and nuclear processes in solar matter
12 p1954 N85-22277

Solar-geophysical data number 479, July 1984. Part 1: (Prompt reports). Data for June 1984, May 1984 and later data
[NASA-CR-175542] 12 p1962 N85-22333

NIMBUS-7 SBUV (Solar Backscatter Ultraviolet) observations of solar UV spectral irradiance variations caused by solar rotation and active-region evolution for the period November 7, 1978 - November 1, 1980
[NASA-CR-175544] 12 p1962 N85-22334

Solar-geophysical data number 483. November 1984. Part 1: (Prompt reports). Data for October 1984, September 1984 and late data
[PB85-147692] 12 p1962 N85-22335

Solar-geophysical data number 483, November 1984. Part 2: (Comprehensive reports). Data for May 1984, December 1981 and miscellanea
[PB85-147700] 12 p1962 N85-22336

Auroral-polar cap environment and its impact on spacecraft plasma interactions 13 p1991 N85-22484

Solar Seismology From Space. A conference at Snowmass, Colorado
[NASA-CR-175661] 14 p2441 N85-25060

Overview of solar seismology: Oscillations as probes of internal structure and dynamics in the Sun
14 p2441 N85-25061

The magneto-optical filter, working principles and recent progress 14 p2442 N85-25066

Observed spatial properties of the solar eigenfunctions and the implications for the existence of resolved multiflets 14 p2443 N85-25074

The hydromagnetics of the Sun — conferences
[ESA-SP-220] 14 p2445 N85-25091

Nonlinear dynamos — solar activity
14 p2447 N85-25106

A consideration of the solar cycle in the light of the behavior of the large active regions
14 p2452 N85-25140

Observations concerning energy balance in solar magnetic regions 14 p2452 N85-25145

About sudden disappearances and reappearances — solar activity 14 p2454 N85-25157

Solar magnetohydrodynamics: Symposium review
14 p2455 N85-25162

Modeling 22-year solar activity cycle within framework of dynamo theory with allowance for primary field
15 p2477 N85-25266

Sixteenth Lunar and Planetary Science Conference. Press abstracts
[NASA-CR-175692] 15 p2680 N85-26548

Bern solar data for January-December 1984
[REPT-51] 15 p2685 N85-26581

Periodicity of variations in galactic cosmic ray fluxes and solar activity parameters near 20th cycle minimum
16 p2720 N85-26791

Dependence of equatorial F-region plasma bubble rise velocity and dynamo electric field on solar cycle
[INPE-3439-PRE/696] 16 p2826 N85-27434

Very large array observations of coronal loops and related observations of solar type stars
[AD-A152027] 16 p2866 N85-27817

Solar activity monitoring satellite (SAMSAT): Impact on space environment services
[PB85-165066] 16 p2866 N85-27818

Solar-Geophysical Data Number 484, December 1984. Part 1 (prompt reports): Data for November 1984, October 1984 and late data
[NASA-CR-175829] 16 p2866 N85-27819

Inferred flows of electric currents in solar active regions 18 p3208 N85-29899

Evidence for submergencew of magnetic flux in a growing active region 18 p3208 N85-29902

Solar-geophysical data no. 485, January 1985. Part 1 (prompt reports): Data for December 1984, November 1984 and late data
[PB85-181360] 20 p3548 N85-32079

Doppler satellite data characteristics
[AD-A154868] 21 p3575 N85-32231

Variation in radiowave propagation conditions in corona during solar activity cycle 22 p3763 N85-33327

Comparisons of the North Polar Cap of Mars and the Earth's Northern Hemisphere snow cover
[NASA-TM-86191] 23 p3989 N85-34728

Precision measurements of solar energetic particle elemental composition
[SH-2.1-4] 23 p3998 N85-34785

Energetic solar particle events
[SH-3.2-2] 23 p4003 N85-34818

A study of periodicities and recurrences in solar activity and cosmic ray modulation
[SH-4.4-14] 23 p4034 N85-35010

Variations of the cosmic ray general component in Antarctica
[SH-4.4-17] 23 p4035 N85-35013

The difference in the energy spectra of galactic cosmic rays at the minima of the 19th and 20th solar activity cycles
[SH-4.4-18] 23 p4035 N85-35014

Cosmic ray variations with the period close to 27 days and their connection with solar activity longitudinal distribution
[SH-4.4-19] 23 p4035 N85-35015

Long-term modulation of galactic cosmic rays in high-energy region
[SH-4.4-22] 23 p4035 N85-35018

Diurnal anisotropy during solar activity cycle twenty and diffusion-convection model
[SH-4.5-7] 23 p4036 N85-35025

Diurnal variations from muon data at Takeyama underground station
[SH-4.5-13] 23 p4037 N85-35030

The modulation features of the long-period cosmic ray variations in connection with the sign change of the general magnetic field of the Sun
[SH-4.5-15] 23 p4037 N85-35032

Cosmic ray density gradient and its dependence on the north-south asymmetry in solar activity
[SH-4.5-17] 23 p4038 N85-35034

Anomalous increase of solar anisotropy above 150GV in 1981-1983
[SH-4.5-18] 23 p4038 N85-35035

Change of cosmic ray anisotropy with solar activity
[SH-4.5-20] 23 p4038 N85-35037

The large scale dynamics of the outer heliosphere and the long-term modulation of galactic cosmic rays
[SH-4.7-3] 23 p4040 N85-35048

Galactic cosmic ray radial gradients and the anomalous He component near maximum solar modulation and to radii beyond 34 AU from the Sun
[SH-4.7-5] 23 p4040 N85-35050

The recovery of the cosmic ray flux from maximum solar modulation at IMP-8 (1 AU) and at Pioneer (R 30 AU)
[SH-4.7-7] 23 p4041 N85-35052

The solar wind effect on cosmic rays and solar activity
[SH-5.1-13] 23 p4043 N85-35066

Solar activity beyond the disk and variations of the cosmic ray gradient
[SH-5.1-23] 23 p4044 N85-35075

Cosmic rays 10Be biennal data and their relationship to aurorae and sunspots
[SH-7.1-1] 23 p4047 N85-35094

SOLAR ACTIVITY EFFECTS

Theoretical study of electron concentration in Venusian atmosphere as function of zenith angle of sun and solar activity in areas of photochemical equilibrium
02 p0163 N85-11104

Scientific contributions in commemoration of Ebro Observatory's 75th anniversary — conference
[ISBN-84-00-05360-X] 04 p0518 N85-13306

Local geomagnetic characteristics of solar activity (Dourbes 1960-1978) 04 p0521 N85-13329

The response of mid-latitude total electron content to solar activity 04 p0522 N85-13336

Solar wind dynamics at small distances from the sun
06 p0823 N85-15227

Solar flare and IMF sector structure effects in the lower ionosphere 11 p1664 N85-20488

The influence of the local solar wind structures on the propagation of low energy particles
12 p1959 N85-22314

Interplanetary shock waves during April and May of 1981 13 p1982 N85-22434

The effects of seeing on noise
14 p2443 N85-25077

The effects of a nearly 100% duty cycle in observations of solar oscillations 14 p2443 N85-25078

Methods for cloud cover estimation
14 p2444 N85-25081

Variability of the structure of the granulation over the solar activity cycle 14 p2447 N85-25100

Nonlinear time-evolution of kink-unstable magnetic flux tubes in the convection zone of the Sun
14 p2447 N85-25105

The first effect of the amplitude of a solar cycle
14 p2452 N85-25143

Variability of the quiet photospheric network
14 p2452 N85-25144

About sudden disappearances and reappearances — solar activity 14 p2454 N85-25157

Multistep orbital correction algorithms for an Earth satellite using low thrust engine
15 p2479 N85-25303

Space-time features of solar cosmic ray penetration into high latitude regions of Earth's magnetosphere based on Intercosmos-19 satellite data 15 p2481 N85-25310

Bursts of relativistic electrons in magnetopause and in outer radiation belt 16 p2722 N85-26801

Some properties of flare-not-associated Forbush decreases
[IFSI-84-13] 20 p3548 N85-32077

Solar radio fluxes as indices of solar activity
[AERONOMICA-ACTA-A-282-1984]
21 p3722 N85-33095

Solar variability observed through changes in solar figure and mean diameter
[DE85-012857] 22 p3860 N85-33900

Search for solar neutrons using NM-64 equipment
[SH-1.4-5] 23 p3995 N85-34765

A search for solar neutrons on a long duration balloon flight
[SH-1.4-6] 23 p3995 N85-34766

On the retention of high-energy protons and nuclei with charges Z or equal to 2 in large solar flares after the process of their acceleration
[SH-2.1-8] 23 p3998 N85-34789

Nucleosynthesis in the terrestrial and solar atmospheres
[SH-2.2-2] 23 p4000 N85-34797

Type 3 solar radio bursts and 3HE-rich events
[SH-2.2-3] 23 p4000 N85-34798

Anomalous low level of cosmic ray intensity decreases observed during 1980
[SH-5.1-15] 23 p4043 N85-35068

When did the average cosmic ray flux increase?
[SH-7.1-4] 23 p4047 N85-35097

Cosmic-ray exposure records and origins of meteorites
[SH-7.1-7] 23 p4047 N85-35099

SOLAR ARRAYS

NT SOLAR BLANKETS

Space know-how, twenty years' space experience
04 p0461 N85-12925

Autonomous momentum management for space station
[NASA-CR-174065] 04 p0462 N85-12931

Autonomous momentum management for space station, exhibit A
[NASA-CR-171256] 04 p0462 N85-12933

FSA field test
[NASA-CR-174114] 04 p0528 N85-13373

Study program for encapsulation materials interface for Flat-plate Solar Array (FSA) project
[NASA-CR-174152] 04 p0530 N85-13385

Trends in space photovoltaic technology
05 p0609 N85-13886

Photovoltaic working group report
05 p0611 N85-13902

A historical overview of the electrical power systems in the US manned and some US unmanned spacecraft
[NASA-CR-174806] 05 p0612 N85-13910
Circuit transients due to negative bias arcs on a high-voltage solar array in low Earth orbit
[NASA-TP-2407] 06 p0780 N85-14858
Safety requirements for wiring systems and connectors for photovoltaic systems
[NASA-CR-174211] 06 p0803 N85-15110
Proceedings of the 23rd Project Integration Meeting
[NASA-CR-174186] 06 p0829 N85-15260
Barriers to achieving high efficiency
06 p0829 N85-15264
Encapsulation design analysis
06 p0829 N85-15268
Polymer-metal interface bond stability
06 p0830 N85-15272
Module flammability research
06 p0830 N85-15274
Performance loss with shorted cells
06 p0832 N85-15294
Investigation of accelerated stress factors and failure/degradation mechanisms
06 p0832 N85-15295
Annual energy spectrum for tracking arrays
06 p0832 N85-15297
Summary of photovoltaic performance models
06 p0832 N85-15298
Proceedings of the 22nd Project Integration Meeting
[DE85-000334] 06 p0833 N85-15302
Demonstration of transparent solar array module design
[NASA-CR-174257] 07 p0992 N85-16302
Manned space station solar array study
[ESA-CR(P)-1941] 09 p1287 N85-18061
Analysis of inverter models and harmonic propagation. Part 1: A physical simulator for large solar cell arrays
[DE85-002312] 09 p1315 N85-18271
Efficient structures for geosynchronous spacecraft solar arrays
[NASA-CR-174448] 10 p1428 N85-19004
Safety requirements for wiring systems and connectors for photovoltaic systems
[NASA-CR-174431] 10 p1477 N85-19324
Analysis of inverter models and harmonic propagation. Part 2: Harmonic propagation
[DE85-000198] 10 p1482 N85-19356
MOD silver metallization for photovoltaics
[NASA-CR-175460] 10 p1510 N85-19526
Seven-year thermal-vacuum real-life test of a solar array drive mechanism manufactured by Marconi Space and Defence Systems (Model No. 002)
[ESA-ESTL-62] 11 p1616 N85-20161
Report of the Electrodynamic Interactions Panel
11 p1645 N85-20363
Control of large collector arrays: The SSPS experience
[DE85-001461] 11 p1675 N85-20553
NASA welding assessment program
[NASA-CR-175512] 12 p1859 N85-21661
Solar powered actuator with continuously variable auxiliary power control
[NASA-CASE-MFS-25637-1] 12 p1876 N85-21769
User's manual for the University of Houston individual heliostat layout and performance code
[DE85-004643] 12 p1882 N85-21808
Interactions between large space power systems and low-Earth-orbit plasmas 13 p1992 N85-22490
The PIX-2 experiment: An overview
13 p1993 N85-22494
Plasma interaction experiment 2 (PIX 2): Laboratory and flight results 13 p1993 N85-22495
Discharges on a negatively biased solar cell array in a charged-particle environment 13 p1994 N85-22499
Space test program of high-voltage solar array-space plasma interactions 13 p1997 N85-22519
Photovoltaic Generators in Space — conferences
[ESA-SP-210] 13 p2005 N85-22565
Thin and ultrathin silicon solar cells for space use
13 p2005 N85-22567
Space solar cells: Adjusting to new demands
13 p2005 N85-22568
Bifacial light sensitive space solar cell
13 p2006 N85-22573
Gallium arsenide arrays versus silicon arrays for space application 13 p2006 N85-22574
Availability of AlGaAs/GaAs solar cells in space
13 p2006 N85-22576
Comparative study of GaAs solar cell potentialities for space applications 13 p2006 N85-22577
Investigation of high output gallium arsenide solar cells 13 p2006 N85-22578
Development of very thin large area GaAs solar cells for space application 13 p2006 N85-22579
GaAs and 3-5 compound solar cells status and prospects for use in space 13 p2007 N85-22580
Development and testing of a spacecraft surface potential monitor 13 p2007 N85-22582
Electrostatic discharge testing on a carbon fiber solar panel structure 13 p2007 N85-22584
In-orbit laser regeneration of the radiation damaged solar arrays 13 p2008 N85-22588
Giotto solar array: Design, manufacture and test
13 p2008 N85-22589
The DFS-Kopernikus solar generator electrical design
13 p2008 N85-22590
The DFS-Kopernikus solar generator
13 p2008 N85-22591
Electrical design of the Intelsat 6 solar generator
13 p2008 N85-22592
Computer aided engineering applied to the design and verification of the generic Advanced Rigid Array (ARA) — solar array 13 p2008 N85-22593
Development and qualification of the electrical part of the Advanced Rigid Array (ARA) — solar array
13 p2008 N85-22594
SPOT solar array 13 p2009 N85-22595
Rigid Solar Generator (GSR) solar arrays
13 p2009 N85-22596
Retractable Rigid Solar Generator (GSR)
13 p2009 N85-22597
Derivation of the Olympus solar array requirements
13 p2009 N85-22598
The Olympus solar array development and test program 13 p2009 N85-22599
The performance of the Olympus power subsystem with its solar array 13 p2009 N85-22601
Survival testing of silicon solar modules
13 p2009 N85-22602
Analysis of optimum front cover thickness for lightweight solar arrays 13 p2010 N85-22606
Problems with electrical interference between solar generators and shunt type regulators
13 p2010 N85-22607
Development of Halley's Comet explorer PLANET-A solar array 13 p2010 N85-22608
Concentrator technologies evaluation for large solar arrays and their application for space stations/platforms
13 p2010 N85-22609
Space Station solar array 13 p2010 N85-22610
Solar array dynamical simulation for illumination and temperature variation 13 p2011 N85-22611
Aspects of low cost module technology — spacecraft solar arrays 13 p2011 N85-22614
Deployment analysis of the Olympus Astromast and comparison with test measurements — solar arrays
13 p2011 N85-22616
NASA photovoltaic research and technology development program for space applications
13 p2011 N85-22617
Study of concentration for space photovoltaic generators 13 p2011 N85-22618
Developments in deployable masts to support flexible solar arrays 13 p2012 N85-22620
Generic design and verification of an Advanced Rigid Array (ARA) — solar array 13 p2012 N85-22621
Growth capabilities of European retractable solar arrays 13 p2012 N85-22625
MSFC data analysis of the SAFE/DAE experiment
14 p2233 N85-23843
Langley Research Center photogrammetric measurements of solar array dynamics: Preliminary results 14 p2233 N85-23844
Solar Array Experiment (SAE) flight experience
14 p2236 N85-23861
Intermediate load modules for test and evaluation
[NASA-CR-175697] 14 p2350 N85-24526
Selection of optimal control program for solar cell panels of Earth satellites 15 p2484 N85-25335
NASA welding assessment program
[NASA-CR-175682] 15 p2568 N85-25844
Module performance and failure analysis area: Flat-plate solar array project
[NASA-CR-175689] 15 p2585 N85-25936
Proposed energy systems for the Brazilian data collection satellite
[INPE-3393-PRE/684] 16 p2731 N85-26856
MOD silver metallization for photovoltaics
[NASA-CR-175773] 16 p2818 N85-27381
Design and development of a linear Fresnel lens air-cooled photovoltaic module and a stand-alone photovoltaic collector array
[DE85-006854] 16 p2819 N85-27391
Relative potentials of concentrating and two-axis tracking flat-plate photovoltaic arrays for central-station applications
[NASA-CR-175669] 17 p2985 N85-28446
Observations of high resistance on slip-rings employing Ag/MoS2/Cu brushes — solar array drives
[ESA-ESTL-70] 18 p3123 N85-29333
Measurements of vector fields with diode array
18 p3204 N85-29660
Using PVFORM, a systems performance model, to determine optimum mounting configurations for flat-plate photovoltaic modules
[DE85-011191] 19 p3306 N85-30495
Multi-kW solar arrays for Earth orbit applications
[NASA-CR-171536] 20 p3406 N85-31139
A dual spin space station design
20 p3408 N85-31152
Frequency domain control design of large space structures: A practical approach
20 p3415 N85-31192
A concept for the intrinsic dielectric strength of electrical insulation materials
[NASA-CR-176040] 20 p3448 N85-31410
Proceedings of the Flat-Plate Solar Array Project Research Forum on High-Efficiency Crystalline Silicon Solar Cells
[NASA-CR-176047] 20 p3478 N85-31615
Activities report of the European Space Tribology Laboratory
[ESA-ESTL-66] 20 p3484 N85-31653
Retractable Rigid Solar Generator (GSR)
[SNIAS-851-440-101] 20 p3484 N85-31654
The SPOT solar array
[SNIAS-851-440-103] 20 p3485 N85-31656
Gallium arsenide arrays versus silicon arrays for space application
[SNIAS-851-440-104] 20 p3485 N85-31657
Study of concentration for space photovoltaic generators
[SNIAS-851-440-105] 20 p3485 N85-31658
Forced convection on solar collector arrays
[DE85-010381] 21 p3585 N85-32267
Proceedings of the 24th Project Integration Meeting
[NASA-CR-176058] 21 p3607 N85-32394
High-efficiency module and array research
21 p3607 N85-32397
Flat-plate module efficiency versus cost tradeoffs
21 p3607 N85-32398
Block V module program 21 p3607 N85-32401
Reliability physics 21 p3608 N85-32402
MOD silver metallization for photovoltaics
21 p3610 N85-32428
The design and development of a constant-speed solar array drive 22 p3798 N85-33519
Features of the solar array drive mechanism for the space telescope 22 p3798 N85-33532
Structural dynamics model and response of the deployable reference configuration space station
[NASA-TM-86386] 22 p3799 N85-33539
Surface voltage gradient role in high voltage solar array-plasma interaction: Center Director's discretionary fund
[NASA-TM-86516] 22 p3805 N85-33567
Photovoltaics technical information guide
[DE85-002924] 22 p3808 N85-33585
Solar maximum: Solar array degradation
[NASA-TM-86194] 23 p3903 N85-34175

SOLAR ATMOSPHERE
Physics of the inner heliosphere 1-10R sub O plasma diagnostics and models
[NASA-CR-174010] 02 p0304 N85-11964
Vector magnetic field analysis of Lorentz forces acting in the solar atmosphere
[AD-A145941] 03 p0449 N85-12652
Kinematics of B and A stars 05 p0741 N85-14766
The radiative hydrodynamics of flare loops heated by impulsive bursts of energetic electrons
05 p0745 N85-14781
Heating in the solar mantle 08 p1233 N85-17769
The calculation of theoretical chromospheric models and the interpretation of solar spectra from rockets and spacecraft
[NASA-CR-174289] 08 p1259 N85-17922
Plasma and nuclear processes in solar matter
12 p1954 N85-22277
Equilibrium model of thin magnetic flux tubes — solar atmosphere 12 p1956 N85-22310
Ultraviolet spectral diagnostics of solar flares and heating events 13 p2205 N85-23675
The hydromagnetics of the Sun — conferences
[ESA-SP-220] 14 p2445 N85-25091
Magnetoconvection: The interaction of convection and small scale magnetic fields — photosphere
14 p2446 N85-25098
Coronal structures 14 p2448 N85-25110
Waves in inhomogeneous media — magnetohydrodynamic waves; solar atmosphere
14 p2449 N85-25116
Science with the Solar Optical Telescope (SOT)
14 p2449 N85-25120
A model for the dynamics of the deep photosphere
14 p2450 N85-25129
Linear models of acoustic waves in sunspot umbrae
14 p2450 N85-25130

Dynamo action of magnetostrophic waves — solar atmosphere 14 p2451 N85-25136

Cyclic flows in the solar convection zone due to the dynamo reaction 14 p2451 N85-25137

Effects of atmospheric stratification on dissipative acoustic and Alfven waves — solar atmosphere 14 p2453 N85-25149

Solar magnetohydrodynamics: Symposium review 14 p2455 N85-25162

Measurements of Solar Vector Magnetic Fields [NASA-CP-2374] 18 p3203 N85-29869

The vector structure of active magnetic fields 18 p3203 N85-29870

On the numerical computation of nonlinear force-free magnetic fields 18 p3203 N85-29871

Modeling solar magnetic structures 18 p3203 N85-29872

Generation and transfer of polarized radiation in the solar atmosphere: Physical mechanisms and magnetic-field diagnostics 18 p3206 N85-29890

Contribution functions for Zeeman-split lines, and line formation in photospheric faculae 18 p3207 N85-29893

Solar photospheric and coronal abundances from solar energetic particle measurements [NASA-CR-176029] 20 p3547 N85-32073

Solar convection [AD-A155214] 21 p3723 N85-33096

Temporal evolution of an energetic electron population in an inhomogeneous medium: Application to solar hard X-ray bursts [SH-1.2-6] 23 p3991 N85-34741

Ultrarelativistic electrons and solar flare gamma-radiation [SH-1.3-11] 23 p3993 N85-34757

Precision measurements of solar energetic particle elemental composition [SH-2.1-4] 23 p3996 N85-34785

Solar Coronal and photospheric abundances from solar energetic particle measurements [SH-2.1-5] 23 p3996 N85-34786

Nucleosynthesis in the terrestrial and solar atmospheres [SH-2.2-2] 23 p4000 N85-34797

Dynamics of the penetration boundaries of solar protons during a strong magnetic storm [SH-6.1-16] 23 p4046 N85-35089

Neutrino production from the solar atmosphere [SH-8.1-9] 23 p4050 N85-35114

SOLAR AUXILIARY POWER UNITS

Features of new solar panels on Salyut-7 02 p0157 N85-11062

SOLAR AZIMUTH

U AZIMUTH

U SOLAR POSITION

SOLAR BLANKETS

Development of a foldline concept for automatic refolding of a flexible blanket (folding analysis) — spaceborne solar generators [ESA-CR(P)-1933] 08 p1179 N85-17428

Design and qualification testing of the Olympus solar array blanket 13 p2009 N85-22600

Blanket integrated cushioning of foldable and retractable solar arrays 13 p2011 N85-22612

Concept for controlled fold by fold deployment and retraction of flexible, foldable solar generators 13 p2011 N85-22613

The Olympus solar array structure and mechanisms 13 p2012 N85-22623

Solar array flight experiment [NASA-TM-86506] 17 p2909 N85-27935

STACBEAM 2 [NASA-CR-176126] 23 p3944 N85-34442

SOLAR CELLS

NT HOMOJUNCTIONS

NT VERTICAL JUNCTION SOLAR CELLS

MOD silver metallization for photovoltaics [NASA-CR-174011] 01 p0026 N85-10163

Development of copper sulfide/cadmium sulfide thin-film solar cells [DE84-004513] 01 p0044 N85-10287

Process Research of Polycrystalline Silicon Material (PROPSM) [NASA-CR-173638] 01 p0067 N85-10446

Liquid cooled, linear focus solar cell receiver [DE84-014446] 01 p0067 N85-10448

The effect of plasma on solar cell array arc characteristics [NASA-TM-86887] 02 p0169 N85-11133

Preparation and properties of evaporated CdTe films compared with single crystal CdTe [DE85-000502] 02 p0222 N85-11452

Research on gallium arsenide diffused junction solar cells [NASA-CR-174057] 02 p0222 N85-11457

Silicon sheet with molecular beam epitaxy for high efficiency solar cells [NASA-CR-174022] 02 p0222 N85-11459

Hydrogen passivation of electrically active defects in crystalline silicon solar cells [DE84-004590] 02 p0223 N85-11461

Research directions and progress in the SERI advanced high efficiency concept program [DE84-004592] 02 p0223 N85-11462

DOE/SERI polycrystalline thin-film photovoltaic research [DE84-004516] 02 p0223 N85-11464

Research on crystalline silicon solar cells [DE84-114591] 02 p0223 N85-11465

Thin film (Al, Ga)As heterojunction solar cells 02 p0258 N85-11691

Cascaded solar photovoltaic cells based on InP-GaInPAs and InP-CdS heterostructures 02 p0268 N85-11749

Development of the production technology of Cu2S/CdS solar generators [BMFT-FB-T-84-137] 03 p0366 N85-12469

Five year research plan, 1984-1988. Photovoltaics: Electricity from sunlight [DE84-013009] 04 p0528 N85-13377

Evaluation of some photovoltaic concentrator solar cell-heat sink coupling materials [DE84-016027] 04 p0529 N85-13378

Silicon for solar cells [DE84-004503] 04 p0529 N85-13381

Comprehensive silicon solar cell computer modeling [NASA-CR-174151] 04 p0530 N85-13386

National Photovoltaics Program Annual Review Meeting, abstracts [DE84-013003] 04 p0530 N85-13390

Trends in space photovoltaic technology 05 p0609 N85-13888

Glow discharge amorphous silicon tin alloys [DE84-013001] 05 p0611 N85-13952

Process research of polycrystalline silicon material (PROPSM) [NASA-CR-174130] 05 p0619 N85-13962

Siemens solar module: Status of the technique, development tendencies 05 p0662 N85-14255

Development and utilization of CdS/Cu2S 05 p0662 N85-14256

Telephoning with light and sun — glass fibers, solar cells 05 p0663 N85-14264

Mains-connected photovoltaic system for a house 05 p0664 N85-14267

Material models and device structures for GaAs solar cells [DE85-000501] 05 p0665 N85-14275

Material models and device structures for GaAs solar cells, introduction 05 p0665 N85-14276

GaAs material properties and models 05 p0665 N85-14277

Anti-reflection coatings materials and models 05 p0665 N85-14278

Comparison of SCAPID/GaAs to experiment 05 p0665 N85-14279

Solar cell coverslide extraction method and apparatus [AD-D011275] 05 p0669 N85-14306

Safety requirements for wiring systems and connectors for photovoltaic systems [NASA-CR-174211] 06 p0803 N85-15110

Development of high-efficiency solar cells on silicon web [NASA-CR-174212] 06 p0828 N85-15259

High-efficiency silicon solar cell research 06 p0829 N85-15261

High-efficiency solar-cell design modeling 06 p0829 N85-15262

Efficiency estimation and sensitivity modeling 06 p0829 N85-15263

MBE growth for high-efficiency silicon solar cells 06 p0829 N85-15265

Investigation of silicon surface passivation by silicon nitride deposition 06 p0829 N85-15266

Development and analysis of silicon solar cells near 20% efficiency 06 p0829 N85-15267

Encapsulation design analysis 06 p0829 N85-15268

Encapsulation materials and processing 06 p0830 N85-15269

Photothermal degradation of encapsulants 06 p0830 N85-15270

Polymer-polymer interface bond stability 06 p0830 N85-15271

Polymer-metal interface bond stability 06 p0830 N85-15272

Predicting electrochemical breakdown in terrestrial photovoltaic modules 06 p0830 N85-15273

Module flammability research 06 p0830 N85-15274

Process research of non-Cz silicon material 06 p0830 N85-15275

Process Research On Polycrystalline Silicon Material (PROPSM) 06 p0830 N85-15276

Evaluation of the ion implantation process for production of solar cells from silicon sheet materials 06 p0831 N85-15281

Laser-assisted solar-cell metallization processing 06 p0831 N85-15282

Miniworkshop on effects of stress and strain in high-speed-growth silicon ribbons 06 p0831 N85-15284

Stress studies in EFG 06 p0831 N85-15285

Advanced dendritic web growth development 06 p0831 N85-15286

Silicon-sheet surface studies 06 p0831 N85-15287

Investigation of structural and electrical properties of low-angle silicon sheet 06 p0831 N85-15288

Semicrystalline casting process development and verification 06 p0832 N85-15289

Electrochemical production of silicon 06 p0832 N85-15290

Analysis of optical and electrical performance of a TCP-coated solar cell 06 p0832 N85-15293

Performance loss with shorted cells 06 p0832 N85-15294

Investigation of accelerated stress factors and failure/degradation mechanisms 06 p0832 N85-15295

Summary of photovoltaic performance models 06 p0832 N85-15296

Proceedings of the 22nd Project Integration Meeting [DE85-000334] 06 p0833 N85-15302

Advances and opportunties in the amorphous silicon research field [DE84-004526] 06 p0833 N85-15304

Recent developments in photovoltaics [DE84-004528] 06 p0833 N85-15305

Results of the 1984 NASA/JPL balloon flight solar cell calibration program [NASA-CR-174270] 07 p0991 N85-16294

Multijunction cells for concentrators: Technology prospects [NASA-CR-174259] 07 p0991 N85-16295

Automated assembly of Gallium Arsenide and 50-micron thick silicon solar cell modules [NASA-CR-174331] 08 p1168 N85-17384

Compilation of Sandia papers contributed to the 17th IEEE Photovoltaic Specialists Conference [DE84-017456] 09 p1315 N85-18267

Analysis of inverter models and harmonic propagation. Part 1: A physical simulator for large solar cell arrays [DE85-002312] 09 p1315 N85-18271

Signal Hill solar-powered repeater report and recommendations [DE85-000487] 09 p1316 N85-18273

Advanced high-efficiency concentrator cells [DE84-013020] 09 p1344 N85-18459

Analysis of inverter models and harmonic propagation. Part 2: Harmonic propagation [DE85-000198] 10 p1482 N85-19356

Intermediate load modules for test and evaluation: Flat-Plate Solar Array Project [NASA-CR-174450] 10 p1506 N85-19512

Silicon film solar cell process [NASA-CR-174446] 10 p1506 N85-19514

Surface and allied studies in silicon solar cells [NASA-CR-175468] 10 p1508 N85-19516

Pulsed excimer laser processing for cost-effective solar cells [NASA-CR-174429] 10 p1509 N85-19517

Mod silver metallization for photovoltaics [NASA-CR-174444] 10 p1509 N85-19518

Investigation of welded interconnection of large area wraparound contacted silicon solar cells [NASA-CR-174438] 10 p1509 N85-19519

Pulsed excimer laser processing for cost-effective solar cells [NASA-CR-175465] 10 p1509 N85-19520

Development of high efficiency solar cells on silicon web [NASA-CR-174435] 10 p1509 N85-19521

Stress studies in EFG [NASA-CR-175464] 10 p1509 N85-19522

Process Research on Polycrystalline Silicon Material (PROPSM) [NASA-CR-175461] 10 p1509 N85-19523

Investigation of accelerated stress factors and failure/degradation mechanisms in terrestrial solar cells [NASA-CR-175469] 10 p1510 N85-19524

Stress-strain analysis of silicon ribbon [NASA-CR-175459] 10 p1510 N85-19525

Mask aligner for solar cell fabrication [AD-D011450] 10 p1510 N85-19529

US Amorphous Silicon Research Project [DE85-000536] 10 p1511 N85-19536
Overview of photovoltaic concentrator technology [DE84-016790] 10 p1512 N85-19539
Solar collection [DE85-000060] 10 p1512 N85-19540
Stress studies in EFG [NASA-CR-175486] 10 p1563 N85-19856
Screen printed interdigitated back contact solar cell [NASA-CASE-LEW-13414-1] 11 p1671 N85-20530
Surface and allied studies in silicon solar cells [NASA-CR-174447] 11 p1671 N85-20531
Lithium counterdoped silicon solar cell [NASA-CASE-LEW-14177-1] 11 p1672 N85-20535
Research on the basic understanding of high efficiency in silicon solar cells [DE85-000507] 11 p1672 N85-20537
Excimer laser annealing to fabricate low cost solar cells [NASA-CR-174394] 11 p1673 N85-20538
Fabrication of monocrystalline GaAs solar cells utilizing NaCl sacrificial substrates [DE84-013016] 11 p1673 N85-20544
Phase 2 fabrication and construction of the Sky Harbor Airport, solar photovoltaic concentrator project [DE85-000019] 11 p1676 N85-20561
The temperature of a glass-encapsulated solar cell estimated from ambient air temperature and global radiation [GKSS-84-E-36] 11 p1676 N85-20563
GaAs and 3-5 compound solar cells status and prospects for use in space [NASA-TM-86960] 12 p1795 N85-21261
International Congress Centrum Berlin report on photovoltaics 12 p1877 N85-21773
Crystallization methods for solar cell silicon 12 p1877 N85-21774
Materials refining for solar cell silicon 12 p1877 N85-21775
Flat-plate silicon for solar cells 12 p1877 N85-21776
Carbothermic production of silicon solar cells using high-purity starting materials 12 p1877 N85-21777
Silicon band spraying technique for solar cells 12 p1877 N85-21778
Development of silicon nitride materials for the casting of solar cell silicon 12 p1878 N85-21779
Photovoltaic solar components 12 p1878 N85-21782
Optimization of silicon-nitride-inversion layer solar cells 12 p1878 N85-21784
Development of new process technologies for solar cells with high efficiency starting from purified silicon 12 p1878 N85-21785
Investigation of the optical properties of solar elements 12 p1879 N85-21786
Pin solar cells made of amorphous silicon 12 p1879 N85-21787
Development of an amorphous silicon panel 12 p1879 N85-21788
Amorphous silicon solar cells with a view to cheap production processes 12 p1879 N85-21789
Production and characterization of amorphous silicon (a-Si:H) as base material for solar cells 12 p1879 N85-21791
Thin-film solar cells from sputtered and vapor-deposited amorphous silicon 12 p1879 N85-21792
Physical-chemical investigations of copper sulfides for use in CdS/Cu2S solar cells 12 p1880 N85-21794
Development of high-efficiency economic systems for photovoltaics 12 p1880 N85-21795
Development of a CdSe thin film solar cell 12 p1880 N85-21796
Development of new solar cells 12 p1880 N85-21797
An investigation of arc discharging on negatively biased dielectric conductor samples in a plasma 13 p1994 N85-22498
Discharges on a negatively biased solar cell array in a charged-particle environment 13 p1994 N85-22499
Photovoltaic Generators in Space — conferences [ESA-SP-210] 13 p2005 N85-22565
History and future views on solar cells of Japanese scientific satellites 13 p2005 N85-22566
Thin and ultrathin silicon solar cells for space use 13 p2005 N85-22567
Space solar cells: Adjusting to new demands 13 p2005 N85-22568
The high voltage silicon cell: A comparative analysis 13 p2005 N85-22569
A 2 x 6 Back Surface Reflection (BSR) silicon solar cell 13 p2005 N85-22570
Experiences with implanted Back Surface Field (BSF) solar cells 13 p2005 N85-22571
A low cost approach with larger diameter silicon wafer — solar cells 13 p2006 N85-22572
Bifacial light sensitive space solar cell 13 p2006 N85-22573
Gallium arsenide arrays versus silicon arrays for space application 13 p2006 N85-22574
Space qualified AlGaAs/GaAs solar cells 13 p2006 N85-22575
Availability of AlGaAs/GaAs solar cells in space 13 p2006 N85-22576
Development of very thin large area GaAs solar cells for space application 13 p2006 N85-22579
GaAlAs-GaAs solar cell development: Prospective for space applications under concentration 13 p2007 N85-22581
Phenomenology of discharges in space: Application to a solar generator — SPOT satellite 13 p2007 N85-22583
Technological process effect on the carrier lifetime degradation of silicon solar cell base layer irradiated by 1 MeV electrons (boron doping case) 13 p2007 N85-22585
The effects of lithium counterdoping on radiation damage and annealing in n(+)p silicon solar cells 13 p2007 N85-22586
Investigation of the degradation of GaAs photovoltaic cells by proton and electron irradiation 13 p2008 N85-22587
The DFS-Kopernikus solar generator electrical design 13 p2008 N85-22590
The DFS-Kopernikus solar generator 13 p2008 N85-22591
Electrical design of the Intelsat 6 solar generator 13 p2008 N85-22592
Development and qualification of the electrical part of the Advanced Rigid Array (ARA) — solar array 13 p2008 N85-22594
Survival testing of silicon solar modules 13 p2009 N85-22602
Calibration of solar cells outside the atmosphere 13 p2009 N85-22603
Inverse behavior of silicon photovoltaic cells 13 p2010 N85-22604
Nonlinearity and spectral mismatch problems of solar cells 13 p2010 N85-22605
Emissivity enhancement of fused silica for space applications — solar cells 13 p2011 N85-22615
NASA photovoltaic research and technology development program for space applications 13 p2011 N85-22617
Improved modeling of the open circuit voltage of solar cells 13 p2011 N85-22619
Isotropic proton irradiation of GaAs solar cells 13 p2012 N85-22622
Annealing of radiation damage in boron and gallium doped silicon solar cells 13 p2012 N85-22624
Fracture mechanics evaluation of GaAs [NASA-CR-175657] 13 p2102 N85-23101
New high-efficiency silicon solar cells [NASA-CR-175643] 13 p2128 N85-23244
Demonstration of feasibility of depositing semiconductor layers using microwave enhanced plasma techniques [NASA-CR-174392] 13 p2163 N85-23421
Some observations of heated gallium arsenide heteroface solar cells [NASA-TM-86388] 14 p2246 N85-23925
Solar cells based on polycrystalline silicon with isothermal potential barriers along grain boundaries 14 p2275 N85-24091
Solar cells with distributed parameters: Current-voltage characteristics under uniform and nonuniform illumination 14 p2275 N85-24093
Characterization of terrestrial solar cells for space applications: Electrical characteristics of thin Westinghouse dendritic web cells as a function of solar intensity, temperature, and incidence angle [NASA-CR-175642] 14 p2349 N85-24516
Silicon-sheet and thin-film cell and module technology potential: Issue study [NASA-CR-175654] 14 p2349 N85-24520
Intermediate load modules for test and evaluation [NASA-CR-175697] 14 p2350 N85-24526
Modelling of photodegradation in solar cell modules of substrate and superstrate design made with ethylene-vinyl acetate as pottant material [NASA-CR-175690] 14 p2350 N85-24527
Laser-assisted solar cell metallization processing [NASA-CR-175686] 14 p2350 N85-24528
Excimer laser annealing to fabricate low cost solar cells [NASA-CR-175702] 14 p2351 N85-24529
Pulsed excimer laser processing for cost-effective solar cells [NASA-CR-175700] 14 p2351 N85-24530
Advanced high-efficiency concentrator cell [DE85-000525] 14 p2351 N85-24533
NASA welding assessment program [NASA-CR-175682] 15 p2568 N85-25844
NASA welding assessment program [NASA-CR-175683] 15 p2568 N85-25845
Electrical research on solar cells and photovoltaic materials [NASA-CR-175699] 15 p2585 N85-25935
Module performance and failure analysis area: Flat-plate solar array project [NASA-CR-175689] 15 p2585 N85-25936
Heavy doping effects in high efficiency silicon solar cells [NASA-CR-175687] 15 p2585 N85-25937
Investigation of silicon surface passivation by silicon nitride film deposition [NASA-CR-175693] 15 p2585 N85-25938
Development of high-efficiency solar cells on silicon web [NASA-CR-175707] 15 p2585 N85-25939
A study of the stability of cadmium sulfide/copper sulfide and cadmium sulfide copper-indium-diselenide solar cells [DE85-002902] 15 p2587 N85-25947
Thin film cadmium telluride and zinc phosphide solar cells [DE85-002904] 15 p2587 N85-25950
Process Research on Polycrystalline Silicon Material (PROPSM) [NASA-CR-175761] 15 p2587 N85-25951
The structural and electronic properties of amorphous silicon based alloy materials [DE85-002909] 15 p2660 N85-26419
Chemical vapor deposition of amorphous semiconductor films [DE85-002917] 15 p2661 N85-26421
Proposed energy systems for the Brazilian data collection satellite [INPE-3393-PRE/664] 16 p2731 N85-26856
Analysis of orbit transfer vehicles for GPS Block 3 satellites [AD-A152021] 16 p2732 N85-26860
Solar elements with distributed parameters 16 p2760 N85-27036
Heavy doping effects in high efficiency silicon solar cells [NASA-CR-175779] 16 p2818 N85-27383
Documentation and solar cell modules [NASA-CR-175769] 16 p2818 N85-27384
Photovoltaic cell reliability research: Investigation of accelerated stress factors and failure-degradation mechanisms in terrestrial solar cells [NASA-CR-175815] 16 p2819 N85-27388
Maintenance of photovoltaic power systems [AD-A152299] 16 p2819 N85-27390
Polycrystalline semiconductor heterojunction modelling (CdS/CuInSe(sub)2) [DE85-002913] 16 p2871 N85-27713
Study of the degradation of short-circuit current and the open-circuit tension of spatial solar cells as a function of the fluency of 1MeV electrons [INPE-3356-PRE/634] 16 p2887 N85-27814
Electrical research on solar cells and photovoltaic materials [NASA-CR-175897] 17 p2986 N85-28452
Comprehensive silicon solar cell computer modeling [NASA-CR-175959] 17 p2987 N85-28461
Report on high intensity solar cells [DE85-008396] 17 p2987 N85-28462
Terrestrial photovoltaic power systems with sunlight concentration [DE85-008398] 17 p2987 N85-28464
Research and developmental study on MIS thin film solar cells of amorphous hydrogenated silicon, part 2 [BMFT-FB-T-84-290] 17 p2988 N85-28467
Zn3P2 as an improved semiconductor for photovoltaic solar cells [DE85-008772] 18 p3097 N85-29171
SERI photovoltaic advanced research and development project: FY 1984 accomplishments [DE85-002939] 18 p3128 N85-29368
Post-deposition heat treatments of CdS/CuInSe2 solar cells [DE85-002943] 18 p3128 N85-29373
Mechanically-stacked multijunction solar cells [DE85-010389] 18 p3129 N85-29377
Research on electrochemical photovoltaic cells [DE85-008775] 18 p3131 N85-29392
Current status of silicon materials research for photovoltaic applications [DE85-008799] 19 p3304 N85-30482
Cadmium sulfide/copper ternary heterojunction cell research [DE85-008778] 19 p3305 N85-30486
Research on the basic understanding of high efficiency in silicon solar cells [DE85-008774] 19 p3305 N85-30487
Optical effects of thin film adhesives in multijunction solar cells [DE85-010120] 19 p3305 N85-30488

High-efficiency, low-cost, passively-cooled PV concentrator module
[DE85-010013] 19 p3305 N85-30490

Design and operation of epitaxial reactor
[DE85-011089] 19 p3306 N85-30491

Block 5 documentation and solar modules
[NASA-CR-176009] 19 p3306 N85-30494

Using PVFORM, a systems performance model, to determine optimum mounting configurations for flat-plate photovoltaic modules
[DE85-011191] 19 p3306 N85-30495

Ink jet printing of silver metallization for photovoltaics
[NASA-CR-176019] 19 p3343 N85-30720

A concept for the intrinsic dielectric strength of electrical insulation materials
[NASA-CR-176040] 20 p3448 N85-31410

An analysis of the feasibility of producing silicon for solar cells by a dichlorosilane/fluidized-bed reactor process
[NASA-CR-176036] 20 p3478 N85-31614

Proceedings of the Flat-Plate Solar Array Project Research Forum on High-Efficiency Crystalline Silicon Solar Cells
[NASA-CR-176047] 20 p3478 N85-31615

Historical perspective of barriers to achieving high-efficiency silicon solar cells
20 p3479 N85-31616

Aspects of silicon bulk lifetimes
20 p3479 N85-31617

Recombination phenomena in high efficiency silicon solar cells 20 p3479 N85-31618

Silicon solar cell efficiency improvement: Status and outlook 20 p3479 N85-31619

Some practical considerations for economical back contact formation on high efficiency solar cells
20 p3479 N85-31620

High-efficiency cell concepts on low-cost silicon sheets 20 p3479 N85-31621

High lifetime solar cell processing and design
20 p3480 N85-31622

Silicon MINP solar cells 20 p3480 N85-31623

High efficiency solar cell research for space applications 20 p3480 N85-31624

Compositional analysis of silicon
20 p3480 N85-31626

Surface passivation and junction formation using low energy hydrogen implants 20 p3480 N85-31628

Measurement of electrical parameters and current components in the bulk of silicon solar cells
20 p3481 N85-31635

Current status of one- and two-dimensional numerical models: Successes and limitations
20 p3482 N85-31636

Application of closed-form solutions to a mesh point field in silicon solar cells 20 p3482 N85-31637

Phenomena simulation for heavy doping and surface recombination velocity 20 p3482 N85-31638

High efficiency large area polysilicon solar cells
20 p3482 N85-31639

High efficiency solar cell processing
20 p3482 N85-31640

Process and design considerations for high-efficiency solar cells 20 p3482 N85-31641

Processing technology for high efficiency silicon solar cells 20 p3483 N85-31642

Texture etching of (100) silicon for solar cells
20 p3483 N85-31643

User handbook for block 5 silicon solar cell modules
[NASA-CR-176043] 20 p3483 N85-31644

Recent improvements in materials for thin GaAs and multibandgap solar cells
[DE85-008800] 20 p3484 N85-31651

Gallium arsenide arrays versus silicon arrays for space application
[SNIAS-851-440-104] 20 p3485 N85-31657

Reduction of radiation damage in solar cells -- spacecraft power supplies
[ESA-CR(P)-2005] 20 p3485 N85-31659

Photovoltaic solar devices
[BMFT-FB-T-84-288] 20 p3485 N85-31660

High-efficiency crystalline silicon technology development 21 p3607 N85-32395

Summary of the high-efficiency crystalline solar cell research forum 21 p3607 N85-32396

High-efficiency module and array research
21 p3607 N85-32397

The future of crystalline silicon technology in the US Department of Energy program
21 p3607 N85-32399

Predicting photothermal field performance
21 p3608 N85-32404

Polymerizable ultraviolet stabilizers
21 p3608 N85-32406

Encapsulation materials research
21 p3608 N85-32407

Topics in electrochemical degradation of photovoltaic modules 21 p3608 N85-32410

Polymer-water interaction studies
21 p3609 N85-32411

Silicon refinement by chemical vapor transport
21 p3609 N85-32412

High-efficiency silicon solar cell research
21 p3609 N85-32417

Physics of heavily doped silicon and solar-cell parameter measurement 21 p3609 N85-32418

Measuring bulk recombination rates and boundary recombination velocities 21 p3609 N85-32419

Studies of oxygen- and carbon-related defects in high-efficiency silicon solar cells
21 p3609 N85-32420

Comprehensive silicon solar-cell computer modeling
21 p3609 N85-32421

Sensitivity analysis of high-efficiency silicon solar-cell design parameters 21 p3610 N85-32422

Silicon surface passivation by silicon nitride deposition
21 p3610 N85-32423

Important loss mechanisms in high-efficiency solar cells 21 p3610 N85-32424

Development of high-efficiency solar cells on silicon web 21 p3610 N85-32425

Simultaneous junction formation
21 p3610 N85-32426

Laser-assisted solar-cell metallization processing
21 p3610 N85-32429

A non-noble front metallization process
21 p3611 N85-32430

Pulsed excimer laser processing for cost-effective solar cells 21 p3611 N85-32432

Excimer laser annealing for fabrication of low-cost solar cells 21 p3611 N85-32433

High-purity silicon crystal growth
21 p3612 N85-32444

Advanced module development overview
21 p3612 N85-32445

Status of high-efficiency module design and fabrication 21 p3612 N85-32446

Photovoltaic module spread-of-flame testing
21 p3612 N85-32448

Improved Nominal Operating Cell Temperature (NOCT) test procedure 21 p3612 N85-32449

Thin-film reliability and engineering overview
21 p3612 N85-32450

Accelerated stress factors and failure/degradation mechanisms in terrestrial solar cells
21 p3613 N85-32451

Failure analysis of thin-film amorphous-silicon solar-cell modules 21 p3613 N85-32452

Reference-cell calibration activities
21 p3613 N85-32453

Solid-melt interface studies of high-speed silicon sheet growth
[NASA-CR-176112] 22 p3751 N85-33249

Block 5 documentation and solar modules
[NASA-CR-176134] 22 p3805 N85-33564

Laser-assisted solar cell metallization processing
[NASA-CR-176124] 22 p3805 N85-33565

Diffusion welding of Cassegrainian concentrator cell stack assemblies
[NASA-CR-176104] 22 p3805 N85-33566

Development of high-efficiency solar cells on silicon web
[NASA-CR-176101] 22 p3805 N85-33568

Ultrasonic seam welding on thin silicon solar cells
[NASA-CR-176116] 22 p3805 N85-33570

Use of low energy hydrogen ion implants in high efficiency crystalline silicon solar cells
[NASA-CR-176109] 22 p3806 N85-33571

An enhanced photoresponse at dislocation subgrain boundaries revealed by X-ray topography of polysilicon solar cells 22 p3806 N85-33572

Photovoltaic energy systems
[DE85-011630] 22 p3807 N85-33581

1985 Amorphous Silicon Review Meeting
[DE85-008794] 22 p3807 N85-33582

Low-cost high-performance silicon concentrator cells
[DE85-008875] 22 p3807 N85-33584

Photovoltaics technical information guide
[DE85-002924] 22 p3808 N85-33585

Solar maximum: Solar array degradation
[NASA-TM-86194] 23 p3903 N85-34175

Flat-plate solar array project process development area process research of non-CZ silicon material
[NASA-CR-176117] 23 p3945 N85-34445

Investigation of test methods, material properties, and processes for solar cell encapsulants
[NASA-CR-176132] 23 p3945 N85-34446

Development of metallization process: FSA project, cells and module formation research area
[NASA-CR-176136] 23 p3945 N85-34447

Dual-chamber plasma deposition of A-Si:H solar cells at high rates using disilane
[DE85-011828] 23 p3946 N85-34451

Practical aspects of photovoltaic technology, applications and cost (revised)
[NASA-CR-174963] 24 p4110 N85-35472

Photovoltaics technology program summary
[DE85-013096] 24 p4112 N85-35483

Design and construction of an advanced power conditioning subsystem for small photovoltaic applications
[DE85-013940] 24 p4113 N85-35485

SOLAR COLLECTORS

NT SOLAR REFLECTORS

Modeling of a second-generation solar-driven Rankine air conditioner
[DE84-015132] 01 p0036 N85-10223

Technical Review of the Solid Particle Receiver Program
[DE84-015161] 01 p0068 N85-10481

Test methods and standards development for active solar heating and cooling systems
[PB84-217447] 03 p0343 N85-12209

Superpure materials research planned
03 p0353 N85-12270

Fluorescent dyes for luminescent solar concentrators
[BMFT-FB-T-84-164] 04 p0480 N85-13061

Concentrator optical characterization using computer mathematical modelling and point source testing
[NASA-CR-174109] 04 p0528 N85-13375

Software used with the flux mapper at the solar parabolic dish test site
[NASA-CR-174108] 04 p0528 N85-13376

Thin polymer film collectors as a contribution to the solar industry
[DE84-015299] 04 p0529 N85-13383

Solar pond overview 05 p0667 N85-14287

Proceedings of the 22nd Project Integration Meeting
[DE85-000334] 06 p0833 N85-15302

Multijunction cells for concentrators: Technology prospects
[NASA-CR-174259] 07 p0991 N85-16295

Antisoiling technology: Theories of surface soiling and performance of antisoiling surface coatings
[NASA-CR-174274] 07 p0991 N85-16296

Performance and cost of energy transport and storage systems for dish applications using reversible chemical reactions
[NASA-CR-174263] 07 p0992 N85-16298

Solar energy conversion based on the principle of fluorescent collectors. Installation of a test collector to deliver several Watts power
[BMFT-FB-T-84-192] 07 p0993 N85-16306

Solar energy conversion based on the principle of fluorescent collectors
[BMFT-FB-T-84-193] 07 p0994 N85-16309

Compilation of Sandia papers contributed to the 17th IEEE Photovoltaic Specialists Conference
[DE84-017456] 09 p1315 N85-18267

NBS (National Bureau of Standards) solar collector durability-reliability test program
[PB85-113603/GAR] 09 p1346 N85-18469

Overview of photovoltaic concentrator technology
[DE84-016790] 10 p1512 N85-19539

Development of mass-producible line-focus tracking concentrating solar collectors. Category 2: Trackers
[DE85-002673] 10 p1512 N85-19543

Photosynthesis of ammonia
[DE85-001482] 11 p1595 N85-20029

Flame spread on combustible solar collector glazing materials
[DE85-002596] 11 p1595 N85-20032

Innovative solar thermal dish technology development
[DE85-002787] 11 p1673 N85-20539

Solar thermal technology
[DE84-013029] 11 p1673 N85-20540

Sol-gel-derived AR coatings for solar receivers
[DE85-000192] 11 p1673 N85-20541

Advanced glazings research
[DE85-000539] 11 p1674 N85-20549

Control of large collector arrays: The SSPS experience
[DE85-001461] 11 p1675 N85-20553

Performance of solar thermal systems with liquid metal MHD conversion
[DE85-002758] 11 p1675 N85-20555

Evaluation of infrared reflectance as a technique fo measuring absorber materials degradation
[DE85-002171] 11 p1729 N85-2087

An investigation of aerowindows for solar receiver
[DE84-010931] 12 p1677 N85-2177

Performance evaluation of an active solar cooling syste utilizing low cost plastic collectors and a evaporatively-cooled absorption chiller
[DE84-010613] 12 p1680 N85-217

NBS solar collector durability/reliability test progra
[DE85-003489] 12 p1681 N85-218

Some solar dish/heat engine design considera
[DE85-003479] 12 p1681 N85-218

User's manual for the University of Houston individual heliostat layout and performance code
[DE85-004843] 12 p1882 N85-21808
Solar process heat: Technology program
[BMFT-FB-T-84-234] 12 p1882 N85-21812
Power from the Sun: Light at night
[PB85-124097] 12 p1883 N85-21814
Ecological observations at the site of the 10 MWe solar thermal power system (1978-1984)
[DE85-004572] 12 p1885 N85-21827
ROSA: A computer model for optical power ratio calculations
[DE85-005174] 13 p2129 N85-23251
Use of heat pipes for heat collection and transmission in solar plants 14 p2265 N85-24037
Selective coatings for solar-to-thermal energy converters 14 p2280 N85-24127
Silicon-sheet and thin-film cell and module technology potential: Issue study
[NASA-CR-175854] 14 p2349 N85-24520
Development and testing of Parabolic Dish Concentrator No. 1
[NASA-CR-175651] 14 p2350 N85-24522
Advanced high-efficiency concentrator cell
[DE85-000525] 14 p2351 N85-24533
An evaluation of thermal storage for liquid-metal, solar thermal receivers
[DE85-002929] 16 p2620 N85-27394
High-altitude testing of selective optical coatings for solar radiators and collectors 17 p2939 N85-28143
Selective coatings for solar heat converters
17 p2939 N85-28144
Relative potentials of concentrating and two-axis tracking flat-plate photovoltaic arrays for central-station applications
[NASA-CR-175889] 17 p2965 N85-28446
Parabolic dish test site: History and operating experience
[NASA-CR-175892] 17 p2985 N85-28447
A program for the calculation of paraboloidal-dish solar thermal power plant performance
[NASA-CR-175874] 17 p2965 N85-28449
Development of mass-producible line-focus tracking concentrating solar collectors. Category 2: Control systems
[DE85-007873] 17 p2987 N85-28459
Shenandoah parabolic dish solar collector
[DE85-008326] 17 p2987 N85-28460
DOE/Sandia point-focus concentrator program, draft
[DE85-008209] 17 p3038 N85-28793
United States participation in International Energy Agency Task IX, Subtask (C): Pyranometry. 1984 participation
[DE85-009615] 18 p3110 N85-29256
Absorber coatings degradation
[DE85-008628] 18 p3126 N85-29367
Airport solar photovoltaic concentrator phase 3
[DE85-006773] 18 p3128 N85-29370
Progress in solar thermal distributed receiver technology
[DE85-008066] 18 p3128 N85-29372
Foamglass solar window collector
[DE85-009197] 18 p3129 N85-29374
Liquid metal thermoelectric converter (LMTEC) for solar applications
[DE85-006405] 18 p3129 N85-29376
Silvered polymer reflectors
[DE85-008782] 18 p3130 N85-29384
Solar Thermal Research Program
[DE85-000514] 18 p3131 N85-29388
10 MWe Solar Thermal Central Receiver Pilot Plant total capitol costs
[DE85-009113] 18 p3131 N85-29390
Thermal performance testing and mathematically modeling of integral collector storage solar hot water systems
[PB85-186906] 18 p3132 N85-29396
Design and operation of solar thermal heat transfer systems
[DE85-009837] 19 p3267 N85-30263
Receiver loss study of optimized solar central receiver systems as a function of receiver thermal loss per unit area
[DE85-010831] 19 p3268 N85-30265
Thermal performance and design of a solid particle cavity receiver
[DE85-010830] 19 p3274 N85-30300
Advanced evacuated tube collectors
[DE85-010271] 19 p3274 N85-30302
High-efficiency, low-cost, passively-cooled PV concentrator module
[DE85-010013] 19 p3305 N85-30490
Calibration of relevant measuring sensors
[DE85-009820] 19 p3306 N85-30492
Proceedings of the Distributed Receiver Solar Thermal Technology Conference
[DE85-010551] 19 p3306 N85-30493
A model for the economic assessment of solar power plants
[DE85-009355] 19 p3381 N85-30977
Solar dynamic systems 20 p3443 N85-31374
View-limiting shrouds for insolation radiometers
[NASA-CR-176041] 20 p3458 N85-31476
Control system for parabolic dish concentrator No. 1
[NASA-CR-176045] 20 p3463 N85-31510
Nomographs for estimating the levelized cost of energy from flat-plate and concentrator photovoltaic systems
[NASA-CR-176048] 20 p3483 N85-31645
Photovoltaic concentrator research status
[DE85-010119] 20 p3483 N85-31647
Self-heating to ignition measurements and computation of critical size for solar energy collector materials
[PB85-183374] 20 p3485 N85-31663
An investigation into the fluidization and heat transfer of low density particles in a fluidized bed with applications
[AD-A155259] 21 p3584 N85-32282
Forced convection on solar collector arrays
[DE85-010381] 21 p3585 N85-32287
Advanced module development overview
21 p3612 N85-32445
Status of high-efficiency module design and fabrication 21 p3612 N85-32446
Module Hipot and ground continuity test results
21 p3612 N85-32447
Photovoltaic module spread-of-flame testing
21 p3612 N85-32448
Improved Nominal Operating Cell Temperature (NOCT) test procedure 21 p3612 N85-32449
Thin-film reliability and engineering overview
21 p3612 N85-32450
Department of Energy gear drive unit final prototype testing and design evaluation
[DE85-003296] 22 p3793 N85-33499
An analysis of the effects of active solar energy system control sensor degradation on system performance
[DE84-013023] 22 p3804 N85-33562
Theory of cellwise optimization for solar central receiver system
[DE85-012586] 22 p3807 N85-33579
Solar central receiver preliminary design studies: Summary and review of contract results
[DE85-011385] 22 p3809 N85-33593
Study of alternative system conversions for the Solar One pilot plant
[DE85-010026] 22 p3809 N85-33594
Long-term goals for solar thermal technology
[DE85-013032] 22 p3809 N85-33597
Optical analysis of parabolic dish concentrators for solar dynamic power systems in space
[NASA-TM-87080] 23 p3903 N85-34176
Vapor phase heat transport concepts
[DE85-009550] 23 p3931 N85-34366
Solar thermal technologies program summary
[DE85-012253] 23 p3945 N85-34449
Solar heat pump
[DE85-011323] 23 p3946 N85-34453
Solar energy education: Renewable energy activities for chemistry and physics
[DE85-010371] 23 p3946 N85-34455
Solar pond technology for Navy applications
[AD-A155877] 24 p4112 N85-35488

SOLAR CONSTANT
Spectroradiometric calibration of the Thematic Mapper and Multispectral Scanner system
[E85-10094] 12 p1874 N85-21756
Global solar oscillations in irradiance and velocity: A comparison 14 p2446 N85-25094

SOLAR CONVERTERS
U SOLAR GENERATORS

SOLAR COOLING
Solar heating and cooling R and D program coordination support
[DE84-013479] 01 p0068 N85-10449
Turbine test report, addendum
[DE84-015130] 02 p0205 N85-11353
Test methods and standards development for active solar heating and cooling systems
[PB84-217447] 03 p0343 N85-12209
Passive solar/Earth sheltered office/dormitory cooling season thermal performance
[DE84-016662] 05 p0669 N85-14308
Performance of the SERI parallel-passage dehumidifier
[DE85-000509] 11 p1672 N85-20536
High performance solar desiccant cooling system: Performance evaluation and research recommendations
[DE85-000508] 11 p1676 N85-20559
A summary and assessment of historical reliability and maintainability data for solar hot water and space conditioning systems
[DE84-004521] 12 p1876 N85-21770
Development of a single-family absorption chiller for use in a solar heating and cooling system, phase 3, volume 2
[DE85-003218] 13 p2130 N85-23253
Testing and further development of a solar absorption cooling plant
[BMFT-FB-T-84-264] 15 p2566 N85-25954
Operation of a low temperature absorption chiller at rating point and at reduced evaporator temperature
[DE85-008308] 16 p2760 N85-27030
Experiments on sorption characteristics of solid desiccant materials for solar desiccant cooling systems
[DE85-000542] 17 p2923 N85-28019
Proceedings of the Distributed Receiver Solar Thermal Technology Conference
[DE85-010551] 19 p3306 N85-30493
Comparative evaluation of ground-coupled heat pumps that use solar energy
[DE85-010950] 20 p3484 N85-31649
Evaporatively cooled chiller for solar air conditioning systems design and field test
[DE84-014154] 20 p3484 N85-31652
Solid desiccant dehumidification systems for residential applications
[PB85-198489] 22 p3755 N85-33279
Advances in open-cycle solid desiccant cooling
[DE85-008797] 22 p3808 N85-33590

SOLAR CORONA
NT CORONAL HOLES
NT CORONAL LOOPS
Studies of solar flares and coronal loops
[AD-A145009] 01 p0130 N85-10898
Study of the solar corona using radio and space observations
[NASA-CR-174034] 02 p0304 N85-11963
Physics of the inner heliosphere 1-10R sub O plasma diagnostics and models
[NASA-CR-174010] 02 p0304 N85-11964
Active regions — and the Solar Maximum Mission
[NASA-CR-170626] 02 p0304 N85-11965
Vector magnetic field analysis of Lorentz forces acting in the solar atmosphere
[AD-A145941] 03 p0449 N85-12852
Magnetic helicity in the solar corona
05 p0745 N85-14780
Structure and evolution of the large scale solar and heliospheric magnetic fields 05 p0746 N85-14782
Distribution of the K-corona over the polar regions of the solar disk: 1965-1983
[PB84-230077] 06 p0835 N85-15317
Meteoritic constraints on processes in the solar nebula 06 p0887 N85-15630
Chemical evolution of the solar nebula: A new model
06 p0887 N85-15631
Homogeneous condensation of gaseous mixtures of Si, Fe, O, N, and C in relative cosmic abundance and implications for astronomical condensation
06 p0887 N85-15632
Dynamic thermal episodes in the protosolar nebula: Development of models from observations on CAI's
06 p0887 N85-15633
The chemistry of rare earth elements in the solar nebula 06 p0889 N85-15643
Differentiated meteorites and the components of chondrites
[NASA-CR-174201] 06 p0890 N85-15649
Polar rain: Solar coronal electrons in the Earth's magnetosphere
[NASA-TM-86150] 07 p1060 N85-16726
Evidence for non-radiative activity in hot stars
08 p1231 N85-17756
Heating in the solar mantle 08 p1233 N85-17769
Coronal and chromospheric physics — Sun, sunspots, and solar limb
[NASA-CR-174290] 08 p1259 N85-17921
Solar Corona Explorer: A mission for the physical diagnosis of the solar corona
[NASA-TM-87416] 10 p1572 N85-19612
Global aspects of stream evolution in the solar wind
[DE85-002207] 11 p1766 N85-21101
Activation of solar flares 12 p1954 N85-22276
Thermal stability of static coronal loops: Part 1: Effects of boundary conditions
[NASA-CR-175495] 12 p1961 N85-22330
A normal incidence, high resolution X-ray telescope for solar coronal observations
[NASA-CR-175622] 13 p2169 N85-23461
Orbital resonances and planetary accretion in the solar nebula 13 p2179 N85-23523
Evolution of grains in a turbulent solar nebula
13 p2179 N85-23525

Research on the early history of the solar system
13 p2180 N85-23527

Physics of the inner heliosphere: Mechanisms, models and observational signatures
[NASA-CR-175632] 13 p2205 N85-23677

The hydromagnetics of the Sun — conferences
[ESA-SP-220] 14 p2445 N85-25091

Coronal structures 14 p2448 N85-25110

The Fe XIII 10747 A and Fe XIV 5303 A coronal emission lines polarization 14 p2448 N85-25111

Mechanisms of magnetic heating of the solar corona
14 p2448 N85-25113

Observational constraints on heating processes — solar corona 14 p2449 N85-25115

Axisymmetric magnetofluidistatic (MFS) equilibria of solar coronal loops: An integral equation approach
14 p2449 N85-25118

Coronal heating by turbulent phase mixed MHD waves — solar corona 14 p2453 N85-25148

The possible role of electrical currents in coronal phenomena 14 p2453 N85-25151

Coronal structures observed at metric wavelengths with the Nancay radioheliograph 14 p2453 N85-25152

Empirical model of the solar corona using solar-cycle related parameters 14 p2453 N85-25153

Harmonic analysis of the solar magnetic field
14 p2454 N85-25154

About sudden disappearances and reappearances — solar activity 14 p2454 N85-25157

Solar maximum mission results on the energetics of the impulsive phase of solar flares 14 p2454 N85-25159

Solar magnetohydrodynamics: Symposium review
14 p2455 N85-25162

Analysis of short-period changes in intensity of hard X-radiation of solar flares registered aboard Venera-13 and Venera-14 spacecraft 16 p2723 N85-26806

Remote sensing of the plasma with time delay measurements (coronal sounding)
16 p2886 N85-27804

The Faraday rotation experiment — solar corona
16 p2886 N85-27805

Very large array observations of coronal loops and related observations of solar type stars
[AD-A152027] 16 p2888 N85-27817

The solar coronal X-ray spectrum 5.5-12 A
[AD-A152334] 17 p3054 N85-28908

Application of the MHD energy principle to magnetostatic atmospheres
[NASA-CR-175967] 18 p3136 N85-29420

Measurements of Solar Vector Magnetic Fields
[NASA-CP-2374] 18 p3203 N85-29869

Magnetic and thermodynamic structure of the solar corona during sunspot minimum
18 p3203 N85-29873

Current evolution in a numerical emerging-magnetic-flux model 18 p3204 N85-29875

Turbulence and wave particle interactions in solar-terrestrial plasmas
[NASA-CR-175970] 18 p3209 N85-29906

Effects of coronal disturbances on the ionization state of the solar wind
[NASA-CR-175997] 19 p3385 N85-31000

Solar photospheric and coronal abundances from solar energetic particle measurements
[NASA-CR-176029] 20 p3547 N85-32073

Contributions to the 19th International Cosmic Ray Conference
[NASA-CR-176060] 21 p3714 N85-33044

Solar coronal and photospheric abundances from solar energetic particle measurements
[PAPER-SH-2.1-5] 21 p3715 N85-33053

Latitude variation of recurrent fluxes in the outer solar system
[SH-4.1-13] 21 p3715 N85-33054

A study of the cyclical variations of coronal holes and their relation to open magnetic fields
[AD-A155251] 21 p3723 N85-33099

Variation in radiowave propagation conditions in corona during solar activity cycle 22 p3763 N85-33327

Relationships between chondritic meteorites and planets 22 p3851 N85-33851

Nebular volatile fractionations associated with chondrule formation 22 p3852 N85-33855

The distribution of compositional classes in the asteroid belt: A cosmochemical fingerprint?
22 p3852 N85-33856

Soft X-Ray Telescope (SXRT)
23 p3900 N85-34159

White Light Coronograph (WLC) and Ultra-Violet Coronal Spectrometer (UVCS) 23 p3901 N85-34161

Prompt acceleration of ions by oblique turbulent shocks in solar flares
[SH-1.1-6] 23 p3989 N85-34733

Study of photon emission by electron capture during solar nuclei acceleration. 3: Photon production evaluations
[SH-1.1-10] 23 p3990 N85-34737

Spectral and spatial properties of solar microflares
[SH-1.2-4] 23 p3991 N85-34740

Two classes of solar energetic particle events associated with impulsive and long duration soft X-ray flares
[SH-1.2-12] 23 p3992 N85-34747

The starting conditions for an optically small solar gamma ray flare
[SH-1.3-2] 23 p3993 N85-34751

Energetic protons from a disappearing solar filament
[SH-1.3-7] 23 p3993 N85-34754

Solar Coronal and photospheric abundances from solar energetic particle measurements
[SH-2.1-5] 23 p3998 N85-34786

Diffusion in the chromosphere and the composition of the solar corona and energetic particles
[SH-2.1-9] 23 p3999 N85-34790

Anomalous abundances of solar energetic particles and coronal gas: Coulomb effects and First Ionization Potential (FIP) ordering
[SH-2.1-10] 23 p3999 N85-34791

Coronal propagation of solar flare particles observed by satellite
[SH-3.1-2] 23 p4001 N85-34807

Coronal propagation of flare associated electrons and protons
[SH-3.1-3] 23 p4001 N85-34808

Peculiarities of propagation of charged particles in solar corona
[SH-3.1-6] 23 p4001 N85-34810

The propagation of solar energetic particles in magnetic channels
[SH-3.2-4] 23 p4003 N85-34820

The flare origin of Forbush decreases not associated with solar flares on the visible hemisphere of the Sun
[SH-5.1-4] 23 p4041 N85-35058

The 4He1H ratios in the chemical compositions of solar flare particles and the primordial solar nebula
[SH-7.1-12] 23 p4048 N85-35104

SOLAR CORPUSCULAR RADIATION

NT SOLAR ELECTRONS
NT SOLAR NEUTRINOS
NT SOLAR PROTONS

Plasma and nuclear processes in solar matter
12 p1954 N85-22277

Solar-geophysical data number 483, November 1984. Part 2: (Comprehensive reports). Data for May 1984, December 1981 and miscellanea
[PB85-147700] 12 p1962 N85-22336

Cyclic changes in barometric coefficient of cosmic ray neutron component 15 p2478 N85-25293

Ninteenth International Cosmic Ray Conference. SH sessions, volume 4
[NASA-CP-2376-VOL-4] 23 p3989 N85-34729

Ninteenth International Cosmic Ray Conference. SH sessions, volume 5
[NASA-CP-2376-VOL-5] 23 p4031 N85-34991

SOLAR COSMIC RAYS

Variation of fast charged particles in event of 22 November 1977 based on Cosmos-900 satellite data
02 p0161 N85-11092

Solar cosmic ray produced neon in lunar soils and their implication for gas-rich meteorite studies
06 p0887 N85-15636

Solar-Geophysical Data. Part 1: (Prompt reports)
[PB85-112068] 11 p1766 N85-21100

Correlated fluctuations of charged particle fluxes and magnetic field according to data from Intercosmos-10 satellite 16 p2722 N85-26802

Solar coronal and photospheric abundances from solar energetic particle measurements
[PAPER-SH-2.1-5] 21 p3715 N85-33053

Differential measurement of cosmic-ray gradient with respect to interplanetary current sheet
[PAPER-SH-4.2-9] 21 p3715 N85-33055

Changes in the energy spectrum of anomalous oxygen and helium during 1977 - 1985
[PAPER-SH-4.6-1] 21 p3715 N85-33056

Solar cycle variations of the anomalous cosmic ray component
[PAPER-SH-4.6-2] 21 p3715 N85-33057

Radial and latitudinal gradients of anomalous oxygen during 1977 - 1985
[PAPER-SH-4.6-4] 21 p3716 N85-33058

Solar modulation and interplanetary gradients of the galactic electron flux, 1977 - 1984
[PAPER-SH-4.7-4] 21 p3716 N85-33059

Source energy spectra from demodulation of solar particle data by interplanetary and coronal transport
[SH-1.3-13] 23 p3994 N85-34758

Ground increase of cosmic ray intensity on February 16, 1984
[SH-1.3-15] 23 p3994 N85-34760

The SCR flare of 16 February 1984 as recorded by the Sayan spectrograph
[SH-1.3-17] 23 p3994 N85-34761

Time extended production of neutrons during a solar flare
[SH-1.4-1] 23 p3994 N85-34762

Further observations of protons resulting from the decay of neutrons ejected by solar flares
[SH-1.4-2] 23 p3994 N85-34763

Suggestions for improving the efficiency of ground-based neutron monitors for detecting solar neutrons
[SH-1.4-3] 23 p3995 N85-34764

Precision measurements of solar energetic particle elemental composition
[SH-2.1-4] 23 p3998 N85-34785

Solar Coronal and photospheric abundances from solar energetic particle measurements
[SH-2.1-5] 23 p3998 N85-34786

Silicon to iron abundances in solar cosmic rays and in the sun
[SH-2.1-6] 23 p3998 N85-34787

Variations in elemental composition of several MEV/nucleon ions observed in interplanetary space
[SH-2.1-7] 23 p3998 N85-34788

The mean ionic charges of N, Ne, MG, SI and S in solar energetic particle events
[SH-2.1-11] 23 p3999 N85-34792

Nucleosynthesis in the terrestrial and solar atmospheres
[SH-2.2-2] 23 p4000 N85-34797

Solar source regions of 3HE-rich particle events
[SH-2.2-4] 23 p4000 N85-34799

The 3HE in solar non-relativistic electron events
[SH-2.2-5] 23 p4000 N85-34800

Elemental abundance differences between nuclei acclerated in CIR shocks and solar flares
[SH-2.2-6] 23 p4000 N85-34801

The heavy ion composition in 3HE-rich solar flares
[SH-2.2-7] 23 p4000 N85-34802

The mean ionic charge of silicon in 3HE-rich solar flares
[SH-2.2-8] 23 p4000 N85-34803

On the connection between the 3HE-enrichment and spectral index of solar energetic particles
[SH-2.2-9] 23 p4001 N85-34804

The plasma mechanism for preferential acceleration of heavy ions
[SH-2.2-10] 23 p4001 N85-34805

Observations of solar energetic particles at a synchronous orbit
[SH-3.1-1] 23 p4001 N85-34806

Coronal propagation of solar flare particles observed by satellite
[SH-3.1-2] 23 p4001 N85-34807

Coronal propagation of flare associated electrons and protons
[SH-3.1-3] 23 p4001 N85-34808

Geometry of the diffusive propagation region in the August 14, 1982 solar electron event
[SH-3.1-5] 23 p4001 N85-34809

Some characteristics of the solar flare event of February 16, 1984
[SH-3.1-7] 23 p4001 N85-34811

Constraints of solar flare particle transport models from anisotropy observations at Voyager 1
[SH-3.1-8] 23 p4002 N85-34812

Determination of the pitch-angle distribution and transverse anisotropy of interplanetary particles
[SH-3.1-11] 23 p4002 N85-34815

Pitch angle distributions of solar energetic particles and the local scattering properties of the interplanetary magnetic field
[SH-3.1-13] 23 p4002 N85-34816

Exponential anisotropy of solar cosmic rays
[SH-3.2-1] 23 p4002 N85-34817

Energetic solar particle events
[SH-3.2-2] 23 p4003 N85-34818

Channeled propagation of solar particles
[SH-3.2-3] 23 p4003 N85-34819

The propagation of solar energetic particles in magnetic channels
[SH-3.2-4] 23 p4003 N85-34820

Radial transport of approximately 1 MeV/nucleon ions during the 22 November 1977 solar particle event
[SH-3.2-5] 23 p4003 N85-34821

Energetic solar particle fluxes out to 3 AU during the 7 May 1978 flare event
[SH-3.2-6] 23 p4003 N85-34822

The local characteristic function of interplanetary particle propagation
[SH-3.2-8] 23 p4003 N85-34823

nvestigation of cosmic ray propagation in interplanetary ace
H-3.2-9] 23 p4004 N85-34824

Diffusion-convection function of cosmic rays
H-3.2-10] 23 p4004 N85-34825

On reflecting boundary behind the Earth's orbit at pagation of fast particles from solar flares
H-3.2-13] 23 p4004 N85-34827

Propagation of the phase of solar modulation
H-4.1-12] 23 p4005 N85-34835

North-south asymmetry in activity on the Sun and cosmic y density gradients
SH-4.2-7] 23 p4007 N85-34845

Gradients and anisotropies of high energy cosmic rays n the outer heliosphere
SH-4.3-7] 23 p4032 N85-34992

IMF-sense-dependent cosmic ray anisotropy produced om diffusion-convection in heliosphere
[SH-4.3-9] 23 p4032 N85-34994

Influence of the neutral sheet on the Swinson's type orth-south anisotropy of cosmic rays
[SH-4.3-10] 23 p4032 N85-34995

Characteristics of cosmic ray pole-equator anisotropy derived from spherical harmonic analysis of neutron monitor data
[SH-4.3-12] 23 p4032 N85-34996

First zonal harmonic component of cosmic ray neutron intensity
[SH-4.3-13] 23 p4032 N85-34997

Cosmic ray intensity distribution perpendicular to solar equatorial plane at 1 A.U. during 1976-83
[SH-4.3-14] 23 p4032 N85-34998

The corotating variation of the north-south anisotropy of cosmic rays
[SH-4.3-15] 23 p4033 N85-34999

Sidereal anisotropy of cosmic rays
[SH-4.4-8] 23 p4034 N85-35006

Cosmic ray intensity variations observed at Matsushiro (220 M.W.E. in depth)
[SH-4.4-9] 23 p4034 N85-35007

Long-term modulation of cosmic rays during solar cycle 21
[SH-4.4-10] 23 p4034 N85-35008

Role of solar flare index in long term modulation of cosmic ray intensity
[SH-4.4-12] 23 p4034 N85-35009

Azimuthal and meridional asymmetries of the solar wind and quasiperiodic variations of intensity of Galactic Cosmic Rays (GCR)
[SH-4.4-20] 23 p4035 N85-35016

Dynamics of two-year cosmic ray variations inferred from the data of spacecraft and stratospheric measurements and from the neutron monitor data in 1959-1981
[SH-4.4-21] 23 p4035 N85-35017

Solar tri-diurnal variation of cosmic rays in a wide range of rigidity
[SH-4.5-3] 23 p4036 N85-35021

Upper cut-off rigidity for corotation anisotropy during solar activity cycles 20 and 21
[SH-4.5-4] 23 p4036 N85-35022

Twenty-two-year cycle of the upper limiting rigidity of Daily waves
[SH-4.5-5] 23 p4036 N85-35023

Solar wind velocity and daily variation of cosmic rays
[SH-4.5-6] 23 p4036 N85-35024

Time and energy dependence of the cosmic ray gradient in the outer heliosphere
[SH-4.7-2] 23 p4040 N85-35047

Frequency spectra of short-period variations of cosmic ray
[SH-5.1-17] 23 p4043 N85-35070

Penetration of solar protons into the Earth's magnetosphere on November 22, 1977
[SH-6.1-15] 23 p4046 N85-35088

Dynamics of the penetration boundaries of solar protons during a strong magnetic storm
[SH-6.1-16] 23 p4046 N85-35089

Solar cosmic ray bursts and solar neutrino fluxes
[SH-8.1-10] 23 p4050 N85-35115

A silicon surface barrier telescope for solar particles identification
[SH-9.1-3] 23 p4050 N85-35118

Strong earthquakes, novae and cosmic ray environment
[SH-10.1-3] 23 p4053 N85-35135

SOLAR CYCLES

NT SUNSPOT CYCLE

Statistical analysis of 11-year and 80-year solar cycles
02 p0161 N85-11095

Statistical properties of geomagnetic pulsations at the Observatory of Fuerstenfeldbruck determined with the aid of pulsation indices. Part 2: Periodicity in the occurrence of pulsations
[REPT-556] 03 p0376 N85-12399

Middle Atmosphere Program. Handbook for MAP, volume 8
[NASA-CR-175478] 11 p1657 N85-20445

Report on the Workshop on Intercomparison of Solar UV Irradiance Measurements and Related Instrument Calibration 11 p1658 N85-20448

Nonlinear time-evolution of kink-unstable magnetic flux tubes in the convection zone of the Sun
14 p2447 N85-25105

Solar and stellar magnetic cycles: Unity and multiplicity 14 p2448 N85-25109

A consideration of the solar cycle in the light of the behavior of the large active regions
14 p2452 N85-25140

Solar cycle variation of ephemeral active regions
14 p2452 N85-25142

The first effect of the amplitude of a solar cycle
14 p2452 N85-25143

Empirical model of the solar corona using solar-cycle related parameters 14 p2453 N85-25153

About sudden disappearances and reappearances — solar activity 14 p2454 N85-25157

Modeling 22-year solar activity cycle within framework of dynamo theory with allowance for primary field
15 p2477 N85-25288

Cyclic changes in barometric coefficient of cosmic ray neutron component 15 p2478 N85-25293

Contributions to the 19th International Cosmic Ray Conference
[NASA-CR-176060] 21 p3714 N85-33044

Solar cycle variations of the anomalous cosmic ray component
[PAPER-SH-4.6-2] 21 p3715 N85-33057

Radial and latitudinal gradients of anomalous oxygen during 1977 - 1985
[PAPER-SH-4.6-4] 21 p3716 N85-33058

Solar modulation and interplanetary gradients of the galactic electron flux, 1977 - 1984
[PAPER-SH-4.7-4] 21 p3716 N85-33059

Solar cycle variation of ephemeral regions
[AD-A154967] 21 p3723 N85-33097

A study of the cyclical variations of coronal holes and their relation to open magnetic fields
[AD-A155251] 21 p3723 N85-33099

Variation in radiowave propagation conditions in corona during solar activity cycle 22 p3763 N85-33327

Elemental abundances in corotating events
[SH-1.5-15] 23 p3997 N85-34778

Solar and interplanetary particles at 2 to 4 MEV during solar cycles 21, solar cycle variations of event sizes, and compositions
[SH-1.5-16] 23 p3997 N85-34779

Cumulative effect of Forbush decreases in the heliospheric modulation during the present solar cycle
[SH-4.1-10] 23 p4005 N85-34833

Cosmic ray north-south anisotropy 1961 - 1983
[SH-4.2-6] 23 p4007 N85-34844

The expected cosmic ray density and stream distributions at the heliolatitudinal asymmetry of solar wind
[SH-4.2-14] 23 p4008 N85-34852

The effect of the neutral sheet structure of the interplanetary magnetic field on cosmic ray distribution in space
[SH-4.2-18] 23 p4008 N85-34855

Spatial distribution of cosmic rays in magnetic cycles of the Sun
[SH-4.2-20] 23 p4009 N85-34857

11- and 22-year variations of the cosmic ray density and of the solar wind speed
[SH-4.2-21] 23 p4009 N85-34858

Difference between even and odd 11-year cycles in cosmic ray intensity
[SH-4.2-22] 23 p4009 N85-34859

An update on the correlation between the cosmic radiation intensity and the geomagnetic AA index
[SH-4.2-24] 23 p4009 N85-34861

Gradients and anisotropies of high energy cosmic rays in the outer heliosphere
[SH-4.3-7] 23 p4032 N85-34992

Long-term modulation of cosmic rays during solar cycle 21
[SH-4.4-10] 23 p4034 N85-35008

Cosmic ray biannual variation
[SH-4.4-15] 23 p4034 N85-35011

The difference in the energy spectra of galactic cosmic rays at the minima of the 19th and 20th solar activity cycles
[SH-4.4-18] 23 p4035 N85-35014

Cosmic ray variations with the period close to 27 days and their connection with solar activity longitudinal distribution
[SH-4.4-19] 23 p4035 N85-35015

Diurnal anisotropy during solar activity cycle twenty and diffusion-convection model
[SH-4.5-7] 23 p4036 N85-35025

Diurnal variations from muon data at Takeyama underground station
[SH-4.5-13] 23 p4037 N85-35030

Solar cycle variations of the anaomalous cosmic ray component
[SH-4.6-2] 23 p4039 N85-35040

Time and energy dependence of the cosmic ray gradient in the outer heliosphere
[SH-4.7-2] 23 p4040 N85-35047

Dimensions of the solar wind cavity and of the region of interplanetary cosmic ray modulation
[SH-4.7-11] 23 p4041 N85-35055

The solar wind effect on cosmic rays and solar activity
[SH-5.1-13] 23 p4043 N85-35066

On the solar cycle variation in the barometer coefficients of high latitude neutron monitors
[SH-6.1-2] 23 p4044 N85-35077

Cosmic ray secular variations in terrestrial records and aurorae
[SH-7.1-3] 23 p4047 N85-35096

When did the average cosmic ray flux increase?
[SH-7.1-4] 23 p4047 N85-35097

Solar neutrino: Flux, cosmic rays and the 11 year solar cycle
[SH-8.1-7] 23 p4049 N85-35112

Solar cosmic ray bursts and solar neutrino fluxes
[SH-8.1-10] 23 p4050 N85-35115

The influences of the galactic cosmic ray on the atmospheric ozone
[SH-10.1-1] 23 p4053 N85-35133

SOLAR DIAMETER

Solar variability observed through changes in solar figure and mean diameter
[DE85-012857] 22 p3880 N85-33900

SOLAR DISK

U SUN

SOLAR DYNAMICS

U HELIOSEISMOLOGY

SOLAR ECLIPSES

Extreme limb profiles of the Sun at far infrared and submillimeter wavelengths 08 p1244 N85-17852

Rocket observations of the ionosphere during the eclipse of 26 February 1979
[NASA-CR-175513] 12 p1888 N85-21850

Effect of solar eclipses on the LAGEOS semimajor axis 20 p3491 N85-31699

SOLAR ELECTRONS

Solar He-3-rich events and non-relativistic electron events: A new association
[NASA-TM-86179] 06 p0890 N85-15652

Polar rain: Solar coronal electrons in the Earth's magnetosphere
[NASA-TM-86150] 07 p1060 N85-16726

The 3HE in solar non-relativistic electron events
[SH-2.2-5] 23 p4000 N85-34800

SOLAR ENERGY

Solar heating and cooling R and D program coordination support
[DE84-013479] 01 p0068 N85-10449

National solar-terrestrial research program
[PB84-216183] 01 p0072 N85-10479

USSR report: Space
[JPRS-USP-84-005] 02 p0156 N85-11060

Features of new solar panels on Salyut-7
02 p0157 N85-11062

Modular photovoltaic array field
[SAND-83-7028] 02 p0222 N85-11454

FSA field test
[NASA-CR-174114] 04 p0528 N85-13373

Experimental and theoretical study of a solar thermochemical receiver module
[NASA-CR-174107] 04 p0528 N85-13374

Joint Indo-German program on solar energy: Parabolic dish program, step 1
[BMFT-FB-T-84-175] 05 p0670 N85-14312

Encapsulation materials and processing
06 p0830 N85-15269

Polymer-polymer interface bond stability
06 p0830 N85-15271

Polymer-metal interface bond stability
06 p0830 N85-15272

Correlations of solar irradiance and daylight illuminance for building energy analysis
[DE85-001736] 06 p0839 N85-15326

National Bureau of Standards passive solar test facility: Instrumentation and site handbook
[PB85-100451/GAR] 07 p0968 N85-16148

Multijunction cells for concentrators: Technology prospects
[NASA-CR-174259] 07 p0991 N85-16295

Evaluation of the measured energy performance of four solar systems
[AD-A147912] 07 p0993 N85-16306

Conference on Singlet Molecular Oxygen (COSMO 84), program and abstracts
[AD-A147281] 07 p1040 N85-16605

Thermal design requirements of a 50-kW zinc/redox flow battery for solar electrical energy storage
[DE84-017088] 09 p1345 N85-18463
Hydrogen from solar energy
[DE85-001914] 10 p1437 N85-19055
Solar thermochemical process interface study
[NASA-CR-174442] 10 p1510 N85-19527
Overview of photovoltaic concentrator technology
[DE84-016790] 10 p1512 N85-19539
Solar collection
[DE85-000060] 10 p1512 N85-19540
Vertical solar louver project
[DE84-017335] 11 p1676 N85-20558
A summary and assessment of historical reliability and maintainability data for solar hot water and space conditioning systems
[DE84-004521] 12 p1676 N85-21770
Large-size fine-granular graphite for solar techniques
12 p1878 N85-21780
Performance evaluation of an active solar cooling system utilizing low cost plastic collectors and an evaporatively-cooled absorption chiller
[DE84-010813] 12 p1880 N85-21798
Latent heat storage technology and application workshop. Summary report: Session 6
[DE85-001097] 12 p1882 N85-21806
Evaluation of ettringite and related compounds for use in solar energy storage
[DE85-003249] 12 p1882 N85-21809
Multi-year plan for Experimental Systems Research: Passive and hybrid solar energy program
[DE85-004696] 12 p1882 N85-21810
Phase change thermal energy storage and the model building codes
[PB85-111201] 12 p1883 N85-21813
Power from the Sun: Light at night
[PB85-124097] 12 p1883 N85-21814
Multiyear plan for experimental systems research passive and hybrid solar energy program
[PB85-146668] 12 p1883 N85-21815
Evaluation of ettringite and related compounds for use in solar energy storage
[PB85-146676] 12 p1883 N85-21816
Ecological observations at the site of the 10 MWe solar thermal power system (1978-1984)
[DE85-004572] 12 p1885 N85-21827
ROSA: A computer model for optical power ratio calculations
[DE85-005174] 13 p2129 N85-23251
A review of development and application of heat pump technology
[CSIR-RR-585] 14 p2300 N85-24241
A bibliography of reports of the Sandia solar thermal distributed receiver systems project
[SAND-84-0313] 16 p2817 N85-27376
A multifunction wall system for application with solar heating and ground cooling
[DE85-006792] 16 p2620 N85-27395
United States participation in International Energy Agency Task IX, Subtask (C): Pyranometry. 1984 participation
[DE85-009615] 18 p3110 N85-29256
Solar pond research at the Los Alamos National Laboratory
[DE85-008631] 18 p3128 N85-29366
Salt-gradient solar ponds
[DE85-008626] 18 p3129 N85-29380
SERI Solar Energy Storage Program: FY 1984
[DE85-002936] 18 p3130 N85-29385
Solar Thermal Research Program
[DE85-000514] 18 p3131 N85-29388
Materials research for passive solar systems: Solid-state phase-change materials
[DE85-006779] 18 p3132 N85-29395
Investigation of the transferability of measures of passive solar energy utilization in the USA to the Federal Republic of Germany
[BMFT-FB-T-84-284] 18 p3132 N85-29396
Electrochromic and thermochromic materials for solar energy applications with emphasis on niobium and vanadium oxides
[DE85-010630] 19 p3249 N85-30147
Thickness-insensitive selective surface paint
[DE85-010566] 19 p3250 N85-30150
Thermal performance and design of a solid particle cavity receiver
[DE85-010630] 19 p3274 N85-30300
Proceedings of the Distributed Receiver Solar Thermal Technology Conference
[DE85-010551] 19 p3306 N85-30493
Renewable technologies program summaries
[DE85-001509] 19 p3307 N85-30500
Recombination phenomena in high efficiency silicon solar cells 20 p3479 N85-31618
High efficiency solar cell processing
20 p3482 N85-31640
Comparative evaluation of ground-coupled heat pumps that use solar energy
[DE85-010950] 20 p3484 N85-31649
Recent improvements in materials for thin GaAs and multibandgap solar cells
[DE85-008600] 20 p3484 N85-31651
Self-heating to ignition measurements and computation of critical size for solar energy collector materials
[PB85-183374] 20 p3485 N85-31663
Proceedings of the 24th Project Integration Meeting
[NASA-CR-176058] 21 p3607 N85-32394
Reliability physics 21 p3608 N85-32402
Failure testing of active solar energy system components
[DE84-013024] 22 p3804 N85-33561
An analysis of the effects of active solar energy system control sensor degradation on system performance
[DE84-013023] 22 p3804 N85-33562
Solar central receiver preliminary design studies: Summary and review of contract results
[DE85-011385] 22 p3809 N85-33593
Study of alternative system conversions for the Solar One pilot plant
[DE85-010026] 22 p3809 N85-33594
Optical analysis of parabolic dish concentrators for solar dynamic power systems in space
[NASA-TM-87080] 23 p3903 N85-34176
Solar thermal technologies program summary
[DE85-012253] 23 p3945 N85-34449
Solar energy education. Renewable energy: A background text
[DE85-010365] 23 p3946 N85-34452
Solar energy education: Renewable energy activities for chemistry and physics
[DE85-010371] 23 p3946 N85-34455
Anomalous abundances of solar energetic particles and coronal gas: Coulomb effects and First Ionization Potential (FIP) ordering
[SH-2.1-10] 23 p3989 N85-34791

SOLAR ENERGY ABSORBERS
Progress on solar absorber selective paint research
[DE84-015536] 04 p0480 N85-13059
Development of a single-family absorption chiller for use in a solar heating and cooling system, phase 3, volume 2
[DE85-003218] 13 p2130 N85-23253
Selective coatings for solar heat converters
17 p2939 N85-28144
Absorber coatings degradation
[DE85-008628] 18 p3128 N85-29367
Solar rocket component study
[AD-A154186] 19 p3227 N85-30007
Electrochromic and thermochromic materials for solar energy applications with emphasis on niobium and vanadium oxides
[DE85-010630] 19 p3249 N85-30147
Thickness-insensitive selective surface paint
[DE85-010566] 19 p3250 N85-30150
Solar dynamic systems 20 p3443 N85-31374

SOLAR ENERGY CONVERSION
NT SOLAR TOTAL ENERGY SYSTEMS
Solar-pumped lasers: A review
02 p0261 N85-11711
Compact welding apparatus with solar power supply
03 p0352 N85-12263
Control and performance of a photovoltaic-thermal energy system 03 p0387 N85-12475
Trends in concentrator, receiver, and storage development for terrestrial applications
05 p0609 N85-13891
The liquid droplet radiator - an ultralightweight heat rejection system for efficient energy conversion in space
05 p0610 N85-13900
Photovoltaic working group report
05 p0611 N85-13902
Stimulation of technologies towards photovoltaic energy conversion 05 p0661 N85-14251
Fundamentals of solar energy conversion based on fluorescence collectors 05 p0662 N85-14256
Utilization of solar energy for the production of hydrogen 05 p0663 N85-14262
Solar energy supplied mobile water purification unit
05 p0664 N85-14270
Material models and device structures for GaAs solar cells
[DE85-000501] 05 p0665 N85-14275
Site-specific research conducted in support of the Salton Sea Solar Pond Project, FY 1982 report
[NASA-CR-174182] 05 p0666 N85-14280
The spectrophotometric method of determining the transmission of solar energy in salt gradient solar ponds
05 p0666 N85-14283
Material selection consideration for solar ponds
05 p0666 N85-14284
Solar pond fluid dynamics and heat transfer
05 p0667 N85-14288
Summary of salt gradient solar pond research
05 p0667 N85-14292
Proceedings of the 23rd Project Integration Meeting
[NASA-CR-174186] 06 p0829 N85-15280
Advances and opportunties in the amorphous silicon research field
[DE84-004526] 06 p0833 N85-15304
Evaluation of the measured energy performance of four solar systems
[AD-A147912] 07 p0993 N85-16306
Solar energy conversion based on the principle of fluorescent collectors. Installation of a test collector to deliver several Watts power
[BMFT-FB-T-84-192] 07 p0993 N85-16308
Solar energy conversion based on the principle of fluorescent collectors
[BMFT-FB-T-84-193] 07 p0994 N85-16309
Heliostat tested 07 p0994 N85-16318
Lunar nuclear power feasibility study
[NASA-CR-171831] 07 p1041 N85-16811
Development of high efficiency solar cells on silicon web
[NASA-CR-174435] 10 p1509 N85-19521
US Amorphous Silicon Research Project
[DE85-000536] 10 p1511 N85-19536
The 35 kilowatt peak power photovoltaic system
[DE85-000189] 10 p1511 N85-19537
Study of low energy density photovoltaic applications under varying rate structures
[DE85-000185] 10 p1511 N85-19538
Solar-gas systems impact analysis study
[PB85-129088] 11 p1616 N85-20163
Solar thermal technology
[DE84-013029] 11 p1673 N85-20540
Energy transfer and photochemistry in biomimetic solar conversion
[PB85-129112] 11 p1677 N85-20586
Photosynthetic water splitting
[DE85-002460] 11 p1690 N85-20627
Solar-assisted hydrogen generation by photoelectrocatalysis
[PB85-149706] 12 p1804 N85-21314
Solar energy converter using surface plasma waves
[NASA-CASE-LEW-13827-1] 12 p1876 N85-21768
Research on microemulsions for storage and conversion of solar energy
[DE85-000161] 12 p1882 N85-21807
A theoretical analysis of solar-driven natural convection energy conversion systems
[DE84-004431] 13 p2128 N85-23245
USSR report: Engineering and equipment
[JPRS-UEQ-84-001] 14 p2265 N85-24034
Drop of coolant temperature in individual components of solar heating system 14 p2265 N85-24035
Power plants of modular construction with quasi-paraboloidal concentrators of solar energy
14 p2266 N85-24036
Selective coatings for solar-to-thermal energy converters 14 p2280 N85-24127
Silicon-sheet and thin-film cell and module technology potential: Issue study
[NASA-CR-175654] 14 p2349 N85-24520
Development and testing of Parabolic Dish Concentrator No. 1
[NASA-CR-175651] 14 p2350 N85-24522
Development of an Organic Rankine-Cycle power module for a small community solar thermal power experiment
[NASA-CR-175650] 14 p2350 N85-24523
Bioenergy, solar biotech research in France, Europe
15 p2536 N85-25846
Eight DOE Solar Photochemistry Research Conference: Proceedings
[DE85-005094] 15 p2587 N85-25948
Space power plants 16 p2724 N85-26813
Solar elements with distributed parameters
16 p2760 N85-27036
A bibliography of reports of the Sandia solar thermal distributed receiver systems project
[SAND-84-0313] 16 p2817 N85-27376
Alternative heat sources for heat pumps
[DE85-007610] 17 p2959 N85-28275
Activity and accomplishments of dish/Stirling electric power system development
[NASA-CR-175841] 17 p2965 N85-28445
Parabolic dish test site: History and operating experience
[NASA-CR-175892] 17 p2965 N85-28447
A program for the calculation of paraboloidal-dish solar thermal power plant performance
[NASA-CR-175674] 17 p2965 N85-28448
Airport solar photovoltaic concentrator phase 3
[DE85-006773] 18 p3128 N85-29370
Foamglass solar window collector
[DE85-009197] 18 p3129 N85-29374

Liquid metal thermoelectric converter (LMTEC) for solar applications
[DE85-008405] 18 p3129 N85-29376
Thermal performance testing and mathematically modeling of integral collector storage solar hot water systems
[PB85-186906] 18 p3132 N85-29398
Advanced evacuated tube collectors
[DE85-010271] 19 p3274 N85-30302
Proceedings of the Distributed Receiver Solar Thermal Technology Conference
[DE85-010551] 19 p3306 N85-30493
Control system for parabolic dish concentrator No. 1
[NASA-CR-176045] 20 p3463 N85-31510
Proceedings of the Flat-Plate Solar Array Project Research Forum on High-Efficiency Crystalline Silicon Solar Cells
[NASA-CR-176047] 20 p3478 N85-31615
Silicon solar cell efficiency improvement: Status and outlook 20 p3479 N85-31619
Nomographs for estimating the levelized cost of energy from flat-plate and concentrator photovoltaic systems
[NASA-CR-176048] 20 p3483 N85-31645
Proceedings of the 24th Project Integration Meeting
[NASA-CR-176058] 21 p3607 N85-32394
Summary of the high-efficiency crystalline solar cell research forum 21 p3607 N85-32396
Silicon refinement by chemical vapor transport
21 p3609 N85-32412
Performance analysis of mixed passive solar heating systems
[DE85-009824] 21 p3613 N85-32455
Prospects for a new kind of synthesis: Assembly of molecular components to achieve functions
[AD-A155023] 21 p3702 N85-32997
Polymer blends for use in photoelectrochemical cells for conversion of solar energy to electricity
[DE85-011602] 22 p3752 N85-33258
Long-term goals for solar thermal technology
[DE85-013032] 22 p3809 N85-33597
Electron photoejection in carbanions
[DE85-011747] 23 p3911 N85-34230
Electron photoejection in carbanions
[DE85-011748] 23 p3912 N85-34237
Practical aspects of photovoltaic technology, applications and cost (revised)
[NASA-CR-174963] 24 p4110 N85-35472

SOLAR FACULAE
U FACULAE

SOLAR FLARES
Studies of solar flares and coronal loops
[AD-A145009] 01 p0130 N85-10898
Solar-geophysical data number 477, May 1984. Part 2: (Comprehensive reports). Data for November 1983, July 1981 and miscellanea. Explanation of data reports issued as number 474 (supplement) February 1984
[PB84-225036] 01 p0131 N85-10900
Solar-geophysical data number 477, May 1984. Part 1: (Prompt reports). Data for April 1984, March 1984 and late data. Explanation of data reports issued as number 474 (supplement) February 1984
[PB84-225028] 01 p0131 N85-10901
Variation of fast charged particles in event of 22 November 1977 based on Cosmos-900 satellite data
02 p0161 N85-11092
Solar flares and laboratory experiments on magnetic reconnection in current sheaths
02 p0162 N85-11099
Energetic electrons in impulsive solar flares
02 p0303 N85-11962
Study of the solar corona using radio and space observations
[NASA-CR-174034] 02 p0304 N85-11963
Active regions — and the Solar Maximum Mission
[NASA-CR-170628] 02 p0304 N85-11965
Vector magnetic field analysis of Lorentz forces acting in the solar atmosphere
[AD-A145941] 03 p0449 N85-12852
Space observations of solar flares
04 p0519 N85-13313
Particle acceleration in two-ribbon flares --- solar flares 04 p0519 N85-13314
The radiative hydrodynamics of flare loops heated by impulsive bursts of energetic electrons
05 p0745 N85-14781
Repulsive force of magnetic clouds during solar flares and magnetospheric substorms
06 p0824 N85-15233
Solar He-3-rich events and non-relativistic electron events: A new association
[NASA-TM-86179] 06 p0890 N85-15652
Temporal and spectral characteristics of solar flare hard X-ray emission
[NASA-TM-86187] 08 p1259 N85-17923
Energy release in solar flares
[NASA-CR-174302] 08 p1259 N85-17924
Directivity of Bremsstrahlung radiation from relativistic beams and the Gamma-Rays from solar flares
[NASA-CR-174433] 10 p1572 N85-19913
Physical aspects of the prediction of solar flares
[NASA-CR-175487] 10 p1572 N85-19915
Effects of the solar-terrestrial environment on satellite operations
[DE85-002413] 11 p1590 N85-20003
Solar-Geophysical Data. Part 1: (Prompt reports)
[PB85-112068] 11 p1766 N85-21100
Activation of solar flares 12 p1954 N85-22276
Neutron and gamma-ray signatures for particle acceleration in solar flares 12 p1954 N85-22278
Forced recognition by nonlinear MHD waves and sequential triggering of solar flares
12 p1956 N85-22291
Signatures of the coalescence instability in solar flares
12 p1956 N85-22293
Solar-geophysical data. Part 2: (Comprehensive reports)
[PB85-112076] 12 p1962 N85-22332
Solar-geophysical data number 479, July 1984. Part 1: (Prompt reports). Data for June 1984, May 1984 and later data
[NASA-CR-175542] 12 p1962 N85-22333
Ultraviolet spectral diagnostics of solar flares and heating events 13 p2205 N85-23675
Solar-geophysical data number 479, August 1981. Part 2: (Comprehensive reports), data for January 1984 and August 1981 and miscellanea. Explanation of data reports issued as number 474 (supplement) February 1984
[NASA-CR-175607] 13 p2205 N85-23679
Diagram of nonstationary rejoining of magnetic force lines 14 p2344 N85-24492
X-ray polarimetry: The measurement of the polarization of solar flare X-rays and the design of a Compton polarimeter 14 p2441 N85-25059
Prominences, two-ribbon flares and coronal transients
14 p2454 N85-25158
Solar maximum mission results on the energetics of the impulsive phase of solar flares 14 p2454 N85-25159
A study of the morphology of solar flares as observed by the hard X-ray imaging spectrometer — Solar Maximum Mission 14 p2454 N85-25160
High resolution hard X-ray spectra of solar and cosmic sources 14 p2455 N85-25163
Pulsations of cosmic ray intensities before increasing flux of relativistic particles from solar flares
15 p2477 N85-25292
Evidence in meteorites for an active early Sun
15 p2680 N85-26550
Satellite research on solar flares
16 p2717 N85-26776
Analysis of short-period changes in intensity of hard X-radiation of solar flares registered aboard Venera-13 and Venera-14 spacecraft 16 p2723 N85-26806
Solar-Geophysical Data Number 484, December 1984. Part 2 (comprehensive reports): Data for June 1984, January 1982 and Miscellanea
[NASA-CR-175826] 16 p2888 N85-27820
Electron-cyclotron maser emission during solar and stellar flares
[NASA-CR-175883] 17 p3054 N85-28907
Turbulence and wave particle interactions in solar-terrestrial plasmas
[NASA-CR-175970] 18 p3209 N85-29906
The influence of the heliospheric current sheet and angular separation on flare accelerated solar wind
[NASA-CR-175962] 18 p3209 N85-29907
The possibility of observing solar neutron events in the lower atmosphere
[NOTA-INTERNA-837] 18 p3209 N85-29908
Effects of coronal disturbances on the ionization state of the solar wind
[NASA-CR-175997] 19 p3365 N85-31000
Solar photospheric and coronal abundances from solar energetic particle measurements
[NASA-CR-176029] 20 p3547 N85-32073
Detection of solar neutrons by ground based neutron monitors
[IFSI-84-11] 20 p3547 N85-32076
Some properties of flare-not-associated Forbush decreases
[IFSI-84-13] 20 p3548 N85-32077
Contributions to the 19th International Cosmic Ray Conference
[NASA-CR-176060] 21 p3714 N85-33044
Precision measurements of solar energetic particle elemental composition
[PAPER-SH-2.1-4] 21 p3715 N85-33052
Solar coronal and photospheric abundances from solar energetic particle measurements
[PAPER-SH-2.1-5] 21 p3715 N85-33053
Soft X-ray polychromator for the Solar Maximum Mission
[NASA-CR-175297] 21 p3723 N85-33096
Heating of the deep chromosphere during solar flares
[AD-A155256] 21 p3723 N85-33100
Search for the north-south asymmetry in solar activity
[AD-A155525] 21 p3724 N85-33102
Radio telescope with 256 antennas built in Siberia
22 p3732 N85-33136
High Resolution Telescope and Spectrograph (HRTS)
23 p3901 N85-34162
Ninteenth International Cosmic Ray Conference. SH sessions, volume 4
[NASA-CP-2376-VOL-4] 23 p3989 N85-34729
The propagation of solar flare particles in a turbulent coronal loop
[SH-1.1-3] 23 p3989 N85-34730
Stochastic particle acceleration in solar flares
[SH-1.1-4] 23 p3989 N85-34731
First-order shock acceleration in solar flares
[SH-1.1-5] 23 p3989 N85-34732
Prompt acceleration of ions by oblique turbulent shocks in solar flares
[SH-1.1-6] 23 p3989 N85-34733
Fast drift kilometric radio bursts and solar proton events
[SH-1.1-7] 23 p3990 N85-34734
Study of photon emission by electron capture during solar nuclei acceleration. 2: Delimitation of conditions for charge transfert establishment
[SH-1.1-9] 23 p3990 N85-34736
Study of photon emission by electron capture during solar nuclei acceleration. 3: Photon production evaluations
[SH-1.1-10] 23 p3990 N85-34737
Study of non-thermal photon production under different scenarios in solar flares. 1: Scenarios and formulations
[SH-1.2-2] 23 p3991 N85-34738
Study of non-thermal photon production under different scenarios in solar flares. 2: The Compton inverse and Bremsstrahlung models and fittings
[SH-1.2-3] 23 p3991 N85-34739
Spectral and spatial properties of solar microflares
[SH-1.2-4] 23 p3991 N85-34740
Temporal evolution of an energetic electron population in an inhomogeneous medium: Application to solar hard X-ray bursts
[SH-1.2-6] 23 p3991 N85-34741
Quantitative analysis of flare accelerated electrons through their hard X-ray and microwave radiation
[SH-1.2-7] 23 p3991 N85-34742
An extended superhot solar flare X-ray source
[SH-1.2-8] 23 p3991 N85-34743
Observations of solar flare photon energy spectra from 20 keV to 7 MeV
[SH-1.2-9] 23 p3992 N85-34744
Ion energy storage for post-flare loops
[SH-1.2-10] 23 p3992 N85-34745
Two types of electron events in solar flares
[SH-1.2-11] 23 p3992 N85-34746
Two classes of solar energetic particle events associated with impulsive and long duration soft X-ray flares
[SH-1.2-12] 23 p3992 N85-34747
A dominant role for protons at the onset of solar flares
[SH-1.2-13] 23 p3992 N85-34748
The energy spectra of solar flare electrons
[SH-1.2-14] 23 p3992 N85-34749
Onset of solar flares as predicted by two-dimensional MHD-models of quiescent prominences
[SH-1.3-1] 23 p3992 N85-34750
The starting conditions for an optically small solar gamma ray flare
[SH-1.3-2] 23 p3993 N85-34751
On the detectability of key-MeV solar protons through their nonthermal Lyman-alpha emission
[SH-1.3-5] 23 p3993 N85-34752
Observations of solar flare gamma-rays and protons
[SH-1.3-6] 23 p3993 N85-34753
Energetic protons from a disappearing solar filament
[SH-1.3-7] 23 p3993 N85-34754
Helios 1 energetic particle observations of the solar gamma ray flare events of 7, 21 June 1980 and 3 June 1982
[SH-1.3-8] 23 p3993 N85-34755
Injection of energetic particles following the gamma-ray flares on June 7, 1980, as observed on Helios 1
[SH-1.3-9] 23 p3993 N85-34756
Ultrarelativistic electrons and solar flare gamma-radiation
[SH-1.3-11] 23 p3993 N85-34757
Source energy spectra from demodulation of solar particle data by interplanetary and coronal transport
[SH-1.3-13] 23 p3994 N85-34758
Spectra of solar proton ground level events using neutron monitor and neutron moderated detector recordings
[SH-1.3-14] 23 p3994 N85-34759

Ground increase of cosmic ray intensity on February 16, 1984
[SH-1.3-15] 23 p3994 N85-34760
The SCR flare of 16 February 1984 as recorded by the Sayan spectrograph
[SH-1.3-17] 23 p3994 N85-34761
Time extended production of neutrons during a solar flare
[SH-1.4-1] 23 p3994 N85-34762
Further observations of protons resulting from the decay of neutrons ejected by solar flares
[SH-1.4-2] 23 p3994 N85-34763
Suggestions for improving the efficiency of ground-based neutron monitors for detecting solar neutrons
[SH-1.4-3] 23 p3995 N85-34764
Search for solar neutrons using NM-64 equipment
[SH-1.4-5] 23 p3995 N85-34765
A search for solar neutrons or a long duration balloon flight
[SH-1.4-6] 23 p3995 N85-34766
Neutral pion production in solar flares
[SH-1.4-7] 23 p3995 N85-34767
High energy neutron and gamma-radiation generated during the solar flares
[SH-1.4-8] 23 p3995 N85-34768
On the angular and energy distribution of solar neutrons generated in P-P reactions
[SH-1.4-9] 23 p3995 N85-34769
Possible detection of flare-generated positrons by Helios 1 on 3 Jun 1982
[SH-1.4-10] 23 p3996 N85-34770
Elemental abundances in corotating events
[SH-1.5-15] 23 p3997 N85-34778
Solar and interplanetary particles at 2 to 4 MEV during solar cycles 21, solar cycle variations of event sizes, and compositions
[SH-1.5-16] 23 p3997 N85-34779
Observation of the fluxes of nuclei with energies 10-20 MEV per nucleon during the solar flare of April 26, 1984
[SH-2.1-1] 23 p3998 N85-34783
Energetic particle observations of the solar-gamma ray/neutron flare events of 3 Jun 1982 and 21 June 1980 isotopic and chemical composition
[SH-2.1-3] 23 p3998 N85-34784
Precision measurements of solar energetic particle elemental composition
[SH-2.1-4] 23 p3998 N85-34785
On the retention of high-energy protons and nuclei with charges Z or equal to 2 in large solar flares after the process of their acceleration
[SH-2.1-8] 23 p3998 N85-34789
The mean ionic charges of N, Ne, MG, SI and S in solar energetic particle events
[SH-2.1-11] 23 p3999 N85-34792
Abundances from solar-flare gamma-ray line spectroscopy
[SH-2.1-13] 23 p3999 N85-34794
Solar flare gamma-ray line spectroscopy
[SH-2.1-14] 23 p3999 N85-34795
Isotopic overabundances and the energetic particle model of solar flares
[SH-2.2-1] 23 p4000 N85-34796
Solar source regions of 3HE-rich particle events
[SH-2.2-4] 23 p4000 N85-34799
Elemental abundance differences between nuclei accelerated in CIR shocks and solar flares
[SH-2.2-6] 23 p4000 N85-34801
The heavy ion composition in 3HE-rich solar flares
[SH-2.2-7] 23 p4000 N85-34802
The mean ionic charge of silicon in 3HE-rich solar flares
[SH-2.2-8] 23 p4000 N85-34803
Coronal propagation of solar flare particles observed by satellite
[SH-3.1-2] 23 p4001 N85-34807
Coronal propagation of flare associated electrons and protons
[SH-3.1-3] 23 p4001 N85-34808
Geometry of the diffusive propagation region in the August 14, 1982 solar electron event
[SH-3.1-5] 23 p4001 N85-34809
Peculiarities of propagation of charged particles in solar corona
[SH-3.1-6] 23 p4001 N85-34810
Some characteristics of the solar flare event of February 16, 1984
[SH-3.1-7] 23 p4001 N85-34811
Constraints of solar flare particle transport models from anisotropy observations at Voyager 1
[SH-3.1-8] 23 p4002 N85-34812
Exponential anisotropy of solar cosmic rays
[SH-3.2-1] 23 p4002 N85-34817
The propagation of solar energetic particles in magnetic channels
[SH-3.2-4] 23 p4003 N85-34820
Radial transport of approximately 1 MeV/nucleon ions during the 22 November 1977 solar particle event
[SH-3.2-5] 23 p4003 N85-34821
Energetic solar particle fluxes out to 3 AU during the 7 May 1978 flare event
[SH-3.2-6] 23 p4003 N85-34822
The local characteristic function of interplanetary particle propagation
[SH-3.2-8] 23 p4003 N85-34823
On reflecting boundary behind the Earth's orbit at propagation of fast particles from solar flares
[SH-3.2-13] 23 p4004 N85-34827
Cumulative effect of Forbush decreases in the heliospheric modulation during the present solar cycle
[SH-4.1-10] 23 p4005 N85-34833
North-south asymmetry in activity on the Sun and cosmic ray density gradients
[SH-4.2-7] 23 p4007 N85-34845
Role of solar flare index in long term modulation of cosmic ray intensity
[SH-4.4-12] 23 p4034 N85-35009
Drift and Forbush decreases
[SH-5.1-2] 23 p4041 N85-35056
The flare origin of Forbush decreases not associated with solar flares on the visible hemisphere of the Sun
[SH-5.1-4] 23 p4041 N85-35056
Longitudinal dependence of the interplanetary perturbation produced by energetic type 4 solar flares and of the associated cosmic ray modulation
[SH-5.1-5] 23 p4042 N85-35059
Spectral analysis of the Forbush decrease of 13 July 1982
[SH-5.1-7] 23 p4042 N85-35061
Study of dominating parameters of high speed solar plasma streams in relation to cosmic ray and geomagnetic storms
[SH-5.1-11] 23 p4042 N85-35064
Anomalous low level of cosmic ray intensity decreases observed during 1980
[SH-5.1-15] 23 p4043 N85-35068
Peculiarities of Galactic Cosmic Ray (GCR) anisotropy variation in connection with the recurrent and sporadic Forbush effects
[SH-5.1-21] 23 p4044 N85-35073
Cosmic ray modulation by high-speed solar wind fluxes
[SH-5.1-22] 23 p4044 N85-35074
Penetration of solar protons into the Earth's magnetosphere on November 22, 1977
[SH-6.1-15] 23 p4046 N85-35088
Solar modulation of cosmic ray intensity and solar flare events inferred from (14)C contents in dated tree rings
[SH-7.1-2] 23 p4047 N85-35095
The 4He1H ratios in the chemical compositions of solar flare particles and the primordial solar nebula
[SH-7.1-12] 23 p4048 N85-35104
Solar neutrinos, solar flares, solar activity cycle and the proton decay
[SH-8.1-8] 23 p4049 N85-35113
Solar cosmic ray bursts and solar neutrino fluxes
[SH-8.1-10] 23 p4050 N85-35115
SONTRAC: A solar neutron track chamber detector
[SH-9.1-12] 23 p4052 N85-35127
A suggested standardized format for cosmic ray ground-level event data
[SH-9.1-15] 23 p4052 N85-35130
Sporadic radio emission connected with a definite manifestation of solar activity in the near Earth space
[SH-10.1-8] 23 p4053 N85-35139
Near Earth space sporadic radio emission busts occurring during sunrise
[SH-10.1-9] 23 p4054 N85-35140
Preliminary results of the Cerenkov EAS flashes the Crimean Astrophysical Observatory
[HE-4.4-17] 24 p4194 N85-36023
High-energy neutrinos from a lunar observatory
[HE-5.3-21] 24 p4207 N85-36112

SOLAR FLUX
Theoretical development of Monte Carlo codes for modeling cumulus cloud fields
[NASA-CR-174083] 02 p0230 N85-11500
Trends in ozone and temperature structure: Comparison of theory and measurements
[DE84-016201] 04 p0539 N85-13428
Detailed performance calculations: Goddard Group, appendix D 05 p0676 N85-14341
MAP/GLOBUS campaign 1983
11 p1658 N85-20447
Response of Earth's atmosphere to increases in solar flux and implications for loss of water from Venus
13 p2178 N85-23518
Convective collapse and overstable oscillations in solar flux tubes 14 p2452 N85-25138
Forecast verification of the 10.7 centimeter solar flux and the Ap daily geomagnetic activity indices
[AD-A152959] 17 p2993 N85-28499
Thermal performance and design of a solid particle cavity receiver
[DE85-010630] 19 p3274 N85-30300
Solar modulation and interplanetary gradients of the galactic electron flux, 1977 - 1984
[PAPER-SH-4.7-4] 21 p3716 N85-33059
The polar caps and the climatic evolution of Mars
22 p3854 N85-33866
Results of ultra-low level 71ge counting for application in the Gallex-solar neutrino experiment at the Gran Sasso Underground Physics Laboratory
[SH-8.1-2] 23 p4049 N85-35106
Correlation between solar neutrino flux and other solar phenomena 23 p4049 N85-35109
A possible mechanism to cause the quasi-biennial variability on the solar neutrino flux
[SH-8.1-5] 23 p4049 N85-35110
The conjecture concerning time variations in the solar neutrino flux
[SH-8.1-6] 23 p4049 N85-35111
Solar neutrino: Flux, cosmic rays and the 11 year solar cycle
[SH-8.1-7] 23 p4049 N85-35112
Solar cosmic ray bursts and solar neutrino fluxes
[SH-8.1-10] 23 p4050 N85-35115

SOLAR FLUX DENSITY
NT SOLAR CONSTANT
Variation of fast charged particles in event of 22 November 1977 based on Cosmos-900 satellite data
02 p0161 N85-11092
Preliminary investigation into using the sun as a source for G/T (Gain to System Noise Temperature) measurements
[PB85-128146] 12 p1952 N85-22265
Peculiarities of propagation of charged particles in solar corona
[SH-3.1-6] 23 p4001 N85-34810
Energetic solar particle fluxes out to 3 AU during the 7 May 1978 flare event
[SH-3.2-6] 23 p4003 N85-34822

SOLAR FURNACES
Superpure materials research planned
03 p0353 N85-12270
Preparation of crystal growth experiments in Spacelab: Si (FSLP), CdTe (D1), ZnS (D1)
[BMFT-FB-W-84-045] 12 p1788 N85-21227
High temperature solar electrothermal processing 2. Zinc from zinc oxide
[AD-A154747] 21 p3562 N85-32159
Decomposition of sulfuric acid using solar thermal energy
[DE85-012266] 21 p3564 N85-32170

SOLAR GENERATORS
NT HOMOJUNCTIONS
NT SOLAR AUXILIARY POWER UNITS
NT SOLAR CELLS
NT VERTICAL JUNCTION SOLAR CELLS
Information package on photovoltaics
05 p0661 N85-14250
Photovoltaic power supply units
05 p0662 N85-14252
Global radiation in West Germany --- solar generators
05 p0662 N85-14253
Development and construction of a prototype photovoltaic energy supply unit
05 p0662 N85-14254
Siemens solar module: Status of the technique, development tendencies 05 p0662 N85-14255
Solar generators made of amorphous silicon
05 p0662 N85-14257
Biaxial tracking solar generator
05 p0663 N85-14259
Photovoltaic 100 kWp pilot plant on the Greek island Kythnos 05 p0664 N85-14266
Mains-connected photovoltaic system for a house
05 p0664 N85-14267
Project Pellworm: Solar electric energy supply for a health center 05 p0664 N85-14268
Realized field tests --- solar generators
05 p0664 N85-14271
Considerations on the dimensioning of photovoltaic supply systems in the low power range
05 p0665 N85-14273
Solar power supplies for ships
05 p0665 N85-14274
A system simulator for the solar generator of artificial satellites
[INPE-3320-TDL/180] 11 p1672 N85-20594
Development and prototype construction of photovoltaic energy supply units 12 p1878 N85-21781
Photovoltaic solar components
12 p1878 N85-21782
Testing and optimization of the production technology of large-surface Cu2S/CdS solar generators
12 p1880 N85-21793

Ecological observations at the site of the 10 MWe solar thermal power system (1978-1984)
[DE85-004572] 12 p1885 N85-21827
Comprehensive evaluation of cost effectiveness of solar electric power plants 14 p2265 N85-24036
Use of heat pipes for heat collection and transmission in solar plants 14 p2265 N85-24037
Power plants of modular construction with quasi-paraboloidal concentrators of solar energy
14 p2266 N85-24038
Parabolic dish test site: History and operating experience
[NASA-CR-175892] 17 p2985 N85-28447
Plastic heliostat enclosure analysis
[DE85-009112] 18 p3130 N85-29387
Thermochemical energy transport using a hydrogen rich working fluid
[AD-D011696] 19 p3233 N85-30042
Calibration of relevant measuring sensors
[DE85-009820] 19 p3306 N85-30492
Advanced module development overview
21 p3612 N85-32445
Module Hipot and ground continuity test results
21 p3612 N85-32447
Thin-film reliability and engineering overview
21 p3612 N85-32450

SOLAR GRANULATION
Variability of the structure of the granulation over the solar activity cycle 14 p2447 N85-25100
Amplification and maintenance of thin magnetic flux tubes by compressible convection — solar magnetism
14 p2447 N85-25104
Stellar granulation 14 p2451 N85-25132
The flux rope models checked by some observations — solar activity 14 p2452 N85-25139
Activities report of the Institute of Astronomy and Astrophysics 17 p3052 N85-28891
Activities report of the Institute of Astronomy and Astrophysics 17 p3052 N85-28892

SOLAR GRAVITATION
Detection of solar gravity mode oscillations
14 p2442 N85-25070
Solar gravity modes from ACRIM-SWM irradiance data
14 p2443 N85-25071
Heliocentric sail problem with variable gravity field reduction 16 p2724 N85-26816

SOLAR HEATING
Solar heating and cooling R and D program coordination support
[DE84-013479] 01 p0068 N85-10449
Test methods and standards development for active solar heating and cooling systems
[PB84-217447] 03 p0343 N85-12209
Superpure materials research planned
03 p0353 N85-12270
A refined computer program for the transient simulation of ground coupled heat pump systems
[DE84-014098] 05 p0637 N85-14088
Passive solar/Earth sheltered office/dormitory cooling season thermal performance
[DE84-016662] 05 p0669 N85-14308
Development of design and economic parameters for passive solar systems
[AD-A147181] 07 p0993 N85-16303
Heat-transfer enhancement in natural convection enclosure flow
[DE84-013048] 09 p1319 N85-18297
Actual versus design performance of solar systems in the National Solar Data Network
[DE85-001190] 09 p1344 N85-18456
Thermal performance testing of passive solar components in NBS (National Bureau of Standards) calorimeter
[PB85-119345/GAR] 09 p1346 N85-18470
Solar collection
[DE85-000060] 10 p1512 N85-19540
A summary and assessment of historical reliability and maintainability data for solar hot water and space conditioning systems
[DE84-004521] 12 p1876 N85-21770
Multiyear plan for experimental systems research passive and hybrid solar energy program
[PB85-146868] 12 p1883 N85-21815
Overview of latent storage for passive solar applications
[DE85-005354] 13 p2129 N85-23249
Development of a single-family absorption chiller for use in a solar heating and cooling system, phase 3, volume 2
[DE85-003218] 13 p2130 N85-23253
Drop of coolant temperature in individual components of solar heating system 14 p2265 N85-24035
Comprehensive evaluation of cost effectiveness of solar electric power plants 14 p2265 N85-24036
Scaling blackbody laser to high powers
[NASA-TM-86395] 14 p2309 N85-24292
Mechanisms of magnetic heating of the solar corona
14 p2448 N85-25113
Heating of coronal loops by tearing turbulence
14 p2448 N85-25114
Observational constraints on heating processes — solar corona 14 p2449 N85-25115
Coronal heating by turbulent phase mixed MHD waves — solar corona 14 p2453 N85-25148
Solar maximum mission results on the energetics of the impulsive phase of solar flares 14 p2454 N85-25159
Solar house, Freiburg
[BMFT-FB-T-84-249] 15 p2588 N85-25953
A multifunction wall system for application with solar heating and ground cooling
[DE85-006792] 16 p2820 N85-27395
Development of mass-producible line-focus tracking concentrating solar collectors. Category 2: Control systems
[DE85-007873] 17 p2987 N85-28459
Foamglass solar window collector
[DE85-009197] 18 p3129 N85-29374
Solar energy for highway uses
[DE84-015653] 18 p3130 N85-29382
Establishment of a methodology for predicting lifetimes in active solar systems
[DE85-006629] 18 p3130 N85-29383
Investigation of the transferability of measures of passive solar energy utilization in the USA to the Federal Republic of Germany
[BMFT-FB-T-84-284] 18 p3132 N85-29396
Solar rocket component study
[AD-A154186] 19 p3227 N85-30007
Comparative evaluation of ground-coupled heat pumps that use solar energy
[DE85-010950] 20 p3484 N85-31649
Geodynamics Branch research program
[NASA-TM-86223] 20 p3489 N85-31688
Soil temperature extrema recovery rates after precipitation cooling 20 p3491 N85-31697
Performance analysis of mixed passive solar heating systems
[DE85-009624] 21 p3613 N85-32455
Laser sealed evacuated window glazings
[DE85-000512] 22 p3754 N85-33273
Failure testing of active solar energy system components
[DE84-013024] 22 p3804 N85-33561
An analysis of the effects of active solar energy system control sensor degradation on system performance
[DE84-013023] 22 p3804 N85-33562
Lopez Energy Alternatives Project
[DE85-010589] 22 p3849 N85-33837
Solar heat pump
[DE85-011323] 23 p3946 N85-34453
Solar system fault detection
[DE85-005987] 23 p3946 N85-34458
Solar pond technology for Navy applications
[AD-A155877] 24 p4112 N85-35488

SOLAR HOUSES
Thermal performance testing of passive solar components in NBS (National Bureau of Standards) calorimeter
[PB85-119345/GAR] 09 p1346 N85-18470
Solar house, Freiburg
[BMFT-FB-T-84-249] 15 p2588 N85-25953
A multifunction wall system for application with solar heating and ground cooling
[DE85-006792] 16 p2820 N85-27395
Investigation of the transferability of measures of passive solar energy utilization in the USA to the Federal Republic of Germany
[BMFT-FB-T-84-284] 18 p3132 N85-29396

SOLAR INSTRUMENTS
NT SPECTROHELIOGRAPHS
Attempts to contruct two-dimensional image of Sun from observations made with RATAN-600 radiotelescope by relay race method 06 p0783 N85-15005
The scanning heliometer 14 p2451 N85-25134

SOLAR LASERS
U SOLAR-PUMPED LASERS

SOLAR LIMB
Extreme limb profiles of the Sun at far infrared and submillimeter wavelengths 08 p1244 N85-17852
Coronal and chromospheric physics — Sun, sunspots, and solar limb
[NASA-CR-174290] 08 p1259 N85-17921
Observed spatial properties of the solar eigenfunctions and the implications for the existence of resolved multiflets 14 p2443 N85-25074
Single-dish high sensitivity determination of solar limb emission at 22 and 44 GHz
[INPE-3545-PRE/758] 19 p3385 N85-30999
An extended superhot solar flare X-ray source
[SH-1.2-8] 23 p3991 N85-34743
Ultrarelativistic electrons and solar flare gamma-radiation
[SH-1.3-11] 23 p3993 N85-34757
Search for solar neutrons using NM-64 equipment
[SH-1.4-5] 23 p3995 N85-34765

SOLAR MAGNETIC FIELD
Structure and evolution of the large scale solar and heliospheric magnetic fields
[NASA-CR-175268] 01 p0130 N85-10897
Solar-geophysical data number 477, May 1984. Part 1: (Prompt reports). Data for April 1984, March 1984 and late data. Explanation of data reports issued as number 474 (supplement) February 1984
[PB84-225028] 01 p0131 N85-10901
Solar flares and laboratory experiments on magnetic reconnection in current sheaths
02 p0162 N85-11099
Study of the solar corona using radio and space observations
[NASA-CR-174034] 02 p0304 N85-11963
Active regions — and the Solar Maximum Mission
[NASA-CR-170628] 02 p0304 N85-11965
Magnetohydrodynamic and gasdynamic theories for planetary bow waves
[NASA-CR-174132] 03 p0448 N85-12850
Structure and evolution of the large scale solar and heliospheric magnetic fields 05 p0746 N85-14782
Energy release in solar flares
[NASA-CR-174302] 08 p1259 N85-17924
Solar-Geophysical Data. Part 1: (Prompt reports)
[PB85-112068] 11 p1766 N85-21100
Magnetospheres in the solar system
12 p1954 N85-22274
Activation of solar flares 12 p1954 N85-22276
What would a dynamo theorist like to know about the dynamics of the solar convection zone?
14 p2441 N85-25062
The magneto-optical filter, working principles and recent progress 14 p2442 N85-25066
Numerical simulations of convectively excited gravity waves 14 p2444 N85-25082
The hydromagnetics of the Sun — conferences
[ESA-SP-220] 14 p2445 N85-25091
Magnetoconvection: The interaction of convection and small scale magnetic fields — photosphere
14 p2446 N85-25098
Magnetic buoyancy instabilities in the convective overshoot zone — Sun 14 p2447 N85-25101
On the structure of magnetic fields in the solar convection zone 14 p2447 N85-25103
Amplification and maintenance of thin magnetic flux tubes by compressible convection — solar magnetism
14 p2447 N85-25104
Nonlinear time-evolution of kink-unstable magnetic flux tubes in the convection zone of the Sun
14 p2447 N85-25105
The Fe XIII 10747 A and Fe XIV 5303 A coronal emission lines polarization 14 p2448 N85-25111
Magnetic instabilities — solar magnetism
14 p2449 N85-25117
The role of differential rotation in magnetic energy storage — coronal loops 14 p2449 N85-25119
Observational aspects of sunspot oscillations
14 p2451 N85-25131
Convective collapse and overstable oscillations in solar flux tubes 14 p2452 N85-25136
The first effect of the amplitude of a solar cycle
14 p2452 N85-25143
Observations concerning energy balance in solar magnetic regions 14 p2452 N85-25145
A study of the material motion into an eruptive prominence — solar prominence
14 p2453 N85-25146
A siphon flow model for Evershed motion — sunspot regions 14 p2453 N85-25147
On running penumbral waves
14 p2453 N85-25150
Harmonic analysis of the solar magnetic field
14 p2454 N85-25154
Magnetic instabilities in solar filaments: Models of twisting motions and ejecta 14 p2454 N85-25156
Magnetic field structures of hard X-ray flares observed by HINOTORI spacecraft — solar flares
14 p2455 N85-25161
Solar magnetohydrodynamics: Symposium review
14 p2455 N85-25162
Elementary sunspot energy model
15 p2476 N85-25287
Modeling 22-year solar activity cycle within framework of dynamo theory with allowance for primary field
15 p2477 N85-25288
The Faraday rotation experiment — solar corona
16 p2886 N85-27805
Measurements of Solar Vector Magnetic Fields
[NASA-CP-2374] 18 p3203 N85-29869

On the numerical computation of nonlinear force-free magnetic fields 18 p3203 N85-29871

Modeling solar magnetic structures
18 p3203 N85-29872

Magnetic and thermodynamic structure of the solar corona during sunspot minimum
18 p3203 N85-29873

Theoretical approach to evolution of solar magnetic field 18 p3204 N85-29874

Current evolution in a numerical emerging-magnetic-flux model 18 p3204 N85-29875

The global structure of magnetic fields which support quiescent prominences 18 p3204 N85-29876

Trends in measurement of solar vector magnetic fields using the Zeeman effect 18 p3204 N85-29877

The solar vector magnetograph of the Okayama Astrophysical Observatory 18 p3205 N85-29882

Vector magnetic field observations with the Haleakala polarimeter 18 p3205 N85-29883

The San Fernando Observatory video Stokes polarimeter 18 p3205 N85-29885

The new solar magnetograph for the Canary Islands Observatory THEMIS 18 p3205 N85-29886

The vector magnetograph of the Sayan Solar Observatory 18 p3206 N85-29887

Multichannel birefringent filter
18 p3206 N85-29888

Diagnostics of vector magnetic fields
18 p3206 N85-29889

Generation and transfer of polarized radiation in the solar atmosphere: Physical mechanisms and magnetic-field diagnostics 18 p3206 N85-29890

Dynamic models of flux tubes in the interpretation of polarization measurements 18 p3206 N85-29891

Least squares inversion of Stokes profiles in the presence of velocity gradients 18 p3207 N85-29892

Effect of polarized radiative transfer on the Hanle magnetic field determination in prominences: Analysis of hydrogen H alpha line observations at Pic-du-Midi
18 p3207 N85-29894

The effect of line damping, magneto-optics and parasitic light on the derivation of sunspot vector magnetic fields
18 p3207 N85-29895

The inference of vector magnetic fields from polarization measurements with limited spectral resolution
18 p3207 N85-29896

Solar monochromatic images in magneto-sensitive spectral lines and maps of vector magnetic fields
18 p3207 N85-29897

Magnetic field-vector measurements in quiescent prominences via the Hanle effect: Analysis of prominences observed at Pic-du-Midi and at Sacramento Peak
18 p3208 N85-29898

Turbulence and wave particle interactions in solar-terrestrial plasmas
[NASA-CR-175970] 18 p3209 N85-29906

Magnetic probing of the solar interior
[NASA-CR-176025] 19 p3385 N85-30998

Solar-geophysical data no. 485, January 1985. Part 1 (prompt reports): Data for December 1984, November 1984 and late data
[PB85-181360] 20 p3548 N85-32079

Differential measurement of cosmic-ray gradient with respect to interplanetary current sheet
[PAPER-SH-4.2-9] 21 p3715 N85-33055

A study of the cyclical variations of coronal holes and their relation to open magnetic fields
[AD-A155251] 21 p3723 N85-33099

Simultaneous Solar Maximum Mission and Very Large Array (VLA) observations of solar active regions
[NASA-CR-176090] 22 p3859 N85-33897

On the possibility of the determining the average mass composition near 10 to the 14th power eV through the solar magnetic field
[OG-5.1-9] 22 p3882 N85-34051

Ultrarelativistic electrons and solar flare gamma-radiation
[SH-1.3-11] 23 p3993 N85-34757

Peculiarities of propagation of charged particles in solar corona
[SH-3.1-6] 23 p4001 N85-34810

Some characteristics of the solar flare event of February 16, 1984
[SH-3.1-7] 23 p4001 N85-34811

Low energy proton bidirectional anisotropies and their relation to transient interplanetary magnetic structures: ISEE-3 observations
[SH-3.1-9] 23 p4002 N85-34813

the role of shock waves in modulation of galactic cosmic rays
[SH-4.1-7] 23 p4005 N85-34831

Cosmic ray intensity and the tilt of the neutral sheet
[SH-4.2-8] 23 p4007 N85-34846

Differential measurement of cosmic-ray gradient with respect to interplanetary current sheet
[SH-4.2-9] 23 p4007 N85-34847

Spatial variation of cosmic rays near the heliospheric current sheet
[SH-4.2-10] 23 p4007 N85-34848

Effects of a wavy neutral sheet on cosmic ray anisotropies
[SH-4.2-11] 23 p4008 N85-34849

Effects of solar magnetic field on cosmic rays
[SH-4.2-12] 23 p4008 N85-34850

Determination of galactic cosmic ray latitudinal gradient using Earth based detectors
[SH-4.2-13] 23 p4008 N85-34851

The expected cosmic ray density and stream distributions at the heliolatitudinal asymmetry of solar wind
[SH-4.2-14] 23 p4008 N85-34852

Latitudinal gradients of cosmic rays and the polarity reversal of the heliospheric magnetic field: A preliminary evaluation
[SH-4.2-16] 23 p4008 N85-34853

The influence of nonstationarity of the solar activity and general solar field on modulation of cosmic rays
[SH-4.2-17] 23 p4008 N85-34854

On the influence of the heliomagnetospheric periphery on the galactic cosmic rays
[SH-4.2-19] 23 p4009 N85-34856

Spatial distribution of cosmic rays in magnetic cycles of the Sun
[SH-4.2-20] 23 p4009 N85-34857

An update on the correlation between the cosmic radiation intensity and the geomagnetic AA index
[SH-4.2-24] 23 p4009 N85-34861

Astrophysical applications of high angular resolution array-telescopes
[OG-9.5-7] 23 p4031 N85-34984

Gradients and anisotropies of high energy cosmic rays in the outer heliosphere
[SH-4.3-7] 23 p4032 N85-34992

Cosmic ray sidereal diurnal variation of galactic origin observed by neutron monitors
[SH-4.4-2] 23 p4033 N85-35000

Long-term modulation of galactic cosmic rays in high-energy region
[SH-4.4-22] 23 p4035 N85-35018

Diurnal variation of galactic cosmic ray intensity on quiet days
[SH-4.5-11] 23 p4037 N85-35029

Long term changes in cosmic ray diurnal variations observed by ion chambers in Hong Kong and Japan
[SH-4.5-14] 23 p4037 N85-35031

The modulation features of the long-period cosmic ray variations in connection with the sign change of the general magnetic field of the Sun
[SH-4.5-15] 23 p4037 N85-35032

Cosmic ray density gradient and its dependence on the north-south asymmetry in solar activity
[SH-4.5-17] 23 p4038 N85-35034

Anomalous increase of solar anisotropy above 150GV in 1981-1983
[SH-4.5-18] 23 p4038 N85-35035

Changes in the energy spectrum of anomalous oxygen and helium during 1977-1985
[SH-4.6-1] 23 p4039 N85-35039

Radial and latitudinal gradients of anomalous oxygen during 1977 - 1985
[SH-4.6-4] 23 p4039 N85-35042

The cosmic ray interplanetary radial gradient from 1972 - 1985
[SH-4.7-1] 23 p4040 N85-35046

The large scale dynamics of the outer heliosphere and the long-term modulation of galactic cosmic rays
[SH-4.7-3] 23 p4040 N85-35048

SOLAR MAXIMUM MISSION

Energetic electrons in impulsive solar flares
02 p0303 N85-11962

Active regions — and the Solar Maximum Mission
[NASA-CR-170628] 02 p0304 N85-11965

Statement of Frank Cepollina, Solar Maximum Repair Mission Project Manager, Goddard Space Flight Center
04 p0461 N85-12930

Space observations of solar flares
04 p0519 N85-13313

Research and technology: Fiscal year 1984 report
[NASA-TM-85231] 12 p1964 N85-22340

Ultraviolet spectral diagnostics of solar flares and heating events 13 p2205 N85-23675

Ultraviolet Spectrometer and Polarimeter (UVSP) software development and hardware tests for the solar maximum mission
[NASA-CR-175279] 14 p2306 N85-24271

Solar gravity modes from ACRIM-SWM irradiance data
14 p2443 N85-25071

Observations of low-degree modes from the solar maximum mission (extended abstract)
14 p2443 N85-25072

Solar maximum mission results on the energetics of the impulsive phase of solar flares 14 p2454 N85-25159

A study of the morphology of solar flares as observed by the hard X-ray imaging spectrometer — Solar Maximum Mission 14 p2454 N85-2516

Examination of returned solar-max surfaces for impacting orbital debris and meteoroids
15 p2661 N85-2655

Soft X-ray polychromator for the Solar Maximum Mission
[NASA-CR-175297] 21 p3723 N85-3309

Solar maximum: Solar array degradation
[NASA-TM-86194] 23 p3903 N85-34175

Monte Carlo calibration of the SMM gamma ray spectrometer for high energy gamma rays and neutrons
[SH-9.1-6] 23 p4051 N85-35121

The 1986 National Aeronautics and Space Administration authorization
[GPO-47-635] 24 p4166 N85-35529

SOLAR MESOSPHERE EXPLORER

Flight experience of Solar Mesosphere Explorer's two nickel-cadmium batteries 20 p3446 N85-3139

SOLAR NEBULA

U SOLAR CORONA

SOLAR NEUTRINOS

Report on solar neutrino experiments
[DE84-014567] 01 p0131 N85-1089

Solar neutrinos: Prospects for detection and implications
[DE84-015522] 02 p0304 N85-11966

Solar neutrino spectroscopy
[DE84-015518] 02 p0304 N85-11968

Chlorine and bromine solar neutrino experiments
[DE84-015720] 02 p0304 N85-11969

Molybdenum solar neutrino experiment
[DE85-003747] 14 p2445 N85-25090

Proposed solar neutrino experiment using (81)Br(nu,e(-e)) (81)Kr
[DE85-004802] 15 p2664 N85-26579

Week interactions of quarks and leptons: Experimental status
[DE85-008171] 18 p3181 N85-29723

Specificity of (71)Ga(p,n) (71)Ge at 35 MeV for Gamow-Teller strength
[DE85-011837] 23 p3971 N85-34615

Ninteenth International Cosmic Ray Conference. SH sessions, volume 5
[NASA-CP-2376-VOL-5] 23 p4031 N85-34991

Results of ultra-low level 71ge counting for application in the Gallex-solar neutrino experiment at the Gran Sasso Underground Physics Laboratory
[SH-8.1-2] 23 p4049 N85-35108

Correlation between solar neutrino flux and other solar phenomena 23 p4049 N85-35109

A possible mechanism to cause the quasi-biennial variability on the solar neutrino flux
[SH-8.1-5] 23 p4049 N85-35110

The conjecture concerning time variations in the solar neutrino flux
[SH-8.1-6] 23 p4049 N85-35111

Solar neutrino: Flux, cosmic rays and the 11 year solar cycle
[SH-8.1-7] 23 p4049 N85-35112

Solar neutrinos, solar flares, solar activity cycle and the proton decay
[SH-8.1-8] 23 p4049 N85-35113

The research program of the Liquid Scintillation Detector (LSD) in the Mont Blanc Laboratory
[HE-5.3-6] 24 p4205 N85-36100

High energy neutrino astronomy with MACRO
[HE-5.3-12] 24 p4206 N85-36106

SOLAR NOISE

U SOLAR RADIO EMISSION

SOLAR OBSERVATORIES

The Ebro Observatory and international scientific organizations 04 p0518 N85-13309

Use of Ebro Observatory data at Word Data Center A for Solar-Terrestrial Physics 04 p0518 N85-13310

Fr. Angelo Secchi, a pioneer in the study of solar-terrestrial relationships 04 p0519 N85-13312

A normal incidence, high resolution X-ray telescope for solar coronal observations
[NASA-CR-175622] 13 p2169 N85-2348

Solar oscillations from two widely separated stations
14 p2446 N85-2509

Science with the Solar and Heliospheric Observatory (SOHO) 14 p2449 N85-2512

Bern solar data for January-December 1984
[REPT-51] 15 p2685 N85-265

Very large array observations of coronal loops an related observations of solar type stars
[AD-A152027] 16 p2888 N85-278

The vector magnetograph of the Sayan So Observatory 18 p3206 N85-298

Solar cycle variation of ephemeral regions
[AD-A154967] 21 p3723 N85-330

Solar adaptive optics
[AD-A155434] 21 p3724 N85-331

Radio telescope with 256 antennas built in Siberia 22 p3732 N85-33136
Coordinated study of solar-terrestrial payloads on space station
[NASA-CR-176160] 23 p3900 N85-34158
Soft X-Ray Telescope (SXRT) 23 p3900 N85-34159
Solar Ultraviolet Spectral Irradiance Monitor (SUSIM) 23 p3901 N85-34160
White Light Coronograph (WLC) and Ultra-Violet Coronal Spectrometer (UVCS) 23 p3901 N85-34161
High Resolution Telescope and Spectrograph (HRTS) 23 p3901 N85-34162
Active Cavity Radiometer (ACR) 23 p3901 N85-34163
Waves in Space Plasmas (WISP) 23 p3901 N85-34164
Space Experiments with Particle Accelerators (SEPAC) 23 p3901 N85-34165
Theoretical and Experimental Beam Plasma Physics (TEBPP) 23 p3901 N85-34166
Recoverable Plasma Diagnostics Package (RPDP) 23 p3902 N85-34167
Electrodynamic tether 23 p3902 N85-34168
Imaging Spectrometric Observatory (ISO) 23 p3902 N85-34169
Atmospheric Emission Photometric Imaging (AEPI) 23 p3902 N85-34170
Magnetospheric multiprobes: MMP/CHEMSAT 23 p3902 N85-34171
Wide Angle Michelson Doppler Imaging Interferometer (WAMDII) 23 p3902 N85-34172
Vehicle Charging And Potential (VCAP) 23 p3902 N85-34173
Initial placement of STO instruments 23 p3902 N85-34174
Development of observational and instrumental techniques in hard X-ray and medium energy gamma-ray astronomy
[NASA-CR-176172] 24 p4168 N85-35841
SOLAR OPTICAL TELESCOPE
Solar optical telescope primary mirror controller
[NASA-CR-174416] 10 p1570 N85-19903
Science with the Solar Optical Telescope (SOT) 14 p2449 N85-25120
SOLAR ORBITS
NT PERIHELIONS
Some considerations on elliptic heliocentric orbits
[INPE-3217-PRE/570] 02 p0297 N85-11926
Heliosynchronism and phasing. Application to the SPOT orbit 05 p0600 N85-13826
Thermal and cryogenic design study for space infrared telescope facility (SIRTF)
[NASA-CR-166613] 07 p0915 N85-15793
Models of angular momentum input to a circum-terrestrial swarm from encounters with heliocentric planetesimals 13 p2179 N85-23521
Analysis of motions of Jupiter's great red spot and white ovals 15 p2670 N85-26472
Heliocentric sail problem with variable gravity field reduction 16 p2724 N85-26816
A comprehensive investigation of the dynamics of micron and submicron lunar ejecta in heliocentric space 19 p3384 N85-30994
Development of observational and instrumental techniques in hard X-ray and medium energy gamma-ray astronomy
[NASA-CR-176172] 24 p4168 N85-35841
SOLAR OSCILLATIONS
Effects of core mixing on solar oscillation frequencies
[DE84-015540] 03 p0449 N85-12853
Nonlocal and nonlinear effects on solar oscillations 09 p1416 N85-18934
Constraints of observations of solar oscillations on solar models with mixing by turbulent diffusion
[DE85-003741] 13 p2205 N85-23678
Solar Seismology From Space. A conference at Snowmass, Colorado
[NASA-CR-175661] 14 p2441 N85-25060
Overview of solar seismology: Oscillations as probes of internal structure and dynamics in the Sun 14 p2441 N85-25061
Solar inverse theory 14 p2441 N85-25063
Rotational inversion from global solar oscillations 14 p2442 N85-25064
Sensitivity of inferred subphotospheric velocity field to mode selection, analysis technique and noise 14 p2442 N85-25065
The magneto-optical filter, working principles and recent progress 14 p2442 N85-25066
Evaluation of a magneto-optical filter and a Fabry-Perot interferometer for the measurement of solar velocity fields from space 14 p2442 N85-25067
The Fourier tachometer 2: An instrument for measuring global solar velocity fields 14 p2442 N85-25068
Observations of intermediate-degree solar oscillations 14 p2442 N85-25069
Detection of solar gravity mode oscillations 14 p2442 N85-25070
Solar gravity modes from ACRIM-SWM irradiance data 14 p2443 N85-25071
Observations of low-degree modes from the solar maximum mission (extended abstract) 14 p2443 N85-25072
Implications of observed frequencies of solar P modes 14 p2443 N85-25073
Observed spatial properties of the solar eigenfunctions and the implications for the existence of resolved multiflets 14 p2443 N85-25074
Optimized response functions for 2-dimensional observations of solar oscillations 14 p2443 N85-25075
The effects of image motion on the l-nu diagram 14 p2443 N85-25076
The effects of seeing on noise 14 p2443 N85-25077
The effects of a nearly 100% duty cycle in observations of solar oscillations 14 p2443 N85-25078
Analysis and interpretation of synthetic time strings of oscillation data 14 p2444 N85-25079
Methods for cloud cover estimation 14 p2444 N85-25081
On the influence of turbulent motions on non-radial oscillations 14 p2444 N85-25083
The stability of the low-degree 5-minute solar oscillations 14 p2444 N85-25084
An excitation mechanism for solar 5-minute oscillation of intermediate and high degree 14 p2444 N85-25085
The resonant count diagram and solar g mode oscillations 14 p2445 N85-25086
Fine structure of solar acoustic oscillations due to rotation 14 p2445 N85-25087
The sensitivity of solar eigenfrequencies to the treatment of the equation of state 14 p2445 N85-25089
Solar oscillations 14 p2445 N85-25092
Solar oscillations from two widely separated stations 14 p2446 N85-25093
Global solar oscillations in irradiance and velocity: A comparison 14 p2446 N85-25094
Oscillatory convection in sunspots 14 p2446 N85-25099
The intern. rotation of the Sun inferred from the rotational splitting of acoustic and gravity mode multiplets 14 p2449 N85-25122
Ten years observations of long-period oscillations of the Sun 14 p2450 N85-25123
The response of the line KI 7699 to the solar oscillations 14 p2450 N85-25124
Conditions of the small oscillations excitation in the different solar models with the mixed core 14 p2450 N85-25126
Linear models of acoustic waves in sunspot umbrae 14 p2450 N85-25130
Observational aspects of sunspot oscillations 14 p2451 N85-25131
The scanning heliometer 14 p2451 N85-25134
The problem of atmospheric turbulence
[NASA-CR-175783] 16 p2832 N85-27464
Activities report of the Institute of Astronomy and Astrophysics 17 p3052 N85-28891
Activities report of the Institute of Astronomy and Astrophysics 17 p3052 N85-28892
Solar variability observed through changes in solar figure and mean diameter
[DE85-012857] 22 p3860 N85-33900
SOLAR PHYSICS
National solar-terrestrial research program
[PB84-216183] 01 p0072 N85-10479
Research and technology, 1984: Marshall Space Flight Center
[NASA-TM-86476] 04 p0590 N85-13765
Heating in the solar mantle 08 p1233 N85-17769
Energy release in solar flares
[NASA-CR-174302] 08 p1259 N85-17924
Solar-geophysical data number 476, April 1984. Part 1: (Prompt reports). Data for March 1984, February 1984 and late data
[PB84-215060] 09 p1416 N85-18936
Solar-geophysical data number 476, April 1984. Part 2: (Comprehensive reports). Data for October 1983, June 1981 and miscellanea
[PB84-215078] 09 p1417 N85-18937
Solar Corona Explorer: A mission for the physical diagnosis of the solar corona
[NASA-TM-87416] 10 p1572 N85-19912
Solar Seismology From Space. A conference at Snowmass, Colorado
[NASA-CR-175661] 14 p2441 N85-25060
Magnetic instabilities — solar magnetism 14 p2449 N85-25117
Science with the Solar Optical Telescope (SOT) 14 p2449 N85-25120
Science with the Solar and Heliospheric Observatory (SOHO) 14 p2449 N85-25121
Solar-Geophysical Data Number 484, December 1984. Part 2 (comprehensive reports): Data for June 1984, January 1982 and Miscellanea
[NASA-CR-175826] 16 p2888 N85-27820
Diagnostics of vector magnetic fields 18 p3206 N85-29889
Evidence for submergencew of magnetic flux in a growing active region 18 p3206 N85-29902
Solar physics applications of computer graphics and image processing 18 p3206 N85-29903
Activities report of the Laboratory of Stellar and Planetary Physics
[G-127] 20 p3544 N85-32052
Solar-geophysical data no. 485, January 1985. Part 1 (prompt reports): Data for December 1984, November 1984 and late data
[PB85-181360] 20 p3548 N85-32079
Activities report of the Aeronomy Department
[G-774-1984] 21 p3633 N85-32569
SOLAR PLANETARY INTERACTIONS
NT SOLAR TERRESTRIAL INTERACTIONS
Response of Earth's atmosphere to increases in solar flux and implications for loss of water from Venus 13 p2178 N85-23518
Development of a global 3-D magnetohydrodynamic computational model for solar wind/cometary and planetary studies
[NASA-CR-175724] 15 p2684 N85-26577
SOLAR PLASMA (RADIATION)
U SOLAR WIND
SOLAR PONDS (HEAT STORAGE)
Site-specific research conducted in support of the Salton Sea Solar Pond Project, FY 1982 report
[NASA-CR-174182] 05 p0666 N85-14280
Laboratory investigations 05 p0666 N85-14281
Analytical models 05 p0666 N85-14282
The spectrophotometric method of determining the transmission of solar energy in salt gradient solar ponds 05 p0666 N85-14283
Material selection consideration for solar ponds 05 p0666 N85-14284
A summary description of a computer program concept for the design and simulation of solar pond electric power generation systems 05 p0666 N85-14285
Salt-gradient solar ponds: Summary of US Department of Energy sponsored research
[NASA-CR-174183] 05 p0667 N85-14286
Solar pond overview 05 p0667 N85-14287
Solar pond fluid dynamics and heat transfer 05 p0667 N85-14288
Review of SERI solar pond work 05 p0667 N85-14289
Salton Sea solar pond power plant design study and regional applicability 05 p0667 N85-14290
Solar pond research at Argonne National Laboratory 05 p0667 N85-14291
Summary of salt gradient solar pond research 05 p0667 N85-14292
Doubly diffusive linear stability with nonconstant gradients
[DE84-013008] 05 p0670 N85-14310
Heat and mass exchange in a partially stratified fluid
[DE85-000526] 10 p1486 N85-19384
Direct-contact condensers for solar pond power production
[DE84-004510] 12 p1876 N85-21771
Solar pond technology for Navy applications
[AD-A155877] 24 p4112 N85-35488
Energy from low temperature differences
[DE85-008817] 24 p4112 N85-35492
SOLAR POSITION
Theoretical study of electron concentration in Venusian atmosphere as function of zenith angle of sun and solar activity in areas of photochemical equilibrium 02 p0163 N85-11104
Integration of multispectral data obtained at different view angles for vegetation analysis 05 p0657 N85-14218
Dark matter near the sun: Simulated star counts and the Oort limit 06 p0880 N85-15592
Simultaneous Earth observations from 2 satellites
[NASA-TM-86204] 16 p2810 N85-27325
Terrain illumination conditions when taking scanning photographs from space 22 p3736 N85-33159
Cosmic ray intensity distribution perpendicular to solar equatorial plane at 1 A.U. during 1976-83
[SH-4.3-14] 23 p4032 N85-34996
SOLAR POWER GENERATION
U SOLAR GENERATORS
SOLAR POWER SATELLITES
Argon ion pollution of the magnetosphere 13 p1998 N85-22523

SOLAR POWER SOURCES
U SOLAR GENERATORS
SOLAR POWERED AIRCRAFT
Mission analysis of solar powered aircraft
[NASA-CR-172583] 20 p3397 N85-31072
SOLAR PROBES
NT HELIOS 1
NT HELIOS 2
SOLAR PROMINENCES
Solar-geophysical data. Part 2: (Comprehensive reports)
[PB85-112076] 12 p1962 N85-22332
A numerical simulation of the formation of solar prominences 14 p2448 N85-25112
A study of the material motion into an eruptive prominence — solar prominence
14 p2453 N85-25146
Energy balance in resistive instabilities — solar prominences 14 p2454 N85-25155
Magnetic instabilities in solar filaments: Models of twisting motions and ejecta 14 p2454 N85-25156
Prominences, two-ribbon flares and coronal transients
14 p2454 N85-25158
The global structure of magnetic fields which support quiescent prominences 18 p3204 N85-29876
Magnetic field-vector measurements in quiescent prominences via the Hanle effect: Analysis of prominences observed at Pic-du-Midi and at Sacramento Peak
18 p3208 N85-29898
Onset of solar flares as predicted by two-dimensional MHD-models of quiescent prominences
[SH-1.3-1] 23 p3992 N85-34750
SOLAR PROPULSION
Proceedings of the AFOSR/AFRPL Rocket Propulsion Research Meeting: Abstracts and Agenda
[AD-A148818] 09 p1288 N85-18085
Solar rocket component study
[AD-A154186] 19 p3227 N85-30007
Mission analysis of solar powered aircraft
[NASA-CR-172583] 20 p3397 N85-31072
SOLAR PROTONS
Entry of solar energetic protons into the distant plasma sheet dependence on distance from the neutral sheet
14 p2357 N85-24567
Magnetosonic waves and their relationship with energetic protons 14 p2368 N85-24635
Latitude variation of recurrent fluxes in the outer solar system
[SH-4.1-13] 21 p3715 N85-33054
The propagation of solar flare particles in a turbulent coronal loop
[SH-1.1-3] 23 p3989 N85-34730
Stochastic particle acceleration in solar flares
[SH-1.1-4] 23 p3989 N85-34731
Fast drift kilometric radio bursts and solar proton events
[SH-1.1-7] 23 p3990 N85-34734
Spectral and spatial properties of solar microflares
[SH-1.2-4] 23 p3991 N85-34740
Ion energy storage for post-flare loops
[SH-1.2-10] 23 p3992 N85-34745
A dominant role for protons at the onset of solar flares
[SH-1.2-13] 23 p3992 N85-34748
The starting conditions for an optically small solar gamma ray flare
[SH-1.3-2] 23 p3993 N85-34751
On the detectability of key-MeV solar protons through their nonthermal Lyman-alpha emission
[SH-1.3-5] 23 p3993 N85-34752
Observations of solar flare gamma-rays and protons
[SH-1.3-6] 23 p3993 N85-34753
Energetic protons from a disappearing solar filament
[SH-1.3-7] 23 p3993 N85-34754
Spectra of solar proton ground level events using neutron monitor and neutron moderated detector recordings
[SH-1.3-14] 23 p3994 N85-34759
On the retention of high-energy protons and nuclei with charges Z or equal to 2 in large solar flares after the process of their acceleration
[SH-2.1-8] 23 p3996 N85-34789
Observations of solar energetic particles at a synchronous orbit
[SH-3.1-1] 23 p4001 N85-34806
Coronal propagation of flare associated electrons and protons
[SH-3.1-3] 23 p4001 N85-34808
Constraints of solar flare particle transport models from anisotropy observations at Voyager 1
[SH-3.1-8] 23 p4002 N85-34812
Low energy proton bidirectional anisotropies and their relation to transient interplanetary magnetic structures: ISEE-3 observations
[SH-3.1-9] 23 p4002 N85-34813
Determination of the pitch-angle distribution and transverse anisotropy of interplanetary particles
[SH-3.1-11] 23 p4002 N85-34815
Channeled propagation of solar particles
[SH-3.2-3] 23 p4003 N85-34819
Energetic solar particle fluxes out to 3 AU during the 7 May 1978 flare event
[SH-3.2-6] 23 p4003 N85-34822
Monte Carlo calculations of relativistic solar proton propagation in interplanetary space
[SH-3.2-11] 23 p4004 N85-34826
Latitude variation of recurrent fluxes in the outer solar system
[SH-4.1-13] 23 p4006 N85-34836
Penetration of solar protons into the Earth's magnetosphere on November 22, 1977
[SH-6.1-15] 23 p4046 N85-35088
Dynamics of the penetration boundaries of solar protons during a strong magnetic storm
[SH-6.1-16] 23 p4046 N85-35089
The influence of the Earth's magnetosphere on the high-energy solar protons
[SH-6.1-22] 23 p4046 N85-35093
Solar neutrinos, solar flares, solar activity cycle and the proton decay
[SH-8.1-6] 23 p4049 N85-35113
SOLAR RADIATION
NT CIRCUMSOLAR RADIATION
NT SOLAR CORPUSCULAR RADIATION
NT SOLAR COSMIC RAYS
NT SOLAR ELECTRONS
NT SOLAR NEUTRINOS
NT SOLAR PROTONS
NT SOLAR RADIO BURSTS
NT SOLAR RADIO EMISSION
NT SOLAR WIND
NT SOLAR X-RAYS
NT SUNLIGHT
NT TYPE 3 BURSTS
NT TYPE 4 BURSTS
Workshop on the Use of Future Multispectral Imaging Capabilities for Lithologic Mapping: Workshop summary
02 p0214 N85-11413
Solar radiation in the ozone layer
04 p0522 N85-13342
Distribution of total solar radiation in Spain
04 p0523 N85-13344
Global radiation in West Germany — solar generators
05 p0662 N85-14253
Plant responses to solar UV-B radiation
05 p0690 N85-14436
Natural interference phenomena affecting spaceborne receivers
[NASA-CR-174256] 07 p0916 N85-15798
Deciduous forest radiation regimes: Effects of forest structure, phenology and Earth-Sun geometry upon their spatial, temporal and spectral variability
[AD-A148804] 07 p0996 N85-16327
NBS (National Bureau of Standards) daylight availability database
[PB84-245745] 07 p1054 N85-16688
Radiation parameterization programs for use in general circulation models
[AD-A148015] 08 p1188 N85-17488
Climate at CRREL (Cold Regions Research and Engineering Laboratory) Hanover, New Hampshire
[AD-A148400] 08 p1189 N85-17495
Weather data for simplified energy calculation methods. Volume 1. Eastern United States: TRY data
[DE85-000493] 09 p1358 N85-18541
Middle Atmosphere Program. Handbook for MAP, volume 7
[NASA-CR-175479] 11 p1656 N85-20437
MSG-7: Atmospheric penetration of solar radiation in the range of Schumann-Runge bands
11 p1657 N85-20443
Middle Atmosphere Program. Handbook for MAP, volume 8
[NASA-CR-175478] 11 p1657 N85-20445
MSG-7: Molecular absorption processes related to the penetration of ultraviolet solar radiation into the middle atmosphere 11 p1658 N85-20449
Ionospheric absorption on 1539 kHz in relation to solar ionizing radiation 11 p1659 N85-20455
Influence of the atmosphere on remotely sensed reflection from vegetation surfaces
[DE85-000658] 11 p1670 N85-20521
Short duration winter-time performances of different passive solar systems
[DE85-000650] 11 p1675 N85-20557
National solar-terrestrial research program, part 1. Solar-terrestrial research for the 1980's, part 2
[AD-A149542] 11 p1681 N85-20591
Microprocessor-controlled rotating shadowband radiometer
[DE85-003633] 12 p1854 N85-21630
Estimating solar radiation for plant simulation models
[E85-10060] 12 p1873 N85-21761
Multi-year plan for Experimental Systems Research: Passive and hybrid solar energy program
[DE85-004698] 12 p1882 N85-21810
NIMBUS-7 SBUV (Solar Backscatter Ultraviolet) observations of solar UV spectral irradiance variations caused by solar rotation and active-region evolution for the period November 7, 1978 - November 1, 1980
[NASA-CR-175544] 12 p1962 N85-22304
Study of integral and spectral direct solar radiation over Atlantic 14 p2341 N85-24475
Supplement to evaluation of satellite derived estimates of solar radiation
[E85-10086] 14 p2346 N85-24506
Evaluation of satellite derived estimates of solar radiation
[E85-10087] 14 p2346 N85-24507
ILUM code: Solar and lunar flux calculations for multi-cloud layered atmospheres
[DE85-005578] 15 p2600 N85-26025
Numerical integration through force discontinuities: Solar radiation pressure 16 p2805 N85-27298
Intercomparison of Radiation Codes in Climate Models (ICRCCM)
[DE85-007251] 16 p2835 N85-27487
Results from the Helios galactic and solar cosmic ray experiment (E7) 16 p2886 N85-27807
Solar radiance models for determination of ERBE scanner filter factor
[NASA-CR-172595] 17 p2995 N85-28513
Preliminary GCM results with a new radiation parameterization 18 p3145 N85-29474
Pacific Northwest solar radiation data
[DE85-009773] 18 p3149 N85-29496
Radiation damage and repair in cells and cell components. Part 2: Physical radiations and biological significance
[DE85-008934] 18 p3152 N85-29518
The possibility of observing solar neutron events in the lower atmosphere
[NOTA-INTERNA-837] 18 p3209 N85-29906
Thermal performance and design of a solid particle cavity receiver
[DE85-010830] 19 p3274 N85-30300
Influence of surface films of petroleum products on conditions for absorption of solar radiation by upper water layer 19 p3289 N85-30396
Stable density stratification solar pond
[NASA-CASE-NPO-15419-2] 19 p3303 N85-30474
View-limiting shrouds for insolation radiometers
[NASA-CR-176041] 20 p3458 N85-31476
Detection of solar neutrons by ground based neutron monitors
[IFSI-84-11] 20 p3547 N85-32076
Clarke Stations and mercurian mass-drivers: Energy for large-scale transportation systems
[DE85-009607] 21 p3560 N85-32145
Calculating solar highlight and shadeless areas for scanning photographs from space and optimizing lighting conditions 22 p3736 N85-33160
Solar energy meteorological research and training program: Region 4
[DE85-011783] 22 p3816 N85-33640
Three dimensional calculation of flux of low energy atmospheric neutrinos
[SH-8.1-11] 23 p4050 N85-35116
Monte Carlo calibration of the SMM gamma ray spectrometer for high energy gamma rays and neutrons
[SH-9.1-6] 23 p4051 N85-35121
Recording system for the solar neutron monitoring a
Mt. Norikura
[SH-9.1-8] 23 p4051 N85-35123
Using the information of cosmic rays to predict influenc
epidemic
[SH-10.1-2] 23 p4053 N85-35134
Space Station Polar Platform: Integrating research and operational missions
[PB85-195279] 24 p4069 N85-3521
SOLAR RADIO BURSTS
NT TYPE 3 BURSTS
NT TYPE 4 BURSTS
Solar-geophysical data number 477, May 1984. Pa
2: (Comprehensive reports). Data for November 198
July 1981 and miscellanea. Explanation of data report
issued as number 474 (supplement) February 1984
[PB84-225036] 01 p0131 N85-109
Solar-geophysical data number 478, June 1984. P
2 (comprehensive reports): Data for December 1983 a
miscellanea
[PB84-243161] 06 p0890 N85-15
Solar-geophysical data number 476, April 1984. P
2: (Comprehensive reports). Data for October 1983, Ju
1981 and miscellanea
[PB84-215078] 09 p1417 N85-18

Solar radio bursts, proton events and geomagnetic activity
[AD-A149018] 10 p1571 N85-19906
Solar-geophysical data. Part 2: (Comprehensive reports)
[PB85-112076] 12 p1962 N85-22332
Solar-geophysical data number 483, November 1984. Part 2: (Comprehensive reports). Data for May 1984, December 1961 and miscellanea
[PB85-147700] 12 p1962 N85-22336
Solar-geophysical data number 479, August 1981. Part 2: (Comprehensive reports), data for January 1984 and August 1981 and miscellanea. Explanation of data reports issued as number 474 (supplement) February 1984
[NASA-CR-175607] 13 p2205 N85-23679
Coronal structures observed at metric wavelengths with the Nancay radioheliograph 14 p2453 N85-25152
The Helios radio astronomy experiment
16 p2886 N85-27803
Microwaves and hard X-rays ultrafast time structures at the impulsive phase of solar bursts
[INPE-3478-PRE/721] 16 p2886 N85-27816
Quenching of the beam-plasma instability by 3-D spectra of large scale density fluctuations
[NASA-CR-175969] 19 p3369 N85-30697
Fast drift kilometric radio bursts and solar proton events
[SH-1.1-7] 23 p3990 N85-34734
Temporal evolution of an energetic electron population in an inhomogeneous medium: Application to solar hard X-ray bursts
[SH-1.2-6] 23 p3991 N85-34741
Two types of electron events in solar flares
[SH-1.2-11] 23 p3992 N85-34746
A dominant role for protons at the onset of solar flares
[SH-1.2-13] 23 p3992 N85-34748
Ground increase of cosmic ray intensity on February 16, 1984
[SH-1.3-15] 23 p3994 N85-34760
Type 3 solar radio bursts and 3HE-rich events
[SH-2.2-3] 23 p4000 N85-34798
The 3HE in solar non-relativistic electron events
[SH-2.2-5] 23 p4000 N85-34800
SOLAR RADIO EMISSION
NT SOLAR RADIO BURSTS
NT TYPE 3 BURSTS
NT TYPE 4 BURSTS
Solar-geophysical data number 477, May 1984. Part 1: (Prompt reports). Data for April 1984, March 1984 and late data. Explanation of data reports issued as number 474 (supplement) February 1984
[PB84-225028] 01 p0131 N85-10901
Attempts to contruct two-dimensional image of Sun from observations made with RATAN-600 radiotelescope by relay race method 06 p0783 N85-15005
Solar-geophysical data number 478, June 1984. Part 1 (prompt reports): Data for May 1984, Apr. 1984, and late data
[PB84-243153] 06 p0890 N85-15653
Solar-geophysical data number 476, April 1984. Part 1: (Prompt reports). Data for March 1984, February 1984 and late data
[PB84-215060] 09 p1416 N85-18936
Solar-Geophysical Data. Part 1: (Prompt reports)
[PB85-112068] 11 p1766 N85-21100
Preliminary investigation into using the sun as a source for G/T (Gain to System Noise Temperature) measurements
[PB85-128148] 12 p1952 N85-22265
A new radio emission at 3 kHz in the outer heliosphere 12 p1959 N85-22312
Solar-geophysical data number 479, July 1984. Part 1: (Prompt reports). Data for June 1984, May 1984 and later data
[NASA-CR-175542] 12 p1962 N85-22333
Solar-geophysical data number 483. November 1984. Part 1: (Prompt reports). Data for October 1984, September 1984 and late data
[PB85-147692] 12 p1962 N85-22335
A synchrotron/inverse Compton interpretation of a solar burst producing fast pulses at lambda 3 mm and hard X-rays 16 p2887 N85-27815
Turbulence and wave particle interactions in solar-terrestrial plasmas
[NASA-CR-175970] 18 p3209 N85-29906
Single-dish high sensitivity determination of solar limb emission at 22 and 44 GHz
[INPE-3545-PRE/758] 19 p3385 N85-30999
Solar-geophysical data no. 485, January 1985. Part 1 (prompt reports): Data for December 1984, November 1984 and late data
[PB85-181360] 20 p3548 N85-32079
Solar radio fluxes as indices of solar activity
[AERONOMICA-ACTA-A-282-1984]
21 p3722 N85-33095
SOLAR RADIO WAVES
U SOLAR RADIO EMISSION
SOLAR RECEIVERS
U SOLAR COLLECTORS
SOLAR REFLECTORS
Joint Indo-German program on solar energy: Parabolic dish program, step 1
[BMFT-FB-T-84-175] 05 p0670 N85-14312
Measurement techniques for evaluating solar reflector materials
[DE85-002194] 10 p1510 N85-19531
Measurement techniques for evaluating solar reflector materials
[PB85-119489] 10 p1512 N85-19541
Accelerated aging of aluminized acrylic solar mirror materials
[DE85-002683] 11 p1612 N85-20136
Electrical research on solar cells and photovoltaic materials
[NASA-CR-175699] 15 p2585 N85-25935
MOD silver metallization for photovoltaics
[NASA-CR-175773] 16 p2818 N85-27381
Silvered polymer reflectors
[DE85-008782] 18 p3130 N85-29384
Plastic heliostat enclosure analysis
[DE85-009112] 18 p3130 N85-29387
MOD silver metallization for photovoltaics
21 p3610 N85-32428
Theory of cellwise optimization for solar central receiver system
[DE85-012586] 22 p3807 N85-33579
SOLAR ROTATION
NIMBUS-7 SBUV (Solar Backscatter Ultraviolet) observations of solar UV spectral irradiance variations caused by solar rotation and active-region evolution for the period November 7, 1978 - November 1, 1980
[NASA-CR-175544] 12 p1962 N85-22334
Solar Seismology From Space. A conference at Snowmass, Colorado
[NASA-CR-175661] 14 p2441 N85-25060
Rotational inversion from global solar oscillations
14 p2442 N85-25064
Analysis and interpretation of synthetic time strings of oscillation data 14 p2444 N85-25079
Fine structure of solar acoustic oscillations due to rotation 14 p2445 N85-25087
On the determination of the solar rotation and indications of the solar differential rotation from an analysis of solar integrated light 14 p2446 N85-25096
Models of solar differential rotation
14 p2446 N85-25097
The solar dynamo and the complex Lorenz equations
14 p2447 N85-25107
The role of differential rotation in magnetic energy storage --- coronal loops 14 p2449 N85-25119
The intern. rotation of the Sun inferred from the rotational splitting of acoustic and gravity mode multiplets
14 p2449 N85-25122
Did the young Sun rotate at 100 km/s
14 p2451 N85-25133
Dynamo action of magnetostrophic waves --- solar atmosphere 14 p2451 N85-25136
Cyclic flows in the solar convection zone due to the dynamo reaction 14 p2451 N85-25137
Stream dynamics between 1 AU and 2 AU: A detailed comparison of observations and theory
[NASA-TM-86086] 15 p2684 N85-26578
The corotating variation of the north-south anisotropy of cosmic rays
[SH-4.3-15] 23 p4033 N85-34999
Cosmic ray power spectral variations. 3: Solar rotation periodicities
[SH-4.4-16] 23 p4034 N85-35012
Study of spectral exponent on quiet and disturbed days
[SH-4.5-10] 23 p4037 N85-35028
SOLAR SAILS
Heliocentric sail problem with variable gravity field reduction 16 p2724 N85-26816
Maximizing the semi-major axis for a freely coning solar sailcraft
[AD-A153175] 17 p2909 N85-27936
SOLAR SEA POWER PLANTS
Temperature sensors for OTEC applications
[DE85-009607] 18 p3110 N85-29254
SOLAR SEISMOLOGY
U HELIOSEISMOLOGY
SOLAR SELECTIVE COATINGS
U SELECTIVE SURFACES
SOLAR SENSORS
Biaxial tracking solar generator
05 p0663 N85-14259
Integration of an Apple 2 Plus computer into an existing dual axis sun tracker system
[AD-A150778] 14 p2404 N85-24823
SOLAR SIMULATION
Isotropic proton irradiation of GaAs solar cells
13 p2012 N85-22622
SOLAR SIMULATORS
Analysis of inverter models and harmonic propagation. Part 1: A physical simulator for large solar cell arrays
[DE85-002312] 09 p1315 N85-18271
SOLAR SPECTRA
Chlorine and bromine solar neutrino experiments
[DE84-015720] 02 p0304 N85-11969
The Fourier tachometer 2: An instrument for measuring global solar velocity fields 14 p2442 N85-25068
Observations of intermediate-degree solar oscillations
14 p2442 N85-25069
Solar oscillations from two widely separated stations
14 p2446 N85-25093
On the determination of the solar rotation and indications of the solar differential rotation from an analysis of solar integrated light 14 p2446 N85-25096
The Fe XIII 10747 A and Fe XIV 5303 A coronal emission lines polarization 14 p2448 N85-25111
Ten years observations of long-period oscillations of the Sun 14 p2450 N85-25123
The response of the line KI 7699 to the solar oscillations 14 p2450 N85-25124
Activities report of the Institute of Astronomy and Astrophysics 17 p3052 N85-28892
The solar coronal X-ray spectrum 5.5-12 A
[AD-A152334] 17 p3054 N85-28906
Simple solar spectral model for direct and diffuse irradiance on horizontal and tilted planes at the Earth's surface for cloudless atmospheres
[DE85-002933] 18 p3137 N85-29424
Multichannel birefringent filter
18 p3206 N85-29888
Diagnostics of vector magnetic fields
18 p3206 N85-29889
Acetonitrile in the Earth's atmosphere: An upper limit deduced from infrared solar spectra
[AERONOMICA-ACTA-A-295-1985]
22 p3813 N85-33623
Application of nonlinear least squares methods to the analysis of solar spectra
[NASA-CR-176122] 22 p3816 N85-33637
Source energy spectra from demodulation of solar particle data by interplanetary and coronal transport
[SH-1.3-13] 23 p3994 N85-34758
Spectra of solar proton ground level events using neutron monitor and neutron moderated detector recordings
[SH-1.3-14] 23 p3994 N85-34759
SOLAR SPECTROMETERS
Middle Atmosphere Program. Handbook for MAP, volume 8
[NASA-CR-175478] 11 p1657 N85-20445
Report on the Workshop on Intercomparison of Solar UV Irradiance Measurements and Related Instrument Calibration 11 p1658 N85-20448
White Light Coronograph (WLC) and Ultra-Violet Coronal Spectrometer (UVCS) 23 p3901 N85-34161
The Jovian electron spectrum: 1978-1984
[SH-1.5-19] 23 p3998 N85-34782
SOLAR STORMS
Interplanetary radio storms. 2: Emission levels and solar wind speed in the range 0.05-0.8 AU
[NASA-TM-84946] 04 p0569 N85-13761
Dynamics of the penetration boundaries of solar protons during a strong magnetic storm
[SH-6.1-16] 23 p4048 N85-35089
SOLAR STREAMS
U SOLAR CORPUSCULAR RADIATION
SOLAR SYSTEM
NT HALLEY'S COMET
Cosmic ray propagation in the local superbubble
[NASA-TM-85030] 03 p0449 N85-12855
Bulk composition of the Moon in the context of models for condensation in the solar nebula
04 p0583 N85-13725
The abundance of deuterium in the outer solar system from ground-based measurements of monodeuterated methane 07 p1060 N85-16725
Airborne Astronomy Symposium. A symposium commemorating the tenth anniversary of operations of the Kuiper Airborne Observatory
[NASA-CP-2353] 08 p1244 N85-17848
Exploring the solar system with stellar occultations
08 p1245 N85-17857
Research and technology, Lyndon B. Johnson Space Center
[NASA-TM-58263] 08 p1262 N85-17929
Future of Ultraviolet Astronomy Based on Six Years of IUE Research
[NASA-CP-2349] 11 p1743 N85-20961
Solar system studies with the IUE: 1982 - 1984
11 p1744 N85-20964

Space research and the new approach to the mechanics of fluid media in cosmos 12 p1953 N85-22271
Magnetospheres in the solar system
12 p1954 N85-22274
Planetary geology in the 1980s
[NASA-SP-467] 13 p2169 N85-23457
Viking radio science data analysis and synthesis
[NASA-CR-175631] 13 p2171 N85-23471
On the origin of Triton and Pluto
13 p2175 N85-23497
Small solar system bodies 13 p2175 N85-23499
Asteroid collisional evolution studies
13 p2176 N85-23501
Impacts in ice: Commissions of solar system crater population 13 p2181 N85-23538
The solar system: Improving knowledge of the system
14 p2396 N85-24782
Formation of the solar system
15 p2677 N85-26532
Statistical theory of planet growth
15 p2678 N85-26534
The propagation of ultraheavy cosmic rays
15 p2685 N85-26582
European space science horizon 2000
[ESA-SP-1070] 16 p2717 N85-26771
The micrometeorite experiment on Helios — inner solar system 16 p2865 N85-27797
The fast individualists in the solar system: Cosmic rays 16 p2866 N85-27806
The study of the physics of cometary nuclei
[NASA-CR-175917] 17 p3054 N85-28905
Gas chromatography: Possible application of advanced instrumentation developed for solar system exploration to space station cabin atmospheres
18 p3157 N85-29551
Volatiles in the outer solar system. 1: Thermodynamics of clathrate hydrates. 2: Ethane ocean on Titan. 3: Evolution of primordial Titan atmosphere
19 p3382 N85-30984
Space research in the United Kingdom: An assessment
[AD-A155334] 21 p3712 N85-33038
Program for observations of Halley's comet
22 p3732 N85-33138
Relationships between chondritic meteorites and planets 22 p3851 N85-33851
Nebular volatile fractionations associated with chondrule formation 22 p3852 N85-33855
What determines the location of satellites and planets? 22 p3853 N85-33858
Volatiles on satellites of the outer solar system
22 p3854 N85-33866
Implications of source abundances of ultraheavy cosmic rays
[OG-7.1-4] 23 p4013 N85-34866
The nature and origin of outer solar system asteroids from reflectance spectrophotometry
24 p4166 N85-35838

SOLAR TEMPERATURE
Solar cycle variations of sunspot temperatures
14 p2452 N85-25141

SOLAR TERRESTRIAL INTERACTIONS
National solar-terrestrial research program
[PB84-216183] 01 p0072 N85-10479
Equatorial energetic distributions of ions of terrestrial radiation belt as function of solar corona temperature response 02 p0160 N85-11087
Fr. Angelo Secchi, a pioneer in the study of solar-terrestrial relationships 04 p0519 N85-13312
Relations between the particle precipitation events in mid-latitudes, the ring current intensity and the polarity of the interplanetary magnetic field
04 p0519 N85-13316
Daily magnetic variations at Ebro, Spain
04 p0520 N85-13325
Helium and hydrogen of the local interstellar mdium observed in the vicinity of the Sun
06 p0873 N85-15540
Middle Atmosphere Program. Handbook for MAP, volume 10
[NASA-CR-175477] 11 p1658 N85-20450
Solar terrestrial influences on the D region as shown by the level of atmospheric radio noise
11 p1664 N85-20486
Geomagnetic disturbances caused by internal atmospheric dynamics 11 p1665 N85-20491
Interplanetary shock waves during April and May of 1981 13 p1982 N85-22434
World ocean level oscillations and their relationship to change in inflow of continental waters
13 p2108 N85-23133
Achievements of the International Magnetospheric Study (IMS) — conference
[ESA-SP-217] 14 p2354 N85-24544
The application of dimensional analysis to the problem of solar wind-magnetosphere energy coupling
14 p2357 N85-24564
Coupling of the solar wind to measures of magnetic activity 14 p2357 N85-24565
The GEOS-2 electric field observations at times of solar wind discontinuities 14 p2360 N85-24584
Solar wind control of electric fields and currents in the magnetosphere and ionosphere
14 p2364 N85-24608
Solar wind control of magnetospheric convection
14 p2365 N85-24615
Solar wind and cosmic rain 15 p2644 N85-26312
Coupling of the solar wind to measures of magnetic activity
[DE85-002415] 15 p2685 N85-26580
Geophysical responses of dynamics of solar wind transition region 16 p2721 N85-26795
Some features of the interplanetary medium during Forbush decreases
[NOTA-INTERNA-636] 18 p3202 N85-29866
Turbulence and wave particle interactions in solar-terrestrial plasmas
[NASA-CR-175970] 18 p3209 N85-29906
Magnetospheric response to solar wind variations
[DE85-010762] 20 p3547 N85-32074
Interaction between an interplanetary shock and the Earth's magnetosphere on 27 August 1978: ISEE-1 electric field and ISEE-2 plasma observations
[IFSI-84-15] 20 p3548 N85-32078
Effect of ions on cloud formation and its role in solar terrestrial relationship 21 p3653 N85-32697
Solar energy meteorological research and training program: Region 4
[DE85-011783] 22 p3816 N85-33640
Space Station Polar Platform: Integrating research and operational missions
[PB85-195279] 24 p4069 N85-35218

SOLAR THERMAL ELECTRIC POWER PLANTS
Development of an Organic Rankine-Cycle power module for a small community solar thermal power experiment
[NASA-CR-175650] 14 p2350 N85-24523
Test results of an organic Rankine-cycle power module for a small community solar thermal power experiment
[NASA-CR-175696] 14 p2350 N85-24524
An evaluation of thermal storage for liquid-metal, solar thermal receivers
[DE85-002929] 16 p2820 N85-27394
Solar Thermal Research Program
[DE85-000514] 18 p3131 N85-29386
Long-term goals for solar thermal technology
[DE85-013032] 22 p3809 N85-33597

SOLAR TOTAL ENERGY SYSTEMS
Shenandoah parabolic dish solar collector
[DE85-008326] 17 p2987 N85-28460

SOLAR VELOCITY
What would a dynamo theorist like to know about the dynamics of the solar convection zone?
14 p2441 N85-25062
The magneto-optical filter, working principles and recent progress 14 p2442 N85-25066

SOLAR WIND
Structure and evolution of the large scale solar and heliospheric magnetic fields
[NASA-CR-175268] 01 p0130 N85-10897
Magnetospheric structures: Uranus and Neptune
02 p0301 N85-11949
The solar wind at 20-30 AU 02 p0301 N85-11950
Physics of the inner heliosphere 1-10R sub O plasma diagnostics and models
[NASA-CR-174010] 02 p0304 N85-11964
Magnetohydrodynamic and gasdynamic theories for planetary bow waves
[NASA-CR-174132] 03 p0448 N85-12850
Magnetohydrodynamic and gasdynamic theories for planetary bow waves
[NASA-CR-174135] 04 p0589 N85-13760
Interplanetary radio storms. 2: Emission levels and solar wind speed in the range 0.05-0.8 AU
[NASA-TM-84946] 04 p0589 N85-13761
Helium and hydrogen of the local interstellar mdium observed in the vicinity of the Sun
06 p0873 N85-15540
Changes of LISM characteristics in the heliospheric interface 06 p0873 N85-15542
Broadening of the interplanetary helium cone structure due to elastic collisions of LISM helium atoms with solar wind ions 06 p0873 N85-15543
Solar wind and cosmic ray irradiation of grains and ices - application to erosion and synthesis of organic compounds in the solar system
06 p0886 N85-15637
Polar rain: Solar coronal electrons in the Earth's magnetosphere
[NASA-TM-86150] 07 p1060 N85-16726
Spicules and surges
[AD-A146785] 07 p1061 N85-16727
Corotating interaction regions in stellar winds: Particle acceleration and non-thermal radio emission in hot stars
08 p1234 N85-17773
Lyman alpha coronagraph research sounding rocket program
[NASA-CR-174376] 09 p1354 N85-18517
Data analysis of electron measurements of the plasma experiment aboard the HELIOS probes
[MPE-185] 09 p1416 N85-18835
Recent investigations at INPE in magnetospheric physics and geomagnetism
[INPE-3260-PRE/603] 10 p1514 N85-19555
Research study of space plasma boundary processes
[NASA-CR-174351] 10 p1558 N85-19623
Effects of the solar-terrestrial environment on satellite operations
[DE85-002413] 11 p1590 N85-20003
Geomagnetic disturbances caused by internal atmospheric dynamics 11 p1665 N85-20491
Application of dimensional analysis to the problem of solar wind-magnetosphere energy coupling
[DE85-002414] 11 p1674 N85-20551
Global aspects of stream evolution in the solar wind
[DE85-002207] 11 p1766 N85-21101
Discovery of the solar wind 12 p1954 N85-22272
Velocity distributions of solar wind ions and electrons
12 p1954 N85-22273
The influence of the local solar wind structures on the propagation of low energy particles
12 p1959 N85-22314
The international VEGA 'Venus-Halley' (1984-1986 experiment: Description and scientific objectives
[NASA-TM-77536] 12 p1960 N85-22324
Development of a Global 3-D magnetohydrodynamic computational model for solar wind-cometary and planetary studies
[NASA-CR-175490] 12 p1962 N85-22331
Solar-geophysical data number 483, November 1984. Part 2: (Comprehensive reports). Data for May 1984, December 1981 and miscellanea
[PB85-147700] 12 p1962 N85-22336
Plans for Interbol satellite experiment
13 p1977 N85-22407
Correlation of interplanetary medium parameters in transition region of high-velocity solar wind streams
13 p1978 N85-22412
Polar plasmas as observed by Dynamics Explorers 1 and 2 13 p1991 N85-22453
Physics of the inner heliosphere: Mechanisms, models and observational signatures
[NASA-CR-175632] 13 p2205 N85-23677
Ultraviolet Spectrometer and Polarimeter (UVSP) software development and hardware tests for the solar maximum mission
[NASA-CR-175279] 14 p2305 N85-24271
The application of dimensional analysis to the problem of solar wind-magnetosphere energy coupling
14 p2357 N85-24564
Coupling of the solar wind to measures of magnetic activity 14 p2357 N85-24565
Particle sources, transport, storage and precipitation — magnetosphere 14 p2359 N85-24576
The GEOS-2 electric field observations at times of solar wind discontinuities 14 p2360 N85-24584
Solar wind control of electric fields and currents in the magnetosphere and ionosphere
14 p2364 N85-24608
Solar wind control of magnetospheric convection
14 p2365 N85-24615
Implications of the global appearance of Pi2 and Pc 3 bursts 14 p2371 N85-24652
Active Magnetospheric Particle Tracing Explorers (AMPTE)
[AD-A151072] 14 p2374 N85-24674
The downshift of electron plasma oscillations in the electron foreshock region
[NASA-CR-175633] 14 p2423 N85-24945
The first effect of the amplitude of a solar cycle
14 p2452 N85-25143
Solar wind and cosmic rain 15 p2644 N85-26312
Development of a global 3-D magnetohydrodynamic computational model for solar wind/cometary and planetary studies
[NASA-CR-175724] 15 p2684 N85-26577
Stream dynamics between 1 AU and 2 AU: A detailed comparison of observations and theory
[NASA-TM-86066] 15 p2684 N85-26578
Coupling of the solar wind to measures of magnetic activity
[DE85-002415] 15 p2685 N85-26580
Instability of solar wind near streamlined bodies
16 p2720 N85-26794
Geophysical responses of dynamics of solar wind transition region 16 p2721 N85-26795

Electric field and energy transfer by magnetopause reconnection
[INPE-3448-PRE/701] 16 p2626 N85-27432

An interplanetary magnetic field ensemble at 1 AU
[NASA-TM-86209] 16 p2682 N85-27784

Direct evidence for solar wind control of Jupiter's hectometer-wavelength radio emission
[NASA-TM-86073] 16 p2683 N85-27790

Ten years solar wind experiments on Helios 1 and Helios 2
16 p2685 N85-27798

Plasma waves in the solar wind: Ten years of Helios observations
16 p2685 N85-27801

Supersonic flow around weak radiation sources
17 p2942 N85-28162

Solar wind observations associated with a slow forward shock wave at 0.31 AU
[MPAE-W-79-84-46] 17 p3055 N85-28909

Shocks in the solar wind between 1 and 8.5 AU: Voyager 1 observations
[NASA-CR-175911] 18 p3209 N85-29905

The influence of the heliospheric current sheet and angular separation on flare accelerated solar wind
[NASA-CR-175962] 18 p3209 N85-29907

More on shock-wave studies with Prognoz-10 satellite
19 p3296 N85-30432

Functions of Prognoz-10: Intercosmos' station explained
19 p3296 N85-30433

Prognoz-10 intercosmos' station launched to study shock waves
19 p3296 N85-30434

Effects of coronal disturbances on the ionization state of the solar wind
[NASA-CR-175997] 19 p3385 N85-31000

Solar-wind magnetosphere energy input functions
[NASA-CR-176021] 19 p3385 N85-31001

Solar photospheric and coronal abundances from solar energetic particle measurements
[NASA-CR-176029] 20 p3547 N85-32073

Magnetospheric response to solar wind variations
[DE85-010762] 20 p3547 N85-32074

Soft X-ray polychromator for the Solar Maximum Mission
[NASA-CR-175297] 21 p3723 N85-33096

Yakutsk Institute's cosmic ray research facility
22 p3732 N85-33135

Spectral measurements of magnetic energy and magnetic helicity between 0.29 and 0.97 AU
[IFSI-85-2] 22 p3850 N85-33844

Magnetotails of the terrestrial planets: A comparative study
22 p3856 N85-33875

Simultaneous Solar Maximum Mission and Very Large Array (VLA) observations of solar active regions
[NASA-CR-176090] 22 p3859 N85-33897

Statistical analyses in the study of solar wind-magnetosphere coupling
[DE85-009596] 22 p3859 N85-33898

White Light Coronograph (WLC) and Ultra-Violet Coronal Spectrometer (UVCS) 23 p3901 N85-34161

Shock and statistical acceleration of energetic particles in the interplanetary medium
[SH-1.5-1] 23 p3996 N85-34771

Pitch angle distributions of 35-1000 keV protons at quasi-perpendicular interplanetary shocks
[SH-1.5-6] 23 p3996 N85-34775

Elemental abundances in corotating events
[SH-1.5-15] 23 p3997 N85-34778

Cosmic ray acceleration by stellar wind. Simulation for heliosphere
[SH-1.5-17] 23 p3997 N85-34780

Low energy proton bidirectional anisotropies and their relation to transient interplanetary magnetic structures: ISEE-3 observations
[SH-3.1-9] 23 p4002 N85-34813

The propagation of solar energetic particles in magnetic channels
[SH-3.2-4] 23 p4003 N85-34820

Effects of a wavy neutral sheet on cosmic ray anisotropies
[SH-4.2-11] 23 p4008 N85-34849

On the influence of the heliomagnetospheric periphery on the galactic cosmic rays
[SH-4.2-19] 23 p4009 N85-34856

An update on the correlation between the cosmic radiation intensity and the geomagnetic AA index
[SH-4.2-24] 23 p4009 N85-34861

Gradients and anisotropies of high energy cosmic rays in the outer heliosphere
[SH-4.3-7] 23 p4032 N85-34992

The corotating variation of the north-south anisotropy of cosmic rays
[SH-4.3-15] 23 p4033 N85-34999

A study of periodicities and recurrences in solar activity and cosmic ray modulation
[SH-4.4-14] 23 p4034 N85-35010

Azimuthal and meridional asymmetries of the solar wind and quasiperiodic variations of intensity of Galactic Cosmic Rays (GCR)
[SH-4.4-20] 23 p4035 N85-35016

Diagnostic of electromagnetic conditions in space using cosmic rays
[SH-4.5-19] 23 p4038 N85-35036

Observation of pick-up ions in the solar wind: Evidence for the source of the anomalous cosmic ray component?
[SH-4.6-5] 23 p4039 N85-35043

On the anomalous component
[SH-4.6-6] 23 p4039 N85-35044

The large-scale modulation of cosmic rays in mid-1982: Its dependence on heliospheric longitude and radius
[SH-4.7-9] 23 p4041 N85-35053

Dimensions of the solar wind cavity and of the region of interplanetary cosmic ray modulation
[SH-4.7-11] 23 p4041 N85-35055

Galactic cosmic ray currents and magnetic field irregularity degree in high-speed solar wind streams
[SH-5.1-9] 23 p4042 N85-35063

Influence of magnetic clouds on cosmic ray intensity variations
[SH-5.1-12] 23 p4042 N85-35065

Peculiarities of Galactic Cosmic Ray (GCR) anisotropy variation in connection with the recurrent and sporadic Forbush effects
[SH-5.1-21] 23 p4044 N85-35073

Cosmic ray modulation by high-speed solar wind fluxes
[SH-5.1-22] 23 p4044 N85-35074

Coupling functions for lead and lead-free neutron monitors from the latitudinal measurements performed in 1982 in the research station Academician Kurchatov
[SH-6.1-1] 23 p4044 N85-35076

Cosmic rays 10Be biennal data and their relationship to aurorae and sunspots
[SH-7.1-1] 23 p4047 N85-35094

Parallel fast-forward shock within 1 AU: Helios-1 and 2 observations
[MPAE-W-79-84-27] 24 p4169 N85-35847

SOLAR WIND VELOCITY

Solar wind dynamics at small distances from the sun
06 p0823 N85-15227

Kinematics of nearby gas and stars
06 p0880 N85-15591

Correlation of interplanetary medium parameters in transition region of high-velocity solar wind streams
13 p1978 N85-22412

Linear filters as a method of real-time prediction of geomagnetic activity
[DE85-010780] 22 p3860 N85-33899

Determination of the pitch-angle distribution and transverse anisotropy of interplanetary particles
[SH-3.1-11] 23 p4002 N85-34815

Evidence for regions of negligible cosmic-ray modulation in the inner heliosphere (10 AU)
[SH-4.1-21] 23 p4006 N85-34840

Determination of galactic cosmic ray latitudinal gradient using Earth based detectors
[SH-4.2-13] 23 p4008 N85-34851

The expected cosmic ray density and stream distributions at the heliolatitudinal asymmetry of solar wind
[SH-4.2-14] 23 p4008 N85-34852

Latitudinal gradients of cosmic rays and the polarity reversal of the heliospheric magnetic field: A preliminary evaluation
[SH-4.2-16] 23 p4008 N85-34853

The effect of the neutral sheet structure of the interplanetary magnetic field on cosmic ray distribution in space
[SH-4.2-18] 23 p4008 N85-34855

11- and 22-year variations of the cosmic ray density and of the solar wind speed
[SH-4.2-21] 23 p4009 N85-34858

The corotating variation of the north-south anisotropy of cosmic rays
[SH-4.3-15] 23 p4033 N85-34999

Long-term modulation of galactic cosmic rays in high-energy region
[SH-4.4-22] 23 p4035 N85-35018

Solar wind velocity and daily variation of cosmic rays
[SH-4.5-6] 23 p4036 N85-35024

The cosmic ray interplanetary radial gradient from 1972 - 1985
[SH-4.7-1] 23 p4040 N85-35046

The recovery of the cosmic ray flux from maximum solar modulation at IMP-8 (1 AU) and at Pioneer (R 30 AU)
[SH-4.7-7] 23 p4041 N85-35052

The large-scale modulation of cosmic rays in mid-1982: Its dependence on heliospheric longitude and radius
[SH-4.7-9] 23 p4041 N85-35053

Nonstationary modulation of galactic cosmic rays in a nonlinear model
[SH-4.7-10] 23 p4041 N85-35054

Study of dominating parameters of high speed solar plasma streams in relation to cosmic ray and geomagnetic storms
[SH-5.1-11] 23 p4042 N85-35064

The solar wind effect on cosmic rays and solar activity
[SH-5.1-13] 23 p4043 N85-35066

SOLAR X-RAYS

Studies of solar flares and coronal loops
[AD-A145009] 01 p0130 N85-10898

Particle acceleration in two-ribbon flares --- solar flares
04 p0519 N85-13314

Temporal and spectral characteristics of solar flare hard X-ray emission
[NASA-TM-86167] 08 p1259 N85-17923

Solar-geophysical data. Part 2: (Comprehensive reports)
[PB85-112076] 12 p1962 N85-22332

Solar-geophysical data number 483, November 1984. Part 2: (Comprehensive reports). Data for May 1984, December 1981 and miscellanea
[PB85-147700] 12 p1962 N85-22336

Solar and stellar coronal plasmas
[NASA-CR-175623] 13 p2205 N85-23676

Solar-geophysical data number 479, August 1981. Part 2: (Comprehensive reports), data for January 1984 and August 1981 and miscellanea. Explanation of data reports issued as number 474 (supplement) February 1984
[NASA-CR-175607] 13 p2205 N85-23679

A study of the morphology of solar flares as observed by the hard X-ray imaging spectrometer --- Solar Maximum Mission 14 p2454 N85-25160

Magnetic field structures of hard X-ray flares observed by HINOTORI spacecraft --- solar flares
14 p2455 N85-25161

Microwaves and hard X-rays ultrafast time structures at the impulsive phase of solar bursts
[INPE-3478-PRE/721] 16 p2886 N85-27816

The solar coronal X-ray spectrum 5.5-12 A
[AD-A152334] 17 p3054 N85-28908

A study of the cyclical variations of coronal holes and their relation to open magnetic fields
[AD-A155251] 21 p3723 N85-33099

Study of non-thermal photon production under different scenarios in solar flares. 1: Scenarios and formulations
[SH-1.2-2] 23 p3991 N85-34738

Study of non-thermal photon production under different scenarios in solar flares. 2: The Compton inverse and Bremsstrahlung models and fittings
[SH-1.2-3] 23 p3991 N85-34739

Spectral and spatial properties of solar microflares
[SH-1.2-4] 23 p3991 N85-34740

Temporal evolution of an energetic electron population in an inhomogeneous medium: Application to solar hard X-ray bursts
[SH-1.2-6] 23 p3991 N85-34741

Quantitative analysis of flare accelerated electrons through their hard X-ray and microwave radiation
[SH-1.2-7] 23 p3991 N85-34742

Two types of electron events in solar flares
[SH-1.2-11] 23 p3992 N85-34746

Two classes of solar energetic particle events associated with impulsive and long duration soft X-ray flares
[SH-1.2-12] 23 p3992 N85-34747

A dominant role for protons at the onset of solar flares
[SH-1.2-13] 23 p3992 N85-34748

Photometric and spectroscopic gamma-ray observations of solar transient phenomena using long duration balloons
[SH-9.1-5] 23 p4051 N85-35120

SOLAR-PUMPED LASERS

Theoretical studies of solar-pumped lasers
[NASA-CR-175801] 16 p2789 N85-27206

SOLDERED JOINTS

The metallurgical processes during the soft soldering of copper and copper alloys and the strength characteristics of soldered joints
[BLL-T6388/BG/WH803/84] 06 p0767 N85-14906

Strength and aging behaviour of soft soldered joints
[BLL-T6385/BG/WH800/84] 07 p0925 N85-15862

Investigation of the creep behaviour of soft soldered joints with solder L-SnAg5 at ambient temperature
[BLL-T6383/BG/WH798/84] 07 p0926 N85-15865

NASA welding assessment program
[NASA-CR-175512] 12 p1859 N85-21661

Aging of gold thick-film solder joints
[DE85-009647] 18 p3077 N85-29037

Drag soldering process control
[DE85-010653] 20 p3433 N85-31301

SOLDERING

Swiss firm improves method for soldering printed circuits 03 p0341 N85-12193

Laser spot welding in the electronics industry
14 p2306 N85-24267

Printed wiring board circuit isolator tool
[AD-D011636] 17 p2968 N85-28333
Method for ultrasonic bonding to soft microelectronic substrates
[NASA-CASE-NPO-16087-1] 18 p3094 N85-29151
Drag soldering process control
[DE85-010853] 20 p3433 N85-31301
Hermetic chip carrier compliant soldering pads
[AD-D011722] 23 p3936 N85-34410

SOLDERS
Special soft solder TK-3 (L-SnCu 3 - DIN 1707)
[BLL-T6384/BG/WH799/84(9022.48)]
06 p0767 N85-14907

SOLENOID VALVES
Locking of Automative Products hydraulic selector valves
[BAE-EXPER/NOTE-459] 15 p2587 N85-25839

SOLENOIDS
Optimum dimensions of power solenoids for magnetic suspension 04 p0489 N85-13116
The generation of rolling moments with the superconducting solenoid model
[NASA-CR-172520] 09 p1283 N85-18068
Virtual cathode oscillator study
[AD-A149268] 10 p1480 N85-19342
In-beam tests of an air-core superconducting-solenoid particle spectrometer
[DE85-004029] 12 p1853 N85-21625
Stability and vibrations of internal windings of high-current superconducting solenoid magnets
[AD-A151465] 15 p2656 N85-26390
Effect of superconducting solenoid model cores on spanwise iron magnet roll control
[NASA-TM-86378] 17 p2905 N85-27915
Optimum dimensions of power solenoids for magnetic suspension
[NASA-TM-77864] 17 p3026 N85-28716
Rotor blade test apperatus
[AD-D011725] 23 p3934 N85-34361
Theoretical and computational research on the focused transport of intense charged particle beams
[DE85-012980] 23 p3972 N85-34821

SOLID ARGON
U SOLIDIFIED GASES

SOLID ELECTROLYTES
Trivalent ion exchange in beta alumina
[AD-A145373] 02 p0172 N85-11151
Study of application of organic semiconductors to electronic components
[BMFT-FB-T-84-142] 02 p0289 N85-11890
Solid electrolytes for medium temperature steam electrolysis
[DE84-014384] 04 p0463 N85-12938
Development and testing of thin film cells for high temperature water vapor electrolysis
[BMFT-FB-T-84-146] 04 p0471 N85-13001
Polyphosphazene solid electrolytes
[AD-A147008] 07 p0931 N85-15902
Ionic and molecular transport in beta- and beta''-alumina
[DE85-000984] 09 p1380 N85-18680
A two photoelectrode solid-state photoelectrochemical cell
[AD-A148982] 10 p1434 N85-19038
High-temperature, solid oxide electrolyte fuel cell power generation system
[DE85-002978] 11 p1675 N85-20552
Solid electrolytes: Mechanisms for achieving optimal conductivity
[AD-A150116] 12 p1801 N85-21296
Production technology of an electrolyte for Na/S batteries
[BMFT-FB-T-84-277] 15 p2550 N85-25742
Degradation phenomena in solid electrolytes
[DE85-007066] 15 p2587 N85-25949
F-cell: The Aspen fuel cell model
[DE85-001975] 18 p3131 N85-29393
Polyethylene imine-metal salt solid electrolyte
[AD-D011676] 19 p3305 N85-30485
Defect interactions at high concentrations in solid oxide electrolytes
[DE85-011824] 22 p3807 N85-33580

SOLID LUBRICANTS
Experimental test program for evaluation of solid lubricant coating as applied to compliant foil gas bearings to 315 deg C
[NASA-CR-174837] 07 p0930 N85-15895
The role of silver in self-lubricating coatings for use at extreme temperatures
[NASA-TM-86943] 11 p1611 N85-20127
Wear reduction by lubricants in confined contacts
14 p2223 N85-23786
Effect of counterface material type and its topography on the tribological properties of polyimide composites
[NASA-TM-87036] 16 p2754 N85-26993
Tooth wear in worm gears in vacuum
16 p2766 N85-27070
Molybdenum disulphide lubrication: A continuation survey, 1981 - 1983
[REPT-84-549] 18 p3082 N85-29065
Friction and wear of solid-lubricated contact in gas turbine engine bearings
[AD-A155042] 21 p3596 N85-32335
Advances in sputtered and ion plated solid film lubrication 22 p3797 N85-33524

SOLID MECHANICS
Proceedings of the 9th Biennial Army Symposium on Solid Mechanics. Advances in Solid Mechanics for Design and Analysis
[AD-A150042] 12 p1867 N85-21710
USSR report: Physics and mathematics
[JPRS-UPM-85-004] 21 p3680 N85-32860

SOLID PHASES
Re-evaluation of phase separation in Ti-Zr-Be metallic glasses
[DE84-015603] 03 p0338 N85-12176
A study of tetrataenite 06 p0885 N85-15623
Speculations on the formation of metallic meteorite phases 06 p0889 N85-15648
Influence of temperatures of reactants on nature of product of solid-phase reactions
[BLL-M-36019-(5828.4)] 07 p0921 NR5-15832
The formation of isolated phase precipitates during the decomposition of high-coercive force Fe-Cr-Co alloys
[BLL-M-36028-(5828.4)] 07 p0924 N85-15855
Kinetics of interaction between carbon and iron oxides of metallized materials in solid phase
[BLL-M-36023-(5828.4)] 07 p0926 N85-15873
Electron-diffraction structural examination of amorphous iron-tin alloys 11 p1604 N85-20084
Investigation of vanadium solid solution and zeta phase regions of vanadium-carbon system
[DE85-002678] 11 p1605 N85-20092
Effect of variable solid phase thermal properties on propellant combustion 13 p2002 N85-22547
Phase separation in polyurethanes: A deuterium NMR study
[AD-A151515] 15 p2505 N85-25451
Detonations of solid explosives
[AD-A152012] 15 p2521 N85-25540
X-ray diffraction study of changes in stress-strain distributions during fatigue of a 2-phase alloy
[AD-A152367] 17 p2930 N85-28087
Solid phase reactions among manganese, potassium perchlorate and barium chromate
[HSE-TRANS-11166] 19 p3237 N85-30071
Fundamental studies of beta phase decomposition modes in titanium alloys
[AD-A154122] 19 p3238 N85-30078

SOLID PROPELLANT COMBUSTION
NT SOLID PROPELLANT IGNITION
An experimental investigation of combustion pressure oscillations in solid fuel ramjets
[AD-A144870] 01 p0024 N85-10147
Critical analysis of nitramine decomposition data. Preliminary comments on autoacceleration and autoinhibition in HMX and RDX decomposition
[AD-A146570] 06 p0774 N85-14946
Analysis of Deflagration to Shock to Detonation Transition (DSDT) in porous energetic solid propellants
08 p1115 N85-17030
Fuel-rich solid propellant boron combustion
[AD-A148522] 08 p1136 N85-17157
Molecular dynamics in nitramines and modified nitramines
[AD-A148515] 08 p1220 N85-17686
Recovery of damaged solid propellants by interrupting burning and crack-propagation processes
[AD-P004343] 10 p1455 N85-19167
Effects of perforation L/D ratio and slotting on stick propellant combustion
[AD-A148854] 10 p1456 N85-19177
Solid propellant combustion diagnostics and automated data retrieval from holograms 13 p1998 N85-22527
Combustion of zirconium carbide
13 p1999 N85-22532
Coupling between velocity oscillations and solid propellant combustion 13 p2000 N85-22536
Mechanism of burning rate enhancement by ferric oxide 13 p2002 N85-22546
Effect of variable solid phase thermal properties on propellant combustion 13 p2002 N85-22547
Mutiple reflection theory for microwave measurement of solid propellant burning rates
13 p2002 N85-22549
In-situ burning rate determination using flash radiography 13 p2002 N85-22550
Molecular dynamics of propellant gases, part 2
13 p2002 N85-22552
Application of atomic fluorescence to measurement of combustion temperature in solid propellants
[AD-A150733] 14 p2263 N85-24021
Components of the combustion gases of propellant charge powders after reaction in the high pressure bomb in the pressure range up to 1000 MPa. Part 1: Nitroglycerine powder GB Pa 125
[ISL-CO-217/83-PT-1] 14 p2264 N85-24027
Solid fuel combustion chamber
[VTH-LR-415] 16 p2741 N85-25918
Solid fuel combustion chamber
[VTH-LR-436] 16 p2741 N85-25919
Solid fuel combustion chamber research in the Netherlands
[VTH-LR-444] 16 p2742 N85-25920
The development of a computational model for a two-dimensional turbulent flow. Part 1: Mathematical background — solid fuel combustion
[VTH-LR-436-PT-1] 16 p2785 N85-27188
Holographic investigation of solid propellant combustion in a two-dimensional motor
[AD-A153546] 18 p3070 N85-28989
Imbedded thermocouples as a solid propellant combustion probe
[AD-A155630] 21 p3564 N85-32187
Closed-bomb combustion of Hivelite-based, Very High Burn Rate (VHBR) propellant
[AD-A155740] 21 p3571 N85-32212

SOLID PROPELLANT IGNITION
The vulnerability of cast double base rocket motors to thermomechanical attack 08 p1115 N85-17033
Response of propellants to high dynamic stresses: The uses of gun launch techniques
08 p1116 N85-17035
Some aspects of the micromechanics of hot spot formation in energetic materials
08 p1116 N85-17036
A two-step bomb to determine the inflammability of propellant charge powders
[ISL-CO-211/83] 14 p2264 N85-24026
Investigation of the choking effect of an inert granular bed on an ignition gas jet charged with particles
[ISL-CO-235/83] 14 p2264 N85-24028
Status of boron combustion research
[AD-A154762] 21 p3563 N85-32180

SOLID PROPELLANT ROCKET ENGINES
A model for grain misalignment in cylindrical port motors
[AD-A144856] 01 p0034 N85-10210
One-dimensional two-phase constant lag flow in combustion chamber of solid propellant rocket motors
[AD-A145679] 02 p0173 N85-11157
Experiments on residual thrust and prediction for upper-stage solid propellant rockets
[NAL-TR-800] 03 p0324 N85-12087
Carbon/carbon rocket motor exit cone reinforcement
[AD-D011360] 07 p0916 N85-15799
Solid propellant Ramrockets 07 p0918 N85-15816
The space shuttle launch vehicle aerodynamic verification challenges 08 p1093 N85-16807
The aerodynamic challenges of SRB recovery
08 p1093 N85-16808
External tank processing from barge to pad
08 p1096 N85-16827
Solid rocket booster retrieval operations
08 p1096 N85-16829
Solid rocket motor certification to meet space shuttle requirements from challenge to achievement
08 p1098 N85-16841
The solid rocket booster auxiliary power unit: Meeting the challenge 08 p1099 N85-16846
Hazard Studies for Solid Propellant Rocket Motors
[AGARD-CP-367] 08 p1114 N85-17025
Review of USAF treatment of solid propellant rocket motor hazards 08 p1114 N85-17027
The vulnerability of cast double base rocket motors to thermomechanical attack 08 p1115 N85-17033
Hazard assessment of a hypothetical large rocket motor 08 p1117 N85-17042
Water impact laboratory and flight test results for the space shuttle solid rocket booster aft skirt
09 p1335 N85-18384
Report on AGARD Meeting: Hazards Studies for Solid Propellant Rocket Motors
[AD-P004340] 10 p1454 N85-19164
Window on science visit to the USA, 21 March - 2
April, 1984 — ramjets and solid propellant rocketry
[VTH-LR-426] 11 p1592 N85-20011
Space Shuttle booster thrust imbalance analysis
[NASA-TM-86493] 12 p1791 N85-2124
Integrated insulation wall assembly — for a solid rocket motor case
[AD-D011553] 12 p1794 N85-2125
Plasticizer system for propellant compositions
[AD-D011502] 12 p1816 N85-213

Plasticizer system for propellant compositions [AD-D011508] 12 p1816 N85-21391
Plasticizer system for propellant compositions [AD-D011516] 12 p1817 N85-21394
Plasticizer system for propellant compositions [AD-D011517] 12 p1817 N85-21395
SRM filament wound case resin characterization studies 12 p1944 N85-22212
Investigation of the effects of NaOH dopant level on the physical and mechanical properties of carbon/phenolic composite material 12 p1945 N85-22213
Nonlinear interactions between vortices and acoustic waves in a rocket combustion chamber 13 p1999 N85-22533
Acoustic energy exchange in sheared mean flows — solid rocket motors 13 p1999 N85-22534
Investigations of reactive and non reactive acoustic boundary layers in porous walled ducts 13 p2000 N85-22535
Comparisons of solid propellant with instability predictions and motor firing experience 13 p2001 N85-22541
Internal fluid mechanism of solid propellant rocket motors 13 p2001 N85-22544
Characterization standards for solid propellant rocket motors [AD-A150250] 13 p2013 N85-22627
Alternate nozzle ablative materials program [NASA-CR-175858] 14 p2246 N85-23924
Ignition, separation of boosters, stages in Ariane 3 14 p2289 N85-24185
A fundamental study of liquid phase particle breakup. Revision [AD-A150791] 14 p2301 N85-24249
AFRPL (Air Force Rocket Propulsion Laboratory) technical objective document FY 85 [AD-A151388] 15 p2495 N85-25389
Analysis of combustion oscillations in heterogeneous systems [AD-A151999] 16 p2745 N85-26942
Surveillance report. Stage 1: Dissected motors-propellants motor number 0012199, phase 15 [AD-A153206] 17 p2916 N85-27973
MM2 LRSLA testing stage 3 propellant [AD-A152540] 17 p2937 N85-28128
Recession of graphitic nozzles in rocket motors 21 p3560 N85-32144
Verification of the SRB motor case pin retainer band tips [NASA-CR-170882] 24 p4070 N85-35220
Results of tests on a specimen of the SRB aft skirt heat shield curtain in the MSFC LRLF [NASA-CR-170883] 24 p4070 N85-35221
Dissected motors-propellants motor number STM-012. Phase 15: Surveillance report, stage 1 [AD-A156068] 24 p4071 N85-35226
Results of tests of K5NA and a revised formulation of EPDM/cork patch material in MSFC Hot Gas Facility [NASA-CR-170890] 24 p4073 N85-35238
Evaluation of SRB phenolic TPS material made by an alternate vendor [NASA-CR-170894] 24 p4073 N85-35240
Space shuttle SRB TPS protective paint test and evaluation in NASA Hot Gas Facility and AEDC Tunnel C [NASA-CR-170884] 24 p4081 N85-35294
Results of tests of Insta-Foam Thermal Protection System (TPS) material for protection of equipment inside the SRB aft skirt [NASA-CR-170892] 24 p4081 N85-35295

SOLID PROPELLANTS
NT CASE BONDED PROPELLANTS
NT COMPOSITE PROPELLANTS
NT DOUBLE BASE ROCKET PROPELLANTS
NT HTPB PROPELLANTS
NT NITRAMINE PROPELLANTS
NT PLASTIC PROPELLANTS
NT SOLID ROCKET PROPELLANTS
Catalyzed low burning rate propellants for upper-stage solid rocket motor [NAL-TR-805] 03 p0339 N85-12181
Special problems of Ramjet with solid fuel 07 p0916 N85-15815
Combustion properties of fuel-rich magnesium propellants with HTPB as binder [FOA-C-20555-D1] 07 p0935 N85-15924
Sensitivity tests for solid propellants in Germany 08 p1115 N85-17028
Modelling the thermal explosion phenomenon in solid propellants: The case of fixed and variable temperatures 08 p1117 N85-17044
Analysis of deflagration to detonation transition in high-energy solid propellants [AD-A148302] 08 p1135 N85-17156
Investigation of the pressure-and velocity-coupled responses of solid propellants using impedance tube method 09 p1300 N85-18168
Antiplane cracks in solid propellants [AD-P004344] 10 p1455 N85-19168
A summary of the mechanism of delayed detonation [AD-P004347] 10 p1455 N85-19171
Curvilinear solid propellant grain [AD-D011457] 10 p1458 N85-19183
Application of fluorescence to measurement of surface temperature in solid propellants 13 p2002 N85-22548
The crystal and molecular structure of a new propellant compound: Triaminoguanidium Azide Nitrate (TAZN) 13 p2002 N85-22551
Non-steady combustion of composite solid propellants [AD-A150827] 14 p2250 N85-23947
A two-step bomb to determine the inflammability of propellant charge powders [ISL-CO-211/83] 14 p2264 N85-24026
Components of the combustion gases of propellant charge powders after reaction in the high pressure bomb in the pressure range up to 1000 MPa. Part 1: Nitroglycerine powder GB Pa 125 [ISL-CO-217/83-PT-1] 14 p2264 N85-24027
Technical instructions for a control operating system of the gas flow installation for the solid fuel combustion chamber [VTH-LR-410] 18 p3118 N85-29302
Closed-bomb combustion of Hivelite-based, Very High Burn Rate (VHBR) propellant [AD-A155740] 21 p3571 N85-32212

SOLID ROCKET BINDERS
Study of HTPB-based SOFRAM fuels [FOA-C-20563-D3] 11 p1614 N85-20150
Amine salts as bonding agents [AD-D011543] 12 p1817 N85-21396

SOLID ROCKET PROPELLANTS
NT DOUBLE BASE ROCKET PROPELLANTS
NT HTPB PROPELLANTS
A model for grain misalignment in cylindrical port motors [AD-A144856] 01 p0034 N85-10210
Combined cycle ramjet engine [AD-D011247] 06 p0760 N85-14859
An optical and mass spectrometric study of the aluminum-oxygen flame [AD-A147434] 07 p0923 N85-15849
Thermophysical property testing using transient techniques [AD-A147085] 07 p1049 N85-16664
Combustion dynamics in rockets [AD-A148478] 08 p1114 N85-17024
Hazard Studies for Solid Propellant Rocket Motors [AGARD-CP-367] 08 p1114 N85-17025
Aims and requirements of NATO group AC/310 08 p1114 N85-17026
Review of USAF treatment of solid propellant rocket motor hazards 08 p1114 N85-17027
Analysis of Deflagration to Shock to Detonation Transition (DSDT) in porous energetic solid propellants 08 p1115 N85-17030
Some aspects of the micromechanics of hot spot formation in energetic materials 08 p1116 N85-17036
Shock and impact response of solid rocket propellants: Experimental and theoretical 08 p1116 N85-17040
Ballistic/detonic transition of propellants 08 p1117 N85-17041
The heat sensitivity of solid propellants 08 p1117 N85-17043
The pressure deflagration limit of solid rocket propellants 08 p1117 N85-17046
Fuel-rich solid propellant boron combustion [AD-A146522] 08 p1136 N85-17157
Recovery of damaged solid propellants by interrupting burning and crack-propagation processes [AD-P004343] 10 p1455 N85-19167
Transition to detonation from rapid-compression (ramp-waves) generated in a burning porous bed [AD-P004345] 10 p1455 N85-19169
Measurement of shock induced reaction in rocket propellants by nanosecond infrared radiometry and photography [AD-P004349] 10 p1456 N85-19173
Analysis of Shock to Detonation Transition (SDT) of porous high energy propellant from ramp-wave compression loading [AD-A149333] 10 p1457 N85-19180
Azido nitramino ether containing solid propellants [AD-D011511] 12 p1816 N85-21392
Plasticizer system for propellant compositions [AD-D011514] 12 p1817 N85-21393
Investigation of the characteristics of the velocity-coupled response functions of solid propellants 13 p2001 N85-22540
Comparisons of solid propellant with instability predictions and motor firing experience 13 p2001 N85-22541
Distributed combustion: A mechanism of acoustic suppression 13 p2001 N85-22543
Chemical kinetics of gas phase decomposition products of nitramine propellants 13 p2003 N85-22558
An apparatus for sizing particulate matter in solid rocket motors [AD-A151282] 15 p2495 N85-25388
Analysis of combustion oscillations in heterogeneous systems [AD-A151999] 16 p2745 N85-26942
Analysis of deflagration to detonation transition in high-energy solid propellants 16 p2757 N85-27010
Surveillance report. Stage 1: Dissected motors-propellants motor number 0012199, phase 15 [AD-A153206] 17 p2916 N85-27973
Holographic investigation of solid propellant combustion in a two-dimensional motor [AD-A153546] 18 p3070 N85-28989
Propellant plasticizer [AD-D011501] 20 p3434 N85-31306

SOLID ROTATION
U ROTATING BODIES

SOLID SOLUTIONS
Determining composition in surface region of semiconductor crystals by method of sudden changes in X-ray photoelectric effect 02 p0267 N85-11746
Producing semiconductor materials by superfast cooling of melt 03 p0354 N85-12274
Investigation of the isothermal precipitation behavior of nickel-base alloys using electrochemical phase extraction [JUEL-1903] 05 p0619 N85-13958
Defective nature of the crystalline lattice of nickel ferrite-based solid solutions [BLL-TRANS-WH-595-(9091.9F)] 10 p1439 N85-19068
Solution growth facility, phase A design study, executive summary — EURECA [RPT/SGF/00014/TER] 11 p1591 N85-20006
Investigation of vanadium solid solution and zeta phase regions of vanadium-carbon system [DE85-002678] 11 p1605 N85-20092
Solid sorbent air sampler [NASA-CASE-MSC-20653-1] 11 p1636 N85-20301
Dissolution of solid solutions in absence of internal mass transfer [BLL-M-36092-(5828.4)] 16 p2748 N85-26959
The precipitation mechanism in a metallic solid solution crystal: Case of the aluminum-copper and aluminum-silver systems [DE85-009981] 18 p3077 N85-29032
Solids mixing in a three phase fluidized bed containing spherically shaped-porous solid particles [PB85-187961] 22 p3765 N85-33453
Cluster variation study of coherent ordering in FCC and BCC solid solutions [AD-A156039] 24 p4079 N85-35280

SOLID STATE
Synthesis and characterization of advanced materials [PB84-215326] 01 p0025 N85-10156
Report on research results in solid state nuclear physics, 1980-1982 [JUEL-SPEZ-250] 03 p0422 N85-12696
Investigations on low-dimensional solid state substances — solitons 03 p0426 N85-12720
Investigation of solid state problems using the hyperfine interaction between static and dynamic internal fields with short live excited probe nuclei 03 p0428 N85-12729
Solid state investigations with nuclear physics methods 03 p0428 N85-12731
Utilization of a tandem accelerator for the investigation of solid state properties by means of heavy ions 03 p0429 N85-12733
Fast ions as probes in solid state research 03 p0430 N85-12740
X-ray and neutron scattering and X-ray spectroscopy for the study of defects in solid state materials 03 p0430 N85-12741
Neutron scattering on macromolecular solid state materials, solutions and melts 03 p0431 N85-12747
Neutron scattering for the investigation of solid state materials, utilization in chemical structures 03 p0432 N85-12752
Nonthermal mechanism for laser annealing of semiconductors and formation of super structure 04 p0487 N85-13109
Solid state research [AD-A147640] 08 p1225 N85-17714
Synthesis chemistry of ceramics by solid-state combustion processes in micro-gravity [DE85-009595] 18 p3081 N85-29061

Solid State Division report on its mission-oriented basic research
[DE85-008788] 19 p3376 N85-30941
SSMIR (Solid State Memory Instrumentation Recorder): A new approach to acquiring data during an aircraft seat/sled ejection sequence
[AD-A154780] 21 p3589 N85-32308
A solid-state framework for terrestrial upper mantles
22 p3858 N85-33878
Solid state high power amplifier for driving the SLC injector klystron
[DE85-013083] 24 p4090 N85-35356
State-of-the-art of solid-state motor controllers
[TI85-008674] 24 p4162 N85-35806
Ionic crystals
[DE85-009462] 24 p4163 N85-35809

SOLID STATE DEVICES
NT AVALANCHE DIODES
NT BIPOLAR TRANSISTORS
NT CHARGE COUPLED DEVICES
NT CHARGE INJECTION DEVICES
NT CHARGE TRANSFER DEVICES
NT CMOS
NT FIELD EFFECT TRANSISTORS
NT GALLIUM ARSENIDE LASERS
NT GERMANIUM DIODES
NT HETEROJUNCTION DEVICES
NT HOMOJUNCTIONS
NT JFET
NT JUNCTION DIODES
NT JUNCTION TRANSISTORS
NT LIGHT EMITTING DIODES
NT METAL OXIDE SEMICONDUCTORS
NT MIM (SEMICONDUCTORS)
NT MIM DIODES
NT MIS (SEMICONDUCTORS)
NT MULTISPECTRAL LINEAR ARRAYS
NT PHOTODIODES
NT PHOTOTRANSISTORS
NT PHOTOVOLTAIC CELLS
NT RUBY LASERS
NT SCHOTTKY DIODES
NT SEMICONDUCTOR DEVICES
NT SEMICONDUCTOR LASERS
NT SILICON CONTROLLED RECTIFIERS
NT SILICON TRANSISTORS
NT SIS (SEMICONDUCTORS)
NT SOLID STATE LASERS
NT THERMISTORS
NT THYRISTORS
NT TRANSISTOR AMPLIFIERS
NT TRANSISTORS
NT VARACTOR DIODES
NT VARISTORS
NT YAG LASERS
Workshop on the Use of Future Multispectral Imaging Capabilities for Lithologic Mapping: Workshop summary
02 p0214 N85-11413
USSR report: Electronics and electrical engineering
[JPRS-UEE-84-014] 03 p0344 N85-12215
The 30 GHz solid state amplifier for low cost low data rate ground terminals
[NASA-CR-174795] 03 p0358 N85-12300
High-speed videography for optical and X-ray imaging
[DE84-012661] 04 p0564 N85-13595
High or low-side solid state relay with current limiting and operational testing
[AD-D011260] 05 p0631 N85-14046
Electronics research at the University of Texas at Austin
[AD-A148800] 07 p0947 N85-15998
Basic research in electronic (JSEP): Joint Services Electronics Program
[AD-A147881] 07 p0948 N85-16007
Solid state research
[NASA-CR-174285] 07 p1048 N85-16656
Photometry with Multi-Anode Microchannel Arrays (MAMAs) and Charge Injection Devices (CIDs)
08 p1252 N85-17909
Filter reflection image guide oscillator and solid state line scanning device
[AD-D011440] 10 p1479 N85-19336
Optical mark reader
[AD-D011462] 10 p1557 N85-19818
A new very high voltage semiconductor switch
[NASA-TM-86957] 11 p1627 N85-20246
Solar energy converter using surface plasma waves
[NASA-CASE-LEW-13827-1] 12 p1876 N85-21788
Semiconductor materials for high frequency solid state sources
[AD-A150020] 12 p1940 N85-22186
Research in the optical sciences
[AD-A150198] 13 p2159 N85-23401
Further developments of CCD line array telecine
[BBC-RD-1985/3] 14 p2293 N85-24217
Basic research in electronics (JSEP)
[AD-A151002] 14 p2298 N85-24230
Annual report on electronics research at the University of Texas at Austin
[AD-A150836] 14 p2415 N85-24901
Development of solid state infrared emitters for gas detection applications
[PB85-148450] 15 p2561 N85-25800
NASA welding assessment program
[NASA-CR-175683] 15 p2568 N85-25845
An advanced solid state pressure transducer for high reliability SSME application 16 p2739 N85-26905
Technology development for thin-film-trace humidity sensors
[BMFT-FB-T-84-268] 17 p2969 N85-28338
Proceedings of the 14th European Solid State Device Research Conference Including Solid State Device Technology, ESSDERC 84
[AD-A153409] 18 p3193 N85-29804
Joint services electronics program
[AD-A154348] 19 p3375 N85-30939
An absolute calibration of the solid state detectors in the narrow band neutrino beam at CERN
[NIKHEF-H/84-10] 20 p3538 N85-32017
Experiments on the influence of active walls on the initial amplitudes and growths of instability waves
[AD-A154630] 21 p3583 N85-32275
Solid state research
[AD-A154783] 21 p3709 N85-33025
TEMO and TEB thermoelectronic devices
22 p3779 N85-33415

SOLID STATE LASERS
NT GALLIUM ARSENIDE LASERS
NT RUBY LASERS
NT YAG LASERS
Peripheral vision displays: The future
01 p0009 N85-10058
Solar-pumped lasers: A review
02 p0261 N85-11711
Optimization of ultrashort pulse generation mode of YAG laser 02 p0262 N85-11713
Improved solid-state laser sources, volume 2
[DE85-000759] 09 p1325 N85-18330
Modern solid state laser materials
[DE85-003685] 10 p1490 N85-19410
Potential of high-average-power solid state lasers
[DE85-003884] 11 p1639 N85-20329
Autostochastic behavior of solid statu ring laser with low frequency periodic loss modulation
11 p1717 N85-20805
Advanced crystalline laser materials
[DE85-003142] 12 p1857 N85-21647
Low jitter trigger for an excimer laser
[DE85-005732] 13 p2097 N85-23080
Research progress on laser crystals in China
13 p2166 N85-23440
Submillimeter-band solid state distributed feedback laser 15 p2644 N85-26307
Spectroscopic investigation of materials for tunable infrared lasers
[AD-A154124] 19 p3272 N85-30291
Pulsed lasers for filming color holographic film images
22 p3761 N85-33426
Trivalent cerium doped crystals as tunable laser systems: Two bad apples
[DE85-008168] 22 p3790 N85-33482

SOLID STATE PHYSICS
USSR report: Physics and mathematics
[JPRS-UPM-84-006] 02 p0256 N85-11676
Research in the theory of condensed matter and elementary particles
[DE85-010447] 20 p3531 N85-31968

SOLID SURFACES
NT CRYSTAL SURFACES
Simulation of contact surface erosion for impact problems 01 p0060 N85-10398
Electron spin polarization effects in low energy electron diffraction, ion neutralization and metastable atom deexcitation at solid surfaces
[DE84-016550] 04 p0572 N85-13649
Macrocyclic poly(tertiary) phosphines for the attachment of metals to surfaces of photodevices
[DE84-015552] 05 p0617 N85-13946
Ion emission from solid surfaces: Comparison of dust impact with other excitations — Giotto mission
14 p2244 N85-23912
Investigation to optimize the passive shock wave/boundary layer control for supercritical airfoil drag reduction
[NASA-CR-175788] 16 p2699 N85-26665
Theory of laser-stimulated surface process. 2: A generalized-master-equation approach to energy transfer between an IR laser, an aspecties and phonons
[AD-A153083] 17 p2970 N85-28344
Statistical mechanics of adsorption and wetting
[DE85-010093] 19 p3269 N85-30271
Effects of laser radiation on surfaces and coatings
[DE85-010475] 22 p3790 N85-33484
Unsteady transonic heat transfer in a transient facility
[NASA-CR-176145] 23 p3930 N85-34384
System maintenance manual for master modeling of aerodynamic surfaces by three-dimensional explicit representation
[NASA-CR-176224] 23 p3956 N85-34517
The dynamics of articulated rigid bodies for purposes of animation 23 p3965 N85-34579

SOLID SUSPENSIONS
Transport properties of multiphase systems
[DE84-015560] 02 p0173 N85-11158
Characteristics of charge transfer in the dispersed phase of electrorheological suspensions
[RAE-TRANS-2125] 19 p3233 N85-30040

SOLID WASTES
Immobilization of toxic waste by embedding it in bitumen
[OEFZS-4277] 07 p0996 N85-16322
FAA policy regarding solid waste disposal facilities
[AD-P004196] 11 p1581 N85-19983
Airport bird hazards associated with solid waste disposal facilities
[AD-P004197] 11 p1581 N85-19984
Field lysimeter facility for evaluating the performance of commercial solidified low-level waste
[DE85-003886] 11 p1727 N85-20863
Large-scale commercial combustion systems for producing energy from municipal solid waste
[DE85-007097] 15 p2587 N85-25946
Measurement of radionuclides in waste packages
[DE85-011674] 22 p3836 N85-33766
Multi-solute subsurface transfer modeling for energy solid wastes: Highlights FY 1984
[DE85-012788] 23 p3966 N85-34591

SOLID-SOLID INTERFACES
Simulation of contact surface erosion for impact problems 01 p0060 N85-10398
Evaluation of interfacial stresses from the amplitude of reflected ultrasonic signal
[DE84-015472] 02 p0276 N85-11796
Electronic structure of semiconductor interfaces
[AD-A147663] 08 p1225 N85-17715
The Si/SiO2 intrinsic states and interface charges. Chapter 1: Origin, properties, models, impact
[HMI-B-413] 09 p1400 N85-18812
Study of metal oxide semiconductor structures by capacitive transient spectroscopy
[ENST-84E011] 11 p1737 N85-20928
Segregation of silicon in alumin-carbon fiber composites 13 p2028 N85-22706
Sliding interfaces with contact-impact in large scale Lagrangian computations
[DE85-006451] 15 p2639 N85-26277

SOLIDIFICATION
NT MELT SPINNING
Low-gravity solidification of cast iron and space technology applications 02 p0151 N85-11022
Directional solidification of flake and nodular cast iron during KC-135 low-g maneuvers
02 p0154 N85-11040
Containerless drop tube solidification and grain refinement of NiAl3 02 p0154 N85-11042
Solidification and crystal growth of solid solution semiconducting alloys 02 p0155 N85-11046
Design and implementation of a low-gravity solidification experiment package for the F-104
02 p0156 N85-11053
A method for evaluating the contamination of steel in relation to the solidification curve
[BLL-M-35735-(5828.4)] 02 p0175 N85-11171
Rapid solidification processing and the control of structure/property relationships
02 p0176 N85-11176
Rapid solidification of steels: Model and commercial alloys 02 p0176 N85-11184
The structure of rapidly solidified nickel-base alloys
02 p0181 N85-11215
Biform resolidification and amorphous phases in a laser and electron beam processed tantalum-iridium alloy
[DE84-013334] 02 p0184 N85-11234
Studies of laser melting and rapid solidification using amorphous silicon
[DE84-014737] 02 p0202 N85-11345
European Scientific Notes, Number 38-9
[AD-A145683] 02 p0306 N85-11875
Weld metal solidification cracking in a carbon-manganese steel 03 p0330 N85-12126
Application of solidification theory to rapid solidification processing
[AD-A145953] 03 p0331 N85-12130
Critical dynamics for continuous rapid solidification processing
[AD-A146071] 03 p0332 N85-12137

NBS (National Bureau of Standards): Materials measurements
[NASA-CR-174038] 03 p0332 N85-12143
Microstructure of ceramics fabricated by unidirectional solidification
[NASA-TM-77423] 03 p0336 N85-12157
The Al-Be system: The effects of RSP on structure and phase relating
[DE84-015604] 04 p0474 N85-13019
Solidification and aging behavior of types 308 and 308CRE stainless steel welds
[DE84-016552] 04 p0476 N85-13029
Inclusion formation during solidification of steels with improved machinability
[BMFT-FB-T-84-160] 05 p0619 N85-13957
Application of solidification theory to rapid solidification processing
[AD-A146619] 06 p0769 N85-14917
Microstructure of rapidly quenched type 308 stainless steel weld filler metal and its implications on rapid solidification processes
[DE85-000930] 06 p0769 N85-14920
Time-resolved studies of ultrarapid solidification of highly undercooled molten silicon formed by pulsed laser irradiation
[DE84-016664] 06 p0813 N85-15164
Experimental and theoretical study of the formation of the 2AB, 3AB, and 9A meteorite chemical groups from the parent liquid 06 p0886 N85-15628
Investigations concerning the magmatic iron meteorites: Static vs. dynamic experiments
06 p0886 N85-15629
The growth of metastable peritectic compounds
[NASA-CR-171289] 07 p0920 N85-15824
The growth of metastable peritectic compounds
[NASA-CR-171290] 07 p0920 N85-15825
Investigation of granules of molybdenum-base alloys obtained with pulsed discharges
[BLL-M-36012-(5828.4)] 07 p0926 N85-15871
SPAR X technical report for experiment 76-22 directional solidification of magnetic composites
[NASA-CR-171271] 07 p0927 N85-15880
Analysis of the heating process of a body in a melt
[BLL-M-36014-(5828.4)] 07 p0956 N85-16057
Grain refining and microstructural modification during solidification
[AD-A147705] 08 p1128 N85-17111
Rapid solidification processing and powder metallurgy of Al alloys
[AD-A148427] 08 p1130 N85-17120
The growth of large diameter single crystals by vertical solidification of the melt
[AD-A148756] 09 p1397 N85-18792
The feasibility of low-G grey solidification of nodular iron in the F-104 experimental furnace package
[NASA-TM-82527] 10 p1426 N85-18996
Research on rapidly solidified alloys
[AD-A149380] 10 p1441 N85-19060
1984 model of binary alloy solidification
[DE85-002497] 11 p1608 N85-20110
Hot melt adhesive attachment pad
[NASA-CASE-LAR-12894-1] 11 p1610 N85-20125
Laser processing of ceramics
[DE85-001184] 11 p1612 N85-20135
Research in surface sciences, disordered materials, and solidification and growth
[PB85-132140] 11 p1737 N85-20927
Experimental determination of systems suitable for study as monotectic binary metallic alloy solidification models
12 p1948 N85-22235
Rapid solidification processing of magnesium alloys
[AD-A150270] 13 p2022 N85-22668
Time-resolved studies of rapid solidification in highly undercooled molten silicon
[DE85-004857] 13 p2036 N85-22765
Dopant incorporation in silicon during nonequilibrium solidification: Comparison of 2 processes
[DE85-005568] 14 p2430 N85-24988
Microstructural characteristics during the controlled solidification of a binary system
[DE85-005200] 15 p2507 N85-25461
Application of solidification theory to rapid solidification processing
[AD-A151251] 15 p2509 N85-25480
Metallurgical characterization of aluminum powder consolidation
[AD-A151990] 15 p2510 N85-25484
Sweden develops new rapid solidification process
15 p2531 N85-25610
Microstructures and properties of rapidly solidified alloys
[NASA-CR-172377] 16 p2746 N85-26961
Rapid solidification of candidate ferritic steels
[DE85-008596] 16 p2750 N85-26971
Use of principle of local equilibrium for assessing diffusional supersaturation during solidification of alloys
[BLL-BISI-TRANS-22487-(9022.06)]
17 p2929 N85-28077
Investigation for low-cost permanent magnets
[AD-A154367] 19 p3260 N85-30212
Consolidated fuel reprocessing program
[DE85-008750] 19 p3366 N85-30871
Linking R and D to problems experienced in solids processing
[AD-A154238] 19 p3380 N85-30968
Concept development evaluation for John Deere/UA STS middeck experiment location
[NASA-CR-171541] 20 p3397 N85-31071
Directional solidification of an eutectic Bi-MnBi alloy
[BLL-M-36270-(5828.4)] 20 p3430 N85-31275
MPS solidification model. Analysis and calculation of macrosegregation in a casting ingot
[NASA-CR-171589] 21 p3566 N85-32178
Polyethylene solidification of low-level wastes
[DE85-012568] 22 p3843 N85-33799
Approximate determination of the extent of the solid-liquid zone
[BLL-M-35829-(5828.4)] 23 p3914 N85-34251
Microstructures in rapidly solidified Ni-Mo alloys
[NASA-TM-87100] 23 p3915 N85-34266
Method for making a low density polyethylene waste form for safe disposal of low level radioactive material
[DE85-006401] 23 p3920 N85-34292

SOLIDIFIED GASES
Understanding the high pressure properties of molecular solids and molecular surfaces deposited on hetrogeneous substrates
[NASA-CR-174262] 07 p1047 N85-16649

SOLIDS
NT SOLIDIFIED GASES
NT THREE DIMENSIONAL BODIES
Synthesis and characterization of advanced materials
[PB84-215326] 01 p0025 N85-10156
13C and 1H NMR (Nuclear Magnetic Resonance) studies of solid polyolefines
[AD-P003909] 01 p0032 N85-10195
NMR (Nuclear Magnetic Resonance) of solid biopolymers
[AD-P003912] 01 p0032 N85-10198
Halfspace representations of extrusions, solids of revolution and pyramids
[DE84-015005] 01 p0104 N85-10700
Finite element analysis of thermoelasticity problems
02 p0208 N85-11369
Mechanism of brittle heat fracture of inhomogeneous solids by high temperature gas jets
02 p0265 N85-11731
Nonlinear acoustics
[AD-A145580] 02 p0276 N85-11796
Constitutive features of solids at shock-wave loading rates
[DE84-015715] 03 p0362 N85-12325
On the co-variant formulation of the law of motion of passive particles in a field of turbulence
[REPT-564] 03 p0377 N85-12407
EXAFS and Moessbauer study of small metal clusters isolated in rare-gas solids
[DE84-015976] 04 p0470 N85-12994
Diffusion of gases in porous solids: Simulation and measurements
[DE84-016292] 04 p0500 N85-13191
High resolution photoacoustic and photothermal imaging 05 p0723 N85-14649
Laser excitation of coupled surface electromagnetic and acoustic waves and of static structures in solids
05 p0723 N85-14652
Measurement of scattering cross sections of liquid and solid hydrogen deuterium and deuterium hydride for thermal neutrons
[DE84-014814] 05 p0727 N85-14671
The concept of solid solvent as processing aid
[AD-A146556] 06 p0771 N85-14934
Transonic flow of elastic medium past slender solid body 06 p0778 N85-14976
Controllable rotation of system of two solid bodies with elastic elements 06 p0780 N85-14988
Motion of heavy symmetric body with flexible bars about stationary point 06 p0780 N85-14989
Theory of harmonic generation of finite amplitude ultrasonic waves in solids of hexagonal symmetry
[AD-A148636] 06 p0860 N85-15465
Optics of solids (surface related) and effect of surface roughness on MOS
[AD-A148883] 07 p0946 N85-15996
A virial equation of state option for the TIGER computer program
[AD-A147490] 07 p1025 N85-16507
Structure of solids surfaces in wear situations
[AD-A148480] 08 p1188 N85-17366
NMR study on rotational fluctuation in solid hydrogen and deuterium 09 p1289 N85-18093
Spontaneous ignition of organic solids by radiant heating 09 p1289 N85-18096
Measurement and control of electrostatic charges on solids in a gaseous suspension
[DE85-001450] 09 p1291 N85-18105
USSR report: Engineering and equipment
[JPRS-UEQ-85-001] 09 p1305 N85-18200
Electromagnetic processing of materials
[AD-A148804] 09 p1311 N85-18241
Stopping powers of solids for low-energy protons
[DE85-001123] 09 p1382 N85-18693
Transport relaxation processes in supercritical fluids
[DE85-002076] 09 p1398 N85-18798
Microscopic determinations of lattice and electronic structures of solids
[DE84-017323] 09 p1399 N85-18806
Theta pinch discharges for solids vaporization and elemental chemical analysis
[DE85-002968] 11 p1733 N85-20899
Explorations into thermodynamics analogies and critical points in reference to gas-solid transport
[DE85-000816] 11 p1738 N85-20929
Photoacoustic effect and its applications
12 p1820 N85-21421
Moving nonlocal crack: Anti-plane shear case
[AD-A149996] 12 p1866 N85-21709
A study of the compatibility of an existing CFD package with a broader class of material constitutions
12 p1945 N85-22219
Division boundary in Al-B composite material with boron in contact with solid and liquid aluminum
13 p2027 N85-22704
USSR report: Engineering and equipment
[JPRS-UEQ-85-003] 13 p2042 N85-22782
Some problems in optimally designing shells of revolution 14 p2278 N85-24114
X-ray emission in heavy ion collisions
[DE85-006350] 14 p2419 N85-24927
Theory and calculations of the electronic structure of solids having directional bonding
[AD-A151062] 14 p2426 N85-24971
Energy trapping, release, and transport in three-dimensional energetic solids and molecular crystals: Theory of defects and impurities
[AD-A151071] 14 p2428 N85-24973
Chaotic dynamics of instabilities in solids
[DE85-004909] 14 p2429 N85-24978
X-ray spectroscopy of solids under pressure
[DE85-006939] 15 p2507 N85-25465
Summary of recent investigations of the mechanical properties of polycrystalline solids
[DE85-006776] 15 p2511 N85-25492
Optical monitoring of photo-acoustic pulse propagation in silicon wafers
[AD-A151333] 15 p2651 N85-26352
Secondary ion mass spectrometry studies of solids and surfaces
[AD-A151744] 16 p2745 N85-26939
Bound and free moisture studies of solid materials by FTNMR
[DE85-003227] 16 p2747 N85-26952
Numerical resolution calculation for elastic-plastic impact problems
[AD-A152292] 16 p2801 N85-27270
Transverse periodic boundary conditions in molecular dynamics with uniaxial strain shock waves
[DE85-006497] 16 p2863 N85-27656
Experiments on sorption characteristics of solid desiccant materials for solar desiccant cooling systems
[DE85-000542] 17 p2923 N85-28019
Free-form design in solid modelling
17 p3004 N85-28569
Boundary to constructive solid geometry mappings: A focus on 2-D issues 17 p3004 N85-28570
A unified representation scheme for solid geometric objects using B-splines (extended abstract)
17 p3006 N85-28585
Diffusion of gases in porous solids: Simulation and measurements
[DE85-008670] 18 p3101 N85-29196
Studies of strain rate effects in the deformation of solids by means of stress pulses and ultrasonic methods
[DE85-009463] 18 p3122 N85-29329
Resolution at its current limit: Applications of the Berkeley ARM
[DE85-009959] 19 p3274 N85-30301
Energy transfer and excimer formation in rare gas solids 19 p3374 N85-30930
Vibrational properties of disordered solids: Far infrared studies
[DE85-010400] 19 p3377 N85-30951
Linking R and D to problems experienced in solids processing
[AD-A154238] 19 p3380 N85-30968

Constitutive modeling of superalloy single crystals and directionally solidified materials
20 p3466 N85-31535

The interactions of composition and stress in crystalline solids
[PB85-179075] 20 p3473 N85-31583

Source characterization of point-like and distributed sources of acoustic emission 20 p3523 N85-31910

X-ray spectroscopy of solids under pressure
[DE85-011486] 22 p3745 N85-33213

Preliminary considerations for the gasdynamic precompression of solid molecular hydrogen
[DE85-013256] 22 p3784 N85-33445

SANCHO: A finite element computer program for the quasistatic, large deformation, inelastic response of two-dimensional solids
[DE85-011456] 22 p3829 N85-33714

Experimental technique for measuring the isentrope of hydrogen to several megabars
[DE85-014332] 24 p4095 N85-35386

Analysis of the nonlinear equations describing the elastic, thermal, and electromagnetic behavior of solids: Existence of solutions of semi-inverse problems
24 p4100 N85-35415

SOLIDS FLOW

Granular Flow Project
[DE85-010015] 19 p3270 N85-30279

Effect of nonuniform size on internal stresses in a rapid, simple shear flow of granular materials. Part 2: Multiple grain sizes
[AD-A154046] 19 p3285 N85-30373

SOLIDUS

Studies on copper alloys containing chromium on the copper side phase diagram
[NASA-TM-77752] 07 p0927 N85-15876

SOLITARY WAVES

Statistical Plasma Physics. Proceedings of the Workshop of the US-Japan Joint Institute for Fusion Theory Program
[IPPJ-669] 02 p0282 N85-11632

Stochastic property of K-dV solitons perturbed by random forces — Korteweg-Devries equation
02 p0283 N85-11643

Chaotic behavior induced by solitons in perturbed integrable systems 02 p0283 N85-11644

Investigations on low-dimensional solid state substances — solitons 03 p0426 N85-12720

Solitons and SEASAT
[AD-A148396] 08 p1176 N85-17414

Mathematical physics approaches to lightning discharge problems
[NASA-TM-86349] 08 p1187 N85-17482

Determination of gravity wave envelope solitons on surface of stratified fluid interacting with wind
14 p2334 N85-24433

Propagation of sound in matter
[AD-A151052] 14 p2416 N85-24906

Soliton energetics in extended Peierls-Hubbard models: A quantum Monte Carlo study
[DE85-005409] 14 p2429 N85-24981

Wave propagation in density stratified fluids
16 p2781 N85-27162

Coherent state description of non-topological solitons and momentum projection
[DE85-007814] 17 p3033 N85-28761

Pattern selection and instability in nonlinear wave equation: An aspect of soliton and chaos
[DE85-009578] 18 p3101 N85-29197

Electromagnetic solitary waves in magnetized plasmas
[DE85-010084] 18 p3190 N85-29788

Theory of soliton waves
[AD-A154784] 21 p3676 N85-32837

SOLITONS

U SOLITARY WAVES

SOLSTICES

Seasonal variations in Triton's atmospheric mass and composition 02 p0301 N85-11948

SOLUBILITY

Effect of toluene on the solubility of biohazardous volatile synthetic organic compounds
[AD-A145186] 01 p0018 N85-10109

An investigation of the solubility and diffusivity of chromium in gallium arsenide
[AD-A144949] 01 p0024 N85-10148

The determination of soluble and insoluble boron in steel by emission spectrometry using an inductively coupled plasma and a scanning monochromator
02 p0180 N85-11211

The behaviour of unstable surfaces: A literature review
[CFD/84/6] 02 p0199 N85-11329

Americium thermodynamic data for the EQ3/6 database
[DE84-017065] 04 p0573 N85-13656

Bicomponent flow problems in rheological fluid mechanics 05 p0635 N85-14073

Transport and relaxation processes in supercritical fluids
[DE84-006591] 05 p0731 N85-14696

Reciprocal solubility of phases in multi-component systems
[BLL-M-36003-(5828.4)] 07 p0926 N85-15870

Studies on copper alloys containing chromium on the copper side phase diagram
[NASA-TM-77752] 07 p0927 N85-15876

SPAR X technical report for experiment 76-22 directional solidification of magnetic composites
[NASA-CR-171271] 07 p0927 N85-15880

Properties of miscible polymer blends
[AD-A147090] 07 p0931 N85-15903

Transport and relaxation processes in supercritical fluids
[DE85-002079] 09 p1398 N85-18797

Transport relaxation processes in supercritical fluids
[DE85-002076] 09 p1398 N85-18798

Vapor pressure studies of the solubilization of hydrocarbons by surfactant micelles
[DE85-004319] 12 p1803 N85-21306

Alloy development, processing and characterization of devitrified titanium base microcrystalline alloys
[AD-A149609] 12 p1806 N85-21327

Application of solidification theory to rapid solidification processing
[AD-A151251] 15 p2509 N85-25480

Method for growth of crystals by pressure reduction of supercritical or subcritical solution
[NASA-CASE-NPO-15772-1] 18 p3192 N85-29800

Microstructures and mechanical properties of microalloyed medium carbon steels
19 p3238 N85-30074

Adhesive evaluation of LARC-TPI and a water-soluble version of LARC-TPI
[NASA-TM-86428] 19 p3248 N85-30136

Advanced fuel cell development
[DE85-009662] 19 p3306 N85-30497

Transport and relaxation processes in supercritical fluids
[DE85-010554] 19 p3358 N85-30816

Development of an impact- and solvent-resistant thermoplastic composite matrix, phase 3
[NASA-CR-172568] 20 p3422 N85-31239

Bubble dynamics in polymer solutions undergoing shear
[AD-A154575] 21 p3568 N85-32193

Measurements of the critical supersaturation of 0.029 to 0.035 micron radius particles at Washington, District of Columbia 21 p3649 N85-32676

Stability of two-dimensional immiscible flow to viscous fingering
[DE85-011403] 23 p3931 N85-34364

SOLUTES

Interaction of solutes with stretched polymers
[AD-A154662] 21 p3589 N85-32196

SOLUTION

Electrochemistry of polymer films not immersed in solution: Electron transfer on an ion budget
[AD-A152969] 17 p2920 N85-27998

SOLUTIONS

NT AQUEOUS SOLUTIONS
NT GAS MIXTURES
NT NUCLEAR EMULSIONS
NT PHOTOGRAPHIC EMULSIONS
NT SOLID SOLUTIONS

Dynamics of polymers in solution and melts
[AD-P003907] 01 p0032 N85-10193

NMR (Nuclear Magnetic Resonance) and macromolecular migration in a melt or in concentrated solutions
[AD-P003908] 01 p0032 N85-10194

A perturbation solution for rigid dumbbell suspensions in steady shear flow
[AD-A144876] 01 p0111 N85-10755

Factor analysis applied to a silane coupling agent on E-glass fiber system
[AD-A145687] 02 p0187 N85-11249

Thermomechanical cracking in layered media from moving friction load
[AD-A146022] 03 p0373 N85-12379

Homomonotone games and monocore solutions, revised
[AD-A146216] 03 p0413 N85-12645

Neutron scattering on macromolecular solid state materials, solutions and melts 03 p0431 N85-12747

Fatal hemorrhagic shock and acetate solutions
[AD-A146754] 07 p1014 N85-16444

On existence and uniqueness of solutions of Hamilton-Jacobi equations
[AD-A147597] 07 p1033 N85-16560

Periodic solutions of prescribed energy for a class of Hamiltonian systems
[AD-A149487] 10 p1548 N85-19764

Rheology of dissemination
[AD-A150006] 12 p1813 N85-2137

A method of calculating periodic solutions of second order dynamical systems
[AD-A149634] 12 p1920 N85-22

Influence of uncompensated solution resistance upon the evaluation of rate constants for rapid electrochemical reactions
[AD-A150657] 14 p2250 N85-22

E-beam-induced fluorescence of excimers in cryogenic solutions
[DE85-010703] 19 p3278 N85-30

Discovery of a nonpropagating hydrodynamic soliton
[AD-A155569] 21 p3582 N85-32

SPLINES. Their equivalence to collocation
[AD-A155250] 21 p3632 N85-32

SOLVATION

Solvent effects upon electrochemical kinetics: Influences of interfacial solvation and solvent relaxation dynamics
[AD-A145624] 02 p0173 N85-1115

Supersonic molecular jet study of the liquid state
[AD-A147416] 09 p1379 N85-18

SOLVENT EXTRACTION

ECUT, Energy Conversion and Utilization Technologies program: Isothermal separation processes update
[NASA-CR-175463] 10 p1433 N85-19

ECUT, Energy Conversion and Utilization Technologies program: Technical and economic assessment of processes for the production of butanol and acetone. Phase 2: Analysis of research advances
[NASA-CR-175471] 10 p1434 N85-1903

Guest molecules in coal
[DE85-010435] 19 p3226 N85-30016

Supercritical solvent extraction of lignite to form carbonaceous chars
[DE85-010159] 19 p3229 N85-30019

Novel analytical approaches to coal beneficiation
[DE85-010437] 19 p3229 N85-30021

The mobile phase in coals: Its nature and modes of release
[DE85-011696] 19 p3230 N85-30026

TRU decontamination of high-level PUREX waste by solvent extraction using a mixed octyl(phenyl)-N,N-diisobutyl-carbamoyl methylphosphine oxide/TBP/NPH (TRUEX) solvent
[DE85-010251] 19 p3235 N85-3005

Consolidated fuel reprocessing program
[DE85-010591] 19 p3358 N85-30816

Consolidated fuel reprocessing program
[DE85-008750] 19 p3366 N85-308

Method for extracting lanthanides and actinides from acid solutions by modification of Purex solvent
[DE85-005763] 23 p3909 N85-342

Separation of uranium from technetium in recovery of spent nuclear fuel
[DE85-006499] 23 p3972 N85-34

SOLVENTS

NT TETRAHYDROFURAN

Solvent effects upon electrochemical kinetics: Influences of interfacial solvation and solvent relaxation dynamics
[AD-A145624] 02 p0173 N85-1115

The concept of solid solvent as processing aid
[AD-A146556] 06 p0771 N85-14

Aspects of solvent toxicity in mixtures
[AD-P004036] 06 p0845 N85-15

Voltammetry and coulometry with immersed thin layer electrodes. Part 1: Model for effects of solution resistivity in linear sweep voltammetry
[AD-A148655] 08 p1159 N85-17

Nebulization reflux concentrator
[NASA-CASE-LAR-13254-1] 11 p1615 N85-20

Process for producing tris s(n-methylamino) methylsilane
[NASA-CASE-MFS-25721-1] 12 p1799 N85-21

Electrochemistry and electrochemical methodology in molten salts
[AD-A149613] 12 p1799 N85-21

Research to explore the feasibility of sulfolanes as electrolytic solvents for rechargeable lithium batteries
[DE85-004345] 12 p1837 N85-21

Noncontinuum solvent effects upon the intrinsic free-energy barrier for electron-transfer reactions
[AD-A150662] 14 p2250 N85-22

Investigation of the structure and dynamics of electrolytes in solvents used for primary and secondary Li-batteries
[AD-A153099] 17 p2954 N85-2

Method for growth of crystals by pressure reduction of supercritical or subcritical solution
[NASA-CASE-NPO-15772-1] 18 p3192 N85-2

Electrochemical studies in liquid crystals
[AD-A154317] 19 p3234 N85-30

Comparison of TT-F-1098 solvent-thinned block fillers with water-thinnable block fillers
[AD-A154207] 19 p3249 N85-30142
Working with flammable solvents, thinners, paints and adhesives
[HSE-TRANS-11086] 19 p3250 N85-30154
Soil extraction kit
[AD-D011736] 22 p3742 N85-33190
Rechargeable lithium-organic electrolyte battery having overcharge protection and method of providing overcharge protection for a lithium-organic electrolyte battery
[AD-D011738] 22 p3806 N85-33575
Organic solvent alteration of hydraulic properties of sedimentary rocks of low permeability: A review
[DE85-012537] 22 p3815 N85-33635
Production of butanol by fermentation in the presence of cocultures of clostridium
[NASA-CASE-NPO-16203-1] 24 p4071 N85-35227

SOMMERFELD WAVES
Image theory for a vertical electric dipole above a wire grid with square cells
[REPT-S-150] 02 p0192 N85-11286
General image theory for the Sommerfeld problem
[REPT-S-154] 02 p0193 N85-11289

SONAR
Detection, classification, and extraction of helicopter-radiated noise
[AD-A145993] 03 p0416 N85-12661
Color and grey scale in sonar displays
05 p0710 N85-14552
Research on nondestructive testing
[AD-A148375] 08 p1171 N85-17380
Technology development for unmanned untethered submersible vehicle systems
[AD-A148794] 09 p1304 N85-18190
Sonars with high noise and clutter rejection for use with adaptive robots
[AD-A151875] 15 p2543 N85-25701
An overview of stochastic signal modeling
[AD-A152144] 16 p2855 N85-27605
HERMIES-1: A mobile robot for navigation and manipulation experiments
[DE85-008852] 18 p3118 N85-29301
Effect of background/foreground color coding on detection in acoustic data displays
[AD-A154105] 19 p3352 N85-30774
The moving thermoacoustic array: A theoretical feasibility study
[AD-A154510] 21 p3699 N85-32980
Planning for VRM: Radar and sonar studies of volcanic terrains on Earth, Venus and Mars
22 p3857 N85-33884
Magnetic search system
[PB85-185106] 23 p3949 N85-34477

SONDES
NT IONOSONDES
NT RADIOSONDES
NT RAWINSONDES
Error analysis of wind determined using a VLF Omega sonde
[WSRL-0361-TM] 06 p0838 N85-15321
Cut-off lows and their influence on the weather in Switzerland
[REPT-45] 10 p1519 N85-19574

SONIC BOOMS
Correlation of predicted and measured sonic boom characteristics from the reentry of STS-1 orbiter
[NASA-TP-2475] 18 p3177 N85-29694

SONIC FLOW
U TRANSONIC FLOW

SONIC SPEED
U ACOUSTIC VELOCITY

SONOHOLOGRAPHY
U ACOUSTICAL HOLOGRAPHY

SOOT
Hot-gas cleanup for molten carbonate fuel cells-dechlorination and soot formation
[DE84-003072] 01 p0068 N85-10450
Analysis and characterization of organic carbon compounds in atmospheric particulate matter
[PB84-232636] 06 p0766 N85-14903
Mechanism of soot formation
[AD-A146817] 07 p0922 N85-15841
Investigation of fuel additive effects on sooting flames
[AD-A149154] 10 p1457 N85-19179
Ionic mechanisms of soot formation in flames
[AD-A150119] 12 p1801 N85-21297
Ideal gas thermodynamic properties for the phenyl, phenoxy, and o-biphenyl radicals
[NASA-TM-83800] 12 p1943 N85-22204
Laser diagnostic analyses of sooting flames
[AD-A150478] 13 p2017 N85-22649
A standard aircraft diffusion flame: Spectral characteristics and a feasibility study for developing an alternate calibration source for aircraft optical fire detection systems
[AD-A150231] 13 p2039 N85-22766
Effects of interactive transport and scavenging of smoke on the calculated temperature change resulting from large amounts of smoke
[DE85-006450] 14 p2378 N85-24684
Shock tube study of the fuel structure effects on the chemical kinetic mechanisms responsible for soot formation, part 2
[NASA-CR-174880] 15 p2504 N85-25444
Studies of the combustion of model fuels with low hydrogen content (pyrolysis of polycyclic aromatics-detection of soot precursors)
[DE85-005422] 15 p2521 N85-25541
An investigation into the soot production processes in a gas turbine engine
[AD-A152710] 17 p2919 N85-27992
Fuel-rich catalytic combustion: A soot-free technique for in situ hydrogen-like enrichment
[NASA-TP-2498] 20 p3423 N85-31244
An analytical and numerical model of radiation heat transfer in direct injection-type diesel combustion
24 p4092 N85-35368

SORBENTS
NT ABSORBENTS
NT ADSORBENTS
Solid sorbent air sampler
[NASA-CASE-MSC-20653-1] 11 p1636 N85-20301
Low pressure storage of methane on interlayered clays for potential vehicular applications
[DE85-006949] 16 p2758 N85-27017

SORPTION
NT ADSORPTION
NT CHEMISORPTION
Development of novel lamps for study of enhanced production of resonance by low-density mercury discharges
[DE84-016889] 05 p0632 N85-14053
Synergistic effects related to surface composition, session summary 06 p0865 N85-15495
Functional and structural changes in human erythrocyte surface after irradiation by UV waves of various wavelenights. Report 2: Adsorption of alcyan blue by external premembranous components
09 p1361 N85-18565
Drifting ice as mechanical factor in purifying and polluting hydrosphere 13 p2106 N85-23132
Evidence that resorption of bone by rat peritonal macrophages occurs in an acidic environment
15 p2612 N85-26096
Experiments on sorption characteristics of solid desiccant materials for solar desiccant cooling systems
[DE85-000542] 17 p2923 N85-28019
Permeation of mixed penetrants through glassy polymer membranes
[AD-A155605] 21 p3570 N85-32207
Biodegradation of jet fuel by aquatic microbial communities
[PB85-191971] 24 p4084 N85-35311

SORTING
U CLASSIFYING

SOT
U SOLAR OPTICAL TELESCOPE

SOUND
U ACOUSTICS

SOUND ABSORPTION
U SOUND TRANSMISSION

SOUND AMPLIFICATION
Study of optical sound generation and amplification
[AD-A147359] 07 p1039 N85-16592

SOUND BARRIER
U ACOUSTIC VELOCITY

SOUND DETECTORS
U SOUND TRANSDUCERS

SOUND FIELDS
Element methods for calculation of sound fields
[RUB-IFM-MITT-41] 05 p0726 N85-14665
Analysis of the surface load and radiated sound of a vibrating airfoil with application to the experiment of Brooks
[NASA-CR-3864] 07 p1038 N85-16590
Optical fibers with reduced pressure sensitivity to high frequency acoustic field
[AD-D011306] 07 p1043 N85-16627
An efficient numerical solution technique for wave propagation in horizontally stratified ocean environments
[AD-A148537] 08 p1190 N85-17502
Behavior of mode frequency characteristics in shallow sea with variation of P-wave veocity in bottom sediment layer and sonic velocity profile in water layer
10 p1498 N85-19457
USSR report: Physics and mathematics
[JPRS-UPM-85-001] 11 p1715 N85-20786
Problem of frequency space variation of sonic field in stratified media 11 p1715 N85-20787
The effects of internal waves on acoustic normal modes
[AD-A150235] 13 p2155 N85-23379
An overview of stochastic signal modeling
[AD-A152144] 16 p2855 N85-27605
The theoretical response of a vertical line array to wind-generated noise in shallow water
[AD-A151730] 16 p2860 N85-27638
Geoacoustic models: Washington state continental margin
[AD-A153761] 18 p3177 N85-29699
On the solution for the sound field in a semi-infinite uniform duct with sheared mean flow
20 p3523 N85-31912
Development of computer programs using the method of images to predict the sound field in a wedge overlaying a fast fluid and comparison with laboratory experiments
[AD-A154580] 21 p3670 N85-32797
The Konstantinov effect and absorption of sound in inhomogeneous media 21 p3680 N85-32861
The sound field of a moving laser-induced acoustic array (theory)
[AD-A154553] 21 p3699 N85-32981

SOUND GENERATORS
Generation of sound by a vortex point in a steady flow of slightly compressible fluid 11 p1715 N85-20789
Acoustic agglomeration methods and apparatus
[NASA-CASE-NPO-15466-1] 12 p1927 N85-22104
An electro-optic spatial light modulator for thermoelastic generation of programmably focused ultrasound
[AD-A152066] 15 p2646 N85-26323
Radiative-collision generation of sound in gases subjected to single-pulse optical excitation
21 p3689 N85-32920

SOUND HOLOGRAPHY
U ACOUSTICAL HOLOGRAPHY

SOUND INTENSITY
Average sound intensity decrease rule in irregular hydroacoustical waveguide 10 p1499 N85-19461
Research on the effect of noise at different times of day: Models, methods and findings
[NASA-CR-3888] 13 p2154 N85-23375
High-frequency acoustic variability in the arctic
[AD-A150550] 13 p2155 N85-23383
Contribution of tonal components to the overall loudness, annoyance and noisiness of noise: Relation between single tones and noise spectral shape
[NASA-CR-3892] 15 p2645 N85-26317
Acoustic propagation in a thermally stratified atmosphere
[NASA-CR-175787] 16 p2860 N85-27636
The Shock and Vibration Digest, volume 17, no. 1
[AD-A151051] 17 p2977 N85-28397
Sound intensity measurement
17 p2977 N85-28398
A study of interior noise levels, noise sources and transmission paths in light aircraft
[NASA-CR-172152] 19 p3350 N85-30766
Spectral methods for the estimation of acoustic intensity, energy density, and surface velocity using a multimicrophone probe 20 p3524 N85-31916

SOUND LOCALIZATION
Foreshortened short-wave scattering on artificial ionospheric inhomogeneities 14 p2340 N85-24468

SOUND MEASUREMENT
U ACOUSTIC MEASUREMENT

SOUND PERCEPTION
U AUDITORY PERCEPTION

SOUND PRESSURE
The acoustic pressure in a wedge-shaped water layer overlying a fast fluid bottom
[AD-A145517] 02 p0276 N85-11795
Determination of the pressure sensitivity of 1 inch condenser microphones
[PTB-AK-28] 05 p0633 N85-14058
An improved source model for aircraft interior noise studies
[NASA-CR-172517] 08 p1217 N85-17668
Effects of vane/blade ratio and spacing on fan noise, volume 1
[NASA-CR-174664] 10 p1553 N85-19791
Influence of pressure on speed of sound in single-phase region of stratifying mixtures 11 p1715 N85-20788
Wind tunnel acoustic study of a propeller installed behind an airplane empennage: Data report
[NASA-CR-177335] 13 p2154 N85-23377
Localization of sources of equivalent noise in fast cold jets, excited and nonexcited
[ISL-CO-201/83] 14 p2416 N85-24910
Wave description of sound propagation through stratified moving atmosphere 15 p2525 N85-25567

SOUND PROPAGATION
Nonlinear propagation in a depth-dependent ocean
[AD-A145079] 01 p0116 N85-10791

The acoustic pressure in a wedge-shaped water layer overlying a fast fluid bottom
[AD-A145517] 02 p0276 N85-11795
USSR report: Life Sciences: Biomedical and behavioral sciences
[JPRS-UBB-84-026] 04 p0543 N85-13457
Amiet shear layer correction with an additional temperature gradient considered: Nomograms for the correction of noise signatures from open jet wind tunnel tests
[DFVLR-MITT-84-11] 05 p0726 N85-14669
Long-distance propagation of infrasound in atmosphere near Earth's surface 06 p0825 N85-15236
Study of optical sound generation and amplification
[AD-A147359] 07 p1039 N85-16592
The Shock and Vibration Digest, volume 16, no. 10
[AD-A147586] 09 p1331 N85-18361
Sound transmission in ducts 09 p1331 N85-18362
Twenty-five sound propagation tests on the continental shelf between Long Island, New York and Cape Canaveral, Florida
[AD-A149669] 12 p1928 N85-22111
Intensity vectors of sound scattering by a spherical shell
[AD-A147847] 13 p2103 N85-23107
Noise measurement flight test: Data/Analyses, hughes 500 D/E helicopter
[AD-A148110] 14 p2219 N85-23758
Fundamental studies of structure borne noise for advanced turboprop applications
[NASA-CR-175737] 15 p2646 N85-26320
Sound propagation through directional internal wave fields
[AD-A151166] 15 p2646 N85-26321
The Shock and Vibration Digest, volume 17, no. 1
[AD-A151051] 17 p2977 N85-28397
Sound intensity measurement
17 p2977 N85-28398
Numerical evaluation of low frequency sound propagation in layered media
[AD-A152690] 17 p3028 N85-28728
Squid detection of acoustomagnetic effects
19 p3373 N85-30924
Amiet shear layer correction with an additional temperature gradient considered: Nomograms for the correction of noise signatures from open jet wind tunnel tests
[ESA-TT-897] 20 p3525 N85-31926

SOUND RANGING
High-frequency acoustic variability in the arctic
[AD-A150550] 13 p2155 N85-23383
Sonars with high noise and clutter rejection for use with adaptive robots
[AD-A151875] 15 p2543 N85-25701

SOUND TRANSDUCERS
NT ELECTROACOUSTIC TRANSDUCERS
NT HYDROPHONES
NT LOUDSPEAKERS
NT MICROPHONES
Acoustic imaging in a water filled metallic pipe — monitoring heat exchangers in nuclear power reactors
[DE84-016051] 09 p1378 N85-18665
Analysis and optimization of parameters of fanned surface acoustic wave transducers
13 p2070 N85-22934
A literature review of EMATs, with stress calculations for simple EMAT geometries
[AERE-R-11415] 15 p2642 N85-26295
Acoustooptic pulse-echo transducer system
[NASA-CR-175919] 17 p2951 N85-28224
The Shock and Vibration Digest, volume 17, no. 1
[AD-A151051] 17 p2977 N85-28397
Sound intensity measurement
17 p2977 N85-28398

SOUND TRANSMISSION
Low-frequency sound absorption measurements in air
[NASA-RP-1128] 02 p0275 N85-11789
Shear-layer correction after Amiet under consideration of additional temperature gradient. Working diagrams for correction of signals
[NASA-TM-77741] 03 p0415 N85-12654
Simple prediction of convergence zone propagation in waters around australia
[AD-A145986] 03 p0416 N85-12659
Coupling of airborne sound into the Earth
[AD-A146231] 03 p0416 N85-12663
A transmission analysis for the use of 2-4 PSK modulation in satellite broadcasting
[ESA-STM-231] 04 p0494 N85-13151
Current and current shear effects in the parabolic approximation for underwater sound channels
[AD-A147833] 07 p1039 N85-16597
Estimate of sound absorption due to magnetoelastic interactions
[AD-A148216] 08 p1218 N85-17671
The susceptibility of aeronautical navigational aids to interference from adjacent-band broadcast transmissions
[BBC-RD-1984/12] 09 p1311 N85-18234
Linear and nonlinear ultrasonic interaction on liquid-solid boundaries
[AD-A148979] 10 p1553 N85-19793
Arctic acoustic propagation model with ice scattering
[AD-A149430] 10 p1553 N85-19795
Simple detonation meter 13 p2077 N85-22971
Ice statistics and acoustic scattering in the Arctic basin
[AD-A150141] 13 p2140 N85-23289
Propagation of sound in matter
[AD-A151013] 14 p2416 N85-24907
Propagation of sound in matter
[AD-A151052] 14 p2416 N85-24908
The theoretical response of a vertical line array to wind-generated noise in shallow water
[AD-A151730] 16 p2860 N85-27638
Development of a modified time delay spectrometry technique for underwater acoustic measurements in a multipath environment
[AD-A152111] 16 p2880 N85-27639
Mobile television radio link
[AD-A152381] 17 p2948 N85-28201
Sound intensity measurement
17 p2977 N85-28398
Numerical evaluation of low frequency sound propagation in layered media
[AD-A152690] 17 p3028 N85-28728
Preliminary investigation of the performance of repeater technology for satellite sound broadcasting
[SSP/017/82] 18 p3092 N85-29137
Study of sound attenuation in sediments
[AD-A153690] 18 p3177 N85-29697
Measured acoustic properties of variable and low density bulk absorbers
[NASA-TM-87065] 19 p3351 N85-30770
Airborne sound transmission loss characteristics of wood-frame construction
[AD-A154174] 20 p3524 N85-31919
Development of computer programs using the method of images to predict the sound field in a wedge overlaying a fast fluid and comparison with laboratory experiments
[AD-A154580] 21 p3670 N85-32797
The Konstantinov effect and absorption of sound in inhomogeneous media 21 p3680 N85-32861
Propagation of sound in a layered laboratory model
[AD-A155141] 21 p3700 N85-32989

SOUND VELOCITY
U ACOUSTIC VELOCITY

SOUND WAVES
NT AERODYNAMIC NOISE
NT AIRCRAFT NOISE
NT ELECTROACOUSTIC WAVES
NT ENGINE NOISE
NT ION ACOUSTIC WAVES
NT JET AIRCRAFT NOISE
NT LAMB WAVES
NT NOISE (SOUND)
NT SONIC BOOMS
NT THERMAL NOISE
Human response to vibroacoustic environments of space vehicles
[NASA-TM-86316] 01 p0116 N85-10789
Acoustic resonator and method of making same
[DE84-014655] 01 p0116 N85-10792
Characteristics of light diffraction by two acoustic waves, one with complex frequency composition
03 p0348 N85-12243
Research in quantitative NDE techniques
[AD-A145990] 03 p0369 N85-12358
Shear-layer correction after Amiet under consideration of additional temperature gradient. Working diagrams for correction of signals
[NASA-TM-77741] 03 p0415 N85-12654
Coupling of airborne sound into the Earth
[AD-A146231] 03 p0416 N85-12663
Optoacoustic spectroscopy
[AD-A145995] 03 p0419 N85-12679
USSR report: Electronics and electrical engineering
[JPRS-UEE-84-010] 04 p0485 N85-13095
Reflection of volume waves in multilayer structures
04 p0485 N85-13097
Vibroacoustic control diagnostics of selected machines based on research on the slide bearing of an automobile engine and the alternator
[ISSN-0208-5658] 05 p0641 N85-14112
Resonant scattering of acoustic waves by elastic spherical shell in fluid 06 p0778 N85-14972
Acoustoelectric interaction in double-layer semiconductors 06 p0786 N85-15023
An extension of the Born inversion method to a depth dependent reference profile
[AD-A146469] 06 p0859 N85-15461
Theory of harmonic generation of finite amplitude ultrasonic waves in solids of hexagonal symmetry
[AD-A146638] 06 p0860 N85-15465
Research on acoustical and optical scattering, optics of bubbles, diffraction catastrophes, laser generation of sound, and shock induced cavitation
[AD-A146703] 06 p0860 N85-15466
On the long range propagation of sound over irregular terrain
[NASA-CR-3862] 07 p1038 N85-16089
Acoustic radiation from single and double ribbed circular cylindrical shells
[AD-A148771] 08 p1219 N85-17676
Radiative amplification of acoustic waves in hot stars
08 p1235 N85-17786
Computation of noise radiation from a free jet perpendicular to its axis via laser anemometry measurements
[ESA-TT-870] 09 p1379 N85-18809
Preliminary results of study of space-time variability of shallow sea on steady acoustical path
10 p1499 N85-19459
USSR report: Physics and mathematics
[JPRS-UPM-85-001] 11 p1715 N85-20786
Problem of frequency space variation of sonic field in stratified media 11 p1715 N85-20787
Phonon-impurity relaxation and acoustic wave absorption in yttrium-aluminum garnet crystals with impurities 11 p1715 N85-20790
Acoustic agglomeration methods and apparatus
[NASA-CASE-NPO-15466-1] 12 p1927 N85-22104
A stochastic-mechanical approach to acoustic pulse propagation in the deep ocean sound channel
[AD-A149598] 12 p1928 N85-22110
Nonlinear interactions between vortices and acoustic waves in a rocket combustion chamber
13 p1999 N85-22533
Generation of longitudinal acoustic waves by modulated helicon waves — nonlinear steady state waves in metals
13 p2090 N85-23049
Intensity vectors of sound scattering by a spherical shell
[AD-A147847] 13 p2103 N85-23107
Numerical results of acoustic radiation, transmission and reflection of steel plate in water
[AMTE(N)-TM-84037] 13 p2155 N85-23376
Properties of materials using acoustic waves
[AD-A150485] 13 p2155 N85-23382
Coupling between velocity oscillations and solid propellant combustion
[AD-A151081] 14 p2247 N85-23927
Generation and development of small-amplitude disturbances in a laminar boundary layer in the presence of an acoustic field
[NASA-TM-77826] 14 p2299 N85-24237
Acoustic radiation from bilaminar plates
14 p2415 N85-24903
Linear models of acoustic waves in sunspot umbrae
14 p2450 N85-25130
Effects of atmospheric stratification on dissipative acoustic and Alfven waves — solar atmosphere
14 p2453 N85-25149
Recording of acoustic wave in gaseous medium with thin-film pyroelectric transducers
15 p2525 N85-25571
Recent progress in the development and application of the parabolic equation
[AD-A151475] 15 p2637 N85-26265
Long range downwind propagation of low-frequency sound
[NASA-TM-86409] 15 p2645 N85-26316
Optical monitoring of photo-acoustic pulse propagation in silicon wafers
[AD-A151333] 15 p2651 N85-26352
An experimental investigation of two-dimensional flame-vortex interactions 16 p2744 N85-26834
Acoustic propagation in a thermally stratified atmosphere
[NASA-CR-175787] 16 p2860 N85-27636
The theoretical response of a vertical line array to wind-generated noise in shallow water
[AD-A151730] 16 p2860 N85-27638
Research and development of subsurface acoustic wave devices for sensor applications
[AD-A152197] 16 p2861 N85-27642
Chemical-acoustic interactions in combustion systems
[AD-A153857] 19 p3233 N85-30046
The acoustic mode in numerical calculations of subsonic combustion
[DE85-010788] 19 p3237 N85-30086
Dual differential interferometer
[NASA-CASE-LAR-12966-1] 19 p3271 N85-30282
Metrology and Oceanology Institutes' underwater acoustics R and D 19 p3289 N85-30394
Propagation of acoustic pulse in atmospheric waveguide 19 p3297 N85-30443

Acoustic particle separation
[NASA-CASE-NPO-155559-1] 19 p3350 N85-30765
Linear time-invariant, space-variant filters and the WKB approximation with applications to underwater acoustic signal processing
[AD-A154250] 19 p3352 N85-30775
Squid detection of acoustomagnetic effects
19 p3373 N85-30924
Optical beam deflection detection of thermal waves in opaque solids 19 p3374 N85-30927
Mean and large-scale turbulence characteristics of the noise-producing region of an acoustically excited round jet 20 p3523 N85-31911
Effects of contact area of an interface on acoustic wave transmission characteristics
[DE85-009935] 20 p3524 N85-31920
Qualitative analysis of sign-bit processing
[AD-A154776] 21 p3671 N85-32804
New approximations and findings of theory of nonlinear acoustic beams 21 p3680 N85-32863
Reflection of acoustic beam from inhomogeneous boundary 21 p3680 N85-32864
Acoustic wave scattering by round cylindrical shell reinforced with stringers 21 p3688 N85-32916
Radiative-collision generation of sound in gases subjected to single-pulse optical excitation
21 p3689 N85-32920
Iteration solution for a submerged force-driven finite cylinder
[AD-A154587] 21 p3699 N85-32982
Acoustic radiation from concentric shells containing an inner fluid
[AD-A155476] 21 p3700 N85-32991
Asymmetry of diffraction orders with light diffraction at surface acoustic wave 22 p3782 N85-33431
A comparison of multipath arrival structures observed in the presence of a surface duct with predictions obtained using classical ray techniques and the parabolic equation method
[AD-A156024] 24 p4145 N85-35696
Search for acoustic signals from high energy cascades
[HE-7.1-1] 24 p4213 N85-36155
Experimental investigation of radiative-acoustic effects in the water by the thermodynamical conditions of Dumand
[HE-7.1-2] 24 p4213 N85-36156
Acoustic detection of air shower cores
[HE-7.1-4] 24 p4213 N85-36158
SOUNDERS
U SOUNDING
SOUNDING
NT ACOUSTIC SOUNDING
NT ATMOSPHERIC SOUNDING
NT BALLOON SOUNDING
NT ECHO SOUNDING
NT IONOSPHERIC SOUNDING
NT MICROWAVE SOUNDING
NT ROCKET SOUNDING
NT SATELLITE SOUNDING
On the Apollo subsatellite evidence for a lunar core
04 p0581 N85-13714
NOAA/NASA joint simulation of AMTS and HIRS
05 p0682 N85-14384
ECMWF/NMC/GLAS joint simulation study
05 p0682 N85-14385
Remote sounding of fields in feed radiators of multi-element antenna system with allowance for interaction with sounding device
06 p0790 N85-15047
Khibiny experiment described
07 p0961 N85-16230
Preliminary results of the oceanographic cruise of USCGC NORTHWIND to the Greenland Sea
[AD-A149802] 12 p1896 N85-21919
Mathematical modeling of two-frequency laser sounding of scattering media 13 p2089 N85-23045
Induction excitation of deep conducting zones
13 p2111 N85-23154
Study of resolution of deep MT soundings by means of physical model 13 p2112 N85-23155
Primary processing of experimental magnetovariation sounding data using spline functions
13 p2115 N85-23175
Disturbances in structure of lower ionosphere at terminators based on results of winde-band LW sounding 14 p2339 N85-24467
Interpretation of directional magnetotelluric soundings by analytical continuation method
14 p2343 N85-24488
High-frequency microwave observations of convective precipitation 15 p2596 N85-26000
Accuracy in determining velocity of fluid movement by Doppler method 19 p3293 N85-30419
Variability of air humidity profiles over ocean determined by lidar sounding 19 p3296 N85-30436
The transient electromagnetic depth sounding technique applied to hydrocarbons and geothermal exploration
[MITT-42] 23 p3949 N85-34476
SOUNDING ROCKETS
Space Research in Japan. National report
01 p0013 N85-10082
Rocket observations 01 p0014 N85-10084
Launch summary for 1978 - 1982 — sounding rockets, space probes, and satellites
[NASA-TM-87375] 04 p0461 N85-12924
Ultrasoft X-ray background observations of the local interstellar medium 06 p0877 N85-15571
Data analysis techniques for vehicle attitudinal, positional and experimental measurements
[AD-A147752] 08 p1188 N85-17484
A study on a medium-sized rocket with Burnout frame
[NAL-TR-821] 09 p1287 N85-18082
Research in extreme ultraviolet and far ultraviolet astronomy
[NASA-CR-174432] 10 p1570 N85-19902
Sounding rocket program Aeronomie. The payload M-I in the project MAP-WINE
[BMFT-FB-W-84-046] 12 p1790 N85-21236
Radar echoes at 2.66 and 40.92 MHz from the mesosphere, part 2.6A 21 p3619 N85-32486
Research in extreme ultraviolet and far ultraviolet astronomy
[NASA-CR-176068] 21 p3716 N85-33060
A normal incidence X-ray telescope sounding rocket payload
[NASA-CR-176169] 24 p4153 N85-35749
SOUTH AFRICA
U REPUBLIC OF SOUTH AFRICA
SOUTH AMERICA
Climate Conference for Latin America and the Caribbean
[WMO-632] 07 p1000 N85-16352
Review of climate problems in Latin America and the Caribbean 07 p1001 N85-16354
Climate and climate data. Report on the workshop held in Brasilia (Argentina) from 11-15 April 1983
07 p1001 N85-16357
The climate in food production in Latin America
07 p1001 N85-16359
The ocean and the dynamics of the tropical atmosphere; its possible predicability 07 p1002 N85-16366
Climatological information and water resources
07 p1002 N85-16367
Energy and climate: Problems in Latin America
07 p1003 N85-16375
Education and training for the climate related activities in Latin America and the Caribbean
07 p1004 N85-16379
Droughts and floods in South America due to the 1982-83 El Nino-southern oscillation episode
[INPE-3408-PRE/677] 09 p1357 N85-18535
Some aspects of atmospheric circulation near South America and interactions with the Antarctic regions
[INPE-3308-PRE/618] 10 p1515 N85-19561
Meridional penetration of frontal systems in South America and its relation to organized convection in the Amazon
[INPE-3407-PRE/676] 10 p1518 N85-19572
El Nino, the capricious child 13 p2106 N85-23121
MAGSAT scalar anomaly map of South America
20 p3473 N85-31586
MAGSAT satellite magnetic anomaly map over South America 20 p3474 N85-31587
SOUTH CAROLINA
Multispectral remote sensing of inland wetlands in South Carolina: Selecting the appropriate sensor
[DE84-013951] 05 p0661 N85-14247
Analysis of data acquired by synthetic aperture radar and LANDSAT Multispectral Scanner over Kershaw County, South Carolina, during the summer season
[E85-10071] 10 p1503 N85-19485
Investigation of radiometric properties of LANDSAT-4 MSS — California, North Carolina, South Carolina, and New England 11 p1666 N85-20500
SOUTH DAKOTA
Image variance and spatial structure in remotely sensed scenes — South Dakota, California, Missouri, Kentucky, Louisiana, Tennessee, District of Columbia, and Oregon
07 p0986 N85-16265
Geodetic accuracy of LANDSAT 4 Multispectral Scanner and Thematic Mapper data — Washington, DC, California, Alabama, South Dakota, and Illinois
11 p1667 N85-20504
SOUTH WEST AFRICA
U NAMIBIA
SOUTHERN CALIFORNIA
Petrology and petrogenesis of Batholitic rocks, San Jacinto Mountains, southern California
05 p0673 N85-14322
Visibility monitoring in the southern California desert for the Department of Defense: Research on operations-limiting visual extinction, RESOLVE protocol
[AD-A146617] 06 p0835 N85-15315
Preliminary assessment of climatic change during late Wisconsin time, southwest Great Basin and vicinity, Arizona, California and Nevada
[DE85-008343] 16 p2836 N85-27488
SOUTHERN HEMISPHERE
NT ANTARCTIC REGIONS
NT ROSS ICE SHELF
Statistical tropical cyclone forecasting techniques for the Southern Hemisphere
[AD-A144752] 01 p0085 N85-10569
Analysis of diabatic heating during FGGE
05 p0683 N85-14393
Structure and energetics of medium-scale atmospheric waves in the southern hemisphere summer
05 p0685 N85-14403
An analysis of the seasonal variations in the water vapor transport fields over the Southern Hemisphere
09 p1356 N85-18531
A new NASA/MSFC mission analysis global cloud cover data base
[NASA-TP-2448] 12 p1893 N85-21878
The ARGOS contribution to the First GARP Global Experiment (FGGE) study of drifting buoys
14 p2325 N85-24371
Observation of polar aurora from the Salyut-6 space station during the great geomagnetic storm of 11-13 Apr. 1981 15 p2477 N85-25291
The South Pacafic convergence zone and energy balance of the southern hemisphere
15 p2593 N85-25960
Motivation for satellite tracking of southern elephant seals Mirounga leonina at sea 16 p2612 N85-27346
X-ray intensification at balloon altitudes of the South Atlantic magnetic anomaly in association with geomagnetic activity
[INPE-3469-PRE/712] 16 p2827 N85-27437
Mechanistic experiments to determine the origin of Southern Hemisphere stationary waves
18 p3143 N85-29461
Quasi stationary states in the Southern Hemisphere
18 p3144 N85-29465
Trends in the Southern Hemisphere
18 p3144 N85-29466
Structure and energetics of medium-scale atmospheric waves in the Southern Hemisphere
20 p3489 N85-31685
SOUTHERN SKY
Dark cloud and globule distribution for galactic longitudes 230 to 360 degrees 06 p0878 N85-15575
Documentation for the machine-readable version of the Cape Photographic Durchmusterung (CPD)
[NASA-TM-87442] 14 p2439 N85-25050
SOVIET SATELLITES
NT COSMOS SATELLITES
NT COSMOS 936 SATELLITE
NT COSMOS 1129 SATELLITE
NT INTERCOSMOS SATELLITES
NT PROGNOZ SATELLITES
NT VENERA SATELLITES
NT VENERA 11 SATELLITE
SOVIET SPACECRAFT
NT LUNIK LUNAR PROBES
NT SALYUT SPACE STATION
NT SOYUZ SPACECRAFT
Cloud cover sampling capability of various satellite combinations for ISCCP 01 p0073 N85-10484
French, Soviets decide to launch Sigma space telescope 03 p0341 N85-12191
The Venus Balloon Project 10 p1465 N85-19243
List of recent Soviet space launches
13 p1985 N85-22457
List of recent Soviet space launches
15 p2489 N85-25361
East Europe report: Science and technology
[JPRS-ESA-84-016] 15 p2533 N85-25624
Flight tests of experimental shuttle craft described
15 p2533 N85-25625
Substorms in energetic radiation belt particles according to data from Meteor artificial Earth satellite
16 p2719 N85-26788
SOVIET UNION
U U.S.S.R.
SOYBEANS
Variation in spectral response of soybeans with respect to illumination, view, and canopy geometry
[E85-10040] 07 p0982 N85-16241
Shortwave infrared detection of vegetation
[E85-10064] 08 p1174 N85-17402
Effect of elevated atmospheric CO2 on plant communities
[DE85-001810] 11 p1678 N85-20576

Mechanical stress regulation of plant growth and development 15 p2610 N85-26087

Modeling the backscattering and transmission properties of vegetation canopies
[E85-10099] 16 p2809 N85-27320

SOYUZ SPACECRAFT

Vitamin metabolism in cosmonauts following short-term flights 01 p0091 N85-10615

Tass reports medical, materials studies aboard Salyut-7 02 p0158 N85-11071

The space flight of the Soviet-Indian crew
[NASA-TM-77615] 12 p1788 N85-21226

Feoktistov says manned lunar, Mars flights lack justification 13 p1985 N85-22452

SPACE ADAPTATION SYNDROME

Physiological considerations of artificial gravity
11 p1645 N85-20366

Prediction of the space adaptation syndrome
11 p1693 N85-20646

Space adaptation syndrome: Incidence and operational implications for the space transportation system program
11 p1695 N85-20655

Shuttle operational test and scientific investigations
14 p2394 N85-24748

SPACE BASED RADAR

Development concerns for satellite-based air traffic control surveillance systems 14 p2230 N85-23816

Measurement of ocean surface currents from space with multi-frequency microwave radars
15 p2539 N85-25672

Primary propulsion of electrothermal, ion and chemical systems for space-based radar orbit transfer
[NASA-TM-87043] 17 p2916 N85-27972

SPACE BASES

NT SPACE COLONIES

Aerojet advanced engine concept
08 p1107 N85-16999

Opening up the future in space with nuclear power
[DE85-002411] 11 p1727 N85-20862

SPACE BIOLOGY

U EXOBIOLOGY

SPACE CAPSULES

Numerical analysis of the 3-dimensional inviscid hypersonic flow around capsule-type bodies by the alternate directional implicit method
[NAL-TR-799] 01 p0002 N85-10012

SPACE CHARGE

Method of splitting for solution of problems in semiconductor physics 02 p0265 N85-11736

Intense non-relativistic cesium ion beam
[DE84-012575] 04 p0560 N85-13566

In-line beam current monitor
[DE84-014054] 04 p0560 N85-13567

Space charge, interfacial kinetics, and electrical response of condensed matter
[AD-A146364] 06 p0765 N85-14893

Low frequency noise in oscillator with limited space-charge accumulation 06 p0786 N85-15024

Measurement of proton autoneutralization potential
[DE85-001752] 06 p0865 N85-15501

Close-spaced high temperature Knudsen flow
[AD-A148477] 08 p1178 N85-17424

Force balance limiting current for charged particle beams
[DE84-016976] 09 p1381 N85-18685

Calculations pertaining to the design of a prebuncher for a 150-MeV electron linear accelerator 3. Comparisons with experimental data
[DE85-002866] 11 p1724 N85-20844

Statistical phenomena in particle beams
[DE85-001050] 12 p1929 N85-22118

Simulation of space charge effects in particle accelerators
[DE85-001626] 12 p1929 N85-22120

High energy facilities advanced projects: Intrabeam scattering for a beam of gold ions
[DE85-000887] 12 p1941 N85-22192

Discharge pulse phenomenology
13 p1995 N85-22509

Effect of space-charge field on output characteristics of O-type oscillators with distributed interaction
13 p2089 N85-23043

Measuring methods of atmospheric electric elements at the Earth's surface during snowfall and investigation of these relationships 15 p2581 N85-25920

Optically triggered transferred-electron device microwave burst and single pulse generators
[AD-D011614] 16 p2778 N85-27141

The design of megawatt gyrotrons
[DE85-007892] 17 p3032 N85-28754

Numerical solutions of the potential distribution within the vacuum region of the FEATRON
[AD-A153683] 18 p3178 N85-29705

A collective interaction klystron specification
[AD-D011704] 19 p3255 N85-30186

Quenching of the beam-plasma instability by 3-D spectra of large scale density fluctuations
[NASA-CR-175969] 19 p3369 N85-30897

Development of power system measurements
[PB85-182582] 20 p3450 N85-31420

Preliminary investigation of dispersion of pollutants in model building wake flows using bipolar space charge
[IC-AERO-84-04] 20 p3487 N85-31671

Electron photoejection in carbanions
[DE85-011747] 23 p3911 N85-34230

Repetitive pulse accelerator technology for light ion inertial confinement fusion
[DE85-012030] 23 p3962 N85-34693

Numerical studies of high current beam compression in heavy ion fusion
[DE85-011674] 24 p4158 N85-35783

Relation between field energy and RMS emittance in intense particle beams
[DE85-012655] 24 p4159 N85-35784

SPACE COLONIES

Feoktistov discusses need for space colonization
13 p1985 N85-22454

Our future in the cosmos: Space
14 p2432 N85-24996

Controlled Ecological Life Support Systems (CELSS)
15 p2688 N85-26604

Historical perspective on the Moon base: The British perspective
[DE85-005905] 17 p2907 N85-27925

SPACE COMMERCIALIZATION

Second Symposium on Space Industrialization — space commercialization
[NASA-CP-2313] 02 p0149 N85-11011

Non-US approaches to space commercialization
02 p0150 N85-11012

Legal considerations and cooperative opportunities for space commercial activities 02 p0150 N85-11013

Financial issues for commercial space ventures: Paying for the dreams 02 p0150 N85-11014

Space industrialization: A national perspective
02 p0150 N85-11015

Land remote sensing commercialization: A status report 02 p0151 N85-11024

Space America's commercial space program
02 p0152 N85-11027

Fluids Experiment Apparatus (FEA)
02 p0155 N85-11048

Commercializing the transfer orbit stage
02 p0155 N85-11049

Space commercialization: Analysis of R and D investments with long time horizons
02 p0155 N85-11052

Advances in electrophoretic separations
02 p0156 N85-11054

Opportunities for commercial organizations
02 p0156 N85-11055

Doing business in space: How to get there from here
02 p0156 N85-11057

Initiatives to promote space commercialization
[GPO-37-551] 02 p0156 N85-11058

Statement of Hon. James M. Beggs, Administrator, NASA, Washington, DC 02 p0156 N85-11059

International cooperation and competition in space
[GPO-38-001] 02 p0295 N85-11911

International cooperation and competition in space. Introduction 02 p0295 N85-11912

Statement of Kenneth S. Pedersen, Director, International Affairs Division, National Aeronautics and Space Administration 02 p0295 N85-11913

Commercial Space Launch Act
[GPO-39-613] 04 p0578 N85-13690

Land Remote-Sensing Commercialization Act
[S-REPT-98-458] 05 p0654 N85-14201

Civilian space stations and the US future in space
[OTA-STI-241] 07 p0914 N85-15781

Issues and findings 07 p0914 N85-15782

Space infrastructure 07 p0914 N85-15783

Toward a goal-oriented civilian space program
07 p0914 N85-15786

Commerce Lab: Mission analysis and payload integration study
[NASA-CR-171272] 08 p1104 N85-16981

International cooperation and competition in civilian space activites
[OTA-ISC-240] 08 p1231 N85-17750

Commerce lab: Mission analysis and payload integration study
[NASA-CR-174381] 10 p1426 N85-18993

West Europe report: Science and technology
[JPRS-WST-85-004] 10 p1460 N85-19204

Commercial space: Europe should have independent strategy 10 p1460 N85-19205

Status of the National Space Transportation System
11 p1712 N85-20772

Commercial space launches
[S-REPT-98-656] 12 p1788 N85-21225

The Ariane launch vehicle is the key of the Europeans to the space market 17 p2908 N85-27901

International space research perspectives of commercialization for German industry
[NASA-TM-77657] 19 p3222 N85-29979

Commerce Lab: Mission analysis payload integration study. Appendix A: Data bases
[NASA-CR-176016] 19 p3224 N85-29980

Insurance and the commercialization of space
[S-PRT-99-18] 20 p3397 N85-31074

Study to encourage and facilitate industrial investment and involvement in space
[NASA-CR-176152] 23 p3898 N85-34147

SPACE COMMUNICATION

NT INTERPLANETARY COMMUNICATION

NT SPACECRAFT COMMUNICATION

JPL highlights, 1983
[NASA-CR-175558] 12 p1951 N85-22256

Interkosmos program of space communication development 15 p2528 N85-25595

Meteorological factors in Earth-Satellite propagation
[NASA-CR-175764] 16 p2769 N85-27090

The Telecommunications and Data Acquisition Report
[NASA-CR-175842] 16 p2770 N85-27094

Synchronizing heavily encoded data in bad weather
16 p2770 N85-27099

A review of tropospheric refraction effects on Earth-to-satellite systems 18 p3107 N85-29236

Interpolation problems in meteor radar analysis, part 7.6A 21 p3626 N85-32529

SPACE COOLING (BUILDINGS)

Thermal energy storage
[DE85-001492] 09 p1344 N85-18454

Experimental testing of cooling by low pressure adsorption in a zeolite
[DE85-007509] 16 p2716 N85-26760

Onset of freezing in residential air-to-air heat exchangers
[DE85-009960] 19 p3267 N85-30259

Advanced heat pump research and development
[DE85-009540] 23 p3932 N85-34372

SPACE DEBRIS

Orbital Debris
[NASA-CP-2360] 12 p1783 N85-21188

NORAD operational system 12 p1783 N85-21189

History of satellite break-ups in space
12 p1783 N85-21190

NORAD's PARCS small satellite tests (1976 and 1978) 12 p1783 N85-21191

Manmade orbital debris studies at NASA Langley
12 p1783 N85-21192

NASA/JSC orbital debris study: Debris model
12 p1783 N85-21193

Proposed preliminary design criteria model environment for the 1990's 12 p1784 N85-21194

Assessment of satellite collision hazards by simulated sampling in space 12 p1784 N85-21195

A model for the evolution of on-orbit manmade debris environment 12 p1784 N85-21196

Geosynchronous satellite collision avoidance
12 p1784 N85-21197

In situ orbital debris experiment concepts
12 p1784 N85-2119

Preliminary design of an Earth-based debris detection system using current technology and existing installations 12 p1784 N85-2119

Use of ground radar to detect reentering debris
12 p1784 N85-2120

Particle size, number, composition and velocity from solid rocket motors 12 p1785 N85-2120

Hypervelocity impacts on Skylab 4/Apollo windows
12 p1785 N85-2120

Survey of probable micrometer-sized Earth-orbital debr fragments in the NASA-JSC cosmic dust samp collection 12 p1785 N85-2120

Impacts on Explorer 46 from an Earth orbi population 12 p1785 N85-2120

In-situ detection of micron-sized dust particles near-Earth space 12 p1785 N85-2120

Hypervelocity impact investigations and meteor shielding experience related to Apollo and Skylab
12 p1785 N85-212

Space debris protection for a reusable orbital tran vehicle 12 p1786 N85-212

Parametric analysis: SOC meteoroid and de protection 12 p1786 N85-212

Space heat rejection radiators: Meteoroid/de consideration 12 p1786 N85-212

A remotely controlled orbiting retriever
12 p1786 N85-21

The international environment UNISPACE '82 and ITU: A relationship between orbit-spectrum reso allocation and orbital debris 12 p1787 N85-21

Orbital debris policy issues: Battelle involvement some personal observations 12 p1787 N85-21

Considerations for policy on man-made debris propagation control 12 p1787 N85-21219
Environment definition, large particles 12 p1787 N85-21220
Modeling 12 p1787 N85-21221
Measurements 12 p1787 N85-21222
Environment definition, small particles, diameter less than or equal to 1 MM 12 p1788 N85-21223
Spacecraft hazard and shielding requirements 12 p1788 N85-21224
Debris impact on Earth-orbiting spacecraft 12 p1948 N85-22234
Analysis of space station operations in the space debris environment [AD-A151872] 15 p2493 N85-25380
What we know about Mars (but otherwise wouldn't) if it is the shergottite parent body 15 p2682 N85-26565
Procedure for estimating orbital debris risks [NASA-TP-2507] 22 p3738 N85-33169

SPACE DENSITY
Probe of the nearby interstellar medium by the vacant line of sight to Beta CMa 06 p0874 N85-15551
Local interstellar extinction with an emphasis on uvby beta results 06 p0875 N85-15559
The dependence of interstellar element depletions on mean space density 11 p1749 N85-20998
X-ray gauge measures areal density variations as small as 0.1% [DE85-003774] 12 p1854 N85-21629
Investigating statistical characteristics of atmospheric background brightness and star background density in equatorial region of celestial sphere 15 p2478 N85-25298

SPACE DIVERSITY
U RECEPTION DIVERSITY

SPACE ENVIRONMENT
U AEROSPACE ENVIRONMENTS

SPACE ENVIRONMENT SIMULATION
NT WEIGHTLESSNESS SIMULATION
Distortional measurement of antennas under space simulation conditions by means of holography 05 p0625 N85-14005
Spontaneous motility of goldfish in absence of terrestrial zeitgebers: Space flight simulation in a mine 05 p0689 N85-14432
Electrostatic wave observation during a space simulation Beam-Plasma-Discharge (BPD) [NASA-CR-174286] 07 p1045 N85-16639
Space environment simulation to test satellite thermal control coatings, volume 1 [CERT-4128-VOL-1] 08 p1109 N85-17012
Space environment simulation to test satellite thermal control coatings. Volume 2: Annex 1 [ESA-CR(P)-1870-VOL-2] 08 p1109 N85-17013
Space environment simulation to test satellite thermal control coatings. Volume 2: Annexes 2, 3, 4 [ESA-CR(P)-1870-VOL-3] 08 p1109 N85-17014
Giotto solar array: Design, manufacture and test 13 p2008 N85-22589
Survival testing of silicon solar modules 13 p2009 N85-22602
Measurements of integral yields of charged secondary particles using neutral beams simulating a cometary fly-by — Giotto mission 14 p2244 N85-23908
ESABASE extension to spacecraft charging analysis. Phase 1: NASCAP software (VAX version) [ESA-CR(P)-1968] 15 p2493 N85-25381
Human productivity experience and undersea habitat design 18 p3159 N85-29563
Experiences with neutral buoyance testing mockups 18 p3159 N85-29571
Space-flight simulations of calcium metabolism using a mathematical model of calcium regulation [NASA-CR-171883] 19 p3328 N85-30621
Measurement of material damping in a simulated space environment 20 p3397 N85-31070
European Space Tribology Laboratory: Facilities, services, capabilities [ESA-BR-12] 20 p3398 N85-31080
The use of perfluoroether lubricants in unprotected space environments 22 p3797 N85-33523
Effects of space radiation on advanced semiconductor devices. Part 3: Further cosmic ray simulation studies of single event upsets and latch-up in CMOS memories [AERE-G-3368-PT-3] 22 p3848 N85-33833
DMSK: A practical 2400-bps receiver for the mobile satellite service: An MSAT-X Report [NASA-CR-176194] 24 p4086 N85-35324

SPACE ENVIRONMENTAL LUBRICATION
U SPACECRAFT LUBRICATION

SPACE ERECTABLE STRUCTURES
Conceptual design and evaluation of selected Space Station concepts: Executive summary [NASA-TM-87382] 02 p0167 N85-11128
Conceptual design and evaluation of selected Space Station concepts, volume 1 [NASA-TM-87383] 02 p0168 N85-11129
Conceptual design and evaluation of selected Space Station concepts, volume 2 [NASA-TM-87384] 02 p0168 N85-11130
Definition of technology development missions for early space stations: Large space structures [NASA-CR-171209] 03 p0323 N85-12084
Large-diameter astromast development [NASA-CR-171201] 03 p0342 N85-12200
Large spaceborne antenna reflectors using inflatable space rigidized structures 05 p0625 N85-14004
Development of a foldline concept for automatic refolding of a flexible blanket (folding analysis) — spaceborne solar generators [ESA-CR(P)-1933] 08 p1179 N85-17428
Ground test article for deployable space structure systems [NASA-CR-171301] 10 p1429 N85-19011
Variable geometry truss concept [REPT-614] 12 p1865 N85-21697
New concepts in deployable beam structures 14 p2232 N85-23832
Space Station structures 14 p2232 N85-23835
Verification for large space structures 14 p2232 N85-23836
MSFC data analysis of the SAFE/DAE experiment 14 p2233 N85-23843
Langley Research Center photogrammetric measurements of solar array dynamics: Preliminary results 14 p2233 N85-23844
Diffraction analysis of mesh deployable reflector antennas 14 p2235 N85-23854
Assembly Concept for Construction of Erectible Space Structure (ACCESS) neutral buoyancy testing results 14 p2236 N85-23862
Definition of technology development missions for early space stations: Large space structures [NASA-CR-171446] 15 p2476 N85-25281
Construction in space 15 p2484 N85-25328
Construction in space [NASA-TM-77630] 15 p2492 N85-25374
Deployable controllable geometry truss beam [NASA-TM-86366] 17 p2909 N85-27934
Solar array flight experiment [NASA-TM-86506] 17 p2909 N85-27935
Application of the ADAMS program to deployable space truss structures [NASA-CR-177927] 19 p3284 N85-30366

SPACE EXPLORATION
NT VIKING MARS PROGRAM
International cooperation and competition in space [GPO-38-001] 02 p0295 N85-11911
Statement of Kenneth S. Pedersen, Director, International Affairs Division, National Aeronautics and Space Administration 02 p0295 N85-11913
Statement of Otho E. Eskin, Director, Office of Advanced Technology, Department of State 02 p0295 N85-11914
Statement of John H. McElroy, Assistant Administrator for Environmental Satellite, Data and Information Services, National Oceanic and Atmospheric Administration 02 p0295 N85-11915
International cooperation and competition in civilian space activities, summary, appendix 1 02 p0295 N85-11916
Space research and the new approach to the mechanics of fluid media in cosmos [TRITA-EPP-84-04] 03 p0447 N85-12844
Mission science value-cost savings from the Advanced Imaging Communication System (AICS) [NASA-CR-174170] 04 p0458 N85-12905
Interstellar mission 04 p0459 N85-12916
NASA's SESAC report on research and analysis in space and Earth sciences 04 p0579 N85-13697
Man in Space: National Historic Landmark Theme Study [PB85-107233/GAR] 07 p0911 N85-15766
Title 2: National Commission on Space (Public Law 98-361) 07 p0915 N85-15791
Reliable software design for avionics and space applications 08 p1065 N85-16751
Spanish language equivalents for a glossary of terms used in the field of space exploration [NASA-TM-87403] 08 p1229 N85-17739
Opening up the future in space with nuclear power [DE85-002411] 11 p1727 N85-20862
A new look at the planets — space probes [AERONOMICA-ACTA-37-1984] 11 p1765 N85-21096
JPL highlights [NASA-CR-175517] 11 p1767 N85-21102
JPL highlights, 1983 [NASA-CR-175558] 12 p1951 N85-22256
Planetary cartography in the next decade (1984 - 1994) [NASA-SP-475] 12 p1960 N85-22323
Activities of the Jet Propulsion Laboratory, 1 January - 31 December 1983 [NASA-CR-175555] 13 p2167 N85-23447
Planetary geology in the 1980s [NASA-SP-467] 13 p2169 N85-23457
Our future in the cosmos: Space 14 p2432 N85-24998
Cometary Astrometry [NASA-CR-175660] 14 p2435 N85-25015
MBB/Erno's views, future plans in aerospace activities 15 p2531 N85-25609
Analysis of the Gran Desierto, Pinacte Region, Sonora, Mexico, via shuttle imaging radar [NASA-CR-175711] 15 p2582 N85-25927
The 1985 long-range program plan [NASA-TM-87464] 15 p2664 N85-26440
Sixteenth Lunar and Planetary Science Conference. Press abstracts [NASA-CR-175692] 15 p2680 N85-26548
USSR report: Space [JPRS-USP-85-004] 16 p2717 N85-26772
Forecasts on long-range development of space programs 16 p2727 N85-26830
US said to seek military advantage in space 16 p2727 N85-26831
East Europe report: Science and technology [JPRS-ESA-85-019] 16 p2767 N85-27077
International cooperation in space exploration 16 p2768 N85-27079
East-West cooperation in outer space [S-HRG-98-1064] 16 p2879 N85-27767
New ESA director on space station, military space 18 p3066 N85-28962
DFVLR study recommends European independence in space systems 18 p3088 N85-29111
Swedish space program includes research satellites 18 p3088 N85-29113
Gas chromatography: Possible application of advanced instrumentation developed for solar system exploration to space station cabin atmospheres 18 p3157 N85-29551
The human role in space (THURIS) 18 p3158 N85-29557
Space ventures and society long-term perspectives [NASA-CR-176012] 19 p3379 N85-30963
Geophysical interpretation of Venus gravity data [NASA-CR-176063] 20 p3547 N85-32071
Far travelers: The exploring machines [NASA-SP-480] 22 p3731 N85-33126
A spacefaring people: Perspectives on early spaceflight [NASA-SP-4405] 23 p4056 N85-35142
Space science and exploration: A historical perspective 23 p4056 N85-35143
The next assignment: The state of the literature on space 23 p4057 N85-35146
The idea of space exploration 23 p4057 N85-35150

SPACE FLIGHT
NT HYPERSONIC REENTRY
NT INTERPLANETARY FLIGHT
NT INTERSTELLAR TRAVEL
NT LONG DURATION SPACE FLIGHT
NT MANNED SPACE FLIGHT
NT SPACE SHUTTLE MISSION 31-C
NT SPACE SHUTTLE MISSION 41-B
NT SPACE SHUTTLE MISSION 41-C
NT SPACE SHUTTLE MISSION 41-G
NT SPACE SHUTTLE MISSION 51-A
NT SPACE SHUTTLE MISSION 51-C
NT SPACE SHUTTLE MISSIONS
NT SPACECRAFT REENTRY
NT VIKING MARS PROGRAM
Vitamin metabolism in cosmonauts following short-term flights 01 p0091 N85-10615
Development of space instrumentation of Intercosmos member countries 02 p0163 N85-11106
Research and technology [NASA-TM-86321] 02 p0305 N85-11973
The human role in space. Volume 1: Executive summary [NASA-CR-171223] 04 p0546 N85-13473
BDLI memorandum on the future of space flight in the Federal Republic of Germany [NASA-TM-77624] 07 p0911 N85-15765
Space motion sickness monitoring experiment: Spacelab 1 11 p1695 N85-20654
Parameters of carbohydrate metabolism and blood serum enzyme activity after short-term spaceflights 12 p1903 N85-21951
Second Soviet-French Symposium on Space Cytology 14 p2386 N85-24699

Food service and nutritional needs
14 p2394 N85-24744

NASA Space Biology Program: 9th Annual Symposium
[NASA-CP-2336] 15 p2605 N85-26054

Effects of weightlessness of Aurelia Ephyra differentiation and statolith synthesis
15 p2605 N85-26056

A detailed analysis of the erythropoietic control system in the human, squirrel, monkey, rat and mouse
[NASA-CR-171879] 15 p2614 N85-26107

Aerosol deposition along the respiratory tract at zero gravity: A theoretical study
[DE85-006703] 15 p2619 N85-26136

Crystal growth from the vapor in low gravity environments
[DE85-009828] 18 p3195 N85-29816

Flow cytometry for health monitoring in space
[DE85-009572] 19 p3329 N85-30625

Maximum likelihood estimation with emphasis on aircraft flight data 20 p3417 N85-31208

Microorganisms in space flight
23 p3951 N85-34490

SPACE FLIGHT FEEDING

Feasibility of producing a range of food products from a limited range of undifferenitiated major food components
[NASA-CR-177329] 07 p1020 N85-16473

Characterization of heat transfer in nutrient materials — space flight feeding
[NASA-CR-171841] 08 p1199 N85-17551

Self-charging metering and dispensing device for fluids
[NASA-CASE-MSC-20275-1] 12 p1848 N85-21595

Food Service and Nutrition for the Space Station
[NASA-CP-2370] 14 p2393 N85-24733

The context for food service and nutrition in the space station 14 p2393 N85-24734

Food service and nutritional needs
14 p2394 N85-24744

Psychobiology and food perception
14 p2394 N85-24745

SPACE FLIGHT STRESS

Distinctions of SPF rats used in experiments aboard biosatellites 07 p1012 N85-16427

Research opportunities in human behavior and performance
[NASA-CR-175473] 10 p1529 N85-19640

Physiological considerations of artificial gravity
11 p1643 N85-20351

Description, validation, and modification of the Guyton model for space-flight applications. Part A. Guyton model of circulatory, fluid and electrolyte control. Part B. Modification of the Guyton model for circulatory, fluid and electrolyte control
[NASA-CR-171876] 15 p2616 N85-26122

Mathematical modeling of fluid-electrolyte alterations during weightlessness
[NASA-CR-171881] 15 p2617 N85-26125

Cardiovascular effects of weightlessness
15 p2686 N85-26607

Psychological issues relevant to astronaut selection for long-duration space flight: A review of the literature
[AD-A154051] 19 p3330 N85-30627

An integrated analysis of the physiological effects of space flight: Executive summary
[NASA-CR-171892] 20 p3506 N85-31796

Mission operations requirements document for D-1 Experiment 102, Vestibular Experiments in Spacelab
[NASA-TM-87495] 21 p3557 N85-32129

Spacelab 1 hematology experiment (INS103): Influence of space flight on erythrokinetics in man
[NASA-TM-58266] 22 p3824 N85-33693

SPACE FLIGHT TRAINING

Cosmonaut Savitskaya says many women in cosmonaut training 16 p2717 N85-26774

SPACE GLIDERS

U LIFTING REENTRY VEHICLES

SPACE GLOSSARIES

Spanish language equivelents for a glossary of terms used in the field of space exploration
[NASA-TM-87403] 08 p1229 N85-17739

Space Transportation System and associated payloads: Glossary, acronyms, and abbreviations
[NASA-RP-1059-REV] 10 p1428 N85-19007

Tenth Conference of Working Group of Socialist Countries on Remote Sensing of Earth under Intercosmos Program 16 p2725 N85-26820

SPACE HABITATS

Overview: Human factors issues in space station architecture 18 p3158 N85-29558

SPACE HEATING (BUILDINGS)

Project Pellworm: Solar electric energy supply for a health center 05 p0664 N85-14266

Review of SERI solar pond work
05 p0667 N85-14289

Passive solar/Earth sheltered office/dormitory cooling season thermal performance
[DE84-016662] 05 p0669 N85-14306

Hanger heating and energy conservation manual
[AD-A147693] 07 p0910 N85-15762

FORTRAN 77 computer program for test procedure calculations of vented heaters
[PB85-109627/GAR] 09 p1305 N85-18198

Thermal energy storage
[DE85-001492] 09 p1344 N85-18454

Actual versus design performance of solar systems in the National Solar Data Network
[DE85-001190] 09 p1344 N85-18456

Optimization of design and control strategies for geothermal space heating systems
[DE85-000496] 09 p1344 N85-18458

Research on heat-exchanger corrosion
[PB85-126316] 11 p1616 N85-20184

A summary and assessment of historical reliability and maintainability data for solar hot water and space conditioning systems
[DE84-004521] 12 p1876 N85-21770

Overview of latent storage for passive solar applications
[DE85-005354] 13 p2129 N85-23249

A review of development and application of heat pump technology
[CSIR-RR-585] 14 p2300 N85-24241

Solar house, Freiburg
[BMFT-FB-T-84-249] 15 p2568 N85-25953

Foamglass solar window collector
[DE85-009197] 18 p3129 N85-29374

Solar energy for highway uses
[DE84-015653] 18 p3130 N85-29382

Onset of freezing in residential air-to-air heat exchangers
[DE85-009960] 19 p3267 N85-30259

Comparative evaluation of ground-coupled heat pumps that use solar energy
[DE85-010950] 20 p3484 N85-31649

Pagosa Springs geothermal project
[DE85-011308] 22 p3807 N85-33583

SPACE INDUSTRIALIZATION

NT SPACE MANUFACTURING
NT SPACE PROCESSING

Second Symposium on Space Industrialization — space commercialization
[NASA-CP-2313] 02 p0149 N85-11011

Space industrialization: A national perspective
02 p0150 N85-11015

Industrial use of land observation satellite systems
02 p0151 N85-11026

Space America's commercial space program
02 p0152 N85-11027

Role of Space Station: The how of space industrialization 02 p0153 N85-11036

Commercial space services 02 p0153 N85-11039

Developing commercial users of space
02 p0154 N85-11044

FRG opinion on Spacelab benefits, space station participation 15 p2532 N85-25618

Space ventures and society long-term perspectives
[NASA-CR-176012] 19 p3379 N85-30963

SPACE INFRARED TELESCOPE FACILITY

Study of application of space telescope science operations software for SIRTF use
[NASA-CR-177337] 09 p1287 N85-18060

Performance of charge-injection-device infrared detector arrays at low and moderate backgrounds
[NASA-TM-86667] 15 p2560 N85-25793

SPACE LABORATORIES

NT MANNED ORBITAL LABORATORIES
NT MANNED ORBITAL RESEARCH LABORATORIES
NT SPACELAB

Commerce Lab: Mission analysis and payload integration study
[NASA-CR-171272] 08 p1104 N85-16961

Botany facility, phase A study. Part 1: Executive summary — EURECA
[BF-DOC-10-VOL-1] 08 p1110 N85-17015

Commerce lab: Mission analysis and payload integration study
[NASA-CR-174381] 10 p1426 N85-18993

Documentation for the West German Federal Cabinet's space policy decision 17 p3051 N85-28886

Life sciences flight experiments program mission science requirements document. The first life sciences dedicated Spacelab mission, part 1
[NASA-TM-87494] 21 p3559 N85-32137

SPACE LAW

Outer space law: A problem of astronautics
[NASA-TM-77760] 07 p1055 N85-16697

Militarization of space activity in United States
15 p2488 N85-25360

SPACE LOGISTICS

Impact of lunar and planetary missions on the space station: Preliminary STS logistics report
[NASA-CR-171837] 09 p1265 N85-18072

In orbit infrastructure. Volume 1: Executive summary — European space programs
[RX011-002/84-VOL-1] 17 p2908 N85-27923

In orbit infrastructure — european space programs
[SNIAS-S/DT-24-996] 18 p3064 N85-28956

SPACE MAINTENANCE

In-orbit laser regeneration of the radiation damaged solar arrays 13 p2006 N85-22588

A concept for a mobile remote manipulator system
14 p2236 N85-23659

In orbit infrastructure. Volume 1: Executive summary — European space programs
[RX011-002/84-VOL-1] 17 p2908 N85-27923

In orbit infrastructure — european space programs
[SNIAS-S/DT-24-996] 18 p3064 N85-28956

Maintenance of long life space systems, volume 1
[MATRA-0316/DX60-VOL-1] 18 p3066 N85-28964

Maintenance of long life space systems, volume 2
[MATRA-0350/DX60-VOL-2] 18 p3066 N85-28965

DFVLR official on areas of US-FRG Space Station cooperation 18 p3086 N85-29091

Space station automation study-satellite servicing. Volume 1: Executive summary
[NASA-CR-171512] 19 p3226 N85-29999

Telepresence work system concepts
22 p3797 N85-33525

A strategy planner for NASA robotics applications
[NASA-CR-175319] 22 p3834 N85-33738

SPACE MANUFACTURING

Non-US approaches to space commercialization
02 p0150 N85-11012

Developing commercial users of space
02 p0154 N85-11044

Statement of Hon. James M. Beggs, Administrator, NASA, Washington, DC 02 p0156 N85-11059

Cosmonauts report on space welding at conference
15 p2484 N85-25320

An analysis of alternate hydrogen sources for lunar manufacture
[DE85-007234] 16 p2884 N85-27792

Low gravity exothermic heating/cooling apparatus
[NASA-CASE-MSC-25707-1] 18 p3104 N85-29214

International space research perspectives of commercialization for German industry
[NASA-TM-77657] 19 p3222 N85-29979

Kidney cell electrophoresis
[NASA-CR-171869] 20 p3496 N85-31745

Prospective uses for diffusion welding in vacuum
22 p3733 N85-33145

Space station automation study. Automation requirements derived from space manufacturing concepts. Volume 1: Executive summary
[NASA-CR-176099] 22 p3738 N85-33170

Space Station automation study. Automation requirements derived from space manufacturing concepts. Volume 2: Technical report
[NASA-CR-176100] 22 p3738 N85-33171

Investment justification of robotic technology in aerospace manufacturing. User's manual
[AD-A156193] 24 p4099 N85-35410

SPACE MECHANICS

NT ASTRODYNAMICS
NT CELESTIAL MECHANICS
NT KEPLER LAWS
NT MINIMUM VARIANCE ORBIT DETERMINATION
NT ORBITAL MECHANICS

Space Mathematics for the Preparation and Development of satellite Exploitation
[ISBN-2-85428-115-2] 14 p2395 N85-24759

The computing facilities of the Toulouse Space Center
14 p2397 N85-24770

Reference systems — in space mechanics
14 p2399 N85-24784

SPACE MISSIONS

NT ASTEROID MISSIONS
NT GIOTTO MISSION
NT SOLAR MAXIMUM MISSION

Space research benefits national economy
02 p0163 N85-11107

Preliminary analysis of space mission applications for electromagnetic launchers
[NASA-CR-174067] 03 p0321 N85-12071

Definition of technology development missions for early space stations: Large space structures
[NASA-CR-171209] 03 p0323 N85-12084

On-orbit support of DARPA-301 payload
[AD-A146897] 07 p0911 N85-15767

The investigation of tethered satellite system dynamics
[NASA-CR-171278] 07 p0912 N85-15772

SHAP (Space Nuclear Auxiliary Power) reactor overview
[AD-A146831] 07 p1041 N85-16612
An optimization method for the preliminary design of interplanetary aerobraking missions
08 p1076 N85-16822
Impact of lunar and planetary missions on the space station
[NASA-CR-171832] 08 p1106 N85-16988
Space Station needs, attributes, and architectural option study
[NASA-CR-174316] 08 p1109 N85-17011
The SIR-B science investigations plan
[NASA-CR-174282] 08 p1143 N85-17208
Impact of lunar and planetary missions on the space station: Preliminary STS logistics report
[NASA-CR-171837] 09 p1265 N85-18072
Data Requirement (DR) MA-03: Payload missions integration — Spacelab payloads
[NASA-CR-171331] 10 p1428 N85-19009
Reed-Solomon code synchronization revisited
10 p1464 N85-19234
Solar Corona Explorer: A mission for the physical diagnosis of the solar corona
[NASA-TM-87416] 10 p1572 N85-19912
Tethered satellite system project overview
11 p1642 N85-20341
Summary presentation of the Science Applications Panel 11 p1644 N85-20355
Summary presentation of the Electrodynamics Interactions Panel 11 p1644 N85-20356
Summary presentation of the Transportation Panel
11 p1644 N85-20357
Summary presentation of the technology and test panel 11 p1644 N85-20360
Results of Space Shuttle flight 41-D
[GPO-39-481] 12 p1791 N85-21243
D-1 report: The first German spacelab mission
[NASA-TM-77637] 13 p1977 N85-22402
Ignition, separation of boosters, stages in Ariane 3
14 p2289 N85-24185
Rendezvous with Saturn's rings
15 p2679 N85-26543
European space science horizon 2000
[ESA-SP-1070] 16 p2717 N85-26771
A SLAM II simulation model for analyzing space station mission processing requirements
[NASA-CR-175664] 16 p2731 N85-26853
Life sciences flight experiments program mission science requirements document. The first life sciences dedicated Spacelab mission, part 1
[NASA-TM-87494] 21 p3559 N85-32137
Space Missions for Automation and Robotics Technologies (SMART) Program
[NASA-TM-86820] 24 p4068 N85-35210

SPACE NAVIGATION
NT INTERPLANETARY NAVIGATION
Planning of navigation measurements using TD criterion for determination of movement of spacecraft by method of least squares 02 p0159 N85-11081
Autonomous navigation of USAF spacecraft
03 p0321 N85-12074
Time comparison with GPS technique and first results with the DFVLR C/A code receiver
[DFVLR-MITT-84-05] 05 p0595 N85-13794
Errors of analog of inertial coordinate systems modeled in astronavigation system 07 p0951 N85-16028
A short note on the high precision navigation of QUASAT 07 p1059 N85-16722
Technical evaluation report on the 46th Symposium of the Avionics Panel on Space System Applications to Tactical Operations
[AGARD-AR-203] 10 p1425 N85-18988
JPL highlights, 1983
[NASA-CR-175558] 12 p1951 N85-22256
The TRANSIT and Global Positioning System (GPS) systems. Precision navigation and localization
14 p2398 N85-24777
Perturbations of Kalman filtering process
15 p2480 N85-25305
Autonomous state determination for an Earth orbiting satellite using horizon and star sensors
[AD-A151827] 15 p2493 N85-25379
Method for evaluating perturbation in algorithms for solving navigational problems 16 p2718 N85-26783
Statistical regularization methods in problem of navigational determination of space vehicle orbits
16 p2719 N85-26784

SPACE OBSERVATIONS (FROM EARTH)
Preliminary design of an Earth-based debris detection system using current technology and existing installations 12 p1784 N85-21199
Use of ground radar to detect reentering debris
12 p1784 N85-21200

Solar Seismology From Space. A conference at Snowmass, Colorado
[NASA-CR-175661] 14 p2441 N85-25060
Planetary Rings. Colloquium 75 — conferences
[ISBN-2-85428-100-4] 15 p2670 N85-26473
Future observations of planetary rings from ground-based observatories and Earth-orbiting satellites
15 p2678 N85-26540
Dust emission of Comet Halley at large heliocentric distances 15 p2681 N85-26556
Activity and magnetic fields on stars from radio observations
[NASA-CR-175966] 18 p3202 N85-29861
Star formation in NGC 7538: Multi-wavelength observations and issues 20 p3545 N85-32063

SPACE PERCEPTION
Theory underlying the peripheral vision horizon device
01 p0006 N85-10048
Cognitive coordinate systems: Accounts of mental rotation and individual differences in spatial ability
[AD-A146149] 03 p0401 N85-12557
Lighting for remote viewing systems
[DE85-001698] 11 p1729 N85-20873
Texture perception and shape from texture
[AD-A154276] 19 p3336 N85-30672

SPACE PHOTOGRAPHY
U SPACEBORNE PHOTOGRAPHY

SPACE PLASMAS
NT SOLAR WIND
NT STELLAR WINDS
Convection of plasma in polar ionosphere, comparison of measurements from Cosmos-184 with model dependent on interplanetary magnetic field vector
02 p0160 N85-11086
The solar wind at 20-30 AU 02 p0301 N85-11950
Impedence measurements on a VLF multi-turn loop antenna in a space plasma simulation chamber
[AD-A145104] 04 p0492 N85-13141
Plasma flow in the near and distant geomagnetic tail
[DE84-014029] 04 p0534 N85-13415
The radiative hydrodynamics of flare loops heated by impulsive bursts of energetic electrons
05 p0745 N85-14781
A warm magnetoactive plasma in a large volume of space 06 p0878 N85-15579
Research study of space plasma boundary processes
[NASA-CR-174351] 10 p1558 N85-19823
Science Applications, part 1 11 p1643 N85-20346
Hydromagnetic precursors of interplanetary plasma burst 13 p1978 N85-22414
One-dimensional model of auroral magnetic force with longitudinal current and cyclotron heating of ions
13 p1980 N85-22424
Interplanetary shock waves during April and May of 1981 13 p1982 N85-22434
Spacecraft-environment interaction: The environmental plasma aspect 13 p1990 N85-22479
Direct measurements of severe spacecraft charging in auroral ionosphere 13 p1991 N85-22480
Polar plasmas as observed by Dynamics Explorers 1 and 2 13 p1991 N85-22483
Auroral-polar cap environment and its impact on spacecraft plasma interactions 13 p1991 N85-22484
Three-dimensional calculation of shuttle charging in polar orbit 13 p1992 N85-22486
Interactions between large space power systems and low-Earth-orbit plasmas 13 p1992 N85-22490
Self-consistent simulation of plasma interactions with secondary-emitting insulators 13 p1993 N85-22492
Surface interactions and high-voltage current collection 13 p1993 N85-22493
The PIX-2 experiment: An overview
13 p1993 N85-22494
Plasma interaction experiment 2 (PIX 2): Laboratory and flight results 13 p1993 N85-22495
Ram-wake effects on plasma current collection of the PIX 2 Langmuir probe 13 p1993 N85-22496
NASCAP simulation of PIX 2 experiments
13 p1993 N85-22497
An investigation of arc discharging on negatively biased dielectric conductor samples in a plasma
13 p1994 N85-22498
Space test program of high-voltage solar array-space plasma interactions 13 p1997 N85-22519
Preliminary investigation of the electrodynamics of a conducting tether 13 p1997 N85-22521
Extation of low-frequency resonance waves by moving conductor in space plasma 13 p2067 N85-22912
Spacecraft environment during the Giotto-Halley encounter: A summary 14 p2246 N85-23921
Observations of auroras and related plasma phenomena by the Kyokko and Jikiken satellite in IMS — EXOS-A and B satellite 14 p2354 N85-24547
Response of magnetospheric substorm activity to changes in the interplanetary magnetized plasma
14 p2357 N85-24563

Measuring electrical field fluctuations by Langmuir Double Probe Method 16 p2720 N85-26789
Geophysical responses of dynamics of solar wind transition region 16 p2721 N85-26795
Determining effective rate of plasma heating in outer equatorial ionosphere using data from ISIS-1 and ISIS-2 satellites 16 p2721 N85-26797
Observations of low energy magnetospheric plasma outside the plasmasphere
[KGI-PREPRINT-075] 20 p3536 N85-32004
Surface voltage gradient role in high voltage solar array-plasma interaction: Center Director's discretionary fund
[NASA-TM-86516] 22 p3805 N85-33567

SPACE PLATFORMS
NT EURECA (ESA)
NT SYNCHRONOUS PLATFORMS
Research study: Studies in atmospheric processes from Space Platforms
[NASA-CR-171176] 01 p0072 N85-10473
Modular experimental platform for science and applications 02 p0152 N85-11031
Selected tether applications in space: An analysis of five selected concepts
[NASA-CR-171222] 04 p0460 N85-12921
Autonomous momentum management for space station
[NASA-CR-174065] 04 p0462 N85-12931
Autonomous momentum management for space station, exhibit A
[NASA-CR-171256] 04 p0462 N85-12933
Tethers open new space options
11 p1642 N85-20340
Earth observations and the polar platform
[NOAA-TR-NESDIS-18] 11 p1669 N85-20517
Space Station
[NASA-EP-211] 12 p1793 N85-21251
Space Technology Experiments Platform (STEP) status: An in-space test facility 14 p2236 N85-23863
Utilization of the polar platform of NASA's Space Station Program for operational Earth observations
[PB85-152502] 14 p2240 N85-23895
MBB/Erno's views, future plans in aerospace activities
15 p2531 N85-25609
Study on the extension of experiment resources in the MAUS project
[BMFT-FB-W-84-051] 15 p2650 N85-26343
Artificial intelligence in space platforms
[AD-A152078] 16 p2651 N85-27578
Comparative study on data system architectures — spacecraft data processing
[ESA-CR(P)-2015] 21 p3675 N85-32828
Initial placement of STO instruments
23 p3902 N85-34174

SPACE POWER REACTORS
NT SPACE POWER UNIT REACTORS
Emerging space nuclear power needs
05 p0608 N85-13882
Technology status of thermionic fuel elements for space nuclear power 05 p0610 N85-13893
Advanced concepts liquid droplet radiator
05 p0610 N85-13899
The liquid droplet radiator - an ultralightweight heat rejection system for efficient energy conversion in space
05 p0610 N85-13900
Lunar nuclear power feasibility study
[NASA-CR-171831] 07 p1041 N85-16611
Interagency program on space nuclear power: Directory of participants in the SP-100 program
[DE85-026339] 08 p1221 N85-17691
Instrumentation and controls evaluation for space nuclear power systems
[DE85-000963] 09 p1383 N85-18695
Safety program considerations for space nuclear reactor systems
[DE85-003295] 10 p1556 N85-19808
Thermionic converter for space reactor described
11 p1621 N85-20206
Opening up the future in space with nuclear power
[DE85-002411] 11 p1727 N85-20862
Space nuclear-power reactor design based on combined neutronic and thermal-fluid analyses
[DE85-002433] 11 p1727 N85-20864
Irradiation effects on fuels for space reactors
[DE84-016460] 12 p1931 N85-22134
Ordered carbon metal alloys for extraterrestrial power systems
[AD-A150661] 14 p2255 N85-23977
Physics effects of accidental submersion of space power reactors in water
[DE85-005020] 15 p2650 N85-26344
Space reactor ground tests, assessment of facility needs
[DE85-006814] 15 p2650 N85-26345

Analysis of alkali liquid metal Rankine space power systems
[DE85-006089] 16 p2741 N85-26917
Load-carrying capabilities of refractory alloys for space reactor power applications
[DE85-010566] 19 p3240 N85-30087
Development of improved thermoelectric materials for space nuclear power systems
[DE85-013079] 22 p3844 N85-33807
SP-100 Thermionic Technology Program
[DE85-012311] 23 p3972 N85-34625
Strategic defense initiative
[DE85-012778] 24 p4150 N85-35735

SPACE POWER UNIT REACTORS
Overview of the 1985 NASA Lewis Research Center SP-100 free-piston Stirling engine activities
[NASA-TM-87026] 16 p2880 N85-27769

SPACE PROBES
NT GALILEO PROBE
NT GALILEO SPACECRAFT
NT GIOTTO MISSION
NT HELIOS 1
NT HELIOS 2
NT JUPITER PROBES
NT LUNIK LUNAR PROBES
NT MARINER 5 SPACE PROBE
NT MARINER 9 SPACE PROBE
NT MARS PROBES
NT PIONEER SPACE PROBES
NT PIONEER 10 SPACE PROBE
NT PIONEER 11 SPACE PROBE
NT VENERA SATELLITES
NT VENERA 11 SATELLITE
NT VENUS PROBES
NT VIKING MARS PROGRAM
NT VIKING SPACECRAFT
Launch summary for 1978 - 1982 — sounding rockets, space probes, and satellites
[NASA-TM-87375] 04 p0461 N85-12924
A priority of space exploration: Observation of Saturn's rings from a Saturn orbiter 15 p2679 N85-26542
Rendezvous with Saturn's rings
15 p2679 N85-26543
Magnetospheric multiprobes: MMP/CHEMSAT
23 p3902 N85-34171
Precision measurements of solar energetic particle elemental composition
[SH-2.1-4] 23 p3998 N85-34765

SPACE PROCESSING
Second Symposium on Space Industrialization — space commercialization
[NASA-CP-2313] 02 p0149 N85-11011
Financial issues for commercial space ventures: Paying for the dreams 02 p0150 N85-11014
Opportunities for space bioprocessing
02 p0150 N85-11018
Potential utilization of glass experiments in space
02 p0151 N85-11020
Preparation of large-particle-size monodisperse latexes in space: The STS-3, STS-4, and STS-7 mission results
02 p0151 N85-11021
Producing gallium arsenide crystals in space
02 p0151 N85-11023
Microgravity containerless processing in long drop tubes 02 p0153 N85-11037
Opportunities for commercial organizations
02 p0156 N85-11055
NBS (National Bureau of Standards): Materials measurements
[NASA-CR-174038] 03 p0332 N85-12143
Bioprocessing in space 05 p0690 N85-14438
Bioprocessing in space 05 p0690 N85-14439
Commerce lab: Mission analysis and payload integration study
[NASA-CR-174381] 10 p1426 N85-18993
The feasibility of low-G grey solidification of nodular iron in the F-104 experimental furnace package
[NASA-TM-82527] 10 p1426 N85-18996
Alloy supercooling on Salyut-7
11 p1604 N85-20083
Development of the sonic pump levitator
[NASA-CR-171382] 12 p1782 N85-21186
Monodisperse Latex Reactor (MLR): A materials processing space shuttle mid-deck payload
[NASA-TM-86487] 12 p1782 N85-21187
Material research in microgravity
[NASA-TM-77628] 14 p2228 N85-23811
Microgravity: A new tool for basic and applied research in space
[EP-212] 16 p2716 N85-26767
Crystallization of aluminum-based alloys in weightlessness 19 p3242 N85-30101
Concept development evaluation for John Deere/UA STS middeck experiment location
[NASA-CR-171541] 20 p3397 N85-31071
Microgravity silicon zoning investigation
[NASA-CR-171531] 20 p3397 N85-31073
German payloads for EURECA 1
[BMFT-FB-W-85-003] 20 p3419 N85-31223
Kidney cell electrophoresis
[NASA-CR-171889] 20 p3496 N85-31745
Task description for the 1983 catalog of tasks for the materials processing in space program
20 p3496 N85-31746
Asymmetric electroosmotic flow and mobility measurements at nonstationary positions in the rectangular chamber 20 p3499 N85-31749
Theoretical prediction of stationary positions in the rectangular chamber during asymmetric electroosmotic flow 20 p3499 N85-31750
A computer program for determining the electrophoretic mobility of cells in a rectangular chamber during asymmetric electroosmotic flow
20 p3499 N85-31751
Evaluation of results of cell electrophoresis experiments on space shuttle STS-3 including pre-flight and post-flight laboratory experiments 20 p3502 N85-31772
Free zone electrophoresis simulation of static column electrophoresis in microgravity on shuttle flight STS-3
20 p3502 N85-31773
Microgravity electrophoresis: A study of the factors that affect free-fluid separation 20 p3502 N85-31774
Pre-flight report on cultured human embryonic kidney cell handling and cell electrophoresis. Prepared prior to continuous-flow electrophoretic separation experiments aboard space shuttle flight STS-8
20 p3503 N85-31775
Properties of electrophoretic fractions of human embryonic kidney cells separated on space shuttle flight STS-8 20 p3503 N85-31776
Study of requirements for and method of multidimensional acoustic imaging — spaceborne experiments
[ESA-CR(P)-2020] 20 p3525 N85-31924
The EURECA solution growth facility conceptual design study. Executive summary
[ESA-CR(P)-2007] 20 p3538 N85-32016

SPACE PROCESSING APPLICATIONS ROCKET
Technological experiments on high-altitude rockets
16 p2725 N85-26818

SPACE PROGRAMS
NT BRAZILIAN SPACE PROGRAM
NT CANADIAN SPACE PROGRAM
NT EUROPEAN SPACE PROGRAMS
NT FRENCH SPACE PROGRAMS
NT INDIAN SPACE PROGRAM
NT JAPANESE SPACE PROGRAM
NT SWEDISH SPACE PROGRAM
NT U.S.S.R. SPACE PROGRAM
Space America's commercial space program
02 p0152 N85-11027
Fokker wants to start new Netherlands space program
03 p0310 N85-11999
Space Nuclear Safety Program
[DE84-016973] 05 p0728 N85-14679
A buyer's guide to space infrastructure
07 p0914 N85-15784
Broadening the debate 07 p0914 N85-15785
Toward a goal-oriented civilian space program
07 p0914 N85-15786
Results of principal NASA studies on space station uses and functional requirements 07 p0914 N85-15787
Title 2: National Commission on Space (Public Law 98-361) 07 p0915 N85-15791
China report: Science and technology
[JPRS-CST-84-039] 11 p1621 N85-20206
PRC journal discusses 'Star Wars' space program
11 p1621 N85-20207
Space Shuttle aerothermodynamic data report, phase C
[NASA-CR-171856] 14 p2241 N85-23697
NASA photography index
[NASA-TM-87457] 15 p2665 N85-26445
East Europe report: Science and technology
[JPRS-ESA-84-032] 16 p2727 N85-26833
Contribution to space program reviewed
16 p2727 N85-26834
Department of Housing and Urban Development-independent agencies appropriations for 1986. Part 6: National Aeronautics and Space Administration
[GPO-47-235] 16 p2879 N85-27768
A spacefaring people: Perspectives on early spaceflight
[NASA-SP-4405] 23 p4056 N85-35142
Space science and exploration: A historical perspective 23 p4056 N85-35143
The next assignment: The state of the literature on space 23 p4057 N85-35146
Opportunities for policy historians: The evolution of the US civilian space program 23 p4057 N85-35147
Space-age Europe, 1957-1980
23 p4057 N85-35148
Space activities in the Soviet Union, Japan, and the People's Republic of China 23 p4057 N85-35149

SPACE RADIATION
U EXTRATERRESTRIAL RADIATION

SPACE RADIATORS
U SPACECRAFT RADIATORS

SPACE RATIONS
Research on zero-gravity botany apparatus
16 p2723 N85-26811

SPACE RENDEZVOUS
NT ORBITAL RENDEZVOUS
Progress-22 docks with Salyut-7
02 p0157 N85-11084
Transportation applications, part 2
11 p1643 N85-20350
Evaluation of OMV ranging and docking systems
12 p1947 N85-22230
National Space Transportation Systems Program mission report
[NASA-TM-87455] 14 p2242 N85-23800
Automatic rendezvous and docking systems functional and performance requirements
[NASA-CR-171866] 15 p2482 N85-25376
Hardware test program for evaluation of baseline range-range rate sensor concept
[NASA-CR-176143] 23 p3933 N85-34377

SPACE SCIENCES
U AEROSPACE SCIENCES

SPACE SHUTTLE ASCENT STAGE
Shuttle navigation status 08 p1092 N85-16901
Debris control design achievements of the booster separation motors 08 p1098 N85-16942
Shuttle system ascent aerodynamic and plume heating 08 p1103 N85-16975
Shuttle/Centaur upper stage capability
11 p1712 N85-20773

SPACE SHUTTLE BOOSTERS
Vibration, acoustic, and shock design and test criteria for components on the Solid Rocket Boosters (SRB), Lightweight External Tank (LWT), and Space Shuttle Main Engines (SSME)
[NASA-RP-1127] 01 p0061 N85-10405
The solid rocket booster auxiliary power unit: Meeting the challenge 08 p1099 N85-16946
Space Shuttle booster thrust imbalance analysis
[NASA-TM-86493] 12 p1791 N85-21241
B-52B/DTV (Drop Test Vehicle) flight test results: Drop test missions
[NASA-CR-171530] 19 p3215 N85-29934
SRB TPS closeout materials characterization
[NASA-CR-170885] 24 p4070 N85-35222
SRB thermal protection systems materials test results in an arc-heated nitrogen environment
[NASA-CR-170881] 24 p4072 N85-35230
Study of NSI and related cable performance during tests performed in the NASA Hot Gas Facility
[NASA-CR-170886] 24 p4101 N85-35423

SPACE SHUTTLE MAIN ENGINE
Rotordynamic analysis of the SSME turbopumps using reduced models
[NASA-CR-171170] 01 p0054 N85-10355
Retardation analytical model to extend service life
[NASA-CR-171177] 01 p0057 N85-10376
Vibration, acoustic, and shock design and test criteria for components on the Solid Rocket Boosters (SRB), Lightweight External Tank (LWT), and Space Shuttle Main Engines (SSME)
[NASA-RP-1127] 01 p0061 N85-10405
An electrochemical study of hydrogen uptake and elimination by bare and gold-plated waspaloy
[NASA-TM-86479] 02 p0182 N85-11222
Non-intrusive speed sensor — space shuttle main engine turbopumps
[NASA-CR-171204] 03 p0364 N85-12331
Analysis of physical-chemical processes governing SSME internal fluid flows
[NASA-CR-171247] 04 p0451 N85-12859
Turbine blade damping study, introduction
04 p0456 N85-12891
Prediction of force coefficients for labyrinth seals
05 p0644 N85-14130
Identification of dynamic coefficients of annular turbulent seals 05 p0644 N85-14133
Analysis of physical-chemical processes governing SSME internal fluid flows
[NASA-CR-174245] 06 p0760 N85-14882
Shuttle avionics software trials, tribulations and success 08 p1090 N85-16891
Man-machine interface and control of the shuttle digital flight system 08 p1091 N85-16894
Space shuttle main engine hardware simulation
08 p1091 N85-16895

SSME lifetime prediction and verification, integrating environments, structures, materials: The challenge 08 p1086 N85-16918

Space shuttle flight readiness firing dress rehearsal for STS-1 08 p1097 N85-16929

Cryogenic propellant management: Integration of design, performance and operational requirements 08 p1098 N85-16939

Space shuttle main engine: Interactive design challenges 08 p1098 N85-16940

Debris control design achievements of the booster separation motors 08 p1098 N85-16942

Computational fluid mechanics utilizing the variational principle of modeling damping seals [NASA-CR-174332] 08 p1161 N85-17325

Assessment of the operating characteristics of the SSME LOX turbopump pump-end bearing [NASA-CR-171287] 08 p1167 N85-17362

Analytical and experimental investigation of rubbing interaction in labyrinth seals for a liquid hydrogen fuel pump — space shuttle main engine [NASA-CR-174657] 09 p1287 N85-18064

The analysis by the lumped parameter method of blade platform friction dampers used in the high pressure fuel turbopump on the space shuttle main engine 09 p1336 N85-18417

SSME thrust chamber simulation using Navier-Stokes equations [NASA-CR-171349] 10 p1430 N85-19017

Thrust chamber performance using Navier-Stokes solution — space shuttle main engine viscous nozzle calculation [NASA-CR-171346] 10 p1430 N85-19019

Preliminary analysis of selected gas dynamic problems – space shuttle main engine main combustion transients and IUS nozzle flow [NASA-CR-171343] 10 p1483 N85-19361

Calculation of flow about posts and powerhead model – space shuttle main engine [NASA-CR-171344] 10 p1483 N85-19362

STS-1 Pogo analysis [NASA-TM-87433] 11 p1591 N85-20007

Using a data base management system for modelling SSME test history data 12 p1944 N85-22211

An investigation of space shuttle main engine shutdown chugging instability 12 p1946 N85-22221

Sensor control of robot arc welding 12 p1948 N85-22233

Evaluation of PHOENICS as a design analysis tool for SSME 12 p1949 N85-22240

Nonlinear rotordynamics analysis [NASA-CR-171425] 13 p1968 N85-22364

High-pressure rocket engine turnaround duct computational fluid dynamics analysis 13 p2003 N85-22556

HPFTP flow diverter analysis [NASA-CR-171424] 13 p2091 N85-23057

Cyclic structural analyses of anisotropic turbine blades for reusable space propulsion systems — ssme fuel turbopump [NASA-TM-86990] 14 p2320 N85-24339

Flow induced vibration of the SSME LOX posts [NASA-CR-175608] 15 p2495 N85-25391

Study of high performance alloy electroforming [NASA-CR-175741] 15 p2508 N85-25473

Advanced High Pressure O2/H2 Technology [NASA-CP-2372] 16 p2733 N85-26862

Thrust chamber life prediction 16 p2733 N85-26865

Manufacturing and producibility technology 16 p2733 N85-26866

Ceramics for advanced O2/H2 application 16 p2734 N85-26868

Vacuum plasma coatings for turbine blades 16 p2734 N85-26869

Material technology 16 p2734 N85-26870

Design overview of fiber-reinforced superalloy composites for the Space Shuttle main engine 16 p2734 N85-26871

Development of hydrogen resistant alloys 16 p2735 N85-26873

Development of new materials for turbopump bearings 16 p2735 N85-26877

Bearings working group 16 p2735 N85-26878

Advanced rocket engine cryogenic turbopump bearing thermal model 16 p2735 N85-26879

Hybrid bearings for LH2 and LO2 turbopumps 16 p2736 N85-26880

Powder metallurgy bearings for advanced rocket engines 16 p2736 N85-26881

Rolling contact fatigue life of chromium ion plated 440C bearing steel 16 p2736 N85-26882

Technical overview structural dynamics 16 p2736 N85-26883

Signal analysis techniques for incipient failure detection in turbomachinery 16 p2736 N85-26884

Flow dynamic environment data base development for the SSME 16 p2736 N85-26885

Turbine blade friction damping study 16 p2736 N85-26886

Preliminary results on passive eddy current damper technology for SSME turbomachinery 16 p2737 N85-26890

Rotor response for transient unbalance changes in a nonlinear simulation 16 p2737 N85-26892

Damping seal verification setup 16 p2738 N85-26893

Damping seals for turbomachinery 16 p2738 N85-26894

Vibration characteristics of the HPOTP (High Pressure Oxygen Turbopump) of the SSME (Space Shuttle Main Engine) 16 p2738 N85-26895

Fluid and gas dynamics 16 p2738 N85-26897

Experimental evaluation of an advanced Space Shuttle main engine hot-gas manifold design concept 16 p2738 N85-26898

Redistribution of the inlet temperature profile through the SSME fuel turbine 16 p2739 N85-26901

Analytical study of flow phenomena in SSME turnaround duct geometries 16 p2739 N85-26902

Instrumentation technology overview 16 p2739 N85-26903

Fiber optic Raman thermometer for Space Shuttle main engine preburner profiling 16 p2739 N85-26904

An advanced solid state pressure transducer for high reliability SSME application 16 p2739 N85-26905

Nonintrusive shaft speed sensor 16 p2740 N85-26906

Flow-induced vibration of the SSME LOX posts: Additional issues [DE85-007339] 16 p2741 N85-26916

Structural Integrity and Durability of Reusable Space Propulsion Systems [NASA-CP-2381] 17 p2910 N85-27941

Overview of aerothermodynamic loads definition study 17 p2910 N85-27942

SSME fuel preburner two-dimensional analysis 17 p2911 N85-27943

SSME turbopump turbine computations 17 p2911 N85-27944

Simulation of multistage turbine flows 17 p2911 N85-27945

New facility to study unsteady wake effects on turbine airfoil heat transfer 17 p2911 N85-27946

Calculation of viscous compressible flows in small gas turbines 17 p2912 N85-27950

Flow-induced vibration of SSME main injector liquid-oxygen posts 17 p2912 N85-27951

Overview of structural response: Probabilistic structural analysis 17 p2912 N85-27952

Composite loads spectra for select space propulsion structural components 17 p2912 N85-27953

Probabilistic structural analysis of SSME turbopump blades: Probabilistic geometry effects 17 p2913 N85-27958

Structural tailoring of SSME blades (vanes) 17 p2913 N85-27960

Cyclic structural analyses of SSME turbine blades 17 p2914 N85-27963

Effects of high mean stress on high-cycle fatigue behavior of PWA 1480 17 p2914 N85-27964

Constitutive cyclic deformation behavior in single-crystal and directionally solidified SSME high-pressure fuel turbopump airfoil materials 17 p2914 N85-27965

Thin-film sensors for space propulsion technology 17 p2915 N85-27968

Optical strain measurement system development 17 p2915 N85-27969

Heat flux sensor calibrator 17 p2915 N85-27970

Feasibility of mapping velocity flow fields in SSME powerhead by laser anemometry techniques 17 p2915 N85-27971

Analysis of physical-chemical processes governing SSME internal fluid flows [NASA-CR-175893] 17 p2957 N85-28261

Research pressure instrumentation for NASA space shuttle main engine [NASA-CR-176014] 19 p3227 N85-30006

SSME seal test program: Test results for hole-pattern damper seals [NASA-CR-171595] 20 p3395 N85-31059

SRB thermal protection systems materials test results in an arc-heated nitrogen environment [NASA-CR-170881] 24 p4072 N85-35236

SPACE SHUTTLE MISSION 31-C

Modular Optoelektronischer Multispektraler Scanner (MOMS), interpretation and evaluation of the MOMS image Arica, West Coast of South America — STS-7 flight 05 p0657 N85-14222

SPACE SHUTTLE MISSION 41-B

National Space Transportation Systems Program mission report [NASA-TM-87454] 14 p2242 N85-23899

Results from radiation monitoring equipment experiment on STS-11 [AD-A152531] 17 p2906 N85-27932

SPACE SHUTTLE MISSION 41-C

National Space Transportation Systems Program mission report [NASA-TM-87455] 14 p2242 N85-23900

SPACE SHUTTLE MISSION 41-G

Atmospheric environment for Space Shuttle (STS-41G) launch [NASA-TM-86486] 07 p0995 N85-16320

SPACE SHUTTLE MISSION 51-A

Atmospheric environment for Space Shuttle (STS-51A) launch [NASA-TM-86497] 12 p1892 N85-21875

SPACE SHUTTLE MISSION 51-C

Atmospheric environment for space shuttle (STS-51C) launch [NASA-TM-86508] 19 p3315 N85-30547

SPACE SHUTTLE MISSIONS

NT SPACE SHUTTLE MISSION 31-C
NT SPACE SHUTTLE MISSION 41-B
NT SPACE SHUTTLE MISSION 41-C
NT SPACE SHUTTLE MISSION 41-G
NT SPACE SHUTTLE MISSION 51-A
NT SPACE SHUTTLE MISSION 51-C

Atmospheric environment for Space Shuttle (STS-41D) launch [NASA-TM-86484] 05 p0679 N85-14356

SPACE SHUTTLE ORBITAL FLIGHT TEST 1

U SPACE TRANSPORTATION SYSTEM 1 FLIGHT

SPACE SHUTTLE ORBITAL FLIGHT TEST 3

U SPACE TRANSPORTATION SYSTEM 3 FLIGHT

SPACE SHUTTLE ORBITAL FLIGHT TEST 4

U SPACE TRANSPORTATION SYSTEM 4 FLIGHT

SPACE SHUTTLE ORBITAL FLIGHT TESTS

U SPACE TRANSPORTATION SYSTEM FLIGHTS

SPACE SHUTTLE ORBITAL FLIGHT 7

U SPACE SHUTTLE MISSION 31-C

SPACE SHUTTLE ORBITAL FLIGHTS

U SPACE TRANSPORTATION SYSTEM FLIGHTS

SPACE SHUTTLE ORBITER 099

U CHALLENGER (ORBITER)

SPACE SHUTTLE ORBITER 101

U ENTERPRISE (ORBITER)

SPACE SHUTTLE ORBITER 102

U COLUMBIA (ORBITER)

SPACE SHUTTLE ORBITER 103

U DISCOVERY (ORBITER)

SPACE SHUTTLE ORBITERS

NT CHALLENGER (ORBITER)
NT COLUMBIA (ORBITER)
NT DISCOVERY (ORBITER)
NT ENTERPRISE (ORBITER)

Structural analysis of the Space Shuttle Orbiter 01 p0061 N85-10401

Space Shuttle Orbiter trimmed center-of-gravity extension study. Volume 8: Effects of configuration modifications on the aerodynamic characteristics of the 140 A/B Orbiter at a Mach number of 5.97 [NASA-TM-72661-VOL-8] 04 p0452 N85-12867

Selected tether applications in space: An analysis of five selected concepts [NASA-CR-171222] 04 p0460 N85-12921

Columbia: The first 5 flights entry heating data series. Volume 1: An overview [NASA-CR-171820] 07 p0913 N85-15777

Effect of aerodynamic and angle-of-attack uncertainties on the May 1979 entry flight control system of the Space Shuttle from Mach 8 to 1.5 [NASA-TP-2365] 07 p0913 N85-15778

Space Shuttle Technical Conference, part 1 [NASA-CP-2342-PT-1] 08 p1090 N85-16889

Evolution of shuttle avionics redundancy management/fault tolerance 08 p1090 N85-16890

Shuttle avionics software trials, tribulations and success 08 p1090 N85-16891

Shuttle avionics software development trials: Tribulations and successes, the backup flight system 08 p1091 N85-16892

SSME digital control design characteristics 08 p1091 N85-16893

Development and implementation of the verification process for the shuttle avionics system 08 p1091 N85-16896

Ground man-machine interfaces for orbiter checkout 08 p1091 N85-16897

Integration of ground and on-board system for terminal count 08 p1092 N85-16898

Integrated design checkout of shuttle payload avionics interfaces 08 p1092 N85-16899

Descent guidance and mission planning for space shuttle 08 p1092 N85-16902
Some effects of digital sampling on orbiter flight control system operation 08 p1092 N85-16903
Space shuttle handling qualities 08 p1092 N85-16904
The development and application of aerodynamic uncertainties: And flight test verification for the space shuttle orbiter 08 p1093 N85-16910
Aerodynamic challenges of ALT 08 p1094 N85-16911
The orbiter air data system 08 p1094 N85-16912
Orbiter structural design and verification 08 p1094 N85-16915
The challenging scales of the bird: Shuttle tile structural integrity 08 p1095 N85-16919
Challenges in the development of the orbiter atmosphere revitalization subsystem 08 p1095 N85-16920
Challenges in the development of the orbiter active thermal control subsystem 08 p1096 N85-16923
Other challenges in the development of the orbiter environmental control hardware 08 p1096 N85-16924
Challenges in the development of the orbiter radiator system 08 p1096 N85-16925
Debris control design achievements of the booster separation motors 08 p1098 N85-16942
Orbital Maneuvering system design evolution 08 p1098 N85-16943
Design evolution of the orbiter reaction control subsystem 08 p1099 N85-16944
Space shuttle orbiter auxiliary power unit development challenges 08 p1099 N85-16945
Space shuttle electrical power generation and reactant supply system 08 p1099 N85-16947
Shuttle S-band communications technical concepts 08 p1099 N85-16948
Shuttle ku-band communications/radar technical concepts 08 p1099 N85-16949
Shuttle payload S-band communications system 08 p1100 N85-16950
TDRSS S-shuttle unique receiver equipment 08 p1100 N85-16951
The Statistical Loop Analyzer (SLA) 08 p1100 N85-16955
Digital scrambling for shuttle communication links: Do drawbacks outweigh advantages? 08 p1101 N85-16956
Electronics systems test laboratory testing of shuttle communications systems 08 p1101 N85-16958
Orbiter wheel and tire certification 08 p1101 N85-16959
Orbiter processing facility: Access platforms Kennedy Space Center, Florida, from challenge to achievement 08 p1102 N85-16968
Payload transportation at KSC 08 p1103 N85-16970
STS payload ground handling mechanism at John F. Kennedy Space Center 08 p1103 N85-16971
The orbiter mate/demate device 08 p1103 N85-16972
In-flight testing of the space shuttle orbiter thermal control system 08 p1103 N85-16974
Thermal design of the space shuttle external tank 08 p1103 N85-16977
Orbiter entry aerothermodynamics 08 p1104 N85-16978
Orbiter thermal protection system 08 p1104 N85-16979
Shuttle on-orbit contamination and environmental effects 08 p1104 N85-16980
Design concept definition study for an improved shuttle waste collection subsystem [NASA-CR-171834] 08 p1198 N85-17546
Improved orbiter waste collection system study [NASA-CR-171830] 08 p1199 N85-17548
Improved orbiter waste collection system study, appendix D [NASA-CR-171833] 08 p1199 N85-17549
Waste collection subsystem study [NASA-CR-171836] 08 p1199 N85-17552
Space Shuttle Orbiter waste collection system conceptual study [NASA-CR-171844] 08 p1199 N85-17553
Space Shuttle Orbiter trimmed center-of-gravity extension study. Volume 9: Effects of configuration modifications on the aerodynamic characteristics of the 140 A/B Orbiter at Mach numbers of 1.5, 2.0, and 2.5 — wind tunnel tests [NASA-TM-72661-VOL-9] 10 p1420 N85-18956
Space Shuttle orbiter trimmed center-of-gravity extension study [NASA-TP-2284] 10 p1428 N85-19003
Study of several factors affecting crew escape trajectories from the Space Shuttle Orbiter at low-subsonic speeds [NASA-TM-86303] 10 p1428 N85-19008
STS-1 Pogo analysis [NASA-TM-87433] 11 p1591 N85-20007
Shuttle tethered satellite system program overview 11 p1642 N85-20342
Results of Space Shuttle flight 41-D [GPO-39-481] 12 p1791 N85-21243
Aerospace Safety Advisory Panel [NASA-TM-87426] 13 p1970 N85-22373
Results of a M = 5.3 heat transfer test of the integrated vehicle using phase-change paint techniques on the 0.0175-scale model 56-OTS in the NASA/Ames Research Center 3.5-foot hypersonic wind tunnel [NASA-CR-167695] 13 p1988 N85-22468
Wakes and differential charging of large bodies in low Earth orbit 13 p1992 N85-22488
Active control technology experience with the Space Shuttle in the landing regime 17 p2903 N85-27900
Shuttle-tethered satellite system definition study. Volume 1: Executive study [NASA-CR-171474] 17 p2907 N85-27924
Numerical computation of space shuttle orbiter flow field [NASA-CR-175912] 18 p3058 N85-28921
Modeling and analysis of pinhole occulter experiment: Initial study phase [NASA-CR-175978] 19 p3272 N85-30267
Use of a hyperbolic grid generation scheme in simulating supersonic viscous flow about three-dimensional winged configuration [NASA-TM-85344] 23 p3893 N85-34116

SPACE SHUTTLE PAYLOADS
NT ATMOSPHERIC GENERAL CIRCULATION EXPERIMENT
NT EARTH RADIATION BUDGET EXPERIMENT
NT OSS-1 PAYLOAD
NT PLASMA INTERACTION EXPERIMENT
NT SPACEBORNE EXPERIMENTS
NT SPACELAB
NT X RAY ASTROPHYSICS FACILITY
Space Research in Japan. National report 01 p0013 N85-10082
SEPAC (space experiments with particle accelerators) 01 p0014 N85-10085
Small Payload Flight Systems (SPFS) 02 p0152 N85-11030
European retrievable carrier (Eureca) and evolutionary space carrier for microgravity, Earth observation and technology demonstration 02 p0152 N85-11032
Project Explorer 02 p0154 N85-11041
Fluids Experiment Apparatus (FEA) 02 p0155 N85-11048
External tank aft cargo carrier 02 p0155 N85-11050
Proceedings of a Workshop on the Applications of Tethers in Space, Volume 1 [NASA-CR-171196] 03 p0322 N85-12076
Proceedings of a Workshop on Applications of Tethers in Space, Volume 2 [NASA-CR-171197] 03 p0322 N85-12077
Continuing issues (FY 1983) concerning military use of the space transportation system [AD-A146091] 03 p0323 N85-12080
The calibration of photographic and spectroscopic films: A densitometric analysis of IIaO film flown aboard the Space Shuttle 3 [NASA-CR-174278] 07 p0962 N85-16101
Lunar nuclear power feasibility study [NASA-CR-171831] 07 p1041 N85-16611
Integrated design checkout of shuttle payload avionics interfaces 08 p1092 N85-16899
Shuttle payload S-band communications system 08 p1100 N85-16950
Payload transportation at KSC 08 p1103 N85-16970
STS payload ground handling mechanism at John F. Kennedy Space Center 08 p1103 N85-16971
Computer aided processing using laser measurements 08 p1103 N85-16973
Shuttle on-orbit contamination and environmental effects 08 p1104 N85-16980
Commerce Lab: Mission analysis and payload integration study [NASA-CR-171272] 08 p1104 N85-16981
Shuttle/Centaur project perspective 08 p1106 N85-16991
Commerce lab: Mission analysis and payload integration study [NASA-CR-174361] 10 p1426 N85-18993
A preliminary study of a cryogenic equivalence principle experiment on Shuttle [NASA-CR-171300] 10 p1426 N85-18994
Commercial space: Europe should have independen strategy 10 p1460 N85-19
British aerospace studies HOTOL satellite launcher 10 p1460 N85-19
Brazilian Remote Sensing Shuttle Experimen (BRESEX): Characteristics and future utilization on satellites [INPE-3313-PRE/620] 10 p1487 N85-19
The BRESEX multispectral camera: Preliminary characteristics [INPE-3357-PRE/635] 10 p1487 N85-19
Space Transportation System (STS) propellan scavenging system study. Volume 1: Technical report [NASA-CR-171848-VOL-1] 11 p1589 N85-20
Tether fundamentals 11 p1643 N85-20
Science Applications, part 1 11 p1643 N85-20
Status of the National Space Transportation System 11 p1712 N85-2077
Monodisperse Latex Reactor (MLR): A materials processing space shuttle mid-deck payload [NASA-TM-86487] 12 p1782 N85-2118
Satellite services and orbital retrieval 12 p1786 N85-21211
Results of Space Shuttle flight 41-D [GPO-39-481] 12 p1791 N85-2124
Report on final recommendations for MPS engineering-science payload [NASA-CR-175659] 13 p1968 N85-2246
Suprathermal plasma observed on STS-3 Mission by plasma diagnostics package 13 p1969 N85-2247
Electron and ion density depletions measured in the STS-3 orbiter wake 13 p1969 N85-2247
Shuttle electrical environment 13 p1990 N85-2247
Interactions measurement payload for Shuttle 13 p1997 N85-2251
Electrostatic forming and testing of polymer films on a 16-foot diameter test fixture [NASA-TM-86328] 13 p2063 N85-22
QUASAT: An orbiting very long baseline interferometer program using large space antenna systems 14 p2230 N85-23
LDR system concepts and technology 14 p2231 N85-23
Development of the 15-meter hoop-column antenna system 14 p2231 N85-23
Box truss development and its application 14 p2231 N85-23
Cable-catenary large antenna concept 14 p2231 N85-23
Large Space Antenna Systems Technology, 1984 [NASA-CP-2368-PT-2] 14 p2233 N85-23
Shuttle payload bay dynamic environments: Summary and conclusion report for STS flights 1-5 and 9 [NASA-CR-175656] 14 p2241 N85-23
Geometric error analysis for shuttle imaging spectrometer experiment [NASA-CR-175665] 14 p2305 N85-24
X-ray polarimetry: The measurement of the polarization of solar flare X-rays and the design of a Compton polarimeter 14 p2441 N85-25
Study on the extension of experiment resources in the MAUS project [BMFT-FB-W-84-051] 15 p2650 N85-26
Space radiation studies for the reporting period, June 1983 - July 1984 [NASA-CR-171411] 15 p2685 N85-26
Microgravity: A new tool for basic and applied research in space [EP-212] 16 p2716 N85-2676
Orbiter middeck/payload standard interfaces contro document [NASA-TM-87473] 16 p2729 N85-28
Space Transportation System. Space shuttle payload flight assignments [NASA-TM-87492] 19 p3224 N85-29
Space Transportation System. Space shuttle payload flight assignments [NASA-TM-87491] 19 p3224 N85-29
On the accuracy of modelling the dynamics of large space structures 19 p3225 N85-29
Evaluation of results of cell electrophoresis experiments on space shuttle STS-3 including pre-flight and post-flight laboratory experiments 20 p3502 N85-3177
Free zone electrophoresis simulation of static column electrophoresis in microgravity on shuttle flight STS-3 20 p3502 N85-3177
Microgravity electrophoresis: A study of the factors that affect free-fluid separation 20 p3502 N85-3177
Properties of electrophoretic fractions of human embryonic kidney cells separated on space shuttle flight STS-8 20 p3503 N85-3177
Appendange deployment mechanism for the Hubble Space Telescope program 22 p3798 N85-33

SPACE SHUTTLE UPPER STAGES
Commercializing the transfer orbit stage 02 p0155 N85-11049
SPACE SHUTTLES
Active control technology experience with the Space Shuttle in the landing regime [NASA-TM-85910] 01 p0012 N85-10071
Results of tests of advanced flexible insulation vortex and flow environments in the North American Aerodynamics Laboratory lowspeed wind tunnel using 0.0405-scale Space Shuttle Orbiter model 16-0 (test OA-308) [NASA-CR-167682] 01 p0015 N85-10098
Vibration, acoustic, and shock design and test criteria for components on the Solid Rocket Boosters (SRB), Lightweight External Tank (LWT), and Space Shuttle Main Engines (SSME) [NASA-RP-1127] 01 p0061 N85-10405
Space Shuttle Environmental Effects: The First 5 Flights [NASA-CR-171812] 01 p0069 N85-10457
Toxicological evaluation of Columbia spacecraft 01 p0094 N85-10631
The evolution of small payload carrier systems 02 p0153 N85-11036
An experimental study of jet impingement on a circular cylinder [AD-A145583] 02 p0198 N85-11326
Shuttle Experimental Radar for Geological Exploration (SERGE) project: Field work relating to the Shuttle Experimental Radar A (SIR-A) in Brazil (phase 2) [NASA-CR-174033] 02 p0219 N85-11444
International cooperation and competition in space [GPO-38-001] 02 p0295 N85-11911
International cooperation and competition in space. Introduction 02 p0295 N85-11912
STS natural environment analysis [NASA-CR-171221] 03 p0322 N85-12079
Charging of the DMSP F-2 spacecraft in the aurora on 10 January 1983 [AD-A146303] 03 p0324 N85-12086
Development of computational fluid dynamics at NASA Ames Research Center [NASA-TM-86021] 04 p0452 N85-12866
Launching systems [CNES-NT-111] 04 p0460 N85-12917
Oil-flow study of a Space Shuttle orbiter tip-fin controller [NASA-TM-86276] 04 p0460 N85-12920
Review of Space Shuttle requirements, operations, and future plans [GPO-39-101] 04 p0461 N85-12927
Statement of Frank Cepollina, Solar Maximum Repair Mission Project Manager, Goddard Space Flight Center 04 p0461 N85-12930
A feasibility study on the use of wind profilers to support Space Shuttle launches [NASA-CR-3861] 04 p0538 N85-13423
Vandenberg space shuttle launch complex [S-HRG-98-1075] 05 p0601 N85-13833
Statement of Edward C. Aldridge, Jr., Under Secretary of the Air Force, Department of the Air Force, accompanied by Lieutenant General Robert W. Bazley, Inspector General and Brigadier General Donald J. Kutyna, Director of Space Systems and Command, Control and Communications, Deputy Chief of Staff, Research, Development and Acquisition 05 p0601 N85-13834
Statement of Honorable James M. Beggs, Administrator, National Aeronautics and Space Administration 05 p0601 N85-13835
A distributed expert system for Space Shuttle flight control 05 p0602 N85-13836
Six degrees of freedom control with each hand? 05 p0700 N85-14492
Searching for impact craters using space shuttle photography 06 p0869 N85-15645
Issues and findings 07 p0914 N85-15782
Space infrastructure 07 p0914 N85-15783
A buyer's guide to space infrastructure 07 p0914 N85-15784
Reduction method for thermal analysis of complex aerospace structures [NASA-TP-2373] 07 p0957 N85-16066
Space Shuttle Technical Conference, part 1 [NASA-CP-2342-PT-1] 08 p1090 N85-16889
Automation of checkout for the shuttle operations era 08 p1092 N85-16900
Shuttle navigation status 08 p1092 N85-16901
Low-speed longitudinal orbiter qualities 08 p1092 N85-16905
The space shuttle ascent vehicle aerodynamic challenges configuration design and data base development 08 p1093 N85-16906
The space shuttle launch vehicle aerodynamic verification challenges 08 p1093 N85-16907
The aerodynamic challenges of SRB recovery 08 p1093 N85-16908
The aerodynamic challenges of the design and development of the space shuttle orbiter 08 p1093 N85-16909
Shuttle structural dynamics characteristics: The analysis and verification 08 p1094 N85-16913
Structural load challenges during space shuttle development 08 p1094 N85-16914
Orbiter structural design and verification 08 p1094 N85-16915
Space shuttle external tank performance improvements: The challenge 08 p1094 N85-16916
Structural and mechanical design challenges of space shuttle solid rocket boosters separation and recovery subsystems 08 p1095 N85-16917
SSME lifetime prediction and verification, integrating environments, structures, materials: The challenge 08 p1095 N85-16918
Challenges of developing an electro-optical system for measuring man's operational envelope 08 p1095 N85-16921
Challenges in the development of the shuttle extravehicular mobility unit 08 p1095 N85-16922
Transition to the space shuttle operations era 08 p1097 N85-16930
Launch processing system concept to reality 08 p1097 N85-16931
Automatic software for controlling cryogenic systems 08 p1097 N85-16932
Mathematical models for space shuttle ground systems 08 p1097 N85-16933
Managing computer-controlled operations 08 p1097 N85-16934
Support systems design and analysis 08 p1097 N85-16935
History, design and performance of the space shuttle hazardous gas detection system 08 p1096 N85-16936
Space Shuttle Technical Conference, part 2 [NASA-CP-2342-PT-2] 08 p1098 N85-16937
Propulsion and power systems perspective 08 p1098 N85-16938
Cryogenic propellant management: Integration of design, performance and operational requirements 08 p1098 N85-16939
Solid rocket motor certification to meet space shuttle requirements from challenge to achievement 08 p1098 N85-16941
The space shuttle program from challenge to achievement: Space exploration rolling on tires 08 p1101 N85-16960
Space shuttle elevon seal panel mechanism 08 p1101 N85-16961
Space shuttle wheels and brakes 08 p1101 N85-16962
The space shuttle orbiter remote manipulator positioning mechanism 08 p1102 N85-16963
An overview of the space remote manipulator system 08 p1102 N85-16964
Space shuttle rudder/speedbrake actuation subsystem 08 p1102 N85-16965
Development of the space shuttle body flap actuation subsystem 08 p1102 N85-16966
Mechanical features of the shuttle rotating service structure 08 p1102 N85-16967
External tank GH2 vent arm 08 p1102 N85-16969
Computer aided processing using laser measurements 08 p1103 N85-16973
Thermal design of the space shuttle solid rocket booster 08 p1103 N85-16976
Impact of activation optimization on the Vandenberg Ground Support System using Q-GERT analysis [AD-A146448] 08 p1105 N85-16986
The design of an ion-neutral mass spectrometer to be used in the Shuttle environment [AD-A146093] 08 p1114 N85-17022
Natural environment analysis [NASA-CR-174330] 08 p1180 N85-17433
Prototype wash water renovation system integration with government-furnished wash fixture [NASA-CR-171829] 08 p1198 N85-17547
Chronology of KSC and KSC related events for 1983 [NASA-TM-87400] 08 p1261 N85-17927
Water impact laboratory and flight test results for the space shuttle solid rocket booster aft skirt 09 p1335 N85-18394
Natural environment analysis [NASA-CR-171333] 10 p1428 N85-19010
Analysis and optimization of small Space Shuttle propulsion platforms [DFVLR-FB-84-28] 10 p1431 N85-19023
Shuttle S-band high gain switched beam breadboard antennas [NASA-CR-171852] 10 p1478 N85-19327
Tethers open new space options 11 p1642 N85-20340
Tethered satellite system project overview 11 p1642 N85-20341
Summary presentation of the Transportation Panel 11 p1644 N85-20357
The Satellite sail 11 p1647 N85-20376
Preflight and postflight motion sickness testing of the Spacelab 1 crew 11 p1694 N85-20652
Space motion sickness monitoring experiment: Spacelab 1 11 p1695 N85-20654
Shuttle software production facility 11 p1701 N85-20694
Shuttle/Centaur upper stage capability 11 p1712 N85-20773
Earth resources research using the Shuttle Imaging Radar system 11 p1713 N85-20779
Aerospace Safety Advisory Panel [NASA-TM-87428] 12 p1774 N85-21135
Space debris protection for a reusable orbital transfer vehicle 12 p1786 N85-21208
Space heat rejection radiators: Meteoroid/debris consideration 12 p1786 N85-21210
A remotely controlled orbiting retriever 12 p1786 N85-21212
Environment definition, small particles, diameter less than or equal to 1 MM 12 p1788 N85-21223
Feasibility of producing commodities and electricity for space shuttle operations at Vandenberg Air Force Base [DCN-84-203-001-80-21] 12 p1789 N85-21230
Advanced research and technology programs for advanced high-pressure oxygen-hydrogen rocket propulsion [NASA-TM-86969] 12 p1789 N85-21231
Study of outgassing and decomposition of space shuttle heat protection tiles, fillers and adhesive [NASA-CR-175565] 12 p1791 N85-21242
Impacts of Space Shuttle thermal protection system tile on F-15 aircraft vertical tile [NASA-TM-85904] 12 p1792 N85-21245
Space Shuttle interactive meteorological data system study [NASA-CR-171418] 12 p1892 N85-21876
Research Reports: 1984 NASA/ASEE Summer Faculty Fellowship Program [NASA-CR-171317] 12 p1944 N85-22210
Characterization of material surfaces exposed to atomic oxygen on space shuttle missions 12 p1946 N85-22220
Ground and flight testing for aircraft guidance and control [AGARD-AG-262] 13 p1966 N85-22350
Feoktistov argues against U.S. space shuttle design concept 13 p1985 N85-22453
Selected tether applications in space: Phase 2. Executive summary [NASA-CR-171421] 13 p1987 N85-22462
Selected tether applications in space: Phase 2 [NASA-CR-171422] 13 p1987 N85-22463
Vibroacoustic study of the NASA Goddard Space Flight Center OSS-1 payload [NASA-CR-175320] 13 p1988 N85-22485
Results of aeroheating DFI and ET design-data test on a 0.0175-scale model 60-OTS conducted in the Von Karman Gas Dynamics Facility (VKF) 40' supersonic and the 50' hypersonic wind tunnels A and C [NASA-CR-167693] 13 p1988 N85-22486
Spacecraft Environmental Interactions Technology, 1983 [NASA-CP-2359] 13 p1989 N85-22470
Space Station technology planning 13 p1989 N85-22471
Vehicle charging on STS-3 Mission 13 p1989 N85-22473
Measured electron contribution to Shuttle plasma environment: Abbreviated update 13 p1990 N85-22476
Laboratory studies of Kapton degradation in an oxygen ion beam 13 p1990 N85-22477
Electron beam charging of Space Shuttle thermal protection system tiles 13 p1990 N85-22478
Interactions measurement payload for Shuttle 13 p1997 N85-22518
Preliminary investigation of the electrodynamics of a conducting tether 13 p1997 N85-22521
Astronaut hazard during free-flight polar EVA 13 p1997 N85-22522
Research opportunities in human behavior and performances [NASA-CR-3886] 13 p2142 N85-23299
Large space antenna technology applied to radar-imaging, rain-rate measurements, and ocean wind sensing 14 p2230 N85-23820
Shuttle attached antenna Flight Experiment Definition Study (FEDS) 14 p2237 N85-23865

Electro-science requirements for shuttle-attached antenna flight experiments 14 p2237 N85-23866
Space Shuttle aerothermodynamic data report, phase C
[NASA-CR-171858] 14 p2241 N85-23897
Surface pressure produced by Space Transportation System flight 41B
[AD-A150793] 14 p2242 N85-23901
Alternate nozzle ablative materials program
[NASA-CR-175658] 14 p2248 N85-23924
Shuttle operational test and scientific investigations
14 p2394 N85-24748
Shuttle communications and tracking systems modeling and TDRSS link simulations studies
[NASA-CR-171861] 15 p2491 N85-25369
Shuttle fleet operations: A simulation analysis
[AD-A151383] 15 p2491 N85-25370
Costs, payload of Ariane, US Space Shuttle compared
15 p2530 N85-25601
Formulation and implementation of nonstationary adaptive estimation algorithm with applications to air-data reconstruction
[NASA-TM-86727] 16 p2706 N85-26699
Active control technology experience with the Space Shuttle in the landing regime 16 p2713 N85-26747
Space Shuttle program communication and tracking systems interface analysis
[NASA-CR-171862] 16 p2729 N85-26841
Cost prediction model for various payloads and instruments for the Space Shuttle Orbiter
[NASA-CR-175761] 16 p2729 N85-26842
Consultative Committee for Space Data Systems. Panel 1: Support
[NASA-CR-175766] 16 p2769 N85-27090
The Bresex multispectral camera: Preliminary characteristics
[INPE-3424-PRE/687] 16 p2787 N85-27195
Shuttle-tethered satellite system definition study extension
[NASA-CR-171473] 17 p2907 N85-27923
Results from radiation monitoring equipment experiment on STS-11
[AD-A152531] 17 p2908 N85-27932
Mathematical modeling and control of a large space structure as applied to a shuttle-antenna configuration
[AD-A153269] 17 p2910 N85-27939
Analysis of heat-transfer measurements from 2 AEDC wind tunnels on the Shuttle external tank
[NASA-CR-171470] 17 p2957 N85-28263
Heating parameter estimation using coaxial thermocouple gages in wind tunnel test articles
[AD-A153039] 17 p2968 N85-28328
Space insurance firms view shuttle, Ariane reliability
18 p3086 N85-29090
British super-shuttle 18 p3087 N85-29104
Astronautical conference hears details on Hermes minishuttle 18 p3088 N85-29112
Internal contamination issues
18 p3156 N85-29543
Space shuttle revitalization system
18 p3157 N85-29548
Publications of the Jet Propulsion Laboratory 1983
[NASA-CR-175979] 18 p3199 N85-29848
Space shuttle molecular and wake vacuum measurements
[NASA-TM-86509] 19 p3222 N85-29978
Hemispherical latching apparatus
[NASA-CASE-MFS-25837-1] 19 p3224 N85-29991
Study of Kapton under simulated shuttle environment
[NASA-CR-176003] 19 p3225 N85-29997
Slide release mechanism — for space shuttle orbiter/external tank connection device
[NASA-CASE-MSC-20080-1] 19 p3279 N85-30334
Insurance and the commercialization of space
[S-PRT-99-16] 20 p3397 N85-31074
Vibration/libration interaction dynamics during the orbiter based deployment of flexible members
20 p3411 N85-31171
Civilian Space Stations and the US future in Space
[OTA-STI-242] 20 p3418 N85-31215
Three-dimensional ballistocardiography in microgravity
20 p3510 N85-31818
Biostack experiments on STS-flights and the impact for man in space 20 p3C10 N85-31821
Pricing options for the space shuttle. Special study
21 p3559 N85-32138
The space shuttle glow
[AD-A154937] 21 p3559 N85-32139
Spacelab 1 hematology experiment (INS103): Influence of space flight on erythrokinetics in man
[NASA-TM-58266] 22 p3624 N85-33693
Results of a study to build a gamma-ray telescope in an external tank
[OG-9.3-3] 23 p4027 N85-34958
Space Missions for Automation and Robotics Technologies (SMART) Program
[NASA-TM-86820] 24 p4068 N85-35210
Results of tests of the SRB aft skirt heat shield curtain in the MSFC Hot Gas Facility
[NASA-CR-170888] 24 p4070 N85-35223
Evaluation of SRB phenolic TPS material made by an alternate vendor
[NASA-CR-170894] 24 p4073 N85-35240
Space shuttle SRB TPS protective paint test and evaluation in NASA Hot Gas Facility and AEDC Tunnel C
[NASA-CR-170884] 24 p4081 N85-35294
Results of tests of Insta-Foam Thermal Protection System (TPS) material for protection of equipment inside the SRB aft skirt
[NASA-CR-170892] 24 p4081 N85-35295
The 1986 National Aeronautics and Space Administration authorization
[GPO-47-635] 24 p4166 N85-35829

SPACE SIMULATORS
Functional capacities of elderly subjects exposed to simulated spaceflight factors 01 p0091 N85-10617

SPACE STATIONS
NT LONG DURATION EXPOSURE FACILITY
NT ORBITAL SPACE STATIONS
NT ORBITING LUNAR STATIONS
NT SALYUT SPACE STATION
NT SKYLAB 3
NT SKYLAB 4
Communications protocols for a fault tolerant, integrated local area network for Space Station applications
[NASA-TM-86304] 01 p0106 N85-10711
Human response to vibroacoustic environments of space vehicles
[NASA-TM-86316] 01 p0116 N85-10789
Office of Technology Assessment
01 p0127 N85-10872
Workshop on Automated Space Station
01 p0127 N85-10873
Second Symposium on Space Industrialization — space commercialization
[NASA-CP-2313] 02 p0149 N85-11011
The computer-communication link for the innovative use of Space Station 02 p0150 N85-11016
Role of Space Station: The how of space industrialization 02 p0153 N85-11036
Commercial space services 02 p0153 N85-11039
Features and uses of progress cargo ships
02 p0157 N85-11061
Conceptual design and evaluation of selected Space Station concepts: Executive summary
[NASA-TM-87382] 02 p0167 N85-11128
Conceptual design and evaluation of selected Space Station concepts, volume 1
[NASA-TM-87383] 02 p0168 N85-11129
Conceptual design and evaluation of selected Space Station concepts, volume 2
[NASA-TM-87384] 02 p0168 N85-11130
An evaluation of grease type ball bearing lubricants operating in various environments
[NASA-TM-86480] 02 p0185 N85-11239
SMP: A solid modeling program
[NASA-CR-172473] 02 p0241 N85-11570
International cooperation and competition in space
[GPO-38-001] 02 p0295 N85-11911
Statement of Kenneth S. Pedersen, Director, International Affairs Division, National Aeronautics and Space Administration 02 p0295 N85-11913
Civilian space stations and the US future in space: Summary
[OTA-STI-242] 03 p0323 N85-12083
Power subsystem automation study
[NASA-CR-171213] 03 p0358 N85-12299
Technologies for space station autonomy
[NASA-CR-174112] 04 p0458 N85-12906
Selected tether applications in space: An analysis of five selected concepts
[NASA-CR-171222] 04 p0460 N85-12921
Definition of technology development missions for early Space Station satellite servicing. Volume 2: Technical
[NASA-CR-171229] 04 p0461 N85-12923
Autonomous momentum management for space station, exhibit A
[NASA-CR-171256] 04 p0462 N85-12933
Regenerative fuel cell energy storage system for a low Earth orbit space station
[NASA-CR-174802] 04 p0527 N85-13371
Research and technology, 1984: Marshall Space Flight Center
[NASA-TM-86476] 04 p0590 N85-13765
Comparative energy storage assessment item
05 p0605 N85-13858
Perspectives on energy storage wheels for space station application 05 p0605 N85-13860
Space Power
[NASA-CP-2352] 05 p0608 N85-13
Space station power system 05 p0608 N85-13
Power for commercial space applications
05 p0608 N85-13
Thermal management technology status
05 p0610 N85-13
Civilian space stations and the US future in space
[OTA-STI-241] 07 p0914 N85-157
Issues and findings 07 p0914 N85-157
Space infrastructure 07 p0914 N85-157
A buyer's guide to space infrastructure
07 p0914 N85-157
Broadening the debate 07 p0914 N85-157
Toward a goal-oriented civilian space program
07 p0914 N85-157
Results of principal NASA studies on space station
and functional requirements 07 p0914 N85-157
The evolution of civilian in-space infrastructure, i.e., space station concepts in the United States
07 p0914 N85-157
International involvement in a civilian space
program 07 p0915 N85-157
Synopsis of the OTA Workshop on Cost
of Civilian Infrastructure (Civilian Space
Elements 07 p0915 N85-157
Financing considerations and Federal budget
07 p0915 N85-157
Space Station truss structures and
considerations
[NASA-TM-86338] 07 p0916 N85-157
Impact of lunar and planetary missions on the
station
[NASA-CR-171632] 08 p1106 N85-169
NASA OAST perspective 08 p1106 N85-169
Space station task force perspective
08 p1106 N85-169
Earth-to-orbit propellant transportation overview
08 p1108 N85-170
Passive storage technologies
08 p1108 N85-170
Active cooling requirements for propellant storage
08 p1108 N85-170
Propellant transfer: Attached depot
08 p1108 N85-170
Space Station needs, attributes, and architectural
study
[NASA-CR-174316] 08 p1109 N85-170
FRG study looks at participation in ESA, US space
station 08 p1141 N85-171
Characterization of heat transfer in nutrient
— space flight feeding
[NASA-CR-171841] 08 p1199 N85-175
Summary of activities of Aeronautics and
Engineering Board
[NASA-CR-174294] 08 p1228 N85-177
Impact of lunar and planetary missions on the
station: Preliminary STS logistics report
[NASA-CR-171837] 09 p1265 N85-180
Space Station engineering and technology
development
[NASA-CR-174363] 09 p1287 N85-180
Commercial space: Europe should have independent
strategy 10 p1460 N85-1
West Europe report: Science and technology
[JPRS-WST-85-008] 11 p1617 N85-201
FRG's DFVLR ready for participation in space
11 p1618 N85-20
Applications of Tethers in Space, volume 1
[NASA-CP-2364] 11 p1642 N85-20
Transportation applications, part 2
11 p1643 N85-20
Summary presentation of the Transportation Panel
11 p1644 N85-20
Summary presentation to the Artificial Gravity Panel
11 p1644 N85-20
Report of the Artificial Gravity Panel
11 p1645 N85-20
Physiological considerations of artificial gravity
11 p1645 N85-20
Some aspects of attitude stability of tethered
stations 11 p1646 N85-20
Charge-to-mass dispersion methods
abrasion-ablation fragmentation models
[NASA-TM-86340] 11 p1726 N85-20
Environment definition, small particles, diameter
than or equal to 1 MM 12 p1788 N85-21
Advanced research and technology programs
advanced high-pressure oxygen-hydrogen
propulsion
[NASA-TM-86968] 12 p1789 N85-21
Space Station
[NASA-EP-211] 12 p1793 N85-21
Aerospace Safety Advisory Panel
[NASA-TM-87426] 13 p1970 N85-22

Feoktistov argues against U.S. space shuttle design concept 13 p1985 N85-22453

Space station systems technology study (add-on task). Volume 1: Executive summary
[NASA-CR-171415] 13 p1986 N85-22459

Advancing automation and robotics technology for the Space Station and for the US economy. Volume 1: Executive overview
[NASA-TM-87566-VOL-1] 13 p1986 N85-22460

Advancing automation and robotics technology for the Space Station and for the US economy, volume 2
[NASA-TM-87566-VOL-2] 13 p1987 N85-22461

Selected tether applications in space: Phase 2. Executive summary
[NASA-CR-171421] 13 p1987 N85-22462

Selected tether applications in space: Phase 2
[NASA-CR-171422] 13 p1987 N85-22463

Space Station technology planning
13 p1989 N85-22471

Space test program of high-voltage solar array-space plasma interactions 13 p1997 N85-22519

Research opportunities in human behavior and performances
[NASA-CR-3886] 13 p2142 N85-23299

Large Space Antenna Systems Technology, 1984
[NASA-CP-2368-PT-2] 14 p2233 N85-23840

Determination of electromagnetic properties of mesh material using advanced radiometer techniques
14 p2235 N85-23855

The space station as a construction base for large space structures 14 p2235 N85-23856

Utilization of space station by the large deployment reflector 14 p2235 N85-23857

Large Deployable Reflector (LDR) requirements for space station accommodations
14 p2236 N85-23858

Utilization of the polar platform of NASA's Space Station Program for operational Earth observations
[PB85-152502] 14 p2240 N85-23895

The context for food service and nutrition in the space station 14 p2393 N85-24734

NASA plans for a space station
14 p2393 N85-24735

Food service management 14 p2393 N85-24736

Alternative food preservation techniques, new technology in food preparation and appropriateness of food supply for the permanently manned space station
14 p2393 N85-24739

Nutritional criteria for military rations and effects of prolonged feeding on acceptability
14 p2394 N85-24742

Food service and nutritional needs
14 p2394 N85-24744

Packaging's contribution for the effectiveness of the space station's food service operation
14 p2394 N85-24746

Packaging for food service 14 p2394 N85-24747

Space station systems technology study (add-on task). Volume 2: Trade study and technology selection
[NASA-CR-171416] 15 p2475 N85-25279

Space station systems technology study (add-on task). Volume 3: Technology advancement program plan
[NASA-CR-171417] 15 p2475 N85-25280

Definition of technology development missions for early space stations: Large space structures
[NASA-CR-171446] 15 p2476 N85-25281

Construction in space
[NASA-TM-77630] 15 p2492 N85-25374

Long-life high performance fuel cell program
[NASA-CR-174874] 15 p2494 N85-25384

Space station propulsion: The advanced development program at Lewis
[NASA-TM-86999] 15 p2494 N85-25386

West Europe report: Science and technology
[JPRS-WST-84-008] 15 p2531 N85-25606

European views differ on space station concept
15 p2531 N85-25608

West Europe report: Science and technology
[JPRS-WST-84-026] 15 p2532 N85-25617

FRG opinion on Spacelab benefits, space station participation 15 p2532 N85-25618

West Europe report: Science and technology
[JPRS-WST-84-010] 15 p2535 N85-25644

A brief description of the two primate experiments to be carried out on SL-4 15 p2687 N85-26597

The NASA Space Station program plans
[NASA-TM-87474] 16 p2730 N85-26846

Spacestation: The next logical step
[NASA-EP-213] 16 p2730 N85-26847

Space Station Engineering and Technology Development
[NASA-CR-175806] 16 p2731 N85-26851

Space Station Spartan study
[NASA-TM-86215] 16 p2731 N85-26852

A SLAM II simulation model for analyzing space station mission processing requirements
[NASA-CR-175664] 16 p2731 N85-26853

Tethered nuclear power for the Space Station
[NASA-TM-87023] 16 p2740 N85-26912

Space Station crew safety alternatives study. Volume 5: Space Station safety plan
[NASA-CR-3858] 17 p2908 N85-27930

Automation and robotics for the National Space Program
[NASA-CR-175881] 17 p2909 N85-27936

Performance analysis of radiation cooled dc transmission lines for high power space systems
[NASA-TM-87040] 17 p2951 N85-28222

Documentation for the West German Federal Cabinet's space policy decision 17 p3051 N85-28886

Space Station crew safety alternatives study. Volume 4: Appendices
[NASA-CR-3857] 18 p3065 N85-28958

An evaluation of oxygen-hydrogen propulsion systems for the Space Station
[NASA-TM-87059] 18 p3067 N85-28971

West Europe report: Science and technology
[JPRS-WST-84-022] 18 p3085 N85-29086

West Europe report: Science and technology
[JPRS-WST-84-031] 18 p3086 N85-29089

DFVLR official on areas of US-FRG Space Station cooperation 18 p3086 N85-29091

FRG weighs ESA participation, budget issues
18 p3088 N85-29110

DFVLR study recommends European independence in space systems 18 p3088 N85-29111

Proceedings of the Seminar on Space Station Human Productivity
[NASA-TM-86673] 18 p3156 N85-29539

Space station crew safety: Human factors interaction model 18 p3156 N85-29540

Space station crew safety alternatives study, third quarter briefing 18 p3156 N85-29541

Statement of contamination problem
18 p3156 N85-29542

Internal contamination issues
18 p3156 N85-29543

Materials and processes control for space applications
18 p3156 N85-29544

Some problems associated with trace contaminant removal systems for spacecabins
18 p3158 N85-29554

Contamination control for increased crew productivity
18 p3158 N85-29555

Human productivity program definition
18 p3158 N85-29556

Overview: Human factors issues in space station architecture 18 p3158 N85-29558

A preliminary human factors planning and design outline of parameters related to space station windows and CCTV monitoring 18 p3158 N85-29559

Human factors issues in space station architecture
18 p3158 N85-29560

Man-machine tradeoff study 18 p3158 N85-29561

Some ideas and questions regarding space station design for human use 18 p3158 N85-29562

Human productivity experience and undersea habitat design 18 p3159 N85-29563

Considerations for space station interior architecture
18 p3159 N85-29564

Human factors in space station architecture: The ECLSS module concept 18 p3159 N85-29565

Habitability sleep accommodations
18 p3159 N85-29566

Customer and mission influence on space station architecture 18 p3159 N85-29567

Space station models, mockups and simulators
18 p3159 N85-29569

Mockups and human productivity studies
18 p3159 N85-29570

Experiences with neutral buoyance testing mockups
18 p3159 N85-29571

Rockwell experience applications to Ames space station mockup habitability/productivity studies
18 p3159 N85-29572

The role of mock-ups in the development of Orbital Replaceable Units (ORU) 18 p3160 N85-29573

International space research perspectives of commercialization for German industry
[NASA-TM-77657] 19 p3222 N85-29979

Space station crew safety alternatives study. Volume 3: Safety impact of human factors
[NASA-CR-3856] 19 p3223 N85-29984

Space station crew safety alternatives study, volume 1
[NASA-CR-3854] 19 p3223 N85-29985

Space station automation study. Volume 2: Technical report. Autonomous systems and assembly
[NASA-CR-171515] 19 p3226 N85-30001

Space station automation study. Volume 1: Executive summary. Autonomous systems and assembly
[NASA-CR-171514] 19 p3226 N85-30002

Flow cytometry for health monitoring in space
[DE85-009572] 19 p3329 N85-30625

Department of Housing and Urban Development-Independent Agencies Appropriation Bill, 1986
[H-REPT-99-212] 19 p3382 N85-30979

Space Station reference configuration description
[NASA-TM-87493] 20 p3408 N85-31146

Space Station man-machine automation trade-off analysis
[NASA-CR-176046] 20 p3408 N85-31147

Automatic assembly of space stations
20 p3409 N85-31153

Space station dynamic modeling, disturbance accommodation, and adaptive control
20 p3409 N85-31154

Space station configuration and flight dynamics identification 20 p3410 N85-31162

Design of multivariable controllers using the Integrated Analysis Capability (IAC) 20 p3412 N85-31172

Attitude control tradeoff study between the use of a flexible beam and a tether configuration for the connection of two bodies in orbit 20 p3412 N85-31174

Space station parametric models
20 p3413 N85-31180

Civilian Space Stations and the US future in Space
[OTA-STI-242] 20 p3418 N85-31215

The 1984 Goddard Space Flight Center Battery Workshop
[NASA-CP-2382] 20 p3443 N85-31371

Regenerative fuel cell systems for space station
20 p3443 N85-31372

Space Station crew safety alternatives study. Volume 2: Threat development
[NASA-CR-3855] 21 p3558 N85-32133

NASA space station automation: AI-based technology review
[NASA-CR-176094] 21 p3558 N85-32134

Automation study for space station subsystems and mission ground support
[NASA-CR-176097] 21 p3559 N85-32136

Space station ECLSS integration analysis: Simplified General Cluster Systems Model, ECLS System Assessment Program enhancements
[NASA-CR-176089] 21 p3670 N85-32796

A survey of structural material issues for a space station
[NASA-TM-86385] 22 p3738 N85-33168

Space station automation study. Automation requirements derived from space manufacturing concepts. Volume 1: Executive summary
[NASA-CR-176099] 22 p3738 N85-33170

Space Station automation study. Automation requirements derived from space manufacturing concepts. Volume 2: Technical report
[NASA-CR-176100] 22 p3738 N85-33171

Space station automation and robotics study. Operator-systems interface
[NASA-CR-176095] 22 p3738 N85-33172

Testimony of Robert A. Frosch before the Subcommittee on HUD and Independent Agencies of the Senate Committee on Appropriations
[NASA-TM-87496] 22 p3738 N85-33173

Statement of Aaron Cohen, Director, Research and Engineering, Johnson Space Center and Chairman, Space Station Advanced Technology Advisory Committee, National Aeronautics and Space Administration, before the Subcommittee on Science, Technology, and Space, Committee on Commerce, Science, and Transportation, United States Senate
[NASA-TM-87497] 22 p3739 N85-33174

Space station automation study: Autonomous systems and assembly, volume 2
[NASA-CR-176092] 22 p3739 N85-33175

Deployable-erectable trade study for space station truss structures
[NASA-TM-87573] 22 p3740 N85-33181

The space station polar platform: NOAA systems considerations and requirements
[NOAA-TR-NESDIS-22] 22 p3740 N85-33182

Structural dynamics model and response of the deployable reference configuration space station
[NASA-TM-86386] 22 p3799 N85-33539

Study to encourage and facilitate industrial investment and involvement in space
[NASA-CR-176152] 23 p3896 N85-34147

Space station rotational equations of motion
[NASA-TP-2511] 23 p3899 N85-34148

Space Station Engineering and Technology Development: Proceedings of the Panel on In-Space Engineering Research and Technology Development
[NASA-CR-176[illegible]] 23 p3899 N85-34153

The role of tethers on space station
[NASA-TM-86519] 23 p3900 N85-34154
Coordinated study of solar-terrestrial payloads on space station
[NASA-CR-176160] 23 p3900 N85-34158
Soft X-Ray Telescope (SXRT)
23 p3900 N85-34159
Solar Ultraviolet Spectral Irradiance Monitor (SUSIM)
23 p3901 N85-34160
White Light Coronograph (WLC) and Ultra-Violet Coronal Spectrometer (UVCS) 23 p3901 N85-34161
High Resolution Telescope and Spectrograph (HRTS)
23 p3901 N85-34162
Active Cavity Radiometer (ACR)
23 p3901 N85-34163
Waves In Space Plasmas (WISP)
23 p3901 N85-34164
Space Experiments with Particle Accelerators (SEPAC) 23 p3901 N85-34165
Theoretical and Experimental Beam Plasma Physics (TEBPP) 23 p3901 N85-34166
Recoverable Plasma Diagnostics Package (RPDP)
23 p3902 N85-34167
Electrodynamic tether 23 p3902 N85-34168
Imaging Spectrometric Observatory (ISO)
23 p3902 N85-34169
Atmospheric Emission Photometric Imaging (AEPI)
23 p3902 N85-34170
Magnetospheric multiprobes: MMP/CHEMSAT
23 p3902 N85-34171
Wide Angle Michelson Doppler Imaging Interferometer (WAMDII) 23 p3902 N85-34172
Vehicle Charging And Potential (VCAP)
23 p3902 N85-34173
Initial placement of STO instruments
23 p3902 N85-34174
Optical analysis of parabolic dish concentrators for solar dynamic power systems in space
[NASA-TM-87080] 23 p3903 N85-34176
Detection of 10 (1) GeV cosmic neutrinos with a space station
[OG-9.4-10] 23 p4030 N85-34977
Technology for large space systems: A bibliography with indexes
[NASA-SP-7046(12)] 24 p4068 N85-35209
Space Missions for Automation and Robotics Technologies (SMART) Program
[NASA-TM-86820] 24 p4068 N85-35210
Space Station Polar Platform: Integrating research and operational missions
[PB85-195279] 24 p4069 N85-35218
The 1986 National Aeronautics and Space Administration authorization
[GPO-47-635] 24 p4166 N85-35829
SPACE STORAGE
Earth-to-orbit propellant transportation overview
08 p1108 N85-17002
Hemispherical latching apparatus
[NASA-CASE-MFS-25837-1] 19 p3224 N85-29991
SPACE SUITS
Flame resistant fibrous materials development
[NASA-CR-167817] 07 p0920 N85-15827
Challenges in the development of the shuttle extravehicular mobility unit 08 p1095 N85-16922
A theoretical method for selecting space craft and space suit atmospheres
[AD-A148219] 08 p1200 N85-17559
Elbow and knee joint for hard space suits and the like
[NASA-CASE-ARC-11610-1] 11 p1687 N85-20666
Shoulder and hip joint for hard space suits and the like
[NASA-CASE-ARC-11543-1] 12 p1910 N85-21986
Torso sizing ring construction for hard space suit
[NASA-CASE-ARC-11616-1] 12 p1910 N85-21987
SPACE SURVEILLANCE (GROUND BASED)
NORAD operational system 12 p1783 N85-21189
SPACE SURVEILLANCE (SPACEBORNE)
NORAD operational system 12 p1783 N85-21189
Computing parameters characterizing possibility of planets falling in star camera field of view during space survey 15 p2467 N85-25351
SPACE SYSTEMS ENGINEERING
U AEROSPACE ENGINEERING
SPACE TECHNOLOGY EXPERIMENTS
Space Technology Experiments Platform (STEP) status: An in-space test facility 14 p2236 N85-23863
SPACE TELESCOPE
U HUBBLE SPACE TELESCOPE
SPACE TOOLS
EVA of cosmonauts Savitskaya and Dzhanibekov
02 p0158 N85-11076
Commentary on hand tool used in cosmonaut EVA
02 p0159 N85-11077
Further details in welding, spray-coating tool
02 p0159 N85-11078
Electric Welding Institute's space-technology test results 03 p0352 N85-12267
Special tools used by cosmonauts in EVA
22 p3731 N85-33129
SPACE TRANSPORTATION
NT CHALLENGER (ORBITER)
NT COLUMBIA (ORBITER)
NT DISCOVERY (ORBITER)
NT ENTERPRISE (ORBITER)
NT SPACE SHUTTLE BOOSTERS
NT SPACE SHUTTLE MISSION 31-C
NT SPACE SHUTTLE MISSION 41-B
NT SPACE SHUTTLE MISSION 41-C
NT SPACE SHUTTLE MISSION 41-G
NT SPACE SHUTTLE MISSION 51-A
NT SPACE SHUTTLE MISSION 51-C
NT SPACE SHUTTLE MISSIONS
NT SPACE SHUTTLE ORBITERS
NT SPACE TRANSPORTATION SYSTEM
Conestoga 2: A low cost commercial space transport system 02 p0153 N85-11033
Winged first stages of space transport appliances
[TUM-RT-TB-84/3] 02 p0167 N85-11125
Possibilities and limits of electromagnetic acceleration in space applications
[ILR-MITT-136] 02 p0193 N85-11292
Verification tests of durable TPS concepts
[NASA-TM-86313] 03 p0323 N85-12065
Space infrastructure 07 p0914 N85-15783
Applications of Tethers in Space, volume 1
[NASA-CP-2364] 11 p1642 N85-20339
Transportation applications, part 1
11 p1643 N85-20349
Report of the Transportation Panel
11 p1645 N85-20364
Optimization of guidance and control using function minimization and NAVSTAR/GPS
[AD-A149956] 12 p1775 N85-21141
Shuttle fleet operations: A simulation analysis
[AD-A151383] 15 p2491 N85-25370
SPACE TRANSPORTATION SYSTEM
NT CHALLENGER (ORBITER)
NT COLUMBIA (ORBITER)
NT DISCOVERY (ORBITER)
NT ENTERPRISE (ORBITER)
NT SPACE SHUTTLE BOOSTERS
NT SPACE SHUTTLE MISSION 31-C
NT SPACE SHUTTLE MISSION 41-B
NT SPACE SHUTTLE MISSION 41-C
NT SPACE SHUTTLE MISSION 41-G
NT SPACE SHUTTLE MISSION 51-A
NT SPACE SHUTTLE MISSION 51-C
NT SPACE SHUTTLE MISSIONS
NT SPACE SHUTTLE ORBITERS
NT SPACE TRANSPORTATION SYSTEM FLIGHTS
National Aeronautics and Space Administration
01 p0127 N85-10671
Legal considerations and cooperative opportunities for space commercial activities 02 p0150 N85-11013
External tank aft cargo carrier
02 p0155 N85-11050
Continuing issues (FY 1983) concerning military use of the space transportation system
[AD-A146091] 03 p0323 N85-12060
Selected tether applications in space: An analysis of five selected concepts
[NASA-CR-171222] 04 p0460 N85-12921
Resident research associateships. Postdoctoral and senior research awards
[NASA-TM-87399] 05 p0734 N85-14717
The aerodynamic challenges of SRB recovery
08 p1093 N85-16906
Space Transportation System and associated payloads: Glossary, acronyms, and abbreviations
[NASA-RP-1059-REV] 10 p1428 N85-19007
Space Transportation System (STS) propellant scavenging system study. Volume 1: Technical report
[NASA-CR-171848-VOL-1] 11 p1589 N85-20000
Space Transportation System (STS) propellant scavenging system study. Volume 2: Supporting research and technology report
[NASA-CR-171849-VOL-2] 11 p1589 N85-20001
Space Transportatioin System (STS) propellant scavenging system study. Volume 3: Cost and work breakdown structure-dictionary
[NASA-CR-171850-VOL-3] 11 p1590 N85-20002
Applications of Tethers in Space, volume 2
[NASA-CP-2365] 11 p1644 N85-20361
Status of the National Space Transportation System
11 p1712 N85-20772
Space Shuttle interactive meteorological data system study
[NASA-CR-171418] 12 p1892 N85-21876
Aerospace Safety Advisory Panel
[NASA-TM-87426] 13 p1970 N85-22373
NASA R and T aerospace plane vehicles: Progress and plans
[NASA-TM-86429] 15 p2491 N85-2
Costs, payload of Ariane, US Space Shuttle compared
15 p2530 N85-2
Telescope in lunar orbit 15 p2562 N85-2
SPACE TRANSPORTATION SYSTEM FLIGHTS
NT SPACE TRANSPORTATION SYSTEM 1 FLIGHT
NT SPACE TRANSPORTATION SYSTEM 3 FLIGHT
NT SPACE TRANSPORTATION SYSTEM 4 FLIGHT
Ground man-machine interfaces for orbiter checkout
08 p1091 N85-1
Overview od STS ground operations/orbiter turnaround STS-1 through STS-7 08 p1096 N85-1
STS atmospheric luminosities
[NASA-CR-175514] 12 p1791 N85-2124
Results of Space Shuttle flight 41-D
[GPO-39-481] 12 p1791 N85-212
Shuttle payload bay dynamic environments: Summary and conclusion report for STS flights 1-5 and 9
[NASA-CR-175856] 14 p2241 N85-2
National Space Transportation Systems Program mission report
[NASA-TM-87456] 14 p2241 N85-2
National Space Transportation Systems Program mission report
[NASA-TM-87454] 14 p2242 N85-2
Surface pressure produced by Space Transportation System flight 41B
[AD-A150793] 14 p2242 N85-2
Recommendations and calculations concerning physical characteristics of the EEVT apparatus
20 p3502 N85-317
Clarke Stations and mercurian mass-drivers: Energy for large-scale transportation systems
[DE85-009607] 21 p3560 N85-32145
SPACE TRANSPORTATION SYSTEM 1 FLIGHT
STS-1 Pogo analysis
[NASA-TM-87433] 11 p1591 N85-20007
SPACE TRANSPORTATION SYSTEM 3 FLIGHT
Get Away Special (GAS) thermal design summary
[X-732-83-8] 15 p2475 N85-2527
SPACE TRANSPORTATION SYSTEM 4 FLIGHT
Shuttle electrical environment
13 p1990 N85-22475
SPACE TRANSPORTATION SYSTEM 11 FLIGHT
Results of Space Shuttle Flight 41-C
[GPO-36-092] 04 p0461 N85-1292
Statement of Captain Robert L. Crippen, USN, Commander of Space Shuttle Flight 41-C; Francis R. Scobee, pilot; Doctor George D. Nelson, Mission Specialist; Terry J. Hart, Mission Specialist; and Doctor James D. Van Hoften, Mission Specialist; accompanied by Frank Cepollina, Solar Maximum Repair Mission Project Manager, Goddard Space Flight Center
04 p0461 N85-1292
Statement of Frank Cepollina, Solar Maximum Repair Mission Project Manager, Goddard Space Flight Center
04 p0461 N85-1293
SPACE VEHICLE CHECKOUT PROGRAM
Integrated design checkout of shuttle payload avionics interfaces 08 p1092 N85-1
Automation of checkout for the shuttle operations era
08 p1092 N85-1
SPACE VEHICLE CONTROL
U SPACECRAFT CONTROL
SPACE VEHICLES
U SPACECRAFT
SPACE WEAPONS
NT LASER WEAPONS
PRC journal discusses 'Star Wars' space program
11 p1621 N85-2
Combat capable space systems for tactical support
11 p1713 N85-2077
High energy lasers: A primer on directed energy weapons for space use
[AD-A151279] 15 p2562 N85-2
US said to seek military advantage in space
16 p2727 N85-2
Military journal on US intelligence satellites
16 p2727 N85-2
Strategic defense initiative
[DE85-012778] 24 p4150 N85-3
SPACE-TIME CONTINUUM
U RELATIVITY
SPACE-TIME FUNCTIONS
Gravitational vacuum 02 p0265 N85-117
Change in relationship of biopotentials of brain zones for various levels of working capacity
07 p1013 N85-1
Algorithm for space-time analysis of data of geomagnetic field
[NASA-TM-77804] 08 p1209 N85-1
Conserved quantities and radiative aspects of asymptotically anti-de Sitter space-times
12 p1956 N85-2

A practical system for collecting reliable data on the space-time behavior of people
[AD-A151174] 15 p2619 N85-26140
Comment on quantum effects on 4-dimensional space-time symmetries
[DE85-007760] 16 p2872 N85-27722
Characteristics of optical information-measurement channels with utilization of scattering effects
22 p3781 N85-33429

SPACE-TIME METRIC
U SPACE-TIME FUNCTIONS

SPACEBORNE ASTRONOMY
Algorithm for astronomical, extended source, signal-to-noise radio calculations
[NASA-TP-2396] 03 p0445 N85-12833
Algorithm for astronomical, point source, signal to noise ratio calculations
[NASA-TP-2397] 03 p0445 N85-12834
Space research and the new approach to the mechanics of fluid media in cosmos
[TRITA-EPP-84-04] 03 p0447 N85-12844
X-ray and ultraviolet observations of BL Lacertae objects 05 p0741 N85-14767
Future studies of the local interstellar medium with Space Telescope and Columbus 06 p0880 N85-15593
Observations of local ISM emission with the Berkeley EUV/FUV shuttle telescope 06 p0880 N85-15594
QUASAT: A VLBI observatory in space — conferences
[ESA-SP-213] 07 p1056 N85-16700
The galaxy scene and QUASAT — VLBI satellite
07 p1056 N85-16703
The QUASAT mission: An overview
07 p1056 N85-16704
Some prospects of space VLBI
07 p1056 N85-16705
QUASAT: Technical aspects of the proposed mission — VLBI satellite 07 p1057 N85-16706
A study on the imaging potential of QUASAT — spaceborne VLBI 07 p1057 N85-16707
Correlator and data processing requirements for QUASAT 07 p1057 N85-16709
Processing system for space VLBI
07 p1057 N85-16711
Testing theories of superluminal motion — QUASAT
07 p1058 N85-16714
QUASAT, gravitational lenses, and studies of the interstellar, intracluster and intergalactic medium
07 p1058 N85-16715
Very Long Base Interferometry (VLBI) in space and X-ray observations of compact sources in active galactic nuclei 07 p1058 N85-16716
The wide-range space radio interferometer
07 p1058 N85-16717
The relevance of QUASAT to the star formation problem 07 p1058 N85-16718
Galactic OH and H2O masers — QUASAT project
07 p1058 N85-16719
Water masers and distance measurements: The impact of QUASAT 07 p1059 N85-16721
A short note on the high precision navigation of QUASAT 07 p1059 N85-16722
Opportunities for high angular and temporal resolutions of galactic objects at radio frequencies — QUASAT
07 p1059 N85-16723
Characteristics of X-ray spectra from galactic and extragalactic X-ray sources 08 p1239 N85-17811
The ROSAT all-sky survey in X-rays
08 p1243 N85-17843
A new look at the planets — space probes
[AERONOMICA-ACTA-37-1984]
11 p1765 N85-21096
X-ray experiment on Prognoz-9 artificial Earth satellite
15 p2478 N85-25295
Planetary Rings. Colloquium 75 — conferences
[ISBN-2-85428-100-4] 15 p2670 N85-26473
Future observations of planetary rings from ground-based observatories and Earth-orbiting satellites
15 p2678 N85-26540
A priority of space exploration: Observation of Saturn's rings from a Saturn orbiter 15 p2679 N85-26542
European space science horizon 2000
[ESA-SP-1070] 16 p2717 N85-26771
IRAS: Space technology from the Netherlands
[B8661841] 17 p2908 N85-27929
Assessment study of liquid content measurement methods applicable to space missions — Infrared Space Observatory
[TU-HH-TRI-ESA-84-2] 17 p2936 N85-28135
Spacelab 2
[NASA-EP-217] 19 p3222 N85-29977
Mapping with QUASAT (quasar satellite) using short observation times
[AD-A155155] 21 p3559 N85-32141
Comments on RS-17 X-ray telescope
22 p3731 N85-33132
Results from Astron orbiting telescope
22 p3732 N85-33134
Mosaic Infrared Sensor for Space Astronomy (MIRSSA)
[NASA-CR-176154] 22 p3786 N85-33456

SPACEBORNE EXPERIMENTS
NT ATMOSPHERIC GENERAL CIRCULATION EXPERIMENT
NT EARTH RADIATION BUDGET EXPERIMENT
NT PLASMA INTERACTION EXPERIMENT
Effect of spaceflight factors on rat bone marrow cells
01 p0092 N85-10620
European retrievable carrier (Eureca) and evolutionary space carrier for microgravity, Earth observation and technology demonstration 02 p0152 N85-11032
The evolution of small payload carrier systems
02 p0153 N85-11036
Fluids Experiment Apparatus (FEA)
02 p0155 N85-11048
Commentary on Salyut-7 electrophoresis, plugging mortar experiments 02 p0158 N85-11072
Tass reports experiments during visiting crew's third day 02 p0158 N85-11073
Commentary on derivation of biological materials, cosmonaut adaptation 02 p0158 N85-11074
Tass reports astrophysical, atmospheric studies on Salyut-7 02 p0158 N85-11075
EVA of cosmonauts Savitskaya and Dzhanibekov
02 p0158 N85-11076
Further details in welding, spray-coating tool
02 p0159 N85-11078
Use of gravitational stabilization in performance of experiments 02 p0160 N85-11084
Research and technology, 1984: Marshall Space Flight Center
[NASA-TM-86476] 04 p0590 N85-13765
Life Sciences Research in Space — conference
[ESA-SP-212] 05 p0689 N85-14425
Bioprocessing in space 05 p0690 N85-14439
Medication interference with space research: An example from a mass-discrimination experiment on Spacelab 1 05 p0695 N85-14472
Computerized sleep staging by detecting eye and hand movement, delta EEG activity and EMG, using portable solid state technique — spaceborne experiments
05 p0695 N85-14475
Overview of German microgravity activities in the field of life science 05 p0696 N85-14476
Space station: New frontier for life sciences in space
05 p0696 N85-14477
Controlled ecological life support system higher plant flight experiments
[NASA-CR-177323] 07 p1020 N85-16471
Botany facility, phase A study. Part 1: Executive summary — EURECA
[BF-DOC-10-VOL-1] 08 p1110 N85-17015
Spaceborne distributed SAR antenna
[NASA-CR-171835] 08 p1150 N85-17259
A method for determining mesoscale dynamic topography
[AD-D011412] 08 p1191 N85-17506
Automatic Monoellipsoidal Mirror Furnace Facility (AMMFF), volume 1 — spaceborne crystal growth
[AMF-RP.100-DS-015-VOL-1] 09 p1285 N85-18073
Development of a 20 GHz modulator for the payload of a satellite for propagation and transmission experiments, including the required converters of the test equipment
[BMFT-FB-W-84-044] 11 p1590 N85-20004
Solution growth facility, phase A design study, executive summary — EURECA
[RPT/SGF/00014/TER] 11 p1591 N85-20006
Alloy supercooling on Salyut-7
11 p1604 N85-20083
Fluid slosh dynamics of surface tension tanks in three axis stabilized spacecraft
[MBB-UR-E-739-84-O] 11 p1634 N85-20291
The space flight of the Soviet-Indian crew
[NASA-TM-77615] 12 p1788 N85-21226
Lyakhov and Aleksandrov on 150-day flight
13 p1977 N85-22405
Comments on Salyut-7 150-day flight
13 p1977 N85-22406
Langley Research Center photogrammetric measurements of solar array dynamics: Preliminary results 14 p2233 N85-23844
Space Technology Experiments Platform (STEP) status: An in-space test facility 14 p2236 N85-23863
Shuttle attached antenna Flight Experiment Definition Study (FEDS) 14 p2237 N85-23865
Electro-science requirements for shuttle-attached antenna flight experiments 14 p2237 N85-23866
National Space Transportation Systems Program mission report
[NASA-TM-87455] 14 p2242 N85-23900
Scientific experiments. Preprocessing of scientific data — spaceborne experiments
14 p2398 N85-24779
Holography in space 15 p2476 N85-25285
Second Soviet-French Symposium on Space Technology 15 p2483 N85-25326
Cosmonauts report on space welding at conference
15 p2484 N85-25329
Paton comments on results of space welding tests
15 p2484 N85-25330
Space brain research in China reported
15 p2537 N85-25657
Importance of gravity for plant growth and behavior
15 p2608 N85-26070
Study on the extension of experiment resources in the MAUS project
[BMFT-FB-W-84-051] 15 p2650 N85-26343
Sixteenth Lunar and Planetary Science Conference. Press abstracts
[NASA-CR-175692] 15 p2680 N85-26548
NASA Ames Summer High School Apprenticeship Research Program
[NASA-TM-86006] 15 p2686 N85-26590
Academician Zuyev notes plans for lasers on spacecraft for atmospheric research 16 p2717 N85-26775
Satellite research on solar flares
16 p2717 N85-26776
Botany facility phase A study. Core payload number 6 EURECA carrier, volume 1
[ESA-CR(P)-1978-VOL-1] 17 p2906 N85-27918
Botany facility phase A study. Core payload number 6 for EURECA carrier, volume 2
[BF-TD-DRD-03-VOL-2] 17 p2906 N85-27919
Long life feasibility study for the shuttle infrared telescope facility
[NASA-CR-3722] 17 p3052 N85-28893
Gas chromatography: Possible application of advanced instrumentation developed for solar system exploration to space station cabin atmospheres
18 p3157 N85-29551
Spacelab 2
[NASA-EP-217] 19 p3222 N85-29977
Space shuttle molecular and wake vacuum measurements
[NASA-TM-86509] 19 p3222 N85-29978
Dynamic response of a flexible space beam
[NASA-TM-86441] 19 p3285 N85-30368
Shuttle Molecular Gun: Smog. Potential experiment for the electrodynamic Tethered Satellite System (TSS) mission
[IFSI-84-17] 20 p3419 N85-31221
Recommendations and calculations concerning physical characteristics of the EEVT apparatus
20 p3502 N85-31769
Experience of science astronaut on the Spacelab-1 mission 20 p3508 N85-31807
Mass-discrimination during prolonged weightlessness
20 p3509 N85-31814
Study of requirements for and method of multidimensional acoustic imaging — spaceborne experiments
[ESA-CR(P)-2020] 20 p3525 N85-31924
Energy spectra of elements with 18 less than or equal to Z less than or equal to 28 between 10 and 300 GeV/amu 20 p3543 N85-32045
Elemental abundances of cosmic rays with Z33 as measured on HEAO-3 20 p3543 N85-32046
Study of proton and neutron activation of metal samples in low Earth orbit
[NASA-CR-171596] 21 p3558 N85-32130
USSR Space Life Sciences Digest
[NASA-CR-3922] 21 p3656 N85-32709
Salyut-7 cosmonauts work with RS-17 and GSPS X-ray telescopes 22 p3731 N85-33131
Results and prospects of physiological research during spaceflights 22 p3732 N85-33139
Effect of substrate moisture on growth and structure of corn leaf 22 p3824 N85-33692
The development of a high energy cosmic ray detector for Spacelab-2
[OG-9.1-8] 23 p4023 N85-34934
The heavy ions in space experiment
[OG-9.1-10] 23 p4023 N85-34936
NASA Developmental Biology Workshop: A summary
[NASA-TM-86756] 24 p4126 N85-35576

SPACEBORNE PHOTOGRAPHY
NT SATELLITE-BORNE PHOTOGRAPHY
Tass reports experiments during visiting crew's third day 02 p0158 N85-11073
The possibility of detection and measurement of cloud structure in the atmosphere of Uranus
02 p0299 N85-11937
Metric camera experiment: Spacelab 1 mission
05 p0658 N85-14229
The photogrammetric camera experiment on Spacelab 1 05 p0658 N85-14230

Searching for impact craters using space shuttle photography 06 p0889 N85-15645
Lyakhov and Aleksandrov on 150-day flight 13 p1977 N85-22405
Experience in automated interpretation of aerospace photographs 13 p1983 N85-22444
Geoindication method for interpreting aerial and space photographs: Status and prospects 13 p1984 N85-22445
Experience in combined special mapping using space information 13 p1984 N85-22449
Study of Volga river delta using space photosurvey materials 15 p2485 N85-25340
Use of space information in petroleum- and gas-prospecting work (example of Southern Mangyshlak) 15 p2485 N85-25341
Example of joint use of data from surface studies and space photographs in investigating dynamics of zone of North Zeravshan seismogenic faults 15 p2485 N85-25342
Relative geological information yield from small-scale multizonal space images (example of Fergana depression and its mountainous margins) 15 p2485 N85-25343
Identifying land use structures of multizonal aerospace photographs using digital data processing 15 p2486 N85-25348
Experience in automation of data processing in interpretation and defining of linear elements from space photographs 15 p2486 N85-25349
Computing parameters characterizing possibility of planets falling in star camera field of view during space survey 15 p2487 N85-25351
Glow of ionospheric F-layer in Line 630 nm determined from photographs taken aboard Salyut-6 orbital station: Interpretation of results 16 p2721 N85-26799
SVIT complex for analysis of space photography 16 p2725 N85-26819
Tenth Conference of Working Group of Socialist Countries on Remote Sensing of Earth under Intercosmos Program 16 p2725 N85-26820
Study and mapping of anthropogenic effect on environment in different regions of USSR on basis of space photographs 16 p2726 N85-26824
Multiple regression analysis of photographic image of soil properties 16 p2726 N85-26825
Analysis of mesofissuring on space photographs: New technique for study of petroleum and gas deposits 16 p2726 N85-26828
Space photographs confirm 40-year-old hydrodynamics discovery 19 p3289 N85-30393
Large format camera photographs: A new tool for understanding arid environments 21 p3604 N85-32379
Terrain illumination conditions when taking scanning photographs from space 22 p3736 N85-33159
Calculating solar highlight and shadeless areas for scanning photographs from space and optimizing lighting conditions 22 p3736 N85-33160
Discrimination of linear contour elements of space photographs based on visual perception model 22 p3736 N85-33161
Mapping of dynamics of deltas by space photography 22 p3737 N85-33163
Comprehensive mapping of arid territories of Arizona using space photography 22 p3737 N85-33164

SPACEBORNE TELESCOPES
NT HUBBLE SPACE TELESCOPE
NT SOLAR OPTICAL TELESCOPE
NT SPACE INFRARED TELESCOPE FACILITY
Optical contacting for gravity probe star tracker [NASA-TM-86475] 01 p0120 N85-10819
Optical analysis of the star-tracker telescope for Gravity Probe [NASA-TM-86474] 01 p0129 N85-10868
The Belikt experiment 02 p0159 N85-11079
West Europe report: Science and technology, no. 166 [JPRS-84845] 03 p0341 N85-12190
French, Soviets decide to launch Sigma space telescope 03 p0341 N85-12191
Choice of orbit for scientific satellites: SIGMA, the submillimeter telescope — Ariane-borne gamma imagery satellite (SIGMA) 05 p0600 N85-13828
Pointing and control system design study for the space infrared telescope facility (SIRTF) [NASA-CR-166612] 07 p0915 N85-15795
SIRTF: The next step [NASA-TM-86663] 07 p1059 N85-16724
SIRTF: The next step 08 p1250 N85-17891
Satellite description 09 p1412 N85-18900
Sixteenth Lunar and Planetary Science Conference. Press abstracts [NASA-CR-175692] 15 p2680 N85-26548
Dall-Null tester for spaceborne applications [AD-A151772] 16 p2881 N85-27779
Long life feasibility study for the shuttle infrared telescope facility [NASA-CR-3722] 17 p3052 N85-28893
The Extended Range X-Ray Telescope center director's discretionary fund report [NASA-TM-86507] 19 p3382 N85-30983
Astron telescope stabilization system 22 p3732 N85-33133
Results from Astron orbiting telescope 22 p3732 N85-33134
Astron X-ray experiment 22 p3732 N85-33137

SPACECRAFT
Space Shuttle Orbiter trimmed center-of-gravity extension study. Volume 8: Effects of configuration modifications on the aerodynamic characteristics of the 140 A/B Orbiter at a Mach number of 5.97 [NASA-TM-72861-VOL-8] 04 p0452 N85-12867
An optimization method for the preliminary design of interplanetary aerobraking missions 08 p1076 N85-16822
On the frontier: Flight research at Dryden 1946-1981 [NASA-SP-4303] 09 p1263 N85-17934
Clarke Stations and mercurian mass-drivers: Energy for large-scale transportation systems [DE85-009607] 21 p3560 N85-32145
Fuel cell applications literature review [DE85-011891] 22 p3809 N85-33592

SPACECRAFT ANTENNAS
Large spaceborne antenna reflectors using inflatable space rigidized structures 05 p0625 N85-14004
Elastic dispersion effects on dynamics and control of large modular antennas — spacecraft antennas 05 p0627 N85-14019
Interleaved array antenna technology development [NASA-CR-171845] 10 p1477 N85-19326
Precision antenna reflector structures 14 p2232 N85-23834
An optimization study to minimize surface distortions of a hoop-column antenna 14 p2232 N85-23837
Structural dynamics analysis 14 p2233 N85-23838
AFWAL space control technology program 14 p2233 N85-23839
Large antenna control methods: Current status and future trends 14 p2234 N85-23845
Application of modern Aperture Integration (AI) and Geometrical Theory of Diffraction (GTD) techniques for analysis of large reflector antennas 14 p2234 N85-23851
Feed system design considerations for large space antenna systems. Part 1: Multiple apertures with non-overlapping feeds 14 p2234 N85-23852
The space station as a construction base for large space structures 14 p2235 N85-23856
Compensator development and examination of performance and robustness [NASA-CR-175703] 15 p2540 N85-25678
Bonded stripline power splitter for ERS-1 [RML-009-84-124] 15 p2550 N85-25740
Application of the ADAMS program to deployable space truss structures [NASA-CR-177927] 19 p3284 N85-30366
Proceedings of the Workshop on Identification and Control of Flexible Space Structures, volume 1 [NASA-CR-176051] 20 p3408 N85-31148
AFWAL control technology programs 20 p3408 N85-31150
Design and evaluation of control systems for large communications satellites 20 p3409 N85-31157
Control of large antennas based on electromagnetic performance criteria 20 p3409 N85-31158
Vibration control experiment design for the 15-m hoop/column antenna 20 p3409 N85-31159
A hardware demonstration of distributed control for a flexible offset-feed antenna 20 p3410 N85-31160
Time-optimal bang-bang slew of rigidized SCOLE configuration 20 p3410 N85-31164
The experimental computer control of a two-dimensional hyperbolic system 20 p3411 N85-31166
Approximation of optimal infinite dimensional compensators for flexible structures 20 p3413 N85-31181
Control of a flexible space antenna: A finite dimensional perspective based on distributed parameter theory 20 p3413 N85-31182
Box truss analysis and technology development. Task 1: Mesh analysis and control [NASA-CR-172570] 23 p3900 N85-34156

SPACECRAFT CABIN ATMOSPHERES
Toxicological evaluation of Columbia spacecraft 01 p0094 N85-10631
Human response to vibroacoustic environments of space vehicles [NASA-TM-86316] 01 p0116 N85-10789
Solid sorbent air sampler [NASA-CASE-MSC-20653-1] 11 p1636 N85-20301
Proceedings of the Seminar on Space Station Human Productivity [NASA-TM-86673] 18 p3156 N85-29539
Internal contamination issues 18 p3156 N85-29543
Extended mission life support systems 18 p3157 N85-29547
Gas chromatography: Possible application of advanced instrumentation developed for solar system exploration to space station cabin atmospheres 18 p3157 N85-29551

SPACECRAFT CABIN SIMULATORS
Space station models, mockups and simulators 18 p3159 N85-29560

SPACECRAFT CABINS
Challenges in the development of the orbiter atmosphere revitalization subsystem 08 p1095 N85-16920
Habitability sleep accommodations 18 p3159 N85-29566

SPACECRAFT CHARGING
SEPAC (space experiments with particle accelerators) 01 p0014 N85-10085
Charging of the DMSP F-2 spacecraft in the aurora on 10 January 1983 [AD-A146303] 03 p0324 N85-12086
Effects of the solar and extraterrestrial environments on space power systems 05 p0610 N85-13896
Rocket body charge neutralization processes in ARAKS experiment (data from two launches) 13 p1980 N85-22428
Spacecraft Environmental Interactions Technology, 1983 [NASA-CP-2359] 13 p1989 N85-22470
Vehicle charging on STS-3 Mission 13 p1989 N85-22473
Electron and ion density depletions measured in the STS-3 orbiter wake 13 p1989 N85-22474
Shuttle electrical environment 13 p1990 N85-22475
Measured electron contribution to Shuttle plasma environment: Abbreviated update 13 p1990 N85-22476
Laboratory studies of Kapton degradation in an oxygen ion beam 13 p1990 N85-22477
Electron beam charging of Space Shuttle thermal protection system tiles 13 p1990 N85-22478
Charging of DMSP/F6 spacecraft in aurora on 10 January 1983 13 p1991 N85-22481
Average and worst-case specifications of precipitating auroral electron environment 13 p1991 N85-22482
Auroral-polar cap environment and its impact on spacecraft plasma interactions 13 p1991 N85-22484
Electric field effects on ion currents in satellite wakes 13 p1991 N85-22485
Three-dimensional calculation of shuttle charging in polar orbit 13 p1992 N85-22486
Polar orbit electrostatic charging of objects in shuttle wake 13 p1992 N85-22487
Wakes and differential charging of large bodies in low Earth orbit 13 p1992 N85-22488
Sheath ionization model of beam emissions from large spacecraft 13 p1992 N85-22489
Interactions between large space power systems and low-Earth-orbit plasmas 13 p1992 N85-22490
Calculation of secondary-electron escape currents from inclined-spacecraft surfaces in a magnetic field 13 p1992 N85-22491
Self-consistent simulation of plasma interactions with secondary-emitting insulators 13 p1993 N85-22492
Surface interactions and high-voltage current collection 13 p1993 N85-22493
The PIX-2 experiment: An overview 13 p1993 N85-22494
Plasma interaction experiment 2 (PIX 2): Laboratory and flight results 13 p1993 N85-22495
Design guidelines for assessing and controlling spacecraft charging effects 13 p1994 N85-22500
Aerospace spacecraft-charging guidelines document 13 p1994 N85-22501
EMI characteristics of a potential control system 13 p1994 N85-22502
Anomalously high potentials observed on ISEE 13 p1994 N85-22503
Characteristics of EMI generated by negative metal-positive dielectric voltage stresses due to spacecraft charging 13 p1995 N85-22505
Laboratory studies of spacecraft response to transient discharge pulses 13 p1995 N85-22506
Development of a continuous broad-energy-spectrum electron source 13 p1995 N85-22507
Automatic charge control system for satellites 13 p1995 N85-22508
Discharge pulse phenomenology 13 p1995 N85-22509

Discharge characteristics of dielectric materials examined in mono-, dual-, and spectral energy electron charging environments 13 p1995 N85-22510
Electron yields from spacecraft materials 13 p1996 N85-22512
Electrical conduction in polymer dielectrics 13 p1996 N85-22514
Spacecraft environmental interactions: A joint Air Force and NASA research and technology program 13 p1997 N85-22517
Interactions measurement payload for Shuttle 13 p1997 N85-22518
Astronaut hazard during free-flight polar EVA 13 p1997 N85-22522
Development and testing of a spacecraft surface potential monitor 13 p2007 N85-22582
Phenomenology of discharges in space: Application to a solar generator — SPOT satellite 13 p2007 N85-22583
Electrostatic discharge testing on a carbon fiber solar panel structure 13 p2007 N85-22584
Measurement of charged secondary particle emission under ion and neutral impact — Giotto mission 14 p2243 N85-23906
Giotto residual ionization 14 p2244 N85-23909
Experimental investigations on ion emission with dust impact on solid surfaces — Giotto spacecraft 14 p2244 N85-23911
Ion emission from solid surfaces: Comparison of dust impact with other excitations — Giotto mission 14 p2244 N85-23912
Electrostatic charging of the Giotto spacecraft due to neutral gas impact 14 p2244 N85-23913
Giotto plasmasheath and wake charging near Halley's Comet: Revised parameters 14 p2245 N85-23915
Simulations of satellite-plasma interaction, including electron space charges — Giotto mission 14 p2245 N85-23916
Anticipated impact plasma problems for the COPERNIC-RPA experiment in the cometary environment — Giotto mission 14 p2245 N85-23917
Plasma environment effects on the Giotto Ion Mass Spectrometer 14 p2245 N85-23919
Electric potential of satellite in electron emitting experiments in initial stage of electron beam injection in steady-state mode 15 p2480 N85-25309
ESABASE extension to spacecraft charging analysis. Phase 1: NASCAP software (VAX version) [ESA-CR(P)-1968] 15 p2493 N85-25381
Preliminary documentation for the polar code [AD-A154125] 19 p3336 N85-30667
Surface voltage gradient role in high voltage solar array-plasma interaction: Center Director's discretionary fund [NASA-TM-86516] 22 p3805 N85-33567
SPACECRAFT COMMUNICATION
Communications protocols for a fault tolerant, integrated local area network for Space Station applications [NASA-TM-86304] 01 p0106 N85-10711
The real world: The user 02 p0150 N85-11017
Pluribus satellite IMP (Interface Message Provision) development mobile access terminal network [AD-A145348] 02 p0190 N85-11269
Timing performance of phase-locked loops in optical pulse position modulation communication systems [AD-A145403] 02 p0190 N85-11271
Telemetry (TM)/telecommand (TC) processor study [ESA-CR(P)-1915] 03 p0323 N85-12081
The Telecommunications and Data Acquisition Report [NASA-CR-174148] 05 p0622 N85-13960
Problems of development of space communication 06 p0793 N85-15067
Demand for satellite-provided domestic communications services up to the year 2000 [NASA-TM-86894] 06 p0798 N85-15099
Spacecraft system study: A study to define the impact of laser communication systems on their host spacecraft [NASA-CR-175272] 07 p0970 N85-16159
Shuttle ku-band communications/radar technical concepts 08 p1099 N85-16949
Shuttle payload S-band communications system 08 p1100 N85-16950
The Communications link analysis and simulation system (CLASS) 08 p1100 N85-16952
The Statistical Loop Analyzer (SLA) 08 p1100 N85-16955
Digital scrambling for shuttle communication links: Do drawbacks outweigh advantages? 08 p1101 N85-16956
Novel applications of the NASA/GSFC Viterbi decoder hardware simulator 08 p1101 N85-16957
Electronics systems test laboratory testing of shuttle communications systems 08 p1101 N85-16958
Coding for reliable satellite communications [NASA-CR-174315] 08 p1150 N85-17257
Pluribus satellite IMP development mobile access terminal network [AD-A147675] 08 p1151 N85-17264
A modified Monte-Carlo technique for the simulation of satellite communication systems [AD-A148669] 08 p1214 N85-17641
Research and technology highlights of the Lewis Research Center [NASA-TM-86899] 08 p1261 N85-17928
Experimental satellite system for determining coordinates of maritime distress 09 p1308 N85-18216
Technical evaluation report on the 46th Symposium of the Avionics Panel on Space System Applications to Tactical Operations [AGARD-AR-203] 10 p1425 N85-18988
Description of amplitude scintillations on a 11 GHz slant path in terms of forward scattering from turbulent layers [FI-455-TBR-76] 11 p1625 N85-20232
Polarization angles of linearly polarized antennas and radio waves in satellite communications [PB85-131613] 11 p1626 N85-20240
Reed-Solomon decoder — applicable to Galileo Project requirements [NASA-CASE-NPO-15982-1] 11 p1690 N85-20680
Tactical operations and space applications 11 p1709 N85-20752
Integrated support of tactical operations by satellite communications 11 p1709 N85-20754
EHF MILSATCOM systems for tactical users 11 p1709 N85-20755
Combat capable space systems for tactical support 11 p1713 N85-20775
Transmission and orbital constraints in space-related programs: Briefing summary 12 p1787 N85-21216
Ionospheric distortions of digital signals with wideband modulation 13 p2072 N85-22945
Space-based antenna measurement system concepts for space station operation 14 p2236 N85-23860
The transpacific experimental sailing by YASEIGO 3 14 p2327 N85-24380
Shuttle communications and tracking systems modeling and TDRSS link simulations studies [NASA-CR-171861] 15 p2491 N85-25369
Pluribus Satellite IMP (Interface Message Provision) development mobile access terminal network [AD-A151201] 15 p2541 N85-25688
Pluribus Satellite IMP (Interface Message Provision) development mobile access terminal network [AD-A151312] 15 p2542 N85-25692
Analysis of space diversity techniques for EHF (Extremely High Frequency) satellite downlinks [AD-A151900] 15 p2544 N85-25705
Adaptation of bit error rate by coding — spacecraft transmissions [ESA-CR(P)-1970] 15 p2545 N85-25711
Space Shuttle program communication and tracking systems interface analysis [NASA-CR-171862] 16 p2729 N85-26841
Consultative Committee for Space Data Systems. Panel 1: Support [NASA-CR-175786] 16 p2769 N85-27090
SESC (Space Environment Services Center) satellite broadcasting 10-year plan [PB85-163541] 16 p2775 N85-27126
Water vapor radiometry research and development phase [NASA-CR-175887] 17 p2995 N85-28512
Optical techniques for signal distribution and control in advanced radar and communication systems 18 p3188 N85-29773
Serial Minimum Shift Keying (SMSK) follow-on study — spacecraft communication [ESA-CR(P)-2026] 20 p3399 N85-31083
Control of flexible structures 20 p3410 N85-31161
Automated testing of developmental satellite communications systems and subsystems [NASA-TM-87070] 20 p3440 N85-31348
Study of the interferences of 2 GHz radio beams with a DORIS system — precise low orbit determination system (DORIS) [CNES-CT/DRT/TIT/RL-84/140-T] 20 p3442 N85-31362
Phase-locked loops for optical homodyne detection, volume 1 — spaceborne receivers [ESA-CR(P)-2029-VOL-1] 20 p3442 N85-31367
Thirty GHz low noise GaAs FET amplifiers — satellite-ground communication [CD.6500686] 20 p3449 N85-31413
A comparison of millimeter wave, direct detect and heterodyne laser intersatellite links [AD-A151964] 20 p3461 N85-31496
Intersatellite optical links: The point ahead angle [CNES-83/DRT/TIT/TR/150] 20 p3533 N85-31984
Automation study for space station subsystems and mission ground support [NASA-CR-176097] 21 p3559 N85-32136
A model for predicting propagation-related DSCS (Defense Communications Engineering Center) margin requirements [AD-A155355] 22 p3756 N85-33281
Satellite links in the ISO architecture: Models and performance evaluation [ENST-84E017] 22 p3756 N85-33284
Variation in radiowave propagation conditions in corona during solar activity cycle 22 p3763 N85-33327
On the principle of uniformity of satellite communications systems 22 p3773 N85-33382
Second-generation mobile satellite system. A conceptual design and trade-off study [NASA-CR-176195] 24 p4086 N85-35325
SPACECRAFT COMPONENTS
NT SPACECRAFT CABINS
NT SPACECRAFT MODULES
Damping synthesis for a spacecraft using substructure and component data [CRC-1365] 03 p0323 N85-12082
Advanced high-power transfer through rotary interfaces 05 p0607 N85-13875
Procedures for testing and evaluating spacecraft-type heat pipes [AD-A146671] 06 p0809 N85-15139
On-orbit support of DARPA-301 payload [AD-A146897] 07 p0911 N85-15767
A total dose characterization of five commercial analog multiplexers [AD-A146886] 07 p0946 N85-15997
Analysis of Nonvolatile Residue (NVR) from spacecraft systems [NASA-TM-86184] 08 p1113 N85-17019
Study in spurious sensitivity of electronics in space [AD-A148386] 08 p1158 N85-17305
The wear of small polyacetal and polymide gears in vacuum — spacecraft gears [ESA-ESTL-058] 08 p1169 N85-17374
Environment definition, large particles 12 p1787 N85-21220
NASA welding assessment program [NASA-CR-175512] 12 p1859 N85-21661
Two-phase fluid thermal transport for spacecraft [AD-A151316] 15 p2493 N85-25378
The G/W handbook for data compilation of irradiation tested electronic components, volume 3 [HMI-B-353-VOL-3] 17 p2956 N85-28258
Evaluation of VLSI technology — space applications [CD.6501702] 18 p3098 N85-29177
The role of mock-ups in the development of Orbital Replaceable Units (ORU) 18 p3160 N85-29573
Results from radiation monitoring equipment experiments on STS-41C, 41D, 41G and 51A [AD-A154676] 21 p3560 N85-32142
Background equatorial astronomical measurements focal plane assembly (refurbished HI STAR SOUTH) [AD-A155215] 21 p3590 N85-32313
SPACECRAFT CONFIGURATIONS
NT SATELLITE CONFIGURATIONS
Space Shuttle wind tunnel testing program [NASA-RP-1125] 02 p0167 N85-11127
Conceptual design and evaluation of selected Space Station concepts: Executive summary [NASA-TM-87382] 02 p0167 N85-11128
Shuttle structural dynamics characteristics: The analysis and verification 08 p1094 N85-16913
Structural load challenges during space shuttle development 08 p1094 N85-16914
Vehicle/engine integration — orbit transfer vehicles 08 p1109 N85-17008
Satellite description 09 p1412 N85-18900
Constellations 11 p1643 N85-20352
Summary presentation of the Constellations Panel 11 p1644 N85-20359
Report of the Constellations Panel 11 p1645 N85-20368
Some aspects of attitude stability of tethered space stations 11 p1646 N85-20369
The ARIANE family 11 p1712 N85-20774
Model control of structural systems [AD-A149734] 12 p1790 N85-21235
On-orbit systems identification of flexible spacecraft Technol., 1984, Pt. 2 p 465-461 14 p2233 N85-23841
Space Technology Experiments Platform (STEP) status: An in-space test facility 14 p2236 N85-23863
Numerical experiments on flexible spacecraft with the aid of the Dynamic Control and Analysis Package (DCAP) [ESA-STM-229] 15 p2493 N85-25382
Incorporating control into the optimal structural design of large flexible space structures [AD-A1528[illegible]] 17 p2909 N85-27937

Space Station reference configuration description
[NASA-TM-87493] 20 p3406 N85-31146
Parametric stiffness control of flexible structures
20 p3414 N85-31167
A study on the control of third generation spacecraft
20 p3415 N85-31196
Nickel-hydrogen spacecraft module configurations study 20 p3447 N85-31401
The space station polar platform: NOAA systems considerations and requirements
[NOAA-TR-NESDIS-22] 22 p3740 N85-33182
Advanced beamed-energy and field propulsion concepts
[NASA-CR-176108] 22 p3741 N85-33186
Spacecraft (Mobile Satellite) configuration design study
[NASA-CR-176153] 23 p3899 N85-34152

SPACECRAFT CONSTRUCTION MATERIALS
Constituent property - composite property relationships in thermoset matrices 04 p0465 N85-12950
Space Station truss structures and construction considerations
[NASA-TM-86338] 07 p0916 N85-15796
SSME lifetime prediction and verification, integrating environments, structures, materials: The challenge
08 p1095 N85-16918
Oxidation protection coatings for polymers
[NASA-CASE-LEW-14072-1] 11 p1611 N85-20129
NASA space materials research
14 p2232 N85-23631
Materials and processes control for space applications
18 p3156 N85-29544
Ion beam sputter-deposited thin film coatings for protection of spacecraft polymers in low Earth orbit
[NASA-TM-87051] 19 p3248 N85-30137
R and D activities of the Structural Sciences Division
20 p3539 N85-32026
A survey of structural material issues for a space station
[NASA-TM-86385] 22 p3738 N85-33168

SPACECRAFT CONTAMINATION
Shuttle on-orbit contamination and environmental effects 08 p1104 N85-16980
Space environment simulation to test satellite thermal control coatings, volume 1
[CERT-4128-VOL-1] 08 p1109 N85-17012
Space environment simulation to test satellite thermal control coatings. Volume 2: Annex 1
[ESA-CR(P)-1870-VOL-2] 08 p1109 N85-17013
Space environment simulation to test satellite thermal control coatings. Volume 2: Annexes 2, 3, 4
[ESA-CR(P)-1870-VOL-3] 08 p1109 N85-17014
Analysis of Nonvolatile Residue (NVR) from spacecraft systems
[NASA-TM-86184] 08 p1113 N85-17019
Minimizing plume contamination production in bipropellant thrusters 13 p2003 N85-22557
Measurement of the nighttime infrared luminosity of Spacelab 1 in the H- and K-bands
[NASA-TM-85972] 14 p2434 N85-25011
Proceedings of the Seminar on Space Station Human Productivity
[NASA-TM-86673] 18 p3156 N85-29539
Statement of contamination problem
18 p3156 N85-29542
Internal contamination issues
18 p3156 N85-29543
Materials and processes control for space applications
18 p3156 N85-29544
Space station trace contaminant control
18 p3157 N85-29550
Mass spectrometry technology at the Jet Propulsion Laboratory (JPL) 18 p3157 N85-29552
Atmosphere monitoring requirements
18 p3158 N85-29553
Some problems associated with trace contaminant removal systems for spacecabins
18 p3158 N85-29554
Contamination control for increased crew productivity
18 p3158 N85-29555
Human productivity program definition
18 p3158 N85-29556
Space shuttle molecular and wake vacuum measurements
[NASA-TM-86509] 19 p3222 N85-29976
Particulate contamination control in clean rooms by particle fallout (PFO) measurements
[ESA-PSS-01-204-ISSUE-1] 20 p3487 N85-31673

SPACECRAFT CONTROL
NT SATELLITE ATTITUDE CONTROL
NT SATELLITE CONTROL
Use of gravitational stabilization in performance of experiments 02 p0160 N85-11084
A user's guide to the Flexible Spacecraft Dynamics and Control Program
[NASA-TM-87389] 03 p0405 N85-12586
Propellant tank resupply system
[AD-D011288] 05 p0603 N85-13848
Torque command steering law for double-gimbaled control moment gyros applied to rotor energy storage
05 p0606 N85-13879
Disturbance propagation in structural networks; control of large space structures 06 p0759 N85-14856
Active nutation control of spacecraft using a magnetic bearing momentum wheel with Vernier gimballing capability
[NAL-TR-8201] 06 p0759 N85-14857
SSME digital control design characteristics
08 p1091 N85-16893
Development and implementation of the verification process for the shuttle avionics system
08 p1091 N85-16896
Summary presentation of the Constellations Panel
11 p1644 N85-20359
The Satellite sail 11 p1647 N85-20376
Attitude data consistence check of rocket payloads
[BMFT-FB-W-84-049] 12 p1790 N85-21239
Stability analysis of flexible spacecraft with PID controller
[CRC-1372] 12 p1792 N85-21247
Radioelectronics and space exploration
12 p1838 N85-21533
Station keeping of geostationary satellites by electric propulsion
[NASA-TM-77820] 14 p2320 N85-24337
Identification and control of structures in space
[NASA-CR-175790] 16 p2731 N85-26850
Artificial intelligence in space platforms
[AD-A152078] 16 p2851 N85-27578
In orbit infrastructure
[DM-51/CC-FL-044-83] 18 p3066 N85-28966
Standard Generic approach for Spacecraft Autonomy and Automation, phase 2 (SGASA-2). Volume 1: Executive summary
[ESA053-1-VOL-1] 18 p3167 N85-29623
Standard Generic Approach for Spacecraft Autonomy and Automation, phase 2 (SGASA-2). Volume 2: Technical report
[ESA053-1-VOL-2] 18 p3167 N85-29624
Standard Generic Approach for Spacecraft Autonomy and Automation, phase 2 (SGASA-2). Volume 3: Appendices
[ESA053-1-VOL-3] 18 p3167 N85-29625
Proceedings of the Workshop on Identification and Control of Flexible Space Structures, volume 1
[NASA-CR-176051] 20 p3408 N85-31148
Control of flexible structures 20 p3410 N85-31161
Design of multivariable controllers using the Integrated Analysis Capability (IAC) 20 p3412 N85-31172
A structural dynamics approach to the simulation of spacecraft control/structure interaction
20 p3412 N85-31173
Proceedings of the Workshop on Identification and Control of Flexible Space Structures, volume 3
[NASA-CR-176053] 20 p3415 N85-31195
A study on the control of third generation spacecraft
20 p3415 N85-31196
Matrix transfer function design for flexible structures: An application 20 p3416 N85-31199
Robust control design for large space structures
20 p3416 N85-31200
On the stability of collocated controllers in the presence or uncertain nonlinearities and other perils
20 p3416 N85-31201
Research and development activities in unified control-structure modeling and design
[NASA-CR-176111] 22 p3740 N85-33180
Space station rotational equations of motion
[NASA-TP-2511] 23 p3899 N85-34148
Hardware math for the 6502 microprocessor
[NASA-TM-86517] 23 p3955 N85-34511
Identification and control of structures in space
[NASA-CR-176175] 24 p4069 N85-35214
TRICCS: A proposed teleoperator/robot integrated command and control system for space applications
[NASA-TM-87577] 24 p4136 N85-35637
Enhancement of the flexible spacecraft dynamics program for open spacecraft
[NASA-CR-175309] 24 p4137 N85-35641

SPACECRAFT DEFENSE
Combat capable space systems for tactical support
11 p1713 N85-20775
Transmission and reflection of laser beams propagating through aerosol clouds in space
[LA-9998-MS] 12 p1856 N85-21638

SPACECRAFT DESIGN
NT SATELLITE DESIGN
Vibration, acoustic, and shock design and test criteria for components on the Solid Rocket Boosters (SRB), Lightweight External Tank (LWT), and Space Shuttle Main Engines (SSME)
[NASA-RP-1127] 01 p0061 N85-10405
Modular experimental platform for science an
applications 02 p0152 N85-11031
External tank aft cargo carrier
02 p0155 N85-11050
Space Shuttle wind tunnel testing program
[NASA-RP-1125] 02 p0167 N85-11127
SMP: A solid modeling program
[NASA-CR-172473] 02 p0241 N85-11570
General Electric composite ring-disk flywheel: Recent and potential developments 05 p0606 N85-13867
Space power management and distribution status and trends 05 p0610 N85-13896
Analytical modeling of spacecraft power systems
05 p0610 N85-13897
Effects of the solar and extraterrestrial environments on space power systems 05 p0610 N85-13898
Aerodynamic characteristics of some lifting reentry concepts applicable to transatmospheric vehicle design studies
[NASA-TM-86331] 06 p0747 N85-14787
Pointing and control system design study for the spa
infrared telescope facility (SIRTF)
[NASA-CR-166612] 07 p0915 N85-15795
Space Shuttle Technical Conference, part 1
[NASA-CP-2342-PT-1] 08 p1090 N85-16889
Shuttle structural dynamics characteristics: The analysis and verification 08 p1094 N85-16913
Structural load challenges during space shuttle development 08 p1094 N85-16914
Orbiter structural design and verification
08 p1094 N85-16915
Space shuttle external tank performance improvements: The challenge 08 p1094 N85-16916
Structural and mechanical design challenges of space shuttle solid rocket boosters separation and recovery subsystems 08 p1095 N85-16917
SSME lifetime prediction and verification, integrating environments, structures, materials: The challenge
08 p1095 N85-16918
Orbiter processing facility: Access platforms Kennedy Space Center, Florida, from challenge to achievement
08 p1102 N85-1696
External tank GH2 vent arm 08 p1102 N85-1696
In-flight testing of the space shuttle orbiter thermal control system 08 p1103 N85-16974
Impact of lunar and planetary missions on the space station
[NASA-CR-171832] 08 p1106 N85-169
OTV fluid mangement systems
08 p1108 N85-17007
Orbital transfer vehicle propulsion issues
08 p1109 N85-17009
Space based OTV servicing 08 p1109 N85-17010
Space Station needs, attributes, and architectural option study
[NASA-CR-174316] 08 p1109 N85-17011
Waste collection subsystem study
[NASA-CR-171836] 08 p1199 N85-17552
Space Shuttle Orbiter waste collection system conceptual study
[NASA-CR-171844] 08 p1199 N85-17553
Vibration analysis of a multipurpose platform
[NAL-TR-803] 09 p1286 N85-18078
Efficient structures for geosynchronous spacecraft solar arrays
[NASA-CR-174448] 10 p1426 N85-19004
Constellations 11 p1643 N85-2035
Study proposal for the possible use of ISS as an aerodynamic facility for aerospace applications
11 p1646 N85-20374
Space heat rejection radiations: Meteoroid/debris consideration 12 p1786 N85-21210
Space Station
[NASA-EP-211] 12 p1793 N85-21251
Design study of an integrated aerobraking orbital transfer vehicle
[NASA-TM-58264] 12 p1795 N85-212
Deployable folded antenna apparatus
[AD-D011503] 12 p1832 N85-214
Debris impact on Earth-orbiting spacecraft
12 p1948 N85-222
Feoktistov recalls period leading to Gagarin spaceflight 13 p1985 N85-2245
Feoktistov argues against U.S. space shuttle desig
concept 13 p1985 N85-224
Feoktistov discusses need for space colonization
13 p1985 N85-224
Report on final recommendations for MP
engineering-science payload
[NASA-CR-175659] 13 p1986 N85-224
Design guidelines for assessing and controll
spacecraft charging effects 13 p1994 N85-22
Uses of composite materials
13 p2027 N85-2
Precision space structures 14 p2232 N85-2

Thermal design of the Giotto spacecraft 14 p2245 N85-23020

Progress of computational fluid dynamics in the world 16 p2691 N85-26612

A study of spacecraft technology and design concepts, volume 1
[NASA-CR-172579-VOL-1] 18 p2730 N85-26844

A study of spacecraft technology and design concepts. Volume 2: Appendices
[NASA-CR-172579-VOL-2] 18 p2730 N85-26845

The NASA Space Station program plans
[NASA-TM-87474] 18 p2730 N85-26846

Spacestation: The next logical step
[NASA-EP-213] 18 p2730 N85-26847

Space Station Spartan study
[NASA-TM-86215] 18 p2731 N85-26852

In orbit infrastructure
[DM-51/CC-FL-044-83] 18 p3066 N85-28966

Astronautical conference hears details on Hermes minishuttle 18 p3066 N85-29112

Proceedings of the Seminar on Space Station Human Productivity
[NASA-TM-86673] 18 p3156 N85-29539

Human factors issues in space station architecture 18 p3158 N85-29560

Considerations for space station interior architecture 18 p3159 N85-29564

Human factors in space station architecture: The ECLSS module concept 18 p3159 N85-29565

Habitability sleep accommodations 18 p3159 N85-29566

Customer and mission influence on space station architecture 18 p3159 N85-29567

Mockups and human productivity studies 18 p3159 N85-29570

Rockwell experience applications to Ames space station mockup habitability/productivity studies 18 p3159 N85-29572

Standard Generic approach for Spacecraft Autonomy and Automation, phase 2 (SGASA-2). Volume 1: Executive summary
[ESA053-1-VOL-1] 18 p3167 N85-29623

Standard Generic Approach for Spacecraft Autonomy and Automation, phase 2 (SGASA-2). Volume 2: Technical report
[ESA053-1-VOL-2] 18 p3167 N85-29624

Standard Generic Approach for Spacecraft Autonomy and Automation, phase 2 (SGASA-2). Volume 3: Appendices
[ESA053-1-VOL-3] 18 p3167 N85-29625

Space station automation study. Volume 2: Technical report. Autonomous systems and assembly
[NASA-CR-171515] 19 p3226 N85-30001

Spacecraft, straight-tube evaporator design
[AD-A154462] 19 p3226 N85-30003

A dual spin space station design 20 p3406 N85-31152

Control of a flexible space antenna: A finite dimensional perspective based on distributed parameter theory 20 p3413 N85-31182

An integrated control and minimum mass structural optimization algorithm for large space structures 20 p3413 N85-31183

ISAAC (Integrated Structural Analysis and Control) via continuum modeling and distributed frequency domain design techniques 20 p3414 N85-31185

Studies toward a manned space station: Participation of European industry in NASA space station (MSS)
[SNIAS-S/DT-Y-25-212] 20 p3418 N85-31217

AUSSAT battery life test program 20 p3446 N85-31395

Research and development activities in unified control-structure modeling and design
[NASA-CR-176111] 22 p3740 N85-33160

Study and realization of a command system adapted to space robotics
[SNIAS-851-440-106] 22 p3740 N85-33183

Evaluation study of mechanical refrigeration systems for application to space missions — infrared astronomy
[SNIAS-1029ACA/LL/V] 22 p3755 N85-33277

SPACECRAFT DOCKING

Tass reports medical, materials studies aboard Salyut-7 02 p0158 N85-11071

Transportation applications, part 2 11 p1643 N85-20350

Evaluation of OMV ranging and docking systems 12 p1947 N85-22230

Swedish equipment for automatic docking in space 15 p2489 N85-25363

Automatic rendezvous and docking systems functional and performance requirements
[NASA-CR-171866] 15 p2492 N85-25376

Astronautical conference hears details on Hermes minishuttle 18 p3066 N85-29112

Docking simulation analysis of range data requirements for the orbital maneuvering vehicle
[NASA-TM-86510] 20 p3407 N85-31143

Space station dynamic modeling, disturbance accommodation, and adaptive control 20 p3409 N85-31154

A modular docking mechanism for in-orbit assembly and spacecraft servicing 22 p3796 N85-33516

Hardware test program for evaluation of baseline range-range rate sensor concept
[NASA-CR-176143] 23 p3933 N85-34377

SPACECRAFT ELECTRONIC EQUIPMENT

Evaluation of test equipment for the detection of contamination on electronic circuits — spacecraft electronics
[ESA-STM-234] 08 p1159 N85-17316

SPACECRAFT ENVIRONMENTS

Toxicological evaluation of Columbia spacecraft 01 p0094 N85-10631

Human response to vibroacoustic environments of space vehicles
[NASA-TM-86316] 01 p0116 N85-10789

Conceptual design and evaluation of selected Space Station concepts, volume 2
[NASA-TM-87384] 02 p0168 N85-11130

An evaluation of grease type ball bearing lubricants operating in various environments
[NASA-TM-86480] 02 p0185 N85-11239

Thermal management technology status 05 p0610 N85-13895

A buyer's guide to space infrastructure 07 p0914 N85-15784

Challenges in the development of the orbiter atmosphere revitalization subsystem 08 p1095 N85-16920

Challenges of developing an electro-optical system for measuring man's operational envelope 08 p1095 N85-16921

Other challenges in the development of the orbiter environmental control hardware 08 p1096 N85-16924

Characterization of heat transfer in nutrient materials — space flight feeding
[NASA-CR-171841] 08 p1199 N85-17551

Physiological considerations of artificial gravity 11 p1643 N85-20351

Aerospace Medicine and Biology: A continuing bibliography with indexes, supplement 267, January 1985
[NASA-SP-7011(267)] 12 p1904 N85-21959

Vibroacoustic study of the NASA Goddard Space Flight Center OSS-1 payload
[NASA-CR-175320] 13 p1988 N85-22465

BLSS: A contribution to future life support 18 p3155 N85-29534

CELSS transportation analysis 18 p3156 N85-29538

Some problems associated with trace contaminant removal systems for spacecabins 18 p3158 N85-29554

Contamination control for increased crew productivity 18 p3158 N85-29555

Human productivity program definition 18 p3158 N85-29556

Some ideas and questions regarding space station design for human use 18 p3158 N85-29562

Publications of the NASA CELSS (Controlled Ecological Life Support Systems) program
[NASA-CR-3911] 19 p3326 N85-30606

Electrophoretic mobilities of erythrocytes in various buffers 20 p3500 N85-31756

Results of Space Experiments in Physiology and Medicine and Informal Briefings by the F-16 Medical Working Group
[AGARD-CP-377] 20 p3507 N85-31805

Some results of the European vestibular experiments in the Spacelab-1 mission 20 p3508 N85-31809

Automation study for space station subsystems and mission ground support
[NASA-CR-176097] 21 p3559 N85-32136

Hydroponics developments for spaceship garden 21 p3663 N85-32754

Mathematical analysis of heart rhythm assessment of distinctive features in adaptation to spaceflight conditions 22 p3733 N85-33142

USSR report: Space Biology and Aerospace Medicine, vol. 19, no. 3, May - June 1985
[JPRS-USB-85-005] 23 p3952 N85-34494

SPACECRAFT EQUIPMENT

NT SPACECRAFT ELECTRONIC EQUIPMENT

Optical contacting for gravity probe star tracker
[NASA-TM-86475] 01 p0120 N85-10819

Definition of technology development missions for early Space Station satellite servicing. Volume 1: Executive summary
[NASA-CR-171228] 04 p0460 N85-12922

Magnetic suspension options for spacecraft inertia-wheel applications 05 p0607 N85-13871

Developments in space power components for power management and distribution 05 p0608 N85-13877

Power transfer from natural emitters to collection apertures at microwave wavelengths
[NASA-CR-174275] 07 p0945 N85-15989

Spaceborne receivers: Basic principles
[NASA-CR-174269] 07 p0946 N85-15990

The Statistical Loop Analyzer (SLA) 08 p1100 N85-16955

Waste collection subsystem study
[NASA-CR-171836] 08 p1199 N85-17552

Space Shuttle Orbiter waste collection system conceptual study
[NASA-CR-171844] 08 p1199 N85-17553

Transient vibration test criteria for spacecraft hardware — galileo spacecraft 09 p1338 N85-18418

High-voltage, high-power, solid-state remote power controllers for aerospace applications
[NASA-TP-2437] 12 p1795 N85-21263

Automated extraction of absorption bands from reflectance spectra 13 p2197 N85-23624

Earth Resources: A continuing bibliography with indexes, issue 45
[NASA-SP-7041(45)] 18 p3123 N85-29336

SPACECRAFT GUIDANCE

NT SATELLITE GUIDANCE

Analysis and simulation of an intertial system (Strapdown) for auxiliary attitude determination by adaptive drift estimation
[INPE-3257-TDL/177] 04 p0454 N85-12882

SPACECRAFT INSTRUMENTS

NT MULTISPECTRAL LINEAR ARRAYS

NT SATELLITE INSTRUMENTS

NT SPACECRAFT POSITION INDICATORS

Natural interference phenomena affecting spaceborne receivers
[NASA-CR-174256] 07 p0916 N85-15796

Reduction of signal modulation caused by polarization in visible optical scanning systems
[AD-D011389] 07 p1042 N85-16820

The design of an ion-neutral mass spectrometer to be used in the Shuttle environment
[AD-A148093] 08 p1114 N85-17022

Multiplex gas chromatography for use in space craft
[NASA-TM-86066] 09 p1290 N85-18097

In-situ detection of micron-sized dust particles in near-Earth space 12 p1785 N85-21205

Microwave blackbodies for spaceborne receivers
[NASA-CR-175647] 13 p2094 N85-23066

Optical system
[NASA-CASE-NPO-15801-1] 13 p2156 N85-23396

Plasma environment effects on the Giotto Ion Mass Spectrometer 14 p2245 N85-23919

Cosmic X-ray physics
[NASA-CR-175906] 17 p3055 N85-28910

Fully redundant mechanical release actuator
[NASA-CASE-LAR-13196-1] 18 p3116 N85-29287

Space optics
[CNES-84/105/T/CT/DRT/TIT/10] 20 p3533 N85-31985

SPACECRAFT LANDING

NT HORIZONTAL SPACECRAFT LANDING

NT MARS LANDING

NT PLANETARY LANDING

Active control technology experience with the Space Shuttle in the landing regime
[NASA-TM-85910] 01 p0012 N85-10071

STS natural environment analysis
[NASA-CR-171221] 03 p0322 N85-12079

Space shuttle handling qualities 08 p1092 N85-16904

Low-speed longitudinal orbiter qualities 08 p1092 N85-16905

Space shuttle main engine: Interactive design challenges 08 p1098 N85-16940

Feoktistov recalls period leading to Gagarin spaceflight 13 p1985 N85-22451

Small solar system bodies 13 p2175 N85-23499

Astronautical conference hears details on Hermes minishuttle 18 p3066 N85-29112

SPACECRAFT LAUNCHING

Tass reports launch of Progress-22 02 p0157 N85-11063

Sweden's Kiruna may be future launch site for satellites 03 p0310 N85-12000

View of Ariane countdown procedures, Kourou launch facilities 03 p0310 N85-12001

STS natural environment analysis
[NASA-CR-171221] 03 p0322 N85-12079

Launching systems
[CNES-NT-11 04 p0460 N85-12917

Launch summary for 1978 - 1982 — sounding rockets, space probes, and satellites
[NASA-TM-87375] 04 p0461 N85-12924

Commercial Space Launch Act [GPO-39-613] 04 p0578 N85-13690
Relationships between Ariane trajectories and satellite orbits 05 p0599 N85-13815
The launch window of a geostationary satellite 05 p0600 N85-13822
Atmospheric environment for Space Shuttle (STS-41D) launch [NASA-TM-86484] 05 p0679 N85-14358
The space shuttle launch vehicle aerodynamic verification challenges 08 p1093 N85-16907
Structural load challenges during space shuttle development 08 p1094 N85-16914
Space shuttle flight readiness firing dress rehearsal for STS-1 08 p1097 N85-16929
Launch processing system concept to reality 08 p1097 N85-16931
Managing computer-controlled operations 08 p1097 N85-16934
Support systems design and analysis 08 p1097 N85-16935
History, design and performance of the space shuttle hazardous gas detection system 08 p1098 N85-16936
Natural environment analysis [NASA-CR-171333] 10 p1428 N85-19010
British aerospace studies HOTOL satellite launcher 10 p1460 N85-19206
Environmental effects of space activities 11 p1678 N85-20577
Atmospheric environment for Space Shuttle (STS-51A) launch [NASA-TM-86497] 12 p1692 N85-21875
Increase in hydrogen emission of upper atmosphere following launches of space vehicles 13 p1981 N85-22431
Feoktistov argues against U.S. space shuttle design concept 13 p1985 N85-22453
List of recent Soviet space launches 13 p1985 N85-22457
China report: Science and technology [JPRS-CST-84-030] 13 p2041 N85-22777
Surface pressure produced by Space Transportation System flight 41B [AD-A150793] 14 p2242 N85-23901
West Europe report: Science and technology [JPRS-WST-85-013] 14 p2289 N85-24183
Ignition, separation of boosters, stages in Ariane 3 14 p2289 N85-24185
Orbital positioning and stationkeeping of geostationary satellites 14 p2397 N85-24772
List of recent Soviet space launches 15 p2489 N85-25361
Calendar of Ariane launches 1984 - 1987 15 p2523 N85-25554
Structure of SYLDA double launch system for Ariane 17 p2946 N85-28185
Ariane space general director on satellite launcher market 18 p3087 N85-29103
Evolution of spacecraft design methods as a function of environmental and geometrical constraints [ESA-CR(P)-2012] 20 p3418 N85-31216
Pricing options for the space shuttle. Special study 21 p3559 N85-32138
The development of staging mechanisms for the Japanese satellite launcher Mu-3SII 22 p3798 N85-33528

SPACECRAFT LUBRICATION
The European Space Tribology Laboratory (ESTL) activities report [ESA-ESTL-61] 05 p0646 N85-14146
The performance of Fomblin Z25 oil in ball bearings operating in vacuum --- spacecraft lubricant [ESA-ESTL-056] 08 p1134 N85-17150
Observations of high resistance on slip-rings employing Ag/MoS2/Cu brushes --- solar array drives [ESA-ESTL-70] 18 p3123 N85-29333
European Space Tribology Laboratory: Facilities, services, capabilities [ESA-BR-12] 20 p3398 N85-31080

SPACECRAFT MAINTENANCE
Satellite servicing: A business opportunity? 02 p0156 N85-11056
Space based OTV servicing 08 p1109 N85-17010
Maintenance of long life space systems, volume 1 [MATRA-0316/DX60-VOL-1] 18 p3066 N85-28964
Maintenance of long life space systems, volume 2 [MATRA-0350/DX60-VOL-2] 18 p3066 N85-28965
Experiences with neutral buoyance testing mockups 18 p3159 N85-29571
The role of mock-ups in the development of Orbital Replaceable Units (ORU) 18 p3160 N85-29573
Technology requirements to be addressed by the NASA Lewis Research Center Cryogenic Fluid Management Facility program [NASA-TM-87048] 19 p3224 N85-29967
A modular docking mechanism for in-orbit assembly and spacecraft servicing 22 p3796 N85-33516

SPACECRAFT MANEUVERS
NT ORBITAL MANEUVERS
Optimal nonlinear feedback control of spacecraft attitude maneuvers 02 p0167 N85-11126
The satellite maneuvers determination department 05 p0599 N85-13820
Application of model following control and estimation techniques to attitude control of maneuvering spacecraft. Part 1: Theory and simulation results [NLR-TR-82116-U-PT-1] 18 p3065 N85-28957
Characteristic elastic systems of time-limited optimal maneuvers 20 p3413 N85-31184
Study and realization of a command system adapted to space robotics [SNIAS-851-440-106] 22 p3740 N85-33183
Identification and control of structures in space [NASA-CR-176175] 24 p4060 N85-35214

SPACECRAFT MODELS
Satellite orbit determination 05 p0598 N85-13813
Satellite attitude determination 05 p0599 N85-13814
Perturbations in geostationary orbit 05 p0600 N85-13824
A model of plasma cloud expansion generated by a dust particle impact --- Giotto mission 14 p2245 N85-23914
The attitude control model tests for the Infrared Astronomical Satellite (IRAS) [B8580071] 18 p3067 N85-28967
Space station models, mockups and simulators 18 p3159 N85-29569
Experiences with neutral buoyance testing mockups 18 p3159 N85-29571
The role of mock-ups in the development of Orbital Replaceable Units (ORU) 18 p3160 N85-29573

SPACECRAFT MODULES
Modular experimental platform for science and applications 02 p0152 N85-11031
Mass analysis of neutral particles and ions released during electrical breakdowns on spacecraft surfaces [NASA-CR-175585] 12 p1793 N85-21250
Space Station structures 14 p2232 N85-23835

SPACECRAFT MOTION
Planning of navigation measurements using TD criterion for determination of movement of spacecraft by method of least squares 02 p0159 N85-11081
Use of gravitational stabilization in performance of experiments 02 p0160 N85-11084
Control of lateral conjectory motion of spacecraft in atmosphere 02 p0160 N85-11085
A user's guide to the Flexible Spacecraft Dynamics and Control Program [NASA-TM-87389] 03 p0405 N85-12586
Positions of relative equilibrium of satellite-gyrostat 16 p2718 N85-26777
Optimum parameters of aerogyroscopic satellite orientation system 16 p2718 N85-26782

SPACECRAFT ORBITAL ASSEMBLY
U ORBITAL ASSEMBLY

SPACECRAFT ORBITS
NT GEOSYNCHRONOUS ORBITS
NT INTERPLANETARY TRANSFER ORBITS
NT PARKING ORBITS
NT POLAR ORBITS
NT SATELLITE ORBITS
NT STATIONARY ORBITS
NT TRANSFER ORBITS
Rapid nonresonant rotation of a spacecraft in nominally periodic orbits in limited 3 body problem 02 p0160 N85-11083
Mars exploration, Venus swingby and conjunction class mission modes, time period 2000 to 2045 [NASA-TM-86477] 02 p0303 N85-11961
Planning for the on-orbit servicing of military spacecraft [AD-A148447] 08 p1104 N85-16963
Summary presentation of the Constellations Panel 11 p1644 N85-20359
Assessment of satellite collision hazards by simulated sampling in space 12 p1784 N85-21195
Models of angular momentum input to a circum-terrestrial swarm from encounters with heliocentric planetesimals 13 p2179 N85-23521
Orbital resonances and planetary accretion in the solar nebula 13 p2179 N85-23523
NASA welding assessment program [NASA-CR-175682] 15 p2568 N85-25844
Telescope in lunar orbit 15 p2682 N85-26568
Life cycle test results of a bipolar nickel hydrogen battery 20 p3448 N85-31406

SPACECRAFT PERFORMANCE
Spacecraft system study: A study to define the impact of laser communication systems on their host spacecraft [NASA-CR-175272] 07 p0970 N85-16159

SPACECRAFT POSITION INDICATORS
Operational experience with ion concentration sensors in orientation systems 13 p1980 N85-22422

SPACECRAFT POWER SUPPLIES
Space power distribution system technology. Volume 3: Test facility design [NASA-CR-171230] 04 p0463 N85-12906
Space nuclear safety program [DE84-015983] 04 p0564 N85-13591
General-purpose heat source development: Safety test program. Postimpact evaluation, design iteration test 2 [DE84-015978] 04 p0564 N85-13592
Technical support services for space and terrestrial systems programs [DE84-009031] 05 p0597 N85-13806
Merits of flywheels for spacecraft energy storage 05 p0605 N85-13867
Inertial storage for satellites 05 p0605 N85-13869
Magnetically suspended flywheel system study 05 p0607 N85-13873
Reaction wheels for kinetic energy storage 05 p0607 N85-13874
Motor/generator and electronic control considerations for energy storage flywheels 05 p0608 N85-13878
Torque command steering law for double-gimbaled control moment gyros applied to rotor energy storage 05 p0608 N85-13879
Space Power [NASA-CP-2352] 05 p0608 N85-13880
Space station power system 05 p0608 N85-13881
Space power for communication satellites beyond 1995 05 p0608 N85-13883
Power for commercial space applications 05 p0608 N85-13884
Missions/planning panel 05 p0609 N85-13886
Radioisotope space power programs 05 p0609 N85-13887
Electrochemistry and storage 05 p0609 N85-13889
Potential of flywheels for spacecraft energy storage 05 p0609 N85-13890
Trends in concentrator, receiver, and storage development for terrestrial applications 05 p0609 N85-13891
Dynamic power systems for power generation 05 p0609 N85-13892
Technology status of thermionic fuel elements for space nuclear power 05 p0610 N85-13893
Space power management and distribution status and trends 05 p0610 N85-13896
Analytical modeling of spacecraft power systems 05 p0610 N85-13897
Effects of the solar and extraterrestrial environments on space power systems 05 p0610 N85-13898
Advanced concepts liquid droplet radiator 05 p0610 N85-13899
The liquid droplet radiator - an ultralightweight heat rejection system for efficient energy conversion in space 05 p0610 N85-13900
Electrodynamic tethers. 1: Power generator in LEO. 2: Thrust for propulsion and power storage 05 p0611 N85-13901
Photovoltaic working group report 05 p0611 N85-13902
Electrochemistry and storage panel report 05 p0611 N85-13903
Dynamic conversion working group summary 05 p0611 N85-13904
Thermoelectric and thermionic conversion technology 05 p0611 N85-13905
Heat rejection working group synopsis 05 p0611 N85-13906
Electrical system technology Working Group (WG) report 05 p0611 N85-13907
Environmental interactions working group report 05 p0611 N85-13908
Advanced and nontraditional concepts working group report 05 p0612 N85-13909
Engineering model system study for a regenerative fuel cell: Study report [NASA-CR-174801] 07 p0991 N85-16
Results of the 1984 NASA/JPL balloon flight solar cell calibration program [NASA-CR-174270] 07 p0991 N85-16
Space shuttle orbiter auxiliary power unit development challenges 08 p1099 N85-16
The solid rocket booster auxiliary power unit: Meeting the challenge 08 p1099 N85-16
Space shuttle electrical power generation and reactant supply system 08 p1099 N85-16
Air Force space technology center space technology Emphasis 84 09 p1333 N85-18
Technology for satellite power conversion [NASA-CR-174335] 09 p1343 N85-19
Opening up the future in space with nuclear power [DE85-002411] 11 p1727 N85-2

GaAs and 3-5 compound solar cells status and prospects r use in space ASA-TM-86960] 12 p1795 N85-21261
General-purpose heat source development: Safety test rogram. Postimpact evaluation, design iteration test 4 LA-10217-SR] 12 p1930 N85-22128
General-purpose heat source development: Safety test rogram. Postimpact evaluation, design iteration test 5 LA-10232-SR] 12 p1931 N85-22129
General-purpose heat source development: Safety test rogram. Postimpact evaluation, design iteration test 1 LA-9660-SR] 12 p1931 N85-22131
Interactions between large space power systems and ow-Earth-orbit plasmas 13 p1992 N85-22490
Photovoltaic Generators in Space — conferences [ESA-SP-210] 13 p2005 N85-22565
History and future views on solar cells of Japanese scientific satellites 13 p2005 N85-22566
Thin and ultrathin silicon solar cells for space use 13 p2005 N85-22567
Space solar cells: Adjusting to new demands 13 p2005 N85-22568
Bifacial light sensitive space solar cell 13 p2006 N85-22573
Space qualified AlGaAs/GaAs solar cells 13 p2006 N85-22575
Availability of AlGaAs/GaAs solar cells in space 13 p2006 N85-22576
Comparative study of GaAs solar cell potentialities for space applications 13 p2006 N85-22577
Investigation of high output gallium arsenide solar cells 13 p2006 N85-22578
Development of very thin large area GaAs solar cells for space application 13 p2006 N85-22579
GaAs and 3-5 compound solar cells status and prospects for use in space 13 p2007 N85-22580
GaAlAs-GaAs solar cell development: Prospective for space applications under concentration 13 p2007 N85-22581
Phenomenology of discharges in space: Application to a solar generator — SPOT satellite 13 p2007 N85-22583
In-orbit laser regeneration of the radiation damaged solar arrays 13 p2008 N85-22588
The DFS-Kopernikus solar generator electrical design 13 p2008 N85-22590
The DFS-Kopernikus solar generator 13 p2008 N85-22591
Electrical design of the Intelsat 6 solar generator 13 p2008 N85-22592
Computer aided engineering applied to the design and verification of the generic Advanced Rigid Array (ARA) — solar array 13 p2008 N85-22593
Development and qualification of the electrical part of the Advanced Rigid Array (ARA) — solar array 13 p2008 N85-22594
SPOT solar array 13 p2009 N85-22595
Rigid Solar Generator (GSR) solar arrays 13 p2009 N85-22596
Retractable Rigid Solar Generator (GSR) 13 p2009 N85-22597
Derivation of the Olympus solar array requirements 13 p2009 N85-22598
The Olympus solar array development and test program 13 p2009 N85-22599
Design and qualification testing of the Olympus solar array blanket 13 p2009 N85-22600
The performance of the Olympus power subsystem with its solar array 13 p2009 N85-22601
Analysis of optimum front cover thickness for lightweight solar arrays 13 p2010 N85-22606
Development of Halley's Comet explorer PLANET-A solar array 13 p2010 N85-22608
Concentrator technologies evaluation for large solar arrays and their application for space stations/platforms 13 p2010 N85-22609
Space Station solar array 13 p2010 N85-22610
Solar array dynamical simulation for illumination and temperature variation 13 p2011 N85-22611
Blanket integrated cushioning of foldable and retractable solar arrays 13 p2011 N85-22612
Concept for controlled fold by fold deployment and retraction of flexible, foldable solar generators 13 p2011 N85-22613
Aspects of low cost module technology — spacecraft solar arrays 13 p2011 N85-22614
Emissivity enhancement of fused silica for space applications — solar cells 13 p2011 N85-22615
NASA photovoltaic research and technology development program for space applications 13 p2011 N85-22617
Study of concentration for space photovoltaic generators 13 p2011 N85-22618
Developments in deployable masts to support flexible solar arrays 13 p2012 N85-22620
Generic design and verification of an Advanced Rigid Array (ARA) — solar array 13 p2012 N85-22621
Growth capabilities of European retractable solar arrays 13 p2012 N85-22625
High output photovoltaic conversion: The quadrispectral project — spacecraft power supplies 13 p2012 N85-22626
Characterization of terrestrial solar cells for space applications: Electrical characteristics of thin Westinghouse dendritic web cells as a function of solar intensity, temperature, and incidence angle [NASA-CR-175642] 14 p2349 N85-24516
Spaceborne power systems preference analyses. Volume 1: Summary [NASA-CR-175644] 14 p2349 N85-24517
Spaceborne power systems preference analyses. Volume 2: Decision analysis [NASA-CR-175645] 14 p2349 N85-24518
Long-life high performance fuel cell program [NASA-CR-174874] 15 p2494 N85-25384
Long-term exposure of pressed plutonium oxide heat sources to aquatic environments [DE85-007385] 15 p2495 N85-25392
Analysis and testing of the thermal properties of space battery cells, phase B, draft [ESA-CR(P)-1971] 15 p2550 N85-25741
Proposed energy systems for the Brazilian data collection satellite [INPE-3393-PRE/684] 16 p2731 N85-26856
Tethered nuclear power for the Space Station [NASA-TM-87023] 16 p2740 N85-26912
Performance analysis of radiation cooled dc transmission lines for high power space systems [NASA-TM-87040] 17 p2951 N85-28222
Multi-kW solar arrays for Earth orbit applications [NASA-CR-171538] 20 p3406 N85-31139
The 1984 Goddard Space Flight Center Battery Workshop [NASA-CP-2382] 20 p3443 N85-31371
Multikilowatt hydrogen-nickel oxide battery system 20 p3443 N85-31373
Solar dynamic systems 20 p3443 N85-31374
System level electrochemical principles 20 p3443 N85-31375
Advances in rechargeable lithium molybdenum disulfide batteries 20 p3444 N85-31376
Geosynchronous performance of a lithium-titanium disulfide battery 20 p3444 N85-31377
RCA's planned test program to compare the performance and life of NiCd cells containing Pellon 2536 in contrast with Pellon 2505 separator material 20 p3445 N85-31385
Failure modes experienced on spacecraft NiCd batteries 20 p3445 N85-31386
Nickel cadmium cell design variable program data analysis 20 p3445 N85-31387
Results of analysis on the design variable cells 20 p3445 N85-31388
Fundamental algorithms of the Goddard battery model 20 p3445 N85-31389
AUSSAT battery life test program 20 p3446 N85-31395
Flight experience of Solar Mesosphere Explorer's two nickel-cadmium batteries 20 p3446 N85-31396
Deep reconditioning of batteries during DSCS 3 flight operations 20 p3446 N85-31397
Design principles for nickel hydrogen cells and batteries 20 p3447 N85-31398
Improved specific energy Ni-H2 cell 20 p3447 N85-31399
Bipolar nickel-hydrogen battery design 20 p3447 N85-31400
Nickel-hydrogen spacecraft module configurations study 20 p3447 N85-31401
Nickel hydrogen bipolar battery electrode design 20 p3447 N85-31402
Nickel-cadmium cell life test 20 p3447 N85-31403
Accelerated and real-time geosynchronous life cycling test performance of nickel-hydrogen batteries 20 p3448 N85-31405
Life cycle test results of a bipolar nickel hydrogen battery 20 p3448 N85-31406
Nickel-hydrogen cell test program summary 20 p3448 N85-31407
The failure mechanism of a nickel electrode in a nickel-hydrogen cell 20 p3448 N85-31408
An industry and government survey: A nickel-hydrogen testing data base 20 p3448 N85-31409
High efficiency solar cell research for space applications 20 p3480 N85-31624
Design principles for nickel-hydrogen cells and batteries [NASA-TM-87037] 20 p3483 N85-31646
Retractable Rigid Solar Generator (GSR) [SNIAS-851-440-101] 20 p3484 N85-31654
Rigid Solar Generator (GSR) solar arrays [SNIAS-851-440-102] 20 p3484 N85-31655
The SPOT solar array [SNIAS-851-440-103] 20 p3485 N85-31656
Study of concentration for space photovoltaic generators [SNIAS-851-440-105] 20 p3485 N85-31658
Reduction of radiation damage in solar cells — spacecraft power supplies [ESA-CR(P)-2005] 20 p3485 N85-31659
Automation study for space station subsystems and mission ground support [NASA-CR-176097] 21 p3559 N85-32136
Solar maximum: Solar array degradation [NASA-TM-86194] 23 p3903 N85-34175
Optical analysis of parabolic dish concentrators for solar dynamic power systems in space [NASA-TM-87080] 23 p3903 N85-34176
STACBEAM 2 [NASA-CR-176126] 23 p3944 N85-34442
General-purpose heat source development: Safety test program. Postimpact evaluation, design iteration test [LA-10034-SR] 23 p3969 N85-34606
Development and characterization of carbon-bonded carbon fiber insulation for radioisotope space power systems [DE85-013365] 24 p4082 N85-35299

SPACECRAFT PRELAUNCH TESTS
U SPACE VEHICLE CHECKOUT PROGRAM

SPACECRAFT PROPULSION
NT ELECTROMAGNETIC PROPULSION
NT ELECTROSTATIC PROPULSION
NT ION PROPULSION
NT MASS DRIVERS (PAYLOAD DELIVERY)
NT PLASMA PROPULSION
NT SOLAR PROPULSION
Mars exploration, Venus swingby and conjunction class mission modes, time period 2000 to 2045 [NASA-TM-86477] 02 p0303 N85-11961
LOX/LH2 propulsion system for launch vehicle upper stage, test results [NASA-TM-77727] 03 p0324 N85-12089
Interstellar mission 04 p0459 N85-12916
Propellant tank resupply system [AD-D011288] 05 p0603 N85-13646
Electrodynamic tethers. 1: Power generator in LEO. 2: Thrust for propulsion and power storage 05 p0611 N85-13901
A historical overview of the electrical power systems in the US manned and some US unmanned spacecraft [NASA-CR-174806] 05 p0612 N85-13910
OTV propulsion tecnology programmatic overview 08 p1107 N85-16997
Drives and benefits overview 08 p1107 N85-16998
Advanced OTV engine concepts 08 p1108 N85-17001
Vehicle/engine integration — orbit transfer vehicles 08 p1109 N85-17008
Orbital transfer vehicle propulsion issues 08 p1109 N85-17009
Design study of an integrated aerobraking orbital transfer vehicle [NASA-TM-58264] 12 p1795 N85-21262
Characterization of terrestrial solar cells for space applications: Electrical characteristics of thin Westinghouse dendritic web cells as a function of solar intensity, temperature, and incidence angle [NASA-CR-175642] 14 p2349 N85-24516
Fiscal year 1986 technical objective document [AD-A151039] 14 p2432 N85-25000
Space station propulsion: The advanced development program at Lewis [NASA-TM-86999] 15 p2494 N85-25386
West Europe report: Science and technology [JPRS-WST-84-009] 15 p2535 N85-25639
Details on spot remote sensing satellite propulsion unit 15 p2535 N85-25640
Advanced energy storage systems [AD-A152244] 16 p2741 N85-26915
Structural Integrity and Durability of Reusable Space Propulsion Systems [NASA-CP-2381] 17 p2910 N85-27941
Composite loads spectra for select space propulsion structural components: Probabilistic load model development 17 p2912 N85-27954
Probabilistic structural analysis theory development 17 p2912 N85-27955
Probabilistic finite element development 17 p2913 N85-27956
Thin-film sensors for space propulsion technology 17 p2915 N85-27968
Experimental research on electrical propulsion [NASA-TM-77876] 18 p3067 N85-28969

SPACECRAFT RADIATORS
Advanced concepts liquid droplet radiator
05 p0610 N85-13899
The liquid droplet radiator - an ultralightweight heat rejection system for efficient energy conversion in space
05 p0610 N85-13900
Heat rejection working group synopsis
05 p0611 N85-13906
Preliminary evaluation of a liquid belt radiator for space applications
[NASA-CR-174807] 07 p0917 N85-15804
Space heat rejection radiatiors: Meteoroid/debris consideration 12 p1786 N85-21210
Advanced radiator concepts
[NASA-TM-87006] 14 p2300 N35-24245
Automation study for space station subsystems and mission ground support
[NASA-CR-176097] 21 p3559 N85-32136
SPACECRAFT RECOVERY
Magnetic spin reduction system for free spinning objects
[NASA-CASE-MFS-25966-1] 02 p0166 N85-11122
Structural and mechanical design challenges of space shuttle solid rocket boosters separation and recovery subsystems 08 p1095 N85-16917
SPACECRAFT REENTRY
NT UNCONTROLLED REENTRY (SPACECRAFT)
Effect of aerodynamic and angle-of-attack uncertainties on the May 1979 entry flight control system of the Space Shuttle from Mach 8 to 1.5
[NASA-TP-2365] 07 p0913 N85-15778
Transportation applications, part 2
11 p1643 N85-20350
Predictions of cardiovascular responses during STS reentry using mathematical models
[NASA-CR-171871] 15 p2616 N85-26119
SPACECRAFT RENDEZVOUS
U SPACE RENDEZVOUS
SPACECRAFT SENSORS
U SPACECRAFT INSTRUMENTS
SPACECRAFT SHIELDING
The challenging scales of the bird: Shuttle tile structural integrity 08 p1095 N85-16919
Hypervelocity impact investigations and meteoroid shielding experience related to Apollo and Skylab
12 p1785 N85-21206
Solid particle environment and protection for the Galileo Orbiter 12 p1786 N85-21207
Space debris protection for a reusable orbital transfer vehicle 12 p1786 N85-21208
Parametric analysis: SOC meteoroid and debris protection 12 p1786 N85-21209
Spacecraft hazard and shielding requirements
12 p1788 N85-21224
Mechanical fastener
[NASA-CASE-LAR-12738-2] 19 p3279 N85-30335
SPACECRAFT STABILITY
In-orbit experiments on IRAS for application to the ISO satellite
[FOK-TR-R-84-057] 03 p0322 N85-12078
Summary presentation of the Constellations Panel
11 p1644 N85-20359
Application Number 3: Using tethers for attitude control 11 p1646 N85-20373
Rotational motion of a satellite
13 p1981 N85-22428
Stability of periodic satellite motions relative to center of mass in circular orbit 16 p2718 N85-26780
Dynamics and control of tethers in elliptical orbits
20 p3399 N85-31067
SPACECRAFT STRUCTURES
Small Payload Flight Systems (SPFS)
02 p0152 N85-11030
Measurement of the inertial constants of a rigid or flexible structure of arbitrary share through a vibration test
[NASA-TM-77557] 02 p0209 N85-11381
Spacecraft structural acoustic studies: Development of structural acoustic design guides
[ESA-CR(P)-1916] 05 p0604 N85-13849
Influence of thermal cycling on the behavior of CFRP material for space structures 05 p0626 N85-14013
Space Shuttle Technical Conference, part 2
[NASA-CP-2342-PT-2] 08 p1096 N85-16937
Thermoviscoelastic analysis of dimensionally stable fiber composite space structures
[AD-A149275] 11 p1593 N85-20021
ACOSS 17 (Active Control of Space Structures)
[AD-A150007] 12 p1793 N85-21253
Elastomer toughened polyimide adhesives — bonding metal and composite material structures for aircraft and spacecraft
[NASA-CASE-LAR-12775-2] 12 p1809 N85-21349
Experimental investigations on ion emission with dust impact on solid surfaces — Giotto spacecraft
14 p2244 N85-23911
Analysis of elastoplastic grids under conditions of variable loads
[REPT-16/1984] 16 p2797 N85-27242
Structure of SYLDA double launch system for Ariane
17 p2946 N85-28185
Finite element thermal-structural analysis of cable-stiffened space structures
[AD-A153822] 18 p3066 N85-28963
R and D activities of the Structural Sciences Division
20 p3539 N85-32026
Effects of environment on spacecraft materials
22 p3733 N85-33144
Research and development activities in unified control-structure modeling and design
[NASA-CR-176111] 22 p3740 N85-33180
SPACECRAFT SURVIVABILITY
A study of spacecraft technology and design concepts. Volume 2: Appendices
[NASA-CR-172579-VOL-2] 16 p2730 N85-26845
SPACECRAFT TELEVISION
NT SATELLITE TELEVISION
Development of TV systems for spacecraft
15 p2484 N85-25332
Optic's institute's development of equipment for comet probe 15 p2484 N85-25333
USSR report: Electronics and electrical engineering
[JPRS-UEE-84-015] 22 p3762 N85-33314
Vatra telvision complex for Salyut orbital space station
22 p3763 N85-33321
SPACECRAFT TRACKING
NT SATELLITE TRACKING
Ocean services user needs assessment. Volume 1: Survey results, conclusions and recommendations
[NASA-CR-174104] 04 p0541 N85-13445
The Western Aeronautical Test Range of NASA Ames Research Center
[NASA-TM-85924] 07 p0909 N85-15756
The Statistical Loop Analyzer (SLA)
08 p1100 N85-16955
The Telecommunications and Data Acquisition Report
[NASA-CR-174366] 10 p1462 N85-19224
Space interception guidance with uncertain factors
13 p2042 N85-22781
Shuttle communications and tracking systems modeling and TDRSS link simulations studies
[NASA-CR-171861] 15 p2491 N85-25369
Space Shuttle program communication and tracking systems interface analysis
[NASA-CR-171862] 16 p2729 N85-26841
Water vapor radiometry research and development phase
[NASA-CR-175887] 17 p2995 N85-28512
Optical receivers using rough reflectors
[NASA-CR-176200] 24 p4154 N85-35750
SPACECRAFT TRAJECTORIES
NT EARTH-VENUS TRAJECTORIES
NT INTERPLANETARY TRAJECTORIES
Mars exploration, Venus swingby and conjunction class mission modes, time period 2000 to 2045
[NASA-TM-86477] 02 p0303 N85-11961
Satellite orbit determination 05 p0598 N85-13813
Relationships between Ariane trajectories and satellite orbits 05 p0599 N85-13815
Optimal multiple-impulse nonlinear orbital rendezvous
08 p1105 N85-16994
Rejection of anomalous observations when determining spacecraft trajectories 13 p1979 N85-22421
Approximate analytic method of calculating trajectories of movement of a flight vehicle in the atmosphere
14 p2279 N85-24121
Optimal space trajectories 14 p2396 N85-24756
SPACECREWS
Thresholds of perception of whole body linear oscillation: Modification by spaceflight 05 p0694 N85-14467
The adaptation of vestibulo-spinal reflexes as a function of spaceflight and their relationship to space motion sickness 05 p0694 N85-14468
Challenges of developing an electro-optical system for measuring man's operational envelope
08 p1095 N85-16921
Results from radiation monitoring equipment experiment on STS-11
[AD-A152531] 17 p2908 N85-27932
Space Station crew safety alternatives study. Volume 4: Appendices
[NASA-CR-3857] 18 p3065 N85-28958
Proceedings of the Seminar on Space Station Human Productivity
[NASA-TM-86673] 18 p3156 N85-29539
Space station crew safety: Human factors interaction model 18 p3156 N85-29540
Space station crew safety alternatives study, third quarter briefing 18 p3156 N85-29541
Internal contamination issues
18 p3156 N85-29543
Human productivity program definition
18 p3156 N85-29
The human role in space (THURIS)
18 p3158 N85-29
Flow cytometry for health monitoring in space
[DE85-009572] 19 p3329 N85-30
Psychological issues relevant to astronaut selection for long-duration space flight: A review of the literature
[AD-A154051] 19 p3330 N85-30
Experience of science astronaut on the Spacelab-1 mission 20 p3506 N85-31
Living aloft: Human requirements for extended spaceflight
[NASA-SP-483] 21 p3666 N85-32
Psychophysiological distinctions of organization and regulation of daily cyclograms of crew activities during long-term spacecraft 22 p3821 N85-33
Results of microbiological studies conducted during operation of Salyut-6 orbital station
22 p3823 N85-33
SPACELAB
Study of proton and neutron activation of metal samples in low Earth orbit
[NASA-CR-171183] 01 p0026 N85-10
PDSS/IMC CIS user's guide
[NASA-CR-171179] 01 p0102 N85-10
Fokker wants to start new Netherlands space program
03 p0310 N85-11
Improving the Spacelab mass memory unit tape layout with a simulation model
[NASA-TM-86483] 05 p0713 N85-1457
Space infrastructure 07 p0914 N85-157
FRG's DFVLR ready for participation in space station
11 p1618 N85-201
Preflight and postflight motion sickness testing of the Spacelab 1 crew 11 p1694 N85-20
Space motion sickness monitoring experiment Spacelab 1 11 p1695 N85-20
D-1 report: The first German spacelab mission
[NASA-TM-77637] 13 p1977 N85-22
National Space Transportation Systems Program mission report
[NASA-TM-87456] 14 p2241 N85-2
NASA plans for a space station
14 p2393 N85-24
Measurement of the nighttime infrared luminosity of Spacelab 1 in the H- and K-bands
[NASA-TM-85972] 14 p2434 N85-25011
European views differ on space station concept
15 p2531 N85-25
MBB/Erno's views, future plans in aerospace activities
15 p2531 N85-25
West Europe report: Science and technology
[JPRS-WST-84-026] 15 p2532 N85-25
FRG opinion on Spacelab benefits, space station participation 15 p2532 N85-25
Infrared telescope
[NASA-CR-171392] 15 p2668 N85-26
Primate experiments on SLS-1
15 p2687 N85-26
A brief description of the two primate experiments to be carried out on SL-4 15 p2687 N85-26
ESA presents plans for European manned space station 18 p3085 N85-29
Spacelab 2
[NASA-EP-217] 19 p3222 N85-29
International space research perspectives of commercialization for German industry
[NASA-TM-77657] 19 p3222 N85-29
Commerce Lab: Mission analysis payload integration study. Appendix A: Data bases
[NASA-CR-176016] 19 p3224 N85-29
Experience of science astronaut on the Spacelab-1 mission 20 p3506 N85-31
The European vestibular experiments of the Spacelab-1 mission 20 p3506 N85-31
Some results of the European vestibular experiments in the Spacelab-1 mission 20 p3506 N85-31
Sleep and wake physiology in weightlessness
20 p3510 N85-31
Mission operations requirements document for D-1 Experiment 102, Vestibular Experiments in Spacelab
[NASA-TM-87495] 21 p3557 N85-32
Spacelab 1 hematology experiment (INS103): Influence of space flight on erythrokinetics in man
[NASA-TM-58266] 22 p3824 N85-3
The 1986 National Aeronautics and Space Administration authorization
[GPO-47-635] 24 p4166 N85-3
SPACELAB PAYLOADS
NT ATMOSPHERIC GENERAL CIRCULATION EXPERIMENT
NT POINTING CONTROL SYSTEMS

The design, fabrication and delivery of a spacelab neutral buoyancy Instrument Pointing System (IPS) mockup — underwater training simulator
[NASA-CR-171233] 04 p0462 N85-12934
Metric camera experiment: Spacelab 1 mission
05 p0658 N85-14229
The photogrammetric camera experiment on Spacelab 1
05 p0658 N85-14230
Spacelab mission D1 Frog statolith experiment STATEX: Hardware family and experiment operational sequence
05 p0669 N85-14426
An automatic device for amphibian egg fertilization in space: Technical aspects and biological requirements
05 p0669 N85-14427
Experiment 1ES031 on Spacelab 1: Are cells sensitive to gravity? — lymphocyte proliferation
05 p0669 N85-14428
Further cell biology experiments with Physarum polycephalum for a reflight of Biorack
05 p0669 N85-14429
Preliminary results of advanced Biostack experiments with plant seeds and spores — cosmic ray effects
05 p0691 N85-14441
The radiobiological advanced Biostack experiment on Spacelab 1 05 p0691 N85-14442
Spacelab 1 experiment: Microorganisms in space hard environment 05 p0691 N85-14443
Three-dimensional ballistocardiography in weightlessness (experiment 1ES 028) — Spacelab
05 p0691 N85-14447
Miniature personal physiological tape recorder (experiment 1ES 30) — Spacelab
05 p0692 N85-14448
The European vestibular experiments in the Spacelab 1 mission 05 p0694 N85-14466
Thresholds of perception of whole body linear oscillation: Modification by spaceflight 05 p0694 N85-14467
The adaptation of vestibulo-spinal reflexes as a function of spaceflight and their relationship to space motion sickness 05 p0694 N85-14468
Caloric stimulation of the vestibular system in microgravity 05 p0695 N85-14469
Sleep physiology in weightlessness (experiment 1ES 030) — Spacelab 05 p0695 N85-14474
Data Requirement (DR) MA-03: Payload missions integration — Spacelab payloads
[NASA-CR-171331] 10 p1428 N85-19009
Middle atmosphere NO and NO2 observed by means of the Spacelab one grille spectrometer
[AERONOMICA-ACTA-A-293-1984]
11 p1680 N85-20588
Future ultraviolet experiments, including FUSE/COLUMBUS 11 p1744 N85-20969
Infrared telescope
[NASA-CR-171392] 15 p2668 N85-26465
Space radiation studies — Spacelab 2 Payload
[NASA-CR-171410] 15 p2685 N85-26584
Long life feasibility study for the shuttle infrared telescope facility
[NASA-CR-3722] 17 p3052 N85-28893
Spacelab 2
[NASA-EP-217] 19 p3222 N85-29977
Commerce Lab: Mission analysis payload integration study. Appendix A: Data bases
[NASA-CR-178016] 19 p3224 N85-29988
Hemispherical latching apparatus
[NASA-CASE-MFS-25837-1] 19 p3224 N85-29991
Gas analysis techniques for human physiological measurements in space — Spacelab
[A/6537] 20 p3507 N85-31803
Activities report of the Aeronomy Department
[G-774-1984] 21 p3633 N85-32569
Detector calibration of the Indian cosmic ray experiment (IONS) in Space-Shuttle Spacelab-13
[SH-9.1-2] 23 p4050 N85-35117

SPACELAB UV-OPTICAL TELESCOPE FACILITY
U STARLAB

SPACERS
Spacer structure
[AD-D011641] 17 p2897 N85-27866

SPACETENNAS
Relationship of spaced antenna and Doppler techniques for velocity measurements (keynote paper), part 3
21 p3619 N85-32488
A simple model for testing the effects of gravity-wave-produced vertical oscillations of scattering irregularities on spaced-antenna, horizontal drift measurements 21 p3619 N85-32489
Potential advantages of the spaced antenna method for operational wind profiling, part 3.1B
21 p3620 N85-32490
Criteria for optimum spacing of spaced antenna, part 3.2A 2. p3620 N85-32491
Accuracy of velocity and power determination by the Doppler method 21 p3620 N85-32493
Interferometer applications of VHF radars, part 3.6A
21 p3621 N85-32497

SPACING
NT AIRCRAFT APPROACH SPACING
The dependence of soil bearing capacity and drawbar pull on the spacing between track
[AD-P004273] 09 p1406 N85-18849
Effects of vane/blade ratio and spacing on fan noise, volume 1
[NASA-CR-174664] 10 p1553 N85-19791
Effects of vane/blade ratio and spacing on fan noise. Volume 2: Data supplement
[NASA-CR-174665] 10 p1553 N85-19792
Variation in the spacing of dislocations in subgrain boundaries with creep strain in Type 304 stainless steel
[DE85-006184] 15 p2511 N85-25493
A heuristic solution to the spacing problem: Maximizing the minimum Euclidean distance among N points in a convex region
[AD-A152116] 16 p2855 N85-27603
Decomposing the joint distribution of several linear combinations of uniform spacings
[AD-A155056] 21 p3677 N85-32845

SPAIN
Scientific contributions in commemoration of Ebro Observatory's 75th anniversary — conference
[ISBN-84-00-05360-X] 04 p0518 N85-13308
Distribution of total solar radiation in Spain
04 p0523 N85-13344
A review of seismicity in peninsular Spain
04 p0523 N85-13349
Structure of the crust and upper mantle of the Iberian continental platform 04 p0523 N85-13350
Deep structure and seismicity in the Catalonia-Pyrenees region 04 p0524 N85-13352
Space research in Spain 08 p1231 N85-17751
A statistical analysis of ice nuclei concentrations at urban and rural sites in Valladolid, Spain
21 p3640 N85-32614

SPALLATION
Investigation of special facilities for a spallation neutron source 03 p0427 N85-12724
Solar cosmic ray produced neon in lunar soils and their implication for gas-rich meteorite studies
06 p0887 N85-15636
Salt action on concrete
[AD-A147812] 07 p0933 N85-15912
Research directed advanced high temperature coating system beyond current state-of-the art systems
[AD-A150696] 14 p2255 N85-23974
Scientific Opportunities with Advanced Facilities for Neutron Scattering
[DE85-012113] 22 p3639 N85-33770
Calculation of improved spallation cross sections
[OG-7.2-23] 23 p4017 N85-34890
Spallogenic origin of nuclei in meteorites
[SH-7.1-10] 23 p4048 N85-35102
Los Alamos high-current proton storage ring
[DE85-012664] 24 p4158 N85-35779

SPALLING
Impact and collisional processes in the solar system
[NASA-CR-174297] 08 p1255 N85-17914
Impact and collisional processes in the solar system
13 p2180 N85-23530
High temperature corrosion of ceramics
[DE85-013481] 24 p4083 N85-35303

SPANWISE BLOWING
NT BLOWING
Low-speed stability and control wind-tunnel investigations of effects of spanwise blowing on fighter flight characteristics at high angles of attack — Langely 12-ft low-speed tunnel and 30- by 60-ft tunnel
[NASA-TP-2431] 14 p2210 N85-23708

SPAR (ROCKET)
U SPACE PROCESSING APPLICATIONS ROCKET

SPARE PARTS
DYNA-SIM: A nonstationary queuing simulation with application to the automated test equipment problem
[AD-A146384] 06 p0857 N85-15450
Managing recoverable aircraft components in the PPB and related processes: Executive summary
[AD-A146806] 07 p1050 N85-16667
A simulation model for Air Launched Cruise Missile engine management
[AD-A147018] 07 p1051 N85-16672
The Air Force can improve its forecasts of aircraft spare parts requirements
[AD-A147911] 07 p1053 N85-16682
Estimating wartime support resource requirements. Statistical and related policy issues
[AD-A147923] 07 p1053 N85-16685
Excessive Air Force inventories result from duplicative spare parts requirements
[AD-A147777] 08 p1228 N85-17734
Automated parts storage and retrieval system positioning device and method
[AD-D011494] 11 p1647 N85-20379
On maximizing the expected lifetime of replaceable systems
[AD-A150003] 12 p1862 N85-21680
Managing recoverable aircraft components in the PPB (Planning, Programming and Budgeting) and related processes. Technical volume
[AD-A152014] 15 p2457 N85-25169
Feasibility of applications of Competition Decision Assist Package (CDAP) to spare parts
[AD-A154716] 21 p3712 N85-33036
Reliability prediction of the series system with spares subject to Weibull failure 24 p4100 N85-35413
DoD Value Engineering conference report. Value Engineering (VE): A tool that benefits line management. Part 4, Workshop B: VE on spare parts
[AD-A156070] 24 p4163 N85-35813

SPARK CHAMBERS
Relation between gamma-ray family and EAS core: Monte-Carlo simulation of EAS core
[HE-3.6-7] 24 p4185 N85-35955
The Nagoya cosmic-ray muon spectrometer 3, part 2: Track detector
[HE-5.2-3] 24 p4202 N85-36081

SPARK DISCHARGES
U ELECTRIC SPARKS

SPARK GAPS
Spark column plasma dynamics model (a first principles model for laser triggered spart gaps)
[AD-A147954] 08 p1166 N85-17354
Low jitter trigger for an excimer laser
[DE85-005732] 13 p2097 N85-23080
Spark gap electrode erosion
[AD-A152802] 17 p2953 N85-28237
Statistical distribution of breakdown voltages in rep-rate spark gaps
[DE85-012813] 24 p4090 N85-35354

SPARK IGNITION
Measurement and analysis of spark ignition engine pressure data to determine heat release profiles
[AD-A144770] 01 p0055 N85-10363
Analysis and simulation of the I C engine Otto cycle using the second law of thermodynamics
02 p0291 N85-11891
FRG ceramic engine components (PET)
08 p1141 N85-17193
Radiation/catalytic augmented combustion
[AD-A148758] 09 p1290 N85-18101
Research and development of alcohol fuel usage in spark ignited engines 09 p1301 N85-18175
Photochemical ignition studies. 1: Laser ignition of flowing premixed gases
[AD-A153048] 17 p2920 N85-28002
Ignition characterization of LOX/hydrocarbon propellants
[NASA-CR-171884] 18 p3083 N85-29070
Ignition characterization of LOX/hydrocarbon propellants
[NASA-CR-171882] 18 p3083 N85-29071
On the low temperature chemistry preceding end gas autoignition
[DE85-010471] 19 p3252 N85-30162
Experimental study of engine knock
[DE85-009851] 22 p3754 N85-33268
Multiparameter conditionally sampled laser velocimetry measurements during flame propagation in a spark ignition engine
[DE85-009850] 22 p3793 N85-33502

SPARK MACHINING
A new theory aiming to define the mechanisms of material removal in electroerosion
[NASA-TM-77875] 18 p3176 N85-29689

SPARK SHADOWGRAPH PHOTOGRAPHY
U SHADOWGRAPH PHOTOGRAPHY

SPARKS
NT ELECTRIC SPARKS
Spectral characteristics of grinding sparks used for identification of scrap metals
[PB85-198570] 24 p4080 N85-35290

SPARTAN SATELLITES
Space Station Spartan study
[NASA-TM-86215] 16 p2731 N85-26852

SPATIAL DEPENDENCIES
The spatial dependence of the Jovian auroral emissions 11 p1759 N85-21068
Spatial dependence of the local diffusion coefficient measured upstream of the November 12, 1978 interplanetary traveling shock
[SH-1.5-12] 23 p3996 N85-34776

SPATIAL DISTRIBUTION
NT STAR DISTRIBUTION
Strain distribution in a type 316/16-8-2 stainless steel weldment during cyclic loading
[DE84-015644] 02 p0210 N85-11384

Dynamics of growth of surface periodic structures when intense light acts on condensed media
02 p0268 N85-11748

The number and distribution of molecular clouds in the inner galaxy 03 p0442 N85-12811

Formation of subsurface Al2O3 layers in aluminum by oxygen ion implantation
[DE84-015599] 04 p0474 N85-13020

On the scale of distances of the galaxy
05 p0737 N85-14735

Local interstellar extinction with an emphasis on uvby beta results 06 p0875 N85-15559

The asteroidal source region of ordinary chondrites
06 p0881 N85-15600

Potential effectiveness of spatial processing in detecting signals against background of interfering reflections
07 p0952 N85-16032

Determination of moments of initial estimate during linear approximation of distribution of ejected impurity
07 p0954 N85-16045

Estimating location parameters in a mixture
07 p0984 N85-16252

Spatial estimation from remotely sensed data via empirical Bayes models 07 p0985 N85-16256

Neutral-current x-distributions
[DE84-016522] 09 p1382 N85-18691

Spatial distribution of auroras and its relationship to geological structure of Norilsk region
10 p1497 N85-19447

Modeling thermal plasma material processing experiments
[DE85-001551] 10 p1560 N85-19838

Mesoscale studies of flow regimes and fluxes of particulate matter in coastal waters
[DE85-003825] 11 p1689 N85-20620

Psychological aspects of phenomenon of spatial synchronization of EEG potential
11 p1691 N85-20632

Short-wavelength observations of HH-2H and HH-24A
11 p1747 N85-20990

Cometary atmospheres: Modeling the spatial distribution of observed neutral radicals
[NASA-CR-175491] 11 p1765 N85-21097

MTF analysis of LANDSAT-4 Thematic Mapper
12 p1871 N85-21737

Technical support for creating an artificial intelligence system for feature extraction and experimental design
[NASA-CR-175286] 12 p1918 N85-22044

Space and time distribtuion of aftershocks
13 p2112 N85-23157

Motion planning with six degrees of freedom
[AD-A150312] 13 p2165 N85-23432

Distribution and properties of large symmetric knobs on Mars 13 p2192 N85-23596

An analytical and numerical study of the interaction of rarefaction waves with area changes in ducts. Part 2: Area enlargements
[UTIAS-273] 14 p2300 N85-24242

Location of continental Permian volcanites of central Asia and its tectonic interpretation
14 p2346 N85-24505

The dawn-dusk asymmetry of particles near the neutral sheet of geomagnetotail 14 p2358 N85-24574

IMS advances in studies of field-aligned currents and their related electrodynamics 14 p2359 N85-24578

The relationship between auroral electrojet and visual aurora 14 p2363 N85-24602

Spatial characteristics of ULF pulsations and their modification by the ionosphere: IMS results
14 p2364 N85-24612

High time-resolution studies of the auroral ionosphere
[AD-A150945] 14 p2409 N85-24850

Charge isolation in a spatial light modulator
[AD-D011581] 15 p2652 N85-26356

Saturn's E ring 15 p2671 N85-26481

Multiple scattering of electromagnetic waves in discrete random media
[AD-A151768] 16 p2772 N85-27112

Study of spatial distribution of auroras
16 p2808 N85-27315

Spatial and temporal visual masking and visibility
[AD-A151968] 16 p2842 N85-27524

Spatial light modulator having a capacitively coupled photoconductor
[AD-D011646] 17 p3037 N85-28790

Cometary atmospheres: Modeling the spatial distribution of observed neutral radicals
[NASA-CR-175882] 17 p3054 N85-28904

Spatial correlations in the decay from an unstable state in the Malthus Verhulst model — laser cavities
[NOTA-INTERNA-832] 18 p3114 N85-29280

Areal coverage of storm precipitation
[NASA-CR-176013] 19 p3315 N85-30550

Influence of particle arrangement on sintering
[AD-A155337] 21 p3599 N85-32352

Interferometer applications of VHF radars, part 3.6A
21 p3621 N85-32497

Aircraft investigations of the distribution of aerosols in the lower troposphere 21 p3647 N85-32659

The distribution of giant salt nuclei inside and outside cloud over the basin of Xin and Jiang
21 p3650 N85-32681

Resource allocation in cerebral specialization of function: Behavioral and electrophysiological studies
[AD-A155092] 21 p3664 N85-32759

Interrelationships among the terrestrial planets
22 p3853 N85-33859

Constraints on the galactic distribution of cosmic rays from the COS-B gamma-ray data
[OG-3.1-6] 22 p3873 N85-33994

SMM detection of interstellar Al-26 gamma radiation
[OG-3.2-1] 22 p3874 N85-34001

The expected cosmic ray density and stream distributions at the heliolatitudinal asymmetry of solar wind
[SH-4.2-14] 23 p4008 N85-34852

Spatial distribution of cosmic rays in magnetic cycles of the Sun
[SH-4.2-20] 23 p4009 N85-34857

Influence of the source distribution on the age distribution of galactic cosmic rays
[OG-8.3-1] 23 p4021 N85-34920

Explanation of the secondary to primary ratio within the continuous Fermi accelerator model
[OG-8.3-2] 23 p4021 N85-34921

The modulation features of the long-period cosmic ray variations in connection with the sign change of the general magnetic field of the Sun
[SH-4.5-15] 23 p4037 N85-35032

On the anomalous component
[SH-4.6-6] 23 p4039 N85-35044

The read-out system of spatial distribution of thermoluminescence in meteorites
[SH-9.1-16] 23 p4052 N85-35131

Noise-sustained structure, intermittency and the Ginzburg-Landau equation
[DE85-009626] 24 p4094 N85-35379

Use of a minimum-ellipse criterion in the study of ion-beam extraction systems
[DE85-012670] 24 p4148 N85-35721

Tskhra-Tskaro complex intended for the investigations of EAS spatial characteristics near axis
24 p4190 N85-35995

Hybrid TLC-pair meter for the Sphinx Project
[HE-5.2-10] 24 p4203 N85-36066

Spatial distribution read-out system for thermoluminescence sheets
[HE-7.1-7] 24 p4213 N85-36161

SPATIAL FILTERING

Effect of hydrogen on formation of energy spectrum of multiply charged and copper ions
02 p0263 N85-11720

Analysis of effectiveness of partial optimization of spatial processing systems 07 p0952 N85-16031

Time and space domain filtering for improved HF communication 10 p1473 N85-19298

Overview of RADC adaptive antenna developments for communications 10 p1474 N85-19299

Method of multivariant intraclass pattern recognition
[AD-D011546] 12 p1818 N85-21405

Acoustooptic cell as space-frequency filter
13 p2090 N85-23051

Analysis and interpretation of synthetic time strings of oscillation data 14 p2444 N85-25079

Jinc-trap resonator
[AD-D011650] 17 p2970 N85-26339

Theoretical principles of vertical subsampling of color difference signals at half the sampling rate — television
[FI-447-TSR-18] 23 p3926 N85-34332

SPATIAL ISOTROPY
U ISOTROPY
U SPATIAL DISTRIBUTION

SPATIAL ORIENTATION
U ATTITUDE (INCLINATION)

SPATIAL RESOLUTION

Geographic science: Executive summary
02 p0214 N85-11408

Geographic science 02 p0214 N85-11409

Geomorphology 02 p0214 N85-11411

Fundamental remote sensing science research program. Part 1: Status report of the mathematical pattern recognition and image analysis project
[E85-10004] 02 p0215 N85-11417

Remote sensing as a mineral prospecting technique
[E85-10010] 02 p0216 N85-11423

Water resources by orbital remote sensing: Examples of applications
[E85-10015] 02 p0217 N85-11428

Vertical coherence along a macroray path in an inhomogeneous anisotropic ocean
[AD-A145992] 03 p0416 N85-12660

Fundamental limitations in antenna resolution by maximum entropy methods
[DE84-017052] 04 p0493 N85-1314

Simulation of optical configurations and sig processing methods in Anger-type neutron-posi scintillation detector
[DE84-012095] 04 p0503 N85-1321

Positron ring system using Anger-type detectors
[DE84-016788] 04 p0503 N85-1321

Investigation of several aspects of LANDSAT 4/5 da quality
[E85-10038] 04 p0525 N85-133

Tomographic reconstruction of axially symmetric obje from a single radiograph
[DE84-016783] 04 p0565 N85-13

Digital comparison and correlation techniques of remo sensing images with differing spatial resolutions
05 p0655 N85-14

A vertically resolved planetary boundary layer
05 p0660 N85-14

Research relative to high spatial resolution passiv microwave sounding systems 05 p0681 N85-14

Diurnal variation harmonics and spatial change in cosmic ray flux 06 p0824 N85-15

Classification of vegetation communities in the Batt Mountain SE quadrangle, Nevada with MSS digital da
[E85-10043] 06 p0826 N85-15

Multi crop area estimation in Idaho using EDITOR
[E85-10054] 06 p0827 N85-15

Rectification of single and multiple frames of sate scanner imagery using points and edges as control
07 p0986 N85-16

The influence of the number of ground control poi on the scene-to-map registration accuracy — Kans Louisiana, Mississipp, and Missouri
07 p0986 N85-16

Image variance and spatial structure in remotely sens scenes — South Dakota, California, Missouri, Kentuc Louisiana, Tennessee, District of Columbia, and Oreg
07 p0986 N85-16

Analysis of subpixel registration
07 p0986 N85-16

Use of the analytic signal in ultrasonic imaging
[DE84-016843] 07 p1039 N85-16

Millimeter wave antenna technology
[AD-A148694] 08 p1155 N85-1729

Resolution enhancement of multichannel microwav imagery from the Nimbus-7 SMMR for maritime rainf analysis
[NASA-CR-174367] 10 p1462 N85-192

X-ray holography of biological specimens
[DE85-002437] 10 p1489 N85-19

Electronic displays: Their strengths and weakness for advanced high performance aircraft
10 p1533 N85-19

LANDSAT scene-to-scene registration accura assessment 11 p1667 N85-20

Geodetic accuracy of LANDSAT 4 Multispectral Scanne and Thematic Mapper data — Washington, DC, Californi Alabama, South Dakota, and Illinois
11 p1667 N85-20

Geometric accuarcy assessment of LANDSAT-4 Multispectral Scanner (MSS) data
11 p1667 N85-20

Wide-angle flat field telescope
[NASA-CASE-GSC-12825-1] 11 p1728 N85-20

Scan angle and detector effects in Thematic Mapp radiometry — Iowa and Arkansas
12 p1871 N85-217

The use of linear feature detection to investig Thematic Mapper data performance and processing
12 p1872 N85-217

Development of high resolution imaging detectors f X-ray astronomy
[NASA-CR-175505] 12 p1953 N85-22

High-resolution SIT TV tube for subnanosecond ima shuttering
[DE85-005189] 13 p2095 N85-23

Impact of Thematic Mapper sensor characteristics o classification accuracy — suburban Washington, D.C., Maryland, and the Chesapeake Bay
13 p2117 N85-231

Quick look analysis of TM data of the Washingt District of Columbia, area 13 p2119 N85-231

Preliminary comparisons of the information content a utility of TM versus MSS data 13 p2120 N85-23

Assessing LANDSAT TM and MSS data for detecti submerged plant communities 13 p2120 N85-23

The use of Thematic Mapper data for land cove discrimination: Preliminary results from the UK SATI programme 13 p2121 N85-23

Preliminary study of information extraction of LANDSA TM data for a suburban/regional test site
13 p2121 N85-23

Comparison of land cover information from LANDSAT Multispectral Scanner (MSS) and airborne Thematic Mapper simulator (TMS) data for hydrologic applications – Clinton River Basin, Michigan
13 p2122 N85-23211

Surface units on Venus derived from Pioneer-Venus altimetry, roughness, and reflectivity measurements
13 p2177 N85-23510

High time-resolution studies of the auroral ionosphere
[AD-A150945] 14 p2409 N85-24850

Spatial resolution of small particles in silane discharge
[AD-A150953] 14 p2423 N85-24948

Observed spatial properties of the solar eigenfunctions and the implications for the existence of resolved multiplets 14 p2443 N85-25074

Looking at more than three dimensions
[DE85-007764] 17 p3009 N85-28600

Image processing: Mathematics, engineering or art
[DE85-007066] 18 p3154 N85-29527

Measurements of vector fields with diode array
18 p3204 N85-29880

Three-dimensional photochemical machining with lasers
[AD-A154711] 21 p3591 N85-32320

Selective population of N = 3 OVIII level during expansion of laser plasma in helium
21 p3688 N85-32914

Hexagonal uniformly redundant arrays for coded-aperture imaging
[OG-9.2-1] 21 p3714 N85-33048

Research in extreme ultraviolet and far ultraviolet astronomy
[NASA-CR-176068] 21 p3716 N85-33060

Advanced instrumentation for Positron Emission Tomography
[DE85-011147] 22 p3840 N85-33779

Adaptive rezoner in a two-dimensional Lagrangian hydrodynamic code
[DE85-010108] 24 p4094 N85-35381

Proportional drift tubes for large area muon detectors
[HE-6.2-11] 24 p4203 N85-36087

SPECIFIC GRAVITY
U DENSITY (MASS/VOLUME)

SPECIFIC HEAT

Accurate measurement of heat capacity by differential scanning calorimetry 04 p0488 N85-12975

Magnetic susceptibility, electrical resistivity, and specific heat of single crystal LaFe-4P-12
[DE84-009979] 04 p0570 N85-13633

The isochoric heat capacity of fluid substances in the critical region. Pre-examinations for a Spacelab experiment
[BMFT-FB-W-84-034] 05 p0723 N85-14650

Thermophysical property testing using transient techniques
[AD-A147065] 07 p1049 N85-16664

Theoretical interpretation of thermal arrest data from differential thermal analysis measurements
12 p1949 N85-22241

Effect of variable solid phase thermal properties on propellant combustion 13 p2002 N85-22547

Characterization-curing-property studies of HBRF 55A resin formulations
[NASA-CR-175836] 16 p2753 N85-26969

Debye temperature and static displacements in LuH sub x single crystals from energy dispersive X-ray diffraction
[DE85-010961] 19 p3376 N85-30946

Basic cryogenics and materials. Phase 1
[NASA-CR-177932] 21 p3572 N85-32215

Dynamics of the melting of chromium-manganese alloys in molten steel
[BLL-M-35850-(5828.4)] 23 p3914 N85-34252

Experimental investigation of radiative-acoustic effects in the water by the thermodynamical conditions of Dumand
[HE-7.1-2] 24 p4213 N85-36156

SPECIFIC IMPULSE

Ion thruster project
[NASA-TM-77726] 07 p0917 N85-15805

SPECIFICATIONS
NT AIRCRAFT SPECIFICATIONS
NT EQUIPMENT SPECIFICATIONS
NT FUNCTIONAL DESIGN SPECIFICATIONS

Tendencies in the development of utilization protocols, seminar report — communication networks
[FUB-11-1983] 01 p0039 N85-10252

Requirements and specifications for cartographic video discs
[AD-A144906] 01 p0049 N85-10325

Logical database processor interface specifications
[PB84-216456] 01 p0105 N85-10705

Investigation of current setting procedures for sector magnets
[CSIR-NAC-83-03] 01 p0117 N85-10795

Manufacturing Methods and Technology (MM/T) specifications for miniature cathode ray tube
[AD-A145597] 02 p0194 N85-11298

APOLLO system requirements specification — electronic document delivery
[ESA-SP-1068] 04 p0494 N85-13150

Improved robotic equipment for radiological emergencies
[DE84-017637] 04 p0509 N85-13249

Quality organization — quality control
[CNES-NT-106] 04 p0511 N85-13257

The ESA product assurance specification system: Explanatory note 04 p0511 N85-13259

Physical database processor preliminary interface specifications
[PB84-217561] 04 p0548 N85-13483

Experimental techniques of formal specifications for the design of tested and reliable computer programs
[ENST-84E007] 05 p0716 N85-14591

Towards a specification of the B programming environment
[CWI-CS-R8406] 05 p0716 N85-14593

Priority rewrite systems — computer programming
[CWI-CS-R8407] 05 p0720 N85-14621

A buyer's guide to space infrastructure
07 p0914 N85-15784

Reliability analysis of local area networks, intermediate report
[BLL-WH-610-(9091.9F)] 07 p1027 N85-16520

Mission-oriented requirements for updating MIL-H-8501. Volume 1: STI proposed structure — military rotorcraft
[NASA-CR-177331-VOL-1] 08 p1088 N85-16877

Mission-oriented requirements for updating MIL-H-8501. Volume 2: STI background and rationale — military rotorcraft
[NASA-CR-177331-VOL-2] 08 p1088 N85-16878

Using the control system design environment in the design of a data link receiver unit for the Coast Guard HH-65A helicopter
[AD-A148624] 08 p1088 N85-16880

Preliminary design criteria and certification test specifications for blast resistant windows
09 p1337 N85-18405

Laser-Electron-Gamma-Source (LEGS)
[DE85-003204] 11 p1638 N85-20322

Object-oriented algebraic specification: Proposal for a notation and 12 examples
[CWI-CS-R8411] 11 p1707 N85-20744

WESF (173)Cs gamma ray sources
[DE85-000676] 11 p1727 N85-20859

GSFC specification electronic data processing magnetic recording tape
[NASA-TM-80599] 12 p1851 N85-21609

Requirements for a database management system
[DE85-004661] 12 p1951 N85-22259

Spacecraft environmental interactions: A joint Air Force and NASA research and technology program
13 p1997 N85-22517

Computer aided draughting in a civil engineering consulting practice 15 p2627 N85-26189

Space reactor ground tests, assessment of facility needs
[DE85-006814] 15 p2650 N85-26345

A description of the process of elaborating man-machine dialog in an aircraft equipped with cathode tubes: Roles and specifications of piloted simulation methods
16 p2696 N85-26658

Water brake convertor: A simple device to convert mechanical energy into heat energy
[DE85-006021] 16 p2716 N85-26766

Orbiter middeck/payload standard interfaces control document
[NASA-TM-87473] 16 p2729 N85-26840

Standards and specifications for geodetic control networks
[PB85-166478] 16 p2816 N85-27374

Avionics data base
[AD-A152415] 17 p2897 N85-27863

The interactive generation of specifications for an onboard software series (GISELE)
17 p2904 N85-27906

Steel Tubes
[BLL-BISI-TRANS-22064-(9022.06)]
17 p2973 N85-28369

Electric Peugeot to have new nickel-iron batteries
18 p3086 N85-29098

Specification of surface roughness over oceans in the GLAS Fourth Order GCM 18 p3142 N85-29455

Atmosphere monitoring requirements
18 p3158 N85-29553

Specification of software quality attributes, volume 1
[AD-A153988] 18 p3163 N85-29593

Specification of software quality attributes. Volume 2: Software quality specification guidebook
[AD-A153989] 18 p3163 N85-29594

Advanced fuel cell development
[DE85-009662] 19 p3306 N85-30497

Maintenance training simulators prime item development specification. Model specification and handbook
[AD-A154106] 19 p3330 N85-30626

Combined function lattices for a 6 GeV synchrotron light source
[DE85-010959] 19 p3367 N85-30885

Standard procedures to be used in specifying basic properties of plastics and polymers
[NPL-DMA(A)-99] 20 p3433 N85-31295

Ultrasonic flowmetering with reflected pulses
[PB85-179885] 20 p3460 N85-31492

The Proust radar 21 p3629 N85-32547

An automated quality assurance surveillance plan for ADP (Automated Data Processing) operations under the Navy's commercial activities program
[AD-A154767] 21 p3671 N85-32802

Portable database driven control system for SPEAR
[DE85-010465] 22 p3830 N85-33720

Stellarator approach to fusion plasma confinement
[DE85-011420] 23 p3984 N85-34704

Specifying and verifying concurrent programs
[AD-A156190] 24 p4136 N85-35652

SLC arc transport system: Magnet design and construction
[DE85-014289] 24 p4159 N85-35789

SPECIMEN GEOMETRY

Influence of test method and material stiffness on the damage produced by low velocity impacts on carbon-epoxy composites No. 45.387/1
[REPT-45.387/1] 03 p0326 N85-12100

Instrumented impact testing machine with reduced specimen oscillation effects
[VTT-290] 04 p0504 N85-13218

Applicability of fatigue strength data obtained from small separately cast specimens on large cast components
05 p0651 N85-14178

Stress intensity factor in a tapered specimen
[NASA-CR-175589] 13 p2102 N85-23099

Fatigue strength of alpha-titanium alloys under cophasal action of variable normal and tangential stresses
15 p2498 N85-25407

A cracked orthotropic sheet stiffened by a semi-infinite orthotropic sheet
[NASA-TP-2455] 21 p3597 N85-32339

Results of an interlaboratory fatigue test program conducted on alloy 800H at room and elevated temperatures
[NASA-CR-174940] 21 p3597 N85-32340

SPECIMENS

X-ray holography of biological specimens
[DE85-002437] 10 p1489 N85-19396

Development of an automated miniature Charpy test method
[DE85-003011] 11 p1652 N85-20405

The preparation of TEM specimens showing oxide scales in transverse cross-section
[AERE-R-11579] 24 p4078 N85-35276

SPECKLE PATTERNS

Laser speckle technique for burner liner strain measurements 02 p0142 N85-10960

Scattering from multi-scale surface — infrared lasers
[RSRE-MEMO-3656] 04 p0505 N85-13222

Measurement of high temperature strain by the laser-speckle strain gauge
[NASA-TM-77751] 07 p0977 N85-16207

Automatic analysis of speckle photographs by microcomputer
[NPL-DITC-47/84] 09 p1322 N85-18308

Image processing instrumentation for speckle interferometry and imaging
[AD-A149308] 11 p1762 N85-21084

Investigations of high resolution imaging through the Earth's atmosphere using speckle interferometry
[AD-A150680] 14 p2439 N85-25053

SPECTRA
NT ABSORPTION SPECTRA
NT ATOMIC SPECTRA
NT BALMER SERIES
NT CONTINUOUS SPECTRA
NT D LINES
NT ELECTROMAGNETIC SPECTRA
NT ELECTRONIC SPECTRA
NT EMISSION SPECTRA
NT ENERGY SPECTRA
NT FRAUNHOFER LINES
NT GAMMA RAY SPECTRA
NT H ALPHA LINE
NT H LINES
NT INFRARED SPECTRA
NT K LINES
NT LINE SPECTRA
NT LYMAN SPECTRA
NT MASS SPECTRA
NT MICROWAVE SPECTRA

NT MOLECULAR SPECTRA
NT NEUTRON SPECTRA
NT NOISE SPECTRA
NT OXYGEN SPECTRA
NT PHOTOLUMINESCENT BANDS
NT PLASMA SPECTRA
NT POWER SPECTRA
NT RADIATION SPECTRA
NT RADIO SPECTRA
NT RAMAN SPECTRA
NT RYDBERG SERIES
NT SCHUMANN-RUNGE BANDS
NT SHOCK SPECTRA
NT SOLAR SPECTRA
NT SPECTRAL BANDS
NT STELLAR SPECTRA
NT UBV SPECTRA
NT ULTRAVIOLET SPECTRA
NT VIBRATIONAL SPECTRA
NT VISIBLE SPECTRUM
NT X RAY SPECTRA

13C and 1H NMR (Nuclear Magnetic Resonance) studies of solid polyolefines
[AD-P003909] 01 p0032 N85-10195

The spatial evolution of t he directional wave spectrum in the Southern Ocean: Its relation to extreme waves in Agulhas Current 08 p1144 N85-17213

Measurement procedures for the radar spectrum engineering criteria
[PB85-119022/GAR] 09 p1313 N85-18254

Surface forward scattering and reflection
[AD-A150115] 12 p1928 N85-22112

Wave directional spectra via ARGOS
16 p2812 N85-27343

One mechanism for generation of wave disturbances in spectra of turbulent flows near ocean surface
19 p3269 N85-30397

Atmospheric planetary wave response to external forcing
[NASA-CR-176000] 19 p3315 N85-30548

A global low order spectral model designed for climate sensitivity studies
[NASA-CR-175999] 19 p3315 N85-30549

Some studies in filtering of atmospheric turbulence
[AD-A154042] 19 p3316 N85-30557

Verification of theoretically computed spectra for a point rotating in a vertical plane
[DE85-011967] 20 p3520 N85-31893

Criteria and algorithms for spectrum parameterization of MST radar signals 21 p3626 N85-32527

Paleoenvironmental investigations at seed cave (Windust cave H-45FR46), Franklin County, Washington
[AD-A154777] 21 p3635 N85-32576

Device for frequency modulation of a laser output spectrum
[DE85-011634] 22 p3790 N85-33479

The 1000 GeV gamma rays from ms pulsars
[OG-2.3-12] 22 p3867 N85-33948

Absolute rigidity spectrum of protons and helium nuclei above 10 GV/c
[OG-4.1-1] 22 p3875 N85-34007

Spectral and spatial properties of solar microflares
[SH-1.2-4] 23 p3991 N85-34740

Relativistic cosmic ray spectra in the full non-linear theory of shock acceleration
[OG-8.1-6] 23 p4018 N85-34896

Master Fit users' guide, version 1.0
[DE85-014199] 24 p4140 N85-35667

SPECTRAL ABSORPTION
U ABSORPTION SPECTRA

SPECTRAL ANALYSIS
U SPECTRUM ANALYSIS

SPECTRAL BANDS
NT ABSORPTION SPECTRA
NT FRAUNHOFER LINES
NT PHOTOLUMINESCENT BANDS
NT SCHUMANN-RUNGE BANDS

Noise jammer discrimination by noise spectral bandwidth
[AD-D011224] 01 p0038 N85-10242

Biophysical and spectral modeling for crop identification and assessment
[E85-10006] 02 p0215 N85-11419

Evaluation of criteria for selecting the spectral attributes of digital LANDSAT MSS imagery for discriminating lithological units in the lower Curaca River Valley, Bahia — Brazil
[E85-10036] 03 p0379 N85-12415

LANDSAT instruments characterization
[E85-10032] 04 p0524 N85-13356

Detection of the J-10 manifold of the pure rotational band of phosphine on Saturn 06 p1245 N85-17855

Study of spectral/radiometric characteristics of the Thematic Mapper for land use applications
[E85-10075] 10 p1504 N85-19489

Prelaunch absolute radiometric calibration of the reflective bands on the LANDSAT-4 protoflight Thematic Mapper 11 p1669 N85-20515

Relative radiometric calibration of LANDSAT TM reflective bands 12 p1869 N85-21725

Evaluation of the radiometric integrity of LANDSAT 4 Thematic Mapper band 6 data 12 p1869 N85-21726

Thermal band characterization of the LANDSAT-4 Thematic Mapper 12 p1869 N85-21727

A preliminary analysis of LANDSAT-4 Thematic Mapper radiometric performance 12 p1870 N85-21730

A preliminary evaluation of LANDSAT-4 Thematic Mapper data for their geometric and radiometric accuracies 12 p1871 N85-21739

Assessment of Thematic Mapper band-to-band registration by the block correlation method
12 p1872 N85-21743

LANDSAT 4 band 6 data evaluation
[E85-10093] 12 p1874 N85-21755

LANDSAT 4 investigations of Thematic Mapper and Multispectral Scanner applications — Drum Mountains, Utah and Tonopath, Nevada
[E85-10095] 12 p1874 N85-21757

Semiconductor materials for high frequency solid state sources
[AD-A150020] 12 p1940 N85-22166

Snow reflectance from Thematic Mapper
13 p2120 N85-23205

Relative accuracy assessment of LANDSAT-4 MSS and TM data for level 1 land cover inventory — Washington, D.C. 13 p2122 N85-23212

Reassignment of the iron (3) absorption bands in the spectra of Mars 13 p2195 N85-23614

Determination of mineral type, abundance, and grain size with remotely obtained reflectance spectra
13 p2196 N85-23623

Reduction of reabsorption effects in scintillators by employing solutes with large Stokes shifts
[DE85-011645] 22 p3838 N85-33767

SPECTRAL EMISSION

Luminous points and breakdown in structure of GaAs transistors 02 p0257 N85-11684

Spectral distribution of radiation in n junctions of GaAs during avalanche breakdown 02 p0258 N85-11686

Scattering models in the microwave regime
[NASA-CR-174001] 04 p0525 N85-13361

A comparison between active and passive sensing of soil moisture from vegetated terrains
04 p0526 N85-13364

Voyager EUV and FUV observations
06 p0875 N85-15554

The unidentified emission features: A study of the Orion Bar and planetary nebulae 08 p1246 N85-17862

Long term variability of the IO torus
11 p1760 N85-21070

Interference immunity of fiber-optic communication lines with spectral multiplexing of channels
13 p2069 N85-22924

Study of integral and spectral direct solar radiation over Atlantic 14 p2341 N85-24475

The use of the spectral matrix in analyzing the propagation characteristics of electromagnetic emissions — magnetosphere 14 p2371 N85-24658

Magnetospheric wave characteristics derived from cross-spectral analysis 14 p2371 N85-24659

Optical radiation emissions from selected sources. Part 2: High intensity discharge lamps
[PB85-149136] 15 p2523 N85-25551

Free electron lasers for the EUV spectral region
[DE85-006804] 15 p2563 N85-25815

Spectroscopic studies of a railgun muzzle flash
[MRL-R-952] 16 p2728 N85-26837

X-ray emission and the winds of cataclysmic variables
[DE85-007663] 17 p3053 N85-28902

Carbon foil secondary electron emission during ion passage through the 40 to 500 keV energy field
[MPE-190] 18 p3184 N85-29747

Recent results of the Los Alamos free-electron laser oscillator experiment
[DE85-010736] 19 p3277 N85-30324

Star formation in NGC 7538: Multi-wavelength observations and issues 20 p3545 N85-32063

Impact of fluctuations in optical properties of atmosphere on the ratio of spectral brightness from remote sensing of agricultural land 22 p3734 N85-33149

Cataloging the spectral brightness coefficients of the forested region of the European territory of the USSR
22 p3735 N85-33155

Direct regression analysis of remote sensing data (using example of grass cover) 22 p3736 N85-33157

A comparison of LANDSAT thematic mapper, multispectral scanner and airborne sensors for mapping the distribution of alteration minerals: Examples from the southwestern United States 24 p4106 N85-35452

Observations of far-infrared transitions between excited states of OH
[NASA-TM-86722] 24 p4167 N85-35833

SPECTRAL ENERGY DISTRIBUTION

Measures of distance between speech signals in the frequency domain — speech recognition
[FUB-5-1984] 01 p0041 N85-10267

Spectral distribution of radiation in n junctions of GaAs during avalanche breakdown 02 p0258 N85-11686

Global aspects of stream evolution in the solar wind
[DE85-002207] 11 p1786 N85-21101

Jet topologies in hadron-hadron collisions
[DE85-001328] 12 p1929 N85-22119

Maximum entropy spectral analysis
[LEOK-TR-1984-08] 14 p2299 N85-24225

A program of ground-based astronomy to complement einstein observations
[AD-A151111] 15 p2668 N85-26466

Recent results of the Los Alamos free-electron laser oscillator experiment
[DE85-010736] 19 p3277 N85-30324

Comparison of simulation with experiment in an RFQ
[DE85-010770] 19 p3349 N85-30757

Requirements for attaining Treanor's distribution of vibrational energy among CO2 levels in CW gasdynamic laser flows
[STN-3] 20 p3461 N85-31499

Some rigorous results concerning spectral theory for ideal MHD
[DE85-013427] 24 p4156 N85-35770

The structure of the shower disk observed at Mt. Norikura
[HE-4.7-1] 24 p4198 N85-36052

Structure of air shower disc near the core
[HE-4.7-2] 24 p4198 N85-36053

A mini-array for large air showers
[HE-4.7-10] 24 p4199 N85-36061

A note on some statistical properties of rise time parameters used in muon arrival time measurements
[HE-4.7-12] 24 p4199 N85-36062

SPECTRAL LINE WIDTH

The X-ray spectrum and time variability of narrow emission line galaxies
[NASA-TM-83859] 03 p0446 N85-12842

Spectral frequency of eigenvalues in optimal problems of stability of cylindrical shells of variable thickness
13 p2047 N85-22815

SPECTRAL LINES
U LINE SPECTRA

SPECTRAL METHODS

Auto-regressive moving average spectral estimation using modified and least squares modified Yule-Walker estimates
[AD-A145516] 02 p0254 N85-11663

Study of CW injection laser with a dispersive external cavity 02 p0270 N85-11760

A pseudospectral Legendre method for hyperbolic equations with an improved stability condition
[NASA-CR-172475] 03 p0410 N85-12617

Effective use of remote sensing products in litigation
[E85-10048] 06 p0827 N85-15250

On the instability of a 3-dimensional attachment line boundary layer: Weakly nonlinear theory and a numerical approach
[NASA-CR-172504] 07 p0957 N85-16063

Autoregressive spectral estimation for two dimensional time series 07 p0985 N85-16258

Data-driven choice of a spectrum estimate: Extending the applicability of cross-validation methods
[DE85-001411] 10 p1437 N85-19056

Spectral methods in time for parabolic problems
[NASA-CR-172539] 11 p1706 N85-20730

Complex symmetric matrices with strongly stable iterates
[NASA-CR-172542] 11 p1706 N85-20731

Simulation of estimating periodicity of seasonally stationary time series
[DE85-003517] 11 p1708 N85-20748

Recovering pointwise values of discontinuous data within spectral accuracy
[NASA-CR-172535] 12 p1919 N85-22049

Synthesis of quasi-optimum algorithms for signal recognition against background of correlated noise employing discrete spectral transformations
13 p2065 N85-23020

Automated extraction of absorption bands from reflectance special 13 p2197 N85-23624

Spectral methods for modeling supersonic chemically reacting flow fields
[NASA-CR-172578] 14 p2300 N85-24240

Analysis of spectral operators in one-dimensional domains
[NASA-CR-172573] 15 p2633 N85-26228

Kolmogorov and scalar spectral regimes in numerical turbulence
[NASA-TM-86699] 17 p2957 N85-28254

On spectral multigrid methods for the time-dependent Navier-Stokes equations
[NASA-CR-172613] 19 p3344 N85-30725
Spectral methods for limited area models
20 p3488 N85-31679
Spectral Theory of Sturm-Liouville Differential Operators: Proceedings of the 1984 Workshop
[DE85-009693] 20 p3520 N85-31890
A review of spectral methods
[NASA-CR-172502] 23 p3929 N85-34350
Study of spectral/radiometric characteristics of the Thematic Mapper for land use applications
[E85-10106] 24 p4107 N85-35464

SPECTRAL NOISE
U WHITE NOISE

SPECTRAL RECONNAISSANCE
Earth resources: A continuing bibliography with indexes
[NASA-SP-7041(44)] 10 p1503 N85-19484
The spot operational remote sensing satellite system: Current status and perspectives
11 p1713 N85-20776
Feature extraction assessment study
[AD-A150189] 13 p2126 N85-23239

SPECTRAL REFLECTANCE
Flight demonstration of new NRL real-time data acquisition system and laser video waveform sampler
[AD-A145126] 01 p0053 N85-10350
Relationships between grass canopy characteristics and LANDSAT Thematic Mapper bands
02 p0213 N85-11402
Botanical sciences team 02 p0214 N85-11407
A comparison between active and passive sensing of soil moisture from vegetated terrains
04 p0526 N85-13364
Spectral reflectance studies on the orientale region of the Moon 06 p0888 N85-15639
Variation in spectral response of soybeans with respect to illumination, view, and canopy geometry
[E85-10040] 07 p0982 N85-16241
Spectral estimators of absorbed photosynthetically active radiation in corn canopies
[E85-10041] 07 p0983 N85-16242
Growth/reflectance model interface for wheat and corresponding model
[E85-10058] 07 p0987 N85-16269
North American vegetation patterns observed with the NOAA-7 advanced very high resolution radiometer — North America
[E85-10062] 08 p1174 N85-17400
Analysis of terrestrial conditions and dynamics
[E85-10063] 08 p1174 N85-17401
Growth and reflectance characteristics of winter wheat canopies
[E85-10080] 10 p1505 N85-19494
Evaluation of infrared reflectance as a technique for measuring absorber materials degradation
[PB85-108488] 11 p1677 N85-20567
Evaluation of infrared reflectance as a technique for measuring absorber materials degradation
[DE85-002171] 11 p1729 N85-20874
Snow reflectance from Thematic Mapper
13 p2120 N85-23205
Multispectral analysis of the Kasei Vallis-Lanae Planum region of Mars 13 p2193 N85-23607
Geologic interpretation of remote sensing data for the Martian volcano, Ascraeus Mons
13 p2194 N85-23608
The search for igneous materials at the Viking landing sites 13 p2194 N85-23609
Basalts of Mars: Constraints on volatile evolution
13 p2194 N85-23610
Zeolites on Mars: Prospects for remote sensing
13 p2195 N85-23615
Remote sensing analyses of localized lunar dark mantle deposits 13 p2195 N85-23616
Spectral reflectance studies of the Orientale basin
13 p2195 N85-23617
Io: Precise comparison of Voyager spectral curves with laboratory measurements 13 p2196 N85-23619
Spectral units on Europa and Ganymede
13 p2196 N85-23621
Determining mineral types and abundances from reflectance measurements 13 p2196 N85-23622
Determination of mineral type, abundance, and grain size with remotely obtained reflectance spectra
13 p2196 N85-23623
Automated extraction of absorption bands from reflectance special 13 p2197 N85-23624
Quantitative analyses of planetary reflectance spectra
13 p2197 N85-23625
Variability of coefficients of spectral brightness of soils
15 p2486 N85-25346
Asteroid amphitrite: Surface composition and prospects for the possible Galileo flyby 15 p2680 N85-26549
Spectral reflectances of natural targets for use in remote sensing studies
[NASA-RP-1139] 19 p3299 N85-30450
Optical effects of thin film adhesives in multijunction solar cells
[DE85-010120] 19 p3305 N85-30488
Regression analysis of aircraft and ground measurement data on vegetation cover 22 p3735 N85-33156
Processing of LANDSAT imagery to map surface mineral alteration on the Alaska Peninsula, Alaska
24 p4106 N85-35455

SPECTRAL RESOLUTION
Reducing spectral dimension of remotely sensed data using principal components analysis and a Peano scanning 02 p0212 N85-11399
Cartography 02 p0214 N85-11412
Fundamental remote sensing science research program. Part 1: Status report of the mathematical pattern recognition and image analysis project
[E85-10004] 02 p0215 N85-11417
Remote sensing as a mineral prospecting technique
[E85-10010] 02 p0216 N85-11423
Water resources by orbital remote sensing: Examples of applications
[E85-10015] 02 p0217 N85-11428
NOAA/NASA joint simulation of AMTS and HIRS
05 p0662 N85-14384
The low-resolution spectra 09 p1413 N85-18907
LANDSAT-4 Science Characterization Early Results. Volume 2, part 1: Thematic Mapper (TM)
[E85-10068] 11 p1668 N85-20508
Spectral characterization of the LANDSAT Thematic Mapper sensors 11 p1669 N85-20514
Atmospheric properties of RU Lupi derived from high- and low-resolution IUE spectra
11 p1754 N85-21031
LANDSAT-4 Science Characterization Early Results. Volume 3, part 2: Thematic Mapper (TM)
[E85-10069] 12 p1869 N85-21724
Thematic Mapper spectral dimensionality and data structure 12 p1871 N85-21736
An analysis of the data obtained by a simultaneous observation of GMS and GMS-2: A study of the difference between the brightness temperatures by GMS and those by GMS-2 12 p1894 N85-21888
Impact of Thematic Mapper sensor characteristics on classification accuracy — suburban Washington, D.C., Maryland, and the Chesapeake Bay
13 p2117 N85-23188
Quick look analysis of TM data of the Washington, District of Columbia, area 13 p2119 N85-23197
Preliminary comparisons of the information content and utility of TM versus MSS data 13 p2120 N85-23202
Assessing LANDSAT TM and MSS data for detecting submerged plant communities 13 p2120 N85-23203
The use of Thematic Mapper data for land cover discrimination: Preliminary results from the UK SATMaP programme 13 p2121 N85-23207
Preliminary study of information extraction of LANDSAT TM data for a suburban/regional test site
13 p2121 N85-23208
Comparison of land cover information from LANDSAT Multispectral Scanner (MSS) and airborne Thematic Mapper simulator (TMS) data for hydrologic applications — Clinton River Basin, Michigan
13 p2122 N85-23211
Automated extraction of absorption bands from reflectance special 13 p2197 N85-23624
Measurements of vector fields with diode array
18 p3204 N85-29880
Mass resolution optimization in a large isotopic composition experiment
[OG-9.1-9] 23 p4023 N85-34935

SPECTRAL SENSITIVITY
SVKD and SVKM-3 seismographs with a low-sensitivity channel
[REPT-553] 03 p0376 N85-12396
SENSIT.FOR: A program for sensitometric reduction
07 p0963 N85-16105
A spectrosensitometer with an absolute calibration
07 p0963 N85-16106
The most effective astronomical photographic emulsions for recording of faint and low-contrast objects
07 p0963 N85-16110
Thematic Mapper. Volume 1: Calibration report flight model, LANDSAT 5
[E85-10059] 07 p0987 N85-16270
Color measurement and discrimination
[NASA-CR-3824] 09 p1365 N85-18579
Spectral characterization of the LANDAT-4 MSS sensors 11 p1666 N85-20499
Investigation of the optical properties of solar elements 12 p1879 N85-21786
LANDSAT-4 Science Characterization Early Results. Volume 4: Applications — agriculture, soils land use, geology, hydrology, wetlands, water quality, biomass identification, and snow mapping
[E85-10070] 13 p2117 N85-23186
A first evaluation of LANDSAT TM data to monitor suspended sediments in lakes — Lake Chicot, Arkansas
13 p2120 N85-23204
Preliminary evaluation of TM for soils information
13 p2121 N85-23206
Comparison of MSS and TM data for landcover classification in the Chesapeake Bay area: A preliminary report — Taylor's Island, Maryland
13 p2121 N85-23210
A global low order spectral model designed for climate sensitivity studies
[NASA-CR-175999] 19 p3315 N85-30549
Paired ion chamber constants for fission gamma-neutron fields
[AD-A155069] 21 p3702 N85-32999

SPECTRAL SIGNATURES
Description of the Dutch-Danish (DUDA) scanner — thermal signatures
[AD-B084893] 01 p0121 N85-10826
Basic principles, methodology, and applications of remote sensing in agriculture
[E85-10016] 02 p0217 N85-11429
Assessment of computer techniques for processing digital LANDSAT MSS data for lithological discrimination of Serra do Ramalho, State of Bahia
[E85-10033] 03 p0378 N85-12412
Ice-soil mixtures: Visual and near-infrared remote sensing techniques
[NASA-CR-174087] 04 p0525 N85-13358
An electronically controlled array for simulation of passive target/background signatures at millimeter wavelengths
[AD-D011456] 10 p1468 N85-19263
Analysis of data acquired by synthetic aperture radar and LANDSAT Multispectral Scanner over Kershaw County, South Carolina, during the summer season
[E85-10071] 10 p1503 N85-19485
Radiometric calibration and processing procedure for reflective bands on LANDSAT-4 protoflight Thematic Mapper 11 p1668 N85-20510
Improved continuum definition in high-background IUE images 11 p1761 N85-21078
Investigations of vegetation and soils information contained in LANDSAT Thematic Mapper and Multispectral Scanner data
[E85-10082] 12 p1873 N85-21747
Remote sensing research for agricultural applications — San Joaquin County, California and Snake River Plain and Twin Falls area, Idaho
[E85-10090] 12 p1873 N85-21752
Overview of TM applications research reports
13 p2117 N85-23187
A concept for the processing and display of Thematic Mapper data 13 p2119 N85-23196
Early results of investigations of LANDSAT 4 Thematic Mapper and Multispectral Scanner applications — Washington, D.C. 13 p2119 N85-23200
Experimental methods for quenching structures in lunar-analog silicate melts: Variations as a function of quench media and composition
13 p2184 N85-23554
Optical 3-D signature device for detecting chemical agents
[AD-D011669] 19 p3272 N85-30293
Physico-geographical regionalization of Caspian lowland based on space survey materials
22 p3736 N85-33162

SPECTRAL THEORY
On a spectral theory of the excitation mechanism of galactic spirals 12 p1955 N85-22284
Simple solar spectral model for direct and diffuse irradiance on horizontal and tilted planes at the Earth's surface for cloudless atmospheres
[DE85-002933] 18 p3137 N85-29424
Approximate inverse spectral transform for the Korteweg-de Vries equation
[PREPRINT-411] 18 p3172 N85-29658
Some rigorous results concerning spectral theory for ideal MHD
[DE85-013427] 24 p4156 N85-35770

SPECTROGRAMS
Tests of the automatic recognition of words spoken by different voices based on collected groups of model binary spectrograms
[ISSN-0208-5658] 05 p0622 N85-13977
Analysis of spacecraft data
[NASA-CR-171587] 21 p3669 N85-32789
Spacecraft-aided research discussed at geology Congress 22 p3734 N85-33147

SPECTROGRAPHS
Future studies of the local interstellar medium with Space Telescope and Columbus 06 p0860 N85-15593
Spectroscopic instrumentation for Tokamak diagnostics 09 p1388 N85-18732
The multi-anode microchannel array detector system: Current status and future prospects
11 p1761 N85-21060
The solar vector magnetograph of the Okayama Astrophysical Observatory 18 p3205 N85-29682
The new solar magnetograph for the Canary Islands Observatory THEMIS 18 p3205 N85-29886
A new study of muons in air showers by NBU air shower array 24 p4190 N85-35997
SPECTROHELIOGRAPHS
The evaluation of a deformable diffraction grating for a stigmatic EUV spectroheliometer
[NASA-CR-174248] 07 p1042 N85-16621
The calculation of theoretical chromospheric models and the interpretation of solar spectra from rockets and spacecraft
[NASA-CR-174269] 08 p1259 N85-17922
Coronal structures observed at metric wavelengths with the Nancay radioheliograph 14 p2453 N85-25152
The San Fernando Observatory video Stokes polarimeter 18 p3205 N85-29885
The new solar magnetograph for the Canary Islands Observatory THEMIS 18 p3205 N85-29886
High Resolution Telescope and Spectrograph (HRTS)
23 p3901 N85-34162
SPECTROHELIOSCOPES
U SPECTROHELIOGRAPHS
SPECTROMETERS
NT FABRY-PEROT SPECTROMETERS
NT GAMMA RAY SPECTROMETERS
NT INFRARED SPECTROMETERS
NT LASER SPECTROMETERS
NT MASS SPECTROMETERS
NT MICROWAVE SPECTROMETERS
NT NEUTRON SPECTROMETERS
NT SOLAR SPECTROMETERS
NT SPECTROHELIOGRAPHS
NT TIME OF FLIGHT SPECTROMETERS
NT ULTRAVIOLET SPECTROMETERS
A high resolution spectroscopic study of the oxygen molecule
[NASA-CR-174061] 02 p0172 N85-11150
Imaging Science Panel. Multispectral Imaging Science Working Group joint meeting with Information Science Panel: Introduction 02 p0213 N85-11406
Multiple object spectroscopy: The MX spectrometer design 02 p0296 N85-11920
Simultaneous measuring absorption spectrometer
[BMFT-FB-T-84-132] 03 p0365 N85-12339
Einstein solid state spectrometer observation of the peculiar red dwarf Wolf 630 AB
[NASA-TM-83947] 03 p0447 N85-12843
Advances in room-temperature solid-state gamma-ray spectrometry
[DE84-015944] 04 p0469 N85-12987
Study of instrument design options for the Columbus spectroscopy mission
[NASA-CR-174072] 04 p0502 N85-13205
LANDSAT instruments characterization
[E85-10028] 05 p0654 N85-14197
Clinical measurements using fiber optics and optrodes
[DE84-015043] 05 p0696 N85-14481
Measurements of X-ray spectra from laser produced plasma 06 p0748 N85-14794
Comparison measurements on optical particle counters
[BLL-DOUNREAY-TR-934-(9091.9F)]
07 p0961 N85-16092
A 150 micron heterodyne spectrometer for airborne astronomy 08 p1249 N85-17887
Tunable heterodyne receiver from 100 micron to 1,000 micron for airborne observations
08 p1249 N85-17888
SIRTF: The next step 08 p1250 N85-17891
Simulation of bent crystal spectrometers
[DE85-002042] 09 p1385 N85-18709
Improved performance for large area triple layer microchannel plate detector for a neutral spectrometer in Doublet III
[DE85-001719] 10 p1488 N85-19395
Application of layered synthetic microstructures to high temperature plasma diagnostics
[DE85-002035] 10 p1559 N85-19828
Research in extreme ultraviolet and far ultraviolet astronomy
[NASA-CR-174432] 10 p1570 N85-19902
Investigation of the output parameters of the pulsed neutron generator NGI-5
[DE85-001823] 11 p1725 N85-20849
Design, construction and initial evaluation of an absolute, time-integrating/time-resolving spectrometer for the diagnostics of pulsed, high temperature plasma X-ray sources in the 100-10,000 eV region
[DE85-003526] 11 p1732 N85-20896
SCATHA (spacecraft charging at high altitudes) plasma interaction experiment: SC-3 high energy particle spectrometer; SC-8 energetic ion composition experiment
[AD-A149726] 12 p1793 N85-21252
Use of the ORACLE DEMS in determining the response of complex scientific instrumentation
[DE85-001742] 12 p1853 N85-21621
Inelastic scattering in condensed matter with high intensity Moessbauer radiation
[DE85-003531] 12 p1854 N85-21627
High resolution diffraction grating
[AD-D011541] 12 p1933 N85-22141
Protons with energies above 30 KeV in Earth's radiation belt at low altitudes during magnetically quiet time close to geomagnetic equator 13 p1980 N85-22423
Rocket body charge neutralization processes in ARAKS experiment (data from two launches)
13 p1980 N85-22426
Reflex attachment for line alignment in spectral diffraction devices 13 p2044 N85-22794
Possibility of mapping active tectonic structures from mercury gas aureoles over sea surface
13 p2113 N85-23162
Effects of focusing on HRS focal-plane polarimeter measurements
[DE85-004627] 13 p2160 N85-23406
Comparison of flame photometer data with total particle volume calculated from laser spectrometer particle count data
[AD-A151008] 14 p2252 N85-23958
Geometric error analysis for shuttle imaging spectrometer experiment
[NASA-CR-175665] 14 p2305 N85-24269
Mossbauer spectrometry: Testing of a new computer based system and its application to a study of an aluminum-iron-cerium alloy
[AD-A151826] 15 p2510 N85-25483
Mirror accessory for line straightening in diffraction spectrometers 16 p2764 N85-27054
New focal plane detector system for the broad range spectrometer
[DE85-005370] 16 p2786 N85-27201
Cryostat and electronic development associated with multi-detector spectrometer systems
[DE85-007624] 16 p2786 N85-27203
Acousto-optical spectrometers at Itapetinga Radio Observatory
[INPE-3479-PRE/722] 16 p2881 N85-27776
Results from a Bragg curve spectrometer
[DE85-007870] 18 p3176 N85-29691
Squid detection of acoustomagnetic effects
19 p3373 N85-30924
A Cerenkov-delta E-Cerenkov detector for high energy cosmic ray isotopes and an accelerator study of Ar-40 and Fe-56 fragmentation
[NASA-CR-176028] 20 p3548 N85-32086
A microprocessor-controlled, multichannel fluorimeter for analysis of sea water
[AD-A154986] 21 p3590 N85-32310
Research in extreme ultraviolet and far ultraviolet astronomy
[NASA-CR-176068] 21 p3716 N85-33060
Program for observations of Halley's comet
22 p3732 N85-33136
Direct regression analysis of remote sensing data (using example of grass cover) 22 p3736 N85-33157
High-resolution spectrum of Cygnus X-1
[OG-2.4-12] 22 p3868 N85-33956
Absolute rigidity spectrum of protons and helium nuclei above 10 GV/c
[OG-4.1-1] 22 p3875 N85-34007
Results of a search for deuterium at 25-50 GC/c using a magnetic spectrometer
[OG-4.2-4] 22 p3878 N85-34024
Galactic antiprotons of 0.2-2 GeV energy
[OG-6.1-11] 22 p3888 N85-34101
Imaging Spectrometric Observatory (ISO)
23 p3902 N85-34169
Investigation of non-intrusive radiometers for entrained gasifier temperature measurement, revision 3
[DE85-011795] 23 p3934 N85-34385
Measurements of Fe and Ar fragmentation cross secions
[OG-7.2-20] 23 p4016 N85-34887
Investigation of cosmic rays in very short time scales
[HE-4.6-7] 24 p4197 N85-36044
A facility for investigation of multiple hadrons at cosmic-ray energies
[HE-4.6-8] 24 p4197 N85-36045
Fast scintillation counter system and performance
[HE-4.6-10] 24 p4197 N85-36047
SPECTROMETRY
U SPECTROMETERS
SPECTROPHOTOMETERS
NT INFRARED SPECTROPHOTOMETERS
NT ULTRAVIOLET SPECTROPHOTOMETERS
Five-minute P modes detected in Doppler shift measurement on Alpha Centauri
08 p1250 N85-1789
Compatibility, contamination and R microspectrophotometry
[DE85-010809] 19 p3273 N85-30297
SPECTROPHOTOMETRY
NT STELLAR SPECTROPHOTOMETRY
Spectrophotometric studies of iodine complexes in an aluminum chloride - butylpyridinium chloride ionic liquid
[AD-A145074] 01 p0024 N85-10150
Physical properties of the satellites of Neptune
02 p0300 N85-11945
Interactions of hydrazine and of hydrazine derivatives with soil constituents and with soils
[AD-A148475] 08 p1122 N85-17074
Spectral characteristics of dust in planetary nebulae
08 p1247 N85-17873
Aromatics determination in middle distillate petroleum fractions by spectrophotometric titration
[PNR-90239] 09 p1293 N85-18120
Observations of cataclysmic variable star winds
11 p1755 N85-21041
The essence of binary star coalescence: A coordinated ground-based photometric and IUE ultraviolet study of FK Comae 11 p1756 N85-21044
Microstructure of Venus cloud layer based on spectrophotometric data from Venera-11 spacecraft
13 p1982 N85-22436
Determining adsorption of surface-active substances by sea bottom deposits 13 p2107 N85-23128
Photometric study of Pluto near perihelion. Part 2: Refinement of rotation period: Color indices
15 p2483 N85-25325
Infrared observations of the Uranian rings
15 p2672 N85-26488
Stellar occultations by Uranus rings on 15 August 1980 and 22 April 1982 15 p2672 N85-26489
Fourier transform infrared spectrophotometric analysis of resin mix stoichiometry, revision 1
[DE85-007272] 16 p2747 N85-26851
Lightcurve CCD spectrophotometry of Pluto
20 p3545 N85-32057
Transparency of water 9n 186 - 500 nm region
21 p3690 N85-32923
The nature and origin of outer solar system asteroids from reflectance spectrophotometry
24 p4168 N85-35838
SPECTROPOLARIMETERS
U POLARIMETERS
SPECTRORADIOMETERS
A comparison of LANDSAT thematic mapper, multispectral scanner and airborne sensors for mapping the distribution of alteration minerals: Examples from the southwestern United States 24 p4106 N85-35452
SPECTROSCOPES
U SPECTROMETERS
SPECTROSCOPIC ANALYSIS
NT FLAME SPECTROSCOPY
Development of a rapid test method for asphalt concrete content determination in hot-mix paving mixtures
[PB84-218692] 03 p0342 N85-12204
Methodology for the collection and analysis of trace metals in atmospheric precipitation
[CM-67] 09 p1350 N85-18481
Beam-foil spectroscopy of highly ionized aluminum atoms 09 p1390 N85-18746
Synchrotron X-ray fluorescence and extended X-ray absorption fine structure analysis
[DE85-003606] 10 p1436 N85-19080
Spectroscopic study of sources and control of impurities in TMX-U: Revision 1
[DE85-004423] 12 p1937 N85-22170
Multiple element neutron-activation analysis of atmospheric aerosols with X-ray and gamma-spectrometric recording of radionuclides formed
13 p2013 N85-22831
Spectroscopic study of gas pollutants in atmosphere over large cities: A review 14 p2341 N85-24475
Spectroscopic analysis of radiation-generated changes in tensile properties of a polyetherimide film
[NASA-TP-2429] 15 p2502 N85-25435
Chemical spectroscopy
[DE85-009594] 18 p3191 N85-29790
Initial results from the Caltech/DSRI balloon-borne isotope experiment
[OG-4.3-8] 21 p3714 N85-33046
Dating Archean zircon by ion microprobe: New light on an old problem 21 p3722 N85-33084

Precision measurements of solar energetic particle elemental composition
[SH-2.1-4] 23 p3998 N85-34785

SPECTROSCOPIC TELESCOPES

Dall-Null tester for spaceborne applications
[AD-A151772] 16 p2881 N85-27779

Stokes parameters modulator for birefringent filters
16 p3205 N85-29884

The new solar magnetograph for the Canary Islands Observatory THEMIS 18 p3205 N85-29886

The vector magnetograph of the Sayan Solar Observatory 18 p3206 N85-29887

A Cerenkov-delta E-Cerenkov detector for high energy cosmic ray isotopes and an accelerator study of Ar-40 and Fe-56 fragmentation
[NASA-CR-176028] 20 p3549 N85-32086

A balloon-borne imaging gamma-ray telescope
[OG-9.2-2] 21 p3714 N85-33049

Balloon-borne video cassette recorders for digital data storage
[OG-9.3-11] 21 p3715 N85-33050

SPECTROSCOPY
NT ABSORPTION SPECTROSCOPY
NT ASTRONOMICAL SPECTROSCOPY
NT AUGER SPECTROSCOPY
NT AURORAL SPECTROSCOPY
NT ELECTRON SPECTROSCOPY
NT FLAME SPECTROSCOPY
NT HOLOGRAPHIC SPECTROSCOPY
NT INFRARED SPECTROSCOPY
NT LASER SPECTROSCOPY
NT MAGNETIC SPECTROSCOPY
NT MASS SPECTROSCOPY
NT MOLECULAR SPECTROSCOPY
NT NUCLEAR RADIATION SPECTROSCOPY
NT OPTICAL EMISSION SPECTROSCOPY
NT OPTOGALVANIC SPECTROSCOPY
NT PHOTOACOUSTIC SPECTROSCOPY
NT PHOTOELECTRON SPECTROSCOPY
NT RAMAN SPECTROSCOPY
NT SPECTROPHOTOMETRY
NT SPECTROSCOPIC ANALYSIS
NT STELLAR SPECTROPHOTOMETRY
NT ULTRASONIC SPECTROSCOPY
NT ULTRAVIOLET SPECTROSCOPY
NT X RAY SPECTROSCOPY

Application of positron annihilation in materials science
[DE84-014733] 02 p0288 N85-11883

Spectroscopic investigations on neutron induced impurity atoms and radiation defects
03 p0430 N85-12742

The present state of the International Star Cluster Photometry Programme 05 p0737 N85-14741

Topics in high resolution spectroscopy of stored ions
[DE85-002093] 06 p0861 N85-15470

A study of structural phase transitions using light scattering techniques
[AD-A147261] 07 p1048 N85-16654

Electrochemical interfaces and electrode processes
[AD-A147414] 09 p1290 N85-18098

Supercritical fluid chromatography/supersonic jet spectroscopy
[DE85-003310] 09 p1292 N85-18115

Beam probe spectroscopic technique for ion temperature and magnetic field measurements
09 p1389 N85-18738

Pulsed photothermal radiometry for remote sensing of spectroscopic and physical properties of thin film
[AD-A149080] 10 p1435 N85-19041

Interim protocol for the automated analysis of semivolatile organic compounds by Gas Chromatography/Fourier Transfer Infrared (GC/FT-IR) spectrometry
[PB85-115186] 11 p1595 N85-20035

KMSF X-ray laser experiments, task no. 2
[DE85-000291] 11 p1640 N85-20335

Coronal spectroscopy in laser plasmas
[DE85-002817] 11 p1730 N85-20880

Research in the optical sciences
[AD-A150196] 13 p2159 N85-23401

Collaborative shock tube studies of benzene pyrolysis
[DE85-006347] 14 p2253 N85-23962

Synthesis and properties of elevated temperature P/M aluminum alloys
[AD-A151031] 14 p2256 N85-23981

Characterization of atomic defects and their aggregates using positron annihilation spectroscopy
[DE85-006206] 14 p2418 N85-24918

Spectroscopy of quasimolecular X-rays with H-like decelerated ions
[DE85-006565] 15 p2649 N85-26337

Proposed solar neutrino experiment using (81)Br(nu,e(-e)) (81)Kr
[DE85-004802] 15 p2684 N85-26579

Spectroscopic investigation of materials for frequency agile laser systems
[AD-A151731] 16 p2790 N85-27208

Nuclear spectroscopic studies
[DE85-006894] 16 p2862 N85-27652

Positron annihilation studies of vacancy formation in tungsten, chromium, and niobium
[DE85-006837] 16 p2871 N85-27710

An investigation of molecular structure of copolymers using positron annihilation spectroscopy
[NASA-TM-86431] 17 p2916 N85-27977

The spectroscopy and reaction kinetics of coordinated unsaturated metal carbonyls
[AD-A153079] 17 p2920 N85-28003

East Europe report: Science and technology
[JPRS-ESA-85-017] 17 p2945 N85-28177

PAS determination of the vacancy formation enthalpy in tungsten
[DE85-010283] 19 p3240 N85-30086

Atomic data for controlled fusion research. Volume 4: Spectroscopic data for iron
[DE85-009658] 19 p3354 N85-30787

Calculation of molecular constants potential energy curves and Franck-Condon factors for lead oxide
[AD-A154521] 21 p3562 N85-32158

Multidimensional luminescence measurements
[AD-A154950] 21 p3563 N85-32162

Basic research in novel inorganic reagents and fluorocarbon chemistry
[AD-A155340] 21 p3564 N85-32165

Aerosol analysis and emission spectrometry with free jets
[DE85-010576] 21 p3564 N85-32168

Electrochemistry of Hexanitroazobenzene (HNAB)
[DE85-010807] 21 p3565 N85-32171

Multi-channel electric aerosol spectrometer
21 p3642 N85-32623

USSR report: Physics and mathematics
[JPRS-UPM-85-004] 21 p3680 N85-32860

Cataloging the spectral brightness coefficients of the forested region of the European territory of the USSR
22 p3735 N85-33155

Supercritical fluid chromatography/supersonic jet spectroscopy
[DE85-007005] 22 p3746 N85-33221

1985 Amorphous Silicon Review Meeting
[DE85-008794] 22 p3807 N85-33582

High-resolution spectroscopic observation of Vela X-1 in the hard X-ray energy range
[OG-2.2-10] 22 p3865 N85-33936

Direct determination of metals in organic matrices by Inductively Coupled Plasma-Atomic Emission Spectrometry (ICP-AES)
[DE85-012015] 23 p3911 N85-34233

Time-resolved spectroscopic studies of detonating heterogeneous explosives
[DE85-009760] 23 p3921 N85-34297

Apparatus and method for the spectrochemical analysis of liquids using the laser spark
[DE85-005749] 23 p3935 N85-34387

Solar flare gamma-ray line spectroscopy
[SH-2.1-14] 23 p3999 N85-34795

Results of ultra-low level 71ge counting for application in the Gallex-solar neutrino experiment at the Gran Sasso Underground Physics Laboratory
[SH-8.1-2] 23 p4049 N85-35108

The read-out system of spatial distribution of thermoluminescence in meteorites
[SH-9.1-16] 23 p4052 N85-35131

Literature search for new physical methods for biological aerosol detection
[AD-A155883] 24 p4128 N85-35592

High-resolution spectroscopy and dynamics of multiphoton processes in atoms and molecules
[AD-A155862] 24 p4147 N85-35714

SPECTRUM ANALYSIS
NT CEPSTRAL ANALYSIS
NT FLAME SPECTROSCOPY
NT MAXIMUM ENTROPY METHOD

Notes on NAC report NAC-83-05: Beam Pulse Length Determination by Spectral Analysis
[CSIR-NAC-83-06] 01 p0119 N85-10816

Giacobini-Zinner comet: Polarimetric and physical observations
[NASA-TM-77771] 01 p0130 N85-10894

Laser on copper and gold vapors with space diversity media 02 p0270 N85-11762

Splitting of surface polariton spectrum by holographic grating 02 p0272 N85-11771

Optical constant determination of thin polymer films in the infrared
[AD-A145669] 02 p0287 N85-11877

Uranus and Neptune
[NASA-CP-2330] 02 p0298 N85-11927

Evaluation of moduli and thicknesses of pavement systems by spectral-analysis-of-surface-waves method
[PB84-219112] 03 p0342 N85-12205

Simultaneous measuring absorption spectrometer
[BMFT-FB-T-84-132] 03 p0365 N85-12339

Signal processing algorithms
[AD-A145748] 03 p0406 N85-12590

Meteorological analysis for clusters of wind turbines
[DE84-013164] 04 p0539 N85-13425

LANDSAT instruments characterization
[E85-10029] 05 p0654 N85-14196

Measurement-technical investigations of wind energy units in the short-time range --- spectrum analysis
05 p0668 N85-14294

Resonant scattering of acoustic waves by elastic spherical shell in fluid 06 p0778 N85-14972

Spectrum of geomagnetic field variations in the range of periods between 1 and 10 years
06 p0821 N85-15215

Asteroid-meteorite connection: Regolith effects implied by lunar reflectance spectra 06 p0888 N85-15640

Laser spectroscopy of alkali atom-tetrahaloethylene reactions
[AD-A147431] 07 p0923 N85-15848

Design of an analog spectrum analyzer for probing experiments
[AD-A147384] 07 p0941 N85-15963

Power spectrum analysis of astronomical photographs digitised with small apertures 07 p0965 N85-16127

Bragg cell spectrum analyzer specification
[AD-D011320] 07 p1044 N85-16629

Data analysis techniques for vehicle attitudinal, positional and experimental measurements
[AD-A147752] 08 p1188 N85-17484

Shock response analysis by personal computer using the extended IFT algorithm 09 p1335 N85-18397

Initialization of Thompson-Pisarenko's algorithm --- sinusoidal signal parameter estimation
[FUB-46-1983] 09 p1375 N85-18641

Confinement of low-energy electrons near metallic surfaces for plasmon generation
[DE85-001119] 09 p1381 N85-18686

Radiation data and standards for Tokamak diagnostics
09 p1390 N85-18742

Relative-entropy minimization with uncertain constraints--theory and application to spectrum analysis
[AD-A149192] 10 p1546 N85-19752

White dwarf stars at ultraviolet wavelengths
11 p1744 N85-20971

Analysis of white dwarf Lyman alpha profiles
11 p1752 N85-21018

Ultraviolet observations of Population 2 Cepheids
11 p1754 N85-21034

LSS 2018: A double-lined spectroscopic binary central star with an extremely large reflection effect
[NASA-CR-175503] 11 p1762 N85-21082

Pseudospectral calculations of two-dimensional transonic flow (Task 1). Numerical investigation of VTOL aerodynamics (Task 2)
[AD-A150123] 12 p1772 N85-21126

Effects of scatterer spacing statistics on ultrasonic backscatter signal spectra
[DE85-003259] 12 p1928 N85-22114

Research in particles and fields
[NASA-CR-175472] 12 p1963 N85-22337

Spectra of incidental interference resulting from nonlinear conversion of signals from transmitters
13 p2073 N85-22950

Efficiency of multitarget signal detection by digital radar data processing devices 13 p2080 N85-22991

Accuracy of random signal spectral parameter estimation against interference background in acoustooptical spectrum analyzers
13 p2090 N85-23052

Determining vector of radiointerferometer base from observations of natural radio emission with narrow spectrum 13 p2112 N85-23158

Relationship between brightness spectrum of photographic image and spectrum of rises on a water surface with waves 13 p2115 N85-23171

Sulfur oxygen processes on Io
13 p2173 N85-23481

Photometric analysis of Jupiter-illuminated images of Io 13 p2196 N85-23620

Maximum entropy spectral analysis
[LEOK-TR-1984-08] 14 p2299 N85-24235

Dynamic spectra of mean monthly values of geomagnetic field elements based on spectral-time analysis data 14 p2344 N85-24496

Remote sensing of directional wave spectra using the surface contour radar
[NASA-TM-84440] 14 p2347 N85-24510

A structural classification of geomagnetic pulsations
14 p2371 N85-24657

The use of the spectral matrix in analyzing the propagation characteristics of electromagnetic emissions — magnetosphere 14 p2371 N85-24658
Magnetospheric wave characteristics derived from cross-spectral analysis 14 p2371 N85-24659
Observations of intermediate-degree solar oscillations
14 p2442 N85-25069
Spectral analysis of diurnal nonuniformity of Earth's rotation 15 p2477 N85-25289
Analysis of spectral characteristics of multilevel digital computing synthesis 15 p2527 N85-25579
Possible uses of tunable diode lasers in infrared spectroscopy
[ESA-TT-869] 15 p2564 N85-25818
A calorimetric approach for measuring emittance and normal spectral absorptance at elevated temperatures
[AD-A151292] 15 p2651 N85-26351
User manual for IMAGER: The DREO (Defence Research Establishment Ottawa) image processing system
[AD-A151754] 15 p2653 N85-26362
Saturn's E-ring in the red spectral region
15 p2671 N85-26480
Asteroid amphitrite: Surface composition and prospects for the possible Galileo flyby 15 p2680 N85-26549
Spectral characteristics of protons at low and high altitudes during geomagnetic storm of 29 July 1977
16 p2719 N85-26786
Multiple regression analysis of photographic image of soil properties 16 p2726 N85-26825
Spectroscopic studies of a railgun muzzle flash
[MRL-R-952] 16 p2728 N85-26837
A phase modulation evaluation procedure for an ARGOS type signal 16 p2811 N85-27336
Development of a modified time delay spectrometry technique for underwater acoustic measurements in a multipath environment
[AD-A152111] 16 p2860 N85-27639
Variability of short term eddy-correlation estimates of mass exchange
[PB85-172641] 18 p3138 N85-29431
Solar monochromatic images in magneto-sensitive spectral lines and maps of vector magnetic fields
18 p3207 N85-29897
Separation of Drude and band-to-band spectra in polyvalent metals
[DE85-010247] 19 p3240 N85-30093
Explosibility of ammonium nitrate
[HSE-TRANS-11111] 19 p3252 N85-30164
Sea water photoluminescence
19 p3292 N85-30415
Comparison of 8 to 12 micrometer and 3 to 5 micrometer CVF transmissometer data with LOWTRAN calculations
[AD-A154218] 19 p3350 N85-30763
Analysis of ferrates and ferrites of three transition metals using Moessbauer effects
[BLL-CE-TRANS-8019-(9022.09)]
20 p3430 N85-31273
Spectral evolution of the pulse of a dual frequency dye laser
[CNES-83/198/T/CT/DRT/TIT/10]
20 p3461 N85-31497
Lightcurve CCD spectrophotometry of Pluto
20 p3545 N85-32057
High resolution evidence for the Garrett-Munk spectrum of stratospheric gravity waves 21 p3622 N85-32503
A relationship between cloud droplet size and CCN critical supersaturation 21 p3649 N85-32677
In-cavity laser IR spectrum analyzer for investigating non-steady-state processes 21 p3685 N85-32894
Spectral-luminescence characteristics and induced emission of Nd-3(+) ion in Gd(2-x)Nd(x)(WO4)3 crystals
21 p3688 N85-32912
Doppler spectrometer for measuring narrow photochemical gaps in inhomogeneously broadened spectra 21 p3689 N85-32921
A balloon-borne imaging gamma-ray telescope
[OG-8.2-2] 21 p3714 N85-33049
Transmitter spectrum analyzer
22 p3774 N85-33389
Binary signal detection in acoustooptic receivers
22 p3782 N85-33430
Acetonitrile in the Earth's atmosphere: An upper limit deduced from infrared solar spectra
[AERONOMICA-ACTA-A-295-1985]
22 p3813 N85-33623
Spectra and positions of galactic gamma-ray sources
[OG-2.5-7] 22 p3866 N85-33963
The universal spectrum of AGNs and QSOs
[OG-2.7-8] 22 p3872 N85-33982
Spectral shape variation of interstellar electrons at high energies
[OG-6.2-7] 22 p3889 N85-34106
On the cosmic ray diffusion in a violent interstellar medium
[OG-7.2-14] 23 p4015 N85-34881
Study of spectral exponent on quiet and disturbed days
[SH-4.5-10] 23 p4037 N85-35028
Spectral analysis of the Forbush decrease of 13 July 1982
[SH-5.1-7] 23 p4042 N85-35061
Proton albedo spectrum observation in low latitude region at Hyderabad, India
[SH-6.1-8] 23 p4045 N85-35082
The application of bispectral analyses to aeroelastic phenomena 24 p4060 N85-35157
The spectrum of cosmic ray muons obtained with 100-ton scintillation detector underground and the analysis of recent experimental data
[HE-5.1-6] 24 p4201 N85-36071
SPECULAR REFLECTION
TM digital image products for applications
11 p1668 N85-20512
Diffraction-limited imaging of space objects 2
[AD-A149344] 11 p1728 N85-20870
Research in image understanding as applied to 3-D tomographic imaging with near optical resolution
[AD-A150096] 12 p1829 N85-21483
Surface forward scattering and reflection
[AD-A150115] 12 p1926 N85-22112
Scheme for measuring specular reflection coefficient at 10.6 microns wavelength with zigzag-path cell and integrating sphere 14 p2275 N85-24097
Aspects of SAR image segmentation
[AD-A154966] 21 p3575 N85-32236
Signal space models for antenna arrays
[AD-A156063] 24 p4067 N85-35335
SPEECH
NT CONVERSATION
NT PHONEMES
NT PHONETICS
NT TALKING
NT WORDS (LANGUAGE)
Status report on speech research. A report on the status and progress of studies on the nature of speech, instrumentation for its investigation, and practical applications
[AD-A145585] 02 p0191 N85-11277
Rech-1 speech synthesizer for man-machine dialog
04 p0543 N85-13456
A comparative study of alternative controls and displays for by the severely physically handicapped
05 p0709 N85-14549
Fast algorithms and specialized architectures
05 p0714 N85-14579
Speech-action interrelationships in operational work
07 p1010 N85-16418
Low-bit rate speech encoders based on Line-Spectrum Frequencies (LSF)
[AD-A150518] 13 p2056 N85-22871
Comparative architectures for a multiple function speech processor
[AD-A150673] 14 p2292 N85-24211
A preliminary investigation into the intelligibility of Microspeech-2, a speech synthesiser
[BAE-BT-12284] 15 p2539 N85-25675
Speech understanding research
[AD-A155462] 21 p3700 N85-32990
SPEECH DISCRIMINATION
U SPEECH RECOGNITION
SPEECH RECOGNITION
A review of selected studies of computerized speech recognition conducted at the Naval Postgraduate School
[AD-A144841] 01 p0037 N85-10235
Classification methods for Italian vowels — speech recognition
[FUB-61-1982] 01 p0039 N85-10248
Description of a semiannual selection procedure of vowel parts of the voice signal using a PDP 11/34 computer
[FUB-4-1983] 01 p0039 N85-10250
Determination of vowel zones in speech — speech recognition
[FUB-16-1983] 01 p0040 N85-10253
Vowel phoneme identification in speech
[FUB-26-1983] 01 p0040 N85-10257
Voice phonetic coding and decoding processes
[FUB-29-1983] 01 p0040 N85-10259
Comparative analysis of the clustering of the LPC coefficients in phoneme recognition
[FUB-39-1983] 01 p0041 N85-10264
Autoregressive nonsteady methods for the analysis and synthesis of the human voice
[FUB-3-1984] 01 p0041 N85-10266
Measures of distance between speech signals in the frequency domain — speech recognition
[FUB-5-1984] 01 p0041 N85-10267
Royal Signals and Radar Establishment speech database recordings 1983: Part 2: Recordings made for automatic speech recognition assessment and research
[RSRE-84008-PT-2] 02 p0190 N85-11267
Identification as a function of familiarity for known voices talking over an unprocessed channel and an LPC (Linear Predictive Coding) voice processor
[AD-A145545] 02 p0191 N85-11278
Implications of artificial intelligence for a user defined technical information system
[AD-P003938] 02 p0248 N85-11618
Wideband integrated voice/data technology
[AD-A146054] 03 p0355 N85-12290
Rech-1 speech synthesizer for man-machine dialog
04 p0543 N85-13456
Tests of the automatic recognition of words spoken by different voices based on collected groups of model binary spectrograms
[ISSN-0208-5658] 05 p0622 N85-13977
VOTAN V5000 speech recognition system performance test report
[AD-A146726] 07 p0939 N85-15950
Literature review of voice recognition and generation technology for Army helicopter applications
[AD-A146878] 07 p0939 N85-15954
Compository speech output (KOSA) with a very large scale integration speech synthesis chip
[FI-13-TBR-18] 07 p0942 N85-15974
Man-machine communication research for robotics reported 08 p1139 N85-17177
Automatic speech recognition in severe environments
[AD-A148481] 08 p1153 N85-17280
A voice-actuated wind tunnel model leak checking system
[NASA-TM-86359] 09 p1263 N85-17936
Speech analysis by parametric methods: A survey
[ENST-84C004] 09 p1313 N85-18251
Overview of leading-edge research at French CNRS lab 11 p1618 N85-20179
Automatic speech recognition in severe environments
[PB85-121697] 12 p1830 N85-21490
Research in continuous speech recognition
[AD-A150474] 13 p2055 N85-22868
Preliminary assessment of the Heuristics H2000 speechlink - speech recognition device — voice data input for Apple 2 computer
[BAE-BT-12276] 15 p2539 N85-25674
A preliminary investigation into the intelligibility of Microspeech-2, a speech synthesiser
[BAE-BT-12284] 15 p2539 N85-25675
A review of speech systems
[BAE-BT-12285] 15 p2539 N85-25676
An introductory study of automatic speech recognition systems
[BAE-BT-12286] 15 p2539 N85-25677
Automation of the process of speech signal segmentation in an analogic-numeric system
[REPT-5/1984] 16 p2768 N85-27082
Implementation of a real-time, interactive, continuous speech recognition system
[AD-A151936] 16 p2773 N85-27117
Evaluating syntactic constraints to speech recognition in a fighter aircraft environment
[AD-A152117] 16 p2773 N85-27119
Wideband integrated voice/data technology
[AD-A152329] 17 p2947 N85-28197
A study of error rates in voice recognition
[AD-A153282] 17 p2949 N85-28211
Study to determine potential flight applications and human factors design guidelines for voice recognition and synthesis systems
[NASA-CR-172590] 20 p3440 N85-31349
A classification vocoder: A very low rate speech transmission by vector quantization of the spectrum
[ENST-84D003] 20 p3441 N85-31356
Speech analysis system for assessing pilots' working fitness 22 p3819 N85-33661
SPEECHES
U LECTURES
SPEED
U VELOCITY
SPEED CONTROL
Use of braking stages for control of turbine speed
09 p1308 N85-18215
Feasibility demonstration of a novel, flat-belt, continuously variable transmission or automotive and electric-hybrid vehicle application
[NASA-CR-174430] 10 p1569 N85-1
Cost comparison of small gas turbines versus electric motors in a variable load industrial application
[PB85-149763] 12 p1837 N85-21530
Pulsewidth modulated speed control of brushless dc motors
[AD-A151966] 16 p2778 N85-27149
Experimental investigation of a variable speed constant frequency electric generating system from a utility perspective
[NASA-CR-174950] 21 p3579 N85-322

SPEED INDICATORS
NT ANEMOMETERS
NT HOT-FILM ANEMOMETERS
NT HOT-WIRE ANEMOMETERS
NT LASER ANEMOMETERS
NT TACHOMETERS
Airspeed sensing pressure valve system
[AD-D011472] 10 p1425 N85-18987
Miniature electrooptical air flow sensor
[NASA-CASE-LAR-13065-1] 11 p1635 N85-20295
Metrological support for remote transport vehicle speedometers 13 p2076 N85-22963
Digital tachometer 22 p3779 N85-33416
Development of contactless sensors for industrial and automotive applications
[BMFT-FB-T-85-031] 24 p4097 N85-35400
SPEED REGULATION
U SPEED CONTROL
SPEED REGULATORS
Speed governor for diesel engine
09 p1307 N85-18214
Investigation of doubly-fed machine in variable speed application
[DE85-004378] 14 p2299 N85-24234
SPEEDOMETERS
U SPEED INDICATORS
SPENT FUELS
Integrated data base program: A status report
[DE84-013604] 05 p0735 N85-14727
Corrosion performance of metals and alloys in a tuff geochemical environment
[DE85-009449] 18 p3077 N85-29033
Binary phase diagram determinations
[DE85-010856] 19 p3235 N85-30058
Experimental program to determine maximum temperatures for dry storage of spent fuel
[DE85-010307] 19 p3236 N85-30060
Physical and chemical changes to rock near electrically heated boreholes at Spent Fuel Test-Climax
[DE85-010834] 19 p3302 N85-30472
Consolidated fuel reprocessing program
[DE85-010591] 19 p3356 N85-30818
Source Term Experiments Project (STEP): Aerosol characterization system
[DE85-010248] 19 p3361 N85-30839
Consolidated fuel reprocessing program
[DE85-008750] 19 p3366 N85-30871
Office of Civilian Radioactive Waste Management
[DE85-012585] 22 p3839 N85-33774
Analytical methods in the purex process
[BLL-DOUNREAY-TR-952(9091.9F)]
24 p4149 N85-35727

SPERMATOCYTES
U GAMETOCYTES
SPERMATOGENESIS
Mammalian tissue sensitivity to long-term exposure to high-intensity stationary magnetic fields
22 p3823 N85-33686

SPHERES
NT CELESTIAL SPHERE
NT CONCENTRIC SPHERES
NT FALLING SPHERES
NT POINCARE SPHERES
NT ROTATING SPHERES
Elastic fields under a spherical indenter
[AD-A146519] 06 p0817 N85-15188
The resistance and mobility functions of two equal spheres in low Reynolds number flow
[AD-A147301] 07 p0959 N85-16080
Temperature prediction in mechanical components, an analytical approach 09 p1327 N85-18339
On detached shock wave of sphere moving with transonic velocities 11 p1622 N85-20215
Optimization of pressure vessels with standard intercepting spheres
[INPE-3276-PRE/600] 11 p1651 N85-20397
Scheme for measuring specular reflection coefficient at 10.6 microns wavelength with zigzag-path cell and integrating sphere 14 p2275 N85-24097
A counterpart of Faxen's formula in potential flow
[REPT-84-09] 17 p2960 N85-28279
Multiple equilibria of the barotropic vorticity equation on a sphere 18 p3146 N85-29475
Method of measuring spherical aberration and apparatus therefor
[AD-D011706] 19 p3387 N85-30882
Solid-state resistance welding cylinders and spheres
[DE85-010064] 20 p3469 N85-31555
SPLINES. Their equivalence to collocation
[AD-A155250] 21 p3632 N85-32566
Combustion-deflagration-detonation transition in a confined spherical powder
[ISL-R-108/84] 22 p3747 N85-33223
Thermal transport measurements of UV laser irradiated spherical targets
[DE85-011038] 23 p3931 N85-34365
Improved flow cytometer measurement of binding assays
[DE85-006407] 23 p3935 N85-34390
SPHERICAL CAPS
Estimation of the depth of a spherical cap in an hydraulic drawing test for some simple conditions of loss of stability
[REPT-4/1984] 16 p2748 N85-26956
SPHERICAL COORDINATES
Comparison of the multigrid and ICCG methods in solving the diffusion equation
[DE84-014409] 02 p0253 N85-11657
Convection schemes for use with curvilinear coordinate systems: A survey
[AD-A147093] 07 p1031 N85-16543
Solution of direct magnetometric problem on spherical Earth 13 p2116 N85-23179
Global coordinate system
[AD-A153878] 19 p3299 N85-30454
Evaluation of coordinate measuring machines
[DE85-011712] 22 p3788 N85-33467
Algorithm for calculation of strain state from measurements of node coordinates of arbitrary curvilinear grid
[BLL-M-36304-(5828.4)] 23 p3940 N85-34422
SPHERICAL HARMONICS
Advantages and limitations of spherical harmonic analyses of geomagnetic data 04 p0519 N85-13318
Geomagnetic secular variation: A jerk in 1970
04 p0521 N85-13329
Comparisons of secular variation in two-dipole and spherical harmonic models with observatory data in Eurasia, 1965-1975 04 p0521 N85-13330
Algorithm for space-time analysis of data on geomagnetic field
[NASA-TM-77804] 08 p1209 N85-17609
Non-radiative energy from differential rotation in hot stars 08 p1234 N85-17778
Isolated systems in general relativity
09 p1400 N85-18813
Time dependent interaction of internal pressure wave with system of two spherical shells
13 p2046 N85-22809
Venus gravity: Global field results
13 p2177 N85-23512
Potential models — Earth gravity
14 p2396 N85-24764
Error spectrum of Goddard satellite models for the gravity field 20 p3491 N85-31704
Characteristics of cosmic ray pole-equator anisotropy derived from spherical harmonic analysis of neutron monitor data
[SH-4.3-12] 23 p4032 N85-34996
Sidereal anisotropy of cosmic rays
[SH-4.4-8] 23 p4034 N85-35006
SPHERICAL PLASMAS
Ion velocity distributions from spherical 1054 nm and 351 nm laser plasmas
[DE85-002816] 10 p1559 N85-19833
Magnetohydrodynamic equilibrium and stability of spheromak with spheroidal plasma-vacuum interface
[IPPJ-732] 23 p3974 N85-34640
SPHERICAL SHELLS
NT SPHERICAL CAPS
Experimental investigation and analysis of oscillations of thin-walled spherical shell during pulse loading
05 p0725 N85-14662
Resonant scattering of acoustic waves by elastic spherical shell in fluid 06 p0778 N85-14972
Tests of the load-bearing and deformation behaviour of reinforced concrete spherical shells under point loading
[BLL-RISLEY-TR-4550-9091.9F)]
06 p0816 N85-15182
Ultrasonic analysis of spherical composite test specimens
[DE85-001591] 07 p0976 N85-16197
Finite element analysis of nonlinear oscillations and flutter of shells of revolution
[AD-A149071] 10 p1496 N85-19440
Radiographic inspection of butt welds described
11 p1620 N85-20198
Time dependent interaction of internal pressure wave with system of two spherical shells
13 p2046 N85-22809
Nonlinear behavior and stability of thin spherical shells subjected to non-axisymmetrical loading
13 p2048 N85-22821
Intensity vectors of sound scattering by a spherical shell
[AD-A147847] 13 p2103 N85-23107
Effect of axisymmetric vibration modes on sensitivity and directivity characteristics of piezoceramic sphere --- hydrophones 15 p2525 N85-25569
Natural vibrations of reinforced spherical shells
17 p2943 N85-28165
Finite elastic deformations of cylindrical and spherical shells under pressure
[OUEL-1549/84] 20 p3470 N85-31559
A mixed pseudospectral/finite difference method for a thermally driven fluid in a nonuniform gravitational field
[NASA-TM-87581] 22 p3783 N85-33436
The effect of power law body forces on a thermally-driven flow between concentric rotating spheres
[NASA-TM-87596] 24 p4093 N85-35374
SPHERICAL WAVES
Design criteria for limited scan antennas at digital microwave line of sight links 10 p1471 N85-19284
Comparison of spherical wave ray tracing and exact boundary value solutions for spherical radomes
[AD-P004353] 12 p1824 N85-21447
Sphericity gauge for wavefront of laser radiation
14 p2275 N85-24098

SPHEROIDS
NT OBLATE SPHEROIDS
Sedimentation of two arbitrarily oriented spheroids in a viscous fluid
[AD-A147303] 07 p0960 N85-16082
Milling of spherical zones in parts
14 p2266 N85-24041
Spheroidal functions: Properties and tabulation. Application to antenna synthesis
14 p2396 N85-24758
Wall effect on lateral migration of spherical particles in a linear shear flow 20 p3452 N85-31432
SPHEROMAKS
Compact toroid development, activity plan for spheromaks
[DE84-016736] 04 p0567 N85-13617
Proceedings of the US-Japan Theory Workshop on 3-D MHD Studies
[DE84-012019] 04 p0568 N85-13620
Magnetohydrodynamic stability of spheromak plasma in toroidal flux conserver with rectangular cross section
[IPPJ-716] 16 p2866 N85-27678
Steady-state spheromak reactor studies
[DE85-009585] 19 p3372 N85-30916
Los Alamos Spheromak Program
[DE85-010748] 20 p3398 N85-31077
Confinement and heating of high beta plasma with emphasis on compact toroids. Compact toroid research
[DE85-011463] 22 p3846 N85-33821
SPHERULES
Neutron activation analysis of stoney spherules from a marine sediment sample 06 p0883 N85-15608
Oxygen isotopes in deep sea spherules
06 p0883 N85-15609
Peculiar spherules from Antarctica and their origin
06 p0883 N85-15612
Fractionation of siderophiles in cosmic spherules and its implications 06 p0884 N85-15613
Survey of probable micrometer-sized Earth-orbital debris fragments in the NASA-JSC cosmic dust sample collection 12 p1785 N85-21203
SPICULES
Spicules and surges
[AD-A146785] 07 p1061 N85-16727
SPIDERS
Gravity perception and cardiac function in the spider
15 p2606 N85-26058

SPIKE ANTENNAS
U MONOPOLE ANTENNAS
SPILLING
Penetration of the atmosphere by flammable mixtures as a result of spillage of LNG on the ground
08 p1179 N85-17432
Methods/materials matrix of ultimate disposal techniques for spilled hazardous materials
[PB85-116853] 12 p1885 N85-21833
Hydrocarbon pool and vapor fire data analysis
[DE85-005857] 15 p2523 N85-25550
Facility for large-scale hazardous gas testing
[DE85-011852] 21 p3564 N85-32169
Description of a test site for large-scale heavy gas dispersion and combustion experiments
[DE85-004987] 23 p3911 N85-34231
Evaluation of source strength and dispersion model predications with data from large nitrogen tetroxide field experiments
[DE85-011855] 23 p3947 N85-34465
MATADOR (Methods for the Analysis of Transport And Deposition Of Radionuclides) code description and user's manual
[TI85-901402] 23 p3966 N85-34592
SPIN
NT ELECTRON CAPTURE
NT ELECTRON SPIN
NT METAL SPINNING
NT NUCLEAR SPIN
NT PARTICLE SPIN
NT SPIN-ORBIT INTERACTIONS
NT SPIN-SPIN COUPLING

Theory of nuclear magnetic relaxation
[AD-P003911] 01 p0032 N85-10197
Analysis of spin echo signals in multi-pulse experiment
06 p0792 N85-15065
A method for estimating the rolling moment due to spin rate for arbitrary planform wings
[NASA-TM-86365] 10 p1425 N85-18990
Thermal traction contact performance evaluation under fully flooded and starved conditions
[NASA-CR-166173] 15 p2568 N85-25648
Spin distributions in heavy ion fusion at and below the Coulomb barrier
[DE85-007617] 17 p3031 N85-28751
Magnetic impurities in superconductors
[DE85-006372] 18 p3196 N85-29825
Neutron scattering study of the heavy fermion system UBe-13
[DE85-010955] 19 p3356 N85-30804

SPIN DYNAMICS
Moment induced by liquid payload during spin-up without a critical layer
[AD-A145716] 02 p0199 N85-11327
Liquid payload moment equations
[AD-A145977] 03 p0362 N85-12319
Application of quantum chemistry of atmospheric chemistry
[AD-A147035] 07 p0922 N85-15843
Theoretical issues involving traps for neutral spin-polarized atoms
[AD-A148035] 08 p1220 N85-17682
Magnetic excitation in CuMn spin glass alloy
[DE85-002564] 10 p1453 N85-19159
Liquid moment on a filled coning cylinder during spin-up: Ad hoc model
[AD-A150280] 13 p2092 N85-23060
Observation of a novel low-lying excited state in zinc complexes
[AD-A150188] 13 p2156 N85-23385
Polar motions measurement study
[AD-A150690] 14 p2372 N85-24664
Theoretical and experimental studies of stabilized metastable helium
[AD-A150706] 14 p2417 N85-24913
Flight investigation of stall, spin and recovery characteristics of a low-wing, single-engine, T-tail light airplane
[NASA-TP-2427] 15 p2470 N85-25248
Use of quaternions in flight mechanics
[AD-A152616] 17 p2899 N85-27875
Lattice actions improved by block-spin renormalisation group and maximally symmetric lattices
[DE85-007416] 17 p3045 N85-28841
Modifications to SOLA-VOF for flow dynamics in spinning cylinders
[AD-A154093] 19 p3265 N85-30250
NMR investigation of crystalline electric field effect on spin-spin relaxation in (Y(1-x)RE(x))Rh4B4
[DE85-010512] 19 p3357 N85-30814
Electron-atom collision studies using optically state selected beams
[DE85-010848] 19 p3368 N85-30888
Spin physics at BNL
[DE85-009768] 20 p3529 N85-31955
Dual towline spin-recovery device
[NASA-CASE-LAR-13076-1] 24 p4066 N85-35200
Studies of the solar mesosphere explorer: Dynamics and horizon sensor performance. Part A: Spin axis precession and atmospheric drag. Part B: Clouds
[NASA-CR-175306] 24 p4069 N85-35213
The NORDA/FNOC (Naval Ocean Research and Development Activity's/Fleet Numerical Oceanography Center) Polar Ice Prediction System (PIPS)-Arctic: A technical description
[AD-A156332] 24 p4126 N85-35577

SPIN EXCHANGE
Polarized internal target apperatus
[DE85-011611] 19 p3354 N85-30793
Electron-atom collision studies using optically state selected beams
[DE85-010848] 19 p3368 N85-30888

SPIN FORGING
U METAL SPINNING

SPIN GLASS
Magnetic excitation in CuMn spin glass alloy
[DE85-002564] 10 p1453 N85-19159
Microstructural and electronic characteristics of metallic spin glasses
[AD-A149959] 12 p1813 N85-21371
Coexistence of antiferromagnetism and spin-glass ordering in the Ising system FeO 55MgO 45Cl2
[DE85-004164] 12 p1942 N85-22197
A numerical investigation of the overlap distribution among pure states in the spin glass phase
[PREPRINT-414] 18 p3172 N85-29659

SPIN REDUCTION
Magnetic spin reduction system for free spinning objects
[NASA-CASE-MFS-25966-1] 02 p0166 N85-11122

SPIN RESONANCE
Dangling bonds and sub-gap optical absorption in silicon
[DE85-011752] 24 p4082 N85-35302

SPIN STABILIZATION
Use of gravitational stabilization in performance of experiments 02 p0160 N85-11084
Hypothetical zero yaw drag trajectory of spinning projectiles between M = 5 and M = 10
[AD-A148899] 10 p1421 N85-18963
Non-contacting electromagnetic de-spin system for Earth orbiting satellites 12 p1946 N85-22225

SPIN WAVES
U MAGNONS

SPIN-LATTICE RELAXATION
Nuclear Magnetic Resonance of Polymeric Materials
[AD-A145078] 01 p0032 N85-10192
13C and 1H NMR (Nuclear Magnetic Resonance) studies of solid polyolefines
[AD-P003909] 01 p0032 N85-10195
Paramagnetic impurity effects in NMR determinations of hydrogen diffusion and electronic structure in metal hydrides. Cerium in YH-2 and LaH-2.25
[DE84-014127] 04 p0472 N85-13005
Anisotropy and relaxation effects of Co2+ ions in LiTi ferrite
[AD-A146550] 06 p0861 N85-15469
Proton NMR and susceptibility measurements in TiCoH/sub x
[DE85-003309] 12 p1807 N85-21336
NMR investigation of crystalline electric field effect on spin-spin relaxation in (Y(1-x)RE(x))Rh4B4
[DE85-010512] 19 p3357 N85-30814

SPIN-ORBIT INTERACTIONS
NT ELECTRON CAPTURE
Magnetic alignment theory and the interpretation of polarization 06 p0880 N85-15590
Inter-zone auger recombination in GaSb laser structures 21 p3662 N85-32875

SPIN-SPIN COUPLING
Novel transport and recombination processes in semiconductors
[AD-A145969] 03 p0433 N85-12757
Vacancy-rearrangement theory in the first Magnus approximation
[DE85-004435] 12 p1930 N85-22123
Finite-perturbation intermediate neglect of differential overlap molecular orbital calculations of nuclear magnetic resonance spin-spin coupling constants for polycyclic aromatic hydrocarbons and aromatic nitrogen heterocyclics
[NASA-TM-87486] 20 p3525 N85-31927

SPINAL CORD
NT SPINE
The position and mobility of the shoulder, spinal column and pelvis in seated subjects
[AD-A153751] 18 p3153 N85-29524

SPINE
An investigation of spinal injury potential from the use of the ACES 2 ejection seat by lower weight female pilots
[AD-A148449] 08 p1196 N85-17537
The clinical and radiological assessment of cervical injury, Annex A 12 p1907 N85-21976

SPINEL
A physical interpretation of the structure and electron-optical data for spinel (MgAl2O4)
[AERE-R-11278] 03 p0434 N85-12767
Anisotropy and relaxation effects of Co2+ ions in LiTi ferrite
[AD-A146550] 06 p0861 N85-15469
Defective nature of the crystalline lattice of nickel ferrite-based solid solutions
[BLL-TRANS-WH-595-(9091.9F)]
10 p1439 N85-19068
Magnetic and structural properties of shock-synthesized zinc ferrite
[DE85-000469] 11 p1736 N85-20915
Oxygen evolution on NiCo2O4 electrodes
17 p2924 N85-28026
Integrated current collector and catalyst support
[DE85-011616] 22 p3761 N85-33311

SPINNING (METALLURGY)
U METAL SPINNING

SPINOR GROUPS
Solutions of field equations in General Relativity with spinor connection 15 p2663 N85-26436

SPIRAL ANTENNAS
Design and measured performance of a broadband Archimedes spiral antenna
[R-NIAS-22] 14 p2290 N85-24194
Radiation and scattering of spiral antennas
[AD-A151929] 16 p2773 N85-27118

SPIRAL GALAXIES
NT BARRED GALAXIES
NT MILKY WAY GALAXY
Molecules in external galaxies
03 p0444 N85-12828
The galactic distribution of open clusters of different ages and the angular velocity of the spiral structure
05 p0737 N85-14737
Excitation of spiral patterns in responsible density wave theory 05 p0740 N85-14764
The correlation between excitation parameter and nebular luminosity for galactic HII regions with application to regions of star formation in M83
05 p0743 N85-14773
The IRAS galaxy 0421+040P06: An active spiral (?) galaxy with extended radio lobes
[NASA-CR-174208] 06 p0871 N85-15536
Large-scale bubble structure of the interstellar medium (ISM) and properties of the Local Spiral Arm (LSA)
06 p0879 N85-15598
A comparison of some photometric parameters of active and normal spiral galaxies 08 p1238 N85-17806
Dust reradiation from NGC 6946
08 p1248 N85-17880
The structure and dynamics of ringed galaxies
09 p1415 N85-18928
On the morphology of spiral modes — disk galaxies
12 p1955 N85-22283
On a spectral theory of the excitation mechanism of galactic spirals 12 p1955 N85-22284
Drift-accretion theory of the spiral structure of galaxies
12 p1957 N85-22298
Some constraints on magnetic fields in galactic spiral arms 12 p1957 N85-22300
The hydrodynamic effects of nuclear active galaxy winds on host galaxies 20 p3545 N85-32062
The galactic gamma-ray distribution and the radial cosmic ray gradient
[OG-3.1-4] 22 p3873 N85-33992
Halo of NGC 4631 and models of cosmic-ray transport
[OG-6.2-3] 22 p3889 N85-34103

SPIRAL WRAPPING
Generated spiral bevel gears: Optimal machine-tool settings and tooth contact analysis
[NASA-TM-87075] 23 p3937 N85-34405

SPLEEN
Distinctions of rat lymphatic organ reactions to acute stress factor during hypokinesia
19 p3324 N85-30596

SPLINE FUNCTIONS
Spline-Galerkin solution of integral equations for 3-body scattering above break-up
[TWISK-327] 01 p0109 N85-10736
Approximation methods for inverse problems involving the vibration of beams with tip bodies
[NASA-CR-172468] 02 p0209 N85-11379
Nonlinear regression with emphasis on spline methods
[AD-A146192] 03 p0412 N85-12633
Application of summability methods to Jackson theorems for splines
[AD-A146256] 03 p0412 N85-12635
Least squares spline regression with block-diagonal variance matrices
[NPL-DITC-40/84] 04 p0554 N85-13523
Multivariate spline methods in surface fitting
07 p0985 N85-16257
A counterexample to a result of Streng and Fix concerning controlled approximation
[AD-A147360] 07 p1032 N85-16550
The stable evaluation of multivariate b-splines
[AD-A147386] 07 p1032 N85-16551
Spline methods for approximating quantile functions and generating random samples
[NASA-TP-2389] 07 p1035 N85-16565
Some qualitative properties of bivariate Euler-Frobenius polynomials
[AD-A149408] 10 p1547 N85-19755
Scattered data interpolation using thin plate splines with tension
[AD-A149803] 12 p1866 N85-21705
A two-dimensional smoothing spline and a regression problem
[AD-A149824] 12 p1921 N85-22067
Spline-based Rayleigh-Ritz methods for the approximation of the natural modes of vibration for flexible beams with tip bodies
[NASA-CR-172566] 13 p2102 N85-23100
Primary processing of experimental magnetovariation sounding data using spline functions
13 p2115 N85-23175
Spline techniques for magnetic fields
[DE85-004919] 14 p2415 N85-24902
The nonlinear analysis of thick composite plates using a cubic spline function 16 p2798 N85-2725

Noise correction on LANDSAT images using a spline-like algorithm
[E85-10098] 16 p2808 N85-27319
An interpolation method with the possibility of first derivative conection
[INPE-3352-PRE/631] 16 p2853 N85-27590
Surface interpolation using weighted splines
[INPE-3387-PRE/658] 16 p2853 N85-27591
Shape preserving spline interpolation
17 p3003 N85-28564
Multivariate spline algorithms for CAGD
17 p3003 N85-28566
Examination of the circle spline routine
17 p3004 N85-28573
Convex interpolating splines of arbitrary degree
17 p3004 N85-28574
A natural bias approach to cardinal spline curves
17 p3004 N85-28575
An intuitive approach to geometric continuity for parametric curves and surfaces (extended abstract)
17 p3005 N85-28579
Urn models and beta-splines
17 p3005 N85-28580
Computer programs for smoothing and scaling airfoil coordinates
[NASA-TM-84656] 20 p3388 N85-31011
Combined state and parameter estimation for a static model of the Maypole (Hoop-Column) antenna suface
20 p3417 N85-31210
SPLINES. Their equivalence to collocation
[AD-A155250] 21 p3632 N85-32566
An intuitive approach to geometric continuity for parametric curves and surfaces
23 p3963 N85-34571
Smoothing surface data by spline functions
[AD-A155829] 24 p4142 N85-35678

SPLINES
Control of rotordynamic instability in a typical gas turbine's power system 05 p0642 N85-14120
Controlled approximation and a characterization of the local approximation order
[AD-A149095] 10 p1546 N85-19750
The definition and computation of a metric on plane curves. The meaning of a face on a geometric model
17 p3004 N85-28571
Spline curves, wire frames and B-value
17 p3006 N85-28587
A robust estimator of location using an adaptive spline model
[AD-A153662] 18 p3174 N85-29676
SPLINES. Their equivalence to collocation
[AD-A155250] 21 p3632 N85-32566

SPLITS (GEOLOGY)
U GEOLOGICAL FAULTS

SPLITTING
Splitting methods for the numerical solution of the incompressible Navier-Stokes equations
[AD-A147463] 07 p1032 N85-16554
Photosynthetic water splitting
[DE85-002460] 11 p1690 N85-20627
Alternative anodic reactions in water splitting
[DE85-004159] 12 p1802 N85-21300
Longitudinal splitting in unidirectional composites, analysis and experiments
[NASA-CR-3881] 13 p2015 N85-22639
Analysis and interpretation of synthetic time strings of oscillation data 14 p2444 N85-25079
Fracture mechanics analysis of cold drawn Si-Cr valve steel
[BLL-BISI-TRANS-22216-(9022.06)]
17 p2978 N85-28405
Study of solute segregation at interfaces using Auger electron spectroscopy
[DE85-005709] 20 p3423 N85-31247

SPOILERS
Investigations on the dynamic loading of wind energy converters with vertical axis and problems of control during starting and overload conditions
[BMFT-FB-T-84-155] 03 p0386 N85-12472
An experimental study of airfoil-spoiler aerodynamics
[NASA-CR-177328] 06 p0748 N85-14796
Repair of composites 06 p1120 N85-17058
Investigation of the turbulent separated flow behind a spoiler
[ISL-CO-240/83] 14 p2213 N85-23726
Calculation of unsteady transonic separated flows by viscous-inviscid interaction 15 p2458 N85-25178
Study of boundary layer separation on a supercritical profile with a spoiler by means of a laser Doppler velocimeter
[ISL-CO-225/84] 23 p3895 N85-34128

SPOKES
The formation of spokes in Saturn's rings
15 p2676 N85-26524
On the role of mother-planet magnetic field in spiral structure explanation of formation of spokes — Saturn rings 15 p2676 N85-26525

SPONTANEOUS COMBUSTION
The reaction of oxygen-nitrogen mixtures with granular activated carbons below the spontaneous ignition temperature
[AD-A149041] 10 p1434 N85-19039
On the low temperature chemistry preceding end gas autoignition
[DE85-010471] 19 p3252 N85-30162

SPONTANEOUS EMISSION
Spontaneous emission by two atoms with different resonance frequencies near a metal surface
[AD-A154115] 19 p3353 N85-30781

SPORADIC E LAYER
Observations and prognosis of HF wave propagation via the sporadic E layer
[UIO-SR-84-04] 03 p0356 N85-12294

SPOT (FRENCH SATELLITE)
Attenuation experimental data bank in the COST 205 project. Structure and management of the final supports
[FUB-5-1983] 01 p0126 N85-10865
Heliosynchronism and phasing. Application to the SPOT orbit 05 p0600 N85-13826
The SPOT data bank system
05 p0659 N85-14236
Evaluation of SPOT simulation data of the S GEOS campaign of the EEC by data of the test sites Freiburg and Staubing (West Germany) 05 p0659 N85-14237
A field control methodology of remotely sensed data for statistical purposes: An example of SPOT simulated data in eastern Belgium — land use statistics
05 p0660 N85-14241
CNES, INRA do joint remote-sensing research
10 p1477 N85-19321
The spot operational remote sensing satellite system: Current status and perspectives
11 p1713 N85-20776
SPOT solar array 13 p2009 N85-22595
Mission analysis and orbit control of the heliosynchronous satellite SPOT
14 p2397 N85-24773
Details on spot remote sensing satellite propulsion unit 15 p2535 N85-25640
DORIS: Prediction in Doppler measurement — satellite onboard measurement
[CNES-CT/DTI/MS/AE/170] 16 p2729 N85-26843
The SPOT solar array
[SNIAS-851-440-103] 20 p3485 N85-31656

SPOT WELDS
Robotization of electric welding processes
03 p0345 N85-12225
Variations in the structure and in the composition of austentic and carbon steel in spot welds
[BLL-BISI-TRANS-21765-(9022.06)]
18 p3073 N85-29007

SPRAY CHARACTERISTICS
Development of holographic particle field data reduction by Fourier analysis
[AD-A148684] 08 p1165 N85-17348
Description of a technique to measure spray distribution in an air stream
[AD-A149780] 12 p1771 N85-21122

SPRAY NOZZLES
Experimental study of the spray characteristics of a research airblast atomizer
[NASA-TM-86911] 07 p0904 N85-15727
An experimental study of spray thruster
[REPT-613] 12 p1845 N85-21578

SPRAYED COATINGS
Air force plasma spray at SA-ALC (San Antonio Air Logistics Center)
[AD-P004004] 03 p0308 N85-11984
An investigation of enhanced capability thermal barrier coating systems for diesel engine components
[NASA-CR-174820] 09 p1298 N85-18154
Infrared-thermal wave scanner for NDE of naval thermal spray coatings
[DE85-002237] 11 p1650 N85-20391
Low cost, sprayed CuInSe2 solar cell research
[DE85-003467] 12 p1881 N85-21799
System for NDH of thermal spray coating bonds
[DE85-007463] 15 p2572 N85-25858
Rocket thrust chamber thermal barrier coatings
16 p2734 N85-26867
Vacuum plasma coatings for turbine blades
16 p2734 N85-26869
Erosion of corrosion-resistant surface treatments on alloy steels
[DE85-006446] 17 p2932 N85-28100
Spray applicator for spraying coatings and other fluids in space
[NASA-CASE-MSC-18852-1] 18 p3115 N85-29283

SPRAYED PROTECTIVE COATINGS
U PROTECTIVE COATINGS
U SPRAYED COATINGS

SPRAYERS
The structure of dilute combusting sprays
[NASA-CR-174838] 07 p0905 N85-15728
Improved sprayer for AN-2 cropdusting work
06 p1068 N85-16769
Development of holographic particle field data reduction by Fourier analysis
[AD-A148684] 08 p1165 N85-17348
Swirling turbulent spray group combustion
09 p1289 N85-18095
Research study of droplet sizing technology leading to the development of an advanced droplet sizing system
[NASA-CR-174839] 12 p1850 N85-21604
Size and velocity distributions of particles and droplets in spray combustion systems
[AD-A150355] 13 p2017 N85-22648
Spray applicator for spraying coatings and other fluids in space
[NASA-CASE-MSC-18852-1] 18 p3115 N85-29283
Spray pyrolysis as a synthetic tool
[AD-A153891] 19 p3234 N85-30047

SPRAYING
NT ARC SPRAYING
NT CROP DUSTING
NT FLAME SPRAYING
NT METAL SPRAYING
NT PLASMA SPRAYING
Silicon band spraying technique for solar cells
12 p1877 N85-21778
MATADOR (Methods for the Analysis of Transport And Deposition Of Radionuclides) code description and user's manual
[TI85-901402] 23 p3966 N85-34592

SPRAYING APPARATUS
U SPRAYERS

SPRAYS
U SPRAYERS

SPREAD F
Kinetic Rayleigh-Taylor instability theory in the ionosphere near equator 13 p2067 N85-22911
Equatorial F-region irregularity latitudinal extension and dynamo electric field
[INPE-3494-PRE/731] 16 p2826 N85-27433

SPREAD SPECTRUM TRANSMISSION
Resistance to HF jamming interference in mobile radio networks by an adaptive, distributed reconfiguration technique
[AD-A145117] 01 p0038 N85-10236
Digital correlator speed improvement by multiplexing
[AD-A145207] 01 p0100 N85-10662
Spread-spectrum communications
[AD-A146135] 03 p0355 N85-12285
Distributed reservation-based code division multiple access
[AD-A147007] 07 p0940 N85-15957
Optimum jamming effects on frequency-hopping M-ary FSK (Frequency-Shift Keying) systems under certain ECCM (Electronic counter-countermeasures) receiver design strategies
[AD-A147766] 08 p1151 N85-17267
AWQPSK: An optimum modulation technique for spread spectrum communication 09 p1311 N85-18235
Fast synchronization model for UHF spread-spectrum communication system 10 p1473 N85-19296
Asynchronous transmission with strong spectral spread 10 p1474 N85-19300
Narrowband spread spectrum systems
10 p1475 N85-19307
Research on adaptive antenna techniques 6
[AD-A149341] 11 p1624 N85-20228
Tactical satellite terminals for land and airborne C3 applications 11 p1710 N85-20760
Detection of angular modulated electromagnetic signals
[AD-D011563] 12 p1623 N85-21437
Spread spectrum mobile radio communications
[AD-A149936] 12 p1829 N85-21477
The performance of a new adaptive filter for digital communications
[AD-A151890] 15 p2543 N85-25702
Measured noise performance of a new method of frequency hopping
[AD-A152679] 17 p2953 N85-28234
Study of a low rate spread spectrum receiver
[ENST-83E015] 20 p3441 N85-31354
Compression of spread spectrum signals on an excessively dispersive channel
[AD-A155184] 21 p3576 N85-32240

SPREADING
Spreading upon compacting of fiber composite materials with porous metal matrix 10 p1443 N85-19096

SPRINGS (ELASTIC)
A gyro sensor block suspension
[AD-D011411] 08 p1154 N85-17284
Elastic compliance of imperfect interfaces: Review and relationship to ultrasonic scattering
[DE85-003068] 11 p1652 N85-20404
Pneumatic clamping device
[AD-D011544] 12 p1858 N85-21656
SPRING: Helical spring design software for microcomputers
[DE85-006200] 15 p2631 N85-26217
Investigation of fatigue strength of spring steel after high-temperature thermomechanical working (HTMW) by helical drawing
[BLL-M-36274-(5828.4)] 20 p3465 N85-31525
SPRINGS (WATER)
Hydrogeochemical investigation of thermal springs in the Black Canyon-Hoover Dam area, Nevada and Arizona
[PB84-202472] 01 p0064 N85-10428
Investigation of mineral and thermomineral springs in the Eifel Mountains regarding thermal indications
[BMFT-FB-T-84-019] 02 p0220 N85-11451
Geothermal assessment of part of the east shore area, Davis and Weber Counties, Utah
[DE84-016817] 09 p1342 N85-18446
Evaluation of low-temperature geothermal potential in Utah and Goshen Valleys and adjacent areas, Utah. Part 2: Water temperature and chemistry
[DE85-009344] 23 p3943 N85-34436
SPUR (REACTORS)
U SPACE POWER UNIT REACTORS
SPUTTERING
NT MAGNETRON SPUTTERING
Sputtering of gold irradiated with thermal neutrons
03 p0429 N85-12738
Effects of monolayer converages on substrate sputtering yields
[DE84-016312] 04 p0476 N85-13033
Ion contrasting chamber for discrimination of grains and textures
[BMFT-FB-T-84-151] 04 p0477 N85-13036
Effects of monolayer coverages on substrate sputtering yields 06 p0865 N85-15496
Synergestic sputtering properties of binary alloys
06 p0865 N85-15497
Optical properties of composite materials
[AD-A146768] 07 p0920 N85-15628
Rivista Tecnica Selenia, volume 9, number 1
07 p0938 N85-15945
Sputtering in thin film technology for optics — laser systems 07 p0938 N85-15948
Structural studies of amorphous Mo-Ge alloys using synchrotron radiation
[DE85-002061] 08 p1131 N85-17125
Synergistic sputtering properties of binary alloys
[DE84-017493] 09 p1297 N85-18148
Application of NbN films to the development of very high field superconducting magnets
[DE85-002729] 10 p1565 N85-19867
Oxidation protection coatings for polymers
[NASA-CASE-LEW-14072-1] 11 p1611 N85-20129
Textured carbon surfaces on copper
[NASA-CASE-LEW-14130-1] 11 p1615 N85-20156
Diamondlike flakes
[NASA-CASE-LEW-13837-2] 12 p1796 N85-21267
Sputter-induced compositional modifications in a Ni-Au alloy
[DE85-002771] 12 p1807 N85-21333
Use of markets to elucidate reacting sputtering processes
[DE85-005723] 13 p2018 N85-22655
Synthesis and characterization of superconducting electronic materials
[AD-A151112] 15 p2659 N85-26409
Measurement of NBLS distributed diode sputter ion pump characteristics
[DE85-006550] 16 p2760 N85-27031
Obtaining amorphous coatings of FeW and Fe-Cr-P-B alloys using laser sputtering
[BLL-BISI-22493-(9022.06)] 17 p2927 N85-28057
Self-sustaining coatings for fusion applications: Copper lithium alloys
[DE85-009740] 18 p3190 N85-29783
Ion beam sputter-deposited thin film coatings for protection of spacecraft polymers in low Earth orbit
[NASA-TM-87051] 19 p3248 N85-30137
Surface effects on sputtered atoms and their angular and energy dependence
[DE85-010506] 19 p3354 N85-30790
Current state of development and expected performance of copper-lithium alloys as an impurity control system in fusion applications
[DE85-009673] 19 p3372 N85-30917
Analysis of beam interaction of the electrical thruster RIT 10 (particle emission) with surfaces
[ESA-TT-826] 20 p3421 N85-31231
Modification of the grain size of sputtered copper with additions of oxygen, krypton, silver, or yttrium
[DE85-010975] 21 p3567 N85-32189
Advances in sputtered and ion plated solid film lubrication 22 p3797 N85-33524
Liquid crystal light valve structures
[NASA-CASE-MSC-20036-1] 22 p3847 N85-33826
Low-energy sputterings with the Monte Carlo Program ACAT
[IPPJ-AM-40] 23 p3982 N85-34690
SPUTTERING GAGES
Thin-film sensors for space propulsion technology
17 p2915 N85-27968
SQUALLS
Short period forecasts in West Africa using Meteosat data 01 p0079 N85-10526
SQUARE WAVES
Square-pulse generator 13 p2075 N85-22959
SQUEEZE FILMS
Effects of fluid inertia and turbulence on force coefficients for squeeze film dampers
05 p0645 N85-14137
Squeeze-film dampers for turbomachinery stabilization
05 p0645 N85-14138
Damping capacity of a sealed squeeze film bearing
05 p0645 N85-14139
Dual clearance squeeze film damper
[NASA-CASE-LEW-13506-1] 22 p3791 N85-33490
SQUEEZING
U COMPRESSING
SQUID (DETECTORS)
The dc SQUID as a tuned radiofrequency amplifier
[DE85-000701] 06 p0805 N85-15123
Ultrasensitive measuring devices
[DE85-000672] 12 p1853 N85-21622
Superconducting gyroscope research
[NASA-CR-171406] 15 p2560 N85-25795
ST VENANT FLEXURE PROBLEM
U SAINT VENANT PRINCIPLE
STABILITY
NT ACOUSTIC INSTABILITY
NT AERODYNAMIC STABILITY
NT AIRCRAFT STABILITY
NT ATTITUDE STABILITY
NT BAROCLINIC INSTABILITY
NT BOUNDARY LAYER STABILITY
NT COMBUSTION STABILITY
NT CONTROL STABILITY
NT DIMENSIONAL STABILITY
NT DIRECTIONAL STABILITY
NT DYNAMIC STABILITY
NT FLAME STABILITY
NT FLOW STABILITY
NT FREQUENCY STABILITY
NT GOERTLER INSTABILITY
NT GYROSCOPIC STABILITY
NT LATERAL STABILITY
NT LONGITUDINAL STABILITY
NT LOW SPEED STABILITY
NT MAGNETOHYDRODYNAMIC STABILITY
NT MAGNETOSPHERIC INSTABILITY
NT MOTION STABILITY
NT ROTARY STABILITY
NT SHELL STABILITY
NT SPACECRAFT STABILITY
NT STATIC STABILITY
NT STORAGE STABILITY
NT STRUCTURAL STABILITY
NT SURFACE STABILITY
NT SYSTEMS STABILITY
NT THERMAL STABILITY
Effect of combined pressure and temperature distortion orientation on high-bypass-ratio turbofan engine stability
[NASA-TM-83771] 01 p0011 N85-10067
Standards for commercially emerging technologies: A preliminary cost-benefit assessment for the Optical Digital data disk (OD3) technology for mass data storage applications
[PB84-223593] 01 p0101 N85-10669
Legendre-Tau approximation for functional differential equations. Part 3: Eigenvalue approximations and uniform stability
[NASA-CR-172447] 01 p0110 N85-10744
Development and flight evaluation of an augmented stability active controls concept: Executive summary
[NASA-CR-166009] 02 p0149 N85-11006
Inorganic composites for space applications
02 p0155 N85-11047
Nonlinear oscillations of 2 body system relative to center of mass in elliptical orbit 02 p0159 N85-11082
Rayleigh-Taylor instability in compressible media
[AD-A145491] 02 p0196 N85-11322
Qualitative results for distributed systems with discrete damping and stiffness with application to control
[AD-A145525] 02 p0209 N85-11382
Relationships between electronic structure and stability of metallic glasses
[AD-A145506] 02 p0287 N85-11874
A simple electronic apparatus for determining the oxidation stability of lubricants and other organic compounds
[AD-A146080] 03 p0338 N85-12172
A comparison of methods for predicting ductile crack growth instability
[AERE-R-11199] 03 p0374 N85-12287
A pseudospectral Legendre method for hyperbolic equations with an improved stability condition
[NASA-CR-172475] 03 p0410 N85-12617
Liquid hydrocarbon fuels from syngas
[DE84-015942] 04 p0482 N85-13069
Stable isotope studies
[DE84-016752] 04 p0562 N85-13583
Development and testing of a 20-kW X-band transmitter with high phase stability 05 p0623 N85-13865
Calibration of noise power transfer standards, measurement uncertainties and long term stability
05 p0630 N85-14035
Rotordynamic Instability Problems in High-Performance Turbomachinery
[NASA-CP-2338] 05 p0642 N85-14116
Full load testing in the platform module prior to tow-out: A case history of subsynchronous instability
05 p0642 N85-14117
Internal hysteresis experienced on a high pressure syn gas compressor 05 p0642 N85-14122
Squeeze-film dampers for turbomachinery stabilization
05 p0645 N85-14138
Normal mode initialization 05 p0680 N85-14372
Stability questions for gravity in 4 and higher dimensions 05 p0734 N85-14716
Polymer-metal interface bond stability
06 p0830 N85-15272
ATA probe beam experiment
[DE84-016017] 06 p0862 N85-15477
Theoretical and experimental study of hydro-elastic instability on the line of shafting of a rotating machine
[BLL-DOUNREAY-TR-937-(9091.9F)]
07 p0972 N85-16174
The pressure deflagration limit of solid rocket propellants 08 p1117 N85-17046
New instabilities in line driven winds
08 p1236 N85-17785
Gain instabilities in photomultipliers: How accurate are photon counting measurements?
08 p1251 N85-17903
Stability of amorphous metals on semiconductor substrates
[DE84-017256] 09 p1295 N85-18134
Computer simulation of multiple stability regions in an internally cooled superconducting conductor and of helium replenishment in a bath-cooled conductor
[DE85-002112] 09 p1399 N85-18805
Stability indicators for front end loaders
[AD-P004293] 09 p1408 N85-18870
Study on controllability and stability of high speed tracked vehicles
[AD-P004302] 09 p1409 N85-18879
Integrated Technology Rotor/Flight Research Rotor (ITR/FRR) concept definition
[NASA-CR-166443] 10 p1423 N85-18978
Integrated Technology Rotor/Flight Research Rotor (ITR/FRR) concept definition
[NASA-CR-166445] 10 p1423 N85-18979
Simulation of the ion-beam-driven drift instability in a magnetic trap, 1
[AD-A149451] 10 p1452 N85-19147
Fluidelastic instability in shell and tube heat exchangers: A framework for a prediction method
[DE84-006518] 10 p1496 N85-19444
Simulation of the ion-beam-driven drift instability in a magnetic trap, 2
[AD-A149452] 10 p1554 N85-19798
Research in nonlinear problems of energy: Informal technical report
[DE85-001529] 11 p1595 N85-20031
Stability evaluation of sulfur dioxide nitric oxide and carbon monoxide gases in cylinders
11 p1648 N85-20387
Complex symmetric matrices with strongly stable iterates
[NASA-CR-172542] 11 p1706 N85-20731
Stability of superconducting composites in a magnetic field
[DE85-002731] 11 p1734 N85-20807
Field validation of statistically-based acceptance plan for bituminous airport pavements. Volume 2: Statistical analysis of Marshall properties of plant-produced bituminous materials
[FAA-PM-84-12-VOL-2] 12 p1781 N85-21181

Field validation of statistically-based acceptance plan for bituminous airport pavements. Volume 4: Computer simulation of multiple acceptance criteria
[FAA-PM-84-12-VOL-4] 12 p1782 N85-21183
Stability of organic audit materials and results of source test analysis audits
[PB85-116184] 12 p1865 N85-21832
Analysis of slope stability, Wilmington to Lindenkohl Canyons, US mid-Atlantic margin
[DE84-012278] 12 p1899 N85-21921
Suppression of tilting instability of a compact torus by energetic particle beams
[IPPJ-705] 12 p1935 N85-22157
Stability of cylindrical shells with one-way constraints
13 p2048 N85-22820
Nonlinear behavior and stability of thin spherical shells subjected to non-axisymmetrical loading
13 p2048 N85-22821
Effect of compliability of hot walls in liquid-propellant engine on low frequency instability
13 p2049 N85-22824
Stability of highly nonlinear oxide-zinc resistors under continuous voltage of industrial frequency
13 p2087 N85-23030
Electrodynamic stability of composite liquid-metal contacts 13 p2087 N85-23031
Stability of turbine runners in sliding bearings under external circulation forces 14 p2272 N85-24074
Stability of vortex structures during separation flow past array of wings 14 p2278 N85-24110
Stability of steady rotation of a cylinder filled with a stratified viscous incompressible fluid
14 p2278 N85-24112
Increasing seam formation stability in electron beam welding of very thick titanium alloys
15 p2500 N85-25420
A study of the stability of cadmium sulfide/copper sulfide and cadmium sulfide copper-indium-diselenide solar cells
[DE85-002902] 15 p2587 N85-25947
Uniqueness and stability in nonlinear elasticity and viscoelasticity
[AD-A151470] 15 p2637 N85-26264
Effects of finite current channel width on the current convective instability
[AD-A151414] 15 p2656 N85-26389
Estimation of the depth of a spherical cap in an hydraulic drawing test for some simple conditions of loss of stability
[REPT-4/1984] 16 p2748 N85-26956
Models of long-period superstructure
[DE85-007659] 16 p2751 N85-26981
A closed loop analysis of POGO instability
[AD-A153121] 17 p2937 N85-28132
Fluid surface behavior in low gravity. Center discretionary fund no. 83-21
[NASA-TP-2486] 17 p2957 N85-28280
Instabilities and chaotic behavior of active and passive laser systems
[AD-A153366] 17 p2971 N85-28346
How a swing behaves
[DE85-008280] 17 p3027 N85-28720
Stability in dynamical systems
[DE85-006698] 17 p3034 N85-28766
Morphological stability and fluid dynamics of vapor crystal growth
[NASA-CR-175879] 17 p3042 N85-28822
Morphological stability and fluid dynamics of vapor crystal growth
[NASA-CR-175880] 17 p3042 N85-28823
Study of the chemical mechanism in lubrication
[DE85-010788] 19 p3228 N85-30013
Optical stability, atmospheric transparency and aerosol absorption 19 p3297 N85-30442
High gain adaptive control of decentralized systems
[DE85-010040] 19 p3339 N85-30688
High gain adaptive control of decentralized systems
[DE85-001566] 19 p3343 N85-30717
Frequency domain control design of large space structures: A practical approach
20 p3415 N85-31192
A control concept for large flexible spacecraft using order reduction techniques 20 p3415 N85-31193
Influence of error of determination of moire isotach orders on the stability of their approximation
[BLL-M-36277-(5828.4)] 20 p3450 N85-31423
Bypass transition to turbulence and research Desiderata 20 p3453 N85-31442
Slow tearing modes: Transitions to instability
20 p3534 N85-31989
Notes on atmospheric stability, turbulence, and its measurements
[AD-A155230] 21 p3637 N85-32588
Two-dimensional simulation of instability growth due to shocks
[DE85-011869] 22 p3784 N85-33442
Tectonic stability and expected ground motion at Yucca Mountain
[DE85-012004] 22 p3814 N85-33629
Saturation of a longitudinal instability due to nonlinearity of the wake field
[DE85-012514] 22 p3837 N85-33761
Compressible two-phase flow instabilities simulated with a hybrid Lagrange-Euler pseudospectral method
[DE85-009904] 23 p3931 N85-34361
Stability of two-dimensional immiscible flow to viscous fingering
[DE85-011403] 23 p3931 N85-34364
Simulation studies on stability of hot electron plasma
23 p3978 N85-34664
Workshop report on Simulation Techniques for Shock Wave Phenomena and Characteristics of Plasmas in Inertial Confinement Fusion
[IPPJ-725] 23 p3979 N85-34670
Instabilities in decelerating supersonic flows with applications to cosmic ray shocks
[OG-8.1-2] 23 p4017 N85-34892
Parametric stability of analytical close-range photogrammetry 24 p4107 N85-35461
Relaxation phenomena and stability of probability densities
[AD-A155923] 24 p4143 N85-35682
Analysis of reactor material experiments investigating oxide fuel crust stability and heat transfer in jet impingement flow
[DE85-012097] 24 p4151 N85-35739

STABILITY AUGMENTATION
Integrated Application of Active Controls (IAAC) technology to an advanced subsonic transport project. ACT/Control/Guidance System study, volume 1
[NASA-CR-165963-VOL-1] 06 p0754 N85-14837
Integrated Application of Active Controls (IAAC) technology to an advanced subsonic transport project. ACT/Control/Guidance System study. Volume 2: Appendices
[NASA-CR-165963-VOL-2] 06 p0754 N85-14838
Leading edge flap system for aircraft control augmentation
[NASA-CASE-LAR-12787-2] 11 p1585 N85-19985
A perspective on superaugmented flight control advantages and problems 16 p2712 N85-26733
Demonstration of relaxed stability on a commercial transport 16 p2713 N85-26745
Multivariable control of a soft coupled space station
20 p3408 N85-31151

STABILITY DERIVATIVES
NT PITCHING MOMENTS
NT ROLLING MOMENTS
NT YAWING MOMENTS
The development of a dynamic model of a generalised combat aircraft with forward wings for the identification of stability and control characteristics
[CAR-84-33] 09 p1280 N85-18050

STABILITY TESTS
NT FLIGHT STABILITY TESTS
NT WIND TUNNEL STABILITY TESTS
Local stability analysis for a planar shock wave
[NASA-TP-2387] 04 p0452 N85-12864
MSFC data analysis of the SAFE/DAE experiment
14 p2233 N85-23643
Langley Research Center photogrammetric measurements of solar array dynamics: Preliminary results 14 p2233 N85-23644
Environmental stability of intercalated graphite fibers
[NASA-TM-87025] 16 p2753 N85-26992
Recent developments in rotary-balance testing of fighter aircraft configurations at NASA Ames Research Center
[NASA-TM-86714] 21 p3551 N85-32090

STABILIZATION
NT SPIN STABILIZATION
NT THREE AXIS STABILIZATION
A high-repetition rate, inductively stabilized, long-pulse excimer laser
[DE84-016827] 04 p0506 N85-13229
Experimental research on electric propulsion. Note 7: Analysis of the performance of an arc-jet driven by means of hydrogen and nitrogen
[NASA-TM-77473] 06 p0760 N85-14861
Beam propagation study: Stabilization of the resistive hose instability in intense electron beams
[AD-A148071] 08 p1220 N85-17684
Stability analysis of flexible spacecraft with PID controller
[CRC-1372] 12 p1792 N85-21247
Stabilization of steady motion of mechanical systems
14 p2280 N85-24122
Mechanical stabilization of austenite against epsilon martensite and its effect on deformation behavior in high manganese steels
[DE85-007654] 17 p2932 N85-29097
Stabilizing force feedback in bio-actuated control systems
[AD-D011634] 17 p3002 N85-28560
Stability of high energy particle plasmas to MHD-like modes
[DE85-007879] 17 p3039 N85-28803
The 3lambda/4 post coupler for drift-tube linacs
[DE85-010753] 20 p3531 N85-31962
Optical output stabilization method for direct current arc lamps
[AD-A154887] 21 p3705 N85-33013
Astron telescope stabilization system
22 p3732 N85-33133
Amplitude stabilization of pulse signals
22 p3762 N85-33320
Optimization of design parameters for alternating current stabilizer based on magnetic suspension
22 p3772 N85-33374
Electron photoejection in carbanions
[DE85-011747] 23 p3911 N85-34230
The balancing of complex linkage mechanisms
23 p3924 N85-34313
Method and apparatus for transfer function simulator for testing complex systems
[NASA-CASE-NPO-15696-1] 23 p3926 N85-34333
Improved method for the stabilization of NaI-photomultiplier gamma detectors against thermal and other drift
[DE85-011830] 23 p3970 N85-34613
Design of dynamic compensators of prescribed pattern
[BU-109] 24 p4142 N85-35674
Spreading the control complexity in decentralized control of interconnected systems
[BU-117] 24 p4144 N85-35688
Decentralized stabilization by high gain feedback
[BU-115] 24 p4144 N85-35689

STABILIZED PLATFORMS
Some notes on a tangent plane oriented heading reference — stabilized platforms
[RAE-TM-IEE-144] 02 p0136 N85-10928
Evaluation of nose, roof, and mast mounted sensor platforms for piloting and sighting, integrated in future combat helicopters 08 p1074 N85-16808
A concept for a mobile remote manipulator system
14 p2236 N85-23659
Estimates of errors of a gyroscope stabilized platform
16 p2763 N85-27050

STABILIZERS (AGENTS)
Micromolecular modeling 21 p3608 N85-32405
Polymerizable ultraviolet stabilizers
21 p3608 N85-32406

STABILIZERS (FLUID DYNAMICS)
NT HORIZONTAL TAIL SURFACES
Advanced composite stabilizer for Boeing 737 aircraft
[NASA-CR-168451] 02 p0137 N85-10934
Advanced manufacturing development of a composite empennage component for L-1011 aircraft
[NASA-CR-165885] 02 p0170 N85-11141
Full-scale testing, production and cost analysis data for the advanced composite stabilizer for Boeing 737 aircraft. Volume 1: Technical summary
[NASA-CR-3649] 05 p0612 N85-13912
Design, ancillary testing, analysis and fabrication data for the advanced composite stabilizer for Boeing 737 aircraft. Volume 1: Technical summary
[NASA-CR-3648] 05 p0612 N85-13913
Design, ancillary testing, analysis and fabrication data for the advanced composite stabilizer for Boeing 737 aircraft, volume 2
[NASA-CR-166011] 05 p0612 N85-13914
Full-scale testing, production and cost analysis data for the advanced composite stabilizer for Boeing 737 aircraft, volume 2
[NASA-CR-166012] 05 p0613 N85-13915
CF-5 vertical stabilizer flight load survey
07 p0895 N85-15673
TUTOR (CL-41A) tail flight load survey
07 p0896 N85-15678
Flutter clearance of the Schweizer 1-36 deep-stall sailplane
[NASA-TM-85917] 22 p3729 N85-33118
A towed instrument vehicle for deep ocean sampling
[AD-A156322] 24 p4125 N85-35576

STABLE OSCILLATIONS
Buildup of oscillations in two-mode gyrotron
06 p0788 N85-15037
Magnetically-localizable, polymerized lipid vesicles and method of disrupting same
[AD-D011666] 19 p3249 N85-30144
Oscillatory solutions of the Peaceman-Rachford alternating direction implicit method and a comparison of methods for the solution of the two dimensional heat diffusion equation
[AD-A154670] 21 p3675 N85-32833

STACKING FAULTS
U CRYSTAL DEFECTS

STACKS

Gas cooled fuel cell systems technology development
[NASA-CR-174732] 07 p0991 N85-16291

Develop and test fuel cell powered on-site integrated total energy systems. Phase 3: Full-scale power plant development
[NASA-CR-174887] 15 p2586 N85-25941

STAGE SEPARATION

Debris control design achievements of the booster separation motors 08 p1098 N85-16942

A theoretical study of two stage thrust augmenting ejectors
[ARL/AERO-R-166] 19 p3218 N85-29954

The development of staging mechanisms for the Japanese satellite launcher Mu-3SII
22 p3798 N85-33528

STAGING (ROCKETS)
U STAGE SEPARATION

STAGNATION FLOW

Physics on aircraft wakes
[NASA-CR-174105] 04 p0453 N85-12871

Laminar jet issuing into stagnant surroundings — PHOENICS code
[PDR/CFDU-IC/15] 04 p0501 N85-13200

Some important problems in unsteady boundary layers including seperation. 2: Unsteady boundary layers close to the stagnation region of slender bodies
[AD-A146964] 07 p0958 N85-16069

Stagnation zone impaction on a simple terrain feature in stable flow 13 p2130 N85-23255

STAGNATION POINT

Preliminary results of a study of the relationship between free stream turbulence and stagnation region heat transfer
[NASA-TM-86884] 02 p0197 N85-11317

Influence of turbulence on erosion by a particle-laden fluid jet
[DE84-014365] 09 p1320 N85-18301

The influence of jet-grid turbulence on heat transfer from the stagnation region of a cylinder in crossflow
[NASA-TM-87011] 15 p2554 N85-25780

Conical stagnation points in the flow around an external corner — delta wings
[VTH-LR-386] 16 p2701 N85-26680

Preliminary results of a study of the relationship between free-stream turbulence and stagnation region heat transfer 20 p3452 N85-31435

Two-dimensional separation in an incompressible fluid — boundary layer separation
[ONERA-RTS-16/3232-RY-060-R]
20 p3456 N85-31459

STAGNATION PRESSURE

Basic studies of multiple free and confined jets
[AD-A149556] 10 p1485 N85-19374

STAGNATION REGION
U STAGNATION POINT

STAINING

Processing of LANDSAT imagery to map surface mineral alteration on the Alaska Peninsula, Alaska
24 p4106 N85-35455

STAINLESS STEELS
NT AUSTENITIC STAINLESS STEELS
NT FERRITIC STAINLESS STEELS
NT MARTENSITIC STAINLESS STEELS

New ferrous metallurgy technology
01 p0019 N85-10114

The oxidation behaviour of a 20 percent Cr/25 percent Ni/Nb stabilized stainless steel in carbon dioxide at high temperatures and its improvement by cerium and yttrium
[AERE-R-11226] 01 p0029 N85-10182

Minor element effects on gas tungsten arc weld penetration
[PB84-222579] 01 p0056 N85-10370

International Conference on Recent Developments in Specialty Steels and Hard Materials. Conference abstracts
[CSIR-S-256] 02 p0176 N85-11177

A review of world wide development in stainless steels
02 p0177 N85-11190

Metalurgy of a 12 percent chromium stainless steel
02 p0178 N85-11195

The effect of replacing molybdenum with vanadium on the corrosion resistant properties of stainless steels
02 p0178 N85-11197

The influence of metallurgical aspects on the pitting corrosion behaviour of high alloy stainless steels
02 p0179 N85-11202

Detection of hydrogen assisted crack growth
[DE84-015920] 02 p0183 N85-11228

Detection of hydrogen assisted crack growth by measurement of modulus changes and acoustic emission
[DE84-015752] 02 p0184 N85-11236

Strain distribution in a type 316/16-8-2 stainless steel weldment during cyclic loading
[DE84-015644] 02 p0210 N85-11384

Diffusion of Cr-51 tracer in Cr-2O-3 and the growth of Cr-2O-3 films
[AERE-R-11314] 03 p0333 N85-12146

A study of precipitation and boron distribution in 20 Cr 25Ni base stainless steels
[AERE-M-3353] 03 p0334 N85-12154

New coatings for high temperature materials protection
[AERE-R-11387] 03 p0339 N85-12180

Subgrains, dislocations and the elevated-temperature strength of type 304 stainless steel
[DE84-001233] 04 p0473 N85-13014

Localized corrosion and stress corrosion cracking behavior of stainless steel weldments
[DE84-016095] 04 p0474 N85-13017

Erosion of multiphase materials
[DE84-015816] 04 p0474 N85-13018

Solidification and aging behavior of types 308 and 308CRE stainless steel welds
[DE84-016552] 04 p0478 N85-13029

Ultrasonic and metallurgical examination of a cracked type 304 stainless steel BWR pipe weldment
[TI84-014968] 04 p0511 N85-13254

Tensile properties and swelling of 20%-cold-worked Type 316 stainless steel irradiated in HFIR
[DE84-014080] 05 p0617 N85-13948

Effects of irradiation fluence and creep on fracture toughness of 347/348 stainless steel
[DE84-016091] 05 p0618 N85-13953

Current and potential transients during localized corrosion of stainless steel
[DE84-014100] 05 p0618 N85-13954

Swelling behavior of titanium-modified AISI 316 alloys
[DE84-013940] 05 p0618 N85-13956

Application of extraction replicas and analytical electron microscopy to precipitate phase studies
[DE85-001253] 06 p0769 N85-14919

Microstructure of rapidly quenched type 308 stainless steel weld filler metal and its implications on rapid solidification processes
[DE85-000930] 06 p0769 N85-14920

Modeling microstructural changes during hot rolling of steels 06 p0798 N85-15096

SANS and TEM studies of carbide precipitation and creep damage in type 304 stainless steel
[DE85-000933] 09 p1296 N85-18139

Stochastic models of pitting corrosion of stainless steels. Part 1: Modelling of the initiation and growth of pits at constant potential
[AERE-R-11146-PT-1] 09 p1298 N85-18151

Picking of stainless steels: A review
[PB85-111979] 10 p1442 N85-19087

Effect of implantation species on the tribological response of stainless steel surfaces
[DE85-003530] 10 p1493 N85-19432

Patterns in the occurrence of the brittle topologically close-packed phases: Al
[DE85-000592] 11 p1607 N85-20106

Chemical cleaning of 304 and 304-L stainless steel surfaces by the nitradd passivation process
[DE85-003714] 11 p1615 N85-20158

Research on heat-exchanger corrosion
[PB85-126316] 11 p1616 N85-20164

Transverse microstructure of an oxide scale formed on a 20 % Cr/25 % Ni niobium stabilized stainless steel
[AERE-R-11034] 12 p1804 N85-21315

Nondestructive testing of stainless steel to improve quality and output efficiency of the processing of ingot and continuous casting
[BMFT-FB-T-84-240] 12 p1808 N85-21345

Local electrochemistry of pitting corrosion in stainless steels
[DE85-005207] 13 p2023 N85-22673

Development of a sintered shim
[DE85-006183] 13 p2025 N85-22685

Use of ferrofluids in machining of metals
13 p2045 N85-22802

Fatigue life, crack initiation, and propagation of 304 stainless steel with non-proportional axialtorsional strain-paths 13 p2101 N85-23094

Studies of the initiation of pitting corrosion on stainless steels
[AERE-M-3400] 14 p2254 N85-23967

Exploratory corrosion tests on alloys in molten salts at 900(0)C
[DE85-000511] 14 p2257 N85-23983

Improvement by cerium and yttrium ion implantation of oxidation behaviour of stabilised stainless steel in carbon dioxide
[AERE-R-11523] 14 p2259 N85-23996

The design and construction of a flow channel and rig for corrosion studies
[AERE-M-3455] 15 p2508 N85-25474

Variation in the spacing of dislocations in subgrain boundaries with creep strain in Type 304 stainless steel
[DE85-006184] 15 p2511 N85-25480

Ignition of metals in high pressure oxygen
16 p2735 N85-26874

Creep-fatigue interaction of notched 304 stainless steel bars 16 p2798 N85-27249

Thermomechanical treatment aimed at the protection of type 316 stainless steel from IGC and IGSCC
[BLL-BISI-TRANS-22498-(9022.06)]
17 p2925 N85-28040

Effect of texture in steel on the susceptibility of hydrogen embrittlement
[BLL-BISI-TRANS-22026-(9022.06)]
17 p2926 N85-28048

Metallurgical means of preventing the corrosion of metal
[BLL-BISI-TRANS-22320-(9022.06)]
17 p2929 N85-28082

Properties of nitrogen containing stainless alloy designed for high resistance to pitting
[DE85-008282] 17 p2931 N85-28086

Experimental and theoretical studies on transport processes in laser welding
[DE84-008572] 17 p2975 N85-28378

Surface degradation of ductile metal in elevated temperature gas-particle streams
[DE85-006428] 18 p3074 N85-29017

Establishment of a methodology for predicting lifetimes in active solar systems
[DE85-008629] 18 p3130 N85-29393

Performance characteristics of gravity-assisted potassium heat pipes
[DE85-010717] 19 p3287 N85-30367

Consolidated fuel reprocessing program
[DE85-008750] 19 p3366 N85-30871

Solid-state resistance welding cylinders and spheres
[DE85-010064] 20 p3469 N85-31556

Machining-induced deformation in stepped specimens of PH 13-8 Mo, 18 nickel maraging steel grade 200T1 and grain-refined HP 9-4-20
[NASA-CR-172450] 21 p3565 N85-32177

Film condensation of steam on externally finned horizontal tubes
[AD-A155642] 21 p3585 N85-32285

Thermodynamic properties of alloys in the Fe-Ti system
[NPL-DMA(A)-96] 22 p3748 N85-33229

Effects of residual stresses and distortion on the nickel 200 and stainless steel 304 weldments
[DE85-011868] 22 p3748 N85-33233

Centrifugal castings of stainless steel spiked with radioactive tracers
[DE85-012003] 22 p3748 N85-33234

Tritium-helium effects in metals
[DE85-011507] 22 p3749 N85-33235

Mechanical properties of plasma arc cut steel
23 p3905 N85-34186

Approximate determination of the extent of the solid-liquid zone
[BLL-M-35829-(5828.4)] 23 p3914 N85-34251

Influence of particle erosion on the microstructural changes in metals and alloys
[TI85-901384] 23 p3917 N85-34276

Stress corrosion cracking susceptibility of types 316NG and 316 stainless steel in an impurity environment
[TI85-006884] 23 p3917 N85-34277

Effect of stainless steel weld overlay cladding on the structural integrity of flawed steel plates in bending, series 1
[TI85-010349] 23 p3939 N85-34418

Analytical ultrasonics for structural materials
[TI85-006132] 23 p3966 N85-34600

Shield design for next-generation, low-neutron-fluence, superconducting tokamaks
[DE85-011409] 23 p3982 N85-34695

Electrochemical method for investigation of the susceptibility of corrosion-resistant steels to intercrystalline corrosion
[BLL-CE-TRANS-8082-(9022.09)]
24 p4077 N85-35269

Effect of temperature and ionic impurities at very low concentrations on stress corrosion cracking of Type 304 stainless steel
[TI85-003048] 24 p4079 N85-35283

X-ray fluorescence analysis of 304L stainless steel
[DE85-013254] 24 p4080 N85-35288

Spectral characteristics of grinding sparks used for identification of scrap metals
[PB85-196570] 24 p4080 N85-35290

Analysis of reactor material experiments investigating oxide fuel crust stability and heat transfer in jet impingement flow
[DE85-012097] 24 p4151 N85-3573

STALLING
Preliminary airworthiness evaluation of the Rutan Aircraft Factory (RAF), Inc. LONG-EZ airplane with external sight
[AD-A145381] 02 p0136 N85-10937

STAMPING
Summaries of press automation conference presented
06 p1139 N85-17173
Calculating reliability and productivity of cold stamping robot complex as queuing system
16 p2761 N85-27039
Experience of sheet stamping robotic complexes
16 p2761 N85-27041
New method for determining stampability of sheet materials
[BLL-BISI-22486-(9022.06)] 17 p2972 N85-28360

STANDARD ATMOSPHERES
U REFERENCE ATMOSPHERES

STANDARD DEVIATION
Battery control and fault detection method
[AD-D011384] 07 p0993 N85-16307
Determination of the laws governing the changes in the standard deviations of the distribution of pollution based on observations of the atmospheric turbulence spectrum and the possibility of simulating it in the laboratory
[BLL-TR-T6373/BG/MRS14883/84]
08 p1179 N85-17431
Positioning accuracy of the ARGOS system in operational use 16 p2811 N85-27335
Derivation of model topography
18 p3141 N85-29449
On the statistical significance of excess events: Remarks of caution and the need for a standard method of calculation
[OG-9.5-10] 23 p4031 N85-34967
Large deviations for the maxima of some random fields
[AD-A155909] 24 p4143 N85-35681

STANDARDIZATION
Increased joint avionics standardization could result in major economies and operational benefits
[AD-A145730] 02 p0139 N85-10945
Standardized efficiency terms: Comparison of some Stirling engine performance figures
[DE84-015407] 02 p0205 N85-11352
SLC nomenclature for beamline components
[DE84-014776] 02 p0279 N85-11816
Standardization of amplitude characteristics of galvanometric seismographs in the KAPG network
[REPT-552] 03 p0375 N85-12395
Standardization of data formats for radar altimeter data 03 p0384 N85-12455
Standardization of flammability tests for hydraulic fluids
[AD-A146468] 06 p0771 N85-14932
Proceedings of the National Bureau of Standards and National Security Agency Workshop on Standardization Issues for Optical Data Disk (OD3) Technology
[PB84-217785] 06 p0848 N85-15383
A standard operating system interface for microcomputer software development
[AD-A146584] 06 p0854 N85-15428
Methodology for evaluating related databases and a computerized algorithm for merging their output
09 p1401 N85-18821
Report on AGARD Meeting: Hazards Studies for Solid Propellant Rocket Motors
[AD-P004340] 10 p1454 N85-19164
Update of thermal conductivity and electrical resistivity of electrolytic iron, tungsten and stainless steel
[PB85-115614] 12 p1803 N85-21311
The ARGOS system and hydrology. Results obtained by ORSTROM and benefits of a degree of standardization 14 p2239 N85-23881
An analysis of data dictionaries and their role in information resource management
[AD-A152134] 16 p2774 N85-27121
NBS physical measurement services
[NBSIR-84-2875] 16 p2859 N85-27633
DOD manual for standard data elements, part 1
[AD-A152201] 16 p2878 N85-27754
High temperature position sensors based on monolithic GaAs Hall IC
[BMFT-FB-T-84-266] 17 p2969 N85-28337
Standard procedures to be used in specifying basic properties of plastics and polymers
[NPL-DMA(A)-99] 20 p3433 N85-31295
Standard series of direct-current motors for regulated electric drives 22 p3772 N85-33375
Development of NATOPS (Naval Air Training and Operating Procedure Standardization) performance software for the H-46D helicopter
[AD-A156069] 24 p4064 N85-35190
Necessary bandwidth and spectral properties of digital modulation
[PB85-165367] 24 p4088 N85-35340
Redefining the scratch standards
[PB85-194736] 24 p4154 N85-35755

STANDARDS
NT FREQUENCY STANDARDS
NT REFERENCE ATMOSPHERES
Compilation of elemental concentration data for NBS (National Bureau of Standards) biological, geological and environmental standard reference materials, 1982
[PB84-218338] 01 p0025 N85-10158
Force standard machines of the National Institutes for Metrology, vol. 2
[PTB-ME-62-VOL-2] 01 p0036 N85-10224
A coaxial noise standard for the 1 GHz to 12.4 GHz frequency range
[PB84-217884] 01 p0042 N85-10272
Requirements and specifications for cartographic video discs
[AD-A144906] 01 p0049 N85-10325
Measurement assurance programs. Part 2: Development and implementation
[PB84-217876] 01 p0051 N85-10338
Measurement assurance programs. Part 1: General introduction
[PB84-217868] 01 p0051 N85-10339
Demonstrating air quality improvements: A review of alternatives
[DE84-014274] 01 p0070 N85-10482
Standards for commercially emerging technologies: A preliminary cost-benefit assessment for the Optical Digital data disk (OD3) technology for mass data storage applications
[PB84-223593] 01 p0101 N85-10669
Analysis of three database system architectures using benchmarks
[PB84-217512] 01 p0105 N85-10706
Automated Data Systems (ADS) documentation standards
[AD-A144867] 01 p0125 N85-10857
Improving technical documents
[AD-B084855] 01 p0126 N85-10866
South African Astronomical Observatory Circulars, no. 7
[SAAOC-7] 01 p0127 N85-10875
Local photometric standards for CaII emission stars
01 p0128 N85-10883
Test methods and standards development for active solar heating and cooling systems
[PB84-217447] 03 p0343 N85-12209
Evolution of the NWC (Naval Weapons Center) thermal standard. Part 5: Thermal standard development and applications
[AD-A146173] 03 p0364 N85-12334
Review of the NAAQS (National Ambient Air Quality Standards) for carbon monoxide: Reassessment of scientific and technical information
[PB84-231315] 03 p0388 N85-12485
Ways to improve management of Federal funded computerized models
[LCD-75-111] 03 p0435 N85-12771
Present practice for the recording of the Earth magnetic field — geophysical observatories
04 p0519 N85-13317
VOC emissions from volatile organic liquid storage tanks: Background information for proposed standards
[PB84-237320] 04 p0532 N85-13403
Special Developments and Methods in High Frequency Measuring Techniques — conferences
[PTB-E-24] 05 p0629 N85-14030
Admittance measurement with twin-T devices in the frequency range between 1 and 300 MHz
05 p0629 N85-14032
Realization of noise power in the microwave range by thermal noise standards 05 p0629 N85-14034
Calibration of noise power transfer standards, measurement uncertainties and long term stability
05 p0630 N85-14035
Voltage dependence of the relative AC-DC transfer difference for HF voltage-transfer standards
05 p0630 N85-14038
A group delay standard for the MHz frequency range
05 p0630 N85-14040
The detection and assessment of defects in automatic ultrasonic inspection
[BLL-RISLEY-TR-4597-(9091.9F)]
05 p0647 N85-14150
Experimentation and measurement
[PB84-233659] 06 p0812 N85-15157
NAAQS (National Ambient Air Quality Standards) Exposure Model (NEM) applied to carbon monoxide
[PB84-242551] 06 p0834 N85-15310
Standard SHEF (Standard Hydrometeorologic Exchange Format) decoder Version 1.1
[PB85-106508/GAR] 06 p0840 N85-15332
Proceedings of the National Bureau of Standards and National Security Agency Workshop on Standardization Issues for Optical Data Disk (OD3) Technology
[PB84-217785] 06 p0848 N85-15383
Prime Computer, Inc., PRIME 750, COBOL-74 Revision 19.3.2
[PB84-227626] 06 p0851 N85-15409
NBS (National Bureau of Standards) and WR62 and WR90 reference noise standards
[PB84-235704] 07 p0942 N85-15977
Estimation of requirements for acceptable noise radiation level of communication transmitters
07 p0949 N85-16017
What should DOE do to help establish voluntary consensus standards for measuring and rating the performance of PV modules?
[NASA-CR-174265] 07 p0992 N85-16297
A superconducting quantum current standard
[NPL-QU-67] 08 p1224 N85-17710
Defect tolerance in pipeline girth welds
[ERS-E.353] 09 p1328 N85-18347
Impact of 810D on dynamic test laboratories
09 p1334 N85-18366
Evaluation of the particulate levels occurring under 1.0/1.2 g/mi nitrogen oxide standards for light duty diesel vehicles and light duty diesel trucks
[PB85-115939/GAR] 09 p1350 N85-18494
Perspective on demonstrations of compliance for high-level waste disposal
[DE85-000989] 09 p1363 N85-18698
Radiation data and standards for Tokamak diagnostics
09 p1390 N85-18742
Proceedings of Colloquium/Workshop on Composite Materials and Structures, Standardization, Qualification, Certification held at washington, D.C. on 8-10 May 1984
[AD-A149039] 10 p1432 N85-19029
Historical cost curves for hydrogen masers and cesium beam frequency and timing standards
10 p1465 N85-19245
Health standards for general vibration
10 p1523 N85-19607
Abstract and index collection
[PB85-119501] 10 p1569 N85-19892
FAA policy regarding solid waste disposal facilities
[AD-P004196] 11 p1581 N85-19963
Magnetic measurements, calibrations, and standards: Report on a survey
[PB85-127627] 11 p1638 N85-20317
Radiation safety of crew and passengers of air transportation in civil aviation. Provisional standards
[NASA-TM-77610] 11 p1692 N85-20638
Prime Computer, Incorporated, PRIME 750, BASICV revision 19.4
[PB85-108074] 11 p1699 N85-20683
Software standards issues — space station software development 11 p1701 N85-20692
Micro focus Cifer 2887 high performance level 2 COBOL; V2.5
[PB85-108959] 11 p1703 N85-20714
Micro focus Cifer 2887 compact level 2 COBOL; V2.5
[PB85-108967] 11 p1703 N85-20715
Metrology for Electronic Technology: A bibliography of NBS (National Bureau of Standards)
[PB85-112895] 12 p1830 N85-21486
Stability of organic audit materials and results of source test analysis audits
[PB85-116184] 12 p1865 N85-21832
Air quality criteria for ozone and other photochemical oxidants. External review draft, volume 2
[PB85-126043] 12 p1886 N85-21836
Air quality criteria for ozone and other photochemical oxidants, external review draft, volume 3
[PB85-126050] 12 p1886 N85-21837
Head/neck injury: Post mortem procedures, Annex B
12 p1907 N85-21977
Journal of Research of the National Bureau of Standards, volume 89, number 2, March - April 1984
[PB85-115426] 12 p1926 N85-22103
A description of the Langley wireframe geometry standard (LaWGS) format
[NASA-TM-85767] 13 p1971 N85-22380
Characterization standards for solid propellant rocket motors
[AD-A150250] 13 p2013 N85-22627
Digital standards conversion: interpolation theory and aperture synthesis
[BBC-RD-1984/20] 13 p2053 N85-22857
Critical current measurements on an NbTi superconducting wire standard reference material
[PB85-118594] 13 p2066 N85-22906
Validation summary report, Burroughs Corporation, 820 FORTRAN release 4.0
[PB84-227792] 13 p2145 N85-23316
Do new aircraft need new technologies and certification rules? 14 p2224 N85-23795

Establishment and maintenance of certification standards for helicopter and turboprop power transmission systems 14 p2224 N85-23796
Safety with industrial manufacturing lasers
14 p2308 N85-24281
Guidelines for development structured FORTRAN programs
[NASA-TM-86407] 14 p2402 N85-24808
Titanium alloys, products, standards listed
15 p2533 N85-25626
New sensor for industrial metrology developed
15 p2538 N85-25665
Standards in process: Foundation and profiles of ISDN (Integrated Services Digital Network) and OSI (Open Systems Interconnection) studies
[PB85-166041/GAR] 15 p2545 N85-25712
Compositional control of plate steels
15 p2565 N85-25826
Papers from the Symposium on Emissions: The Value of Incentives and Guidelines for Control
[S-336] 15 p2590 N85-25967
Management of vacuum leak-detection processes, standards and calibration
[DE85-006705] 16 p2758 N85-27202
Standards and specifications for geodetic control networks
[PB85-166478] 16 p2816 N85-27374
Review of national emission standards for mercury
[PB85-153906] 16 p2822 N85-27406
Mapping principles for the standards interface for computer aided design
[PB85-177905] 16 p2849 N85-27566
NBS physical measurement services
[NBSIR-84-2876] 16 p2859 N85-27633
DoD manual for standard data elements, part 2
[AD-A152202] 16 p2878 N85-27755
DoD manual for standard data elements, part 3
[AD-A152203] 16 p2878 N85-27756
NBS (National Bureau of Standards) research reports
[PB85-127421] 16 p2879 N85-27764
Development of new circuit symbols for binary logic elements
[MBB-Z-39/85-O] 17 p3014 N85-28640
State Weights and Measures Laboratories: Program handbook
[PB85-183356] 18 p3111 N85-29263
Development of guidelines for setting physiological and hygienic standards for noise levels in aerospace medicine 19 p3323 N85-30584
A systematic determination of skill and simulator requirements for airline transport pilot certification
[AD-A154135] 19 p3330 N85-30630
Liquid metal reactor programs: Safeguards and program assurance
[DE85-010621] 19 p3331 N85-30635
Standards Committee activities of the National Bureau of Standards: 1984 highlights
[PB85-183382] 19 p3350 N85-30764
Auto fuel efficiency standards, part 2
[GPO-41-189] 20 p3435 N85-31309
The 1982 National Measurement Requirements Survey
[NMRC-83-01-SUMM] 20 p3436 N85-31321
Journal of Research of the National Bureau of Standards, volume 90, number 1, January - February 1985
[PB85-179083] 20 p3522 N85-31908
Improved coordinate measuring machine calibration and control
[DE85-012053] 21 p3590 N85-32315
Digital matched filter 22 p3765 N85-33339
Modeling of auto exhaust smog chamber data for EKMA development
[PB85-186492] 22 p3813 N85-33619
Development of solid thorium-232 reference materials
[DE85-011453] 22 p3841 N85-33785
Recommendations for the design and equipping of engineering metrology laboratories
[NPL-MOM-22] 23 p3898 N85-34145
Redefining the scratch standards
[PB85-194736] 24 p4154 N85-35755

STANDING WAVES
Tides and tidal currents of the inland waters of Western Washington
[PB84-237379] 06 p0842 N85-15346
Standing wave pattern of HF radio waves in the ionospheric reflection region. Part 1: General formules
[UIO-SR-84-05-PT-1] 09 p1313 N85-18253
Observation of standing spinwaves in thin Fe-films by means of Raman spectroscopy
[DE85-003036] 11 p1735 N85-20913
Nonrelativistic Kapitza-Dirac scattering
[AD-A150622] 13 p2159 N85-23405
Magnetic pulsations recorded in northern Scandinavia during the IMS; a study of Pc 4-5 events
14 p2370 N85-24847
Nonrelativistic Kapitza-Dirac scattering
[AD-A150649] 14 p2417 N85-24911

STANDS
U SUPPORTS

STANNIDES
NT NIOBIUM STANNIDES

STAPHYLOCOCCUS
Structural-functional changes in bacterial cells under spaceflight conditions 16 p2724 N85-26812

STAR CLUSTERS
NT PRAESEPE STAR CLUSTERS
NT VIRGO GALACTIC CLUSTER
Observations of four Beta Cephei stars in NGC6231
01 p0126 N85-10877
Search for white dwarf companions of cool stars with peculiar element abundances
[NASA-CR-174030] 02 p0297 N85-11923
Studies of extragalactic RR Lyrae stars
03 p0444 N85-12831
An infrared study of the bi-polar outflow region GGD 12-15
[NASA-TM-86655] 03 p0445 N85-12835
Fifth Conference on Star Clusters and Associations and Their Relation to the Evolution of the Galaxy
[PUBL-56] 05 p0736 N85-14732
Structural properties of open star clusters and their relation to the galaxy 05 p0736 N85-14733
Open star clusters and the evolution of the galactic disk 05 p0736 N85-14734
The galactic distribution of open clusters of different ages and the angular velocity of the spiral structure
05 p0737 N85-14737
On collective effects in the rotation of stars in clusters and associations 05 p0737 N85-14739
A search for possible members of open clusters among known Ap stars 05 p0737 N85-14740
The present state of the International Star Cluster Photometry Programme 05 p0737 N85-14741
The Lund catalogue of open cluster parameters
05 p0738 N85-14742
Collective processes and formation of star clusters
05 p0738 N85-14743
The distribution of dust in the region of the Rosette Nebula and MON OB2 association
05 p0739 N85-14753
Proper motions and kinematical properties of Orion trapezium type stellar systems 05 p0739 N85-14755
On the most probable number of flare stars in the Pleiades field 05 p0739 N85-14756
Hyades moving group 05 p0740 N85-14757
The influence of stellar luminosity and temperature calibration on the determination of the initial mass function 05 p0740 N85-14760
High sensitivity, high angular resolution far-infrared photometry from the KAO 08 p1246 N85-17867
International Ultraviolet Explorer observations of amorphous hot galaxies
[NASA-CR-174354] 10 p1571 N85-19904
Ultraviolet studies of the young populous cluster NGC 2100 in the LMC 11 p1748 N85-20995
Processes and problems in secondary star formation
[DE85-003623] 12 p1960 N85-22322
A study of W Serpentis binaries: SX Cassiopeiae, RX Cassiopeiae, and W Serpentis 20 p3544 N85-32053
Far-infrared observations of young clusters embedded in the R Coronae Austrinae and RHO Ophiuchi dark clouds
[NASA-TM-86681] 24 p4167 N85-35834

STAR DISTRIBUTION
Lessons from the globular cluster NGC 5466
05 p0738 N85-14749
Galactic orbits of globular clusters
05 p0739 N85-14750
The fragmentation of molecular clouds and the IMF
05 p0740 N85-14759
Automated star counts in nebulous areas
07 p0967 N85-16137
International Ultraviolet Explorer observations of amorphous hot galaxies
[NASA-CR-174354] 10 p1571 N85-19904
Discriminant analysis of pulsar groups in the diagram P versus P 12 p1960 N85-22319
Processes and problems in secondary star formation
[DE85-003623] 12 p1960 N85-22322
The color excesses of classical cepheids and the structure of our galaxy 13 p2169 N85-23459
The structure and angular momentum content of dark clouds 14 p2439 N85-25054
A star camera aspect system suitable for use in balloon experiments
[OG-9.3-10] 23 p4028 N85-34965

STAR FIELDS
U STAR DISTRIBUTION

STAR TRACKERS
NT CCD STAR TRACKER
Optical contacting for gravity probe star tracker
[NASA-TM-86475] 01 p0120 N85-10819
Optical analysis of the star-tracker telescope for Gravity Probe
[NASA-TM-86474] 01 p0129 N85-10898
The de Tifini star pointer characterization and conclusions on the 1982 transmediterranean flight
[CESR-83-1070] 02 p0139 N85-10946
Optimization of orientation in navigation by two heavenly bodies 07 p0951 N85-16027
The UKIRT centre section structural investigation -- United Kingdom Infrared Telescope (UKIRT)
[UKIRT-22] 09 p1414 N85-18820
Integration of an Apple 2 Plus computer into an existing dual axis sun tracker system
[AD-A150778] 14 p2404 N85-24823
Autonomous state determination for an Earth orbiting satellite using horizon and star sensors
[AD-A151827] 15 p2493 N85-25379
Charge Injection Device (CID) used as a photodector: Implementation and performance. Application to light source tracking (stars, lasers)
[CNES-83/CT/DRT/TIT/OE/146]
20 p3533 N85-31983

STAR TRACKING
U STAR TRACKERS

STARCHES
Synthesis and characterization of novel polymers from non-petroleum sources for use in enhanced oil recovery
[DE85-010922] 19 p3250 N85-30151

STARFIGHTER AIRCRAFT
U F-104 AIRCRAFT

STARK EFFECT
Stark broadening of H(-) resonances in large electric fields
[DE84-016974] 04 p0496 N85-13154
The adsorption of acrylonitrile at a gold electrode: An EMIRS measurement of the electrochemical stark effect
[AD-A148664] 08 p1123 N85-17082
X-ray line broadening of a diagnostic in laser produced plasma
[DE85-001170] 10 p1560 N85-19841

STARLAB
Future ultraviolet experiments, including FUSE/COLUMBUS 11 p1744 N85-20986

STARLIFTER AIRCRAFT
U C-141 AIRCRAFT

STARS
NT A STARS
NT B STARS
NT BINARY STARS
NT BLACK HOLES (ASTRONOMY)
NT BLUE STARS
NT CARBON STARS
NT CATACLYSMIC VARIABLES
NT CEPHEID VARIABLES
NT COMPANION STARS
NT COOL STARS
NT DWARF NOVAE
NT DWARF STARS
NT EARLY STARS
NT ECLIPSING BINARY STARS
NT FLARE STARS
NT GIANT STARS
NT HERBIG-HARO OBJECTS
NT HERCULES NOVA
NT HOT STARS
NT INFRARED STARS
NT LATE STARS
NT M STARS
NT MAGNETIC STARS
NT MAIN SEQUENCE STARS
NT METALLIC STARS
NT NEUTRON STARS
NT NOVAE
NT O STARS
NT PECULIAR STARS
NT PRAESEPE STAR CLUSTERS
NT PRE-MAIN SEQUENCE STARS
NT PROTOSTARS
NT PULSARS
NT RADIO STARS
NT RED DWARF STARS
NT RED GIANT STARS
NT REFERENCE STARS
NT STELLAR GRAVITATION
NT SUBDWARF STARS
NT SUBGIANT STARS
NT SUN
NT SUPERGIANT STARS
NT SUPERMASSIVE STARS
NT SUPERNOVAE
NT SYMBIOTIC STARS
NT T TAURI STARS
NT VARIABLE STARS
NT WHITE DWARF STARS

NT WOLF-RAYET STARS
NT X RAY BINARIES
NT ZETA AURIGAE STAR

UEV photometry of E region standard stars of intermediate brightness 01 p0128 N85-10879

Observations of the pulsating hydrogen: Deficient star BD+13 deg 3224, during 1980 - 1981
01 p0128 N85-10882

Local photometric standards for CaII emission stars
01 p0128 N85-10883

Documentation for the machine-readable version of the ANS Ultraviolet Photometry Catalogue of Point Sources (Wesselius et al 1982)
[NASA-TM-87379] 03 p0406 N85-12589

Studies of extragalactic RR Lyrae stars
03 p0444 N85-12831

Documentation for the machine-readable version of the MK classification extension catalogue Morris-Kennedy (1983)
[NASA-TM-87372] 04 p0549 N85-13491

Documentation for the machine-readable version of the Perth 75: A Catalogue of Positions of 2589 FK4 and FK4S Stars (Nikoloff and Hog 1982)
[NASA-TM-87376] 04 p0549 N85-13492

Documentation for the machine-readable version of the AGK3 Star Catalogue of Positions and Proper Motions North of -2 deg .5 declination (Dieckvoss and Collaborators 1975)
[NASA-TM-87378] 04 p0549 N85-13493

Collective processes and formation of star clusters
05 p0738 N85-14743

Iron core collapse models of Type 2 supernovae
[DE84-013909] 05 p0743 N85-14775

Local interstellar extinction with an emphasis on uvby beta results 06 p0875 N85-15559

Do the arching HI filaments show in local reddening data? 06 p0876 N85-15561

Radio and UV observations of high latitude HI
06 p0879 N85-15583

Narrow absorption components in Be star winds
08 p1232 N85-17760

Ultraviolet spectral morphology of O-type stellar winds
08 p1232 N85-17762

Airborne Astronomy Symposium. A symposium commemorating the tenth anniversary of operations of the Kuiper Airborne Observatory
[NASA-CP-2353] 08 p1244 N85-17848

History of photometric precision
08 p1250 N85-17893

Photometric precision needed for planetary detection
08 p1250 N85-17894

Five-minute P modes detected in Doppler shift measurement on Alpha Centauri
08 p1250 N85-17895

Atmospheric limitations in stellar seismology: Should we measure radial velocity or brightness fluctuations?
08 p1251 N85-17899

The atmospheric extinction problem
08 p1251 N85-17901

Reduction to outside the atmosphere and statistical tests used in Geneva photometry 08 p1251 N85-17902

A CCD system for photometry of direct and spectroscopic images 08 p1252 N85-17904

Elemental abundances of mercury-manganese stars and the population 2 type star HD 109995
[NASA-CR-174298] 08 p1255 N85-17913

A comparative study of dust and young stars in three small galaxies 09 p1415 N85-18928

IUE observations of blue horizontal branch globular clusters and UV-bright stars 11 p1748 N85-20992

The UV extinction laws in two very young clusters, NGC 6530 in the galaxy and NGC 2100 in the LMC
11 p1748 N85-20994

The central star of NGC 40 11 p1751 N85-21013

Chromospheric emission lines in high-resolution LWR spectra (220 - 3000 alpha) of gamma CRU (M3 3) and alpha ORI (M2 lab) 11 p1758 N85-21058

Active late-type stars and the applicability of coronal loop models 11 p1758 N85-21059

Co-rotating interaction regions in stellar winds
11 p1758 N85-21060

IUE low-dispersion reference atlas
11 p1760 N85-21073

IUE observations of faint standard stars for calibration of the space telescope 11 p1761 N85-21076

A survey of Mg II h and k emission in near-solar type stars
[NASA-CR-175572] 12 p1953 N85-22269

University of Cambridge Institute of Astronomy report of activities 13 p2170 N85-23464

Activities report of the Institute for Astronomy and Astrophysics
[MITT-5] 14 p2434 N85-25012

Documentation for the machine-readable version of the Cape Photographic Durchmusterung (CPD)
[NASA-TM-87442] 14 p2439 N85-25050

Very large array observations of coronal loops and related observations of solar type stars
[AD-A152027] 16 p2688 N85-27817

Activities report of the Institute of Astronomy
20 p3545 N85-32059

Star formation in NGC 7538: Multi-wavelength observations and issues 20 p3545 N85-32063

Basic formulae for the computation of the deflection of the vertical from astronomical star observations
[AD-A154912] 21 p3605 N85-32390

Neutrino-antineutrino annihilation around collapsing star
[OG-1.1-10] 22 p3861 N85-33911

Search for gamma rays of energy 10(15) eV from Cygnus X-3
[OG-2.1-1] 22 p3862 N85-33919

Observation of an excess of cosmic ray muons of energies 2 TeV from the direction of Cygnus X-3
[OG-2.1-3] 22 p3863 N85-33920

Muon content of gamma ray induced EAS from Cygnus X-3
[OG-2.1-4] 22 p3863 N85-33921

Gamma rays of energy or = 10(15) eV from Cyg X-3
[OG-2.1-5] 22 p3863 N85-33922

The capability of the existing network of installations for detecting the antineutrino burst from collapsing stars
[HE-5.3-13] 24 p4206 N85-36107

STARTERS
NT ENGINE STARTERS

STARTING

Control system design language implementation of a gas turbine starting controller
[AD-A147896] 07 p0905 N85-15732

Comparative visualization of accelerating flow around various bodies, starting from rest
[AD-P004159] 09 p1264 N85-17944

Engine wear and cold startability of methanol fueled engines.
[DE85-001208] 11 p1647 N85-20381

STATE EQUATIONS
U EQUATIONS OF STATE

STATE ESTIMATION

Hybrid state estimation approach to multiobject tracking for airborne surveillance radars
[AD-A148459] 08 p1153 N85-17279

STATE VECTORS

Optimum design for nonlinear shock mounts for transient inputs 09 p1334 N85-18390

High level languages in protocol specification and verification
[FUB-51-1983] 09 p1370 N85-18611

Computer program TRAMP: Inclusion of state space facilities and the analysis of non-linear elements
[BAE-BT-12643] 15 p2626 N85-26181

Fundamental equivalence of generalised state space systems
[MATHEMATICS-RESEARCH-182]
15 p2642 N85-26293

Adaptive filtering for large space structures: A closed-form solution 20 p3417 N85-31206

STATIC AERODYNAMIC CHARACTERISTICS

The aerodynamics of bluff bodies in turbulent shear layers 05 p0593 N85-13780

Experimental techniques and instrumentation for bluff body aerodynamics 05 p0593 N85-13781

Automatic correction of static characteristics of measurement channel of digital oscillograph
06 p0795 N85-15083

Static longitudinal stability and control characteristics of the Fokker F27 Friendship calculated by simple handbook methods
[VTH-LR-394] 16 p2711 N85-26728

STATIC CHARACTERISTICS
NT STATIC AERODYNAMIC CHARACTERISTICS

Structural analysis of the Space Shuttle Orbiter
01 p0061 N85-10401

Static and dynamic characteristics of materials with beam-microstructure 03 p0370 N85-12361

Sensitivity analysis of discrete structural systems: A survey
[NASA-TM-86333] 06 p0817 N85-15186

Treatment of general boundary conditions and point-wise state variable constraints in optimum design for static and dynamic response
09 p1330 N85-18356

Electrothermal transducer with short time constant
13 p2088 N85-23040

Method of static measurements of absolute scattering matrix of radar targets 22 p3762 N85-33316

STATIC DEFORMATION

NIKE3D: An implicit, finite-deformation, finite element code for analyzing the static and dynamic response of three-dimensional solids, revision 1
[DE84-017161] 04 p0514 N85-13277

Consolidation theory with consideration of frame plasticity
[REPT-8/1984] 16 p2796 N85-27240

Liquid-metal transducers for strain measurement during in-pile materials testing 17 p2945 N85-28176

The static aeroelasticity of a composite wing
18 p3121 N85-29321

Mechanical properties of aligned short carbon fiber reinforced PES and PI laminates
[ESA-TT-898] 20 p3422 N85-31240

STATIC ELECTRICITY

International Aerospace and Ground Conference on Lightning and Static Electricity. 1984 technical papers. Supplement
[NASA-CP-2356] 07 p0999 N85-16343

STATIC FIRING

Qualification of an electrothermal hydrazine thruster with a vacuum thrust of 0.5 to 2.0 N
[BMFT-FB-W-84-043] 07 p0917 N85-15808

Space shuttle flight readiness firing dress rehearsal for STS-1 08 p1097 N85-16929

STATIC LOADS

Strength of welded joints in VT23 alloy upon repeated static loading 01 p0020 N85-10120

Interactive buckling of thin-walled structural components under static and dynamic loads
01 p0059 N85-10392

Study of delamination cracking under static and cyclic loads of carbon-epoxy composite materials
[REPT-42-727/F] 03 p0327 N85-12102

Free-edge failures of composite laminates
04 p0467 N85-12971

Characterization of fiber optic cables under large tensile loads
[DE84-016816] 05 p0651 N85-14180

Stability of hollow shafts under torsion
06 p0780 N85-14986

Tests of the load-bearing and deformation behaviour of reinforced concrete spherical shells under point loading
[BLL-RISLEY-TR-4550-9091.9F)]
06 p0816 N85-15182

Preliminary report on tests of tensile specimens with a part-through surface notch for a filament wound graphite/epoxy material
[NASA-CR-172545] 10 p1431 N85-19026

Sensitivity of titanium alloys to stress concentration during repeated static loads 11 p1602 N85-20074

Elastic compliance of imperfect interfaces: Review and relationship to ultrasonic scattering
[DE85-003068] 11 p1652 N85-20404

Yield joint condition for three-dimensional I-beams
[ILR-MITT-137] 12 p1867 N85-21716

Some problems in optimally designing shells of revolution 14 p2278 N85-24114

Investigation to optimize the passive shock wave/boundary layer control for supercritical airfoil drag reduction
[NASA-CR-175788] 16 p2699 N85-26665

Forced structural response using component mode synthesis
[DE85-008479] 19 p3287 N85-30383

Static and cyclic behavior of semi-rigid steel beam-column connections
[PB85-194363] 24 p4103 N85-35433

STATIC PRESSURE
NT HYDROSTATIC PRESSURE

Effect of combined pressure and temperature distortion orientation on high-bypass-ratio turbofan engine stability
[NASA-TM-83771] 01 p0011 N85-10067

High temperature static strain sensor development program 02 p0141 N85-10959

Effects of inlet distortion on a static pressure probe mounted on the engine hub in an F-15 airplane
[NASA-TP-2411] 13 p1974 N85-22394

Transition detection using surface pressure holes
14 p2212 N85-23722

Measurement of turbofan-turbojet thrust from tailpipe static pressure
[AD-A154036] 19 p3220 N85-29967

On the evaluation of boundary layer measurements on boattailed bodies of revolution in axisymmetric compressible subsonic flow
[ESA-TT-883] 20 p3457 N85-31471

Static high pressure study of nitric oxide chemistry: Proposed mechanism for nitric oxide detonation
[DE85-010795] 22 p3746 N85-33220

Explosive containment study
[DE85-0117[illegible]] 22 p3753 N85-33267

STATIC STABILITY
NT DIMENSIONAL STABILITY
NT SHELL STABILITY
NT STRUCTURAL STABILITY

Integrated Application of Active Controls (IAAC) technology to an advanced subsonic transport project-longitudinal handling qualities study of a relaxed-stability airplane
[NASA-CR-3660] 02 p0148 N85-11005

Generation and evolution of diabatic planetary waves in continuously stratified atmosphere with Ekman dissipation 09 p1364 N85-18515

Approximate neutral point of a subsonic canard aircraft
[NASA-TM-86694] 15 p2482 N85-25205

Numerical experiments of jet streak ageostrophic circulations using pseudo-geostrophic initialization and perspectives 15 p2590 N85-25969

Realisation of relaxed static stability on a commercial transport 16 p2713 N85-26746

Demonstration of relaxed static stability on a commercial transport 17 p2903 N85-27898

Realisation of relaxed static stability on a commercial transport 17 p2903 N85-27899

STATIC TESTS
NT STATIC FIRING

Initial sailplane project: The RP-1
04 p0468 N85-12976

Static jet noise test results of four 0.35 scale-model QCGAT mixer nozzles
[NASA-TM-86871] 04 p0558 N85-13551

Measuring methods to determine the static and dynamic behavior of wind energy converters
05 p0688 N85-14297

Static internal performance of single-expansion-ramp nozzles with various combinations of internal geometric parameters
[NASA-TM-86270] 06 p0749 N85-14797

Using a data base management system for modelling SSME test history data 12 p1944 N85-22211

Modifications to the nozzle test chamber to extend nozzle static-test capability
[NASA-TM-86388] 15 p2464 N85-25216

Static investigation of several yaw vectoring concepts on nonaxisymmetric nozzles
[NASA-TP-2432] 18 p3058 N85-28924

Static and cyclic behavior of semi-rigid steel beam-column connections
[PB85-194363] 24 p4103 N85-35433

STATICS
NT ELECTROSTATICS
NT HYDROSTATICS

Numerical solution of one-dimensional nonlinear problems of statics for elastic beams and shells under rigid constraints 17 p2943 N85-28166

Method of solving problems of statics for multilayer shells of revolution 17 p2943 N85-28167

Scattering by distributions of small thin particles
19 p3253 N85-30172

STATIONARY ORBITS

Non-stable motions and instability in stellar associations 05 p0739 N85-14754

Construction and functioning of extended orbital systems 16 p2724 N85-26814

Geostationary orbit capacity study
[REPT-44-3558] 18 p3091 N85-29134

STATIONKEEPING

Stationkeeping strategies for geostationary satellites
05 p0600 N85-13625

The investigation of tethered satellite system dynamics
[NASA-CR-171278] 07 p0912 N85-15772

Station keeping of geostationary satellites by electric propulsion
[NASA-TM-77820] 14 p2320 N85-24337

Moored buoy stationkeeping and location system
14 p2331 N85-24416

Orbital positioning and stationkeeping of geostationary satellites 14 p2397 N85-24772

Artificial intelligence in space platforms
[AD-A152078] 16 p2851 N85-27578

STATIONS
NT AUTOMATIC WEATHER STATIONS
NT CREW STATIONS
NT CREW WORKSTATIONS
NT EARTH TERMINALS
NT EOSS
NT GLOBAL TRACKING NETWORK
NT GROUND STATIONS
NT HYDROELECTRIC POWER STATIONS
NT LONG DURATION EXPOSURE FACILITY
NT ORBITAL SPACE STATIONS
NT ORBITING LUNAR STATIONS
NT PAYLOAD STATIONS
NT POLYSTATION DOPPLER TRACKING SYSTEM
NT SALYUT SPACE STATION
NT SPACE STATIONS
NT TRACKING STATIONS
NT WEATHER STATIONS
NT WORKSTATIONS

Sector suite man-machine functional capabilities and performance requirements
[AD-A146881] 10 p1531 N85-19647

Use of mobile surface station for synchronous satellite measurements in seismological research
13 p1984 N85-22447

Applications, specifications of Robotron CAD-CAM work stations 15 p2537 N85-25661

Deployment of a regional array in Norway
[AD-A154120] 19 p3313 N85-30536

STATISTICAL ANALYSIS
NT AMPLITUDE DISTRIBUTION ANALYSIS
NT ANALYSIS OF VARIANCE
NT BIVARIATE ANALYSIS
NT CORRELATION COEFFICIENTS
NT COVARIANCE
NT DISCRIMINANT ANALYSIS (STATISTICS)
NT FACTOR ANALYSIS
NT GOODNESS OF FIT
NT KOLMOGOROFF-SMIRNOFF TEST
NT LIKELIHOOD RATIO
NT MAXWELL-BOLTZMANN DENSITY FUNCTION
NT MULTIVARIATE STATISTICAL ANALYSIS
NT NONPARAMETRIC STATISTICS
NT NORMAL DENSITY FUNCTIONS
NT ORTHOGONALITY
NT PEARSON DISTRIBUTIONS
NT POISSON DENSITY FUNCTIONS
NT PROBABILITY DENSITY FUNCTIONS
NT PROBABILITY DISTRIBUTION FUNCTIONS
NT QUANTILES
NT RANK TESTS
NT RAYLEIGH DISTRIBUTION
NT REGRESSION ANALYSIS
NT REGRESSION COEFFICIENTS
NT SEQUENTIAL ANALYSIS
NT STANDARD DEVIATION
NT STATISTICAL CORRELATION
NT STATISTICAL DECISION THEORY
NT STATISTICAL TESTS
NT VARIANCE (STATISTICS)
NT WEIBULL DENSITY FUNCTIONS

Equation of state study for polar fluids
[PB84-222801] 01 p0025 N85-10157

Measurement assurance programs. Part 2: Development and implementation
[PB84-217876] 01 p0051 N85-10338

Simulation uses of the exponential distribution
[AD-A144940] 01 p0112 N85-10756

Harmonizable, Cramer, and Karhunen classes of processes
[AD-A144984] 01 p0113 N85-10767

An integral inequality with applications to order statistics
[AD-A145081] 01 p0113 N85-10770

Optimizing search with positive information feedback
[CSIR-TWISK-313] 01 p0125 N85-10855

Some statistical characteristics of atmospheric optical thickness in visible spectral range
02 p0164 N85-11109

A study of environmental characterization of conventional and advanced aluminum alloys for selection and design. Phase 2: The breaking load test method
[NASA-CR-172387-PHASE-2] 02 p0182 N85-11219

Seminar on Principal Components Analysis in the Atmospheric and Earth Sciences
[CSIR-S-334] 02 p0211 N85-11388

What is principal components analysis?
02 p0211 N85-11389

Principal components: A review
02 p0211 N85-11390

Application of correspondence analysis to meteorological data 02 p0211 N85-11393

A principal component analysis of eastern Transvaal seasonal rainfall, 1950 to 1981
02 p0212 N85-11395

The application of principal component analysis in a study of rainfall 02 p0212 N85-11396

Spatial relationships in stream flow residuals
02 p0212 N85-11397

The application of principal components analysis to LANDSAT MSS data 02 p0212 N85-11398

Northern Hemisphere atlas of 1-minute rainfall rates
[AD-A145411] 02 p0231 N85-11508

Weighted distributions arising out of methods of ascertainment
[AD-A145615] 02 p0252 N85-11648

Fluctuations in parameters of light beam along path with reflection in turbulent atmosphere
02 p0263 N85-11722

Spread-spectrum communications
[AD-A146135] 03 p0355 N85-12265

Statistical properties of geomagnetic pulsations at the Observatory of Fuerstenfeldbruck determined with the aid of pulsation indices. Part 2: Periodicity in the occurrence of pulsations
[REPT-558] 03 p0376 N85-12599

GASP cloud- and particle-encounter statistics and their application to LFC aircraft studies. Volume 2: Appendixes
[NASA-TM-85835-VOL-2] 03 p0395 N85-12522

Statistical analysis of some traveling salesman algorithms
[AD-A145786] 03 p0410 N85-12620

A building blocks approach to statistical databases
03 p0437 N85-12782

Test report no. 17.208: Statistics of the basic characteristics of carbon-epoxy composites
[DGT-23.426/A] 04 p0468 N85-12979

Analysis of frequency-selective integrated circuits in system of normal coordinates 04 p0489 N85-13119

Thermal shock as a carbide grade development tool
[DE84-016939] 04 p0509 N85-13251

Design and implementation of a modular program system for statistical analyses
[IKE-4-114] 04 p0551 N85-13503

Satellite orbit determination 05 p0598 N85-13613

Synthesis of load-time histories resulting from statistical analysis 05 p0650 N85-14171

Some techniques in image processing
05 p0721 N85-14629

Approximating the percentage points of Greenwood's statistic with Cornish-Fisher expansions
[CWI-MS-R8405] 05 p0721 N85-14634

Methodology for economic evaluation of process technologies in the early research and development stages
[DE84-015863] 05 p0736 N85-14731

Statistics from the operation of the low-level wind shear alert system (LLWAS) during the Joint Airport Weather Studies (JAWS) Project
[DOT/FAA/PM-84/32] 06 p0750 N85-14804

Annual review of aircraft accident data: US general aviation, calendar year, 1981
[PB84-230960] 06 p0750 N85-14805

Statistical analysis of visual wave observations and gage/radar measurements
[AD-A148358] 06 p0798 N85-15100

Information-theoretic properties of languages and their grammars
[AD-A146668] 06 p0799 N85-15106

Frequency and motion of western North Pacific tropical cyclones
[PB85-106466/GAR] 06 p0839 N85-15331

Statistical filtering as method for detecting transcrustal acoustic anomalies 07 p0962 N85-16237

An evaluation and comparison of vertical profile data from the VISSR Atmospheric Sounder (VAS)
[NASA-TP-2425] 07 p1000 N85-16351

Lattice statistics
[AD-A146662] 07 p1029 N85-16530

A complete characterization of triply balanced matrices with applications to survey sampling
[AD-A147083] 07 p1031 N85-16542

Model robust response surface designs: Scaling 2-level factorials
[AD-A147 94] 07 p1033 N85-16558

On the power functions of test statistics in order restricted inference
[AD-A147126] 07 p1035 N85-16566

FAA (Federal Aviation Administration) statistical handbook of aviation, calendar year 1983
[AD-A148171] 08 p1067 N85-16760

An analysis of robust and efficient priors associated with a finite Bayesian model for compliance testing
[AD-A148497] 08 p1213 N85-17635

Antisampling for estimation: An overview
[AD-A148545] 08 p1216 N85-17659

A statistical evaluation of the limitations of single-channel intermediate-band photoelectric stellar photometry 08 p1251 N85-17900

An objective error measure for the comparison of calculated and measured transient response histories
09 p1335 N85-18395

Field studies of run-up generated by wind waves on dissipative beaches
[AD-A148793] 09 p1350 N85-18548

Computing environments for data analysis. Part 1. Introduction
[AD-A148677] 09 p1373 N85-18632

Computing environments for data analysis. Part 2. Hardware
[AD-A148678] 09 p1374 N85-18633

Estimating the scale parameter of an exponential distribution from a sample of time-censored r-th order statistics
[AD-A148060] 09 p1375 N85-18644

Simple approximate variances for b-letter values. A sampling enquiry: Supplement
[DE85-001410] 09 p1376 N85-18647

Issues in sensitivity and statistical analysis of large-scale, computer-based models
[PB85-116317/GAR] 09 p1376 N85-18650

Evaluation of the birdstrike threat to the F-15 present fleet, rapid deployment force, and dual role fighter transparencies
[AD-A148954] 10 p1421 N85-18966

Factors influencing the ball milling of Si3N4 in water
[NASA-TM-86932] 10 p1450 N85-19136

The ambiguity function of random binary-phase-coded waveforms
[AD-A148906] 10 p1466 N85-19249

TRAN-STAT: Statistics for environmental studies
[DE85-000829] 10 p1513 N85-19547

Frozen precipitation and concurrent weather: A case study for Munchen-Riem, West Germany
[AD-A149227] 10 p1519 N85-19577

Robust Kalman filtering and its applications
[AD-A149044] 10 p1550 N85-19775

Worldwide birdstrike statistics of Lufthansa German Airlines
[AD-P004183] 11 p1579 N85-19945

Microscopic identification of feathers in order to improve birdstrike statistics
[AD-P004187] 11 p1579 N85-19950

Statistical theory of fragmentation processes
[DE85-002206] 11 p1653 N85-20414

National Performance Audit Program ambient air audits of analytical proficiency
[PB85-138204] 11 p1680 N85-20586

User's guide for the computer program response factor (REFAC)
[PB85-138600] 11 p1705 N85-20726

Checking the shape of discrete distributions
[DE85-000177] 11 p1706 N85-20733

An exact solution to the 2 point OC (Operating-Characteristic) curve determination
[AD-A148120] 11 p1706 N85-20746

An IUE high-resolution atlas of O-type spectra
11 p1760 N85-21074

General aviation activity and avionics survey
[AD-A149572] 12 p1769 N85-21103

Field validation of statistically-based acceptance plan for bituminous airport pavements. Volume 1: Correlation analysis of Marshall properties of laboratory-compacted specimens
[FAA-PM-84-12-VOL-1] 12 p1781 N85-21180

Field validation of statistically-based acceptance plan for bituminous airport pavements. Volume 2: Statistical analysis of Marshall properties of plant-produced bituminous materials
[FAA-PM-84-12-VOL-2] 12 p1781 N85-21181

Field validation of statistically-based acceptance plan for bituminous airport pavements. Volume 3: Statistical analysis of 3 methods for determining maximum specific gravity of bituminous concrete mixtures
[FAA-PM-84-12-VOL-3] 12 p1781 N85-21182

Field validation of statistically-based acceptance plan for bituminous airport pavements. Volume 4: Computer simulation of multiple acceptance criteria
[FAA-PM-84-12-VOL-4] 12 p1782 N85-21183

Field validation of statistically-based acceptance plan for bituminous airport pavements. Volume 5: Summary of validation studies
[FAA-PM-84-12-VOL-5] 12 p1782 N85-21184

Preliminary review of statistical treatment of S-glass/epoxy stress rupture data
[AD-A149810] 12 p1797 N85-21275

Algorithm for statistical simulation of electromagnetic compatibility characteristics of high-frequency transmission channels in radioelectronic facilities
12 p1842 N85-21560

Statistics of french Armee de l'air ejections 1970 - 1980 12 p1906 N85-21971

List of head/neck injury on ejection in the German Armed Forces from 1972-1981 12 p1906 N85-21972

General saddlepoint approximations with applications to l-statistics
[AD-A150073] 12 p1924 N85-22096

Surface forward scattering and reflection
[AD-A150115] 12 p1928 N85-22112

Statistical phenomena in particle beams
[DE85-001050] 12 p1929 N85-22118

A statistical approach to vendor selection
[AD-A149781] 12 p1950 N85-22249

Motion of symmetrical satellite with flexible viscoelastic rods about center of mass in circular orbit
13 p1979 N85-22420

Ice statistics and acoustic scattering in the Arctic basin
[AD-A150141] 13 p2140 N85-23289

Microcomputer: Controlled statistics analyzer
[BLL-CE-TRANS-7971-(9022.09)]
13 p2144 N85-23306

Bootstrapping the Kalman filter
[AD-A150509] 13 p2153 N85-23370

Informative geometry of probability spaces
[AD-A150510] 13 p2153 N85-23371

Unsupervised classification of global radar units on Venus 13 p2196 N85-23632

Estimate of fatigue stability of gas-turbine engine compressor vanes in probabilistic aspect
14 p2287 N85-24169

Statistical/Trend analysis of the marine atmospheric boundary layer model
[AD-A151053] 14 p2374 N85-24673

Circulation statistics based on FGGE (First GARP Global Experiment) level 3-B analyses produced by GFDL (Geophysics Fluid Dynamics Laboratory)
[PB85-149318] 14 p2379 N85-24688

Boundary crossing probabilities and statistical applications
[AD-A151027] 14 p2411 N85-24869

Shuttle fleet operations: A simulation analysis
[AD-A151383] 15 p2491 N85-25370

Statistical techniques for signal processing
[AD-A151231] 15 p2541 N85-25690

Nonparametric detection of narrowband signals
[AD-A151290] 15 p2542 N85-25691

Statistical analysis of partial discharge inception in high voltage 15 p2546 N85-25715

Recent VAS imaging/sounding research
15 p2597 N85-26004

Interactive graphical data analysis
[DE85-005946] 15 p2631 N85-26215

Higher order residual analysis for nonlinear time series with autoregressive correlation structures
[AD-A149232] 15 p2636 N85-26257

Intermediate term forecasting techniques for management
[AD-A151370] 15 p2637 N85-26262

Statistical comparison of pooled nitrogen washout data of various altitude decompression response groups
[NASA-TM-58265] 15 p2639 N85-26278

Statistical analysis techniques for small sample sizes
[NASA-CR-171872] 15 p2639 N85-26279

Point processes associated with extreme value theory
[AD-A151211] 15 p2640 N85-26280

Statistical aspects of reliability, maintainability and availability
[AD-A151228] 15 p2640 N85-26282

Scattered data interpolation and approximation
[DE85-007495] 15 p2641 N85-26290

Lectures on probability and statistics
[DE85-007079] 15 p2641 N85-26291

An evaluation of the performance of a new storm tracking methodology
[AD-A152234] 16 p2835 N85-27484

Circulation statistics from January and July: Simulation with the NCAR (National Center for Atmospheric Research) community climate model (CCMOB)
[PB85-165637] 16 p2837 N85-27497

Statistical study of the dynamic analysis of the workload in the A310 certification campaign
16 p2844 N85-27531

Locally-weighted-regression scatter-plot smoothing (LOWESS): A graphical exploratory data analysis technique
[AD-A152239] 16 p2855 N85-27609

Multivariable statistical modelling and its application
16 p2857 N85-27617

Mutli-particle quantum mechanics obeying fractional statistics
[DE85-007830] 16 p2873 N85-27723

Data management issues of statistical databases
[DE85-007616] 16 p2879 N85-27763

The effect of microalloying with calcium and magnesium on the plasticity of Poldi AKN 20 Ni-based alloy
[BLL-BISI-TRANS-2174-(9022.09)]
17 p2929 N85-28075

Computing environments for data analysis. Part 1: Introduction
[DE85-007919] 17 p3009 N85-28603

Computing environments for data analysis. Part 2: Hardware
[DE85-008320] 17 p3009 N85-28604

Computer program for prediction of capture maneuver probability for an on-off reaction controlled upper stage
[NASA-CR-165937] 17 p3010 N85-28611

Software environment for conducting interactive statistical analysis
[AD-A153378] 17 p3012 N85-28626

Improved statistical analysis method for prediction of maximum inlet distortion
[AD-A153767] 18 p3083 N85-28947

Statistical fracture theories for brittle materials
[AD-A153530] 18 p3121 N85-29324

Intercomparison of sea-surface temperature anomaly fields 18 p3140 N85-29440

A comparison of the bounded derivative and the normal mode initialization methods using real data
18 p3144 N85-29483

Pacific Northwest solar radiation data
[DE85-009773] 18 p3149 N85-29496

Towards a statistical analysis of genetic sequences data with particular reference to protein sequences
[AD-A153605] 18 p3152 N85-29515

Accepting error to make less error
[AD-A153949] 18 p3171 N85-29651

Extrapolation methods for multi-dimensional quadrature of singular and regular integrand functions
[DE85-009665] 18 p3172 N85-29655

Cavityless optical bistability in systems of two-level atoms 18 p3186 N85-29764

Corrosion fatigue cooperative testing program statistical analysis
[AD-A153886] 19 p3238 N85-30077

Diagnosis of vertical motions from VAS retrievals during a convective outbreak
[NASA-CR-171569] 19 p3316 N85-30554

Precipitation estimation using collocated GOES satellite and surface data
[AD-A154248] 19 p3317 N85-30559

Workshop on objective analysis: Analysis strategies for field-dependent estimation
[PB85-179901] 19 p3318 N85-30569

Troposphere-stratosphere (surface-55 km) monthly general circulation statistics for the Northern Hemisphere-four year averages
[NASA-TM-86182] 20 p3495 N85-31730

A cluster analysis method for identification of subpopulations of cells in flow cytometric list-mode arrays 20 p3503 N85-31779

A guide to the statistical analysis of the results of linear and nonlinear least-squares data fitting
[NPL-DITC-53/84] 20 p3521 N85-31895

Reliability of void detection in structural ceramics using scanning laser acoustic microscopy
[NASA-TM-87035] 21 p3597 N85-32337

Signal statistics of the radar echoes: Angle-of-arrival statistics, part 2.2A 21 p3618 N85-32482

A statistical analysis of ice nuclei concentrations at urban and rural sites in Valladolid, Spain
21 p3640 N85-32614

A statistical study of CCN concentration in subequatorial climate: The particular case of the tropical wet forest
21 p3649 N85-32673

An error-dependent model of instrument-scanning behavior in commercial airline pilots
[NASA-CR-3908] 21 p3665 N85-32765

Theory of soliton waves
[AD-A154784] 21 p3676 N85-32837

Optimization of sampling in statistical physics experiments 21 p3698 N85-32975

Enhancing precision of remote temperature sensing data from satellites under cloudy atmospheric conditions
22 p3734 N85-33148

Logical and physical modeling and design of scientific and statistical databases for energy research
[DE85-008081] 22 p3833 N85-33737

Statistical analyses in the study of solar wind-magnetosphere coupling
[DE85-009596] 22 p3859 N85-33898

Observations of the Crab Nebula at energies 4.10(11)
[OG-2.3-1] 22 p3865 N85-33938

Statistical pooling method of fatigue data for reliability design 23 p3906 N85-34196

Theoretical and experimental analyses of the performance of two-color laser ranging systems
[NASA-CR-176159] 23 p3936 N85-34397

On the statistical significance of excess events: Remarks of caution and the need for a standard method of calculation
[OG-9.5-10] 23 p4031 N85-34987

A new statistic for the analysis of circular data in gamma-ray astronomy
[OG-9.5-13] 23 p4031 N85-34989

Rigidity spectrum of Forbush decrease
[SH-5.1-6] 23 p4042 N85-35060

Methods and software for cosmic ray scintillation studies
[SH-9.1-17] 23 p4052 N85-35132

Statistical distribution of breakdown voltages in rep-rate spark gaps
[DE85-012813] 24 p4090 N85-35354

Users guide for optimum interpolation method of global data assimilation
[AD-A155929] 24 p4138 N85-35646

Risk analysis and sensitivity: Antithesis or synthesis
[B8562444] 24 p4144 N85-35687

STATISTICAL COMMUNICATION THEORY
U COMMUNICATION THEORY

STATISTICAL CORRELATION
Assessment of Thematic Mapper band-to-band registration by the block correlation method
12 p1872 N85-21743
More precise curve of dependence between density and velocity of longitudinal waves in consolidated crust and top of mantle in oceanic structures
13 p2110 N85-23143
Solar radio fluxes as indices of solar activity
[AERONOMICA-ACTA-A-282-1984]
21 p3722 N85-33095
Estimate of signal-to-interference energy ratio in discrete-data transmission 22 p3776 N85-33398
The relationship between personality and performance
24 p4129 N85-35800

STATISTICAL DECISION THEORY
Markovian control problems: Functional equations and algorithms
[MCTH-97] 01 p0107 N85-10717
Total positivity. A review
[AD-A145205] 01 p0114 N85-10771
A note on validity generalization procedures
[AD-A150065] 12 p1924 N85-22085
Generation and termination of binary decision trees for nonparametric multiclass classification
[AD-A151361] 15 p2640 N85-26283

STATISTICAL DISTRIBUTIONS
NT BRIGHTNESS DISTRIBUTION
NT PEARSON DISTRIBUTIONS
NT PROBABILITY DISTRIBUTION FUNCTIONS
NT RAYLEIGH DISTRIBUTION
A simple transport model 02 p0284 N85-11853
On the Edgeworth expansion for the sum of a function of uniform spacings
[CWI-MS-R8404] 05 p0719 N85-14619
A monotonicity property of the power function of multivariate tests
[CWI-MS-R8406] 05 p0721 N85-14635
Lower level inference control in statistical database systems
[DE84-016005] 05 p0735 N85-14729
On the most probable number of flare stars in the Pleiades field 05 p0739 N85-14756
Blood pressure levels of active pilots compared with those of air traffic controllers
[AD-A146645] 06 p0846 N85-15373
Distributions of extreme values of sequences of autocorrelated random variables
[PB84-240746] 06 p0858 N85-15456
On a random difference equation for matrices and a characterization of the gamma distribution
[AD-A146858] 07 p1029 N85-16529
The effect of assumptions about cost element probability distributions on operating and support cost risk analysis
[AD-A147553] 07 p1036 N85-16576
A numerical analysis of sampling plans based on prior distribution and costs
[AD-A147718] 08 p1210 N85-17616
Stochastic dynamic analysis of a structure with frictional joints 09 p1337 N85-18406
Morphology of keV-electrons in the Earth's magnetosphere as observed by GEOS 1
[DRI-3-84] 09 p1350 N85-18496
MTI system simulation and clutter output statistics
[AD-A149193] 10 p1467 N85-19255
Scrawl plots, and letter and bletter strips
[DE85-001409] 11 p1707 N85-20739
Tests of fit based on normalized spacings
[AD-A149749] 12 p1921 N85-22062
General saddlepoint approximations with applications to l-statistics
[AD-A150073] 12 p1924 N85-22086
Stable measures and processes in statistical physics
[AD-A149592] 12 p1926 N85-22098
Skewed stable variables and processes
[AD-A150549] 13 p2153 N85-23372
Average spacing for rings of individual multi-ring basins is 2.0(0.5)D 13 p2182 N85-23541
A note on equivalent random theory
[CWI-OS-R8410] 14 p2412 N85-24872
A statistical approach to relaxation in glassy materials
[AD-A151285] 15 p2518 N85-25524
On limiting empirical distribution function of the eigenvalues of a multivariate F matrix, revised
[AD-A151885] 15 p2641 N85-26286
On asymptotic joint distribution of the eigenvalues of the noncentral manova matrix for nonnormal populations
[AD-A151886] 15 p2642 N85-26294
Brownian motion with quadratic killing and some implications: Revision
[AD-A151323] 15 p2642 N85-26296
Multinomial form of the solution of problems of the statistics of elastic rectangular disks
[REPT-17/1984] 16 p2797 N85-27244
Inequalities for distributions with increasing failure rate
[AD-A152812] 17 p2976 N85-28390
Statistical interpretation of the ECMWF model using MOS to predict surface wind and temperature
[WSR-2] 17 p2995 N85-28515
Estimating random integrals from noisy observations: Sampling designs and their performance
[AD-A152926] 17 p3025 N85-28702
A collection of probability distributions
[AD-A153128] 17 p3025 N85-28704
Recent measurements in turbulent jet flames at Sandia Combustion Research Facility 20 p3424 N85-31254
The distribution of the number of empty cells in a generalized random allocation scheme
[AD-A154806] 21 p3677 N85-32841
Decomposing the joint distribution of several linear combinations of uniform spacings
[AD-A155056] 21 p3677 N85-32845
Antistarshapedness, dispersiveness and mixtures
[AD-A155583] 21 p3678 N85-32849
Phonetic transcription statistics: Constitution and statistical utilization
[ENST-85D001] 22 p3756 N85-33285
Search for bursts in air shower data
[OG-5.3-10] 22 p3865 N85-34076
Statistical distribution of breakdown voltages in rep-rate spark gaps
[DE85-012813] 24 p4090 N85-35354
Large deviations for the maxima of some random fields
[AD-A155909] 24 p4143 N85-35681
The model of independent particles emission in the multiparticle production theory
[HE-3.2-10] 24 p4179 N85-35916

STATISTICAL MECHANICS
Fluctuation spectrum for linear gyroviscous MHD
[IPP-6/237] 01 p0121 N85-10828
Equipartition threshold in nonlinear large Hamiltonian systems: The Fermi-Pasta-Ulam model
[NOTA-INTERNA-819] 02 p0255 N85-11670
Statistical Plasma Physics. Proceedings of the Workshop of the US-Japan Joint Institute for Fusion Theory Program
[IPPJ-689] 02 p0282 N85-11832
Large deviations for processes with independent increments
[AD-A147293] 08 p1210 N85-17610
Reduction of the wavepacket: How long does it take?
[DE84-016778] 09 p1400 N85-18815
Stable measures and processes in statistical physics
[AD-A149592] 12 p1926 N85-22098
Detonation behavior of LX-14 and PBX-9404: Theoretical aspect
[DE85-010036] 18 p3084 N85-29076
Statistical mechanics of adsorption and wetting
[DE85-010093] 19 p3269 N85-30271
Physical concepts in the development of constitutive equations 20 p3467 N85-31537
Cluster variation study of coherent ordering in FCC and BCC solid solutions
[AD-A156039] 24 p4079 N85-35280

STATISTICAL MOMENTS
U DISTRIBUTION MOMENTS

STATISTICAL PROBABILITY
U PROBABILITY THEORY

STATISTICAL TESTS
NT KOLMOGOROFF-SMIRNOFF TEST
NT RANK TESTS
Probability distribution of leadtime demand
[AD-A144952] 01 p0113 N85-10766
Neuro-linguistic programming: Eye movements as indicators of representational systems
[AD-A147541] 07 p1016 N85-16454
Prematurely terminated sequential tests for MIL-STD 781C
[AD-A148417] 08 p1216 N85-17657
Reduction to outside the atmosphere and statistical tests used in Geneva photometry 08 p1251 N85-17902
The asymptotic behavior of the likelihood ratio statistic for testing a shift in mean in a sequence of independent normal variates
[AD-A149329] 10 p1550 N85-19779
A non-parametric probability density estimator and some applications
[AD-A151853] 15 p2641 N85-26287
Asymptotic expansions of the distribution of test statistics associated with several two parameter exponential distributions
[AD-A151906] 15 p2641 N85-26289
An empirical comparison of the accuracy of univariate and multivariate corrections for range restriction
[AD-A153071] 17 p3019 N85-28670
A collection of probability distributions
[AD-A153128] 17 p3025 N85-28704
Effect of some estimators on a large sample approximation to the non-null distribution of the pearson chi-square statistic
[AD-A153515] 18 p3173 N85-29673
Detection of multivariate outliers with dispersion slippage in elliptically symmetric distributions
[AD-A153785] 18 p3174 N85-29677
Corrosion fatigue cooperative testing program statistical analysis
[AD-A153886] 19 p3238 N85-30077
Performance envelopes and optimal appropriateness measurement
[AD-A154129] 19 p3330 N85-30629
Equipercentile test equating: The effects of presmoothing and postsmoothing on the magnitude of sample-dependent errors
[AD-A154110] 19 p3347 N85-30746

STATISTICAL WEATHER FORECASTING
A short-term forecast model for thunderstorm rotation
01 p0061 N85-10542
Short-term forecasting using a REMOS approach -- regime model output statistics (REMOS)
01 p0061 N85-10544
On probability forecasts for temperature
01 p0064 N85-10565
Severe weather statistics STADTS decoder (SXW) and plotter (SWY)
[PB84-213693] 01 p0086 N85-10576
Forecast of the northeastern drought by the method of periodicities: Use and abuses
[INPE-3109-PRE/506] 02 p0230 N85-11502
Statistical interpretation of NWP model output: An overview of techniques used and results achieved
[REPT-551.509.313] 02 p0231 N85-11503
Development of guidance forecasts at the Royal Netherlands Metorological Institute (KNMI). Part 1: General information
[KNMI-TR-54-PT-1] 08 p1190 N85-17499
Development of guidance forecasts at the Royal Netherlands Meteorological Institute (KNMI). Part 2: Extreme wind speed at IJmuiden
[KNMI-TR-54-PT-2] 08 p1190 N85-17500
On the relationship between maximum surface temperature and various parameters; with reference to objective forecasting
[KNMI-TR-58] 12 p1897 N85-21906
A weather service for agriculture
16 p2830 N85-27450
On the interannual variability of the Indian monsoon and the Southern Oscillation 20 p3495 N85-31728
An evaluation of discretized conditional probability and linear regression threshold techniques in model output statistics forecasting of cloud amount and ceiling over the North Atlantic Ocean
[AD-A155100] 21 p3636 N85-32581
Tunisian climate seen through a Markov process
[CT-585] 23 p3950 N85-34482
An atmospheric boundary layer model forced by the operational ECMWV-model
[WSR-3] 24 p4120 N85-35541
Users guide for optimum interpolation method of global data assimilation
[AD-A155929] 24 p4138 N85-35648
Two methods of global data assimilation
[AD-A155961] 24 p4143 N85-35684

STATISTICS
Computer equipment for research in statistics
[AD-A145755] 03 p0406 N85-1259
On the weak limits of elementary symmetric polynomials
[CWI-MS-R8407] 05 p0719 N85-14620
Principal curves and surfaces
[AD-A148833] 09 p1375 N85-18646

STATOR BLADES
Study of controlled diffusion stator blading
[NASA-CR-167995] 09 p1281 N85-18058
Development of a rotor wake-vortex model, volume 1
[NASA-CR-174849] 16 p2699 N85-26886

STATORS
Energy efficient engine component development and integration program
[NASA-CR-170034] 02 p0146 N85-10980
Analysis for leakage and rotordynamic coefficients of surface roughened tapered annular gas seals
05 p0644 N85-14135
Development of a Navier-Stokes rotor and stator analysis
[AD-A146967] 07 p0958 N85-16070
Magnetic noise in single-machine rotating frequency converters 13 p2077 N85-22[illegible]
Transient technique for measuring heat transfer coefficients on stator airfoils in a jet engine environment
[NASA-TM-87005] 15 p2560 N85-25794
Spacer structure
[AD-D011641] 17 p2897 N85-27896
Damping seal for turbomachinery
[NASA-CASE-MFS-25342-2] 19 p3280 N85-30341
Induction motors with minimum waste of magnetic iron
22 p3772 N85-33377

Magnetic field and equivalent circuit of induction motors with shielded poles 22 p3772 N85-33578

STAYS
U GUY WIRES

STEADY FLOW
NT COUETTE FLOW

A perturbation solution for rigid dumbbell suspensions in steady shear flow
[AD-A144876] 01 p0111 N85-10755

Random processes and magnetohydrodynamic turbulence 02 p0271 N85-11767

Numerical calculation of steady turbulent flows in adverse pressure gradients
[CFD/83/9] 04 p0501 N85-13195

Bicomponent flow problems in rheological fluid mechanics 05 p0635 N85-14073

An experimental study of airfoil-spoiler aerodynamics
[NASA-CR-177328] 06 p0748 N85-14796

Dynamic response of electromagnetic current meters
[PB84-229731] 06 p0842 N85-15344

Contamination and distortion of steady flow field induced by discrete frequency in aircraft gas turbines
[AD-A147092] 07 p0958 N85-16073

Existence of slow steady flows of viscoelastic fluids with differential constitutive equations
[AD-A147240] 07 p0959 N85-16077

Steady flow model user's guide
[DE85-002001] 08 p1163 N85-17337

On the shedding of vorticity at separation
[AD-P004166] 09 p1265 N85-17951

Theoretical investigation of dynamic stall using a momentum integral method
[AD-P004170] 09 p1266 N85-17955

A turbulent closure model for the free atmosphere
09 p1351 N85-18502

Recent developments and open problems in the mathematical theory of viscoelasticity
[AD-A149043] 10 p1545 N85-19742

Generation of sound by a vortex point in a steady flow of slightly compressible fluid 11 p1715 N85-20789

The split-coefficient matrix method for supersonic three dimensional flow 12 p1821 N85-21425

Internal fluid mechanism of solid propellant rocket motors 13 p2001 N85-22544

Stabilization of steady motion of mechanical systems
14 p2280 N85-24122

An analytical and numerical study of the interaction of rarefaction waves with area changes in ducts. Part 2: Area enlargements
[UTIAS-273] 14 p2300 N85-24242

Contribution to the theory of stationary separation areas
[NASA-TM-77825] 14 p2300 N85-24244

Nonlinear problems in flight dynamics involving aerodynamic bifurcations
[NASA-TM-86706] 15 p2462 N85-25206

Pseudo-unsteady systems for steady inviscid flows
[ESA-TT-877] 15 p2558 N85-25782

Boundary layer at moving cylinder surface
16 p2765 N85-27084

Upwind-difference methods for aerodynamic problems governed by the Euler equations
[REPT-84-23] 17 p2893 N85-27834

Method of calculating separation flow of subsonic gas stream around wings 17 p2942 N85-28161

Steady, incompressible, inviscid flow through a finite collapsible tube under longitudinal tension
[REPT-84-01] 17 p2959 N85-28278

The method of residual minimization in compressible steady flows
[AD-A153924] 18 p3100 N85-29193

Numerical simulation of potential flow in transonic steady regimes 20 p3369 N85-31016

Data set 9: LANN wing. Pitching oscillation
20 p3390 N85-31030

High Re separated flow solutions using the Navier-Stokes and approximate equations
[AD-A152252] 20 p3454 N85-31451

Optimization of a numerical method to calculate elliptic flows
[ESA-TT-889] 20 p3457 N85-31472

STEADY STATE

Three degree of freedom steady state point performance program: Updated version 1
[CSIR-NIAST-83/48] 01 p0001 N85-10005

Forced vibrations of friction-damped beam structures in two dimensions
[UDR-TM-82-08] 04 p0456 N85-12892

Multiple steady states for characteristic initial value problems
[NASA-CR-172486] 06 p0749 N85-14800

Effect of steady-state temperature distortion on inlet flow to a high-bypass-ration turbofan engine
[NASA-TM-86896] 07 p0904 N85-15725

On vortex transport in turbine channels
09 p1308 N85-18217

Identification of vibration parameters of flexible structures 09 p1331 N85-18360

Permanent magnet motors
[DE85-000860] 10 p1482 N85-19355

Initial testing of a variable-stroke Stirling engine
[NASA-TM-86875] 10 p1569 N85-19895

A simple model of electron beam initiated dielectric breakdown 13 p1996 N85-22516

Internal fluid mechanism of solid propellant rocket motors 13 p2001 N85-22544

Confidence intervals using the regenerative method for simulation output analysis
[AD-A150147] 13 p2149 N85-23343

A research program in active control/aeroelasticity
[NASA-CR-175674] 14 p2218 N85-23752

Stability of steady modes of motion by axis of rotating wheel in nonlinear bearings 14 p2279 N85-24117

Stability of permanent rotation modes of asymmetric heavy solid body 14 p2279 N85-24118

Stability of steady motions of dynamically symmetrical solid at a triangular libration point
14 p2279 N85-24120

Stabilization of steady motion of mechanical systems
14 p2280 N85-24122

Ergodicity and Steady-State-Equilibrium conditions for Markov chains
[AD-A151038] 14 p2409 N85-24854

Steady state solution of the Fokker-Planck equation combined with unidirectional quasilinear diffusion under detailed balance conditions
[DE85-004917] 14 p2425 N85-24959

Is there more than one steady state for NOx?
15 p2687 N85-26593

Rotor blade flap-lag stability and response in forward flight in turbulent flows 16 p2705 N85-26886

Numerical analysis of flow non-uniformity in the hot gas manifold of the Space Shuttle main engine
16 p2738 N85-26899

Luminescence probe studies of ionomers. I: Steady-state measurements from nafion membrane
[AD-A152475] 17 p3029 N85-28730

Limit theorems for the method of replication
[AD-A153541] 18 p3170 N85-29642

Stationary properties and switching characteristics of dispersive optical bistability in CuCl
18 p3186 N85-29763

Steady-state spheromak reactor studies
[DE85-009585] 19 p3372 N85-30916

Aspects of silicon bulk lifetimes
20 p3479 N85-31617

MPS solidification model. Analysis and calculation of macrosegregation in a casting ingot
[NASA-CR-171589] 21 p3566 N85-32178

Weak shock waves propagating in fluid-gas mixtures
[AD-A154759] 21 p3584 N85-32276

Radar echoes at 2.66 and 40.92 MHz from the mesosphere, part 2.6A 21 p3619 N85-32486

Generalized formulation of a class of explicit and implicit TVD schemes
[NASA-TM-86775] 21 p3675 N85-32830

On the dependence of the convergence of Gummel's algorithm on the regularity of the solution
[AD-A154626] 21 p3675 N85-32832

Quasi-steady-state melting mode during combined laser irradiation of semiconductor materials
21 p3682 N85-32874

Establishment of steady-state power level in pulse-periodic excimer laser 21 p3685 N85-32896

A system of magnetohydrodynamic-type equations
21 p3693 N85-32946

On one nonlinear problem of laser thermochemistry
21 p3697 N85-32971

Chemical evolution of the Earth: Equilibrium or disequilibrium process? 21 p3721 N85-33088

Soft X-ray polychromator for the Solar Maximum Mission
[NASA-CR-175297] 21 p3723 N85-33096

Scientific Opportunities with Advanced Facilities for Neutron Scattering
[DE85-012113] 22 p3839 N85-33770

Transports studies of ECH and ICRH-heated bumpy torus plasma in NBT-1M 23 p3978 N85-34662

Analytic and numerical calculations of the ambipolar electric field in a stellarator 23 p3978 N85-34665

Numerical descriptions of cosmic-ray transport
[SH-4.1-3] 23 p4004 N85-34829

The 1973-1984 solar modulation of cosmic ray nuclei
[SH-4.1-16] 23 p4006 N85-34836

Exact solutions for sporadic acceleration of cosmic rays
[OG-8.3-7] 23 p4022 N85-34925

Stochastic particle acceleration in flaring stars
[OG-8.3-9] 23 p4022 N85-34927

The geostatistical approach to the inverse problem in two-dimensional steady state groundwater modeling
24 p4107 N85-35462

STEADY STATE CREEP

Transverse vibration and buckling of a cantilevered beam with tip body under constant axial base acceleration
[NASA-CR-175567] 12 p1864 N85-21694

Steady-state reaction of three-layered cylindrical shell to effect of moving load 13 p2047 N85-22611

Short term determination of the creep properties of high temperature materials
[CRIF-MT-160] 20 p3432 N85-31288

Design and fabrication of durable owner-built wind turbine blades
[DE85-009200] 20 p3484 N85-31650

STEADY STATE FLOW
U EQUILIBRIUM FLOW

STEAM

Solid electrolytes for medium temperature steam electrolysis
[DE84-014384] 04 p0463 N85-12938

Hydrogen production employing high-temperature solid oxide cells
[DE84-014559] 06 p0786 N85-14901

Open-cycle vapor compression heat pump
[PB85-101475/GAR] 06 p0775 N85-14951

Experiment on triggered fragmentation on a molten copper droplet in water
[BLL-WH-602-(9091.9F)] 08 p1125 N85-17091

Hydrogen flame acceleration and transition to detonation
[DE85-000611] 12 p1802 N85-21299

Steam generator tube vibration tests
[DE85-003599] 12 p1867 N85-21712

Experimental study of steam condensation on water in countercurrent flow in presence of inert gases
[DE84-013028] 12 p1881 N85-21800

Dependents of velocity distribution in exit section of converging channel on shape of inlet channel in regulating valve 14 p2277 N85-24106

Response of steam-water mixtures to pressure transients
[DE85-010798] 19 p3267 N85-30262

Geothermal hydrogen and health in Rotorua, New Zealand
[DE85-901283] 19 p3301 N85-30467

Film condensation of steam on externally finned horizontal tubes
[AD-A155642] 21 p3585 N85-32285

Method for determining depth and shape of a sub-surface conductive object
[DE85-006502] 23 p3935 N85-34389

Control system for fluid heated steam generator
[DE85-005734] 23 p3939 N85-34417

Calculations on the feasibility of ultrasonic inspection of steam generator tubing in pressurized water reactors
[AERE-R-10960] 23 p3940 N85-34419

Downstream behavior of volatile fission product species
[DE85-012124] 23 p3971 N85-34617

Pressure measurements in a hydrogen combustion environment: Hydrogen-air combustion test series 1 and 2 in the FITS tank, volume 1
[TI85-009899] 24 p4076 N85-35259

Heat transfer coefficients for particles in liquid in axially rotating cans 24 p4093 N85-35370

Steamflood pilots in the O'Connell Ranch field and the T-4 Ranch field
[DE85-901363] 24 p4108 N85-35468

STEAM GENERATORS
U BOILERS

STEAM TURBINES

Advanced technology cogeneration system conceptual design study: Closed cycle gas turbines
[NASA-CR-168222] 07 p0992 N85-16300

Low leakage turbine shaft seals for advanced combined cycle systems
[AD-A149372] 10 p1492 N85-19420

Development and test of a high COP Rankine heat pump for generation of process steam. Phase 2: Fabrication and test
[DE85-002600] 11 p1632 N85-20275

Axial bearings with lever-type equalizer system
14 p2267 N85-24048

Group technology for working turbine drive wheel disks 14 p2269 N85-24061

Selection of bearing type for large steam turbines
14 p2271 N85-24069

Estimating defectiveness buildup during service in metal of welded runner in low-pressure cylinder of turbine
14 p2271 N85-24070

Some problems in improving reliability and accuracy of regulators with hydraulic amplifiers in main channel of power turbine 14 p2271 N85-24071

Stability of turbine runners in sliding bearings under external circulation forces 14 p2272 N85-24074

Causes and means of prevention of erosion of exit edges of drive vanes in final stages of K-300-240 turbine
14 p2272 N85-24076

Computer code calculations of the TMI-2 accident: Initial and boundary conditions [DE86-012813] 24 p4140 N85-35666

STEEL STRUCTURES

Delayed fracture of high-strength steels in spherical tanks for LP gas [BLL-RISLEY-TR-4926-(9091.9F)] 01 p0026 N85-10162

The use of vanadium in low alloy structural steels 02 p0180 N85-11207

Processes to increase the fatigue life of constructions with already initiated cracks 05 p0650 N85-14176

Mechanical properties of Shielded Metal Arc (SMA) and Submerged Arc (SA) welded joints for quenched and tempered steel StE 470. [VTT-319] 09 p1328 N85-18346

Investigation of steel structures ucing ultrasonic waves [BR93258] 13 p2101 N85-23091

Pressure welding of corrosion-resistant steel with AMg6 aluminum 15 p2501 N85-25426

Durability of joints of 30KhGSA and 12Kh18N10T steels made by diffusion welding 15 p2501 N85-25428

Welding technology and organisation in steel construction 15 p2566 N85-25828

Effects of the phase compositions of cast low-pearlite steels micro-alloyed with vanadium and titanium of their structure and properties [BLL-BISI-TRANS-22301-(9022.06)] 17 p2928 N85-28067

Initial imperfection surveys on conical shells at Hoechst AG [VTH-LR-407] 17 p2981 N85-28429

Experimental and theoretical assessment of a new technique for the non-destructive evaluation of laminated panels [AD-A155622] 21 p3562 N85-32155

Monotonous stress-strain properties of structural steel subjected to nonstationary repetitive pre-loading 23 p3904 N85-34185

Safety and reliability of steel structural materials under random service impact loads 23 p3906 N85-34197

STEELS
NT AUSTENITIC STAINLESS STEELS
NT CARBON STEELS
NT CHROMIUM STEELS
NT FERRITIC STAINLESS STEELS
NT HIGH STRENGTH STEELS
NT LOW CARBON STEELS
NT MARAGING STEELS
NT MARTENSITIC STAINLESS STEELS
NT NICKEL STEELS
NT STAINLESS STEELS

Material degradation in heavy steel plates caused by bending with a laser [AD-A144784] 01 p0052 N85-10343

The effect of 2 strength reducing techniques on the ultimate tensile strength of AISI 4130 steel: Rocket motor case venting [AD-A145526] 02 p0169 N85-11134

Energy-saving technological methods of obtaining controlled atmospheres [BLL-M-35724-(5828.4)] 02 p0171 N85-11145

A method for evaluating the contamination of steel in relation to the solidification curve [BLL-M-35735-(5828.4)] 02 p0175 N85-11171

Rapid solidification of steels: Model and commercial alloys 02 p0176 N85-11184

Design of strong, ductile, duplex low alloy steels 02 p0177 N85-11189

The adhesion of hard and wear resistant coatings 02 p0179 N85-11203

The constitution as the basis for recent and future developments of wear resistant materials 02 p0179 N85-11205

Recent developments on the role of molybdenum in irons and steels 02 p0180 N85-11206

The use of vanadium in low alloy structural steels 02 p0180 N85-11207

An investigation into the superhardening effect in molybdenum-free steel with specific reference to alloy substitution 02 p0180 N85-11209

The influence of rare Earth elements on the temper embrittlement behaviour and mechanical properties of a low alloy steel 02 p0180 N85-11210

The determination of soluble and insoluble boron in steel by emission spectrometry using an inductively coupled plasma and a scanning monochromator 02 p0180 N85-11211

The role of molybdenum as an alloy element in adhesive wear resistance 02 p0181 N85-11212

Contributions to the 7th International Acoustic Emission Symposium [AD-A145368] 02 p0275 N85-11792

Stress corrosion of pressure vessel steel A533-B in high temperature water [BLL-RISLEY-TR-4600-(9091.9F)] 03 p0330 N85-12125

Weld metal solidification cracking in a carbon-manganese steel 03 p0330 N85-12126

Mechanical properties of a leaded, resulfurized, rephosphorized steel in various thermo/mechanical conditions [PB84-216464] 03 p0333 N85-12144

Related studies to cathodic protection of reinforced concrete structures [PB84-218114] 03 p0333 N85-12145

Causes of strength reduction in welded titanium-steel joints 03 p0352 N85-12262

Evaluation of ferritic alloy Fe-2 1/4Cr-1Mo after neutron irradiation: Irradiation creep and swelling [DE84-014647] 04 p0474 N85-13022

Corrosion resistance of nitrided low-alloy steels [PB84-235027] 04 p0477 N85-13040

Effect of lubricant extreme-pressure additives on surface fatigue life of AISI 9310 spur gears [NASA-TP-2406] 04 p0507 N85-13234

Response of ferritic steels to nonsteady loading at elevated temperatures [DE84-014280] 04 p0513 N85-13272

Impact toughness of wire after cold deformation and annealing [BLL-M-35941-(5828.4)] 05 p0615 N85-13930

Reproducibility of readings from oxygen concentration elements [BLL-M-35920-(5828.4)] 05 p0616 N85-13941

Inclusion formation during solidification of steels with improved machinability [BMFT-FB-T-84-160] 05 p0619 N85-13957

Fatigue behavior of sintered steels and measurement criteria for sintered prefabricated parts 05 p0650 N85-14174

Influence of the shape and distribution of inclusions of the fatigue strength of bearing steels in rotary bending [BLL-PNR-90243-(8019.3153)] 06 p0768 N85-14912

Strain rate effects and temperature history effects for three different tempers of 4340 VAR steel [AD-A146372] 06 p0768 N85-14915

Improvement of the ladle deoxidizing of Al-killed steel [BMFT-FB-T-84-172] 06 p0769 N85-14923

Measuring the corrosion rate of reinforcing steel in concrete [PB84-244532] 06 p0770 N85-14925

Effect of crack-tip region constraint on fracture in the ductile-to-brittle transition [PB84-237395] 06 p0770 N85-14926

Effect of external magnetic field on characteristics of current-carrying steel tape 06 p0788 N85-15034

Prediction of forming limit diagrams for deep drawing 06 p0796 N85-15089

Characterizing X-ray machines [AD-A146532] 06 p0862 N85-15481

Testing of non-alloyed and low-alloyed steels for their behaviour with respect to intercrystalline stress corrosion cracking [BLL-RISLEY-TR-4546-(9091.9F)] 07 p0925 N85-15861

Comparison of the sensitivities of ultrasonic, radiographic and acoustic emission test methods for the examination of a thick weld [BLL-RISLEY-TR-4547-(9091.9F)] 07 p0975 N85-16194

A hydrogen partitioning model for hydrogen assisted crack growth [AD-A147385] 07 p0978 N85-16214

Verification of the fatigue properties of (small) wind turbines [NLR-MP-83055-U] 07 p0994 N85-16311

Effect of microstructure and trapping on the hydrogen embrittlement susceptibility of a ti-bearing HSLA steel [AD-A148610] 08 p1130 N85-17122

Electrodes for repairing power engineering equipment made from creep resisting steel [BLL-CE-TRANS-8064-(9022.09)] 08 p1167 N85-17360

Implantation of Ti + C for reduced friction and wear of steels [DE85-001606] 09 p1295 N85-18135

Effect of temperature on the stress-relaxation response of a pressure vessel steel [TI85-003588] 09 p1339 N85-18424

Results of an EPRG round robin test programme with DWTT specimens — drop weight test (DWTT);pipe steels [ERS-E.365] 09 p1341 N85-18432

New method for heat treatment of metals 10 p1446 N85-19110

Influence of laser hardening on mechanical properties of type 45 steel with various preliminary heat treatments 10 p1446 N85-19111

Optimization of production of composite diamond-containing materials using titanium carbide-steel alloys 10 p1446 N85-19113

Fracture resistance of surface layer with technological defects under cyclical loading 10 p1448 N85-19129

Influence of melting conditions on strength of transition zone between steel and composite material 10 p1450 N85-19133

The effect of filler wire and flux compositions on the microstructure and properties of microalloyed steel weld metal [AD-A149529] 10 p1492 N85-19423

USSR report: Materials science and metallurgy [JPRS-UMS-84-005] 11 p1597 N85-20044

Method of constructing diagram of bimetal fatigue failure 11 p1599 N85-20058

Residual stress after laser processing 11 p1600 N85-20065

Effect of silicon and titanium properties on Ni8Co9Mo5Ti steel 11 p1601 N85-20069

Distribution of hydrogen in multi-layer welded joints of alloyed steels 11 p1603 N85-20079

Hydrogen attack of steel [DE85-002645] 11 p1606 N85-20113

Ion-beam nitriding of steels [NASA-CASE-LEW-14104-1] 12 p1805 N85-21324

Hydrogen embrittlement of cadmium-plated ultra-high strength steels in paint strippers [ARL/MAT-R-117] 12 p1806 N85-21326

Characterization of lubricated bearing surfaces operated under high loads [NASA-TM-86964] 12 p1811 N85-21357

Steel castings by the electroslag casting technique [DE85-003812] 12 p1819 N85-21409

Delayed cracking strength of experimental grades of 42 CD 4 steel in aqueous H2S surroundings [BLL-T6419/BG/LRS/LRST738/84] 13 p2020 N85-22658

USSR report: Materials science and metallurgy [JPRS-UMS-85-002] 13 p2025 N85-22688

Specifics of laser heat treatment of high steel tools 13 p2029 N85-22714

Comparison of dynamic-tension and constant-load strength characteristics of heat-resistant materials 13 p2030 N85-22722

Mechanical properties and brittle fracture resistance of welded multilayer elements for high pressure vessels 13 p2033 N85-22736

Structure and mechanical characteristics of heterogeneous joints produced by laser welding 13 p2034 N85-22742

New tooling for plasma cutting technology 13 p2051 N85-22842

Case depth on flanks of gears for helicopter gearboxes 14 p2222 N85-23780

The effect of water chemistry on the rates of hydrogen generation for galvanized steel corrosion at post-loca conditions [NUREG/CR-3361] 14 p2253 N85-23960

Fracture toughness of HY-130 steel weld metals [AD-A150841] 14 p2255 N85-23976

Laser cutting: A new tool for shipbuilding 14 p2308 N85-24285

Titanium diffusion method prevents metal corrosion 15 p2514 N85-25510

The influence of abrasive blast cleaning and corrosion inhibitors on protective paint coatings 15 p2517 N85-25522

Electrically conductive polymer concrete overlays [DE85-006728] 15 p2522 N85-25549

Studies of ferritic filler metals for welding 9 percent nickel steel 15 p2565 N85-25825

Compositional control of plate steels 15 p2565 N85-25826

SHAFT: Interactive shaft design program [DE85-007333] 15 p2568 N85-25850

Sizing capability of automated ultrasonic time-of-flight diffraction in thick section steel and aspects of reliable inspection in practice [AERE-R-11548] 15 p2571 N85-25855

The effect of overload cycles on fatigue crack propagation in structural steels 15 p2577 N85-25897

Grain boundary composition and intergranular fracture of steels. Volume 1: Detection of grain boundary segregation in steels [DE85-006850] 15 p2662 N85-26428

Rolling contact fatigue life of chromium ion plated 440C bearing steel 16 p2736 N85-26802

Determination of permissible heating rate of metal [BLL-M-36107-(5828.4)] 16 p2748 N85-26857

Study of oscillations of composite cylindrical shells using a dynamic stiffness technique 16 p2766 N85-27066

Full statistical characteristics of microdeformation
[BLL-M-36076-(5828.4)] 16 p2798 N85-27254

An X-ray study of residual stresses in narrow groove TIG weldments
[DE85-006485] 16 p2802 N85-27274

Weldability of micro-alloy steels as reaction of structure and inclusions
[BLL-BISI-TRANS-22196-(9022.06)] 17 p2924 N85-28027

Physio-chemical mechanisms of the processes of the formation of globular inclusions in ball-bearing metal
[BLL-BISI-TRANS-22235-(9022.06)] 17 p2924 N85-28030

Forming of coating protection system: Mechanism of paint-coating anti-corrosion protection of steel
[BLL-BISI-TRANS-22081-(9022.06)] 17 p2925 N85-28033

Corrosion characteristics of some steels produced through a self-cleaning rotating electrode
[BLL-BISI-TRANS-22046-(9022.06)] 17 p2925 N85-28034

Thermomechanical softening treatment for bearing and tool steels
[BLL-BISI-TRANS-22432-(9022.06)] 17 p2925 N85-28035

X-ray crystallography of steel U8 after pulsed laser hardening
[BLL-BISI-22444-(9022.06)] 17 p2925 N85-28038

Steels with improved machinability
[BLL-BISI-22341-(9022.06)] 17 p2927 N85-28061

Textural transformations taking place during heat and mechanical treatment in triplex steels
[BLL-BISI-TRANS-22404-(9022.06)] 17 p2927 N85-28063

Microstructure and mechanical properties of rare-earths-microalloyed high-speed tool steel
[BLL-BISI-TRANS-22043-(9022.06)] 17 p2928 N85-28064

Physical properties of steels and their temperature dependence
[BLL-BISI-TRANS-22285-(9022.06)] 17 p2928 N85-28065

Study on mechanism of surface deformation induced by stress corrosion cracking
[BLL-BISI-TRANS-21896-(9022.06)] 17 p2928 N85-28066

Influence of structural state and alloy content of austenite on formation of martensitic phases in steels
[BLL-BISI-TRANS-22385-(9022.06)] 17 p2928 N85-28068

Effect of the agressive action of soil on metallic pipelines. New possibilities for the passive and active corrosion protection
[BLL-BISI-TRANS-21630-(9022.06)] 17 p2928 N85-28070

Influence of manganese and heat treatment on structure and properties of Fe-0.1 percent-C-14 percent Cr-based steels
[BLL-BISI-TRANS-22299-(9022.06)] 17 p2928 N85-28071

Part played by non-metallic inclusions during deformation and fracture of steel with different grain sizes
[BLL-BISI-TRANS-22321-(9022.06)] 17 p2928 N85-28072

Influence of eutectic silicate inclusions on micro-processes during deformation and fracture of 12GS steel
[BLL-BISI-TRANS-22296-(9022.06)] 17 p2929 N85-28073

Examination of steels by chemical analysis for quality assurance
[BLL-BISI-TRANS-22068-(9022.06)] 17 p2929 N85-28074

Influence of preliminary thermomechanical treatment on depth and hardness of nitrided layers
[BLL-BISI-TRANS-22488-(9022.06)] 17 p2929 N85-28078

Mechanical stabilization of austenite against epsilon martensite and its effect on deformation behavior in high manganese steels
[DE85-007654] 17 p2932 N85-28097

Temperature and manganese content dependences of tensile deformation in iron-high manganese binary alloys
[DE85-007656] 17 p2932 N85-28098

Hydrogen degradation of pipeline steels
[DE85-008930] 17 p2932 N85-28101

Welding of 11 458.1 steel in shielding atmospheres
[BLL-BISI-TRANS-21763-(9022.06)] 17 p2972 N85-28353

Submerged arc welding of new Czechoslovak micro-alloy steels
[BLL-BISI-TRANS-22193-(9022.06)] 17 p2972 N85-28356

Application of 4-wire submerged arc method to welding UOE pipe
[BLL-BISI-TRANS-22417-(9022.06)] 17 p2972 N85-28358

Examples of application of machinability tests
[BLL-BISI-TRANS-22346-(9022.06)] 17 p2973 N85-28363

Assessing the machinability of gearwheel steels during manufacture
[BLL-BISI-TRANS-22343-(9902.06)] 17 p2973 N85-28365

Steel Tubes
[BLL-BISI-TRANS-22084-(9022.06)] 17 p2973 N85-28369

Quality testing to the specifications of the Stahl-Eisen-Pruefblatt 1570/71 using an automatic image analysis system
[BLL-BISI-TRANS-22253-(9022.06)] 17 p2976 N85-28385

Tests of low-cycle fatigue of elected steels of class 11
[BLL-BISI-TRANS-22039-(9022.06)] 17 p2978 N85-28404

On validity of threshold values of fatigue strength of steel structures
[BLL-BISI-TRANS-22192-(9022.06)] 17 p2978 N85-28408

Investigations of the material factors in the adiabatic shearing of steels
[AD-A153084] 17 p2979 N85-28418

Critical conditions for failure in materials subjected to high rates of loading
[AD-A153135] 17 p2980 N85-28420

World iron ore reserves
[BLL-BISI-TRANS-22280-(9022.06)] 17 p2983 N85-28435

Strength versus toughness relation in Fe-high manganese alloys
[DE85-007682] 18 p3074 N85-29013

Specimen thickness effects for elastic-plastic CTOD toughness of A36 steel
[DE85-006992] 18 p3077 N85-29038

Magnetic steels with the lowest specific total losses
[BMFT-FB-T-84-263] 18 p3078 N85-29042

Behavior of reinforced concrete at elevated temperatures
[DE85-009032] 18 p3123 N85-29332

Effect of matrix composition on steel fiber reinforced concrete properties 19 p3230 N85-30028

Welding of steel-aluminum cooling panels for the holds of refrigerator vessels 19 p3246 N85-30129

Study of intermediate velocity penetration of steel spheres into deep aluminum targets
[DE85-010419] 19 p3287 N85-30385

Contribution to the modelling of the gas carburizing process for steels
[BLL-OA-TRANS-3205-(6196.300)] 20 p3428 N85-31263

Effects of humidity cycles on the corrosion of galvanised reinforcements in carbonated and uncarbonated mortars
[BLL-CE-TRANS-8039-(9022.09)] 20 p3430 N85-31272

Joining of sintered composite TiC-steel materials by welding
[BLL-M-36253-(5828.4)] 20 p3461 N85-31502

Investigation of fatigue strength of spring steel after high-temperature thermomechanical working (HTMW) by helical drawing
[BLL-M-36274-(5828.4)] 20 p3465 N85-31525

Theoretical modelling of the electro-chemistry in a corrosion fatigue crack. Part 2: Mathematical aspects of associated unsteady reaction equations
[NPL-DMA(A)-100-PT-2] 20 p3465 N85-31529

Assessment of dynamic test methods for the measurement of fracture toughness — steels
[OUEL-1561/85] 20 p3470 N85-31565

Decomposition of sulfuric acid using solar thermal energy
[DE85-012288] 21 p3564 N85-32170

Understanding and laboratory prediction of the atmospheric corrosion behavior of steels and of non-ferrous metals and alloys
[AD-A154642] 21 p3566 N85-32179

Development of improved dynamic failure models
[AD-A155686] 21 p3600 N85-32354

Rapid analysis of steels using laser-based techniques
[DE85-010747] 22 p3748 N85-33232

Management of Corrosion
[AGARD-LS-141] 22 p3749 N85-33238

Corrosion management strategies for aircraft and related systems 22 p3749 N85-33239

Induction motors with minimum waste of magnetic iron 22 p3772 N85-33377

The study of the effect of residual microimpurities on the fatigue strength of 55S2 steel
[BLL-M-36317-(5828.4)] 23 p3913 N85-34246

Special features of the fracture of ball-bearing steel close to non-metallic inclusion eutectics
[BLL-M-35809-(5828.4)] 23 p3914 N85-34258

Properties of tungsten-free steel for cutting tools
[BLL-M-35808-(5828.4)] 23 p3915 N85-34259

Chromium-base powder alloys for welding cladding layer of bimetal
[BLL-M-35776-(5828.4)] 23 p3915 N85-34260

The properties of VSt3sp inoculated steel
[BLL-M-35894-(5828.4)] 23 p3915 N85-34263

Hydrogen embrittlement testing
[DE85-007352] 23 p3916 N85-34273

Decomposition of martensite in R6M5 and R6AM5 steels after direct immersion in liquid nitrogen
[BLL-M-36305] 24 p4077 N85-35268

Tests on zirconium nitride coatings applied to SW 18 steel using the chemical vapor deposition method 24 p4078 N85-35271

The dynamic strain ageing of A533B class 1 nuclear pressure vessel steel
[AERE-R-11485] 24 p4078 N85-35274

The character of observed porosity and its possible effects on rolling contact fatigue life of M-50 steel
[AD-A155930] 24 p4079 N85-35279

Effect of prior warm rolling on the retained austenite content and hardening response of VIM-VAR (vacuum-induction melted-vacuum-arc remelted) AISI M-50 steel
[AD-A156145] 24 p4079 N85-35281

STEEP GRADIENT AIRCRAFT
U V/STOL AIRCRAFT

STEEPEST ASCENT METHOD
U STEEPEST DESCENT METHOD

STEEPEST DESCENT METHOD

Use of shanks transformation for speeding up adaptation process in antenna arrays 07 p0951 N85-16029

Some plant location problems — computer networks
[FUB-14-1984] 22 p3835 N85-33746

STEEPNESS
U SLOPES

STEERABLE ANTENNAS

Simulation of the performance of adaptively controlled Navstar antennas in battlefield scenarios 10 p1472 N85-19292

An electronically-steerable active receiving array for h.f.
[BBC-RD-1985/2] 12 p1822 N85-21430

Concepts and cost trade-offs for land vehicle antennas in satellite mobile communications
[NASA-CR-175731] 15 p2540 N85-25680

A simulation study of jammer nulling trade-offs in a reactively steered adaptive array
[AD-A153461] 18 p3090 N85-29124

A planar version of a 4.0 gigahertz reactively steered adaptive array
[AD-A156029] 24 p4087 N85-35330

STEERING

Tracking servo compensator with rate aiding
[AD-D011372] 07 p0942 N85-15971

Development of a soil-wheel interaction model
[AD-P004259] 09 p1404 N85-18835

The guidelines to design the lever turning gears in articulated vehicles
[AD-P004301] 09 p1409 N85-18878

Study on controllability and stability of high speed tracked vehicles
[AD-P004302] 09 p1409 N85-18879

Forces on undriven, angled wheels
[AD-P004303] 09 p1409 N85-18880

Influence of tire on resistance and steering forces of tires
[AD-P004306] 09 p1410 N85-18883

Basic study on the turning resistance of track
[AD-P004307] 09 p1410 N85-18884

Study on steerability of articulated tracked vehicles
[AD-P004308] 09 p1410 N85-18885

Skid steering of wheeled and tracked vehicles: Analysis with Coulomb friction assumptions
[AD-A149826] 12 p1860 N85-21664

Practicality of electronic beam steering for MST/ST radars, part 6.2A 21 p3624 N85-32516

Iris tilting and RF steering in the SLAC Linac
[DE85-011704] 22 p3841 N85-33783

STELLAR (STAR TRACKER)
U CCD STAR TRACKER

STELLAR ACTIVITY
NT FACULAE
NT SOLAR ACTIVITY
NT SOLAR FLARES
NT SOLAR PROMINENCES
NT SOLAR STORMS
NT SPICULES
NT STELLAR FLARES
NT SUNSPOTS

Non-stable motions and instability in stellar associations 05 p0739 N85-14754

Study of the pulsations of the ZZ Ceti stars
09 p1414 N85-18923
The vertical structure and stability of alpha model accretion disks 09 p1417 N85-18936
Radiative ion beams: Hot stellar reactions in the laboratory
[DE85-001570] 11 p1722 N85-20833
Solar and stellar coronal plasmas
[NASA-CR-175623] 13 p2205 N85-23676
Solar and stellar magnetic cycles: Unity and multiplicity 14 p2448 N85-25109
Stellar surface phenomena: A spectroscopic study of the RS canum venaticorum binaries
15 p2669 N85-26467
Activity and magnetic fields on stars from radio observations
[NASA-CR-175966] 18 p3202 N85-29861
Search for stellar collapse with the MACRO detector at Gran Sasso
[HE-5.3-11] 24 p4206 N85-36105

STELLAR ATMOSPHERES
NT CHROMOSPHERE
NT SOLAR ATMOSPHERE
Outer atmospheres of giant and supergiant stars
[NASA-CR-174165] 04 p0580 N85-13703
RS CV sub n binary systems
[NASA-CR-174164] 04 p0580 N85-13704
The distribution of dust in the region of the Rosette Nebula and MON OB2 association
05 p0739 N85-14753
On the content of nitrogen in atmospheres of late giants derived from molecular bands on NH in the UV spectral range 05 p0740 N85-14761
Stability of stellar disk and ratio of halo to disk masses in the galaxy 05 p0740 N85-14763
Theoretical studies of chromospheres and winds in cool stars
[NASA-CR-174204] 06 p0880 N85-15596
Homogeneous condensation of gaseous mixtures of Si, Fe, O, N, and C in relative cosmic abundance and implications for astronomical condensation
06 p0887 N85-15632
The Origin of Nonradiative Heating/Momentum in Hot Stars
[NASA-CP-2358] 08 p1231 N85-17755
Evidence for non-radiative activity in hot stars
08 p1231 N85-17756
Evidence for non-radiative activity in stars with T sub eff 10000 K 08 p1231 N85-17757
Nonthermal radio emission and the HR diagram
08 p1232 N85-17763
Departures from LTE populations versus anomalous abundances: The effects of heating
08 p1234 N85-17776
Is the ratio of observed X-ray luminosity to bolometric luminosity in early-type stars really a constant?
08 p1234 N85-17777
Magnetic effects in the heating and modification of flows in the outer stellar atmospheres with application to early type star case 08 p1235 N85-17783
Summary of the origin of nonradiative heating/momentum in hot stars
08 p1236 N85-17789
Outer atmospheres of cool stars observed with IUE
11 p1744 N85-20968
Carbon, silicon, and oxygen in the white dwarf star GD 40 11 p1752 N85-21017
The solar stellar connection in the far ultraviolet
11 p1757 N85-21055
A progress report on the analysis of long exposure SWP high resolution spectra of cool stars
11 p1758 N85-21057
Active late-type stars and the applicability of coronal loop models 11 p1758 N85-21059
Observations of Cygnus X-3 above 10(15) eV from 1979 - 1984
[OG-2.1-6] 22 p3863 N85-33923
On gamma and neutrino radiation from Cyg X-3
[OG-2.1-7] 22 p3863 N85-33924
X-ray spectra of bursting neutron stars
23 p3981 N85-34686
The HEAO-2 Guest Investigator Program: Non-linear growth of instabilities in line-driven stellar winds
[NASA-CR-176168] 24 p4168 N85-35840

STELLAR COLOR
Ultraviolet studies of the young populous cluster NGC 2100 in the LMC 11 p1748 N85-20995
The color excesses of classical cepheids and the structure of our galaxy 13 p2169 N85-23459

STELLAR COMPOSITION
Collective processes and formation of star clusters
05 p0738 N85-14743
Evolution of globular clusters
05 p0738 N85-14746
On the content of nitrogen in atmospheres of late giants derived from molecular bands on NH in the UV spectral range 05 p0740 N85-14761
Large-scale bubble structure of the interstellar medium (ISM) and properties of the Local Spiral Arm (LSA)
06 p0879 N85-15588
Magellanic cloud objects 11 p1744 N85-20965
The usual hot stars in unusual galaxies
11 p1745 N85-20975
IUE and Voyager observations of very hot O-type subdwarfs 11 p1751 N85-21010
Analysis of high-depression IUE spectra of subdwarf B stars 11 p1751 N85-21011
Ultraviolet and optical spectroscopy and polarimetry of the helium weak star HD 21699: Evidence for a magnetically controlled stellar wind
11 p1759 N85-21065
Magnetospheres and winds in the helium weak stars: Observations of C 5 in upper main sequence CP stars
11 p1759 N85-21066
IUE spectrophotometry of helium weak and silicon stars 11 p1759 N85-21067
Search for stellar collapse with the MACRO detector at Gran Sasso
[HE-5.3-11] 24 p4206 N85-36105

STELLAR CORES
Evolution of globular clusters
05 p0738 N85-14746
Brightness distribution in globular clusters derived by the narrow-slit scanning method
05 p0738 N85-14748
Lessons from the globular cluster NGC 5466
05 p0739 N85-14749
The fate of globular clusters 05 p0739 N85-14751
Solar oscillations 14 p2445 N85-25092
Mixing in the solar interior 14 p2446 N85-25095
Conditions of the small oscillations excitation in the different solar models with the mixed core
14 p2450 N85-25126

STELLAR CORONAS
NT CORONAL LOOPS
NT SOLAR CORONA
Outer atmospheres of giant and supergiant stars
[NASA-CR-174165] 04 p0580 N85-13703
A search for possible members of open clusters among known Ap stars 05 p0737 N85-14740
Stability of stellar disk and ratio of halo to disk masses in the galaxy 05 p0740 N85-14763
Evidence for non-radiative activity in stars with T sub eff 10000 K 08 p1231 N85-17757
Coronal temperatures 08 p1233 N85-17766
The scaling of coronal models from one star to another 08 p1233 N85-17771
Overheated open coronal regions
08 p1234 N85-17772
Non-radiative energy from differential rotation in hot stars 08 p1234 N85-17778
A leaky waveguide model for MHD wave driven winds from coronal holes 08 p1235 N85-17781
X-ray coronae of late type stars: Theoretical implications 11 p1742 N85-20953
Coronal effects of the winds of early-type stars
11 p1749 N85-21002
Solar and stellar coronal plasmas
[NASA-CR-175623] 13 p2205 N85-23676
A program of ground-based astronomy to complement einstein observations
[AD-A151111] 15 p2668 N85-26466
The kinematic and radial properties of normal luminous SC galaxies 20 p3545 N85-32061

STELLAR DOPPLER SHIFT
U DOPPLER EFFECT
U EXTRATERRESTRIAL RADIATION

STELLAR ENVELOPES
Numerical models of the spectral appearance of protostellar envelopes 03 p0442 N85-12816
Shapes of wind driven circumstellar shells
03 p0443 N85-12821
Theoretical studies of chromospheres and winds in cool stars
[NASA-CR-174204] 06 p0880 N85-15596
Active phenomena in the pre-main sequence star AB AUR 08 p1233 N85-17765
IUE and ESO observations of the P Cyg star AG Carinae and its ring nebula 11 p1750 N85-21006
Ultraviolet observations of circumstellar matter in Algol type binary systems 11 p1756 N85-21043
Circumstellar material in Algols and Serpentids
11 p1757 N85-21051
Ultraviolet, radio and X-ray observations of hybrid stars 11 p1759 N85-21063
Electrons and positrons from expanding supernova envelopes in dense clouds
[OG-6.2-9] 22 p3669 N85-34108

STELLAR EVOLUTION
NT STELLAR MASS ACCRETION
Variations of the H and K emission lines of singly ionized calcium in the eclipsing binary star system AR Lacertae
02 p0296 N85-11921
Solar neutrinos: Prospects for detection and implications
[DE84-015522] 02 p0304 N85-11968
Star Formation Workshop
[ROE-OR-13] 03 p0441 N85-12809
Distribution and properties of molecular clouds in the galaxy 03 p0442 N85-12810
Compact infrared sources: Protostars before IRAS
03 p0442 N85-12812
IRAS observations of galactic star formation
03 p0442 N85-12813
Far-infrared observations of some regions of star formation 03 p0442 N85-12814
Open cluster formation --- stellar evolution
03 p0442 N85-12815
Numerical models of the spectral appearance of protostellar envelopes 03 p0442 N85-12816
Spherical accretion onto a protostellar core
03 p0442 N85-12817
Masers associated with regions of recent star formation 03 p0443 N85-12820
Shapes of wind driven circumstellar shells
03 p0443 N85-12821
The rotation of B-type stars and processes of star formation 03 p0443 N85-12823
The significance of comets for star formation
03 p0443 N85-12824
Star formation in interacting galaxies
03 p0444 N85-12826
Infrared mapping of galaxian centers: Star forming regions with kiloparsec scale sizes
03 p0444 N85-12827
Molecules in external galaxies
03 p0444 N85-12828
Future theoretical needs in studies of star formation
03 p0444 N85-12829
Age groups and composite diagrams for young open clusters 05 p0737 N85-1473
The behaviour of brighter binaries and yellow giants in open clusters 05 p0737 N85-1473
The present state of the International Star Cluste Photometry Programme 05 p0737 N85-1474
Binaries and evolution of globular clusters
05 p0738 N85-1474
Evolution of globular clusters
05 p0738 N85-1474
Evolution of globular clusters
05 p0738 N85-1474
Non-stable motions and instability in stella associations 05 p0739 N85-1475
The evolution of a sparse stellar system
05 p0740 N85-1475
The fragmentation of molecular clouds and the IMF
05 p0740 N85-1475
On the content of nitrogen in atmospheres of late giant derived from molecular bands on NH in the UV spectra range 05 p0740 N85-1476
The velocity-age relation for B and A stars
05 p0740 N85-1476
Kinematics of B and A stars 05 p0741 N85-147
The correlation between excitation parameter an nebular luminosity for galactic HII regions with applicatio to regions of star formation in M83
05 p0743 N85-1477
The relevance of QUASAT to the star formatio problem 07 p1058 N85-1671
The Origin of Nonradiative Heating/Momentum in Ho Stars
[NASA-CP-2358] 08 p1231 N85-177
Active inner regions of isolated galaxies
08 p1237 N85-177
On the surface density of X-ray selected BL Lacert objects 08 p1240 N85-178
Active galactic nuclei and their cosmological evolutio
08 p1243 N85-178
Star formation in globules 08 p1247 N85-178
Far infrared observations of molecular clouds in the out galaxy 08 p1247 N85-178
Far infrared emission from galaxies
08 p1248 N85-178
Starbursts in galaxies: Implications of molecular a far-infrared observations 08 p1248 N85-178
Spectroscopic observations of selected ste systems
[NASA-CR-174286] 08 p1255 N85-17
On the progenitors of white dwarfs
[NASA-CR-174376] 09 p1413 N85-18
Boundary conditions for the paleoenvironme Chemical and physical processes in the pre-solar neb — molecular clouds, interstellar matter, and abundan
[NASA-CR-174370] 10 p1570 N85-19
Fragmentation and turbulence in collapsing gas clo
[DE85-003745] 11 p1633 N85-20

Future of Ultraviolet Astronomy Based on Six Years of IUE Research
[NASA-CP-2349] 11 p1743 N85-20961
Hot stars: Six years of progress
11 p1743 N85-20963
Magellanic cloud objects 11 p1744 N85-20965
Interacting binary systems 11 p1744 N85-20967
UV observations and results on pre-main sequence stars 11 p1744 N85-20970
The usual hot stars in unusual galaxies
11 p1745 N85-20975
IUE observations of blue horizontal branch globular clusters and UV-bright stars 11 p1748 N85-20992
Mass distribution and evolutionary scheme for central stars of planetary nebulae 11 p1751 N85-21012
Hydrodynamic simulations of recurrent novae
11 p1753 N85-21025
Old and new neutron stars
[DE85-002716] 11 p1762 N85-21085
The luminosity distribution of pulsars
12 p1959 N85-22317
All-Union conference of radio astronomers
13 p1977 N85-22408
Dynamics of long-period comets
13 p2176 N85-23506
The Formation of preplanetary disks from the collapse of rotating molecular cloud cores
13 p2180 N85-23526
Research on the early history of the solar system
13 p2180 N85-23527
Numerical study of a two-fluid hydrodynamical model of interstellar medium and population 1 stars
14 p2440 N85-25055
Molybdenum solar neutrino experiment
[DE85-003747] 14 p2445 N85-25090
Did the young Sun rotate at 100 km/s
14 p2451 N85-25133
Formation of the solar system
15 p2677 N85-26532
Did bosonic sneutrino stars ever exist
[PREPRINT-421] 18 p3202 N85-29867
The kinematic and radial properties of normal luminous SC galaxies 20 p3545 N85-32061
Star formation in NGC 7538: Multi-wavelength observations and issues 20 p3545 N85-32063
Search for the universal ancestors
[NASA-SP-477] 21 p3667 N85-32777
Noble gases and the early history of the Earth: Inappropriate paradigms and assumptions inhibit research and communication 21 p3719 N85-33075
Search for stellar collapse with the MACRO detector at Gran Sasso
[HE-5.3-11] 24 p4206 N85-36105

STELLAR FIELDS
U STAR DISTRIBUTION

STELLAR FLARES
NT SOLAR FLARES
Light variations of the B-type star HD 160202
08 p1232 N85-17761
X-ray activity in pre-main sequence stars
08 p1233 N85-17764
Outer atmospheres of cool stars observed with IUE
11 p1744 N85-20968
The solar stellar connection in the far ultraviolet
11 p1757 N85-21055

STELLAR GRAVITATION
Some evidence for large gravitational redshift in Seyfert galaxy NGC 4151
[OG-2.7-11] 22 p3872 N85-33984

STELLAR LUMINOSITY
The influence of stellar luminosity and temperature calibration on the determination of the initial mass function 05 p0740 N85-14760
Unidentified IRAS sources: Ultrahigh luminosity galaxies
[NASA-CR-174207] 06 p0872 N85-15537
Observations of highly-ionized interstellar iron
06 p0876 N85-15565
Some aspects of active galactic nuclei
07 p1056 N85-16702
Light variations of the B-type star HD 160202
08 p1232 N85-17761
Stellar winds: Observational evidence for a hot-cool star connection 08 p1233 N85-17768
On the role played by lines in radiatively driven stellar winds depending on the position of the stars in the HR diagram 08 p1236 N85-17787
A new estimate of the local luminosity function of Seyfert 1 nuclei 08 p1237 N85-17796
Star formation in globules 08 p1247 N85-17868
Far infrared observations of molecular clouds in the outer galaxy 08 p1247 N85-17869
SIRTF: The next step 08 p1250 N85-17891
The ground based photometric limitations to the search for light variations due to 5-minute solar-type oscillations in other stars 08 p1251 N85-17898
IUE observations of blue horizontal branch globular clusters and UV-bright stars 11 p1748 N85-20992
Ultraviolet studies of the young populous cluster NGC 2100 in the LMC 11 p1748 N85-20995
Superionized species and winds in low luminosity B and Be stars 11 p1749 N85-21003
Betegeuse at maximum luminosity
11 p1756 N85-21061
IUE low-dispersion reference atlas
11 p1760 N85-21073
An IUE high-resolution atlas of O-type spectra
11 p1760 N85-21074
IUE observations of faint standard stars for calibration of the space telescope 11 p1761 N85-21076
Dynamics of elliptical galaxies and the r sup 1/4 luminosity law 12 p1955 N85-22262
The luminosity distribution of pulsars
12 p1959 N85-22317
Formation of optical-line emitting regions in the jets of SS433 12 p1959 N85-22318
Observations concerning energy balance in solar magnetic regions 14 p2452 N85-25145
Investigating statistical characteristics of atmospheric background brightness and star background density in equatorial region of celestial sphere
15 p2476 N85-25298
The ultraviolet spectra of intermediate redshift quasars
20 p3544 N85-32056
The kinematic and radial properties of normal luminous SC galaxies 20 p3545 N85-32061

STELLAR MAGNETIC FIELDS
NT SOLAR MAGNETIC FIELD
Theory tested by means of the stars — viability of the alpha-omega dynamo model 08 p1233 N85-17770
Bipolar flows and X-ray emission from young stellar object 08 p1234 N85-17779
Magnetic effects in the heating and modification of flows in the outer stellar atmospheres with application to early type star case 08 p1235 N85-17783
Transport properties of the outer crust of magnetic neutron stars 09 p1415 N85-18927
Ultraviolet and optical spectroscopy and polarimetry of the helium weak star HD 21669: Evidence for a magnetically controlled stellar wind
11 p1759 N85-21065
The modelling of latitudinal gradients in the solar wind in the outer solar system 12 p1947 N85-22231
The axisymmetric pulsar magnetosphere
12 p1955 N85-22279
Nonlinear waves in the magnetosphere of pulsars
12 p1955 N85-22281
Thermal convection and magnetic fields in accretion disks of black holes 12 p1955 N85-22285
About static and dynamic solutions of the aligned rotator model --- pulsar magnetospheres
12 p1958 N85-22306
Solar and stellar magnetic cycles: Unity and multiplicity 14 p2448 N85-25109
The generation of magnetic fields by a flow with chaotic streamlines 14 p2451 N85-25135
Activity and magnetic fields on stars from radio observations
[NASA-CR-175966] 18 p3202 N85-29861
Observations of Cygnus X-3 above 10(15) eV from 1979 - 1984
[OG-2.1-6] 22 p3863 N85-33923

STELLAR MAGNITUDE
South African Astronomical Observatory Circulars, no. 7
[SAAOC-7] 01 p0127 N85-10875
Extending magnitude standards to faint stars with a sub-beam prism 07 p0965 N85-16124
Sub-beam prism used at the Bosscha Schmidt telescope 07 p0965 N85-16125
Astronomers' problems with the calibration of Schmidt plates 07 p0965 N85-16126
A statistical evaluation of the limitations of single-channel intermediate-band photoelectric stellar photometry 08 p1251 N85-17900
Documentation for the machine-readable version of the Cordoba Durchmusterung (CD)
[NASA-TM-87441] 14 p2439 N85-25049

STELLAR MASS
NT STELLAR GRAVITATION
Gravitational vacuum 02 p0265 N85-11734
The behaviour of brighter binaries and yellow giants in open clusters 05 p0737 N85-14738
On the role played by lines in radiatively driven stellar winds depending on the position of the stars in the HR diagram 08 p1236 N85-17787
Multiline transfer and the dynamics of stellar winds
08 p1236 N85-17788
Spectroscopic observations of selected stellar systems
[NASA-CR-174288] 08 p1255 N85-17915
UV observations and results on pre-main sequence stars 11 p1744 N85-20970
Mass distribution and evolutionary scheme for central stars of planetary nebulae 11 p1751 N85-21012
Three short-period binaries seen at high-dispersion UX ARI, IOTA TRI and HA5110 11 p1756 N85-21047
The Formation of preplanetary disks from the collapse of rotating molecular cloud cores
13 p2180 N85-23526
Relevance of cosmic gamma rays to the mass of gas in the galaxy
[OG-3.1-8] 22 p3874 N85-33996

STELLAR MASS ACCRETION
Spherical accretion onto a protostellar core
03 p0442 N85-12817
Age groups and composite diagrams for young open clusters 05 p0737 N85-14736
Accretion in the zeta Aurigae and 32 Cygni shock cones 11 p1754 N85-21036
Orbital resonances and planetary accretion in the solar nebula 13 p2179 N85-23523
Research on the early history of the solar system
13 p2180 N85-23527
Thermal and magnetic properties of neutron stars
16 p2880 N85-27774
X-ray spectra of bursting neutron stars
23 p3981 N85-34686

STELLAR MASS EJECTION
Solar-geophysical data number 477, May 1984. Part 2: (Comprehensive reports). Data for November 1983, July 1981 and miscellanea. Explanation of data reports issued as number 474 (supplement) February 1984
[PB84-225036] 01 p0131 N85-10900
Nonradial pulsation and mass loss in early B stars
08 p1232 N85-17759
Bipolar ejection of matter from hot stars
08 p1233 N85-17767
Nonradiative heating and enhanced mass-loss due to shear turbulence in massive hot stars
08 p1235 N85-17780
Further investigation of mass loss phenomena in hot white dwarfs and O subdwarfs 11 p1751 N85-21014
Mechanical energy release by protostars to molecular clouds 12 p1957 N85-22302

STELLAR MODELS
Variations of the H and K emission lines of singly ionized calcium in the eclipsing binary star system AR Lacertae
02 p0296 N85-11921
Thermal effects in stellar pulsations
02 p0297 N85-11925
Numerical models of the spectral appearance of protostellar envelopes 03 p0442 N85-12816
Shapes of wind driven circumstellar shells
03 p0443 N85-12821
Particle acceleration in two-ribbon flares --- solar flares 04 p0519 N85-13314
Time dependent effects at the foot of the chromosphere
[NASA-CR-174143] 04 p0589 N85-13762
The fragmentation of molecular clouds and the IMF
05 p0740 N85-14759
Iron core collapse models of Type 2 supernovae
[DE84-013909] 05 p0743 N85-14775
The radiative hydrodynamics of flare loops heated by impulsive bursts of energetic electrons
05 p0745 N85-14781
Chemical evolution of the solar nebula: A new model
06 p0887 N85-15631
Dynamic thermal episodes in the protosolar nebula: Development of models from observations on CAI's
06 p0887 N85-15633
Narrow absorption components in Be star winds
08 p1232 N85-17760
Ultraviolet spectral morphology of O-type stellar winds
08 p1232 N85-17762
Active phenomena in the pre-main sequence star AB AUR 08 p1233 N85-17765
Bipolar ejection of matter from hot stars
08 p1233 N85-17767
Theory tested by means of the stars — viability of the alpha-omega dynamo model 08 p1233 N85-17770
The scaling of coronal models from one star to another 08 p1233 N85-17771
A leaky waveguide model for MHD wave driven winds from coronal holes 08 p1235 N85-17781
Transport properties of the outer crust of magnetic neutron stars 09 p1415 N85-18927
A comparative study of dust and young stars in three small galaxies 09 p1415 N85-18928
IUE observations of blue horizontal branch globular clusters and UV-bright stars 11 p1748 N85-20992
The fading of R coronae borealis
11 p1753 N85-21029
Active late-type stars and the applicability of coronal loop models 11 p1758 N85-21059

Thermal stability of static coronal loops: Part 1: Effects of boundary conditions
[NASA-CR-175495] 12 p1961 N85-22330
Theoretical and observational studies of stellar activity 13 p2171 N85-23468
Constraints of observations of solar oscillations on solar models with mixing by turbulent diffusion
[DE85-003741] 13 p2205 N85-23678
Numerical study of a two-fluid hydrodynamical model of interstellar medium and population 1 stars 14 p2440 N85-25065
Models of solar differential rotation 14 p2446 N85-25097
Amplification and maintenance of thin magnetic flux tubes by compressible convection --- solar magnetism 14 p2447 N85-25104
The solar dynamo and the complex Lorenz equations 14 p2447 N85-25107
A numerical simulation of the formation of solar prominences 14 p2448 N85-25112
Conditions of the small oscillations excitation in the different solar models with the mixed core 14 p2450 N85-25126
Linear models of acoustic waves in sunspot umbrae 14 p2450 N85-25130
The flux rope models checked by some observations --- solar activity 14 p2452 N85-25139
Empirical model of the solar corona using solar-cycle related parameters 14 p2453 N85-25153
Modeling 22-year solar activity cycle within framework of dynamo theory with allowance for primary field 15 p2477 N85-25288
Activities report of the Institute of Astronomy and Astrophysics 17 p3052 N85-28692
Self-consistent models for the X-ray emission from supernova remnants 20 p3548 N85-32082

STELLAR MOTIONS
NT STELLAR OSCILLATIONS
NT STELLAR ROTATION
Documentation for the machine-readable version of the Perth 75: A Catalogue of Positions of 2589 FK4 and FK4S Stars (Nikoloff and Hog 1982)
[NASA-TM-87376] 04 p0549 N85-13492
Documentation for the machine-readable version of the AGK3 Star Catalogue of Positions and Proper Motions North of -2 deg .5 declination (Dieckvoss and Collaborators 1975)
[NASA-TM-87378] 04 p0549 N85-13493
Evolution of globular clusters 05 p0738 N85-14745
Investigation of central parts of globular clusters, performed in PUlkovo 05 p0738 N85-14747
Non-stable motions and instability in stellar associations 05 p0739 N85-14754
Proper motions and kinematical properties of Orion trapezium type stellar systems 05 p0739 N85-14755
Hyades moving group 05 p0740 N85-14757
The evolution of a sparse stellar system 05 p0740 N85-14758
Radiative amplification of acoustic waves in hot stars 08 p1235 N85-17786
The relationship between radio structures and stellar dynamics of nearby elliptical galaxies 08 p1236 N85-17794
Documentation for the machine readable version of the Yale Catalogue of the Positions and Proper Motions of Stars between Declinations -60 deg and -70 deg (Fallon 1983)
[NASA-TM-87443] 14 p2439 N85-25051
Solar convection
[AD-A155214] 21 p3723 N85-33098

STELLAR OCCULTATION
Catalogue of observations of total occultations of stars by the Moon for the years 1972 to 1980 and of grazing occultations for the years 1963 to 1980
[BULL-192] 05 p0741 N85-14766
Exploring the solar system with stellar occultations 08 p1245 N85-17857
Occultations of stars and radio sources by comets: Predictions and observing prospects 14 p2437 N85-25034
The rings of Uranus 15 p2672 N85-26486
Stellar occultations by Uranus rings on 15 August 1980 and 22 April 1982 15 p2672 N85-26489
Rings around Neptune? 15 p2672 N85-26491
Structure and dynamics of Saturn's rings as seen by the Voyager stellar occultation 15 p2673 N85-26494
The C ring of Saturn: A high resolution view of some of its structure 15 p2673 N85-26495
The eccentric ringlet at 1.29 R sub S --- Saturn radius (RS) 15 p2673 N85-26496
Voyager UVS observations of stellar occultations by the rings of Saturn --- ultraviolet spectrometer (UVS) 15 p2673 N85-26497
Occultation detection of a Neptune ring segment 15 p2681 N85-26558
The 13 November 1984 occultation of BD +08 deg 0471 by (1) Ceres
[NASA-CR-176108] 23 p3987 N85-34725

STELLAR OSCILLATIONS
NT SOLAR OSCILLATIONS
The ground based photometric limitations to the search for light variations due to 5-minute solar-type oscillations in other stars 08 p1251 N85-17898
Atmospheric limitations in stellar seismology: Should one measure radial velocity or brightness fluctuations? 08 p1251 N85-17899
Energy relations on the small oscillations excitation in the stars 14 p2450 N85-25125
Quasiperiodic oscillations in bright galactic-bulge X-ray sources
[NASA-CR-176138] 23 p3987 N85-34723

STELLAR PARALLAX
Astrometric applications of the Mt. Stromlo PDS 1010A --- microdensitometer 07 p0967 N85-16136

STELLAR PHYSICS
NT SOLAR PHYSICS

STELLAR RADIATION
NT STELLAR WINDS
Fast Hartmann method for problems in astronomical adaptive optics 02 p0161 N85-11094
Masers associated with regions of recent star formation 03 p0443 N85-12820
Stability of stellar disk and ratio of halo to disk masses in the galaxy 05 p0740 N85-14763
Voyager EUV and FUV observations 06 p0875 N85-15554
Natural interference phenomena affecting spaceborne receivers
[NASA-CR-174256] 07 p0916 N85-15798
Radiative amplification of acoustic waves in hot stars 08 p1235 N85-17786
Multiline transfer and the dynamics of stellar winds 08 p1236 N85-17788
A survey of fast X-ray transients using the HEAO A-1 Sky Survey experiment 09 p1411 N85-18895
Radio emission from RS CVn binary systems 09 p1417 N85-18939
Coordinated ultraviolet and visual observations of Omega Orionis 1982-1983 11 p1750 N85-21007
A survey of Mg II h and k emission in near-solar type stars
[NASA-CR-175572] 12 p1953 N85-22269
Activity and magnetic fields on stars from radio observations
[NASA-CR-175966] 18 p3202 N85-29861
The radiation of the Vela pulsar 20 p3548 N85-32080
Microburst of TeV gamma rays from the Crab pulsar
[OG-2.3-4] 22 p3866 N85-33941
Secondary periodicities of microbursts of TeV gamma rays from the Crab pulsar
[OG-2.3-5] 22 p3866 N85-33942
Gamma-ray line emission from Al-26 produced by Wolf-Rayet stars
[OG-3.2-5] 22 p3875 N85-34003
Electrons and positrons from expanding supernova envelopes in dense clouds
[OG-6.2-9] 22 p3889 N85-34108
Investigations of the cyclotron resonance effects in the X ray spectrum of the neutron star Hercules X-1
[MPE-191] 22 p3890 N85-34112
Low-excitation Herbig-Haro objects and interstellar extinction
[NASA-CR-176142] 23 p3968 N85-34726

STELLAR ROTATION
NT SOLAR ROTATION
The rotation of B-type stars and processes of star formation 03 p0443 N85-12823
On collective effects in the rotation of stars in clusters and associations 05 p0737 N85-14739
Corotating interaction regions in stellar winds: Particle acceleration and non-thermal radio emission in hot stars 08 p1234 N85-17773
Winds from rotating, magnetic, hot stars 08 p1234 N85-17775
Non-radiative energy from differential rotation in hot stars 08 p1234 N85-17778
Nonradiative heating and enhanced mass-loss due to shear turbulence in massive hot stars 08 p1235 N85-17780
Search for millisecond rotational periods in some low-mass X-ray binaries observed by EXOSAT 11 p1741 N85-20949
Rotational modulation of chromospheric emission in cool giants and hybrid stars 11 p1750 N85-21064
The structure and angular momentum content of dark clouds 14 p2439 N85-25054
Study of the parameters affecting the collapse of a rotating protostellar cloud 24 p4168 N85-35837

STELLAR SPECTRA
NT SOLAR SPECTRA
Local photometric standards for CaII emission stars 01 p0128 N85-10960
A spectroscopic survey of 113 nearby red dwarf stars 01 p0129 N85-10966
Compact infrared sources: Protostars before IRAS 03 p0442 N85-12812
Far-infrared observations of some regions of star formation 03 p0442 N85-12814
Numerical models of the spectral appearance of protostellar envelopes 03 p0442 N85-12816
Masers associated with regions of recent star formation 03 p0443 N85-12820
RS CV sub n binary systems
[NASA-CR-174164] 04 p0560 N85-13704
Observations of highly-ionized interstellar iron 06 p0876 N85-15585
Modelling the local interstellar medium as a supernova remnant in a multiphase gas 06 p0879 N85-15586
The Torun measuring system for astronomical spectra 07 p0966 N85-16130
Spectrophotometry of cool stars from objective prism spectra 07 p0966 N85-16134
Narrow absorption components in Be star winds 08 p1232 N85-17760
Coronal temperatures 08 p1233 N85-17766
Departures from LTE populations versus anomalous abundances: The effects of heating 08 p1234 N85-17776
On the role played by lines in radiatively driven stellar winds depending on the position of the stars in the HR diagram 08 p1236 N85-17787
Multiline transfer and the dynamics of stellar winds 08 p1236 N85-17788
Optical studies of X-ray selected Active Galactic Nuclei (AGN) in the direction of the Large Magellanic Cloud (LMC) 08 p1237 N85-17797
Carbon stars: There is no such thing as a dead leg 08 p1247 N85-17871
Mid-infrared spectroscopy of planetary nebulae 08 p1247 N85-17872
Image quality on the KAO 08 p1249 N85-17885
High precision measurement of stellar radial velocity variations 08 p1250 N85-17886
Experimental determination of the 1 sigma(+) state electron-dipole-moment function of carbon monoxide up to a large internuclear separation
[NASA-TM-85979] 09 p1379 N85-18870
Contributions of the X-ray astronomy group --- conference
[MPE-PREPRINT-29] 11 p1742 N85-20852
X-ray coronae of late type stars: Theoretical implications 11 p1742 N85-20853
Simultaneous EXOSAT and optical observations of the pulsing X-ray binary H2252-035 / AO Psc 11 p1743 N85-20858
Spectral studies of low-mass X-ray binaries observed by EXOSAT 11 p1743 N85-20859
EXOSAT observations of 4U1705-44 --- X ray binary 11 p1743 N85-20860
Further investigation of mass loss phenomena in hot white dwarfs and O subdwarfs 11 p1751 N85-21014
IUE spectrophotometry of the hot helium-rich PG1159 DO degenerates 11 p1751 N85-21015
Self-consistent recalibration of IUE determination of hot DA white dwarf effective temperatures 11 p1751 N85-21016
Carbon, silicon, and oxygen in the white dwarf star GD 40 11 p1752 N85-21017
Analysis of white dwarf Lyman alpha profiles 11 p1752 N85-21018
The outburst and long term behavior of the triple period cataclysmic variable TV Col 11 p1752 N85-21021
FP Cygni profiles in HL CMa 11 p1752 N85-21022
New results on PU VUL 11 p1753 N85-21023
The UV extinction of HR 5999 11 p1753 N85-210
Variability of ultraviolet emission lines in the carbon st
TX Psc 11 p1753 N85-2102
Temporal UV emission from the peculiar star F
Puppis 11 p1753 N85-210
Three short-period binaries seen at high-dispersion U
ARI, IOTA TRI and HA5110 11 p1756 N85-210
The eclipsing binary U Sagittae: Evidence for C
processing and mass exchange in the past 11 p1757 N85-210
A search for the spectroscopic binary companions
Polaris using IUE spectra 11 p1757 N85-210
Co-rotating interaction regions in stellar winds 11 p1758 N85-21
Ultraviolet, radio and X-ray observations of hy
stars 11 p1759 N85-21
Rotational modulation of chromospheric emission in c
giants and hybrid stars 11 p1750 N85-21

Magnetospheres and winds in the helium weak stars: Observations of C 5 in upper main sequence CP stars
11 p1759 N85-21066
IUE low-dispersion reference atlas
11 p1760 N85-21073
An IUE high-resolution atlas of O-type spectra
11 p1760 N85-21074
Statistical classification of IUE low-dispersion stellar spectra: Progress report 11 p1760 N85-21075
Stellar ultraviolet flux distributions in the 912-1200 A wavelength range 11 p1762 N85-21081
The ultraviolet excess of quasars 3: The highly polarized quasars PKS 0736+017 and PKS 1510-089
[NASA-CR-175576] 12 p1953 N85-22266
A survey of Mg II h and k emission in near-solar type stars
[NASA-CR-175572] 12 p1953 N85-22269
Plasma processes in Herbig-Haro objects
12 p1957 N85-22301
Formation of optical-line emitting regions in the jets of SS433 12 p1959 N85-22318
Solar and stellar coronal plasmas
[NASA-CR-175623] 13 p2205 N85-23676
Documentation for the machine-readable version of the Stellar Spectrophotometric Atlas, 3130 A lambda 10800 A of Gunn and Stryker (1983)
[NASA-TM-87437] 14 p2438 N85-25045
Documentation for the machine-readable version of A Library of Stellar Spectra (Jacoby, Hunter and Christian 1984)
[NASA-TM-87438] 14 p2438 N85-25046
Documentation for the machine-readable version of A Finding List for the Multiplet Tables of NSRDS-NBS 3, Sections 1-10 (Adelman, Adelman, Fischel and Warren 1984)
[NASA-TM-87440] 14 p2438 N85-25048
Did the young Sun rotate at 100 km/s
14 p2451 N85-25133
Stellar surface phenomena: A spectroscopic study of the RS canum venaticorum binaries
15 p2669 N85-26467
Activities report of the Institute of Astronomy and Astrophysics 17 p3052 N85-28892
A study of W Serpentis binaries: SX Cassiopeiae, RX Cassiopeiae, and W Serpentis 20 p3544 N85-32053
Investigations of the cyclotron resonance effects in the X ray spectrum of the neutron star Hercules X-1
[MPE-191] 22 p3890 N85-34112
The cosmic ray interplanetary radial gradient from 1972 - 1985
[SH-4.7-1] 23 p4040 N85-35046
The HEAO-2 Guest Investigator Program: Non-linear growth of instabilities in line-driven stellar winds
[NASA-CR-176168] 24 p4168 N85-35840

STELLAR SPECTROPHOTOMETRY
Local photometric standards for CaII emission stars
01 p0128 N85-10883
Photoelectric photometry of globular cluster giants
01 p0128 N85-10884
Spectroscopic data for globular cluster giants. 1: Stars of the red giant tip 01 p0128 N85-10885
Einstein solid state spectrometer observation of the peculiar red dwarf Wolf 630 AB
[NASA-TM-83947] 03 p0447 N85-12843
Astronomical photography 1984 — conferences
[ROE-OR-14] 07 p0962 N85-16102
The Malin effect in stellar photography
07 p0966 N85-16131
Some applications of signal-to-noise in photographic stellar photometry 07 p0966 N85-16132
Stellar photographic photometry using a double wedge technique with a focal reducer system
07 p0966 N85-16133
Spectrophotometry of cool stars from objective prism spectra 07 p0966 N85-16134
Summary of the origin of nonradiative heating/momentum in hot stars
08 p1236 N85-17789
A comparison of some photometric parameters of active and normal spiral galaxies 08 p1238 N85-17806
Five-minute P modes detected in Doppler shift measurement on Alpha Centauri
08 p1250 N85-17895
A statistical evaluation of the limitations of single-channel intermediate-band photoelectric stellar photometry 08 p1251 N85-17900
A CCD system for photometry of direct and spectroscopic images 08 p1252 N85-17904
Ultraviolet spectroscopy of selected astronomical sources
[NASA-CR-174379] 09 p1413 N85-18912
UKIRT spectro-photometry system — United Kingdom Infrared Telescope (UKIRT)
[UKIRT-23] 09 p1414 N85-18921
The central star of NGC 40 11 p1751 N85-21013
IUE spectrophotometry of the hot helium-rich PG1159 DO degenerates 11 p1751 N85-21015
Eclipse observations of Epsilon Aurigae
11 p1755 N85-21037
IUE spectrophotometry of helium weak and silicon stars 11 p1759 N85-21067
IUE observations of faint standard stars for calibration of the space telescope 11 p1761 N85-21076
Calibrations of wavelengths in SWP echelle spectra
11 p1761 N85-21077
Documentation for the machine-readable version of the Stellar Spectrophotometric Atlas, 3130 A lambda 10800 A of Gunn and Stryker (1983)
[NASA-TM-87437] 14 p2438 N85-25045
Activities report of the Institute of Astronomy and Astrophysics 17 p3052 N85-28891
Activities report of the Institute of Astronomy and Astrophysics 17 p3052 N85-28892
The San Fernando Observatory video Stokes polarimeter 18 p3205 N85-29885
Photometric and spectroscopic gamma-ray observations of solar transient phenomena using long duration balloons
[SH-9.1-5] 23 p4051 N85-35120

STELLAR STRUCTURE
Age groups and composite diagrams for young open clusters 05 p0737 N85-14736
The dynamical evolution of the environment of an OB association 05 p0739 N85-14752
Proper motions and kinematical properties of Orion trapezium type stellar systems 05 p0739 N85-14755
On the most probable number of flare stars in the Pleiades field 05 p0739 N85-14756
The velocity-age relation for B and A stars
05 p0740 N85-14762
The nature of the soft X-ray emitting region in the direction of the North Polar spur
06 p0877 N85-15568
HEAO-1 diffuse soft X-ray sky maps
06 p0877 N85-15570
The X-ray structure of the Crab Nebula
11 p1741 N85-20946
The X-ray structure of the Crab Nebula
11 p1742 N85-20954
Research on the early history of the solar system
13 p2180 N85-23527
Overview of solar seismology: Oscillations as probes of internal structure and dynamics in the Sun
14 p2441 N85-25061
Solar inverse theory 14 p2441 N85-25063
The hydromagnetics of the Sun — conferences
[ESA-SP-220] 14 p2445 N85-25091
Coronal structures 14 p2448 N85-25110
Solar magnetohydrodynamics: Symposium review
14 p2455 N85-25162
Activities report of the Institute of Astronomy and Astrophysics 17 p3052 N85-28891
Activities report of the Laboratory of Stellar and Planetary Physics
[G-127] 20 p3544 N85-32052
The kinematic and radial properties of normal luminous SC galaxies 20 p3545 N85-32061
A possible mechanism to cause the quasi-biennial variability on the solar neutrino flux
[SH-8.1-5] 23 p4049 N85-35110

STELLAR TEMPERATURE
Thermal effects in stellar pulsations
02 p0297 N85-11925
The influence of stellar luminosity and temperature calibration on the determination of the initial mass function 05 p0740 N85-14760
The Origin of Nonradiative Heating/Momentum in Hot Stars
[NASA-CP-2358] 08 p1231 N85-17755
Coronal temperatures 08 p1233 N85-17766
Stellar winds: Observational evidence for a hot-cool star connection 08 p1233 N85-17768
Heating in the solar mantle 08 p1233 N85-17769
Overheated open coronal regions
08 p1234 N85-17772
Transport properties of the outer crust of magnetic neutron stars 09 p1415 N85-18927
The UV extinction laws in two very young clusters, NGC 6530 in the galaxy and NGC 2100 in the LMC
11 p1748 N85-20994
Ultraviolet studies of the young populous cluster NGC 2100 in the LMC 11 p1748 N85-20995
Stellar winds in the young galactic cluster NGC 6530
11 p1750 N85-21004
IUE and Voyager observations of very hot O-type subdwarfs 11 p1751 N85-21010
Self-consistent recalibration of IUE determination of hot DA white dwarf effective temperatures
11 p1751 N85-21016
Cooling of neutron stars with hyperons
[DE85-004641] 13 p2171 N85-23472

STELLAR WINDS
Helium atoms in interstellar and interplanetary media, part 3: Temperature and velocity of interstellar wind
02 p0160 N85-11068
Relation of core structure to high velocity outflow in G35.2-0.74 and other molecular clouds
03 p0443 N85-12818
Molecular hydrogen emission associated with high velocity flows. A tracer for low velocity shocks
03 p0443 N85-12819
Shapes of wind driven circumstellar shells
03 p0443 N85-12821
The dynamical evolution of the environment of an OB association 05 p0739 N85-14752
Stromgren trails of hot white dwarfs
06 p0879 N85-15589
Theoretical studies of chromospheres and winds in cool stars
[NASA-CR-174204] 06 p0880 N85-15596
Observations of nonthermal radio emission from early-type stars 08 p1232 N85-17758
Narrow absorption components in Be star winds
08 p1232 N85-17760
Ultraviolet spectral morphology of O-type stellar winds
08 p1232 N85-17762
X-ray activity in pre-main sequence stars
08 p1233 N85-17764
Stellar winds: Observational evidence for a hot-cool star connection 08 p1233 N85-17768
Corotating interaction regions in stellar winds: Particle acceleration and non-thermal radio emission in hot stars
08 p1234 N85-17773
Synchrotron emission from chaotic stellar winds
08 p1234 N85-17774
Winds from rotating, magnetic, hot stars
08 p1234 N85-17775
Is the ratio of observed X-ray luminosity to bolometric luminosity in early-type stars really a constant?
08 p1234 N85-17777
Nonradiative heating and enhanced mass-loss due to shear turbulence in massive hot stars
08 p1235 N85-17780
A leaky waveguide model for MHD wave driven winds from coronal holes 08 p1235 N85-17781
Radiatively driven winds and what they imply: A review of radiative driven instabilities and their importance in hot stars 08 p1235 N85-17782
Effect of scattering on instabilities in line-driven stellar winds 08 p1235 N85-17784
New instabilities in line driven winds
08 p1235 N85-17785
On the role played by lines in radiatively driven stellar winds depending on the position of the stars in the HR diagram 08 p1236 N85-17787
Multiline transfer and the dynamics of stellar winds
08 p1236 N85-17788
Collimated winds from active galactic nuclei
08 p1241 N85-17832
Centrifugally driven magnetohydrodynamic (MHD) winds and the nonthermal emission regions in Active Galactic Nuclei (AGN) 08 p1242 N85-17835
Duelling winds: A model for broad-line regions — galactic nuclei 08 p1242 N85-17837
Far-infrared photometry of low-mass pre-main-sequence stars with broad CO wings 08 p1246 N85-17866
Spectroscopic observations of selected stellar systems
[NASA-CR-174288] 08 p1255 N85-17915
Combined ultraviolet studies of astronomical sources
[NASA-CR-174361] 09 p1413 N85-18910
Hot stars: Six years of progress
11 p1743 N85-20963
Coronal effects of the winds of early-type stars
11 p1749 N85-21002
Superionized species and winds in low luminosity B and Be stars 11 p1749 N85-21003
Stellar winds in the young galactic cluster NGC 6530
11 p1750 N85-21004
Main sequence B stars with strong winds
11 p1750 N85-21005
FP Cygni profiles in HL CMa
11 p1752 N85-21022
Atmospheric properties of RU Lupi derived from high- and low-resolution IUE spectra
11 p1754 N85-21031
The stellar wind in the BO V-type eclipsing binary Y Cygni 11 p1755 N85-21040
Observations of cataclysmic variable star winds
11 p1755 N85-21041
Chromospheric emission lines in high-resolution LWR spectra (220 - 3000 alpha) of gamma CRU (M3 3) and alpha ORI (M2 Iab) 11 p1758 N85-21058
Co-rotating interaction regions in stellar winds
11 p1758 N85-21060
Ultraviolet, radio and X-ray observations of hybrid stars 11 p1759 N85-21063

Ultraviolet and optical spectroscopy and polarimetry of the helium weak star HD 21699: Evidence for a magnetically controlled stellar wind
11 p1759 N85-21065

Magnetospheres and winds in the helium weak stars: Observations of C 5 in upper main sequence CP stars
11 p1759 N85-21066

Old and new neutron stars
[DE85-002716] 11 p1762 N85-21085

The modelling of latitudinal gradients in the solar wind in the outer solar system 12 p1947 N85-22231

Plasma processes in Herbig-Haro objects
12 p1957 N85-22301

An analytic model for hydromagnetospheres — stellar winds; pulsars; cosmic jets 12 p1959 N85-22313

Processes and problems in secondary star formation
[DE85-003623] 12 p1960 N85-22322

Winds in cataclysmic variable stars
[DE85-006706] 15 p2669 N85-26470

X-ray emission and the winds of cataclysmic variables
[DE85-007663] 17 p3053 N85-28902

The hydrodynamic effects of nuclear active galaxy winds on host galaxies 20 p3545 N85-32062

Excess gamma-rays in the direction of the rho Ophiuchi cloud: An exotic object?
[OG-2.5-1] 22 p3868 N85-33958

Evidence for a dynamical halo around the edge-on galaxy NGC 4631
[OG-6.2-1] 22 p3889 N85-34102

Possible origin of the anomalous component of cosmic rays
[SH-4.6-7] 23 p4039 N85-35045

The HEAO-2 Guest Investigator Program: Non-linear growth of instabilities in line-driven stellar winds
[NASA-CR-176168] 24 p4188 N85-35840

STELLARATORS

Elimination of stochasticity in stellarators
02 p0282 N85-11639

Proceedings of the US-Japan Theory Workshop on 3-D MHD Studies
[DE84-012019] 04 p0568 N85-13620

Zero-current, high beta stelleration equilibria with rotational transform profile control
[DE84-016635] 04 p0568 N85-13624

Monte Carlo studies of transport in stellarators
[DE84-017633] 04 p0568 N85-13625

MHD equilibrium and stability for stellarator/torsatron configurations
[DE85-001139] 09 p1391 N85-18750

Electron cyclotron resonance heating system for the stellarator W 7-AS
[IPF-84-5] 09 p1395 N85-18779

Wave absorption and transport studies on Electron Cyclotron Resonance (ECR) heated stellarator plasmas in W 7-A
[IPF-84-9] 09 p1395 N85-18782

Fusion Energy Division
[DE85-001701] 11 p1731 N85-20884

Activities report of the Institute of Plasma Research
11 p1733 N85-20903

TOKASTAR: A Tokamak stellarator hybrid with possible bean-shaped operation
[IPPJ-718] 16 p2866 N85-27680

I. F. S. (Institute for Fusion Studies) Newsletter, Volume 4, Number 1
[DE85-007917] 17 p3040 N85-28809

Recent progress in stellarator reactor conceptual design
[DE85-009592] 18 p3169 N85-29780

Alternating current OHMIC heating in a toroidal stellarator 20 p3534 N85-31988

Cyclotron absorption of fast magnetosonic wave in stellarator 21 p3693 N85-32945

Method and apparatus for maintaining equilibrium in a helical axis stellarator
[DE85-011626] 22 p3845 N85-33815

Proceedings of the US-Japan Workshop on Transport in Open-Ended Systems
[IPPJ-727] 23 p3975 N85-34644

Analytic and numerical calculations of the ambipolar electric field in a stellarator 23 p3978 N85-34665

Behavior of helically-trapped fast ion orbits in heliotron E 23 p3978 N85-34666

Advanced Toroidal Facility (ATF)
[DE85-011567] 23 p3983 N85-34699

Stellarator approach to fusion plasma confinement
[DE85-011420] 23 p3984 N85-34704

Confinement and heating of high beta plasmas with emphasis on compact toroids
[DE85-011459] 24 p4155 N85-35761

STELLITE (TRADEMARK)

Interaction of high-cycle and low-cycle fatigue of Haynes 188 alloy at 1400 F deg 17 p2913 N85-27961

STEMS

Gravitropism in leafy dicot stems
15 p2610 N85-26086

STEP FAULTS

U GEOLOGICAL FAULTS

STEPPES

Snow cover in the Siberian forest-steppe
[NASA-TM-77914] 23 p3943 N85-34435

STEREOCHEMISTRY

Synthesis of stereoisomeric - metal complexes using phase-transfer catalysis and photochemical transforms
[AD-A145787] 03 p0331 N85-12134

A metal-catalyzed rearrangement of alkene-alkynes and the stereochemistry of metallacyclobutene ring opening
[AD-A149084] 10 p1435 N85-19042

Chemical applications of topology and group theory. 18: Polyhedral isomerizations of seven-coordinate complexes
[AD-A149461] 10 p1436 N85-19047

STEREOGRAPHY

U STEREOPHOTOGRAPHY

STEREOPHONICS

Psychological and physiological basis of stereophonic effect 15 p2526 N85-25574

STEREOPHOTOGRAPHY

An overview of Multispectral Electro-Optical Stereo Scanner (MEOSS) mission 04 p0458 N85-12908

The Monocular Electro-Optical Stereo Scanner Experiment (MEOSS) 04 p0459 N85-12910

Hierarchical data structures and algorithms for digital stereoscopical mensuration 08 p1175 N85-17410

Determining grasp points using photometric stereo and the PRISM binocular stereo system
[AD-A147782] 08 p1222 N85-17697

A generalized ordering constraint for stereo correspondence
[AD-A149182] 10 p1467 N85-19390

Processing of underwater photographs
10 p1499 N85-19462

The position and mobility of the shoulder, spinal column and pelvis in seated subjects
[AD-A153751] 18 p3153 N85-29524

Use of stereographic projection in marine geodesy
19 p3294 N85-30421

Large format camera photographs: A new tool for understanding arid environments
21 p3604 N85-32379

Progress report on a new search for free e/3 quarks in the cores of 10(15) - 10(16) eV air showers
[HE-6.2-15] 24 p4212 N85-36151

STEREOSCOPIC PHOTOGRAPHY

U STEREOPHOTOGRAPHY

STEREOSCOPY

NT STEREOPHOTOGRAPHY

SIR-B cartography and stereo topographic mapping
08 p1147 N85-17234

Automatic terrain elevation mapping and registration
08 p1148 N85-17242

Hurricane structure and dynamics from stereoscopic and infrared satellite observations and radar data
15 p2594 N85-25988

STERILIZATION EFFECTS

NT CHEMICAL EFFECTS
NT DECONTAMINATION
NT THERMAL DEGRADATION

STERNS

U AFTERBODIES

STEROIDS

NT ALDOSTERONE
NT CORTICOSTEROIDS
NT CORTISONE
NT HYDROXYCORTICOSTEROID

Modulation of the cytosolic androgen receptor in striated muscle by sex steroids
[NASA-CR-174173] 04 p0545 N85-13466

STIFF STRUCTURES

U RIGID STRUCTURES

STIFFENING

Design proposals for torsional buckling of stiffeners
[AD-A144783] 01 p0062 N85-10409

An experimental investigation into the dynamic response of a stiffened flat plate loaded impulsively by an underwater shockwave
[AD-A151321] 15 p2578 N85-25903

Finite element thermal-structural analysis of cable-stiffened space structures
[AD-A153822] 18 p3086 N85-28963

Design of transversely stiffenend FRP panels under compressive load — fiber reinforced plastic (FRP) ships
[AMTE(S)-R-84104] 23 p3940 N85-34424

STIFFNESS

Comparison of numerical techniques for integration of stiff ordinary differential equations arising in combustion chemistry
[NASA-TP-2372] 01 p0011 N85-10065

The theory of elastic modulus of fabric composites and its examination by experiments
[NAL-TR-808] 01 p0022 N85-10133

Influence of test method and material stiffness on the damage produced by low velocity impacts on carbon-epoxy composites No. 45.387/1
[REPT-45.387/1] 03 p0326 N85-12100

Interactions among system stiffness, wear and vibrations 03 p0370 N85-12364

Hydrodynamic impeller stiffness, damping, and inertia in the rotordynamics of centrifugal flow pumps
05 p0643 N85-14125

Theoretical approach to labyrinth seal forces - cross-coupled stiffness of a straight-through labyrinth seal 05 p0643 N85-14127

Experimental investigation of lateral forces induced by flow through model labyrinth glands
05 p0643 N85-14128

Dynamic stiffness characteristics of high eccentricity ratio bearings and seals by perturbation testing
05 p0645 N85-14141

A review of imperfection sensitivity of stiffened shells
[AD-A147311] 07 p0978 N85-16213

A gyro sensor block suspension
[AD-D011411] 08 p1154 N85-17284

Modelling and identification of the structural properties of an astromast
[CRC-1374] 09 p1329 N85-18382

Theory versus experiment for the rotordynamic coefficients of annular gas seals. Part 2: Constant clearance and convergent-tapered geometry
[NASA-CR-174413] 10 p1491 N85-19416

Predicting stability of full-scale composite constructions of the basis of stiffness 11 p1599 N85-20054

Elastic compliance of imperfect interfaces: Review and relationship to ultrasonic scattering
[DE85-003068] 11 p1652 N85-20404

Experimental stiffness of tapered bore seals
[NASA-TM-86978] 15 p2568 N85-25847

Effect of internal pressure on flexibility and stress intensification factors for pipe elbows analyzed by the finite element method
[AD-A151161] 15 p2578 N85-25901

Study of oscillations of composite cylindrical shells using a dynamic stiffness technique 16 p2766 N85-27096

Friction and wear behavior of aluminum and composite I-beam stiffened airplane skins
[NASA-TM-86418] 17 p2895 N85-27852

Design of helicopter rotor blades for optimum dynamic characteristics
[NASA-CR-176076] 20 p3393 N85-31044

Vibrational stabilization of flexible structures
20 p3414 N85-31186

Stiffness control of large space structures
20 p3414 N85-31189

An overview of latest model reduction and control methods of large flexible space structures
20 p3414 N85-31191

Thermomechanically induced pre- and postbuckling of general structure 20 p3467 N85-31540

Shear-stress distribution and shear stiffness in the case represented by a non-homogeneous cross-section, of any shape, but composed of an orthotropic material, when subjected to a shear force
[DRIC-T-7430] 20 p3469 N85-31554

Appiication of traction drives as servo mechanisms
22 p3797 N85-33620

The properties of thin-section, four-point-contact ball bearings in space 22 p3797 N85-33621

An introduction to finite elements
23 p3924 N85-34319

STIFFNESS MATRIX

Recursive calculation of curved finite element stiffness matrices
[CSIR-TWISK-303] 01 p0108 N85-10726

Parallel triangularization of substructured finite element problems
[NASA-CR-172466] 02 p0241 N85-11899

An algorithm for assembly of stiffness matrices into a compacted data structure
[AD-A146727] 07 p1023 N85-16482

Finite axisymmetric deformation of a thin shell of revolution 16 p2798 N85-27251

Parametric stiffness control of flexible structures
20 p3414 N85-31187

Automated dynamic analytical model improvement for damped structures
[NASA-CR-177945] 23 p3941 N85-34425

Constrained stiffness matrix adjustment using mode data
[AD-A155988] 24 p4143 N85-35895

STIGMATISM

Electrostatic astigmatic tubular lens
21 p3695 N85-32555

STILLS

Alcohol fuel from Ohio farms: An introduction
[TI-84-901290] 05 p0621 N85-13970

STIMULANTS
NT ATROPINE
NT NOREPINEPHRINE
STIMULATED EMISSION
NT WATER MASERS
Four-photon resonant third harmonic generation
[DE85-010070] 19 p3367 N85-30883
STIMULATED EMISSION DEVICES
NT ARGON LASERS
NT ATMOSPHERIC LASERS
NT CARBON DIOXIDE LASERS
NT CARBON LASERS
NT CARBON MONOXIDE LASERS
NT CHEMICAL LASERS
NT CONTINUOUS WAVE LASERS
NT DF LASERS
NT DYE LASERS
NT EXCIMER LASERS
NT FREE ELECTRON LASERS
NT GALLIUM ARSENIDE LASERS
NT GAS LASERS
NT GASDYNAMIC LASERS
NT GLASS LASERS
NT HCN LASERS
NT HELIUM-NEON LASERS
NT HF LASERS
NT HIGH POWER LASERS
NT HYDROGEN MASERS
NT INFRARED LASERS
NT INJECTION LASERS
NT INTERSTELLAR MASERS
NT IODINE LASERS
NT KRYPTON FLUORIDE LASERS
NT LASERS
NT MASERS
NT METAL VAPOR LASERS
NT NEODYMIUM LASERS
NT NITROGEN LASERS
NT NOVA LASER SYSTEM
NT NUCLEAR PUMPED LASERS
NT ORGANIC LASERS
NT PLASMADYNAMIC LASERS
NT PULSED LASERS
NT Q SWITCHED LASERS
NT RAMAN LASERS
NT RARE GAS-HALIDE LASERS
NT RING LASERS
NT RUBY LASERS
NT SEMICONDUCTOR LASERS
NT SOLAR-PUMPED LASERS
NT SOLID STATE LASERS
NT TEA LASERS
NT TRAVELING WAVE MASERS
NT TUNABLE LASERS
NT TWO-WAVELENGTH LASERS
NT ULTRASHORT PULSED LASERS
NT ULTRAVIOLET LASERS
NT WATER MASERS
NT WAVEGUIDE LASERS
NT X RAY LASERS
NT XENON CHLORIDE LASERS
NT XENON FLUORIDE LASERS
NT YAG LASERS
STIMULATION
NT AUDITORY STIMULI
NT SENSORY STIMULATION
Space-time characteristics of radiation of single-mode injection lasers 02 p0269 N85-11758
Effect of triphthasine and elenium on changes in evoked bioelectrical activity of the brain exposed to stationary magnetic field 19 p3325 N85-30601
STIMULI
Laboratory note: Effect on sleep latency of pre-sleep AEP (Auditory Evoked Potential) procedures
[AD-A147620] 08 p1194 N85-17527
STIRLING CYCLE
Free-piston Stirling engine development
[PB84-237767] 01 p0056 N85-10369
Liquid-piston Stirling machines
[DE84-014256] 02 p0205 N85-11351
Standardized efficiency terms: Comparison of some Stirling engine performance figures
[DE84-015407] 02 p0205 N85-11352
Stirling material technology
[NASA-TM-86888] 04 p0472 N85-13007
Linear harmonic analysis for Stirling machines and second law analysis of four important losses
[DE84-016595] 04 p0573 N85-13655
Linear harmonic analysis of Stirling engine thermodynamics
[DE84-016646] 04 p0574 N85-13657
Overview of waste heat utilization systems
[NASA-TM-86901] 04 p0578 N85-13692
Dynamic power systems for power generation
05 p0609 N85-13892
Dynamic conversion working group summary
05 p0611 N85-13904
Stirling engine development, state of the art, possible engine applications and suitability in comparison to established plants and systems
[BMFT-FB-T-84-196] 05 p0646 N85-14149
Effect of water on hydrogen permeability — Stirling engines
[NASA-TM-86904] 06 p0761 N85-14864
Phase 1-A development kinematic Sterling/Rankine commercial gas-fired heat pump research program
[PB85-100931/GAR] 07 p0936 N85-15926
Initial testing of a variable-stroke Stirling engine
[NASA-TM-86875] 10 p1569 N85-19895
Introducing engine innovations: An examination of future markets for Brayton and Stirling automotive engines
[DE84-016319] 11 p1647 N85-20382
Magentically actuated compressor
[NASA-CASE-GSC-12799-1] 12 p1818 N85-21404
Gas-fired duplex free-piston Stirling refrigerator
12 p1819 N85-21413
Some solar dish/heat engine design considerations
[DE85-003479] 12 p1881 N85-21802
Parameters of symmetric rhombic drive mechanism for single-cylinder Stirling engine 14 p2271 N85-24072
Overview of the 1985 NASA Lewis Research Center SP-100 free-piston Stirling engine activities
[NASA-TM-87028] 16 p2680 N85-27759
Activity and accomplishments of dish/Stirling electric power system development
[NASA-CR-175841] 17 p2965 N85-28445
Simplified analysis of Stirling engines and heat pumps
[DE85-008753] 17 p2966 N85-28457
Report to Congress on the Automotive Technology Development Program
[DE85-005840] 17 p3052 N85-28890
Free-piston Stirling engine/linear alternator 1000-hour endurance test
[NASA-CR-174771] 19 p3304 N85-30481
STOCHASTIC PROCESSES
NT MARKOV CHAINS
NT MARKOV PROCESSES
NT RANDOM PROCESSES
NT RANDOM WALK
Theory of nuclear magnetic relaxation
[AD-P003911] 01 p0032 N85-10197
Some weak and strong laws of large numbers for d(0,1) -valued random variables
[AD-A144845] 01 p0111 N85-10754
Simulation uses of the exponential distribution
[AD-A144940] 01 p0112 N85-10756
On the Pontryagin principle for stochastic optimal control
[TWISK-328] 01 p0112 N85-10762
Stochastic properties of a sequence of interfailure times under minimal repair and under revival
[AD-A145003] 01 p0113 N85-10769
Asynchronous discrete control of continuous processes
[AD-A145570] 02 p0189 N85-11282
Asymptotically optimal adaptive control
[AD-A145666] 02 p0249 N85-11629
Limit theory for the sample covariance and correlation functions of moving averages
[AD-A145488] 02 p0251 N85-11642
Maximum likelihood estimation of the survival functions of N stochastically ordered random variables
[AD-A145429] 02 p0254 N85-11662
On the rate of mean convergence of finite linear predictors of multivariate stationary stochastic processes
[AD-A145609] 02 p0254 N85-11664
Diffusion and intermittency in an extended one-dimensional maps 02 p0282 N85-11834
Long time correlation and stochastic diffusion in the standard map 02 p0282 N85-11835
Stochasticity and transport in Hamiltonian systems
02 p0282 N85-11836
Long-time tail in the two-wave model
02 p0282 N85-11837
Stochastic property of K-dV solitons perturbed by random forces — Korteweg-Devries equation
02 p0283 N85-11843
Stable distribution and Levy process in fractal turbulence 02 p0283 N85-11846
On-line fatigue life prediction under stochastic loading by the time series modeling 03 p0370 N85-12362
Regenerative simulation methods for local area computer networks
[AD-A146197] 03 p0409 N85-12612
Return difference feedback design for robust uncertainty tolerance in stochastic multivariable control systems
[AD-A145861] 03 p0411 N85-12624
Vertical coherence along a macroray path in an inhomogeneous anisotropic ocean
[AD-A145992] 03 p0416 N85-12660
A stochastic model for optimizing the consumption and exploration of nonrenewable natural resources
[INPE-2770-PRE/343] 03 p0440 N85-12804
Accounting for error stochasticity in terminal homing of aircraft 04 p0489 N85-13115
Stochastic cell model for hadronic multiparticle distributions
[DE84-016480] 04 p0562 N85-13578
Stochastic does not equal ad hoc — theories of lunar origin 04 p0586 N85-13741
Evaluation of the stochastic drift of rate-integrating gyros as preparation for the analysis of laser gyro drift measurements
[ESA-TT-827] 05 p0639 N85-14099
Coupling of multidirectional diffusions by reflection
[CTH-MATH-1984-20] 05 p0719 N85-14613
An on-line parameter estimation algorithm for counting process observations
[CWI-OS-R8406] 05 p0721 N85-14632
Information flow in event-driven large-scale systems
[DE84-014167] 05 p0735 N85-14728
Studies in statistical signal processing
[AD-A147130] 07 p0940 N85-15959
The Shock and Vibration Digest, volume 16, no. 9
[AD-A146779] 07 p0976 N85-16200
Techniques for nonlinear random vibration problems
07 p0977 N85-16201
Estimation for a semimartingale regression model using the method of sieves
[AD-A146809] 07 p1028 N85-16527
Numerical methods and approximation and modelling problems in stochastic control theory
[AD-A146927] 07 p1029 N85-16533
The symmetry group and exponents of operator stable probability measures
[AD-A147187] 07 p1035 N85-16566
Limiting distributions of functionals of Markov chains
[AD-A147632] 07 p1036 N85-16577
Local dependence and point processes of exceedances in stationary sequences
[AD-A147859] 07 p1036 N85-16578
Robust prediction and interpolation for vector stationary processes, part 3
[AD-A147860] 07 p1036 N85-16579
Infinite order autoregressive representations of multivariate stationary stochastic processes
[AD-A147863] 07 p1036 N85-16580
On modeling the performance and reliability of multi-mode computer systems
[AD-A148444] 08 p1208 N85-17599
Optimal stochastic LQ control with measurements displaced in time
[OUEL-1547/84] 08 p1209 N85-17605
Large deviations for processes with independent increments
[AD-A147293] 08 p1210 N85-17610
Asymptotic methods for the analysis, estimation, and control of stochastic dynamic systems
[AD-A147758] 08 p1211 N85-17618
Extended Stochastic Petri Nets: Applications and analysis
[AD-A148439] 08 p1213 N85-17633
Bounding the stochastic performance of continuum structure functions 1
[AD-A148621] 08 p1213 N85-17640
Methods and applications of time series analysis. Part 2: Linear stochastic models
[AD-A147292] 08 p1214 N85-17645
Research in stochastic processes
[AD-A148622] 08 p1216 N85-17660
Stochastic models of pitting corrosion of stainless steels. Part 1: Modeling of the initiation and growth of pits at constant potential
[AERE-R-11146-PT-1] 09 p1298 N85-18151
Stochastic dynamic analysis of a structure with frictional joints 09 p1337 N85-18408
Modeling stochastic wind loads on vertical axis wind turbines
[DE85-001148] 09 p1340 N85-18426
SPADE: Series-parallel directed acyclic graph evaluator
[AD-A148458] 09 p1368 N85-18592
Nicolai maps and stochastic observables from a coupling constant flow
[BONN-HE-84-26] 09 p1376 N85-18653
Data-driven choice of a spectrum estimate: Extending the applicability of cross-validation methods
[DE85-001411] 10 p1437 N85-19058
UHF communications through forested propagation channels 10 p1470 N85-19260
A non-hypoelliptic Dirichlet problem from stochastics
10 p1537 N85-19687
Research in adaptive and decentralized control
[AD-A146964] 10 p1543 N85-19728

Bounding the stochastic performance of continuum structure functions 2
[AD-A149458] 10 p1548 N85-19762
Stochastic methods for the description of multiparticle production
[DE84-009981] 10 p1556 N85-19810
Stochastic runaway of dynamical systems
[IPP-6/244] 11 p1708 N85-20745
Bayesian analysis of time series 1: Householder transformation analyses
[DE85-004449] 11 p1708 N85-20749
Autostochastic behavior of solid state ring laser with low frequency periodic loss modulation
11 p1717 N85-20805
Stochastic convective-dispersive transport model for wastes disposed at the 106-mile ocean disposal site
[PB85-116176] 12 p1885 N85-21831
The effect of stochastic surface heat fluxes on the climatology of the seasonal thermocline
[AD-A149957] 12 p1889 N85-21857
Distributed asynchronous deterministic and stochastic gradient optimization algorithms: Revision
[AD-A149997] 12 p1921 N85-22068
Rates of convergence of semistochastic approximation procedures for solving stochastic optimization problems
12 p1924 N85-22088
A stochastic-mechanical approach to acoustic pulse propagation in the deep ocean sound channel
[AD-A149598] 12 p1928 N85-22110
Statistical phenomena in particle beams
[DE85-001050] 12 p1929 N85-22118
An analysis of a dynamic project cost problem
[CSIR-TWISK-338] 13 p2149 N85-23341
The design of a unified package for the solution of stochastic petri net models
[AD-A150326] 13 p2151 N85-23354
Regenerative stochastic Petri nets
[AD-A150343] 13 p2151 N85-23355
Regenerative simulation of non-Markovian stochastic systems
[AD-A150344] 13 p2153 N85-23367
Application of the maximum entropy/optimal projection control design approach for large space structures
14 p2234 N85-23849
Studies of the initiation of pitting corrosion on stainless steels
[AERE-M-3400] 14 p2254 N85-23967
Dynamic stochastic model of long-period variability of ocean surface temperature 14 p2334 N85-24437
Parameter estimation in stochastic dynamic systems
14 p2395 N85-24754
Ergodicity and Steady-State-Equilibrium conditions for Markov chains
[AD-A151038] 14 p2409 N85-24854
Estimation of optimum scores for partition detectors using stochastic approximation techniques
14 p2411 N85-24865
Stochastic pursuit-evasion differential games in the plane
[CSIR-TWISK-343] 14 p2412 N85-24875
Kinematic dynamo theory for an arbitrary mean flow
14 p2448 N85-25108
Boundary of modulation diffusion and stochastic instability of high energy protons in inner radiation belt
15 p2482 N85-25316
Theory and Applications of State Estimation. NRIMS Summer Seminar Series
[CSIR-SWISK-37] 15 p2635 N85-26244
Nonlinear estimation 15 p2635 N85-26245
The Kalman filter 15 p2635 N85-26246
Linear filtering with non-Gaussian initial conditions
15 p2635 N85-26247
Truncated nonlinear filters 15 p2635 N85-26249
Some aspects of decentralized Kalman filtering
15 p2635 N85-26250
Tracking filters 15 p2635 N85-26252
Point processes associated with extreme value theory
[AD-A151211] 15 p2640 N85-26280
Inference and state estimation for stochastic point processes
[AD-A151216] 15 p2640 N85-26281
Stochastic modeling of planetary ring systems
15 p2675 N85-26516
Graphic simulation of a machine-repairman model
[AD-A151761] 16 p2694 N85-26633
Characteristic functionals of stochastic wave processes
[REPT-14/1984] 16 p2768 N85-27084
Some new results on the discrete-time Riccati Equation and their use in the design of optimal regulators and observer-estimators
[AD-A151934] 16 p2854 N85-27597
An application of Markov chains to the problem of migration in inventory systems
[AD-A151954] 16 p2857 N85-27618
Probabilistic finite element development
17 p2913 N85-27956
On the exceedance point process for a stationary sequence
[AD-A152627] 17 p3018 N85-28665
Extension of three theorems of Fourier series on the disc to the torus
[AD-A153017] 17 p3019 N85-28669
On stochastic integral representation of stable processes with sample paths in Banach spaces
[AD-A152927] 17 p3025 N85-28703
Maximum flow in planar networks with exponentially distributed arc capacities
[AD-A153158] 17 p3026 N85-28710
I. F. S. (Institute for Fusion Studies) Newsletter, Volume 4, Number 1
[DE85-007917] 17 p3040 N85-28809
A global optimization algorithm using stochastic differential equations
[AD-A153526] 18 p3161 N85-29583
Limit behaviour for stochastic monotonicity and applications
[AD-A153814] 18 p3170 N85-29648
High performance asynchronous limited sensing algorithms for CSMA and CSMA-CD channels
[AD-A153919] 18 p3171 N85-29650
Performance evaluation of stochastic timed decision-free Petri Nets
[AD-A153987] 18 p3171 N85-29652
Numerical simulation of the transient by the unstable state in a Lotka-Volterra model
[NOTA-INTERNA-833] 18 p3175 N85-29684
Stochastic resonance in the Landau-Ginzburg equation
[PREPRINT-430] 18 p3175 N85-29685
Short and long-term robot feedback
[PB85-180735] 19 p3281 N85-30347
Use of adjoint equations in problems of evaluating state of random hydrodynamic fields
19 p3289 N85-30398
Method for computing evolution of random hydropdynamic fields on basis of adjoint equations
19 p3292 N85-30412
Expected utility, penalty functions, and duality in stochastic nonlinear programming, revised
[AD-A154034] 19 p3335 N85-30660
An overview of latest model reduction and control methods of large flexible space structures
20 p3414 N85-31191
Routing algorithms and stochastic analysis for large communications networks
[AD-A154654] 21 p3573 N85-32225
A simulation of weather in 3D space
[AD-A155221] 21 p3636 N85-32586
SIGMA - A stochastic-integration global minimization algorithm
[AD-A154878] 21 p3671 N85-32806
Relating corrosion maintenance to environmental factors 22 p3750 N85-33247
Stochastic groundwater flow modeling using the second-order method
[DE85-011250] 22 p3802 N85-33556
Modeling and measurement of fault-tolerant multiprocessors
[NASA-CR-3920] 22 p3833 N85-33732
Frame buffer algorithms for stochastic models
23 p3957 N85-34525
Specifying stochastic objects in a hierarchical graphics system 23 p3957 N85-34526
Stochastic particle acceleration in flaring stars
[OG-8.3-9] 23 p4022 N85-34927
On the statistical significance of excess events: Remarks of caution and the need for a standard method of calculation
[OG-9.5-10] 23 p4031 N85-34967

STOICHIOMETRY
Effect of oxidizing medium and heat treatment on stoichiometry of ZnSe crystal surface
03 p0353 N85-12272
Catalytic oxidation by transition metal ions in zeolites
[AD-A146828] 07 p0922 N85-15842
Homogeneous reaction involving components of different redox couples. 2: Polarographic studies of the interactions of alkali metal cations with anthracene and fluoroanthene dianions in N,N-dimethylformamide and acetonitrile
[AD-A148667] 08 p1124 N85-17085
Study of self-propagating condensed phase reactions TiB(2) synthesis
[AD-A153198] 17 p2921 N85-28006
New examples of clusters, extended metal-metal bonding and interstitial derivatives
[DE85-005926] 17 p3044 N85-28837
Combustion characterization of coals for industrial applications
[DE85-010673] 19 p3228 N85-30014
Lithium cell reactions
[AD-A154429] 19 p3306 N85-30[illegible]
Survey of mixing in metal/insulator systems
[DE85-011938] 23 p3985 N85-34714
CO + H2 reaction over nitrogn-modified iron catalysts
[DE85-013791] 24 p4072 N85-35[illegible]
Size and shape dependence of CO adsorption sites on sapphire supported Fe microcrystals
[NASA-CR-176171] 24 p4160 N85-357[illegible]

STOKES FLOW
A counterpart of Faxen's formula in potential flow
[REPT-84-09] 17 p2960 N85-28[illegible]

STOKES LAW (FLUID MECHANICS)
Experiments on controlled, unsteady, separated turbulent boundary layers
[AD-P004172] 09 p1268 N85-17[illegible]

STOKES LAW OF RADIATION
Modifications to a propagation model for the combined refraction-diffraction of stokes waves; shallow water, large angle and breaking wave effects
[AD-A151426] 15 p2586 N85-25[illegible]
Measurements of vector fields with diode array
18 p3204 N85-29[illegible]
Dynamic models of flux tubes in the interpretation of polarization measurements 18 p3206 N85-29[illegible]
Contribution functions for Zeeman-split lines, and line formation in photospheric faculae
18 p3207 N85-[illegible]
The effect of line damping, magneto-optics and parasitic light on the derivation of sunspot vector magnetic fields
18 p3207 N85-29[illegible]

STOKES THEOREM (VECTOR CALCULUS)
Measurements of vector fields with diode array
18 p3204 N85-29[illegible]
Analysis of the new polarimeter for the Marshall Space Flight Center vector magnetograph
18 p3205 N85-29[illegible]
The solar vector magnetograph of the Okayama Astrophysical Observatory 18 p3205 N85-29[illegible]

STOL AIRCRAFT
U SHORT TAKEOFF AIRCRAFT

STONES (ROCKS)
U ROCKS

STONY METEORITES
NT ALLENDE METEORITE
NT CARBONACEOUS CHONDRITES
NT CARBONACEOUS METEORITES
NT CHONDRITES
NT PANTAR CHONDRITES
NT TEKTITES
Origin of mesosiderites as a natural consequence of planet formation 15 p2683 N85-26574

STOPCOCKS
U COCKS

STOPPING POWER
Stopping powers of solids for low-energy protons
[DE85-001123] 09 p1382 N85-18[illegible]
Slowing down of charged particles by the bound electrons in a plasma — ion beams, nuclear fusion
[LP-209] 14 p2419 N85-24[illegible]

STORABLE PROPELLANTS
NT AIRCRAFT FUELS
Space Transportation System (STS) propellant scavenging system study. Volume 1: Technical report
[NASA-CR-171848-VOL-1] 11 p1589 N85-20000
Space Transportation System (STS) propellant scavenging system study. Volume 2: Supporting research and technology report
[NASA-CR-171849-VOL-2] 11 p1589 N85-20001
Surveillance report. Stage 1: Dissected motors-propellants motor number 0012190, phase 15
[AD-A153206] 17 p2916 N85-27[illegible]

STORAGE
Depot modernization at the Defense Logistics Agency
[AD-P004008] 03 p0308 N85-11[illegible]
Changes in spectral properties of detached leaves
[E85-10042] 07 p0983 N85-18[illegible]
Characterization and selection of polymer materials for binary munitions storage. Part 2: Characterization of LLDPE resins
[AD-A148324] 08 p1133 N85-17144

STORAGE BATTERIES
NT LEAD ACID BATTERIES
NT NICKEL CADMIUM BATTERIES
NT NICKEL HYDROGEN BATTERIES
NT NICKEL ZINC BATTERIES
NT SILVER HYDROGEN BATTERIES
NT ZINC-BROMIDE BATTERIES
NT ZINC-CHLORINE BATTERIES
Electrochemistry and storage
05 p0609 N85-13[illegible]
Electrochemistry and storage panel report
05 p0611 N85-13[illegible]
Energy storage for stationary and mobile operation as a buffer of power supply from additive energy sources
05 p0663 N85-14[illegible]

Rechargeable lithium cell
[AD-D011302] 07 p0993 N85-16304

Polymer electrolytes: An investigation of some poly (N-propylaziridine)/lithium salt compositions
[RAE-TR-84036] 08 p1131 N85-17130

BBC of Switzerland develops electric car
08 p1141 N85-17192

Status of French research in plastic batteries
15 p2530 N85-25603

Calcium/thionyl chloride battery technology
[AD-A151975] 15 p2586 N85-25945

Maintenance of photovoltaic power systems
[AD-A152299] 16 p2819 N85-27390

Regenerative fuel cell systems for space station
20 p3443 N85-31372

System level electrochemical principles
20 p3443 N85-31375

Advances in rechargeable lithium molybdenum disulfide batteries 20 p3444 N85-31376

Geosynchronous performance of a lithium-titanium disulfide battery 20 p3444 N85-31377

Rechargeable lithium-organic electrolyte battery having overcharge protection and method of providing overcharge protection for a lithium-organic electrolyte battery
[AD-D011738] 22 p3806 N85-33575

Solar heat pump
[DE85-011323] 23 p3946 N85-34453

STORAGE RINGS (PARTICLE ACCELERATORS)

The Berkeley mini-collider
[DE84-014594] 01 p0118 N85-10808

Self potentials of an electron ring in a torus for large ring displacement from the minor axis
[AD-A146088] 03 p0421 N85-12691

Positron ring system using Anger-type detectors
[DE84-016788] 04 p0503 N85-13212

A normal-incidence monochromator branch line on the FEL-undulator for experimental studies in the 5 to 30 eV region
[DE84-014379] 04 p0505 N85-13225

ASP: A new PEP experiment to measure single photons
[DE84-015732] 04 p0560 N85-13563

Tune shifts for coasting beams crossing at small angles
[DE84-017174] 04 p0562 N85-13579

Instrumentation at national facilities for synchrotron radiation topography
[DE84-016256] 04 p0564 N85-13593

Crossing point conditions, quadrupole gradients and drift space lengths
[DE85-003223] 11 p1721 N85-20825

Electron storage ring beam lifetime dependence on pressure and pumping speed
[DE85-003208] 11 p1724 N85-20845

Review of polarized proton beam techniques and a report on the workshop on polarized beams
[DE85-004390] 12 p1930 N85-22127

Intense, broadband, pulsed I-R source at the National Synchrotron Light Source
[DE84-010542] 12 p1935 N85-22154

Study of the potential usefulness of superfine holographic x-ray gratings in AXAF and astrophysics in general 12 p1945 N85-22215

Electronics Engineering Department EE Technical Review
[UCRL-50025-84-1] 13 p2063 N85-22887

Application of permanent magnets in accelerators and electron storage rings
[DE85-004981] 15 p2642 N85-26297

Energy dependence of the emittance of damping ring beams
[DE85-007080] 15 p2649 N85-26341

Measurement of NSLS distributed diode sputter ion pump characteristics
[DE85-006550] 16 p2760 N85-27031

Proceedings of the Workshop on Polarized Targets in Storage Rings
[DE85-002704] 16 p2862 N85-27653

Distortion functions
[DE85-007511] 16 p2862 N85-27655

Calculations of beam dynamics in Sandia linear electron accelerators, 1984
[DE85-010417] 18 p3180 N85-29719

Coherent X-rays and vacuum-ultraviolet radiation from storage-ring-based undulators and free electron lasers
[DE85-009968] 18 p3183 N85-29738

Experience with a high-brightness storage ring: The NSLS 750 MeV VUV ring
[DE85-010547] 18 p3190 N85-29787

Present and future directions of atomic physics research with multiply-charged ions at Brookhaven National Laboratory
[DE85-010860] 19 p3354 N85-30788

Experiments with stored heavy ions
[DE85-009076] 19 p3356 N85-30802

Guide to the Main Ring DO overpass
[DE85-011722] 20 p3531 N85-31963

Saturation of a longitudinal instability due to nonlinearity of the wake field
[DE85-012514] 22 p3837 N85-33761

Multiple-frequency electron cyclotron heating of hot electron rings in EBT-1
[DE85-011302] 23 p3983 N85-34701

Forty-five years of e(+)e(-) annihilation physics: 1956 to 2001
[DE85-013052] 24 p4149 N85-35723

Breeding new light into old machines (and new)
[DE85-013055] 24 p4155 N85-35763

Vacuum system for the Argonne 6 GeV synchrotron light source
[DE85-012286] 24 p4157 N85-35773

Los Alamos high-current proton storage ring
[DE85-012664] 24 p4158 N85-35779

Accelerator physics measurements at the damping ring
[DE85-013373] 24 p4159 N85-35785

TOSCA calculations and measurements for the SLAC SLC damping ring dipole magnet
[DE85-014366] 24 p4160 N85-35793

STORAGE STABILITY

Storage life of thermal detents
[DE84-016934] 04 p0476 N85-13030

Storage stability of jet fuels
[AD-A146360] 06 p0773 N85-14943

Microspots on spectroscopic plates — astronomical photography 07 p0964 N85-16113

Passive storage technologies
08 p1108 N85-17003

Mechanisms of heat and mass transfer across a double-diffusive interface
[PB85-148468] 12 p1848 N85-21594

Prediction of the long term stability of polyester-based recording media
[PB85-160133] 14 p2262 N85-24019

Conservation of turbines by inhibited air
14 p2268 N85-24054

Alternative food preservation techniques, new technology in food preparation and appropriateness of food supply for the permanently manned space station
14 p2393 N85-24739

Solid state hydrogen pumping and storage material
[AD-D011610] 16 p2757 N85-27011

Surveillance report. Stage 1: Dissected motors-propellants motor number 0012199, phase 15
[AD-A153206] 17 p2916 N85-27973

Additional experiments relative to the shelf life of Li(Si)/FeS2 thermal batteries
[DE85-008482] 18 p3095 N85-29162

Review of zirconium-zircaloy pyrophoricity
[DE85-011169] 23 p3916 N85-34270

Dissected motors-propellants motor number STM-012. Phase 15: Surveillance report, stage 1
[AD-A156099] 24 p4071 N85-35226

STORAGE TANKS

Insulating polymer concrete
[DE84-017239] 04 p0480 N85-13057

VOC emissions from volatile organic liquid storage tanks: Background information for proposed standards
[PB84-237320] 04 p0532 N85-13403

Shock testing of a nitrogen tank (Cryo diffusion type 220 VLR) on the middle weight shock stand
[NASA-TM-77747] 06 p0817 N85-15183

Risks in the transport and storage of liquefied natural gas. Sub-project 5-2: Investigation into building damage
[BLL-RISLEY-TR-4608-(9091.9F)]
07 p0935 N85-15926

Passive Orbital Disconnect Strut (PODS 3) structural test program
[NASA-CR-177325] 08 p1113 N85-17020

High temperature sensible heat storage options
[DE85-000534] 18 p3129 N85-29375

Mixtures experiment where the amount of the mixture is a factor under study
[DE85-010974] 19 p3250 N85-30153

Cultural data base implementation study and computer-aided scene modeling system users manual
[AD-A154232] 19 p3333 N85-30646

Oil tank electrostatic charging report
[DRIC-T-6867] 20 p3436 N85-31319

Results of variable enthalpy tests of CPR-488 TIP panels in MSFC Hot Gas Facility
[NASA-CR-170869] 24 p4072 N85-35237

STORE RELEASE

U EXTERNAL STORE SEPARATION

STORM DAMAGE

Effects of a lightning strike on a civil defense operation center
[FOA-A-30035-A3] 02 p0232 N85-11514

Hurricane Alicia, Galveston and Houston, Texas, 17-18 August 1983
[PB84-237056] 04 p0541 N85-13441

California coastal erosion and storm damage during the winter 1982 - 1983, a reconnaissance report
[PB85-121706] 10 p1521 N85-19591

STORMS

NT CYCLOGENESIS
NT CYCLONES
NT DUST STORMS
NT HURRICANES
NT IONOSPHERIC STORMS
NT MAGNETIC STORMS
NT POLAR SUBSTORMS
NT RAINSTORMS
NT SNOWSTORMS
NT SOLAR STORMS
NT STORMS (METEOROLOGY)
NT SUDDEN IONOSPHERIC DISTURBANCES
NT THUNDERSTORMS
NT TORNADOES
NT TROPICAL STORMS
NT TYPHOONS

Effect of mountain wave dynamics on orographic storms
[DE84-014713] 04 p0540 N85-13433

Probable maximum flood estimation - Eastern United States
[AD-A146536] 06 p0839 N85-15324

Behavior and characteristics of storm cold outflows
09 p1356 N85-18529

Mesoscale storm and dry period parameters from hourly precipitation data: Program documentation
[DE85-001366] 09 p1357 N85-18538

Hurricane alicia storm surge and wave data
[AD-A149668] 12 p1895 N85-21896

Mesoscale analysis and modeling group
15 p2596 N85-26001

Review of VAS demonstration
15 p2596 N85-26002

Impact of soil moisture in organizing a severe storm outbreak 15 p2597 N85-26009

Role of frontal circulations and gravity waves in initiating convective storm systems 15 p2598 N85-26010

An evaluation of the performance of a new storm tracking methodology
[AD-A152234] 16 p2835 N85-27484

Centralized Storm Information System (CSIS)
[NASA-CR-175898] 17 p2994 N85-28506

A report from the Space Science and Engineering Center, the University of Wisconsin-Madison, Madison, Wisconsin 17 p2994 N85-28507

Test and evaluation plan for the Centralized Storm Information System 17 p2994 N85-28508

CSIS test and evaluation 17 p2994 N85-28509

Functional and performance requirements of the next NOAA-Kasas City computer system
17 p2994 N85-28510

Convective storm downdraft outflows detected by NASA/MSFC's Airborne 10.6 micron pulsed Doppler Lidar System
[NASA-CR-3898] 17 p2995 N85-28511

A numerical study of the Pacific polar low
[AD-A153777] 18 p3140 N85-29495

The temporal evolution of a small auroral substorm as viewed from high altitudes with Dynamics Explorer 1
[NASA-CR-176064] 20 p3493 N85-31718

Radio-frequency radiation of storm clouds
21 p3692 N85-32939

STORMS (METEOROLOGY)

NT DUST STORMS
NT HURRICANES
NT POLAR SUBSTORMS
NT RAINSTORMS
NT SNOWSTORMS
NT THUNDERSTORMS
NT TORNADOES
NT TROPICAL STORMS
NT TYPHOONS

Energy correlation between natural extra-low-frequency noises at various frequencies 06 p0784 N85-15010

Spring program summary, 198[illegible]
[PB84-222223] 06 p0839 N85-15330

The rationale and suggested approaches for research geosynchronous satellite measurements for severe storm and mesoscale investigations
[NASA-TM-86185] 09 p1356 N85-18532

The influence of soil moisture distribution on the severe-storm environment of the southern Great Plains: A numerical study of the SESAME 4 case
09 p1357 N85-18534

Cut-off lows and their influence on the weather in Switzerland
[REPT-45] 10 p1519 N85-19574

Varying structure and intensity change characteristics of 4 Western North Pacific tropical cyclones
[AD-A1496[illegible]] 12 p1895 N85-21895

Model sensitivity studies of major east coast storms
15 p2598 N85-26016

Justification and plan for participation in GALE
15 p2599 N85-26017

The seasonal cycle of storminess as measured by band-pass fluctuations 18 p3144 N85-29467

Environmental Research Laboratories publication abstracts, FY 1984
[PB85-180594] 19 p3313 N85-30540

A probabilistic forecasting model of tropical cyclone-generated storm surge for a straight coastline
19 p3314 N85-30544

Areal coverage of storm precipitation
[NASA-CR-176013] 19 p3315 N85-30550

STORMSAT SATELLITE

The rationale and suggested approaches for research geosynchronous satellite measurements for severe storm and mesoscale investigations
[NASA-TM-86185] 09 p1356 N85-18532

The effect of the arbitrary level assignment of satellite cloud motion wind vectors on wind analyses in the pre-thunderstorm environment
[NASA-TM-86186] 10 p1517 N85-19565

STOSS-AND-LEE TOPOGRAPHY

U GLACIAL DRIFT

STOWAGE (ONBOARD EQUIPMENT)

Hemispherical latching apparatus
[NASA-CASE-MFS-25837-1] 19 p3224 N85-29991

STRAIGHT WINGS

U RECTANGULAR WINGS

STRAIN AGING

U PRECIPITATION HARDENING

STRAIN DISTRIBUTION

U STRESS CONCENTRATION

STRAIN ENERGY METHODS

The effect of cross-link density on the toughening mechanism of elastomer-modified epoxies
04 p0465 N85-12951

Numerical investigation of the micromechanics of composite fracture 04 p0467 N85-12970

Toughening mechanism in elastomer-modified epoxy resins, part 2
[NASA-CR-3852] 04 p0478 N85-13046

Stress intensity factors for corner cracks at holes located near an edge
[FFA-TN-1984-20] 04 p0514 N85-13279

Residual thermal and moisture influences on the strain energy release rate analysis of edge delamination
[NASA-TM-86437] 20 p3422 N85-31238

Finite elastic deformations of cylindrical and spherical shells under pressure
[OUEL-1549/84] 20 p3470 N85-31559

Stored energy and structural failure
[OUEL-1564/85] 20 p3471 N85-31567

STRAIN FATIGUE

U FATIGUE (MATERIALS)

STRAIN GAGE ACCELEROMETERS

Navy operational loads data sources and systems
07 p0895 N85-15668

STRAIN GAGES

High temperature static strain sensor development program 02 p0141 N85-10959

Instrumentation techniques for measuring large, high rate strains with foil resistance strain gages
[AD-A146248] 03 p0364 N85-12337

Semiconductor-type transducer with universal strain gauge for measurement of low pressures
04 p0489 N85-13116

A preliminary study of using a strain-gauged balance and parameter estimation techniques for the determination of aerodynamic forces on a model in a very short duration wind tunnel
[AD-A146473] 06 p0810 N85-15145

Structural load measurements on a Northrop NF-5A
07 p0894 N85-15667

Tornado: Structural Usage Monitoring System (SUMS) 07 p0896 N85-15680

Diffusion in metals under high mechanical strain and acceleration
[JUEL-1913] 07 p0928 N85-15887

The constant current strain gauge bridge
[ARL/STRUC-TM-385] 07 p0952 N85-16097

Six-component strain gage block scale 167-6B. Part 1: Calibration, September 1983
[F+W-FO-1699] 07 p0968 N85-16143

Residual stresses at small diffusion welds
[DE84-014982] 07 p0974 N85-16189

Measurement of high temperature strain by the laser-speckle strain gauge
[NASA-TM-77751] 07 p0977 N85-16207

Recommendations for the use of Ni-Cr-base alloy extensometers for measurement of creep strain
[NPL-DMA(A)-81] 08 p1164 N85-17342

Pressure measurements in a hydrogen combustion environment: An evaluation of 3 pressure transducers
[TI85-003845] 09 p1323 N85-18312

Resistance foil strain gage technology as applied to composite materials
[NASA-CR-3872] 10 p1431 N85-19024

Thin film strain transducer --- suitable for in-flight measurement of scientific balloon strain
[NASA-CASE-WLP-10055-2] 12 p1849 N85-21598

Evaluation results of the 700 deg C Chinese strain gauges --- for gas turbine engine
[NASA-TM-86973] 12 p1860 N85-21606

MFTF sensor verification computer program
[DE85-004452] 12 p1916 N85-22020

Root stresses in conformal gears-strain gauge and photoelastic investigations 14 p2223 N85-23787

Effect of drag behind nozzle array on its force and energy characteristics 14 p2277 N85-24107

An experimental investigation into the dynamic response of a stiffened flat plate loaded impulsively by an underwater shockwave
[AD-A151321] 15 p2578 N85-25903

A strain gauge manual
[AD-A151802] 16 p2787 N85-27197

Optical strain measurement system development
17 p2915 N85-27969

Liquid-metal transducers for strain measurement during in-pile materials testing 17 p2945 N85-28176

R and D activities of the Systems Engineering Division
20 p3540 N85-32027

The compliance of end effector force sensors for robot manipulator control 24 p4096 N85-35406

Carbon fiber strainmeter studies in southern California
[PB85-196889] 24 p4118 N85-35528

STRAIN HARDENING

Strain hardening and strain aging in Fe-Al-Mn alloys
02 p0178 N85-11196

High temperature low-cycle fatigue mechanisms in single crystals of nickel-based superalloy Mar-M 200
[NASA-CR-174739] 03 p0331 N85-12130

The influence of porosity on the deformation and fracture of alloys
[AD-A148766] 08 p1130 N85-17124

Ultrasonic characterization of advanced composite flywheels
[DE85-000188] 11 p1593 N85-20026

Influence of work-hardening on the Portevin-LeChatelier effect
[DE85-002505] 11 p1605 N85-20093

Structural basis for the mechanical properties of polyethienes
[PB85-149771] 11 p1613 N85-20142

Measurement of material properties to Mbar pressures using time-resolved shock wave techniques
[DE85-007319] 15 p2558 N85-25780

Slideline verification for multilayer pressure vessels and piping analysis including strain hardening
[DE85-005816] 22 p3801 N85-33549

STRAIN MEASUREMENT

Laser speckle technique for burner liner strain measurements 02 p0142 N85-10960

Device for measuring relative axial expansion of turbine rotor employing space-vector tracking method
06 p0776 N85-14962

Advanced fatigue monitoring on service aircraft
07 p0895 N85-15671

Experiences obtained from service fatigue monitoring exercises 07 p0895 N85-15672

Residual stresses at small diffusion welds
[DE84-014982] 07 p0974 N85-16189

Recommendations for the use of Ni-Cr-base alloy extensometers for measurement of creep strain
[NPL-DMA(A)-81] 08 p1164 N85-17342

Resistance foil strain gage technology as applied to composite materials
[NASA-CR-3872] 10 p1431 N85-19024

Thin film strain transducer --- suitable for in-flight measurement of scientific balloon strain
[NASA-CASE-WLP-10055-2] 12 p1849 N85-21598

Fibre composite laminated plate analysis using a card programmable calculator (HP41C/CV)
[NIAST-83/88] 13 p2103 N85-23106

Some advances in experimentation supporting development of viscoplastic constitutive models
[NASA-CR-174855] 16 p2799 N85-27260

Liquid-metal transducers for strain measurement during in-pile materials testing 17 p2945 N85-28176

Fatigue strength of Inconel 625 plate and weldments used in the DIII-D configuration vacuum vessel
[DE85-008276] 17 p2981 N85-28427

Inhomogeneous deformation: The theory and geological application of finite strain compatibility
19 p3312 N85-30532

Some advances in experimentation supporting development of viscoplastic constitutive models
20 p3468 N85-31545

Algorithm for calculation of strain state from measurements of node coordinates of arbitrary curvilinear grid
[BLL-M-36304-(5828.4)] 23 p3940 N85-34422

Strain measurement using point recognition picture processing
[DRIC-T-7407] 24 p4101 N85-35421

1983 review of experimental stress and strain analysis
[DRIC-T-7469] 24 p4101 N85-35422

STRAIN RATE

Reliability considerations for the total strain range version of strainrange partitioning
[NASA-CR-174757] 02 p0209 N85-11380

Instrumentation techniques for measuring large, high rate strains with foil resistance strain gages
[AD-A146248] 03 p0364 N85-12337

Horizontal-strain observations in the Shumagin Island and Yakataga seismic gaps, Alaska
04 p0515 N85-13297

Strain rate effects and temperature history effects for three different tempers of 4340 VAR steel
[AD-A146372] 06 p0766 N85-14815

The role of microstructure in the modelling of plastic flow in P/M superalloys at forging temperatures and strain rate 06 p0796 N85-15080

The influence of strain rate and porosity on the deformation and fracture of titanium and nickel
[AD-A148670] 08 p1130 N85-17123

Deformation and fracture of P/M (Powder/Metallurgy) titanium alloys
[AD-A148672] 09 p1294 N85-18128

Models for shock damage to marine structural materials 09 p1336 N85-18400

Cavitation phenomenon in superplastic creep
[DE85-001716] 10 p1441 N85-19083

Behavior of fiber-reinforced composites under dynamic tension
[AD-A150619] 13 p2015 N85-22941

Effect of oxygen on mechanical properties of Nb-V alloy
[DE85-002681] 14 p2256 N85-23962

Influence of pretreatment, environment and strain rate on stress corrosion cracking of the aluminum alloy 7075-T6
[VTH-LR-433] 16 p2752 N85-26995

Conformational and mechanical properties at high strain rates
[AD-A153401] 17 p2950 N85-28272

Studies of strain rate effects in the deformation of solids by means of stress pulses and ultrasonic methods
[DE85-009463] 18 p3122 N85-29329

Short term determination of the creep properties of high temperature materials
[CRIF-MT-160] 20 p3432 N85-31289

Synthesis and characterization of copolyimides with varying flexibilizing groups
[NASA-TM-86416] 20 p3433 N85-31296

Viscoplasticity based on overstress with a differential growth law for the equilibrium stress
20 p3466 N85-31532

Fundamental investigations of failure during superplastic forming process
[AD-A154647] 21 p3568 N85-32194

Strain rate sensitivity estimation from high velocity impact data
[AD-A154703] 21 p3599 N85-32247

Influence of particle arrangement on sintering
[AD-A155337] 21 p3599 N85-32262

On high strain rate fragmentation of a closed vessel
23 p3904 N85-34187

Experimental study on time and temperature dependent behavior of crack growth in viscoelastic strip
23 p3905 N85-34193

Effect of strain rate on the initial failure of notched GRP laminates 23 p3906 N85-34214

Carbon fiber strainmeter studies in southern California
[PB85-196889] 24 p4118 N85-35528

Simulation of lattice damage due to dynamic loading
[DE85-008468] 24 p4162 N85-35800

STRAIN SOFTENING

U PLASTIC DEFORMATION

STRAITS

Internal waves in marine straits
[PREPRINT-415] 18 p3151 N85-2951

STRAKES

Flight mechanics analysis of dynamic derivatives of t
Dornier variable wind tunnel model
[ESA-TT-854] 11 p1577 N85-19

STRANGE ATTRACTORS

A case of a not-so-strange strange attractor
[CWI-AM-R8406] 08 p1214 N85-17

STRANGENESS

A holographic streamer chamber for relati
nucleus-nucleus collision experiments
24 p4147 N85-3

STRAPDOWN INERTIAL GUIDANCE

Analysis and simulation of an intertial system (Strapdown) for auxiliary attitude determination by adaptive drift estimation
[INPE-3257-TDL/177] 04 p0454 N85-12882

Flight testing of Litton laser gyro strapdown system LTN-90 for general aviation
[DFVLR-MITT-84-16] 07 p0901 N85-15709

Standard Attitude Heading Reference System (SAHRS) full scale development program
08 p1073 N85-16804

A discussion of coning errors exhibited by inertial navigation systems
[RAE-TM-RAD-NAV-243] 08 p1082 N85-16854

Implementation of an inertial navigation algorithm using a limited wordlength microprocessor for a strapdown navigation computer
[BAE-BT-12782] 15 p2468 N85-25234

Navigation: Accounting for copy
16 p2695 N85-26641

Preguidance and piloting with the aid of composite inertial sensors 16 p2696 N85-26646

Autofocus motion compensation for synthetic aperture radar and its compatibility with strapdown inertial navigation sensors on highly maneuverable aircraft
[AD-A151940] 16 p2704 N85-26693

Simulation of gyrocompassing alignment and calibration of strapdown inertial navigation system in a swaying vehicle
[DFVLR-MITT-84-20] 17 p2895 N85-27850

The DREO (Defence Research Establishment Ottawa) Inertial Navigation Laboratory: Development and test capabilities
[AD-A154425] 19 p3216 N85-29945

Simulations of strapdown-system errors and error compensation methods — transport aircraft navigation
[DFVLR-MITT-84-22] 20 p3392 N85-31040

Flight testing the Litton LTN 90 laser gyro strapdown system for civil aviation
[ESA-TT-904] 20 p3392 N85-31042

Test evaluation of the Honeywell GG1111 Single-Degree-of-Freedom (SDF) strapdown gyroscope
[AD-A154768] 21 p3589 N85-32307

STRAPS

Retroreflective armbands: Influences of wearing mode, aging and other factors on the visibility distance
[IZF-1984-28] 14 p2422 N85-24942

Verification of the SRB motor case pin retainer band tips
[NASA-CR-170882] 24 p4070 N85-35220

STRATA

NT SUBSTRATES

Boundary condition effects in the energy loss spectrum of layered systems
[NOTA-INTERNA-802] 02 p0289 N85-11887

Problem of frequency space variation of sonic field in stratified media 11 p1715 N85-20787

Mechanisms of heat and mass transfer across a double-diffusive interface
[PB85-148468] 12 p1848 N85-21594

Regions of propagation of short-wave perturbations in spherical layer of rotating fluid 13 p2107 N85-23130

Radar echoes at 2.66 and 40.92 MHz from the mesosphere, part 2.6A 21 p3619 N85-32486

STRATEGIC MATERIALS

Research and development requirements for ion implantation
[AD-P003951] 02 p0286 N85-11867

Use of ion implantation to modify the corrosion behavior of metals
[AD-P003953] 02 p0286 N85-11869

Guayule research
[GPO-29-562] 04 p0477 N85-13042

The B2 aluminides as alternative materials
[NASA-TM-86937] 10 p1440 N85-19076

Preliminary SPR thermal model description and results for WH-11 and BM-4
[DE85-013171] 23 p3931 N85-34360

Applications of the mineral resources data system and the international strategic minerals inventory in mineral-resource assessments by region and commodity
24 p4105 N85-35451

Mineral resources programs 24 p4106 N85-35456

The Conterminous United States Mineral Assessment Program 24 p4106 N85-35458

STRATEGY

A strategy for the adjustment and analysis of densification networks — geodetic networks
[SER-C-295] 01 p0063 N85-10420

The effect of strategy in second order manual control on resource competition with a sturnberg memory search task
[AD-A150965] 14 p2391 N85-24727

Equilibrium solutions, stabilities and dynamics of Lanchester's equations with optimization of initial force commitments
[AD-A151510] 15 p2637 N85-26266

An incremental multigrid strategy for the fluid dynamics equations
[AD-A151953] 16 p2783 N85-27172

Space Station crew safety alternatives study. Volume 4: Appendices
[NASA-CR-3857] 18 p3065 N85-28958

Strategic use of business graphics: A stakeholder approach 23 p3963 N85-34566

Arms control and The President's Strategic Defense Initiative
[AD-A156334] 24 p4068 N85-35212

STRATIFICATION

NT ATMOSPHERIC STRATIFICATION

NT INTERCALATION

Doubly diffusive linear stability with nonconstant gradients
[DE84-013008] 05 p0670 N85-14310

Heat and mass exchange in a partially stratified fluid
[DE85-000528] 10 p1486 N85-19384

Stratified charge rotary aircraft engine technology enablement program
[NASA-CR-174812] 12 p1778 N85-21163

Horizontal coherence of temperature microstructure in upper ocean layer 13 p2109 N85-23139

Wave propagation in density stratified fluids
16 p2781 N85-27162

The effect of the Benthic Boundary Layer on the physics of intense mesoscale eddies
[AD-A153193] 17 p2958 N85-28270

Arctic mixed layer dynamics
[AD-A153582] 18 p3150 N85-29505

Buoyant jet entrainment in stratified fluids
19 p3263 N85-30238

Numerical modeling of subsurface communication
[DE85-012618] 21 p3577 N85-32249

Turbulent structure of stably stratified nocturnal slope flows
[AD-A155845] 24 p4123 N85-35559

Analysis of two-parameter constant background born inversion for acoustic synthetic data
[AD-A156394] 24 p4145 N85-35698

STRATIFIED FLOW

Numerical calculations of stratified Ekman layer flow over ridges with a finite element model
[DE84-014482] 04 p0499 N85-13179

On the classification and nonlinear solution of one type of stratified shear flow
[AD-A148832] 09 p1319 N85-18295

Thermal striping downstream of a horizontal elbow under thermally stratified transient flow conditions
[DE84-014687] 09 p1320 N85-18302

Some approximations of geophysical hydrodynamics
14 p2336 N85-24448

Modeling of shear flow in a stratified fluid
14 p2340 N85-24469

Buildup of oscillation of bodies in stratified fluid
17 p2941 N85-28157

Numerical techniques for steady two-dimensional transcritical stratified flow problems, with an application to the intermediate field dynamics of ocean thermal energy conversion plants
[DE85-008347] 18 p3151 N85-29509

Natural convection experiments in a stratified liquid-saturated porous medium
[DE85-009003] 20 p3455 N85-31457

Some remarks on the constitutive equations of stratified gas-liquid flow
[EME-137] 20 p3456 N85-31466

Resolution of thermal striping issue downstream of a horizontal pipe elbow in stratified pipe flow
[DE85-006195] 21 p3586 N85-32292

Some aspects of internal gravity waves in a multi-layered moving stratified flow 24 p4092 N85-35369

STRATIFIED LAYERS

U STRATA

STRATIGRAPHY

Geothermal resources of the Laramie, Hanna, and Shirley Basins, Wyoming
[DE84-016104] 01 p0064 N85-10423

Seismic discrimination of a geothermal field: Cerro Prieto
[DE84-014581] 01 p0064 N85-10425

Erosion and sedimentation chronology of three watersheds in Maryland
[PB84-207356] 01 p0071 N85-10467

Paleoenvironmental interpretation of the upper cretaceous Point Lookout sandstone: Implications for shoreline progradation and basin tectonic history, San Juan basin, New Mexico 02 p0227 N85-11486

Stratigraphy, petrology, and tectonic setting of the Alisitos Group, Baja California, Mexico
03 p0389 N85-124

Stratigraphy, sedimentology and tectonic significance of the Upper Cretaceous Virginian Ridge formation, Method Basin, Washington: Implications for tectonic history of the North Cascades 03 p0390 N85-12494

Geographic and stratigraphic distribution of Miocene palynomorphs in north Idaho 03 p0390 N85-12498

Late quarterly glaciolacustrine and vegetational history of the Copper River Basin, south-central Alaska
03 p0391 N85-12499

The Kanayut Conglomerate in the westernmost Brooks Range, Alaska 04 p0516 N85-13289

Newly recognized sedimentary environments in the Shelikof Formation, Alaska 04 p0516 N85-13292

Stratigraphy, petrology, and structure of the Pingston terrane, Mount Hayes C-5 and C-6 quadrangles, eastern Alaska Range, Alaska 04 p0517 N85-13301

Geothermal resource assessment for North Dakota
[DE84-016128] 04 p0526 N85-13367

Some methodological aspects of study of layer associations in continents and oceans
06 p0820 N85-15205

Geothermal assessment of a portion of the Escalante Valley, Utah
[DE84-015964] 06 p0828 N85-15257

Time series analysis programs for stratigraphic data
[AD-A146627] 06 p0854 N85-15429

Quaternary stratigraphy of the lower Iowa and Cedar River Valleys, southeast Iowa 09 p1352 N85-18504

Stratigraphy of early ordovician El Paso group of the southern Hueco Mountains, Hudspeth County, Texas
09 p1353 N85-18510

Part 1. Stratigraphy, structure and petrology of the Peterborough 1.5-minute quadrangle, New Hampshire and part 2. Graphite textural and isotropic variations in plutonic rocks, south-central New Hampshire
09 p1353 N85-18511

Structure and stratigraphy of Midterhuken Peninsula, Bellsund, West Spitsbergen 09 p1353 N85-18513

Quaternary stratigraphy, geochronology and carbon isotope geology of alluvial deposits in the Texas panhandle 09 p1353 N85-18514

SIR-A imagery in geologic studies of the Sierra Madre Oriental, northeastern Mexico. Part 1 (Regional stratigraphy): The use of morphostratigraphic units in remote sensing mapping
[NASA-CR-175457] 10 p1505 N85-19497

Study of stratigraphy of the Precambrian Soviet Baltic shield 13 p2110 N85-23148

Reflected wave travel-time curves in stratified media with vertically heterogeneous layers and slightly sloping curved boundaries 13 p2114 N85-23167

Assessment of computer based geologic mapping of rock units in the LANDSAT-4 scene of northern Death Valley, California 13 p2119 N85-23196

Dark halo craters and the thickness of grooved terrain on Ganymede 13 p2173 N85-23484

Valles Marineris basin beds: A complex story
13 p2201 N85-23652

Mars: Stratigraphy of western highlands and polar regions 13 p2201 N85-23653

Evaluating structure-forming role of late Paleozoic and Mesozoic-Cenozoic tectonic movements in Baltic Sea region 14 p2337 N85-24450

Shales and other argillaceous strata in the United States
[DE85-010453] 18 p3125 N85-29353

Stratigraphic analysis of Pennsylvania rocks using hierarchy of transgressive-regressive units
19 p3312 N85-30531

Paleoenvironmental investigations at seed cave (Windust cave H-45FR46), Franklin County, Washington
[AD-A154777] 21 p3635 N85-32576

Sulfur transformations at the hydrogen sulfide/oxygen interface in stratified waters and in cyanobacterial mats
21 p3657 N85-32715

The Aravalli sequence of Rajasthan, India: A Precambrian continental margin?
21 p3720 N85-33064

Lithology and stratigraphy of drill holes completed during 1984 in LANL use areas of Yucca Flat, Nevada Test Site, volume 6
[DE85-010695] 22 p3815 N85-33631

Bedrock geology of the Brattleboro Quadrangle, Vermont-New Hampshire
[DE85-011027] 22 p3815 N85-33634

Geology and petroleum resources of basins in western China
[DE85-013038] 23 p3948 N85-34469

Seismic stratigraphic analysis of the Mississippi Fan
24 p4115 N85-35507

STRATOCUMULUS CLOUDS

Conditions governing the formation of stratocumulus clouds over the western Atlantic during cold air outbreaks
[AD-A146760] 07 p1004 N85-16383

The physics of the marine stratocumulus-capped mixed layer 15 p2583 N85-25979

STRATOPAUSE
Coupling between the thermosphere and the stratosphere: The role of nitric oxide
11 p1662 N85-20472

STRATOSPHERE
A comparison of 2- and 3-dimensional transport within a stratospheric circulation model
02 p0227 N85-11485
Solar radiation in the ozone layer
04 p0522 N85-13342
Trends in ozone and temperature structure: Comparison of theory and measurements
[DE84-016201] 04 p0539 N85-13428
Comparison of wind derived from the LIMS (Limb Infrared Monitor of the Stratosphere) satellite instrument with rocket observations
[NASA-CR-174083] 04 p0541 N85-13444
Aspects of the comparison of stratospheric trace species measurements with photochemical models
[DE84-017028] 05 p0672 N85-14317
Utilization of SAGE aerosol profiles in the analysis of Mauna Loa stratospheric lidar data
[NASA-CR-174198] 05 p0675 N85-14332
Jet stream errors and tropospheric-stratospheric interactions in the GLAS general circulation model
05 p0683 N85-14392
Nature of short-period variations of cosmic rays in stratosphere 06 p0823 N85-15224
Study of infrared atmospheric emission
[AD-A147517] 07 p0998 N85-16336
Optical studies of nitrogen oxides in the stratosphere
08 p1183 N85-17455
Satellite stratospheric aerosol measurement validation
[NASA-TM-86003] 08 p1187 N85-17479
Generation and evolution of diabatic planetary waves in continuously stratified atmosphere with Ekman dissipation 09 p1354 N85-18515
Stratospheric concentration of nitric acid, ozone and carbonyl sulfide: Measurement of nitric acid absorption in the Q branch of the V4 band as a function of temperature
[ESA-TT-864] 09 p1355 N85-18524
Airborne lidar measurements of El Chichon stratospheric aerosols, October 1982 to November 1982
[NASA-RP-1136] 10 p1514 N85-19550
Aerosol limb absorption --- stratosphere
[NASA-TM-77733] 10 p1515 N85-19562
Health assessment document for carbon tetrachloride
[PB85-124196] 10 p1528 N85-19638
PMP-2: Equatorial wave dynamics
11 p1655 N85-20422
Middle Atmosphere Program. Handbook for MAP, volume 5
[NASA-CR-175481] 11 p1656 N85-20434
A catalogue of dynamic parameters describing the variability of the middle stratosphere during the northern winters 11 p1656 N85-20435
Middle Atmosphere Program. Handbook for MAP, volume 7
[NASA-CR-175479] 11 p1656 N85-20437
PMP-1 report: The fourth winter of PMP-1, 1981 - 1982: A winter with several interesting features
11 p1657 N85-20441
Workshop on Comparison of Data and Derived Dynamical Quantities During Northern Hemisphere (PMP-1) Winters 11 p1657 N85-20444
MAP/GLOBUS campaign 1983
11 p1658 N85-20447
Abnormal circulation changes in the winter stratosphere, detected through variations of D region ionospheric absorption 11 p1659 N85-20458
Midwinter disturbances in the middle atmosphere
11 p1661 N85-20465
Large scale winter time disturbances in meteor winds over central and eastern Europe
11 p1661 N85-20467
VHF radar observations in the stratosphere and mesosphere during a stratospheric warming
11 p1661 N85-20468
Changes in the ozone content over central Europe during reversals of stratospheric circulation in late winter
11 p1661 N85-20469
Aspects of planetary wave transports in the middle atmosphere 11 p1661 N85-20471
Coupling between the thermosphere and the stratosphere: The role of nitric oxide
11 p1662 N85-20472
Lidar observations of stratospheric aerosol over Mauna Loa Observatory, 1974 - 1981
[PB85-115061] 11 p1662 N85-20597
The Jovian Stratosphere in the ultraviolet
11 p1760 N85-21069
Measurement of nuclear lines with a dual Ge(Li) telescope aboard a stratospheric balloon
[INPE-3380-TDL/185] 11 p1762 N85-21083
Chemical kinetics and photochemical data for use in stratospheric modeling. Evaluation number 6
[NASA-CR-175584] 12 p1888 N85-21849
Observation of cosmic ray flux variations in stratosphere 13 p1981 N85-22430
Calibration of solar cells outside the atmosphere
13 p2009 N85-22603
A theoretical study of the ozone quasi-biennial oscillation in the tropical stratosphere 13 p2132 N85-23264
One-dimensional nonstationary model of photochemical transformations of gas impurities in stratosphere
14 p2342 N85-24484
High altitude sampling program: Radioactivity in the stratosphere
[DE85-005924] 14 p2374 N85-24676
The source of stratospheric NO and N2O
[NASA-CR-175713] 15 p2588 N85-25956
SAM 2 measurements of the polar stratospheric aerosol, volume 5
[NASA-RP-1140] 15 p2590 N85-25970
Wave dynamics and transport in the stratosphere
[NASA-CR-175789] 16 p2823 N85-27413
Stratospheric ClO: In-situ detection with a new approach 16 p2824 N85-27416
The copper vapor laser 16 p2824 N85-27417
Research and development of new instruments
16 p2824 N85-27418
Water vapor 16 p2824 N85-27420
Role and fate of ozone in the atmosphere
16 p2824 N85-27421
SAM II measurements of the polar stratospheric aerosol. Volume 6: April to October 1981
[NASA-RP-1141] 16 p2825 N85-27422
Investigation of the reaction system NOX/ClOX/HOX under tropospheric and stratospheric conditions
[BPT-11/84] 18 p3137 N85-29427
Photochemical processes in the lower stratosphere (ozone layer) 18 p3148 N85-29490
Circulation and transport in the middle atmosphere: Troposphere and lower atmosphere
18 p3148 N85-29491
Development of a technique for in situ detection of stratospheric nitrogen dioxide 19 p3312 N85-30534
Short meridional scale anomalies in the lower stratosphere and upper troposphere
20 p3489 N85-31684
Troposphere-stratosphere (surface-55 km) monthly general circulation statistics for the Northern Hemisphere-four year averages
[NASA-TM-86182] 20 p3495 N85-31730
Tropospheric-stratospheric exchange, part 1.1A
21 p3615 N85-32468
Gravity waves from the stratosphere to the mesosphere, part 1.3B 21 p3616 N85-32471
A numerical analysis of transient planetary waves and the vertical structure in a meso-strato-troposphere model, part 1.4A 21 p3617 N85-32473
Vertical transport in the atmosphere: Measurement capabilities and requirements of VHF radars, part 1.6A
21 p3617 N85-32476
Morphology of the scattering targets: Fresnel and turbulent mechanisms, part 2.1A
21 p3618 N85-32481
Antenna induced range smearing in MST radars
21 p3620 N85-32495
High resolution evidence for the Garrett-Munk spectrum of stratospheric gravity waves 21 p3622 N85-32503
Relationship of isolated turbulent regions to the general turbulent background, part 4.4A
21 p3623 N85-32506
Estimation of vertical diffusion from observations of Atmospheric turbulence layers, part 4.4B
21 p3623 N85-32507
Further developments of EISCAT as an MST radar
21 p3627 N85-32534
Urbana radar systems: Possibilities and limitations
21 p3628 N85-32540
Millstone Hill radar: Capabilities for S/T observations
21 p3629 N85-32548
The Ponape ST radar 21 p3629 N85-32549
Measurements of vertical velocity over flat terrain by ST radar and other related uses of the radar data set
21 p3630 N85-32550
Activities report of the Aeronomy Department
[G-774-1984] 21 p3633 N85-32569
A new hypothesis for the observed vertical distribution of atmospheric aerosols 21 p3645 N85-32646
Theoretical studies of structure and stability of hydrates of atmospheric sulfur species 21 p3650 N85-32684
Ozone during sudden stratospheric warming: A three-dimensional simulation
[AERONOMICA-ACTA-A-292-1984]
22 p3813 N85-33621
Voigt line profile computation of infrared lines in the stratosphere and mesosphere
[AERONOMICA-ACTA-A-294-1985]
22 p3813 N85-3362
A comparison of calculated and measured background noise rates in hard X-ray telescopes at balloon altitude
[OG-9.3-7] 23 p4028 N85-349
Dynamics of two-year cosmic ray variations inferred from the data of spacecraft and stratospheric measurements and from the neutron monitor data in 1959-1981
[SH-4.4-21] 23 p4035 N85-35017
Diurnal effect in cosmic rays at middle latitudes according to stratospheric measurements
[SH-4.5-8] 23 p4036 N85-350

STRATOSPHERIC AEROSOL & GAS EXPERIMENT
U SAGE SATELLITE

STRATOTANKER AIRCRAFT
U C-135 AIRCRAFT

STRATUS CLOUDS
An operational numerical model for prediction of fog and stratus 01 p0080 N85-10537
A 1-dimensional model with a sub-grid scale condensation scheme for stratiform clouds and fog
01 p0080 N85-10538
An operational forecasting system for stratus and fog with sodar 01 p0081 N85-10539
Fog advection in the Namib 16 p2831 N85-27454
Transport and formation of summertime cloud condensation nuclei over the Arctic Ocean
21 p3651 N85-328

STREAK CAMERAS
Fore-optics systems designed for electronic streak cameras using fiber optics
[DE84-014525] 02 p0281 N85-11830
A means of extending streak camera recording into the important 1300-1600 nm wavelength regime: Parametric frequency upconversion
[DE84-015666] 04 p0503 N85-13208
High-bandwidth multichannel fiber optic system for measuring gamma rays
[DE84-014526] 04 p0564 N85-13596
Characterization of electronic streak tubes including one with internal CCD readout
[DE84-016823] 05 p0639 N85-14098
A microchannel plate streak camera
[DE84-016536] 06 p0811 N85-15153
Approaches to ultrafast neutron detectors
[DE85-001206] 11 p1636 N85-20307
Photonic methods of high speed analog data recording
[DE84-016723] 11 p1637 N85-20308
Neutron streak camera electron gun design
[DE85-000620] 11 p1637 N85-20315
Microchannel plate streak camera
[DE85-011604] 20 p3458 N85-31481
Coordinated research program in pulsed power physics
[AD-A154629] 21 p3679 N85-328

STREAK PHOTOGRAPHY
Developments of optical fast-gated imaging systems
[DE84-016170] 04 p0502 N85-13204
Measuring transient radiation effects in optical fibers
[DE84-015044] 04 p0565 N85-1359
Improvements in avalanche-transistor sweep circuitry for electrooptic streak cameras
[DE84-016195] 06 p0811 N85-15155
Approaches to ultrafast neutron detectors
[DE85-001206] 11 p1636 N85-20307
Design, construction and initial evaluation of an absolute, time-integrating/time-resolving spectrometer for the diagnostics of pulsed, high temperature plasma X-ray sources in the 100-10,000 eV region
[DE85-003526] 11 p1732 N85-209
Streak tube characterization
[DE85-009674] 17 p2956 N85-282

STREAM FUNCTIONS (FLUIDS)
Some numerical analyses of flows with separation
16 p2692 N85-28616
A stream function approach to solving the conservative Euler equations for transonic flows
24 p4059 N85-3515

STREAMLINE FLOW
U LAMINAR FLOW

STREAMLINED BODIES
NT FAIRINGS
An experimental and analytical study of the aerodynamic interference effects between two Sears-Haack bodies at Mach 2.7
[NASA-TM-85729] 16 p2700 N85-289
Instability of solar wind near streamlined bodies
16 p2720 N85-2879

STREAMLINING
Transonic merging separated flows
[AD-A150867] 14 p2213 N85-237

STREAMS
NT GAS STREAMS

Potential for acidification of six remote ponds in the White Mountains of New Hampshire
[PB84-207349] 02 p0225 N85-11475
Post-Laramide history of North Central Wyoming
08 p1181 N85-17444
Theoretical study of collective ion acceleration in the Luce diode
[AD-A150107] 12 p1929 N85-22116
Late Tertiary and Quaternary river systems of the eastern Sahara as mapped on shuttle radar and LANDSAT images 13 p2199 N85-23641
The ionospheric O+ streams in the magnetotail between 22 RE and 6 RE 14 p2360 N85-24582
Applications of Kalman filtering and recursive least-squares in river flow modelling
15 p2636 N85-26254
Towards a uniform topological treatment of streams and functions on streams
[CWI-CS-R8422] 17 p3014 N85-28639
On the origin of streamwise vortices in a turbulent boundary layer
[AD-A153651] 18 p3100 N85-29166
Geomorphic analyses from space imagery
21 p3603 N85-32374
Hydrology
[PB85-182954] 23 p3944 N85-34440

STRENGTH
Fundamentals of microcrack nucleation mechanics
[NASA-CR-3851] 07 p0975 N85-16195

STRENGTH OF MATERIALS
U MECHANICAL PROPERTIES

STRESS (PHYSIOLOGY)
NT ACCELERATION STRESSES (PHYSIOLOGY)
NT CENTRIFUGING STRESS
Effect of short-term hypokinesia on rat opioid system reaction 01 p0093 N85-10625
The role of physical and physiological capacities and their modification on the tolerance to various stress experienced by Air Force personnel
[AD-A145779] 03 p0400 N85-12550
Endocrine responses to nonhypotensive gravitational stress: Vasopressin and aldosterone
05 p0693 N85-14459
Endocrine responses to hypotensive gravitational stress: Catecholamines, pancreatic polypeptide, and vasopressin 05 p0693 N85-14460
Blood pressure levels of active pilots compared with those of air traffic controllers
[AD-A146645] 06 p0846 N85-15373
An atropinized heat-stressed rat model: Dose response effects and pharmacokinetics
[AD-A146851] 07 p1011 N85-16423
Change in relationship of biopotentials of brain zones for various levels of working capacity
07 p1013 N85-16438
Human factors survey: C-5 pilots
[AD-A147106] 07 p1020 N85-16477
Tolerance endpoint for evaluating the effects of heat stress in dogs
[AD-A148104] 08 p1192 N85-17511
Thermoregulatory responses during exercise at graded hypohydration levels
[AD-A147733] 08 p1195 N85-17526
Advanced development of an active neuromusculature response to mechanical stress
[AD-A148436] 08 p1196 N85-17536
Study of bodily functional status and quality of controlling action of power unit operators with various intensities of labor 09 p1362 N85-18569
The physiology of ultradian rhythms and their role in affecting disease resistance
[AD-A148642] 09 p1363 N85-18575
Work physiology of operating personnel at power plants in arid regions 10 p1523 N85-19606
Effects of overall vibration and noise on operational personnel 10 p1523 N85-19608
Skeletal muscle metabolism during exercise is influenced by heat acclimation
[AD-A148845] 10 p1527 N85-19632
LBNP training of crew members on main missions aboard Salyut-6 orbital station 12 p1901 N85-21938
Main component method used to study variations of cardiovascular parameters 12 p1901 N85-21939
Distinctive morphological manifestations of acute stress reaction in adrenal cortex of hypokinetic rats
12 p1902 N85-21944
Brain mechanisms underlying individual differences in reaction to stress: An animal model
[AD-A150195] 13 p2143 N85-23301
Exercise-heat strain during hypohydration: Interaction with heat acclimation and aerobic fitness
[AD-A151023] 14 p2389 N85-24717
Mechanical stress regulation of plant growth and development 15 p2610 N85-26087
A detailed analysis of the erythropoietic control system in the human, squirrel, monkey, rat and mouse
[NASA-CR-171879] 15 p2614 N85-26107
Description, validation, and modification of the Guyton model for space-flight applications. Part A. Guyton model of circulatory, fluid and electrolyte control. Part B. Modification of the Guyton model for circulatory, fluid and electrolyte control
[NASA-CR-171876] 15 p2616 N85-26122
The behavior of renal-regulating hormones during hypogravic stress
[NASA-CR-171877] 15 p2616 N85-26123
What is being done to control motion sickness?
15 p2687 N85-26599
Plasma hormonal responses at graded hypohydration levels during exercise/heat stress
[AD-A153681] 18 p3153 N85-29523
Distinctions of rat lymphatic organ reactions to acute stress factor during hypokinesia
19 p3324 N85-30586
Phenomenon of universal rosette-forming cell stimulation by extreme stress 20 p3505 N85-31789
Anatomy of stress 20 p3505 N85-31791
Physical training and G tolerance
20 p3511 N85-31824
Status of the air traffic control system
[GPO-40-343] 21 p3554 N85-32107
Regulation of physical activity in antiorthostatic position by acting on adrenosympathetic and hypophyseo-adrenocortical systems
22 p3824 N85-33689
Thermal stress suffered by tank crews working in summer heat
[DRIC-T-7492] 22 p3826 N85-33698
Determination of individual tolerance in hyperbaric oxygen 23 p3954 N85-34507
Report of Amphibian Development Group
24 p4127 N85-35583
Weight loss, rectal temperature and heart rates following the 1984 Boston Marathon
[AD-A155984] 24 p4132 N85-35612

STRESS (PSYCHOLOGY)
The role of physical and physiological capacities and their modification on the tolerance to various stress experienced by Air Force personnel
[AD-A145779] 03 p0400 N85-12550
Catecholamine excretion and subjective ratings of tension during autogenic training and mental stress
[REPT-172] 05 p0697 N85-14483
Blood pressure levels of active pilots compared with those of air traffic controllers
[AD-A146645] 06 p0846 N85-15373
Job and family stress as predictors of pilot health, job satisfaction and performance
[AD-A142176] 07 p1018 N85-16464
Human factors survey: C-5 pilots
[AD-A147106] 07 p1020 N85-16477
An investigation of the relationship between stressful life events and psychological, behavioral and physiological outcomes
[AD-A147754] 08 p1197 N85-17541
Decision making in stressful conditions: A model based on the coping perspective
[FOA-C-55064-H3] 08 p1229 N85-17738
Effect of modulated ultrahigh frequency field on behavior and hormone level in female rats under emotional stress
09 p1361 N85-18562
Research opportunities in human behavior and performance
[NASA-CR-175473] 10 p1529 N85-19640
NASA: Model development for human factors interfacing
[NASA-CR-175584] 12 p1910 N85-21985
Psychological issues relevant to astronaut selection for long-duration space flight: A review of the literature
[AD-A154051] 19 p3330 N85-30627
Phenomenon of universal rosette-forming cell stimulation by extreme stress 20 p3505 N85-31789
Anatomy of stress 20 p3505 N85-31791
Status of the air traffic control system
[GPO-40-343] 21 p3554 N85-32107
Operator's functional comfort zone when controlling moving object 22 p3821 N85-33670
Regulation of physical activity in antiorthostatic position by acting on adrenosympathetic and hypophyseo-adrenocortical systems
22 p3824 N85-33689

STRESS ANALYSIS
NT BOUNDARY ELEMENT METHOD
NT X RAY STRESS ANALYSIS
Design proposals for torsional buckling of stiffeners
[AD-A144783] 01 p0062 N85-10409
Improved multiaxial creep-rupture strength criterion
[DE84-014273] 01 p0062 N85-10413
The 3-D inelastic analysis methods for hot section components: Brief description 02 p0143 N85-10972
Directional nature of strengthening during thermomechanical treatment
[BLL-M-35746-(5829.4)] 02 p0175 N85-11174
Environment-induced embrittlement: Effect of impurity segregation and state of stress
[DE84-015436] 02 p0184 N85-11235
Stress analysis of pin-loaded orthotropic plates using orthotropic photoelasticity 02 p0207 N85-11366
Materials properties, loads, and stress analysis, Spartan REM: Appendix A
[NASA-CR-171092] 02 p0208 N85-11375
A digital algorithm for composite laminate analysis: FORTRAN, Revised
[AD-A145833] 03 p0326 N85-12096
Sour-gas cracking in ferritic steels
[AERE-R-10908] 03 p0333 N85-12148
Evaluation of laterally loaded laminated glass units by theory and experiment
[PB84-216423] 03 p0339 N85-12179
Fatigue limit analysis involving biaxial stress components 03 p0370 N85-12363
Dispersion forces of solids under stress. Chemisorption under stress
[AD-A146171] 03 p0373 N85-12380
Stress relief cracking studies of 2 1/4Cr1Mo steel
[AERE-R-11111] 03 p0374 N85-12388
Characterization of stressed metals using acoustic shear waves 05 p0648 N85-14159
Stress studies of EFG
[NASA-CR-174078] 06 p0651 N85-14179
Encapsulation design analysis
06 p0829 N85-15266
Strain analysis of the Leoville chondrite and conditions in asteroidal interiors 06 p0895 N85-15620
A study of interply layer effects on the free-edge stress field of angleplied laminates
[NASA-TM-86924] 07 p0919 N85-15822
A theoretical view on the stress analysis of fully inflated parachute canopies
[AD-A148367] 08 p1078 N85-16835
Contact behavior, impact response and damage in graphite-epoxy laminates subjected to initial stresses
08 p117 N85-17386
A study of constitutive relations for polycrystalline aluminum during finite dynamic plastic deformation
08 p1172 N85-17388
Determination of the elastic constants of inhomogeneous materials with X-ray diffraction
[AD-A148469] 08 p1173 N85-17393
A simple engineering treatment of center cracked tension panels in the regime of nonlinear fracture mechanics under plane stress conditions
[GKSS-84-E-38] 08 p1173 N85-17396
Thermal-stress analysis for a wood composite blade
[NASA-CR-174794] 08 p1178 N85-17421
Evaluation of laterally loaded laminated glass units by theory and experiment
[PB85-111532/GAR] 09 p1300 N85-18166
East Europe report: Science and technology
[JPRS-ESA-85-008] 10 p1480 N85-19200
Methodology for stress analysis of heavy metal plate
10 p1480 N85-19203
Statistical study of anthropogenic seismic noise with IVK-7 computer system 10 p1503 N85-19483
Stress studies in EFG
[NASA-CR-175464] 10 p1509 N85-19522
Stress studies in EFG
[NASA-CR-175486] 10 p1563 N85-19856
Comparison of methods for predicting fiber stresses in a cracked Kevlar/epoxy monolayer
[DE84-016118] 11 p1593 N85-20022
Application of hysteresis modelling to the non-destructive inspection of stress
[DE85-003081] 11 p1650 N85-20383
USSR report: Physics and mathematics
[JPRS-UPM-85-001] 11 p1715 N85-20786
Advanced stress analysis methods applicable to turbine engine structures
[NASA-CR-175573] 12 p1778 N85-21165
Finite element analysis of problems associated with life enhancement techniques
[ARL/STRUC-R-404] 12 p1862 N85-21676
Symmetric primal-dual variational formulations of coupled dynamic systems: Three-dimensional elasticity, shells, fluid-structure interaction
[ONERA-1983-91] 12 p1863 N85-21684
3-D inelastic analysis methods for hot section components (base program) -- turbine blades, turbine vanes, and combustor liners
[NASA-CR-174700] 12 p1863 N85-21686
Transverse vibration and buckling of a cantilevered beam with tip body under constant axial base acceleration
[NASA-CR-175567] 12 p1864 N85-21694
On the stress analysis of bonded inserts
[ARL/STRUC-R-407] 12 p1865 N85-21698

STRESS CALCULATIONS

Scattered data interpolation using thin plate splines with tension
[AD-A149803] 12 p1886 N85-21705
Texture independent determination of residual stress in polycrystalline aggregates using Rayleigh waves
[AERE-R-11483] 12 p1943 N85-22203
A study of the compatibility of an existing CFD package with a broader class of material constitutions
12 p1945 N85-22219
Root stresses in conformal gears-strain gauge and photoelastic investigations 14 p2223 N85-23787
Analysis of slabs-on-grade for a variety of loading and support conditions
[AD-A150965] 14 p2264 N85-24030
Reduction of free-edge stress concentration
[AD-A150732] 14 p2321 N85-24340
Stress in axially symmetrical heavy metal projectiles during discharge — numerical simulation
[ISL-CO-219/83] 14 p2321 N85-24345
Stress and efficiency studies
[NASA-CR-175686] 14 p2351 N85-24531
Crack growth direction in unidirectional off-axis graphite epoxy
[NASA-CR-175752] 15 p2502 N85-25433
The accuracy of approximate solutions in the analysis of fracture of composites
[NASA-CR-175738] 15 p2503 N85-25437
Reduced-chromium stainless steel substitutes containing silicon and aluminum
[PB85-160786] 15 p2513 N85-25502
Acoustic emission of semiconductor devices
15 p2529 N85-25593
Symmetric composite laminate stress analysis
15 p2575 N85-25876
Structural analysis of electronic assembly housing
[DE85-005794] 15 p2580 N85-25913
Enhanced thermal-structural analysis by integrated finite elements
[AD-A151103] 15 p2636 N85-26258
The physical effects of different stress situations on graphite/epoxy compounds 15 p2687 N85-26594
Impact of magnetic isolation on pointing system performance in the presence of structural flexibility
[NASA-CR-172481] 16 p2732 N85-26861
Determination of permissible heating rate of metal
[BLL-M-36107-(5828.4)] 16 p2748 N85-26957
In plane stress analysis
[NASA-CR-175775] 16 p2799 N85-27259
Component-specific modeling
[NASA-CR-174765] 16 p2799 N85-27261
Effects of high mean stress on high-cycle fatigue behavior of PWA 1480 17 p2914 N85-27964
First passage times for combinations of random loads
[AD-A153275] 17 p2960 N85-28423
Mechanics of composite materials, theory and application
[VTH-LR-431] 18 p3123 N85-29334
Effect of edge distance on yield initiation in a remotely loaded half-plane containing interference-fit disc of the same material
[ARL/STRUC-R-413] 19 p3285 N85-30369
Computational methods in advanced stress and durability analyses
[AD-A154119] 19 p3286 N85-30375
On design of off-axis specimens
[AD-A154326] 19 p3286 N85-30379
Strain-path modeling for geo-materials
[AD-A154378] 19 p3286 N85-30380
Effects of high mean stress on the high-cycle fatigue behavior of PWA 1480
[NASA-CR-176020] 19 p3287 N85-30388
Micromechanism of fracture for stage 1 hydrogen-induced crack growth
[DE85-010027] 19 p3288 N85-30390
The location of stress in clothing
[AD-A154423] 19 p3331 N85-30633
Effect of speed and press fit on fatigue life of roller-bearing inner-race contact
[NASA-TP-2486] 20 p3463 N85-31511
Construction of constraint equation for stresses and strains
[BLL-M-36239-(5828.4)] 20 p3465 N85-31524
Load transfer by analytical methods
[SNIAS-851-111-109] 20 p3470 N85-31561
Journal of Research of the National Bureau of Standards, volume 89, no. 6, November - December 1984
[PB85-179042] 20 p3472 N85-31580
Development and test of advanced composite components. Center Directors discretionary fund program
[NASA-TM-86512] 21 p3561 N85-32147
The shearing contribution in transformation toughening of brittle materials
[AD-A154656] 21 p3566 N85-32195
Matrix fracture in fiber-reinforced ceramics
[AD-A154704] 21 p3569 N85-32197
User's guide for computer program CGFAG, Concrete General Flexure Analysis with Graphics
[AD-A155555] 21 p3570 N85-32204
Dynamic fracture of concrete and other heterogeneous materials
[AD-A154513] 21 p3596 N85-32343
Stress and buckling analysis 21 p3611 N85-32439
Remote temperature-set-point controller
[DE85-011614] 22 p3787 N85-33459
Shear wave transducer for boreholes
[DE85-011662] 22 p3787 N85-33461
Proceedings of the Mechanisms Conference, volume 1 23 p3923 N85-34309
The use of ultrasound to monitor incipient failure of rolling element bearings 23 p3924 N85-34317
Inertial stresses and deformations in mechanisms
23 p3924 N85-34320
Thermal stress analysis of a new turbine shroud seal concept
[NASA-TM-87082] 23 p3938 N85-34406
Design of transversely stiffenend FRP panels under compressive load — fiber reinforced plastic (FRP) ships
[AMTE(S)-R-84104] 23 p3940 N85-34424
The stress pattern analysis of coarse grain titanium specimens
[PNR-90250] 23 p3942 N85-34433
Damage induced stress redistribution in composite laminates 24 p4072 N85-35235
Development of a high strength isothermally heat-treated nodular iron road wheel arm
[AD-A155755] 24 p4099 N85-35408
Stress analysis of axisymmetric sandwich shells of variable thickness 24 p4101 N85-35419
1983 review of experimental stress and strain analysis
[DRIC-T-7469] 24 p4101 N85-35422
On size effects in plane stress crack-growth resistance
[AD-A155926] 24 p4102 N85-35426
Simplified procedures for the evaluation of settlements in sands due to earthquake shaking
[PB85-197887] 24 p4118 N85-35527
Establishment of a Computer-Aided Design (CAD)-Computer-Aided Manufacturing (CAM) process for the production of cold forged gears
[AD-A155756] 24 p4137 N85-35644
The finite element-difference method
24 p4141 N85-35672

STRESS CALCULATIONS
U STRESS ANALYSIS

STRESS CONCENTRATION
Finite element modelling of buried structures
01 p0061 N85-10403
Distributions of fatigue life and fatigue strength in notched specimens of a carbon 8-harness-satin laminate
[NAL-TR-809T] 01 p0061 N85-10407
Benchmark notch test for life prediction
02 p0140 N85-10953
Effect of stress concentrations in composite structures
[NASA-CR-173876] 02 p0170 N85-11140
Strain distribution in a type 316/16-8-2 stainless steel weldment during cyclic loading
[DE84-015644] 02 p0210 N85-11384
Modeling the stress field in laminated composite plates near discontinuities
[PB84-219237] 03 p0327 N85-12103
Viscoplastic finite element analysis of rapid fracture
03 p0370 N85-12365
Flow-based analyses of metal deformation processes: An overview 06 p0796 N85-15087
Disc fatigue life predictions for gas turbine engines
07 p0907 N85-15743
Fundamentals of microcrack nucleation mechanics
[NASA-CR-3851] 07 p0975 N85-16195
Stresses in pin-loaded orthotropic plates using photoelasticity
[NASA-CR-172498] 07 p0977 N85-16204
Modeling localized stress fields in composite laminates
[AD-A148530] 08 p1120 N85-17056
Finite element calculation for a Y-joint and comparison of results with strain measurements
[BLL-RISLEY-TR-4526-(9091.9F)]
08 p1171 N85-17381
Influence of setting angle of jet cooling nozzles on temperature and stress state of a turbine wheel
09 p1306 N85-18208
The fracture mechanics of a slit crack with crack-tip dual zones 09 p1332 N85-18371
Integrated Technology Rotor/Flight Research Rotor (ITR/FRR) concept definition
[NASA-CR-166443] 10 p1423 N85-18978
Stress concentration due to axial tension of loaded nonsymmetric-shaped grooves
[AD-A149425] 10 p1496 N85-19442
Stress studies in EFG
[NASA-CR-174441] 10 p1506 N85-19515
Stress-strain analysis of silicon ribbon
[NASA-CR-175459] 10 p1510 N85-19525
Residual stress after laser processing
11 p1600 N85-20065
Sensitivity of titanium alloys to stress concentration during repeated static loads 11 p1602 N85-20074
Effect of stress concentration fatigue resistance of refractory nickel alloys under asymmetrical multicycle loading, communication 1 11 p1604 N85-20086
Local strain redistribution corrections for a simplified inelastic analysis procedure based on an elastic finite-element analysis
[NASA-TP-2421] 11 p1651 N85-20396
On local total strain redistribution using a simplified cyclic inelastic analysis based on an elastic solution
[NASA-TM-86913] 12 p1864 N85-21690
Stresses in a half-plane containing either a pressurized hole or an interference-fit disc
[ARL/STRUC-R-409] 12 p1865 N85-21700
Elastic response of a half-plane to a bonded interference-fit disc of the same material
[ARL/STRUC-R-406] 12 p1865 N85-21701
Moving nonlocal crack: Anti-plane shear case
[AD-A149996] 12 p1866 N85-21709
Fracture analysis of cracks in complete cylindrical shells
[AD-A150091] 12 p1867 N85-21711
Reliability of structural brittle materials
12 p1946 N85-22222
Shape optimization for minimal stress concentration
13 p2101 N85-23083
On Hybrid and mixed finite element methods
[NASA-CR-175551] 13 p2101 N85-23096
Elasticity solution of an adhesively bonded joint
[NASA-CR-175591] 13 p2101 N85-23097
Advanced life analysis methods. Volume 2: Crack growth analysis methods for attachment lugs
[AD-A150420] 13 p2103 N85-23109
Role of residual stresses in stress corrosion cracking in alloy 600 tubes. Part 1: Determination of throughwall residual stresses and their modification by transient heat treatment
[DE85-004648] 14 p2257 N85-23989
Reaction of piezoceramic shell to concentrated forces
14 p2279 N85-24115
Reduction of free-edge stress concentration
[AD-A150732] 14 p2321 N85-24340
Elastic-plastic analysis for cyclic loading using a linearized yield condition
[PB85-149607] 14 p2322 N85-24346
Finite element model for creep in composite masonry
[PB85-150324] 14 p2322 N85-24347
Evaluation of stress concentration coefficients in butt-welded joints with displaced edges
15 p2501 N85-25425
The effects of pin elasticity, clearance, and friction on the stresses in a pin-loaded orthotropic plate
[NASA-CR-175816] 16 p2743 N85-26927
Experimentally determined distribution of stress around a horizontally loaded model pile in dense sand
[CE-43] 16 p2796 N85-27239
In plane stress analysis
[NASA-CR-175775] 16 p2799 N85-27259
Accuracy of the calculated stress field around a craze
[DE85-005520] 16 p2801 N85-27272
An X-ray diffraction study of the residual stress-strain distribution in shot-peened 2-phase brass
[AD-A152416] 17 p2930 N85-28086
Natural vibrations of reinforced spherical shells
17 p2943 N85-28165
Cyclic torsion of a circular cylinder and its residual stress distribution
[AD-A153347] 17 p2960 N85-28424
Numerical analysis of end effects in symmetric laminated plates
[NAL-TR-850] 18 p3068 N85-28977
Strain fields for aluminum at different tooling temperatures and extrusion ratios
[DE85-008257] 18 p3075 N85-29020
Fatigue behavior of unidirectional FP-Al composites with circular holes
[AD-A153466] 18 p3121 N85-29322
Mechanics of composite materials, theory and application
[VTH-LR-431] 18 p3123 N85-29334
Effect of thermochemical processing on fatigue resistance of titanium alloys 19 p3244 N85-30112
Residual stress distributions in (plastically) surface deformed two-phase materials 19 p3283 N85-30354
Multiaxial fatigue and fracture: A literature review
[ARL/STRUC-R-410] 19 p3285 N85-30370
Effects of high mean stress on the high-cycle fatigue behavior of PWA 1480
[NASA-CR-176020] 19 p3287 N85-30388

Inhomogeneous deformation: The theory and geological application of finite strain compatibility
19 p3312 N85-30532

Integral constraints on stress energy perturbations in general relativity and applications to cosmology
19 p3383 N85-30985

Two simplified procedures for predicting cyclic material response from a strain history 20 p3467 N85-31543

A clamped rectangular plate containing a crack
[NASA-CR-177925] 20 p3469 N85-31552

Shear-stress distribution and shear stiffness in the case represented by a non-homogeneous cross-section, of any shape, but composed of an orthotropic material, when subjected to a shear force
[DRIC-T-7430] 20 p3469 N85-31554

On the variation of the stress intensity factor along the front of a surface flaw
[OUEL-1565/85] 20 p3471 N85-31568

The interactions of composition and stress in crystalline solids
[PB85-179075] 20 p3473 N85-31583

Mechanics of near tip microcracking in brittle material
[AD-A154684] 21 p3598 N85-32346

Stress concentration in the elastoplastic state and residual stress after unloading
[AD-A155628] 21 p3600 N85-32356

Stress and efficiency studies in EFG
[NASA-CR-176125] 22 p3751 N85-33251

The stress distribution in pin-loaded orthotropic plates
[NASA-CR-176146] 22 p3800 N85-33547

Fractographic analysis for nonpropagating conditions of fatigue crack at high stress ratios in mild steel
23 p3905 N85-34194

Multiaxial stress analysis taking account of penetration depth of X-rays. A solution by means of polynomial approximation 23 p3907 N85-34204

Stress distribution of fiberglass reinforced plastic beam with a delamination under three-point bending
23 p3908 N85-34210

Stresses and strains in a plate resulting from two closely-spaced interference-fit fasteners
[ARL/STRUC-TM-409] 23 p3941 N85-34429

The stress pattern analysis of coarse grain titanium specimens
[PNR-90250] 23 p3942 N85-34433

Geophysical-geological studies of possible extensions of the New Madrid fault zone
[TI85-901341] 23 p3949 N85-34475

Damage induced stress redistribution in composite laminates 24 p4072 N85-35235

Static and cyclic behavior of semi-rigid steel beam-column connections
[PB85-194363] 24 p4103 N85-35433

The finite element-difference method
24 p4141 N85-35672

STRESS CORROSION

NT STRESS CORROSION CRACKING

Influence of nitrogen on the sensitization, corrosion, mechanical, and microstructural properties of austenitic stainless steels
[DE84-015134] 01 p0028 N85-10177

A study of environmental characterization of conventional and advanced aluminum alloys for selection and design. Phase 1: Literature review
[NASA-CR-172387-PHASE-1] 02 p0181 N85-11218

Corrosion of brass in potable water service
[CETIM-100390] 04 p0477 N85-13037

In-situ stress relief of expanded alloy 600 steam generator tubing
[DE84-014560] 04 p0513 N85-13273

Stress relief of transition zones
[DE85-000234] 11 p1653 N85-20411

The effect of stress and hot corrosion on nickel-base superalloys
[AD-A154722] 21 p3566 N85-32181

Automatic capability to store and retrieve component data and to calculate structural integrity of these components
[DE85-012429] 22 p3831 N85-33728

STRESS CORROSION CRACKING

A study of environmental characterization of conventional and advanced aluminum alloys for selection and design. Phase 1: Literature review
[NASA-CR-172387-PHASE-1] 02 p0181 N85-11218

A study of environmental characterization of conventional and advanced aluminum alloys for selection and design. Phase 2: The breaking load test method
[NASA-CR-172387-PHASE-2] 02 p0182 N85-11219

Stress corrosion of pressure vessel steel A533-B in high temperature water
[BLL-RISLEY-TR-4600-(9091.9F)]
03 p0330 N85-12125

Localized corrosion and stress corrosion cracking behavior of stainless steel weldments
[DE84-016095] 04 p0474 N85-13017

Fractographic study of stress corrosion cracking of SUS 304 stainless steel in various environments
[BLL-RISLEY-TR-4598-(9091.9F)]
05 p0615 N85-13928

Influence of the mechanical and electrochemical characteristics of austenitic and austenoferritic steels on the propagation rate and morphology of stress corrosion cracking
[BLL-RISLEY-TR-4545-(9091.9F)]
06 p0767 N85-14906

Testing of non-alloyed and low-alloyed steels for their behaviour with respect to intercrystalline stress corrosion cracking
[BLL-RISLEY-TR-4546-(9091.9F)]
07 p0925 N85-15861

Stochastic models of pitting corrosion of stainless steels. Part 1: Modelling of the initiation and growth of pits at constant potential
[AERE-R-11146-PT-1] 09 p1298 N85-18151

Contributions of segregated phosphorus to the intergranular stress corrosion cracking of nickel
[DE85-003112] 11 p1606 N85-20099

Stress corrosion cracking and oxidation characteristics of boride-strengthened microcrystalline iron and nickel based alloys
[AD-A149805] 12 p1806 N85-21328

Stress corrosion cracking behavior of tungsten heavy alloys
[AD-A149843] 12 p1806 N85-21329

Role of segregated P and S in intergranular stress corrosion cracking of nickel
[DE85-004547] 13 p2024 N85-22679

Advanced life analysis methods. Volume 1: Cracking data survey and NDI (nondestructive inspection) assessment for attachment lugs
[AD-A150419] 13 p2103 N85-23108

The role of hydrogen in the stress corrosion failure of high strength Al-Zn-Mg alloys
[AD-A150891] 14 p2256 N85-23978

Role of residual stresses in stress corrosion cracking in alloy 600 tubes. Part 1: Determination of throughwall residual stresses and their modification by transient heat treatment
[DE85-004648] 14 p2257 N85-23988

Anode formation of passivating films on titanium alloy at temperatures up to 200 deg C
15 p2515 N85-25519

Microscopic study of the influence of impurities on interface bonding
[AD-A151725] 16 p2743 N85-26928

Influence of pretreatment, environment and strain rate on stress corrosion cracking of the aluminum alloy 7075-T6
[VTH-LR-433] 16 p2752 N85-26985

Corrosion characteristics of some steels produced through a self-cleaning rotating electrode
[BLL-BISI-TRANS-22046-(9022.06)]
17 p2925 N85-28034

The synergistic actions of stress corrosion cracking and corrosion fatigue
[BLL-BISI-TRANS-22334-(9022.06)]
17 p2926 N85-28045

Study on mechanism of surface deformation induced by stress corrosion cracking
[BLL-BISI-TRANS-21896-(9022.06)]
17 p2928 N85-28066

Tendency of selected low-carbon steels to corrosion cracking in nitrates
[BLL-BISI-TRANS-22262-(9022.06)]
18 p3073 N85-29006

Marine corrosion
[AD-A153843] 18 p3074 N85-29012

Publications of the Jet Propulsion Laboratory 1983
[NASA-CR-175979] 18 p3199 N85-29848

Effect of multi-functional inhibitors on the electrochemistry within corrosion crack
19 p3238 N85-30075

Resistance to corrosion fatigue in aluminum alloy 1561 in sea water 19 p3243 N85-30108

Kinetics of H-induced stress corrosion cracking. Part 1: Important features of cracking in respect of high strength steels
[BLL-BISI-TRANS-(9022.06)] 19 p3282 N85-30350

Theoretical modelling of the electro-chemistry in a corrosion fatigue crack. Part 2: Mathematical aspects of associated unsteady reaction equations
[NPL-DMA(A)-100-PT-2] 20 p3465 N85-31529

Stress corrosion of ceramic materials
[AD-A155020] 21 p3570 N85-32202

Current requirements for the design and maintenance against corrosion of UK military aircraft
22 p3750 N85-33244

Relating corrosion maintenance to environmental factors 22 p3750 N85-33247

The influence of temperature on static and dynamic SCC crack growth behavior in aluminum alloy
23 p3905 N85-34190

A fractographic study on mode 2 and mode 3 SCC crack growth in an Al-Zn-Mg alloy 23 p3905 N85-34191

Stress corrosion cracking susceptibility of types 316NG and 316 stainless steel in an impurity environment
[TI85-006884] 23 p3917 N85-34277

Effect of temperature and ionic impurities at very low concentrations on stress corrosion cracking of Type 304 stainless steel
[TI85-003048] 24 p4079 N85-35283

STRESS CYCLES

Distributions of fatigue life and fatigue strength in notched specimens of a carbon 8-harness-satin laminate
[NAL-TR-809T] 01 p0061 N85-10407

Comparison between cycle ergometers with different mechanical braking systems
[FOA-C-54058-H1] 07 p0975 N85-16193

Compaction of sand using ordinary off-road vehicles
[AD-P004297] 09 p1409 N85-18674

Two simplified procedures for predicting cyclic material response from a strain history 20 p3467 N85-31543

Simplified procedures for the evaluation of settlements in sands due to earthquake shaking
[PB85-197887] 24 p4118 N85-35527

STRESS DISTRIBUTION

U STRESS CONCENTRATION

STRESS FUNCTIONS

Recent advances in hybrid/mixed finite elements
[NASA-CR-175574] 12 p1863 N85-21687

Fillet weld stress using finite element methods
15 p2576 N85-25884

STRESS INTENSITY FACTORS

Stress-derivative control of keystoning deformation in finite element codes 01 p0058 N85-10385

Crack tip opening displacement for work hardening materials
[GKSS-84-E-26] 01 p0063 N85-10415

Stress intensity factors for a circular ring with uniform array of radial cracks of unequal depth
[AD-A145893] 03 p0372 N85-12377

Stress intensity factors for corner cracks at holes located near an edge
[FFA-TN-1984-20] 04 p0514 N85-13279

Elastodynamic stress intensity factors of an interface finite-width crack
[DE84-016908] 06 p0817 N85-15190

Experimental compliance calibration of the NASA Lewis Research Center Mode 2 fatigue specimen
[NASA-TM-86908] 07 p0977 N85-16205

Circumferential cracks in cylindrical shells
09 p1330 N85-18354

finite element analysis of bi-material systems with applications in hydraulic fracturing
09 p1332 N85-18369

The fracture mechanics of a slit crack with crack-tip dual zones 09 p1332 N85-18371

Crack problems for bonded nonhomogeneous materials under antiplane shear loading
[NASA-CR-172532] 10 p1495 N85-19438

Fracture analysis of notched composites
[NASA-CR-172563] 11 p1593 N85-20020

On the stress analysis of bonded inserts
[ARL/STRUC-R-407] 12 p1865 N85-21698

The residual strength of cracked specimens representing a section of the mirage into wing main spar
[ARL/STRUC-R-408] 12 p1865 N85-21699

Effect of phase state of TiC-NiTi powder composite materials on nature of failure and mechanical properties
13 p2027 N85-22702

Stress intensity factor in a tapered specimen
[NASA-CR-175589] 13 p2102 N85-23099

Crack propagation under constant and variable stress amplitudes: A comparison of calculations based on the Striation spacing and tests 14 p2320 N85-24336

On residual stresses and stress intensity factors in composite materials 15 p2572 N85-25859

Transition region for corner cracks at holes
[AD-A151835] 15 p2579 N85-25908

Study to optimize Cr-Mo steels to resist hydrogen and temper embrittlement
[DE85-005492] 17 p2932 N85-28096

Crack propetion in unidirectional laminates by the stress intensity factors 18 p3121 N85-29320

Fracture of laminated composite materials
19 p3230 N85-30030

Kinetics of H-induced stress corrosion cracking. Part 1: Important features of cracking in respect of high strength steels
[BLL-BISI-TRANS-(9022.06)] 19 p3282 N85-30350

Fracture mechanics formulas on microcomputers
[NASA-TM-77850] 19 p3284 N85-30362

On the variation of the stress intensity factor along the front of a surface flaw
[OUEL-1565/85] 20 p3471 N85-31568

A cracked orthotropic sheet stiffened by a semi-infinite orthotropic sheet
[NASA-TP-2455] 21 p3597 N85-32339
On the methods to determine the stress intensity factors in boundary element method 23 p3905 N85-34189
Time and temperature dependence of fracture surface in soft epoxy resin 23 p3908 N85-34213
Nonlinear adhesive behavior effects in a cracked orthotropic sheet stiffened by a semi-infinite orthotropic sheet
[NASA-TM-87584] 23 p3941 N85-34426
Stress-intensity factors for circumferential surface cracks in pipes and rods under tension and bending loads
[NASA-TM-87594] 24 p4101 N85-35424
STRESS MEASUREMENT
Composite laminate optimization program suitable for microcomputers 01 p0059 N85-10389
Evaluation of interfacial stresses from the amplitude of reflected ultrasonic signal
[DE84-015472] 02 p0276 N85-11798
Back stress in dislocation creep. Part 1: Basic concepts and measuring techniques
[NASA-TM-77773] 07 p0977 N85-16206
Measurement of stress in clothing: A literature review and methods selected
[AD-A147674] 08 p1132 N85-17132
Piezoelectric stress transducer used for measurements of explosions in hard rock 11 p1638 N85-20316
The measurement of residual stresses using ultrasonics
[AERE-R-11415] 12 p1868 N85-21722
Load carrying capacity of double circular arc gears
14 p2221 N85-23776
Evaluation of the blind hole drilling method for the measurement of residual stress
[AD-A151459] 15 p2579 N85-25905
Surface shear stress characteristics in turbulent flows
19 p3211 N85-29914
Development of an NBS (National Bureau of Standards) polymer gage for dynamic soil stress measurement
[PB85-208494] 24 p4118 N85-35526
STRESS PROPAGATION
Wave propagation in heterogeneous media
[AD-A150800] 14 p2321 N85-24341
Constitutive modeling for blast-induced wave propagation
[AD-A153576] 18 p3099 N85-29187
On the variation of the stress intensity factor along the front of a surface flaw
[OUEL-1565/85] 20 p3471 N85-31568
STRESS RATIO
Fractographic analysis for nonpropagating conditions of fatigue crack at high stress ratios in mild steel
23 p3905 N85-34194
STRESS RELAXATION
Equibiaxial extension of two polymer melts: Polystyrene and low density polyethylene
[AD-A144893] 01 p0032 N85-10200
Stress relief cracking studies of 2 1/4Cr1Mo steel
[AERE-R-11111] 03 p0374 N85-12388
Free volume considerations in thermoplastic and thermosetting resins 04 p0465 N85-12952
In-situ stress relief of expanded alloy 600 steam generator tubing
[DE84-014560] 04 p0513 N85-13273
Effect of temperature on the stress-relaxation response of a pressure vessel steel
[DE85-003588] 09 p1339 N85-18424
Stress relief of transition zones
[DE85-000234] 11 p1653 N85-20411
Rheology of dissemination
[AD-A150006] 12 p1813 N85-21373
MM2 LRSLA testing stage 3 propellant
[AD-A152540] 17 p2937 N85-28128
A state variable approach to transient creep deformation in stress reduction experiments
[DE85-009492] 18 p3122 N85-29331
Mechanics of near tip microcracking in brittle material
[AD-A154884] 21 p3598 N85-32346
STRESS RELIEVING
Stress-relieving interlayers for bituminous resurfacings
[PB85-136885] 12 p1820 N85-21415
Possible use of rapid heating for improving mechanical properties of titanium alloys 15 p2498 N85-25409
Local heat treatment of welded joints of pipes and rotary vessels 17 p2924 N85-28028
Welding of 11 458.1 steel in shielding atmospheres
[BLL-BISI-TRANS-21763-(9022.06)]
17 p2972 N85-28353
STRESS RUPTURE STRENGTH
U CREEP RUPTURE STRENGTH
STRESS TENSORS
Analysis of the nonlinear equations describing the elastic, thermal, and electromagnetic behavior of solids: Existence of solutions of semi-inverse problems
24 p4100 N85-35415
STRESS WAVES
Excitation modes and parameters of stress waves in metal exposed to single laser pulses
10 p1446 N85-19109
Piezoelectric stress transducer used for measurements of explosions in hard rock 11 p1638 N85-20316
Stress waves in an isotropic elastic plate excited by a circular transducer
[NASA-CR-3877] 11 p1650 N85-20390
Application of homomorphic signal processing to stress wave factor analysis
[NAS 1.26:174671] 12 p1861 N85-21673
Wave propagation in heterogeneous media
[AD-A150800] 14 p2321 N85-24341
Altimetry data and the elastic stress tensor of subduction zones
[NASA-CR-175796] 16 p2825 N85-27425
Interaction of large amplitude stress waves in layered elastic-plastic materials
[AD-A153519] 18 p3121 N85-29323
A study of the stress wave factor technique for the characterization of composite materials
[NASA-CR-174870] 19 p3231 N85-30035
Behaviors of stress waves in a conical bar
23 p3904 N85-34182
STRESS-STRAIN DIAGRAMS
Dependence of microplasticity of beryllium on grain size and heat treatment 03 p0353 N85-12273
The cyclic stress-strain behavior of nickel-base superalloy poly- and single crystals
14 p2254 N85-23969
STRESS-STRAIN DISTRIBUTION
U STRESS CONCENTRATION
STRESS-STRAIN RELATIONSHIPS
Benchmark notch test for life prediction
02 p0140 N85-10953
Viscoplastic finite element analysis of rapid fracture
03 p0370 N85-12365
Investigation of toughened neat resins and their relations to advanced composite mechanical properties
04 p0464 N85-12949
Strain rate effects and temperature history effects for three different tempers of 4340 VAR steel
[AD-A146372] 06 p0768 N85-14915
Strength analysis of fan-shaped wing considering temperature deformation and creep deformations
06 p0779 N85-14983
Analysis of thin-walled airframe members in geometrically nonlinear statement
06 p0780 N85-14985
Miniworkshop on effects of stress and strain in high-speed-growth silicon ribbons
06 p0831 N85-15284
A study of Reynolds-stress closure model
[NASA-CR-174342] 08 p1161 N85-17324
Deformation and fracture of P/M (Powder/Metallurgy) titanium alloys
[AD-A148672] 08 p1294 N85-18128
On solving nonlinear problems of aircraft structural mechanical design 09 p1309 N85-18223
Verification and application of the Iosipescu shear test method
[NASA-CR-174346] 09 p1333 N85-18376
Evaluation of failure criterion for graphite/epoxy fabric laminates
[NASA-CR-172547] 10 p1431 N85-19025
Microstrain analysis in bent single crystal silicon by double crystal X-ray topography technique
[DE85-000422] 10 p1564 N85-19863
Local strain redistribution corrections for a simplified inelastic analysis procedure based on an elastic finite-element analysis
[NASA-TP-2421] 11 p1651 N85-20396
A solution method for nonlinear dynamic analysis of shell structures
[AD-A149846] 12 p1866 N85-21708
A study of the compatibility of an existing CFD package with a broader class of material constitutions
12 p1945 N85-22219
Behavior of fiber-reinforced composites under dynamic tension
[AD-A150619] 13 p2015 N85-22641
Dissipation of energy in composite material
13 p2027 N85-22703
Method of calculating strength of joint produced by cold welding of aluminum under discrete loading
13 p2034 N85-22743
Determination of stresses and deformations in linearly elastic conical shell subjected to aerodynamic loading and heating 13 p2047 N85-22812
Theoretical and experimental investigation of mechanically fastened composites
[AD-A150961] 14 p2248 N85-23035
Strength computation of thin walled shell by discreet-continuous model 14 p2288 N85-24181
A preliminary investigation into transverse fracture of unidirectional fiber composites
[AERE-R-11494] 15 p2503 N85-25436
Superplasticity in a thermo-mechanically processed Aluminum-10.2%Mg-0.52%Mn alloy
[AD-A152016] 15 p2510 N85-25485
Dependence of plasticity of VT1-00 titanium alloy on microstructure 15 p2515 N85-25516
Compressive strength of epoxy resin chocks subjected to elevated temperatures
[AD-A152018] 15 p2519 N85-25532
On thermomechanical testing in support of constitutive equation development for high temperature alloys
[NASA-CR-174879] 15 p2577 N85-25894
Fiber reinforcemant of gun propellant
[AD-A152296] 16 p2757 N85-27014
Stressed-strained state of tubular shells under uniformly distributed pressure 16 p2766 N85-27067
Stressed state of multilayer thick-walled longitudinally corrugated cylinders 16 p2766 N85-27069
Cyclic structural analyses of SSME turbine blades
17 p2914 N85-27963
X-ray diffraction study of changes in stress-strain distributions during fatigue of a 2-phase alloy
[AD-A152367] 17 p2930 N85-28067
An X-ray diffraction study of the residual stress-strain distribution in shot-peened 2-phase brass
[AD-A152418] 17 p2930 N85-28086
State of stress and penetration of plastic deformation in forming
[BLL-BISI-22199-(9022.06)] 17 p2977 N85-28396
Cyclic torsion of a circular cylinder and its residual stress distribution
[AD-A153347] 17 p2980 N85-28424
Finite element thermal-structural analysis of cable-stiffened space structures
[AD-A153822] 18 p3066 N85-28963
Strain fields for aluminum at different tooling temperatures and extrusion ratios
[DE85-008257] 18 p3075 N85-29020
Transient dynamic solutions of some half space problems by the boundary element method
19 p3283 N85-30360
Effect of nonuniform size on internal stresses in a rapid, simple shear flow of granular materials. Part 1: Two grain sizes
[AD-A154045] 19 p3285 N85-30372
Strain-path modeling for geo-materials
[AD-A154378] 19 p3286 N85-30380
The initiation and growth of adiabatic shear bands
[AD-A154459] 19 p3287 N85-30382
Inhomogeneous deformation: The theory and geological application of finite strain compatibility
19 p3312 N85-30532
Residual thermal and moisture influences on the strain energy release rate analysis of edge delamination
[NASA-TM-86437] 20 p3422 N85-31238
On elastic-plastic fracture criterion
20 p3465 N85-31528
Finite element analysis of notch behavior using a state variable constitutive equation 20 p3466 N85-31548
Component-specific modeling
[NASA-CR-174925] 21 p3556 N85-32119
Effects of weak interfaces on thermostructural behavior of carbon-carbon composites
[AD-A155330] 21 p3562 N85-32154
Fundamental investigations of failure during superplastic forming process
[AD-A154647] 21 p3566 N85-32194
Hertzian contact in two and three dimensions
[NASA-TP-2473] 21 p3586 N85-32201
Analysis of stress-strain relationships in silicon ribbon
21 p3611 N85-32408
Stress and efficiency studies in EFG
[NASA-CR-176125] 22 p3751 N85-33051
Remote temperature-set-point controller
[DE85-011614] 22 p3787 N85-33459
Monotonous stress-strain properties of structural steel subjected to nonstationary repetitive pre-loading
23 p3904 N85-34185
Development and application of a unified viscoelastic constitutive model for the prediction of material response under thermomechanical loading
24 p4101 N85-35420
1983 review of experimental stress and strain analysis
[DRIC-T-7469] 24 p4101 N85-35422
STRESS-STRAIN-TIME RELATIONS
The stress-strain-time graph of rheological soils and its application
[AD-P004286] 09 p1407 N85-1

Constitutive modeling for blast-induced wave propagation
[AD-A153576] 18 p3099 N85-29187

STRESSES
NT AXIAL STRESS
NT COMBINED STRESS
NT CRITICAL LOADING
NT RESIDUAL STRESS
NT REYNOLDS STRESS
NT SHEAR STRESS
NT TENSILE STRESS
NT THERMAL STRESSES
NT TORSIONAL STRESS
NT TRIAXIAL STRESSES
NT VIBRATIONAL STRESS
Equivalent damage: A critical assessment
02 p0140 N85-10952
Response of propellants to high dynamic stresses: The uses of gun launch techniques
[DE84-013223] 02 p0188 N85-11259
Large-area sheet task advanced dendritic web growth development
[NASA-CR-174021] 02 p0223 N85-11463
Stress intensity factors for a circular ring with uniform array of radial cracks of unequal depth
[AD-A145893] 03 p0372 N85-12377
Dispersion forces of solids under stress. Chemisorption under stress
[AD-A146171] 03 p0373 N85-12380
Bulletin of the Faculty of Engineering, Hokkaido University, no. 123
[ISSN-0385-602-X] 04 p0482 N85-13075
Estimation of dynamic stresses around the shot point by scale model experiment 04 p0482 N85-13076
Longevity of thin-walled engine parts subjected to transient stresses under creep conditions
06 p0777 N85-14966
Stresses and strains in lithosphere caused by Earth's thermoconvective oscillations 06 p0822 N85-15217
Free surface effects on the wake of a flat plate
[AD-A146966] 07 p0956 N85-16071
Computer program for determining induced stresses and consolidation settlements (CSETT)
[AD-A146730] 07 p1023 N85-16493
Response of propellants to high dynamic stresses: The uses of gun launch techniques
08 p1116 N85-17035
Modeling localized stress fields in composite laminates
[AD-A148630] 08 p1120 N85-17056
The fracture mechanics of a slit crack with crack-tip dual zones 09 p1332 N85-18371
NOAA OTEC CWP (National Oceanic and Atmospheric Administration Ocean Thermal Energy Conversion Cold Water Pipe) at-sea test. Volume 3, part 1: Tabulation of the power spectra for selected channels
[PB84-238955] 09 p1346 N85-18467
Stresses in situ generating by bulldozers
[AD-P004270] 09 p1405 N85-18846
Finite element analysis of ground deformation beneath moving track loads
[AD-P004271] 09 p1405 N85-18847
Investigation of accelerated stress factors and failure/degradation mechanisms in terrestrial solar cells
[NASA-CR-175409] 10 p1510 N85-19524
Fractographic features of titanium alloy fatigue failure under repeated static stress and high frequency vibration 11 p1601 N85-20070
Characteristics of EMI generated by negative metal-positive dielectric voltage stresses due to spacecraft charging 13 p1985 N85-22505
Load capacity of cages of roller bearings for planet wheels 14 p2221 N85-23775
On the corner singularity of a 3-D Griffith crack
[AD-A150889] 14 p2321 N85-24342
Magnetohydrodynamic considerations for the design of self-cooled liquid-metal fusion reactor blankets
[DE85-000242] 14 p2425 N85-24957
Yield stress determination from miniaturized disk bend test data
[DE85-008495] 18 p3122 N85-29330
Interim rock mass properties and conditions for analyses of a repository in crystalline rock
[DE85-010700] 18 p3125 N85-29352
Implications about in situ stress at Yucca Mountain
[DE85-008066] 18 p3126 N85-29356
Measurement and calculation of the mechanical response of a highly fractured rock
[DE85-008421] 18 p3127 N85-29362
A multiphase continuum model to describe dynamic loading effects in nonlinear porous media
[DE85-010102] 19 p3301 N85-30463
The location of stress in clothing
[AD-A154423] 19 p3331 N85-30633
Comparative analysis of laboratory and fullscale experimental data for metal flow displacements and speeds
[BLL-M-36286-(5828.4)] 20 p3430 N85-31276
Machining-induced deformation in stepped specimens of PH 13-8 Mo, 18 nickel maraging steel grade 200T1 and grain-refined HP 9-4-20
[NASA-CR-172450] 21 p3565 N85-32177
Sintering studies project
[AD-A154750] 21 p3572 N85-32216
Thin-film reliability and engineering overview
21 p3612 N85-32450
Temperature sensitivity of fiber-optic transmission line
22 p3764 N85-33331
Slideline verification for multilayer pressure vessels and piping analysis including strain hardening
[DE85-005816] 22 p3801 N85-33549
Damage induced stress redistribution in composite laminates 24 p4072 N85-35235

STRETCHING
Equibiaxial extension of two polymer melts: Polystyrene and low density polyethylene
[AD-A144893] 01 p0032 N85-10200
Finite element method calculation of a necking tension specimen including heat transfer influence
[RUB-IFM-MITT-40] 05 p0648 N85-14162
Thermal stress-dependent dilation of concrete
[DE84-014688] 11 p1653 N85-20412
Critical events in inelastic deformation of glassy polymers in adsorptive medium
13 p2014 N85-22634

STRIATION
The role of finite parallel length on the stability of barium clouds
[AD-A146972] 07 p0996 N85-16328
Application of optical and electron microscopic techniques in the fractographic determination of fatigue crack growth rates 14 p2320 N85-24334
Crack propagation under constant and variable stress amplitudes: A comparison of calculations based on the Striation spacing and tests 14 p2320 N85-24336
Striation free doped silicon
[AD-A155730] 22 p3847 N85-33827

STRINGERS
Tensile strength of composite sheets with unidirectional stringers and crack-like damage: A brief report
[NASA-TM-86310] 02 p0170 N85-11139
A cracked orthotropic sheet stiffened by a semi-infinite orthotropic sheet
[NASA-TP-2455] 21 p3597 N85-32339
Acoustic wave scattering by round cylindrical shell reinforced with stringers 21 p3686 N85-32916
Nonlinear adhesive behavior effects in a cracked orthotropic sheet stiffened by a semi-infinite orthotropic sheet
[NASA-TM-87584] 23 p3941 N85-34426

STRIP TRANSMISSION LINES
NT MICROSTRIP TRANSMISSION LINES
A generalized solution to a class of printed circuit antennas
[AD-A145626] 02 p0191 N85-11278
A coaxial cavity gunn oscillator using probe coupled microstrip
[AD-D011437] 10 p1479 N85-19334
Bonded stripline power splitter for ERS-1
[RML-009-84-124] 15 p2550 N85-25740
Research on superconductive signal-processing devices
[AD-A152703] 17 p2953 N85-28235
MMIC devices for active phased array antennas
[NASA-CR-176015] 19 p3254 N85-30177
Application of field similitude theory to calculation of stripline heating 22 p3780 N85-33419
Power flow evaluations for HERMES 3
[DE85-013116] 24 p4158 N85-35769

STROBOSCOPES
Orbit extrapolation — satellite orbits
05 p0598 N85-13811
Characteristics of digital range finder with stroboscopic discretization 22 p3762 N85-33319

STRONG INTERACTIONS (FIELD THEORY)
Experimental studies of diffractive phenomena
[DE85-006812] 17 p3031 N85-28749
Dependence of the average spatial and energy characteristics of the hadron-lepton cascade on the strong interaction parameters at superhigh energies
24 p4188 N85-35977

STRONGLY COUPLED PLASMAS
Many-body correlations in strongly-coupled plasmas
02 p0284 N85-11850
Local fields in strongly coupled plasmas
[DE84-013375] 04 p0567 N85-13611
Spatial resolution of small particles in silane discharge
[AD-A150953] 14 p2423 N85-24948
Equations of state of strongly coupled plasma mixtures
[DE85-006163] 15 p2657 N85-26393
Enhanced thermal coupling by a repetitively pulsed laser
[AD-A154435] 19 p3276 N85-30317
Activities of Rutgers - The State University Department of Mathematics
[AD-A154158] 19 p3370 N85-30904
Strong coupling effects on bound states in plasmas
[AD-A154353] 19 p3370 N85-30905
Low frequency instabilities driven by an ion temperature anisotropy
[AD-A154902] 21 p3707 N85-33016

STRONTIUM
NT STRONTIUM 90

STRONTIUM COMPOUNDS
NT STRONTIUM FLUORIDES
NT STRONTIUM TITANATES

STRONTIUM FLUORIDES
Feasibility of melt casting strontium fluoride to produce high-density heat sources
[DE85-009429] 18 p3130 N85-29361

STRONTIUM ISOTOPES
NT STRONTIUM 90

STRONTIUM TITANATES
A study of structural phase transitions using light scattering techniques
[AD-A147261] 07 p1048 N85-16654
Planar ferroelectric microcapacitors for microwave devices 13 p2087 N85-23032

STRONTIUM 90
Environmental surveillance at Los Alamos during 1984
[DE85-011886] 22 p3811 N85-33605
Estimation of Sr90 and Cs137 activity introduced and accumulation in the Po basin until 1983
[CISE-2515] 22 p3813 N85-33617

STROUHAL NUMBER
Periodic vortex shedding in the supersonic wake of a planar plate
[NASA-TM-77854] 15 p2463 N85-25207

STRUCTURAL ANALYSIS
NT DYNAMIC STRUCTURAL ANALYSIS
NT ENERGY METHODS
NT EQUILIBRIUM METHODS
NT FLUTTER ANALYSIS
NT MATRIX METHODS
NT STRAIN ENERGY METHODS
A study of bituminous pavements to determine a correlation between pavement structure designs and tripping of asphalt cement
[PB84-217751] 01 p0037 N85-10231
Broadband transverse field interaction continuous beam amplifier
[AD-D011229] 01 p0043 N85-10279
Application of concurrent processing to structural dynamic response computations
01 p0057 N85-10380
Initial experience with distributing structural calculations among computers operating in parallel
01 p0058 N85-10381
Structural analysis of the Space Shuttle Orbiter
01 p0061 N85-10401
Finite element modelling of buried structures
01 p0061 N85-10403
On the computer analysis of structures and mechanical systems 01 p0061 N85-10404
Development of advanced constitutive model for reinforced concrete
[AD-A145050] 01 p0062 N85-10411
Turbine Engine Hot Section Technology (HOST)
[NASA-TM-83022] 02 p0140 N85-10951
Nonlinear structural and life analyses of a turbine blade 02 p0141 N85-10954
Nonlinear structural and life analyses of a combustor liner 02 p0141 N85-10955
Component-specific modeling
02 p0143 N85-10971
The 3-D inelastic analysis methods for hot section components: Brief description 02 p0143 N85-10972
Constitutive model development for isotropic materials
02 p0144 N85-10975
Validation of structural analysis methods using the in-house liner cyclic rigs 02 p0146 N85-10987
Quasi-Newton algorithms for large scale nonlinear systems 02 p0208 N85-11370
Optical waveguide spatial filters
[AD-A145674] 02 p0260 N85-11825
Biaxial constitutive equation development for single crystals
[NASA-CR-174056] 02 p0286 N85-11862
Study of structure of sponge titanium varieties
03 p0350 N85-12256
Constituent properties and interrelationships
04 p0467 N85-12964

Bulletin of the Faculty of Engineering, Hokkaido University, no. 123
[ISSN-0385-602-X] 04 p0482 N85-13075
Implication structures for generalized implication matrix in ISM 04 p0483 N85-13079
Design, ancillary testing, analysis and fabrication data for the advanced composite stabilizer for Boeing 737 aircraft, volume 2
[NASA-CR-166011] 05 p0612 N85-13914
Analytical thermal formulations for antenna dishes — satellite antennas 05 p0627 N85-14017
Structure errors in system identification
05 p0700 N85-14495
USSR report: Engineering and equipment
[JPRS-UEQ-84-007] 06 p0775 N85-14954
Iterative method of calculating strength of airframe members using finite element method
06 p0775 N85-14955
Sensitivity analysis of discrete structural systems: A survey
[NASA-TM-86333] 06 p0817 N85-15186
Encapsulation design analysis
06 p0829 N85-15268
CF-5 vertical stabilizer flight load survey
07 p0895 N85-15673
Keeping up with operational loads in the French Air Force: Defining new equipment
07 p0896 N85-15681
USAF approach to airborne structural data recording: Airborne Data Acquisition Multifunction System (ADAMS)
07 p0897 N85-15683
Engine cyclic durability by analysis and material testing 07 p0907 N85-15744
Flutter control with unsteady aerodynamic models
[AD-A147858] 07 p0909 N85-15753
Reduction method for thermal analysis of complex aerospace structures
[NASA-TP-2373] 07 p0957 N85-16066
A review of imperfection sensitivity of stiffened shells
[AD-A147311] 07 p0978 N85-16213
Advances in composites technology
[NASA-TM-86353] 08 p1118 N85-17046
Composites with a periodic structure, mathematical analysis and numerical treatment
[AD-A148301] 08 p1119 N85-17053
Mechanical properties of adhesively bonded aluminum structures protected with hydration inhibitors
[AD-A148123] 08 p1133 N85-17139
Computational methods for nonlinear dynamics problems in solid and structural mechanics
[AD-A148352] 08 p1172 N85-17382
Vibration analysis of a multipurpose platform
[NAL-TR-803] 09 p1286 N85-18078
Treatment of general boundary conditions and point-wise state variable constraints in optimum design for static and dynamic response
09 p1330 N85-18358
NASA Lewis Research Center/University Graduate Research Program on Engine Structures
[NASA-TM-86916] 09 p1333 N85-18375
The Shock and Vibration Bulletin 54. Part 2: Ship shock, shock and blast and ground shock
[AD-A148132] 09 p1334 N85-18386
Assessment of seismic survivability
09 p1336 N85-18402
Penetration of short duration airblast into protective structures 09 p1336 N85-18404
A pole-free reduced-order characteristic determinant method for linear vibration analysis based on sub-structuring 09 p1336 N85-18412
Determination of shear coefficient of a general beam cross section by finite element method
09 p1336 N85-18413
Applications of the Heavy-Iron Rutherford Backscattering Spectrometry (HIRBS) to the analysis of contact structures on GaAs and Ge
[DE85-000671] 10 p1564 N85-19861
SANS studies of polymers
[DE85-002471] 11 p1612 N85-20134
A new rheological model for concrete structural analysis
[DE84-014743] 11 p1653 N85-20413
Innovative solar thermal dish technology development
[DE85-002787] 11 p1673 N85-20539
Alternative approximation concepts for space frame synthesis
[NASA-CR-172526] 12 p1776 N85-21150
Nonlinear analysis for high-temperature multilayered fiber composite structures — turbine blades
[NASA-TM-83754] 12 p1797 N85-21273
Symmetric primal-dual variational formulations of coupled dynamic systems: Three-dimensional elasticity, shells, fluid-structure interaction
[ONERA-1983-91] 12 p1863 N85-21684
3-D inelastic analysis methods for hot section components (base program) — turbine blades, turbine vanes, and combustor liners
[NASA-CR-174700] 12 p1863 N85-21686
On local total strain redistribution using a simplified cyclic inelastic analysis based on an elastic solution
[NASA-TM-86913] 12 p1864 N85-21690
Time marching numerical solution of the dynamic response of nonlinear systems
[NAF-AN-25] 12 p1865 N85-21696
A solution method for large deformation contact problems
[AD-A148642] 12 p1866 N85-21707
A solution method for nonlinear dynamic analysis of shell structures
[AD-A148646] 12 p1866 N85-21708
Geometrically nonlinear analysis of laminated elastic structures
[NASA-CR-175609] 12 p1868 N85-21720
Systems vulnerability and lethality in the development phase
[AD-A149737] 12 p1924 N85-22089
Simple theoretical models for composite rotor blades
[NASA-CR-175620] 13 p1971 N85-22382
Specifics of kinetics of polymorphous conversion upon heating of low carbon steels 13 p2030 N85-22721
Machine analysis of resonance characteristics of plate-type radio electronic equipment constructions
13 p2085 N85-23018
Operational loads measurement: A philosophy and its implementation — aircraft structures
[AD-A149445] 13 p2144 N85-23308
Raman structural studies of the nickel electrode
[NASA-CR-175619] 13 p2162 N85-23414
Meteoroidal impacts, plasma, fine structure of ringlets and spokes on Saturn's ring B 13 p2174 N85-23490
The olivine asteroids: Discovery, mineralogy, and relationship to pallasites 13 p2175 N85-23500
Research on composite materials for structural design
[AD-A150802] 14 p2260 N85-24004
Unified constitutive material models for nonlinear finite-element structural analysis — gas turbine engine blades and vanes
[NASA-TM-86985] 14 p2320 N85-24338
Cyclic structural analyses of anisotropic turbine blades for reusable space propulsion systems — same fuel turbopump
[NASA-TM-86990] 14 p2320 N85-24339
Finite Element Methods in South Africa 1983 — conference
[S-332] 14 p2410 N85-24863
On the structure of the turbulent vortex
15 p2463 N85-25213
Automatic Dynamic Aircraft Modeler (ADAM), volume 1
[AD-A151410] 15 p2471 N85-25252
NASA R and T aerospace plane vehicles: Progress and plans
[NASA-TM-86429] 15 p2491 N85-25368
Definition of ground test for verification of large space structure control
[NASA-CR-171438] 15 p2492 N85-25377
Thirteenth NASTRAN Users' Colloquium
[NASA-CP-2373] 15 p2573 N85-25863
New enhancements in April 85 NASTRAN release
15 p2573 N85-25864
Improved accuracy in solid isoparametric elements using selectively reduced integration 15 p2573 N85-25865
Crack elements for COSMIC/NASTRAN
15 p2573 N85-25866
A 4-node bilinear isoparametric element in Rockwell NASTRAN 15 p2573 N85-25867
Layered composite analysis capability
15 p2573 N85-25868
NPLOT: An interactive plotting program for NASTRAN finite element models 15 p2573 N85-25869
COSMIC/NASTRAN-PATRAN interface
15 p2574 N85-25870
Two interactive graphics postprocessors for NASTRAN 15 p2574 N85-25871
An unusual application of NASTRAN contour plotting capability 15 p2574 N85-25872
CADS: A Computer Aided Design System
15 p2574 N85-25876
Learjet Model 55 wing analysis with landing loads
15 p2575 N85-25883
Fillet weld stress using finite element methods
15 p2576 N85-25884
The structural finite element model of the C-5A
15 p2576 N85-25885
Using NASTRAN to model missile inertia loads
15 p2576 N85-25886
Experience with free bodies 15 p2576 N85-25887
NASTRAN analysis comparison to shock tube tests used to simulate nuclear overpressures
15 p2576 N85-25888
Direct transient analysis of a fuze assembly by axisymmetric solid elements 15 p2576 N85-25890
Transient analysis of a magnetic heat pump
15 p2576 N85-25891
Vibration and buckling of rotating, pretwisted, preconed beams including Coriolis effects
[NASA-TM-87004] 15 p2577 N85-25893
Structures and Dynamics Division research and technology plans for FY 1985 and accomplishments for FY 1984
[NASA-TM-86417] 15 p2577 N85-25895
Elastic-workhardening SDF (Single-Degree-of-Freedom) system subjected to random blast excitations
[AD-A151666] 15 p2579 N85-25909
Structural analysis of electronic assembly housing
[DE85-005794] 15 p2580 N85-25913
GEMINI: A computer program for two and three dimensional linear static and seismic structural analysis, CDC 7600 version
[DE85-007496] 15 p2631 N85-26219
Enhanced thermal-structural analysis by integrated finite elements
[AD-A151103] 15 p2636 N85-26258
Methods of first wall structural analysis with applications to the long pulse commercial Tokamak reactor design
[DE85-004915] 15 p2657 N85-26397
ESP (External-Stores Program): A pilot computer program for determining flutter-critical external-store configurations. Volume 1: User's manual
[AD-A152268] 16 p2710 N85-26725
A study of structural concepts for ultralightweight spacecraft
[NASA-CR-175765] 16 p2730 N85-26848
Nonlinear structural analysis for fiber-reinforced superalloy turbine blades 16 p2737 N85-26887
Adaptation of continuous beams and the method of optimizing the flexibility of their elastic supports. Theorem on maximal adaptation loading, supplement
[REPT-10/1984-SUPPL] 16 p2797 N85-27241
Optimal modeling with a minimum of local distortion
[REPT-18/1984] 16 p2797 N85-27243
A computer analysis program for interfacing thermal and structural codes
[NASA-TM-87021] 16 p2800 N85-27284
USAF damage tolerant design handbook: Guidelines for the analysis and design of damage tolerant aircraft structures, revision B
[AD-A153161] 17 p2896 N85-27858
Probabilistic structural analysis theory development
17 p2912 N85-27955
Probabilistic finite element: Variational theory
17 p2913 N85-27957
Probabilistic structural analysis of SSME turbopump blades: Probabilistic geometry effects
17 p2913 N85-27958
Cyclic structural analyses of SSME turbine blades
17 p2914 N85-27963
Coherent structure reflective turbulent viscous flow modeling
[AD-A153086] 17 p2958 N85-28267
The Shock and Vibration Digest, volume 17, no. 1
[AD-A151051] 17 p2977 N85-28397
Continuum modeling of latticed structures
17 p2977 N85-28399
First passage times for combinations of random loads
[AD-A153275] 17 p2980 N85-28423
Structural analysis of terrane accretions in the eastern Brooks Range and adjacent areas in central Alaska and Canada
[DE85-008279] 17 p2993 N85-2850
Implementation of a general finite element code on an IBM PC compatible microcomputer
[AD-A152881] 17 p3011 N85-2881
Sample problems for STAGSC-1
[AD-A153142] 17 p3012 N85-2882
Finite element thermal-structural analysis of cable-stiffened space structures
[AD-A153822] 18 p3066 N85-2890
Constitutive modeling for blast-induced wa propagation
[AD-A153576] 18 p3086 N85-2918
Structural Analysis
[DFVLR-MITT-84-21] 18 p3120 N85-2931
Research on structural analysis at the DFVLR Brunswick 18 p3120 N85-2931
Field consistency and the finite element analysis o multifield structural problems 18 p3120 N85-2931
Low-energy electron diffraction experiment and theo
[DE85-009967] 18 p3195 N85-2982
Action of plasma and explosion products on alumina
19 p3242 N85-3010
Structural analysis and cost estimate of an eight-le space frame as a support structure for horizontal axis wi turbines
[NASA-TM-83470] 19 p3264 N85-30

Large deflections of a cantilever beam under arbitrarily directed tip load
[NASA-TM-86442] 19 p3284 N85-30363
Underwater shock-induced responses of stiffened flat plates: An investigation into the predictive capabilities of the USA-STAGS code
[AD-A154245] 19 p3286 N85-30377
Seismic pipe support construction practices
[DE85-001316] 19 p3287 N85-30386
Three-dimensional finite element impact analysis of a nuclear waste truck cask
[DE85-010653] 19 p3288 N85-30389
Fire performance of interstitial space construction system
[NBSIR-85-3158] 20 p3436 N85-31318
Activities report of the Laboratory of Mechanics and Energetics 20 p3437 N85-31328
A numerical algorithm for endochronic plasticity and comparison with experiment 20 p3467 N85-31539
Two simplified procedures for predicting cyclic material response from a strain history 20 p3467 N85-31543
Detection of internal structure by scattered light intensity: Application to kidney cell sorting
20 p3503 N85-31777
Efficient solution methods for nonlinear finite element analysis 20 p3519 N85-31886
Iteration solution for a submerged force-driven finite cylinder
[AD-A154587] 21 p3699 N85-32962
SANCHO: A finite element computer program for the quasistatic, large deformation, inelastic response of two-dimensional solids
[DE85-011456] 22 p3829 N85-33714
Intermittent motion 23 p3925 N85-34323
Software for mechanism design
23 p3925 N85-34324
Kinematic analysis of Hurricane Frederick (1979) using satellite, aircraft and rawinsonde data
[NASA-CR-176167] 24 p4119 N85-35533
A new method of differential structural analysis of gamma-family basic parameters
[HE-3.6-3] 24 p4184 N85-35952

STRUCTURAL BASINS
NT MISSOURI RIVER BASIN (US)
NT RIVER BASINS
NT WATERSHEDS
Predicting fracturing zones in Caspian depression subsalt deposits on basis of space information and geological-geophysical data 02 p0164 N85-11111
Marine geological and geophysical investigations of the Antarctic Continental Margin, 1984
[GS-CIRC-935] 02 p0212 N85-11400
Late quaternary glacial cycles in the Bahamian deep basins and in the adjacent Atlantic Ocean
02 p0226 N85-11476
Geophysical investigations of the central part of Niger State, Nigeria 03 p0390 N85-12496
Martian impact basins: Morphology differences and tectonic provinces
[NASA-CR-174074] 03 p0448 N85-12847
Reconnaissance geology of the northern part of the Unalakleet quadrangle 04 p0516 N85-13291
Paleomagnetic latitude of paleocene volcanic rocks of the Cantwell Formation, central Alaska
04 p0517 N85-13302
CO-2-silica geothermometer for low temperature geothermal resource assessment, with application to resources in the Safford Basin, Arizona
[DE84-013958] 04 p0534 N85-13411
Directional properties of circular Maria: Interpretation in the context of a testable gravitational capture model for lunar origin 04 p0586 N85-13743
Effect of lithology and climate on the morphology of drainage basins in northwestern Colorado
[PB84-226238] 06 p0828 N85-15258
Spectral reflectance studies on the orientale region of the Moon 06 p0888 N85-15639
New data on presence of ores in salt dome structures of Dnieper-Donets Basin 07 p0981 N85-16234
Deep water mass circulation in the Western Alboran Basin: Measurements in July and September 1980 (Alboran I experiment)
[AD-A148566] 08 p1191 N85-17504
Petrography, diagenesis and depositional models of the St. Louis limestone, valmeyeran (middle Mississippian), Illinois Basin, USA 09 p1352 N85-18506
Diagenesis of niagaran (middle silurian) pinnacle reefs, northwest Michigan 09 p1352 N85-18508
Mercury 09 p1411 N85-18890
Moon 09 p1411 N85-18893
Evolution of sedimentation basins in Earth's history
10 p1497 N85-19451
Post-carboniferous tectonics in the Anadarko Basin, Oklahoma: Evidence from side-looking radar imagery
[NASA-CR-175458] 10 p1505 N85-19498
Crustal stretching and subsidence in sedimentary eastern Switzerland and permo-carboniferous basins in the continental United States
[DE85-000622] 11 p1681 N85-20592
Lithologic and environmental atlas of Berea Sandstone (Mississippian) in the Appalachian Basin
[PB85-129039] 11 p1682 N85-20600
Review of problems in lithology
13 p2113 N85-23160
Average spacing for rings of individual multi-ring basins ie 2.0(0.5)D 13 p2182 N85-23541
Ring-diameter ratios for multi-ring basins average 2.0(0.5)D 13 p2182 N85-23542
Ripple ring basins on Ganymede and Callisto
13 p2183 N85-23547
Fluvial drainage basins and valley networks: Eastern Margaritifer Sinus, Mars 13 p2190 N85-23586
Spectral reflectance studies of the Orientale basin
13 p2195 N85-23617
The deep structure of lunar basins: Clues to the understanding of basin formation and modification
13 p2200 N85-23647
Valles Marineris basin beds: A complex story
13 p2201 N85-23652
Global tectonics on Ganymede
13 p2202 N85-23659
Preliminary assessment of climatic change during late Wisconsin time, southwest Great Basin and vicinity, Arizona, California and Nevada
[DE85-008343] 16 p2836 N85-27488
Tidal rectification in lateral viscous boundary layers of a semienclosed basin
[CWI-AM-R8415] 17 p2960 N85-28284
Geoacoustic models: Washington state continental margin
[AD-A153701] 18 p3177 N85-29699
Flood-runoff forecasting with HEC1F
[AD-A154286] 19 p3300 N85-30456
An objective analysis technique for extrapolating tidal fields 20 p3493 N85-31715
Great Lakes hydrometeorologic and hydraulic data needs 20 p3496 N85-31739
Lunar and Martian impact basins: Exposed records of terrestrial bombardment? 21 p3721 N85-33090
Geothermal resources of the Laramie, Hanna and Shirley Basins, Wyoming
[DE85-005005] 23 p3943 N85-34436
Hydrology
[PB85-182954] 23 p3944 N85-34440
Geology and petroleum resources of basins in western China
[DE85-013038] 23 p3948 N85-34469
Geothermal resources of the Washakie and Great Divide basins, Wyoming
[DE85-013004] 24 p4112 N85-35491
Depositional systems and coal occurrence in the Fort Union Formation (Paleocene), Powder River Basin, Wyoming and Montana 24 p4114 N85-35505
Geology: Structural history and fluvial geomorphology of the southern Death Valley Fault Zone, Inyo and San Bernardino Counties, California
24 p4114 N85-35506

STRUCTURAL BEAMS
U BEAMS (SUPPORTS)

STRUCTURAL DESIGN
NT PRESSURE VESSEL DESIGN
The Influence of Large Scale Computing on Aircraft Structural Design
[AGARD-R-706] 01 p0007 N85-10040
Initial postbuckling analysis of elastoplastic thin-shear structures 01 p0059 N85-10393
Interactive aircraft flight control and aeroelastic stabilization
[NASA-CR-174025] 02 p0148 N85-11003
Structural design guidelines for heliports
[FAA-PM-84-23] 02 p0149 N85-11010
Design of alternate launch and recovery surfaces for environmental effects
[AD-A145800] 03 p0320 N85-12066
Design, ancillary testing, analysis and fabrication data for the advanced composite stabilizer for Boeing 737 aircraft. Volume 1: Technical summary
[NASA-CR-3648] 05 p0612 N85-13913
Structural design and thermal stability of TELE-X antenna tower 05 p0627 N85-14016
The need for a dedicated public service helicopter design 06 p0753 N85-14828
Cross-shaped aperture synthesis system
06 p0782 N85-14999
Space Station truss structures and construction considerations
[NASA-TM-86338] 07 p0916 N85-15796
Design procedures for fiber composite structural components: Panels subjected to combined in-plane loads
[NASA-TM-86909] 07 p0919 N85-15823
Aeroproyekt develops improved runway surfacing
08 p1068 N85-16770
Orbiter structural design and verification
08 p1094 N85-16915
Space shuttle external tank performance improvements: The challenge 08 p1094 N85-16916
Structural and mechanical design challenges of space shuttle solid rocket boosters separation and recovery subsystems 08 p1095 N85-16917
Orbiter processing facility: Access platforms Kennedy Space Center, Florida, from challenge to achievement
08 p1102 N85-16966
Passive Orbital Disconnect Strut (PODS 3) structural test program
[NASA-CR-177325] 08 p1113 N85-17020
Finite element computation of structural design sensitivity analysis 09 p1330 N85-18353
Design oriented identification of critical points in transient response 09 p1330 N85-18357
Optimization of vibrating beams including the effects of coupled bending and torsional modes
09 p1331 N85-18364
Reflections on trends in dynamics: The Navy's perspective 09 p1334 N85-18382
Direct energy minimization approach to whipping analysis of pressure hulls 09 p1335 N85-18393
Assessment of seismic survivability
09 p1336 N85-18402
Design and construction details of the FRX-C/T device: A compact toroid plasma translation experiment
[DE85-001527] 09 p1390 N85-18749
Heat transfer and mechanical interactions in fusion nuclear systems
[DE84-016233] 09 p1392 N85-18761
Versator divertor experiment: Preliminary designs
[DE84-017159] 09 p1393 N85-18769
Sealing assembly
[AD-D011463] 10 p1452 N85-19151
Characteristics of the elevation drive suspension of the 64-meter antennas 10 p1464 N85-19240
SSPS-CRS advanced sodium receiver: Construction experience report
[DE85-000825] 10 p1511 N85-19533
Innovative solar thermal dish technology development
[DE85-002787] 11 p1673 N85-20539
Developments in deployable masts to support flexible solar arrays 13 p2012 N85-22620
Generic design and verification of an Advanced Rigid Array (ARA) — solar array 13 p2012 N85-22621
The Olympus solar array structure and mechanisms
13 p2012 N85-22623
Experimental investigation of crippling strength of Chinese aluminum alloy (LY12CZ) sections
13 p2041 N85-22779
Shape optimization for minimal stress concentration
13 p2101 N85-23093
Precision space structures 14 p2232 N85-23833
Research on composite materials for structural design
[AD-A150802] 14 p2260 N85-24004
Invariant system of technological preparation of production 14 p2268 N85-24056
Mechanical aspects of interfaces and surfaces in ceramic containing systems
[AD-A151978] 15 p2519 N85-25530
Design of shear deformable antisymmetric angle-ply laminates to maximize the fundamental frenquency and frequency separation
[CSIR-TWISK-333] 15 p2577 N85-25892
Creep ratcheting simplified methods experience from structural design of elevated temperature components
[DE85-007433] 15 p2580 N85-25915
A literature review of EMATs, with stress calculations for simple EMAT geometries
[AERE-R-11415] 15 p2642 N85-26295
Structural design and kinematic configuration of two-armed robots 16 p2761 N85-27037
Design and construction of a computer controlled mirothermocouple probe for the study of buoyant jets
[AD-A152224] 16 p2788 N85-27199
Numerical optimization algorithm for engineering problems using microcomputer
[AD-A152135] 16 p2847 N85-27554
The application of computer aided structural optimization to the design of aircraft components
[MBB-UT-21/84-O] 16 p2873 N85-27728
Some aspects of how to design cost-effective flight control systems
[MBB-LKE-32/S/PUB/143] 16 p2873 N85-27729
Design and construction of a CW ND:YAG laser using a single elliptical cavity and water cooled krypton arc lamp pumping
[AD-A152657] 17 p2970 N85-28340
Engineering significance of fatigue thresholds and short fatigue cracks for structural design
[NLR-MP-84001-U] 17 p2981 N85-28430

Structural design of the Sandia 34-meter vertical-axis wind turbine
[DE85-011146] 18 p3116 N85-29300
Impact dynamics research on composite transport structures
[NASA-TM-86391] 19 p3284 N85-30367
Fatigue characterization of fabricated ship details for design
[SSC-318] 19 p3285 N85-30371
Operational results for the experimental DOE/NASA Mod-OA wind turbine project
[NASA-TM-83517] 19 p3304 N85-30479
Physical dimensions of humans; values; the effect of clothing, working clothes and protective equipment on the design of work places
[HSE-TRANS-10866] 19 p3331 N85-30636
Design of aggressive superconducting TFCX magnet systems
[DE85-010003] 19 p3376 N85-30943
Fire performance of interstitial space construction system
[NBSIR-85-3158] 20 p3436 N85-31318
Structural dynamics model and response of the deployable reference configuration space station
[NASA-TM-86386] 22 p3799 N85-33539
A rational approach to cam design
23 p3923 N85-34311

STRUCTURAL DESIGN CRITERIA
Energy efficient engine combustor test hardware detailed design report
[N^SA-CR-167945] 02 p0140 N85-10950
Structural analysis 02 p0143 N85-10969
Materials properties, loads, and stress analysis, Spartan REM: Appendix A
[NASA-CR-171092] 02 p0208 N85-11375
Computer models and output, Spartan REM: Appendix B
[NASA-CR-171093] 02 p0208 N85-11376
Large-diameter astromast development
[NASA-CR-171201] 03 p0342 N85-12200
DCS (Defense Communications System) network synchronization design criteria
[AD-A148251] 03 p0356 N85-12289
Design of electromagnetic bearing for vibration control of flexible transmission shaft 05 p0645 N85-14136
Technical Workshop: Advanced Helicopter Cockpit Design
[NASA-CP-2351] 06 p0750 N85-14806
Superaugmented rotorcraft program
06 p0750 N85-14807
High-efficiency silicon solar cell research
06 p0829 N85-15261
High-efficiency solar-cell design modeling
06 p0829 N85-15262
Barriers to achieving high efficiency
06 p0829 N85-15264
Evaluation of operational loads to verify structural design 07 p0896 N85-15677
Special problems of Ramjet with solid fuel
07 p0918 N85-15815
Solid propellant Ramrockets 07 p0918 N85-15816
Damping capacity of multilayer tube during torsion
[BLL-M-36011-(5828.4)] 07 p0977 N85-16202
Design criteria for small wind turbines
[NLR-MP-83054-U] 07 p0994 N85-16310
Calculated parameters for the initial part of an accelerator with high-frequency quadrupole focusing
[RAE-TRANS-2122] 07 p1040 N85-16600
The aerodynamic challenges of the design and development of the space shuttle orbiter
08 p1093 N85-16909
Structural load challenges during space shuttle development 08 p1094 N85-16914
Propulsion and power systems perspective
08 p1096 N85-16936
Space shuttle main engine: Interactive design challenges 08 p1096 N85-16940
Shipboard shock response of the model structure DSM: Experimental results versus responses predicted by eight participants 09 p1335 N85-18392
Preliminary design criteria and certification test specifications for blast resistant windows
09 p1337 N85-18405
Over the wing propeller
[NASA-CASE-LAR-13134-1] 11 p1584 N85-19980
Space Transportation System (STS) propellant scavenging system study. Volume 3: Cost and work breakdown structure-dictionary
[NASA-CR-171850-VOL-3] 11 p1590 N85-20002
Calculations pertaining to the design of a prebuncher for a 150-MeV electron linear accelerator 3: Comparisons with experimental data
[DE85-002986] 11 p1724 N85-20844
Image lobe analysis for large radomes
[AD-P004359] 12 p1825 N85-21453
Broadband thermoplastic radomes
[AD-P004369] 12 p1827 N85-21463
Study for the optimization of a transport aircraft wing for maximum fuel efficiency. Volume 1: Methodology, criteria, aeroelastic model definition and results
[NASA-CR-172551] 13 p1971 N85-22378
Verification for large space structures
14 p2232 N85-23836
An optimization study to minimize surface distortions of a hoop-column antenna 14 p2232 N85-23837
Experimental facility for studying MHD effects in liquid metal cooled blankets
[DE85-000683] 14 p2423 N85-24943
Definition of technology development missions for early space stations: Large space structures
[NASA-CR-171446] 15 p2476 N85-25281
Oxygen-hydrogen thrusters for Space Station auxiliary propulsion systems
[NASA-CR-175891] 15 p2494 N85-25383
Concepts and cost trade-offs for land vehicle antennas in satellite mobile communications
[NASA-CR-175731] 15 p2540 N85-25580
Multikilowatt hydrogen-nickel oxide battery system
[DE85-003339] 15 p2550 N85-25737
Two-phase flow in centrifugal pumps
[BLL-CE-TRANS-8085-(9022.09)]
15 p2605 N85-26053
Computers in the determination of rainfall septh-duration-frequencies in Natal
15 p2627 N85-26188
Radiation effects on structural materials
[DE85-007032] 15 p2649 N85-26338
A scanning optical microprobe for infrared detector measurement
[AD-A151746] 15 p2653 N85-26361
Synthesis study: Validation of a gust generator in the presence of a model in a wind tunnel
[ONERA-RT-16/5106-RY-051]
16 p2701 N85-26678
Bearings working group 16 p2735 N85-26878
Hybrid bearings for LH2 and LO2 turbopumps
16 p2736 N85-26880
Rotordynamics 16 p2737 N85-26888
Research in the field of rib stiffened shell stability
16 p2766 N85-27066
Deployable controllable geometry truss beam
[NASA-TM-86366] 17 p2909 N85-27934
Overview of structural response: Probabilistic structural analysis 17 p2912 N85-27952
A ten channel temperature controller
[AD-A152664] 17 p2967 N85-28326
Frangibility of obstacles at airports
[NLR-MP-84002-U] 17 p2981 N85-28431
On the accuracy of modelling the dynamics of large space structures 19 p3225 N85-29995
The dynamics and control of large flexible space structures, 8
[NASA-CR-175986] 19 p3225 N85-29996
Analysis of rotorcraft crash dynamics for development of improved crashworthiness design criteria
[FAA-CT-85-11] 20 p3391 N85-31031
SPAR improved structural-fluid dynamic analysis capability
[NASA-CR-171549] 20 p3454 N85-31449
A model parameter extraction procedure applicable to linear time-invariant dynamic systems
[NASA-CR-176120] 22 p3835 N85-33747
Design of transversely stiffenend FRP panels under compressive load -- fiber reinforced plastic (FRP) ships
[AMTE(S)-R-84104] 2. p3840 N85-34424

STRUCTURAL DYNAMICS
U DYNAMIC STRUCTURAL ANALYSIS

STRUCTURAL ENGINEERING
STARS: A general-purpose finite element computer program for analysis of engineering structures
[NASA-RP-1129] 02 p0209 N85-11378
Activities report of the Department of Engineering
03 p0342 N85-12202
Underground engineering (selected articles)
[AD-A141053] 04 p0483 N85-13082
Earthquake engineering facilities and instrumentation
[PB84-231661] 04 p0504 N85-13220
Orbiter processing facility: Access platforms Kennedy Space Center, Florida, from challenge to achievement
08 p1102 N85-16968
On solving nonlinear problems of aircraft structural mechanical design 09 p1309 N85-18223
FRG firms jump into market for auto, aircraft ceramics
09 p1309 N85-18225
Reflections on trends in dynamics: The Navy's perspective 09 p1334 N85-18382
Solutions to structural dynamics problems
09 p1334 N85-18384
The Shock and Vibration Bulletin 54. Part 3: Structural dynamics, machinery dynamics and vibration problems
[AD-A148133] 09 p1337 N85-18406
System software for the finite element machine
[NASA-CR-3870] 09 p1372 N85-186
Planning for greater-confinement disposal
[DE85-002143] 09 p1383 N85-186
Hydrodynamic flow structures in quantum field theory
[DE84-015513] 09 p1401 N85-188
Geometric Hamiltonian structures and perturbation theory
[DE85-002006] 11 p1707 N85-2073
Proceedings of the 9th Biennial Army Symposium on Solid Mechanics. Advances in Solid Mechanics for Design and Analysis
[AD-A150042] 12 p1867 N85-21710
Computer-Aided Structural Engineering (CASE) project. Seepage analysis of confined flow problems by the method of fragments (CFRAG)
[AD-A150015] 12 p1875 N85-2178
New concepts in deployable beam structures
14 p2232 N85-238
Technology for large space systems: A bibliography with indexes, supplement 11
[NASA-SP-7046(11)] 15 p2475 N85-2527
Automatic Dynamic Aircraft Modeler (ADAM) for the computer program NASTRAN 15 p2574 N85-25875
Symmetric composite laminate stress analysis
15 p2575 N85-25876
Symposium on Computers in Civil Engineering 1983
[CSIR-S-298] 15 p2626 N85-26182
Programme development: A state of the art
15 p2626 N85-26185
Progress through cooperation and exchange of ideas and experiences 15 p2626 N85-26186
An approach for user controlled reinforced concrete design optimization 15 p2627 N85-26187
Computers in the determination of rainfall septh-duration-frequencies in Natal
15 p2627 N85-2618
A study of spacecraft technology and design concepts, volume 1
[NASA-CR-172579-VOL-1] 16 p2730 N85-2684
Incorporating control into the optimal structural design of large flexible space structures
[AD-A152858] 17 p2909 N85-2793
Research on structural analysis at the DFVLR, Brunswick 18 p3120 N85-29314
Cultural data base implementation study and computer-aided scene modeling system users manual
[AD-A154232] 19 p3333 N85-3064
Mechanical considerations in cw linacs
[DE85-010726] 19 p3363 N85-3085
Field testing of a lightweight relocatable structure in a temperate environment
[AD-A155171] 21 p3589 N85-3235
Proceedings of the 24th Project Integration Meeting
[NASA-CR-176058] 21 p3607 N85-3238
Designing a graphics application interface
23 p3964 N85-34574

STRUCTURAL FAILURE
Development of failure criterion for Kevlar-epoxy fabric laminates
[NASA-CR-172465] 02 p0170 N85-1113
Studies on reliability of structural systems
02 p0206 N85-1136
Formulation and solution methods for classical problems of static buckling
[CETIM-101010] 04 p0514 N85-1328
Nonlinear deformation and static linear buckling of structures under pressure
[CETIM-11-E-350] 04 p0514 N85-13281
TUTOR (CL-41A) tail flight load survey
07 p0896 N85-1567
Steel containment buckling
[DE85-003744] 13 p2103 N85-23111
Study of failure mechanism of fibrous composition materials taking into account physicochemical reactions of components 19 p3243 N85-3010
Effect of matrix plasticity on durability of fibrous composition materials 19 p3243 N85-30107
Fatigue resistance of VT3-1 titanium alloy related to surface cold working 19 p3245 N85-3012
Effect of protective method on cyclic durability and nature of failure of titanium alloy welded joints
19 p3245 N85-30122
Fatigue characterization of fabricated ship details for design
[SSC-318] 19 p3285 N85-3037
Stored energy and structural failure
[OUEL-1564/85] 20 p3471 N85-315
Automatic capability to store and retrieve component data and to calculate structural integrity of these components
[DE85-012429] 22 p3831 N85-337
Safety and reliability of steel structural materials under random service impact loads 23 p3906 N85-341
Effect of strain rate on the initial failure of notched GR laminates 23 p3908 N85-342

Three-dimensional finite element failure model for predicting failure in fibre reinforced bolted joints
[BR94778] 23 p3940 N85-34423

STRUCTURAL FATIGUE
U FATIGUE (MATERIALS)

STRUCTURAL FOUNDATIONS
U FOUNDATIONS

STRUCTURAL MATERIALS
U CONSTRUCTION MATERIALS

STRUCTURAL MEMBERS
NT ANISOTROPIC PLATES
NT BEAMS (SUPPORTS)
NT CANTILEVER BEAMS
NT CANTILEVER PLATES
NT CIRCULAR PLATES
NT COLUMNS (SUPPORTS)
NT CURVED BEAMS
NT ELASTIC PLATES
NT FLAT PLATES
NT I BEAMS
NT LONGERONS
NT MEMBRANE STRUCTURES
NT METAL PLATES
NT ORTHOTROPIC PLATES
NT PERFORATED PLATES
NT PLATES (STRUCTURAL MEMBERS)
NT POROUS PLATES
NT RECTANGULAR BEAMS
NT REINFORCED PLATES
NT SKIN (STRUCTURAL MEMBER)
NT STRAKES
NT STRINGERS
NT STRUTS
NT TRUSSES
NT WING PANELS

Research on large, highly accurate, inflatable reflectors
[AD-A145080] 01 p0016 N85-10099

Radiation effects on structural materials
[DE84-014771] 01 p0029 N85-10178

Design proposals for torsional buckling of stiffeners
[AD-A144783] 01 p0062 N85-10409

Report of the Department of Aerospace Engineering
03 p0307 N85-11977

Analysis of thin-walled airframe members in geometrically nonlinear statement
06 p0780 N85-14965

Thermally isolated structural support link
[AD-D011349] 07 p0972 N85-16176

The Shock and Vibration Digest, volume 16, no. 10
[AD-A147588] 09 p1331 N85-18361

The Shock and Vibration Bulletin 54. Part 2: Ship shock, shock and blast and ground shock
[AD-A148132] 09 p1334 N85-18388

Models for shock damage to marine structural materials 09 p1336 N85-18400

Adjustment structure
[AD-D011461] 10 p1459 N85-19193

Viscoplastic constitutive relationships with dependence on thermomechanical history
[NASA-CR-174836] 12 p1864 N85-21691

An overview of the MIL-HDBK-5 program
[AD-A147788] 14 p2254 N85-23970

Daze fasteners
[NASA-CASE-LAR-13009-1] 18 p3116 N85-29285

Viscoplasticity based on overstress with a differential growth law for the equilibrium stress
20 p3466 N85-31532

A comparison of smooth specimen and analytical simulation techniques for notched members at elevated temperatures 20 p3468 N85-31546

Poly-functional building material from fiberglass (its fabrication and properties) 23 p3908 N85-34209

A simple but systematic CSG system
23 p3963 N85-34569

Analytical ultrasonics for structural materials
[TI85-006132] 23 p3966 N85-34600

User's guide: A computer program for strength analysis of non-hydraulic concrete structural elements. Report 2. Strength design of reinforced concrete column sections (PCAUC)
[AD-A156393] 24 p4102 N85-35429

STRUCTURAL PROPERTIES (GEOLOGY)

Geothermal resources of the Laramie, Hanna, and Shirley Basins, Wyoming
[DE84-016104] 01 p0064 N85-10423

Predicting fracturing zones in Caspian depression subsalt deposits on basis of space information and geological-geophysical data 02 p0164 N85-11111

Hypothesis on the origin of lineaments in the LANDSAT and SLAR images of precambrian soil in the low Contas River Valley (southern Bahia)
[E85-10007] 02 p0215 N85-11420

Systematic data interpretation of remote sensing in the reception of hydrocarbons, volume 1
[E85-10008] 02 p0215 N85-11421

Shuttle Experimental Radar for Geological Exploration (SERGE) project: Field work relating to the Shuttle Experimental Radar A (SIR-A) in Brazil (phase 2)
[NASA-CR-174033] 02 p0219 N85-11444

Interior structure of Uranus 02 p0299 N85-11939

Mars-Earth geographical comparisons: A pictorial view
[NASA-TM-86166] 02 p0302 N85-11957

The colloidal chemistry of ceramic clays
[NASA-TM-77734] 03 p0336 N85-12163

Seismology in rockburst research
[REPT-551] 03 p0375 N85-12394

Franciscan and related rocks of southern Humbolt County, northern California coast ranges: Analysis of structure, tectonics, sedimentary petrology, paleogeography, depositional histroy, and thermal maturity 03 p0390 N85-12495

Geophysical investigations of the central part of Niger State, Nigeria 03 p0390 N85-12496

Multispectral and geomorphic studies of processed Voyager 2 images of Europa
[NASA-CR-174075] 03 p0448 N85-12848

Structural observations in the Circle quadrangle, Yukon-Tanana Upland, Alaska 04 p0517 N85-13298

Structure of the crust and upper mantle of the Iberian continental platform 04 p0523 N85-13350

Deep structure beneath the Pyrenees
04 p0524 N85-13351

Deep structure and seismicity in the Catalonia-Pyrenees region 04 p0524 N85-13352

Methods for correlating geological, geochemical and geophysical data with satellite imagery in central Ireland
05 p0655 N85-14208

A multiple approach in remote sensing for structural and lithological mapping by use Modular Optoelectronic Multispectral Scanner (MOMS)/LANDSAT/Heat Capacity Mapping Mission (HCMM) data
05 p0660 N85-14244

Geology and resources of the Tar Sand Triangle, southeastern Utah
[DE84-012017] 05 p0677 N85-14346

Documentation of earthquake algorithms
[PB84-235324] 05 p0677 N85-14351

Summaries of physical research in the geosciences
[DE85-001882] 06 p0818 N85-15194

Deep structure of terrestrial crust and upper mantle in southeastern Siberia and Far East according geological-geophysical data 06 p0821 N85-15212

Geological, structural, and geomorphological analyses from SIR-B 08 p1145 N85-17226

Structural investigation of the Canadian Shield by orbital radar and LANDSAT 08 p1147 N85-17236

Structural investigation of the Grenville Province by radar and other imaging and nonimaging sensors
08 p1147 N85-17237

Delineation of major geologic structures in Turkey using SIR-B data 08 p1149 N85-17249

Structure and stratigraphy of Midterhuken Peninsula, Bellsund, West Spitsbergen 09 p1353 N85-18513

Vertical movements and structure formation within island systems of northeast Asia 10 p1501 N85-19471

Basic structural features and probable mechanism of formation of the Kuril Island system
10 p1501 N85-19472

Mesozoic magmatism of Mongolian-Okhotsk Belt and its possible geodynamic interpretation
10 p1502 N85-19481

Geological reasons for change in intensity of linear magnetic anomalies of the Kursk magnetic anomaly
[NASA-TM-77824] 10 p1514 N85-19552

Crustal stretching and subsidence in sedimentary eastern Switzerland and permo-carboniferous basins in the continental United States
[DE85-000622] 11 p1681 N85-20592

Workshop on Remote Sensing/Lineament Applications for Energy Extraction
[DE84-009291] 12 p1875 N85-21763

The origin and evolution of terrestrial and Martian rock labyrinths
[NASA-CR-175511] 12 p1961 N85-22326

Review of problems in lithology
13 p2113 N85-23160

Normal and anomalous geothermal fields and their relationship to hierarchy of geological bodies
13 p2113 N85-23163

Planetary geology in the 1980s
[NASA-SP-467] 13 p2160 N85-23457

Io: Generation of silicate magma by shear melting at the base of a basaltic lithosphere
13 p2172 N85-23476

Topographic evidence for shield volcanism on Io
13 p2172 N85-23478

Sulfur volcanoes on Io? 13 p2173 N85-23479

Patterns of fracture and tidal stresses due to nonsynchronous rotation: Implications for fracturing on Europa 13 p2173 N85-23483

Formation of bright terrain bands on Ganymede by unstable lithosphere extension 13 p2173 N85-23485

Progress on studies of early intense cratering
13 p2181 N85-23536

Impacts in ice: Commissions of solar system crater population 13 p2181 N85-23538

Problems in recovering crater production functions
13 p2182 N85-23539

The nature of Martian flow ejecta craters
13 p2183 N85-23545

Distribution and properties of large symmetric knobs on Mars 13 p2192 N85-23596

Planetary analogs in Antarctica: Icy satellites
13 p2193 N85-23605

Lithologic and structural control on slope morphology in the Valles Marineris 13 p2201 N85-23651

Three-layer generic Ganymedes: Structure and evolution 13 p2202 N85-23657

Lineaments on Ganymede: New evidence for late tectonic activity 13 p2202 N85-23658

Tectonics of the Valhalla structure on Callisto
13 p2202 N85-23662

Mars geologic mapping: A review and new concepts
13 p2202 N85-23663

Geology of the Ganymede quadrangle Jg7
13 p2203 N85-23665

Structure and origin of Martian satellites
15 p2483 N85-25323

Use of space information in petroleum- and gas-prospecting work (example of Southern Mangyshlak)
15 p2485 N85-25341

Interpretation of space photolineaments
15 p2487 N85-25353

Analysis of the Gran Desierto, Pinacte Region, Sonora, Mexico, via shuttle imaging radar
[NASA-CR-175711] 15 p2582 N85-25927

Nd-isotopic evidence for the origin of the Sudbury complex by meteoritic impact 15 p2660 N85-26554

Inversion of Rayleigh wave group velocities from high-explosive tests
[AD-A152172] 16 p2763 N85-27175

System of interpretation of remote sensing data when hydrocarbons are present, volume 2
[INPE-3087-TDL/162-VOL-2] 16 p2810 N85-27326

Surface exploration geophysics applied to the Moon
[DE85-006714] 16 p2884 N85-27793

The Shock and Vibration Digest, volume 17, no. 2
[AD-A153129] 17 p2977 N85-28400

The effects of seismic waves
17 p2978 N85-28401

Yearbook of the Bureau of Mineral Resources, Geology and Physics: Geoscientific research, resource assessment, and database development, 1 Jul. 1983 to 30 Jun. 1984
[BMR-84] 17 p2989 N85-28474

Proceedings of the 1980 Workshop of the International Association of Seismology and Physics of the Earth's Interior on the Seismic Modeling of Laterally Varying Structures: Contributions based on data from the 1978 Saudi Arabian refraction profile
[GS-CIRC-937] 17 p2989 N85-28476

Preliminary interpretation of Saudi Arabian seismic refraction data 17 p2989 N85-28477

Explanation of Russian models: Saudi Arabian seismic refraction profile 17 p2991 N85-28487

Geoacoustic models: Washington state continental margin
[AD-A153781] 18 p3177 N85-29699

Transport properties of Topopah Spring tuff
[DE85-010448] 19 p3270 N85-30278

Tectonic structure features of some deep faults in Atlantic and Pacific Oceans (according to deep seismic sounding-reflected waves method data)
19 p3295 N85-30428

Physical and chemical changes to rock near electrically heated boreholes at Spent Fuel Test-Climax
[DE85-010834] 19 p3302 N85-30472

Structural and tectonic history of the Golconda allochton, southern Toiyabe Range, Nevada
19 p3312 N85-30529

Comparative study of fracture planes computed from topography and lineaments from imagery with structures and mineralization in the magnetic belt of Washington State
[DE85-010972] 20 p3477 N85-31608

Global Mega-Geomorphology
[NASA-CP-2312] 2 p3600 N85-32357

Andrean examples of mega-geomorphology themes
21 p3602 N85-32367

Lunar and Martian impact basins: Exposed records of terrestrial bombardment? 21 p3721 N85-33090

Earth's primordial differentiation, and its after-effects
21 p3722 N85-33092

Compressional environment in the location and orientation of planetary dorsa and terrestrial earthquake fault structures 22 p3857 N85-33885

Structural development of the west-central Grant Range, Nye County, Nevada 24 p4115 N85-35508
Crustal structure in southern California from array data
24 p4115 N85-35512

STRUCTURAL RELIABILITY
Studies on reliability of structural systems
02 p0206 N85-11362
Assuring structural integrity in Army systems
[NASA-CR-175492] 11 p1651 N85-20398
Axiomatic characterizations of continuum structure functions
[AD-A149817] 12 p1866 N85-21706
Overview of structural response: Probabilistic structural analysis 17 p2912 N85-27952
Reactor pressure vessel steels ASME SA533B and SA508 C 1.2
[VTT-340] 22 p3794 N85-33507
Safety and reliability of steel structural materials under random service impact loads 23 p3906 N85-34197
Statistical pooling method of fatigue data for reliability design 23 p3906 N85-34198

STRUCTURAL RIGIDITY
U STRUCTURAL STABILITY

STRUCTURAL STABILITY
NT SHELL STABILITY
Effects of cobalt, boron, and zirconium on the microstructure of Udimet 738
[NASA-CR-174762] 01 p0027 N85-10166
Structural stability of nickel heat resistant alloys at high temperatures 03 p0350 N85-12251
Section 1. Method of determining mode shapes and natural frequencies of the NASA unmodified test structure. Section 2. Continuous beam closed from solution to the NASA-LSS astromast torsional vibration, appendix E
05 p0603 N85-13844
The problem of protecting the structure of a packet composite of optimal thinwall elements
10 p1444 N85-19101
Methodology for stress analysis of heavy metal plate
10 p1460 N85-19203
Influence of plastic deformation on structural stability of nichrome-tungsten composite materials
11 p1599 N85-20060
Stability of viscoelastic constructions subjected to steady random compressing loads 11 p1720 N85-20819
Behavior of buried flexible cylinders under the influence of nonuniform hoop compression
[PB85-116523] 12 p1868 N85-21718
MSFC data analysis of the SAFE/DAE experiment
14 p2233 N85-23843
Langley Research Center photogrammetric measurements of solar array dynamics: Preliminary results 14 p2233 N85-23844
Structural changes with one- and two-stage aging of alloys Ti-Al-Mo-Fe and Ti-Zr-V-Al-Sn
15 p2499 N85-25415
USSR report: Engineering and equipment
[JPRS-UEQ-84-006] 16 p2760 N85-27035
Stability of anisotropic cylindrical sandwich shells
16 p2766 N85-27065
Research in the field of rib stiffened shell stability
16 p2766 N85-27068
Structural stability and bifurcation in conical flow fields
[VTH-LR-424] 16 p2803 N85-27282
Injection laser structure design
[AD-A153210] 17 p2971 N85-28345
The Shock and Vibration Digest, volume 17, no. 1
[AD-A151051] 17 p2977 N85-28397
Continuum modeling of latticed structures
17 p2977 N85-28399
The Shock and Vibration Digest, volume 17, no. 2
[AD-A153129] 17 p2977 N85-28400
Recent progress in the dynamic plastic behaviour of structures, part 4 17 p2978 N85-28402
Constitutive modeling for blast-induced wave propagation
[AD-A153576] 18 p3099 N85-29187
On the accuracy of modelling the dynamics of large space structures 19 p3225 N85-29995
The dynamics and control of large flexible space structures, 8
[NASA-CR-175986] 19 p3225 N85-29996
New directions in asymptotically stable finite-dimensional adaptive control of linear distributed parameter systems 20 p3412 N85-31177
Vibrational stabilization of flexible structures
20 p3414 N85-31188
A systematic plan for the continued study of dimensional stability of metallic alloys considered for the fabrication of cryogenic wind tunnel models
[NASA-CR-172440] 21 p3565 N85-32172

STRUCTURAL STRAIN
Design sensitivity analysis of an antisymmetric angle-ply laminate
[CSIR-TWISK-318] 01 p0021 N85-10128
Advanced fatigue monitoring on service aircraft
07 p0895 N85-15671
Experiences obtained from service fatigue monitoring exercises 07 p0895 N85-15672
CF-5 vertical stabilizer flight load survey
07 p0895 N85-15673
Tornado: Structural Usage Monitoring System (SUMS) 07 p0896 N85-15680
Flight parameters recording for structure fatigue life monitoring 07 p0896 N85-15682
A literature survey of ground load statistics for landing gear fatigue design purposes
[FFA-TN-1984-39] 09 p1280 N85-18054
Modal analysis of structural systems involving nonlinear coupling 09 p1337 N85-18409
Fatigue-creep interaction in + or - 45 deg carbon-resin composites --- aircraft construction materials
[ONERA-RT/40/7086/M] 11 p1594 N85-20027
Optimal modeling with a minimum of local distortion
[REPT-18/1984] 16 p2797 N85-27243
Multinomial form of the solution of problems of the statistics of elastic rectangular disks
[REPT-17/1984] 16 p2797 N85-27244
Recent progress in the dynamic plastic behaviour of structures, part 4 17 p2978 N85-28402
Torsion-tension coupling in rods
18 p3120 N85-29315
Stored energy and structural failure
[OUEL-1564/85] 20 p3471 N85-31567

STRUCTURAL VIBRATION
NT BENDING VIBRATION
NT FLUTTER
NT LINEAR VIBRATION
NT MISSILE VIBRATION
NT SELF INDUCED VIBRATION
NT SUBSONIC FLUTTER
NT SUPERSONIC FLUTTER
NT TORSIONAL VIBRATION
NT TRANSONIC FLUTTER
A rigid body mechanism in structural dynamics
02 p0206 N85-11361
Power flow between non-conservatively coupled oscillators
[ISVR-TR-125] 02 p0209 N85-11377
Simulation of vibration processes in damped structures with allowance for temperature-frequency characteristics of vibration absorbing materials
02 p0257 N85-11660
Normal mode method of solving problem forced oscillations of rib-reinforced shell of revolution in liquid
02 p0273 N85-11781
Theoretical and experimental modal analysis of a rotor test rig --- shipboard equipment
[AMTE(N)-TM-83079] 03 p0371 N85-12370
Comparison of free component mode synthesis techniques using MSC/NASTRAN
[DE84-014451] 04 p0514 N85-13278
Response measurements for two building structures excited by noise from a large horizontal axis wind turbine generator
[NASA-CR-172482] 04 p0558 N85-13552
Definition of ground test for Large Space Structure (LSS) control verification, appendix G
05 p0603 N85-13845
The Shock and Vibration Digest, volume 16, no. 11
[AD-A148466] 08 p1171 N85-17382
Modelling and identification of the structural properties of an astromast
[CRC-1374] 09 p1329 N85-18352
The Shock and Vibration Bulletin 54. Part 1: Welcome, keynote address, invited papers MIL-STD-810D, MIL-STD-810D panel session
[AD-A148131] 09 p1333 N85-18377
Keynote address 09 p1333 N85-18378
Least favorable response of inelastic structures
09 p1336 N85-18398
Leakage-flow induced vibrations of a chimney structure suspended in a liquid flow --- nuclear reactors
09 p1339 N85-18420
Assessing expired fatigue life in large turbine shafts
[DE84-016676] 09 p1340 N85-18427
Flow-induced tube vibration thresholds in heat exchangers from shellside water tests
[DE84-006603] 11 p1652 N85-20407
The effect of an elastic foundation and of dissipative forces on the stability of fluid conveying pipes
[TAE-56] 12 p1863 N85-21686
Planar dynamics of a uniform beam with rigid bodies affixed to the ends
[NASA-CR-175566] 12 p1864 N85-21693
A quantitative comparison of active and passive damping for large space structures
[UTIAS-TN-249] 13 p1998 N85-22524
Spline-based Rayleigh-Ritz methods for the approximation of the natural modes of vibration for flexible beams with tip bodies
[NASA-CR-172566] 13 p2102 N85-23109
Applications of the conformal mapping method to the solution of mechanical vibrations problems
13 p2102 N85-23100
Structural dynamics analysis 14 p2233 N85-23839
MSFC data analysis of the SAFE/DAE experiment
14 p2233 N85-23843
Langley Research Center photogrammetric measurements of solar array dynamics: Preliminary results 14 p2233 N85-23844
La Recherche Aerospatiale Bimonthly Bulletin Number 1984-3, 220/May-June
[ESA-TT-862] 16 p2695 N85-26808
Internal resonance in nonlinear vibrating systems
[REPT-15/1984] 16 p2797 N85-27245
On the wind-induced vibrations of a mass-spring system
[REPT-84-04] 17 p2981 N85-28428
Vibration/libration interaction dynamics during the orbiter based deployment of flexible members
20 p3411 N85-31171
Experimental and theoretical assessment of a new technique for the non-destructive evaluation of laminated panels
[AD-A155622] 21 p3562 N85-32155
Fixed gain and adaptive techniques for rotorcraft vibration control
[NASA-CR-177344] 22 p3728 N85-33111
Flutter clearance of the Schweizer 1-36 deep-stall sailplane
[NASA-TM-85917] 22 p3729 N85-33118

STRUCTURAL WEIGHT
Ultralightweight oxygen container
[PB84-220730] 01 p0036 N85-10228
Space shuttle external tank performance improvements: The challenge 08 p1094 N85-16916
A study of structural concepts for ultralightweight spacecraft
[NASA-CR-175765] 16 p2730 N85-26940
Multi-kW solar arrays for Earth orbit applications
[NASA-CR-171538] 20 p3406 N85-31139

STRUCTURES
Bounding the stochastic performance of continuum structure functions 2
[AD-A149458] 10 p1548 N85-19702

STRUTS
Stall elimination and restart enhancement device
[AD-D011217] 01 p0010 N85-10082
Influence of strut cross-section on strut radiation of reflector antennas
[FI-455-TBR-39] 03 p0357 N85-12286
Passive Orbital Disconnect Strut (PODS 3) structural test program
[NASA-CR-177325] 08 p1113 N85-17020
Variable length strut with longitudinal compliance and locking capability
[NASA-CASE-MFS-25907-1] 23 p3937 N85-34401

STS
U SPACE TRANSPORTATION SYSTEM

STS-1
U SPACE TRANSPORTATION SYSTEM 1 FLIGHT

STS-3
U SPACE TRANSPORTATION SYSTEM 3 FLIGHT

STS-4
U SPACE TRANSPORTATION SYSTEM 4 FLIGHT

STS-7
U SPACE SHUTTLE MISSION 31-C

STS-11
U SPACE SHUTTLE MISSION 41-B

STS-13
U SPACE SHUTTLE MISSION 41-C

STS-17
U SPACE SHUTTLE MISSION 41-G

STS-19
U SPACE SHUTTLE MISSION 51-A

STS-20
U SPACE SHUTTLE MISSION 51-C

STUDENTS
Project Explorer 02 p0154 N85-11041
Designing an expert system for training automotive electrical troubleshooting
[AD-P003926] 02 p0246 N85-11806
Training guide for scientific and engineering trainees 1984
[AD-A147983] 08 p1198 N85-17542
Satellite communications and amateur radio
12 p1838 N85-21534
NASA Ames Summer High School Apprenticeship Research Program
[NASA-TM-86006] 15 p2686 N85-26590
The impact of group processing on achievement in cooperative learning groups
[AD-A153166] 17 p3001 N85-28651

Oral discussion, group-to-individual transfer and achievement in cooperative learning groups
[AD-A153209] 17 p3001 N85-28552
Summer High School Apprenticeship Research Program (SHARP) of the National Aeronautics and Space Administration
[NASA-CR-175791] 17 p3046 N85-28840
STUDIES
U INVESTIGATION
STURM-LIOUVILLE OPERATOR
U STURM-LIOUVILLE THEORY
STURM-LIOUVILLE THEORY
Spectral Theory of Sturm-Liouville Differential Operators: Proceedings of the 1984 Workshop
[DE85-009693] 20 p3520 N85-31890
STYRENES
NT POLYSTYRENE
Volatile organic emissions from adhesives with indoor applications
[DE84-015965] 05 p0620 N85-13966
Control technology for fiber reinforced plastics industry at AMF Hatteras Yachts, New Bern Division, New Bern, North Carolina
[PB85-109015] 10 p1460 N85-19196
Influence of hydrogen bonding in block copolymers and their blends 13 p2036 N85-22752
Damage development during low cycle fatigue of carbon-black loaded SBR
[DE85-006234] 15 p2519 N85-25533
Stabilized unsaturated polyesters
[NASA-CASE-NPO-16103-1] 18 p3078 N85-29043
SUBARCTIC REGIONS
Current inventory of anthropogenic carbon dioxide in the North Pacific Subarctic Gyre
[PB85-187938] 24 p4125 N85-35570
SUBASSEMBLIES
Multistage spent particle collector and a method for making same
[NASA-CASE-LEW-13914-1] 22 p3791 N85-33489
SUBCARRIER WAVES
U CARRIER WAVES
SUBCIRCUITS
U CIRCUITS
U SUBASSEMBLIES
SUBCRITICAL FLOW
Performance of two transonic airfoil wind tunnels utilizing limited ventilation 03 p0313 N85-12020
Method for growth of crystals by pressure reduction of supercritical or subcritical solution
[NASA-CASE-NPO-15772-1] 18 p3192 N85-29800
SUBDUCTION (GEOLOGY)
Oceanic plateaus, anomalous subduction, and the accretion of buoyant features at convergent margins
05 p0688 N85-14422
Kuril-Aleutian subduction 19 p3290 N85-30402
Thermal evolution of coastal California with implications for hydrocarbon maturation 24 p4115 N85-35509
A dynamic model of Venus's gravity field
[NASA-CR-176173] 24 p4169 N85-35845
SUBDWARF STARS
Observations of the O-type subdwarf eclipsing binary system LB 3459 (AA Dor) 01 p0126 N85-10881
Ultraviolet spectroscopy of selected astronomical sources
[NASA-CR-174379] 09 p1413 N85-18912
IUE and Voyager observations of very hot O-type subdwarfs 11 p1751 N85-21010
Analysis of high-depression IUE spectra of subdwarf B stars 11 p1751 N85-21011
Further investigation of mass loss phenomena in hot white dwarfs and O subdwarfs 11 p1751 N85-21014
Studies of hot B subdwarfs. Part 2: Energy distributions of three bright sdB/sdOB stars in the 950-5500 angstrom range
[NASA-CR-175854] 16 p2881 N85-27775
SUBGIANT STARS
Evidence for non-radiative activity in stars with T sub eff 10000 K 06 p1231 N85-17757
A search for white-dwarf companions of subgiant CH stars 11 p1752 N85-21019
SUBGRAVITY
U REDUCED GRAVITY
SUBJECTS
Energy data base: Subject categories and scope
[DE84-017376] 17 p3050 N85-28881
SUBLATTICES
U LATTICES (MATHEMATICS)
SUBLAYERS
U SUBSTRATES
SUBLIMATION
Synergisms in surface erosion, session summary
06 p0864 N85-15493
Synergistic effects related to surface composition, session summary 06 p0865 N85-15495
SUBLIMINAL STIMULI
Subliminal communication technology
[GPO-38-833] 05 p0622 N85-13979
SUBMARINE CABLES
Metallized synthetic cable
[AD-D011283] 05 p0628 N85-14023
SUBMARINES
The development of a method for the shock-resistant securing of large batteries in submarines
09 p1335 N85-18391
Research on ocean floor electrical surveys
[AD-A148831] 12 p1889 N85-21920
The body burden of organic vapors in artificial air trial measurements aboard a moored submarine
[AD-A149698] 12 p1910 N85-21988
Ventilation flow: Submerged
18 p3156 N85-29545
Preliminary results of an ALVIN dive program on active hydrothermal vents at the southern Juan de Fuca Ridge
24 p4106 N85-35454
SUBMERGED BODIES
NT DIVING (UNDERWATER)
NT UNDERWATER RESEARCH LABORATORIES
The low frequency behaviour of an immersed structure at a standstill in a high density fluid with free surface
[TP-1983-31] 13 p2103 N85-23105
SUBMERGING
Modernization of IDTs-6 ultrasonic installation
[BLL-M-35716-(5828.4)] 02 p0206 N85-11356
Comparison of simulation of weightlessness by Head Down Tilt (HDT) and Water Immersion (WI)
05 p0692 N85-14454
Hemodynamics and plasma arginine vasopressin during water immersion in normal men
05 p0693 N85-14458
Physics effects of accidental submersion of space power reactors in water
[DE85-005020] 15 p2650 N85-26344
SUBMERSIBLE AIRCRAFT
Robust rate control system designs for a submersible
[AD-A144792] 01 p0111 N85-10753
SUBMILLIMETER WAVES
Detection of submillimeter polarization in the Orion Nebula
[NASA-TM-86013] 04 p0579 N85-13700
Choice of orbit for scientific satellites: SIGMA, the submillimeter telescope --- Ariane-borne gamma imagery satellite (SIGMA) 05 p0600 N85-13828
A new free electron laser using a relativistic beam with spiralling electron
[AD-D011318] 07 p0971 N85-16165
Far infrared and submillimeter observations of the giant planets 08 p1245 N85-17856
Far-infrared spectroscopy of interstellar gas
08 p1245 N85-17858
First results of submillimeter polarimetry
08 p1246 N85-17861
Instrumentation for submillimeter polarimetry
08 p1250 N85-17889
A new generation of sub mm telescopes, made of carbon fiber reinforced plastic 08 p1250 N85-17890
Absorption of radiation by water vapor in windows of relative transparency of 95-145 micrometer range
13 p2076 N85-22968
Submillimeter-band solid state distributed feedback laser 15 p2644 N85-26307
Submillimeter local oscillators for spaceborne heterodyne applications
[NASA-RP-1147] 19 p3226 N85-30005
Double photon excitation of high-Rydberg atoms as a long-lived submillimeter detector
[NASA-CASE-NPO-16372-1] 19 p3352 N85-30779
SUBREFLECTORS
Microwave surface resistivity of several materials at ambient temperature 10 p1463 N85-19226
Design procedure for the new 70-meter antenna subreflector positioner 10 p1463 N85-19232
Subreflector focusing techniques applied to new DSS-15 and DSS-45 34-meter antennas
10 p1464 N85-19233
Electromagnetic scattering by arbitrarily shaped reflectors: Subreflector efficiency
[AD-A149224] 15 p2541 N85-25687
SUBROUTINE LIBRARIES (COMPUTERS)
ZTL: A subroutine package for the IBM personal computer to support the Ziatech ZT1488 IEEE-488 controller
[LA-10141-MS] 12 p1913 N85-22010
TRANIO: A subroutine package for the IBM personal computer to support the transfer 6002 CAMAC crate controller
[LA-10145-MS] 12 p1914 N85-22015
Using MATHLIB on the IBM computer and sundry plotting examples with a taste of IMSL
[DE85-011395] 19 p3340 N85-30695
SUBROUTINES
Description and use of the single-color transmissometer plume diagnostic code A32CODE
[AD-A146181] 03 p0325 N85-12090
High altitude chemically reacting gas particle mixtures. Volume 2: Program manual for RAMP2 --- rocket nozzle and orbital plume flow fields
[NASA-CR-171827] 07 p0916 N85-15802
On the generation of random variables for radar simulation purposes 07 p0936 N85-15947
Some scientific subroutines in LISP
[AD-A147869] 07 p1026 N85-16515
Computer center CDC libraries/NSRD (subprograms)
[AD-A146792] 08 p1206 N85-17593
Three-dimensional, direct and vectorized elliptic solvers for various boundary conditions
[AD-B088266L] 08 p1206 N85-17595
Calibration of thermocouples based on two state points of water and BS 4937; part 5, 1974
09 p1324 N85-18317
Solutions to structural dynamics problems
09 p1334 N85-18384
Modeling relationships using groups and items
09 p1367 N85-18591
Monitoring the execution of plans in SIPE (System for Interactive Planning and Execution) monitoring
[AD-A149138] 10 p1544 N85-19731
A computer system for generating single and double sampling plans for attributes data
[AD-A149548] 11 p1701 N85-20696
Standardized format for computer series
[PB85-108668] 11 p1706 N85-20724
DOS 21: PCDOS 2.0 support subroutine package for the IBM personal computer
[LA-10142-MS] 12 p1914 N85-22012
HGRAPH: A subroutine package for the IBM personal computer to support the Hercules Graphic Card
[LA-10144-MS] 12 p1914 N85-22013
ZTLCK: A subroutine package for the IBM personal computer to support the Ziatech ZT1488 real time clock
[LA-10146-MS] 12 p1914 N85-22014
Programs for dynamic loading of precompiled subroutine packages, especially for applications with the Watfiv compiler
[DFVLR-MITT-84-18] 12 p1917 N85-22035
BLAS (Basic Linear Algebra Subroutines), linear algebra modules and supercomputers
[AD-A151504] 15 p2628 N85-26199
A general purpose scatter storage subsystem and a comparison of hashing methods
[NASA-CR-175814] 16 p2845 N85-27542
Proposal for an extended set of FORTRAN Basic Linear Algebra subprograms
[DE85-007241] 16 p2848 N85-27562
A set of subroutines for masked three-dimensional plotting with rotations
[MEAH-33] 20 p3514 N85-31846
Evaluation and implementation of a functional microprogram generator
[AD-A155164] 21 p3674 N85-32823
A versatile computer package for mechanism analysis
23 p3924 N85-34314
Software for mechanism design
23 p3925 N85-34324
A quickly tested Pascal random number generator for microcomputers
[AD-A156059] 24 p4136 N85-35633
CRAYCDC
[NASA-CR-177374] 24 p4137 N85-35639
CDCCRAY
[NASA-CR-177375] 24 p4137 N85-35640
SUBSETS (MATHEMATICS)
U SET THEORY
SUBSIDENCE
Results from geopressured-geothermal subsidence studies
[DE84-016279] 09 p1354 N85-18520
Crustal stretching and subsidence in sedimentary eastern Switzerland and permo-carboniferous basins in the continental United States
[DE85-000622] 11 p1681 N85-20592
Evolution of the oceanic upper mantle and effects on sea floor subsidence geoid height and heat flow
19 p3319 N85-30575
SUBSONIC AIRCRAFT
Energy efficient engine component development and integration program
[NASA-CR-170034] 02 p0146 N85-10990
Technology developments for laminar boundary layer control on subsonic transport aircraft
08 p1071 N85-16787

SUBSONIC FLOW
PAN AIR: A computer program for predicting subsonic or supersonic linear potential flows about arbitrary configurations using a higher order panel method. Volume 3: Case manual (version 1.0)
[NASA-CR-3253] 02 p0135 N85-10922
Further development of a transonic cascade analysis
[AD-A145410] 02 p0198 N85-11319
Flow calculation on a thin wing, with specific attention to separation point at the trailing edge
[FTW-FO-1721] 05 p0694 N85-13787
PROGRAM VSAERO: A computer program for calculating the non-linear aerodynamic characteristics of arbitrary configurations: User's manual
[NASA-CR-166476] 06 p0749 N85-14802
Basic instability mechanisms in chemically reacting subsonic and supersonic flows
[AD-A148408] 08 p1122 N85-17071
Calculations for aerodynamic characteristics on a 3-D lifting body in a subsonic flow using boundary element method
[NAL-TR-835] 09 p1272 N85-17998
A locally linearized panel method for tran-/subsonic flow past an oscillating wing 11 p1622 N85-20212
Aerodynamic behavior of ventilated wind tunnel walls
13 p1988 N85-22363
Investigation of parabolic computational techniques for internal high-speed viscous flows
[NASA-CR-172555] 13 p2091 N85-23056
Approximate neutral point of a subsonic canard aircraft
[NASA-TM-86694] 15 p2462 N85-25205
Static and dynamic pressure measurements on a NACA 0012 airfoil in the Ames High Reynolds Number Facility
[NASA-TP-2485] 17 p2691 N85-27023
Propulsion efficiency of vibrating bodies in subsonic gas stream 17 p2942 N85-28159
Method of calculating separation flow of subsonic gas stream around wings 17 p2942 N85-28161
Supersonic flow around weak radiation sources
17 p2942 N85-28162
On the evaluation of boundary layer measurements on boattailed bodies of revolution in axisymmetric compressible subsonic flow
[ESA-TT-883] 20 p3457 N85-31471
A comparison of laser Doppler anemometry and probe measurements within the boundary layer of an airfoil at subsonic flow
[ISL-CO-219/84] 23 p3895 N85-34127
SUBSONIC FLUTTER
Numerical simulation of the subsonic wing-rock phenomenon 03 p0320 N85-12064
SUBSONIC SPEED
Empirical formulas for the prediction of the base pressure of missile bodies at subsonic velocities
[DFVLR-FB-84-23] 03 p0316 N85-12044
Aileron effectiveness for a subsonic transport model with a high-aspect-ratio supercritical wing
[NASA-TM-85674] 07 p0898 N85-15695
Natural unsteadiness of a separation bubble behind a backward-facing step
[AD-P004176] 09 p1267 N85-17961
A computer program for the drag prediction of subsonic, turbine powered aircraft in the en-route configuration
[VTH-LR-412] 16 p2701 N85-26881
Analysis of unsteady pressure measurements on a supercritical airfoil with a harmonically oscillating trailing edge flap at subsonic and transonic speeds
[DFVLR-FB-84-49] 17 p2893 N85-27837
Subsonic and transonic aerodynamics of a wraparound fin configuration
[AD-A153646] 18 p3059 N85-28927
Empirical formulas for the prediction of the base pressure of missile bodies at subsonic velocities
[ESA-TT-893] 20 p3399 N85-31082
SUBSONIC WIND TUNNELS
Effect of boundary layers on solid walls in three-dimensional subsonic wind tunnels
03 p0313 N85-12023
Analytical modeling of circuit aerodynamics in the new NASA Lewis wind tunnel
[NASA-TM-86912] 07 p0897 N85-15686
Six-component strain gage block scale 167-6B. Part 1: Calibration, September 1983
[F+W-FO-1609] 07 p0968 N85-16143
Aeronautical facilities catalogue. Volume 1: Wind tunnels
[NASA-RP-1132] 10 p1426 N85-18991
Wall interference estimation of the NAL's two-dimensional wind tunnel
[NAL-TR-829] 10 p1426 N85-18992
Harbin's subsonic, transonic wind tunnel detailed
14 p2263 N85-24143
SUBSTANCES
U MATERIALS
SUBSTITUTES
Use of ion implantation to modify the corrosion behavior of metals
[AD-P003953] 02 p0286 N85-11869
General studies on composite materials. Evaluation of auxiliary products of national origin
[SNIAS-2500/DCI-PR/84] 03 p0326 N85-12101
Polyimide resin characteristics, test
[DGT-24.322] 04 p0479 N85-13049
Effects of heteroatom substituents on the properties of 1,2-dioxetanes
[AD-A148727] 09 p1290 N85-18100
The B2 aluminides as alternative materials
[NASA-TM-86937] 10 p1440 N85-19076
Partial replacement of chromium in austenitic stainless steels by molybdenum, copper, and vanadium, report of investigations 1984
[PB85-116506] 12 p1809 N85-21346
Substituent effects on the electrical conductivities of the phenazine derivatives
[NASA-TM-77792] 14 p2249 N85-23936
SUBSTITUTION
U SUBSTITUTES
SUBSTRATES
Acoustic resonator and method of making same
[DE84-014655] 01 p0116 N85-10792
Cleaning procedures of laser mirror substrates
[DFVLR-MITT-84-06] 05 p0640 N85-14108
Ultrasonic girth weld evaluation for aluminum substrate of spherical Kevlar-epoxy test specimens
[DE85-001592] 06 p0816 N85-15181
Elastodynamic stress intensity factors of an interface finite-width crack
[DE84-016908] 06 p0817 N85-15190
Substrate preparation for thin film deposition: A survey
[DE84-016119] 06 p0866 N85-15514
Deposition of titanium nitride coatings by reactive evaporation and electrically activated reactive evaporation
[BLL-TRANS-5043-(9091.9F)] 07 p0925 N85-15858
Slow wave circuit with shaped dielectric substrate
[AD-D011386] 07 p0946 N85-15986
Aluminum nitride insulator for 3-5 MIS (Metal-Insulator-Semiconductor) applications
[AD-A147842] 07 p1049 N85-16662
Stability of amorphous metals on semiconductor substrates
[DE84-017256] 09 p1295 N85-18134
Effects of MAR-M247 substrate (modified) composition on coating oxidation coating/substrate interdiffusion -- protective coatings for hot section components of gas turbine engines
[NASA-CR-174851] 10 p1440 N85-19073
Adsorption thermodynamics and surface transport of metal catalyst poisons
[DE85-002868] 10 p1441 N85-19084
Investigation of welded interconnection of large area wraparound contacted silicon solar cells
[NASA-CR-174436] 10 p1509 N85-19519
Low temperature deposition of nickel films
[AD-D011569] 12 p1805 N85-21319
A process to produce fine line metallic collection patterns on semiconductors devices
[NASA-CASE-NPO-16413-1] 12 p1805 N85-21325
Distributed Gunn effect devices; a numerical analysis of microstrip circuits on thin active GaAs substrates
[FOA-C-30383-E] 12 p1837 N85-21527
Influence of substrate heating and thermal annealing on the surface crystallinity in single Si crystals implanted with high doses of (16)O
[DE85-005264] 13 p2164 N85-23428
High-temperature X-ray diffraction study of coating-substrate compatibility in yttria-coated graphite
[DE85-005916] 14 p2262 N85-24016
Investigation of the MBE growth of InSb and novel quantum well structures
[AD-A151014] 14 p2427 N85-24969
NASA welding assessment program
[NASA-CR-175682] 15 p2568 N85-25844
Investigation of basic characteristics of laser heating in thermoluminescence and of laser-stimulated luminescence
[AD-A152143] 16 p2790 N85-27212
Glassy metals: New highly resistant material
[BLL-BISI-TRANS-21764-(9022.06)]
17 p2926 N85-28049
Properties of chromate coatings formed on electrolytic zinc substrates
[BLL-BISI-TRANS-22349-(9022.06)]
17 p2926 N85-28052
The structure of ion plated films in relation to coating properties
[NASA-TM-87055] 18 p3085 N85-29085
Method for ultrasonic bonding to soft microelectronic substrates
[NASA-CASE-NPO-16087-1] 18 p3094 N85-29161
Investigation of superlattice device structures
[NASA-CR-3903] 18 p3094 N85-29162
Silicide conductors reliability research
[AD-A153768] 18 p3095 N85-29157
An experimental study of the pressure in a fast bottom beneath the apex of an overlying fluid wedge
[AD-A153618] 18 p3177 N85-29686
Integrated electrooptical components using dielectric substrates 18 p3187 N85-29787
Process for the epitaxial deposition of 3-5 compounds utilizing a binary alloy as the metallic source
[AD-D011663] 18 p3193 N85-29801
Glow discharge deposition at high rates using disilane
[DE85-010236] 19 p3263 N85-30295
Increased voltage photovoltaic cell
[NASA-CASE-NPO-16155-1] 19 p3303 N85-30475
Microwave SAW (Surface Acoustic Wave) monochromator
[AD-D011718] 21 p3590 N85-32011
Thin-film reliability and engineering overview
21 p3612 N85-32450
Rationale in the selection of corrosion protective coating systems 22 p3750 N85-33242
Thermoelectric generator and method for the fabrication thereof
[DE85-011650] 22 p3760 N85-33302
Electron beam enhanced surface modification for making highly resolved structures
[DE85-011609] 22 p3760 N85-33305
Effect of substrate moisture on growth and structure of corn leaf 22 p3824 N85-33882
Liquid crystal light valve structures
[NASA-CASE-MSC-20036-1] 22 p3847 N85-33826
Thermal barrier coating system
[NASA-CASE-LEW-14057-1] 24 p4072 N85-35233
Oxidation resistant slurry coating for carbon-based materials
[NASA-CASE-LEW-13923-1] 24 p4077 N85-35267
Wear-resistant coatings for tools intended for cold working
[BLL-RISLEY-TR-5040-(9091.9F)]
24 p4081 N85-35293
Advanced detectors and signal processing
[NASA-CR-176193] 24 p4088 N85-35343
Solid neon sources for plasma and X-ray lasers
[DE85-011347] 24 p4098 N85-35402
SUBSTRUCTURES
Damping synthesis for a spacecraft using substructure and component data
[CRC-1365] 03 p0323 N85-12082
Full-scale crash-test evaluation of two load-limiting subfloors for general aviation airframes
[NASA-TP-2380] 04 p0512 N85-13267
An effective substructure technique applied to crack problems 18 p3121 N85-29319
A substructure coupling procedure applicable to general linear time-invariant dynamic systems
[NASA-CR-176144] 22 p3800 N85-33542
SUBTROPICAL REGIONS
U TEMPERATE REGIONS
U TROPICAL REGIONS
SUBURBAN AREAS
A comparison of metropolitan and non-metropolitan employment characteristics: Indications of the size of non-metropolitan mobile communication services user classes
[NASA-CR-175646] 13 p2053 N85-22855
Assessment of the role of nitrogen oxides in nonurban ozone formation
[PB85-173880] 19 p3311 N85-30524
SUCROSE
The use of moments of momentum to account for crystal habits
[NASA-CR-3907] 20 p3421 N85-31232
SUCTION
Hybrid laminar flow control study
[NASA-CR-165930] 02 p0137 N85-10933
Approximate solution of a laminar flow over a flat pla
with suction and pressure gradient
[AD-A145482] 02 p0198 N85-1132
Drag reduction due to boundary-layer control b
combined blowing and suction 08 p1070 N85-1678
Design studies of thick laminar flow airfoils for low spee
flight employing turbulent boundary layer suction over th
rear part 08 p1070 N85-1678
Turbulent drag reduction research
08 p1071 N85-167
Active and passive shock/boundary layer interactio
control on supercritical airfoils 08 p1072 N85-167
Air intake efficiency at zero speed and lip suction
jet engines
[BAE-KRS-N-GEN-303] 09 p1272 N85-179

Calibration of sonic valves for the laminar flow control, leading-edge flight test
[NASA-TP-2423] 14 p2210 N85-23707
SUD AVIATION AIRCRAFT
NT CONCORDE AIRCRAFT
SUDAN
SIR-B analysis of the Precambrian shield of Sudan and Egypt: Penetration studies and subsurface mapping
08 p1145 N85-17219
SUDDEN IONOSPHERIC DISTURBANCES
Solar-geophysical data number 476, April 1984. Part 1: (Prompt reports). Data for March 1984, February 1984 and late data
[PB84-215060] 09 p1416 N85-18936
Solar flare and IMF sector structure effects in the lower ionosphere 11 p1684 N85-20486
Solar-geophysical data number 483. November 1984. Part 1: (Prompt reports). Data for October 1984, September 1984 and late data
[PB85-147692] 12 p1962 N85-22335
SUDDEN STORM COMMENCEMENTS
A simulation experiment of a rapidly developed medium scale cyclone 01 p0079 N85-10530
Solar-geophysical data number 479, July 1984. Part 1: (Prompt reports). Data for June 1984, May 1984 and later data
[NASA-CR-175542] 12 p1962 N85-22333
Observations during a magnetosphere substorm triggered by a Storm Sudden Commencement (SSC): A case study 14 p2361 N85-24586
Sudden Storm Commencement (SSC) associated hydromagnetic variations at geosynchronous altitude and on the ground 14 p2369 N85-24642
SUGAR BEETS
Multi crop area estimation in Idaho using EDITOR
[E85-10054] 06 p0827 N85-15251
SUGAR CANE
Development and testing of a rural credit supervision system at the level of counties and rural properties utilizing remote sensing techniques
[E85-10018] 02 p0217 N85-11431
SUGARS
NT GALACTOSE
NT GLUCOSE
NT PENTOSE
NT RIBOSE
NT SUCROSE
Production of butanol by fermentation in the presence of cocultures of clostridium
[NASA-CASE-NPO-16203-1] 24 p4071 N85-35227
SUITS
NT PRESSURE SUITS
NT SPACE SUITS
SULFATES
NT SODIUM SULFATES
The concentration of sulfate in broken cloud layers
[DE85-000228] 11 p1678 N85-20574
Applicability of laboratory kinetics studies to the evaluation of aqueous phase atmospheric oxidation of sulfur-4
[DE85-000586] 12 p1863 N85-21819
Studies of the mechanisms and rates with which nitrogen species are incorporated into cloud water and precipitation
[PB85-144350] 12 p1896 N85-21914
Chemical weathering of soils from the dry valleys of Antarctica: A terrestrial analog of Martian weathering processes 13 p2197 N85-23628
A comparative evaluation of the effects of acid precipitation, natural acid production and harvesting of cation removal from forests
[DE85-005254] 15 p2589 N85-25961
Qualitative and quantitative examination of the performance of regional air quality models representing different modeling approaches
[DE85-010508] 19 p3310 N85-30518
Sulfates in marine aerosols over the tropical Western Pacific Ocean 21 p3651 N85-32690
Granulometric study of the acidity and sulfate excess in marine aerosols 21 p3652 N85-32691
Geology and geochemistry of sulfide and sulfate deposition 21 p3658 N85-32723
Phototrophic bacteria and their role in the biogeochemical sulfur cycle 21 p3660 N85-32735
Sulfur reduction in sediments of marine and evaporite environments 21 p3661 N85-32742
Thermodynamic data for mineral technology
[PB85-184331] 22 p3803 N85-33560
Effects of H2S on molten carbonate fuel cells. Literature review on the impact of SO2 in the oxidant supplied to molten carbonate fuel cells
[DE85-011698] 22 p3808 N85-33586
Environmental surveillance at Los Alamos during 1984
[DE85-011666] 22 p3811 N85-33605
Effects of acid rain on forest nutrient status
[DE85-012488] 23 p3947 N85-34463
Throughfall rate and chemistry studies: Whiteface Mountain
[DE85-012407] 23 p3947 N85-34464
Incorporating meteorological data into receptor analysis: RAPS (Regional Air Pollution Study) revisited
[PB85-189944] 24 p4114 N85-35503
A new drawing technique for nylon 6 by reversible plasticization with iodine
[AD-A156272] 24 p4102 N85-35803
SULFATION
Molecular orbital studies in oxidation: Sulfate formation and metal-metal oxide adhesion
[NASA-CR-176070] 21 p3565 N85-32174
Adsorption of O2, SO2, and SO3 on nickel oxide. Mechanism for sulfate formation
[NASA-CR-176072] 21 p3565 N85-32175
SULFIDATION
Behavior of pressurized tubes of candidate alloys in a simulated low-Btu environment
[DE85-003403] 09 p1296 N85-18141
SULFIDES
NT BARIUM SULFIDES
NT CADMIUM SULFIDES
NT CALCIUM SULFIDES
NT CARBON DISULFIDE
NT COPPER SULFIDES
NT DISULFIDES
NT HYDROGEN SULFIDE
NT MOLYBDENUM DISULFIDES
NT POLYSULFIDES
NT PYRITES
NT TROILITE
NT ZINC SULFIDES
Research on electroluminescence in thin film yttrium oxysulfide
[AD-A146909] 07 p1037 N85-16582
Quality testing to the specifications of the Stahl-Eisen-Pruefblatt 1570/71 using an automatic image analysis system
[BLL-BISI-TRANS-22253-(9022.06)]
17 p2976 N85-28365
Lithium-alloy/iron sulfide battery design studies
[DE85-007991] 18 p3131 N85-29389
The global sulfur cycle
[NASA-TM-87570] 21 p3656 N85-32710
Sulfur diagenesis in marine sediments
21 p3658 N85-32721
Geology and geochemistry of sulfide and sulfate deposition 21 p3658 N85-32723
Sulfate-reducing bacteria: Microbiology and physiology 21 p3659 N85-32732
Structure and physiology of Beggiatoa and Thiothrix
21 p3659 N85-32734
Enrichments for phototrophic bacteria and characterization by morphology and pigment analysis
21 p3660 N85-32738
Interactions among sulfide-oxidizing bacteria
21 p3661 N85-32741
Sulfur reduction in sediments of marine and evaporite environments 21 p3661 N85-32742
Microbial communities and microprofiles of sulfide and oxygen of alum rock sulfur springs
21 p3661 N85-32746
Microbial colonization and growth on metal sulfides and other mineral surfaces 21 p3662 N85-32747
Thermodynamic data for mineral technology
[PB85-184331] 22 p3803 N85-33560
Special features of the fracture of ball-bearing steel close to non-metallic inclusion eutectics
[BLL-M-35609-(5828.4)] 23 p3914 N85-34258
Some geophysical guides to ore in southern and southwestern Alaska 24 p4103 N85-35438
Massive sulfide deposits from the southern Juan de Fuca Ridge 24 p4105 N85-35446
SULFONATES
An investigation of chemiluminescent reactions
[AD-A148460] 08 p1122 N85-17073
Luminescence probe studies of ionomers. 2. Steady-state measurements from sulfonated polyethylene and teflon membranes
[AD-A152233] 16 p2755 N85-27000
Development and evaluation of sulfonated polysulfone membranes for the zinc-ferricyanide battery
[DE85-009104] 24 p4090 N85-35357
SULFONES
Characterization of a thermoplastic polyimidesulfone
[NASA-TM-86358] 10 p1450 N85-19135
Characterization of acetylene-terminated resin cure states
[AD-A149463] 10 p1452 N85-19148
Process for preparing solvent resistant, thermoplastic aromatic poly(imidesulfone)
[NASA-CASE-LAR-12858-2] 11 p1610 N85-20124
Research to explore the feasibility of sulfolanes as electrolytic solvents for rechargeable lithium batteries
[DE85-004345] 12 p1837 N85-21525
Fracture surface analysis in composite and titanium bonding: Part 1: Titanium bonding
[NASA-CR-175750] 15 p2502 N85-25434
Polyaromatic ether-sulfone-ketones with fluoro-substituted-p-cyclophane units as cross-linking sites
[AD-D011649] 17 p2933 N85-28105
Mechanical properties of aligned short carbon fiber reinforced PES and PI laminates
[ESA-TT-898] 20 p3422 N85-31240
Synthesis and properties of arylethersulfone thermoset systems
[AD-A154811] 21 p3569 N85-32198
SULFUR
Surface segregation of sulfur during oscillatory pin-on-plate wear studies of precious metal electrical contact alloys. 1: Friction and electrical contact resistance
[DE84-006962] 02 p0195 N85-11303
Mechanical properties of a leaded, resulfurized, rephosphorized steel in various thermo/mechanical conditions
[PB84-216464] 03 p0333 N85-12144
Determination of halogens and sulfur in organic compounds and polymers by combustion-ion chromatography
[DE84-016186] 05 p0614 N85-13921
Effects of heteroatom substituents on the properties of 1,2-dioxetanes
[AD-A148727] 09 p1290 N85-18100
Non-photochemical interactions of sulfur and nitrogen compounds in acid deposition
[DE84-016141] 10 p1513 N85-19646
Implications of the presence of S2 in cometary ice
11 p1760 N85-21072
Sulfur volcanoes on Io? 13 p2173 N85-23479
Sulfur oxygen processes on Io
13 p2173 N85-23481
Diagrams of chemical and electrochemical equilibria in the presence of oxygen and sulphur
[AD-A150929] 14 p2251 N85-23953
Trends of petroleum fuels
[DE85-000116] 14 p2263 N85-24023
Systematic nomenclature of the nitrogen, oxygen and sulfur functional polycyclic aromatic hydrocarbons
[DE85-007426] 17 p2916 N85-27974
Gas phase ion-molecule chemistry of carbon, nitrogen and oxygen compounds
[AD-A152876] 17 p2919 N85-27996
Part played by non-metallic inclusions during deformation and fracture of steel with different grain sizes
[BLL-BISI-TRANS-22321-(9022.06)]
17 p2928 N85-28072
Study of the explosive combustion of drops of sulphur at high temperatures
[HSE-TRANS-11182] 19 p3252 N85-30183
Advanced fuel cell development
[DE85-009662] 19 p3306 N85-30497
Sulfur activation at the Little Boy-Comet Critical Assembly: A replica of the Hiroshima bomb
[DE85-010261] 20 p3527 N85-31938
Theoretical studies of structure and stability of hydrates of atmospheric sulfur species 21 p3650 N85-32684
Variations of particulate sulfur concentrations in a coastal atmospheric environment in connection with the change of air masses origin 21 p3652 N85-32692
The global sulfur cycle
[NASA-TM-87570] 21 p3656 N85-32710
Sulfur transformations at the hydrogen sulfide/oxygen interface in stratified waters and in cyanobacterial mats
21 p3657 N85-32715
Cytochromes and iron sulfur proteins in sulfur metabolism of phototrophic bacteria
21 p3657 N85-32718
Carbon and sulfur cycling through geologic time
21 p3658 N85-32720
Ecophysiology of phototrophic sulfur bacteria in lakes: Vertical distribution of planktonic populations
21 p3658 N85-32722
Sulfur cycling in freshwater sediments
21 p3658 N85-32726
Some thoughts on GAIA and the sulfur cycle
21 p3658 N85-32727
Sulfur and carbon cycling in organic-rich marine sediments 21 p3659 N85-32729
Possible roles of manganese redox chemistry in the sulfur cycle 21 p3659 N85-32731
Phototrophic bacteria and their role in the biogeochemical sulfur cycle 21 p3660 N85-32735
The role of sulfur in osmoregulation and salinity tolerance in cyanobacteria, algae, and plants
21 p3660 N85-32736
Sulfur cycling and metabolism of phototrophic and filamentous sulfur bacteria 21 p3660 N85-32737

Anaerobic reduction of elemental sulfur by Chromatium vinosum and Beggiatoa alba 21 p3660 N85-32739

Sulfur Cycle 21 p3662 N85-32748

Multiphoton production and detection of atoms
[AD-A156661] 21 p3702 N85-33000

A new analysis of cosmic ray isotopes at 3 GeV/n from HEA03-C2 data
[OG-4.3-6] 22 p3679 N85-34031

Circumstellar shells of late-type stars: A study at millimeter and infrared wavelengths
24 p4167 N85-35836

SULFUR COMPOUNDS
NT BARIUM SULFIDES
NT CADMIUM SULFIDES
NT CALCIUM SULFIDES
NT CARBON DISULFIDE
NT COPPER SULFIDES
NT DISULFIDES
NT HYDROGEN SULFIDE
NT MOLYBDENUM DISULFIDES
NT ORGANIC SULFUR COMPOUNDS
NT POLYSULFIDES
NT PYRITES
NT SODIUM SULFATES
NT SULFATES
NT SULFIDES
NT SULFONATES
NT SULFONES
NT SULFUR DIOXIDES
NT SULFUR FLUORIDES
NT SULFUR OXIDES
NT SULFURIC ACID
NT THIAZINE (TRADEMARK)
NT THIOLS
NT TROILITE
NT ZINC SULFIDES

Environmental Research Division report: Atmospheric physics
[DE85-009659] 18 p3133 N85-29404

SULFUR DIOXIDES

Estimation of the potential and probable source regions for acid precipitation
[DE84-015119] 02 p0225 N85-11472

Stability evaluation of sulfur dioxide nitric oxide and carbon monoxide gases in cylinders
11 p1646 N85-20367

Effect of elevated atmospheric CO2 on plant communities
[DE85-001610] 11 p1678 N85-20576

National Acid Precipitation Assessment Program. Report to the President and Congress (1983)
[PB85-116713] 11 p1679 N85-20581

Continued research in mesoscale air pollution simulation modeling. Volume 5: Refinements in numerical analysis, transport, chemistry, and pollutant removal
[PB85-137362] 11 p1680 N85-20585

National Performance Audit Program ambient air audits of analytical proficiency
[PB85-138204] 11 p1680 N85-20586

Evaluation of complex terrain air quality simulation models
[PB85-119465] 12 p1686 N85-21835

Gas phase ion-molecule chemistry of carbon, nitrogen and oxygen compounds
[AD-A152676] 17 p2919 N85-27996

Absolute calibrations of SO2 and NO analyzers by photographic methods
[DFVLR-MITT-85-02] 17 p2994 N85-28504

Methods for simulating gas phase SO2 oxidation in atmospheric models
[PB85-173110] 18 p3135 N85-29418

Qualitative and quantitative examination of the performance of regional air quality models representing different modeling approaches
[DE85-010508] 19 p3310 N85-30518

Historic emissions of sulfur and nitrogen oxides in the U.S. from 1900 to 1980. Volume 1: Results
[PB85-191195] 20 p3487 N85-31674

Historic emissions of sulfur and nitrogen oxides in the U.S. from 1900 to 1980. Volume 2: Data
[PB85-191203] 20 p3487 N85-31675

Modeling of chemical transformations of SO(x) and NO(x) in the polluted atmosphere: An overview of approaches and current status
[PB85-173169] 20 p3487 N85-31677

Experimental studies of the formation of Aitken nuclei in the atmosphere 21 p3644 N85-32641

Effects of H2S on molten carbonate fuel cells. Literature review on the impact of SO2 in the oxidant supplied to molten carbonate fuel cells
[DE85-011698] 22 p3806 N85-33586

The 1984 environmental monitoring program report for Idaho National Engineering Laboratory site
[DE85-011209] 22 p3812 N85-33611

Forecasting future industrial SO2 and NC/sub x/ emissions, revised 23 p3947 N85-34461

Throughfall rate and chemistry studies: Whiteface Mountain
[DE85-012407] 23 p3947 N85-34464

SULFUR FLUORIDES

Recent advances in gaseous dielectrics
[DE84-014279] 02 p0196 N85-11304

Green River air quality model development: Meteorological and tracer data, July/August 1982. Field study in Brush Valley, Colorado
[DE84-014975] 02 p0225 N85-11474

The use of tracers for the study of atmospheric chemical and physical transformation processes
[DE84-015267] 05 p0671 N85-14313

Transport and relaxation processes in supercritical fluids
[DE84-006591] 05 p0731 N85-14698

Atmospheric wind and diffusion from analysis of an SF6 release at 350 km altitude
[AD-A147965] 08 p1185 N85-17471

Pseudo-stationary oblique-shock-wave reflections in a polyatomic gas, sulfur hexafluoride
[UTIAS-TN-253] 12 p1845 N85-21577

Predischarge parameters of SF6-CO2 determined by laser 15 p2584 N85-25821

SULFUR OXIDES
NT SULFUR DIOXIDES

Evaluation of recent SO/sub x/and NO/sub x/ emission inventories
[DE85-002649] 11 p1677 N85-20570

Reduction of pollutant formation in combustion processes
[DE85-010181] 19 p3309 N85-30512

Safety of Li-SOCl2 cells 20 p3444 N85-31383

Adsorption of O2, SO2, and SO3 on nickel oxide. Mechanism for sulfate formation
[NASA-CR-176072] 21 p3565 N85-32175

Environmental surveillance at Los Alamos during 1984
[DE85-011866] 22 p3811 N85-33605

SULFURIC ACID

Laboratory evaluation of microwave absorption properties under simulated conditions for planetary atmospheres
[NASA-CR-174060] 02 p0303 N85-11960

Sulfuric acid chemical heat pump program, March - November 1982
[DE84-017436] 09 p1320 N85-18304

Solar thermochemical process interface study
[NASA-CR-174442] 10 p1510 N85-19527

Study of the formation of sulfuric acid aerosols
[DE85-008102] 17 p2922 N85-28011

Oxygen isotopic study of the oxidation of SO2 by H2O2 in the atmosphere
[DE85-004017] 17 p2968 N85-28468

Rapid estimation of concentration of aromatic classes in middistillate fuels by high-performance liquid chromatography
[NASA-TP-2495] 20 p3434 N85-31307

Decomposition of sulfuric acid using solar thermal energy
[DE85-012288] 21 p3564 N85-32170

Aerobic sulfur-oxidizing bacteria: Environmental selection and diversification 21 p3656 N85-32712

Synthesis of 2,4,8,10-tetroxaspiro5,5undecane
[NASA-CASE-ARC-11243-2] 22 p3741 N85-33187

Determination of the viscosity number of thermoplastics in dilute solution; polyamides (PA)
[NASA-TM-77673] 24 p4061 N85-35296

SUMMARIES
NT ABSTRACTS

Beyond fault trees to fault graphs
[DE84-017022] 09 p1370 N85-18608

Summaries of FY 1984 engineering research
[DE85-006273] 15 p2664 N85-26442

Experimental plasma research: Plasma summaries
[DE85-008116] 17 p3039 N85-28805

Photovoltaic Systems Development Project: An activity summary
[DE85-009994] 18 p3129 N85-29379

Activities at the Lunar and Planetary Institute
[NASA-CR-175914] 18 p3201 N85-29859

Standards Committee activities of the National Bureau of Standards: 1984 highlights
[PB85-183382] 19 p3350 N85-30764

A research program to reduce the interior noise in general aviation aircraft, index and summary
[NASA-CR-176178] 24 p4145 N85-35695

SUMMER

Combining radar and satellite data for the localization and identification of summer convection
01 p0077 N85-10509

Forecast impact of components of the FGGE observing system 05 p0681 N85-14373

Structure and energetics of medium-scale atmospheric waves in the southern hemisphere summer
05 p0685 N85-14403

Sea breeze-induced mesoscale systems and severe weather
[NASA-CR-174317] 08 p1187 N85-17480

The 500 millibar sign frequency teleconnection charts: Summer
[PB85-111359] 11 p1696 N85-20913

Sector analysis of relevant meteorological parameters for long range transport of air pollutants
[NR-27] 12 p1693 N85-21882

Collection and use of lightning strike data in the western US during summer 1983
[PB85-110534] 12 p1697 N85-21907

Variation of Arctic cloud cover in summer
[DE85-004507] 13 p2139 N85-22285

The BALSAMINE experiment
14 p2236 N85-23876

Radiative forcing of the southwest summer monsoon (a satellite perspective) 15 p2593 N85-25881

The use of radar in determining precipitation processes in the BEWMEX area 16 p2831 N85-27455

Evaluation of the area and severity of last night's frosts
[REPT-109] 16 p2833 N85-27473

Structure and energetics of medium-scale atmospheric waves in the Southern Hemisphere
20 p3489 N85-31686

Agricultural weather report for the Ijsselmeer polders in the 1984 summer season; a verification report
[KNMI-TR-61] 20 p3496 N85-31737

Aircraft observations of condensation and ice nuclei at a tropical station 21 p3640 N85-32813

Transport and formation of summertime cloud condensation nuclei over the Arctic Ocean
21 p3651 N85-32886

SUMS

On an algorithm for Pythagorean sums and its connection with continued fractions
[NPL-DITC-42/84] 05 p0716 N85-14603

Sequential minimization for sum of squares of unknown functions
[DE85-004162] 11 p1707 N85-20736

SUN

Estimating sunspot number
[NASA-TM-86471] 01 p0130 N85-10898

Report on solar neutrino experiments
[DE84-014567] 01 p0131 N85-10899

The mapping of the Sun at 8 mm wavelength and tracking of the active regions in the period 23 May - 5 June 1983
[REPT-S-149] 02 p0297 N85-11924

Active regions — and the Solar Maximum Mission
[NASA-CR-170628] 02 p0304 N85-11965

Chlorine and bromine solar neutrino experiments
[DE84-015720] 02 p0304 N85-11969

Time dependent effects at the foot of the chromosphere
[NASA-CR-174143] 04 p0589 N85-13702

Structure and evolution of the large scale solar and heliospheric magnetic fields 05 p0746 N85-14782

Distribution of the K-corona over the polar regions of the solar disk: 1965-1983
[PB84-230077] 06 p0835 N85-15317

Local Interstellar Medium. International Astronomical Union Colloquium No. 81
[NASA-CP-2345] 06 p0872 N85-15539

Helium and hydrogen of the local interstellar mdium observed in the vicinity of the Sun
06 p0873 N85-15540

Absorption line studies and the distribution of neutral gas in the local interstellar medium
06 p0873 N85-15544

Synthesis of data on the local interstellar medium
06 p0874 N85-15545

Meteoritic constraints on processes in the solar nebula 06 p0887 N85-15630

Chemical evolution of the solar nebula: A new model
06 p0887 N85-15631

Dynamic thermal episodes in the protosolar nebula: Development of models from observations on CAI's
06 p0887 N85-15633

Solar He-3-rich events and non-relativistic electron events: A new association
[NASA-TM-86179] 06 p0890 N85-15652

Variation in spectral response of soybeans with respect to illumination, view, and canopy geometry
[E85-10040] 07 p0982 N85-16241

Spicules and surges
[AD-A146785] 07 p1061 N85-16727

Sun-aligned polar cap auroral arcs
[AD-A146052] 08 p1185 N85-17472

Extreme limb profiles of the Sun at far infrared and submillimeter wavelengths 08 p1244 N85-17652

Coronal and chromospheric physics — Sun, sunspots, and solar limb
[NASA-CR-174290] 08 p1259 N85-17921

Evidence for a solar companion star
[DE85-002069] 10 p1571 N85-18907

User's guide for the Nimbus 7 ERB Solar Analysis Tape (ESAT)
[NASA-TM-86143] 10 p1572 N85-19814
National solar-terrestrial research program, part 1. Solar-terrestrial research for the 1980's, part 2
[AD-A149542] 11 p1681 N85-20591
Herstmonceux observations of the Sun, planets and Moon, 1957 - 1982
[BULL-193] 11 p1762 N85-21087
Plasma and nuclear processes in solar matter 12 p1954 N85-22277
Helium atoms in interstellar and interplanetary space. II: Determination of direction of interstellar gas motion relative to Sun 13 p1980 N85-22425
Relationship between seismic status of Earth and relative position of bodies in sun-earth-moon system 14 p2345 N85-24499
Ionization equilibrium and equation of state in the solar interior 14 p2445 N85-25088
The hydromagnetics of the Sun --- conferences
[ESA-SP-220] 14 p2445 N85-25091
Mixing in the solar interior 14 p2446 N85-25095
Did the young Sun rotate at 100 km/s 14 p2451 N85-25133
Solar magnetohydrodynamics: Symposium review 14 p2455 N85-25162
Apparent thichness of Saturn's rings from the observations of the ring plane crossing 15 p2671 N85-26477
Formation of the solar system 15 p2677 N85-26532
Evidence in meteorites for an active early Sun 15 p2680 N85-26550
Stokes parameters modulator for birefringent filters 18 p3205 N85-29884
The San Fernando Observatory video Stokes polarimeter 18 p3205 N85-29885
The new solar magnetograph for the Canary Islands Observatory THEMIS 18 p3205 N85-29886
Multichannel birefringent filter 18 p3206 N85-29888
Solar convection
[AD-A155214] 21 p3723 N85-33098
Heating of the deep chromosphere during solar flares
[AD-A155256] 21 p3723 N85-33100
Search for the north-south asymmetry in solar activity
[AD-A155525] 21 p3724 N85-33102
Terrain illumination conditions when taking scanning photographs from space 22 p3736 N85-33159
On the possibility of the determining the average mass composition near 10 to the 14th power eV through the solar magnetic field
[OG-5.1-9] 22 p3882 N85-34051
Coordinated study of solar-terrestrial payloads on space station
[NASA-CR-176160] 23 p3900 N85-34158
Soft X-Ray Telescope (SXRT) 23 p3900 N85-34159
Solar Ultraviolet Spectral Irradiance Monitor (SUSIM) 23 p3901 N85-34160
White Light Coronograph (WLC) and Ultra-Violet Coronal Spectrometer (UVCS) 23 p3901 N85-34161
High Resolution Telescope and Spectrograph (HRTS) 23 p3901 N85-34162
Active Cavity Radiometer (ACR) 23 p3901 N85-34163
Sidereal anisotropies in the median rigidity range 60-600GV in 1978-1983
[SH-4.4-3] 23 p4033 N85-35001
The sidereal semi-diurnal variation observed at high zenith angles at Mawson, 1968-1984, and the polarity of the solar main field
[SH-4.4-6] 23 p4033 N85-35004
A study of periodicities and recurrences in solar activity and cosmic ray modulation
[SH-4.4-14] 23 p4034 N85-35010
Results of ultra-low level 71ge counting for application in the Gallex-solar neutrino experiment at the Gran Sasso Underground Physics Laboratory
[SH-8.1-2] 23 p4049 N85-35108
Correlation between solar neutrino flux and other solar phenomena 23 p4049 N85-35109
A possible mechanism to cause the quasi-biennial variability on the solar neutrino flux
[SH-8.1-5] 23 p4049 N85-35110
The conjecture concerning time variations in the solar neutrino flux
[SH-8.1-6] 23 p4049 N85-35111
Solar neutrino: Flux, cosmic rays and the 11 year solar cycle
[SH-8.1-7] 23 p4049 N85-35112
Solar neutrinos, solar flares, solar activity cycle and the proton decay
[SH-8.1-8] 23 p4049 N85-35113
Neutrino production from the solar atmosphere
[SH-8.1-9] 23 p4050 N85-35114
Solar cosmic ray bursts and solar neutrino fluxes
[SH-8.1-10] 23 p4050 N85-35115
A silicon surface barrier telescope for solar particles identification
[SH-9.1-3] 23 p4050 N85-35118
Photometric and spectroscopic gamma-ray observations of solar transient phenomena using long duration balloons
[SH-9.1-5] 23 p4051 N85-35120
Monte Carlo calibration of the SMM gamma ray spectrometer for high energy gamma rays and neutrons
[SH-9.1-6] 23 p4051 N85-35121

SUN SENSORS
U SOLAR SENSORS

SUNLIGHT
Structure of temperature field based on observations of refraction from high meteorological mast 06 p0819 N85-15199
The temperature of a glass-encapsulated solar cell estimated from ambient air temperature and global radiation
[GKSS-84-E-36] 11 p1676 N85-20563
On the determination of the solar rotation and indications of the solar differential rotation from an analysis of solar integrated light 14 p2446 N85-25096
Terrestrial photovoltaic power systems with sunlight concentration
[DE85-006396] 17 p2967 N85-28464
Solar energy for highway uses
[DE84-015653] 18 p3130 N85-29382
Electricity from sunlight: The emergence of photovoltaics, revised edition
[DE85-002920] 19 p3307 N85-30502

SUNRISE
The investigation of short wave signal structure in the vicinity of the caustic by means of a high-directed antenna
[PR-194] 03 p0354 N85-12277
Computing worldwide sunrise, sunset, moonrise, moonset and twilight times using 5 WWPs 105-3 and 105-4
[AD-A148049] 08 p1189 N85-17490

SUNSET
The investigation of short wave signal structure in the vicinity of the caustic by means of a high-directed antenna
[PR-194] 03 p0354 N85-12277
Computing worldwide sunrise, sunset, moonrise, moonset and twilight times using 5 WWPs 105-3 and 105-4
[AD-A148049] 08 p1189 N85-17490

SUNSPOT CYCLE
Estimating sunspot number
[NASA-TM-86471] 01 p0130 N85-10896
Solar cycle variations of sunspot temperatures 14 p2452 N85-25141
Dependence of equatorial F-region plasma bubble rise velocity and dynamo electric field on solar cycle
[INPE-3439-PRE/696] 16 p2826 N85-27434
Magnetic and thermodynamic structure of the solar corona during sunspot minimum 18 p3203 N85-29873
Equitorial scintillations: Advances since ISEA-6
[AD-A154962] 21 p3631 N85-32559
Difference between even and odd 11-year cycles in cosmic ray intensity
[SH-4.2-22] 23 p4009 N85-34859
An update on the correlation between the cosmic radiation intensity and the geomagnetic AA index
[SH-4.2-24] 23 p4009 N85-34861

SUNSPOTS
Estimating sunspot number
[NASA-TM-86471] 01 p0130 N85-10896
Solar-geophysical data number 477, May 1984. Part 1: (Prompt reports). Data for April 1984, March 1984 and late data. Explanation of data reports issued as number 474 (supplement) February 1984
[PB84-225026] 01 p0131 N85-10901
Coronal and chromospheric physics --- Sun, sunspots, and solar limb
[NASA-CR-174290] 08 p1259 N85-17921
Geomagnetic disturbances caused by internal atmospheric dynamics 11 p1665 N85-20491
Oscillatory convection in sunspots 14 p2446 N85-25099
Linear models of acoustic waves in sunspot umbrae 14 p2450 N85-25130
Observational aspects of sunspot oscillations 14 p2451 N85-25131
The flux rope models checked by some observations --- solar activity 14 p2452 N85-25139
Solar cycle variation of ephemeral active regions 14 p2452 N85-25142
A siphon flow model for Evershed motion --- sunspot regions 14 p2453 N85-25147
Elementary sunspot energy model 15 p2476 N85-25287
Stokes parameters modulator for birefringent filters 18 p3205 N85-29884
Least squares inversion of Stokes profiles in the presence of velocity gradients 18 p3207 N85-29892
The effect of line damping, magneto-optics and parasitic light on the derivation of sunspot vector magnetic fields 18 p3207 N85-29895
Comparisons of simultaneous vector magnetograms 18 p3208 N85-29900
Solar cycle variation of ephemeral regions
[AD-A154967] 21 p3723 N85-33097
High Resolution Telescope and Spectrograph (HRTS) 23 p3901 N85-34162
Anomalous low level of cosmic ray intensity decreases observed during 1980
[SH-5.1-15] 23 p4043 N85-35068
Cosmic rays 10Be biennal data and their relationship to aurorae and sunspots
[SH-7.1-1] 23 p4047 N85-35094
Correlation between solar neutrino flux and other solar phenomena 23 p4049 N85-35109
Solar neutrino: Flux, cosmic rays and the 11 year solar cycle
[SH-8.1-7] 23 p4049 N85-35112
Solar neutrinos, solar flares, solar activity cycle and the proton decay
[SH-8.1-8] 23 p4049 N85-35113
Using the information of cosmic rays to predict influence epidemic
[SH-10.1-2] 23 p4053 N85-35134

SUPERALLOYS
U HEAT RESISTANT ALLOYS

SUPERCHARGERS
Ceramic turbochargers: A case study of a near-term application of high-strength ceramics
[DE85-006495] 17 p2975 N85-28379
Future of ceramic turbochargers: Promises and pitfalls
[DE85-006209] 17 p2975 N85-28380

SUPERCHARGING
U SUPERCHARGERS

SUPERCOMPUTERS
NT CRAY COMPUTERS
Supercomputers and VLSI: The effect of large scale integration on computer architecture
[AD-A145406] 02 p0239 N85-11555
Gauge Theory on a Lattice, 1984: Proceedings
[DE84-014856] 02 p0291 N85-11892
Development of the NLTSS operating system
[DE84-013702] 05 p0714 N85-14576
Vector computer memory bank contention
[NASA-CR-177342] 09 p1376 N85-18649
Computational plasma physics and supercomputers
[DE85-001739] 09 p1393 N85-18766
Developments in the simulation of compressible inviscid and viscous flow on supercomputers
[NASA-TM-86674] 11 p1575 N85-19924
Bottleneckology: Evaluating supercomputers
[DE85-005574] 13 p2145 N85-23315
Very large least squares problems and supercomputers
[AD-A151270] 15 p2623 N85-26162
Supercomputers and symbolic computation
[AD-A151376] 15 p2623 N85-26166
Role of supercomputers in energy research programs
[DE85-006865] 15 p2624 N85-26172
BLAS (Basic Linear Algebra Subroutines), linear algebra modules and supercomputers
[AD-A151504] 15 p2628 N85-26199
Lattice overview
[DE85-007282] 15 p2662 N85-26427
Recent advances in supercomputers 16 p2693 N85-26625
Computational plasma physics and supercomputers, revision 1
[DE85-007228] 16 p2867 N85-27687
France's use of Cray 1, plans for national supercomputer 18 p3086 N85-29093
Proceedings of the Argonne Workshop on Programming the Next Generation of Supercomputers
[DE85-008348] 19 p3343 N85-30718
The NAS kernel benchmark program
[NASA-TM-86711] 21 p3670 N85-32795
The impact of supercomputers on experimentation: A view from a national laboratory
[NASA-TM-86822] 23 p3955 N85-34510
Vector calculation of particle code 23 p3981 N85-34688

SUPERCONDUCTING MAGNETS
Materials studies for magnetic fusion energy applications at low temperatures, 7
[DE84-013487] 01 p0122 N85-10837
Superconducting magnet for probing eddy currents in dynamic models 04 p0489 N85-13117

Two-rotor alternators with superconductor field winding 06 p0795 N85-15082

High-performance TF coil design for the Toroidal Fusion Core Experiment (TFCX) [DE85-001127] 08 p1159 N85-17315

Design and operating experience of an ac-dc power converter for a superconducting magnetic energy storage unit [DE84-014041] 09 p1316 N85-18275

Fracture toughness of austenitic stainless steel weld metal at 4 K [DE84-016638] 09 p1340 N85-18425

Computer simulation of multiple stability regions in an internally cooled superconducting conductor and of helium replenishment in a bath-cooled conductor [DE85-002112] 09 p1399 N85-18805

Experience highlights from the design and manufacture of US LCT coils [DE84-017504] 10 p1482 N85-19354

Application of NbN films to the development of very high field superconducting magnets [DE85-002729] 10 p1565 N85-19867

Magnetic heat pump feasibility assessment [DE85-002806] 11 p1632 N85-20276

Development of high field Nb-Ti accelerator dipoles [DE85-000621] 11 p1714 N85-20782

Crossing point conditions, quadrupole gradients and drift space lengths [DE85-003223] 11 p1721 N85-20825

Stability of superconducting composites in a magnetic field [DE85-002731] 11 p1734 N85-20907

In-beam tests of an air-core superconducting-solenoid particle spectrometer [DE85-004029] 12 p1853 N85-21625

Superconducting magnet technology for accelerators [DE85-004192] 12 p1926 N85-22102

Design considerations for a 100 kW CW, 140 GHz gyrotron oscillator [DE85-005282] 13 p2066 N85-22904

High-field dipoles for future accelerators [DE85-002315] 13 p2157 N85-23391

Special purpose materials for fusion application [DE85-005346] 14 p2424 N85-24950

Stability and vibrations of internal windings of high-current superconducting solenoid magnets [AD-A151465] 15 p2656 N85-26390

Effect of superconducting solenoid model cores on spanwise iron magnet roll control [NASA-TM-86378] 17 p2905 N85-27915

Experience with oepration of a large magnet system in the international fusion superconducting magnet test facility [DE85-009288] 17 p3027 N85-28721

Handbook on superconductivity: The large-scale applications. Chapter 4 [DE85-008170] 17 p3044 N85-28838

Reciprocating magnetic refrigerator employing tandem porous matrices within a reciprocating displacer [NASA-CASE-NPO-16257-1] 18 p3085 N85-29082

Tokamak ignition/burn experimental research device [DE85-009999] 18 p3190 N85-29785

High harmonic rectangular gyrotron 19 p3256 N85-30189

Computer studies of the quench behavior of an SSC model-dipole [DE85-010633] 19 p3360 N85-30829

Design of aggressive superconducting TFCX magnet systems [DE85-010003] 19 p3376 N85-30943

Cryogenics for the Superconducting Super Collider: Workshop Proceedings [DE85-010951] 20 p3437 N85-31327

Superconducting toroidal field coil current densities for the TFCX [DE85-010285] 20 p3530 N85-31959

140 GHz gyrotron development program [DE85-010348] 20 p3537 N85-32013

Design improvements and cost reductions for a 5000 MWh superconducting Magnetic Energy Storage plant [DE85-010572] 22 p3847 N85-33830

Shield design for next-generation, low-neutron-fluence, superconducting tokamaks [DE85-011409] 23 p3982 N85-34695

A high resolution gas Cerenkov detector for the superconducting magnet facility [OG-9.1-6] 23 p4023 N85-34932

Enhanced heat transfer computations for internally cooled cable superconductor [DE85-011897] 24 p4095 N85-35383

Effect of Cu4Ti compound formation on the characteristics of NbTi accelerator magnet wire [DE85-014226] 24 p4159 N85-35788

SUPERCONDUCTING POWER TRANSMISSION

Operational test results of a prototype superconducting power transmission system and their extrapolation to the performance of a large system [DE85-006731] 16 p2779 N85-27153

SUPERCONDUCTING QUANTUM INTERFEROMETERS

U SQUID (DETECTORS)

SUPERCONDUCTIVITY

NT KONDO EFFECT

Considerations regarding the choice of beam parameters and IP configuration for the SSC [DE84-014532] 01 p0118 N85-10803

Low temperature properties of Mo/Mi superlattices [DE84-014729] 02 p0288 N85-11881

Mossbauer effect and contactless conductivity studies of superconducting actinides intermetallics and hydrides. Mossbauer high pressure studies 03 p0430 N85-12743

Formation of superconductive Al(GeSi) alloys by low temperature laser quenching methods [DE84-016667] 04 p0474 N85-13021

Strong-coupling superconductivity of Mg in proximity to Ta [DE84-015462] 04 p0569 N85-13627

Report of the reference designs study group on the superconducting super collider [DE84-015567] 04 p0569 N85-13630

Superconducting NbTi and Pb(Cu) bandpass filters 05 p0623 N85-13986

Phase diagrams of organic superconductors [DE84-016219] 05 p0731 N85-14699

Actinides, the narrowest bands [DE84-016463] 05 p0733 N85-14710

ASC 1984 Applied Superconductivity Conference [DE84-016204] 06 p0866 N85-15521

Fast granular superconducting bolometer [AD-D011332] 07 p0961 N85-16093

Electronic structure, chemical bonding, and superconductivity of silver films on germanium [AD-A147720] 08 p1128 N85-17112

Structure-property relationships in intercalated graphite [AD-A147949] 08 p1219 N85-17680

A superconducting quantum current standard [NPL-QU-67] 08 p1224 N85-17710

The generation of rolling moments with the superconducting solenoid model [NASA-CR-172520] 09 p1283 N85-18068

Status of RF superconductivity at Argonne National Laboratory [DE85-002145] 09 p1312 N85-18245

Operational characteristics of a 1000 MVA superconducting power transmission system [DE85-000232] 09 p1314 N85-18263

Characterization of Nb-8 wt % Al wires by analytical electron microscopy [DE85-002726] 10 p1442 N85-19086

Metrology for Electronic Technology: A bibliography of NBS (National Bureau of Standards) [PB85-112895] 12 p1830 N85-21486

Rotating squid magnetometers and gradiometers [AD-D011529] 12 p1849 N85-21600

The UFe4P12 and CeFe4P12: Non-metallic isotopes of superconducting LaFe4P12 [DE85-003724] 12 p1942 N85-22195

Critical current measurements on an NbTi superconducting wire standard reference material [PB85-118594] 13 p2066 N85-22906

Outlook for realization of proximity effect and Josephson direct current in helium-2 13 p2074 N85-22956

Microstructural study on the processing and properties of high-field A15 superconducting materials [DE85-004652] 13 p2164 N85-23423

Synthesis and characterization of superconducting electronic materials [AD-A151112] 15 p2659 N85-26409

Superconducting traveling wave accelerators [DE85-006247] 15 p2661 N85-26424

Electronic transport in Mo/Ni superlattice [DE85-006835] 15 p2661 N85-26425

The superconducting cavity stability ruby maser oscillator 17 p2967 N85-28324

Handbook on superconductivity: The large-scale applications. Chapter 4 [DE85-008170] 17 p3044 N85-28838

Simultaneous phase and frequency control of a three-phase inductor-convertor bridge [DE85-006197] 18 p3096 N85-29164

Some comments on SSC physics [DE85-008444] 18 p3179 N85-29712

Magnetic impurities in superconductors [DE85-008372] 18 p3196 N85-29825

Magnetoconductance in aluminum films, wires, and cylinders 19 p3374 N85-30928

Critical current density and microstructural state of an internal tin multifilementary superconducting wire [DE85-009966] 22 p3761 N85-33308

Physics Division annual review, 1 April 1983 - 31 March 1984 [ANL-84-24] 23 p3969 N85-34602

Magnitude and range of the RKKy interaction in SmRh4B4 [DE85-012284] 23 p3965 N85-34712

Design considerations for personnel access penetrations for the superconducting super collider [DE85-013027] 24 p4162 N85-35807

SUPERCONDUCTORS

Conversion of microwave signals by superconducting films in the resistive state [NASA-TM-77595] 01 p0123 N85-10843

Experiments with phase transitions at very high pressure [NASA-CR-174029] 02 p0172 N85-11148

Calculation of critical temperature for Nb-Cu multilayer film superconductor [AD-A144321] 02 p0274 N85-11788

Theory of the double critical state in type-2 superconductors [DE84-015461] 02 p0269 N85-11866

Radiation induced defects in superconductors of type 2 03 p0429 N85-12734

ASC 1984 Applied Superconductivity Conference [DE84-016204] 06 p0866 N85-15521

Superconducting rotor dynamics [AD-A147176] 07 p0947 N85-16000

Forces on neutral atoms due to electromagnetic fields [AD-A148984] 07 p1040 N85-16603

Short range order-long range order in superconducting materials [AD-A148764] 08 p1227 N85-17724

Subcable test facility [DE85-002103] 09 p1315 N85-18269

Thermally induced quasiparticle branch imbalance in thin film superconductors 09 p1396 N85-18786

Computer simulation of multiple stability regions in an internally cooled superconducting conductor and of helium replenishment in a bath-cooled conductor [DE85-002112] 09 p1399 N85-18805

Report of the Technology and Test Panel 11 p1646 N85-20370

Stability of superconducting composites in a magnetic field [DE85-002731] 11 p1734 N85-20907

Thin film technology of high-critical-temperature superconducting electronics [AD-A150010] 12 p1940 N85-22185

Measurement of the induced moment magnetic form factor of a heavy fermion superconductor [DE85-004165] 12 p1942 N85-22194

Survey of the state-of-the-art of miniature cryocoolers for superconductive devices [AD-A150319] 13 p2041 N85-22774

Critical current measurements on an NbTi superconducting wire standard reference material [PB85-118594] 13 p2066 N85-22906

Spectral evaluation of irregularity of superconducting coaxial cables 13 p2082 N85-23000

Winding insulation in electromagnetic systems for Tokamak reactor plants 13 p2087 N85-23035

Improvement in magnetic field properties of vanadium-gallium superconductors by enhancement of spin-orbit scattering [DE85-002893] 13 p2164 N85-23422

Tunneling in magnetic superconducting systems [AD-A150677] 14 p2426 N85-24963

High field RF superconductivity: To pulse or not to pulse [DE85-004381] 14 p2429 N85-24977

Superconducting gyroscope research [NASA-CR-171406] 15 p2560 N85-25795

Stability and vibrations of internal windings of high-current superconducting solenoid magnets [AD-A151465] 15 p2656 N85-26390

Synthesis and characterization of superconducting electronic materials [AD-A151112] 15 p2659 N85-26409

Approximate closed-form expression for the electron-scattering-induced interaction between magnetic flux lines and grain boundaries [DE85-004699] 15 p2660 N85-26417

Research on design of cryotransformers and its prospects for the future [AD-A152400] 17 p2952 N85-28230

Research on superconductive signal-processing devices [AD-A152703] 17 p2953 N85-28235

Measuring structure functions at SSC energies [DE85-007515] 17 p3031 N85-28746

Operation of HFTF to test the MIT 12 T coil [DE85-010409] 18 p3195 N85-29821

Magnetic impurities in superconductors
[DE85-008372] 18 p3196 N85-29825
Superconducting electronic film structures
[AD-A154196] 19 p3259 N85-30207
Flux pinning and flux flow studies in superconductors using flux flow noise techniques
[DE85-010814] 19 p3376 N85-30945
Detector problems at the SSC
[DE85-010217] 21 p3703 N85-33007
Cryogenic system for the University of Washington Superconducting Booster
[DE85-010604] 22 p3754 N85-33274
Magnetic shielding with superconductors based on niobium-tin compounds 22 p3771 N85-33370
Magnitude and range of the RKKy interaction in SmRh4B4
[DE85-012284] 23 p3985 N85-34712
Flux-line lattice anisotropy in V3Si: Observation and interpretation
[DE85-011935] 23 p3985 N85-34713
Center for Electronics and Electrical Engineering technical progress bulletin covering center programs, July-September with 1985 CEEE events calendar
[PB85-191393] 24 p4091 N85-35383
SUPERCOOLING
NT CRYOGENIC COOLING
Rapid solidification processing and the control of structure/property relationships
02 p0176 N85-11178
Frazil ice formation
[AD-A147425] 07 p0988 N85-16279
Alloy supercooling on Salyut-7
11 p1604 N85-20083
The nucleation of ice crystals during the freezing of large supercooled drops 21 p3640 N85-32806
SUPERCRITICAL AIRFOILS
NT SUPERCRITICAL WINGS
Effect of upstream sidewall boundary layer removal on an airfoil test — conducted in Langley 0.3-m transonic cryogenic tunnel 03 p0313 N85-12019
Steady- and unsteady-pressure measurements on a supercritical-wing model with oscillating control surfaces at subsonic and transonic speeds
[NASA-TM-84543] 08 p1077 N85-16831
Investigation to optimize the passive shock wave/boundary layer control for supercritical airfoil drag reduction
[NASA-CR-175788] 16 p2699 N85-26665
High Reynolds number tests of a NASA SC(3)-0712(B) airfoil in the Langley 0.3-meter transonic cryogenic tunnel
[NASA-TM-86371] 19 p3213 N85-29926
Pressure distribution from high Reynolds number tests of a NASA SC(3)-0712(B) airfoil in the Langley 0.3-meter transonic cryogenic tunnel
[NASA-TM-86370] 19 p3213 N85-29927
Data set 9: LANN wing. Pitching oscillation
20 p3390 N85-31030
SUPERCRITICAL FLOW
Performance of two transonic airfoil wind tunnels utilizing limited ventilation 03 p0313 N85-12020
Joined wing transonic design and test validation
[AD-A148355] 08 p1078 N85-16834
Supercritical fluid chromatography/supersonic jet spectroscopy
[DE85-003310] 09 p1292 N85-18115
Transport and relaxation processes in supercritical fluids
[DE85-002079] 09 p1398 N85-18797
Transport relaxation processes in supercritical fluids
[DE85-002076] 09 p1398 N85-18798
Nested subcritical flows within supercritical systems
[NASA-TM-86980] 12 p1845 N85-21574
Separating polymer solutions using high pressure LCST Lower Critical Solution Temperature) phenomena
[AD-A151538] 15 p2518 N85-25528
Static and dynamic pressure measurements on a NACA 0012 airfoil in the Ames High Reynolds Number Facility
[NASA-TP-2485] 17 p2891 N85-27823
Methods for design aerodynamics of modern transport aircraft
[DFVLR-FB-85-05] 17 p2893 N85-27838
Transport and relaxation processes in supercritical fluids
[DE85-010554] 19 p3358 N85-30816
SUPERCRITICAL FLUIDS
Transport and relaxation processes in supercritical fluids
[DE84-006591] 05 p0731 N85-14698
Electrochemistry in near-critical and supercritical fluids. I. Ammonia
[AD-A146429] 06 p0765 N85-14894
Transport and relaxation processes in supercritical fluids
[DE85-002079] 09 p1398 N85-18797
Transport relaxation processes in supercritical fluids
[DE85-002076] 09 p1398 N85-18798
Method for growth of crystals by pressure reduction of supercritical or subcritical solution
[NASA-CASE-NPO-15772-1] 18 p3192 N85-29800
Micro-scale methods for characterization of supercritical fluid extraction and fractionation processes
[DE85-010968] 20 p3455 N85-31456
Supercritical fluid chromatography/supersonic jet spectroscopy
[DE85-007005] 22 p3746 N85-33221
SUPERCRITICAL PRESSURES
Transport and relaxation processes in supercritical fluids
[DE84-006591] 05 p0731 N85-14698
Comparison of analytical and experimental steadyand unsteady-pressure distributions at Mach number 0.78 for a high-aspect-ratio supercritical wing model with oscillating control surfaces
[NASA-TM-84589] 07 p0899 N85-15697
Polymer solution-supercritical fluid behavior
[AD-A154514] 21 p3568 N85-32192
SUPERCRITICAL WINGS
Transonic wing and far field test data on a high aspect ratio transport wing for three dimensional computational method evaluation 01 p0004 N85-10021
Experimental trim drag values and flow-field measurements for a wide-body transport model with conventional and supercritical wings
[NASA-TP-2071] 02 p0135 N85-10920
Aileron effectiveness for a subsonic transport model with a high-aspect-ratio supercritical wing
[NASA-TM-85674] 07 p0898 N85-15695
Comparison of analytical and experimental steadyand unsteady-pressure distributions at Mach number 0.78 for a high-aspect-ratio supercritical wing model with oscillating control surfaces
[NASA-TM-84589] 07 0899 N85-15697
Installed nacelle drag-improvement tests of an M = 0.8 turboprop transport configuration
[NASA-TM-84302] 07 p0902 N85-15716
Active and passive shock/boundary layer interaction control on supercritical airfoils 08 p1072 N85-16795
The NYU inverse swept wing code
[NASA-CR-3662] 08 p1077 N85-16830
Transonic steady- and unsteady-pressure measurements on a high-aspect-ratio supercritical-wing model with oscillating control surfaces
[NASA-TM-81888] 09 p1273 N85-18003
Subsonic and transonic pressure measurements on a high-aspect-ratio supercritical-wing model with oscillating control surfaces
[NASA-TM-83201] 09 p1273 N85-18004
Measured unsteady transonic aerodynamic characteristics of an elastic supercritical wing with an oscillating control surface
[NASA-TM-86376] 12 p1771 N85-21116
Unsteady transonic pressure measurements on a semi-span wind-tunnel model of a transport-type supercritical wing (Lann model). Part 2: Pressure distributions (plotted) and plots of the vibration modes
[AD-A130488] 12 p1846 N85-21579
Preliminary development of an approximation procedure for supercritical wing design optimization applications
[AD-A150177] 13 p1972 N85-22383
Transonic pressure distributions on a two-dimensional 0012 and supercritical MBB-A3 profile oscillating in heave and pitch 15 p2457 N85-25173
Analysis of transonic aerodynamic characteristics for a supercritical airfoil oscillating in heave, pitch and with oscillating flap 15 p2458 N85-25175
Experience with transonic unsteady aerodynamic calculations 15 p2458 N85-25176
The development of unsteady transonic 3-D full potential code and its aeroelastic applications
15 p2460 N85-25187
Aerodynamic research in preparation for a new Dutch transport aircraft with supercritical wings
[B8580077] 17 p2893 N85-27836
Analysis of unsteady pressure measurements on a supercritical airfoil with a harmonically oscillating trailing edge flap at subsonic and transonic speeds
[DFVLR-FB-84-49] 17 p2893 N85-27837
Pressure distribution data from tests of 2.29 M (7.5 feet) span EET high-lift transport aircraft model in the Ames 12-foot pressure tunnel
[NASA-TM-84517] 19 p3211 N85-29912
Low-speed tests of a high-aspect-ratio, supercritical-wing transport model equipped with a high-lift flap system in the Langley 4- by 7-meter and Ames 12-foot pressure tunnels
[NASA-TP-2097] 20 p3388 N85-31010
Transonic calculations for a flexible supercritical wing and comparison with experiment
[NASA-TM-86439] 20 p3388 N85-31012
An experimental investigation of propfan installations on an upswept supercritical wing at transonic Mach numbers
[NASA-CR-172605] 20 p3388 N85-31013
Extension of the small perturbations method in three-dimensional transonic, unsteady flow to the case of real wings
[ONERA-NT-17/3064-RY-070-R]
20 p3389 N85-31017
Verification of calculation methods for unsteady airloads in the precipitation of transonic flutter
[NLR-MP-84016-U] 20 p3390 N85-31027
The application of laser anemometry to the study of transonic shock boundary-layer interactions
[ISL-CO-204/84] 20 p3396 N85-31067
Study of boundary layer separation on a supercritical profile with a spoiler by means of a laser Doppler velocimeter
[ISL-CO-225/84] 23 p3895 N85-34128
SUPERFLUID FLOW
U SUPERFLUIDITY
SUPERFLUIDITY
Momentum distributions in superfluid helium: Bose condensate fraction
[DE84-014676] 05 p0731 N85-14700
Thermal and cryogenic design study for space infrared telescope facility (SIRTF)
[NASA-CR-166613] 07 p0915 N85-15793
Critical velocities in He II for independently varied superfluid and normal fluid velocities
09 p1396 N85-18784
Turbulence in pure superfluid flow
09 p1397 N85-18790
Germanium resistance thermometer calibration at superfluid helium temperatures
12 p1947 N85-22228
Outlook for realization of proximity effect and Josephson direct current in helium-2 13 p2074 N85-22956
Entropy of He 2 and universality near the superfluid in He(4) 19 p3378 N85-30957
SUPERGIANT STARS
Outer atmospheres of giant and supergiant stars
[NASA-CR-174165] 04 p0580 N85-13703
Theoretical studies of chromospheres and winds in cool stars
[NASA-CR-174204] 06 p0880 N85-15596
The spectroscopic antics of S 18/SMC
11 p1750 N85-21008
Ultraviolet analysis of the peculiar F supergiant HD 112374 11 p1754 N85-21035
Egress spectra of the new eclipsing supergiant 22 Vulfeculae 11 p1755 N85-21039
Multi-year and possibly periodic variations in the UV spectrum of 58 Pegasi 11 p1756 N85-21046
IUE and optical observations of LMC X-ray binaries
11 p1757 N85-21050
MU Sagittarii and Beta Lyrae: Combined IUE/Voyager observations 11 p1757 N85-21052
A search for the spectroscopic binary companions of Polaris using IUE spectra 11 p1757 N85-21053
Betegeuse at maximum luminosity
11 p1758 N85-21061
SUPERHEATING
An investigation into the superhardening effect in molybdenum-free steel with specific reference to alloy substitution 02 p0180 N85-11209
Anomalies of aluminum structure and properties
13 p2026 N85-22693
Vapor explosions in superheated liquids and fundamental studies of the physics of detonation
[AD-A151362] 15 p2504 N85-25447
Effects of ambient pressure on the instability of a liquid boiling explosively at the superheat limit
[DE85-009476] 23 p3932 N85-34370
SUPERHETERODYNE RECEIVERS
Construction of a superheterodyne receiver for 10 micron waves to be put on a Cassegrain optics telescope for spectroscopic research on the Mars and Venus atmospheres
[MPE-183] 06 p0872 N85-15538
High-frequency input device for superheterodyne radio receiver with wideband preselector
12 p1839 N85-21540
SUPERHIGH FREQUENCIES
Development and testing of a 20-kW X-band transmitter with high phase stability 05 p0623 N85-13985
Electrical consequences of mechanical antenna characteristics 05 p0625 N85-14006
The Finnish approach to microwave remote sensing of snow 05 p0656 N85-14212
Shuttle S-band communications technical concepts
08 p1099 N85-16948
Shuttle ku-band communications/radar technical concepts 08 p1099 N85-16949
Shuttle payload S-band communications system
08 p1100 N85-16950

TDRSS S-shuttle unique receiver equipment
08 p1100 N85-16951

Shuttle S-band high gain switched beam breadboard antennas
[NASA-CR-171852] 10 p1478 N85-19327

Description of amplitude scintillations on a 11 GHz slant path in terms of forward scattering from turbulent layers
[FI-455-TBR-76] 11 p1625 N85-20232

Minimization of system vulnerability in Naval satellite communication networks 11 p1710 N85-20758

Satellite reception of reentry vehicle telemetry
[AD-A151651] 15 p2492 N85-25372

Development and flight test of a helicopter, X-band, portable precision landing system concept
[NASA-TM-86710] 16 p2710 N85-26721

Radar study of the melting layer
[ESA-CR(P)-1974] 17 p2997 N85-28527

Channel multiplexers for broadcast satellite transponders in the 12 GHz band
[NHK-LABS-NOTE-310] 18 p3090 N85-29122

The HURRA, a high resolution experimental radar system broadband receiver
[FOA-C-30375-E1] 18 p3091 N85-29132

Measurement of permittivity and permeability of microwave materials
[AD-D011656] 18 p3176 N85-29688

Design of a shuttle-borne SAR for the DFVLR's planning study
[ERYS-019/84] 20 p3419 N85-31218

Paired ion chamber constants for fission gamma-neutron fields
[AD-A155069] 21 p3702 N85-32999

On total cross sections and slopes at superhigh energies
[HE-1.1-4] 24 p4170 N85-35652

SUPERHYBRID MATERIALS
NT GRAPHITE-EPOXY COMPOSITES

Fabrication and quality assurance processes for superhybrid composite fan blades
[NASA-TM-83354] 06 p0763 N85-14882

SUPERIMPOSITION (MATHEMATICS)
U SUPERPOSITION (MATHEMATICS)

SUPERLATTICES

Low temperature properties of Mo/Mi superlattices
[DE84-014729] 02 p0288 N85-11881

Folded acoustic and quantized optic phonons in semiconductor superlattices
[AD-A145935] 03 p0433 N85-12756

Electron and hole effective masses for two-dimensional transport in strained-layer superlattices
[DE84-016222] 04 p0570 N85-13637

Single crystal semiconductor multilayers for electrically active optical interference filters
[DE84-015614] 04 p0571 N85-13640

Photoluminescence studies of Ga(As,P) strained-layer superlattices
[DE84-015709] 05 p0731 N85-14701

InAsSb strained-layer superlattices (SLSs) for long wavelength detector applications
[DE84-016111] 05 p0732 N85-14706

Theoretical investigation of device aspects of semiconductor superlattices
[AD-A146641] 06 p0867 N85-15509

Strained-layer superlattice emitter and detector structures using modulation-doped active regions
[DE85-000064] 06 p0867 N85-15511

The growth and properties of semiconductor strained-layer superlattices
[DE84-012979] 06 p0868 N85-15515

Silicon superlattices. 2: Si-Ge heterostructures and MOS systems
[NASA-CR-174287] 08 p1224 N85-17711

Ionic and molecular transport in beta- and beta''-alumina
[DE85-000984] 09 p1380 N85-18680

Theory of silicon superlattices: Band structure and mobility enhancement 09 p1396 N85-18789

Semiconductor superlattice photodetectors
[NASA-CR-174347] 09 p1397 N85-18791

Radiation effects in Straind-Layer Superlattice (SLS) structures
[DE85-001713] 09 p1398 N85-18799

Effect of hydrostatic pressure on trapping centers in strained-layer superlattice structures
[DE85-001362] 09 p1399 N85-18807

Ion-implantation doping of strained-layer superlattices
[DE85-001903] 09 p1400 N85-18811

Ion implanted lateral in 2Ga 8As/GaAs strained-layer superlattice photodector
[DE85-001365] 10 p1563 N85-19659

Ferromagnetic resonance in a Ni-Mo superlattice
[DE85-003039] 11 p1735 N85-20911

Electronic structure of silicon superlattices
[NASA-CR-175536] 11 p1736 N85-20916

AlAs/GaAs superlattice barrier unipolar diode structure
[DE85-001904] 11 p1736 N85-20921

Evaluation of implantation-disordering of (InGa)As/GaAs strained-layer superlattices
[DE85-003533] 12 p1942 N85-22200

Ion implantation disorder in strained-layer superlattices
[DE85-004466] 14 p2430 N85-24984

InGaAs/GaAs, Strained-Layer Superlattice (SLS), junction photodetectors, LED's, injection LASER's and FET's for optoelectronic IC applications
[DE85-001940] 14 p2430 N85-24986

Novel materials properties of strained-layer superlattices
[DE85-003676] 14 p2430 N85-24989

Strained-layer superlattices and strain-induced light holes
[DE85-003675] 14 p2431 N85-24990

Models of long-period superstructure
[DE85-007659] 16 p2751 N85-26981

Morphology of GaAs/sub 1-x/P/sub x/ superlattices grown by MOCVD and chloride VPE
[DE85-002944] 17 p3045 N85-28842

Theoretical investigation of material characteristics of semiconductor superlattices
[AD-A154126] 19 p3375 N85-30938

Doping superlattices in organometallic VPE InP
[AD-A155151] 21 p3710 N85-33029

Optical properties of heterostructures and superlattices
[AD-A156243] 24 p4162 N85-35602

SUPERMASSIVE STARS

Radiative ion beams: Hot stellar reactions in the laboratory
[DE85-001570] 11 p1722 N85-20833

SUPERNOVA REMNANTS

Non-local origin of a substantial portion of the soft X-ray background 06 p0877 N85-15567

Modelling the local interstellar medium as a supernova remnant in a multiphase gas 06 p0879 N85-15585

Non equilibrium ionization in the local hot bubble
06 p0879 N85-15587

X-ray spectra of supernova remnants
[NASA-TM-86169] 09 p1413 N85-18909

Combined ultraviolet studies of astronomical sources
[NASA-CR-174361] 09 p1413 N85-18910

Supernova remnants and the carbon abundance in M33 11 p1745 N85-20972

A soft X-ray survey of galactic supernova remnants with the Einstein Observatory 14 p2434 N85-25013

A rocket-borne X-ray observation of SN1006 with the imaging gas scintillation proportional counter
14 p2435 N85-25014

Interstellar Al-26 and excess Mg-26
15 p2680 N85-26551

Self-consistent models for the X-ray emission from supernova remnants 20 p3548 N85-32082

On some problems of gamma-astronomy
[OG-2.7-15] 22 p3873 N85-33988

Local interstellar medium and gamma-ray astronomy
[OG-3.1-1] 22 p3873 N85-33989

Excess gamma rays from the Loop I supernova remnant
[OG-3.1-10] 22 p3874 N85-33998

The electron spectra in the synchrotron nebula of the supernova remnant G 29.7-0.3
[OG-6.2-10] 22 p3889 N85-34109

Cosmic ray secondary nuclei and the structure of the galaxy
[OG-7.2-4] 23 p4014 N85-34876

On the cosmic ray diffusion in a violent interstellar medium
[OG-7.2-14] 23 p4015 N85-34881

Acceleration of cosmic rays in supernova-remnants
[OG-8.1-9] 23 p4018 N85-34899

Onion-shell model for cosmic ray electrons and radio synchrotron emission in supernova remnants
[OG-8.1-10] 23 p4018 N85-34900

Approximate supernova remnant dynamics with cosmic ray production
[OG-8.1-12] 23 p4019 N85-34901

Interstellar (Na-22) as a possible source of the excess (Ne-22) in the galactic cosmic ray
[OG-8.2-12] 23 p4020 N85-34908

The origins of cosmic rays and quantum effects on gravity
[OG-8.2-15] 23 p4020 N85-34911

SUPERNOVAE

A search for low luminosity pulsars and its implications for the pulsar luminosity functions
02 p0296 N85-11919

Supernova envelope shock origin of cosmic rays: A review
[DE84-016479] 04 p0590 N85-13763

Iron core collapse models of Type 2 supernovae
[DE84-013909] 05 p0743 N85-14775

Research in nuclear astrophysics: Stellar collapse and supernovae
[DE84-015559] 05 p0743 N85-14776

Distances of local clouds from optical line observations 06 p0875 N85-15558

A model of the soft X-ray background as a blast wave viewed from inside 06 p0879 N85-15586

Processes and problems in secondary star formation
[DE85-003623] 12 p1960 N85-22322

A program of ground-based astronomy to complement einstein observations
[AD-A151111] 15 p2668 N85-26466

The soft X-ray background as a supernova blast wave viewed from inside: Solar abundance models
[NASA-CR-175767] 16 p2687 N85-27813

Spectral evolution of gamma-rays from adiabatically expanding sources in dense clouds
[OG-2.5-2] 22 p3869 N85-33959

Supernova explosion in dense clouds in the galaxy and the COS-B gamma-ray sources
[OG-2.5-3] 22 p3869 N85-33960

Diffuse galactic annihilation radiation from supernova nucleosynthesis
[OG-3.2-8] 22 p3875 N85-34004

Electrons and positrons from expanding supernova envelopes in dense clouds
[OG-6.2-9] 22 p3889 N85-34108

A very important process of nucleosynthesis in stars
[OG-7.1-11] 23 p4014 N85-34872

A numerical study of diffusive shock acceleration of cosmic rays in supernova shocks
[OG-8.2-2] 23 p4019 N85-34903

Do supernovae of type 1 paly a role in cosmic-ray production?
[OG-8.2-5] 23 p4019 N85-34905

The nucleosynthesis of deterium and helium-3
[OG-8.2-18] 23 p4020 N85-34914

Nuclear reactions in shock wave front during supernova events
[OG-8.2-19] 23 p4021 N85-34915

Propagation of injected cosmic rays under distributed reacceleration
[OG-8.3-3] 23 p4021 N85-34922

Propagation of cosmic rays and new evidence for distributed acceleration
[OG-8.3-5] 23 p4022 N85-34924

SUPEROXIDES
U INORGANIC PEROXIDES

SUPERPLASTICITY

Evaluation of the role of diffusion creep in superplastic deformation 01 p0021 N85-10127

Cavitation phenomenon in superplastic creep
[DE84-015484] 04 p0513 N85-13271

Cavitation phenomenon in superplastic creep
[DE85-001716] 10 p1441 N85-19083

Study of superplastic alloys based on Al-Zn-Ca
10 p1442 N85-19092

MBB uses superplastic forming, diffusion bonding for alloys 11 p1618 N85-20177

Dependence of superplastic flow on state of grain boundaries 13 p2025 N85-22869

Aluminum alloy ATs5K5 (5% Zn + 5% Ca) for superplastic forming 13 p2026 N85-22887

Characteristics and applications of superplastic materials for aeronautics
[MBB-BB-565/84-O] 16 p2873 N85-27727

Precision die forging of blades or gas turbines
17 p2940 N85-28146

Effects of annealing treatments on superplasticity in a thermomechanically processed Aluminum-10.2%Mg-0.52%Mn
[AD-A154414] 19 p3239 N85-30080

The effect of alloy additions on superplasticity in thermomechanically processed high magnesium aluminum-magnesium alloys
[AD-A155142] 21 p3567 N85-32184

SUPERPOSITION (MATHEMATICS)

A limit theorem for the superposition of renewal processes
[CWI-MS-R8408] 05 p0722 N85-14636

Magnetic field calculation for ideal conductors by method of equivalent currents 06 p0788 N85-15035

Mathematical modeling of wave fields by superimposition of boundary waves in reflected earthquake waves method 10 p1501 N85-19476

Normal mode calculations for fuselage type intricate structures by regarding them as systems with superposed constraints 13 p2048 N85-22817

SUPERPRESSURE BALLOONS

Location and data collection for long stratospheric balloon flights 14 p2326 N85-24377

SUPERSATURATION

Chemical engineering principles of constant temperature-constant supersaturation growth of potassium dihydrogen phosphate (KDP) crystals
[DE84-017081] 04 p0571 N85-13645

Use of principle of local equilibrium for assessing diffusional supersaturation during solidification of alloys
[BLL-BISI-TRANS-22487-(9022.06)]
17 p2929 N85-28077

Experimental investigation of properties of ice-forming reagents 21 p3639 N85-32602

The effect of supersaturation, temperature and particle size on ice-nucleating ability of atmospheric aerosol
21 p3639 N85-32604

On the efficiency of the mechanism of ice particles formation in the vapor supersaturation field around a freezing droplet 21 p3639 N85-32606

Supersaturation spect A of Ice Nuclei at different locations in Europe and over the North-Atlantic
21 p3640 N85-32615

Supersaturation obtained in a condensation nucleus counter 21 p3642 N85-32624

Analysis of performance of dynamic thermal diffusion chamber 21 p3642 N85-32625

Critical supersaturations with respect to water for fast condensation-freezing ice nucleation
21 p3643 N85-32632

A simple model to investigate the activation process in waterclouds 21 p3649 N85-32675

Measurements of the critical supersaturation of 0.029 to 0.035 micron radius particles at Washington, District of Columbia 21 p3649 N85-32676

A relationship between cloud droplet size and CCN critical supersaturation 21 p3649 N85-32677

Fog activation and supersaturation
21 p3650 N85-32678

SUPERSONIC AIRCRAFT
NT B-70 AIRCRAFT
NT CONCORDE AIRCRAFT
NT F-8 AIRCRAFT
NT F-14 AIRCRAFT
NT F-15 AIRCRAFT
NT F-16 AIRCRAFT
NT F-17 AIRCRAFT
NT F-104 AIRCRAFT
NT F-106 AIRCRAFT
NT F-111 AIRCRAFT
NT JAGUAR AIRCRAFT
NT MIG AIRCRAFT
NT MIRAGE AIRCRAFT
NT MIRAGE 3 AIRCRAFT
NT RF-4 AIRCRAFT
NT SUPERSONIC TRANSPORTS
NT X-15 AIRCRAFT

An engine trade study for a supersonic STOVL fighter-attack aircraft, volume 1
[NASA-CR-166304] 02 p0133 N85-10910

F-7 supersonic day fighter viewed — Jian-7 aircraft
06 p0747 N85-14791

A-5 supersonic attack aircraft described — Qiang-5 aircraft 06 p0747 N85-14792

Details of export A-5 close-support aircraft given --- Qiang-5 aircraft 06 p0748 N85-14793

Preliminary performance of a vertical-attitude takeoff and landing, supersonic cruise aircraft concept having thrust vectoring integrated into the flight control system
[NASA-CR-172530] 10 p1423 N85-18977

Details of export A-5 close-support aircraft given
10 p1424 N85-18983

Some aspects of the design of a fly-by-wire flying control system for a supersonic V/STOL fighter aircraft
[COLL-AERON-8413] 12 p1780 N85-21175

Study of an efficient long-range Mach 2.7 supersonic transport configuration concept
[NASA-TM-86414] 21 p3554 N85-32110

SUPERSONIC AIRFOILS

Experimental and theoretical study of the longitudinal aerodynamic characteristics of delta and double-delta wings at Mach numbers of 1.60, 1.90, and 2.16
[NASA-TP-2433] 19 p3213 N85-29922

Effect of leading-edge load constraints on the design and performance of supersonic wings
[NASA-TP-2446] 19 p3213 N85-29923

A theory of quasi-conical solutions of noninteger degree — flow fields on supersonic wings
[UTH-LR-420] 20 p3390 N85-31024

SUPERSONIC BOUNDARY LAYERS

Development of artificially produced perturbations in supersonic boundary layer 21 p3683 N85-32879

SUPERSONIC COMBUSTION RAMJET ENGINES

Ramjets with supersonic combustion
07 p0918 N85-15817

Computational analysis of scramjet dual mode operation
[NASA-CR-174250] 07 p0956 N85-16060

Langley Mach 4 scramjet test facility
[NASA-TM-86277] 08 p1089 N85-16883

Investigation of parabolic computational techniques for internal high-speed viscous flows
[NASA-CR-172555] 13 p2091 N85-23056

SUPERSONIC CRUISE AIRCRAFT RESEARCH

Supersonic cruise technology
[NASA-SP-472] 18 p3057 N85-28912

Application of an aerodynamic analysis method including attainable thrust estimates to low speed leading-edge flap design for supersonic cruise vehicles
[NASA-CR-165843] 19 p3212 N85-29918

SUPERSONIC DIFFUSERS

The role of convective perturbations in supercritical inlet oscillations 13 p2004 N85-22563

SUPERSONIC FLIGHT

Selection of air intake parameters for supersonic-flow operation 13 p2051 N85-22837

Supersonic cruise technology
[NASA-SP-472] 18 p3057 N85-28912

China has developed a new version of fighter aircraft
[AD-A155293] 21 p3555 N85-32118

SUPERSONIC FLOW

Implementation of the supersonic triplet singularity into the USTORE computer code
[CSIR-NIAST-83/47] 01 p0001 N85-10006

PAN AIR: A computer program for predicting subsonic or supersonic linear potential flows about arbitrary configurations using a higher order panel method. Volume 3: Case manual (version 1.0)
[NASA-CR-3253] 02 p0135 N85-10922

Study of the structure of turbulent shear flows at supersonic speeds and high Reynolds number
[NASA-CR-174144] 04 p0452 N85-12865

Wall adaptation at Mach 1.2 — wind tunnel tests
[ONERA-RTS-26/3075-AY-402]
04 p0453 N85-12873

Friction and heat exchange in laminar and turbulent boundary layers with axisymmetrical bodies exposed to heterogeneous supersonic flow
05 p0724 N85-14655

Numerical method for computing supersonic flow over wings of flight vehicles 05 p0725 N85-14659

Supersonic nonlinear potential analysis
[NASA-CR-172456] 07 p0897 N85-15685

An investigation of vortex-induced aerodynamic characteristics of supersonic cruise configurations
[NASA-CR-174299] 07 p0898 N85-15690

A second-order accurate parabolized Navier-Stokes algorithm for internal flows
[NASA-CR-174258] 07 p0956 N85-16059

Recent advances in computational methods to solve the high-lift multi-component airfoil problem
08 p1066 N85-16774

First derivatives of flow quantities behind two-dimensional, nonuniform supersonic flow over a convex corner
[NASA-TM-86272] 08 p1077 N85-16828

Basic instability mechanisms in chemically reacting subsonic and supersonic flows
[AD-A148406] 08 p1122 N85-17071

A numerical study of several supersonic flows
09 p1272 N85-17995

A first-order Green's function approach to supersonic oscillatory flow: A mixed analytic and numeric treatment
[NASA-CR-172207] 09 p1273 N85-18002

Microwave discharge in a supersonic flow for the excitation of a gas dynamic CO laser
[ESA-TT-833] 09 p1326 N85-18337

A shock wave capability for the improved Two-Dimensional Kinetics (TDK) computer program
[NASA-CR-171302] 10 p1483 N85-19360

Comparison of two-dimensional laser and hot-wire velocimetry for a supersonic turbulent boundary layer
11 p1576 N85-19927

LOVEL-84: A LOw-VELocity aerodynamic heating code for flat plates, wedges, and cones
[DE85-002604] 11 p1576 N85-19933

Characteristics of flow of oscillatory-relaxing gas in nozzles with constant cross-sections in throat region
11 p1716 N85-20794

Determination of the drag of free flying particles in supersonic flow with a pulsed laser
12 p1773 N85-21129

The split-coefficient matrix method for supersonic three dimensional flow 12 p1821 N85-21425

Investigation of parabolic computational techniques for internal high-speed viscous flows
[NASA-CR-172555] 13 p2091 N85-23056

Spectral methods for modeling supersonic chemically reacting flow fields
[NASA-CR-172578] 14 p2300 N85-24240

Developement of a theoretical model to describe the interaction between electric discharge and supersonic flow of a pulsed CO laser
[DFVLR-FB-84-45] 14 p2310 N85-24301

A semi-empirical unsteady transonic method with supersonic free stream 15 p2458 N85-25179

A computer program to calculate the supersonic flow over a solid cone in air or water
[AD-A151102] 15 p2484 N85-25217

Numerical calculation of subsonic jets in crossflow with reduced numerical diffusion
[NASA-TM-87003] 15 p2472 N85-25263

Characteristics of heat exchange in the region of injection into a supersonic high-temperature flow
[NASA-TM-77833] 15 p2555 N85-25762

An experimental and analytical study of the aerodynamic interference effects between two Sears-Haack bodies at Mach 2.7
[NASA-TM-85729] 16 p2700 N85-26673

Measurements of the symmetric aerodynamic coefficients for flat faced cylinders in the angle of attack regime 0 to 90 deg for transonic and supersonic speeds
[FFA-TN-1984-04] 16 p2700 N85-26675

Supersonic flow around blunt wedge
17 p2942 N85-28158

Experimental and theoretical study of the longitudinal aerodynamic characteristics of delta and double-delta wings at Mach numbers of 1.60, 1.90, and 2.16
[NASA-TP-2433] 19 p3213 N85-29922

Effect of leading-edge load constraints on the design and performance of supersonic wings
[NASA-TP-2446] 19 p3213 N85-29923

A first-order time-domain Green's function approach to supersonic unsteady flow
[NASA-CR-172208] 19 p3214 N85-29930

A theory of quasi-conical solutions of noninteger degree — flow fields on supersonic wings
[UTH-LR-420] 20 p3390 N85-31024

A supersonic potential gradient method for the calculation of unsteady aerodynamic pressures on harmonically oscillating wings
[DFVLR-FB-85-11] 20 p3390 N85-31026

Requirements for attaining Treanor's distribution of vibrational energy among CO2 levels in CW gasdynamic laser flows
[STN-3] 20 p3461 N85-31499

Use of a hyperbolic grid generation scheme in simulating supersonic viscous flow about three-dimensional winged configuration
[NASA-TM-85344] 23 p3893 N85-34116

Instabilities in decelerating supersonic flows with applications to cosmic ray shocks
[OG-8.1-2] 23 p4017 N85-34892

Finite analytic solutions of supersonic flows in two-dimensional non-symmetrical channels
24 p4059 N85-35154

Unsteady flow in a supersonic cascade with two in-passage shocks
[NASA-CR-3925] 24 p4060 N85-35158

Supersonic flow with feeding of energy
[NASA-TM-77912] 24 p4061 N85-35163

Deceleration of a supersonic flow behind a curved shock wave with isentropic precompression
[NASA-TM-77920] 24 p4061 N85-35164

SUPERSONIC FLOW INLETS
U SUPERSONIC INLETS

SUPERSONIC FLUTTER

A comparison of measured and predicted unsteady pressure on a fan blade in unstalled supersonic flutter
[PNR-90223] 08 p1079 N85-16839

SUPERSONIC INLETS

An inviscid computational method for supersonic inlets
[AD-A145997] 03 p0316 N85-12042

A mixed finite difference analysis of the internal and external transonic flow fields of inlets with centerbody
11 p1619 N85-20192

SUPERSONIC JET FLOW

Density distribution in supersonic jet discharged into vacuum from nozzle with bevel tip
02 p0269 N85-11757

Aeroacoustic data for high Reynolds number supersonic axisymmetric jets
[NASA-TM-86296] 07 p1038 N85-16587

Supercritical fluid chromatography/supersonic jet spectroscopy
[DE85-003310] 09 p1292 N85-18115

Parametric study of autooscillation upon flow of supersonic jet into cylindrical cavity
16 p2765 N85-27060

SUPERSONIC NOZZLES

Calculation of an unsteady transonic flow with shock waves and separation in Laval nozzles
[MPIS-14/1984] 14 p2213 N85-23728

An experimental study of clustered, two-dimensional rocket nozzles
[AD-A151889] 15 p2495 N85-25390

Impact starting of plane nozzles with wide divergence angle 17 p2941 N85-28156

SUPERSONIC SPEEDS

Observations from varying the lift and drag inputs to a noise prediction method for supersonic helical tip speed propellers
[NASA-TM-83797] 01 p0115 N85-10788

best copy available

Supersonic Tactical Missile (STM) radome development
[AD-P004360] 12 p1825 N85-21454
Supersonic aerodynamic characteristics of canard, tailless, and aft-tail configurations for 2 wing planforms
[NASA-TP-2434] 17 p2891 N85-27822
Supersonic cruise technology
[NASA-SP-472] 18 p3057 N85-28912
Lee-side flow over delta wings at supersonic speeds
[NASA-TP-2430] 19 p3212 N85-29921
Two approaches for the prediction of plume-induced separation
[AD-A154098] 19 p3215 N85-29935

SUPERSONIC TEST APPARATUS
Analysis of heat-transfer measurements from 2 AEDC wind tunnels on the Shuttle external tank
[NASA-CR-171470] 17 p2957 N85-28263

SUPERSONIC TRANSPORTS
NT CONCORDE AIRCRAFT
Effects of leading-edge devices on the low-speed aerodynamic characteristics of a highly-swept arrow-wing
[NASA-CR-172531] 13 p1968 N85-22365
Supersonic cruise technology
[NASA-SP-472] 18 p3057 N85-28912
Study of an efficient long-range Mach 2.7 supersonic transport configuration concept
[NASA-TM-86414] 21 p3554 N85-32110

SUPERSONIC WAKES
Wakes and differential charging of large bodies in low Earth orbit 13 p1992 N85-22488
Periodic vortex shedding in the supersonic wake of a planar plate
[NASA-TM-77854] 15 p2483 N85-25207

SUPERSONIC WIND TUNNELS
Investigation of light source and scattering medium related to vapor-screen flow visualization in a supersonic wind tunnel
[NASA-TM-86290] 06 p0810 N85-15144
The S2MA wind tunnel at the Modane-Avrieux aerodynamic test center
[ESA-TT-862] 09 p1284 N85-18071
Aeronautical facilities catalogue. Volume 1: Wind tunnels
[NASA-RP-1132] 10 p1426 N85-18891
Transonic and supersonic wind tunnel tests on control effectiveness on schematic missile configurations
[FFA-TN-1983-20] 20 p3389 N85-31020
Transonic and supersonic wind tunnel tests on control effectiveness on schematic missile configurations: Supplement
[FFA-TN-1983-20-SUPPL] 20 p3389 N85-31021
Supersonic flow with feeding of energy
[NASA-TM-77912] 24 p4061 N85-35163

SUPERSONICS
Supersonic cruise technology
[NASA-SP-472] 18 p3057 N85-28912

SUPINE POSITION
Effect of body position and immobilization on intensity of spatial illusions in weightlessness
22 p3821 N85-33672
Investigation of spectrum of human bile acids during 120-day antiorthostatic hypokinesia
22 p3821 N85-33674
Vascular mechanisms of adaptation to antiorthostatic position 22 p3822 N85-33675
Cerebral hemodynamics and ventricular function in -15 deg antiorthostatic position 22 p3822 N85-33676
Effect of short-term antiorthostatic hypokinesia on dynamics of cardiorespiratory parameters during graded physical exercise 22 p3822 N85-33677
Investigation of some aspects of amino acid metabolism in man during brief exposure to antiorthostatic hypokinesia combined with ultraviolet radiation
22 p3822 N85-33678

SUPPLEMENTS
NASA Thesaurus supplement: A 3-part cumulative supplement to the 1982 edition of the NASA Thesaurus
[NASA-SP-7051(SUPPL-2)] 03 p0437 N85-12785

SUPPLYING
Chronic fuel shortages in Volga civil aviation administration 15 p2461 N85-25198

SUPPORT SYSTEMS
NT CLOSED ECOLOGICAL SYSTEMS
NT EMERGENCY LIFE SUSTAINING SYSTEMS
NT GROUND SUPPORT SYSTEMS
NT LIFE SUPPORT SYSTEMS
Air Force Human Resources Laboratory report: Fiscal year, 1983
[AD-A145647] 02 p0238 N85-11548
Constraint-based scheduling in an intelligent logistics support system: An artificial intelligence approach
[AD-A145613] 02 p0293 N85-11900
The human role in space. Volume 2: Research analysis and technology report
[NASA-CR-171224] 04 p0546 N85-13474
UH-60A external stores support system fixed provision fairings drag determination
[AD-A147168] 07 p0902 N85-15719
Acquisition planning at the Defense Communications Agency
[AD-A146877] 07 p1051 N85-16669
Lateral support system for canister-launched missile
[AD-D011369] 08 p1106 N85-16967
Close air support mission: Development of a unitary measure of pilot performance
[AD-A149285] 11 p1697 N85-20665
JESS facility modification and environmental/power plans
[NASA-CR-175665] 14 p2227 N85-23607
The development of a programming support system for rapid prototyping. Tasks 2 and 3
[AD-A151549] 15 p2629 N85-26202
Logical design of a decision support system to forecast technology, prices and costs for the national communications system
[AD-A152330] 17 p2948 N85-28198

SUPPORTS
NT PYLONS
Small Payload Flight Systems (SPFS)
02 p0152 N85-11030
The evolution of small payload carrier systems
02 p0153 N85-11038
Heavy duty precision pan and tilt head
[AD-A146669] 04 p0509 N85-13246
Dynamic testing of NOVA laser switchyard tower
[DE84-014450] 05 p0640 N85-14103
Thermally isolated structural support link
[AD-D011349] 07 p0972 N85-16176
Flexible line support assembly
[AD-D011391] 07 p0972 N85-16177
High efficiency electron beam gun foil support
[AD-D011434] 08 p1159 N85-17312
Two-dimensional shock response of a mass on energy-absorbing shock mounts
09 p1334 N85-18389
Optimum design for nonlinear shock mounts for transient inputs 09 p1334 N85-18390
Gear case vibration isolation in a geared turbine generator 09 p1338 N85-18414
Hydrostatic bearing pad maximum load and overturning conditions for the 70-meter antenna
10 p1465 N85-19241
Precise bearing support ditherer
[AD-D011470] 10 p1493 N85-19428
Remote pivot decoupler pylon: Wing/store suppression
[NASA-CASE-LAR-13173-1] 11 p1584 N85-19981
Portable pallet weighing apparatus
[NASA-CASE-GSC-12789-1] 11 p1635 N85-20294
Support structures for optical components in the Laser Demonstration Facility
[DE85-008879] 17 p2971 N85-28349
Production of thin-walled electricity welded tubes with reduced internal flash
[BLL-BISI-TRANS-22381-(9022.06)]
17 p2973 N85-28364
Buckling and bracing of cantilevers
[CE-42] 17 p2979 N85-28413
Low-profile fastener
[AD-D011667] 19 p3280 N85-30343
Seismic pipe support construction practices
[DE85-901315] 19 p3287 N85-30386
Properties of Ti-6Al-4V spun formed fuze supports
[DE85-011968] 22 p3792 N85-33498
STACBEAM 2
[NASA-CR-176126] 23 p3944 N85-34442

SUPPRESSION
U RETARDING

SUPPRESSORS
NT ECHO SUPPRESSORS
Isolated load switching with surge suppression
[AD-D011218] 01 p0042 N85-10274
Reverse wave suppression in unstable ring resonator
[AD-A146825] 07 p0939 N85-15952
Development of a 30 GHz/1 kW broadband traveling wave tube with suppression of band edge oscillations
[BMFT-FB-W-84-035] 07 p0948 N85-16011
The ac power line protection for an IEEE 587 Class B environment 07 p1000 N85-16347
Improved operation of transversely exited N2O lasers
[AD-D011488] 10 p1400 N85-19409
Measurements of distributed combustion
13 p2001 N85-22542
Distributed combustion: A mechanism of acoustic suppression 13 p2001 N85-22543
The design and operation of a simple low-speed flutter-suppression model
[AD-A151610] 15 p2474 N85-25269
Suppression of vibration effects on piezoelectric crystal resonators
[AD-D011625] 16 p2778 N85-27142

SURFACE ACOUSTIC WAVE DEVICES
Conductor structure for thick film electrical device
[AD-D011240] 01 p0043 N85-10281
Radio frequency probing apparatus for surface acoustic wave devices
[AD-D011230] 01 p0050 N85-10327
Multiple passband transducers for tone selection from a frequency comb generator
[RSRE-MEMO-3647] 02 p0194 N85-11296
Laser excitation of coupled surface electromagnetic and acoustic waves and of static structures in solids
05 p0723 N85-14652
Dutch institutes do research in tactile visual robot sensors 09 p1310 N85-18228
Compensation of skew passband of a SAW filter using predistortion 12 p1821 N85-21422
Improvement of VHF(MB) model
[AD-A150087] 12 p1829 N85-21480
SAW oscillator with digital compensation for the temperature related frequency changes
[AD-D011537] 12 p1833 N85-21500
Monolithic thin film SAW (Surface Acoustic Wave) structures
[AD-A149782] 12 p1835 N85-21511
Optimal synthesis of surface acoustic wave filters
13 p2070 N85-22933
Analysis and optimization of parameters of fanned surface acoustic wave transducers
13 p2070 N85-22934
Experimental study of high-stability oscillator with surface-acoustic-wave resonator in feedback loop
13 p2090 N85-23053
Optical processing in radon space
[AD-A150289] 13 p2159 N85-23402
Surface acoustic wave structure and volume waves
15 p2525 N85-25568
System of phase-lock automatic frequency control with acoustoelectronic convolver 15 p2526 N85-25573
Development of a Digitally Compensated SAW Oscillator (DCSO) to provide temperature stable frequency
[AD-A151907] 15 p2549 N85-25730
Compensation of acoustic wave devices
[AD-D011582] 15 p2646 N85-26322
Vapor sensing by means of a ZnO-on-Si surface acoustic wave resonator
[DE85-003250] 15 p2646 N85-26324
Research and development of subsurface acoustic wave devices for sensor applications
[AD-A152197] 16 p2861 N85-27642
Derated application of parts for (Electronic Systems Division) systems development. Revision
[AD-A153299] 17 p2955 N85-28248
Passivation on high Q acoustic strain sensor for accelerometer
[AD-A153565] 18 p3177 N85-29695
Surface acoustic wave devices as chemical vapor microsensors
[AD-A153752] 18 p3177 N85-29698
Investigation of fast reaction SAW (Surface Acoustic Wave) accelerometer
[AD-A153876] 19 p3216 N85-29943
Gas sensing with surface acoustic wave devices
[DE85-009125] 20 p3524 N85-31921
Microwave SAW (Surface Acoustic Wave) monochromator
[AD-D011718] 21 p3590 N85-32311

SURFACE COOLING
Picosecond laser pulse interactions with metallic and semiconductor surfaces
[AD-A149112] 10 p1490 N85-19405
Unsteady heat transfer due to time-dependent free stream velocity 17 p2911 N85-27947

SURFACE CRACKS
Detection of cracks in a plastics pipe joint by reflection holography
[NPL-DMA(A)-87/MOM-70] 04 p0502 N85-13202
Behavior of pressurized tubes of candidate alloys in a simulated low-Btu environment
[DE85-003403] 09 p1296 N85-18141
Development of surface cracks in AMg6 alloy under low-cycle loading conditions 10 p1442 N85-19089
Evaluation of machining damage in brittle materials
[DE85-001794] 11 p1612 N85-20136
Modifications of flight by flight load sequences to provide for good fracture surface readability
14 p2319 N85-24330
On the use of marker loads and replicas for measuring growth rates for small cracks 14 p2319 N85-24331
On Rayleigh waves and Rayleigh wave extension of surface micro-cracks 15 p2572 N85-25860
Accuracy of the calculated stress field around a crack
[DE85-005520] 16 p2801 N85-27272

Field theory analysis using the finite element method to determine the deliberation curves of three dimensional fracture mechanics specimens with a semicircular surface crack applying the electrical direct current potential method for crack depth measurement
[GKSS-84-E-53] 17 p2982 N85-28434

SURFACE DEFECTS
Exploratory development of advanced surface flaw detection methods
[AD-A148757] 09 p1281 N85-18060
Low power microprocessor based measurements system for determining the integrity of coatings on buried pipelines
[ERS-E.380] 09 p1324 N85-18323
Defect tolerance in pipeline girth welds
[ERS-E.353] 09 p1328 N85-18347
GaAlAs Sb APD optimization
[AD-A149406] 10 p1480 N85-19344
Study of metal oxide semiconductor structures by capacitive transient spectroscopy
[ENST-84E011] 11 p1737 N85-20926
Correlation of uniaxial and biaxial fracture strengths of ceramics
[DE85-003779] 14 p2261 N85-24011
Practical surface methods 14 p2316 N85-24314
Study on mechanism of surface deformation induced by stress corrosion cracking
[BLL-BISI-TRANS-21896-(9022.06)] 17 p2928 N85-28066
On the variation of the stress intensity factor along the front of a surface flaw
[OUEL-1565/85] 20 p3471 N85-31568
Surface passivation and junction formation using low energy hydrogen implants 20 p3480 N85-31628
Redefining the scratch standards
[PB85-194736] 24 p4154 N85-35755

SURFACE DIFFUSION
Surface diffusion of high temperature vapors in porous alumina
[DE84-015968] 04 p0479 N85-13053
Technique for measuring surface diffusion by laser-beam-localized surface photochemistry
[DE85-007885] 18 p3113 N85-29273
Micro-reactions of metal contacts on various types of GaAs surfaces
[AD-A153650] 18 p3193 N85-29806
The use of the glistening surface concept in rough surface scattering
[AD-A154922] 21 p3575 N85-32234
An analysis of physical optics models for rough surface scattering
[AD-A154960] 21 p3575 N85-32235
Mean flow and turbulence in complex terrain
[AD-A155138] 21 p3636 N85-32583

SURFACE DISTORTION
An optimization study to minimize surface distortions of a hoop-column antenna 14 p2232 N85-23837
Electromagnetic analysis for surface tolerance effects on large space antennas 14 p2234 N85-23850
Lidar ER2 (ozone). Crystal characterization for harmonic conversion — laser systems
[CERT-2/6129-00] 16 p2872 N85-27717
Moving random surfaces and correlation analysis
[CRC-1384] 19 p3253 N85-30168

SURFACE EFFECT SHIPS
Detection, classification, and extraction of helicopter-radiated noise
[AD-A145993] 03 p0416 N85-12661
Analysis of head motion during simulated, rough water operation of a 2200 ton surface effect ship
11 p1695 N85-20656
Seakeeping and vibration tests of the Coast Guard 110 foot surface effect ship SEA BIRD class (WSES)
[AD-A154150] 19 p3252 N85-30166

SURFACE ENERGY
Numerical simulations of fuel droplet flows using a Lagrangian triangular mesh
[AD-A146087] 03 p0362 N85-12320
The chemical nature of the fiber/resin interface in composite materials 04 p0465 N85-12953
Effects of high energy radiation on the mechanical properties of epoxy-graphite fiber reinforced composites
[NASA-CR-174314] 08 p1118 N85-17047
Measurements of the surface energy budget in the southern Gobi Desert of China, and in the Rocky Mountains of Colorado
[NASA-CR-175506] 12 p1888 N85-21847
Fluorinated polyesters
[AD-D011611] 16 p2753 N85-26988
Fracture toughness of MgCr(sub)2O(sub)4-ZrO(sub)2
[DE85-007945] 17 p2917 N85-27982
New adatom model for Si(11) 7X7 and Si(111)Ge 5X5 reconstructed surfaces 20 p3480 N85-31625
Effect of precipitation variables on the specific surface and explosion characteristics of pentaerythritol tetranitrate
[DE85-009620] 23 p3922 N85-34302

SURFACE FINISHING
Electro-spark case-hardening of contoured surfaces
01 p0035 N85-10216
Publications of Center for Manufacturing Engineering (of the National Bureau of Standards), 1978-1983
[PB84-224526] 01 p0036 N85-10228
The use of ion implantation for materials processing
[AD-A145436] 02 p0287 N85-11873
DoD Robotics Application Workshop Proceedings
[AD-A145867] 03 p0307 N85-11978
Air force, robotic painting
[AD-P004006] 03 p0308 N85-11986
The development of CVD oxide coatings for the protection of metal surfaces — chemical vapor deposition (CVD) 03 p0332 N85-12142
Surface coatings for low emittance in the thermal surveillance band
[MRL-R-937] 03 p0336 N85-12158
Laser balancing system for high material removal rates
[NASA-CR-174731] 03 p0365 N85-12341
Contamination problems during surface cleaning for thermocompression bonding
[DE84-013066] 04 p0475 N85-13023
Ion beam and laser induced surface modifications
[DE84-016569] 04 p0571 N85-13642
A review of metallic surface treatments for corrosion mitigation
[AD-A146701] 06 p0769 N85-14916
Influence of shot-peening methods on surface quality and service life of bearings 06 p0776 N85-14960
Ceramic fabrication process before firing-surface treatment of ceramic powder
[NASA-TM-77437] 08 p1131 N85-17129
Process development for the production of technically high quality monocrystalline diamond grits
[BMFT-FB-T-84-204] 08 p1138 N85-17166
Initial investigation of cryogenic wind tunnel model filler materials
[NASA-TM-86363] 09 p1283 N85-18069
Antifriction nickel-phosphorous coatings on aluminum alloy products 09 p1309 N85-18221
Survey of the finish characteristics of machined optical surfaces
[DE85-001343] 09 p1385 N85-18708
Estimate of quality of aluminum alloy surface preparation for arc welding 10 p1449 N85-19128
Textured carbon surfaces on copper
[NASA-CASE-LEW-14130-1] 11 p1615 N85-20156
Diamondlike flakes
[NASA-CASE-LEW-13837-2] 12 p1796 N85-21267
Ion-beam nitriding of steels
[NASA-CASE-LEW-14104-1] 12 p1805 N85-21324
A process to produce fine line metallic collection patterns on semiconductors devices
[NASA-CASE-NPO-16413-1] 12 p1805 N85-21325
Sputter-induced compositional modifications in a Ni-Au alloy
[DE85-002771] 12 p1807 N85-21333
New application possibilities for clad steel by reducing surface treatment expenditure and by using improved welding technology
[BMFT-FB-T-84-236] 12 p1861 N85-21672
Innovative research in the design and operation of large telescopes for space: Aspects of giant telescopes in space
[NASA-CR-175626] 13 p2170 N85-23482
New technology of finish cutting teeth in large gear blanks 14 p2267 N85-24047
Laser surface treatments 14 p2308 N85-24284
Mechanical properties of TiN deposits obtained by PVD and TiN, TiC, TiC + TiN obtained by CVD
[BLL-RISLEY-TR-5097-(9091.9F)] 15 p2508 N85-25471
Electrochemical behavior of amorphous alloys based on iron, cobalt and nickel in H3PO4 solutions alone and mixed with HF 15 p2513 N85-25505
The influence of abrasive blast cleaning and corrosion inhibitors on protective paint coatings
15 p2517 N85-25522
New material, process spins off from Volvo LCP 2000 program 15 p2536 N85-25648
Investigation of silicon surface passivation by silicon nitride film deposition
[NASA-CR-175693] 15 p2585 N85-25938
Interaction of liquid crystals with inhomogeneous surfaces
[AD-A151557] 15 p2660 N85-26413
MOD silver metallization for photovoltaics
[NASA-CR-175773] 16 p2818 N85-27381
Surface modification of solids
[DE85-007543] 16 p2871 N85-27715
Corrosion characteristics of some steels produced through a self-cleaning rotating electrode
[BLL-BISI-TRANS-22046-(9022.06)] 17 p2925 N85-28034
Properties of chromate coatings formed on electrolytic zinc substrates
[BLL-BISI-TRANS-22349-(9022.06)] 17 p2926 N85-28052
Mechanical interactions of rough surfaces
[DE85-005653] 18 p3118 N85-29299
Atomized magnetism-aluminum protective coatings
19 p3244 N85-30116
New metal coating method developed
21 p3568 N85-32191
Reliability of void detection in structural ceramics using scanning laser acoustic microscopy
[NASA-TM-87035] 21 p3597 N85-32337
MOD silver metallization for photovoltaics
21 p3610 N85-32428
Implementation of polymer impregnation as a bridge deck sealant
[PB85-185718] 22 p3753 N85-33265
Performance improvements from surfacing in aero engine components
[PNR-90257] 23 p3897 N85-34142
Towards the development of technological processes for the preparation of cadmium plated steel articles
[BLL-M-36315-(5828.4)] 23 p3913 N85-34248
Results of tests of weathered K5NA closeout material in the MSFC Hot Gas Facility
[NASA-CR-170893] 24 p4073 N85-35239
Wear-resistant coatings for tools intended for cold working
[BLL-RISLEY-TR-5040-(9091.9F)] 24 p4081 N85-35293
Size and shape dependence of CO adsorption sites on sapphire supported Fe microcrystals
[NASA-CR-176171] 24 p4160 N85-35794

SURFACE GEOMETRY
Semianalytic modeling of aerodynamic shapes
[NASA-TP-2413] 12 p1771 N85-21120
A deformation analysis of flat flexible gear and its equation of original curved surfaces
[NASA-TM-77493] 12 p1659 N85-21660

SURFACE INTERACTIONS
U SURFACE REACTIONS

SURFACE IONIZATION
Computerized study of several electrostatic, surface-ionization ion-source configurations
[DE85-001512] 11 p1721 N85-20823
Sputter-induced compositional modifications in a Ni-Au alloy
[DE85-002771] 12 p1807 N85-21333
Ion emission from solid surfaces: Comparison of dust impact with other excitations — Giotto mission
14 p2244 N85-23912
A model of plasma cloud expansion generated by a dust particle impact — Giotto mission
14 p2245 N85-23914
Fluorescence quenching by metal semiconductor and insulator surfaces 19 p3374 N85-30929

SURFACE LAYERS
NT MONOMOLECULAR FILMS
The influence of surface layers on the friction and wear behavior of materials 01 p0054 N85-10357
Non-oxide ceramics: A new class of engineering materials 02 p0179 N85-11199
Characterization of amorphous surface layers in Fe implanted with Ti and C
[DE84-014980] 02 p0289 N85-11885
Thermomechanical cracking in layered media from moving friction load
[AD-A146022] 03 p0373 N85-12379
Aeroproyekt develops improved runway surfacing
06 p1068 N85-16770
Moessbauer study of amorphous Fe(67)Co(18)B(14)S(1)
[AERE-R-11526] 11 p1737 N85-20928
The effect of Xe underlayers on the surface enhanced Raman scattering of pyridine on cold silver
[AD-A150109] 12 p1801 N85-21294
Some unique aspects of fouling on copper as compared to titanium or nickel
[AD-A150072] 12 p1806 N85-21332
Role of passive surface films on corrosion fatigue crack initiation
[DE85-000436] 14 p2257 N85-23985
Most important geochemical barrier zones in ocean (with example of Atlantic Ocean basin)
14 p2343 N85-24491
Fracture surface analysis in composite and titanium bonding: Part 1: Titanium bonding
[NASA-CR-175750] 15 p2502 N85-25434
The theoretical response of a vertical line array to wind-generated noise in shallow water
[AD-A151730] 16 p2860 N85-27638

Investigation of reaction layer formation in high-load capacity lubricating oils
[MPA-83-01] 17 p2975 N85-28381
A survey of the turbulence in the marine surface layer for the operation of low-Reynolds number aircraft
[AD-A154133] 19 p3316 N85-30558
Surface wave modes of a multilayered medium backed by a perfectly conducting ground plane: Computation of propagation constants
[DE85-011454] 22 p3829 N85-33715
Method of precisely modifying predetermined surface layers of a workpiece by cluster ion impact therewith
[DE85-006519] 23 p3984 N85-34710

SURFACE NAVIGATION
Terrain navigation concepts for autonomous vehicles
[AD-A144994] 01 p0005 N85-10031
NAVSTAR GPS (Global Positioning System) marine receiver performance analysis
[AD-A146414] 06 p0753 N85-14831
Use of three omega radionavigation system position lines for solving problems in marine geodesy
13 p2107 N85-23131
Checking on the position of navigation marker buoys by the ARGOS system 16 p2813 N85-27354

SURFACE PRESSURE
U PRESSURE

SURFACE PROPERTIES
NT ADHESION
NT ADSORPTIVITY
NT COEFFICIENT OF FRICTION
NT INTERFACIAL TENSION
NT SKIN TEMPERATURE (NON-BIOLOGICAL)
NT SPECTRAL REFLECTANCE
NT SURFACE CRACKS
NT SURFACE DEFECTS
NT SURFACE ENERGY
NT SURFACE ROUGHNESS
NT SURFACE STABILITY
NT SURFACE TEMPERATURE
NT WALL TEMPERATURE
Test measurements of the 100 m telescope at lambda = 7 mm
[TR-18] 01 p0129 N85-10890
Dynamics of growth of surface periodic structures when intense light acts on condensed media
02 p0268 N85-11748
Design of alternate launch and recovery surfaces for environmental effects
[AD-A145800] 03 p0320 N85-12066
Polycyclic aromatic hydrocarbons on the inner surfaces of copper tubing
[AD-A145979] 03 p0337 N85-12169
Vertical coherence along a macroray path in an inhomogeneous anisotropic ocean
[AD-A145992] 03 p0416 N85-12660
HgCdTe surface and defect study program
[AD-A146343] 03 p0434 N85-12764
Effect of a thermal gradient applied to a sinusoidal surface profile
[DE84-015649] 03 p0434 N85-12765
Surface diffusion of high temperature vapors in porous alumina
[DE84-015968] 04 p0479 N85-13053
Reflection of volume waves in multilayer structures
04 p0485 N85-13097
Surface structure determination with ARPEFS
[DE84-016904] 04 p0571 N85-13644
Biosphere/atmosphere interactions
05 p0679 N85-14364
Laser excitation of coupled surface electromagnetic and acoustic waves and of static structures in solids
05 p0723 N85-14652
Characterization of surface electronic properties of semi-insulating InP
[AD-A146553] 06 p0866 N85-15507
Solid state, surface and catalytic properties of oxides
[DE85-002096] 06 p0867 N85-15512
Surface studies of Nb, its compounds, and coatings
[DE84-017353] 06 p0868 N85-15516
Test your contacts by measuring their constriction resistance
[BLL-WH-611-(9091.9F)] 07 p0944 N85-15978
Effect of five lubricants on life of AISI 9310 spur gears
[NASA-TP-2419] 07 p0962 N85-16099
Theoretical study of laser-induced surface excitations on a grating
[AD-A147855] 07 p0972 N85-16172
Antisoiling technology: Theories of surface soiling and performance of antisoiling surface coatings
[NASA-CR-174274] 07 p0991 N85-16296
Preparation and evaluation of ZnSe and ZnS sub X Se sub 1-x epitaxial layers on Ge substrates for applications in surface passivation and heterojunction devices
[AD-A147432] 07 p1048 N85-16657
Optimization of technical catalysts with the help of surface analysis
[BMFT-FB-T-84-225] 08 p1124 N85-17086
Australian Multiexperimental Assessment of SIR-B (AMAS) 08 p1148 N85-17243
Investigations of vacuum ultraviolet and soft X-ray lasers
[AD-A148277] 08 p1167 N85-17358
Structure of solids surfaces in wear situations
[AD-A148480] 08 p1166 N85-17366
Research on nondestructive testing
[AD-A148375] 08 p1171 N85-17380
Determining grasp points using photometric stereo and the PRISM binocular stereo system
[AD-A147782] 08 p1222 N85-17697
Flow separation induced by periodic aerodynamic interference
[AD-P004174] 09 p1286 N85-17959
Surface mechanical properties and wear behavior of ion implanted TIB2
[DE85-001130] 09 p1295 N85-18133
Calculating heat transfer coefficients for turbine profiles taking surface curvature and elevated flow turbulence into account 09 p1307 N85-18212
Nondestructive characterization of semiconductor surfaces and interfaces 09 p1329 N85-18349
Effective antireflection coatings of transparent polymeric materials by gas-phase surface fluorination
[DE84-013027] 09 p1385 N85-18711
Surface and allied studies in silicon solar cells
[NASA-CR-175468] 10 p1508 N85-19516
Optical second harmonic generation for surface studies
[DE85-000670] 11 p1640 N85-20333
Classical rainbow scattering of alkali ions on metal surfaces. Application to the investigation of unknown surface structures
[MPIS-10/1984] 11 p1726 N85-20854
Measurement of the configuration of a concave surface by the interference of reflected light
[NASA-TM-77796] 11 p1728 N85-20867
Surface physics instrumentation
[AD-A149304] 11 p1728 N85-20869
Surface physics and crystallography
[DE85-003128] 11 p1735 N85-20910
Laser studies of chemical dynamics at the gas-solid interface
[DE84-017590] 11 p1736 N85-20920
Runway rubber removal specification development field evaluation procedures development
[FAA-PM-84-27] 12 p1781 N85-21179
Solar-assisted hydrogen generation by photoelectrocatalysis
[PB85-149706] 12 p1804 N85-21314
Tribological properties of boron nitride synthesized by ion beam deposition
[NASA-TM-86962] 12 p1810 N85-21355
Evaluation of corrosion-erosion behavior of various ceramic materials
[AD-A149756] 12 p1812 N85-21367
Surface-slip equations for multicomponent nonequilibrium air flow
[NASA-TM-85820] 12 p1845 N85-21573
Planar dynamics of a uniform beam with rigid bodies affixed to the ends
[NASA-CR-175566] 12 p1864 N85-21693
Problem of diffraction by wavy surface: Comparison of numerical methods of solution
13 p2079 N85-22985
Method for processing broad-profile data
13 p2117 N85-23185
Dipole active surface vibrational resonances on clean and hydrogen covered Ni(110)
[AD-A150546] 13 p2163 N85-23420
Study and estimation of planet-crossing asteroid populations: Discoveries and analysis
13 p2175 N85-23498
The olivine asteroids: Discovery, mineralogy, and relationship to palasites 13 p2175 N85-23500
Surfaces of asteroids and cometary nuclei
13 p2176 N85-23503
Venus surface composition from radio/radar measurements 13 p2177 N85-23509
Surface structures of Hawaiian lavas
13 p2186 N85-23566
Significant parameters of the behavior and of the surface damage of the lubricated Hertzian contact: An application to gears 14 p2222 N85-23783
Fatigue fracture topography 14 p2318 N85-24323
Determination of temperature and degree of roughness of sea and land surfaces by microwave radiometric polarization measurements 14 p2334 N85-24432
X-ray emission in heavy ion collisions
[DE85-006350] 14 p2419 N85-24927
Monte Carlo lattice models for adsorbed polymer conformation
[NASA-TP-2453] 14 p2426 N85-24961
Residual oxygen pressure in contact gap upon diffusion welding of titanium 15 p2499 N85-25418
Surface composition, properties and thermal stability of massive and fine metallic glasses
15 p2513 N85-25509
Mechanisms of buildup and properties of aluminum coatings on heat-resistant nickel alloys
15 p2513 N85-25506
Development of high-efficiency solar cells on silicon web
[NASA-CR-175707] 15 p2565 N85-25869
Threshold electron studies of gas-surface interactions
[AD-A151271] 15 p2647 N85-25928
Diagnostics of a glow discharge used to produce hydrogenated amorphous silicon films
[DE85-002914] 15 p2661 N85-26420
Secondary ion mass spectrometry studies of solids and surfaces
[AD-A151744] 16 p2745 N85-26939
Free-surface phenomena under low- and zero-gravity conditions
[NASA-CR-175835] 16 p2782 N85-27166
Inversion of Rayleigh wave group velocities from high-explosive tests
[AD-A152172] 16 p2783 N85-27175
Surface exploration geophysics applied to the Moon
[DE85-006714] 16 p2884 N85-27763
Interaction of high-cycle and low-cycle fatigue of Haynes 188 alloy at 1400 F deg 17 p2913 N85-27861
Coadsorption studies on transition metals
[PB85-183713] 18 p3072 N85-29003
Predicting microfracture in ceramics via a microcontact model
[DE85-005654] 18 p3081 N85-29080
Studies on surface processes during friction and wear
[AD-A153509] 18 p3117 N85-29296
Surface hydrologic characteristics of proposed repository locations in the Palo Duro Basin of the Texas Panhandle
[DE85-010530] 18 p3126 N85-29355
Effect of surface state on durability of aluminized boron fibers 19 p3244 N85-30115
Moving random surfaces and correlation analysis
[CRC-1384] 19 p3253 N85-30186
Residual stress distributions in (plastically) surface deformed two-phase materials 19 p3283 N85-30356
Solid surface characterization by contact angle measurements
[FOA-C-40209-C,B2] 20 p3459 N85-31488
Nitridation of SiO2 for surface passivation
20 p3480 N85-31627
Using ship wake patterns to evaluate SAR (Synthetic Aperture Radar) ocean wave imaging mechanisms. Joint US-Canadian Ocean Wave Investigation Project
[AD-A154633] 21 p3573 N85-32223
Toward the theory of acoustic scattering on uneven free surface 21 p3680 N85-32882
Acoustic radiation from concentric shells containing an inner fluid
[AD-A155476] 21 p3700 N85-32991
Considerations of large scale impact and the early Earth 21 p3718 N85-33070
Solar cycle variation of ephemeral regions
[AD-A154967] 21 p3723 N85-33097
Anti wear property of two phasic metal composite
23 p3906 N85-34199
Infrared studies of the influence of alkali metals on the C-O bond in chemisorbed carbon monoxide
[DE85-005306] 23 p3911 N85-34232
Method for preparing hydride configurations and reactive metal surface
[DE85-006443] 23 p3917 N85-34274
Redefining the scratch standards
[PB85-194736] 24 p4154 N85-35755
Size and shape dependence of CO adsorption sites on sapphire supported Fe microcrystals
[NASA-CR-176171] 24 p4160 N85-35794
Electronic structure and lattice dynamics of dimensionally constrained and disordered solids
[AD-A155927] 24 p4161 N85-35797

SURFACE REACTIONS
Plasma surface interactions in magnetic fusion systems
[DE84-015255] 01 p0123 N85-10842
Surface production of negative hydrogen ions
[AD-A145437] 02 p0277 N85-11801
Ceramic powder for sintering materials
[NASA-TM-77434] 03 p0336 N85-12168
One-dimensional model of thin films. Analysis of aluminum surface 03 p0350 N85-12254
Comparison of wide aperture and short residence time ion lenses
[DE84-015274] 03 p0420 N85-12685

The 6th International Summer Institute in Surface Science 1983)
[AD-A146253] 03 p0434 N85-12762
Low energy ion-molecule reaction dynamics and chemiionization kinetics
[DE84-015881] 04 p0559 N85-13562
Hydrogen absorption on (110) tungsten planes at 30 K: An atom-probe field-ion microscope study
[DE84-015659] 04 p0560 N85-13565
Effects of surface interactions and mechanical properties of PBXs (plastic bonded explosives) on explosive sensitivity
[AD-A146368] 06 p0773 N85-14944
Structure of adsorbed monolayers. The surface chemical bond
[DE84-016879] 06 p0861 N85-15471
Proceedings of Workshop on Synergistic Effects in Surface Phenomena Related to Plasma-Wall Interactions
[IPPJ-AM-35] 06 p0864 N85-15486
Synergistic effects in fusion machines, session summary 06 p0864 N85-15489
Plasma surface interaction processes and possible synergisms 06 p0864 N85-15490
Synergisms in hydrogen recycling, session summary
06 p0864 N85-15491
Steady state hydrogen transport in solids
06 p0864 N85-15492
Synergisms in surface erosion, session summary
06 p0864 N85-15493
Synergism in materials erosion due to multispecies impact 06 p0864 N85-15494
Synergistic effects related to surface composition, session summary 06 p0865 N85-15495
Effects of monolayer coverages on substrate sputtering yields 06 p0865 N85-15496
Plasma-surface interactions in large tandem mirror devices, MFTF-B
[DE85-001753] 06 p0865 N85-15499
Vibrational spectroscopy of chemisorption phenomena on model catalyst surfaces
[AD-A146753] 07 p0922 N85-15840
Phase-dissipative mechanisms for laser-induced surface desorption-dissociation processes
[AD-A147961] 08 p1121 N85-17065
Estimation of the rate of electron transfers between 2 contacting polymer surfaces
[AD-A148416] 08 p1122 N85-17072
Optimization of technical catalysts with the help of surface analysis
[BMFT-FB-T-84-225] 08 p1124 N85-17086
Hydrogen trapping, diffusion, and recombination in austenitic stainless steels
[DE85-001871] 09 p1294 N85-18129
Low and moderate temperature oxidation of atomically clean nickel, chromium and Ni-Cr alloys
[DE84-017350] 09 p1295 N85-18131
Ion beam studies of hydrogen in metals
[DE84-017422] 09 p1297 N85-18145
Two-dimensional modeling of conduction-mode laser welding
[DE85-001804] 09 p1327 N85-18341
Plasma surface interaction processes and possible synergisms
[DE85-001861] 09 p1391 N85-18752
Reactivity of ion implanted silicon carbide
[DE85-001543] 09 p1399 N85-18802
Fundamental aspects on ion-beam surface modification: Defect production and migration processes
[DE85-000093] 09 p1399 N85-18804
Characterization of erosion of metallic materials under cavitation attack in a mineral oil
[NASA-TM-86934] 10 p1440 N85-19075
Composition and method for cleaning embedded soil from surfaces having low gloss coatings
[AD-D011465] 10 p1459 N85-19194
Plasma states near surface of metal irradiated by CO2 laser
11 p1719 N85-20815
Studies of silicon-refractory metal interfaces: Photoemission study of interface formation and compound nucleation
[AD-A150075] 12 p1800 N85-21293
Three-dimensional calculation of shuttle charging in polar orbit 13 p1992 N85-22486
Confinement properties of high energy density plasmas in the Wisconsin levitated octupole
13 p2161 N85-23408
Hydrogen on impurity-covered iron surfaces
14 p2254 N85-23968
Practical surface methods 14 p2316 N85-24314
Self-substaining low-Z coatings for impurity control. Part 1: General considerations
[DE85-000427] 14 p2425 N85-24956
C2H(n) fragments on metal surfaces
[AD-A151474] 15 p2505 N85-25449
Studies of metal/carbon surface chemistry
[DE85-005513] 15 p2507 N85-25463
Numerical modeling of gas dynamic phenomena during supersonic flow of viscous gas in channel with electrical flow discharge 15 p2643 N85-26304
Neutralization and excitation in low-energy ion-surface collisions
[AD-A151568] 15 p2660 N85-26414
Effects of surface chemistry on hot corrosion life
[NASA-CR-174915] 16 p2708 N85-26711
The role of surface generated radicals in catalytic combustion 17 p2898 N85-27869
Corrosion Research Center of the University of Minnesota
[DE85-009416] 18 p3075 N85-29022
Technique for measuring surface diffusion by laser-beam-localized surface photochemistry
[DE85-007885] 18 p3113 N85-29273
Micro-reactions of metal contacts on various types of GaAs surfaces
[AD-A153650] 18 p3193 N85-29806
Method for predicting the performance of cathode materials
[AD-D011665] 19 p3257 N85-30198
Perturbative treatment of quasi-resonant proton neutralization at alkali-halide surfaces
[AD-A154143] 19 p3356 N85-30806
Elementary processes in the catalytic combustion of methane (mechanism, intermediates, and controlling reactions)
[PB85-188357] 20 p3436 N85-31316
Overlap integrals for atom-metal surface interactions
[AD-A155038] 21 p3702 N85-32998
Method for measuring surface activity of silicon nitride powder
[NASA-TM-77906] 24 p4073 N85-35242
Prediction of plasticity characteristics for three-dimensional fracture specimens comparison with experiment
[AD-A156425] 24 p4102 N85-35430

SURFACE ROUGHNESS

Turbulent boundary layers over rough surfaces hypersonic flow
[AD-A145040] 01 p0003 N85-10016
Terrain analysis procedural guide for surface configuration
[AD-A145637] 02 p0219 N85-11446
The chemical nature of the fiber/resin interface in composite materials 04 p0465 N85-12953
Analysis for leakage and rotordynamic coefficients of surface roughened tapered annular gas seals
05 p0644 N85-14135
Intensification of convective heat transfer by means of artificial surface roughness 06 p0778 N85-14975
Effect of asperity interactions on scuffing
[AD-A146544] 06 p0814 N85-15170
Optics of solids (surface related) and effect of surface roughness on MOS
[AD-A146883] 07 p0946 N85-15996
Interactive digital image processing for terrain data extraction
[AD-A148580] 08 p1176 N85-17417
On the virtual wall height in open channel flow with large relative roughness 09 p1303 N85-18188
Theory of resonant light scattering from a rough surface 09 p1383 N85-18701
Comparison of measured and simulated ride comfort for an agricultural tractor and influence of travel speed and tyre-inflation pressure on dynamic response
[AD-P004281] 09 p1407 N85-18857
Characteristics of farm field profiles as sources of tractor vibration
[AD-P004282] 09 p1407 N85-18858
Scanning photoacoustic microscopy of aluminum with aluminum oxide, roughness standards and rubber
[AD-A149460] 10 p1441 N85-19081
Mechanical interactions of rough surfaces
[DE85-000614] 10 p1494 N85-19434
An experimental investigation of microstrip properties on soft substrates from 2 to 40 GHz
[NASA-TM-86961] 11 p1624 N85-20224
Wind-tunnel research on the mechanics of plumes in the atmospheric surface layer
[AD-A150019] 12 p1846 N85-21584
Electromagnetic Acoustic Transducers (EMATs) for erosion monitoring
[DE85-004834] 12 p1854 N85-21628
Surface forward scattering and reflection
[AD-A150115] 12 p1928 N85-22112
A posteriori increase of resolving power of optical system forming averaged monochromatic images
13 p2082 N85-23003
Effects of fracture roughness on fluid flow through a single deformable fracture
[DE85-004593] 13 p2092 N85-23062
Calculations of microwave brightness temperature of rough soil surfaces: Bare field
[NASA-TM-86200] 13 p2123 N85-23221
Microwave remote sensing of soil moisture
13 p2125 N85-23235
A systematic study of light scattering by irregularly shaped particles
[AD-A150192] 13 p2159 N85-23400
Unsupervised classification of global radar units on Venus 13 p2198 N85-23632
Mapping and geological analysis of Mercury and Venus radar ranging data 13 p2198 N85-23633
Mars radar catalog 13 p2198 N85-23636
Statistics of Aeolian surface of Mars
13 p2199 N85-23637
Investigation of the conditions for tripping transition with roughness elements and their influence on boundary layer development 14 p2212 N85-23720
The characteristics of surface roughness important to gear and rolling bearing problems
14 p2222 N85-23782
Quantitative roughness analysis of treated surfaces with higher-class finish by methods of X-ray reflectometry
14 p2282 N85-24136
Effect of flight sequences in complex load histories on crack front marking 14 p2318 N85-24326
Generation of marker lines on fatigue fracture surfaces 14 p2319 N85-24328
Proceedings of the 9th US Air Force and the Federal Republic of Germany Data Exchange Agreement Meeting. Viscous and Interacting Flow Field Effects
[AD-A153020] 17 p2958 N85-28266
Mechanical interactions of rough surfaces
[DE85-005653] 18 p3118 N85-29299
Specification of surface roughness over oceans in the GLAS Fourth Order GCM 18 p3142 N85-29455
Influence of land-surface roughness on atmospheric circulation and rainfall: A sensitivity study with a GCM
18 p3146 N85-29479
Measurement of mode interaction due to waveguide surface roughness
[AD-A154039] 19 p3255 N85-30183
Using ship wake patterns to evaluate SAR (Synthetic Aperture Radar) ocean wave imaging mechanisms. Joint US-Canadian Ocean Wave Investigation Project
[AD-A154633] 21 p3573 N85-32223
The use of the glistening surface concept in rough surface scattering
[AD-A154922] 21 p3575 N85-32234
An analysis of physical optics models for rough surface scattering
[AD-A154960] 21 p3575 N85-32235
Surface roughness effects in elastohydrodynamic contacts
[NASA-TP-2488] 21 p3595 N85-32329
Toward the theory of acoustic scattering on uneven free surface 21 p3680 N85-32862

SURFACE ROUGHNESS EFFECTS

Numerical forecast of pressure field by considering the mutual influence of orography, thermal nonhomogeneity and surface friction 01 p0060 N85-10534
Proposal for wall function for friction and heat transfer in the presence of roughness and mass transfer
[CFD/84/12] 04 p0501 N85-13196
Scattering from multi-scale surface — infrared lasers
[RSRE-MEMO-3656] 04 p0505 N85-13222
Scattering of electromagnetic waves by surface with small asperities 06 p0784 N85-15013
Approach to solution of diffraction problem for waves at rough surface 06 p0784 N85-15014
Development of an artificial boundary layer for different outlet flows 14 p2212 N85-23719
Energy reflection coefficient for H+ ions at energies between 10 and 80 keV
[DE85-007547] 16 p2883 N85-27662
Comparison of findings of theories describing reflection from real surface with experiments in region of ultrasoft X-radiation 21 p3694 N85-32950

SURFACE STABILITY

The behaviour of unstable surfaces: A literature review
[CFD/84/6] 02 p0199 N85-11329
Development of a preliminary ALRS stabilized material pavement analysis system (SPAS)
[AD-A147116] 07 p0910 N85-15760
Soil compliance influence on tyre performance
[AD-P004260] 09 p1404 N85-18836
Quality control in soil compaction by behaviours of exciter
[AD-P004295] 09 p1406 N85-18872
Adsorption thermodynamics and surface transport of metal catalyst poisons
[DE85-002668] 10 p1441 N85-19084
Experiments on the influence of active walls on the initial amplitudes and growths of instability waves
[AD-A154630] 21 p3583 N85-32275
Instability and chaotic behavior in a free-surface flow
[AD-A154879] 21 p3584 N85-32279
Interfacial bonding stability 21 p3608 N85-32409

SURFACE TEMPERATURE
NT SKIN TEMPERATURE (NON-BIOLOGICAL)
NT WALL TEMPERATURE
The Martian climate: Energy balance models with CO2/H2O atmospheres
[NASA-CR-174073] 03 p0448 N85-12849
The need for integrating ground thermal measurements with thermal aircraft imagery 05 p0660 N85-14243
Satellite definition of the bio-optical and thermal variation of coastal eddies associated with the African current
[AD-A147910] 07 p0989 N85-16282
Laser-initiated combustion studies on metallic alloys in pressurized oxygen
[PB85-128114] 10 p1436 N85-19066
Analytical fuel property effects: Small combustors, phase 2
[NASA-CR-174848] 10 p1456 N85-19175
A model for forecasting runway surface temperature and verification with subjective forecasts
[TR-28] 10 p1518 N85-19569
Thermal investigation of an electrical high-current arc with porous gas-cooled anode
[NASA-TM-77769] 11 p1627 N85-20245
Applications of pulsed-laser techniques and thermographic phosphors to dynamic thermometry of rotating surfaces
[DE85-000403] 11 p1639 N85-20328
Hot radome boresight error measurements
[AD-P004364] 12 p1826 N85-21458
The effect of stochastic surface heat fluxes on the climatology of the seasonal thermocline
[AD-A149957] 12 p1869 N85-21857
Oceanic role in terrestrial climate
[DE85-004422] 12 p1896 N85-21904
On the relationship between maximum surface temperature and various parameters; with reference to objective forecasting
[KNMI-TR-58] 12 p1897 N85-21905
Application of fluorescence to measurement of surface temperature in solid propellants
13 p2002 N85-22548
Estimation of regional evapotranspiration using remotely sensed land surface temperature. Part 1: Measurement of evapotranspiration at the Environmental Research Center and determination of Priestley-Taylor parameter
13 p2125 N85-23233
Estimation of regional evapotranspiration using remotely sensed land surface temperature. Part 2: Application of equilibrium evaporation model to estimate evapotranspiration by remote sensing technique — Japan 13 p2125 N85-23234
Testing an energy balance model for estimating actual evapotranspiration using remotely sensed data — Hannover, West Germany barley and wheat fields
13 p2125 N85-23236
A method for estimating soil moisture availability
[NASA-CR-175606] 13 p2126 N85-23238
Fabrication of ceramic substrate-reinforced and free forms
[NASA-TM-86994] 14 p2247 N85-23926
Application of atomic fluorescence to measurement of combustion temperature in solid propellants
[AD-A150733] 14 p2263 N85-24021
Seven-wavelength pyrometer for determining surface temperature of ablation materials
[NASA-TM-77832] 14 p2305 N85-24268
Dynamic stochastic model of long-period variability of ocean surface temperature 14 p2334 N85-24437
Choice of optimum pairs of spectral intervals for IR-range survey of Earth's surface 15 p2486 N85-25344
Numerical simulation of boundary layer excitation by surface heating/cooling
[NASA-CR-172575] 15 p2554 N85-25756
Annual cycle. Part 1: The annual variation of surface temperatures over the United States and Canada
[PB85-147676] 15 p2600 N85-26026
Raman studies of surface temperature in laser-heated semiconductors
[AD-A151377] 15 p2659 N85-26412
Regularities in recent changes in surface air temperature and atmospheric precipitation fields
16 p2807 N85-27311
Evaluation of the area and severity of last night's frosts
[REPT-109] 16 p2833 N85-27473
Simulation of a synchronously coupled atmosphere-ocean prediction model
[AD-A152020] 16 p2835 N85-27482
A GCM study of the atmospheric response to tropical SST anomalies 18 p3146 N85-29477
Temperature and surface damage under lubricated sliding-rolling contacts 19 p3280 N85-30338
Facility for large-scale hazardous gas testing
[DE85-011852] 21 p3564 N85-32169
Surface temperature distribution along a thin liquid layer due to thermocapillary convection
[NASA-TM-87115] 23 p3930 N85-34357
SURFACE TENSION
U INTERFACIAL TENSION
SURFACE TO SURFACE MISSILES
NT CRUISE MISSILES
NT INTERCONTINENTAL BALLISTIC MISSILES
NT MINUTEMAN ICBM
NT POLARIS MISSILES
Dissected motors-propellants motor number STM-012. Phase 15: Surveillance report, stage 1
[AD-A156088] 24 p4071 N85-35226
SURFACE TREATMENT
U SURFACE FINISHING
SURFACE VEHICLES
NT AIRCRAFT CARRIERS
NT AUTOMATED GUIDEWAY TRANSIT VEHICLES
NT AUTOMATED TRANSIT VEHICLES
NT AUTOMOBILES
NT BOATS
NT ELECTRIC AUTOMOBILES
NT ELECTRIC HYBRID VEHICLES
NT ELECTRIC MOTOR VEHICLES
NT LIFEBOATS
NT LUNOKHOD LUNAR ROVING VEHICLES
NT MOTOR VEHICLES
NT ROCKET PROPELLED SLEDS
NT ROVING VEHICLES
NT SLEDS
NT SURFACE EFFECT SHIPS
NT TANK TRUCKS
NT TANKER SHIPS
NT TANKS (COMBAT VEHICLES)
NT TRACKED VEHICLES
NT TRACTORS
NT TRANSPORTER
NT TRUCKS
NT WALKING MACHINES
Terrain navigation concepts for autonomous vehicles
[AD-A144994] 01 p0005 N85-10031
Study of annoyance due to urban automobile traffic. Annex 4: A catalog of the characteristics of noise at different measuring points
[NASA-TM-77516] 03 p0387 N85-12478
Synthesis of transit practice: Diesel fuel quality and effects of fuel additives
[PB84-235688] 05 p0621 N85-13973
Vehicle anchoring system
[AD-D011292] 06 p0815 N85-15173
Automatic land vehicle navigation using road map data
[DE84-017178] 09 p1278 N85-18043
Calculation of the area covered by mobile radio systems using geographic data stored in a computer
[FUB-43-1983] 09 p1312 N85-18247
The experimental performance of an off-road vehicle utilizing a semi-active suspension — off-road motorcyles
09 p1339 N85-18421
Modelling of off-road tyres and soil for improved traction
[AD-P004258] 09 p1404 N85-18834
Development of a soil-wheel interaction model
[AD-P004259] 09 p1404 N85-18835
Soil compliance influence on tyre performance
[AD-P004260] 09 p1404 N85-18836
The rolling resistance and sinkage of towed dual wheel combination in sand
[AD-P004261] 09 p1404 N85-18837
Performance prediction of pneumatic tyres on sand
[AD-P004262] 09 p1404 N85-18838
Traction forces of drive tyre on the compacted soil
[AD-P004264] 09 p1404 N85-18840
Prediction of in-sand tire and wheeled vehicle drawbar performance
[AD-P004265] 09 p1404 N85-18841
Designing off-road vehicles with good ride behaviour
[AD-P004267] 09 p1405 N85-18843
Ride comfort of off-road vehicles
[AD-P004279] 09 p1406 N85-18855
Proceedings of the 8th International Conference on the Performance of Off-Road Vehicles and Machines, volume 2
[AD-A148835] 09 p1407 N85-18859
Study of the motion of agricultural vehicles on steep grass-covered slopes
[AD-P004290] 09 p1408 N85-18867
Pressure tests in soil below tires of agricultural vehicles
[AD-P004294] 09 p1408 N85-18871
Smoother terrain-machine
[AD-P004296] 09 p1409 N85-18873
Compaction of sand using ordinary off-road vehicles
[AD-P004297] 09 p1409 N85-18874
Flotation tires and subsurface compaction
[AD-P004299] 09 p1409 N85-18876
The guidelines to design the lever turning gears in articulated vehicles
[AD-P004301] 09 p1409 N85-18878
Influence of tire on resistance and steering forces of tires
[AD-P004306] 09 p1410 N85-18883
Planning of air cushion transport vehicles
14 p2285 N85-24180
Hybrid propulsion technologies for urban bus transit
[PB85-157469] 16 p2880 N85-27773
Evaluation of semiconductor devices for Electric and Hybrid Vehicle (EHV) ac-drive applications, volume 1
[NASA-CR-176118] 23 p3927 N85-34
Visual position determination for autonomous vehicle navigation
[AD-A156007] 24 p4063 N85-35181
SURFACE WATER
Water resources data, Mississippi, water year 1982
[PB84-224559] 01 p0065 N85-10434
Water resources data, Florida, water year 1982. Volume 4: Northwest Florida
[PB84-223445] 01 p0066 N85-10437
Isolation, concentration and subsequent analysis by capillary gas chromatography of trace amounts of organophosphorus compounds from aqueous samples
[AD-B089301L] 12 p1803 N85-21329
A preliminary analysis of LANDSAT-4 Thematic Mapper radiometric performance 12 p1870 N85-21730
Literature review for development of the master analytical scheme for organic compounds in water
[PB85-152674] 15 p2507 N85-25486
Analysis of suspended sediment distributions in the surface waters of Delaware Bay using remote sensing of optical properties 15 p2582 N85-25826
Operation guiding light-scientific program and field plan. The pilot field experiment for NORDA project chemical dynamics in ocean frontal areas
[AD-A153765] 18 p3150 N85-29507
Microwave hydrology: A trilogy
[NASA-CR-176042] 20 p3477 N85-31603
Global environmental transport models for tritium
[DE85-011437] 22 p3816 N85-33639
Hydrology
[PB85-182954] 23 p3944 N85-34440
SURFACE WAVES
NT BAROCLINIC WAVES
NT CAPILLARY WAVES
NT ELECTROMAGNETIC SURFACE WAVES
NT GRAVITY WAVES
NT RIPPLES
NT SOMMERFELD WAVES
Transformation of heterogeneous surface waves by skewed streams 02 p0259 N85-11697
Evaluation of moduli and thicknesses of pavement systems by spectral-analysis-of-surface-waves method
[PB84-219112] 03 p0342 N85-12205
Propagation of acoustic shear waves through active periodic structure 04 p0490 N85-13125
Slow surface magnetoplasma waves in oblique magnetic field 07 p0952 N85-16004
The investigation of selected oceanographic applications of spaceborne synthetic-aperture radar
08 p1146 N85-17233
SEASAT 3 and 4
[AD-A148343] 08 p1152 N85-17274
Second order Bragg scattering in a SAR
[AD-A148395] 08 p1152 N85-17275
Evolution of nonlinear wave groups on water of slowly-varying depth
[AD-A147947] 08 p1162 N85-17329
Short range order-long range order in superconducting materials
[AD-A148764] 08 p1227 N85-17724
The effects of surface waves on RF discharge pumped lasers
[AD-A149689] 12 p1856 N85-21640
Solar energy converter using surface plasma waves
[NASA-CASE-LEW-13827-1] 12 p1876 N85-21768
Surface wave excitation study
[DE85-005301] 13 p2056 N85-22875
Results of an initial trial of a satellite telemetering buoy measuring near surface current
16 p2812 N85-27346
Surface waveseismic yields as measured by the Regional Seismic Test Network
[DE85-010532] 18 p3137 N85-29425
Surface acoustic wave devices as chemical vapor microsensors
[AD-A153752] 18 p3177 N85-29689
Theoretical investigations of the propagation and interactions of surface waves
[AD-A153548] 18 p3185 N85-29753
Microwave bandstop filter
[AD-D011716] 19 p3261 N85-30222
Dual differential interferometer
[NASA-CASE-LAR-12966-1] 19 p3271 N85-30282

Discovery of a nonpropagating hydrodynamic soliton
[AD-A155569] 21 p3582 N85-32268

Large-time behavior of viscous surface waves
[AD-A154806] 21 p3584 N85-32276

Upward continuation of surface gravity anomalies
[AD-A154973] 21 p3631 N85-32560

Solid state research
[AD-A154763] 21 p3709 N85-33025

Asymmetry of diffraction orders with light diffraction at surface acoustic wave 22 p3782 N85-33431

Numerical experiment of elastic wave propagation by framework model
[DRIC-T-7482] 22 p3795 N85-33511

Surface wave modes of a multilayered medium backed by a perfectly conducting ground plane: Computation of propagation constants
[DE85-011454] 22 p3829 N85-33715

Heterodyne holographic interferometry for visualization of surface acoustic waves
[AD-A155405] 22 p3836 N85-33753

Second Colloquim on the Scattering of Ultrasonic Waves
[AD-A156298] 24 p4145 N85-35697

SURFACES

Surface chemistry of palladium
[DE84-014572] 02 p0173 N85-11163

Determining composition in surface region of semiconductor crystals by method of sudden changes in X-ray photoelectric effect 02 p0267 N85-11746

Incompressible lifting-surface aerodynamics for a rotor-stator combination
[NASA-TM-83767] 03 p0316 N85-12039

Choice of criteria for rejection of insulating components in high-voltage surge equipment
06 p0785 N85-15021

Free-surface boundary layer and the origin of bow vortices
[AD-A147427] 07 p0960 N85-16083

Model robust response surface designs: Scaling 2-level factorials
[AD-A147494] 07 p1033 N85-16556

A free shear layer prediction of the turbulent wake of a flat plate towed below a free surface
[AD-A148699] 09 p1319 N85-18293

Experimental investigation of a turbulent incompressible boundary layer on a curved wall
11 p1577 N85-19936

Surface physics instrumentation
[AD-A149304] 11 p1728 N85-20869

The construction of curves and surfaces using numerical optimization techniques 17 p3003 N85-28565

A survey of patch methods 17 p3003 N85-28567

Some negative results in N-sided patches
17 p3004 N85-28572

Unsteady transonic flow calculations for interfering lifting surface configurations
[NASA-TM-86432] 19 p3214 N85-29931

Experimental method for measuring positronium reflection from surfaces
[DE85-010949] 20 p3531 N85-31967

Removable cleanable antireflection shield
[AD-D011735] 22 p3844 N85-33810

Block-implicit calculations of three-dimensional laminar flow in strongly curved ducts
[DE85-003047] 23 p3931 N85-34363

Acoustical absorption coefficient in a diffuse field of a plane, rectangular material of finite dimensions placed on an infinite perfectly reflecting surface
[NRC/CNR-TT-2113] 23 p3968 N85-34599

SURFACTANTS

Vapor pressure studies of the solubilization of hydrocarbons by surfactant micelles
[DE85-004319] 12 p1803 N85-21306

Turbulent flows of surfacant solutions
[AD-B089137L] 13 p2092 N85-23058

Determining adsorption of surface-active substances by sea bottom deposits 13 p2107 N85-23128

On the question to the effect of surfactants on the spectrum of cloud drops in the process of their condensation growth 21 p3650 N85-32679

SURGERY

Applications of CdTe to nuclear medicine
[DE85-011877] 23 p3952 N85-34492

SURGES

Isolated load switching with surge suppression
[AD-D011218] 01 p0042 N85-10274

A model for the propagation of the westward traveling surge
[TRITA-EPP-84-03] 03 p0393 N85-12515

Surge transient simulation in turbo-jet engine
05 p0596 N85-13796

Surge and stall in centrifugal compressors
05 p0637 N85-14087

Circuit transients due to negative bias arcs on a high-voltage solar array in low Earth orbit
[NASA-TP-2407] 06 p0760 N85-14858

Allowable surge currents and failure mechanisms in semiconductor power devices in various modes of operation 06 p0795 N85-15080

Spicules and surges
[AD-A146785] 07 p1061 N85-16727

On one design principle of surge protector for gas turbine engine compressor 09 p1306 N85-18206

Electromagnetic pulse (EMP) interaction with electric power systems. Power Systems Technology Program
[DE85-000166] 09 p1312 N85-18244

Observation of a westward travelling surge from satellites at low, medium and high altitudes
[NASA-TM-87434] 09 p1342 N85-18442

A survey of fast X-ray transients using the HEAO A-1 Sky Survey experiment 09 p1411 N85-18895

Flashover failures from wet-wire arcing and tracking
[AD-A149055] 10 p1478 N85-19332

A theory of post-stall transients in multistage axial compression systems
[NASA-CR-3878] 12 p1771 N85-21117

Hurricane storm surge research
[GPO-40-048] 12 p1893 N85-21880

Hurricane alicia storm surge and wave data
[AD-A149668] 12 p1895 N85-21896

Surge strength of symmetric cable with monolithic polyethylene insulation of quads
13 p2082 N85-23001

Transients during the switching of SF6-insulated isolating switches
[BLL-CE-TRANS-7986-(9022.09)]
15 p2546 N85-25713

An investigation of hydraulic transients in combination free surface and pressurized flows
19 p3264 N85-30239

Resolution of thermal striping issue downstream of a horizontal pipe elbow in stratified pipe flow
[DE85-006195] 21 p3586 N85-32292

Nonlinear spectroscopy
[AD-A154708] 21 p3704 N85-33010

Exploring results of the possibility on detecting cosmic ray particles by acoustic way
[HE-7.1-3] 24 p4213 N85-36157

SURVEILLANCE

NT SPACE SURVEILLANCE (GROUND BASED)
NT SPACE SURVEILLANCE (SPACEBORNE)

Hybrid state estimation approach to multiobject tracking for airborne surveillance radars
[AD-A148459] 08 p1153 N85-17279

TCAS II: Design and validation of the high-traffic-density surveillance subsystem
[DOT/FAA/PM-84/5] 13 p1970 N85-22375

Surveillance program for the dissection and analysis of explosive and pyrotechnic components
[DE85-006105] 16 p2757 N85-27016

An automated quality assurance surveillance plan for ADP (Automated Data Processing) operations under the Navy's commercial activities program
[AD-A154767] 21 p3671 N85-32802

Power density and threshold control strategies for radar track initiation
[AD-A155357] 22 p3756 N85-33282

Evaluation of nuclear detonation location capability under high attack scenario
[AD-A155761] 24 p4149 N85-35729

SURVEILLANCE RADAR

NT MULTISTATIC RADAR

Design and realization of a multiradar tracking system for air traffic control
[ENST-84E010] 09 p1279 N85-18044

The use of small mobile radars to detect, monitor, and quantify bird movements
[AD-P004188] 11 p1580 N85-19951

On the altitudinal distribution of birds and bird strikes in the Netherlands
[AD-P004189] 11 p1580 N85-19952

Method and means for providing frequency agile operation of MTI (Moving Target Indicator) radar
[AD-D011561] 12 p1823 N85-21436

Development concerns for satellite-based air traffic control surveillance systems 14 p2230 N85-23816

Multi-bistatic radar for short range surveillance
[BAE-BT-10603] 15 p2539 N85-25673

The effects of subrefractive layers and elevated ducts on airborne radar and ESM (Electronic Surveillance Measures)
[AD-A155524] 21 p3637 N85-32592

SURVEYING

U SURVEYS

SURVEYS

NT GEODETIC SURVEYS
NT GEOLOGICAL SURVEYS

Chemical heat pump state-of-the-art survey
[DE84-013552] 01 p0048 N85-10312

A survey and evaluation of software quality assurance
[AD-A147552] 07 p1026 N85-16510

A complete characterization of triply balanced matrices with applications to survey sampling
[AD-A147083] 07 p1031 N85-16542

Manufacturing costs, equipment needs and technological opportunities among small and medium-size manufacturers
[DE85-000479] 09 p1304 N85-18193

Practical application of earth resistivity methods in phase 2 of the installation restoration program
[AD-P004148] 09 p1348 N85-18484

Benthic boundary layer, IOS observational programme: Discovery Gap measurements, March 1984 — Institute of Oceanographic Sciences (IOS)
[ISO-180] 09 p1359 N85-18552

Atlas of snow and ice resources
10 p1497 N85-19449

MAP-related activities in the United States
11 p1655 N85-20427

General aviation activity and avionics survey
[AD-A149572] 12 p1769 N85-21103

A community survey of helicopter noise annoyance conducted under controlled noise exposure conditions
[NASA-TM-86400] 13 p2154 N85-23374

Research on the effect of noise at different times of day: Models, methods and findings
[NASA-CR-3888] 13 p2154 N85-23375

Development, achievements in China's cartography work 13 p2166 N85-23434

A constant altitude flight survey method for mapping atmospheric ambient pressures and systematic radar errors
[NASA-TM-86733] 19 p3217 N85-29951

SURVIVAL

Maximum likelihood estimation of the survival functions of N stochastically ordered random variables
[AD-A145429] 02 p0254 N85-11[illegible]2

Conditional regression models for transient state survival analysis
[AD-A147872] 07 p1034 N85-16563

Effects of pyridostigmine on psychomotor and visual performance
[AD-A148553] 08 p1196 N85-17539

Assessment of seismic survivability
09 p1336 N85-18402

Effect of prolonged hunger during experimental hikes
11 p1692 N85-20637

Proportional odds models for survival data and estimates using ranks
[MATHEMATICS-RESEARCH-172]
12 p1923 N85-22080

Survival of microorganisms and bacterial predation in nature
[AD-A153574] 18 p3152 N85-29514

Effects of long-term low-level radiofrequency radiation exposure on rats. Volume 8: Evaluation of longevity, cause of death, and histopathological findings
[AD-A154283] 19 p3327 N85-30610

Aviation safety (aircraft passenger survivability and cabin safety)
[GPO-39-847] 23 p3895 N85-34130

SURVIVAL EQUIPMENT

Evaluation of survival straws (pocket purifier)
[AD-A146240] 03 p0328 N85-12114

SUSCEPTIBILITY (MAGNETISM)

U MAGNETIC PERMEABILITY

SUSPENDING (HANGING)

NT MAGNETIC SUSPENSION

Test methods for cable cars
[CETIM-1-5K-45-1] 04 p0515 N85-13262

A gyro sensor block suspension
[AD-D011411] 08 p1154 N85-17284

A Lagrange-D'Alembert formulation of the equations of motion of a helicopter carrying an externally suspended load
[NASA-TM-85864] 12 p1776 N85-21149

Precise mounting of instruments in universal suspension with skewed axes 14 p2273 N85-24083

Constant fiber number during skeletal muscle atrophy and modified arachidonate metabolism during hypertrophy 15 p2609 N85-26078

Blood pressure responses and mineral ocorticoid levels in the suspended rat model for weightlessness
15 p2609 N85-26079

SUSPENSION SYSTEMS (VEHICLES)

The experimental performance of an off-road vehicle utilizing a semi-active suspension — off-road motorcyles
09 p1339 N85-18421

A theoretical investigation of an active suspension system for wheeled tractors
[AD-P004268] 09 p1405 N85-18844

Low-profile fastener
[AD-D011667] 19 p3280 N85-30343

Damping of suspension oscillations for stratospheric balloon experiments
[MPE-IR-42 20 p3463 N85-31517

SWAGING

Development of intercalated wire and cable
[AD-A146502] 06 p0774 N85-14948

SWALLOWING

Tritium hazard via the ingestion pathway
[DE85-012897] 24 p4133 N85-35618

SWAMPS

U MARSHLANDS

SWATH WIDTH

Cartography 02 p0214 N85-11412

SAR swath widening techniques — satellite radar
[BL-6198] 20 p3441 N85-31358

SWEAT

Evaluation of a field expedient technique for sweat sample collection
[AD-A151916] 16 p2641 N85-27521

SWEAT COOLING

Advanced liner-cooling techniques for gas turbine combustors
[NASA-TM-86952] 12 p1770 N85-21115

Exercise-heat strain during hypohydration: Interaction with heat acclimation and aerobic fitness
[AD-A151023] 14 p2389 N85-24717

SWEATING

U PERSPIRATION

SWEDEN

PROMIS 600: The pilot project for the future Swedish weather service 01 p0083 N85-10560

A pilot study of future research on seismic hazards in Sweden
[FOA-C-20544-T1] 02 p0229 N85-11496

Sweden's Kiruna may be future launch site for satellites 03 p0310 N85-12000

Space research in Sweden 03 p0321 N85-12073

Seismicity of southern Sweden
[FOA-C-20543-T1] 07 p0998 N85-16340

Ground truth for SIR-B images obtained by SIR system 8 impulse radar 08 p1149 N85-17251

Finnair, LOT, SAS reps in USSR on present operations, plans 09 p1278 N85-18035

Scania, ASEA of Sweden use robots for all production phases 09 p1310 N85-18229

Overview of major Swedish institutions in polymer research 11 p1592 N85-20014

Catastrophic-flood features in Swedish Lapland as a terrestrial analog for Martian channel flows
13 p2190 N85-23587

Hydrological data collection from Swedish mountain areas 14 p2327 N85-24388

Sweden develops new rapid solidification process
15 p2531 N85-25610

Sweden invents new ceramic for more durable cutting tools 15 p2536 N85-25645

Swedish space program includes research satellites
18 p3088 N85-29113

Possible use of the COSPAS/SARSAT system within the Swedish mountain rescue organization
20 p3401 N85-31100

Human factors engineering contracts in Sweden: An overview
[FOA-C-56043-H2] 20 p3513 N85-31836

SWEDISH SPACE PROGRAM

Swedish equipment for automatic docking in space
15 p2489 N85-25363

SWEEP CIRCUITS

Improvements in avalanche-transistor sweep circuitry for electrooptic streak cameras
[DE84-016195] 06 p0811 N85-15155

SWEEP EFFECT

Design of a basic profile for a low sweep airfoil. Part 2: Experimental investigation on the DFVLR-W1 airfoil profile in the Brunswick transonic wind tunnel
[DFVLR-FB-85-01-PT-2] 17 p2892 N85-27833

SWEEP FREQUENCY

Simple sweep frequency generator
13 p2075 N85-22960

SWELLING

Evaluation of ferritic alloy Fe-2 1/4Cr-1Mo after neutron irradiation: Irradiation creep and swelling
[DE84-014647] 04 p0474 N85-13022

Tensile properties and swelling of 20%-cold-worked Type 316 stainless steel irradiated in HFIR
[DE84-014080] 05 p0617 N85-13948

Swelling behavior of titanium-modified AISI 316 alloys
[DE84-013940] 05 p0618 N85-13956

Mechanisms of elevated temperature rupture in single phase ceramics
[DE85-000697] 09 p1299 N85-18156

Swelling behavior of manganese-bearing AISI 216 steel
[DE85-005712] 15 p2512 N85-25495

The physical effects of different stress situations on graphite/epoxy compounds 15 p2687 N85-26594

Swelling behavior of titanium-modified AISI 316 alloys
[DE85-007470] 16 p2752 N85-26982

An investigation of the irradiation swelling mechanisms in refractory metals at high temperatures
[AD-A154149] 19 p3238 N85-30079

SWEPT FORWARD WINGS

The development of a dynamic model of a generalised combat aircraft with forward wings for the identification of stability and control characteristics
[CAR-84-33] 09 p1280 N85-18050

Active control of forward swept wings with divergence and flutter aeroelastic instabilities
09 p1282 N85-18063

Multivariable control law design for the X-29 aircraft
[AD-A151828] 15 p2472 N85-25259

Active control of forward swept wings with divergence and flutter aeroelastic instabilities
[AD-A151837] 15 p2474 N85-25270

Some effects of sweep direction and strakes for wings with sharp leading edges
[CA-8421] 17 p2892 N85-27826

X-29 digital flight control system design
17 p2901 N85-27889

The static aeroelasticity of a composite wing
18 p3121 N85-29321

SWEPT WINGS

NT DELTA WINGS
NT SWEPT FORWARD WINGS
NT SWEPTBACK WINGS

Experiments suitable for wind tunnel wall interference assessment/correction 03 p0313 N85-12021

Design of a basic airfoil for a slightly swept wing. Part 1: Theoretical transonic airfoil design
[DFVLR-FB-84-19-PT-1] 03 p0316 N85-12043

Experimental study on transonic flutter characteristics of sweptback wing with core composite plates having different fiber orientations
[NAL-TR-827] 06 p0756 N85-14842

Application of two and three-dimensional criteria for calculating transitions and boundary layers over swept wings 08 p1070 N85-16783

Full scale experiments into the use of large eddy breakup devices for drag reduction on aircraft
08 p1071 N85-16790

Joined wing transonic design and test validation
[AD-A148355] 08 p1078 N85-16834

Unsteady stall penetration of an oscillating swept wing
[AD-P004156] 09 p1264 N85-17941

Effects of leading-edge devices on the low-speed aerodynamic characteristics of a highly-swept arrow-wing
[NASA-CR-172531] 13 p1968 N85-22365

Calculation of vortex-flap aerodynamic characteristics
[NASA-CR-175624] 13 p1969 N85-22367

Calculation of unsteady transonic flow around a high swept wing 15 p2459 N85-25184

La Recherche Aerospatiale Bimonthly Bulletin, Number 1984-4, 221/July-August
[ESA-TT-884] 16 p2695 N85-26637

On the effect of wing taper and sweep direction on leading edge transition
[CA-8425] 17 p2892 N85-27827

Effect of leading-edge load constraints on the design and performance of supersonic wings
[NASA-TP-2446] 19 p3213 N85-29923

Selecting step sizes in sensitivity analysis by finite differences
[NASA-TM-86382] 22 p3799 N85-33538

SWEPTBACK WINGS

NT DELTA WINGS

Experience with transonic unsteady aerodynamic calculations 15 p2458 N85-25176

Some effects of sweep direction and strakes for wings with sharp leading edges
[CA-8421] 17 p2892 N85-27826

Experimental and theoretical study of the longitudinal aerodynamic characteristics of delta and double-delta wings at Mach numbers of 1.60, 1.90, and 2.16
[NASA-TP-2433] 19 p3213 N85-29922

Design of a basic airfoil for a slightly swept wing. Part 1: Theoretical transonic airfoil design
[ESA-TT-892] 20 p3394 N85-31054

SWINGBY TECHNIQUE

Mars exploration, Venus swingby and conjunction class mission modes, time period 2000 to 2045
[NASA-TM-86477] 02 p0303 N85-11961

SWIRLING

Design of swirled axisymmetric turbulent jets
05 p0724 N85-14657

Rayleigh and Raman scattering for density in a swirling flow combustor 08 p1120 N85-17060

Swirling turbulent spray group combustion
09 p1269 N85-18095

Workshop report: Swirl Enhanced Combustion
13 p2005 N85-22564

Turbulence characteristics of swirling flowfields
[NASA-CR-174918] 16 p2709 N85-26717

Flow modifying device
[NASA-CASE-LEW-13562-2] 24 p4065 N85-35195

SWIRLING WAKES

U TURBULENT WAKES

SWITCHES

NT CAPACITANCE SWITCHES
NT ELECTRIC RELAYS
NT ELECTRIC SWITCHES
NT FLUID SWITCHING ELEMENTS
NT SWITCHING CIRCUITS
NT THERMOSTATS

LED multifunction keyboard engineering study
[AD-A145199] 01 p0010 N85-10061

Simulation study of a new inverse-pinch high Coulomb transfer switch
[NASA-CR-172420] 02 p0194 N85-11294

Vacuum inductive pulsed power compression for inertial confinement fusion
[DE84-010935] 03 p0421 N85-12860

High-temperature optically activated GaAs power switching for aircraft digital electronic control
[NASA-CR-174711] 04 p0457 N85-12901

Storage life of thermal detents
[DE84-016934] 04 p0476 N85-13030

Magnetic and photoconductive repetitive rail-gun opening switches
[DE84-017080] 04 p0496 N85-13163

Integrated power devices with three-dimensional connection for automation systems
06 p0794 N85-15077

Switchable zero order diffraction gratings as light valves
[AD-A147575] 07 p1044 N85-16633

Centrifuge tests to provide closure bounds for switches subjected to random vibration
[DE85-002003] 10 p1482 N85-19357

A new very high voltage semiconductor switch
[NASA-TM-86957] 11 p1627 N85-20246

Wide angle phased array dome lens antenna with a reflection/transmission switch
[AD-D011562] 12 p1833 N85-21502

KAM-250 antenna switch 13 p2068 N85-22916

Picosecond photoconductive devices for 10 Gbit/s optoelectronic switching 18 p3187 N85-29770

Development of a resistive load for PBFA 2 rimfire gas switch simultaneity and laser triggering tests
[DE85-011080] 19 p3365 N85-30889

The plasma erosion opening switch
[AD-A154942] 21 p3580 N85-32259

Coordinated research program in pulsed power physics
[AD-A154629] 21 p3679 N85-32858

Operational window for a plasma erosion opening switch used for voltage multiplication on pulsed power generators
[AD-A155482] 21 p3707 N85-33020

Electro-optic harmonic conversion to switch a laser beam out of a cavity
[DE85-011619] 22 p3790 N85-33483

Multiple-stage integrating accelerometer
[DE85-006505] 23 p3935 N85-34388

Photoconductive pulse power switches: A review
[DE85-014125] 24 p4091 N85-35360

SWITCHING

NT MICROWAVE SWITCHING
NT PACKET SWITCHING
NT PACKET TRANSMISSION

DC switching regulated power supply for driving an inductive load
[DE84-014238] 01 p0044 N85-10285

Formation of reference signals in laser-type gas analyzers with mechanical switching of optical channels
06 p0787 N85-15027

High-speed power thyristors with excellent switching and load characteristics 06 p0793 N85-15070

NBS (National Bureau of Standards) switching radiometers
[PB84-235894] 07 p0968 N85-16147

Stereo decoder without subcarrier restoration
13 p2068 N85-22921

Energy considerations in second breakdown
[AD-A152389] 17 p2952 N85-28229

Pursuit tracking performance and flash disruption: The effects of training the non-dominant eye on target reacquisition
[AD-A153404] 17 p2990 N85-28541

Picosecond photoconductive devices for 10 Gbit/s optoelectronic switching 18 p3187 N85-29770

Experimental demonstration of an optoelectronic switch matrix for satellite-switched TDMA signals in the 0.3-4.0 GHz band
[CRC-TN-717] 19 p3253 N85-30170

Control of energy-storage dc-to-dc converters: The large-signal time-domain approach
19 p3257 N85-3018

Switchable zero order diffraction gratings as light valves
[AD-A154471] 20 p3533 N85-31981
Plasma erosion opening switch
[DE85-011364] 20 p3535 N85-31996
The plasma erosion opening switch
[AD-A154942] 21 p3580 N85-32259
Model that predicts pulse charged gas switching breakdown phenomena
[DE85-013119] 22 p3761 N85-33313

SWITCHING CIRCUITS
NT FLUID SWITCHING ELEMENTS
Isolated load switching with surge suppression
[AD-D011218] 01 p0042 N85-10274
Noise isolation system for high-speed circuits
[DE84-014229] 01 p0043 N85-10283
High or low-side solid state relay with current limiting and operational testing
[AD-D011260] 05 p0631 N85-14046
Power MOS fast switching techniques
[DE84-015046] 05 p0732 N85-14707
Trends in development of bipolar power transistors
06 p0793 N85-15072
Fast switching driver for inductive load, such as a phase shifter
[AD-D011368] 08 p1143 N85-17207
Development of photoconductive power switch technology
[DE85-001514] 09 p1315 N85-18270
Surface and allied studies in silicon solar cells
[NASA-CR-174447] 11 p1671 N85-20531
Power circuit utilizing self-excited Hall effect switch means
[AD-D011505] 12 p1832 N85-21496
Transients during the switching of SF6-insulated isolating switches
[BLL-CE-TRANS-7986-(9022.09)]
15 p2546 N85-25713
Development of a butterfly multiprocessor test bed description of butterfly components
[AD-A153692] 18 p3095 N85-29155
Stationary properties and switching characteristics of dispersive optical bistability in CuCl
18 p3186 N85-29763
Experimental demonstration of an optoelectronic switch matrix for satellite-switched TDMA signals in the 0.3-4.0 GHz band
[CRC-TN-717] 19 p3253 N85-30170
Fast transient behavior of thyristor switches
[AD-A154109] 19 p3259 N85-30206
Performance of the butterfly processor-memory interconnection in a vector environment
[DE85-007931] 19 p3261 N85-30224
T/R switch design for short-range measurements, part 8.1A 21 p3624 N85-32515
Coordinated research program in pulsed power physics
[AD-A154629] 21 p3679 N85-32858
Switching power supply
[DE85-005993] 22 p3761 N85-33312
Capacitance measuring device
[DE85-011643] 22 p3767 N85-33460
Series-counterpulse repetitive-pulse inductive storage circuit
[DE85-006436] 23 p3928 N85-34342

SWITCHING ELEMENTS
U SWITCHING CIRCUITS

SWITCHING THEORY
Onboard demand scheduling of a multibeam SS/TDMA satellite with integrated circuit and packet switching
14 p2229 N85-23812
Automation of development of software for switching units that are implemented in the form of multiprocessor systems on a microcomputer base
14 p2401 N85-24802

SWITZERLAND
Deformation mechanisms associated with mesoscopic kinkbands, Jura Mountains (Switzerland) and Chaines Subalpines (France) 03 p0389 N85-12492
West Europe report: Science and technology
[JPRS-WST-84-007] 15 p2530 N85-25600

SYMBIOSIS
From microbial communities to cells
21 p3559 N85-32728

SYMBIOTIC STARS
Fluorescent excitation of Fe 2, Mn 2, Ti 2, N 1 lines by V 4, N 5, O 6: Emission lines in the spectra of symbiotic stars and Seyfert galaxies 11 p1746 N85-20984
IUE observations of the jet emission feature in R Aquarii 11 p1747 N85-20988
Physical models for the UV continua of symbiotic stars
11 p1756 N85-21048

SYMBOLIC PROGRAMMING
Representation and refinement of visual specifications in PegaSys
[AD-A148733] 09 p1368 N85-18598
Supercomputers and symbolic computation
[AD-A151376] 15 p2623 N85-26186
Use of REDUCE 2 for symbolic programming
[INPE-3355-PRE/633] 16 p2846 N85-27544
Tenth-order expansion formulae for the orbital eccentricity function K (sub lpq)(e) obtained using a symbolic algebraic manipulation system
[AD-A153754] 18 p3170 N85-29647

SYMBOLS
Information-theoretic properties of languages and their grammars
[AD-A146688] 06 p0799 N85-15106
Symbol structure, information content and visual form: A carto-semiotic theory of map signs
09 p1342 N85-18439
FLAD user's manual: FLAD file contents
[AD-A148700] 09 p1368 N85-18594
Automatic symbolic solution of Markov chains
[AD-A150476] 13 p2153 N85-23369
Symbol stream combining in a convolutionally coded system 16 p2771 N85-27101
Development of new circuit symbols for binary logic elements
[MBB-Z-39/85-O] 17 p3014 N85-28640
Proposal for the systematic naming of mesons and baryons
[DE85-008453] 17 p3035 N85-28773

SYMMETRICAL BODIES
NT AXISYMMETRIC BODIES
NT BODIES OF REVOLUTION
NT CELESTIAL SPHERE
NT CONCENTRIC SPHERES
NT CONICAL BODIES
NT CYLINDRICAL BODIES
NT ELLIPSOIDS
NT FAIRINGS
NT FALLING SPHERES
NT PARABOLIC BODIES
NT POINCARE SPHERES
NT ROTATING CYLINDERS
NT ROTATING SPHERES
NT SLENDER CONES
NT SPHERES
NT STREAMLINED BODIES
NT TORUSES
Two lunar global asymmetries
04 p0585 N85-13734
Motion of heavy symmetric body with flexible bars about stationary point 06 p0780 N85-14969
Dynamics of solid body with ellipsoidal cavity containing magnetic fluid 14 p2279 N85-24116
Stability of steady motions of dynamically symmetrical solid at a triangular libration point
14 p2279 N85-24120
The Mises yield condition for thin rotationally symmetric shells
[BLL-BISI-TRANS-22047-(9022.06)]
17 p2976 N85-28409
Magnetic field and equivalent circuit of induction motors with shielded poles 22 p3772 N85-33378

SYMMETRY
NT BROKEN SYMMETRY
Searching for top, Higgs, and supersymmetry: The minimum invariant mass technique
[DE84-014539] 01 p0119 N85-10813
Nonlinear symmetrization of picosecond pulses in optical fibers 02 p0264 N85-11725
On the weak limits of elementary symmetric polynomials
[CWI-MS-R8407] 05 p0719 N85-14620
On the nature of the baryon asymmetry
[NASA-TM-86156] 05 p0746 N85-14784
Downwash in the plane of symmetry of an elliptically loaded wing
[NASA-TP-2414] 07 p0898 N85-15693
The symmetry group and exponents of operator stable probability measures
[AD-A147187] 07 p1035 N85-16568
A numerical approach for the vibration analysis of an axisymmetric shell structure with a nonuniform edge constraint
[AD-A149286] 11 p1651 N85-20402
Complex symmetric matrices with strongly stable iterates
[NASA-CR-172542] 11 p1706 N85-20731
Ultraviolet divergences and supersymmetric theories
[DE85-001649] 11 p1729 N85-20875
Simulating supersymmetry at the SSC
[DE85-000699] 11 p1736 N85-20917
Accidental degeneracies, hidden supersymmetries, and spectrum-generating superalgebras
[DE85-003547] 11 p1738 N85-20930
Efficient heating and confinement of ions in an axisymmetric magnetic mirror supplemented with dc electric field
[IPPJ-707] 12 p1935 N85-22160
Determining geometrical divergence using seismic observation data 14 p2343 N85-24489
Determination of symmetry of immediate surroundings in amorphous Co-P alloys 15 p2496 N85-25398
Effect of axisymmetric vibration modes on sensitivity and directivity characteristics of piezoceramic sphere — hydrophones 15 p2525 N85-25569
Antenna with outboard exciter for 3.4-13.25 GHz frequency range 15 p2526 N85-25577
Temperature: Curvature relationships for unsymmetric graphite-epoxy laminates
[VPI-E-85-08] 16 p2743 N85-26926
On residual stress in an elastic body
16 p2798 N85-27248
Chemical applications of topology and group theory. 17: An information theoretical approach to polyhedral symmetry
[AD-A152821] 17 p2919 N85-27995
Lattice actions improved by block-spin renormalisation group and maximally symmetric lattices
[DE85-007416] 17 p3045 N85-28841
Hamiltonian picture of the free electron laser and unitary symmetries
[PREPRINT-436] 18 p3114 N85-29281
Detection of multivariate outliers with dispersion slippage in elliptically symmetric distributions
[AD-A153765] 18 p3174 N85-29677
Weak interactions of quarks and leptons: Experimental status
[DE85-006171] 18 p3181 N85-29723
Distribution of density in closed-impression die forging of axisymmetrical products from metal powders
19 p3245 N85-30118
Boson-fermion symmetries in the W-Pt region
[DE85-009755] 19 p3362 N85-30845
Primordial inflation and supergravity
[DE85-009538] 19 p3383 N85-30989
Theoretical prediction of stationary positions in the rectangular chamber during asymmetric electroosmotic flow 20 p3499 N85-31750
New O(6) region near A = 130 and the interplay of triaxiality and gamma-softness in the IBA
[DE85-010957] 20 p3530 N85-31961
Remarks on nucleon-nucleon hard scattering
[NIKHEF-H/84-14] 20 p3532 N85-31979
Possibility of developing charged-particle energy analyzer based on hyperboloidal axisymmetrical lens
21 p3691 N85-32933

SYMMETRY BREAKING
U BROKEN SYMMETRY

SYMPATHETIC NERVOUS SYSTEM
Natural electrical activity of human sympathetic nerve fibers, recorded from body surface
07 p1013 N85-16433
Regulation of physical activity in antiorthostatic position by acting on adrenosympathetic and hypophyseo-adrenocortical systems
22 p3824 N85-33689

SYMPATHOMIMETICS
U ADRENERGICS

SYMPHONIE SATELLITES
Clock synchronization by the Symphonie and Laser Synchronization from Stationary Orbit (LASSO) geostationary satellites 14 p2398 N85-24778

SYMPTOMS
U SIGNS AND SYMPTOMS

SYNAPSES
Natural electrical activity of human sympathetic nerve fibers, recorded from body surface
07 p1013 N85-16433
Direct assessment of synaptic modification rules
[AD-A148376] 08 p1196 N85-17534
Effects of hypothermia on brain metabolism
11 p1692 N85-20636
A model for generalization and specification by single neurons
[AD-A150871] 14 p2391 N85-24724

SYNCHRONISM
NT BIT SYNCHRONIZATION
NT FREQUENCY SYNCHRONIZATION
DCS (Defense Communications System) network synchronization design criteria
[AD-A146251] 03 p0356 N85-12289
Adaptive mutual interference suppression method
[AD-D011288] 05 p0628 N85-14024
Experiences with nonsynchronous forced vibration in centrifugal compressors 05 p0642 N85-14119
Digital raster timing encoder-decoder
[AD-D011279] 06 p0804 N85-15120
Reed-Solomon code synchronization revisited
10 p1464 N85-19234
Fast synchronization model for UHF spread-spectrum communication system 10 p1473 N85-19296
A technical solution to fadings in tactical satellite digital transmissions 10 p1473 N85-19297

Asynchronous transmission with strong spectral spread 10 p1474 N85-19300

Design of a semi-custom integrated circuit for the SLAC SLC timing control system
[DE85-003091] 11 p1629 N85-20258

Psychological aspects of phemomenon of spatial synchronization of EEG potential
11 p1691 N85-20632

Investigation of influence of communications link and synchronization error on noise tolerance of group transmission of binary information based on orthogonal Walsh function 13 p2086 N85-23026

Location and synchronization — space-time coordinates 14 p2397 N85-24768

Constructing unifying frameworks for the study of distributed system and algorithms
[AD-A151287] 15 p2637 N85-26261

Synchronizing heavily encoded data in bad weather
16 p2770 N85-27099

Symbol stream combining in a convolutionally coded system 16 p2771 N85-27101

UHF IRIG G distribution system
17 p2965 N85-28306

Precise time transfer using MKIII VLBI technology
17 p2966 N85-28310

Time synchronization experiments with APPLE
17 p2967 N85-28323

New GOES satellite synchronized time code generation 18 p3109 N85-29247

The time and frequency comparisons via Loran-C and National TV Network in Yugoslavia
18 p3109 N85-29248

Introduction to programming multiple-processor computers
[DE85-010274] 18 p3164 N85-29599

Balanced system for ranging and synchronization between satellite pairs
[AD-D011697] 19 p3224 N85-29992

Phase locked loop synchronization for direct detection optical PPM communication systems
[NASA-CR-176026] 19 p3254 N85-30178

Development of a resistive load for PBFA 2 rimfire gas switch simultaneity and laser triggering tests
[DE85-011080] 19 p3365 N85-30869

Globally-asynchronous locally-synchronous systems
[AD-A154624] 21 p3573 N85-32222

Consensus in the presence of partial synchrony (Preliminary version)
[AD-A154705] 21 p3670 N85-32799

A new fault-tolerant algorithm for clock synchronization
[AD-A154771] 21 p3676 N85-32836

SYNCHRONIZATION
U SYNCHRONISM

SYNCHRONIZERS

Hydraulic forces on a centrifugal impeller undergoing synchronous whirl 05 p0643 N85-14124

Instrument to synchronize Thomson scattering diagnostic measurements with MHD activity in a Tokamak
[DE85-012082] 23 p3964 N85-34706

SYNCHRONOUS DETECTORS
U CORRELATORS

SYNCHRONOUS MOTORS

Operational behavior of wind energy converters. Control and dynamic and types of generators, volume 1
[BMFT-FB-T-84-154-VOL-1] 03 p0386 N85-12470

Operational behavior of wind energy converters: Control and dynamic and types of generators, volume 2
[BMFT-FB-T-84-154-VOL-2] 03 p0386 N85-12471

The performance of an alternating-current thyristor-controlled motor 15 p2546 N85-25716

SYNCHRONOUS PLATFORMS

Full load testing in the platform module prior to tow-out: A case history of subsynchronous instability
05 p0642 N85-14117

Vibration analysis of a multipurpose platform
[NAL-TR-803] 09 p1286 N85-18078

Concentrator technologies evaluation for large solar arrays and their application for space stations/platforms
13 p2010 N85-22609

JANUS: An autonomous platform optimized for SARSAT type missions 20 p3406 N85-31135

The space station polar platform: NOAA systems considerations and requirements
[NOAA-TR-NESDIS-22] 22 p3740 N85-33182

SYNCHRONOUS SATELLITES
NT AEROS SATELLITE
NT ANIK SATELLITES
NT GOES SATELLITES
NT GOES 5
NT MIRANDA SATELLITE
NT SIRIO SATELLITE
NT STORMSAT SATELLITE

The past, present, and anticipated future contributions of geosynchronous satellites to short range prediction
01 p0076 N85-10503

Charging of the DMSP F-2 spacecraft in the aurora on 10 January 1983
[AD-A146303] 03 p0324 N85-12086

The launch window of a geostationary satellite
05 p0600 N85-13822

Perturbations in geostationary orbit
05 p0600 N85-13824

Stationkeeping strategies for geostationary satellites
05 p0600 N85-13825

Debris in the geostationary orbit ring, the endless shooting gallery: The necessity for a disposal policy
12 p1786 N85-21214

Navy tactical applications guide. Volume 4. Part 1. Eastern North Pacific weather analysis and forecast applications
[AD-A150097] 12 p1896 N85-21900

In-orbit laser regeneration of the radiation damaged solar arrays 13 p2006 N85-22588

The DFS-Kopernikus solar generator electrical design
13 p2006 N85-22590

The DFS-Kopernikus solar generator
13 p2006 N85-22591

Station keeping of geostationary satellites by electric propulsion
[NASA-TM-77820] 14 p2320 N85-24337

Orbital positioning and stationkeeping of geostationary satellites 14 p2397 N85-24772

A FORTRAN program for deep space sensor analysis
[AD-A151700] 15 p2489 N85-25366

A simulation experiment on the impact of geostationary temperature retrievals in numerical models
15 p2597 N85-26005

Study of a medium term flexible fixed satellite service mission
[DM51/CC-IM-0165.83] 18 p3091 N85-29136

A 406 MHz ELT processor for geostationary satellites — Emergency Locator Transmitter (ELT)
20 p3403 N85-31114

Navigation data for Emergency Position Indicating Radio Beacons (EPIRBs) 20 p3403 N85-31115

International prototype network in Dubna experimental satellite communications system
22 p3773 N85-33383

SYNCHROPHASING

An improved source model for aircraft interior noise studies
[NASA-CR-172517] 08 p1217 N85-17668

SYNCHROTRON RADIATION

Applications of synchrotron X-ray diffraction topography to fractography
[DE84-016257] 04 p0513 N85-13274

Instrumentation at national facilities for synchrotron radiation topography
[DE84-016256] 04 p0564 N85-13593

Electron spectrometry experiments with the use of synchrotron radiation
[DE85-001286] 07 p1041 N85-16610

Structural studies of amorphous Mo-Ge alloys using synchrotron radiation
[DE85-002061] 08 p1131 N85-17125

Synchrotron emission from chaotic stellar winds
08 p1234 N85-17774

Application of tunable monochromatic synchrotron radiation to the quantitative determination of trace elements
[DE85-001271] 09 p1291 N85-18106

Radio emission from RS CVn binary systems
09 p1417 N85-18939

Synchrotron X-ray fluorescence and extended X-ray absorption fine structure analysis
[DE85-003606] 10 p1438 N85-19063

Linear, position-sensitive X-ray detector used for real-time calculations of small-angle scattering parameters with submillisecond resolution
[DE85-002530] 10 p1489 N85-19401

Surface physics and crystallography
[DE85-003128] 11 p1735 N85-20910

Major facilities for materials research and related disciplines
[PB85-108850] 11 p1739 N85-20934

Multifrequency observations of BL LAC objects and violently variable quasars 11 p1746 N85-20981

Coordinated multifrequency observations of the BL LAC objects MRK 180, MRK 421, and MRK 501
11 p1746 N85-20983

Betatron-synchrotron detrapping in a tapered wiggler free electron laser
[AD-A149686] 12 p1856 N85-21642

Resonance between betatron and synchrotron oscillations in a free electron laser: A 3-D numerical study
[AD-A150059] 12 p1857 N85-21645

Intense, broadband, pulsed I-R source at the National Synchrotron Light Source
[DE84-010542] 12 p1936 N85-22154

Angle-resolved photoemission study of AuGa2 and AuIn2 intermetallic compounds
[AD-A150000] 12 p1940 N85-221

EXAFS of monolayers on silver electrodes: SSRL proposal number 717M
[AD-A150623] 13 p2018 N85-22

Threshold double photoionization of argon with synchrotron radiation
[AD-A150615] 13 p2157 N85-2

Noninductive current drive in Tokamaks
[DE85-005427] 14 p2424 N85-24

Application of permanent magnets in accelerators and electron storage rings
[DE85-004981] 15 p2642 N85-2

Measurement of NSLS distributed diode sputter ion pump characteristics
[DE85-006550] 16 p2760 N85-27

A synchrotron/inverse Compton interpretation of a solar burst producing fast pulses at lambda 3 mm and hard X-rays 16 p2887 N85-2761

Polymer Research at Synchrotron Radiation Sources: Symposium Proceedings
[DE85-008488] 18 p3081 N85-2

VUV synchrotron light as a technique for studying the interface quality and properties of thin overlayers
[DE85-009822] 19 p3262 N85-3

Present and future directions of atomic physics research with multiply-charged ions at Brookhaven National Laboratory
[DE85-010960] 19 p3354 N85-30

Frequent observations of extragalactic compact sources at 24 GHz 19 p3386 N85-31

The Silica Aerogel Detector (SAD) story — Cherenkov detector
[USIP-84-14] 20 p3459 N85-31

Permanent magnets for production and use of high energy particle beams
[DE85-009934] 20 p3522 N85-31

Microscopic control of semiconductor surface oxidation
[AD-A154799] 21 p3709 N85-33

Photoionization of alkali and alkaline earth atoms: Na and Mg
[DE85-011812] 22 p3837 N85-33

Saturation of a longitudinal instability due to nonlinearity of the wake field
[DE85-012514] 22 p3837 N85-33

On the emission region of gamma ray bursts
[OG-1.1-4] 22 p3861 N85-33

The electron spectra in the synchrotron nebula of the supernova remnant G 29.7-0.3
[OG-6.2-10] 22 p3869 N85-34

Onion-shell model for cosmic ray electrons and radio synchrotron emission in supernova remnants
[OG-8.1-10] 23 p4018 N85-34

Dissociative and double photoionization cross sections of NO from threshold to 120 A
[NASA-CR-176185] 24 p4147 N85-357

Exit channels of autoionization resonances in atoms
[DE85-012299] 24 p4149 N85-357

Breeding new light into old machines (and new)
[DE85-013055] 24 p4155 N85-357

Accelerator physics measurements at the damping ring
[DE85-013373] 24 p4159 N85-357

SYNCHROTRONS
NT STORAGE RINGS (PARTICLE ACCELERATORS)

Design study of the vacuum pump of the ESRP — synchrotron radiation
[NIKHEF-MTG-21] 08 p1138 N85-171

A study of the K-edge absorption spectra of selected vanadium compounds
[AD-A149334] 10 p1435 N85-19

First- and second-order charged particle optics
[DE85-006310] 14 p2421 N85-24

Future accelerator studies of high energy heavy ion collisions
[DE85-005885] 15 p2650 N85-2

Experiments with light ions at CERN super proton synchrotron
[DE85-007625] 17 p3031 N85-28

Alternating gradient synchrotron
[DE85-005950] 17 p3033 N85-28

Muon spin rotation studies 17 p3042 N85-28

3d calculations of a fixed field alternating gradient synchrotron magnet
[DE85-002742] 18 p3183 N85-29

Experience with a high-brightness storage ring: The NSLS 750 MeV VUV ring
[DE85-010547] 18 p3190 N85-29

Slow extraction of LAMPF 2
[DE85-010744] 19 p3356 N85-30

Combined function lattices for a 6 GeV synchrotron light source
[DE85-010959] 19 p3367 N85-30885
Longitudinal tune control in synchrotrons
[DE85-010745] 20 p3527 N85-31937
Spin physics at BNL
[DE85-009768] 20 p3529 N85-31955
Tailored vacuum chambers for ac magnets
[DE85-010767] 21 p3591 N85-32319
High-energy Physics Institute building 3-trillion-ev accelerator 21 p3691 N85-32934
Heavy ion medical accelerator options
[DE85-011204] 22 p3841 N85-33784
Commissioning the polarized beam in the AGS
[DE85-010958] 22 p3841 N85-33788
Robinson instability and beam loading
[DE85-013301] 24 p4151 N85-35737
Vacuum system for the Argonne 6 GeV synchrotron light source
[DE85-012286] 24 p4157 N85-35773
SYNCOPE
NT BLACKOUT (PHYSIOLOGY)
SYNDROMES
U SIGNS AND SYMPTOMS
SYNOPTIC MEASUREMENT
Empirical and modeled synoptic cloud climatology of the Arctic Ocean
[NASA-CR-175626] 13 p2137 N85-23272
Diagnostics of severe convection and subsynoptic scale ageostrophic circulations
[NASA-CR-171581] 21 p3634 N85-32571
SYNOPTIC METEOROLOGY
Application of automatic pattern methods in very-short-range forecasting 01 p0078 N85-10521
Short-term forecasting using a REMOS approach --- regime model output statistics (REMOS)
01 p0081 N85-10544
Investigation of summertime convection over the upper Current River valley of southeast Missouri
[PB84-222369] 01 p0086 N85-10578
The identification of rain-bearing synoptic systems through principal component analysis
02 p0212 N85-11394
The application of principal component analysis in a study of rainfall 02 p0212 N85-11396
Bibliography of climate textbooks and studies
[WCP-84] 02 p0231 N85-11505
The METEOSAT exploitation project, operational use of a remote sensing system 05 p0658 N85-14223
Use of photographs of meteorologic satellites in synoptic analysis
[SESIT-5] 05 p0679 N85-14357
The use of available potential energy to evaluate two GLAS FGGE data sets 05 p0682 N85-14387
The influence of synoptic scales on low-frequency modes of variability 05 p0687 N85-14412
Distribution of the K-corona over the polar regions of the solar disk: 1965-1983
[PB84-230077] 06 p0835 N85-15317
Synoptical observations of snow depths at Dutch meteorological stations, 1956 - 1977
[KNMI-TR-51] 07 p1006 N85-16407
Sea breeze-induced mesoscale systems and severe weather
[NASA-CR-174317] 08 p1187 N85-17480
Development of guidance forecasts at the Royal Netherlands Metorological Institute (KNMI). Part 1: General information
[KNMI-TR-54-PT-1] 08 p1190 N85-17499
Some aspects of atmospheric circulation near South America and interactions with the Antarctic regions
[INPE-3308-PRE/618] 10 p1515 N85-19561
Oceanographic and meteorological research based on the data products of SEASAT
[E85-10091] 12 p1874 N85-21753
AFOS (Automation of Field Operations and Service) surface observation decoding
[PB85-137586] 12 p1898 N85-21913
Sea breeze-induced mesoscale systems and severe weather 15 p2598 N85-26012
Development of a graphic system: Example using the outline of synoptic charts
[INPE-3296-PRE/611] 16 p2810 N85-27327
Fog advection in the Namib 16 p2831 N85-27454
A graphic system for drawing synoptic maps by computer
[INPE-3215-PRE/566] 16 p2834 N85-27474
SINOGRAFO: A system for influencing and forecasting weather
[INPE-3349-PRE/628] 16 p2834 N85-27475
Statistical interpretation of the ECMWF model using MOS to predict surface wind and temperature
[WSR-2] 17 p2995 N85-28515
Towards a study of synoptic-scale variability of the California current system
[NASA-CR-175671] 17 p2997 N85-28529
Atmospheric cross sections for the Arctic gas and aerosol sampling program, March - April 1983
[NASA-CR-176027] 19 p3314 N85-30541
On the state of knowledge on meteorologically caused icing of aircraft in clouds
[ESA-TT-861] 20 p3496 N85-31736
Frequency and site selection criteria for MST radars, part 5.1A 21 p3624 N85-32512
SYNTAX
NT WORDS (LANGUAGE)
Model theory for infinitely deep languages
[ISSN-0355-0087] 01 p0101 N85-10674
PROGEN: An incremental programming environment
[NRIMS-TWISK-315] 02 p0241 N85-11566
Research in knowledge representation for natural language understanding
[AD-A145807] 03 p0409 N85-12613
Toward a principle-based parser
[AD-A147637] 08 p1202 N85-17585
Speech analysis by parametric methods: A survey
[ENST-84C004] 09 p1313 N85-18251
An algorithm for generating abstract syntax trees
[NASA-CR-172541] 12 p1912 N85-22003
The four forms of omega
[AD-A149694] 12 p1915 N85-22020
The design and implementation of a syntax directed editor for a space constrained microcomputer
[AD-A151313] 15 p2623 N85-26163
Evaluating syntactic constraints to speech recognition in a fighter aircraft environment
[AD-A152117] 16 p2773 N85-27119
Research in knowledge representation for natural language understanding
[AD-A152260] 16 p2851 N85-27579
The design, implementation and application of a table-driven syntax-directed editor
[AD-A154234] 19 p3336 N85-30670
Survey of Ada (Trademark)-based PDLs (Program Design Language)
[AD-A154402] 19 p3338 N85-30680
Speech understanding research
[AD-A155462] 21 p3700 N85-32990
Research on distributed artificial intelligence
[AD-A155356] 22 p3833 N85-33733
SYNTHESIS
Electrochemistry of Hexanitroazobenzene (HNAB)
[DE85-010807] 21 p3565 N85-32171
SYNTHESIS (CHEMISTRY)
A method for obtaining new cyclical imides of derivative benzimidazoles
[AD-A145042] 01 p0017 N85-10106
Method of obtaining polychalcones
[AD-A145051] 01 p0018 N85-10107
Method of obtaining polybenzimidazopyrrolones
[AD-A145140] 01 p0018 N85-10108
Synthesis of pentafluorotellurium hypofluorite
[AD-D011212] 01 p0023 N85-10139
Two silicon phthalocyanines and a silicon naphthalocyanine: Synthesis, electrochemistry and electrogenerated chemiluminescence
[AD-A144760] 01 p0023 N85-10145
Synthesis and characterization of advanced materials
[PB84-215326] 01 p0025 N85-10156
Powder containing 2H-type silicon carbide produced by reacting silicon dioxide and carbon powder in nitrogen atmosphere in the presence of aluminum
[NASA-TM-77597] 01 p0027 N85-10167
Transition metal carbene complexes
[AD-A144879] 01 p0028 N85-10173
Method for the preparation of poly(carbonyl fluoride) oligomers
[AD-D011207] 01 p0030 N85-10184
Preparation and properties of single crystals of hydrogen bis(phthalocyaninato) neodymium(3)
[AD-A144933] 01 p0123 N85-10846
Recent progress in BGO development for high resolution calorimetry
[MPI-PAE/EXP-E1-129] 01 p0124 N85-10848
A new heat-resistant polymer from dimer diamine bismaleimide. Part 1: Preparation and free radical cure of dimer diamine bismaleimide
[AD-A145664] 02 p0186 N85-11247
The 7-Amino-4,6-Dinitrobenzofuroxan, an insensitive high explosive
[AD-A145665] 02 p0188 N85-11257
Synthesis of stereoisomeric - metal complexes using phase-transfer catalysis and photochemical transforms
[AD-A145787] 03 p0331 N85-12134
Syntheses of polyhedranes and polyhedral carboranes
[AD-A146076] 03 p0340 N85-12187
Thermoplastic/melt-processable polyimides
04 p0466 N85-12961
Matrix synthesis and characterization
04 p0467 N85-12965
Study of catalysts and mechanisms in synthesis reactions
[DE84-015025] 04 p0470 N85-12990
Physics and design of advanced infrared bolometers and photoconductors
[DE84-016683] 04 p0503 N85-13213
Low temperature synthesis of polycaproamide copolymers grafted with polydimethylaminothylmethacrylate
06 p0761 N85-14868
Synthesis of reinforced composite threads based on polymer mixtures 06 p0761 N85-14869
Synthesis of antimicrobial chemical fibers and fibrous materials containing quaternary ammonium compounds and their utilization 06 p0762 N85-14872
A silicon phthalocyanine and a silicon naphthalocyanine: Synthesis, electrochemistry, and electrogenerated chemiluminescence
[AD-A146441] 06 p0765 N85-14895
Polymerization and halogen scrambling behavior of phenyl-substituted cyclotriphosphazenes
[AD-A146366] 06 p0771 N85-14930
Synthesis of film-forming electron-accepting polymers
[AD-A146430] 06 p0771 N85-14931
Solar wind and cosmic ray irradiation of grains and ices - application to erosion and synthesis of organic compounds in the solar system
06 p0888 N85-15637
Pseudo-p-1,2,2,9,9,10,10-octofluoro (2,2)-p-cyclophane bis-acid chloride
[AD-D011393] 07 p0919 N85-15818
Structural and synthetic organosilicon chemistry
[AD-A147101] 07 p0919 N85-15820
Synthesis and properties of Hexachloromolybdates(5) and related species
[AD-A139599] 07 p0924 N85-15852
Fluorinated diacrylic esters
[AD-D011328] 07 p0929 N85-15889
Polyphosphazene solid electrolytes
[AD-A147006] 07 p0931 N85-15902
Synthesis and characterization of unique liquid crystalline block copolyesters. A proposal for a polymer research center at the Atlanta University
[AD-A147280] 07 p0932 N85-15907
New synthesis of phosphazene polymers
[AD-A147567] 07 p0933 N85-15910
Elastomers and other organic composites
[AD-A147624] 08 p1131 N85-17131
Synthesis and characterization of a 1,4 Polybutadiene/isotactic polypropylene block copolymer
[AD-A148199] 08 p1133 N85-17142
The synthesis and characterization of Poly(Oxy(2-Methyl-1,3-Phenylene) Methyl-1,3 -Phenylene) Oxyterephthaloyl)Oxy
[AD-A148269] 08 p1133 N85-17143
Properties of ultra-violet cured poly(dimethylsiloxane)-urea acrylates
[AD-A148570] 08 p1134 N85-17146
Poly(dimethylsiloxane)-polyurethane elastomers: Synthesis and properties of segmented copolymers and related zwitterionomers
[AD-A148571] 08 p1134 N85-17147
Metal-support interactions: The effect of catalyst preparation on catalytic activity
[DE84-017425] 09 p1293 N85-18118
Continuous organic electrochemical synthesis
[DE85-001400] 10 p1437 N85-19057
Stable polymeric carbon radicals. Part 2: Attempts at the preparation of polyradicals of the triphenylmethyl type linked by P-phenylene units
[NASA-TM-77799] 10 p1450 N85-19134
Method for making heterocyclic block copolymers
[AD-D011446] 10 p1451 N85-19143
Polymer electrolytes: An investigation of some poly (N-propylaziridine)/lithium salt compositions
[AD-A149444] 10 p1452 N85-19146
Method for synthesizing indium phosphide
[AD-D011475] 10 p1563 N85-19655
Studies of the kinetics and mechanisms of ammonia synthesis and hydrodesulfurization on metal single crystal surfaces
[DE85-001650] 11 p1595 N85-20030
Investigation of structure-permeability relationships of silicone polymer membranes
[PB85-148476] 11 p1596 N85-20038
Solar fuel synthesis based on colloidal and particulate semiconductors
[PB85-129104] 11 p1614 N85-20152
The synthesis, structural characterization and reactions of closo-Rhodacarborane Anions containing a formal d8 metal vertex 1,2
[AD-A149640] 12 p1799 N85-21285
Fire resistant polymers based on 1-(diorgano oxyphosphonyl)methyl-2,4- and 2,6-diamino benzenes
[NASA-CASE-ARC-11512-2] 12 p1811 N85-21362

Scale-up of vanadium trineodecanoate
[AD-A149935] 12 p1813 N85-21370
Plasticizer system for propellant compositions
[AD-D011502] 12 p1816 N85-21390
Plasticizer system for propellant compositions
[AD-D011506] 12 p1816 N85-21391
Plasticizer system for propellant compositions
[AD-D011517] 12 p1817 N85-21395
Ideal gas thermodynamic properties for the phenyl, phenoxy, and o-biphenyl radicals
[NASA-TM-83800] 12 p1843 N85-22204
Synthesis and characterization of poly(vinylidene fluoride)
[AD-A150291] 13 p2037 N85-22759
Geomagnetic field dynamics 13 p2116 N85-23162
Preparations of methoxynitrophenazines and their photoconductivities
[NASA-TM-77775] 14 p2247 N85-23929
Synthesis and properties of elevated temperature P/M aluminum alloys
[AD-A151031] 14 p2258 N85-23991
Synthesis of hydrophobic, crosslinkable resins
[AD-A150658] 14 p2290 N85-24002
Investigation of the MBE growth of InSb and novel quantum well structures
[AD-A151014] 14 p2427 N85-24999
Comparative sinterability of combustion synthesized and commercial titanium carbides
[DE85-006255] 15 p2512 N85-25498
A soluble linear Schiff-base coordination polymer containing eight-coordinate zirconium(4)
[AD-A151446] 15 p2518 N85-25527
Synthesis of phenols from metal-carbynes and diynes
[AD-A151913] 16 p2754 N85-26997
Micelle-derived catalysts for extended Schulz-Flory
[DE85-005858] 17 p2922 N85-28012
Polyaromatic ether-sulfone-keytones with fluoro-substituted-p-cyclophane units as cross-linking sites
[AD-D011649] 17 p2933 N85-28106
Preparation of silicon carbide-silicon nitride fibers by the pyrolysis of polycarbosilazane precursors
[NASA-TM-86505] 17 p2933 N85-28107
New examples of clusters, extended metal-metal bonding and interstitial derivatives
[DE85-005926] 17 p3044 N85-28637
Phenoxy resins containing pendent ethynyl groups and cured resins obtained therefrom
[NASA-CASE-LAR-13262-1] 18 p3066 N85-28973
The conversion of smaller borane fragments to larger structures. Systematics of boron hydride reactions
[AD-A153443] 18 p3070 N85-28985
New synthetic routes to boron cage compounds
[AD-A153554] 18 p3071 N85-28991
Study of synthesis gas conversion over metal oxides
[DE85-010136] 18 p3072 N85-28999
Synthesis chemistry of ceramics by solid-state combustion processes in micro-gravity
[DE85-009595] 18 p3091 N85-29061
Liquid hydrocarbon fuels from syngas
[DE85-009813] 19 p3228 N85-30017
Spray pyrolysis as a synthetic tool
[AD-A153891] 19 p3234 N85-30047
Metallophthalocyanine dimers incorporating five atom covalent bridges
[AD-A154365] 19 p3234 N85-30051
New approaches to functionalized fluorocarbons
[AD-A154205] 19 p3248 N85-30141
Synthesis and characterization of novel polymers from non-petroleum sources for use in enhanced oil recovery
[DE85-010922] 19 p3250 N85-30151
Design and chemical synthesis of iodine-containing molecules for application to solar-pumped I* lasers
[NASA-CR-176010] 19 p3275 N85-30310
Development of an impact- and solvent-resistant thermoplastic composite matrix, phase 3
[NASA-CR-172568] 20 p3422 N85-31239
Synthesis and characterization of copolyimides with varying flexibilizing groups
[NASA-TM-86416] 20 p3433 N85-31296
Propellant plasticizer
[AD-D011501] 20 p3434 N85-31306
Synthesis and properties of arylethersulfone thermoset systems
[AD-A154811] 21 p3569 N85-32198
Synthesis of energetic materials
[AD-A154887] 21 p3571 N85-32210
Origin of life 21 p3667 N85-32713
The composition of the primitive atmosphere and the synthesis of organic compounds on the early Earth
21 p3717 N85-33065
Synthesis of 2,4,8,10-tetroxaspiro5,5undecane
[NASA-CASE-ARC-11243-2] 22 p3741 N85-33187
Electrolytic synthesis of colored eta alumina film
23 p3906 N85-34201
Fire-resistant phosphorus containing polyimides and copolyimides
[NASA-CASE-ARC-11522-2] 23 p3918 N85-34290
Preparation of ethylenediamine dinitrate
[DE85-006423] 23 p3922 N85-34305
Ethylenediamine salt of 5-nitrotetrazole and preparation
[DE85-005738] 23 p3923 N85-34306
Synthesis of ultrafine ceramic and metallic powders in a thermal argon rf plasma
[DE85-009834] 23 p3983 N85-34696
FTIR studies of hydrocarbon synthesis on Pd/ZSM5 catalysts
[DE85-012430] 24 p4071 N85-35230
System for the continuous generation of phosphorous aerosols from red phosphorus-butyl rubber
[DE85-013527] 24 p4072 N85-35232

SYNTHESIZERS
Rech-1 speech synthesizer for man-machine dialog
04 p0543 N85-13456
Optimal design efforts in Shanghai described
13 p1972 N85-22386
Analysis of spectral characteristics of multilevel digital computing synthesis 15 p2527 N85-25579
A preliminary investigation into the intelligibility of Microspeech-2, a speech synthesizer
[BAE-BT-12284] 15 p2539 N85-25675

SYNTHETIC APERTURE RADAR
NT SIDE-LOOKING RADAR
Ultrasonic synthetic aperture focusing using unfocused pulse-echo transducers
[AERE-R-11230] 01 p0057 N85-10374
Production of optically correlated SEASAT-A (SEA satellite) SAR (Synthetic Aperture Radar) imagery at DREO (Defence Research Establishment Ottawa)
[AD-A145970] 03 p0355 N85-12281
Aspects and applications of SAR (Synthetic Aperture Radar) imagery for mensuration
[AD-A146301] 03 p0356 N85-12290
Structural aspects of SAR antenna for Japanese Earth Resources Satellite 1 05 p0626 N85-14007
Technology for the ERS-1 SAR antenna
05 p0626 N85-14008
Multispectral (X and C band) crop classification with synthetic aperture radar (SAR-580) optical data
05 p0657 N85-14217
Metric evaluation of SAR-580 optical images for cartographic purposes 05 p0659 N85-14231
The wide-range space radio interferometer
07 p1058 N85-16717
The use of digital spaceborne SAR data for the delineation of surface features indicative of malaria vector breeding habitats 08 p1146 N85-17230
The investigation of selected oceanographic applications of spaceborne synthetic-aperture radar
08 p1146 N85-17233
SIR-B cartography and stereo topographic mapping
08 p1147 N85-17234
Investigation of SIR-B images for lithologic mapping
08 p1148 N85-17241
Automatic terrain elevation mapping and registration
08 p1148 N85-17242
Australian Multiexperimental Assessment of SIR-B (AMAS) 09 p1148 N85-17243
German Radar Observation Shuttle Experiment (ROSE) 08 p1148 N85-17245
SAR internal wave signature experiment
08 p1149 N85-17253
Information extraction and transmission techniques for spaceborne synthetic aperture radar images
[NASA-CR-174341] 08 p1150 N85-17256
Spaceborne distributed SAR antenna
[NASA-CR-171835] 08 p1150 N85-17259
Extraction of structural information from radar signals
[FOA-C-30370-E1] 08 p1165 N85-17292
The use of synthetic aperture radar imagery to detect hazards to navigation
[AD-A149324] 10 p1422 N85-18971
Interleaved array antenna technology development
[NASA-CR-171845] 10 p1477 N85-19326
China report: Science and technology
[JPRS-CST-84-032] 11 p1621 N85-20202
Optical processor for synthetic aperture radar
11 p1621 N85-20203
Quantization study for ERS-1 wave mode
[DFVLR-FB-84-39] 11 p1625 N85-20234
A modern approach of a synthetic aperture radar processor and its technological aspects
11 p1713 N85-20778
Earth resources research using the Shuttle Imaging Radar system 11 p1713 N85-20779
JPL highlights
[NASA-CR-175517] 11 p1767 N85-21102
The imaging of internal waves by the SEASAT-A synthetic aperture radar
[AD-A149808] 12 p1875 N85-21761
The imaging of internal waves by the SEASAT-A synthetic aperture radar
[ARE(PORTLAND)TN-720/84]
13 p2054 N85-22860
Edge detection in SAR imagery using gradient operators — synthetic aperture radar (SAR)
[AD-A149411] 13 p2054 N85-22862
Synthetic aperture radar simulation study
[AD-A151000] 14 p2293 N85-24214
Synthetic aperture radar data processing
14 p2398 N85-24780
SEASAT report
[AD-A151283] 15 p2553 N85-25931
Autofocus motion compensation for synthetic aperture radar and its compatibility with strapdown inertial navigation sensors on highly maneuverable aircraft
[AD-A151940] 16 p2704 N85-26883
Application of artificial intelligence (AI) to radar image understanding
[AD-A152519] 17 p3017 N85-28864
The multiple processor machine for image processing, volume 5
[ESA-CR(P)-1976-VOL-5] 18 p3164 N85-29803
Computer simulation of the effects of a distributed array antenna on synthetic aperture rarler images
[NASA-CR-171888] 19 p3254 N85-30176
Design of a shuttle-borne SAR for the DFVLR's planning study
[ERYS-019/84] 20 p3419 N85-31216
SAR swath widening techniques — satellite radar
[BL-6198] 20 p3441 N85-31358
Synthetic aperture radar data processing — satellite-borne radar
[CNES-198-T-CT/DRT/TIT/RL]
20 p3442 N85-31383
Digital signal processing for spaceborne synthetic aperture radar
[FOA-C-30381-E1] 20 p3442 N85-31384
Deterministic and random phase noise of oscillators — synthetic aperture radar
[ESA-TT-848] 20 p3449 N85-31415
Using ship wake patterns to evaluate SAR (Synthetic Aperture Radar) ocean wave imaging mechanisms. Joint US-Canadian Ocean Wave Investigation Project
[AD-A154633] 21 p3573 N85-32223
Aspects of SAR image segmentation
[AD-A154965] 21 p3575 N85-32236
Basic properties and interpretation of synthesized radar images of sea waves with long synthetization time
22 p3773 N85-33084
Method and apparatus for Delta Kappa synthetic aperture radar measurement of ocean current
[NASA-CASE-NPO-15704-1] 23 p3925 N85-34327
AMI calibration study. Volume 1: SAR calibration. Volume 2: Ground Targets. Volume 3: Scatterometer calibration — Active Microwave Instrument (AMI) ERS-1
[C2248/4/4-VOL-1] 23 p3936 N85-34394

SYNTHETIC APERTURES
Electromagnetic-acoustic-transducer
e system for thick-weld inspection
[PB84-219492] 01 p0051 N85-10028
Aperture synthesis for radioastronomy
06 p0781 N85-14982
Place of aperture synthesis in general theory of antennas (review) 06 p0781 N85-14983
Method of aperture synthesis: Fundamental relations and data processing in aperture synthesis systems (review) 06 p0781 N85-14984
Aperture synthesis (review) 06 p0781 N85-14985
Modern radioastronomical aperture synthesis systems (review) 06 p0782 N85-14987
Metric-wave and decimetric-wave aperture synthesis systems (review) 06 p0782 N85-14988
Cross-shaped aperture synthesis system
06 p0782 N85-14989
Decimetric-wave aperture synthesis system at Scientific Research Institute of Radiophysics
06 p0782 N85-15000
Phase problem in aperture synthesis systems
06 p0782 N85-15002
Approximating true radioluminance distribution from observations on aperture synthesis systems
06 p0783 N85-15003
Synthesis of radio image on RATAN-600 radiotelescope 06 p0783 N85-15004
Attempts to contruct two-dimensional image of Sun from observations made with RATAN-600 radiotelescope by relay race method 06 p0783 N85-15006
Invariance of mean-square effective area of synthesized apertures 06 p0784 N85-15009
Emerging technology of synthetic aperture focusing to ultrasonic testing
[DE85-000373] 09 p1378 N85-18884
Digital standards conversion: Interpolation theory and aperture synthesis
[BBC-RD-1984/20] 13 p2053 N85-22857

Analysis and interpretation of synthetic time strings of oscillation data 14 p2444 N85-25079
Spectral information from gapped data. A comparison of technique 14 p2444 N85-25080
Synthetic aperture side-looking radar image adjustment 16 p2606 N85-27304
Advanced ultrasonic imaging of piping in Dresden and Vermont Yankee reactors
[TI85-010049] 20 p3464 N85-31520
Optical synthetic aperture techniques
[AD-A156151] 24 p4154 N85-35752

SYNTHETIC FIBERS
NT CERAMIC FIBERS
NT GLASS FIBERS
NT NYLON (TRADEMARK)
Method of obtaining polybenzimidazopyrrolones
[AD-A145140] 01 p0018 N85-10106
New type of unique frequency laser communications
[AD-A145126] 01 p0038 N85-10239
Thermoplastic-carbon fiber hybrid yarn
[NASA-CR-3849] 03 p0325 N85-12093
Metallized synthetic cable
[AD-D011263] 05 p0628 N85-14023
Properties of polycaproamide fibers modified by grafted polyacrylonitrile 06 p0761 N85-14867
Low temperature synthesis of polycaproamide copolymers grafted with polydimethylaminothylmethacrylate
06 p0761 N85-14868
Synthesis of reinforced composite threads based on polymer mixtures 06 p0761 N85-14869
Comparison of methods for predicting fiber stresses in a cracked Kevlar/epoxy monolayer
[DE84-016118] 11 p1593 N85-20022
Diamond cutters' grinders 13 p2051 N85-22841
Mechanics of polymers and composites: Research opportunities
[DE85-007052] 15 p2503 N85-25442
Fatigue of synthetic fibers for marine rope applications
[MIT-R84-2] 17 p2979 N85-28414
Fatigue behavior of synthetic fibers, yarns and ropes
17 p2979 N85-28415
The effects of sea water and concentrated salt solutions on the fatigue of nylon 6,6 fibers
17 p2979 N85-28416
Substitution of asbestos by aramid fibers and fiber blends in industrial textiles and composites with organic binders
[BMFT-FB-T-85-006] 23 p3920 N85-34294

SYNTHETIC FUELS
NT GASOHOL (FUEL)
Mechanisms of syncrude-synfuel degradation
[DE84-015206] 01 p0034 N85-10212
The status of synthetic fuels and cost-shared energy R and D facilities
[GPO-36-903] 03 p0339 N85-12182
Inertial confinement fusion: Present status and future potential
[DE84-016177] 04 p0567 N85-13616
The infrastructure for a surge in synfuels production: The potential role of the AE and C industry and of owner operators
[RAND/N-2172-SFC] 09 p1301 N85-18170
Test report for Getty Synthetic Fuels, Inc., Calumet City, Illinois
[PB85-119493] 10 p1459 N85-19191
Synthetic fuels policy
[GPO-34-227] 11 p1613 N85-20143
Trifunctional catalysts for conversion of syngas to alcohols
[DE85-004577] 13 p2040 N85-22771
Current alternative energy research and development in Illinois
[PB85-163137] 16 p2820 N85-27397
Linking R and D to problems experienced in solids processing
[AD-A154236] 19 p3380 N85-30968
Improved catalysts for liquid hydrocarbon fuels from syngas
[DE85-011062] 20 p3421 N85-31234
A comparison of two bench scale tests of fuel low temperature flow properties
[AD-A154477] 20 p3435 N85-31311
Biomass thermochemical conversion program
[DE85-011607] 21 p3572 N85-32213
Seventh Symposium on Biotechnology for Fuels and Chemicals: Program and abstracts
[DE85-011197] 22 p3742 N85-33192
Aspects of high-resolution gas chromatography as applied to the analysis of hydrocarbon fuels and other complex organic mixtures. Volume 1
[AD-A156154] 24 p4076 N85-35257

SYNTHETIC METALS
The replacement of precious metal thick film inks using conductive polymer technology
[AD-A152002] 16 p2749 N85-26965

SYNTHETIC RESINS
NT ACRYLIC RESINS
NT EPOXY RESINS
NT KEVLAR (TRADEMARK)
NT NYLON (TRADEMARK)
NT PHENOLIC RESINS
NT POLYAMIDE RESINS
NT POLYESTER RESINS
NT POLYETHER RESINS
NT POLYMETHYL METHACRYLATE
NT THERMOPLASTIC FILMS
NT THERMOPLASTIC RESINS
NT THERMOSETTING RESINS
NT VINYL COPOLYMERS
Fundamental studies of composite toughness
04 p0464 N85-12948
Polymeric liner selection for military waste impoundments
[AD-P004143] 09 p1348 N85-18479
Evaluation of the PSP resin as a precursor of carbon
[ONERA-RT-11/1764-M] 16 p2744 N85-26932
The replacement of precious metal thick film inks using conductive polymer technology
[AD-A152002] 16 p2749 N85-26965
Ambient air contamination: Characterization and detection techniques 18 p3157 N85-29546

SYNTHETIC RUBBERS
NT CHLOROPRENE RESINS
NT ELASTOMERS
NT VULCANIZED ELASTOMERS
Damage development during low cycle fatigue of carbon-black loaded SBR
[DE85-006234] 15 p2519 N85-25533
System for the continuous generation of phosphorous aerosols from red phosphorus-butyl rubber
[DE85-013527] 24 p4072 N85-35232

SYSTEM EFFECTIVENESS
Energy-saving technological methods of obtaining controlled atmospheres
[BLL-M-35724-(5828.4)] 02 p0171 N85-11145
Investigation of the gas-content of gas-liquid systems
[BLL-M-35748-(5828.4)] 02 p0171 N85-11146
NASA Redox Storage System Development Project
[NASA-TM-83677] 03 p0385 N85-12465
Holographic displacement analysis with fiber optics
[AD-A146185] 03 p0420 N85-12680
Maintenance Management Information and Control System (MMICS): Administrative boon or burden
[AD-A145762] 03 p0438 N85-12790
Advancement of remote systems technology: Past perspectives and future plans
[DE84-016710] 04 p0509 N85-13250
Effectiveness of agricultural aviation
04 p0544 N85-13460
Operation of aviation support bases
04 p0544 N85-13461
Flying qualities and control system characteristics for superaugmented aircraft
[NASA-CR-170419] 05 p0596 N85-13800
Analytical models 05 p0666 N85-14282
Army aviation today and tomorrow
06 p0751 N85-14810
Survey relating to the implementation of cost/schedule control systems criteria within the Department of Defense and industry
[AD-A146664] 06 p0870 N85-15526
Reverse wave suppression in unstable ring resonator
[AD-A146825] 07 p0939 N85-15952
Analysis of effectiveness of partial optimization of spatial processing systems 07 p0952 N85-16031
Nondestructive tests and fracture mechanics investigations in the Component Integrity Research Programme
[BLL-RISLEY-TR-4541-(9091.9F)]
07 p0976 N85-16199
Evaluation of the measured energy performance of four solar systems
[AD-A147912] 07 p0993 N85-16306
Lunar nuclear power feasibility study
[NASA-CR-171831] 07 p1041 N85-16611
S-3A ballast block final design and engineering tests
[AD-A147685] 08 p1080 N85-16842
A study of Air Force Quality Circle program effectiveness as viewed through facilitator's perceptions
[AD-A147633] 08 p1170 N85-17377
Comparative usefulness of flue gas oxygen and carbon dioxide analysis
[BLL-TRANS-T6358/BG/WH783/84]
08 p1179 N85-17430
Strategic management for organizational effectiveness. The effect of human resource planning on retention and related issues, volume 1
[AD-A149398] 10 p1566 N85-19674
Strategic management for organizational effectiveness. The effect of human resource planning on retention and related issues, volume 2
[AD-A149399] 10 p1566 N85-19675
A computer-based gaming system for assessing recognition performance (RECOG)
[AD-A149752] 12 p1915 N85-22022
Transmission efficiency measurements and correlations with physical characteristics of the lubricant
14 p2222 N85-23781
Problems regarding the practical evaluation of efficiency of worm gears 14 p2224 N85-23793
Axial bearings with lever-type equalizer system
14 p2267 N85-24048
Analysis of team performance in a programmed environment
[NASA-CR-175634] 14 p2392 N85-24728
Combinatorial performance/cost analysis of an autonomous navigation system for aircraft
16 p2695 N85-26640
Construction and functioning of extended orbital systems 16 p2724 N85-26814
Proposal of a method for evaluating accuracy of estimated impulse response of a system
16 p2759 N85-27024
Operational test results of a prototype superconducting power transmission system and their extrapolation to the performance of a large system
[DE85-006731] 16 p2779 N85-27153

SYSTEM FAILURES
Artificial intelligence approaches to monitoring system integrity
[AD-P003930] 02 p0246 N85-11610
Ballpark reliability estimation techniques
[AD-A145971] 03 p0369 N85-12357
Material flow in the manufacturing system: Fault-diagnosis systems as support for the maintenance of highly automated manufacturing systems
[PNR-90238] 09 p1371 N85-18618
EOS (electrical overstress) protection for VLSI (Very Large Scale Integration) devices
[AD-A150333] 13 p2064 N85-22891
Parallel test method for LSI (Large Scale Integration) microprocessors
[AD-A150237] 13 p2144 N85-23310
Contribution of instrumentation and control software to system reliability
[DE85-004693] 13 p2149 N85-23340
Some critical factors that limit the effectiveness of machine intelligence technology in military systems applications
[AD-A150684] 14 p2407 N85-24836
Automation of servicibility of radio-relay station equipment 15 p2527 N85-25582
Determining availability characteristics of DSN data systems using discrepancy report data
16 p2772 N85-27109
How to handle failures in advanced flight control systems of future transport aircraft 17 p2904 N85-27905
Dynamic considerations for control of closed life support systems 18 p3155 N85-29537
Materials and processes control for space applications
18 p3156 N85-29544
Problems and solutions in analyzing partial-reflection drift data by correlation techniques
21 p3626 N85-32529
Failure testing of active solar energy system components
[DE84-013024] 22 p3804 N85-33561

SYSTEM GENERATED ELECTROMAGNETIC PULSES
Laboratory studies of spacecraft response to transient discharge pulses 13 p1995 N85-22506
Discharge pulse phenomenology
13 p1995 N85-22509
Electron yields from spacecraft materials
13 p1996 N85-22512

SYSTEM IDENTIFICATION
Time invariant memoryless nonlinear systems identification method
[FUB-9-1983] 01 p0114 N85-10773
Nonlinear system identification methodology development based on F-4S flight test data analysis
[AD-A146289] 03 p0318 N85-12053
Structure errors in system identification
05 p0700 N85-14496
The practical identification of systems with nonlinearities
[RR-264] 08 p1209 N85-17607
Identification of dynamic systems, theory and formulation
[NASA-RP-1138] 10 p1551 N85-19784
Three algorithms for parametric frequency domain system identification
[DE85-002801] 11 p1706 N85-20736

Application of the system identification technique to goal-directed saccades
[AD-A150132] 12 p1906 N85-21967
Proposal of a method for evaluating accuracy of estimated impulse response of a system
16 p2759 N85-27024
Identification of gust input and gust response characteristics from Do 28 TNT flight test data
[DFVLR-FB-84-48] 17 p2900 N85-27881
Space station configuration and flight dynamics identification 20 p3410 N85-31162
Large space structure flight experiment
20 p3410 N85-31163
Experiments in structural dynamics and control using a grid 20 p3410 N85-31165
Optimal sensor locations for structural identification
20 p3417 N85-31209
Combined state and parameter estimation for a static model of the Maypole (Hoop-Column) antenna suface
20 p3417 N85-31210
Experimental verification of identification algorithms for control of flexible structures 20 p3418 N85-31211
An Eigensystem Realization Algorithm (ERA) for modal parameter identification and model reduction
20 p3418 N85-31212
Numerical experimentation with maximum likelihood identification in static distributed systems
20 p3418 N85-31214
A system identification package for VAX and LSI 11
[OUEL-1569/85] 20 p3516 N85-31862
An overview of nonlinear systems identification
[RR-271] 20 p3520 N85-31894
On the choice of parameterization for identification
[OUEL-1554/84] 20 p3522 N85-31904
Multishaker modal testing
[NASA-CR-176139] 22 p3800 N85-33544
Lectures of a Flight Mechanics Conference — conferences
[ESA-TT-831] 24 p4061 N85-35165
The effect of instrumentation system parameters on the results of a flight mechanical system identification
24 p4061 N85-35170

SYSTEMS ANALYSIS
NT SYSTEM IDENTIFICATION
Modelling the demand for construction
[CSIR-TWISK-322] 01 p0035 N85-10218
On the computer analysis of structures and mechanical systems 01 p0061 N85-10404
Time invariant memoryless nonlinear systems identification method
[FUB-9-1983] 01 p0114 N85-10773
Information requirements analysis: An application
[AD-A144896] 01 p0125 N85-10858
Energy efficient engine. Volume 1: Component development and integration program
[NASA-CR-173084] 02 p0146 N85-10992
Computing the reliability of k out of n systems
[AD-A145505] 02 p0206 N85-11357
Aeroelastic stability analysis with interacting structural nonlinearities 02 p0207 N85-11364
A prospectus for Thematic Mapper research in the Earth sciences
[E85-10003] 02 p0215 N85-11416
Systems analysis for microcomputer acquisitions
[AD-A145447] 02 p0239 N85-11556
Diagnosis based on description of structure and function
[AD-P003919] 02 p0245 N85-11599
A representation for the functioning of devices that supports compilation of expert problem solving structures: An extended summary
[AD-P003921] 02 p0245 N85-11601
Artificial intelligence approaches to monitoring system integrity
[AD-P003930] 02 p0246 N85-11610
DELTA: An expert system for diesel electric locomotive repair
[AD-P003941] 02 p0248 N85-11621
The ACE (Automated Cable Expert) experiment: Initial evaluation of an expert system for preventive maintenance
[AD-P003943] 02 p0248 N85-11623
The application of artificial intelligence to a maintenance and diagnostic information system
[AD-P003945] 02 p0249 N85-11625
On the requirements of expert systems for fault isolation
[AD-P003947] 02 p0249 N85-11627
Gain-phase structures for linear multivariable systems
[RR-256] 02 p0256 N85-11674
Preliminary analysis of space mission applications for electromagnetic launchers
[NASA-CR-174087] 03 p0321 N85-12071
The human operator and system effectiveness
[AD-A146326] 03 p0402 N85-12563
Introduction to the subjective transfer function approach to analyzing systems
[AD-A145817] 03 p0436 N85-12774
Design of a scientific information collation and dissemination system, volumes 1 thru 3
[AD-A146002] 03 p0438 N85-12791
Development and demonstration of a vertical axis wind turbine POWERHOUSE
[DE84-901449] 04 p0527 N85-13389
Evaluation of automated decisionmaking methodologies and development of an integrated robotic system simulation
[NASA-CR-172401] 04 p0552 N85-13516
Linear harmonic analysis for Stirling machines and second law analysis of four important losses
[DE84-016595] 04 p0573 N85-13655
ECUT energy data reference series: Lightweight materials for ground transportation
[DE84-015269] 05 p0621 N85-13974
Detailed performance calculations: Goddard Group, appendix D 05 p0676 N85-14341
New uses for sensitivity analysis: How different movement tasks effect limb model parameter sensitivity
05 p0706 N85-14529
Operational requirements - system concepts
06 p0752 N85-14823
NAVSTAR GPS (Global Positioning System) marine receiver performance analysis
[AD-A146414] 06 p0753 N85-14831
The theory of optimal confidence limits for systems reliability with counterexamples for results on optimal confidence limits for series systems
[AD-A147236] 07 p1031 N85-16546
Software testing in an Ada programming environment
08 p1065 N85-16748
Impact of activation optimization on the Vandenberg Ground Support System using Q-GERT analysis
[AD-A148448] 08 p1105 N85-16986
The description of large systems
[AD-A148072] 08 p1205 N85-17586
Asymptotic methods for the analysis, estimation, and control of stochastic dynamic systems
[AD-A147758] 08 p1211 N85-17618
Representation and refinement of visual specifications in PegaSys
[AD-A148733] 09 p1368 N85-18596
Analysis and optimization of small Space Shuttle propulsion platforms
[DFVLR-FB-84-29] 10 p1431 N85-19023
A decision model for selection of microcomputers and operating systems
[AD-A149076] 10 p1538 N85-19694
Predicting the performance of distributed knowledge-based systems: A modeling approach
[AD-A149021] 10 p1545 N85-19738
TSS Satellite overview 11 p1642 N85-20343
The use of analytical models to interpret data properly
[ERS-E.341] 11 p1651 N85-20399
The use of analytical models to interpret measured data properly. 1. General background theory
11 p1651 N85-20400
Advanced concepts in systems analysis and simulation
[DE85-002726] 11 p1702 N85-20701
Needs, opportunities, and options for large scale systems research
[DE85-002664] 11 p1709 N85-20750
Reliability analysis of automatic systems
[VTT-301] 12 p1863 N85-21682
Needs, opportunities, and options for large scale systems research
[DE85-004642] 12 p1925 N85-22091
Reluctance and doubly-excited reluctance motors
[DE85-003585] 13 p2065 N85-22900
Cooling performance improvement of a horizontal ground coupled heat pump
[DE85-002470] 13 p2093 N85-23065
SIGPI: A user's manual for the fast computation of the probabilistic performance of a complex system
[DE85-005447] 13 p2148 N85-23336
Automatic symbolic solution of Markov chains
[AD-A150476] 13 p2153 N85-23369
Application of the Hardman methodology to the Single Channel Ground-Airborne Radio System (SINCGARS)
[NASA-CR-175694] 14 p2218 N85-23756
Model and controller reduction of uncertain systems using covariance equivalent realizations
14 p2243 N85-23902
Some recent developments in systems reliability
[AD-A150661] 14 p2317 N85-24318
Space Mathematics for the Preparation and Development of satellite Exploitation
[ISBN-2-85428-115-2] 14 p2395 N85-24753
Introduction to methods of evaluating the operational reliability of complex systems: Application to satellite control ground support 14 p2397 N85-24771
Identification of dynamic systems
[AGARD-AG-300-VOL-2] 15 p2470 N85-2524
Space station systems technology study (add-on task
Volume 3: Technology advancement program plan
[NASA-CR-171417] 15 p2475 N85-252
Logic analyzer survey and reviews
[BAE-881/ELO/1645] 15 p2621 N85-2615
An extension of a microcomputer based system fo
analysis of line drawing quantization schemes
[AD-A152008] 15 p2624 N85-2617
Computer program TRAMP: Inclusion of state spac
facilities and the analysis of non-linear elements
[BAE-BT-12643] 15 p2626 N85-2618
Computer science and technology: A guide t
performance evaluation of database systems
[PB85-155794] 15 p2631 N85-2621
Design of a variable-focal-length optical system
[NASA-CR-175710] 15 p2651 N85-2634
A database design for the Brazilian Air Force Flying Uni
Operational Control System
[AD-A151848] 15 p2666 N85-2645
Analysis and specification of a universal data model for distributed data base systems
[AD-A151856] 15 p2666 N85-2645
The evolutive state: A new definition of system state to include sequencing of events
16 p2696 N85-2664
An evaluation of thermal storage for liquid-metal, solar thermal receivers
[DE85-002929] 16 p2820 N85-2739
Central solar heating plants with seasonal storage. Evaluation of systems concepts based on heat storage in aquifers
[DE85-006788] 16 p2820 N85-2739
An ultrasensitive and element specific photoionization detection system for environmental analysis
[AD-A153365] 17 p2968 N85-2833
System analysis of a field Army Topographic Support System
[AD-A153318] 17 p2984 N85-2843
System Analysis for the Huntsville Operation Support Center, Distributed Computer System
[NASA-CR-171506] 17 p3015 N85-2864
An examination of alternative forms of fit in contingency theory
[AD-A152602] 17 p3047 N85-2865
The concept of fit in contingency theory
[AD-A152603] 17 p3047 N85-2865
Experimental philosophy leading to a small scale digital data base of the conterminous United States for designing experiments with remotely sensed data
[NASA-TM-85009] 17 p3049 N85-2887
Guidance on planning and implementing computer system reliability
[PB85-177996] 18 p3161 N85-2958
An operational analysis of system calibration
[AD-A153556] 18 p3170 N85-2964
Alternative theories of inference in expert systems for image analysis
[AD-A153649] 18 p3170 N85-2964
Instrument Systems Analysis and Verification Facility (ISAVF) users guide
[NASA-TM-86226] 19 p3223 N85-2998
Automatic ac/dc thermal voltage converter and ac voltage calibration system
[PB85-182574] 19 p3274 N85-3000
Modeling water resources systems for water quality
[AD-A154288] 19 p3300 N85-30457
A Lotus 1-2-3 based system reliability program
[DE85-010533] 19 p3340 N85-30701
ZOG/VINSON technology demonstration project system description. Volume 1
[AD-A154211] 19 p3342 N85-30713
A systems analysis of the erythropoietic responses to weightlessness. Volume 1: Mathematical model simulations of the erythropoietic responses to weightlessness
[NASA-CR-171890] 20 p3506 N85-3179
A systems analysis of the erythropoietic responses to weightlessness. Volume 2: Description of the model of erythropoiesis regulation. Part A: Model for regulation of erythropoiesis. Part B: Detailed description of the model for regulation of erythropoiesis
[NASA-CR-171891] 20 p3506 N85-3179
A numerical study of Taylor-Vortex flow
[AD-A154787] 21 p3584 N85-3227
The optimality of lower confidence limits for the reliability of series systems obtained by the method of key test results or other related techniques
[AD-A154880] 21 p3597 N85-3233
Space station ECLSS integration analysis: Simplified General Cluster Systems Model, ECLS System Assessment Program enhancements
[NASA-CR-176089] 21 p3670 N85-3279

A comprehensive study of the AFIT (Air Force Institute of Technology) software development environment
[AD-A155450] 21 p3672 N85-32812

Survival function of hypo-exponential distributions
[AD-A155518] 21 p3672 N85-32814

Determination of sensitivity functions for discrete dynamic systems from results of function modeling on digital computer 22 p3769 N85-33359

An evaluation of a class of practical optimization techniques for structural dynamics applications
[PB85-195766] 24 p4103 N85-35434

Prototyping with data dictionaries for requirements analysis
[AD-A156303] 24 p4139 N85-35654

SYSTEMS COMPATIBILITY

Documentation for DIGLIB: Device independent graphics library
[DE84-017385] 04 p0550 N85-13500

Software for special functions
[DE85-004684] 12 p1917 N85-22033

Basic EMC (Electromagnetic Compatibility) technology advancement for C3 systems: Model revision for IEMCAP (Intrasystem Electromagnetic Compatibility Analysis Program)
[AD-A150795] 14 p2292 N85-24208

The evolutive state: A new definition of system state to include sequencing of events
16 p2696 N85-26643

SYSTEMS DESIGN

U SYSTEMS ENGINEERING

SYSTEMS ENGINEERING

NT COMPUTER SYSTEMS DESIGN

NT CONTROL SYSTEMS DESIGN

A production peripheral vision display system
01 p0010 N85-10059

A multipurpose weather radar network
01 p0077 N85-10510

Hardware implementation of a support system for the 2501 Western digital LSI, complete controller of the second level, first version of the CCITT 25 (CAP) recommendations
[FUB-60-1982] 01 p0100 N85-10666

ADS: A FORTRAN program for automated design synthesis, version 1.00
[NASA-CR-172460] 01 p0102 N85-10684

System engineering and integration contract for implementation of the National Airspace System Plan. Volume 2: Section 5.0
[AD-A145710] 02 p0137 N85-10929

Avionics Integrity Program (Avip). Volume 2: Hardware case studies
[AD-A145689] 02 p0139 N85-10944

Combustion system for radiation investigations
02 p0145 N85-10986

Software engineering environments for mission critical applications: STARS alternative programmatic approaches
[AD-A145285] 02 p0241 N85-11571

The need for improvements in weapon system maintenance: What can AI (Artificial Intelligence) contribute?
[AD-P003913] 02 p0244 N85-11593

Diagnosis via causal reasoning: Paths of interaction and the locality principle
[AD-P003920] 02 p0245 N85-11600

An expert system for representing procedural knowledge
[AD-P003923] 02 p0245 N85-11603

Optical waveguide spatial filters
[AD-A145674] 02 p0260 N85-11825

Characteristics of systems engineering in aviation science research
[AD-A145602] 02 p0292 N85-11899

Activities report of the Department of Engineering
03 p0342 N85-12202

Automation of assembly of electrical products
03 p0346 N85-12226

Interactions among system stiffness, wear and vibrations 03 p0370 N85-12384

The ERS-1 radar altimeter: An overview
03 p0379 N85-12421

Automating software design metrics
[AD-A145869] 03 p0407 N85-12598

An input translator for a computer-aided design system
[AD-A146337] 03 p0408 N85-12605

System status display information
[NASA-CR-172347] 04 p0455 N85-12889

Study of instrument design options for the Columbus spectroscopy mission
[NASA-CR-174072] 04 p0502 N85-13205

Expert systems in design and manufacture
[DE84-005522] 04 p0550 N85-13496

Dynamics and controls working group summary
05 p0604 N85-13854

Self-tuning controller design and implementation
[OUEL-1535/84] 05 p0621 N85-13975

A generalized LQG approach to self-tuning control. Part 1: Aspects of design. Part 2: Implementation and simulation
[OUEL-1536/84] 05 p0622 N85-13976

Avionics technology - system concepts
06 p0753 N85-14824

Attack helicopter (AH-1T) cockpit systems integration
06 p0753 N85-14826

Workshop on Computer Architecture
[AD-A146455] 06 p0847 N85-15378

Architecture, design, and system; performance assessment and development methodology for computer-based systems. Volume 1: Methodology description, discussion, and assessment
[AD-A146577] 06 p0847 N85-15379

Implementation of a Zilog Z-80 base realization library for the computer systems design environment
[AD-A146359] 06 p0853 N85-15423

A framework for the development of Navy computer-based systems: Combat system architecture and combat system engineering put into perspective
[AD-A146460] 06 p0856 N85-15445

United States Air force aircraft modification process: A system dynamics analysis
[AD-A146854] 07 p0893 N85-15659

The investigation of tethered satellite system dynamics
[NASA-CR-171278] 07 p0912 N85-15772

Future database machine architectures
[AD-A146786] 07 p1022 N85-16481

Software test handbook
[AD-A146844] 07 p1024 N85-16498

Program visualization: Graphics support for software development
[AD-A146887] 07 p1024 N85-16499

Technical performance measurement handbook
[AD-A147314] 07 p1052 N85-16675

Automatic briefing and mission management systems for battlefield support 08 p1073 N85-16799

Development and flight test of a helicopter compact, portable, precision landing system concept
08 p1076 N85-16821

Transition to the space shuttle operations era
08 p1097 N85-16930

Launch processing system concept to reality
08 p1097 N85-16931

Automatic software for controlling cryogenic systems
08 p1097 N85-16932

Support systems design and analysis
08 p1097 N85-16935

Orbital Maneuvering system design evolution
08 p1098 N85-16943

Design evolution of the orbiter reaction control subsystem 08 p1099 N85-16944

Space shuttle orbiter auxiliary power unit development challenges 08 p1099 N85-16945

Space shuttle electrical power generation and reactant supply system 08 p1099 N85-16947

Design study of the vacuum pump of the ESRP --- synchrotron radiation
[NIKHEF-MTG-21] 08 p1138 N85-17167

A cometary ion mass spectrometer
[NASA-CR-174328] 08 p1164 N85-17343

Design and fabrication of a CCD camera for use with relay optics in solar X-ray astronomy
[NASA-CR-174334] 08 p1164 N85-17344

Approaches to structuring the software development process
[AD-A147694] 08 p1205 N85-17582

Complexity, testability, and fault analysis of digital, analog and hybrid systems
[AD-A148465] 08 p1213 N85-17634

Design of mismatched Smith predictors using plant step data
[RR-263] 08 p1217 N85-17664

Open-cycle centrifugal vapor-compression heat pump
[PB85-113405/GAR] 09 p1328 N85-18348

Large electrostatic accelerators
[DE85-001120] 09 p1382 N85-18689

Stability indicators for front end loaders
[AD-P004293] 09 p1408 N85-18870

Study on steerability of articulated tracked vehicles
[AD-P004308] 09 p1410 N85-18885

Distributed data processing design methodology
[AD-A148888] 10 p1537 N85-19692

Ada in mission critical system acquisition: A guidebook
[AD-A149271] 10 p1540 N85-19710

Methodology investigation software testing of multiprocessor systems
[AD-A149446] 10 p1541 N85-19714

Improving engineering system design by formal decomposition, sensitivity analysis, and optimization
[NASA-TM-86377] 10 p1551 N85-19785

The EURECA Automatic Gradient Heating Facility (AGHF), phase A study
[ESA-CR(P)-1939] 11 p1591 N85-20005

Shuttle tethered satellite system program overview
11 p1642 N85-20342

US MILSATCOM: Present and future
11 p1709 N85-20753

Integrated control system engineering support
[AD-A149742] 12 p1780 N85-21177

China report: Science and technology
[JPRS-CST-85-008] 12 p1820 N85-21416

Systems research on China in year 2000
12 p1820 N85-21418

Needs, opportunities, and options for large scale systems research
[DE85-004642] 12 p1925 N85-22091

Derivation of the Olympus solar array requirements
13 p2009 N85-22598

Optimal allocation of components in parallel-series and series-parallel systems
[AD-A150169] 13 p2144 N85-23309

Performance evaluation of distributed systems with unbalanced flows: An analysis of the INFOPLEX data storage hierarchy
[AD-A150528] 13 p2147 N85-23328

LEXICON: A structured modeling system for optimization
[AD-A150538] 13 p2147 N85-23329

Operation and maintenance requirements of the Army Remotely Piloted Vehicle (RPV)
[NASA-CR-175714] 14 p2218 N85-23755

Application of the Hardman methodology to the Single Channel Ground-Airborne Radio System (SINCGARS)
[NASA-CR-175694] 14 p2218 N85-23756

Advanced life analysis methods. Volume 5: Executive summary and damage tolerance criteria recommendations for attachment lugs
[AD-A151017] 14 p2219 N85-23761

Model and controller reduction of uncertain systems using covariance equivalent realizations
14 p2243 N85-23902

Some recent developments in systems reliability
[AD-A150661] 14 p2317 N85-24318

Sensitivities of projected 1980 photovoltaic system costs to major system cost drivers
[NASA-CR-175669] 14 p2349 N85-24519

Some critical factors that limit the effectiveness of machine intelligence technology in military systems applications
[AD-A150684] 14 p2407 N85-24836

Response to NAS plan audit report recommendations
[FAA-ES-85-1] 15 p2488 N85-25235

Standards in process: Foundation and profiles of ISDN (Integrated Services Digital Network) and OSI (Open Systems Interconnection) studies
[PB85-165041/GAR] 15 p2545 N85-25712

A critical review of selected recent advancements in arc welding equipment and processes
15 p2566 N85-25833

Research in the design of high-performance reconfigurable systems
[NASA-CR-175705] 15 p2621 N85-26153

Design specifications for IMAGER: The DREO (Defence Research Establishment Ottawa) image processing system
[AD-A151752] 15 p2624 N85-26168

Future directions in computers
15 p2626 N85-26183

Evaluating computer-communication networks with simulation techniques
[AD-A151852] 15 p2632 N85-26222

Design and implementation of the digital engineering laboratory distributed database management system
[AD-A151694] 15 p2665 N85-26450

Design adequacy: An effectiveness factor
16 p2695 N85-26642

The evolutive state: A new definition of system state to include sequencing of events
16 p2696 N85-26643

Simulation: A tool for cost-effective systems design and live test reduction 16 p2698 N85-26657

Cost-effective missile guidance through distributed architecture and standard processes
16 p2698 N85-26662

Technical evaluation report on the Flight Mechanics Symposium on Active Control Systems: Review, Evaluation and Projections
[AGARD-AR-220] 16 p2711 N85-26730

X-29A digital flight control system design
16 p2712 N85-26736

ACT flight research experience
16 p2713 N85-26741

Operational and developmental experience with the F/A-18A digital flight control system
16 p2713 N85-26742

Flight testing and development of the F/A-18A digital flight control system 16 p2713 N85-26743

Construction and functioning of extended orbital systems 16 p2724 N85-26814

Spacecraft configuration study for second generation mobile satellite system
[NASA-CR-175774] 16 p2730 N85-26849

Historical perspectives on information transmission engineering 16 p2759 N85-27023

Automated CPX support system preliminary design phase
[NASA-CR-175784] 16 p2769 N85-27091

Fatigue criterion to system design, life and reliability
[NASA-TM-87017] 16 p2793 N85-27226

Development of graphical time response using the OPTSYSX program
[AD-A152221] 16 p2848 N85-27557

Evaluation of Ada (trademark) as a communications programming language, volume 1
[AD-A152314] 16 p2848 N85-27559

Analysis of control system from a viewpoint of desired pole placement and desired degree of robustness
[AD-A152627] 17 p2899 N85-27876

The gust simulation apparatus of the 3m x 3m low speed wind tunnel of the DFVLR in Goettingen, West Germany
[DFVLR-FB-85-04] 17 p2906 N85-27920

Engineering robot actions in a computer integrated manufacturing environment
[CWI-CS-R8415] 17 p2938 N85-28139

Performance analysis of the DSN baseband assembly (Bba) Real-Time Combiner (RTC)
[NASA-CR-175878] 17 p2946 N85-28190

NASA guidelines for assuring the adequacy and appropriateness of security safeguards in sensitive applications
[NASA-CR-175489] 17 p3007 N85-28593

The touch panel system: Design and development
[AD-A153014] 17 p3008 N85-28596

A test methodology for an automated and interactive software development environment
[AD-A152857] 17 p3011 N85-28618

Impurity control and vacuum pumping system design and analysis for next-generation Tokamaks
[DE85-009291] 17 p3041 N85-28815

Complete development and implement AFIT/ENG database management system, volume 1
[AD-A153043] 17 p3048 N85-28866

The development of information systems at NLR
[B8580079] 17 p3051 N85-28884

Evaluation of a fault tolerant system for an integrated avionics sensor configuration with TSRV flight data
[NASA-CR-172589] 18 p3062 N85-28941

LFMR definition study
[AD-A153691] 18 p3090 N85-29126

System design of multi-layer (3-dimensional) integrated circuits
[AD-A153468] 18 p3094 N85-29154

The system design of a rubidium maser frequency standard 18 p3106 N85-29232

Fuel cells: A bibliography
[DE85-004565] 18 p3128 N85-29371

Development of molten carbonate fuel cell power plant, volume 1
[DE85-006743] 18 p3131 N85-29394

Materials and processes control for space applications
18 p3156 N85-29544

Guidance on planning and implementing computer system reliability
[PB85-177996] 18 p3161 N85-29581

Annotated bibliography of recent papers on software engineering environments
[PB85-191385] 18 p3165 N85-29607

Activities of Istituto Elettrotecnico Nazionale Galileo Ferraris 18 p3199 N85-29845

Space station automation study. Volume 2: Technical report. Autonomous systems and assembly
[NASA-CR-171515] 19 p3226 N85-30001

Automatic ac/dc thermal voltage converter and ac voltage calibration system
[PB85-182574] 19 p3274 N85-30304

Forced structural response using component mode synthesis
[DE85-008479] 19 p3287 N85-30383

Design and implementation of an intelligence database
[AD-A154095] 19 p3381 N85-30973

Proceedings of the Workshop on Identification and Control of Flexible Space Structures, volume 1
[NASA-CR-176051] 20 p3406 N85-31148

Control of flexible structures 20 p3410 N85-31161

Space station configuration and flight dynamics identification 20 p3410 N85-31162

ISAAC (Integrated Structural Analysis and Control) via continuum modeling and distributed frequency domain design techniques 20 p3414 N85-31165

New measurement solutions for low frequency systems 20 p3437 N85-31325

Study of terrestrial mobile systems for personal communications
[MCS-8436] 20 p3441 N85-31357

Improved specific energy Ni-H2 cell
20 p3447 N85-31399

Evaporatively cooled chiller for solar air conditioning systems design and field test
[DE84-014154] 20 p3484 N85-31652

Proceedings of the 1st Workshop for the Design of Expert System Partial Differential Equation Solvers
[AD-A154192] 20 p3515 N85-31853

RESO: Expert system applied to company computer networks
[ENST-84E016] 20 p3518 N85-31874

Decentralized control synthesis method for large-scale interconnected systems
[DE85-000748] 20 p3518 N85-31878

The development of complex systems
20 p3539 N85-32021

R and D programmes at the National Aeronautical Laboratory
[AR-22] 20 p3539 N85-32022

R and D activities of the Systems Engineering Division
20 p3540 N85-32027

Development of reduced order models for control system design using the OPTSYSX program
[AD-A154552] 21 p3556 N85-32124

The documentation assistant: An intelligent system for documentation
[AD-A154709] 21 p3670 N85-32800

A comprehensive study of the AFIT (Air Force Institute of Technology) software development environment
[AD-A155450] 21 p3672 N85-32812

Evaluation of a software design approach: Develop a threat resolution module in Ada (trademark)
[AD-A155599] 21 p3672 N85-32815

Distributed name management
[AD-A154785] 21 p3712 N85-33037

System for computer-aided design of analog electronic circuits 22 p3768 N85-33353

Integrated Support Software System (ISSS)
[AD-A155715] 22 p3829 N85-33710

Portable database driven control system for SPEAR
[DE85-010465] 22 p3830 N85-33720

Flat is not necessarily good
[DE85-012819] 22 p3830 N85-33723

Space Station Engineering and Technology Development: Proceedings of the Panel on In-Space Engineering Research and Technology Development
[NASA-CR-176110] 23 p3899 N85-34153

A methodology for the design of testable custom large-scale integrated circuits
[AD-A156098] 24 p4090 N85-35351

Wind turbine noise: Prediction tools and design parameter dependence 24 p4110 N85-35477

Recommendations for content revision and alternate delivery modes for the Human Engineering Guide to Equipment Design (HEGED)
[AD-A155781] 24 p4134 N85-35624

An approach to determining computer security requirements for Navy systems
[AD-A155750] 24 p4135 N85-35627

SYSTEMS FOR NUCLEAR AUXILIARY POWER

U SNAP

SYSTEMS INTEGRATION

PROFS: An approach to improved operational weather services — Program for Regional Observing and Forecasting Services (PROFS) 01 p0083 N85-10555

Numerical algorithms and parallel tasking
[AD-A145090] 01 p0104 N85-10693

Avionics Integrity Program (Avip). Volume 2: Hardware case studies
[AD-A145689] 02 p0139 N85-10944

Supercomputers and VLSI: The effect of large scale integration on computer architecture
[AD-A145408] 02 p0239 N85-11555

AFHRL (Air Force Human Resources Laboratory) program for artificial intelligence applications to maintenance and training
[AD-P003931] 02 p0247 N85-11611

Developments in Soviet robot technology viewed
04 p0491 N85-13127

Superaugmented rotorcraft program
06 p0750 N85-14807

HH-65A Dolphin digital integrated avionics
06 p0751 N85-14815

Integrated cockpit design for the Army helicopter improvement program 06 p0751 N85-14816

Integrated navigation systems: Where are we headed?
[AD-A146425] 06 p0753 N85-14832

Setting time standards at NISTARS (Naval Integrated Storage and Retrieval System)
[AD-A146371] 06 p0870 N85-15529

The design and development of an integrated core system for battlefield helicopters
08 p1074 N85-16811

Evolution toward a multi-bus architecture for Army helicopter avionic systems 08 p1074 N85-16812

Integration of sensor fusion in advanced helicopter cockpit design 08 p1074 N85-16813

Development, production and testing of central control and display unit for helicopters
[BMFT-FB-W-84-039] 08 p1085 N85-16871

Integrated design checkout of shuttle payload avionics interfaces 08 p1092 N85-16890

Managing computer-controlled operations
08 p1097 N85-16934

Support systems design and analysis
08 p1097 N85-16936

Robotics research, integration overview presented. Application objectives cited 08 p1142 N85-17201

Coordinated research in robotics and integrated manufacturing
[AD-A148204] 08 p1168 N85-17365

Cognitive asymmetry and occupation. Computer programmers, students, and bank personnel, part 1 and part 2
[AD-A147125] 08 p1197 N85-17540

Towards an ideal database server for office automation environments
[AD-A148184] 08 p1229 N85-17742

Integrated technology rotor/flight research rotor hub concept definition
[NASA-CR-166447] 09 p1280 N85-18061

Data Requirement (DR) MA-03: Payload missions integration — Spacelab payloads
[NASA-CR-171331] 10 p1428 N85-19009

MATRA has Europe's largest white room for satellites
10 p1477 N85-19320

A safety evaluation of the relocation of the ACM (Air Combat Maneuver) panel in the F-14 ( )/AIP (Avionics Integration Program)
[AD-A149596] 12 p1777 N85-21158

Dual band radome wall design
[AD-P004357] 12 p1825 N85-21451

Integrated digital networks
[AD-A150605] 13 p2056 N85-22873

Invariant system of technological preparation of production 14 p2268 N85-24056

Integrated control system for FMS components
14 p2285 N85-24158

Response to NAS plan audit report recommendations
[FAA-ES-85-1] 15 p2468 N85-25235

Space station systems technology study (add-on task). Volume 3: Technology advancement program plan
[NASA-CR-171417] 15 p2475 N85-25280

Standards in process: Foundation and profiles of ISDN (Integrated Services Digital Network) and OSI (Open Systems Interconnection) studies
[PB85-165041/GAR] 15 p2545 N85-25712

Computerized biophysical data acquisition system for motion sickness studies
[AD-A151691] 15 p2618 N85-26131

Computers and the consulting engineer
15 p2626 N85-26184

The STOL and maneuver technology program integrated control system development 17 p2905 N85-27910

An evaluation of oxygen-hydrogen propulsion systems for the Space Station
[NASA-TM-87059] 18 p3067 N85-28971

Investigation of fast reaction SAW (Surface Acoustic Wave) accelerometer
[AD-A153876] 19 p3216 N85-29943

Local automation model software benchmarking: Test plan
[AD-A154349] 19 p3337 N85-30676

High gain adaptive control of decentralized systems
[DE85-010040] 19 p3339 N85-30686

Performance improvements of a highly integrated digital electronic control system for an F-15 airplane
[NASA-TM-86748] 21 p3556 N85-32120

High temperature electronics technology: Life test report
[AD-A154681] 21 p3580 N85-32257

Characteristics of a numerical fluid dynamics simulator
[DE85-009602] 21 p3586 N85-32290

Qualification needs for advanced integrated aircraft
[NASA-TM-86731] 22 p3729 N85-33119

Digital matched filter 22 p3765 N85-33339

The integrated manual and automatic control of complex flight systems
[NASA-CR-176166] 24 p4066 N85-35201

Analog, still without fear
[AD-A155920] 24 p4089 N85-35348

SYSTEMS MANAGEMENT

On some common interests among reliability, inventory and queuing
[AD-A145595] 02 p0251 N85-11646

Research in data management and system reliability
[AD-A145496] 03 p0436 N85-12773
Computer aided processing using laser measurements
08 p1103 N85-16973
Training guide for scientific and engineering trainees 1984
[AD-A147963] 08 p1196 N85-17542
Research and Modeling of Supervisory Control Behavior, report of a workshop
[AD-A149621] 12 p1950 N85-22248
Management aspects of software maintenance
[AD-A152035] 16 p2847 N85-27550
Management control systems and interdependencies: An empirical study
[AD-A152280] 16 p2876 N85-27746
Cost savings from multiyear contracting
[AD-A153564] 18 p3197 N85-29834
NASA Space controls research and technology program 20 p3408 N85-31149
Program Manager: The journal of the defense systems management college, volume 14, number 2, March-April 1985
[AD-A154219] 20 p3540 N85-32031
Navy information systems: Planning, policy, organization, and management
[PB85-176113] 20 p3541 N85-32038
NASA space station automation: AI-based technology review
[NASA-CR-176094] 21 p3558 N85-32134
Analysis of spacecraft data
[NASA-CR-171597] 21 p3669 N85-32790
User commands for product design and system management
[DE85-011706] 22 p3830 N85-33721

SYSTEMS SIMULATION
Optimizing search with positive information feedback
[CSIR-TWISK-313] 01 p0125 N85-10855
ERS-1 radar altimeter system performance evaluation and calibration 03 p0383 N85-12451
Simplified planar model of ground test verification structure, appendix B 05 p0603 N85-13841
Elimination of uncontrollable rigid body mode, appendix C 05 p0603 N85-13842
Evaluation of SPOT simulation data of the S GEOS campaign of the EEC by data of the test sites Freiburg and Staubing (West Germany) 05 p0659 N85-14237
A digital piloting system for the combat helicopter
08 p1074 N85-16806
A simulator for studying helicopter weapons systems
08 p1075 N85-16816
The use of simulation for the technical and economic evaluation of flexible manufacturing systems. Part 2: Results of the simulation
[PNR-90233-PT-2] 09 p1371 N85-18614
MTI system simulation and clutter output statistics
[AD-A149193] 10 p1467 N85-19255
TVENT1P user's manual, a computer code for analyzing tornado induced gas dynamic transients in flow networks
[DE85-002346] 10 p1486 N85-19379
The noise of laser diodes with modulated injection current
[FI-465-TBR-23] 11 p1625 N85-20233
The use of analytical models to interpret measured data properly. 1. General background theory
11 p1651 N85-20400
A system simulator for the solar generator of artificial satellites
[INPE-3320-TDL/180] 11 p1672 N85-20534
Solar array dynamical simulation for illumination and temperature variation 13 p2011 N85-22611
Transition fixing and simulation of high Reynolds number flow at transonic velocities 14 p2212 N85-23721
System theoretic description of physical systems
[CWI-TRACT-3] 14 p2414 N85-24894
Space station systems technology study (add-on task). Volume 3: Technology advancement program plan
[NASA-CR-171417] 15 p2475 N85-25280
Manipulation and simulation of general robots using the zero-position description 15 p2567 N85-25838
Simulation: A tool for cost-effective systems design and live test reduction 16 p2698 N85-26657
A description of the process of elaborating man-machine dialog in an aircraft equipped with cathode tubes: Roles and specifications of piloted simulation methods
16 p2698 N85-26658
A complete inference system for regular processes with silent moves
[CWI-CS-R8420] 17 p3014 N85-28638
Simulations of strapdown-system errors and error compensation methods — transport aircraft navigation
[DFVLR-MITT-84-22] 20 p3392 N85-31040
Reduced order models and simulation data in control systems design
[RR-267] 20 p3463 N85-31516
Linear system structure and cone containment for bilinear systems
[RR-268] 20 p3519 N85-31879
Design of simulation experiments
[FEW-123] 20 p3519 N85-31885
Regression metamodel summarization of model behavior
[FEW-120] 20 p3522 N85-31902
On the interpretation of variables — simulation and regression models
[FEW-136] 20 p3522 N85-31903
Performance of rolling ball and isometric joystick on a 2-D target alignment task
[RSRE-MEMO-3695] 22 p3826 N85-33699
Discrete simulation models - their role in the design, development and management of inventory control systems
[PNR-90249] 23 p3986 N85-34719

SYSTEMS STABILITY
Aeroelastic stability analysis with interacting structural nonlinearities 02 p0207 N85-11364
The dimensional stability of advanced composite antenna reflectors: Analytical and test evaluation — satellite antennas 05 p0626 N85-14014
Effects of transport delays of manual control system performance 05 p0701 N85-14498
Relaxation times for queueing systems
[CWI-OS-R8407] 05 p0719 N85-14618
The stability of an infinite elastic pipe with uniform mean flow
[AD-A148686] 08 p1161 N85-17326
Brief outline of analytic stability studies of magnetically insulated systems — bibliobiographies
[DE85-000212] 09 p1393 N85-18765
Contribution to the study of perturbational stabilization
[ONERA-NT-1984-1] 11 p1714 N85-20781
Instabilities and the fine structure of Saturn's rings
15 p2676 N85-26520
Stability and feasibility of model ecosystems
[PREPRINT-431] 18 p3134 N85-29408

T

T TAURI STARS
Bipolar molecular outflows: T Tauri stars and Herbig-Haro objects 03 p0446 N85-12837
UV observations and results on pre-main sequence stars 11 p1744 N85-20970
Atmospheric properties of RU Lupi derived from high- and low-resolution IUE spectra
11 p1754 N85-21031
Mechanical energy release by protostars to molecular clouds 12 p1957 N85-22302

T-33 AIRCRAFT
A preliminary flight evaluation of the peripheral vision display using the NT-33A aircraft
[AD-A145123] 01 p0010 N85-10060

TABLES (DATA)
NT MATHEMATICAL TABLES
Water resources data, Maryland and Delaware, water year 1983
[PB84-225135] 01 p0065 N85-10431
Water resources data, California, water year 1982. Volume 4: Northern central valley basins and the Great Basin from Honey Lake Basin to Oregon state line
[PB84-225127] 01 p0065 N85-10432
Water resources data, California, water year 1982. Volume 2: Pacific slope basins from Arroyo Grande to Oregon state line except Central Valley
[PB84-224708] 01 p0065 N85-10433
Water resources data, Virginia, water year 1983
[PB84-224542] 01 p0066 N85-10435
Water resources data, Ohio, water year 1983. Volume 2: St. Lawrence River basin statewide project data
[PB84-223676] 01 p0066 N85-10436
A building blocks approach to statistical databases
03 p0437 N85-12782
Tide tables 1985, high and low water predictions, central and western Pacific Ocean and Indian Ocean
[PB84-238393] 04 p0542 N85-13451
Tide tables 1985. High and low ater predictions: Europe and West Coast of Africa including the Mediterranean Sea
[PB84-230093] 06 p0841 N85-15343
Safe decompression schedules for caisson workers
[PB85-103612/GAR] 07 p1017 N85-16463
Experimental study of main rotor tip geometry and tail rotor interactions in hover. Volume 2: Run log and tabulated data
[NASA-CR-177336-VOL-2] 13 p1965 N85-22345
A model for large sparse contingency tables
[AD-A150320] 13 p2151 N85-23350
An atlas of pure water vapor spectra from 500 to 5000/cm, volume 1
[AD-A151756] 15 p2505 N85-25454
Bern solar data for January-December 1984
[REPT-51] 15 p2685 N85-26581
Summary of Meteorological Observations, Surface (SMOS), Dallas, Texas
[AD-A150599] 16 p2835 N85-27480
Climatological data of stations in the Netherlands No. 11: Frequency tables and tables with runs according to measurements at principal climatological stations 1961-1980, sunshine stations 1956-1980, precipitation stations 1951-1980
[KNMI-150-11] 18 p3149 N85-29499
Bayesian full rank marginalization for 2-way contingency tables
[AD-A153841] 18 p3171 N85-29649
Atomic data for controlled fusion research. Volume 4: Spectroscopic data for iron
[DE85-009658] 19 p3354 N85-30787
Tables of generalized hydrogen diffusion profiles and permeating fluxes for fusion applications
[DE85-008876] 19 p3372 N85-30919
Compendum of unsteady aerodynamic measurements, addendum 1
[AGARD-R-702-ADD-1] 20 p3390 N85-31028
Phonetic transcription statistics: Constitution and statistical utilization
[ENST-85D001] 22 p3756 N85-33285

TABLETS
A multi-touch three dimensional touch-sensitive tablet (executive summary) 23 p3961 N85-34553

TABS (CONTROL SURFACES)
Aircraft rotor blade with passive tuned tab
[NASA-CASE-ARC-11444-1] 19 p3217 N85-29947

TABULATING
U TABULATION PROCESSES

TABULATION PROCESSES
(NAT)Fe(n,n'x) spectra at 65.5 MeV
[AD-A155776] 24 p4150 N85-35730

TACAN
Shuttle navigation status 08 p1092 N85-16901
Distance Measuring Equipment (DME), general
[AD-A152585] 17 p2895 N85-27846

TACHOMETERS
The removal, mechanical handling and installation procedures for declination tachometer and Itek encoder — United Kingdom Infrared Telescope
[UKIRT-17] 09 p1414 N85-18915
Two-stage gyrocompass 14 p2273 N85-24080
The Fourier tachometer 2: An instrument for measuring global solar velocity fields 14 p2442 N85-25068
Digital tachometer 22 p3779 N85-33416

TACHYONS
Results of a search for monopoles and tachyons in horizontal cosmic ray flux
[HE-6.1-3] 24 p4209 N85-36129
Search for tachyons associated with extensive air showers in the ground level cosmic radiation
[HE-6.2-13] 24 p4212 N85-36149

TACTICAL AIR NAVIGATION
U TACAN

TACTICS
Increased joint avionics standardization could result in major economies and operational benefits
[AD-A145730] 02 p0139 N85-10945
Intelligent interfaces for tactical airborne platforms
06 p0752 N85-14820
A framework for the development of Navy computer-based systems: Combat system architecture and combat system engineering put into perspective
[AD-A146460] 06 p0856 N85-15445
Human factors and training research in military organizations and systems
[AD-A146832] 07 p1020 N85-16475
Close air support mission: Development of a unitary measure of pilot performance
[AD-A149285] 11 p1697 N85-20665
Combat capable space systems for tactical support
11 p1713 N85-20775
Supersonic Tactical Missile (STM) radome development
[AD-P004360] 12 p1825 N85-21454
Equilibrium solutions, stabilities and dynamics of Lanchester's equations with optimization of initial force commitments
[AD-A151510] 15 p2637 N85-26266
Transceiver test device
[AD-D011728] 22 p3786 N85-33458

TACTILE DISCRIMINATION
Dutch institutes do research in tactile visual robot sensors 08 p1310 N85-18228
Short and long-term robot feedback
[PB85-180735] 19 p3281 N85-30347

TACTILE SENSATION
U TOUCH

TAGGING
U MARKING

TAIL ASSEMBLIES
An experimental study on the induced normal force on tail-fins due to wing-tail interference
[NAL-TR-814] 03 p0318 N85-12051
Experiences obtained from service fatigue monitoring exercises 07 p0895 N85-15672
TUTOR (CL-41A) tail flight load survey
07 p0896 N85-15678
All-composite Airbus empennage
07 p0936 N85-15931
Wind tunnel accoustic study of a propeller installed behind an airplane empennage: Data report
[NASA-CR-177335] 13 p2154 N85-23377
Description of a computer program treating transonic steady state aeroelastic effects for a canard or tail airplane
[FFA-TN-1983-23] 16 p2700 N85-26674
The influence of helicopter tail shape on drag: An aerodynamic study using a low speed wind tunnel
[AD-A156304] 24 p4062 N85-35174
TAIL MOUNTINGS
U TAIL ASSEMBLIES
TAIL PLANES
U HORIZONTAL TAIL SURFACES
TAIL ROTORS
NT HELICOPTER TAIL ROTORS
Aircraft accident report, Western Helicopters, Inc., Bell UH-1B, N87701, Valencia, California, July 23, 1982
[PB84-910414] 05 p0594 N85-13789
An experimental investigation of the chopping of helicopter main rotor tip vortices by the tail rotor
[NASA-CR-177338] 13 p2154 N85-23376
TAIL SURFACES
NT HORIZONTAL TAIL SURFACES
TAILLESS AIRCRAFT
NT F-106 AIRCRAFT
NT MIRAGE 3 AIRCRAFT
TAILORING
U DESIGN
TAILS (ASSEMBLIES)
U TAIL ASSEMBLIES
TAIWAN
Sedimentary and tectonic evolution of the western Taiwan foredeep 03 p0389 N85-12491
Crustal dynamics studies in China
[NASA-CR-175617] 13 p2132 N85-23265
TAKEOFF
Preliminary airworthiness evaluation of the Rutan Aircraft Factory (RAF), Inc. LONG-EZ airplane with external sight
[AD-A145381] 02 p0138 N85-10937
Performance capabilities of the C-5 and C-17 cargo aircraft
[AD-A145518] 02 p0138 N85-10939
Insight. Background information for multipurpose pilots: Flight phenomena 02 p0138 N85-10940
To take off and to land safely, Hoechst 1678 for ice and snow free runways 05 p0595 N85-13791
Airport activity statistics of certificated route air carriers
[AD-A148472] 08 p1061 N85-16846
Optimum performance parameters for ski-jump operations of USAF fighter aircraft
[AD-A148532] 08 p1064 N85-16867
Boundary layer transition control for takeoff and landing configurations 14 p2211 N85-23714
Trajectory measurements for take-off and landing tests and other short-range applications, volume 16
[AGARD-AG-160-VOL-16] 15 p2561 N85-25801
The use of pressure sensing taps on the aircraft wing as sensor for flight control systems
16 p2698 N85-26660
Probabilistic computer model of optimal runway turnoffs
[NASA-CR-172549] 16 p2715 N85-26760
A system for take-off and landing measurements (STALINS)
[B8560072] 17 p2895 N85-27849
Addition of flexible body option to the TOLA computer program, part 1
[NASA-CR-132732-1] 17 p2896 N85-27855
Addition of flexible body option to the TOLA computer program. Part 2: User and programmer documentation
[NASA-CR-132732-2] 17 p2896 N85-27856
Wind tunnel results of advanced high speed propellers in the takeoff, climb and landing operating regimes
[NASA-TM-87054] 19 p3213 N85-29925
TAKEOFF RUNS
Probabilistic computer model of optimal runway turnoffs
[NASA-CR-172549] 16 p2715 N85-26760
TALKING
NT WORDS (LANGUAGE)
Post fire interview: Development and field validation of the behavioral sequence interview technique
[NBS-GCR-84-477] 04 p0454 N85-12881
TANDEM ROTOR HELICOPTERS
NT CH-47 HELICOPTER
TANDEM WING AIRCRAFT
Parametric study of a canard-configured transport using conceptual design optimization
[NASA-TP-2400] 11 p1584 N85-19979
TANGENTS
Cores of tangent cones and Clarke's tangent cone
[CSIR-TWISK-314] 01 p0108 N85-10727
TANK TRUCKS
Some stability and control problems with trailed farm tankers on slopes
[AD-P004291] 09 p1408 N85-18868
TANKER SHIPS
A crew exposure study. Phase II. Volume 2. At sea. Part A
[AD-A155233] 21 p3686 N85-32774
Further studies on liquid sloshing
[PB85-198695] 24 p4095 N85-35388
TANKS (COMBAT VEHICLES)
Assuring structural integrity in Army systems
[NASA-CR-175492] 11 p1651 N85-20398
Ground evaluation of helicopter air-to-air warfare
13 p1967 N85-22360
Improvements in tank tread assemblies
[NASA-CASE-NPO-16321-1] 18 p3117 N85-29291
Production verification of the acoustic emission weld monitor
[AD-A154168] 20 p3464 N85-31519
Thermal stress suffered by tank crews working in summer heat
[DRIC-T-7492] 22 p3626 N85-33696
TANKS (CONTAINERS)
NT CYLINDRICAL TANKS
NT EXTERNAL TANKS
NT FUEL TANKS
NT PROPELLANT TANKS
NT STORAGE TANKS
NT WING TANKS
Ultralightweight oxygen container
[PB84-220730] 01 p0036 N85-10226
The analysis of tank calibration data from several runs
[DE84-015529] 02 p0200 N85-11337
Analysis of seismic sloshing of reactor tanks considering submerged components and seismic isolation
[DE85-010499] 19 p3269 N85-30273
Elastomers used in aeronautics industry
[SNIAS-851-551-103] 20 p3434 N85-31304
TANTALUM
Strong-coupling superconductivity of Mg in proximity to Ta
[DE84-015482] 04 p0569 N85-13627
The effect of tantalum on the structure/properties of two polycrystalline nickel-base superalloys: B-1900 + Hf MAR-M247
[NASA-CR-174847] 09 p1294 N85-18127
Stability of amorphous metals on semiconductor substrates
[DE84-017256] 09 p1295 N85-18134
Wavecode constitutive models: Nonhomogeneous mixtures
[DE85-000836] 12 p1798 N85-21278
Gigantic lithium deposit discovered in France
14 p2289 N85-24184
Ultra-trace analysis of sinter tantalum with SIMS
[BLL-RARDE-TR-1220-(7291.7965)]
23 p3913 N85-34245
TANTALUM ALLOYS
Biform resolidification and amorphous phases in a laser and electron beam processed tantalum-iridium alloy
[DE84-013334] 02 p0184 N85-11234
Effects of MAR-M247 substrate (modified) composition on coating oxidation coating/substrate interdiffusion --- protective coatings for hot section components of gas turbine engines
[NASA-CR-174851] 10 p1440 N85-19073
TANTALUM COMPOUNDS
Positron measurements in 2H-TaSe2 crystals
[DE85-010507] 20 p3529 N85-31949
TAPE RECORDERS
Miniature personal physiological tape recorder (experiment 1ES 30) --- Spacelab
05 p0692 N85-14448
Operating time meter for tape recorder
12 p1838 N85-21537
Playback amplifier with high interference immunity
13 p2077 N85-22970
Operation of autotracking system in various video playback modes 16 p2764 N85-27055
Module for interfacing microprocessors and microcomputer 22 p3774 N85-33390
TAPER
U TAPERING
TAPERED WINGS
U SWEPT WINGS
TAPERING
Parabolic tapers for overmoded waveguides
[DE84-014237] 01 p0039 N85-10247
Reducing grating lobes due to subarray amplitude tapering
[AD-D011723] 23 p3927 N85-34339
TAPES
Evaluation and prediction of long-term environmental effects of nonmetallic materials
[NASA-CR-171353] 10 p1450 N85-19137
TAR SANDS
Aviation turbine fuels from tar sands bitumen and heavy oils. Part 1: Process analysis
[AD-A151319] 15 p2521 N85-25539
Subsurface petroleum geology of Santa Rosa sandstone (Triassic), northeast New Mexico
[TI85-901364] 19 p3313 N85-30538
TARE (DATA REDUCTION)
U DATA REDUCTION
TARGET ACQUISITION
The prediction of observer responses from photometric data on smoke screens; an analysis of the Oldebroek 2 trials, May 1981
[IZF-1984-21] 01 p0095 N85-10642
Description of the Dutch-Danish (DUDA) scanner -- thermal signatures
[AD-B084893] 01 p0121 N85-10825
Army aviation today and tomorrow
06 p0751 N85-14810
Radar echo enhancement using surface reflections
[AD-A146970] 07 p0939 N85-15955
Binocular overlap in a fiber optic helmet mounted display
[AD-P004331] 09 p1270 N85-17965
Synthesis of digital nonrecursive band-elimination filters for moving-target selectors 12 p1840 N85-21545
Efficiency of multitarget signal detection by digital radar data processing devices 13 p2060 N85-22991
Operation and maintenance requirements of the Army Remotely Piloted Vehicle (RPV)
[NASA-CR-175714] 14 p2218 N85-23755
An MRTD-compatible bar pattern response model for TV and direct view sighting systems
[BAE-BT-12090] 15 p2620 N85-26146
Optimizing the specifications for an air-surface laser system 16 p2696 N85-26644
Performance of rolling ball and isometric joystick on a 2-D target alignment task
[RSRE-MEMO-3695] 22 p3826 N85-33699
TARGET PENETRATION
U TERMINAL BALLISTICS
TARGET RECOGNITION
Content, variety, and augmentation of simulated visual scenes for teaching air-to-ground attack
[AD-A145218] 01 p0013 N85-10080
Joint services electronics program
[AD-A145065] 01 p0042 N85-10276
The perceptual quality of smoke screens: An analysis of the Oldebroek 2 trials, May 1981
[IZF-1984-20] 01 p0095 N85-10641
Digital correlator speed improvement by multiplexing
[AD-A145207] 01 p0100 N85-10662
Using gross outline features in long range target identification
[FOA-C-53018-H2] 02 p0237 N85-11543
About ambiguity and Q-functions
[AD-A145293] 02 p0250 N85-11636
Design of edge detectors for reduced images
[AD-A145700] 02 p0252 N85-11653
Distributed sensor networks
[AD-A146209] 03 p0355 N85-12256
The development of new methods for solving the target identification or inverse scattering problem for time-harmonic acoustic and electromagnetic waves
[AD-A145821] 03 p0415 N85-12657
Visibility of various target-background color combinations under different chromatic ambient illuminations
[AD-A146348] 03 p0420 N85-12684
Color and grey scale in sonar displays
05 p0710 N85-14502
Optimization of moving-target selection radar devices for nonGaussian signals for stationary targets
06 p0789 N85-15040
Radar echo enhancement using surface reflections
[AD-A146970] 07 p0939 N85-15955
Target detection using microwave irradiances from natural sources: A passive, local and global surveillance system
[NASA-CR-174260] 07 p0946 N85-15991
Human factors and training research in military organizations and systems
[AD-A146832] 07 p1020 N85-16475
Multi target tracking by dynamic scene analysis
[AD-A148922] 10 p1466 N85-19250

Optical implementation of the synthetic discriminant function
[AD-A149582] 10 p1557 N85-19617
Automatic pickup of trajectory by method of sequential analysis taking into account deviation of radar markers from center of strobe 12 p1836 N85-21535
Research on ocean floor electrical surveys
[AD-A149831] 12 p1899 N85-21920
The accuracy in calculations of intervisibility with digital terrain models — digital models
[FOA-C-20557-D8(E1)] 12 p1909 N85-21983
Moving target detection 13 p2067 N85-22915
Visual simulation requirements for aircraft aspect recognition at real world distances
[AD-A151040] 14 p2228 N85-23810
Digital computer applications of Kalman filter in target tracking
[AD-A150770] 14 p2404 N85-24821
Eye movement in response to single and multiple targets
[AD-A151115] 15 p2617 N85-26126
Visual search strategy predictions: The use of aspect ratio as a cue
[BAE-BT-12585] 15 p2619 N85-26138
Poisson and multinomial shadowing processes
[AD-A151600] 15 p2640 N85-26286
An investigation into generalised matched filter techniques
[BAE-BR-12971] 15 p2651 N85-26348
Low-resolution target classification from a staring infrared sensor
[AD-A151690] 15 p2652 N85-26358
Design adequacy: An effectiveness factor
16 p2695 N85-26642
Scene analysis using recursive frequency domain correlation with energy normalization
[AD-A151777] 16 p2854 N85-27596
A mathematical model for calculating detection probability of a diffusion target
[AD-A152026] 16 p2854 N85-27601
Target discrimination using infrared techniques: Theoretical considerations
[AD-A154070] 19 p3350 N85-30762
Feedforward-feedback control logic for robust target-tracking 20 p3436 N85-31317
Radar target identification through electromagnetic scattering studies
[AD-A154596] 21 p3573 N85-32220
Broadside scattering of a tubular cylinder for evaluation of target identification
[AD-A155739] 21 p3577 N85-32248
Bayesian vs MAP multiple model adaptive estimation for field of view expansion in tracking airborne targets
[AD-A155466] 21 p3679 N85-32855
Selectivity of weight compensator of passive interference to unknown velocities of detectable targets
22 p3762 N85-33317
Hardware test program for evaluation of basline range-range rate sensor concept
[NASA-CR-176143] 23 p3933 N85-34377

TARGET SIMULATORS
Docking simulation analysis of range data requirements for the orbital maneuvering vehicle
[NASA-TM-86510] 20 p3407 N85-31143

TARGET THICKNESS
A method for the evaluation of the residual energy of a metallic fragment after perforation of a thin target
[ISL-R-113/83] 16 p2794 N85-27233

TARGETS
NT LASER TARGETS
NT PARTICLE ACCELERATOR TARGETS
NT RADAR TARGETS
A production system model of capturing reactive moving targets 05 p0705 N85-14524
Analysis of the impact of a deformable missile model on a deformable obstruction
[BLL-RISLEY-TR-8534-(9091.9F)]
06 p0859 N85-15459
Electro-optical target detection
[AD-D011366] 07 p1042 N85-16617
The value and utility of inflight onboard simulation
[AD-A146033] 08 p1198 N85-17543
An electronically controlled array for simulation of passive target/background signatures at millimeter wavelengths
[AD-D011456] 10 p1468 N85-19263
Nose and inlet duct radomes for the firebolt aerial target
[AD-P004375] 12 p1827 N85-21469
Experimental test of the three subaperture method for estimating target elevation angle
[AD-A149687] 12 p1851 N85-21614
Shallow magma targets in the western US
[DE85-003274] 12 p1881 N85-21803
Variable flexing device for targets in internal beams of charged particle accelerators 13 p2044 N85-22797
Microwave blackbodies for spaceborne receivers
[NASA-CR-175647] 13 p2094 N85-23068
Eye movement in response to single and multiple targets
[AD-A151115] 15 p2617 N85-26126
Angular tracking error in A phase comparison monopulse tracking radar: A critical review and extension of the phase front distortion approach
[AD-A152628] 17 p2949 N85-28205
Tracking algorithm performance analysis program (TRAPP)
[DE85-007304] 17 p3009 N85-28601
Study of intermediate velocity penetration of steel spheres into deep aluminum targets
[DE85-010419] 19 p3287 N85-30385
Spectral reflectances of natural targets for use in remote sensing studies
[NASA-RP-1139] 19 p3299 N85-30450
Polarized internal target apparatus
[DE85-011611] 19 p3354 N85-30793
Ion beam-plasma interactions
[DE85-010202] 19 p3371 N85-30913
Moving finite element method for ICF target implosion
23 p3980 N85-34675
Target observability for satellite-based sensors
[AD-A156139] 24 p4069 N85-35217

TASK COMPLEXITY
The design and use of subtasks in part training and their relationship to the whole task
05 p0711 N85-14559
On choosing between two probabilistic choice sub-models in a dynamic multitask environment
05 p0711 N85-14563
No fatigue effect on blink rate
05 p0712 N85-14564

TASKS
NT AUDITORY TASKS
NT VISUAL TASKS
Comprehension of instructions for operating devices
[AD-A145263] 01 p0098 N85-10653
Ada (trademark) training curriculum. Real-time concepts I303 teacher's guide
[AD-A145093] 01 p0104 N85-10694
Decision tree rating scales for workload estimation: Theme and variations
[NASA-CR-174062] 02 p0237 N85-11544
Models of natural intelligence in fault diagnosis tasks: Implications for training and aiding of maintenance personnel
[AD-P003927] 02 p0246 N85-11607
Helicopter pilot performance for discrete-maneuver flight tasks 05 p0702 N85-14502
Psychological issues in online adaptive task allocation
05 p0704 N85-14516
Twentieth Annual Conference on Manual Control, volume 2
[NASA-CP-2341-VOL-2] 05 p0707 N85-14535
Performance enhancements under dual-task conditions 05 p0707 N85-14537
The effects of task structure on time-sharing efficiency and resource allocation optimality
05 p0711 N85-14562
Multiple resources and display formatting: The implications of task integration in a simulated air traffic control task
[AD-A150713] 14 p2292 N85-24205
The effect of strategy in second order manual control on resource competition with a sternberg memory search task
[AD-A150985] 14 p2391 N85-24727
Shape with and without redundant colour as coding mechanism for simulated radar displays in a time-extended simple vigilance task
[AD-A151683] 16 p2844 N85-27533
Resource allocation in cerebral specialization of function: Behavioral and electrophysiological studies
[AD-A155092] 21 p3664 N85-32759
Conceptualizing in assembly tasks
[AD-A155564] 21 p3665 N85-32770

TASMANIA
Sidereal variations deep underground in Tasmania
[SH-4.4-4] 23 p4033 N85-35002

TATB
Sensitivity and performance characterization of DINGU
[DE85-010750] 22 p3754 N85-33269
Friction, impact, and electrostatic discharge sensitivities of energetic materials
[DE85-013321] 24 p4083 N85-35309

TAXIING
New airport ground traffic control system planned
03 p0310 N85-12006
A feasibility study for using low boiling point fluids to change aircraft tire deflection
[AD-A152096] 16 p2706 N85-26701

TAXONOMY
Fungi of Mt. Babia Gora. 1: Mycoflora of forests
[NASA-TM-77484] 02 p0234 N85-11522
Asteroid taxonomy from cluster analysis of Photometry
09 p1411 N85-16897
Microalgae culture collection, 1984-1985
[DE84-013035] 11 p1690 N85-20626
Microplankton species assemblages at the Scripps Pier from March to November 1983 during the 1982-1984 El Nino event
[NASA-CR-175553] 12 p1699 N85-21926
Asteroid compositional rings: Clues to the compositions of primordial planetesimals in the middle solar system
15 p2678 N85-26537
A new taxonomy for distributed computer systems based upon operating system structure
[NASA-TM-86436] 19 p3342 N85-30709

TAYLOR INSTABILITY
Large-scale bubble structure of the interstellar medium (ISM) and properties of the Local Spiral Arm (LSA)
06 p0879 N85-15588
Kinetic Rayleigh-Taylor instability theory in the ionosphere near equator 13 p2067 N85-22911
Applications of Canuto's method to Rayleigh-Taylor-initiated turbulence
[DE85-010835] 18 p3102 N85-29202

TAYLOR SERIES
Stress-derivative control of keystoning deformation in finite element codes 01 p0058 N85-10385
Model diagnosis in two-way tables by means of row and column Euclidean maps
[CSIR-TWISK-307] 01 p0108 N85-10730
Upwind compact finite difference schemes
[CSIR-TWISK-334] 01 p0110 N85-10742
Determination of nonlinear viscoelasticity parameters for polymeric and composite materials by numerical methods
[AD-A145311] 02 p0185 N85-11240
Kinematics of nearby gas and stars
06 p0880 N85-15591
First derivatives of flow quantities behind two-dimensional, nonuniform supersonic flow over a convex corner
[NASA-TM-86272] 08 p1077 N85-16828
A series expansion study of the Navier-Stokes equations
[DFVLR-FB-84-34] 09 p1321 N85-18306
Efficiency of algorithms for gas-air channel diagnostics in gas turbine engines based on gas thermodynamic parameters 13 p2048 N85-22823
An incremental multigrid strategy for the fluid dynamics equations
[AD-A151953] 16 p2783 N85-27172
On the equivalent bilinearization of nonlinear controlled delay systems
[RR-272] 20 p3519 N85-31880

TAYLOR THEOREM
U TAYLOR SERIES

TAYLOR-GOERTLER INSTABILITY
U GOERTLER INSTABILITY

TDMA
U TIME DIVISION MULTIPLE ACCESS

TDR SATELLITES
TDRSS S-shuttle unique receiver equipment
08 p1100 N85-16951
The Communications link analysis and simulation system (CLASS) 08 p1100 N85-16952
Modeling techniques used in the communications link analysis and simulation system (CLASS)
08 p1100 N85-16953
Validation of the communications link analysis and simulation system (CLASS) 08 p1100 N85-16954
Digital scrambling for shuttle communication links: Do drawbacks outweigh advantages?
08 p1101 N85-16956
SIR-B coverage 08 p1143 N85-17211

TEA LASERS
Carbon dioxide laser radar for monitoring atmospheric transmittance and atmospheric aerosol
09 p1354 N85-18518
Improved operation of transversely excited N2O lasers
[AD-D011488] 10 p1490 N85-19409
Absorption of ozone molecules in strong field of tea CO2 injection laser 11 p1718 N85-20806
Obtaining amorphous coatings of FeW and Fe-Cr-P-B alloys using laser sputtering
[BLL-BISI-22493-(9022.06)] 17 p2927 N85-28057

TEACHING
U EDUCATION

TEAMS
Model of team organization and behavior and team description method
[AD-A147540] 07 p1053 N85-16880
Team dimensions: Their identity, their measurement and their relationships
[AD-A149662] 12 p1908 N85-21978

Assessing the behavior and performance of teams in organizations: The case of air transport crews
[AD-A150359] 13 p2143 N85-23302
Analysis of team performance in a programmed environment
[NASA-CR-175634] 14 p2392 N85-24728

TEARING
Impact dynamics research on composite transport structures
[NASA-TM-86391] 19 p3284 N85-30367
On size effects in plane stress crack-growth resistance
[AD-A155926] 24 p4102 N85-35426

TEARING MODES (PLASMAS)
Proceedings of the US-Japan Theory Workshop on 3-D MHD Studies
[DE84-012019] 04 p0566 N85-13620
Role of multiple helicity nonlinear interaction of tearing modes in dynamo and anomalous thermal transport in the Reversed Pitch Field
[DE85-002176] 10 p1560 N85-19639
Forced recognition by nonlinear MHD waves and sequential triggering of solar flares
12 p1956 N85-22291
Heating of coronal loops by tearing turbulence
14 p2448 N85-25114
Energy balance in resistive instabilities — solar prominences 14 p2454 N85-25155

TECHNETIUM
Molybdenum solar neutrino experiment
[DE85-003747] 14 p2445 N85-25090
Separation of uranium from technetium in recovery of spent nuclear fuel
[DE85-006499] 23 p3972 N85-34627
Elemental technetium as a cosmic-ray clock
[OG-7.1-9] 23 p4013 N85-34870

TECHNICAL WRITING
Improving technical documents
[AD-B084855] 01 p0126 N85-10866
The characteristics of generation and the rate of distribution for science and technology information in our country (China)
[AD-A141037] 04 p0575 N85-13671
Write while you work: Painless technical writing for Sandia engineers
[DE84-010669] 04 p0577 N85-13679
European Scientific Notes. Volume 39, number 1
[AD-A149498] 10 p1568 N85-19886
The potential for advanced computerized aids for comprehensible writing of technical documents
[AD-A150501] 13 p2055 N85-22870
Coping with computer terminology
[DE85-006076] 18 p3161 N85-29579
Standard procedures to be used in specifying basic properties of plastics and polymers
[NPL-DMA(A)-99] 20 p3433 N85-31295

TECHNIQUES
U METHODOLOGY

TECHNOLOGICAL FORECASTING
NT DELPHI METHOD (FORECASTING)
NT PATTERN METHOD (FORECASTING)
NT PROFILE METHOD (FORECASTING)
The future of satellite remote sensing: A worldwide assessment and prediction 02 p0151 N85-11025
Tactical missiles technologies. Research and prospectives
[SNIAS-841-320-101] 04 p0461 N85-12925
Perspectives of remote sensing at the end of the decade 05 p0659 N85-14238
Integrated Application of Active Controls (IAAC) technology to an advanced subsonic transport project. ACT/Control/Guidance System study, volume 1
[NASA-CR-165963-VOL-1] 06 p0754 N85-14837
A modified unit commitment and generation control for utilities with large wind generation penetrations
[DE84-015362] 06 p0806 N85-15129
Robotic technology: An assessment and forecast
[AD-A146672] 06 p0815 N85-15171
The application of a technology index to aircraft turbine engine cost estimating relationships
[AD-A147701] 08 p1087 N85-16874
The aircraft engine of the future
[PNR-90226] 08 p1087 N85-16875
USSR report: Machine tools and metalworking equipment
[JPRS-UMM-84-021] 08 p1136 N85-17168
Technology planning for flexible manufacturing systems 08 p1139 N85-17170
Developments in gas metering technology
[ERS-E.348] 09 p1321 N85-18307
Long-range electronics program outlined
11 p1700 N85-20687
Software technology within NASA
11 p1701 N85-20695
Technological and economic assessment of advanced ceramic materials. Volume 1: Summary and conclusions
[PB85-113082] 12 p1815 N85-21383
Technological and economic assessment of advanced ceramic materials. Volume 6: A case study of ceramic cutting tools
[PB85-113132] 12 p1815 N85-21387
GaAlAs-GaAs solar cell development: Prospective for space applications under concentration
13 p2007 N85-22581
Growth capabilities of European retractable solar arrays 13 p2012 N85-22625
FORTRAN in the 90's
[DE85-006154] 13 p2148 N85-23332
Inferences of future operations drawn from past and present applications of drifting buoys
14 p2323 N85-24356
Accomplishments of science by the year 2000
14 p2432 N85-24996
Fiscal year 1986 technical objective document
[AD-A151039] 14 p2432 N85-25000
A decision support methodology for space technology advocacy
[AD-A151395] 15 p2476 N85-25283
Future information technology, 1984: Telecommunications
[NBS/SP-500/119] 16 p2678 N85-27762
In orbit infrastructure. Volume 1: Executive summary — European space programs
[RX011-002/84-VOL-1] 17 p2908 N85-27928
Aluminum-lithium alloys: The answer of the aluminum industry to the threat of advanced fiber-reinforced materials
[VTH-LR-406] 17 p2932 N85-28102
Logical design of a decision support system to forecast technology, prices and costs for the national communications system
[AD-A152330] 17 p2948 N85-28196
Air Force technical objective document FY 86
[AD-A152730] 17 p3047 N85-28855
In orbit infrastructure — european space programs
[SNIAS-S/DT-24-996] 18 p3064 N85-28956
Outside users payload model
[NASA-CR-176011] 19 p3223 N85-29986
Technology for increasing the uranium-235 isotopic abundance in natural uranium feed on a productive scale
[DE85-011252] 19 p3357 N85-30610
Space ventures and society long-term perspectives
[NASA-CR-176012] 19 p3379 N85-30963
Evolution of spacecraft design methods as a function of environmental and geometrical constraints
[ESA-CR(P)-2012] 20 p3418 N85-31216
Structure and functions of ultra-thin films of organic compounds
[DRIC-T-7481] 22 p3741 N85-33188
Telecommunications forecast for ITU Region 2 to the year 1995
[NASA-TM-87077] 23 p3899 N85-34150
Towards the year 2000: Developments in inspection and product assurance to be anticipated during the next 15 years — aircraft engines
[PNR-90258] 23 p3940 N85-34421

TECHNOLOGIES
NT BIOTECHNOLOGY
NT ENERGY TECHNOLOGY
NT GEOTHERMAL TECHNOLOGY
NT MARINE TECHNOLOGY
NT MILITARY TECHNOLOGY
NT REACTOR TECHNOLOGY
Primer on the registration of technical information in industry 03 p0436 N85-12786
Development of robot technology in Shanghai surveyed 04 p0492 N85-13134
China report: Science and technology
[JPRS-CST-84-042] 06 p0747 N85-14789
East Europe report: Science and technology
[JPRS-ESA-85-005] 09 p1377 N85-18659
China report: Science and technology
[JPRS-CST-84-037] 10 p1424 N85-18982
West Europe report: Science and technology
[JPRS-WST-85-005] 11 p1592 N85-20013
China report: Science and technology
[JPRS-CST-84-026] 11 p1619 N85-20189
China report: Science and technology
[JPRS-CST-85-006] 12 p1820 N85-21416
Impacts of robotic and flexible manufacturing technologies on manufacturing costs and employment
[AD-A150060] 12 p1860 N85-21668
An open-ended future: In defense of a new humanism
[NASA-TM-77613] 12 p1944 N85-22209
Oversight review of the five-year outlook report on science and technology
[GPO-41-058] 12 p1949 N85-22243
Space Technology Experiments Platform (STEP) status: An in-space test facility 14 p2236 N85-2
USSR report: Engineering and equipment
[JPRS-UEQ-84-005] 14 p2285 N85-24137
The Impact of Science on Society
[NASA-SP-482] 14 p2431 N85-249
The legacy of science 14 p2432 N85-249
West Europe report: Science and technology
[JPRS-WST-85-014] 15 p2489 N85-250
East European report: Science and technology
[JPRS-ESA-85-010] 15 p2524 N85-25
USSR report: Electronics and electrical engineering
[JPRS-UEE-85-005] 15 p2524 N85-25
China report: Science and technology
[JPRS-CST-85-009] 15 p2530 N85-25
West Europe report: Science and technology
[JPRS-WST-84-020] 15 p2534 N85-25
West Europe report: Science and technology
[JPRS-WST-84-003] 15 p2534 N85-25
China report: Science and technology
[JPRS-CST-85-010] 15 p2564 N85-25
The development and implementation of advanced welding technology 15 p2565 N85-25
A study of spacecraft technology and design concepts, volume 1
[NASA-CR-172579-VOL-1] 16 p2730 N85-26
The Department of Defense statement on the Science and Technology Program by Colonel Donald I. Carter, USAF Acting Deputy Under Secretary of Defense for Research and Advanced Technology before the Subcommittee on Research and Development of the Committee on Armed Services of the United States House of Representatives, 99th Congress, first session
[AD-A152467] 17 p3046 N85-2885
The outlook for Soviet advanced technologies
[AD-P004564] 17 p3048 N85-2885
Technology and Soviet political choices
[AD-P004566] 17 p3048 N85-2886
Management of large-scale technology
23 p4057 N85-3514
EPALIT: A data management system applied to the control and retrieval of technical reports
[PB85-193068] 24 p4166 N85-355

TECHNOLOGY ASSESSMENT
Aeronautics Technology Possibilities for 2000: Report of a workshop
[NASA-CR-174018] 01 p0001 N85-1000
Development trends and requirements of propulsion system technology for civil aircraft
01 p0011 N85-100
Satellite reconnaissance
[AD-B085034] 01 p0015 N85-100
Technical Review of the Solid Particle Receiver Program
[DE84-015181] 01 p0068 N85-104
A subjective evaluation of the PROFS operational workstation based upon a real-time forecasting experiment in summer 1983 — Program for Regional Observing and Forecasting Services (PROFS) 01 p0083 N85-105
Interactive computer display systems in nowcasting
01 p0083 N85-105
Fusion and its future in Illinois
[DE84-014686] 01 p0122 N85-106
Office of Technology Assessment
01 p0127 N85-106
Foreign civil aviation competition: 1976 summary and implications
[NASA-TM-X-73907] 02 p0133 N85-109
Role of research aircraft in technology development
[NASA-TM-85913] 02 p0137 N85-109
The future of satellite remote sensing: A worldwide assessment and prediction 02 p0151 N85-1102
Developing commercial users of space
02 p0154 N85-1104
Advances in electrophoretic separations
02 p0156 N85-1105
Opportunities for commercial organizations
02 p0156 N85-1105
Doing business in space: How to get there from here
02 p0156 N85-1105
Space research benefits national economy
02 p0163 N85-1110
The Multispectral Imaging Science Working Group. Volume 1: Executive summary
[E85-10001] 02 p0213 N85-1140
The Multispectral Imaging Science Working Group. Volume 2: Working group reports
[E85-10002] 02 p0213 N85-1140
Information Science Panel joint meeting with Imaging Science Panel 02 p0214 N85-1141
A prospectus for Thematic Mapper research in the Earth sciences
[E85-10003] 02 p0215 N85-1141
A report on the training course at Fortaleza (Ceara)
[E85-10013] 02 p0216 N85-1142

DOD related software technology requirements, practices, and prospects for the future
[AD-A145493] 02 p0242 N85-11575

The microprocessor control of a motor-alternator
[RAE-TM-NAV-ENG-1023(L)] 02 p0244 N85-11591

Artificial intelligence applications to maintenance
[AD-P003914] 02 p0244 N85-11594

An overview of the Joint Logistics Commanders Automatic Test Equipment Panel
[AD-P003916] 02 p0244 N85-11596

Narrowband tunable dye laser with amplifier pumped by powerful nitrogen laser 02 p0262 N85-11716

Auditory information systems in military aircraft: Current configurations versus the state of the art
[AD-A145469] 02 p0275 N85-11794

Proceedings of the Ion Implantation for Army Needs Workshop
[AD-A145474] 02 p0286 N85-11863

Review of the University of Manchester Ion Implantation Conference
[AD-P003950] 02 p0286 N85-11866

Research and technology
[NASA-TM-86321] 02 p0305 N85-11973

Preliminary analysis of space mission applications for electromagnetic launchers
[NASA-CR-174067] 03 p0321 N85-12071

Civilian space stations and the US future in space: Summary
[OTA-STI-242] 03 p0323 N85-12083

Sensor technology for second, third generation industrial robots. Optical sensor applications
03 p0342 N85-12198

Improving operational reliability and productivity of robotized technological complexes
03 p0346 N85-12227

New welding equipment for mechanized welding and trends in further development 03 p0352 N85-12264

Dynamic and other secondary benefits of compressed air energy storage
[DE84-015571] 03 p0386 N85-12468

Interstellar mission 04 p0459 N85-12916

Definition of technology development missions for early Space Station satellite servicing. Volume 2: Technical
[NASA-CR-171229] 04 p0461 N85-12923

Tactical missiles technologies. Research and prospectives
[SNIAS-841-320-101] 04 p0461 N85-12925

Electroforming of nickel
[SNIAS-841-501-101] 04 p0484 N85-13085

Metal oxide semiconductors power transistors
[CNES-84/QPE/FT/190] 04 p0496 N85-13166

China report: Science and technology
[JPRS-CST-84-001] 04 p0557 N85-13545

Present status, future prospects of domestic acoustical instruments 04 p0557 N85-13548

Value analysis — industrial competition
[CNES-NT-110] 04 p0577 N85-13684

Electromechanical/electromagnetics working group summary 05 p0604 N85-13852

A summary of the 1983 Integrated Flywheel Technology Workshop 05 p0605 N85-13855

Merits of flywheels for spacecraft energy storage
05 p0605 N85-13857

Evaluating NASA technology programs in terms of private sector impacts 05 p0608 N85-13885

Missions/planning panel 05 p0609 N85-13886

Basic investigation concerning the applicability of multispectral radiation data from microwave radiometry measurements to geoscientific objectives of remote sensing
[ESA-TT-846] 05 p0628 N85-14027

Metric evaluation of SAR-580 optical images for cartographic purposes 05 p0659 N85-14231

The role of expert systems in remote sensing
05 p0661 N85-14246

Solar pond overview 05 p0667 N85-14287

Bioprocessing in space 05 p0690 N85-14439

An overview of some monoplanar missile programs
[NASA-TM-86330] 06 p0747 N85-14786

Aperture synthesis (review) 06 p0781 N85-14995

Robotic technology: An assessment and forecast
[AD-A146672] 06 p0815 N85-15171

Civilian space stations and the US future in space
[OTA-STI-241] 07 p0914 N85-15781

Toward a goal-oriented civilian space program
07 p0914 N85-15786

Comparative investigation of three commercial radiosonde systems
[KNMI-TR-53] 07 p1009 N85-16409

The application of a technology index to aircraft turbine engine cost estimating relationships
[AD-A147701] 08 p1087 N85-16874

Low lift-to-drag aero-assisted orbit transfer vehicles
08 p1107 N85-16994

Flight crew training technology: A review
09 p1275 N85-18010

West Europe report: Science and technology
[JPRS-WST-85-003] 09 p1309 N85-18224

Configuration study for a 30 GHz monolithic receive array: Technical assessment
[NASA-CR-174897] 09 p1311 N85-18238

Impact of 810D on dynamic test laboratories
09 p1334 N85-18386

State and development of the machine-tool industry in Japan. Part 2: Flexible manufacturing systems
[PNR-90236-PT-2] 09 p1371 N85-18617

NASA new technology identification and evaluation
[NASA-CR-174368] 09 p1403 N85-18832

DOE/ORNL electric systems program overview
[DE85-003334] 10 p1459 N85-19197

Overview of photovoltaic concentrator technology
[DE84-016790] 10 p1512 N85-19539

Measurement techniques for evaluating solar reflector materials
[PB85-119469] 10 p1512 N85-19541

High energy pulsed particle accelerator
[AD-A149247] 10 p1554 N85-19797

Technological and economic assessment of advanced ceramic materials. Volume 3: A case study of ceramic capacitors
[PB85-113108] 11 p1613 N85-20141

The response of explosive systems to thermal stimuli: A state-of-the-art assessment
[DE85-000919] 11 p1614 N85-20148

Institute director surveys industrial automation drive
11 p1617 N85-20167

Developments in GDR metal forming technology assessed 11 p1617 N85-20168

Thermophysical properties of matter
11 p1620 N85-20199

Progress toward free-electron lasers for applications
[DE85-002208] 11 p1639 N85-20326

Technology and test 11 p1643 N85-20353

Where are we going in tethers
11 p1644 N85-20354

Introducing engine innovations: An examination of future markets for Brayton and Stirling automotive engines
[DE84-016319] 11 p1647 N85-20382

Exploratory assessment of second generation robotics and sensor-based systems
[PB85-132793] 11 p1648 N85-20388

High performance solar desiccant cooling system: Performance evaluation and research recommendations
[DE85-000508] 11 p1676 N85-20559

Software technology within NASA
11 p1701 N85-20695

Technological and economic assessment of advanced ceramic materials. Volume 2: A case study of ceramics in heat engine applications
[PB85-113090] 12 p1815 N85-21384

Technological and economic assessment of advanced ceramic materials. Volume 5: A case study of ceramic toxic and combustible gas sensors
[PB85-113124] 12 p1815 N85-21386

High-technology ceramics in Japan
[PB85-125029] 12 p1815 N85-21389

Latent heat storage technology and application workshop. Summary report: Session 6
[DE85-001097] 12 p1882 N85-21806

Multiyear plan for experimental systems research passive and hybrid solar energy program
[PB85-146868] 12 p1883 N85-21815

1984 science and technology posture hearing with the director of the Office of Science and Technology Policy
[GPO-41-060] 12 p1949 N85-22244

The high voltage silicon cell: A comparative analysis
13 p2005 N85-22569

Gallium arsenide arrays versus silicon arrays for space application 13 p2006 N85-22574

Availability of AlGaAs/GaAs solar cells in space
13 p2006 N85-22576

Comparative study of GaAs solar cell potentialities for space applications 13 p2006 N85-22577

Survival testing of silicon solar modules
13 p2009 N85-22602

Aspects of low cost module technology — spacecraft solar arrays 13 p2011 N85-22614

Study of concentration for space photovoltaic generators 13 p2011 N85-22618

Isotropic proton irradiation of GaAs solar cells
13 p2012 N85-22622

Recent trends in particle size analysis techniques
[NASA-TM-77735] 13 p2017 N85-22645

Survey of the state-of-the-art of miniature cryocoolers for superconductive devices
[AD-A150319] 13 p2041 N85-22774

Nation said to rank high with 15 satellites
13 p2041 N85-22778

USSR report: Machine tools and metalworking equipment
[JPRS-UMM-85-005] 13 p2051 N85-22839

Technologies to sustain tropical forest resources
[TI85-901065] 13 p2126 N85-23241

Spatial acquisition algorithms and systems for intersatellite optical communication links
[AD-A150794] 14 p2292 N85-24207

The 1981 transatlantic boat race contribution for marine meteorological measurements 14 p2324 N85-24361

Miscellaneous ARGOS maritime applications — yacht races 14 p2327 N85-24383

Drifting buoy studies for weather applications
14 p2329 N85-24396

USSR report: Cybernetics, computers, and automation technology
[JPRS-UCC-85-002] 14 p2400 N85-24794

Investigation of technology needs for avoiding helicopter pilot error related accidents
[NASA-CR-3895] 15 p2465 N85-25220

European views differ on space station concept
15 p2531 N85-25608

East Europe report: Science and technology
[JPRS-ESA-85-018] 15 p2537 N85-25658

Soviet Institute director on GDR-USSR welding technology 15 p2538 N85-25662

Mathematical aspect of welding technology research discussed 15 p2538 N85-25663

Applicability of modular versus universal robots discussed 15 p2538 N85-25664

Multi-bistatic radar for short range surveillance
[BAE-BT-10603] 15 p2539 N85-25673

Welding techniques in pressure part technology
15 p2566 N85-25835

Biotechnology in Japan
[PB85-169464] 15 p2315 N85-26113

Supercomputers and symbolic computation
[AD-A151376] 15 p2623 N85-26166

USSR report: Cybernetics, computers and automation technology
[JPRS-UCC-85-003] 15 p2625 N85-26174

Protective coatings for aircraft structures: A review
[VTH-LR-413] 16 p2706 N85-26704

The state-of-the-art and future of flight control systems 16 p2712 N85-26732

Forecasts on long-range development of space programs 16 p2727 N85-26830

US said to seek military advantage in space
16 p2727 N85-26831

Instrumentation technology overview
16 p2739 N85-26903

East Europe report: Science and technology
[JPRS-ESA-85-019] 16 p2767 N85-27077

Preliminary technology utilization assessment of the robotic fruit harvester
[NASA-CR-175834] 16 p2844 N85-27532

Flight test support aircraft Advanced Technologies Testing Aircraft System (ATTAS) for the DFVLR
[MBB-FE-732/S/PUB/154] 16 p2874 N85-27730

The Helios missions 16 p2884 N85-27795

Controller requirements for uncoupled aircraft motion, volume 1
[AD-A153173] 17 p2900 N85-27878

Glassy metals: New highly resistant material
[BLL-BISI-TRANS-21764-(9022.06)]
17 p2926 N85-28049

USSR report: Science and technology policy
[JPRS-UST-85-008] 17 p3049 N85-28872

General laws of development of technology
17 p3049 N85-28875

Advanced vehicle systems assessment. Volume 1: Executive summary
[NASA-CR-175876] 17 p3051 N85-28887

West European report: Science and technology
[JPRS-WST-84-036] 18 p3066 N85-28960

Conservation and substitution technology for critical metals in bearings and related components for industrial equipment and opportunities for improved bearing performance
[PB85-176246] 18 p3082 N85-29069

West Europe report: Science and technology
[JPRS-WST-84-022] 18 p3085 N85-29086

France's use of Cray 1, plans for national supercomputer 18 p3086 N85-29093

Preliminary investigation of the performance of repeater technology for satellite sound broadcasting
[SSP/017/82] 18 p3092 N85-29137

Evaluation of VLSI technology — space applications
[CD.6501702] 18 p3098 N85-29177

New technologies to improve laboratory testing
[DE85-008151] 18 p3110 N85-29257

Small central receiver Brayton cycle study
[DE85-008882] 18 p3126 N85-29369

Progress in solar thermal distributed receiver technology
[DE85-006066] 18 p3128 N85-29372

Progress in radar meteorology
18 p3146 N85-29486

Direct digital control study
[AD-A153685] 18 p3167 N85-29621
Sub-committee on advanced technology and technology transfer
[AD-A153645] 18 p3198 N85-29836
Current activities and background of technology transfer and exchange program at Lawrence Livermore National Laboratory
[DE85-009526] 18 p3199 N85-29843
Space station automation study-satellite servicing, volume 2
[NASA-CR-171513] 19 p3226 N85-30000
New form of graphite 19 p3243 N85-30111
The Federal Wind Program at NASA Lewis Research Center
[NASA-TM-83480] 19 p3304 N85-30478
Uniform cost-estimation method for biomass production and conversion technologies
[DE85-011714] 19 p3380 N85-30970
The application of laser anemometry to the study of transonic shock boundary-layer interactions
[ISL-CO-204/84] 20 p3396 N85-31067
Specific aspects of maritime search and rescue in French metropolitan and overseas territories: Expected benefits from a detection and location of distress system by satellites 20 p3401 N85-31097
Possible use of the COSPAS/SARSAT system within the Swedish mountain rescue organization
20 p3401 N85-31100
Maritime mobile satellite techniques as an integral part of the Future Global Maritime Distress and Safety System (FGMDSS): The position of the Federal Republic of Germany 20 p3406 N85-31136
Advanced (unfloated) gyros for satellite control
[ESA-CR(P)-2010] 20 p3419 N85-31222
An overview of measurement solutions for digital systems 20 p3437 N85-31326
SAR swath widening techniques — satellite radar
[BL-6196] 20 p3441 N85-31358
A survey of unified constitutive theories
20 p3466 N85-31531
Moire interferometric measurement of relative displacements in dovetail joints
[OUEL-1563/85] 20 p3471 N85-31566
Gas hydrates
[DE85-001986] 20 p3477 N85-31607
Millimetre wave pulse technology — satellite mapping
[ESA-CR(P)-2004] 20 p3478 N85-31611
Gallium arsenide arrays versus silicon arrays for space application
[SNIAS-851-440-104] 20 p3485 N85-31657
Study of concentration for space photovoltaic generators
[SNIAS-851-440-105] 20 p3485 N85-31658
The Department of Defense report on the technology base and support of university research
[AD-A154309] 20 p3540 N85-32030
Renewable energy research and development outlook, volume 1
[DE85-011577] 20 p3540 N85-32033
GAO (General Accounting Office) assessment of DOD's Very High Speed Integrated Circuits (VHSIC) technology program
[AD-A155109] 21 p3581 N85-32261
Space station ECLSS integration analysis: Simplified General Cluster Systems Model, ECLS System Assessment Program enhancements
[NASA-CR-176089] 21 p3670 N85-32796
Detector problems at the SSC
[DE85-010217] 21 p3703 N85-33007
Advanced beamed-energy and field propulsion concepts
[NASA-CR-176108] 22 p3741 N85-33186
Military hydrology. Report 9: State-of-the-art review and annotated bibliography of dam-breach flood forecasting
[AD-A155383] 22 p3801 N85-33553
Low-head hydroelectric power demonstration project: City of Gonzales, Texas
[DE85-010403] 22 p3809 N85-33595
Photovoltaic industry progress through 1984
[DE85-013029] 22 p3809 N85-33596
The development of titanium production in the USSR
[BLL-OA-TRANS-3226-(6196.3)]
23 p3913 N85-34244
Vapor phase heat transport concepts
[DE85-009550] 23 p3931 N85-34366
SP-100 Thermionic Technology Program
[DE85-012311] 23 p3972 N85-34625
Analysis of incompressible cascade flows using state-of-the-art computer programs
[AD-A155850] 24 p4062 N85-35173
Energy Efficient Engine Program technology benefit/cost study, volume 2
[NASA-CR-174766-VOL-2] 24 p4066 N85-35196
Technology for large space systems: A bibliography with indexes
[NASA-SP-7046(12)] 24 p4086 N85-35209
State-of-the-art construction technology for deep tunnels and shafts in rock
[AD-A156362] 24 p4099 N85-35411
Practical aspects of photovoltaic technology, applications and cost (revised)
[NASA-CR-174963] 24 p4110 N85-35472
A Programmable Automatic Noise Data and Other Related parameter Acquisition system (PANDORA) — wind energy converters 24 p4111 N85-35479
Visit to test facility Stoetten (West Germany) May 9, 1984, including the Voith Wind Energy Converter (WEC) 520 turbine. The annual production of various wind energy plants in selected locations 24 p4112 N85-35487

TECHNOLOGY TRANSFER
NT AEROSPACE TECHNOLOGY TRANSFER
PROFS: An approach to improved operational weather services — Program for Regional Observing and Forecasting Services (PROFS) 01 p0083 N85-10555
Project COST 72 (The European weather radar project) today 01 p0084 N85-10561
Factors critical to the implementation of self-paced instruction: A background review
[AD-A145143] 01 p0097 N85-10648
Integrated computer-aided manufacturing (ICAM) architecture. Part 3, volume 8: Technology transfer
[AD-A144732] 01 p0103 N85-10689
Energy efficient engine. Volume 2. Appendix A: Component development and integration program
[NASA-CR-173085] 02 p0146 N85-10991
Opportunities for commercial organizations
02 p0156 N85-11055
Development of space instrumentation of Intercosmos member countries 02 p0163 N85-11106
Remote sensing applications program
[E85-10022] 02 p0218 N85-11435
Artificial Intelligence in Maintenance: Proceedings of the Joint Services Workshop
[AD-A145349] 02 p0244 N85-11592
AGARD Highlights
[AGARD-HIGHLIGHTS-84/2] 02 p0305 N85-11972
Proceedings of a Workshop on Applications of Tethers in Space, Executive Summary
[NASA-CR-171195] 03 p0322 N85-12075
Dynamics and controls working group summary
05 p0604 N85-13854
Land Remote-Sensing Commercialization Act
[S-REPT-98-458] 05 p0654 N85-14201
The availability of Japanese scientific and technical information in the United States
[GPO-35-241] 05 p0735 N85-14726
Naval surface weapons center technology transfer report (FY83)
[AD-A146501] 06 p0871 N85-15534
Propulsion and power systems perspective
08 p1096 N85-16938
Microwave radiometric studies of composition and structure 08 p1183 N85-17456
Study of application of space telescope science operations software for SIRTF use
[NASA-CR-177337] 09 p1287 N85-18080
Emerging role of the national laboratory in the development and transfer of materials technology
[DE85-001252] 09 p1288 N85-18086
West Europe report: Science and technology
[JPRS-WST-85-003] 09 p1309 N85-18224
NASA new technology identification and evaluation
[NASA-CR-174368] 09 p1403 N85-18832
West Europe report: Science and technology
[JPRS-WST-85-004] 10 p1460 N85-19204
French research minister on policy, technology transfer 11 p1618 N85-20182
China report: Science and technology
[JPRS-CST-84-040] 11 p1623 N85-20219
Oversight review of the five-year outlook report on science and technology
[GPO-41-058] 12 p1949 N85-22243
Transfer of technology
[S-REPT-98-684] 12 p1949 N85-22246
Transfer of technology
[S-HRG-98-986] 12 p1949 N85-22247
The availability of Japanese scientific and technical information in the United States
[GPO-39-478] 12 p1951 N85-22254
Technology transfer to the Middle East
[PB85-127744] 12 p1952 N85-22264
China report: Science and technology
[JPRS-CST-85-003] 13 p2166 N85-23433
West Europe report: Science and technology
[JPRS-WST-85-013] 14 p2289 N85-24183
East Europe report: Science and technology
[JPRS-ESA-85-015] 14 p2289 N85-24189
West Europe report: Science and technology
[JPRS-WST-84-007] 15 p2530 N85-25600
China report: Science and technology
[JPRS-CST-85-007] 15 p2533 N85-25821
Energy Data Base: Subject thesaurus permutated listing, Revision 6, appendix
[DE84-016963] 15 p2666 N85-26464
China report: Science and Technology
[JPRS-CST-85-012] 16 p2806 N85-27300
Bioengineering and rehabilitation: Windows of opportunity past, present and future
[NASA-EP-216] 16 p2841 N85-27318
Soviet space programs, 1976-1980 (with supplementary data through 1983). Part 3: Unmanned space activities
[S-PRT-98-235-PT-3] 16 p2879 N85-27765
The significance of Helios for Europe
16 p2886 N85-27508
West Europe report: Science and technology
[JPRS-WST-84-024] 17 p2945 N85-28183
Technology and Soviet political choices
[AD-P004566] 17 p3046 N85-28881
Close encounters with S/T (science and technology) in the Soviet Union
[AD-P004570] 17 p3048 N85-28884
Catalog of research projects at Lawrence Berkeley Laboratory, 1985
[DE85-008679] 17 p3049 N85-28888
Report to Congress on the Automotive Technology Development Program
[DE85-005640] 17 p3052 N85-28890
West European report: Science and technology
[JPRS-WST-84-036] 18 p3066 N85-28980
West Europe report: Science and technology
[JPRS-WST-84-032] 18 p3086 N85-29095
Results of Italian research in high power lasers
18 p3086 N85-29097
US restrictions on technology transfer reviewed
18 p3088 N85-29115
Photovoltaic Systems Development Project: An activity summary
[DE85-009994] 18 p3129 N85-29379
Sub-committee on advanced technology and technology transfer
[AD-A153645] 18 p3198 N85-29836
Current activities and background of technology transfer and exchange program at Lawrence Livermore National Laboratory
[DE85-009526] 18 p3199 N85-29843
U.S.-China conference on science policy
[PB85-176345] 19 p3380 N85-30671
West Europe report: Science and technology
[JPRS-WST-85-020] 20 p3438 N85-31333
Evaluative report on the Institute for Computer Science and Technology, National Bureau of Standards, fiscal year 1984
[PB85-176097] 20 p3514 N85-31648
Spin-offs from technical scientific infrastructures, no. 1
20 p3540 N85-32034
Spin-offs from technical commercial infrastructures, no. 2 20 p3540 N85-32035
Photovoltaics technical information guide
[DE85-002924] 22 p3806 N85-33385
Technology transfer report: Feasibility study for the use of geothermal brine in the Ashdod area, Israel
[DE85-013316] 22 p3810 N85-33398
New innovative businesses from industry. Experiences in the Netherlands in the successful transfer of technology from university to industry 22 p3849 N85-33843
Proceedings of the 14th Army Science Conference. Volume 3: Principal authors P through Z
[AD-A149202] 24 p4144 N85-35591
Electronic information management and productivity
[DE85-013362] 24 p4164 N85-35818

TECHNOLOGY UTILIZATION
PROFS: An approach to improved operational weather services — Program for Regional Observing and Forecasting Services (PROFS) 01 p0083 N85-10555
Canada report to COSPAR 01 p0131 N85-10906
Industrial use of land observation satellite systems
02 p0151 N85-11028
Agribusiness and space: No limits to growth
02 p0152 N85-11029
Economic evaluation of space survey materials use in land improvement engineering field work
02 p0165 N85-11115
A prospectus for Thematic Mapper research in the Earth sciences
[E85-10003] 02 p0215 N85-11418
A report on the training course at Fortaleza (Ceara)
[E85-10013] 02 p0216 N85-11426
Applications of remote sensing techniques to oceanography and sea ice
[FOA-B-80004-M7] 02 p0220 N85-11448
On applying AI (Artificial Intelligence) to maintenance and troubleshooting
[AD-P003915] 02 p0244 N85-11595

AI (Artificial Intelligence) approaches to troubleshooting
[AD-P003918] 02 p0245 N85-11598
Navy programs on ion implantation for materials modification
[AD-P003952] 02 p0286 N85-11868
Requirements and special problems of land altimetry — satellite altimetry 03 p0380 N85-12430
The applications of fibre optics in gas turbine engine instrumentation
[PNR-90209] 03 p0420 N85-12687
The Uniform Science and Technology Research and Development Utilization Act
[GPO-36-327] 04 p0577 N85-13685
Uniform Science and Technology Research and Development Utilization Act
[H-REPT-98-983-PT-1] 04 p0577 N85-13686
Rotating assembly working group summary
05 p0604 N85-13851
Fundamentals and applications of the six port measuring technique — reflectometer 05 p0630 N85-14029
Stirling engine development, state of the art, possible engine applications and suitability in comparison to established plants and systems
[BMFT-FB-T-84-196] 05 p0646 N85-14149
Contributions to remote sensing : Applications of thermal infrared
[COMMUN-34/1984] 05 p0654 N85-14196
Methodological research in connection with the handling of LANDSAT satellite data for archaeology
05 p0655 N85-14207
Remote sensing data in support of conventional data
05 p0659 N85-14232
ERS-1 and its potential for industrial utilization
05 p0659 N85-14235
Utilization possibilities of photovoltaics in the private sector 05 p0664 N85-14272
ASC 1984 Applied Superconductivity Conference
[DE84-016204] 06 p0868 N85-15521
Integrated technology wing study (oral presentation)
[NASA-CR-169497] 07 p0902 N85-15718
Impressions from a study tour in Finland concerning fiber reinforced plastics, June 1984
[FOA-C-20552-D2(E4,F9)] 07 p0921 N85-15831
Where to next in astronomical photography? — tabular grain emulsions 07 p0964 N85-16114
Use of minicomputers for the formation of hydrological data banks 07 p1001 N85-16358
Possibilities and impossibilities of microcomputer systems
[AD-1984-904] 07 p1028 N85-16522
Research and technology, 1984 report
[NASA-TM-83096] 07 p1061 N85-16730
Research and technology, Lyndon B. Johnson Space Center
[NASA-TM-58263] 08 p1262 N85-17929
Manufacturing costs, equipment needs and technological opportunities among small and medium-size manufacturers
[DE85-000479] 09 p1304 N85-18193
Computers and education
[GPO-28-378] 10 p1537 N85-19689
Magnetic heat pump feasibility assessment
[DE85-002806] 11 p1632 N85-20276
Tactical operations and space applications
11 p1709 N85-20752
Technological and economic assessment of advanced ceramic materials: Volume 4: A case study of integrated optic devices
[PB85-113116] 12 p1815 N85-21385
Applications of Tethers in Space
[NASA-CP-2366] 12 p1859 N85-21659
New application possibilities for clad steel by reducing surface treatment expenditure and by using improved welding technology
[BMFT-FB-T-84-236] 12 p1861 N85-21672
Latent heat storage technology and application workshop. Summary report: Session 6
[DE85-001097] 12 p1882 N85-21806
Space solar cells: Adjusting to new demands
13 p2005 N85-22568
Metal-semiconductor phase transition and its application
[DRIC-T-7149] 13 p2021 N85-22665
Role of optical disk at computing centers
[DE85-005124] 13 p2145 N85-23314
Physicists' role in new technological development discussed 13 p2166 N85-23436
Economic mechanism of integration of science, production 13 p2167 N85-23443
Technology and Economics, Inc. Technology Application Team
[NASA-CR-175830] 13 p2168 N85-23454
Riga Institute seeking faster introduction of new technology 14 p2208 N85-23686
Possible technological answers to new design requirements for power transmission systems
14 p2222 N85-23779
Piezoelectric plastics — polyvinyl fluoride
[ISL-CO-202/83] 14 p2262 N85-24017
Group technology for working turbine drive wheel disks 14 p2269 N85-24061
Remote sensing: New tool for China's geologists
14 p2283 N85-24141
Applications of ultrasonic technology
14 p2283 N85-24144
Minister B. V. Balmont on status of automation drive
14 p2284 N85-24151
Application possibilities of laser Doppler anemometry in the investigation of the transonic interaction between shock wave and boundary layer
[ISL-R-131/83] 14 p2304 N85-24265
Utilization of microchannel plates in the flash X-ray technique
[ISL-CO-228/83] 14 p2306 N85-24275
Lasers in the domains of ultrashort-time phenomena physics and ballistics
[ISL-CO-236/83] 14 p2310 N85-24299
Inferences of future operations drawn from past and present applications of drifting buoys
14 p2323 N85-24356
The 1981 transatlantic boat race contribution for marine meteorological measurements 14 p2324 N85-24361
Miscellaneous ARGOS maritime applications — yacht races 14 p2327 N85-24383
The Effect of Computers on the Generation and Use of Technical Data
[NBSIR-84-2907] 14 p2400 N85-24792
Accomplishments of science by the year 2000
14 p2432 N85-24996
Our future in the cosmos: Computers
14 p2432 N85-24997
Performance testing and system characterization. DOE hybrid test vehicle, phase 3
[NASA-CR-175668] 14 p2434 N85-25010
Roundtable on effective use of flight simulators
15 p2460 N85-25190
Holography in space 15 p2476 N85-25285
French robotics research at Grenoble labs
15 p2523 N85-25555
West Europe report: Science and technology
[JPRS-WST-84-014] 15 p2536 N85-25647
An introductory study of automatic speech recognition systems
[BAE-BT-12286] 15 p2539 N85-25677
Industrial applications of pattern recognition and image processing 15 p2622 N85-26157
Summaries of FY 1984 engineering research
[DE85-006273] 15 p2664 N85-26442
Aspects of application of ACT systems for pilot workload alleviation 16 p2712 N85-26734
Uses of laser technology described
16 p2768 N85-27080
Function of remote sensing in Brazil
[INPE-3314-PRE/621] 16 p2810 N85-27329
Status of computer aided mapping in hydrographic services 16 p2815 N85-27366
Surveying and optical tooling technologies combined to align a skewed beamline at the LAMPF accelerator
[DE85-005902] 16 p2864 N85-27664
Characteristics and applications of superplastic materials for aeronautics
[MBB-BB-565/84-O] 16 p2873 N85-27727
New materials and techniques for aircraft structures
[B8580074] 17 p2897 N85-27861
Automation and robotics for the National Space Program
[NASA-CR-175881] 17 p2909 N85-27936
Aluminum-lithium alloys: The answer of the aluminum industry to the threat of advanced fiber-reinforced materials
[VTH-LR-406] 17 p2932 N85-28102
Hot Isostatic Pressing (HIP): Techniques, applications and economical use
[JUEL-SPEZ-288] 17 p2939 N85-28141
USSR report: Engineering and equipment
[JPRS-UEQ-85-004] 17 p2939 N85-28142
Applications of robots in machine tool industry reviewed 17 p2946 N85-28189
Catalog of research projects at Lawrence Berkeley Laboratory, 1985
[DE85-008679] 17 p3049 N85-28869
General laws of development of technology
17 p3049 N85-28875
Results of Italian research in high power lasers
18 p3086 N85-29097
Some applications of aeronautical engineering in the construction of yachts
[NLR-MP-83042-U] 20 p3394 N85-31052
Existing and potential INMARSAT capabilities for the Future Global Maritime Distress and Safety System
20 p3402 N85-31110
Solar dynamic systems 20 p3443 N85-31374
The role of scientific ballooning for exploration of the magnetosphere
[TRITA-EPP-84-07] 20 p3494 N85-31724
A systematic plan for the continued study of dimensional stability of metallic alloys considered for the fabrication of cryogenic wind tunnel models
[NASA-CR-172449] 21 p3565 N85-32172
Deep sea mega-geomorphology: Progress and problems 21 p3602 N85-32369
Use of the synoptic view: Examples from Earth and other planets 21 p3602 N85-32371
Statement of Aaron Cohen, Director, Research and Engineering, Johnson Space Center and Chairman, Space Station Advanced Technology Advisory Committee, National Aeronautics and Space Administration, before the Subcommittee on Science, Technology, and Space, Committee on Commerce, Science, and Transportation, United States Senate
[NASA-TM-87497] 22 p3739 N85-33174
High powered epicyclic gears: Some recent development 23 p3924 N85-34316
Energy Efficient Engine Program technology benefit/cost study, volume 1
[NASA-CR-174766-VOL-1] 24 p4066 N85-35197
Motor glider meteorology 24 p4121 N85-35543

TECTONIC MOVEMENT
U TECTONICS

TECTONICS
Seismotectonic nature of some annular photoanomalies registered by remote methods 02 p0164 N85-11110
Hypothesis on the origin of lineaments in the LANDSAT and SLAR images of precambrian soil in the low Contas River Valley (southern Bahia)
[E85-10007] 02 p0215 N85-11420
Paleoenvironmental interpretation of the upper cretaceous Point Lookout sandstone: Implications for shoreline progradation and basin tectonic history, San Juan basin, New Mexico 02 p0227 N85-11486
Vertical crustal movements in southern California, 1974 to 1978
[GS-CIRC-905] 02 p0228 N85-11491
Heat flow map of Europe: Brief summary of the geophysical implications
[REPT-582] 03 p0377 N85-12405
Stratigraphy, petrology, and tectonic setting of the Alisitos Group, Baja California, Mexico
03 p0389 N85-12488
Stratigraphy, sedimentology and tectonic significance of the Upper Cretaceous Virginian Ridge formation, Method Basin, Washington: Implications for tectonic history of the North Cascades 03 p0390 N85-12494
Franciscan and related rocks of southern Humbolt County, northern California coast ranges: Analysis of structure, tectonics, sedimentary petrology, paleogeography, depositional histroy, and thermal maturity 03 p0390 N85-12495
Geophysical investigations of the central part of Niger State, Nigeria 03 p0390 N85-12496
Martian impact basins: Morphology differences and tectonic provinces
[NASA-CR-174074] 03 p0448 N85-12847
Horizontal-strain observations in the Shumagin Island and Yakataga seismic gaps, Alaska
04 p0515 N85-13287
Deep structure and seismicity in the Catalonia-Pyrenees region 04 p0524 N85-13352
Archean sedimentation and tectonics in southern Africa
[NASA-CR-174156] 04 p0533 N85-13408
Models for volcanic processes in Long Valley, California: Testing by continental drilling
[DE84-014943] 04 p0534 N85-13414
Priorities for a national program of continental drilling for scientific purposes 04 p0534 N85-13418
A tectonic and metamorphic history of the north-central Klamath Mountains, California 05 p0673 N85-14323
Tectonic history of a continent: Island arc boundary, west-central Idaho 05 p0673 N85-14324
Geology, petrology, and tectonic setting of the Mafic rocks of the 1480 Ma old granite-rhyolite terrane of Missouri, USA 05 p0674 N85-14327
Sedimentation, structure and tectonics of the Umpqua group (paleocene to early eocene), southwestern Oregon 05 p0676 N85-14354
Earthquakes and tectonics of Pacific Ocean margins
06 p0820 N85-15206
Some trends in the modern Earth sciences — plate tectonics and Earth's crust 06 p0820 N85-15207
Boundary velocities of mohorovicic discontinuity and upper mantle structure of Pacific Ocean bed
06 p0821 N85-15211

General model of earthquakes and the place of warnings in it 07 p0981 N85-16232
Model of earthquake mechanism 07 p0982 N85-16236
Tectonic, volcanic, and climatic geomorphology study of the Sierras Pampeanas Andes, northwestern Argentina 08 p1144 N85-17215
Structure and stratigraphy of Midterhuken Peninsula, Bellsund, West Spitsbergen 09 p1353 N85-18513
Mercury 09 p1411 N85-18890
Venus 09 p1411 N85-18891
Earth 09 p1411 N85-18892
Utilization of mobile VLBI for geodetic measurements 10 p1486 N85-19248
Localization of destruction process 10 p1500 N85-19470
Vertical movements and structure formation within island systems of northeast Asia 10 p1501 N85-19471
Study of tectonic earthquake precursors by geodetic methods 10 p1502 N85-19479
Mesozoic magmatism of Mongolian-Okhotsk Belt and its possible geodynamic interpretation 10 p1502 N85-19481
Post-carboniferous tectonics in the Anadarko Basin, Oklahoma: Evidence from side-looking radar imagery [NASA-CR-175458] 10 p1505 N85-19498
Tectonic lineaments in the cenozoic volcanics of southern Guatemala: Evidence for a broad continental plate boundary zone [NASA-CR-175456] 10 p1505 N85-19499
Crustal stretching and subsidence in sedimentary eastern Switzerland and permo-carboniferous basins in the continental United States [DE85-000622] 11 p1681 N85-20592
Use of paleomagnetic data in tectonic analysis of oceanic structures 13 p2108 N85-23135
Review of problems in lithology 13 p2113 N85-23160
Possibility of mapping active tectonic structures from mercury gas aureoles over sea surface 13 p2113 N85-23162
Geomagnetic precursors of intensive earthquakes in the 1-0.-2 Hz frequency range of geomagnetic pulsations 13 p2116 N85-23178
A tectonic model of an incipient spreading center and its margins: The Northern Red Sea and the Dead Sea rift 13 p2140 N85-23286
Venus chasmata: A lithosphere stretching model 13 p2178 N85-23516
Terrestrial analog studies for Martian patterned ground 13 p2190 N85-23590
Terrestrial analogs for planetary wrinkle ridges 13 p2199 N85-23644
Planetary interior modeling and tectonic implications 13 p2200 N85-23649
Elysium region, Mars: Tests of lithospheric loading models for the formation of tectonic features 13 p2200 N85-23650
Kasei Vallis of Mars: Dating the interplay of tectonics and geomorphology 13 p2201 N85-23654
Creep of ice: Further studies 13 p2201 N85-23655
Lineaments on Ganymede: New evidence for late tectonic activity 13 p2202 N85-23658
Global tectonics on Ganymede 13 p2202 N85-23659
Tectonics of the Galileo Regio on Ganymede 13 p2202 N85-23660
Importance of the tectonic motions on Ganymede 13 p2202 N85-23661
Tectonics of the Valhalla structure on Callisto 13 p2202 N85-23662
Evaluating structure-forming role of late Paleozoic and Mesozoic-Cenozoic tectonic movements in Baltic Sea region 14 p2337 N85-24450
Location of continental Permian volcanites of central Asia and its tectonic interpretation 14 p2346 N85-24505
Example of joint use of data from surface studies and space photographs in investigating dynamics of zone of North Zeravshan seismogenic faults 15 p2485 N85-25342
Periodic cometary showers: Real or imaginary? 15 p2680 N85-26555
Analysis of mesofissuring on space photographs: New technique for study of petroleum and gas deposits 16 p2726 N85-26829
A travel-time interpretation of the 1978 seismic refraction profile in the Kingdom of Saudi Arabia 17 p2991 N85-28486
Natural gas anomaly in bottom waters of South China Sea 19 p3290 N85-30399
Microstructural analysis of Pacific Ocean and Indian Ocean ultrabasites 19 p3291 N85-30405
Density characteristics of asthenosphere in Atlantic Ocean 19 p3294 N85-30423
Tectonic structure features of some deep faults in Atlantic and Pacific Oceans (according to deep seismic sounding-reflected waves method data) 19 p3295 N85-30428
Highly important features of regional tectonics of Earth's Arctic sector 19 p3298 N85-30449
Structural and tectonic history of the Golconda allochton, southern Tolyabe Range, Nevada 19 p3312 N85-30529
Euro-African MAGSAT anomaly-tectonic observations 20 p3475 N85-31596
Long-wavelength magnetic and gravity anomaly correlations on Africa and Europe 20 p3476 N85-31597
Continental magnetic anomaly constraints on continental reconstruction 20 p3476 N85-31599
Regional magnetic anomaly constraints on continental rifting 20 p3476 N85-31600
Geodynamics Branch research program [NASA-TM-86223] 20 p3489 N85-31688
Contemporary plate motions from LAGEOS 20 p3489 N85-31689
The global VLBI fiducial network 20 p3490 N85-31690
First epoch measurements by Mark III VLBI of the San Andreas Fault experiment baseline 20 p3490 N85-31691
Geophysical interpretation of satellite laser ranging measurements 20 p3490 N85-31692
Geologic and hydrologic characterization and evaluation of the basin and range province relative to the disposal of high-level radioactive waste. Part 3: Geologic and hydrologic evaluation [GS-CIRC-904-A] 20 p3526 N85-31934
Global Mega-Geomorphology [NASA-CP-2312] 21 p3600 N85-32357
Global geomorphology 21 p3601 N85-32359
Quantitative analysis in megageomorphology 21 p3603 N85-32376
Techniques, problems and uses of mega-geomorphological mapping 21 p3604 N85-32378
Planetary perspective. Report of Working Group Number 4 21 p3605 N85-32385
A review of tectonic aspects of the Limpopo belt and other Archean high-grade gneissic terranes 21 p3720 N85-33080
Use of space photographs for analysis of structural and dynamic conditions of formation of ancient phlogopite and apatite deposits 22 p3735 N85-33153
Crustal Dynamics Project: Catalogue of site information [NASA-TM-86218] 22 p3801 N85-33552
Tectonic stability and expected ground motion at Yucca Mountain [DE85-012004] 22 p3814 N85-33629
Subduction zone tectonic studies to develop concepts for the occurrence of sediment subduction [DE85-011794] 22 p3815 N85-33632
Impact processes and their implications for planetary formation and early evolution 22 p3853 N85-33860
Planetary surface processes: A review 22 p3855 N85-33869
A solid-state framework for terrestrial upper mantles 22 p3856 N85-33878
Crustal development in the terrestrial planets 22 p3856 N85-33879
Contrasts in evolution of Venus and Earth 22 p3857 N85-33880
Compressional environment in the location and orientation of planetary dorsa and terrestrial earthquake fault structures 22 p3857 N85-33885
Geology and petroleum resources of basins in western China [DE85-013038] 23 p3948 N85-34469
Some recent deposit modeling efforts 24 p4106 N85-35453
Seismic stratigraphic analysis of the Mississippi Fan 24 p4115 N85-35507
A dynamic model of Venus's gravity field [NASA-CR-176173] 24 p4189 N85-35845

TEETH
Spiral bevel and circular arc helical gears: Tooth contact analysis and the effect of misalignment on circular arc helical gears [NASA-TM-87013] 20 p3395 N85-31060

TEFLON (TRADEMARK)
An experimental investigation of microstrip properties on soft substrates from 2 to 40 GHz [NASA-TM-86961] 11 p1624 N85-20224
Spectral evaluation of irregularity of superconducting coaxial cables 13 p2082 N85-23000
Method for ultrasonic bonding to soft microelectronic substrates [NASA-CASE-NPO-16087-1] 18 p3094 N85-29151
Elliptical X-ray analyzer spectrograph application to a laser-produced plasma [DE85-013790] 24 p4097 N85-35098

TEKTITES
Microtektite discovered in Beijing [NASA-TM-77765] 01 p0130 N85-10085

TELECHIRICS
U REMOTE HANDLING

TELECOMMUNICATION
NT AIRCRAFT COMMUNICATION
NT BROADCASTING
NT CODE DIVISION MULTIPLE ACCESS
NT COLOR TELEVISION
NT COMMUNICATION
NT DATA LINKS
NT DEFENSE COMMUNICATIONS SATELLITE SYSTEM
NT DEFENSE COMMUNICATIONS SYSTEM (DCS)
NT DEMAND ASSIGNMENT MULTIPLE ACCESS
NT ELECTRONIC MAIL
NT FACSIMILE COMMUNICATION
NT FREQUENCY DIVISION MULTIPLE ACCESS
NT GROUND-AIR-GROUND COMMUNICATION
NT INTERPLANETARY COMMUNICATION
NT LINE OF SIGHT COMMUNICATION
NT MULTICHANNEL COMMUNICATION
NT MULTIPLE ACCESS
NT OPTICAL COMMUNICATION
NT PCM TELEMETRY
NT PULSE COMMUNICATION
NT RADIO COMMUNICATION
NT RADIO RELAY SYSTEMS
NT RADIO TELEMETRY
NT RADIOTELEPHONES
NT SATELLITE TELEVISION
NT SELECTIVE DISSEMINATION OF INFORMATION
NT SHIP TO SHORE COMMUNICATION
NT SINGLE CHANNEL PER CARRIER TRANSMISSION
NT SPACE COMMUNICATION
NT SPACECRAFT ANTENNAS
NT SPACECRAFT COMMUNICATION
NT SPACECRAFT TELEVISION
NT TELEMETRY
NT TELEPHONY
NT TIME DIVISION MULTIPLE ACCESS
NT VIDEO COMMUNICATION
NT VOICE COMMUNICATION
NT VOICE DATA PROCESSING
NT WIDEBAND COMMUNICATION
NT WIRELESS COMMUNICATION
Tendencies in the development of utilization protocols, seminar report — communication networks [FUB-11-1983] 01 p0039 N85-10252
Availability of transmission systems in continental and intercontinental connections — telecommunication [FUB-33-1983] 01 p0040 N85-10261
Hardware implementation of a support system for the 2501 Western digital LSI, complete controller of the second level, first version of the CCITT 25 (CAP) recommendations [FUB-80-1982] 01 p0100 N85-10086
An investigation of the use, cost, perceived value and social context of telecommunications tools in two-year college libraries in the southeastern United States 02 p0293 N85-11901
DCS (Defense Communications System) network synchronization design criteria [AD-A146251] 03 p0356 N85-12289
Five-year plan for meeting the automatic data processing and telecommunications needs of the Federal Government. Volume 1: Planning strategies [PB84-214501] 03 p0436 N85-12777
Federal Telecommunications Privacy Act of 1984 [H-REPT-98-815] 03 p0441 N85-12907
Mission science value-cost savings from the Advanced Imaging Communication System (AICS) [NASA-CR-174170] 04 p0458 N85-12905
China report: Science and technology [JPRS-CST-84-003] 04 p0491 N85-13132
New telecommunications optical fiber developed 04 p0492 N85-13135
The Telecom 1 satellite telecommunication system 04 p0493 N85-13147
USSR report: Electronics and electrical engineering [JPRS-UEE-84-011] 06 p0789 N85-15042
Problems of development of space communication 06 p0793 N85-15087
US objectives generally achieved at broadcasting satellite international conference. Improvements can help in future conferences [PB84-235316] 06 p0800 N85-15109
USSR report: Electronics and electrical engineering [JPRS-UEE-84-016] 07 p0949 N85-15014
USSR report: Electronics and electrical engineering [JPRS-UEE-84-017] 07 p0951 N85-16025

Life cycle cost management master plan for the Defense Communications Agency
[AD-A146876] 07 p1050 N85-16668
Acquisition planning at the Defense Communications Agency
[AD-A146877] 07 p1051 N85-16669
On the complexity of distributed decision problems
[AD-A147174] 07 p1052 N85-16674
East Europe report: Science and technology
[JPRS-ESA-84-046] 08 p1139 N85-17176
Telecommunications equipment at 1984 Leipzig Spring Fair 08 p1140 N85-17179
Compilation of annual reports of the Navy ELF (Extremely Low Frequency) communications system ecological monitoring program. Volume 1: Tabs A-E
[AD-A148326] 08 p1152 N85-17272
Compilation of annual reports of the Navy ELF (Extremely Low Frequency) communications system ecological monitoring program (1983). Volume 2: Tabs F-J
[AD-A148327] 08 p1152 N85-17273
A modified Monte-Carlo technique for the simulation of satellite communication systems
[AD-A148689] 08 p1214 N85-17641
Calculation of cumulative distributions and detection probabilities in communications and optics
[AD-A147781] 08 p1215 N85-17650
Star on the horizon: The emergence of the direct broadcast satellite in American mass communications
[AD-A148819] 09 p1312 N85-18242
Study of factors affecting an HF/VHF direct broadcasting satellite service
[PB85-120689/GAR] 09 p1313 N85-18255
The Telecommunications and Data Acquisition Report
[NASA-CR-174366] 10 p1462 N85-19224
A system for measuring the characteristics of the ionospheric channel by digital transmissions
10 p1472 N85-19287
An H.F. simulator for use with real time channel evaluation systems 10 p1473 N85-19293
Worldwide report: Telecommunications policy, research and development
[JPRS-TTP-85-002] 10 p1475 N85-19309
NTT (Nippon Telegraph and Telephone Public Corporation) develops new optical fiber
10 p1476 N85-19311
Worldwide report: Telecommunications policy, research and development
[JPRS-TTP-85-006] 10 p1476 N85-19314
Spectrum resource assessment of the 7125-8500 MHz band
[PB85-127413] 11 p1626 N85-20242
Spectrum resource assessment of the fixed and mobile services in the 947-17,700 MHz band, phase 1
[PB85-126268] 11 p1626 N85-20243
East Europe report: Scientific affairs
[JPRS-ESA-84-006] 11 p1700 N85-20684
Communications software for Olympics Micromation Computer System
[PB85-109510] 11 p1704 N85-20723
Base communications issues for the 1960s
[AD-A149764] 12 p1828 N85-21474
Digital channel efficiency model
[AD-A150084] 12 p1829 N85-21479
Sample size and precision in communication performance measurements
[PB85-1143270] 12 p1830 N85-21488
Algorithm for statistical simulation of electromagnetic compatibility characteristics of high-frequency transmission channels in radioelectronic facilities
12 p1842 N85-21560
Computer and communications security and privacy
[GPO-39-741] 12 p1911 N85-21994
A concatenated coding scheme for error control
[NASA-CR-175504] 12 p1912 N85-22001
Oversight review of the five-year outlook report on science and technology
[GPO-41-068] 12 p1949 N85-22243
Technology transfer to the Middle East
[PB85-127744] 12 p1952 N85-22264
Integrated digital networks
[AD-A150605] 13 p2056 N85-22873
USSR report: Electronics and electrical engineering
[JPRS-UEE-85-001] 13 p2078 N85-22976
Analysis of interference caused by interfering radio signals in communications systems with frequency separation of telephone channels and frequency modulation 13 p2086 N85-23025
Further developments of CCD line array telecine
[BBC-RD-1985/3] 14 p2293 N85-24217
Interactive communication channel
[AD-D011580] 15 p2542 N85-25695
Wideband fiber optic communications link
[AD-A151704] 15 p2542 N85-25697
Standards in process: Foundation and profiles of ISDN (Integrated Services Digital Network) and OSI (Open Systems Interconnection) studies
[PB85-165041/GAR] 15 p2545 N85-25712
Future information technology, 1984 telecommunications
[PB85-165850] 15 p2624 N85-26173
Thin Route Project 15 p2687 N85-26598
Communications 15 p2687 N85-26600
The Record of Electrical and Communication Engineering Conversazione, volume 53, no. 2, November 1984
[ISSN-0385-7719] 16 p2758 N85-27022
Historical perspectives on information transmission engineering 16 p2759 N85-27023
Optical non-line-of-sight covert, secure high data communication system
[AD-D011607] 16 p2769 N85-27087
Satellite provided customer promises services, a forecast of potential domestic demand through the year 2000. Volume 4: Sensitivity analysis
[NASA-CR-174662] 16 p2769 N85-27092
Future information technology, 1984: Telecommunications
[NBS/SP-500/119] 16 p2878 N85-27762
National Telecommunications and Information Administration authorization
[GPO-38-660] 16 p2879 N85-27766
East Europe report: Science and technology
[JPRS-ESA-85-017] 17 p2945 N85-28177
Radiometer integrated into a communication terminal
[AD-A151746] 17 p2947 N85-28195
Logical design of a decision support system to forecast technology, prices and costs for the national communications system
[AD-A152330] 17 p2948 N85-28198
ELF (Extremely Low Frequency) communications system ecological monitoring program: Measurements of ELF electromagnetic fields for site selection and characterization, 1983
[AD-A153120] 17 p2949 N85-28209
Moon bounce communications to small terminals
[AD-A153297] 17 p2950 N85-28212
Discrete mathematics for communications systems
[AD-A152814] 17 p3018 N85-28664
Rome Development Center Air Force technical objective document C3I FY-86
[AD-A152476] 17 p3047 N85-28851
Study of a medium term flexible fixed satellite service mission
[DM51/CC-IM-0185.83] 18 p3091 N85-29136
Maser and secondary clock in telecommunications networks 18 p3106 N85-29246
Publications of the Jet Propulsion Laboratory 1983
[NASA-CR-175979] 18 p3199 N85-29848
Implementation of a serial communication process for a fault tolerant, real time, multitransputer operating system
[AD-A154237] 19 p3343 N85-30714
Antenna pointing of large flexible telecommunications spacecraft 20 p3409 N85-31156
Basic EMC (Electromagnetic Compatibility) technology advancement for C3 systems. Volume 1B: Demodulation radio frequency interference effects in operational amplifier circuits
[AD-A154121] 20 p3440 N85-31350
Scientific report of the Department of Systems and Communications
[ENST-84D002] 20 p3441 N85-31355
An analysis of physical optics models for rough surface scattering
[AD-A154960] 21 p3575 N85-32235
Security controls in the Stockpoint Logistics Integrated Communications Environment (SPLICE)
[AD-A155536] 21 p3576 N85-32244
Parameter estimation in communication system tracking satellite observations
[AD-A155137] 21 p3636 N85-32582
A model for predicting propagation-related DSCS (Defense Communications Engineering Center) margin requirements
[AD-A155355] 22 p3758 N85-33281
USSR report: Electronics and electrical engineering
[JPRS-UEE-84-003] 22 p3773 N85-33381
Telecommunication market research processing
[ENST-83E018] 23 p3926 N85-34331
Interprocess communication
[AD-A156337] 24 p4088 N85-35337
Proceedings of the 14th Army Science Conference. Volume 3: Principal authors P through Z
[AD-A149202] 24 p4144 N85-35691

TELECONFERENCING
Software for interactive on-line conferences
[AD-A154742] 21 p3670 N85-32801

TELEGRAPH SYSTEMS
Transient processes in tuned amplifier during phase-shift keying with smooth phase variation
15 p2527 N85-25581

TELEGRAPHY
U TELEGRAPH SYSTEMS

TELEMETERS
U TELEMETRY

TELEMETRY
NT PCM TELEMETRY
NT RADIO TELEMETRY
High-data-rate wide-angle underwater acoustic telemetry system
[DE84-015696] 02 p0233 N85-11519
Signal characteristics of an underwater explosive acoustic telemetry system
[DE84-016653] 05 p0726 N85-14668
Pulse code modulation telemetry: Properties of various binary modulation types
[AD-A147214] 07 p0913 N85-15780
An autonomous roving vehicle for the planet Mars: A summary of over 15 years of research
[RPI-TR-MP-83] 07 p0973 N85-16179
A variable length and sensor spacing thermistor array
[AD-D011416] 08 p1113 N85-17017
Development of the TT and C station equipment at INPE
[INPE-3327-PRE/625] 10 p1427 N85-18999
Directory of range data conversion and processing systems
[AD-A148996] 10 p1427 N85-19001
Telemetry systems of Interkosmos satellites
11 p1617 N85-20173
An overview of the Thematic Mapper geometric correction system 11 p1668 N85-20511
Wind-weighting for sounding rockets with a telemetry system
[NASA-TP-2438] 12 p1792 N85-21246
Remote control of an impact demonstration vehicle
[NASA-TM-85925] 14 p2225 N85-23797
Hydrometric telemetry in Canada
14 p2239 N85-23882
Programming for Pioneer 12 15 p2688 N85-26606
Present stage of utilization of the ARGOS system by the ORSTOM hydrological service for hydrometric data collection 16 p2813 N85-27348
Use of a network of telemetered meteorological stations for prediction of the distribution of an atmospheric tracer
16 p2831 N85-27458
Telemetry system for the transmission of data from projectiles during the acceleration phase in the gun barrel
[ISL-CO-207/84] 22 p3739 N85-33178
Development of an adjustable buoyancy balloon tracer of atmospheric motion. Phase 1: Systems design and demonstration of feasibility
[PB85-185817] 22 p3817 N85-33648
Design, development and operation of a high simultaneous capacity digital telemetry system — turbomachine blade flutter
[PNR-90261] 23 p3899 N85-34151
Miniature infra-red data acquisition and telemetry system
[NASA-CR-177953] 24 p4096 N85-35390

TELEOPERATOR MANEUVERING SYSTEM
U TELEOPERATORS

TELEOPERATORS
Review of teleoperator research
05 p0703 N85-14511
Translational control of a graphically simulated robot arm by kinematic rate equations that overcome elbow joint singularity
[NASA-TP-2376] 06 p0856 N85-15446
Transportation applications, part 2
11 p1643 N85-20350
Real time algorithms for robotic control of teleoperators
[DE85-001137] 11 p1647 N85-20380
Investigation of dynamics of manipulator with elastic sections 13 p2048 N85-22619
Hand controllers for teleoperation. A state-of-the-art technology survey and evaluation
[NASA-CR-175890] 17 p3002 N85-28559
Analysis of remote operating systems for space-based servicing operations, volume 1
[NASA-CR-171885] 19 p3225 N85-29993
Analysis of remote operating systems for space-based servicing operations. Volume 2: Study results
[NASA-CR-171886] 19 p3225 N85-29994
Space station automation study-satellite servicing. Volume 1: Executive summary
[NASA-CR-171512] 19 p3226 N85-29999
Space station automation study-satellite servicing, volume 2
[NASA-CR-171513] 19 p3226 N85-30000

Manipulators in teleoperation
[DE85-010563] 20 p3512 N85-31833
NASA space station automation: AI-based technology review
[NASA-CR-176094] 21 p3558 N85-32134
NASA space station automation: AI-based technology review. Executive summary
[NASA-CR-176096] 21 p3558 N85-32135
Space station automation and robotics study. Operator-systems interface
[NASA-CR-176095] 22 p3738 N85-33172
Space station automation study: Autonomous systems and assembly, volume 2
[NASA-CR-176092] 22 p3739 N85-33175
Telepresence work system concepts
22 p3797 N85-33525
Dual arm master controller development
22 p3797 N85-33526
Space Missions for Automation and Robotics Technologies (SMART) Program
[NASA-TM-86620] 24 p4068 N85-35210

TELEPHONES
NT RADIOTELEPHONES
Energy supply problems for emergency telephones
05 p0663 N85-14265
A single optical fiber telephone system
[AD-D011293] 06 p0799 N85-15107
Fast data and voice transmission for mobile services with high immunity against multipath and co-channel interference 10 p1475 N85-19306

TELEPHONY
RF characteristics of the hoop column antenna for the land mobile satellite system mission
[NASA-CR-3842] 02 p0189 N85-11264
The ACE (Automated Cable Expert) experiment: Initial evaluation of an expert system for preventive maintenance
[AD-P003943] 02 p0248 N85-11623
Analog voice processing for FM transmission in a telephone channel
[INPE-2798-PRE/359] 03 p0354 N85-12279
Telephoning with light and sun — glass fibers, solar cells 05 p0663 N85-14264
Energy supply problems for emergency telephones
05 p0663 N85-14265
A single optical fiber telephone system
[AD-D011293] 06 p0799 N85-15107
Equipment for multiplexing multichannel radio-relay lines of communication
[AD-A148402] 08 p1153 N85-17276
Low voltage two wire to four wire telephone circuit converter apparatus
[AD-D011449] 10 p1468 N85-19261
Self-adaptive echo cancellation for telephony
[ENST-84E013] 20 p3441 N85-31353

TELESCOPES
NT ASTRONOMICAL TELESCOPES
NT GAMMA RAY TELESCOPES
NT HELIOMETERS
NT HUBBLE SPACE TELESCOPE
NT INFRARED TELESCOPES
NT PARTICLE TELESCOPES
NT PYROHELIOMETERS
NT RADIO TELESCOPES
NT REFLECTING TELESCOPES
NT REFRACTING TELESCOPES
NT SCHMIDT CAMERAS
NT SCHMIDT TELESCOPES
NT SOLAR OPTICAL TELESCOPE
NT SPACE INFRARED TELESCOPE FACILITY
NT SPACEBORNE TELESCOPES
NT SPECTROSCOPIC TELESCOPES
NT ULTRAVIOLET TELESCOPES
NT X RAY TELESCOPES
Direct view helmet mounted telescope
[AD-D011291] 06 p0755 N85-14839
Dual-secondary mirror Cassegrain optical system
[AD-D011273] 06 p0862 N85-15478
Helmet mounted telescope
[AD-D011355] 07 p1019 N85-16467
Evaluation of nose, roof, and mast mounted sensor platforms for piloting and sighting, integrated in future combat helicopters 08 p1074 N85-16808
On the unique capabilities of the Hubble space telescope for studies of ROSAT deep-survey X-ray sources
08 p1243 N85-17846
A CCD system for photometry of direct and spectroscopic images 08 p1252 N85-17904
Utilization of mobile VLBI for geodetic measurements
10 p1466 N85-19246
Wide-angle flat field telescope
[NASA-CASE-GSC-12825-1] 11 p1728 N85-20868
Utilization of space station by the large deployment reflector 14 p2235 N85-23857
Laser beam shaping system with reduced objective diameter 14 p2275 N85-24095
Aberration characteristics of plane-parallel compensator plate 14 p2276 N85-24100
Astometry at La Silla 14 p2436 N85-25025
Evaluation of a magneto-optical filter and a Fabry-Perot interferometer for the measurement of solar velocity fields from space 14 p2442 N85-25067
An MRTD-compatible bar pattern response model for TV and direct view sighting systems
[BAE-BT-12090] 15 p2620 N85-26146
Stress analysis of the space telescope focal plane structure joint
[NASA-CR-175797] 16 p2803 N85-27284
Holographic corrector in objective with compound main mirror 17 p2941 N85-28153
Trends in measurement of solar vector magnetic fields using the Zeeman effect 18 p3204 N85-29877
The San Fernando Observatory video Stokes polarimeter 18 p3205 N85-29885
Multichannel birefringent filter
18 p3206 N85-29888
Grazing incidence beam expander
[DE85-010784] 19 p3368 N85-30889
Cosmic ray charge and energy spectrum measurements using a new large area Cerenkov x dE/dx telescope
[OG-4.1-5] 22 p3676 N85-34011
High Resolution Telescope and Spectrograph (HRTS)
23 p3901 N85-34162
Angular resolution of air-shower array-telescopes
[OG-9.5-6] 23 p4030 N85-34963
New Matsushiro underground cosmic ray station (220 M.W.E. in depth)
[SH-9.1-14] 23 p4052 N85-35129
Upper limit on magnetic monopole flux from Baksan experiment
[HE-6.1-11] 24 p4210 N85-36136

TELESCOPING STRUCTURES
U FOLDING STRUCTURES

TELEVISION CAMERAS
East Europe report: Science and technology
[JPRS-ESA-84-030] 01 p0101 N85-10670
Underwater television equipment described
01 p0101 N85-10672
Television camera video level control system
[NASA-CASE-MSC-18578-1] 12 p1821 N85-21427
Italy's Fiat uses Sweden's Asea seeing robot
15 p2536 N85-25650
Electronic detection and concealment of film dirt
[BBC-RD-1985/4] 15 p2538 N85-25667
The San Fernando Observatory video Stokes polarimeter 18 p3205 N85-29885
A digital contour-corrector for a high-definition TV camera
[NHK-LABS-NOTE-311] 19 p3254 N85-30179
LI481 and LI482 vidicons for two-tube color TV cameras with improved image quality 22 p3764 N85-33333
Electronic imaging system and technique
[DE85-005740] 23 p3935 N85-34393
Spatial distribution read-out system for thermoluminescence sheets
[HE-7.1-7] 24 p4213 N85-36161

TELEVISION EQUIPMENT
NT IMAGE DISSECTOR TUBES
NT TELEVISION CAMERAS
NT TELEVISION RECEIVERS
Videotex and weather services: Finnish applications
01 p0084 N85-10567
Television animation store: Recording pictures on a parallel transfer magnetic disc
[BBC-RD-1984/17] 10 p1462 N85-19220
Lighting for remote viewing systems
[DE85-001698] 11 p1729 N85-20873
Device for controlling operation of lithicon cathode-ray memory tube 12 p1839 N85-21542
Welder training/welder testing
[BLL-WI-TRANS-683-(9312.57)]
16 p2792 N85-27223

TELEVISION RECEIVERS
Correlating and adaptive digital filters
[BMFT-FB-T-84-299] 15 p2551 N85-25744
Improved high performance television receiver
[PB85-170751] 18 p3092 N85-29139
East Europe report: Science and technology. Selections on CSSR computer technology
[JPRS-ESA-84-017] 21 p3668 N85-32781

TELEVISION RECEPTION
BBC receiving terminal for the European orbital test satellite
[BBC-RD-1984/15] 08 p1142 N85-17205
Satellite broadcasting: The performance of C-MAC in a hardware simulation of a DBS transmission chain
[BBC-RD-1984/9] 08 p1143 N85-17206
Problems relevant to town incoming radio TV links
[NASA-TM-77623] 08 p1150 N85-17255
Subjective evaluation of the effect of noise and interference on frequency modulated NTSC television signals
[CRC-1367] 09 p1310 N85-18230
Horizontal deflection TS-257
13 p2069 N85-22926
Timing accuracy of LF and TV synchronization techniques 17 p2961 N85-28288
Retinally stabilized differential resolution television display
[NASA-CASE-NPO-15432-1] 18 p3089 N85-29117
GROWIAN: First observations of the environmental impact at the GROWIAN site — wind energy converter
24 p4110 N85-35478
Television interference at the Maglarp (Sweden) wind turbine 24 p4111 N85-35480
Television interference measurement at Kalkugnen (Sweden) test windmill 24 p4111 N85-35481

TELEVISION SYSTEMS
NT COLOR TELEVISION
NT SATELLITE TELEVISION
NT SPACECRAFT TELEVISION
Videotex and weather services: Finnish applications
01 p0084 N85-10567
East Europe report: Science and technology
[JPRS-ESA-84-030] 01 p0101 N85-10670
Underwater television equipment described
01 p0101 N85-10672
Selection of parameters for image decomposition by television system for recognition of group of point sources 06 p0785 N85-15018
Teletrack: A special effect
[BBC-RD-1984/10] 06 p0796 N85-15097
US objectives generally achieved at broadcasting satellite international conference. Improvements can help in future conferences
[PB84-235316] 06 p0800 N85-15109
Digital raster timing encoder-decoder
[AD-D011279] 06 p0804 N85-15120
Estimation of the impulse response of television channels from digitized waveforms
[CRC-1376] 12 p1822 N85-21429
Television animation store: Digital chroma, key and mixer units
[BBC-RD-1984/16] 12 p1824 N85-21442
Electronic generation of text for television
[BBC-RD-1984/14] 13 p2053 N85-22856
Superfine laser position control using statistically enhanced resolution in real time
[DE85-005643] 15 p2564 N85-25817
An MRTD-compatible bar pattern response model for TV and direct view sighting systems
[BAE-BT-12090] 15 p2620 N85-26146
Mobile television radio link
[AD-A152381] 17 p2948 N85-28201
Investigation into the use of the TV magnifier in the Netherlands
[HSE-TRANS-11142] 20 p3533 N85-31996
Space Experiments with Particle Accelerators (SEPAC) 23 p3901 N85-34165
Computer animation in distance teaching
23 p3965 N85-34581

TELEVISION TRANSMISSION
Television transmission in frequency modulation
04 p0493 N85-13146
Subjective evaluation of the effect of noise and interference on frequency modulated NTSC television signals
[CRC-1367] 09 p1310 N85-18230
Brussels Satellite Convention
[S-EXEC-REPT-98-52] 12 p1790 N85-21234
Estimation of the impulse response of television channels from digitized waveforms
[CRC-1376] 12 p1822 N85-21429
Digital standards conversion: Interpolation theory and aperture synthesis
[BBC-RD-1984/20] 13 p2053 N85-22857
Horizontal deflection TS-257
13 p2069 N85-22926
Development of TV systems for spacecraft
15 p2484 N85-25332
Mobile television radio link
[AD-A152381] 17 p2948 N85-28201
Timing accuracy of LF and TV synchronization techniques 17 p2961 N85-28288
Unattended TV time transfer results
17 p2964 N85-28305
Improved high performance television receiver
[PB85-170751] 18 p3092 N85-29139
The time and frequency comparisons via Loran-C and National TV Network in Yugoslavia
18 p3109 N85-29248

TELLEGEN THEORY
U GYRATORS
U NETWORK ANALYSIS
U NETWORK SYNTHESIS

TELLURIC CURRENTS
Directional analysis of wave packets of magnetotelluric field 14 p2344 N85-24495
TELLURIDES
NT CADMIUM TELLURIDES
NT INDIUM TELLURIDES
NT LEAD TELLURIDES
NT MERCURY TELLURIDES
NT TIN TELLURIDES
TELLURIUM
Time resolved calorimetry of 30 nm Te-films during laser annealing
[AD-A145047] 01 p0052 N85-10346
Optical bistability in Cd(x)Hg(1-x)Te
18 p3186 N85-29760
TELLURIUM COMPOUNDS
NT CADMIUM TELLURIDES
NT INDIUM TELLURIDES
NT LEAD TELLURIDES
NT MERCURY TELLURIDES
NT TIN TELLURIDES
Synthesis of pentafluorotellurium hypofluorite
[AD-D011212] 01 p0023 N85-10139
TEMPERATE REGIONS
The response of mid-latitude total electron content to solar activity 04 p0522 N85-13336
Monthly and seasonal climatology over the global tropics and subtropics for the decade 1973 to 1983. Volume 1: 200 mb winds
[AD-A148521] 06 p0638 N85-15322
Precipitation characteristics of a dual mesoscale convective complex
[PB84-226711] 06 p0640 N85-15337
Chemical, biological, and physical measurements from the subtropical western North Atlantic Ocean. Summer 1982, USNS Lynch, cruise 710-82
[AD-A153823] 18 p3201 N85-29857
TEMPERATURE
NT AMBIENT TEMPERATURE
NT ATMOSPHERIC TEMPERATURE
NT BODY TEMPERATURE
NT BRIGHTNESS TEMPERATURE
NT COMBUSTION TEMPERATURE
NT CRITICAL TEMPERATURE
NT CURIE TEMPERATURE
NT FLAME TEMPERATURE
NT FLASH POINT
NT GAS TEMPERATURE
NT HIGH TEMPERATURE
NT IGNITION TEMPERATURE
NT INLET TEMPERATURE
NT ION TEMPERATURE
NT IONOSPHERIC TEMPERATURE
NT LOW TEMPERATURE
NT LUNAR TEMPERATURE
NT NEEL TEMPERATURE
NT NOISE TEMPERATURE
NT OCEAN TEMPERATURE
NT OPERATING TEMPERATURE
NT PLANETARY TEMPERATURE
NT PLASMA TEMPERATURE
NT ROOM TEMPERATURE
NT SATELLITE TEMPERATURE
NT SEA SURFACE TEMPERATURE
NT SKIN TEMPERATURE (BIOLOGY)
NT SKIN TEMPERATURE (NON-BIOLOGICAL)
NT SOLAR TEMPERATURE
NT STELLAR TEMPERATURE
NT SURFACE TEMPERATURE
NT TRANSITION TEMPERATURE
NT ULTRALOW TEMPERATURES
NT WALL TEMPERATURE
NT WATER TEMPERATURE
Deuteron NMR (Nuclear Magnetic Resonance) in relation to the glass transition in polymers
[AD-P003910] 01 p0032 N85-10196
Allowable surge currents and failure mechanisms in semiconductor power devices in various modes of operation 06 p0795 N85-15080
Homogeneous condensation of gaseous mixtures of Si, Fe, O, N, and C in relative cosmic abundance and implications for astronomical condensation
06 p0867 N85-15632
Temperature variation of laser mirror stability criteria
10 p1445 N85-19108
Decaying particles do not heat up the Universe
[DE85-002191] 11 p1763 N85-21091
Temperature responses of composite panels
[AD-A150053] 12 p1798 N85-21277
Digital temperature and velocity control of mach 0.3 atmospheric pressure durability testing burner rigs in long time, unattended cyclic testing
[NASA-TM-86959] 12 p1805 N85-21321
Externally compensated crystal oscillator (ECXO) study
[AD-A150335] 13 p2064 N85-22893
Structure and properties of ion-implanted Al sub 2 O sub 3
[DE85-005374] 14 p2430 N85-24987
Adjustment of the frequency-temperature characteristics of crystal oscillators
[AD-D011588] 15 p2548 N85-25726
Monthly and seasonal weather outlook for mid-January to mid-February 1985, volume 39, number 2, January 15, 1985
[PB85-164572] 16 p2837 N85-27500
Monthly and seasonal weather outlook for February 1985, volume 39, number 3, January 30, 1985
[PB85-159424] 16 p2838 N85-27502
Urban climate and air hygiene before, during, and after the lifework of Hellmut Berg. Overview of a branch of applied meteorology 18 p3147 N85-29487
TEMPERATURE COMPENSATION
Development of a polymer pressure gage with temperature compensation 03 p0365 N85-12340
Dynamic polymer pressure transducer with temperature compensation
[AD-D011373] 07 p0967 N85-16142
Dielectric resonator oscillators with digital temperature compensation
[AD-D011715] 19 p3261 N85-30221
Development of a temperature-compensated hot-film anemometer system for boundary-layer transition detection on high-performance aircraft
[NASA-TM-86732] 22 p3730 N85-33121
TEMPERATURE CONTROL
Programmable digital temperature controller apparatus
[AD-D011221] 01 p0049 N85-10319
Thermal management technology status
05 p0610 N85-13895
Determining lamp/ballast system performance with a temperature-controlled integrating chamber
[DE84-014606] 05 p0631 N85-14049
Thermoregulatory consequences of long-term microwave exposure at controlled ambient temperatures
[PB84-236603] 05 p0697 N85-14484
Procedures for testing and evaluating spacecraft-type heat pipes
[AD-A146671] 06 p0809 N85-15139
Development of a preprototype times wastewater recovery subsystem, addendum
[NASA-CR-171823] 07 p1019 N85-16468
Space shuttle main engine: Interactive design challenges 08 p1096 N85-16940
In-flight testing of the space shuttle orbiter thermal control system 08 p1103 N85-16974
Active cooling requirements for propellant storage
08 p1106 N85-17004
Propellant transfer: Attached depot
08 p1108 N85-17005
Thermoregulatory responses during exercise at graded hypohydration levels
[AD-A147733] 08 p1195 N85-17528
Transmissive Dewar cooling chamber for optically pumped semiconductor ring lasers
[AD-D011550] 12 p1855 N85-21636
High temperature acoustic levitator
[NASA-CASE-NPO-16022-1] 12 p1927 N85-22105
Thermal design of the Giotto spacecraft
14 p2245 N85-23920
Erosion of corrosion-resistant surface treatments on alloy steels
[DE85-008446] 17 p2932 N85-28100
A ten channel temperature controller
[AD-A152664] 17 p2967 N85-28326
Microprocessor controlled temperature chassis
[DE85-008392] 17 p3009 N85-28602
Heat management system for aircraft
[AD-D011658] 18 p3061 N85-28936
Advanced thermal barrier system bond coatings for use on Ni, Co-, and Fe-base alloy substrates
[NASA-TM-87062] 20 p3431 N85-31283
Remote temperature-set-point controller
[DE85-011614] 22 p3787 N85-33459
Electronic temperature equalizer
[PB85-181485] 22 p3789 N85-33475
Feedback regulated induction heater for a flowing fluid
[DE85-006506] 23 p3939 N85-34414
TEMPERATURE DEPENDENCE
Thermal fatigue of gas turbine engine blades made of material based on silicon nitride and silicon carbide
01 p0019 N85-10115
Critical point wetting drop tower experiment
02 p0155 N85-11045
NBS (National Bureau of Standards): Materials measurements
[NASA-CR-174038] 03 p0332 N85-12143
Time-temperature dependence of the strength of commercial zirconia ceramics
[AD-A146233] 03 p0336 N85-12173
Magnetic properties of and superfine interactions in amorphous Fe-Cr-Co-Si-B alloys
03 p0349 N85-12248
Energy of stacking fault and dislocation structure of titanium alloys 03 p0351 N85-12259
Electric properties of neovolcanic rocks of central and east Slovakia
[REPT-568] 03 p0376 N85-12401
Nondestructive evaluation of residual stress in low-carbon steel, introduction 04 p0512 N85-13265
Kohn anomaly in metastable fcc lanthanum at low temperatures
[DE84-015459] 04 p0569 N85-13628
Chemical engineering principles of constant temperature-constant supersaturation growth of potassium dihydrogen phosphate (KDP) crystals
[DE84-017081] 04 p0571 N85-13645
Thermal diffusivity and conductivity of chromium-manganese alloying compositions
[BLL-M-35925-(5828.4)] 05 p0616 N85-13938
Electronic bandstructure of an incommensurate crystal
[DE84-016891] 05 p0733 N85-14714
Effects of temperature on the response time of thermocouples and resistance thermometers
[DE84-016855] 06 p0811 N85-15154
Anisotropy and microstructure of rare earth permanent magnet materials
[AD-A146549] 06 p0859 N85-15460
Structural relaxation and isoconfigurational flow of a metallic glass near equilibrium
[AD-A147688] 07 p0933 N85-15915
Nondestructive measurement of bulk residual stresses
[AD-A147063] 07 p0978 N85-16211
A hydrogen partitioning model for hydrogen assisted crack growth
[AD-A147365] 07 p0978 N85-16214
Temperature dependence of the crystal structures of Nylon 11
[AD-A147563] 07 p1049 N85-16661
The heat sensitivity of solid propellants
08 p1117 N85-17043
Low temperature properties of CeOs2 in the C14 and C15 crystallographic Laves phases
[DE85-003754] 10 p1564 N85-19866
Effects of hydrogen on magnetic properties of amorphous zirconium alloys
[DE85-003303] 11 p1607 N85-20107
Applications of pulsed-laser techniques and thermographic phosphors to dynamic thermometry of rotating surfaces
[DE85-000403] 11 p1639 N85-20328
Direct measurement of the temperature dependence of the velocity of the reaction of deuterium atoms with vibration-excited hydrogen molecules
[MPIS-12/1984] 11 p1726 N85-20856
Study of the kinetics of hydrogenation using aged catalysts
[DE85-004373] 12 p1802 N85-21302
The UFe4P12 and CeFe4P12: Non-metallic isotopes of superconducting LaFe4P12
[DE85-003724] 12 p1942 N85-22195
Combustion kinetics of metal atoms and metallic radicals over wide temperature ranges 13 p1999 N85-22530
Orientation and temperature dependence of some mechanical properties of the single-crystal nickel-base superalloy Rene N4. 3: Tension-compression anisotropy
[NASA-TM-86982] 13 p2021 N85-22660
Magnetic studies of Ni3Al(Fe) compounds
[DE85-005262] 13 p2025 N85-22686
Division boundary in Al-B composite material with boron in contact with solid and liquid aluminum
13 p2027 N85-22704
Temperature dependence of propagation of high-current electron beam through drift space
13 p2079 N85-22982
Change of electrical characteristics of radio-frequency cables under thermal effect 13 p2081 N85-22999
Photovoltaic cells of InP-CdS heterojunction type and their temperature characteristics under A-M illumination
14 p2275 N85-24092
Dependence of parameters of silicon photovoltaic cells on temperature and light intensity
14 p2275 N85-24094
Characterization of terrestrial solar cells for space applications: Electrical characteristics of thin Westinghouse dendritic web cells as a function of solar intensity, temperature, and incidence angle
[NASA-CR-175642] 14 p2349 N85-24516
Temperature variation of resistivity of certain alloys based on transition and simple metals in amorphous and crystalline states 15 p2496 N85-25399
Thermoregulatory and vestibular systems in the rat
15 p2610 N85-26082

Special features of the temperature dependence of the capillary constant in the vicinity of the critical point
[BLL-T6438/BG/LRS/LRST750/85] 16 p2859 N85-27632

Mechanical properties of polycrystalline alpa titanium
[BLL-BISI-TRANS-21923-(9022.06)] 17 p2924 N85-28029

Physical properties of steels and their temperature dependence
[BLL-BISI-TRANS-22285-(9022.06)] 17 p2928 N85-28065

Temperature and manganese content dependences of tensile deformation in iron-high manganese binary alloys
[DE85-007656] 17 p2932 N85-28098

The temperature dependence of diffracted beam intensities in atom-surface scattering
[AD-A152762] 17 p3029 N85-28736

The effect of temperature on the corrosion-erosion of 9Cr1Mo steel
[DE85-008507] 18 p3076 N85-29030

Development and testing of the variable vertical resolution Fourth Order GCM 18 p3142 N85-29453

Improvements in the energy resolution and high-count-rate performance of bismuth germanate
[DE85-010763] 19 p3240 N85-30092

High temperature Raman studies of phase transitions in thin film dielectrics
[DE85-010973] 19 p3263 N85-30234

Fatigue-crack propagation behavior of alloy A-286
[DE85-007460] 19 p3288 N85-30391

Method for determining Wagner parameters of interaction of first and second orders
[BLL-M-36261-(5828.4)] 20 p3430 N85-31278

LEO life testing with different charge control
20 p3448 N85-31393

A survey of unified constitutive theories
20 p3486 N85-31531

Positron measurements in 2H-TaSe2 crystals
[DE85-010507] 20 p3529 N85-31949

Remarks on preparation of indandione detection reagents
[NASA-TM-77905] 21 p3560 N85-32146

Absorption of laser radiation in substance with absorption coefficient depending linearly upon temperature 21 p3694 N85-32953

The influence of temperature on static and dynamic SCC crack growth behavior in aluminum alloy
23 p3905 N85-34190

Experimental study on time and temperature dependent behavior of crack growth in viscoelastic strip
23 p3905 N85-34193

Time and temperature dependence of fracture surface in soft epoxy resin 23 p3906 N85-34213

Shape memory effect in uranium-niobium alloys below room temperature
[DE85-012964] 23 p3916 N85-34288

Study of photon emission by electron capture during solar nuclei acceleration, 1: Temperature-dependent cross section for charge changing processes
[SH-1.1-6] 23 p3990 N85-34735

Aqueous volatile weak electrolyte equilibria to 300 C
[DE85-013840] 24 p4076 N85-35261

TEMPERATURE DIFFERENCES

U TEMPERATURE GRADIENTS

TEMPERATURE DISTRIBUTION

Manual of phosphoric acid fuel cell stack three-dimensional model and computer program
[NASA-CR-174722] 01 p0067 N85-10447

Numerical forecast of pressure field by considering the mutual influence of orography, thermal nonhomogeneity and surface friction 01 p0080 N85-10534

Alpine meteorology: Translations of classic contributions by Wagner, A., Ekhart, E. and Defant, F.
[DE84-014929] 01 p0085 N85-10574

Analytical modeling of random thermal fluctuations in the NORDA high-frequency sound scattering facility
[AD-A145024] 01 p0116 N85-10790

Numerical analysis of flow and heat transfer in the VAFB LOX storage Dewar tank
[NASA-CR-171203] 02 p0197 N85-11315

Temperature structures and infrared-derived properties of the atmosphere of Uranus and Neptune
02 p0296 N85-11931

Open cycle OTEC thermal-hydraulic systems analysis and parametric studies
[DE84-013011] 04 p0530 N85-13391

Analysis of diabatic heating during FGGE
05 p0683 N85-14393

Structure of temperature field based on observations of refraction from high meteorological mast
06 p0819 N85-15199

Allowing for the temperature field in the wall thickness of checkerwork in thermal calculation
[BLL-M-36015-(5828.4)] 07 p0956 N85-16058

Influence of setting angle of jet cooling nozzles on temperature and stress state of a turbine wheel
09 p1306 N85-18208

Two-dimensional modeling of conduction-mode laser welding
[DE85-001804] 09 p1327 N85-18341

Transport properties of the outer crust of magnetic neutron stars 09 p1415 N85-18927

Stress studies in EFG
[NASA-CR-174441] 10 p1508 N85-19515

Mathematical simulation of thermal prrocesses involved in electron-beam treatment 12 p1843 N85-21565

Dilution jet configurations in a reverse flow combustor
[NASA-CR-174888] 13 p1974 N85-22392

Effects of temperature variation among droplets in an evaporating fuel spray 13 p2004 N85-22562

Horizontal coherence of temperature microstructure in upper ocean layer 13 p2109 N85-23139

Analysis of NIMBUS-7 SMMR data — Hokkaido, Japan snow cover 13 p2125 N85-23232

Thermal and thermoelastic effects in rolling/sliding contacts
[AD-A150435] 13 p2165 N85-23429

Qualification of the T2 wind tunnel in cryogenic operation. A: Thermal field, preliminary study of a schematic model
[NASA-TM-77781] 14 p2227 N85-23805

Railgun conductor heating from multiple current pulses
[DE85-005333] 14 p2265 N85-24031

Estimating defectiveness buildup during service in metal of welded runner in low-pressure cylinder of turbine
14 p2271 N85-24070

Structure of cold film in water-air boundary layer
14 p2335 N85-24443

The photospheric temperature structure of magnetic flux tubes 14 p2447 N85-25102

Development of a temperature measurement system with application to a jet in a cross flow experiment
[NASA-CR-174896] 15 p2472 N85-25262

Hermetic sealing of nonlubricated gas seal and friction characteristics, chapter 7
[DE85-006375] 15 p2569 N85-25851

Density characteristics of asthenosphere in Atlantic Ocean 19 p3294 N85-30423

Short meridional scale anomalies in the lower stratosphere and upper troposphere
20 p3469 N85-31684

High pressure working mode of hollow cathode arc discharges
[NASA-TM-77880] 20 p3535 N85-31992

Temperature field around a spherical, cylindrical, and needle-shaped crystal, growing in a pre-cooled melt
[NASA-TM-77889] 20 p3537 N85-32011

Quasi-steady-state melting mode during combined laser irradiation of semiconductor materials
21 p3682 N85-32874

On one nonlinear problem of laser thermochemistry
21 p3697 N85-32971

Enhancing precision of remote temperature sensing data from satellites under cloudy atmospheric conditions
22 p3734 N85-33148

Surface temperature distribution along a thin liquid layer due to thermocapillary convection
[NASA-TM-87115] 23 p3930 N85-34357

Interaction of trace elements and welding parameters on GTA weld shape
[DE85-004046] 24 p4080 N85-35284

Heat transfer coefficients for particles in liquid in axially rotating cans 24 p4093 N85-35370

A two-phase flow and heat transfer model for zero gravity
[AD-A156097] 24 p4094 N85-35377

Response of a BWR Mark 2 containment vessel head to loads beyond the design basis
[DE85-010524] 24 p4103 N85-35432

TEMPERATURE EFFECTS

Interpolation formulas for viscosity of six gases: Air, nitrogen, carbon dioxide, helium, argon and oxygen
[PB84-217801] 01 p0026 N85-10161

Stability of bromine intercalated graphite fibers
[NASA-TM-86859] 01 p0031 N85-10187

13C and 1H NMR (Nuclear Magnetic Resonance) studies of solid polyolefines
[AD-P003909] 01 p0032 N85-10195

Platinum thin film resistors as accurate and stable temperature sensors
[NASA-TM-77728] 01 p0049 N85-10322

Inorganic composites for space applications
02 p0155 N85-11047

The silane interphase of composites: Effects of process conditions on gamma-aminopropyltriethoxysilane
[AD-A145578] 02 p0171 N85-11143

Thermodynamics of reactions of deoxidation of nickel melts
[BLL-M-35729-(5828.4)] 02 p0175 N85-11168

The influence of metallurgical aspects on the pitting corrosion behaviour of high alloy stainless steels
02 p0179 N85-11202

Microstructure and creep behaviour at elevated temperature of unidirectionally solidified eutectic nickel base superalloys 02 p0181 N85-11216

Stability of heated boundary layers
02 p0196 N85-11311

Complex formation and temperature stability of electrophysical properties of GaAs seminsulating single crystals 02 p0258 N85-1166

Contributions to the 7th International Acoustic Emission Symposium
[AD-A145368] 02 p0275 N85-11792

The effect of temperature on the radiation induced losses of large diameter GPS (Germanium phosphosilicate) and GBS core optical fibers
[AD-A145409] 02 p0280 N85-11823

Long-term thermal aging of 2 graphite-polyimide composite materials
[NASA-TP-2369] 03 p0325 N85-12094

Effects of prior austenite and ferrite grain size on fracture properties of a plain carbon steel
[AD-A146276] 03 p0332 N85-12136

Effect of a thermal gradient applied to a sinusoidal surface profile
[DE84-015649] 03 p0434 N85-12765

Experimental and theoretical studies of moisture and temperature effects on the mechanical properties of graphite/epoxy laminates and neat resins
04 p0467 N85-12969

Tap noise-pressure fluctuations. Study of the acoustic behavior of hydraulic equipment in buildings as a function of the temperature
[CETIM-11-H-337] 04 p0502 N85-13201

The effect of temperature and pressure on the composition density of alkaline metals
[BLL-M-35940-(5828.4)] 05 p0616 N85-13934

Tensile properties and swelling of 20%-cold-worked Type 316 stainless steel irradiated in HFIR
[DE84-014080] 05 p0617 N85-13948

Additives for heat engine coal slurry fuels
[DE84-016434] 05 p0621 N85-13971

Site-specific research conducted in support of the Salton Sea Solar Pond Project, FY 1982 report
[NASA-CR-174182] 05 p0686 N85-14260

Strain rate effects and temperature history effects for three different tempers of 4340 VAR steel
[AD-A146372] 06 p0768 N85-14915

Impact of temperature on cycle life of globe ISOA EV-3000 lead-acid batteries
[DE84-015840] 06 p0805 N85-15126

Effects of temperature on the response time of thermocouples and resistance thermometers
[DE84-016855] 06 p0811 N85-15154

Special features of the deformation of molybdenum at high temperatures
[BLL-M-36027-(5828.4)] 07 p0924 N85-15856

Kinetics of interaction between carbon and iron oxides of metallized materials in solid phase
[BLL-M-36023-(5828.4)] 07 p0926 N85-15873

The relationship between radiation sensitivity and redox equilibria — glass processing variables
[AD-A147216] 07 p0932 N85-15906

Effects of low temperatures on the growth and unfrozen water content of an aquatic plant
[AD-A147107] 07 p1011 N85-16424

Biochemical evaluation of bodily influence of high and low temperatures 07 p1014 N85-16441

On reversion phenomena in Cu-Zr-Cr alloys
[NASA-TM-77791] 08 p1125 N85-17092

Application of electricity to the reheating of metals prior to forming. Forging, lamination, induction
[BLL-TR-T6399/BG/MRS14903/84]
08 p1137 N85-17160

Departures from LTE populations versus anomalous abundances: The effects of heating
08 p1234 N85-17776

Effect of temperature on the stress-relaxation response of a pressure vessel steel
[TI85-003588] 09 p1339 N85-18424

Influence of temperature on wear resistance of detonation coatings of alloy powders
10 p1447 N85-19116

Study of the volumetric changes in VT23 alloy upon heating 10 p1448 N85-19123

Evaluation and prediction of long-term environmental effects of nonmetallic materials
[NASA-CR-171353] 10 p1450 N85-19137

Investigation of welded interconnection of large area wraparound contacted silicon solar cells
[NASA-CR-174438] 10 p1509 N85-19519

Heat stress and personal protective equipment
[DE85-003552] 10 p1532 N85-19652

Evaluation of residual stress in laminated metallic composites 11 p1598 N85-20052

Effect of temperature and deformation rate on hardness of copper 11 p1605 N85-20090

Non-isothermal irradiation creep of nickel alloys Inconel 706 and PE-16
[DE85-000842] 11 p1607 N85-20102

Micrographic and fractographic examination of alloys 2214 and 2024 for conditions which would cause burning of the metal on being put into solution, trial 17/175
[DGT-23.419] 11 p1609 N85-20117

The response of explosive systems to thermal stimuli: A state-of-the-art assessment
[DE85-000919] 11 p1614 N85-20148

Electrical and thermal performance during charging and discharging a Phase 1 gel cell battery
[PB85-114312] 11 p1677 N85-20565

Vapor pressure studies of the solubilization of hydrocarbons by surfactant micelles
[DE85-004319] 12 p1803 N85-21306

Performance assessment of Class 1E pressure transmitters subjected to environmental stresses
[DE85-001623] 12 p1854 N85-21626

Evaluation of ettringite and related compounds for use in solar energy storage
[PB85-146876] 12 p1883 N85-21816

Preventive effect of acute heat factors during hypokinesia 12 p1902 N85-21945

Effects of temperature variation among droplets in an evaporating fuel spray 13 p2004 N85-22562

Solar array dynamical simulation for illumination and temperature variation 13 p2011 N85-22611

Study of effective physiological temperature
13 p2042 N85-22780

Cooling performance improvement of a horizontal ground coupled heat pump
[DE85-002470] 13 p2093 N85-23065

Thermal and thermoelastic effects in rolling/sliding contacts
[AD-A150435] 13 p2165 N85-23429

Io: Generation of silicate magma by shear melting at the base of a basaltic lithosphere
13 p2172 N85-23476

Characteristics of basaltic lava flows on Venus
13 p2177 N85-23508

Terrestrial analog studies for Martian patterned ground
13 p2190 N85-23590

Effect of elevated-temperature neutron irradiation on fracture toughness of ceramics
[DE85-000652] 14 p2261 N85-24010

Drop of coolant temperature in individual components of solar heating system 14 p2265 N85-24035

Stability of turbine runners in sliding bearings under external circulation forces 14 p2272 N85-24074

Effects of interactive transport and scavenging of smoke on the calculated temperature change resulting from large amounts of smoke
[DE85-006450] 14 p2378 N85-24684

Influences of thermal spikes in ion beam mixing
[DE85-006130] 14 p2419 N85-24924

Peltier heat of a small polaron in a magnetic semiconductor
[DE85-000470] 14 p2430 N85-24983

Effect of deep cooling on crack resistance and low-temperature hardening of aluminum alloys
15 p2496 N85-25396

Effects of primary recoil energy on the production rate of mobile defects during elevated temperature irradiation
[DE85-006218] 15 p2511 N85-25489

Ion beam mixing of marker layers in Al and Si
[DE85-006227] 15 p2511 N85-25490

Anode formation of passivating films on titanium alloy at temperatures up to 200 deg C
15 p2515 N85-25519

Compressive strength of epoxy resin chocks subjected to elevated temperatures
[AD-A152018] 15 p2519 N85-25532

Development of a Digitally Compensated SAW Oscillator (DCSO) to provide temperature stable frequency
[AD-A151907] 15 p2549 N85-25730

Modeling of midwest severe thunderstorms
15 p2596 N85-25995

Qualification of a wall gage for the SIMA wagon, adapted to the test of half models motorized by compressed air turbines — SIMA wind tunnel
[ONERA-PV-1/6068-GY] 16 p2701 N85-26677

Ca-Ga, Sr-Ga and Ba-Ga binary systems
[DE85-006454] 16 p2751 N85-26980

Screening ceramic materials for intense radiant heat applications
[DE85-006989] 16 p2756 N85-27006

Thermal consequences of localized SAR from RFR exposures 16 p2775 N85-27130

Effects of temperature on remotely sensed mafic mineral absorption features 16 p2809 N85-27323

High-thermal-gradient superalloy crystal growth
17 p2914 N85-27956

Influence of temperature in melting and casting on quality of medium-alloy steel
[BLL-BISI-TRANS-22310-(9902.06)]
17 p2936 N85-28137

Effects of level broadening on the magnetothermal oscillations in two-dimensional electron systems
[AD-A152639] 17 p3029 N85-28732

Tendency of selected low-carbon steels to corrosion cracking in nitrates
[BLL-BISI-TRANS-22262-(9022.06)]
18 p3073 N85-29006

Aging study of copper alloy 172
[DE85-009848] 18 p3075 N85-29023

Preliminary results of the Inconel 617 optimization program. Advanced gas cooled reactor materials program
[DE85-006235] 18 p3075 N85-29024

The effect of temperature on the corrosion-erosion of 9Cr1Mo steel
[DE85-006507] 18 p3076 N85-29030

Aging of gold thick-film solder joints
[DE85-009847] 18 p3077 N85-29037

The effects of extreme temperatures on thermocouples
[DE85-008650] 18 p3110 N85-29258

Electrochemical and morphological study of the effect of temperature on the restructuring and loss of capacity of alkaline battery electrodes
[DE85-006869] 18 p3129 N85-29378

Effects of thermal fluctuations on systems with small surface tension
[PREPRINT-437] 18 p3152 N85-29520

Burner rig corrosion of SiC at 1000 deg C
[NASA-TM-87061] 19 p3227 N85-30011

Diffusion welding of incompatible materials
19 p3245 N85-30121

Effect of heating temperature in a vacuum on state of surface layers of welded OT4 titanium alloy
19 p3245 N85-30123

Comparison and evaluation of field and numerical results from the Site A heater test at Avery Island
[DE85-010625] 19 p3268 N85-30269

An investigation of cementation and carbonitriding by means of ionic bombardment
[BLL-OA-TRANS-3203-(6196.300)]
20 p3429 N85-31265

A study of the effect of a mismatch in gamma and gamma prime phase lattice spacings on the high temperature strength characteristics of dispersion-hardened nickel alloys
[BLL-CE-TRANS-8048-(9022.09)]
20 p3430 N85-31279

Cells for measuring thermoelectromotive force and electrical resistance of metals in temperature range of 20-950 degrees Celsius
[BLL-M-36240-(5828.4)] 20 p3457 N85-31473

Nonlinear Constitutive Relations for High Temperature Application, 1984
[NASA-CP-2369] 20 p3465 N85-31530

Micromechanics of high temperature deformation and failure 20 p3466 N85-31534

On the use of internal state variables in thermoviscoplastic constitutive equations
20 p3466 N85-31536

Oxygen and carbon impurities and related defects in silicon 20 p3481 N85-31631

Friction and wear of solid-lubricated contact in gas turbine engine bearings
[AD-A155042] 21 p3596 N85-32335

Interfacial bonding stability 21 p3606 N85-32409

Temperature sensitivity of fiber-optic transmission line
22 p3764 N85-33331

Thermal stress suffered by tank crews working in summer heat
[DRIC-T-7492] 22 p3826 N85-33698

Design analysis for a repository in crystalline rock
[DE85-011802] 22 p3839 N85-33771

The influence of temperature on the composition density of the transition metals
[BLL-M-35896-(5826.4)] 23 p3915 N85-34262

Evaluation of source strength and dispersion model predications with data from large nitrogen tetroxide field experiments
[DE85-011855] 23 p3947 N85-34465

Studies in thermo-hydro-chemical transport in porous and fractured media
[DE85-012555] 23 p3949 N85-34473

Thermally induced chemical migration: A natural analog approach
[DE85-012308] 23 p3949 N85-34474

Pressure measurements in a hydrogen combustion environment: Hydrogen-air combustion test series 1 and 2 in the FITS tank, volume 1
[TI85-009899] 24 p4076 N85-35258

Effect of temperature and ionic impurities at very low concentrations on stress corrosion cracking of Type 304 stainless steel
[TI85-003048] 24 p4079 N85-35283

Search for acoustic signals from high energy cascades
[HE-7.1-1] 24 p4213 N85-36155

Experimental investigation of radiative-acoustic effects in the water by the thermodynamical conditions of Dumand
[HE-7.1-2] 24 p4213 N85-36156

TEMPERATURE FIELDS
U TEMPERATURE DISTRIBUTION

TEMPERATURE GRADIENTS
NT THERMOCLINES

Selecting the proper ceramic material for a regenerator experiencing large temperature gradients
[AD-A144796] 01 p0032 N85-10199

Method for calculating linear shrinkage and expansion of metals and alloys
[BLL-M-35747-(5828.4)] 02 p0175 N85-11173

Shear-layer correction after Amiet under consideration of additional temperature gradient. Working diagrams for correction of signals
[NASA-TM-77741] 03 p0415 N85-12654

Effect of a thermal gradient applied to a sinusoidal surface profile
[DE84-015649] 03 p0434 N85-12765

Numerical modeling of the atmosphere
05 p0680 N85-14370

Amiet shear layer correction with an additional temperature gradient considered: Nomograms for the correction of noise signatures from open jet wind tunnel tests
[DFVLR-MITT-84-11] 05 p0726 N85-14869

Modelling temperature changes during hot working operations 06 p0798 N85-15095

Stresses and strains in lithosphere caused by Earth's thermoconvective oscillations 06 p0822 N85-15217

Temperature distortion generator for turboshaft engine testing
[NASA-TM-83748] 07 p0893 N85-15656

A diffuser heat transfer code
[AD-A149270] 10 p1430 N85-19022

Discovery about temperature fluctuations in turbulent air flows 10 p1500 N85-19466

The EURECA Automatic Gradient Heating Facility (AGHF), phase A study
[ESA-CR(P)-1939] 11 p1591 N85-20005

Fluid temperature and concentration gradient measurement study — for spaceborne experiments
[CISE-R/FL/1/04] 11 p1637 N85-20309

Winter anomaly of the lower ionosphere and its possible causes 11 p1660 N85-20459

Winter anomaly 1982/83 in comparison with earlier winters (1960-82) 11 p1660 N85-20461

Heat flux in Lorentzian plasma
[IPPJ-704] 12 p1935 N85-22158

Turbulence measurements in shock induced flows
13 p2091 N85-23055

Fine structure of vertical distribution of light attenuation index of sea water 13 p2109 N85-23140

Characteristics of basaltic lava flows on Venus
13 p2177 N85-23508

Estimating defectiveness buildup during service in metal of welded runner in low-pressure cylinder of turbine
14 p2271 N85-24070

Preliminary report on the results of hydrological measurements in the southern Tyrrhenian Sea, in the Messina strait and in the western Ionian sea
[PREPRINT-433] 14 p2382 N85-24693

Sea ice, climate and Fram Strait
15 p2603 N85-26042

Scheme for atmospheric thermal sensing from satellites with enhanced vertical resolution
16 p2726 N85-26823

Arctic mixed layer dynamics
[AD-A153582] 18 p3150 N85-29505

The thermal calculation of opaque heat screens
[BLL-M-36273-(5828.4)] 20 p3450 N85-31421

DHC: A diurnal heat capacity program for microcomputers
[DE85-009545] 20 p3516 N85-31659

Amiet shear layer correction with an additional temperature gradient considered: Nomograms for the correction of noise signatures from open jet wind tunnel tests
[ESA-TT-897] 20 p3525 N85-31926

A positron annihilation Doppler broadening study of niobium
[DE85-010287] 20 p3527 N85-31936

Temperature measurements on small droplets
21 p3653 N85-32699

Electronic temperature equalizer
[PB85-181485] 22 p3789 N85-33475

Approximate determination of the extent of the solid-liquid zone
[BLL-M-35329-(5828.4)] 23 p3914 N85-34251
Control system for fluid heated steam generator
[DE85-005734] 23 p3939 N85-34417
Integral representation for nonlinear heat transport
23 p3961 N85-34683
Evaluation of low-temperature geothermal potential in north-central Box Elder County, Utah
[DE85-009541] 24 p4112 N85-35490
Comparative analysis of operational forecasts versus actual weather conditions in airline flight planning, volume 4
[NASA-CR-167865] 24 p4120 N85-35537
TEMPERATURE INDICATORS
U INDICATING INSTRUMENTS
U TEMPERATURE MEASURING INSTRUMENTS
TEMPERATURE INSTRUMENTS
U TEMPERATURE MEASURING INSTRUMENTS
TEMPERATURE INVERSIONS
NT CENTRIFUGING STRESS
NT INTERFACIAL TENSION
Green River air quality model development: Meteorological and tracer data, July/August 1982. Field study in Brush Valley, Colorado
[DE84-014975] 02 p0225 N85-11474
Stresses and strains in lithosphere caused by Earth's thermoconvective oscillations 06 p0822 N85-15217
Effect of steady-state temperature distortion on inlet flow to a high-bypass-ration turbofan engine
[NASA-TM-86896] 07 p0904 N85-15725
Thermal deformation of flexible rotors in friction bearings 14 p2280 N85-24123
The temperature fluctuation in stable stratification above snow cover 15 p2581 N85-25918
Average collisional vibrational energy transfer quantities and the inversion temperature
[AD-A152674] 17 p3029 N85-28733
Reports from the German Meteorological Service. No. 167: Results of aerological soundings in the model area upper Rhine: Heat release project upper Rhine area, part 3
[ISBN-3-88148-216-4] 23 p3950 N85-34479
Analytic solutions of inverse heat conduction problems
24 p4092 N85-35367
TEMPERATURE MEASUREMENT
Effect of combined pressure and temperature distortion orientation on high-bypass-ratio turbofan engine stability
[NASA-TM-83771] 01 p0011 N85-10067
A thermodynamic surface for the critical region of ethylene
[PB84-217850] 01 p0025 N85-10159
Description of the Dutch-Danish (DUDA) scanner --- thermal signatures
[AD-B084893] 01 p0121 N85-10826
An interactive computer code for calculation of gas-phase chemical equilibrium (EQLBRM)
[NASA-CR-168337] 02 p0140 N85-10948
Dynamic gas temperature measurement system
02 p0141 N85-10958
Spectroradiometric calibration of the Thematic Mapper and Multispectral Scanner system
[E85-10026] 02 p0218 N85-11439
Large-area sheet task advanced dendritic web growth development
[NASA-CR-174021] 02 p0223 N85-11463
A temperature climatology for New York State
03 p0394 N85-12517
Evaluation of thermocouple junction temperature
[DE84-015159] 04 p0502 N85-13206
Development of a feasibility model for a thin-film precision power meter
[BMFT-FB-T-84-161] 04 p0504 N85-13217
Climate-chamber experiments to improve pilots' work conditions 04 p0543 N85-13454
Improved apparatus and techniques for high temperature and pressure deformation of crystalline materials
[DE84-016049] 04 p0569 N85-13629
Applications of TOMS ozone data and clustering techniques in satellite soundings
05 p0681 N85-14379
Fidelity of satellite soundings
05 p0682 N85-14383
Computer program to compute soil thermal conductivity from transient temperature measurements
[PB85-100550] 07 p0996 N85-16341
Revised Uniform Summary of Surface Weather Observations (RUSSWO). Spangdahlem AB, Germany, parts A-F
[AD-A147166] 07 p1006 N85-16392
Ground-based measurements of mesosphere temperatures by optical means
08 p1183 N85-17453
Application of Fabry-Perot spectrometers for measurement of upper atmosphere temperatures and winds 08 p1183 N85-17454
Lidar studies of temperature and density using Rayleigh scattering 08 p1184 N85-17459
Lidar studies of the alkali metals
08 p1184 N85-17460
Measurements of sediment temperatures, conductivity and heat flow in the North Atlantic and their relevance to radioactive waste disposal
[IOS-172] 09 p1359 N85-18551
Materials physics
[DE84-017103] 09 p1377 N85-18658
Investigation of surface tension phenomena using the KC-135 aircraft
[NASA-TM-82506] 10 p1426 N85-18995
Investigation of fuel additive effects on sooting flames
[AD-A149154] 10 p1457 N85-19179
1984 AFOSR Research Meeting on Diagnostics of Reacting Flow held at New Haven, Connecticut on 21-22 March 1984
[AD-A149023] 10 p1484 N85-19367
Problems in high temperature thermocouple thermometry
[DE85-000808] 10 p1486 N85-19397
Satellite support to the Sierra Cooperative Pilot Project: 1979/80 and 1980/81
[PB85-115079] 10 p1520 N85-19583
Fluid temperature and concentration gradient measurement study --- for spaceborne experiments
[CISE-R/FL/1/04] 11 p1637 N85-20309
The temperature of a glass-encapsulated solar cell estimated from ambient air temperature and global radiation
[GKSS-84-E-36] 11 p1676 N85-20563
Ferromagnetic resonance in a Ni-Mo superlattice
[DE85-003039] 11 p1735 N85-20911
Ionic mechanisms of soot formation in flames
[AD-A150119] 12 p1801 N85-21297
Method of and apparatus for measuring temperature and pressure --- atmospheric sounding
[NASA-CASE-GSC-12558-1] 12 p1856 N85-21639
Method of measuring sea surface water temperature with a satellite including wideband passive synthetic-aperture multichannel receiver
[NASA-CASE-NPO-15651-1] 12 p1869 N85-21723
Dilution jet configurations in a reverse flow combustor
[NASA-CR-174888] 13 p1974 N85-22392
Application of fluorescence to measurement of surface temperature in solid propellants
13 p2002 N85-22546
Radiosodar system for remote synchronous measurements of wind speed, temperature and its fluctuations 13 p2110 N85-23145
Modulation of light energy transduction in photosynthesis
[DE85-004711] 13 p2141 N85-23292
Analysis and interpretation of observations of airglow at 297 nm in the Venus thermosphere
13 p2172 N85-23473
Qualification of the T2 wind tunnel in cryogenic operation. A: Thermal field, preliminary study of a schematic model
[NASA-TM-77781] 14 p2227 N85-23805
Application of atomic fluorescence to measurement of combustion temperature in solid propellants
[AD-A150733] 14 p2263 N85-24021
Advanced diagnostics for reacting flows
[AD-A150675] 14 p2301 N85-24246
Seven-wavelength pyrometer for determining surface temperature of ablation materials
[NASA-TM-77832] 14 p2305 N85-24266
Possible multiple atmospheric thermal modes with time scale on order of one month 14 p2333 N85-24430
Determination of temperature and degree of roughness of sea and land surfaces by microwave radiometric polarization measurements 14 p2334 N85-24432
Monthly and Seasonal Weather Outlook for mid-December 1984 mid-January 1985, volume 38, number 24, 14 December 1984
14 p2379 N85-24667
Development of a temperature measurement system with application to a jet in a cross flow experiment
[NASA-CR-174896] 15 p2472 N85-25262
System for NDH of thermal spray coating bonds
[DE85-007463] 15 p2572 N85-25858
A simulation experiment on the impact of geostationary temperature retrievals in numerical models
15 p2597 N85-26005
Utilization of satellite data in mesoscale modeling of severe weather 15 p2597 N85-26007
The validation of sea surface temperatures determined from AVHRR data using in situ data recovered via system ARGOS 16 p2812 N85-27342
Observations of airglow O2(1-Sigma) atmospheric band at 8645 A and the rotational temperature at 23 deg S
[INPE-3378-PRE/653] 16 p2826 N85-27435
High resolution spectroscopy of C13O18 in gas mixtures
[AD-A152625] 17 p2919 N85-27891
NMR manometer for measuring high pressures at liquid-helium temperatures 17 p2944 N85-28171
Apparatus for measuring velocity of sound in fluids
17 p2944 N85-28175
Observations of surface water temperature in the Netherlands since 1860: Statistics
[KNMI-WR-84-3] 17 p2997 N85-28531
Observations of surface water temperature in the Netherlands since 1860: Tables for light vessels
[KNMI-WR-84-4] 17 p2998 N85-28532
Observations of surface water temperature in the Netherlands since 1860: Series from KNMI-RWS
[KNMI-WR-84-5] 17 p2998 N85-28533
Automatic liquid-metal temperature monitoring with the use of immersed transducers
[BLL-BISI-TRANS-22427-(9022.06)]
18 p3104 N85-29215
Applications of fuzzy clustering techniques to stratified by tropopause MSU temperature retrievals
18 p3141 N85-29444
Temperature sensitive oscillator
[NASA-CASE-GSC-12958-1] 19 p3258 N85-30201
Method for thermal monitoring subcutaneous tissue
[NASA-CASE-LAR-13028-1] 19 p3328 N85-30818
Intermittency, conditional sampling and turbulent combustion 20 p3424 N85-31249
Application of the Diffusion Raman Anti-Stokes Coherent (DRASC) method to a SNECMA combustion chamber
[YKC-3086/84] 20 p3425 N85-31250
Short-time spectroscopic measurement of the temperature of solids
[ISL-CO-202/84] 20 p3459 N85-31486
DHC: A diurnal heat capacity program for microcomputers
[DE85-009545] 20 p3516 N85-31859
In-situ measurement of wall thermal performance: Data interpretation and apparatus design recommendations
[DE85-011979] 21 p3586 N85-32289
Temperature measurements on small droplets
21 p3653 N85-32690
Application of field similitude theory to calculation of stripline heating 22 p3760 N85-33418
IEA-SSPS CRS calibration report: Calibration of relevant measuring sensors
[DE85-010174] 22 p3788 N85-33468
Electronic temperature equalizer
[PB85-181485] 22 p3789 N85-33475
Measurement and correlation of jet fuel viscosities at low temperatures
[NASA-CR-174911] 23 p3921 N85-34295
Preliminary SPR thermal model description and results for WH-11 and BM-4
[DE85-013171] 23 p3931 N85-34380
Investigation of non-intrusive radiometers for entrained gasifier temperature measurement, revision 3
[DE85-011795] 23 p3934 N85-34385
Control system for fluid heated steam generator
[DE85-005734] 23 p3939 N85-34417
Measurement and interpretation of electron angle at MABE beam stop
[DE85-011918] 23 p3963 N85-34498
Electron irradiation of N type cadmium telluride
[AD-A156117] 24 p4161 N85-35801
TEMPERATURE MEASURING INSTRUMENTS
NT BATHYTHERMOGRAPHS
NT PYROMETERS
NT RESISTANCE THERMOMETERS
NT TEMPERATURE PROBES
NT THERMOCOUPLE PYROMETERS
NT THERMOMETERS
Thermosonde and UHF radar measurements of C2 sub n at Westford, Massachusetts - July 1981
[AD-A145398] 02 p0190 N85-11270
Evolution of the NWC (Naval Weapons Center) thermal standard. Part 5: Thermal standard development and applications
[AD-A146173] 03 p0364 N85-12234
External cavity diode laser sensor
[AD-D011341] 07 p0969 N85-16192
Fluid temperature and concentration gradient measurement study --- for spaceborne experiments
[CISE-R/FL/1/04] 11 p1637 N85-20309
Automatic liquid-metal temperature monitoring with the use of immersed transducers
[BLL-BISI-TRANS-22427-(9022.06)]
18 p3104 N85-29215
TEMPERATURE PROBES
Germanium resistance thermometer calibration at superfluid helium temperatures
12 p1947 N85-22228
TEMPERATURE PROFILES
Use of ground based microwave radiometers for nowcasting 01 p0078 N85-10517

CHORDS: A new temperature or sound speed profile thinning algorithm
[AD-A145464] 02 p0275 N85-11793
Water vapor profile retrievals from the HIRS/MSU satellite sounder 05 p0681 N85-14378
Diurnal and seasonal patterns of temperature and wind flow in the planetary boundary layer for ten locations in complex terrain
[PB85-106698/GAR] 06 p0840 N85-15333
An evaluation and comparison of vertical profile data from the VISSR Atmospheric Sounder (VAS)
[NASA-TP-2425] 07 p1000 N85-16351
The pressure deflagration limit of solid rocket propellants 08 p1117 N85-17046
Determination of ion temperature and rotation velocity profiles by visible, UV and X-ray spectroscopy on Doublet 3 09 p1388 N85-18734
Stress-strain analysis of silicon ribbon
[NASA-CR-175459] 10 p1510 N85-19525
Thermal investigation of an electrical high-current arc with porous gas-cooled anode
[NASA-TM-77789] 11 p1627 N85-20245
Effect of input distributions on the probabilistic fracture mechanics analysis of reactor pressure vessels
[DE85-000632] 11 p1652 N85-20403
Winter anomaly of the lower ionosphere and its possible causes 11 p1660 N85-20459
Theoretical analysis of condensation in the presence of noncondensable gases as applied to open cycle OTEC condensers
[DE84-015609] 11 p1675 N85-20556
Monthly and seasonal weather outlook for October 1984, volume 38, number 19, 29 September 1984
[PB85-113538] 11 p1687 N85-20610
Monthly and seasonal weather outlook for mid-October to mid-November 1984, volume 38, number 20, 13 October 1984
[PB85-113546] 11 p1687 N85-20611
Co-rotating interaction regions in stellar winds
11 p1758 N85-21060
Analysis of selective chopper radiometer data
[NASA-CR-175157] 12 p1895 N85-21894
Two-dimensional numerical model of sensible and latent heat transport in an irrigated field under advective conditions 13 p2131 N85-23261
Radiation-dominated snowmelt on Mars
13 p2191 N85-23592
The effect of air holes on combustor liner wall temperature profile: Experiments
[NAL-TR-840] 15 p2504 N85-25443
Real-time enhancement of a climatology or forecast of ocean thermal structure using observed ocean temperatures
[AD-A151118] 15 p2604 N85-26049
Acoustic propagation in a thermally stratified atmosphere
[NASA-CR-175787] 16 p2860 N85-27636
An investigation into the soot production processes in a gas turbine engine
[AD-A152710] 17 p2919 N85-27992
Energy deposition and its effects on the E+ capture section at Sector 20
[DE85-010964] 18 p3182 N85-29727
Imbedded thermocouples as a solid propellant combustion probe
[AD-A155630] 21 p3564 N85-32167
Application of nonlinear least squares methods to the analysis of solar spectra
[NASA-CR-176122] 22 p3816 N85-33637
Turbulent structure of stably stratified nocturnal slope flows
[AD-A155845] 24 p4123 N85-35559

TEMPERATURE SCALES
A comparison of two bench scale tests of fuel low temperature flow properties
[AD-A154477] 20 p3435 N85-31311
Self-study manual on optical radiation measurements. Part 1: Concepts. Chapter 12: Blackbodies, blackbody radiation, and temperature scales
[PB85-195303] 24 p4154 N85-35754

TEMPERATURE SENSORS
NT THERMISTORS
Platinum thin film resistors as accurate and stable temperature sensors
[NASA-TM-77728] 01 p0049 N85-10322
Fiber optic, Fabry-Perot high temperature sensor
[NASA-CR-174712] 04 p0564 N85-13594
Temperature sensors for OTEC applications
[DE85-009807] 18 p3110 N85-29254
On-line temperature sensor
[DE85-011641] 22 p3787 N85-33465
Materials and process development for microcomputer-compatible pressure, temperature, and position sensors
[BMFT-FB-T-85-024] 24 p4097 N85-35399

TEMPERING
Study to optimize Cr-Mo steels to resist hydrogen and temper embrittlement. A study of carbides formed in low alloy Cr-Mo steels
[DE84-015208] 01 p0029 N85-10179
Wear properties of rapidly solidified surfaces of a pseudo-binary Fe-TiC alloy 02 p0179 N85-11204
Effect of tempering on the strength and toughness of 2 1/4 Cr-1 Mo steel weldments
[DE85-003618] 09 p1296 N85-18140
Residual stress after laser processing
11 p1600 N85-20065
Phase transformations in vanadium alloys of titanium during quenching and tempering
11 p1602 N85-20073
Kinetics of reaction of metals and non-metals during diffusion welding 11 p1602 N85-20076
Effect of mill run and temper variations on barrier anodic film format ion on 6061 aluminum alloy
[DE85-000447] 11 p1608 N85-20112
Effect of aluminum on nature of titanium alloy failure
15 p2498 N85-25411
Powder-metallurgy alloys and steels
[BLL-BISI-TRANS-22239-(9022.06)]
17 p2926 N85-28050
The characteristic structure of weld metal of high temperature alloy X20CrMoV 121
[BLL-BISI-TRANS-21623-(9022.06)]
17 p2928 N85-28069
Study to optimize Cr-Mo steels to resist hydrogen and temper embrittlement
[DE85-005492] 17 p2932 N85-28096
Application of the unloading compliance methods in fracture toughness measurements of a quenched and tempered steel
[BLL-CE-TRANS-7953-(9022.09)]
20 p3465 N85-31523

TEMPLATES
Computer-generated latitude and longitude templates for rapid determination of geographic positions in Alaska
04 p0516 N85-13288
Mask aligner for solar cell fabrication
[AD-D011450] 10 p1510 N85-19529

TEMPORAL DISTRIBUTION
Specifics of dynamics of brain biopotentials under the influence of complex audible communicative signals
07 p1014 N85-16440
Space and time distribtuion of aftershocks
13 p2112 N85-23157
The relationship between auroral electrojet and visual aurora 14 p2363 N85-24602
Elemental analysis of aerosols in Transvaal urban and power-producing areas using time and size-resolved samples 16 p2829 N85-27443
Resource allocation in cerebral specialization of function: Behavioral and electrophysiological studies
[AD-A155092] 21 p3664 N85-32759
Temporal variations of the anomalous oxygen component, 1977 - 1984
[SH-4.6-3] 23 p4039 N85-35041

TEMPORAL RESOLUTION
Fundamental remote sensing science research program. Part 1: Status report of the mathematical pattern recognition and image analysis project
[E85-10004] 02 p0215 N85-11417
Water resources by orbital remote sensing: Examples of applications
[E85-10015] 02 p0217 N85-11428
Time-resolved spectroscopy of evanescent-wave excited fluorescence
[DE84-015213] 04 p0473 N85-13013
Time-resolved tomographic images of a relativistic electron beam
[DE84-015021] 04 p0565 N85-13597
Opportunities for high angular and temporal resolutions of galactic objects at radio frequencies — QUASAT
07 p1059 N85-16723
LANDSAT scene-to-scene registration accuracy assessment 11 p1667 N85-20502
Geometric accuarcy assessment of LANDSAT-4 Multispectral Scanner (MSS) data
11 p1667 N85-20505
Spectral methods in time for parabolic problems
[NASA-CR-172539] 11 p1706 N85-20730
Fast times at high temperatures
[DE85-003306] 12 p1943 N85-22205
Time-resolved studies of rapid solidification in highly undercooled molten silicon
[DE85-004857] 13 p2036 N85-22765
Observed spatial properties of the solar eigenfunctions and the implications for the existence of resolved multiflets 14 p2443 N85-25074
Time-resolving electron temperature diagnostic for ALCATOR C
[DE85-004916] 16 p2868 N85-27690

TENNESSEE
Image variance and spatial structure in remotely sensed scenes — South Dakota, California, Missouri, Kentucky, Louisiana, Tennessee, District of Columbia, and Oregon
07 p0966 N85-16265

TENSILE CREEP
Morphological changes of gamma prime precipitates in nickel-base superalloy single crystals
[NASA-TM-83696] 01 p0026 N85-10165
Mechanisms of elevated temperature rupture in single phase ceramics
[DE85-000697] 09 p1299 N85-18158
Fatigue-creep interaction in + or - 45 deg carbon-resin composites — aircraft construction materials
[ONERA-RT/40/7086/M] 11 p1594 N85-20027

TENSILE DEFORMATION
Structure and properties of titanium alloys after isothermal deformation at low speeds
03 p0351 N85-12260
Strength analysis of fan-shaped wing considering temperature deformation and creep deformations
06 p0779 N85-14963
The influence of porosity on the deformation and fracture of alloys
[AD-A148766] 08 p1130 N85-17124
Influence of work-hardening on the Portevin-LeChatelier effect
[DE85-002505] 11 p1605 N85-20093

TENSILE PROPERTIES
Tensile properties and swelling of 20%-cold-worked Type 316 stainless steel irradiated in HFIR
[DE84-014080] 05 p0617 N85-13948
Characterization of fiber optic cables under large tensile loads
[DE84-016816] 05 p0651 N85-14180
Characterization of newly developed conductive composites
[AD-A146852] 06 p0764 N85-14884
Weldability and mechanical property characterization of weld clad alloy 800H tubesheet forging
[DE85-001737] 11 p1609 N85-20116
Structural basis for the mechanical properties of polyethienes
[PB85-149771] 11 p1613 N85-20142
Steel castings by the electroslag casting technique
[DE85-003812] 12 p1819 N85-21409
Effects of neutron irradiation at 450(0)C and 16 dpa on the properties of various commercial copper alloys
[DE85-005716] 13 p2024 N85-22684
Spectroscopic analysis of radiation-generated changes in tensile properties of a polyetherimide film
[NASA-TP-2429] 15 p2502 N85-25435
Temperature and manganese content dependences of tensile deformation in iron-high manganese binary alloys
[DE85-007656] 17 p2932 N85-28098
Preliminary results of the Inconel 617 optimization program. Advanced gas cooled reactor materials program
[DE85-006235] 18 p3075 N85-29024
Influence of recrystallization and solution on the tenecity of the 7010 and 7475 alloys. Olygocyclic fatigue of the 7010 alloy
[ONERA-RT-19/5069-M] 20 p3432 N85-31269
Numerical study of tensile fracture in plane stress
[ONERA-RT-22/7169-RY-070-R]
20 p3470 N85-31563
Effects of weak interfaces on thermostructural behavior of carbon-carbon composites
[AD-A155330] 21 p3562 N85-32154
Fracture behavior of aluminum composites reinforced with fiber 23 p3907 N85-34207
Apparatus producing constant cable tension for intermittent demand
[DE85-006434] 23 p3938 N85-34412
Effect of thermal ageing on the mechanical properties of PWR pressure vessel steels and weldments
[AERE-R-11460] 24 p4078 N85-35275
Microshrink, tensile properties, and the detection of microshrink
[AD-A155875] 24 p4079 N85-35278

TENSILE STRENGTH
The effect of 2 strength reducing techniques on the ultimate tensile strength of AISI 4130 steel: Rocket motor case venting
[AD-A145526] 02 p0169 N85-11134
Tensile strength of composite sheets with unidirectional stringers and crack-like damage: A brief report
[NASA-TM-86310] 02 p0170 N85-11139
Resistance of Navy shipboard outerwear garments and fire-resistant fabrics to extreme heat
[AD-A145414] 02 p0238 N85-11546
Effects of tin on microstructure and mechanical behavior of Inconel 718
[NASA-TM-86866] 03 p0330 N85-12129

Test report no. 17.206: Statistics of the basic characteristics of carbon-epoxy composites
[DGT-23.426/A] 04 p0468 N85-12979
Tensile properties and swelling of 20%-cold-worked Type 316 stainless steel irradiated in HFIR
[DE84-014060] 05 p0617 N85-13948
Influence of the shape and distribution of inclusions of the fatigue strength of bearing steels in rotary bending
[BLL-PNR-90243-(8019.3153)] 06 p0768 N85-14912
Strength and aging behaviour of soft soldered joints
[BLL-T6385/BG/WH800/84] 07 p0925 N85-15862
On heat-treatable copper-chromium alloy, 1
[NASA-TM-77753] 07 p0927 N85-15879
Mechanical property data 7050-t736511 alloy
[AD-A147365] 07 p0928 N85-15882
Imide modified epoxy matrix resins
[NASA-CR-174695] 07 p0930 N85-15892
Laboratory investigation on adhesives for Naval facilities construction
[AD-A147453] 07 p0932 N85-15909
Hydrogen embrittlement of nickel
[AD-A148322] 08 p1129 N85-17119
Tensile test of pressureless-sintered silicon nitride at elevated temperature
[NASA-TM-77777] 08 p1172 N85-17390
Effect of tempering on the strength and toughness of 2 1/4 Cr-1 Mo steel weldments
[DE85-003618] 09 p1296 N85-18140
Ti-6Al-4V alloy castings prepared in zircon sand molds and the effect of hot isostatic pressing
[PB85-109932/GAR] 09 p1298 N85-18150
Studies of structure and mechanical properties of carbon-reinforced plastic based on spirally reinforced filler 10 p1444 N85-19100
Influence of extension rate on strength and deformation characteristics of titanium alloys over a broad temperature range 10 p1448 N85-19121
Effects of chromium and aluminum on mechanical and oxidation properties of iron-nickel-base superalloys based on CG-27
[NASA-TP-2443] 12 p1805 N85-21323
The strength and characteristics of VPPA welded 2219-T87 aluminum alloy 12 p1948 N85-22224
Structural strenght of strip D16T aluminum alloy with low copper and magnesium content
13 p2025 N85-22691
New deformable secondary aluminum alloys
13 p2026 N85-22694
Effect of operating medium on cyclic durability of AD33-W composite 13 p2029 N85-22716
Analysis of strength and ductility of welded joints in AMtsS and AMg5 aluminum alloys
13 p2033 N85-22737
Experimental investigation of crippling strength of Chinese aluminum alloy (LY12CZ) sections
13 p2041 N85-22779
Effect of oxygen on mechanical properties of Nb-V alloy
[DE85-002681] 14 p2256 N85-23982
Cast-iron technology: Metallographic and mechanical testing results
[DE85-002684] 14 p2257 N85-23984
Environmental effects on the tensile strength of chemically vapor deposited silicon carbide fibers
[NASA-TM-86981] 14 p2259 N85-24000
Hydrogen resistance of VT1-0 titanium under 150 MPa pressure at room temperature 15 p2499 N85-25414
Development of high strength ship hull steel for high heat input welding — controlled rolling and accelerated cooling 15 p2565 N85-25827
Tensile and fracture toughness properties of Mirage III spars
[AR-003-019] 15 p2578 N85-25899
Magnetic method of inspecting mechanical properties of general purpose tubes
[BLL-M-36084-(5828.4)] 16 p2796 N85-27235
Mechanical properties of lunar materials under anhydrous, hard vacuum conditions: Applications of lunar glass structural components
[DE85-006682] 16 p2801 N85-27271
SRB filament wound case material property study
[NASA-CR-171469] 17 p2910 N85-27940
Role of hydrogen and structure on CMSX-2
17 p2915 N85-27967
High tensile strength, punchable, hot rolled strips with good plasticity
[BMFT-FB-T-84-256] 18 p3078 N85-29040
Load-carrying capabilities of refractory alloys for space reactor power applications
[DE85-010566] 19 p3240 N85-30067
Long range ordered alloys modified by addition of niobium and cerium
[DE85-011661] 20 p3431 N85-31285
Orientation and strength of semi-crystalline polymers
20 p3432 N85-31294
Long-term strength of glass fibre/phenolic resin composites
[NPL-DMA(A)-88] 22 p3742 N85-33195
Tensile fatigue of glass fibers and composites with conventional and surface compressed fibers
[RR-84-4] 22 p3742 N85-33196
Strength properties of glassfiber reinforced thermoplastics 23 p3908 N85-34212
Study on fracture behavior of epoxy resin
23 p3909 N85-34216
Effects of temperature on the tensile strength and elastic modulus of composite material
[AD-A156112] 24 p4075 N85-35251
Crystallization of Polyetheretherketone (PEEK) in carbon fiber composites
[AD-A156316] 24 p4075 N85-35252
Effect of microstructure on the fatigue behavior of Fe-C-X alloys
[DE85-011749] 24 p4080 N85-35265

TENSILE STRESS
Contributions to the 7th International Acoustic Emission Symposium
[AD-A145368] 02 p0275 N85-11792
Stress concentration due to axial tension of loaded nonsymmetric-shaped grooves
[AD-A149425] 10 p1496 N85-19442
Tether fundamentals 11 p1643 N85-20345
Simplified theory for the behaviour of buried flexible cylinders under the influence of uniform hoop compression
[PB85-116531] 11 p1654 N85-20419
Longitudinal splitting in unidirectional composites, analysis and experiments
[NASA-CR-3881] 13 p2015 N85-22639
Orientation and temperature dependence of some mechanical properties of the single-crystal nickel-base superalloy Rene N4. 3: Tension-compression anisotropy
[NASA-TM-86962] 13 p2021 N85-22680
Origin of Martian polygonal terrain: Preliminary results
13 p2191 N85-23591
Determination of permissible heating rate of metal
[BLL-M-36107-(5828.4)] 16 p2748 N85-26957
Magnetic method of inspecting mechanical properties of general purpose tubes
[BLL-M-36084-(5828.4)] 16 p2796 N85-27235
Matrix fracture in fiber-reinforced ceramics
[AD-A154704] 21 p3569 N85-32197
A continuous damage model based on stepwise-stress creep rupture tests
[NASA-CR-174941] 21 p3597 N85-32341
Apparatus producing constant cable tension for intermittent demand
[DE85-006434] 23 p3938 N85-34412

TENSILE TESTS
Tensile and crack propagation tests on aluminum alloys of the 2000 and 7000 series in laminated plate and forged products
[M2-678300] 03 p0373 N85-12383
Composite materials characterization and development at AFWAL 04 p0464 N85-12944
Finite element method calculation of a necking tension specimen including heat transfer influence
[RUB-IFM-MITT-40] 05 p0646 N85-14162
Special features of the deformation of molybdenum at high temperatures
[BLL-M-36027-(5828.4)] 07 p0924 N85-15856
Tensile testing of SiC whiskers
[DE85-003712] 11 p1593 N85-20025
Strength properties of unidirectionally reinforced hybrid composites 11 p1599 N85-20056
Reduced-chromium stainless steel substitutes containing silicon and aluminum
[PB85-160786] 15 p2513 N85-25502
Magnetic method of inspecting mechanical properties of general purpose tubes
[BLL-M-36084-(5828.4)] 16 p2796 N85-27235
MM2 LRSLA testing stage 3 propellant
[AD-A152540] 17 p2937 N85-28128
Short term determination of the creep properties of high temperature materials
[CRIF-MT-160] 20 p3432 N85-31288
Graphite/PMR polyimide composites with improved toughness
[NASA-TM-87081] 21 p3561 N85-32148
Tensile testing apparatus
[NASA-CASE-LAR-13243-1] 23 p3933 N85-34375
Effect of temperature and ionic impurities at very low concentrations on stress corrosion cracking of Type 304 stainless steel
[TI85-003048] 24 p4079 N85-35283

TENSIOMETERS
A strain gauge manual
[AD-A151802] 16 p2787 N85-27197

TENSION
Psychological states (mood, affect or emotion) experienced by JASDF pilots through flying duties. 2: Flying conditions causing pilots psychological disturbances 01 p0090 N85-10[illegible]
Evaluation of failure criterion for graphite/epoxy fabric laminates
[NASA-CR-172547] 10 p1431 N85-19025

TENSOR ANALYSIS
Linear and bilinear infinite-dimensional representations of finite-dimensional nonlinear systems
[RR-259] 02 p0254 N85-11681
Trust region methods for minimization
[AD-A147073] 07 p1030 N85-16540
Alternatives for jet engine control
[NASA-CR-175831] 16 p2709 N85-26713
Alternatives for jet engine control
[NASA-CR-175832] 16 p2709 N85-26714
Alternatives for jet engine control
[NASA-CR-175833] 16 p2709 N85-26715
Boundary layer and parabolic flows
[DFVLR-FB-84-46] 17 p2960 N85-28[illegible]
Reduction techniques for infinite-dimensional Hamiltonian systems: Some ideas and applications
[PREPRINT-424] 18 p3173 N85-2[illegible]

TENSOR FIELDS
U TENSORS

TENSORS
NT STRESS TENSORS
Linear conformal gravitation 02 p0265 N85-11735
Microwave measurement of the complex dielectric tensor at anisotropic slab materials
[DE84-017050] 04 p0493 N85-13144
Interacting Boson approximation
[DE85-003016] 22 p3837 N85-33756
Scalar/Vector potential formulation for compressible viscous unsteady flows
[NASA-CR-3921] 23 p3893 N85-34113

TEREPHTHALATE
NT POLYETHYLENE TEREPHTHALATE

TERMINAL BALLISTICS
Penetrator/armour interactions: Background to Australian work
[MRL-R-936] 03 p0367 N85-12353
An introduction to fuzzy regression analysis with a ballistic application
[AD-A146093] 03 p0411 N85-12629
Nondestructive deceleration of a rocket sled — target penetration tests
[FOA-C-20549-D3] 07 p0912 N85-15771
A computerized study of rigid cones penetrating aluminum targets
[FOA-C-20561-D4] 11 p1648 N85-20384
An orthogonal grid technique for studying internal deformation and energy absorption in target penetration
[AD-A149989] 12 p1860 N85-21[illegible]
OMEGA: An optronic device to measure the incidence angle of a projectile
[ISL-CO-207/83] 14 p2306 N85-24274
A method for the evaluation of the residual energy of a metallic fragment after perforation of a thin target
[ISL-R-113/83] 16 p2794 N85-27[illegible]
Holographic assembly for measuring velocity fields of supersonic ballistic splinters at a large distance
[ISL-CO-203/84] 20 p3459 N85-314[illegible]
Numerical simulation of interior and terminal ballistics phenomena. Investigation of the effects of the parameters and application examples
[ISL-R-112/84] 22 p3631 N85-33731
Presentation of numerical simulation work in terminal ballistics using a few examples. Applications of the calculation model Program for Elastoplastic Simulation of Impacts (PEPSI) of the Franco-German Research Institute Saint Louis (ISL)
[ISL-CO-209/84] 22 p3634 N85-33741
Experimental data for characterizing perforating impacts. Fragmentation processes
[AD-A156370] 24 p4102 N85-35427

TERMINAL GUIDANCE
NT LASER GUIDANCE
Dual mode radio frequency-infrared frequency system
[AD-D011402] 08 p1081 N85-1[illegible]
Integration of ground and on-board system for terminal count 08 p1092 N85-1[illegible]
AN investigation into the control limitations of a bank to turn missile in the terminal homing phase
[AD-A152193] 16 p2704 N85-2[illegible]
Dispersion sensitivity of the eight inch advanced range munitions technology projectile due to wind and minor thrust errors
[AD-A152145] 16 p2727 N85-2[illegible]
Automatic assembly of space stations
20 p3409 N85-31153

TERMINALS

BBC receiving terminal for the European orbital test satellite
[BBC-RD-1984/15] 08 p1142 N85-17205

TERMINATOR LINES

Near Earth space sporadic radio emission busts occurring during sunrise
[SH-10.1-9] 23 p4054 N85-35140

TERMINOLOGY

An operational system for subject switching between controlled vocabularies: A computational linguistics approach
[NASA-CR-3838] 02 p0293 N85-11903

Error and uncertainty — metrology
[NPL-DPMA-2] 08 p1137 N85-17161

Online database search strategies and thesaural relationship models 09 p1402 N85-18822

Systematic nomenclature of the nitrogen, oxygen and sulfur functional polycyclic aromatic hydrocarbons
[DE85-007426] 17 p2916 N85-27974

Coping with computer terminology
[DE85-006076] 18 p3161 N85-29579

Spanish language equivalents for a glossary of terms used in the field of space exploration
[NASA-TM-86211] 19 p3379 N85-30961

Re-evaluation of cosmic ray cutoff terminology
[SH-6.1-11] 23 p4045 N85-35084

TERNARY ALLOYS

Re-evaluation of phase separation in Ti-Zr-Be metallic glasses
[DE84-015603] 03 p0338 N85-12176

Zero-flux planes and flux reversals in multicomponent diffusion
[DE84-015212] 05 p0618 N85-13950

High temperature properties of equiatomic FeAl with ternary additions
[NASA-TM-86936] 10 p1439 N85-19072

Clustering and ordering in 3-5 alloys
[AD-A150604] 13 p2022 N85-22670

Influence of composition on the microstructural evolution and mechanical properties of irradiated Fe-Ni-Cr ternaries
[DE85-007462] 17 p2931 N85-28094

Amorphous alloys of ion-implanted Fe-Ti-C
[DE85-010656] 19 p3360 N85-30834

A fractographic study on mode 2 and mode 3 SCC crack growth in an Al-Zn-Mg alloy 23 p3905 N85-34191

Enthalpies of formation of liquid Fe-Ce-Si and Fe-Ce-Al three-component alloys
[BLL-M-36296-(5828.4)] 23 p3913 N85-34247

TERNARY SYSTEMS

Transport properties and distribution functions in 3-5 semiconductors
[AD-A147525] 07 p1049 N85-16660

Formation of a limiting composition in the preparation of ternary 3-5 semiconductors by the VPE (Vapor Phase Epitaxy) Hydride technique
[AD-A147639] 08 p1225 N85-17713

High temperature properties of equiatomic FeAl with ternary additions
[NASA-TM-86938] 10 p1439 N85-19072

A study of interdiffusion in beta + gamma/gamma + gamma prime Ni-Cr-Al
[NASA-CR-174852] 11 p1597 N85-20041

Characterization of high temperature electrically conducting oxides
[DE85-004296] 12 p1803 N85-21307

Process for making a heterojunction source-drain insulated gate field-effect transistors utilizing diffusion to form the lattice
[AD-D011536] 12 p1939 N85-22176

A study of liquid-vapor equilibria of the bromine-hydrobromic acid-water system
[NASA-TM-77748] 14 p2249 N85-23940

Dual species ion implantation of ternary compounds based on In-Ga-As
[AD-D011617] 16 p2869 N85-27696

Three body abrasive wear in various metal combinations 23 p3906 N85-34200

TERNARY SYSTEMS (DIGITAL)

U DIGITAL SYSTEMS

TERRACES (LANDFORMS)

NT PIEDMONTS
NT PLATEAUS

Quaternary stratigraphy of the lower Iowa and Cedar River Valleys, southeast Iowa 09 p1352 N85-18504

Morphology and mechanics of terraces in lunar craters
13 p2182 N85-23543

Newly discovered Martian impact basins
13 p2182 N85-23544

Interaction of Martian flow ejecta blankets with pre-existing impact craters: Morphological observations
13 p2183 N85-23546

TERRAIN

A one-level mesoscale model suitable for nowcasting and short-term forecasting in regions of complex terrain
01 p0061 N85-10541

Digital Terrain Elevation Data (DTED) anomaly removal through the use of an interactive Fourier frequency filtering process
[AD-A145433] 02 p0219 N85-11445

Digital elevation models improve processing of Alaskan gravity data 04 p0515 N85-13285

Stratigraphy, petrology, and structure of the Pingston terrane, Mount Hayes C-5 and C-6 quadrangles, eastern Alaska Range, Alaska 04 p0517 N85-13301

Relationship between model complexity and data base quality for complex terrain tracer experiments
[DE84-015022] 04 p0539 N85-13429

Potential geological natural landmarks of the East Gulf Coastal Plain
[PB84-230317] 06 p0835 N85-15316

Simple mesoscale models for operational use in regions of topographic and thermal forcing: Development and evaluation
[AD-A146667] 06 p0839 N85-15325

On the long range propagation of sound over irregular terrain
[NASA-CR-3862] 07 p1038 N85-16569

Automatic terrain elevation mapping and registration
08 p1148 N85-17242

Interactive digital image processing for terrain data extraction
[AD-A146580] 08 p1176 N85-17417

Soil compliance influence on tyre performance
[AD-P004260] 09 p1404 N85-18836

Dynamic simulation of track laying vehicles
[AD-P004266] 09 p1405 N85-18842

A comparison between a conventional method and an improved method for predicting tracked vehicle performance
[AD-P004276] 09 p1406 N85-18852

Effect of hitch positions on the performance of track-grouser systems
[AD-P004277] 09 p1406 N85-18853

Ride comfort of off-road vehicles
[AD-P004279] 09 p1406 N85-18855

Further development in ride quality assessment
[AD-P004280] 09 p1406 N85-18856

Comparison of measured and simulated ride comfort for an agricultural tractor and influence of travel speed and tyre-inflation pressure on dynamic response
[AD-P004281] 09 p1407 N85-18857

Characteristics of farm field profiles as sources of tractor vibration
[AD-P004282] 09 p1407 N85-18858

Smoother terrain-machine
[AD-P004298] 09 p1409 N85-18873

Natural environment analysis
[NASA-CR-171333] 10 p1428 N85-19010

A comparison between predicted and measured propagation loss in the VHF/UHF range in rugged terrain 10 p1471 N85-19285

Control of mammals at airports
[AD-P004192] 11 p1580 N85-19957

Landscape management on airports for reduction of bird populations
[AD-P004194] 11 p1581 N85-19960

Inexpensive multipurpose landscaping
11 p1581 N85-19961

Atmospheric diffusion in hilly region on middle reaches of the Chang Jiang 11 p1620 N85-20196

Mean flow and turbulence in complex terrain NPS (Naval Postgraduate School)/Vandenberg measurement system
[AD-A150184] 13 p2138 N85-23274

The ASCOT Data Analysis Workshop
[DE85-004407] 13 p2139 N85-23283

Low altitude texture comparison data base and smooth shaded texture
[AD-A150342] 13 p2146 N85-23323

Dark halo craters and the thickness of grooved terrain on Ganymede 13 p2173 N85-23484

Formation of bright terrain bands on Ganymede by unstable lithosphere extension 13 p2173 N85-23485

Basaltic pressure ridges: Formation and relationship to flow emplacement 13 p2186 N85-23567

Paleohydrologic implications of valley networks of Mars 13 p2190 N85-23585

Relative time-scale for channeling events within chaotic terrains, Margaritifer Sinus, Mars
13 p2190 N85-23589

Terrestrial analog studies for Martian patterned ground
13 p2190 N85-23590

Origin of Martian polygonal terrain: Preliminary results
13 p2191 N85-23591

Investigations of the Mars cratered terrain: Smooth plains boundary in the eastern equatorial region
13 p2191 N85-23596

Martian fretted terrain morphometry interpreted using principal components analysis 13 p2192 N85-23597

Distribution and properties of large symmetric knobs on Mars 13 p2192 N85-23598

Enigmatic hills of the mottled plains, Mare Acidalium quadrangle (MC-4), Mars 13 p2192 N85-23599

Importance of the tectonic motions on Ganymede
13 p2202 N85-23661

Evaluation of carrying capacity and landscape damage in northern Kenya by multistage remote sensing
[DFVLR-FB-84-47] 14 p2347 N85-24514

A study of terrain reductions, density anomalies and geophysical inversion methods in gravity field modelling
[AD-A150768] 14 p2373 N85-24686

Technical development to improve satellite sounding over radiatively complex terrain
[NASA-CR-175746] 15 p2583 N85-25929

Mean conditions and turbulence statistics at Vandenberg AFB, California
[AD-A151366] 15 p2665 N85-26449

Radar return from vegetation covered terrains
[INPE-3470-PRE/713] 16 p2770 N85-27093

A study of the effect of gently varying terrain on atmospheric flow near the surface
16 p2823 N85-27411

Structural analysis of terrane accretions in the eastern Brooks Range and adjacent areas in central Alaska and Canada
[DE85-008279] 17 p2993 N85-28501

Application of artificial intelligence (AI) to radar image understanding
[AD-A152519] 17 p3017 N85-28654

The AFTI/F16 terrain-aided navigation system
[DE85-008411] 18 p3060 N85-28935

Influence of land surface processes on the Indian monsoon: A numerical study 18 p3146 N85-29478

Influence of land-surface roughness on atmospheric circulation and rainfall: A sensitivity study with a GCM
18 p3146 N85-29479

Categorization of nocturnal drainage flows within the Brush Creek valley in western Colorado and the variability of sigma theta in complex terrain
[DE85-011291] 19 p3300 N85-30461

MELSAR: A mesoscale air quality model for complex terrain. Volume 2: Appendices
[DE85-010991] 19 p3310 N85-30519

The use of the glistening surface concept in rough surface scattering
[AD-A154922] 21 p3575 N85-32234

Geomorphological similarity and uniqueness
21 p3601 N85-32361

Ancient landscapes: Their nature and significance for the question of inheritance 21 p3601 N85-32364

Landscape inheritance: Report of Working Group Number 2 21 p3604 N85-32383

Process thresholds: Report of Working Group Number 3 21 p3604 N85-32384

Microcomputer processing of LANDSAT Thematic Mapper data for the acquisition of military tactical terrain data
[AD-A154781] 21 p3605 N85-32389

Mean flow and turbulence in complex terrain
[AD-A155138] 21 p3636 N85-32583

A transportable, machine oriented library of european sky and terrain radiance distributions with contemporary radiometric and meteorological profiles
[AD-A155254] 21 p3637 N85-32590

A review of tectonic aspects of the Limpopo belt and other Archean high-grade gneissic terranes
21 p3720 N85-33060

Implementation of the SITAN algorithm in the digital terrain management and display system
[DE85-010659] 22 p3729 N85-33115

Terrain illumination conditions when taking scanning photographs from space 22 p3736 N85-33159

MELSAR: A mesoscale air quality model for complex terrain. Volume 1: Overview, technical description and user's guide
[DE85-010943] 22 p3811 N85-33608

Evaluation of the 2DFLOW and hybrid complex-terrain dispersion models with the 1980 ASCOT data base from the Geysers
[DE85-012960] 22 p3812 N85-33613

A user-friendly computer-aided construction of boundaries 23 p3962 N85-34564

Three-dimensional gravity ideal body studies in rough terrain
[DE85-014097] 24 p4118 N85-35525

Turbulent structure of stably stratified nocturnal slope flows
[AD-A155845] 24 p4123 N85-35559

TERRAIN ANALYSIS

Geomorphology 02 p0214 N85-11411

Terrain analysis procedural guide for surface configuration
[AD-A145637] 02 p0219 N85-11446

Remote sensing for landforms and soils in the arid southwest United States 03 p0378 N85-12410

Comparison between tracer measurements and model calculations for nighttime drainage flows in complex terrain
[DE84-014709] 04 p0539 N85-13431

Atmospheric studies in complex terrain
[DE84-008553] 05 p0676 N85-14345

A brief investigation into the validity of SEASAT radar altimeter data acquired over land
[AD-A146560] 06 p0827 N85-15254

Evaluation of the L-band scattering characteristics of volcanic terrain in aid of lithologic identification, assessment of SIR-B calibration, and development of planetary geomorphic analogs 08 p1146 N85-17232

Investigation of SIR-B images for lithologic mapping
08 p1148 N85-17241

Mathematical aspects of digital terrain information; Report from International Society for Photogrammetry and Remote Sensing (ISPRS) working group 3:3, 1980 - 1984 — photogrammetry 08 p1175 N85-17407

Natural environment analysis
[NASA-CR-174330] 08 p1180 N85-17433

Automated and interactive data base generation
[AD-P004316] 09 p1268 N85-17970

CIG (Computer image generation) data bases in an instance: Bits and pieces
[AD-P004318] 09 p1269 N85-17972

The generation of three-dimensional data bases using a building block approach
[AD-P004319] 09 p1269 N85-17973

SIR-A imagery in geologic studies of the Sierra Madre Oriental, northeastern Mexico. Part 1 (Regional stratigraphy): The use of morphostratigraphic units in remote sensing mapping
[NASA-CR-175457] 10 p1505 N85-19497

The accuracy in calculations of intervisibility with digital terrain models — digital models
[FOA-C-20557-D8(E1)] 12 p1909 N85-21983

Stagnation zone impaction on a simple terrain feature in stable flow 13 p2130 N85-23255

Using SM-4 Omega system in checking and editing digital terrain information 15 p2487 N85-25350

Structural analysis of terrane accretions in the eastern Brooks Range and adjacent areas in central Alaska and Canada
[DE85-008279] 17 p2993 N85-28501

Scattering from foliage covered terrain
[AD-A154724] 21 p3574 N85-32228

Planning for VRM: Radar and sonar studies of volcanic terrains on Earth, Venus and Mars
22 p3857 N85-33884

TERRAIN FOLLOWING AIRCRAFT

Observations of physiological and psychological effects of terrain following flight based on in-flight test experience 10 p1532 N85-19657

TERRESTRIAL MAGNETISM

U GEOMAGNETISM

TERRESTRIAL PLANETS

NT EARTH (PLANET)
NT MARS (PLANET)
NT MERCURY (PLANET)
NT VENUS (PLANET)

Development of a Global 3-D magnetohydrodynamic computational model for solar wind-cometary and planetary studies
[NASA-CR-175490] 12 p1962 N85-22331

Accumulation of the terrestrial planets
13 p2179 N85-23524

Implications of convection in the Moon and the terrestrial planets 13 p2183 N85-23548

Terrestrial Planets: Comparative Planetology
[NASA-CR-176093] 22 p3851 N85-33849

Noble gases in meteorites and terrestrial planets
22 p3851 N85-33850

Terrestrial Xe isotopic contraints on the early history of the Earth 22 p3852 N85-33852

Oxidation states of iron in the terrestrial planets: Evidence and implications for accretion models
22 p3852 N85-33854

The distribution of compositional classes in the asteroid belt: A cosmochemical fingerprint?
22 p3852 N85-33856

Late-stage planetesimals: How big?
22 p3852 N85-33857

What determines the location of satellites and planets? 22 p3853 N85-33858

Interrelationships among the terrestrial planets
22 p3853 N85-33859

Impact processes and their implications for planetary formation and early evolution 22 p3853 N85-33860

Origin of the atmosphere and hydrosphere of the terrestrial planets 22 p3853 N85-33863

A solid-state framework for terrestrial upper mantles
22 p3856 N85-33878

Crustal development in the terrestrial planets
22 p3856 N85-33879

Magnetic field generation in the cores of terrestrial bodies 22 p3859 N85-33894

TERRESTRIAL RADIATION

A sphere-scanning radiometer for rapid directional measurements of sky and ground radiance: The PARABOLA field instrument
[NASA-TM-86171] 03 p0363 N85-12329

Simple formula to estimate carbon dioxide gas effect in radiation balance of underlying surface
06 p0823 N85-15226

Deciduous forest radiation regimes: Effects of forest structure, phenology and Earth-Sun geometry upon their spatial, temporal and spectral variability
[AD-A146804] 07 p0996 N85-16327

Diurnal variations in terrestrial magnetic field and structure of magnetosphere 14 p2344 N85-24493

Comparison of measurement and simulation results of radiation temperatures applied to the thermal mapping of Munich
[DFVLR-FB-85-06] 17 p2964 N85-28442

Ion waves generated by ion loss-cone distributions or drifting particles
[KGI-PREPRINT-070] 20 p3549 N85-32087

Empirical model for the Earth's cosmic ray shadow at 400 KM: Prohibited cosmic ray access
[SH-6.1-14] 23 p4046 N85-35087

Cosmic ray secular variations in terrestrial records and aurorae
[SH-7.1-3] 23 p4047 N85-35096

TESSERAL HARMONICS

Geopotential harmonics of order 15 and 30, from analysis of the orbit of satellite 1971-10B
[RAE-TR-84006] 02 p0165 N85-11121

Individual geopotential coefficients of order 15 and 30, from resonant satellite orbits
[RAE-TR-84021] 08 p1105 N85-16985

TEST BEDS

U TEST EQUIPMENT

TEST CHAMBERS

NT ANECHOIC CHAMBERS
NT HYPERBARIC CHAMBERS
NT PRESSURE CHAMBERS
NT VACUUM CHAMBERS

Natural exposure versus chamber simulation
[AD-A149536] 10 p1495 N85-19437

An environmentally-controlled extended-use small animal hypobaric chamber
[AD-A153735] 19 p3221 N85-29974

A prototype test chamber for fit testing of protective masks in the field
[FOA-C-40206-C1(C2)] 20 p3512 N85-31834

Analysis of performance of dynamic thermal diffusion chamber 21 p3642 N85-32625

A thermal diffusion chamber for the measurement of cloud condensation nuclei 21 p3642 N85-32627

Stable generation of highly monodisperse aerosols
21 p3642 N85-32628

Development of a chemical kinetic mechanism for the US EPA (Environmental Protection Agency) regional oxidant model
[PB85-185858] 22 p3813 N85-33618

Modeling of auto exhaust smog chamber data for EKMA development
[PB85-186492] 22 p3813 N85-33619

Multidimensional analysis of data obtained in experiments with X-ray emulsion chambers and extensive air showers
[HE-3.6-2] 24 p4184 N85-35951

TEST EQUIPMENT

Economic model of calibration improvements for automatic test equipment
[PB84-217827] 01 p0051 N85-10335

A machine for weight-lift testing
[AD-A146816] 07 p0973 N85-16182

Random pattern tracking acceleration tolerance tester
[AD-D011404] 07 p1017 N85-16459

Heater block assembly for use in thermal oxidation testing of jet fuel
[AD-D011430] 08 p1123 N85-17077

Seven-wavelength pyrometer for determining surface temperature of ablation materials
[NASA-TM-77832] 14 p2305 N85-24268

Electromagnetic inspection of wire ropes using sensor arrays
[AD-A155412] 22 p3795 N85-33509

The design and analysis of single flank transmission error testor for loaded gears
[NASA-CR-176163] 23 p3937 N85-34404

TEST FACILITIES

NT ANECHOIC CHAMBERS
NT BLOWDOWN WIND TUNNELS
NT CASCADE WIND TUNNELS
NT CRYOGENIC WIND TUNNELS
NT ENVIRONMENTAL LABORATORIES
NT HYDRAULIC TEST TUNNELS
NT HYPERSONIC WIND TUNNELS
NT LOW SPEED WIND TUNNELS
NT ROCKET TEST FACILITIES
NT SLOTTED WIND TUNNELS
NT SUBSONIC WIND TUNNELS
NT SUPERSONIC WIND TUNNELS
NT TEST RANGES
NT TEST STANDS
NT TRANSONIC WIND TUNNELS
NT WIND TUNNELS

Aeronautical systems technology needs: Escape, rescue and survival, test facilities and test equipment and training-simulation equipment
[AD-A145059] 01 p0001 N85-10002

Characteristics of controlled-oscillating annular cascade test facility with Freon gas
[NAL-TR-812] 01 p0003 N85-10014

Evaluation of hollow fiber ultrafiltration as a pretreatment for reverse osmosis desalinaton of seawater
[PB84-212406] 01 p0026 N85-101

The NBS tri-directional test facility
[PB84-217462] 01 p0051 N85-1033

HOST liner cyclic facilities: Facility description
02 p0146 N85-10

Atmospheric and pressurized low speed wind tunnel performance and cost comparisons
[ARL/AERO-R-160] 02 p0149 N85-110

Performance of a large area flash chamber prototype
[NOTA-INTERNA-807] 02 p0201 N85-112

Accelerated stress facility 1976-1983
[AD-A146101] 03 p0359 N85-12

Space power distribution system technology. Volume 3: Test facility design
[NASA-CR-171230] 04 p0463 N85-12

Calibration and use of filter test facility orifice plates
[DE84-016851] 04 p0500 N85-1319

The European Space Tribology Laboratory (ESTL) activities report
[ESA-ESTL-61] 05 p0646 N85-1414

Measuring system and data evaluation methods of the test field for wind energy units at Pellworm
05 p0668 N85-142

High pressure combustion test facility for gas turbine research
[NAL-TR-801] 06 p0757 N85-14

Heat transfer results and operational characteristics of the NASA Lewis Research Center Hot Section Cascade Test Facility
[NASA-TM-86890] 06 p0808 N85-1513

Advanced mass spectrometers for hydrogen isotope analyses
[DE85-000716] 06 p0811 N85-1515

Visibility monitoring in the southern California desert for the Department of Defense: Research on operations-limiting visual extinction, RESOLVE protocol
[AD-A146617] 06 p0835 N85-15315

The Western Aeronautical Test Range of NASA Ames Research Center
[NASA-TM-85924] 07 p0909 N85-157

Facility safety study
[NASA-CR-174280] 07 p0910 N85-157

Equipment for preflight test of an Electronic Countermeasures (ECM) avionic system
07 p0939 N85-15

National Bureau of Standards passive solar test facility: instrumentation and site handbook
[PB85-100451/GAR] 07 p0968 N85-161

Langley Mach 4 scramjet test facility
[NASA-TM-86277] 08 p1069 N85-16

Electronics systems test laboratory testing of shuttle communications systems 08 p1101 N85-16

Sensitiveness and explosiveness assessment at Perme Waltham Abbey 08 p1115 N85-170

On the frontier: Flight research at Dryden 1946-19
[NASA-SP-4303] 09 p1263 N85-17

Activities at Mil Experimental Design Bureau
09 p1278 N85-18

High pressure combustion test facility for gas turbine research
[NAL-TR-801] 09 p1283 N85-18

NASA-VCOSS dynamic test facility
[NASA-TM-86491] 10 p1427 N85-18

Ground test experiment for large space structures
[NASA-TM-86489] 10 p1429 N85-190

Theory versus experiment for the rotordynamic coefficients of annular gas seals. Part 1: Test facility and apparatus
[NASA-CR-174409] 10 p1491 N85-194

Facilities for studing radiation damage in nonmetals during irradiation
[DE85-000590] 10 p1554 N85-198

New air supply-prime mover facility for engine tests detailed 11 p1621 N85-20

Use of laser flow visualization techniques in reactor component thermal-hydraulic studies
[DE84-014768] 11 p1639 N85-20330
Major facilities for materials research and related disciplines
[PB85-106850] 11 p1739 N85-20934
A history of full-scale testing of aircraft structures at the National Aeronautical Establishment
[NAE-AN-24] 12 p1777 N85-21153
Heat Cycle Research Experimental Program report, FY-84
[DE85-003558] 12 p1882 N85-21811
AIRLAB: A laboratory for flight-crucial-electronics system research 13 p1968 N85-22362
Activities of the Jet Propulsion Laboratory, 1 January - 31 December 1983
[NASA-CR-175555] 13 p2167 N85-23447
Electric vehicle test program: INEL transition qualification test plan
[DE85-005171] 13 p2169 N85-23456
Welcome to the Saclay Propeller Testing Center
[NASA-TM-77648] 14 p2225 N85-23799
Dynamic verification of large space structures
14 p2234 N85-23847
Modifications to the nozzle test chamber to extend nozzle static-test capability
[NASA-TM-86368] 15 p2464 N85-25216
The design and construction of a flow channel and rig for corrosion studies
[AERE-M-3455] 15 p2508 N85-25474
French consulting firm develops own robotics
15 p2535 N85-25642
Parameterization of a transient electromagnetic facility and test antennas from transient data
[DE85-006231] 15 p2545 N85-25710
Influence of surface roughness on compressor blades at high reynolds number in a two-dimensional cascade
[AD-A151655] 15 p2557 N85-25777
Space reactor ground tests, assessment of facility needs
[DE85-006814] 15 p2650 N85-26345
An assessment of the suitability of the BHGA structural test rig for aerodynamic testing of hang gliders
[CA-8506] 17 p2896 N85-27853
Rotorcraft research testing in the National Full-Scale Aerodynamics Complex at NASA Ames Research Center
[NASA-TM-86687] 17 p2896 N85-27854
Experience with oepration of a large magnet system in the international fusion superconducting magnet test facility
[DE85-009288] 17 p3027 N85-28721
An Impurity Control Test Facility (ICTF) for the study of fusion reactor/plasma edge materials
[DE85-007946] 17 p3040 N85-28810
Research test facility for evaporation and combustion of alternative jet fuels at high air temperatures
[AD-A153630] 18 p3083 N85-29073
New technologies to improve laboratory testing
[DE85-008151] 18 p3110 N85-29257
Operation of HFTF to test the MIT 12 T coil
[DE85-010409] 18 p3195 N85-29621
The DREO (Defence Research Establishment Ottawa) Inertial Navigation Laboratory: Development and test capabilities
[AD-A154425] 19 p3216 N85-29945
Opacity control technique for jet engine test cells
[AD-D011668] 19 p3220 N85-29968
Air Force bid sample testing 20 p3437 N85-31323
MFTF-(alpha) + T shield design
[DE85-010496] 20 p3529 N85-31948
Simulation of automatic control of MFTF-B neutral beams
[DE85-010640] 20 p3530 N85-31960
MHD generator CDIF
[DE85-011389] 20 p3536 N85-32001
Decomposition of sulfuric acid using solar thermal energy
[DE85-012288] 21 p3564 N85-32170
Georgetown University Photovoltaic Higher Education National Exemplar Facility (PHENEF)
21 p3607 N85-32400
Low temperature experimental capability for use with gas guns
[DE65-010418] 22 p3801 N85-33548
Description of a test site for large-scale heavy gas dispersion and combustion experiments
[DE85-004987] 23 p3911 N85-34231
The 1984 biotic studies of Yucca Mountain, Nevada test site, Nye County, Nevada
[DE85-011715] 23 p3951 N85-34487
Design and testing of an energy-absorbing crewseat for the F/FB-111 aircraft. Volume 2: Data from seat testing
[NASA-CR-3917] 24 p4084 N85-35184
A study of the control of particulate emissions from turbine engine test cells 24 p4067 N85-35205

TEST FIRING
NT STATIC FIRING
A metallographic investigation of rotating bands for 7.5 cm artillery projectiles
[FOA-C-20551-D2] 07 p0929 N85-15888
Using a data base management system for modelling SSME test history data 12 p1944 N85-22211
Detonation velocity measurements of the explosives Detasheet C and Amatol
[AD-A152298] 16 p2757 N85-27015
Use of the computer programa PARA 80 to study results from firing the railgun ERGS-1M
[MRL-R-900] 22 p3738 N85-33167
A 1984 environmental summary: Sandia National Laboratories Tonopah Test Range, Tonopah, Nevada
[DE85-011145] 22 p3812 N85-33612

TEST RANGES
The Western Aeronautical Test Range of NASA Ames Research Center
[NASA-TM-85924] 07 p0909 N85-15756
A 1984 environmental summary: Sandia National Laboratories Tonopah Test Range, Tonopah, Nevada
[DE85-011145] 22 p3812 N85-33612

TEST STANDS
DFVLR rotorcraft: Construction and engineering
[NASA-TM-77740] 01 p0006 N85-10035
HOST liner cyclic facilities: Facility description
02 p0146 N85-10986
Possibilities of increasing the simulation quality of multiaxial test stands — vehicle testing
05 p0649 N85-14169
Synthesis of load-time histories resulting from statistical analysis 05 p0650 N85-14171
A tracked vehicle test plant for the simulation of dynamic operation
[AD-P004305] 09 p1410 N85-18882
The detonation of aerosols and vapors of combustible substances under controlled conditions. Part 1: Construction of a test installation
[ISL-R-109/83-PT-1] 14 p2254 N85-23966
Test devices for aeronautical research and technology
[NASA-TM-77651] 17 p2905 N85-27914
Data processing on the rotor test stand at DFVLR in Brunswick: Microprogrammable interfaces and array processor as key components in a PDP 11 real time data acquisition and processing system
[DFVLR-MITT-85-03] 17 p2906 N85-27921
Comparison of simulation with experiment in an RFQ
[DE85-010770] 19 p3349 N85-30757
The design and analysis of single flank transmission error testor for loaded gears
[NASA-CR-176163] 23 p3937 N85-34404

TEST VEHICLES
NT FLIGHT TEST VEHICLES
Energy efficient engine ICLS Nacelle detail design report
[NASA-CR-167870] 02 p0146 N85-10993
A functional vehicle for autonomous mobile robot research
[AD-A150052] 12 p1860 N85-21666
Test plan for performance testing of the Eaton AC-3 electric vehicle
[DE85-011954] 23 p3927 N85-34341

TESTERS
U TEST EQUIPMENT

TESTING
U TESTS

TESTING MACHINES
U TEST EQUIPMENT

TESTS
Experiments on the influence of active walls on the initial amplitudes and growths of instability waves
[AD-A154630] 21 p3583 N85-32275

TETHERED BALLOONS
Preliminary investigation of the electrodynamics of a conducting tether 13 p1997 N85-22521

TETHERED SATELLITES
Proceedings of a Workshop on Applications of Tethers in Space, Executive Summary
[NASA-CR-171195] 03 p0322 N85-12075
Proceedings of a Workshop on the Applications of Tethers in Space, Volume 1
[NASA-CR-171196] 03 p0322 N85-12076
Proceedings of a Workshop on Applications of Tethers in Space, Volume 2
[NASA-CR-171197] 03 p0322 N85-12077
Global matrix of thermospheric density values for selected solar/geomagnetic conditions and spacecraft orbital attitudes
[NASA-TM-86478] 04 p0533 N85-13409
Electrodynamic tethers. 1: Power generator in LEO. 2: Thrust for propulsion and power storage
05 p0611 N85-13901
The investigation of tethered satellite system dynamics
[NASA-CR-171278] 07 p0912 N85-15772
Investigation of dynamic noise affecting geodynamics information in a tethered subsatellite
[NASA-CR-174292] 08 p1174 N85-17405
Applications of Tethers in Space, volume 1
[NASA-CP-2364] 11 p1642 N85-20339
Tethers open new space options
11 p1642 N85-20340
Tethered satellite system project overview
11 p1642 N85-20341
Shuttle tethered satellite system program overview
11 p1642 N85-20342
TSS Satellite overview 11 p1642 N85-20343
Satellite module design 11 p1642 N85-20344
Tether fundamentals 11 p1643 N85-20345
Science Applications, part 1 11 p1643 N85-20346
Science Applications, part 2 11 p1643 N85-20347
Transportation applications, part 2
11 p1643 N85-20350
Technology and test 11 p1643 N85-20353
Summary presentation of the Science Applications Panel 11 p1644 N85-20355
Summary presentation of the technology and test panel 11 p1644 N85-20360
Applications of Tethers in Space, volume 2
[NASA-CP-2365] 11 p1644 N85-20361
Space science and applications
11 p1644 N85-20362
Report of the Electrodynamic Interactions Panel
11 p1645 N85-20363
Report of the Technology and Test Panel
11 p1646 N85-20370
Pultrusion process for fabrication of tethers (preliminary concepts) 11 p1646 N85-20371
Instrumentation for Application Number 1: Mass spectrometric analysis of the boundary layer associated with the tethered satellite 11 p1646 N85-20372
Application Number 3: Using tethers for attitude control 11 p1646 N85-20373
Study proposal for the possible use of ISS as an aerodynamic facility for aerospace applications
11 p1646 N85-20374
Transport processes in the upper atmosphere
11 p1646 N85-20375
Applications of Tethers in Space
[NASA-CP-2366] 12 p1859 N85-21659
Excitation of low-frequency plasma waves by a conducting, tethered satellite 13 p2171 N85-23470
The investigation of tethered satellite system dynamics
[NASA-CR-171433] 15 p2492 N85-25375
The investigation of tethered satellite system dynamics
[NASA-CR-175855] 16 p2731 N85-26854
Shuttle-tethered satellite system definition study extension
[NASA-CR-171473] 17 p2907 N85-27923
Shuttle-tethered satellite system definition study. Volume 1: Executive study
[NASA-CR-171474] 17 p2907 N85-27924
Dynamics and control of tethers in elliptical orbits
20 p3399 N85-31087
Shuttle Molecular Gun: Smog. Potential experiment for the electrodynamic Tethered Satellite System (TSS) mission
[IFSI-84-17] 20 p3419 N85-31221
Investigation of dynamic noise affecting geodynamics information in a tethered subsatellite
[NASA-CR-176031] 20 p3476 N85-31602
Recoverable Plasma Diagnostics Package (RPDP)
23 p3902 N85-34167
Electrodynamic tether 23 p3902 N85-34168
The investigation of tethered satellite system dynamics
[NASA-CR-176180] 24 p4069 N85-35215

TETHERING
Selected tether applications in space: An analysis of five selected concepts
[NASA-CR-171222] 04 p0460 N85-12921
Propellant transfer: Tethered depot
08 p1108 N85-17006
Applications of Tethers in Space, volume 1
[NASA-CP-2364] 11 p1642 N85-20339
Tethers open new space options
11 p1642 N85-20340
Electrodynamic interactions 11 p1643 N85-20348
Transportation applications, part 1
11 p1643 N85-20349
Physiological considerations of artificial gravity
11 p1643 N85-20351
Constellations 11 p1643 N85-20352
Where are we going in tethers
11 p1644 N85-20354

Summary presentation of the Science Applications Panel 11 p1644 N85-20355
Summary presentation of the Electrodynamics Interactions Panel 11 p1644 N85-20356
Summary presentation of the Transportation Panel 11 p1644 N85-20357
Summary presentation to the Artificial Gravity Panel 11 p1644 N85-20358
Summary presentation of the Constellations Panel 11 p1644 N85-20359
Summary presentation of the technology and test panel 11 p1644 N85-20360
Report of the Transportation Panel 11 p1645 N85-20364
Report of the Artificial Gravity Panel 11 p1645 N85-20365
Physiological considerations of artificial gravity 11 p1645 N85-20366
Artificial gravity: Tethers and containers 11 p1645 N85-20367
Report of the Constellations Panel 11 p1645 N85-20368
Some aspects of attitude stability of tethered space stations 11 p1646 N85-20369
The Satellite sail 11 p1647 N85-20376
A functional vehicle for autonomous mobile robot research [AD-A150052] 12 p1860 N85-21666
Selected tether applications in space: Phase 2. Executive summary [NASA-CR-171421] 13 p1987 N85-22462
Selected tether applications in space: Phase 2 [NASA-CR-171422] 13 p1987 N85-22463
Preliminary assessment of power-generating tethers in space and of propulsion for their orbit maintenance 13 p1997 N85-22520
Preliminary investigation of the electrodynamics of a conducting tether 13 p1997 N85-22521
Attitude control tradeoff study between the use of a flexible beam and a tether configuration for the connection of two bodies in orbit 20 p3412 N85-31174
The role of tethers on space station [NASA-TM-86519] 23 p3900 N85-34154

TETHERLINES
Electrodynamic tethers. 1: Power generator in LEO. 2: Thrust for propulsion and power storage 05 p0611 N85-13901
Tether fundamentals 11 p1643 N85-20345
Pultrusion process for fabrication of tethers (preliminary concepts) 11 p1646 N85-20371
Applications of Tethers in Space [NASA-CP-2366] 12 p1859 N85-21659
Stratospheric ClO: In-situ detection with a new approach 16 p2824 N85-27416
Shuttle-tethered satellite system definition study. Volume 1: Executive study [NASA-CR-171474] 17 p2907 N85-27924
Non-backdriveable free wheeling coupling [NASA-CASE-MSC-20475-1] 18 p3116 N85-29290
Dynamics and control of tethers in elliptical orbits 20 p3399 N85-31087

TETRACHLOROMETHANE
U CARBON TETRACHLORIDE

TETRAGONS
NT RECTANGLES

TETRAHYDROFURAN
Development of a lithium secondary battery separator 20 p3444 N85-31378

TETRANITROTETRAZACYCLOOCTANE
U HMX

TETROONS
U SUPERPRESSURE BALLOONS

TEXAS
Hurricane Alicia, Galveston and Houston, Texas, 17-18 August 1983 [PB84-237056] 04 p0541 N85-13441
Stratigraphy of early ordovician El Paso group of the southern Hueco Mountains, Hudspeth County, Texas 09 p1353 N85-18510
On the formation of the nocturnal coastal surface wind speed maximum 09 p1356 N85-18528
Radioactive waste isolation in salt: Peer review of the Office of Nuclear Waste Isolation's report on the organic geochemistry of deep groundwaters from the Palo Duro Basin, Texas [DE85-001439] 10 p1556 N85-19811
Analysis of SMIRR data for volcanic and sedimentary terrains of the trans-Pecos region, Texas 13 p2197 N85-23626
Report on regional groundwater flow modeling for the Palo Duro Basin, Texas [DE85-007490] 16 p2815 N85-27370
Surface hydrologic characteristics of proposed repository locations in the Palo Duro Basin of the Texas Panhandle [DE85-010530] 18 p3126 N85-29355

TEXTILES
Improved uniformity of viscous textile fibers obtained by altering drying procedures 06 p0762 N85-14871
Synthesis of antimicrobial chemical fibers and fibrous materials containing quaternary ammonium compounds and their utilization 06 p0762 N85-14872
Preparation of fire-resistant infusible polycaproamide fiber 06 p0763 N85-14877
Ceramic fabric material testing [DE84-012014] 09 p1300 N85-18165
Italy invents robot to compete with Asea, Hitachi 15 p2535 N85-25643
Substitution of asbestos by aramid fibers and fiber blends in industrial textiles and composites with organic binders [BMFT-FB-T-85-006] 23 p3920 N85-34294
Re-designing a mechanism for higher speed: A case history from textile machinery 23 p3923 N85-34310
A versatile computer package for mechanism analysis 23 p3924 N85-34314

TEXTS
Formats for numerical and textual data in data processing [DFVLR-MITT-84-07] 04 p0551 N85-13504
Electronic generation of text for television [BBC-RD-1984/14] 13 p2053 N85-22856
The acquisition of procedures from text. A production-system analysis of transfer of training [AD-A151029] 14 p2392 N85-24732
A network-based approach to text handling for the online scientific community 15 p2664 N85-26444
NAPGEN: Automatic NAPLPS page generator 23 p3964 N85-34575

TEXTURES
Visual representations subserving texture perception [AD-A145412] 02 p0236 N85-11538
Ion contrasting chamber for discrimination of grains and textures [BMFT-FB-T-84-151] 04 p0477 N85-13036
Late oligocene gabbro near Ketchikan, southeastern Alaska 04 p0518 N85-13307
Microstructure, texture and formability of thin aluminium sheets 06 p0798 N85-15068
Size dependence of chondrule textural types 06 p0882 N85-15606
Texture classification using autoregressive filtering 07 p0984 N85-16254
A wind-tunnel study of the saltation of heterogeneous (size, density) sands 08 p1182 N85-17449
Optical flow and texture variables useful in detecting decelerating and accelerating self-motion [AD-A148718] 09 p1384 N85-18703
Microwave remote sensing of soil moisture 13 p2125 N85-23235
Low altitude texture comparison data base and smooth shaded texture [AD-A150342] 13 p2146 N85-23323
Textural transformations taking place during heat and mechanical treatment in triplex steels [BLL-BISI-TRANS-22404-(9022.06)] 17 p2927 N85-28063
Texture perception and shape from texture [AD-A154276] 19 p3336 N85-30672

TF-34 ENGINE
Nonlinear global stability analysis of compressor stall phenomena [NASA-CR-174906] 19 p3219 N85-29960

TFX AIRCRAFT
U F-111 AIRCRAFT

THAILAND
Ex-minister urges communications satellite development 10 p1476 N85-19316
Communications satellite needs examined 10 p1476 N85-19317
Satellite-computer interface 10 p1476 N85-19318

THALAMUS
Influence of limboreticular complex on some reactions of rabbits 19 p3326 N85-30607

THALLIUM
Abundancies of Ni, Cr, CO and major elements in the silicate portion of the Moon: Constraints from primary lunar magmas 04 p0582 N85-13720

THAWING
U MELTING

THEMATIC MAPPING
Evaluating effectiveness of using space information in specialized hydrogeological research 02 p0164 N85-11114
Technological approach to automation of specialized processing of survey data 02 p0165 N85-11118
Relationships between grass canopy characteristics and LANDSAT Thematic Mapper bands 02 p0213 N85-11402
The Multispectral Imaging Science Working Group. Volume 1: Executive summary [E85-10001] 02 p0213 N85-11404
The Multispectral Imaging Science Working Group. Volume 2: Working group reports [E85-10002] 02 p0213 N85-11405
Geographic science: Executive summary 02 p0214 N85-11408
Geographic science 02 p0214 N85-11409
Land use/land cover 02 p0214 N85-11410
Geomorphology 02 p0214 N85-11411
Cartography 02 p0214 N85-11412
A prospectus for Thematic Mapper research in the Earth sciences [E85-10003] 02 p0215 N85-11416
Executive report: Results of the IRGA-CNPq/INPE experimental project [E85-10011] 02 p0216 N85-11424
Remote sensing applied to forest resources [E85-10012] 02 p0216 N85-11425
A report on the training course at Fortaleza (Ceara) [E85-10013] 02 p0216 N85-11426
Basic principles, methodology, and applications of remote sensing in agriculture [E85-10016] 02 p0217 N85-11429
Mapping land use changes in the carboniferous region of Santa Catarina, report 2 [E85-10017] 02 p0217 N85-11430
Remote sensing applications program [E85-10022] 02 p0218 N85-11435
Application of digital analysis of MSS to agro-environmental studies [E85-10024] 02 p0218 N85-11437
Thematic mapping of likely target areas for the occurence of cassiterite in the Serra do Mocambo (GO) granitic massifs using LANDSAT 2 digital imaging [E85-10027] 02 p0219 N85-11440
The mapping of the Sun at 8 mm wavelength and tracking of the active regions in the period 23 May - 5 June 1983 [REPT-S-149] 02 p0297 N85-11904
Assessment of computer techniques for processing digital LANDSAT MSS data for lithological discrimination of Serra do Ramalho, State of Bahia [E85-10033] 03 p0378 N85-12412
LANDSAT instruments characterization [E85-10029] 05 p0654 N85-14199
Integration of multiple thematic data with LANDSAT data: Some results about the feasibility of Mediterranean land cover inventories 05 p0655 N85-14205
The integrated use of digital cartographic data and remotely sensed imagery 05 p0655 N85-14209
Monitoring and mapping global vegetation cover using data from meteorological satellites 05 p0656 N85-14211
Statistics and mapping of land uses by means of LANDSAT MSS imagery 05 p0657 N85-14219
The use of Thematic Mapper data for land cover survey 05 p0657 N85-14220
Metric evaluation of SAR-580 optical images for cartographic purposes 05 p0659 N85-14231
Combining Heat Capacity Mapping Mission (HCMM) LANDSAT and thematic map information into a unique high precision merged multichannel system – climatology 05 p0660 N85-14239
A field control methodology of remotely sensed data for statistical purposes: An example of SPOT simulated data in eastern Belgium — land use statistics 05 p0660 N85-14241
Evaluation of SIR-B imagery for geologic and geomorphic mapping, hydrology, and oceanography in Australia 08 p1146 N85-17229
Structural investigation of the Grenville Province by radar and other imaging and nonimaging sensors 08 p1147 N85-17237
Investigation of SIR-B images for lithologic mapping 08 p1148 N85-17241
Analysis of terrestrial conditions and dynamics [E85-10063] 08 p1174 N85-17401
Advanced technology for hydrographic mapping [FOA-C-30371-E1] 08 p1176 N85-17418
Analysis of data acquired by synthetic aperture radar and LANDSAT Multispectral Scanner over Kershaw County, South Carolina, during the summer season [E85-10071] 10 p1503 N85-19485
Study of spectral/radiometric characteristics of the Thematic Mapper for land use applications [E85-10075] 10 p1504 N85-19489
Spectroradiometric calibration of the Thematic Mapper and Multispectral Scanner system [E85-10077] 10 p1504 N85-19491
Thematic Mapper: Design through flight evaluation [E85-10078] 10 p1504 N85-19492
LANDSAT-4 Science Characterization Early Results. Volume 2, part 1: Thematic Mapper (TM) [E85-10068] 11 p1668 N85-20508
An overview of LANDSAT-4 and the Thematic Mapper 11 p1668 N85-20509

Radiometric calibration and processing procedure for reflective bands on LANDSAT-4 protoflight Thematic Mapper 11 p1668 N85-20510

An overview of the Thematic Mapper geometric correction system 11 p1668 N85-20511

TM digital image products for applications 11 p1668 N85-20512

Canadian plans for Thematic Mapper data 11 p1668 N85-20513

Characterization of radiometric calibration of LANDSAT-4 reflective bands 11 p1669 N85-20516

LANDSAT-4 Science Characterization Early Results. Volume 3, part 2: Thematic Mapper (TM) [E85-10069] 12 p1869 N85-21724

Thermal band characterization of the LANDSAT-4 Thematic Mapper 12 p1869 N85-21727

A preliminary assessment of LANDSAT-4 Thematic Mapper data — Windsor, Ontario and Medicine Hat areas, Canada 12 p1869 N85-21728

Preliminary evaluation of the radiometric calibration of LANDSAT-4 Thematic Mapper data by the Canada Centre for Remote Sensing 12 p1870 N85-21729

A preliminary analysis of LANDSAT-4 Thematic Mapper radiometric performance 12 p1870 N85-21730

A preliminary evaluation of LANDSAT-4 Thematic Mapper data for their geometric and radiometric accuracies 12 p1871 N85-21739

Spatial resolution estimation of LANDSAT-4 Thematic Mapper data 12 p1872 N85-21741

An analysis of the high frequency vibrations in early Thematic Mapper scenes 12 p1872 N85-21742

Tests of low-frequency geometric distortions in LANDSAT 4 images 12 p1872 N85-21744

Investigation of TM band-to-band registration using the JSC registration processor 12 p1872 N85-21745

Geodetic accuracy of LANDSAT 4 Multispectral Scanner and Thematic Mapper data 12 p1873 N85-21746

Investigations of vegetation and soils information contained in LANDSAT Thematic Mapper and Multispectral Scanner data [E85-10082] 12 p1873 N85-21747

Remote sensing research for agricultural applications — San Joaquin County, California and Snake River Plain and Twin Falls area, Idaho [E85-10090] 12 p1873 N85-21752

LANDSAT 4 band 6 data evaluation [E85-10093] 12 p1874 N85-21755

Spectroradiometric calibration of the Thematic Mapper and Multispectral Scanner system [E85-10094] 12 p1874 N85-21756

LANDSAT 4 investigations of Thematic Mapper and Multispectral Scanner applications — Drum Mountains, Utah and Tonopath, Nevada [E85-10095] 12 p1874 N85-21757

Review of computer mapping and display techniques applicable to regional analysis [DE85-003545] 12 p1875 N85-21764

Experience in combined special mapping using space information 13 p1984 N85-22449

LANDSAT-4 Science Characterization Early Results. Volume 4: Applications — agriculture, soils land use, geology, hydrology, wetlands, water quality, biomass identification, and snow mapping [E85-10070] 13 p2117 N85-23186

Overview of TM applications research reports 13 p2117 N85-23187

Impact of Thematic Mapper sensor characteristics on classification accuracy — suburban Washington, D.C., Maryland, and the Chesapeake Bay 13 p2117 N85-23188

Analysis and evaluation of the LANDSAT-4 MSS and TM sensors and ground data processing systems: Early results 13 p2117 N85-23189

Characterization of LANDSAT-4 TM and MSS image quality for the interpretation of California's agricultural resources — Central Valley 13 p2118 N85-23190

Evaluation of Thematic Mapper performance as applied to hydrocarbon exploration — Ontario, Canada; Cement, Oklahoma; and Death Valley, California 13 p2118 N85-23191

Geologic utility of LANSDAT-4 TM data — Death Valley, California and the Silver Bell area of southern Arizona 13 p2118 N85-23192

An initial analysis of LANDSAT-4 Thematic Mapper data for the discrimination of agricultural, forested wetlands, and urban land cover — Poinsett County, Arkansas; and Reelfoot Lake and Union City, Tennessee 13 p2118 N85-23193

Preliminary evaluation of Thematic Mapper image data quality 13 p2118 N85-23194

Assessment of computer based geologic mapping of rock units in the LANDSAT-4 scene of northern Death Valley, California 13 p2119 N85-23195

A concept for the processing and display of Thematic Mapper data 13 p2119 N85-23196

Quick look analysis of TM data of the Washington, District of Columbia, area 13 p2119 N85-23197

Remote sensing of coastal wetlands biomass using Thematic Mapper wavebands — Lewes, Delaware 13 p2119 N85-23198

A preliminary comparison of the information content of data from the LANDSAT 4 Thematic Mapper and Multispectral Scanner — Arkansas 13 p2119 N85-23199

Early results of investigations of LANDSAT 4 Thematic Mapper and Multispectral Scanner applications — Washington, D.C. 13 p2119 N85-23200

Thematic Mapper data quality and performance assessment in renewable resources/agriculture/remote sensing 13 p2120 N85-23201

Preliminary comparisons of the information content and utility of TM versus MSS data 13 p2120 N85-23202

A first evaluation of LANDSAT TM data to monitor suspended sediments in lakes — Lake Chicot, Arkansas 13 p2120 N85-23204

Snow reflectance from Thematic Mapper 13 p2120 N85-23205

Preliminary evaluation of TM for soils information 13 p2121 N85-23206

Preliminary study of information extraction of LANDSAT TM data for a suburban/regional test site 13 p2121 N85-23208

Comparative techniques used to evaluate Thematic Mapper data for land cover classification in Logan County, West Virginia 13 p2121 N85-23209

Comparison of MSS and TM data for landcover classification in the Chesapeake Bay area: A preliminary report — Taylor's Island, Maryland 13 p2121 N85-23210

Comparison of land cover information from LANDSAT Multispectral Scanner (MSS) and airborne Thematic Mapper simulator (TMS) data for hydrologic applications — Clinton River Basin, Michigan 13 p2122 N85-23211

Relative accuracy assessment of LANDSAT-4 MSS and TM data for level 1 land cover inventory — Washington, D.C. 13 p2122 N85-23212

An investigation of several aspects of LANDSAT-5 data quality — Palmer County, Shelby, mt; White sands, NM; Great Salt Lake, UT; San Matted Bridge and Sacramento, California [E85-10096] 13 p2122 N85-23214

Studies on physical properties of snow based on multi channel microwave radiometer 13 p2125 N85-23231

Analysis of NIMBUS-7 SMMR data — Hokkaido, Japan snow cover 13 p2125 N85-23232

CNPq/INPE LANDSAT system: Report of activities from October 1, 1983 to September 30, 1984 — Brazil [E85-10097] 16 p2608 N85-27318

Shuttle imaging radar-A (SIR-A) data analysis — geology of the Ozark Plateau of southern Missouri, land use in western Illinois, and vegetation types at Koonamore Station, Australia [NASA-CR-175785] 16 p2609 N85-27324

Raster or vector processing. Experience with the application of programs for the construction of thematic maps with boundary design in the Lower Saxony (West Germany) Land Administration for ground research 16 p2615 N85-27365

Microcomputer processing of LANDSAT Thematic Mapper data for the acquisition of military tactical terrain data [AD-A154781] 21 p3605 N85-32389

Comprehensive mapping of arid territories of Arizona using space photography 22 p3737 N85-33164

How map designers can represent their ideas in thematic maps: Effective user interfaces for thematic map design 23 p3962 N85-34562

LANDSAT-4/5 image data quality analysis [E85-10105] 24 p4107 N85-35463

Study of spectral/radiometric characteristics of the Thematic Mapper for land use applications [E85-10106] 24 p4107 N85-35464

Geology and geomorphology of the Roraima group, southeastern Venezuela 24 p4115 N85-35511

THEODOLITES

Testing of a field portable GPS (Global Positioning System) geodetic receiver [AD-A148336] 08 p1082 N85-16859

Experience in use of optical theodolite for machine construction 14 p2267 N85-24049

THEOREM PROVING

Cores of tangent cones and Clarke's tangent cone [CSIR-TWISK-314] 01 p0108 N85-10727

Boundary behavior of analytic functions, analytic wave front sets and the intersection problem of Ehrenpreis [PREPRINT-809] 01 p0114 N85-10778

Simplified proofs of some basic theorems for quasiregular mappings 10 p1535 N85-19677

The Chinese remainder theorem and multi-PRF radars [AD-A141375] 13 p2054 N85-22656

THEOREMS

NT BAYES THEOREM
NT BERNOULLI THEOREM
NT DUALITY THEOREM
NT EQUIPARTITION THEOREM
NT EXISTENCE THEOREMS
NT FLOQUET THEOREM
NT GAUSS-MARKOV THEOREM
NT POYNTING THEOREM
NT RECIPROCITY THEOREM
NT SIMILARITY THEOREM
NT STOKES THEOREM (VECTOR CALCULUS)
NT UNIQUENESS THEOREM
NT VIRIAL THEOREM

Cores of tangent cones and Clarke's tangent cone [CSIR-TWISK-314] 01 p0108 N85-10727

A non-commutative quasi subadditive ergodic theorem [AD-A146810] 07 p1037 N85-16581

A theorem on the optimal allocation of effort [AD-A148028] 08 p1211 N85-17623

Signal reconstruction from Fourier transform sign information [AD-A148039] 08 p1211 N85-17624

Dynamics and control of general linear lumped-parameter systems 09 p1372 N85-18623

Computing the Kac determinant using dual mode techniques and more about the No-ghost theorem [DE85-001329] 09 p1375 N85-18640

Simplified proofs of some basic theorems for quasiregular mappings 10 p1535 N85-19677

Statistical analysis techniques for small sample sizes [NASA-CR-171872] 15 p2639 N85-26279

Extension of three theorems of Fourier series on the disc to the torus [AD-A153017] 17 p3019 N85-28669

Central limit theorems in the area of large deviations for some dependent random variables [AD-A153125] 17 p3043 N85-28631

Some relations among directions of curves at an invariant point on a thermodynamic phase diagram 19 p3312 N85-30530

A note on a theorem of R. Duffin [AD-A154786] 21 p3676 N85-32838

A system of magnetohydrodynamic-type equations 21 p3693 N85-32946

THEORETICAL PHYSICS

NT NEWTON THEORY
NT QUANTUM THEORY

Research program in theoretical high-energy physics [DE84-013717] 01 p0119 N85-10817

USSR report: Physics and mathematics [JPRS-UPM-84-006] 02 p0256 N85-11676

Research in elementary particle physics [DE84-013520] 02 p0279 N85-11815

Theoretical studies in tandem mirror physics [DE84-015634] 04 p0566 N85-13604

Activities report in nuclear physics 05 p0728 N85-14880

Testing theories of superluminal motion — QUASAT 07 p1058 N85-16714

Experimental and theoretical high energy physics [DE85-000844] 11 p1726 N85-20858

Theoretical nuclear physics [DE85-003466] 12 p1932 N85-22135

Research in theoretical physics [DE85-004286] 12 p1944 N85-22207

Theoretical aspects of electroweak and other interactions in medium-energy nuclear physics [DE85-003821] 13 p2157 N85-23392

Research in theoretical nuclear physics [DE85-006172] 14 p2418 N85-24920

Field near the front of a signal in a waveguide accomplished with dispersive plasma [REPT-11/1984] 16 p2768 N85-27083

Activities report in nuclear physics and particle acceleration 20 p3532 N85-31977

Bergson and the unification of the sciences [DE85-009961] 20 p3538 N85-32018

USSR report: Physics and mathematics [JPRS-UPM-85-004] 21 p3680 N85-32860

THEORIES

On the validation of computer science theories [AD-A148637] 08 p1203 N85-17572

THERAPY

NT CHEMOTHERAPY
NT RADIATION THERAPY

Influence of activation of ASFS-2 on human emotional status 08 p1194 N85-17522

Management of vibration sickness in coal mines by hyperbaric oxygenation 10 p1523 N85-19609

Comparative assessment of different treatment modalities in miners with vibration- and noise-induced disease 10 p1524 N85-19610

Management of microcirculatory disorders in vibration sickness 10 p1524 N85-19811
Modulated sinusoidal currents in management of vibration sickness 10 p1524 N85-19812
THERMAL ABSORPTION
Selective coatings for solar-to-thermal energy converters 14 p2280 N85-24127
Thickness-insensitive selective surface paint
[DE85-010566] 19 p3250 N85-30150
Heat-mass flow enhancement system for a metal hydride assembly
[DE85-010696] 22 p3763 N85-33441
THERMAL AGITATION
U THERMAL ENERGY
THERMAL ANALYSIS
Energy efficient engine combustor test hardware detailed design report
[NASA-CR-167945] 02 p0140 N85-10950
Simulation of solidification in a Bridgman cell
[NASA-CR-3843] 02 p0197 N85-11314
HIP glassmaking for high nitrogen compositions in the Y-Si-Al-O-N system
[DE84-015546] 03 p0336 N85-12175
An experimental investigation and numerical simulation of the thermomechanical phenomena in compressor rotor tip rubbing 03 p0367 N85-12352
Technical activities 1983, Office of Nondestructive Evaluation
[PB84-217074] 03 p0370 N85-12360
Accurate measurement of heat capacity by differential scanning calorimetry 04 p0468 N85-12975
Thermal and mechanical analysis of major components for the advanced adiabatic diesel engine
04 p0506 N85-13243
Special soft solder TK-3 (L-SnCu 3 - DIN 1707)
[BLL-T6364/BG/WH799/84(9022.48)]
06 p0767 N85-14907
Semicrystalline casting process development and verification 06 p0832 N85-15289
Reduction method for thermal analysis of complex aerospace structures
[NASA-TP-2373] 07 p0957 N85-16066
A critical analysis of ocean thermal analysis models in operation at FNOC (Fleet Numerical Oceanography Centers)
[AD-A148731] 09 p1359 N85-18547
Development of media for dynamic latent heat storage for the low-temperature range. Part 1: Thermal analyses of selected salt hydrate systems
[NASA-TM-77776] 10 p1507 N85-19510
Theoretical interpretation of thermal arrest data from differential thermal analysis measurements
12 p1949 N85-22241
Applications of high pressure differential scanning calorimetry to aviation fuel thermal stability research
[NASA-TM-87002] 14 p2249 N85-23941
NASTRAN's application in agricultural engineering
15 p2575 N85-25880
Analysis of physical-chemical processes governing SSME internal fluid flows
[NASA-CR-175893] 17 p2957 N85-28261
Electrical conductivity and phase diagram of binary alloys. 21: The system palladium-chromium
[NASA-TM-77863] 18 p3073 N85-29009
Binary phase diagram determinations
[DE85-010856] 19 p3235 N85-30058
Improved Nominal Operating Cell Temperature (NOCT) test procedure 21 p3612 N85-32449
THERMAL BATTERIES
Synthesis and properties of Hexachloromolybdates(5) and related species
[AD-A139599] 07 p0924 N85-15852
Thermal design requirements of a 50-kW zinc/redox flow battery for solar electrical energy storage
[DE84-017088] 09 p1345 N85-18463
Robotic thermal battery pellet fabrication
[DE85-007755] 16 p2779 N85-27154
Additional experiments relative to the shelf life of Li(Si)/FeS2 thermal batteries
[DE85-008482] 18 p3095 N85-29162
Burn front velocity as a function of pellet density in iron-potassium perchlorate heat powders
[DE85-011448] 21 p3572 N85-32214
THERMAL BLOOMING
Ground-up-to-Space (GUTS) laser propagation code description and manual
[AD-A150783] 14 p2309 N85-24295
Ship-to-ship propagation: Maritime data analyses
[AD-A155484] 21 p3592 N85-32325
THERMAL BOUNDARY LAYER
Qualification of the T2 wind tunnel in cryogenic operation. A: Thermal field, preliminary study of a schematic model
[NASA-TM-77781] 14 p2227 N85-23805
Structure of cold film in water-air boundary layer
14 p2335 N85-24443
THERMAL CONDUCTIVITY
Simulation of solidification in a Bridgman cell
[NASA-CR-3843] 02 p0197 N85-11314
Thermal conductivity of iron/potassium perchlorate heat powder
[DE84-017071] 04 p0476 N85-13035
Thermal conductivity and interface resistance of particle-filled silicone resin
[DE84-011681] 04 p0479 N85-13056
Insulating polymer concrete
[DE84-017239] 04 p0480 N85-13057
Geothermal studies in Alaska: Conditions at Prudhoe Bay 04 p0516 N85-13290
Thermal properties of soils and soils testing
[DE84-015312] 04 p0525 N85-13360
Megaregolith thickness, heat flow, and the bulk composition of the Moon 04 p0583 N85-13723
High temperature thermoelectric energy conversion
05 p0610 N85-13894
Thermal contact conductance measurements on Doublet 3 armor tile traphite
[DE8⁴-013554] 05 p0613 N85-13916
Thermal diffusivity and conductivity of chromium-manganese alloying compositions
[BLL-M-35925-(5828.4)] 05 p0616 N85-13938
Salt-gradient solar ponds: Summary of US Department of Energy sponsored research
[NASA-CR-174183] 05 p0667 N85-14286
Solar pond research at Argonne National Laboratory
05 p0667 N85-14291
Thermal conductivity of aluminum, copper, iron and tungsten for temperature from 1 K to the melting point
[PB84-235878] 06 p0770 N85-14924
Test your contacts by measuring their constriction resistance
[BLL-WH-611-(9091.9F)] 07 p0944 N85-15978
Analysis of the heating process of a body in a melt
[BLL-M-36014-(5828.4)] 07 p0956 N85-16057
Thermal evaporation in blast waves: A model for aneurism formation in the NRL (Naval Research Laboratory) LASER-HANE simulation experiment
[AD-A147006] 07 p0978 N85-16210
Computer program to compute soil thermal conductivity from transient temperature measurements
[PB85-100550] 07 p0996 N85-16341
Wave absorption and transport studies on Electron Cyclotron Resonance (ECR) heated stellarator plasmas in W 7-A
[IPF-84-9] 09 p1395 N85-18782
Transport properties of the outer crust of magnetic neutron stars 09 p1415 N85-18927
Analysis of compact heat exchanger performance
[DE84-012624] 10 p1485 N85-19377
Some specifics of methods for mass detailed studies of rock heat conductivity 10 p1502 N85-19477
U, Th, K content, heat production and thermal conductivity of Sao Paulo, Brazil continental shelf sediments: A reconnaissance work
[INPE-3401-PRE/670] 10 p1515 N85-19558
Generation of Alfven waves due to thermal modulation of the electrical conductivity
[AD-A149389] 10 p1558 N85-19826
Thickness effect in low-density insulation
[DE85-003065] 11 p1631 N85-20273
Theoretical and experimental analysis of vertical, concentric-tube ground-coupled heat exchangers
[DE85-000474] 11 p1633 N85-20286
Operational characteristics of the OMEGA short-wavelength laser fusion facility
[DE85-002819] 11 p1640 N85-20334
Temperature responses of composite panels
[AD-A150053] 12 p1798 N85-21277
Update of thermal conductivity and electrical resistivity of electrolytic iron, tungsten and stainless steel
[PB85-115814] 12 p1803 N85-21311
Simulation of thermal and electromagnetic processes in induction plasmatrons 12 p1841 N85-21552
Effect of variable solid phase thermal properties on propellant combustion 13 p2002 N85-22547
Thermally stimulated conductivity in semi-insulating gallium arsenide 13 p2088 N85-23036
Time resolved X-ray studies during pulsed laser irradiation of Ge
[DE85-005263] 13 p2097 N85-23083
Electrical and thermal transport property studies of high-temperature thermoelectric materials
[AD-A150167] 13 p2163 N85-23417
H-division materials physics progress
[DE85-004990] 13 p2165 N85-23430
Electrical and thermal transport property studies of high-temperature thermoelectric materials
[AD-A150900] 14 p2427 N85-24967
Transformation toughened ceramics: A potential material for light diesel engine applications
[AD-A151413] 15 p2518 N85-25525
Transformation toughened ceramics: A potential material for light diesel engine application
[AD-A151421] 15 p2518 N85-2552
Directional thermal conductivities of graphite-epoxy composites: 0/90 and 0/+ or - 45/90
[AD-A152209] 16 p2743 N85-26
Characterization-curing-property studies of HBRF 55A resin formulations
[NASA-CR-175836] 16 p2753 N85-26
Conducting a thermal conductivity survey
[NASA-CR-175792] 16 p2782 N85-2718
In situ Tuff water migration/heater experiment
[DE85-010415] 18 p3101 N85-292
Development of a high-temperature coolant for advanced diesel engines
[AD-A153680] 18 p3117 N85-292
Thermophysical properties correlations and pseudocomponent characterization parameter estimation for fossil fluids
[DE85-009297] 19 p3230 N85-3002
Clearing of polydisperse aqueous aerosol by laser radiation pulses 19 p3296 N85-3044
Approximate solution to the problem of heating massive bodies by radiation
[BLL-M-36272-(5828.4)] 20 p3450 N85-3142
Basic cryogenics and materials. Phase 1
[NASA-CR-177932] 21 p3572 N85-3221
In-situ measurement of wall thermal performance: Data interpretation and apparatus design recommendations
[DE85-011979] 21 p3586 N85-322
The design, construction and operation of a large-area, high-temperature, thermal conductance apparatus – furnace insulation
[NPL-DMA(A)-84] 22 p3786 N85-3345
The properties of thin-section, four-point-contact ball bearings in space 22 p3797 N85-3352
Development of improved thermoelectric materials for space nuclear power systems
[DE85-013079] 22 p3844 N85-33
Poly-functional building material from fiberglass (its fabrication and properties) 23 p3906 N85-34
Finding the roots of the transcendental equations in problems in determining the thermal conductivity of spheres with heterogeneous boundary conditions
[BLL-M-35878-(5828.4)] 23 p3929 N85-3434
Calculation of roots of transcendental equations in problems of determining thermal conductivity of cylinder with non-uniform boundary conditions
[BLL-M-35788-(5828.4)] 23 p3929 N85-343
Sequential regularization solution of the inverse heat conduction problem
[DE85-010657] 23 p3931 N85-343
Confinement experiments on ISX-B
[DE85-012346] 23 p3984 N85-347
THERMAL CONTROL COATINGS
Optimization of the NiCrAl-Y/ZrO-Y2O3 thermal barrier system
[NASA-TM-86905] 07 p0927 N85-158
Evaluation of colorless polyimide film for thermal control coating applications
[NASA-TM-86341] 07 p0930 N85-158
Challenges in the development of the orbiter active thermal control subsystem 08 p1096 N85-16
Thermal design of the space shuttle solid rocket booster 08 p1103 N85-16
Thermal design of the space shuttle external tank
08 p1103 N85-16
Space environment simulation to test satellite thermal control coatings, volume 1
[CERT-4128-VOL-1] 08 p1109 N85-17012
Space environment simulation to test satellite thermal control coatings. Volume 2: Annex 1
[ESA-CR(P)-1870-VOL-2] 08 p1109 N85-17013
Space environment simulation to test satellite thermal control coatings. Volume 2: Annexes 2, 3, 4
[ESA-CR(P)-1870-VOL-3] 08 p1109 N85-17014
An investigation of enhanced capability thermal barrier coating systems for diesel engine components
[NASA-CR-174820] 09 p1298 N85-18154
Antifriction properties of gas thermal coatings of clad carbine powders 10 p1447 N85-19115
Influence of temperature on wear resistance of detonation coatings of alloy powders
10 p1447 N85-19116
Method of determining thermal stability of heat-resistant coatings on graphite 10 p1447 N85-19117
Contactless determination of the conductivity of the white paint PCB-Z — Giotto spacecraft thermal control coating 14 p2243 N85-239
Rocket thrust chamber thermal barrier coatings
16 p2734 N85-26
Vacuum plasma coatings for turbine blades
16 p2734 N85-26
Erosion of corrosion-resistant surface treatments on alloy steels
[DE85-008446] 17 p2932 N85-28100

Advanced thermal barrier system bond coatings for use n Ni, Co-, and Fe-base alloy substrates
ASA-TM-87062] 20 p3431 N85-31283
Energy efficient engine, high pressure turbine thermal rrier coating. Support technology report
ASA-CR-168037] 24 p4066 N85-35199
RMAL CONVECTION
FREE CONVECTION
RMAL CURRENTS
CONVECTIVE FLOW
RMAL CYCLING TESTS
HOST instrumentation R and D program overview
02 p0141 N85-10957
Validation of structural analysis methods using the n-house liner cyclic rigs 02 p0146 N85-10987
HOST liner cyclic facilities: Facility description
02 p0146 N85-10988
Influence of thermal cycling on the behavior of CFRP aterial for space structures 05 p0626 N85-14013
In-flight evalution of LCF life consumption of critical rotor omponents subjected to high transient thermal stress
07 p0906 N85-15734
Ion implantation and laser processing of III-V compound emiconductors with applications to the fabrication of icrowave devices
[AD-A146846] 07 p1047 N85-16851
Damage to boron fibers during thermal cycling and nnealing 10 p1445 N85-19107
NASA welding assessment program
[NASA-CR-175512] 12 p1859 N85-21661
Change in microstructure of heat-resistant nickel alloys pon thermal cycling in a current of gas
13 p2031 N85-22725
The cyclic stress-strain behavior of nickel-base uperalloy poly- and single crystals
14 p2254 N85-23969
Rocket thrust chamber thermal barrier coatings
16 p2734 N85-26867
Downdraw extrusion of ULE(TM) glass
[AD-A153783] 18 p3079 N85-29048
Thermal-cycle testing of the G-tunnel heated block
[DE85-008408] 18 p3126 N85-29359
Effect of heating temperature in a vacuum on state of urface layers of welded OT4 titanium alloy
19 p3245 N85-30123
Electrical resistivity and hysteresis of the equiatomic nickel-titanium alloy near the martensitic transformation temperature 23 p3904 N85-34181
X-ray measurement of thermal stresses in tungsten fiber-copper composites 23 p3907 N85-34205
ERMAL DECOMPOSITION
NT PYROLYSIS
Fire retardant cellulosehydrate fibers
06 p0761 N85-14870
Critical analysis of nitramine decomposition data. Preliminary comments on autoacceleration and autoinhibition in HMX and RDX decomposition
[AD-A146570] 06 p0774 N85-14946
Description and operation of a thermal decomposition unit-gas chromatographic system
[PB84-246362] 07 p0968 N85-16146
Synthesis, static and reactive characterization of supported organometallics
[DE85-004285] 12 p1808 N85-21340
The use of hydrazine as an alternate source of energy
[NASA-CR-175535] 12 p1817 N85-21397
A computer controlled mass spectrometer system for investigating the decomposition of non-metallic materials under atmospheric conditions 12 p1948 N85-22237
Kinetics of mechanism of the thermal decomposition of dimethylnitramine and dimethylnitrosamine
13 p2004 N85-22559
Theory of relaxation processes in decomposing polymer materials during high-intensity convective heating
13 p2028 N85-22710
Metallic and metalloceramic coating by thermal decomposition
[NASA-TM-86992] 13 p2036 N85-22755
HERMAL DEFOCUSING
U THERMAL BLOOMING
HERMAL DEGRADATION
Thermal ageing studies of 9%Cr 1%Mo steel
[AERE-R-11109] 03 p0333 N85-12149
Liquid phase products and solid deposit formation from thermally stressed model jet fuels
[NASA-TM-86874] 04 p0481 N85-13066
Pathophysiological study of poisoning due to thermal degradation of materials — aircraft cabins
[CERMA-84-15] 11 p1692 N85-20640
Material thermolysis product toxicity: Definition of a hazard evaluation methodology
[CERMA-84-08] 11 p1692 N85-20641
Evaluation of infrared reflectance as a technique for measuring absorber materials degradation
[DE85-002171] 11 p1729 N85-20874
Laboratory studies of Kapton degradation in an oxygen ion beam 13 p1990 N85-22477
Structure-property relationships in polymeric matrix materials
[AD-A153929] 18 p3080 N85-29050
Absorber coatings degradation
[DE85-008628] 18 p3128 N85-29367
CP DDT detonators. 4: Thermal aging
[DE85-011172] 19 p3251 N85-30160
Photothermal degradation studies of encapsulants
21 p3608 N85-32403
Micromolecular modeling 21 p3608 N85-32405
THERMAL DIFFUSION
Stresses and strains in lithosphere caused by Earth's thermoconvective oscillations 06 p0822 N85-15217
Noncontact photo-thermal probe-beam deflection measurement of thermal diffusivity in an confined hot gas
[AD-A147481] 07 p0971 N85-16170
Analysis of performance of dynamic thermal diffusion chamber 21 p3642 N85-32625
A thermal diffusion chamber for the measurement of cloud condensation nuclei 21 p3642 N85-32627
THERMAL DIFFUSIVITY
Noncontact photo-thermal probe-beam deflection measurement of thermal diffusivity in an confined hot gas
[AD-A147481] 07 p0971 N85-16170
Optical beam deflection detection of thermal waves in opaque solids 19 p3374 N85-30927
Characterization of the optical and thermal properties of matter by photothermal techniques
[DE85-012607] 24 p4076 N85-35260
THERMAL DISSOCIATION
Jet fuel property changes and their effect on producibility and cost in the U.S., Canada, and Europe
[NASA-CR-174840] 16 p2757 N85-27012
THERMAL EFFECTS
U TEMPERATURE EFFECTS
THERMAL EFFICIENCY
U THERMODYNAMIC EFFICIENCY
THERMAL EMISSION
NT THERMIONIC EMISSION
Surface coatings for low emittance in the thermal surveillance band
[MRL-R-937] 03 p0336 N85-12156
Absorption and emission of EUV radiation by the local ISM 06 p0876 N85-15563
Exploration of the solar system by airborne astronomy
08 p1244 N85-17851
Continuous laminar smoke generator
[NASA-CASE-LAR-13014-1] 12 p1781 N85-21178
Hot spots on Io: Correlation of infrared emission and visible reflectance 13 p2172 N85-23475
Pressed boride cathodes
[NASA-TM-77821] 17 p2918 N85-27964
THERMAL ENERGY
Control and performance of a photovoltaic-thermal energy system 03 p0387 N85-12475
Possibilities of conjugating binary solutions for thermal energy storage
[DE84-016704] 04 p0531 N85-13392
Deputy Minister discusses plans for geothermal power
07 p0994 N85-16313
Electrodynamic interactions 11 p1643 N85-20348
Solar Thermal Research Program
[DE85-000514] 18 p3131 N85-29388
Advanced evacuated tube collectors
[DE85-010271] 19 p3274 N85-30302
Thermal Energy Storage Program annual operating plan FY 1985
[DE85-008745] 19 p3307 N85-30499
Decomposition of sulfuric acid using solar thermal energy
[DE85-012288] 21 p3564 N85-32170
Design and development of a linear thermal actuator
22 p3796 N85-33518
Study of alternative system conversions for the Solar One pilot plant
[DE85-010026] 22 p3609 N85-33594
Heat transfer coefficients for particles in liquid in axially rotating cans 24 p4093 N85-35370
THERMAL ENERGY STORAGE
U HEAT STORAGE
THERMAL ENVIRONMENTS
Thermal management technology status
05 p0610 N85-13895
In-flight testing of the space shuttle orbiter thermal control system 08 p1103 N85-16974
NASA welding assessment program
[NASA-CR-175683] 15 p2568 N85-25845
Thermal annealing of Fe implanted Al2O3 in oxidizing and reducing environment: Revised version
[DE85-007546] 16 p2752 N85-26963
The study of thermal forecasting for gliding
16 p2830 N85-27453
Downdraw extrusion of ULE(TM) glass
[AD-A153783] 18 p3079 N85-29048
Improved Nominal Operating Cell Temperature (NOCT) test procedure 21 p3612 N85-32449
Filament wound structures in PSP carbon composite
[RV10/84424] 22 p3743 N85-33198
A kinetic model for predicting oxidative degradation rates in combined radiation-thermal environments
[TI85-002629] 24 p4100 N85-35414
THERMAL EXPANSION
Self-similar expansion of dense matter due to heat transfer by nonlinear conduction
[MPQ-81] 01 p0046 N85-10297
Method for calculating linear shrinkage and expansion of metals and alloys
[BLL-M-35747-(5828.4)] 02 p0175 N85-11173
Thermal deformation measurements of heat-resistant structural materials for aircraft by electro optical displacement transducer
[NAL-TR-810] 03 p0325 N85-12092
Investigation of the relations between neat resin and advanced composite mechanical properties. Volume 1: Results
[NASA-CR-172303] 05 p0612 N85-13911
The dimensional stability of advanced composite antenna reflectors: Analytical and test evaluation --- satellite antennas 05 p0626 N85-14014
Thermal stress-dependent dilation of concrete
[DE84-014668] 11 p1653 N85-20412
Fracture mechanics evaluation of GaAs
[NASA-CR-175657] 13 p2102 N85-23101
Extreme precision antenna reflector study results
14 p2232 N85-23830
Density and thermal expansion measurements of several mixed oxide glasses in the solid and liquid regions
[DE85-006134] 14 p2261 N85-24014
Enhanced thermal-structural analysis by integrated finite elements
[AD-A151103] 15 p2636 N85-26258
Low-temperature thermal expansion of glass
15 p2645 N85-26315
Thermal expansion effects in electrical transport in amorphous metals
[AD-A152477] 17 p2930 N85-28089
Daze fasteners
[NASA-CASE-LAR-13009-1] 18 p3116 N85-29285
Thermal-cycle testing of the G-tunnel heated block
[DE85-008408] 18 p3126 N85-29359
Thermal expansion coefficients of a 30% glass fiber filled PEEK pyrotechnic charge holder
[DE85-010805] 19 p3251 N85-30155
Thermal expansion of selected graphite reinforced polyimide-, epoxy-, and glass-matrix composite
[NASA-TM-87572] 21 p3561 N85-32149
Temperature sensitivity of fiber-optic transmission line
22 p3764 N85-33331
Design and development of a linear thermal actuator
22 p3796 N85-33518
Hermetic chip carrier compliant soldering pads
[AD-D011722] 23 p3938 N85-34410
Search for acoustic signals from high energy cascades
[HE-7.1-1] 24 p4213 N85-36155
Experimental investigation of radiative-acoustic effects in the water by the thermodynamical conditions of Dumand
[HE-7.1-2] 24 p4213 N85-36156
Acoustic detection of air shower cores
[HE-7.1-4] 24 p4213 N85-36158
THERMAL FATIGUE
Stress corrosion of pressure vessel steel A533-B in high temperature water
[BLL-RISLEY-TR-4600-(9091.9F)]
03 p0330 N85-12125
Cumulative damage modeling of fatigue crack growth
07 p0907 N85-15741
Engine cyclic durability by analysis and material testing 07 p0907 N85-15744
Thermal-mechanical fatigue crack growth in Inconel X-750
[NASA-CR-174740] 07 p0927 N85-15877
Analytical and experimental investigation of rubbing interaction in labyrinth seals for a liquid hydrogen fuel pump — space shuttle main engine
[NASA-CR-174657] 09 p1287 N85-18084
Fatigue resistance of welded joints of high strength steels produced by electron beam welding
10 p1449 N85-19127
High-thermal-gradient superalloy crystal growth
17 p2814 N85-27366
Gas turbines: Operating conditions, material selection and development
[NLR-MP-83046-U] 20 p3395 N85-31062
Basic cryogenics and materials. Phase 1
[NASA-CR-177332] 21 p3572 N85-32215

THERMAL GRAVIMETRY
U THERMOGRAVIMETRY
THERMAL INSTABILITY
Ionospheric and magnetospheric modifications caused by VLF waves
[AD-A148210] 08 p1186 N85-17475
THERMAL INSULATION
Insulating polymer concrete
[DE84-017239] 04 p0460 N85-13057
Description of the insulation system for the Langley 0.3-Meter Transonic Cryogenic Tunnel
[NASA-TM-86274] 07 p0909 N85-15755
Thermal and mechanical properties of polyurethane foams and a survey of insulating concretes at cryogenic temperatures
[PB85-100949/GAR] 07 p0934 N85-15918
Thermal design of the space shuttle external tank
08 p1103 N85-16977
FRG ceramic engine components (PET)
08 p1141 N85-17193
A systems analysis of alternative concepts for aircrew cold weather clothing
[AD-A148805] 09 p1365 N85-18580
Insulation bonding test system
[NASA-CASE-MFS-25862-1] 11 p1610 N85-20126
Thickness effect in low-density insulation
[DE85-003065] 11 p1631 N85-20273
Envelope thermal test unit: Technical description
[DE84-012254] 11 p1674 N85-20548
Integrated insulation wall assembly — for a solid rocket motor case
[AD-D011553] 12 p1794 N85-21257
Environmental cycling of cellulosic thermal insulation and its influence on fire performance
[DE85-004295] 13 p2041 N85-22776
Development of a polystyrene insulation system
[DE85-006950] 16 p2784 N85-27180
Heat resistant sheathed insulated electrical conductors
[AD-D011644] 17 p2951 N85-28219
Ceramic coatings for heat engine materials: Status and future needs
[DE85-006759] 18 p3080 N85-29053
Ceramic coatings for heat engine materials
[DE85-005238] 18 p3080 N85-29054
Design and operation of solar thermal heat transfer systems
[DE85-009837] 19 p3267 N85-30263
Performance analysis of mixed passive solar heating systems
[DE85-009624] 21 p3613 N85-32455
The design, construction and operation of a large-area, high-temperature, thermal conductance apparatus — furnace insulation
[NPL-DMA(A)-84] 22 p3786 N85-33455
Carbon/carbon combustor external insulation
[AD-D011719] 23 p3910 N85-34224
High temperature structural insulating material
[DE85-006361] 23 p3920 N85-34291
SRB attach ring phenolic TPS fishtail seal evaluation tests
[NASA-CR-170887] 24 p4098 N85-35407
Study of NSI and related cable performance during tests performed in the NASA Hot Gas Facility
[NASA-CR-170886] 24 p4101 N85-35423
THERMAL MAPPING
Application of digital analysis of MSS to agro-environmental studies
[E85-10024] 02 p0218 N85-11437
Contributions to remote sensing : Applications of thermal infrared
[COMMUN-34/1984] 05 p0854 N85-14196
The need for integrating ground thermal measurements with thermal aircraft imagery 05 p0860 N85-14243
The use of principal components analysis techniques Nimbus-7 coastal zone color scanner data to define mesoscale ocean features through a warm humid atmosphere
[AD-A148567] 08 p1176 N85-17416
Examples of environment services: Hydrological and pollution measurements in the Po River (Italy)
[CISE-2209] 11 p1679 N85-20578
Evaluation of the radiometric quality of the TM data using clustering, linear transformations and multispectral distance measures — Illinois 12 p1870 N85-21731
Geologic interpretation of remote sensing data for the Martian volcano, Ascraeus Mons
13 p2194 N85-23608
Water-ice clouds on Mars: Location and seasonal variation 13 p2194 N85-23611
Proposed use of system ARGOS with data buoys for calibration of thermal infrared imagery of North British waters for sea surface temperature maps
14 p2240 N85-23889
Temperature anomalies above ore bodies
14 p2345 N85-24500
Comparison of measurement and simulation results of radiation temperatures applied to the thermal mapping of Munich
[DFVLR-FB-85-06] 17 p2964 N85-28442
Modeling of geothermal systems
[DE85-012553] 23 p3943 N85-34439
THERMAL NEUTRONS
Method and apparatus for determining the content and distribution of a thermal neutron absorbing material in an object
[DE84-014319] 01 p0117 N85-10801
Fine structure analysis with thermal neutrons and development and construction of a multidetector system
03 p0422 N85-12686
Sputtering of gold irradiated with thermal neutrons
03 p0429 N85-12736
Two phases of neutron production in the POSEIDON plasma focus
[IPF-84-10] 09 p1395 N85-18783
Apparatus and method for identification of matrix materials in which transuranic elements are embedded using thermal neutron capture gamma-ray emission
[DE85-011659] 22 p3786 N85-33454
Properties of 10 (18)-10 (19)eV EAS at far core distance
[HE-4.7-3] 24 p4198 N85-36054
THERMAL NOISE
Realization of noise power in the microwave range by thermal noise standards 05 p0629 N85-14034
Adaptive antenna arrays for weak interfering signals
[NASA-CR-174336] 08 p1150 N85-17258
Mathematical model of discriminator for signals with fluctuations and thermal noise 13 p2072 N85-22943
An excitation mechanism for solar 5-minute oscillation of intermediate and high degree
14 p2444 N85-25065
THERMAL PLASMAS
Bremsstrahlung radiation from longitudinal plasma waves caused by subthermal electrons in plasma
02 p0264 N85-11730
Power law X- and gamma-ray emission from relativistic thermal plasmas 08 p1241 N85-17829
Physics of nonmagnetic relativistic thermal plasmas
09 p1386 N85-18715
Modeling thermal plasma material processing experiments
[DE85-001551] 10 p1560 N85-19638
Excitation of impurities by heavy particles and radiative losses of thermonuclear plasma
11 p1719 N85-20816
Plasma processing of materials
[AD-A152398] 17 p3039 N85-28800
Thermal ion heating in the vicinity of the plasmapause
[NASA-CR-176030] 20 p3535 N85-31993
A retarding ion mass spectrometer for the Dynamics Explorer-1
[NASA-CR-171588] 21 p3589 N85-32303
Integral representation for nonlinear heat transport
23 p3981 N85-34683
Synthesis of ultrafine ceramic and metallic powders in a thermal argon rf plasma
[DE85-009634] 23 p3983 N85-34696
THERMAL POWER
U TURBOGENERATORS
THERMAL PROPERTIES
U THERMODYNAMIC PROPERTIES
THERMAL PROTECTION
Testing of three different flight suits in fire environment — fuel fire
[FOA-C-59012-H1] 02 p0238 N85-11552
Verification tests of durable TPS concepts
[NASA-TM-86313] 03 p0323 N85-12085
Integral boost, heat protection, port covers and transition 07 p0918 N85-15813
Space Shuttle Technical Conference, part 2
[NASA-CP-2342-PT-2] 08 p1098 N85-16937
Thermal design of the space shuttle solid rocket booster 08 p1103 N85-16976
Orbiter thermal protection system
08 p1104 N85-16979
Rolls-Royce experience with thermal barrier coatings — in aircraft engines
[PNR-90222] 08 p1135 N85-17152
Process for preparing essentially colorless polyimide film containing phenoxy-linked diamines
[NASA-CASE-LAR-13353-1] 11 p1611 N85-20128
Study of outgassing and decomposition of space shuttle heat protection tiles, fillers and adhesive
[NASA-CR-175565] 12 p1791 N85-21242
Impacts of Space Shuttle thermal protection system tile on F-15 aircraft vertical tile
[NASA-TM-85904] 12 p1792 N85-21245
Process for preparing highly optically transparent-colorless armomatic polyimide film
[NASA-CASE-LAR-13351-1] 12 p1811 N85-21380
Electron beam charging of Space Shuttle thermal protection system tiles 13 p1990 N85-22478
National Space Transportation Systems Program mission report
[NASA-TM-87454] 14 p2242 N85-23696
Development of acceptance criteria for batches of silane primer for external tank thermal protection system bonding applications
[NASA-CR-171428] 14 p2259 N85-23898
Seven-wavelength pyrometer for determining surface temperature of ablation materials
[NASA-TM-77832] 14 p2305 N85-24288
Development of acceptance criteria for batches of silane primer for external tank thermal protection system bonding applications
[NASA-CR-171436] 15 p2518 N85-25523
Development of acceptance criteria for batches of silane primer for external tank thermal protection system bonding applications
[NASA-CR-175850] 16 p2754 N85-26985
Artificial and natural icing tests YEH-60A quick fix helicopter
[AD-A155147] 21 p3555 N85-32118
Experimental aerodynamic heating to simulated space shuttle tiles in laminar and turbulent boundary layers with variable flow angles at a nominal Mach number of 7
[NASA-TP-2307] 23 p3929 N85-34351
Upgrading auxiliary facility outleakage and combustion detection
[DE85-012796] 23 p3934 N85-34388
Investigation of experimental lightweight firewall materials for A/C engine bay applications
[AD-A155765] 24 p4062 N85-35175
Verification of the SRB motor case pin retainer band tips
[NASA-CR-170882] 24 p4070 N85-35220
SRB TPS closeout materials characterization
[NASA-CR-170885] 24 p4070 N85-35222
Results of tests of the SRB aft skirt heat shield curtain in the MSFC Hot Gas Facility
[NASA-CR-170888] 24 p4070 N85-35223
Results of tests of MTA-2 TPS on the SRB hold-down bolt blast container
[NASA-CR-170891] 24 p4070 N85-35224
SRB thermal protection systems materials test results in an arc-heated nitrogen environment
[NASA-CR-170881] 24 p4072 N85-35236
Results of tests of K5NA and a revised formulation of EPDM/cork patch material in MSFC Hot Gas Facility
[NASA-CR-170890] 24 p4073 N85-35238
Results of tests of weathered K5NA closeout material in the MSFC Hot Gas Facility
[NASA-CR-170893] 24 p4073 N85-35239
Evaluation of SRB phenolic TPS material made by an alternate vendor
[NASA-CR-170894] 24 p4073 N85-35240
Space shuttle SRB TPS protective paint test and evaluation in NASA Hot Gas Facility and AEDC Tunnel C
[NASA-CR-170884] 24 p4081 N85-35294
Results of tests of Insta-Foam Thermal Protection System (TPS) material for protection of equipment inside the SRB aft skirt
[NASA-CR-170892] 24 p4081 N85-35295
THERMAL RADIATION
Thick film radiation detector
[AD-D011211] 01 p0048 N85-10318
Infrared thermal radiation of Venus
02 p0163 N85-11101
Investigation of cloud feedback in the GLAS model
05 p0685 N85-14404
Modeling influence of three layer cloud cover on outgoing thermal radiation 06 p0825 N85-15242
The adsorption of CO and oxygen on Cu layers on a W(110) surface
[AD-A147345] 07 p0923 N85-15847
Support for the Naval Research Laboratory Passive Microwave Clutter Analysis Program
[AD-A146771] 07 p0939 N85-15951
Self-generated magnetic fields and thermal flux inhibition
[AD-A147405] 07 p0971 N85-16166
Thermal radiation hazards from Liquified Petroleum Gas (LPG) fireballs
[VTT-304] 09 p1293 N85-18132
Influence of aerosol on formation of outgoing thermal radiation 14 p2342 N85-24483
Lidar and radiometer observations of thunderstorm tops 15 p2595 N85-25994
Technique to reduce scattered light in optical systems
[AD-D011597] 18 p3185 N85-29752
Enhanced thermal coupling by a repetitively pulsed laser
[AD-A154435] 19 p3276 N85-30317

Nuclear thermal transmittance in the atmosphere using LOWTRAN-6 computer code
[AD-A154669] 21 p3630 N85-32553
Enhancing precision of remote temperature sensing data from satellites under cloudy atmospheric conditions
22 p3734 N85-33146
Instrumentation for sensing moisture content of material using a transient thermal pulse
[NASA-CASE-NPO-15493-2] 23 p3933 N85-34373
Fire research publications, 1984
[PB85-208502] 24 p4166 N85-35827

THERMAL RESISTANCE
Silicon nitride powder
[NASA-TM-77731] 01 p0022 N85-10132
Thermal conductivity and interface resistance of particle-filled silicone resin
[DE84-011681] 04 p0479 N85-13056
High specific heat dielectrics and Kapicza resistance at dielectric boundaries
[AD-A148476] 08 p1217 N85-17666
Vapor pressure and evaporation rate of certain heat-resistant compounds in a vacuum at high temperatures
[NASA-TM-77807] 10 p1434 N85-19036
Oxidation of PT-7M and OT4-1 titanium alloys in air
11 p1600 N85-20063
Thermal barrier coating system
[NASA-CASE-LEW-13324-2] 12 p1796 N85-21266
Fire resistant polymers based on 1-(diorgano oxyphosphonyl)methyl-2,4- and 2,6-diamino benzenes
[NASA-CASE-ARC-11512-2] 12 p1811 N85-21362
Fire and heat resistant laminating resins based on maleimido and citraconimido substituted 1-(diorgano oxyphosphonyl)methyl-2,4- and 2,6-diaminobenzenes
[NASA-CASE-ARC-11533-1] 12 p1812 N85-21364
Temperature-insensitive optical fibers
[AD-D011551] 12 p1933 N85-22142
Possibility of producing monolithic composite materials based on niobium carbide 13 p2028 N85-22707
System for forming and focusing high current beam of deuterium ions 13 p2045 N85-22798
Measurement of internal thermal resistance for quality control of semiconductor devices
13 p2074 N85-22953
Heat resistant Carbon Fiber Reinforced Plastics (CFRP) hardening equipment
[MBB/LFA33/CFK/PUB/007] 17 p2916 N85-27976
Dispersion-strengthened powder-metallurgical chromium steels
[BLL-BISI-TRANS-22323-(9022.06)]
17 p2929 N85-28081
Investigations of the material factors in the adiabatic shearing of steels
[AD-A153084] 17 p2979 N85-28418
A simple power meter for high energy pulsed lasers
[AD-D011661] 18 p3113 N85-29271
Thermodynamics of high temperature materials
[AD-A154269] 19 p3378 N85-30958
Solid-state resistance welding cylinders and spheres
[DE85-010064] 20 p3469 N85-31555
Investigation of experimental lightweight firewall materials for A/C engine bay applications
[AD-A155765] 24 p4062 N85-35175

THERMAL RESOURCES
NT GEOTHERMAL RESOURCES
NT GEYSERS
The United States Geological Survey in Alaska: Accomplishments during 1983
[USGS-CIRC-945] 23 p3948 N85-34468

THERMAL SHIELDING
U HEAT SHIELDING

THERMAL SHOCK
Thermal shock as a carbide grade development tool
[DE84-016939] 04 p0509 N85-13251
Impact of NDE unreliability on pressure vessel fracture predictions
[DE84-015586] 05 p0647 N85-14151
Computation of thermal shock-free straightening conditions for aluminum-magnesium alloy welded structures 10 p1449 N85-19131
Possibility of producing monolithic composite materials based on niobium carbide 13 p2028 N85-22707
Dispersed-metal-toughened alumina
[NASA-CR-174687] 13 p2037 N85-22758
Creep ratcheting simplified methods experience from structural design of elevated temperature components
[DE85-007433] 15 p2580 N85-25915

THERMAL SIMULATION
Simulation of the coupled atmospheric and oceanic boundary layer model during MILDEX
[AD-A155166] 21 p3655 N85-32705

THERMAL STABILITY
NT TEMPERATURE DEPENDENCE
Development of new and improved polymer matrix resin systems, phase 1
[NASA-CR-166595] 01 p0017 N85-10104
Heat treatment of welded joints in OT4 and VT20 titanium alloys 01 p0020 N85-10119
Stability of bromine intercalated graphite fibers
[NASA-TM-86859] 01 p0031 N85-10167
A new heat-resistant polymer from dimer diamine bismaleimide. Part 1: Preparation and free radical cure of dimer diamine bismaleimide
[AD-A145664] 02 p0186 N85-11247
External fuel vaporization study, phase 2
[NASA-CR-174079] 02 p0187 N85-11252
The KZD-85 engine test. Engine type: 1 cylinder, 2 stroke motor 2100 Husquarna
[FWE-FO-1717] 02 p0205 N85-11354
Study of application of organic semiconductors to electronic components
[BMFT-FB-T-84-142] 02 p0289 N85-11890
Reinforcement of molybdenum disilicide with nematic crystals of aluminum oxide 03 p0353 N85-12269
Construction of a bacterium to convert cellulose to ethanol
[TI84-901639] 04 p0481 N85-13068
Thermally stable thermoset resin compositions
[AD-D011274] 05 p0620 N85-13963
Structural design and thermal stability of TELE-X antenna tower 05 p0627 N85-14016
Vaporization behavior, phase equilibria, and thermodynamic stabilities of nickel phosphides
[AD-A146663] 06 p0765 N85-14697
Hazard Studies for Solid Propellant Rocket Motors
[AGARD-CP-367] 08 p1114 N85-17025
Heater block assembly for use in thermal oxidation testing of jet fuel
[AD-D011430] 08 p1123 N85-17077
Phase formation and stability in the pseudobinary Ni3Al-Ni3V alloy system
[DE85-001117] 09 p1296 N85-18143
Strength and failure of ceramic-metallic material
10 p1446 N85-19112
Method of determining thermal stability of heat-resistant coatings on graphite 10 p1447 N85-19117
Study of advanced fuel system concepts for commercial aircraft and engines
[NASA-CR-174752] 10 p1456 N85-19176
A review of hazard assessment procedures for liquid gun propellants
[AD-A149470] 10 p1457 N85-19182
Properties and thermal stabilities of amorphous transition metal hydrides
[DE85-002117] 11 p1607 N85-20104
High-temperature-stable detonators
[DE85-005188] 12 p1818 N85-21402
SAW oscillator with digital compensation for the temperature related frequency changes
[AD-D011537] 12 p1833 N85-21500
Stability of three-layer glass-reinforced plastic shells of rotation 13 p2047 N85-22813
NASA space materials research
14 p2232 N85-23831
Some observations of heated gallium arsenide heteroface solar cells
[NASA-TM-86368] 14 p2246 N85-23925
Applications of high pressure differential scanning calorimetry to aviation fuel thermal stability research
[NASA-TM-87002] 14 p2249 N85-23941
Surface composition, properties and thermal stability of massive and fine metallic glasses
15 p2513 N85-25506
Thermal stability of titanium alloys after cold plastic deformation 15 p2515 N85-25515
Simulation studies for surfaces and materials strength
[NASA-CR-175766] 16 p2800 N85-27262
Thermally stable elastomers: Review of silarylene-siloxane polymers and polysilmethylenes
[AD-A152323] 17 p2934 N85-28111
Atomic hydrogen maser measurements with wall surfaces of carbon tetrafluoride
18 p3108 N85-29243
Graphite/PMR polyimide composites with improved toughness
[NASA-TM-87061] 21 p3561 N85-32148
Basic research in novel inorganic reagents and fluorocarbon chemistry
[AD-A155340] 21 p3564 N85-32165
Basic cryogenics and materials. Phase 1
[NASA-CR-177932] 21 p3572 N85-32215
Experimental characterization and stability of salt- and nonsalt-containing grouts and mortars (BCT-1F- and BCT-1FF-related)
[DE85-012339] 22 p3753 N85-33263
Review of zirconium-zircaloy pyrophoricity
[DE85-011169] 23 p3916 N85-34270
A theoretical study of non-adiabatic surface effects for a model in the NTF cryogenic wind tunnel
[NASA-CR-3924] 23 p3929 N85-34352

THERMAL STRESSES
Burner liner thermal/structural load modelling
02 p0143 N85-10970
Features of plastic deformation and fracture of EP 741 nickel alloy under thermal strain
03 p0349 N85-12250
Liquid phase products and solid deposit formation from thermally stressed model jet fuels
[NASA-TM-86874] 04 p0481 N85-13066
In-flight evalution of LCF life consumption of critical rotor components subjected to high transient thermal stress
07 p0906 N85-15734
Monitoring engine thermal stresses
07 p0906 N85-15735
Thermal-stress analysis for a wood composite blade
[NASA-CR-174794] 08 p1178 N85-17421
Thermal striping downstream of a horizontal elbow under thermally stratified transient flow conditions
[DE84-014687] 09 p1320 N85-18302
The response of explosive systems to thermal stimuli: A state-of-the-art assessment
[DE85-000919] 11 p1614 N85-20148
Thermal stress-dependent dilation of concrete
[DE84-014688] 11 p1653 N85-20412
Temperature responses of composite panels
[AD-A150053] 12 p1798 N85-21277
Stress compensation crystal device
[AD-D011497] 12 p1941 N85-22189
Optimization of overall dimensions of enclosures for low-voltage devices and equipment
13 p2087 N85-23033
Estimating defectiveness buildup during service in metal of welded runner in low-pressure cylinder of turbine
14 p2271 N85-24070
Enhanced thermal-structural analysis by integrated finite elements
[AD-A151103] 15 p2636 N85-26258
Thrust chamber life prediction
16 p2733 N85-26865
Finite element thermal-structural analysis of cable-stiffened space structures
[AD-A153822] 18 p3086 N85-28963
Daze fasteners
[NASA-CASE-LAR-13009-1] 18 p3116 N85-29285
Gas turbines: Operating conditions, material selection and development
[NLR-MP-83046-U] 20 p3395 N85-31082
Accelerated stress factors and failure/degradation mechanisms in terrestrial solar cells
21 p3613 N85-32451
Effects of residual stresses and distortion on the nickel 200 and stainless steel 304 weldments
[DE85-011868] 22 p3748 N85-33233
X-ray measurement of thermal stresses in tungsten fiber-copper composites 23 p3907 N85-34205
Influence of cyclic thermal loading on internal stress in casted epoxy resin 23 p3908 N85-34211
Thermal stress analysis of a new turbine shroud seal concept
[NASA-TM-87082] 23 p3938 N85-34406
Mach 14 flow restrictor thermal stress analysis
[AD-A156215] 24 p4067 N85-35208

THERMAL VACUUM TESTS
Seven-year thermal-vacuum real-life test of a solar array drive mechanism manufactured by Marconi Space and Defence Systems (Model No. 002)
[ESA-ESTL-62] 11 p1616 N85-20161

THERMALIZATION (ENERGY ABSORPTION)
Monte Carlo simulation of thermalization of subexcitation electrons in molecular hydrogen
[NAL-TR-815T] 01 p0117 N85-10798
Efficient heating and confinement of ions in an axisymmetric magnetic mirror supplemented with dc electric field
[IPPJ-707] 12 p1935 N85-22180
Monte Carlo simulation of thermalization of subexcitation electrons in He, Ne, Ar, Kr and Xe
[NAL-TR-843T] 18 p3178 N85-29702

THERMICONS
Preliminary study for an IR-vidicon for the 8 to 14 micron range, phase 1
[BMFT-FB-W-84-025] 05 p0633 N85-14067

THERMIONIC CATHODES
Pressed boride cathodes
[NASA-TM-77821] 17 p2918 N85-27984
The effect of metal overlayers of thermionic dispenser cathodes
[AD-A154795] 21 p3701 N85-32995

THERMIONIC CONVERSION SYSTEMS
U THERMIONIC POWER GENERATION

THERMIONIC CONVERTERS
NT SOLAR BLANKETS
Technology status of thermionic fuel elements for space nuclear power 05 p0610 N85-13893
China report: Science and technology
[JPRS-CST-84-039] 11 p1621 N85-20206

Thermionic converter for space reactor described
11 p1621 N85-20208
SP-100 Thermionic Technology Program
[DE85-012311] 23 p3972 N85-34825
THERMIONIC EMISSION
AlAs/GaAs superlattice barrier unipolar diode structure
[DE85-001904] 11 p1736 N85-20921
THERMIONIC EMITTERS
Technology status of thermionic fuel elements for space nuclear power 05 p0610 N85-13883
Research on thermionic plasmas
[AD-A150683] 14 p2423 N85-24944
Multi-channel pulser for the SLC thermionic electron source
[DE85-014222] 24 p4160 N85-35792
THERMIONIC POWER GENERATION
Thermoelectric and thermionic conversion technology
05 p0611 N85-13905
Close-spaced high temperature Knudsen flow
[AD-A148477] 08 p1178 N85-17424
High thermal power density heat transfer apparatus providing electrical isolation at high temperature using heat pipes
[NASA-CASE-LEW-12950-2] 18 p3098 N85-29179
Thermionic photovoltaic energy converter
[NASA-CASE-LEW-14077-1] 23 p3944 N85-34441
THERMIONIC REACTORS
U ION ENGINES
THERMISTORS
A variable length and sensor spacing thermistor array
[AD-D011416] 08 p1113 N85-17017
Temperature sensors for OTEC applications
[DE85-009807] 18 p3110 N85-29254
THERMITES
Thermite and Fe/KClO4: Some thermodynamic calculations
[DE84-016945] 04 p0573 N85-13653
Consolidation of thermites by pressing and sintering
[DE84-016943] 09 p1297 N85-18146
Parameters affecting hot wire ignition of thermite mixtures
[DE84-016941] 09 p1301 N85-18176
A program to develop thermite reactions to produce refractory borides and carbides
[AD-A148972] 10 p1434 N85-19037
Thermal profiles of thermite reactions
[DE85-003306] 10 p1438 N85-19061
THERMOCHEMICAL PROPERTIES
NT HEAT OF FORMATION
NT HEAT OF FUSION
NT HEAT OF VAPORIZATION
Compiled and thermodynamic data sources for aqueous and biochemical systems: An annotated bibliography, 1930 - 1983
[PB85-137693] 12 p1944 N85-22208
Influence of thermochemical treatment on properties of low-carbon steel
[BLL-BISI-TRANS-22410-(9022.06)]
17 p2927 N85-28055
Hydrolysis, formation and ionization constants at 25(0)C, and at high temperature-high ionic strength
[DE85-010645] 19 p3236 N85-30061
THERMOCHEMISTRY
NT AEROTHERMOCHEMISTRY
Experimental and theoretical study of a solar thermochemical receiver module
[NASA-CR-174107] 04 p0528 N85-13374
Blanket materials for fusion reactors: Comparisons of thermochemical performance
[DE84-016240] 04 p0566 N85-13622
Laminar heat-transfer distributions on biconics at incidence in hypersonic-hypervelocity flows
[NASA-TP-2213] 07 p0957 N85-16065
Application of computer methods for calculation of multicomponent phase diagrams of high temperature structural ceramics
[AD-A148138] 08 p1133 N85-17140
Dynamics and mechanisms of catalytic processes and hot chemistry
[DE85-002899] 09 p1292 N85-18114
Carbon vaporization/condensation effects
[NASA-TM-87430] 10 p1436 N85-19048
Some specifics of methods for mass detailed studies of rock heat conductivity 10 p1502 N85-19477
Solar thermochemical process interface study
[NASA-CR-174442] 10 p1510 N85-19527
Direct contact heat recovery from molten salt
[DE85-002830] 11 p1674 N85-20550
Combustion kinetics of metal atoms and metallic radicals over wide temperature ranges 13 p1999 N85-22530
Mechanical properties of TiN deposits obtained by PVD and TiN, TiC, TiC + TiN obtained by CVD
[BLL-RISLEY-TR-5097-(9091.9F)]
15 p2508 N85-25471
Gas phase ion-molecule chemistry of carbon, nitrogen and oxygen compounds
[AD-A152676] 17 p2919 N85-27996
Elementary reactions of importance in oxidation, combustion ignition and flame inhibitions
[AD-A153139] 17 p2921 N85-28004
Influence of preliminary thermomechanical treatment on depth and hardness of nitrided layers
[BLL-BISI-TRANS-22488-(9022.06)]
17 p2929 N85-28078
Alcohol Fuels Program technical review, spring 1984
[DE85-002919] 17 p2938 N85-28134
Light scattering and spectroscopic studies of polymerization processes
[AD-A153407] 18 p3069 N85-28984
Thermochemical energy transport using a hydrogen rich working fluid
[AD-D011696] 19 p3233 N85-30042
Theoretical studies of combustion chemistry
[DE85-010284] 19 p3237 N85-30069
High temperature solar electrothermal processing 2. Zinc from zinc oxide
[AD-A154747] 21 p3562 N85-32159
Biomass thermochemical conversion program
[DE85-011667] 21 p3572 N85-32213
Process for improving the quality of epitaxial silicon films grown on insulating substrates
[AD-D011730] 22 p3847 N85-33828
Thermodynamics of the corrosion of chromium in molten carbonates
[DE85-011407] 24 p4079 N85-35282
THERMOCHROMATIC MATERIALS
Electrochromic and thermochromic materials for solar energy applications with emphasis on niobium and vanadium oxides
[DE85-010630] 19 p3249 N85-30147
THERMOCLINES
The effect of stochastic surface heat fluxes on the climatology of the seasonal thermocline
[AD-A149957] 12 p1869 N85-21857
Frontal nature of Cromwell Current
14 p2336 N85-24445
Local mechanism of equatorial countercurrents
14 p2336 N85-24446
Most important geochemical barrier zones in ocean (with example of Atlantic Ocean basin)
14 p2343 N85-24491
Real-time enhancement of a climatology or forecast of ocean thermal structure using observed ocean temperatures
[AD-A151118] 15 p2604 N85-26049
Thermal evolution of coastal California with implications for hydrocarbon maturation 24 p4115 N85-35509
THERMOCOUPLE PYROMETERS
Thin-film sensors for space propulsion technology
17 p2915 N85-27968
THERMOCOUPLES
Dynamic gas temperature measurement system
02 p0141 N85-10958
Evaluation of thermocouple junction temperature
[DE84-015159] 04 p0502 N85-13206
Field installed brazed thermocouple feedthroughs for high vacuum experiments
[DE84-013556] 04 p0503 N85-13207
Development of a feasibility model for a thin-film precision power meter
[BMFT-FB-T-84-161] 04 p0504 N85-13217
Effects of temperature on the response time of thermocouples and resistance thermometers
[DE84-016855] 06 p0811 N85-15154
High temperature thermocouple and heat flux gauge using a unique thin film-hardware hot juncture
[NASA-TM-86898] 07 p0962 N85-16096
Calibration of thermocouples based on two state points of water and BS 4937; part 5, 1974
09 p1324 N85-18317
Problems in high temperature thermocouple thermometry
[DE85-000608] 10 p1488 N85-19397
Advanced thin film thermocouples
[NASA-CR-175541] 12 p1850 N85-21607
Performance of Chromel versus Alumel and Nicrosil versus Nisil thermocouple assemblies in vacuum and argon between 1000 deg C and 1200 deg C
[DE85-000610] 12 p1853 N85-21624
Results of aeroheating DFI and ET design-data test on a 0.0175-scale model 60-OTS conducted in the Von Karman Gas Dynamics Facility (VKF) 40' supersonic and the 50' hypersonic wind tunnels A and C
[NASA-CR-167693] 13 p1988 N85-22466
Low temperature calibration fixture
[DE85-003969] 13 p2094 N85-23071
Qualification of the T2 wind tunnel in cryogenic operation. A: Thermal field, preliminary study of a schematic model
[NASA-TM-77781] 14 p2227 N85-23805
Thermocouple modeling
[DE85-005172] 14 p2306 N85-24273
Development of a temperature measurement system with application to a jet in a cross flow experiment
[NASA-CR-174696] 15 p2472 N85-25262
Design and construction of a computer controlled mirothermocouple probe for the study of buoyant jets
[AD-A152224] 16 p2788 N85-27190
A ten channel temperature controller
[AD-A152664] 17 p2967 N85-28228
Heating parameter estimation using coaxial thermocouple gages in wind tunnel test articles
[AD-A153039] 17 p2968 N85-28229
The effects of extreme temperatures on thermocouples
[DE85-008650] 18 p3110 N85-29258
Imbedded thermocouples as a solid propellant combustion probe
[AD-A155630] 21 p3564 N85-32167
Resolution of thermal striping issue downstream of a horizontal pipe elbow in stratified pipe flow
[DE85-006195] 21 p3586 N85-32292
Failure mechanisms in metal-sheathed thermocouples
[DE85-011929] 21 p3590 N85-32317
IEA-SSPS CRS calibration report: Calibration of relevant measuring sensors
[DE85-010174] 22 p3788 N85-33486
THERMODYNAMIC COUPLING
Survey of mixing in metal/insulator systems
[DE85-011938] 23 p3985 N85-34714
THERMODYNAMIC CYCLES
NT BRAYTON CYCLE
NT CARNOT CYCLE
NT OTTO CYCLE
NT RANKINE CYCLE
NT STIRLING CYCLE
Liquid-piston Stirling machines
[DE84-014255] 02 p0205 N85-11351
Standardized efficiency terms: Comparison of some Stirling engine performance figures
[DE84-015407] 02 p0205 N85-11352
Noise reduction of the exhaust from pneumatic tools
[BMFT-FB-HA-83-021] 02 p0276 N85-11786
Magnetic heat pump cycles for industrial waste heat recovery
[DE84-017016] 04 p0499 N85-13183
Evaluation of heat engine for hybrid vehicle application
[NASA-CR-174163] 04 p0508 N85-13245
Heat cycle research program
[DE84-017015] 09 p1344 N85-18455
Initial results for supercritical cycle experiments using pure and mixed-hydrocarbon working fluids
[DE84-017006] 09 p1345 N85-18460
Available energy method for evaluating thermodynamic performance of heat pump systems
[DE84-017223] 09 p1400 N85-18814
DOE/ORNL electric systems program overview
[DE85-003334] 10 p1459 N85-19197
Initial testing of a variable-stroke Stirling engine
[NASA-TM-86875] 10 p1569 N85-19885
Heat Cycle Research Experimental Program report, FY-84
[DE85-003558] 12 p1882 N85-21811
Power plants of modular construction with quasi-paraboloidal concentrators of solar energy
14 p2266 N85-24038
A mathematical model of reciprocating combustion engine dynamics for the diagnosis of deficient energy conversion 19 p3280 N85-30330
Adiabatic thermal models for planetary bodies
22 p3857 N85-33881
THERMODYNAMIC EFFICIENCY
Combustion modeling of a 2 cylinder cycle reciprocating engine
[AD-A144782] 01 p0055 N85-10364
Available energy method for evaluating thermodynamic performance of heat pump systems
[DE84-017223] 09 p1400 N85-18814
Influence of fuel properties on gas turbine combustion performance
[AD-A151464] 15 p2504 N85-25440
Development of a coal-water slurry-fueled diesel engine for industrial cogeneration. Task 1.0 topical report: Thermodynamic analysis
[DE85-010455] 19 p3236 N85-30082
Historical perspective of barriers to achieving high-efficiency silicon solar cells
20 p3479 N85-31616
Fuel cell applications literature review
[DE85-011891] 22 p3809 N85-33592
THERMODYNAMIC EQUILIBRIUM
An interactive computer code for calculation of gas-phase chemical equilibrium (EQLBRM)
[NASA-CR-168337] 02 p0140 N85-10946

Thermodynamic conditions of the Earth's atmosphere with pollution processes 04 p0523 N85-13345

ECUT, Energy Conversion and Utilization Technologies program: Isothermal separation processes update
[NASA-CR-175483] 10 p1433 N85-19033

Adsorption thermodynamics and surface transport of metal catalyst poisons
[DE85-002668] 10 p1441 N85-19084

Nucleation of phase transitions in the vicinity of phase boundary. Part 1: Comparison of various idolated mechanisms. Part 2: Coupled cluster growth processes
[N-0206-5658] 12 p1938 N85-22174

Compiled and thermodynamic data sources for aqueous and biochemical systems: An annotated bibliography, 1930 - 1983
[PB85-137693] 12 p1944 N85-22206

Thermodynamic calculations of equilibrium states in metal-carbon-hydrogen-oxygen system
[BLL-BISI-TRANS-22092-(9022.06)]
17 p3045 N85-28844

The interactions of composition and stress in crystalline solids
[PB85-179075] 20 p3473 N85-31583

Current understanding of point defects and diffusion processes in silicon 20 p3481 N85-31632

Condensation properties of atmospheric aerosol
21 p3649 N85-32672

THERMODYNAMIC PROPERTIES

NT CRITICAL POINT
NT CRITICAL PRESSURE
NT CRITICAL TEMPERATURE
NT EMISSIVITY
NT ENTHALPY
NT ENTROPY
NT FREE ENERGY
NT HEAT OF FORMATION
NT HEAT OF FUSION
NT HEAT OF VAPORIZATION
NT MELTING POINTS
NT PYROELECTRICITY
NT SPECIFIC HEAT
NT SUPERCRITICAL PRESSURES
NT SURFACE ENERGY
NT THERMAL CONDUCTIVITY
NT THERMAL DIFFUSION
NT THERMAL DIFFUSIVITY
NT THERMAL EXPANSION
NT THERMAL INSTABILITY
NT THERMAL STABILITY
NT THERMOCHEMICAL PROPERTIES
NT THERMOPHYSICAL PROPERTIES
NT VAPOR PRESSURE
NT VOLATILITY

Combustion gas properties I-ASTM jet A fuel and dry air
[NASA-TP-2359] 01 p0010 N85-10064

Granular boundary segregation in low-alloyed titanium-vanadium alloys 01 p0019 N85-10117

A thermodynamic surface for the critical region of ethylene
[PB84-217850] 01 p0025 N85-10159

Thermodynamic properties of isobutane-isopentane mixtures from -40 to +600(0)F and up to 1000 psia
[DE84-015137] 01 p0124 N85-10850

Dynamic gas temperature measurement system
02 p0141 N85-10958

Laser speckle technique for burner liner strain measurements 02 p0142 N85-10963

Thermodynamics of reactions of deoxidation of nickel melts
[BLL-M-35729-(5828.4)] 02 p0175 N85-11168

A case study of a convective outbreak using VAS-derived thermodynamic parameters
[AD-A145560] 02 p0232 N85-11512

NBS (National Bureau of Standards): Materials measurements
[NASA-CR-174038] 03 p0332 N85-12143

Surface coatings for low emittance in the thermal surveillance band
[MRL-R-937] 03 p0336 N85-12158

Critical evaluation of binary rare Earth diagrams
[DE84-014880] 04 p0470 N85-12991

Electrochemical investigations of novel electrode materials
[DE84-014352] 04 p0495 N85-13158

Thermal properties of soils and soils testing
[DE84-015312] 04 p0525 N85-13360

Thermite and Fe/KClO4: Some thermodynamic calculations
[DE84-016945] 04 p0573 N85-13653

Americium thermodynamic data for the EQ3/6 database
[DE84-017065] 04 p0573 N85-13656

Analytical thermal formulations for antenna dishes — satellite antennas 05 p0627 N85-14017

Strain rate effects and temperature history effects for three different tempers of 4340 VAR steel
[AD-A146372] 06 p0768 N85-14915

Effects of surface interactions and mechanical properties of PBXs (plastic bonded explosives) on explosive sensitivity
[AD-A146388] 06 p0773 N85-14944

Aerodynamic and thermal characteristics of stellate bodies in hypersonic flow of rarefied gas at angle of attack 06 p0778 N85-14974

Thermodynamical characteristics of heat storage reactors using metal hydrides
[NAL-TR-822] 06 p0869 N85-15524

Thermal and mechanical properties of polyurethane foams and a survey of insulating concretes at cryogenic temperatures
[PB85-100949/GAR] 07 p0934 N85-15918

Thermal evaporation in blast waves: A model for aneurism formation in the NRL (Naval Research Laboratory) LASER-HANE simulation experiment
[AD-A147006] 07 p0978 N85-16210

A virial equation of state option for the TIGER computer program
[AD-A147490] 07 p1025 N85-16507

Temperature dependence of the crystal structures of Nylon 11
[AD-A147563] 07 p1049 N85-16661

Computer program for calculation of complex chemical equilibrium compositions and applications. Supplement 1: Transport properties
[NASA-TM-86885] 07 p1049 N85-16663

In-flight testing of the space shuttle orbiter thermal control system 08 p1103 N85-16974

Photoacoustic microscopy of oxygen contaminated titanium alloys
[AD-P004127] 08 p1127 N85-17102

A research proposal for the theoretical study of the thermodynamic and transport properties of dense plasmas
[AD-A148040] 08 p1224 N85-17708

Proceedings of the AFOSR/AFRPL Rocket Propulsion Research Meeting: Abstracts and Agenda
[AD-A148818] 09 p1288 N85-18085

Thermodynamic properties of aqueous NaCl from 273 to 823 K with estimates for higher temperatures
[DE85-000392] 09 p1292 N85-18116

Physical characterization of magma
[DE85-000568] 09 p1354 N85-18519

Materials physics
[DE84-017103] 09 p1377 N85-18658

Acoustic microscopy at cryogenic temperatures
[AD-A148755] 09 p1384 N85-18704

Magnetic fusion energy plasma interactive and high heat flux components. Volume 2: Technical assessment of the critical issues and problem areas in high heat flux materials and component development
[DE85-001155] 09 p1393 N85-18764

Pulsed photothermal radiometry for remote sensing of spectroscopic and physical properties of thin film
[AD-A149080] 10 p1435 N85-19041

Quasi-thermodynamic prediction of hydrogen reemission behavior from titanium films
[DE85-003667] 10 p1564 N85-19864

Application of Monte Carlo and molecular dynamics methods to the calculation of thermodynamic properties of molten salts
[AD-A148897] 10 p1565 N85-19869

Thermophysical properties of porous fiber materials
11 p1601 N85-20068

The physical modelling of transition metal alloying: The roles that different levels of theory play
[DE85-000591] 11 p1607 N85-20105

Report of the Technology and Test Panel
11 p1646 N85-20370

User's manual for GRIZZLY
[DE85-001405] 11 p1702 N85-20702

Novel photo-thermal technique for flow and spectroscopic measurements in a dense aerosol stream
[AD-A149745] 12 p1800 N85-21287

Chemical approach for controlling nadimide cure temperature and rate
[NASA-CASE-LEW-13770-5] 12 p1810 N85-21352

Fine-grained, isotropic graphite for use as NBS (National Bureau of Standards) thermophysical property RM's from 5 to 2500 K
[PB85-112886] 12 p1814 N85-21381

Mathematical simulation of thermal prrocesses involved in electron-beam treatment 12 p1843 N85-21565

Nonnal coordinate monolithic crystal filter
[AD-D011498] 12 p1941 N85-22188

Ideal gas thermodynamic properties for the phenyl, phenoxy, and o-biphenyl radicals
[NASA-TM-83800] 12 p1943 N85-22204

Green's function solution of the Kondo problems and universality of the thermodynamic properties
[DE85-002739] 12 p1943 N85-22206

Efficiency of algorithms for gas-air channel diagnostics in gas turbine engines based on gas thermodynamic parameters 13 p2048 N85-22823

Thermodynamic and kinetic studies of pulsed laser annealing from transient conductivity measurements
[DE85-003677] 13 p2096 N85-23078

Thermal response of aircraft cabin ceiling materials during a post-crash, external fuel-spill, fire scenario
[PB85-145647] 14 p2220 N85-23764

Thermal deformation of flexible rotors in friction bearings 14 p2280 N85-24123

Analysis and testing of the thermal properties of space battery cells, phase B, draft
[ESA-CR(P)-1971] 15 p2550 N85-25741

On thermomechanical testing in support of constitutive equation development for high temperature alloys
[NASA-CR-174879] 15 p2577 N85-25894

Development of new materials for turbopump bearings
16 p2735 N85-26877

Effect of nickel addition on the thermal, magnetic and magnetomechanical properties of Fe(80)B(15)Si(5)
[AD-A152281] 16 p2749 N85-26967

Computer program for the calculation of multicomponent convective diffusion deposition rates from chemically frozen boundary layer theory
[NASA-CR-168329] 16 p2781 N85-27164

Design and construction of a computer controlled mirothermocouple probe for the study of buoyant jets
[AD-A152224] 16 p2788 N85-27199

The study of thermal forecasting for gliding
16 p2830 N85-27453

Thermal and magnetic properties of neutron stars
16 p2880 N85-27774

Investigation of heat transfer to a turbine blade cascade using a shock tube
[AD-A153090] 17 p2898 N85-27871

Thermodynamic analysis of the plasma nitriding of ferrovanadium
[BLL-BISI-TRANS-22237-(9022.06)]
17 p2924 N85-28032

Analysis and modeling for thermal focal plane arrays
[AD-A153156] 17 p2968 N85-28329

Thermodynamic calculations of equilibrium states in metal-carbon-hydrogen-oxygen system
[BLL-BISI-TRANS-22092-(9022.06)]
17 p3045 N85-28844

High-temperature oxidation of alloys in mixed oxidants
[DE85-009706] 18 p3077 N85-29035

Preparation of sinteractive silicon nitride powders
[BMFT-FB-T-84-303] 18 p3082 N85-29066

Reliability derating procedures
[AD-A153744] 18 p3119 N85-29309

Materials research for passive solar systems: Solid-state phase-change materials
[DE85-008779] 18 p3132 N85-29395

Growth mechanism and properties of the thermal and anodic oxides of the 3-5 compound semiconductors
[AD-A153408] 18 p3193 N85-29803

Electronic states in silicon and on its interfaces
[AD-A153664] 18 p3193 N85-29807

Thermodynamic properties of liquid Li-Ph, Na-Pb and K-Plc]b alloys: Similarities and Differences
[DE85-004074] 18 p3197 N85-29830

Thermodynamic systematics of oxides of americium, curium and neighboring elements
[DE85-009704] 18 p3197 N85-29831

Thermophysical properties correlations and pseudocomponent characterization parameter estimation for fossil fluids
[DE85-009297] 19 p3230 N85-30024

Self-developing polysilane deep-UV resists: Photochemistry, photophysics and submicron lithography
[DE85-007606] 19 p3237 N85-30067

Structure and properties of VT23 alloy welded joints after thermocyclic processing 19 p3246 N85-30125

Thermo-mechanical and thermal behavior of high-temperature structural materials
[AD-A154154] 19 p3266 N85-30251

Activities of Rutgers - The State University Department of Mathematics
[AD-A154158] 19 p3370 N85-30904

Thermodynamics of high temperature materials
[AD-A154269] 19 p3378 N85-30956

Special materials: Carbons
[SNIAS-851-551-104] 20 p3421 N85-31235

Method for determining Wagner parameters of interaction of first and second orders
[BLL-M-36261-(5828.4)] 20 p3430 N85-31278

Meteorological weapons
[AD-A154735] 21 p3835 N85-32575

Numerical modeling of sea ice dynamics and ice thickness characteristics
[AD-A154600] 21 p3854 N85-32700

Thermodynamic data for mineral technology
[PB85-184331] 22 p3803 N85-33560

Refractive indices and thermo-optic coefficients of nonlinear crystals isomorphic to KH2PO4
[DE85-012968] 22 p3847 N85-33831
Experimental evaluation of the thermodynamic properties of concentrated aqueous potassium hydroxide solutions
[DE85-010626] 23 p3912 N85-34238
Calculation of activities of components in liquid alloys of iron with yttrium
[BLL-M-35868-(5828.4)] 23 p3914 N85-34253
Design and lubrication of high-speed rolling-element bearings
[NASA-TM-87107] 23 p3938 N85-34409
Determination of properties of zeolite/refrigerant combinations for solar refrigeration systems
[DE85-012009] 23 p3945 N85-34448
Characterization of the optical and thermal properties of matter by photothermal techniques
[DE85-012607] 24 p4076 N85-35260
Analysis of the nonlinear equations describing the elastic, thermal, and electromagnetic behavior of solids: Existence of solutions of semi-inverse problems
24 p4100 N85-35415

THERMODYNAMICS
NT AEROTHERMODYNAMICS
NT COMBUSTION PHYSICS
Compressibility and fugacity of gaseous hydrogen
[NLR-TR-83079-U] 01 p0025 N85-10154
Theory of nonlocal elasticity and some applications
[AD-A145201] 01 p0062 N85-10412
Reduction of nonlinear problems to Schroedinger or heat equations: Formation of Kepler orbits, singular solutions for hydrodynamical equations
[REPT-72] 01 p0129 N85-10892
Thermodynamics of decarburization of niobium-bearing high-alloy melts
[BLL-M-35726-(5828.4)] 02 p0175 N85-11169
Thermodynamic calculations and the chemical vapour deposition of hard materials 02 p0179 N85-11200
Analysis and simulation of the I C engine Otto cycle using the second law of thermodynamics
02 p0291 N85-11691
Thermomechanical cracking in layered media from moving friction load
[AD-A146022] 03 p0373 N85-12379
Difference schemes for equations of Schrodinger type
[AD-A145812] 03 p0410 N85-12622
The development of new methods for solving the target identification or inverse scattering problem for time-harmonic acoustic and electromagnetic waves
[AD-A145821] 03 p0415 N85-12657
Thermodynamics and phase equilibria in the vandium-silicon system
[AD-A145870] 03 p0435 N85-12769
Thermodynamic study of CO2-organic compound interaction at high pressures and temperatures
[DE84-015777] 04 p0573 N85-13654
Linear harmonic analysis for Stirling machines and second law analysis of four important losses
[DE84-016595] 04 p0573 N85-13655
Linear harmonic analysis of Stirling engine thermodynamics
[DE84-016646] 04 p0574 N85-13657
On experimental equations of state for Boson gases
[PTB-ME-61] 04 p0574 N85-13659
Answering thermodynamic questions with three-dimensional viscous flow calculations
05 p0636 N85-14081
Variational principles in thermoplasticity. Part 2: Coupled thermomechanical processes
[RUB-IFM-MITT-37-PT-2] 05 p0648 N85-14161
Process Modeling Applied to Metal Forming and Thermomechanical Processing
[AGARD-LS-137] 06 p0796 N85-15086
Intercomparison between West Germany and US thermodynamic codes
[AD-A146622] 06 p0869 N85-15525
Aqueous alteration of meteorite parent bodies: Possible role of unfrozen water and the Antarctic meteorite analogy 06 p0884 N85-15617
Interaction between chromium oxide and carbon
[BLL-M-36002-(5828.4)] 07 p0926 N85-15867
Target detection using microwave irradiances from natural sources: A passive, local and global surveillance system
[NASA-CR-174260] 07 p0946 N85-15991
Assessment of the operating characteristics of the SSME LOX turbopump pump-end bearing
[NASA-CR-171287] 08 p1167 N85-17362
Impact and collisional processes in the solar system
[NASA-CR-174297] 08 p1255 N85-17914
A thermal-mechanical model of deflagration-to-detonation in granular energetic materials
[AD-P004346] 10 p1455 N85-19170
Thermodynamics of the reactive flow model
[DE85-004405] 10 p1565 N85-19670
Explorations into thermodynamics analogies and critical points in reference to gas-solid transport
[DE85-000816] 11 p1738 N85-20929
Viscoplastic constitutive relationships with dependence on thermomechanical history
[NASA-CR-174836] 12 p1864 N85-21691
Atmospheric environment for Space Shuttle (STS-51A) launch
[NASA-TM-86497] 12 p1892 N85-21875
Clustering and ordering in 3-5 alloys
[AD-A150604] 13 p2022 N85-22670
Thermodynamics of copper-nickel alloys containing aluminum, silicon, titanium, and chromium relative to their use in ceramic brazing
[DE85-004767] 13 p2023 N85-22674
Some unique features of isentrophic flow of gas under high pressures 13 p2043 N85-22788
Impact and collisional processes in the solar system
13 p2180 N85-23530
Theoretical thermodynamics of mixtures at high pressures 13 p2183 N85-23550
Chemical-mechanical interaction in gears
14 p2223 N85-23785
Thermodynamic calculations and the chemical vapour deposition of hard materials 14 p2431 N85-24991
Get Away Special (GAS) thermal design summary
[X-732-83-8] 15 p2475 N85-25278
Separating polymer solutions using high pressure LCST Lower Critical Solution Temperature) phenomena
[AD-A151538] 15 p2518 N85-25528
Entropy production during fatigue as a criterion for failure. A local theory of fracture in engineering materials
[AD-A151289] 15 p2578 N85-25902
Numerical simulation of North Atlantic Sea ice variability, 1951 - 1980 15 p2603 N85-26040
Origin of the Greenland ice sheet
15 p2604 N85-26046
USSR report: Physics and mathematics
[JPRS-UPM-85-003] 15 p2642 N85-26300
Stream dynamics between 1 AU and 2 AU: A detailed comparison of observations and theory
[NASA-TM-86086] 15 p2664 N85-26576
Analytical fuel property effects--small combustors
[NASA-CR-174738] 16 p2708 N85-26700
Study of the kinetics and thermodynamics of hydrogen in Pd-based alloys
[DE85-007341] 16 p2750 N85-26969
Eigenvalue approximation methods for quantum lattice Hamiltonians 16 p2858 N85-27627
Dynamic creep buckling: Analysis of shell structures subjected to time-dependent mechanical and thermal loading 17 p2913 N85-27959
Designing for fiber composite structural durability in hygrothermomechanical environment
[NASA-TM-87045] 17 p2917 N85-27978
Silica problem in the design of geothermal power plants
[DE85-008245] 17 p2986 N85-28453
Homogeneous processes of atmospheric interest
[NASA-CR-175770] 17 p2989 N85-28475
Effects of level broadening on the magnetothermal oscillations in two-dimensional electron systems
[AD-A152639] 17 p3029 N85-28732
Rolling contact fatigue testing of thermomechanically processed M-50 steel
[AD-A153640] 18 p3122 N85-29327
Implications about in situ stress at Yucca Mountain
[DE85-008068] 18 p3126 N85-29356
Solar rocket component study
[AD-A154186] 19 p3227 N85-30007
Thermo-mechanical and thermal behavior of high-temperature structural materials
[AD-A154154] 19 p3266 N85-30251
Evaluation of the eigenvalue method in the solution of transient heat conduction problems
[AD-A154434] 19 p3266 N85-30256
Thermodynamic study of CO2-organic compound interaction at high pressures and temperatures
[DE85-010999] 19 p3268 N85-30266
Some relations among directions of curves at an invariant point on a thermodynamic phase diagram
19 p3312 N85-30530
Thermodynamics of high temperature materials
[AD-A154269] 19 p3378 N85-30958
Thermomigration in porous media. Study of the development of a drying zone 20 p3456 N85-31462
Physical concepts in the development of constitutive equations 20 p3467 N85-31537
Effects of weak interfaces on thermostructural behavior of carbon-carbon composites
[AD-A155330] 21 p3562 N85-32154
Polymer solution-supercritical fluid behavior
[AD-A154514] 21 p3568 N85-32192
Sintering studies project
[AD-A154750] 21 p3572 N85-32216
The sound field of a moving laser-induced acoustic array (theory)
[AD-A154553] 21 p3699 N85-32961
Chemical evolution of the Earth: Equilibrium or disequilibrium process? 21 p3721 N85-33088
Technical assessment of thermal-hydraulics for high heat flux fusion components
[DE85-013178] 23 p3930 N85-34369
Thermodynamics of the corrosion of chromium in molten carbonates
[DE85-011407] 24 p4079 N85-35282
Hadron thermodynamics in relativistic nuclear collisions
[HE-1.1-6] 24 p4171 N85-35856

THERMOELASTICITY
Finite element analysis of thermoelasticity problems
02 p0206 N85-11369
New aspects of thermoelastic contact
[AD-A147554] 07 p0979 N85-16217
An electro-optic spatial light modulator for thermo-elastic generation of programmably focused ultrasound
[AD-A149078] 10 p1553 N85-19794
Translational and extensional energy release rates (the J- and M-integrals) for a crack layer in thermoelasticity
[NASA-CR-174872] 12 p1863 N85-21685
Effects of triazine components on physicochemical properties of polybutadiene: urethane block copolymers
13 p2014 N85-22626
A review of path-independent integrals in elastic-plastic fracture mechanics, task 4
[NASA-CR-174956] 22 p3799 N85-33541

THERMOELECTRIC CONVERSION SYSTEMS
U THERMOELECTRIC POWER GENERATION

THERMOELECTRIC GENERATORS
NT SOLAR SEA POWER PLANTS
Space nuclear safety program
[DE84-015074] 04 p0463 N85-12939
Space nuclear safety program
[DE84-015064] 04 p0463 N85-12940
Technical support services for space and terrestrial systems programs
[DE84-009031] 05 p0597 N85-13606
Radioisotope space power programs
05 p0609 N85-13887
Power flattening techniques for radioisotopic thermoelectric generators
[AD-A146365] 06 p0833 N85-15299
Development of a preprototype times wastewater recovery subsystem, addendum
[NASA-CR-171823] 07 p1019 N85-16468
General-purpose heat source development: Safety test program. Postimpact evaluation, design iteration test 4
[LA-10217-SR] 12 p1930 N85-22128
Development of advanced thermoelectric materials
[NASA-CR-175684] 14 p2351 N85-24532
Long-term exposure of pressed plutonium oxide heat sources to aquatic environments
[DE85-007365] 15 p2495 N85-25392
LPCVD tungsten deposition on Si-Ge alloy
[DE85-005588] 16 p2750 N85-26970
Liquid metal thermoelectric converter (LMTEC) for solar applications
[DE85-008405] 18 p3129 N85-29376
Thermoelectric generator and method for the fabrication thereof
[DE85-011650] 22 p3760 N85-33302

THERMOELECTRIC MATERIALS
Electrical and thermal transport property studies of high-temperature thermoelectric materials
[AD-A150167] 13 p2163 N85-23417
Development of advanced thermoelectric materials
[NASA-CR-175684] 14 p2351 N85-24532
Electrical and thermal transport property studies of high-temperature thermoelectric materials
[AD-A150900] 14 p2427 N85-24967
Development of improved thermoelectric materials for space nuclear power systems
[DE85-013079] 22 p3844 N85-33907

THERMOELECTRIC POWER GENERATION
Emerging space nuclear power needs
05 p0606 N85-13882
High temperature thermoelectric energy conversion
05 p0610 N85-13884
Thermoelectric and thermionic conversion technology
05 p0611 N85-13885
Power flattening techniques for radioisotopic thermoelectric generators
[AD-A146365] 06 p0833 N85-15299
General-purpose heat source development: Safety test program. Postimpact evaluation, design iteration test 5
[LA-10232-SR] 12 p1931 N85-22129
General-purpose heat source development: Safety test program. Postimpact evaluation, design iteration test 1
[LA-9660-SR] 12 p1931 N85-22131

Spaceborne power systems preference analyses. Volume 2: Decision analysis
[NASA-CR-175645] 14 p2349 N85-24518

THERMOELECTRICITY
Mechanisms of electrical conductivity in olivine
[DE84-014333] 04 p0495 N85-13159
Power flattening techniques for radioisotopic thermoelectric generators
[AD-A146365] 06 p0833 N85-15299
Evaluation of the thermoelectric method for determination of interstitial gases in titanium
[AD-P004132] 08 p1127 N85-17107
Thermally induced quasiparticle branch imbalance in thin film superconductors 09 p1396 N85-18786
Electrothermal transducer with short time constant
13 p2066 N85-23040
Electrical and thermal transport property studies of high-temperature thermoelectric materials
[AD-A150167] 13 p2163 N85-23417
Transport studies of several novel organic conductors
[DE85-003950] 14 p2420 N85-24979
Thermo-electric valve
[AD-D011682] 19 p3252 N85-30165
Cells for measuring thermoelectromotive force and electrical resistance of metals in temperature range of 20-950 degrees Celsius
[BLL-M-36240-(5828.4)] 20 p3457 N85-31473

THERMOGRAMS
U RECORDING INSTRUMENTS
U TEMPERATURE MEASURING INSTRUMENTS

THERMOGRAPHY
Infrared thermography of burn front propagation in heat powders
[DE85-003307] 10 p1438 N85-19060
Thermal profiles of thermite reactions
[DE85-003308] 10 p1438 N85-19061
Fast times at high temperatures
[DE85-003306] 12 p1943 N85-22205

THERMOGRAVIMETRY
Development of acceptance criteria for batches of silane primer for external tank thermal protection system bonding applications
[NASA-CR-171286] 04 p0478 N85-13043
Instruments for characterization of carbon black and polymers
[AD-A146475] 06 p0810 N85-15146
Applications of high pressure differential scanning calorimetry to aviation fuel thermal stability research
[NASA-TM-87002] 14 p2249 N85-23941
Supercritical solvent extraction of lignite to form carbonaceous chars
[DE85-010159] 19 p3229 N85-30019

THERMOHYDRAULICS
Thermohydrodynamic model: Hydrothermal system, shallowly seated magma chamber
13 p2115 N85-23173
Coolant mixing in LMFBR rod bundles and outlet plenum mixing transients
[DE85-010336] 19 p3268 N85-30268
Technical assessment of thermal-hydraulics for high heat flux fusion components
[DE85-013178] 23 p3930 N85-34359
Mathematical modeling of ultimate heat sink cooling ponds
[TI85-009747] 23 p3932 N85-34369
Ocean thermal energy conversion
[DE85-012291] 23 p3946 N85-34456
MATADOR (Methods for the Analysis of Transport And Deposition Of Radionuclides) code description and user's manual
[TI85-901402] 23 p3966 N85-34592

THERMOLUMINESCENCE
The observation of a single thermoluminescence glow peak described by kinetics more general than the usual 1st and 2nd order kinetics
[DE84-014697] 02 p0173 N85-11160
Investigation of basic characteristics of laser heating in thermoluminescence and of laser-stimulated luminescence
[AD-A152143] 16 p2790 N85-27212
Dosimeasurements with thermoluminescence dosimeters at a Febetron 701, 600 kV in room 022 of the Interuniversity Reactor Institute (IRI)
[IRI-190-84-02] 18 p3111 N85-29262
Symposium on Luminescent Radiation Receivers and Converters 19 p3295 N85-30430
Research on the experimental verification of dosimetry calculations
[DE85-011282] 19 p3331 N85-30637
Error evaluation in measurements with thermoluminescent dosimeters
[ISS-T-84/6] 22 p3788 N85-33471
The read-out system of spatial distribution of thermoluminescence in meteorites
[SH-9.1-16] 23 p4052 N85-35131
Detection threshold energy of high energy cascade showers using thermoluminescence PTFE-sheet and hot-gas reader
[HE-7.1-5] 24 p4213 N85-36159
Application of thermoluminescence for detection of cascade shower 1: Hardware and software of reader system
[HE-7.1-6] 24 p4213 N85-36160
Spatial distribution read-out system for thermoluminescence sheets
[HE-7.1-7] 24 p4213 N85-36161
Application of thermoluminescence for detection of cascade shower 2: Detection of cosmic ray cascade shower at Mount Fuji
[HE-7.1-12] 24 p4214 N85-36162

THERMOMAGNADYNAMICS
U THERMOMAGNETIC EFFECTS

THERMOMAGNETIC EFFECTS
Thermomagnetic generator
[DE84-017018] 04 p0530 N85-13388
The formation of isolated phase precipitates during the decomposition of high-coercive force Fe-Cr-Co alloys
[BLL-M-36028-(5828.4)] 07 p0924 N85-15855

THERMOMAGNETISM
U THERMOMAGNETIC EFFECTS

THERMOMECHANICAL TREATMENT
Directional nature of strengthening during thermomechanical treatment
[BLL-M-35746-(5828.4)] 02 p0175 N85-11174
Cavitation phenomenon in superplastic creep
[DE84-015484] 04 p0513 N85-13271
The creep and creep rupture of SMC-R50 under different thermomechanical conditions 05 p0648 N85-14160
Back stress in dislocation creep. Part 1: Basic concepts and measuring techniques
[NASA-TM-77773] 07 p0977 N85-16206
Developing procedures for thermomechanical processing of high-durability VT22 titanium alloy
13 p2031 N85-22726
Compositional control of plate steels
15 p2565 N85-25826
Fatigue life, fatigue crack propagation and fracture toughness study of 7075 aluminum alloy subjected to thermomechanical processing 15 p2573 N85-25862
Analysis of shell type structures subjected to time dependent mechanical and thermal loading
[NASA-CR-175747] 15 p2577 N85-25896
Multiaxial and thermomechanical fatigue considerations in damage tolerant design
[NASA-TM-87022] 16 p2749 N85-26964
Thermomechanical softening treatment for bearing and tool steels
[BLL-BISI-TRANS-22432-(9022.06)]
17 p2925 N85-28035
Thermomechanical treatment aimed at the protection of type 316 stainless steel from IGC and IGSCC
[BLL-BISI-TRANS-22496-(9022.06)]
17 p2925 N85-28040
Investigation of fatigue strength of spring steel after high-temperature thermomechanical working (HTMW) by helical drawing
[BLL-M-36274-(5828.4)] 20 p3465 N85-31525
Thermomechanical deformation in the presence of metallurgical changes 20 p3466 N85-31533
Thermomechanically induced pre- and postbuckling of general structure 20 p3467 N85-31540
Development and application of a unified viscoelastic constitutive model for the prediction of material response under thermomechanical loading
24 p4101 N85-35420

THERMOMECHANICS
U THERMODYNAMICS

THERMOMETERS
NT RESISTANCE THERMOMETERS
Heat flux sensors for burner liners and turbine blades and vanes 02 p0142 N85-10961
Digital thermometer with linearizer on slide wire
07 p0954 N85-16049
Germanium resistance thermometer calibration at superfluid helium temperatures
12 p1947 N85-22228
Low temperature calibration fixture
[DE85-003969] 13 p2094 N85-23071
The gamma thermometer: A new type of fixed internal instrumentation developed by EDF
[BLL-CE-TRANS-8080-(9022.09)]
15 p2560 N85-25791
Fiber optic Raman thermometer for Space Shuttle main engine preburner profiling 16 p2739 N85-26904

THERMOMETRY
U TEMPERATURE MEASUREMENT

THERMONUCLEAR ENERGY
U THERMONUCLEAR POWER GENERATION

THERMONUCLEAR EXPLOSIONS
On the design of a global detection system for airborne radioactivity
[CM-68] 20 p3487 N85-31670

THERMONUCLEAR POWER GENERATION
SPECTER: Neutron damage calculations for materials irradiations
[DE85-005791] 18 p3180 N85-29716
Modeling and experiments on tritium permeation in fusion reactor blankets
[DE85-008439] 18 p3183 N85-29741
Tokamak ignition/burn experimental research device
[DE85-009999] 18 p3190 N85-29785
Alloy development for irradiation performance
[DE85-010454] 19 p3240 N85-30091
Report to the Working Group on Technology, Growth and Employment
[DE85-010320] 19 p3372 N85-30920
Nuclear data needs for fusion energy development
[DE85-010445] 20 p3536 N85-32000
Technical assessment of thermal-hydraulics for high heat flux fusion components
[DE85-013178] 23 p3930 N85-34359

THERMONUCLEAR REACTIONS
NT CONTROLLED FUSION
NT NUCLEAR FUSION
Ion-density correlations and enhancement of thermonuclear reaction rate in dense, inertially confined fusion plasmas 02 p0284 N85-11849
Solar neutrinos: Prospects for detection and implications
[DE84-015522] 02 p0304 N85-11968
Inertial confinement fusion: Present status and future potential
[DE84-016177] 04 p0567 N85-13616
X-ray bursts: Observation versus theory
[NASA-CR-174415] 10 p1573 N85-19916
Numerical analysis of thermonuclear detonation in dense plasma 11 p1719 N85-20814
Fusion Energy Division
[DE85-001701] 11 p1731 N85-20884
Whist code calculations of ignition margin in an ignition Tokamak
[DE85-009507] 18 p3190 N85-29784
Advances in ICF power reactor design
[DE85-010030] 19 p3361 N85-30841
X-ray spectra of bursting neutron stars
23 p3981 N85-34686

THERMOPHILES
Construction of a bacterium to convert cellulose to ethanol
[TI84-901639] 04 p0481 N85-13068

THERMOPHILIC PLANTS
NT BLUE GREEN ALGAE

THERMOPHYSICAL PROPERTIES
NT CRITICAL POINT
NT CRITICAL PRESSURE
NT CRITICAL TEMPERATURE
NT EMISSIVITY
NT HEAT OF FUSION
NT MELTING POINTS
NT PYROELECTRICITY
NT SPECIFIC HEAT
NT SUPERCRITICAL PRESSURES
NT TEMPERATURE DEPENDENCE
NT THERMAL CONDUCTIVITY
NT THERMAL DIFFUSION
NT THERMAL DIFFUSIVITY
NT THERMAL STABILITY
NT VAPOR PRESSURE
NT VOLATILITY
USSR report: Materials science and metallurgy, no. 93
[JPRS-84810] 01 p0018 N85-10110
Solidification and crystal growth of solid solution semiconducting alloys 02 p0155 N85-11046
Exothermic processes in solids under low temperatures, their physics and their cryogenic implications
[JUEL-1919] 03 p0414 N85-12651
PRIAMUS, a computer program for the calculation of thermophysical properties of gas mixtures containing O2, N2, CO, CO2, He, H2O, H2, CH4
[JUEL-1916] 04 p0472 N85-13002
National Bureau of Standards passive solar test facility: Instrumentation and site handbook
[PB85-100451/GAR] 07 p0968 N85-16148
Thermophysical property testing using transient techniques
[AD-A147085] 07 p1049 N85-16664
Weldability of alloy ABM1 to alloy 1201
11 p1603 N85-20080
China report: Science and technology
[JPRS-CST-84-025] 11 p1620 N85-20197
Thermophysical properties of matter
11 p1620 N85-20199

Fine-grained, isotropic graphite for use as NBS (National Bureau of Standards) thermophysical property RM's from 5 to 2500 K
[PB85-112886] 12 p1614 N85-21381
Simulation of thermal and electromagnetic processes in induction plasmatrons 12 p1641 N85-21552
Nested subcritical flows within supercritical systems
[NASA-TM-86960] 12 p1645 N85-21574
Thermophysical properties of working fluids for binary geothermal cycles
[DE85-000385] 12 p1681 N85-21804

THERMOPHYSICS
U THERMODYNAMICS

THERMOPLASTIC FILMS
Induction heating gun
[NASA-CASE-LAR-13181-1] 18 p3085 N85-29083

THERMOPLASTIC RESINS
NT THERMOPLASTIC FILMS
Thermoplastic-carbon fiber hybrid yarn
[NASA-CR-3849] 03 p0325 N85-12093
Constituent property - composite property relationships in thermoset matrices 04 p0465 N85-12950
Free volume considerations in thermoplastic and thermosetting resins 04 p0465 N85-12952
Solvent resistant thermoplastic composite matrices
04 p0466 N85-12960
Thermoplastic/melt-processable polyimides
04 p0466 N85-12961
Aliphatic-aromatic heterocyclics as potential thermoplastics for composite matrices
04 p0466 N85-12962
Characterization of a thermoplastic polyimidesulfone
[NASA-TM-86358] 10 p1450 N85-19135
Characterization and adhesive bonding of poly(etheretherketone) resins and composites
[DE85-002526] 11 p1593 N85-20023
Hot melt adhesive attachment pad
[NASA-CASE-LAR-12894-1] 11 p1610 N85-20125
Broadband thermoplastic radomes
[AD-P004369] 12 p1627 N85-21463
Stability of three-layer glass-reinforced plastic shells of rotation 13 p2047 N85-22813
Finland, Sweden cooperate in composites research
17 p2946 N85-28184
Phenoxy resins containing pendent ethynyl groups and cured resins obtained therefrom
[NASA-CASE-LAR-13262-1] 18 p3068 N85-28973
Laminated thermoplastic radome
[AD-D011684] 18 p3079 N85-29045
Adhesive evaluation of LARC-TPI and a water-soluble version of LARC-TPI
[NASA-TM-86428] 19 p3248 N85-30136
Development of an impact- and solvent-resistant thermoplastic composite matrix, phase 3
[NASA-CR-172568] 20 p3422 N85-31239
Structure-property relationships in thermoplastic elastomers. Part 3: Segmented polyacetal-polyurethanes
[AD-A154897] 21 p3569 N85-32200
Strength properties of glassfiber reinforced thermoplastics 23 p3906 N85-34212
Determination of the viscosity number of thermoplastics in dilute solution; polyamides (PA)
[NASA-TM-77673] 24 p4061 N85-35296

THERMOPLASTICITY
Nonlinear structural and life analyses of a combustor liner 02 p0141 N85-10955
Variational principles in thermoplasticity. Part 2: Coupled thermomechanical processes
[RUB-IFM-MITT-37-PT-2] 05 p0646 N85-14161
Finite element method calculation of a necking tension specimen including heat transfer influence
[RUB-IFM-MITT-40] 05 p0648 N85-14162
Structure-property relationships in thermoplastic elastomers. Part 1: Segmented polyether-polyurethanes
[AD-A148043] 08 p1133 N85-17138
Characterization of novel binders based on energetic thermoplastic elastomers
[AD-A148993] 10 p1451 N85-19139
Thermoset-thermoplastic aromatic polyamide containing N-propargyl groups
[NASA-CASE-LAR-12723-1] 11 p1610 N85-20123
Process for preparing solvent resistant, thermoplastic aromatic poly(imidesulfone)
[NASA-CASE-LAR-12858-2] 11 p1610 N85-20124
Chemoviscosity modeling for thermosetting resins, 2
[NASA-CR-177958] 24 p4073 N85-35243

THERMOREGULATION
Thermoregulatory consequences of long-term microwave exposure at controlled ambient temperatures
[PB84-236603] 05 p0697 N85-14484
Effects of body mass and morphology on thermal responses in water
[AD-A147558] 07 p1016 N85-16455
Specifics of human thermal regulatory reactions upon exposure to coriolis acceleration
10 p1525 N85-19617
Sleep deprivation and exercise tolerance
[AD-A150586] 13 p2142 N85-23296
Exercise-heat strain during hypohydration: Interaction with heat acclimation and aerobic fitness
[AD-A151023] 14 p2389 N85-24717
Thermoregulatory and vestibular systems in the rat
15 p2610 N85-26082
Mathematical models relating to human thermoregulation: Basic assumptions, validation, and application. Parts A and B
[AD-A151558] 15 p2616 N85-26130
Primate experiments on SLS-1
15 p2687 N85-26592
Microwave radiation and thermoregulation
[AD-A155718] 22 p3818 N85-33654
Electroanesthesia as a means of controlling cold stress of local hypothermia 22 p3823 N85-33687

THERMOSETTING RESINS
NT EPOXY RESINS
NT KEVLAR (TRADEMARK)
NT NYLON (TRADEMARK)
NT PHENOLIC RESINS
NT POLYAMIDE RESINS
Chemoviscosity modeling for thermosetting resins - I
[NASA-CR-172443] 03 p0326 N85-12096
Constituent property - composite property relationships in thermoset matrices 04 p0465 N85-12950
Free volume considerations in thermoplastic and thermosetting resins 04 p0465 N85-12952
Thermally stable thermoset resin compositions
[AD-D011274] 05 p0620 N85-13963
The use of microdielectrometry in monitoring the cure of resins and composites
[AD-A148619] 08 p1119 N85-17055
Synthesis of hydrophobic, crosslinkable resins
[AD-A150658] 14 p2260 N85-24002
NASA/aircraft industry standard specification for graphite fiber toughened thermoset resin composite material
[NASA-RP-1142] 16 p2742 N85-26923
Structure-property relationships in polymeric matrix materials
[AD-A153929] 18 p3080 N85-29050
Synthesis and properties of arylethersulfone thermoset systems
[AD-A154811] 21 p3569 N85-32198
Chemoviscosity modeling for thermosetting resins, 2
[NASA-CR-177958] 24 p4073 N85-35243

THERMOSIPHONS
Investigation of crisis phenomena in thermosyphons with internal heat-dissipation
[BLL-M-35765-(5828.4)] 02 p0197 N85-11313

THERMOSPHERE
NT TURBOPAUSE
Global matrix of thermospheric density values for selected solar/geomagnetic conditions and spacecraft orbital attitudes
[NASA-TM-86478] 04 p0533 N85-13409
Dynamics of the low-latitude thermosphere and ionosphere 09 p1351 N85-18501
Middle Atmosphere Program. Handbook for MAP, volume 10
[NASA-CR-175477] 11 p1658 N85-20450
Coupling between the thermosphere and the stratosphere: The role of nitric oxide
11 p1662 N85-20472
Basic features of global circulation in the mesopause lower thermosphere region 11 p1662 N85-20475
Investigation of aeronomic processes on the basis of ionospheric sporadic E 11 p1663 N85-20482
High time resolution thermospheric temperature and wind studies in the Arctic
[AD-A150114] 12 p1890 N85-21860
Experiment for measuring electric fields within the sounding rocket project Energy Budget
[BMFT-FB-W-84-048] 12 p1891 N85-21866
Models of the upper atmosphere
12 p1945 N85-22217
Analysis and interpretation of observations of airglow at 297 nm in the Venus thermosphere
13 p2172 N85-23473
Mechanism of formation of low temperatures in nighttime Venusian thermosphere 16 p2723 N85-26807
Thermospheric winds observed by OI6300A Doppler shifts at 23 deg S in the Brazilian sector
[INPE-3384-RPE/470] 16 p2834 N85-27479
Circulation and transport in the middle atmosphere: Mesosphere and lower thermosphere
18 p3148 N85-29492
Additional possibilities of radiometeor azimuthal method for measuring wind velocity in lower thermosphere
19 p3296 N85-30438
Venus thermospheric circulation
[PB85-180420] 19 p3384 N85-30097
Further developments of EISCAT as an MST radar
21 p3627 N85-32634

THERMOSTABILITY
U THERMAL STABILITY

THERMOSTATS
German payloads for EURECA 1
[BMFT-FB-W-85-003] 20 p3419 N85-31223
TEMO and TEB thermoelectronic devices
22 p3779 N85-33415

THERMOTROPISM
U ANISOTROPY
U TEMPERATURE EFFECTS

THERMOVISCOELASTICITY
Thermoviscoelastic analysis of dimensionally stable fiber composite space structures
[AD-A149275] 11 p1593 N85-20021
The initiation and growth of adiabatic shear bands
[AD-A154459] 19 p3267 N85-30082

THESAURI
An operational system for subject switching between controlled vocabularies: A computational linguistics approach
[NASA-CR-3838] 02 p0283 N85-11903
NASA Thesaurus supplement: A 3-part cumulative supplement to the 1982 edition of the NASA Thesaurus
[NASA-SP-7051(SUPPL-2)] 03 p0437 N85-12785
Online database search strategies and thesaural relationship models 09 p1402 N85-18822
Keyword thesaurus: A list of terms and codes to identify areas of interest for research and other types of sponsored programs (revised October 1984)
[PB85-136893] 10 p1566 N85-19880
NASA Thesaurus supplement, a three part cumulative supplement to the 1982 edition of the NASA Thesaurus
[NASA-SP-7051(SUPPL-3)] 14 p2432 N85-25002
Energy data base: Subject thesaurus
[DE84-010568] 16 p2878 N85-27761

THETA PINCH
The origin of plasma rotation in the early phase of an FRC produced by a reversed field theta pinch
[IPPJ-698] 06 p0863 N85-15482
Theta pinch discharges for solids vaporization and elemental chemical analysis
[DE85-002968] 11 p1733 N85-20990

THIAZINE (TRADEMARK)
The electrochemistry of azine, oxazine and thiazine dyes
[AD-A152394] 17 p2918 N85-27890

THICK FILMS
Conductor structure for thick film electrical device
[AD-D011240] 01 p0043 N85-10281
Thick film radiation detector
[AD-D011211] 01 p0046 N85-10318
Structural studies of sputtered MOS(2) films by angle-resolved photoelectron spectroscopy
[AD-A146052] 03 p0433 N85-12759
Transport processes during the growth of oxide films at elevated temperature
[AERE-R-11293] 03 p0434 N85-12766
Qualification of a thick film hybrid
[BMFT-FB-W-84-024] 04 p0497 N85-13170
Viscosity measurements for thick-film pastes
06 p0831 N85-15280
The replacement of precious metal thick film inks using conductive polymer technology. Phase 1: Feasibility study
[AD-A147814] 07 p0933 N85-15913
Ink jet printing of silver metallization for photovoltaics
[NASA-CR-175798] 15 p2586 N85-25943
The replacement of precious metal thick film inks using conductive polymer technology
[AD-A152002] 16 p2749 N85-26965
MOD silver metallization for photovoltaics
[NASA-CR-175773] 16 p2818 N85-27581
MOD silver metallization for photovoltaics
21 p3610 N85-32428

THICK PLATES
On some exact solutions in elastostatics in terms of harmonic functions 09 p1332 N85-18367
Assessment of effectiveness of electron beam welding of titanium alloys up to 40 mm in thickness by vertical or horizontal beam 11 p1603 N85-20078
Method of separately determining electrophysical properties of bulky conductor 13 p2073 N85-22961
Method of fabricating acceleration resistant crystal resonators and acceleration resistant crystal resonators so formed
[AD-D011630] 16 p2778 N85-27146
The nonlinear analysis of thick composite plates using a cubic spline function 16 p2798 N85-27252
A refinement of the transverse shear deformation theory for multilayered anisotropic plates
[STN-5] 20 p3471 N85-31671

THICK WALLS
Allowing for the temperature field in the wall thickness of checkerwork in thermal calculation
[BLL-M-38015-(5828.4)] 07 p0956 N85-16058
Development of a floating element wall shear transducer
[AD-A148450] 08 p1164 N85-17348
Radiographic inspection of butt welds described
11 p1620 N85-20198
Methods of first wall structural analysis with applications to the long pulse commercial Tokamak reactor design
[DE85-004915] 15 p2657 N85-26397
Experimental study of collapse of thick-walled tube under external pressure and axial force
23 p3904 N85-34186
THICKNESS
Evaluation of moduli and thicknesses of pavement systems by spectral-analysis-of-surface-waves method
[PB84-219112] 03 p0342 N85-12205
Variation of resin properties through the thickness of cured samples 04 p0468 N85-12974
Synthesis study of nondestructive testing devices for use in overlay thickness design of flexible pavements
[PB84-218080] 06 p0774 N85-14950
Stability of circular cylindrical shell with piecewise constant thickness subjected to radial pressure
06 p0779 N85-14982
Method for non contacting gauging of the wall thickness of tubes by backscattering radiation
[OEFZS-4274] 07 p0968 N85-16144
Lithography radiation effects study
[AD-A149552] 10 p1468 N85-19260
New method for studying surface crack growth in laminated polymer composite materials
11 p1598 N85-20051
Thickness effect in low-density insulation
[DE85-003065] 11 p1631 N85-20273
Liquid thickness gage
[NASA-CASE-LAR-13342-1] 11 p1635 N85-20297
AEM with a convergent beam
[DE85-000667] 11 p1714 N85-20784
An investigation of compressible flows over open cavities including shear layer thickness effects
[AD-A150086] 12 p1847 N85-21588
Analysis of optimum front cover thickness for lightweight solar arrays 13 p2010 N85-22606
Composition and thickness of oxide coatings on granule surfaces of aluminum alloys 13 p2030 N85-22719
Spectral frequency of eigenvalues in optimal problems of stability of cylindrical shells of variable thickness
13 p2047 N85-22815
Thickness of ridged plains materials in Hesperia Planum, Mars 13 p2185 N85-23561
Apparent thichness of Saturn's rings from the observations of the ring plane crossing
15 p2671 N85-26477
Specimen thickness effects for elastic-plastic CTOD toughness of A36 steel
[DE85-006992] 18 p3077 N85-29038
Electrodynamic transducers for ultrasonic reception
18 p3119 N85-29306
Effect of confinement on failure in 95 TATB/5 KEL-F
[DE85-010790] 19 p3251 N85-30158
Heat flow through ocean floor and its relationship to lithosphere structure and thickness
19 p3294 N85-30422
X-ray diffractometric measurements and calculations of limiting values of discrepancy between lattices and layer thicknesses, preventing generation of dislocations during growth of multilayer heterostructures
21 p3681 N85-32866
The longitudinal thickness of air-shower fronts
[OG-9.5-1] 23 p4030 N85-34978
Solid neon sources for plasma and X-ray lasers
[DE85-011347] 24 p4098 N85-35402
THIN AIRFOILS
NT THIN WINGS
Aerodynamics of airfoils subject to 3-dimensional periodic gusts
[AD-A145149] 01 p0003 N85-10018
Technology for pressure-instrumented thin airfoil models, phase 1
[NASA-CR-3891] 14 p2227 N85-23804
THIN FILMS
NT ENERGY ABSORPTION FILMS
NT FERROMAGNETIC FILMS
NT MONOMOLECULAR FILMS
Research on large, highly accurate, inflatable reflectors
[AD-A145080] 01 p0016 N85-10099
Analysis of glow discharges for understanding the process of film formation
[NASA-TM-83750] 01 p0022 N85-10138
Platinum thin film resistors as accurate and stable temperature sensors
[NASA-TM-77728] 01 p0049 N85-10322
Time resolved calorimetry of 30 nm Te-films during laser annealing
[AD-A145047] 01 p0052 N85-10346
Conversion of microwave signals by superconducting films in the resistive state
[NASA-TM-77595] 01 p0123 N85-10843
Preparation and properties of evaporated CdTe films compared with single crystal CdTe
[DE85-000502] 02 p0222 N85-11452
DOE/SERI polycrystalline thin-film photovoltaic research
[DE84-004516] 02 p0223 N85-11464
Thin film (Al, Ga)As heterojunction solar cells
02 p0258 N85-11691
Materials modification by ion beam mixing
[AD-P003948] 02 p0286 N85-11864
Relationships between electronic structure and stability of metallic glasses
[AD-A145506] 02 p0287 N85-11874
Diffusion of Cr-51 tracer in Cr-2O-3 and the growth of Cr-2O-3 films
[AERE-R-11314] 03 p0333 N85-12146
Twisted domain wall in very thin magnetic films with perpendicular anisotropy 03 p0350 N85-12252
Effect of heat treatment on phase composition and crystal structure of thin WSi2 films on silicon substrates
03 p0350 N85-12253
One-dimensional model of thin films. Analysis of aluminum surface 03 p0350 N85-12254
Development of the production technology of Cu2S/CdS solar generators
[BMFT-FB-T-84-137] 03 p0386 N85-12469
Dielectric and optical properties of sputtered thin films
[AD-A146210] 03 p0420 N85-12681
Fast ions as probes in solid state research
03 p0430 N85-12740
Center for dielectric studies
[AD-A146183] 03 p0434 N85-12761
The effect of thin-film growth mode on XPS/UPS/AES intensities
[AD-A146284] 03 p0434 N85-12763
Transport processes during the growth of oxide films at elevated temperature
[AERE-R-11293] 03 p0434 N85-12766
Research activities of the Illinois University Coordinated Science Laboratory
[AD-A145589] 03 p0449 N85-12856
Contamination problems during surface cleaning for thermocompression bonding
[DE84-013066] 04 p0475 N85-13023
Development of a feasibility model for a thin-film precision power meter
[BMFT-FB-T-84-161] 04 p0504 N85-13217
Thin polymer film collectors as a contribution to the solar industry
[DE84-015299] 04 p0529 N85-13383
Advanced amorphous materials for photovoltaic conversion
[DE84-017198] 04 p0529 N85-13384
Development and utilization of CdS/Cu2S
05 p0662 N85-14256
Contamination analysis of Ti-O2 thin films deposited using ion assisted deposition
[DE84-014944] 05 p0732 N85-14705
Stability of lubricant film in gas dynamic bearing
06 p0778 N85-14977
Recording holograms on thin films of titanium dioxide
06 p0789 N85-15039
Oxide charge characteristics of low temperature MOS (Metal-Oxide-Silicon) oxide films
[AD-A146447] 06 p0803 N85-15113
Amorphous metallic layers in Si metallization systems
06 p0830 N85-15277
Recent developments in photovoltaics
[DE84-004528] 06 p0833 N85-15305
Electronic transport processes in refractory metal silicides
[AD-A146495] 06 p0861 N85-15468
Effects of monolayer coverages on substrate sputtering yields 06 p0865 N85-15496
Synergestic sputtering properties of binary alloys
06 p0865 N85-15497
Arc-evaporated carbon films: Optical properties and electron mean free paths
[DE85-001246] 06 p0867 N85-15510
Substrate preparation for thin film deposition: A survey
[DE84-016119] 06 p0868 N85-15514
Evaluation of colorless polyimide film for thermal control coating applications
[NASA-TM-86341] 07 p0930 N85-15894
Sputtering in thin film technology for optics — laser systems 07 p0938 N85-15948
Fast granular superconducting bolometer
[AD-D011332] 07 p0961 N85-16093
High temperature thermocouple and heat flux gauge using a unique thin film-hardware hot juncture
[NASA-TM-86898] 07 p0962 N85-16096
Research on electroluminescence in thin film yttrium oxysulfide
[AD-A146909] 07 p1037 N85-16582
Electronic structure, chemical bonding, and electron conductivity of thin-film transition-metal silicides
[AD-A147721] 08 p1226 N85-17718
Thin film transistors for addressing flat panel displays
[BMFT-FB-T-84-210] 08 p1227 N85-17726
An inexpensive vector thin film magnetometer
[AD-A148725] 09 p1323 N85-18310
Light scattering studies of lower dimensional colloidal particle and critical fluid systems
[DE85-002087] 09 p1377 N85-18654
Thermally induced quasiparticle branch imbalance in thin film superconductors 09 p1396 N85-18786
Amorphous materials and recrystallization
[DE85-001873] 09 p1398 N85-18801
Pulsed photothermal radiometry for remote sensing of spectroscopic and physical properties of thin film
[AD-A149080] 10 p1435 N85-19041
Bondability of Al-Si thin film in thermosonic gold wire bonding — integrated circuits
[NASA-TM-77795] 10 p1439 N85-19071
Lithography radiation effects study
[AD-A149552] 10 p1468 N85-19260
Mod silver metallization for photovoltaics
[NASA-CR-174444] 10 p1509 N85-19518
Use of alternative solvents for low-temperature LPE growth of CdTe films
[AD-A149418] 10 p1562 N85-19853
Photon scattering and interaction analysis of interfacial corrosion and catalysis
[DE85-002534] 11 p1606 N85-20114
Deposition of diamondlike carbon films
[NASA-CASE-LEW-14080-1] 11 p1615 N85-20153
Chemically amplified laser direct-writing of aluminum
[DE85-000308] 11 p1639 N85-20324
Fabrication of monocrystalline GaAs solar cells utilizing NaCl sacrificial substrates
[DE84-013016] 11 p1673 N85-20544
Observation of standing spinwaves in thin Fe-films by means of Raman spectroscopy
[DE85-003036] 11 p1735 N85-20913
A computer simulation of thin film nucleation and growth: The Volmer-Weber case
[NASA-TM-86968] 12 p1796 N85-21264
A process to produce fine line metallic collection patterns on semiconductors devices
[NASA-CASE-NPO-16413-1] 12 p1805 N85-21325
Monolithic thin film SAW (Surface Acoustic Wave) structures
[AD-A149782] 12 p1835 N85-21511
Advanced thin film thermocouples
[NASA-CR-175541] 12 p1850 N85-21607
Ultrasensitive measuring devices
[DE85-000672] 12 p1853 N85-21622
Development of a CdSe thin film solar cell
12 p1880 N85-21796
Thin film technology of high-critical-temperature superconducting electronics
[AD-A150010] 12 p1940 N85-22185
Mass spectra of neutral particles released during electrical breakdown of thin polymer films
13 p1996 N85-22511
Microscopic magnetic structure of multiple bilayers of thin films of Fe and Ge
[DE85-004188] 13 p2024 N85-22682
Structure of amorphous films of alloys based on Fe, condensed from laser erosion products
13 p2035 N85-22749
Planar ferroelectric microcapacitors for microwave devices 13 p2087 N85-23032
Non-linear optical techniques for visible and UV lasers and thin film deposition
[AD-A150489] 13 p2096 N85-23077
Silicon-sheet and thin-film cell and module technology potential: Issue study
[NASA-CR-175654] 14 p2349 N85-24520
Tunneling in magnetic superconducting systems
[AD-A150677] 14 p2426 N85-24963
Ferroelectric tungsten bronze bulk crystals and epitaxial thin films for electro-optic device applications
[AD-A151044] 14 p2427 N85-24970
Structure of condensed aluminum thin film metallizations 15 p2512 N85-25501
Recording of acoustic wave in gaseous medium with thin-film pyroelectric transducers
15 p2525 N85-25571
Thin film cadmium telluride and zinc phosphide solar cells
[DE85-002904] 15 p2587 N85-25950
In situ thin film measurements
[AD-A151379] 15 p2652 N85-26353

Experimental and theoretical study of the infrared reflectance of thin oxide films on metals
[DE85-006799] 15 p2653 N85-26386
Applications of piezoelectric and pyroelectric thin films: Opportunities for Langmuir-Blodgett technology
[AD-A149239] 15 p2659 N85-26408
Synthesis and characterization of superconducting electronic materials
[AD-A151112] 15 p2659 N85-26409
In situ thin film measurement
[AD-A151365] 15 p2659 N85-26411
Fundamental studies of growth, doping and transformation in beta silicon carbide
[AD-A152047] 15 p2660 N85-26416
Characterization of thin films and layered structures using X-ray absorption and reflection at grazing incidence
[DE85-006560] 15 p2662 N85-26429
Thin-film polycrystalline silicon research
[DE85-002908] 15 p2663 N85-26434
Thin-film sensors for space propulsion technology
17 p2915 N85-27968
In situ HVEM studies of electron beam-driven composition changes in thin film alloys: Displacement-rate gradient effects
[DE85-007992] 17 p2931 N85-28092
Thin films properties of sputtered niobium silicide on SiO2, Si3N4 and on n+ poly-Si
[AD-A152378] 17 p2952 N85-28228
Technology development for thin-film-trace humidity sensors
[BMFT-FB-T-84-268] 17 p2969 N85-28338
Research and developmental study on MIS thin film solar cells of amorphous hydrogenated silicon, part 2
[BMFT-FB-T-84-290] 17 p2986 N85-28467
The structure of ion plated films in relation to coating properties
[NASA-TM-87055] 18 p3085 N85-29085
Dynamics of thin-film breakup in a constricted pore
[DE85-006442] 18 p3101 N85-29199
SERI photovoltaic advanced research and development project: FY 1984 accomplishments
[DE85-002939] 18 p3128 N85-29368
Thin layered interference mirrors to reduce radiation damage
[DE85-009763] 18 p3185 N85-29756
Ion beam sputter-deposited thin film coatings for protection of spacecraft polymers in low Earth orbit
[NASA-TM-87051] 19 p3248 N85-30137
Mechanical protection of DLC films on fused silica slides
[NASA-TM-87056] 19 p3248 N85-30138
Method for production of ceramic oxide and carbide bodies by polymer inclusion and decomposition
[DE85-011668] 19 p3250 N85-30152
Thin film phase transition materials development program
[AD-A154260] 19 p3259 N85-30209
VUV synchrotron light as a technique for studying the interface quality and properties of thin overlayers
[DE85-009822] 19 p3262 N85-30227
High temperature Raman studies of phase transitions in thin film dielectrics
[DE85-010973] 19 p3263 N85-30234
Cadmium sulfide/copper ternary heterojunction cell research
[DE85-006778] 19 p3305 N85-30486
Optical effects of thin film adhesives in multijunction solar cells
[DE85-010120] 19 p3305 N85-30488
Photoeffects of semiconductor electrolyte interfaces
[AD-A154163] 20 p3449 N85-31411
Nitridation of SiO2 for surface passivation
20 p3480 N85-31627
Recent improvements in materials for thin GaAs and multibandgap solar cells
[DE85-008800] 20 p3484 N85-31651
New metal coating method developed
21 p3568 N85-32191
Multilayer capacitor dielectrics produced from metallo-organic precursors
[AD-A154592] 21 p3580 N85-32254
Development of wide band recording materials
[AD-A154961] 21 p3589 N85-32309
Microwave-enhanced thin-film deposition
21 p3611 N85-32431
Failure analysis of thin-film amorphous-silicon solar-cell modules 21 p3613 N85-32452
Electrotransport in thin films
[AD-A155584] 21 p3710 N85-33034
Structure and functions of ultra-thin films of organic compounds
[DRIC-T-7481] 22 p3741 N85-33188
Examination of anisotropic films by resonance method
22 p3778 N85-33412
Advances in sputtered and ion plated solid film lubrication 22 p3797 N85-33524
1985 Amorphous Silicon Review Meeting
[DE85-008794] 22 p3807 N85-33582
Development and demonstration of a spiral-wound thin-film composite membrane system for the economical production of oxygen-enriched air, phase 4
[DE85-012380] 23 p3920 N85-34288
Polarisation insensitive achromatic cube beamsplitter — binocular microscopes
[NPL-MOM-72] 23 p3973 N85-34630

THIN PLATES
A triangular finite element for thin plates and shells
01 p0058 N85-10386
Composite laminate optimization program suitable for microcomputers 01 p0059 N85-10389
Scattering of H10-mode wave by narrow conducting plate inside rectangular waveguide
06 p0788 N85-15036
Microstructure, texture and formability of thin aluminium sheets 06 p0796 N85-15088
Silicon-sheet surface studies
06 p0831 N85-15287
Investigation of structural and electrical properties of low-angle silicon sheet 06 p0831 N85-15288
Static and dynamic fracture toughness characterization of SA508 forging and SA533B welded plate — pressure vessel steels
[CISE-2256] 08 p1131 N85-17127
The problem of protecting the structure of a packet composite of optimal thinwall elements
10 p1444 N85-19101
Assessment of effectiveness of electron beam welding of titanium alloys up to 40 mm in thickness by vertical or horizontal beam 11 p1603 N85-20078
Potential of high-average-power solid state lasers
[DE85-003884] 11 p1639 N85-20329
A new model for thin plates with rapidly varying thickness. Part 3: Comparison of different scalings
[AD-A149748] 12 p1866 N85-21704
Scattered data interpolation using thin plate splines with tension
[AD-A149603] 12 p1866 N85-21705
Experimental and numerical analysis of electric currents and electromagnetic blunting of cracks in thin plates
[AD-A150418] 13 p2022 N85-22669
Breakdown of thin plates by radiation
13 p2028 N85-22709
Pre- and post-processing for stream-function eddy current calculations
[AD-A150417] 13 p2065 N85-22896
Measurement of damping of graphite epoxy materials
[NASA-CR-175663] 14 p2248 N85-23931
The effect of low sheet thicknesses on the fracture toughness of an Al alloy (7075-T6) — Aramid Reinforced Aluminum Laminate (ARALL)
[VTH-LR-425] 16 p2752 N85-26964
A method for the evaluation of the residual energy of a metallic fragment after perforation of a thin target
[ISL-R-113/83] 16 p2794 N85-27233
An experimental study of the magnetoelastic bending of thin plates made of soft ferromagnetic material
19 p3282 N85-30352
Method of preparing thin porous sheets of ceramic material
[DE85-006399] 24 p4082 N85-35300

THIN WALLED SHELLS
A triangular finite element for thin plates and shells
01 p0058 N85-10386
Initial postbuckling analysis of elastoplastic thin-shear structures 01 p0059 N85-10393
Numerical improvement of asymptotic solutions and nonlinear shell analysis 05 p0648 N85-14156
Nonlinear finite element analysis of elastic and elastic-plastic buckling of cylinders under complex combined loads 09 p1332 N85-18373
The problem of protecting the structure of a packet composite of optimal thinwall elements
10 p1444 N85-19101
A new NDE (Non-Destructive Evaluation) capability for thin-shelled structures
[AD-A149625] 12 p1862 N85-21676
Elasticity formulas for thin-walled shells with piezoceramic layers 13 p2047 N85-22816
Fabrication of ceramic substrate-reinforced and free forms
[NASA-TM-86994] 14 p2247 N85-23926
Strength computation of thin walled shell by discreet-continuous model 14 p2266 N85-24161
Dynamic creep buckling: Analysis of shell structures subjected to time-dependent mechanical and thermal loading 17 p2913 N85-27959
Initial imperfection surveys on conical shells at Hoechst AG
[VTH-LR-407] 17 p2981 N85-28429

THIN WALLS
Interactive buckling of thin-walled structural components under static and dynamic loads
01 p0059 N85-10382
Analysis of thin-walled airframe members in geometrically nonlinear statement
06 p0780 N85-14866
Stability of hollow shafts under torsion
06 p0780 N85-14868
Effect of protective medium on durability and fracture structure on seam zones of thin-walled titanium articles produced by diffusion welding 13 p2033 N85-22738
Theory of diaphragm light modulators with electrical input signal 13 p2062 N85-23002
Head-on scattering of a tubular cylinder of finite length for radar target identification purposes
[AD-A155606] 21 p3577 N85-32246

THIN WINGS
ESP (External-Stores Program): A pilot computer program for determining flutter-critical external-store configurations. Volume 2: Final report on program enhancement and delivery
[AD-A152269] 16 p2711 N85-26728
A computational method for wings of arbitrary planform
[AD-A153788] 18 p3059 N85-28929
A supersonic potential gradient method for the calculation of unsteady aerodynamic pressures on harmonically oscillating wings
[DFVLR-FB-85-11] 20 p3390 N85-31026

THINNERS
U SOLVENTS

THIOLS
Formation of high molecular weight products from benzene during boundary lubrication
[NASA-TM-86966] 13 p2017 N85-22644
Distribution and abundance of organic thiols
21 p3857 N85-32717

THOMAS-FERMI MODEL
Theoretical thermodynamics of mixtures at high pressures 13 p2183 N85-23550

THOMAS-FERMI THEORY
U THOMAS-FERMI MODEL

THOMSON EFFECT
U THERMOELECTRICITY

THOMSON SCATTERING
A high transmission, 20 channel polychromator for the Thomson scattering diagnostic of TORTUR 3 — plasma diagnostics
[REPT-84-156] 03 p0422 N85-12694
Lidar-Thomson scattering — nuclear fusion
[IPP-1/299] 08 p1221 N85-17693
Feasibility of alpha particle measurement by CO2 laser Thomson scattering
[DE85-001764] 09 p1326 N85-18334
Lidar-Thomson scattering — Joint European Torus
[IPF-84-3] 09 p1394 N85-18777
Feasibility of alpha particle measurement by CO2 laser Thomson scattering
[DE85-004938] 13 p2097 N85-23081
System for lower hybrid current startup
15 p2654 N85-26373
Electron temperature measurements from induced toroidal current in ELMO Bumpy Torus scale
[DE85-008549] 18 p3189 N85-29776
Thomson scattering on Elmo Bumpy Torus
[DE85-010584] 20 p3527 N85-31941
Instrument to synchronize Thomson scattering diagnostic measurements with MHD activity in a Tokamak
[DE85-012082] 23 p3964 N85-34708

THORIUM
NT THORIUM ISOTOPES
Contribution to the radiogeology of Sao Roque, SP, granites
[INPE-3076-PRE/492] 03 p0391 N85-12500
U, Th, K content, heat production and thermal conductivity of Sao Paulo, Brazil continental shelf sediments: A reconnaissance work
[INPE-3401-PRE/670] 10 p1515 N85-18559
Uranium, thorium isotopic analyses and uranium-series ages of calcite and opal and stable isotopic compositions of calcite from drill cores UE25a no. 1, USR G-2 and USW G-3/GU-3, Yucca Mountain, Nevada
[DE85-013039] 23 p3948 N85-34471

THORIUM ISOTOPES
Development of solid thorium-232 reference materials
[DE85-011453] 22 p3841 N85-33765

THORIUM 228
U THORIUM ISOTOPES

THORIUM 230
U THORIUM ISOTOPES

THORIUM 234
U THORIUM ISOTOPES

THORON
U RADON ISOTOPES

THREADS
Improvement of gas-tightness of OTTG and TBO-5 threaded pipe couplings
[BLL-M-35993-(5828.4)] 07 p0972 N85-16175
The design and development of a spacecraft appendage tie down mechanism 22 p3797 N85-33522
THREAT EVALUATION
Dual band radome wall design
[AD-P004357] 12 p1825 N85-21451
Generation of flight paths using heuristic search
[AD-A151949] 16 p2704 N85-26694
Fiber reinforcement of gun propellant
[AD-A152296] 16 p2757 N85-27014
Space Station crew safety alternatives study. Volume 5: Space Station safety plan
[NASA-CR-3858] 17 p2906 N85-27930
Space station crew safety alternatives study. Volume 3: Safety impact of human factors
[NASA-CR-3856] 19 p3223 N85-29984
Space station crew safety alternatives study, volume 1
[NASA-CR-3854] 19 p3223 N85-29985
Space Station crew safety alternatives study. Volume 2: Threat development
[NASA-CR-3855] 21 p3558 N85-32133
Evaluation of a software design approach: Develop a threat resolution module in Ada (trademark)
[AD-A155599] 21 p3672 N85-32815
THREE AXIS STABILIZATION
Fluid slosh dynamics of surface tension tanks in three axis stabilized spacecraft
[MBB-UR-E-739-84-O] 11 p1634 N85-20291
The attitude control model tests for the Infrared Astronomical Satellite (IRAS)
[B8580071] 18 p3067 N85-28967
THREE BODY PROBLEM
Sturmian expansion approximation to three-body scattering
[CSIR-TWISK-309] 01 p0109 N85-10731
Spline-Galerkin solution of integral equations for 3-body scattering above break-up
[TWISK-327] 01 p0109 N85-10738
Rapid nonresonant rotation of a spacecraft in nominally periodic orbits in limited 3 body problem
02 p0160 N85-11063
Quasi-three dimensional modeling of functionally-integrated elements of large-scale integrated circuits 04 p0490 N85-13122
The restricted problem of 2 + N bodies
09 p1414 N85-18925
Lagrangian solutions in photogravitational restricted circular three-body problem 13 p1979 N85-22416
Computation of elliptical functions in problems of celestial mechanics 13 p1979 N85-22418
Stability of steady motions of dynamically symmetrical solid at a triangular libration point
14 p2279 N85-24120
On an assymetric choice for a cluster expansion of the three-body problem
[CSIR-TWISK-339] 14 p2408 N85-24844
Applications of three-body resonances to satellites and planetary rings 15 p2676 N85-26518
Integrable cases of restricted doubly averaged 3-body problem 16 p2718 N85-26778
The 6 pi-periodic solutions of plane restricted elliptical 3-body problem in neighborhood of libration points
16 p2718 N85-26779
Configuration space Faddeev calculations
[DE85-005813] 16 p2872 N85-27721
THREE DIMENSIONAL BODIES
Recent advances in hybrid/mixed finite elements
[NASA-CR-175574] 12 p1863 N85-21687
Three-dimensional sensing and interpretation
[AD-A150890] 14 p2311 N85-24304
Three-dimensional photochemical machining with lasers
[AD-A154711] 21 p3591 N85-32320
On the dependence of the convergence of Gummel's algorithm on the regularity of the solution
[AD-A154628] 21 p3675 N85-32832
Mathematical modeling of ultimate heat sink cooling ponds
[TI85-009747] 23 p3932 N85-34369
A simple but systematic CSG system
23 p3963 N85-34569
Building an octree from a set of parallelepipeds
23 p3964 N85-34572
Low cost geometric modelling system for CAM
23 p3964 N85-34578
Generative design in architecture using an expert system 23 p3965 N85-34582
THREE DIMENSIONAL BOUNDARY LAYER
On the instability of a 3-dimensional attachment line boundary layer: Weakly nonlinear theory and a numerical approach
[NASA-CR-172504] 07 p0957 N85-16063
Theoretical contributions to transonic flow analysis for transport aircraft
[BMFT-FB-W-84-036] 08 p1078 N85-16838
A 3-dimensional turbulent boundary layer upstream and around a junction vortex flow 08 p1160 N85-17319
A finite difference method for inverse mode calculations of a three-dimensional boundary layer
[ESA-TT-869] 09 p1274 N85-18007
Influence of turbulence of incident stream on three dimensional boundary layer 14 p2278 N85-24113
An exploratory investigation of sharp fin-induced shock wave/turbulent boundary layer interactions at high shock strengths
[AD-A151571] 15 p2556 N85-25772
Three-Dimensional Boundary Layers
[AGARD-R-719] 15 p2558 N85-25784
Three-dimensional boundary layers and shear flows activities at ONERA/CERT 15 p2558 N85-25785
Three-dimensional boundary layers: A report on work in Germany 15 p2559 N85-25786
Three-dimensional boundary layer research at NLR
15 p2559 N85-25787
Brief review of current work in the UK on three dimensional boundary layers 15 p2559 N85-25788
Problems and opportunities with three-dimensional boundary layers — aircraft, missile, and ship components 15 p2559 N85-25789
Three-dimensional wing boundary layer analysis program BLAY and its application
16 p2694 N85-26632
THREE DIMENSIONAL FLOW
NT SECONDARY FLOW
Numerical analysis of the 3-dimensional inviscid hypersonic flow around capsule-type bodies by the alternate directional implicit method
[NAL-TR-799] 01 p0002 N85-10012
Aerodynamics of airfoils subject to 3-dimensional periodic gusts
[AD-A145149] 01 p0003 N85-10018
Transonic wing and far field test data on a high aspect ratio transport wing for three dimensional computational method evaluation 01 p0004 N85-10021
Oil flow patterns of separated flow on a hemispherical cylinder at incidence
[DFVLR-FB-84-20] 01 p0048 N85-10313
Characteristic boundary conditions for three-dimensional transonic unsteady aerodynamics
[NASA-TM-86292] 02 p0134 N85-10915
Three dimensional separation and vortex formation
02 p0196 N85-11306
Two- and three-dimensional model and wall data from a flexible-walled transonic test section
03 p0312 N85-12015
A data base for three-dimensional all-interference code evaluation 03 p0312 N85-12017
Minimization of wall interference for three-dimensional models with two-dimensional wall adaptation — wind tunnel walls
[VKI-TN-149] 03 p0321 N85-12070
Turbomachinery blade design using advanced calculation methods
[PNR-90218] 04 p0456 N85-12896
Fundamental study of three dimensional two phase flow in combustion systems
[AD-A142886] 04 p0496 N85-13177
Flow calculation on a thin wing, with specific attention to separation point at the trailing edge
[FTW-FO-1721] 05 p0594 N85-13787
Accuracy of preparation of three-dimensional reference grid
[BLL-M-35921-(5828.4)] 05 p0616 N85-13939
Answering thermodynamic questions with three-dimensional viscous flow calculations
05 p0636 N85-14081
Theoretical approach to labyrinth seal forces - cross-coupled stiffness of a straight-through labyrinth seal 05 p0643 N85-14127
Turbulent bubbles behind airfoils and wings at high angle of attack 08 p1069 N85-16779
Aerodynamic issues in the design of high-lift systems for transport aircraft 08 p1069 N85-16780
Application of two and three-dimensional criteria for calculating transitions and boundary layers over swept wings 08 p1070 N85-16783
Application of the vortex-lattice concept to flows with smooth-surface separation 08 p1160 N85-17320
Research done at DERAT (October 1982 through September 1983); summary of principal results obtained
[NASA-TM-77786] 08 p1228 N85-17730
Three-dimensional vortex methods
[DE85-000391] 09 p1320 N85-18299
Averaging effects in models of three-dimensional two-phase flows
[AD-A149313] 10 p1484 N85-19371
Developments in the simulation of compressible inviscid and viscous flow on supercomputers
[NASA-TM-86674] 11 p1575 N85-19924
Three-dimensional analysis of heat transfer and gas flow in a radiant furnace
[DE84-011732] 11 p1633 N85-20284
A study of degenerate and nondegenerate critical points in three-dimensional flow fields
[DFVLR-FB-84-36] 11 p1633 N85-20288
Dynamic investigations of a spherical tank structure filled with liquid using ANSYS three-dimensional fluid elements
[MBB-UR-E-737-83-O] 11 p1654 N85-20418
Three-dimensional unsteady lifting surface theory in the subsonic range
[NASA-TM-77812] 12 p1770 N85-21111
The split-coefficient matrix method for supersonic three dimensional flow 12 p1821 N85-21425
A three-dimensional spectral algorithm for simulations of transition and turbulence
[NASA-CR-172561] 12 p1845 N85-21575
Solution of the three-dimensional Navier-Stokes equations for a steady laminar horseshoe vortex flow
[AD-A149851] 12 p1846 N85-21582
Turbulent convecting flow in a square duct with a 180 deg bend: An experimental and numerical study
[AD-A149960] 12 p1846 N85-21583
Experimental studies of Quasi-Two-Dimensional and three-dimensional viscous interaction regions induced by skewed-shock and swept-shock boundary layer interactions
[AD-A150080] 12 p1847 N85-21587
Robust calculation of three-dimensional transonic potential flow based on the nonlinear gas multigrid method and a mixed incomplete lower upper decomposition/strongly implicit procedure (ILU/SIP) algorithm
[NLR-MP-84003-U] 12 p1848 N85-21593
On the solution of the three-dimensional flowfield about a flow-through nacelle
[NASA-TM-87448] 13 p1969 N85-22371
Preliminary development of an approximation procedure for supercritical wing design optimization applications
[AD-A150177] 13 p1972 N85-22383
Calculation of three-dimensional, viscous flow through turbomachinery blade passages by parabolic marching
[NASA-TM-86984] 14 p2211 N85-23711
Mixing, chemical reaction and flow field development in ducted rockets
[DE85-004083] 14 p2247 N85-23928
Fundamental study of three dimensional two phase flow in combustion systems
[AD-A150739] 14 p2250 N85-23945
Discrete models for the numerical analysis of time-dependent multidimensional gas dynamics
[NASA-CR-172574] 14 p2300 N85-24239
Three-dimensional current systems and electric fields during active aurora 14 p2362 N85-24599
The generation of three-dimensional body-fitted coordinate systems for viscous flow problems
[AD-A150861] 14 p2408 N85-24848
Unsteady transonic aerodynamic and aeroelastic calculations about airfoils and wings
15 p2459 N85-25185
Natural convection in cylindrical containers
15 p2555 N85-25763
Two computational methods for cascade flows
16 p2692 N85-26617
Numerical example of three-dimensional flying object in shockless transonic flow 16 p2693 N85-26623
Turbulence characteristics of swirling flowfields
[NASA-CR-174918] 16 p2709 N85-26717
Study of the primary zone of gas turbine hearths
[ONERA-RTS-22/3256-EY] 16 p2709 N85-26719
Numerical analysis of flow non-uniformity in the hot gas manifold of the Space Shuttle main engine
16 p2738 N85-26899
Fuel and oxidizer turbine loss analysis
16 p2739 N85-26900
Redistribution of the inlet temperature profile through the SSME fuel turbine 16 p2739 N85-26901
Report on regional groundwater flow modeling for the Palo Duro Basin, Texas
[DE85-007490] 16 p2815 N85-27370
A three-dimensional turbulent separated flow and related mesurements
[NASA-CR-175913] 18 p3098 N85-29181
A method for computing the core flow in three-dimensional leading-edge vortices
[NASA-TM-87489] 19 p3214 N85-29932
KIVA: A computer program for two- and three-dimensional fluid flows with chemical reactions and fuel sprays
[DE85-010334] 19 p3339 N85-30693
Numerical simulation of potential flow in transonic steady regimes 20 p3389 N85-31016

Extension of the small perturbations method in three-dimensional transonic, unsteady flow to the case of real wings
[ONERA-NT-17/3084-RY-070-R] 20 p3389 N85-31017
An implicit finite-difference code for a two-equation turbulence model for three-dimensional flows
[NASA-TM-86752] 20 p3454 N85-31448
A new finite element approach: Progress in inviscid flow computations
[NASA-TM-86434] 20 p3454 N85-31450
Three-Dimensional Techniques Applied to Internal Flows in Propulsion Systems
[AGARD-LS-140] 21 p3586 N85-32293
An analysis of flow models: From Navier-Stokes to potential flow equations 21 p3587 N85-32295
Computation of three-dimensional, inviscid, rotational flows 21 p3587 N85-32296
An elliptic calculation procedure for 3-D viscous flow 21 p3587 N85-32297
A 3-D Euler method for internal transonic flows computation with a multi-domain approach 21 p3587 N85-32298
Performance evaluation of flow in turbomachinery blade rows 21 p3587 N85-32299
Numerical solution of the Navier-Stokes equations for 3-D internal flows: An emerging capability 21 p3588 N85-32300
Simulation of complex three-dimensional flows
[NASA-TM-86773] 21 p3675 N85-32831
A three-dimensional viscous flow analysis for the helicopter tip vortex generation problem
[NASA-CR-3906] 23 p3893 N85-34114
Integral equation formulation for three-dimensional unsteady transonic flow
[ARL/STRUC-R-416] 23 p3894 N85-34119
Block-implicit calculations of three-dimensional laminar flow in strongly curved ducts
[DE85-003047] 23 p3931 N85-34363
System maintenance manual for master modeling of aerodynamic surfaces by three-dimensional explicit representation
[NASA-CR-178224] 23 p3956 N85-34517
Unsteady flow in a supersonic cascade with two in-passage shocks
[NASA-CR-3925] 24 p4060 N85-35158
General design method for 3-dimensional, potential flow fields. Part 2: Computer program DIN3D1 for simple, unbranched ducts
[NASA-CR-3926] 24 p4060 N85-35159
The lateral distributions of charged particles of energy greater than 0.3 E sub crit in electron-photon cascades in lead and air
[HE-3.6-10] 24 p4185 N85-35957

THREE DIMENSIONAL MOTION
NT SECONDARY FLOW
NT THREE DIMENSIONAL FLOW
Recognition of complex 3-dimensional objects using 3-dimensional moment invariants
[AD-A148119] 08 p1212 N85-17625
Ill-posed problems and regularization analysis in early vision
[AD-A147753] 08 p1222 N85-17696
Collision detection for moving polyhedra
[AD-A148961] 10 p1544 N85-19735
Cyclic industrial robots with mechanical energy storing devices: Multipositional system with one or several degrees of freedom 13 p2045 N85-22803
Stability of Rossby waves within framework of three-component analysis 13 p2109 N85-23142
New method for compensating and measuring any motion of three-dimensional objects in holographic interferometry
[ISL-CO-216/84] 22 p3789 N85-33474
Three-dimensional hydrodynamic hot-spot model
[DE85-009587] 23 p3922 N85-34301
Computation of three-dimensional shock wave and boundary-layer interactions
[NASA-TM-86780] 24 p4093 N85-35372
Analytical-numerical methods of calculations of energy and three-dimensional particle distributions in electromagnetic cascades
[HE-3.5-13] 24 p4184 N85-35950
On mini-cluster observed by Chacaltaya emulsion chamber experiment
[HE-3.6-12] 24 p4185 N85-35959
Peculiarities of gamma-quanta distribution at 20 TeV energy
[HE-3.7-10] 24 p4186 N85-35967

THRESHOLD CURRENTS
Determination of threshold and maximum operating electric stresses for selected high voltage insulation. Task 3: Investigation of high voltage capacitor insulation
[DE84-017051] 09 p1316 N85-18274
Threshold electron studies of gas-surface interactions
[AD-A151271] 15 p2647 N85-26328
Inter-zone auger recombination in GaSb laser structures 21 p3882 N85-32875

THRESHOLD DETECTORS (DOSIMETERS)
Search for anomalous C-jets in Chacaltaya emulsion chamber experiment
[HE-3.2-5] 24 p4179 N85-35913
Exotic interactions among C-jets and Pb-jets
[HE-3.2-6] 24 p4179 N85-35914
Detection threshold energy of high energy cascade showers using thermoluminescence PTFE-sheet and hot-gas reader
[HE-7.1-5] 24 p4213 N85-36159

THRESHOLD GATES
High-power gate turn-off thyristors 06 p0793 N85-15071

THRESHOLD LOGIC
Estimation of the threshold in fatigue crack initiation models: A Bayesian approach
[AD-A144847] 01 p0062 N85-10410

THRESHOLD SHIFT
U THRESHOLDS

THRESHOLDS
Analysis of threshold effects during estimation of arrival time of optical signals 07 p0951 N85-16030
The role of nuclei size in transient cavitation threshold measurements
[AD-A148334] 08 p1162 N85-17332
Optimal threshold and weight sorting of elevation angle readings under conditions of fadeouts of a directed signal 12 p1840 N85-21547
An evaluation of discretized conditional probability and linear regression threshold techniques in model output statistics forecasting of visibility over the north Atlantic Ocean
[AD-A151955] 16 p2857 N85-27619
Threshold effects and cellular recognition
[DE85-010816] 19 p3327 N85-30614

THRESHOLDS (PERCEPTION)
Thresholds of perception of whole body linear oscillation: Modification by spaceflight 05 p0694 N85-14467
Inner ear characteristics during 7 day antiorthostatic bedrest (6 deg head down tilt) 05 p0695 N85-14470
Quantitative measurement of human auditory acuity 10 p1524 N85-19614
Auditory impairment and the onset of disability and handicap in noise-induced hearing loss
[ISVR-TR-126] 20 p3507 N85-31801
Thresholds for detection of linear oscillation following prolonged weightlessness 20 p3508 N85-31810
Auditory fatigue caused by exposure to different frequency sounds presented at equivalent intensity
[ISL-R-101/84] 20 p3525 N85-31923

THROATS
Multiple steady states for characteristic initial value problems
[NASA-CR-172486] 06 p0749 N85-14800
Mixing characteristics of an underexpanded multiple jet ejector
[AD-A148557] 10 p1485 N85-19375
Characteristics of flow of oscillatory-relaxing gas in nozzles with constant cross-sections in throat region 11 p1716 N85-20794

THROTTLING
Nonintrusive shaft speed sensor 16 p2740 N85-26908

THRUST
NT JET THRUST
NT LOW THRUST
NT ROCKET THRUST
NT VARIABLE THRUST
Three degree of freedom steady state point performance program: Updated version 1
[CSIR-NIAST-83/48] 01 p0001 N85-10005
Development of the Engineering Test Satellite-3 (ETS-3) ion engine system
[NASA-TM-77538] 01 p0017 N85-10101
Energy efficient engine ICLS engine bearings, drives and configuration: Detail design report
[NASA-CR-167871] 02 p0147 N85-10997
Thrust characterization of very high burning rate propellants
[AD-A145891] 03 p0340 N85-12186
On selecting bypass mixers for turbofan engines 09 p1306 N85-18207
An investigation of the driving wheel thrust of paddy field tractors
[AD-P004284] 09 p1407 N85-18861
Summary presentation of the Electrodynamics Interactions Panel 11 p1644 N85-20356
Report of the Electrodynamic Interactions Panel 11 p1645 N85-20363
Application of an aerodynamic analysis method including attainable thrust estimates to low speed leading-edge flap design for supersonic cruise vehicles
[NASA-CR-165843] 19 p3212 N85-29918
Measurement of turbofan-turbojet thrust from tailpipe static pressure
[AD-A154036] 19 p3220 N85-29967
Docking simulation analysis of range data requirements for the orbital maneuvering vehicle
[NASA-TM-86510] 20 p3407 N85-31143
Voyager 0.2-lbf thruster valve assembly short pulse test report
[NASA-CR-176121] 22 p3741 N85-33186

THRUST AUGMENTATION
An engine trade study for a supersonic STOVL fighter-attack aircraft, volume 1
[NASA-CR-166304] 02 p0133 N85-10910
Viscous-inviscid aerodynamic analysis of two-dimensional thrust augmentors
[NASA-CR-177321] 04 p0451 N85-12881
An experimental investigation of two-dimensional thrust augmenting ejectors, part 1
[NASA-CR-174111] 04 p0456 N85-12884
A theoretical study of two stage thrust augmenting ejectors
[ARL/AERO-R-166] 19 p3218 N85-29954
Discussion of the paper, Some Aspects of Propulsion for the Augmenter-Wing Concept, by D. C. Whittley
[NASA-TM-77884] 22 p3727 N85-33108

THRUST BEARINGS
Comparison of predicted and measured friction for a tilt-pad thrust bearing with crown and roughness under hydrodynamic and mixed lubrication
[AD-A145752] 03 p0371 N85-12371
Axial bearings with lever-type equalizer system 14 p2267 N85-24048
Work of axial bearing under dynamic loading 14 p2288 N85-24182
Calculation of friction at spherical bearing journals in turbomachines 17 p2940 N85-28150

THRUST CHAMBERS
Extended performance technology study 30-cm thruster
[NASA-CR-168259] 07 p0917 N85-15806
SSME thrust chamber simulation using Navier-Stokes equations
[NASA-CR-171349] 10 p1430 N85-19017
Thrust chamber performance using Navier-Stokes solution --- space shuttle main engine viscous nozzle calculation
[NASA-CR-171346] 10 p1430 N85-19018
Effective specific impulse of secondary flow injected into a rocket nozzle
[NAL-TR-848T] 18 p3067 N85-28970

THRUST CONTROL
NT THRUST VECTOR CONTROL
Aircraft thrust control scheme for terrain following system
[AD-D011387] 07 p0901 N85-15711
Design evolution of the orbiter reaction control subsystem 08 p1099 N85-16944

THRUST DISTRIBUTION
Space Shuttle booster thrust imbalance analysis
[NASA-TM-86493] 12 p1791 N85-21241

THRUST FAULTS
U GEOLOGICAL FAULTS

THRUST LOADS
Calculation of friction at spherical bearing journals in turbomachines 17 p2940 N85-28150
Characteristics of a confined jet thrust vector control nozzle
[AD-A153087] 17 p2958 N85-28259

THRUST MEASUREMENT
Vacuum chamber pressure effects on thrust measurements of low Reynolds number nozzles
[NASA-TM-86955] 12 p1794 N85-21259
Measurement of turbofan-turbojet thrust from tailpipe static pressure
[AD-A154036] 19 p3220 N85-29967
Two-plane balance and slip-ring design 22 p3799 N85-33538

THRUST POWER
U THRUST

THRUST REVERSAL
Experimental study of aerodynamic shielding of turbojet engine air intake against exhaust gases 09 p1307 N85-18210

THRUST VECTOR CONTROL
Gyrodynamic fixture for measuring thrust force components
[AD-D011256] 06 p0760 N85-14860
The solid rocket booster auxiliary power unit: Meeting the challenge 08 p1099 N85-16946
Static internal performance of a two-dimensional convergent nozzle with thrust-vectoring capability up to 60 deg
[NASA-TP-2391] 10 p1419 N85-18851

Preliminary performance of a vertical-attitude takeoff and landing, supersonic cruise aircraft concept having thrust vectoring integrated into the flight control system
[NASA-CR-172530] 10 p1423 N85-18977

Relative control effectiveness technique with application to airplane control coordination
[NASA-TP-2416] 14 p2218 N85-23753

Minimum time turns using vectored thrust
[AD-A151693] 15 p2471 N85-25256

Characteristics of a confined jet thrust vector control nozzle
[AD-A153067] 17 p2958 N85-28268

Static investigation of several yaw vectoring concepts on nonaxisymmetric nozzles
[NASA-TP-2432] 18 p3058 N85-28924

Thrust vectoring apparatus for maneuvering missile in flight
[AD-D011693] 19 p3226 N85-30004

THRUSTORS

Modeling the exhaust of the pulsed plasma thruster
[AD-A155344] 21 p3707 N85-33018

THUNDERSTORMS

On the nowcasting of mountain-generated thunderstorm systems 01 p0074 N85-10489

The microburst as a hazard to aviation: Structure, mechanisms, and nowcasting 01 p0074 N85-10491

A scheme for the delineation and extrapolation of thunderstorms from GOES satellite data
01 p0076 N85-10507

A lightning detection system in Sweden
01 p0078 N85-10519

A short-term forecast model for thunderstorm rotation
01 p0081 N85-10542

Nowcasting using lightning location techniques
01 p0084 N85-10568

Investigation of summertime convection over the upper Current River valley of southeast Missouri
[PB84-222389] 01 p0086 N85-10578

A case study of a convective outbreak using VAS-derived thermodynamic parameters
[AD-A145560] 02 p0232 N85-11512

Effects of a lightning strike on a civil defense operation center
[FOA-A-30035-A3] 02 p0232 N85-11514

NASA thunderstorm overflight program: Atmospheric electricity research. An overview report on the optical lightning detection experiment for spring and summer 1983
[NASA-TM-86468] 03 p0363 N85-12330

Investigations of severe/tornadic thunderstorm development and evolution based on satellite and AVE/SESAME/VAS data
[NASA-CR-174154] 04 p0536 N85-13424

Aircraft accident report Air Canada, Lockheed L-1011, C-FTNJ, near Charleston, South Carolina, November 24, 1983
[PB84-910413] 05 p0594 N85-13790

Synoptic observations of the radio noise background in the frequency range 150-180 kHz to provide design data for the low frequency communications designer
[AD-A147438] 07 p0941 N85-15965

Sea breeze-induced mesoscale systems and severe weather
[NASA-CR-174317] 08 p1187 N85-17480

Direct-strike lightning photographs, swept-flash attachment patterns, and flight conditions for storm hazards 1982
[NASA-TM-86347] 12 p1892 N85-21877

Mesoscale Atmospheric Processes Research Program Science Review
[NASA-TM-87465] 15 p2594 N85-25987

Anvil structure of severe thunderstorms
15 p2595 N85-25993

Lidar and radiometer observations of thunderstorm tops 15 p2595 N85-25994

Modeling of midwest severe thunderstorms
15 p2596 N85-25995

Satellite detection of severe thunderstorms
15 p2596 N85-25996

Severe storm detection with passive 37 GHz observations 15 p2596 N85-25997

Soil moisture and evapotranspiration estimates based on satellite data 15 p2596 N85-25998

Sea breeze-induced mesoscale systems and severe weather 15 p2598 N85-26012

Comparison of wind velocity in thunderstorms determined from measurements by a ground-based Doppler radar and an F-106B airplane
[NASA-TM-86348] 16 p2703 N85-26687

Fluid-dynamic model of a downburst
[UTIAS-271] 16 p2829 N85-27441

The electric current densities beneath thunderstorms
20 p3494 N85-31726

Thunderstorm phenomena and weather radar scanning strategies
[DOT/FAA/PM-85/14] 21 p3634 N85-32573

THYMUS GLAND

Distinctions of rat lymphatic organ reactions to acute stress factor during hypokinesia
19 p3324 N85-30596

THYRATRONS

Non-self-maintained high-voltage low-pressure discharge 13 p2088 N85-23037

THYRISTORS

NT SILICON CONTROLLED RECTIFIERS

High-speed power thyristors with excellent switching and load characteristics 06 p0793 N85-15070

High-power gate turn-off thyristors
06 p0793 N85-15071

High-speed power devices with field control
06 p0794 N85-15073

New methods of fast switching of high power by means of semiconductor devices 06 p0794 N85-15075

Allowable surge currents and failure mechanisms in semiconductor power devices in various modes of operation 06 p0795 N85-15080

Semiconductor submicrosecond power commutator switches 06 p0795 N85-15081

Analysis of inverter models and harmonic propagation. Part 3. Transient processes in inverter models
[DE85-000191] 10 p1510 N85-19530

High-voltage, high-power, solid-state remote power controllers for aerospace applications
[NASA-TP-2437] 12 p1795 N85-21263

New types of power supplies for ultrasonic processing equipment 12 p1843 N85-21566

The performance of an alternating-current thyristor-controlled motor 15 p2546 N85-25716

Fast transient behavior of thyristor switches
[AD-A154109] 19 p3259 N85-30206

Standard series of direct-current motors for regulated electric drives 22 p3772 N85-33375

Photothyristor optrons and optron microcircuits, part 1
22 p3781 N85-33424

THYROID GLAND

Structural changes in thyroid due to high-altitude adaptation in Kirghizia 22 p3820 N85-33666

TID

U TRAVELING IONOSPHERIC DISTURBANCES

TIDAL OSCILLATION

U TIDES

TIDAL WAVES

Tide tables 1985, high and low water predictions, central and western Pacific Ocean and Indian Ocean
[PB84-238393] 04 p0542 N85-13451

Recent observations of tides and tidal currents from the northeastern Bering Sea shelf
[PB84-241785] 04 p0543 N85-13452

Rip in White Sea 19 p3290 N85-30401

An objective analysis technique for extrapolating tidal fields 20 p3493 N85-31715

TIDE POWERED GENERATORS

Progress in developing tidal electric power plants reported 07 p0994 N85-16314

TIDES

NT ATMOSPHERIC TIDES
NT EARTH TIDES
NT LUNAR TIDES

Tide tables 1985. High and low ater predictions: Europe and West Coast of Africa including the Mediterranean Sea
[PB84-230093] 06 p0841 N85-15343

Spectral model for subtidal variability in the Chesapeake Bay
[PB84-226679] 06 p0842 N85-15345

Tides and tidal currents of the inland waters of Western Washington
[PB84-237379] 06 p0842 N85-15346

Monitoring of the tidal dynamics of the Dutch Waddensea by SIR-B 08 p1147 N85-17235

Altimetry, orbits and tides
[E85-10066] 08 p1174 N85-17404

Field-work report: Medway Estuary, 28 June - 18 July 1983
[RNC/NS/TR8] 13 p2041 N85-22773

Stability of the Galilean satellites in deep orbital resonance 13 p2172 N85-23477

Two-cycle mechanism of dissipation of tidal energy in ocean 14 p2335 N85-24436

Tidal breakup and origin of the Uranian ring system
15 p2676 N85-26535

Tidal rectification in lateral viscous boundary layers of a semienclosed basin
[CWI-AM-R8415] 17 p2960 N85-28284

Dynamic theory of polar tide 19 p3292 N85-30414

An objective analysis technique for extrapolating tidal fields 20 p3493 N85-31715

Ocean tidal parameters from LAGEOS
20 p3493 N85-31716

Interactions of galaxies and their nuclear activity
20 p3545 N85-32060

Reverification of the Chesapeake Bay model
[AD-A155486] 21 p3655 N85-32706

Coastal erosion along Monterey Bay
[AD-A155610] 21 p3655 N85-32707

On the importance of viscous dissipation in Io
22 p3855 N85-33873

Bibliography on tidal hydraulics. Report 2. Supplement 9: Supplementary material compiled from June 1980 - June 1983. Tidal flows in rivers and harbors
[AD-A155990] 24 p4125 N85-35574

TIG WELDING

U GAS TUNGSTEN ARC WELDING

TIGHTNESS

Improvement of gas-tightness of OTTG and TBO-5 threaded pipe couplings
[BLL-M-35993-(5826.4)] 07 p0972 N85-16175

TILES

Thermal contact conductance measurements on Doublet 3 armor title traphite
[DE84-013554] 05 p0613 N85-13916

The challenging scales of the bird: Shuttle tile structural integrity 08 p1095 N85-16919

Study of outgassing and decomposition of space shuttle heat protection tiles, fillers and adhesive
[NASA-CR-175565] 12 p1791 N85-21242

Photovoltaic roofing tile systems
12 p1878 N85-21783

Electron beam charging of Space Shuttle thermal protection system tiles 13 p1990 N85-22478

Mechanical fastener
[NASA-CASE-LAR-12738-2] 19 p3278 N85-30335

Experimental aerodynamic heating to simulated space shuttle tiles in laminar and turbulent boundary layers with variable flow angles at a nominal Mach number of 7
[NASA-TP-2307] 23 p3929 N85-34351

TILT

U ATTITUDE (INCLINATION)

TILT ROTOR AIRCRAFT

Speed benefits of tilt-rotor designs for LHX
[NASA-CR-166437] 07 p0902 N85-15717

Helicopter aeromechanics: Introduction and historical review 18 p3057 N85-28914

TILTING

U ATTITUDE (INCLINATION)

TILTING ROTORS

Speed benefits of tilt-rotor designs for LHX
[NASA-CR-166437] 07 p0902 N85-15717

TILTMETERS

Soil tilt measurement: First results of the comparative analysis of the response of two different tiltmeters
[NOTA-INTERNA-818] 02 p0228 N85-11494

TIMBER IDENTIFICATION

Remote sensing applications program
[E85-10022] 02 p0218 N85-11435

An initial analysis of LANDSAT-4 Thematic Mapper data for the discrimination of agricultural, forested wetlands, and urban land cover — Poinsett County, Arkansas; and Reelfoot Lake and Union City, Tennessee
13 p2118 N85-23193

TIMBER INVENTORY

Some principles of plant resources evaluation using remotely sensed data 04 p0543 N85-13459

Forest cover monitoring by remote sensing in Great Britain 05 p0656 N85-14214

TIME

NT EPHEMERIS TIME
NT FLIGHT TIME
NT REACTION TIME
NT RELAXATION TIME
NT RESPONSE TIME (COMPUTERS)
NT SIDEREAL TIME
NT UNIVERSAL TIME

Microseism level, time variations at Turkmen seismic stations studied 07 p0981 N85-16231

Efficient computation of optimal time for transaction processing in a database system
[AD-A147568] 07 p1054 N85-16693

A theorem on the optimal allocation of effort
[AD-A148028] 08 p1211 N85-17623

A power transformation exponential regression model for censored failure time data
[AD-A148377] 08 p1212 N85-17632

Historical cost curves for hydrogen masers and cesium beam frequency and timing standards
10 p1465 N85-19245

Space and time variations and turbopause dynamical structure 11 p1663 N85-20483

High time resolution thermospheric temperature and wind studies in the Arctic
[AD-A150114] 12 p1890 N85-21860

Annals of the New York Academy of Sciences, Volume 423 — timing and time perception
[AD-A150031] 12 p1909 N85-21961

The measurement of human time estimating ability using a modified jerison device
[AD-A151870] 15 p2620 N85-26141

Piloted simulation of an algorithm for onboard control of time-optimal intercept
[NASA-TP-2445] 18 p3063 N85-28949

Proceedings of the Sixteenth Annual Precise Time and Time Interval (PTTI) Applications and Planning Meeting
[NASA-TM-87561] 18 p3105 N85-29221

The Rubidium-Crystal Oscillator Hybrid Development Program 18 p3106 N85-29230

The timing of noise-sensitive activities in residential areas
[NASA-CR-177937] 20 p3524 N85-31918

The sound field of a moving laser-induced acoustic array (theory)
[AD-A154553] 21 p3699 N85-32981

Digital matched filter 22 p3765 N85-33339

Dual optical mechanical position tracker
[AD-D011739] 22 p3844 N85-33811

An internally consistent gamma ray burst time history phenomenology
[OG-1.2-6] 22 p3862 N85-33916

TIME CONSTANT

Control of lateral conjectory motion of spacecraft in atmosphere 02 p0160 N85-11065

Development of a temperature measurement system with application to a jet in a cross flow experiment
[NASA-CR-174896] 15 p2472 N85-25262

Sub-optimal control of nonlinear flexible space structures 20 p3414 N85-31190

TIME DELAY

U TIME LAG

TIME DEPENDENCE

Time variability of directionality properties of pulsed EB-EDL (Electron Beam-Electric Discharge Laser) N2-CO2 lasers
[AD-A145546] 02 p0202 N85-11344

Time-temperature dependence of the strength of commercial zirconia ceramics
[AD-A146233] 03 p0336 N85-12173

Optimum replacement of a system subject to shocks
[AD-A145611] 03 p0372 N85-12374

A proposed reference set of scenarios for radiatively active atmospheric constituents
[DOE/NBB-0066] 03 p0386 N85-12483

Time-dependent chemistry of molecular clouds 03 p0443 N85-12822

Time dependent effects at the foot of the chromosphere
[NASA-CR-174143] 04 p0569 N85-13762

Volatility of vanadium from a candidate fusion tractor alloy
[DE84-015277] 05 p0618 N85-13955

Titanium-potassium heat pipe corrosion studies
[DE84-015526] 05 p0637 N85-14090

Components of the time variation of sea surface height from SEASAT altimeter data 05 p0658 N85-14227

The effect of pressure on the mechanical properties of polymers. Part 2: Measurement of the time-dependent Poisson's ratio
[DE85-002139] 06 p0772 N85-14936

Splitting methods for the numerical solution of the incompressible Navier-Stokes equations
[AD-A147463] 07 p1032 N85-16554

Effect of integration time on precision of absorbances measured with a diode array UV-VIS spectrophotometer
[AD-A146952] 07 p1043 N85-16624

A moving finite element method for time dependent partial differential equations with error estimation and refinement
[AD-A147719] 08 p1210 N85-17617

Can the singularity be removed in time-dependent flows?
[AD-P004165] 09 p1265 N85-17950

Influence of normalized frequency on time-dependent aerodynamic characteristics of vane blading profiles 09 p1306 N85-18204

Numerical investigation of phase change heat transfer in a horizontal cylinder including effects of natural convection 09 p1318 N85-18286

The vertical structure and stability of alpha model accretion disks 09 p1417 N85-18936

Electromagnetic braking of a metallic projectile in flight
[AD-A149424] 10 p1480 N85-19345

Mechanisms of damage accumulation in time-dependent cyclic deformation
[DE85-001004] 10 p1496 N85-19443

The relevance of averaging period to wind power measurements and efficiency of Wind Energy Conversion Systems (WECS)
[GKSS-84-E-35] 11 p1676 N85-20582

X-ray spectroscopy of laser-produced plasmas
[DE85-002170] 11 p1733 N85-20897

Unsteady flows around 3-dimensional wings
[AD-A149993] 12 p1772 N85-21124

Study of the kinetics of hydrogenation using aged catalysts
[DE85-004373] 12 p1802 N85-21302

Rheology of dissemination
[AD-A150006] 12 p1813 N85-21373

Surface forward scattering and reflection
[AD-A150115] 12 p1923 N85-22112

Research program on the effect of pressure on the mechanical properties of polymers, part 2
[DE85-000995] 13 p2037 N85-22761

Time-dependent flow of stream swirled in vortex chamber 13 p2043 N85-22786

Time dependent interaction of internal pressure wave with system of two spherical shells 13 p2046 N85-22800

Time-resolved ellipsometry and reflectivity measurements of the optical properties of silicon during pulsed excimer laser irradiation
[DE85-005091] 13 p2096 N85-23079

Nonrelativistic Kapitza-Dirac scattering
[AD-A150622] 13 p2159 N85-23405

Discrete models for the numerical analysis of time-dependent multidimensional gas dynamics
[NASA-CR-172574] 14 p2300 N85-24239

High time-resolution studies of the auroral ionosphere
[AD-A150945] 14 p2409 N85-24850

Nonrelativistic Kapitza-Dirac scattering
[AD-A150649] 14 p2417 N85-24911

A study of the time dependence in fracture processes relating to service prediction of adhesive joints and advanced composites
[AD-A152064] 15 p2579 N85-25910

Gravity perception and response in shoot of cereal grasses 15 p2611 N85-26091

A practical system for collecting reliable data on the space-time behavior of people
[AD-A151174] 15 p2619 N85-26140

Time dependent and steady-state solutions of the electron energy distribution in a weakly ionized gas subject to an ac or dc electric field
[AD-A151829] 15 p2656 N85-26391

Identification and control of structures in space
[NASA-CR-175790] 16 p2731 N85-26850

An incremental multigrid strategy for the fluid dynamics equations
[AD-A151953] 16 p2783 N85-27172

Some advances in experimentation supporting development of viscoplastic constitutive models
[NASA-CR-174855] 16 p2799 N85-27260

Evaluation of an algorithm for the solution of the time-dependent Euler equations
[AD-A151993] 16 p2854 N85-27600

Optimum convection conditions for Czochralski growth of semiconductors
[INPE-3395-PRE/665] 16 p2870 N85-27703

Analysis of time dependent dielectric failures
[AD-A153200] 17 p2954 N85-28243

New time and frequency services at the National Bureau of Standards 17 p2961 N85-28289

Distributed elections in a ring of processors using Archimedean time
[CWI-CS-R8416] 17 p3016 N85-28653

The temperature dependence of diffracted beam intensities in atom-surface scattering
[AD-A152762] 17 p3029 N85-28736

Model computations of radon, and radon decay product, concentrations in an open system; the Hewlett-Packard 41C program RNSS, version 02
[IRI-190-83-12] 17 p3035 N85-28775

The strategy for time dependent quantum mechanical calculations using a Gaussian wave packet representation of the wave function
[AD-A152709] 17 p3046 N85-28845

Drift mobilities by time-of-flight methods and time-dependent phototransport in the nanosecond regime in amorphous semiconductors
[DE85-008729] 18 p3194 N85-29815

A first-order time-domain Green's function approach to supersonic unsteady flow
[NASA-CR-172206] 19 p3214 N85-29930

On spectral multigrid methods for the time-dependent Navier-Stokes equations
[NASA-CR-172613] 19 p3344 N85-30725

Exact invariants in resonance form for time-dependent potentials
[DE85-010733] 19 p3346 N85-30739

Some advances in experimentation supporting development of viscoplastic constitutive models 20 p3468 N85-31545

Time-implicit Monte-Carlo collision algorithm for particle-in-cell electron transport models
[DE85-010758] 20 p3521 N85-31900

Source-term considerations for a potential radioactive-waste repository located in unsaturated tuff
[DE85-010090] 20 p3529 N85-31953

Magnetospheric response to solar wind variations
[DE85-010762] 20 p3547 N85-32074

Variations in the small-scale galactic magnetic field and short time-scale intensity variations of extragalactic radio sources 20 p3549 N85-32084

Use of MMLE3 to determine lower order equivalent systems in the time domain
[AD-A154700] 21 p3554 N85-32112

MPS solidification model. Analysis and calculation of macrosegregation in a casting ingot
[NASA-CR-171589] 21 p3566 N85-32178

In-situ measurement of wall thermal performance: Data interpretation and apparatus design recommendations
[DE85-011979] 21 p3586 N85-32236

Mean flow and turbulence in complex terrain
[AD-A155138] 21 p3636 N85-32583

Calculation of steady and unsteady airfoil flow fields via the Navier-Stokes equations
[NASA-CR-3899] 22 p3727 N85-33106

Analysis of solution of Bloch's equations in time domain 22 p3771 N85-33371

Model projections of time-dependent response to increasing carbon dioxide
[DE85-013326] 22 p3816 N85-33841

Implicit Monte Carlo methods and non-equilibrium Marshak wave radiative transport
[DE85-010711] 22 p3835 N85-33743

Multiple collision solutions for time-dependent neutron transport in slabs of finite thickness
[OEFZS-4312] 22 p3838 N85-33782

Evidence for long-term variability in the ultra high energy photon flux from Cygnus X-3
[OG-2.1-10] 22 p3863 N85-33926

Variability in the high energy gamma ray emission from Cyg X-3 over a two-year period (1983 - 1984) at E 4 x 10(11) eV
[OG-2.1-11] 22 p3864 N85-33927

Experimental study on time and temperature dependent behavior of crack growth in viscoelastic strip 23 p3905 N85-34183

Time and temperature dependence of fracture surface in soft epoxy resin 23 p3906 N85-34213

Preliminary SPR thermal model description and results for WH-11 and BM-4
[DE85-013171] 23 p3931 N85-34360

Compressible two-phase flow instabilities simulated with a hybrid Lagrange-Euler pseudospectral method
[DE85-009904] 23 p3931 N85-34361

Thermal transport measurements of UV laser irradiated spherical targets
[DE85-011038] 23 p3931 N85-34365

New semi-implicit method for solving the time-dependent conservation equations for incompressible flow
[DE85-010926] 23 p3931 N85-34367

Guiding center distribution function and longitudinal invariant 23 p3978 N85-34660

The dependence of solar modulation on the sign of the cosmic ray particle charge
[SH-4.2-23] 23 p4009 N85-34860

Time-dependent nonlinear cosmic ray shocks confirming abstract
[OG-8.1-3] 23 p4017 N85-34883

Selfsimilar time dependent shock structures
[OG-8.1-4] 23 p4017 N85-34894

A new approach to evaluate gamma-ray measurements
[OG-9.5-11] 23 p4031 N85-34986

Diagnostic of electromagnetic conditions in space using cosmic rays
[SH-4.5-19] 23 p4038 N85-35036

Time and energy dependence of the cosmic ray gradient in the outer heliosphere
[SH-4.7-2] 23 p4040 N85-35047

Identification and control of structures in space
[NASA-CR-176175] 24 p4069 N85-35214

Subcritical fracture propagation in rocks: An examination using the methods of fracture mechanics and non-destructive testing 24 p4116 N85-35518

Time-dependent response of the climate to increasing atmospheric carbon dioxide 24 p4119 N85-35532

DEPTH-CHARGE static and time-dependent perturbation/sensitivity system for nuclear reactor core analysis, revision 1
[DE85-013103] 24 p4139 N85-35659

A graph theoretic procedure for the design of feedback patterns
[REPT-110] 24 p4142 N85-35873

Decentralized stabilization by high gain feedback
[BU-115] 24 p4144 N85-35880

Structure of air shower disc near the core
[HE-4.7-2] 24 p4198 N85-36050

Longitudinal development of muons in large air showers studies from the arrival time distributions measured at 900m above sea level
[HE-4.7-4] 24 p4199 N85-36085

Arrival time distributions of electrons in air showers with primary energies above 10 (18)eV observed at 900m above sea level
[HE-4.7-5] 24 p4199 N85-36056

A note on some statistical properties of rise time parameters used in muon arrival time measurements
[HE-4.7-12] 24 p4199 N85-36062

Study of the time-differentiated particle flux density at various distances from EAS axis
[HE-4.7-15] 24 p4200 N85-36065

TIME DISCRIMINATION

Estimating number, time and length; a baseline study
05 p0695 N85-14473

TIME DIVISION MULTIPLE ACCESS

SLIM TDMA ANIK B pilot project
[CRC-REPT-1366] 03 p0354 N35-12278

The Telecom 1 satellite telecommunication system
04 p0493 N85-13147

Analytical modeling of a polling protocol — airline information network
[ENST-84H001] 09 p1277 N85-18029

Multimission advanced configurations study — telecommunication satellites
[MATRA-DM.51/CC/FL/0151.83]
12 p1790 N85-21237

Assessment of effectiveness of signal-code constructions in time division-multi-access satellite systems 13 p2066 N85-22906

Onboard demand scheduling of a multibeam SS/TDMA satellite with integrated circuit and packet switching
14 p2220 N85-23812

TIME DIVISION MULTIPLEXING

Digital correlator speed improvement by multiplexing
[AD-A145207] 01 p0100 N85-10662

Multiplexing the ethernet interface among VAX/VMS users
[AD-A145539] 02 p0243 N85-11568

Contribution to the study and realization of the CARTHAGE multiservice local network
[ENST-84E006] 05 p0716 N85-14595

Electro-optic techniques for VLSI interconnect
18 p3188 N85-29774

TIME FUNCTIONS

Long-time tail in the two-wave model
02 p0282 N85-11837

Determination of crustal and upper mantle structure from analysis of broadband teleseismic P-waveforms
08 p1181 N85-17440

Effects of heterogeneities on the propagation, scattering and attenuation of seismic waves and the characterization of seismic source
[AD-A148284] 08 p1186 N85-17476

Reflected wave travel-time curves in stratified media with vertically heterogeneous layers and slightly sloping curved boundaries 13 p2114 N85-23167

Optimal sensor locations for structural identification
20 p3417 N85-31209

Use of MMLE3 to determine lower order equivalent systems in the time domain
[AD-A154700] 21 p3554 N85-32112

Art of programming programmable microcalculators: Calculation of response from current values of action
22 p3767 N85-33348

SIG: A general-purpose signal processing program. User's manual: Revision 1
[DE85-013035] 24 p4140 N85-35662

TIME LAG

A nonlinear filter for compensating for time delays in manual control systems 05 p0700 N85-14493

A method for measuring the effective throughput time delay in simulated displays involving manual control
05 p0701 N85-14497

Effects of transport delays of manual control system performance 05 p0701 N85-14498

Measurements of pilot time delay as influenced by controller characteristics and vehicles time delays
05 p0701 N85-14500

Optimal stochastic LQ control with measurements displaced in time
[OUEL-1547/84] 08 p1209 N85-17605

A note on the prediction error for small time lags into the future
[AD-A148221] 08 p1215 N85-17654

Adaptive signal processing for radio communications
10 p1473 N85-19295

In-flight investigation of the effects of time delay in control system on flying qualities in landing approach
[DFVLR-FB-84-35] 11 p1586 N85-19989

Signal propagation delay, wire length distribution and the efficiency of VLSI circuits
[CWI-CS-R8412] 11 p1630 N85-20266

Circuit topology, signal propagation delay and the efficiency of VLSI circuits
[CWI-CS-R8414] 11 p1630 N85-20267

On the application of compatibility checking techniques to dynamic flight test data
[ARL/AERO-R-161] 12 p1776 N85-21151

The effects of cooling on delay-time limits in IC's
14 p2297 N85-24224

Wavelength dependent, tunable, optical time delay system for electrical signals
[AD-D011584] 15 p2548 N85-25725

Mode dependent, optical time delay system for electrical signals
[AD-D011596] 15 p2653 N85-26363

Digital RF delay line for ECM (electronic countermeasure) look-through
[AD-A152120] 16 p2774 N85-27120

Topics in time delay estimation
[AD-A152231] 16 p2855 N85-27607

Proceedings of the Fifteenth Annual Precise Time and Time Interval (PTTI) Applications and Planning Meeting
[AD-A149163] 17 p2961 N85-28287

Timing accuracy of LF and TV synchronization techniques 17 p2961 N85-28288

International time comparison by a GPS timing receiver 17 p2962 N85-28293

First results of GPS time transfer to Australia
17 p2962 N85-28294

The role of a low Earth orbiter in intercontinental time synchronization via GPS satellites
17 p2964 N85-28306

Ionospheric limitations to time transfer by satellite
18 p3107 N85-29234

Atmospheric limitations to clock synchronization at microwave frequencies 18 p3107 N85-29236

Probabilistic analysis of combinational circuits with random delays 19 p3257 N85-30192

Use of MMLE3 to determine lower order equivalent systems in the time domain
[AD-A154700] 21 p3554 N85-32112

In-flight evaluation of pure time delays in pitch and roll
[NASA-TM-86744] 21 p3556 N85-32123

Robust detection and classification of regional seismic signals using a two mode/two stage cascaded adaptive arma (CAARMA) model
[AD-A154710] 21 p3630 N85-32554

Sub-luminal pulses from cosmic ray air showers
[HE-4.7-13] 24 p4200 N85-36063

TIME MARCHING

Spectral methods in time for parabolic problems
[NASA-CR-172539] 11 p1706 N85-20730

Time marching numerical solution of the dynamic response of nonlinear systems
[NAF-AN-25] 12 p1865 N85-21696

Thermodynamic evaluation of transonic compressor rotors using the finite volume approach
[NASA-CR-175811] 16 p2708 N85-26712

TIME MEASUREMENT

Timing performance of phase-locked loops in optical pulse position modulation communication systems
[AD-A145403] 02 p0190 N85-11271

Late Paleozoic and early Mesozoic radiolarians in the Circle quadrangle, east-central Alaska
04 p0517 N85-13297

Time comparison with GPS technique and first results with the DFVLR C/A code receiver
[DFVLR-MITT-84-05] 05 p0595 N85-13794

References in space and time
05 p0598 N85-13809

Measurements of pilot time delay as influenced by controller characteristics and vehicles time delays
05 p0701 N85-14500

Mobility and trapping time measurements in HgI2
[DE84-015954] 06 p0869 N85-15522

Effects of aircraft and flight parameters on energy-efficient profile descents in time-based metered traffic
[NASA-CR-172338-ADD] 07 p0901 N85-15706

Construction, testing of 1-MW nitrogen laser
08 p1140 N85-17182

A system for measuring the characteristics of the ionospheric channel by digital transmissions
10 p1472 N85-19287

Operating time meter for tape recorder
12 p1838 N85-21537

Location and synchronization — space-time coordinates 14 p2397 N85-24768

Development of simulation procedures for VLSI systems (timing simulation)
[BMFT-FB-T-84-297] 15 p2550 N85-25743

Analysis of short-period changes in intensity of hard X-radiation of solar flares registered aboard Venera-13 and Venera-14 spacecraft 16 p2723 N85-26806

Proceedings of the Fifteenth Annual Precise Time and Time Interval (PTTI) Applications and Planning Meeting
[AD-A149163] 17 p2961 N85-28287

Recent improvements in the atomic time scales of the National Bureau of Standards 17 p2962 N85-28290

Improved master clock reference system at USNO
17 p2963 N85-28300

Spread spectrum time transfer experiment via INTELSAT 17 p2964 N85-28304

Timing-system design considerations for a mobile astrolabe 17 p2965 N85-28309

Clock characterization tutorial
17 p2965 N85-28311

Methods for optimal recursive estimation of non-stationary time series, applications to atomic time and frequency metrology 17 p2965 N85-28312

Kalman filter estimates of the NAVSTAR satellite clock parameters 17 p2965 N85-28315

The measurement of linear frequency drift in oscillators 17 p2966 N85-28316

A plan for the development of inertial reconstruction of initial state clock (IRIS) 17 p2966 N85-28317

Prospects for atomic frequency standards
18 p3105 N85-29222

Time transfer techniques: Historical overview, current practices and future capabilities
18 p3108 N85-29245

Maintenance of time and frequency in the Jet Propulsion Laboratory's Deep Space Network using the Global Positioning System 18 p3109 N85-29249

Using GPS and VLBI technology to maintain 14 digit synchronization 18 p3109 N85-29250

Performance test results of a low cost GPS time and frequency monitor 18 p3109 N85-29252

Drift mobilities by time-of-flight methods and time-dependent phototransport in the nanosecond regime in amorphous semiconductors
[DE85-008729] 18 p3194 N85-29815

Time comparisons using the Global Positioning System (GPS). Method and first results obtained using the DFVLR C/A receiver
[ESA-TT-894] 20 p3480 N85-31490

Investigation of space-time structure of glow of laser plasma colliding with flat screen
21 p3693 N85-32947

The sound field of a moving laser-induced acoustic array (theory)
[AD-A154553] 21 p3699 N85-32981

Method of characterizing critical timing paths and analyzing timing related failure modes in very large scale integrated circuits
[AD-D011731] 22 p3759 N85-33298

Hit-size effectiveness theory applied to high doses of low LET radiation for pink mutations in Tradescantia
[DE85-011835] 22 p3819 N85-33657

Observations of Cygnus X-3 above 10(15) eV from 1979 - 1984
[OG-2.1-6] 22 p3863 N85-33923

On gamma and neutrino radiation from Cyg X-3
[OG-2.1-7] 22 p3863 N85-33924

Observations of the Crab Nebula at energies 4.10(11)
[OG-2.3-1] 22 p3865 N85-33938

Spectra and positions of galactic gamma-ray sources
[OG-2.5-7] 22 p3869 N85-33963

Mini and super mini arrays for the study of highest energy cosmic rays
[OG-9.4-9] 23 p4029 N85-34976

Shower disc sampling and the angular resolution of gamma-ray shower detectors
[OG-9.5-2] 23 p4030 N85-34980

The use of the McIlwain L-parameter to estimate cosmic ray vertical cutoff rigidities for different epochs of the geomagnetic field
[SH-6.1-12] 23 p4045 N85-35085

Characterization of microstrip discontinuities in the time and frequency domains
[NASA-CR-176190] 24 p4088 N85-35342

The system of EAS time analysis
[HE-4.4-10] 24 p4193 N85-36018

TIME MEASURING INSTRUMENTS

NT ATOMIC CLOCKS
NT AUTONOMOUS SPACECRAFT CLOCKS
NT CHRONOMETERS
NT CLOCKS
NT TIMING DEVICES

Optical pin apparatus for measuring the arrival time and velocity of shock waves and particles
[DE84-014501] 01 p0120 N85-10824

The steering of GPS time 17 p2964 N85-28301

Spread spectrum time transfer experiment via INTELSAT 17 p2964 N85-28304

TIME OF FLIGHT SPECTROMETERS

Time-of-flight spectroscopy of ionic and metastable fragments from dissociating molecules
[AD-A148088] 08 p1220 N85-17683

A compact time-of-flight energy analyzer of high resolution — for Tokamaks
[REPT-84-154] 09 p1324 N85-18316

An operational test of a time-of-flight analyzer at the ASDEX Tokamak
[REPT-84-155] 09 p1324 N85-18319

In-beam tests of an air-core superconducting-solenoid particle spectrometer
[DE85-004029] 12 p1653 N85-21625

Carbon foil secondary electron emission during ion passage through the 40 to 500 keV energy field
[MPE-190] 18 p3184 N85-29747

Time-resolved energy spectrum of the ion beam generated in the plasma focus 19 p3369 N85-30692

Gas composition and molecule velocity in the detonation products of pentaerythritol tetranitrate (PETN) in expansion in a high vacuum container. Analysis by mass spectroscopy and time of flight spectrometry
[ISL-R-109/84] 22 p3747 N85-33226

An improved time of flight gamma-ray telescope to monitor diffuse gamma-ray in the energy range 5 MeV - 50 MeV
[OG-9.3-2] 23 p4027 N85-34957

The Nagoya cosmic-ray muon spectrometer 3, part 1: Preliminary observations
[HE-5.2-2] 24 p4202 N85-36080

The Nagoya cosmic-ray muon spectrometer 3, part 2: Track detector
[HE-5.2-3] 24 p4202 N85-36081

The Nagoya cosmic-ray muon spectrometer 3, part 3: Automatic film scanning equipment
[HE-5.2-4] 24 p4202 N85-36082

The Nagoya cosmic-ray muon spectrometer 3, part 4: Track reconstruction method
[HE-5.2-5] 24 p4202 N85-36083

TIME OPTIMAL CONTROL

Optimal control of waiting time in a M/G/1 queue
[INPE-2767-PRE/340] 02 p0255 N85-11671

Development and certification of a new stall warning and avoidance system 05 p0702 N85-14507

Inverse modelling to obtain head movement controller signal 05 p0705 N85-14525

A control model: Interpretation of Fitts' law
05 p0706 N85-14526

Improvement of the transient response in the finite settling time control
[NAL-TR-823] 06 p0757 N85-14843

Minimum time turns using vectored thrust
[AD-A151693] 15 p2471 N85-25256

High specific power aircraft turn maneuvers: Tradeoff of time-to-turn versus change in specific energy
[AD-A151701] 15 p2471 N85-25257

Wavelength dependent, tunable, optical time delay system for electrical signals
[AD-D011584] 15 p2548 N85-25725

TIME RESPONSE

Machine computation of delay and capacitance of transistor structures of subnanosecond large integrated circuits 04 p0490 N85-13120

Generalization of discrete Fourier transform for interpolation in time domain 22 p3775 N85-33396

Generalization of discrete Fourier transformation for interpolation in time domain 22 p3776 N85-33400

TIME SERIES ANALYSIS

Kolmogorov-Smirnov goodness-of-fit test: Corrected for use with EEG-like data
[AD-A144711] 01 p0110 N85-10745

Influential observations in time series
[AD-A144719] 01 p0112 N85-10763

Estimation in nonlinear time series model II: Some nonstationary series
[AD-A145709] 02 p0255 N85-11668

On-line fatigue life prediction under stochastic loading by the time series modeling 03 p0370 N85-12362

Time series modeling of human operator dynamics in manual control tasks 05 p0699 N85-14488

Statistical time series models of pilot control with applications to instrument discrimination
05 p0700 N85-14489

Utilization of historic information in an optimisation task 05 p0700 N85-14490

Time series analysis programs for stratigraphic data
[AD-A146627] 06 p0854 N85-15429

Electronics research at the University of Texas at Austin
[AD-A146900] 07 p0947 N85-15996

Autoregressive spectral estimation for two dimensional time series 07 p0985 N85-16256

The ocean and the dynamics of the tropical atmosphere; its possible predicability 07 p1002 N85-16366

A factor analysis for time series
[AD-A147495] 07 p1036 N85-16574

Time series analysis of closed-loop pilot vehicle dynamics 08 p1067 N85-16876

Robust linear filtering for multivariable stationary time series, part 3
[AD-A148169] 08 p1212 N85-17627

Methods and applications of time series analysis. Part 2: Linear stochastic models
[AD-A147292] 08 p1214 N85-17645

On the ergodicity of bilinear time series models and some applications
[AD-A148032] 08 p1215 N85-17651

Internal variables in the lattice for cholesky factorization. Kalman filtering and model identification
[AD-A149431] 10 p1547 N85-19757

Modelling and residual analysis of nonlinear auto-regressive time series in exponential variables
[AD-A149047] 10 p1550 N85-19776

Asymptotic distributions of the sample mean, autocovariances and autocorrelations of long-memory time series
[AD-A149409] 10 p1551 N85-19781

Statistical analysis of autoregressive spectral estimates for noise corrupted autoregressive series
[AD-A149543] 11 p1706 N85-20747

Simulation of estimating periodicity of seasonally stationary time series
[DE85-003517] 11 p1706 N85-20748

Bayesian analysis of time series 1: Householder transformation analyses
[DE85-004449] 11 p1706 N85-20749

Analysis of selective chopper radiometer data
[NASA-CR-175157] 12 p1895 N85-21894

A review of some aspects of robust inference for time series
[AD-A149706] 12 p1923 N85-22082

Approaches and algorithms for robust signal processing 13 p2062 N85-22878

Markov method for simulating non-Gaussian wind speed time series
[DE85-003450] 13 p2139 N85-23284

Studies of the initiation of pitting corrosion on stainless steels
[AERE-M-3400] 14 p2254 N85-23967

Dynamic spectra of mean monthly values of geomagnetic field elements based on spectral-time analysis data 14 p2344 N85-24496

Annual report on electronics research at the University of Texas at Austin
[AD-A150636] 14 p2415 N85-24901

Analysis and interpretation of synthetic time strings of oscillation data 14 p2444 N85-25079

Spectral information from gapped data. A comparison of technique 14 p2444 N85-25080

A comparison of alternative analytic models for event related potential records
[AD-A151977] 15 p2618 N85-26134

A practical system for collecting reliable data on the space-time behavior of people
[AD-A151174] 15 p2619 N85-26140

Kalman filtering and exponential smoothing in economics 15 p2635 N85-26248

Higher order residual analysis for nonlinear time series with autoregressive correlation structures
[AD-A149232] 15 p2636 N85-26257

Study of longitudinal landing flying qualities evaluation using pilot model theory
[AD-A152194] 16 p2706 N85-26702

A Markov method for simulating non-Gaussian wind speed time series
[DE85-007131] 16 p2835 N85-27485

Methods for optimal recursive estimation of non-stationary time series, applications to atomic time and frequency metrology 17 p2965 N85-28312

Towards a study of synoptic-scale variability of the California current system
[NASA-CR-175871] 17 p2997 N85-28529

Transverse vorticity measurements in an excited two-dimensional mixing layer 19 p3264 N85-30241

Rayleigh scattering for density measurements in premixed flames: One point, time series data
20 p3424 N85-31253

Numerical considerations in the development and implementation of constitutive models
20 p3467 N85-31541

Magnetospheric response to solar wind variations
[DE85-010762] 20 p3547 N85-32074

On the spectrum of atmospheric velocity fluctuations seen by MST/ST radar and their interpretation
21 p3622 N85-32504

On the transformation regularities of time series of solid aerosol concentrations in the surface atmospheric layer
21 p3645 N85-32648

Kalman filter time series analysis of gamma-ray data from NaI(T1) detectors for the ND6620 computer
[AD-A154905] 21 p3705 N85-33014

The conjecture concerning time variations in the solar neutrino flux
[SH-8.1-6] 23 p4049 N85-35111

Methods and software for cosmic ray scintillation studies
[SH-8.1-17] 23 p4052 N85-35132

Signal space models for antenna arrays
[AD-A156063] 24 p4087 N85-35335

TIME SHARING

Normal approximation for response time in a processor-shared computer system model
[AD-A144997] 01 p0103 N85-10680

The effects of task structure on time-sharing efficiency and resource allocation optimality
05 p0711 N85-14582

Passive maser using timesharing for control of the cavity and control of the oscillator on the line of stimulated emission
[AD-D011326] 07 p0969 N85-16151

Development and evaluation of a Fault-Tolerant Multiprocessor (FTMP) computer. Volume 2: FTMP software
[NASA-CR-166072] 19 p3341 N85-30706

TIME SIGNALS

Portable real-time clock
[AD-A146218] 03 p0364 N85-12338

Digital raster timing encoder-decoder
[AD-D011279] 06 p0804 N85-15120

Clock synchronization by the Symphonie and Laser Synchronization from Stationary Orbit (LASSO) geostationary satellites 14 p2398 N85-24778

Maintenance of time and frequency in the DSN using the global positioning system 16 p2771 N85-27105

Proceedings of the Fifteenth Annual Precise Time and Time Interval (PTTI) Applications and Planning Meeting
[AD-A149163] 17 p2961 N85-28287

Timing accuracy of LF and TV synchronization techniques 17 p2961 N85-28288

New time and frequency services at the National Bureau of Standards 17 p2961 N85-28289

Recent improvements in the atomic time scales of the National Bureau of Standards 17 p2962 N85-28290

Automation of Precise Time Reference Stations (PTRS) 17 p2962 N85-28291

International time comparison by a GPS timing receiver 17 p2962 N85-28293

A new precision time and frequency source for stationary PTTI applications 17 p2963 N85-28297

On-orbit frequency stability analysis of the GPS NAVSTAR's 3 and 4 rubidium clocks and NAVSTAR's 5 and 6 cesium clocks 17 p2963 N85-28298

Improved master clock reference system at USNO
17 p2963 N85-28300

The steering of GPS time 17 p2964 N85-28301

Test results for prototype GPS rubidium clocks
17 p2964 N85-28302

Spread spectrum time transfer experiment via INTELSAT 17 p2964 N85-28304

Unattended TV time transfer results
17 p2964 N85-28305

The role of a low Earth orbiter in intercontinental time synchronization via GPS satellites
17 p2964 N85-28306

Timing of spacecraft data: Time accuracy requirements and timing facilities of the European Space Agency (ESA) 17 p2964 N85-28307

UHF IRIG G distribution system
17 p2965 N85-28308

Precise time transfer using MKIII VLBI technology
17 p2965 N85-28310

Kalman filter estimates of the NAVSTAR satellite clock parameters 17 p2965 N85-28315

Time synchronization experiments with APPLE
17 p2967 N85-28323

Prospects for atomic frequency standards
18 p3105 N85-29222

Atmospheric limitations to clock synchronization at microwave frequencies 18 p3107 N85-29226

Relationship between Allan variances and Kalman Filter parameters 18 p3107 N85-29228

Development of hydrogen masers for K-3 VLBI system
18 p3108 N85-29229

TIMERS

U TIMING DEVICES

TIMING

U TIME MEASUREMENT

TIMING DEVICES

Proceedings of the Fifteenth Annual Precise Time and Time Interval (PTTI) Applications and Planning Meeting
[AD-A149163] 17 p2961 N85-28287

New time and frequency services at the National Bureau of Standards 17 p2961 N85-28289

Recent improvements in the atomic time scales of the National Bureau of Standards 17 p2962 N85-28290

International time comparison by a GPS timing receiver 17 p2962 N85-28293

International time transfer and portable clock evaluation using GPS timing receivers: Preliminary results
17 p2964 N85-28303

Prospects for atomic frequency standards
18 p3105 N85-29222

Atmospheric limitations to clock synchronization at microwave frequencies 18 p3107 N85-29226

Development of hydrogen masers for K-3 VLBI system
18 p3108 N85-29239
New GOES satellite synchronized time code generation 18 p3109 N85-29247
Numerical optical computing at the Ohio State University 18 p3188 N85-29775

TIN
Thematic mapping of likely target areas for the occurence of cassiterite in the Serra do Mocambo (GO) granitic massifs using LANDSAT 2 digital imaging
[E85-10027] 02 p0219 N85-11440
Study of vibrational energy transfer at a liquid tin surface
[AD-A145741] 02 p0277 N85-11804
Effects of tin on microstructure and mechanical behavior of inconel 718
[NASA-TM-86866] 03 p0330 N85-12129
Geology and geochemical evolution of the Lost River, Alaska, tin deposit 04 p0533 N85-13405
Float zone experiments in space
[NASA-CR-171284] 07 p0911 N85-15786
Investigations into the improvement of processing of Bolivian tin ores
[BMFT-FB-T-84-184] 07 p0917 N85-15807
Interpretation of 119 Sn isomer shifts and 3d 5/2-core-level shifts based on Dirac-Slater calculations on a number of ionic states
[USIP-85-06] 20 p3532 N85-31973
Development of metallization process: FSA project, cells and module formation research area
[NASA-CR-176136] 23 p3945 N85-34447
The Conterminous United States Mineral Assessment Program 24 p4106 N85-35458
The Alaska Mineral Resources Assessment Program
24 p4107 N85-35460

TIN ALLOYS
Electron-irradiated effects in metals
[DE84-016989] 09 p1297 N85-18147
Electron-diffraction structural examination of amorphous iron-tin alloys 11 p1604 N85-20084
Properties of Ti alloyed multifilamentary Nb3Sn wires by internal tin process
[DE85-003212] 12 p1941 N85-22191
Basis and pyramidal slipping in single crystals of alpha-alloy Ti-Al-Sn 13 p2032 N85-22730
Critical current density and microstructural state of an internal tin multifilamentary superconducting wire
[DE85-009966] 22 p3761 N85-33308

TIN COMPOUNDS
NT NIOBIUM STANNIDES
NT TIN OXIDES
NT TIN TELLURIDES
Magnetization measurements on multifilamentary Nb3Sn and NbTi conductors
[DE85-001237] 11 p1737 N85-20923
Marine environmental quality assessment program, five-year plan (FY 1984 - 1986)
[AD-A154715] 21 p3613 N85-32459

TIN OXIDES
Process for preparation of crosslinked poly(tri-n-butyltin) methacrylate with simultaneous particle size reduction
[AD-D011313] 07 p0932 N85-15905
Development of materials for open-cycle MHD
[DE84-017293] 09 p1393 N85-18770

TIN TELLURIDES
The behavior of Pb(1-x)Sn(x)Te semiconductor laser diodes in a magnetic field
[AD-A145431] 02 p0287 N85-11872

TIP DRIVEN ROTORS
Experimental study of main rotor tip geometry and tail rotor interactions in hover. Volume 1. Text and figures
[NASA-CR-177336-VOL-1] 13 p1965 N85-22344
Experimental study of main rotor tip geometry and tail rotor interactions in hover. Volume 2: Run log and tabulated data
[NASA-CR-177336-VOL-2] 13 p1965 N85-22345
Application of two-dimensional unsteady aerodynamic to a free-tip rotor response analysis
[NASA-CR-177348] 19 p3215 N85-29933
Performance comparison between NACA 23024 and NACA 64(3)-618 airfoil configurated rotors for horizontal-axis wind turbines
[NASA-TM-83471] 19 p3303 N85-30477

TIP SPEED
Shutdown characteristics of the Mod-O wind turbine with aileron controls
[NASA-TM-86918] 07 p0992 N85-16299
Study of controlled diffusion stator blading
[NASA-CR-167995] 09 p1281 N85-18058
Further comparison of wind tunnel and airplane acoustic data for advanced design high speed propeller models
[NASA-TM-86935] 12 p1927 N85-22106
Energy efficient engine. Fan and quarter-stage component performance report
[NASA-CR-168070] 23 p3897 N85-34141

TIPS
NT BLADE TIPS
NT CRACK TIPS
NT WING TIPS
Approximation methods for inverse problems involving the vibration of beams with tip bodies
[NASA-CR-172468] 02 p0209 N85-11379

TIRES
NT AIRCRAFT TIRES
Predictor model for seasonal variations in skid resistance. Volume 2: Comprehensive report
[PB84-226620] 01 p0037 N85-10230
Numerical analysis of some problems related to the mechanics of pneumatic tires: Finite deformation/rolling contact of a viscoelastic cylinder and finite deformation of cord-reinforced rubber composites
01 p0060 N85-10397
Orbiter wheel and tire certification
08 p1101 N85-16959
Modelling of off-road tyres and soil for improved traction
[AD-P004258] 09 p1404 N85-18834
Soil compliance influence on tyre performance
[AD-P004260] 09 p1404 N85-18836
Performance prediction of pneumatic tyres on sand
[AD-P004262] 09 p1404 N85-18838
Effects of slip on energy distribution between tyre and soil
[AD-P004263] 09 p1404 N85-18839
Traction forces of drive tyre on the compacted soil
[AD-P004264] 09 p1404 N85-18840
Prediction of in-sand tire and wheeled vehicle drawbar performance
[AD-P004265] 09 p1404 N85-18841
Comparison of measured and simulated ride comfort for an agricultural tractor and influence of travel speed and tyre-inflation pressure on dynamic response
[AD-P004281] 09 p1407 N85-18857
Proceedings of the 8th International Conference on the Performance of Off-Road Vehicles and Machines, volume 2
[AD-A148635] 09 p1407 N85-18859
Pressure tests in soil below tires of agricultural vehicles
[AD-P004294] 09 p1408 N85-18871
Flotation tires and subsurface compaction
[AD-P004299] 09 p1409 N85-18876
Forces on undriven, angled wheels
[AD-P004303] 09 p1409 N85-18880
Influence of tire on resistance and steering forces of tires
[AD-P004306] 09 p1410 N85-18883
Tire inflation/deflation system
[AD-D011459] 10 p1493 N85-19426
Tire deflation mechanism
[AD-D011460] 10 p1493 N85-19427
Techniques to analyze vehicle coastdown data
[DE85-005159] 12 p1772 N85-21127

TIROS N SERIES SATELLITES
NT NOAA 6 SATELLITE
Report of the First Session of the International Working Group on Data Management for the International Satellite Cloud Climatology Project (ISCCP)
[WCP-42] 01 p0073 N85-10483
ISCCP Cloud Algorithm Intercomparison Workshop
01 p0073 N85-10485
ISSCP Cloud Algorithm Intercomparison Workshop
01 p0073 N85-10486
A comparison of TIROS-N series satellite data and LANDSAT data over Scotland 05 p0656 N85-14210
The ARGOS Platform Transmitter Terminals (PTTs)
14 p2237 N85-23672
Hydrometric telemetry in Canada
14 p2239 N85-23882
Data Collection and Platform Location by Satellite: ARGOS Users' Conference 14 p2239 N85-23883
Some experience from ARGOS stations in the open sea 14 p2240 N85-23891
The experience of the Swedish Meteorological and Hydrological Institute (SMHI) with the ARGOS system
[PM-U1/81] 14 p2240 N85-23892
Improvements brought about to the system since 1978 and statements on future development
14 p2323 N85-24349
New directions in ARGOS instrumentation at Polar Research Lab (PRL) 14 p2323 N85-24350
Automatic weather stations in Antarctica
14 p2324 N85-24360
NOAA'S role in support of service ARGOS
14 p2328 N85-24394
Long term drifting float for measuring mean oceanic circulation using ARGOS system
16 p2811 N85-27339
Availability of the ARGOS system based on the orbital characteristics of the TIROS-N satellites — oceanographic/meteorological data
16 p2813 N85-27352
Location and data collection satellite system ARGOS. User's guide — satellite based localization
16 p2816 N85-27371

TIROS PROJECT
Data Collection and Platform Location by Satellite: ARGOS Users' Conference 14 p2237 N85-23669
The ARGOS system status report after 2 years operation 14 p2237 N85-23670
System performance, data distribution and technical files — ARGOS project 14 p2237 N85-23671
The ARGOS VHF direct readout mini-station and CML-80-MP data collection Platform Transmitter Terminals (PTTs) 14 p2238 N85-23673
The ARGOS system status report
14 p2239 N85-23884
Equipment for the ARGOS system from Eidsvoll Electronics A.S. 14 p2239 N85-23885
ARGOS VHF direct readout mini-station
14 p2239 N85-23886
The ARGOS system after 3 years operation
14 p2325 N85-24368
The ARGOS program — satellite based localization
14 p2397 N85-24775

TIROS SATELLITES
NT TIROS N SERIES SATELLITES
Satellites and politics: Weather, communications, and earth resources 23 p4057 N85-35144

TISSUES (BIOLOGY)
NT EPITHELIUM
Determination of bound water in biological tissue and energy dissipated in bound water by low level microwaves
[AD-A143101] 03 p0399 N85-12547
Alterations in skeletal muscle with disuse atrophy
[NASA-CR-174195] 06 p0843 N85-15349
Interactions of ketones and hexacarbons
[AD-P004019] 06 p0843 N85-15353
Workshop on membrane biophysics
[AD-A148236] 08 p1192 N85-17512
Bioelectrochemistry 2: Membrane phenomena
[AD-A149132] 10 p1522 N85-19602
Characteristics of human masseter under conditions of hypokinesia 11 p1691 N85-20630
Morphological study of monkeys submitted to antiorthostatic hypokinesia 12 p1902 N85-21942
Gravitropism in leafy dicot stems
15 p2610 N85-26086
Chemicals identified in human biological media, a data base. Volume 6, part 2: Records 7586-8694
[DE85-006767] 18 p3154 N85-29528
Method for thermal monitoring subcutaneous tissue
[NASA-CASE-LAR-13026-1] 19 p3329 N85-30618
Development anmd testing of electrophoresis solutions. Task I.1: Development of optimal buffer system
20 p3500 N85-31755
Physical chemical state of water in living cells
[AD-A154566] 21 p3662 N85-32749

TITAN
Do the satellites of Uranus control its magnetosphere?
02 p0301 N85-11952
Outer satellite atmospheres: Their nature and planetary interactions
[NASA-CR-174146] 04 p0589 N85-13759
Extended atmospheres of outer planet satellites and comets
[NASA-CR-174398] 09 p1416 N85-18933
Research in planetary studies and operation of Mauna Kea Observatory
[NASA-CR-175616] 13 p2169 N85-23460
Giant planets and their satellites: Cosmochemistry, evolution and structure 13 p2175 N85-23494
Extended atmospheres of outer planet satellites and comets
[NASA-CR-175673] 14 p2440 N85-25058
The eccentric ringlet at 1.29 R sub S — Saturn radius (RS) 15 p2673 N85-26496
Volatiles in the outer solar system. 1: Thermodynamics of clathrate hydrates. 2: Ethane ocean on Titan. 3: Evolution of primordial Titan atmosphere
19 p3382 N85-30964

TITAN CENTAUR LAUNCH VEHICLE
Assessment of candidate-expendable launch vehicles for large payloads
[NASA-CR-175540] 14 p2237 N85-23667

TITANATES
NT BARIUM TITANATES
NT LEAD ZIRCONATE TITANATES
NT PEROVSKITES
NT PIEZOELECTRIC CERAMICS
NT STRONTIUM TITANATES

TITANIUM

Optimization of mechanical/corrosion properties of Ticode-12 plate and sheet. Part 1: Compositional effects, stage 1
[DE84-015935] 02 p0184 N85-11231

Characterization of amorphous surface layers in Fe implanted with Ti and C
[DE84-014960] 02 p0289 N85-11865

Study of structure of sponge titanium varieties
03 p0350 N85-12256

Structural recrystallization in titanium
03 p0351 N85-12258

Causes of strength reduction in welded titanium-steel joints 03 p0352 N85-12262

Effect of oxide coated thickness on thermal ignition of titanium-based pyrotechnics
[DE84-013061] 04 p0461 N85-13065

Oxygen diffusion from anodic surface oxide films on titanium subhydride studies by auger electron spectroscopy and electron energy loss spectroscopy
[DE84-016942] 04 p0572 N85-13648

Testing of production of silicon-titanium-magnesium alloying composition
[BLL-M-35904-(5828.4)] 05 p0616 N85-13937

Nitriding of titanium and its alloys by N2, NH3 or mixtures of N2 + H2 in a dc arc plasma at low pressures (or = to torr)
[NASA-TM-83803] 06 p0814 N85-15168

Evaluation of the alkaline peroxide pre-bond surface treatment for titanium
[AD-A147352] 07 p0928 N85-15881

Ultrasonic evaluation of titanium contamination with correlation techniques
[AD-P004126] 08 p1126 N85-17101

Feasibility study to demonstrate detection of low levels of oxygen contaminant in titanium using eddy current and ultrasonic NDE (Nondestructive Evaluation) techniques
[AD-P004129] 08 p1127 N85-17104

Neutron activation analysis of titanium with oxygen contamination
[AD-P004134] 08 p1128 N85-17109

The influence of strain rate and porosity on the deformation and fracture of titanium and nickel
[AD-A148670] 08 p1130 N85-17123

Implantation of Ti + C for reduced friction and wear of steels
[DE85-001606] 09 p1295 N85-18135

Fiber composite materials with titanium matrix
10 p1445 N85-19105

Kinetics of saturation of porous titanium with low melting point metals 10 p1446 N85-19114

Quasi-thermodynamic prediction of hydrogen reemission behavior from titanium films
[DE85-003667] 10 p1564 N85-19864

USSR report: Materials science and metallurgy
[JPRS-UMS-84-005] 11 p1597 N85-20044

Structure and properties of copper-titanium-aluminum composites obtained by thermoreactive sintering
11 p1600 N85-20061

Effect of silicon and titanium properties on Ni8Co9Mb5Ti steel 11 p1601 N85-20069

Mechanism of titanium impact on brittle tendency in delayed deformation of martensite-aging steels
11 p1604 N85-20087

Chemisorption theory: Adsorption on copper-nickel alloys and titanium surface embrittlement
[DE85-001815] 12 p1807 N85-21334

Rational use of tatanium in nonferrous metallurgy
13 p2031 N85-22728

Studies of electrical properties of surface films and localization during electrochemical dimensional working of titanium 13 p2032 N85-22729

Study of structural changes of dual-phase titanium alloy during shock wave loading 15 p2496 N85-25408

Possible use of rapid heating for improving mechanical properties of titanium alloys 15 p2498 N85-25409

Study of oxidized surface coating on titanium after annealing 15 p2498 N85-25412

Residual oxygen pressure in contact gap upon diffusion welding of titanium 15 p2499 N85-25418

Titanium diffusion method prevents metal corrosion
15 p2514 N85-25510

Inhibiting titanium corrosion in hot nitrogen nitrate solutions using sulfate ions 15 p2514 N85-25511

Hydrogen induced crack growth in Grade-12 Titanium
[BNL-NUREG-35598] 16 p2751 N85-26976

Experimental investigation of the pulsed photoacoustic effect produced on a solid surface
[AD-A152114] 16 p2860 N85-27640

Mechanical properties of polycrystalline alpa titanium
[BLL-BISI-TRANS-21923-(9022.06)]
17 p2924 N85-28029

Study of the influence of metallurgical factors on fatigue and fracture of aerospace structural materials
[AD-A153913] 18 p3122 N85-29326

The physical and mechanical properties of near-equiatomic titanium-nickel
19 p3237 N85-30072

Microstructures and mechanical properties of microalloyed medium carbon steels
19 p3238 N85-30074

The microstructural state of Nb3Sn in a multifilamentary titanium doped bronze-process wire
[DE85-010979] 19 p3240 N85-30089

Vacuum pressure welding of commercial titanium with 2Kh13 and 12Kh18N10T steels
19 p3246 N85-30124

Producing titanium-sapphire items by solid-phase bonding through aluminum gasket
19 p3246 N85-30127

Electrochemical reduction of titanium in dimethyl sulphoxide
[BLL-OA-TRANS-3225-(6196.300)]
20 p3429 N85-31267

Long range ordered alloys modified by addition of niobium and cerium
[DE85-011661] 20 p3431 N85-31285

Precision measurements of solar energetic particle elemental composition
[PAPER-SH-2.1-4] 21 p3715 N85-33052

Properties of Ti-6Al-4V spun formed fuze supports
[DE85-011968] 22 p3792 N85-33498

Joint design for improved fatigue life of diffusion-bonded box-stiffened panels
[NASA-TP-2480] 22 p3799 N85-33537

The development of titanium production in the USSR
[BLL-OA-TRANS-3226-(6196.3)]
23 p3913 N85-34244

Calculating the interatomic pair potential allowing for resonance interaction in titanium, nickel and vanadium
[BLL-M-35843-(5828.4)] 23 p3913 N85-34249

The properties of VSt3sp inoculated steel
[BLL-M-35894-(5828.4)] 23 p3915 N85-34263

An X-ray diffraction study of titanium oxidation
[NASA-CR-176263] 23 p3915 N85-34264

Applications of the mineral resources data system and the international strategic minerals inventory in mineral-resource assessments by region and commodity
24 p4105 N85-35451

TITANIUM ALLOYS

NT NITINOL ALLOYS

Granular boundary segregation in low-alloyed titanium-vanadium alloys 01 p0019 N85-10117

Influence of annealing on properties of AT3 alloy welded joints 01 p0019 N85-10118

Heat treatment of welded joints in OT4 and VT20 titanium alloys 01 p0020 N85-10119

Strength of welded joints in VT23 alloy upon repeated static loading 01 p0020 N85-10120

Fracture toughness characteristics of welded joints in VT65 and AT6 titanium alloys 01 p0020 N85-10121

Nonlinear ultrasonic characterization of oxygen impurities in titanium, 2
[AD-A144857] 01 p0027 N85-10171

Effect of microstructure and trapping on the hydrogen embrittlement susceptibility of a titanium bearing HSLA steel 02 p0174 N85-11166

Re-evaluation of phase separation in Ti-Zr-Be metallic glasses
[DE84-015603] 03 p0338 N85-12176

Kinetics of fatigue factor of AT3 titanium alloys in air, distilled water and 3.5% aqueous NaCl solution
03 p0350 N85-12255

Structure of two-phase titanium alloys with different microstructures 03 p0351 N85-12257

Energy of stacking fault and dislocation structure of titanium alloys 03 p0351 N85-12259

Structure and properties of titanium alloys after isothermal deformation at low speeds
03 p0351 N85-12260

Structure and ductility of fracture of joints produced by electron-beam welding of VT6ch titanium alloy parts
03 p0351 N85-12261

Fatigue crack propagation in metastable titanium alloys
[AD-A145824] 03 p0372 N85-12376

The TA6Zr5D (IMI 685) characterization in strain controlled tests. (Specimens obtained from a forged spinning wheel) no. M4-45870
[M4-45870] 03 p0373 N85-12384

Swelling behavior of titanium-modified AISI 316 alloys
[DE84-013940] 05 p0618 N85-13956

Flow-based analyses of metal deformation processes: An overview 06 p0796 N85-15087

Pulsed electric discharge laser technology. Electron beam window foil material
[AD-A146420] 06 p0813 N85-15162

Nitriding of titanium and its alloys by N2, NH3 or mixtures of N2 + H2 in a dc arc plasma at low pressures (or = to torr)
[NASA-TM-83803] 06 p0814 N85-15168

Disc fatigue life predictions for gas turbine engines
07 p0907 N85-1574

Titanium Matrix/Continuous Fiber/Continuous fibe composite interface interactions and their influence o mechanical properties
[AD-A147504] 07 p0920 N85-1582

Study of residual stresses introduced into TA6ZrD (68 cylinders by quenching
[BLL-PNR-90240-(8019.3153)]
07 p0925 N85-1585

Pulsed electric discharge laser technology. Electro beam window foil material
[AD-A147488] 07 p0972 N85-1617

Proceedings of the 2nd Workshop on Nondestructive Evaluation (NDE) of Titanium Alloys
[AD-A147626] 08 p1125 N85-1709

NDE (Nondestructive Evaluation) of oxygen contaminated titanium alloys and weldments
[AD-P004121] 08 p1126 N85-1709

Effects of oxygen on the microstructure and propertie of titanium 6211 alloys
[AD-P004122] 08 p1126 N85-17097

Nonlinear ultrasonic characterization of oxygen impurities in titanium
[AD-P004123] 08 p1126 N85-17098

Effects of oxygen-contamination-induced microstructural changes on the reverberation of ultrasound in Ti-6211 alloys
[AD-P004124] 08 p1126 N85-17099

Acoustical characterization of Ti-6211 weldments and oxygen contamination Ti-6211 plate
[AD-P004125] 08 p1126 N85-17100

Photoacoustic microscopy of oxygen contaminated titanium alloys
[AD-P004127] 08 p1127 N85-17102

High resolution acoustic microstructural characterization of titanium with interstitial contamination
[AD-P004128] 08 p1127 N85-17103

Evaluation of interstitial gas contamination in titanium alloys using induced magnetic field analysis
[AD-P004130] 08 p1127 N85-17105

Electromagnetic NDE of interstitial contamination in titanium alloy weldments
[AD-P004131] 08 p1127 N85-17106

Evaluation of the thermoelectric method for determination of interstitial gases in titanium
[AD-P004132] 08 p1127 N85-17107

Measurement of oxygen contamination in titanium alloy ingots by fast neutron activation analysis
[AD-P004133] 08 p1128 N85-17108

Nondestructive evaluation of titanium alloys. ESCA (Electron Spectroscopy for Chemical Analysis), ISS (Ion Scattering Spectroscopy), and SIMS (Secondary Ion Mass Spectrometry) examination of titanium alloy solid surfaces
[AD-P004135] 08 p1128 N85-17110

Effect of microstructure and trapping on the hydrogen embrittlement susceptibility of a ti-bearing HSLA steel
[AD-A148610] 08 p1130 N85-17122

Deformation and fracture of P/M (Powder/Metallurgy) titanium alloys
[AD-A148672] 09 p1294 N85-18128

Ion implantation of surgical Ti-6Al-4V alloy
[DE85-000943] 09 p1296 N85-18142

Ti-6Al-4V alloy castings prepared in zircon sand molds and the effect of hot isostatic pressing
[PB85-109932/GAR] 09 p1298 N85-18150

Study of residual stresses introduced into TA6ZrD (685) cylinders by quenching --- compressor disk alloy
[PNR-90240] 09 p1341 N85-18435

Impact toughness of composites with layered microstructure of OT4 titanium alloy
10 p1445 N85-19104

Optimization of production of composite diamond-containing materials using titanium carbide-steel alloys 10 p1446 N85-19113

Influence of extension rate on strength and deformation characteristics of titanium alloys over a broad temperature range 10 p1448 N85-19121

Kinetics of oxidation of titanium alloy upon heating to 1000 deg C 10 p1448 N85-19122

Kinetics of joint formation during diffusion welding of VT5 titanium alloys 10 p1448 N85-19125

Calculation of mode field in electron beam welding of VT6 titanium alloy 10 p1449 N85-19129

Oxidation of PT-7M and OT4-1 titanium alloys in air
11 p1600 N85-20060

Fractographic features of titanium alloy fatigue failure under repeated static stress and high frequency vibration 11 p1601 N85-20070

Effect of hydrogen on fatigue of VT6 alloy
11 p1601 N85-20071

Dependence of mechanical properties of large VT3-1 alloy forgings on microstructure parameters
11 p1602 N85-20072

Phase transformations in vanadium alloys of titanium during quenching and tempering 11 p1602 N85-20073
Sensitivity of titanium alloys to stress concentration during repeated static loads 11 p1602 N85-20074
Improving operational properties of titanium alloys by diffusion siliciding 11 p1602 N85-20075
Assessment of effectiveness of electron beam welding of titanium alloys up to 40 mm in thickness by vertical or horizontal beam 11 p1603 N85-20078
Amorphous Ni-Ti alloys: A new method of synthesis [DE85-002744] 11 p1605 N85-20094
MBB uses superplastic forming, diffusion bonding for alloys 11 p1618 N85-20177
Method for refining microstructures of cast titanium articles [AD-D011518] 12 p1804 N85-21318
Alloy development, processing and characterization of devitrified titanium base microcrystalline alloys [AD-A149609] 12 p1806 N85-21327
Proton NMR and susceptibility measurements in TiCoH/sub x [DE85-003309] 12 p1807 N85-21336
Comparison of the fatigue resistance (initiation, propagation) of cast TA6V with hot rolled TA6V — titanium alloy [DGT-25369-PT-1] 12 p1808 N85-21341
Properties of Ti alloyed multifilamentary Nb3Sn wires by internal tin process [DE85-003212] 12 p1941 N85-22191
Effect of phase state of TiC-NiTi powder composite materials on nature of failure and mechanical properties 13 p2027 N85-22702
Decomposition of VTAN alloy solid solution upon irradiation and thermal aging 13 p2029 N85-22712
High temperature antifriction properties of Ti sub 1-sub xNb sub x C sub 0.5N sub 0.5 alloys 13 p2029 N85-22715
Developing procedures for thermomechanical processing of high-durability VT22 titanium alloy 13 p2031 N85-22726
Influence of annealing on cyclic and short-term strength of thin sheets of VT1-0 titanium and OTR4 alloy 13 p2031 N85-22727
Basis and pyramidal slipping in single crystals of alpha-alloy Ti-Al-Sn 13 p2032 N85-22730
Specifics of structure and mechanical properties of metastable beta-titanium alloys after deformation and aging 13 p2032 N85-22731
Properties of welded joints in argon arc welding of titanium alloy using a protective coating 13 p2032 N85-22733
Thermal hardening of welded joints in titanium alloys with various structures 13 p2032 N85-22734
Effect of protective medium on durability and fracture structure on seam zones of thin-walled titanium articles produced by diffusion welding 13 p2033 N85-22736
Technological parameters of diffusion welding processes in honeycomb titanium alloy structures 13 p2033 N85-22739
Fatigue strength of alpha-titanium alloys under cophasal action of variable normal and tangential stresses 15 p2498 N85-25407
Study of structural changes of dual-phase titanium alloy during shock wave loading 15 p2498 N85-25408
Possible use of rapid heating for improving mechanical properties of titanium alloys 15 p2498 N85-25409
Effect of annealing procedures on structure and properties of VT6 alloy with initial large-grained structure 15 p2498 N85-25410
Effect of aluminum on nature of titanium alloy failure 15 p2498 N85-25411
Resistance of hydrogenated alpha-titanium alloys to corrosion-fatigue fracture 15 p2499 N85-25413
Hydrogen resistance of VT1-0 titanium under 150 MPa pressure at room temperature 15 p2499 N85-25414
Ways of improving level and stability of mechanical characteristics of diffusion-welded joints of OT4 titanium alloy 15 p2499 N85-25417
Brittle fracture resistance of electron beam-welded joints in titanium Alpha alloys 15 p2500 N85-25419
Increasing seam formation stability in electron beam welding of very thick titanium alloys 15 p2500 N85-25420
Development of coating for protection of backside of seam in welding of titanium alloys 15 p2500 N85-25421
Thermocompression welding of parts made from AMts and VT1 alloys 15 p2501 N85-25430
USSR report: Materials science and metallurgy [JPRS-UMS-85-004] 15 p2513 N85-25503
Hardening of titanium alloy electric-arc welded joints 15 p2514 N85-25513
Mechanical properties of cast Martensitic high-strength multicomponent titanium alloys 15 p2514 N85-25514
Thermal stability of titanium alloys after cold plastic deformation 15 p2515 N85-25515
Dependence of plasticity of VT1-00 titanium alloy on microstructure 15 p2515 N85-25516
Structure and properties of VT20L titanium alloy with 0.1-0.3 percent content 15 p2515 N85-25517
Effect of initial structure on texture of pressed titanium alloy bars 15 p2515 N85-25518
Anode formation of passivating films on titanium alloy at temperatures up to 200 deg C 15 p2515 N85-25519
West Europe report: Science and technology [JPRS-WST-84-012] 15 p2523 N85-25552
MBB uses new CFC form tool for titanium alloy air intake 15 p2523 N85-25553
Titanium alloys, products, standards listed 15 p2533 N85-25626
Solid state bonding of molybdenum and TZM [BLL-T6439/BG/LRS/LRST751/85] 16 p2792 N85-27220
Effects of the phase compositions of cast low-pearlite steels micro-alloyed with vanadium and titanium of their structure and properties [BLL-BISI-TRANS-22301-(9022.06)] 17 p2928 N85-28067
Titanium metal-matrix composites [AD-D011643] 17 p2930 N85-28086
The disordering process in an L12 ordered alloy [DE85-008152] 17 p2931 N85-28093
Fundamental studies of beta phase decomposition modes in titanium alloys [AD-A154122] 19 p3238 N85-30078
Wear improvement in titanium alloys by ion implantation [AD-D011694] 19 p3239 N85-30081
Effect of thermochemical processing on fatigue resistance of titanium alloys 19 p3244 N85-30112
Determining partial molar volume of hydrogen in titanium alloys 19 p3245 N85-30119
Fatigue resistance of VT3-1 titanium alloy related to surface cold working 19 p3245 N85-30120
Effect of protective method on cyclic durability and nature of failure of titanium alloy welded joints 19 p3245 N85-30122
Effect of heating temperature in a vacuum on state of surface layers of welded OT4 titanium alloy 19 p3245 N85-30123
Fatigue resistance of homogeneous and heterogeneous welded joints of TS5 titanium alloy 19 p3246 N85-30126
concentration variation of work function of alloys in the system nickel-titanium-aluminum 19 p3247 N85-30134
CO adsorption on (111) and (100) surfaces of the Pt sub 3 Ti alloy. Evidence for parallel binding and strong activation of CO [NASA-CR-176077] 21 p3565 N85-32176
Fundamental investigations of failure during superplastic forming process [AD-A154847] 21 p3568 N85-32194
Thermodynamic properties of alloys in the Fe-Ti system [NPL-DMA(A)-96] 22 p3748 N85-33229
Electrical resistivity and hysteresis of the equiatomic nickel-titanium alloy near the martensitic transformation temperature 23 p3904 N85-34181
Influence of particle erosion on the microstructural changes in metals and alloys [TI85-901384] 23 p3917 N85-34276
Laser welding of 6Al-4V titanium alloy [DE85-012019] 23 p3938 N85-34413
The stress pattern analysis of coarse grain titanium specimens [PNR-90250] 23 p3942 N85-34433

TITANIUM BORIDES
Development and testing of TiB2, used as cathode material in Al-electrolysis cells [BMFT-FB-T-84-176] 05 p0633 N85-14060
Surface mechanical properties and wear behavior of ion implanted TiB2 [DE85-001130] 09 p1295 N85-18133
Secondary fluorescence effects on X-ray microanalysis [DE85-005565] 15 p2506 N85-25457
Study of self-propagating condensed phase reactions TiB(2) synthesis [AD-A153196] 17 p2921 N85-26006

TITANIUM CARBIDES
New titanium carbide grade for metal cutting 02 p0181 N85-11214
Optimization of production of composite diamond-containing materials using titanium carbide-steel alloys 10 p1446 N85-19113
Antifriction properties of gas thermal coatings of clad carbine powders 10 p1447 N85-19115
Particulate toughened silicon carbide [DE85-004797] 13 p2016 N85-22643
Comparative sinterability of combustion synthesized and commercial titanium carbides [DE85-006255] 15 p2512 N85-25498
Joining of sintered composite TiC-steel materials by welding [BLL-M-36253-(5828.4)] 20 p3461 N85-31502

TITANIUM CHLORIDES
Electrochemical behaviour of TiCl4 solutions in low melting point organic media [BLL-OA-TRANS-3174-(6196.3)] 06 p0764 N85-14888
Electrochemical reduction of titanium in dimethyl sulphoxide [BLL-OA-TRANS-3225-(6196.300)] 20 p3429 N85-31267
The determination of dinitrotoluene in single base propellants [AD-A154672] 21 p3571 N85-32209

TITANIUM COMPOUNDS
NT BARIUM TITANATES
NT LEAD ZIRCONATE TITANATES
NT PEROVSKITES
NT PIEZOELECTRIC CERAMICS
NT RUTILE
NT STRONTIUM TITANATES
NT TITANIUM BORIDES
NT TITANIUM CARBIDES
NT TITANIUM CHLORIDES
NT TITANIUM NITRIDES
NT TITANIUM OXIDES
Critical current measurements on an NbTi superconducting wire standard reference material [PB85-118594] 13 p2066 N85-22906
The mechanisms of phenylacetylene polymerization by molybdenum and titanium initiators [AD-A150993] 14 p2260 N85-24007
Pressure-dependence of TiS(2) and TiSe(2) bandstructures [AD-A151200] 15 p2659 N85-26410
New catalysts and new electrolytes for acid fuel cells [DE85-009940] 19 p3307 N85-30498
Geosynchronous performance of a lithium-titanium disulfide battery 20 p3444 N85-31377
The development of titanium production in the USSR [BLL-OA-TRANS-3226-(6196.3)] 23 p3913 N85-34244
Development of metallization process: FSA project, cells and module formation research area [NASA-CR-176136] 23 p3945 N85-34447

TITANIUM DIOXIDE
U TITANIUM OXIDES

TITANIUM NITRIDES
Deposition of titanium nitride coatings by reactive evaporation and electrically activated reactive evaporation [BLL-TRANS-5043-(9091.9F)] 07 p0925 N85-15858
Structural distortions of ultra-dispersed titanium nitride powders 13 p2029 N85-22717
Gear-cutting tools made of ultra high speed steel coated with TiN [BLL-RISLEY-TR-5109-(9091.9F)] 15 p2567 N85-25837
New metal coating method developed 21 p3568 N85-32191

TITANIUM OXIDES
NT RUTILE
The development of CVD oxide coatings for the protection of metal surfaces — chemical vapor deposition (CVD) 03 p0332 N85-12142
Contamination analysis of Ti-O2 thin films deposited using ion assisted deposition [DE84-014944] 05 p0732 N85-14705
Recording holograms on thin films of titanium dioxide 06 p0789 N85-15039
Time resolved Raman studies of laser induced damage in TiO2 optical coatings [DE85-003166] 11 p1640 N85-20332
Degradation mechanisms in ceramic dielectrics [AD-A149791] 12 p1813 N85-21369
Electron stimulated desorption and the role of secondary electrons [AD-A150974] 14 p2252 N85-23955
Fracture surface analysis in composite and titanium bonding: Part 1: Titanium bonding [NASA-CR-175750] 15 p2502 N85-25434
Photoeffects of semiconductor electrolyte interfaces [AD-A154163] 20 p3449 N85-31411
Characterization of catalysis with metal-support effects and of the species adsorbed on their surfaces [DE85-012254] 24 p4096 N85-35394

TITRATION
Mononitration of durene [NASA-TM-77774] 06 p0765 N85-14892

Aromatics determination in middle distillate petroleum fractions by spectrophotometric titration
[PNR-00239] 09 p1293 N85-18123
Computer-assisted Gran titration procedure for strong acid determination
[DE85-006601] 15 p2507 N85-25462
Increase of total CO2 in the World ocean
[DE85-007756] 23 p3950 N85-34484

TNT (TRINITROTOLUENE)
U TRINITROTOLUENE

TOBACCO
Plant cell cultures in biological space experiments
05 p0690 N85-14434

TOKAMAK DEVICES
MHD instabilities in simple plasma configuration
[AD-A144936] 01 p0121 N85-10629
Polarized electron cyclotron emission in the Tokapole 2 Tokamak
[DE84-014953] 01 p0122 N85-10636
Plasma surface interactions in magnetic fusion systems
[DE84-015255] 01 p0123 N85-10642
Measuring local ion energy distribution function in Tuman-3 Tokamak plasma 02 p0271 N85-11766
Relaxation of plasma rotation in a Tokamak in the presence of extraneous forces and corrugation of the magnetic field
[DE84-015628] 02 p0284 N85-11854
Theory of resistive ballooning modes in Tokamaks
[DE84-015626] 04 p0566 N85-13606
Internal helical mode m = 1 of a Tokamak in the plateau and banana regimes
[DE84-015623] 04 p0566 N85-13607
Fusion plasma theory. Task 1: Magnetic confinement fusion plasma theory
[DE84-014941] 04 p0566 N85-13608
Fusion plasma theory. Task 3: Auxiliary heating in Tokamaks and tandem mirrors
[DE84-014940] 04 p0566 N85-13609
Rotation of a tenuous plasma with a high toroidal velocity in a Tokamak
[DE84-012990] 04 p0567 N85-13615
High-Beta Tokamak research
[DE84-016470] 04 p0568 N85-13618
High-Beta plasma theory
[DE84-016471] 04 p0568 N85-13619
Proceedings of the US-Japan Theory Workshop on 3-D MHD Studies
[DE84-012019] 04 p0568 N85-13620
Imaging polarimeter-interferometer arrays for Tokamak measurements
[DE84-015916] 05 p0730 N85-14693
Passive stabilization of vertical instability in Tokamak reactor 06 p0775 N85-14958
Generation of suprathermal electrons during plasma current startup by lower hybrid waves in a Tokamak
[IPPJ-697] 06 p0863 N85-15483
Alpha-particle diagnostics with high energy neutral beams
[IPPJ-695] 06 p0863 N85-15485
Limits of possible operation of the R-Tokamak due to ideal MHD instabilities
[IPPJ-694] 06 p0863 N85-15486
Experimental results on Tokamak beta limits from ISX-B
[DE84-015372] 07 p1046 N85-16644
High-performance TF coil design for the Toroidal Fusion Core Experiment (TFCX)
[DE85-001127] 08 p1159 N85-17315
Subcable test facility
[DE85-002103] 09 p1315 N85-18269
A compact time-of-flight energy analyzer of high resolution --- for Tokamaks
[REPT-84-154] 09 p1324 N85-18318
An operational test of a time-of-flight analyzer at the ASDEX Tokamak
[REPT-84-155] 09 p1324 N85-18319
Slow wave antenna coupling to ion Bernstein waves for plasma heating in ICRF
[AD-B089084L] 09 p1386 N85-18717
Proceedings on US-Japan Workshop on Tokamak Diagnostics by X-ray, VUV and Optical Radiations
[IPPJ-703] 09 p1386 N85-18719
X-rays spectroscopy on the PLT and TFTR Tokamaks
09 p1386 N85-18720
Radial profiles of high resolution X-ray spectra from the Alcator C Tokamak 09 p1387 N85-18723
Recent activities on JIPP T-IIU Tokamak
09 p1387 N85-18724
Impurity control by additional current rise and gas puffing during ICRF heating in JIPP T-IIU Tokamak
09 p1387 N85-18725
X-ray spectroscopy of high-Z and high-density plasmas 09 p1387 N85-18726
Spectra of highly-ionized atoms for the diagnostics of the new generation of Tokamaks
09 p1388 N85-18730
Sources, densities, and transport of impurities in neutral-beam injected Tokamaks
09 p1388 N85-18731
Spectroscopic instrumentation for Tokamak diagnostics 09 p1388 N85-18732
Determination of ion temperature and rotation velocity profiles by visible, UV and X-ray spectroscopy on Doublet 3 09 p1388 N85-18734
Transport experiments in the Texas experimental Tokamak 09 p1389 N85-18741
Radiation data and standards for Tokamak diagnostics
09 p1390 N85-18742
Impact of atomic data on Tokamak modeling
09 p1390 N85-18743
Compilation of atomic data for diagnostics of Tokamak
09 p1390 N85-18744
Beam-foil spectroscopy of highly ionized aluminum atoms 09 p1390 N85-18746
MHD equilibrium and stability for stellarator/torsatron configurations
[DE85-001139] 09 p1391 N85-18750
Extended abstract: Ergodic magnetic limiter experiments on TEXT with a 7/3 resonance
[DE85-001390] 09 p1391 N85-18754
Discharge initiation experiments in the Tokapole II Tokamak
[DE84-017345] 09 p1391 N85-18755
Experimental investigations of driven Alfven wave resonances in a Tokamak plasma using carbon dioxide laser interferometry
[DE85-001049] 09 p1392 N85-18758
Effects of q and high beta on Tokamak stability
[DE84-016650] 09 p1393 N85-18767
Background calculations for the measurement of the ion temperature in a deuterium plasma
[DE84-016546] 09 p1393 N85-18768
Versator divertor experiment: Preliminary designs
[DE84-017159] 09 p1393 N85-18769
Studies on impurity control and hydrogen pumping with chromium gettering in ISX-B
[DE85-001896] 09 p1394 N85-18771
The energy spectra of slowed-down neutrals from the heating beams in ASDEX --- tokamak
[REPT-84-157] 09 p1394 N85-18772
Sequentially-framing soft X-ray pinhole camera for Tokamak plasma studies
[DE85-001717] 10 p1489 N85-19399
CO2 laser interferometer array for Big Dee
[DE85-001718] 10 p1490 N85-19411
Far-infrared interferometry/polarimetry on the ISX-B Tokamak
[DE84-015401] 10 p1558 N85-19627
Space-time statistics of the turbulence in a Tokamak edge plasma
[DE85-002667] 10 p1559 N85-19634
A proposed method for fast determination of plasma parameters
[IPP-1/228] 11 p1730 N85-20677
Fusion Energy Division
[DE85-001701] 11 p1731 N85-20684
FIR interferometer/polarimeter system on ISX-B Tokamak
[DE85-001129] 11 p1731 N85-20687
Control of surface composition and hydrogen recycling by plasma conditioning
[DE85-001859] 11 p1731 N85-20689
Driven global Alfven eigenmodes
[DE85-001056] 11 p1732 N85-20690
Fluctuations and transport in fusion plasmas
[DE85-003612] 11 p1732 N85-20693
Determination of experimental Tokamak plasma properties using maximum entropy analysis
[DE85-001723] 12 p1936 N85-22165
Tritium catalyzed deuterium Tokamaks
[DE85-004825] 12 p1936 N85-22166
Observations of bulk electron heating due to return current in a tokamak discharge started up by lower hybrid waves
[IPPJ-708] 12 p1937 N85-22172
Winding insulation in electromagnetic systems for Tokamak reactor plants 13 p2087 N85-23035
Lower hybrid heating and current drive, and ion cyclotron heating experiments on the Alcator C and the Versator II Tokamaks
[DE85-004918] 13 p2161 N85-23412
East Europe report: Science and technology
[JPRS-ESA-85-015] 14 p2289 N85-24189
Design, theoretical innovations in Tokamaks systems
14 p2289 N85-24190
Noninductive current drive in Tokamaks
[DE85-005427] 14 p2424 N85-24951
ICRF antenna coupling theory for a cylindrically stratified plasma
[DE85-004960] 14 p2424 N85-24952
Self-substaining low-Z coatings for impurity control. Part 1: General considerations
[DE85-000427] 14 p2425 N85-24956
Magnetohydrodynamic considerations for the design of self-cooled liquid-metal fusion reactor blankets
[DE85-000242] 14 p2425 N85-24957
Breakthrough in container confinement of ultracold neutrons 15 p2644 N85-26311
Annual Review, April 1983 - March 1984
[ISSN-0547-1567] 15 p2654 N85-26369
Scientific activities. A: Reacting plasma physics. 1: Introduction and overview 15 p2654 N85-26370
Outline of alternative design of R-Tokamak
15 p2654 N85-26371
Plasma heating 15 p2654 N85-26372
Preparatory experiments. 1: JIPP T-IIU
15 p2654 N85-26374
MHD fluctuations in ISX-B
[DE85-004800] 15 p2657 N85-26386
New directions in Tokamak reactors
[DE85-002548] 15 p2657 N85-26396
Methods of first wall structural analysis with applications to the long pulse commercial Tokamak reactor design
[DE85-004915] 15 p2657 N85-26397
Toroidal equilibrium with low frequency wave driven currents
[DE85-005790] 15 p2658 N85-26401
Self-sustaining low-Z coatings for fusion applications 2: - copper-lithium
[DE85-002553] 15 p2658 N85-26403
Ballooning beta limits of dee and bean shaped Tokamaks
[IPPJ-713] 16 p2866 N85-27678
TOKASTAR: A Tokamak stellarator hybrid with possible bean-shaped operation
[IPPJ-718] 16 p2866 N85-27680
Computational plasma physics and supercomputers, revision 1
[DE85-007228] 16 p2867 N85-27687
Spherical torus, compact fusion at low field
[DE85-006983] 16 p2867 N85-27689
Time-resolving electron temperature diagnostic for ALCATOR C
[DE85-004916] 16 p2868 N85-27690
A four-field model for Tokamak plasma dynamics
[DE85-007111] 16 p2868 N85-27694
Coupled plasma-neutral transport model for the scrape-off region
[DE85-007559] 16 p2868 N85-27695
Tokamak systems code
[DE85-008147] 16 p2869 N85-27696
Accelerator-based plasma-wall interaction studies on the TEXTOR Tokamak
[DE85-007540] 17 p3040 N85-28606
Tokamak fusion core experiment maintenance study
[DE85-008040] 17 p3040 N85-28613
The transport of neutral H, D, T and He and O in the boundary layers of a Tokamak plasma
[REPT-84-153] 17 p3041 N85-28617
New concept for a wall detector for alpha particles
[DE85-009037] 18 p3183 N85-29740
Whist code calculations of ignition margin in an ignition Tokamak
[DE85-009507] 18 p3190 N85-29784
Tokamak ignition/burn experimental research device
[DE85-009969] 18 p3190 N85-29785
Feasibility study of a fission-suppressed Tokamak fusion breeder
[DE85-009099] 18 p3190 N85-29786
Toroidal viscosity and ambipolarity in the neoclassical transport theory of axisymmetric tori
[DE85-010622] 19 p3358 N85-30620
TFCK shielding optimization
[DE85-010503] 19 p3359 N85-30626
Magnetic fusion 1985: What next?
[DE85-009953] 19 p3365 N85-30666
Impurity and particle control systems for tokamak reactor experiments
[DE85-006124] 19 p3366 N85-30673
ICRF antenna coupling and wave propagation in a tokamak plasma 19 p3369 N85-30680
Effects of a radial electric field on tokamak edge turbulence
[DE85-010401] 19 p3371 N85-30910
Ballooning instabilities on a magnetic separatrix
[DE85-010655] 19 p3372 N85-30915
Neutronics activities for next generation devices
[DE85-010488] 20 p3527 N85-31909
Superconducting toroidal field coil current densities for the TFCX
[DE85-010285] 20 p3530 N85-31959

Runaway electrons and plasma turbulence in current ramping by lower hybrid waves in tokamak plasmas
[DE85-011390] 20 p3535 N85-31997
Injection of hydrogen macroparticles into T-10 tokamak 21 p3692 N85-32937
Influence of ECR-heating on MHD activity of plasma in tokamak-10 installation 21 p3694 N85-32949
System and method of operating toroidal magnetic confinement devices
[DE85-011670] 22 p3845 N85-33814
Possibility of potential generation by lower hybrid wave 23 p3977 N85-34654
Observation of mode-converted by ion Bernstein wave by an HCN laser scattering
[IPPJ-724] 23 p3979 N85-34668
Compact DT fusion spherical tori at modest field
[DE85-011568] 23 p3982 N85-34692
Experimental measurements of the ion cyclotron antennas' coupling and RF characteristics
[DE85-011569] 23 p3982 N85-34694
Shield design for next-generation, low-neutron-fluence, superconducting tokamaks
[DE85-011409] 23 p3982 N85-34695
Observation of helical sawtooth oscillations in a tokamak
[DE85-012062] 23 p3983 N85-34703
ECH tokamak
[DE85-012074] 23 p3984 N85-34707
Neutral pumping rates for a next step tokamak ignition device
[DE85-012780] 24 p4157 N85-35776
Generalized reduced fluid model with finite ion-gyroradius effects
[DE85-013123] 24 p4157 N85-35777
Resonance localization in tokamaks excited with ICRF waves
[DE85-014559] 24 p4160 N85-35791

TOLERANCES (MECHANICS)
NT IMPACT TOLERANCES
Development of powder metallurgy 2XXX series Al alloys for high temperature aircraft structural applications
[NASA-CR-172408] 02 p0182 N85-11220
Array sidelobes, error tolerance, gain, and beamwidth
[AD-A147004] 07 p0940 N85-15956
Tolerance synthesis of multilayer radome walls
07 p0953 N85-16041
Advances in composites technology
[NASA-TM-86353] 08 p1118 N85-17048
Defect tolerance in pipeline girth welds
[ERS-E.353] 09 p1328 N85-18347
Construction tolerances for low loss, dielectric coated, metallic waveguide for transmission optical radiation
[DE85-004056] 10 p1558 N85-19822
Method for increasing linearity of load cell
11 p1623 N85-20221
Advanced life analysis methods. Volume 1: Cracking data survey and NDI (nondestructive inspection) assessment for attachment lugs
[AD-A150419] 13 p2103 N85-23108
Advanced life analysis methods. Volume 2: Crack growth analysis methods for attachment lugs
[AD-A150420] 13 p2103 N85-23109
Advanced life analysis methods. Volume 4: Tabulated test data for attachment lugs
[AD-A151016] 14 p2219 N85-23760
Advanced life analysis methods. Volume 5: Executive summary and damage tolerance criteria recommendations for attachment lugs
[AD-A151017] 14 p2219 N85-23761
Dimensions of smooth mating parts with protective coatings 14 p2280 N85-24124
Multiaxial and thermomechanical fatigue considerations in damage tolerant design
[NASA-TM-87022] 16 p2749 N85-26964
Probabilistic structural analysis of SSME turbopump blades: Probabilistic geometry effects
17 p2913 N85-27958

TOLERANCES (PHYSIOLOGY)
NT ACCELERATION TOLERANCE
NT ALTITUDE TOLERANCE
NT COLD TOLERANCE
NT HEAT TOLERANCE
NT HUMAN TOLERANCES
NT RADIATION TOLERANCE
General resistance of organism of rats under hypokinesia 05 p0694 N85-14462
A crew exposure study. Volume 1: Offshore
[AD-A146884] 07 p1015 N85-16449
Effects of restricted water intake on performance in a cold environment
[AD-A146904] 07 p1015 N85-164[illegible]
Aviation-related cardiorespiratory effects of blood donation in female pilots
[AD-A148045] 08 p1195 N85-17529
Analysis of head motion during simulated, rough water operation of a 2200 ton surface effect ship
11 p1695 N85-20656
The current status of the RAF programme of desensitisation for motion sick aircrew
11 p1695 N85-20658
Role of mental work in human tolerance in total-body vibration 12 p1901 N85-21940
Investigation of adaptive distinctions of mechanism of controlled glycemia in Macaca rhesus monkeys
12 p1902 N85-21946
Multiple regression method used to assess animal adaptation to hypoxic hypoxia 12 p1902 N85-21947
The medical results of human exposures to radio frequency radiation
[AD-A149718] 12 p1905 N85-21962
Sleep deprivation and exercise tolerance
[AD-A150180] 13 p2142 N85-23295
Sleep deprivation and exercise tolerance
[AD-A150566] 13 p2142 N85-23296
Sleep deprivation and exercise tolerance
[AD-A150626] 13 p2142 N85-23297
Simulation of a G-tolerance curve using the pulsatile cardiovascular model
[NASA-CR-171873] 15 p2616 N85-26120
Fluid-electrolyte responses during prolonged space flight: A review and interpretation of significant findings
[NASA-CR-171878] 15 p2617 N85-26124
Functional impairment and structureal cervical injuries in human surrogates
[PB85-167436] 15 p2619 N85-26137
Effects of dehydration or cold exposure and restricted fluid intake upon cognitive performance
[AD-A151973] 16 p2842 N85-27525
An in vitro method for the screening of trichothecene mycotoxin cytotoxicity and the study of mycotoxin countermeasures
[AD-A153663] 18 p3152 N85-29517
Acclimatization to far north 20 p3506 N85-31792
The role of sulfur in osmoregulation and salinity tolerance in cyanobacteria, algae, and plants
21 p3660 N85-32736
A crew exposure study. Phase II. Volume 2. At sea. Part A
[AD-A155233] 21 p3686 N85-32774
Effects of low level carbon monoxide (CO) on tracking and monitoring. An attempt to replicate the findings of Putz et al. (1976) protocol 2
[AD-A155722] 22 p3825 N85-33694
Tolerance to +Gz and +Gx accelerations of individuals in older age groups in good health and with early signs of arteriosclerosis 23 p3952 N85-34496

TOLLMEIN-SCHLICHTING WAVES
Generation and development of small-amplitude disturbances in a laminar boundary layer in the presence of an acoustic field
[NASA-TM-77826] 14 p2299 N85-24237

TOLUENE
Effect of toluene on the solubility of biohazardous volatile synthetic organic compounds
[AD-A145188] 01 p0018 N85-10109
Deuteron NMR (Nuclear Magnetic Resonance) in relation to the glass transition in polymers
[AD-P003910] 01 p0032 N85-10196
Influence of structural parameters of zeolite catalysts on their activity and selectivity
[BMFT-FB-T-83-253] 03 p0329 N85-12119
Determination of Toluene's degradation products under simulated atmospheric conditions
05 p0674 N85-14331
Research in phase transfer catalysis
[AD-A148286] 08 p1121 N85-17068
Supersonic molecular jet study of the liquid state
[AD-A147416] 09 p1379 N85-18671
Polymer solution-supercritical fluid behavior
[AD-A154514] 21 p3568 N85-32192
Thermal reactions of aromatics with CaO
[DE85-010688] 22 p3742 N85-33193
Modeling of auto exhaust smog chamber data for EKMA development
[PB85-186492] 22 p3813 N85-33619
Carcinogenesis of nitrated toluenes and benzenes skin and lung tumor assays in mice
[AD-A155723] 22 p3818 N85-33655
Studies in photochemical smog chemistry. 1: Atmospheric chemistry of toulene. 2: Analysis of chemical reaction mechanisms for photochemical smog
24 p4113 N85-35497

TOMOGRAPHY
NT COMPUTER AIDED TOMOGRAPHY
Tomographic reconstruction of neutron radiograph images
[AD-A145682] 02 p0280 N85-11826
Time-resolved tomographic images of a relativistic electron beam
[DE84-015021] 04 p0565 N85-13597
Tomographic reconstruction of axially symmetric objects from a single radiograph
[DE84-016783] 04 p0565 N85-13599
Field implementation of geophysical diffraction tomography
[DE84-017594] 09 p1343 N85-18449
Acoustic tomographic reconstrution of anomalies in three-dimensional bodies
[DE84-017035] 09 p1378 N85-18666
Simultaneous determination of cerebral blood flow and partition coefficient with a freely diffusable tracer
[DE85-001226] 11 p1690 N85-20625
Reconstruction of a 3-dimensional transonic rotor flow field from holographic interferogram data
[NASA-TM-86690] 12 p1770 N85-21112
Research in image understanding as applied to 3-D tomographic imaging with near optical resolution
[AD-A150096] 12 p1829 N85-21483
A new NDE (Non-Destructive Evaluation) capability for thin-shelled structures
[AD-A149625] 12 p1862 N85-21678
NDE methods for green ceramics
[DE85-004019] 13 p2036 N85-22766
Optical processing in radon space
[AD-A150289] 13 p2159 N85-23402
Axial topography from digitized real time radiography
[DE85-006767] 18 p3091 N85-29130
Three-dimensional and tomographic imaging device for X-ray and gamma-ray emitting objects
[NASA-CASE-GSC-12851-1] 19 p3271 N85-30281
Preliminary evaluation of alterant geophysical tomography in welded tuff
[DE85-010626] 19 p3302 N85-30469
Arctic acoustic tomography MIZEX 84
[AD-A154426] 19 p3320 N85-30580
Biology and Medicine Division
[DE85-010638] 19 p3327 N85-30613
Radiation interactions for tomography
[DE85-008961] 19 p3355 N85-30799
Advanced instrumentation for Positron Emission Tomography
[DE85-011147] 22 p3840 N85-33779

TONOMETRY
U INTRAOCULAR PRESSURE
U PRESSURE MEASUREMENT

TONUS
U MUSCULAR TONUS

TOOLING
New tooling for plasma cutting technology
13 p2051 N85-22842
MBB automates aircraft production in many FRG facilities 14 p2289 N85-24188
An analysis of machine tool systems suitable for laser profiling 14 p2308 N85-24282

TOOLS
NT BORING MACHINES
NT DRILL BITS
NT GRINDING MACHINES
NT LATHES
NT MACHINE TOOLS
NT MILLING MACHINES
NT SAWS
NT SPACE TOOLS
NT TURRET LATHES
Utility of the M.I.T. (Massachusetts Institute of Technology) underwater stud welding gun
[AD-A144793] 01 p0055 N85-10365
Prediction accuracy of the torques for rotary tillage by an analog tool
[AD-P004288] 09 p1406 N85-18865
Connection system — insuring against loss of a tool component without using multiple tethers
[NASA-CASE-MSC-20319-1] 12 p1857 N85-21649
Aircraft skin penetrator and agent applicator. Volume 2: Test and evaluation
[AD-A151609] 15 p2466 N85-25225
Gear-cutting tools made of ultra high speed steel coated with TiN
[BLL-RISLEY-TR-5109-(9091.9F)]
15 p2567 N85-25837
Classification and types of diamond wear in honing
15 p2567 N85-25842
Printed wiring board circuit isolator tool
[AD-D011638] 17 p2968 N85-28333
The blind and the paralyzed. The notion of the tool revealed and integrated in a different organization environment
[SNIAS-851-422-104] 20 p3513 N85-31835
Action of wear-inhibiting Al2O3-coatings when applied to hard metal cutting tools
[BLL-RISLEY-TR-5041-(9091.9F)]
24 p4081 N85-35292
Wear-resistant coatings for tools intended for cold working
[BLL-RISLEY-TR-5040-(9091.9F)]
24 p4081 N85-35293

TOPEX
Topex Gravity Model Development Team activities during fiscal year 1984
[NASA-TM-86208] 16 p2804 N85-27285
Status of the observational data sets — TOPEX
16 p2804 N85-27286
Satellite selection criteria 16 p2804 N85-27288
Optical best arc RMS test results
16 p2804 N85-27290
Ocean tide models for Topex analysis
16 p2805 N85-27291
Radial orbit error spectrum for Topex
16 p2805 N85-27292
The size of a gravitational field model for Topex
16 p2805 N85-27293
Numerical integration through force discontinuities: Solar radiation pressure 16 p2805 N85-27296
Station coordinates and Earth rotation parameters from Lageos laser ranging 16 p2806 N85-27299
TOPEX error budget 20 p3493 N85-31717

TOPOGRAPHY
NT LUNAR TOPOGRAPHY
NT TERRAIN
The SANCOR programme on coastal processes, April 1982 - March 1988
[REPT-68] 01 p0069 N85-10455
Investigation of summertime convection over the upper Current River valley of southeast Missouri
[PB84-222389] 01 p0086 N85-10578
The application of principal component analysis in a study of rainfall 02 p0212 N85-11396
Geomorphology 02 p0214 N85-11411
Cartography 02 p0214 N85-11412
Hypothesis on the origin of lineaments in the LANDSAT and SLAR images of precambrian soil in the low Contas River Valley (southern Bahia)
[E85-10007] 02 p0215 N85-11420
Terrain analysis procedural guide for surface configuration
[AD-A145637] 02 p0219 N85-11446
Satellite altimetry for sea-surfacing topography determination and geoid improvement
03 p0382 N85-12444
Modelling of altimeter tracking over topographical surfaces — satellite antennas 03 p0383 N85-12450
The structure of the Iceland-Faeroe ridge, derived from geophysical measurements
[DRIC-T-7255] 03 p0397 N85-12535
Comparison between tracer measurements and model calculations for nighttime drainage flows in complex terrain
[DE84-014709] 04 p0539 N85-13431
The 1984 NASA/ASEE summer faculty fellowship program
[NASA-CR-174138] 04 p0574 N85-13663
Mars polar volatiles: Topographic and geologic setting
[NASA-CR-174089] 04 p0581 N85-13708
Atmospheric studies in complex terrain
[DE84-008553] 05 p0676 N85-14345
Potential geological natural landmarks of the East Gulf Coastal Plain
[PB84-230317] 06 p0835 N85-15316
Statistical relationships between meteorological data stations and implications to diagnostic models in complex terrain
[DE84-014380] 06 p0839 N85-15328
Relationship between forest clearing and biophysical factors in tropical environments: Implications for the design of a forest change monitoring approach — Costa Rica
[E85-10051] 07 p0983 N85-16247
A Computer-generated topographic display system for navigation and mission planning in helicopters
08 p1073 N85-16800
SIR-B interferometric topography
08 p1145 N85-17224
Interlobate comparison of glacial-depositional style as evidenced by small-relief glacial landscape features in Illinois, Indiana, and Ohio, utilizing SIR-B
08 p1146 N85-17231
SIR-B cartography and stereo topographic mapping
08 p1147 N85-17234
Monitoring of the tidal dynamics of the Dutch Waddensea by SIR-B 08 p1147 N85-17235
Application and calibration of the subsurface mapping capability of SIR-B in desert regions
08 p1148 N85-17244
Mathematical aspects of digital terrain information; Report from International Society for Photogrammetry and Remote Sensing (ISPRS) working group 3:3, 1980 - 1984 — photogrammetry 08 p1175 N85-17407
Post-Laramide history of North Central Wyoming
08 p1181 N85-17444
A method for determining mesoscale dynamic topography
[AD-D011412] 08 p1191 N85-17506
Gravity anomaly map of Mars and Moon and analysis of Venus gravity field: New analysis procedures
[NASA-CR-174295] 08 p1258 N85-17919
The pleistocene geology of Vilas County, Wisconsin
09 p1353 N85-18509
Venus 09 p1411 N85-18891
A comparison between predicted and measured propagation loss in the VHF/UHF range in rugged terrain 10 p1471 N85-19285
Climate of Salt Lake City, Utah
[PB85-123875] 10 p1521 N85-19589
Application of SLF (Standard Linear Format) to digital hydrographic products
[AD-A149509] 10 p1522 N85-19596
Microstrain analysis in bent single crystal silicon by double crystal X-ray topography technique
[DE85-000422] 10 p1564 N85-19863
Analysis of slope stability, Wilmington to Lindenkohl Canyons, US mid-Atlantic margin
[DE84-012278] 12 p1899 N85-21921
Planetary cartography in the next decade (1984 - 1994)
[NASA-SP-475] 12 p1960 N85-22323
Physiography of the Martian west equatorial uplift
12 p1961 N85-22325
Hypsometric features on Venus
13 p1983 N85-22439
Evaluating accuracy in orientation of topographic photograph and satellite-centered direction from star photograph 13 p1983 N85-22442
Development, achievements in China's cartography work 13 p2166 N85-23434
Topographic evidence for shield volcanism on Io
13 p2172 N85-23478
The support of long wavelength loads on Venus
13 p2178 N85-23515
Newly discovered Martian impact basins
13 p2182 N85-23544
Mapping structures characteristic of the highland boundary scarp on Mars 13 p2191 N85-23595
Mercury radar altimetry: A preliminary analysis
13 p2196 N85-23631
Unsupervised classification of global radar units on Venus 13 p2196 N85-23632
Mapping and geological analysis of Mercury and Venus radar ranging data 13 p2198 N85-23633
Correction and geological analysis of lunar 3.8 cm radar data 13 p2198 N85-23634
Mars radar catalog 13 p2198 N85-23636
The deep structure of lunar basins: Clues to the understanding of basin formation and modification
13 p2200 N85-23647
Mars: Stratigraphy of western highlands and polar regions 13 p2201 N85-23653
The Galilean Satellite Geological Mapping Program, 1984 13 p2203 N85-23664
Fatigue Crack Topography
[AGARD-CP-376] 14 p2318 N85-24321
Fatigue fracture topography 14 p2318 N85-24323
A study of terrain reductions, density anomalies and geophysical inversion methods in gravity field modelling
[AD-A150788] 14 p2373 N85-24666
Studies of deformation in niobium by X-ray topographic methods
[AD-A150726] 14 p2427 N85-24965
Contamination of the fetch-limited directional wave spectrum by waves emanating from an embayment
[NASA-TM-84441] 15 p2604 N85-26048
Tenth Conference of Working Group of Socialist Countries on Remote Sensing of Earth under Intercosmos Program 16 p2725 N85-26820
Reports on cartography and geodesy. Series 1: Original reports, no. 94
[ISSN-0469-4236] 16 p2814 N85-27357
Use of vector processors in cartographic raster data processing, with special regard to the AP-120B vector processor 16 p2814 N85-27358
Testing of scanner-assisted revision of the topographic map 1:25,000 (TK 25) 16 p2814 N85-27359
Automatic engraving of map frames in the revision of the TK 25, 1:25,000 topographical map
16 p2814 N85-27362
Groundwater model for an island aquifer: Bribie Island groundwater study
[CE-44] 16 p2821 N85-27396
System analysis of a field Army Topographic Support System
[AD-A153318] 17 p2964 N85-28439
A discussion of adaptive grids and their applicability in numerical hydrodynamic modeling
[AD-A151843] 17 p3017 N85-28659
Derivation of model topography
18 p3141 N85-29449
Sigma filter 18 p3142 N85-29450
Comparison of two orographical data sets for the GLAS Fourth Order GCM 18 p3142 N85-29452
Engineering geology of selected areas, US army engineer division, lower Mississippi valley. The American bottom area, MO-IL. Volume 1
[AD-A154258] 19 p3299 N85-30455
Sand dispersion from an ephemeral river delta on the wave-dominated central California coast
[AD-A154352] 19 p3300 N85-30458
Stratigraphic analysis of Pennsylvania rocks using hierarchy of transgressive-regressive units
19 p3312 N85-30531
Evolution of the oceanic upper mantle and effects on sea floor subsidence geoid height and heat flow
19 p3319 N85-30575
HANDTC: A FORTRAN program to calculate inner-zone terrain corrections
[DE85-011196] 19 p3340 N85-30609
Video discs - what are they and where do they fit in?
[AD-A154166] 20 p3458 N85-31479
Comparative study of fracture planes computed from topography and lineaments from imagery with structures and minuralization in the magnetic belt of Washington State
[DE85-010972] 20 p3477 N85-31608
The application of computer imaging techniques to ocean topography and geophysical data
20 p3492 N85-31711
Geophysical interpretation of Venus gravity data
[NASA-CR-176063] 20 p3547 N85-32071
The measurement of strain fields by X-ray topographic contour mapping
[AD-A154870] 21 p3599 N85-32345
Geomorphological similarity and uniqueness
21 p3601 N85-32361
Regional landform thresholds
21 p3601 N85-32362
Some observations on paleogeomorphology
21 p3601 N85-32363
Ancient landscapes: Their nature and significance for the question of inheritance 21 p3601 N85-32364
Quantitative analysis in megageomorphology
21 p3603 N85-32376
Landscape inheritance: Report of Working Group Number 2 21 p3604 N85-32383
Process thresholds: Report of Working Group Number 3 21 p3604 N85-32384
Frequency and site selection criteria for MST radars, part 5.1A 21 p3624 N85-32512
Upward continuation of surface gravity anomalies
[AD-A154973] 21 p3631 N85-32580
An enhanced photoresponse at dislocation subgrain boundaries revealed by X-ray topography of polysilicon solar cells 22 p3806 N85-33572
Planetary surface processes: A review
22 p3855 N85-33869
Evaluation: Close-range photogrammetry for slope inventory and monitoring
[PB85-192755] 24 p4108 N85-35470
Three-dimensional gravity ideal body studies in rough terrain
[DE85-014097] 24 p4118 N85-35525

TOPOLOGY
NT FIXED POINTS (MATHEMATICS)
NT HOMOTOPY THEORY
NT LINKS (MATHEMATICS)
NT METRIC SPACE
Planarity criteria in electromagnetic topology
[AD-A145279] 01 p0036 N85-10241
Birkhoff orbits for non-monotone twist maps
[AD-A144718] 01 p0110 N85-10747
Fractals: From snow flakes to galactic clusters
[NOTA-INTERNA-796] 02 p0296 N85-11916
A topological approach to database theory
03 p0437 N85-12781
Lectures on generalized solutions to the minimal surface equation
[DE84-016882] 05 p0722 N85-149
Invariant measures and the equicontinuous structure relation 1
[CWI-PM-R8403] 05 p0723 N85-149
Invariant measures and the equicontinuous structure relation 2: The relative case
[CWI-PM-R8404] 05 p0723 N85-149
Disturbance propagation in structural networks; control of large space structures 06 p0759 N85-14
Chemical applications of topology and group theory. 18: Polyhedral isomerizations of seven-coordinate complexes
[AD-A149461] 10 p1436 N85-19
Advanced inverter technology
[AD-A149335] 10 p1480 N85-19
A circuit grammer for operational amplifier design
[AD-A149566] 10 p1481 N85-19
Diffeomorphic approximation of quasiconformal and quasisymmetric homeomorphisms
10 p1536 N85-19

Shielded enclosures for experimental studies of shielding topology
[AD-A149292] 11 p1624 N85-20227
Circuit topology, signal propagation delay and the efficiency of VLSI circuits
[CWI-CS-R8414] 11 p1630 N85-20267
Annals of the Fourier Institute, volume 34, no. 4
11 p1698 N85-20668
Topological triviality of versal unfoldings of complete intersections 11 p1699 N85-20678
The origin and evolution of terrestrial and Martian rock labyrinths
[NASA-CR-175511] 12 p1961 N85-22326
Relationship between topological and magnetic order in small metal clusters
[AD-A150547] 13 p2016 N85-22651
Method for processing broad-profile data
13 p2117 N85-23165
Surfaces with canonical hyperplane sections
[CWI-TRACT-1] 14 p2410 N85-24856
Topology and Order Structures, part 2
[MCT-169-PT-2] 14 p2413 N85-24879
Twenty questions on ordered spaces
14 p2413 N85-24880
A note on perfect normality in generalized ordered spaces 14 p2413 N85-24881
Metrization theorems for continuous images of compact ordered spaces 14 p2413 N85-24882
A pathological homogeneous subspace of the real line
14 p2413 N85-24883
A note on topological groups with dense orderable subspaces 14 p2413 N85-24884
The Kappa sub n property in small Omega sub 1 trees
14 p2413 N85-24885
On compactifications of generalized order GO-spaces
14 p2413 N85-24886
The orderability of compact scattered spaces
14 p2413 N85-24887
Submetrizable topologies on the ordinals
14 p2414 N85-24888
When is a GO-space JO(2)? 14 p2414 N85-24889
Local bases and product partial order II
14 p2414 N85-24890
Mappings of finite oscillations at local separating points 14 p2414 N85-24891
Orderable subspaces of compact F-spaces
14 p2414 N85-24892
Fake topological Hilbert spaces and characterizations of dimension in terms of negligibility
[CWI-TRACT-2] 14 p2414 N85-24893
Isoparametric 3-D finite element mesh generation using interactive computer graphics 15 p2574 N85-25873
Point processes associated with extreme value theory
[AD-A151211] 15 p2640 N85-26280
Mathematical programming in computer network design
[AD-A152275] 16 p2848 N85-27558
A study of topologies and protocols for fiber optic local area network
[NASA-CR-175771] 16 p2864 N85-27669
Chemical applications of topology and group theory. 17: An information theoretical approach to polyhedral symmetry
[AD-A152821] 17 p2919 N85-27995
The definition and computation of a metric on plane curves. The meaning of a face on a geometric model
17 p3004 N85-28571
Some negative results in N-sided patches
17 p3004 N85-28572
Contouring trivariate data 17 p3005 N85-28582
On the definition of topological susceptibility via lattice anomalous Ward identities and its perturbative tail
[PREPRINT-416] 18 p3184 N85-29744
Nested dissection on a mesh-connected processor array
[AD-A154088] 19 p3342 N85-30711
Global Mega-Geomorphology
[NASA-CP-2312] 21 p3600 N85-32357
Broadcasting topology and routing information in computer networks
[AD-A155668] 21 p3674 N85-32827
Synthesis of metrico-topological model for layout of topology of large-scale-integration arrays
22 p3781 N85-33427
Graph-theoretical exorcism
[DE85-011916] 23 p3955 N85-34512
Cosmic ray secondary nuclei and the structure of the galaxy
[OG-7.2-4] 23 p4014 N85-34876
Alfven wave scattering and the secondary to primary ratio
[OG-7.2-9] 23 p4015 N85-34878
Edge detection and geometric methods in computer vision
[AD-A155873] 24 p4135 N85-35630

TORCHES
Cosmonauts report on space welding at conference
15 p2484 N85-25329
Paton comments on results of space welding tests
15 p2484 N85-25330

TORNADO AIRCRAFT
U MRCA AIRCRAFT

TORNADOES
Recent examples of mesoscale numerical forecasts of severe weather events along the east coast
[NASA-TM-86172] 03 p0395 N85-12523
Investigations of severe/tornadic thunderstorm development and evolution based on satellite and AVE/SESAME/VAS data
[NASA-CR-174154] 04 p0538 N85-13424
TVENT1P user's manual, a computer code for analyzing tornado induced gas dynamic transients in flow networks
[DE85-002346] 10 p1486 N85-19379
Hurricane Research Division, fiscal year 1984 programs, fiscal year 1985 projections 16 p2836 N85-27491
J. P. Finley: The first severe storms forecaster
[PB85-17453] 19 p3318 N85-30566
Automated cell detection as a mesocyclone precursor tool
[AD-A154952] 21 p3635 N85-32577
Real-time automated detection of mesocyclones and tornado vortex signatures
[AD-A154968] 21 p3635 N85-32578

TOROIDAL PLASMAS
Means of varying conditions in the expanded boundary divertor without affecting energy confinement
[DE84-013840] 01 p0122 N85-10836
Plasma drift equilibrium (gyration) in toroidal systems with complex magnetic-field geometry
[DE84-015627] 01 p0122 N85-10839
Destruction of magnetic surfaces in three-dimensional MHD equilibria 02 p0282 N85-11838
Elimination of stochasticity in stellarators
02 p0282 N85-11839
Study of plasma convection and wall interactions in magnetic confinement systems
[DE84-013959] 03 p0421 N85-12692
Compact toroid development, activity plan for spheromaks
[DE84-016736] 04 p0567 N85-13617
Monte Carlo studies of transport in stellarators
[DE84-017633] 04 p0588 N85-13625
Elma Bumpy Torus physics
[DE84-015909] 05 p0730 N85-14694
Generation of suprathermal electrons during plasma current startup by lower hybrid waves in a Tokamak
[IPPJ-697] 06 p0863 N85-15483
Shear-Alfven dynamics of toroidally confined plasmas, part A
[DE85-001590] 06 p0866 N85-15502
X-rays spectroscopy on the PLT and TFTR Tokamaks
09 p1386 N85-18720
Recent activities on JIPP T-IIU Tokamak
09 p1387 N85-18724
Density measurements of atomic hydrogen in NBT-IM by laser-induced fluorescence spectroscopy
09 p1389 N85-18739
Transport experiments in the Texas experimental Tokamak 09 p1389 N85-18741
Design and construction details of the FRX-C/T device: A compact toroid plasma translation experiment
[DE85-001527] 09 p1390 N85-18749
Discharge initiation experiments in the Tokapole II Tokamak
[DE84-017345] 09 p1391 N85-18755
Effects of q and high beta on Tokamak stability
[DE84-016850] 09 p1393 N85-18767
Analysis of Jovian low frequency radio emissions
[NASA-CR-174449] 10 p1571 N85-19906
Observations of low frequency plasma fluctuations in ELMC Bumpy Torus
[DE85-003796] 11 p1732 N85-20895
Long term variability of the IO torus
11 p1760 N85-21070
The continuous spectrum of an axisymmetric equilibrium with a mixed poloidal and toroidal magnetic field with gravity included 14 p2450 N85-25126
Preparatory experiments. 1: JIPP T-IIU
15 p2654 N85-26374
Toroidal equilibrium with low frequency wave driven currents
[DE85-005790] 15 p2658 N85-26401
Spherical torus, compact fusion at low field
[DE85-006983] 16 p2867 N85-27689
Time-resolving electron temperature diagnostic for ALCATOR C
[DE85-004916] 16 p2868 N85-27690
Comparison study of toroidal-field divertors for a compact reversed-field pinch reactor
[DE85-009591] 18 p3189 N85-29781
Toroidal viscosity and ambipolarity in the neoclassical transport theory of axisymmetric tori
[DE85-010822] 19 p3358 N85-30820
Poloidal variations in toroidal fusion reactor wall power loadings
[DE85-009505] 19 p3362 N85-30848
Radiation-cooled helicity-injecting reversed field pinch formed with relativistic electrons
[IPPJ-721] 19 p3370 N85-30901
System and method of operating toroidal magnetic confinement devices
[DE85-011670] 22 p3845 N85-33614
Compact DT fusion spherical tori at modest field
[DE85-011568] 23 p3982 N85-34692
Advanced Toroidal Facility (ATF)
[DE85-011567] 23 p3983 N85-34699
Observation of helical sawtooth oscillations in a tokamak
[DE85-012062] 23 p3983 N85-34703
Proposed FRX-D experiment
[DE85-012766] 24 p4158 N85-35778

TOROIDAL SHELLS
Poloidal variations in toroidal fusion reactor wall power loadings
[DE85-009505] 19 p3362 N85-30848
Alternating current OHMIC heating in a toroidal stellerator 20 p3534 N85-31988

TOROIDS
Self potentials of an electron ring in a torus for large ring displacement from the minor axis
[AD-A146086] 03 p0421 N85-12691
The evaluation of a deformable diffraction grating for a stigmatic EUV spectroheliometer
[NASA-CR-174248] 07 p1042 N85-16621
Experience highlights from the design and manufacture of US LCT coils
[DE84-017504] 10 p1482 N85-19354
Experience with oepration of a large magnet system in the international fusion superconducting magnet test facility
[DE85-009268] 17 p3027 N85-28721
Recent progress in stellarator reactor conceptual design
[DE85-009592] 18 p3189 N85-29780
TFCK shielding optimization
[DE85-010503] 19 p3359 N85-30826
Steady-state spheromak reactor studies
[DE85-009585] 19 p3372 N85-30916
Design of aggressive superconducting TFCX magnet systems
[DE85-010003] 19 p3376 N85-30943
Confinement and heating of high beta plasma with emphasis on compact toroids. Compact toroid research
[DE85-011463] 22 p3846 N85-33821

TORPEDO ENGINES
NT TURBOROCKET ENGINES

TORQUE
Cylinder power fault diagnosis in military diesel engines
[TT-8405] 01 p0053 N85-10354
The in-flight estimation and indication of cumulative fatigue damage to helicopter gears
[ARL/AERO-R-164] 03 p0317 N85-12050
Autonomous momentum management for space station
[NASA-CR-174085] 04 p0462 N85-12931
Autonomous momentum management for space station, exhibit A
[NASA-CR-171256] 04 p0462 N85-12933
Torque command steering law for double-gimbaled control moment gyros applied to rotor energy storage
05 p0608 N85-13879
Speed governor for diesel engine
09 p1307 N85-18214
Prediction accuracy of the torques for rotary tillage by an analog tool
[AD-P004268] 09 p1406 N85-18865
Antenna axis drive torques for the 70-meter antenna
10 p1464 N85-19237
Advanced gearbox technology in small turbo propeller engines 14 p2221 N85-23771
Influence of axial shaft load on operation of magnetoelastic torque transducer
14 p2270 N85-24065
Selection of optimum corrections torque for vertical gyro according to special-purpose program
14 p2273 N85-24082
Superconducting gyroscope research
[NASA-CR-171406] 15 p2560 N85-25795
How a shepherd guides a sheep herd — satellite-planetary ring interaction
15 p2674 N85-26503
Calculation of friction at spherical bearing journals in turbomachines 17 p2940 N85-28150
Load-induced rotordynamic instabilities in turbomachinery 19 p3280 N85-30340

Estimation of dynamic rotor loads for the rotor systems research aircraft: Methodology development and validation
[NASA-CR-177362] 20 p3393 N85-31045
Test evaluation of the Honeywell GG1111 Single-Degree-of-Freedom (SDF) strapdown gyroscope
[AD-A154768] 21 p3589 N85-32307
Drag-compensated, precision-powered hinge system
22 p3796 N85-33517
Application of traction drives as servo mechanisms
22 p3797 N85-33520
The properties of thin-section, four-point-contact ball bearings in space 22 p3797 N85-33521
Two-plane balance and slip-ring design
22 p3799 N85-33536
Dual towline spin-recovery device
[NASA-CASE-LAR-13076-1] 24 p4066 N85-35200

TORQUE CONVERTERS
Advanced inverter technology
[AD-A149335] 10 p1460 N85-19343

TORQUE MEASURING APPARATUS
U TORQUEMETERS

TORQUE MOTORS
Brush and commutator segment torquer motor
[AD-D011726] 23 p3927 N85-34340

TORQUEMETERS
Torque sensor
[AD-D011276] 05 p0639 N85-14096
Load-induced rotordynamic instabilities in turbomachinery 19 p3280 N85-30340
Two-plane balance and slip-ring design
22 p3799 N85-33536
Development of contactless sensors for industrial and automotive applications
[BMFT-FB-T-85-031] 24 p4097 N85-35400

TORQUERS
A dual spin space station design
20 p3408 N85-31152

TORSION
Design proposals for torsional buckling of stiffeners
[AD-A144783] 01 p0062 N85-10409
Fatigue in composite materials
04 p0467 N85-12968
Initial sailplane project: The RP-1
04 p0468 N85-12976
A geometrical theory of spin motion
[DE84-016537] 04 p0574 N85-13658
Damping capacity of multilayer tube during torsion
[BLL-M-36011-(5828.4)] 07 p0977 N85-16202
Modelling and identification of the structural properties of an astromast
[CRC-1374] 09 p1329 N85-18352
Evaluation of failure criterion for graphite/epoxy fabric laminates
[NASA-CR-172547] 10 p1431 N85-19025
Rheology of dissemination
[AD-A150006] 12 p1813 N85-21373
Fatigue damage and small crack growth during biaxial loading 16 p2797 N85-27247
Buckling and bracing of cantilevers
[CE-42] 17 p2979 N85-28413
Torsion-tension coupling in rods
18 p3120 N85-29315
Application of traction drives as servo mechanisms
22 p3797 N85-33520

TORSIONAL STRESS
Stability of hollow shafts under torsion
06 p0760 N85-14986
Steady-state reaction of three-layered cylindrical shell to effect of moving load 13 p2047 N85-22811
Influence of axial shaft load on operation of magnetoelastic torque transducer
14 p2270 N85-24065
Twisting of segmental shafts
14 p2279 N85-24119
On the radial structure of planetary rings
15 p2675 N85-26512
An improved torsional method for determining the fracture toughness of stiff materials and of adhesive joints
[AD-A152091] 16 p2800 N85-27267

TORSIONAL VIBRATION
Cylinder power fault diagnosis in military diesel engines
[TT-8405] 01 p0053 N85-10354
Damping capacity of multilayer tube during torsion
[BLL-M-36011-(5828.4)] 07 p0977 N85-16202
Measurement and evaluation of the loading of shafts by torsional vibrations 07 p0980 N85-16222
Optimization of vibrating beams including the effects of coupled bending and torsional modes
09 p1331 N85-18364
A pole-free reduced-order characteristic determinant method for linear vibration analysis based on sub-structuring 09 p1336 N85-18412
Effect of coupled torsional-flexural vibration of a geared shaft system on the dynamic tooth load
09 p1336 N85-18415
Precision measurement of torsional oscillations induced by gear errors 09 p1336 N85-18416
Journal of Research of the National Bureau of Standards, volume 89, number 2, March - April 1984
[PB85-115426] 12 p1926 N85-22103

TORSO
Torso sizing ring construction for hard space suit
[NASA-CASE-ARC-11616-1] 12 p1910 N85-21987
Torso restraint system
[AD-D011609] 16 p2702 N85-26684

TORUSES
A modeling analysis program for the JPL Table Mountain Io sodium cloud data
[NASA-CR-175493] 11 p1681 N85-20589
Torus data flow for parallel computation of missized matrix problems
[DE85-008761] 17 p3026 N85-28715
Alternating current OHMIC heating in a toroidal stellerator 20 p3534 N85-31988
Effect of ECH and ICH on ambipolar potential in NBT-1M 23 p3978 N85-34661
Transports studies of ECH and ICRH-heated bumpy torus plasma in NBT-1M 23 p3978 N85-34662
Simulation studies on stability of hot electron plasma
23 p3978 N85-34664
Behavior of helically-trapped fast ion orbits in heliotron E 23 p3978 N85-34666
Observation of mode-converted by ion Bernstein wave by an HCN laser scattering
[IPPJ-724] 23 p3979 N85-34668

TOTAL ENERGY SYSTEMS
NT SOLAR TOTAL ENERGY SYSTEMS
Develop and test fuel cell powered on-site integrated total energy systems. Phase 3: Full-scale power plant development
[NASA-CR-174687] 15 p2586 N85-25941

TOUCH
NT TACTILE DISCRIMINATION
The acquisition, processing, and use of tactile sensor data in robot control 05 p0641 N85-14114
The touch panel system: Design and development
[AD-A153014] 17 p3008 N85-28596
Ergonomic problems regarding the interactive touch input via screens in onboard and ground-based flight control
[NASA-TM-77814] 20 p3512 N85-31832
Issues and techniques in touch-sensitive tablet input (executive summary) 23 p3960 N85-34543
A multi-touch three dimensional touch-sensitive tablet (executive summary) 23 p3961 N85-34553

TOUGHNESS
NT NOTCH SENSITIVITY
A study of vacuum melting to increase the toughness of maraging steels
[AD-A145017] 01 p0028 N85-10175
Fundamental studies of structure property relationship in transformation toughened ceramics
[DE84-015344] 01 p0033 N85-10204
Microstructural basis of strength and toughness in hardmetals 02 p0177 N85-11165
The inter-relation of microstructure, toughness and fatigue crack growth behaviour in WC-Co hardmetals
02 p0177 N85-11168
Design of strong, ductile, duplex low alloy steels
02 p0177 N85-11169
Tough Composite Materials
[NASA-CP-2334] 04 p0463 N85-12941
Fundamental studies of composite toughness
04 p0464 N85-12948
Development of a heterogeneous laminating resin
04 p0465 N85-12956
Constituent properties and interrelationships
04 p0467 N85-12964
Inclusion formation during solidification of steels with improved machinability
[BMFT-FB-T-84-160] 05 p0619 N85-13957
Imide modified epoxy matrix resins
[NASA-CR-174695] 07 p0930 N85-15892
Effect of tempering on the strength and toughness of 2 1/4 Cr-1 Mo steel weldments
[DE85-003818] 09 p1296 N85-18140
Interlaminar fracture toughness in resin matrix composites
[AD-A150565] 13 p2015 N85-22640
Particulate toughened silicon carbide
[DE85-004797] 13 p2016 N85-22643
Simultaneous chemical vapor deposition of SiC-dispersed phase composites
[DE85-007751] 16 p2744 N85-26931
Strength versus toughness relation in Fe-high manganese alloys
[DE85-007682] 18 p3074 N85-29013
Aging study of copper alloy 172
[DE85-009846] 18 p3075 N85-29023
Specimen thickness effects for elastic-plastic CTOD toughness of A36 steel
[DE85-006992] 18 p3077 N85-29038
The mechanics of internal stress and microcrack toughening mechanisms in ceramics
[AD-A154049] 19 p3248 N85-30139
Controlled indentation flaws for the construction of toughness and fatigue master maps
[PB85-179067] 20 p3473 N85-31582
Graphite/PMR polyimide composites with improved toughness
[NASA-TM-87061] 21 p3561 N85-32146
Development of a high strength isothermally heat-treated nodular iron road wheel arm
[AD-A155755] 24 p4099 N85-35408

TOWED BODIES
A dynamical model for a towed linear sonar antenna
[REPT-6-84] 04 p0512 N85-13263
The rolling resistance and sinkage of towed dual wheel combination in sand
[AD-P004261] 09 p1404 N85-18837
A Lagrange-D'Alembert formulation of the equations of motion of a helicopter carrying an externally suspended load
[NASA-TM-85864] 12 p1770 N85-21149
A towed instrument vehicle for deep ocean sampling
[AD-A156322] 24 p4125 N85-35576

TOWED TARGETS
U TARGETS
U TOWED BODIES

TOWERS
NT AIRPORT TOWERS
Some considerations on Aeroelastic instabilities caused by coupling between propeller-type rotor and its supporting structure
[NAL-TR-804] 01 p0003 N85-10013
Structural design and thermal stability of TELE-X antenna tower 05 p0627 N85-14016
Dynamic testing of NOVA laser switchyard tower
[DE84-014450] 05 p0640 N85-14103
A novel type of stayed tower for wind turbines
[ISD-295] 15 p2587 N85-25952
Structural analysis and cost estimate of an eight-leg space frame as a support structure for horizontal axis wind turbines
[NASA-TM-83470] 19 p3284 N85-30361
New corrosion protection concept for very high voltage line towers
[BLL-OA-TRANS-2691-(6196.300)]
20 p3429 N85-31270

TOWING
Compaction of sand using ordinary off-road vehicles
[AD-P004297] 09 p1409 N85-18874

TOWNSEND DISCHARGE
NT GAS DISCHARGES

TOXIC DISEASES
NT CARBON MONOXIDE POISONING
NT LEAD POISONING
Proceedings of the 14th Conference on Environmental Toxicology
[AD-A146400] 06 p0843 N85-15350
Neurotoxicology: A new scientific challenge
[AD-P004017] 06 p0843 N85-15351

TOXIC HAZARDS
Effect of toluene on the solubility of biohazardous volatile synthetic organic compounds
[AD-A145168] 01 p0018 N85-10109
Polychlorinated biphenyls (PCBs) in transit system electrical equipment
[PB84-222207] 01 p0045 N85-10291
The pyrolysis toxic gas analysis of aircraft interior materials
[AD-A146285] 03 p0328 N85-12115
A biological sensor for the detection of toxicants
[AD-D011304] 07 p0967 N85-16141
Toxic hazards research
[AD-A147857] 07 p1011 N85-16425
A scanning alarm electronic processor
[AD-D011419] 08 p1158 N85-17309
Strategies for preparing and submitting a part B application for a DoD facility
[AD-P004139] 09 p1347 N85-18475
Practical application of earth resistivity methods in phase 2 of the installation restoration program
[AD-P004148] 09 p1348 N85-18484
The Hazardous Materials Technical Center
[AD-P004149] 09 p1349 N85-18485
Protocol for aquifer cleanup decision making at military installations
[AD-P004151] 09 p1349 N85-18487
Analysis of geohydrologic data by kriging
[AD-P004152] 09 p1349 N85-18488

Test report for Getty Synthetic Fuels, Inc., Calumet City, Illinois
[PB85-119493] 10 p1459 N85-19191
Improved techniques for removal of sediments contaminated with hazardous materials
[PB85-116093] 11 p1679 N85-20580
Methods/materials matrix of ultimate disposal techniques for spilled hazardous materials
[PB85-116653] 12 p1885 N85-21833
Assessment of hazardous waste surface impoundment technology case studies and perspectives of experts
[PB85-117059] 12 p1886 N85-21834
Summary report of the Workshop on Structure Activity Concepts in Environmental Sciences
[PB85-137339] 12 p1887 N85-21841
Effect of high ammonia content in closed environment on some parameters of human nitrogen and carbohydrate metabolism against background of a controlled diet
12 p1903 N85-21946
Analysis and model/data comparisons of large-scale releases of nitrogen tetroxide
[DE85-009989] 18 p3133 N85-29406
Toxic hazards tests for vehicles and other equipment
[AD-A149164] 20 p3506 N85-31797
Hydrazine and the F-16 20 p3511 N85-31826
Space Station crew safety alternatives study. Volume 2: Threat development
[NASA-CR-3855] 21 p3558 N85-32133
Review of hazardous waste cleanup and disposal efforts at Tinker Air Force Base
[GPO-43-294] 21 p3613 N85-32457
Hazardous air pollutants
[GPO-43-064] 21 p3613 N85-32458
Emergency modeling of hazardous air pollutants
[AD-A155441] 21 p3614 N85-32461
Air force technical objective document, Aerospace Medical Division, Fiscal Year 1986
[AD-A155195] 21 p3664 N85-32762
A crew exposure study. Phase II. Volume 2. At sea. Part A
[AD-A155233] 21 p3666 N85-32774
Practical consequences of the assessment of different energy health risks
[DE85-004536] 22 p3825 N85-33696
Proceedings of the 7th Joint Panel Meeting of the UJNR Panel on Fire Research and Safety
[PB85-199545] 24 p4085 N85-35317
Land Disposal of Hazardous Waste
[PB85-196378] 24 p4113 N85-35500

TOXICITY
NT CARBON MONOXIDE POISONING
NT LEAD POISONING
Aquatic plant control research program. Evaluation of Fusarium roseum Culmorum as a biological control agent for Hydrilla verticillata
[AD-A145228] 01 p0069 N85-10459
Toxicological evaluation of Columbia spacecraft
01 p0094 N85-10631
Modeling effects of toxicants on aquatic systems
[DE84-016594] 04 p0531 N85-13396
Toxicology and metabolism of nickel compounds
[DE84-014919] 05 p0696 N85-14478
The toxicity of complex mixtures
[AD-P004033] 06 p0844 N85-15363
Toxicology of natural and man-made toxicants in drinking water
[AD-P004035] 06 p0845 N85-15365
Aspects of solvent toxicity in mixtures
[AD-P004036] 06 p0845 N85-15366
Toxic hazards research
[AD-A147857] 07 p1011 N85-16425
A crew exposure study. Volume 1: Offshore
[AD-A146684] 07 p1015 N85-16449
Acute oral toxicity (LD50) of 4-nitrophenyl monochloromethyl (Phenyl) phosphinate (TA009) in male rats
[AD-A148337] 08 p1192 N85-17513
Manned testing of two closed-circuit oxygen underwater breathing apparatus: US Navy Emerson Rig and Fenzy PO.68
[AD-A148300] 08 p1200 N85-17580
Role of biological assessment in effluent control
[PB85-116101] 12 p1885 N85-21830
Toxicity, mutagenesis and aging due to endogenous oxygen radicals
[AD-A150121] 12 p1900 N85-21928
Determination of toxicity of combustion products of habitability foams concurrently with flammability studies of these materials
[AD-A149647] 12 p1905 N85-21961
Chemical characterization and toxicologic evaluation of airborne mixtures. Inhalation toxicology of diesel fuel obscurant aerosol in Sprague-Dawley rats. Phase 3. Subchronic exposures
[AD-A150100] 12 p1905 N85-21966
Interaction of metals and metalloids with biomembranes
[DE85-004902] 13 p2141 N85-23293
Toxicity of TNT wastewaters to aquatic organisms. Volume 4: Chronic toxicity of 2,4-dinitrotoluene and condensate water
[AD-A153536] 18 p3132 N85-29400
Formation and fate of toxic chemicals in California's atmosphere
[PB85-172609] 18 p3134 N85-29414
An in vitro method for the screening of trichothecene mycotoxin cytotoxicity and the study of mycotoxin countermeasures
[AD-A153663] 18 p3152 N85-29517
Chemicals identified in human biological media, a data base. Volume 6, part 2: Records 7588-8894
[DE85-006767] 18 p3154 N85-29528
Information science in toxicology
[DE85-007746] 18 p3200 N85-29851
Pollutant body burdens and reproduction in Platichthys stellatus from San Francisco Bay
[DE85-010407] 19 p3308 N85-30509
Polyesters: A review of the literature on products of combustion and toxicity
[NBSIR-85-3139] 20 p3433 N85-31298
Hydrazine and the F-16 20 p3511 N85-31826
Distribution and abundance of organic thiols
21 p3657 N85-32717
Effects of low level carbon monoxide (CO) on tracking and monitoring. An attempt to replicate the findings of Putz et al. (1976) protocol 2
[AD-A155722] 22 p3825 N85-33694
Anaerobic microbial transformations in subsurface environments: Project description
[DE85-012789] 23 p3951 N85-34486
Estimating risks of lead-induced hemoglobin decrements under conditions of uncertainty: Methodology, pilot judgments and illustrative calculations
[DE85-012293] 23 p3952 N85-34493

TOXICITY AND SAFETY HAZARD
Portable microprocessor-controlled instrument for sensing, identifying and monitoring gaseous chemicals
[DE84-013431] 04 p0504 N85-13214
Immobilization of toxic waste by embedding it in bitumen
[OEFZS-4277] 07 p0995 N85-16322
Health assessment document for carbon tetrachloride
[PB85-124196] 10 p1526 N85-19636
Material thermolysis product toxicity: Definition of a hazard evaluation methodology
[CERMA-84-08] 11 p1692 N85-20641
Use of environmental health-risk analysis for managing toxic substances
[DE85-008964] 18 p3160 N85-29574

TOXICOLOGY
Proceedings of the 14th Conference on Environmental Toxicology
[AD-A146400] 06 p0843 N85-15350
Neurotoxicology: A new scientific challenge
[AD-P004017] 06 p0843 N85-15351
Review of the toxicokinetics of n-hexane
[AD-P004018] 06 p0843 N85-15352
Interactions of ketones and hexacarbons
[AD-P004019] 06 p0843 N85-15353
Molecular mechanisms of n-hexane neurotoxicity
[AD-P004020] 06 p0843 N85-15354
Pathology and axonal transport in hexacarbon neuropathies
[AD-P004021] 06 p0843 N85-15355
Organophosphorus-induced delayed neurotoxicity: Syndrome and experimental models
[AD-P004022] 06 p0844 N85-15356
Chemistry and metabolism of delayed neurotoxic organophosphorus esters
[AD-P004023] 06 p0844 N85-15357
Pathology of organophosphorus-induced delayed neurotoxicity
[AD-P004024] 06 p0844 N85-15358
Electrophysiologic changes in organophosphorus-induced delayed neurotoxicity
[AD-P004025] 06 p0844 N85-15359
Biochemistry and pathogenic hypotheses of organophosphorus-induced delayed neurotoxicity
[AD-P004026] 06 p0844 N85-15360
Critical overview of hexacarbons and organophosphates
[AD-P004027] 06 p0844 N85-15361
Pharmacokinetic interactions of mixtures
[AD-P004032] 06 p0844 N85-15362
The toxicity of complex mixtures
[AD-P004033] 06 p0844 N85-15363
Teratogenicity studies of carbaryl and malathion alone and in combination in various laboratory animals
[AD-P004034] 06 p0845 N85-15364
Toxicology of natural and man-made toxicants in drinking water
[AD-P004035] 06 p0845 N85-15365
Aspects of solvent toxicity in mixtures
[AD-P004036] 06 p0845 N85-15366
An update on the capabilities of the Air Force Computerized Occupational Health Program (COHP)
[AD-P004037] 06 p0845 N85-15367
The epidemiology and toxicology of Agent Orange
[AD-P004038] 06 p0845 N85-15368
Early detection of environmental exposure
[AD-P004039] 06 p0845 N85-15369
USSR report: Life sciences. Biomedical and behavioral sciences
[JPRS-UBB-84-015] 07 p1010 N85-16416
Material thermolysis product toxicity: Definition of a hazard evaluation methodology
[CERMA-84-08] 11 p1692 N85-20641
Air quality criteria for ozone and other photochemical oxidants. External review draft, volume 4
[PB85-126068] 12 p1886 N85-21838
Chemical characterization and toxicologic evaluation of airborne mixtures. Inhalation toxicology of diesel fuel obscurant aerosol in Sprague-Dawley rats. Phase 3. Subchronic exposures
[AD-A150100] 12 p1905 N85-21966
Role and fate of ozone in the atmosphere
16 p2824 N85-27421
Information science in toxicology
[DE85-007746] 18 p3200 N85-29851
Molecular toxicology of chromatin: The role of Poly(ADP-Ribose) in gene control
[AD-A154415] 19 p3327 N85-30611
EPA (Environmental Protection Agency) research program guide, FY-1985, October 1, 1984 - September 30, 1985
[PB85-181881] 20 p3487 N85-31676

TOXINS AND ANTITOXINS
Induction of immunity to toxins with anti-idiotypic antibody
[AD-A146793] 07 p1014 N85-16445
Bibliography of venomous and poisonous marine animals and their toxins
[AD-A148409] 08 p1192 N85-17514
Structural-functional changes in bacterial cells under spaceflight conditions 16 p2724 N85-26812
An in vitro method for the screening of trichothecene mycotoxin cytotoxicity and the study of mycotoxin countermeasures
[AD-A153663] 18 p3152 N85-29517
Differences in susceptibility of inbred mice to bacillus anthracis
[AD-A155646] 21 p3662 N85-32750

TRACE CONTAMINANTS
Aircraft measurements of tracer gas during the 1983 cross Appalachian tracer experiment (CAPTEX)
[DE84-015292] 04 p0531 N85-13395
Atmospheric tracer experiments in a deep narrow valley
[PB84-234590] 04 p0532 N85-13402
Cross-Appalachian Tracer Experiment (CAPTEX '83)
[PB84-236641] 06 p0834 N85-15307
Modeling of turbulent dispersion of neutral and buoyant contaminants released from two dimensional sources --- air pollution
[VKI-TN-150] 08 p1180 N85-17436
Methodology for the collection and analysis of trace metals in atmospheric precipitation
[CM-67] 09 p1350 N85-18401
Nebulization reflux concentrator
[NASA-CASE-LAR-13254-1] 11 p1615 N85-20154
One-dimensional nonstationary model of photochemical transformations of gas impurities in stratosphere
14 p2342 N85-24484
Vertical redistribution of a pollutant tracer due to cumulus convection
[PB85-172971] 18 p3134 N85-29415
Diffusion of trace gases in the ground level boundary layer 18 p3148 N85-29489
Internal contamination in the space station
18 p3157 N85-29549
Space station trace contaminant control
18 p3157 N85-29550
Some problems associated with trace contaminant removal systems for spacecabins
18 p3158 N85-29554
Contamination control for increased crew productivity
18 p3158 N85-29555
Human productivity program definition
18 p3158 N85-29556
X-ray fluorescence analysis of uranium concentrates
[DE85-013189] 24 p4148 N85-35717

TRACE ELEMENTS
Minor element effects on gas tungsten arc weld penetration
[PB84-222579] 01 p0056 N85-10370

Green River air quality model development: Meteorological and tracer data, July/August 1982. Field study in Brush Valley, Colorado
[DE84-014976] 02 p0225 N85-11474
COST 50 - materials for gas turbines, part 1 and 2 3UK9
[NPL-DMA(A)-74] 05 p0617 N85-13943
The effect of trace elements on the properties at high temperature of a Ni-Cr-base alloy
05 p0617 N85-13944
The use of tracers for the study of atmospheric chemical and physical transformation processes
[DE84-015267] 05 p0671 N85-14313
Aspects of the comparison of stratospheric trace species measurements with photochemical models
[DE84-017028] 05 p0672 N85-14317
The Georges Bank monitoring program 1983: Analysis of trace metals in bottom sediments
[CIRC-915] 05 p0686 N85-14423
Dark matter near the sun: Simulated star counts and the Oort limit 06 p0880 N85-15562
Atmospheric heating of meteorites: Results from nuclear track studies 06 p0882 N85-15607
Application of tunable monochromatic synchrotron radiation to the quantitative determination of trace elements
[DE85-001271] 09 p1291 N85-18106
Tracer diffusion in an ordered alloy: Application of the path probability and Monte Carlo methods
[DE85-002766] 14 p2257 N85-23986
Resonant coherent anti-Stokes Raman scattering
[ESA-TT-876] 15 p2507 N85-25466
Trace metal determinations in nickel-plating baths by polarographic methods
[DE85-007084] 15 p2511 N85-25488
Upper-air data collection during CAPTEX
[DE85-006300] 16 p2827 N85-27438
Use of a network of telemetered meteorological stations for prediction of the distribution of an atmospheric tracer
16 p2831 N85-27458
An ultrasensitive and element specific photoionization detection system for environmental analysis
[AD-A153365] 17 p2968 N85-28332
Data base of all known, published data on trace elements in oil shale and its products
[DE85-003399] 18 p3126 N85-29357
Elemental tracers of source regions of contaminants in precipitation
[DE85-007366] 18 p3133 N85-29407
Atmospheric Tracer Workshop
[DE85-010573] 20 p3486 N85-31668
Marine aerosols at the Dutch North Sea coast: Size distributions and fractionation of trace elements
21 p3648 N85-32664
Anorthositic oceanic crust in the Archean Earth
21 p3719 N85-33077
Ultra-trace analysis of sinter tantalum with SIMS
[BLL-RARDE-TR-1220-(7291.7965)]
23 p3913 N85-34245
Evaluation of low-temperature geothermal potential in Utah and Goshen Valleys and adjacent areas, Utah. Part 2: Water temperature and chemistry
[DE85-009344] 23 p3943 N85-34436
The identification of compounds in mustard hydrolysate
[AD-A156361] 24 p4076 N85-35256
Interaction of trace elements and welding parameters on GTA weld shape
[DE85-004046] 24 p4080 N85-35284
Elemental tracers of source regions of contaminants in precipitation
[DE85-012858] 24 p4113 N85-35499
TRACERS
Analysis techniques for tracer studies of oxidation
[NASA-CR-174796] 03 p0336 N85-12162
Relationship between model complexity and data base quality for complex terrain tracer experiments
[DE84-015022] 04 p0539 N85-13429
A new physical Lagrangian tracer
[DE84-016212] 05 p0687 N85-14419
Mechanisms of impurity diffusion in rutile
[DE84-014741] 06 p0786 N85-14902
Air quality assessment model validation in complex terrain
[AD-A147690] 08 p1180 N85-17434
Chlorine isotopes as environmental tracers in Columbia River basalt groundwaters
[DE85-011392] 19 p3302 N85-30473
Atmospheric Tracer Workshop
[DE85-010573] 20 p3486 N85-31668
A strategy for calibrating atmospheric transport models
[CSIRO-DAR-TP-9] 24 p4116 N85-35518
TRACKED VEHICLES
Proceedings of the International Conference on the Performance of Off-Road Vehicles and Machines, (8th), volume 1
[AD-A148834] 09 p1403 N85-18833
Dynamic simulation of track laying vehicles
[AD-P004266] 09 p1405 N85-18842
Stresses in situ generating by bulldozers
[AD-P004270] 09 p1405 N85-18846
Finite element analysis of ground deformation beneath moving track loads
[AD-P004271] 09 p1405 N85-18847
A rig for testing the soft soil performance of track systems
[AD-P004272] 09 p1405 N85-18848
The dependence of soil bearing capacity and drawbar pull on the spacing between track
[AD-P004273] 09 p1406 N85-18849
The dynamic interaction between track and soil
[AD-P004274] 09 p1406 N85-18850
Analysis of ground pressure distribution beneath tracked model with respect to external loading
[AD-P004275] 09 p1406 N85-18851
A comparison between a conventional method and an improved method for predicting tracked vehicle performance
[AD-P004276] 09 p1406 N85-18852
Effect of hitch positions on the performance of track-grouser systems
[AD-P004277] 09 p1406 N85-18853
Grouser effect studies
[AD-P004278] 09 p1406 N85-18854
Proceedings of the 8th International Conference on the Performance of Off-Road Vehicles and Machines, volume 2
[AD-A148635] 09 p1407 N85-18859
Mobility of the small combine (track type) on soft ground-relationship between the position of the center of gravity and the mobility
[AD-P004285] 09 p1407 N85-18862
Study on controllability and stability of high speed tracked vehicles
[AD-P004302] 09 p1409 N85-18879
A tracked vehicle test plant for the simulation of dynamic operation
[AD-P004305] 09 p1410 N85-18882
Basic study on the turning resistance of track
[AD-P004307] 09 p1410 N85-18884
Study on steerability of articulated tracked vehicles
[AD-P004308] 09 p1410 N85-18885
Skid steering of wheeled and tracked vehicles: Analysis with Coulomb friction assumptions
[AD-A149826] 12 p1860 N85-21664
Improvements in tank tread assemblies
[NASA-CASE-NPO-16321-1] 18 p3117 N85-29291
TRACKING (POSITION)
NT CCD STAR TRACKER
NT INFRARED TRACKING
NT OPTICAL TRACKING
NT POLYSTATION DOPPLER TRACKING SYSTEM
NT PURSUIT TRACKING
NT RADAR TRACKING
NT RADIO TRACKING
NT RANGE AND RANGE RATE TRACKING
NT SATELLITE TRACKING
NT SPACECRAFT TRACKING
NT STAR TRACKERS
NT WILDLIFE RADIOLOCATION
Distributed sensor networks
[AD-A146209] 03 p0355 N85-12296
Biaxial tracking solar generator
05 p0663 N85-14259
Model estimation and identification of manual controller objectives in complex tracking tasks
05 p0700 N85-14494
Types of tracking errors induced by concurrent secondary manual task 05 p0711 N85-14561
Device for measuring relative axial expansion of turbine rotor employing space-vector tracking method
06 p0776 N85-14962
Annual energy spectrum for tracking arrays
06 p0832 N85-15297
Stereo Electro-optical Tracking System (SETS)
[NASA-CR-172471] 07 p0962 N85-16096
Automatic camera tracking for remote manipulators
[DE85-001897] 07 p0974 N85-16187
An interactive FORTRAN program for determining reliability of pseudo-range geodetic point positioning using the global positioning system
[AD-A147133] 07 p0988 N85-16275
Random pattern tracking acceleration tolerance tester
[AD-D011404] 07 p1017 N85-16459
JPL Robotics Laboratory computer vision software library
[NASA-CR-174272] 07 p1023 N85-16491
Ocean acoustics
[AD-A147062] 07 p1038 N85-16891
Dual mode scanner-tracker
[AD-D011417] 08 p1113 N85-17016
Deep water mass circulation in the Western Alboran Basin: Measurements in July and September 1980 (Alboran I experiment)
[AD-A148586] 08 p1191 N85-17504
Mobility of the small combine (track type) on soft ground-relationship between the position of the center of gravity and the mobility
[AD-P004285] 09 p1407 N85-18862
Development of mass-producible line-focus tracking concentrating solar collectors. Category 2: Trackers
[DE85-002673] 10 p1512 N85-19
Wind-weighting for sounding rockets with a telemetry system
[NASA-TP-2438] 12 p1792 N85-21246
Observational study of transport in the free troposphere
[PB85-144145] 12 p1867 N85-21845
Numerical methods for tracking interfaces
[LA-9917-MS] 12 p1919 N85-22052
Technical manual: Description and operation Stereo Tracking System
[DE85-004807] 13 p2094 N85-23070
Main features of Antarctic Ocean circulation as revealed by satellite tracking of icebergs
14 p2325 N85-24372
Some methods of computing platform transmitter terminal location estimates — ARGOS system; whale tracking 14 p2332 N85-2442
Digital computer applications of Kalman filter in target tracking
[AD-A150770] 14 p2404 N85-24821
Investigation of a failure detection/identification system for a tactical aircraft navigation system
[AD-A151846] 15 p2469 N85-25240
Swedish equipment for automatic docking in space
15 p2489 N85-2538
Sonars with high noise and clutter rejection for use with adaptive robots
[AD-A151875] 15 p2543 N85-25701
Automatic tracking of crack growth via finite elements
16 p2797 N85-27248
An evaluation of the performance of a new storm tracking methodology
[AD-A152234] 16 p2835 N85-27484
Development of mass-producible line-focus tracking concentrating solar collectors. Category 2: Control systems
[DE85-007673] 17 p2987 N85-28459
Automatic detection of gust fronts
[FAA-PM-85-11] 17 p2995 N85-28516
Tracking algorithm performance analysis program (TRAPP)
[DE85-007304] 17 p3009 N85-28601
Adaptive aiding for symbiotic human-computer control: Conceptual model and experimental approach
[AD-A153870] 19 p3332 N85-30644
Department of Energy gear drive unit final prototype testing and design evaluation
[DE85-003296] 22 p3793 N85-3349
Airborne cloud tracking measurements during the Three Mile Island nuclear station accident, Middletown, Pennsylvania. Date of survey: March - June 1979
[DE85-012080] 22 p3816 N85-336
Operator's functional comfort zone when controlling moving object 22 p3821 N85-33670
Effects of low level carbon monoxide (CO) on tracking and monitoring. An attempt to replicate the findings of Putz et al. (1976) protocol 2
[AD-A155722] 22 p3825 N85-33
Comparative analysis of operational forecasts versus actual weather conditions in airline flight planning, volume 1
[NASA-CR-167662] 24 p4119 N85-35
Comparative analysis of operational forecasts versus actual weather conditions in airline flight planning, volume 2
[NASA-CR-167663] 24 p4119 N85-35
TRACKING AND DATA RELAY SATELLITES
U TDR SATELLITES
TRACKING ANTENNAS
U DIRECTIONAL ANTENNAS
TRACKING FILTERS
Design and performance of sampled data loops f subcarrier and carrier tracking 05 p0623 N85-13
Improved carrier tracking by smoothing estimators
05 p0623 N85-13
Algorithm for tracking maneuvering object w ambiguous measurements 06 p0791 N85-15
Tristatic tracking filter used by the mult measurement system
[AD-A146665] 07 p0911 N85-15

Synthesis of digital nonrecursive band-elimination filters for moving-target selectors 12 p1840 N85-21545
Synthesis of optimum algorithms for secondary processing 13 p2080 N85-22992
Investigation of a failure detection/identification system for a tactical aircraft navigation system
[AD-A151846] 15 p2469 N85-25240
Theory and Applications of State Estimation. NRIMS Summer Seminar Series
[CSIR-SWISK-37] 15 p2635 N85-26244
Tracking filters 15 p2635 N85-26252
Estimation of maneuvering targets
15 p2636 N85-26253
Synthesis of adaptive filters for tracking radio systems
22 p3763 N85-33325

TRACKING NETWORKS
NT DEEP SPACE NETWORK
NT GLOBAL TRACKING NETWORK
NT MATTS (SYSTEMS)
NT POLYSTATION DOPPLER TRACKING SYSTEM
NT RADAR NETWORKS
Evaluation of the RSTN (Regional Seismic Test Network) network and further improvement to automatic association
[AD-A146395] 06 p0835 N85-15312
Distributed sensor networks
[AD-A147636] 08 p1151 N85-17262

TRACKING PROBLEM
Suppression of biodynamic interference by adaptive filtering 05 p0706 N85-14530
Models for the effects of G-seat cuing on roll-axis tracking performance 05 p0707 N85-14532
Some effects of digital sampling on orbiter flight control system operation 08 p1092 N85-16903

TRACKING RADAR
Turnaround control for mechanically scanned radar antennas
[AD-D011236] 01 p0039 N85-10246
A proof-of-principle getaway special free-flying satellite demonstration 02 p0155 N85-11051
Avionics Flight Evaluation System (AFES)
13 p1967 N85-22357
Angular tracking error in A phase comparison monopulse tracking radar: A critical review and extension of the phase front distortion approach
[AD-A152628] 17 p2949 N85-28205

TRACKING STATIONS
NT GLOBAL TRACKING NETWORK
NT POLYSTATION DOPPLER TRACKING SYSTEM
Survey of VLF-OMEGA transmissions received during summer at Antarctic peninsula
[INPE-3399-PRE/666] 10 p1462 N85-19223

TRACKING STUDIES
U TRACKING (POSITION)

TRACKS
An evaluation of the 64-meter antenna radial bearing for use on the 70-meter antenna
10 p1464 N85-19236

TRACTION
Modelling of off-road tyres and soil for improved traction
[AD-P004258] 09 p1404 N85-18834
Soil compliance influence on tyre performance
[AD-P004260] 09 p1404 N85-18836
Traction forces of drive tyre on the compacted soil
[AD-P004264] 09 p1404 N85-18840
The stress-strain-time graph of rheological soils and its application
[AD-P004286] 09 p1407 N85-18863
Thermal traction contact performance evaluation under fully flooded and starved conditions
[NASA-CR-168173] 15 p2566 N85-25848
Rolling, slip and traction measurements on low modulus materials
[NASA-CR-174909] 22 p3791 N85-33491
Application of traction drives as servo mechanisms
22 p3797 N85-33520

TRACTORS
NT TRACKED VEHICLES
Converting gasoline farm tractors to run efficiently on farm-produced alcohol
[DE84-015796] 02 p0205 N85-11350
Effects of slip on energy distribution between tyre and soil
[AD-P004263] 09 p1404 N85-18839
A theoretical investigation of an active suspension system for wheeled tractors
[AD-P004268] 09 p1405 N85-18844
Increase in performance and improvement of ride comfort of self-propelled construction machinery by reducing pitch and vertical vibration
[AD-P004269] 09 p1405 N85-18845
Comparison of measured and simulated ride comfort for an agricultural tractor and influence of travel speed and tyre-inflation pressure on dynamic response
[AD-P004281] 09 p1407 N85-18857
Characteristics of farm field profiles as sources of tractor vibration
[AD-P004282] 09 p1407 N85-18858
The research of driving wheel with movable lugs of the paddy field floating tractor
[AD-P004283] 09 p1407 N85-18860
An investigation of the driving wheel thrust of paddy field tractors
[AD-P004284] 09 p1407 N85-18861
Behaviour of soil under a lugged wheel
[AD-P004287] 09 p1407 N85-18864
The analysis on the dynamic performance of a single lug
[AD-P004289] 09 p1408 N85-18866
Some stability and control problems with trailed farm tankers on slopes
[AD-P004291] 09 p1408 N85-18868
Control of tractors on sloping ground
[AD-P004292] 09 p1408 N85-18869
Tractor power selection with compaction constraints
[AD-P004300] 09 p1409 N85-18877
Turning behaviour of articulated frame steering tractor
[AD-P004304] 09 p1409 N85-18881

TRACTS
U SITES

TRADEOFFS
Hydrologic and economic models for watershed evaluation and research
[PB84-222371] 01 p0066 N85-10438
BIT/BITE tradeoff analysis model
[AD-A149345] 11 p1701 N85-20697
High specific power aircraft turn maneuvers: Tradeoff of time-to-turn versus change in specific energy
[AD-A151701] 15 p2471 N85-25257
Trade-off between land vehicle antenna cost and gain for satellite mobile communications
[NASA-CR-175732] 15 p2540 N85-25661
Space Station man-machine automation trade-off analysis
[NASA-CR-176046] 20 p3408 N85-31147

TRADESCANTIA
Hit-size effectiveness theory applied to high doses of low LET radiation for pink mutations in Tradescantia
[DE85-011835] 22 p3819 N85-33657

TRAFFIC
NT AIR TRAFFIC
Study of annoyance due to urban automobile traffic
[NASA-TM-77514] 01 p0069 N85-10458
Study of annoyance due to urban automobile traffic. Annex 4: A catalog of the characteristics of noise at different measuring points
[NASA-TM-77516] 03 p0387 N85-12478
Patterns of behavior in lodgings exposed to traffic noise
[NASA-TM-77750] 03 p0387 N85-12479
Proceedings of the 8th International Conference on the Performance of Off-Road Vehicles and Machines, volume 2
[AD-A148635] 09 p1407 N85-18859
Basic study on the turning resistance of track
[AD-P004307] 09 p1410 N85-18884
Base communications issues for the 1980s
[AD-A149764] 12 p1828 N85-21474
Overlays for plain jointed concrete pavements
[PB85-156297] 15 p2523 N85-25557
An electron microscopic study of urban aerosol
21 p3651 N85-32689

TRAFFIC CONTROL
NT AIR TRAFFIC CONTROL
NT AUTOMATED EN ROUTE ATC
NT RADAR APPROACH CONTROL
US Army human Engineering Laboratory Communications Survey: A Pilot Study (HELCOMS-PS)
[AD-A151434] 15 p2521 N85-25544

TRAILERS
Some stability and control problems with trailed farm tankers on slopes
[AD-P004291] 09 p1408 N85-18868

TRAILING EDGE FLAPS
Pressure distribution data from tests of 2.29 M (7.5 feet) span EET high-lift transport aircraft model in the Ames 12-foot pressure tunnel
[NASA-TM-84517] 19 p3211 N85-29912
Low-speed tests of a high-aspect-ratio, supercritical-wing transport model equipped with a high-lift flap system in the Langley 4- by 7-meter and Ames 12-foot pressure tunnels
[NASA-TP-2097] 20 p3388 N85-31010

TRAILING EDGES
Experimental studies of transonic airfoil trailing edge and wake flowfield properties 05 p0592 N85-13773
Simultaneous flow visualization and unsteady lift measurement on an oscillating lifting surface
[AD-P004157] 09 p1264 N85-17942
Current status of trailing edge loss calculation for a turbine blade
[PNR-90244] 09 p1282 N85-18061
Aerodynamic heating rate distributions induced by trailing edge controls on hypersonic aircraft configurations at Mach 8
[NASA-TM-87453] 13 p1989 N85-22370
Low-speed characteristics of a circulation control airfoil with AFT camber and a spiral trailing edge
[AD-A150851] 14 p2213 N85-23725
Turbulent flow of fluid near trailing edge of plate in stream at zero angle of attack 16 p2764 N85-27067
Flame acceleration mechanisms under conditions of partial confinement
[PB85-184083] 18 p3073 N85-29004
Analysis of the turbulent near wake at a sharp trailing edge 20 p3387 N85-31006
Trailing edge flow and aerodynamic sound. Part 1: Tonal pressure and velocity fluctuations. Part 2: Random pressure and velocity fluctuations
[AD-A154947] 21 p3552 N85-32097
On the application of a hairpin vortex model of wall turbulence to trailing edge noise prediction
[NASA-CR-177938] 22 p3726 N85-33109
A design procedure to modify the trailing edge upper surface pressure gradient of a given aerofoil
[GU-AERO-8408] 23 p3894 N85-34120
Reflection plane tests of a wind turbine blade tip section with ailerons
[NASA-TM-87018] 23 p3945 N85-34444

TRAILS
U TRACKS

TRAINEES
U STUDENTS

TRAINERS
U TRAINING DEVICES

TRAINING
U EDUCATION

TRAINING AIRCRAFT
NT CL-41 AIRCRAFT
NT DH 115 AIRCRAFT
NT JAGUAR AIRCRAFT
NT JET PROVOST AIRCRAFT
NT T-33 AIRCRAFT
Analysis of the flow field about a T-45 using PANAIR
[AD-A145611] 07 p0899 N85-15898
Can the Aggressors continue to be effective in the F-5E?
[AD-A146661] 07 p1019 N85-16465
Collision avoidance for Naval training aircraft
[FAA-PM-84-4] 12 p1774 N85-21136
Aircraft structure for application to training aircraft
[CH-635286-A5] 15 p2469 N85-25244
RAFTS: A T-38 replacement for the 21st century
[AD-A156103] 24 p4065 N85-35191

TRAINING ANALYSIS
Factors critical to the implementation of self-paced instruction: A background review
[AD-A145143] 01 p0097 N85-10648
Artificial intelligence contributions to training and maintenance
[AD-P003934] 02 p0247 N85-11614
An analysis of the technical training of enlisted minuteman missile maintenance personnel
[AD-A147078] 07 p0912 N85-15775
Pilot education and safety awareness programs
09 p1277 N85-18026

TRAINING DEVICES
Aeronautical systems technology needs: Escape, rescue and survival, test facilities and test equipment and training-simulation equipment
[AD-A145059] 01 p0001 N85-10002
Training effectiveness evaluation and utilization demonstration of a low cost cockpit procedures trainer
[AD-A145179] 01 p0013 N85-10078
Factors critical to the implementation of self-paced instruction: A background review
[AD-A145143] 01 p0097 N85-10648
Ada (trademark) training curriculum. Real-time concepts I303 teacher's guide
[AD-A145093] 01 p0104 N85-10694
Ada (trademark) training curriculum. Software engineering for managers m101 teacher's exercise guide
[AD-A145094] 01 p0104 N85-10695
GUIDON
[AD-P003925] 02 p0246 N85-11605
Designing an expert system for training automotive electrical troubleshooting
[AD-P003926] 02 p0246 N85-11606
The psychology of technical devices and technical discourse
[AD-P003929] 02 p0246 N85-11609
Artificial intelligence contributions to training and maintenance
[AD-P003934] 02 p0247 N85-11614

Training capabilities test of Electronics Equipment Maintenance Trainer (EEMT): Findings and conclusions
[AD-A146075] 03 p0359 N85-12302
Information Center handbook
[PB84-211341] 03 p0439 N85-12795
Determining training device requirements in Army aviation systems 05 p0711 N85-14558
The design and use of subtasks in part training and their relationship to the whole task
05 p0711 N85-14559
Simulating speed and height cues in the C-130 weapon system trainer
[AD-P004313] 09 p1268 N85-17967
Dynamic training devices in CRM training
09 p1276 N85-18018
Use of airplanes for loft training
09 p1276 N85-18019
Cockpit resources management and the theory of the situation 09 p1276 N85-18022
Cockpit resource management training
09 p1276 N85-18023
Simulation 09 p1277 N85-18024
Low cost training aids and devices
09 p1277 N85-18025
Pilot education and safety awareness programs
09 p1277 N85-18026
Initiative uses of aircraft for flight training
09 p1277 N85-18027
Study of cognitive styles of students in automated teaching system 10 p1525 N85-19620
New flight simulators at Vnukovo permit less in-flight training 12 p1769 N85-21107
Maintenance training simulators prime item development specification. Model specification and handbook
[AD-A154108] 19 p3330 N85-30628
Models for multidimensional tests and hierarchically structured training materials
[AD-A155231] 21 p3665 N85-32769

TRAINING EVALUATION
Training effectiveness evaluation and utilization demonstration of a low cost cockpit procedures trainer
[AD-A145179] 01 p0013 N85-10078
Factors critical to the implementation of self-paced instruction: A background review
[AD-A145143] 01 p0097 N85-10648
Overview of training and aiding
[AD-P003917] 02 p0245 N85-11597
Individual differences in automatic and controlled information processing
[AD-A146245] 03 p0401 N85-12559
An analysis of the technical training of enlisted minuteman missile maintenance personnel
[AD-A147078] 07 p0912 N85-15775
Concept paper for the development of a DOD Ada (trademark) software engineering education and training plan
[AD-A148774] 08 p1206 N85-17592
Simulation 09 p1277 N85-18024
Low cost training aids and devices
09 p1277 N85-18025
Innovative approaches to recurrent training
09 p1277 N85-18028
Research needs on the interaction between information systems and their users: Report of a workshop
[PB85-121523] 10 p1568 N85-19891
NASA Ames Summer High School Apprenticeship Research Program
[NASA-TM-86006] 15 p2686 N85-26590
A review of safety practices and safety training for the explosives field
[AD-A152295] 16 p2759 N85-27028
Welder training/welder testing
[BLL-WI-TRANS-683-(9312.57)]
16 p2792 N85-27223
Guidelines of the Federal Minister of Transportation for the formation and examination of airline personnel, part 4 17 p3002 N85-28556
The use of flight simulators in measuring and improving training effectiveness
[AD-A153817] 18 p3064 N85-28954
Simulation for human factors research. A central question: Fidelity 18 p3159 N85-29568
Microcomputers in transportation: Software and source book, February 1985
[PB85-181022] 20 p3517 N85-31868

TRAINING SIMULATORS
NT COCKPIT SIMULATORS
NT FLIGHT SIMULATORS
NT SPACECRAFT CABIN SIMULATORS
The design, fabrication and delivery of a spacelab neutral buoyancy Instrument Pointing System (IPS) mockup --- underwater training simulator
[NASA-CR-171233] 04 p0482 N85-12934
The use of flight simulators in measuring and improving training effectiveness
[AD-A153817] 18 p3064 N85-28954
Maintenance training simulators prime item development specification. Model specification and handbook
[AD-A154108] 19 p3330 N85-30628

TRAJECTORIES
NT ABORT TRAJECTORIES
NT ASCENT TRAJECTORIES
NT BALLISTIC TRAJECTORIES
NT DESCENT TRAJECTORIES
NT EARTH-VENUS TRAJECTORIES
NT ELECTRON TRAJECTORIES
NT INTERORBITAL TRAJECTORIES
NT INTERPLANETARY TRAJECTORIES
NT MISSILE TRAJECTORIES
NT PARTICLE TRAJECTORIES
NT REENTRY TRAJECTORIES
NT ROUND TRIP TRAJECTORIES
NT SPACECRAFT TRAJECTORIES
Moment induced by liquid payload during spin-up without a critical layer
[AD-A145716] 02 p0199 N85-11327
Trajectory estimation using combined time-of-arrival and velocity measurements
[DE84-015872] 02 p0242 N85-11582
Arctic ice island and sea ice movements and mechanical properties
[DE84-016323] 04 p0542 N85-13450
A numerical investigation of planetesimal collision trajectories with a Moon accumulating in Earth orbit
04 p0586 N85-13740
A Generalized Escape System Simulation (GESS) computer program. Volume 2: GESS programmer's manual, version 2
[AD-A148363] 08 p1081 N85-16845
An investigation of the driving wheel thrust of paddy field tractors
[AD-P004284] 09 p1407 N85-18861
Electromagnetic braking of a metallic projectile in flight
[AD-A149424] 10 p1480 N85-19345
Atmospheric profile imprint in firewall ablation coefficient 11 p1662 N85-20473
A user's manual for AMEER flight path trajectory simulation code
[DE85-006580] 15 p2472 N85-25260
Numerical calculation of subsonic jets in crossflow with reduced numerical diffusion
[NASA-TM-87003] 15 p2472 N85-25263
Inference and state estimation for stochastic point processes
[AD-A151216] 15 p2640 N85-26281
Dispersion sensitivity of the eight inch advanced ramjet munitions technology projectile due to wind and minor thrust errors
[AD-A152145] 16 p2727 N85-26835
The mean trajectory approximation for charge and energy transfer processes at surfaces
[AD-A152708] 17 p3043 N85-28830
Lattice actions improved by block-spin renormalisation group and maximally symmetric lattices
[DE85-007416] 17 p3045 N85-28841
Global coordinate system
[AD-A153876] 19 p3299 N85-30454
Effect of vertical shear on regional-scale trajectories in near-frontal conditions
[DE85-007554] 19 p3317 N85-30561
Emittance growth caused by current variation in a beam-transport channel
[DE85-010743] 19 p3363 N85-30849
Use of a minimum-ellipse criterion in the study of ion-beam extraction systems
[DE85-012670] 24 p4148 N85-35721

TRAJECTORY ANALYSIS
Trajectory estimation using combined time-of-arrival and velocity measurements
[DE84-015872] 02 p0242 N85-11582
Relationships between Ariane trajectories and satellite orbits 05 p0590 N85-13815
Interplanetary trajectories 05 p0600 N85-13827
Algorithm for tracking manuevering object with ambiguous measurements 06 p0791 N85-15057
Flow visualization study of the effect of injection hole geometry on an inclined jet in crossflow
[NASA-TM-86936] 11 p1631 N85-20269
Rejection of anomalous observations when determining spacecraft trajectories 13 p1979 N85-22421
Approximate analytic method of calculating trajectories of movement of a flight vehicle in the atmosphere
14 p2279 N85-24121
Space Mathematics for the Preparation and Development of satellite Exploitation
[ISBN-2-85428-115-2] 14 p2395 N85-24753
Orbit reconstitution --- satellite orbits
14 p2396 N85-24765
Towards the Halley Comet 14 p2399 N85-24783
Minimax problem of estimating trajectory parameters in continuous formulation 15 p2479 N85-25301
Computer program for prediction of capture maneuve probability for an on-off reaction controlled upper stag
[NASA-CR-165937] 17 p3010 N85-2861
The role of thermal motions of air particles for firebal
[PUBL-59] 17 p3053 N85-2890
Calculation of trajectories of detached wind turbin blades and prediction of site risk levels associated wi failures of HAWT's 24 p4110 N85-3547

TRAJECTORY CONTROL
NT TRAJECTORY OPTIMIZATION
Space interception guidance with uncertain factors
13 p2042 N85-2278
User's manual of the BNDSCO computer program fo solving constrained optimal control problems
[DFVLR-MITT-85-05] 20 p3516 N85-3186
A method of accurizing rail guns
[LA-10028-MS] 22 p3737 N85-3316

TRAJECTORY MEASUREMENT
Trajectory estimation using combined time-of-arrival an velocity measurements
[DE84-015872] 02 p0242 N85-1158
Rejection of anomalous observations when determining spacecraft trajectories 13 p1979 N85-2242
Trajectory measurements for take-off and landing tes and other short-range applications, volume 16
[AGARD-AG-160-VOL-16] 15 p2561 N85-2580
Method for evaluating perturbation in algorithms fo solving navigational problems 16 p2718 N85-2678

TRAJECTORY OPTIMIZATION
Interplanetary trajectories 05 p0600 N85-1382
Optimal multiple-impulse nonlinear orbital rendezvous
08 p1105 N85-1698
Planning of minimum-time trajectories for robot arm
[AD-A148956] 10 p1492 N85-1941
Algorithm for determining optimal three impuls point-to-orbit transfer with limited transfer time
13 p1979 N85-2241
Synthesis of optimum algorithms for secondar processing 13 p2080 N85-2299
Optimal space trajectories 14 p2396 N85-2479
Minimum time turns using vectored thrust
[AD-A151693] 15 p2471 N85-2525
A numerical study of the mean trajectory approximatio in a non-adiabatic process
[AD-A152763] 17 p3030 N85-2873
Piloted simulation of an algorithm for onboard contr of time-optimal intercept
[NASA-TP-2445] 18 p3063 N85-2894
SIGMA - A stochastic-integration global minimizatio algorithm
[AD-A154878] 21 p3671 N85-3280

TRANQUILIZERS
Primate equilibrium performance and diazepam: A behavioral tolerance effect
[AD-A145157] 01 p0094 N85-1063

TRANSATMOSPHERIC VEHICLES
NASA R and T aerospace plane vehicles: Progre and plans
[NASA-TM-86429] 15 p2491 N85-2539

TRANSCEIVERS
U TRANSMITTER RECEIVERS

TRANSCENDENTAL FUNCTIONS
NT EXPONENTIAL FUNCTIONS
NT LOGARITHMS
NT PERIODIC FUNCTIONS
NT TANGENTS
On the spherical derivative of a meromorphic functio with a Nevanlinna deficient value
10 p1535 N85-1967
Solutions of problems of miller and rubel
10 p1536 N85-1968
Collision detection for moving polyhedra
[AD-A148961] 10 p1544 N85-1973
Arithmetic and elementary functions on mini an microcomputers 14 p2396 N85-2476
Calculation of roots of transcendental equations f problems of determining thermal conductivity of cylind with non-uniform boundary conditions
[BLL-M-35788-(5828.4)] 23 p3929 N85-3434

TRANSDUCERS
NT ELECTROACOUSTIC TRANSDUCERS
NT ELECTRONIC TRANSDUCERS
NT HYDROPHONES
NT IMAGE TRANSDUCERS
NT INTERDIGITAL TRANSDUCERS
NT LOUDSPEAKERS
NT MAGNETIC TRANSDUCERS
NT MICROPHONES
NT MODE TRANSFORMERS
NT PIEZOELECTRIC GAGES
NT PIEZOELECTRIC TRANSDUCERS
NT PIEZORESISTIVE TRANSDUCERS
NT PRESSURE SENSORS
NT SOUND TRANSDUCERS
NT TORQUERS
NT ULTRASONIC WAVE TRANSDUCERS

A miniature urethane molded acoustic transducer
[AD-A146459] 06 p0804 N85-15114
Unsteady pressure measurements on a biconvex airfoil in a transonic oscillating cascade
[NASA-TM-86914] 07 p0896 N85-15689
Digital thermometer with linearizer on slide wire
07 p0954 N85-16049
Ultrasonic transducers, performance variability, design, and manufacturing procedures
[AD-A146575] 08 p1158 N85-17306
Development of a floating element wall shear transducer
[AD-A148450] 08 p1164 N85-17346
Modeling of real UT transducer field/flaw interactions
[DE85-000341] 09 p1329 N85-18351
Stress waves in an isotropic elastic plate excited by a circular transducer
[NASA-CR-3877] 11 p1650 N85-20390
Compensation of skew passband of a SAW filter using predistortion 12 p1621 N85-21422
Thin film strain transducer --- suitable for in-flight measurement of scientific balloon strain
[NASA-CASE-WLP-10055-2] 12 p1849 N85-21598
Rocket body charge neutralization processes in ARAKS experiment (data from two launches)
13 p1980 N85-22426
Programmable filter with fanned interdigital surface acoustic wave transducer 13 p2083 N85-23008
Electrothermal transducer with short time constant
13 p2088 N85-23040
Influence of axial shaft load on operation of magnetoelastic torque transducer
14 p2270 N85-24065
Transducer of linear displacements
14 p2281 N85-24130
A transduction path method of solid state sensor analysis and investigation
[AD-A152123] 16 p2870 N85-27707
Liquid-metal transducers for strain measurement during in-pile materials testing 17 p2945 N85-28176
Automatic liquid-metal temperature monitoring with the use of immersed transducers
[BLL-BISI-TRANS-22427-(9022.06)]
18 p3104 N85-29215
Gravity enhanced acoustic levitation method and apparatus
[NASA-CASE-NPO-16147-1-CU]
18 p3177 N85-29693
Microwave bandstop filter
[AD-D011716] 19 p3261 N85-30222
Fiber optic sensors operating at dc
[AD-D011674] 19 p3271 N85-30283
Fiber optics in transient radiation fields
[DE85-010721] 19 p3368 N85-30886
Wideband disturbance accomodation in precision flexible space structures 20 p3415 N85-31194
Ultrasonic flowmetering with reflected pulses
[PB85-179885] 20 p3460 N85-31492
R and D activities of the Systems Engineering Division
20 p3540 N85-32027
Experimental and theoretical assessment of a new technique for the non-destructive evaluation of laminated panels
[AD-A155622] 21 p3562 N85-32155
Shear wave transducer for boreholes
[DE85-011882] 22 p3787 N85-33461
Device for frequency modulation of a laser output spectrum
[DE85-011634] 22 p3790 N85-33479
Non-bonded ultrasonic transducer
[DE85-011006] 22 p3794 N85-33504
Electromagnetic inspection of wire ropes using sensor arrays
[AD-A155412] 22 p3795 N85-33509
Fast shutter apparatus
[DE85-006501] 23 p3928 N85-34343
Acoustic cross-correlation flowmeter for solid-gas flow
[DE85-005988] 23 p3935 N85-34391
A multi-touch three dimensional touch-sensitive tablet (executive summary) 23 p3961 N85-34553

TRANSEQUATORIAL PROPAGATION
Propagation and amplification of Ion Cyclotron Waves (ICW's) in a multicomponent plasma. The Earth magnetosphere as a giant maser for Alfven waves
14 p2368 N85-24634

TRANSFER
U TRANSFERRING

TRANSFER FUNCTIONS
NT MODULATION TRANSFER FUNCTION
NT OPTICAL TRANSFER FUNCTION
Definition of acceptable levels of mismatch for equivalent systems of augmented CTOL (Conventional Take-Off and Landing) aircraft
[AD-A145619] 02 p0149 N85-11007
Gain-phase structures for linear multivariable systems
[RR-256] 02 p0256 N85-11674
Dual (GaAl) As-heterostructure based injection laser traveling wave amplifier 02 p0261 N85-11706
Transfer function of multilayered magnetooptical space-time modulator 02 p0264 N85-11726
CONTROL: A suite of interactive transfer-function analysis programs
[OUEL-1527/84] 03 p0408 N85-12609
Coupling of airborne sound into the Earth
[AD-A146231] 03 p0416 N85-12663
Introduction to the subjective transfer function approach to analyzing systems
[AD-A145817] 03 p0436 N85-12774
Investigation of several aspects of LANDSAT 4/5 data quality
[E85-10038] 04 p0525 N85-13357
Mars polar volatiles: Topographic and geologic setting
[NASA-CR-174089] 04 p0581 N85-13708
A very efficient transfer function bounding technique on bit error rate for Viterbi decoded, rate 1/N convolutional codes 05 p0624 N85-13991
Derivation of recursive digital filters by the step-invariant and the ramp-invariant transformations
[AD-A146500] 06 p0857 N85-15452
EMC (Electromagnetic compatibility) spec criteria in Volterra systems
[AD-A147659] 08 p1151 N85-17263
Optically induced intervalence-band transitions in germanium by the absorption of 1.06 micrometers picosecond pulses
[DE85-000946] 09 p1399 N85-18803
Further results on rate 1/N convolutional code constructions with minimum required SNR criterion
10 p1464 N85-19235
Imaging through a multiple scattering medium
[DE85-002051] 10 p1557 N85-19821
Journal of Research of the National Bureau of Standards, volume 89, number 2, March - April 1984
[PB85-115426] 12 p1926 N85-22103
Modal synthesis of multidimensional PI-regulators for objects with inertial sections 14 p2270 N85-24064
Tutorial discussion of electronic sampling systems for recording wide-bandwidth transient signals
[DE85-006577] 15 p2549 N85-25735
Development of graphical pole-zero, root-locus, Bode, Nyquist, and Nichols responses using the OPTSYSX program
[AD-A152148] 16 p2847 N85-27555
Generalised translation invariance and systems theory
[CRM-8501] 17 p3017 N85-28657
An interactive computer aid for the design and analysis of linear, single input/single output digital and continuous control systems
[AD-A153704] 18 p3162 N85-29589
A study of interior noise levels, noise sources and transmission paths in light aircraft
[NASA-CR-172152] 19 p3350 N85-30766
Matrix transfer function design for flexible structures: An application 20 p3416 N85-31199
Basic EMC (Electromagnetic Compatibility) technology advancement for C3 systems. Volume 1B: Demodulation radio frequency interference effects in operational amplifier circuits
[AD-A154121] 20 p3440 N85-31350
Synthesis of high-speed devices using integrated operational amplifiers 22 p3781 N85-33428
Method and apparatus for transfer function simulator for testing complex systems
[NASA-CASE-NPO-15896-1] 23 p3926 N85-34333
A multi-touch three dimensional touch-sensitive tablet (executive summary) 23 p3961 N85-34553

TRANSFER OF TRAINING
China report: Science and technology
[JPRS-CST-85-003] 13 p2166 N85-23433
The role of prior knowledge in operating equipment from written instructions
[AD-A151007] 14 p2392 N85-24730
The acquisition of procedures from text. A production-system analysis of transfer of training
[AD-A151029] 14 p2392 N85-24732

TRANSFER ORBITS
NT INTERPLANETARY TRANSFER ORBITS
Commercializing the transfer orbit stage
02 p0155 N85-11049
Relationships between Ariane trajectories and satellite orbits 05 p0599 N85-13815
Satellite positioning — in geosynchronous orbit
05 p0600 N85-13823
Transportation applications, part 1
11 p1643 N85-20349
Space debris protection for a reusable orbital transfer vehicle 12 p1786 N85-21208
The long term behaviour of Earth orbits and the implications for debris control 12 p1786 N85-21213
Radiation exposure and performance of multiple burn LEO-GEO orbit transfer trajectories
[NASA-TM-86946] 12 p1788 N85-21228
Algorithm for determining optimal three impulse point-to-orbit transfer with limited transfer time
13 p1979 N85-22419
Optimal space trajectories 14 p2396 N85-24756
Manrating orbital transfer vehicle propulsion
[NASA-TM-87019] 15 p2494 N85-25385
Telescope in lunar orbit 15 p2682 N85-26568
Analysis of orbit transfer vehicles for GPS Block 3 satellites
[AD-A152021] 16 p2732 N85-26860
Primary propulsion of electrothermal, ion and chemical systems for space-based radar orbit transfer
[NASA-TM-87043] 17 p2916 N85-27972
Optimal low thrust transfer using a first-order perturbation model
[AD-A154761] 21 p3676 N85-32835

TRANSFERRING
Voltage dependence of the relative AC-DC transfer difference for HF voltage-transfer standards
05 p0630 N85-14038
Chemical and photographic evaluation of rigid explosive transfer lines
[AD-A149303] 11 p1613 N85-20145
A new technique for system-to-system transfer of surface data 17 p3007 N85-28589

TRANSFORM INTEGRALS
U INTEGRAL TRANSFORMATIONS

TRANSFORMATION TENSORS
U TENSORS

TRANSFORMATIONS
Tests of fit based on normalized spacings
[AD-A149749] 12 p1921 N85-22062
Transformation of charged particle beams by concentrating electro-optical systems
21 p3690 N85-32925

TRANSFORMATIONS (MATHEMATICS)
NT COORDINATE TRANSFORMATIONS
NT FAST FOURIER TRANSFORMATIONS
NT HOUSEHOLDER TRANSFORMATIONS
NT INTEGRAL TRANSFORMATIONS
NT LAPLACE TRANSFORMATION
Reducing spectral dimension of remotely sensed data using principal components analysis and a Peano scanning 02 p0212 N85-11399
Utilization of interpolation and transformation for the compression of digital image data
[INPE-3061-PRE/479] 02 p0240 N85-11566
Lie-transformation action principle for classical plasma dynamics
[DE84-014576] 02 p0285 N85-11858
Comparison of free component mode synthesis techniques using MSC/NASTRAN
[DE84-014451] 04 p0514 N85-13278
Derivation of recursive digital filters by the step-invariant and the ramp-invariant transformations
[AD-A146500] 06 p0857 N85-15452
New technology high efficiency and high stability color motion video compression system
[AD-A147523] 07 p0941 N85-15968
Use of shanks transformation for speeding up adaptation process in antenna arrays 07 p0951 N85-16029
A power transformation exponential regression model for censored failure time data
[AD-A148377] 08 p1212 N85-17632
Modeling relationships using groups and items
09 p1367 N85-18591
Investigation of three-dimensional mesh generation with precise controls
[AD-A148759] 09 p1374 N85-18636
Diffeomorphic approximation of quasiconformal and quasisymmetric homeomorphisms
10 p1536 N85-19678
A conformal mapping suitable for problems involving interaction between given geometries and known far fields
[AD-A149050] 10 p1545 N85-19744
Triple matrix product optical processors using combined time-and-space integration
[AD-D011483] 10 p1557 N85-19820
Bayesian analysis of time series 1: Householder transformation analyses
[DE85-004449] 11 p1708 N85-20749
Functional equation for the embedding of a homomorphism of the interval into a flow
[DE85-000655] 11 p1713 N85-20780
Nonlinear sigma-models and integration methods
[DE85-004447] 12 p1922 N85-22071
Harmonic analysis and Radon transforms on pencils of geodesics
[CWI-PM-R8413] 12 p1922 N85-22074
A simple and efficient algorithm to compute tail probabilities from transforms
[AD-A150928] 14 p2409 N85-24849

The omni-transform in single-channel queues
[AD-A151019] 14 p2409 N85-24852
Control of a flexible beam
[DE85-007243] 15 p2580 N85-25914
Old and new in Moebius groups
15 p2634 N85-26235
Solution to eigenvalue problems of antisymmetric cross-ply and antisymmetric angle-ply laminated plates using affine transformations
[AD-A153040] 17 p2917 N85-27980
Curved finite elements and curve approximation
17 p3007 N85-28590
Investigation and implementation of a tree transformation system for user friendly programming
[AD-A152716] 17 p3011 N85-28617
Generalised translation invariance and systems theory
[CRM-8501] 17 p3017 N85-28657
On approximating a set-valued function locally
[AD-A153540] 18 p3170 N85-29641
On the transformation of derivatives of distributions on surfaces
[PREPRINT-434] 18 p3173 N85-29670
Application of Floquet theory to helicopter blade flapping stability
[AD-A154460] 19 p3218 N85-29952
Nonlinear dynamics: A personal perspective
[DE85-010962] 20 p3521 N85-31899

TRANSFORMERS
NT MODE TRANSFORMERS
NT VOLTAGE CONVERTERS (AC TO AC)
Developments in space power components for power management and distribution 05 p0608 N85-13877
Pulse transformer package for impedance matching a laser diode to a transmission line
[AD-D011499] 12 p1855 N85-21632
Design and performance of etched polarisation transformers for microwave frequencies
[R-NIAS-26] 14 p2297 N85-24218
Detection and location of partial discharges in transformer windings using electrical methods
15 p2551 N85-25750
Research on design of cryotransformers and its prospects for the future
[AD-A152400] 17 p2952 N85-28230
High voltage isolation transformer
[NASA-CASE-GSC-12817-1] 18 p3093 N85-29146
Design and testing of a pulsed current transformer
[AD-A154228] 19 p3259 N85-30208
T/R switch design for short-range measurements, part 6.1A 21 p3624 N85-32515
Calculation of external magnetic field of a shielded transformer 22 p3771 N85-33373

TRANSFORMS
U TRANSFORMATIONS (MATHEMATICS)

TRANSIENT HEATING
NT PULSE HEATING
NT SHOCK HEATING
Instrumentation for sensing moisture content of material using a transient thermal pulse
[NASA-CASE-NPO-15493-2] 23 p3933 N85-34373

TRANSIENT LOADS
NT BLAST LOADS
NT GUST LOADS
NT IMPACT LOADS
NT LANDING LOADS
NT SHOCK LOADS
Transient vibration test criteria for spacecraft hardware — galileo spacecraft 09 p1338 N85-18418
Crack growth geometry in aluminum alloy sheet material under flight simulation loading. 1: A comparison between TWIST and miniTWIST FALSTAFF and short FALSTAFF. 2: Effect of truncating high loads
[VTH-LR-441] 11 p1609 N85-20119
Symmetric primal-dual variational formulations of coupled dynamic systems: Three-dimensional elasticity, shells, fluid-structure interaction
[ONERA-1983-91] 12 p1863 N85-21684
Analysis of shell type structures subjected to time dependent mechanical and thermal loading
[NASA-CR-175747] 15 p2577 N85-25896
Transient behavior of a single-blade horizontal-axis wind turbine
[MBB-UD-421/84-O] 16 p2875 N85-27737

TRANSIENT OSCILLATIONS
Thresholds of perception of whole body linear oscillation: Modification by spaceflight 05 p0694 N85-14467
Transient voltage oscillations in coils
[DE85-006715] 15 p2550 N85-25738
Analysis of transient radiation upset in a 16K SRAM
[DE85-009442] 23 p3965 N85-34586

TRANSIENT PRESSURES
Finite element method for a class of viscoelastic flows in deforming domains applied to jet breakup
[DE84-014571] 04 p0500 N85-13186
Surge transient simulation in turbo-jet engine
05 p0596 N85-13796
Experimental investigations of the unsteady turbulent friction behavior with pressure impulses in a circular pipe
[IWAWI-MITT-102] 18 p3103 N85-29210
Response of steam-water mixtures to pressure transients
[DE85-010799] 19 p3267 N85-30262

TRANSIENT RESPONSE
A generalized mathematical solution for transient off tracking of single vehicles and truck combinations
[DM-2] 01 p0107 N85-10719
The transient behavior of networks with infinite server nodes
[CWI-OS-R8406] 05 p0722 N85-14640
Improvement of the transient response in the finite settling time control
[NAL-TR-823] 06 p0757 N85-14843
Sensitivity analysis of discrete structural systems: A survey
[NASA-TM-86333] 06 p0817 N85-15186
Data and results of a laboratory investigation of microprocessor upset caused by simulated lightning-induced analog transients
07 p0999 N85-16345
Transient response of a small-signal microwave GaAs FET to X-rays
[DE85-000066] 09 p1315 N85-18265
The Shock and Vibration Bulletin 54. Part 2: Ship shock, shock and blast and ground shock
[AD-A148132] 09 p1334 N85-18388
Two-dimensional shock response of a mass on energy-absorbing shock mounts
09 p1334 N85-18389
Optimum design for nonlinear shock mounts for transient inputs 09 p1334 N85-18390
An objective error measure for the comparison of calculated and measured transient response histories
09 p1335 N85-18395
Analysis of inverter models and harmonic propagation. Part 3. Transient processes in inverter models
[DE85-000191] 10 p1510 N85-19530
Analysis of the transient response of temporal artery blood flow data relative to various anti-G suit pressure schedules 10 p1533 N85-19680
TRACR3D: A model of flow and transport in porous/fractured media
[LA-9667-MS] 12 p1845 N85-21576
Symmetric primal-dual variational formulations of coupled dynamic systems: Three-dimensional elasticity, shells, fluid-structure interaction
[ONERA-1983-91] 12 p1863 N85-21684
Laboratory studies of spacecraft response to transient discharge pulses 13 p1995 N85-22506
Hydrodynamic simulation of transient processes in injection system of aircraft engines during pump unswirling 13 p2050 N85-22829
Transient analysis of loaded thin-wire antennas and transmission lines 13 p2053 N85-22852
Research efforts in support of resonance extraction studies. Volume 1: Improvement and validation of TWFD (Thin-Wire Frequency-Domain): A thin-wire frequency-domain scattering code
[AD-A150296] 13 p2054 N85-22864
Tutorial discussion of electronic sampling systems for recording wide-bandwidth transient signals
[DE85-008577] 15 p2549 N85-25735
Transient analysis of a magnetic heat pump
15 p2576 N85-25891
Continuum modeling of latticed structures
17 p2977 N85-28399
A state variable approach to transient creep deformation in stress reduction experiments
[DE85-009492] 18 p3122 N85-29331
Dynamical study of flat plates by nonlinear elasticity theory
[STN-8] 20 p3471 N85-31572
Analysis of the transient response of temporal artery blood flow data relative to various anti-G suit pressure schedules
[AD-A155242] 21 p3666 N85-32775
Numerical simulation of nonisothermal transient processes in GaAs diode structures
22 p3767 N85-33350
Synthesis of high-speed devices using integrated operational amplifiers 22 p3781 N85-33428
Substructure coupling in the frequency domain
[NASA-CR-176140] 22 p3800 N85-33543
The transient electromagnetic depth sounding technique applied to hydrocarbons and geothermal exploration
[MITT-42] 23 p3949 N85-34476

TRANSIENTS (SURGES)
U SURGES

TRANSISTOR AMPLIFIERS
Isolated load switching with surge suppression
[AD-D011216] 01 p0042 N85-10274
Dual-gate MESFET variable gain constant output power amplifier
[AD-D011334] 07 p0945 N85-15992
Playback amplifier with high interference immunity
13 p2077 N85-22970
KT3127A, KT3128A transistors
22 p3779 N85-33414

TRANSISTOR CIRCUITS
Machine computation of delay and capacitance of transistor structures of subnanosecond large integrated circuits 04 p0490 N85-13120
Computer investigation of effects of high injection in transistor large integrated circuit structures
06 p0793 N85-15088
Transistor-transistor logic microcircuit tester
12 p1842 N85-21556
Recommendation on use of series K157UL1 microcircuits 13 p2071 N85-22996
USSR report: Electronics and electrical engineering
[JPRS-UEE-84-015] 22 p3762 N85-33314
Noise in stages and in interstage couplings of various transistor circuits 22 p3765 N85-33334

TRANSISTOR LOGIC
Development of a planar heterojunction bipolar transistor for very high speed logic
[AD-A150374] 13 p2064 N85-22895

TRANSISTOR-TRANSISTOR-LOGIC INTEG CIRCUITS
U TTL INTEGRATED CIRCUITS

TRANSISTORS
NT BIPOLAR TRANSISTORS
NT FIELD EFFECT TRANSISTORS
NT JFET
NT JUNCTION TRANSISTORS
NT PHOTOTRANSISTORS
NT SILICON TRANSISTORS
Solution of the Boltzmann transport equations for a permeable base transistor
[AD-A144969] 01 p0112 N85-10757
Electron traps in the GaAs permeable base transistor
[AD-A145399] 02 p0287 N85-11871
Circuit engineering and technological optimization of very high speed LSI logic elements and transistor structures 03 p0347 N85-12237
Developments in space power components for power management and distribution 05 p0608 N85-13877
Qualitative of analysis of MOS circuits
[AD-A149267] 10 p1480 N85-19341
Code lock with microcircuit 13 p2071 N85-22935
Study of 1/f noise in solids
[AD-A151069] 14 p2428 N85-24972
Computer-aided identification of complete constitution model of transistor structure for design of subnanosecond large-scale-integrated circuits 15 p2529 N85-25594
Energy considerations in second breakdown
[AD-A152389] 17 p2952 N85-28229
Leading-edge microelectronics research at Sweden's Chalmers 20 p3438 N85-31337
Millimetre wave pulse technology — satellite mapping
[ESA-CR(P)-2004] 20 p3478 N85-31611

TRANSIT SATELLITES
The TRANSIT and Global Positioning System (GPS) systems. Precision navigation and localization
14 p2398 N85-24777

TRANSITION
Deuteron NMR (Nuclear Magnetic Resonance) in relation to the glass transition in polymers
[AD-P003910] 01 p0032 N85-10196

TRANSITION FLOW
First cryogenic test of the CAST 7 profile in the T2 wind tunnel. Comparison with calculations — airfoils
[ONERA-RTS-58/1685-AY-035-D]
04 p0577 N85-13682
Transition and mixing in axisymmetric jets and vortex rings 05 p0591 N85-13769
Boundary layer control by transition fixing — conference
[DFVLR-MITT-84-17] 14 p2211 N85-23712
Investigation of the conditions for tripping transition with roughness elements and their influence on boundary layer development 14 p2212 N85-23720
Transition fixing and simulation of high Reynolds number flow at transonic velocities 14 p2212 N85-23721
Investigations of the experimental detection of boundary layer transitions 14 p2213 N85-23723
Cone drag in the transition from continuum to free molecular flow
[OUEL-1536/84] 20 p3390 N85-31023
Experimental observation of transition behavior on a flat plate 20 p3452 N85-31437
Development of a temperature-compensated hot-film anemometer system for boundary-layer transition detection on high-performance aircraft
[NASA-TM-86732] 22 p3730 N85-33121
Nozzle wall roughness effects on free-stream noise and transition in the pilot low-disturbance tunnel
[NASA-TM-86389] 23 p3930 N85-34355

TRANSITION METALS
NT CADMIUM
NT CHROMIUM
NT CHROMIUM ISOTOPES
NT COBALT
NT COBALT 60
NT GOLD
NT HAFNIUM
NT IRIDIUM
NT IRON
NT IRON ISOTOPES
NT IRON 59
NT MANGANESE
NT MANGANESE ISOTOPES
NT MOLYBDENUM
NT NICKEL
NT NICKEL ISOTOPES
NT NIOBIUM
NT OSMIUM
NT OSMIUM ISOTOPES
NT PALLADIUM
NT PLATINUM
NT REFRACTORY METALS
NT RHENIUM
NT RHODIUM
NT RUTHENIUM
NT SCANDIUM
NT SCANDIUM ISOTOPES
NT SILVER
NT TANTALUM
NT TECHNETIUM
NT TITANIUM
NT TUNGSTEN
NT VANADIUM
NT YTTRIUM
NT ZINC
NT ZIRCONIUM
The oxidation of transition-metal ions by molecular oxygen
[BLL-M-29593-(5828.4)] 02 p0175 N85-11172
Calculations of optical properties of transition metals
[BLL-M-35744-(5828.4)] 02 p0175 N85-11175
Lattice dilation in metal-hydrogen systems
[BLL-M-35758-(5825.4)] 02 p0176 N85-11176
Lattice defects in body centered cubic transition metals 03 p0427 N85-12727
Evidence for d-band conduction in metallic glasses containing transition metal elements
[DE84-014822] 04 p0570 N85-13635
Theoretical methods for the study of transition metals in crystals
[DE84-015606] 05 p0732 N85-14709
Electronic and magnetic properties of transition-metal surfaces, interfaces and overlayers
[DE84-016886] 05 p0733 N85-14713
A nonnoble front metallization process
06 p0830 N85-15279
Theoretical research program to study transition metal trimers and embedded clusters
[NASA-CR-174296] 08 p1125 N85-17093
Electronic structure, chemical bonding, and electron conductivity of thin-film transition-metal silicides
[AD-A147721] 08 p1226 N85-17716
Comparisons between computed and observed grain boundary structures and properties in metals
[DE85-002596] 10 p1442 N85-19085
Properties and thermal stabilities of amorphous transition metal hydrides
[DE85-002117] 11 p1607 N85-20104
The physical modelling of transition metal alloying: The roles that different levels of theory play
[DE85-000591] 11 p1607 N85-20105
Studies of metal/carbon surface chemistry
[DE85-005513] 15 p2507 N85-25463
Synthesis and characterization of superconducting electronic materials
[AD-A151112] 15 p2659 N85-26409
Transitional metal activation and functionalization of C-H bonds
[DE85-006816] 16 p2746 N85-26949
Survey of experimental and theoretical electron-impact ionization cross sections for transition metal ions in low stages of ionization
[DE85-007605] 16 p2863 N85-27656
Thermodynamic analysis of the plasma nitriding of ferrovanadium
[BLL-BISI-TRANS-22237-(9022.06)]
17 p2924 N85-28032
Clusters of transition metal atoms
[AD-A153126] 17 p3030 N85-28740
New examples of clusters, extended metal-metal bonding and interstitial derivatives
[DE85-005926] 17 p3044 N85-28837
Coadsorption studies on transition metals
[PB85-183713] 18 p3072 N85-29003
Local density theory of heats of formation and short-range order parameters in substitutionally disordered alloys
[DE85-009611] 18 p3075 N85-29021
Transition metal catalyzed transformations of unsaturated molecules
[DE85-009531] 18 p3080 N85-29055
Spectroscopic investigation of materials for tunable infrared lasers
[AD-A154124] 19 p3272 N85-30291
The influence of temperature on the composition density of the transition metals
[BLL-M-35896-(5826.4)] 23 p3915 N85-34262
Noble metals as incipient transition metals
[DE85-013283] 24 p4080 N85-35286

TRANSITION POINTS
Combustion-deflagration-detonation transition in a confined spherical powder
[ISL-R-108/84] 22 p3747 N85-33223
Combustion-deflagration-detonation transition
[ISL-CO-221/84] 22 p3747 N85-33225

TRANSITION PRESSURE
Experiments with phase transitions at very high pressure
[NASA-CR-174029] 02 p0172 N85-11148
Analysis of Shock to Detonation Transition (SDT) of porous high energy propellant from ramp-wave compression loading
[AD-A149333] 10 p1457 N85-19180

TRANSITION PROBABILITIES
Studies of the chemistry of vibrationally and electronically excited species in planetary upper atmospheres
[NASA-CR-174134] 03 p0449 N85-12851
Absolute transition probabilities of lines in the spectra of astrophysical atoms, molecules, and ions
[NASA-CR-174141] 04 p0580 N85-13705
Radiation data and standards for Tokamak diagnostics
09 p1390 N85-18742
Sensitivity of conditions for lumping finite Markov chains
[AD-A152122] 16 p2855 N85-27604
Field theory of the metal-insulator transitions in restricted symmetries
[NOTA-INTERNA-829] 18 p3196 N85-29826
Variational transition state theory
[DE85-010685] 19 p3235 N85-30059
Probabilistic analysis of automatic control systems for detection systems 22 p3765 N85-33335
Vacuum ultraviolet laser
[DE85-011632] 22 p3790 N85-33478

TRANSITION TEMPERATURE
Nuclear Magnetic Resonance of Polymeric Materials
[AD-A145078] 01 p0032 N85-10192
Structural evolution during the gel to glass conversion
[DE84-014954] 06 p0772 N85-14939
Ferromagnetism in metals at finite temperatures
[DE85-000698] 09 p1377 N85-18656
Connector/nitinol delta contact force device
[AD-D011467] 10 p1481 N85-19349
Development of media for dynamic latent heat storage for the low-temperature range. Part 1: Thermal analyses of selected salt hydrate systems
[NASA-TM-77778] 10 p1507 N85-19510
Synthesis and properties of arylethersulfone thermoset systems
[AD-A154811] 21 p3569 N85-32198
Importance and significance of transition temperatures
[AD-A154871] 21 p3569 N85-32199

TRANSITS
NT THEODOLITES

TRANSLATING
NT MACHINE TRANSLATION
The portable LISP translation tool
[AD-A149765] 12 p1915 N85-22023
The design and analysis of a complete hierarchical interface for the multi-backend database system
[AD-A151550] 15 p2629 N85-26203
Spanish language equivalents for a glossary of terms used in the field of space exploration
[NASA-TM-86211] 19 p3379 N85-30961

TRANSLATIONAL MOTION
NT SECONDARY FLOW
NT THREE DIMENSIONAL FLOW
NT THREE DIMENSIONAL MOTION
Translational control of a graphically simulated robot arm by kinematic rate equations that overcome elbow joint singularity
[NASA-TP-2376] 06 p0856 N85-15446
Processing dynamic image sequences from a moving sensor
[AD-A149984] 12 p1934 N85-22148
Absolute movement of Pacific Ocean plate during last 120 million years 13 p2107 N85-23126
The unsteady boundary layer on an elliptic cylinder following the impulsive onset of translational and rotational motion — dynamic stall 14 p2209 N85-23699
Construction of conditionally periodic solutions of problem of reciprocating motion of axially symmetric satellite of triaxial planet 15 p2480 N85-25304

TRANSLUCENCE
Light transmitting window assembly
[NASA-CASE-MSC-18417-1] 18 p3165 N85-29750

TRANSLUNAR SPACE
U INTERPLANETARY SPACE

TRANSMISSION
NT ACOUSTIC PROPAGATION
NT AERODYNAMIC HEAT TRANSFER
NT CODE DIVISION MULTIPLE ACCESS
NT CONDUCTIVE HEAT TRANSFER
NT CONVECTIVE HEAT TRANSFER
NT DATA TRANSMISSION
NT DEMULTIPLEXING
NT DIFFRACTION PROPAGATION
NT ELECTRIC POWER TRANSMISSION
NT ELECTROMAGNETIC WAVE TRANSMISSION
NT FREQUENCY DIVISION MULTIPLE ACCESS
NT FREQUENCY DIVISION MULTIPLEXING
NT GROUND WAVE PROPAGATION
NT HALOS
NT HEAT TRANSFER
NT HEAT TRANSMISSION
NT HYPERSONIC HEAT TRANSFER
NT IONOSPHERIC PROPAGATION
NT LAMINAR HEAT TRANSFER
NT LIGHT SCATTERING
NT LIGHT TRANSMISSION
NT MICROWAVE ATTENUATION
NT MICROWAVE TRANSMISSION
NT MULTIPATH TRANSMISSION
NT MULTIPLE ACCESS
NT MULTIPLEXING
NT PCM TELEMETRY
NT RADAR TRANSMISSION
NT RADIATIVE HEAT TRANSFER
NT RADIO TRANSMISSION
NT SATELLITE TRANSMISSION
NT SCATTER PROPAGATION
NT SELF PROPAGATION
NT SHOCK WAVE PROPAGATION
NT SHORT WAVE RADIO TRANSMISSION
NT SIGNAL TRANSMISSION
NT SINGLE CHANNEL PER CARRIER TRANSMISSION
NT SINGLE SIDEBAND TRANSMISSION
NT SOUND TRANSMISSION
NT SPREAD SPECTRUM TRANSMISSION
NT STRESS PROPAGATION
NT TELEPHONY
NT TELEVISION TRANSMISSION
NT TIME DIVISION MULTIPLEXING
NT TRANSEQUATORIAL PROPAGATION
NT TURBULENT HEAT TRANSFER
NT WAVE PROPAGATION
NT WAVELENGTH DIVISION MULTIPLEXING
Characterization of atmospheric conditions along transmission paths from a remotely piloted vehicle
[AD-A145527] 02 p0232 N85-11511
A new leaky wave antenna for millimeter waves based on the groove guide
[AD-A146428] 06 p0799 N85-15102
Multiple scattering effects on transmission through the atmosphere
[AD-A147527] 07 p0941 N85-15969
Low-loss flexible dielectric waveguide for millimeter-wave transmission and its application to devices
[AD-A147648] 07 p0946 N85-16006
Temperature dependence of propagation of high-current electron beam through drift space
13 p2079 N85-22982
Journal of Research of the National Bureau of Standards, volume 90, number 1, January - February 1985
[PB85-179083] 20 p3522 N85-31906
Conjugated symmetrical coupler curves, produced by 4-bar linkages having the same transmission angles
23 p3924 N85-34322
Hologram-like transmission of pictures
23 p3961 N85-34552

TRANSMISSION CIRCUITS
Interface structures for millimeter-wave circuits
[AD-A146557] 06 p0804 N85-15118
Beam forming network
[NASA-CASE-NPO-15743-1] 18 p3069 N85-29118

TRANSMISSION EFFICIENCY
Effects of transport delays of manual control system performance 05 p0701 N85-14498
Automated radome testing
[AD-P004362] 12 p1826 N85-21456

Recommendation on use of series K157UL1 microcircuits 13 p2071 N85-22936
Interference immunity of optical radar system with phased antenna array 15 p2526 N85-25575
Land mobile satellite transmission measurements at 869 MHz: Selected results from the dedicated stratospheric balloon experiment of November 12 and 13, 1984 [NASA-CR-175734] 15 p2541 N85-25685
A brief comparison of Egyptian with West German atmospheric transmission data in the 8 to 11.5 micron waveband [BAE-BT-12829] 15 p2594 N85-25963
Meteorological factors in Earth-Satellite propagation [NASA-CR-175764] 16 p2789 N85-27089
Correlation of rheological characteristics of lubricants with transmission efficiency measurements [NASA-TM-86988] 19 p3280 N85-30342
Serial Minimum Shift Keying (SMSK) follow-on study -- spacecraft communication [ESA-CR(P)-2026] 20 p3399 N85-31083

TRANSMISSION LINES
NT BEAM WAVEGUIDES
NT CIRCULAR WAVEGUIDES
NT COAXIAL CABLES
NT COMMUNICATION CABLES
NT FLUID TRANSMISSION LINES
NT MICROSTRIP TRANSMISSION LINES
NT OPTICAL WAVEGUIDES
NT PLASMAGUIDES
NT POWER LINES
NT RECTANGULAR WAVEGUIDES
NT STRIP TRANSMISSION LINES
NT SUBMARINE CABLES
NT UNDERGROUND TRANSMISSION LINES
NT WAVEGUIDES
Broadband transverse field interaction continuous beam amplifier [AD-D011229] 01 p0043 N85-10279
Transverse field interaction multibeam amplifier [AD-D011241] 01 p0043 N85-10282
Laboratory evaluation of Electromagnetic Pulse (EMP) hardness testing concepts for electrical conduit systems [AD-A145466] 02 p0190 N85-11273
Fiber cable in optical system with brightness amplifier 02 p0263 N85-11724
Electrical parameters in 60-Hz biological exposure systems and their measurement: A primer [PB84-217793] 03 p0400 N85-12548
Development of intercalated wire and cable [AD-A146502] 06 p0774 N85-14949
Safety requirements for wiring systems and connectors for photovoltaic systems [NASA-CR-174211] 06 p0803 N85-15110
Holographic directional coupler for fiber optic systems [AD-D011365] 07 p0937 N85-15939
Multiwavelength bidirectional coupler-decouplers [AD-A147009] 07 p1043 N85-16625
Operational characteristics of a 1000 MVA superconducting power transmission system [DE85-000232] 09 p1314 N85-18263
Feasiblity study for a 34 GHz (Ka band) gyroamplifier [NASA-CR-174439] 10 p1477 N85-19325
Experimental investigation of certain beam transport issues in a pulsed transmission line linear accelerator [DE85-002310] 10 p1555 N85-19805
Effect of interfacial characteristics of metal clad polymeric substrates on electrical high frequency interconnection performance [NASA-TM-86948] 11 p1624 N85-20223
Effects of electromagnetic fields produced by high voltage transmission lines [DE85-900034] 11 p1625 N85-20230
Calculation of transmission line impedances using the ANSYS finite element program [DE84-016715] 11 p1629 N85-20261
A process to produce fine line metallic collection patterns on semiconductors devices [NASA-CASE-NPO-16413-1] 12 p1805 N85-21325
Pulse transformer package for impedance matching a laser diode to a transmission line [AD-D011499] 12 p1855 N85-21632
Transient analysis of loaded thin-wire antennas and transmission lines 13 p2053 N85-22852
Interference immunity of fiber-optic communication lines with spectral multiplexing of channels 13 p2069 N85-22924
AL-124 light-emitting diode in 30 Mbit/s fiber-optic communication line 13 p2069 N85-22925
Synthesis of low-pass filters using coupled lines with unmatched loads 13 p2071 N85-22938
Possibilities of aerial electric prospecting by long cable method for detecting poorly conducting strata 13 p2115 N85-23177
A compact, aperture-matched, balanced transmission line antenna [R-NIAS-28] 14 p2290 N85-24196
Basic EMC (Electromagnetic Compatibility) technology advancement for C3 systems. Volume 4E: Modeling of transmission lines. A comparison of lumped-circuit iterative models and the transmission line model [AD-A150652] 14 p2291 N85-24201
Preliminary estimation of mutual interference between fixed satellite service systems 15 p2523 N85-25586
Asymptotic solutions of MHD equations with finite conductivity [REPT-12/1984] 16 p2652 N85-27581
Multiconductor flat cable [AD-D011635] 17 p2950 N85-28218
Performance analysis of radiation cooled dc transmission lines for high power space systems [NASA-TM-87040] 17 p2951 N85-28222
Reliability report for communication networks [AD-A153764] 18 p3090 N85-29127
Electrical line source and point source interactions with anomalies in the ground [DE85-009777] 18 p3095 N85-29161
Energizing arrangement for charge coupled device control electrodes [AD-D011712] 19 p3261 N85-30220
Development of power system measurements [PB85-182582] 20 p3450 N85-31420
Ultrasonic flowmetering with reflected pulses [PB85-179885] 20 p3460 N85-31492
Fin line filters technology and electronic warfare [AD-A154975] 21 p3576 N85-32237
Microcomputer network: Investigation and implementation [AD-A155631] 21 p3674 N85-32826
Temperature sensitivity of fiber-optic transmission line 22 p3764 N85-33331
Maximally flat approximation of attenuation characteristics of coupled-line filters 22 p3775 N85-33393
Injector losses on Mite [DE85-012356] 24 p4090 N85-35355
RFQ modeling computer program [DE85-012665] 24 p4140 N85-35661

TRANSMISSION LOSS
Performance loss with shorted cells 06 p0832 N85-15294
Analytic models for radiation induced loss in optical fibers 2: A physical model [AD-A147442] 07 p1044 N85-16632
Optical frequency domain reflectometry 08 p1222 N85-17695
Studies on reactive mufflers. Part 2: Mufflers with air flow 09 p1303 N85-18184
Propagation measurements for land-mobile satellite services in the 800 MHz band [CRC-TN-724] 09 p1310 N85-18231
Propagation measurements for land-mobile satellite systems at 1541 MHz [CRC-TN-723] 09 p1310 N85-18232
Subcable test facility [DE85-002103] 09 p1315 N85-18269
A critical analysis of ocean thermal analysis models in operation at FNOC (Fleet Numerical Oceanography Centers) [AD-A148731] 09 p1359 N85-18547
A comparison between predicted and measured propagation loss in the VHF/UHF range in rugged terrain 10 p1471 N85-19285
Construction tolerances for low loss, dielectric coated, metallic waveguide for transmission optical radiation [DE85-004056] 10 p1558 N85-19822
Measurements and predictions of HF ground wave radio propagation over irregular, inhomogeneous terrain [PB85-110666] 12 p1830 N85-21487
Noise transmission loss of a rectangular plate in an infinite baffle [NASA-TP-2398] 12 p1927 N85-22109
Optical reflectometer for multimode fiber lightpipes 13 p2075 N85-22961
Ice statistics and acoustic scattering in the Arctic basin [AD-A150141] 13 p2140 N85-23289
Development of a modified time delay spectrometry technique for underwater acoustic measurements in a multipath environment [AD-A152111] 16 p2860 N85-27639
Effects of Formvar coating and copper-nickel outer sheath on the ac losses of multi-strand subsize cables [DE85-010413] 18 p3096 N85-29166
Airborne sound transmission loss characteristics of wood-frame construction [AD-A154174] 20 p3524 N85-31919

TRANSMISSIONS (MACHINE ELEMENTS)
The in-flight estimation and indication of cumulative fatigue damage to helicopter gears [ARL/AERO-R-164] 03 p0317 N85-12050
The monitoring of machines [CETIM-15-J-041] 04 p0510 N85-13253
Investigation on experimental techniques to detect, locate and quantify gear noise in helicopter transmissions [NASA-CR-3847] 08 p1217 N85-17667
Feasibility demonstration of a novel, flat-belt, continuously variable transmission or automotive and electric-hybrid vehicle application [NASA-CR-174430] 10 p1569 N85-19894
Design of tightening device and calculation of forces in manipulator transmissions with base-drive mounted 13 p2046 N85-22804
Gears and Power Transmission Systems for Helicopters and Turboprops [AGARD-CP-369] 14 p2220 N85-23765
Summary of drive-train component technology in helicopters 14 p2220 N85-23766
Current transmission systems 14 p2220 N85-23767
Helicopter transmission lubricants 14 p2220 N85-23768
Special power train requirements for the next generation of rotary-wing aircraft 14 p2220 N85-23769
A state of the art assessment of turboprop transmission technology and projected needs for the next generation 14 p2220 N85-23770
The helicopter transmission design process 14 p2221 N85-23772
Software for designing teeth for reduction gears and transmissions 14 p2221 N85-23773
Fine filtration: An attractive route towards lower helicopter operating costs 14 p2221 N85-23774
Manufacturing considerations related to aircraft gearboxes 14 p2222 N85-23776
Possible technological answers to new design requirements for power transmission systems 14 p2222 N85-23779
Transmission efficiency measurements and correlations with physical characteristics of the lubricant 14 p2222 N85-23781
Problems of elastic hydrodynamic lubrication of helicopter transmission gears 14 p2222 N85-23784
Evolution of the design techniques for helicopter main transmission gearboxes 14 p2223 N85-23789
Do new aircraft need new technologies and certification rules? 14 p2224 N85-23795
Establishment and maintenance of certification standards for helicopter and turboprop power transmission systems 14 p2224 N85-23796
A system-level mathematical model for evaluation of power train performance of load-leveled electric-vehicles [NASA-CR-175652] 14 p2434 N85-25009
Correlation of rheological characteristics of lubricants with transmission efficiency measurements [NASA-TM-86988] 19 p3280 N85-30342
Estimation of dynamic rotor loads for the rotor systems research aircraft: Methodology development and validation [NASA-CR-177362] 20 p3393 N85-31045
The design and analysis of single flank transmission error testor for loaded gears [NASA-CR-176163] 23 p3937 N85-34404

TRANSMISSIVITY
Seasonal variations of reflexibility and transmissibility of ULF waves propagating through the ionosphere of geomagnetic mid-latitudes [REPT-560] 03 p0376 N85-12403
Fine structure of vertical distribution of light attenuation index of sea water 13 p2109 N85-23140
The geostatistical approach to the inverse problem in two-dimensional steady state groundwater modeling 24 p4107 N85-35482

TRANSMISSOMETERS
Atmospheric transmissometer [AD-D011540] 12 p1932 N85-22140
Comparison of 8 to 12 micrometer and 3 to 5 micrometer CVF transmissometer data with LOWTRAN calculations [AD-A154218] 19 p3350 N85-30763

TRANSMITTANCE
Changes in spectral properties of detached leaves [E85-10042] 07 p0983 N85-16243
Carbon dioxide laser radar for monitoring atmospheric transmittance and atmospheric aerosol 09 p1354 N85-18516
An HF communications frequency-management procedure for forecasting the frequency of optimum transmission [AD-A149191] 10 p1467 N85-19254
A new CO2 transmittance parameterization and its impact on the GLA GCM 18 p3146 N85-29476
Measurement of permittivity and permeability of microwave materials [AD-D011656] 18 p3176 N85-29886
Light transmitting window assembly [NASA-CASE-MSC-18417-1] 18 p3185 N85-29750

Comparison of 8 to 12 micrometer and 3 to 5 micrometer CVF transmissometer data with LOWTRAN calculations
[AD-A154218] 19 p3350 N85-30763
Ship-to-ship propagation: Maritime data analyses
[AD-A155484] 21 p3592 N85-32325
Nuclear thermal transmittance in the atmosphere using LOWTRAN-6 computer code
[AD-A154669] 21 p3630 N85-32553
Characteristic modes for slots in a ground plane TE case
[AD-A155757] 24 p4086 N85-35326
Feasibility study of radar-transmitting materials
[AD-A155839] 24 p4087 N85-35329
Linear absorption and scattering of laser beams
[AD-A156167] 24 p4098 N85-35401

TRANSMITTER RECEIVERS
Quartz filter transceiver 12 p1838 N85-21538
Firefighters' communication transceiver test plan
[NASA-CR-171419] 13 p2053 N85-22854
Transceiver test device
[AD-D011728] 22 p3786 N85-33458

TRANSMITTERS
NT EMERGENCY LOCATOR TRANSMITTERS
NT IONOSONDES
NT RADAR TRANSMITTERS
NT RADIO BEACONS
NT RADIO TRANSMITTERS
NT RADIOSONDES
NT RADIOTELEPHONES
NT RAWINSONDES
NT REPEATERS
NT TRANSMITTER RECEIVERS
Lightweight, broadband Rayleigh wave transducer
[AD-D011345] 07 p1037 N85-16584
A variable length and sensor spacing thermistor array
[AD-D011416] 08 p1113 N85-17017
Methodical approaches to determination of sanitation protective zone dimensions around TV centers and TV retransmitters 09 p1361 N85-18563
Data acquisition, measurement devices at 1984 Leipzig Spring Fair 09 p1376 N85-18631
Performance assessment of Class 1E pressure transmitters subjected to environmental stresses
[DE85-001623] 12 p1854 N85-21626
A compact, aperture-matched, balanced transmission line antenna
[R-NIAS-28] 14 p2290 N85-24196
Satellite reception of reentry vehicle telemetry
[AD-A151851] 15 p2492 N85-25372
Cophasal horizontal wideband array antennas for transmitting with asymmetric output
15 p2526 N85-25576
Measurement results from a balloon experiment simulating land mobile satellite transmissions
[NASA-CR-175740] 15 p2540 N85-25683
On the throughput of channel access algorithms with limited sensing
[AD-A151984] 15 p2630 N85-26208
Digital RF delay line for ECM (electronic countermeasure) look-through
[AD-A152120] 16 p2774 N85-27120
A communications link for an implantable electrode array
[AD-A152238] 16 p2840 N85-27510
High switching speed electrically tuned microwave magnetic resonance devices
[AD-D011699] 19 p3260 N85-30217
Multitrunk high-frequency multiplexing of antenna-waveguide channels 22 p3774 N85-33385
Transmitter spectrum analyzer
22 p3774 N85-33389
Microcomputer controlled image processor
[AD-D011734] 22 p3833 N85-33735

TRANSONIC AIRCRAFT
U SUPERSONIC AIRCRAFT

TRANSONIC COMPRESSORS
A finite element method for the solution of two-dimensional transonic flows in cascades
[PNR-90216] 03 p0316 N85-12045
Study of controlled diffusion stator blading
[NASA-CR-167995] 09 p1281 N85-18058

TRANSONIC FLIGHT
Joined wing transonic design and test validation
[AD-A148355] 08 p1078 N85-16834
Experiences with transition fixation in the high-speed regime at NLR 14 p2211 N85-23715
Design of a basic airfoil for a slightly swept wing. Part 1: Theoretical transonic airfoil design
[ESA-TT-892] 20 p3394 N85-31054

TRANSONIC FLOW
An experimental study of the transonic equivalence rule with lift, part 2
[AR-LR-614-PT-2] 01 p0001 N85-10004
Development and applications of algorithms for calculating the transonic flow about harmonically oscillating wings
[NASA-CR-172376] 01 p0002 N85-10007
Computational methods for complex flowfields
[AD-A145219] 01 p0004 N85-10019
Transonic flow analysis for rotors. Part 1: Three-dimensional quasi-steady, full-potential calculation
[NASA-TP-2375-PT-1] 02 p0134 N85-10914
Further development of a transonic cascade analysis
[AD-A145410] 02 p0198 N85-11319
Inverse design technique for cascades
[NASA-CR-3836] 03 p0311 N85-12008
Performance of two transonic airfoil wind tunnels utilizing limited ventilation 03 p0313 N85-12020
Experiments suitable for wind tunnel wall interference assessment/correction 03 p0313 N85-12021
Development in UK of a method for calculating tunnel wall corrections from flow measurements
03 p0314 N85-12026
Design of a basic airfoil for a slightly swept wing. Part 1: Theoretical transonic airfoil design
[DFVLR-FB-84-19-PT-1] 03 p0316 N85-12043
A finite element method for the solution of two-dimensional transonic flows in cascades
[PNR-90216] 03 p0316 N85-12045
Investigations of boundary layers in the Emmen Federal Aircraft works transonic tunnel, Switzerland
[FW-FO-1641] 04 p0453 N85-12877
Comparative flow calculation on transonic cone/cylinder standard models in connection with the wall interference problem
[FW-FO-1689] 04 p0453 N85-12878
A local slot boundary condition for transonic flow calculations in slotted-wall test sections of wind tunnels
[FFA-TN-1984-34] 04 p0453 N85-12879
Investigation for the improvement of the transonic tunnel working section of the Emmen Federal Aircraft Works (Switzerland)
[FW-FO-1681] 04 p0458 N85-12904
Simulation of separated transonic airfoil flow by finite-difference viscous-inviscid interaction
05 p0591 N85-13768
The numerical simulation of steady transonic rotational flow using a dual potential formulation
05 p0591 N85-13770
Experimental studies of transonic airfoil trailing edge and wake flowfield properties 05 p0592 N85-13773
Transonic jets: A numerical approach in the hodograph plane 05 p0592 N85-13774
Navier-Stokes computational study of axisymmetric transonic turbulent flows with a two-equation model of turbulence 05 p0634 N85-14068
Development of the code NSFOIL for analyzing high Reynolds number transonic flow around an airfoil
[NAL-TR-816] 06 p0749 N85-14801
A theoretical design method for 3-dimensional transonic wings
[NAL-TR-830] 06 p0754 N85-14834
Transonic flow of elastic medium past slender solid body 06 p0778 N85-14976
Review of requirements and status of simulation and scaling of transonic, viscous flows
[AD-A146357] 06 p0808 N85-15137
A comparative study of the nonuniqueness problem of the potential equation
[NASA-TP-2385] 07 p0898 N85-15694
An exploratory study of finite difference grids for transonic unsteady aerodynamics
[NASA-TM-84583] 07 p0899 N85-15696
A method for solving the inverse problem of transonic cascade flow
[AD-A146739] 07 p0899 N85-15698
Transonic shock interaction with a tangentially-injected turbulent boundary layer 08 p1072 N85-16796
Shock waves in transonic flows at moderate Reynolds Number 08 p1076 N85-16823
Vectorizable multigrid algorithms for transonic flow calculations
[NASA-CR-174326] 08 p1077 N85-16827
Research into topics in transonic flow theory
[AD-A148526] 08 p1078 N85-16837
Theoretical contributions to transonic flow analysis for transport aircraft
[BMFT-FB-W-84-036] 08 p1078 N85-16838
Analysis of inviscid transonic flow around an airfoil by diagonal form of IAF scheme
[NAL-TR-831] 10 p1420 N85-18955
Effects of airfoil shape, thickness, camber, and angle of attack on calculated transonic unsteady airloads
[NASA-TM-86320] 10 p1420 N85-18957
Efficient self-consistent viscous-inviscid solutions for unsteady transonic flow
[NASA-TM-86335] 10 p1420 N85-18959
Unsteady transonic flow calculations for two-dimensional canard-wing configurations with aeroelastic applications
[NASA-TM-86375] 10 p1420 N85-18960
Viscous effects on transonic airfoil stability and response
[NASA-TM-86374] 10 p1421 N85-18961
Unsteady transonic pressure measurements on a semispan wind-tunnel model of a transport-type supercritical wing (Lann model). Part 2: Pressure distributions (plotted) and plots of the vibration modes
[AD-A130488] 10 p1421 N85-18965
Contribution to the study of a numerical implicit method for solving the Euler equations
[ESA-TT-872] 10 p1549 N85-19771
A fast algorithm of the finite difference method for computation of the transonic flow past an arbitrary airfoil with the conservative full-potential equation
11 p1619 N85-20191
A mixed finite difference analysis of the internal and external transonic flow fields of inlets with centerbody
11 p1619 N85-20192
A locally linearized panel method for tran-/subsonic flow past an oscillating wing 11 p1622 N85-20212
Transonic pressure distribution computations of a flexible wing 11 p1622 N85-20213
On relaxation of transonic flows around zero-lift airfoils and convergence of self-correcting wing tunnels
11 p1622 N85-20214
Finite difference computation of the flow around airfoils in two-dimensional transonic slotted wall wind tunnel
11 p1623 N85-20216
Reconstruction of a 3-dimensional transonic rotor flow field from holographic interferogram data
[NASA-TM-86690] 12 p1770 N85-21112
Transonic interactions of unsteady vortical flows
[NASA-TM-86658] 12 p1770 N85-21113
Measured unsteady transonic aerodynamic characteristics of an elastic supercritical wing with an oscillating control surface
[NASA-TM-86376] 12 p1771 N85-21116
Pseudospectral calculations of two-dimensional transonic flow (Task 1). Numerical investigation of VTOL aerodynamics (Task 2)
[AD-A150123] 12 p1772 N85-21126
Unsteady transonic pressure measurements on a semi-span wind-tunnel model of a transport-type supercritical wing (Lann model). Part 2: Pressure distributions (plotted) and plots of the vibration modes
[AD-A130488] 12 p1846 N85-21579
Robust calculation of three-dimensional transonic potential flow based on the nonlinear gas multigrid method and a mixed incomplete lower upper decomposition/strongly implicit procedure (ILU/SIP) algorithm
[NLR-MP-84003-U] 12 p1848 N85-21593
Preliminary development of an approximation procedure for supercritical wing design optimization applications
[AD-A150177] 13 p1972 N85-22383
F-14A aircraft high-speed flow simulations
[NASA-CR-172559] 14 p2209 N85-23702
Calibration of sonic valves for the laminar flow control, leading-edge flight test
[NASA-TP-2423] 14 p2210 N85-23707
Recent transonic unsteady pressure measurements at the NASA Langley Research Center
[NASA-TM-86408] 14 p2210 N85-23710
The influence of transition strips on the pressure distribution on transonic profiles
14 p2212 N85-23718
Transition fixing and simulation of high Reynolds number flow at transonic velocities 14 p2212 N85-23721
Transonic merging separated flows
[AD-A150667] 14 p2213 N85-23724
Calculation of an unsteady transonic flow with shock waves and separation in Laval nozzles
[MPIS-14/1984] 14 p2213 N85-23728
Application possibilities of laser Doppler anemometry in the investigation of the transonic interaction between shock wave and boundary layer
[ISL-R-131/83] 14 p2304 N85-24265
Transonic Unsteady Aerodynamics and its Aeroelastic Applications
[AGARD-CP-374] 15 p2457 N85-25171
Transonic pressure distributions on a two-dimensional 0012 and supercritical MBB-A3 profile oscillating in heave and pitch 15 p2457 N85-25173
Numerical studies of unsteady transonic flow over oscillating airfoil 15 p2458 N85-25174
Analysis of transonic aerodynamic characteristics for a supercritical airfoil oscillating in heave, pitch and with oscillating flap 15 p2458 N85-25175
Calculation of harmonic aerodynamic forces of aerofoils and wings from the Euler equations
15 p2458 N85-25177

Calculation of unsteady transonic separated flows by viscous-inviscid interaction 15 p2458 N85-25178

A semi-empirical unsteady transonic method with supersonic free stream 15 p2458 N85-25179

Improvement and extension of a numerical procedure for the three dimensional unsteady transonic flows
15 p2459 N85-25181

Application of time-linearized methods to oscillating wings in transonic flow and flutter
15 p2459 N85-25182

Computation of unsteady transonic flows about two-dimensional and three-dimensional AGARD standard configurations 15 p2459 N85-25183

Calculation of unsteady transonic flow around a high swept wing 15 p2459 N85-25184

Unsteady transonic aerodynamic and aeroelastic calculations about airfoils and wings
15 p2459 N85-25185

The development of unsteady transonic 3-D full potential code and its aeroelastic applications
15 p2460 N85-25187

A new implicit plus minus splitting method for the solution of the Euler equations in the transonic flow regime
15 p2461 N85-25200

Transonic aerodynamic and aeroelastic characteristics of a variable sweep wing
[NASA-TM-86677] 15 p2462 N85-25203

Numerical analyses in aerodynamic design of aero-engine fan 16 p2692 N85-26618

Numerical example of three-dimensional flying object in shockless transonic flow 16 p2693 N85-26623

A numerical design method for three-dimensional transonic wings 16 p2694 N85-26631

Description of a computer program treating transonic steady state aeroelastic effects for a canard or tail airplane
[FFA-TN-1983-23] 16 p2700 N85-26674

Measurements of the symmetric aerodynamic coefficients for flat faced cylinders in the angle of attack regime 0 to 90 deg for transonic and supersonic speeds
[FFA-TN-1984-04] 16 p2700 N85-26675

Numerical solution of transonic normal shock wave-boundary layer interaction using the Bohning-Zierop model — wind tunnel flow
[VTH-LR-416] 16 p2701 N85-26683

Numerical study of porous airfoils in transonic flow
[NASA-TM-86713] 17 p2892 N85-27828

Transonic Mach number determination in a blow-down wind tunnel with solid walls and a downstream throat
[VTH-LR-402] 17 p2893 N85-27835

Navier-Stokes computational study of axisymmetric transonic turbulent flows with a two-equation model of turbulence
[AD-A152653] 17 p2958 N85-28265

Proceedings of the 9th US Air Force and the Federal Republic of Germany Data Exchange Agreement Meeting, Viscous and Interacting Flow Field Effects
[AD-A153020] 17 p2958 N85-28266

Subsonic and transonic aerodynamics of a wraparound fin configuration
[AD-A153646] 18 p3059 N85-28927

Flow quality of National Aerospace Laboratory two-dimensional transonic wind tunnel. Part 3: Flow turbulence level and measuring method
[NAL-TR-842-PT-3] 18 p3064 N85-28952

Hyperbolic phenomena in the flow of viscoelastic fluids
[AD-A153533] 18 p3099 N85-29186

Inviscid analysis of two supercritical laminar-flow-control airfoils at design and off-design conditions
[NASA-TM-84657] 19 p3212 N85-29920

Unsteady transonic flow calculations for interfering lifting surface configurations
[NASA-TM-86432] 19 p3214 N85-29931

Selected topics in experimental aeroelasticity at the NASA Langley Research Center
[NASA-TM-86436] 19 p3284 N85-30364

Floating shock-fitting in transonic potential flow calculations 20 p3387 N85-31007

Calculation of transonic flows around an aircraft configuration with motorized nacelle
[SNIAS-851-111-106] 20 p3387 N85-31008

Transonic calculations for a flexible supercritical wing and comparison with experiment
[NASA-TM-86439] 20 p3388 N85-31012

Numerical simulation of potential flow in transonic steady regimes 20 p3389 N85-31016

Data set 9: LANN wing. Pitching osuilation
20 p3390 N85-31030

The application of laser anemometry to the study of transonic shock boundary-layer interactions
[ISL-CO-204/84] 20 p3396 N85-31067

R and D activities of the Aerodynamics Division
20 p3539 N85-32023

Calculation of transonic steady and oscillatory pressures on a low aspect ratio model and comparison with experiment
[NASA-TM-86449] 21 p3551 N85-32092

Notes on unsteady transonic cascade flows
[AD-A154829] 21 p3552 N85-32096

Design of a generator for near-tangential transonic swirling outflow
[AD-A155163] 21 p3584 N85-32260

An elliptic calculation procedure for 3-D viscous flow
21 p3587 N85-32297

Exact solutions of singular equations for viscous transonic flows 21 p3683 N85-32882

Integral equation formulation for three-dimensional unsteady transonic flow
[ARL/STRUC-R-416] 23 p3894 N85-34119

A review of spectral methods
[NASA-CR-172502] 23 p3929 N85-34350

Unsteady transonic heat transfer in a transient facility
[NASA-CR-176145] 23 p3930 N85-34354

System maintenance manual for master modeling of aerodynamic surfaces by three-dimensional explicit representation
[NASA-CR-178224] 23 p3956 N85-34517

A stream function approach to solving the conservative Euler equations for transonic flows
24 p4059 N85-35156

Numerical studies of 2-dimensional flows
[NASA-CR-3930] 24 p4060 N85-35160

TRANSONIC FLUTTER

Experimental study on transonic flutter characteristics of sweptback wing with core composite plates having different fiber orientations
[NAL-TR-827] 06 p0756 N85-14842

A study of transonic flutter of a two-dimensional airfoil using the U-g and p-k methods
[LR-615] 12 p1771 N85-21121

Experience with transonic unsteady aerodynamic calculations 15 p2458 N85-25176

A semi-empirical unsteady transonic method with supersonic free stream 15 p2458 N85-25179

A study of transonic flutter of a two-dimensional airfoil using the U-g and p-k methods
[AD-A151463] 15 p2473 N85-25268

Numerical simulation of transonic flutter of a high-aspect ratio transport wing 16 p2694 N85-26630

Selected topics in experimental aeroelasticity at the NASA Langley Research Center
[NASA-TM-86436] 19 p3284 N85-30364

Verification of calculation methods for unsteady airloads in the precipitation of transonic flutter
[NLR-MP-84016-U] 20 p3390 N85-31027

TRANSONIC INLETS

U SUPERSONIC INLETS

TRANSONIC SPEED

Effect of upstream sidewall boundary layer removal on an airfoil test — conducted in Langley 0.3-m transonic cryogenic tunnel 03 p0313 N85-12019

Asymptotic methods for wind tunnel wall corrections at transonic speed 03 p0313 N85-12022

Effect of a variable camber and twist wing at transonic Mach numbers
[NASA-TM-86281] 04 p0452 N85-12869

Prediction of cruciform all-movable control characteristics at transonic speeds
[AD-A147291] 08 p1078 N85-16832

On detached shock wave of sphere moving with transonic velocities 11 p1622 N85-20215

Analysis of unsteady pressure measurements on a supercritical airfoil with a harmonically oscillating trailing edge flap at subsonic and transonic speeds
[DFVLR-FB-84-49] 17 p2893 N85-27837

Flow quality of National Aerospace Laboratory two-dimensional transonic wind tunnel. Part 3: Flow turbulence level and measuring method
[NAL-TR-842-PT-3] 18 p3064 N85-28952

An experimental investigation of propfan installations on an upswept supercritical wing at transonic Mach numbers
[NASA-CR-172605] 20 p3388 N85-31013

Development of a temperature-compensated hot-film anemometer system for boundary-layer transition detection on high-performance aircraft
[NASA-TM-86732] 22 p3730 N85-33121

TRANSONIC WIND TUNNELS

Pressure distributions measured on research wing M100 mounted on an axisymmetric body
01 p0004 N85-10023

Pressure distributions measured on research wing M86 mounted on an axisymmetric body
01 p0004 N85-10024

The data processing system of the NAL 2m x 2m transonic wind tunnel
[NAL-TR-811] 01 p0012 N85-10075

Computations for the 16-foot transonic tunnel, NASA, Langley Research Center
[NASA-TM-86319] 02 p0149 N85-11009

Wind Tunnel Wall Interference Assessment and Correction, 1983
[NASA-CP-2319] 03 p0311 N85-12011

Wall interference measurements for three-dimensional models in transonic wind tunnels: Experimental difficulties 03 p0311 N85-12012

Survey of ONERA activities on adaptive-wall applications and computation of residual corrections
03 p0312 N85-12013

Two- and three-dimensional model and wall data from a flexible-walled transonic test section
03 p0312 N85-12015

Assessment of lift- and blockage-induced wall interference in a three-dimensional adaptive-wall tunnel
03 p0312 N85-12016

A data base for three-dimensional all-interference code evaluation 03 p0312 N85-12017

Investigations of flow field perturbations induced on slotted transonic-tunnel walls 03 p0312 N85-12018

Review of the advanced technology airfoil test program in the 0.3-meter transonic cryogenic tunnel
03 p0315 N85-12033

Some experience with Barnwell-Sewall type correction to two-dimensional airfoil data 03 p0315 N85-12034

Adaptation of a four-wall interference assessment/correction procedure for airfoil tests in the 0.3-m TCT 03 p0315 N85-12036

Parametric determination of blockage interference of 3-dimensional models in the Emmen Federal Aircraft works transonic tunnel (Switzerland)
[FW-FO-1636] 04 p0453 N85-12876

Investigation for the improvement of the transonic tunnel working section of the Emmen Federal Aircraft Works (Switzerland)
[FW-FO-1681] 04 p0456 N85-12904

Description of the insulation system for the Langley 0.3-Meter Transonic Cryogenic Tunnel
[NASA-TM-86274] 07 p0909 N85-15756

Flow quality of NAL 2-dimensional transonic wind tunnel. Part 2: Extensive and systematic pressure fluctuations study in the settling chamber, test section and second throat of the NAL 2-D transonic wind tunnel
[NAL-TR-836-PT2] 09 p1283 N85-18066

The S2MA wind tunnel at the Modane-Avrieux aerodynamic test center
[ESA-TT-862] 09 p1284 N85-18071

Aeronautical facilities catalogue. Volume 1: Wind tunnels
[NASA-RP-1132] 10 p1426 N85-18991

Finite difference computation of the flow around airfoils in two-dimensional transonic slotted wall wind tunnel
11 p1623 N85-20216

Exploratory flutter test in a cryogenic wind tunnel
[NASA-TM-86380] 12 p1863 N85-21569

Calibration of wind tunnel flow quality
13 p1976 N85-22390

Harbin's subsonic, transonic wind tunnel detailed
14 p2283 N85-24143

Measurements in the flow field of a cylinder with a laser transit anemometer and a drag rake in the Langley 0.3 m transonic cryogenic tunnel
[NASA-TM-86399] 14 p2305 N85-24270

Mathematical modeling of the AEDC (Arnold Engineering Development Center) propulsion wind tunnel (16T)
[AD-A151293] 15 p2475 N85-25275

Investigation to optimize the passive shock wave/boundary layer control for supercritical airfoil drag reduction
[NASA-CR-175786] 16 p2699 N85-26665

A curved test section for research on transonic shock wave-boundary layer interaction
[VTH-LR-414] 16 p2701 N85-26682

Study on needs for a magnetic suspension system operating with a transonic wind tunnel
[NASA-CR-3900] 16 p2715 N85-26759

Design of a basic profile for a low sweep airfoil. Part 2: Experimental investigation on the DFVLR-W1 airfoil profile in the Brunswick transonic wind tunnel
[DFVLR-FB-85-01-PT-2] 17 p2892 N85-27833

Transonic Mach number determination in a blow-down wind tunnel with solid walls and a downstream throat
[VTH-LR-402] 17 p2893 N85-27835

Flow quality of National Aerospace Laboratory two-dimensional transonic wind tunnel. Part 3: Flow turbulence level and measuring method
[NAL-TR-842-PT-3] 18 p3064 N85-28952

On power effecient operation of the 2m x 2m transonic wind tunnel at the National Aerospace Laboratory
[NAL-TR-847] 18 p3064 N85-28953

High Reynolds number tests of a NASA SC(3)-0712(B) airfoil in the Langley 0.3-meter transonic cryogenic tunnel
[NASA-TM-86371] 19 p3213 N85-2[illegible]

Transonic and supersonic wind tunnel tests on control effectiveness on schematic missile configurations
[FFA-TN-1983-20] 20 p3369 N85-31020
Transonic and supersonic wind tunnel tests on control effectiveness on schematic missile configurations: Supplement
[FFA-TN-1983-20-SUPPL] 20 p3369 N85-31021
Sidewall boundary-layer effects in two-dimensional airfoil testing
[NASA-CR-176034] 20 p3396 N85-31065

TRANSONICS
U TRANSONIC FLOW

TRANSPARENCE
Method for measuring haze in transparencies
[AD-D011233] 01 p0120 N85-10623
Effect of aberration in optical system on illuminance distribution over image of strip in semicoherent light
06 p0777 N85-14970
Evaluation of colorless polyimide film for thermal control coating applications
[NASA-TM-86341] 07 p0930 N85-15894
Demonstration of transparent solar array module design
[NASA-CR-174257] 07 p0992 N85-16302
Aircraft transparency bird impact analysis using the MAGNA computer program
[AD-P004186] 11 p1579 N85-19946
Process for preparing essentially colorless polyimide film containing phenoxy-linked diamines
[NASA-CASE-LAR-13353-1] 11 p1611 N85-20128
Process for preparing highly optically transparent-colorless armomatic polyimide film
[NASA-CASE-LAR-13351-1] 12 p1811 N85-21360
Progress on transparent yttria
[AD-P004370] 12 p1827 N85-21464
Effect of transparent coatings on generation of laser-induced shock waves in metals
13 p2026 N85-22711
Nonuniform interference coatings with thickness-dependent refractive index
14 p2281 N85-24131
Error in laser correlation wind speed meters resulting from variable atmospheric transparency
14 p2338 N85-24457
Choice of optimum pairs of spectral intervals for IR-range survey of Earth's surface 15 p2486 N85-25344
Measurement of ultrasonic fields in transparent media using a scanning differential interferometer
[NASA-CR-175921] 17 p3028 N85-28726
Light transmitting window assembly
[NASA-CASE-MSC-18417-1] 18 p3185 N85-29750
Optical stability, atmospheric transparency and aerosol absorption 19 p3297 N85-30442
The measurement of aircraft windscreen haze and its effect on visual performance
[AD-A154949] 21 p3555 N85-32114
Transparency of water in 186 - 500 nm region
21 p3590 N85-32923
Digital holographic synthesis of pattern-forming transparencies for ring antenna arrays
22 p3763 N85-33326
Implicit Monte Carlo methods and non-equilibrium Marshak wave radiative transport
[DE85-010711] 22 p3835 N85-33743

TRANSPARENT MATERIALS
U TRANSPARENCE

TRANSPIRATION
Study of deposition control using transpiration
[DE85-002339] 10 p1485 N85-19378
Study of deposition control using transpiration
[DE85-003463] 11 p1585 N85-19984
Pressure drop and coefficients of internal heat transfer necessary for transpiration cooling
13 p2050 N85-22831
Small gas turbine combustor study: Fuel injector performance in a transpiration-cooled liner
[NASA-TM-86989] 15 p2473 N85-25264
Study of a constricted electric arc cooled by transpiration
[NASA-TM-77846] 17 p3038 N85-28798

TRANSPIRATION COOLING
U SWEAT COOLING

TRANSPLANTATION
The EM algorithm for censored data
[AD-A148136] 08 p1212 N85-17626

TRANSPONDERS
Investigation of the ice dynamics in the marginal ice zone
[AD-A146729] 07 p1009 N85-16411
Margin leveling algorithm for fully saturated satellite transponder with CDMA (Code Division Multiple Access) signalling
[AD-A151710] 15 p2543 N85-25699
Channel multiplexers for broadcast satellite transponders in the 12 GHz band
[NHK-LABS-NOTE-310] 18 p3090 N85-29122
Performance interface document for the S-band diplexer for space users of NASA networks
[NASA-TM-86224] 23 p3900 N85-34155

TRANSPORT AIRCRAFT
NT A-310 AIRCRAFT
NT A-320 AIRCRAFT
NT ALADIN 2 AIRCRAFT
NT BOEING 727 AIRCRAFT
NT BOEING 737 AIRCRAFT
NT BOEING 747 AIRCRAFT
NT BOEING 767 AIRCRAFT
NT C-5 AIRCRAFT
NT C-135 AIRCRAFT
NT C-141 AIRCRAFT
NT CARGO AIRCRAFT
NT CH-47 HELICOPTER
NT CONCORDE AIRCRAFT
NT DC 8 AIRCRAFT
NT DC 9 AIRCRAFT
NT DC 10 AIRCRAFT
NT DHC 2 AIRCRAFT
NT EUROPEAN AIRBUS
NT F-27 AIRCRAFT
NT L-1011 AIRCRAFT
NT UH-60A HELICOPTER
Design of a digital ride quality augmentation system for commuter aircraft
[NASA-CR-172419] 01 p0006 N85-10037
Analysis of a transport fuselage section drop test
01 p0060 N85-10400
Experimental trim drag values and flow-field measurements for a wide-body transport model with conventional and supercritical wings
[NASA-TP-2071] 02 p0135 N85-10920
Advanced composite stabilizer for Boeing 737 aircraft
[NASA-CR-168451] 02 p0137 N85-10934
Aircraft surface coatings
[NASA-CR-3861] 02 p0137 N85-10935
Simulator study of flight characteristics of several large, dissimilar, cargo transport airplanes during approach and landing
[NASA-TP-2357] 02 p0148 N85-11002
Integrated Application of Active Controls (IAAC) technology to an advanced subsonic transport project-longitudinal handling qualities study of a relaxed-stability airplane
[NASA-CR-3660] 02 p0148 N85-11005
Design of a basic airfoil for a slightly swept wing. Part 1: Theoretical transonic airfoil design
[DFVLR-FB-84-19-PT-1] 03 p0316 N85-12043
Flutter parametric studies of cantilevered twin-engine-transport type wing with and without winglet. Volume 1: Low-speed investigations
[NASA-CR-172410-VOL-1] 04 p0513 N85-13269
Flight test results on stall characteristics of a large jet transport
[NAL-TR-817] 06 p0754 N85-14835
Integrated Application of Active Controls (IAAC) technology to an advanced subsonic transport project. ACT/Control/Guidance System study, volume 1
[NASA-CR-165963-VOL-1] 06 p0754 N85-14837
Integrated Application of Active Controls (IAAC) technology to an advanced subsonic transport project. ACT/Control/Guidance System study. Volume 2: Appendices
[NASA-CR-165963-VOL-2] 06 p0754 N85-14838
Ground-effect analysis of a jet transport airplane
[NASA-TM-85920] 07 p0897 N85-15667
Integrated technology wing study (oral presentation)
[NASA-CR-169497] 07 p0902 N85-15718
Design and test requirements for development of today's engines 07 p0906 N85-15737
Documentation and separate test program development is most important for test/maintenance
08 p1065 N85-16745
Aerodynamic issues in the design of high-lift systems for transport aircraft 08 p1069 N85-16780
Technology developments for laminar boundary layer control on subsonic transport aircraft
08 p1071 N85-16787
Theoretical contributions to transonic flow analysis for transport aircraft
[BMFT-FB-W-84-036] 08 p1078 N85-16838
The visibility climatology of McMurdo Sound-Williams Field, Antarctica
[AD-A148108] 08 p1189 N85-17492
Initiative uses of aircraft for flight training
09 p1277 N85-18027
Review of engine ingestions to wide body transport aircraft
[AD-P004185] 11 p1579 N85-19947
New runway enables IL-76 flights to Tenkeli in far north 12 p1769 N85-21106
Integrated paratroop door
[AD-D011507] 12 p1776 N85-21146
Analytically redundant output feedback scheme for reduction of structural loads of a flexible transport aircraft
[TT-8303] 12 p1777 N85-21154
Guidance and control research flight testing with HFB 320 test aircraft 13 p1967 N85-22355
Study for the optimization of a transport aircraft wing for maximum fuel efficiency. Volume 1: Methodology, criteria, aeroelastic model definition and results
[NASA-CR-172551] 13 p1971 N85-22378
China report: Science and technology
[JPRS-CST-84-008] 13 p1972 N85-22384
Improved Y-11 general-purpose transport designated Y-12 13 p1972 N85-22385
Assessing the behavior and performance of teams in organizations: The case of air transport crews
[AD-A150359] 13 p2143 N85-23302
Experiences with transition fixation in the high-speed regime at NLR 14 p2211 N85-23715
Demonstration of relaxed stability on a commercial transport 16 p2713 N85-26745
Realisation of relaxed static stability on a commercial transport 16 p2713 N85-26746
Wing buffeting active control testing on a transport aircraft configuration in a large sonic tunnel
16 p2714 N85-26750
How to handle failures in advanced flight control systems of future transport aircraft 16 p2714 N85-26752
Methods for design aerodynamics of modern transport aircraft
[DFVLR-FB-85-05] 17 p2893 N85-27838
Friction and wear behavior of aluminum and composite I-beam stiffened airplane skins
[NASA-TM-86418] 17 p2895 N85-27852
Demonstration of relaxed static stability on a commercial transport 17 p2903 N85-27898
Realisation of relaxed static stability on a commercial transport 17 p2903 N85-27899
Wing buffeting active control testing on a transport aircraft configuration in a large sonic windtunnel
17 p2904 N85-27903
How to handle failures in advanced flight control systems of future transport aircraft 17 p2904 N85-27905
Advanced secondary power system for transport aircraft
[NASA-TP-2463] 18 p3062 N85-28944
Pressure distribution data from tests of 2.29 M (7.5 feet) span EET high-lift transport aircraft model in the Ames 12-foot pressure tunnel
[NASA-TM-84517] 19 p3211 N85-29912
Nacelle/pylon/wing integration on a transport model with a natural laminar flow nacelle
[NASA-TP-2439] 19 p3213 N85-29924
Crew systems and flight station concepts for a 1995 transport aircraft
[NASA-CR-166068] 19 p3221 N85-29973
Low-speed tests of a high-aspect-ratio, supercritical-wing transport model equipped with a high-lift flap system in the Langley 4- by 7-meter and Ames 12-foot pressure tunnels
[NASA-TP-2097] 20 p3388 N85-31010
Seat experiments for the full-scale transport aircraft controlled impact demonstration
[AD-A155024] 21 p3553 N85-32106
Energy efficient transport technology: Program summary and bibliography
[NASA-RP-1135] 22 p3729 N85-33116
Application of frequency domain handling qualities criteria to the longitudinal landing task
[NASA-TM-86728] 22 p3730 N85-33124
Development of an energy-absorbing passenger seat for a transport aircraft 22 p3796 N85-33515
Guidelines for the evaluation of visual approach slope indicators
[ARL/SYS-R-32] 23 p3896 N85-34132
Ground-based and in-flight simulator studies of flight characteristics of a twin-fuselage passenger transport airplane during approach and landing
[NASA-TP-2451] 23 p3898 N85-34144

TRANSPORT COEFFICIENTS
U TRANSPORT PROPERTIES

TRANSPORT PROPERTIES
NT ATMOSPHERIC CONDUCTIVITY
NT CARRIER MOBILITY
NT DIFFUSION COEFFICIENT
NT EDDY VISCOSITY
NT ELECTRICAL RESISTIVITY
NT ELECTRON MOBILITY
NT GAS VISCOSITY
NT GASEOUS DIFFUSION
NT GASEOUS SELF-DIFFUSION
NT HOLE MOBILITY
NT IONIC MOBILITY
NT IONOSPHERIC CONDUCTIVITY
NT KONDO EFFECT
NT MAGNETORESISTIVITY

NT PHOTOCONDUCTIVITY
NT PLASMA CONDUCTIVITY
NT SUPERCONDUCTIVITY
NT THERMAL CONDUCTIVITY
NT THERMAL DIFFUSIVITY
NT VISCOSITY

Plasma surface interactions in magnetic fusion systems
[DE84-015255] 01 p0123 N85-10842

Transport properties of multiphase systems
[DE84-015560] 02 p0173 N85-11159

Electrocatalysis of fuel cell reactions: Investigation of alternate electrolytes
[NASA-CR-174753] 02 p0222 N85-11455

Diffusion and intermittency in an extended one-dimensional maps 02 p0282 N85-11834

Stochasticity and transport in Hamiltonian systems
02 p0282 N85-11836

Fundamental electronic properties of donor-type graphite intercalated compounds
[AD-A146148] 03 p0326 N85-12099

Electrochemical and surface science research on fuel cells
[DE84-015962] 03 p0359 N85-12307

Static and quasielastic neutron scattering for the investigation of structure, dynamics and transport properties of lipid layers and lipid/protein compounds
03 p0432 N85-12753

Novel transport and recombination processes in semiconductors
[AD-A145989] 03 p0433 N85-12757

Transport processes during the growth of oxide films at elevated temperature
[AERE-R-11293] 03 p0434 N85-12766

High temperature thermoelectric energy conversion
05 p0610 N85-13894

Three dimensional global modeling of atmospheric CO2 05 p0652 N85-14189

Transport and relaxation processes in supercritical fluids
[DE84-006591] 05 p0731 N85-14698

Pathology and axonal transport in hexacarbon neuropathies
[AD-P004021] 06 p0843 N85-15355

Electronic transport processes in refractory metal silicides
[AD-A146495] 06 p0861 N85-15466

Preparation and electronic properties of MoS(2) and WS(2) single crystals grown in the presence of cobalt
[AD-A146508] 06 p0866 N85-15506

Strained-layer superlattice emitter and detector structures using modulation-doped active regions
[DE85-000064] 06 p0867 N85-15511

Anomalous electronic transport in boron carbides
[DE84-015620] 06 p0868 N85-15518

Transport properties and distribution functions in 3-5 semiconductors
[AD-A147525] 07 p1049 N85-16660

Computer program for calculation of complex chemical equilibrium compositions and applications. Supplement 1: Transport properties
[NASA-TM-86885] 07 p1049 N85-16663

Application of electrochemical engineering methods and theory to solving corrosion and adhesion problems with organic coatings
[AD-A147799] 08 p1129 N85-17115

The fundamentals of dislocation transport of hydrogen in bcc iron
[AD-A148143] 08 p1129 N85-17117

A research proposal for the theoretical study of the thermodynamic and transport properties of dense plasmas
[AD-A148040] 08 p1224 N85-17706

Resistivity of alloys
[DE85-000806] 09 p1296 N85-18136

Analysis of geohydrologic data by kriging
[AD-P004152] 09 p1349 N85-18488

Ionic and molecular transport in beta- and beta''-alumina
[DE85-000984] 09 p1360 N85-18580

Transport experiments in the Texas experimental Tokamak 09 p1369 N85-18741

Transport relaxation processes in supercritical fluids
[DE85-002076] 09 p1398 N85-18796

Transport properties of the outer crust of magnetic neutron stars 09 p1415 N85-18927

Finite-(beta) optimization of tandem mirrors
[DE85-002658] 10 p1560 N85-19835

Transport processes in the upper atmosphere
11 p1646 N85-20375

MCNP code
[DE85-002565] 11 p1702 N85-20705

TRACR3D: A model of flow and transport in porous/fractured media
[LA-9667-MS] 12 p1845 N85-21576

ELECT groundwater transport research code
[DE85-003284] 12 p1884 N85-21824

Stochastic convective-dispersive transport model for wastes disposed at the 106-mile ocean disposal site
[PB85-116176] 12 p1885 N85-21831

S3-3 ONR-118 data analysis
[AD-A149725] 12 p1889 N85-21855

User's guide for TWOHEX: A code package for two-dimensional, neutral-particle transport in equilateral triangular meshes
[DE85-004482] 12 p1930 N85-22125

The ASCOT Data Analysis Workshop
[DE85-004407] 13 p2139 N85-23283

Electrical and thermal transport property studies of high-temperature thermoelectric materials
[AD-A150167] 13 p2163 N85-23417

Transport properties of silica thermally grown on silicon
[AD-A150304] 13 p2163 N85-23418

Ion transporting composite membranes. 1: Nafion impregnated gore-tex
[AD-A151020] 14 p2252 N85-23980

Electrical and thermal transport property studies of high-temperature thermoelectric materials
[AD-A150900] 14 p2427 N85-24967

Transport studies of several novel organic conductors
[DE85-003950] 14 p2429 N85-24979

Experimental check of ion transport mechanism in Earth's radiation belt with exposure to nonsteady-state electric fields 15 p2480 N85-25306

Two-phase fluid thermal transport for spacecraft
[AD-A151316] 15 p2493 N85-25378

Mixing across a gas-gas interface
[AD-A151471] 15 p2556 N85-25770

Development of algorithms for using satellite meteorological data sets to study global transport of stratospheric aerosols and ozone
[NASA-CR-172540] 15 p2591 N85-25974

Polyamines as possible modulators of gravity induced calcium transport in plants 15 p2606 N85-26060

Electrical resistivity in amorphous metals: Consequences of phonon ineffectiveness in the diffraction model
[AD-A152130] 16 p2779 N85-27150

Computer program for the calculation of multicomponent convective diffusion deposition rates from chemically frozen boundary layer theory
[NASA-CR-168329] 16 p2781 N85-27164

Coupled plasma-neutral transport model for the scrape-off region
[DE85-007559] 16 p2868 N85-27695

Polycrystalline semiconductor heterojunction modelling (CdS/CuInSe(sub)2)
[DE85-002913] 16 p2871 N85-27713

Variability of short term eddy-correlation estimates of mass exchange
[PB85-172641] 18 p3138 N85-29431

Turbulent transport and length scale measurement experiments with comfined coaxial jets
[NASA-CR-174831] 19 p3265 N85-30245

Transport properties of Topopah Spring tuff
[DE85-010448] 19 p3270 N85-30278

Sand dispersion from an ephemeral river delta on the wave-dominated central California coast
[AD-A154352] 19 p3300 N85-30458

Monte Carlo electron/photon transport
[DE85-010799] 19 p3364 N85-30861

Hadley circulation in planetary atmospheres
20 p3546 N85-32067

Silicon refinement by chemical vapor transport
21 p3609 N85-32412

Influence of chemical form, feeding regimen, and animal species on the gastrointestinal absorption of plutonium
[DE85-010291] 21 p3662 N85-32751

Electrotransport in thin films
[AD-A155584] 21 p3710 N85-33034

The relation between the age of the subconducting slab and the recycling of sediments into the mantle
21 p3717 N85-33063

Comments on two matters related to turbulent combustion 22 p3743 N85-33204

New and revised methods of purifying mercuric iodide
[DE85-011684] 22 p3749 N85-33237

Estimation of Sr90 and Cs137 activity introduced and accumulation in the Po basin until 1983
[CISE-2515] 22 p3813 N85-33617

Subduction zone tectonic studies to develop concepts for the occurrence of sediment subduction
[DE85-011794] 22 p3815 N85-33632

Nuclear data for MCNP
[DE85-010794] 22 p3840 N85-33782

Proceedings of the US-Japan Workshop on Transport in Open-Ended Systems
[IPPJ-727] 23 p3975 N85-34644

Potential effect in transport due to non-axisymmetric confining field 23 p3975 N85-34645

Radial transport phenomena for TMX-upgrade
23 p3976 N85-34647

Induced azimuthal electric field effects on tandem transport and ambipolarity 23 p3976 N85-34650

Radial transport caused by collision
23 p3976 N85-34652

Bounce resonance heating and radial transport of electrons 23 p3977 N85-34655

Electron dynamics and transport in a mirror field
23 p3977 N85-34656

Azimuthal uniformity and current balance study of ICRH-produced plasma in RFC-XXM
23 p3977 N85-34659

Effect of ECH and ICH on ambipolar potential in NBT-1M 23 p3978 N85-34661

Transports studies of ECH and ICRH-heated bumpy torus plasma in NBT-1M 23 p3978 N85-34662

Workshop report on Simulation Techniques for Shock Wave Phenomena and Characteristics of Plasmas in Inertial Confinement Fusion
[IPPJ-725] 23 p3979 N85-34670

Helios 1 energetic particle observations of the solar gamma ray flare events of 7, 21 June 1980 and 3 June 1982
[SH-1.3-8] 23 p3993 N85-34755

Source energy spectra from demodulation of solar particle data by interplanetary and coronal transport
[SH-1.3-13] 23 p3994 N85-34756

Constraints of solar flare particle transport models from anisotropy observations at Voyager 1
[SH-3.1-8] 23 p4002 N85-34812

Radial transport of approximately 1 MeV/nucleon ions during the 22 November 1977 solar particle event
[SH-3.2-5] 23 p4003 N85-34821

Cosmic-ray transport in the galactic magnetosphere
[OG-7.2-17] 23 p4016 N85-34884

Subseasonal variability in a two-level atmospheric general circulation model 24 p4114 N85-35504

A strategy for calibrating atmospheric transport models
[CSIRO-DAR-TP-9] 24 p4116 N85-35518

Calculation of heavy-ion tracks in liquid water
[DE85-012101] 24 p4149 N85-35725

Beam intensity increases at the intense pulsed neutron source accelerator
[DE85-012377] 24 p4155 N85-35764

Neutral pumping rates for a next step tokamak ignition device
[DE85-012780] 24 p4157 N85-35776

TRANSPORT THEORY
NT CHAPMAN-ENSKOG THEORY
NT MIXING LENGTH FLOW THEORY

Solution of contaminant transport equations using an orthogonal-upstream finite element scheme
[DE84-014266] 01 p0070 N85-10469

Experimental observation of neoclassical currents
[DE84-015113] 01 p0122 N85-10834

A finite element projection method for the solution of particle transport problems with anisotropic scattering
[AD-A145382] 02 p0250 N85-11637

A simple transport model 02 p0284 N85-11653

On the co-variant formulation of the law of motion of passive particles in a field of turbulence
[REPT-564] 03 p0377 N85-12407

Proceedings of a Workshop on Atmospheric Research Needs for the Western United States
[DE84-015069] 04 p0534 N85-13412

Parallel processing of numerical transport algorithms
[DE84-016825] 04 p0555 N85-13534

Theoretical studies of Field-Reversed Configurations (FRC) and experimental study of the FRC during translation
[DE84-016467] 04 p0566 N85-13600

Fusion plasma theory. Task 3: ECRH and transport modeling in tandem mirrors and divertor physics
[DE84-014939] 04 p0567 N85-13612

Rotation of a tenuous plasma with a high toroidal velocity in a Tokamak
[DE84-012990] 04 p0567 N85-13615

Monte Carlo studies of transport in stellarators
[DE84-017633] 04 p0568 N85-13625

Theoretical investigations relevant to magnetic fusion research
[DE85-001777] 06 p0866 N85-15508

Hydrologic characteristics of the Mediterranean and Black Sea 07 p0981 N85-16238

The (20)Ne interaction in extended matter
[NASA-TM-86312] 07 p1061 N85-16739

Spectroscopic measurement on Heliotron E
09 p1387 N85-18722

Radial profiles of high resolution X-ray spectra from the Alcator C Tokamak 09 p1387 N85-18723

Applied mathematics of transport theory
[DE85-000846] 11 p1633 N85-20280

Finite element method for solving neutron transport problems
[DE85-001075] 11 p1722 N85-20829
ITS: The Integrated TIGER Series of coupled electron/photon Monte Carlo transport codes
[DE85-003719] 11 p1725 N85-20847
Magnetic fluctuations, field reversal maintenance, and anomalous thermal transport in the reversed field pinch
[DE85-003604] 11 p1732 N85-20892
Fluctuations and transport in fusion plasmas
[DE85-003612] 11 p1732 N85-20893
A linear characteristic-nodal transport method for the two-dimensional (X,Y)-geometry multigroup discrete ordinates equations over an arbitrary triangle mesh
[LA-10092-T] 12 p1913 N85-22008
Polar cap formation on Ganymede
13 p2174 N85-23486
Active Magnetospheric Particle Tracing Explorers (AMPTE)
[AD-A151072] 14 p2374 N85-24674
Synthetic acceleration of coarse-mesh S/sub n/ transport calculations
[DE84-014721] 14 p2409 N85-24855
Image formation in terms of the transport equation
[DE85-004993] 15 p2653 N85-26365
Limiting profiles in contaminant transport through porous media — ground water pollution
[REPT-84-31] 17 p2960 N85-28282
Projected discrete ordinates methods for numerical transport problems
[DE85-005632] 17 p3020 N85-28678
Augmented weighted diamond force of the linear nodal scheme for Cartesian coordinate systems
[DE85-005631] 17 p3020 N85-28679
Examination of a method for predicting the properties of railgun plasmas
[AR-004-322] 17 p3039 N85-28799
Electron multiple, plural and single scattering
[DE85-010325] 18 p3181 N85-29721
Low plasma edge temperatures for the self-pumped limiter
[DE85-010155] 18 p3189 N85-29782
MCNP: A general Monte Carlo code for neutron and photon transport
[DE85-010764] 19 p3348 N85-30753
Low-discrepancy point sets in transport codes
[DE85-010786] 19 p3348 N85-30755
Toroidal viscosity and ambipolarity in the neoclassical transport theory of axisymmetric tori
[DE85-010622] 19 p3358 N85-30820
A new slab geometry radiation transport differencing scheme
[DE85-006681] 19 p3366 N85-30874
Monte Carlo learning-biasing experiment with intelligent random numbers
[DE85-010713] 22 p3834 N85-33742
Collisional transport for a superthermal ion species in a plasma
[DE85-011943] 22 p3845 N85-33818
Theoretical and computational research on the focused transport of intense charged particle beams
[DE85-0129[illegible]] 23 p3972 N85-34621
Why do leaky-box models work so fine?
[OG-7.2-8] 23 p4014 N85-34877
Exact solutions for sporadic acceleration of cosmic rays
[OG-8.3-7] 23 p4022 N85-34925
Relativistic transport theory for cosmic-rays
[OG-8.3-8] 23 p4022 N85-34926
TRANSPORT VEHICLES
Test methods for cable cars
[CETIM-1-5K-45-1] 04 p0515 N85-13282
TRANSPORTATION
NT AIR TRANSPORTATION
NT CHALLENGER (ORBITER)
NT COLUMBIA (ORBITER)
NT DISCOVERY (ORBITER)
NT ENTERPRISE (ORBITER)
NT MARINE TRANSPORTATION
NT RAIL TRANSPORTATION
NT SPACE SHUTTLE BOOSTERS
NT SPACE SHUTTLE MISSION 31-C
NT SPACE SHUTTLE MISSION 41-B
NT SPACE SHUTTLE MISSION 41-C
NT SPACE SHUTTLE MISSION 41-G
NT SPACE SHUTTLE MISSION 51-A
NT SPACE SHUTTLE MISSION 51-C
NT SPACE SHUTTLE MISSIONS
NT SPACE SHUTTLE ORBITERS
NT SPACE TRANSPORTATION
NT SPACE TRANSPORTATION SYSTEM
NT URBAN TRANSPORTATION
Summary of activities pertaining to utilization of grant purchase of batteries for electric van
[DE84-015793] 02 p0195 N85-11305
USSR report: Transportation
[JPRS-UTR-84-029] 03 p0310 N85-12002
Proceedings of a Workshop on the Applications of Tethers in Space, Volume 1
[NASA-CR-171196] 03 p0322 N85-12076
Proceedings of a Workshop on Applications of Tethers in Space, Volume 2
[NASA-CR-171197] 03 p0322 N85-12077
ECUT energy data reference series: Lightweight materials for ground transportation
[DE84-015269] 05 p0621 N85-13974
Determining training device requirements in Army aviation systems 05 p0711 N85-14556
Risks in the transport and storage of liquefied natural gas. Sub-project 5-2: Investigation into building damage
[BLL-RISLEY-TR-4606-(9091.9F)]
07 p0935 N85-15926
USSR report: Transportation
[JPRS-UTR-85-001] 08 p1067 N85-16763
USSR report: Transportation
[JPRS-UTR-85-003] 09 p1277 N85-18032
The Hazardous Materials Technical Center
[AD-P004149] 09 p1349 N85-18485
Electric-Hybrid Vehicle (E-HV) demonstration-test project
[DE85-002370] 10 p1570 N85-19899
Transportation
[JPRS-UTR-85-004] 12 p1769 N85-21105
Current development, applications of airships in USSR
12 p1769 N85-21109
USSR report: Transportation
[JPRS-UTR-84-015] 15 p2460 N85-25192
US Army human Engineering Laboratory Communications Survey: A Pilot Study (HELCOMS-PS)
[AD-A151434] 15 p2521 N85-25544
Structures and Dynamics Division research and technology plans for FY 1985 and accomplishments for FY 1984
[NASA-TM-86417] 15 p2577 N85-25895
USSR report: Transportation
[JPRS-UTR-84-025] 17 p2894 N85-27841
Test devices for aeronautical research and technology
[NASA-TM-77651] 17 p2905 N85-27914
Tribological sinks: Money down the drain
[DE85-010019] 17 p2974 N85-28376
Microcomputers in transportation: Software and source book, February 1985
[PB85-181022] 20 p3517 N85-31886
Shuttle car loading system
[NASA-CASE-NPO-15949-1] 23 p3987 N85-34722
TRANSPORTATION ENERGY
Hybrid propulsion technologies for urban bus transit
[PB85-157469] 16 p2860 N85-27773
TRANSPORTATION NETWORKS
Relationship between forest clearing and biophysical factors in tropical environments: Implications for the design of a forest change monitoring approach — Costa Rica
[E85-10051] 07 p0983 N85-16247
Microwave methods for paving
[DE85-004194] 14 p2265 N85-24032
Information technology applications in voluntary sector transport operations. SP1: Objectives and programme of work
[TT-8501] 15 p2667 N85-26457
Design and implementation of an interactive route editor 23 p3962 N85-34559
TRANSPORTER
An air-breathing ballistic space transporter for Europe
[NASA-TM-77645] 12 p1792 N85-21244
TRANSURANIUM ELEMENTS
NT AMERICIUM
NT AMERICIUM ISOTOPES
NT AMERICIUM 241
NT CALIFORNIUM ISOTOPES
NT CURIUM
NT CURIUM 244
NT PLUTONIUM
NT PLUTONIUM ISOTOPES
NT PLUTONIUM 238
NT PLUTONIUM 239
Volume compressibilities of transuranium elements compounds, especially of neptunium compounds
03 p0431 N85-12744
TRU decontamination of high-level PUREX waste by solvent extraction using a mixed octyl(phenyl)-N,N-diisobutyl-carbamoyl methylphosphine oxide/TBP/NPH (TRUEX) solvent
[DE85-010251] 19 p3235 N85-30054
Apparatus and method for identification of matrix materials in which transuranic elements are embedded using thermal neutron capture gamma-ray emission
[DE85-011659] 22 p3786 N85-33454
TRANSVERSE ACCELERATION
Axisymmetrical oscillations of shell systems subjected to impulse loads 13 p2047 N85-22614
Relation between gamma-ray family and EAS core: Monte-Carlo simulation of EAS core
[HE-3.6-7] 24 p4185 N85-35955
Structured events in Pamir carbon X-ray chambers
[HE-3.7-7] 24 p4186 N85-35965
Structure of air shower disc near the core
[HE-4.7-2] 24 p4198 N85-36053
TRANSVERSE OSCILLATION
A Galerkin method for the estimation of parameters in hybrid systems governing the vibration of flexible beams with tip bodies
[NASA-CR-172537] 10 p1544 N85-19734
TRANSVERSE VIBRATION
U TRANSVERSE OSCILLATION
TRANSVERSE WAVES
Acoustoelectric interaction in double-layer semiconductors 06 p0786 N85-15023
Quantitative acoustic emission techniques
[AERE-R-11262] 07 p0977 N85-16203
Tunable microwave transversal filters
[AD-A148370] 08 p1158 N85-17304
Automated TEM (Transverse electromagnetic) cell calibration system
[PB85-134377] 11 p1638 N85-20319
Explosive transverse electric field and particle acceleration during magnetic collapse — cosmic plasma
12 p1956 N85-22202
Surface acoustic wave structure and volume waves
15 p2525 N85-25568
Transverse periodic boundary conditions in molecular dynamics with uniaxial strain shock waves
[DE85-006497] 16 p2863 N85-27656
Guided-mode launching in a slab waveguide by way of diffraction at the edge of a conducting screen residing on one surface of the slab
[AD-A154686] 21 p3575 N85-32232
Transverse momentum distribution of pion deg in the fragmentation region of super high energy interactions
24 p4180 N85-35921
Radio wave emitted by an extensive air showers in 10KHz to 1MHz region
[HE-4.6-15] 24 p4198 N85-36051
TRANSVERSELY EXCITED ATMOSPHERIC LASERS
U TEA LASERS
TRAPATT DIODES
U AVALANCHE DIODES
TRAPPED MAGNETIC FIELDS
Simulation of the ion-beam-driven drift instability in a magnetic trap, 1
[AD-A149451] 10 p1452 N85-19147
Simulation of the ion-beam-driven drift instability in a magnetic trap, 2
[AD-A149452] 10 p1554 N85-19798
Beam trapping in high current cyclic accelerators with strong focusing fields
[AD-A151392] 15 p2648 N85-26331
TRAPPED PARTICLES
NT INNER RADIATION BELT
NT MAGNETICALLY TRAPPED PARTICLES
NT OUTER RADIATION BELT
NT PROTON BELTS
NT RADIATION BELTS
Laser cooling and trapping of neutral atoms
[AD-A146046] 03 p0366 N85-12345
Charge trapping in low temperature MOS (Metal-Oxide-Silicon) oxides
[AD-A146450] 06 p0860 N85-15467
Simulation of the ion-beam-driven drift instability in a magnetic trap, 2
[AD-A149452] 10 p1554 N85-19798
SCATHA (spacecraft charging at high altitudes) plasma interaction experiment: SC-3 high energy particle spectrometer; SC-8 energetic ion composition experiment
[AD-A149728] 12 p1793 N85-21252
S3-3 ONR-118 data analysis
[AD-A149725] 12 p1869 N85-21855
Intermolecular energy transfer between the individual zero-field levels of triplet traps in an orientationally disordered solid
[AD-A150751] 14 p2417 N85-24914
Reduction of the trapping of positrons in dislocated single crystals of iron when charged with hydrogen
[DE85-010235] 19 p3377 N85-30950
Proton ring trapping in a magnetic mirror
20 p3534 N85-31990
CYLTRAN calculations of electron effects on XD detectors
[LA-10264-MS] 23 p3969 N85-34601
HgCdTe surface and defect study program
[AD-A156079] 24 p4161 N85-35799
TRAPPING
Trapping for Newtonian diffusion processes
[REPT-73] 01 p0130 N85-10893

Effect of microstructure and trapping on the hydrogen embrittlement susceptibility of a titanium bearing HSLA steel 02 p0174 N85-11166
Impurity trapping during gas phase epitaxy of gallium arsenide 02 p0257 N85-11686
Deceleration, cooling, and trapping of atoms
[AD-A146234] 03 p0418 N85-12672
Mobility and trapping time measurements in HgI2
[DE84-016954] 06 p0869 N85-15522
Effect of microstructure and trapping on the hydrogen embrittlement susceptibility of a ti-bearing HSLA steel
[AD-A148610] 08 p1130 N85-17122
Hydrogen trapping, diffusion, and recombination in austenitic stainless steels
[DE85-001871] 09 p1294 N85-18129
Effect of hydrostatic pressure on trapping centers in strained-layer superlattice structures
[DE85-001362] 09 p1399 N85-18807
Enhanced diffusion from interstitial trapping during solid-phase-epitaxial growth of silicon alloys
[DE85-001285] 12 p1941 N85-22193
Trapping model analysis of annihilation line narrowing in some plastically deformed metals and alloys
[AERE-R-10593] 14 p2258 N85-23995
Energy trapping, release, and transport in three-dimensional energetic solids and molecular crystals: Theory of defects and impurities
[AD-A151071] 14 p2428 N85-24973
Frequency and time standards based on stored ions
18 p3105 N85-29223
Theory of positron annihilation in vacancies in concentrated disordered alloys
[DE85-010267] 18 p3183 N85-29734
Carrier loss in dispersive transport in amorphous semiconductors
[DE85-009122] 18 p3194 N85-29811
Trapping of ion conics by downward parallel electric fields
[AD-A155306] 21 p3633 N85-32568

TRAPS
Electron traps in the GaAs permeable base transistor
[AD-A145399] 02 p0267 N85-11871
Characterization of ion implanted deuterium traps in nickel by equilibration with deuterium gas
[DE84-014958] 02 p0288 N85-11879
Deceleration, cooling, and trapping of atoms
[AD-A146234] 03 p0418 N85-12672
Forces on neutral atoms due to electromagnetic fields
[AD-A146984] 07 p1040 N85-16803
Theoretical issues involving traps for neutral spin-polarized atoms
[AD-A148035] 08 p1220 N85-17682

TRAVELING IONOSPHERIC DISTURBANCES
Medium- and large-scale wave disturbances and heterogeneities of electron concentration in outer ionosphere in middle and low latitudes
06 p0825 N85-15241
Dispersion properties of moving ionospheric perturbations 07 p0952 N85-16036
On the dynamics of the westward traveling surge
14 p2364 N85-24607

TRAVELING SALESMAN PROBLEM
Statistical analysis of some traveling salesman algorithms
[AD-A145766] 03 p0410 N85-12620
The traveling salesman problem on a graph and some related integer polyhedra
[AD-A147953] 08 p1211 N85-17621
Local search in routing problems with time windows
[CWI-OS-R8409] 12 p1922 N85-22075

TRAVELING SOLVENT METHOD
Automatic Monoellipsoidal Mirror Furnace Facility (AMMFF), volume 1 — spaceborne crystal growth
[AMF-RP.100-DS-015-VOL-1] 09 p1265 N85-18073

TRAVELING WAVE MASERS
Millimeter-wave range masers: A review
13 p2089 N85-23042
Propagation and amplification of Ion Cyclotron Waves (ICW's) in a multicomponent plasma. The Earth magnetosphere as a giant maser for Alfven waves
14 p2366 N85-24634

TRAVELING WAVE MODULATION
Advanced infrared laser modulator development
[NASA-CR-172479] 06 p0862 N85-15479

TRAVELING WAVE TUBES
NT HELITRONS
Dual (GaAl) As-heterostructure based injection laser traveling wave amplifier 02 p0261 N85-11708
Spectrally matched modulation of radiation of injection laser in traveling-wave amplifier below 2 GHz
02 p0262 N85-11712
Millimeter-wave travelling-wave IMPATT diode
[AD-A146545] 06 p0804 N85-15117
Development of a 30 GHz/1 kW broadband traveling wave tube with suppression of band edge oscillations
[BMFT-FB-W-84-035] 07 p0948 N85-16011
Traveling wave tube for broadcast satellites
10 p1475 N85-19310
Design of low loss helix circuits for interference fitted and brazed circuits
[NASA-CR-168313] 10 p1478 N85-19328
Construction techniques of a molecular hydrogen laser
[AD-A152929] 17 p2970 N85-28343

TRAVELING WAVES
NT SOLITARY WAVES
On the asymptotic analysis of travelling shocks and phase boundaries in elastic bars
[AD-A147239] 07 p0959 N85-16076
Performance ranges of helical antenna made of conductor with extra bends 12 p1836 N85-21536
Behavior of small ferromagnetic particles in travelling magnetic field 12 p1843 N85-21584
Reflected wave travel-time curves in stratified media with vertically heterogeneous layers and slightly sloping curved boundaries 13 p2114 N85-23167
Dynamic response of shells and plates subjected to variable magnitude traveling loads
16 p2796 N85-27250
Experiments on the influence of active walls on the initial amplitudes and growths of instability waves
[AD-A154630] 21 p3583 N85-32275

TRAYS
A robotic system for preparing reagent and dilution vials
[DE85-008262] 16 p2793 N85-27231

TREADS
Improvements in tank tread assemblies
[NASA-CASE-NPO-16321-1] 18 p3117 N85-29291

TREE RING DATING
U DENDROCHRONOLOGY

TREES (MATHEMATICS)
NT FAULT TREES
Model-based probabilistic reasoning for electronics troubleshooting
[AD-P003937] 02 p0247 N85-11617
Synthesis of tree-structured computing systems through use of closures
[AD-A150502] 13 p2147 N85-23326
Parallel update of minimum spanning trees in logarithmic time
[AD-A150497] 13 p2151 N85-23357
The Kappa sub n property in small Omega sub 1 trees
14 p2413 N85-24885
Generation and termination of binary decision trees for nonparametric multiclass classification
[AD-A151361] 15 p2640 N85-26283
Investigation and implementation of a tree transformation system for user friendly programming
[AD-A152716] 17 p3011 N85-28617
Embedding graphs in lines, trees and grids
19 p3334 N85-30652
A theoretical and empirical analysis of coherent ray-tracing 23 p3957 N85-34524
A new approach to linear quadtrees
23 p3961 N85-34550

TREES (PLANTS)
NT CONIFERS
NT DECIDUOUS TREES
Nonparametric analysis of Minnesota spruce and aspen tree data and LANDSAT data 07 p0984 N85-16253
Simulating responses to expected climate change in eastern North America: Applications to decision-making in the forest industry
[DE85-001272] 07 p1006 N85-16406
UHF radiowave propagation through forests
[AD-A149518] 10 p1467 N85-19256
Response of unmanaged forests to CO2-induced climate change: Available information, initial tests and data requirements
[DOE/NSB-0053] 12 p1883 N85-21817
Combined effects of atmospheric deposition, internal acid production, and harvesting on nutrient gains and losses from forest ecosystems
[DE85-002325] 12 p1884 N85-21821
Areas with forest soils sensitive to acidic deposition under alternative damage hypotheses
[DE85-005257] 13 p2130 N85-23257
Use of forest modeling to project acid rain effects
[DE85-005251] 16 p2821 N85-27400
Interactive effects of acid rain and gaseous air pollutants on natural terrestrial vegetation
[DE85-005255] 16 p2821 N85-27401
Screening Prosopis (mesquite) species for biofuel production on semi-arid lands
[DE85-010048] 19 p3302 N85-30471
Insights into the phylogenetic positions of photosynthetic bacteria obtained from 5S rRNA and 16S rRNA sequence data 21 p3658 N85-32719
Effects of acid rain on forest nutrient status
[DE85-012486] 23 p3947 N85-34463

TREMORS
Study of earthquake preparation processes from distribution of weak tremor epicenters
14 p2345 N85-24501

TRENDS
Future directions in operations research
[REPT-84-24] 17 p3026 N85-28711
Avionics and civil aircraft systems: The present and the future
[SNIAS-851-111-104] 20 p3392 N85-31038
Evolution of spacecraft design methods as a function of environmental and geometrical constraints
[ESA-CR(P)-2012] 20 p3418 N85-31216

TRESCA FLOW
Removal of singularities in Tresca and Mohr-Coulomb yield functions
[OUEL-1526/84] 03 p0413 N85-12642

TRIAMINOGUANIDINIUM AZIDE
The crystal and molecular structure of a new propellant compound: Triaminoguanidium Azide Nitrate (TAZN)
13 p2002 N85-22551

TRIAMINOTRINITROBENZENE
U TATB

TRIANGULAR WINGS
U DELTA WINGS

TRIANGULATION
A triangular finite element for thin plates and shells
01 p0058 N85-10398
The 1980 diagnostic adjustment of the German main triangulation network. 4: Network adjustment (part 3)
[SER-B-267-PT-3-MITT-168] 11 p1665 N85-20494
The 1980 diagnostic adjustment of the German main triangulation network. 4: Network adjustment (part 1)
[SER-B-267-PT-1-MITT-168] 11 p1670 N85-20525
The 1980 diagnostic adjustment of the German main triangulation network. 4: Network adjustment (part 2)
[SER-B-267-PT-2-MITT-168] 11 p1670 N85-20528
The 6 pi-periodic solutions of plane restricted elliptical 3-body problem in neighborhood of libration points
16 p2718 N85-26779
Standards and specifications for geodetic control networks
[PB85-166478] 16 p2816 N85-27374

TRIAXIAL STRESSES
Creep deformation of compacted decomposed granite soils 09 p1303 N85-18187
Influence of grain size distribution on the undrained dynamic properties of saturated sand
[PB85-102382/GAR] 09 p1305 N85-18197

TRIAXIALITY
U TRIAXIAL STRESSES

TRIBOLOGY
Plasma variables and tribological properties of coatings in low pressure (0.1 - 10.0 torr) plasma systems
[NASA-TM-83796] 02 p0189 N85-11281
Microscopic aspects of the effect of friction reducers at the lubrication limit
[NASA-TM-77413] 03 p0367 N85-12354
Roller crosshead analysis 04 p0507 N85-13229
The European Space Tribology Laboratory (ESTL) activities report
[ESA-ESTL-61] 05 p0646 N85-14146
Effect of asperity interactions on scuffing
[AD-A146544] 06 p0814 N85-15170
Tribological properties of graphite-fiber-reinforced, partially fluorinated polyimide composites
[NASA-TM-86826] 09 p1296 N85-18153
Effect of implantation species on the tribological response of stainless steel surfaces
[DE85-003530] 10 p1493 N85-19432
The role of silver in self-lubricating coatings for use at extreme temperatures
[NASA-TM-86943] 11 p1611 N85-20127
Tribological properties of boron nitride synthesized by ion beam deposition
[NASA-TM-86962] 12 p1810 N85-21355
Tribological systems as applied to aircraft engines
[NASA-TM-86965] 12 p1858 N85-21857
Thermal and thermoelastic effects in rolling/sliding contacts
[AD-A150435] 13 p2165 N85-23429
Gears and Power Transmission Systems for Helicopters and Turboprops
[AGARD-CP-369] 14 p2220 N85-23765
Chemical-mechanical interaction in gears
14 p2223 N85-23785
Wear reduction by lubricants in confined contacts
14 p2223 N85-23786
Summaries of FY 1984 engineering research
[DE85-006273] 15 p2664 N85-26442
Effect of counterface material type and its topography on the tribological properties of polyimide composites
[NASA-TM-87036] 16 p2754 N85-26983
Tribological sinks: Money down the drain
[DE85-010019] 17 p2974 N85-28376

European Space Tribology Laboratory: Facilities, services, capabilities
[ESA-BR-12] 20 p3398 N85-31080

Activities report of the European Space Tribology Laboratory
[ESA-ESTL-66] 20 p3484 N85-31653

Hertzian contact in two and three dimensions
[NASA-TP-2473] 21 p3596 N85-32331

Aluminum work function: Effect of oxidation, mechanical scraping and ion bombardment
[NASA-TM-87079] 23 p3915 N85-34265

TRICHLORIDES
U CHLORIDES

TRIGGER CIRCUITS

Low jitter trigger for an excimer laser
[DE85-005732] 13 p2097 N85-23080

Construction techniques of a molecular hydrogen laser
[AD-A152628] 17 p2970 N85-28343

Coordinated research program in pulsed power physics
[AD-A154629] 21 p3679 N85-32858

Fast shutter apparatus
[DE85-006501] 23 p3926 N85-34343

Synchronous timing of multi-energy fast beam extraction during a single AGS cycle
[DE85-011629] 24 p4158 N85-35781

Arrival time distributions of electrons in air showers with primary energies above 10 (18)eV observed at 900m above sea level
[HE-4.7-5] 24 p4199 N85-36056

Methods for roof-top mini-arrays
[HE-4.7-7] 24 p4199 N85-36058

Progress report on a new search for free e/3 quarks in the cores of 10(15) - 10(16) eV air showers
[HE-6.2-15] 24 p4212 N85-36151

TRIGGERS
U ACTUATORS

TRIGONOMETRIC FUNCTIONS
NT TANGENTS

TRIM (BALANCE)
U AERODYNAMIC BALANCE

TRIMERS

Polymerization and halogen scrambling behavior of phenyl-substituted cyclotriphosphazenes
[AD-A146366] 06 p0771 N85-14930

Theoretical research program to study transition metal trimers and embedded clusters
[NASA-CR-174298] 08 p1125 N85-17093

TRIMETHYL COMPOUNDS

Effects of heteroatom substituents on the properties of 1,2-dioxetanes
[AD-A148727] 09 p1290 N85-18100

TRINITROTOLUENE

Treatment of wastewater (red water) resulting from TNT (trinitrotoluene) purification
[AD-P004148] 09 p1348 N85-18482

Voltammetric analysis of ordnance materials. Part 2: A portable digital voltammeter for use with a silver wire working electrode
[AD-A152480] 17 p2967 N85-28325

Toxicity of TNT wastewaters to aquatic organisms. Volume 4: Chronic toxicity of 2,4-dinitrotoluene and condensate water
[AD-A153536] 18 p3132 N85-29400

TRINITROTRIAZOCYCLOHEXANE
U RDX

TRIODES

Textured carbon surfaces on copper
[NASA-CASE-LEW-14130-1] 11 p1615 N85-20156

Multi-channel pulser for the SLC thermionic electron source
[DE85-014222] 24 p4160 N85-35792

TRIPHENYLS

Stable polymeric carbon radicals. Part 2: Attempts at the preparation of polyradicals of the triphenylmethyl type linked by P-phenylene units
[NASA-TM-77799] 10 p1450 N85-19134

TRIPLE AXIS SPECTROMETERS
U NEUTRON SPECTROMETERS

TRIPLET EXCITATION
U ATOMIC ENERGY LEVELS

TRIPLET STATE
U ATOMIC ENERGY LEVELS

TRIPROPELLANTS
U LIQUID ROCKET PROPELLANTS

TRITIUM

Blanket materials for fusion reactors: Comparisons of thermochemical performance
[DE84-016240] 04 p0568 N85-13622

Evaluation of arctic test of improved tritium radioluminescent lighting
[DE84-014867] 05 p0597 N85-13805

Tritium catalyzed deuterium Tokamaks
[DE85-004825] 12 p1936 N85-22166

Scientific activities. A: Reacting plasma physics. 1: Introduction and overview 15 p2654 N85-26370

Two-dimensional TBR calculations for conceptual compact reversed-field pinch reactor blanket
[DE85-007636] 17 p3040 N85-28812

Use of environmental health-risk analysis for managing toxic substances
[DE85-008964] 18 p3160 N85-29574

New concept for a wall detector for alpha particles
[DE85-009037] 18 p3183 N85-29740

Modeling and experiments on tritium permeation in fusion reactor blankets
[DE85-008439] 18 p3183 N85-29741

Counter current extraction system for tritium recovery from 17Li-83Pb
[DE85-010519] 19 p3240 N85-30090

Quantitative passive technique for assay of near-surface tritium in materials
[DE85-010661] 19 p3360 N85-30833

Tritium system design for the mirror reactors FPD-1, FPD-2 and FPD-3
[DE85-010490] 19 p3363 N85-30852

Current state of development and expected performance of copper-lithium alloys as an impurity control system in fusion applications
[DE85-009673] 19 p3372 N85-30917

Tables of generalized hydrogen diffusion profiles and permeating fluxes for fusion applications
[DE85-008876] 19 p3372 N85-30919

MFTF-(alpha) + T shield design
[DE85-010496] 20 p3529 N85-31948

Tritium technology review
[DE85-010504] 21 p3703 N85-33006

Tritium-helium effects in metals
[DE85-011507] 22 p3749 N85-33235

Environmental surveillance at Los Alamos during 1984
[DE85-011886] 22 p3811 N85-33605

The 1984 environmental monitoring report, Sandia National Laboratories, Albuquerque, New Mexico
[DE85-011175] 22 p3811 N85-33607

Technology of off-gas treatment for liquid-fed ceramic melters
[DE85-012467] 22 p3812 N85-33610

Global environmental transport models for tritium
[DE85-011437] 22 p3816 N85-33639

Ultraviolet radiation-damage absorption peak in solid deuterium-tritium, revision 1
[DE85-012969] 22 p3844 N85-33806

Key issues of fusion nuclear technology development (FINESSE)
[DE85-012599] 22 p3845 N85-33817

Compact DT fusion spherical tori at modest field
[DE85-011566] 23 p3982 N85-34692

Tritium hazard via the ingestion pathway
[DE85-012897] 24 p4133 N85-35618

TRITON

Physical properties of Neptune and Triton inferred from the Orbit of Triton 02 p0300 N85-11942

Physical properties of the satellites of Neptune
02 p0300 N85-11945

Seasonal variations in Triton's atmospheric mass and composition 02 p0301 N85-11948

Research in planetary studies and operation of Mauna Kea Observatory
[NASA-CR-175618] 13 p2169 N85-23460

On the origin of Triton and Pluto
13 p2175 N85-23497

TRIVALENT IONS

Trivalent ion exchange in beta alumina
[AD-A145373] 02 p0172 N85-11151

Trivalent cerium doped crystals as tunable laser systems: Two bad apples
[DE85-008168] 22 p3790 N85-33482

TROILITE

The low-energy secondary cosmic ray flux: Detectors in iron meteorites 06 p0887 N85-15635

TROMBE WALLS

Short duration winter-time performances of different passive solar systems
[DE85-000650] 11 p1675 N85-20557

Thickness-insensitive selective surface paint
[DE85-010566] 19 p3250 N85-30150

Performance analysis of mixed passive solar heating systems
[DE85-009624] 21 p3613 N85-32455

TROPICAL METEOROLOGY

Planetary scale interactions 05 p0684 N85-14397

Diagnostics of rainfall anomalies in the nordeste during the global weather experiment 05 p0685 N85-14405

Frequency and motion of western North Pacific tropical cyclones
[PB85-106466/GAR] 06 p0839 N85-15331

Ocean and climate, an example. The interannual variability of the tropical Pacific Ocean
07 p1002 N85-16365

The ocean and the dynamics of the tropical atmosphere: its possible predicability 07 p1002 N85-16366

The Amazon and climate 07 p1003 N85-16376

Meridional penetration of frontal systems in South America and its relation to organized convection in the Amazon
[INPE-3407-PRE/676] 10 p1518 N85-19572

Accuracy of typhoon center determined by GMS imagery 12 p1894 N85-21887

Tropical Oceans-Global Atmosphere (TOGA) experiment planning for the Brazilian participation in TOGA global climate program
[INPE-3499-PRE/735] 16 p2834 N85-27477

Tropical ozone: Seasonal variations in the troposphere at 6 deg S
[INPE-3555-PRE/766] 19 p3313 N85-30535

Mariners weather log, volume 29, number 1, winter 1985
[PB85-177483] 19 p3318 N85-30570

Mariners weather log, volume 28, number 4, fall 1984
[PB85-178408] 19 p3318 N85-30571

Southern oscillation/El Nino excitation of the Earth's Chandler wobble 20 p3490 N85-31686

Forecast of Atlantic seasonal hurricane activity for 1985 20 p3495 N85-31732

Tropical Ocean and Global Atmosphere (TOGA) heat exchange project: A summary report
[NASA-CR-176038] 20 p3496 N85-31738

TROPICAL REGIONS
NT AMAZON REGION (SOUTH AMERICA)

Resonance model of Pc3 in subtropical regions — geomagnetism 04 p0520 N85-13323

Monthly and seasonal climatology over the global tropics and subtropics for the decade 1973 to 1983. Volume 1: 200 mb winds
[AD-A146521] 06 p0838 N85-15322

Razrezy program research in the tropical Atlantic
07 p0981 N85-16229

Relationship between forest clearing and biophysical factors in tropical environments: Implications for the design of a forest change monitoring approach — Costa Rica
[E85-10061] 07 p0983 N85-16247

Natural exposure versus chamber simulation
[AD-A149538] 10 p1495 N85-19437

Slow motions in the tropical troposphere
13 p2131 N85-23262

A theoretical study of the ozone quasi-biennial oscillation in the tropical stratosphere 13 p2132 N85-23264

Cumulus effects on the large-scale vorticity and momentum fields in the tropical atmosphere
13 p2137 N85-23270

Surface currents in the tropical Pacific during 1979-1980 using drifting buoys 14 p2323 N85-24354

The Tropical Ocean and Global Atmosphere program (TOGA) 14 p2330 N85-24411

Deuteron whistlers at low latitudes in the low altitude topside ionosphere 14 p2366 N85-24625

Low-latitude ducted whistlers observed at Sanya, Hainan, China 14 p2367 N85-24626

Whistler observation at Okinawa, Japan during the IMS 14 p2367 N85-24627

Biophysical evaluation of the wet globe temperature index (Botsball) at high air movements and constant dew point temperature
[AD-A151065] 14 p2378 N85-24683

Chemical, biological, and physical measurements from the subtropical western North Atlantic Ocean. Summer 1982, USNS Lynch, cruise 710-82
[AD-A153823] 18 p3201 N85-29857

Tropical ozone: Seasonal variations in the troposphere at 6 deg S
[INPE-3555-PRE/766] 19 p3313 N85-30535

An examination of the Southern Oscillation in the upper troposheric tropical and subtopical wind field
20 p3488 N85-31680

Moist barotropic instability in the tropics
20 p3489 N85-31683

Aircraft observations of condensation and ice nuclei at a tropical station 21 p3640 N85-32613

Formation of particles in the air of the humid tropical forests 21 p3644 N85-32639

A statistical study of CCN concentration in subequatorial climate: The particular case of the tropical wet forest
21 p3649 N85-32673

Properties of forest derived cloud condensation nuclei
21 p3650 N85-32682

Sulfates in marine aerosols over the tropical Western Pacific Ocean 21 p3651 N85-32690

Observation of energy spectrum of electron albedo in low latitude region at Hyderabad, India
[SH-6.1-7] 23 p4045 N85-35081

Proton albedo spectrum observation in low latitude region at Hyderabad, India
[SH-6.1-8] 23 p4045 N85-35082

Mean cloudiness over the global tropics from satellite observations
[AD-A156188] 24 p4123 N85-35561

TROPICAL STORMS
NT HURRICANES
NT TYPHOONS
Digital radar data as an aid in nowcasting in Hong Kong 01 p0079 N85-10525
Statistical tropical cyclone forecasting techniques for the Southern Hemisphere
[AD-A144752] 01 p0085 N85-10569
A tropical cyclone precipitation estimation technique using geostationary satellite data
[PB84-226703] 01 p0086 N85-10579
Summary of 1984 Atlantic seasonal tropical cyclone activity and verification of author's forecast
03 p0395 N85-12520
A possible mechanism for the diurnal oscillations of tropical cyclones 09 p1356 N85-18530
Tropical cyclone data tape for the Eastern and Central North Pacific Basins, 1949-1983: Contents, limitations and uses
[PB85-110054] 10 p1520 N85-19585
Intensification of tropical instabilities
[AD-A149985] 12 p1896 N85-21899
Mesoscale Atmospheric Processes Research Program Science Review
[NASA-TM-87486] 15 p2594 N85-25987
Monitoring tropical cyclone growth using GOES VISSR/VAS and Nimbus-7 TOMS data
15 p2595 N85-25989
Convection modeling and application to severe storms
15 p2595 N85-25991
Forecast of Atlantic seasonal hurricane activity for 1985 16 p2833 N85-27470
Technique that uses satellite, radar, and conventional data for analyzing and short-range forecasting of precipitation from extratropical cyclones
[PB85-164994] 16 p2837 N85-27499
Characteristics of North Indian Ocean tropical cyclone activity
[AD-A153085] 17 p2997 N85-28524
Forecasting of tropical cyclone motion using an EOF (Empirical Orthogonal Function) representation of wind forcing
[AD-A155034] 21 p3636 N85-32580
TROPICS
U TROPICAL REGIONS
TROPISM
NT GEOTROPISM
NT GRAVITROPISM
Polyamines as possible modulators of gravity induced calcium transport in plants 15 p2606 N85-26060
Calcium and calmodulin localization in gravitropically-responding plant organs
15 p2606 N85-26061
Role of Ca++ in shoot gravitropism — avena
15 p2607 N85-26065
Gravistimulus production in roots of corn
15 p2607 N85-26066
A possible explanation of why gravitropic growth is detected earlier than straight growth
15 p2607 N85-26067
Gravitropism in leafy dicot stems
15 p2610 N85-26086
Mutant peas as probes in the understanding of growth and gravitropism 15 p2611 N85-26088
TROPOPAUSE
Applications of TOMS ozone data and clustering techniques in satellite soundings
05 p0681 N85-14379
Applications of fuzzy clustering techniques to stratified by tropopause MSU temperature retrievals
18 p3141 N85-29444
Comparison of tropopause altitude determination by the Platteville Radar, Sunset Radar and the NWS Rawinsonde 21 p3617 N85-32477
Practical use of a tropopause height determination algorithm on an MST radar data set, part 1.8B
21 p3618 N85-32479
The Ponape ST radar 21 p3629 N85-32549
TROPOSPHERE
The inducement of planetary boundary layer mass convergence associated with varying vorticity beneath tropospheric wind maximum 01 p0074 N85-10494
Observed rate of tropospheric diffusion
[DE84-016047] 02 p0224 N85-11470
Assessment of Techniques for Measuring Tropospheric H sub x O sub y
[NASA-CP-2332] 05 p0675 N85-14336
Assessment of Techniques for Measuring Tropospheric H sub x O sub y: Summary 05 p0675 N85-14337
Detailed performance calculations: Goddard Group, appendix D 05 p0676 N85-14341
Detailed performance calculations: Georgia Institute of Technology Group, appendix E
05 p0676 N85-14342
Detailed performance calculations: Harvard Group, appendix G 05 p0676 N85-14344
Jet stream errors and tropospheric-stratospheric interactions in the GLAS general circulation model
05 p0683 N85-14392
Linear studies of stationary, extratropical anomalies in the troposphere 05 p0686 N85-14410
Revised Uniform Summary of Surface Weather Observations (RUSSWO). Spangdahlem AB, Germany, parts A-F
[AD-A147166] 07 p1006 N85-16392
Tropospheric and ionospheric phase perturbations and Doppler frequency shift effects
[AD-A148579] 08 p1154 N85-17283
Propagation of wide bandwidth signals in a tropospheric ducting system 10 p1469 N85-19271
Observational study of transport in the free troposphere
[PB85-144145] 12 p1887 N85-21845
Global tropospheric chemistry: A plan for action
[NASA-CR-175545] 12 p1891 N85-21865
Varying structure and intensity change characteristics of 4 Western North Pacific tropical cyclones
[AD-A149826] 12 p1895 N85-21895
Intensification of tropical instabilities
[AD-A149985] 12 p1896 N85-21899
Slow motions in the tropical troposphere
13 p2131 N85-23262
Cumulus cloud venting of mixed layer ozone
[NASA-TM-87429] 13 p2132 N85-23269
Cumulus effects on the large-scale vorticity and momentum fields in the tropical atmosphere
13 p2137 N85-23270
Comparison of observations of orographic disturbances in the troposphere and upper atmosphere
14 p2341 N85-24479
Survey of developments in tropospheric communication apparatus 15 p2528 N85-25567
An investigation of tropospheric ions
16 p2823 N85-27412
Radon concentration inversion in the troposphere: Still unexplained
[INPE-3380-PRE/638] 16 p2826 N85-27431
The seasonal cycle of atmospheric CO in the Southern Hemisphere 16 p2830 N85-27447
A review of tropospheric refraction effects on Earth-to-satellite systems 18 p3107 N85-29235
Field measurements with the TAMS-2B and development of methods for measuring HCHO, HC3 and HONO in real air
[PB85-172955] 18 p3135 N85-29419
Investigation of the reaction system NOX/ClOX/HOX under tropospheric and stratospheric conditions
[BPT-11/84] 18 p3137 N85-29427
Circulation and transport in the middle atmosphere: Troposphere and lower atmosphere
18 p3148 N85-29491
Tropical ozone: Seasonal variations in the troposphere at 6 deg S
[INPE-3555-PRE/766] 19 p3313 N85-30535
Short meridional scale anomalies in the lower stratosphere and upper troposphere
20 p3489 N85-31684
Troposphere-stratosphere (surface-55 km) monthly general circulation statistics for the Northern Hemisphere-four year averages
[NASA-TM-86182] 20 p3495 N85-31730
Meteorological and aeronomical requirements for MST radar networks (keynote paper), part 1
21 p3615 N85-32467
Tropospheric-stratospheric exchange, part 1.1A
21 p3615 N85-32468
A numerical analysis of transient planetary waves and the vertical structure in a meso-strato-troposphere model, part 1.4A 21 p3617 N85-32473
Performance of the Colorado wind-profiling network, part 1.5A 21 p3617 N85-32475
Vertical transport in the atmosphere: Measurement capabilities and requirements of VHF radars, part 1.6A
21 p3617 N85-32476
Morphology of the scattering targets: Fresnel and turbulent mechanisms, part 2.1A
21 p3618 N85-32481
Antenna induced range smearing in MST radars
21 p3620 N85-32495
Frequency and site selection criteria for MST radars, part 5.1A 21 p3624 N85-32512
Urbana radar systems: Possibilities and limitations
21 p3628 N85-32540
Progress and plans for the Colorado Wind Profiler Network 21 p3628 N85-32542
Millstone Hill radar: Capabilities for S/T observations
21 p3629 N85-32548
The Ponape ST radar 21 p3629 N85-32549
Measurements of vertical velocity over flat terrain by ST radar and other related uses of the radar data set
21 p3630 N85-32550
Eleventh International Conference on Atmospheric Aerosols, Condensation and Ice Nuclei, volume 1
[PB85-182400] 21 p3644 N85-32636
A new hypothesis for the observed vertical distribution of atmospheric aerosols 21 p3645 N85-32646
On the mechanisms responsible for the formation of typical size spectra and vertical distribution of tropospheric aerosol particles 21 p3645 N85-32647
Application of Particle Induced X-ray Emission analysis (PIXE) to aerosol long range transport studies
21 p3648 N85-32665
Aircraft observations of cloud condensation nuclei in maritime and continental environments
21 p3650 N85-32680
Sulfur Cycle 21 p3662 N85-32746
TROPOSPHERIC SCATTERING
Field coherence function in layerwise nonhomogeneous troposphere 06 p0784 N85-15012
Influence of propagation in digital wireless beam, microwave links 10 p1470 N85-19277
Measurements and predictions of multipath dispersion for troposcatter links 10 p1472 N85-19289
Tropospheric scatter communication system having angle diversity
[AD-D011448] 14 p2291 N85-24200
Microwave propagation studies, measurements and education in Surabaya, Indonesia
[B8464633] 24 p4088 N85-35335
TROPOSPHERIC WAVES
NT PLANETARY WAVES
Tropospheric gravity waves observed by three closely spaced ST radars 21 p3623 N85-32509
Elimination of range-aliased echoes in the VHF radars
21 p3625 N85-32521
TROUBLESHOOTING
U MAINTENANCE
TROUGHS
Prediction of wave height of wind-generated seas in finite water depth
[AD-A145996] 03 p0396 N85-12539
The origin and evolution of terrestrial and Martian rock labyrinths
[NASA-CR-175511] 12 p1961 N85-22326
TRUCKS
NT TANK TRUCKS
A generalized mathematical soluation for transient off tracking of single vehicles and truck combinations
[DM-2] 01 p0107 N85-10718
Evaluation of the particulate levels occurring under 1.0/1.2 g/mi nitrogen oxide standards for light duty diesel vehicles and light duty diesel trucks
[PB85-115939/GAR] 09 p1350 N85-18494
Comparison of measured and simulated ride comfort for an agricultural tractor and influence of travel speed and tyre-inflation pressure on dynamic response
[AD-P004281] 09 p1407 N85-18867
Electric vehicle demonstration project
[DE85-003124] 11 p1741 N85-20944
Test plan for acceptance, verification and performance testing of the Bedford Lucas Chloride Electric Van. Part 1: Acceptance and verification testing at EG and G Automotive Research. Part 2: INEL performance testing, revision 1
[DE85-005157] 17 p3051 N85-28866
Three-dimensional finite element impact analysis of a nuclear waste truck cask
[DE85-010653] 19 p3266 N85-30380
TRUNCATION (MATHEMATICS)
U APPROXIMATION
TRUNCATION ERRORS
Crack growth geometry in aluminum alloy sheet material under flight simulation loading. 1: A comparison between TWIST and miniTWIST FALSTAFF and short FALSTAFF. 2: Effect of truncating high loads
[VTH-LR-441] 11 p1609 N85-20119
Sigma filter 18 p3142 N85-29460
TRUNKS (LINES)
U TRANSMISSION LINES
TRUNNIONS
U SHAFTS (MACHINE ELEMENTS)
TRUSSES
The evolution of small payload carrier systems
02 p0153 N85-11036
Effects of member imperfections on the behavior of space trusses 02 p0207 N85-11363
Conceptual design for scaled truss antenna flight experiment
[NASA-TM-85804] 04 p0462 N85-12932
Space Station truss structures and construction considerations
[NASA-TM-86338] 07 p0916 N85-15796
Alternative approximation concepts for space frame synthesis
[NASA-CR-172526] 12 p1776 N85-21150
Variable geometry truss concept
[REPT-614] 12 p1865 N85-21687

Synchronously deployable tetrahedral truss reflector
14 p2231 N85-23827
Deployable controllable geometry truss beam
[NASA-TM-86366] 17 p2909 N85-27934
Buckling and post-buckling behavior of sparsely connected built-up columns 19 p3283 N85-30358
Application of the ADAMS program to deployable space truss structures
[NASA-CR-177927] 19 p3284 N85-30366
Environmental background measurement program
[AD-A153860] 19 p3319 N85-30577
Parametric stiffness control of flexible structures
20 p3414 N85-31187
Deployable-erectable trade study for space station truss structures
[NASA-TM-87573] 22 p3740 N85-33181
Structural dynamics model and response of the deployable reference configuration space station
[NASA-TM-86386] 22 p3799 N85-33539
Box truss analysis and technology development. Task 1: Mesh analysis and control
[NASA-CR-172570] 23 p3900 N85-34156

TRYPSIN
Effects of method of detachment on electrophoretic mobility of mammalian cells grown in monolayer culture
20 p3500 N85-31757

TRYPTOPHAN
Laboratory note: Effect on sleep latency of pre-sleep AEP (Auditory Evoked Potential) procedures
[AD-A147620] 08 p1194 N85-17527

TSUNAMI WAVES
Catalog of submarine volcanoes and hydrological phenomena associated with volcanic events: 1500 BC to 31 Dec. 1899
[PB85-117984] 12 p1891 N85-21869
Atmospherically forced, coastally trapped, long period gravity waves off the south coast of southern Africa
16 p2832 N85-27461
Plane Tsunami wave caused by elastic oscillations of ocean floor 19 p3290 N85-30403

TTL INTEGRATED CIRCUITS
AL-124 light-emitting diode in 30 Mbit/s fiber-optic communication line 13 p2069 N85-22025

TUBE ANODES
On-line monitoring of the true corrosion rate in problems related to power plants
[CISE-2335] 08 p1131 N85-17126

TUBE CATHODES
NT COLD CATHODES
NT HOT CATHODES
NT PHOTOCATHODES
NT THERMIONIC CATHODES
Improved materials and processes of dispenser cathodes
[AD-A148810] 09 p1314 N85-18262
The effect of metal overlayers of thermionic dispenser cathodes
[AD-A154795] 21 p3701 N85-32995

TUBE HEAT EXCHANGERS
Internal heat transfer and pressure drop measurements in a variously baffled shell and tube heat exchanger
03 p0380 N85-12310
Fluidelastic instability in shell and tube heat exchangers: A framework for a prediction method
[DE84-006518] 10 p1498 N85-19444
Acoustic resonance in heat exchanger tube banks
[DE85-004395] 11 p1632 N85-20261
Flow-induced tube vibration thresholds in heat exchangers from shellside water tests
[DE84-006603] 11 p1652 N85-20407
Computer-aided thermohydraulic design of TEMA type E shell and tube heat exchangers for use in low pressure, liquid-to-liquid, single phase applications
[AD-A153779] 18 p3100 N85-29191

TUBES
Apparatus for producing diamond-like carbon flakes
[NASA-CASE-LEW-13837-3] 11 p1615 N85-20155
Dynamic models of flux tubes in the interpretation of polarization measurements 18 p3206 N85-29891
Electrostatic astigmatic tubular lens
21 p3895 N85-32955

TUBING
U PIPES (TUBES)

TUMBLING MOTION
Optimal open loop and nonlinear feedback control for remote orbital capture
[AD-A151967] 16 p2732 N85-26859

TUMORS
NT CANCER
NT LEUKEMIAS
Radiation physics, biophysics, and radiation biology
[DE84-014865] 09 p1360 N85-18557
Carcinogenesis of nitrated toluenes and benzenes skin and lung tumor assays in mice
[AD-A155723] 22 p3818 N85-33655

TUNABLE LASERS
Tunable CW semiconductor platelet laser
[AD-D011215] 01 p0052 N85-10341
Using two-beam interference method for measuring wavelength of tunable pulse lasers
02 p0272 N85-11772
Advanced infrared laser modulator development
[NASA-CR-172479] 06 p0862 N85-15479
Visible and ultraviolet lasers based on excimer transitions in the homonuclear halogens
[AD-D011311] 07 p0971 N85-16163
A new free electron laser using a relativistic beam with spiralling electron
[AD-D011316] 07 p0971 N85-16165
Characterization of CNRS Fizeau wedge laser tuner
[NASA-CR-174357] 09 p1325 N85-18328
Carbon dioxide laser radar for monitoring atmospheric transmittance and atmospheric aerosol
09 p1354 N85-18516
Developments and applications of laser fluorescence spectroscopy for studies of particle behaviours in fusion plasmas 09 p1369 N85-18735
Optically bistable devices using semiconductor materials
[AD-A149551] 11 p1628 N85-20253
Progress toward free-electron lasers for applications
[DE85-002208] 11 p1639 N85-20326
Portable remote laser sensor for methane leak detection
[NASA-CASE-NPO-15790-1] 12 p1865 N85-21631
Advanced crystalline laser materials
[DE85-003142] 12 p1857 N85-21647
Principle and design of a medium-enhanced free-electron laser 15 p2561 N85-25802
Calculations of collision-induced optical gain in high density mixtures of D2 or HD with a buffer gas
[AD-A151372] 15 p2648 N85-26330
Spectroscopic investigation of materials for frequency agile laser systems
[AD-A151731] 16 p2790 N85-27208
High resolution spectroscopy of C13O16 in gas mixtures
[AD-A152625] 17 p2919 N85-27991
The construction and study of improved Al(x)Ga(1-x)As-GaAs heterostructure devices
[AD-A153264] 17 p2954 N85-28244
Digital control of diode laser for atmospheric spectroscopy
[NASA-CASE-NPO-16000-1] 18 p3112 N85-29264
Intense ion beam diode diagnostics using a tunable dye laser
[DE85-006079] 18 p3113 N85-29272
Measurement of radical species concentrations and polycyclic aromatic hydrocarbons in flames by fluorescence and absorption using a tunable dye laser
[DE85-006624] 18 p3113 N85-29274
Field measurements with the TAMS-2B and development of methods for measuring HCHO, HC3 and HONO in real air
[PB85-172955] 18 p3135 N85-29419
Spectroscopic investigation of materials for tunable infrared lasers
[AD-A154124] 19 p3272 N85-30291
Lifetime and quenching measurements of C2H emission produced by vacuum ultraviolet photolysis of C2H2
[DE85-010769] 19 p3278 N85-30330
Generation of single nanosecond high-contrast radiation pules (lambda = 10.6 micrometers)
21 p3684 N85-32886
Lasing on LiF:F(-)2 - dye centers with transverse pumping 21 p3684 N85-32890
Tunable lasers with high conversion efficiency
21 p3687 N85-32906
Identification of vibrational-rotational transitions of Os-192O4 within frequency tuning limits of high pressure CO2 waveguide laser 21 p3689 N85-32917
Trivalent cerium doped crystals as tunable laser systems: Two bad apples
[DE85-008168] 22 p3790 N85-33482
High-resolution spectroscopy and dynamics of multiphoton processes in atoms and molecules
[AD-A155862] 24 p4147 N85-35714

TUNDRA
The ecology of tundra ponds of the Arctic coastal plain: A community profile
[TI85-900650] 15 p2589 N85-25958

TUNERS
NT WAVEGUIDE TUNERS
Characterization of CNRS Fizeau wedge laser tuner
[NASA-CR-174357] 09 p1325 N85-18328
Imaging apparatus for transverse electrode electro-optic tunable filter
[AD-D011524] 12 p1832 N85-21497
Wavelength dependent, tunable, optical time delay system for electrical signals
[AD-D011584] 15 p2548 N85-25725

TUNGSTATES
Spectral-luminescence characteristics and induced emission of Nd-3(+) ion in Gd(2-x)Nd(x)(WO4)3 crystals
21 p3698 N85-32912
Electronic structure and lattice dynamics of dimensionally constrained and disordered solids
[AD-A156927] 24 p4161 N85-35797

TUNGSTEN
Microstructural basis of strength and toughness in hardmetals 02 p0177 N85-11185
Magnetic properties of the cobalt matrix in WC-Co compacts 02 p0177 N85-11186
The inter-relation of microstructure, toughness and fatigue crack growth behaviour in WC-Co hardmetals
02 p0177 N85-11188
Hydrogen absorption on (110) tungsten planes at 30 K: An atom-probe field-ion microscope study
[DE84-015659] 04 p0560 N85-13565
Thermal conductivity of aluminum, copper, iron and tungsten for temperature from 1 K to the melting point
[PB84-235878] 06 p0770 N85-14924
The adsorption of CO and oxygen on Cu layers on a W(110) surface
[AD-A147345] 07 p0923 N85-15847
Influence of volumetric fiber content on some matrix damage factors during thermal cycling of tungsten-EI 765 composite 10 p1443 N85-19097
Influence of melting conditions on strength of transition zone between steel and composite material
10 p1450 N85-19133
Influence of plastic deformation on structural stability of nichrome-tungsten composite materials
11 p1599 N85-20060
Negative lithium emission from a tungsten surface in a plasma
[DE85-003456] 12 p1936 N85-22167
Gigantic lithium deposit discovered in France
14 p2289 N85-24184
Ferroelectric tungsten bronze bulk crystals and epitaxial thin films for electro-optic device applications
[AD-A151044] 14 p2427 N85-24970
Influence of oxygen traces on the properties of tungsten heavy metals
[BLL-RARDE-TR-1177-(7291.7965)]
15 p2508 N85-25470
Corrosion inhibitor formulation for molybdenum, tungsten and other metals
[AD-D011593] 15 p2510 N85-25486
LPCVD tungsten deposition on Si-Ge alloy
[DE85-005588] 16 p2750 N85-26970
Positron annihilation studies of vacancy formation in tungsten, chromium, and niobium
[DE85-006837] 16 p2871 N85-27710
Continued development and testing of tungsten controlled porosity dispenser cathodes
[AD-A152595] 17 p2931 N85-28090
Influence of microstructure on mechanical properties in cemented tungsten-carbides 19 p3230 N85-30029
PAS determination of the vacancy formation enthalpy in tungsten
[DE85-010283] 19 p3240 N85-30086
Properties of tungsten-free steel for cutting tools
[BLL-M-35808-(5828.4)] 23 p3915 N85-34259
Detonation in tungsten-loaded HMX
[DE85-009606] 23 p3922 N85-34299
Dynamic compaction of a monosized spherical tungsten powder
[DE85-014808] 24 p4080 N85-35289
Applications of the mineral resources data system and the international strategic minerals inventory in mineral-resource assessments by region and commodity
24 p4105 N85-35451
The Conterminous United States Mineral Assessment Program 24 p4106 N85-35458

TUNGSTEN ALLOYS
The Palmqvist test and its applications in WC-Co alloys 02 p0177 N85-11187
Ultrasonic inspection of alloyed tungsten bars
[AD-A148900] 10 p1495 N85-19435
Fabrication and properties of tungsten heavy metal alloys containing 30% - 90% tungsten
[DE85-000152] 11 p1607 N85-20103
Stress corrosion cracking behavior of tungsten heavy alloys
[AD-A149843] 12 p1806 N85-21329
Development of reduced activation alloys for fusion service: Draft
[DE85-007464] 18 p3074 N85-29014

TUNGSTEN CARBIDES
Microstructure and deformation aspects of some specialty steels and hard metals
02 p0176 N85-11182
Erosion of sintered WC-Co alloys
02 p0179 N85-11201
Erosion of multiphase materials
[DE84-015816] 04 p0474 N85-13018

Calibration method for acoustic scattering measurements using a spherical target
[AD-D011521] 12 p1927 N85-22106

Phase size distribution in WC/Co hardmetal
[NPL-DMA(A)-93] 20 p3431 N85-31281

TUNGSTEN COMPOUNDS
NT TUNGSTATES
NT TUNGSTEN CARBIDES

Preparation and electronic properties of MoS(2) and WS(2) single crystals grown in the presence of cobalt
[AD-A146506] 06 p0866 N85-15506

TUNGSTEN INERT GAS WELDING
U GAS TUNGSTEN ARC WELDING

TUNING

A high resolution spectroscopic study of the oxygen molecule
[NASA-CR-174061] 02 p0172 N85-11150

Tunable microwave transversal filters
[AD-A148370] 08 p1158 N85-17304

Approximate models in multivariable process control: An inverse Nyquist array and robust tuning regulator interpretation
[RR-261] 08 p1216 N85-17663

Integrated circuit tunable cavity oscillator
[AD-D011474] 10 p1481 N85-19351

Precision tunable resonant microwave cavity
[NASA-CASE-LEW-13935-1] 11 p1626 N85-20248

Aircraft rotor blade with passive tuned tab
[NASA-CASE-ARC-11444-1] 19 p3217 N85-29947

Longitudinal tune control in synchrotrons
[DE85-010745] 20 p3527 N85-31937

Gradiental adaptive corrector with optimum tuning step 22 p3776 N85-33403

Tuning system for capacitively loaded 1/4 accelerating cavity
[DE85-012516] 24 p4091 N85-35358

TUNISIA

Tunisian climate seen through a Markov process
[CT-585] 23 p3950 N85-34482

TUNNEL DIODES

Spectroscopy of surface adsorbed molecules
[DE85-009452] 17 p3034 N85-28768

TUNNEL RESISTORS
U ELECTRON TUNNELING
U RESISTORS

TURBIDITY

Active remote sensing of ocean parameters, an engineering study 02 p0213 N85-11403

Influence scattering and Q in the lithosphere
[AD-A150939] 14 p2293 N85-24213

Visibility of small objects in turbid atmosphere
14 p2342 N85-24482

Rapid rate-kinetic turbidometric assay for quantitation of antiviral complement-fixing antibodies
[AD-A153644] 18 p3152 N85-29516

Determination of low chloride values in Rocky Flats scrub alloy solutions and other complex matrices
[DE85-011506] 23 p3911 N85-34234

TURBINE BLADES

The effect of channel convergence on heat transfer in a passage with short pin fins
[NASA-TM-83801] 01 p0046 N85-10303

Nonlinear structural and life analyses of a turbine blade 02 p0141 N85-10954

Heat flux sensors for burner liners and turbine blades and vanes 02 p0142 N85-10961

Studies on the hot corrosion of a nickel-base superalloy, Udimet 700
[NASA-TM-86882] 02 p0163 N85-11224

Preliminary results of a study of the relationship between free stream turbulence and stagnation region heat transfer
[NASA-TM-86884] 02 p0197 N85-11317

A finite element method for the solution of two-dimensional transonic flows in cascades
[PNR-90216] 03 p0316 N85-12045

Materials for advanced turbine engines. Project 2: Rene 150 directionally solidified superalloy turbine blades, volume 2
[NASA-CR-167993] 03 p0319 N85-12059

Cyclic endurance testing of the RB211-22B cast HP turbine blade --- high pressure (HP)
[PNR-90210] 03 p0320 N85-12063

A study of the effect of wake-passing on turbine blades
[OUEL-1515/84] 03 p0363 N85-12326

Turbine blade damping study
[NASA-CR-171255] 04 p0456 N85-12890

Turbine blade damping study, introduction
04 p0456 N85-12891

Forced vibrations of friction-damped beam structures in two dimensions
[UDR-TM-82-08] 04 p0456 N85-12892

COST 50 - materials for gas turbines, part 1 and 2 ЭUK9
[NPL-DMA(A)-74] 05 p0617 N85-13943

The microstructural characteristics of revert superalloys --- for turbine blades
05 p0617 N85-13945

Use of least-squares method for estimating errors of turbine blade type parts during fabrication
06 p0776 N85-14963

Random vibrations of aircraft engine blades
06 p0777 N85-14967

Turbine blade test cascade modifications and orations, August 1982 - April 1983
[DE84-009268] 06 p0833 N85-15303

Problems and possibilities for life extension in gas turbine components 07 p0907 N85-15742

Experiences with the material bevaviour and high temperature low cycle fatigue life prediction of the IN 738 blading alloy 07 p0908 N85-15746

Cyclic endurance testing of the RB211-22B cast HP turbine blade 07 p0908 N85-15747

Verification of life prediction through component testing 07 p0908 N85-15748

Repair welding and brazing procedures for turbine components and investigation of the brazing behavior of thin filler foils
[MTU-TB-908/84] 07 p0974 N85-16190

SSME lifetime prediction and verification, integrating environments, structures, materials: The challenge
08 p1095 N85-16918

Thermal-stress analysis for a wood composite blade
[NASA-CR-174794] 08 p1178 N85-17421

Life assessment and damage tolerance of wind turbines
[AD-B088148L] 08 p1179 N85-17427

Current status of trailing edge loss calculation for a turbine blade
[PNR-90244] 09 p1282 N85-18061

Replaceable blade turbine and stationary specimen corrosion testing facility
[NASA-TM-86931] 09 p1294 N85-18126

USSR report: Engineering and equipment
[JPRS-UEQ-85-001] 09 p1305 N85-18200

Designing the profile of turbine blades using an iteration technique 09 p1305 N85-18201

Calculating secondary nonviscous gas flows in spatial cascades of turbines 09 p1305 N85-18202

Influence of secondary flow rate on dynamic stresses in turbine rotor blades 09 p1306 N85-18205

Experimental study of influence of size of upper and lower laps on operational efficiency of centripetal full-inlet air driven microturbines 09 p1307 N85-18211

Calculating heat transfer coefficients for turbine profiles taking surface curvature and elevated flow turbulence into account 09 p1307 N85-18212

Correction of engraving stamp for forming blanks of gas turbine engine blades 09 p1307 N85-18213

Determination of blade service life under irregular loading conditions 09 p1309 N85-18222

The analysis by the lumped parameter method of blade platform friction dampers used in the high pressure fuel turbopump on the space shuttle main engine
09 p1338 N85-18417

One-piece HPTR blade squealer tip
[AD-D011452] 10 p1425 N85-18989

Nonlinear analysis for high-temperature multilayered fiber composite structures --- turbine blades
[NASA-TM-83754] 12 p1797 N85-21273

High pressure turbine rotor two-piece blade retainer
[AD-D011498] 12 p1858 N85-21653

Cooled turbine blade tip closure
[AD-D011525] 12 p1858 N85-21654

Computer analysis of wind turbine blade dynamic loads
[DE85-000530] 12 p1867 N85-21714

Energy losses at leading edge of turbine blade during multirow jet cooling 13 p2049 N85-22826

effect of gas stream sweeping past the effluent of a perforated plate on heat transfer inside the perforations
13 p2051 N85-22836

Mechanization and automation of production processes in turbine building 14 p2269 N85-24057

Construction of profiles of intermediate blade sections from master profiles given on conical surfaces
14 p2272 N85-24075

Automating the study of error in discrete aerodynamic fairing design 14 p2288 N85-24176

Unified constitutive material models for nonlinear finite-element structural analysis --- gas turbine engine blades and vanes
[NASA-TM-86985] 14 p2320 N85-24338

Cyclic structural analyses of anisotropic turbine blades for reusable space propulsion systems --- ssme fuel turbopump
[NASA-TM-86990] 14 p2320 N85-24339

Advanced High Pressure O2/H2 Technology
[NASA-CP-2372] 16 p2733 N85-26862

Vacuum plasma coatings for turbine blades
16 p2734 N85-26869

Material technology 16 p2734 N85-26870

Design overview of fiber-reinforced superalloy composites for the Space Shuttle main engine
16 p2734 N85-26871

Materials for advanced rocket engine turbopump turbine blades 16 p2734 N85-26872

High-pressure hydrogen testing of single crystal superalloys for advanced rocket engine turbopump turbine blades 16 p2735 N85-26875

Turbine blade friction damping study
16 p2736 N85-26886

Nonlinear structural analysis for fiber-reinforced superalloy turbine blades 16 p2737 N85-26887

Redistribution of the inlet temperature profile through the SSME fuel turbine 16 p2739 N85-26901

Reusable rocket engine turbopump condition monitoring 16 p2740 N85-26907

Response of a wind turbine blade to seismic and turbulent wind excitations 16 p2817 N85-27375

Investigation of heat transfer to a turbine blade cascade using a shock tube
[AD-A153090] 17 p2898 N85-27871

Testing of materials and coatings for jet engine components under simulated operational conditions
[B8580073] 17 p2899 N85-27873

SSME turbopump turbine computations
17 p2911 N85-27944

Probabilistic structural analysis of SSME turbopump blades: Probabilistic geometry effects
17 p2913 N85-27958

Structural tailoring of SSME blades (vanes)
17 p2913 N85-27960

Cyclic structural analyses of SSME turbine blades
17 p2914 N85-27963

Effects of high mean stress on high-cycle fatigue behavior of PWA 1480 17 p2914 N85-27964

Post-stall wind tunnel data for NACA 44XX series airfoil sections
[DE85-002946] 18 p3060 N85-28601

Long-Term Materials Test Program
[DE85-003248] 18 p3077 N85-29034

Acoustic noise associated with the MOD-1 wind turbine: its source, impact, and control
[DE85-002947] 18 p3178 N85-29700

Turbine blade-tip clearance excitation forces
[NASA-CR-171534] 19 p3220 N85-29963

Effect of prolonged high temperature on durability of coated high-temperature nickel alloys
19 p3243 N85-30105

Effects of high mean stress on the high-cycle fatigue behavior of PWA 1480
[NASA-CR-176020] 19 p3287 N85-30399

Realization by vapor deposition of turbine blades covered with a silicon nitride layer
20 p3395 N85-31061

Preliminary results of a study of the relationship between free-stream turbulence and stagnation region heat transfer 20 p3452 N85-31435

Influence of moisture and elevated temperature on the fatigue properties of WTS-3 glass fiber blade material -- wind turbine blade (WTS-3)
[FFA-TN-1984-58] 20 p3470 N85-31558

Design and fabrication of durable owner-built wind turbine blades
[DE85-009200] 20 p3484 N85-31650

R and D activities of the Propulsion Division
20 p3539 N85-32025

Component-specific modeling
[NASA-CR-174925] 21 p3556 N85-32119

Three-Dimensional Techniques Applied to Internal Flows in Propulsion Systems
[AGARD-LS-140] 21 p3586 N85-32289

A 3-D Euler method for internal transonic flows computation with a multi-domain approach
21 p3587 N85-32298

Calculation of 3-D flow without numerical mixing
21 p3588 N85-32301

Local heat-transfer measurements on a large-scale-model turbine blade airfoil using a composite of a heater element and liquid crystals
[NASA-TM-86900] 22 p3782 N85-33435

Design, development and operation of a high simultaneous capacity digital telemetry system -- turbomachine blade flutter
[PNR-90261] 23 p3899 N85-34151

Calculation of trajectories of detached wind turbine blades and prediction of site risk levels associated with failures of HAWT's 24 p4110 N85-35475

TURBINE ENGINES
NT GAS TURBINE ENGINES
NT J-52 ENGINE
NT J-85 ENGINE
NT JET ENGINES
NT RAMJET ENGINES
NT SUPERSONIC COMBUSTION RAMJET ENGINES

NT TURBOFAN ENGINES
NT TURBOJET ENGINES
NT TURBOPROP ENGINES
Chemistry of fuel deposits and sediments and their precursors [NASA-CR-174778] 01 p0034 N85-10209
HOST instrumentation R and D program overview 02 p0141 N85-10957
Hot section laser anemometry 02 p0142 N85-10962
Laser anemometer optimization 02 p0142 N85-10963
Turbine heat transfer 02 p0142 N85-10964
Life prediction and constitutive behavior: Overview 02 p0143 N85-10973
Dilution jet mixing 02 p0145 N85-10985
Combustion system for radiation investigations 02 p0145 N85-10986
Validation of structural analysis methods using the in-house liner cyclic rigs 02 p0146 N85-10987
HOST liner cyclic facilities: Facility description 02 p0146 N85-10988
Energy efficient engine. Low pressure turbine test hardware detailed design report [NASA-CR-167956] 02 p0147 N85-10994
Materials for advanced turbine engines. Project 2: Rene 150 directionally solidified superalloy turbine blades, volume 2 [NASA-CR-167993] 03 p0319 N85-12059
Heat transfer and pressure drop in blade cooling channels with turbulence promoters [NASA-CR-3837] 03 p0381 N85-12315
Parametric estimates of propulsion system maintenance manhours [AD-A147120] 07 p0894 N85-15662
Improvement of the corrosion resistance of turbine engine bearings [AD-A147430] 07 p0905 N85-15731
Engine Cyclic Durability by Analysis and Testing [AGARD-CP-368] 07 p0905 N85-15733
The application of a technology index to aircraft turbine engine cost estimating relationships [AD-A147701] 08 p1067 N85-16874
Design description of a microprocessor based Engine Monitoring and Control unit (EMAC) for small turboshaft [NASA-TM-86860] 09 p1263 N85-17935
Experimental and analytical study of ceramic-coated turbine-tip shroud seals for small turbine engines [NASA-TM-86881] 09 p1281 N85-18057
An analytic model of gas turbine engine installations [AD-A146708] 09 p1281 N85-18059
USSR report: Engineering and equipment [JPRS-UEQ-85-001] 09 p1305 N85-18200
Use of braking stages for control of turbine speed 09 p1308 N85-18215
Advanced stress analysis methods applicable to turbine engine structures [NASA-CR-175573] 12 p1778 N85-21165
Pressure drop and coefficients of internal heat transfer necessary for vanepiration cooling 13 p2050 N85-22831
Composition and photochemical reactivity of turbine engine exhaust [AD-A150558] 13 p2130 N85-23256
Design of piping for oil drain from turbine bearings 14 p2271 N85-24073
Ignition/combustion processes 16 p2740 N85-26909
New facility to study unsteady wake effects on turbine airfoil heat transfer 17 p2911 N85-27948
USSR report: Engineering and equipment [JPRS-UEQ-85-004] 17 p2939 N85-28142
Flow characteristics of a partially submerged liquid pickup [DE85-006744] 17 p2950 N85-28276
Improved statistical analysis method for prediction of maximum inlet distortion [AD-A153767] 18 p3063 N85-28947
Ceramic Technology for Advanced Heat Engines Project [DE85-006755] 18 p3080 N85-29052
Ceramic coatings for heat engine materials: Status and future needs [DE85-006750] 18 p3080 N85-29053
Ceramic coatings for heat engine materials [DE85-005238] 18 p3080 N85-29054
Component-specific modeling [NASA-CR-174925] 21 p3556 N85-32119
Energy efficient engine, high pressure turbine thermal barrier coating. Support technology report [NASA-CR-168037] 24 p4066 N85-35199
A study of the control of particulate emissions from turbine engine test cells 24 p4067 N85-35205

TURBINE PUMPS
Rotordynamic analysis of the SSME turbopumps using reduced models [NASA-CR-171170] 01 p0054 N85-10365
Non-intrusive speed sensor — space shuttle main engine turbopumps [NASA-CR-171204] 03 p0364 N85-12331
Analysis of physical-chemical processes governing SSME internal fluid flows [NASA-CR-174245] 06 p0760 N85-14862
Assessment of the operating characteristics of the SSME LOX turbopump pump-end bearing [NASA-CR-171267] 08 p1167 N85-17362
Calculation of flow about posts and powerhead model — space shuttle main engine [NASA-CR-171344] 10 p1483 N85-19362
Cyclic structural analyses of anisotropic turbine blades for reusable space propulsion systems — same fuel turbopump [NASA-TM-86990] 14 p2320 N85-24339
Advanced High Pressure O2/H2 Technology [NASA-CP-2372] 16 p2733 N85-26862
Ceramics for advanced O2/H2 application 16 p2734 N85-26868
Design overview of fiber-reinforced superalloy composites for the Space Shuttle main engine 16 p2734 N85-26871
Materials for advanced rocket engine turbopump turbine blades 16 p2734 N85-26872
Development of new materials for turbopump bearings 16 p2735 N85-26877
Bearings working group 16 p2735 N85-26878
Advanced rocket engine cryogenic turbopump bearing thermal model 16 p2735 N85-26879
Hybrid bearings for LH2 and LO2 turbopumps 16 p2736 N85-26880
Rolling contact fatigue life of chromium ion plated 440C bearing steel 16 p2736 N85-26882
Signal analysis techniques for incipient failure detection in turbomachinery 16 p2736 N85-26884
Turbine blade friction damping study 16 p2736 N85-26886
Preliminary results on passive eddy current damper technology for SSME turbomachinery 16 p2737 N85-26890
Damping seal verification setup 16 p2738 N85-26893
Damping seals for turbomachinery 16 p2738 N85-26894
Vibration characteristics of the HPOTP (High Pressure Oxygen Turbopump) of the SSME (Space Shuttle Main Engine) 16 p2738 N85-26895
Analytical study of flow phenomena in SSME turnaround duct geometries 16 p2739 N85-26902
Reusable rocket engine turbopump condition monitoring 16 p2740 N85-26907
Nonintrusive shaft speed sensor 16 p2740 N85-26908
SSME fuel preburner two-dimensional analysis 17 p2911 N85-27943
SSME turbopump turbine computations 17 p2911 N85-27944
Probabilistic structural analysis of SSME turbopump blades: Probabilistic geometry effects 17 p2913 N85-27958
Cyclic structural analyses of SSME turbine blades 17 p2914 N85-27963
Constitutive cyclic deformation behavior in single-crystal and directionally solidified SSME high-pressure fuel turbopump airfoil materials 17 p2914 N85-27965
Improved turbopump dynamics [NASA-TM-86514] 20 p3462 N85-31509

TURBINE WHEELS
Unsteady aerodynamic response of cascades and turborotors 03 p0319 N85-12058
Comparison between the properties of conventional wrought and powder metallurgical alloys for turbine disc applications 07 p0906 N85-15739
Problems and possibilities for life extension in gas turbine components 07 p0907 N85-15742
Clearance flow-generated transverse forces at the rotors of thermal turbomachines [NASA-TM-77292] 07 p0973 N85-16180
Influence of setting angle of jet cooling nozzles on temperature and stress state of a turbine wheel 09 p1306 N85-18208
Causes and means of prevention of erosion of exit edges of drive vanes in final stages of K-300-240 turbine 14 p2272 N85-24076
Some problems of optimum journal design for disk-drum rotors under antisymmetric loading 14 p2286 N85-24167
Properties and microstructures for dual alloy combinations of three superalloys with alloy 901 [NASA-TM-86987] 16 p2749 N85-26963
Aerodynamic forces developing in channels between vanes in turbine drive wheels 16 p2765 N85-27082
Unsteady heat transfer due to time-dependent free stream velocity 17 p2911 N85-27947
Experimental measurements and analysis of heat transfer and gas dynamics in a rotating turbine stage 17 p2911 N85-27949
A comparison of experimental and theoretical results for rotordynamic coefficients of four annular gas seals [NASA-CR-176086] 21 p3596 N85-32332

TURBINES
NT GAS TURBINES
NT SHROUDED TURBINES
NT STEAM TURBINES
NT WIND TURBINES
Characteristics of controlled-oscillating annular cascade test facility with Freon gas [NAL-TR-812] 01 p0003 N85-10014
Energy efficient engine high pressure turbine ceramic shroud support technology report [NASA-CR-168038] 02 p0147 N85-10996
Further development of a transonic cascade analysis [AD-A145410] 02 p0198 N85-11319
Turbine test report, addendum [DE84-015130] 02 p0205 N85-11353
Device for measuring relative axial expansion of turbine rotor employing space-vector tracking method 06 p0776 N85-14962
Influence of secondary flow rate on dynamic stresses in turbine rotor blades 09 p1306 N85-18205
On vortex transport in turbine channels 09 p1308 N85-18217
Gear case vibration isolation in a geared turbine generator 09 p1338 N85-18414
Assessing expired fatigue life in large turbine shafts [DE84-016676] 09 p1340 N85-18427
Initial results for supercritical cycle experiments using pure and mixed-hydrocarbon working fluids [DE84-017008] 09 p1345 N85-18460
Fabrication of turbine parts with transportable tools 14 p2267 N85-24046
Conservation of turbines by inhibited air 14 p2268 N85-24054
Manufacture of drive wheel vanes for hydraulic turbines on program controlled machine tools 14 p2269 N85-24058
Dependents of velocity distribution in exit section of converging channel on shape of inlet channel in regulating valve 14 p2277 N85-24106
Study of axial bearings without oil bath with radial cooling of blocks 14 p2286 N85-24164
Unsteady gas dynamics problems related to flight vehicles [AD-A151187] 15 p2464 N85-25218
Aviation turbine fuels from tar sands bitumen and heavy oils. Part 1: Process analysis [AD-A151319] 15 p2521 N85-25539
Exploratory wind-tunnel investigation of a wingtip-mounted vortex turbine for vortex energy recovery [NASA-TP-2468] 16 p2699 N85-26667
Qualification of a well gage for the SIMA wagon, adapted to the test of half models motorized by compressed air turbines — SIMA wind tunnel [ONERA-PV-1/8068-GY] 16 p2701 N85-26677
Water brake convertor: A simple device to convert mechanical energy into heat energy [DE85-006021] 16 p2716 N85-26766
Fuel and oxidizer turbine loss analysis 16 p2739 N85-26900
USSR report: Engineering and equipment [JPRS-UEQ-84-006] 16 p2760 N85-27035
Quasi-steady vibrations of a rotating shaft grazing an obstacle: Spiral vibration [BLL-CE-TRANS-7962-(9022.09)] 16 p2790 N85-27256
Ceramic turbochargers: A case study of a near-term application of high-strength ceramics [DE85-006495] 17 p2975 N85-28379
Method for driving two-phase turbines with enhanced efficiency [NASA-CASE-NPO-15037-2] 18 p3115 N85-29282
Variable cycle engine for high altitude aircraft [AD-D011705] 19 p3221 N85-29989
Combustor turbulence 20 p3452 N85-31434
Heat transfer in aeropropulsion systems [NASA-TM-87066] 20 p3453 N85-31444
Microprocessor control design for a low-head crossflow turbine [AD-A155477] 21 p3556 N85-32121
Observations of the use of the setapoint detector [AD-A15453[illegible]] 21 p3571 N85-32208

TURBOCHARGERS
U SUPERCHARGERS
U TURBOCOMPRESSORS

TURBOCOMPRESSORS
Energy efficient engine component development and integration program
[NASA-CR-170034] 02 p0146 N85-10990
Full load testing in the platform module prior to tow-out: A case history of subsynchronous instability
05 p0642 N85-14117
Current problems in turbomachinery fluid dynamics
[AD-A147127] 07 p0958 N85-16074
Study of residual stresses introduced into TA6ZrD (685) cylinders by quenching --- compressor disk alloy
[PNR-90240] 09 p1341 N85-18435
A theory of post-stall transients in multistage axial compression systems
[NASA-CR-3878] 12 p1771 N85-21117
Some unique features in operation of two-stage turbojet engine with afterburner 13 p2049 N85-22828
HPFTP flow diverter analysis
[NASA-CR-171424] 13 p2091 N85-23057
T700 cutter life improvement program
[AD-A150450] 13 p2099 N85-23069
Simulation of multistage turbine flows
17 p2911 N85-27945
Unsteady flow in multistage turbines
17 p2911 N85-27946
Precision die forging of blades or gas turbines
17 p2940 N85-28148
Ceramic turbochargers: A case study of a near-term application of high-strength ceramics
[DE85-006495] 17 p2975 N85-28379
Future of ceramic turbochargers: Promises and pitfalls
[DE85-006209] 17 p2975 N85-28380
TURBOCONVERTERS
U TURBOGENERATORS
TURBOELECTRIC CONVERSION
U TURBOGENERATORS
TURBOFAN AIRCRAFT
NT A-7 AIRCRAFT
NT BOEING 727 AIRCRAFT
NT BOEING 737 AIRCRAFT
NT BOEING 767 AIRCRAFT
NT C-141 AIRCRAFT
NT CONCORDE AIRCRAFT
NT CV-990 AIRCRAFT
NT DC 8 AIRCRAFT
NT F-111 AIRCRAFT
Aerodynamic detuning analysis of an unstalled supersonic turbofan cascade
[NASA-TM-87001] 16 p2700 N85-26670
A computer program for the drag prediction of subsonic, turbine powered aircraft in the en-route configuration
[VTH-LR-412] 16 p2701 N85-26681
TURBOFAN ENGINES
NT TF-34 ENGINE
Characteristics of controlled-oscillating annular cascade test facility with Freon gas
[NAL-TR-812] 01 p0003 N85-10014
Stall elimination and restart enhancement device
[AD-D011217] 01 p0010 N85-10062
Development trends and requirements of propulsion system technology for civil aircraft
01 p0011 N85-10066
Effect of combined pressure and temperature distortion orientation on high-bypass-ratio turbofan engine stability
[NASA-TM-83771] 01 p0011 N85-10067
Energy efficient engine. Volume 1: Component development and integration program
[NASA-CR-173084] 02 p0146 N85-10992
Energy efficient engine ICLS engine bearings, drives and configuration: Detail design report
[NASA-CR-167871] 02 p0147 N85-10997
Turbofan noise generation. Volume 2: Computer programs
[NASA-CR-167952] 02 p0275 N85-11791
Static jet noise test results of four 0.35 scale-model QCGAT mixer nozzles
[NASA-TM-86871] 04 p0558 N85-13551
Applications of finite and wave envelope element approximations to acoustic radiation from turbofan engine inlets in flight 05 p0726 N85-14664
Effect of steady-state temperature distortion on inlet flow to a high-bypass-ration turbofan engine
[NASA-TM-86896] 07 p0904 N85-15725
Flow measurement device
[AD-D011432] 08 p1168 N85-17369
Research and development for semi-spherical inflow control device
[NAL-TR-833] 09 p1281 N85-18056
On selecting bypass mixers for turbofan engines
09 p1306 N85-18207
Preliminary performance of a vertical-attitude takeoff and landing, supersonic cruise aircraft concept having thrust vectoring integrated into the flight control system
[NASA-CR-172530] 10 p1423 N85-18977
Fluctuating pressures on fan blades of a turbofan engine, flight test investigation
[NASA-TP-2381] 10 p1553 N85-19790
Review of engine ingestions to wide body transport aircraft
[AD-P004185] 11 p1579 N85-19947
On the solution of the three-dimensional flowfield about a flow-through nacelle
[NASA-TM-87448] 13 p1969 N85-22371
Effects of inlet distortion on a static pressure probe mounted on the engine hub in an F-15 airplane
[NASA-TP-2411] 13 p1974 N85-22394
Hover test results of a small-scale twin-tilt nacelle model
[NASA-TM-86665] 14 p2210 N85-23706
Performance and surge limits of a TF30-P-3 turbofan engine/axisymmetric mixed-compression inlet propulsion system at Mach 2.5
[NASA-TP-2461] 15 p2472 N85-25261
Transient technique for measuring heat transfer coefficients on stator airfoils in a jet engine environment
[NASA-TM-87005] 15 p2560 N85-25794
Spacer structure
[AD-D011641] 17 p2897 N85-27866
Fan noise suppression in turbofan engines
[B8580076] 17 p2898 N85-27872
DEAN: A program for dynamic engine analysis
[NASA-TM-87033] 18 p3062 N85-28945
Energy efficient engine component development and integration program
[NASA-CR-172846] 19 p3219 N85-29958
Fault detection and accommodation testing on an F100 engine in an F-15 airplane
[NASA-TM-86735] 19 p3219 N85-29962
Measurement of turbofan-turbojet thrust from tailpipe static pressure
[AD-A154036] 19 p3220 N85-29967
Energy Efficient Engine Program technology benefit/cost study, volume 1
[NASA-CR-174766-VOL-1] 24 p4066 N85-35197
Energy Efficient Engine Program technology benefit/cost study, volume 2
[NASA-CR-174766-VOL-2] 24 p4066 N85-35198
TURBOFANS
Energy efficient engine component development and integration program
[NASA-CR-170034] 02 p0146 N85-10990
Turbofan noise generation. Volume 2: Computer programs
[NASA-CR-167952] 02 p0275 N85-11791
CFM 56-2. Oligocyclic fatigue of the turbofan disk: Dimensionning and tests for verification and improvements 07 p0908 N85-15750
Structural response of a rotating bladed disk to rotor whirl
[NASA-CR-175605] 13 p1973 N85-22391
Energy efficient engine. Fan and quarter-stage component performance report
[NASA-CR-168070] 23 p3897 N85-34141
TURBOGENERATORS
Operating experience with potassium systems --- thermal power stations
[OEFZS-4275] 03 p0387 N85-12473
Monitoring environmental and related performance parameters for a Rankine-cycle turbine electric generator utilizing geothermal energy at the Gila Hot Springs, New Mexico
[DE84-901772] 09 p1345 N85-18465
Conceptual design of a 10 MW shore-based OTEC plant
[DE84-015808] 10 p1511 N85-19532
USSR report: Engineering and equipment
[JPRS-UEQ-84-001] 14 p2265 N85-24034
Study of axial bearings without oil bath with radial cooling of blocks 14 p2286 N85-24164
Conceptual design of a fixed-pitch wind turbine generator system rated at 400 kilowatts
[NASA-CR-174877] 18 p3127 N85-29363
ASME performance test on TVA Sequoyah unit 1
[DE85-901316] 19 p3358 N85-30815
TURBOJET AIRCRAFT
U JET AIRCRAFT
TURBOJET ENGINE CONTROL
Man-vehicle systems research facility advanced aircraft flight simulator throttle mechanism
22 p3798 N85-33527
TURBOJET ENGINES
NT J-52 ENGINE
NT J-85 ENGINE
NT TURBOFAN ENGINES
NT TURBOPROP ENGINES
Surge transient simulation in turbo-jet engine
05 p0596 N85-13796
Exploratory development of advanced surface flaw detection methods
[AD-A148757] 09 p1281 N85-18060
Experimental study of aerodynamic shielding of turbojet engine air intake against exhaust gases
09 p1307 N85-18210
Experimental study of ceramic coated tip seals for turbojet engines
[NASA-TM-86939] 10 p1483 N85-19363
Propagation of three-dimensional turbulent jet from lobar nozzle through surrounding stream
13 p2042 N85-22785
Exergetical analysis of turbojet engine cycle
13 p2049 N85-22825
Some unique features in operation of two-stage turbojet engine with afterburner 13 p2049 N85-22828
Influence of fuel properties on gas turbine combustion performance
[AD-A151464] 15 p2504 N85-25446
Transient technique for measuring heat transfer coefficients on stator airfoils in a jet engine environment
[NASA-TM-87005] 15 p2560 N85-25794
Preliminary wind tunnel study of the influence of a jet on the unsteady aerodynamics of a turbojet engine
[ONERA-RT-12/5115-RY-230-R-231G]
16 p2701 N85-26679
Measurement of turbofan-turbojet thrust from tailpipe static pressure
[AD-A154036] 19 p3220 N85-29967
Variable cycle engine for high altitude aircraft
[AD-D011705] 19 p3221 N85-29969
China has developed a new version of fighter aircraft
[AD-A155293] 21 p3555 N85-32118
TURBOMACHINE BLADES
NT COMPRESSOR BLADES
NT ROTOR BLADES (TURBOMACHINERY)
NT STATOR BLADES
NT TURBINE BLADES
Characteristics of controlled-oscillating annular cascade test facility with Freon gas
[NAL-TR-812] 01 p0003 N85-10014
Analysis of turbomachine blades: A review
02 p0208 N85-11374
Model equation for simulating flows in multistage turbomachinery
[NASA-TM-86869] 03 p0315 N85-12036
Performance deterioration of cascades exposed to solid particles 03 p0319 N85-12057
Unsteady aerodynamic response of cascades and turborotors 03 p0319 N85-12058
Turbomachinery blade design using advanced calculation methods
[PNR-90218] 04 p0456 N85-12896
Incorporation of viscous-inviscid interactions in turbomachinery design
[PNR-90219] 04 p0457 N85-12897
Modelling viscous flow in turbomachinery
[PNR-90220] 04 p0457 N85-12898
An improved computer model for prediction of axial gas turbine performance losses
[NASA-CR-174246] 07 p0904 N85-15724
Tailored airfoils for vertical axis wind turbines
[DE85-004628] 12 p1772 N85-21128
Current problems in turbomachinery fluid dynamics
[AD-A150533] 13 p1974 N85-22397
Experimental and analytical investigation of fan flow interaction with downstream struts
[NASA-CR-175756] 15 p2462 N85-25201
A study of internal and distributed damping for vibrating turbomachiner blades
[NASA-CR-175901] 17 p2898 N85-27868
Unsteady heat transfer due to time-dependent free stream velocity 17 p2911 N85-27947
Experimental measurements and analysis of heat transfer and gas dynamics in a rotating turbine stage
17 p2911 N85-27949
Composite loads spectra for select space propulsion structural components 17 p2912 N85-27953
Directionally solidified gas turbine alloys
[PNR-90264] 23 p3917 N85-34279
TURBOMACHINERY
NT CENTRIFUGAL COMPRESSORS
NT CENTRIFUGAL PUMPS
NT GAS TURBINES
NT SHROUDED TURBINES
NT STEAM TURBINES
NT TURBINE PUMPS
NT TURBINES
NT TURBOCOMPRESSORS
NT TURBOFANS
NT TURBOGENERATORS
NT WIND TURBINES
Advanced blade tip seal system, volume 2
[NASA-CR-167851] 02 p0147 N85-10999
Model equation for simulating flows in multistage turbomachinery
[NASA-TM-86869] 03 p0315 N85-12036
Performance deterioration of cascades exposed to solid particles 03 p0319 N85-12057

Unsteady aerodynamic response of cascades and turborotors
03 p0319 N85-12056

Comparative review of laser Doppler and laser two-focus anemometry in turbomachinery applications
[VKI-TM-34] 03 p0367 N85-12350

Incorporation of viscous-inviscid interactions in turbomachinery design
[PNR-90219] 04 p0457 N85-12897

Modelling viscous flow in turbomachinery
[PNR-90220] 04 p0457 N85-12898

Rotordynamic Instability Problems in High-Performance Turbomachinery
[NASA-CP-2338] 05 p0642 N85-14116

Analysis of dynamic characteristics of fluid force induced by labyrinth seal 05 p0643 N85-14129

Prediction of force coefficients for labyrinth seals
05 p0644 N85-14130

An iwatsubo-based solution for labyrinth seals - comparison with experimental results
05 p0644 N85-14131

Preliminary investigation of labyrinth packing pressure drops at onset of swirl-induced rotor instability
05 p0644 N85-14132

Identification of dynamic coefficients of annular turbulent seals 05 p0644 N85-14133

Effects of fluid inertia and turbulence on force coefficients for squeeze film dampers
05 p0645 N85-14137

Squeeze-film dampers for turbomachinery stabilization
05 p0645 N85-14138

Influence of stationary components on unsteady flow in industrial centrifugal compressors
05 p0645 N85-14140

USSR report: Engineering and equipment
[JPRS-UEQ-84-007] 06 p0775 N85-14954

The use of an optical data acquisition system for bladed disk vibration analysis
[NASA-TM-86891] 06 p0817 N85-15184

Development of a Navier-Stokes rotor and stator analysis
[AD-A146967] 07 p0958 N85-16070

Clearence flow-generated transverse forces at the rotors of thermal turbomachines
[NASA-TM-77292] 07 p0973 N85-16180

Turbo fluid machinery and diffusers
[NASA-TM-77467] 08 p1167 N85-17363

Calculating secondary nonviscous gas flows in spatial cascades of turbines 09 p1305 N85-18202

Analysis of experimental shaft seal data for high-performance turbomachines, as for Space Shuttle main engines
[NASA-TM-86928] 12 p1844 N85-21569

Current problems in turbomachinery fluid dynamics
[AD-A150533] 13 p1974 N85-22397

Future directions in aeropropulsion technology
[NASA-TM-87010] 14 p2207 N85-23685

Experimental and analytical investigation of fan flow interaction with downstream struts
[NASA-CR-175756] 15 p2462 N85-25201

Material technology 16 p2734 N85-26870

Monitoring of turbo-machines by shaft vibration measurement
[BLL-CE-TRANS-7900-(9022.09)]
16 p2799 N85-27255

Simulation of multistage turbine flows
17 p2911 N85-27945

Vibrations of rotors connected through couplings with backlash 17 p2940 N85-28147

Calculation of friction at spherical bearing journals in turbomachines 17 p2940 N85-28150

Load-induced rotordynamic instabilities in turbomachinery 19 p3280 N85-30340

Damping seal for turbomachinery
[NASA-CASE-MFS-25842-2] 19 p3280 N85-30341

Numerical and experimental investigation of turbomachinery rotor flow fields
20 p3451 N85-31429

A device for generating motive force through the expansion of a non-elastic dense fluid
[NASA-TM-77664] 20 p3454 N85-31446

Three-Dimensional Techniques Applied to Internal Flows in Propulsion Systems
[AGARD-LS-140] 21 p3586 N85-32293

An analysis of flow models: From Navier-Stokes to potential flow equations 21 p3587 N85-32295

Calculation of 3-D flow without numerical mixing
21 p3588 N85-32301

A comparison of experimental and theoretical results for rotordynamic coefficients of four annular gas seals
[NASA-CR-176086] 21 p3596 N85-32332

A geometric modeller for turbomachinery applications
23 p3962 N85-34556

TURBOPAUSE

Space and time variations and turbopause dynamical structure 11 p1663 N85-20483

Turbopause as source of internal gravity waves
16 p2808 N85-27314

TURBOPROP AIRCRAFT

NT F-27 AIRCRAFT
NT OV-1 AIRCRAFT

Observations from varying the lift and drag inputs to a noise prediction method for supersonic helical tip speed propellers
[NASA-TM-83797] 01 p0115 N85-10766

Installed nacelle drag-improvement tests of an M = 0.8 turboprop transport configuration
[NASA-TM-84302] 07 p0902 N85-15716

Transmission error measurements in gearbox development 14 p2224 N85-23794

Establishment and maintenance of certification standards for helicopter and turboprop power transmission systems 14 p2224 N85-23796

Fundamental studies of structure borne noise for advanced turboprop applications
[NASA-CR-175737] 15 p2648 N85-26320

A computer program for the drag prediction of subsonic, turbine powered aircraft in the en-route configuration
[VTH-LR-412] 16 p2701 N85-26681

Effects of propeller rotation direction on airplane interior noise levels
[NASA-TP-2444] 19 p3350 N85-30767

TURBOPROP ENGINES

An improved source model for aircraft interior noise studies
[NASA-CR-172517] 08 p1217 N85-17668

Analytical fuel property effects: Small combustors, phase 2
[NASA-CR-174846] 10 p1456 N85-19175

Gears and Power Transmission Systems for Helicopters and Turboprops
[AGARD-CP-369] 14 p2220 N85-23765

A state of the art assessment of turboprop transmission technology and projected needs for the next generation
14 p2220 N85-23770

Advanced gearbox technology in small turbo propeller engines 14 p2221 N85-23771

Fatigue life analysis of a turboprop reduction gearbox
[NASA-TM-87014] 16 p2793 N85-27228

Wind tunnel results of advanced high speed propellers in the takeoff, climb and landing operating regimes
[NASA-TM-87054] 19 p3213 N85-29925

Low-speed wind-tunnel tests of an advanced eight-bladed propeller
[NASA-TM-86364] 19 p3214 N85-29928

Large-scale Advanced Propfan (LAP) program
[NASA-TM-87067] 19 p3220 N85-29964

Two-plane balance and slip-ring design
22 p3799 N85-33536

TURBOPUMPS

U TURBINE PUMPS

TURBOROCKET ENGINES

Aerojet advanced engine concept
08 p1107 N85-16999

TURBOROTORS

U TURBINE WHEELS

TURBOSHAFTS

Temperature distortion generator for turboshaft engine testing
[NASA-TM-83748] 07 p0893 N85-15656

Variable cycle engine for high altitude aircraft
[AD-D011705] 19 p3221 N85-29969

TURBULENCE

NT ATMOSPHERIC TURBULENCE
NT CLEAR AIR TURBULENCE
NT GUSTS
NT HOMOGENEOUS TURBULENCE
NT ISOTROPIC TURBULENCE
NT LOW LEVEL TURBULENCE
NT MAGNETOHYDRODYNAMIC TURBULENCE
NT PLASMA TURBULENCE

Limiting effects during turbulent combustion
02 p0274 N85-11784

Chaotic behavior induced by solitons in perturbed integrable systems 02 p0283 N85-11844

Vorticity amplification in viscous flow around a body
03 p0360 N85-12309

Heat transfer and pressure drop in blade cooling channels with turbulence promoters
[NASA-CR-3837] 03 p0361 N85-12315

Numerical studies of unsteady transonic flow over an oscillating airfoil
[NASA-TM-86011] 03 p0361 N85-12316

On the co-variant formulation of the law of motion of passive particles in a field of turbulence
[REPT-564] 03 p0377 N85-12407

A spatial model of wind shear and turbulence for flight simulation 03 p0395 N85-12518

Automatic recognition and turbuling objects
[AD-A145908] 03 p0419 N85-12676

The role of freestream turbulence scale in subsonic flow separation
[NASA-CR-174172] 04 p0452 N85-12870

Laminar separation bubble with transition: Prediction test with local interaction
[BLL-PNR-90231-(8019.3153)]
06 p0808 N85-15132

Characteristic scale of inner mixing layers in stably stratified atmosphere 06 p0824 N85-15235

A scanning laser velocimeter for turbulence research
[NASA-CR-172493] 07 p0897 N85-15686

The structure of dilute combusting sprays
[NASA-CR-174838] 07 p0905 N85-15728

Dynamical characteristics of weak turbulence
[AD-A147186] 07 p0959 N85-16075

Turbulence measurement interferometer apparatus
[AD-D011377] 07 p0970 N85-16156

Recent advances in computational methods to solve the high-lift multi-component airfoil problem
08 p1066 N85-16774

Basic instability mechanisms in chemically reacting subsonic and supersonic flows
[AD-A148408] 08 p1122 N85-17071

Nonradiative heating and enhanced mass-loss due to shear turbulence in massive hot stars
08 p1235 N85-17780

Analysis of pressure gradient-velocity correlation in turbulent, premixed flames 09 p1272 N85-17994

Flame propagation and stabilization studies using Rayleigh scattering and laser Doppler velocimetry
[AD-A148602] 09 p1290 N85-18102

Turbulent premixed flame study
[DE85-003220] 09 p1292 N85-18112

A free shear layer prediction of the turbulent wake of a flat plate towed below a free surface
[AD-A148699] 09 p1319 N85-18293

Natural environment analysis
[NASA-CR-171333] 10 p1428 N85-19010

Effects of a periodic disturbance on structure and mixing in turbulent shear layers and wakes
[AD-A149278] 10 p1484 N85-19370

Internal Gravity Waves and Small-Scale Turbulence: Proceedings of the 2nd 'Aha Huliko'a Hawaiian Winter Workshop
[AD-A149510] 10 p1522 N85-19597

Fragmentation and turbulence in collapsing gas clouds
[DE85-003745] 11 p1633 N85-20282

Pre-turbulence: Transitional Laminar-turbulent flows
11 p1716 N85-20793

Frequency spectra of turbulent pulsations in stability of laminar boundary layer 11 p1716 N85-20795

Fluctuations and transport in fusion plasmas
[DE85-003612] 11 p1732 N85-20893

Theory of resistivity-gradient-driven turbulence
[DE85-002175] 11 p1733 N85-20898

Skin friction measurements for 2 relatively thick airfoil sections at high Reynolds number
[AD-A150021] 12 p1772 N85-21125

Time and space variability of turbulent concentration fluctuations
[AD-A149963] 12 p1896 N85-21896

Methods of progressing waves in turbulent media with applications to acoustics
[AD-A149599] 12 p1920 N85-22055

Plasma performance of TFCX and jet with sawtoothing
[DE85-003335] 12 p1936 N85-22168

Processes and problems in secondary star formation
[DE85-003623] 12 p1960 N85-22322

Intensity fluctuations of focused laser beam during reflection in turbulent atmosphere
13 p2078 N85-22975

Mean flow and turbulence in complex terrain NPS (Naval Postgraduate School)/Vandenberg measurement system
[AD-A150184] 13 p2136 N85-23274

Evolution of grains in a turbulent solar nebula
13 p2179 N85-23525

Estimating unsteady aerodynamic forces on a cascade in a three-dimensional turbulence field
[NASA-TM-86701] 14 p2209 N85-23704

Factors affecting dwell times on digital displaying
[NASA-TM-86406] 14 p2390 N85-24722

On the influence of turbulent motions on non-radial oscillations 14 p2444 N85-25083

Numerical studies of unsteady transonic flow over oscillating airfoil 15 p2458 N85-25174

Studies on the interference of wings and propeller slipstreams
[NASA-CR-175753] 15 p2463 N85-25210

An experimental study of hairpin-type vortices as a potential flow structure of turbulent boundary layers
15 p2553 N85-25751

Mixing across a gas-gas interface
[AD-A151471] 15 p2556 N85-25770

High-capacity real-time computer system for processing hydrophysical data 15 p2625 N85-26178

Measurement and theory of turbulence in RR Lyrae [DE85-005899] 15 p2669 N85-26471
Voyage to Uranus 15 p2687 N85-26596
Observations, theoretical ideas and modeling of turbulent flows: Past, present and future [NASA-TM-86679] 16 p2782 N85-27167
A Markov method for simulating non-Gaussian wind speed time series [DE85-007131] 16 p2835 N85-27485
Kolmogorov and scalar spectral regimes in numerical turbulence [NASA-TM-86699] 17 p2957 N85-28264
Parameterization of subgrid-scale fluxes in mesoscale meteorological models [AD-A153016] 17 p2996 N85-28523
Flame acceleration mechanisms under conditions of partial confinement [PB85-184083] 18 p3073 N85-29004
Applications of Canuto's method to Rayleigh-Taylor-initiated turbulence [DE85-010835] 18 p3102 N85-29202
An experimental investigation of curvature and freestream turbulence effects on heat transfer and fluid mechanics in transitional boundary layer flows 19 p3264 N85-30240
Experimental determination of the mixing frequency parameter for coalescence/dispersion modeling of turbulent combustion [DE85-011468] 19 p3270 N85-30280
Excitation of turbulence by density waves [NASA-CR-3905] 19 p3314 N85-30546
Measurements of folded path optical scintillation using a corner cube, a cat's eye and a flat mirror reflector [AD-A154044] 19 p3367 N85-30679
Ion-acoustic double layer in a magnetic picket fence configuration [INPE-3552-PRE/764] 19 p3369 N85-30898
Two-point theory of current-driven ion-cyclotron turbulence [DE85-010114] 19 p3372 N85-30918
Transition in Turbines [NASA-CP-2386] 20 p3452 N85-31433
Preliminary results of a study of the relationship between free-stream turbulence and stagnation region heat transfer 20 p3452 N85-31435
Flat-plate transition 20 p3452 N85-31436
Sandia Cooperative Group on the Aerothermochemistry of Turbulent Combustion [DE85-004720] 20 p3455 N85-31453
Sandia Cooperative Group on the Aerothermochemistry of Turbulent Combustion [DE85-007493] 20 p3455 N85-31454
Progress in the development of a two-fluid model of turbulence: A set of 42 lecture panels [CFD/84/20] 20 p3457 N85-31469
Verification of theoretically computed spectra for a point rotating in a vertical plane [DE85-011967] 20 p3520 N85-31893
Mean and large-scale turbulence characteristics of the noise-producing region of an acoustically excited round jet 20 p3523 N85-31911
R and D activities of the Propulsion Division 20 p3539 N85-32025
Large eddy structures in transitional and turbulent flames [AD-A154520] 21 p3562 N85-32157
Experiments on the influence of active walls on the initial amplitudes and growths of instability waves [AD-A154630] 21 p3583 N85-32275
Velocity and transient measurements in a shock tube using a hot-wire anemometer [AD-A154664] 21 p3589 N85-32305
Observations of mesospheric turbulence by rocket probe and VHF radar, part 2.4A 21 p3619 N85-32484
Mesospheric measurements of irregularity patches using a 3-antenna interferometer, part 3.6B 21 p3621 N85-32498
Techniques for the study of gravity waves and turbulence (keynote paper), part 4 21 p3621 N85-32499
Spectral measurements of turbulence and gravity waves, part 4.2A 21 p3622 N85-32501
Relationship of isolated turbulent regions to the general turbulent background, part 4.4A 21 p3623 N85-32506
Multiparameter conditionally sampled laser velocimetry measurements during flame propagation in a spark ignition engine [DE85-009850] 22 p3793 N85-33502
A simulation of high energy cosmic ray propagation 1 [OG-5.4-1] 22 p3865 N85-34078
Interstellar turbulence, random density variations, and scintillation measurements [OG-7.2-13] 23 p4015 N85-34880
On the cosmic ray diffusion in a violent interstellar medium [OG-7.2-14] 23 p4015 N85-34881
The role of cosmic rays in magnetic hydrodynamics of interstellar medium [OG-7.2-15] 23 p4015 N85-34882
Noise-sustained structure, intermittency and the Ginzburg-Landau equation [DE85-009626] 24 p4094 N85-35379
Study of the parameters affecting the collapse of a rotating protostellar cloud 24 p4168 N85-35837

TURBULENCE EFFECTS
Application of two and three-dimensional criteria for calculating transitions and boundary layers over swept wings 08 p1070 N85-16783
Magnetohydrodynamic (MHD) turbulence in radio galaxies 12 p1958 N85-22305
Influence of turbulence of incident stream on three dimensional boundary layer 14 p2276 N85-24113
An excitation mechanism for solar 5-minute oscillation of intermediate and high degree 14 p2444 N85-25085
The effects of atmospheric turbulence on an air-to-air optical communication link [AD-A151840] 15 p2543 N85-25700
A three-dimensional turbulent separated flow and related mesurements [NASA-CR-175913] 18 p3096 N85-29181
Radio wave scattering and intermittency of turbulence in the atmosphere 19 p3288 N85-30392
Radio wave scattering and turbulence intermittence in atmosphere 19 p3298 N85-30446
The Terrain-Responsive Atmospheric Code (TRAC) for plume growth and dispersion in complex terrain [DE85-010541] 19 p3309 N85-30513
Fluctuations in light intensity during backscattering in turbulent medium 21 p3695 N85-32956
Compressible two-phase flow instabilities simulated with a hybrid Lagrange-Euler pseudospectral method [DE85-009904] 23 p3931 N85-34361
The physical and empirical basis for a specific clear-air turbulence risk index [NASA-CR-178522] 24 p4120 N85-35540

TURBULENCE METERS
Lidar measurements of structural characteristics of atmospheric turbulence 06 p0824 N85-15229
Turbulence measurements in shock induced flows 13 p2091 N85-23055
Surface shear stress characteristics in turbulent flows 19 p3211 N85-29914

TURBULENT BOUNDARY LAYER
Turbulent boundary layers over rough surfaces hypersonic flow [AD-A145040] 01 p0003 N85-10016
An integral method for analyzing incompressible two dimensional turbulent boundary layers with separation 02 p0196 N85-11309
Design, manufacture, and testing of compliant coatings for reduction of turbulent drag [AD-A145510] 02 p0198 N85-11323
Similarity criteria of spectra of pressure pulsations of turbulent boundary layer near wall 02 p0258 N85-11679
Developed turbulent flow under conditions of internal and external problems 02 p0260 N85-11700
Geometric characteristics of turbulent boundary layer separation upon action with direct shock wave in conical flows 02 p0269 N85-11755
A study of the critical layer in a rotating liquid payload [AD-A146094] 03 p0362 N85-12321
Laminar and turbulent boundary layers in a plane of symmetry [AD-A146261] 03 p0362 N85-12323
Turbulent boundary layers with secondary flow [NASA-TM-77494] 04 p0498 N85-13176
The aerodynamics of bluff bodies in turbulent shear layers 05 p0583 N85-13780
Friction and heat exchange in laminar and turbulent boundary layers with axisymmetrical bodies exposed to heterogeneous supersonic flow 05 p0724 N85-14655
Channel constructed to provide well defined boundary layers for vorticity optical probe measurements [AD-A146679] 06 p0809 N85-15140
Design studies of thick laminar flow airfoils for low speed flight employing turbulent boundary layer suction over the rear part 08 p1070 N85-16786
On the relaxation of a turbulent boundary layer after an encounter with a forward facing step 08 p1071 N85-16789
Full scale experiments into the use of large eddy breakup devices for drag reduction on aircraft 08 p1071 N85-16790
Oblique shock wave-turbulent boundary layer interaction on a porous wall with suction 08 p1072 N85-16794
Transonic shock interaction with a tangentially-injected turbulent boundary layer 08 p1072 N85-16796
A 3-dimensional turbulent boundary layer upstream and around a junction vortex flow 08 p1160 N85-17319
Aerothermal tests of a 12.5 percent cone at Mach 6.7 for various Reynolds numbers, angles of attack and nose shapes — conducted in Langley 8-foot high temperature tunnel [NASA-TP-2345] 08 p1161 N85-17322
Comparison of techniques to measure the low wavenumber wall pressure spectrum of a turbulent boundary layer [AD-A148074] 08 p1162 N85-17331
Development of a floating element wall shear transducer [AD-A148450] 08 p1164 N85-17346
Some structural features of unsteady separating turbulent shear flows [AD-P004164] 09 p1265 N85-17949
Experiments on controlled, unsteady, separated turbulent boundary layers [AD-P004172] 09 p1266 N85-17957
A finite difference method for inverse mode calculations of a three-dimensional boundary layer [ESA-TT-80[illegible]] 09 p1274 N85-18007
Comparison of two-dimensional laser and hot-wire velocimetry for a supersonic turbulent boundary layer 11 p1576 N85-19927
Experimental investigation of a turbulent incompressible boundary layer on a curved wall 11 p1577 N85-19936
Finite difference method for solving turbulent boundary layer equations 11 p1619 N85-20193
A survey of the turbulent drag reduction using passive devices [NMI-R-193] 11 p1630 N85-20288
Flight-measured laminar boundary-layer transition phenomena including stability theory analysis [NASA-TP-2417] 12 p1771 N85-21118
A study of the turbulent layer in the water at an air-water interface 14 p2378 N85-24679
An experimental study of hairpin-type vortices as a potential flow structure of turbulent boundary layers 15 p2553 N85-25751
Computational models of the viscous sublayer and limiting behavior of turbulence near a wall [AD-A151198] 15 p2556 N85-25767
An exploratory investigation of sharp fin-induced shock wave/turbulent boundary layer interactions at high shock strengths [AD-A151571] 15 p2556 N85-25772
Viscous effects on blast wave flowfields [AD-A152013] 15 p2558 N85-25779
Three-dimensional boundary layers and shear flows activities at ONERA/CERT 15 p2558 N85-25785
Three-dimensional boundary layer research at NLR 15 p2559 N85-25787
Brief review of current work in the UK on three dimensional boundary layers 15 p2559 N85-25788
Thermodynamic evaluation of transonic compressor rotors using the finite volume approach [NASA-CR-175811] 16 p2708 N85-26712
An experimental study of compressible turbulent reattaching free shear layers 16 p2781 N85-27161
Vortex studies relating to boundary layer turbulence and noise [NASA-TM-87475] 16 p2782 N85-27169
Theoretical investigation of three-dimensional shock wave turbulent boundary layer interactions. Part 3 [AD-A152251] 16 p2783 N85-27177
An experimental investigation of the interaction between a shock wave and a turbulent boundary layer on a convex wall [VTH-LR-428] 16 p2785 N85-27187
Navier-Stokes computational study of axisymmetric transonic turbulent flows with a two-equation model of turbulence [AD-A152653] 17 p2958 N85-28265
Numerical simulation of unsteady motion in a turbulent mixing layer [NAL-TR-849T] 18 p3099 N85-29183
On the origin of streamwise vortices in a turbulent boundary layer [AD-A153651] 18 p3100 N85-29188
An experimental study of plane mixing layer development [NASA-TM-86696] 19 p3221 N85-29971
Transverse vorticity measurements in an excited two-dimensional mixing layer 19 p3264 N85-30241
Acrosswind response of towers and stacks of circular cross-section 19 p3282 N85-30354
A survey of the turbulence in the marine surface layer for the operation of low-Reynolds number aircraft [AD-A154133] 19 p3316 N85-30558
Analysis of the turbulent near wake at a sharp trailing edge 20 p3387 N85-31006
The effects of microbubbles on turbulent boundary layer skin friction 20 p3451 N85-31425
Transition in Turbines [NASA-CP-2386] 20 p3452 N85-31433

Transition in a disturbed environment 20 p3452 N85-31436

Experimental observation of transition behavior on a flat plate 20 p3452 N85-31437

On the evaluation of boundary layer measurements on boattailed bodies of revolution in axisymmetric compressible subsonic flow [ESA-TT-883] 20 p3457 N85-31471

Trailing edge flow and aerodynamic sound. Part 1: Tonal pressure and velocity fluctuations. Part 2: Random pressure and velocity fluctuations [AD-A154947] 21 p3552 N85-32097

An evaluation of four methods of numerical analysis for two-dimensional airfoil flows [AD-A155202] 21 p3552 N85-32098

Recession of graphitic nozzles in rocket motors 21 p3560 N85-32144

Investigations of micro-turbulence in the bottom of the boundary layer [AD-A155148] 21 p3636 N85-32585

Thermal contraction of current flow through electrode turbulent boundary layer 21 p3690 N85-32926

On the application of a hairpin vortex model of wall turbulence to trailing edge noise prediction [NASA-CR-177938] 22 p3728 N85-33109

Experimental aerodynamic heating to simulated space shuttle tiles in laminar and turbulent boundary layers with variable flow angles at a nominal Mach number of 7 [NASA-TP-2307] 23 p3929 N85-34351

A three-dimensional turbulent boundary layer undergoing transverse strain and streamwise pressure gradient [NASA-TM-86768] 23 p3930 N85-34358

Adverse pressure gradient and separating turbulent boundary-layer flows: The effect of disequilibrium in initial conditions 24 p4059 N85-35155

Vortex boundary-layer interactions [NASA-CR-176192] 24 p4093 N85-35373

Pressure cross spectra in turbulent boundary layers in water [AD-A156153] 24 p4094 N85-35378

TURBULENT DIFFUSION

Engineering method of calculating a turbulent diffusion flame [BLL-M-35761-(5828.4)] 02 p0171 N85-11147

On the co-variant formulation of the law of motion of passive particles in a field of turbulence [REPT-564] 03 p0377 N85-12407

Combustion driven oscillation of ducted diffusion flame 09 p1289 N85-18094

Influence of turbulence on erosion by a particle-laden fluid jet [DE84-014365] 09 p1320 N85-18301

Atmospheric diffusion in hilly region on middle reaches of the Chang Jiang 11 p1620 N85-20196

Continued research in mesoscale air pollution simulation modeling. Volume 6. Further studies in the modeling of microscale phenomena [PB85-137370] 12 p1887 N85-21844

Constraints of observations of solar oscillations on solar models with mixing by turbulent diffusion [DE85-003741] 13 p2205 N85-23678

An equation of profile of snow drift density during snowfall 15 p2561 N85-25919

Field validation of 6-particle puff model [DE85-004073] 15 p2589 N85-25962

Estimation of vertical diffusion from observations of Atmospheric turbulence layers, part 4.4B 21 p3623 N85-32507

MST radar data management 21 p3627 N85-32532

Application of a turbulent closure model to the parameterization of the vertical diffusion of heat, momentum, and humidity in the ECMWF model --- European Center for Medium Term Weather Forecasting (ECMWF) [MITT-41] 24 p4095 N85-35387

TURBULENT FLOW

NT CAVITATION FLOW

A review and analysis of boundary layer transition data for turbine application [NASA-TM-86880] 01 p0047 N85-10306

Analytical modeling of random thermal fluctuations in the NORDA high-frequency sound scattering facility [AD-A145024] 01 p0116 N85-10790

Accelerated convergence for incompressible flow calculations [NASA-TM-86863] 02 p0140 N85-10949

Direct numerical simulation of curved turbulent channel flow [NASA-TM-85974] 02 p0197 N85-11316

Preliminary results of a study of the relationship between free stream turbulence and stagnation region heat transfer [NASA-TM-86884] 02 p0197 N85-11317

The CMC/3DPNS computer program for prediction of three-dimensional, subsonic, turbulent aerodynamic juncture region flow. Volume 3: Programmers' manual [NASA-CR-165998] 02 p0197 N85-11318

Design, manufacture, and testing of compliant coatings for reduction of turbulent drag [AD-A145510] 02 p0198 N85-11323

Computer simulation techniques for turbulent flows [CFD/84/11] 02 p0199 N85-11331

Developed turbulent flow under conditions of internal and external problems 02 p0260 N85-11700

Laminar-to-turbulent flow transition under influence of acoustic oscillations 02 p0260 N85-11701

Second order modeling of scalar turbulent flows 03 p0360 N85-12311

The structure of the vorticity field in turbulent channel flow. Part 2: Study of ensemble-averaged fields [NASA-TM-86657] 03 p0361 N85-12317

Numerical simulations of compliant material response to turbulent flow, revision 1 [AD-A145801] 03 p0372 N85-12373

Study of the structure of turbulent shear flows at supersonic speeds and high Reynolds number [NASA-CR-174144] 04 p0452 N85-12865

Fundamental study of three dimensional two phase flow in combustion systems [AD-A142886] 04 p0498 N85-13177

Numerical calculation of steady turbulent flows in adverse pressure gradients [CFD/83/9] 04 p0501 N85-13195

Progress in the development of a two-fluid model of turbulence for near-wall flows, part 1 [CFD/84/7-PT-1] 04 p0501 N85-13196

Progress in the development of a two-fluid model of turbulence for near-wall flows. Part 3: Preliminary investigation of a stably-stratified boundary layer [CFD/84/9-PT-3] 04 p0501 N85-13197

Navier-Stokes computational study of axisymmetric transonic turbulent flows with a two-equation model of turbulence 05 p0634 N85-14066

Direct numerical simulation of curved turbulent channel flow 05 p0635 N85-14072

Experiments on the structure of turbulent reattaching flow 05 p0635 N85-14074

Identification of dynamic coefficients of annular turbulent seals 05 p0644 N85-14133

Analysis and testing for rotordynamic coefficients of turbulent annular seals with different, directionally homogeneous surface-roughness treatment for rotor and stator elements 05 p0644 N85-14134

Effects of fluid inertia and turbulence on force coefficients for squeeze film dampers 05 p0645 N85-14137

A three-dimensional axisymmetric calculation procedure for turbulent flows in a radial vaneless diffuser [NASA-TM-86903] 06 p0749 N85-14798

Investigation of the local mass transfer of a laminar and turbulent falling liquid film [BLL-T6368/BG/WH792/84] 06 p0807 N85-15130

Channel constructed to provide well defined boundary layers for vorticity optical probe measurements [AD-A146679] 06 p0809 N85-15140

A scanning laser velocimeter for turbulence research [NASA-CR-172493] 07 p0897 N85-15686

Studies of the wall shear stress in a turbulent pulsating pipe flow [AD-A146772] 07 p0957 N85-16068

Turbulence measurement interferometer apparatus [AD-D011377] 07 p0970 N85-16156

Ionospheric turbulence: Interchange instabilities and chaotic fluid behavior [AD-A147810] 07 p0996 N85-16337

Turbulent drag reduction research 08 p1071 N85-16788

Combustion in high speed air flows [AD-A148371] 08 p1122 N85-17070

The two-fluid model of turbulence applied to combustion phenomena [CFD/84/15] 08 p1124 N85-17089

Computation of flow and heat transfer in flow around a 180 deg bend [AD-A148065] 08 p1162 N85-17330

A 2-dimensional second order closure model of the upper atmosphere 08 p1182 N85-17450

Closure problem and numerical studies of turbulence 08 p1209 N85-17608

Research done at DERAT (October 1982 through September 1983); summary of principal results obtained [NASA-TM-77786] 08 p1228 N85-17730

USSR report: Engineering and equipment [JPRS-UEQ-85-001] 09 p1305 N85-18200

Calculating heat transfer coefficients for turbine profiles taking surface curvature and elevated flow turbulence into account 09 p1307 N85-18212

Analysis of sudden expansion flow in a two-dimensional duct with and without side-wall injection using the k-epsilon turbulence model 09 p1317 N85-18282

Turbulent bouyant flow and pressure variations around a circular cylinder in a cross uniform flow near the ground 09 p1318 N85-18287

The sensitivity analysis in k-epsilon turbulence modeling applied to jet flows 09 p1318 N85-18288

A turbulent closure model for the free atmosphere 09 p1351 N85-18502

Turbulence in pure superfluid flow 09 p1397 N85-18790

A multistage time-stepping scheme for the Navier-Stokes equations [NASA-CR-172527] 10 p1483 N85-19365

Momentum and heat transfers in a complex, but well-defined turbulent fluid flow [DE85-002857] 10 p1486 N85-19381

Discovery about temperature fluctuations in turbulent air flows 10 p1500 N85-19466

Modeling turbulent flow in compressible fluids: Metrological aspects --- conferences 11 p1575 N85-19926

Characterization of jet turbulence using infrared radiometry 11 p1576 N85-19928

Laser Raman techniques for studying flows and flames 11 p1576 N85-19929

Experimental approach to terms within grids --- turbulent flow calculations 11 p1576 N85-19930

Fourier densitometry: A new optical method for measuring density fluctuations by Rayleigh scattering --- turbulent jets 11 p1576 N85-19932

Research in nonlinear problems of energy: Informal technical report [DE85-001529] 11 p1595 N85-20031

Numerical simulation of turbulent reacting flows [DE84-016777] 11 p1632 N85-20278

Calculation of oscillating turbulent flows in open channels [KU-SFB-80/T/226] 11 p1633 N85-20289

Pre-turbulence: Transitional Laminar-turbulent flows 11 p1716 N85-20793

An investigation of turbulence mechanisms in V/STOL upwash flow fields [AD-A149786] 12 p1772 N85-21123

Investigation of flowfields found in typical combustor geometries [NASA-CR-3869] 12 p1779 N85-21167

Two-dimensional measurements of OH concentration and temperature in reactive flows [AD-A149649] 12 p1800 N85-21292

Kinetics of nitric oxide formation in laminar and turbulent methane combustion [PB85-149696] 12 p1804 N85-21313

Application of large eddy interaction model to channel flow [NASA-TM-86691] 12 p1844 N85-21572

Theoretical and empirical studies of the basic structure of turbulent shear flows, including separated flows and effects of wall curvature [AD-A149657] 12 p1846 N85-21580

Turbulent convecting flow in a square duct with a 180 deg bend: An experimental and numerical study [AD-A149969] 12 p1846 N85-21583

Time and space variability of turbulent concentration fluctuations [AD-A149963] 12 p1896 N85-21898

Hydrodynamic stability problem formulated by numerical solutions of the Navier-Stokes equations 12 p1946 N85-22223

Turbulent flows of surfacant solutions [AD-B089137L] 13 p2092 N85-23056

Flow-induced vibrations of a circular cylinder duo to turbulent internal flows [DE85-002766] 13 p2103 N85-23110

Evolution of set of Rossby waves toward anisotropic equilibrium state 13 p2109 N85-23141

Investigation of the turbulent separated flow behind a spoiler [ISL-CO-240/83] 14 p2213 N85-23726

Turbulent flow around circular cylinder uniformly rotating in infinite incompressible fluid 14 p2277 N85-24109

Hydraulic drag of rod with artificial microroughness in longitudinal flow 14 p2278 N85-24111

Calculating boundary layer on profile with laminar and turbulent flow zone 14 p2286 N85-24177

Problem of reduction to ideal tube in experimental aerodynamics 14 p2286 N85-24179

Block-implicit multigrid solution of Navier-Stokes equations in primitive variables [DE85-004071] 14 p2301 N85-24250

Energy structure of atmospheric boundary layer above waves 14 p2335 N85-24442

Modeling of shear flow in a stratified fluid 14 p2340 N85-24469

Unsteady transonic aerodynamic and aeroelastic calculations about airfoils and wings 15 p2459 N85-25185
Analysis of selected problems involving vortical flows [NASA-CR-177347] 15 p2463 N85-25212
On the structure of the turbulent vortex 15 p2463 N85-25213
Heat transfer and fluid mechanics measurements in the turbulent reattaching flow behind a backward-facing step 15 p2553 N85-25753
A critical evaluation of various turbulence models as applied to internal fluid flows [NASA-TP-2474] 15 p2554 N85-25757
The influence of jet-grid turbulence on heat transfer from the stagnation region of a cylinder in crossflow [NASA-TM-87011] 15 p2554 N85-25760
Turbulence effects on a glow discharge as derived from continuity and energy considerations [AD-A151836] 15 p2557 N85-25775
An experimental study of the noise generated by vaporous cavitation in turbulent shear flows produced by confined orifice plates 15 p2645 N85-26316
La Recherche Aerospatiale Bimonthly Bulletin Number 1984-3, 220/May-June [ESA-TT-882] 16 p2695 N85-26636
Low Reynolds number vehicles [AGARD-AG-288] 16 p2699 N85-26666
Rotor blade flap-lag stability and response in forward flight in turbulent flows 16 p2705 N85-26698
Thermodynamic evaluation of transonic compressor rotors using the finite volume approach [NASA-CR-175811] 16 p2708 N85-26712
Confined turbulent swirling recirculating flow predictions [NASA-CR-174917] 16 p2709 N85-26716
Turbulence characteristics of swirling flowfields [NASA-CR-174918] 16 p2709 N85-26717
Turbulent flow of fluid near trailing edge of plate in stream at zero angle of attack 16 p2784 N85-27057
Observations, theoretical ideas and modeling of turbulent flows: Past, present and future [NASA-TM-86679] 16 p2782 N85-27167
Dynamic response of fluid transmission lines [AD-A151926] 16 p2782 N85-27171
Study of the coupling between average, coherent and turbulent fields in a circular excited free jet [ISL-R-115/83] 16 p2785 N85-27184
Computation model of turbulent free flow: Application to axisymmetric jets [ISL-R-126/83] 16 p2785 N85-27185
The development of a computational model for a two-dimensional turbulent flow. Part 1: Mathematical background — solid fuel combustion [VTH-LR-436-PT-1] 16 p2785 N85-27188
A study of the effect of gently varying terrain on atmospheric flow near the surface 16 p2823 N85-27411
An introduction to vortex breakdown and vortex core bursting [NAE-AN-28] 17 p2892 N85-27829
SSME turbopump turbine computations 17 p2911 N85-27944
An experimental investigation of a turbulent junction vortex [NASA-CR-175915] 17 p2957 N85-28259
Heat transfer in pipes [NASA-TM-77838] 17 p2957 N85-28262
Navier-Stokes computational study of axisymmetric transonic turbulent flows with a two-equation model of turbulence [AD-A152653] 17 p2958 N85-28265
Coherent structure reflective turbulent viscous flow modeling [AD-A153086] 17 p2958 N85-28267
A three-dimensional turbulent separated flow and related measurements [NASA-CR-175913] 18 p3098 N85-29181
Surface shear stress characteristics in turbulent flows 19 p3211 N85-29914
Nacelle/pylon/wing integration on a transport model with a natural laminar flow nacelle [NASA-TP-2439] 19 p3213 N85-29924
Decay of a coherent scalar disturbance in a turbulent flow [NASA-TM-86700] 19 p3264 N85-30244
Turbulent transport and length scale measurement experiments with confined coaxial jets [NASA-CR-174831] 19 p3265 N85-30245
One mechanism for generation of wave disturbances in spectra of turbulent flows near ocean surface 19 p3289 N85-30397
A study of the turbulent layer in the water at an air-water interface [AD-A154117] 19 p3319 N85-30578
Sandia Cooperative Group on the Aerothermochemistry of Turbulent Combustion. Discussion record of fourth meeting [DE85-004720] 20 p3423 N85-31248
Intermittency, conditional sampling and turbulent combustion 20 p3424 N85-31249
Conditional modelling in turbulent shear flows 20 p3424 N85-31250
The microstructure approach to conserved scalar pdf models 20 p3424 N85-31251
Rayleigh scattering for density measurements in premixed flames: One point, time series data 20 p3424 N85-31253
Blowout of turbulent diffusion flames 20 p3425 N85-31256
Non-equilibrium effects in turbulent diffusion flames 20 p3425 N85-31258
Vortex simulation of v-shaped flame 20 p3425 N85-31259
Mechanisms of exhaust pollutants and plume formation in continuous combustion [AD-A154169] 20 p3435 N85-31310
The effect of injection-stream turbulence on film cooling effectiveness and heat transfer coefficients 20 p3451 N85-31424
Turbulent reacting flows 20 p3451 N85-31427
A mathematical analysis of the effect of free stream turbulence on the Blasius boundary layer 20 p3451 N85-31430
Combustor turbulence 20 p3452 N85-31434
Heat transfer and fluid mechanics measurements in transitional boundary layer flows 20 p3453 N85-31439
A review and analysis of boundary layer transition data for turbine application 20 p3453 N85-31440
Turbulent solutions of equations of fluid motion 20 p3453 N85-31441
An implicit finite-difference code for a two-equation turbulence model for three-dimensional flows [NASA-TM-86752] 20 p3454 N85-31448
On the multifractal nature of fully developed turbulence and chaotic systems [PREPRINT-413] 20 p3455 N85-31458
Progress in the development of a two-fluid model of turbulence: A set of 42 lecture panels [CFD/84/20] 20 p3457 N85-31469
Optimization of a numerical method to calculate elliptic flows [ESA-TT-889] 20 p3457 N85-31472
Injection of drag reducing additives into turbulent water flows: Two-component velocity measurements and mixing length model predictions [AD-A154604] 21 p3583 N85-32274
Numerical solutions of turbulent models for flow over a flat plate with angle of attack [DE85-010360] 21 p3585 N85-32286
Determination of billows and other turbulent structures, part 4.1A 21 p3621 N85-32500
Recent results at the Sunset radar 21 p3627 N85-32536
Theoretical foundations of turbulent flows 21 p3683 N85-32880
On the application of a hairpin vortex model of wall turbulence to trailing edge noise prediction [NASA-CR-177936] 22 p3728 N85-33109
Sandia Cooperative Group on the Aerothermochemistry of Turbulent Combustion. Discussion record of the second meeting [DE85-007493] 22 p3743 N85-33203
Comments on two matters related to turbulent combustion 22 p3743 N85-33204
Pressure correlations in turbulent reacting flows 22 p3744 N85-33205
Second order modelling in non-constant density flows 22 p3744 N85-33206
Turbulent mixing and combustion 22 p3744 N85-33207
Jet flows: Modelling and experiments 22 p3744 N85-33208
Simultaneous measurement of velocity and density in a turbulent nonpremixed flame 22 p3744 N85-33209
Vortex dynamics simulation of conserved scalar dissipation 22 p3745 N85-33210
Nonequilibrium chemistry in an isothermal turbulent flow 22 p3745 N85-33211
Modeling of turbulent recirculating combusting flows 22 p3745 N85-33212
Turbulence modelling for the prediction of turbulent jets: Wakes and plumes [CFD/84/5] 22 p3784 N85-33447
The calculation of two-dimensional buoyant surface jets with the k-W model of turbulence --- kinetic energy-vorticity fluctuations (k-W) [CFD/84/21] 22 p3785 N85-33448
Experimental aerodynamic heating to simulated space shuttle tiles in laminar and turbulent boundary layers with variable flow angles at a nominal Mach number of 7 [NASA-TP-2307] 23 p3929 N85-34351
A study of the second and third order closure models of turbulence for prediction of separated shear flows [NASA-CR-176127] 23 p3929 N85-34353
Adverse pressure gradient and separating turbulent boundary-layer flows: The effect of disequilibrium in initial conditions 24 p4059 N85-35155
Prediction of turbulent internal recirculating flows with K-epsilon models 24 p4092 N85-35366
Studies on effects of boundary conditions in confined turbulent flow predictions [NASA-CR-3929] 24 p4093 N85-35371
Turbulent structure of stably stratified nocturnal slope flows [AD-A155845] 24 p4123 N85-35559
Two-point closure study of covariance budgets for turbulent Rayleigh-Benard convection [PB85-189108] 24 p4124 N85-35566

TURBULENT HEAT TRANSFER
A study of the effect of wake-passing on turbine blades [OUEL-1515/84] 03 p0363 N85-12325
Convective heat transfer coefficients for pipe flow with curvature induced secondary motion 09 p1318 N85-18285
An experimental investigation of flap turbulent heat transfer and pressure characteristics in hypersonic flow 12 p1821 N85-21426
Coupling between velocity oscillations and solid propellant combustion [AD-A151081] 14 p2247 N85-23927
Design and construction of a computer controlled mirothermocouple probe for the study of buoyant jets [AD-A152224] 16 p2786 N85-27199
Experimental investigation of turbulent heat transfer in straight and curved rectangular ducts [AD-A154413] 19 p3266 N85-30255
Bypass transition to turbulence and research Desiderata 20 p3453 N85-31442
Scale seperation closure and Alfven wave turbulence [DE85-013124] 24 p4095 N85-35385

TURBULENT JETS
The properties of plane turbulent buoyant jet [NAL-TR-798] 01 p0046 N85-10304
Characteristics of a turbulent plane offset jet 02 p0196 N85-11310
An experimental study of jet impingement on a circular cylinder [AD-A145583] 02 p0198 N85-11326
Mass and momentum transport in a turbulent buoyant vertical axisymmetric jet 05 p0635 N85-14070
Design of swirled axisymmetric turbulent jets 05 p0724 N85-14657
The properties of a round turbulent buoyant jet [NAL-TR-826] 06 p0806 N85-15136
Turbulent jet flow in a channel with a circulation region 09 p1306 N85-18216
An experimental study of single and multiple turbulent buoyant jets in crossflow 09 p1317 N85-18281
Deflected jet experiments in a turbulent combustor flowfield [NASA-CR-174863] 13 p1973 N85-22390
Behavior of turbulent gas jets in an axisymmetric confinement [NASA-CR-174829] 15 p2473 N85-25265
An experimental investigation of unexcited and exicted elliptic jets 15 p2554 N85-25755
Buoyant jet entrainment in stratified fluids 19 p3263 N85-30238
Conditional modelling in turbulent shear flows 20 p3424 N85-31250
Recent measurements in turbulent jet flames at Sandia Combustion Research Facility 20 p3424 N85-31254
Assessment of superlayer contribution to the conserved scalar PDF in a hydrogen turbulent jet diffusion flame 20 p3425 N85-31255
Strong turbulence chemistry interaction in a piloted turbulent jet diffusion flame 20 p3425 N85-31257
Jet flows: Modelling and experiments 22 p3744 N85-33208
Turbulence modelling for the prediction of turbulent jets: Wakes and plumes [CFD/84/5] 22 p3784 N85-33447

TURBULENT MIXING
Further developments of a nongradient theory of premixed turbulent flames [NAL-TR-802T] 01 p0023 N85-10143
Experiments on turbulent mixing and chemical reactions in a liquid mixing layer 02 p0134 N85-10912
Effects of core mixing on solar oscillation frequencies [DE84-015540] 03 p0449 N85-12853

Long range effect of turbulent pressure pulsations in plane-parallel flows at different velocities with various flame fronts 09 p1308 N85-18220
Mixing chemical reaction and flow field development in ducted rockets
[DE85-002710] 11 p1501 N85-20009
Propagation of three-dimensional turbulent jet from lobar nozzle through surrounding stream
13 p2042 N85-22785
Time-dependent flow of stream swirled in vortex chamber 13 p2043 N85-22786
Behavior of turbulent gas jets in an axisymmetric confinement
[NASA-CR-174829] 15 p2473 N85-25265
An experimental investigation of confined, multiple, turbulent jet mixing with recirculation — flow distribution in combustors with injection plates
15 p2555 N85-25764
Mixing across a gas-gas interface
[AD-A151471] 15 p2556 N85-25770
Kolmogorov and scaler spectral regimes in numerical turbulence
[NASA-TM-86699] 17 p2957 N85-28264
Numerical simulation of unsteady motion in a turbulent mixing layer
[NAL-TR-849T] 18 p3099 N85-29183
Transverse vorticity measurements in an excited two-dimensional mixing layer 19 p3264 N85-30241
Destruction of density jumps in ocean by turbulence
19 p3291 N85-30407
Slow chemistry effects in a turbulent mixing layer
20 p3424 N85-31252
Recent measurements in turbulent jet flames at Sandia Combustion Research Facility 20 p3424 N85-31254
Strong turbulence chemistry interaction in a piloted turbulent jet diffusion flame 20 p3425 N85-31257
Mechanisms of exhaust pollutants and plume formation in continuous combustion
[AD-A154169] 20 p3435 N85-31310
An experimental investigation of confined, multiple, turbulent jet mixing with recirculation
20 p3451 N85-31426
Errors and parameterizations of sub-grid scale processes in regional-scale atmospheric models
20 p3488 N85-31682
Mean and large-scale turbulence characteristics of the noise-producing region of an acoustically excited round jet 20 p3523 N85-31911
Vertical transport in the atmosphere: Measurement capabilities and requirements of VHF radars, part 1.6A
21 p3617 N85-32476
Morphology of the scattering targets: Fresnel and turbulent mechanisms, part 2.1A
21 p3618 N85-32481
Turbulent mixing and combustion
22 p3744 N85-33207
Jet flows: Modelling and experiments
22 p3744 N85-33208
TURBULENT WAKES
NT PROPELLER SLIPSTREAMS
NT SLIPSTREAMS
A study of the effect of wake-passing on turbine blades
[OUEL-1515/84] 03 p0363 N85-12326
Experimental studies of transonic airfoil trailing edge and wake flowfield properties 05 p0592 N85-13773
Wake flow behind bluff bodies
05 p0593 N85-13783
A free shear layer prediction of the turbulent wake of a flat plate towed below a free surface
[AD-A148699] 09 p1319 N85-18293
Method for the prediction of the installation aerodynamics of a propfan at subsonic speeds
[NASA-CR-3887] 13 p1969 N85-22369
Calculating isothermal flow in wake beyond injection zone 14 p2287 N85-24175
Periodic vortex shedding in the supersonic wake of a planar plate
[NASA-TM-77854] 15 p2463 N85-25207
Development of a rotor wake-vortex model, volume 1
[NASA-CR-174849] 16 p2699 N85-26668
New facility to study unsteady wake effects on turbine airfoil heat transfer 17 p2911 N85-27948
Turbulent wake of a submerged flat plate
[AD-A153776] 18 p3100 N85-29190
Acrosswind response of towers and stacks of circular cross-section 19 p3282 N85-30354
Analysis of the turbulent near wake at a sharp trailing edge 20 p3387 N85-31006
Turbulence modeling in a two-dimensional wake
20 p3452 N85-31431
Trailing edge flow and aerodynamic sound. Part 1: Tonal pressure and velocity fluctuations. Part 2: Random pressure and velocity fluctuations
[AD-A154947] 21 p3552 N85-32097
Turbulence modelling for the prediction of turbulent jets: Wakes and plumes
[CFD/84/5] 22 p3784 N85-33447
Laser Doppler Anemometer (LDA) measurements in the turbulent near-wake of blunt bodies
[ISL-CO-212/84] 22 p3785 N85-33450
TURING MACHINES
One queue or two pushdown stores take square time on a one-head tape unit
[CWI-CS-R8406] 05 p0717 N85-14601
Counting is easy — Turing machines
[CWI-CS-R8423] 17 p3009 N85-28606
TURKEY
Delineation of major geologic structures in Turkey using SIR-B data 08 p1149 N85-17249
TURNAROUND (STS)
Overview od STS ground operations/orbiter turnaround STS-1 through STS-7 08 p1096 N85-16926
TURNING FLIGHT
Robust rate control system designs for a submersible
[AD-A144792] 01 p0111 N85-10753
High specific power aircraft turn maneuvers: Tradeoff of time-to-turn versus change in specific energy
[AD-A151701] 15 p2471 N85-25257
TURRET LATHES
Production turret lathe retrofitted with robot
10 p1461 N85-19214
TURTLES
Transatlantic migration study of the leathery turtle using the ARGOS system. Transatlantic turtle race
14 p2326 N85-24379
TUTOR AIRCRAFT
U CL-41 AIRCRAFT
TVC (CONTROL)
U THRUST VECTOR CONTROL
TWILIGHT GLOW
Twilight intensity variation of the infrared hydroxyl airglow 11 p1663 N85-20481
TWINNING
The growth of twins and twin lamellae in synthetic diamond crystals 02 p0181 N85-11213
Development of high-efficiency solar cells on silicon web
[NASA-CR-174212] 06 p0826 N85-15259
Method of fabricating acceleration resistant crystal resonators and acceleration resistant crystal resonators so formed
[AD-D011630] 16 p2778 N85-27145
TWISTED WINGS
Effect of a variable camber and twist wing at transonic Mach numbers
[NASA-TM-86281] 04 p0452 N85-12869
Detailed pressure distribution measurements obtained on several configurations of an aspect-ratio-7 variable twist wing
[NASA-TM-86308] 10 p1419 N85-18950
TWISTING
Indications of twist in the Epsilon rings of Uranus
15 p2672 N85-26490
Effects of shepherd conjunctions on Saturn's F-ring
15 p2675 N85-26511
TWO BODY ORBITS
U TWO BODY PROBLEM
TWO BODY PROBLEM
Nonlinear oscillations of 2 body system relative to center of mass in elliptical orbit 02 p0159 N85-11082
Constraints on the origin of viscoelastic bodies
04 p0584 N85-13732
Accumulation of the terrestrial planets
13 p2179 N85-23524
TWO DIMENSIONAL BODIES
Forced vibrations of friction-damped beam structures in two dimensions
[UDR-TM-82-08] 04 p0456 N85-12892
Current status of one- and two-dimensional numerical models: Successes and limitations
20 p3482 N85-31636
On the dependence of the convergence of Gummel's algorithm on the regularity of the solution
[AD-A154628] 21 p3675 N85-32832
Adaptive rezoner in a two-dimensional Lagrangian hydrodynamic code
[DE85-010108] 24 p4094 N85-35381
Use of a minimum-ellipse criterion in the study of ion-beam extraction systems
[DE85-012670] 24 p4148 N85-35721
TWO DIMENSIONAL BOUNDARY LAYER
Stability of heated boundary layers
02 p0196 N85-11311
Boundary condition effects in the energy loss spectrum of layered systems
[NOTA-INTERNA-802] 02 p0289 N85-11887
Influence of turbulence of incident stream on three dimensional boundary layer 14 p2278 N85-24113
Stability calculations of the two-dimensional boundary layer along a concave wall: Part 1: A numerical method of solution for the simultaneous ordinary differential equations governing disturbances
[NAL-TR-841] 15 p2554 N85-25758
TWO DIMENSIONAL FLOW
NT COUETTE FLOW
An integral method for analyzing incompressible two dimensional turbulent boundary layers with separation
02 p0196 N85-11309
Stability of heated boundary layers
02 p0196 N85-11311
Large structure in the far wakes of two-dimensional bluff bodies 05 p0592 N85-13771
Unsteady flow characteristics in the near-wake of a two-dimensional obstacle
[NASA-TM-77782] 07 p0897 N85-15684
Laminar flow over a backward-facing step
[AD-A147469] 07 p0960 N85-16084
Unsteady free-convection heat transfer inside an annular cavity
[CFD/84/16] 08 p1163 N85-17339
Weakly-reflective boundary conditions for two-dimensional shallow water flow problems
[PUBL-322] 08 p1163 N85-17341
Modeling of turbulent dispersion of neutral and buoyant contaminants released from two dimensional sources — air pollution
[VKI-TN-150] 08 p1180 N85-17436
A 2-dimensional second order closure model of the upper atmosphere 08 p1182 N85-17450
Flow instabilities in transonic small disturbance theory
[NASA-TM-86251] 09 p1273 N85-18000
Analysis of sudden expansion flow in a two-dimensional duct with and without side-wall injection using the k-epsilon turbulence model 09 p1317 N85-18282
Numerical predictions for unsteady viscous flow past an array of cylinders 09 p1318 N85-18284
SSME thrust chamber simulation using Navier-Stokes equations
[NASA-CR-171349] 10 p1430 N85-19017
Transonic interactions of unsteady vortical flows
[NASA-TM-86658] 12 p1770 N85-21113
Pseudospectral calculations of two-dimensional transonic flow (Task 1). Numerical investigation of VTOL aerodynamics (Task 2)
[AD-A150123] 12 p1772 N85-21126
Numerical integration of the unsteady full-potential equation with applications to transonic flow about a two-dimensional airfoil
[NLR-MP-84022-U] 12 p1773 N85-21130
Experimental studies of Quasi-Two-Dimensional and three-dimensional viscous interaction regions induced by skewed-shock and swept-shock boundary layer interactions
[AD-A150080] 12 p1847 N85-21587
A linear characteristic-nodal transport method for the two-dimensional (X,Y)-geometry multigroup discrete ordinates equations over an arbitrary triangle mesh
[LA-10092-T] 12 p1913 N85-22006
Propagation of three-dimensional turbulent jet from lobar nozzle through surrounding stream
13 p2042 N85-22785
Evolution of set of Rossby waves toward anisotropic equilibrium state 13 p2109 N85-23141
Stability of Rossby waves within framework of three-component analysis 13 p2109 N85-23142
Wave motion of three-component medium under load moving on plane boundary 14 p2277 N85-24105
Discrete models for the numerical analysis of time-dependent multidimensional gas dynamics
[NASA-CR-172574] 14 p2300 N85-24239
Laser anemometry two dimensional measurement of velocity fluctuations in an excited jet
[ISL-CO-213/83] 14 p2302 N85-24254
Unsteady transonic aerodynamic and aeroelastic calculations about airfoils and wings
15 p2459 N85-25185
A finite element, Navier-Stokes study of the confined, laminar flow over a downstream facing step
15 p2553 N85-25754
Influence of surface roughness on compressor blades at high reynolds number in a two-dimensional cascade
[AD-A151855] 15 p2557 N85-25777
The development of a computational model for a two-dimensional turbulent flow. Part 1: Mathematical background — solid fuel combustion
[VTH-LR-436-PT-1] 16 p2785 N85-27188
Supersonic flow around weak radiation sources
17 p2942 N85-28162
Flow quality of National Aerospace Laboratory two-dimensional transonic wind tunnel. Part 3: Flow turbulence level and measuring method
[NAL-TR-842-PT-3] 18 p3064 N85-28952

Time-averaged and time-dependent computations of isothermal flowfields in a centerbody combustor
[AD-A153662] 18 p3100 N85-29169
Screening phase transitions in two-dimensional Coulomb gas
[NOTA-INTERNA-830] 18 p3192 N85-29798
Use of a two-dimensional flow model to quantify aquatic habitat
[AD-A154267] 19 p3266 N85-30253
KIVA: A computer program for two- and three-dimensional fluid flows with chemical reactions and fuel sprays
[DE85-010334] 19 p3339 N85-30693
A numerical method for the solution of the inverse problem in external aerodynamics
[STN-7] 20 p3390 N85-31025
Turbulent reacting flows 20 p3451 N85-31427
Turbulence modeling in a two-dimensional wake
20 p3452 N85-31431
Two-dimensional separation in an incompressible fluid --- boundary layer separation
[ONERA-RTS-16/3232-RY-060-R]
20 p3456 N85-31459
An evaluation of four methods of numerical analysis for two-dimensional airfoil flows
[AD-A155202] 21 p3552 N85-32098
Finite element methods for viscoelastic flow
[AD-A154877] 22 p3783 N85-33437
Two-dimensional simulation of instability growth due to shocks
[DE85-011869] 22 p3784 N85-33442
Turbulence modelling for the prediction of turbulent jets: Wakes and plumes
[CFD/84/5] 22 p3784 N85-33447
The calculation of two-dimensional bucyant surface jets with the k-W model of turbulence --- kinetic energy-vorticity fluctuations (k-W)
[CFD/84/21] 22 p3785 N85-33448
Unsteady flow in a supersonic cascade with two in-passage shocks
[NASA-CR-3925] 24 p4060 N85-35158
Numerical studies of 2-dimensional flows
[NASA-CR-3930] 24 p4060 N85-35160

TWO DIMENSIONAL JETS
Large amplitude forcing of a high speed 2-dimensional jet
[NASA-CR-175646] 13 p1974 N85-22393

TWO FLUID MODELS
Progress in the development of a two-fluid model of turbulence for near-wall flows, part 1
[CFD/84/7-PT-1] 04 p0501 N85-13196
Progress in the development of a two-fluid model of turbulence for near-wall flows. Part 3: Preliminary investigation of a stably-stratified boundary layer
[CFD/84/9-PT-3] 04 p0501 N85-13197
The two-fluid model of turbulence applied to combustion phenomena
[CFD/84/15] 08 p1124 N85-17089
Direct electron and ion fluid computation of high electrostatic fields in dense inhomogeneous plasma with subsequent nonlinear optical and dynamical laser interaction 15 p2656 N85-26388
Progress in the development of a two-fluid model of turbulence: A set of 42 lecture panels
[CFD/84/20] 20 p3457 N85-31469

TWO PHASE FLOW
Void fraction measurements performed in a vertical large diameter tube compared to different predicting correlations
[GKSS-84-E-24] 01 p0048 N85-10315
Visualization of the diverging two-phase flow pattern in a horizontal T-junction with vertical branch
[GKSS-84-E-25] 01 p0048 N85-10316
Investigation of the gas-content of gas-liquid systems
[BLL-M-35748-(5828.4)] 02 p0171 N85-11146
One-dimensional two-phase constant lag flow in combustion chamber of solid propellant rocket motors
[AD-A145679] 02 p0173 N85-11157
Investigation of crisis phenomena in thermosyphons with internal heat-dissipation
[BLL-M-35765-(5828.4)] 02 p0197 N85-11313
Combustion waves in dispersed-2-phase mixtures
[CFD/84/13] 04 p0472 N85-13003
Fundamental study of three dimensional two phase flow in combustion systems
[AD-A142666] 04 p0498 N85-13177
Similarity considerations in 1-component 2-phase flow
[DE84-016370] 04 p0499 N85-13184
Deterministic sensitivity analysis of two-phase flow systems: Forward and adjoint methods
[DE84-016276] 04 p0499 N85-13185
Theoretical description of film boiling in a two phase flow calculation
[IKE-2-66] 05 p0636 N85-14092
VORT: A computer code for bubbly two-phase flow
[DE84-017076] 06 p0809 N85-15142
Flow of nitrogen-pressurized Halon 1301 in fire extinguishing systems
[NASA-CR-174271] 07 p0900 N85-15701
Influence of turbulence on erosion by a particle-laden fluid jet
[DE84-014365] 09 p1320 N85-18301
Averaging effects in models of three-dimensional two-phase flows
[AD-A149313] 10 p1484 N85-19371
TRACR3D: A model of flow and transport in porous/fractured media
[LA-9667-MS] 12 p1845 N85-21576
Two-phase flow in geothermal systems
[DE85-004692] 12 p1848 N85-21591
Fundamental study of three dimensional two phase flow in combustion systems
[AD-A150739] 14 p2250 N85-23945
A fundamental study of liquid phase particle breakup. Revision
[AD-A150791] 14 p2301 N85-24249
Two-phase fluid thermal transport for spacecraft
[AD-A151316] 15 p2493 N85-25378
Application of the Van Leer method to the solution of one-dimensional volume fraction equations
[CFD/84/17] 15 p2558 N85-25781
Two-phase flow in centrifugal pumps
[BLL-CE-TRANS-8065-(9022.09)]
15 p2605 N85-26053
Measurements of two-phase exhaust flow parameters of a small caliber gun associated with muzzle flash phenomena
[ISL-CO-212/83] 16 p2784 N85-27182
Flow characteristics of a partially submerged liquid pickup
[DE85-008744] 17 p2959 N85-28276
Two phase discharge of liquefied gases through pipes. Field experiments with ammonia and theoretical model
[FOA-B-40139-C1] 18 p3103 N85-29209
Method for driving two-phase turbines with enhanced efficiency
[NASA-CASE-NPO-15037-2] 18 p3115 N85-29282
Effect of nonuniform size on internal stresses in a rapid, simple shear flow of granular materials. Part 2: Multiple grain sizes
[AD-A154046] 19 p3285 N85-30373
Droplet deposition in vertical two-phase flow
[CFD/84/22] 20 p3456 N85-31460
Intermittent gas-liquid flow modeling in horizontal or weakly inclined pipes
[EME-132] 20 p3456 N85-31465
Some remarks on the constitutive equations of stratified gas-liquid flow
[EME-137] 20 p3456 N85-31466
Enthalpy transients in fractured two-phase geothermal systems
[DE85-011988] 22 p3808 N85-33587
Compressible two-phase flow instabilities simulated with a hybrid Lagrange-Euler pseudospectral method
[DE85-009904] 23 p3931 N85-34361
Stability of two-dimensional immiscible flow to viscous fingering
[DE85-011403] 23 p3931 N85-34364
A two-phase flow and heat transfer model for zero gravity
[AD-A156097] 24 p4094 N85-35377

TWO PHASE SYSTEMS
U BINARY SYSTEMS (MATERIALS)

TWO REFLECTOR ANTENNAS
Attempts to contruct two-dimensional image of Sun from observations made with RATAN-600 radiotelescope by relay race method 06 p0783 N85-15005
The 20 GHz proof-of-concept test model results for a multiple scan beam dual reflector antenna
[NASA-CR-174268] 07 p0938 N85-15944
BBC receiving terminal for the European orbital test satellite
[BBC-RD-1984/15] 08 p1142 N85-17205
Interpolation methods for GTD analysis of shaped reflectors 10 p1463 N85-19231

TWO-WAVELENGTH LASERS
Spectral evolution of the pulse of a dual frequency dye laser
[CNES-83/168/T/CT/DRT/TIT/10]
20 p3461 N85-31497
High-power two-frequency CW dye laser
21 p3686 N85-32900

TYPE 3 BURSTS
Interplanetary radio storms. 2: Emission levels and solar wind speed in the range 0.05-0.8 AU
[NASA-TM-84946] 04 p0589 N85-13761
Arguments for fundamental emission by the parametric process L yields T + S in interplanetary type III bursts --- langmuir, electromagnetic, ion acoustic waves (L, T, S) 12 p1958 N85-22311
Evidence concerning the generation mechanism of solar type 3 radio bursts 16 p2886 N85-27802
Type 3 solar radio bursts and 3HE-rich events
[SH-2.2-3] 23 p4000 N85-34796

TYPE 4 BURSTS
The longitudinal asymmetry of the interplanetary perturbation producing Forbush decreases
[IFSI-84-18] 20 p3546 N85-32066
Interplanetary disturbances during Forbush decreases
[IFSI-84-10] 20 p3547 N85-32075
The flare origin of Forbush decreases not associated with solar flares on the visible hemisphere of the Sun
[SH-5.1-4] 23 p4041 N85-35058

TYPEWRITERS
The representation of action plans in long term memory 05 p0709 N85-14545

TYPHOONS
Frequency and motion of western North Pacific tropical cyclones
[PB85-106466/GAR] 06 p0839 N85-15331
Meteorological Satellite Center Technical Note No. 10, 1984
[MSC-TN-10] 12 p1894 N85-21884
On the relative motion of typhoons: In the case of Typhoon 8305 and Typhoons 8306 and 8307
12 p1894 N85-21885
On the error of typhoon intensity estimation by means of IR Dvorak technique occurring when the eye is very small 12 p1894 N85-21886
Accuracy of typhoon center determined by GMS imagery 12 p1894 N85-21887
Hurricane Research Division, fiscal year 1984 programs, fiscal year 1985 projections 16 p2836 N85-27491

U

U TUBES
U MANOMETERS

U.S.S.R.
Development of powder metallurgy in various sections of USSR 01 p0019 N85-10116
Report on high-precision jig-boring machines
01 p0035 N85-10215
Growth, future of Soviet robotics sector analyzed
01 p0035 N85-10217
USSR report: Space
[JPRS-USP-84-005] 02 p0156 N85-11060
Features and uses of progress cargo ships
02 p0157 N85-11061
USSR report: Physics and mathematics
[JPRS-UPM-84-006] 02 p0256 N85-11676
USSR report: Transportation
[JPRS-UTR-84-028] 03 p0310 N85-12002
Ministry wants better commo facilities for agroaviation
03 p0310 N85-12003
Start-2 ATC system installation progresses at Leningrad 03 p0311 N85-12007
USSR report: Electronics and electrical engineering
[JPRS-UEE-84-014] 03 p0344 N85-12215
Bibliography of Soviet laser developments, number 65, May - June 1983
[AD-A146189] 03 p0366 N85-12347
USSR report: Electronics and electrical engineering
[JPRS-UEE-84-010] 04 p0485 N85-13095
USSR report: Physics and mathematics
[JPRS-UPM-84-007] 05 p0723 N85-14651
Manganese in recent sediments of Ukrainian SSR Black Sea shelf 06 p0819 N85-15200
Thermal energy resources of thermal waters in Kazakhstan 06 p0820 N85-15208
Deep structure of terrestrial crust and upper mantle in southeastern Siberia and Far East according geological-geophysical data 06 p0821 N85-15212
Automated Lavina collects data on snow
07 p0980 N85-16224
New data on presence of ores in salt dome structures of Dnieper-Donets Basin 07 p0981 N85-16234
Deep structure of Western Siberia
07 p0981 N85-16235
Deputy Minister discusses plans for geothermal power
07 p0994 N85-16313
USSR report: Life sciences. Biomedical and behavioral sciences
[JPRS-UBB-84-027] 07 p1012 N85-16426
USSR report: Transportation
[JPRS-UTR-85-001] 08 p1067 N85-16763
Director on institute's civil aviation projects
08 p1067 N85-16764
International projects, other work of Aeroproyekt Institute 08 p1068 N85-16767
Designer on civil aircraft design trends in USSR
08 p1068 N85-16768
Regional and seasonal variations in snow-cover density in the USSR
[AD-A148429] 08 p1189 N85-17496

USSR report: Life sciences. Biomedical and behavioral sciences
[JPRS-UBB-85-001] 08 p1193 N85-17515
USSR report: Transportation
[JPRS-UTR-85-003] 09 p1277 N85-18032
First deputy minister on 1984 civil aviation performance 09 p1277 N85-18033
Collegium on aviation fuel conservation efforts
09 p1278 N85-18034
Activities at Mil Experimental Design Bureau
09 p1278 N85-18036
Improvements under way at Gorkiy airport
09 p1278 N85-18040
USSR report: Engineering and equipment
[JPRS-UEQ-85-001] 09 p1305 N85-18200
USSR report: Life sciences. Biomedical and behavioral sciences
[JPRS-UBB-85-007] 09 p1362 N85-18566
USSR report: Materials science and metallurgy
[JPRS-UMS-84-008] 10 p1442 N85-19088
French commentary on Soviet industrial espionage
10 p1481 N85-19210
Types of placer formation of eastern Arctic shelf
10 p1498 N85-19452
Relationship of gold content to gravity fields in Far East 10 p1501 N85-19475
USSR report: Life sciences. Biomedical and behavioral sciences
[JPRS-UBB-85-008] 10 p1523 N85-19605
USSR report: Life sciences. Biomedical and behavioral sciences
[JPRS-UBB-85-011] 10 p1525 N85-19616
USSR report: Life sciences. Biomedical and behavioral sciences
[JPRS-UBB-85-009] 10 p1526 N85-19625
Soviet National Middle Atmosphere Program
11 p1655 N85-20428
USSR report: Physics and mathematics
[JPRS-UPM-85-001] 11 p1715 N85-20786
Transportation
[JPRS-UTR-85-004] 12 p1769 N85-21105
Current development, applications of airships in USSR
12 p1769 N85-21109
New method of reconstructing conditions of recent differentiation of oil and gas in the Amudarya Basin (based on results of interpretation of space photographs)
13 p1984 N85-22446
Current plans for development of chemical industry
13 p2014 N85-22633
USSR report: Electronics and electrical engineering
[JPRS-UEE-85-002] 13 p2066 N85-22907
Possibilities of aerial electric prospecting by long cable method for detecting poorly conducting strata
13 p2115 N85-23177
Minister Bugayev on civil aviation in 1984, plans for 1985 14 p2208 N85-23689
1st deputy minister on civil aviation support of economy 14 p2208 N85-23690
Deputy minister on civil aviation fuel conservation efforts 14 p2208 N85-23691
Deputy minister on civil aviation construction projects
14 p2208 N85-23692
Improvements in personnel needed for better flight safety 14 p2208 N85-23693
USSR report: Engineering and equipment
[JPRS-UEQ-84-005] 14 p2285 N85-24157
Results of comparison of long-wave radiation fluxes measured by Soviet and Japanese actinometric radiosounds 14 p2333 N85-24427
Second Soviet-French Symposium on Space Cytology
14 p2386 N85-24699
USSR report: Cybernetics, computers, and automation technology
[JPRS-UCC-85-002] 14 p2400 N85-24794
The astrometry network of observers in USSR
14 p2436 N85-25029
USSR report: Transportation
[JPRS-UTR-85-008] 15 p2460 N85-25189
Official on Soviet research in deicing techniques
15 p2460 N85-25191
USSR report: Transportation
[JPRS-UTR-84-015] 15 p2460 N85-25192
Civil air code international flights section explained
15 p2460 N85-25194
Study of Volga river delta using space photosurvey materials 15 p2485 N85-25340
Use of space information in petroleum- and gas-prospecting work (example of Southern Mangyshlak)
15 p2485 N85-25341
USSR report: Materials science and metallurgy
[JPRS-UMS-85-001] 15 p2496 N85-25395
USSR report: Electronics and electrical engineering
[JPRS-UEE-85-005] 15 p2524 N85-25565
USSR report: Cybernetics, computers and automation technology
[JPRS-UCC-85-003] 15 p2625 N85-26174
USSR report: Physics and mathematics
[JPRS-UPM-85-003] 15 p2642 N85-26300
USSR report: Space
[JPRS-USP-85-004] 16 p2717 N85-26772
Study and mapping of anthropogenic effect on environment in different regions of USSR on basis of space photographs 16 p2726 N85-26824
USSR report: Engineering and equipment
[JPRS-UEQ-84-006] 16 p2760 N85-27035
Cloud-seeding for regulating precipitation in Moscow area 16 p2807 N85-27306
USSR report: Transportation
[JPRS-UTR-84-026] 17 p2894 N85-27841
Science and Technology in the Soviet Union
[AD-A152828] 17 p3047 N85-28856
Soviet weapons development and the scientific community
[AD-P004562] 17 p3047 N85-28857
Computing in the Soviet general economy: An introductory overview
[AD-P004563] 17 p3047 N85-28858
The outlook for Soviet advanced technologies
[AD-P004564] 17 p3048 N85-28859
Social and political problems in Soviet basic research
[AD-P004565] 17 p3048 N85-28860
Technology and Soviet political choices
[AD-P004566] 17 p3048 N85-28861
Technology and technical efficiency in the Soviet Union: Dominant patterns of constrained optimization in a noncompetitive economic regime
[AD-P004567] 17 p3048 N85-28862
The revolution in military affairs and the Soviet system
[AD-P004568] 17 p3048 N85-28863
Close encounters with S/T (science and technology) in the Soviet Union
[AD-P004570] 17 p3048 N85-28864
R/D contracts in the Soviet Union
[AD-P004569] 17 p3048 N85-28865
Permafrost, seasonally frozen ground, snow cover and vegetation in the USSR
[AD-A153628] 18 p3124 N85-29346
Search and rescue at sea in the USSR
20 p3400 N85-31094
COSPAS-SARSAT demonstration and evaluation phase: COSPAS tests in the USSR and their results
20 p3405 N85-31130
Microwave hydrology: A trilogy
[NASA-CR-176042] 20 p3477 N85-31603
on the transport of large condensation nuclei in the atmosphere at various altitudes over the territory of the USSR 21 p3653 N85-32698
USSR Space Life Sciences Digest
[NASA-CR-3922] 21 p3656 N85-32709
USSR report: Electronics and electrical engineering
[JPRS-UEE-84-003] 22 p3773 N85-33381
The development of titanium production in the USSR
[BLL-OA-TRANS-3226-(6196.3)]
23 p3913 N85-34244
Space activities in the Soviet Union, Japan, and the People's Republic of China 23 p4057 N85-35149

U.S.S.R. SPACE PROGRAM
Soviet space programs, 1976-1980, with supplementary data through 1983. Part 2: Manned space programs and space life sciences
[S-REPT-98-235-PT-2] 01 p0014 N85-10088
Tass reports medical, materials studies aboard Salyut-7 02 p0158 N85-11071
25th anniversary of the Gagarin Cosmonaut Training Center
[NASA-TM-77644] 09 p1286 N85-18076
The space flight of the Soviet-Indian crew
[NASA-TM-77615] 12 p1788 N85-21226
USSR report: Space Biology and Aerospace Medicine, volume 18, no. 6, November - December 1984
[JPRS-USB-85-002] 12 p1900 N85-21931
Feoktistov says manned lunar, Mars flights lack justification 13 p1985 N85-22452
U.S., Soviet space program aims contrasted
13 p1985 N85-22455
USSR report: Space
[JPRS-USP-85-003] 15 p2476 N85-25284
List of recent Soviet space launches
15 p2489 N85-25361
Interkosmos program of space communication development 15 p2528 N85-25585
Forecasts on long-range development of space programs 16 p2727 N85-26830
International cooperation in space exploration
16 p2766 N85-27079
Soviet space programs, 1976-1980 (with supplementary data through 1983). Part 3: Unmanned space activities
[S-PRT-98-235-PT-3] 16 p2879 N85-27765

U-2 AIRCRAFT
NASA thunderstorm overflight program: Atmospheric electricity research. An overview report on the optical lightning detection experiment for spring and summer 1983
[NASA-TM-86468] 03 p0363 N85-12330
Discovery of nuclear tracks in interplanetary dust
06 p0889 N85-15647

UBV SPECTRA
UBV photometry of E region stars: Some intercomparisons 01 p0126 N85-10880

UDIMET ALLOYS
The response of cobalt-free Udimet 700 type alloy to modified heat treatments
[NASA-TM-86942] 11 p1597 N85-20043

UH-1 HELICOPTER
Navigation and flight director guidance for the NASA/FAA helicopter MLS curved approach flight test program
[NASA-CR-177350] 16 p2704 N85-26691

UH-60A HELICOPTER
UH-60A external stores support system fixed provision fairings drag determination
[AD-A147186] 07 p0902 N85-15719
A comparison of lightning and nuclear electromagnetic pulse response of a helicopter 07 p1000 N85-16349
Assessment of simulation fidelity using measurements of piloting technique in flight 08 p1075 N85-16817

UHTREX (NUCLEAR REACTORS)
U HIGH TEMPERATURE NUCLEAR REACTORS

UK SATELLITES
NT MIRANDA SATELLITE
UK Skynet 4 communications satellites
11 p1710 N85-20757
Minimization of system vulnerability in Naval satellite communication networks 11 p1710 N85-20758

ULM (LIGHT MODULATION)
U ULTRASONIC LIGHT MODULATION

ULTRA SHORT WAVE RADIO EQUIPMENT
U VERY HIGH FREQUENCY RADIO EQUIPMENT

ULTRAHIGH FREQUENCIES
Wave multiple scattering by a finite number of unclosed circular cylinders
[NASA-TM-77593] 01 p0037 N85-10232
VHF/UHF radar and its application in nowcasting
01 p0078 N85-10516
DRG theory on the basis of a discrete interaction model
[PR-215] 03 p0358 N85-12297
Shuttle S-band communications technical concepts
08 p1099 N85-16948
Using the global positioning system (GPS) phase observable for relative geodesy: Modeling, processing, and results 09 p1341 N85-18437
Dissemination of ERS-1 low bit rate data and the use of L-band receiving stations
[NLR-TR-83049-U] 09 p1358 N85-18542
Effect of modulated ultrahigh frequency field on behavior and hormone level in female rats under emotional stress
09 p1361 N85-18562
Broad-band UHF dipole array
[NASA-TM-86373] 10 p1462 N85-19222
UHF radiowave propagation through forests
[AD-A149518] 10 p1467 N85-19256
UHF communications through forested propagation channels 10 p1470 N85-19280
Measurements of propagation at 900 MHz in an urban zone for establishing a digital radiomobile system
10 p1472 N85-19288
Shuttle S-band high gain switched beam breadboard antennas
[NASA-CR-171852] 10 p1478 N85-19327
Assessment of satellite power flux-density limits in the 2025-2300 MHz frequency range, part 2
[PB85-101244] 11 p1625 N85-20236
Spectrum resource assessment of the fixed and mobile services in the 947-17,700 MHz band, phase 1
[PB85-128288] 11 p1626 N85-20243
The ARGOS Platform Transmitter Terminals (PTTs)
14 p2237 N85-23872
Propagation considerations in land mobile satellite transmission
[NASA-CR-175733] 15 p2540 N85-25684
Optimal frequencies for broadcast transmitters in the UHF domain: Report
[TUM-M8404] 16 p2769 N85-27088
A phase modulation evaluation procedure for an ARGOS type signal 16 p2811 N85-27336
FAA (Federal aviation administration) assessment of satellite concepts and aviation spectrum requirements
[AD-A152331] 17 p2948 N85-28199
Measurements of VHF/UHF radio propagation in a maritime temperate climate
[CRC-1360] 18 p3089 N85-29119
Improved high performance television receiver
[PB85-170751] 18 p3092 N85-29139

Dielectric resonator stabilized microstrip oscillator
[AD-D011706] 19 p3261 N85-30219

The CCIR satellite EPIRB coordinated trials programme --- Emergency Position Indicating Radio Beacon (EPIRB); International Radio Consultative Committee (CCIR) 20 p3402 N85-31111

The International Radio Consultative Committee (CCIR) recommended satellite Emergency Position Indicating Radio Beacon (EPIRB) system operating through geostationary satellites at 1.6 GHz
20 p3402 N85-31112

A 406 MHz geostationary satellite SARSAT experiment 20 p3403 N85-31113

A 406 MHz ELT processor for geostationary satellites --- Emergency Locator Transmitter (ELT)
20 p3403 N85-31114

Evolution of 406 MHz Search and Rescue (SAR) processor 20 p3403 N85-31116

A micro/PDP-11 system for 406 MHz COSPAS/SARSAT processing 20 p3403 N85-31117

Search and rescue satellite (SARSAT) error analysis of the 406 MHz system 20 p3403 N85-31118

The 121.5/243 MHz ELT identification — Emergency Locator Transmitter (ELT) 20 p3404 N85-31119

SARSAT 406 MHz system technical evaluation
20 p3404 N85-31124

SARSAT 121.5/243 MHz technical evaluation
20 p3405 N85-31126

Potential advantages of the spaced antenna method for operational wind profiling, part 3.1B
21 p3620 N85-32490

Hadron cross sections at ultra high energies and unitarity bounds on diffraction dissociation
[HE-1.1-3] 24 p4170 N85-35851

1Single particle momentum and angular distributions in hadron-hadron collisions at ultrahigh energies
[HE-1.2-1] 24 p4171 N85-35860

ULTRAHIGH VACUUM

Precision manipulator heating and cooling apparatus for use in UHV systems with sample transfer capability
[NASA-CASE-LAR-13040-1] 18 p3116 N85-29286

Space shuttle molecular and wake vacuum measurements
[NASA-TM-86509] 19 p3222 N85-29978

ULTRALIGHT AIRCRAFT

Parachute extraction device for ultralight gliders
[CH-643499-A5] 16 p2699 N85-26663

ULTRALOW FREQUENCIES

U EXTREMELY LOW RADIO FREQUENCIES

ULTRALOW TEMPERATURES

Thermal and mechanical properties of polyurethane foams and a survey of insulating concretes at cryogenic temperatures
[PB85-100949/GAR] 07 p0934 N85-15918

ULTRASHORT PULSED LASERS

Coherent amplification of ultrasonic pulses in activated crystals 05 p0724 N85-14653

Clock synchronization by the Symphonie and Laser Synchronization from Stationary Orbit (LASSO) geostationary satellites 14 p2398 N85-24778

Optical inhomogeneities in a nanosecond-pulse iodine photodissociation laser with slow UV radiation pumping
21 p3686 N85-32902

ULTRASONIC CLEANING

Cleaning procedures of laser mirror substrates
[DFVLR-MITT-84-06] 05 p0640 N85-14108

ULTRASONIC FLAW DETECTION

Ultrasonic synthetic aperture focusing using unfocused pulse-echo transducers
[AERE-R-11230] 01 p0057 N85-10374

Modernization of IDTs-6 ultrasonic installation
[BLL-M-35716-(5828.4)] 02 p0206 N85-11356

High-frequency asymptotic behavior of reflected and transmitted waves during scattering of sound by hollow elastic sphere filled with fluid 02 p0266 N85-11738

Identification of pulse-echo rays in austenitic steels
[AERE-R-11265] 03 p0369 N85-12356

Ultrasonic and metallurgical examination of a cracked type 304 stainless steel BWR pipe weldment
[TI84-014966] 04 p0511 N85-13254

Defect detection threshold in riveted joints, test report no.44-833/F --- in aircraft 04 p0511 N85-13260

The detection and assessment of defects in automatic ultrasonic inspection
[BLL-RISLEY-TR-4597-(9091.9F)]
05 p0647 N85-14150

Pulse-echo method for flaw detection in concrete
[PB84-234509] 06 p0775 N85-14953

NDE (Nondestructive Evaluation) of oxygen contaminated titanium alloys and weldments
[AD-P004121] 08 p1126 N85-17096

Leak monitoring in high pressure preheaters by a noninvasive ultrasonic method
[CISE-2373] 11 p1650 N85-20394

Leak detection by acoustic emission monitoring in power plant high pressure preheaters
[CISE-2392] 11 p1650 N85-20395

Defect characterisation and monitoring by acoustic emission
[AERE-R-11409] 12 p1863 N85-21683

An amplitude correlation and differencing method for the monitoring of flaws in repeat ultrasonic inspections
[AERE-R-11416] 15 p2571 N85-25854

Sizing capability of automated ultrasonic time-of-flight diffraction in thick section steel and aspects of reliable inspection in practice
[AERE-R-11548] 15 p2571 N85-25855

Laser-based non-destructive testing techniques for the ultrasonic characterization of sub-surface flaws
[AERE-R-11562] 15 p2572 N85-25856

Nondestructive tests of ceramic components for aircraft turbines 16 p2709 N85-26718

Echo-responses from crack-like two-dimensional reflectors in focused ultrasonic fields. Ultrasonic crack tip method for the determination of crack depth
[BLL-BISI-22062-(9022.06)] 16 p2796 N85-27236

Ultrasonic testing of carbon fiber reinforced plastics (CFRP) using pattern recognition methods
[MBB-BB-563/84-0] 16 p2873 N85-27726

Ultrasonic flaw detector with microcomputer interpretation
[BMFT-FB-T-84-272] 17 p2977 N85-28395

Detecting and analyzing crack defects
[BLL-BISI-TRANS-22062-(9022.06)]
17 p3027 N85-28723

Echo-responses from crack-like two-dimensional reflectors in focused ultrasonic fields
17 p3027 N85-28724

Ultrasonic crack tip method for the determination of crack depth 17 p3028 N85-28725

Ultrasonic testing of tubes
[BLL-BISI-TRANS-22337-(9022.06)]
18 p3119 N85-29304

Characteristic features of testing equipment: Application to the ultrasonic inspection of tubes
18 p3119 N85-29305

Study of an ultrasonic detection method to inspect bonding effects in light alloy bonded structures, test report no. 43-954/F --- aircraft structures
[PV-43-954/F] 22 p3795 N85-33510

Ultrasonic inspection of carbon fiber reinforced plastic by means of sample-recognition methods
[NASA-TM-77896] 24 p4074 N85-35245

ULTRASONIC LIGHT MODULATION

Four-wave hypersonic reversing mirrors in saturated mode 11 p1719 N85-20812

ULTRASONIC RADIATION

Polarization of ultrasound transmitted through boundary of magnetically inactive and equatorially magnetized media 02 p0257 N85-11682

Theory of harmonic generation of finite amplitude ultrasonic waves in solids of hexagonal symmetry
[AD-A146636] 06 p0860 N85-15465

Superlattice ultrasonic wave generator
[AD-D011363] 07 p1036 N85-16585

Effects of scatterer spacing statistics on ultrasonic backscatter signal spectra
[DE85-003259] 12 p1928 N85-22114

Investigations of ultrasonic wave interactions at boundaries separating anisotropic materials
[DE85-003506] 13 p2155 N85-23384

Connection between time- and frequency-domain three-dimensional inverse problems for the Schroedinger equation
[DE85-005914] 15 p2639 N85-26274

An electro-optic spatial light modulator for thermoelastic generation of programmably focused ultrasound
[AD-A152066] 15 p2646 N85-26323

Acoustooptic pulse-echo transducer system
[NASA-CR-175919] 17 p2951 N85-28224

Dual differential interferometer
[NASA-CASE-LAR-12966-1] 19 p3271 N85-30262

Method for thermal monitoring subcutaneous tissue
[NASA-CASE-LAR-13028-1] 19 p3328 N85-30618

Development of ultrasonic modeling techniques for the study of crustal inhomogeneities
[AD-A155206] 21 p3632 N85-32565

Second Colloquim on the Scattering of Ultrasonic Waves
[AD-A156298] 24 p4145 N85-35697

Exploring results of the possibility on detecting cosmic ray particles by acouctic way
[HE-7.1-3] 24 p4213 N85-36157

ULTRASONIC SCANNERS

Study and realization of a Doppler system with pulsed, directional, multiport (128) emission and sequential signal treatment — ultrasonic echography, blood flow
[ENST-84E006] 05 p0639 N85-14102

Ultrasonic measurements, X-ray photographs and image processing
[BLL-RISLEY-TR-4586-(9091.9F)]
07 p1037 N85-16583

Measurement of ultrasonic fields in transparent media using a scanning differential interferometer
[NASA-CR-175921] 17 p3028 N85-28726

Study of requirements for and method of multidimensional acoustic imaging --- spaceborne experiments
[ESA-CR(P)-2020] 20 p3525 N85-31924

ULTRASONIC SPECTROSCOPY

Second Colloquim on the Scattering of Ultrasonic Waves
[AD-A156298] 24 p4145 N85-35697

ULTRASONIC TESTS

Nonlinear ultrasonic characterization of oxygen impurities in titanium, 2
[AD-A144657] 01 p0027 N85-10171

Ultrasonic nondestructive evaluation, microstructure, and mechanical property interrelations
[NASA-TM-86876] 01 p0056 N85-10371

Evaluation of interfacial stresses from the amplitude of reflected ultrasonic signal
[DE84-015472] 02 p0276 N85-11798

Technical activities 1983, Office of Nondestructive Evaluation
[PB84-217074] 03 p0370 N85-12380

Nondestructive evaluation of residual stress in low-carbon steel, introduction 04 p0512 N85-13265

Nondestructive determination of mechanical properties --- aluminum alloys 04 p0512 N85-13266

Measurement of the preloading of bolted joints by the ultrasonic method
[CETIM-1-5H-38-6] 04 p0558 N85-13556

Ultrasonic girth weld evaluation for aluminum substrate of spherical Kevlar-epoxy test specimens
[DE85-001592] 06 p0816 N85-15181

Nondestructive inspection: Improved capabilities of technicians
[AD-A147368] 07 p0975 N85-16196

Ultrasonic analysis of spherical composite test specimens
[DE85-001591] 07 p0976 N85-16197

Use of the analytic signal in ultrasonic imaging
[DE84-016843] 07 p1039 N85-16598

Effects of oxygen-contamination-induced microstructural changes on the reverberation of ultrasound in Ti-6211 alloys
[AD-P004124] 08 p1126 N85-17099

Ultrasonic evaluation of titanium contamination with correlation techniques
[AD-P004126] 08 p1126 N85-17101

Modeling of real UT transducer field/flaw interactions
[DE85-000341] 09 p1329 N85-18351

Emerging technology of synthetic aperture focusing for ultrasonic testing
[DE85-000373] 09 p1378 N85-18864

Ultrasonic inspection of alloyed tungsten bars
[AD-A148900] 10 p1495 N85-19435

Ultrasonic analysis of Kevlar-epoxy filament wound spherical test specimens
[DE85-005198] 11 p1593 N85-20024

Ultrasonic large-diameter pipe weld testing installations 11 p1603 N85-20081

Quantitative non-destructive evaluation of damage in composite materials using transmitted and reflected ultrasound
[NASA-CR-175550] 12 p1796 N85-21269

The role of dislocations in ultrasonic attenuation
[AERE-R-11384] 12 p1804 N85-21317

Application of homomorphic signal processing to stress wave factor analysis
[NAS 1.26:174871] 12 p1861 N85-21673

Defect characterisation and monitoring by acoustic emission
[AERE-R-11409] 12 p1863 N85-21683

The measurement of residual stresses using ultrasonics
[AERE-R-11415] 12 p1888 N85-21722

Effects of scatterer spacing statistics on ultrasonic backscatter signal spectra
[DE85-003259] 12 p1928 N85-22114

Investigation of steel structures using ultrasonic waves
[BR93258] 13 p2101 N85-23091

Standing of industrial radiography in South Africa
14 p2316 N85-24311

Ultrasonic non-destructive testing technique
14 p2316 N85-24313

Laser-based non-destructive testing techniques for the ultrasonic characterization of sub-surface flaws
[AERE-R-11562] 15 p2572 N85-25856

An electro-optic spatial light modulator for thermoelastic generation of programmably focused ultrasound
[AD-A152066] 15 p2646 N85-26323

Ultrasonic dispersion of soils for routine particle size analysis: Recommended procedures
[DE85-006530] 16 p2861 N85-27643
Ultrasonic test evaluation of the insert bond on hermetic connectors
[DE85-006394] 18 p3120 N85-29310
Grain structure identification by ultrasound frequency averaging and deconvolution
[AD-A154332] 19 p3352 N85-30777
Advanced ultrasonic imaging of piping in Dresden and Vermont Yankee reactors
[TI85-010049] 20 p3464 N85-31520
The use of ultrasound to monitor incipient failure of rolling element bearings 23 p3924 N85-34317
Calculations on the feasibility of ultrasonic inspection of steam generator tubing in pressurized water reactors
[AERE-R-10960] 23 p3940 N85-34419
Quantitative non-destructive evaluation of composite materials based on ultrasonic wave propagation
[NASA-CR-176176] 24 p4074 N85-35244
ULTRASONIC WAVE TRANSDUCERS
Multiple passband transducers for tone selection from a frequency comb generator
[RSRE-MEMO-3647] 02 p0194 N85-11295
Qualification of noninvasive systems for on-line leak detection in high pressure feed water preheaters
[CISE-2341] 04 p0558 N85-13555
New types of power supplies for ultrasonic processing equipment 12 p1843 N85-21586
Piezoelectric and electrostatic polymeric transducers for acoustic emission detection
[AD-A150883] 14 p2306 N85-24272
A multi-element ultrasonic ranging array
[AD-A150698] 14 p2416 N85-24906
Ultrasonic testing of tubes
[BLL-BISI-TRANS-22337-(9022.06)]
18 p3119 N85-29304
Electrodynamic transducers for ultrasonic reception
18 p3119 N85-29306
The use of ultrasound to monitor incipient failure of rolling element bearings 23 p3924 N85-34317
ULTRASONIC WAVES
U ULTRASONIC RADIATION
ULTRASONIC WELDING
Non-destructive testing of HF-welded pipe
[BLL-BISI-TRANS-22182-(9022.06)]
17 p2976 N85-28388
Ultrasonic seam welding on thin silicon solar cells
[NASA-CR-176116] 22 p3805 N85-33570
ULTRASONICS
Collapse of cavitation bubbles between two walls in ultrasonic field 02 p0266 N85-11739
Propagation of acoustic shear waves through active periodic structure 04 p0490 N85-13125
Optical method of measuring velocity of shear waves
06 p0787 N85-15029
Nondestructive measurement of bulk residual stresses
[AD-A147063] 07 p0978 N85-16211
Optical fibers with reduced pressure sensitivity to high frequency acoustic field
[AD-D011306] 07 p1043 N85-16627
Nonlinear ultrasonic characterization of oxygen impurities in titanium
[AD-P004123] 08 p1126 N85-17098
Ultrasonic transducers, performance variability, design, and manufacturing procedures
[AD-A148575] 08 p1158 N85-17306
Journal of Research of the National Bureau of Standards, Volume 89, Number 1, January-February, 1984
[PB84-235530] 08 p1262 N85-17931
An electro-optic spatial light modulator for thermo-elastic generation of programmably focused ultrasound
[AD-A149078] 10 p1553 N85-19794
Stress waves in an isotropic elastic plate excited by a circular transducer
[NASA-CR-3877] 11 p1650 N85-20390
Elastic compliance of imperfect interfaces: Review and relationship to ultrasonic scattering
[DE85-003068] 11 p1652 N85-20404
Dynamic world modeling for an intelligent mobile robot using a rotating ultra-sonic ranging device
[AD-A149979] 12 p1775 N85-21143
Continuous measurement of zircaloy corrosion in air with an ultrasonic corrosion monitor
[DE85-003663] 12 p1807 N85-21337
Journal of Research of the National Bureau of Standards, volume 89, number 2, March - April 1984
[PB85-115426] 12 p1926 N85-22103
Elastic wave scattering from cavities and sound inclusions analyzed by the resonance method
[AD-A150315] 13 p2155 N85-23381
Applications of ultrasonic technology
14 p2263 N85-24144
A multi-element ultrasonic ranging array
[AD-A150698] 14 p2416 N85-24906
Ultrasonic SH wave velocity in textured aluminum plates
[AERE-R-11516] 15 p2509 N85-25475
Sonars with high noise and clutter rejection for use with adaptive robots
[AD-A151875] 15 p2543 N85-25701
The development of a transducer system for the accurate measurement of ultrasonic phase delay of SH plate waves
[AERE-R-11598] 15 p2559 N85-25790
Ultrasonic characterization of porosity: Theory
[DE85-005922] 15 p2646 N85-26325
Evaluation of experimental epoxy monomers
[NASA-TM-87476] 16 p2754 N85-26996
Creating a Mobile Autonomous Robot Research System (MARRS)
[AD-A151963] 16 p2793 N85-27229
Method for ultrasonic bonding to soft microelectronic substrates
[NASA-CASE-NPO-16087-1] 18 p3094 N85-29151
Electrodynamic transducers for ultrasonic reception
18 p3119 N85-29306
Ultrasonic testing of plates containing edge cracks
[NASA-CR-3904] 18 p3119 N85-29307
Dual differential interferometer
[NASA-CASE-LAR-12966-1] 19 p3271 N85-30282
Method for thermal monitoring subcutaneous tissue
[NASA-CASE-LAR-13028-1] 19 p3328 N85-30618
Grain structure identification by ultrasound frequency averaging and deconvolution
[AD-A154332] 19 p3352 N85-30777
Ultrasonic flowmetering with reflected pulses
[PB85-179865] 20 p3460 N85-31492
Propagation and reflection of a finite amplitude ultrasonic beam including harmonic content: A numeric model
20 p3523 N85-31914
Reliability of void detection in structural ceramics using scanning laser acoustic microscopy
[NASA-TM-87035] 21 p3587 N85-32337
USSR report: Electronics and electrical engineering
[JPRS-UEE-84-003] 22 p3773 N85-33381
Non-bonded ultrasonic transducer
[DE85-011006] 22 p3794 N85-33504
Analytical ultrasonics for structural materials
[TI85-006132] 23 p3968 N85-34600
Sound speed measurements in liquid oxygen-liquid nitrogen mixtures
[NASA-TP-2464] 24 p4083 N85-35307
ULTRAVIOLET ABSORPTION
Solar radiation in the ozone layer
04 p0522 N85-13342
Measuring EUV line emission from the hot interstellar medium 06 p0880 N85-15595
Cumulus cloud venting of mixed layer ozone
[NASA-TM-87429] 13 p2132 N85-23269
Multiple product channels in the collision free UV photodissociation of 2-nitropropane
[AD-A150686] 14 p2251 N85-23951
Studies on radiative collisional and ultraviolet lasers
[AD-A151004] 14 p2310 N85-24296
Ground-based remote sensing of atmospheric pollution 16 p2832 N85-27462
Micromolecular modeling 21 p3606 N85-32405
Heating of the deep chromosphere during solar flares
[AD-A155256] 21 p3723 N85-33100
Ultraviolet radiation-damage absorption peak in solid deuterium-tritium, revision 1
[DE85-012969] 22 p3844 N85-33806
ULTRAVIOLET ASTRONOMY
UBV photometry of E region stars: Some intercomparisons 01 p0128 N85-10880
Ultraviolet observations of Uranus and Neptune below 3000 Angstrom 02 p0298 N85-11932
Documentation for the machine-readable version of the ANS Ultraviolet Photometry Catalogue of Point Sources (Wesselius et al 1982)
[NASA-TM-87379] 03 p0406 N85-12589
Observations of local ISM emission with the Berkeley EUV/FUV shuttle telescope 06 p0880 N85-15594
X-ray and UV Emission from Active Galactic Nuclei — conference
[MPE-184] 08 p1236 N85-17790
Ultraviolet spectroscopy of selected astronomical sources
[NASA-CR-174379] 09 p1413 N85-18912
Future of Ultraviolet Astronomy Based on Six Years of IUE Research
[NASA-CP-2349] 11 p1743 N85-20961
IUE absorption line studies of highly ionized interstellar gas 11 p1743 N85-20962
Hot stars: Six years of progress
11 p1743 N85-20963
Ultraviolet and X-ray observations of active galactic nuclei: Constraints on models of the broad emission line region 11 p1744 N85-20966
Interacting binary systems 11 p1744 N85-20967
Outer atmospheres of cool stars observed with IUE
11 p1744 N85-20968
Future ultraviolet experiments, including FUSE/COLUMBUS 11 p1744 N85-20969
UV observations and results on pre-main sequence stars 11 p1744 N85-20970
White dwarf stars at ultraviolet wavelengths
11 p1744 N85-20971
Supernova remnants and the carbon abundance in M33 11 p1745 N85-20972
Comments on the origins and variations of carbon and nitrogen in the ISM of galaxies as evident from IUE spectroscopy of H 2 regions 11 p1745 N85-20973
IUE spectroscopy of extragalactic H H regions
11 p1745 N85-20974
The usual hot stars in unusual galaxies
11 p1745 N85-20975
Highly ionized gas associated with the small Magellanic cloud 11 p1745 N85-20976
Galactic absorption lines measured from the IUE low dispersion spectra of active galaxies
11 p1745 N85-20977
Observations of Mg 1 and Mg 2 in the local ISM
11 p1748 N85-20997
Observations of RR Lyrae and X Arietis with the IUE satellite 11 p1754 N85-21030
The spatial dependence of the Jovian auroral emissions 11 p1759 N85-21068
Ultraviolet observations of Uranus and Neptune below 3000 A 11 p1760 N85-21071
Stellar ultraviolet flux distributions in the 912-1200 A wavelength range 11 p1762 N85-21081
Current ideas on the nature of comets
14 p2435 N85-25017
Winds in cataclysmic variable stars
[DE85-006708] 15 p2669 N85-26470
Research in extreme ultraviolet and far ultraviolet astronomy
[NASA-CR-176068] 21 p3716 N85-33060
Astron X-ray experiment 22 p3732 N85-33137
ULTRAVIOLET LASERS
Interaction of UV-laser radiation with molecular surface-films
[AD-A146311] 03 p0366 N85-12349
Development of prototypes for versatile fast discharge systems for pulsed gas lasers, especially excimer lasers
[BMFT-FB-T-84-174] 06 p0813 N85-15165
Visible and ultraviolet lasers based on excimer transitions in the homonuclear halogens
[AD-D011311] 07 p0971 N85-16163
Investigations of vacuum ultraviolet and soft X-ray lasers
[AD-A148277] 08 p1167 N85-17358
Laser-Electron-Gamma-Source (LEGS)
[DE85-003204] 11 p1638 N85-20322
Operational characteristics of the OMEGA short-wavelength laser fusion facility
[DE85-002619] 11 p1640 N85-20334
Non-linear optical techniques for visible and UV lasers and thin film deposition
[AD-A150489] 13 p2096 N85-23077
Studies on radiative collisional and ultraviolet lasers
[AD-A151004] 14 p2310 N85-24296
Laser with a hollow copper cathode
[ISL-R-119/83] 14 p2310 N85-24300
The application of laser resonance saturation to the development of efficient short wavelength lasers
[AD-A153951] 18 p3113 N85-29270
Vacuum ultraviolet laser
[DE85-011632] 22 p3790 N85-33478
Thermal transport measurements of UV laser irradiated spherical targets
[DE85-011036] 23 p3931 N85-34365
ULTRAVIOLET LIGHT
U ULTRAVIOLET RADIATION
ULTRAVIOLET MICROSCOPY
Interaction of solutes with stretched polymers
[AD-A154662] 21 p3569 N85-32196
ULTRAVIOLET PHOTOMETRY
Documentation for the machine-readable version of the ANS Ultraviolet Photometry Catalogue of Point Sources (Wesselius et al 1982)
[NASA-TM-87379] 03 p0406 N85-12589
Local interstellar extinction with an emphasis on uvby beta results 06 p0875 N85-15559
Research in extreme ultraviolet and far ultraviolet astronomy
[NASA-CR-176068] 21 p3716 N85-33060
ULTRAVIOLET RADIATION
NT EXTREME ULTRAVIOLET RADIATION
NT FAR ULTRAVIOLET RADIATION
NT LYMAN ALPHA RADIATION
Temporal and spatial variations in the intensity of ultraviolet emissions from Jupiter and the Io torus
03 p0448 N85-12846

Absolute transition probabilities of lines in the spectra of astrophysical atoms, molecules, and ions
[NASA-CR-174141] 04 p0580 N85-13705
Search for the radiative decay of a cosmic relic particle with IUE
[PREPRINT-410] 04 p0580 N85-13707
Plant responses to solar UV-B radiation
05 p0690 N85-14436
Properties of ultra-violet cured poly(dimethylsiloxane)-urea acrylates
[AD-A148570] 08 p1134 N85-17146
Active inner regions of isolated galaxies
08 p1237 N85-17795
The unidentified emission features: A study of the Orion Bar and planetary nebulae 08 p1246 N85-17862
Effect of ultraviolet radiation on transparent polymer films as determined using in situ FTIR-RA spectroscopy. Volume 2: Photophysics of poly(vinylidene fluoride) films
[DE84-013040] 09 p1299 N85-18159
Functional and structural changes in human erythrocyte surface after irradiation by UV waves of various wavelengths. Report 1: Expression of ABO and Rheaus system antigen 09 p1361 N85-18564
Functional and structural changes in human erythrocyte surface after irradiation by UV waves of various wavelentghts. Report 2: Adsorption of alcyan blue by external premembranous components
09 p1361 N85-18565
Design of VUV monochromator systems
09 p1388 N85-18733
Genetic effects of microwave exposure on mammalian cells in vitro. Volume 2, Appendix B: Cytogenetics and growth kinetics data, 1.2 GHz
[AD-A148867] 10 p1522 N85-19600
Parametric processes in underdense UV laser-produced plasmas
[DE85-002812] 10 p1559 N85-19630
Temperature-dependent surface states and transitions of Si(111)-7x7
[AD-A149156] 10 p1562 N85-19650
Report on the Workshop on Intercomparison of Solar UV Irradiance Measurements and Related Instrument Calibration 11 p1658 N85-20448
MSG-7: Molecular absorption processes related to the penetration of ultraviolet solar radiation into the middle atmosphere 11 p1658 N85-20449
The variation of galactic interstellar extencion in the ultraviolet 11 p1749 N85-21000
Interstellar extinction in the nucleus of H PER
11 p1749 N85-21001
New results on PU VUL 11 p1753 N85-21023
Temporal UV emission from the peculiar star RX Puppis 11 p1753 N85-21026
Effect of ultraviolet radiation on transparent polymer films as determined using in situ FTIR-RA spectroscopy. Volume 1: Photodegradation of transparent polymer films
[DE84-013039] 12 p1814 N85-21377
Determination of ionospheric electron density profiles from satellite UV (ultraviolet) emission measurements
[AD-A150734] 14 p2373 N85-24667
Photoreactivation and other ultraviolet/visible light effects on DNA in human skin
[DE85-005135] 14 p2390 N85-24719
Evaluation of pyrotechnic fire suppression system for six pyrotechnic compositions
[AD-A152905] 17 p2937 N85-28130
Definition of requirements for injection locking of pulsed UV lasers
[DE85-010126] 18 p3113 N85-29275
The photochemical oxidation of GaAs
[AD-A153669] 19 p3233 N85-30045
Method for the preparation of photochromic insulating crystals
[DE85-011606] 19 p3262 N85-30229
Lidar techniques for search and rescue
[DE85-009586] 19 p3278 N85-30327
Molecular toxicology of chromatin: The role of Poly(ADP-Ribose) in gene control
[AD-A154415] 19 p3327 N85-30611
Photon-counting image sensors for the ultraviolet
[NASA-CR-176062] 20 p3458 N85-31478
Polymerizable ultraviolet stabilizers
21 p3608 N85-32406
Photoinduced active sites on ice nucleating aerosol of silver iodide 21 p3639 N85-32601
Excimer-laser generator of powerful UV picosecond pulses synchronized with picosecond pulses in visible and IR bands 21 p3686 N85-32903
Investigation of some aspects of amino acid metabolism in man during brief exposure to antiorthostatic hypokinesia combined with ultraviolet radiation
22 p3822 N85-33678
Ultraviolet radiation-damage absorption peak in solid deuterium-tritium, revision 1
[DE85-012969] 22 p3844 N85-33806
Solar Ultraviolet Spectral Irradiance Monitor (SUSIM)
23 p3901 N85-34160
Process for functionalizing alkanes
[DE85-006420] 23 p3909 N85-34219
Using the information of cosmic rays to predict influence epidemic
[SH-10.1-2] 23 p4053 N85-35134
The 2nd European Conference on Atomic and Molecular Physics
[AD-A155863] 24 p4148 N85-35715
Surface discharges as intense photon sources in the extreme ultraviolet
[DE85-012593] 24 p4158 N85-35762

ULTRAVIOLET SPECTRA
Search for the radiative decay of a cosmic relic particle with IUE
[PREPRINT-410] 04 p0580 N85-13707
X-ray and ultraviolet observations of BL Lacertae objects 05 p0741 N85-14767
Observations of absorption lines from highly ionized atoms 06 p0876 N85-15562
Ultraviolet spectral morphology of O-type stellar winds
08 p1232 N85-17762
The ultraviolet spectra of the narrow line active galaxies NGC 3081 and NGC 4507 08 p1237 N85-17799
UV and X-ray observations of AGN: Two comparisons with other wave lengths — Active Galactic Nuclei (AGN)
08 p1240 N85-17819
Extended atmospheres of outer planet satellites and comets
[NASA-CR-174338] 08 p1258 N85-17916
Excimer laser photofragmentation of organophosphonates. 1: Detection of the PO radical from dimethyl methyl phosphonate (DMMP)
[AD-A149471] 10 p1490 N85-19407
International Ultraviolet Explorer observations of amorphous hot galaxies
[NASA-CR-174354] 10 p1571 N85-19904
Structure of the Seyfert broad line region and absorption region of NGC 4151 11 p1746 N85-20978
The UV spectra of intermediate redshift quasars
11 p1746 N85-20980
Very recent IUE observations of 2 BL lacertae objects
11 p1746 N85-20982
A model for the variable continuum of the Seyfert 1 galaxy NGC 5548 11 p1747 N85-20985
IUE observations of planetary nebulae in the Magellenic Clouds 11 p1747 N85-20986
IUE observations of the jet emission feature in R Aquarii 11 p1747 N85-20988
The changing ultraviolet spectrum of Herbig-Haro object No. 1 11 p1747 N85-20989
Short-wavelength observations of HH-2H and HH-24A
11 p1747 N85-20990
Ultraviolet studies of the young populous cluster NGC 2100 in the LMC 11 p1748 N85-20995
IUE observations of interstellar lines
11 p1748 N85-20996
High-velocity interstellar gas in the line-of-sight to HD 50896 11 p1749 N85-20999
Coronal effects of the winds of early-type stars
11 p1749 N85-21002
Superionized species and winds in low luminosity B and Be stars 11 p1749 N85-21003
Main sequence B stars with strong winds
11 p1750 N85-21005
IUE and ESO observations of the P Cyg star AG Carinae and its ring nebula 11 p1750 N85-21006
Coordinated ultraviolet and visual observations of Omega Orionis 1982-1983 11 p1750 N85-21007
The spectroscopic antics of S 18/SMC
11 p1750 N85-21008
An episodic red-wing structure of SiIV, lambda 1394A, in gamma Cas 11 p1750 N85-21009
IUE and Voyager observations of very hot O-type subdwarfs 11 p1751 N85-21010
Analysis of high-depression IUE spectra of subdwarf B stars 11 p1751 N85-21011
The fading of R coronae borealis
11 p1753 N85-21029
Observations of RR Lyrae and X Arietis with the IUE satellite 11 p1754 N85-21030
Atmospheric properties of RU Lupi derived from high- and low-resolution IUE spectra
11 p1754 N85-21031
Mg 2 emission of Pop. 2 long-period Cepheids
11 p1754 N85-21032
Blue companions of Cepheids
11 p1754 N85-21033
Ultraviolet observations of Population 2 Cepheids
11 p1754 N85-21034
Ultraviolet analysis of the peculiar F supergiant HD 112374 11 p1754 N85-21035
Eclipse observations of Epsilon Aurigae
11 p1755 N85-21037
The stellar wind in the BO V-type eclipsing binary Y Cygni 11 p1755 N85-21040
Multi-year and possibly periodic variations in the UV spectrum of 56 Pegasi 11 p1756 N85-21046
Physical models for the UV continua of symbiotic stars
11 p1756 N85-21048
MU Sagittarii and Beta Lyrae: Combined IUE/Voyager observations 11 p1757 N85-21052
Chromospheric activity in M giants
11 p1757 N85-21056
A progress report on the analysis of long exposure SWP high resolution spectra of cool stars
11 p1758 N85-21057
Chromospheric emission lines in high-resolution LWR spectra (220 - 3000 alpha) of gamma CRU (M3 3) and alpha ORI (M2 lab) 11 p1758 N85-21058
Rotational modulation of chromospheric emission in cool giants and hybrid stars 11 p1759 N85-21064
Ultraviolet and optical spectroscopy and polarimetry of the helium weak star HD 21669: Evidence for a magnetically controlled stellar wind
11 p1759 N85-21065
IUE spectrophotometry of helium weak and silicon stars 11 p1759 N85-21067
The Jovian Stratosphere in the ultraviolet
11 p1760 N85-21069
Long term variability of the IO torus
11 p1760 N85-21070
IUE low-dispersion reference atlas
11 p1760 N85-21073
An IUE high-resolution atlas of O-type spectra
11 p1760 N85-21074
Statistical classification of IUE low-despersion stellar spectra: Progress report 11 p1760 N85-21075
The ultraviolet excess of quasars 3: The highly polarized quasars PKS 0736+017 and PKS 1510-089
[NASA-CR-175576] 12 p1953 N85-22268
A survey of Mg II h and k emission in near-solar type stars
[NASA-CR-175572] 12 p1953 N85-22269
Plasma processes in Herbig-Haro objects
12 p1957 N85-22301
NIMBUS-7 SBUV (Solar Backscatter Ultraviolet) observations of solar UV spectral irradiance variations caused by solar rotation and active-region evolution for the period November 7, 1978 - November 1, 1980
[NASA-CR-175544] 12 p1962 N85-22334
A survey for galactic plane ultraviolet-excess objects: Space densities for white dwarfs, subdwarfs, and cataclysmic variables 13 p2169 N85-23458
Ultraviolet spectral diagnostics of solar flares and heating events 13 p2205 N85-23675
Self-developing polysilane deep-UV resists: Photochemistry, photophysics and submicron lithography
[DE85-007608] 19 p3237 N85-30067
The ultraviolet spectra of intermediate redshift quasars
20 p3544 N85-32056

ULTRAVIOLET SPECTROGRAPHS
U ULTRAVIOLET SPECTROMETERS

ULTRAVIOLET SPECTROMETERS
Oblique focus ICCD laboratory evaluation
[NASA-CR-174205] 06 p0862 N85-15460
Voyager EUV and FUV observations
06 p0875 N85-15554
A new generation of spectrometer designs for ultraviolet astronomy 11 p1761 N85-21079
Ozone Correlative Measurements Workshop
[NASA-CP-2362] 13 p2105 N85-23112
Scientific requirements for ozone measurements
13 p2105 N85-23113
Method for determining the number of correlative measurements required to validate the SBUV/2 ozone retrievals 13 p2105 N85-23114
Ultraviolet Spectrometer and Polarimeter (UVSP) software development and hardware tests for the solar maximum mission
[NASA-CR-175279] 14 p2305 N85-24271
Measurements with an auroral spectrometer in the Energy Budget Campaign
[BMFT-FB-W-84-050] 14 p2374 N85-24677
Voyager UVS observations of stellar occultations by the rings of Saturn — ultraviolet spectrometer (UVS)
15 p2673 N85-26497
French and West German equipment for Vega Project
16 p2722 N85-26805
Ground-based remote sensing of atmospheric pollution 16 p2832 N85-27462
Studies of hot B subdwarfs. Part 2: Energy distributions of three bright sdB/sdOB stars in the 950-5500 angstrom range
[NASA-CR-175854] 16 p2881 N85-27775
Solar Ultraviolet Spectral Irradiance Monitor (SUSIM)
23 p3901 N85-34160
High Resolution Telescope and Spectrograph (HRTS)
23 p3901 N85-34162

ULTRAVIOLET SPECTROPHOTOMETERS
Effect of integration time on precision of absorbances measured with a diode array UV-VIS spectrophotometer
[AD-A146952] 07 p1043 N85-16624
Winds in cataclysmic variable stars
[DE85-006708] 15 p2669 N85-26470
ULTRAVIOLET SPECTROSCOPY
Optical and UV emission of active galactic nuclei
08 p1236 N85-17791
Determination of ion temperature and rotation velocity profiles by visible, UV and X-ray spectroscopy on Doublet 3
09 p1366 N85-18734
UV observations of epsilon aurigae during ingress and totality 11 p1755 N85-21038
Egress spectra of the new eclipsing supergiant 22 Vulfeculae 11 p1755 N85-21039
Ultraviolet spectroscopy of the interacting binary U Sagittae 11 p1755 N85-21042
The essence of binary star coalescence: A coordinated ground-based photometric and IUE ultraviolet study of FK Comae 11 p1756 N85-21044
Strange F + Be binary star systems
11 p1756 N85-21045
Characterization of multiphoton ionization processes in the ultraviolet
[AD-A151427] 15 p2652 N85-26354
Transparency of water 9n 186 - 500 nm region
21 p3690 N85-32923
The 2nd European Conference on Atomic and Molecular Physics
[AD-A155863] 24 p4148 N85-35715
ULTRAVIOLET TELESCOPES
Observations of local ISM emission with the Berkeley EUV/FUV shuttle telescope 06 p0880 N85-15594
UMBRAS
Linear models of acoustic waves in sunspot umbrae
14 p2450 N85-25130
Solar cycle variations of sunspot temperatures
14 p2452 N85-25141
UNCONSCIOUSNESS
NT BLACKOUT (PHYSIOLOGY)
UNCONTROLLED REENTRY (SPACECRAFT)
Natural atmospheric reentry --- satellite orbit decay
05 p0600 N85-13829
Orbital debris policy issues: Battelle involvement and some personal observations 12 p1787 N85-21218
Natural reentry of satellites 14 p2397 N85-24774
UNDERCARRIAGES
Deflection model of a CT4-A undercarriage
[AD-A149776] 12 p1777 N85-21156
Selection of effective arrangement of heavy undercarriage systems for use with concrete runways
14 p2285 N85-24158
UNDERGROUND ACOUSTICS
Sidereal variations deep underground in Tasmania
[SH-4.4-4] 23 p4033 N85-35002
The effect of the interplanetary magnetic field on sidereal variations observed at medium depth underground detectors
[SH-4.4-5] 23 p4033 N85-35003
Corrected sidereal anisotropy for underground moons
[SH-4.4-7] 23 p4033 N85-35005
Cosmic ray intensity variations observed at Matsushiro (220 M.W.E. in depth)
[SH-4.4-9] 23 p4034 N85-35007
UNDERGROUND EXPLOSIONS
Seismology 1983: Nuclear test ban verification, earthquake and Earth resource investigation
[FOA-C-20537-T1] 02 p0229 N85-11495
Micro-deformation of quartz under dynamic action and its applications 11 p1620 N85-20201
Surface waveseismic yields as measured by the Regional Seismic Test Network
[DE85-010532] 18 p3137 N85-29425
A multiphase continuum model to describe dynamic loading effects in nonlinear porous media
[DE85-010102] 19 p3301 N85-30463
Seismic discrimination
[AD-A154167] 20 p3494 N85-31722
Experimental and analytic characterization of nonlinear seismic attenuation
[AD-A154760] 21 p3631 N85-32556
Investigation of the lightning vulnerability of nuclear explosive test systems at the Nevada Test Site
[DE85-011761] 24 p4124 N85-35563
Ground motion measurements for the QUESO nuclear event
[DE85-014806] 24 p4151 N85-35743
UNDERGROUND STORAGE
Hybrid system for producing and storing ice
[DE84-017474] 09 p1304 N85-18195
Natural convection experiments about a finite-length cylindrical heat source in a liquid-saturated porous medium
[DE84-012657] 09 p1320 N85-18298
Nevada nuclear waste storage investigations preliminary repository concepts report
[DE85-002132] 09 p1383 N85-18696
Rock mechanics: Issues and research needs in the disposal of wastes in hydraulic fractures
[DE85-001399] 10 p1556 N85-19809
Index to published geologic maps in the region around the potential Yucca Mountain nuclear waste repository site, southern Nye County, Nevada
[DE85-000260] 11 p1669 N85-20518
Underground pumped hydroelectric storage
[DE85-000288] 11 p1676 N85-20560
Consolidation around a point heat source
[PB85-116549] 11 p1682 N85-20601
High-level waste processing and disposal
[DE85-003564] 11 p1728 N85-20865
Shallow land burial technology: Humid
[DE85-004432] 12 p1932 N85-22136
Occurrence of uranium in ground water in the vicinity of the US Department of Energy Feed Materials Production Center, Fernald, Ohio
[DE85-010340] 19 p3364 N85-30862
Preliminary SPR thermal model description and results for WH-11 and BM-4
[DE85-013171] 23 p3931 N85-34360
UNDERGROUND STRUCTURES
Finite element modelling of buried structures
01 p0061 N85-10403
Study for a large area underground detector made with organic scintillators for searching for magnetic monopoles
[NOTA-INTERNA-814] 02 p0201 N85-11339
An underground search for massive slow particles (hunting Grand Unified Theory (GUT) monopoles)
[NOTA-INTERNA-821] 02 p0292 N85-11894
Underground engineering (selected articles)
[AD-A141053] 04 p0483 N85-13082
Development of the GASCOPACT (R) pipe and cable tracer
[ERS-E.340] 09 p1324 N85-18320
GASCOPACT: A new approach to pipe and cable location
[ERS-E.383] 09 p1325 N85-18324
Simplified theory for the behaviour of buried flexible cylinders under the influence of uniform hoop compression
[PB85-116531] 11 p1654 N85-20419
Behavior of buried flexible cylinders under the influence of nonuniform hoop compression
[PB85-116523] 12 p1868 N85-21718
Constitutive modeling for blast-induced wave propagation
[AD-A153576] 18 p3090 N85-29187
Commercial feasibility of underground gasification of Texas lignite to produce synthetic gas
[DE85-001998] 18 p3127 N85-29361
Literature survey of underground construction methods for application to hardened facilities
[AD-A155212] 21 p3599 N85-32351
Method for determining depth and shape of a sub-surface conductive object
[DE85-006502] 23 p3935 N85-34389
New Matsushiro underground cosmic ray station (220 M.W.E. in depth)
[SH-9.1-14] 23 p4052 N85-35129
An underground cosmic ray muon telescope for observation of cosmic ray anisotropy
24 p4196 N85-36037
A possible EAS array above the Soudan 2 detector
[HE-4.6-9] 24 p4197 N85-36046
Upper limit on magnetic monopole flux from Baksan experiment
[HE-6.1-11] 24 p4210 N85-36136
UNDERGROUND TRANSMISSION LINES
The HEMP (High-altitude Electromagnetic Pulse) response of a long transmission line buried in the earth
[AD-A146517] 06 p0800 N85-15108
Development of the GASCOPACT (R) pipe and cable tracer
[ERS-E.340] 09 p1324 N85-18320
GASCOPACT: A new approach to pipe and cable location
[ERS-E.383] 09 p1325 N85-18324
UNDERWATER ACOUSTICS
A description and discussion of FREDDEX oceanographic measurements
[AD-A145032] 01 p0068 N85-10596
The numerical solution of the Helmholtz equation for wave propagation problems in underwater acoustics
[NASA-CR-172454] 02 p0250 N85-11634
The acoustic pressure in a wedge-shaped water layer overlying a fast fluid bottom
[AD-A145517] 02 p0276 N85-11795
Acoustic scattering cross sections for truly composite wind-wave surfaces. Scattering without bubbles
[AD-A145672] 03 p0415 N85-12655
Signal characteristics of an underwater explosive acoustic telemetry system
[DE84-016853] 05 p0726 N85-14668
Wave-wave interactions, microseisms, and infrasonic ambient noise in the ocean
[AD-A146529] 06 p0859 N85-15463
Research on acoustical and optical scattering, optics of bubbles, diffraction catastrophes, laser generation of sound, and shock induced cavitation
[AD-A146703] 06 p0860 N85-15466
Ocean acoustics
[AD-A147082] 07 p1038 N85-16591
Arctic marine acoustics
[AD-A147492] 07 p1039 N85-16594
Current and current shear effects in the parabolic approximation for underwater sound channels
[AD-A147833] 07 p1039 N85-16597
An efficient numerical solution technique for wave propagation in horizontally stratified ocean environments
[AD-A148537] 08 p1190 N85-17502
SAI (Science Applications, Inc.) Interim Scattering Model/Ice (SISM/ICE)
[AD-A148596] 08 p1213 N85-17638
A broadband matching network
[AD-D011406] 08 p1219 N85-17675
A 3-dimensional mass conserving element for compressible flows
[NASA-CR-172513] 09 p1373 N85-18626
Specifics of backscattering of sound by bottom of bank in open sea 10 p1499 N85-19460
Average sound intensity decrease rule in irregular hydroacoustical waveguide 10 p1499 N85-19461
Linear and nonlinear ultrasonic interaction on liquid-solid boundaries
[AD-A148979] 10 p1553 N85-19793
A stochastic-mechanical approach to acoustic pulse propagation in the deep ocean sound channel
[AD-A149598] 12 p1928 N85-22110
Twenty-five sound propagation tests on the continental shelf between Long Island, New York and Cape Canaveral, Florida
[AD-A149869] 12 p1928 N85-22111
Numerical results of acoustic radiation, transmission and reflection of steel plate in water
[AMTE(N)-TM-84037] 13 p2155 N85-23378
Vertical discrimination in the sound channel
[AD-A150254] 13 p2155 N85-23380
Recent progress in the development and application of the parabolic equation
[AD-A151475] 15 p2637 N85-26265
Development of a modified time delay spectrometry technique for underwater acoustic measurements in a multipath environment
[AD-A152111] 16 p2860 N85-27639
Multiple array processors for ocean acoustic problems
[AD-A152174] 16 p2860 N85-27641
Metrology and Oceanology Institutes' underwater acoustics R and D 19 p3289 N85-30394
Arctic acoustic tomography MIZEX 84
[AD-A154426] 19 p3320 N85-30580
Well-posedness of one-way wave equations and absorbing boundary conditions
[NASA-CR-172619] 19 p3345 N85-30727
Development of computer programs using the method of images to predict the sound field in a wedge overlaying a fast fluid and comparison with laboratory experiments
[AD-A154580] 21 p3670 N85-32797
The moving thermoacoustic array: A theoretical feasibility study
[AD-A154510] 21 p3699 N85-32980
Discrete-element acoustic analysis of submerged structures using doubly asymptotic approximations
[AD-A154959] 21 p3700 N85-32987
A random layer model for reflection from ocean bottom sediments
[AD-A155019] 21 p3700 N85-32988
Propagation of sound in a layered laboratory model
[AD-A155141] 21 p3700 N85-32989
Understanding coherence losses incurred by bottom-retained signals
[AD-A155559] 21 p3701 N85-32992
Mean intensity of wave reflected by wavefront reversing mirror in turbulent medium 22 p3762 N85-33432
Pressure cross spectra in turbulent boundary layers in water
[AD-A156153] 24 p4094 N85-35378
A comparison of multipath arrival structures observed in the presence of a surface duct with predictions obtained using classical ray techniques and the parabolic equation method
[AD-A156024] 24 p4145 N85-35696
UNDERWATER BREATHING APPARATUS
Manned testing of two closed-circuit oxygen underwater breathing apparatus: US Navy Emerson Rig and Fenzy PO.68
[AD-A148300] 08 p1200 N85-17560

The use of austenitic stainless steel versus monel (Ni-cu) alloy in pressurized Gaseous Oxygen (GOX) life support systems
[AD-A156305] 24 p4134 N85-35625

UNDERWATER ENGINEERING
Utility of the M.I.T. (Massachusetts Institute of Technology) underwater stud welding gun
[AD-A144793] 01 p0055 N85-10365
French firms develop artificial intelligence robot
03 p0341 N85-12192
Evaluation of the Kerie Cable thermal arc cutting equipment
[AD-A147813] 07 p0974 N85-16186
Underwater pipeline: Welding by high frequency induction
[BLL-WI-TRANS-682-(9312.57)]
16 p2792 N85-27221
The dynamics of slack marine cables
[AD-A156022] 21 p3599 N85-32349

UNDERWATER EXPLOSIONS
Signal characteristics of an underwater explosive acoustic telemetry system
[DE84-016653] 05 p0726 N85-14666
The development of a method for the shock-resistant securing of large batteries in submarines
09 p1335 N85-18391
Shipboard shock response of the model structure DSM: Experimental results versus responses predicted by eight participants 09 p1335 N85-18392
An experimental investigation into the dynamic response of a stiffened flat plate loaded impulsively by an underwater shockwave
[AD-A151321] 15 p2578 N85-25903
Underwater shock-induced responses of stiffened flat plates: An investigation into the predictive capabilities of the USA-STAGS code
[AD-A154245] 19 p3286 N85-30377
An investigation into the comparisons of the underwater shock effects on a stiffened flat plate to the predictive nature of a computer model
[AD-A155612] 21 p3600 N85-32355

UNDERWATER PHOTOGRAPHY
East Europe report: Science and technology
[JPRS-ESA-84-030] 01 p0101 N85-10670
Underwater television equipment described
01 p0101 N85-10672
The use of in-situ photography in studies of the deep-sea benthos at IOS — Institute of Oceanographic Sciences (IOS)
[IOS-182] 09 p1360 N85-18553
Processing of underwater photographs
10 p1499 N85-19462

UNDERWATER PHYSIOLOGY
Hyperbaric physiology (status and prospects)
08 p1194 N85-17521
Hydrogen-oxygen (hydrox) breathing at 1.3MPa
[FOA-C-58015-H1] 09 p1364 N85-18577
Pressure chamber simulation of 450-meter dive
20 p3505 N85-31788

UNDERWATER RESEARCH LABORATORIES
Preliminary results of an ALVIN dive program on active hydrothermal vents at the southern Juan de Fuca Ridge
24 p4106 N85-35454

UNDERWATER RESOURCES
Maritime prospecting, mining discussed
07 p0960 N85-16226
Technical and cost analyses of manganese nodule processing techniques and their significant variations
[PB85-146615] 14 p2258 N85-23992
Massive sulfide deposits from the southern Juan de Fuca Ridge 24 p4105 N85-35446

UNDERWATER SOUND
U UNDERWATER ACOUSTICS

UNDERWATER STRUCTURES
Discrete-element acoustic analysis of submerged structures using doubly asymptotic approximations
[AD-A154959] 21 p3700 N85-32987

UNDERWATER TESTS
The design, fabrication and delivery of a spacelab neutral buoyancy Instrument Pointing System (IPS) mockup — underwater training simulator
[NASA-CR-171233] 04 p0462 N85-12934
NOAA OTEC CWP (National Oceanic and Atmospheric Administration Ocean Thermal Energy Conversion Cold Water Pipe) at-sea test. Volume 3, part 1: Tabulation of the power spectra for selected channels
[PB84-236955] 09 p1346 N85-18467
The Deep Drifter Program — deep ocean sensors
14 p2329 N85-24400
Predicting electrical performance parameters of underwater cables 22 p3775 N85-33391
Modular detector for deep underwater registration of muons and muon groups
[HE-5.4-15] 24 p4208 N85-36125

UNDERWATER VEHICLES
NT SUBMARINES
NT UNDERWATER RESEARCH LABORATORIES
Technology development for unmanned untethered submersible vehicle systems
[AD-A148794] 09 p1304 N85-18190
The ARGOS system aboard research vehicles: 1981 experiment aboard the Le Suroit oceanographic vessel and the outlook
[CNEXO/DFT/OPNAV/82-06] 14 p2327 N85-24382
Environmental background measurement program
[AD-A153660] 19 p3319 N85-30577
A towed instrument vehicle for deep ocean sampling
[AD-A156322] 24 p4125 N85-35576

UNIAXIAL STRAIN
U AXIAL STRAIN

UNIFIED FIELD THEORY
On the nature of the baryon asymmetry
[NASA-TM-86156] 05 p0746 N85-14784
Thin end of the wedge
[DE84-016439] 09 p1401 N85-18816
Supersymmetric inflationary cosmology
[DE85-001332] 09 p1415 N85-18929
Experimental and theoretical high energy physics
[DE85-000844] 11 p1726 N85-20858
Superheavy magnetic monopoles and the standard cosmology
[DE85-003922] 15 p2686 N85-26587
Dark matter, galaxies, and large scale structure in the universe
[DE85-008053] 16 p2882 N85-27786
Study for a large area acrylic scintillator detector — magnetic monopoles
[NOTA-INTERNA-827] 18 p3097 N85-29174
Cosmology in theories with extra dimensions
18 p3202 N85-29864
The dimensional reduction transition
[DE85-003948] 19 p3383 N85-30990
Charge 4/3 leptons in cosmic rays
[HE-6.2-14] 24 p4212 N85-36150

UNIFORM FLOW
NT BLASIUS FLOW
Comparison of uniform perturbation solutions and numerical solutions for some potential flows past slender bodies
[NASA-CR-172485] 06 p0749 N85-14799

UNIPOLAR TRANSISTORS
U FIELD EFFECT TRANSISTORS

UNIQUENESS
On existence and uniqueness of solutions of Hamilton-Jacobi equations
[AD-A147597] 07 p1033 N85-16560
Existence, uniqueness and stability conditions for general finite element methods in linear elasticity
09 p1332 N85-18372
Hamilton-Jacobi equations in infinite dimensions. Part 1. Uniqueness of viscosity solutions
[AD-A149094] 10 p1546 N85-19749
Construction of solutions for two-dimensional Riemann problems
[DE85-003136] 10 p1549 N85-19770
Uniqueness and stability in nonlinear elasticity and viscoelasticity
[AD-A151470] 15 p2637 N85-26264

UNIQUENESS THEOREM
On two concepts of fundamental matching
[CSIR-TWISK-335] 01 p0110 N85-10743
Existance and non-uniqueness of similarity solutions of a boundary layer problem
[NASA-CR-172503] 07 p0957 N85-16064

UNITED KINGDOM
NT ENGLAND
The United Kingdom Meteorological Office mesoscale forecasting system 01 p0080 N85-10533
Revised Uniform Summary of Surface Weather Observations (RUSSWO). Alconbury RAF United Kingdom, parts A-F
[AD-A146913] 07 p1004 N85-16384
Revised Uniform Summary of Surface Weather Observations (RUSSWO). Mildenhall RAF, United Kingdom, parts A-F
[AD-A146915] 07 p1005 N85-16386
Air traffic management concepts for the UK in the 1990's: A review of recent RSRE work
[AD-A147850] 08 p1082 N85-16853
United Kingdom report on space research
08 p1231 N85-17752
Innovation in British industry (notably the aircraft industry) and its value: Collected papers
[BAE-KRS-N-GEN-286] 09 p1263 N85-17933
Assessment of wave power available at key United Kingdom sites
[IOS-186] 09 p1346 N85-18466
British aerospace studies HOTOL satellite launcher
10 p1480 N85-19206
Meteorological and oceanographic support during the Falklands conflict 11 p1712 N85-20769
A review of fatality, impairment of consciousness and head and neck injury on Royal Air Force ejections 1968-1981 12 p1907 N85-21975
Brief review of current work in the UK on three dimensional boundary layers 15 p2559 N85-25786
Information technology applications in voluntary sector transport operations. SP1: Objectives and programme of work
[TT-8501] 15 p2667 N85-26457
British super-shuttle 18 p3087 N85-29104
The contribution of an operational SAR satellite system to the UK SAR organisation — search and rescue (SAR)
20 p3400 N85-31095
UK experience with COSPAS-SARSAT and INMARSAT distress systems 20 p3406 N85-31132
Environmental aspects of large-scale wind-power systems in the UK 24 p4110 N85-35478

UNITED KINGDOM SATELLITES
U UK SATELLITES

UNITED NATIONS
International cooperation in remote sensing applications 05 p0656 N85-14209

UNITED STATES
NT ALABAMA
NT ALASKA
NT ARIZONA
NT ARKANSAS
NT CALIFORNIA
NT COLORADO
NT CONNECTICUT
NT DELAWARE
NT FLORIDA
NT GEORGIA
NT HAWAII
NT IDAHO
NT ILLINOIS
NT INDIANA
NT IOWA
NT KANSAS
NT KENTUCKY
NT LOUISIANA
NT MAINE
NT MARYLAND
NT MASSACHUSETTS
NT MICHIGAN
NT MISSISSIPPI
NT MISSOURI
NT MONTANA
NT NEBRASKA
NT NEVADA
NT NEW HAMPSHIRE
NT NEW JERSEY
NT NEW MEXICO
NT NEW YORK
NT NORTH CAROLINA
NT NORTH DAKOTA
NT OHIO
NT OKLAHOMA
NT OREGON
NT PENNSYLVANIA
NT SOUTH CAROLINA
NT SOUTH DAKOTA
NT TENNESSEE
NT TEXAS
NT UTAH
NT VIRGINIA
NT WASHINGTON
NT WISCONSIN
NT WYOMING
Geology and geomorphology of the southern central Blue Ridge: An indexed bibliography
[PB84-225119] 01 p0072 N85-10480
The south-central United States magnetic anomaly
[E85-10025] 02 p0218 N85-11438
International cooperation and competition in space
[GPO-38-001] 02 p0295 N85-11911
Statement of Otho E. Eskin, Director, Office of Advanced Technology, Department of State
02 p0295 N85-11914
Statement of John H. McElroy, Assistant Administrator for Environmental Satellite, Data and Information Services, National Oceanic and Atmospheric Administration
02 p0295 N85-11915
International cooperation and competition in civilian space activities, summary, appendix 1
02 p0295 N85-11916
NESDIS international activities, appendix 2
02 p0295 N85-11917
US energy for the rest of the century, 1984 edition
[PB84-207406] 04 p0531 N85-13393
The evolution of civilian in-space infrastructure, i.e., space station concepts in the United States
07 p0914 N85-15788

International involvement in a civilian space station program 07 p0915 N85-15789

Synopsis of the OTA Workshop on Cost Containment of Civilian Infrastructure (Civilian Space Station) Elements 07 p0915 N85-15790

Title 2: National Commission on Space (Public Law 98-361) 07 p0915 N85-15791

Financing considerations and Federal budget impacts 07 p0915 N85-15792

Government contract contingent liabilities. The anti-deficiency act, and the hobgoblin of little minds [AD-A147919] 07 p1053 N85-16684

Evaluation of the radar response to land surfaces and volumes: Examination of theoretical models, target statistics, and applications 08 p1149 N85-17250

Outlook for expanding the Federal research in progress system [AD-A148354] 08 p1229 N85-17737

High-technology ceramics in Japan [TIB5-900369] 09 p1299 N85-18157

Comparison of energy storage systems in the United States chilled water versus two types of ice storage systems [DE85-001102] 09 p1344 N85-18452

Petrography, diagenesis and depositional models of the St. Louis limestone, valmeyeran (middle Mississippian), Illinois Basin, USA 09 p1352 N85-18506

Birds and airport agriculture in the conterminous United States: A review of literature [AD-P004208] 11 p1583 N85-19975

The FAA grant-in-aid assurances: FAR part 139, and airport hazards [AD-P004209] 11 p1583 N85-19976

MAP-related activities in the United States 11 p1655 N85-20427

Shallow magma targets in the western US [DE85-003274] 12 p1881 N85-21803

Response of unmanaged forests to CO2-induced climate change: Available information, initial tests and data requirements [DOE/NSB-0053] 12 p1883 N85-21817

A review of neck injury and impaired consciousness associated with US Navy ejections 1 January 1969 - 31 December 1979 12 p1906 N85-21973

Twenty-five sound propagation tests on the continental shelf between Long Island, New York and Cape Canaveral, Florida [AD-A149869] 12 p1928 N85-22111

Militarization of space activity in United States 15 p2488 N85-25360

Military journal on US intelligence satellites 16 p2727 N85-26832

AWS (Air Weather Service) climatic briefs: North America [AD-A152161] 16 p2835 N85-27483

Great Lakes winter weather and ice conditions for 1982-83 [PB85-165009] 16 p2837 N85-27498

Potential climatic impacts of increasing atmospheric CO2 with emphasis on water availability and hydrology in the United States [NASA-TM-87479] 17 p2995 N85-28517

Close encounters with S/T (science and technology) in the Soviet Union [AD-P004570] 17 p3048 N85-28864

Experimental philosophy leading to a small scale digital data base of the conterminous United States for designing experiments with remotely sensed data [NASA-TM-85009] 17 p3049 N85-28877

US restrictions on technology transfer reviewed 18 p3088 N85-29115

Shales and other argillaceous strata in the United States [DE85-010453] 18 p3125 N85-29353

The COSPAS/SARSAT demonstration and evaluation. Results of the first year in the United States 20 p3405 N85-31128

The south-central United States magnetic anomaly 20 p3474 N85-31591

The south-central United States magnetic anomaly 20 p3475 N85-31592

Helicopter noise survey for selected cities in the contiguous US [AD-A154893] 21 p3699 N85-32985

Magnetic Fusion Program plan [DE85-009861] 22 p3846 N85-33823

The role of regional subsurface geochemistry in resource assessment in the central United States 24 p4104 N85-35440

New silver resource map of the United States: Potential for increased domestic silver production 24 p4105 N85-35445

Early and middle Cenozoic volcanic synthesis 24 p4105 N85-35449

UNITY

Partitions of unity and approximation [AD-A144717] 01 p0110 N85-10746

UNIVAC COMPUTERS

NT UNIVAC 1100 SERIES COMPUTERS

Sperry Univac System 80, Model 6, OS/3 BASIC, Version 10.01 [PB85-108066] 10 p1542 N85-19722

UNIVAC 1100 SERIES COMPUTERS

R and D activities of the Computer Centre 20 p3540 N85-32029

UNIVERSAL TIME

Universal time effects in polar ionosphere 14 p2338 N85-24461

UNIVERSE

Decaying particles do not heat up the Universe [DE85-002191] 11 p1763 N85-21091

Cosmology, galactic astronomy and elementary particle physics 12 p1956 N85-22289

Dark matter, galaxies, and large scale structure in the universe [DE85-008053] 16 p2882 N85-27786

Constructing a bit string universe [DE85-008317] 18 p3197 N85-29829

UNIVERSITIES

An investigation of the use, cost, perceived value and social context of telecommunications tools in two-year college libraries in the southeastern United States 02 p0293 N85-11901

Improving the research infrastructure at US universities and colleges [GPO-35-290] 04 p0574 N85-13661

Research report 1979-1982. Part 2: Projects [ISBN-3-7983-0960-4] 04 p0575 N85-13667

Optical computer studies at UK's Heriot-Watt University 09 p1309 N85-18227

NASA Lewis Research Center/University Graduate Research Program on Engine Structures [NASA-TM-86916] 09 p1333 N85-18375

Renewal request for high energy physics at Texas A and M University [DE85-004469] 11 p1724 N85-20843

Research in surface sciences, disordered materials, and solidification and growth [PB85-132140] 11 p1737 N85-20927

Air Force Academy Aeronautics Digest [AD-A149814] 12 p1769 N85-21104

Academic science and engineering: R and D funds, fiscal year 1982 (detailed statistical tables) [PB85-154763] 15 p2664 N85-26443

Selected university laboratory needs in support of national security [AD-A153511] 18 p3197 N85-29833

NASA initiatives with historically black colleges and universities [NASA-EP-210] 19 p3379 N85-30960

The Department of Defense report on the technology base and support of university research [AD-A154309] 20 p3540 N85-32030

Spin-offs from technical scientific infrastructures, no. 1 20 p3540 N85-32034

The Naval Postgraduate School Flight Mechanics Laboratory: A feasibility study [AD-A154578] 21 p3557 N85-32127

New innovative businesses from industry. Experiences in the Netherlands in the successful transfer of technology from university to industry 22 p3849 N85-33843

UNIVERSITY PROGRAM

Canada report to COSPAR 01 p0131 N85-10906

Summary and analysis of hearing on improving the research infrastructure at US universities and colleges [GPO-36-854] 04 p0574 N85-13660

UNLOADING

Mechanical features of the shuttle rotating service structure 08 p1102 N85-16967

New applications for robot loaders, unloaders 08 p1139 N85-17175

Mathematical model for rollout of planet roving vehicle from landing craft 15 p2484 N85-25334

Application of the unloading compliance methods in fracture toughness measurements of a quenched and tempered steel [BLL-CE-TRANS-7953-(9022.09)] 20 p3465 N85-31523

Responses of skeletal muscle to unloading, a review [NASA-CR-176177] 24 p4128 N85-35594

UNMANNED SPACECRAFT

NT BIOSATELLITES
NT EXOSAT SATELLITE
NT GALILEO PROBE
NT GALILEO SPACECRAFT
NT GEODETIC SATELLITES
NT GEOS 1 SATELLITE
NT GEOS 2 SATELLITE
NT GEOS 3 SATELLITE
NT GIOTTO MISSION
NT HEAO 1
NT HEAO 2
NT HEAO 3
NT HELIOS 1
NT HELIOS 2
NT JUPITER PROBES
NT LAGEOS (SATELLITE)
NT LUNIK LUNAR PROBES
NT MARINER 5 SPACE PROBE
NT MARINER 9 SPACE PROBE
NT MARS PROBES
NT NAVIGATION SATELLITES
NT NAVSTAR SATELLITES
NT PASSIVE SATELLITES
NT PIONEER SPACE PROBES
NT PIONEER VENUS SPACECRAFT
NT PIONEER 10 SPACE PROBE
NT PIONEER 11 SPACE PROBE
NT SOLAR OBSERVATORIES
NT SPACE PROBES
NT TRANSIT SATELLITES
NT VENERA SATELLITES
NT VENERA 11 SATELLITE
NT VENUS PROBES
NT VOYAGER 1 SPACECRAFT
NT VOYAGER 2 SPACECRAFT

Winged first stages of space transport appliances [TUM-RT-TB-84/3] 02 p0167 N85-11125

A study of spacecraft technology and design concepts, volume 1 [NASA-CR-172579-VOL-1] 16 p2730 N85-26844

A study of spacecraft technology and design concepts. Volume 2: Appendices [NASA-CR-172579-VOL-2] 16 p2730 N85-26845

Soviet space programs, 1976-1980 (with supplementary data through 1983). Part 3: Unmanned space activities [S-PRT-98-235-PT-3] 16 p2879 N85-27765

Far travelers: The exploring machines [NASA-SP-480] 22 p3731 N85-33126

Noiseless coding for the Gamma Ray spectrometer [NASA-CR-176201] 24 p4069 N85-35219

UNSATURATION (CHEMISTRY)

Stabilized unsaturated polyesters [NASA-CASE-NPO-16103-1] 18 p3078 N85-29043

UNSTEADY FLOW

NT OSCILLATING FLOW

Development and applications of algorithms for calculating the transonic flow about harmonically oscillating wings [NASA-CR-172376] 01 p0002 N85-10007

A study of the effect of wake-passing on turbine blades [OUEL-1515/84] 03 p0363 N85-12326

Evaluation of the unsteady effects for a class of wind turbines 05 p0592 N85-13772

Experiences with nonsynchronous forced vibration in centrifugal compressors 05 p0642 N85-14119

Two-dimensional unsteady analysis of fluid forces on a whirling centrifugal impeller in a volute 05 p0643 N85-14126

Influence of stationary components on unsteady flow in industrial centrifugal compressors 05 p0645 N85-14140

An experimental study of airfoil-spoiler aerodynamics [NASA-CR-177328] 06 p0748 N85-14796

Unsteady flow characteristics in the near-wake of a two-dimensional obstacle [NASA-TM-77762] 07 p0897 N85-15684

A scanning laser velocimeter for turbulence research [NASA-CR 172493] 07 p0897 N85-15686

Comparison of analytical and experimental steadyand unsteady-pressure distributions at Mach number 0.78 for a high-aspect-ratio supercritical wing model with oscillating control surfaces [NASA-TM-84589] 07 p0899 N85-15697

Some important problems in unsteady boundary layers including separation. 2: Unsteady boundary layers close to the stagnation region of slender bodies [AD-A146964] 07 p0958 N85-16069

A comparison of measured and predicted unsteady pressure on a fan blade in unstalled supersonic flutter [PNR-90223] 08 p1079 N85-16839

Proceedings of the workshop on unsteady separated flow held at the United States Air Force Academy on August 10-11, 1983 [AD-A148249] 09 p1263 N85-17937

Wing rock flow phenomena [AD-P004154] 09 p1264 N85-17939

Potential applications of forced unsteady flows [AD-P004155] 09 p1264 N85-17940

Numerical solution of the Navier-Stokes equations for unsteady separated flows [AD-P004161] 09 p1265 N85-17946

Unsteady aerodynamic loading of an airfoil due to vortices released intermittently from its upper surface [AD-P004162] 09 p1265 N85-17947

Can the singularity be removed in time-dependent flows?
[AD-P004165] 09 p1265 N85-17950

Unsteady separated flow: Forced and common vorticity about oscillating airfoils
[AD-P004167] 09 p1265 N85-17952

Unsteady separated flows: Generation and use by insects
[AD-P004168] 09 p1266 N85-17953

Theoretical study of non-linear unsteady aerodynamics of a non-rigid lifting body
[AD-P004169] 09 p1266 N85-17954

Theoretical investigation of dynamic stall using a momentum integral method
[AD-P004170] 09 p1266 N85-17955

Preliminary results from the unsteady airfoil model USTAR2
[AD-P004171] 09 p1266 N85-17956

Experiments on controlled, unsteady, separated turbulent boundary layers
[AD-P004172] 09 p1266 N85-17957

Flow separation induced by periodic aerodynamic interference
[AD-P004174] 09 p1266 N85-17959

Numerical predictions for unsteady viscous flow past an array of cylinders 09 p1318 N85-18284

On the flow processes in sharply inclined and stalled airfoils in parallel movement and rotation
[NASA-TM-77509] 10 p1419 N85-18952

Unsteady transonic flow calculations for two-dimensional canard-wing configurations with aeroelastic applications
[NASA-TM-86375] 10 p1420 N85-18960

A probe for direct measurement of flow direction
[ESA-TT-853] 11 p1637 N85-20310

Parachute inflation dynamics
11 p1715 N85-20792

Unsteady aerodynamic characterization of a military aircraft in vertical gusts
[NASA-TM-77810] 12 p1770 N85-21110

Three-dimensional unsteady lifting surface theory in the subsonic range
[NASA-TM-77812] 12 p1770 N85-21111

Transonic interactions of unsteady vortical flows
[NASA-TM-86658] 12 p1770 N85-21113

Unsteady flows around 3-dimensional wings
[AD-A149993] 12 p1772 N85-21124

Numerical integration of the unsteady full-potential equation with applications to transonic flow about a two-dimensional airfoil
[NLR-MP-84022-U] 12 p1773 N85-21130

Estimating unsteady aerodynamic forces on a cascade in a three-dimensional turbulence field
[NASA-TM-86701] 14 p2209 N85-23704

Recent transonic unsteady pressure measurements at the NASA Langley Research Center
[NASA-TM-86408] 14 p2210 N85-23710

Calculation of an unsteady transonic flow with shock waves and separation in Laval nozzles
[MPIS-14/1984] 14 p2213 N85-23728

Interactions of unstable shear layers with leading edges and associated pressure fields 14 p2299 N85-24236

Stability of an oscillating boundary layer
[NASA-TM-77827] 14 p2299 N85-24238

Unsteady flows in a tube with combustion reaction
[ISL-R-118/83] 14 p2303 N85-24261

Transonic Unsteady Aerodynamics and its Aeroelastic Applications
[AGARD-CP-374] 15 p2457 N85-25171

Trends in computational capabilities for fluid dynamics
15 p2457 N85-25172

Transonic pressure distributions on a two-dimensional 0012 and supercritical MBB-A3 profile oscillating in heave and pitch 15 p2457 N85-25173

Analysis of transonic aerodynamic characteristics for a supercritical airfoil oscillating in heave, pitch and with oscillating flap 15 p2458 N85-25175

Experience with transonic unsteady aerodynamic calculations 15 p2458 N85-25176

Calculation of unsteady transonic separated flows by viscous-inviscid interaction 15 p2458 N85-25178

A semi-empirical unsteady transonic method with supersonic free stream - 15 p2458 N85-25179

Improvement and extension of a numerical procedure for the three dimensional unsteady transonic flows
15 p2459 N85-25181

Computation of unsteady transonic flows about two-dimensional and three-dimensional AGARD standard configurations 15 p2459 N85-25183

Calculation of unsteady transonic flow around a high swept wing 15 p2459 N85-25184

The development of unsteady transonic 3-D full potential code and its aeroelastic applications
15 p2460 N85-25187

Unsteady analysis of rotor blade tip flow
[NASA-CR-3868] 15 p2462 N85-25202

Transonic aerodynamic and aeroelastic characteristics of a variable sweep wing
[NASA-TM-86677] 15 p2462 N85-25203

Numerical solutions of 3-dimensional Navier-Stokes equations for closed bluff-bodies
[NASA-CR-175755] 15 p2636 N85-26255

Recent progress in computational aerodynamics
16 p2693 N85-26626

LDA study of non-steady flame propagation in a constant volume duct
[DE85-007233] 16 p2746 N85-26948

Experimental investigations of prismatic cylinders in flow with harmonic pulsations
[KU-SFB-210/E/4] 16 p2785 N85-27186

Background noise measurements from jet exit vanes designed to reduced flow pulsations in an open-jet wind tunnel
[NASA-TM-86383] 17 p2906 N85-27916

Unsteady flow in multistage turbines
17 p2911 N85-27946

New facility to study unsteady wake effects on turbine airfoil heat transfer 17 p2911 N85-27948

Numerical simulation of unsteady motion in a turbulent mixing layer
[NAL-TR-849T] 18 p3099 N85-29183

Experimental investigations of the unsteady turbulent friction behavior with pressure impulses in a circular pipe
[IWAWI-MITT-102] 18 p3103 N85-29210

A first-order time-domain Green's function approach to supersonic unsteady flow
[NASA-CR-172208] 19 p3214 N85-29930

Unsteady transonic flow calculations for interfering lifting surface configurations
[NASA-TM-86432] 19 p3214 N85-29931

Verification of calculation methods for unsteady airloads in the precipitation of transonic flutter
[NLR-MP-84016-U] 20 p3390 N85-31027

Compendium of unsteady aerodynamic measurements, addendum 1
[AGARD-R-702-ADD-1] 20 p3390 N85-31028

Data set 9: LANN wing. Pitching oscillation
20 p3390 N85-31030

Nonnewtonian, unsteady flow in a convergent divergent duct 20 p3456 N85-31463

Identification of unsteady aerodynamics and aeroelastic integro-differential systems
[NASA-TM-86749] 21 p3678 N85-32851

Toward the propagation of waves in unsteady media
21 p3683 N85-32881

One method of solving the problem of unsteady heat exchange of a body and its ablation
22 p3733 N85-33146

Scalar/Vector potential formulation for compressible viscous unsteady flows
[NASA-CR-3921] 23 p3893 N85-34113

Integral equation formulation for three-dimensional unsteady transonic flow
[ARL/STRUC-R-416] 23 p3894 N85-34119

Modelling of unsteady, incompressible separation on an aerofoil using an inviscid flow algorithm
[GU-AERO-8412] 23 p3894 N85-34122

Unsteady transonic heat transfer in a transient facility
[NASA-CR-176145] 23 p3930 N85-34354

Unsteady flow in a supersonic cascade with two in-passage shocks
[NASA-CR-3925] 24 p4060 N85-35158

UNSTEADY STATE

Autoregressive nonsteady methods for the analysis and synthesis of the human voice
[FJB-3-1984] 01 p0041 N85-10266

Instability in semiconductors exposed to ionizing radiation 02 p0267 N85-11747

Full load testing in the platform module prior to tow-out: A case history of subsynchronous instability
05 p0642 N85-14117

Subsynchronous vibrations in a high pressure centrifugal compressor: A case history 05 p0642 N85-14118

Control of rotordynamic instability in a typical gas turbine's power system 05 p0642 N85-14120

Experimental on-stream elimination of resonant whirl in a large centrifugal compressor 05 p0642 N85-14121

MPS solidification model. Analysis and calculation of macrosegregation in a casting ingot
[NASA-CR-171589] 21 p3566 N85-32178

Toward the propagation of waves in unsteady media
21 p3683 N85-32881

UNSWEPT WINGS

NT RECTANGULAR WINGS

Turbulent bubbles behind airfoils and wings at high angle of attack 08 p1069 N85-16779

UP-CONVERTERS

Distortion of temporal characteristics during parametric up-conversion of ultrashort laser pulses
11 p1717 N85-20803

UPDRAFTS

U VERTICAL AIR CURRENTS

UPGRADING

The properties of VSt3sp inoculated steel
[BLL-M-35894-(5828.4)] 23 p3915 N85-34283

UPLINKING

Polarization angles of linearly polarized antennas and radio waves in satellite communications
[PB85-131613] 11 p1626 N85-20240

Remote control of an impact demonstration vehicle
[NASA-TM-85925] 14 p2225 N85-23797

The IRAS end-to-end data system
[NLR-MP-83056-U] 17 p3051 N85-28883

Receive shaping filter manufacture --- QPSK uplinks
[ESA-CR(P)-1996] 20 p3449 N85-31412

UPPER AIR

U UPPER ATMOSPHERE

UPPER ATMOSPHERE

NT D REGION
NT E REGION
NT EXOSPHERE
NT F REGION
NT F 2 REGION
NT GEOMAGNETIC TAIL
NT IONOSPHERE
NT LOWER IONOSPHERE
NT MAGNETOPAUSE
NT MAGNETOSPHERE
NT MESOPAUSE
NT MESOSPHERE
NT SPORADIC E LAYER
NT THERMOSPHERE
NT TURBOPAUSE
NT UPPER IONOSPHERE

MERIT: A man/computer data management and enhancement system for upper air nowcasting/forecasting in the United States --- Minimum Energy Routes using Interactive Techniques (MERIT)
01 p0083 N85-10558

Aeronomy 02 p0298 N85-11930

Upper Atmosphere Research Satellite (UARS) trade analysis
[NASA-CR-175269] 07 p0912 N85-15774

A 2-dimensional second order closure model of the upper atmosphere 08 p1182 N85-17450

Application of Fabry-Perot spectrometers for measurement of upper atmosphere temperatures and winds 08 p1183 N85-17454

The influence of deep cumulus convection on large-scale flow during AVE/SESAME 1, 10-11 April 1979
09 p1355 N85-18526

Survey of VLF-OMEGA transmissions received during summer at Antarctic peninsula
[INPE-3399-PRE/666] 10 p1462 N85-19223

Upper atmosphere research at INPE
[INPE-3281-PRE/604] 10 p1515 N85-19557

Brazil future plans in upper atmosphere research in Antarctica
[INPE-3400-PRE/669] 10 p1515 N85-19559

Transport processes in the upper atmosphere
11 p1646 N85-20375

Orographic disturbances of upper atmosphere emissions 11 p1663 N85-20480

Increase in hydrogen emission of upper atmosphere following launches of space vehicles
13 p1981 N85-22431

Comparison of observations of orographic disturbances in the troposphere and upper atmosphere
14 p2341 N85-24479

Magnetospheric effects on the upper atmosphere
14 p2365 N85-24616

Investigation of the daytime lunar atmosphere
[NASA-CR-175636] 14 p2440 N85-25057

Atmospheric density model 16 p2805 N85-27297

Full shadow phenomenon in Earth's upper atmosphere 16 p2808 N85-27316

Homogeneous processes of atmospheric interest
[NASA-CR-175770] 17 p2989 N85-28475

Observations of mesospheric turbulence by rocket probe and VHF radar, part 2.4A 21 p3619 N85-32484

The MU radar now partly in operation
21 p3628 N85-32543

Geologic processes on Venus: An update
22 p3857 N85-33883

Wide Angle Michelson Doppler Imaging Interferometer (WAMDII) 23 p3902 N85-34172

Additional flux of particles and albedo-electrons in upper atmosphere
[SH-6.1-6] 23 p4045 N85-35080

Space Station Polar Platform: Integrating research and operational missions
[PB85-195279] 24 p4069 N85-35218

UPPER IONOSPHERE

NT F REGION
NT F 2 REGION

Medium- and large-scale wave disturbances and heterogeneities of electron concentration in outer ionosphere in middle and low latitudes
06 p0825 N85-15241
Spreading of greatly extended inhomogeneities in upper ionsphere 14 p2339 N85-24462
Determining effective rate of plasma heating in outer equatorial ionosphere using data from ISIS-1 and ISIS-2 satellites 16 p2721 N85-26797

UPPER STAGE ROCKET ENGINES
Experiments on residual thrust and prediction for upper-stage solid propellant rockets
[NAL-TR-800] 03 p0324 N85-12087
LOX/LH2 propulsion system for launch vehicle upper stage, test results
[NASA-TM-77727] 03 p0324 N85-12089
Shuttle/Centaur project perspective
08 p1106 N85-16991
Shuttle/Centaur upper stage capability
11 p1712 N85-20773

UPPER SURFACE BLOWING
A study of lift characteristics of an upper surface blown jetwing with a rectangular nozzle
05 p0591 N85-13767
Low-speed wind tunnel tests of the NAL fan-jet STOL research aircraft model with ground simulation by tangential blowing
[NAL-TR-828] 10 p1423 N85-18976

UPSTREAM
Effect of upstream sidewall boundary layer removal on an airfoil test — conducted in Langley 0.3-m transonic cryogenic tunnel 03 p0313 N85-12019

UPWASH
Integral equation of lifting surfaces in Laplace domain and analytic continuation of its pressure kernel
[NAL-TR-795T] 01 p0002 N85-10009
An investigation of turbulence mechanisms in V/STOL upwash flow fields
[AD-A149786] 12 p1772 N85-21123
Fuselage upwash effects on RSRA rotor systems
[NASA-CR-177349] 20 p3368 N85-31015

UPWELLING
U UPWELLING WATER

UPWELLING WATER
Salinity driven oceanographic upwelling
[DE85-011664] 22 p3818 N85-33652

URANIUM
NT URANIUM ISOTOPES
NT URANIUM 235
Progress in lead/uranium zircon studies of lower paleozoic rocks of the southern Alexander terrane
04 p0518 N85-13304
U, Th, K content, heat production and thermal conductivity of Sao Paulo, Brazil continental shelf sediments: A reconnaissance work
[INPE-3401-PRE/670] 10 p1515 N85-19558
Approaches to ultrafast neutron detectors
[DE85-001206] 11 p1636 N85-20307
Compact L-edge densitometer for uranium concentration assay
[DE85-010344] 18 p3110 N85-29261
Occurrence of uranium in ground water in the vicinity of the US Department of Energy Feed Materials Production Center, Fernald, Ohio
[DE85-010340] 19 p3364 N85-30862
Reaction of uranium and the fluorocarbon FC-75
[DE85-012322] 22 p3843 N85-33802
Shape memory effect in uranium-niobium alloys below room temperature
[DE85-012964] 23 p3916 N85-34268
Method for preparing hydride configurations and reactive metal surface
[DE85-006443] 23 p3917 N85-34274
Uranium, thorium isotopic analyses and uranium-series ages of calcite and opal and stable isotopic compositions of calcite from drill cores UE25a no. 1, USR G-2 and USW G-3/GU-3, Yucca Mountain, Nevada
[DE85-013039] 23 p3948 N85-34471
Separation of uranium from technetium in recovery of spent nuclear fuel
[DE85-006499] 23 p3972 N85-34627
Lead and uranium group abundances in cosmic rays
[OG-7.1-3] 23 p4013 N85-34865
X-ray fluorescence analysis of uranium concentrates
[DE85-013189] 24 p4148 N85-35717
Measurement of uranium enrichment for gaseous uranium at low pressure
[DE85-012697] 24 p4150 N85-35733
Stopping relativistic Xe, Ho, Au and U nuclei in nuclear emulsions 24 p4173 N85-35876

URANIUM ALLOYS
Cerium compounds in the fashion of the light actinides
[DE84-014642] 04 p0475 N85-13024
The corrosion resistance of zinc coatings on depleted uranium and uranium alloys
[DE85-007216] 15 p2510 N85-25487
Neutron scattering study of the heavy fermion system UBe-13
[DE85-010955] 19 p3356 N85-30804
Experimental attempt to achieve microstructure variations through temperature/time permutations for a nonwrought powder metallurgy uranium-6 niobium alloy
[DE85-013166] 23 p3916 N85-34272

URANIUM CARBIDES
Loss-of-flow transient characterization in carbide-fueled LMFBRs
[DE85-009552] 19 p3269 N85-30270

URANIUM COMPOUNDS
NT URANIUM CARBIDES
NT URANIUM FLUORIDES
Growth and magnetic investigations of single crystals of intermetallic compounds of rare earths and uranium — magnetic properties 03 p0425 N85-12712
Measurement of uranium enrichment for gaseous uranium at low pressure
[DE85-012697] 24 p4150 N85-35733

URANIUM FLUORIDES
Liquid-phase compositions from vapor-phase analyses 2: Adaptation of the Prausnitz program to UF6 and some of its potential impurities
[DE85-011521] 21 p3673 N85-32819

URANIUM ISOTOPES
NT URANIUM 235
Methodology for economic evaluation of process technologies in the early research and development stages
[DE84-015863] 05 p0736 N85-14731
Environmental surveillance at Los Alamos during 1984
[DE85-011886] 22 p3811 N85-33605
The 1984 environmental monitoring report, Sandia National Laboratories, Albuquerque, New Mexico
[DE85-011175] 22 p3811 N85-33607
Gamma-ray line intensities for depleted uranium
[DE85-012674] 22 p3843 N85-33804

URANIUM 235
Technology for increasing the uranium-235 isotopic abundance in natural uranium feed on a productive scale
[DE85-011252] 19 p3357 N85-30810
Application of evaluated fission-product delayed-neutron precursor data in reactor kinetics calculations
[DE85-012728] 23 p3972 N85-34624
Measurement of uranium enrichment for gaseous uranium at low pressure
[DE85-012697] 24 p4150 N85-35733

URANUS (PLANET)
NT URANUS RINGS
Uranus and Neptune
[NASA-CP-2330] 02 p0298 N85-11927
The origin and evolution of Uranus and Neptune
02 p0298 N85-11928
Atmospheres of Uranus and Neptune
02 p0298 N85-11929
Aeronomy 02 p0298 N85-11930
Temperature structures and infrared-derived properties of the atmosphere of Uranus and Neptune
02 p0298 N85-11931
Interior structure of Uranus 02 p0299 N85-11939
Rotational properties of Uranus and Neptune
02 p0299 N85-11940
Oblatenesses of Uranus and Neptune
02 p0300 N85-11941
Origin and evolution of the Uranian and Neptunian satellites: Some dynamical considerations
02 p0300 N85-11943
Composition, structure and evolution of Uranian and Neptunian satellites 02 p0300 N85-11944
Physical properties of the Uranian satellites
02 p0300 N85-11946
Satellite masses in the Uranus and Neptune systems
[PSI-CONTRIB-196] 02 p0301 N85-11947
Magnetospheric structures: Uranus and Neptune
02 p0301 N85-11949
Magnetosphere, rings, and moons of Uranus
02 p0301 N85-11951
Do the satellites of Uranus control its magnetosphere?
02 p0301 N85-11952
The structure of the Uranian rings and the search for rings around Neptune 02 p0302 N85-11954
Infrared images of the Uranian rings
02 p0302 N85-11955
Dynamics of the Uranian rings
02 p0302 N85-11956
Research in planetary studies and operation of Mauna Kea Observatory
[NASA-CR-175618] 13 p2169 N85-23460
Giant planets and their satellites: Cosmochemistry, evolution and structure 13 p2175 N85-23494
The structure and composition of Uranus and Neptune
13 p2175 N85-23495
Studies of icy bodies: Uranian satellites and cometary nuclei 13 p2175 N85-23496
Voyage to Uranus 15 p2687 N85-26596
Magnetospheres of the outer planets
[AD-A154354] 19 p3384 N85-30996

URANUS ATMOSPHERE
Properties of the upper tropospheres of Uranus and Neptune derived from observations at visible to near-infrared wavelengths 02 p0298 N85-11933
Near infrared imaging of Uranus and Neptune
02 p0299 N85-11934
A review of the millimeter and centimeter observations of Uranus 02 p0299 N85-11935
Atmospheric dynamics of Uranus and Neptune: Theoretical considerations 02 p0299 N85-11936
The possibility of detection and measurement of cloud structure in the atmosphere of Uranus
02 p0299 N85-11937
Ultraviolet observations of Uranus and Neptune below 3000 A 11 p1760 N85-21071
Possible period of Jovian activity and possibility of seasons 16 p2723 N85-26810
Monodeurated methane in the outer solar system. 2. Its detection on Uranus at 1.6 microns
[NASA-CR-175762] 16 p2882 N85-27782

URANUS RINGS
Magnetosphere, rings, and moons of Uranus
02 p0301 N85-11951
The structure of the Uranian rings and the search for rings around Neptune 02 p0302 N85-11954
Infrared images of the Uranian rings
02 p0302 N85-11955
Dynamics of the Uranian rings
02 p0302 N85-11956
The rings of Uranus 15 p2672 N85-26486
Inclinations of the Uranian rings
15 p2672 N85-26487
Infrared observations of the Uranian rings
15 p2672 N85-26488
Stellar occultations by Uranus rings on 15 August 1980 and 22 April 1982 15 p2672 N85-26489
Indications of twist in the Epsilon rings of Uranus
15 p2672 N85-26490
The gravitational interaction between inclined, elliptical rings --- Uranus rings 15 p2675 N85-26514
On planetary rings as sources and sinks of magnetospheric plasmas 15 p2677 N85-26526
Tidal breakup and origin of the Uranian ring system
15 p2678 N85-26535
Future studies of planetary rings by spaceprobes
15 p2679 N85-26541

URBAN AREAS
U CITIES

URBAN DEVELOPMENT
Department of Housing and Urban Development, and certain independent agencies appropriations for fiscal year 1985, part 2
[S-REPT-98-889-PT-2] 01 p0127 N85-10870
National Aeronautics and Space Administration
01 p0127 N85-10871
Study of the urban evolution of Brasilia with the use of LANDSAT data
[E85-10101] 16 p2809 N85-27321

URBAN PLANNING
Nationwide urban runoff program. Relationship of urban runoff to land use and groundwater resources
[PB85-114692] 10 p1506 N85-19505
Experience of the Institute of Space Research with the use of remote sensing in urban planning studies
[INPE-3159-PRE/533] 16 p2880 N85-27770
Hydrodynamics and sanitation
[CT-579] 20 p3487 N85-31672

URBAN RESEARCH
Study of annoyance due to urban automobile traffic
[NASA-TM-77514] 01 p0069 N85-10458
Land use/land cover 02 p0214 N85-11410
Astronomy and sodium lighting
[RAND/N-2089-RC] 09 p1413 N85-18914
An initial analysis of LANDSAT-4 Thematic Mapper data for the discrimination of agricultural, forested wetlands, and urban land cover — Poinsett County, Arkansas; and Reelfoot Lake and Union City, Tennessee
13 p2118 N85-23193
Urban vehicle research project
[DE85-005444] 17 p3052 N85-28889
The timing of noise-sensitive activities in residential areas
[NASA-CR-177937] 20 p3524 N85-31918
Solar energy meteorological research and training program: Region 4
[DE85-011783] 22 p3816 N85-33640

URBAN TRANSPORTATION
Electric and hybrid vehicle demonstration project
[DE84-014622] 06 p0871 N85-15535
ElectriFleet Project
[DE85-001598] 10 p1570 N85-19898
Electric vehicle demonstration project
[DE85-003124] 11 p1741 N85-20344

In-vehicle evaluation of the Globe EV 2300 lead-acid, Delco Remy 150 nickel-zinc, and Eagle-Picher NIF 270 nickel-iron battery systems
[NASA-CR-175653] 14 p2349 N85-24521

Hybrid propulsion technologies for urban bus transit
[PB85-157469] 16 p2880 N85-27773

UREAS

Crystalline structure of urea ice sheets used in modeling experiments in the CRREL test basin
[AD-A148434] 08 p1226 N85-17722

Long term durability of urea formaldehyde glued joints removed from Vampire aircraft
[AD-A149053] 10 p1424 N85-18985

URETHANES

A miniature urethane molded acoustic transducer
[AD-A146459] 06 p0804 N85-15114

Plasticizer system for propellant compositions
[AD-D011502] 12 p1816 N85-21390

Plasticizer system for propellant compositions
[AD-D011517] 12 p1817 N85-21395

URINALYSIS

Circadian dynamics of potassium excretion in urine as related to working on one and two shifts
19 p3325 N85-30598

URINE

Urokinase production by electrophoretically separated cultured human embryonic kidney cells
20 p3501 N85-31765

A critical synopsis: Continuous growth of proximal tubular kidney epithelial cells in hormone-supplemented serum-free medium 20 p3501 N85-31767

The Fibrin slide assay for detecting urokinase activity in human fetal kidney cells 20 p3502 N85-31768

Composition and dynamics of bacteriocenosis associated with algae in human life-support systems
22 p3823 N85-33684

USA (UNITED STATES)

U UNITED STATES

USER MANUALS (COMPUTER PROGRAMS)

High frequency radar software reference manual for Product Two
[PB84-210079] 01 p0041 N85-10270

Manual of phosphoric acid fuel cell power plant optimization model and computer program
[NASA-CR-174721] 01 p0067 N85-10445

IAC user manual
[NASA-CR-175300] 01 p0102 N85-10677

PDSS/IMC CIS user's guide
[NASA-CR-171179] 01 p0102 N85-10682

MICROSCOPE: A software system for multivariate analysis
[AD-A144720] 01 p0103 N85-10688

HULL users' manual
[AD-A145000] 01 p0103 N85-10691

AGS-880 menu system user guide
[DE84-014338] 01 p0104 N85-10699

PASCAL-MP algebraic and numerical manipulator for polynomials
[INPE-3229-TDL/176] 02 p0240 N85-11562

SMILE user's guide: A macro preprocessor for extending FORTRAN
[DE84-015984] 02 p0243 N85-11584

Programmer's guide for ASKF 77: A tool for programming of dialogs in FORTRAN and PASCAL
[FOA-C-30366-E1] 02 p0243 N85-11585

A user's guide to the Flexible Spacecraft Dynamics and Control Program
[NASA-TM-87389] 03 p0405 N85-12586

Computer center introductory reference manual for CDC CYBER
[AD-A145796] 03 p0406 N85-12593

Effective date (E-DATE) model documentation. Changes to reflect model enhancement
[AD-A146050] 03 p0407 N85-12599

NATFREQ users manual: A FORTRAN 4 program for computing natural frequencies, mode shapes and drag coefficients for taut strumming cables with attached masses and spring-mass combinations
[AD-A146058] 03 p0407 N85-12600

Advanced Ada (trademark)
[AD-A146257] 03 p0407 N85-12602

Real-time Ada (trademark)
[AD-A146258] 03 p0407 N85-12603

Turbine blade damping study
[NASA-CR-171255] 04 p0456 N85-12890

Users manual for a computer program for dynamic response analysis of bladed systems
[UDR-TR-84-38] 04 p0456 N85-12893

NIKE3D: An implicit, finite-deformation, finite element code for analyzing the static and dynamic response of three-dimensional solids, revision 1
[DE84-017161] 04 p0514 N85-13277

Users manual for BRGLM: Interactive general linear model regression, version 3
[DE84-017386] 04 p0550 N85-13501

Preliminary user's guide for BIGONE on the Cray
[DE84-017075] 04 p0568 N85-13623

Automated Library Search System (ALSS) user's manual
[DE84-015952] 04 p0576 N85-13672

Computer programs to predict induced effects of jets exhausting into a crossflow
[NASA-CR-166591] 05 p0592 N85-13776

PROGRAM VSAERO: A computer program for calculating the non-linear aerodynamic characteristics of arbitrary configurations: User's manual
[NASA-CR-166476] 06 p0749 N85-14802

VLSI design tools, reference manual, release 2.0
[AD-A146444] 06 p0803 N85-15112

Investigative findings of image enhancement techniques
[AD-A146392] 06 p0853 N85-15424

High altitude chemically reacting gas particle mixtures. Volume 3: Computer code user's and applications manual — rocket nozzle and orbital plume flow fields
[NASA-CR-171828] 07 p0917 N85-15803

Interactive Signal Analysis Software (ISAS). User's manual
[AD-A146999] 07 p1022 N85-16485

RATFOR user's guide version 2.0
[NASA-CR-166601] 07 p1023 N85-16490

NYU Ada/Ed user's guide: Version 1.4 for VAX/VMS systems
[AD-A146759] 07 p1024 N85-16495

NOISEMAP 4.4 computer program update, operator's manual, addendum 1
[AD-A147091] 07 p1025 N85-16503

FORTRAN version of the quantitative energy-dispersive electron beam X-ray analysis program FRAME C
[PB84-240936] 07 p1027 N85-16519

A FORTRAN plotting package for graphic VDUs
[AD-A148489] 08 p1204 N85-17577

MC68CRX cross-assembler users manual
[AD-A148031] 08 p1205 N85-17584

Operating system for a real-time multiprocessor propulsion system simulator. User's manual
[NASA-TP-2426] 08 p1207 N85-17596

Boring information and subsurface data base package user's guide
[AD-A148623] 08 p1230 N85-17747

Computer center CDC libraries/utility (programs)
[AD-A148680] 09 p1368 N85-18593

FLAD user's manual: FLAD file contents
[AD-A148700] 09 p1368 N85-18594

User's guide to MIX: A computer code for fitting mixture distributions to data
[DE85-001451] 09 p1369 N85-18603

User/programmer guide for UCMD 108 multi-vertex polyarc/path integrity verifier
[DE84-017173] 09 p1369 N85-18604

User's manual: Menu-driven data graphing program for the Tektronix 7912AD and 7612D transient digitizer system
[DE85-002151] 09 p1370 N85-18610

UKIRT spectro-photometry system — United Kingdom Infrared Telescope (UKIRT)
[UKIRT-23] 09 p1414 N85-18921

TVENT1P user's manual, a computer code for analyzing tornado induced gas dynamic transients in flow networks
[DE85-002346] 10 p1486 N85-19379

Ada (trademark) primer
[AD-A148855] 10 p1539 N85-19703

FORTRAN 66 analyser: User's manual
[PB85-111748] 10 p1542 N85-19724

User's manual for GRIZZLY
[DE85-001405] 11 p1702 N85-20702

User's guide for the computer program response factor (REFAC)
[PB85-138600] 11 p1705 N85-20726

A GC/MS (Gas Chromatograph/Mass Spectrometer) data management process. Part 1: User's guide, version 1.0
[PB85-116051] 12 p1803 N85-21309

NOAA-AISC user's guide for implementing CERES maize model for large area yield estimation
[E85-10083] 12 p1873 N85-21748

User's guide to the TAMW wheat model as implemented on the IBM 360/195 computer
[E85-10084] 12 p1873 N85-21749

NOAA-AISC user's guide for implementing CERES wheat model for large area yield estimation
[E85-10085] 12 p1873 N85-21750

User's manual for the University of Houston individual heliostat layout and performance code
[DE85-004643] 12 p1882 N85-21808

A user's guide to sensitivity testing on computer models at Los Alamos National Laboratory
[LA-10104-M] 12 p1914 N85-22018

Implementation of the computer program-system MOSS (Map Overlay and Statistical System) on a VAX-11 series computer under VMS
[AD-A149612] 12 p1914 N85-22019

User's guide for NPSOL (Version 2.1): A FORTRAN package for quadratic programming
[AD-A150078] 12 p1916 N85-22028

METC VAX-IBM guide to ASPEN
[DE85-001974] 12 p1916 N85-22031

VAX-ASPEN installation guide
[DE85-001973] 12 p1916 N85-22032

Microcomputers in transit: A software handbook
[PB85-136414] 12 p1918 N85-22042

User's guide for TWOHEX: A code package for two-dimensional, neutral-particle transport in equilateral triangular meshes
[DE85-004482] 12 p1930 N85-22125

ROSA: A computer model for optical power ratio calculations
[DE85-005174] 13 p2129 N85-23251

M68000 RNF text formatter user's manual
[NASA-TM-86327] 13 p2146 N85-23320

SIGPI: A user's manual for the fast computation of the probabilistic performance of a complex system
[DE85-005447] 13 p2148 N85-23336

User's and programmer's guide to the mechanics of moving finite element code
[DE85-006165] 13 p2152 N85-23365

User's guide to calibration of analog electronic controllers in HVAC systems
[AD-A150803] 14 p2298 N85-24229

Users guide: The LaRC human-operator-simulator-based pilot model
[NASA-TM-86367] 14 p2390 N85-24721

The HORNE reasoning system, revision
[AD-A150983] 14 p2405 N85-24827

Computer Visual System (CVS) reference manual
[DE85-006328] 14 p2407 N85-24837

Automatic Dynamic Aircraft Modeler (ADAM), volume 1
[AD-A151410] 15 p2471 N85-25252

A user's manual for AMEER flight path trajectory simulation code
[DE85-006580] 15 p2472 N85-25260

A new NASTRAN capability for data reduction
15 p2574 N85-25874

The interactive plotting program: GRAPH
[AD-A151371] 15 p2623 N85-26165

Design specifications for IMAGER: The DREO (Defence Research Establishment Ottawa) image processing system
[AD-A151752] 15 p2624 N85-26168

Backend control processor for a multi-processor relational database computer system
[AD-A151892] 15 p2624 N85-26169

Programming the digital computer ODRA-1204 in MOST-2 language
[NASA-TM-87462] 15 p2627 N85-26191

Advanced life analysis methods. Volume 6: User's manual for LUGRO computer program to predict crack growth in attachment lugs
[AD-A151235] 15 p2628 N85-26195

Preliminary design of the Ada programming support environment configuration manager
[AD-A151845] 15 p2629 N85-26206

GEMINI: A computer program for two and three dimensional linear static and seismic structural analysis, CDC 7600 version
[DE85-007496] 15 p2631 N85-26218

User manual for IMAGER: The DREO (Defence Research Establishment Ottawa) image processing system
[AD-A151754] 15 p2653 N85-26362

ESP (External-Stores Program): A pilot computer program for determining flutter-critical external-store configurations. Volume 1: User's manual
[AD-A152268] 16 p2710 N85-26725

An interactive computer package for use with simulation models which performs multidimensional sensitivity analysis by employing the techniques of response surface methodology
[AD-A151956] 16 p2846 N85-27548

Users manual for coordinate generation code CRDSRA
[NASA-CR-172584] 17 p2891 N85-27824

User's manual for airfoil flow field computer code SRAIR
[NASA-CR-172585] 17 p2891 N85-27825

Airport and airway system cost allocation model. Volume 7: User's manual
[AD-A152877] 17 p2906 N85-27917

FLOWPLOT 2: A fluid dynamics and heat transfer plotting package
[DE85-009802] 17 p2959 N85-28277

Documentation of PHOTO: A user's manual for the analysis of photographic and X-ray negatives
[AD-A152968] 17 p2967 N85-28327

COSMIC Software Catalog, 1985 edition
[NASA-CR-174070] 17 p3010 N85-28608

Real-Time Multiprocessor Programming Language (RTMPL) user's manual
[NASA-TP-2422] 17 p3010 N85-28610

VULTURE manual
[DE85-008873] 17 p3013 N85-28631

ODIN: An extensible software environment. Report and user's reference manual
[DE65-006459] 18 p3164 N85-29600

Nimbus 7 Coastal Zone Color Scanner (CZCS). Level 2 data product users' guide
[NASA-TM-86202] 19 p3299 N85-30452

An interim user's manual for the advanced scavenging module version 1.2
[PB85-173904] 19 p3318 N85-30572

Cultural data base implementation study and computer-aided scene modeling system users manual
[AD-A154232] 19 p3333 N85-30646

MC TRICOMP user's guide
[AD-A154339] 19 p3337 N85-30673

BP (Basic Processor) TRICOMP user's guide
[AD-A154340] 19 p3337 N85-30674

VAX TRICOMP user's guide
[AD-A154341] 19 p3337 N85-30675

Computer Performance Modeling Tool (CPMT)
[AD-A154438] 19 p3338 N85-30682

T sub EX font tables
[DE85-011394] 19 p3339 N85-30687

Apollo multiplexer operations manual
[DE85-011293] 19 p3343 N85-30719

Nonequilibrium air radiation (Nequair) program: User's manual
[NASA-TM-86707] 19 p3353 N85-30780

User's guide for the Mk-3 D-coronameter data system
[PB85-181204] 19 p3385 N85-31002

A set of subroutines for masked three-dimensional plotting with rotations
[MEAH-33] 20 p3514 N85-31846

SCAP: A Shaped Charge Analysis Program. User's manual for SCAP 1.0
[DE85-011182] 20 p3515 N85-31854

User's manual of the BNDSCO computer program for solving constrained optimal control problems
[DFVLR-MITT-85-05] 20 p3516 N85-31865

Manual for the computer program for the Gaussian plume model with percentile calculations
[KNMI-TR-60] 20 p3517 N85-31867

Tip vortex computer code SRATIP. User's guide
[NASA-CR-172603] 21 p3551 N85-32093

User's guide for computer program CGFAG, Concrete General Flexure Analysis with Graphics
[AD-A155555] 21 p3570 N85-32204

BLAF: A blast field reconstruction program from pressure histories
[AD-A155300] 21 p3585 N85-32283

CARE 3 user friendly interface user's guide
[NASA-CR-172608] 21 p3669 N85-32791

Research on an expert system for database operation of simulation-emulation math models. Volume 2, Phase 1: Results
[NASA-CR-176088] 21 p3669 N85-32793

Praxis release notes, version 7.3
[DE85-011862] 21 p3673 N85-32820

Aerodynamic analysis of a horizontal axis wind turbine by use of helical vortex theory, volume 2: Computer program users manual
[NASA-CR-174921] 22 p3804 N85-33563

QKPLT users guide, version 2.0
[L-10094-M] 22 p3828 N85-33707

CARE 3 MENU maintenance manual
[NASA-CR-172609] 22 p3828 N85-33708

DECODE: A software manual for use with the Serial ASCII Instrumentation Loop (SAIL) system
[AD-A155358] 22 p3828 N85-33709

SMACS: A system of computer programs for probabilistic seismic analysis of structures and subsystems. Volume 1: User's manual
[DE85-011853] 22 p3830 N85-33724

User's operating procedures. Volume 1: Scout project information programs
[NASA-CR-177948] 23 p3956 N85-34518

User's operating procedures. Volume 1: Scout project financial analysis program
[NASA-CR-177949] 23 p3956 N85-34519

User's guide to the MATHEW/ADPIC models
[DE85-012952] 23 p3966 N85-34587

User's manual for the FLORA equilibrium and stability code
[DE85-013182] 23 p3966 N85-34590

Development of NATOPS performance software for the SH-3D and SH-3H helicopters
[AD-A156140] 24 p4065 N85-35192

User's guide: A computer program for strength analysis of non-hydraulic concrete structural elements. Report 2. Strength design of reinforced concrete column sections (PCAUC)
[AD-A156393] 24 p4102 N85-35429

Users guide for optimum interpolation method of global data assimilation
[AD-A155929] 24 p4138 N85-35648

SIG: A general-purpose signal processing program. User's manual: Revision 1
[DE85-013035] 24 p4140 N85-35662

LOCAT: A data retrieval program
[AD-A156004] 24 p4165 N85-35822

USER REQUIREMENTS

User requirements for very-short-range weather forecasts: Some key issues 01 p0084 N85-10562

Benefits resulting from tailored very-short-range forecasts in Sweden 01 p0084 N85-10564

Some aspects of matching nowcasting and Very-Short-Range Forecasting (VSRF) products with the need of a multilingual community of a mountainous country — Swiss Alps 01 p0084 N85-10566

Evaluating a scientific workstation computer
[DE84-014764] 01 p0100 N85-10663

AGS-880 menu system user guide
[DE84-014338] 01 p0104 N85-10699

Microcomputer management guidelines
[PB84-212174] 01 p0105 N85-10704

Information requirements analysis: An application
[AD-A144896] 01 p0125 N85-10858

Implications of artificial intelligence for a user defined technical information system
[AD-P003938] 02 p0248 N85-11618

An effective graphics user interface for rules and inference mechanisms
[AD-P003942] 02 p0248 N85-11622

Intelligent information retrieval from on-line technical documentation
[AD-P003946] 02 p0249 N85-11626

Design of a scientific information collation and dissemination system, volumes 1 thru 3
[AD-A146002] 03 p0438 N85-12791

Definition of technology development missions for early Space Station satellite servicing. Volume 2: Technical
[NASA-CR-171229] 04 p0461 N85-12923

Calms processor (CALMPRO) user's guide
[PB84-229467] 04 p0540 N85-13439

User-oriented development and production of integrated circuits in small and medium quantities
[BMFT-FB-T-84-171] 05 p0633 N85-14059

ERS-1 and its potential for industrial utilization
05 p0659 N85-14235

Civil law enforcement missions
06 p0751 N85-14812

Specification of a transport protocol for computer communications. Volume 1: Overview and Services. Volume 2: Class 2 protocol. Volume 3: Class 4 protocol
[PB84-222850] 06 p0848 N85-15380

Specification of a transport protocol for computer communications. Volume 4: Service specifications. Volume 5: Guidance for the implementor. Volume 6: Guidance for implementation selection
[PB84-222868] 06 p0848 N85-15385

Specification of a transport protocol for computer communications. Volume 7: Testing OSL protocols, a compendium of papers. Volume 8: User's guide to the testing system for implementations of the ICST transport protocol. Volume 9: A test suite for implementations of the ICST transport protocol. Volume 10: Specification of a remote scenario interpreter for implementations of the ICST transport protocol
[PB84-222876] 06 p0848 N85-15386

Beginner's guide to blocked records on magnetic tape
[DE85-001691] 06 p0855 N85-15433

Design and analysis of an SQL (Structured Query Language) interface for a multi-backend database system
[AD-A146534] 06 p0856 N85-15447

Commerce Laboratory: Mission analysis payload integration study
[NASA-CR-171298] 07 p0911 N85-15764

Results of principal NASA studies on space station uses and functional requirements 07 p0914 N85-15787

What do we want: Increased speed, resolution, contrast or DOE? — astronomical photography
07 p0964 N85-16115

Climatological information and water resources
07 p1002 N85-16367

Mental models and cooperative problem solving with expert systems
[AD-A147843] 07 p1021 N85-16479

A study of the relationship between user attitudes and the success of the MAJCOM and AFRCE work information management system
[AD-A146956] 07 p1051 N85-16671

ATE user's view on design for maintainability
08 p1064 N85-16737

Commerce Lab: Mission analysis. Payload integration study
[NASA-CR-171285] 08 p1104 N85-16982

Shuttle/Centaur project perspective
08 p1106 N85-16991

Space Station needs, attributes, and architectural option study
[NASA-CR-174316] 08 p1109 N85-17011

Space Station engineering and technology development
[NASA-CR-174383] 09 p1267 N85-18079

Commerce lab: Mission analysis and payload integration study
[NASA-CR-174381] 10 p1426 N85-18993

Sector suite man-machine functional capabilities and performance requirements
[AD-A148881] 10 p1531 N85-19647

Microcomputers in transit: A hardware handbook
[PB65-113660] 10 p1536 N85-19700

Research needs on the interaction between information systems and their users: Report of a workshop
[PB85-121523] 10 p1568 N85-19891

Development of computer centers, equipment described: Problems of computer centers
11 p1700 N85-20686

GPS system field testing 11 p1711 N85-20762

Evaluation of the vocabulary switching systems
[PB85-127157] 12 p1951 N85-22260

Introduction to the Space Physics Analysis Network (SPAN)
[NASA-TM-86499] 14 p2290 N85-24198

Commercial data base management system for geonames data base
[AD-A150835] 14 p2433 N85-25007

Study on needs for a magnetic suspension system operating with a transonic wind tunnel
[NASA-CR-3900] 16 p2715 N85-26759

Design of computer-related workstations in relation to job functions and productivity
[AD-A151938] 16 p2844 N85-27534

Management considerations for an information center
[AD-A151774] 16 p2875 N85-27742

Personal computer aided decision analysis
[AD-A151911] 16 p2875 N85-27743

Further development of high voltage SIPMOS FET's to fulfill market needs
[BMFT-FB-T-84-255] 17 p3045 N85-28843

Automated Weather Observing System (AWOS) demonstration program
[AD-A153463] 18 p3148 N85-29493

BREED: A CDC-7600 computer program for the automation of breeder reactor design analysis (LWBR Development Program)
[DE85-010327] 19 p3338 N85-30686

SPAR improved structural-fluid dynamic analysis capability
[NASA-CR-171549] 20 p3454 N85-31449

Design guidelines for user-system interface software
[AD-A154907] 21 p3671 N85-32807

The effect of communication-language designs on software specifications
[AD-A155173] 21 p3672 N85-32809

Praxis release notes, version 7.3
[DE85-011862] 21 p3673 N85-32820

The flow of scientific and technical information in the US Army Research Laboratories
[AD-A155050] 21 p3713 N85-33043

Fracture detection and characterization for geothermal reservoir definition
[DE85-008677] 22 p3815 N85-33630

DECODE: A software manual for use with the Serial ASCII Instrumentation Loop (SAIL) system
[AD-A155358] 22 p3828 N85-33709

Product definition: Technical specification of needs
[SNIAS-851-430-104] 23 p3910 N85-34228

Graphics interaction in databases
23 p3958 N85-34534

A model for graphics interface tool development
23 p3960 N85-34545

Using percent-done program indicators to enhance user interfaces 23 p3960 N85-34546

Architecture of languages for large CAD systems development 23 p3962 N85-34557

How map designers can represent their ideas in thematic maps: Effective user interfaces for thematic map design
23 p3962 N85-34562

UTAH

Summary of salt gradient solar pond research
05 p0667 N85-14292

Geology and resources of the Tar Sand Triangle, southeastern Utah
[DE84-012017] 05 p0677 N85-14346

best copy available

A geographic information system for resource managers based on multi-level remote sensing data
[E85-10047] 06 p0827 N85-15249
Geothermal assessment of a portion of the Escalante Valley, Utah
[DE84-016964] 06 p0828 N85-15257
Detecting agricultural to urban land use change from multi-temporal MSS digital data --- Salt Lake County, Utah
[E85-10049] 07 p0983 N85-16245
An integrated remote sensing approach for identifying ecological range sites --- parker mountain
[E85-10050] 07 p0983 N85-16246
Revised Uniform Summary of Surface Weather Observations (RUSSWO). Hill AFB, Utah, parts A-F
[AD-A147184] 07 p1006 N85-16395
Petrography, sedimentology, diagenesis, and reservoir characteristics of some Pennsylvanian phylloid algal limestones: Kansas and Utah, USA
09 p1352 N85-18507
Assessment of LANDSAT for rangeland mapping, Rush Valley, Utah
[E85-10072] 10 p1503 N85-19486
An integrated GIS/remote sensing data base in North Cache soil conservation district, Utah: A pilot project for the Utah Department of Agriculture's RIMS (Resource Inventory and Monitoring System)
[E85-10073] 10 p1504 N85-19487
LANDSAT 4 investigation of Thematic Mapper and Multispectral Scanner applications
[E85-10076] 10 p1504 N85-19490
Climate of Salt Lake City, Utah
[PB85-123875] 10 p1521 N85-19589
Low-temperature geothermal assessment of the Jordan Valley Salt Lake County, Utah
[DE85-000616] 11 p1670 N85-20524
Aeromagnetic and radiometric signatures of a possible porphyry system in the western Tusher Mountains, Utah
24 p4103 N85-35437
Evaluation of low-temperature geothermal potential in north-central Box Elder County, Utah
[DE85-009541] 24 p4112 N85-35490

UTILITIES
Analysis of wind energy systems for selected electric utilities
[DE84-013025] 04 p0530 N85-13389
Photovoltaic Systems Development and Evaluation Projects Integration Meeting
[DE84-008530] 11 p1673 N85-20542
Experimental investigation of a variable speed constant frequency electric generating system from a utility perspective
[NASA-CR-174950] 21 p3579 N85-32251

UTILITY AIRCRAFT
NT BO-105 HELICOPTER
NT DO-28 AIRCRAFT
NT P-531 HELICOPTER
NT U-2 AIRCRAFT
NT UH-1 HELICOPTER
NT UH-60A HELICOPTER

UTILIZATION
NT COAL UTILIZATION
NT GEOTHERMAL ENERGY UTILIZATION
NT LASER APPLICATIONS
NT LASER CUTTING
NT LASER FUSION
NT REUSE
NT WASTE ENERGY UTILIZATION
NT WASTE UTILIZATION
NT WINDPOWER UTILIZATION
The Palmqvist test and its applications in WC-Co alloys 02 p0177 N85-11187
Radio telemetry formula applications. A practical users guide
[AD-A146247] 03 p0356 N85-12286
Technical order managers handbook: Utilization assessment
[AD-A147579] 07 p1055 N85-16694
Space station propulsion: The advanced development program at Lewis
[NASA-TM-86999] 15 p2494 N85-25386
Mathematical programming in the Netherlands
[REPT-ARW-03-THE-BDK/ORS/83/10]
20 p3517 N85-31866
Applications of CdTe to nuclear medicine
[DE85-011877] 23 p3952 N85-34492

UV CETI STARS
U FLARE STARS

UV LASERS
U ULTRAVIOLET LASERS

V

V BAND
U EXTREMELY HIGH FREQUENCIES

V/STOL AIRCRAFT
NT BO-105 HELICOPTER
NT CH-47 HELICOPTER
NT FLYING PLATFORMS
NT HELICOPTERS
NT MILITARY HELICOPTERS
NT P-531 HELICOPTER
NT RIGID ROTOR HELICOPTERS
NT ROTARY WING AIRCRAFT
NT SHORT TAKEOFF AIRCRAFT
NT TILT ROTOR AIRCRAFT
NT UH-1 HELICOPTER
NT UH-60A HELICOPTER
NT VERTICAL TAKEOFF AIRCRAFT
Inlet and airframe compatibility for a V/STOL fighter/attack aircraft with top-mounted inlets
[NASA-TM-84252] 01 p0003 N85-10015
Computer programs to predict induced effects of jets exhausting into a crossflow
[NASA-CR-166591] 05 p0592 N85-13776
An investigation of turbulence mechanisms in V/STOL upwash flow fields
[AD-A149786] 12 p1772 N85-21123
Some aspects of the design of a fly-by-wire flying control system for a supersonic V/STOL fighter aircraft
[COLL-AERON-8413] 12 p1780 N85-21175
Special course on V/STOL aerodynamics: An assessment of European jet lift aircraft
[AGARD-R-710-ADDENDUM] 15 p2460 N85-25166
Future of V/STOL aircraft systems: A survey of opinions
[NASA-TM-86669] 18 p3061 N85-26937

VACANCIES (CRYSTAL DEFECTS)
Application of positron annihilation in materials science
[DE84-014733] 02 p0266 N85-11663
Investigation of the interaction of atoms with lattice defects using probe methods 03 p0429 N85-12737
Defective nature of the crystalline lattice of nickel ferrite-based solid solutions
[BLL-TRANS-WH-595-(9091.9F)]
10 p1439 N85-19068
Resolvability of defect ensembles with positron annihilation studies
[DE85-010041] 18 p3196 N85-29823
PAS determination of the vacancy formation enthalpy in tungsten
[DE85-010283] 19 p3240 N85-30086

VACCINES
Induction of immunity to toxins with anti-idiotypic antibody
[AD-A146793] 07 p1014 N85-16445
Progress, goals in biotechnology summarized
17 p2945 N85-28182
Genetic and physiological control of protective antigen synthesis by bacillus anthracis
[AD-A156324] 24 p4133 N85-35617

VACUUM
NT HIGH VACUUM
NT ULTRAHIGH VACUUM
The Boltzmann equation: Global existence for a rare gas in an infinite vacuum
[PREPRINT-78] 01 p0124 N85-10851
Gravitational vacuum 02 p0265 N85-11734
Simulation of the interaction of single-pulsed optical lasers with targets in a vacuum
[DE84-016476] 06 p0640 N85-14107
Performance of Chromel versus Alumel and Nicrosil versus Nisil thermocouple assemblies in vacuum and argon between 1000 deg C and 1200 deg C
[DE85-000610] 12 p1853 N85-21624
Review of anode phenomena in vacuum arcs
[DE85-002736] 12 p1926 N85-22101
High temperature antifriction properties of Ti sub 1-sub xNb sub x C sub 0.5N sub 0.5 alloys
13 p2029 N85-22715
ANTENA user guide
[DE85-004961] 14 p2424 N85-24953
Spray applicator for spraying coatings and other fluids in space
[NASA-CASE-MSC-18652-1] 18 p3115 N85-29283
Magnetics calculations for an ELMO Bumpy Square
[DE85-010442] 18 p3191 N85-29792
The photochemical oxidation of GaAs
[AD-A153689] 19 p3233 N85-30045
Prospective uses for diffusion welding in vacuum
22 p3733 N85-33145
The 2nd European Conference on Atomic and Molecular Physics
[AD-A155863] 24 p4148 N85-35715
SU(2) x U(1) vacuum and the Centauro events
24 p4175 N85-35885

VACUUM APPARATUS
NT ION PUMPS
NT IONIZATION GAGES
NT MOLECULAR PUMPS
NT VACUUM CHAMBERS
NT VACUUM FURNACES
NT VACUUM PUMPS
High temperature ultra-high vacuum infrared window seal
[AD-D011333] 07 p0929 N85-15890
Cryogenic glass-to-metal seal
[AD-D011370] 07 p0933 N85-15911
Metal vapor arc switch electromagnetic accelerator technology
[NASA-CR-174380] 09 p1314 N85-18259
Instrumentation for particle-beams research using excited merging beams
[AD-A154155] 19 p3356 N85-30907
Effective brightness of zero-point fluctuations of the electromagnetic vacuum accompanying parametric scattering of light 21 p3694 N85-32951

VACUUM CHAMBERS
Final magnetic shimming of vacuum chamber suspension holes on the sector magnets
[CSIR-NAC-83-02] 01 p0117 N85-10798
Electrostatic wave observation during a space simulation Beam-Plasma-Discharge (BPD)
[NASA-CR-174286] 07 p1045 N85-16639
Tailored vacuum chambers for ac magnets
[DE85-010767] 21 p3591 N85-32319
Dual-chamber plasma deposition of A-Si:H solar cells at high rates using disilane
[DE85-011828] 23 p3946 N85-34451
Monitoring dosage of volatile compounds in tests at low barometric pressure 23 p3954 N85-34506
Size effects of vacuum chamber for H- (D-) ion volume production by sheet plasma 1
[IPPJ-731] 23 p3974 N85-34639

VACUUM DEPOSITION
Apparatus for producing diamond-like carbon flakes
[NASA-CASE-LEW-13837-3] 11 p1615 N85-20155
Diamondlike flakes
[NASA-CASE-LEW-13837-2] 12 p1796 N85-21267
Peculiarities of MgF2 film formation and optimization of MgF2 film deposition process 14 p2261 N85-24132
In situ thin film measurements
[AD-A151379] 15 p2652 N85-26353
Synthesis and characterization of superconducting electronic materials
[AD-A151112] 15 p2659 N85-26409
Vacuum plasma coatings for turbine blades
16 p2734 N85-26869
New metal coating method developed
21 p3568 N85-32191
Advances in sputtered and ion plated solid film lubrication 22 p3797 N85-33524
Polarisation insensitive achromatic cube beamsplitter --- binocular microscopes
[NPL-MOM-72] 23 p3973 N85-34630

VACUUM EFFECTS
Density distribution in supersonic jet discharged into vacuum from nozzle with bevel tip
02 p0269 N85-11757
Spacelab 1 experiment: Microorganisms in space hard environment 05 p0691 N85-14443
Evaluation and prediction of long-term environmental effects of nonmetallic materials
[NASA-CR-171353] 10 p1450 N85-19137
Cutting structural materials in vacuum
14 p2266 N85-24165
Mechanical properties of lunar materials under anhydrous, hard vacuum conditions: Applications of lunar glass structural components
[DE85-006682] 16 p2801 N85-27271
Effective specific impulse of secondary flow injected into a rocket nozzle
[NAL-TR-848T] 18 p3067 N85-26970
Prospective uses for diffusion welding in vacuum
22 p3733 N85-33145

VACUUM FURNACES
West Europe report: Science and technology
[JPRS-WST-84-008] 15 p2531 N85-25606
France develops new continuous vacuum treatment method 15 p2531 N85-25611
Studies on the processing methods for extraterrestrial materials
[NASA-CR-175778] 16 p2716 N85-26768

VACUUM GAGES
NT IONIZATION GAGES

VACUUM MELTING
A study of vacuum melting to increase the toughness of maraging steels
[AD-A145017] 01 p0028 N85-10175
Effect of prior warm rolling on the retained austenite content and hardening response of VIM-VAR (vacuum-induction melted-vacuum-arc remelted) AISI M-50 steel
[AD-A156145] 24 p4079 N85-35281
X-ray fluorescence analysis of 304L stainless steel
[DE85-013254] 24 p4080 N85-35288

VACUUM PUMPS
NT ION PUMPS
NT MOLECULAR PUMPS
Electron storage ring beam lifetime dependence on pressure and pumping speed
[DE85-003206] 11 p1724 N85-20845
Impurity control and vacuum pumping system design and analysis for next-generation Tokamaks
[DE85-009291] 17 p3041 N85-28815
VACUUM SYSTEMS
Design study of the vacuum pump of the ESRP --- synchrotron radiation
[NIKHEF-MTG-21] 08 p1138 N85-17167
Electron storage ring beam lifetime dependence on pressure and pumping speed
[DE85-003206] 11 p1724 N85-20845
Measurement of NSLS distributed diode sputter ion pump characteristics
[DE85-006550] 16 p2760 N85-27031
Management of vacuum leak-detection processes, standards and calibration
[DE85-006705] 16 p2788 N85-27202
Vacuum interface flashover with bipolar electric fields
[DE85-012027] 22 p3755 N85-33275
Supermite vacuum interface design
[DE85-012861] 22 p3837 N85-33759
Ultrahigh vacuum system of the heavy ion transport line at Brookhaven
[DE85-011838] 22 p3840 N85-33778
Key issues of fusion nuclear technology development (FINESSE)
[DE85-012599] 22 p3845 N85-33817
Experimental lithium system
[DE85-013252] 24 p4094 N85-35382
High vacuum portable pumping station suitable for accelerator use
[DE85-011840] 24 p4155 N85-35759
Vacuum system for the Argonne 6 GeV synchrotron light source
[DE85-012286] 24 p4157 N85-35773
Neutral pumping rates for a next step tokamak ignition device
[DE85-012780] 24 p4157 N85-35776
VACUUM TESTS
NT THERMAL VACUUM TESTS
The performance of Fomblin Z25 oil in ball bearings operating in vacuum --- spacecraft lubricant
[ESA-ESTL-056] 08 p1134 N85-17150
The wear of small polyacetal and polymide gears in vacuum --- spacecraft gears
[ESA-ESTL-058] 08 p1169 N85-17374
Vapor pressure and evaporation rate of certain heat-resistant compounds in a vacuum at high temperatures
[NASA-TM-77807] 10 p1434 N85-19036
Measurement of damping of graphite epoxy materials
[NASA-CR-176073] 21 p3596 N85-32334
VACUUM TUBE OSCILLATORS
NT CATHODE RAY TUBES
NT COLD CATHODE TUBES
NT GAS DISCHARGE TUBES
NT HELITRONS
NT KLYSTRONS
NT MAGNETRONS
NT MICROWAVE OSCILLATORS
NT MICROWAVE TUBES
NT PHOTOMULTIPLIER TUBES
NT PICTURE TUBES
NT THERMICONS
NT THYRATRONS
NT TRAVELING WAVE TUBES
NT VIDICONS
VACUUM TUBES
NT CATHODE RAY TUBES
NT COLD CATHODE TUBES
NT GAS DISCHARGE TUBES
NT HELITRONS
NT KLYSTRONS
NT MAGNETRONS
NT MICROWAVE OSCILLATORS
NT MICROWAVE TUBES
NT PHOTOMULTIPLIER TUBES
NT PICTURE TUBES
NT THERMICONS
NT THYRATRONS
NT TRAVELING WAVE TUBES
NT VIDICONS
Laser welder for fabricating neutron tubes
[DE85-009865] 17 p2974 N85-28377
Advanced evacuated tube collectors
[DE85-010271] 19 p3274 N85-30302
VACUUM ULTRAVIOLET RADIATION
U FAR ULTRAVIOLET RADIATION
VALENCE
Actinides, the narrowest bands
[DE84-016463] 05 p0733 N85-14710
Basic studies of atomic dynamics
[DE84-015661] 09 p1380 N85-18675
Angle-resolved photoemission study of AuGa2 and AuIn2 intermetallic compounds
[AD-A150000] 12 p1940 N85-22183
The Valence- and conduction-band structure of the sapphire (1102) surface
[AD-A150001] 12 p1940 N85-22184
Mixed valence materials
[AD-A151009] 14 p2252 N85-23959
Strained-layer superlattices and strain-induced light holes
[DE85-003675] 14 p2431 N85-24990
VALIDATION
U PROVING
VALIDITY
AFOS (Automation of Field Operations and Services)-ERA forecast verification, September 1984
[PB85-137578] 12 p1897 N85-21912
A note on validity generalization procedures
[AD-A150085] 12 p1924 N85-22085
VALKYRIE AIRCRAFT
U B-70 AIRCRAFT
VALLEYS
NT DEATH VALLEY (CA)
NT IMPERIAL VALLEY (CA)
NT SACRAMENTO VALLEY (CA)
Paleohydrology and geomorphology of selected reaches of the upper Wabash Valley, Indiana
02 p0226 N85-11481
Love and Rayleigh waves in irregular ground
04 p0523 N85-13348
Atmospheric tracer experiments in a deep narrow valley
[PB84-234590] 04 p0532 N85-13402
Geothermal assessment of a portion of the Escalante Valley, Utah
[DE84-015964] 06 p0828 N85-15257
Towing tank studies of stratified flow over ridges and valleys
[DE84-011418] 06 p0839 N85-15329
A numerical method for interface problems in elastodynamics
[NASA-TM-86488] 08 p1172 N85-17391
Mesozoic ophiolific olistostromes and Cenozoic imbricate thrust faulting in the northern California coast ranges: Geology of the Mysterious Valley area, Napa County 08 p1182 N85-17445
Low-temperature geothermal assessment of the Jordan Valley Salt Lake County, Utah
[DE85-000616] 11 p1670 N85-20524
Paleohydrologic implications of valley networks of Mars 13 p2190 N85-23585
Geomorphology and geology of the Southwestern Margaritifer Sinus and Argyre regions of Mars. Part 1: Geological and geomorphological overview
13 p2192 N85-23600
Geomorphology and geology of the Southwestern Margaritifer Sinus and Argyre regions of Mars. Part 3: Valley types and distribution 13 p2193 N85-23602
Late Tertiary and Quaternary river systems of the eastern Sahara as mapped on shuttle radar and LANDSAT images 13 p2199 N85-23641
The rifted margin of Saudi Arabia
17 p2990 N85-28483
VALMET: A valley air pollution model
[DE85-010820] 21 p3614 N85-32463
VALSALVA EXERCISE
Main component method used to study variations of cardiovascular parameters 12 p1901 N85-21939
VALSALVA MANEUVER
U VALSALVA EXERCISE
VALUE
NT Q VALUES
Point processes associated with extreme value theory
[AD-A151211] 15 p2640 N85-26280
Computing the singular value decomposition of a product of two matrices
[DE85-006977] 16 p2859 N85-27631
VALUE ENGINEERING
Introduction to the subjective transfer function approach to analyzing systems
[AD-A145817] 03 p0436 N85-12774
Value analysis --- industrial competition
[CNES-NT-110] 04 p0577 N85-13684
Mini-Seminar on Non-Destructive Testing
[CSIR-TSD-0009/83] 14 p2316 N85-24308
New materials needs in aeronautics
[SNIAS-851-502-101] 22 p3729 N85-33120
DOD Value Engineering Conference report. Value Engineering (VE): A tool that benefits line management held at Leesburg, Virginia on 1-2 November 1984. Part 1. Executive summary
[AD-A156067] 24 p4163 N85-35810
DOD Value Engineering Conference report. Value Engineering (VE): A tool that benefits line management held at Leesburg, Virginia on 1-2 November 1984. Part 2. Plenary session
[AD-A156068] 24 p4163 N85-35811
DoD Value Engineering conference report. Value Engineering (VE): A tool that benefits line management. Part 3, Workshop A: VE in the program office
[AD-A156069] 24 p4163 N85-35812
DoD Value Engineering conference report. Value Engineering (VE): A tool that benefits line management. Part 4, Workshop B: VE on spare parts
[AD-A156070] 24 p4163 N85-35813
DoD Value Engineering conference report. Value Engineering (VE): A tool that benefits line management. Part 5, Workshop C: VEP/VECP administration, negotiation, and implementation
[AD-A156071] 24 p4163 N85-35814
DoD Value Engineering conference report. Value Engineering (VE): A tool that benefits line management. Part 6, Workshop D: VE training-orientation
[AD-A156072] 24 p4164 N85-35815
DoD Value Engineering conference report. Value Engineering (VE): A tool that benefits line management. Part 7, Workshop E: VE in construction and architect engineer contracts
[AD-A156073] 24 p4164 N85-35816
VALVES
NT AUTOMATIC CONTROL VALVES
NT COCKS
NT CONTROL VALVES
NT DAMPERS (VALVES)
NT FUEL VALVES
NT GAS VALVES
NT PRESSURE REGULATORS
NT SOLENOID VALVES
Back end valves: History and modifications
[DE84-009272] 05 p0646 N85-14145
Turbine blade test cascade modifications and orations, August 1982 - April 1983
[DE84-009268] 06 p0833 N85-15303
Airspeed sensing pressure valve system
[AD-D011472] 10 p1425 N85-18987
Tire inflation/deflation system
[AD-D011459] 10 p1493 N85-19426
Tire deflation mechanism
[AD-D011460] 10 p1493 N85-19427
Performance of the 10 KSI Wilson valve breech
[DE85-000258] 10 p1493 N85-19430
Pneumatic clamping device
[AD-D011544] 12 p1858 N85-21656
Hydraulic characteristics of reduction installation valves 14 p2269 N85-24060
Dependents of velocity distribution in exit section of converging channel on shape of inlet channel in regulating valve 14 p2277 N85-24106
Fracture mechanics analysis of cold drawn Si-Cr valve steel
[BLL-BISI-TRANS-22216-(9022.06)]
17 p2978 N85-28405
Automatic volume calibration system
[DE85-006955] 18 p3102 N85-29204
Moisture content and gas sampling device
[NASA-CASE-MSC-18666-1] 18 p3103 N85-29213
Linear motion valve
[NASA-CASE-MSC-20148-1] 18 p3115 N85-29284
Thermo-electric valve
[AD-D011682] 19 p3252 N85-30165
Sobolev-Poincare's inequality and the Neumann problem for u sub t = divergence of the absolute value of the gradient u to the p-2 power x the gradient u
[AD-A154788] 21 p3676 N85-32839
Automatic rotary valve actuator
[DE85-012797] 22 p3794 N85-33505
Reactant pressure differential control for fuel cell gases
[NASA-CASE-MSC-2[illegible]7-2] 23 p3937 N85-34403
VAMPIRE AIRCRAFT
U DH 115 AIRCRAFT
VAN ALLEN RADIATION BELTS
U RADIATION BELTS
VAN DER WAAL FORCES
Infrared excitation of clusters and ions of atmospheric interest
[DE85-002098] 10 p1516 N85-19564
Explorations into thermodynamics analogies and critical points in reference to gas-solid transport
[DE85-000816] 11 p1738 N85-20929
Many-body processes in atomic and molecular physics
[DE85-009750] 19 p3354 N85-30791
VANADIUM
Granular boundary segregation in low-alloyed titanium-vanadium alloys 01 p0019 N85-10117
The effect of replacing molybdenum with vanadium on the corrosion resistant properties of stainless steels
02 p0176 N85-11197

Electrolytic lapping technique for vanadium
[DE84-014710] 02 p0183 N85-11227
Review: Role of refractory metal alloys in fusion reactor applications
[AERE-R-11317] 03 p0422 N85-12695
Thermodynamics and phase equilibria in the vandium-silicon system
[AD-A145870] 03 p0435 N85-12769
Preparation of low-silicon vanadium metal
[DE84-014818] 04 p0476 N85-13031
Volatility of vanadium from a candidate fusion tractor alloy
[DE84-015277] 05 p0618 N85-13955
Investigation of vanadium solid solution and zeta phase regions of vanadium-carbon system
[DE85-002678] 11 p1605 N85-20092
Improvement in magnetic field properties of vanadium-gallium superconductors by enhancement of spin-orbit scattering
[DE85-002893] 13 p2164 N85-23422
Thermodynamic analysis of the plasma nitriding of ferrovanadium
[BLL-BISI-TRANS-22237-(9022.06)] 17 p2924 N85-28032
Microstructures and mechanical properties of microalloyed medium carbon steels
19 p3238 N85-30074
Properties of Ti-6Al-4V spun formed fuze supports
[DE85-011968] 22 p3792 N85-33498
Method for preparing high purity vanadium
[DE85-006412] 23 p3913 N85-34242
Calculating the interatomic pair potential allowing for resonance interaction in titanium, nickel and vanadium
[BLL-M-35843-(5828.4)] 23 p3913 N85-34249
Flux-line lattice anisutropy in V3Si: Observation and interpretation
[DE85-011935] 23 p3985 N85-34713
Applications of the mineral resources data system and the international strategic minerals inventory in mineral-resource assessments by region and commodity
24 p4105 N85-35451

VANADIUM ALLOYS
The use of vanadium in low alloy structural steels
02 p0180 N85-11207
Ion implantation of surgical Ti-6Al-4V alloy
[DE85-000943] 09 p1296 N85-18142
Ti-6Al-4V alloy castings prepared in zircon sand molds and the effect of hot isostatic pressing
[PB85-109932/GAR] 09 p1298 N85-18150
Phase transformations in vanadium alloys of titanium during quenching and tempering
11 p1602 N85-20073
Partial replacement of chromium in austenitic stainless steels by molybdenum, copper, and vanadium, report of investigations 1984
[PB85-116506] 12 p1809 N85-21346
Decomposition of VTAN alloy solid solution upon irradiation and thermal aging 13 p2029 N85-22712
Effect of oxygen on mechanical properties of Nb-V alloy
[DE85-002681] 14 p2256 N85-23982
Conversions in amorphous zirconium-vanadium alloy
15 p2496 N85-25400
Effects of the phase compositions of cast low-pearlite steels micro-alloyed with vanadium and titanium of their structure and properties
[BLL-BISI-TRANS-22301-(9022.06)] 17 p2928 N85-28067
The disordering process in an L12 ordered alloy
[DE85-006152] 17 p2931 N85-28093
Development of reduced activation alloys for fusion service: Draft
[DE85-007464] 18 p3074 N85-29014
Long range ordered alloys modified by addition of niobium and cerium
[DE85-011661] 20 p3431 N85-31285
Reliability of welds to repair defects in cast components made from CrMoV steel
[BLL-CE-TRANS-8054-(9022.09)] 20 p3461 N85-31501

VANADIUM COMPOUNDS
NT VANADIUM OXIDES
Scale-up of vanadium trineodecanoate
[AD-A149935] 12 p1813 N85-21370

VANADIUM OXIDES
A study of the K-edge absorption spectra of selected vanadium compounds
[AD-A149334] 10 p1435 N85-19045
Metal-semiconductor phase transition and its application
[DRIC-T-7149] 13 p2021 N85-22665
Electrochromic and thermochromic materials for solar energy applications with emphasis on niobium and vanadium oxides
[DE85-010630] 19 p3249 N85-30147
Thin film phase transition materials development program
[AD-A154260] 19 p3259 N85-30209
Photoeffects of semiconductor electrolyte interfaces
[AD-A154163] 20 p3449 N85-31411
The Konstantinov effect and absorption of sound in inhomogeneous media 21 p3680 N85-32861

VANELESS DIFFUSERS
Vaneless diffusers — flow in centrigal compressors
05 p0637 N85-14084
Lateral fluid forces acting on a whirling centrifugal impeller in vaneless and vaned diffuser
05 p0643 N85-14123
A three-dimensional axisymmetric calculation procedure for turbulent flows in a radial vaneless diffuser
[NASA-TM-86903] 06 p0749 N85-14796

VANES
NT GUIDE VANES
NT JET VANES
NT WIND VANES
Heat flux sensors for burner liners and turbine blades and vanes 02 p0142 N85-10961
Studies on the hot corrosion of a nickel-base superalloy, Udimet 700
[NASA-TM-86882] 02 p0183 N85-11224
Preliminary results of a study of the relationship between free stream turbulence and stagnation region heat transfer
[NASA-TM-86884] 02 p0197 N85-11317
Comparison of options for reduction of noise in the test section of the NASA Langley 4x7m wind tunnel, including reduction of nozzle area
[NASA-CR-172446-VOL-2] 05 p0726 N85-14667
Replaceable blade turbine and stationary specimen corrosion testing facility
[NASA-TM-86931] 09 p1294 N85-18126
Effects of vane/blade ratio and spacing on fan noise, volume 1
[NASA-CR-174664] 10 p1553 N85-19791
Effects of vane/blade ratio and spacing on fan noise. Volume 2: Data supplement
[NASA-CR-174665] 10 p1553 N85-19792
Manufacture of drive wheel vanes for hydraulic turbines on program controlled machine tools
14 p2269 N85-24058
Causes and means of prevention of erosion of exit edges of drive vanes in final stages of K-300-240 turbine
14 p2272 N85-24076
Prediction of vortex-induced loads on wind-tunnel turning vanes
[NASA-TM-86678] 15 p2462 N85-25204
Vortex shedding flowmeters for liquids at high flow velocities 16 p2740 N85-26906
Aerodynamic forces developing in channels between vases in turbine drive wheels 16 p2765 N85-27062
Long-Term Materials Test Program
[DE85-003248] 18 p3077 N85-29034
Preliminary results of a study of the relationship between free-stream turbulence and stagnation region heat transfer 20 p3452 N85-31435
Design of a generator for near-tangential transonic swirling outflow
[AD-A155163] 21 p3584 N85-32280

VANS
U TRUCKS

VAPOR DEPOSITION
NT VACUUM DEPOSITION
Hot hollow cathode gun assembly
[DE84-014312] 01 p0121 N85-10832
Chemical vapor deposition of amorphous silicon films produced by using higher order silanes
[DE84-004519] 01 p0123 N85-10847
Laser spectroscopy and gas-phase chemistry in CVD
[DE84-014959] 02 p0173 N85-11156
Thermodynamic calculations and the chemical vapour deposition of hard materials 02 p0179 N85-11200
The development of CVD oxide coatings for the protection of metal surfaces — chemical vapor deposition (CVD) 03 p0332 N85-12142
Deposition in the human lung during respiration of small particles suspended in the air
[BLL-RISLEY-TR-5021-(9091.9F)] 03 p0400 N85-12549
CVD parameter study using strategy of experimentation
[DE84-015900] 04 p0473 N85-13011
Development of a polysilicon process based on chemical vapor deposition of dichlorosilane in an advanced Siemen's reactor
[NASA-CR-174146] 04 p0483 N85-13083
Glow discharge amorphous silicon tin alloys
[DE84-013001] 05 p0616 N85-13952
Creep of chemically vapor deposited SiC fibers
[NASA-TM-86897] 06 p0763 N85-14876
Electrical properties of 10-50 nm TEOS (Tetraethoxysilane) LPCVD (Low Pressure Chemical Vapor Deposition) films
[AD-A146416] 06 p0803 N85-15111
Investigation of silicon surface passivation by silicon nitride deposition 06 p0829 N85-15266
Preparation and electronic properties of MoS(2) and WS(2) single crystals grown in the presence of cobalt
[AD-A146506] 06 p0866 N85-15506
Alloys and method of making
[AD-D011337] 07 p0927 N85-15874
Method of preparing single crystalline cubic silicon carbide layers
[AD-D011305] 07 p1046 N85-16653
Preparation and evaluation of ZnSe and ZnS sub X Se sub 1-x epitaxial layers on Ge substrates for applications in surface passivation and heterojunction devices
[AD-A147432] 07 p1048 N85-16657
Fabrication of ceramic-ceramic composites by chemical vapor deposition
[DE85-000981] 09 p1296 N85-18155
Advanced high-efficiency concentrator cells
[DE84-013020] 09 p1344 N85-18459
Fabrication of fiber-reinforced ceramic composites by chemical vapor infiltration
[DE85-003609] 11 p1611 N85-20132
Chemically amplified laser direct-writing of aluminum
[DE85-000308] 11 p1639 N85-20324
Development of a polysilicon process based on chemical vapor deposition of dichlorosilane in an advanced Siemen's reactor
[NASA-CR-174445] 11 p1672 N85-20532
Fabrication of monocrystalline GaAs solar cells utilizing NaCl sacrificial substrates
[DE84-013016] 11 p1673 N85-20544
High-temperature, solid oxide electrolyte fuel cell power generation system
[DE85-002978] 11 p1675 N85-20552
Method for the preparation of epitaxial films of mercury cadmium telluride
[AD-D011532] 12 p1938 N85-22175
Environmental effects on the tensile strength of chemically vapor deposited silicon carbide fibers
[NASA-TM-86981] 14 p2259 N85-24000
Laser-assisted solar cell metallization processing
[NASA-CR-175686] 14 p2350 N85-24526
Producible alternative to CdTe for epitaxy (PACE-2) of LWIR (Long Wave Infrared) HgCdTe
[AD-A150678] 14 p2426 N85-24964
Thermodynamic calculations and the chemical vapour deposition of hard materials 14 p2431 N85-24991
Mechanical properties of TiN deposits obtained by PVD and TiN, TiC, TiC + TiN obtained by CVD
[BLL-RISLEY-TR-5097-(9091.9F)] 15 p2508 N85-25471
Vapor sensing by means of a ZnO-on-Si surface acousti
wave resonator
[DE85-003250] 15 p2646 N85-2632
Fundamental studies of growth, doping an
transformation in beta silicon carbide
[AD-A152047] 15 p2660 N85-2641
Chemical vapor deposition of amorphous semiconducto
films
[DE85-002917] 15 p2661 N85-2642
Computer program for the calculation of multicomponen
convective diffusion deposition rates from chemical
frozen boundary layer theory
[NASA-CR-168329] 16 p2781 N85-2716
Morphology of GaAs/sub 1-x/P/sub x/ superlattice
grown by MOCVD and chloride VPE
[DE85-002944] 17 p3045 N85-288
Corrosion resistant coating
[NASA-CASE-NPO-15928-1] 18 p3073 N85-290
Limiting processes laser CVD
[DE85-008846] 18 p3114 N85-292
Crystal growth from the vapor in low gra
environments
[DE85-009628] 18 p3195 N85-298
Chemistry and physics of silicon-based amorph
semiconductors
[DE85-001931] 19 p3377 N85-30
Realization by vapor deposition of turbine bla
covered with a silicon nitride layer
20 p3395 N85-31
New metal coating method developed
21 p3568 N85-32
Improved process for the preparation of fiber-reinfor
ceramic composites by chemical vapor deposition
[DE85-011584] 22 p3752 N85-33
1985 Amorphous Silicon Review Meeting
[DE85-008794] 22 p3807 N85-3
An impact-induced terrestrial atmosphere and iron-
reactions during accretion of the Earth
22 p3854 N85-3

Tests on zirconium nitride coatings applied to SW 18 steel using the chemical vapor deposition method
24 p4078 N85-35271

VAPOR GENERATORS
U VAPORIZERS

VAPOR JETS
A new theory aiming to define the mechanisms of material removal in electroerosion
[NASA-TM-77875] 18 p3176 N85-29689

VAPOR LIQUID EQUILIBRIUM
U LIQUID-VAPOR EQUILIBRIUM

VAPOR PHASE EPITAXY
Impurity trapping during gas phase epitaxy of gallium arsenide 02 p0257 N85-11686
Preparation and evaluation of ZnSe and ZnS sub X Se sub 1-x epitaxial layers on Ge substrates for applications in surface passivation and heterojunction devices
[AD-A147432] 07 p1048 N85-16657
Formation of a limiting composition in the oreparation of ternary 3-5 semiconductors by the VPE (Vapor Phase Epitaxy) Hydride technique
[AD-A147639] 08 p1225 N85-17713
Fundamental studies of growth, doping and transformation in beta silicon carbide
[AD-A149339] 10 p1562 N85-19851
Preparation of crystal growth experiments in Spacelab: Si (FSLP), CdTe (D1), ZnS (D1)
[BMFT-FB-W-84-045] 12 p1788 N85-21227
1.5 to 1.7 micrometers LEDs (Light-Emitting Diode)
[AD-A149685] 12 p1834 N85-21508
Process for the epitaxial deposition of III-V compounds utilizing a continuous in-situ hydrogen chloride etch
[AD-D011557] 12 p1939 N85-22177
Morphological stability and fluid dynamics of vapor crystal growth
[NASA-CR-175879] 17 p3042 N85-28822
Morphological stability and fluid dynamics of vapor crystal growth
[NASA-CR-175880] 17 p3042 N85-28823
Development of photodetectors
[AD-A153773] 18 p3095 N85-29158
Process for the epitaxial deposition of 3-5 compounds utilizing a binary alloy as the metallic source
[AD-D011683] 18 p3193 N85-29801
Doping superlattices in organometallic VPE InP
[AD-A155151] 21 p3710 N85-33029

VAPOR PHASES
CREKID: A computer code for transient, gas-phase combustion of kinetics
[NASA-TM-83806] 01 p0011 N85-10068
NaK chemiluminescence
[AD-A146077] 03 p0326 N85-12110
Sintering behavior of ultrafine silicon carbide powders obtained by vapor phase reaction
[NASA-TM-77422] 03 p0336 N85-12161
Numerical modelling of the drying of porous materials
[DE84-013056] 04 p0499 N85-13181
Attempted measurement of gaseous H-2O-2 in the ambient atmosphere
[DE85-001937] 06 p0834 N85-15306
Reactions of metal ions and their cluster in the gas phase using laser ionization: Ion cyclotron resonance spectroscopy
[DE84-016491] 09 p1293 N85-18120
Effective antireflection coatings of transparent polymeric materials by gas-phase surface fluorination
[DE84-013027] 09 p1385 N85-18711
Desorption efficiences of vapor phase polynuclear aromatic compounds on solid adsorbents
[DE85-001303] 10 p1436 N85-19052
Determination of vapor phase content when metals are struck by laser radiation pulses of various densities
10 p1445 N85-19106
Numerical simulations of liquid propellant combustion instability: Onset and growth
[DE85-000743] 10 p1458 N85-19186
Analysis of phase composition of products of laser destruction of metallic surfaces
11 p1600 N85-20064
Chemical kinetics of gas phase decomposition products of nitramine propellants 13 p2003 N85-22558
Procedure for certifying quantity of volatile organic compounds emitted by paint, ink and other coatings
[PB85-159044] 15 p2520 N85-25537
Vapor sensing by means of a ZnO-on-Si surface acoustic wave resonator
[DE85-003250] 15 p2646 N85-26324
Research on the kinetics of phase changes in solids
[AD-A152367] 17 p2918 N85-27989
Gas phase ion-molecule chemistry of carbon, nitrogen and oxygen compounds
[AD-A152876] 17 p2919 N85-27996
The decomposition of gas phase formaldehyde by plasma discharge
[AD-A153202] 17 p2921 N85-28007
Chemical transformation modules for Eulerian acid deposition models. Volume 1: The gas-phase chemistry
[PB85-173714] 18 p3072 N85-29001
Electron irradiation of light emitting diodes
[AD-A154441] 19 p3260 N85-30213
Chemical transformation in acid rain. Volume 1: New methodologies for sampling and analysis of gas-phase peroxide
[PB85-173425] 19 p3311 N85-30527
Reactions of metal ions and their clusters in the gas phase using laser ionization-ion cyclotron resonance spectroscopy
[DE85-009478] 19 p3361 N85-30838
Modeling of chemical transformations of SO(x) and NO(x) in the polluted atmosphere: An overview of approaches and current status
[PB85-173169] 20 p3487 N85-31677
Liquid-phase compositions from vapor-phase analyses 2: Adaptation of the Prausnitz program to UF6 and some of its potential impurities
[DE85-011521] 21 p3673 N85-32819
Microwave semiconductor research: Materials, devices and circuits and gallium arsenide ballistic electron transistors
[AD-A154698] 21 p3709 N85-33024
Method for preparing Pb-(beta)-aluminum ceramic
[DE85-011665] 22 p3752 N85-33256
Volatile loss following very large impacts
22 p3853 N85-33862
Volatiles on satellites of the outer solar system
22 p3854 N85-33868
Vapor phase heat transport concepts
[DE85-009550] 23 p3931 N85-34366
Heats of formation of gas phase organosulfur molecules, radicals and ions measured by PEPICO and application of (17)O and (33)S NMR spectroscopy to structure determination of organosulfur compounds
[DE85-010558] 24 p4071 N85-35229

VAPOR PRESSURE
Mathematical models for the boiling diagram of the ideal two-component mixture
[DFVLR-FB-84-22] 04 p0471 N85-13000
Stable isotope studies
[DE84-016752] 04 p0562 N85-13583
Metal vapor arc switch electromagnetic accelerator technology
[NASA-CR-174380] 09 p1314 N85-18259
Vapor pressure and evaporation rate of certain heat-resistant compounds in a vacuum at high temperatures
[NASA-TM-77807] 10 p1434 N85-19036
Vapor pressure studies of the solubilization of hydrocarbons by surfactant micelles
[DE85-004319] 12 p1803 N85-21306
Trends of petroleum fuels
[DE85-000116] 14 p2263 N85-24023
Entropy of He 2 and universality near the superfluid in He(4) 19 p3378 N85-30957

VAPORIZATION HEAT
U HEAT OF VAPORIZATION

VAPORIZERS
NT EVAPORATORS
Nonlinear control model of an H2O steam reactor
[DFVLR-FB-84-30] 07 p0975 N85-16192
Solar thermochemical process interface study
[NASA-CR-174442] 10 p1510 N85-19527
Continuous laminar smoke generator
[NASA-CASE-LAR-13014-1] 12 p1781 N85-21178
Forced convective, nonequilibrium, post-CHF heat transfer experiment data and correlation comparison report
[TI85-009331] 23 p3932 N85-34371

VAPORIZING
NT BOILING
NT COAL GASIFICATION
NT EVAPORATION
NT EVAPOTRANSPIRATION
NT FILM BOILING
NT FLASHING (VAPORIZING)
NT NUCLEATE BOILING
NT PROPELLANT EVAPORATION
NT SUBLIMATION
NT TRANSPIRATION
Vaporization behavior of chromium phosphides. The solid 2-phase regions CrP-Cr12P7, Cr12P7-Cr3P, and Cr3P-Cr
[AD-A145481] 02 p0172 N85-11152
Volatile elements in and on lunar volcanic glasses: What do they tell us about lunar genesis?
04 p0584 N85-13728
Vaporization behavior, phase equilibria, and thermodynamic stabilities of nickel phosphides
[AD-A146683] 06 p0765 N85-14897
Methanol vaporization: Effects on volumetric efficiency and on determination of optimum fuel delivery system
[PB84-243914] 09 p1302 N85-18181
Initial results for supercritical cycle experiments using pure and mixed-hydrocarbon working fluids
[DE84-017008] 09 p1345 N85-18460
Carbon vaporization/condensation effects
[NASA-TM-87430] 10 p1436 N85-19048
Dissociated methanol citation
[DE85-000505] 10 p1458 N85-19166
Analysis of phase composition of products of laser destruction of metallic surfaces
11 p1600 N85-20064
Theta pinch discharges for solids vaporization and elemental chemical analysis
[DE85-002968] 11 p1733 N85-20899
Studies on the processing methods for extraterrestrial materials
[NASA-CR-175778] 16 p2716 N85-26768
Crystal growth from the vapor in low gravity environments
[DE85-009628] 18 p3195 N85-29816
Effects of ambient pressure on the instability of a liquid boiling explosively at the superheat limit
[DE85-009476] 23 p3932 N85-34370
Monitoring dosage of volatile compounds in tests at low barometric pressure 23 p3954 N85-34506

VAPORS
NT METAL VAPORS
NT SODIUM VAPOR
NT WATER VAPOR
Experimental and theoretical study of condensation in multicomponent vapors
[DE84-015610] 02 p0174 N85-11164
VOC emissions from volatile organic liquid storage tanks: Background information for proposed standards
[PB84-237320] 04 p0532 N85-13403
Pharmacokinetic interactions of mixtures
[AD-P004032] 06 p0844 N85-15362
Mass spectrometry/mass spectrometry as a screening method for detecting explosive vapors
[DE85-001276] 09 p1292 N85-18110
Experimental and theoretical study of condensation in multicomponent vapors
[DE85-000843] 10 p1485 N85-19376
Photo-thermal detection of the onset of photo-chemical nucleation (laser-snow) in vapor
[AD-A150111] 12 p1801 N85-21295
The detonation of aerosols and vapors of combustible substances under controlled conditions. Part 1: Construction of a test installation
[ISL-R-109/83-PT-1] 14 p2254 N85-23966
Vapor explosions in superheated liquids and fundamental studies of the physics of detonation
[AD-A151362] 15 p2504 N85-25447
Development of a new faster process for the fabrication of ceramic fiber-reinforced ceramic composites by chemical vapor infiltration
[DE85-007550] 16 p2756 N85-27007
Performance of an active/passive hybrid solar system utilizing vapor transport
[DE85-008627] 17 p2988 N85-28466
Dynamics of vapor explosions
[DE85-008845] 18 p3101 N85-29194
Surface acoustic wave devices as chemical vapor microsensors
[AD-A153752] 18 p3177 N85-29698
Vapor-screen technique for flow visualization in the Langley Unitary Plan Wind Tunnel
[NASA-TM-86384] 19 p3214 N85-29929
Catalytic hydrotreatment studies with model compounds
[DE85-010187] 19 p3236 N85-30064
Enhanced thermal coupling by a repetitively pulsed laser
[AD-A154435] 19 p3276 N85-30317
Laser-induced fluorescence measurement of vapor concentration surrounding evaporating droplets
[DE85-009409] 19 p3277 N85-30320
Status of boron combustion research
[AD-A154762] 21 p3563 N85-32160
Silicon refinement by chemical vapor transport
21 p3609 N85-32412
A crew exposure study. Phase II. Volume 2. At sea. Part A
[AD-A155233] 21 p3666 N85-32774
Photofragment fluorescence as a sensitive probe for gas-phase alkali compounds and their photochemistry
[DE85-010707] 22 p3746 N85-33219
New and revised methods of purifying mercuric iodide
[DE85-011684] 22 p3749 N85-33237
Drying of pulverized material with heated condensible vapor
[DE85-011656] 22 p3783 N85-33438

VARACTOR DIODES
Maser cavity servo-tuning system
[NASA-CASE-NPO-15890-1-CU]
18 p3093 N85-29143

VARACTORS
U VARACTOR DIODES

VARIABILITY
Variability of major organic components in aircraft fuels. Volume 3: Sample data package for the reference JP-4 fuel
[AD-A145483] 02 p0188 N85-11254
Climatological variability in modeling of long-term regional transport and deposition of air pollutants
[DE84-014726] 04 p0539 N85-13430
An analysis of kinetic response variability
05 p0707 N85-14533
A survey for photometric variability from space
08 p1251 N85-17897
Evaluating the variability of ceramics with X-ray fluorescence
[DE85-002028] 10 p1453 N85-19155
Variability of cardiac rhythm during information loading
10 p1525 N85-19619
Middle Atmosphere Program. Handbook for MAP. volume 5
[NASA-CR-175481] 11 p1656 N85-20434
A catalogue of dynamic parameters describing the variability of the middle stratosphere during the northern winters 11 p1656 N85-20435
Long term variability of the IO torus
11 p1760 N85-21070
Ozone Correlative Measurements Workshop
[NASA-CP-2362] 13 p2105 N85-23112
Scientific requirements for ozone measurements
13 p2105 N85-23113
Influence of spatial variability of hydraulic characteristics of soils on surface parameters obtained from remote sensing data in infrared and microwaves
[NASA-TM-77902] 20 p3477 N85-31604
Observations of Cygnus X-3 above 10(15) eV from 1979 - 1984
[OG-2.1-6] 22 p3863 N85-33923
Variability in the high energy gamma ray emission from Cyg X-3 over a two-year period (1983 - 1984) at E 4 x 10(11) eV
[OG-2.1-11] 22 p3864 N85-33927
A search in the COS-B data base for correlated time variability in regions containing objects of interest
[OG-2.5-9] 22 p3869 N85-33964
Effect of precipitation variables on the specific surface and explosion characteristics of pentaerythritol tetranitrate
[DE85-009620] 23 p3922 N85-34302

VARIABLE AREA WINGS
U TRAILING EDGE FLAPS

VARIABLE CYCLE ENGINES
Supersonic cruise technology
[NASA-SP-472] 18 p3057 N85-28912
Variable cycle engine for high altitude aircraft
[AD-D011705] 19 p3221 N85-29969

VARIABLE GEOMETRY STRUCTURES
Variable geometry Darrieus wind machine
[PB84-207281] 01 p0068 N85-10453
Variable geometry truss concept
[REPT-614] 12 p1865 N85-21697
Stability of cylindrical shells with variable thickness under external pressure 17 p2943 N85-28164

VARIABLE LIFT
U LIFT

VARIABLE MASS SYSTEMS
The fragmentation of molecular clouds and the IMF
05 p0740 N85-14759
The influence of stellar luminosity and temperature calibration on the determination of the initial mass function 05 p0740 N85-14760

VARIABLE PITCH PROPELLERS
Circulation control propellers for general aviation, including a BASIC computer program
[NASA-CR-165968] 19 p3219 N85-29959

VARIABLE STARS
NT CATACLYSMIC VARIABLES
NT CEPHEID VARIABLES
NT DWARF NOVAE
NT HERCULES NOVA
NT NOVAE
NT SUPERNOVAE
NT SYMBIOTIC STARS
NT T TAURI STARS
Simultaneous photometry and radial velocities of dwarf cepheids and Delta Scuti stars
01 p0128 N85-10878
Spectroscopic data for globular cluster giants. 1: Stars of the red giant tip 01 p0128 N85-10885
Nonradial pulsation and mass loss in early B stars
08 p1232 N85-17759
EXO 1102.8+2539, an X-ray variable Active Galactic Nucleus (AGN) 08 p1239 N85-17816
A statistical evaluation of the limitations of single-channel intermediate-band photoelectric stellar photometry 08 p1251 N85-17900
Study of the pulsations of the ZZ Ceti stars
09 p1414 N85-18923
White dwarf stars at ultraviolet wavelengths
11 p1744 N85-20971
IUE observations of the jet emission feature in R Aquarii 11 p1747 N85-20988
IUE and ESO observations of the P Cyg star AG Carinae and its ring nebula 11 p1750 N85-21006
Coordinated ultraviolet and visual observations of Omega Orionis 1982-1983 11 p1750 N85-21007
The outburst and long term behavior of the triple period cataclysmic variable TV Col 11 p1752 N85-21021
New results on PU VUL 11 p1753 N85-21023
The UV extinction of HR 5999
11 p1753 N85-21026
The fading of R coronae borealis
11 p1753 N85-21029
Observations of RR Lyrae and X Arietis with the IUE satellite 11 p1754 N85-21030
Atmospheric properties of RU Lupi derived from high- and low-resolution IUE spectra
11 p1754 N85-21031
Mg 2 emission of Pop. 2 long-period Cepheids
11 p1754 N85-21032
Blue companions of Cepheids
11 p1754 N85-21033
Observations of cataclysmic variable star winds
11 p1755 N85-21041
Three short-period binaries seen at high-dispersion UX ARI, IOTA TRI and HA5110 11 p1756 N85-21047
A model for eclipsing cataclysmic variables
13 p2171 N85-23467
Offerings of the Astronomical Institute of Bonn
15 p2667 N85-26459
Photoelectric observations of the eclipsing binary V 836 Cygni
[REPT-98] 15 p2668 N85-26462
Measurement and theory of turbulence in RR Lyrae
[DE85-005899] 15 p2669 N85-26471
Long-term observations of Cyg X-3 with Vela 5B
[DE85-005556] 15 p2686 N85-26586
Galactic gamma-ray sources, SNOBs, and giant H2 regions
[OG-2.5-4] 22 p3869 N85-33961

VARIABLE SWEEP WINGS
Transonic aerodynamic and aeroelastic characteristics of a variable sweep wing
[NASA-TM-86677] 15 p2482 N85-25203

VARIABLE THRUST
Orbital maneuvers with finite thrust. Volume 1: Mathematical formulation, numerical methods, catalog concept
[ESA-CR(P)-1910-VOL-1] 06 p0758 N85-14848
Orbit maneuvers with finite thrust. Volume 2: Reference manual, part 1
[ESA-CR(P)-1910-VOL-2-PT-1]
06 p0758 N85-14849
Orbit maneuvers with finite thrust. Volume 3: User's guide, part 2
[ESA-CR(P)-1910-VOL-3-PT-2]
06 p0758 N85-14850
Orbit maneuvers with finite thrust. Volume 3: Reference catalog, parts 1 and 2
[ESA-CR(P)-1910-VOL-3-PT-1/2]
06 p0758 N85-14851
Orbit maneuvers with finite thrust. Volume 3: Reference catalog, part 3
[ESA-CR(P)-1910-VOL-3-PT-3]
06 p0758 N85-14852

VARIANCE (STATISTICS)
NT ANALYSIS OF VARIANCE
NT BIVARIATE ANALYSIS
NT COVARIANCE
NT MULTIVARIATE STATISTICAL ANALYSIS
NT REGRESSION ANALYSIS
Construction of a confidence region for linear functions with unknown parameters
[CTH-MATH-1984-17] 05 p0721 N85-14630
Geostatistics for resource and reserve estimation
[PB85-105781/GAR] 07 p0989 N85-16286
Scrawl plots, and letter and blotter strips
[DE85-001409] 11 p1707 N85-20739
Optimal designs for comparisons between two sets of treatments
[AD-A150621] 13 p2152 N85-23360
Censored observations, repeated measures and mixed effects models: An approach using the EM algorithm and normal errors
[MATHEMATICS-RESEARCH-183]
15 p2636 N85-26256
Studies in quality improvement. Part 1: Dispersion effects from fractional designs, revised
[AD-A153516] 18 p3119 N85-29306

VARIATION METHOD
U CALCULUS OF VARIATIONS

VARIATIONAL PRINCIPLES
Variational principles in thermoplasticity. Part 2: Coupled thermomechanical processes
[RUB-IFM-MITT-37-PT-2] 05 p0648 N85-14161
Surface reconstruction preserving discontinuities
[AD-A146741] 07 p1026 N85-16526
The principle of virtual work and associated variational principles
[ESA-TT-873] 09 p1340 N85-18428
Symmetric primal-dual variational formulations of coupled dynamic systems: Three-dimensional elasticity, shells, fluid-structure interaction
[ONERA-1983-91] 12 p1863 N85-21684
On Hybrid and mixed finite element methods
[NASA-CR-175551] 13 p2101 N85-23096
On an iterative scheme for the solution of constrained variational equations
[CSIR-TWISK-341] 13 p2149 N85-23342
Lyapunov stability of very simple steady solutions of prognostic systems 14 p2333 N85-24429
Finite element methods in space mathematics
14 p2396 N85-24757
Axisymmetric magnetofluidistatic (MFS) equilibria of solar coronal loops: An integral equation approach
14 p2449 N85-25118
Variational bounds on Darcy's constant
[DE85-006636] 15 p2580 N85-25916
Variational bounds on Darcy's constant
[DE85-008959] 18 p3101 N85-29195

VARIATIONS
NT ANNUAL VARIATIONS
NT DIURNAL VARIATIONS
NT GEOMAGNETIC PULSATIONS
NT MAGNETIC VARIATIONS
NT NOCTURNAL VARIATIONS
NT PERIODIC VARIATIONS
NT SECULAR VARIATIONS
NT WIND VARIATIONS
Measurement of areal mass variation in Rayleigh-Taylor unstable targets
[AD-A145541] 02 p0198 N85-11325
Determination of geoid undulations and ocean heights from ERS-1 radar altimetry data
03 p0381 N85-12432
Spectral model for subtidal variability in the Chesapeake Bay
[PB84-226679] 06 p0842 N85-15345
Efficient scores, variance decompositions and Monte Carlo swindles
[AD-A146673] 06 p0858 N85-15456
Fluctuation phenomena studies in chemically sensitive field effect transistors. Part 2: Corrosion of silicon oxynitride
[AD-A148227] 08 p1157 N85-17302
The ground based photometric limitations to the search for light variations due to 5-minute solar-type oscillations in other stars 08 p1251 N85-17898
NMR study on rotational fluctuation in solid hydrogen and deuterium 09 p1289 N85-18093
Discovery about temperature fluctuations in turbulent air flows 10 p1500 N85-19466
Twilight intensity variation of the infrared hydroxyl airglow 11 p1663 N85-20481
Space and time variations and turbopause dynamical structure 11 p1663 N85-20483
Variability of ultraviolet emission lines in the carbon star TX Psc 11 p1753 N85-21027
The portable LISP translation tool
[AD-A149765] 12 p1915 N85-22023
Observation of cosmic ray flux variations in stratosphere 13 p1981 N85-22430
Variations in resistivity of upper crustal layer
13 p2113 N85-23184
Method for processing broad-profile data
13 p2117 N85-23185
The relationship between marine aerosol particles and satellite-detected radiance 13 p2131 N85-23263
VAS/model impact study 15 p2597 N85-26006
Measuring electrical field fluctuations by Langmuir Double Probe Method 16 p2720 N85-26789
Probabilistic finite element: Variational theory
17 p2913 N85-27957
Energy sources of the dominant frequency dependent 3-dimensional atmospheric modes
18 p3143 N85-29462
On the characterization of nonnegatively estimable linear combinations of variance components
[AD-A153786] 18 p3174 N85-29678
Emittance growth caused by current variation in a beam-transport channel
[DE85-010743] 19 p3363 N85-30849
Intermittency, conditional sampling and turbulent combustion 20 p3424 N85-31249
Magnetospheric response to solar wind variations
[DE85-010762] 20 p3547 N85-32074

On the transformation regularities of time series of solid aerosol concentrations in the surface atmospheric layer
21 p3645 N85-32648
Object identification and manipulation using silhouette moments
[AD-A154755] 21 p3705 N85-33011
Optical output stabilization method for direct current arc lamps
[AD-A154987] 21 p3705 N85-33013
Impact of fluctuations in optical properties of atmosphere on the ratio of spectral brightness from remote sensing of agricultural land 22 p3734 N85-33149
Gamma-ray burst variability above 4 MeV
[OG-1.2-7] 22 p3862 N85-33917
Cosmic ray intensity variations at primary rigidities near 1900 GV
[OG-5.3-0] 22 p3885 N85-34075
The final COS-B database: In-flight calibration of instrumental parameters
[OG-9.3-9] 23 p4028 N85-34964
The effect of the interplanetary magnetic field on sidereal variations observed at medium depth underground detectors
[SH-4.4-5] 23 p4033 N85-35003
Corrected sidereal anisotropy for underground moons
[SH-4.4-7] 23 p4033 N85-35005
Sidereal anisotropy of cosmic rays
[SH-4.4-8] 23 p4034 N85-35006
A study of periodicities and recurrences in solar activity and cosmic ray modulation
[SH-4.4-14] 23 p4034 N85-35010
Altitude variations of cosmic-ray soft and hard components observed by airborne detectors
[SH-6.1-5] 23 p4045 N85-35079
The effects of parameter variation on helicopter performance
[AD-A156027] 24 p4064 N85-35169
Cluster variation study of coherent ordering in FCC and BCC solid solutions
[AD-A156039] 24 p4079 N85-35280
The measurement of nitrogen oxide (NO, NO2) exchange over plant/soil surfaces
[CSIRO-DAR-TP-8] 24 p4127 N85-35587
Muon fluctuation studies of EAS 10(17) eV
[HE-4.3-9] 24 p4191 N85-36003

VARIOMETERS
Primary processing of experimental magnetovariation sounding data using spline functions
13 p2115 N85-23175

VARISTORS
Advanced metal oxide varistor concepts
[DE84-016677] 09 p1316 N85-18276
Effects of processing chemistry on electrical properties of high field ZnO varistors
[DE85-007688] 17 p2956 N85-28254
A study of Co and Mn in ZnO varistors
[DE85-011193] 19 p3263 N85-30233
Long-term research in Japan: Amorphous metals, metal oxide varistors, high-power semiconductors and superconducting generators
[DE85-010827] 22 p3748 N85-33230

VARNISHES
Evaluation of properties of varnishes, exterior stains and exterior primers
[PB84-243948] 06 p0772 N85-14940

VASCULAR SYSTEM
NT ARTERIES
NT BLOOD VESSELS
NT VEINS
Modulated sinusoidal currents in management of vibration sickness 10 p1524 N85-19612
Specifics of human thermal regulatory reactions upon exposure to coriolis acceleration
10 p1525 N85-19617

VASOCONSTRICTION
Endocrine responses to hypotensive gravitational stress: Catecholamines, pancreatic polypeptide, and vasopressin 05 p0693 N85-14460

VASOMOTOR NERVOUS SYSTEM
U NERVOUS SYSTEM

VATOL AIRCRAFT
Preliminary performance of a vertical-attitude takeoff and landing, supersonic cruise aircraft concept having thrust vectoring integrated into the flight control system
[NASA-CR-172530] 10 p1423 N85-18977
Ground effect on helicopter aerodynamics and stability
20 p3395 N85-31063

VAX COMPUTERS
NT VAX-11 SERIES COMPUTERS
NT VAX-11/780 COMPUTER
Introduction to LBL graphics
[DE85-000389] 09 p1369 N85-18600
Scientific data bases on a VAX-11/780 running VMS
[DE85-007925] 16 p2678 N85-27760
Report on the SLC control system
[DE85-013076] 24 p4148 N85-35722

VAX-11 SERIES COMPUTERS
NT VAX-11/780 COMPUTER
Digital Equipment Corp., VAX-11/782, VAX FORTRAN version 4.0
[PB84-227701] 03 p0405 N85-12582
Implementation of the computer program-system MOSS (Map Overlay and Statistical System) on a VAX-11 series computer under VMS
[AD-A149612] 12 p1914 N85-22019
A system identification package for VAX and LSI 11
[OUEL-1569/85] 20 p3516 N85-31862
Parallel processing on the Livermore VAX 11/780-4 parallel processor system with compatability to Cray Research, Inc. (CRI) multitasking, version 1
[DE85-011656] 23 p3967 N85-34595

VAX-11/780 COMPUTER
Multiplexing the ethernet interface among VAX/VMS users
[AD-A145539] 02 p0243 N85-11580
Digital Equipment Corporation VAX Ada Compiler Version T0.8-2 VAX-11/785, 11/750, 11/730, using VMS, Version 4.0 and MicroVAX 1, using MicroVMS Version 1.0
[AD-A149375] 10 p1538 N85-19696
Integrated Support Software System (ISSS)
[AD-A155715] 22 p3829 N85-33710

VCE
U VARIABLE CYCLE ENGINES

VCO
U VOLTAGE CONTROLLED OSCILLATORS

VECTOR ANALYSIS
NT COLLINEARITY
NT COPLANARITY
NT VORTICITY
Cores of tangent cones and Clarke's tangent cone
[CSIR-TWISK-314] 01 p0106 N85-10727
Constrained optimization using iterated partial Kuhn-Tucker vectors
[AD-A145476] 02 p0251 N85-11641
Wind shear measuring on board an airliner
[NASA-TM-77463] 03 p0395 N85-12521
Techniques for vector quantization
[AD-A147052] 07 p1030 N85-16539
Belief structures
[AD-A147526] 07 p1036 N85-16575
Robust prediction and interpolation for vector stationary processes, part 3
[AD-A147660] 07 p1036 N85-16579
Development of a 20/30 GHz receiving station for propagation experiments with L-SAT
[AD-A148261] 08 p1152 N85-17271
A moving finite element method for time dependent partial differential equations with error estimation and refinement
[AD-A147719] 08 p1210 N85-17617
Vectorization and implementation of an efficient multigrid algorithm for the solution of elliptic partial differential equations
[AD-A149049] 10 p1545 N85-19743
Characteristic vector analysis of inflection ratio spectra: New technique for analysis of ocean color data
[NASA-TP-2426] 13 p2126 N85-23237
Dynamics of solid body with ellipsoidal cavity containing magnetic fluid 14 p2279 N85-24116
Proposal for an extended set of FORTRAN Basic Linear Algebra subprograms
[DE85-007241] 16 p2648 N85-27562
The role of ellipticity and normality assumptions in formulating live-boundary conditions in elasticity
[AD-A153475] 18 p3168 N85-29630
Magnetic field-vector measurements in quiescent prominences via the Hanle effect: Analysis of prominences observed at Pic-du-Midi and at Sacramento Peak
18 p3206 N85-29898
Inferred flows of electric currents in solar active regions 18 p3206 N85-29899
Comparisons of simultaneous vector magnetograms
18 p3208 N85-29900
Evidence for submergencew of magnetic flux in a growing active region 18 p3208 N85-29902
Graphic displays of vector magnetograph data
18 p3209 N85-29904
High accuracy digital acousto-optic matrix computer
[AD-D011692] 19 p3343 N85-30716
Vector calculation of particle code
23 p3981 N85-34688
Invariant tests and likelihood ratio tests for multivariate elliptically contoured distributions
[AD-A155844] 24 p4142 N85-35679

VECTOR CALCULUS
U VECTOR SPACES

VECTOR CONTROL
U DIRECTIONAL CONTROL

VECTOR MESONS
Skyrmions and vector mesons: A symmetric approach
[DE84-015297] 04 p0563 N85-13584
Does low-energy physics depend on the potential of a heavy Higgs-particle
[NIKHEF-H/85-1] 22 p3838 N85-33763

VECTOR SPACES
NT ADJOINTS
NT BANACH SPACE
NT CANONICAL FORMS
NT EIGENVALUES
NT EIGENVECTORS
NT HILBERT SPACE
NT JORDAN FORM
NT MATRICES (MATHEMATICS)
NT SOBOLEV SPACE
NT STATE VECTORS
NT STIFFNESS MATRIX
NT STOKES THEOREM (VECTOR CALCULUS)
NT VECTORS (MATHEMATICS)
NT VORTICITY
Aerospatiale's experimentations of vectorization on supercomputers for aircraft structural problems
01 p0007 N85-10041
Comparative analysis of the clustering of the LPC coefficients in phoneme recognition
[FUB-39-1983] 01 p0041 N85-10264
Trilinear alternating forms on a vector space of dimension 7
[CWI-PM-R8402] 05 p0722 N85-14844
Schubert varieties are arithmetically Cohen-Macaulay
16 p2653 N85-27592
The vector potential in a branched Riemann space
[VTH-LR-395] 16 p2656 N85-27614
The global structure of magnetic fields which support quiescent prominences 18 p3204 N85-29876
A classification vocoder: A very low rate speech transmission by vector quantization of the spectrum
[ENST-84D003] 20 p3441 N85-31356
Study of new computing algorithms for supercomputers. Application to parallel processing computation
[SNIAS-440-070/84] 20 p3516 N85-31860
Simulation of complex three-dimensional flows
[NASA-TM-86773] 21 p3675 N85-32831
On the convergence of an iterative formulation of the electromagnetic scattering from an infinite grating of thin wires 24 p4085 N85-35319

VECTORS (MATHEMATICS)
NT EIGENVECTORS
NT STATE VECTORS
NT VORTICITY
Some concepts in multi-criteria optimization
[CSIR-TWISK-299] 01 p0108 N85-10722
What is principal components analysis?
02 p0211 N85-11389
The information in the minor principal components
02 p0211 N85-11391
Techniques for vector quantization
[AD-A147052] 07 p1030 N85-16539
Determining vector of radiointerferometer base from observations of natural radio emission with narrow spectrum 13 p2112 N85-23156
Schur-Ostrowski theorems for functionals on l1(0,1)
[AD-A150193] 13 p2150 N85-23346
Organization of conveyor processing of vector commands in multiprocessor computer systems with a reorganizable structure 14 p2401 N85-24799
Spline techniques for magnetic fields
[DE85-004919] 14 p2415 N85-24902
Recent trends in software technology for vector processors 16 p2691 N85-26615
Recent developments in nonlinear normal mode initialization 18 p3142 N85-29451
Developement of an optimum interpolation analysis method for the CYBER 205 18 p3143 N85-29456
Measurements of Solar Vector Magnetic Fields
[NASA-CP-2374] 18 p3203 N85-29869
The vector structure of active magnetic fields
18 p3203 N85-29870
Trends in measurement of solar vector magnetic fields using the Zeeman effect 18 p3204 N85-29877
Measurements of vector fields with diode array
18 p3204 N85-29880
Analysis of the new polarimeter for the Marshall Space Flight Center vector magnetograph
18 p3205 N85-29881
The solar vector magnetograph of the Okayama Astrophysical Observatory 18 p3205 N85-29882
Generation and transfer of polarized radiation in the solar atmosphere: Physical mechanisms and magnetic-field diagnostics 18 p3206 N85-29890
Optimizing data access in the LAMPF control system
[DE85-012653] 24 p4140 N85-35663

VEGA LAUNCH VEHICLE
Kovtunenko comments on Vega flight plan, instrumentation 15 p2482 N85-25318

VEGA PROJECT
The Venus Balloon Project 10 p1465 N85-19243

The international VEGA 'Venus-Halley' (1984-1986 experiment: Description and scientific objectives 12 p1960 N85-22324 [NASA-TM-77536]
USSR report: Space 13 p1977 N85-22403 [JPRS-USP-85-001]
Comments on Vega mission 15 p2482 N85-25319
Press conference on flight of Vega spacecraft 15 p2482 N85-25320
TASS update on flights of Vega-1 and Vega-2 16 p2722 N85-26803
Kovtunenko discuses Vega Project 16 p2722 N85-26804
French and West German equipment for Vega Project 16 p2722 N85-26805

VEGA ROCKET VEHICLE
U VEGA LAUNCH VEHICLE

VEGETABLES
NT POTATOES
Multi crop area estimation in Idaho using EDITOR 06 p0827 N85-15251 [E85-10054]
Packaging for food service 14 p2394 N85-24747

VEGETATION
NT CANOPIES (VEGETATION)
The Multispectral Imaging Science Working Group. Volume 1: Executive summary 02 p0213 N85-11404 [E85-10001]
The Multispectral Imaging Science Working Group. Volume 2: Working group reports 02 p0213 N85-11405 [E85-10002]
Botanical sciences team 02 p0214 N85-11407
Late quarterly glaciolacustrine and vegetational history of the Copper River Basin, south-central Alaska 03 p0391 N85-12499
Scattering models in the microwave regime 04 p0525 N85-13361 [NASA-CR-174001]
Scattering from randomly oriented scatterers of arbitrary shape in the low-frequency limit with application to vegetation 04 p0525 N85-13362
Scattering from randomly oriented circular discs with application to vegetation 04 p0525 N85-13363
A comparison between active and passive sensing of soil moisture from vegetated terrains 04 p0526 N85-13364
Monitoring and mapping global vegetation cover using data from meteorological satellites 05 p0656 N85-14211
Integration of multispectral data obtained at different view angles for vegetation analysis 05 p0657 N85-14218
Classification of vegetation communities in the Battle Mountain SE quadrangle, Nevada with MSS digital data 06 p0826 N85-15246 [E85-10043]
An integrated LANDSAT/ancillary data classification of desert rangeland 06 p0826 N85-15248 [E85-10046]
An integrated remote sensing approach for identifying ecological range sites — parker mountain 07 p0963 N85-16246 [E85-10050]
Microwave and optical remote sensing of forest vegetation 08 p1146 N85-17226
Remote sensing of soil moisture 08 p1149 N85-17252
North American vegetation patterns observed with the NOAA-7 advanced very high resolution radiometer — North America 08 p1174 N85-17400 [E85-10062]
Shortwave infrared detection of vegetation 08 p1174 N85-17402 [E85-10064]
An integrated GIS/remote sensing data base in North Cache soil conservation district, Utah: A pilot project for the Utah Department of Agriculture's RIMS (Resource Inventory and Monitoring System) 10 p1504 N85-19487 [E85-10073]
Preliminary evaluation of the airborne imaging spectrometer for vegetation analysis 10 p1505 N85-19496 [NASA-CR-174440]
Vegetation analysis for arid lands geobotany 10 p1506 N85-19500 [NASA-CR-175455]
Thematic Mapper spectral dimensionality and data structure 12 p1871 N85-21736
Investigations of vegetation and soils information contained in LANDSAT Thematic Mapper and Multispectral Scanner data 12 p1873 N85-21747 [E85-10082]
Air quality criteria for ozone and other photochemical oxidants, external review draft, volume 3 12 p1886 N85-21837 [PB85-126050]
Preliminary comparisons of the information content and utility of TM versus MSS data 13 p2120 N85-23202
The microwave propagation and backscattering characteristics of vegetation — wheat, sorghum, soybeans and corn fields in Kansas 13 p2122 N85-23213 [E85-10086]
Microwave remote sensing of soil moisture 13 p2125 N85-23235
Atlas of archived vegetation, land-use and seasonal Albedo data sets 14 p2346 N85-24508 [NASA-TM-86199]
Soil moisture and evapotranspiration estimates based on satellite data 15 p2596 N85-25996
Use of Goudrian model in studying laws of reflection in vegetation-soil system in optical range. 2: Influence of illumination conditions on spectral brightness coefficients 16 p2726 N85-26827
Microwave model prediction and verifications for vegetated terrain 16 p2809 N85-27322 [E85-10102]
Function of remote sensing in Brazil 16 p2810 N85-27329 [INPE-3314-PRE/621]
Impact of ozone on vegetation 16 p2821 N85-27403 [PB85-159937]
Airphoto interpretation of vegetation and landforms for soil mapping 17 p2983 N85-28436
Permafrost, seasonally frozen ground, snow cover and vegetation in the USSR 18 p3124 N85-29346 [AD-A153628]
Influence of land surface processes on the Indian monsoon: A numerical study 18 p3146 N85-29478
Space imagery and some geomorphological problems of the Guiana Shield, South America 21 p3602 N85-32368

VEGETATION GROWTH
NT CROP GROWTH
Remote sensing applied to forest resources 02 p0216 N85-11425 [E85-10012]
Terrestrial nitrogen cycles: Some unanswered questions 05 p0653 N85-14192
Image texture study for the operational meteorological satellites NOAA 6 and NOAA 7 and its variation with time. Application to the Beauce region 05 p0661 N85-14249 [ENST-84E009]
Simulating responses to expected climate change in eastern North America: Applications to decision-making in the forest industry 07 p1008 N85-16406 [DE85-001272]
Effects of low temperatures on the growth and unfrozen water content of an aquatic plant 07 p1011 N85-16424 [AD-A147107]
Controlled ecological life support system higher plant flight experiments 07 p1020 N85-16471 [NASA-CR-177323]
Spectral characterization of the LANDAT-4 MSS sensors 11 p1666 N85-20499
NOAA-AISC user's guide for implementing CERES wheat model for large area yield estimation 12 p1873 N85-21750 [E85-10085]
Estimating solar radiation for plant simulation models 12 p1873 N85-21751 [E85-10089]
Modular plant culture systems for life support functions 12 p1895 N85-21924 [NASA-CR-171853]
Transduction of the root gravitropic stimulus: Can apical calcium regulate auxin distribution? 15 p2606 N85-26063
Attempts to localize and identify the gravity sensing device of plant seedlings 15 p2607 N85-26064
Daylily as a system to study effects of space flight on plant development 15 p2607 N85-26068
Importance of gravity for plant growth and behavior 15 p2608 N85-26070
Mechanical stress regulation of plant growth and development 15 p2610 N85-26087
Mutant peas as probes in the understanding of growth and gravitropism 15 p2611 N85-26088
Plant growth biophysics: The basis for growth asymmetry induced by gravity 15 p2611 N85-26089
An indirect role for ethylene in shoot-inversion release of apical dominance in Pharbitis nil 15 p2611 N85-26090
Gravity perception and response in shoot of cereal grasses 15 p2611 N85-26091
Participation of ethylene in two modes of gravistimulation of shoots 15 p2613 N85-26101
Isolation of hybridomas for golgi-associated proteins and a plant calmodulin 15 p2613 N85-26103
Differential wall growth in gravistimulated corn roots: Its timing and regulation 15 p2614 N85-26105
Use of forest modeling to project acid rain effects 16 p2821 N85-27400 [DE85-005251]
Hydroponics developments for spaceship garden 21 p3663 N85-32754
Regression analysis of aircraft and ground measurement data on vegetation cover 22 p3735 N85-33156

VEGETATIVE INDEX
Effects of atmospheric water vapor and clouds on NOAA (National Oceanic and Atmospheric Administration) AVHRR (Advanced Very High Resolution Radiometer) satellite data 02 p0280 N85-11824 [AD-A145425]
Remote sensing of coastal wetlands biomass using Thematic Mapper wavebands — Lewes, Delaware 13 p2119 N85-23198

VEHICLE WHEELS
Performance evaluation of automotive wheel bearing greases 03 p0337 N85-12168 [AD-A145946]
Orbiter wheel and tire certification 08 p1101 N85-16959
Prediction of in-sand tire and wheeled vehicle drawbar performance 09 p1404 N85-18841 [AD-P004265]
Proceedings of the 8th International Conference on the Performance of Off-Road Vehicles and Machines, volume 2 09 p1407 N85-18859 [AD-A148635]
The research of driving wheel with movable lugs of the paddy field floating tractor 09 p1407 N85-18860 [AD-P004283]
An investigation of the driving wheel thrust of paddy field tractors 09 p1407 N85-18861 [AD-P004284]
Behaviour of soil under a lugged wheel 09 p1407 N85-18864 [AD-P004287]
The analysis on the dynamic performance of a single lug 09 p1408 N85-18866 [AD-P004289]
A simple prediction model for soil compaction under various wheel loads and geometries as an aid to vehicle design 09 p1409 N85-18875 [AD-P004298]
The guidelines to design the lever turning gears in articulated vehicles 09 p1409 N85-18878 [AD-P004301]
Skid steering of wheeled and tracked vehicles: Analysis with Coulomb friction assumptions 12 p1880 N85-21684 [AD-A149826]

VEHICULAR TRACKS
Improvements in tank tread assemblies [NASA-CASE-NPO-16321-1] 18 p3117 N85-29291

VEINS
Reaction of cerebral ventricles to antiorthostatic position and occlusion of jugular veins 01 p0093 N85-10626
Effect of maximum physical load on oxygen-transport properties of blood 01 p0093 N85-10627
The influence of angiotensin on the maintenance of venous tone. The effect of Lower Body Negative Pressure (LBNP) and angiotensin blockade 05 p0693 N85-14457
Hemodynamics and plasma arginine vasopressin during water immersion in normal man 05 p0693 N85-14458

VELA SATELLITES
X-ray emission from Centaurus A — Vela 5B; radio galaxy 08 p1229 N85-17813
Long-term observations of Cyg X-3 with Vela 5B 15 p2686 N85-26586 [DE85-005556]

VELOCITY
NT ACOUSTIC VELOCITY
NT AIRSPEED
NT ANGULAR VELOCITY
NT CRITICAL VELOCITY
NT EXHAUST VELOCITY
NT FLOW VELOCITY
NT GROUND SPEED
NT GROUP VELOCITY
NT HIGH SPEED
NT HYPERSONIC SPEED
NT LIGHT SPEED
NT LOW SPEED
NT ORBITAL VELOCITY
NT PHASE VELOCITY
NT PROPAGATION VELOCITY
NT RADIAL VELOCITY
NT RELATIVISTIC VELOCITY
NT ROTOR SPEED
NT SOLAR VELOCITY
NT SOLAR WIND VELOCITY
NT SUBSONIC SPEED
NT SUPERSONIC SPEEDS
NT TIP SPEED
NT TRANSONIC SPEED
NT WIND VELOCITY
Turbine test report, addendum 02 p0205 N85-11353 [DE84-015130]
The influence of inert particulate material on the properties of RDX/polyethylene wax compositions 03 p0336 N85-12159 [MRL-R-929]
Dynamic compression and volatile release of carbonates 03 p0391 N85-12504 [NASA-CR-174076]
Speed test results and hardware/software study of computational speed problem, appendix D 05 p0603 N85-13843
Transonic flow of elastic medium past slender solid body 06 p0778 N85-14976

Speed benefits of tilt-rotor designs for LHX
[NASA-CR-166437] 07 p0902 N85-15717
Free surface effects on the wake of a flat plate
[AD-A146966] 07 p0958 N85-16071
Nondestructive measurement of bulk residual stresses
[AD-A147063] 07 p0978 N85-16211
A low perturbation electron injector for cyclic accelerators
[AD-D011312] 07 p1040 N85-16604
Investigation of the pressure-and velocity-coupled responses of solid propellants using impedance tube method 09 p1300 N85-18168
Metallographic grinding efficiency
[DE85-001520] 09 p1304 N85-18194
The axial velocity spread acceptance of free electron lasers
[AD-A149024] 10 p1489 N85-19403
Initial velocity of the emerging free boundary in a two-phase Stefan problem with imposed flux
[DE85-003813] 11 p1631 N85-20272
Digital temperature and velocity control of mach 0.3 atmospheric pressure durability testing burner rigs in long time, unattended cyclic testing
[NASA-TM-86959] 12 p1805 N85-21321
Speed and accuracy in automated manufacture
[DE85-003913] 12 p1819 N85-21410
Basic studies of gases for fast switches
[AD-A149828] 12 p1835 N85-21514
The performance of an alternating-current thyristor-controlled motor 15 p2546 N85-25716
Empirical development of ground acceleration, velocity and displacement for accidental explosions at J5 or the proposed large altitude rocket cell at Arnold Engineering Development Center
[DE85-008324] 16 p2758 N85-27020
BLAF: A blast field reconstruction program from pressure histories
[AD-A155300] 21 p3585 N85-32283
Numerical solutions of turbulent models for flow over a flat plate with angle of attack
[DE85-010380] 21 p3585 N85-32286
Horizontal and vertical structure of velocity, potential vorticity and energy in the gulf stream
[AD-A154753] 21 p3655 N85-32702
Experimental studies of chemical reactivity during shock initiation of hexanitrostilbene
[DE85-011726] 22 p3754 N85-33270
The design and development of a constant-speed solar array drive 22 p3796 N85-33519
Detonation in tungsten-loaded HMX
[DE85-009606] 23 p3922 N85-34299
Comparison of experimental data on detonation velocity and Chapman-Jouget pressure vs initial HE density with predictions from Ree's model equation of state
[DE85-007266] 23 p3922 N85-34304
Design and lubrication of high-speed rolling-element bearings
[NASA-TM-87107] 23 p3938 N85-34409
Crustal structure in southern California from array data
24 p4115 N85-35512

VELOCITY COUPLING

Coupling between velocity oscillations and solid propellant combustion 13 p2000 N85-22536
Coupled acoustic and hydrodynamic wave instabilities
13 p2000 N85-22538
Investigation of the characteristics of the velocity-coupled response functions of solid propellants
13 p2001 N85-22540
Analysis of combustion oscillations in heterogeneous systems
[AD-A151999] 16 p2745 N85-26942
Measurement of mode interaction due to waveguide surface roughness
[AD-A154039] 19 p3255 N85-30183

VELOCITY DISTRIBUTION

Monte Carlo simulation of thermalization of subexcitation electrons in molecular hydrogen
[NAL-TR-815T] 01 p0117 N85-10798
Numerical analysis of flow and heat transfer in the VAFB LOX storage Dewar tank
[NASA-CR-171203] 02 p0197 N85-11315
NLR activities in the field of wind tunnel wall interference 03 p0313 N85-12024
On the co-variant formulation of the law of motion of passive particles in a field of turbulence
[REPT-564] 03 p0377 N85-12407
Laser anemometer study of separated flow on wing profiles
[ISL-CO-214/83] 04 p0453 N85-12872
Finite element method for a class of viscoelastic flows in deforming domains applied to jet breakup
[DE84-014571] 04 p0500 N85-13186
Study of the velocity-acoustic pressure correlation in a cold jet, centered on the sign and the amplitude of the velocity fluctuations
[ISL-R-124/83] 04 p0501 N85-13193
Experiments on the structure of turbulent reattaching flow 05 p0635 N85-14074
The evolution of a sparse stellar system
05 p0740 N85-14758
The fragmentation of molecular clouds and the IMF
05 p0740 N85-14759
The velocity-age relation for B and A stars
05 p0740 N85-14762
Stability of stellar disk and ratio of halo to disk masses in the galaxy 05 p0740 N85-14763
Laminar separation bubble with transition: Prediction test with local interaction
[BLL-PNR-90231-(8019.3153)]
06 p0808 N85-15132
Molecular clouds within 100 pc
06 p0877 N85-15573
The smallest sizes of diffuse interstellar clouds
06 p0878 N85-15578
Kinematics of nearby gas and stars
06 p0880 N85-15591
Dark matter near the sun: Simulated star counts and the Oort limit 06 p0880 N85-15592
Calculation of the velocity field generated by a helicopter main and tail rotors in hover
[AD-A147731] 08 p1078 N85-16833
On the virtual wall height in open channel flow with large relative roughness 09 p1303 N85-18188
Determination of total pressure losses in stepped annular diffusors with curvilinear outer walls and uniform velocity field at inlet 09 p1306 N85-18203
Feasibility of alpha particle measurement by CO2 laser Thomson scattering
[DE85-001764] 09 p1326 N85-18334
Monte Carlo simulation of electron thermalization in rare gases
[NAL-TR-834T] 09 p1375 N85-18643
Determination of ion temperature and rotation velocity profiles by visible, UV and X-ray spectroscopy on Doublet 3 09 p1388 N85-18734
Behavior of mode frequency characieristics in shallow sea with variation of P-wave veocity in bottom sediment layer and sonic velocity profile in water layer
10 p1498 N85-19457
Surface-slip equations for multicomponent nonequilibrium air flow
[NASA-TM-85820] 12 p1845 N85-21573
Velocity distributions of solar wind ions and electrons
12 p1954 N85-22273
Plasma in the clusters of galaxies
12 p1957 N85-22299
Dilution jet configurations in a reverse flow combustor
[NASA-CR-174888] 13 p1974 N85-22392
Size and velocity distributions of particles and droplets in spray combustion systems
[AD-A150355] 13 p2017 N85-22648
More precise curve of dependence between density and velocity of longitudinal waves in consolidated crust and top of mantle in oceanic structures
13 p2110 N85-23143
Progress on Experimental impact studies
13 p2181 N85-23534
Ring-diameter ratios for multi-ring basins average 2.0(0.5)D 13 p2182 N85-23542
Dependents of velocity distribution in exit section of converging channel on shape of inlet channel in regulating valve 14 p2277 N85-24106
Effect of drag behind nozzle array on its force and energy characteristics 14 p2277 N85-24107
Laser anemometry two dimensional measurement of velocity fluctuations in an excited jet
[ISL-CO-213/83] 14 p2302 N85-24254
Visualization of velocity fields with Doppler images
[ISL-CO-218/83] 14 p2302 N85-24256
Energy structure of atmospheric boundary layer above waves 14 p2335 N85-24442
Localization of sources of equivalent noise in fast cold jets, excited and nonexcited
[ISL-CO-201/83] 14 p2416 N85-24910
Sensitivity of inferred subphotospheric velocity field to mode selection, analysis technique and noise
14 p2442 N85-25065
The effects of image motion on the l-nu diagram
14 p2443 N85-25076
The effects of seeing on noise
14 p2443 N85-25077
Global solar oscillations in irradiance and velocity: A comparison 14 p2446 N85-25094
Investigation of potential and viscous flow effects contributing to dynamic stall
[AD-A151696] 15 p2557 N85-25773
Study of the coupling between average, coherent and turbulent fields in a circular excited free jet
[ISL-R-115/83] 16 p2785 N85-27184
Multinomial form of the solution of problems of the statistics of elastic rectangular disks
[REPT-17/1984] 16 p2797 N85-27244
Feasibility of mapping velocity flow fields in SSME powerhead by laser anemometry techniques
17 p2915 N85-27971
Least squares inversion of Stokes profiles in the presence of velocity gradients 18 p3207 N85-29892
Generation of capillary instabilities by external disturbances in a liquid jet
[NASA-TM-87041] 19 p3265 N85-30246
Geometry, velocity structure and penetration depths of descending slabs in the western Pacific
19 p3319 N85-30574
A comparison of laser Doppler anemometry and probe measurements within the boundary layer of an airfoil at subsonic flow
[ISL-CO-219/84] 23 p3695 N85-34127
Real time analysis of PETN detonation products
[DE85-009581] 23 p3922 N85-34303
Collisional relaxation of electron tail distribution
[IPPJ-729] 23 p3974 N85-34635
Electron loss process and cross section of multiply charged ions by neutral atoms 23 p3981 N85-34685
High resolution Cherenkov detectors for cosmic ray isotope experiment
[OG-9.1-4] 23 p4023 N85-34930
Workshop Proceedings: Interpretation of Seismic Wave Propagation in Laterally Heterogeneous Structures
[BMR-258] 24 p4118 N85-35530
Analysis of two-parameter constant background born inversion for acoustic synthetic data
[AD-A156394] 24 p4145 N85-35698

VELOCITY FIELDS

U VELOCITY DISTRIBUTION

VELOCITY MEASUREMENT

NT WIND VELOCITY MEASUREMENT

Optical pin apparatus for measuring the arrival time and velocity of shock waves and particles
[DE84-014501] 01 p0120 N85-10824
Hot section laser anemometry
02 p0142 N85-10962
Laser anemometer optimization
02 p0142 N85-10963
Trajectory estimation using combined time-of-arrival and velocity measurements
[DE84-015872] 02 p0242 N85-11582
Project review on geophysical and ocean sound speed profile inversion
[AD-A145717] 02 p0276 N85-11797
Non-intrusive speed sensor — space shuttle main engine turbopumps
[NASA-CR-171204] 03 p0364 N85-12331
Hyades moving group 05 p0740 N85-14757
Kinematics of B and A stars 05 p0741 N85-14766
Optical method of measuring velocity of shear waves
06 p0787 N85-15029
Axisymmetric electromagnetic field influence on the characteristic velocity of an arc-jet
[NASA-TM-77475] 07 p0936 N85-15942
Experiments on controlled, unsteady, separated turbulent boundary layers
[AD-P004172] 09 p1266 N85-17957
Analysis of pressure gradient-velocity correlation in turbulent, premixed flames 09 p1272 N85-17994
Velocity measurements in a 3D shock wave laminar boundary layer interaction. Part 1: Low speed 2D LDV measurements
[AD-A149533] 10 p1485 N85-19373
Study of submicron particle size distributions by laser Doppler measurement of Brownian motion
[AD-A149139] 10 p1487 N85-19386
Ion velocity distributions from spherical 1054 nm and 351 nm laser plasmas
[DE85-002816] 10 p1559 N85-19633
Comparison of two-dimensional laser and hot-wire velocimetry for a supersonic turbulent boundary layer
11 p1576 N85-19927
Experimental investigation of a turbulent incompressible boundary layer on a curved wall
11 p1577 N85-19936
Assessment of satellite collision hazards by simulated sampling in space 12 p1784 N85-21195
In situ orbital debris experiment concepts
12 p1784 N85-21198
Use of ground radar to detect reentering debris
12 p1784 N85-21200
Solid particle receiver experiments: Velocity measurements
[DE85-000257] 12 p1853 N85-21623
Dilution jet configurations in a reverse flow combustor
[NASA-CR-174888] 13 p1974 N85-22392
Large space antenna technology applied to radar-imaging, rain-rate measurements, and ocean wind sensing 14 p2230 N85-23820
Laser anemometry two dimensional measurement of velocity fluctuations in an excited jet
[ISL-CO-213/83] 14 p2302 N85-24254

Interferometric velocity measurements in ballistics [ISL-CO-239/83] 14 p2306 N85-24276
New methods for interpreting seismic time fields in media with variable velocities 14 p2343 N85-24490
A brief summary of results derived from Scandinavian Twin Auroral Radar Experiment (STARE) observations during IMS — Ionospheric electric fields 14 p2362 N85-24595
The Fourier tachometer 2: An instrument for measuring global solar velocity fields 14 p2442 N85-25068
Investigation of a failure detection/identification system for a tactical aircraft navigation system [AD-A151846] 15 p2469 N85-25240
An experimental technique for the study of velocity profiles in a laminar jet using a pulsed nitrogen laser [AD-A151496] 15 p2556 N85-25771
Voyage to Uranus 15 p2687 N85-26596
Method of calculating separation flow of subsonic gas stream around wings 17 p2942 N85-28161
Apparatus for measuring velocity of sound in fluids 17 p2944 N85-28175
Least squares inversion of Stokes profiles in the presence of velocity gradients 18 p3207 N85-29892
Geomagnetic velocimeter [AD-D011672] 19 p3218 N85-29953
Effect of confinement on failure in 95 TATB/5 KEL-F [DE85-010790] 19 p3251 N85-30158
Improved fluid flow meter for measuring the rate of fluid flow in a conduit [NASA-CASE-MFS-28030-1] 19 p3271 N85-30286
Using synchro-ballistic cameras to determine the velocity and spin rate of high-velocity projectiles [DE85-010829] 19 p3367 N85-30884
Velocity visualization in gaseous flows [NASA-CR-174954] 20 p3453 N85-31445
Holographic assembly for measuring velocity fields of supersonic ballistic splinters at a large distance [ISL-CO-203/84] 20 p3459 N85-31487
New optical satellite data 20 p3492 N85-31705
Free-zone electrophoresis of animal cells. 1: Experiments on cell-cell interactions 20 p3499 N85-31754
Improvement of vertical velocity measurements, part 3.4B 21 p3620 N85-32494
Problems and solutions in analyzing partial-reflection drift data by correlation techniques 21 p3626 N85-32529
Simultaneous measurement of velocity and density in a turbulent nonpremixed flame 22 p3744 N85-33209
Optical-fiber/microprocessor-based remote velocity sensor [DE85-010071] 22 p3788 N85-33470
Nonsimultaneous coupled laser velocimeter measurement technique: Error prediction for spatially noncoincident measurements [NASA-TM-86718] 23 p3934 N85-34379
Noise-sustained structure, intermittency and the Ginzburg-Landau equation [DE85-009626] 24 p4094 N85-35379
Determination of vertical air velocity using measurements of the aircraft motion 24 p4121 N85-35545

VELOCITY MODULATION
Velocity-changing collisional effects in nonlinear atomic spectroscopy and photon echo decay in gases [NASA-CR-174159] 04 p0559 N85-13559
Profile of a relativistic electron beam propagated through a linear wiggler and an axial guide field [AD-A154403] 19 p3353 N85-30783

VELOCITY PROFILES
U VELOCITY DISTRIBUTION

VENERA SATELLITES
NT VENERA 11 SATELLITE
Results on volcanism, surface geology from Venera-15, -16 15 p2482 N85-25321

VENERA 11 SATELLITE
Microstructure of Venus cloud layer based on spectrophotometric data from Venera-11 spacecraft 13 p1982 N85-22436

VENTILATION
Hangar destratification investigation [AD-A145049] 01 p0012 N85-10076
Performance of two transonic airfoil wind tunnels utilizing limited ventilation 03 p0313 N85-12020
Interaction between lung mechanics and gas exchange by low volume high frequency pulmonary ventilation in patients with respiratory failure [AD-A146604] 06 p0646 N85-15372
Active and passive shock/boundary layer interaction control on supercritical airfoils 08 p1072 N85-16795
TVENT1P user's manual, a computer code for analyzing tornado induced gas dynamic transients in flow networks [DE85-002346] 10 p1486 N85-19379
Theoretical and experimental investigations of dust loaded flow fields in industrial halls [BMFT-FB-HA-84-044] 12 p1819 N85-21411
Spirolit-2 instrument used to test pulmonary ventilation 12 p1903 N85-21950
New control design principles based on measured performance and energy analysis of HVAC (Heating, Ventilating, and Air-Conditioning) systems [AD-A151708] 15 p2522 N85-25546
Ventilation flow: Submerged 18 p3156 N85-29545

VENTING
The effect of 2 strength reducing techniques on the ultimate tensile strength of AISI 4130 steel: Rocket motor case venting [AD-A145526] 02 p0169 N85-11134
External tank GH2 vent arm 08 p1102 N85-16969
Cumulus cloud venting of mixed layer ozone [NASA-TM-87429] 13 p2132 N85-23269
Opacity control technique for jet engine test cells [AD-D011666] 19 p3220 N85-29968

VENTS
Numerical simulations of the effect of floor and ceiling venting on fire and smoke spread in aircraft cabins [PB85-178333] 19 p3216 N85-29939
Preliminary results of an ALVIN dive program on active hydrothermal vents at the southern Juan de Fuca Ridge 24 p4106 N85-35454

VENTURI TUBES
Certain optimal parameters of high-velocity Venturi ejection tubes [BLL-M-35924-(5828.4)] 05 p0634 N85-14066

VENUS (PLANET)
NT VENUS SURFACE
Infrared thermal radiation of Venus 02 p0163 N85-11101
Impact cratering: The process and its effects on planetary evolution — and silicate-carbonate reactions on Venus [NASA-CR-174016] 02 p0226 N85-11488
Mars exploration, Venus swingby and conjunction class mission modes, time period 2000 to 2045 [NASA-TM-86477] 02 p0303 N85-11961
Gravity anomaly map of Mars and Moon and analysis of Venus gravity field: New analysis procedures [NASA-CR-174295] 08 p1258 N85-17919
The geology of the terrestrial planets [NASA-SP-469] 09 p1410 N85-18888
Venus 09 p1411 N85-18891
The Venus Balloon Project 10 p1465 N85-19243
The international VEGA 'Venus-Halley' (1984-1986 experiment: Description and scientific objectives [NASA-TM-77536] 12 p1960 N85-22324
Volcanism on Venus as connecting link 13 p1982 N85-22433
Preliminary photomaps of Venus surface in the Maxwell Mountains and adjacent areas 13 p1982 N85-22438
Analysis and interpretation of observations of airglow at 297 nm in the Venus thermosphere 13 p2172 N85-23473
Characteristics of basaltic lava flows on Venus 13 p2177 N85-23508
Venus surface composition from radio/radar measurements 13 p2177 N85-23509
Surface units on Venus derived from Pioneer-Venus altimetry, roughness, and reflectivity measurements 13 p2177 N85-23510
Classification of circular features on Venus 13 p2177 N85-23511
Venus gravity: Global field results 13 p2177 N85-23512
Geophysical interpretation of Venus gravity data 13 p2178 N85-23513
Gravity field of Venus and comparison with Earth 13 p2178 N85-23514
The support of long wavelength loads on Venus 13 p2178 N85-23515
Venus chasmata: A lithosphere stretching model 13 p2178 N85-23516
A statistical treatment of the regional slope characteristics of Venus and Earth 13 p2178 N85-23517
The effect of particle density on aeolian transport 13 p2189 N85-23581
Potential bedforms on Venus: Wind tunnel simulations 13 p2189 N85-23583
Analyses of radar images of small craters 13 p2199 N85-23642
Planetary interior modeling and tectonic implications 13 p2200 N85-23649
TASS update on flights of Vega-1 and Vega-2 16 p2722 N85-26803
Kovtunenko discuses Vega Project 16 p2722 N85-26804
French and West German equipment for Vega Project 16 p2722 N85-26805
Venus thermospheric circulation [PB85-180420] 19 p3384 N85-30997
Geophysical interpretation of Venus gravity data [NASA-CR-176063] 20 p3547 N85-32071
Extended atmospheres of outer planet satellites and comets [NASA-CR-176137] 22 p3851 N85-33846
Venus, Earth and Mars: Present bounds on similarities and differences in bulk composition 22 p3856 N85-33876
Contrasts in evolution of Venus and Earth 22 p3857 N85-33880
Geologic processes on Venus: An update 22 p3857 N85-33883
Planning for VRM: Radar and sonar studies of volcanic terrains on Earth, Venus and Mars 22 p3857 N85-33884
Dynamic compensation of Venus's geoid: A comparison with Earth 22 p3858 N85-33888
Admittance functions from Venus vertical gravity and modes of topographic support 22 p3858 N85-33889
A dynamic model of Venus's gravity field [NASA-CR-176173] 24 p4160 N85-35845

VENUS ATMOSPHERE
NT VENUS CLOUDS
Two-level model for formation of night ionosphere of Venus from radio occulation experiments 02 p0162 N85-11100
H2O profile in lower atmosphere of Venus based on effective radiation flux measurements 02 p0163 N85-11102
Change in Venusian atmosphere absorption coefficient with altitude 02 p0163 N85-11103
Theoretical study of electron concentration in Venusian atmosphere as function of zenith angle of sun and solar activity in areas of photochemical equilibrium 02 p0163 N85-11104
Laboratory evaluation of microwave absorption properties under simulated conditions for planetary atmospheres [NASA-CR-174060] 02 p0303 N85-11960
Studies of the chemistry of vibrationally and electronically excited species in planetary upper atmospheres [NASA-CR-174134] 03 p0449 N85-12851
Construction of a superheterodyne receiver for 10 micron waves to be put on a Cassegrain optics telescope for spectroscopic research on the Mars and Venus atmospheres [MPE-183] 06 p0872 N85-15538
Exploration of the solar system by airborne astronomy 08 p1244 N85-17851
Response of Earth's atmosphere to increases in solar flux and implications for loss of water from Venus 13 p2178 N85-23518
The effect of particle density on aeolian transport 13 p2189 N85-23581
Mechanism of formation of low temperatures in nighttime Venusian thermosphere 16 p2723 N85-26807
Venus thermospheric circulation [PB85-180420] 19 p3384 N85-30997
Water loss from Venus: Implications for the Earth's early atmosphere 21 p3721 N85-33067
Laboratory evaluation and application of microwave absorption properties under simulated conditions for planetary atmospheres [NASA-CR-176078] 22 p3851 N85-33847

VENUS CLOUDS
Microstructure of Venus cloud layer based on spectrophotometric data from Venera-11 spacecraft 13 p1982 N85-22436

VENUS PROBES
NT MARINER 5 SPACE PROBE
NT VENERA SATELLITES
NT VENERA 11 SATELLITE
Kovtunenko comments on Vega flight plan, instrumentation 15 p2482 N85-25318
Comments on Vega mission 15 p2482 N85-25319
Press conference on flight of Vega spacecraft 15 p2482 N85-25320
Results on volcanism, surface geology from Venera-15, -16 15 p2482 N85-25321
Interpretation of Venus gravitational anomalies 15 p2483 N85-25322
Laboratory evaluation and application of microwave absorption properties under simulated conditions for planetary atmospheres [NASA-CR-176078] 22 p3851 N85-33847

VENUS RADAR ECHOES
Progress in planetary radarclinometry 13 p2198 N85-23630

VENUS SURFACE
Venus 09 p1411 N85-18891
Visualization of radar altimetry data for Venus 13 p1982 N85-22437
Preliminary photomaps of Venus surface in the Maxwell Mountains and adjacent areas 13 p1982 N85-22438

Hypsometric features on Venus
13 p1983 N85-22439

Volcanism and rift formation in Beta Regio, Venus: New radar results 13 p2176 N85-23507

Characteristics of basaltic lava flows on Venus
13 p2177 N85-23508

Venus surface composition from radio/radar measurements 13 p2177 N85-23509

Surface units on Venus derived from Pioneer-Venus altimetry, roughness, and reflectivity measurements
13 p2177 N85-23510

Classification of circular features on Venus
13 p2177 N85-23511

Venus gravity: Global field results
13 p2177 N85-23512

Geophysical interpretation of Venus gravity data
13 p2178 N85-23513

The support of long wavelength loads on Venus
13 p2178 N85-23515

Venus chasmata: A lithosphere stretching model
13 p2178 N85-23516

A statistical treatment of the regional slope characteristics of Venus and Earth
13 p2178 N85-23517

Potential bedforms on Venus: Wind tunnel simulations
13 p2189 N85-23583

Microdunes and other aeolian bedforms on Venus: Wind tunnel simulations 13 p2189 N85-23584

Unsupervised classification of global radar units on Venus 13 p2198 N85-23632

Analyses of radar images of small craters
13 p2199 N85-23642

Geological analyses of the surface of Venus and Mars from lander spacecraft images and orbital radar observations 19 p3384 N85-30993

Geophysical interpretation of Venus gravity data
[NASA-CR-176063] 20 p3547 N85-32071

VERBAL COMMUNICATION

Crew communication as a factor in aviation accidents
05 p0710 N85-14555

A full mission simulator study of aircrew performances: The measurement of crew coordination and decisionmaking factors and their relationships to flight task performances 05 p0710 N85-14556

Communication on the flight deck
05 p0711 N85-14557

Neuro-linguistic programming: Eye movements as indicators of representational systems
[AD-A147541] 07 p1016 N85-16454

Multiple resources and brain laterality
[AD-A148912] 10 p1530 N85-19643

Verbal information processing paradigms: A review of theory and methods
[AD-A153229] 17 p3050 N85-28880

VERIFICATION (PROVING)
U PROVING

VERTEBRAE

Analysis of long bone and vertebral failure patterns
[AD-A154796] 21 p3663 N85-32758

VERTEBRAL COLUMN

The effects of helicopter vibration on the spinal system
[AD-A148274] 03 p0402 N85-12562

Analysis of long bone and vertebral failure patterns
[AD-A154796] 21 p3663 N85-32758

VERTEBRATES
NT AMPHIBIA
NT BABOONS
NT BEARS
NT BIRDS
NT CATS
NT DEER
NT DOGS
NT DOLPHINS
NT FISHES
NT FROGS
NT GUINEA PIGS
NT HUMAN BEINGS
NT MAMMALS
NT MICE
NT MONKEYS
NT PRIMATES
NT RABBITS
NT RATS
NT SEALS (ANIMALS)
NT SHARKS
NT SHEEP
NT TURTLES
NT WHALES

VERTICAL AIR CURRENTS

Diurnal and seasonal patterns of temperature and wind flow in the planetary boundary layer for ten locations in complex terrain
[PB85-106698/GAR] 06 p0840 N85-15333

The sensitivity of mesoscale cyclogenesis forecasts to detailed three-dimensional isentropic initial analyses and varied vertical model resolution
15 p2598 N85-26015

The study of thermal forecasting for gliding
16 p2830 N85-27453

Approximate method for computing wind velocity in atmosphere 19 p3298 N85-30444

Tropospheric gravity waves observed by three closely spaced ST radars 21 p3623 N85-32509

Thunderstorm phenomena and weather radar scanning strategies
[DOT/FAA/PM-85/14] 21 p3634 N85-32573

Determination of vertical air velocity using measurements of the aircraft motion
24 p4121 N85-35545

Measurements for the determination of the vertical structure of the convective boundary layer — atmospheric boundary layer 24 p4122 N85-35550

VERTICAL ATTITUDE TAKEOFF-LANDING AIRCRAFT
U VATOL AIRCRAFT

VERTICAL DISTRIBUTION
NT STAR DISTRIBUTION

Wave phase velocity in a wind gradient — gravity waves 04 p0523 N85-13343

The z-dependence of the spin temperature of HI
06 p0878 N85-15580

Measurements of H2O in Jupiter's atmosphere from 5 microns airborne observations 08 p1244 N85-17854

The vertical structure and stability of alpha model accretion disks 09 p1417 N85-18938

Aerosol limb absorption — stratosphere
[NASA-TM-77733] 10 p1515 N85-19562

Measurement of the vertical gradient of the semidiurnal tidal wind phase in winter at the 95 km level
11 p1662 N85-20478

Peat resources of Maine. Volume 1: Aroostook County
[DE85-004196] 11 p1669 N85-20519

Peat resources of Maine. Volume 4: Southern and western Maine
[DE85-004198] 11 p1670 N85-20520

Special features of computations of vertical distribution of concentration of suspended sediments under marine conditions 13 p2106 N85-23125

An equation of profile of snow drift density during snowfall 15 p2581 N85-25919

An experimental study of brine upward migration in thin sea ice 15 p2582 N85-25923

Vertical redistribution of a pollutant tracer due to cumulus convection
[PB85-172971] 18 p3134 N85-29415

Development and testing of the variable vertical resolution Fourth Order GCM 18 p3142 N85-29453

Parameterization of surface fluxes in the VVR Fourth Order GCM 18 p3142 N85-29454

Observations of mesospheric turbulence by rocket probe and VHF radar, part 2.4A 21 p3619 N85-32484

Visibility and vertical structure measurements in southern Germany
[AD-A154714] 21 p3635 N85-32574

A new hypothesis for the observed vertical distribution of atmospheric aerosols 21 p3645 N85-32646

On the mechanisms responsible for the formation of typical size spectra and vertical distribution of tropospheric aerosol particles 21 p3645 N85-32647

Drying of pulverized material with heated condensible vapor
[DE85-011656] 22 p3783 N85-33438

Application of nonlinear least squares methods to the analysis of solar spectra
[NASA-CR-176122] 22 p3816 N85-33637

Estimating the change in asymptotic direction due to secular changes in the geomagnetic field
[SH-6.1-13] 23 p4045 N85-35086

Partitioning of the vertical turbulent energy transport into positive and negative contributions — meteorology
24 p4122 N85-35551

Aircraft measurements during the Bonn Experiment (BONEX 1) — meteorology 24 p4122 N85-35552

VERTICAL FINS
U FINS

VERTICAL JUNCTION SOLAR CELLS

Apparatus for etching vertical junction solar cell wafers
[AD-D011653] 17 p2984 N85-28443

VERTICAL LANDING

Why vertical landing — aircraft
[BAE-KRS-N-GEN-301] 09 p1279 N85-18048

VERTICAL MOTION

Vertical crustal movements in southern California, 1974 to 1978
[GS-CIRC-905] 02 p0228 N85-11491

Increase in performance and improvement of ride comfort of self-propelled construction machinery by reducing pitch and vertical vibration
[AD-P004269] 09 p1405 N85-18845

Vertical movements and structure formation within island systems of northeast Asia 10 p1501 N85-19471

Diagnosis of vertical motions from VAS retrievals during a convective outbreak
[NASA-CR-171569] 19 p3316 N85-30554

A simple model for testing the effects of gravity-wave-produced vertical oscillations of scattering irregularities on spaced-antenna, horizontal drift measurements 21 p3619 N85-32489

Estimation of vertical diffusion from observations of Atmospheric turbulence layers, part 4.4B
21 p3623 N85-32507

VERTICAL ORIENTATION

Observations of the vertical structure of the eddy field in the Kuroshio extension
[AD-A145178] 01 p0089 N85-10599

Mass and momentum transport in a turbulent buoyant vertical axisymmetric jet 05 p0635 N85-14070

Lateral fluid forces acting on a whirling centrifugal impeller in vaneless and vaned diffuser
05 p0643 N85-14123

Experimental investigation of lateral forces induced by flow through model labyrinth glands
05 p0643 N85-14128

The growth of large diameter single crystals by vertical solidification of the melt
[AD-A148756] 09 p1397 N85-18792

Along-track deflection of the vertical from SEASAT: GEBCO (General Bathymetric Chart of the Oceans) overlays
[PB85-129641] 12 p1876 N85-21767

Vertical discrimination in the sound channel
[AD-A150254] 13 p2155 N85-23380

High-frequency acoustic variability in the arctic
[AD-A150550] 13 p2155 N85-23383

Six-inch HYGE vertical impact facility
[AD-A150665] 14 p2228 N85-23809

Observation of precipitating clouds by a vertically pointing radar at Morino in the Iburi District, Hokkaido, Japan 15 p2582 N85-25922

Scheme for atmospheric thermal sensing from satellites with enhanced vertical resolution
16 p2726 N85-26823

The theoretical response of a vertical line array to wind-generated noise in shallow water
[AD-A151730] 16 p2860 N85-27638

Structural design of the Sandia 34-meter vertical-axis wind turbine
[DE85-011146] 18 p3118 N85-29300

Natural convection in square partitioned enclosures
[AD-A153707] 18 p3197 N85-29828

Improvement of vertical velocity measurements, part 3.4B 21 p3620 N85-32494

Determination of horizontal and vertical wavelengths of gravity waves in the mesosphere by spaced wind measurements 21 p3623 N85-32510

Trapping of ion conics by downward parallel electric fields
[AD-A155306] 21 p3633 N85-32568

Visibility and vertical structure measurements in southern Germany
[AD-A154714] 21 p3635 N85-32574

Horizontal and vertical structure of velocity, potential vorticity and energy in the gulf stream
[AD-A154753] 21 p3655 N85-32702

Admittance functions from Venus vertical gravity and modes of topographic support 22 p3858 N85-33889

VERTICAL PERCEPTION

Prediction of seasickness susceptibility
11 p1693 N85-20647

Amyloplast sedimentation kinetics in corn roots
15 p2606 N85-26059

Polyamines as possible modulators of gravity induced calcium transport in plants 15 p2606 N85-26060

Role of Ca + + in shoot gravitropism — avena
15 p2607 N85-26065

A possible explanation of why gravitropic growth is detected earlier than straight growth
15 p2607 N85-26067

Dissociation of autonomic and sensory vestibular reactions 23 p3953 N85-34501

VERTICAL STABILIZERS
U STABILIZERS (FLUID DYNAMICS)

VERTICAL TAILS
U STABILIZERS (FLUID DYNAMICS)
U TAIL ASSEMBLIES

VERTICAL TAKEOFF AIRCRAFT
NT FLYING PLATFORMS

An engine trade study for a supersonic STOVL fighter-attack aircraft, volume 1
[NASA-CR-166304] 02 p0133 N85-10910

Simulation evaluation of two VTOL control/display systems in IMC approach and shipboard landing [NASA-TM-85996] 06 p0756 N85-14841
Circulation control: A bibliography of DTNSRDC research and selected outside references: Update [AD-A146966] 07 p0893 N85-15661
International aviation (selected articles) [AD-A148704] 08 p1067 N85-16762
Pseudospectral calculations of two-dimensional transonic flow (Task 1). Numerical investigation of VTOL aerodynamics (Task 2) [AD-A150123] 12 p1772 N85-21126
Analysis of control system from a viewpoint of desired pole placement and desired degree of robustness [AD-A152627] 17 p2699 N85-27876

VERTICAL TAKEOFF AND LANDING
U VERTICAL LANDING

VERTICES
U APEXES

VERY HIGH FREQUENCIES
VHF/UHF radar and its application in nowcasting 01 p0078 N85-10516
Study of factors affecting an HF/VHF direct broadcasting satellite service [PB85-120889/GAR] 09 p1313 N85-18255
Improvement of VHF(MB) model [AD-A150087] 12 p1829 N85-21480
A fully distributed approach to the design of a 16 K bit/sec VHF packet radio network [AD-A141282] 13 p2054 N85-22859
Alternatives for satellite sound broadcast systems at HF and VHF 14 p2229 N85-23815
The ARGOS VHF direct readout mini-station and CML-80-MP data collection Platform Transmitter Terminals (PTTs) 14 p2236 N85-23873
ARGOS VHF direct readout mini-station 14 p2239 N85-23886
Generalized graph coloring: A frequency assignment method for VHF broadcasting [TUM-M8405] 16 p2844 N85-27535
Measurements of VHF/UHF radio propagation in a maritime temperate climate [CRC-1380] 18 p3069 N85-29119
Field antenna handbook [AD-A155204] 21 p3576 N85-32242
A modified Fresnel scattering model for the parameterization of Fresnel returns, part 2.3A 21 p3618 N85-32483
Observations of mesospheric turbulence by rocket probe and VHF radar, part 2.4A 21 p3619 N85-32484
Usefulness of multifrequency MST radar measurements, part 2.6B 21 p3619 N85-32487
Potential advantages of the spaced antenna method for operational wind profiling, part 3.1B 21 p3620 N85-32490
Improvement of vertical velocity measurements, part 3.4B 21 p3620 N85-32494
Interferometer applications of VHF radars, part 3.6A 21 p3621 N85-32497
Testing and optimizing MST coaxial collinear arrays, part 6.4A 21 p3625 N85-32518
Elimination of range-aliased echoes in the VHF radars 21 p3625 N85-32521
A note on the proposed UK VHF radar 21 p3629 N85-32545
Radar wind profilers in the Colorado network [PB85-185486] 22 p3817 N85-33647

VERY HIGH FREQUENCY RADIO EQUIPMENT
Preliminary investigation of the performance of repeater technology for satellite sound broadcasting [SSP/017/82] 18 p3092 N85-29137

VERY HIGH SPEED INTEGRATED CIRCUITS
U VHSIC (CIRCUITS)

VERY LARGE SCALE INTEGRATION
Routing the power and ground wires on a VLSI chip [AD-A145356] 02 p0194 N85-11296
The application of microprocessors in the command and control of satellites by the MECB stations [INPE-3282-RPE/466] 02 p0239 N85-11553
Supercomputers and VLSI: The effect of large scale integration on computer architecture [AD-A145406] 02 p0239 N85-11555
Circuit engineering and technological optimization of very high speed LSI logic elements and transistor structures 03 p0347 N85-12237
Application of a silicon compiler to VLSI (Very Large Scale Integrated circuits) design of digital pipelined multipliers [AD-A146328] 03 p0403 N85-12569
VLSI (Very Large Scale Integration) design tools reference manual, release 1.0 [AD-A146273] 03 p0408 N85-12604
Ion beam lithography [BMFT-FB-T-84-182] 04 p0504 N85-13219
VLSI architectures for the multiplication of integers modulo a Fermat number 05 p0624 N85-13993
Practical application of electron beam testing in LSI and VLSI circuits [BMFT-FB-T-84-185] 05 p0633 N85-14061
VLSI design tools, reference manual, release 2.0 [AD-A146444] 06 p0803 N85-15112
Specialized silicon compilers for language recognition [AD-A146526] 06 p0853 N85-15425
Built-in test and self repair mechanisms in a digital correlator integrated circuit 08 p1064 N85-16741
Electronics component R and D, production capability reviewed 08 p1140 N85-17181
Electrical characterization of VLSI (Very Large Scale Integration) memories [AD-A147657] 08 p1156 N85-17296
Restructurable VLSI program [AD-A148145] 08 p1157 N85-17301
DDL system: Design systhesis of digital systems [NASA-CR-170759] 09 p1366 N85-18584
Researchers, projects at French intelligent machine center 10 p1460 N85-19207
Siemens' CAD system designs VLSI circuits 10 p1461 N85-19209
Research into self-timed VLSI circuits [AD-A149140] 10 p1479 N85-19339
Method of examining microcircuit patterns [NASA-CASE-NPO-16299-1] 11 p1628 N85-20250
Signal propagation delay, wire length distribution and the efficiency of VLSI circuits [CWI-CS-R8412] 11 p1630 N85-20266
Design of a bit-sliced processor array with built-in-self-test [AD-A149785] 12 p1835 N85-21513
Built-in tests for VLSI (Very Large Scale Integration) finite-state machines [AD-A149784] 12 p1911 N85-21997
X-ray lithography and VLSI circuits 13 p2052 N85-22846
Periodic binary sequence generators: VLSI circuits considerations [NASA-CR-175649] 13 p2063 N85-22886
EOS (electrical overstress) protection for VLSI (Very Large Scale Integration) devices [AD-A150333] 13 p2064 N85-22891
UW/NW (University of Washington/Northwest) VLSI Consortium [AD-A150740] 14 p2404 N85-24818
Developments in microelectronics: Past and future 15 p2530 N85-25597
Designing VLSI (Very Large Scale Integrated) circuits for testability [AD-A151834] 15 p2549 N85-25729
Development of simulation procedures for VLSI systems (timing simulation) [BMFT-FB-T-84-297] 15 p2550 N85-25743
Influence and possibilities of Very Large Scale Integration (VLSI) in pattern recognition and image processing 15 p2622 N85-26160
Techniques for computing the DFT using the residue Fermat number systems and VLSI 16 p2770 N85-27097
An integrated UNIX-based CAD system for the design and testing of custom VLSI chips 16 p2771 N85-27102
System design of automated VLSI (Very Large Scale Integrated) test station and implementation of selected system aspects [AD-A151961] 16 p2778 N85-27147
Radiation hardening for VLSI applications [DE85-005493] 16 p2780 N85-27155
VLSI workshop and project: February - November 1982 [WSRL-0374-TR] 17 p2951 N85-28223
Restructurable VLSI (Very large scale integration) program [AD-A152340] 17 p2951 N85-28226
Efficient VLSI (Very Large Scale Integration) fault simulation [AD-A152661] 17 p2953 N85-28233
VLSI (Very large scale integrated circuits) device reliability models [AD-A153268] 17 p2954 N85-28245
Speed-up techniques for complementary metal oxide semiconductor very large scale integration [AD-A152466] 17 p3043 N85-28829
Microstore: The Stanford analog memory unit [DE85-005534] 18 p3095 N85-29160
Evaluation of VLSI technology — space applications [CD.6501702] 18 p3098 N85-29177
The use of VLSI technology for the real-time generation of graphics displays: A proposal [AD-A153766] 18 p3160 N85-29578
Electro-optic techniques for VLSI interconnect 18 p3188 N85-29774
Split-cross-bridge resistor for testing for proper fabrication of integrated circuits [NASA-CASE-NPO-16021-1] 19 p3256 N85-30187
A single chip VLSI architecture for radar signal processing 19 p3257 N85-30195
A comparison of the radiation hardness of various VLSI technologies for defense applications [DE85-006973] 19 p3263 N85-30236
Fault-tolerant computing research [AD-A154082] 19 p3342 N85-30710
Implementation of a serial communication process for a fault tolerant, real time, multitransputer operating system [AD-A154237] 19 p3343 N85-30714
VLSI structures for numerical and digital signal processing computations 20 p3439 N85-31340
Basic development of a 1.5 micrometer very large scale integrated technique, part 1-4 [BMFT-FB-T-85-032-PT-1-4] 20 p3449 N85-31417
VLSI (Very Large Scale Integrated) tutorials through the video-computer courseware implementation system [AD-A155889] 24 p4135 N85-35631
Computer Aided Design (CAD) methods for very large scale integration systems [BMFT-FB-T-85-029] 24 p4141 N85-35668

VERY LONG BASE INTERFEROMETRY
Measurement of pulsar parallax by Very Long Baseline Interferometry 03 p0444 N85-12830
The Telecommunications and Data Acquisition Report [NASA-CR-174149] 05 p0622 N85-13980
Submilliarcsecond VLBI using compact close pairs of radio sources: Error analysis 05 p0622 N85-13981
VLBI solutions for the time variation of DSN baselines: 1978 - 1983 05 p0623 N85-13983
The performance of differential VLBI delay during interplanetary cruise 05 p0623 N85-13984
VLBI system (BLK I) IF-video down conversion design 05 p0625 N85-13996
Interferometry with decametric waves (review) 06 p0781 N85-14996
Software for Crimea-Pushchino radiointerferometer 06 p0783 N85-15007
Primary data processing in very long baseline radiointerferometer 06 p0783 N85-15008
QUASAT: A VLBI observatory in space — conferences [ESA-SP-213] 07 p1056 N85-16700
The galaxy scene and QUASAT — VLBI satellite 07 p1056 N85-16703
The QUASAT mission: An overview 07 p1056 N85-16704
Some prospects of space VLBI 07 p1056 N85-16705
QUASAT: Technical aspects of the proposed mission — VLBI satellite 07 p1057 N85-16706
A study on the imaging potential of QUASAT — spaceborne VLBI 07 p1057 N85-16707
Potential affiliate stations to work with the EVN — European VLBI Network; QUASAT 07 p1057 N85-16708
Correlator and data processing requirements for QUASAT 07 p1057 N85-16709
Limitation of VLBI angular resolution 07 p1057 N85-16710
Processing system for space VLBI 07 p1057 N85-16711
Testing theories of superluminal motion — QUASAT 07 p1058 N85-16714
QUASAT, gravitational lenses, and studies of the interstellar, intracluster and intergalactic medium 07 p1058 N85-16715
Very Long Base Interferometry (VLBI) in space and X-ray observations of compact sources in active galactic nuclei 07 p1058 N85-16716
The wide-range space radio interferometer 07 p1058 N85-16717
The relevance of QUASAT to the star formation problem 07 p1058 N85-16718
Galactic OH and H2O masers — QUASAT project 07 p1058 N85-16719
Water masers and distance measurements: The impact of QUASAT 07 p1059 N85-16721
A short note on the high precision navigation of QUASAT 07 p1059 N85-16722
Opportunities for high angular and temporal resolutions of galactic objects at radio frequencies — QUASAT 07 p1059 N85-16723
Very long base interferometry (VLBI) and X-ray observations of complete samples of radio selected active galactic nuclei 08 p1243 N85-17847
VLBI observations of compact double radio sources 09 p1417 N85-18940
The Telecommunications and Data Acquisition Report [NASA-CR-174366] 10 p1462 N85-19224
Arcsecond positions for milliarcsecond VLBI nuclei of extragalactic radio sources. Part 3: 74 sources 10 p1463 N85-19225
The accuracy of radio interferometric measurements of Earth rotation 10 p1465 N85-19246

Utilization of mobile VLBI for geodetic measurements 10 p1466 N85-19248

Studies of galactic HI in 21-centimeter absorption 13 p2170 N85-23466

QUASAT: An orbiting very long baseline interferometer program using large space antenna systems 14 p2230 N85-23822

Antenna Technology for QUASAT application — radio antenna for very long base interferometry missions 14 p2231 N85-23828

Observation model and parameter partials for the JPL VLBI parameter estimation software MASTERFIT-F 2.0 [NASA-CR-175640] 14 p2347 N85-24509

Station coordinates and Earth rotation parameters from Lageos laser ranging 16 p2806 N85-27299

Basic research for the geodynamics program [NASA-CR-175751] 16 p2825 N85-27424

Precise time transfer using MKIII VLBI technology 17 p2965 N85-28310

Using GPS and VLBI technology to maintain 14 digit synchronization 18 p3109 N85-29250

New stations supporting crustal dynamics project VLBI measurements 20 p3491 N85-31701

New VLBI technology developments 20 p3491 N85-31702

Comparing SLR and VLBI geodetic parameters 20 p3491 N85-31703

Milliarcsecond morphology of the twin quasar 0957 + 56A,B: The view through a gravitational lens 20 p3544 N85-32054

Mapping with QUASAT (quasar satellite) using short observation times [AD-A155155] 21 p3559 N85-32141

Crustal dynamics project data analysis fixed station VLBI geodetic results [NASA-TM-86229] 21 p3615 N85-32465

Crustal Dynamics Project: Catalogue of site information [NASA-TM-86218] 22 p3801 N85-33552

VERY LOW FREQUENCIES

The case for concern about very low frequency fields from visual display terminals: The need for further research and shielding of VDTs [CCOHS-P83-2E] 02 p0234 N85-11526

Impedance measurements on a VLF multi-turn loop antenna in a space plasma simulation chamber [AD-A145104] 04 p0492 N85-13141

Human reactions to ELF (Extremely Low Frequency) electric and magnetic fields. An annotated bibliography of current literature, fourth edition [PB84-230358] 04 p0545 N85-13472

Infralow-frequency digital phase meter 06 p0787 N85-15031

Ionospheric and magnetospheric modifications caused by VLF waves [AD-A148210] 08 p1188 N85-17475

Survey of VLF-OMEGA transmissions received during summer at Antarctic peninsula [INPE-3399-PRE/666] 10 p1462 N85-19223

The ULF/ELF/VLF electromagnetic fields generated in a sea of finite depth by elevated dipole sources [AD-A149638] 12 p1828 N85-21470

A new radio emission at 3 kHz in the outer heliosphere 12 p1959 N85-22312

VLF emissions observed by ISIS Satellites during the IMS 14 p2366 N85-24621

VLF wave-particle interaction experiments by EXOS-B/Siple station transmissions 14 p2366 N85-24622

Magnetospheric wave characteristics derived from cross-spectral analysis 14 p2371 N85-24659

Hazards of VLF electromagnetic fields 16 p2776 N85-27136

VLF (Very low frequency) workshop held at San Diego California, 24-25 January 1985 [AD-A154652] 21 p3573 N85-32224

Numerical modeling of subsurface communication [DE85-012818] 21 p3577 N85-32249

VESTA ASTEROID

Asteroid collisional evolution studies 13 p2176 N85-23501

VESTIBULAR NYSTAGMUS

Caloric stimulation of the vestibular system in microgravity 05 p0695 N85-14469

Problems of space biology. Volume 50: Nystagmometry for evaulation of the status of the vestibular function [NASA-TM-77616] 14 p2385 N85-24694

VESTIBULAR TESTS

The European vestibular experiments in the Spacelab 1 mission 05 p0694 N85-14466

Thresholds of perception of whole body linear oscillation: Modification by spaceflight 05 p0694 N85-14467

The adaptation of vestibulo-spinal reflexes as a function of spaceflight and their relationship to space motion sickness 05 p0694 N85-14468

Caloric stimulation of the vestibular system in microgravity 05 p0695 N85-14469

Visual-vestibular interaction in human motion perception 05 p0695 N85-14471

Thermoregulatory and vestibular systems in the rat 15 p2610 N85-26082

Influence of limboreticular complex on some reactions of rabbits 19 p3326 N85-30607

The European vestibular experiments of the Spacelab-1 mission 20 p3506 N85-31808

Some results of the European vestibular experiments in the Spacelab-1 mission 20 p3506 N85-31809

Spatial orientation in weightlessness and readaptation to Earth's gravity 20 p3509 N85-31811

Mission operations requirements document for D-1 Experiment 102, Vestibular Experiments in Spacelab [NASA-TM-87495] 21 p3557 N85-32129

Effect of experimental motion sickness on postrotory nystagmus and counterrotation illusion 22 p3824 N85-33690

Dissociation of autonomic and sensory vestibular reactions 23 p3953 N85-34501

VESTIBULES

The development of the vestibular apparatus under conditions of weightlessness [NASA-TM-77517] 07 p1011 N85-16422

Neurophysiological correlates of motion sickness: Role of vestibulocerebellum and 'vomiting center' reanalyzed 11 p1693 N85-20643

Influence of gravitoinertial force level on apparent magnitude of coriolis cross-coupled angular accelerations and motion sickness 11 p1693 N85-20644

Vestibular and oculomotor function during Gz variations 11 p1693 N85-20645

Quantitation of Na+, K+-ATPase enzyme activity in tissues of the mammalian vestibular system 15 p2613 N85-26102

Anatomy of the vestibulo-automatic outflow to the gut 15 p2614 N85-26106

Mission operations requirements document for D-1 Experiment 102, Vestibular Experiments in Spacelab [NASA-TM-87495] 21 p3557 N85-32129

Effect of experimental motion sickness on postrotory nystagmus and counterrotation illusion 22 p3824 N85-33690

Dissociation of autonomic and sensory vestibular reactions 23 p3953 N85-34501

VETERINARY MEDICINE

USSR report: Life sciences. Biomedical and behavioral sciences [JPRS-UBB-84-015] 07 p1010 N85-16416

VFR (RULES)

U VISUAL FLIGHT RULES

VHF OMNIRANGE NAVIGATION

Use of microprocessor techniques and new antenna systems to improve the navigation aids very high frequency omnidirectional radar (VOR), Doppler VOR and Instrument Landing System (ILS) [BMFT-FB-W-84-026] 02 p0137 N85-10930

Evaluation of radio navigation systems and their configuration with respect to minimum cost [ESA-TT-847] 20 p3392 N85-31043

VHSIC (CIRCUITS)

Circuit engineering and technological optimization of very high speed LSI logic elements and transistor structures 03 p0347 N85-12237

USSR report: Electronics and electrical engineering [JPRS-UEE-84-010] 04 p0485 N85-13095

Life cycle cost model for very high speed integrated circuits [AD-A147798] 08 p1157 N85-17296

Signal propagation delay, wire length distribution and the efficiency of VLSI circuits [CWI-CS-R8412] 11 p1630 N85-20266

Circuit topology, signal propagation delay and the efficiency of VLSI circuits [CWI-CS-R8414] 11 p1630 N85-20267

Research in the design of high-performance reconfigurable systems [NASA-CR-175705] 15 p2621 N85-26153

VLSI (Very large scale integrated circuits) device reliability models [AD-A153268] 17 p2954 N85-28245

GAO (General Accounting Office) assessment of DOD's Very High Speed Integrated Circuits (VHSIC) technology program [AD-A155109] 21 p3581 N85-32261

VIBRATION

NT BENDING VIBRATION
NT COMBUSTION VIBRATION
NT FLUTTER
NT FORCED VIBRATION
NT FREE VIBRATION
NT LATTICE VIBRATIONS
NT LINEAR VIBRATION
NT MISSILE VIBRATION
NT POGO EFFECTS
NT RANDOM VIBRATION
NT RESONANT VIBRATION
NT SELF INDUCED VIBRATION
NT STRUCTURAL VIBRATION
NT SUBSONIC FLUTTER
NT SUPERSONIC FLUTTER
NT TORSIONAL VIBRATION
NT TRANSONIC FLUTTER

Helicopter rotor blade design for minimum vibration [NASA-CR-3825] 01 p0006 N85-10032

Rotordynamic analysis of the SSME turbopumps using reduced models [NASA-CR-171170] 01 p0054 N85-10355

Human response to vibroacoustic environments of space vehicles [NASA-TM-86316] 01 p0116 N85-10780

The Shock and Vibration Digest, volume 16, no. 8 [AD-A145653] 02 p0208 N85-11372

Analysis of turbomachine blades: A review 02 p0208 N85-11374

Approximation methods for inverse problems involving the vibration of beams with tip bodies [NASA-CR-172466] 02 p0209 N85-11379

Interactions among system stiffness, wear and vibrations 03 p0370 N85-12364

Studies of the chemistry of vibrationally and electronically excited species in planetary upper atmospheres [NASA-CR-174134] 03 p0449 N85-12851

Structural properties of amorphous metals by Raman scattering [DE84-016947] 04 p0475 N85-13027

Computation of the nonequilibrium flow in a gasdynamic laser [AD-A141022] 04 p0505 N85-13224

Vibration data analysis system for SNLA area 3 reference manual [DE84-016207] 04 p0514 N85-13275

Subsynchronous vibrations in a high pressure centrifugal compressor: A case history 05 p0642 N85-14118

Experiences with nonsynchronous forced vibration in centrifugal compressors 05 p0642 N85-14119

Internal hysteresis experienced on a high pressure syn gas compressor 05 p0642 N85-14122

Experimental investigation of lateral forces induced by flow through model labyrinth glands 05 p0643 N85-14128

An iwatsubo-based solution for labyrinth seals - comparison with experimental results 05 p0644 N85-14131

Influence of stationary components on unsteady flow in industrial centrifugal compressors 05 p0645 N85-14140

Propulsive efficiency of vibrating wing in supersonic flow 05 p0724 N85-14656

Linear problem of harmonic vibrator acting at supercritical frequencies in subsonic boundary layer 06 p0779 N85-14978

F-8 refueling boom ground vibration test [NASA-TM-84914] 07 p0902 N85-15713

Analysis of the surface load and radiated sound of a vibrating airfoil with application to the experiment of Brooks [NASA-CR-3864] 07 p1036 N85-16590

Development of a pressure transducer for usage in high temperature and vibration environments. Phase 1: Feasibility investigation [AD-A148695] 08 p1165 N85-17349

Eigenvalues of rotating machinery 08 p1167 N85-17361

Vibration analysis of a multipurpose platform [NAL-TR-803] 09 p1286 N85-18078

Identification of vibration parameters of flexible structures 09 p1331 N85-18360

Coriolis effects on the vibrations of rotating beams, plates and shells 09 p1331 N85-18366

Impact of 810D on dynamic test laboratories 09 p1334 N85-18386

The Shock and Vibration Bulletin 54. Part 2: Ship shock, shock and blast and ground shock [AD-A148132] 09 p1334 N85-18388

Direct energy minimization approach to whipping analysis of pressure hulls 09 p1335 N85-18393

The Shock and Vibration Bulletin 54. Part 3: Structural dynamics, machinery dynamics and vibration problems [AD-A148133] 09 p1337 N85-18406

Increase in performance and improvement of ride comfort of self-propelled construction machinery by reducing pitch and vertical vibration [AD-P004269] 09 p1405 N85-18845

Ride comfort of off-road vehicles [AD-P004279] 09 p1406 N85-18855

Further development in ride quality assessment [AD-P004280] 09 p1406 N85-18856

Characteristics of farm field profiles as sources of tractor vibration
[AD-P004282] 09 p1407 N85-18858
Integrated Technology Rotor/Flight Research Rotor (ITR/FRR) concept definition study
[NASA-CR-166444] 10 p1424 N85-18981
Fluidelastic instability in shell and tube heat exchangers: A framework for a prediction method
[DE84-006518] 10 p1496 N85-19444
Health standards for general vibration
10 p1523 N85-19607
Effects of overall vibration and noise on operational personnel 10 p1523 N85-19608
Acta Aeronautica et Astronautic Sinica (selected articles)
[AD-A148830] 11 p1575 N85-19922
Fractographic features of titanium alloy fatigue failure under repeated static stress and high frequency vibration 11 p1601 N85-20070
Model testing and analysis of NOVA laser structures
[DE84-017569] 11 p1638 N85-20321
On the coupling of an anchored flame with an acoustic field
[COLL-AERON-8434] 12 p1799 N85-21282
Applications of vibration analysis to the condition monitoring of rolling element bearings
[ARL/AERO-R-163] 12 p1859 N85-21663
An analysis of the high frequency vibrations in early Thematic Mapper scenes 12 p1872 N85-21742
Nonlinear rotordynamics analysis
[NASA-CR-171425] 13 p1968 N85-22364
Normal mode calculations for fuselage type intricate structures by regarding them as systems with superposed constraints 13 p2048 N85-22617
The Shock and Vibration Digest, volume 16, no. 12
[AD-A150594] 13 p2102 N85-23102
Machine tool vibrations: A review
13 p2102 N85-23104
Flow-induced vibrations of a circular cylinder due to turbulent internal flows
[DE85-002766] 13 p2103 N85-23110
Condition monitoring of helicopter gearboxes using automatic vibration analysis techniques
14 p2223 N85-23790
Gear noise origins 14 p2224 N85-23791
Transmission error measurements in gearbox development 14 p2224 N85-23794
Some problems in improving reliability and accuracy of regulators with hydraulic amplifiers in main channel of power turbine 14 p2271 N85-24071
Oscillations of gas turbine installation rotors under operating conditions 14 p2272 N85-24077
Abatement of noise and vibration in pipelines of hydro systems 14 p2276 N85-24102
Effect of apparent fluid masses on natural vibration frequencies of impellers of multistage centrifugal pumps
14 p2277 N85-24108
Recent developments in the dynamics of advanced rotor systems
[NASA-TM-86669] 14 p2317 N85-24320
Flow induced vibration of the SSME LOX posts
[NASA-CR-175606] 15 p2495 N85-25391
Frequency/period estimation and adaptive rejection of periodic disturbances
[AD-A149229] 15 p2632 N85-26226
Raman scattering of light in epitaxial films of solid phosphide-gallium arsenide solutions
15 p2643 N85-26301
Stability and vibrations of internal windings of high-current superconducting solenoid magnets
[AD-A151465] 15 p2656 N85-26390
Identification and control of structures in space
[NASA-CR-175790] 16 p2731 N85-26850
The effect of inaccuracies in structural models on the control of large space structures
[AD-A151794] 16 p2732 N85-26858
Flow dynamic environment data base development for the SSME 16 p2736 N85-26885
Vibration characteristics of the HPOTP (High Pressure Oxygen Turbopump) of the SSME (Space Shuttle Main Engine) 16 p2738 N85-26895
Flow-induced vibration of the SSME LOX posts: Additional issues
[DE85-007339] 16 p2741 N85-26916
Measurement of damping of graphite expoxy materials
[NASA-CR-175793] 16 p2743 N85-26925
Suppression of vibration effects on piezoelectric crystal resonators
[AD-D011625] 16 p2778 N85-27142
Quasi-steady vibrations of a rotating shaft grazing an obstacle: Spiral vibration
[BLL-CE-TRANS-7962-(9022.09)]
16 p2799 N85-27256
Quantum statistical theory of vibrational dynamics in a laser-driven admolecule-surface system
[AD-A152022] 16 p2872 N85-27719
Natural vibrations of reinforced spherical shells
17 p2943 N85-28165
DOE/ANL/HTRI heat exchanger tube vibration data bank: Addendum 5
[DE85-007730] 17 p2960 N85-28425
Telescoping low vibration pulling mechanism for Czochralski crystal growth
[AD-D011655] 17 p3044 N85-28838
Turbine blade-tip clearance excitation forces
[NASA-CR-171534] 19 p3220 N85-29963
Forced structural response using component mode synthesis
[DE85-008479] 19 p3287 N85-30383
Vibration control experiment design for the 15-m hoop/column antenna 20 p3409 N85-31159
Time-optimal bang-bang slew of rigidized SCOLE configuration 20 p3410 N85-31164
Numerical and experimental evaluation for single-axis control of an LSS laboratory model
20 p3411 N85-31168
On the measurement of material damping in a simulated space environment 20 p3411 N85-31169
A phase-locked frequency multiplier for the signal averaging of the vibration of the Wessex helicopter input spiral bevel pinion
[AD-A154914] 21 p3555 N85-32113
Proposal for modifications to the Wessex helicopter main rotor gearbox vibration monitoring program
[AD-A155196] 21 p3555 N85-32117
Calculation of molecular constants potential energy curves and Franck-Condon factors for lead oxide
[AD-A154521] 21 p3562 N85-32158
Development of a temperature-compensated hot-film anemometer system for boundary-layer transition detection on high-performance aircraft
[NASA-TM-86732] 22 p3730 N85-33121
A modal parameter extraction procedure applicable to linear time-invariant dynamic systems
[NASA-CR-176120] 22 p3835 N85-33747
Accelerator vibration issues
[DE85-010766] 22 p3842 N85-33791
Dual optical mechanical position tracker
[AD-D011739] 22 p3844 N85-33811
Generated spiral bevel gears: Optimal machine-tool settings and tooth contact analysis
[NASA-TM-87075] 23 p3937 N85-34405
Nonlinear flap-lag-extensional vibrations of rotating, pretwisted, preconed beams including Coriolis effects
[NASA-TM-87102] 23 p3941 N85-34427
Laboratory vibration schedules
[AD-A155856] 24 p4064 N85-35188
Vibrations of free hollow circular cylindrical bodies
24 p4100 N85-35418
A normal incidence X-ray telescope sounding rocket payload
[NASA-CR-176169] 24 p4153 N85-35749

VIBRATION DAMPERS
U VIBRATION ISOLATORS

VIBRATION DAMPING
Modular design attitude control system
[NASA-CR-171182] 01 p0016 N85-10096
Highlights of the Institute of Sound and Vibration Research 01 p0131 N85-10905
Simulation of vibration processes in damped structures with allowance for temperature-frequency characteristics of vibration absorbing materials
02 p0257 N85-11680
Basic study of bladed disk structural response
[AD-A146226] 03 p0319 N85-12061
An appraisal of an out-of-phase feed-back system for the variation of damping of dynamic wind-tunnel models
[NMI-189] 03 p0320 N85-12065
Turbine blade damping study
[NASA-CR-171255] 04 p0456 N85-12890
Turbine blade damping study, introduction
04 p0456 N85-12891
Forced vibrations of friction-damped beam structures in two dimensions
[UDR-TM-82-08] 04 p0456 N85-12892
Experiments in control of flexible structures with uncertain parameters 05 p0602 N85-13837
Damping capacity of a sealed squeeze film bearing
05 p0645 N85-14139
F-8 refueling boom ground vibration test
[NASA-TM-84914] 07 p0902 N85-15713
Study to eliminate ground resonance using active controls
[NASA-CR-166609] 07 p0902 N85-15715
Damping capacity of multilayer tube during torsion
[BLL-M-36011-(5828.4)] 07 p0977 N85-16202
Photoemission, vibrational and stimulated desorption studies of metal-semiconductor interfaces and of chemisorbed atoms and molecules
[AD-A147709] 08 p1225 N85-17717
Shock response analysis by personal computer using the extended IFT algorithm 09 p1335 N85-18397
Experimental investigation of vibroimpact of two cantilever beams 09 p1336 N85-18399
The Shock and Vibration Bulletin 54. Part 3: Structural dynamics, machinery dynamics and vibration problems
[AD-A148133] 09 p1337 N85-18406
Structural modifications by viscoelastic elements
09 p1337 N85-18407
Stochastic dynamic analysis of a structure with frictional joints 09 p1337 N85-18408
The experimental performance of an off-road vehicle utilizing a semi-active suspension — off-road motorcyles
09 p1339 N85-18421
A theoretical investigation of an active suspension system for wheeled tractors
[AD-P004268] 09 p1405 N85-18844
Variable friction secondary seal for face seals
[NASA-CASE-LEW-14170-1] 11 p1647 N85-20377
The effect of an elastic foundation and of dissipative forces on the stability of fluid conveying pipes
[TAE-563] 12 p1663 N85-21668
A quantitative comparison of active and passive damping for large space structures
[UTIAS-TN-249] 13 p1998 N85-22524
Dynamic verification of large space structures
14 p2234 N85-23847
Passive and Active Control of Space Structures (PACOSS) 14 p2234 N85-23848
ACOSS 11 (Active Control Of Space Structures)
[AD-A150639] 14 p2246 N85-23922
Measurement of damping of graphite epoxy materials
[NASA-CR-175663] 14 p2248 N85-23931
Selection of bearing type for large steam turbines
14 p2271 N85-24069
Modeling and control of large flexible structures, phase 1
[AD-A150736] 14 p2403 N85-24817
Preliminary results on passive eddy current damper technology for SSME turbomachinery
16 p2737 N85-26890
A study of internal and distributed damping for vibrating turbomachiner blades
[NASA-CR-175901] 17 p2898 N85-27868
Stressed-strained state of tightening buckles in sectional runners of gas turbines 17 p2940 N85-28149
Continuum modeling of latticed structures
17 p2977 N85-28399
Vibration control of rotor shaft
[NASA-TM-87053] 18 p3117 N85-29292
Spillover minimization: An approach for actuators and sensors placement in distributed parameter study
[INPE-3525-PRE/746] 19 p3272 N85-30269
Variable force, eddy-current or magnetic damper
[NASA-CASE-LEW-13717-1] 19 p3279 N85-30333
A dual spin space station design
20 p3408 N85-31152
Stiffness control of large space structures
20 p3414 N85-31189
Sub-optimal control of nonlinear flexible space structures 20 p3414 N85-31190
Adaptive filtering for large space structures: A closed-form solution 20 p3417 N85-31206
A comparison of experimental and theoretical results for rotordynamic coefficients of four annular gas seals
[NASA-CR-176086] 21 p3596 N85-32332
Modelling and parameter estimation for distributed vibratory systems
[AD-A154518] 21 p3598 N85-32344
Fixed gain and adaptive techniques for rotorcraft vibration control
[NASA-CR-177344] 22 p3728 N85-33111
Flutter clearance of the Schweizer 1-36 deep-stall sailplane
[NASA-TM-85917] 22 p3729 N85-33118
A substructure coupling procedure applicable to general linear time-invariant dynamic systems
[NASA-CR-176144] 22 p3800 N85-33542
Multishaker modal testing
[NASA-CR-176139] 22 p3800 N85-33544

VIBRATION EFFECTS
NT POGO EFFECTS
Singular asymptotic expansions in nonlinear rotordynamics
[NASA-CR-174012] 01 p0017 N85-10100
The effects of helicopter vibration on the spinal system
[AD-A146274] 03 p0402 N85-12562
Experimental investigation of vibroimpact of two cantilever beams 09 p1336 N85-18399
Structural modifications by viscoelastic elements
09 p1337 N85-18407
Propeller propulsion system integration: State of technology survey
[NASA-CR-3882] 12 p1771 N85-21119
Role of mental work in human tolerance in total-body vibration 12 p1901 N85-21940

Singular asymptotic expansions in nonlinear rotordynamics 12 p1945 N85-22218
Suppression of vibration effects on piezoelectric crystal resonators
[AD-D011625] 16 p2778 N85-27142
Dual species ion implantation of ternary compounds based on In-Ga-As
[AD-D011617] 16 p2869 N85-27698
Flow-induced vibration of SSME main injector liquid-oxygen posts 17 p2912 N85-27951
Vibrations of rotors connected through couplings with backlash 17 p2940 N85-28147
Stressed-strained state of tightening buckles in sectional runners of gas turbines 17 p2940 N85-28149
A mechanical model of the human body and its application 24 p4129 N85-35596

VIBRATION ISOLATORS
Extended aeroelastic analysis for helicopter rotors with prescribed hub motion and blade appended penduluum vibration absorbers
[NASA-CR-172455] 03 p0315 N85-12038
Optimum design for nonlinear shock mounts for transient inputs 09 p1334 N85-18390
Gear case vibration isolation in a geared turbine generator 09 p1338 N85-18414
The analysis by the lumped parameter method of slade platform friction dampers used in the high pressure fuel turbopump on the space shuttle main engine
09 p1338 N85-18417
Vibrational loading mechanism of unitized corrugated containers with cushions and non-load-bearing contents
09 p1339 N85-18419
Vibration isolated cold plate assembly
[AD-D011444] 10 p1484 N85-19368
Evaluation of air and ground launched cruise missile navigational element containers
[AD-A149654] 12 p1774 N85-21138
Vibration isolator actuator
[AD-D011574] 14 p2321 N85-24343
Helicopter rotor
[CH-637890-A5] 15 p2470 N85-25245
Frequency/period estimation and adaptive rejection of periodic disturbances
[AD-A149229] 15 p2632 N85-26226
Preliminary results on passive eddy current damper technology for SSME turbomachinery
16 p2737 N85-26890
Consolidation theory with consideration of frame plasticity
[REPT-9/1984] 16 p2796 N85-27240
Aircraft rotor blade with passive tuned tab
[NASA-CASE-ARC-11444-1] 19 p3217 N85-29947
Variable force, eddy-current or magnetic damper
[NASA-CASE-LEW-13717-1] 19 p3279 N85-30333
Fast scintillation counter preamplifier for the observation of Linsley effect
[HE-4.7-9] 24 p4199 N85-36060
A mini-array for large air showers
[HE-4.7-10] 24 p4199 N85-36061

VIBRATION MEASUREMENT
The monitoring of machines
[CETIM-15-J-041] 04 p0510 N85-13253
Measuring large amplitudes of mechanical vibrations with laser interferometers 06 p0787 N85-15028
Emitted vibration measurement device and method
[NASA-CASE-MFS-25981-1] 11 p1635 N85-20299
Applications of the vibration probe to localized current measurements
[DE85-004702] 13 p2023 N85-22675
Ultrafast holography using optical fibers
[ISL-CO-238/83] 16 p2788 N85-27204
Monitoring of turbo-machines by shaft vibration measurement
[BLL-CE-TRANS-7900-(9022.09)]
16 p2799 N85-27255
Measurement of damping of graphite epoxy materials
[NASA-CR-176073] 21 p3596 N85-32334

VIBRATION METERS
NT SEISMOGRAPHS
System for automatic recording of vibration parameters 14 p2262 N85-24135

VIBRATION MODE
Helicopter rotor blade design for minimum vibration
[NASA-CR-3825] 01 p0006 N85-10032
Theoretical and experimental modal analysis of a rotor test rig — shipboard equipment
[AMTE(N)-TM-83079] 03 p0371 N85-12370
The use of an optical data acquisition system for bladed disk vibration analysis
[NASA-TM-86891] 06 p0817 N85-15184
The Shock and Vibration Digest, volume 16, no. 10
[AD-A147588] 09 p1331 N85-18361
A review of approximate methods for determining the vibrational modes of membranes
09 p1331 N85-18363
Optimization of vibrating beams including the effects of coupled bending and torsional modes
09 p1331 N85-18364
Leakage-flow-induced vibration of a tube-in-tube slip joint
[DE84-007301] 11 p1652 N85-20406
Unsteady transonic pressure measurements on a semi-span wind-tunnel model of a transport-type supercritical wing (Lann model). Part 2: Pressure distributions (plotted) and plots of the vibration modes
[AD-A130488] 12 p1846 N85-21579
Spline-based Rayleigh-Ritz methods for the approximation of the natural modes of vibration for flexible beams with tip bodies
[NASA-CR-172566] 13 p2102 N85-23100
Effect of axisymmetric vibration modes on sensitivity and di rectivity characteristics of piezoceramic sphere — hydrophones 15 p2525 N85-25569
Ultrafast holography using optical fibers
[ISL-CO-238/83] 16 p2788 N85-27204
A natural modes formulation and modal identities for structures with linear viscous damping
[CRC-1382] 18 p3120 N85-29312

VIBRATION PROTECTION
U VIBRATION ISOLATORS

VIBRATION SIMULATORS
The changing vibration simulation for military ground vehicles 09 p1334 N85-18387

VIBRATION TESTING MACHINES
U VIBRATION SIMULATORS

VIBRATION TESTS
NT DAMPING TESTS
Vibration, acoustic, and shock design and test criteria for components on the Solid Rocket Boosters (SRB), Lightweight External Tank (LWT), and Space Shuttle Main Engines (SSME)
[NASA-RP-1127] 01 p0061 N85-10405
F-8 refueling boom ground vibration test
[NASA-TM-84914] 07 p0902 N85-15713
Transient vibration test criteria for spacecraft hardware — galileo spacecraft 09 p1338 N85-18418
Flow-induced tube vibration thresholds in heat exchangers from shellside water tests
[DE84-006603] 11 p1652 N85-20407
Steam generator tube vibration tests
[DE85-003599] 12 p1867 N85-21712
Vibroacoustic study of the NASA Goddard Space Flight Center OSS-1 payload
[NASA-CR-175320] 13 p1988 N85-22465
Investigation of gas-turbine engine blower impeller vibrations with change in engine intake conditions
14 p2287 N85-24170
Vibrations of rotors connected through couplings with backlash 17 p2940 N85-28147
Seakeeping and vibration tests of the Coast Guard 110 foot surface effect ship SEA BIRD class (WSES)
[AD-A154150] 19 p3252 N85-30166

VIBRATIONAL FREQUENCIES
U VIBRATIONAL SPECTRA

VIBRATIONAL RELAXATION
U MOLECULAR RELAXATION

VIBRATIONAL SPECTRA
Vibrational power transmission of an idealised gearbox
[ISVR-TR-124] 02 p0204 N85-11346
Optimizing CW CO2 lasers with respect to output power in different bands 02 p0271 N85-11768
Structure of vibrational spectrum and selection rules in Raman and hyper-Raman light scattering spectra of inorganic glasses 02 p0271 N85-11789
Molecular beam scattering 03 p0417 N85-12666
Investigation on experimental techniques to detect, locate and quantify gear noise in helicopter transmissions
[NASA-CR-3847] 08 p1217 N85-17667
Quantum mechanical and semiclassical approaches to molecular dynamics
[DE85-003458] 10 p1555 N85-19803
An analysis of short-to-medium-range seismic attenuation tests using a multilayered viscoelastic seismic propagation model
[AD-A149771] 12 p1869 N85-21856
Adsorption site, adsorption energy and normal vibration frequency of H/Ni(100) via total energy calculations
[AD-A150555] 13 p2156 N85-23368
Observation of surface vibrational resonances on (110) surfaces of FCC metals
[AD-A150469] 13 p2163 N85-23419
Dipole active surface vibrational resonances on clean and hydrogen covered Ni(110)
[AD-A150546] 13 p2163 N85-23420
Calculations of collision-induced optical gain in high-density mixtures of D2 or HD with a buffer gas
[AD-A151372] 15 p2648 N85-26330
A measurement of the vibrational band strength for the upsilon sub 3 band of the HO2 radical
[NASA-CR-175858] 16 p2744 N85-26936
Vibrational spectra of a-Fe(.78)P(.22) by inelastic neutron scattering
[DE85-008298] 17 p2922 N85-28016
Investigation of several low-lying levels of X doublet pi state of NCO using argon laser excited fluorescence
[AD-A153693] 18 p3071 N85-28994
Vibrational properties of disordered solids: Far infrared studies
[DE85-010400] 19 p3377 N85-30951
Requirements for attaining Treanor's distribution of vibrational energy among CO2 levels in CW gasdynamic laser flows
[STN-3] 20 p3481 N85-31499
Modelling and parameter estimation for distributed vibratory systems
[AD-A154518] 21 p3598 N85-32344
Time-resolved spectroscopic studies of detonating heterogeneous explosives
[DE85-009760] 23 p3921 N85-34297
The photodissociation of acetylene at 193.3 NM
[AD-A155775] 24 p4075 N85-35255
Circumstellar shells of late-type stars: A study at millimeter and infrared wavelengths
24 p4167 N85-35836

VIBRATIONAL STRESS
Influence of secondary flow rate on dynamic stresses in turbine rotor blades 09 p1306 N85-18205
Comparison of measured and simulated ride comfort for an agricultural tractor and influence of travel speed and tyre-inflation pressure on dynamic response
[AD-P004281] 09 p1407 N85-18857
Investigation of gas-turbine engine blower impeller vibrations with change in engine intake conditions
14 p2287 N85-24170

VIBRATORY LOADS
Damping capacity of multilayer tube during torsion
[BLL-M-36011-(5828.4)] 07 p0977 N85-16202
Measurement and evaluation of the loading of shafts by torsional vibrations 07 p0980 N85-16222
Vibrational loading mechanism of unitized corrugated containers with cushions and non-load-bearing contents
09 p1339 N85-18419

VIBROMETERS
U VIBRATION METERS

VIDEO COMMUNICATION
Videotex and weather services: Finnish applications
01 p0084 N85-10567
Video concepts in CRM training
09 p1276 N85-18015
Combined processing method and matched filter for discrete composite frequency phase-shift keyed signal
13 p2070 N85-22931
Development of thin film hybrid IC active filter for video band use
[NHK-LABS-NOTE-312] 18 p3094 N85-29153
Optical multiplexing on monomode fibers
[ENST-83E016] 20 p3533 N85-31982

VIDEO DATA
Flight demonstration of new NRL real-time data acquisition system and laser video waveform sampler
[AD-A145126] 01 p0053 N85-10350
Videotex and weather services: Finnish applications
01 p0084 N85-10567
High-speed videography for optical and X-ray imaging
[DE84-012661] 04 p0564 N85-13595
Atmospheric wind and diffusion from analysis of an SF6 release at 350 km altitude
[AD-A147965] 08 p1185 N85-17471
Producing high scene content with perspective validity
[AD-P004314] 09 p1268 N85-17968
Automated and interactive data base generation
[AD-P004316] 09 p1268 N85-17970
Geographic subdivision and top level data structures, Columbus, Magellan, and expanding CIG (Computer Image Generation) horizons
[AD-P004317] 09 p1268 N85-17971
CIG (Computer image generation) data bases in an instance: Bits and pieces
[AD-P004318] 09 p1269 N85-17972
Extracting digital data from a bus and multiplexing it with a video signal
[AD-D011491] 11 p1636 N85-20302
Television animation store: Digital chroma, key and mixer units
[BBC-RD-1984/16] 12 p1824 N85-21442
Performance of time-position discriminator of composite signal 13 p2072 N85-22941
Evaluating identifiability in remote sensing problems
15 p2486 N85-25347
Processing speech for analysis using optical Fourier techniques
[AD-A151898] 15 p2544 N85-25704
Design issues in video disc map display
[AD-A153531] 18 p3109 N85-29253
Video discs - what are they and where do they fit in?
[AD-A154166] 20 p3458 N85-31479

Balloon-borne video cassette recorders for digital data storage
[OG-9.3-11] 21 p3715 N85-33050
Relaxation techniques
[AD-A156248] 24 p4133 N85-35621
Aeronautical Systems Division Manufacturing/Quality assurance orientation
[AD-A156128] 24 p4164 N85-35817

VIDEO DISKS
Requirements and specifications for cartographic video discs
[AD-A144906] 01 p0049 N85-10325
Analog disc recorder system: Operator's reference manual
[DE84-016926] 04 p0503 N85-13209
Low altitude high speed flight simulation using video disc technology
[AD-P004312] 09 p1268 N85-17966
Design issues in video disc map display
[AD-A153531] 18 p3109 N85-29253
Video discs - what are they and where do they fit in?
[AD-A154166] 20 p3458 N85-31479
Realizing the full potential of the video disc for mapping applications
[AD-A154966] 21 p3606 N85-32391
Electronic file system on an SM 90 minicomputer: The SARDE project
[ENST-84E018] 22 p3828 N85-33705
Balloon-borne video cassette recorders for digital data storage
[OG-9.3-11] 23 p4028 N85-34966

VIDEO EQUIPMENT
NT PICTURE TUBES
Development of a dynamic radiographic capability using high-speed video
[DE84-016477] 04 p0511 N85-13256
Visual systems for remotely controlled vehicles
05 p0703 N85-14512
VICOM technical description
[REPT-611-0012-REV-A] 08 p1202 N85-17563
Television animation store: Recording pictures on a parallel transfer magnetic disc
[BBC-RD-1984/17] 10 p1462 N85-19220
Video animation system
[DE85-005494] 14 p2405 N85-24831
Operation of autotracking system in various video playback modes 16 p2764 N85-27055
Atmospheric Emission Photometric Imaging (AEPI)
23 p3902 N85-34170

VIDEO SIGNALS
Transient currents of ideally conducting body of revolution with transient diffraction
06 p0785 N85-15019
Electrooptical sensor for automatic detection of objects 06 p0789 N85-15040
New technology high efficiency and high stability color motion video compression system
[AD-A147523] 07 p0941 N85-15968
Analysis of threshold effects during estimation of arrival time of optical signals 07 p0951 N85-16030
Extracting digital data from a bus and multiplexing it with a video signal
[AD-D011491] 11 p1636 N85-20302
Television camera video level control system
[NASA-CASE-MSC-18578-1] 12 p1821 N85-21427
Operation of autotracking system in various video playback modes 16 p2764 N85-27055
Hardware test program for evaluation of baseline range-range rate sensor concept
[NASA-CR-175794] 16 p2787 N85-27193
Synthesis of optimum receiver and processor for interfering radio pulse signals 22 p3769 N85-33361

VIDICONS
NT RETURN BEAM VIDICONS
NT THERMICONS
Programmable optical sensor
[AD-D011244] 02 p0281 N85-11829
Mars polar volatiles: Topographic and geologic setting
[NASA-CR-174089] 04 p0581 N85-13706
The development of new techniques in laser spectroscopy 19 p3233 N85-30041
LI481 and LI482 vidicons for two-tube color TV cameras with improved image quality 22 p3764 N85-33333

VIEW EFFECTS
Integration of multispectral data obtained at different view angles for vegetation analysis
05 p0657 N85-14218

VIEWING
NT FIELD OF VIEW
Improved radiographic viewing system
[AD-A147587] 07 p1016 N85-16456
Double window viewing chamber assembly
[NASA-CASE-MFS-28057-1] 18 p3063 N85-28951

VIKING LANDER SPACECRAFT
NT VIKING LANDER 1
Conclusion of Viking Lander Imaging Investigation: Picture catalog of experiment data record
[NASA-RP-1137] 11 p1765 N85-21099
The search for igneous materials at the Viking landing sites 13 p2194 N85-23609

VIKING LANDER 1
Analysis of the Viking Lander 1 surface wind vector for sols 45 to 375
[NASA-CR-174349] 09 p1416 N85-18932
Observed changes at Viking Lander 1
13 p2188 N85-23575

VIKING MARS PROGRAM
The Mars ancient cratered terrain, smooth plains boundary: Implications of Viking color data for evolution of the Amenthes Region 15 p2682 N85-26564

VIKING ORBITER SPACECRAFT
Geomorphic classification of Icelandic and Martian volcanoes: Limitations of comparative planetology research from LANDSAT and Viking orbiter images
21 p3603 N85-32372

VIKING SPACECRAFT
NT VIKING LANDER SPACECRAFT
NT VIKING LANDER 1
NT VIKING ORBITER SPACECRAFT
Participation in the Mars Data Analysis Program: Analysis of cloud forms in Viking and Mariner 9 images
[NASA-CR-175604] 13 p2204 N85-23673

VIKING 1 SPACECRAFT
NT VIKING LANDER SPACECRAFT
NT VIKING LANDER 1
NT VIKING ORBITER SPACECRAFT

VIKING 2 SPACECRAFT
NT VIKING LANDER SPACECRAFT
NT VIKING ORBITER SPACECRAFT

VINYL COPOLYMERS
Vinyl citrates from citric acid as new monomers
[BMFT-FB-T-83-256] 03 p0336 N85-12178
Ferroelectric homopolymer PVF2 and P (VDF-TrFe) copolymers 24 p4089 N85-35347

VINYL CYANIDE
U ACRYLONITRILES

VINYL ETHYLENE
U BUTADIENE

VINYL POLYMERS
NT POLYVINYL FLUORIDE
Development of new and improved polymer matrix resin systems, phase 1
[NASA-CR-166595] 01 p0017 N85-10104
Dynamic polymer pressure transducer with temperature compensation
[AD-D011373] 07 p0967 N85-16142
Chiral polymers
[AD-A150366] 13 p2037 N85-22760
A new large-scale, high-resolution multicolor software display concept
[AD-A155404] 22 p3827 N85-33703
Development and demonstration of a spiral-wound thin-film composite membrane system for the economical production of oxygen-enriched air, phase 4
[DE85-012380] 23 p3920 N85-34288
High temperature polymer concrete
[DE85-005756] 23 p3920 N85-34290

VINYL RADICAL
(Vinyloxy)fluorocyclotriphosphazenes
[AD-A147448] 07 p0924 N85-15850

VINYLIDENE
Synthesis and characterization of poly(vinylidene fluoride)
[AD-A150291] 13 p2037 N85-22759
C2H(n) fragments on metal surfaces
[AD-A151474] 15 p2505 N85-25449

VIOLENCE
NT ATTACKING (ASSAULTING)

VIRGINIA
Late precambrian to ordovician metamorphism and orogenesis in the Blue Ridge and western Piedmont, Virginia Appalachians 09 p1352 N85-18503
Intraband radiometric performance of the LANDSAT 4 Thematic Mapper — Washington, DC, Arkansas, Massachusetts, Virginia, and Arizona
12 p1871 N85-21738

VIRGO GALACTIC CLUSTER
Virgo cluster as a high energy cosmic rays source
[OG-5.4-8] 22 p3886 N85-34085

VIRGO STAR CLUSTER
U VIRGO GALACTIC CLUSTER

VIRIAL COEFFICIENTS
A virial equation of state option for the TIGER computer program
[AD-A147490] 07 p1025 N85-16507
Measurement of gas compressibility factor data for natural gas and synthetic gas components and their mixtures
[PB85-129047] 11 p1614 N85-20151
Observations of current pulsations of characteristics in atmosphere with period of about 1.5 hours
14 p2341 N85-24480

VIRIAL THEOREM
On experimental equations of state for Boson gases
[PTB-ME-61] 04 p0574 N85-13659
Potential at atomic boundaries in the TF (or TFD) model and equations of states 12 p1820 N85-21419

VIRTUAL PROPERTIES
The principle of virtual work and associated variational principles
[ESA-TT-873] 09 p1340 N85-18428

VIRUSES
Molecular interactions of high energy fuels and jet fuels with oncogenic viruses and endogenous viruses
[AD-A145484] 02 p0188 N85-11255
The effects of simulated weightlessness on susceptibility to viral and bacterial infections using a murine model
15 p2613 N85-26100
Using the information of cosmic rays to predict influence epidemic
[SH-10.1-2] 23 p4053 N85-35134

VISCERA
NT ADRENAL GLAND
NT BLADDER
NT INTESTINES
NT KIDNEYS
NT LIVER
NT LUNGS
NT ORGANS
NT PANCREAS
NT PARATHYROID GLAND
NT PITUITARY GLAND
NT RECTUM
NT SPLEEN
NT THYMUS GLAND
NT THYROID GLAND

VISCOELASTIC DAMPING
A quantitative comparison of active and passive damping for large space structures
[UTIAS-TN-249] 13 p1998 N85-22524
Finite element prediction of loss factors for structures with frequency-dependent damping treatments
15 p2576 N85-25889

VISCOELASTIC FLOW
U VISCOELASTICITY

VISCOELASTICITY
NT PHOTOVISCOELASTICITY
NT THERMOVISCOELASTICITY
Nuclear Magnetic Resonance of Polymeric Materials
[AD-A145078] 01 p0032 N85-10192
NMR (Nuclear Magnetic Resonance) and macromolecular migration in a melt or in concentrated solutions
[AD-P003908] 01 p0032 N85-10194
On wave propagation in linear viscoelasticity
[AD-A144739] 01 p0111 N85-10750
Determination of nonlinear viscoelasticity parameters for polymeric and composite materials by numerical methods
[AD-A145311] 02 p0185 N85-11240
Acceleration waves 02 p0207 N85-11367
Accelerated viscoelastic characterization of T300/5208 graphite-epoxy laminates 03 p0325 N85-12091
Numerical simulations of compliant material response to turbulent flow, revision 1
[AD-A145801] 03 p0372 N85-12373
Finite element method for a class of viscoelastic flows in deforming domains applied to jet breakup
[DE84-014571] 04 p0500 N85-13186
Dynamics of liquid filament breakup
[DE84-016008] 04 p0500 N85-13187
Constraints on the origin of viscoelastic bodies
04 p0584 N85-13732
Existence of slow steady flows of viscoelastic fluids with differential constitutive equations
[AD-A147240] 07 p0959 N85-16077
Study of reaction kinetics and development of elastic properties in network polymerization systems by the impulse technique
[AD-A148187] 08 p1133 N85-17141
An efficient numerical solution technique for wave propagation in horizontally stratified ocean environments
[AD-A148537] 08 p1190 N85-17502
A finite element analysis of viscoelastic materials with varying time scales 09 p1330 N85-18355
Structural modifications by viscoelastic elements
09 p1337 N85-18407
Recent developments and open problems in the mathematical theory of viscoelasticity
[AD-A149043] 10 p1545 N85-19742
Single integral constitutive equations for viscoelastic fluids
[AD-A149410] 10 p1547 N85-19756
Stability of viscoelastic constructions subjected to steady random compressing loads 11 p1720 N85-20619

Accelerated viscoelastic characterization of T300-5208 graphite-epoxy laminates [NASA-CR-3871] 12 p1797 N85-21271

Algorithm for the simulation of transient viscoelastic flows with free surfaces [DE85-002713] 12 p1848 N85-21590

Journal of Research of the National Bureau of Standards, volume 89, number 2, March - April 1984 [PB85-115426] 12 p1926 N85-22103

Mechanics of polymers and composites: Research opportunities [DE85-007052] 15 p2503 N85-25442

Fracture problems in power law viscoelastic materials [AD-A149221] 15 p2578 N85-25900

Uniqueness and stability in nonlinear elasticity and viscoelasticity [AD-A151470] 15 p2637 N85-26264

Dynamic response of shells and plates subjected to variable magnitude traveling loads 16 p2798 N85-27250

Vortices in non-Newtonian fluids [AD-A153169] 17 p2958 N85-28269

Theoretical and experimental studies of the mechanics of viscoelastic liquids [AD-A153505] 18 p3070 N85-28987

Hyperbolic phenomena in the flow of viscoelastic fluids [AD-A153533] 18 p3099 N85-29186

Prediction of lifetime for ceramic materials in the elastic and viscoelastic region by fracture mechanical methods [ESA-TT-825] 20 p3434 N85-31305

Finite element methods for viscoelastic flow [AD-A154877] 22 p3783 N85-33437

Experimental study on time and temperature dependent behavior of crack growth in viscoelastic strip 23 p3905 N85-34193

Viscoelastic behavior of short-fiber composite materials [DE85-011233] 23 p3910 N85-34225

Three-dimensional finite deformation viscoelastic model accounting for damage effects [DE85-012951] 24 p4139 N85-35660

VISCOMETRY

Interpolation formulas for viscosity of six gases: Air, nitrogen, carbon dioxide, helium, argon and oxygen [PB84-217801] 01 p0026 N85-10161

VISCOPLASTIC FLOW

U VISCOPLASTICITY

VISCOPLASTICITY

Viscoplastic finite element analysis of rapid fracture 03 p0370 N85-12365

Life prediction at high temperature under multiaxial loading 07 p0907 N85-15745

Viscoplastic constitutive relationships with dependence on thermomechanical history [NASA-CR-174836] 12 p1864 N85-21691

On thermomechanical testing in support of constitutive equation development for high temperature alloys [NASA-CR-174879] 15 p2577 N85-25894

Uniqueness and stability in nonlinear elasticity and viscoelasticity [AD-A151470] 15 p2637 N85-26264

Some advances in experimentation supporting development of viscoplastic constitutive models [NASA-CR-174855] 16 p2799 N85-27260

Interaction of large amplitude stress waves in layered elastic-plastic materials [AD-A153519] 18 p3121 N85-29323

Nonlinear Constitutive Relations for High Temperature Application, 1984 [NASA-CP-2369] 20 p3465 N85-31530

Viscoplasticity based on overstress with a differential growth law for the equilibrium stress 20 p3466 N85-31532

Constitutive modeling of superalloy single crystals and directionally solidified materials 20 p3466 N85-31535

On the use of internal state variables in thermoviscoplastic constitutive equations 20 p3466 N85-31536

Physical concepts in the development of constitutive equations 20 p3467 N85-31537

Some advances in experimentation supporting development of viscoplastic constitutive models 20 p3468 N85-31545

Creep crack growth predictions in INCO 718 using a continuum damage model 20 p3469 N85-31551

Short-time creep of ice [NRC/CNR-TT-2111] 23 p3941 N85-34428

Development and application of a unified viscoelastic constitutive model for the prediction of material response under thermomechanical loading 24 p4101 N85-35420

VISCOSITY

NT EDDY VISCOSITY

NT GAS VISCOSITY

Interpolation formulas for viscosity of six gases: Air, nitrogen, carbon dioxide, helium, argon and oxygen [PB84-217801] 01 p0026 N85-10161

Laminar flow heat exchangers. Viscosity induced non-uniform flow [AD-A144777] 01 p0047 N85-10307

External fuel vaporization study, phase 2 [NASA-CR-174079] 02 p0187 N85-11252

An investigation of the suitability of using a Sieglaff-McKelvey high shear rate melt rheometer for the measurement of low viscosity polymer solutions [AD-A146275] 03 p0338 N85-12174

Numerical simulations of fuel droplet flows using a Lagrangian triangular mesh [AD-A146087] 03 p0362 N85-12320

Development of acceptance criteria for batches of silane primer for external tank thermal protection system bonding applications [NASA-CR-171266] 04 p0478 N85-13043

Toughening mechanism in elastomer-modified epoxy resins, part 2 [NASA-CR-3852] 04 p0478 N85-13046

A simple extension to multidimensional problems of the artificial viscosity due to Lapidus 06 p0806 N85-15134

Viscosity measurements for thick-film pastes 06 p0831 N85-15280

Structural relaxation and isoconfigurational flow of a metallic glass near equilibrium [AD-A147868] 07 p0933 N85-15915

Viscosity solutions of Hamilton-Jacobi equations at the boundary [AD-A147444] 07 p1032 N85-16553

On existence and uniqueness of solutions of Hamilton-Jacobi equations [AD-A147597] 07 p1033 N85-16560

Research into topics in transonic flow theory [AD-A148526] 08 p1078 N85-16837

A Van Leer shock capturing algorithm for the Euler equations [AD-A148761] 08 p1163 N85-17335

New discovery in supersonic flight research 09 p1278 N85-18041

Metallographic grinding efficiency [DE85-001520] 09 p1304 N85-18194

Blood viscosity responses to acute exercise and aerobic conditioning in women 09 p1363 N85-18573

Neumann type boundary conditions for Hamilton-Jacobi equations [AD-A149069] 10 p1546 N85-19746

Hamilton-Jacobi equations in infinite dimensions. Part 1. Uniqueness of viscosity solutions [AD-A149094] 10 p1546 N85-19749

Structure-phase state and properties of high-durability VAL8 alloy 11 p1597 N85-20046

Trends of petroleum fuels [DE85-000116] 14 p2263 N85-24023

Mixing in the solar interior 14 p2446 N85-25095

Models of solar differential rotation 14 p2446 N85-25097

Possible use of rapid heating for improving mechanical properties of titanium alloys 15 p2498 N85-25409

Mean free paths, viscosity, and the limitations of perfect fluid hydrodynamics in the description of the quark-gluon plasma [DE85-005501] 15 p2649 N85-26339

Viscosity in Saturn's rings 15 p2674 N85-26507

Characterization-curing-property studies of HBRF 55A resin formulations [NASA-CR-175836] 16 p2753 N85-26989

Aerodynamic performance of a wing in ground effect using the PANAIR program [AD-A153303] 17 p2892 N85-27832

Evaluation of used crankcase oils using computerized infrared spectrometry [AD-A152993] 17 p2920 N85-27999

Thermophysical properties correlations and pseudocomponent characterization parameter estimation for fossil fluids [DE85-009297] 19 p3230 N85-30024

Synthesis and characterization of novel polymers from non-petroleum sources for use in enhanced oil recovery [DE85-010922] 19 p3250 N85-30151

On spectral multigrid methods for the time-dependent Navier-Stokes equations [NASA-CR-172613] 19 p3344 N85-30725

Floating shock-fitting in transonic potential flow calculations 20 p3387 N85-31007

Large-time behavior of viscous surface waves [AD-A154805] 21 p3584 N85-32278

Thermophysical properties of fluids for the gas industry [PB85-196471] 22 p3747 N85-33227

Dynamic compensation of Venus's geoid: A comparison with Earth 22 p3858 N85-33888

Method for controlling the viscosity of siloxane oils [DE85-011586] 23 p3909 N85-34221

Measurement and correlation of jet fuel viscosities at low temperatures [NASA-CR-174911] 23 p3921 N85-34295

Chemoviscosity modeling for thermosetting resins, 2 [NASA-CR-177958] 24 p4073 N85-35243

Determination of the viscosity number of thermoplastics in dilute solution; polyamides (PA) [NASA-TM-77673] 24 p4081 N85-35296

Study of the parameters affecting the collapse of a rotating protostellar cloud 24 p4168 N85-35837

VISCOUS DAMPING

NT VISCOELASTIC DAMPING

Results for second order hyperbolic systems with viscous dumping [AD-A151100] 15 p2555 N85-25765

Viscosity in Saturn's rings 15 p2674 N85-26507

A natural modes formulation and modal identities for structures with linear viscous damping [CRC-1382] 18 p3120 N85-29312

VISCOUS DRAG

Aircraft drag reduction technology 08 p1070 N85-16782

Numerical study of large-eddy breakup and its effect on the drag characteristics of boundary layers [NASA-CR-3884] 12 p1797 N85-21272

VISCOUS FLOW

NT BOUNDARY LAYER FLOW

NT BOUNDARY LAYER SEPARATION

NT COUETTE FLOW

NT REATTACHED FLOW

NT SECONDARY FLOW

NT SEPARATED FLOW

NT STOKES FLOW

Prediction of aerodynamic characteristics of fighter wings at high angles of attack [AD-A145107] 01 p0003 N85-10017

Gas flow environment and heat transfer nonrotating 3D program 02 p0142 N85-10966

Nonsteady motion of solid sphere in compressible viscous fluid 02 p0269 N85-11753

Model equation for simulating flows in multistage turbomachinery [NASA-TM-86869] 03 p0315 N85-12036

Vorticity amplification in viscous flow around a body 03 p0360 N85-12309

Viscous-inviscid aerodynamic analysis of two-dimensional thrust augmentors [NASA-CR-177321] 04 p0451 N85-12861

Numerical calculations of stratified Ekman layer flow over ridges with a finite element model [DE84-014482] 04 p0499 N85-13179

Bicomponent flow problems in rheological fluid mechanics 05 p0635 N85-14073

Answering thermodynamic questions with three-dimensional viscous flow calculations 05 p0636 N85-14081

Review of requirements and status of simulation and scaling of transonic, viscous flows [AD-A146357] 06 p0806 N85-15137

Analytical modeling of circuit aerodynamics in the new NASA Lewis wind tunnel [NASA-TM-86912] 07 p0897 N85-15686

Recent advances in computational methods to solve the high-lift multi-component airfoil problem 08 p1068 N85-16774

Aerodynamic issues in the design of high-lift systems for transport aircraft 08 p1069 N85-16780

Research done at DERAT (October 1982 through September 1983); summary of principal results obtained [NASA-TM-77786] 08 p1228 N85-17730

Theoretical study of non-linear unsteady aerodynamics of a non-rigid lifting body [AD-P004169] 09 p1266 N85-17954

Numerical approach for the aerodynamic analysis if airfoils with laminar separation [NASA-CR-172496] 09 p1273 N85-18001

Numerical predictions for unsteady viscous flow past an array of cylinders 09 p1318 N85-18284

Viscous effects on transonic airfoil stability and response [NASA-TM-86374] 10 p1421 N85-18961

Thrust chamber performance using Navier-Stokes solution — space shuttle main engine viscous nozzle calculation [NASA-CR-171346] 10 p1430 N85-19019

A multistage time-stepping scheme for the Navier-Stokes equations [NASA-CR-172527] 10 p1483 N85-19365

Flow and plasticity via nonequilibrium molecular dynamics [DE85-001011] 10 p1555 N85-19804

Calculation of three-dimensional, viscous flow through turbomachinery blade passages by parabolic marching [NASA-TM-86984] 14 p2211 N85-23711

Stability of steady rotation of a cylinder filled with a stratified viscous incompressible fluid
14 p2276 N85-24112

Computations for segmented radial bearings
14 p2288 N85-24180

Contribution to the theory of stationary separation areas
[NASA-TM-77825] 14 p2300 N85-24244

The generation of three-dimensional body-fitted coordinate systems for viscous flow problems
[AD-A150861] 14 p2406 N85-24848

Numerical calculation of subsonic jets in crossflow with reduced numerical diffusion
[NASA-TM-87003] 15 p2472 N85-25263

Investigation of potential and viscous flow effects contributing to dynamic stall
[AD-A151696] 15 p2557 N85-25773

Viscous effects on blast wave flowfields
[AD-A152013] 15 p2558 N85-25779

Numerical solutions of 3-dimensional Navier-Stokes equations for closed bluff-bodies
[NASA-CR-175755] 15 p2636 N85-26255

A numerical procedure on three-dimensional parabolic flow in duct 16 p2692 N85-26620

Computational aerodynamics in designing aircraft
16 p2693 N85-26622

Recent progress in computational aerodynamics
16 p2693 N85-26626

The role of computational fluid dynamics in aeronautical engineering 16 p2694 N85-26629

Numerical analysis of flow non-uniformity in the hot gas manifold of the Space Shuttle main engine
16 p2738 N85-26899

Proceedings of the 9th US Air Force and the Federal Republic of Germany Data Exchange Agreement Meeting. Viscous and Interacting Flow Field Effects
[AD-A153020] 17 p2958 N85-28266

A second-order pressure-correction method for viscous incompressible flow
[REPT-84-15] 17 p2960 N85-28280

Numerical computation of space shuttle orbiter flow field
[NASA-CR-175912] 18 p3058 N85-28921

Instability at the interface between two shearing fluids in a channel
[AD-A153532] 18 p3099 N85-29185

Application of computational fluid dynamics to complex inlet ducts
[NASA-TM-87060] 19 p3265 N85-30247

Viscous flows in rotating pipes with internal cavities and related vortex breakdowns
[NASA-TM-86761] 20 p3454 N85-31447

A new finite element approach: Progress in inviscid flow computations
[NASA-TM-86434] 20 p3454 N85-31450

Tip vortex computer code SRATIP. User's guide
[NASA-CR-172603] 21 p3551 N85-32093

Large-time behavior of viscous surface waves
[AD-A154805] 21 p3584 N85-32278

Computation of three-dimensional, inviscid, rotational flows 21 p3587 N85-32296

A 3-D Euler method for internal transonic flows computation with a multi-domain approach
21 p3587 N85-32298

Exact solutions of singular equations for viscous transonic flows 21 p3683 N85-32882

On the importance of viscous dissipation in Io
22 p3855 N85-33873

Scalar/Vector potential formulation for compressible viscous unsteady flows
[NASA-CR-3921] 23 p3893 N85-34113

A three-dimensional viscous flow analysis for the helicopter tip vortex generation problem
[NASA-CR-3906] 23 p3893 N85-34114

Stability of two-dimensional immiscible flow to viscous fingering
[DE85-011403] 23 p3931 N85-34364

Elastohydrodynamic lubrication calculations used as a tool to study scuffing
[NASA-TM-87097] 23 p3938 N85-34408

Cooling high intensity atomic hydrogen beams to liquid helium temperatures
[DE85-012515] 24 p4148 N85-35716

VISCOUS FLUIDS

Fluctuation spectrum for linear gyroviscous MHD
[IPP-6/237] 01 p0121 N85-10828

Wave propagation in compliant tubes containing a heat-conducting viscous fluid
[WTHD-163] 05 p0638 N85-14094

Sedimentation of two arbitrarily oriented spheroids in a viscous fluid
[AD-A147303] 07 p0960 N85-16062

Analysis of the surface load and radiated sound of a vibrating airfoil with application to the experiment of Brooks
[NASA-CR-3864] 07 p1036 N85-16590

Boundary layer at moving cylinder surface
16 p2765 N85-27064

Theoretical and experimental studies of the mechanics of viscoelastic liquids
[AD-A153505] 18 p3070 N85-28967

Instability at the interface between two shearing fluids in a channel
[AD-A153532] 18 p3099 N85-29185

Couette flow of two fluids between concentric cylinders
[AD-A155827] 24 p4093 N65-35376

VISIBILITY

Shipboard measurement of cloud bases and average surface visibility with an eye-safe lidar
[AD-A144889] 01 p0052 N85-10345

Joint probability of selected cloud and visibility thresholds around Koblenz, Germany
[AD-A145294] 02 p0231 N85-11506

Air-to-air visual acquisition performance with TCAS 2
[FAA-PM-84-17] 02 p0236 N85-11537

Visibility of various target-background color combinations under different chromatic ambient illuminations
[AD-A146348] 03 p0420 N85-12684

Revised Uniform Summary of Surface Weather Observations (RUSSWO). Alconbury RAF United Kingdom, parts A-F
[AD-A146913] 07 p1004 N85-16384

Revised Uniform Summary of Surface Weather Observations (RUSSWO). McChord AFB, Washington, parts A-F
[AD-A146914] 07 p1005 N85-16385

Revised Uniform Summary of Surface Weather Observations (RUSSWO). Mildenhall RAF, United Kingdom, parts A-F
[AD-A146915] 07 p1005 N85-16386

Revised Uniform Summary of Surface Weather Observations (RUSSWO). Dobbins AFB, Georgia, parts A-F
[AD-A146916] 07 p1005 N85-16387

Experiments in forecasting atmospheric marine horizontal visibility using model output statistics with conditional probabilities of discretized parameters
[AD-A147574] 07 p1008 N85-16404

Evaluation of nose, roof, and mast mounted sensor platforms for piloting and sighting, integrated in future combat helicopters 08 p1074 N85-16806

The visibility climatology of McMurdo Sound-Williams Field, Antarctica
[AD-A148106] 08 p1189 N85-17492

Selecting one among the many: A simple network implementing shifts in selective visual attention
[AD-A148989] 10 p1530 N85-19644

Analysis of a visual performance experiment
[DE85-000710] 10 p1530 N85-19645

Impact of aerosols on visibility and climate: A report prepared for Panel 3, Environmental Impact, of the NATO/CCMS Air Pollution Pilot Study on Air Pollution Control Strategies and Impact Modelling
[PB85-106744] 12 p1897 N85-21906

The accuracy in calculations of intervisibility with digital terrain models — digital models
[FOA-C-20557-D6(E1)] 12 p1909 N85-21983

Visibility of small objects in turbid atmosphere
14 p2342 N85-24482

Retroreflective armbands: Influences of wearing mode, aging and other factors on the visibility distance
[IZF-1984-28] 14 p2422 N85-24942

Determination of the observation conditions of celestial bodies with the aid of the DISPO system
[NAS 1.15:77632] 14 p2438 N85-25044

Comparison of some West German cloud height and visibility data — weapon test sites
[BAE-BT-12734] 15 p2593 N85-25982

Poisson and multinomial shadowing processes
[AD-A151600] 15 p2640 N85-26286

Air quality benefit analysis for Los Angeles and San Francisco based on housing values and visibility
[PB85-166049] 16 p2822 N85-27409

Spatial and temporal visual masking and visibility
[AD-A151968] 16 p2842 N85-27524

An evaluation of discretized conditional probability and linear regression threshold techniques in model output statistics forecasting of visibility over the north Atlantic Ocean
[AD-A151955] 16 p2857 N85-27619

Quality assurance for RESOLVE (Research on Operations-Limiting Visual Extinction). A visibility study in the California desert
[AD-A152383] 17 p2992 N85-28494

The measurement of aircraft windscreen haze and its effect on visual performance
[AD-A154949] 21 p3555 N85-32114

Forecasting atmospheric visibility over the summer north Atlantic using the principal discriminant method
[AD-A155537] 21 p3637 N85-32593

Ice fog as an electro-optical obscurant
[AD-A155059] 21 p3705 N85-33015

Immediate visibility after red and white adaptation
[AD-A156271] 24 p4132 N85-35616

VISIBLE INFRARED SPIN SCAN RADIOMETER

An evaluation and comparison of vertical profile data from the VISSR Atmospheric Sounder (VAS)
[NASA-TP-2425] 07 p1000 N85-16351

VISSR infrared calibration by means of calculated radiances 12 p1894 N85-21889

GMS operational calibration procedure and status
12 p1895 N85-21893

Sea surface temperatures from VAS MSI data
[NASA-CR-175706] 14 p2382 N85-24689

Review of VAS demonstration
15 p2596 N85-26002

Nowcasting applications of VAS
15 p2597 N85-26003

VISIBLE RADIATION
U LIGHT (VISIBLE RADIATION)

VISIBLE SPECTRUM

Spectral components at visual and infrared wavelengths in active galactic nuclei
[NASA-CR-174133] 03 p0445 N85-12832

IUE and ESO observations of the P Cyg star AG Carinae and its ring nebula 11 p1750 N85-21006

Coordinated ultraviolet and visual observations of Omega Orionis 1982-1983 11 p1750 N85-21007

The spectroscopic antics of S 18/SMC
11 p1750 N85-21008

Ultraviolet and optical spectroscopy and polarimetry of the helium weak star HD 21699: Evidence for a magnetically controlled stellar wind
11 p1759 N85-21065

Non-linear optical techniques for visible and UV lasers and thin film deposition
[AD-A150489] 13 p2096 N85-23077

Spectral units on Europa and Ganymede
13 p2196 N85-23621

Spectral reflectance of carbonate minerals and rocks in the visible and near infrared (0.35 - 2.55 microns) and its applications in carbonate petrology
[NASA-CR-175763] 15 p2591 N85-25973

Estimation of convective rainfall from visible and infrared satellite data 15 p2596 N85-25999

In situ thin film measurements
[AD-A151379] 15 p2652 N85-26353

Alkali atom - SbCl(5) reactions: Blue-green chemiluminescence from an inverted population in SbCl
[AD-A154371] 19 p3276 N85-30315

Absorption and scattering properties of aerosols of aggregated particles in the infrared spectral region
[AD-A155475] 21 p3637 N85-32591

Transparency of water 9n 186 - 500 nm region
21 p3690 N85-32923

The ISAVF opto-mechanical test bed
[NASA-TM-87505] 24 p4067 N85-35206

VISION
NT BINOCULAR VISION
NT COLOR VISION
NT NIGHT VISION
NT PERIPHERAL VISION

Pattern reversal visual evoked potentials and reaction time
[CSIR-SR-PERS-354] 01 p0097 N85-10644

Development and evaluation of a performance-based test of saccadic and vestibulo-ocular control
[AD-A145367] 02 p0237 N85-11545

Visually evoked responses from non-occipital areas of the human cortex
[AD-A146079] 03 p0400 N85-12553

Visual selective attention
[AD-A146220] 03 p0401 N85-12558

Spatiotemporal characteristics of visual localization
[AD-A148013] 08 p1200 N85-17555

Ill-posed problems and regularization analysis in early vision
[AD-A147753] 08 p1222 N85-17696

Human assembly time versus levels of visual and tactile sensory input: Experimental results for five devices
[AD-A149982] 12 p1909 N85-21980

Italy's Fiat uses Sweden's Asea seeing robot
15 p2536 N85-25650

Vision algorithms and psychophysics
[AD-A151888] 15 p2620 N85-26142

Retinally stabilized differential resolution television display
[NASA-CASE-NPO-15432-1] 18 p3089 N85-29117

Discovery regarding visual neuron adaptation applicable to robot use 20 p3504 N85-31786

Some results of the European vestibular experiments in the Spacelab-1 mission 20 p3508 N85-31809

Visual phenomena produced by binocularly disparate dynamic visual noise
[AD-A154758] 21 p3663 N85-32757

The development and evaluation of color display systems for airborne applications. Phase 1: Fundamental visual, perceptual, and display system considerations
[FAA/PM-85-19] 22 p3826 N85-33700
Heuristic rules for visualization
23 p3965 N85-34584

VISUAL ACUITY
Using gross outline features in long range target identification
[FOA-C-53018-H2] 02 p0237 N85-11543
Electrophysiological correlates of Vernier acuity in human visual cortex
[AD-A146533] 06 p0846 N85-15371
Immediate visibility after red and white adaptation
[AD-A156271] 24 p4132 N85-35616

VISUAL AIDS
Dialog system of preparation and presentation of visual information 10 p1526 N85-19622

VISUAL CONTROL
The two modes of visual processing: Implications for spatial orientation 01 p0008 N85-10047
Neurocognitive pattern analysis of an auditory and visual numeric motor control task. Part 1: Development of methods
[AD-A146609] 09 p1364 N85-18578
Guidelines for the evaluation of visual approach slope indicators
[ARL/SYS-R-32] 23 p3896 N85-34132

VISUAL DISCRIMINATION
The two modes of visual processing: Implications for spatial orientation 01 p0008 N85-10047
A human visual system investigation applicable to image contour coding
[FUB-36-1983] 01 p0095 N85-10640
The perceptual quality of smoke screens: An analysis of the Oldebroek 2 trials, May 1981
[IZF-1984-20] 01 p0095 N85-10641
The prediction of observer responses from photometric data on smoke screens; an analysis of the Oldebroek 2 trials, May 1981
[IZF-1984-21] 01 p0095 N85-10642
Discriminability of signals from noise in a dynamic stereoscopic space
[AD-A148406] 08 p1196 N85-17535
Color measurement and discrimination
[NASA-CR-3824] 09 p1365 N85-18579
Human assembly time versus levels of visual and tactile sensory input: Experimental results for five devices
[AD-A149982] 12 p1909 N85-21960
Visual search strategy predictions: The use of aspect ratio as a cue
[BAE-BT-12565] 15 p2619 N85-26138
Individual observer data for the 1955 Stiles-Burch 2 deg pilot investigation — color vision
[NPL-QU-68] 20 p3512 N85-31830
An error-dependent model of instrument-scanning behavior in commercial airline pilots
[NASA-CR-3908] 21 p3665 N85-32785
Discrimination of linear contour elements of space photographs based on visual perception model
22 p3736 N85-33161

VISUAL DISPLAYS
U DISPLAY DEVICES

VISUAL FIELDS
The two modes of visual processing: Implications for spatial orientation 01 p0008 N85-10047

VISUAL FLIGHT RULES
National airspace review: Airport radar service area operational confirmation report
[DOT/FAA/AT-84/2] 07 p0901 N85-15707
Analysis of estimation algorithms for CDTI and CAS applications
[NASA-CR-172444] 13 p1973 N85-22387

VISUAL OBSERVATION
Procedures for precap visual inspection
[NASA-RP-1122] 04 p0495 N85-13156
Statistical analysis of visual wave observations and gage/radar measurements
[AD-A146358] 06 p0798 N85-15100
The state of the art in printed wiring board inspection
[AD-A149871] 12 p1862 N85-21679
An MRTD-compatible bar pattern response model for TV and direct view sighting systems
[BAE-BT-12090] 15 p2620 N85-26146
A preliminary human factors planning and design outline of parameters related to space station windows and CCTV monitoring 18 p3158 N85-29559

VISUAL PERCEPTION
NT SPACE PERCEPTION
NT VISUAL DISCRIMINATION
The Malcolm horizon: History and future
01 p0008 N85-10046
The peripheral visual cue assessment facility at Ames Research Center 01 p0008 N85-10050
Peripheral vision displays: The future
01 p0009 N85-10058
Image signals encoding techniques oriented towards the reduction of perceptive redundance
[FUB-23-1983] 01 p0040 N85-10256
Effects of repetitive, small-spot, incoherent light flashes on pursuit tracking performance
[AD-A144848] 01 p0095 N85-10637
Inhibition of return: Neural basis and function
[AD-A145242] 01 p0098 N85-10652
The effect of sleep loss on the human visual event-related potential
[AD-A145364] 02 p0234 N85-11526
Eyelid motion sequences predictive of decision errors
[AD-A145702] 02 p0235 N85-11531
Air-to-air visual acquisition performance with TCAS 2
[FAA-PM-84-17] 02 p0236 N85-11537
Visual representations subserving texture perception
[AD-A145412] 02 p0236 N85-11538
Toward a computational neuropsychology of high-level vision
[AD-A145711] 02 p0236 N85-11540
The Beatrice experiment and the luminance concept in Dante
[NOTA-INTERNA-823] 02 p0281 N85-11831
A mathematical model of visual perception regarding peripheral vision and its application to the Hermann's illusion 04 p0483 N85-13080
Visual-vestibular interaction in human motion perception 05 p0695 N85-14471
Representing multidimensional systems using visual displays 05 p0711 N85-14560
Central regulation of sensory flow in human visual system 07 p1013 N85-16435
Lateral specifics of visual perception
07 p1013 N85-16436
Testing changes in visual function due to orbital environment
[AD-A147259] 07 p1016 N85-16453
Vision by man and machine: How the brain processes visual information may be suggested by studies in computer vision (and vice versa)
[AD-A147890] 07 p1017 N85-16458
Discriminability of signals from noise in a dynamic stereoscopic space
[AD-A148406] 08 p1196 N85-17535
Spatiotemporal characteristics of visual localization
[AD-A148013] 08 p1200 N85-17555
The IMAGE 3 Conference Proceedings
[AD-A148636] 09 p1267 N85-17962
Altitude control using action-demanding interactive displays: Toward an active psychophysics
[AD-P004311] 09 p1267 N85-17965
Considerations in an optical variable acuity display system
[AD-P004323] 09 p1269 N85-17977
Progress report on an eye-slaved area-of-interest visual display
[AD-P004326] 09 p1270 N85-17980
Baffled eye and confounded brain or using visual illusions to train blind pilots
[AD-P004332] 09 p1271 N85-17986
Global optical metrics for self-motion perception
[AD-P004333] 09 p1271 N85-17987
AVTS (Advanced Visual Technology System): A high fidelity visual simulator
[AD-P004338] 09 p1271 N85-17992
Restructuring of the process of visual recognition as perception conditions alter 10 p1526 N85-19624
Multiple resources and brain laterality
[AD-A148912] 10 p1530 N85-19643
Selecting one among the many: A simple network implementing shifts in selective visual attention
[AD-A148989] 10 p1530 N85-19644
Some effects of display format variables on the perception of aircraft spatial orientation
10 p1534 N85-19666
A method for reduction of ambiguity in segmentation of images
[INPE-3394-TDL/186] 11 p1697 N85-20664
The accuracy in calculations of intervisibility with digital terrain models — digital models
[FOA-C-20557-D8(E1)] 12 p1909 N85-21983
Visual simulation requirements for aircraft aspect recognition at real world distances
[AD-A151040] 14 p2228 N85-23810
The effect of set size on color matching
[AD-A150699] 14 p2388 N85-24713
Visual recognition of simple objects by a connection network
[AD-A151043] 14 p2389 N85-24718
Survey of remote sensing techniques for wave measurement
[NASA-TM-84429] 15 p2583 N85-25928
A portable battery for objective, non-obstrusive measures of human performances
[NASA-CR-171868] 15 p2586 N85-25942
Vision algorithms and psychophysics
[AD-A151888] 15 p2620 N85-26142
Spatial and temporal visual masking and visibility
[AD-A151966] 16 p2842 N85-27524
Perception of roll rate from an artificial horizon and peripheral displays
[VTH-LR-403] 17 p3002 N85-28557
Effect of background/foreground color coding on detection in acoustic data displays
[AD-A154105] 19 p3352 N85-30774
The measurement of aircraft windscreen haze and its effect on visual performance
[AD-A154949] 21 p3555 N85-32114
Visual phenomena produced by binocularly disparate dynamic visual noise
[AD-A154758] 21 p3663 N85-32757
Discrimination of linear contour elements of space photographs based on visual perception model
22 p3736 N85-33161
Heterodyne holographic interferometry for visualization of surface acoustic waves
[AD-A155405] 22 p3836 N85-33753
Image synthesis: Optical identity or pictorial communication? 23 p3963 N85-34565
Heuristic rules for visualization
23 p3965 N85-34584
Visual impact of GROWIAN and resulting recommendations for siting of large wind energy converters 24 p4112 N85-35486
Matched filtering of visual evoked potentials to detect acceleration (+Gz) induced blackout
[AD-A155912] 24 p4131 N85-35609
The human engineering eye movement measurement research facility
[AD-A156099] 24 p4132 N85-35613
Immediate visibility after red and white adaptation
[AD-A156271] 24 p4132 N85-35616

VISUAL PHOTOMETRY
The prediction of observer responses from photometric data on smoke screens; an analysis of the Oldebroek 2 trials, May 1981
[IZF-1984-21] 01 p0095 N85-10642
Photometric study of the Saturn E ring
15 p2671 N85-26483
A manual of methods for the continuous flow determination of ammonia, nitrate-nitrite, phosphate and silicate in seawater
[IOS-177] 23 p3913 N85-34243

VISUAL SIGNALS
Discriminability of signals from noise in a dynamic stereoscopic space
[AD-A148406] 08 p1196 N85-17535
Changing system and display concepts and their impact on aircrew performance 10 p1533 N85-19665

VISUAL STIMULI
The two modes of visual processing: Implications for spatial orientation 01 p0008 N85-10047
The peripheral visual cue assessment facility at Ames Research Center 01 p0008 N85-10050
Pattern reversal visual evoked potentials and reaction time
[CSIR-SR-PERS-354] 01 p0097 N85-10644
Neural control of the direction of covert visual orienting
[AD-A145189] 01 p0097 N85-10650
An in-flight investigation of a twin fuselage configuration in approach and landing
[NASA-CR-172366] 05 p0596 N85-13801
Spontaneous motility of goldfish in absence of terrestrial zeitgebers: Space flight simulation in a mine
05 p0689 N85-14432
Use of linear perspective scene cues in a simulated height regulation task 05 p0704 N85-14517
Cockpit window edge proximity effects on judgements of horizon vertical displacement
05 p0704 N85-14518
Mean and random errors of visual roll rate perception from central and peripheral visual displays
05 p0704 N85-14519
Direction judgement errors in perspective displays
05 p0705 N85-14520
The interaction of focused attention with flow-field sensitivity 05 p0705 N85-14521
Accuracy of system step response roll magnitude estimation from central and peripheral visual displays and simulator cockpit motion 05 p0705 N85-14522
Lateral specifics of visual perception
07 p1013 N85-16436
Visual evoked potentials with disrupted functioning of nonspecific cerebral systems 07 p1013 N85-16437
Random pattern tracking acceleration tolerance tester
[AD-D011404] 07 p1017 N85-16459
Functional inter-hemisphere asymmetry in recognition of visual stimuli of various classes
08 p1193 N85-17517

Spatiotemporal characteristics of visual localization
[AD-A148013] 08 p1200 N85-17555
Determination of functional mobility of human nervous system with the PNN-3 instrument
10 p1525 N85-19618
Susceptibility of cat and squirrel monkey to motion sickness induced by visual stimulation: Correlation with susceptibility to vestibular stimulation
11 p1694 N85-20650
Visual simulation requirements for aircraft aspect recognition at real world distances
[AD-A151040] 14 p2226 N85-23810
The effect of set size on color recognition
[AD-A150958] 14 p2391 N85-24726
Visual phenomena produced by binocularly disparate dynamic visual noise
[AD-A154758] 21 p3663 N85-32757

VISUAL TASKS
Effects of repetitive, small-spot, incoherent light flashes on pursuit tracking performance
[AD-A144848] 01 p0095 N85-10637
The effect of set size on color matching
[AD-A150899] 14 p2388 N85-24713

VISUAL TRACKING
U OPTICAL TRACKING

VISUALIZATION OF FLOW
U FLOW VISUALIZATION

VITAMIN D
U CALCIFEROL

VITAMIN K
U PHYLLOQUINONE

VITAMINS
NT CALCIFEROL
NT PHYLLOQUINONE
Vitamin metabolism in cosmonauts following short-term flights 01 p0091 N85-10615
The effects of prolonged feeding meal, ready-to-eat (MRE) operational rations
[AD-A154763] 21 p3686 N85-32773

VITREOUS MATERIALS
Microtektite discovered in Beijing
[NASA-TM-77765] 01 p0130 N85-10695
Effect of light pulses on film of chalcogenide vitreous semiconductors 02 p0258 N85-11687

VITRIFICATION
Stabilization of contaminated soils by in situ vitrification
[AD-P004144] 09 p1348 N85-18480
High level radioactive waste vitrification process equipment component testing
[DE85-011143] 19 p3273 N85-30296
Development of HWVP melter/turntable components for canyon-remote maintenance and replacement
[DE85-010308] 19 p3273 N85-30298
Technology of off-gas treatment for liquid-fed ceramic melters
[DE85-012467] 22 p3812 N85-33610

VLASOV EQUATIONS
Hamiltonian and Lagrangian theory of gyrokinetic equations 02 p0283 N85-11845
Theory of ponderomotive forces
02 p0283 N85-11847
Covariant Poisson brackets for classical fields
[DE85-010085] 18 p3171 N85-29654
High harmonic rectangular gyrotron
19 p3256 N85-30189
Guiding center distribution function and longitudinal invariant 23 p3978 N85-34663
Numerical solutions of the Vlasov equation
23 p3979 N85-34672

VLBI
U VERY LONG BASE INTERFEROMETRY

VLSI
U VERY LARGE SCALE INTEGRATION

VOCODERS
Literature review of voice recognition and generation technology for Army helicopter applications
[AD-A148878] 07 p0939 N85-15954
Comparative architectures for a multiple function speech processor
[AD-A150673] 14 p2292 N85-24211
Survey of narrow band vocoder technology
[AD-A151919] 16 p2773 N85-27114
The design of an adaptive predictive coder using a single-chip digital signal processor
[AD-A152461] 17 p2952 N85-28231
A classification vocoder: A very low rate speech transmission by vector quantization of the spectrum
[ENST-84D003] 20 p3441 N85-31356

VOICE COMMUNICATION
NT TELEPHONY
NT VOICE DATA PROCESSING
Improvement of the narrowband linear predictive coder. Part 2: Synthesis improvements
[AD-A145031] 01 p0038 N85-10237
Interaction of voice and data traffic in a packet switching communication network and virtual circuit
[FUB-63-1982] 01 p0039 N85-10249
Voice communication handling in X 25 packet switching networks
[FUB-30-1983] 01 p0040 N85-10260
Royal Signals and Radar Establishment speech database recordings 1983: Part 2: Recordings made for automatic speech recognition assessment and research
[RSRE-84008-PT-2] 02 p0190 N85-11267
Identification as a function of familiarity for known voices talking over an unprocessed channel and an LPC (Linear Predictive Coding) voice processor
[AD-A145545] 02 p0191 N85-11276
Technological institute director views artificial intelligence 03 p0341 N85-12197
Wideband integrated voice/data technology
[AD-A146054] 03 p0355 N85-12283
Hearing protection and speech intelligibility of two nonstandard inflight communication headsets
[AD-A146110] 03 p0355 N85-12284
Rech-1 speech synthesizer for man-machine dialog
04 p0543 N85-13456
VOTAN V5000 speech recognition system performance test report
[AD-A146726] 07 p0939 N85-15950
Literature review of voice recognition and generation technology for Army helicopter applications
[AD-A148878] 07 p0939 N85-15954
Man-machine communication research for robotics reported 08 p1139 N85-17177
Transmission scheduling to reduce convex delay costs in packet networks
[AD-A148451] 08 p1153 N85-17278
A voice-actuated wind tunnel model leak checking system
[NASA-TM-86359] 09 p1263 N85-17936
EHF air-to-air communications
10 p1469 N85-19273
Fast data and voice transmission for mobile services with high immunity against multipath and co-channel interference 10 p1475 N85-19306
Overview of leading-edge research at French CNRS lab 11 p1618 N85-20179
Base communications issues for the 1980s
[AD-A149764] 12 p1828 N85-21474
Automatic speech recognition in severe environments
[PB85-121697] 12 p1830 N85-21490
Tubes and transistors in audio amplifiers
12 p1837 N85-21532
Low-bit rate speech encoders based on Line-Spectrum Frequencies (LSF)
[AD-A150518] 13 p2056 N85-22871
Interference effects of vocalization on dual task performance
[AD-A150687] 14 p2291 N85-24203
Secure digital speech communication
[AD-D011572] 14 p2293 N85-24215
A preliminary investigation into the intelligibility of Microspeech-2, a speech synthesiser
[BAE-BT-12284] 15 p2539 N85-25675
Wideband integrated voice/data technology
[AD-A152329] 17 p2947 N85-28197
Oral discussion, group-to-individual transfer and achievement in cooperative learning groups
[AD-A153209] 17 p3001 N85-28552
Secure digital voice communications in the Defense Data Network (DDN)
[AD-A154677] 21 p3574 N85-32226
Interactive on-line conferences
[AD-A154723] 21 p3574 N85-32227
Application of adaptive noise cancellation to Coast Guard voice communications
[AD-A154798] 21 p3574 N85-32230
Software for interactive on-line conferences
[AD-A154742] 21 p3670 N85-32801
Speech analysis system for assessing pilots' working fitness 22 p3819 N85-33661

VOICE CONTROL
Voice command weapons launching system
[AD-D011378] 07 p0937 N85-15940
Automatic speech recognition in severe environments
[PB85-121697] 12 p1830 N85-21490
A description of the process of elaborating man-machine dialog in an aircraft equipped with cathode tubes: Roles and specifications of piloted simulation methods
16 p2698 N85-26858
Wideband integrated voice/data technology
[AD-A152329] 17 p2947 N85-28197
Study to determine potential flight applications and human factors design guidelines for voice recognition and synthesis systems
[NASA-CR-172590] 20 p3440 N85-31349

VOICE DATA PROCESSING
Classification methods for Italian vowels — speech recognition
[FUB-61-1982] 01 p0039 N85-10248
Description of a semiannual selection procedure of vowel parts of the voice signal using a PDP 11/34 computer
[FUB-4-1983] 01 p0039 N85-10250
Determination of vowel zones in speech — speech recognition
[FUB-16-1983] 01 p0040 N85-10253
Vowel phoneme identification in speech
[FUB-26-1983] 01 p0040 N85-10257
Voice phonetic coding and decoding processes
[FUB-29-1983] 01 p0040 N85-10259
Voice communication handling in X 25 packet switching networks
[FUB-30-1983] 01 p0040 N85-10260
Autoregressive nonsteady methods for the analysis and synthesis of the human voice
[FUB-3-1984] 01 p0041 N85-10266
Measures of distance between speech signals in the frequency domain — speech recognition
[FUB-5-1984] 01 p0041 N85-10267
Analog voice processing for FM transmission in a telephone channel
[INPE-2798-PRE/359] 03 p0354 N85-12279
Voice data processing in packet switching modes
[FUB-44-1983] 09 p1312 N85-18248
Speech analysis by parametric methods: A survey
[ENST-84C004] 09 p1313 N85-18251
Automatic speech recognition in severe environments
[PB85-121697] 12 p1830 N85-21490
Comparative architectures for a multiple function speech processor
[AD-A150673] 14 p2292 N85-24211
Preliminary assessment of the Heuristics H2000 speechlink - speech recognition device — voice data input for Apple 2 computer
[BAE-BT-12276] 15 p2539 N85-25674
A review of speech systems
[BAE-BT-12285] 15 p2539 N85-25676
Processing speech for analysis using optical Fourier techniques
[AD-A151898] 15 p2544 N85-25704
Wideband integrated voice/data technology
[AD-A152329] 17 p2947 N85-28197
A method and apparatus for operating on companded PCM voice data
[NASA-CASE-KSC-11285-1] 18 p3089 N85-29120
A classification vocoder: A very low rate speech transmission by vector quantization of the spectrum
[ENST-84D003] 20 p3441 N85-31356
Introduction to adaptive techniques for voice signal processing
[FUB-52-1983] 22 p3756 N85-33267

VOID RATIO
Void fraction measurements performed in a vertical large diameter tube compared to different predicting correlations
[GKSS-84-E-24] 01 p0048 N85-10315
A note on the G-space version of Glicksberg's theorem
[CWI-PM-R8405] 08 p1217 N85-17665

VOIDS
Radiation effects on structural materials
[DE84-014771] 01 p0029 N85-10178
Induction voidmeter
[DE84-014321] 01 p0050 N85-10329
Experimental determination of the critical cavity radius in Fe-10% Cr for ion irradiation
[DE84-016570] 04 p0571 N85-13646
Collapse and removal of discontinuities in joint zone during diffusion welding 11 p1602 N85-20077
Effect of diaphragm leakage on turbine stage characteristics 14 p2286 N85-24168
Swelling behavior of titanium-modified AISI 316 alloys
[DE85-007470] 16 p2752 N85-26962
Theory of positron annihilation in vacancies in concentrated disordered alloys
[DE85-010267] 18 p3183 N85-29734
Determination of the vacancy formation enthalpy in chromium by positron annihilation
[DE85-010286] 19 p3239 N85-30084
Reliability of void detection in structural ceramics using scanning laser acoustic microscopy
[NASA-TM-87035] 21 p3597 N85-32337

VOIGT EFFECT
Voigt line profile computation of infrared lines in the stratosphere and mesosphere
[AERONOMICA-ACTA-A-294-1985]
22 p3813 N85-33622

VOLATILITY
Effect of toluene on the solubility of biohazardous volatile synthetic organic compounds
[AD-A145188] 01 p0018 N85-10109

Dynamic compression and volatile release of carbonates
[NASA-CR-174076] 03 p0391 N85-12504
Origin of the Moon: Constraints from volatile elements 04 p0584 N85-13727
Volatility of vanadium from a candidate fusion tractor alloy
[DE84-016277] 05 p0618 N85-13955
Volatile organic emissions from adhesives with indoor applications
[DE84-015965] 05 p0620 N85-13966
Volatility of in-use gasoline and gasoline-methanol blends
[PB85-117976] 10 p1459 N85-19189
Magmas as selective filters of volatiles between planetary mantles and surfaces
13 p2185 N85-23557
Procedure for certifying quantity of volatile organic compounds emitted by paint, ink and other coatings
[PB85-159044] 15 p2520 N85-25537
Limiting factor of flame propagation in mono-sized sprays of low-volatility fuels
[NAL-TR-839T] 15 p2521 N85-25538
Volatiles in the outer solar system. 1: Thermodynamics of clathrate hydrates. 2: Ethane ocean on Titan. 3: Evolution of primordial Titan atmosphere
19 p3382 N85-30984
Nebular volatile fractionations associated with chondrule formation 22 p3852 N85-33855
Volatile loss following very large impacts
22 p3853 N85-33862
Volatiles on satellites of the outer solar system
22 p3854 N85-33868
Monitoring dosage of volatile compounds in tests at low barometric pressure 23 p3954 N85-34506

VOLATILIZATION
U VAPORIZING

VOLCANICS
U VOLCANOLOGY

VOLCANOES
NT MARS VOLCANOES
The petrology and geochemistry of high cascade volcanics in southern Washington: Mount Saint Helens volcano and the Indian Heaven basalt field
02 p0227 N85-11487
Geology and geochemistry of early Tertiary submarine volcanic rocks of the Aleutian Islands, and their bearing on the development of the Aleutian Island Arc
03 p0389 N85-12493
Reconnaissance geology of the northern part of the Unalakleet quadrangle 04 p0516 N85-13291
Paleomagnetic latitude of paleocene volcanic rocks of the Cantwell Formation, central Alaska
04 p0517 N85-13302
Paleogene volcanic rocks of the Matanuska Valley area and the displacement history of the Castle Mountain fault 04 p0518 N85-13303
Models for volcanic processes in Long Valley, California: Testing by continental drilling
[DE84-014943] 04 p0534 N85-13414
Satellite photographs suggest arctic volcano
07 p0982 N85-16239
Evaluation of the L-band scattering characteristics of volcanic terrain in aid of lithologic identification, assessment of SIR-B calibration, and development of planetary geomorphic analogs 08 p1146 N85-17232
Correlation and petrological interpretation of abyssal and terrestrial tephra layers 09 p1353 N85-18512
Tectonic lineaments in the cenozoic volcanics of southern Guatemala: Evidence for a broad continental plate boundary zone
[NASA-CR-175456] 10 p1505 N85-19499
Airborne lidar measurements of El Chichon stratospheric aerosols, October 1982 to November 1982
[NASA-RP-1136] 10 p1514 N85-19550
Catalog of submarine volcanoes and hydrological phenomena associated with volcanic events: 1500 BC to 31 Dec. 1899
[PB85-117984] 12 p1891 N85-21869
Volcanism on Venus as connecting link
13 p1982 N85-22433
Sulfur volcanoes on Io? 13 p2173 N85-23479
Geomorphic classification of lava flows on Io
13 p2173 N85-23480
Volcanism and rift formation in Beta Regio, Venus: New radar results 13 p2176 N85-23507
Volcanic debris flows in the Elysium region of Mars
13 p2185 N85-23560
Estimates of lava eruption rates at Alba Patera, Mars
13 p2185 N85-23562
Thermal infrared observations of lava flows during the 1984 Mauna Loa eruption 13 p2186 N85-23564
Field measurements of the 1983 Royal Gardens lava flows, Kilauea Volcano, and 1984 Mauna Loa lava flows, Hawaii 13 p2186 N85-23565
Surface structures of Hawaiian lavas
13 p2186 N85-23566
Morphologic evolution of the Mount St. Helens crater area, Washington 13 p2187 N85-23568
Volcanism of the Colorado Plateau (basin and range transition): Implications for crustal processes
13 p2187 N85-23569
The geology of East Butte, a rhyolitic volcanic dome on the Eastern Snake River Plain, Idaho
13 p2187 N85-23570
A silicic shield volcano in Bolivia
13 p2187 N85-23572
Submarine volcanic eruptions and potential analogs for Venus 13 p2187 N85-23573
Terrestrial analogs for planetary wrinkle ridges
13 p2199 N85-23644
Skywave radar detectability of volcanic aerosols
[AD-A151448] 15 p2542 N85-25694
The impact ejection of living organisms into space
15 p2682 N85-26566
Closer look at lunar volcanism
[DE85-006663] 15 p2683 N85-26576
Evolution of stratospheric aerosol size distribution from ground-based radiometric measurements: A study of El Chichon aerosol
[DE85-007555] 16 p2827 N85-27439
Thermal-cycle testing of the G-tunnel heated block
[DE85-008406] 18 p3126 N85-29359
Pacific Northwest solar radiation data
[DE85-009773] 18 p3149 N85-29496
Influence of underwater volcanic mountains of Atlantic on microplankton distribution 19 p3294 N85-30424
Melt zones beneath five volcanic complexes in California: An assessment of shallow magma occurrences
[DE85-010644] 19 p3305 N85-30489
Source-term considerations for a potential radioactive-waste repository located in unsaturated tuff
[DE85-010090] 20 p3529 N85-31953
Data analysis for lidar and quartz crystal microbalance systems
[NASA-CR-172601] 21 p3615 N85-32464
Changes in the organic material in lakes in the blast zone of Mount St. Helens, Washington: Hydrologic effects of the eruptions
[GS-CIRC-850-1] 21 p3630 N85-32551
Early and middle Cenozoic volcanic synthesis
24 p4105 N85-35449
Preliminary results of an ALVIN dive program on active hydrothermal vents at the southern Juan de Fuca Ridge
24 p4106 N85-35454

VOLCANOLOGY
Magnetic characteristics of some volcanic rocks of the west Carpathians
[REPT-557] 03 p0376 N85-12400
Electric properties of neovolcanic rocks of central and east Slovakia
[REPT-558] 03 p0376 N85-12401
Volatile elements in and on lunar volcanic glasses: What do they tell us about lunar genesis?
04 p0584 N85-13728
Tectonic, volcanic, and climatic geomorphology study of the Sierras Pampeanas Andes, northwestern Argentina 08 p1144 N85-17215
Structure of Iceland and ocean floor spreading
13 p2112 N85-23159
Magmatism in continent-ocean transition zone (development of ideas of A. N. Zavaritskiy)
13 p2113 N85-23161
Planetary geology in the 1980s
[NASA-SP-467] 13 p2169 N85-23457
Reports of the Planetary Geology and Geophysics Program, 1984
[NASA-TM-87563] 13 p2172 N85-23474
Topographic evidence for shield volcanism on Io
13 p2172 N85-23478
Estimates of lava eruption rates at Alba Patera, Mars
13 p2185 N85-23562
Emplacement of long lava flows on Mauna Loa (Hawaii) and Alba (Mars) 13 p2186 N85-23563
Thermal infrared observations of lava flows during the 1984 Mauna Loa eruption 13 p2186 N85-23564
Volcanism of the Colorado Plateau (basin and range transition): Implications for crustal processes
13 p2187 N85-23569
The geology of Mt. Hope, a silicic volcanic center in West Central Arizona 13 p2187 N85-23571
Hydrovolcanism 13 p2188 N85-23574
Results on volcanism, surface geology from Venera-15, -16 15 p2482 N85-25321
Closer look at lunar volcanism
[DE85-006663] 15 p2683 N85-26576
Andrean examples of mega-geomorphology themes
21 p3602 N85-32367
Planetary surface processes: A review
22 p3855 N85-33869
Planning for VRM: Radar and sonar studies of volcanic terrains on Earth, Venus and Mars
22 p3857 N85-33884
Workshop on Recent Research in the Valles Caldera
[DE85-010569] 23 p3949 N85-34472

VOLT-AMPERE CHARACTERISTICS
Planar ferroelectric microcapacitors for microwave devices 13 p2067 N85-23032
Solar cells with distributed parameters: Current-voltage characteristics under uniform and nonuniform illumination 14 p2275 N85-24093
Pressed boride cathodes
[NASA-TM-77821] 17 p2918 N85-27984
Electrochemistry of Hexanitroazobenzene (HNAB)
[DE85-010807] 21 p3565 N85-32171

VOLTAGE
U ELECTRIC POTENTIAL

VOLTAGE BREAKDOWN
U ELECTRICAL FAULTS

VOLTAGE CONTROLLED OSCILLATORS
Analog to digital converter
[AD-D011338] 07 p0945 N85-15983
Image line voltage controlled oscillator with replaceable components
[AD-D011436] 10 p1479 N85-19333
Wide-band phase locked loop amplifier apparatus
[AD-D011720] 23 p3927 N85-34337

VOLTAGE CONVERTERS (AC TO AC)
Automatic ac/dc thermal voltage converter and ac voltage calibration system
[PB85-182574] 19 p3274 N85-30304
Outline of CCVT (Coupling Capacitor Voltage Transformer) calibration procedure, EPRI-NBS (Electric Power Research Institute/National Bureau of Standards) prototype system. Supplement to EPRI report EL-890 (Field Calibration System for CCVTs, April 1978)
[PB85-182566] 20 p3450 N85-31418

VOLTAGE CONVERTERS (DC TO DC)
Control of energy-storage dc-to-dc converters: The large-signal time-domain approach
19 p3257 N85-30196

VOLTAGE GENERATORS
NT PHOTOVOLTAIC CELLS

VOLTAGE MEASUREMENT
U ELECTRICAL MEASUREMENT

VOLTAGE REGULATORS
Problems with electrical interference between solar generators and shunt type regulators
13 p2010 N85-22607
Autonomous uninterruptable power supply apparatus
[AD-D011571] 14 p2298 N85-24232
Method of improving dynamic characteristics of DC voltage stabilizers with compound regulation
15 p2528 N85-25589
Spark gap electrode erosion
[AD-A152802] 17 p2953 N85-28237
High voltage isolation transformer
[NASA-CASE-GSC-12817-1] 18 p3093 N85-29146
Batteryless magneto-driven portable radiac
[DE85-011622] 22 p3760 N85-33300

VOLTAGE VARIATION INDICATORS
U VOLTMETERS

VOLTERRA EQUATIONS
Linear autonomous retarded functional differential equations; a sharp version of Henry's theorem
[CWI-AM-R8405] 05 p0720 N85-14625
EMC (Electromagnetic compatibility) spec criteria in Volterra systems
[AD-A147659] 08 p1151 N85-17263
Stability results for discrete Volterra equations: Numerical experiments
[CWI-NM-R8409] 11 p1707 N85-20743
Solving Volterra integral equations with ODE codes
[DE85-011216] 19 p3346 N85-30740

VOLTMETERS
China report: Science and technology
[JPRS-CST-84-001] 04 p0557 N85-13545
Present status, future prospects of domestic acoustical instruments 04 p0557 N85-13548
Pulsed-power system diagnostics: Electromagnetic data interpretation along pulse lines
[AD-A146807] 06 p0810 N85-15148
Microprocessor-controlled anodic stripping voltammeter for trace metal analysis in tap water
[DE85-002781] 12 p1852 N85-21619
Application of modulated hydrodynamic voltammetry to the study of anodic electrocatalysis
[DE85-004182] 13 p2018 N85-22653
R, L, C, G measurement 21 p3668 N85-32784

VOLUME
NT BODY VOLUME (BIOLOGY)
The analysis of tank calibration data from several runs
[DE84-015529] 02 p0200 N85-11337
Characteristics of aerosol volume distributions measured at Meppen, W. Germany
[AD-A146138] 03 p0396 N85-12528

Free volume considerations in thermoplastic and thermosetting resins 04 p0465 N85-12952
Reflection of volume waves in multilayer structures 04 p0485 N85-13097
Precision volume measuring system
[DE85-002589] 11 p1636 N85-20305
Optimization of pressure vessels with standard intercepting spheres
[INPE-3276-PRE/800] 11 p1651 N85-20397
Application of the Van Leer method to the solution of one-dimensional volume fraction equations
[CFD/84/17] 15 p2558 N85-25781
Determining partial molar volume of hydrogen in titanium alloys 19 p3245 N85-30119

VOLUMETRIC ANALYSIS
Chemistry of ore-forming fluids 24 p4103 N85-35436

VOLUMETRIC EFFICIENCY
Methanol vaporization: Effects on volumetric efficiency and on determination of optimum fuel delivery system
[PB84-243914] 09 p1302 N85-18181

VOMITING
Neurophysiological correlates of motion sickness: Role of vestibulocerebellum and 'vomiting center' reanalyzed 11 p1693 N85-20643
Prediction of the space adaptation syndrome 11 p1693 N85-20646

VON MISES THEORY
U STRESS FUNCTIONS

VOR SYSTEMS
U VHF OMNIRANGE NAVIGATION

VORTEX ALLEVIATION
Wake effects on the aerodynamic performance of horizontal axis wind turbines
[NASA-CR-174920] 18 p3127 N85-29364

VORTEX AVOIDANCE
Experimental research on electric propulsion. Note 7: Analysis of the performance of an arc-jet driven by means of hydrogen and nitrogen
[NASA-TM-77473] 06 p0760 N85-14861

VORTEX BREAKDOWN
Turbulent drag reduction research 08 p1071 N85-16788
Full scale experiments into the use of large eddy breakup devices for drag reduction on aircraft 08 p1071 N85-16790
Experimental investigation of a breakdown criterion for a vortex in an incompressible flow — delta wing
[ONERA-RT-27/1147-AY] 11 p1577 N85-19935
La Recherche Aerospatiale Bimonthly Bulletin, Number 1984-4, 221/July-August
[ESA-TT-884] 16 p2695 N85-26637
An introduction to vortex breakdown and vortex core bursting
[NAE-AN-28] 17 p2892 N85-27829
Viscous flows in rotating pipes with internal cavities and related vortex breakdowns
[NASA-TM-86761] 20 p3454 N85-31447

VORTEX COLUMNS
U VORTICES

VORTEX DISTURBANCES
U VORTICES

VORTEX FLAPS
The lateral-directional characteristics of a 74-degree Delta wing employing gothic planform vortex flaps
[NASA-CR-3848] 03 p0311 N85-12009
Calculation of vortex-flap aerodynamic characteristics
[NASA-CR-175624] 13 p1969 N85-22367
Investigation of the Vortex Tab
[NASA-CR-172586] 15 p2463 N85-25209

VORTEX FLOW
U VORTICES

VORTEX GENERATION
U VORTEX GENERATORS

VORTEX GENERATORS
An experimental investigation of the parallel blade-vortex interaction
[NASA-TM-86005] 05 p0592 N85-13777
On the generation of trailing vortices by surface mounted obstacles 05 p0593 N85-13785
On vortex transport in turbine channels 09 p1308 N85-18217
Generation of a pair of symmetric eddies behind a slender axisymmetric body with pitch angle
[ISL-R-121/83] 11 p1577 N85-19934
An experimental investigation of two-dimensional flame-vortex interactions 16 p2744 N85-26934
Vortex generating flow passage design for increased film cooling effectiveness
[NASA-CASE-LEW-14039-1] 22 p3782 N85-33433
Wingtip vortex propeller
[NASA-CASE-LAR-13019-1] 24 p4065 N85-35194
Vortex boundary-layer interactions
[NASA-CR-176192] 24 p4093 N85-35373

VORTEX RINGS
Transition and mixing in axisymmetric jets and vortex rings 05 p0591 N85-13769

VORTEX SHEDDING
An experimental study of airfoil-spoiler aerodynamics
[NASA-CR-177328] 06 p0748 N85-14796
Wing rock flow phenomena
[AD-P004154] 09 p1264 N85-17939
Unsteady aerodynamic loading of an airfoil due to vortices released intermittently from its upper surface
[AD-P004162] 09 p1265 N85-17947
A Navier-Stokes calculation of the airfoil dynamic stall process
[AD-P004163] 09 p1265 N85-17948
On the shedding of vorticity at separation
[AD-P004166] 09 p1265 N85-17951
Acoustic resonance in heat exchanger tube banks
[DE85-004395] 11 p1632 N85-20281
Nonlinear interactions between vortices and acoustic waves in a rocket combustion chamber 13 p1999 N85-22533
Acoustic energy exchange in sheared mean flows — solid rocket motors 13 p1999 N85-22534
Periodic vortex shedding in the supersonic wake of a planar plate
[NASA-TM-77854] 15 p2463 N85-25207
Vortex shedding flowmeters for liquids at high flow velocities 16 p2740 N85-26906
Trailing edge flow and aerodynamic sound. Part 1: Tonal pressure and velocity fluctuations. Part 2: Random pressure and velocity fluctuations
[AD-A154947] 21 p3552 N85-32097

VORTEX SHEETS
Physics on aircraft wakes
[NASA-CR-174105] 04 p0453 N85-12871
Unsteady flows around 3-dimensional wings
[AD-A149993] 12 p1772 N85-21124
A study of aerodynamic control in stalled flight leading-edge vortex formation analysis
[AD-A153758] 18 p3059 N85-28928
A method for computing the core flow in three-dimensional leading-edge vortices
[NASA-TM-87489] 19 p3214 N85-29932
Vortex sheet modeling with higher order curved panels 20 p3451 N85-31428
A panel method study of vortex sheets with special emphasis on sheets of axisymmetric geometry
[NASA-CR-177365] 21 p3552 N85-32095

VORTEX STREETS
NT KARMAN VORTEX STREET

VORTEX TUBES
U HILSCH TUBES
U VORTICES

VORTICES
NT WING TIP VORTICES
On vortex bursting
[NASA-TM-77587] 01 p0002 N85-10008
Results of tests of advanced flexible insulation vortex and flow environments in the North American Aerodynamics Laboratory lowspeed wind tunnel using 0.0405-scale Space Shuttle Orbiter model 16-0 (test OA-309)
[NASA-CR-167692] 01 p0015 N85-10096
Stability of fluid flow in a cylindrical annulus
[NASA-TM-77720] 01 p0046 N85-10300
Review of some vortex relations
[NASA-CR-172452] 01 p0046 N85-10302
Induction voidmeter
[DE84-014321] 01 p0050 N85-10329
Observations of the vertical structure of the eddy field in the Kuroshio extension
[AD-A145178] 01 p0089 N85-10599
Numerical studies of mesoscale eddies using quasigeostrophic and primitive equation ocean models
[PB84-214048] 01 p0089 N85-10602
Experiments on turbulent mixing and chemical reactions in a liquid mixing layer 02 p0134 N85-10912
Force and moment measurements on a 74 deg delta wing with an apex flap
[NASA-CR-166081] 02 p0134 N85-10918
VORCOR: A computer program for calculating characteristics of wings with edge vortex seperation by using a vortex-filament and-core model
[NASA-CR-165902] 02 p0135 N85-10921
Three dimensional separation and vortex formation 02 p0196 N85-11306
Flow visualization study of a vortex-wing interaction
[NASA-TM-86656] 03 p0316 N85-12040
Interaction between an airfoil and a streamwise vortex
[AD-A145823] 03 p0316 N85-12041
Vorticity amplification in viscous flow around a body 03 p0360 N85-12309
Vortex-generating coolant-flow-passage design for increased film-cooling effectiveness and surface coverage
[NASA-TP-2388] 03 p0361 N85-12314
The structure of the vorticity field in turbulent channel flow. Part 2: Study of ensemble-averaged fields
[NASA-TM-86657] 03 p0361 N85-12317
Eddy detection in the Norwegian, Greenland, and Barents Seas with a radar altimeter 03 p0382 N85-12442
Particle entrainment in a compressible vortex
[ISL-CO-230/83] 04 p0500 N85-13192
The numerical simulation of steady transonic rotational flow using a dual potential formulation 05 p0591 N85-13770
An experimental investigation of the parallel blade-vortex interaction
[NASA-TM-86005] 05 p0592 N85-13777
On the generation of trailing vortices by surface mounted obstacles 05 p0593 N85-13785
Aircraft accident report Air Canada, Lockheed L-1011, C-FTNJ, near Charleston, South Carolina, November 24, 1983
[PB84-910413] 05 p0594 N85-13790
The effect of grazing flow on the impedance of the Helmholtz resonator 05 p0635 N85-14076
A collection of flow visualization techniques used in the Aerodynamic Research Branch
[NASA-TM-85998] 06 p0808 N85-15135
Channel constructed to provide well defined boundary layers for vorticity optical probe measurements
[AD-A146679] 06 p0809 N85-15140
VORT: A computer code for bubbly two-phase flow
[DE84-017076] 06 p0809 N85-15142
Large-eddy simulation. Guidelines for its application to planetary boundary layer research
[AD-A146381] 06 p0890 N85-15651
An investigation of vortex-induced aerodynamic characteristics of supersonic cruise configurations
[NASA-CR-174299] 07 p0898 N85-15690
Numerical studies of interacting vortices
[NASA-TM-86325] 07 p0957 N85-16062
Current problems in turbomachinery fluid dynamics
[AD-A147127] 07 p0958 N85-16074
Free-surface boundary layer and the origin of bow vortices
[AD-A147427] 07 p0960 N85-16083
Laminar flow over a backward-facing step
[AD-A147469] 07 p0960 N85-16084
Interactions between mean flow and finite-amplitude mesoscale eddies in a barotropic ocean
[AD-A147249] 07 p1009 N85-16413
Modelling circulation control by blowing — airfoils 08 p1069 N85-16778
Full scale experiments into the use of large eddy breakup devices for drag reduction on aircraft 08 p1071 N85-16790
Helicopter model rotor-blade vortex interaction impulsive noise: Scalability and parametric variations
[NASA-TM-86007] 08 p1077 N85-16826
Prediction of dynamic stall characteristics using advanced non-linear panel methods
[AD-A148453] 08 p1078 N85-16836
New Zealand SIR-B science investigations 08 p1144 N85-17218
A 3-dimensional turbulent boundary layer upstream and around a junction vortex flow 08 p1160 N85-17319
Application of the vortex-lattice concept to flows with smooth-surface separation 08 p1160 N85-17320
Secondary flow in cascades
[AD-A148415] 08 p1162 N85-17333
A 2-dimensional second order closure model of the upper atmosphere 08 p1182 N85-17450
Unsteady aerodynamic loading of an airfoil due to vortices released intermittently from its upper surface
[AD-P004162] 09 p1265 N85-17947
Unsteady seperated flow: Forced and common vorticity about oscillating airfoils
[AD-P004167] 09 p1265 N85-17952
New discovery in supersonic flight research 09 p1278 N85-18041
Three-dimensional vortex methods
[DE85-000391] 09 p1320 N85-18299
Turbulence in pure superfluid flow 09 p1397 N85-18790
A study for calculating rotor loads using free vortex concept 11 p1620 N85-20194
A study of eddy-mean flow interactions using Eliassen-Palm diagnostics: FGGE SOP-1 data and the NASA GLAS general circulation model compared
[NASA-CR-175508] 11 p1686 N85-20604
Frequency spectra of turbulent pulsations in stability of laminar boundary layer 11 p1716 N85-20795
Transonic interactions of unsteady vortical flows
[NASA-TM-86658] 12 p1770 N85-21113
Numerical study of large-eddy breakup and its effect on the drag characteristics of boundary layers
[NASA-CR-3884] 12 p1797 N85-21272

A calculation of slender delta wing with leading-edge separation by quasi-vortex-lattice method 12 p1821 N85-21423

Calculation of the flow around thick wings with separation vortices 12 p1821 N85-21424

Solution of the three-dimensional Navier-Stokes equations for a steady laminar horseshoe vortex flow [AD-A149851] 12 p1846 N85-21582

A supplement study on the subsynoptic cloud system off the south coast of Japan 12 p1895 N85-21892

Study for prediction of rotor/wake/fuselage interference, part 1 [NASA-CR-177340-VOL-1] 13 p1965 N85-22346

Study for prediction of rotor/wake/fuselage interference. Part 2: Program users guide [NASA-CR-177340-VOL-2] 13 p1966 N85-22347

Method for the prediction of the installation aerodynamics of a propfan at subsonic speeds [NASA-CR-3887] 13 p1969 N85-22369

Deflected jet experiments in a turbulent combustor flowfield [NASA-CR-174863] 13 p1973 N85-22390

Propagation of three-dimensional turbulent jet from lobar nozzle through surrounding stream 13 p2042 N85-22785

Time-dependent flow of stream swirled in vortex chamber 13 p2043 N85-22786

Experimentally determined characteristics of vortex heaters 13 p2050 N85-22833

Grid generation for a pump collector [AD-A150217] 13 p2092 N85-23059

Double and inverse Taylor-Hogg vortices in a stratified ocean 13 p2108 N85-23137

An experimental investigation of the chopping of helicopter main rotor tip vortices by the tail rotor [NASA-CR-177338] 13 p2154 N85-23376

Computations of two-dimensional airfoil-vortex interactions — helicopter rotor flowfields [NASA-CR-3885] 14 p2210 N85-23709

Stability of vortex structures during separation flow past array of wings 14 p2278 N85-24110

Experimental and theoretical investigation of the motion of particles in a compressible vortex [ISL-R-129/83] 14 p2303 N85-24264

Modeling evolution of unstable geostropic eddies in barotropic ocean 14 p2336 N85-24447

Hydromagnetic vortices: An interpretation for dawnside events as on December 11, 1977 — magnetotail 14 p2371 N85-24653

Prediction of vortex-induced loads on wind-tunnel turning vanes [NASA-TM-86678] 15 p2462 N85-25204

An exploratory study of apex fence flaps on a 74 deg delta wing [NASA-CR-172463] 15 p2463 N85-25208

Analysis of selected problems involving vortical flows [NASA-CR-177347] 15 p2463 N85-25212

On the structure of the turbulent vortex 15 p2463 N85-25213

Flow past a flat plat with a vortex/sink combination [JIAA-TR-58] 15 p2464 N85-25215

An experimental study of hairpin-type vortices as a potential flow structure of turbulent boundary layers 15 p2553 N85-25751

Stability calculations of the two-dimensional boundary layer along a concave wall: Part 1: A numerical method of solution for the simultaneous ordinary differential equations governing disturbances [NAL-TR-841] 15 p2554 N85-25758

Vortex dynamics [AD-A151278] 15 p2637 N85-26260

Dust devils on Mars 15 p2683 N85-26573

La Recherche Aerospatiale Bimonthly Bulletin Number 1984-2, 219/March-April [ESA-TT-878] 16 p2694 N85-26635

Exploratory wind-tunnel investigation of a wingtip-mounted vortex turbine for vortex energy recovery [NASA-TP-2468] 16 p2699 N85-26667

Development of a rotor wake-vortex model, volume 1 [NASA-CR-174849] 16 p2699 N85-26668

An experimental investigation of two-dimensional flame-vortex interactions 16 p2744 N85-26934

Vortex studies relating to boundary layer turbulence and noise [NASA-TM-87475] 16 p2782 N85-27169

An experimental investigation of a turbulent junction vortex [NASA-CR-175915] 17 p2957 N85-28259

Vortices in non-Newtonian fluids [AD-A153169] 17 p2958 N85-28269

The effect of the Benthic Boundary Layer on the physics of intense mesoscale eddies [AD-A153193] 17 p2958 N85-28270

Tidal rectification in lateral viscous boundary layers of a semienclosed basin [CWI-AM-R8415] 17 p2960 N85-28284

Kinetic energy and vorticity of lee cyclones [MITT-40] 17 p2993 N85-28502

Flame acceleration mechanisms under conditions of partial confinement [PB85-184083] 18 p3073 N85-29004

On the origin of streamwise vortices in a turbulent boundary layer [AD-A153651] 18 p3100 N85-29188

Turbulent wake of a submerged flat plate [AD-A153776] 18 p3100 N85-29190

The hydrosynclastic infundibulum [AD-A153849] 18 p3100 N85-29192

Transient eddies in the UCLA GCM 18 p3145 N85-29470

Singularity solutions for ellipsoids in Low-Reynolds-Number flows: With applications to the calculation of hydrodynamic interactions in suspensions of ellipsoids [AD-A153503] 18 p3168 N85-29632

Wake effects of the aerodynamic performance of horizontal axis wind turbines 19 p3211 N85-29915

Aerodynamic analysis of a horizontal axis wind turbine by use of helical vortex theory. Volume 1: Theory [NASA-CR-168054] 19 p3212 N85-29916

Lee-side flow over delta wings at supersonic speeds [NASA-TP-2430] 19 p3212 N85-29921

A method for computing the core flow in three-dimensional leading-edge vortices [NASA-TM-87469] 19 p3214 N85-29932

Transverse vorticity measurements in an excited two-dimensional mixing layer 19 p3264 N85-30241

Shock waves in adjacent engine inlets [ISL-R-104/84] 20 p3396 N85-31068

Vortex simulation of v-shaped flame 20 p3425 N85-31259

Viscous flows in rotating pipes with internal cavities and related vortex breakdowns [NASA-TM-86761] 20 p3454 N85-31447

Large eddy structures in transitional and turbulent flames [AD-A154520] 21 p3562 N85-32157

Determination of billows and other turbulent structures, part 4.1A 21 p3621 N85-32500

On the application of a hairpin vortex model of wall turbulence to trailing edge noise prediction [NASA-CR-177938] 22 p3728 N85-33109

Vortex dynamics simulation of conserved scalar dissipation 22 p3745 N85-33210

Drying of pulverized material with heated condensible vapor [DE85-011656] 22 p3783 N85-33438

Aerodynamic analysis of a horizontal axis wind turbine by use of helical vortex theory, volume 2: Computer program users manual [NASA-CR-174921] 22 p3804 N85-33563

A three-dimensional viscous flow analysis for the helicopter tip vortex generation problem [NASA-CR-3906] 23 p3893 N85-34114

Comments on the prediction of dynamic stall [GU-AERO-8501] 23 p3894 N85-34125

VORTICITY

The inducement of planetary boundary layer mass convergence associated with varying vorticity beneath tropospheric wind maximum 01 p0074 N85-10494

Spatial and temporal interpolation of NEROS radiosonde winds [PB84-232545] 04 p0540 N85-13438

Numerical modeling of the atmosphere 05 p0680 N85-14370

Channel constructed to provide well defined boundary layers for vorticity optical probe measurements [AD-A146679] 06 p0809 N85-15140

Calculating secondary nonviscous gas flows in spatial cascades of turbines 09 p1305 N85-18202

Behavior and characteristics of storm cold outflows 09 p1356 N85-18529

A frozen vorticity approach to the axisymmetric strong interaction problem [AD-A149101] 10 p1484 N85-19369

Planetary scale circulation anomalies associated with droughts over northeast Brazil [INPE-3351-PRE/630] 10 p1518 N85-19570

Cumulus effects on the large-scale vorticity and momentum fields in the tropical atmosphere 13 p2137 N85-23270

Natural convection in cylindrical containers 15 p2555 N85-25763

Numerical experiments of jet streak ageostrophic circulations using pseudo-geostrophic initialization and perspectives 15 p2590 N85-25969

The vector potential in a branched Riemann space [VTH-LR-395] 16 p2856 N85-27614

Transverse vorticity measurements using an array of four hot-wire probes [FSFL-R-85-006] 18 p3099 N85-29184

On Fofonoff's mode 18 p3145 N85-29471

Transverse vorticity measurements in an excited two-dimensional mixing layer 19 p3264 N85-30241

Horizontal and vertical structure of velocity, potential vorticity and energy in the gulf stream [AD-A154753] 21 p3655 N85-32702

Maintenance of blocking anticyclones in a general circulation model [PB85-190866] 24 p4124 N85-35567

VORTICITY EQUATIONS

Hyperbolic phenomena in the flow of viscoelastic fluids [AD-A153533] 18 p3099 N85-29186

Multiple equilibria of the barotropic vorticity equation on a sphere 18 p3146 N85-29475

A numerical study of Taylor-Vortex flow [AD-A154787] 21 p3584 N85-32277

The calculation of two-dimensional buoyant surface jets with the k-W model of turbulence — kinetic energy-vorticity fluctuations (k-W) [CFD/84/21] 22 p3785 N85-33446

VORTICITY TRANSPORT HYPOTHESIS

Behavior of small ferromagnetic particles in traveling magnetic field 12 p1843 N85-21564

VOWELS

Classification methods for Italian vowels — speech recognition [FUB-61-1982] 01 p0039 N85-10248

Description of a semiannual selection procedure of vowel parts of the voice signal using a PDP 11/34 computer [FUB-4-1983] 01 p0039 N85-10250

Determination of vowel zones in speech — speech recognition [FUB-16-1983] 01 p0040 N85-10253

Vowel phoneme identification in speech [FUB-26-1983] 01 p0040 N85-10257

VOYAGER PROJECT

Uranus and Neptune [NASA-CP-2330] 02 p0298 N85-11927

Atmospheric dynamics of Uranus and Neptune: Theoretical considerations 02 p0299 N85-11936

Charged particle erosion of icy satellites: Coronal atmospheres and surface redistribution 03 p0448 N85-12845

Multispectral and geomorphic studies of processed Voyager 2 images of Europa [NASA-CR-174075] 03 p0448 N85-12848

Mission science value-cost savings from the Advanced Imaging Communication System (AICS) [NASA-CR-174170] 04 p0458 N85-12905

The performance of differential VLBI delay during interplanetary cruise 05 p0623 N85-13984

Lower atmospheric composition of Jupiter from Voyager infrared measurements [NASA-CR-174196] 05 p0745 N85-14779

Analysis of Jovian decametric data: Study of radio emission mechanisms [NASA-CR-174206] 08 p1258 N85-17917

MU Sagittarii and Beta Lyrae: Combined IUE/Voyager observations 11 p1757 N85-21052

Radio scintillations observed during atmospheric occultations of Voyager: Internal gravity waves at Titan and magnetic field orientations at Jupiter and Saturn [NASA-CR-175554] 12 p1961 N85-22327

Sulfur volcanoes on Io? 13 p2173 N85-23479

Geomorphic classification of lava flows on Io 13 p2173 N85-23480

Sulfur oxygen processes on Io 13 p2173 N85-23481

The violet absorber on Io: Disulfur monoxide derivatives 13 p2173 N85-23482

Dark halo craters and the thickness of grooved terrain on Ganymede 13 p2173 N85-23484

Formation of bright terrain bands on Ganymede by unstable lithosphere extension 13 p2173 N85-23485

Investigations of planetary ring phenomena 13 p2174 N85-23487

Dynamical studies of Saturn's rings 13 p2174 N85-23489

Jupiter/Voyager data analysis [NASA-CR-175723] 15 p2679 N85-26545

Stream dynamics between 1 AU and 2 AU: A detailed comparison of observations and theory [NASA-TM-86086] 15 p2684 N85-26578

Voyager 0.2-lbf thruster valve assembly short pulse test report [NASA-CR-176121] 22 p3741 N85-33185

VOYAGER 1 SPACECRAFT

Voyager EUV and FUV observations 06 p0875 N85-15554

Hot spots on Io: Correlation of infrared emission and visible reflectance 13 p2172 N85-23475

The eccentric ringlet at 1.29 R sub S — Saturn radius (RS) 15 p2673 N85-26496

Voyager UVS observations of stellar occultations by the rings of Saturn — ultraviolet spectrometer (UVS) 15 p2673 N85-26497

Voyager planetary radio astronomy: Grain and particle impacts shot noise in Saturn's ring plane 15 p2673 N85-26498

Shocks in the solar wind between 1 and 8.5 AU: Voyager 1 observations
[NASA-CR-175911] 18 p3209 N85-29905

Analysis of Jovian decametric data: Study of radio emission mechanisms
[NASA-CR-176057] 22 p3651 N85-33846

The energy spectrum of Jovian electrons in interplanetary space
[SH-1.5-18] 23 p3997 N85-34781

VOYAGER 2 SPACECRAFT

Pioneer 10 and Voyager observations of the interstellar medium in scattered emission of the He 584 A and H Lya 1216 A lines 06 p0873 N85-15541

Voyager EUV and FUV observations 06 p0875 N85-15554

Patterns of fracture and tidal stresses due to nonsynchronous rotation: Implications for fracturing on Europa 13 p2173 N85-23483

Voyager UVS observations of stellar occultations by the rings of Saturn — ultraviolet spectrometer (UVS) 15 p2673 N85-26497

Voyager planetary radio astronomy: Grain and particle impacts shot noise in Saturn's ring plane 15 p2673 N85-26498

Future studies of planetary rings by spaceprobes 15 p2679 N85-26541

Voyage to Uranus 15 p2687 N85-26596

Cosmic ray modulation and turbulent interaction regions near 11 AU
[NASA-TM-86193] 18 p3209 N85-29909

Acceleration of ions and electrons to near-cosmic ray energies in a perpendicular shock: The January 6, 1978 event
[SH-1.5-4] 23 p3996 N85-34773

The energy spectrum of Jovian electrons in interplanetary space
[SH-1.5-18] 23 p3997 N85-34781

VTOL
U VERTICAL LANDING

VTOL AIRCRAFT
U VERTICAL TAKEOFF AIRCRAFT

VULCANIZATES
U VULCANIZED ELASTOMERS

VULCANIZED ELASTOMERS

Simple EOS for the silicone rubber Sylgard 184
[DE85-001394] 12 p1814 N85-21376

Development of nitrile rubbers and foams having a high static modulus and low creep
[BR91465] 14 p2259 N85-24001

VULNERABILITY

The vulnerability of cast double base rocket motors to thermomechanical attack 08 p1115 N85-17033

A methodology for the determination of rotary wing aircraft vulnerabilities in air-to-air combat simulation
[AD-A148964] 10 p1424 N85-18984

Survivable local area network
[AD-D011453] 10 p1468 N85-19262

Minimization of system vulnerability in Naval satellite communication networks 11 p1710 N85-20758

Systems vulnerability and lethality in the development phase
[AD-A149737] 12 p1924 N85-22089

Elastic-workhardening SDF (Single-Degree-of-Freedom) system subjected to random blast excitations
[AD-A151866] 15 p2579 N85-25909

Survivable ground base sensor
[AD-D011647] 17 p2950 N85-28213

Literature survey of underground construction methods for application to hardened facilities
[AD-A155212] 21 p3599 N85-32351

Investigation of the lightning vulnerability of nuclear explosive test systems at the Nevada Test Site
[DE85-011761] 24 p4124 N85-35563

W

W WINGS
U VARIABLE SWEEP WINGS

W-R STARS
U WOLF-RAYET STARS

WAFERS

Ion beam lithography
[BMFT-FB-T-84-182] 04 p0504 N85-13219

Silicon-sheet surface studies 06 p0831 N85-15287

Restructurable VLSI program
[AD-A148145] 08 p1157 N85-17301

Pulsed excimer laser processing for cost-effective solar cells
[NASA-CR-174429] 10 p1509 N85-19517

Pulsed excimer laser processing for cost-effective solar cells
[NASA-CR-175465] 10 p1509 N85-19520

Stress studies in EFG
[NASA-CR-175464] 10 p1509 N85-19522

Lithium counterdoped silicon solar cell
[NASA-CASE-LEW-14177-1] 11 p1672 N85-20535

Factors affecting SOS (Silicon-On-Sapphire) yield and reliability
[AD-A150004] 12 p1835 N85-21515

Ingot slicing machine and method
[NASA-CASE-NPO-15483-1] 12 p1857 N85-21650

A low cost approach with larger diameter silicon wafer — solar cells 13 p2006 N85-22572

Multifunctional elements for integrated optics 13 p2068 N85-22918

Time-resolved reflectivity measurement of extrinsic silicon during pulsed laser irradiation
[AD-A150350] 13 p2159 N85-23403

Uses of, experiences in production of custom designed IC's 17 p2945 N85-28180

Interfacial bonding stability 21 p3608 N85-32409

Sixty GHz IMPATT diode development
[NASA-CR-174989] 22 p3756 N85-33293

WAKEFULNESS

Effects of partial deprivation of slow-wave sleep on sleep-wakefulness cycles 10 p1524 N85-19613

Sleep and wake physiology in weightlessness 20 p3510 N85-31819

WAKES
NT AIRCRAFT WAKES
NT HELICOPTER WAKES
NT LAMINAR WAKES
NT NEAR WAKES
NT PROPELLER SLIPSTREAMS
NT SLIPSTREAMS
NT SUPERSONIC WAKES
NT TURBULENT WAKES

Turbofan noise generation. Volume 2: Computer programs
[NASA-CR-167952] 02 p0275 N85-11791

Large structure in the far wakes of two-dimensional bluff bodies 05 p0592 N85-13771

Energy spread in SLC linac with Landau damping
[DE84-016259] 05 p0727 N85-14675

SEASAT 3 and 4
[AD-A148343] 08 p1152 N85-17274

Second order Bragg scattering in a SAR
[AD-A148395] 08 p1152 N85-17275

Solitons and SEASAT
[AD-A148396] 08 p1176 N85-17414

Preliminary results from the unsteady airfoil model USTAR2
[AD-P004171] 09 p1266 N85-17956

A study for calculating rotor loads using free vortex concept 11 p1620 N85-20194

Unsteady flows around 3-dimensional wings
[AD-A149993] 12 p1772 N85-21124

Electron and ion density depletions measured in the STS-3 orbiter wake 13 p1989 N85-22474

Polar orbit electrostatic charging of objects in shuttle wake 13 p1992 N85-22487

Ram-wake effects on plasma current collection of the PIX 2 Langmuir probe 13 p1993 N85-22496

Oscillating airfoils and their wake
[NASA-TM-77831] 14 p2209 N85-23701

Prediction of vortex-induced loads on wind-tunnel turning vanes
[NASA-TM-86676] 15 p2462 N85-25204

Analysis of selected problems involving vortical flows
[NASA-CR-177347] 15 p2463 N85-25212

On the structure of the turbulent vortex 15 p2463 N85-25213

SEASAT report
[AD-A151283] 15 p2583 N85-25931

A study of aerodynamic control in stalled flight leading-edge vortex formation analysis
[AD-A153758] 18 p3059 N85-28928

Wake effects on the aerodynamic performance of horizontal axis wind turbines
[NASA-CR-174920] 18 p3127 N85-29364

Space shuttle molecular and wake vacuum measurements
[NASA-TM-86509] 19 p3222 N85-29978

Preliminary investigation of dispersion of pollutants in model building wake flows using bipolar space charge
[IC-AERO-84-04] 20 p3487 N85-31671

Using ship wake patterns to evaluate SAR (Synthetic Aperture Radar) ocean wave imaging mechanisms. Joint US-Canadian Ocean Wave Investigation Project
[AD-A154633] 21 p3573 N85-32223

WALKING

Locomotion research for the analysis of the human gait and for the determination of the maximum loads of the pelvis-leg skeleton. Volume 1: Two-dimensional analysis
[BMFT-FB-T-83-187-VOL-1] 02 p0236 N85-11535

Locomotion research for the analysis of the human gait and for the determination of the maximum loads of the pelvis-leg skeleton. Volume 2: Three-dimensional analysis
[BMFT-FB-T-83-188-VOL-2] 02 p0236 N85-11536

The energy cost of women walking and running in shoes and boots
[AD-A151022] 14 p2389 N85-24716

Diet of first Soviet expedition on Mount Everest 19 p3323 N85-30586

WALKING MACHINES

Machine Mechanics Institute builds walking vehicle 04 p0543 N85-13455

Control of walking: Local control and real time systems 05 p0715 N85-14583

3D (Three-Dimensional) sensor for adaptive suspension vehicle
[AD-A150921] 14 p2311 N85-24305

WALL FLOW

Design, manufacture, and testing of compliant coatings for reduction of turbulent drag
[AD-A145510] 02 p0198 N85-11323

Similarity criteria of spectra of pressure pulsations of turbulent boundary layer near wall 02 p0256 N85-11679

Developed turbulent flow under conditions of internal and external problems 02 p0260 N85-11700

Progress in wind tunnel wall interference assessment/correction procedures at the NAE 03 p0314 N85-12025

Tunnel constraint for a jet in crossflow 03 p0314 N85-12027

Interference from slotted walls 03 p0314 N85-12028

Wind tunnel wall interference correction for aircraft models 03 p0314 N85-12029

Determination of equivalent model geometry for tunnel wall interference assessment/correction 03 p0314 N85-12031

Minimization of wall interference for three-dimensional models with two-dimensional wall adaptation — wind tunnel walls
[VKI-TN-149] 03 p0321 N85-12070

Wall effects on the slow steady motion of a particle in a viscous incompressible fluid
[PREPRINT-828] 03 p0363 N85-12327

Wall influence corrections in wind tunnels: Blockage correction according to the wall pressure signature method
[FW-FO-1613] 04 p0453 N85-12875

Parametric determination of blockage interference of 3-dimensional models in the Emmen Federal Aircraft works transonic tunnel (Switzerland)
[FW-FO-1636] 04 p0453 N85-12876

A local slot boundary condition for transonic flow calculations in slotted-wall test sections of wind tunnels
[FFA-TN-1984-34] 04 p0453 N85-12879

Investigation for the improvement of the transonic tunnel working section of the Emmen Federal Aircraft Works (Switzerland)
[FW-FO-1681] 04 p0458 N85-12904

Turbulent boundary layers with secondary flow
[NASA-TM-77494] 04 p0498 N85-13176

Progress in the development of a two-fluid model of turbulence for near-wall flows, part 1
[CFD/84/7-PT-1] 04 p0501 N85-13196

Progress in the development of a two-fluid model of turbulence for near-wall flows. Part 3: Preliminary investigation of a stably-stratified boundary layer
[CFD/84/9-PT-3] 04 p0501 N85-13197

Proposal for wall function for friction and heat transfer in the presence of roughness and mass transfer
[CFD/84/12] 04 p0501 N85-13198

Experiments on the structure of turbulent reattaching flow 05 p0635 N85-14074

Studies of the wall shear stress in a turbulent pulsating pipe flow
[AD-A146772] 07 p0957 N85-16068

Corrections for attached sidewall boundary-layer effects in 2-dimensional airfoil testing
[NASA-CR-3673] 09 p1272 N85-17997

Experimental investigation of a turbulent incompressible boundary layer on a curved wall 11 p1577 N85-19936

An investigation of turbulence mechanisms in V/STOL upwash flow fields
[AD-A149786] 12 p1772 N85-21123

A three-dimensional spectral algorithm for simulations of transition and turbulence
[NASA-CR-172561] 12 p1845 N85-21575

An experimental investigation of the interaction between a shock wave and a turbulent boundary layer on a convex wall
[VTH-LR-426] 16 p2785 N85-27187

Adaptive wall wind tunnels and wall interference correction methode
[DFVLR-IB-222-84-A-37] 17 p2905 N85-27912

Coherent structure reflective turbulent viscous flow modeling
[AD-A153086] 17 p2958 N85-28267

Wall effect on lateral migration of spherical particles in a linear shear flow 20 p3452 N85-31432

Injection of drag reducing additives into turbulent water flows: Two-component velocity measurements and mixing length model predictions
[AD-A154604] 21 p3583 N85-32274

Experiments on the influence of active walls on the initial amplitudes and growths of instability waves
[AD-A154630] 21 p3583 N85-32275

WALL JETS

Modelling circulation control by blowing — airfoils
08 p1069 N85-18778

WALL PRESSURE

Experimental study of Mach reflection of weak shock waves 02 p0260 N85-11703

Wind tunnel wall interference in closed, ventilated and adaptive test sections 03 p0312 N85-12014

Experiments suitable for wind tunnel wall interference assessment/correction 03 p0313 N85-12021

Tunnel constraint for a jet in crossflow
03 p0314 N85-12027

An inerference assessment approach for a three-dimensional slotted tunnel with sparse wall pressure data 03 p0314 N85-12030

Review of the advanced technology airfoil test program in the 0.3-meter transonic cryogenic tunnel
03 p0315 N85-12033

Singularity model for the analysis of wall interference in closed wind tunnels according to the wall pressure signature method (blockage and lift)
[FW-FO-1612] 04 p0453 N85-12874

Comparative flow calculation on transonic cone/cylinder standard models in connection with the wall interference problem
[FW-FO-1689] 04 p0453 N85-12878

Comparison of techniques to measure the low wavenumber wall pressure spectrum of a turbulent boundary layer
[AD-A148074] 08 p1162 N85-17331

Experimental investigation of a turbulent incompressible boundary layer on a curved wall
11 p1577 N85-19336

Sidewall boundary-layer effects in two-dimensional airfoil testing
[NASA-CR-176034] 20 p3396 N85-31065

WALL TEMPERATURE

Laminar flow heat exchangers. Viscosity induced non-uniform flow
[AD-A144777] 01 p0047 N85-10307

High temperature thermocouple and heat flux gauge using a unique thin film-hardware hot juncture
[NASA-TM-86898] 07 p0962 N85-16096

The effect of air holes on combustor liner wall temperature profile: Experiments
[NAL-TR-840] 15 p2504 N85-25443

Study of a constricted electric arc cooled by transpiration
[NASA-TM-77846] 17 p3036 N85-28798

Numerical solutions of turbulent models for flow over a flat plate with angle of attack
[DE85-010380] 21 p3585 N85-32286

WALLS

NT NOZZLE WALLS
NT POROUS WALLS
NT THICK WALLS
NT THIN WALLS
NT TROMBE WALLS
NT WIND TUNNEL WALLS

Development of a floating element wall shear transducer
[AD-A144794] 01 p0049 N85-10324

Direct numerical simulation of curved turbulent channel flow
[NASA-TM-85974] 02 p0197 N85-11316

Performance of two transonic airfoil wind tunnels utilizing limited ventilation 03 p0313 N85-12020

Modeling of propulsive jet plumes--extension of modeling capabilities by utilizing wall curvature effects
[AD-A146262] 03 p0362 N85-12324

Complex frequency analysis of damped thin-walled beams with open cross sections
03 p0371 N85-12366

Architecture of dermatophyte cell Walls: Electron microscopic and biochemical analysis
[NASA-TM-77441] 03 p0399 N85-12546

Study of plasma convection and wall interactions in magnetic confinement systems
[DE84-013959] 03 p0421 N85-12692

Laminar flame propagation/quench for a parallel-wall duct
[DE84-009773] 04 p0470 N85-12993

Response measurements for two building structures excited by noise from a large horizontal axis wind turbine generator
[NASA-CR-172482] 04 p0558 N85-13552

JPL in-house fluidized-bed reactor research
06 p0832 N85-15291

Proceedings of Workshop on Synergistic Effects in Surface Phenomena Related to Plasma-Wall Interactions
[IPPJ-AM-35] 06 p0864 N85-15488

Synergistic effects in fusion machines, session summary 06 p0864 N85-15489

Plasma surface interaction processes and possible synergisms 06 p0864 N85-15490

Synergisms in hydrogen recycling, session summary
06 p0864 N85-15491

Steady state hydrogen transport in solids
06 p0864 N85-15492

Synergisms in surface erosion, session summary
06 p0864 N85-15493

Synergistic effects related to surface composition, session summary 06 p0865 N85-15495

Effects of monolayer coverages on substrate sputtering yields 06 p0865 N85-15496

Synergestic sputtering properties of binary alloys
06 p0865 N85-15497

Tolerance synthesis of multilayer radome walls
07 p0953 N85-16041

Oblique shock wave-turbulent boundary layer interaction on a porous wall with suction 08 p1072 N85-16794

Transonic shock interaction with a tangentially-injected turbulent boundary layer 08 p1072 N85-16796

Studies on seismic earth pressure of cohesive backfill
09 p1303 N85-18186

Determination of total pressure losses in stepped annular diffusors with curvilinear outer walls and uniform velocity field at inlet 09 p1306 N85-18203

Plasma surface interaction processes and possible synergisms
[DE85-001861] 09 p1391 N85-18752

Heat transfer and mechanical interactions in fusion nuclear systems
[DE84-016233] 09 p1392 N85-18761

OTEC (Ocean Thermal Energy Conversion) Cold Water Pipe At-Sea Test Program. Phase 2: Suspended pipe test
[PB85-119931] 10 p1512 N85-19542

Envelope thermal test unit: Technical description
[DE84-012254] 11 p1674 N85-20548

Vibrational relaxation in H-2 molecules by wall collisions: Applications to negative ion source processes
[DE85-000852] 11 p1721 N85-20828

Control of surface composition and hydrogen recycling by plasma conditioning
[DE85-001859] 11 p1731 N85-20889

Integrated insulation wall assembly — for a solid rocket motor case
[AD-D011553] 12 p1794 N85-21257

Method and apparatus for mapping the distribution of chemical elements in an extended medium
[NASA-CASE-GSC-12808-1] 12 p1798 N85-21279

Theoretical and empirical studies of the basic structure of turbulent shear flows, including separated flows and effects of wall curvature
[AD-A149657] 12 p1846 N85-21580

Turbulent convecting flow in a square duct with a 180 deg bend: An experimental and numerical study
[AD-A149969] 12 p1846 N85-21583

Apparatus and method to keep the walls of a free-space reactor free from deposits of solid materials
[NASA-CASE-NPO-15851-1] 12 p1858 N85-21652

Experimental studies of low temperature surface interactions of atomic hydrogen using maser technique
[AD-A150216] 13 p2017 N85-22647

Optimization of overall dimensions of enclosures for low-voltage devices and equipment
13 p2067 N85-23033

Overview of latent storage for passive solar applications
[DE85-005354] 13 p2129 N85-23249

Confinement properties of high energy density plasmas in the Wisconsin levitated octupole
13 p2161 N85-23408

Heat transfer to vertical flat plates in a rectangular gas-fluidized bed
[AD-A150785] 14 p2301 N85-24248

Stability calculations of the two-dimensional boundary layer along a concave wall: Part 1: A numerical method of solution for the simultaneous ordinary differential equations governing disturbances
[NAL-TR-841] 15 p2554 N85-25758

Plasma-wall interactions in tandem mirror machines
[DE85-006387] 15 p2657 N85-26399

Accelerator-based plasma-wall interaction studies on the TEXTOR Tokamak
[DE85-007540] 17 p3040 N85-28806

Atomic hydrogen maser measurements with wall surfaces of carbon tetrafluoride
18 p3108 N85-29243

New concept for a wall detector for alpha particles
[DE85-009037] 18 p3183 N85-29740

Airborne sound transmission loss characteristics of wood-frame construction
[AD-A154174] 20 p3524 N85-31919

Wall flames and implications for upward flame spread
[FAA-CT-85-2] 21 p3553 N85-32103

Construction of University of Missouri, Rolla's full scale cloud simulation chamber and applied research
[AD-A154682] 21 p3557 N85-32128

In-situ measurement of wall thermal performance: Data interpretation and apparatus design recommendations
[DE85-011979] 21 p3586 N85-32289

WALSH FUNCTION

Algorithm in Walsh function basis for analysis of integrated microcircuits on MOS-structures
13 p2083 N85-23006

Use of Walsh functions for calculating characteristics of digital fitiers with impulse response of finite duration
13 p2083 N85-23011

Investigation of influence of communications link and synchronization error on noise tolerence of group transmission of binary information based on orthogonal Walsh function 13 p2086 N85-23026

WAR GAMES

Command control group behaviors. Objective 1: A methodology for and identification of command control group behaviors
[AD-A145690] 02 p0191 N85-11279

Automated CPX support system preliminary design phase
[NASA-CR-175784] 16 p2769 N85-27091

An extended two-target differential game model for medium-range air combat game analysis
[NASA-CR-175968] 18 p3175 N85-29687

WARFARE

NT ANTISHIP WARFARE
NT ANTISUBMARINE WARFARE
NT CHEMICAL WARFARE
NT COMBAT
NT ELECTRONIC WARFARE

Materials for emergency repair of runways
[AD-A146139] 03 p0320 N85-12068

A framework for the development of Navy computer-based systems: Combat system architecture and combat system engineering put into perspective
[AD-A146460] 06 p0856 N85-15445

Can the Aggressors continue to be effective in the F-5E?
[AD-A146861] 07 p1019 N85-16465

The value and utility of inflight onboard simulation
[AD-A148033] 08 p1196 N85-17543

A methodology for the determination of rotary wing aircraft vulnerabilities in air-to-air combat simulation
[AD-A148984] 10 p1424 N85-18984

Servo operated anti-G suit pressurization system
[AD-D011468] 10 p1531 N85-19651

Impact of future aircombat characteristics on pilot performance and cockpit design
10 p1533 N85-19661

PRC journal discusses 'Star Wars' space program
11 p1621 N85-20207

Military applications of meteorological satellite (METSAT) data 11 p1711 N85-20767

Civil weather satellite systems
11 p1711 N85-20768

Meteorological and oceanographic support during the Falklands conflict 11 p1712 N85-20769

Development of satellite data presentation for environmental forecasting 11 p1712 N85-20770

Ground evaluation of helicopter air-to-air warfare
13 p1967 N85-22360

Visual simulation requirements for aircraft aspect recognition at real world distances
[AD-A151040] 14 p2228 N85-23810

Equilibrium solutions, stabilities and dynamics of Lanchester's equations with optimization of initial force commitments
[AD-A151510] 15 p2637 N85-26266

Equipment development for rapid detection of microorganisms in air and water
[FOA-A-40046-B2] 18 p3134 N85-29410

Transceiver test device
[AD-D011728] 22 p3786 N85-33456

Arms control and The President's Strategic Defense Initiative
[AD-A158334] 24 p4068 N85-35212

WARHEADS
Penguin warhead safety tests
08 p1115 N85-17031
Calculation through Fault Tree Analysis of the probability of a warhead being armed prior to launch
[AD-P004339] 10 p1454 N85-19163
Preventing explosive propagation in racks or containers of tactical missiles
[AD-P004342] 10 p1455 N85-19166
WARMING
U HEATING
WARNING DEVICES
U WARNING SYSTEMS
WARNING SIGNALS
U WARNING SYSTEMS
WARNING SYSTEMS
NT MINE DETECTORS
Flight phase status monitor study. Phase 1: Systems concepts
[DOT/FAA/PM-84/18] 03 p0317 N85-12048
A model for the effectiveness of aircraft alerting and warning systems 05 p0702 N85-14506
Development and certification of a new stall warning and avoidance system 05 p0702 N85-14507
Statistics from the operation of the low-level wind shear alert system (LLWAS) during the Joint Airport Weather Studies (JAWS) Project
[DOT/FAA/PM-84/32] 06 p0750 N85-14604
Human factors in cockpit automation
06 p0752 N85-14819
A biological sensor for the detection of toxicants
[AD-D011304] 07 p0967 N85-16141
Battery control and fault detection method
[AD-D011384] 07 p0993 N85-16307
LPI-radar for helicopter obstacle warning
08 p1074 N85-16810
History, design and performance of the space shuttle hazardous gas detection system
08 p1098 N85-16936
A scanning alarm electronic processor
[AD-D011419] 08 p1158 N85-17309
The use of synthetic aperture radar imagery to detect hazards to navigation
[AD-A149324] 10 p1422 N85-18971
Large natural geophysical events: Planetary planning
[DE85-000859] 11 p1763 N85-21092
Extraction of signals from background interference with unknown parameters in quantized sample
13 p2084 N85-23013
Helicopter user survey: Traffic alert and collision avoidance system (TCAS)
[FAA-PM-85-6] 15 p2466 N85-25236
Preliminary airworthiness evaluation of a National Aeronautics and Space Administration automated stall warning system for an OV-1 aircraft
[AD-A152010] 16 p2707 N85-26706
Reusable rocket engine turbopump condition monitoring 16 p2740 N85-26907
Information presentation in power plant control rooms
[VTT-320] 16 p2864 N85-27668
Seismic discrimination
[AD-A154167] 20 p3494 N85-31722
Function of a device for detection of biological aerosols in field testing
[FOA-C-40194-B2] 20 p3504 N85-31782
Automated cell detection as a mesocyclone precursor tool
[AD-A154952] 21 p3635 N85-32577
ARAC status report, 1985
[DE85-012835] 22 p3810 N85-33603
Solar system fault detection
[DE85-005987] 23 p3946 N85-34456
An approach to determining computer security requirements for Navy systems
[AD-A155750] 24 p4135 N85-35627
WARPAGE
Determination of shear coefficient of a general beam cross section by finite element method
09 p1336 N85-18413
WASHING
In situ washing procedures for the UKIRT 3.8 meter primary mirror — United Kingdom Infrared Telescope (UKIRT)
[UKIRT-20] 09 p1414 N85-18918
Control of acid deposition precursors through dry scrubbing
[DE85-010281] 19 p3235 N85-30056
WASHINGTON
Glacier dynamics and the development of glacial landforms in the eastern Puget lowland, Washington
03 p0389 N85-12490
Stratigraphy, sedimentology and tectonic significance of the Upper Cretaceous Virginian Ridge formation, Methow Basin, Washington: Implications for tectonic history of the North Cascades 03 p0390 N85-12494
Tides and tidal currents of the inland waters of Western Washington
[PB84-237379] 06 p0842 N85-15346
Revised Uniform Summary of Surface Weather Observations (RUSSWO). McChord AFB, Washington, parts A-F
[AD-A146914] 07 p1005 N85-16385
Preliminary survey of wind generation in Washington: Site studies and selected wind speed data
[DE85-000058] 09 p1345 N85-18462
Structural morphology and associated strain within parts of the US section of the Kootenay Arc, NE, Washington
09 p1352 N85-18505
Changes in the organic material in lakes in the blast zone of Mount St. Helens, Washington: Hydrologic effects of the eruptions
[GS-CIRC-850-1] 21 p3630 N85-32551
WASHOUT (RADIOACTIVITY)
U FALLOUT
WASPALOY
An electrochemical study of hydrogen uptake and elimination by bare and gold-plated waspaloy
[NASA-TM-86479] 02 p0182 N85-11222
Possibilities for a more accurate life prediction of components — gas turbine disks
07 p0976 N85-16198
WASTE DISPOSAL
NT HAZARDOUS MATERIAL DISPOSAL (IN SPACE)
Depot modernization at the Defense Logistics Agency
[AD-P004008] 03 p0306 N85-11968
Crystalline rocks of the northeastern United States
[DE84-013674] 05 p0677 N85-14347
Description and operation of a thermal decomposition unit-gas chromatographic system
[PB84-246362] 07 p0968 N85-16146
Design concept definition study for an improved shuttle waste collection subsystem
[NASA-CR-171834] 08 p1198 N85-17546
Improved orbiter waste collection system study
[NASA-CR-171830] 08 p1199 N85-17548
Improved orbiter waste collection system study, appendix D
[NASA-CR-171833] 08 p1199 N85-17549
Waste collection subsystem study
[NASA-CR-171836] 08 p1199 N85-17552
Space Shuttle Orbiter waste collection system conceptual study
[NASA-CR-171844] 08 p1199 N85-17553
Ground-water level data and preliminary potentiometric-surface maps, Yucca Mountain and vicinity, Nye County, Nevada
[DE85-001771] 09 p1343 N85-18448
Proceedings of the Environmental Systems Symposium (13th) held at Bethesda, Md., 20-22 March 1984
[AD-A148194] 09 p1346 N85-18471
Strategies for preparing and submitting a part B application for a DoD facility
[AD-P004139] 09 p1347 N85-18475
Assessment of environmental costs at ordnance activities
[AD-P004140] 09 p1347 N85-18476
Remedial action of hazardous waste US Army Corps of Engineers, Anniston, Alabama
[AD-P004141] 09 p1347 N85-18477
Polymeric liner selection for military waste impoundments
[AD-P004143] 09 p1348 N85-18479
Applying an innovative approach to field investigations at a remedial action site
[AD-P004145] 09 p1348 N85-18481
The Hazardous Materials Technical Center
[AD-P004149] 09 p1349 N85-18485
Community relations activities at Department of Defense sites
[AD-P004150] 09 p1349 N85-18486
Protocol for aquifer cleanup decision making at military installations
[AD-P004151] 09 p1349 N85-18487
Analysis of geohydrologic data by kriging
[AD-P004152] 09 p1349 N85-18488
Consideration of future climatic changes in three geologic settings
[DE85-001704] 09 p1357 N85-18537
Measurements of sediment temperatures, conductivity and heat flow in the North Atlantic and their relevance to radioactive waste disposal
[IOS-172] 09 p1359 N85-18551
An assessement of biological processes close to the sea bed in a slope region and its significance to the assessment of sea-bed disposal of radioactive waste
[IOS-185] 09 p1360 N85-18554
Rockwell Hanford operations defense waste and byproducts management
[DE85-000553] 09 p1382 N85-18694
Nevada nuclear waste storage investigations preliminary repository concepts report
[DE85-002132] 09 p1383 N85-18696
Planning for greater-confinement disposal
[DE85-002143] 09 p1383 N85-18697
Perspective on demonstrations of compliance for high-level waste disposal
[DE85-000969] 09 p1383 N85-18698
Commission operation. National Low-Level Radioactive Waste Management Program
[DOE/LLW-33T] 09 p1383 N85-18699
Rock mechanics: Issues and research needs in the disposal of wastes in hydraulic fractures
[DE85-001399] 10 p1556 N85-19809
FAA policy regarding solid waste disposal facilities
[AD-P004196] 11 p1581 N85-19963
Airport bird hazards associated with solid waste disposal facilities
[AD-P004197] 11 p1581 N85-19964
Effectiveness of an overhead wire barrier in deterring gulls from feeding at a sanitary landfill
[AD-P004199] 11 p1582 N85-19966
Effectiveness of an overhead wire barrier system in reducing gull use at the BFI Jedburg sanitary landfill, Berkeley and Dorchester counties, South Carolina
[AD-P004200] 11 p1582 N85-19967
Effect of host-rock dissolution and precipitation on permeability in a nuclear waste repository in tuff
[DE85-000675] 11 p1727 N85-20860
Radioactive waste isolation in salt: Peer review of the D'Appolonia report on schematic designs for penetration seals for a repository in the Permian Basin, Texas
[DE85-000693] 11 p1727 N85-20861
Field lysimeter facility for evaluating the performance of commercial solidified low-level waste
[DE85-003886] 11 p1727 N85-20863
High-level waste processing and disposal
[DE85-003564] 11 p1728 N85-20865
ELECT groundwater transport research code
[DE85-003284] 12 p1884 N85-21824
Role of biological assessment in effluent control
[PB85-116101] 12 p1885 N85-21830
Stochastic convective-dispersive transport model for wastes disposed at the 106-mile ocean disposal site
[PB85-116176] 12 p1885 N85-21831
Methods/materials matrix of ultimate disposal techniques for spilled hazardous materials
[PB85-116853] 12 p1885 N85-21833
Assessment of hazardous waste surface impoundment technology case studies and perspectives of experts
[PB85-117059] 12 p1886 N85-21834
Shallow land burial technology: Humid
[DE85-004432] 12 p1932 N85-22136
Research and development related to the Nevada nuclear waste storage investigations
[DE85-002303] 12 p1932 N85-22138
Application of far-field models to the disposal of nuclear waste in geologic formations
[DE85-005489] 14 p2420 N85-24932
Protecting the nation's groundwater from contamination, volume 1
[PB85-154201] 15 p2590 N85-25965
Protecting the nation's groundwater from contamination, volume 2
[PB85-154219] 15 p2590 N85-25966
Shales and other argillaceous strata in the United States
[DE85-010453] 18 p3125 N85-29353
Region-to-area screening methodology for the Crystalline Repository Project
[DE85-009892] 18 p3125 N85-29354
Implications about in situ stress at Yucca Mountain
[DE85-008068] 18 p3126 N85-29356
Thermal-cycle testing of the G-tunnel heated block
[DE85-008408] 18 p3126 N85-29359
Advanced regenerative environmental control and life support systems: Air and water regeneration
18 p3155 N85-29535
Radionuclide mobility in the shallow portion of an active high-temperature geothermal system
[DE85-010293] 18 p3182 N85-29729
Experimental program to determine maximum temperatures for dry storage of spent fuel
[DE85-010307] 19 p3236 N85-30060
Hydrolysis, formation and ionization constants at 25(0)C, and at high temperature-high ionic strength
[DE85-010645] 19 p3236 N85-30061
Mixtures experiment where the amount of the mixture is a factor under study
[DE85-010974] 19 p3250 N85-30153
Reference data source documentation for performance assessment studies, Basalt Waste Isolation Project, Hanford Site, Washington
[DE85-010543] 19 p3301 N85-30466

Preliminary evaluation of alterant geophysical tomography in welded tuff
[DE85-010826] 19 p3302 N85-30469
Petrologic and geochemical characterization of the Topopah Spring Member of the Paintbrush Tuff: Outcrop samples used in waste package experiments
[DE85-010449] 19 p3302 N85-30470
Environmental Sciences Division report
[DE85-010452] 19 p3308 N85-30506
Radioactive liquid wastes discharged to ground in the 200 areas during 1984
[DE85-010819] 19 p3310 N85-30517
Analysis of leachate production in closed hazardous waste landfills
[DE85-010978] 19 p3310 N85-30520
Bulk and thermal properties of the functional Tuffaceous Beds in holes USW G-1, UE-25 no. 1, and USW G-2, Yucca Mountain, Nevada
[DE85-011181] 19 p3365 N85-30866
Dispersal From Deep Ocean Sources: Physical and Related Scientific Processes
[DE85-010420] 20 p3497 N85-31740
Development of processes for the inclusion of radioactive waste in glass-metal compounds and ceramic materials
[BLL-CE-TRANS-8014-(9022.09)]
20 p3526 N85-31931
Geologic and hydrologic characterization and evaluation of the basin and range province relative to the disposal of high-level radioactive waste. Part 1: Introduction and guidelines
[GS-CIRC-904-A] 20 p3526 N85-31932
Geologic and hydrologic characterization and evaluation of the basin and range province relative to the disposal of high-level radioactive waste. Part 2: Geologic and hydrologic characterization
[GS-CIRC-904-B] 20 p3526 N85-31933
Geologic and hydrologic characterization and evaluation of the basin and range province relative to the disposal of high-level radioactive waste. Part 3: Geologic and hydrologic evaluation
[GS-CIRC-904-A] 20 p3526 N85-31934
Source-term considerations for a potential radioactive-waste repository located in unsaturated tuff
[DE85-010090] 20 p3529 N85-31953
Review of hazardous waste cleanup and disposal efforts at Tinker Air Force Base
[GPO-43-294] 21 p3613 N85-32457
Centrifugal castings of stainless steel spiked with radioactive tracers
[DE85-012003] 22 p3748 N85-33234
WIPP horizon in situ permeability measurements
[DE85-012687] 22 p3802 N85-33557
Technology of off-gas treatment for liquid-fed ceramic melters
[DE85-012467] 22 p3812 N85-33610
Corrosion resistant storage container for radioactive material
[DE85-011666] 22 p3838 N85-33765
Office of Civilian Radioactive Waste Management
[DE85-012585] 22 p3839 N85-33774
Review of zirconium-zircaloy pyrophoricity
[DE85-011169] 23 p3916 N85-34270
Method for making a low density polyethylene waste form for safe disposal of low level radioactive material
[DE85-006401] 23 p3920 N85-34292
Research at the Institute of Oceanographic Sciences related to the possible disposal of radioactive waste on or beneath the seafloor
[IOS-204] 23 p3973 N85-34628
Simulated effects of increased recharge on the ground-water flow system of Yucca Mountain and vicinity, Nevada-California
[DE85-012985] 24 p4108 N85-35469
Land Disposal of Hazardous Waste
[PB85-196376] 24 p4113 N85-35500

WASTE ENERGY UTILIZATION
Evaluation of selected advanced heat exchangers for waste heat recuperation of high temperature streams
[DE84-016299] 04 p0499 N85-13180
Magnetic heat pump cycles for industrial waste heat recovery
[DE84-017016] 04 p0499 N85-13183
Detailed performance analysis of the A.A.D. - concept B 04 p0507 N85-13237
Overview of waste heat utilization systems
[NASA-TM-86901] 04 p0578 N85-13692
Challenges in the development of the orbiter radiator system 08 p1096 N85-16925
Available energy method for evaluating thermodynamic performance of heat pump systems
[DE84-017223] 09 p1400 N85-18814
Comparative evaluation of three alternative power cycles for waste heat recovery from the exhaust of adiabatic diesel engines
[NASA-TM-86953] 20 p3542 N85-32043
Feasibility study for small group water desalination equipment
[AD-A155106] 21 p3563 N85-32164
Woven heat exchanger
[DE85-011633] 22 p3783 N85-33439
Advanced regenerative heat recovery system
[PB85-199602] 24 p4064 N85-35315

WASTE HEAT
Evaluation of selected advanced heat exchangers for waste heat recuperation of high temperature streams
[DE84-016299] 04 p0499 N85-13180
Magnetic heat pump cycles for industrial waste heat recovery
[DE84-017016] 04 p0499 N85-13183
Open-cycle vapor compression heat pump
[PB85-101475/GAR] 06 p0775 N85-14951
Available energy method for evaluating thermodynamic performance of heat pump systems
[DE84-017223] 09 p1400 N85-18814
Development and test of a high COP Rankine heat pump for generation of process steam. Phase 2: Fabrication and test
[DE85-002600] 11 p1632 N85-20275
Technology for industrial waste heat recovery by organic Rankine cycle systems
[DE85-006719] 18 p3102 N85-29206
Comparative evaluation of three alternative power cycles for waste heat recovery from the exhaust of adiabatic diesel engines
[NASA-TM-86953] 20 p3542 N85-32043
Woven heat exchanger
[DE85-011633] 22 p3783 N85-33439
Energy from low temperature differences
[DE85-006817] 24 p4112 N85-35492

WASTE TREATMENT
HS and E environmental sciences
[DE84-016183] 05 p0672 N85-14314
Immobilization of toxic waste by embedding it in bitumen
[OEFZS-4277] 07 p0995 N85-16322
Proceedings of the Environmental Systems Symposium (13th) held at Bethesda, Md., 20-22 March 1984
[AD-A148194] 09 p1346 N85-18471
Strategies for preparing and submitting a part B application for a DoD facility
[AD-P004139] 09 p1347 N85-18475
Stabilization of contaminated soils by in situ vitrification
[AD-P004144] 09 p1348 N85-18480
Treatment of wastewater (red water) resulting from TNT (trinitrotoluene) purification
[AD-P004146] 09 p1348 N85-18482
Rockwell Hanford operations defense waste and byproducts management
[DE85-000553] 09 p1382 N85-18694
Hydrolysis of plastic wastes with the aim of recovering and reprocessing the starting components (recycling)
[BMFT-FB-T-84-250] 12 p1885 N85-21828
Controlled Ecological Life Support Systems (CELSS)
15 p2688 N85-26604
Survey of CELSS concepts and preliminary research in Japan 18 p3155 N85-29533
Publications of the NASA CELSS (Controlled Ecological Life Support Systems) program
[NASA-CR-3911] 19 p3326 N85-30608
Anaerobic microbial transformations in subsurface environments
[DE85-012790] 22 p3819 N85-33659
Method for extracting lanthanides and actinides from acid solutions by modification of Purex solvent
[DE85-005763] 23 p3909 N85-34220

WASTE UTILIZATION
Development of a preprototype times wastewater recovery subsystem, addendum
[NASA-CR-171823] 07 p1019 N85-16468
Technology for industrial waste heat recovery by organic Rankine cycle systems
[DE85-006719] 18 p3102 N85-29206
Qualitative comparison of fusion reactor materials for waste handling and disposal
[DE85-010473] 19 p3360 N85-30830

WASTE WATER
Development of a preprototype times wastewater recovery subsystem
[NASA-CR-171815] 03 p0388 N85-12480
Addendum: Development of a preprototype times wastewater recovery subsystem
[NASA-CR-171816] 03 p0388 N85-12481
Development of a preprototype times wastewater recovery subsystem: Appendices
[NASA-CR-171817] 03 p0388 N85-12482
Mechanism and process of flocculation by polymeric flocculant 09 p1303 N85-18185
Polymeric liner selection for military waste impoundments
[AD-P004143] 09 p1348 N85-18479
Treatment of wastewater (red water) resulting from TNT (trinitrotoluene) purification
[AD-P004146] 09 p1348 N85-18482
Removal of heavy metals by artificial wetlands
[PB85-116127] 10 p1513 N85-19548
Literature review for development of the master analytical scheme for organic compounds in water
[PB85-152874] 15 p2507 N85-25466
Toxicity of TNT wastewaters to aquatic organisms. Volume 4: Chronic toxicity of 2,4-dinitrotoluene and condensate water
[AD-A153536] 18 p3132 N85-29400
EPA (Environmental Protection Agency) research program guide, FY-1985, October 1, 1984 - September 30, 1985
[PB85-181861] 20 p3487 N85-31676
The degradation of pollutants in water and waste water by means of electron or gamma irradiation
[OEFZS-4317] 22 p3812 N85-33615

WASTES
NT FECES
NT GARBAGE
NT HUMAN WASTES
NT INDUSTRIAL WASTES
NT LIQUID WASTES
NT METABOLIC WASTES
NT RADIOACTIVE WASTES
NT SOLID WASTES
NT URINE
NT WASTE WATER
Proceedings of the Environmental Systems Symposium (13th) held at Bethesda, Md., 20-22 March 1984
[AD-A148194] 09 p1346 N85-18471
Strategies for preparing and submitting a part B application for a DoD facility
[AD-P004139] 09 p1347 N85-18475
Location of volatile buried wastes by field portable instrumentation
[AD-P004147] 09 p1346 N85-18483
Practical application of earth resistivity methods in phase 2 of the installation restoration program
[AD-P004148] 09 p1348 N85-18484
Organic solvent alteration of hydraulic properties of sedimentary rocks of low permeability: A review
[DE85-012537] 22 p3815 N85-33635

WATCHES
U CLOCKS

WATER
NT COASTAL WATER
NT COLD WATER
NT FRESH WATER
NT GROUND WATER
NT INLAND WATERS
NT NEARSHORE WATER
NT POTABLE WATER
NT SEA WATER
NT SHALLOW WATER
NT SPRINGS (WATER)
NT SURFACE WATER
NT WASTE WATER
Compilation of elemental concentration data for NBS (National Bureau of Standards) biological, geological and environmental standard reference materials, 1982
[PB84-218338] 01 p0025 N85-10156
Resonant frequencies and mode shapes for single and double cylindrical shells
[AD-A144778] 01 p0062 N85-10406
Effect of fluid and salt supplements to food allowance on endurance of head-to-pelvis accelerations following 7-day dry immersion and under ordinary motor activity conditions 01 p0092 N85-10618
Determination of bound water in biological tissue and energy dissipated in bound water by low level microwaves
[AD-A143101] 03 p0399 N85-12547
Prediction of long term strength of glass reinforced plastics in wet environments
[NPL-DMA(A)-80] 04 p0477 N85-13041
Ice-soil mixtures: Visual and near-infrared remote sensing techniques
[NASA-CR-174087] 04 p0525 N85-13358
Effect of water on hydrogen permeability — Stirling engines
[NASA-TM-86904] 06 p0761 N85-14864
Deuterium diffusion in a soil-water-ice mixture
[AD-A148457] 08 p1176 N85-17415
Ground-based measurements of mesosphere temperatures by optical means
08 p1183 N85-17453
A method for automatic water mass classification
[AD-D011405] 08 p1191 N85-17505
Prototype wash water renovation system integration with government-furnished wash fixture
[NASA-CR-171829] 08 p1198 N85-17547
Measurements of H2O in Jupiter's atmosphere from 5 microns airborne observations 08 p1244 N85-17854

Water impact laboratory and flight test results for the space shuttle solid rocket booster aft skirt
09 p1335 N85-18394
A model for the climatic behavior of water on Mars
09 p1415 N85-18931
Factors influencing the ball milling of Si3N4 in water
[NASA-TM-86932] 10 p1450 N85-19136
Water absorption and conductivity in poly(ethylene oxide)-lithium tetrafluoroborate films
[AD-A147969] 10 p1450 N85-19138
A 10/sup 11/W high current pulse electron beam accelerator described 11 p1620 N85-20200
Photosynthetic water splitting
[DE85-002460] 11 p1690 N85-20627
Alternative anodic reactions in water splitting
[DE85-004159] 12 p1802 N85-21300
Parametric evaluation of ball milling of SiC in water
[NASA-TM-86974] 12 p1811 N85-21356
Microprocessor-controlled anodic stripping voltammeter for trace metal analysis in tap water
[DE85-002781] 12 p1852 N85-21619
Development and evaluation of a procedure for the rapid analysis of fresh concrete
[AD-A149741] 12 p1866 N85-21703
Gas-liquid chemistry of natural waters, volume 2
[DE85-002457] 12 p1884 N85-21823
Polar cap formation on Ganymede
13 p2174 N85-23486
The evolution of CO2 on Mars
13 p2185 N85-23558
Hydrovolcanism 13 p2188 N85-23574
Mars: Long term changes in the state and distribution of H2O 13 p2191 N85-23593
Radar and the detection of liquid water on Mars
13 p2199 N85-23636
Ammonia formation caused by the presence of water in the wet grinding of silicon nitride powder
[NASA-TM-77746] 14 p2249 N85-23937
Long-term exposure of pressed plutonium oxide heat sources to aquatic environments
[DE85-007385] 15 p2495 N85-25392
The effects of water and hydrogen on materials used in integrated circuit packages
[AD-A151893] 15 p2518 N85-25529
Physics effects cf accidental submersion of space power reactors in water
[DE85-005020] 15 p2650 N85-26344
The Martian climate: Energy balance models with CO2/H2O atmospheres
[NASA-CR-175722] 15 p2679 N85-26547
Mars: Seasonally variable radar reflectivity
15 p2683 N85-26570
Combustion and micro-explosion of water/oil emulsions in high pressure environments
[AD-A152960] 17 p2919 N85-27997
Alternative heat sources for heat pumps
[DE85-007610] 17 p2959 N85-28275
Inspection evaluation and repair of the flawed feedwater nozzle of the 50 MWe Dodewaard GKN boiling water reactor
[ISBN-90-353-0017-3] 17 p2977 N85-28394
Potential climatic impacts of increasing atmospheric CO2 with emphasis on water availability and hydrology in the United States
[NASA-TM-87479] 17 p2995 N85-28517
Modeling and experiments on tritium permeation in fusion reactor blankets
[DE85-008439] 18 p3183 N85-29741
Adhesive evaluation of LARC-TPI and a water-soluble version of LARC-TPI
[NASA-TM-86428] 19 p3248 N85-30136
Response of steam-water mixtures to pressure transients
[DE85-010798] 19 p3267 N85-30262
Activities of the Wind Energy Programme
20 p3540 N85-32028
Two-phase flow visualization in a transparent, atmospheric pressure, boiling water loop
[DE84-016857] 21 p3586 N85-32288
Polymer-water interaction studies
21 p3609 N85-32411
Mechanism of heterogeneous deposition ice nucleation near water-saturation 21 p3638 N85-32597
Ice nucleation of single water droplet by silver iodide: A laboratory observation 21 p3643 N85-32630
Critical supersaturations with respect to water for fast condensation-freezing ice nucleation
21 p3643 N85-32632
Monte Carlo studies of H2O layers adsorbed on a model basal face of AgI 21 p3643 N85-32633
Cloud condensation on insoluble particles
21 p3648 N85-32670
Interactions among sulfide-oxidizing bacteria
21 p3661 N85-32741
Physical chemical state of water in living cells
[AD-A154566] 21 p3662 N85-32749
Transparency of water 9n 186 - 500 nm region
21 p3690 N85-32923
Activation analysis of natural water using neutrons of various energies 21 p3690 N85-32924
Nonsaturable microdryer
[DE85-005760] 23 p3946 N85-34457
Multi-solute subsurface transfer modeling for energy solid wastes: Highlights FY 1984
[DE85-012788] 23 p3966 N85-34591
Pressure cross spectra in turbulent boundary layers in water
[AD-A156163] 24 p4094 N85-35378
Calculation of heavy-ion tracks in liquid water
[DE85-012101] 24 p4149 N85-35725
Observation of EAS using a large water tank
24 p4189 N85-35986
An experiment to detect gut monopoles
[HE-6.1-7] 24 p4210 N85-36133

WATER BALANCE
The water balance and climate — Amazon region
07 p1003 N85-16370
Modeling interception of rainfall by forests and the role of interception in the water balance
[DE85-002822] 12 p1884 N85-21825
Fluid metabolism of monkeys during two-week antiorthostatic hypokinesia 12 p1902 N85-21943

WATER CIRCULATION
NT COASTAL CURRENTS
NT EL NINO
NT GULF STREAM
NT OCEAN CURRENTS
NT WATER CURRENTS
Synthesis of current measurements in Puget Sound, Washington. Volume 1: Index to current measurements made in Puget Sound from 1908-1980 with daily and record averages for selected measurements
[PB84-214105] 01 p0069 N85-10603
Deep water mass circulation in the Western Alboran Basin: Measurements in July and September 1980 (Alboran I experiment)
[AD-A148566] 08 p1181 N85-17504
North Atlantic Deep Water Formation
[NASA-CP-2367] 15 p2601 N85-26028
Review of North Atlantic source waters
15 p2601 N85-26029
Deep water formation 15 p2601 N85-26030
Destruction of density jumps in ocean by turbulence
19 p3291 N85-30407

WATER COLOR
Analysis of suspended sediment distributions in the surface waters of Delaware Bay using remote sensing of optical properties 15 p2582 N85-25926

WATER CONSUMPTION
Uncertainty in water resource planning: An economic evaluation of a water use reduction alternative
[PB84-202605] 01 p0065 N85-10430

WATER CONTENT
U MOISTURE CONTENT

WATER COOLED REACTORS
NT BOILING WATER REACTORS
NT LIGHT WATER REACTORS
NT PRESSURIZED WATER REACTORS
NT ZERO POWER REACTORS
Emerging technology of synthetic aperture focusing for ultrasonic testing
[DE85-000373] 09 p1378 N85-18664
Technical assessment of thermal-hydraulics for high heat flux fusion components
[DE85-013176] 23 p3930 N85-34359

WATER COOLING
U LIQUID COOLING

WATER CURRENTS
NT COASTAL CURRENTS
NT EL NINO
NT GULF STREAM
NT OCEAN CURRENTS
Spectral model for subtidal variability in the Chesapeake Bay
[PB84-226679] 06 p0842 N85-15345
Slope water intrusions within the nearshore waters off Long Island, New York
[DE85-001386] 09 p1359 N85-18549
Analysis of flow within the coastal boundary layer off Long Island, New York
[DE85-001384] 09 p1359 N85-18550
Field-work report: Medway Estuary, 28 June - 18 July 1983
[RNC/NS/TR8] 13 p2041 N85-22773
Temporal and spatial scales of Labrador Sea water formation 15 p2601 N85-26031
Frequency of recurrence and critical conditions for generation of Langmuir circulations
19 p3291 N85-30409

WATER DEPTH
Satellite altimetric measurements of lake levels
03 p0383 N85-12447
Evolution of nonlinear wave groups on water of slowly-varying depth
[AD-A147947] 08 p1162 N85-17329

WATER EROSION
Paleohydrology and geomorphology of selected reaches of the upper Wabash Valley, Indiana
02 p0226 N85-11481
Experiments and analyses of the formation of erosional scour marks with implications to the origin of the Martian outflow channels 13 p2190 N85-23586

WATER FLOW
Water resources data for Maine, water year 1983
[PB84-225143] 01 p0066 N85-10440
Water resources data for Ohio, water year 1983. Volume 1: Ohio River basin
[PB84-224690] 01 p0066 N85-10441
Water resources data for Michigan, water year 1983
[PB84-225176] 01 p0066 N85-10442
Coso Monitoring Program, January 1981 through December 1983
[AD-A147894] 07 p0998 N85-16338
Subcooled flow boiling at high heat flux
[OUEL-1540/84] 08 p1163 N85-17338
Weakly-reflective boundary conditions for two-dimensional shallow water flow problems
[PUBL-322] 08 p1163 N85-17341
Analysis of geohydrologic data by kriging
[AD-P004152] 09 p1349 N85-18468
World ocean level oscillations and their relationship to change in inflow of continental waters
13 p2108 N85-23133
A computer program to calculate the supersonic flow over a solid cone in air or water
[AD-A151102] 15 p2464 N85-25217
Applications of Kalman filtering and recursive least-squares in river flow modelling
15 p2636 N85-26254
Tidal rectification in lateral viscous boundary layers of a semienclosed basin
[CWI-AM-R8415] 17 p2960 N85-28284
The hydrosynclastic infundibulum
[AD-A153849] 18 p3100 N85-29192
Injection of drag reducing additives into turbulent water flows: Two-component velocity measurements and mixing length model predictions
[AD-A154604] 21 p3583 N85-32274
Reverification of the Chesapeake Bay model
[AD-A155486] 21 p3655 N85-32706
Computer and water-model simulation of flow through poppet valves
[CFD/85/2] 22 p3785 N85-33449
Military hydrology. Report 9: State-of-the-art review and annotated bibliography of dam-breach flood forecasting
[AD-A155363] 22 p3801 N85-33553
Stochastic groundwater flow modeling using the second-order method
[DE85-011250] 22 p3802 N85-33556
National program for inspection of non-federal dams. Woodward reservoir dam (VT 00209), Connecticut River Basin, Plymouth, Vermont. Phase 1 inspection report
[AD-A156256] 24 p4144 N85-35693

WATER HEATING
Test methods and standards development for active solar heating and cooling systems
[PB84-217447] 03 p0343 N85-12209
Qualification of noninvasive systems for on-line leak detection in high pressure feed water preheaters
[CISE-2341] 04 p0558 N85-13555
Actual versus design performance of solar systems in the National Solar Data Network
[DE85-001190] 09 p1344 N85-18456
A review of development and application of heat pump technology
[CSIR-RR-585] 14 p2300 N85-24241
Thermal performance testing and mathematically modeling of integral collector storage solar hot water systems
[PB85-186906] 18 p3132 N85-29398
Energy and Technology Review
[DE85-011767] 21 p3716 N85-33061
Advanced heat pump research and development
[DE85-009540] 23 p3932 N85-34372

WATER IMMERSION
Effects of body mass and morphology on thermal responses in water
[AD-A147558] 07 p1016 N85-16455

WATER INJECTION
Geothermal wells drilled in Transcarpathians
07 p0994 N85-16315
Description of a technique to measure spray distribution in an air stream
[AD-A149780] 12 p1771 N85-21122
Estimation of gas turbine engine boost provided by injecting water behind compressor
13 p2051 N85-22838

Steamflood pilots in the O'Connell Ranch field and the T-4 Ranch field
[DE85-901363] 24 p4106 N85-35488

WATER JETS
U HYDRAULIC JETS

WATER LANDING
NT DITCHING (LANDING)
Air carrier overwater emergency equipment and procedures
[PB85-917006] 21 p3553 N85-32105
Aircraft accident report: World Airways Inc., Flight 30H, McDonnell Douglas DC-10-30CF, N113WA, Boston-Logan International Airport, Boston, Massachusetts, January 23, 1982
[PB85-910406] 22 p3728 N85-33114

WATER MANAGEMENT
Water resources data, Mississippi, water year 1982
[PB84-224559] 01 p0065 N85-10434
Water resources data for Maine, water year 1983
[PB84-225143] 01 p0066 N85-10440
Water resources data for Ohio, water year 1983. Volume 1: Ohio River basin
[PB84-224690] 01 p0066 N85-10441
Remote sensing applications program
[E85-10022] 02 p0218 N85-11435
Water Science and Technology Board
[PB84-216571] 03 p0384 N85-12460
Photovoltaic pump systems 05 p0664 N85-14269
The ARGOS system and hydrology. Results obtained by ORSTROM and benefits of a degree of standardization 14 p2239 N85-23881
Hydrometric telemetry in Canada
14 p2239 N85-23882
Water quantity and quality research for the Rhine Meuse estuary
[PUBL-325] 17 p2988 N85-28470
Great Lakes hydrometeorologic and hydraulic data needs 20 p3496 N85-31739
Empirical methods for predicting eutrophication in impoundments. Report 3. Phase 2. Model refinements
[AD-A155483] 21 p3614 N85-32462

WATER MASERS
Masers associated with regions of recent star formation 03 p0443 N85-12820
Galactic OH and H2O masers — QUASAT project
07 p1058 N85-16719
Water maser outburst 07 p1058 N85-16720
Water masers and distance measurements: The impact of QUASAT 07 p1059 N85-16721

WATER POLLUTION
NT OIL POLLUTION
Solution of contaminant transport equations using an orthogonal-upstream finite element scheme
[DE84-014266] 01 p0070 N85-10463
Response of algal populations to changes in stream water quality
[PB84-202464] 01 p0070 N85-10465
Acid Deposition: Processes of Lake Acidification
[PB84-216175] 01 p0070 N85-10466
The use of fixed-bed adsorber models to predict the fluxes of toxic substances in groundwaters and soil environments
[PB84-202563] 01 p0071 N85-10468
Reverse osmosis treatment to control inorganic and volatile organic contamination
[PB84-223528] 01 p0071 N85-10470
East Europe report: Science and technology
[JPRS-ESA-84-029] 01 p0115 N85-10783
Radiotracer studies of the dispersion of solid pollutants in marine and estuarial environment: Measurement of diffusion coefficients and the phenomenon of dispersion by currents
[BLL-DRIC-TRANS-7104-(3623.66)]
02 p0224 N85-11468
Potential for acidification of six remote ponds in the White Mountains of New Hampshire
[PB84-207349] 02 p0225 N85-11475
Polycyclic aromatic hydrocarbons on the inner surfaces of copper tubing
[AD-A145979] 03 p0337 N85-12169
NODC/1983: National Oceanographic Data Center report
[PB84-222231] 04 p0542 N85-13449
Fate and disposition of trichloroethylene in surface soils
[AD-A147916] 07 p0995 N85-16321
Remote sensing of rice fields and sea pollution by SIR-B 08 p1145 N85-17222
Applying an innovative approach to field investigations at a remedial action site
[AD-P004145] 09 p1348 N85-18481
Protocol for aquifer cleanup decision making at military installations
[AD-P004151] 09 p1349 N85-18487
Intrusion of radioactive industrially polluted water from North Sea into central Baltic Sea
10 p1496 N85-19454
Removal of heavy metals by artificial wetlands
[PB85-116127] 10 p1513 N85-19546
Examples of environment services: Hydrological and pollution measurements in the Po River (Italy)
[CISE-2299] 11 p1679 N85-20576
Isolation, concentration and subsequent analysis by capillary gas chromatography of trace amounts of organophosphorus compounds from aqueous samples
[AD-B089301L] 12 p1803 N85-21306
Role of biological assessment in effluent control
[PB85-116101] 12 p1885 N85-21830
Standard analytical procedures of the NOAA National Analytical Facility, 1984-85: Extractable toxic organic compounds
[PB85-126282] 12 p1887 N85-21840
Determining adsorption of surface-active substances by sea bottom deposits 13 p2107 N85-23128
Protecting the nation's groundwater from contamination, volume 1
[PB85-154201] 15 p2590 N85-25965
Protecting the nation's groundwater from contamination, volume 2
[PB85-154219] 15 p2590 N85-25966
Acid rain: Effects on fish and wildlife
[PB85-154672] 16 p2821 N85-27402
Limiting profiles in contaminant transport through porous media — ground water pollution
[REPT-84-31] 17 p2960 N85-28282
Radiation-induced degradation of trichloroethylene and tetrachloroethylene in drinking water
[OEFZS-4298] 18 p3134 N85-29409
Equipment development for rapid detection of microorganisms in air and water
[FOA-A-40046-B2] 18 p3134 N85-29410
Pollutant body burdens and reproduction in Platichthys stellatus from San Francisco Bay
[DE85-010407] 19 p3306 N85-30509
Radioactive liquid wastes discharged to ground in the 200 areas during 1984
[DE85-010619] 19 p3310 N85-30517
State-of-the-art of aquifer restoration. Volume 1: Sections 1 through 8
[PB85-181071] 20 p3478 N85-31612
State-of-the-art of aquifer restoration. Volume 2: Appendices A through G
[PB85-181089] 20 p3478 N85-31613
Chemoreception and detection of micropollutants by means of a telemetric bionic detector
[DRIC-T-7460] 22 p3810 N85-33600
Acid rain in Europe
[COMMITTEE-PRINT-99-F] 22 p3810 N85-33601
The 1984 effluent and environmental monitoring report for the Bettis Atomic Power Laboratory
[DE85-011533] 22 p3810 N85-33602
Environmental summary for calendar year 1984
[DE85-012020] 22 p3810 N85-33604
The 1984 environmental monitoring report, Sandia National Laboratories, Albuquerque, New Mexico
[DE85-011175] 22 p3811 N85-33607
The degradation of pollutants in water and waste water by means of electron or gamma irradiation
[OEFZS-4317] 22 p3812 N85-33615

WATER PRESSURE
Fine structure of vertical distribution of light attenuation index of sea water 13 p2109 N85-23140

WATER PURIFICATION
U WATER TREATMENT

WATER QUALITY
Application guide for Hydrological Simulation Program FORTRAN (HSPF)
[PB84-215763] 01 p0064 N85-10427
Major institutional arrangements affecting ground water in New York state
[PB84-202506] 01 p0065 N85-10429
Water resources data, Florida, water year 1982. Volume 4: Northwest Florida
[PB84-223445] 01 p0066 N85-10437
Water resources data for Maine, water year 1983
[PB84-225143] 01 p0066 N85-10440
Water resources data for Ohio, water year 1983. Volume 1: Ohio River basin
[PB84-224690] 01 p0066 N85-10441
Water resources data for Michigan, water year 1983
[PB84-225176] 01 p0066 N85-10442
Response of algal populations to changes in stream water quality
[PB84-202464] 01 p0070 N85-10465
Acid Deposition: Processes of Lake Acidification
[PB84-216175] 01 p0070 N85-10466
Multispectral Imaging Science Working Group for Hydrologic Science: Executive summary
02 p0214 N85-11414
Water resources data for California, water year 1982. Volume 1: Southern Great Basin from Mexican border to Mono Lake Basin and Pacific Slope Basins from Tijuana River to Santa Maria River
[PB84-220870] 03 p0384 N85-12461
Water resources data for Florida, water year 1982. Volume 3A: Southwest Florida surface water
[PB84-223080] 03 p0384 N85-12462
Water resources data for Nebraska, water year 1982
[PB84-223668] 03 p0385 N85-12463
Water resources data for California, water year 1982. Volume 3: Southern Central Valley Basins and Great Basins from Walker River to Truckee River
[PB84-223726] 03 p0385 N85-12464
In-lake water quality management for Lake Eureka: Highlights of third year (1983) operation
[PB85-104149/GAR] 07 p0990 N85-16289
Climate and water quality 07 p1002 N85-16368
Development of a preprototype times wastewater recovery subsystem, addendum
[NASA-CR-171823] 07 p1019 N85-16468
Water resources data for Alabama, water year 1983
[PB85-123842] 10 p1507 N85-19507
Water resources data for Illinois, water year 1983. Volume 1: Illinois except Illinois River Basin
[PB85-125755] 10 p1507 N85-19508
Monitoring approaches for assessing quality of high altitude lakes: Colorado Flat Tops Wilderness Area
[PB85-117232] 11 p1679 N85-20579
Role of biological assessment in effluent control
[PB85-116101] 12 p1885 N85-21830
Drifting ice as mechanical factor in purifying and polluting hydrosphere 13 p2106 N85-23132
A first evaluation of LANDSAT TM data to monitor suspended sediments in lakes — Lake Chicot, Arkansas
13 p2120 N85-23204
Literature review for development of the master analytical scheme for organic compounds in water
[PB85-152874] 15 p2507 N85-25468
Water quantity and quality research for the Rhine Meuse estuary
[PUBL-325] 17 p2988 N85-28470
Surface hydrologic characteristics of proposed repository locations in the Palo Duro Basin of the Texas Panhandle
[DE85-010530] 18 p3126 N85-29355
Toxicity of TNT wastewaters to aquatic organisms. Volume 4: Chronic toxicity of 2,4-dinitrotoluene and condensate water
[AD-A153536] 18 p3132 N85-29400
Modeling water resources systems for water quality
[AD-A154288] 19 p3300 N85-30457
Annual environmental monitoring report, January-December 1984
[DE85-011689] 20 p3486 N85-31665
EPA (Environmental Protection Agency) research program guide, FY-1985, October 1, 1984 - September 30, 1985
[PB85-181881] 20 p3487 N85-31676
Offshore oceanographic and environmental monitoring services for the Strategic Petroleum Reserve, volume 3
[DE85-009907] 20 p3497 N85-31741
Empirical methods for predicting eutrophication in impoundments. Report 3. Phase 2. Model refinements
[AD-A155483] 21 p3614 N85-32462
Soil extraction kit
[AD-D011736] 22 p3742 N85-33190
The 1984 effluent and environmental monitoring report for the Bettis Atomic Power Laboratory
[DE85-011533] 22 p3810 N85-33602
Environmental surveillance at Los Alamos during 1984
[DE85-011886] 22 p3811 N85-33605
The 1984 environmental monitoring report, Sandia National Laboratories, Albuquerque, New Mexico
[DE85-011175] 22 p3811 N85-33607
Legionnaires' disease bacteria in power plant cooling systems: Phase 2
[DE85-011546] 22 p3825 N85-33695

WATER RECLAMATION
Development of a preprototype times wastewater recovery subsystem
[NASA-CR-171815] 03 p0388 N85-12480
Addendum: Development of a preprototype times wastewater recovery subsystem
[NASA-CR-171816] 03 p0388 N85-12481
Development of a preprototype times wastewater recovery subsystem: Appendices
[NASA-CR-171817] 03 p0388 N85-12482
Development of a preprototype times wastewater recovery subsystem, addendum
[NASA-CR-171823] 07 p1019 N85-16468
Prototype wash water renovation system integration with government-furnished wash fixture
[NASA-CR-171829] 08 p1196 N85-17547

Space station ECLSS integration analysis: Simplified General Cluster Systems Model, ECLS System Assessment Program enhancements
[NASA-CR-176069] 21 p3670 N85-32796
Experimental validation of allowable concentrations of sodium and potassium in recycled drinking water
22 p3823 N85-33685

WATER RECOVERY
U WATER RECLAMATION

WATER RESOURCES
NT AQUIFERS
Major institutional arrangements affecting ground water in New York state
[PB84-202506] 01 p0065 N85-10429
Uncertainty in water resource planning: An economic evaluation of a water use reduction alternative
[PB84-202605] 01 p0065 N85-10430
Water resources data, Maryland and Delaware, water year 1983
[PB84-225135] 01 p0065 N85-10431
Water resources data, California, water year 1982. Volume 4: Northern central valley basins and the Great Basin from Honey Lake Basin to Oregon state line
[PB84-225127] 01 p0065 N85-10432
Water resources data, California, water year 1982. Volume 2: Pacific slope basins from Arroyo Grande to Oregon state line except Central Valley
[PB84-224708] 01 p0065 N85-10433
Water resources data, Mississippi, water year 1982
[PB84-224559] 01 p0065 N85-10434
Water resources data, Virginia, water year 1983
[PB84-224542] 01 p0066 N85-10435
Water resources data, Ohio, water year 1983. Volume 2: St. Lawrence River basin statewide project data
[PB84-223676] 01 p0066 N85-10436
Water resources data, Florida, water year 1982. Volume 4: Northwest Florida
[PB84-223445] 01 p0066 N85-10437
Water resources data for Maine, water year 1983
[PB84-225143] 01 p0066 N85-10440
Water resources data for Ohio, water year 1983. Volume 1: Ohio River basin
[PB84-224690] 01 p0066 N85-10441
Water resources data for Michigan, water year 1983
[PB84-225176] 01 p0066 N85-10442
Estuaries of the Cape. Part 2: Synopses of available information on individual systems. Report 13: Silvermine (CSW 3)
[CSIR-RR-412-PT-2] 01 p0086 N85-10582
Water resources by orbital remote sensing: Examples of applications
[E85-10015] 02 p0217 N85-11428
Water resources data for Florida, water year 1983. Volume 3B: Southwest Florida ground water
[PB84-220862] 03 p0384 N85-12459
Water Science and Technology Board
[PB84-216571] 03 p0384 N85-12460
Water resources data for California, water year 1982. Volume 1: Southern Great Basin from Mexican border to Mono Lake Basin and Pacific Slope Basins from Tijuana River to Santa Maria River
[PB84-220870] 03 p0384 N85-12461
Water resources data for Florida, water year 1982. Volume 3A: Southwest Florida surface water
[PB84-223080] 03 p0384 N85-12462
Water resources data for Nebraska, water year 1982
[PB84-223668] 03 p0385 N85-12463
Water resources data for California, water year 1982. Volume 3: Southern Central Valley Basins and Great Basins from Walker River to Truckee River
[PB84-223726] 03 p0385 N85-12464
Activities of the Coastal Research Center
[PB84-231323] 05 p0672 N85-14320
Climatological information and water resources
07 p1002 N85-16367
Water and climate, study of one case
07 p1002 N85-16369
The water balance and climate — Amazon region
07 p1003 N85-16370
Closed-loop concepts for the Army: Water conservation, recycle, and reuse
[AD-A148839] 09 p1365 N85-18581
Water resources data for Alabama, water year 1983
[PB85-123842] 10 p1507 N85-19507
Water resources data for Illinois, water year 1983. Volume 1: Illinois except Illinois River Basin
[PB85-125755] 10 p1507 N85-19508
Water resources data for Colorado, water year 1983. Volume 1: Missouri River Basin, Arkansas River Basin and Rio Grande Basin
[PB85-123859] 11 p1671 N85-20528
Water resources data for Colorado, water year 1983. Volume 2: River Basin above Dolores River
[PB85-123867] 11 p1671 N85-20529
Building a functional, integrated GIS/remote sensing resource analysis and planning system — Utah
[E85-10092] 12 p1874 N85-21754
Hydrology and climatic conditions in Greenland
14 p2327 N85-24387
Protecting the nation's groundwater from contamination, volume 1
[PB85-154201] 15 p2590 N85-25965
Groundwater model for an island aquifer: Bribie Island groundwater study
[CE-44] 16 p2821 N85-27396
Water quantity and quality research for the Rhine Meuse estuary
[PUBL-325] 17 p2986 N85-28470
Modeling water resources systems for water quality
[AD-A154266] 19 p3300 N85-30457
Radioactive liquid wastes discharged to ground in the 200 areas during 1984
[DE85-010819] 19 p3310 N85-30517
Microwave hydrology: A trilogy
[NASA-CR-176042] 20 p3477 N85-31603
Great Lakes hydrometeorologic and hydraulic data needs
20 p3496 N85-31739
Feasibility study for small group water desalination equipment
[AD-A155106] 21 p3563 N85-32164

WATER RUNOFF
Remote Sensing of Snow and Evapotranspiration
[NASA-CP-2363] 13 p2123 N85-23223
General report of the researches of snowpack properties, snowmelt runoff and evapotranspiration in Japan
13 p2124 N85-23225
Snowmelt-runoff model utilizing remotely-sensed data
13 p2124 N85-23226
Snowmelt runoff model in Japan
13 p2124 N85-23227
Distribution of snow and maximum snow water equivalent obtained by LANDSAT data and degree day method
13 p2124 N85-23229

WATER TABLES
Ground-water level data and preliminary potentiometric-surface maps, Yucca Mountain and vicinity, Nye County, Nevada
[DE85-001771] 09 p1343 N85-18448

WATER TAKEOFF AND LANDING AIRCRAFT
NT SEAPLANES

WATER TEMPERATURE
NT OCEAN TEMPERATURE
NT SEA SURFACE TEMPERATURE
Water resources data for Michigan, water year 1983
[PB84-225176] 01 p0066 N85-10442
Forecasting water temperature decline and freeze-up in rivers
[AD-A147068] 07 p0987 N85-16274
Coso Monitoring Program, January 1981 through December 1983
[AD-A147894] 07 p0998 N85-16338
Geothermal assessment of part of the east shore area, Davis and Weber Counties, Utah
[DE84-016817] 09 p1342 N85-18446
Water resources data for Illinois, water year 1983. Volume 1: Illinois except Illinois River Basin
[PB85-125755] 10 p1507 N85-19508
Fine structure of vertical distribution of light attenuation index of sea water
13 p2109 N85-23140
A first evaluation of LANDSAT TM data to monitor suspended sediments in lakes — Lake Chicot, Arkansas
13 p2120 N85-23204
Physiochemically controlled scour jet array system
[AD-D011688] 19 p3308 N85-30505
Evaluation of low-temperature geothermal potential in Utah and Goshen Valleys and adjacent areas, Utah. Part 2: Water temperature and chemistry
[DE85-009344] 23 p3943 N85-34438
Geothermal resources of the Washakie and Great Divide basins, Wyoming
[DE85-013004] 24 p4112 N85-35491

WATER TREATMENT
An evaluation of the electrodialysis reversal process (Edr) for the desalination of brackish water from the Omaruru delta (SWA/Namibia)
01 p0023 N85-10141
Operating experiences of reverse osmosis plants treating Rand Water Board (RWB) water: Pitfalls and problems
01 p0023 N85-10142
Reverse osmosis treatment to control inorganic and volatile organic contamination
[PB84-223528] 01 p0071 N85-10470
Ultrafiltration as pretreatment for the preparation of drinking water by reverse osmosis onboard ships
[PML-1984-32] 01 p0098 N85-10654
Evaluation of survival straws (pocket purifier)
[AD-A146240] 03 p0328 N85-12114
Development of a preprototype times wastewater recovery subsystem
[NASA-CR-171815] 03 p0388 N85-12480
Addendum: Development of a preprototype times wastewater recovery subsystem
[NASA-CR-171816] 03 p0388 N85-12481
Development of a preprototype times wastewater recovery subsystem: Appendices
[NASA-CR-171817] 03 p0388 N85-12482
Solar energy supplied mobile water purification unit
05 p0664 N85-14270
USSR report: Chemistry
[JPRS-UCH-84-012] 06 p0761 N85-14865
In-lake water quality management for Lake Eureka: Highlights of third year (1983) operation
[PB85-104149/GAR] 07 p0990 N85-16289
Development of a preprototype times wastewater recovery subsystem, addendum
[NASA-CR-171823] 07 p1019 N85-16468
Prototype wash water renovation system integration with government-furnished wash fixture
[NASA-CR-171829] 08 p1198 N85-17547
Mechanism and process of flocculation by polymeric flocculant
09 p1303 N85-18165
Treatment of wastewater (red water) resulting from TNT (trinitrotoluene) purification
[AD-P004146] 09 p1348 N85-18482
Removal of heavy metals by artificial wetlands
[PB85-116127] 10 p1513 N85-19548
Radiation-induced degradation of trichloroethylene and tetrachloroethylene in drinking water
[OEFZS-4296] 18 p3134 N85-29409
Hydrodynamic solutions for the diffusion of components in confined media
20 p3456 N85-31464
State-of-the-art of aquifer restoration. Volume 1: Sections 1 through 8
[PB85-181071] 20 p3478 N85-31612
State-of-the-art of aquifer restoration. Volume 2: Appendices A through G
[PB85-181089] 20 p3478 N85-31613
Oxidation of formaldehyde solutions used for the preservation of reverse osmosis membranes
[PB85-185585] 22 p3742 N85-33194
The degradation of pollutants in water and waste water by means of electron or gamma irradiation
[OEFZS-4317] 22 p3812 N85-33615
Experimental validation of allowable concentrations of sodium and potassium in recycled drinking water
22 p3823 N85-33685

WATER TUNNEL TESTS
Design, manufacture, and testing of compliant coatings for reduction of turbulent drag
[AD-A145510] 02 p0198 N85-11323
Multi-ducted inlet combustor research and development
[AD-A153753] 18 p3063 N85-28946
Circulation control lift generation experiment: Hardware development
22 p3799 N85-33535

WATER TUNNELS
U HYDRAULIC TEST TUNNELS

WATER VAPOR
H2O profile in lower atmosphere of Venus based on effective radiation flux measurements
02 p0163 N85-11102
The water vapor resistances of some clothing assemblies used by flying personnel of the Swedish Armed Forces: A series of model studies
[FOA-C-59011-H1] 02 p0238 N85-11551
Effects of atmospheric water vapor and clouds on NOAA (National Oceanic and Atmospheric Administration) AVHRR (Advanced Very High Resolution Radiometer) satellite data
[AD-A145425] 02 p0260 N85-11824
Measurement of range-resolved water vapor concentration by coherent CO2 differential absorption lidar
[PB84-236892] 04 p0535 N85-13420
Development and evaluation of cloud water collectors
[PB84-232529] 04 p0540 N85-13437
Aspects of the comparison of stratospheric trace species measurements with photochemical models
[DE84-017028] 05 p0672 N85-14317
Comparison of optimum interpolation and Cressman analyses
05 p0680 N85-14371
Water vapor profile retrievals from the HIRS/MSU satellite sounder
05 p0681 N85-14378
Studies of atmospheric water in storms with the Nimbus 7 scanning multichannel microwave radiometer
05 p0682 N85-14382
Hydrogen production employing high-temperature solid oxide cells
[DE84-014559] 06 p0766 N85-14901
Nonlinear control model of an H2O steam reactor
[DFVLR-FB-84-30] 07 p0975 N85-16192
Continuum absorption by H2O in the 700-1200 cm(-1) and 2400-280 cm(-1) windows
[AD-A147391] 07 p0997 N85-16334
The atmospheric extinction problem
08 p1251 N85-17901

An analysis of the seasonal variations in the water vapor transport fields over the Southern Hemisphere
09 p1356 N85-18531

Effect of water vapor and water droplets on the RAM-1 (Real-Time Aerosol Monitor): Preliminary results
[PB85-109429] 11 p1637 N85-20313

Electrochemical cell to measure corrosion rates in noncondensing environments
[DE85-003148] 12 p1807 N85-21338

The effects of atmospheric water vapor on infrared propagation
[AD-A150030] 12 p1934 N85-22150

An atlas of nitrogen-broadened water vapor spectra from 500 to 5000 cm(-1), volume 1
[AD-A150527] 13 p2018 N85-22650

Absorption of radiation by water vapor in windows of relative transparency of 95-145 micrometer range
13 p2076 N85-22968

Below-room-temperature water-vapor continuum absorption within the 8- to 10 micron atmospheric transmission window
[TR-0084(4945-09)-1] 13 p2132 N85-23266

A study of liquid-vapor equilibria of the bromine-hydrobromic acid-water system
[NASA-TM-77748] 14 p2249 N85-23940

Diffusion of water vapor in Carbon Fiber Reinforced Plastics (CFRP). Measurement of the diffusion coefficient under influence of concentration
[DFVLR-FB-84-41] 14 p2262 N85-24018

Determining atmosphere moisture content from differences in two-frequency microwave radiation measurements 14 p2341 N85-24474

Study of integral and spectral direct solar radiation over Atlantic 14 p2341 N85-24475

Biophysical evaluation of the wet globe temperature index (Botsball) at high air movements and constant dew point temperature
[AD-A151065] 14 p2378 N85-24683

An atlas of pure water vapor spectra from 500 to 5000/cm, volume 1
[AD-A151756] 15 p2505 N85-25454

Development of hydrogen resistant alloys
16 p2735 N85-26873

An atlas of pure water vapor spectra from 500 to 5000/cm, Volume 2
[AD-A151757] 16 p2745 N85-26940

Water vapor 16 p2824 N85-27420

Precipitable water in the atmosphere, determined from surface dewpoint values 16 p2831 N85-27457

Atmospheric frontal zone studies
[NASA-CR-175293] 16 p2833 N85-27469

Experimental and theoretical study of condensation in multicomponent vapors
[DE85-009357] 17 p2923 N85-28021

Water vapor radiometry research and development phase
[NASA-CR-175887] 17 p2995 N85-28512

Comparison of optimum interpolation and Cressman analyses 18 p3141 N85-29448

Ship-to-ship propagation: Maritime data analyses
[AD-A155484] 21 p3592 N85-32325

On the efficiency of the mechanism of ice particles formation in the vapor supersaturation field around a freezing droplet 21 p3639 N85-32606

Basic ice nucleation mechanisms on mono and microcrystals and ice forming nuclei. Theoretical analysis and experimental results achieved in the laboratory over the past ten years: Review paper
21 p3642 N85-32629

A simple model to investigate the activation process in waterclouds 21 p3649 N85-32675

The interaction of polynuclear aromatic hydrocarbons PAH's with water vapor and their role as condensation nuclei in the formation of haze and fog
21 p3652 N85-32695

Distinctions in formation of microflora on construction materials used in habitable pressurized compartments
22 p3823 N85-33683

Potential spin-offs of the carbon dioxide observational platform system (CO-OPS) for remote sensing opportunities
[NASA-TP-2510] 23 p3899 N85-34149

Millimeter-wave propagation in moist air: Model versus path data
[AD-A156040] 24 p4087 N85-35331

Air chemistry measurements 2
[AD-A156041] 24 p4117 N85-35520

WATER VEHICLES

NT AIRCRAFT CARRIERS
NT BOATS
NT LIFEBOATS
NT SHIPS
NT SUBMARINES
NT SURFACE EFFECT SHIPS
NT TANKER SHIPS
NT UNDERWATER RESEARCH LABORATORIES
NT UNDERWATER VEHICLES

Corrosion problems in the Canadian maritime forces
[AD-A151594] 15 p2509 N85-25481

WATER WAVES

NT TIDAL WAVES

Return wave heights off South Uist estimated from seven years of data
[IOS-164] 01 p0089 N85-10601

Paleoenvironmental interpretation of the upper cretaceous Point Lookout sandstone: Implications for shoreline progradation and basin tectonic history, San Juan basin, New Mexico 02 p0227 N85-11486

Ocean wave parameters extraction using satellite short-pulse radar altimeters 03 p0380 N85-12425

The impact of satellite altimeter data on wave research 03 p0380 N85-12427

International banking of satellite and in-situ wave data by the Marine Information and Advisory Services (MIAS)
03 p0381 N85-12434

Impact of ERS-1 observations on wave forecasting in the North Sea 03 p0381 N85-12437

Intercomparison of GEOS 3/SEASAT wave data and wave model data 03 p0381 N85-12438

Extraction of wave period from altimeter data
03 p0382 N85-12439

Simulation of wavefronts returned by realistic surfaces
03 p0383 N85-12448

The altimeter as a support to the scatterometer in the representation of winds and derived wave fields in coastal waters and enclosed seas: A research at its onset
03 p0383 N85-12453

The estimation of persistance statistics from cumulative probabilities of wave height
[NMI-R183] 03 p0397 N85-12534

Prediction of wave height of wind-generated seas in finite water depth
[AD-A145996] 03 p0398 N85-12539

Parameterizing extreme still water levels and waves in design level studies
[IOS-183] 03 p0398 N85-12542

Statistical analysis of visual wave observations and gage/radar measurements
[AD-A146358] 06 p0798 N85-15100

Two-dimensional lake wave prediction system
[PB84-231034] 06 p0841 N85-15342

Wave-wave interactions, microseisms, and infrasonic ambient noise in the ocean
[AD-A146529] 06 p0859 N85-15463

The interpretation of SIR-B imagery of surface waves and other oceanographic features using in-situ, meteorological satellite, and infrared satellite data
08 p1143 N85-17212

The spatial evolution of t he directional wave spectrum in the Southern Ocean: Its relation to extreme waves in Agulhas Current 08 p1144 N85-17213

Evolution of nonlinear wave groups on water of slowly-varying depth
[AD-A147947] 08 p1162 N85-17329

Assessment of wave power available at key United Kingdom sites
[IOS-186] 09 p1346 N85-18466

Field studies of run-up generated by wind waves on dissipative beaches
[AD-A148793] 09 p1359 N85-18548

Quantization study for ERS-1 wave mode
[DFVLR-FB-84-39] 11 p1625 N85-20234

The imaging of internal waves by the SEASAT-A synthetic aperture radar
[AD-A149808] 12 p1875 N85-21761

Hurricane alicia storm surge and wave data
[AD-A149688] 12 p1895 N85-21896

Relationship between brightness spectrum of photographic image and spectrum of rises on a water surface with waves 13 p2115 N85-23171

Fourier transform of wave data on ARGOS buoys
14 p2323 N85-24351

Low-frequency oscillations of sea level and group structure of wind waves 14 p2335 N85-24441

Remote sensing of directional wave spectra using the surface contour radar
[NASA-TM-84440] 14 p2347 N85-24510

Water wave propagation over uneven bottoms
[AD-A151450] 15 p2556 N85-25769

Survey of remote sensing techniques for wave measurement
[NASA-TM-84429] 15 p2583 N85-25928

Contamination of the fetch-limited directional wave spectrum by waves emanating from an embayment
[NASA-TM-84441] 15 p2604 N85-26048

Deepwater wind wave growth with fetch and duration
[AD-A151604] 15 p2604 N85-26051

Sound propagation through directional internal wave fields
[AD-A151168] 15 p2646 N85-26321

Wave directional spectra via ARGOS
16 p2612 N85-27343

Routine wave and meteorological measurements in offshore areas using ARGOS data surveillance
16 p2612 N85-27344

Atmospherically forced, coastally trapped, long period gravity waves off the south coast of southern Africa
16 p2832 N85-27461

Internal waves in marine straits
[PREPRINT-415] 18 p3151 N85-29510

A laser slope gauge and a spar buoy wave gauge: Tools for the validation of microwave remote sensors
[AD-A154038] 19 p3272 N85-30290

One mechanism for generation of wave disturbances in spectra of turbulent flows near ocean surface
19 p3289 N85-30397

Plane Tsunami wave caused by elastic oscillations of ocean floor 19 p3290 N85-30403

Discovery of a nonpropagating hydrodynamic soliton
[AD-A155569] 21 p3582 N85-32268

Coastal erosion along Monterey Bay
[AD-A155610] 21 p3655 N85-32707

Theory of soliton waves
[AD-A154784] 21 p3676 N85-32837

Basic properties and interpretation of synthesized radar images of sea waves with long synthetization time
22 p3773 N85-33384

Atlantic coast hindcast. Phase 2: Wave information, additional extremal estimates
[AD-A156137] 24 p4125 N85-35575

WATERPROOFING

Shallow land burial technology: Humid
[DE85-004432] 12 p1932 N85-22136

Results of the AFRSI rewaterproofing systems screening test in the NASA/Ames Research Center (ARC) 2 x 2-foot transonic wind tunnel
[NASA-CR-167694] 13 p1988 N85-22467

Land vehicle corrosion management
22 p3750 N85-33246

WATERSHEDS

Hydrologic and economic models for watershed evaluation and research
[PB84-222371] 01 p0066 N85-10438

Erosion and sedimentation chronology of three watersheds in Maryland
[PB84-207356] 01 p0071 N85-10467

Estuaries of the Cape. Part 2: Synopses of available information on individual systems. Report 13: Silvermine (CSW 3)
[CSIR-RR-412-PT-2] 01 p0086 N85-10582

Estuaries of the Cape. Part 2: Synopses of available information on individual systems. Report no. 16: Eerste (CSW 6)
[CSIR-RR-415-PT-2] 01 p0087 N85-10585

Potential for acidification of six remote ponds in the White Mountains of New Hampshire
[PB84-207349] 02 p0225 N85-11475

The 1984 NASA/ASEE summer faculty fellowship program
[NASA-CR-174138] 04 p0574 N85-13663

Multispectral remote sensing of inland wetlands in South Carolina: Selecting the appropriate sensor
[DE84-013951] 05 p0661 N85-14247

Identification and characterization of watershed models for evaluation of impacts of climate change on hydrology
[DE85-008575] 18 p3125 N85-29348

Synthetic rainfall and its use in hydrologic modeling
19 p3314 N85-30542

Geologic and hydrologic characterization and evaluation of the basin and range province relative to the disposal of high-level radioactive waste. Part 1: Introduction and guidelines
[GS-CIRC-904-A] 20 p3526 N85-31932

Hydrology
[PB85-182954] 23 p3944 N85-34440

WATERWAVE ENERGY

Assessment of wave power available at key United Kingdom sites
[IOS-186] 09 p1346 N85-18466

Evaluation of wave energy resources on the French Atlantic seaboard 14 p2325 N85-24369

WATERWAVE ENERGY CONVERSION

Research recommendations for ac interfacing between electric utility transmission and distribution systems and wind, photovoltaics, and OTEC energy systems
[DE85-002942] 18 p3096 N85-29169

WATERWAYS

NT HARBORS

WATTMETERS

Development of a feasibility model for a thin-film precision power meter
[BMFT-FB-T-84-161] 04 p0504 N85-13217

The Mk. : NPL digital sampling ac wattmeter
[NPL-DES-82] 22 p3758 N85-33290

WAVE AMPLIFICATION
Radiative amplification of acoustic waves in hot stars
06 p1235 N85-17786
Propagation and amplification of Ion Cyclotron Waves (ICW's) in a multicomponent plasma. The Earth magnetosphere as a giant maser for Alfven waves
14 p2366 N85-24634
Microwave tubes: Literature survey no. 5 comprising year 1983
[FOA-C-30377-E] 15 p2550 N85-25739
Amplification of electromagnetic wave by electron stream with negative velocity differences
21 p3692 N85-32941
Electromagnetic wave amplification during cyclotron resonance in a medium 21 p3693 N85-32942
WAVE ATTENUATION
NT ACOUSTIC ATTENUATION
NT MANDELSTAM REPRESENTATION
NT RADAR ATTENUATION
NT RADIO ATTENUATION
NT SHOCK WAVE ATTENUATION
Atmospheric channel performance measurements at 10 to 100 GHz
[PB84-211325] 01 p0042 N85-10271
Elastic wave propagation through polycrystals
[DE84-016772] 04 p0558 N85-13554
Measuring transient radiation effects in optical fibers
[DE84-015044] 04 p0565 N85-13596
Applicability of log-normal model to probabilistic description of quasi-pulse interference
13 p2064 N85-23014
Effects of contact area of an interface on acoustic wave transmission characteristics
[DE85-009935] 20 p3524 N85-31920
Maximally flat approximation of attenuation characteristics of coupled-line filters
22 p3775 N85-33393
WAVE DIFFRACTION
Scattering of electromagnetic waves by plasma half-space after initiation of motion
02 p0264 N85-11729
Diffraction of plane polarized waves by noncircular cylindrical cavity 02 p0269 N85-11754
Diffraction of electromagnetic wave by screen of arbitrary shape 02 p0273 N85-11778
Diffraction of plane electromagnetic waves on semiinfinite grid of parallel conductors arranged at angle to its edge 03 p0344 N85-12217
Ionospheric scintillation: A brief review
04 p0522 N85-13337
Scattering of electromagnetic waves by surface with small asperities 06 p0784 N85-15013
Approach to solution of diffraction problem for waves at rough surface 06 p0784 N85-15014
Optimization piezoelectric transducer width of acousto-optical devices 07 p0950 N85-16024
Spontaneous diffraction of sequence of supershort light pulses in dye solution 11 p1718 N85-20811
Measurement of the configuration of a concave surface by the interference of reflected light
[NASA-TM-77796] 11 p1726 N85-20867
Diffraction of plane TM-wave on continuously irregular elliptical plasma 13 p2067 N85-22914
Calculation of amplitude-phase characteristics of signal scattered obliquely on meteor trail
13 p2073 N85-22948
Intensity fluctuations of focused laser beam during reflection in turbulent atmosphere
13 p2078 N85-22975
Problem of diffraction by wavy surface: Comparison of numerical methods of solution
13 p2079 N85-22985
Diffraction of periodic grounding system of finite length
13 p2081 N85-22994
Accuracy of random signal spectral parameter estimation against interference background in acoustooptical spectrum analyzers
13 p2090 N85-23052
An examination of the use of wave packets for the calculation of atom diffraction by surface
[AD-A152760] 17 p3029 N85-28735
Asymmetry of diffraction orders with light diffraction at surface acoustic wave 22 p3782 N85-33431
Holoswitch
[AD-A155841] 24 p4096 N85-35392
WAVE DISPERSION
Elastic dispersion effects on dynamics and control of large modular antennas — spacecraft antennas
05 p0627 N85-14019
Dispersion curves for normal waves in cylindrical shell and conditions for spatial coincidence in vicinity of critical frequencies 06 p0778 N85-14973
Structure of frequency modulated and phase-shift keyed signals reflected from ionosphere at near-critical frequencies 07 p0952 N85-16035
Dispersion properties of moving ionospheric perturbations 07 p0952 N85-16036
Measurements and predictions of multipath dispersion for troposcatter links 10 p1472 N85-19289
Observations of RR Lyrae and X Arietis with the IUE satellite 11 p1754 N85-21030
Magnetostatic-wave propagation in a finite YIG-Loaded rectangular waveguide
[AD-A150332] 13 p2055 N85-22865
Intensity fluctuations of focused laser beam during reflection in turbulent atmosphere
13 p2078 N85-22975
Generation and propagation of electron cyclotron harmonic waves 14 p2367 N85-24630
Theoretical studies of electric cyclotron harmonic (ECH) waves based on experimental data from GEOS 1
14 p2367 N85-24631
Modifications to a propagation model for the combinded refraction-diffraction of stokes waves; shallow water, large angle and breaking wave effects
[AD-A151426] 15 p2556 N85-25766
A method of solving the dispersion equation for electrostatic electron waves in magnetized plasma
[KGI-PREPRINT-071] 16 p2869 N85-27687
Beam diffusion in linear ionospheric layer
21 p3695 N85-32958
Methods for measuring and analyzing dispersion properties of multimode fiber optic lightpipes (a review)
21 p3695 N85-32960
Optical image of bounded objects
21 p3697 N85-32968
Observation of mode-converted by ion Bernstein wave by an HCN laser scattering
[IPPJ-724] 23 p3979 N85-34688
Transient analysis of electromagnetic reflection from dispersive materials
[PB85-200186] 24 p4154 N85-35753
WAVE DRAG
NT INTERFERENCE DRAG
An investigation of vortex-induced aerodynamic characteristics of supersonic cruise configurations
[NASA-CR-174299] 07 p0896 N85-15690
WAVE EQUATIONS
NT DIRAC EQUATION
NT EIKONAL EQUATION
NT KORTEWEG-DEVRIES EQUATION
NT LAME WAVE EQUATIONS
NT SCHROEDINGER EQUATION
Integral of wave kinetic equation of drift waves
02 p0283 N85-11848
Current status of blast wave theory and computations. Volume 2: The quasi-similar solution
[AD-A146538] 06 p0806 N85-15136
Nonlinear wave propagation
[AD-A148114] 08 p1152 N85-17269
Solitons and SEASAT
[AD-A148396] 08 p1176 N85-17414
An invariant measure for the equation u sub tt - u sub xx + u3 = O
[AD-A147300] 08 p1210 N85-17612
High order difference schemes with reduced dispersion for hyperbolic differential equations
[CWI-NM-R8408] 11 p1634 N85-20293
Research in theoretical nuclear physics
[DE85-004349] 12 p1932 N85-22137
A mathematical formulation of the Scole control problem, part 1
[NASA-CR-172581] 14 p2243 N85-23903
Wave description of sound propagation through stratified moving atmosphere 15 p2525 N85-25567
Scattering of sounds by piezoceramic cylindrical shell near rigid surface 17 p2943 N85-28168
Pattern selection and instability in nonlinear wave equation: An aspect of soliton and chaos
[DE85-009578] 18 p3101 N85-29197
Reverberation effects on directionality and response of stationary monopole and dipole sources in a wind tunnel
[NASA-TM-87063] 20 p3453 N85-31443
Wave propagation and methods of solution of the wave equation for moving disturbances sources
[ESA-TT-824] 20 p3522 N85-31906
Qualitative analysis of sign-bit processing
[AD-A154776] 21 p3671 N85-32804
Generalized string amplitude and wave equation for hadrons
[DE85-011492] 22 p3842 N85-33798
Absorbing boundary conditions for exterior problems
[NASA-CR-177944] 24 p4142 N85-35676
WAVE EXCITATION
NT ACOUSTIC EXCITATION
Investigation of RF excited CW CO2 waveguide lasers
[NASA-CR-174106] 04 p0505 N85-13221
Surface wave excitation study
[DE85-005301] 13 p2056 N85-22875
Numerical simulations of convectively excited gravity waves 14 p2444 N85-25082
An excitation mechanism for solar 5-minute oscillation of intermediate and high degree
14 p2444 N85-25085
Antenna with outboard exciter for 3.4-13.25 GHz frequency range 15 p2526 N85-25577
Study of the coupling between average, coherent and turbulent fields in a circular excited free jet
[ISL-R-115/83] 16 p2785 N85-27184
Vibrational stabilization of flexible structures
20 p3414 N85-31188
Excitation of some alkaline Earth-like ions
[DE85-010737] 20 p3529 N85-31951
WAVE FRONT DEFORMATION
Fast Hartmann method for problems in astronomical adaptive optics 02 p0161 N85-11094
Degenerate four-wave mixing lineshapes in sodium vapor under pulsed excitation
[AD-A148211] 08 p1222 N85-17698
WAVE FRONT RECONSTRUCTION
Algorithms for reconstruction of partially known, band limited Fourier transform pairs from noisy data
[AD-A150194] 13 p2150 N85-23347
Methods for design aerodynamics of modern transport aircraft
[DFVLR-FB-85-05] 17 p2893 N85-27838
WAVE FRONTS
NT SHOCK FRONTS
Boundary behavior of analytic functions, analytic wave front sets and the intersection problem of Ehrenpreis
[PREPRINT-809] 01 p0114 N85-10778
Simulation of wavefronts returned by realistic surfaces
03 p0383 N85-12448
Performance of Bayes-optimal angle-of-arrival estimators
[AD-A146594] 06 p0858 N85-15454
Modeling of real UT transducer field/flaw interactions
[DE85-000341] 09 p1329 N85-18351
Experimental investigation of wavefront conjugation during Mandelstam-Brillouin scattering of focused laser beams in condensed media 11 p1716 N85-20796
Four-wave hypersonic reversing mirrors in saturated mode 11 p1719 N85-20812
Double pinhole spatial phase correlator apparatus
[AD-D011495] 11 p1729 N85-20872
Ruby wavefront-conjugation laser for obtaining high temperature plasma 13 p2044 N85-22795
Sphericity gauge for wavefront of laser radiation
14 p2275 N85-24096
Stability of high energy particle plasmas to MHD-like modes
[DE85-007879] 17 p3039 N85-28803
Mean intensity of wave reflected by wavefront reversing mirror in turbulent medium 22 p3782 N85-33432
Heterodyne holographic interferometry for visualization of surface acoustic waves
[AD-A155405] 22 p3836 N85-33753
The longitudinal thickness of air-shower fronts
[OG-9.5-1] 23 p4030 N85-34978
WAVE FUNCTIONS
NT MOLECULAR ORBITALS
Sturmian expansion approximation to three-body scattering
[CSIR-TWISK-309] 01 p0109 N85-10731
Dirac single particle wave functions in inelastic electron scattering
[DE84-015129] 02 p0279 N85-11814
Long-time tail in the two-wave model
02 p0282 N85-11837
Oscillator strengths for OII ions
[NASA-CR-174153] 04 p0559 N85-13558
Aharonov-Bohm effect in absorption of electromagnetic wave 06 p0786 N85-15022
An extension of the multiconfiguration Hartree-Foc program for continuum functions
[DE85-002080] 09 p1379 N85-1867
Quasiparticle aggregation in the Fractional Quantum Hal Effect
[DE85-001574] 10 p1565 N85-1986
Computer modeling of vibrational energy levels o potential laser candidates (diatomic molecules)
[AD-A151765] 16 p2790 N85-2720
Microscopic analysis of angular momentum projecte HFB-states in terms of interacting bosons
[DE85-007629] 16 p2863 N85-2786
The strategy for time dependent quantum mechanic calculations using a Gaussian wave packet representatio of the wave function
[AD-A152709] 17 p3046 N85-2884
Experimental and theoretical investigations of ope resonators — precipitation measurement
[DFVLR-FB-85-12] 20 p3449 N85-3141
Excitation of some alkaline Earth-like ions
[DE85-010737] 20 p3529 N85-3195
Overlap integrals for atom-metal surface interactio
[AD-A155038] 21 p3702 N85-329

WAVE GENERATION
Waves and instabilities in collisionless shocks
[AD-A146689] 06 p0881 N85-15597
Superlattice ultrasonic wave generator
[AD-D011363] 07 p1038 N85-16585
Evolution of nonlinear wave groups on water of slowly-varying depth
[AD-A147947] 08 p1162 N85-17329
Generation of longitudinal acoustic waves by modulated helicon waves — nonlinear steady state waves in metals
13 p2090 N85-23049
Generation and development of small-amplitude disturbances in a laminar boundary layer in the presence of an acoustic field
[NASA-TM-77826] 14 p2299 N85-24237
Pc 1-2 pulsations and related phenomena: A review — geomagnetic pulsations 14 p2364 N85-24611
Generation and propagation of electron cyclotron harmonic waves 14 p2367 N85-24630
Microwave tubes: Literature survey no. 5 comprising year 1983
[FOA-C-30377-E] 15 p2550 N85-25739
On gravitational waves 16 p2759 N85-27026
Millimeter wave generation by relativistic electron beams
[AD-A153860] 18 p3179 N85-29708
Ion waves generated by ion loss-cone distributions or drifting particles
[KGI-PREPRINT-070] 20 p3549 N85-32087

WAVE INTERACTION
NT SHOCK WAVE INTERACTION
Broadband transverse field interaction continuous beam amplifier
[AD-D011229] 01 p0043 N85-10279
Chaotic behavior induced by solitons in perturbed integrable systems 02 p0283 N85-11844
Wave-wave interactions, microseisms, and infrasonic ambient noise in the ocean
[AD-A146529] 06 p0859 N85-15463
Ionospheric and magnetospheric modifications caused by VLF waves
[AD-A148210] 08 p1186 N85-17475
PMP-2: Equatorial wave dynamics
11 p1655 N85-20422
Coupling between velocity oscillations and solid propellant combustion 13 p2000 N85-22536
Measurements of distributed combustion
13 p2001 N85-22542
Stability of Rossby waves within framework of three-component analysis 13 p2109 N85-23142
An analytical and numerical study of the interaction of rarefaction waves with area changes in ducts. Part 2: Area enlargements
[UTIAS-273] 14 p2300 N85-24242
ICRF antenna coupling theory for a cylindrically stratified plasma
[DE85-004960] 14 p2424 N85-24952
The resonant count diagram and solar g mode oscillations 14 p2445 N85-25086
Interaction of large amplitude stress waves in layered elastic-plastic materials
[AD-A153519] 18 p3121 N85-29323
Guided and radiation wave interactions in periodic dielectric waveguides 19 p3253 N85-30173
Frequency-spreading coupler
[AD-D011663] 19 p3258 N85-30200
Finite-perturbation intermediate neglect of differential overlap molecular orbital calculations of nuclear magnetic resonance spin-spin coupling constants for polycyclic aromatic hydrocarbons and aromatic nitrogen heterocyclics
[NASA-TM-87486] 20 p3525 N85-31927
Wave/particle interactions in the plasma sheet
[NASA-CR-171537] 20 p3547 N85-32072
Some recent developments in the interpretation of MST radar returns from clear air (keynote paper), part 2
21 p3618 N85-32480
Computation of three-dimensional shock wave and boundary-layer interactions
[NASA-TM-86780] 24 p4093 N85-35372
Resonance localization in tokamaks excited with ICRF waves
[DE85-014559] 24 p4160 N85-35791

WAVE MOTION
U WAVES

WAVE OSCILLATORS
U OSCILLATORS

WAVE PACKETS
Reduction of the wavepacket: How long does it take?
[DE84-016778] 09 p1400 N85-18815
Directional analysis of wave packets of magnetotelluric field 14 p2344 N85-24495
Propagation of wave packet in a dissipative dielectric medium
[IPPJ-710] 15 p2655 N85-26385
An examination of the use of wave packets for the calculation of atom diffraction by surface
[AD-A152760] 17 p3029 N85-28735
The strategy for time dependent quantum mechanical calculations using a Gaussian wave packet representation of the wave function
[AD-A152709] 17 p3046 N85-28845
Electrostatic ion cyclotron instability due to a nonuniform electric field perpendicular to the external magnetic field
[AD-A155474] 21 p3707 N85-33019

WAVE PROPAGATION
NT ACOUSTIC PROPAGATION
NT DIFFRACTION PROPAGATION
NT GROUND WAVE PROPAGATION
NT HALOS
NT IONOSPHERIC PROPAGATION
NT LIGHT SCATTERING
NT MANDELSTAM REPRESENTATION
NT SCATTER PROPAGATION
NT SHOCK WAVE PROPAGATION
NT TRANSEQUATORIAL PROPAGATION
Implementation of the supersonic triplet singularity into the USTORE computer code
[CSIR-NIAST-83/47] 01 p0001 N85-10006
Problems on the diffraction and propagation of waves (selected articles)
[AD-A145139] 01 p0038 N85-10240
Atmospheric channel performance measurements at 10 to 100 GHz
[PB84-211325] 01 p0042 N85-10271
Transverse field interaction multibeam amplifier
[AD-D011241] 01 p0043 N85-10282
On wave propagation in linear viscoelasticity
[AD-A144739] 01 p0111 N85-10750
Fast waves near the lower hybrid frequency
[DE84-015217] 01 p0123 N85-10841
Acceleration waves 02 p0207 N85-11367
Finite element analysis of thermoelasticity problems
02 p0208 N85-11369
Paleoenvironmental interpretation of the upper cretaceous Point Lookout sandstone: Implications for shoreline progradation and basin tectonic history, San Juan basin, New Mexico 02 p0227 N85-11486
The propagation and growth of whistler mode waves generated by electron beams in Earth's bow shock
[AD-A145572] 02 p0228 N85-11492
The numerical solution of the Helmholtz equation for wave propagation problems in underwater acoustics
[NASA-CR-172454] 02 p0250 N85-11634
Polarization of ultrasound transmitted through boundary of magnetically inactive and equatorially magnetized media 02 p0257 N85-11682
Propagation of longitudinal elastic waves in multilayered half-space 02 p0273 N85-11779
Stochastic property of K-dV solitons perturbed by random forces — Korteweg-Devries equation
02 p0283 N85-11843
Computer molecular dynamics of 2-D water (ice) structures under shock
[AD-A145818] 03 p0372 N85-12375
Specific phenomena associated with the propagation of seismic waves in central Europe
[REPT-548] 03 p0375 N85-12391
Hole shots along refraction profile R4/78 recorded at the temporary seismic station near Stary Plzenec (west Bohemia)
[REPT-549] 03 p0375 N85-12392
Seasonal variations of reflexibility and transmissibility of ULF waves propagating through the ionosphere of geomagnetic mid-latitudes
[REPT-560] 03 p0376 N85-12403
Finite-difference synthetic seismograms for SH waves
[AD-A145834] 03 p0392 N85-12506
Millimeter-wave propagation and remote sensing of the atmosphere
[AD-A146339] 03 p0393 N85-12512
Coupling of airborne sound into the Earth
[AD-A146231] 03 p0416 N85-12663
Gyrotron beam generation with helical magnetic fields
[AD-A145987] 03 p0417 N85-12670
Studies of ignition and combustion wave propagation in exothermic systems using high-speed photography
[DE84-016482] 04 p0471 N85-12995
Digital radio link: Wave propagation measurements using narrow band technique
[FOA-C-30364-E2] 04 p0494 N85-13152
Wave phase velocity in a wind gradient — gravity waves 04 p0523 N85-13343
Elastic wave propagation through polycrystals
[DE84-016772] 04 p0558 N85-13554
Wave propagation in compliant tubes containing a heat-conducting viscous fluid
[WTHD-163] 05 p0638 N85-14094
Characteristic impedance of a porous center during transmission of quasi-static sinusoidal vibrations
[ISSN-0208-5658] 05 p0647 N85-14155
Signal characteristics of an underwater explosive acoustic telemetry system
[DE84-016653] 05 p0726 N85-14668
Disturbance propagation in structural networks; control of large space structures 06 p0759 N85-14856
Acoustoelectric interaction in double-layer semiconductors 06 p0786 N85-15023
Investigating phase structure of electromagnetic field in local inhomogeneities by modeling method
06 p0822 N85-15220
Longitudinal current before westward propagating auroral band 06 p0823 N85-15223
Limits of applicability of long wave theory in studies of oscillations of n-layer fluid 06 p0824 N85-15234
Theory of harmonic generation of finite amplitude ultrasonic waves in solids of hexagonal symmetry
[AD-A146636] 06 p0860 N85-15465
Reverse wave suppression in unstable ring resonator
[AD-A146825] 07 p0939 N85-15952
A quasi-optical method for measuring the complex permittivity of materials
[AD-A147483] 07 p0941 N85-15966
Multiple scattering effects on transmission through the atmosphere
[AD-A147527] 07 p0941 N85-15969
Slow surface magnetoplasma waves in oblique magnetic field 07 p0952 N85-16034
Transformation of electromagnetic waves in plasma with randomly-heterogeneous magnetic field
07 p0953 N85-16039
Quantitative acoustic emission techniques
[AERE-R-11262] 07 p0977 N85-16203
Nonlinear waves in a rod. Results for incompressible elastic materials
[AD-A147485] 07 p0979 N85-16216
Nonlinear wave propagation study
[AD-A147011] 07 p0996 N85-16329
Short period guided waves over oceanic and continental paths
[AD-A147053] 07 p0997 N85-16331
On the long range propagation of sound over irregular terrain
[NASA-CR-3862] 07 p1038 N85-16589
Electrostatic wave observation during a space simulation Beam-Plasma-Discharge (BPD)
[NASA-CR-174286] 07 p1045 N85-16639
Acoustical characterization of Ti-6211 weldments and oxygen contamination Ti-6211 plate
[AD-P004125] 08 p1126 N85-17100
Nonlinear wave propagation
[AD-A148114] 08 p1152 N85-17269
Propagation and scattering considerations for the 0.2-3.0 GHz frequency range for a space-based radar
[AD-A148504] 08 p1153 N85-17282
Tunable microwave transversal filters
[AD-A148370] 08 p1158 N85-17304
On seismic waves 08 p1171 N85-17383
Effects of heterogeneities on the propagation, scattering and attenuation of seismic waves and the characterization of seismic source
[AD-A148284] 08 p1186 N85-17476
An efficient numerical solution technique for wave propagation in horizontally stratified ocean environments
[AD-A148537] 08 p1190 N85-17502
Optical wave propagation and imaging in the atmosphere 08 p1222 N85-17694
Short range order-long range order in superconducting materials
[AD-A148764] 08 p1227 N85-17724
A leaky waveguide model for MHD wave driven winds from coronal holes 08 p1235 N85-17781
Wave propagation in periodic, composite structures
09 p1332 N85-18370
Penetration of short duration airblast into protective structures 09 p1336 N85-18404
Acoustic tomographic reconstrution of anomalies in three-dimensional bodies
[DE84-017035] 09 p1378 N85-18666
UHF radiowave propagation through forests
[AD-A149518] 10 p1467 N85-19256
Propagation of electromagnetic fields along the sea/sea-bed interface
[AD-A149523] 10 p1467 N85-19257
Propagation Influences on Digital Transmission Systems: Problems and Solutions
[AGARD-CP-363] 10 p1469 N85-19269
Propagation of wide bandwidth signals in a tropospheric ducting system 10 p1469 N85-19271
Influence of propagation in digital wireless beam, microwave links 10 p1470 N85-19277
Design criteria for limited scan antennas at digital microwave line of sight links 10 p1471 N85-19284
A comparison between predicted and measured propagation loss in the VHF/UHF range in rugged terrain 10 p1471 N85-19285

A review of transmission and channel evaluation techniques for digital communication systems
10 p1474 N85-19301

Shock propagation in the exhaust gas handling system of the proposed large altitude rocket cell: Methods and preliminary analysis
[DE85-003055] 11 p1591 N85-20010

Digital controller for the Wave Propagation Laboratory's VHF and UHF wind-profiling radars
[PB85-112142] 11 p1626 N85-20238

Soviet National Middle Atmosphere Program
11 p1655 N85-20428

Seasonal characteristics of mesospheric plasma and their transitions 11 p1660 N85-20464

Midwinter disturbances in the middle atmosphere
11 p1661 N85-20465

Numerical investigation of propagation of radiation pulse at xxx 11 p1718 N85-20809

Wavecode constitutive models: Nonhomogeneous mixtures
[DE85-000636] 12 p1798 N85-21278

Waveform control and application of detonation wave in explosives 12 p1820 N85-21420

Aerosol multiple-scanning code, ASCAT
[LA-10046-MS] 12 p1823 N85-21440

Double reference pulsed phase locked loop (DRP-2L-2)
[NASA-CASE-LAR-13310-1] 12 p1824 N85-21441

Survivable propagation
[AD-A150070] 12 p1829 N85-21478

An analysis of short-to-medium-range seismic attenuation tests using a multilayered viscoelastic seismic propagation model
[AD-A149771] 12 p1889 N85-21856

Structure and forcing of teleconnection patterns occurring in general circulation model simulations
[DE85-002434] 12 p1890 N85-21862

Methods of progressing waves in turbulent media with applications to acoustics
[AD-A149599] 12 p1920 N85-22055

Magnetostatic-wave propagation in a finite YIG-Loaded rectangular waveguide
[AD-A150332] 13 p2055 N85-22665

Two-and-one-half dimensional in-plane wave propagation
[AD-A150467] 13 p2055 N85-22667

USSR report: Electronics and electrical engineering
[JPRS-UEE-85-002] 13 p2066 N85-22907

Mode control and wavelength tuning in open ended Michelson interferometric semiconductor laser
13 p2095 N85-23073

Applications of the conformal mapping method to the solution of mechanical vibrations problems
13 p2102 N85-23103

Regions of propagation of short-wave perturbations in spherical layer of rotating fluid 13 p2107 N85-23130

Geomagnetic precursors of intensive earthquakes in the 1-0.-2 Hz frequency range of geomagnetic pulsations
13 p2116 N85-23178

Seismic waves and dispersion relations
13 p2116 N85-23181

Vertical discrimination in the sound channel
[AD-A150254] 13 p2155 N85-23380

Investigations of ultrasonic wave interactions at boundaries separating anisotropic materials
[DE85-003506] 13 p2155 N85-23384

Wave propagation in heterogeneous media
[AD-A150800] 14 p2321 N85-24341

Possibility of retrieving dynamics of reflected wave method records beneath low-velocity zone
14 p2346 N85-24503

Generation and propagation of electron cyclotron harmonic waves 14 p2367 N85-24630

Regional seismic wave propagation
[AD-A150801] 14 p2373 N85-24671

Surface acoustic wave structure and volume waves
15 p2525 N85-25566

Water wave propagation over uneven bottoms
[AD-A151450] 15 p2556 N85-25769

Reflection and transmission of flexural waves at discontinuities 15 p2572 N85-25861

Contamination of the fetch-limited directional wave spectrum by waves emanating from an embayment
[NASA-TM-84441] 15 p2604 N85-26048

Recent progress in the development and application of the parabolic equation
[AD-A151475] 15 p2637 N85-26265

Field near the front of a signal in a waveguide accomplished with dispersive plasma
[REPT-11/1984] 16 p2768 N85-27083

Characteristic functionals of stochastic wave processes
[REPT-14/1984] 16 p2768 N85-27084

Wave propagation in density stratified fluids
16 p2781 N85-27162

Two-dimensional beat wave acceleration simulation
[DE85-005961] 16 p2791 N85-27214

Principles of wave formation along web of H-beams
[BLL-M-36041-(5828.4)] 16 p2798 N85-27253

Numerical resolution calculation for elastic-plastic impact problems
[AD-A152292] 16 p2801 N85-27270

Born inversion with a stratified reference velocity
[AD-A149222] 16 p2853 N85-27594

Research and development of subsurface acoustic wave devices for sensor applications
[AD-A152197] 16 p2861 N85-27642

Propagation of non-axisymmetric elastic waves through shell with filler under radial load at one end
17 p2943 N85-28169

Radiometer integrated into a communication terminal
[AD-A151746] 17 p2947 N85-28195

A transport theory of millimeter wave propagation in woods and forests
[AD-A151883] 17 p2947 N85-28196

The weighting function for scintillation on a folded path
[AD-A152659] 17 p2949 N85-28206

A crustal section for the Arabian Shield and adjacent Red Sea margin derived from first-arrival data
17 p2990 N85-28480

Measurements of VHF/UHF radio propagation in a maritime temperate climate
[CRC-1380] 18 p3089 N85-29119

Some further aspects of the influence of raindrop-size distributions on millimeter-wave propagation
[PB85-168334] 18 p3092 N85-29138

Hyperbolic phenomena in the flow of viscoelastic fluids
[AD-A153533] 18 p3099 N85-29186

Constitutive modeling for blast-induced wave propagation
[AD-A153576] 18 p3099 N85-29187

Propagation of gravity waves in the atmosphere and around critical levels
[KNMI-WR-85-1] 18 p3137 N85-29428

On the global distribution of three-dimensional Eliassen-Palm fluxes by stationary waves
18 p3145 N85-29469

Anderson localization for large disorder or low energy
[PREPRINT-426] 18 p3176 N85-29692

Theoretical investigations of the propagation and interactions of surface waves
[AD-A153548] 18 p3185 N85-29753

Measurement of mode interaction due to waveguide surface roughness
[AD-A154039] 19 p3255 N85-30183

Clearing of polydisperse aqueous aerosol by laser radiation pulses 19 p3296 N85-30445

Use of Omega radio navigation system in geophysical work in Antarctica 19 p3298 N85-30448

Linear time-invariant, space-variant filters and the WKB approximation with applications to underwater acoustic signal processing
[AD-A154250] 19 p3352 N85-30775

Heating of electrons in a high density tokamak by a micro-wave near second harmonic frequency
[DE85-010682] 19 p3359 N85-30822

Application of single and multiple scattering techniques to optical properties of dielectric media
19 p3366 N85-30877

ICRF antenna coupling and wave propagation in a tokamak plasma 19 p3369 N85-30893

Electromagnetic lateral waves in layered media
19 p3369 N85-30894

Localization of waves in a disordered medium
19 p3373 N85-30926

Scattering models in signal processing
20 p3439 N85-31339

Field antenna handbook
[AD-A155204] 21 p3576 N85-32242

Numerical modeling of subsurface communication
[DE85-012816] 21 p3577 N85-32249

Dynamic fracture of concrete and other heterogeneous materials
[AD-A154513] 21 p3598 N85-32343

Gravity waves from the stratosphere to the mesosphere, part 1.3B 21 p3616 N85-32471

Gravity-wave spectra in the atmosphere observed by MST radar, part 4.2B 21 p3622 N85-32502

Experimental and analytic characterization of nonlinear seismic attenuation
[AD-A154760] 21 p3631 N85-32556

Development of ultrasonic modeling techniques for the study of crustal inhomogeneities
[AD-A155206] 21 p3632 N85-32565

The effects of subrefractive layers and elevated ducts on airborne radar and ESM (Electronic Surveillance Measures)
[AD-A155524] 21 p3637 N85-32592

New approximations and findings of theory of nonlinear acoustic beams 21 p3680 N85-32863

Reflection of acoustic beam from inhomogeneous boundary 21 p3680 N85-32864

Toward the propagation of waves in unsteady media
21 p3683 N85-32881

Laser radiation propagation in inertialess nonlinear medium 21 p3686 N85-32898

Variation in radiowave propagation conditions in corona during solar activity cycle 22 p3763 N85-33327

USSR report: Electronics and electrical engineering
[JPRS-UEE-84-003] 22 p3773 N85-33381

Calculating dominant (quasi-t) mode group velocity in shielded microstrip line 22 p3780 N85-33422

Gradient scaling for nonuniform meshes
[DE85-009625] 22 p3784 N85-33443

Numerical experiment of elastic wave propagation by framework model
[DRIC-T-7462] 22 p3795 N85-33511

Surface wave modes of a multilayered medium backed by a perfectly conducting ground plane: Computation of propagation constants
[DE85-011454] 22 p3829 N85-33715

A measurement of the cosmic ray elements C to Fe in the two energy intervals 0.5-2.0 GeV/n and 20-60 GeV/n
[OG-4.1-6] 22 p3876 N85-34012

Interstellar propagation and the isotopic composition of hydrogen in the galactic cosmic rays
[OG-4.2-1] 22 p3877 N85-34021

Galactic propagation models consistent with the cosmic ray lifetime derived from Be-10 measurements
[OG-4.3-1] 22 p3878 N85-34026

Implications of new measurements of O-16 + p + C-12,13, N-14,15 for the abundances of C, N isotopes at the cosmic ray source
[OG-4.3-2] 22 p3878 N85-34027

A simulation of high energy cosmic ray propagation 1
[OG-5.4-1] 22 p3885 N85-34078

Behaviors of stress waves in a conical bar
23 p3904 N85-34182

Computational study on excitation, propagation and 3 omega -heating due to the ion Bernstein wave
[IPPJ-733] 23 p3975 N85-34641

Cosmic ray modulatin and merged interaction regions
[SH-4.1-11] 23 p4005 N85-34834

Propagation of the phase of solar modulation
[SH-4.1-12] 23 p4005 N85-34835

Cosmic ray modulation in a random anisotropic magnetic field
[SH-4.1-20] 23 p4006 N85-34839

Diffusion of strongly magnetized cosmic ray particles in a turbulent medium
[OG-7.2-16] 23 p4015 N85-34883

Measurements of the fragmentation of (40)Ar, (28)Si and (12)C in CH2C and H targets between 300 and 1500 MeV/nuc at the Bevalac
[OG-7.2-19] 23 p4016 N85-34886

Interactions of heavy nuclei, Kr, Xe and Ho, in light targets
[OG-7.2-21] 23 p4016 N85-34888

Perturbation-iteration theory for analyzing microwave striplines
[NASA-CR-176189] 24 p4085 N85-35321

Millimeter-wave propagation in moist air: Model versus path data
[AD-A156040] 24 p4087 N85-35331

Workshop Proceedings: Interpretation of Seismic Wave Propagation in Laterally Heterogeneous Structures
[BMR-258] 24 p4118 N85-35530

A comparison of multipath arrival structures observed in the presence of a surface duct with predictions obtained using classical ray techniques and the parabolic equation method
[AD-A156024] 24 p4145 N85-35696

Propagation of cosmic rays through the atmosphere in the quark-gluon strings model 24 p4173 N85-35873

WAVE RADIATION

U ELECTROMAGNETIC RADIATION

WAVE REFLECTION

NT MACH REFLECTION

An improved analytical theory of Rossby wave driven Eulerian and Lagrangian mean flows along non-zonal barriers with application to the Hawaiian Ridge
[AD-A144951] 01 p0086 N85-10593

Scattering matrix of antenna array with Joule losses in radiators 06 p0791 N85-15053

An extension of the Born inversion method to a depth dependent reference profile
[AD-A146469] 06 p0859 N85-15461

Reflection theorems for some anisotropic media
07 p0953 N85-16038

Application of homomorphic signal processing to stress wave factor analysis
[NAS 1.26:174871] 12 p1861 N85-21673

Three-mirror open resonator for millimeter wave band
13 p2077 N85-22972
Interference flux during reflection of heterogeneous waves 13 p2078 N85-22977
Axial focusing of signal from distant point radiator reflected twice in deep paraboloid
13 p2078 N85-22979
Experimental verification of beam deflection from hybrid reflector antenna within wide-angle sector
13 p2079 N85-22984
Water wave propagation over uneven bottoms
[AD-A151450] 15 p2556 N85-25769
Reflection and transmission of flexural waves at discontinuities 15 p2572 N85-25861
Results of simultaneous measurements of absorption and polarization of radio waves reflected from ionosphere 16 p2807 N85-27313
Kirchhoff modeling via wave equation datuming
[AD-A152399] 17 p3028 N85-28727
Most desirable terrain, e.g., flat vs valley location, part 5.1B 21 p3624 N85-32513
A random layer model for reflection from ocean bottom sediments
[AD-A155019] 21 p3700 N85-32988
Transient analysis of electromagnetic reflection from dispersive materials
[PB85-200186] 24 p4154 N85-35753

WAVE RESISTANCE
Nonrelativistic Kapitza-Dirac scattering
[AD-A150649] 14 p2417 N85-24911
Reactanceless synthesized impedance bandpass amplifier
[NASA-CASE-GSC-12788-1] 18 p3093 N85-29145

WAVE SCATTERING
NT ACOUSTIC SCATTERING
NT ATMOSPHERIC SCATTERING
NT ELECTROMAGNETIC SCATTERING
NT HALOS
NT LIGHT SCATTERING
NT MICROWAVE SCATTERING
NT MIE SCATTERING
NT RAMAN SPECTRA
NT RAYLEIGH SCATTERING
NT REVERBERATION
NT THOMSON SCATTERING
NT TROPOSPHERIC SCATTERING
NT X RAY SCATTERING
Wave multiple scattering by a finite number of unclosed circular cylinders
[NASA-TM-77593] 01 p0037 N85-10232
Wave guide branchings (n-port) types of representation of linear, time-independent and sourceless n-ports
[NASA-TM-77770] 01 p0037 N85-10233
Scattering of plane wave on cylindrical shell in low-frequency region 02 p0256 N85-11677
Transformation of heterogeneous surface waves by skewed streams 02 p0259 N85-11697
Modeling rain polarization effects to millimeter wave frequencies
[PB84-231042] 03 p0357 N85-12296
Elastic compliance of imperfect interfaces: Review and relationship to ultrasonic scattering
[DE85-003068] 11 p1652 N85-20404
Calculation of amplitude-phase characteristics of signal scattered obliquely on meteor trail
13 p2073 N85-22948
Use of Bigaussian approximation to describe fading in scattering communications channel
13 p2084 N85-23017
Elastic wave scattering from an interface crack in a layered half space 13 p2101 N85-23095
Scattering of elastic waves on fractures randomly distributed in a three-dimensional medium
13 p2111 N85-23151
Nonrelativistic Kapitza-Dirac scattering
[AD-A150649] 14 p2417 N85-24911
Field near the front of a signal in a waveguide accomplished with dispersive plasma
[REPT-11/1984] 16 p2768 N85-27083
A transport theory of millimeter wave propagation in woods and forests
[AD-A151883] 17 p2947 N85-28196
The temperature dependence of diffracted beam intensities in atom-surface scattering
[AD-A152762] 17 p3029 N85-28736
Laser forward and backscattering in particulate media
[AD-A154138] 19 p3275 N85-30312
Application of single and multiple scattering techniques to optical properties of dielectric media
19 p3366 N85-30877
Optical beam deflection detection of thermal waves in opaque solids 19 p3374 N85-30927
Scattering models in signal processing
20 p3439 N85-31339
Development of ultrasonic modeling techniques for the study of crustal inhomogeneities
[AD-A155206] 21 p3632 N85-32565
Acoustic wave scattering by round cylindrical shell reinforced with stringers 21 p3686 N85-32916
Investigation of ion-acoustic plasma turbulence in field of powerful electromagnetic wave by CO2-laser radiation scattering 21 p3691 N85-32935
Characteristics of optical information-measurement channels with utilization of scattering effects
22 p3781 N85-33429
Method and apparatus for Delta Kappa synthetic aperture radar measurement of ocean current
[NASA-CASE-NPO-15704-1] 23 p3925 N85-34327
Attenuation properties of the Petatlan region, Mexico, and a local magnitude scale for microearthquakes in this area 24 p4116 N85-35513
Second Colloquim on the Scattering of Ultrasonic Waves
[AD-A156298] 24 p4145 N85-35697

WAVEFORMS
NT PULSE AMPLITUDE
NT PULSE DURATION
NT SAWTOOTH WAVEFORMS
NT SQUARE WAVES
Flight demonstration of new NRL real-time data acquisition system and laser video waveform sampler
[AD-A145126] 01 p0053 N85-10350
Detection and estimation of image contours
[FUB-35-1983] 01 p0112 N85-10760
Notes on NAC report NAC-83-05: Beam Pulse Length Determination by Spectral Analysis
[CSIR-NAC-83-06] 01 p0119 N85-10816
Simulation of wavefronts returned by realistic surfaces
03 p0383 N85-12448
Acoustic emission waveforms in a half space
[AD-A148322] 03 p0417 N85-12664
Beam profiling in gigawatt 1064-nm lasers used in research on optical materials at Livermore
[DE84-087226] 04 p0506 N85-13223
On estimating the phase of periodic waveform in additive Gaussian noise, part 2 05 p0622 N85-13982
Pulsed-power system diagnostics: Electromagnetic data interpretation along pulse lines
[AD-A146807] 06 p0810 N85-15148
Electromagnetic resonances of cylinders and aircraft model with resistive wires
[NASA-CR-174203] 06 p0838 N85-15319
Theoretical and experimental analyses of laser altimeters for barometric measurements over the ocean
08 p1165 N85-17351
Determination of crustal and upper mantle structure from analysis of broadband teleseismic P-waveforms
08 p1181 N85-17440
The ambiguity function of random binary-phase-coded waveforms
[AD-A148906] 10 p1466 N85-19249
Transient waveform acquisition system for the ELMO Bumpy Torus
[DE85-000154] 11 p1733 N85-20901
Waveform control and application of detonation wave in explosives 12 p1820 N85-21420
Estimation of the impulse response of television channels from digitized waveforms
[CRC-1376] 12 p1822 N85-21429
The use of a high-speed 12-bit A/D converter for digital sampling of communication signal carriers
[AD-A150578] 13 p2056 N85-22872
Invariance of probability characteristics of detector to shape of optical pulse signals 13 p2090 N85-23048
Generation of longitudinal acoustic waves by modulated helicon waves — nonlinear steady state waves in metals
13 p2090 N85-23049
Secure digital speech communication
[AD-D011572] 14 p2293 N85-24215
Modifications to a propagation model for the combinded refraction-diffraction of stokes waves; shallow water, large angle and breaking wave effects
[AD-A151428] 15 p2556 N85-25768
A comparison of alternative analytic models for event related potential records
[AD-A151977] 15 p2618 N85-26134
An analysis of jamming effects on noncoherent digital receivers
[AD-A153791] 18 p3090 N85-29128
Huffman-coded pulse compression waveforms
[AD-A155322] 21 p3576 N85-32243
Transceiver test device
[AD-D011728] 22 p3786 N85-33458
Fast scintillation counter system and performance
[HE-4.6-10] 24 p4197 N85-36047
Search for acoustic signals from high energy cascades
[HE-7.1-1] 24 p4213 N85-36155

WAVEGUIDE ANTENNAS
NT HORN ANTENNAS
Analysis of flat finite antenna consisting of waveguide radiators 06 p0790 N85-15048
A new leaky wave antenna for millimeter waves based on the groove guide
[AD-A146428] 06 p0799 N85-15102

WAVEGUIDE FILTERS
Dual mode directionally coupled band reject filter apparatus
[AD-D011359] 07 p0945 N85-15984
Optimal synthesis of surface acoustic wave filters
13 p2070 N85-22933
Fin line filters technology and electronic warfare
[AD-A154975] 21 p3576 N85-32237
Waveguide dielectric millimeter band filter with enhanced selectivity 22 p3780 N85-33421

WAVEGUIDE LASERS
Investigation of RF excited CW CO2 waveguide lasers
[NASA-CR-174106] 04 p0505 N85-13221
Life study of RF excited Hg arc lamps and CO2 waveguide lasers
[AD-A149616] 12 p1856 N85-21640
Ground slot waveguide laser
[AD-D011600] 15 p2563 N85-25813

WAVEGUIDE TUNERS
Micro-waveguide transformers of coherent optical signals 07 p0950 N85-16022

WAVEGUIDE WINDOWS
Analysis of waveguide discontinuities by the method of moments
[AD-A151499] 15 p2547 N85-25721

WAVEGUIDES
NT BEAM WAVEGUIDES
NT CIRCULAR WAVEGUIDES
NT OPTICAL WAVEGUIDES
NT PLASMAGUIDES
NT RECTANGULAR WAVEGUIDES
Wave guide branchings (n-port) types of representation of linear, time-independent and sourceless n-ports
[NASA-TM-77770] 01 p0037 N85-10233
Parabolic tapers for overmoded waveguides
[DE84-014237] 01 p0039 N85-10247
Biaxial-crystal laser with waveguide resonator
02 p0262 N85-11717
Using fiber-optics light guides in diagnosing intense shock waves 02 p0272 N85-11773
Scattering of electromagnetic waves in flat waveguide with bilateral diaphragms 03 p0347 N85-12235
The S-matrix and acoustic signal structure in simple and compound waveguides
[PP-583] 03 p0415 N85-12652
Implementing waveguide bandwidth six-port reflectometer circuits at millimetric wavelengths
[RSRE-MEMO-3878] 04 p0495 N85-13155
Technology for the ERS-1 SAR antenna
05 p0626 N85-14008
Field coherence function in layerwise nonhomogeneous troposphere 06 p0784 N85-15012
Interface structures for millimeter-wave circuits
[AD-A146557] 06 p0804 N85-15118
Investigating phase structure of electromagnetic field in local inhomogeneities by modeling method
06 p0822 N85-15220
Advanced infrared laser modulator development
[NASA-CR-172479] 06 p0862 N85-15479
MMIC devices for active phased array antennas
[NASA-CR-174281] 07 p0938 N85-15943
NBS (National Bureau of Standards) and WR62 and WR90 reference noise standards
[PB84-235704] 07 p0942 N85-15977
Investigation of planar waveguides and components for millimeter-wave integrated circuits
[AD-A147380] 07 p0948 N85-16005
Low-loss flexible dielectric waveguide for millimeter-wave transmission and its application to devices
[AD-A147848] 07 p0948 N85-16006
Acoustic transducers for fast reactor instrumentation
[BLL-RISLEY-TR-4979-(P091.9F)]
07 p0961 N85-16091
Upgrading flexible infrared waveguides
[AD-A146763] 07 p0970 N85-16160
A leaky waveguide model for MHD wave driven winds from coronal holes 08 p1235 N85-17781
The Shock and Vibration Digest, volume 16, no. 10
[AD-A147588] 09 p1331 N85-18361
Sound transmission in ducts 09 p1331 N85-18362
Multihole couplers for overmoded waveguide systems
[IPF-83-8] 09 p1394 N85-18773
Design of mode converters from TE circular om modes in circular waveguides to TE rectangular mo modes in rectangular waveguides for high power applications in the frequency range 1 to 30 GHz
[IPF-84-7] 09 p1395 N85-18781
Interleaved array antenna technology development
[NASA-CR-171845] 10 p1477 N85-19326

Design of low loss helix circuits for interference fitted and brazed circuits
[NASA-CR-168313] 10 p1478 N85-19328
Filter reflection image guide oscillator and solid state line scanning device
[AD-D011440] 10 p1479 N85-19336
Integrated circuit tunable cavity oscillator
[AD-D011474] 10 p1481 N85-19351
Average sound intensity decrease rule in irregular hydroacoustical waveguide 10 p1499 N85-19461
Construction tolerances for low loss, dielectric coated, metallic waveguide for transmission optical radiation
[DE85-004056] 10 p1558 N85-19822
Numerical methods for analyzing electromagnetic scattering
[NASA-CR-175507] 12 p1823 N85-21438
Single-cavity SLED device
[DE85-002587] 12 p1929 N85-22117
Variational and moment method solutions of the fields in a parallel-plate waveguide-aperture system
[DE85-006288] 13 p2057 N85-22676
A 60 GHz 200 kW CW gyrotron with high output mode purity
[DE85-005263] 13 p2066 N85-22905
Diffraction of periodic grounding system of finite length
13 p2081 N85-22994
Microstrip comb array design
[R-NIAS-24] 14 p2290 N85-24195
Millimeter-wave diffraction devices and materials
[AD-A150876] 14 p2418 N85-24917
Space processing of acoustic signals in plane-parallel waveguide — antenna arrays 15 p2525 N85-25572
Analysis of the electromagnetic scattering from an inlet geometry with lossy walls
[NASA-CR-175743] 15 p2541 N85-25686
Analysis of waveguide discontinuities by the method of moments
[AD-A151499] 15 p2547 N85-25721
Monolithic planar doped barrier limiter
[AD-D011578] 15 p2548 N85-25723
Waveguide phenomena in dense relaxing gases and their use in chemical and gas-dynamic lasers
15 p2644 N85-26308
Field near the front of a signal in a waveguide accomplished with dispersive plasma
[REPT-11/1984] 16 p2768 N85-27083
Design of the waveguide for microwave heating of solid lithium ceramic blankets
[DE85-009776] 17 p2935 N85-28120
Fiber optics in high dose radiation fields
[DE85-008649] 18 p3185 N85-29755
Analysis of systems of waveguide discontinuities by the method of moments 19 p3253 N85-30171
Guided and radiation wave interactions in periodic dielectric waveguides 19 p3253 N85-30173
Measurement of mode interaction due to waveguide surface roughness
[AD-A154039] 19 p3255 N85-30183
High harmonic rectangular gyrotron
19 p3256 N85-30189
Frequency-spreading coupler
[AD-D011683] 19 p3258 N85-30200
A computation of fin-line impedance
[AD-A154080] 19 p3258 N85-30204
Controlled-linewidth laser source
[AD-D011681] 19 p3274 N85-30306
Propagation of acoustic pulse in atmospheric waveguide 19 p3297 N85-30443
Guided-mode launching in a slab waveguide by way of diffraction at the edge of a conducting screen residing on one surface of the slab
[AD-A154686] 21 p3575 N85-32232
Multitrunk high-frequency multiplexing of antenna-waveguide channels 22 p3774 N85-33385
Miniature two-mode filters 22 p3775 N85-33394
Strongly coupled millimeter-band waveguide directional couplers 22 p3779 N85-33418
Fundamentals of radio optical theory of resonant and directional quasi-optical devices
22 p3780 N85-33420
Normal modes in an overmoded circular waveguide coated with lossy material
[NASA-CR-176186] 24 p4085 N85-35320

WAVELENGTH DIVISION MULTIPLEXING
Multiwavelength bidirectional coupler-decouplers
[AD-A147009] 07 p1043 N85-16625
NGC 2024: Multi-wavelength infrared and radio observations 08 p1246 N85-17865
Optical multiplexing on monomode fibers
[ENST-83E016] 20 p3533 N85-31982

WAVELENGTHS
Influence of radiation wavelength on elastic pulse shape during laser excitation 02 p0257 N85-11681
The 248 nm - new short wavelength for pumping lasers employing vapors of complex molecules
02 p0261 N85-11705
Using two-beam interference method for measuring wavelength of tunable pulse lasers
02 p0272 N85-11772
Variability of Neptune 02 p0299 N85-11936
Extinction by dielectric particles at optical and infrared wavelengths
[AD-A146305] 03 p0413 N85-12640
Wavelength coded image transmission and holographic optical elements
[AD-A146490] 06 p0810 N85-15147
Calibrations of wavelengths in SWP echelle spectra
11 p1761 N85-21077
Enhancing the performance of a high-gain free electron laser operating at millimeter wavelengths
[DE85-000862] 12 p1857 N85-21646
Phase function, backscatter, extinction, and absorption for standard radiation atmosphere and El Chichon aerosol models at visible and near-infrared wavelengths
[NASA-TM-86379] 12 p1892 N85-21674
Regions of propagation of short-wave perturbations in spherical layer of rotating fluid 13 p2107 N85-23130
Development of global model for atmospheric backscatter at CO2 wavelengths
[NASA-CR-175679] 15 p2591 N85-25971
Population inversion in laser-initiated vacuum arcs
[AD-A151958] 16 p2790 N85-27210
An evaluation and preparation of ferromagnetic liquid composites for use at millimeter wavelengths
[AD-A153939] 18 p3069 N85-28960
The application of laser resonance saturation to the development of efficient short wavelength lasers
[AD-A153951] 18 p3113 N85-29270
Development and application of a high power ND-glass laser instrument
[AD-A154366] 19 p3276 N85-30314
Reduced to pole long-wavelength magnetic anomalies of Africa and Europe 20 p3475 N85-31595
Long-wavelength magnetic and gravity anomaly correlations on Africa and Europe
20 p3476 N85-31597
Increase of antenna area instead of transmitter power, part 6.3A 21 p3624 N85-32517
Investigation of reproducibility of emission wavelength of helium-neon laser with external neon absorption cell (0.63 micrometers) 21 p3663 N85-32884

WAVES
A numerical method for interface problems in elastodynamics
[NASA-TM-86488] 06 p1172 N85-17391
Special features of computations of vertical distribution of concentration of suspended sediments under marine conditions 13 p2106 N85-23125
Energy structure of atmospheric boundary layer above waves 14 p2335 N85-24442
High-frequency wind wave spectrum in storm basin
14 p2336 N85-24444
The development of a transducer system for the accurate measurement of ultrasonic phase delay of SH plate waves
[AERE-R-11596] 15 p2559 N85-25790
Behavior of the porous bed in a combustion-deflagration-detonation transition
[ISL-CO-220/84] 22 p3747 N85-33224
Shear wave transducer for boreholes
[DE85-011662] 22 p3787 N85-33461

WEAK ENERGY INTERACTIONS
NT WEAK INTERACTIONS (FIELD THEORY)
Results on weak current from CHARM collaboration --- neutrino interactions
[NOTA-INTERNA-810] 02 p0279 N85-11817
Theoretical aspects of electroweak and other interactions in medium-energy nuclear physics
[DE85-003621] 13 p2157 N85-23392
Strong-coupling approximations
[DE85-007829] 19 p3353 N85-30785
Search for neutrino oscillations at the Brookhaven AGS
[DE85-009766] 20 p3530 N85-31957
Effects of CP violation in SU(2) sub L x SU(2) sub R x U(1) electroweak models
[DE85-010801] 20 p3531 N85-31965

WEAK INTERACTIONS (FIELD THEORY)
Thin end of the wedge
[DE84-016439] 09 p1401 N85-18816
Shell-model Lanczos-method studies of the Gamow-Teller strength function in astrophysics
[DE85-004205] 11 p1763 N85-21093
Theoretical nuclear physics
[DE85-003466] 12 p1932 N85-22135
Weak interactions of quarks and leptons: Experimental status
[DE85-008171] 18 p3181 N85-29723
The effects of weak turublence on parametric processes in an unmagnetized plasma 19 p3369 N85-30896
Phenomenology of the standard and nonstandard Higgs particles
[USIP-85-03] 20 p3532 N85-31971
Systematics of quark mass matrices in the Standard Electroweak Model
[USIP-85-05] 20 p3532 N85-31972
Spatial parity violation in elastic neutron-nuclei interaction channel 21 p3691 N85-32932
Does low-energy physics depend on the potential of a heavy Higgs-particle
[NIKHEF-H/85-1] 22 p3838 N85-33763

WEAPON SYSTEMS
NT LASER WEAPONS
NT MISSILE SYSTEMS
Analysis of on-board CIG (Computer Image Generator) applications for aircrew training
[AD-A145214] 01 p0013 N85-10079
Directed energy missile defense in space
[PB84-210111] 01 p0015 N85-10095
The need for improvements in weapon system maintenance: What can AI (Artificial Intelligence) contribute?
[AD-P003913] 02 p0244 N85-11593
Artificial intelligence applications to maintenance
[AD-P003914] 02 p0244 N85-11594
Knowledge based tools for electronic equipment maintenance
[AD-P003940] 02 p0248 N85-11620
Avionics/crew station integration
06 p0752 N85-14818
Attack helicopter (AH-1T) cockpit systems integration
06 p0753 N85-14826
ILIR task of digital recoil travel measurement system
[AD-A147102] 07 p0967 N85-16140
An analysis of the effect of process controls on productivity and weapon system costs in DoD procurement
[AD-A147496] 07 p1052 N85-16678
Estimating wartime support resource requirements. Statistical and related policy issues
[AD-A147923] 07 p1053 N85-16685
Effective life cycle software support: A study in discipline and versatility 08 p1065 N85-16746
A weapon system design approach to diagnostics
08 p1066 N85-16752
A simulator for studying helicopter weapons systems
08 p1075 N85-16816
On estimating the cost growth of weapon systems
[AD-A147297] 08 p1230 N85-17749
Simulating speed and height cues in the C-130 weapon system trainer
[AD-P004313] 09 p1268 N85-17967
Air Force space technology center space technology: Emphasis 84 09 p1333 N85-18381
Assuring structural integrity in Army systems
[NASA-CR-175492] 11 p1651 N85-20398
BIT/BITE tradeoff analysis model
[AD-A149345] 11 p1701 N85-20697
Supersonic Tactical Missile (STM) radome development
[AD-P004360] 12 p1825 N85-21454
Air combat simulation: Methods, models, trends
13 p1967 N85-22359
Using NASTRAN to model missile inertia loads
15 p2576 N85-25866
Studies of electro-optical attenuation in the vicinity of cloud base
[AD-A151745] 15 p2653 N85-26360
Design adequacy: An effectiveness factor
16 p2695 N85-26642
Design-To-Cost (DTC) methodology to achieve affordable avionics 16 p2696 N85-26645
Military journal on US intelligence satellites
16 p2727 N85-26832
Presentations at the Tri-Service Cloud Modeling Workshop (2nd), held at the Naval Surface Weapons Center, White Oak, Maryland, 26-27 June 1984, volume 1
[AD-A152735] 17 p2996 N85-28522
The Department of Defense statement on the Science and Technology Program by Colonel Donald I. Carter, USAF Acting Deputy Under Secretary of Defense for Research and Advanced Technology before the Subcommittee on Research and Development of the Committee on Armed Services of the United States House of Representatives, 99th Congress, first session
[AD-A152467] 17 p3046 N85-28850
Soviet weapons development and the scientific community
[AD-P004562] 17 p3047 N85-28857
The revolution in military affairs and the Soviet system
[AD-P004568] 17 p3048 N85-28863
Assessment of computer resource management plan for division support weapon system
[AD-A154142] 19 p3342 N85-30712

Producibility Engineering and Planning (PEP): Program management guidelines
[AD-A153730] 19 p3379 N85-30966
Cost and schedule implications of multinational coproduction
[AD-A154358] 19 p3380 N85-30969
SAFEORD: Safety of explosive ordnance databank
[AD-A154058] 19 p3380 N85-30972
Meteorological weapons
[AD-A154735] 21 p3635 N85-32575
Next generation gunship
[AD-A156361] 24 p4065 N85-35193
Proceedings of the 14th Army Science Conference. Volume 3: Principal authors P through Z
[AD-A149202] 24 p4144 N85-35691

WEAPONS
NT ARTILLERY
NT GUNS (ORDNANCE)
NT LASER WEAPONS
NT NUCLEAR WEAPONS
NT SPACE WEAPONS
NT WARHEADS
Evolution of the NWC (Naval Weapons Center) thermal standard. Part 5: Thermal standard development and applications
[AD-A146173] 03 p0364 N85-12334
Naval surface weapons center technology transfer report (FY83)
[AD-A146501] 06 p0871 N85-15534
Design of explosive logic elements
[DE84-009611] 11 p1614 N85-20146
China report: Science and technology
[JPRS-CST-84-025] 11 p1620 N85-20197
Phenomenology of microwave coupling, part 1
[DE85-003097] 11 p1624 N85-20229
Theory of lethality
[DE85-000457] 11 p1721 N85-20826
A proportional-plus-integral controller for a particle beam weapon
[AD-A153213] 17 p3035 N85-28778
Toxic hazards tests for vehicles and other equipment
[AD-A149164] 20 p3506 N85-31797

WEAPONS DELIVERY
Content, variety, and augmentation of simulated visual scenes for teaching air-to-ground attack
[AD-A145218] 01 p0013 N85-10080

WEAPONS DEVELOPMENT
Soviet weapons development and the scientific community
[AD-P004562] 17 p3047 N85-28857
Technology and technical efficiency in the Soviet Union: Dominant patterns of constrained optimization in a noncompetitive economic regime
[AD-P004587] 17 p3048 N85-28862

WEAR
Structure and wear workshop colloquium
01 p0054 N85-10356
The influence of surface layers on the friction and wear behavior of materials 01 p0054 N85-10357
The influence of the carbide distribution on the abrasive wear of ledeburitic chromium steels
01 p0054 N85-10359
Structure and abrasive resistance of iron based alloys rich in hardening components 01 p0054 N85-10360
Friction and wear of polymers and polymer composite materials 01 p0054 N85-10361
Friction, wear and structure of heterogeneous materials 01 p0055 N85-10362
Wear properties of rapidly solidified surfaces of a pseudo-binary Fe-TiC alloy 02 p0179 N85-11204
The constitution as the basis for recent and future developments of wear resistant materials
02 p0179 N85-11205
Surface segregation of sulfur during oscillatory pin-on-plate wear studies of precious metal electrical contact alloys. 1: Friction and electrical contact resistance
[DE84-006962] 02 p0195 N85-11303
Lubricity of well-characterized jet and broad-cut fuels by ball-on-cylinder machine
[NASA-TM-83807] 03 p0339 N85-12183
Interactions among system stiffness, wear and vibrations 03 p0370 N85-12364
Wear and corrosion of components under stress and subjected to motion
[AD-A145781] 03 p0372 N85-12372
Effect of humidity on fretting wear of several pure metals
[NASA-TP-2403] 04 p0472 N85-13006
Microstructural effects in abrasive wear
[DE84-016155] 04 p0509 N85-13247
Wear of anodic oxide films on aluminum alloys in cryogenic liquids
[NAL-TR-818] 06 p0768 N85-14914
Effects of silver and group 2 fluorides addition to plasma sprayed chromium carbide high temperature solid lubricant for foil gas bearing to 650 deg C
[NASA-TM-86895] 06 p0770 N85-14928
A study of wear characteristics due to pressure for hydraulic fixed displacement vane pumps
[AD-A146023] 06 p0814 N85-15169
Mechanical aspects of high temperature coatings
07 p0906 N85-15749
Fundamental tribological properties of ceramics
[NASA-TM-86915] 07 p0930 N85-15893
Surface effects of corrosive media on hardness, friction, and wear of materials
[NASA-TM-83711] 07 p0930 N85-15896
Effect of five lubricants on life of AISI 9310 spur gears
[NASA-TP-2419] 07 p0962 N85-16099
Structure of solids surfaces in wear situations
[AD-A148480] 08 p1168 N85-17366
The wear of small polyacetal and polymide gears in vacuum — spacecraft gears
[ESA-ESTL-058] 08 p1169 N85-17374
Surface mechanical properties and wear behavior of ion implanted TiB2
[DE85-001130] 09 p1295 N85-18133
Implantation of Ti + C for reduced friction and wear of steels
[DE85-001606] 09 p1295 N85-18135
Influence of temperature on wear resistance of detonation coatings of alloy powders
10 p1447 N85-19116
Characteristics of the elevation drive suspension of the 64-meter antennas 10 p1464 N85-19240
Effect of implantation species on the tribological response of stainless steel surfaces
[DE85-003530] 10 p1493 N85-19432
Engine wear and cold startability of methanol fueled engines.
[DE85-001208] 11 p1647 N85-20381
Ion-beam nitriding of steels
[NASA-CASE-LEW-14104-1] 12 p1805 N85-21324
Tribological systems as applied to aircraft engines
[NASA-TM-86965] 12 p1858 N85-21657
Applications of vibration analysis to the condition monitoring of rolling element bearings
[ARL/AERO-R-163] 12 p1859 N85-21663
Rational use of tatanium in nonferrous metallurgy
13 p2031 N85-22728
Durability of VT16 alloy compounds obtained by diffusion welding 13 p2034 N85-22740
Sliding seal materials for adiabatic engines
[NASA-CR-174893] 13 p2037 N85-22757
Use of optical techniques in studies of wear rates of anodized aluminum and polymer coatings on aluminum
14 p2259 N85-23997
Sweden invents new ceramic for more durable cutting tools 15 p2536 N85-25645
Classification and types of diamond wear in honing
15 p2567 N85-25842
Metal armatures for railguns
[AD-A152129] 16 p2728 N85-26838
Reusable rocket engine turbopump condition monitoring 16 p2740 N85-26907
Effects of wear on structure-sensitive magnetic properties of ceramic ferrite in contact with magnetic tape
[NASA-TM-87007] 16 p2753 N85-26991
Effect of counterface material type and its topography on the tribological properties of polyimide composites
[NASA-TM-87036] 16 p2754 N85-26993
Breakway friction and dynamic friction/wear measurements of various ceramic materials from 25 C (75 F) to 650 C (1200 F)
[NASA-CR-174803] 16 p2754 N85-26994
Tooth wear in worm gears in vacuum
16 p2766 N85-27070
Extreme evaluation of reliability indices for components of metallurgical equipment
[BLL-M-36070-(5828.4)] 16 p2796 N85-27234
Friction and wear behavior of aluminum and composite I-beam stiffened airplane skins
[NASA-TM-86418] 17 p2895 N85-27852
Tribological sinks: Money down the drain
[DE85-010019] 17 p2974 N85-28376
Studies on surface processes during friction and wear
[AD-A153509] 18 p3117 N85-29296
Wear improvement in titanium alloys by ion implantation
[AD-D011694] 19 p3239 N85-30081
Microstructure-abrasive wear characteristics of low carbon dual phase steels
[DE85-010988] 19 p3239 N85-30083
Geothermal COMPAX drill hit development
[DE85-011353] 20 p3469 N85-31556
Rolling, slip and traction measurements on low modulus materials
[NASA-CR-174909] 22 p3791 N85-33491
Application of traction drives as servo mechanisms
22 p3797 N85-33520
Three body abrasive wear in various metal combinations 23 p3906 N85-34200

WEAR INHIBITORS
The role of molybdenum as an alloy element in adhesive wear resistance 02 p0181 N85-11212
The effect of heat treatment on wear resistance of gas-plasma eutectic coatings
[BLL-M-35756-(5828.4)] 03 p0329 N85-12122
Deposition of titanium nitride coatings by reactive evaporation and electrically activated reactive evaporation
[BLL-TRANS-5043-(9091.9F)] 07 p0925 N85-15858
Effect of zero-wear in friction pairs operating in abrasive media 13 p2045 N85-22801
Wear reduction by lubricants in confined contacts
14 p2223 N85-23786
Gear-cutting tools made of ultra high speed steel coated with TiN
[BLL-RISLEY-TR-5109-(9091.9F)]
15 p2567 N85-25837
Non-contact hydrostatic bearings
16 p2762 N85-27046
Lubricant and additive effects on spur gear fatigue life
[NASA-TM-87044] 17 p2974 N85-28373
Physical-mechanical characteristics and wear resistance of coatings applied by microarc oxidation
19 p3242 N85-30104
Anti wear property of two phasic metal composite
23 p3906 N85-34199
Action of wear-inhibiting Al2O3-coatings when applied to hard metal cutting tools
[BLL-RISLEY-TR-5041-(9091.9F)]
24 p4081 N85-35292
Wear-resistant coatings for tools intended for cold working
[BLL-RISLEY-TR-5040-(9091.9F)]
24 p4081 N85-35293

WEAR TESTS
The monitoring of machines
[CETIM-15-J-041] 04 p0510 N85-13253
The wear of small polyacetal and polymide gears in vacuum — spacecraft gears
[ESA-ESTL-058] 08 p1169 N85-17374
Implantation of Ti + C for reduced friction and wear of steels
[DE85-001606] 09 p1295 N85-18135
Cutting structural materials in vacuum
14 p2286 N85-24165
Classification and types of diamond wear in honing
15 p2567 N85-25842
Determination of wear intensity and resource of crankshafts and cylinder liners of ZIL-130 and ZMZ-53 engines
[BLL-BISI-TRANS-21393-(9022.06)]
17 p2972 N85-28355
Examples of application of machinability tests
[BLL-BISI-TRANS-22346-(9022.06)]
17 p2973 N85-28363
Lubricant and additive effects on spur gear fatigue life
[NASA-TM-87044] 17 p2974 N85-28373
Sintering reactions, structure and properties of a cobalt free nonconventional hard material
[DE85-007704] 18 p3076 N85-29025
Study of the chemical mechanism in lubrication
[DE85-010768] 19 p3228 N85-30013
Mechanical protection of DLC films on fused silica slides
[NASA-TM-87056] 19 p3248 N85-30138

WEATHER
NT COLD WEATHER
NT HOT WEATHER
National solar-terrestrial research program
[PB84-216183] 01 p0072 N85-10479
Weather satellite products in the Flight Service Automation System (FSAS)
[AD-A146520] 06 p0759 N85-14855
Revised Uniform Summary of Surface Weather Observations (RUSSWO). Alconbury RAF United Kingdom, parts A-F
[AD-A146913] 07 p1004 N85-16384
Revised Uniform Summary of Surface Weather Observations (RUSSWO). McChord AFB, Washington, parts A-F
[AD-A146914] 07 p1005 N85-16385
Revised Uniform Summary of Surface Weather Observations (RUSSWO). Mildenhall RAF, United Kingdom, parts A-F
[AD-A146915] 07 p1005 N85-16386
Revised Uniform Summary of Surface Weather Observations (RUSSWO). Dobbins AFB, Georgia, parts A-F
[AD-A146916] 07 p1005 N85-16387

Revised Uniform Summary of Surface Weather Observations (RUSSWO). Shemya AFB, Alaska, parts A-F
[AD-A146917] 07 p1005 N85-16388
Revised Uniform Summary of Surface Weather Observations (RUSSWO). Pope AFB, Fayetteville, North Carolina, parts A-F
[AD-A146918] 07 p1005 N85-16389
Revised Uniform Summary of Surface Weather Observations (RUSSWO). Sondestrom AB, Greenland, parts A-F
[AD-A146919] 07 p1005 N85-16390
Revised Uniform Summary of Surface Weather Observations (RUSSWO). England AFB, Alexandria, Lousiana, parts A-F
[AD-A146920] 07 p1006 N85-16391
Revised Uniform Summary of Surface Weather Observations (RUSSWO). Spangdahlem AB, Germany, parts A-F
[AD-A147166] 07 p1006 N85-16392
Limited surface observations climatic summary (LISOCS). Hohenfels, AAF, West Germany
[AD-A147167] 07 p1006 N85-16393
Revised Uniform Summary of Surface Weather Observations (RUSSWO). Offutt AFB, Nebraska, parts A-F
[AD-A147183] 07 p1006 N85-16394
Revised Uniform Summary of Surface Weather Observations (RUSSWO). Hill AFB, Utah, parts A-F
[AD-A147184] 07 p1006 N85-16395
Revised Uniform Summary of Surface Weather Observations (RUSSWO). Parts A-F: Homestead AFB, Florida
[AD-A147203] 07 p1007 N85-16396
Propagation and scattering considerations for the 0.2-3.0 GHz frequency range for a space-based radar
[AD-A148504] 08 p1153 N85-17282
Two-dimensional modeling for lineal and areal probabilities of weather conditions
[AD-A147970] 08 p1188 N85-17486
Denver ARTCC (Air Route Traffic Control Center) evaluation of PROFS (Program for Regional Observing and Forecasting Services) mesoscale weather products
[PB85-120301/GAR] 09 p1279 N85-18045
Revised Uniform Summary of Surface Weather Observations (RUSSWO). Parts A-F Zweibrucken AB, Germany
[AD-A147165] 09 p1357 N85-18536
Weather data for simplified energy calculation methods. Volume 4: United States, WYEC data
[DE85-000491] 09 p1357 N85-18539
Equations and algorithms for meteorological applications in air weather service
[AD-A146894] 10 p1519 N85-19575
OBLOG: Designed to create and maintain a 49 hour observation log file
[PB85-109526] 10 p1519 N85-19579
Monthly and Seasonal Weather Outlook for November, 1984, Volume 38, Number 27, October 30, 1984
[PB85-118800] 10 p1521 N85-19588
Digital and color energy maps for graphic display of hourly data
[DE85-000526] 11 p1673 N85-20543
Weather data for simplified energy calculation methods. Volume 2: Middle United States. TRY data
[DE85-000494] 11 p1687 N85-20608
Monthly and seasonal weather outlook for October 1984, volume 38, number 19, 29 September 1984
[PB85-113538] 11 p1687 N85-20610
Monthly and seasonal weather outlook for January 1985, volume 39, number 1
[PB85-148799] 12 p1898 N85-21915
El Nino, the capricious child 13 p2106 N85-23121
Possibility of determining atmospheric weather parameters by radio and radiooptical measurements of refraction of cosmic sources 13 p2110 N85-23148
Summary of Meteorological Observations, Surface (SMOS), Fallon, Nevada
[AD-A150481] 13 p2138 N85-23276
Summary of Meteorological Observations, Surface (SMOS) Camp Pendleton, California
[AD-A150482] 13 p2138 N85-23277
Summary of Meteorological Observations, Surface (SMOS), Bermuda
[AD-A150537] 13 p2138 N85-23278
Summary of Meteorological Observations, Surface (SMOS), Alameda, California
[AD-A150609] 13 p2138 N85-23281
An introduction to USAFETAC (USAF Environmental Technical Applications Center)
[AD-A150971] 14 p2378 N85-24662
The impact of weather on aviation safety
[GPO-35-520] 16 p2703 N85-26685
Regularities in recent changes in surface air temperature and atmospheric precipitation fields
16 p2807 N85-27311
Effect of precipitation on wind turbine performance
[NASA-TM-86986] 16 p2818 N85-27385
AWS (Air Weather Service) climatic briefs: Asia
[AD-A151944] 16 p2835 N85-27481
Comparison of circulation statistics based on FGGE (First GARP Global Experiment) level 3-B analyses produced by GFDL (Geophysics Fluid Dynamics Laboratory) and ECMWF (European Centre for Medium Range Weather Forecasts) for special observing periods
[PB85-153848] 16 p2836 N85-27492
Monthly and seasonal weather outlook for mid-January to mid-February 1985, volume 39, number 2, January 15, 1985
[PB85-164572] 16 p2837 N85-27500
Monthly and seasonal weather outlook for February 1985, volume 39, number 3, January 30, 1985
[PB85-159424] 16 p2838 N85-27502
Flying in spite of the weather
[NLR-MP-84021-U] 17 p2895 N85-27847
Air Weather Service (AWS) climatic briefs: Europe
[AD-A152528] 17 p2996 N85-28519
Experiments on the assimilation of patches of data using a barotropic model 18 p3140 N85-29441
Mariners weather log, volume 29, number 1, winter 1985
[PB85-177483] 19 p3318 N85-30570
Mariners weather log, volume 28, number 4, fall 1984
[PB85-178406] 19 p3318 N85-30571
Middle Atmosphere Program. Handbook for MAP. Volume 14: URSI/SCOSTEP Workshop on Technical Aspects of MST Radar
[NASA-CR-176085] 21 p3615 N85-32466
Investigations of micro-turbulence in the bottom of the boundary layer
[AD-A155146] 21 p3636 N85-32585
A simulation of weather in 3D space
[AD-A155221] 21 p3636 N85-32586
Satellites and politics: Weather, communications, and earth resources 23 p4057 N85-35144

WEATHER CHARTS
U METEOROLOGICAL CHARTS

WEATHER CONDITIONS
U WEATHER

WEATHER CONTROL
U WEATHER MODIFICATION

WEATHER DATA RECORDERS
Thermosonde C2N measurements in Hawaii--August 1982
[AD-A148016] 08 p1189 N85-17489
Annual cycle. Part 1: The annual variation of surface temperatures over the United States and Canada
[PB85-147676] 15 p2600 N85-26026
Fog advection in the Namib 16 p2831 N85-27454

WEATHER FORECASTING
NT LONG RANGE WEATHER FORECASTING
NT NOWCASTING
NT NUMERICAL WEATHER FORECASTING
NT STATISTICAL WEATHER FORECASTING
Operational evaluation of 5 cm Doppler radar. Two contributions: Review of WSR-74C Doppler radar operations at WSO Montgomery, Alabama (April 1982 - August 1983). The Johnson-Effect resolving ambiguous Doppler velocities
[PB84-207521] 01 p0041 N85-10269
Large-scale ocean-atmosphere interactions in the mid-latitudes and equatorial regions: A literature review
[CSIR-T/SEA-8302] 01 p0073 N85-10482
Remote sensing of atmospheric particulates: Technological innovation and physical limitations in applications to short-range weather prediction
[NSF ATM-82-09684] 01 p0077 N85-10511
The use of dual polarisation radar for observing and predicting convective activity 01 p0077 N85-10512
The PROMIS Doppler radar system; design and operational experience 01 p0077 N85-10513
Nowcasting with Doppler radar: The forecaster-computer relationship
01 p0077 N85-10514
PROFS: An approach to improved operational weather services — Program for Regional Observing and Forecasting Services (PROFS) 01 p0083 N85-10555
Statistical tropical cyclone forecasting techniques for the Southern Hemisphere
[AD-A144752] 01 p0085 N85-10569
Setting hurricane conditions of readiness with high confidence
[AD-A144785] 01 p0085 N85-10570
Automated aircraft icing forecast technique
[AD-A144853] 01 p0085 N85-10571
Some aspects of post-frontal convective areas along the west coast of the united states
[AD-A144895] 01 p0085 N85-10572
Investigation of summertime convection over the upper Current River valley of southeast Missouri
[PB84-222389] 01 p0086 N85-10578
Joint probability of selected cloud and visibility thresholds around Koblenz, Germany
[AD-A145284] 02 p0231 N85-11506
Handbook for sea ice analysis and forecasting
[AD-A145286] 02 p0233 N85-11516
Report of the Division of Atmospheric Physics, 1980-1983 03 p0391 N85-12501
Plotting TDL coastal wind forecasts
[PB84-220789] 03 p0397 N85-12533
Use of photographs of meteorologic satellites in synoptic analysis
[SESIT-5] 05 p0679 N85-14357
Very short range statistical forecasting of automated weather observations
[DOT/FAA/PM-84/31] 05 p0679 N85-14359
Global Scale Atmospheric Processes Research Program Review
[NASA-CP-2344] 05 p0679 N85-14360
GLAS fourth order model 05 p0679 N85-14361
Massively parallel processor 05 p0680 N85-14366
Studies of atmospheric water in storms with the Nimbus 7 scanning multichannel microwave radiometer
05 p0682 N85-14382
The influence of synoptic scales on low-frequency modes of variability 05 p0687 N85-14412
Convective scale weather analysis and forecasting
[NASA-CR-174185] 06 p0838 N85-15320
Marners weather log, volume 28, no. 3, July-August-September 1984
[PB85-107266] 06 p0840 N85-15334
Trends in skill and accuracy of National Weather Service pop forecasts
[PB84-229053] 06 p0840 N85-15335
Environmental research laboratories (of the National Oceanic and Atmospheric Administration) programs and plans: FY 1983 programs and FY 1984 plans
[PB84-226729] 06 p0840 N85-15336
AFOS (Automation of Field Operations and Services) display of MDR (Manually Digitized Radar) data on local map backgrounds
[PB84-220797] 06 p0840 N85-15338
NOAA (National Oceanic and Atmospheric Administration) Aircraft Satellite Data Link (ASDL)
[PB84-243773] 07 p0942 N85-15976
Automated Lavina collects data on snow
07 p0960 N85-16224
Experiments in forecasting atmospheric marine horizontal visibility using model output statistics with conditional probabilities of discretized parameters
[AD-A147574] 07 p1008 N85-16404
The 500 millibar sign frequency teleconnection charts: Winter
[PB85-106276/GAR] 07 p1009 N85-16410
Estimations of diabatic heating for an explosively-developing maritime cyclone
[AD-A147678] 08 p1188 N85-17483
Two-dimensional modeling for lineal and areal probabilities of weather conditions
[AD-A147970] 08 p1188 N85-17486
A scheme for short-term prediction of hydrometeors using advection and physical forcing
[AD-A148011] 08 p1188 N85-17487
Index of Air Weather Service technical publications, 1 July 1983-30 June 1984
[AD-A148051] 08 p1189 N85-17491
The visibility climatology of McMurdo Sound-Williams Field, Antarctica
[AD-A148108] 08 p1189 N85-17492
Denver ARTCC (Air Route Traffic Control Center) evaluation of PROFS (Program for Regional Observing and Forecasting Services) mesoscale weather products
[PB85-120301/GAR] 09 p1279 N85-18045
Rain volume estimation over areas using satellite and radar data
[NASA-CR-174434] 10 p1518 N85-19568
Frozen precipitation and concurrent weather: A case study for Munchen-Riem, West Germany
[AD-A149227] 10 p1519 N85-19577
Monthly and Seasonal Weather Outlook for November, 1984, Volume 38, Number 27, October 30, 1984
[PB85-118800] 10 p1521 N85-19588
Climate of Salt Lake City, Utah
[PB85-123875] 10 p1521 N85-19589
Hurricane plotting program
[PB85-121432] 10 p1521 N85-19592
Improved models for increasing wind penetration, economics and operating reliability
[NASA-CR-175538] 11 p1674 N85-20545
Monthly and seasonal weather outlook for mid-October to mid-November 1984, volume 38, number 20, 13 October 1984
[PB85-113546] 11 p1687 N85-20611
The 500 millibar sign frequency teleconnection charts: Fall
[PB85-110930] 11 p1687 N85-20612

The 500 millibar sign frequency teleconnection charts: Summer
[PB85-111359] 11 p1688 N85-20613

The 500 millibar sign frequency teleconnection charts: Spring
[PB85-111367] 11 p1688 N85-20614

Isentropic objective analysis
[PB85-112167] 11 p1688 N85-20617

Use and interpretation of isentropic analyses
[PB85-132694] 11 p1688 N85-20618

Development of satellite data presentation for environmental forecasting 11 p1712 N85-20770

21 Layer troposphere-stratosphere climate model
[NASA-TM-86163] 12 p1892 N85-21871

Space Shuttle interactive meteorological data system study
[NASA-CR-171418] 12 p1892 N85-21876

Hurricane storm surge research
[GPO-40-046] 12 p1893 N85-21880

On the error of typhoon intensity estimation by means of IR Dvorak technique occurring when the eye is very small 12 p1894 N85-21886

Varying structure and intensity change characteristics of 4 Western North Pacific tropical cyclones
[AD-A149628] 12 p1895 N85-21895

Navy tactical applications guide. Volume 4. Part 1. Eastern North Pacific weather analysis and forecast applications
[AD-A150097] 12 p1896 N85-21900

FTASUM: Aviation forecast summaries
[PB85-112977] 12 p1897 N85-21908

SAOSUM: A short summary of observations
[PB85-120384] 12 p1897 N85-21909

Preliminary results of associating cloud-to-ground lightning with surface convergence and radar reflectivity at Kennedy Space Center in 1983
[NASA-CR-175543] 12 p1897 N85-21910

TRAJ: Single station trajectory plot
[PB85-135002] 12 p1897 N85-21911

AFOS (Automation of Field Operations and Service) surface observation decoding
[PB85-137586] 12 p1898 N85-21913

New atmospheric sensor analysis study
[NASA-CR-171426] 13 p2094 N85-23069

Summary of Meteorological Observations Surface (SMOS), Sigonella, Sicily/Navy
[AD-A150539] 13 p2138 N85-23260

Tactical deployment of satellite-reporting drifting data buoys for environmental data acquisition
14 p2332 N85-24423

Influence of interaction between ocean and atmosphere on intensity of moving tropical cyclone
14 p2333 N85-24431

Monthly and Seasonal Weather Outlook for mid-December 1984 mid-January 1985, volume 38, number 24, 14 December 1984
14 p2379 N85-24687

Convection modeling and application to severe storms
15 p2595 N85-25991

Mesoscale analysis and modeling group
15 p2596 N85-26001

Nowcasting applications of VAS
15 p2597 N85-26003

Recent failures of weather satellites
[S-HRG-98-1070] 16 p2731 N85-26855

Lightweight aerological radiosonde MARZ
16 p2807 N85-27309

Symposium on Atmospheric Sciences in South Africa
[CSIR-S-331] 16 p2829 N85-27442

The study of thermal forecasting for gliding
16 p2830 N85-27453

Use of a network of telemetered meteorological stations for prediction of the distribution of an atmospheric tracer
16 p2831 N85-27458

Forecast of Atlantic seasonal hurricane activity for 1985 16 p2833 N85-27470

A survey of major east coast snowstorms, 1960-1983. Part 2: Case studies of eighteen storms
[NASA-TM-86196] 16 p2833 N85-27472

SINOGRAFO: A system for influencing and forecasting weather
[INPE-3349-PRE/628] 16 p2834 N85-27475

Simulation of a synchronously coupled atmosphere-ocean prediction model
[AD-A152020] 16 p2835 N85-27482

Hurricane Research Division, fiscal year 1984 programs, fiscal year 1985 projections 16 p2836 N85-27491

SCPP (Sierra Cooperative Pilot Project) Forecasting Support 16 p2837 N85-27493

Evaluation of the PROFS (Program for Regional Observing and Forecasting Services) 1982, real-time forecast experiment
[PB85-159747] 16 p2837 N85-27495

Technique that uses satellite, radar, and conventional data for analyzing and short-range forecasting of precipitation from extratropical cyclones
[PB85-164994] 16 p2837 N85-27499

Centralized Storm Information System (CSIS)
[NASA-CR-175898] 17 p2994 N85-28506

A report from the Space Science and Engineering Center, the University of Wisconsin-Madison, Madison, Wisconsin 17 p2994 N85-28507

Test and evaluation plan for the Centralized Storm Information System 17 p2994 N85-28508

CSIS test and evaluation 17 p2994 N85-28509

Functional and performance requirements of the next NOAA-Kasas City computer system
17 p2994 N85-28510

Spectral decomposition and verification of NOGAPS 500MB medium-range forecasts
[AD-A152550] 17 p2996 N85-28520

Weather radar studies
[AD-A152563] 17 p2996 N85-28521

Airborne research meteorological data collected by the National Hurricane Research Laboratory (Hurricane Research Division/AOML) during the 1982-1983 hurricane seasons: Inventory and availability
[PB85-163681] 17 p2997 N85-28528

Research Review, 1983
[NASA-TM-86219] 18 p3139 N85-29433

Forecast impact simulation studies
18 p3139 N85-29435

The contrasting Northern Hemisphere winters of 1980-81 and 1981-82 18 p3144 N85-29468

Some recent developments in numerical modelling at ECMWF 18 p3147 N85-29481

Automated Weather Observing System (AWOS) demonstration program
[AD-A153463] 18 p3148 N85-29493

Environmental Research Laboratories (of the National Oceanic and Atmospheric Administration) programs and plans: FY 1984 programs and FY 1985 plans
[PB85-171494] 18 p3149 N85-29501

Application of climatological analysis to minimize air pollution impacts in California
[PB85-172963] 18 p3149 N85-29502

Isotropic plotter
[PB85-175651] 18 p3150 N85-29504

Monthly and seasonal weather outlook for mid-March to mid-April 1985, March 14, 1985, volume 39, no. 6
[PB85-174751] 19 p3317 N85-30565

J. P. Finley: The first severe storms forecaster
[PB85-17453] 19 p3318 N85-30566

VIDTEX
[PB85-175669] 19 p3318 N85-30567

Forecast of Atlantic seasonal hurricane activity for 1985 20 p3495 N85-31732

Carbon dioxide and climate: Potential impacts
[DE85-009473] 20 p3496 N85-31734

Automated cell detection as a mesocyclone precursor tool
[AD-A154952] 21 p3635 N85-32577

Forecasting of tropical cyclone motion using an EOF (Empirical Orthogonal Function) representation of wind forcing
[AD-A155034] 21 p3636 N85-32580

Monthly and seasonal weather outlook for April 1985, March 30, 1985, volume 39, no. 7
[PB85-183804] 22 p3817 N85-33648

Dynamics of Mesoscale Weather Systems: 1984 Summer Colloguium
[PB85-186266] 22 p3817 N85-33649

Application of a turbulent closure model to the parameterization of the vertical diffusion of heat, momentum, and humidity in the ECMWF model — European Center for Medium Term Weather Forecasting (ECMWF)
[MITT-41] 24 p4095 N85-35387

Comparative analysis of operational forecasts versus actual weather conditions in airline flight planning, volume 1
[NASA-CR-167862] 24 p4119 N85-35534

Comparative analysis of operational forecasts versus actual weather conditions in airline flight planning, volume 2
[NASA-CR-167863] 24 p4119 N85-35535

Comparative analysis of operational forecasts versus actual weather conditions in airline flight planning, volume 3
[NASA-CR-167864] 24 p4120 N85-35536

Comparative analysis of operational forecasts versus actual weather conditions in airline flight planning, volume 4
[NASA-CR-167865] 24 p4120 N85-35537

Comparative analysis of operational forecasts versus actual weather conditions in airline flight planning: Summary report
[NASA-CR-167866] 24 p4120 N85-35538

A preliminary intercomparison between numerical upper wind forecasts and research aircraft measurements of jet streams
[NASA-CR-167884] 24 p4120 N85-35539

The physical and empirical basis for a specific clear-air turbulence risk index
[NASA-CR-178522] 24 p4120 N85-35540

Project Skywater, 1983-84 SCPP (Sierra Cooperative Pilot Project) data inventory
[PB85-187052] 24 p4124 N85-35565

Surface cyclogenesis as indicated by satellite imagery
[PB85-191815] 24 p4124 N85-35566

Program for Regional Observing and Forecasting Services (PROFS)
[PB85-188050] 24 p4124 N85-35569

WEATHER FRONTS
U FRONTS (METEOROLOGY)

WEATHER MAPS
U METEOROLOGICAL CHARTS

WEATHER MODIFICATION
NT CLOUD DISPERSAL
NT CLOUD SEEDING
NT RAINMAKING

International Conference on Physics of Clouds
06 p0819 N85-15198

The management of atmospheric resources in food production 07 p1002 N85-16362

Satellite support to the Sierra Cooperative Pilot Project: 1979/80 and 1980/81
[PB85-115079] 10 p1520 N85-19583

Ice multiplication in summertime cumulus clouds in the BEWMEX area 16 p2829 N85-27445

Effects of cloud seeding on precipitation development in cumulus clouds 16 p2831 N85-27456

Meteorological weapons
[AD-A154735] 21 p3635 N85-32575

Experimental studies of the kinetics of deposition nucleation on an ice nucleant used in weather modification 21 p3638 N85-32598

Ice nucleating characteristics of Capparis Aphylla, an Indian herb 21 p3641 N85-32619

Project Skywater, 1983-84 SCPP (Sierra Cooperative Pilot Project) data inventory
[PB85-187052] 24 p4124 N85-35565

WEATHER RADAR
U METEOROLOGICAL RADAR

WEATHER STATIONS
NT AUTOMATIC WEATHER STATIONS

The climate of Denmark. Summaries of observations from light vessels. 3: Sea temperature
[ISBN-87-7478-215-0] 01 p0073 N85-10481

The pluviometric recording stations in the 11 GHz radio link at Invioletella Monte S. Pancrazio — Italy
[FUB-6-1983] 01 p0086 N85-10575

Use of prototyping for man-machine interface requirements definition on the AWDS (Automated Weather Distribution System) program
[AD-A146033] 03 p0396 N85-12526

Acquisition and storage of Cabauw measurements: A system proposal
[KNMI-TR-48] 04 p0540 N85-13434

Statistical relationships between meteorological data stations and implications to diagnostic models in complex terrain
[DE84-014380] 06 p0839 N85-15328

Mariners weather log, volume 28, no. 3, July-August-September 1984
[PB85-107266] 06 p0840 N85-15334

Automated Lavina collects data on snow
07 p0980 N85-16224

Climate of Salt Lake City, Utah
[PB85-123875] 10 p1521 N85-19589

Cabauw (Netherlands) meteorological data tapes 1973-1984: Description of instrumentation and data processing for continuous measurements
[KNMI-WR-84-6] 14 p2379 N85-24685

Wind observation station description for Den Helder (period 1843-1972) and De Kooy (period 1955-1980)
[KNMI-TR-42] 14 p2379 N85-24686

Fog advection in the Namib 16 p2831 N85-27454

Use of a network of telemetered meteorological stations for prediction of the distribution of an atmospheric tracer
16 p2831 N85-27458

Ground-based remote sensing of atmospheric pollution 16 p2832 N85-27462

AWS (Air Weather Service) climatic briefs: North America
[AD-A152161] 16 p2835 N85-27483

SCPP (Sierra Cooperative Pilot Project) data collection and analysis. Volume 1: Executive summary
[PB85-156051] 16 p2837 N85-27494

Evaluation of the PROFS (Program for Regional Observing and Forecasting Services) 1982, real-time forecast experiment
[PB85-159747] 16 p2837 N85-27495

Climatological data of stations in the Netherlands No. 11: Frequency tables and tables with runs according to measurements at principal climatological stations 1961-1980, sunshine stations 1956-1980, precipitation stations 1951-1980
18 p3149 N85-29409
[KNMI-150-11]
Reports from the German Meteorological Service. No. 166: The optimal spectral density of climatological station networks
23 p3950 N85-34476
[ISBN-3-88148-214-8]

WEATHERING
Impact cratering: The process and its effects on planetary evolution — and silicate-carbonate reactions on Venus
02 p0228 N85-11488
[NASA-CR-174016]
Durability and behavior of prestressed concrete beams. Posttensioned concrete beam investigation, supplemental laboratory tests of beams exposed from 1961 to 1962
09 p1304 N85-18191
[AD-A146821]
NBS solar collector durability/reliability test program
12 p1881 N85-21801
[DE85-003489]
Planetary analogs in Antarctica: Mars
13 p2193 N85-23604
Iron oxides of Mars: Evidence for contemporary weathering
13 p2195 N85-23613
New corrosion protection concept for very high voltage line towers
[BLL-OA-TRANS-2691-(6196.300)]
20 p3429 N85-31270

WEATHERPROOFING
New corrosion protection concept for very high voltage line towers
[BLL-OA-TRANS-2691-(6196.300)]
20 p3429 N85-31270

WEBBING
Large-area sheet task advanced dendritic web growth development
02 p0223 N85-11463
[NASA-CR-174021]

WEBS (MEMBRANES)
U MEMBRANES

WEBS (SHEETS)
Development of high-efficiency solar cells on silicon web
06 p0828 N85-15259
[NASA-CR-174212]
Advanced dendritic web growth development
06 p0831 N85-15286
Aircraft barricade
07 p0910 N85-15761
[AD-D011316]
Solid/melt interface studies of high-speed silicon sheet growth
14 p2350 N85-24525
[NASA-CR-175696]
Development of high-efficiency solar cells on silicon web
15 p2585 N85-25939
[NASA-CR-175707]
Stress and efficiency studies in EFG
22 p3751 N85-33251
[NASA-CR-176125]
Instrumentation for sensing moisture content of material using a transient thermal pulse
[NASA-CASE-NPO-15493-2] 23 p3933 N85-34373
Flat-plate solar array project process development area process research of non-CZ silicon material
23 p3945 N85-34445
[NASA-CR-176117]

WEBS (SUPPORTS)
Principles of wave formation along web of H-beams
[BLL-M-36041-(5828.4)] 16 p2796 N85-27253

WEDGE FLOW
Pseudo-stationary oblique-shock-wave reflections in a polyatomic gas, sulfur hexafluoride
12 p1845 N85-21577
[UTIAS-TN-253]
Tabular and graphical solutions of regular and Mach reflections in pseudo-stationary frozen and vibrational-equilibrium flows, part 1
23 p3893 N85-34117
[UTIAS-283-PT-1]
Tabular and graphical solutions of regular and Mach reflections in pseudo-stationary frozen and vibrational-equilibrium flows, part 2
23 p3894 N85-34118
[UTIAS-283-PT-2]

WEDGES
Aircraft chocks
01 p0012 N85-10077
[AD-A145135]
Wedge with crack in bielastic medium
02 p0273 N85-11780
Design of two-mirror scanner with axes of rotation not in plane of mirrors
06 p0777 N85-14969
Modeling of large-scale accretionary wedge and thin-skinned trust-and-fold belt mechanics
08 p1181 N85-17442
Experimental study of the effect of moist environments on epoxy resin chocks
15 p2568 N85-25849
[AD-A152052]
An experimental study of the pressure in a fast bottom beneath the apex of an overlying fluid wedge
18 p3177 N85-29696
[AD-A153618]

WEIBEL INSTABILITY
Reliability prediction of the series system with spares subject to Weibull failure
24 p4100 N85-35413

WEIBULL DENSITY FUNCTIONS
Return wave heights off South Uist estimated from seven years of data
01 p0089 N85-10601
[IOS-164]
The estimation of persistance statistics from cumulative probabilities of wave height
03 p0397 N85-12534
[NMI-R183]
Brownian motion with quadratic killing and some implications: Revision
15 p2642 N85-26296
[AD-A151323]
Rolling contact fatigue testing of thermomechanically processed M-50 steel
18 p3122 N85-29327
[AD-A153640]
On the confidence limits for Weibull reliability and quantiles: The case of maximum likelihood estimation from small size censored samples
20 p3521 N85-31896
[REPT-84-RR-345]
Weibull distribution based on maximum likelihood with interval inspection data
21 p3678 N85-32647
[NASA-TM-86515]
Reliability of two sintered silicon nitride materials
23 p3919 N85-34284
[NASA-TM-87092]

WEIGHT (MASS)
NT ATOMIC WEIGHTS
NT BIOMASS
NT BODY WEIGHT
NT STRUCTURAL WEIGHT
Silicon nitride powder
01 p0022 N85-10132
[NASA-TM-77731]
Potential of flywheels for spacecraft energy storage
05 p0609 N85-13690
A machine for weight-lift testing
07 p0973 N85-16182
[AD-A146816]
Advances in composites technology
08 p1118 N85-17048
[NASA-TM-86353]
Primer for mass metrology
09 p1305 N85-18199
[PB85-121424/GAR]
The optimal control and design of a flexible manipulator arm
09 p1327 N85-18340
A study of the effect of mass loading on the shock environment
09 p1336 N85-18401
Tractor power selection with compaction constraints
09 p1409 N85-18877
[AD-P004300]
Integrated Technology Rotor/Flight Research Rotor (ITR/FRR) concept definition study
10 p1424 N85-18961
[NASA-CR-166444]
State measurement laboratories: Program description (part 1). Directory (part 2)
11 p1739 N85-20935
[PB85-137651]
Gears and Power Transmission Systems for Helicopters and Turboprops
14 p2220 N85-23765
[AGARD-CP-369]
Advanced gearbox technology in small turbo propeller engines
14 p2221 N85-23771
The physical effects of different stress situations on graphite/epoxy compounds
15 p2687 N85-26594
Some aspects of how to design cost-effective flight control systems
16 p2695 N85-26639
Study of Kapton under simulated shuttle environment
19 p3225 N85-29997
[NASA-CR-176003]
Preliminary sizing and performance of aircraft
21 p3554 N85-32111
[NASA-TM-86357]
On high strain rate fragmentation of a closed vessel
23 p3904 N85-34187

WEIGHT FACTORS
U WEIGHT (MASS)

WEIGHT INDICATORS
NT MICROBALANCES
Rain rate meter
07 p0999 N85-16342
[AD-D011381]
Numerical analysis of the first static calibration of the RSRA helicopter active-isolator rotor balance system
08 p1083 N85-16863
[NASA-TM-85975]
Effect of superconducting solenoid model cores on spanwise iron magnet roll control
17 p2905 N85-27915
[NASA-TM-86378]

WEIGHT MEASUREMENT
Portable pallet weighing apparatus
[NASA-CASE-GSC-12789-1] 11 p1635 N85-20294

WEIGHT REDUCTION
Flight simulation fatigue crack propagation in metal/carbon-epoxy laminates
01 p0063 N85-10416
[NLR-TR-83006-U]
Modern structural materials. Present situation and evolution prospects — aircraft materials
04 p0455 N85-12686
[SNIAS-842-551-101]
Space shuttle external tank performance improvements: The challenge
06 p1094 N85-16916
Preventing explosive propagation in racks or containers of tactical missiles
10 p1455 N85-19166
[AD-P004342]
Development of Halley's Comet explorer PLANET-A solar array
13 p2010 N85-22608
Filmwise condensation of steam on low integral-finned tubes
16 p2783 N85-27176
[AD-A152220]
Application of lightweight composite materials to naval weapons systems
18 p3069 N85-28981
[PB85-173607]
Multi-kW solar arrays for Earth orbit applications
20 p3406 N85-31139
[NASA-CR-171538]
Aeroelastic constraints for a wing weight minimization procedure
23 p3895 N85-34126
[FFA-TN-1985-4]

WEIGHTING FUNCTIONS
Solution of contaminant transport equations using an orthogonal-upstream finite element scheme
01 p0070 N85-10463
[DE84-014266]
A combined logistic regression and Zionts-Wallenius methodology for multiple criteria linear programming
01 p0102 N85-10679
[TWISK-314]
A weighted polynomial inequality
01 p0110 N85-10741
[CSIR-TWISK-332]
Definition of acceptable levels of mismatch for equivalent systems of augmented CTOL (Conventional Take-Off and Landing) aircraft
02 p0149 N85-11007
[AD-A145619]
Weighted distributions arising out of methods of ascertainment
02 p0252 N85-11648
[AD-A145615]
Long-range predictive control using weighting-sequence models
04 p0553 N85-13521
[OUEL-1542/84]
Synthesis of systems for coherent weighted signal processing against background of correlated interference
06 p0790 N85-15045
A noise-suppressing digital frequency meter
06 p0796 N85-15084
An adaptive Fast Fourier Transform weighting technique to increase small target sensitivity
08 p1154 N85-17286
[AD-D011424]
On the binary weight distribution of some Reed-Solomon codes
09 p1373 N85-18628
[NASA-CR-174375]
Optimal threshold and weight sorting of elevation angle readings under conditions of fadeouts of a directed signal
12 p1840 N85-21547
Investigation of the numerical method of moments for digital computer determination of differential equations
15 p2638 N85-26268
[AD-A151896]
Locally-weighted-regression scatter-plot smoothing (LOWESS): A graphical exploratory data analysis technique
16 p2855 N85-27609
[AD-A152239]
The weighting function for scintillation on a folded path
17 p2949 N85-28206
[AD-A152659]
Fuzzy hierarchical analysis
17 p3021 N85-28685
[DE85-008149]
Experimental investigations of the unsteady turbulent friction behavior with pressure impulses in a circular pipe
18 p3103 N85-29210
[IWAWI-MITT-102]
Evaluation of densities and distributions via hermite and generalized laguerre series employing high-order expansion coefficients determined recursively via moments or cumulants
18 p3175 N85-29682
[AD-A153950]
MCNP variance reduction overview
19 p3346 N85-30741
[DE85-010765]
Measurements of folded path optical scintillation using a corner cube, a cat's eye and a flat mirror reflector
19 p3367 N85-30879
[AD-A154044]
Monte Carlo learning-biasing experiment with intelligent random numbers
22 p3834 N85-33742
[DE85-010713]

WEIGHTLESSNESS
Second All-Union Seminar on Hydromechanics and Heat and Mass Exchange in Weightlessness, summaries of reports
01 p0047 N85-10305
[NASA-TM-77590]
Circulatory orthostatic instability: Role of deconditioning of resistive vessels
01 p0091 N85-10612
Hemopoiesis in rats submitted to weightlessness
01 p0091 N85-10613
Compensatory and adaptive regional hemodynamic reactions to weightlessness during long-term spaceflights
01 p0091 N85-10616
Effect of spaceflight factors on rat bone marrow cells
01 p0092 N85-10620
Developing commercial users of space
02 p0154 N85-11044
Post buckling behavior of a circular rod constrained within a circular cylinder
02 p0207 N85-11385
A survey of space biology and space medicine
04 p0545 N85-13466
[ESA-BR-17]
Three-dimensional ballistocardiography in weightlessness (experiment 1ES 028) — Spacelab
05 p0691 N85-14447
The European vestibular experiments in the Spacelab 1 mission
05 p0694 N85-14466
Sleep physiology in weightlessness (experiment 1ES 030) — Spacelab
05 p0695 N85-14474

The effect of part-simulation of weightlessness on human control of bilateral teleoperation: Neuromotor considerations 05 p0703 N85-14510

The development of the vestibular apparatus under conditions of weightlessness
[NASA-TM-77517] 07 p1011 N85-16422

Distinctions of SPF rats used in experiments aboard biosatellites 07 p1012 N85-16427

Testing changes in visual function due to orbital environment
[AD-A147259] 07 p1016 N85-16453

Controlled ecological life support system higher plant flight experiments
[NASA-CR-177323] 07 p1020 N85-16471

Gravity and biological systems: Emphasis on human physiology
[ESA-BR-21] 09 p1360 N85-18558

Physiological considerations of artificial gravity
11 p1645 N85-20366

Influence of gravitoinertial force level on apparent magnitude of coriolis cross-coupled angular accelerations and motion sickness 11 p1693 N85-20644

Space adaptation syndrome: Incidence and operational implications for the space transportation system program
11 p1695 N85-20655

USSR report: Space Biology and Aerospace Medicine, volume 18, no. 6, November - December 1984
[JPRS-USB-85-002] 12 p1900 N85-21931

External respiration, gas exchange and energy expenditures of man in weightlessness
12 p1900 N85-21932

Circadian rhythm of human body temperature during spaceflights 12 p1901 N85-21934

Comparative analysis of effects of weightlessness and its models on velocity and strength properties and tone of human skeletal muscles 12 p1901 N85-21936

LBNP training of crew members on main missions aboard Salyut-6 orbital station 12 p1901 N85-21938

Human lung fluid content during 7-day head-down tilt
12 p1902 N85-21941

Fluid metabolism of monkeys during two-week antiorthostatic hypokinesia 12 p1902 N85-21943

Parameters of carbohydrate metabolism and blood serum enzyme activity after short-term spaceflights
12 p1903 N85-21951

Alterations in gut transport of minerals and in binding proteins during simulated weightlessness
[NASA-CR-175637] 14 p2388 N85-24709

Effects of weightlessness of Aurelia Ephyra differentiation and statolith synthesis
15 p2605 N85-26056

Transduction of the root gravitropic stimulus: Can apical calcium regulate auxin distribution?
15 p2606 N85-26063

Daylily as a system to study effects of space flight on plant development 15 p2607 N85-26068

The role of vitamin D in the bone changes associated with simulated weightlessness 15 p2608 N85-26072

Quantitative alterations in the function of bone forming cells due to reduced weight bearing
15 p2609 N85-26075

Blood pressure responses and mineral ocorticoid levels in the suspended rat model for weightlessness
15 p2609 N85-26079

Development and maturation of the neuromuscular junciton in cell culture under conditions of simulated zero-gravity 15 p2611 N85-26093

Effects of simulated weightlessness on mammalian development. Part 2: Meiotic maturation of mouse oocytes during clinostat rotation 15 p2612 N85-26094

Evidence that resorption of bone by rat peritonal macrophages occurs in an acidic environment
15 p2612 N85-26098

The effects of simulated weightlessness on susceptibility to viral and bacterial infections using a murine model
15 p2613 N85-26100

Analysis of head-down tilt as an analog of weightlessness using a mathematical simulation model
[NASA-CR-171870] 15 p2616 N85-26118

Predictions of cardiovascular responses during STS reentry using mathematical models
[NASA-CR-171871] 15 p2616 N85-26119

Simulation of a G-tolerance curve using the pulsatile cardiovascular model
[NASA-CR-171873] 15 p2616 N85-26120

Description, validation, and modification of the Guyton model for space-flight applications. Part A. Guyton model of circulatory, fluid and electrolyte control. Part B. Modification of the Guyton model for circulatory, fluid and electrolyte control
[NASA-CR-171876] 15 p2616 N85-26122

The behavior of renal-regulating hormones during hypogravic stress
[NASA-CR-171877] 15 p2616 N85-26123

Fluid-electrolyte responses during prolonged space flight: A review and interpretation of significant findings
[NASA-CR-171878] 15 p2617 N85-26124

Mathematical modeling of fluid-electrolyte alterations during weightlessness
[NASA-CR-171881] 15 p2617 N85-26125

Aerosol deposition along the respiratory tract at zero gravity: A theoretical study
[DE85-006703] 15 p2619 N85-26136

Primate experiments on SLS-1
15 p2687 N85-26592

USSR report: Space
[JPRS-USP-85-004] 16 p2717 N85-26772

Free-surface phenomena under low- and zero-gravity conditions
[NASA-CR-175835] 16 p2782 N85-27166

Free-surface phenomena under low- and zero-gravity conditions
[NASA-CR-175865] 17 p2907 N85-27922

Changes in bone structure and metabolism during simulated weightlessness: Endocrine and dietary factors
[NASA-CR-175961] 18 p3153 N85-29521

Crystal growth from the vapor in low gravity environments
[DE85-009628] 18 p3195 N85-29816

Crystallization of aluminum-based alloys in weightlessness 19 p3242 N85-30101

Cosmonauts' postural reactions after long-term missions aboard Salyut-6 orbital station 19 p3323 N85-30585

A systems analysis of the erythropoietic responses to weightlessness. Volume 1: Mathematical model simulations of the erythropoietic responses to weightlessness
[NASA-CR-171890] 20 p3506 N85-31794

A systems analysis of the erythropoietic responses to weightlessness. Volume 2: Description of the model of erythropoiesis regulation. Part A: Model for regulation of erythropoiesis. Part B: Detailed description of the model for regulation of erythropoiesis
[NASA-CR-171891] 20 p3506 N85-31795

An integrated analysis of the physiological effects of space flight: Executive summary
[NASA-CR-171892] 20 p3506 N85-31796

Results of Space Experiments in Physiology and Medicine and Informal Briefings by the F-16 Medical Working Group
[AGARD-CP-377] 20 p3507 N85-31805

Thresholds for detection of linear oscillation following prolonged weightlessness 20 p3508 N85-31810

Spatial orientation in weightlessness and readaptation to Earth's gravity 20 p3509 N85-31811

Reinterpretation of otolith input as a primary factor in space motion sickness 20 p3509 N85-31812

Postural adjustments associated with arm movements in weightlessness 20 p3509 N85-31813

Mass-discrimination during prolonged weightlessness
20 p3509 N85-31814

Changes in cardiovascular function: Weightlessness and ground-based studies 20 p3509 N85-31815

Cardiovascular research in space: Problems and results 20 p3510 N85-31817

Sleep and wake physiology in weightlessness
20 p3510 N85-31819

Sensitivity of human lymphocytes to microgravity in-vitro 20 p3510 N85-31820

Mission operations requirements document for D-1 Experiment 102, Vestibular Experiments in Spacelab
[NASA-TM-87495] 21 p3557 N85-32129

Analysis of the transient response of temporal artery blood flow data relative to various anti-G suit pressure schedules
[AD-A155242] 21 p3666 N85-32775

Intracardiac hemodynamics and human heart function in simulated weightlessness 22 p3733 N85-33140

Mechanisms of osteodystrophy in weightlessness
22 p3733 N85-33143

USSR report: Space Biology and Aerospace Medicine, volume 19, no. 2, March - April 1985
[JPRS-USB-85-004] 22 p3820 N85-33667

Labyrinthine and extralabyrinthine mechanisms of development of motion sickness in weightlessness
22 p3821 N85-33668

Effect of body position and immobilization on intensity of spatial illusions in weightlessness
22 p3821 N85-33672

Vascular mechanisms of adaptation to antiorthostatic position 22 p3822 N85-33675

Cerebral hemodynamics and ventricular function in -15 deg antiorthostatic position 22 p3822 N85-33676

Effect of short-term antiorthostatic hypokinesia on dynamics of cardiorespiratory parameters during graded physical exercise 22 p3822 N85-33677

Investigation of some aspects of amino acid metabolism in man during brief exposure to antiorthostatic hypokinesia combined with ultraviolet radiation
22 p3822 N85-33678

General description of experiment dealing with rat ontogenesis aboard Cosmos-1514 biosatellite
22 p3822 N85-33679

Morphological study of antiorthostatic hypokinesia in monkeys 22 p3822 N85-33680

Rat plasma hormone levels following flight aboard Cosmos-1129 biosatellite 22 p3823 N85-33681

Morphological manifestations of hemodynamic changes in lungs of monkeys submitted to antiorthostatic hypokinesia 22 p3824 N85-33686

Effect of substrate moisture on growth and structure of corn leaf 22 p3824 N85-33692

Spacelab 1 hematology experiment (INS103): Influence of space flight on erythrokinetics in man
[NASA-TM-58266] 22 p3824 N85-33693

Fluid-electrolyte metabolism and renal function in cosmonauts following 185-day spaceflight
23 p3952 N85-34495

Effect of hypokinesia and +Gz accelerations on transport function of human blood
23 p3952 N85-34497

Effect of water immersion of parameters of central hemodynamics in individuals over 45 years old
23 p3953 N85-34499

Rat skeletal muscles with simulation of physiological effects of weightlessness (morphological study)
23 p3953 N85-34502

Lipogenesis in rat liver after flight aboard Cosmos-1129 biosatellite 23 p3954 N85-34508

Problems of aviation and space medicine and psychology discussed at 14th Gagarin lectures
23 p3954 N85-34509

A two-phase flow and heat transfer model for zero gravity
[AD-A156097] 24 p4094 N85-35377

The use of a laser Doppler velocimeter in a standard flammability tube
[NASA-CR-174960] 24 p4096 N85-35389

Possible mechanism for changes in glycogen metabolism in unloaded soleus muscle
[NASA-CR-176184] 24 p4127 N85-35588

Response of amino acids in hindlimb muscles to recovery from hypogravity and unloading by tail-cast suspension
[NASA-CR-176183] 24 p4128 N85-35589

Muscle protein and glycogen responses to recovery from hypogravity and unloading by tail-cast suspension
[NASA-CR-176181] 24 p4128 N85-35591

Cardiovascular responses to orthostatism and weightlessness 24 p4130 N85-35601

WEIGHTLESSNESS SIMULATION

Influence of simulated weightlessness on the motility of the acellular slime mold Physarum polycephalum
05 p0689 N85-14430

Plant cell cultures in biological space experiments
05 p0690 N85-14434

The use of horizontal clinostats in studies of plant statocyte development 05 p0690 N85-14435

Left heart ventricular function during a 7 day zero-g simulation (6 deg head down tilt)
05 p0691 N85-14446

Physical performance capacity after a 7 day head-down tilt (-6 deg) 05 p0692 N85-14451

Leg volume changes. Responses to Lower Body Negative Pressure (LBNP) during 7 days of zero-g simulation (6 deg Head-Down Tilt (HDT))
05 p0692 N85-14452

Heart rate variability during 7 day head-down tilt (6 deg) 05 p0692 N85-14453

Comparison of simulation of weightlessness by Head Down Tilt (HDT) and Water Immersion (WI)
05 p0692 N85-14454

Hemodynamics and plasma arginine vasopressin during water immersion in normal man
05 p0693 N85-14458

Glucose tolerance in trained and untrained subjects during head-down tilt (6 deg) 05 p0693 N85-14461

Inner ear characteristics during 7 day antiorthostatic bedrest (6 deg head down tilt) 05 p0695 N85-14470

The role of gravity on the reproduction of arabidopsis plants 15 p2607 N85-26069

The salutary effect of dietary calcium on bone mass in a rat model of simulated weightlessness
15 p2608 N85-26073

Actual and simulated weightlessness inhibit osteogenesis in long bone metaphysis by different mechanisms 15 p2608 N85-26074

Cardiovascular effects of weightlessness
15 p2686 N85-26607

Chromosome aberrations in Crepis capillaris exposed to gamma radiation and clinostat
19 p3325 N85-30600

Morphological study of primate hypothalamus and hypophysis after experiment with antiorthostatic hypokinesia 19 p3325 N85-30603

Study of the cardiovascular system in microgravity: Results and perspectives 20 p3509 N85-31616

WELD STRENGTH

Strength of welded joints in VT23 alloy upon repeated static loading 01 p0020 N85-10120

Fracture toughness characteristics of welded joints in VT65 and AT6 titanium alloys 01 p0020 N85-10121

Influence of residual stresses resulting from manufacturing on the fatigue strength of welded joints
05 p0650 N85-14177

Repair welding and brazing procedures for turbine components and investigation of the brazing behavior of thin filler foils
[MTU-TB-906/84] 07 p0974 N85-16190

Static and dynamic fracture toughness characterization of SA508 forging and SA533B welded plate — pressure vessel steels
[CISE-2258] 08 p1131 N85-17127

Mechanical properties of Shielded Metal Arc (SMA) and Submerged Arc (SA) welded joints for quenched and tempered steel StE 470.
[VTT-319] 09 p1328 N85-18346

Defect tolerance in pipeline girth welds
[ERS-E.353] 09 p1328 N85-18347

The effect of filler wire and flux compositions on the microstructure and properties of microalloyed steel weld metal
[AD-A149529] 10 p1492 N85-19423

Kinetics of reaction of metals and non-metals during diffusion welding 11 p1602 N85-20076

Collapse and removal of discontinuities in joint zone during diffusion welding 11 p1602 N85-20077

Weldability of alloy ABM1 to alloy 1201
11 p1603 N85-20080

Effects of neutron irradiation on the fracture properties of HT-9 weld
[DE85-001068] 12 p1807 N85-21339

Influence of welding defects at melting boundary on static strength of welded joint in large-diameter pipe
13 p2033 N85-22735

Technological parameters of diffusion welding processes in honeycomb titanium alloy structures
13 p2033 N85-22739

Durability of joints of 30KhGSA and 12Kh18N10T steels made by diffusion welding 15 p2501 N85-25428

Mechanical properties of welded joints of 1201 aluminum alloy 15 p2502 N85-25431

Fillet weld stress using finite element methods
15 p2576 N85-25884

Paton Institute expert on GDR-USSR welding research
16 p2768 N85-27078

Local heat treatment of welded joints of pipes and rotary vessels
[BLL-BISI-TRANS-22197-(9022.06)]
17 p2972 N85-28354

Technical information: Weldability of stainless steel. Part 1: Austenitic stainless steel
[BLL-BISI-TRANS-22456-(9022.06)]
17 p2973 N85-28362

Load-carrying capabilities of refractory alloys for space reactor power applications
[DE85-010566] 19 p3240 N85-30067

Structure and properties of VT23 alloy welded joints after thermocyclic processing 19 p3246 N85-30125

Diffusion welding of Cassegrainian concentrator cell stack assemblies
[NASA-CR-176104] 22 p3805 N85-33566

Ultrasonic seam welding on thin silicon solar cells
[NASA-CR-176116] 22 p3805 N85-33570

WELD TESTS

Electromagnetic-acoustic-transducer
e system for thick-weld inspection
[PB84-219492] 01 p0051 N85-10336

Prediction of weld defects using welding condition data
[VTT-HR-264] 03 p0370 N85-12359

Comparative investigation of testing methods to determine hot crack susceptibility during welding
[BAM-ERP-2415] 07 p0979 N85-16218

Static and dynamic fracture toughness characterization of SA508 forging and SA533B welded plate — pressure vessel steels
[CISE-2258] 08 p1131 N85-17127

Mechanical properties of Shielded Metal Arc (SMA) and Submerged Arc (SA) welded joints for quenched and tempered steel StE 470.
[VTT-319] 09 p1328 N85-18346

Ultrasonic large-diameter pipe weld testing installations 11 p1603 N85-20081

Structure of transient zone in diffusion welding of TsTS-19 piezoceramic with AMg6 alloy
11 p1603 N85-20082

Effects of neutron irradiation on the fracture properties of HT-9 weld
[DE85-001068] 12 p1807 N85-21339

The strength and characteristics of VPPA welded 2219-T87 aluminum alloy 12 p1946 N85-22224

Paton comments on results of space welding tests
15 p2484 N85-25330

Durability of joints of 30KhGSA and 12Kh18N10T steels made by diffusion welding 15 p2501 N85-25428

Weldability of Ni3Al-type aluminide alloys
[DE85-006932] 15 p2512 N85-25496

Welder training/welder testing
[BLL-WI-TRANS-883-(9312.57)]
16 p2792 N85-27223

Local heat treatment of welded joints of pipes and rotary vessels
[BLL-BISI-TRANS-22197-(9022.06)]
17 p2972 N85-28354

Statistical models used in analyzing the quality of welded tubes
[BLL-BISI-TRANS-22232-(9022.06)]
17 p2976 N85-28384

Non-destructive testing of HF-welded pipe
[BLL-BISI-TRANS-22182-(9022.06)]
17 p2976 N85-28388

Mechanical properties of Shielded Metal Arc (SMA) and Submerged Arc (SA) welded joints in a steel Raex 386 P Arctic
[VTT-339] 22 p3801 N85-33551

WELDABILITY

Weldability of aged heat resistant nickel alloys
01 p0021 N85-10125

Effect of iron on the performance of IN 625 weld deposits
[BR91456] 06 p1169 N85-17376

Weldability of alloy ABM1 to alloy 1201
11 p1603 N85-20080

Weldability and mechanical property characterization of weld clad alloy 800H tubesheet forging
[DE85-001737] 11 p1609 N85-20116

The strength and characteristics of VPPA welded 2219-T87 aluminum alloy 12 p1946 N85-22224

Laser spot welding in the electronics industry
14 p2308 N85-24287

Weldability of Ni3Al-type aluminide alloys
[DE85-006932] 15 p2512 N85-25496

Development of high strength ship hull steel for high heat input welding — controlled rolling and accelerated cooling 15 p2565 N85-25827

Relationships between microstructure and microfissuring in alloy 718 16 p2735 N85-26876

Paton Institute expert on GDR-USSR welding research
16 p2768 N85-27078

Weldability of micro-alloy steels as reaction of structure and inclusions
[BLL-BISI-TRANS-22196-(9022.06)]
17 p2924 N85-28027

High-strength weldable steel 03G4N2MAF Sh with improved ductility
[BLL-BISI-TRANS-22233-(9022.06)]
17 p2924 N85-28031

Stainless steels: Application and welding
[BLL-BISI-TRANS-22357-(9022.06)]
17 p2927 N85-28059

Welding of 11 458.1 steel in shielding atmospheres
[BLL-BISI-TRANS-21763-(9022.06)]
17 p2972 N85-28353

Submerged arc welding of new Czechoslovak micro-alloy steels
[BLL-BISI-TRANS-22193-(9022.06)]
17 p2972 N85-28356

Technical information: Weldability of stainless steel. Part 1: Austenitic stainless steel
[BLL-BISI-TRANS-22456-(9022.06)]
17 p2973 N85-28362

Tests of low-cycle fatigue of elected steels of class 11
[BLL-BISI-TRANS-22039-(9022.06)]
17 p2976 N85-28404

Weldability/microstructure relationships of high nickel alloys for header applications
[DE85-009337] 19 p3241 N85-30094

Plasma arc welding, equipment, installation and process control
[DE85-008481] 19 p3373 N85-30921

Ultrasonic seam welding on thin silicon solar cells
[NASA-CR-176116] 22 p3805 N85-33570

WELDED JOINTS

NT SPOT WELDS

Influence of annealing on properties of AT3 alloy welded joints 01 p0019 N85-10118

Heat treatment of welded joints in OT4 and VT20 titanium alloys 01 p0020 N85-10119

Strength of welded joints in VT23 alloy upon repeated static loading 01 p0020 N85-10120

Fracture toughness characteristics of welded joints in VT65 and AT6 titanium alloys 01 p0020 N85-10121

Suppressing porosity in weld joints of 1420 aluminum alloy 01 p0020 N85-10123

Effect of welding method on corrosion resistance of welded compositions made of 1201 alloy
01 p0020 N85-10124

Research on high-strength steels with an improved resistance against weld cracking
[AD-A144830] 01 p0027 N85-10170

Electromagnetic-acoustic-transducer
e system for thick-weld inspection
[PB84-219492] 01 p0051 N85-10336

Minor element effects on gas tungsten arc weld penetration
[PB84-222579] 01 p0056 N85-10370

Materials studies for magnetic fusion energy applications at low temperatures, 7
[DE84-013487] 01 p0122 N85-10837

Design, construction, demonstration and delivery of an automated narrow gap welding system
[AD-A145497] 02 p0204 N85-11346

Strain distribution in a type 316/16-8-2 stainless steel weldment during cyclic loading
[DE84-015644] 02 p0210 N85-11384

Effect of rhenium on the structure and properties of the weld metal of a molybdenum alloy
[NASA-TM-77491] 03 p0330 N85-12128

Causes of strength reduction in welded titanium-steel joints 03 p0352 N85-12262

Localized corrosion and stress corrosion cracking behavior of stainless steel weldments
[DE84-016095] 04 p0474 N85-13017

Solidification and aging behavior of types 308 and 308CRE stainless steel welds
[DE84-016552] 04 p0476 N85-13029

Influence of residual stresses resulting from manufacturing on the fatigue strength of welded joints
05 p0650 N85-14177

Ultrasonic girth weld evaluation for aluminum substrate of spherical Kevlar-epoxy test specimens
[DE85-001592] 06 p0816 N85-15181

Residual stresses at small diffusion welds
[DE84-014982] 07 p0974 N85-16189

Comparison of the sensitivities of ultrasonic, radiographic and acoustic emission test methods for the examination of a thick weld
[BLL-RISLEY-TR-4547-(9091.9F)]
07 p0975 N85-16194

Ultrasonic evaluation of titanium contamination with correlation techniques
[AD-P004126] 08 p1126 N85-17101

Electrodes for repairing power engineering equipment made from creep resisting steel
[BLL-CE-TRANS-8064-(9022.09)]
08 p1167 N85-17360

Effect of tempering on the strength and toughness of 2 1/4 Cr-1 Mo steel weldments
[DE85-003818] 09 p1298 N85-18140

Mechanical properties of Shielded Metal Arc (SMA) and Submerged Arc (SA) welded joints for quenched and tempered steel StE 470.
[VTT-319] 09 p1328 N85-18346

Fracture toughness of austenitic stainless steel weld metal at 4 K
[DE84-016638] 09 p1340 N85-18425

Kinetics of joint formation during diffusion welding of VT5 titanium alloys 10 p1448 N85-19125

Fatigue resistance of welded joints of high strength steels produced by electron beam welding
10 p1449 N85-19127

Estimate of quality of aluminum alloy surface preparation for arc welding 10 p1449 N85-19128

Calculation of mode field in electron beam welding of VT6 titanium alloy 10 p1449 N85-19129

Diffusion welding with forced deformation of heat-resistant nickel-based dispersion hardened alloy
10 p1449 N85-19130

Collapse and removal of discontinuities in joint zone during diffusion welding 11 p1602 N85-20077

Assessment of effectiveness of electron beam welding of titanium alloys up to 40 mm in thickness by vertical or horizontal beam 11 p1603 N85-20078

Distribution of hydrogen in multi-layer welded joints of alloyed steels 11 p1603 N85-20079

Ultrasonic large-diameter pipe weld testing installations 11 p1603 N85-20081

Structure of transient zone in diffusion welding of TsTS-19 piezoceramic with AMg6 alloy
11 p1603 N85-20082

China report: Science and technology
[JPRS-CST-84-025] 11 p1620 N85-20197

Radiographic inspection of butt welds described
11 p1620 N85-20198

NASA welding assessment program
[NASA-CR-175512] 12 p1859 N85-21661

The strength and characteristics of VPPA welded 2219-T87 aluminum alloy 12 p1946 N85-22224

Problem of pore formation mechanism in welded joints of aluminum alloys in the system aluminum-magnesium-lithium 13 p2032 N85-22732
Properties of welded joints in argon arc welding of titanium alloy using a protective coating
13 p2032 N85-22733
Thermal hardening of welded joints in titanium alloys with various structures 13 p2032 N85-22734
Influence of welding defects at melting boundary on static strength of welded joint in large-diameter pipe
13 p2033 N85-22735
Mechanical properties and brittle fracture resistance of welded multilayer elements for high pressure vessels
13 p2033 N85-22736
Analysis of strength and ductility of welded joints in AMtsS and AMg5 aluminum alloys
13 p2033 N85-22737
Effect of protective medium on durability and fracture structure on seam zones of thin-walled titanium articles produced by diffusion welding 13 p2033 N85-22738
Durability of VT16 alloy compounds obtained by diffusion welding 13 p2034 N85-22740
Structure and mechanical characteristics of heterogeneous joints produced by laser welding
13 p2034 N85-22742
Method of calculating strength of joint produced by cold welding of aluminum under discrete loading
13 p2034 N85-22743
Effect of moisture in inert gases on density of seam metal and on mechanical characteristics of welded joints of aluminum and aluminum alloys
13 p2034 N85-22744
Automatic multi-layer welding of thick cylindrical structures under flux 13 p2035 N85-22746
Softening of metal near seam during welding of heat-resistant nickel alloys 13 p2035 N85-22747
Microstructure and properties of ferrous alloy weldments
[DE85-005582] 14 p2257 N85-23987
Laser spot welding in the electronics industry
14 p2306 N85-24287
Ways of improving level and stability of mechanical characteristics of diffusion-welded joints of OT4 titanium alloy 15 p2499 N85-25417
Structure and mechanical properties of dispersion-hardened nickel alloy joints welded by diffusion 15 p2500 N85-25422
Evaluation of stress concentration coefficients in butt-welded joints with displaced edges
15 p2501 N85-25425
Pressure welding of corrosion-resistant steel with AMg6 aluminum 15 p2501 N85-25426
Durability of joints of 30KhGSA and 12Kh18N10T steels made by diffusion welding 15 p2501 N85-25428
Contact point and seam welding of heat-resistant alloys 15 p2501 N85-25429
Thermocompression welding of parts made from AMts and VT1 alloys 15 p2501 N85-25430
Mechanical properties of welded joints of 1201 aluminum alloy 15 p2502 N85-25431
Effect of protective atmosphere composition on durability of welded joints of niobium alloys
15 p2502 N85-25432
Hardening of titanium alloy electric-arc welded joints
15 p2514 N85-25513
Evaluation of the corrosion properties of aluminum alloy 5083 weldments
[DE85-007729] 16 p2751 N85-26977
Method of investigating accumulations of damage to weld joints in the case of low-cycle creep
[BLL-CE-TRANS-8088-(9022.09)]
16 p2792 N85-27219
Special features of the one-sided automatic welding of structures of Al-Mg alloys 16 p2792 N85-27222
Sources of improvement in quality of contact butt welding of wire
[BLL-M-36085-(5828.4)] 16 p2793 N85-27225
An X-ray study of residual stresses in narrow groove TIG weldments
[DE85-006485] 16 p2802 N85-27274
Local heat treatment of welded joints of pipes and rotary vessels 17 p2924 N85-28028
Welding of 11 456.1 steel in shielding atmospheres
[BLL-BISI-TRANS-21763-(9022.06)]
17 p2972 N85-28353
Local heat treatment of welded joints of pipes and rotary vessels
[BLL-BISI-TRANS-22197-(9022.06)]
17 p2972 N85-28354
Formation of a fine structure during shock wave welding
[BLL-BISI-TRANS-22401-(9022.06)]
17 p2973 N85-28368
Examination of the regions of the joint of sheets bonded by the explosive welding technique
[BLL-BISI-TRANS-22352-(9022.06)]
17 p2973 N85-28370
Differential between crack and pseudo-crack indications by means of objective magnetic flux leakage testing
[BLL-BISI-TRANS-22033-(9022.06)]
17 p2976 N85-28386
Inspection of welds and the factors improving its effectiveness in welded structure fabrication
[BLL-BISI-TRANS-22194-(9022.06)]
17 p2976 N85-28387
Non-destructive testing of HF-welded pipe
[BLL-BISI-TRANS-22182-(9022.06)]
17 p2976 N85-28388
The fatigue properties of welds at low temperature, according to the type of steel
[BLL-BISI-TRANS-22455-(9022.06)]
17 p2978 N85-28410
Fatigue strength of Inconel 625 plate and weldments used in the DIII-D configuration vacuum vessel
[DE85-008276] 17 p2981 N85-28427
Fatigue behavior of HY-130 steel weldments containing fabrication discontinuities
[AD-A153630] 18 p3122 N85-29326
Effect of protective method on cyclic durability and nature of failure of titanium alloy welded joints
19 p3245 N85-30122
Vacuum pressure welding of commercial titanium with 2Kh13 and 12Kh18N10T steels
19 p3246 N85-30124
Structure and properties of VT23 alloy welded joints after thermocyclic processing 19 p3246 N85-30125
Fatigue resistance of homogeneous and heterogeneous welded joints of TS5 titanium alloy
19 p3246 N85-30126
Hot cracking of austenitic stainless steels: The debut of the Sigmajig
[DE85-010560] 20 p3431 N85-31287
Determination of local deformation during explosive welding
[BLL-M-36279-(5828.4)] 20 p3462 N85-31503
Production verification of the acoustic emission weld monitor
[AD-A154168] 20 p3464 N85-31519
Effects of residual stresses and distortion on the nickel 200 and stainless steel 304 weldments
[DE85-011888] 22 p3748 N85-33233
Mechanical properties of Shielded Metal Arc (SMA) and Submerged Arc (SA) welded joints in a steel Raex 386 P Arctic
[VTT-339] 22 p3801 N85-33551
Gas shielding apparatus
[DE85-005992] 23 p3939 N85-34416
X-ray fluorescence analysis of 304L stainless steel
[DE85-013254] 24 p4080 N85-35268

WELDED STRUCTURES
NT STEEL STRUCTURES
Weld metal solidification cracking in a carbon-manganese steel 03 p0330 N85-12126
Ultrasonic and metallurgical examination of a cracked type 304 stainless steel BWR pipe weldment
[TI84-014968] 04 p0511 N85-13254
NDE (Nondestructive Evaluation) of oxygen contaminated titanium alloys and weldments
[AD-P004121] 08 p1126 N85-17096
Effects of oxygen-contamination-induced microstructural changes on the reverberation of ultrasound in Ti-6211 alloys
[AD-P004124] 08 p1126 N85-17099
Acoustical characterization of Ti-6211 weldments and oxygen contamination Ti-6211 plate
[AD-P004125] 08 p1126 N85-17100
Electromagnetic NDE of interstitial contamination in titanium alloy weldments
[AD-P004131] 08 p1127 N85-17106
Computation of thermal shock-free straightening conditions for aluminum-magnesium alloy welded structures 10 p1449 N85-19131
Institute's contribution to Soviet welding technology noted 16 p2767 N85-27072
Local heat treatment of welded joints of pipes and rotary vessels
[BLL-BISI-TRANS-22197-(9022.06)]
17 p2972 N85-28354
Steel Tubes
[BLL-BISI-TRANS-22064-(9022.06)]
17 p2973 N85-28369
Inspection of welds and the factors improving its effectiveness in welded structure fabrication
[BLL-BISI-TRANS-22194-(9022.06)]
17 p2976 N85-28387
Hot cracking of austenitic stainless steels: The debut of the Sigmajig
[DE85-010560] 20 p3431 N85-31287

WELDING
NT ARC WELDING
NT BRAZING
NT COLD WELDING
NT DIFFUSION WELDING
NT ELECTRIC WELDING
NT ELECTRON BEAM WELDING
NT ELECTROSLAG WELDING
NT EXPLOSIVE WELDING
NT FRICTION WELDING
NT FUSION WELDING
NT GAS TUNGSTEN ARC WELDING
NT LASER WELDING
NT LOW TEMPERATURE BRAZING
NT PLASMA ARC WELDING
NT PRESSURE WELDING
NT ULTRASONIC WELDING
Future robotics program at San Antonio ALC (Air Logistics Center)
[AD-P004011] 03 p0309 N85-11991
USSR report: Materials science and metallurgy
[JPRS-UMS-84-007] 03 p0348 N85-12244
Compact welding apparatus with solar power supply
03 p0352 N85-12263
Comparative investigation of testing methods to determine hot crack susceptibility during welding
[BAM-ERP-2415] 07 p0979 N85-16216
Robotics application in construction industry assessed
08 p1139 N85-17178
Technical data on new engineering products
10 p1460 N85-19201
Interaction between a crack and a soft inclusion
[NASA-CR-172533] 10 p1495 N85-19439
Investigation of welded interconnection of large area wraparound contacted silicon solar cells
[NASA-CR-174438] 10 p1509 N85-19519
USSR report: Materials science and metallurgy
[JPRS-UMS-84-005] 11 p1597 N85-20044
Evaluation of residual stress in laminated metallic composites 11 p1598 N85-20052
Chemical cleaning of 304 and 304-L stainless steel surfaces by the nitradd passivation process
[DE85-003714] 11 p1615 N85-20158
Automatic multi-layer welding of thick cylindrical structures under flux 13 p2035 N85-22746
USSR report: Materials science and metallurgy
[JPRS-UMS-85-001] 15 p2496 N85-25395
USSR report: Materials science and metallurgy
[JPRS-UMS-85-004] 15 p2513 N85-25503
Soviet Institute director on GDR-USSR welding technology 15 p2536 N85-25662
Applicability of modular versus universal robots discussed 15 p2536 N85-25664
Welding technology: Japan --- Conference
[ISBN-0-85300177-4] 15 p2565 N85-25823
The development and implementation of advanced welding technology 15 p2565 N85-25824
Studies of ferritic filler metals for welding 9 percent nickel steel 15 p2565 N85-25825
Application of new welding technology in the fabrication of nuclear power plant 15 p2566 N85-25829
NASA welding assessment program
[NASA-CR-175683] 15 p2568 N85-25845
Special features of the one-sided automatic welding of structures of Al-Mg alloys 16 p2792 N85-27222
Hazards in welding due to oxygen changes in the workplace atmosphere
[BLL-WI-TRANS-684-(9312.57)]
16 p2792 N85-27224
The characteristic structure of weld metal of high temperature alloy X20CrMoV 121
[BLL-BISI-TRANS-21623-(9022.06)]
17 p2928 N85-28069
Formation of a fine structure during shock wave welding
[BLL-BISI-TRANS-22401-(9022.06)]
17 p2973 N85-28368
Principal quality assurance measures in the manufacture of HF-welded high-pressure linepipe
[BLL-BISI-TRANS-21690-(9022.06)]
17 p2976 N85-28389
Fatigue crack propagation characteristics and fatigue fracture toughness in 780 MPa grade high strength steel weldments at low temperature
[BLL-BISI-TRANS-22369-(9022.06)]
17 p2979 N85-28411
Alignment and assembly tool for very large diameter cylinders
[NASA-CASE-MFS-28001-1] 18 p3116 N85-29289
Brittle fracture behaviour of cold formed, welded 10mm to 20 mm thick plate manufactured from plain carbon structural steels
[BLL-BISI-TRANS-21676-(9022.06)]
18 p3120 N85-29311

Chemical composition and kinetics of libration of gases upon welding of aluminum alloys
19 p3247 N85-30131
Reliability of welds to repair defects in cast components made from CrMoV steel
[BLL-CE-TRANS-8054-(9022.09)]
20 p3461 N85-31501
Joining of sintered composite TiC-steel materials by welding
[BLL-M-36253-(5828.4)] 20 p3461 N85-31502
Production verification of the acoustic emission weld monitor
[AD-A154168] 20 p3464 N85-31519
Analytical simulation of weld effects in creep range
20 p3468 N85-31550
United States Army welding research and development topical and coordination meeting
[AD-A155834] 24 p4099 N85-35409

WELDING MACHINES
Compact welding apparatus with solar power supply
03 p0352 N85-12263
New welding equipment for mechanized welding and trends in further development 03 p0352 N85-12264
Laser and diffusion welding equipment R and D
03 p0352 N85-12265
Design features, applications of new robots
08 p1139 N85-17174
Characterization of the heat source distribution of a typical GTAW welding arc
[DE85-004322] 12 p1861 N85-21670
Automatic multi-layer welding of thick cylindrical structures under flux 13 p2035 N85-22746
Cosmonauts report on space welding at conference
15 p2484 N85-25329
Paton comments on results of space welding tests
15 p2484 N85-25330
Sources of improvement in quality of contact butt welding of wire
[BLL-M-36085-(5828.4)] 16 p2793 N85-27225
Laser welder for fabricating neutron tubes
[DE85-009965] 17 p2974 N85-28377

WELLS
Similarity considerations in 1-component 2-phase flow
[DE84-016370] 04 p0499 N85-13184
Geothermal wells drilled in Transcarpathians
07 p0994 N85-16315
Geothermal assessment of part of the east shore area, Davis and Weber Counties, Utah
[DE84-016817] 09 p1342 N85-18446
Technical support for geopressured-geothermal well activities in Louisiana
[DE85-010462] 18 p3102 N85-29203
Hot Dry Rock Geothermal Energy Developement Program
[DE85-010570] 19 p3268 N85-30264
Lost circulation in geothermal wells: Research and development status
[DE85-009836] 19 p3268 N85-30267
Linear boundary detection using pressure buildup tests
[DE85-009926] 22 p3784 N85-33444
Geologic, technical, and economic sensitivity analysis in support of the GRI (Gase Research Institute) tight gas reservoirs project area
[PB85-192276] 22 p3802 N85-33559
Proposed resource evaluation plan. Salton Sea scientific drilling program
[DE85-011294] 22 p3815 N85-33633
Method for determining depth and shape of a sub-surface conductive object
[DE85-006502] 23 p3835 N85-34389
Depletion modeling of liquid dominated geothermal reservoirs
[DE85-009923] 23 p3943 N85-34437
Evaluation of low-temperature geothermal potential in north-central Box Elder County, Utah
[DE85-008541] 24 p4112 N85-35490

WEST GERMANY
Colloquium about Joint Projects within DFVLR/ISRO Cooperation
[DFVLR-MITT-84-12] 04 p0458 N85-12907
Presentation of Indian Space Research Organization (ISRO)/DFVLR cooperation 04 p0459 N85-12912
German domestic scheduled air transport in the year 2000
[ESA-TT-828] 05 p0595 N85-13792
Global radiation in West Germany --- solar generators
05 p0662 N85-14253
Overview of German microgravity activities in the field of life science 05 p0696 N85-14476
BDLI memorandum on the future of space flight in the Federal Republic of Germany
[NASA-TM-77624] 07 p0911 N85-15765
Revised Uniform Summary of Surface Weather Observations (RUSSWO). Spangdahlem AB, Germany, parts A-F
[AD-A147166] 07 p1006 N85-16392
Limited surface observations climatic summary (LISOCS). Hohenfels, AAF, West Germany
[AD-A147167] 07 p1006 N85-16393
Activities report on West German civil airports. Part 1: Text
[ISBN-3-87977-055-7-PT-1] 08 p1090 N85-16887
Activities report for the West German Civil Airports. Part 2: Tables
[ISBN-3-87977-055-7-PT-2] 08 p1090 N85-16888
The Prandtl Hergesell project of a national research establishment for aeronautics
[ESA-TT-835] 09 p1272 N85-17993
Space research in the Federal Republic of Germany
09 p1285 N85-18074
Activities report of the Department of Applied Research 78 for satellite geodesy of the Technical University, Munich
[ASTRON-GEODAET-ARB-45]
09 p1342 N85-18440
Revised Uniform Summary of Surface Weather Observations (RUSSWO). Parts A-F Zweibrucken AB, Germany
[AD-A147165] 09 p1357 N85-18536
Activities report in aerospace in West Germany
[ISSN-0070-3966] 09 p1418 N85-18947
FRG's DFVLR ready for participation in space station
11 p1618 N85-20176
The 1980 diagnostic adjustment of the German main triangulation network. 4: Network adjustment (part 3)
[SER-B-267-PT-3-MITT-168] 11 p1665 N85-20494
The 1980 diagnostic adjustment of the German main triangulation network. 4: Network adjustment (part 1)
[SER-B-267-PT-1-MITT-168] 11 p1670 N85-20525
The 1980 diagnostic adjustment of the German main triangulation network. 4: Network adjustment (part 2)
[SER-B-267-PT-2-MITT-168] 11 p1670 N85-20526
List of head/neck injury on ejection in the German Armed Forces from 1972-1981 12 p1906 N85-21972
D-1 report: The first German spacelab mission
[NASA-TM-77637] 13 p1977 N85-22402
West Europe report: Science and technology
[JPRS-WST-84-007] 15 p2530 N85-25600
Three-dimensional boundary layers: A report on work in Germany 15 p2559 N85-25786
Comparison of some West German cloud height and visibility data --- weapon test sites
[BAE-BT-12734] 15 p2593 N85-25982
A brief comparison of Egyptian with West German atmospheric transmission data in the 8 to 11.5 micron waveband
[BAE-BT-12829] 15 p2594 N85-25983
Proceedings of the 9th US Air Force and the Federal Republic of Germany Data Exchange Agreement Meeting, Viscous and Interacting Flow Field Effects
[AD-A153020] 17 p2958 N85-28266
Investigation of air pollution impact in Eastern Bavaria: Measurement results from August and September, 1984
[DFVLR-FB-85-03] 17 p2988 N85-28471
Documentation for the West German Federal Cabinet's space policy decision 17 p3051 N85-28886
Investigation of the transferability of measures of passive solar energy utilization in the USA to the Federal Republic of Germany
[BMFT-FB-T-84-284] 18 p3132 N85-29396
International space research perspectives of commercialization for German industry
[NASA-TM-77657] 19 p3222 N85-29979
Maritime mobile satellite techniques as an integral part of the Future Global Maritime Distress and Safety System (FGMDSS): The position of the Federal Republic of Germany 20 p3406 N85-31136
Reports from the German Meteorological Service. No. 167: Results of aerological soundings in the model area upper Rhine: Heat release project upper Rhine area, part 3
[ISBN-3-88148-216-4] 23 p3950 N85-34479
Special questions of siting wind turbine arrays and networks --- West Germany 24 p4111 N85-35484

WEST INDIES
NT CUBA
NT PUERTO RICO

WEST PAKISTAN
U BANGLADESH

WESTLAND AIRCRAFT
NT P-531 HELICOPTER

WESTLAND P-531 HELICOPTER
U P-531 HELICOPTER

WETLANDS
Multispectral remote sensing of inland wetlands in South Carolina: Selecting the appropriate sensor
[DE84-013951] 05 p0661 N85-14247
Removal of heavy metals by artificial wetlands
[PB85-116127] 10 p1513 N85-19548
An initial analysis of LANDSAT-4 Thematic Mapper data for the discrimination of agricultural, forested wetlands, and urban land cover --- Poinsett County, Arkansas; and Reelfoot Lake and Union City, Tennessee
13 p2118 N85-23193
Remote sensing of coastal wetlands biomass using Thematic Mapper wavebands --- Lewes, Delaware
13 p2119 N85-23198
Comparison of MSS and TM data for landcover classification in the Chesapeake Bay area: A preliminary report --- Taylor's Island, Maryland
13 p2121 N85-23210

WETNESS
U MOISTURE CONTENT

WETTABILITY
Preliminary evaluation of a liquid belt radiator for space applications
[NASA-CR-174807] 07 p0917 N85-15804
Contact angle and surface tension measurements of a five-ring polyphenyl ether
[NASA-TM-86927] 07 p0930 N85-15897

WETTING
Critical point wetting drop tower experiment
02 p0155 N85-11045
The chemical nature of the fiber/resin interface in composite materials 04 p0465 N85-12953
A nonmobile front metallization process
06 p0830 N85-15279
Investigation of surface tension phenomena using the KC-135 aircraft
[NASA-TM-82506] 10 p1426 N85-18995
Factors influencing the ball milling of Si3N4 in water
[NASA-TM-86932] 10 p1450 N85-19136
Modeling of transient heat pipe operation
[NASA-CR-175496] 12 p1844 N85-21571
Examination of the contact wetting angle in the vicinity of critical temperature
[BLL-T6416/BG/CRS/LR-ST735/84]
13 p2091 N85-23054
Statistical mechanics of adsorption and wetting
[DE85-010093] 19 p3269 N85-30271
Mechanics of a gaseous film barrier to lubricant wetting of elastohydrodynamically lubricated conjunctions
[NASA-TP-2500] 21 p3595 N85-32330

WHALES
Tracking whale migrations with the ARGOS satellite system 14 p2330 N85-24403
Some methods of computing platform transmitter terminal location estimates --- ARGOS system; whale tracking 14 p2332 N85-24420
The ARGOS system ured for tracking gray whales
14 p2332 N85-24421
The ARGOS system used for tracking gray whales
16 p2812 N85-27347

WHEAT
Multi crop area estimation in Idaho using EDITOR
[E85-10054] 06 p0827 N85-15251
Growth/reflectance model interface for wheat and corresponding model
[E85-10058] 07 p0987 N85-16269
Growth and reflectance characteristics of winter wheat canopies
[E85-10080] 10 p1505 N85-19494
User's guide to the TAMW wheat model as implemented on the IBM 360/195 computer
[E85-10084] 12 p1873 N85-21749
NOAA-AISC user's guide for implementing CERES wheat model for large area yield estimation
[E85-10085] 12 p1873 N85-21750
Modeling the backscattering and transmission properties of vegetation canopies
[E85-10099] 16 p2809 N85-27320
Regression analysis of aircraft and ground measurement data on vegetation cover 22 p3735 N85-33156

WHEATSTONE BRIDGES
The constant current strain gauge bridge
[ARL/STRUC-TM-385] 07 p0962 N85-16097
Developing a flowmeter for streams with high solids content
[DE84-016643] 09 p1323 N85-18316
Instrumentation for sensing moisture content of material using a transient thermal pulse
[NASA-CASE-NPO-15493-2] 23 p3933 N85-34373

WHEEL BRAKES
Development of carbon based brake lining materials without asbestos content in the form of carbon-carbon composites and carbon-metal or carbon-carbide composites
[BMFT-FB-T-85-014] 18 p3082 N85-29067

WHEELS
NT COUNTER-ROTATING WHEELS
NT FLYWHEELS
NT REACTION WHEELS
NT TURBINE WHEELS
NT VEHICLE WHEELS

Grease versus oil lubrication of wheel bearings in Army equipment
[AD-A147546] 07 p0973 N85-16184
Space shuttle wheels and brakes
08 p1101 N85-16962
Development of a soil-wheel interaction model
[AD-P004250] 09 p1404 N85-18835
The rolling resistance and sinkage of towed dual wheel combination in sand
[AD-P004261] 09 p1404 N85-18837
Forces on undriven, angled wheels
[AD-P004303] 09 p1409 N85-18880
An evaluation of the 64-meter antenna radial bearing for use on the 70-meter antenna
10 p1464 N85-19236
Manufacture of drive wheel vanes for hydraulic turbines on program controlled machine tools
14 p2269 N85-24058
Modernization of running gear of crane
14 p2286 N85-24163
Assessing the machinability of gearwheel steels during manufacture
[BLL-BISI-TRANS-22343-(9902.06)]
17 p2973 N85-28365
Non-backdriveable free wheeling coupling
[NASA-CASE-MSC-20475-1] 18 p3116 N85-29290
Development of a high strength isothermally heat-treated nodular iron road wheel arm
[AD-A155755] 24 p4099 N85-35408

WHIP ANTENNAS
HF broadband whip antenna evaluation
[AD-A149527] 10 p1467 N85-19258

WHIRL
U ROTATION

WHIRL INSTABILITY
U ROTARY STABILITY

WHIRLING
U ROTATION

WHISKER COMPOSITES
Fabrication of SiC whiskers and composites
[DE85-002038] 09 p1289 N85-18091
Tensile testing of SiC whiskers
[DE85-003712] 11 p1593 N85-20025
Particulate and whisker toughened alumina composites
[DE85-005239] 16 p2743 N85-26930

WHISKERS (CRYSTALS)
Tensile testing of SiC whiskers
[DE85-003712] 11 p1593 N85-20025

WHISTLERS
The propagation and growth of whistler mode waves generated by electron beams in Earth's bow shock
[AD-A145572] 02 p0228 N85-11492
Inference of equatorial field-line integrated electron density values using whistlers
[AD-A145822] 03 p0392 N85-12507
Asymptotic orbit theory for trapped electrons in inhomogeneous Whistler field
[AD-A146178] 03 p0392 N85-12510
Three dimensional ray tracing of the Jovian magnetosphere in the low frequency range
[NASA-CR-175462] 10 p1571 N85-19909
Excitation of low-frequency plasma waves by a conducting, tethered satellite 13 p2171 N85-23470
Deuteron whistlers at low latitudes in the low altitude topside ionosphere 14 p2366 N85-24625
Low-latitude ducted whistlers observed at Sanya, Hainan, China 14 p2367 N85-24626
Whistler observation at Okinawa, Japan during the IMS 14 p2367 N85-24627
Whistler mode waves near the plasmapause: Results from the IMS VLF experiment at Halley, Antarctica
14 p2367 N85-24628

WHITE DWARF STARS
Search for white dwarf companions of cool stars with peculiar element abundances
[NASA-CR-174030] 02 p0297 N85-11923
Voyager EUV and FUV observations
06 p0875 N85-15554
Stromgren trails of hot white dwarfs
06 p0879 N85-15589
Ultraviolet spectroscopy of selected astronomical sources
[NASA-CR-174379] 09 p1413 N85-18912
On the progenitors of white dwarfs
[NASA-CR-174378] 09 p1413 N85-18913
Study of the pulsations of the ZZ Ceti stars
09 p1414 N85-18923
White dwarf stars at ultraviolet wavelengths
11 p1744 N85-20971
Mass distribution and evolutionary scheme for central stars of planetary nebulae 11 p1751 N85-21012
Further investigation of mass loss phenomena in hot white dwarfs and O subdwarfs 11 p1751 N85-21014
Self-consistent recalibration of IUE determination of hot DA white dwarf effective temperatures
11 p1751 N85-21016
Carbon, silicon, and oxygen in the white dwarf star GD 40 11 p1752 N85-21017
Analysis of white dwarf Lyman alpha profiles
11 p1752 N85-21018
A search for white-dwarf companions of subgiant CH stars 11 p1752 N85-21019
The white dwarf companion of the mild BA star Xi1 Cet 11 p1752 N85-21020
The outburst and long term behavior of the triple period cataclysmic variable TV Col 11 p1752 N85-21021
Hydrodynamic simulations of recurrent novae
11 p1753 N85-21025
Egress spectra of the new eclipsing supergiant 22 Vulleculae 11 p1755 N85-21039
A survey for galactic plane ultraviolet-excess objects: Space densities for white dwarfs, subdwarfs, and cataclysmic variables 13 p2169 N85-23458
Photoelectric observations of the dwarf nova VW Hydri during the November 1977 supermaximum
[REPT-97] 15 p2667 N85-26461
On gamma and neutrino radiation from Cyg X-3
[OG-2.1-7] 22 p3863 N85-33924

WHITE LIGHT HOLOGRAPHY
White-light optical information processing and holography
[AD-A146938] 07 p0967 N85-16138
The utilization of optical fibers in holography
[ISL-R-102/83] 16 p2787 N85-27196

WHITE NOISE
NT THERMAL NOISE
Non-Gaussian approach for parametric random vibration of non-linear structures 01 p0060 N85-10395
Spectral noise density and random errors of pulse frequency characteristic meters
03 p0346 N85-12231
Flight test technique for evaluation of gust load alleviation analysis methodology
[NASA-TM-86344] 06 p0754 N85-14833
On the probability density of signal-to-noise ratio in an improved adaptive detector, part 1
[AD-A148856] 10 p1550 N85-19772
Statistical analysis of autoregressive spectral estimates for noise corrupted autoregressive series
[AD-A149543] 11 p1708 N85-20747
Methods of digital correction for channels of multichannel radar receivers 13 p2082 N85-23005
On the probability density of signal-to-noise ratio in an improved detector
[AD-A152529] 17 p2952 N85-28232
Random vibration of nonlinear, parametrically excited systems 19 p3262 N85-30351
Noise in stages and in interstage couplings of various transistor circuits 22 p3765 N85-33334
Nonlinear filtration of clutter 22 p3777 N85-33404

WICKS
Monogroove heat pipe design: Insulated liquid channel with bridging wick
[NASA-CASE-MSC-20497-1] 16 p3098 N85-29180

WIDE ANGLE LENSES
A second generation WAVIDS (Wide Angle Virtual Image Display System)
[AD-P004328] 09 p1270 N85-17982
Wide-angle optics with strong magnetic fields for efficient generation of secondary-particle beams
[DE85-007727] 18 p3179 N85-29713
Evidence for long-term variability in the ultra high energy photon flux from Cygnus X-3
[OG-2.1-10] 22 p3863 N85-33926

WIDEBAND
U BROADBAND

WIDEBAND COMMUNICATION
Interference immunity of digital equipment for coherent processing of wideband signals
04 p0486 N85-13100
Digital simulation of communications channels: An overview 10 p1472 N85-19290
Fast synchronization model for UHF spread-spectrum communication system 10 p1473 N85-19296
Overview of RADC adaptive antenna developments for communications 10 p1474 N85-19299
Ionospheric distortions of digital signals with wideband modulation 13 p2072 N85-22945
Cophasal horizontal wideband array antennas for transmitting with asymmetric output
15 p2526 N85-25576
Adaptation of bit error rate by coding — spacecraft transmissions
[ESA-CR(P)-1970] 15 p2545 N85-25711

WIENER FILTERING
Recursive algorithms for adaptive arrays based on estimates
[REPT-5-84] 01 p0107 N85-10718

WIENER HOPF EQUATIONS
Random equations in aerodynamics
[NASA-CR-174279] 06 p1077 N85-16825

WIGGLER MAGNETS
A free electron laser with two-component wiggler
11 p1623 N85-20217
Progress toward free-electron lasers for applications
[DE85-002206] 11 p1639 N85-20326
Note of the dynamic behavior of a magnet system suspended by a thin fiber, with special reference to the Quartz Horizontal Magnetometer (QHM)
[DMI-GEOPHYS-PAPERS-R-70]
11 p1714 N85-20785
Application of permanent magnets in accelerators and electron storage rings
[DE85-004981] 15 p2642 N85-26297
Permanent magnets for production and use of high energy particle beams
[DE85-009934] 20 p3522 N85-31905
Electron trajectories in a combined wiggler and alternating gradient quadrupole field
[DE85-010727] 22 p3842 N85-33794
Breeding new light into old machines (and new)
[DE85-013055] 24 p4155 N85-35763

WIGHTMAN THEORY
U FIELD THEORY (PHYSICS)
U QUANTUM THEORY
U RELATIVISTIC THEORY

WIGNER COEFFICIENT
A packed storage program for angular momentum coupling coefficients
[TWISK-316] 01 p0102 N85-10680
The ambiguity function and the Wigner distribution
[AD-A150095] 12 p1829 N85-21482

WILDLIFE
NT BABOONS
NT BIRDS
NT MONKEYS
Control of mammals at airports
[AD-P004192] 11 p1580 N85-19957
Airport site selection and design
[AD-P004193] 11 p1581 N85-19959
Acid rain: Effects on fish and wildlife
[PB85-154672] 16 p2821 N85-27402

WILDLIFE RADIOLOCATION
Tracking pelagic dolphins by satellite
14 p2324 N85-24364
Polar bear telemetry results from the Nimbus-6 system
14 p2325 N85-24365
Development of ARGOS platforms for tracking of basking sharks. Cetorhinus maximus
14 p2326 N85-24378
Transatlantic migration study of the leathery turtle using the ARGOS system. Transatlantic turtle race
14 p2326 N85-24379
Tracking whale migrations with the ARGOS satellite system 14 p2330 N85-24403
Drifting buoy development and future programs — Japanese ARGOS program 14 p2330 N85-24406
Some methods of computing platform transmitter terminal location estimates — ARGOS system; whale tracking 14 p2332 N85-24420
The ARGOS system used for tracking gray whales
14 p2332 N85-24421
Motivation for satellite tracking of southern elephant seals Mirounga leonina at sea 16 p2812 N85-27346
The ARGOS system used for tracking gray whales
16 p2812 N85-27347

WINCHES
The orbiter mate/demate device
08 p1103 N85-16972
Improvements in linked-spar motion-compensated lifting system
[AD-D011413] 08 p1138 N85-17165

WIND (METEOROLOGY)
NT CYCLOGENESIS
NT GEOSTROPHIC WIND
NT GROUND WIND
NT GUSTS
NT JET STREAMS (METEOROLOGY)
NT MONSOONS
NT SEA BREEZE
NT SQUALLS
NT WINDS ALOFT
Alpine meteorology: Translations of classic contributions by Wagner, A., Ekhart, E. and Defant, F.
[DE84-014929] 01 p0085 N85-10574
Microburst wind structure and evaluation of Doppler radar for wind shear detection
[DOT/FAA/PM-84/29] 02 p0230 N85-11501
Wind shear measuring on board an airliner
[NASA-TM-77463] 03 p0395 N85-12521
Plotting TDL coastal wind forecasts
[PB84-220789] 03 p0397 N85-12533

Aircraft measurements of tracer gas during the 1983 cross Appalachian tracer experiment (CAPTEX)
[DE84-015292] 04 p0531 N85-13395

Effect of mountain wave dynamics on orographic storms
[DE84-014713] 04 p0540 N85-13433

Comparison of wind derived from the LIMS (Limb Infrared Monitor of the Stratosphere) satellite instrument with rocket observations
[NASA-CR-174083] 04 p0541 N85-13444

Investigation of satellite measurements in the presence of clouds, forcing influences on clouds and feedback to the large scale following convection
05 p0662 N85-14381

Large scale rossby waves during FGGE
05 p0664 N85-14396

Statistical relationships between meteorological data stations and implications to diagnostic models in complex terrain
[DE84-014360] 06 p0839 N85-15328

Limited surface observations climatic summary (LISOCS). Camp Casey, Tong Du Chon, Korea
[AD-A147204] 07 p1007 N85-16397

Limited surface observatins climatic summary (LISOCS). Ansbeck AHP, Germany
[AD-A147205] 07 p1007 N85-16398

Studies of coastal mesoscale winds using SIR-B
08 p1147 N85-17238

MWR, Meteor Wind Radars 08 p1184 N85-17462

Development of guidance forecasts at the Royal Netherlands Meteorological Institute (KNMI). Part 2: Extreme wind speed at IJmuiden
[KNMI-TR-54-PT-2] 08 p1190 N85-17500

Modeling stochastic wind loads on vertical axis wind turbines
[DE85-001148] 09 p1340 N85-18426

The wobble of the Earth and the low frequency dynamics of the ocean 09 p1358 N85-18546

Field studies of run-up generated by wind waves on dissipative beaches
[AD-A148793] 09 p1359 N85-18548

MAP in Japan: Organization and projects
11 p1655 N85-20425

MAP activities in Hungary 11 p1657 N85-20440

Variation of derived mesospheric nitric oxide in relation to wind and temperature in winter
11 p1658 N85-20452

Large scale winter time disturbances in meteor winds over central and eastern Europe
11 p1661 N85-20467

VHF radar observations in the stratosphere and mesosphere during a stratospheric warming
11 p1661 N85-20468

Changes in the ozone content over central Europe during reversals of stratospheric circulation in late winter
11 p1661 N85-20469

Some aspects of general circulation and tides in the middle atmosphere 11 p1661 N85-20470

Meteor wind results from Atlanta, USA, and Ramey, Puerto Rico 11 p1662 N85-20474

Basic features of global circulation in the mesopause lower thermosphere region 11 p1662 N85-20475

Winds and waves (4 min - 11 yrs) in the upper middle atmosphere (60-110 km) at Saskatoon, Canada (52 deg N, 107 deg W): MF radar (2.2 MHz) soundings 1973 - 1983 11 p1662 N85-20476

Measurement of the vertical gradient of the semidiurnal tidal wind phase in winter at the 95 km level
11 p1662 N85-20478

Stratwarm effects in the ionospheric D region wind field 11 p1663 N85-20479

Orographic disturbances of upper atmosphere emissions 11 p1663 N85-20480

Turbulence parameters impacting dispersion in an urban convection boundary layer
[PB85-116036] 11 p1682 N85-20598

High time resolution thermospheric temperature and wind studies in the Arctic
[AD-A150114] 12 p1890 N85-21860

Los Alamos MINI-Review: Tracking Antarctic winds
[DE85-004597] 12 p1896 N85-21903

Summary of Meteorological Observations Surface (SMOS), Sigonella, Sicily/Navy
[AD-A150539] 13 p2138 N85-23280

Summary of Meteorological Observations, Surface (SMOS), Alameda, California
[AD-A150609] 13 p2138 N85-23281

Determination of gravity wave envelope solitons on surface of stratified fluid interacting with wind
14 p2334 N85-24433

High-frequency wind wave spectrum in storm basin
14 p2336 N85-24444

Field of point source of low-frequency sound in atmosphere with altitudinally nonuniform wind
15 p2524 N85-25566

Nowcasting applications of VAS
15 p2597 N85-26003

Wind modelling for increased aircraft operational efficiency 16 p2697 N85-26652

Use of a network of telemetered meteorological stations for prediction of the distribution of an atmospheric tracer
16 p2831 N85-27456

A Markov method for simulating non-Gaussian wind speed time series
[DE85-007131] 16 p2835 N85-27485

Propagation of gravity waves in the atmosphere and around critical levels
[KNMI-WR-85-1] 18 p3137 N85-29426

Analysis of ocean surface wind fields using SEASAT-A scatterometer data 18 p3139 N85-29434

Application of climatological analysis to minimize air pollution impacts in California
[PB85-172963] 18 p3149 N85-29502

A survey of the turbulence in the marine surface layer for the operation of low-Reynolds number aircraft
[AD-A154133] 19 p3316 N85-30556

A survey of wind and turbulence modeling methods
[AD-A154470] 20 p3496 N85-31733

Aeolian geomorphology from the global perspective
21 p3603 N85-32373

Diagnostics of severe convection and subsynoptic scale ageostrophic circulations
[NASA-CR-171581] 21 p3634 N85-32571

Notes on atmospheric stability, turbulence, and its measurements
[AD-A155230] 21 p3637 N85-32588

Radar wind profilers in the Colorado network
[PB85-185486] 22 p3817 N85-33647

Evaluation of source strength and dispersion model predications with data from large nitrogen tetroxide field experiments
[DE85-011865] 23 p3947 N85-34485

Program for Regional Observing and Forecasting Services (PROFS)
[PB85-108050] 24 p4124 N85-35569

WIND CIRCULATION
U ATMOSPHERIC CIRCULATION

WIND DIRECTION

Multisensor satellite data integration for sea surface wind speed and direction determination
[NASA-CR-174162] 04 p0542 N85-13446

Development and verification of MCD-2 and MOD-OA simulation models
[DE84-017389] 04 p0550 N85-13499

A diagnostic approach to obtaining planetary boundary layer winds using satellite-derived thermal data
05 p0674 N85-14330

Climate at CRREL (Cold Regions Research and Engineering Laboratory) Hanover, New Hampshire
[AD-A148400] 08 p1189 N85-17495

Analysis of the Viking Lander 1 surface wind vector for sols 45 to 375
[NASA-CR-174349] 09 p1416 N85-18932

Isentropic objective analysis
[PB85-112167] 11 p1688 N85-20617

Portable Automated Mesonet (PAM) data from the 1980 experiment in Anderson Creek Valley
[DE85-004361] 13 p2139 N85-23282

Analysis of the inflow and air-sea interactions in hurricane Frederic 15 p2595 N85-25990

Mean conditions and turbulence statistics at Vandenberg AFB, California
[AD-A151366] 15 p2665 N85-26449

Urban climate and air hygiene before, during, and after the lifework of Hellmut Berg. Overview of a branch of applied meteorology 18 p3147 N85-29487

Acrosswind response of towers and stacks of circular cross-section 19 p3262 N85-30354

Practicality of electronic beam steering for MST/ST radars, part 6.2A 21 p3624 N85-32516

Mean flow and turbulence in complex terrain
[AD-A155138] 21 p3636 N85-32583

WIND EFFECTS

Natural environment analysis
[NASA-CR-171333] 10 p1428 N85-19010

Cut-off lows and their influence on the weather in Switzerland
[REPT-45] 10 p1519 N85-19574

Study of pollutant dispersion in an urban street canyon
[DE85-002648] 11 p1677 N85-20571

Algorithms for automatic four-dimensional aircraft guidance, considering the momentary wind situation
[DFVLR-FB-84-40] 12 p1775 N85-21148

Evaluating wind flow around buildings on heliport placement
[FAA-PM-84-25] 12 p1893 N85-21881

On the wind error of the Finnish raingauge
[REPT-37] 12 p1893 N85-21883

The clinical and biomedical evaluation of trauma and fatalities associated with aircrew ejection and crash. A Working Group report
[AGARD-AR-194] 12 p1906 N85-21969

Introduction: The clinical and biomedical evaluation for trauma and fatalities associated with aircrew ejection and crash 12 p1906 N85-21970

List of head/neck injury on ejection in the German Armed Forces from 1972-1981 12 p1906 N85-21972

Portable Automated Mesonet (PAM) data from the 1980 experiment in Anderson Creek Valley
[DE85-004361] 13 p2139 N85-23282

Seasonal and secular variation of the Solis Lacus albedo feature: Relation to the Martian dust-transport cycle
13 p2188 N85-23576

The effect of particle density on aeolian transport
13 p2189 N85-23581

A comparison of terrestrial saltation flux in the laboratory and the field 13 p2189 N85-23582

Statistics of Aeolian surface of Mars
13 p2199 N85-23637

Sea-ice motion in response to geostrophic winds
14 p2323 N85-24357

Local mechanism of equatorial countercurrents
14 p2336 N85-24446

Sound propagation studies for a large horizontal axis wind turbine
[NASA-CR-172564] 14 p2415 N85-24904

Sea breeze-induced mesoscale systems and severe weather 15 p2596 N85-26012

Dynamic and aeroelastic action of guy cables
[VTT-16] 16 p2802 N85-27276

Response of a wind turbine blade to seismic and turbulent wind excitations 16 p2817 N85-27375

On the wind-induced vibrations of a mass-spring system
[REPT-84-04] 17 p2981 N85-28428

Experimental and theoretical determination of the wing-induced lateral wind on the tail surfaces in oscillating rolling motion. Part 2: Theoretical investigations for calculation of the lateral wind
[IFD-1/84-PT-2] 18 p3061 N85-28940

Experiments on the assimilation of patches of data using a barotropic model 18 p3140 N85-29441

Study of drift currents in initial stage of generation of wind waves by laser Doppler anemometer
19 p3291 N85-30408

Frequency of recurrence and critical conditions for generation of Langmuir circulations
19 p3291 N85-30409

Sea surface radio emission at wavelengths 0.86 and 1.3 cm near Brewster angle 19 p3293 N85-30418

Comparative analysis of operational forecasts versus actual weather conditions in airline flight planning, volume 4
[NASA-CR-167865] 24 p4120 N85-35537

WIND ENERGY
U WINDPOWER UTILIZATION

WIND EROSION

Venus 09 p1411 N85-18891

Observed changes at Viking Lander 1
13 p2188 N85-23575

Seasonal and secular variation of the Solis Lacus albedo feature: Relation to the Martian dust-transport cycle
13 p2188 N85-23576

Eolian erosion on Mars: Three scales
13 p2188 N85-23577

Planetary analogs in Antarctica: Mars
13 p2193 N85-23604

WIND MEASUREMENT
NT WIND VELOCITY MEASUREMENT

Detailed analysis of the structure of local wind systems in Canterbury, New Zealand 01 p0075 N85-10501

The altimeter as a support to the scatterometer in the representation of winds and derived wave fields in coastal waters and enclosed seas: A research at its onset
03 p0383 N85-12453

Wind shear measuring on board an airliner
[NASA-TM-77463] 03 p0395 N85-12521

A feasibility study on the use of wind profilers to support Space Shuttle launches
[NASA-CR-3861] 04 p0538 N85-13423

Spatial and temporal interpolation of NEROS radiosonde winds
[PB84-232545] 04 p0540 N85-13438

Measurement-Technical Investigations of Wind Energy Units
[JUEL-SPEZ-244] 05 p0667 N85-14293

Measurement-technical investigations of wind energy units in the short-time range — spectrum analysis
05 p0668 N85-14294

Measurement-technical problems in the investigation of wind energy units 05 p0668 N85-14295

Measuring system and data evaluation methods of the test field for wind energy units at Pellworm
05 p0668 N85-14296

Measuring methods to determine the static and dynamic behavior of wind energy converters
05 p0668 N85-14297
Measuring-technical investigation of wind energy units from the control-technical, electrical and energetic point of view 05 p0668 N85-14301
Existing measuring systems for wind energy units
05 p0669 N85-14302
Measuring techniques in the measuring program for the windpowered unit GROWIAN 05 p0669 N85-14303
Application of Fabry-Perot spectrometers for measurement of upper atmosphere temperatures and winds 08 p1183 N85-17454
Partial reflection spaced antenna wind measurements
08 p1185 N85-17467
D1 LF wind measurements in the 90 to 100 km height range 08 p1185 N85-17468
Data catalog for the 1982 DFVLR observational Foehn experiment — alpine wind
[DFVLR-FB-84-33] 09 p1358 N85-18543
The effect of the arbitrary level assignment of satellite cloud motion wind vectors on wind analyses in the pre-thunderstorm environment
[NASA-TM-86186] 10 p1517 N85-19565
Cut-off lows and their influence on the weather in Switzerland
[REPT-45] 10 p1519 N85-19574
An evaluation of wind measurements by four Doppler sodars
[PB85-115301] 10 p1520 N85-19586
Measurement of the vertical gradient of the semidiurnal tidal wind phase in winter at the 95 km level
11 p1662 N85-20478
Stratwarm effects in the ionospheric D region wind field 11 p1663 N85-20479
Improved models for increasing wind penetration, economics and operating reliability
[NASA-CR-175536] 11 p1674 N85-20545
The relevance of averaging period to wind power measurements and efficiency of Wind Energy Conversion Systems (WECS)
[GKSS-84-E-35] 11 p1676 N85-20562
Wind-weighting for sounding rockets with a telemetry system
[NASA-TP-2438] 12 p1792 N85-21246
Atmosphere ice-ocean interactions in the Antarctic (IAGO) 14 p2326 N85-24375
An overview of NDBC drifting buoy development programs — NOAA Data Buoy Center (DBC)
14 p2332 N85-24422
Low-frequency oscillations of sea level and group structure of wind waves 14 p2335 N85-24441
Experimental results of temperature-wind soundings of the atmosphere by the radio acoustical method
14 p2340 N85-24471
Wind observation station description for Den Helder (period 1843-1972) and De Kooy (period 1955-1980)
[KNMI-TR-42] 14 p2379 N85-24686
Application of infrared radiometers for airborne detection of clear air turbulence and low level wind shear, airborne infrared low level wind shear detection test
[NASA-CR-175725] 15 p2594 N85-25965
Wind modelling for increased aircraft operational efficiency 16 p2697 N85-26652
Analysis of the NASA/MSFC airborne Doppler lidar results from San Gorgonio Pass, California
[NASA-CR-3901] 16 p2832 N85-27463
Influence of coherent mesoscale structures on satellite-based Doppler lidar wind measurements
[NASA-CR-175853] 16 p2833 N85-27467
Analysis of ocean surface wind fields using SEASAT-A scatterometer data 18 p3139 N85-29434
Using regression analysis for determining air data sensor errors by means of an inertial navigation system
[ESA-TT-886] 20 p3392 N85-31041
Tropical Ocean and Global Atmosphere (TOGA) heat exchange project: A summary report
[NASA-CR-176038] 20 p3496 N85-31736
Facility for large-scale hazardous gas testing
[DE85-011852] 21 p3564 N85-32169
Performance of the Colorado wind-profiling network, part 1.5A 21 p3617 N85-32475
Potential advantages of the spaced antenna method for operational wind profiling, part 3.1B
21 p3620 N85-32490
Determination of horizontal and vertical wavelengths of gravity waves in the mesosphere by spaced wind measurements 21 p3623 N85-32510
Elimination of range-aliased echoes in the VHF radars
21 p3625 N85-32521
Data base for the Colorado profiling network
21 p3627 N85-32533
Verification of Doppler sodar measurements — atmospheric boundary layer
[KNMI-WR-85-2] 22 p3817 N85-33645

WIND PRESSURE
The relevance of averaging period to wind power measurements and efficiency of Wind Energy Conversion Systems (WECS)
[GKSS-84-E-35] 11 p1676 N85-20562
The theoretical response of a vertical line array to wind-generated noise in shallow water
[AD-A151730] 16 p2660 N85-27638

WIND PROFILES
Structural design guidelines for heliports
[FAA-PM-84-23] 02 p0149 N85-11010
Wave phase velocity in a wind gradient — gravity waves 04 p0523 N85-13343
A feasibility study on the use of wind profilers to support Space Shuttle launches
[NASA-CR-3861] 04 p0536 N85-13423
Spatial and temporal interpolation of NEROS radiosonde winds
[PB84-232545] 04 p0540 N85-13438
Calms processor (CALMPRO) user's guide
[PB84-229467] 04 p0540 N85-13439
Error analysis of wind determined using a VLF Omega sonde
[WSRL-0361-TM] 06 p0838 N85-15321
Diurnal and seasonal patterns of temperature and wind flow in the planetary boundary layer for ten locations in complex terrain
[PB85-106698/GAR] 06 p0840 N85-15333
Atmospheric environment for Space Shuttle (STS-41G) launch
[NASA-TM-86486] 07 p0995 N85-16320
Natural environment analysis
[NASA-CR-174330] 08 p1180 N85-17433
Global scale diagnoses of FGGE data
[NASA-CR-174356] 09 p1356 N85-18533
Spring changeover of the middle atmosphere circulation compared with rocket wind data up to 80 km
11 p1661 N85-20466
Measurement of the vertical gradient of the semidiurnal tidal wind phase in winter at the 95 km level
11 p1662 N85-20478
Stratwarm effects in the ionospheric D region wind field 11 p1663 N85-20479
Phased antenna array for wind profiling applications
[PB85-132884] 12 p1837 N85-21529
Oceanographic and meteorological research based on the data products of SEASAT
[E85-10091] 12 p1874 N85-21753
High time resolution thermospheric temperature and wind studies in the Arctic
[AD-A150114] 12 p1890 N85-21860
Atmospheric environment for Space Shuttle (STS-51A) launch
[NASA-TM-86497] 12 p1892 N85-21875
Preliminary study of inphase gusts and moment force wind loads over the first 150 meters at KSC, Florida
[NASA-TM-86501] 13 p2137 N85-23273
Thermospheric winds observed by OI6300A Doppler shifts at 23 deg S in the Brazilian sector
[INPE-3384-RPE/470] 16 p2834 N85-27479
Analysis of ocean surface wind fields using SEASAT-A scatterometer data 18 p3139 N85-29434
Specification of surface roughness over oceans in the GLAS Fourth Order GCM 18 p3142 N85-29455
Additional possibilities of radiometeor azimuthal method for measuring wind velocity in lower thermosphere
19 p3296 N85-30438
The micrometeorology of an Amazonian rainforest
[INPE-3515-PRE/740] 19 p3315 N85-30551
An examination of the Southern Oscillation in the upper troposheric tropical and subtopical wind field
20 p3488 N85-31680
Performance of the Colorado wind-profiling network, part 1.5A 21 p3617 N85-32475
Potential advantages of the spaced antenna method for operational wind profiling, part 3.1B
21 p3620 N85-32490
High resolution evidence for the Garrett-Munk spectrum of stratospheric gravity waves 21 p3622 N85-32503
On the spectrum of atmospheric velocity fluctuations seen by MST/ST radar and their interpretation
21 p3622 N85-32504
Relationship of isolated turbulent regions to the general turbulent background, part 4.4A
21 p3623 N85-32506
Testing and optimizing MST coaxial collinear arrays, part 6.4A 21 p3625 N85-32518
Elimination of range-aliased echoes in the VHF radars
21 p3625 N85-32521
Data base for the Colorado profiling network
21 p3627 N85-32533
Recent results at the Sunset radar
21 p3627 N85-32536
Progress and plans for the Colorado Wind Profiler Network 21 p3628 N85-32542
Method and apparatus for four-beam radar
[PB85-181477] 22 p3757 N85-33299
Verification of Doppler sodar measurements — atmospheric boundary layer
[KNMI-WR-85-2] 22 p3817 N85-33645
Radar wind profilers in the Colorado network
[PB85-185486] 22 p3817 N85-33647
User's guide to the MATHEW/ADPIC models
[DE85-012952] 23 p3966 N85-34587
Determination of vertical air velocity using measurements of the aircraft motion
24 p4121 N85-35545
Control variables in vertical wind determination using simple flight-mechanical equations
24 p4121 N85-35546

WIND SHEAR
The microburst as a hazard to aviation: Structure, mechanisms, and nowcasting 01 p0074 N85-10491
Microburst wind structure and evaluation of Doppler radar for wind shear detection
[DOT/FAA/PM-84/29] 02 p0230 N85-11501
A spatial model of wind shear and turbulence for flight simulation 03 p0395 N85-12518
Wind shear measuring on board an airliner
[NASA-TM-77463] 03 p0395 N85-12521
Conditional symmetric instability and mesoscale rainbands 05 p0678 N85-14356
Jet stream errors and tropospheric-stratospheric interactions in the GLAS general circulation model
05 p0683 N85-14392
Statistics from the operation of the low-level wind shear alert system (LLWAS) during the Joint Airport Weather Studies (JAWS) Project
[DOT/FAA/PM-84/32] 06 p0750 N85-14804
Critical conditions for the automatic control of landing from decision height in variable winds
[UTIAS-284] 06 p0753 N85-14830
Combined effects of baroclinic and barotropic instability in a nonlinear low order model
[DM-41] 09 p1358 N85-18544
The effect of the arbitrary level assignment of satellite cloud motion wind vectors on wind analyses in the pre-thunderstorm environment
[NASA-TM-86186] 10 p1517 N85-19565
Wind shear detection technology
[GPO-38-920] 12 p1893 N85-21879
Intensification of tropical instabilities
[AD-A149985] 12 p1896 N85-21899
Total energy-rate feedback for automatic glide-slope tracking during wind-shear penetration
[NASA-TP-2412] 14 p2226 N85-23801
Long nonlinear waves in layers of sudden changes in wind velocity 14 p2340 N85-24470
Application of infrared radiometers for airborne detection of clear air turbulence and low level wind shear, airborne infrared low level wind shear detection test
[NASA-CR-175725] 15 p2594 N85-25965
Radar turbulence estimates. Effects of wind shear and reflectivity factor gradients
[AD-A151876] 15 p2599 N85-26023
The use of pressure sensing taps on the aircraft wing as sensor for flight control systems
16 p2698 N85-26660
Contributions on the subject of longitudinal movements of aircraft in wind shears
[NASA-TM-77837] 18 p3139 N85-29432
Effect of vertical shear on regional-scale trajectories in near-frontal conditions
[DE85-007554] 19 p3317 N85-30561
A survey of wind and turbulence modeling methods
[AD-A154470] 20 p3496 N85-31733

WIND TUNNEL APPARATUS
Preliminary results using a rapid photographic wake traverse system — in a wind tunnel
[RAE-TM-AERO-1987] 02 p0200 N85-11332
Measurement data acquisition and processing system for wind rotor measurements in the wind channel of Bremen University 05 p0668 N85-14298
Procedural aspects of testing aerodynamic models with combustion in high-enthalpy transient-mode installations
05 p0725 N85-14658
Analytical and physical modeling program for the NASA Lewis Research Center's Altitude Wind Tunnel (AWT)
[NASA-TM-86919] 07 p0909 N85-15757
The NASA Altitude Wind Tunnel (AWT): Its role in advanced icing research and development
[NASA-TM-86920] 07 p0910 N85-15758
Six-component strain gage block scale 167-6B. Part 1: Calibration, September 1983
[F+W-FO-1699] 07 p0968 N85-16143
Numerical analysis of the first static calibration of the RSRA helicopter active-isolator rotor balance system
[NASA-TM-86975] 08 p1063 N85-16863
A new fast response probe for diffusion studies in atmospheric air — pollution modeling
[IC-AERO-84-01] 08 p1180 N85-17437

The S2MA wind tunnel at the Modane-Avrieux aerodynamic test center
[ESA-TT-862] 09 p1284 N85-18071
Development of an artificial boundary layer for different outlet flows 14 p2212 N85-23719
Investigation of the conditions for tripping transition with roughness elements and their influence on boundary layer development 14 p2212 N85-23720
Transition detection using surface pressure holes
14 p2212 N85-23722
Investigations of the experimental detection of boundary layer transitions 14 p2213 N85-23723
Prediction of vortex-induced loads on wind-tunnel turning vanes
[NASA-TM-86678] 15 p2462 N85-25204
The ONERA establishment at Cannes in the service of aeronautical research
[ESA-TT-875] 15 p2475 N85-25276
Qualification of a wall gage for the SIMA wagon, adapted to the test of half models motorized by compressed air turbines — SIMA wind tunnel
[ONERA-PV-1/8068-GY] 16 p2701 N85-26677
Study on needs for a magnetic suspension system operating with a transonic wind tunnel
[NASA-CR-3800] 16 p2715 N85-26759
An automatic traversing system for Laser Doppler Anemometer (LDA) applications to wind tunnels and to free jets
[ISL-CO-225/83] 16 p2836 N85-27490
Construction 1976-1980: Design, manufacturing, calibration of the German-Dutch wind tunnel (DNW)
17 p2905 N85-27913
Effect of superconducting solenoid model cores on spanwise iron magnet roll control
[NASA-TM-86378] 17 p2905 N85-27915
Cryogenic test technology, 1984
[AGARD-AR-212] 18 p3088 N85-29116
A computer-controlled traverse gear for the Oxford wind engineering research group's 4 metre x 2 metre wind tunnel
[OUEL-1525/84] 20 p3463 N85-31514
Gust simulation for flight mechanical wind tunnel tests
24 p4062 N85-35172

WIND TUNNEL BALANCES
U WEIGHT INDICATORS
U WIND TUNNEL APPARATUS

WIND TUNNEL CALIBRATION
Wind tunnel calibration of a hemispherical head angle of attack and angle of sideslip indicator
[FFA-TN-1984-11] 02 p0135 N85-10923
Langley Mach 4 scramjet test facility
[NASA-TM-86277] 08 p1089 N85-16883
Calibration of wind tunnel flow quality
13 p1976 N85-22399
A preliminary investigation of the dynamic force-calibration of a magnetic suspension and balance system
[NASA-CR-172580] 14 p2228 N85-23808

WIND TUNNEL MODELS
Pressure distributions measured on research wing M100 mounted on an axisymmetric body
01 p0004 N85-10023
Problem of reduction to ideal wind tunnel in experimental aerodynamics 02 p0260 N85-11702
An appraisal of an out-of-phase feed-back system for the variation of damping of dynamic wind-tunnel models
[NMI-189] 03 p0320 N85-12065
Singularity model for the analysis of wall interference in closed wind tunnels according to the wall pressure signature method (blockage and lift)
[FW-FO-1612] 04 p0453 N85-12874
Comparative flow calculation on transonic cone/cylinder standard models in connection with the wall interference problem
[FW-FO-1689] 04 p0453 N85-12878
Manufacturing report of an augmented lift, variable deflection half wing
[ONERA-RT-25/1736-AY-108-A]
05 p0581 N85-13766
Procedural aspects of testing aerodynamic models with combustion in high-enthalpy transient-mode installations
05 p0725 N85-14858
A preliminary study of using a strain-gauged balance and parameter estimation techniques for the determination of aerodynamic forces on a model in a very short duration wind tunnel
[AD-A146473] 06 p0810 N85-15145
Analysis of the flow field about a T-45 using PANAIR
[AD-A146811] 07 p0889 N85-15699
Experiences with the use of a side-strut model support system for high angles of attack in the Trinsonik wind tunnel TMK
[DFVLR-MITT-84-09] 07 p0910 N85-15763
Joined wing transonic design and test validation
[AD-A148355] 08 p1078 N85-16834
A voice-actuated wind tunnel model leak checking system
[NASA-TM-86359] 09 p1263 N85-17936
The generation of rolling moments with the superconducting solenoid model
[NASA-CR-172520] 09 p1283 N85-18068
Initial investigation of cryogenic wind tunnel model filler materials
[NASA-TM-86363] 09 p1283 N85-18069
Unsteady transonic pressure measurements on a semispan wind-tunnel model of a transport-type supercritical wing (Lann model). Part 2: Pressure distributions (plotted) and plots of the vibration modes
[AD-A130488] 10 p1421 N85-18965
Wall interference estimation of the NAL's two-dimensional wind tunnel
[NAL-TR-829] 10 p1426 N85-18992
Flight mechanics analysis of dynamic derivatives of the Dornier variable wind tunnel model
[ESA-TT-854] 11 p1577 N85-19937
Technology for pressure-instrumented thin airfoil models, phase 1
[NASA-CR-3891] 14 p2227 N85-23804
An exploratory study of apex fence flaps on a 74 deg delta wing
[NASA-CR-172483] 15 p2463 N85-25206
The design and operation of a simple low-speed flutter-suppression model
[AD-A151610] 15 p2474 N85-25269
Synthesis study: Validation of a gust generator in the presence of a model in a wind tunnel
[ONERA-RT-16/5108-RY-051]
16 p2701 N85-26678
The application of numerical control (NC) in manufacturing wind tunnel models
[B8580078] 17 p2939 N85-28140
Analysis of heat-transfer measurements from 2 AEDC wind tunnels on the Shuttle external tank
[NASA-CR-171470] 17 p2957 N85-28263
Heating parameter estimation using coaxial thermocouple gages in wind tunnel test articles
[AD-A153039] 17 p2968 N85-28328
Materials and techniques for model construction
[NASA-CR-172620] 20 p3396 N85-31066
Experiences with the use of a side-strut model support system for high angles for attack in the TMK Trinsonik Wind Tunnel
[ESA-TT-895] 20 p3396 N85-31069
Preliminary investigation of dispersion of pollutants in model building wake flows using bipolar space charge
[IC-AERO-84-04] 20 p3487 N85-31671
A systematic plan for the continued study of dimensional stability of metallic alloys considered for the fabrication of cryogenic wind tunnel models
[NASA-CR-172449] 21 p3565 N85-32172
Machining-induced deformation in stepped specimens of PH 13-8 Mo, 18 nickel maraging steel grade 200T1 and grain-refined HP 9-4-20
[NASA-CR-172450] 21 p3565 N85-32177
Two-plane balance and slip-ring design
22 p3799 N85-33536

WIND TUNNEL STABILITY TESTS
Experimental and theoretical determination of the wing-induced lateral wind on the tail surfaces in oscillating rolling motion. Part 1: Application of the Mobile Oscillating Derivatives (MOD) on an experimental part
[IFD-1/84-PT-1] 18 p3061 N85-28839

WIND TUNNEL TESTS
Transonic wing and far field test data on a high aspect ratio transport wing for three dimensional computational method evaluation 01 p0004 N85-10021
Transonic wing and far field test data on a moderate aspect ratio wing for three dimensional computational method evaluation 01 p0004 N85-10022
Pressure distributions measured on research wing M100 mounted on an axisymmetric body
01 p0004 N85-10023
Pressure distributions measured on research wing M86 mounted on an axisymmetric body
01 p0004 N85-10024
DFVLR rotorcraft: Construction and engineering
[NASA-TM-77740] 01 p0006 N85-10035
Results of tests of advanced flexible insulation vortex and flow environments in the North American Aerodynamics Laboratory lowspeed wind tunnel using 0.0405-scale Space Shuttle Orbiter model 16-0 (test OA-309)
[NASA-CR-167692] 01 p0015 N85-10096
Planer jets impinging on various obstacles and some modes of flow oscillation
[MPIS-MITT-78] 01 p0048 N85-10317
Data input, processing and presentation — helicopter rotor balance measurement
[NASA-TM-77739] 01 p0125 N85-10856
Design and wind tunnel evaluation of a symmetric airfoil series for large wind turbine applications
[NASA-CR-174784] 02 p0135 N85-10919
Results of winglet development studies for DC-10 derivatives
[NASA-CR-3677] 02 p0138 N85-10936
Space Shuttle wind tunnel testing program
[NASA-RP-1125] 02 p0167 N85-11127
Experimental study of Mach reflection of weak shock waves 02 p0260 N85-11703
Analysis of noise measured from a propeller in a wake
[NASA-TP-2358] 02 p0274 N85-11786
Wall interference measurements for three-dimensional models in transonic wind tunnels: Experimental difficulties 03 p0311 N85-12012
Survey of ONERA activities on adaptive-wall applications and computation of residual corrections
03 p0312 N85-12013
Assessment of lift- and blockage-induced wall interference in a three-dimensional adaptive-wall tunnel
03 p0312 N85-12016
Wind tunnel wall interference correction for aircraft models 03 p0314 N85-12029
Determination of equivalent model geometry for tunnel wall interference assessment/correction
03 p0314 N85-12031
Experiences with a high-blockage model tested in the NASA Ames 12-foot pressure wind tunnel
03 p0315 N85-12032
Experimental and predicted heating distributions for biconics at incidence in air at Mach 10
[NASA-TP-2334] 03 p0361 N85-12313
Laser anemometer study of separated flow on wing profiles
[ISL-CO-214/83] 04 p0453 N85-12872
Wall adaptation at Mach 1.2 — wind tunnel tests
[ONERA-RTS-26/3075-AY-402]
04 p0453 N85-12873
Singularity model for the analysis of wall interference in closed wind tunnels according to the wall pressure signature method (blockage and lift)
[FW-FO-1612] 04 p0453 N85-12874
Wall influence corrections in wind tunnels: Blockage correction according to the wall pressure signature method
[FW-FO-1613] 04 p0453 N85-12875
Parametric determination of blockage interference of 3-dimensional models in the Emmen Federal Aircraft works transonic tunnel (Switzerland)
[FW-FO-1636] 04 p0453 N85-12876
Investigations of boundary layers in the Emmen Federal Aircraft works transonic tunnel, Switzerland
[FW-FO-1641] 04 p0453 N85-12877
Comparative flow calculation on transonic cone/cylinder standard models in connection with the wall interference problem
[FW-FO-1689] 04 p0453 N85-12878
Flight and wind-tunnel comparisons of the inlet-airframe interaction of the F-15 airplane
[NASA-TP-2374] 04 p0455 N85-12884
Evaluation of the Langley 4- by 7-meter tunnel for propeller noise measurements
[NASA-TM-85721] 04 p0558 N85-13553
First cryogenic test of the CAST 7 profile in the T2 wind tunnel. Comparison with calculations — airfoils
[ONERA-RTS-58/1685-AY-035-D]
04 p0577 N85-13682
Amiet shear layer correction with an additional temperature gradient considered: Nomograms for the correction of noise signatures from open jet wind tunnel tests
[DFVLR-MITT-84-11] 05 p0726 N85-14869
Static internal performance of single-expansion-ramp nozzles with various combinations of internal geometric parameters
[NASA-TM-86270] 06 p0749 N85-14797
A preliminary study of using a strain-gauged balance and parameter estimation techniques for the determination of aerodynamic forces on a model in a very short duration wind tunnel
[AD-A146473] 06 p0810 N85-15145
Effects of body shape on the aerodynamics of a body of revolution at Mach numbers from 1.6 to 4.6
[NASA-TM-86345] 07 p0893 N85-15657
Analytical modeling of circuit aerodynamics in the new NASA Lewis wind tunnel
[NASA-TM-86912] 07 p0897 N85-15688
Aileron effectiveness for a subsonic transport model with a high-aspect-ratio supercritical wing
[NASA-TM-85674] 07 p0898 N85-15695
The UH-1H helicopter icing flight test program: An overview
[NASA-TM-86925] 07 p0900 N85-15702
Installed nacelle drag-improvement tests of an M = 0.8 turboprop transport configuration
[NASA-TM-84302] 07 p0902 N85-15716

Analytical and physical modeling program for the NASA Lewis Research Center's Altitude Wind Tunnel (AWT)
[NASA-TM-86919] 07 p0909 N85-15757

The NASA Altitude Wind Tunnel (AWT): Its role in advanced icing research and development
[NASA-TM-86920] 07 p0910 N85-15758

Stereo Electro-optical Tracking System (SETS)
[NASA-CR-172471] 07 p0962 N85-16098

Investigations into the effects of scale and compressibility on lift and drag in the RAE 5m pressurized low-speed wind tunnel 08 p1066 N85-16773

Results of S5 CH tests with an ARL (Aerospace Research Laboratory) cascade
[NASA-TM-77510] 08 p1069 N85-16882

A wind-tunnel study of the saltation of heterogeneous (size, density) sands 08 p1182 N85-17449

Research done at DERAT (October 1982 through September 1983); summary of principal results obtained
[NASA-TM-77766] 08 p1228 N85-17730

Corrections for attached sidewall boundary-layer effects in 2-dimensional airfoil testing
[NASA-CR-3873] 09 p1272 N85-17997

Effect of jet exit vanes on flow pulsations in an open-jet wind tunnel
[NASA-TM-86299] 09 p1273 N85-17999

Subsonic and transonic pressure measurements on a high-aspect-ratio supercritical-wing model with oscillating control surfaces
[NASA-TM-83201] 09 p1273 N85-18004

The Altitude Wind Tunnel (AWT): A unique facility for propulsion system and adverse weather testing
[NASA-TM-86921] 09 p1283 N85-18067

Static internal performance of a two-dimensional convergent nozzle with thrust-vectoring capability up to 60 deg
[NASA-TP-2391] 10 p1419 N85-18951

Space Shuttle Orbiter trimmed center-of-gravity extension study. Volume 9: Effects of configuration modifications on the aerodynamic characteristics of the 140 A/B Orbiter at Mach numbers of 1.5, 2.0, and 2.5 — wind tunnel tests
[NASA-TM-72861-VOL-9] 10 p1420 N85-18956

Unsteady transonic pressure measurements on a semispan wind-tunnel model of a transport-type supercritical wing (Lann model). Part 2: Pressure distributions (plotted) and plots of the vibration modes
[AD-A130488] 10 p1421 N85-18965

Low-speed wind tunnel tests of the NAL fan-jet STOL research aircraft model with ground simulation by tangential blowing
[NAL-TR-828] 10 p1423 N85-18976

Study of several factors affecting crew escape trajectories from the Space Shuttle Orbiter at low-subsonic speeds
[NASA-TM-86303] 10 p1428 N85-19008

Post stall airfoil data for wind turbines: Wind tunnel test results
[DE85-004052] 10 p1511 N85-19534

Fluctuating pressures on fan blades of a turbofan engine, flight test investigation
[NASA-TP-2381] 10 p1553 N85-19790

Wind-tunnel investigation of a full-scale canard-configured general aviation airplane
[NASA-TP-2382] 11 p1575 N85-19925

Flight mechanics analysis of dynamic derivatives of the Dornier variable wind tunnel model
[ESA-TT-854] 11 p1577 N85-19937

Unsteady aerodynamic characterization of a military aircraft in vertical gusts
[NASA-TM-77810] 12 p1770 N85-21110

Measured unsteady transonic aerodynamic characteristics of an elastic supercritical wing with an oscillating control surface
[NASA-TM-86376] 12 p1771 N85-21116

Unsteady transonic pressure measurements on a semi-span wind-tunnel model of a transport-type supercritical wing (Lann model). Part 2: Pressure distributions (plotted) and plots of the vibration modes
[AD-A130488] 12 p1846 N85-21579

Exploratory flutter test in a cryogenic wind tunnel
[NASA-TM-86380] 12 p1863 N85-21689

Further comparison of wind tunnel and airplane acoustic data for advanced design high speed propeller models
[NASA-TM-86935] 12 p1927 N85-22108

Dynamic wind tunnel testing for active control research 13 p1966 N85-22352

Dynamic wind-tunnel testing of active controls by the NASA Langley Research Center
13 p1966 N85-22353

Effects of leading-edge devices on the low-speed aerodynamic characteristics of a highly-swept arrow-wing
[NASA-CR-172531] 13 p1968 N85-22365

Investigations into the effects of scale and compressibility on lift and drag in the RAE 5m pressurised low-speed wind tunnel
[RAE-TM-AERO-2006] 13 p1969 N85-22372

Deflected jet experiments in a turbulent combustor flowfield
[NASA-CR-174863] 13 p1973 N85-22390

Cryogenic wind tunnels: A selected annotated bibliography
[NASA-TM-86346] 13 p1976 N85-22401

Results of aeroheating DFI and ET design-data test on a 0.0175-scale model 60-OTS conducted in the Von Karman Gas Dynamics Facility (VKF) 40' supersonic and the 50' hypersonic wind tunnels A and C
[NASA-CR-167693] 13 p1988 N85-22466

Results of the AFRSI rewaterproofing systems screening test in the NASA/Ames Research Center (ARC) 2 x 2-foot transonic wind tunnel
[NASA-CR-167694] 13 p1988 N85-22467

Results of a M = 5.3 heat transfer test of the integrated vehicle using phase-change paint techniques on the 0.0175-scale model 56-OTS in the NASA/Ames Research Center 3.5-foot hypersonic wind tunnel
[NASA-CR-167695] 13 p1988 N85-22468

CARD's low-speed wind tunnel described
13 p2052 N85-22849

Wind tunnel acoustic study of a propeller installed behind an airplane empennage: Data report
[NASA-CR-177335] 13 p2154 N85-23377

The effect of particle density on aeolian transport
13 p2189 N85-23581

Potential bedforms on Venus: Wind tunnel simulations
13 p2189 N85-23583

Microdunes and other aeolian bedforms on Venus: Wind tunnel simulations 13 p2189 N85-23584

Estimating unsteady aerodynamic forces on a cascade in a three-dimensional turbulence field
[NASA-TM-86701] 14 p2209 N85-23704

Low-speed stability and control wind-tunnel investigations of effects of spanwise blowing on fighter flight characteristics at high angles of attack — Langely 12-ft low-speed tunnel and 30- by 60-ft tunnel
[NASA-TP-2431] 14 p2210 N85-23706

Recent transonic unsteady pressure measurements at the NASA Langley Research Center
[NASA-TM-86408] 14 p2210 N85-23710

Boundary layer control by transition fixing — conference
[DFVLR-MITT-84-17] 14 p2211 N85-23712

Problems of the application of wind tunnel results to aerodynamic performance of large aircraft
14 p2211 N85-23713

Transition fixing on wings in industrial wind tunnels and associated problems 14 p2212 N85-23717

Transition detection using surface pressure holes
14 p2212 N85-23722

Investigations of the experimental detection of boundary layer transitions 14 p2213 N85-23723

Investigation of the aerodynamic forces on bluff bodies at high Reynolds numbers
[DFVLR-MITT-84-19] 14 p2213 N85-23727

Qualification of the T2 wind tunnel in cryogenic operation. B: Flow fluctuations, particle detection and qualification
[NASA-TM-77782] 14 p2227 N85-23806

Space Shuttle aerothermodynamic data report, phase C
[NASA-CR-171858] 14 p2241 N85-23897

China report: Science and technology
[JPRS-CST-84-012] 14 p2283 N85-24140

Harbin's subsonic, transonic wind tunnel detailed
14 p2283 N85-24143

Transonic pressure distributions on a two-dimensional 0012 and supercritical MBB-A3 profile oscillating in heave and pitch 15 p2457 N85-25173

Analysis of transonic aerodynamic characteristics for a supercritical airfoil oscillating in heave, pitch and with oscillating flap 15 p2458 N85-25175

An exploratory study of apex fence flaps on a 74 deg delta wing
[NASA-CR-172483] 15 p2463 N85-25208

Investigation of the Vortex Tab
[NASA-CR-172586] 15 p2463 N85-25209

Behavior of turbulent gas jets in an axisymmetric confinement
[NASA-CR-174829] 15 p2473 N85-25265

Experiments in dilution jet mixing effects of multiple rows and non-circular orifices
[NASA-TM-86996] 15 p2473 N85-25266

The ONERA establishment at Cannes in the service of aeronautical research
[ESA-TT-875] 15 p2475 N85-25276

An evaluation of proposed acoustic treatments for the NASA LaRC 4 x 7 meter wind tunnel
[NASA-CR-172577] 15 p2646 N85-26319

La Recherche Aerospatiale Bimonthly Bulletin Number 1984-2, 219/March-April
[ESA-TT-879] 16 p2694 N85-26635

Low Reynolds number vehicles
[AGARD-AG-288] 16 p2699 N85-26666

Exploratory wind-tunnel investigation of a wingtip-mounted vortex turbine for vortex energy recovery
[NASA-TP-2468] 16 p2699 N85-26667

An experimental and analytical study of the aerodynamic interference effects between two Sears-Haack bodies at Mach 2.7
[NASA-TM-85729] 16 p2700 N85-26673

Measurements of the symmetric aerodynamic coefficients for flat faced cylinders in the angle of attack regime 0 to 90 deg for transonic and supersonic speeds
[FFA-TN-1984-04] 16 p2700 N85-26675

Measurements in low pressure flow using an electronic beam detector — wind tunnel tests
16 p2701 N85-26676

Synthesis study: Validation of a gust generator in the presence of a model in a wind tunnel
[ONERA-RT-16/5108-RY-051]
16 p2701 N85-26678

Preliminary wind tunnel study of the influence of a jet on the unsteady aerodynamics of a turbojet engine
[ONERA-RT-12/5115-RY-230-R-231G]
16 p2701 N85-26679

Wing buffeting active control testing on a transport aircraft configuration in a large sonic tunnel
16 p2714 N85-26750

An experimental study of compressible turbulent reattaching free shear layers 16 p2761 N85-27161

Wing tunnel investigation of dynamic stall of an NACA 0018 airfoil oscillating in pitch
[NAE-AN-27] 17 p2892 N85-27830

Design of a basic profile for a low sweep airfoil. Part 2: Experimental investigation on the DFVLR-W1 airfoil profile in the Brunswick transonic wind tunnel
[DFVLR-FB-85-01-PT-2] 17 p2892 N85-27833

Rotorcraft research testing in the National Full-Scale Aerodynamics Complex at NASA Ames Research Center
[NASA-TM-86687] 17 p2896 N85-27854

Wing buffeting active control testing on a transport aircraft configuration in a large sonic windtunnel
17 p2904 N85-27903

Background noise measurements from jet exit vanes designed to reduced flow pulsations in an open-jet wind tunnel
[NASA-TM-86383] 17 p2906 N85-27916

The gust simulation apparatus of the 3m x 3m low speed wind tunnel of the DFVLR in Goettingen, West Germany
[DFVLR-FB-85-04] 17 p2906 N85-27920

Analysis of heat-transfer measurements from 2 AEDC wind tunnels on the Shuttle external tank
[NASA-CR-171470] 17 p2957 N85-28263

Heating parameter estimation using coaxial thermocouple gages in wind tunnel test articles
[AD-A153039] 17 p2968 N85-28328

Wind-tunnel evaluation of a 21-percent-scale powered model of a prototype advanced scout helicopter
[NASA-TP-2420] 18 p3056 N85-28923

Static investigation of several yaw vectoring concepts on nonaxisymmetric nozzles
[NASA-TP-2432] 18 p3058 N85-28924

Gust load alleviation of a cantilevered rectangular elastic wing. Wind tunnel experiment and analysis
[NAK-TR-86] 18 p3063 N85-28950

Cryogenic test technology, 1984
[AGARD-AR-212] 18 p3088 N85-29116

Activities of the Department of Aerospace Engineering
18 p3199 N85-29844

Inviscid analysis of two supercritical laminar-flow-control airfoils at design and off-design conditions
[NASA-TM-84657] 19 p3212 N85-29920

Effect of leading-edge load constraints on the design and performance of supersonic wings
[NASA-TP-2446] 19 p3213 N85-29923

Nacelle/pylon/wing integration on a transport model with a natural laminar flow nacelle
[NASA-TP-2439] 19 p3213 N85-29924

High Reynolds number tests of a NASA SC(3)-0712(B) airfoil in the Langley 0.3-meter transonic cryogenic tunnel
[NASA-TM-86371] 19 p3213 N85-29926

Pressure distribution from high Reynolds number tests of a NASA SC(3)-0712(B) airfoil in the Langley 0.3-meter transonic cryogenic tunnel
[NASA-TM-86370] 19 p3213 N85-29927

Low-speed wind-tunnel tests of an advanced eight-bladed propeller
[NASA-TM-86364] 19 p3214 N85-29928

A numerical solution of a nonisothermal wall using the two-dimensional Navier-Stokes equations
[AD-A1[illegible]167] 19 p3266 N85-30257

Acrosswind response of towers and stacks of circular cross-section 19 p3282 N85-30354

Selected topics in experimental aeroelasticity at the NASA Langley Research Center
[NASA-TM-86436] 19 p3284 N85-30364

Computer program for plotting and fairing wind-tunnel data
[NASA-TM-85848] 20 p3387 N85-31009

Low-speed tests of a high-aspect-ratio, supercritical-wing transport model equipped with a high-lift flap system in the Langley 4- by 7-meter and Ames 12-foot pressure tunnels
[NASA-TP-2097] 20 p3388 N85-31010

Real scale test of the Petit Canard aircraft in the number 3 section, 47 sqm, of the SIMA wind tunnel, May 1984
[ONERA-PV-1/0772-GY] 20 p3389 N85-31016

Aerodynamic measurement of the wind flow in the number two section of the SIMA wind tunnel
[ONERA-PV-1/8136-GY] 20 p3389 N85-31019

Transonic and supersonic wind tunnel tests on control effectiveness on schematic missile configurations
[FFA-TN-1983-20] 20 p3389 N85-31020

Transonic and supersonic wind tunnel tests on control effectiveness on schematic missile configurations: Supplement
[FFA-TN-1983-20-SUPPL] 20 p3389 N85-31021

Data set 8: ZKP wing, oscillating aileron
20 p3390 N85-31029

Reverberation effects on directionality and response of stationary monopole and dipole sources in a wind tunnel
[NASA-TM-87063] 20 p3453 N85-31443

Preliminary wind tunnel experiments to investigate the effect of heat transfer on the dispersion of cold dense gases
[OUEL-1546/84] 20 p3456 N85-31467

Amiet shear layer correction with an additional temperature gradient considered: Nomograms for the correction of noise signatures from open jet wind tunnel tests
[ESA-TT-897] 20 p3525 N85-31826

Aerodynamic characteristics of the standard dynamics model in coning motion at Mach 0.6
[NASA-TM-86717] 21 p3552 N85-32094

Wind tunnel drag evaluations of helicopter nose sections
[AD-A155489] 21 p3553 N85-32100

The collected data for ramp function tests on a NACA 23012 aerofoil. Volume 1: Description and pressure data
[GU-AERO-8413-VOL-1] 23 p3894 N85-34123

An investigation into the three-dimensional stall development on a modified NACA 23012 aerofoil
[GU-AERO-8414] 23 p3894 N85-34124

Prediction of the flow-field interference induced by the long-range laser velocimeter in the Ames 40- by 80-foot and the 80- by 120-foot wind tunnels
[NASA-TM-86763] 23 p3896 N85-34146

Reflection plane tests of a wind turbine blade tip section with ailerons
[NASA-TM-87018] 23 p3945 N85-34444

Presentation of the acoustic and aerodynamic results of the Aladin 2 concept qualification testing
[NASA-TM-77863] 24 p4060 N85-35161

Gust simulation for flight mechanical wind tunnel tests
24 p4062 N85-35172

The influence of helicopter tail shape on drag: An aerodynamic study using a low speed wind tunnel
[AD-A158304] 24 p4062 N85-35174

Miniature infra-red data acquisition and telemetry system
[NASA-CR-177953] 24 p4096 N85-35390

WIND TUNNEL WALLS

Wind Tunnel Wall Interference Assessment and Correction, 1983
[NASA-CP-2319] 03 p0311 N85-12011

Wall interference measurements for three-dimensional models in transonic wind tunnels: Experimental difficulties 03 p0311 N85-12012

Survey of ONERA activities on adaptive-wall applications and computation of residual corrections
03 p0312 N85-12013

Wind tunnel wall interference in closed, ventilated and adaptive test sections 03 p0312 N85-12014

Two- and three-dimensional model and wall data from a flexible-walled transonic test section
03 p0312 N85-12015

Assessment of lift- and blockage-induced wall interference in a three-dimensional adaptive-wall tunnel
03 p0312 N85-12016

A data base for three-dimensional all-interference code evaluation 03 p0312 N85-12017

Effect of upstream sidewall boundary layer removal on an airfoil test — conducted in Langley 0.3-m transonic cryogenic tunnel 03 p0313 N85-12019

Experiments suitable for wind tunnel wall interference assessment/correction 03 p0313 N85-12021

Asymptotic methods for wind tunnel wall corrections at transonic speed 03 p0313 N85-12022

Effect of boundary layers on solid walls in three-dimensional subsonic wind tunnels
03 p0313 N85-12023

NLR activities in the field of wind tunnel wall interference 03 p0313 N85-12024

Progress in wind tunnel wall interference assessment/correction procedures at the NAE
03 p0314 N85-12025

Development in UK of a method for calculating tunnel wall corrections from flow measurements
03 p0314 N85-12026

Tunnel constraint for a jet in crossflow
03 p0314 N85-12027

Interference from slotted walls
03 p0314 N85-12028

Adaptation of a four-wall interference assessment/correction procedure for airfoil tests in the 0.3-m TCT 03 p0315 N85-12035

Minimization of wall interference for three-dimensional models with two-dimensional wall adaptation — wind tunnel walls
[VKI-TN-149] 03 p0321 N85-12070

Wall adaptation at Mach 1.2 — wind tunnel tests
[ONERA-RTS-26/3075-AY-402]
04 p0453 N85-12873

Singularity model for the analysis of wall interference in closed wind tunnels according to the wall pressure signature method (blockage and lift)
[FW-FO-1612] 04 p0453 N85-12874

Wall influence corrections in wind tunnels: Blockage correction according to the wall pressure signature method
[FW-FO-1613] 04 p0453 N85-12875

Parametric determination of blockage interference of 3-dimensional models in the Emmen Federal Aircraft works transonic tunnel (Switzerland)
[FW-FO-1636] 04 p0453 N85-12876

A local slot boundary condition for transonic flow calculations in slotted-wall test sections of wind tunnels
[FFA-TN-1984-34] 04 p0453 N85-12879

On the relaxation of a turbulent boundary layer after an encounter with a forward facing step
06 p1071 N85-16789

Wall interference estimation of the NAL's two-dimensional wind tunnel
[NAL-TR-829] 10 p1426 N85-18992

Aerodynamic behavior of ventilated wind tunnel walls
13 p1966 N85-22363

Unsteady gas dynamics problems related to flight vehicles
[AD-A151167] 15 p2464 N85-25218

Wind tunnel wall interference
[AD-A151212] 15 p2474 N85-25273

A curved test section for research on transonic shock wave-boundary layer interaction
[VTH-LR-414] 16 p2701 N85-26682

Adaptive wall wind tunnels and wall interference correction methods
[DFVLR-IB-222-84-A-37] 17 p2905 N85-27912

Effect of ground and/or ceiling planes on thrust of rotors in hover
[NASA-TM-86754] 20 p3388 N85-31014

Reverberation effects on directionality and response of stationary monopole and dipole sources in a wind tunnel
[NASA-TM-87063] 20 p3453 N85-31443

WIND TUNNELS

NT BLOWDOWN WIND TUNNELS
NT CASCADE WIND TUNNELS
NT CRYOGENIC WIND TUNNELS
NT HYPERSONIC WIND TUNNELS
NT LOW SPEED WIND TUNNELS
NT SLOTTED WIND TUNNELS
NT SUBSONIC WIND TUNNELS
NT SUPERSONIC WIND TUNNELS
NT TRANSONIC WIND TUNNELS

Investigations of boundary layers in the Emmen Federal Aircraft works transonic tunnel, Switzerland
[FW-FO-1641] 04 p0453 N85-12877

Evaluation of the Langley 4- by 7-meter tunnel for propeller noise measurements
[NASA-TM-85721] 04 p0558 N85-13553

Sources, paths, and concepts for reduction of noise in the test section of the NASA Langley 4x7m wind tunnel
[NASA-CR-172446-VOL-1] 05 p0726 N85-14866

Comparison of options for reduction of noise in the test section of the NASA Langley 4x7m wind tunnel, including reduction of nozzle area
[NASA-CR-172446-VOL-2] 05 p0726 N85-14867

Ultrasound instrumentation for the 7 inch Mach seven tunnel
[NASA-CR-174277] 07 p1036 N85-16586

On relaxation of transonic flows around zero-lift airfoils and convergence of self-correcting wing tunnels
11 p1622 N85-20214

The ONERA establishment at Cannes in the service of aeronautical research
[ESA-TT-875] 16 p2475 N85-25276

Post-stall wind tunnel data for NACA 44XX series airfoil sections
[DE85-002048] 18 p3060 N85-28931

Vapor-screen technique for flow visualization in the Langley Unitary Plan Wind Tunnel
[NASA-TM-86384] 19 p3214 N85-29929

Practical aspects of laser holographic interferometry in wind tunnels
[NASA-TM-86786] 23 p3933 N85-34378

Langley aeronautics and space test highlights, 1984
[NASA-TM-87585] 23 p4057 N85-35151

WIND TURBINES

Some considerations on Aeroelastic instabilities caused by coupling between propeller-type rotor and its supporting structure
[NAL-TR-804] 01 p0003 N85-10013

Variable geometry Darrieus wind machine
[PB84-207281] 01 p0068 N85-10453

Design and wind tunnel evaluation of a symmetric airfoil series for large wind turbine applications
[NASA-CR-174764] 02 p0135 N85-10919

Aileron controls for wind turbine applications
[NASA-TM-86867] 02 p0222 N85-11458

Development and demonstration of a vertical axis wind turbine POWERHOUSE
[DE84-901449] 04 p0527 N85-13369

Tailored airfoils for vertical axis wind turbines
[DE84-013618] 04 p0529 N85-13380

Analysis of wind energy systems for selected electric utilities
[DE84-013025] 04 p0530 N85-13389

Meteorological analysis for clusters of wind turbines
[DE84-013164] 04 p0539 N85-13425

Subhourly wind forecasting techniques for wind turbine operations
[DE84-016205] 04 p0539 N85-13427

Development and verification of MOD-2 and MOD-OA simulation models
[DE84-017369] 04 p0550 N85-13499

Response measurements for two building structures excited by noise from a large horizontal axis wind turbine generator
[NASA-CR-172482] 04 p0558 N85-13552

Evaluation of the unsteady effects for a class of wind turbines 05 p0592 N85-13772

Measurement-Technical Investigations of Wind Energy Units
[JUEL-SPEZ-244] 05 p0667 N85-14293

Measurement-technical investigations of wind energy units in the short-time range — spectrum analysis
05 p0668 N85-14294

Measurement-technical problems in the investigation of wind energy units 05 p0668 N85-14295

VOITH: Wind energy converter WEC 520
05 p0668 N85-14299

Shutdown characteristics of the Mod-O wind turbine with aileron controls
[NASA-TM-86918] 07 p0992 N85-16299

Development of large wind energy power generation system
[NASA-TM-77779] 07 p0992 N85-16301

Design criteria for small wind turbines
[NLR-MP-83054-U] 07 p0994 N85-16310

Verification of the fatigue properties of (small) wind turbines
[NLR-MP-83055-U] 07 p0994 N85-16311

Detection of low frequency impulsive noise from large wind turbine generators
[NASA-CR-172511] 07 p1038 N85-16566

Blade technology program for large wind turbines, phase 1
[BMFT-FB-T-84-217] 08 p1179 N85-17426

Life assessment and damage tolerance of wind turbines
[AD-B088148L] 08 p1179 N85-17427

Modeling stochastic wind loads on vertical axis wind turbines
[DE85-001148] 09 p1340 N85-18426

Preliminary survey of wind generation in Washington: Site studies and selected wind speed data
[DE85-000058] 09 p1345 N85-18462

Variable speed generator technology options for wind turbine generators
[RR-84-4] 10 p1478 N85-19331

Post stall airfoil data for wind turbines: Wind tunnel test results
[DE85-004052] 10 p1511 N85-19534

Rocky Flats Wind Energy Research Center FY 1983 report
[DE85-004500] 10 p1511 N85-19535

Mini-model testing of wind turbines using novel excitation
[DE85-000666] 11 p1654 N85-20417

Improved models for increasing wind penetration, economics and operating reliability
[NASA-CR-175536] 11 p1674 N85-20545

Tailored airfoils for vertical axis wind turbines
[DE85-004628] 12 p1772 N85-21128

Computer analysis of wind turbine blade dynamic loads
[DE85-000530] 12 p1867 N85-21714

Aerodynamic research efforts at SERI Wind Energy Research Center at Rocky Flats
[DE85-000529] 12 p1881 N85-21805

Development of large, horizontal-axis wind turbines
[NASA-TM-86950] 13 p2128 N85-23242

Structural design of the Sandia 34-M Vertical Axis Wind Turbine
[DE85-002631] 13 p2129 N85-23247

Investigation of doubly-fed machine in variable speed application
[DE85-004378] 14 p2299 N85-24234

Sound propagation studies for a large horizontal axis wind turbine
[NASA-CR-172564] 14 p2415 N85-24904

NASTRAN-based software for the structural dynamic analysis of vertical and horizontal axis wind turbines
[DE85-001712] 15 p2580 N85-25911

Inviscid upwind finite difference model for two dimensional vertical axis wind turbines
15 p2585 N85-25933

A novel type of stayed tower for wind turbines
[ISD-295] 15 p2587 N85-25952

Response of a wind turbine blade to seismic and turbulent wind excitations 16 p2817 N85-27375

Effect of precipitation on wind turbine performance
[NASA-TM-86986] 16 p2818 N85-27385

Transient behavior of a single-blade horizontal-axis wind turbine
[MBB-UD-421/84-O] 16 p2875 N85-27737

Wind energy systems: Program summary for fiscal year, 1983
[DE85-002927] 17 p2985 N85-28451

Field test report of the Department of Energy's 100-kW vertical axis wind turbine
[DE85-006475] 17 p2987 N85-28458

A 5-year research plan, 1985-1990. Wind energy technology: Generating power from the wind
[DE85-006427] 17 p2987 N85-28463

Post-stall wind tunnel data for NACA 44XX series airfoil sections
[DE85-002948] 18 p3060 N85-28931

Structural design of the Sandia 34-meter vertical-axis wind turbine
[DE85-011146] 18 p3118 N85-29300

Conceptual design of a fixed-pitch wind turbine generator system rated at 400 kilowatts
[NASA-CR-174877] 18 p3127 N85-29363

Wake effects on the aerodynamic performance of horizontal axis wind turbines
[NASA-CR-174920] 18 p3127 N85-29364

Government review of the Mod-2 wind turbine (as-built)
[NASA-TM-86983] 18 p3127 N85-29365

Acoustic noise associated with the MOD-1 wind turbine: its source, impact, and control
[DE85-002947] 18 p3178 N85-29700

Wake effects of the aerodynamic performance of horizontal axis wind turbines 19 p3211 N85-29915

Aerodynamic analysis of a horizontal axis wind turbine by use of helical vortex theory. Volume 1: Theory
[NASA-CR-168054] 19 p3212 N85-29916

Structural analysis and cost estimate of an eight-leg space frame as a support structure for horizontal axis wind turbines
[NASA-TM-83470] 19 p3284 N85-30361

Analytical model for predicting emergency shutdown of a two-bladed horizontal axis wind turbine
[NASA-TM-83472] 19 p3303 N85-30476

Performance comparison between NACA 23024 and NACA 64(3)-618 airfoil configurated rotors for horizontal-axis wind turbines
[NASA-TM-83471] 19 p3303 N85-30477

The Federal Wind Program at NASA Lewis Research Center
[NASA-TM-83480] 19 p3304 N85-30478

Operational results for the experimental DOE/NASA Mod-OA wind turbine project
[NASA-TM-83517] 19 p3304 N85-30479

Influence of moisture and elevated temperature on the fatigue properties of WTS-3 glass fiber blade material — wind turbine blade (WTS-3)
[FFA-TN-1984-58] 20 p3470 N85-31558

Design and fabrication of durable owner-built wind turbine blades
[DE85-009200] 20 p3484 N85-31650

Wind energy in the north Netherlands region
20 p3485 N85-31661

Wind turbines and environment management
[CP-MEMO-1983-11] 20 p3485 N85-31662

Verification of theoretically computed spectra for a point rotating in a vertical plane
[DE85-011967] 20 p3520 N85-31893

Experimental investigation of a variable speed constant frequency electric generating system from a utility perspective
[NASA-CR-174950] 21 p3579 N85-32251

Aerodynamic analysis of a horizontal axis wind turbine by use of helical vortex theory, volume 2: Computer program users manual
[NASA-CR-174921] 22 p3804 N85-33563

Reflection plane tests of a wind turbine blade tip section with ailerons
[NASA-TM-87018] 23 p3945 N85-34444

General environmental aspects of large scale wind energy utilization 24 p4110 N85-35474

Calculation of trajectories of detached wind turbine blades and prediction of site risk levels associated with failures of HAWT's 24 p4110 N85-35475

GROWIAN: First observations of the environmental impact at the GROWIAN site — wind energy converter
24 p4110 N85-35476

Wind turbine noise: Prediction tools and design parameter dependence 24 p4110 N85-35477

Environmental Monitoring Burger Hill, Orkney wind turbine generator site and similar work at other UK WTG sites 24 p4111 N85-35482

Siting of large scale wind turbines in Denmark
24 p4111 N85-35483

Special questions of siting wind turbine arrays and networks — West Germany 24 p4111 N85-35484

Environmental aspects of the Netherlands wind farm project 24 p4111 N85-35485

Visit to test facility Stoetten (West Germany) May 9, 1984, including the Voith Wind Energy Converter (WEC) 520 turbine. The annual production of various wind energy plants in selected locations 24 p4112 N85-35487

WIND VANES

R and D activities of the Systems Engineering Division
20 p3540 N85-32027

WIND VARIATIONS

Development and verification of MCD-2 and MOD-OA simulation models
[DE84-017389] 04 p0550 N85-13499

WIND VELOCITY

NT SOLAR WIND VELOCITY

Helium atoms in interstellar and interplanetary media, part 3: Temperature and velocity of interstellar wind
02 p0160 N85-11086

Fastest-mile wind speeds in Hurricane Alicia
[PB84-220771] 03 p0397 N85-12532

Bipolar molecular outflows: T Tauri stars and Herbig-Haro objects 03 p0446 N85-12837

Subhourly wind forecasting techniques for wind turbine operations
[DE84-016205] 04 p0539 N85-13427

Multisensor satellite data integration for sea surface wind speed and direction determination
[NASA-CR-174162] 04 p0542 N85-13446

Development and verification of MCD-2 and MOD-OA simulation models
[DE84-017389] 04 p0550 N85-13499

Study of the improvement in analyzing passive microwave remote sensing data by integrated use of ground data 05 p0658 N85-14226

A diagnostic approach to obtaining planetary boundary layer winds using satellite-derived thermal data
05 p0674 N85-14330

Variability of short-term eddy-correlation estimates of mass exchange
[DE84-007271] 05 p0677 N85-14349

Atmospheric wind and diffusion from analysis of an SF6 release at 350 km altitude
[AD-A147965] 08 p1185 N85-17471

Climate at CRREL (Cold Regions Research and Engineering Laboratory) Hanover, New Hampshire
[AD-A148400] 08 p1189 N85-17495

Regional and seasonal variations in snow-cover density in the USSR
[AD-A148429] 08 p1189 N85-17496

Preliminary survey of wind generation in Washington: Site studies and selected wind speed data
[DE85-000058] 09 p1345 N85-18462

Dynamics of the low-latitude thermosphere and ionosphere 09 p1351 N85-18501

On the formation of the nocturnal coastal surface wind speed maximum 09 p1356 N85-18528

Analysis of the Viking Lander 1 surface wind vector for sols 45 to 375
[NASA-CR-174349] 09 p1416 N85-18932

Antenna axis drive torques for the 70-meter antenna
10 p1464 N85-19237

Tropical cyclone data tape for the Eastern and Central North Pacific Basins, 1949-1983: Contents, limitations and uses
[PB85-110054] 10 p1520 N85-19565

A catalogue of dynamic parameters describing the variability of the middle stratosphere during the northern winters 11 p1656 N85-20435

Wind: Measuring for energy
[DE85-900227] 11 p1667 N85-20607

Observations of cataclysmic variable star winds
11 p1755 N85-21041

Study of effective physiological temperature
13 p2042 N85-22780

Preliminary study of inphase gusts and moment force wind loads over the first 150 meters at KSC, Florida
[NASA-TM-86501] 13 p2137 N85-23273

Portable Automated Mesonet (PAM) data from the 1980 experiment in Anderson Creek Valley
[DE85-004361] 13 p2139 N85-23282

Markov method for simulating non-Gaussian wind speed time series
[DE85-003450] 13 p2139 N85-23284

Design considerations for high-altitude, long-endurance, microwave-powered aircraft
[NASA-TM-86403] 14 p2218 N85-23751

Large space antenna technology applied to radar-imaging, rain-rate measurements, and ocean wind sensing 14 p2230 N85-23820

Low-frequency oscillations of sea level and group structure of wind waves 14 p2335 N85-24441

Error in laser correlation wind speed meters resulting from variable atmospheric transparency
14 p2338 N85-24457

Long nonlinear waves in layers of sudden changes in wind velocity 14 p2340 N85-24470

Wave description of sound propagation through stratified moving atmosphere 15 p2525 N85-25567

Mean conditions and turbulence statistics at Vandenberg AFB, California
[AD-A151366] 15 p2665 N85-26449

Comparison of wind velocity in thunderstorms determined from measurements by a ground-based Doppler radar and an F-106B airplane
[NASA-TM-86348] 16 p2703 N85-26667

Formulation and implementation of nonstationary adaptive estimation algorithm with applications to air-data reconstruction
[NASA-TM-86727] 16 p2706 N85-26699

Variability of short term eddy-correlation estimates of mass exchange
[PB85-172641] 18 p3136 N85-29431

Urban climate and air hygiene before, during, and after the lifework of Hellmut Berg. Overview of a branch of applied meteorology 18 p3147 N85-29487

Utilization of the SEASAT scatterometer winds for ocean mixed layer modeling
[AD-A153748] 18 p3150 N85-29506

Study of drift currents in initial stage of generation of wind waves by laser Doppler anemometer
19 p3291 N85-30408

Approximate method for computing wind velocity in atmosphere 19 p3296 N85-30444

Comparison of wind and turbulence measurements from Doppler lidar and instrumented aircraft
[NASA-CR-171535] 20 p3495 N85-31729

Improved Nominal Operating Cell Temperature (NOCT) test procedure 21 p3612 N85-32449

Synoptic-scale dynamics with vertical velocity, part 1.8A 21 p3617 N85-32476

Relationship of spaced antenna and Doppler techniques for velocity measurements (keynote paper), part 3
21 p3619 N85-32488

Effects of line-of-sight velocity on spaced-antenna measurements, part 3.5A 21 p3621 N85-32496

Use of the VAD technique and measurements of momentum flux in the stratosphere at Arecibo, part 4.3A
21 p3622 N85-32505

Tropospheric gravity waves observed by three closely spaced ST radars 21 p3623 N85-32509

Data base for the Colorado profiling network
21 p3627 N85-32533

Status of the Jicamarca radar
21 p3627 N85-32535

Recent results at the Sunset radar
21 p3627 N85-32536

Mean flow and turbulence in complex terrain
[AD-A155138] 21 p3636 N85-32583

Method and apparatus for four-beam radar
[PB85-181477] 22 p3757 N85-33289

Air-sea interaction with SSM/I and altimeter
[NASA-CR-176105] 22 p3816 N85-33650

Comparative analysis of operational forecasts versus actual weather conditions in airline flight planning, volume 1
[NASA-CR-167862] 24 p4119 N85-35534

Comparative analysis of operational forecasts versus actual weather conditions in airline flight planning, volume 2
[NASA-CR-167563] 24 p4119 N85-35535
Comparative analysis of operational forecasts versus actual weather conditions in airline flight planning, volume 3
[NASA-CR-167564] 24 p4120 N85-35536
Comparative analysis of operational forecasts versus actual weather conditions in airline flight planning, volume 4
[NASA-CR-167565] 24 p4120 N85-35537
Comparative analysis of operational forecasts versus actual weather conditions in airline flight planning: Summary report
[NASA-CR-167566] 24 p4120 N85-35538

WIND VELOCITY MEASUREMENT
Performance evaluation and estimation of a laser time-of-flight velocimeter 03 p0363 N85-12326
Wind speed determination from radar altimeters
03 p0380 N85-12424
Laser Doppler Anemometer (LDA) wind velocity measurements: Possibilities for measurements on windpower units 05 p0668 N85-14300
Wind sheltering correction — anemometry
[KNMI-TR-52] 07 p1009 N85-16406
Recent methods for calibrating the anemometry of helicopters at low speeds 08 p1074 N85-16809
Radiosodar system for remote synchronous measurements of wind speed, temperature and its fluctuations 13 p2110 N85-23145
Science opportunities using the NASA scatterometer on N-ROSS
[NASA-CR-175639] 13 p2123 N85-23222
Intermediate results of the NORDSEE experiment
[AD-A151363] 15 p2542 N85-25693
The use of pressure sensing taps on the aircraft wing as sensor for flight control systems
16 p2698 N85-26560
Conducting a wind sensing study
[NASA-CR-175782] 16 p2832 N85-27465
Feasibility study on Laser Doppler Anemometer (LDA) wind velocity measurements using pulsed visible laser light
[ISL-CO-224/83] 16 p2836 N85-27489
Additional possibilities of radiometeor azimuthal method for measuring wind velocity in lower thermosphere
19 p3296 N85-30438
Aerodynamic measurement of the wind flow in the number two section of the SIMA wind tunnel
[ONERA-PV-1/8138-GY] 20 p3389 N85-31019
Relationship of spaced antenna and Doppler techniques for velocity measurements (keynote paper), part 3
21 p3619 N85-32488
The Adelaide VHF radar: Capabilities and future plans
21 p3629 N85-32546
Millstone Hill radar: Capabilities for S/T observations
21 p3629 N85-32548
Air-sea interaction with SSM/I and altimeter
[NASA-CR-176105] 22 p3818 N85-33650
Kinematic analysis of Hurricane Frederick (1979) using satellite, aircraft and rawinsonde data
[NASA-CR-176167] 24 p4119 N85-35533
Control variables in vertical wind determination using simple flight-mechanical equations
24 p4121 N85-35546
The principles of wind measurement with the help of aircraft 24 p4123 N85-35558

WINDING
NT FILAMENT WINDING
NT WIRE WINDING
Stability and vibrations of internal windings of high-current superconducting solenoid magnets
[AD-A151465] 15 p2656 N85-26390
Optimization of design parameters for alternating current stabilizer based on magnetic suspension
22 p3772 N85-33374
Apparatus producing constant cable tension for intermittent demand
[DE85-006434] 23 p3938 N85-34412

WINDMILLS (WINDPOWERED MACHINES)
Investigations on the dynamic loading of wind energy converters with vertical axis and problems of control during starting and overload conditions
[BMFT-FB-T-84-155] 03 p0386 N85-12472
Government review of the Mod-2 wind turbine (as-built)
[NASA-TM-86963] 18 p3127 N85-29365
Aerodynamic analysis of a horizontal axis wind turbine by use of helical vortex theory. Volume 1: Theory
[NASA-CR-168054] 19 p3212 N85-29916
Activities of the Wind Energy Programme
20 p3540 N85-32028
Television interference measurement at Kalkugnen (Sweden) test windmill 24 p4111 N85-35481

WINDOWS (APERTURES)
Response measurements for two building structures excited by noise from a large horizontal axis wind turbine generator
[NASA-CR-172482] 04 p0558 N85-13552
Cockpit window edge proximity effects on judgements of horizon vertical displacement
05 p0704 N85-14516
Preliminary design criteria and certification test specifications for blast resistant windows
09 p1337 N85-18405
Calculation of Si(Li) X-ray detector efficiencies
[DE85-002732] 10 p1489 N85-19400
Hypervelocity impacts on Skylab 4/Apollo windows
12 p1785 N85-21202
Millimeter wave dielectric property measurement of gyrotron window materials
[DE85-004430] 12 p1802 N85-21304
Improvements in glazings: SERI materials research in progress
[DE84-013049] 12 p1814 N85-21378
Double window viewing chamber assembly
[NASA-CASE-MFS-28057-1] 18 p3083 N85-28951
A preliminary human factors planning and design outline of parameters related to space station windows and CCTV monitoring 18 p3158 N85-29559
Light transmitting window assembly
[NASA-CASE-MSC-18417-1] 18 p3185 N85-29750
Laser sealed evacuated window glazings
[DE85-000512] 22 p3754 N85-33273
Diamondlike carbon protective coatings for IR materials
[NASA-TM-87083] 23 p3973 N85-34631

WINDOWS (INTERVALS)
NT LASER WINDOWS
NT LAUNCH WINDOWS
The Jovian atmospheric window at 2.7 microns: A search for H2S
[NASA-TM-86661] 03 p0445 N85-12636
The effects of a nearly 100% duty cycle in observations of solar oscillations 14 p2443 N85-25076
China report: Science and technology
[JPRS-CST-85-007] 15 p2533 N85-25621
Professional Committee on Solid Propulsion hold conference 15 p2533 N85-25623
Extent to which least-squares cross-validation minimizes integrated square error in nonparametric density estimation
[AD-A153789] 18 p3174 N85-29679
Search of the VAXintosh customizing VMS V4.0 for DCL windows
[DE85-011306] 22 p3831 N85-33729

WINDPOWER UTILIZATION
Aileron controls for wind turbine applications
[NASA-TM-86867] 02 p0222 N85-11458
Operational behavior of wind energy converters. Control and dynamic and types of generators, volume 1
[BMFT-FB-T-84-154-VOL-1] 03 p0386 N85-12470
Operational behavior of wind energy converters: Control and dynamic and types of generators, volume 2
[BMFT-FB-T-84-154-VOL-2] 03 p0386 N85-12471
Investigations on the dynamic loading of wind energy converters with vertical axis and problems of control during starting and overload conditions
[BMFT-FB-T-84-155] 03 p0386 N85-12472
Analysis of wind energy systems for selected electric utilities
[DE84-013025] 04 p0530 N85-13389
Measurement-Technical Investigations of Wind Energy Units
[JUEL-SPEZ-244] 05 p0667 N85-14293
Measurement-technical problems in the investigation of wind energy units 05 p0668 N85-14295
Measuring system and data evaluation methods of the test field for wind energy units at Pellworm
05 p0668 N85-14296
Measuring-technical investigation of wind energy units from the control-technical, electrical and energetic point of view 05 p0668 N85-14301
Wind-powered electric generation runway lighting system demonstration project
[DE84-014962] 05 p0670 N85-14311
Development of large wind energy power generation system
[NASA-TM-77779] 07 p0992 N85-16301
Preliminary survey of wind generation in Washington: Site studies and selected wind speed data
[DE85-000058] 09 p1345 N85-18462
Rocky Flats Wind Energy Research Center FY 1983 report
[DE85-004500] 10 p1511 N85-19535
Improved models for increasing wind penetration, economics and operating reliability
[NASA-CR-175536] 11 p1674 N85-20545
Wind generator for Solar Office Complex, Luna Vocational Technical Institute, Las Vegas, New Mexico
[DE85-900103] 11 p1674 N85-20547
The relevance of averaging period to wind power measurements and efficiency of Wind Energy Conversion Systems (WECS)
[GKSS-84-E-35] 11 p1676 N85-20562
Wind: Measuring for energy
[DE85-900227] 11 p1687 N85-20607
Aerodynamic research efforts at SERI Wind Energy Research Center at Rocky Flats
[DE85-000529] 12 p1881 N85-21805
The transpacific experimental sailing by YASEIGO 3
14 p2327 N85-24380
Wind energy technology program summary
[DE85-007349] 16 p2820 N85-27392
Transient behavior of a single-blade horizontal-axis wind turbine
[MBB-UD-421/84-O] 16 p2875 N85-27737
Wind energy systems: Program summary for fiscal year, 1983
[DE85-002927] 17 p2965 N85-28451
Field test report of the Department of Energy's 100-kW vertical axis wind turbine
[DE85-006475] 17 p2967 N85-28458
A 5-year research plan, 1985-1990. Wind energy technology: Generating power from the wind
[DE85-008427] 17 p2967 N85-28463
Research recommendations for ac interfacing between electric utility transmission and distribution systems and wind, photovoltaics, and OTEC energy systems
[DE85-002942] 18 p3096 N85-29169
Government review of the Mod-2 wind turbine (as-built)
[NASA-TM-86963] 18 p3127 N85-29365
Aerodynamic analysis of a horizontal axis wind turbine by use of helical vortex theory. Volume 1: Theory
[NASA-CR-168054] 19 p3212 N85-29916
The Federal Wind Program at NASA Lewis Research Center
[NASA-TM-83480] 19 p3304 N85-30478
Renewable technologies program summaries
[DE85-001509] 19 p3307 N85-30500
Wind energy in the north Netherlands region
20 p3485 N85-31661
Wind turbines and environment management
[CP-MEMO-1983-11] 20 p3485 N85-31662
Verification of theoretically computed spectra for a point rotating in a vertical plane
[DE85-011967] 20 p3520 N85-31693
R and D programmes at the National Aeronautical Laboratory
[AR-22] 20 p3539 N85-32022
Activities of the Wind Energy Programme
20 p3540 N85-32028
Wind energy battery storage, phase 2
[DE85-009753] 23 p3945 N85-34450
Solar energy education. Renewable energy: A background text
[DE85-010365] 23 p3946 N85-34452
Implementing agreement for cooperation in the development of large scale wind energy conversion systems
[JUEL-SPEZ-278] 24 p4110 N85-35473
General environmental aspects of large scale wind energy utilization 24 p4110 N85-35474
GROWIAN: First observations of the environmental impact at the GROWIAN site — wind energy converter
24 p4110 N85-35476
Environmental aspects of large-scale wind-power systems in the UK 24 p4110 N85-35478
Environmental Monitoring Burger Hill, Orkney wind turbine generator site and similar work at other UK WTG sites 24 p4111 N85-35482
Visit to test facility Stoetten (West Germany) May 9, 1984, including the Voith Wind Energy Converter (WEC) 520 turbine. The annual production of various wind energy plants in selected locations 24 p4112 N85-35487

WINDPOWERED GENERATORS
Operational behavior of wind energy converters. Control and dynamic and types of generators, volume 1
[BMFT-FB-T-84-154-VOL-1] 03 p0386 N85-12470
Operational behavior of wind energy converters: Control and dynamic and types of generators, volume 2
[BMFT-FB-T-84-154-VOL-2] 03 p0386 N85-12471
Development and demonstration of a vertical axis wind turbine POWERHOUSE
[DE84-901449] 04 p0527 N85-13369
Measurement-Technical Investigations of Wind Energy Units
[JUEL-SPEZ-244] 05 p0667 N85-14293
Measurement-technical investigations of wind energy units in the short-time range — spectrum analysis
05 p0668 N85-14294
Measurement-technical problems in the investigation of wind energy units 05 p0668 N85-14295

Measuring system and data evaluation methods of the test field for wind energy units at Pellworm
05 p0668 N85-14296

Measuring methods to determine the static and dynamic behavior of wind energy converters
05 p0668 N85-14297

Measurement data acquisition and processing system for wind rotor measurements in the wind channel of Bremen University 05 p0668 N85-14298

Laser Doppler Anemometer (LDA) wind velocity measurements: Possibilities for measurements on windpower units 05 p0668 N85-14300

Measuring-technical investigation of wind energy units from the control-technical, electrical and energetic point of view 05 p0668 N85-14301

Existing measuring systems for wind energy units
05 p0669 N85-14302

Measuring techniques in the measuring program for the windpowered unit GROWIAN 05 p0669 N85-14303

Measuring and control tasks in OPTIWA
05 p0669 N85-14304

The upwind power plant Manzanares
05 p0669 N85-14305

Wind-powered electric generation runway lighting system demonstration project
[DE84-014962] 05 p0670 N85-14311

A modified unit commitment and generation control for utilities with large wind generation penetrations
[DE84-015362] 06 p0806 N85-15129

Development of large wind energy power generation system
[NASA-TM-77779] 07 p0992 N85-16301

A preliminary assessment of environmental noise from large Wind Energy Conversion Systems (WECS) based on experiences from Swedish prototypes
[FFA-TN-1984-48] 09 p1379 N85-18666

Variable speed generator technology options for wind turbine generators
[RR-84-4] 10 p1478 N85-19331

Wind generator for Solar Office Complex, Luna Vocational Technical Institute, Las Vegas, New Mexico
[DE85-900103] 11 p1674 N85-20547

Development of large, horizontal-axis wind turbines
[NASA-TM-86950] 13 p2126 N85-23242

Field test report of the Department of Energy's 100-kW vertical axis wind turbine
[DE85-008475] 17 p2987 N85-28458

Government review of the Mod-2 wind turbine (as-built)
[NASA-TM-86983] 18 p3127 N85-29365

Structural analysis and cost estimate of an eight-leg space frame as a support structure for horizontal axis wind turbines
[NASA-TM-83470] 19 p3284 N85-30361

The Federal Wind Program at NASA Lewis Research Center
[NASA-TM-83480] 19 p3304 N85-30478

Operational results for the experimental DOE/NASA Mod-OA wind turbine project
[NASA-TM-83517] 19 p3304 N85-30479

Activities of the Wind Energy Programme
20 p3540 N85-32028

Implementing agreement for cooperation in the development of large scale wind energy conversion systems
[JUEL-SPEZ-278] 24 p4110 N85-35473

General environmental aspects of large scale wind energy utilization 24 p4110 N85-35474

Calculation of trajectories of detached wind turbine blades and prediction of site risk levels associated with failures of HAWT's 24 p4110 N85-35475

GROWIAN: First observations of the environmental impact at the GROWIAN site — wind energy converter
24 p4110 N85-35476

Wind turbine noise: Prediction tools and design parameter dependence 24 p4110 N85-35477

Environmental aspects of large-scale wind-power systems in the UK 24 p4110 N85-35478

A Programmable Automatic Noise Data and Other Related parameter Acquisition system (PANDORA) — wind energy converters 24 p4111 N85-35479

Television interference at the Maglarp (Sweden) wind turbine 24 p4111 N85-35480

Environmental Monitoring Burger Hill, Orkney wind turbine generator site and similar work at other UK WTG sites 24 p4111 N85-35482

Special questions of siting wind turbine arrays and networks — West Germany 24 p4111 N85-35484

Environmental aspects of the Netherlands wind farm project 24 p4111 N85-35485

Visual impact of GROWIAN and resulting recommendations for siting of large wind energy converters 24 p4112 N85-35486

Visit to test facility Stoetten (West Germany) May 9, 1984, including the Voith Wind Energy Converter (WEC) 520 turbine. The annual production of various wind energy plants in selected locations 24 p4112 N85-35487

WINDPOWERED PUMPS

Activities of the Wind Energy Programme
20 p3540 N85-32028

WINDS ALOFT

NT GEOSTROPHIC WIND
NT JET STREAMS (METEOROLOGY)

A feasibility study on the use of wind profilers to support Space Shuttle launches
[NASA-CR-3861] 04 p0538 N85-13423

Cut-off lows and their influence on the weather in Switzerland
[REPT-45] 10 p1519 N85-19574

Atmospheric environment for space shuttle (STS-51C) launch
[NASA-TM-86508] 19 p3315 N85-30547

WINDSCREENS

U WINDSHIELDS

WINDSHIELDS

Method for measuring haze in transparencies
[AD-D011233] 01 p0120 N85-10823

Evaluation of the birdstrike threat to the F-15 present fleet, rapid deployment force, and dual role fighter transparencies
[AD-A148954] 10 p1421 N85-18966

Avoiding serious bird strike incidents
[AD-P004178] 11 p1578 N85-19940

1983 Air Force bird strikes
[AD-P004182] 11 p1579 N85-19944

Aircraft transparency bird impact analysis using the MAGNA computer program
[AD-P004186] 11 p1579 N85-19948

Bird impact evaluation of the F/RF-4 transparency system 11 p1579 N85-19949

The measurement of aircraft windscreen haze and its effect on visual performance
[AD-A154949] 21 p3555 N85-32114

WING CAMBER

Automatic flight control modes for the AFTI/F-111 mission adaptive wing aircraft 17 p2905 N85-27909

WING FLAPS

NT LEADING EDGE FLAPS
NT LEADING EDGE SLATS
NT TRAILING EDGE FLAPS
NT VORTEX FLAPS

Force and moment measurements on a 74 deg delta wing with an apex flap
[NASA-CR-166081] 02 p0134 N85-10918

Recent progress of development and understanding of high lift systems 08 p1066 N85-16772

Analysis of transonic aerodynamic characteristics for a supercritical airfoil oscillating in heave, pitch and with oscillating flap 15 p2458 N85-25175

Airfoil wing with flap
[CH-634787-A5] 15 p2469 N85-25243

Simulator study of the stall departure characteristics of a light general aviation airplane with and without a wing-leading-edge modification
[NASA-TM-86309] 15 p2470 N85-25250

WING FLOW METHOD TESTS

Flow visualization study of a vortex-wing interaction
[NASA-TM-86656] 03 p0316 N85-12040

Transition fixing on wings in industrial wind tunnels and associated problems 14 p2212 N85-23717

Transonic calculations for a flexible supercritical wing and comparison with experiment
[NASA-TM-86439] 20 p3388 N85-31012

WING LOADING

Design of a digital ride quality augmentation system for commuter aircraft
[NASA-CR-172419] 01 p0006 N85-10037

Numerical simulation of the subsonic wing-rock phenomenon 03 p0320 N85-12064

Crack resistance of pressed and rolled semifinished goods of aluminum alloys used in load-bearing aircraft wing structures 03 p0348 N85-12245

Flight test technique for evaluation of gust load alleviation analysis methodology
[NASA-TM-86344] 06 p0754 N85-14833

Structural load measurements on a Northrop NF-5A
07 p0894 N85-15667

Downwash in the plane of symmetry of an elliptically loaded wing
[NASA-TP-2414] 07 p0898 N85-15593

WING NACELLE CONFIGURATIONS

Installed nacelle drag-improvement tests of an M = 0.8 turboprop transport configuration
[NASA-TM-84302] 07 p0902 N85-15716

Nacelle/pylon/wing integration on a transport model with a natural laminar flow nacelle
[NASA-TP-2439] 19 p3213 N85-29924

WING OSCILLATIONS

Graphics software for the display of body deformation motion
[FW-FO-1640] 04 p0456 N85-12888

Propulsive efficiency of vibrating wing in supersonic flow 05 p0724 N85-14656

Wing rock flow phenomena
[AD-P004154] 09 p1264 N85-17939

Transonic steady- and unsteady-pressure measurements on a high-aspect-ratio supercritical-wing model with oscillating control surfaces
[NASA-TM-81888] 09 p1273 N85-18003

A locally linearized panel method for tran-/subsonic flow past an oscillating wing 11 p1622 N85-20212

Oscillating airfoils and their wake
[NASA-TM-77831] 14 p2209 N85-23701

Transonic Unsteady Aerodynamics and its Aeroelastic Applications
[AGARD-CP-374] 15 p2457 N85-25171

Analysis of transonic aerodynamic characteristics for a supercritical airfoil oscillating in heave, pitch and with oscillating flap 15 p2458 N85-25175

Calculation of harmonic aerodynamic forces of aerofoils and wings from the Euler equations
15 p2458 N85-25177

A semi-empirical unsteady transonic method with supersonic free stream 15 p2458 N85-25179

Application of time-linearized methods to oscillating wings in transonic flow and flutter
15 p2459 N85-25182

The development of unsteady transonic 3-D full potential code and its aeroelastic applications
15 p2460 N85-25187

Propulsion efficiency of vibrating bodies in subsonic gas stream 17 p2942 N85-28159

Data set 9: LANN wing. Pitching oscillation
20 p3390 N85-31030

WING PANELS

Solar Array Experiment (SAE) flight experience
14 p2236 N85-23661

WING PLANFORMS

NT DELTA WINGS
NT SWEPT FORWARD WINGS
NT SWEPTBACK WINGS
NT VARIABLE SWEEP WINGS

A method for estimating the rolling moment due to spin rate for arbitrary planform wings
[NASA-TM-86365] 10 p1425 N85-18990

Calculation of the flow around thick wings with separation vortices 12 p1821 N85-21424

Supersonic aerodynamic characteristics of canard, tailless, and aft-tail configurations for 2 wing planforms
[NASA-TP-2434] 17 p2891 N85-27822

Some effects of sweep direction and strakes for wings with sharp leading edges
[CA-8421] 17 p2892 N85-27826

A method to calculate the parameters of wings of arbitrary planform
[AD-A152669] 17 p2892 N85-27831

WING PROFILES

NT WING SPAN

Laser anemometer study of separated flow on wing profiles
[ISL-CO-214/83] 04 p0453 N85-12672

Manufacturing report of an augmented lift, variable deflection half wing
[ONERA-RT-25/1736-AY-108-A]
05 p0591 N85-13766

Numerical method for computing supersonic flow over wings of flight vehicles 05 p0725 N85-14659

Integrated technology wing study (oral presentation)
[NASA-CR-169497] 07 p0902 N85-15718

Transition fixing in the high speed range for the development of civil aircraft wings
14 p2211 N85-23716

The influence of transition strips on the pressure distribution on transonic profiles
14 p2212 N85-23718

Investigation of the conditions for tripping transition with roughness elements and their influence on boundary layer development 14 p2212 N85-23720

Studies on the interference of wings and propeller slipstreams
[NASA-CR-175753] 15 p2463 N85-25210

Unsteady transonic flow calculations for interfering lifting surface configurations
[NASA-TM-86432] 19 p3214 N85-29931

Low-speed tests of a high-aspect-ratio, supercritical-wing transport model equipped with a high-lift flap system in the Langley 4- by 7-meter and Ames 12-foot pressure tunnels
[NASA-TP-2097] 20 p3366 N85-31010

A numerical method for the solution of the inverse problem in external aerodynamics
[STN-7] 20 p3390 N85-31025

Design of a basic airfoil for a slightly swept wing. Part 1: Theoretical transonic airfoil design
[ESA-TT-892] 20 p3394 N85-31054

WING ROOTS
Optimum design of nonplanar wings: Minimum induced drag for a given lift and wing root bending moment
[NAL-TR-797] 01 p0002 N85-10011

WING SLATS
U LEADING EDGE SLATS

WING SPAN
Integrated technology wing study (oral presentation)
[NASA-CR-169497] 07 p0902 N85-15716
Aerodynamic analysis of a horizontal axis wind turbine by use of helical vortex theory, volume 2: Computer program users manual
[NASA-CR-174921] 22 p3804 N85-33563

WING TANKS
Fuel containment and damage tolerance in large composite primary aircraft structures
[NASA-CR-166083] 19 p3231 N85-30032

WING TIP VORTICES
Prediction of aerodynamic characteristics of fighter wings at high angles of attack
[AD-A145107] 01 p0003 N85-10017
Aerodynamic improvements by discrete wing tip jets
[AD-A148981] 10 p1421 N85-18964
Investigation of the Vortex Tab
[NASA-CR-172586] 15 p2463 N85-25209
Interaction of a turbulent vortex with a lifting surface
15 p2464 N85-25214
Tip vortex computer code SRATIP. User's guide
[NASA-CR-172603] 21 p3551 N85-32093

WING TIPS
Integrated technology wing study (oral presentation)
[NASA-CR-169497] 07 p0902 N85-15716
Determination of corrections to flow direction measurements obtained with a wing-tip mounted sensor
[NASA-CR-174412] 10 p1421 N85-18962
Exploratory wind-tunnel investigation of a wingtip-mounted vortex turbine for vortex energy recovery
[NASA-TP-2468] 16 p2699 N85-26667
Wingtip vortex propeller
[NASA-CASE-LAR-13019-1] 24 p4065 N85-35194

WINGED VEHICLES
An overview of some monoplanar missile programs
[NASA-TM-86330] 06 p0747 N85-14786

WINGLETS
Optimum design of nonplanar wings: Minimum induced drag for a given lift and wing root bending moment
[NAL-TR-797] 01 p0002 N85-10011
Natural laminar flow airfoil design considerations for winglets on low-speed airplanes
[NASA-CR-3853] 04 p0452 N85-12863
Flutter parametric studies of cantilevered twin-engine-transport type wing with and without winglet. Volume 1: Low-speed investigations
[NASA-CR-172410-VOL-1] 04 p0513 N85-13269
Flutter parametric studies of cantilevered twin-engine transport type wing with and without winglet. Volume 2: Transonic and density effect investigations
[NASA-CR-172410-VOL-2] 04 p0513 N85-13270
Study of winglets applied to biplanes
[NASA-TM-86350] 08 p1083 N85-16862
DC-10 winglet flight evaluation
[NASA-CR-3704] 19 p3217 N85-29949

WINGS
NT AEROELASTIC RESEARCH WINGS
NT BEARINGLESS ROTORS
NT CAMBERED WINGS
NT DELTA WINGS
NT FIXED WINGS
NT FLEXIBLE WINGS
NT LIFTING ROTORS
NT LOW ASPECT RATIO WINGS
NT RECTANGULAR WINGS
NT RIGID ROTORS
NT RIGID WINGS
NT ROTARY WINGS
NT SLENDER WINGS
NT SUPERCRITICAL WINGS
NT SWEPT FORWARD WINGS
NT SWEPT WINGS
NT SWEPTBACK WINGS
NT THIN WINGS
NT TILTING ROTORS
NT TIP DRIVEN ROTORS
NT TWISTED WINGS
NT UNSWEPT WINGS
NT VARIABLE SWEEP WINGS
Integral equation of lifting surfaces in Laplace domain and analytic continuation of its pressure kernel
[NAL-TR-795T] 01 p0002 N85-10009
Optimum design of nonplanar wings: Minimum induced drag for a given lift and wing root bending moment
[NAL-TR-797] 01 p0002 N85-10011
Deposition in the human lung during respiration of small particles suspended in the air
[BLL-RISLEY-TR-5021-(9091.9F)]
03 p0400 N85-12549
A study of lift characteristics of an upper surface blown jetwing with a rectangular nozzle
05 p0591 N85-13767
Reduction method for thermal analysis of complex aerospace structures
[NASA-TP-2373] 07 p0957 N85-16066
Recent progress of development and understanding of high lift systems 08 p1068 N85-16772
Design of an airfoil leading edge slat using an inverse aerodynamic calculation method
08 p1069 N85-16777
Aerodynamic issues in the design of high-lift systems for transport aircraft 08 p1069 N85-16780
An update of the Canada/USA augmentor-wing project 08 p1070 N85-16781
Aerodynamic-structural study of canard wing, dual wing, and conventional wing systems for general aviation applications
[NASA-CR-172529] 08 p1077 N85-16829
Theory of wing rock 09 p1262 N85-18064
Unsteady transonic flow calculations for two-dimensional canard-wing configurations with aeroelastic applications
[NASA-TM-86375] 10 p1420 N85-18960
Remote pivot decoupler pylon: Wing/store suppression
[NASA-CASE-LAR-13173-1] 11 p1584 N85-19961
A locally linearized panel method for tran-/subsonic flow past an oscillating wing 11 p1622 N85-20212
Fatigue crack propagation in mirage 1110 wing main spar specimens and the effects of spectrum truncation on life
[ARL/STRUC-R-405] 12 p1776 N85-21152
Study for the optimization of a transport aircraft wing for maximum fuel efficiency. Volume 1: Methodology, criteria, aeroelastic model definition and results
[NASA-CR-172551] 13 p1971 N85-22378
Some optimization problems in static aeroelasticity for wings made of composite materials
14 p2277 N85-24104
Computation of unsteady transonic flows about two-dimensional and three-dimensional AGARD standard configurations 15 p2459 N85-25183
The application of transonic unsteady methods for calculation of flutter airloads 15 p2460 N85-25186
Studies on the interference of wings and propeller slipstreams
[NASA-CR-175753] 15 p2463 N85-25210
Aircraft structure for application to training aircraft
[CH-635286-A5] 15 p2469 N85-25244
Learjet Model 55 wing analysis with landing loads
15 p2575 N85-25883
Computational aerodynamics for aircraft wing design
16 p2693 N85-26627
A numerical design method for three-dimensional transonic wings 16 p2694 N85-26631
Hypersonic nonequilibrium gas flow past zero-aspect wing 16 p2765 N85-27083
Wing buffeting active control testing on a transport aircraft configuration in a large sonic windtunnel
17 p2904 N85-27903
Method of calculating separation flow of subsonic gas stream around wings 17 p2942 N85-28161
Further investigations to improve the fatigue life of the Mirage 1110 wing main span
[ARL/STRUC-TM-397] 18 p3061 N85-28938
Gust load alleviation of a cantilevered rectangular elastic wing. Wind tunnel experiment and analysis
[NAK-TR-86] 18 p3063 N85-28950
Application of an aerodynamic analysis method including attainable thrust estimates to low speed leading-edge flap design for supersonic cruise vehicles
[NASA-CR-165843] 19 p3212 N85-29918
Data set 8: ZKP wing, oscillating aileron
20 p3390 N85-31029
Data set 9: LANN wing. Pitching oscillation
20 p3390 N85-31030
Vortex sheet modeling with higher order curved panels
20 p3451 N85-31428
R and D activities of the Structural Sciences Division
20 p3539 N85-32026
Aerodynamic characteristics of a distinct wing-body configuration at Mach 6: Experiment, theory, and the hypersonic isolation principle
[NASA-TP-2467] 22 p3727 N85-33107
Aeroelastic constraints for a wing weight minimization procedure
[FFA-TN-1985-4] 23 p3895 N85-34126
Fuel containment and damage tolerance for large composite primary aircraft structures. Phase 1: Testing
[NASA-CR-166091] 24 p4073 N85-35241

WINTER
The winter anomaly in ionospheric absorption (with special reference to the results obtained in Spain)
04 p0522 N85-13338
Possible anomaly prediction system for the middle atmosphere — ionospheric absorption
04 p0522 N85-13339
Mean maximum mixing heights for northern Asia for the winter of 1978
[DE84-015980] 05 p0672 N85-14315
Forecast impact of components of the FGGE observing system 05 p0681 N85-14373
Results of the carbon monoxide study in Washington, D.C. and Denver, Colorado, in the winter of 1982-83
[PB84-230069] 06 p0834 N85-15309
Trends in skill and accuracy of National Weather Service pop forecasts
[PB84-229053] 06 p0840 N85-15335
The 500 millibar sign frequency teleconnection charts: Winter
[PB85-106276/GAR] 07 p1009 N85-16410
Regional and seasonal variations in snow-cover density in the USSR
[AD-A148429] 08 p1189 N85-17496
Frozen precipitation and concurrent weather: A case study for Munchen-Riem, West Germany
[AD-A149227] 10 p1519 N85-19577
Precipitation gage network operations for wintertime research in the Central Sierra Nevada
[PB85-115020] 10 p1520 N85-19582
Ground-based snow and ice crystal observation system used in Sierra Nevada winter orographic storms
[PB85-115343] 10 p1520 N85-19584
California coastal erosion and storm damage during the winter 1982 - 1983, a reconnaissance report
[PB85-121705] 10 p1521 N85-19591
PMP-1: A coordinated study of the behavior of the middle atmosphere in winter 11 p1654 N85-20421
The Middle Atmosphere Program: Winter in Northern Europe (MAP/WINE) 11 p1655 N85-20429
Middle Atmosphere Program. Handbook for MAP, volume 5
[NASA-CR-175461] 11 p1656 N85-20434
A catalogue of dynamic parameters describing the variability of the middle stratosphere during the northern winters 11 p1656 N85-20435
Middle Atmosphere Program. Handbook for MAP, volume 7
[NASA-CR-175479] 11 p1656 N85-20437
Winter in Northern Europe (WINE) project
11 p1657 N85-20439
PMP-1 report: The fourth winter of PMP-1, 1981 - 1982: A winter with several interesting features
11 p1657 N85-20441
Workshop on Comparison of Data and Derived Dynamical Quantities During Northern Hemisphere (PMP-1) Winters 11 p1657 N85-20444
The first winter of MAP-dynamics, 1982-1983: A winter with three different warming periods
11 p1657 N85-20446
Variation of derived mesospheric nitric oxide in relation to wind and temperature in winter
11 p1658 N85-20452
Abnormal circulation changes in the winter stratosphere, detected through variations of D region ionospheric absorption 11 p1659 N85-20458
Winter anomaly of the lower ionosphere and its possible causes 11 p1660 N85-20459
Autumn and winter anomalies in ionospheric absorption as measured by riometers 11 p1660 N85-20460
Winter anomaly 1982/83 in comparison with earlier winters (1960-82) 11 p1660 N85-20461
A model of the influence of neutral air dynamics on the seasonal variation in the low ionosphere
11 p1660 N85-20462
Explanation of the normal winter anomaly from the seasonal variation of short wave absorption
11 p1660 N85-20463
Midwinter disturbances in the middle atmosphere
11 p1661 N85-20465
Large scale winter time disturbances in meteor winds over central and eastern Europe
11 p1661 N85-20467
Changes in the ozone content over central Europe during reversals of stratospheric circulation in late winter
11 p1661 N85-20469
Measurement of the vertical gradient of the semidiurnal tidal wind phase in winter at the 95 km level
11 p1662 N85-20478
Stratwarm effects in the ionospheric D region wind field 11 p1663 N85-20479
Middle Atmosphere Program. Handbook for MAP. Volume 12: Coordinated Study of the Behavior of the Middle Atmosphere in Winter (PMP-1) Workshops
[NASA-CR-175475] 11 p1665 N85-20492

Short duration winter-time performances of different passive solar systems
[DE85-000850] 11 p1675 N85-20557
Sector analysis of relevant meteorological parameters for long range transport of air pollutants
[NR-27] 12 p1893 N85-21862
Mountain barrier baroclinity effects on surface winds along the Alaskan Arctic coast 14 p2236 N85-23877
Data collection and winter ice dynamics in the Beaufort Sea 14 p2236 N85-23878
Response of winter forecasts made with the GLA Fourth Order GCM to Changes in the horizontal grid resolution
18 p3143 N85-29456
Energy sources of the dominant frequency dependent 3-dimensional atmospheric modes
18 p3143 N85-29462
The contrasting Northern Hemisphere winters of 1980-81 and 1981-82 18 p3144 N85-29468
Transient eddies in the UCLA GCM
18 p3145 N85-29470
Circulation and transport in the middle atmosphere: Troposphere and lower atmosphere
18 p3146 N85-29491
Airborne measurements of atmospheric ice nuclei
21 p3640 N85-32612
Snow cover in the Siberian forest-steppe
[NASA-TM-77914] 23 p3943 N85-34435
Project Skywater, 1983-84 SCPP (Sierra Cooperative Pilot Project) data inventory
[PB85-187052] 24 p4124 N85-35565

WIRE
NT ELECTRIC WIRE
NT EXPLODING WIRES
NT GUY WIRES
Finitely conducting, infinitely long, cylindrical wire in the presence of a plane wave (EMP)
[DE84-015363] 02 p0192 N85-11282
Impact toughness of wire after cold deformation and annealing
[BLL-M-35941-(5828.4)] 05 p0615 N85-13930
Galvanized wire protected against corrosion by chromate passivization
[BLL-M-35906-(5828.4)] 05 p0616 N85-13936
Development of intercalated wire and cable
[AD-A146502] 06 p0774 N85-14949
Electromagnetic resonances of cylinders and aircraft model with resistive wires
[NASA-CR-174203] 06 p0838 N85-15319
Electromagnetic inspection of wire ropes using sensor arrays
[AD-A148317] 08 p1170 N85-17379
Characterization of Nb-8 wt % Al wires by analytical electron microscopy
[DE85-002726] 10 p1442 N85-19086
Double pinch-push contact insertion end-effector
[AD-D011485] 10 p1459 N85-19196
Effectiveness of an overhead wire barrier in deterring gulls from feeding at a sanitary landfill
[AD-P004199] 11 p1582 N85-19966
Multiple parallel wires above a finitely conducting plane earth in the presence of a plane wave (EMP)
[DE85-001116] 11 p1625 N85-20231
A moment solution for an arbitrary configuration of partly shielded wires above a ground plane
[AD-A149762] 12 p1828 N85-21473
Method and apparatus for detecting acoustic emissions from metal matrix wire
[AD-D011556] 12 p1927 N85-22107
Investigation of the conditions for tripping transition with roughness elements and their influence on boundary layer development 14 p2212 N85-23720
Basic EMC (Electromagnetic Compatibility) technology advancement for C3 systems: Model revision for IEMCAP (Intrasystem Electromagnetic Compatibility Analysis Program)
[AD-A150795] 14 p2292 N85-24208
Research on design of cryotransformers and its prospects for the future
[AD-A152400] 17 p2952 N85-28230
Basic EMC (Electromagnetic compatibility) technology advancement for C3 systems. Volume 4D: Modeling crosstalk in balanced twisted pairs
[AD-A153678] 18 p3090 N85-29125
The microstructural state of Nb3Sn in a multifilamentary titanium doped bronze-process wire
[DE85-010979] 19 p3240 N85-30089
Electromagnetic inspection of wire ropes using sensor arrays
[AD-A155412] 22 p3795 N85-33509
Features of the solar array drive mechanism for the space telescope 22 p3796 N85-33532
Towards the development of technological processes for the preparation of cadmium plated steel articles
[BLL-M-36315-(5828.4)] 23 p3913 N85-34248
Apperatus producing constant cable tension for intermittent demand
[DE85-006434] 23 p3938 N85-34412
Effect of Cu4Ti compound formation on the characteristics of NbTi accelerator magnet wire
[DE85-014226] 24 p4159 N85-35786

WIRE BRIDGE CIRCUITS
NT WHEATSTONE BRIDGES
Modular detonator device
[AD-D011232] 03 p0340 N85-12184

WIRE CLOTH
Explosion-proof properties and hydraulic resistance of fire-barrier elements based on knitted metallic screens
11 p1601 N85-20067
Flow through very porous screens
[NASA-TP-2436] 11 p1631 N85-20270
Flow around rotating and nonmoving circular cylinder near flat screen. Report 1: Aerodynamic forces in cylinder 16 p2765 N85-27059

WIRE MESH
U WIRE CLOTH

WIRE WINDING
Detection and location of partial discharges in transformer windings using electrical methods
15 p2551 N85-25750

WIRELESS COMMUNICATION
NTT (Nippon Telegraph and Telephone Public Corporation) develops new optical fiber
10 p1476 N85-19311

WIRING
NT BEAM LEADS
Bondability of Al-Si thin film in thermosonic gold wire bonding — integrated circuits
[NASA-TM-77795] 10 p1439 N85-19071
Safety requirements for wiring systems and connectors for photovoltaic systems
[NASA-CR-174431] 10 p1477 N85-19324
Reducing gull use of some attractions near airports
[AD-P004195] 11 p1581 N85-19962

WIRING SYSTEMS
U WIRING

WISCONSIN
Compilation of annual reports of the Navy ELF (Extremely Low Frequency) communications system ecological monitoring program. Volume 1: Tabs A-E
[AD-A148326] 08 p1152 N85-17272
Compilation of annual reports of the Navy ELF (Extremely Low Frequency) communications system ecological monitoring program (1983). Volume 2: Tabs F-J
[AD-A148327] 08 p1152 N85-17273
Glacial geology of Barron County, Wisconsin
09 p1351 N85-18500
The pleistocene geology of Vilas County, Wisconsin
09 p1353 N85-18509
Rationale and basic design for experimental acidification of a lake ecosystem in Northern Wisconsin
[PB85-116077] 12 p1885 N85-21829

WOLF-RAYET STARS
Observations of nonthermal radio emission from early-type stars 08 p1232 N85-17758
Departures from LTE populations versus anomalous abundances: The effects of heating
08 p1234 N85-17776
Spectroscopic observations of selected stellar systems
[NASA-CR-174288] 08 p1255 N85-17915
High-velocity interstellar gas in the line-of-sight to HD 50896 11 p1749 N85-20999
Gamma-ray line emission from Al-26 produced by Wolf-Rayet stars
[OG-3.2-5] 22 p3875 N85-34003
Neutron-rich nuclei in cosmic rays and Wolf-Rayet stars
[OG-8.2-6] 23 p4019 N85-34906
Bursting star formation and the overabundance of Wolf-Rayet stars
[OG-8.2-8] 23 p4019 N85-34907

WOLFRAM
U TUNGSTEN

WOMEN
U FEMALES

WOOD
NT CORK (MATERIALS)
NT PLYWOOD
Thermal-stress analysis for a wood composite blade
[NASA-CR-174794] 08 p1178 N85-17421
Flash pyrolysis of biomass with reactive and non-reactive gases
[DE85-010962] 19 p3306 N85-30496
Airborne sound transmission loss characteristics of wood-frame construction
[AD-A154174] 20 p3524 N85-31919

WOODEN STRUCTURES
Seismic performance of low-rise light-framed wood buildings 08 p1171 N85-17384

WOOL
Properties of polycaproamide fibers modified by grafted polyacrylonitrile 06 p0761 N85-14867
Pathophysiological study of poisoning due to thermal degradation of materials — aircraft cabins
[CERMA-84-15] 11 p1692 N85-20640

WORD PROCESSING
Bulletin of the Faculty of Engineering, Hokkaido University, no. 123
[ISSN-0385-602-X] 04 p0482 N85-13075
Document interchange format
[PB84-217033] 07 p1027 N85-16517
M68000 RNF text formatter user's manual
[NASA-TM-86327] 13 p2146 N85-23320
The Record of Electrical and Communication Engineering Conversazione, volume 53, no. 2, November 1984
[ISSN-0385-7719] 16 p2758 N85-27022
The design of an English word-processor for scientific and technical use in which superscripts, subscripts and Greek characters are operated by screen-edit. 3
16 p2759 N85-27025
A procedure for communications with PDP-10 and PDP-11 (IS/1 UNIX) type computers through use of CPT word processing equipment, revision 1
[DE85-007596] 16 p2845 N85-27540

WORDS (LANGUAGE)
Keyword thesaurus: A list of terms and codes to identify areas of interest for research and other types of sponsored programs (revised October 1984)
[PB85-136893] 10 p1566 N85-19890
Spanish language equivalents for a glossary of terms used in the field of space exploration
[NASA-TM-86211] 19 p3379 N85-30961

WORK
NT PHYSICAL WORK
An update on the capabilities of the Air Force Computerized Occupational Health Program (COHP)
[AD-P004037] 06 p0845 N85-15367
Human aspects in office automation
[PB84-240738] 06 p0847 N85-15376
The principle of virtual work and associated variational principles
[ESA-TT-873] 09 p1340 N85-18428
Sector suite man-machine functional capabilities and performance requirements
[AD-A148881] 10 p1531 N85-19647
Computing environments for data analysis. Part 1: Introduction
[DE85-007919] 17 p3009 N85-28603
Computing environments for data analysis. Part 2: Hardware
[DE85-008320] 17 p3009 N85-28604

WORK CAPACITY
Work capacity of heat and electric power plant operations working 12 hour day and night shifts
09 p1362 N85-18567
Human assembly time versus levels of visual and tactile sensory input: Experimental results for five devices
[AD-A149982] 12 p1909 N85-21960
The relationship between performance and satisfaction: A utility analysis
[AD-A152342] 17 p3000 N85-28546
Cosmonauts' cardiovascular system function during long-term orbital flights aboard Salyut-6 station
22 p3733 N85-33141
Responses of skeletal muscle to unloading, a review
[NASA-CR-176177] 24 p4126 N85-35594
Physiological responses to unvarying (steady) and 2-2-1 shifts: Miami International Flight Service Station
[AD-A155751] 24 p4133 N85-35619

WORK FUNCTIONS
Amorphous metallic layers in Si metallization systems
06 p0830 N85-15277
Energy relations on the small oscillations excitation in the stars 14 p2450 N85-25125
concentration variation of work function of alloys in the system nickel-titanium-aluminum
19 p3247 N85-30134
Study of nonlinear distortion in microwave amplifiers using Schottky gate field effect transistors
22 p3780 N85-33423

WORK HARDENING
NT STRAIN HARDENING
Crack tip opening displacement for work hardening materials
[GKSS-84-E-28] 01 p0063 N85-10415
Work hardening of simple two phase composites
[DE84-014629] 04 p0468 N85-12978
Effect on work-hardening in dynamic deformation of beryllium
[DE85-002691] 11 p1608 N85-20111

WORK-REST CYCLE
Effects of partial deprivation of slow-wave sleep on sleep-wakefulness cycles 10 p1524 N85-19613

Human performance in continuous/sustained operations and the demands of extended work/rest schedules. An annotated bibliography
[AD-A155619] 21 p3686 N85-32771
Psychophysiological distinctions of organization and regulation of daily cyclograms of crew activities during long-term spacecraft 22 p3821 N85-33669
Physiological responses to unvarying (steady) and 2-2-1 shifts: Miami International Flight Service Station
[AD-A155751] 24 p4133 N85-35619

WORKING FLUIDS
NT FERROFLUIDS
Technical Review of the Solid Particle Receiver Program
[DE84-015181] 01 p0068 N85-10451
Method and apparatus for determining the content and distribution of a thermal neutron absorbing material in an object
[DE84-014319] 01 p0117 N85-10801
Analysis of dynamic characteristics of fluid force induced by labyrinth seal 05 p0643 N85-14129
Working medium for sorption heat pumps
[BLL-T6960/BG/WH785/84] 06 p0807 N85-15131
Preliminary evaluation of a liquid belt radiator for space applications
[NASA-CR-174807] 07 p0917 N85-15804
Initial results for supercritical cycle experiments using pure and mixed-hydrocarbon working fluids
[DE84-017008] 09 p1345 N85-18460
Performance of solar thermal systems with liquid metal MHD conversion
[DE85-002758] 11 p1675 N85-20555
Leak detectors for organic Rankine cycle power plants: On-line and manual methods
[DE85-002792] 12 p1652 N85-21617
Thermophysical properties of working fluids for binary geothermal cycles
[DE85-000385] 12 p1681 N85-21804
Effect of operating medium on cyclic durability of AD33-W composite 13 p2029 N85-22716
Advanced radiator concepts
[NASA-TM-87008] 14 p2300 N85-24245
Intrinsically irreversible acoustic heat engines
[DE85-007672] 19 p3270 N85-30276

WORKLOADS (PSYCHOPHYSIOLOGY)
An investigation of the use of steady-state evoked potentials for human performance and workload assessment and control
[AD-A145727] 02 p0237 N85-11541
Decision tree rating scales for workload estimation: Theme and variations
[NASA-CR-174062] 02 p0237 N85-11544
Measuring workload differences between short-term memory and long-term memory scenarios in a simulated flight environment 05 p0703 N85-14513
POPCORN: A supervisory control simulation for workload and performance research
05 p0704 N85-14515
Twentieth Annual Conference on Manual Control, volume 2
[NASA-CP-2341-VOL-2] 05 p0707 N85-14535
Measurement of workload: Physics, psychophysics, and metaphysics 05 p0708 N85-14539
Subjective workload assessment and voluntary control of effort in a tracking task 05 p0708 N85-14540
Decision tree rating scales for workload estimation: Theme and variations 05 p0708 N85-14541
Assessing the subjective workload of directional orientation tasks 05 p0708 N85-14542
Classification systems for individual differences in multiple-task performance and subjective estimates of workload 05 p0708 N85-14543
Measuring pilot workload in a moving-base simulator. Part 2: Building levels of workload
05 p0712 N85-14566
The Sternberg task as a workload metric in flight handling qualities research 05 p0712 N85-14568
Blood pressure levels of active pilots compared with those of air traffic controllers
[AD-A146645] 06 p0846 N85-15373
Dynamic training devices in CRM training
09 p1276 N85-18018
Research at automated ATC Scientific-Experimental Center 09 p1278 N85-18037
Improvement of workload estimation techniques in piloting tasks
[NASA-CR-174374] 10 p1531 N85-19646
Aircrew and avionics: Friends or Foes?
10 p1532 N85-19654
Impact of future aircombat characteristics on pilot performance and cockpit design
10 p1533 N85-19661
Grasp of information by the pilot in future combat aircraft 10 p1533 N85-19662
Pilot workload, performance and aircraft control automation 10 p1534 N85-19670
Aircrew-aircraft integration issues in future US Army helicopters 10 p1535 N85-19672
Operations concept for the advanced automation system man-machine interface
[AD-A149797] 12 p1774 N85-21139
Human assembly time versus levels of visual and tactile sensory input: Experimental results for five devices
[AD-A149982] 12 p1909 N85-21980
Plans for adaptation research during Antarctic expedition 14 p2333 N85-24426
Complex program of ergonomic studies Pilot described 14 p2386 N85-24698
Analysis of team performance in a programmed environment
[NASA-CR-175834] 14 p2392 N85-24728
Dual-task timesharing using a projected attitude display (Malcolm horizon)
[AD-A150789] 14 p2395 N85-24750
Mental workload measurement: Event-related potentials and ratings of workload and fatigue
[NASA-CR-177354] 15 p2619 N85-26139
A comparison of pictorial and speech warning messages in the modern cockpit
[AD-A151917] 16 p2707 N85-26706
Aspects of application of ACT systems for pilot workload alleviation 16 p2712 N85-26734
Statistical study of the dynamic analysis of the workload in the A310 certification campaign
16 p2844 N85-27531
Aspects of application of ACT systems for pilot workload alleviation 17 p2901 N85-27887
The relationship between performance and satisfaction: A utility analysis
[AD-A152342] 17 p3000 N85-28546
Investigation of biochemical and psychological parameters of air traffic controllers in prestart state before beginning to work 19 p3325 N85-30599
Adaptive aiding for symbiotic human-computer control: Conceptual model and experimental approach
[AD-A153870] 19 p3332 N85-30644
Guide on workload forecasting
[PB85-177632] 19 p3341 N85-30704
Speech analysis system for assessing pilots' working fitness 22 p3819 N85-33661
Cardiorespiratory function and work performance during adaptation to industrial labor in midalpine conditions
22 p3820 N85-33665
Models for assessing workload of aircrews on long distance flights 24 p4129 N85-35599
Physiological responses to unvarying (steady) and 2-2-1 shifts: Miami International Flight Service Station
[AD-A155751] 24 p4133 N85-35619

WORKSTATIONS
Extension of the software development workbench to include microcomputer workstations
[AD-A151903] 15 p2630 N85-26207
Design of computer-related workstations in relation to job functions and productivity
[AD-A151938] 16 p2844 N85-27534
NASA space station automation: AI-based technology review. Executive summary
[NASA-CR-176096] 21 p3558 N85-32135

WORLD
U EARTH (PLANET)

WORLD DATA CENTERS
Use of Ebro Observatory data at Word Data Center A for Solar-Terrestrial Physics 04 p0518 N85-13310
On the study of ionospheric disturbances
04 p0522 N85-13335

WORLD METEOROLOGICAL ORGANIZATION
Review of climate problems in Latin America and the Caribbean 07 p1001 N85-16354
The potential contributions of the World Climate Program (WCP) to the economies of developing countries
07 p1003 N85-16371
International list of selected, supplementary and auxiliary ships — WMO
[WMO-47-ED-84] 11 p1687 N85-20609
Commission for Marine Meteorology
[WMO-640] 20 p3496 N85-31735
The 2nd World Meteorological Association Regional Association (Asia), 8th session
[WMO-642] 22 p3817 N85-33643

WRAPAROUND CONTACT SOLAR CELLS
U SOLAR CELLS

WRINKLING
NT FLANGE WRINKLING

WRIST
Kinematic rate control of simulated robot hand at or near wrist singularity
[NASA-TP-2440] 16 p2851 N85-27575
The compliance of end effector force sensors for robot manipulator control 24 p4096 N85-35406

WROUGHT ALLOYS
Characterization of modified 9 r-1 Mo steel sand castings
[DE85-012057] 24 p4080 N85-35287

WU-2 AIRCRAFT
U U-2 AIRCRAFT

WYOMING
Geothermal resources of the Laramie, Hanna, and Shirley Basins, Wyoming
[DE84-016104] 01 p0064 N85-10423
Subsurface temperatures in northeastern Wyoming measured by bottom hole temperature records
[TI84-901610] 04 p0534 N85-13413
Chronologic and climatic control on soil development, northern Bighorn Basin, Wyoming and Montana
08 p1161 N85-17443
Post-Laramide history of North Central Wyoming
08 p1161 N85-17444
Geothermal resources of the Laramie, Hanna and Shirley Basins, Wyoming
[DE85-005005] 23 p3943 N85-34436
Depositional systems and coal occurrence in the Fort Union Formation (Paleocene), Powder River Basin, Wyoming and Montana 24 p4114 N85-35505

X

X BAND
U SUPERHIGH FREQUENCIES

X RAY ABSORPTION
EXAFS studies of sodium silicate glasses containing dissolved actinides
[DE84-015835] 04 p0479 N85-13051
Extended X-ray absorption fine structure (Exafs) studies of the actinides
[DE84-015833] 04 p0559 N85-13561
X-ray absorption in perfect crystals
[DE84-016034] 05 p0732 N85-14708
Measurement of soft X-ray absorption spectra with a fluorescent ion chamber detector
[AD-A142213] 07 p0922 N85-15838
Synchrotron X-ray fluorescence and extended X-ray absorption fine structure analysis
[DE85-003606] 10 p1438 N85-19063
Characterization of thin films and layered structures using X-ray absorption and reflection at grazing incidence
[DE85-006580] 15 p2662 N85-26429

X RAY ANALYSIS
NT LAUE METHOD
X-radiography of slices of the Allende Meteorite
06 p0885 N85-15622
FORTRAN version of the quantitative energy-dispersive electron beam X-ray analysis program FRAME C
[PB84-240936] 07 p1027 N85-16519
Recent investigations at INPE in magnetospheric physics and geomagnetism
[INPE-3280-PRE/603] 10 p1514 N85-19555
K and L-shell cross-sections for X-ray microanalysis in an AEM
[DE85-002733] 11 p1721 N85-20822
The clinical and radiological assessment of cervical injury, Annex A 12 p1907 N85-21976
Head/neck injury: Post mortem procedures, Annex B
12 p1907 N85-21977
In-situ burning rate determination using flash radiography 13 p2002 N85-22550
EXAFS of monolayers on silver electrodes: SSRL proposal number 717M
[AD-A150623] 13 p2018 N85-22652
Application of field X-ray: Radiometric analysis in exploratory geology and means for its improvement
13 p2115 N85-23176
Uniaxial orientation of linear low density polyethylene
[AD-A151037] 14 p2261 N85-24009
Flash radiography 14 p2317 N85-24316
Studies of deformation in niobium by X-ray topographic methods
[AD-A150726] 14 p2427 N85-24965
Secondary fluorescence effects on X-ray microanalysis
[DE85-005565] 15 p2506 N85-25457
La Recherche Aerospatiale Bimonthly Bulletin Number 1984-3, 220/May-June
[ESA-TT-882] 16 p2695 N85-26636
Elemental analysis of aerosols in Transvaal urban and power-producing areas using time and size-resolved samples 16 p2829 N85-27443
Atom location by electron channeling analysis
[DE85-007549] 16 p2872 N85-27716
East Europe report: Science and technology
[JPRS-ESA-85-017] 17 p2945 N85-28177
Proton induced X-ray emission method, its application in analytics 17 p2945 N85-28178

Cosmic X-ray physics
[NASA-CR-175806] 17 p3055 N85-28910
X-ray satellite
[NASA-TM-77896] 20 p3407 N85-31144
Application of Particle Induced X-ray Emission analysis (PIXE) to aerosol long range transport studies
21 p3648 N85-32066
An enhanced photoresponse at dislocation subgrain boundaries revealed by X-ray topography of polysilicon solar cells 22 p3806 N85-33572
X-ray residual stress analysis on the coarse grain of copper and its application to the brazed copper
23 p3907 N85-34202
Study on the correlation between grinding conditions and residual stresses in ground surface of steel by the X-ray method 23 p3907 N85-34203
X-ray measurement of thermal stresses in tungsten fiber-copper composites 23 p3907 N85-34205
X-ray fluorescence analysis of 304L stainless steel
[DE85-013254] 24 p4080 N85-35286
Detection threshold energy of high energy cascade showers using thermoluminescence PTFE-sheet and hot-gas reader
[HE-7.1-5] 24 p4213 N85-36159
Application of thermoluminescence for detection of cascade shower 2: Detection of cosmic ray cascade shower at Mount Fuji
[HE-7.1-12] 24 p4214 N85-36162
X RAY APPARATUS
NT X RAY TUBES
DoD Robotics Application Workshop Proceedings
[AD-A145867] 03 p0307 N85-11976
Robotics in nondestructive inspection at Sacramento Air Logistics Center
[AD-P004012] 03 p0309 N85-11992
Characterizing X-ray machines
[AD-A148532] 06 p0862 N85-15481
X rays from the aurora
[AD-A148828] 08 p1186 N85-17477
Flash X-ray diffraction
[ISL-CO-227/84] 23 p3936 N85-34396
X RAY ASTRONOMY
NT X RAY BINARIES
NT X RAY SOURCES
Rocket observations 01 p0014 N85-10084
Study of a coded mask telescope for astronomical measurements in the hard X-ray domain
[MPE-182] 01 p0129 N85-10889
X-ray observations of the Seyfert 1 galaxies AKN120 and MCG8-11-11
[NASA-TM-86063] 03 p0446 N85-12839
A large scale height galactic component of the diffuse 2-60 keV background
[NASA-TM-83837] 03 p0446 N85-12841
A model of the soft X-ray background as a blast wave viewed from inside 06 p0879 N85-15586
Very Long Base Interferometry (VLBI) in space and X-ray observations of compact sources in active galactic nuclei 07 p1056 N85-16716
Design and fabrication of a CCD camera for use with relay optics in solar X-ray astronomy
[NASA-CR-174334] 08 p1164 N85-17344
Theory tested by means of the stars — viability of the alpha-omega dynamo model 08 p1233 N85-17770
X-ray and UV Emission from Active Galactic Nuclei — conference
[MPE-184] 08 p1236 N85-17790
X-ray emission from active galactic nuclei
08 p1238 N85-17806
EXOSAT observations of active galactic nuclei
08 p1238 N85-17809
Very long base interferometry (VLBI) and X-ray observations of complete samples of radio selected active galactic nuclei 08 p1243 N85-17847
X-ray bursts: Observation versus theory
[NASA-CR-174415] 10 p1573 N85-18916
Contributions of the X-ray astronomy group — conference
[MPE-PREPRINT-28] 11 p1741 N85-20947
Contributions of the X-ray astronomy group — conference
[MPE-PREPRINT-29] 11 p1742 N85-20952
Development of high resolution imaging detectors for X-ray astronomy
[NASA-CR-175505] 12 p1953 N85-22266
X-ray astronomy and plasma astrophysics
12 p1956 N85-22288
Solar and stellar coronal plasmas
[NASA-CR-175623] 13 p2205 N85-23676
Solar maximum mission results on the energetics of the impulsive phase of solar flares 14 p2454 N85-25159
Professional Committee on Solid Propulsion hold conference 15 p2533 N85-25623
A program of ground-based astronomy to complement einstein observations
[AD-A151111] 15 p2668 N85-26466
Spectral constraints on models of gas in clusters of galaxies
[NASA-TM-86188] 15 p2669 N85-26468
Analysis of short-period changes in intensity of hard X-radiation of solar flares registered aboard Venera-13 and Venera-14 spacecraft 16 p2723 N85-26806
Optical pulsar in the Large Magellanic Cloud remnant 0540-69.2
[DE85-006707] 16 p2883 N85-27788
The soft X-ray background as a supernova blast wave viewed from inside: Solar abundance models
[NASA-CR-175767] 16 p2887 N85-27813
Observation of the Crab nebula in the hard X-ray
[MPE-186] 17 p3053 N85-28897
Axion mass limits from pulsar X-rays
[DE85-010634] 18 p3202 N85-29865
The Extended Range X-Ray Telescope center director's discretionary fund report
[NASA-TM-86507] 19 p3362 N85-30983
X-ray satellite
[NASA-TM-77882] 20 p3407 N85-31145
The design, development, testing, fabrication, calibration and integration of a High Resolution Imager (HRI) for the Roentgen Satellite (ROSAT)
[NASA-CR-175302] 22 p3741 N85-33184
Cyg X-3: Not seen in high-energy gamma rays by COS-B
[OG-2.2-2] 22 p3864 N85-33929
Relevance of the observation of UHE gammas to hard X-ray astronomy
[OG-2.2-6] 22 p3865 N85-33932
High-resolution spectroscopic observation of Vela X-1 in the hard X-ray energy range
[OG-2.2-10] 22 p3866 N85-33936
Quasiperiodic oscillations in bright galactic-bulge X-ray sources
[NASA-CR-176138] 23 p3987 N85-34723
Lapex: A Phoswich balloon experiment for hard X-ray astronomy
[OG-9.3-1] 23 p4027 N85-34956
Research of advanced techniques for X-ray detectors and telescopes with applications to rockets and the LAMAR facility
[NASA-CR-176161] 23 p4054 N85-35141
X RAY ASTROPHYSICS FACILITY
Natural environment design criteria for the Advanced X-ray Astrophysics Facility (AXAF) definition and preliminary design
[NASA-TM-86481] 01 p0014 N85-10089
Study of the potential usefulness of superfine holographic x-ray gratings in AXAF and astrophysics in general 12 p1945 N85-22215
X RAY BINARIES
Search for millisecond rotational periods in some low-mass X-ray binaries observed by EXOSAT
11 p1741 N85-20949
Spectral studies of low-mass X-ray binaries observed by EXOSAT 11 p1743 N85-20959
IUE and optical observations of LMC X-ray binaries
11 p1757 N85-21050
Ultra high energy gamma rays, cosmic rays and neutrinos from accreting degenerate stars
[OG-2.2-5] 22 p3864 N85-33931
500 TeV gamma rays from Hercules X-1
[OG-2.2-7] 22 p3865 N85-33933
High-resolution spectroscopic observation of Vela X-1 in the hard X-ray energy range
[OG-2.2-10] 22 p3866 N85-33936
X RAY DENSITY MEASUREMENT
Non-local origin of a substantial portion of the soft X-ray background 06 p0877 N85-15567
X-ray gauge measures areal density variations as small as 0.1%
[DE85-003774] 12 p1854 N85-21629
X RAY DIFFRACTION
Applications of synchrotron X-ray diffraction topography to fractography
[DE84-016257] 04 p0513 N85-13274
X-ray polarization in highly oriented pyrolytic graphite
[DE84-015573] 05 p0613 N85-13917
Microstructural origins of hot spots in RDX explosive and a reference inert material
[AD-A146665] 06 p0774 N85-14947
Mossbauer spectroscopy and X-ray diffraction of samples from the Santa Catharina iron meteorite
06 p0885 N85-15624
Gallium arsenide compounds tested nondestructively with X-rays 07 p0936 N85-15934
X-ray and backscattering analysis of ion implantation phenomena in GaAs and related compounds
[AD-A147449] 07 p1048 N85-16659
Temperature dependence of the crystal structures of Nylon 11
[AD-A147563] 07 p1049 N85-16661
Structural studies of amorphous Mo-Ge alloys using synchrotron radiation
[DE85-002061] 08 p1131 N85-17125
Determination of the elastic constants of inhomogeneous materials with X-ray diffraction
[AD-A148469] 08 p1173 N85-17393
Application of layered synthetic microstructures to high temperature plasma diagnostics
[DE85-002035] 10 p1569 N85-19826
Microscopic magnetic structure of multiple bilayers of thin films of Fe and Ge
[DE85-004186] 13 p2024 N85-22662
Characterization of supported metal catalysts by imaging, microdiffraction and microanalysis techniques
[DE85-005587] 14 p2253 N85-23961
Structural, morphological and optical characteristics of KGd(WO4)2 crystals 14 p2280 N85-24126
Crystallinity determination by curvefit procedure for a semi-crystalline polymer
[NASA-TM-86412] 15 p2517 N85-25520
Ca-Ga, Sr-Ga and Ba-Ga binary systems
[DE85-006454] 16 p2751 N85-26980
X-ray crystallography of steel U8 after pulsed laser hardening
[BLL-BISI-22444-(9022.06)] 17 p2925 N85-28036
X-ray diffraction study of changes in stress-strain distributions during fatigue of a 2-phase alloy
[AD-A152367] 17 p2930 N85-28087
An X-ray diffraction study of the residual stress-strain distribution in shot-peened 2-phase brass
[AD-A152418] 17 p2930 N85-28086
The synthesis and structure of polyphosphazenes
[AD-A153134] 17 p2934 N85-28112
Properties of defects in Hg(1-x)Cd(x)Te
[AD-A153243] 17 p3044 N85-28835
Age hardening and atomic structure of an aluminum-6 at. % silver alloy
[DE85-009977] 18 p3077 N85-29031
A new high-resolution pickup tube for live X-ray topography
[NHK-LABS-NOTE-309] 18 p3193 N85-29802
Application of the reference intensity method to coal analysis
[DE85-009526] 19 p3228 N85-30015
Highly dispersed metal atoms in zeolites
[DE85-010515] 19 p3354 N85-30792
Debye temperature and static displacements in LuH sub x single crystals from energy dispersive X-ray diffraction
[DE85-010961] 19 p3376 N85-30946
Modification of the grain size of sputtered copper with additions of oxygen, krypton, silver, or yttrium
[DE85-010975] 21 p3567 N85-32189
The measurement of strain fields by X-ray topographic contour mapping
[AD-A154870] 21 p3599 N85-32348
Quantitative determination of mineral composition by powder X-ray diffraction
[DE85-011654] 22 p3760 N85-33301
An X-ray diffraction study of titanium oxidation
[NASA-CR-176263] 23 p3915 N85-34264
Flash X-ray diffraction
[ISL-CO-227/84] 23 p3936 N85-34396
X RAY FLUORESCENCE
Synchrotron X-ray fluorescence and extended X-ray absorption fine structure analysis
[DE85-003606] 10 p1436 N85-19063
Evaluating the variability of ceramics with X-ray fluorescence
[DE85-002028] 10 p1453 N85-19155
Highly dispersed metal atoms in zeolites
[DE85-010515] 19 p3354 N85-30792
Variations of particulate sulfur concentrations in a coastal atmospheric environment in connection with the change of air masses origin 21 p3652 N85-32692
X-ray fluorescence analysis of 304L stainless steel
[DE85-013254] 24 p4080 N85-35286
Measurement of uranium enrichment for gaseous uranium at low pressure
[DE85-012697] 24 p4150 N85-35733
X RAY IMAGERY
Development of a dynamic radiographic capability using high-speed video
[DE84-016477] 04 p0511 N85-13256
FLACS: A new sensitometer for measurement of extreme low intensity reciprocity in a controlled environment — X-ray films 07 p0963 N85-16104
The physical implications of an isothermal model for the hot intracluster medium
[NASA-TM-86174] 11 p1763 N85-21089
Development of high resolution imaging detectors for X-ray astronomy
[NASA-CR-175505] 12 p1953 N85-22266
New developments in industrial radiography
14 p2317 N85-24317

Documentation of PHOTO: A user's manual for the analysis of photographic and X-ray negatives
[AD-A152966] 17 p2967 N85-28327
A new high-resolution pickup tube for live X-ray topography
[NHK-LABS-NOTE-309] 18 p3193 N85-29802
Development of observational and instrumental techniques in hard X-ray and medium energy gamma-ray astronomy
[NASA-CR-176172] 24 p4168 N85-35841
High sensitive X-ray films to detect electron showers in 100 GeV region
[HE-3.1-13] 24 p4178 N85-35911
X-ray film chamber with carbon target of Tien-Shan complex array 24 p4179 N85-35915
A new method of differential structural analysis of gamma-family basic parameters
[HE-3.6-3] 24 p4184 N85-35952

X RAY INSPECTION
Quantitative roughness analysis of treated surfaces with higher-class finish by methods of X-ray reflectometry
14 p2282 N85-24136

X RAY IRRADIATION
Lithography radiation effects study
[AD-A149552] 10 p1468 N85-19280
Hit-size effectiveness theory applied to high doses of low LET radiation for pink mutations in Tradescantia
[DE85-011836] 22 p3819 N85-33857
Applications of holography to X-ray imaging
[DE85-010664] 23 p3934 N85-34364
The read-out system of spatial distribution of thermoluminescence in meteorites
[SH-9.1-16] 23 p4052 N85-35131
Neutrino astronomy and the atmospheric background
[HE-5.3-17] 24 p4207 N85-36111

X RAY LASERS
Particle physics
[DE84-013834] 05 p0727 N85-14673
Estimate of nuclear-pumped X-ray laser mechanism
06 p0748 N85-14795
Investigations of vacuum ultraviolet and soft X-ray lasers
[AD-A148277] 08 p1167 N85-17358
Imploding plasma X-ray laser research
[DE85-000057] 09 p1326 N85-18331
KMSF X-ray laser experiments, task no. 1
[DE85-001002] 11 p1639 N85-20325
KMSF X-ray laser experiments, task no. 2
[DE85-000291] 11 p1640 N85-20335
Time resolved X-ray studies during pulsed laser irradiation of Ge
[DE85-005263] 13 p2097 N85-23083
Population inversion in laser-initiated vacuum arcs
[AD-A151968] 16 p2790 N85-27210
Progress in inertial fusion at LLNL
[DE85-010831] 19 p3277 N85-30321
Strong coupling effects on bound states in plasmas
[AD-A154353] 19 p3370 N85-30905
Novette diagnostic support
[DE85-012937] 23 p3934 N85-34383
Photoionization-pumped, Ne 2, X-ray laser studies project
[DE85-012973] 23 p3936 N85-34399
Summary of activities, 1983
[LBL-18500] 23 p3969 N85-34605
Solid neon sources for plasma and X-ray lasers
[DE85-011347] 24 p4098 N85-35402

X RAY SCATTERING
High energy-resolution inelastic X-ray scattering
[DE84-014565] 01 p0118 N85-10604
X-ray and neutron scattering and X-ray spectroscopy for the study of defects in solid state materials
03 p0430 N85-12741
Microstructural analysis of ion containing polymers
[DE85-001584] 10 p1453 N85-19157
Magnetic X-ray scattering studies of the rare Earth metal holmium
[DE85-003606] 12 p1807 N85-21335
Comparison of findings of theories describing reflection from real surface with experiments in region of ultrasoft X-radiation 21 p3694 N85-32950
On gamma and neutrino radiation from Cyg X-3
[OG-2.1-7] 22 p3863 N85-33924
Gamma rays of 0.3 to 30 MeV from PSR 0531+21
[OG-2.3-8] 22 p3866 N85-33945

X RAY SOURCES
NT X RAY BINARIES
X-ray observations of the Seyfert 1 galaxies AKN120 and MCG8-11-11
[NASA-TM-80663] 03 p0446 N85-12839
On syntheses of the X-ray background with power-law sources
[NASA-TM-82173] 03 p0446 N85-12840
Einstein solid state spectrometer observation of the peculiar red dwarf Wolf 630 AB
[NASA-TM-83947] 03 p0447 N85-12843
Ultrasoft X-ray background observations of the local interstellar medium 06 p0877 N85-15571
Preliminary results on the ultraviolet observations of a complete X-ray selected sample of Active Galactic Nuclei (AGN) — HEAO 2 06 p1237 N85-17800
The extragalactic nature of H0323+022
06 p1237 N85-17802
Spatially resolved optical spectroscopy of the radio jet of the X-ray galaxy NGC 2110 06 p1238 N85-17804
X-ray surveys of quasars with the Einstein observatory
06 p1238 N85-17807
Characteristics of X-ray spectra from galactic and extragalactic X-ray sources 06 p1239 N85-17811
EXO 1102.8+2039, an X-ray variable Active Galactic Nucleus (AGN) 06 p1239 N85-17816
Comments on the physics of active galactic nuclei
06 p1240 N85-17823
The ROSAT all-sky survey in X-rays
06 p1243 N85-17843
The ROSAT XUV wide field camera
06 p1243 N85-17844
On the unique capabilities of the Hubble space telescope for studies of ROSAT deep-survey X-ray sources
06 p1243 N85-17846
A survey of fast X-ray transients using the HEAO A-1 Sky Survey experiment 09 p1411 N85-18895
X-ray emission from Centaurus A
[DE85-002030] 09 p1417 N85-18943
Design, construction and initial evaluation of an absolute, time-integrating/time-resolving spectrometer for the diagnostics of pulsed, high temperature plasma X-ray sources in the 100-10,000 eV region
[DE85-003526] 11 p1732 N85-20896
The X-ray structure of the Crab Nebula
11 p1741 N85-20948
Search for millisecond rotational periods in some low-mass X-ray binaries observed by EXOSAT
11 p1741 N85-20949
Optical and X-ray observations of 4U2129+47/V1727 CYG in a quiescent state 11 p1742 N85-20950
EXOSAT observations of the galactic bulge X-ray source GX17+2 — X ray binary star 11 p1742 N85-20951
The X-ray structure of the Crab Nebula
11 p1742 N85-20954
Recent results on the Crab Pulsar X-ray light curve
11 p1742 N85-20955
EXOSAT observations of the 35d intensity variations of Her X-1 — X ray binary source
11 p1742 N85-20956
Pulse phase spectroscopy of Her X-1 with EXOSAT — X ray binary source 11 p1743 N85-20957
Simultaneous EXOSAT and optical observations of the pulsing X-ray binary H2252-035 / AO Psc
11 p1743 N85-20958
Spectral studies of low-mass X-ray binaries observed by EXOSAT 11 p1743 N85-20959
EXOSAT observations of 4U1705-44 — X ray binary
11 p1743 N85-20960
Very recent IUE observations of 2 BL lacertae objects
11 p1746 N85-20982
Considerations for upgrading modifications to the Marshall Space Flight Center's X-ray calibration facility
12 p1946 N85-22226
X-ray experiment on Prognoz-9 artificial Earth satellite
15 p2478 N85-25295
Optical observations of HEAO-B objects
17 p3052 N85-28695
A high energy X-ray study of the galactic center
[AD-A153852] 18 p3202 N85-29862
One-frequency laser interferometer using the optic fiber as a polarization-independent interference phase detector
[DE85-010644] 19 p3277 N85-30326
Salyut-7 cosmonauts work with RS-17 and GSPS X-ray telescopes 22 p3731 N85-33131
Comments on RS-17 X-ray telescope
22 p3731 N85-33132
Astron X-ray experiment 22 p3732 N85-33137
Observation of hard X-rays from the Crab pulsar and A0535+26
[OG-2.3-7] 22 p3866 N85-33944
Search for periodicities near 59 s in the COS-B gamma-ray data of 2CG195+04 (Geminga)
[OG-2.4-3] 22 p3867 N85-33950
A search in the COS-B data base for correlated time variability in regions containing objects of interest
[OG-2.5-9] 22 p3869 N85-33964
Radio observations of four anticenter 2CG gamma-ray sources
[OG-2.5-10] 22 p3869 N85-33965
Balloon observations of hard X-rays from some galactic X-ray sources
[OG-2.5-11] 22 p3870 N85-33966
Further studies of X-ray structure of the Perseus cluster
[OG-2.5-12] 22 p3870 N85-33967
Observation of gamma-rays from LMC X-4 above 10(16) eV
[OG-2.6-10] 22 p3870 N85-33972
The 4U 0115+63: Another energetic gamma ray binary pulsar
[OG-2.6-11] 22 p3870 N85-33973
Balloon observations of hard X-rays from NGC 4151 and an X-ray transient source
[OG-2.7-6] 22 p3871 N85-33979
An extended superhot solar flare X-ray source
[SH-1.2-8] 23 p3991 N85-34743
Capabilities of the GRO/BATSE for monitoring of discrete sources
[OG-9.2-16] 23 p4026 N85-34955
Lapex: A Phoswich balloon experiment for hard X-ray astronomy
[OG-9.3-1] 23 p4027 N85-34956

X RAY SPECTRA
X-ray observations of the Seyfert 1 galaxies AKN120 and MCG8-11-11
[NASA-TM-80663] 03 p0446 N85-12839
On syntheses of the X-ray background with power-law sources
[NASA-TM-82173] 03 p0446 N85-12840
The X-ray spectrum and time variability of narrow emission line galaxies
[NASA-TM-83559] 03 p0446 N85-12842
Secondary fluorescence effects on X-ray microanalysis
[DE84-016600] 05 p0618 N85-13951
Non-LTE considerations in spectral diagnostics of thermal transport and implosion experiments
[DE84-015187] 05 p0730 N85-14689
X-ray and ultraviolet observations of BL Lacertae objects 05 p0741 N85-14767
Measurements of X-ray spectra from laser produced plasma 06 p0748 N85-14794
The nature of the soft X-ray emitting region in the direction of the North Polar spur
06 p0877 N85-15568
HEAO-1 diffuse soft X-ray sky maps
06 p0877 N85-15570
Ultrasoft X-ray background observations of the local interstellar medium 06 p0877 N85-15571
Evidence for non-radiative activity in stars with T sub eff 10000 K 06 p1231 N85-17757
Coronal temperatures 06 p1233 N85-17766
Effect of scattering on instabilities in line-driven stellar winds 06 p1235 N85-17784
Radiative amplification of acoustic waves in hot stars
06 p1235 N85-17786
X-ray emission from active galactic nuclei
06 p1236 N85-17806
Soft X-ray emission from BL Lac objects
06 p1239 N85-17810
Characteristics of X-ray spectra from galactic and extragalactic X-ray sources 06 p1239 N85-17811
X-ray emission from PKS 2155-304 — BL Lac object
06 p1239 N85-17812
X-ray emission from Centaurus A — Vela 5B; radio galaxy 06 p1239 N85-17813
X-ray spectra of accretion disks — active galactic nuclei 06 p1239 N85-17814
The X-ray spectra of NGC 4151 — Seyfert galaxy
06 p1239 N85-17815
One to eight month X-ray light curves for active extragalactic objects 06 p1239 N85-17817
The high energy X-ray spectrum of 3C 273 — quasar
06 p1240 N85-17818
UV and X-ray observations of AGN: Two comparisons with other wave lengths — Active Galactic Nuclei (AGN)
06 p1240 N85-17819
The X-ray properties of high-redshift, optically selected QSOs 06 p1240 N85-17821
On the surface density of X-ray selected BL Lacertae objects 06 p1240 N85-17822
An inverse Compton model of the X-ray emission in Seyfert galaxies 06 p1241 N85-17827
Power law X- and gamma-ray emission from relativistic thermal plasmas 06 p1241 N85-17829
Pair production at moderate optical depths — galactic nuclei X ray spectra 06 p1241 N85-17830
X-ray spectra of accretion disks — active galactic nuclei 06 p1242 N85-17836
The origin of the X-ray background
06 p1243 N85-17841
Temporal and spectral characteristics of solar flare hard X-ray emission
[NASA-TM-86187] 06 p1259 N85-17923
Application of tunable monochromatic synchrotron radiation to the quantitative determination of trace elements
[DE85-001271] 09 p1291 N85-18106
X-ray spectra of supernova remnants
[NASA-TM-86169] 09 p1413 N85-18909

Sequentially-framing soft X-ray pinhole camera for Tokamak plasma studies
[DE85-001717] 10 p1469 N85-19399
Design, construction and initial evaluation of an absolute, time-integrating/time-resolving spectrometer for the diagnostics of pulsed, high temperature plasma X-ray sources in the 100-10,000 eV region
[DE85-003526] 11 p1732 N85-20896
Contributions of the X-ray astronomy group — conference
[MPE-PREPRINT-29] 11 p1742 N85-20952
X-ray coronae of late type stars: Theoretical implications 11 p1742 N85-20953
EXOSAT observations of the 35d intensity variations of Her X-1 — X ray binary source
11 p1742 N85-20956
Spectral studies of low-mass X-ray binaries observed by EXOSAT 11 p1743 N85-20959
IUE and optical observations of LMC X-ray binaries
11 p1757 N85-21050
X-ray emission from active galactic nuclei
[NASA-TM-86175] 11 p1763 N85-21088
Plasma in the clusters of galaxies
12 p1957 N85-22299
A soft X-ray survey of galactic supernova remnants with the Einstein Observatory 14 p2434 N85-25013
High resolution hard X-ray spectra of solar and cosmic sources 14 p2455 N85-25163
Spectroscopy of quasimolecular X-rays with H-like decelerated ions
[DE85-006565] 15 p2649 N85-26337
Spectral constraints on models of gas in clusters of galaxies
[NASA-TM-86188] 15 p2669 N85-26488
X-ray emission and the winds of cataclysmic variables
[DE85-007663] 17 p3053 N85-28902
The solar coronal X-ray spectrum 5.5-12 A
[AD-A152334] 17 p3054 N85-28908
Opticals constant at X-ray wavelengths
[DE85-009743] 19 p3355 N85-30795
Simultaneous Solar Maximum Mission and Very Large Array (VLA) observations of solar active regions
[NASA-CR-176090] 22 p3859 N85-33897
CEN A observation at MeV-energies
[OG-2.7-7] 22 p3871 N85-33980
Investigations of the cyclotron resonance effects in the X ray spectrum of the neutron star Hercules X-1
[MPE-101] 22 p3890 N85-34112
Workshop report on Simulation Techniques for Shock Wave Phenomena and Characteristics of Plasmas in Inertial Confinement Fusion
[IPPJ-725] 23 p3979 N85-34670
X-ray spectra of bursting neutron stars
23 p3981 N85-34686
Multiple inner shell vacancies in laser-irradiated Au plasma 23 p3981 N85-34687
Helios 1 energetic particle observations of the solar gamma ray flare events of 7, 21 June 1980 and 3 June 1982
[SH-1.3-8] 23 p3993 N85-34755
Injection of energetic particles following the gamma-ray flares on June 7, 1980, as observed on Helios 1
[SH-1.3-9] 23 p3993 N85-34756
Multidimensional analysis of data obtained in experiments with X-ray emulsion chambers and extensive air showers
[HE-3.6-2] 24 p4184 N85-35951

X RAY SPECTROGRAPHY
U X RAY SPECTROSCOPY

X RAY SPECTROMETRY
U X RAY SPECTROSCOPY

X RAY SPECTROSCOPY
The X-ray Absorption Coefficient Fine Structure (EXAFS) study on precipitates in AlCu
[DESY-SR-84-15] 01 p0025 N85-10153
X-ray and neutron scattering and X-ray spectroscopy for the study of defects in solid state materials
03 p0430 N85-12741
Space observations of solar flares
04 p0519 N85-13313
Non equilibrium ionization in the local hot bubble
06 p0879 N85-15587
Measurement of soft X-ray absorption spectra with a fluorescent ion chamber detector
[AD-A142213] 07 p0922 N85-15836
An auroral X-ray imaging spectrometer
[AD-A147756] 08 p1185 N85-17469
Simulation of bent crystal spectrometers
[DE85-002042] 09 p1385 N85-18709
X-rays spectroscopy on the PLT and TFTR Tokamaks
09 p1386 N85-18720
Radial profiles of high resolution X-ray spectra from the Alcator C Tokamak 09 p1387 N85-18723
Soft X-ray spectroscopy of laser produced plasmas
09 p1387 N85-18727
X-ray spectroscopy of high-Z and high-density plasmas 09 p1387 N85-18728
Determination of ion temperature and rotation velocity profiles by visible, UV and X-ray spectroscopy on Doublet 3 09 p1388 N85-18734
X-ray spectra of supernova remnants
[NASA-TM-86169] 09 p1413 N85-18909
Characterization of CO binding sites on Rh(111) and Rh(331) surfaces by XPS and LEED (Low Energy Electron Diffraction): Comparison to EELS (Electron Energy Loss Spectroscopy) results
[AD-A149331] 10 p1435 N85-19044
Synchrotron X-ray fluorescence and extended X-ray absorption fine structure analysis
[DE85-003606] 10 p1438 N85-19063
Calculation of Si(Li) X-ray detector efficiencies
[DE85-002732] 10 p1469 N85-19400
X-ray spectroscopy of laser-produced plasmas
[DE85-002170] 11 p1733 N85-20897
Pulse phase spectroscopy of Her X-1 with EXOSAT — X ray binary source 11 p1743 N85-20957
Description of the SSB/A (Special Sensor B/Aerospace X-ray spectrometer
[AD-A150040] 12 p1790 N85-21236
Some unique aspects of fouling on copper as compared to titanium or nickel
[AD-A150072] 12 p1806 N85-21332
Development and application of low energy X-ray and electron physics
[AD-A149963] 12 p1926 N85-22099
The Valence- and conduction-band structure of the sapphire (1102) surface
[AD-A150001] 12 p1940 N85-22184
Magnetic field structures of hard X-ray flares observed by HINOTORI spacecraft — solar flares
14 p2455 N85-25161
X-ray spectroscopy of solids under pressure
[DE85-006939] 15 p2507 N85-25465
Soft X-ray diagnostics of laser-produced plasmas (HALNA) 15 p2655 N85-26382
Cosmic X-ray physics
[NASA-CR-175906] 17 p3055 N85-28910
Proceedings of the Fifth International Conference on Nuclear Methods in Environmental and Energy Research
[DE84-017345] 19 p3310 N85-30521
An empirical technique to measure X-ray production and detection efficiencies in the analytical electron microscope
[DE85-010270] 19 p3361 N85-30837
Chemical structure of interfaces
20 p3460 N85-31629
CCD-based X-ray spectrometry for on-line determination of laser plasma electron temperature
21 p3692 N85-32938
Soft X-ray polychromator for the Solar Maximum Mission
[NASA-CR-175297] 21 p3723 N85-33096
Salyut-7 cosmonauts work with RS-17 and GSPS X-ray telescopes 22 p3731 N85-33131
Astron X-ray experiment 22 p3732 N85-33137
X-ray spectroscopy of solids under pressure
[DE85-011486] 22 p3745 N85-33213
Thermal transport measurements of UV laser irradiated spherical targets
[DE85-011036] 23 p3931 N85-34365
Elliptical X-ray analyzer spectrograph application to a laser-produced plasma
[DE85-013790] 24 p4097 N85-35396
Size and shape dependence of CO adsorption sites on sapphire supported Fe microcrystals
[NASA-CR-176171] 24 p4160 N85-35794

X RAY STRESS ANALYSIS
Multiaxial stress analysis taking account of penetration depth of X-rays. A solution by means of polynomial approximation 23 p3907 N85-34204

X RAY TELESCOPES
A normal incidence, high resolution X-ray telescope for solar coronal observations
[NASA-CR-174145] 04 p0579 N85-13689
Considerations for upgrading modifications to the Marshall Space Flight Center's X-ray calibration facility
12 p1946 N85-22226
A normal incidence, high resolution X-ray telescope for solar coronal observations
[NASA-CR-175622] 13 p2169 N85-23461
A rocket-borne X-ray observation of SN1006 with the imaging gas scintillation proportional counter
14 p2435 N85-25014
The Extended Range X-Ray Telescope center director's discretionary fund report
[NASA-TM-86507] 19 p3382 N85-30963
Salyut-7 cosmonauts work with RS-17 and GSPS X-ray telescopes 22 p3731 N85-33131
Comments on RS-17 X-ray telescope
22 p3731 N85-33132
Astron X-ray experiment 22 p3732 N85-33137
Coordinated study of solar-terrestrial payloads on space station
[NASA-CR-176160] 23 p3900 N85-34158
Soft X-Ray Telescope (SXRT)
23 p3900 N85-34159
A comparison of calculated and measured background noise rates in hard X-ray telescopes at balloon altitude
[OG-9.3-7] 23 p4026 N85-34962
A normal incidence X-ray telescope sounding rocket payload
[NASA-CR-176169] 24 p4153 N85-35749

X RAY TUBES
Considerations for upgrading modifications to the Marshall Space Flight Center's X-ray calibration facility
12 p1946 N85-22226

X RAYS
NT COSMIC X RAYS
NT SOLAR X-RAYS
Determining composition in surface region of semiconductor crystals by method of sudden changes in X-ray photoelectric effect 02 p0267 N85-11746
Experimental capabilities and prospects for measuring soft X-ray photoabsorption
[DE84-015486] 02 p0278 N85-11813
Energetic electrons in impulsive solar flares
02 p0303 N85-11952
Flash radiography as a quantitative tool
[DE84-016465] 04 p0503 N85-13211
Real space solution to the phase problem in X-ray crystallography: ALCAMPS (Ames Laboratory Computer-aided Analysis of Multi-solution Patterson Superpositions)
[DE84-015476] 04 p0572 N85-13651
A neutral gas jet in a low velocity shock front at the boundary of the Draco Nebula 06 p0878 N85-15576
Improved radiographic viewing system
[AD-A147587] 07 p1016 N85-16456
X rays from the aurora
[AD-A148628] 08 p1186 N85-17477
X-ray activity in pre-main sequence stars
08 p1233 N85-17764
Is the ratio of observed X-ray luminosity to bolometric luminosity in early-type stars really a constant?
08 p1234 N85-17777
Non-radiative energy from differential rotation in hot stars 08 p1234 N85-17778
Bipolar flows and X-ray emission from young stellar object 08 p1234 N85-17779
A microchannel plate pinhole camera for 20 to 100 keV X-ray imaging
[DE85-001572] 10 p1468 N85-19396
X-ray holography of biological specimens
[DE85-002437] 10 p1469 N85-19398
Coronal effects of the winds of early-type stars
11 p1749 N85-21002
Development and application of low energy X-ray and electron physics
[AD-A149963] 12 p1926 N85-22099
X-ray lithography and VLSI circuits
13 p2062 N85-22846
Utilization of microchannel plates in the flash X-ray technique
[ISL-CO-226/83] 14 p2306 N85-24275
Basic principles of industrial radiography
14 p2316 N85-24310
Auroral X-rays and equatorial electrons in the morning sector — substorm 14 p2361 N85-24590
On the location of the source for X-ray microbursts
14 p2361 N85-24591
Workshop report on new directions in soft X-ray photoabsorption
[DE85-006150] 14 p2419 N85-24923
X-ray emission in heavy ion collisions
[DE85-006360] 14 p2419 N85-24927
X-ray polarimetry: The measurement of the polarization of solar flare X-rays and the design of a Compton polarimeter 14 p2441 N85-25059
Annual Review, April 1983 - March 1984
[ISSN-0547-1567] 15 p2654 N85-26369
An X-ray study of residual stresses in narrow groove TIG weldments
[DE85-006485] 16 p2802 N85-27274
Software for reflectivity calculations of X-ray mirrors, revision 1
[DE85-006642] 16 p2867 N85-27688
A synchrotron/inverse Compton interpretation of a solar burst producing fast pulses at lambda 3 mm and hard X-rays 16 p2887 N85-27815
Documentation of PHOTO: A user's manual for the analysis of photographic and X-ray negatives
[AD-A152966] 17 p2967 N85-28327
Coherent X-rays and vacuum-ultraviolet radiation from storage-ring-based undulators and free electron lasers
[DE85-009968] 18 p3163 N85-29736

Design consideration for the X-ray Cerenkov experiment
[AD-A153696] 18 p3189 N85-29777
Three-dimensional and tomographic imaging device for X-ray and gamma-ray emitting objects
[NASA-CASE-GSC-12851-1] 19 p3271 N85-30281
Symposium on Luminescent Radiation Receivers and Converters 19 p3295 N85-30430
Opticals constant at X-ray wavelengths
[DE85-008743] 19 p3355 N85-30795
An empirical technique to measure X-ray production and detection efficiencies in the analytical electron microscope
[DE85-010270] 19 p3361 N85-30837
Comparison of findings of theories describing reflection from real surface with experiments in region of ultrasoft X-radiation 21 p3694 N85-32950
Contributions to the 19th International Cosmic Ray Conference
[NASA-CR-176080] 21 p3714 N85-33044
Salyut-7 cosmonauts work with RS-17 and GSPS X-ray telescopes 22 p3731 N85-33131
Results from Astron orbiting telescope
22 p3732 N85-33134
Gamma-ray burst variability above 4 MeV
[OG-1.2-7] 22 p3862 N85-33917
Observations on TeV gamma rays from Geminga and PSR 0950+08
[OG-2.4-6] 22 p3868 N85-33953
Balloon observations of hard X-rays from some galactic X-ray sources
[OG-2.5-11] 22 p3870 N85-33966
Further studies of X-ray structure of the Perseus cluster
[OG-2.5-12] 22 p3870 N85-33967
Some evidence for large gravitational redshift in Seyfert galaxy NGC 4151
[OG-2.7-11] 22 p3872 N85-33984
Spectrum of the gamma-ray diffuse component observed from HEAO-1
[OG-3.1-12] 22 p3874 N85-34000
Applications of holography to X-ray imaging
[DE85-010984] 23 p3934 N85-34384
Quasiperiodic oscillations in bright galactic-bulge X-ray sources
[NASA-CR-176138] 23 p3987 N85-34723
A position sensitive phoswich hard X-ray detector system
[OG-9.3-12] 23 p4028 N85-34967
Generation of stimulated emission in the soft X-ray range by nonlinear processes with excimer lasers
[DE85-012465] 24 p4098 N85-35403
On a possibility of inelasticity partial coefficient K sub gamma determination in pi C and pi Pb interactions at 10 to the 14th power eV (experiment PAMIR 1)
[HE-1.1-12] 24 p4171 N85-35859
Experiment Pamir-3. Coplanar emission of high energy gamma-quanta at interaction of hadrons with nuclei of air atoms at energies above 10 to the 7th power GeV
[HE-1.4-12] 24 p4177 N85-35899
Hadrons registration in emulsion chamber with carbon block
[HE-3.7-3] 24 p4186 N85-35962
Structured events in Pamir carbon X-ray chambers
[HE-3.7-7] 24 p4186 N85-35965
Ultra high energy events in ECHOS series and primary energy spectrum
[HE-3.7-9] 24 p4188 N85-35966

X-15 AIRCRAFT
Low-speed longitudinal orbiter qualities
08 p1092 N85-16905

X-29 AIRCRAFT
Multivariable control law design for the X-29 aircraft
[AD-A151828] 15 p2472 N85-25259
X-29 digital flight control system design
17 p2901 N85-27889

XB-70 AIRCRAFT
U B-70 AIRCRAFT

XBQM-108A AIRCRAFT
U VATOL AIRCRAFT

XENON
NT XENON ISOTOPES
NT XENON 129
Where is the Earth's missing xenon?
06 p0888 N85-15641
Kinetic studies following state selective laser excitations
[DE85-007173] 15 p2564 N85-25816
Double photon excitation of high-Rydberg atoms as a long-lived submillimeter detector
[NASA-CASE-NPO-16372-1] 19 p3352 N85-30779
Energy transfer and excimer formation in rare gas solids 19 p3374 N85-30930
Powerful XeCl excimer electric discharge laser with good temporal stability and fast response time
21 p3688 N85-32911
Interactions of heavy nuclei, Kr, Xe and Ho, in light targets
[OG-7.2-21] 23 p4016 N85-34888
Stopping relativistic Xe, Ho, Au and U nuclei in nuclear emulsions 24 p4173 N85-35876
Experimental basis for the models of cascade propagation in atmosphere
[HE-3.6-6] 24 p4186 N85-35954

XENON CHLORIDE LASERS
Electric discharge excitation and energy source integration
[AD-A151502] 15 p2562 N85-25806
Discharge characteristics of high-pressure, fast-discharge XeCl excimer laser
15 p2564 N85-25820

XENON FLUORIDE LASERS
Investigation of plasma processes in electronic transition lasers
[AD-A148862] 12 p1834 N85-21506

XENON ISOTOPES
NT XENON 129
The I-Pu-Xe age of the Moon
04 p0584 N85-13729
The degassing history of the Earth: Noble gas studies of Archaean cherts and zero age glassy submarine basalts 21 p3718 N85-33072
Nuclear reactions in shock wave front during supernova events
[OG-8.2-19] 23 p4021 N85-34915

XENON 129
When did the average cosmic ray flux increase?
[SH-7.1-4] 23 p4047 N85-35097

Y

YAG (GARNET)
U YTTRIUM-ALUMINUM GARNET

YAG LASERS
Optical recording of information on paper by CO2 and YAG-lasers 02 p0261 N85-11710
Optimization of ultrashort pulse generation mode of YAG laser 02 p0262 N85-11713
Anomalies in frequency characteristics of solid-state ring laser 02 p0271 N85-11765
Laser balancing system for high material removal rates
[NASA-CR-174731] 03 p0365 N85-12341
Design and testing of a refractive laser beam homogenizer
[AD-A146897] 07 p0970 N85-16162
Highly efficient Nd:YAG lasers for free-space optical communications 10 p1463 N85-19229
Solid state luminescent light filters for neodymium lasers 11 p1716 N85-20799
Lasing characertistics of YAG: Nd(3+)-laser with LiF passive shutter with F2 color centers
11 p1717 N85-20802
Stability of temporal and energy parameters of picosecond lanthanum beryllate laser
11 p1717 N85-20804
Neodymium YAG laser pumped with radiation from high frequency electrodeless discharge
13 p2044 N85-22796
Laser Welding, Cutting and Surface Treatment
14 p2306 N85-24278
Laser welding in the manufacture of heart pacemakers
14 p2306 N85-24286
Lasers in the nuclear industry
14 p2309 N85-24289
Laser drilling of aeroengine components
14 p2309 N85-24290
Future trends in the use of lasers in manufacturing
14 p2309 N85-24291
Amplification of scattered induced radiation flux in high-gain laser rods 15 p2644 N85-26309
Raman studies of surface temperature in laser-heated semiconductors
[AD-A151377] 15 p2659 N85-26412
Conducting a wind sensing study
[NASA-CR-175782] 16 p2832 N85-27465
Feasibility study on Laser Doppler Anemometer (LDA) wind velocity measurements using pulsed visible laser light
[ISL-CO-224/83] 16 p2836 N85-27489
Design and construction of a CW ND:YAG laser using a single elliptical cavity and water cooled krypton arc lamp pumping
[AD-A152657] 17 p2970 N85-28340
Laser machining and some applications
[NHK-LABS-NOTE-307] 18 p3112 N85-29266
Development and application of a high power ND-glass laser instrument
[AD-A154366] 19 p3276 N85-30314
Choice of optimum saturating absorber for YAG passive mode-locking laser 21 p3685 N85-32893
Operation of solid state lasers exposed to electron beam 21 p3685 N85-32895
Passive Q-modulation of optical cavities by KCl crystals containing OH(-) -ions 21 p3686 N85-32915
Holographic cinematography with the help of a pulse YAG laser
[ISL-CO-213/84] 22 p3788 N85-33472
Cineholography
[ISL-CO-214/84] 22 p3788 N85-33473

YANG-MILLS FIELDS
Supersymmetric Yang-Mills fields as an integrable system and connections with other non-linear systems
[DE84-013231] 04 p0556 N85-13539

YARNS
The effects of radial yarns, 3-dimensionally reinforced carbon-carbon composite
[AD-A144751] 01 p0022 N85-10134
Thermoplastic-carbon fiber hybrid yarn
[NASA-CR-3849] 03 p0325 N85-12093

YAW
Robust rate control system designs for a submersible
[AD-A144792] 01 p0111 N85-10753
Oil-flow study of a Space Shuttle orbiter tip-fin controller
[NASA-TM-86276] 04 p0450 N85-12920
Hypothetical zero yaw drag trajectory of spinning projectiles between M = 5 and M = 10
[AD-A148698] 10 p1421 N85-18963
Static investigation of several yaw vectoring concepts on nonaxisymmetric nozzles
[NASA-TP-2432] 18 p3058 N85-28924

YAWING MOMENTS
Liquid moment on a filled coning cylinder during spin-up: Ad hoc model
[AD-A150280] 13 p2092 N85-23060

YAWMETERS
U ATTITUDE INDICATORS
U YAW

YEAST
Microbial ecology of extreme environments: Antarctic yeasts and growth in substrate-limited habitats
[NASA-CR-175810] 16 p2839 N85-27509
Microbial ecology of extreme environments: Antarctic yeasts and growth in substrate-limited habitats
[NASA-CR-176005] 19 p3226 N85-30609

YF-17 AIRCRAFT
U F-17 AIRCRAFT

YHU-1 HELICOPTER
U UH-1 HELICOPTER

YIELD
Crop yield forecasting 07 p1001 N85-16360
NOAA-AISC user's guide for implementing CERES maize model for large area yield estimation
[E85-10083] 12 p1873 N85-21748
Electron yields from spacecraft materials
13 p1996 N85-22512
Surface waveseismic yields as measured by the Regional Seismic Test Network
[DE85-010532] 18 p3137 N85-29425

YIELD POINT
Removal of singularities in Tresca and Mohr-Coulomb yield functions
[OUEL-1526/84] 03 p0413 N85-12642
A simple engineering treatment of center cracked tension panels in the regime of nonlinear fracture mechanics under plane stress conditions
[GKSS-84-E-38] 08 p1173 N85-17396
The influence of mechanical damage on transmission pipeline integrity
[ERS-E.351] 09 p1340 N85-18431
Recent studies of the significance of mechanical damage in pipelines
[ERS-E.367] 09 p1341 N85-18433
Dynamic pressure test unit-ratio method
[AD-D011486] 10 p1488 N85-19392
Yield joint condition for three-dimensional I-beams
[ILR-MITT-137] 12 p1867 N85-21716
Magnetic method of inspecting mechanical properties of general purpose tubes
[BLL-M-36084-(5828.4)] 16 p2796 N85-27235
Fuel containment and damage tolerance in large composite primary aircraft structures
[NASA-CR-166083] 19 p3231 N85-30032
Effect of edge distance on yield initiation in a remotely loaded half-plane containing interference-fit disc of the same material
[ARL/STRUC-R-413] 19 p3285 N85-30369
Fuel containment and damage tolerance for large composite primary aircraft structures. Phase 1: Testing
[NASA-CR-166091] 24 p4073 N85-35241

YIELD STRENGTH
NT MICROYIELD STRENGTH
Multiaxial yield behavior of 1100 aluminum following various magnitudes of prestrain
[DE84-013904] 05 p0617 N85-13949

Defining effect of hardening on mean yield strength in deformation zone
[BLL-M-35804-(5828.4)] 05 p0647 N85-14154
Yield joint condition for three-dimensional I-beams
[ILR-MITT-137] 12 p1867 N85-21716
Structural strenght of strip D16T aluminum alloy with low copper and magnesium content
13 p2025 N85-22691
New deformable secondary aluminum alloys
13 p2026 N85-22694
Experimental investigation of crippling strength of Chinese aluminum alloy (LY12CZ) sections
13 p2041 N85-22779
Effect of oxygen on mechanical properties of Nb-V alloy
[DE85-002881] 14 p2256 N85-23982
Cast-iron technology: Metallographic and mechanical testing results
[DE85-002884] 14 p2257 N85-23984
Elastic-plastic analysis for cyclic loading using a linearized yield condition
[PB85-149607] 14 p2322 N85-24346
Magnetic method of inspecting mechanical properties of general purpose tubes
[BLL-M-36084-(5828.4)] 16 p2796 N85-27235
The Mises yield condition for thin rotationally symmetric shells
[BLL-BISI-TRANS-22047-(9022.06)]
17 p2976 N85-28409
Strength versus toughness relation in Fe-high manganese alloys
[DE85-007682] 18 p3074 N85-29013
Aging study of copper alloy 172
[DE85-009848] 18 p3075 N85-29023
Yield stress determination from miniaturized disk bend test data
[DE85-009485] 18 p3122 N85-29330
Effect of edge distance on yield initiation in a remotely loaded half-plane containing interference-fit disc of the same material
[ARL/STRUC-R-413] 19 p3285 N85-30369
Fatigue-crack growth and ductile fracture toughness behavior of ASTM A387 Grade 91 steel
[DE85-008495] 20 p3431 N85-31286
Mechanical properties of plasma arc cut steel
23 p3905 N85-34186
YIG (GARNET)
U YTTRIUM-IRON GARNET
YJ-85 ENGINE
U J-85 ENGINE
YOUNG MODULUS
U MODULUS OF ELASTICITY
YTTERBIUM
Optimization of the NiCrAl-Y/ZrO-Y2O3 thermal barrier system
[NASA-TM-86905] 07 p0927 N85-15878
Thermal barrier coating system
[NASA-CASE-LEW-14057-1] 24 p4072 N85-35233
YTTRIUM
High-temperature erosion of plasma-sprayed, yttria-stabilized zirconia in a simulated turbine environment
[NASA-TP-2406] 04 p0478 N85-13045
Compatibility experiments of facilities, materials, and propellants for electrothermal thrusters
[NASA-TM-86956] 12 p1795 N85-21260
Magnetovolume effects in some Y-Ni intermetallic compounds
[ISSN-0066-2003] 13 p2021 N85-22663
Improvement by cerium and yttrium ion implantation of oxidation behaviour of stabilised stainless steel in carbon dioxide
[AERE-R-11523] 14 p2259 N85-23996
A study of adherent oxide scales
[AD-A155554] 21 p3567 N85-32186
Modification of the grain size of sputtered copper with additions of oxygen, krypton, silver, or yttrium
[DE85-010975] 21 p3567 N85-32189
Calculation of activities of components in liquid alloys of iron with yttrium
[BLL-M-35868-(5828.4)] 23 p3914 N85-34253
Influence of yttrium on eutectoid transformation in irons
[BLL-M-35787-(5828.4)] 24 p4078 N85-35270
YTTRIUM COMPOUNDS
NT YTTRIUM OXIDES
NT YTTRIUM-ALUMINUM GARNET
NT YTTRIUM-IRON GARNET
Research on electroluminescence in thin film yttrium oxysulfide
[AD-A146909] 07 p1037 N85-16582
YTTRIUM OXIDES
Fundamental studies of structure property relationship in transformation toughened ceramics
[DE84-015344] 01 p0033 N85-10204
Study of the reactive-element effect in oxidation of Fe-Cr alloys using transverse section analytical electron microscopy
[DE84-016237] 04 p0571 N85-13641
Densification of submicron YSZ (Yttria-Stabilized Zirconia) powders with alumina and borate additives
[AD-A148620] 10 p1482 N85-19150
Progress on transparent yttria
[AD-P004370] 12 p1827 N85-21484
High-temperature X-ray diffraction study of coating-substrate compatibility in yttria-coated graphite
[DE85-006916] 14 p2282 N85-24016
Passivation on high Q acoustic strain sensor for accelerometer
[AD-A153565] 18 p3177 N85-29695
Process for improving the quality of epitaxial silicon films grown on insulating substrates
[AD-D011730] 22 p3847 N85-33626
YTTRIUM-ALUMINUM GARNET
Phonon-impurity relaxation and acoustic wave absorption in yttrium-aluminum garnet crystals with impurities 11 p1715 N85-20790
Electron-oscillatory spectra of yttrium-erbium-aluminum garnet of crystals and their role in laser pumping
11 p1715 N85-20791
YTTRIUM-IRON GARNET
Symmetry of exchange interaction in crystalline magnetic films 02 p0259 N85-11694
YUGOSLAVIA
The time and frequency comparisons via Loran-C and National TV Network in Yugoslavia
18 p3109 N85-29248
YUH-1 HELICOPTER
U UH-1 HELICOPTER
YUH-60A HELICOPTER
U UH-60A HELICOPTER

Z

ZEEMAN EFFECT
Development of novel lamps for study of enhanced production of resonance by low-density mercury discharges
[DE84-015890] 05 p0632 N85-14053
EPR linewidth studies of unpaired electrons at the Si-SiO2
[DE84-016727] 05 p0733 N85-14712
Nonlinear optical studies of rydberg atoms using degenerate four-wave mixing
[AD-A146827] 07 p1043 N85-16623
Basic studies of atomic dynamics
[DE84-015861] 09 p1380 N85-18675
Trends in measurement of solar vector magnetic fields using the Zeeman effect 18 p3204 N85-29877
Contribution functions for Zeeman-split lines, and line formation in photospheric faculae
18 p3207 N85-29893
ZENER DIODES
U AVALANCHE DIODES
ZENITH
Winter anomaly 1982/83 in comparison with earlier winters (1960-82) 11 p1660 N85-20461
Development of a portable zenith chamber and its use on the 47th parallel
[SER-C-287] 11 p1741 N85-20946
Simultaneous Earth observations from 2 satellites
[NASA-TM-86204] 16 p2810 N85-27325
The thickness of the shower disc as observed in showers produced by primaries above 10 (19)eV
[HE-4.7-6] 24 p4199 N85-36057
Thickness of the particle swarm in cosmic ray air showers
[HE-4.7-14] 24 p4200 N85-36064
Energy spectrum of cascades generated by muons in Baksan underground scintillation telescope
[HE-5.1-15] 24 p4202 N85-36077
Geophysical searches for three-neutrino oscillations
[HE-5.3-9] 24 p4205 N85-36103
ZEOLITES
Influence of structural parameters of zeolite catalysts on their activity and selectivity
[BMFT-FB-T-83-253] 03 p0329 N85-12119
Neutron diffraction studies of the hydrogen bonding and water molecules in zeolites
[DE84-016431] 06 p0766 N85-14900
Catalytic oxidation by transition metal ions in zeolites
[AD-A146828] 07 p0922 N85-15842
Advanced NMR characterization of zeolite catalysts
[DE85-000456] 09 p1291 N85-18104
Cation promotion effects in zeolite-supported F-T catalysts
[DE85-001706] 09 p1291 N85-18106
Zeolites on Mars: Prospects for remote sensing
13 p2195 N85-23615
Chemical weathering of soils from the dry valleys of Antarctica: A terrestrial analog of Martian weathering processes 13 p2197 N85-23628
Experimental testing of cooling by low pressure adsorption in a zeolite
[DE85-007509] 16 p2716 N85-26763
Correlation of zeolite ZSM-5 acid strength with catalytic activity and selectivity
[DE85-005415] 17 p2922 N85-28013
High resolution powder diffraction
[DE85-006287] 17 p2922 N85-28015
Cation promotion effects in zeolite-supported F-T catalysts
[DE85-009969] 19 p3233 N85-30044
Advanced NMR characterization of zeolite catalysts
[DE85-010143] 19 p3363 N85-30853
Rigid zeolite containing polyurethane foams
[DE85-008406] 23 p3919 N85-34286
Determination of properties of zeolite/refrigerant combinations for solar refrigeration systems
[DE85-012009] 23 p3945 N85-34448
FTIR studies of hydrocarbon synthesis on Pd/ZSM5 catalysts
[DE85-012430] 24 p4071 N85-35230
ZERO CROSSINGS
U ROOTS OF EQUATIONS
ZERO GRAVITY
U WEIGHTLESSNESS
ZERO LIFT
On relaxation of transonic flows around zero-lift airfoils and convergence of self-correcting wing tunnels
11 p1622 N85-20214
ZERO POINT ENERGY
Effective brightness of zero-point fluctuations of the electromagnetic vacuum accompanying parametric scattering of light 21 p3684 N85-32961
Evaluation of parameters for particles acceleration by the zero-point field of quantum electrodynamics
[OG-8.2-16] 23 p4020 N85-34912
ZERO POWER REACTORS
Monte Carlo alpha calculation
[DE85-010720] 19 p3349 N85-30758
Sulfur activation at the Little Boy-Comet Critical Assembly: A replica of the Hiroshima bomb
[DE85-010261] 20 p3527 N85-31938
ZETA AURIGAE STAR
Accretion in the zeta Aurigae and 32 Cygni shock cones 11 p1754 N85-21036
Egress spectra of the new eclipsing supergiant 22 Vulfeculae 11 p1755 N85-21039
ZETA PINCH
Finite orbit analysis for long wavelength modes in a plasma with a hot component
[DE85-006896] 15 p2666 N85-26404
ZINC
Universal binding energy relations in metallic adhesion
[NASA-TM-86869] 03 p0331 N85-12132
Alabama Tin Belt: Metallogenesis and mineral resource evaluation. Year-end report
[DE84-901335] 07 p0989 N85-16283
Thermal design requirements of a 50-kW zinc/redox flow battery for solar electrical energy storage
[DE84-017068] 09 p1345 N85-18463
Humidity effects on adhesion of nickel-zinc ferrite in elastic contact with magnetic tape and itself
[NASA-TP-2449] 12 p1811 N85-21359
Research on separators for alkaline zinc batteries
[DE85-003082] 12 p1836 N85-21523
New deformable secondary aluminum alloys
13 p2026 N85-22694
Aluminum alloy ATs5K5 (5% Zn + 5% Ca) for superplastic forming 13 p2026 N85-22697
Observation of a novel low-lying excited state in zinc complexes
[AD-A150188] 13 p2156 N85-23365
Thin film cadmium telluride and zinc phosphide solar cells
[DE85-002904] 15 p2587 N85-25950
Characteristics of polyacrylic acid-complexed zinc phosphate conversion films deposited on metal surfaces
[DE85-004057] 16 p2750 N85-26974
New approaches to functionalized fluorocarbons
[AD-A154205] 19 p3248 N85-30141
Photoelectronic properties of zinc phosphide crystals and heterojunctions
[DE85-008777] 19 p3307 N85-30501
Zinc: Biological effects. Facts and fiction
[USIP-84-12] 20 p3507 N85-31798
Plasma mass and effective inductance in a small railgun
[AD-A154644] 21 p3589 N85-32304
Environmental surveillance at Los Alamos during 1984
[DE85-011888] 22 p3811 N85-33605
The Conterminous United States Mineral Assessment Program 24 p4106 N85-35458

ZINC ALLOYS
Sea water rope batteries
[AD-A144775] 01 p0042 N85-10275
Application of the diffraction model to amorphous magnesium zinc alloys
[AD-A147389] 07 p0888 N85-18883
Influence of excess phases on fracture toughness of cast aluminum-magnesium-zinc alloy
10 p1442 N85-19091
Study of superplastic alloys based on Al-Zn-Ca
10 p1442 N85-19092
The role of hydrogen in the stress corrosion failure of high strength Al-Zn-Mg alloys
[AD-A150891] 14 p2258 N85-23976
Temperature variation of resistivity of certain alloys based on transition and simple metals in amorphous and crystalline states 15 p2496 N85-25399
Thermal expansion effects in electrical transport in amorphous metals
[AD-A152477] 17 p2930 N85-28089
Study of phase equilibria and crystallization processes in Al-Zn-Mg alloy systems 19 p3241 N85-30098
Resistance to corrosion fatigue in aluminum alloy 1561 in sea water 19 p3243 N85-30108
ZINC CHLORIDES
Transport in aqueous battery systems
[DE85-007246] 17 p2955 N85-28251
ZINC COATINGS
Galvanized wire protected against corrosion by chromate passivization
[BLL-M-35908-(5828.4)] 05 p0816 N85-13936
High strength steel sheet with dual phase structure
[BMFT-FB-T-84-219] 12 p1806 N85-21342
Corrosion of aircraft Al and Al-Zn ion plated steel fasteners 13 p2021 N85-22666
The effect of water chemistry on the rates of hydrogen generation for galvanized steel corrosion at post-loca conditions
[NUREG/CR-3361] 14 p2253 N85-23963
The corrosion resistance of zinc coatings on depleted uranium and uranium alloys
[DE85-007216] 15 p2510 N85-25487
New corrosion protection concept for very high voltage line towers
[BLL-OA-TRANS-2891-(8196.300)]
20 p3429 N85-31270
Effects of humidity cycles on the corrosion of galvanised reinforcements in carbonated and uncarbonated mortars
[BLL-CE-TRANS-8039-(9022.09)]
20 p3430 N85-31272

ZINC COMPOUNDS
NT ZINC CHLORIDES
NT ZINC OXIDES
NT ZINC SELENIDES
NT ZINC SULFIDES
The alpha-form of the hydroxides of bivalent metals
[NASA-TM-77506] 04 p0473 N85-13009
Magnetic and structural properties of shock-synthesized zinc ferrite
[DE85-000469] 11 p1736 N85-20915
Properties of chromate coatings formed on electrolytic zinc substrates
[BLL-BISI-TRANS-22349-(9022.06)]
17 p2926 N85-28052

ZINC NICKEL BATTERIES
U NICKEL ZINC BATTERIES
ZINC OXIDES
Solid state, surface and catalytic properties of oxides
[DE85-002096] 06 p0867 N85-15512
Advanced metal oxide varistor concepts
[DE84-016677] 09 p1316 N85-18276
Stability of highly nonlinear oxide-zinc resistors under continuous voltage of industrial frequency
13 p2087 N85-23030
Vapor sensing by means of a ZnO-on-Si surface acoustic wave resonator
[DE85-003250] 15 p2546 N85-26324
Effects of processing chemistry on electrical properties of high field ZnO varistors
[DE85-007668] 17 p2958 N85-28254
A study of Co and Mn in ZnO varistors
[DE85-011193] 19 p3263 N85-30233
Gas sensing with surface acoustic wave devices
[DE85-009125] 20 p3524 N85-31921
High temperature solar electrothermal processing 2. Zinc from zinc oxide
[AD-A154747] 21 p3562 N85-32158
Development and evaluation of sulfonated polysulfone membranes for the zinc-ferricyanide battery
[DE85-009104] 24 p4090 N85-35357
ZINC SELENIDES
Effect of oxidizing medium and heat treatment on stoichiometry of ZnSe crystal surface
03 p0353 N85-12272

Zn3P2 as an improved semiconductor for photovoltaic solar cells
[DE85-008772] 18 p3097 N85-29171
ZINC SULFIDES
Laser induced damage of zinc sulphide
[BAE-ST-13363] 15 p2562 N85-25803
Zn3P2 as an improved semiconductor for photovoltaic solar cells
[DE85-008772] 18 p3097 N85-29171
Prospects for parallel nonlinear optical signal processing using GaAs etalons and ZnS interference filters
18 p3187 N85-29765
Vectorial electron transfer on designed surfaces
[PB85-204600] 24 p4076 N85-35263
ZINC-BROMIDE BATTERIES
Prospects for advanced storage battery technologies
[DE84-015706] 09 p1348 N85-18484
ZINC-CHLORINE BATTERIES
Baseline cycle testing of a 500-kWh zinc chloride battery at the Battery Energy Storage Test (BEST) Facility
[DE85-008946] 17 p2955 N85-28249
Transport in aqueous battery systems
[DE85-007246] 17 p2955 N85-28251
ZIRCALOYS (TRADEMARK)
Continuous measurement of zircaloy corrosion in air with an ultrasonic corrosion monitor
[DE85-003660] 12 p1807 N85-21337
ZIRCONIUM
Effects of cobalt, boron, and zirconium on the microstructure of Udimet 738
[NASA-CR-174762] 01 p0027 N85-10166
High-temperature erosion of plasma-sprayed, yttria-stabilized zirconia in a simulated turbine environment
[NASA-TP-2406] 04 p0476 N85-13045
A soluble linear Schiff-base coordination polymer containing eight-coordinate zirconium(4)
[AD-A151446] 15 p2518 N85-25527
Characterization of the fatigue and slow crack growth behavior of partially stabilized zirconia ceramics
[DE85-005240] 17 p2934 N85-28113
Long range ordered alloys modified by addition of niobium and cerium
[DE85-011661] 20 p3431 N85-31285
Chemical constraints on the evolution of Archean continental crust 21 p3722 N85-33093
Thermal barrier coating system
[NASA-CASE-LEW-14057-1] 24 p4072 N85-35233
ZIRCONIUM ALLOYS
NT ZIRCALOYS (TRADEMARK)
Re-evaluation of phase separation in Ti-Zr-Be metallic glasses
[DE84-015603] 03 p0338 N85-12176
On reversion phenomena in Cu-Zr-Cr alloys
[NASA-TM-77791] 08 p1125 N85-17092
Effects of hydrogen on magnetic properties of amorphous zirconium alloys
[DE85-003303] 11 p1607 N85-20107
Conversions in amorphous zirconium-vanadium alloy
15 p2496 N85-25400
Manufacturing process to reduce large grain growth in zirconium alloys
[DE85-011649] 23 p3915 N85-34267
ZIRCONIUM CARBIDES
Combustion of zirconium carbide
13 p1999 N85-22532
Measurements of distributed combustion
13 p2001 N85-22542

ZIRCONIUM COMPOUNDS
NT ZIRCONIUM CARBIDES
NT ZIRCONIUM HYDRIDES
NT ZIRCONIUM NITRIDES
NT ZIRCONIUM OXIDES
Progress in lead/uranium zircon studies of lower paleozoic rocks of the southern Alexander terrane
04 p0518 N85-13304
Dating Archean zircon by ion microprobe: New light on an old problem 21 p3722 N85-33094
ZIRCONIUM HYDRIDES
Effects of hydrogen on magnetic properties of amorphous zirconium alloys
[DE85-003303] 11 p1607 N85-20107
ZIRCONIUM NITRIDES
Corrosion study on zirconium refractory coatings. 1: Oxidation of zirconium nitride coatings by oxygen
[BLL-RISLEY-TR-5044-(9091.9F)]
07 p0925 N85-15857
Tests on zirconium nitride coatings applied to SW 18 steel using the chemical vapor deposition method
24 p4078 N85-35271

ZIRCONIUM OXIDES
Fundamental studies of structure property relationship in transformation toughened ceramics
[DE84-015344] 01 p0033 N85-10204
Microfluorescence studies of zirconium oxide
[DE84-016116] 03 p0329 N85-12118

Time-temperature dependence of the strength of commercial zirconia ceramics
[AD-A148239] 03 p0336 N85-12173
An investigation of enhanced capability thermal barrier coating systems for diesel engine components
[NASA-CR-174620] 09 p1298 N85-18154
Study of charge transport in the thermoelectret state of some ceramics and glasses
[DE85-001763] 09 p1300 N85-18163
Densification of submicron YSZ (Yttria-Stabilized Zirconia) powders with alumina and borate additives
[AD-A148820] 10 p1452 N85-19150
Laser processing of ceramics
[DE85-001184] 11 p1612 N85-20135
High-temperature, solid oxide electrolyte fuel cell power generation system
[DE85-002876] 11 p1675 N85-20552
Transformation toughened ceramics: A potential material for light diesel engine applications
[AD-A151413] 15 p2518 N85-25525
Rocket thrust chamber thermal barrier coatings
16 p2734 N85-26867
Fracture toughness of MgCr(sub)2O(sub)4-ZrO(sub)2
[DE85-007945] 17 p2917 N85-27982
Indirect brazing of structural ceramics for uncooled diesels
[DE85-005589] 17 p2935 N85-28116
Microstructure-mechanical property relationships in transformation-toughened ceramics
[DE85-008722] 17 p2935 N85-28117
Study of synthesis gas conversion over metal oxides
[DE85-010136] 18 p3072 N85-28989
Process for improving the quality of epitaxial silicon films grown on insulating substrates
[AD-D011730] 22 p3647 N85-33828
ZODIACAL DUST
Zodiacal light: A replica of the interplanetary dust cloud — Helios space probe 16 p2665 N85-27796
ZODIACAL LIGHT
Zodiacal light: A replica of the interplanetary dust cloud — Helios space probe 16 p2665 N85-27796
ZONAL HARMONICS
Diurnal variation harmonics and spatial change in cosmic ray flux 06 p0824 N85-15230
First zonal harmonic component of cosmic ray neutron intensity
[SH-4.3-13] 23 p4032 N85-34997
ZONE MELTING
Stress studies of EFG
[NASA-CR-174078] 05 p0651 N85-14179
German payloads for EURECA 1
[BMFT-FB-W-85-003] 20 p3419 N85-31223
Striation free doped silicon
[AD-A155730] 22 p3647 N85-33827
ZONE REFINING
U ZONE MELTING
ZONES
U REGIONS
ZPR REACTORS
U ZERO POWER REACTORS

VOLUME 23 NUMBERS 1-6

NATIONAL AERONAUTICS AND SPACE ADMINISTRATION U.S.A.

Scientific and Technical Aerospace Reports

Abstracts **January – March 1985**

TABLE OF CONTENTS

STAR Issue	*Page*
1	1
2	133
3	307
4	451
5	591
6	747

VOLUME 23 NUMBERS 7-12

Scientific and Technical Aerospace Reports

Abstracts April – June 1985

TABLE OF CONTENTS

STAR Issue *Page*
7 893
8 1063
9 1263
10 1419
11 1575
12 1769

VOLUME 23 NUMBERS 13-18

Scientific and Technical Aerospace Reports

Abstracts **July – September 1985**

TABLE OF CONTENTS

STAR Issue	*Page*
13	**1965**
14	**2207**
15	**2457**
16	**2691**
17	**2891**
18	**3057**

VOLUME 23 NUMBERS 19-24

Scientific and Technical Aerospace Reports

NATIONAL AERONAUTICS AND SPACE ADMINISTRATION U.S.A.

Abstracts **October – December 1985**

TABLE OF CONTENTS

STAR Issue *Page*
19 3211
20 3387
21 3551
22 3727
23 3893
24 4059

☆U.S. GOVERNMENT PRINTING OFFICE:1986-498-188 42457

FEDERAL DEPOSITORY LIBRARY PROGRAM

The Federal Depository Library Program provides Government publications to designated libraries throughout the United States. The Regional Depository Libraries listed below receive and retain at least one copy of nearly every Federal Government publication, either in printed or microfilm form, for use by the general public. These libraries provide reference services and inter-library loans; however, they are *not* sales outlets. You may wish to ask your local library to contact a Regional Depository to help you locate specific publications, or you may contact the Regional Depository yourself.

ARKANSAS STATE LIBRARY
One Capitol Mall
Little Rock, AR 72201
(501) 371-2326

AUBURN UNIV. AT MONTGOMERY LIBRARY
Documents Department
Montgomery, AL 36193
(205) 279-9110, ext. 253

UNIV. OF ALABAMA LIBRARY
Documents Dept.—Box S
University, AL 35486
(205) 348-7369

DEPT. OF LIBRARY, ARCHIVES AND PUBLIC RECORDS
Third Floor—State Cap.
1700 West Washington
Phoenix, AZ 85007
(602) 255-4121

UNIVERSITY OF ARIZONA LIB.
Government Documents Dept.
Tucson, AZ 85721
(602) 626-5233

CALIFORNIA STATE LIBRARY
Govt. Publications Section
P.O. Box 2037
Sacramento, CA 95809
(916) 322-4572

UNIV. OF COLORADO LIB.
Government Pub. Division
Campus Box 184
Boulder, CO 80309
(303) 492-8834

DENVER PUBLIC LIBRARY
Govt. Pub. Department
1357 Broadway
Denver, CO 80203
(303) 571-2131

CONNECTICUT STATE LIBRARY
Government Documents Unit
231 Capitol Avenue
Hartford, CT 06106
(203) 566-4971

UNIV. OF FLORIDA LIBRARIES
Library West
Documents Department
Gainesville, FL 32611
(904) 392-0367

UNIV. OF GEORGIA LIBRARIES
Government Reference Dept.
Athens, Ga 30602
(404) 542-8951

UNIV. OF HAWAII LIBRARY
Govt. Documents Collection
2550 The Mall
Honolulu, HI 96822
(808) 948-8230

UNIV. OF IDAHO LIBRARY
Documents Section
Moscow, ID 83843
(208) 885-6344

ILLINOIS STATE LIBRARY
Information Services Branch
Centennial Building
Springfield, IL 62706
(217) 782-5185

INDIANA STATE LIBRARY
Serials Documents Section
140 North Senate Avenue
Indianapolis, IN 46204
(317) 232-3686

UNIV. OF IOWA LIBRARIES
Govt. Documents Department
Iowa City, IA 52242
(319) 353-3318

UNIVERSITY OF KANSAS
Doc. Collect—Spencer Lib.
Lawrence, KS 66045
(913) 864-4662

UNIV. OF KENTUCKY LIBRARIES
Govt. Pub. Department
Lexington, KY 40506
(606) 257-3139

LOUISIANA STATE UNIVERSITY
Middleton Library
Govt. Docs. Dept.
Baton Rouge, LA 70803
(504) 388-2570

LOUISIANA TECHNICAL UNIV. LIBRARY
Documents Department
Ruston, LA 71272
(318) 257-4962

UNIVERSITY OF MAINE
Raymond H. Fogler Library
Tri-State Regional Documents Depository
Orono, ME 04469
(207) 581-1680

UNIVERSITY OF MARYLAND
McKeldin Lib.—Doc. Div.
College Park, MD 20742
(301) 454-3034

BOSTON PUBLIC LIBRARY
Government Docs. Dept.
Boston, MA 02117
(617) 536-5400 ext. 226

DETROIT PUBLIC LIBRARY
Sociology Department
5201 Woodward Avenue
Detroit, MI 48202
(313) 833-1409

MICHIGAN STATE LIBRARY
P.O. Box 30007
Lansing, MI 48909
(517) 373-0640

UNIVERSITY OF MINNESOTA
Government Pubs. Division
409 Wilson Library
309 19th Avenue South
Minneapolis, MN 55455
(612) 373-7813

UNIV. OF MISSISSIPPI LIB.
Documents Department
University, MS 38677
(601) 232-5857

UNIV. OF MONTANA
Mansfield Library
Documents Division
Missoula, MT 59812
(406) 243-6700

NEBRASKA LIBRARY COMM.
Federal Documents
1420 P Street
Lincoln, NE 68508
(402) 471-2045
In cooperation with University of Nebraska-Lincoln

UNIVERSITY OF NEVADA LIB.
Govt. Pub. Department
Reno, NV 89557
(702) 784-6579

NEWARK PUBLIC LIBRARY
5 Washington Street
Newark, NJ 07101
(201) 733-7812

UNIVERSITY OF NEW MEXICO
Zimmerman Library
Government Pub. Dept.
Albuquerque, NM 87131
(505) 277-5441

NEW MEXICO STATE LIBRARY
Reference Department
325 Don Gaspar Avenue
Santa Fe, NM 87501
(505) 827-2033, ext. 22

NEW YORK STATE LIBRARY
Empire State Plaza
Albany, NY 12230
(518) 474-5563

UNIVERSITY OF NORTH CAROLINA AT CHAPEL HILL
Wilson Library
BA SS Documents Division
Chapel Hill, NC 27515
(919) 962-1321

UNIVERSITY OF NORTH DAKOTA
Chester Fritz Library
Documents Department
Grand Forks, ND 58202
(701) 777-2617, ext. 27
(In cooperation with North Dakota State Univ. Library)

STATE LIBRARY OF OHIO
Documents Department
65 South Front Street
Columbus, OH 43215
(614) 462-7051

OKLAHOMA DEPT. OF LIB.
Government Documents
200 NE 18th Street
Oklahoma City, OK 73105
(405) 521-2502

OKLAHOMA STATE UNIV. LIB.
Documents Department
Stillwater, OK 74078
(405) 624-6546

PORTLAND STATE UNIV. LIB.
Documents Department
P.O. Box 1151
Portland, OR 97207
(503) 229-3673

STATE LIBRARY OF PENN.
Government Pub. Section
P.O. Box 1601
Harrisburg, PA 17105
(717) 787-3752

TEXAS STATE LIBRARY
Public Services Department
P.O. Box 12927—Cap. Sta.
Austin, TX 78753
(512) 471-2996

TEXAS TECH UNIV. LIBRARY
Govt. Documents Department
Lubbock, TX 79409
(806) 742-2268

UTAH STATE UNIVERSITY
Merrill Library, U.M.C. 30
Logan, UT 84322
(801) 750-2682

UNIVERSITY OF VIRGINIA
Alderman Lib.—Public Doc.
Charlottesville, VA 22901
(804) 924-3133

WASHINGTON STATE LIBRARY
Documents Section
Olympia, WA 98504
(206) 753-4027

WEST VIRGINIA UNIV. LIB.
Documents Department
Morgantown, WV 26506
(304) 293-3640

MILWAUKEE PUBLIC LIBRARY
814 West Wisconsin Avenue
Milwaukee, WI 53233
(414) 278-3000

ST. HIST LIB. OF WISCONSIN
Government Pub. Section
816 State Street
Madison, WI 53706
(608) 262-4347

WYOMING STATE LIBRARY
Supreme Ct. & Library Bld.
Cheyenne, WY 82002
(307) 777-6344

National Aeronautics and
Space Administration
Code NIT-4
Washington, D.C.
20546
Official Business
Penalty for Private Use, $300

SPECIAL FOURTH-CLASS RATE
POSTAGE & FEES PAID
NASA
WASHINGTON, D.C.
PERMIT No. G 27

NASA

POSTMASTER: If Undeliverable (Section 158
Postal Manual) Do Not Return